SELDIN AND GIEBISCH'S THE KIDNEY

Physiology and Pathophysiology

FIFTH EDITION

Edited by

ROBERT J. ALPERN
MICHAEL J. CAPLAN
ORSON W. MOE

Volume 1

SELDIN AND GIEBISCH'S THE KIDNEY

PHYSIOLOGY AND PATHOPHYSIOLOGY

FIFTH EDITION

ELSEVIER science & technology books

Companion Web Site:

http://booksite.elsevier.com/9780123814623

Seldin and Giebisch's The Kidney: Physiology and Pathophysiology, fifth edition

Robert J. Alpern, Orson W. Moe and Michael Caplan, Editors

Resources for Professors:

- All figures from the book available as both Power Point slides and .jpeg files

TOOLS FOR ALL YOUR TEACHING NEEDS
textbooks.elsevier.com

ACADEMIC PRESS

To adopt this book for course use, visit http://textbooks.elsevier.com.

SELDIN AND GIEBISCH'S THE KIDNEY

PHYSIOLOGY AND PATHOPHYSIOLOGY

FIFTH EDITION

VOLUME 1

ROBERT J. ALPERN
Yale University School of Medicine
New Haven, CT, USA

ORSON W. MOE
The University of Texas Southwestern Medical Center at Dallas
Dallas, TX, USA

MICHAEL CAPLAN
Yale University School of Medicine, New Haven, CT, USA

ELSEVIER

AMSTERDAM • BOSTON • HEIDELBERG • LONDON
NEW YORK • OXFORD • PARIS • SAN DIEGO
SAN FRANCISCO • SINGAPORE • SYDNEY • TOKYO

Academic Press is an imprint of Elsevier

Academic Press is an imprint of Elsevier

32 Jamestown Road, London NW1 7BY, UK
225 Wyman Street, Waltham, MA 02451, USA
525 B Street, Suite 1800, San Diego, CA 92101-4495, USA

Fifth edition 2013

Copyright © 2013 Elsevier Inc. All rights reserved

No part of this publication may be reproduced, stored in a retrieval system or transmitted in any form or by any means electronic, mechanical, photocopying, recording or otherwise without the prior written permission of the publisher

Permissions may be sought directly from Elsevier's Science & Technology Rights Department in Oxford, UK: phone (+44) (0) 1865 843830; fax (+44) (0) 1865 853333; email: permissions@elsevier.com. Alternatively, visit the Science and Technology Books website at www.elsevierdirect.com/rights for further information

Notice
No responsibility is assumed by the publisher for any injury and/or damage to persons or property as a matter of products liability, negligence or otherwise, or from any use or operation of any methods, products, instructions or ideas contained in the material herein. Because of rapid advances in the medical sciences, in particular, independent verification of diagnoses and drug dosages should be made

Medicine is an ever-changing field. Standard safety precautions must be followed, but as new research and clinical experience broaden our knowledge, changes in treatment and drug therapy may become necessary or appropriate. Readers are advised to check the most current product information provided by the manufacturer of each drug to be administered to verify the recommended dose, the method and duration of administrations, and contraindications. It is the responsibility of the treating physician, relying on experience and knowledge of the patient, to determine dosages and the best treatment for each individual patient. Neither the publisher nor the authors assume any liability for any injury and/or damage to persons or property arising from this publication

British Library Cataloguing-in-Publication Data
A catalogue record for this book is available from the British Library

Library of Congress Cataloging-in-Publication Data
A catalog record for this book is available from the Library of Congress

ISBN : 978-0-12-381462-3 (set)
ISBN : 978-0-12-397207-1 (volume 1)
ISBN : 978-0-12-397208-8 (volume 2)

For information on all Academic Press publications
visit our website at elsevierdirect.com

Typeset by MPS Ltd.
www.adi-mps.com

Printed and bound in United States of America

12 13 14 15 16 10 9 8 7 6 5 4 3 2 1

Dedication

This book is dedicated to Steven C. Hebert. Steve was at his heart a kidney physiologist, applying cutting edge technologies to address the most fundamental concepts of kidney function and disease. He was an extraordinary scientist, clinician, mentor, leader and friend.

This page intentionally left blank

CONTENTS

VOLUME 1

Foreword xiii
Preface xv
List of Contributors xvii

I
EPITHELIAL AND NONEPITHELIAL TRANSPORT AND REGULATION

1. Epithelial Cell Structure and Polarity 3
KARL S. MATLIN AND MICHAEL J. CAPLAN

2. Mechanisms of Ion Transport across Cell Membranes 45
LUIS REUSS AND GUILLERMO A. ALTENBERG

3. Renal Ion-Translocating ATPases 67
DOMINIQUE ELADARI, UDO HASLER AND ERIC FÉRAILLE

4. Mechanisms of Water Transport Across Cell Membranes and Epithelia 95
GUILLERMO A. ALTENBERG AND LUIS REUSS

5. Cell Volume Control 121
FLORIAN LANG

6. Solute Transport, Energy Consumption, and Production in the Kidney 143
TAKASHI SEKINE AND HITOSHI ENDOU

7. Electrophysiological Analysis of Transepithelial Transport 177
HENRY SACKIN AND LAWRENCE G. PALMER

8. Renal Ion Channels, Electrophysiology of Transport, and Channelopathies 217
JAMES D. STOCKAND

9. Microvascular Permeability and the Exchange of Water and Solutes Across Microvascular Walls 263
C. CHARLES MICHEL

10. External Balance of Electrolytes and Acids and Alkali 291
MAN S. OH

11. Renal Cilia Structure, Function, and Physiology 319
JAY N. PIECZYNSKI AND BRADLEY K. YODER

12. Intercellular Junctions 347
ALAN S.L. YU, FIONA HANNER AND JÁNOS PETI-PETERDI

13. Principles of Cell Signaling 369
LLOYD CANTLEY

14. Scaffolding Proteins in Transport Regulation 405
PAUL A. WELLING

15. The Renin–Angiotensin System 427
THU H. LE, STEVEN D. CROWLEY, SUSAN B. GURLEY AND THOMAS M. COFFMAN

16. Neural Control of Renal Function 451
EDWARD J. JOHNS AND ULLA C. KOPP

17. Eicosanoids and Renal Function 487
MATTHEW D. BREYER, RAYMOND C. HARRIS AND RICHARD M. BREYER

18. Extracellular Nucleotides and Renal Function 511
DAVID G. SHIRLEY, MATTHEW A. BAILEY, SCOTT S.P. WILDMAN, FREDERICK W.K. TAM AND ROBERT J. UNWIN

19. Paracrine Regulation of Renal Function by Dopamine 539
PEDRO A. JOSE, ROBIN A. FELDER AND GILBERT M. EISNER

II

STRUCTURAL AND FUNCTIONAL ORGANIZATION OF THE KIDNEY

20. Structural Organization of the Mammalian Kidney 595
WILHELM KRIZ AND BRIGITTE KAISSLING

21. Biophysical Basis of Glomerular Filtration 693
SCOTT C. THOMSON AND ROLAND C. BLANTZ

22. Glomerular Cell Biology 721
YOSHIRO MAEZAWA, DAVIDE CINA AND SUSAN E. QUAGGIN

23. Function of the Juxtaglomerular Apparatus: Control of Glomerular Hemodynamics and Renin Secretion 757
JÜRGEN B. SCHNERMANN AND HAYO CASTROP

24. Renal Cortical and Medullary Microcirculations: Structure and Function 803
THOMAS L. PALLONE AND CHUNHUA CAO

25. Molecular and Cellular Mechanisms of Kidney Development 859
KEVIN T. BUSH, HIROYUKI SAKURAI AND SANJAY K. NIGAM

26. Molecular and Cellular Mechanisms of Glomerular Capillary Development 891
JEFFREY H. MINER AND DALE R. ABRAHAMSON

27. Postnatal Renal Development 911
MICHEL BAUM, JYOTHSNA GATTINENI AND LISA M. SATLIN

28. Renal Hyperplasia and Hypertrophy 933
PAUL T. BRINKKOETTER, SIAN V. GRIFFIN AND STUART J. SHANKLAND

29. Stem Cells and Generation of New Cells in the Adult Kidney 959
JUAN A. OLIVER AND QAIS AL-AWQATI

III

FLUID AND ELECTROLYTE REGULATION AND DYSREGULATION

30. Epithelial Na^+ Channels 983
SHAOHU SHENG, KENNETH R. HALLOWS AND THOMAS R. KLEYMAN

31. Anion Channels 1019
OWEN M. WOODWARD AND WILLIAM B. GUGGINO

32. Physiology and Pathophysiology of the NaCl Co-Transporters in the Kidney 1047
GERARDO GAMBA

33. Sodium and Chloride Transport: Proximal Nephron 1081
ALAN M. WEINSTEIN

34. Sodium Chloride Transport in the Loop of Henle, Distal Convoluted Tubule, and Collecting Duct 1143
GERARDO GAMBA, WENHUI WANG AND LAURENT SCHILD

35. Mineralocorticoid Action in the Aldosterone Sensitive Distal Nephron 1181
OLIVIER STAUB AND JOHANNES LOFFING

36. Inherited Disorders of Renal Salt Homeostasis: Insights from Molecular Genetics Studies 1213
UTE I. SCHOLL AND RICHARD P. LIFTON

37. Natriuretic Hormones 1241
DAVID L. VESELY

38. Pathophysiology of Sodium Retention and Wastage 1283
BIFF F. PALMER, ROBERT J. ALPERN AND DONALD W. SELDIN

39. Physiology and Pathophysiology of Hypertension 1319
JOHN E. HALL, JOEY P. GRANGER AND MICHAEL E. HALL

40. Physiology and Pathophysiology of Diuretic Action 1353
DAVID H. ELLISON

41. Aquaporin Water Channels in Mammalian Kidney 1405
SØREN NIELSEN, TAE-HWAN KWON, HENRIK DIMKE, MARTIN SKOTT AND JØRGEN FRØKLÆR

42. Thirst and Vasopressin 1441
GARY L. ROBERTSON

43. The Urine Concentrating Mechanism and Urea Transporters 1463
JEFF M. SANDS AND HAROLD E. LAYTON

44. Hyponatremia 1511
RICHARD H. STERNS, STEPHEN M. SILVER AND J. KEVIN HIX

45. Hypernatremic States 1541
CHRISTOPHER J. RIVARD, WEI WANG AND LAURENCE CHAN

46. Polyuria and Diabetes Insipidus 1571
DANIEL G. BICHET

47. The Molecular Biology of Renal K^+ Channels 1601
WENHUI WANG AND CHOU-LONG HUANG

48. Extrarenal Potassium Metabolism 1629
VAIBHAV SAHNI, ALEKSANDRA GMURCZYK AND ROBERT M. ROSA

49. Regulation of K^+ Excretion 1659
GERHARD MALNIC, GERHARD GIEBISCH, SHIGEAKI MUTO, WENHUI WANG, MATTHEW A. BAILEY AND LISA M. SATLIN

50. Physiopathology of Potassium Deficiency 1717
FRANCESCO TREPICCIONE, MIRIAM ZACCHIA AND GIOVAMBATTISTA CAPASSO

VOLUME 2

Foreword xiii
Preface xv
List of Contributors xvii

51. Clinical Disorders of Hyperkalemia 1741
KAMEL S. KAMEL, SHIH-HUA LIN, SUNG-SEN YANG AND MITCHELL HALPERIN

52. Control of Intracellular pH 1773
MARK O. BEVENSEE AND WALTER F. BORON

53. SLC4 Sodium-Driven Bicarbonate Transporters 1837
IRA KURTZ

54. The SLC4 Anion Exchanger Gene Family 1861
ANDREW K. STEWART AND SETH L. ALPER

55. Cellular Mechanisms of Renal Tubular Acidification 1917
L. LEE HAMM, ROBERT J. ALPERN AND PATRICIA A. PREISIG

56. Chemoreceptors, Breathing and pH 1979
EUGENE NATTIE

57. Renal Ammonium Ion Production and Excretion 1995
NORMAN P. CURTHOYS

58. Clinical Syndromes of Metabolic Alkalosis 2021
ORSON W. MOE, ROBERT J. ALPERN AND DONALD W. SELDIN

59. Clinical Syndromes of Metabolic Acidosis 2049
RETO KRAPF, DONALD W. SELDIN AND ROBERT J. ALPERN

60. Respiratory Acid–Base Disorders 2113
NICOLAOS E. MADIAS AND HORACIO J. ADROGUÉ

61. Mechanisms and Disorders of Magnesium Metabolism 2141
KARL P. SCHLINGMANN, GARY A. QUAMME AND MARTIN KONRAD

62. Calcium Channels 2167
JOOST G.J. HOENDEROP AND RENÉ J.M. BINDELS

63. The Calcium-Sensing Receptor 2187
EDWARD M. BROWN, STEVEN C. HEBERT, DANIELA RICCARDI AND JOHN P. GEIBEL

64. Renal Calcium Metabolism 2225
JOSÉ F. BERNARDO AND PETER A. FRIEDMAN

65. The Hormonal Regulation of Calcium Metabolism 2249
PETER J. TEBBEN AND RAJIV KUMAR

66. Disorders of Calcium Metabolism 2273
CRISTINA DUMITRU AND JOHN WYSOLMERSKI

67. Pathogenesis and Treatment of Nephrolithiasis 2311
FREDRIC L. COE, ANDREW EVAN AND ELAINE WORCESTER

68. Proximal Tubular Handling of Phosphate 2351
HEINI MURER, IAN C. FORSTER, NATI HERNANDO AND JÜRG BIBER

69. Clinical Disturbances of Phosphate Homeostasis 2369
THERESA J. BERNDT AND RAJIV KUMAR

70. Glucose Reabsorption in The Kidney 2393
CHARLES S. HUMMEL AND ERNEST M. WRIGHT

71. Kidney Transport of Amino Acids and Oligopeptides, and Aminoacidurias 2405
SIMONE M.R. CAMARGO, VICTORIA MAKRIDES, ROBERT KLETA AND FRANÇOIS VERREY

72. Organic Anion and Cation Transporters in Renal Elimination of Drugs 2425
GERHARD BURCKHARDT AND HERMANN KOEPSELL

73. Renal Filtration, Transport, and Metabolism of Albumin and Albuminuria 2457
ERIK ILSØ CHRISTENSEN, RIKKE NIELSEN AND HENRIK BIRN

IV
PATHOPHYSIOLOGY OF RENAL DISEASE

74. Physiologic Principles in the Clinical Evaluation of Electrolyte, Water, and Acid–Base Disorders 2477
DANIEL BATLLE, SHELDON CHEN AND SYED K. HAQUE

75. Biomarkers for Assessment of Renal Function During Acute Kidney Injury 2513
PRASAD DEVARAJAN

76. Pathophysiology of Acute Kidney Injury 2527
BRUCE A. MOLITORIS AND ASIF SHARFUDDIN

77. Ischemic Renal Disease 2577
CHRISTOPHER J. COOPER, LANCE D. DWORKIN AND WILLIAM L. HENRICH

78. Pathophysiology and Pathogenesis of Diabetic Nephropathy 2605
SHELDON CHEN, CHARBEL KHOURY AND FUAD N. ZIYADEH

79. Renal Failure in Cirrhosis 2633
PERE GINÈS, ANDRÉS CÁRDENAS AND ROBERT W. SCHRIER

80. Autosomal Dominant Polycystic Kidney Disease 2645
STEFAN SOMLO, VICENTE E. TORRES AND MICHAEL J. CAPLAN

81. Renal Physiology and Disease in Pregnancy 2689
MARSHALL D. LINDHEIMER, KIRK P. CONRAD AND S. ANANTH KARUMANCHI

82. Immune and Inflammatory Glomerular Diseases 2763
ANUP MANOHARON, JEFFREY R. SCHELLING, MATTHEW DIAMOND, MOONJA CHUNG-PARK, MICHAEL MADAIO AND JOHN R. SEDOR

83. Immunologic Mechanisms of Vasculitis 2817
JONATHON W. HOMEISTER, J. CHARLES JENNETTE AND RONALD J. FALK

84. Genetic Abnormalities in Glomerular Function 2847
YOAV SEGAL AND CLIFFORD E. KASHTAN

85. Cellular Mechanisms of Drug Nephrotoxicity 2889
ROBERT JAMES WALKER AND ZOLTÁN HUBA ENDRE

86. Role of Glomerular Mechanical Stress in the Pathogenesis of Chronic Kidney Disease 2933
CLARICE KAZUE FUJIHARA AND ROBERTO ZATZ

87. Role of Proteinuria in the Progression of Renal Disease 2961
MAURO ABBATE, DANIELA MACCONI, GIUSEPPE REMUZZI AND CARLA ZOJA

88. The Inflammatory Response to Ischemic Acute Renal Injury 2985
CHRISTOPHER Y. LU

89. Catalytic (Labile) Iron in Kidney Disease 3007
MOHAN RAJAPURKAR, RADHAKRISHNA BALIGA AND SUDHIR V. SHAH

90. Chronic Kidney Disease: Pathophysiology and the Influence of Dietary Protein 3021
BIRUH T. WORKENEH AND WILLIAM E. MITCH

91. Management of Calcium and Bone Disease in Renal Patients 3073
L. DARRYL QUARLES

92. Hematopoiesis and the Kidney 3087
ARMIN KURTZ, ROLAND H. WENGER AND KAI-UWE ECKARDT

93. Individualizing the Dialysate to Address Electrolyte Disturbances in the Dialysis Patient 3125
BIFF F. PALMER

94. Homeostasis of Solute and Water by the Transplanted Kidney 3151
J. HAROLD HELDERMAN, HEIDI SCHAEFER, ANTHONY J. LANGONE AND SIMIN GORAL

95. Renal Disposition of Drugs and Translation to Dosing Strategies 3185
PÄR MATSSON, KATHLEEN M. GIACOMINI AND D. CRAIG BRATER

Index 3215

This page intentionally left blank

Foreword

The focus of these volumes ever since the publication of the first edition in 1985 has been on renal physiology, conceived broadly as the analysis of those processes by which the kidney maintains the volume and composition of the body in the face of varied intake, physiologic alterations and pathologic disturbances. The text began with a detailed exploration of the basic mechanisms and their regulation that underlie the exchanges of water and electrolytes across cell membranes of the body. The mechanisms used by the kidney to make appropriate renal homeostatic adjustments were next presented.

In the early texts the renal response was attributed to the whole organ rather than to discrete molecular processes. It was the application of the methods and theories of the generalizing sciences, physics and chemistry, to biologic systems that, in subsequent additions, facilitated a reduction of the explanatory system to the more basic level of molecular biology, thereby providing a more comprehensive understanding of the basic processes that permit the physiologic adjustments.

In this 5th edition, such new and powerful disciplines as genetics and cell biology have been deployed to deepen and widen further the explanatory framework. Not only have previous chapters been extensively updated, but new chapters have been added to incorporate additional disciplines. Individual chapters, for example, now provide detailed treatment of the significance of cilia; the role of stem cells is now given special consideration. Finally, there has been a significant expansion of the section of pathophysiology, incorporating the newer findings of cell biology and genetics.

In a sense, this new edition represents a significant advancement in the march of reduction to a more fundamental level of understanding of the normal and deranged function of the kidney.

Donald W. Seldin
Gerhard H Giebisch

This page intentionally left blank

Preface

As described in its preface, the first edition of *The Kidney*: *Physiology and Pathophysiology*, published in 1985, focused on renal physiology, "conceived broadly as the study of those processes by which the kidney maintains the volume and composition of the body in the face of physiologic demands and pathologic disturbances." As noted in the fourth edition, science has since then become more reductionist, an evolution that has been reflected in the content of subsequent editions. Dissection of physiologic phenomena at the level of organs and cells has been enriched by descriptions of the roles of individual molecules. While this trend in science has continued, it has been complemented by a renewed focus on integrating these molecular functions to define their roles in cellular and organ physiology, as well as their role in body homeostasis and disease. A complete understanding of physiologic and pathophysiologic processes must include knowledge of individual molecules, as well as their integration into homeostatic systems that function to maintain body composition. A thorough understanding of physiologic mechanisms endows us with a greater understanding of pathophysiology and disease. Reciprocally, an understanding of disease states furnishes us with valuable information about normal physiology. The present edition continues to focus on describing the present state of knowledge of the molecules and the systems that contribute to normal physiologic function of the kidney, and the homeostatic mechanisms subserved by the kidney.

The present edition also concentrates on how these mechanisms malfunction, resulting in the diseased state. Again we will address the pathophysiology of disease states from the molecular to the system level. One of the appealing features of nephrology is the ability to utilize our understanding of normal physiology to elucidate principles of pathophysiology, and secondarily develop rational approaches to the diagnosis, treatment, and prevention of disease. Thus, the clinician addressing a patient with a fluid and electrolyte disorder need not memorize a list of possible causes or algorithms, but can logically deduce a solution through a thorough understanding of kidney function. As science continues to evolve, our understanding of the pathophysiologic basis of disease can now be applied to a much broader set of ailments. We continue, therefore, to broaden the scope of this book so as to place greater emphasis on mechanisms of disease.

The first section of the textbook begins with general principles of epithelial and non-epithelial transport and regulation. This extensive section of the book continues a tradition established in the first edition, but extends it to include a more extensive discussion of transport regulation.

The second section of the book describes the organization of the kidney with an increased emphasis on the glomerulus, as this field continues to evolve. There follows an in-depth review of renal growth and development, including a discussion of the role of stem cells in the kidney.

This is then followed by Section Three, describing mechanisms of fluid and electrolyte regulation and dysregulation. In no other book can one find this subject addressed with the depth and thoroughness found in this textbook. The Fifth Edition includes a more in-depth discussion of recently described families of transporters, integrating this information to describe their role in physiologic and pathophysiologic processes.

Section Four, the pathophysiology of renal disease, has been extended as our knowledge of renal dysfunctions and their contribution to renal ailments has expanded. Many chapters deal with common everyday clinical issues, but are presented in the context of pathophysiologic mechanisms. A series of chapters focus on mechanisms of progression of renal disease, as the importance of interrupting or forestalling this progression has assumed great importance in clinical nephrology. A thorough understanding of the roles of glomerular pressure, proteinuria, inflammation, and oxidants will help researchers and clinicians prevent renal failure, decreasing the need for dialysis and transplant.

The evolution of our understanding of kidney function and dysfunction derives from sequential discoveries made by a series of investigators, each benefiting from the accomplishments of their predecessors. The same can be said for this textbook. Originally conceived by two of the greatest renal physiologists of the twentieth century, Donald Seldin and Gerhard

Giebisch, it was passed on to Steve Hebert and one of the present editors. As the present editors, it is our hope to continue the book's commitment to science, and its role in our understanding and practice of nephrology, and in so doing to honor the previous editors for all that they have contributed to the book, to nephrology, to epithelial physiology, and to science in general.

List of Contributors

Dale R. Abrahamson, PhD Department of Anatomy and Cell Biology, University of Kansas Medical Center, Kansas City, KS, USA

Qais Al-Awqati, MB, ChB Departments of Medicine and Physiology, Columbia University, New York, NY, USA

Robert J. Alpern, MD Office of the Dean Yale, University School of Medicine, New Haven, CT, USA

Guillermo A. Altenberg, MD, PhD Department of Cell Physiology and Molecular Biophysics, and Center for Membrane Protein Research, Texas Tech University Health Sciences Center, Lubbock, Texas, TX, USA

Matthew A. Bailey, PhD British Heart Foundation Centre for Cardiovascular Science, University of Edinburgh, UK

Michel Baum, MD Departments of Pediatrics and Internal Medicine, University of Texas Southwestern Medical Center, Dallas, TX, USA

Daniel G. Bichet, MD, MSc Hôpital du Sacré-Coeur de Montréal, Departments of Medicine and Physiology, University of Montreal, Montréal, Québec, Canada

Roland C. Blantz, MD University of California and VA San Diego Healthcare System, San Diego, CA, USA

Matthew D. Breyer, PhD Biotechnology Discovery Research Eli Lilly and Company Indianapolis, IN and Division of Nephrology, Department of Medicine, Vanderbilt University, Nashville, TN

Richard M. Breyer Division of Nephrology, Department of Medicine, Vanderbilt University, Nashville, TN, USA

Paul T. Brinkkoetter University Hospital Cologne, Cologne, Germany

Kevin T. Bush, PhD Department of Pediatrics University of California San Diego, La Jolla, CA, USA

Lloyd Cantley, MD Section of Nephrology, Department of Internal Medicine, Yale University School of Medicine, New Haven, CT, USA

Chunhua Cao, MD, PhD Division of Nephrology, Department of Medicine, University of Maryland at Baltimore, Baltimore, MD, USA

Giovambattista Capasso, MD Chair of Nephrology, Department of Internal Medicine, Faculty of Medicine, Second University of Naples, Italy

Hayo Castrop, PhD Institute of Physiology, University of Regensburg, Germany

Laurence Chan, MD, PhD, FRCP University of Colorado Denver, Aurora, Colorado, USA

Davide Cina Samuel Lunenfeld Research Institute, Mount Sinai Hospital and Institute of Medical Science, Toronto, Ontario, Canada

Thomas M. Coffman, MD Division of Nephrology, Department of Medicine, Duke University and Durham VA Medical Centers, Durham, North Carolina, USA, Cardiovascular and Metabolic Disorders Research Program, Duke-NUS, Singapore

Steven D. Crowley, MD Division of Nephrology, Department of Medicine, Duke University and Durham VA Medical Centers, Durham, North Carolina, USA

Henrik Dimke, MSc Department of Biomedicine, University of Aarhus, Aarhus, Denmark; The Samuel Lunenfeld Research Institute, Mt. Sinai Hospital, Toronto, Ontario, Canada

Gilbert M. Eisner, Mb Georgetown University Medical Center, USA

Dominique Eladari, MD, PhD INSERM U872, Centre de Recherche des Cordeliers, Paris, France

David H. Ellison, MD Oregon Health & Science University & VA Medical Center, Portland, OR, USA

Hitoshi Endou, MD, PhD Department of Pharmacology and Toxicology, Kyorin University School of Medicine, Tokyo, Japan

Robin A. Felder, PhD University of Virginia Health Sciences Center, USA

Eric Féraille, MD, PhD Department of Cell Physiology and Metabolism and Service of Nephrology, University Medical Center, Geneva, Switzerland

Jørgen Frøkiær, MD, DMSc Water and Salt Research Center, Department of Clinical Physiology, Aarhus University Hospital-Skejby, Aarhus N, Denmark

Gerardo Gamba, MD, PhD Molecular Physiology Unit, Department of Nephrology and Mineral Metabolism, Instituto Nacional de Ciencias Médicas y Nutrición Salvador Zubirán, and Instituto de Investigaciones Biomédicas, Universidad Nacional Autónoma de México, Mexico City, Mexico

Jyothsna Gattineni, MD Department of Pediatrics, University of Texas Southwestern Medical Center, Dallas, TX, USA

Gerhard Giebisch, MD Dept. of Cellular & Molecular Physiology, Yale University School of Medicine, New Haven, CT, USA

Aleksandra Gmurczyk, MD The Feinberg School of Medicine, Northwestern University, Chicago, IL, USA

Joey P. Granger, PhD Department of Physiology and Biophysics and Department of Medicine, University of Mississippi Medical Center, MS, USA

Sian V. Griffin, MD University Hospital Wales, Health Park, Cardiff, Wales

William B. Guggino, PhD Department of Physiology, The Johns Hopkins University School of Medicine, Baltimore, MD, USA

Susan B. Gurley, MD, PhD Division of Nephrology, Department of Medicine, Duke University and Durham VA Medical Centers, Durham, North Carolina, USA

John E. Hall, PhD Department of Physiology and Biophysics and Department of Medicine, University of Mississippi Medical Center, MS, USA

Michael E. Hall, MD Department of Physiology and Biophysics and Department of Medicine, University of Mississippi Medical Center, MS, USA

Kenneth R. Hallows, MD, PhD Renal-Electrolyte Division, Department of Medicine and Department of Cell Biology and Physiology, University of Pittsburgh, Pittsburgh, PA, USA

Fiona Hanner Department of Physiology and Biophysics and Zilkha Neurogenetic Institute, University of Southern California Keck School of Medicine, Los Angeles, CA, USA

Raymond C. Harris, MD Division of Nephrology, Department of Medicine, Vanderbilt University, Nashville, TN, USA

Udo Hasler Department of Cell Physiology and Metabolism and Service of Nephrology, University Medical Center, Geneva, Switzerland

J. Kevin Hix, MD University of Rochester School of Medicine and Dentistry, Rochester, New York, USA

Chou-Long Huang, MD, PhD University of Texas, Southwestern Medical Center, Dallas, TX, USA

Edward J. Johns, BSc, PhD, DSc Department of Physiology, University College Cork, Cork, Republic of Ireland

Pedro A. Jose, MD, PhD Division of Nephrology, Department of Medicine, University of Maryland School of Medicine, USA

Brigitte Kaissling Institute for Anatomy, University of Zürich, Switzerland

Thomas R. Kleyman, MD Renal-Electrolyte Division, Department of Medicine and Department of Cell Biology and Physiology, University of Pittsburgh, Pittsburgh, PA, USA

Ulla C. Kopp, PhD Departments of Internal Medicine & Pharmacology, University of Iowa Carver College of Medicine, Iowa City, IA, USA

Wilhelm Kriz Department of Anatomy and Developmental Biology, Medical Faculty Mannheim, University of Heidelberg, Mannheim, Germany

Tae-Hwan Kwon Department of Biochemistry and Cell Biology, School of Medicine, Kyungpook National University, Taegu, Korea

Florian Lang Department of Physiology, University of Tübingen, Tübingen, Germany

Harold E. Layton Department of Mathematics, Duke University, Durham, NC, USA

Thu H. Le, MD Division of Nephrology, Department of Medicine, University of Virginia, Charlottesville, VA, USA

Richard P. Lifton Departments of Genetics and Internal Medicine, Howard Hughes Medical Institute, Yale University School of Medicine, New Haven, CT, USA

Johannes Loffing Institute of Anatomy, University of Zurich, Zurich, Switzerland

Yoshiro Maezawa Samuel Lunenfeld Research Institute, Mount Sinai Hospital, Toronto, Ontario, Canada

Gerhard Malnic Universidade de Sao Paulo, Instituto de Ciencias Biomedicas, Departamento de Fisiologie e Biofisica, Sao Paulo, Brazil

Karl S. Matlin, PhD Laboratory of Epithelial Pathobiology, Department of Surgery, University of Chicago, IL, USA

C. Charles Michel Department of Bioengineering, Imperial College, London, UK

Jeffrey H. Miner, PhD Department of Medicine, Renal Division, Washington University School of Medicine, St. Louis, MO, USA

Shigeaki Muto, MD, PhD Universidade de Sao Paulo, Instituto de Ciencias Biomedicas, Departamento de Fisiologie e Biofisica, Sao Paulo, Brazil

Søren Nielsen, MD, PhD Water and Salt Research Center, Department of Biomedicine, University of Aarhus, Aarhus, Denmark

Sanjay K. Nigam, MD Departments of Pediatrics, Cellular and Molecular Medicine, Medicine (Division of Nephrology and Hypertension), and Bioengineering, University of California San Diego, La Jolla, CA, USA

Man S. Oh, MD State University of New York, Downstate Medical Center, Brooklyn, NY, USA

Juan A. Oliver Department of Medicine, Columbia University, New York, NY, USA

Thomas L. Pallone, MD Division of Nephrology, Department of Medicine, University of Maryland at Baltimore, Baltimore, MD, USA

Biff F. Palmer, MD Professor of Internal Medicine, Department of Internal Medicine, Division of Nephrology, University of Texas Southwestern Medical Center, Dallas, TX, USA

Lawrence G. Palmer, PhD Department of Physiology & Biophysics, Weill Medical College of Cornell University, New York City NY, USA

János Peti-Peterdi, MD, PhD Department of Physiology and Biophysics and Zilkha Neurogenetic Institute, University of Southern California Keck School of Medicine, Los Angeles, CA, USA

Jay N. Pieczynski Department of Cell Biology, University of Alabama at Birmingham, Birmingham, AL, USA

Susan E. Quaggin Samuel Lunenfeld Research Institute, Mount Sinai Hospital; Institute of Medical Science; Division of Nephrology, St. Michael's Hospital University of Toronto, Toronto, Ontario, Canada

Luis Reuss, MD Department of Cell Physiology and Molecular Biophysics, and Center for Membrane Protein Research, Texas Tech University Health Sciences Center, Lubbock, Texas, TX, USA

Christopher J. Rivard, PhD University of Colorado Denver, Aurora, Colorado, USA

Gary L. Robertson, MD The Feinberg Medical School of Medicine, Northwestern University, Chicago, IL, USA

Robert M. Rosa, MD The Feinberg School of Medicine, Northwestern University, Chicago, IL, USA

Henry Sackin, PhD Department of Physiology & Biophysics, Rosalind Franklin University/The Chicago Medical School, North Chicago, IL, USA

Vaibhav Sahni, MD The Feinberg School of Medicine, Northwestern University, Chicago, IL, USA

Hiroyuki Sakurai, MD Department of Pharmacology and Toxicology, Kyorin University School of Medicine, Mitaka, Tokyo, Japan

Jeff M. Sands, MD Renal Division, Department of Medicine, Emory University School of Medicine, Atlanta, GA, USA

Lisa M. Satlin, MD Departments of Pediatrics and Medicine, Mount Sinai School of Medicine, New York, NY, USA

Laurent Schild Département de Pharmacologie et de Toxicologie, Université de Lausanne, Lausanne, Switzerland

Jürgen B. Schnermann, MD National Institute of Diabetes, and Digestive and Kidney Diseases, National Institutes of Health, Bethesda, MD, USA

Ute I. Scholl, MD Departments of Genetics and Internal Medicine, Howard Hughes Medical Institute, Yale University School of Medicine, New Haven, CT, USA

Takashi Sekine, MD Department of Pediatrics, Toho University School of Medicine, Ohashi Hospital, Tokyo, Japan

Donald W. Seldin, MD Department of Internal Medicine, University of Texas Southwestern Medical Center, Dallas, TX, USA

Stuart J. Shankland, MD University of Washington, Seattle, Washington, USA

Shaohu Sheng, MD Renal-Electrolyte Division, Department of Medicine, University of Pittsburgh, Pittsburgh, PA, USA

David G. Shirley, PhD UCL Centre for Nephrology, University College London Medical School, UK

Stephen M. Silver, MD Clinical Professor of Medicine, University of Rochester School of Medicine and Dentistry, Rochester, New York, USA

Martin Skott Department of Biomedicine, University of Aarhus, Aarhus, Denmark

Olivier Staub Department of Pharmacology & Toxicology, University of Lausanne, Lausanne, Switzerland

Richard H. Sterns, MD Rochester General Hospital and University of Rochester School of Medicine and Dentistry, Rochester, New York, USA

James D. Stockand, PhD Department of Physiology, University of Texas Health Science Center, San Antonio, TX, USA

Frederick W.K. Tam, PhD, FRCP Kidney and Transplant Institute, Imperial College School of Medicine, UK

Scott C. Thomson, MD University of California and VA San Diego Healthcare System, San Diego, CA, USA

Francesco Trepiccione Chair of Nephrology, Department of Internal Medicine, Faculty of Medicine, Second University of Naples, Italy

Robert J. Unwin, PhD, FRCP UCL Centre for Nephrology, University College London Medical School, UK

David L. Vesely, MD, PhD University of South Florida Cardiac Hormone Center, and James A. Haley Veterans Medical Center, Tampa, FL, USA

Wei Wang, MD University of Colorado Denver, Aurora, Colorado, USA

Wenhui Wang, MD Department of Pharmacology, New York Medical College, Valhalla, NY, USA

Alan M. Weinstein, MD Department of Physiology and Biophysics, Weill Medical College of Cornell University, New York, NY, USA

Paul A. Welling, MD Department of Physiology, University of Maryland School of Medicine, Baltimore, MD, USA

Scott S.P. Wildman, PhD Medway School of Pharmacy, The Universities of Kent and Greenwich at Medway, UK

Owen M. Woodward Department of Physiology, The Johns Hopkins University School of Medicine, Baltimore, MD, USA

Bradley K. Yoder, PhD Department of Cell Biology, University of Alabama at Birmingham, Birmingham, AL, USA

Alan S.L. Yu, MB, BChir Division of Nephrology and Hypertension, and The Kidney Institute, University of Kansas Medical Center, Kansas City, KS, USA

Miriam Zacchia Chair of Nephrology, Department of Internal Medicine, Faculty of Medicine, Second University of Naples, Italy

This page intentionally left blank

SECTION 1

EPITHELIAL AND NONEPITHELIAL TRANSPORT AND REGULATION

This page intentionally left blank

CHAPTER

1

Epithelial Cell Structure and Polarity

Karl S. Matlin[1] *and Michael J. Caplan*[2]

[1]Laboratory of Epithelial Pathobiology, Department of Surgery, University of Chicago, IL, USA
[2]Department of Cellular and Molecular Physiology, Yale University School of Medicine, New Haven, CT, USA

INTRODUCTION

Many of the chapters in this volume are devoted to the mechanisms through which the nephron is able to convert the glomerular filtrate into concentrated urine that is responsive to the metabolic status of the organism as a whole. The multifactorial nature of this problem means it needs to be treated at several levels of resolution. A meaningful description of renal tubular functions requires an understanding of the nephron's properties as an integrated tissue, as well as those of its constituent parts, including the cells and molecules that contribute to its transport functions.

As detailed elsewhere in this volume, the nephron is a remarkably heterogeneous structure. Throughout its length, the renal tubule is notable for the marked variations in the morphologic and physiologic properties of its epithelial cells, reflecting the numerous and diverse responsibilities that neighboring segments are called on to fulfill. At the tissue level, the function of the kidney is critically dependent on the geometry and topography of the nephron. The precise juxtaposition of various epithelial cell types, which manifest distinct fluid and electrolyte transport capabilities, in large measure specifies the course of modifications to which the glomerular filtrate is exposed. This dependence on geometry also extends to renal function at the cellular level.

The Nature and Physiologic Implications of Epithelial Polarity

Despite their variations in form and function, all of the epithelial cells that line the nephron share at least one fundamental characteristic. Like their relatives in other tissues, all epithelial cells are polarized. The plasma membranes of polarized epithelial cells are divided into two morphologically and biochemically distinct domains.[1–6] In the case of the nephron, the apical surfaces of the epithelial cells face the tubular lumen. The basolateral surface rests on the epithelial basement membrane, and is in contact with the interstitial fluid compartment. The lipid and protein components of these two contiguous plasmalemmal domains are almost entirely dissimilar.[1–6] It is precisely these differences that account for the epithelial cell's capacity to mediate the vectorial transport of solutes and fluid against steep concentration gradients. Thus, the subcellular geometry of renal epithelial cells is critical to renal function.

The principal cell of the collecting tubule provides a useful illustration of the importance of biochemical polarity for renal function. As described in other contributions to this volume, the principal cell is required to resorb sodium against a very steep concentration gradient. It accomplishes this task through the carefully controlled placement of ion pumps and channels.[7–9] The basolateral plasma membrane of the principal cell, like that of most polarized epithelial cells, possesses a large complement of Na^+/K^+-ATPase. This basolateral sodium pump catalyzes the energetically unfavorable transport of three sodium ions out of the cell in exchange for two potassium ions, through the consumption of the energy embodied in one molecule of ATP.[10] The apical surface of the principal cell lacks sodium pump, but is equipped with a sodium channel, which allows sodium ions to move passively down their concentration gradient.[11] Through the action of the sodium pump the intracellular sodium concentration is kept low and the driving forces across the apical membrane favor the influx of sodium from the tubular fluid through the apical sodium channels. Thus, the combination of a basolateral Na^+/K^+-ATPase and an apical sodium channel lead to the vectorial movement of

Seldin and Giebisch's The Kidney, Fifth Edition.
DOI: http://dx.doi.org/10.1016/B978-0-12-381462-3.00001-X

© 2013 Elsevier Inc. All rights reserved.

sodium from the tubule lumen to the interstitial space against its electrochemical gradient. This elegant mechanism is critically dependent upon the principal cell's biochemical polarity. If the sodium pump and the sodium channel occupied the same plasmalemmal domain, then the gradients generated by the former could not be profitably exploited by the latter. Thus, the vectorial resorption or secretion of solutes or fluid is predicated upon the asymmetric distribution of transport proteins in polarized epithelial cells.

The fact that epithelial cells manifest biochemical polarity implies that they are endowed with the capacity to generate and maintain differentiated subdomains of their cell surface membranes.[1–6] Newly synthesized membrane proteins must be targeted to the appropriate cell surface domain, and retained there following their delivery. During tissue development, cell division, and wound healing, plasmalemmal domains must be delimited and their biochemical character established. Clearly, specialized machinery and pathways must exist through which this energetically unfavorable compositional asymmetry can be supported. The nature of these specializations has been the subject of intense study for decades. While firm answers are not yet available, a number of fascinating model systems have been developed, and valuable insights have emerged. This chapter will focus on what is known of the processes through which tubular epithelial cells create their polarized geometry.

EPITHELIAL CELL STRUCTURE: MORPHOLOGY AND PHYSIOLOGY

The renal tubular epithelium is composed of a remarkably varied collection of cell types, ranging from the highly specialized glomerular epithelial cells with foot processes that faciliate filtration of the blood through the basement membrane, to the simple squamous epithelium of the loop of Henle. A detailed delineation of its morphologic diversity is beyond the scope of this chapter. However, certain essential features are shared among all cell types in the tubular epithelium and, indeed, most other epithelial cell types found in the body. Among these are a differentiated, microvillar apical surface facing the tubular lumen, a lateral surface specialized for cell–cell interactions and regulation of transepithelial permeability, and a basal surface that adheres to the basement membrane. Furthermore, as described previously, the basolateral plasma membrane is particularly important in ion transport, because it is the location of the Na^+/K^+-ATPase and the cell is able to modulate its surface area in response to the transport activity of individual cell types. The cell–cell adhesive relationships are responsible for the integrity of the epithelium, and also dictate the permeability of the epithelium to small molecules that, in part, give each segment of the epithelium its physiological identity. Furthermore, adhesion of epithelial cells to each other and to the basement membrane sends spatial signals to the cells essential for the establishment and maintenance of epithelial cell polarity. In the following sections the morphology and functional composition of the apical and basolateral domains of the plasma membrane will be described, after detailing the nature of the junctional complex that mediates cell–cell adhesion.

The Junctional Complex

All epithelial cells, including those of the kidney tubule, are joined together along the lateral surfaces by a series of intercellular junctions first noted by their characteristic ultrastructural appearance and relative locations on the lateral plasma membrane.[12,13] These include the tight junction or *zonula occludens*, the adherens junction (*zonula adherens* or intermediate junction), desmosomes, and gap junctions. In most mammalian epithelia the tight junction is located at the apical-most edge of the lateral membrane closely followed by the adherens junction. Desmosomes and gap junctions have less specific locations on the lateral membrane. Desomosomes and gap junctions will be described briefly, followed by a more comprehensive description of tight junctions and adherens junctions, because of their essential functions in the organization, physiology, and morphogenesis of epithelia.

Desmosomes are large, multiprotein complexes primarily responsible for the mechanical strength of cell–cell interactions.[14] They are formed after the assembly of adherens and tight junctions. By transmission electron microscopy they appear as discrete, focal concentrations of dense material in the cytoplasm of adjacent cells, as well as in the intercellular space.[13] In contrast to adherens and tight junctions, desmosomes do not form an adhesive belt around the entire epithelial cell, but are a kind of "spot weld" at various points on adjacent lateral membranes. They are composed of both integral membrane proteins of the cadherin family called desmogleins and desmocollins, and peripheral membrane proteins known as desmoplakins, as well as a variety of other protein constituents.[14] Adjacent cells adhere to each other through cadherin-mediated interactions. The peripheral components then provide mechanical stability to this interaction, via keratin intermediate filaments in the cytoplasm of each cell.[15] Ultrastructurally, these appear as a mass of hair-like protrusions interacting in parallel with each plaque and then splaying out into the cytoplasm.[13,14]

In this manner, desmosomes link all cells in the epithelium. While there is evidence that desmosomal components may play an active role in regulating some aspects of cell−cell adhesion and even gene expression,[16] in general their function is considered to be relatively passive.

Gap junctions are so named because of the characteristic 3 nm gap between adjacent cells that is evident using transmission electron microscopy.[17,18] Examination of freeze-fracture specimens, which permits visualization of the internal topography of membranes, reveals the gap junction as a discrete array of intramembranous particles or connexons.[17,18] Each connexon is composed of five identical connexins, a family of transmembrane proteins. Connexons on adjacent cells interact through their extracytoplasmic domains to form a series of low-resistance channels. These permit the passage of small molecules of less than 1 kDa, linking neighboring cells in the epithelium both electrically and metabolically. In the kidney, it is likely that gap junctions play important roles during morphogenesis and repair, although their precise functions have not been investigated in detail.[17,18]

Among the numerous functions subserved by epithelia, perhaps the most important is that of a barrier between the intra- and extracorporeal spaces. In the case of the kidney, the extracorporeal space is defined by the lumen of the renal tubule. That the chemical composition of urine differs substantially from that of the interstitial extracellular fluid bathing the epithelial basement membranes is evidence that the barrier provided by the tubular epithelium is tight to both small and large molecules. There are two components to this barrier, arranged in parallel.[19−21] The first is comprised of the apical and basolateral membranes of the epithelial cells, which together serve as a pair of series resistances to the flow of solutes across the epithelia. The second barrier is provided by the tight junction or *zonula occludens* that controls movement of molecules between the cells along the so-called paracellular pathway.[20−29]

The tight junction defines a border between the apical and basolateral plasma membranes. In columnar and cuboidal cells of the renal epithelium, it is found at the apical extremity of the lateral membrane and in the plane of the apical surface. Analysis by transmission electron microscopy originally suggested that the tight junction is a zone of partial fusion between the plasma membranes of adjacent cells.[13] Although this is no longer believed to be the case (see below), the ultrastructure of the junctions is consistent with this interpretation. When cells that have been treated with osmium are examined at high magnification, their membranes are distinguished by a characteristic pattern. The two leaflets of the lipid bilayer appear as a "unit membrane," defined by a pair of darkly stained parallel lines separated from one another by 5−10 nm.[30] In areas corresponding to the tight junction, the four parallel lines representing the two unit membrane of adjacent cells are replaced by three lines, which led to the suggestion that the two outer leaflets contributed by the neighboring cells have in some way merged to form a new trilaminar membrane structure.[12]

The putative outer leaflet fusion suggested by morphologic studies received some support from examination of lipid mobility in polarized epithelial cells. The mobility of outer leaflet lipids is restricted by the tight junction.[31,32] Labeled lipid probes inserted into the outer leaflets of epithelial apical or basolateral plasma membranes have unimpeded mobility within their respective domains, but cannot cross the tight junction.[31,32] Furthermore, outer leaflet lipids are unable to diffuse between neighboring epithelial cells through the tight junction. In contrast, inner leaflet lipids can apparently move freely between the two plasma membrane domains, suggesting that the tight junction presents no barrier to their diffusion. These observations are consistent with a model of the tight junction, in which the outer leaflets of the lipid bilayer participate in the formation of some junctional structure, while the inner leaflet remains unperturbed. These results also suggest that the lipid composition of the apical inner leaflet is necessarily identical to that of the basolateral one, because any differences would quickly be randomized by diffusion. Thus, the differences in lipid compositions of the apical and basolateral surfaces alluded to in the introduction to this chapter must be entirely contributed by the constituents of the outer leaflet.[32,33]

Electron microscopy has provided further insights into the structure of the tight junction. Examination of freeze-fracture replicas of epithelial cells reveals the tight junction to be composed of continuous branching and interwoven strands that surround the entire perimeter of the cell.[34] These strands appear as elevations in the P or cytoplasmic fracture face, and are matched by grooves in the E or external face. In some cell types the strands have a fibrillar appearance, and no discrete subunit structure can be resolved. In other cell types, and in samples not fixed with glutaraldehyde, the strands can appear more as a series of particles.[34] Although some early models postulated that the strands were composed of unusually structured lipids, it is now certain that they are primarily composed of integral membrane proteins (see below). Observations of a number of cell types with different amounts of transepithelial electrical resistance revealed a rough correlation between the number and complexity of the anastomosing strands and the degree of transepithelial electrical resistance. While this correlation certainly exists in at least some epithelia,[35] the amount of

resistance is now known to be a function of the specific complement of proteins making up tight junctions in different cells.

The first tight junction protein identified was, appropriately, ZO-1 (*zonula occludens*-1).[36] ZO-1, however, turned out to be a cytoplasmic peripheral membrane protein, suggesting that other, integral transmembrane proteins capable of mediating cell−cell contact and the intermembrane permeability barrier must exist. Shortly thereafter, occludin, a multispanning membrane protein, was identified, followed by many other proteins.[21] It is now clear that the tight junction is an extremely complex structure composed of at least three different families of transmembrane proteins including: multiple claudins; occludin and other members of the MARVEL family; and the junctional adhesion molecules or JAMS.[21] Additional peripheral membrane proteins are also part of the tight junction, including ZO-1, -2, and -3, and cingulins. It is also evident that the functions of these protein complexes extend beyond regulating solute permeability to participation in epithelial cell polarization.[37]

Claudins are the most important tight junctional proteins controlling paracellular permeability of small molecules.[38−43] They are the major protein constituent of the tight junctional strands seen in freeze-fracture; expression of claudins in fibroblasts produces characteristic strands and promotes cell−cell adhesion.[21,38,41,43−45] The claudin family consists of at least 24 members in mammals. All are tetraspanning transmembrane proteins of 20−27 kD, with two extracellular loops. With one exception, the cytoplasmic C-terminal sequence of claudins interacts with ZO-1, -2, and -3. Interacting claudins on neighboring epithelial cells create charge selective channels, with the overall permeability of the tight junction to ions dependent on the particular mix of claudins expressed in the cell.[21,44] This was illustrated dramatically in the renal epithelial cell line MDCK (Madin−Darby canine kidney) when expression of claudin 8, in addition to other endogenous claudins, reduced the paracellular movement of mono- and divalent cations without affecting the permeability of anions or uncharged solute molecules.[46] In the kidney tubular epithelium, cells of the proximal tubule, which has a transepithelial electrical resistance of 6−10 Ωcm^2, express claudins 2, 6, 9, 10, and 11, while cells of the collecting duct, with a much higher resistance of 1000 Ωcm^2, express claudins 3, 4, 6, 7, 8, 10, and 14[29,47] (Figure 1.1). Other cell types along the nephron express other combinations, yielding a range of increasing resistances in the proximal-to-distal direction[29,47] (Figure 1.1).

The selective barrier created primarily by claudins is sometimes referred to as the "pore pathway," because it permits movement only of small ions and other uncharged small solute molecules. However, in at least some epithelia, there is also a kind of "leak pathway" that allows passage of larger molecules, including macromolecules.[21] The nature of the leak pathway and its regulation is poorly understood. Occludin, which is also a tetraspanning membrane protein unrelated to claudins, may play a role in the leak pathway, together with ZO-1 and the actin cytoskeleton. Even though it is counterintuitive, an electrically tight pore pathway can co-exist with an active leak pathway, although the molecular and structural basis of this has not been fully clarified.[21]

The tight junction is a structure whose function is highly dependent on interactions between integral and peripheral components and the actin cytoskeleton. ZO-1 and its family members are perhaps the most important class of proteins linking the various tight junctional proteins together.[36,48,49] ZO-1 contains multiple PDZ (PSD95-Dlg-ZO-1) protein interaction domains. These bind to both claudins and JAMs, while other regions of the molecule bind to occludin and actin. ZO-1 is also capable of binding to components usually identified with adherens junctions, and to a wide variety of signaling molecules.[21] While it is still valid to view the regulation of paracellular permeability as the primary function of the tight junction, it is more appropriate to think of the overall structure as a component of a larger apical junctional complex responsible for a multiplicity of adhesive, signaling, and membrane trafficking functions.

Originally, the tight junction was looked at as a stable, static structure in intact epithelia. Recent results using, among other approaches, expression of fluorescent tight junction proteins in cultured and intact epithelia, indicate that, in fact, the tight junction is highly dynamic.[50] In the intestine, the epithelial leak pathway will open to permit uptake of glucose beyond the capacity of the Na^+-glucose transporter in the apical membrane. This process is controlled by the actomyosin cytoskeleton, since drug-induced actin depolymerization, as well as activation of myosin light chain kinase (MLCK), compromises the epithelial barrier.[50−52] Breakdown in the barrier is accompanied by simultaneous endocytosis of occludin, both implicating occludin in the regulation of the leak pathway and further demonstrating the cell's capacity to reshape the junction. Tumor necrosis factor (TNF), which is involved in the pathogenesis of Crohn's disease, will cause barrier breakdown through a mechanism also dependent on MLCK.[50] Although these studies of tight junction plasticity have concentrated on the intestine, it would be surprising if similar mechanisms were not operable in the renal tubular epithelium, especially in the proximal tubule which morphologically resembles intestinal absorptive cells, and where uptake of a variety of filtered materials occurs.

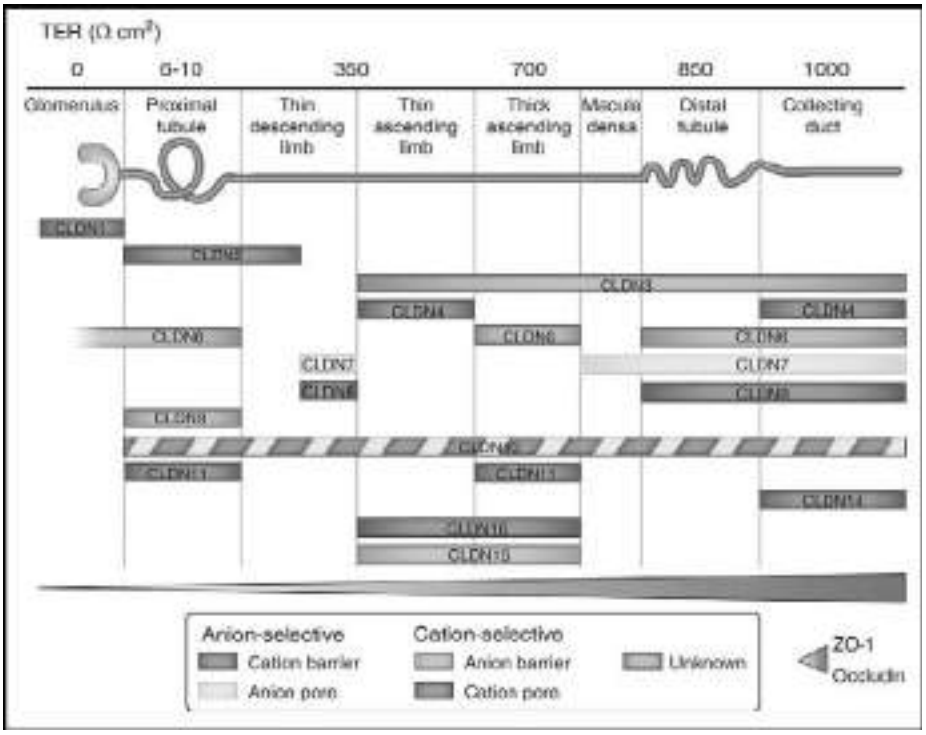

FIGURE 1.1 **The relationship between transepithelial resistance and claudin subtype expression along the nephron.** *(Reprinted from ref. [29].)*

The adherens junction, or *zonula adherens*, forms a belt just below the tight junction in most epithelial cells, connecting them via extracellular interactions and cytoplasmic linkages to the actin cytoskeleton (Figure 1.2). In the electron microscope, adherens junctions appear as a dense, somewhat amorphous concentration of submembranous staining, with a mass of impinging actin filaments.[13] The major adhesive component of the adherens junction is E-cadherin.[25,53,54] E-cadherin is a single-pass transmembrane protein that consists of a series of calcium-binding extracellular or EC repeat domains, and a cytoplasmic tail that interacts with members of the catenin family. In adherent cells E-cadherin is concentrated in the adherens junction, but can also be more diffusely distributed over the lateral plasma membrane. Adhesion between cells occurs through *trans* interactions between the EC1 domains contributed by different cells in the presence of calcium, which maintains the proper conformation of the extracellular part of E-cadherin. Interactions occur initially through individual molecules, but are then consolidated and strengthened through lateral interactions of individual units.

The stability of E-cadherin-mediated adhesion is dependent on the binding of catenins to the cytoplasmic tail of E-cadherin.[25,54] P120-catenin binds to a specific octapeptide located in the cytoplasmic juxtamembranous part of the cytoplasmic tail, and appears to be responsible for maintaining the stability of E-cadherin in the membrane, preventing its endocytosis and degradation. It is also involved in signaling related to cell motility, and is a substrate for the Src-receptor tyrosine kinase. The second catenin that associates with E-cadherin is β-catenin, which binds to the carboxy terminus of the cytoplasmic tail in a phosphorylation-dependent manner.[25,54] Certain serine phosphorylations of E-cadherin increase the affinity of the β-catenin–E-cadherin interaction, while phosphorylation of serines on β-catenin disrupt the interaction with E-cadherin, and with α-catenin. In addition to its role in cell–cell adhesion, β-catenin is itself an important signaling molecule that is capable of entering the nucleus and regulating transcription of genes related to cell proliferation and differentiation.[16,55,56] Its function in transcription is carefully regulated by the Wnt signaling pathway by keeping the cytoplasmic concentration of β-catenin low, either through its interaction with E-cadherin or through its degradation by a mechanism dependent on a cytoplasmic "destruction complex" and ubiquitination.

In the adherens junction, β-catenin serves as a bridge between E-cadherin and α-catenin that, in turn, interacts with the actin cytoskeleton. In this manner, cell–cell adhesion through the adherens junction is given both a degree of mechanical stability and mobility through actomyosin contraction.[54] Originally the β-catenin–α-catenin–actin interaction was believed to be somewhat static, but recent evidence indicates that it is very dynamic. Alpha-catenin can exist as either a monomer or dimer, with the monomer able to bind β-catenin, but not actin, and the dimer able to bind actin, but not β-catenin. Three pools then exist in the cell: a monomer

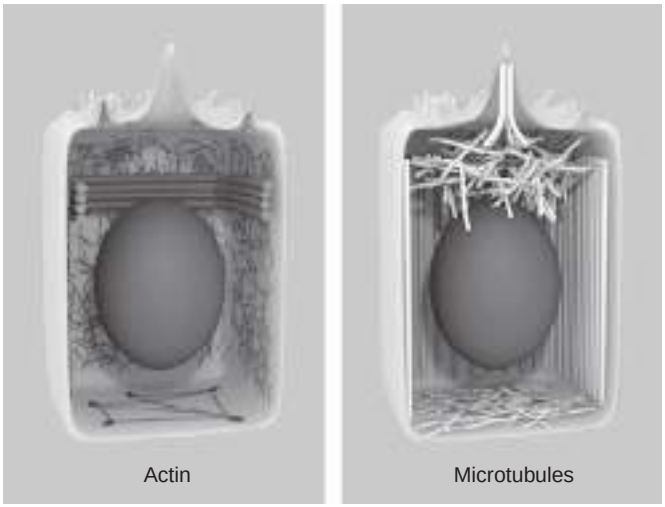

FIGURE 1.2 **The distribution of actin filaments and microtubules in polarized renal epithelial cells, based on the Madin–Darby canine kidney (MDCK) cell line.** *(Images courtesy of Jonathan Bowen and Elias T. Spoliotis, Drexel University, Philadelphia, Pennsylvania.)*

pool bound to β-catenin; a free cytoplasmic monomer pool; and a dimer pool bound to actin. As the adherens junction forms and consolidates, a high concentration of monomers is transported to a localized site on the membrane through β-catenin interactions. This then drives dimer formation and a dynamic linkage to the actin cytoskeleton. Localized concentration of α-catenin dimers can also inhibit Arp2/3, a mediator of actin branching essential for cell migration, and thus facilitate the transformation from a migrating cell to an adherent polarized cell during processes such as injury repair.[54] The recognition that the adherens junction is dynamic and plays a role in cell motility has helped to transform our view of epithelia from that of a static sheet of cells to one of interlocking cells capable of constant motion and remodeling, all the while maintaining a precise permeability barrier between the inside and outside compartments of the body.

The Apical Microvillar Surface

The apical brush border membrane is perhaps best epitomized by the one that graces the epithelial cells of the proximal tubule. Named for its appearance, the proximal tubular brush border is comprised of densely packed parallel microvilli which rise like the bristles of a brush from the level of the tight junctions to a height of 1 to 1.3 μm. The proximal tubular brush border is by far the most luxuriant to be found in the nephron; although the apical membranes of other renal epithelial cell types are endowed with small collections of microvillus-like structures, much less is known about the structural specializations characteristic of the apical membranes of more distal renal epithelial cells.[57]

The functions subserved by apical microvilli are not entirely clear. Certainly their most dramatic and obvious effect upon the properties of the apical membrane is manifest as a tremendous amplification of the apical membrane surface area. For the proximal tubule this amplification is in the order of 20-fold.[58,59] As is the case for the epithelia of the small intestine, it is through this redundancy that the proximal tubular epithelial cells markedly increase the efficiency of both their absorptive and degradative functions.

Physiologically, the proximal tubule is responsible for the resorption of ~60% of the filtered load of fluid and solutes.[60] Furthermore, it mediates the digestion of essentially all of the polysaccharides and peptides present in the glomerular filtrate, and transports the resultant sugars and amino acids from the lumen to the interstitial fluid space.[58] It is apparent, therefore, that the epithelial cells of the proximal tubule must be specially equipped, in order to cope efficiently with the comparatively enormous quantities of fluid and substrates that rapidly transit this nephron segment. The presence of an extravagant brush border greatly increases the fraction of the tubular fluid that comes into close contact with the enzymatic and transport systems arrayed on the microvillar surfaces prior to its passage from this tubule segment into the descending loop of Henle. Concomitantly, it proportionally multiplies the number of enzymatic and transport systems available to modify the substrates dissolved in the tubular fluid. Thus, the brush border membrane provides the scaffolding for the relatively massive arsenal of enzymatic and transport machinery required to accomplish the proximal tubule's function as a high-capacity and high-throughput absorptive system.

Ultrastructurally, a microvillus is composed of a bundle of ~19 parallel thin filaments that are linked to one another and to the overlying surface membrane by protein cross bridges.[61,62] The thin filaments extend well beyond the base of the microvillus, and are anchored in a dense matrix of fibers oriented parallel to the plane of the membrane. This meshwork, referred to as the terminal web, underlies the entire apical surface and anastomses with the filaments that radiate from the lateral desmosomes and zonulae adherens (Figure 1.2). The functional implications of these structural arrangements have become clearer as their components have been biochemically identified.[63,64]

The thin filaments that form the microvillar core are composed of actin[61,65] (Figure 1.2). Ultrastructural studies employing heavy meromyosin reveal that all of the filaments in the bundle share a single polarity, and are oriented with their nucleating end towards the microvillar tip. At their termination in the microvillar tip the filaments are received by an electron-dense cap whose molecular identity has yet to be established.[61]

As they emerge from the base of the microvillus, the actin filaments are caught up in the fibers of the terminal web (Figure 1.2). Fodrin, or non-erythroid spectrin, comprises one of the major components of this network.[61,64,66] It appears to function beneath the brush border as an actin fiber cross-linker. Another of the chief constituents of this fibrillar matrix is a non-muscle form of myosin II that belongs to the same myosin subfamily as its skeletal muscle counterpart. Bipolar myosin thick filaments appear to interact with the actin filaments as they sweep out of the microvillar sheath to join the terminal web.[61,65,67] Paired anti-parallel myosin filaments cross-link the actin filaments of neighboring microvilli to one another, forming a connection which bears close comparison to the actin−myosin arrangement characteristic of the striated muscle sarcomere. The analogy is strengthened by the presence in the microvillar rootlet of tropomyosin, a protein that functions in skeletal muscle to regulate the interaction between actin and myosin.[67,68]

This marked molecular similarity between the terminal web and the skeletal muscle contractile unit prompted speculation that this arrangement might also be functionally homologous. A number of investigators have postulated that activation of myosin-based contraction at the microvillar base might lead to microvillar shortening.[69] Repetitive activation of such a mechanism would lead to a piston-like extension and retraction of these membranous processes, which in turn might stir the surrounding tubular fluid. Such a mixing motion is certainly teleologically appealing, in that it would help to ensure that the tubular fluid is uniformly exposed to the enzymatic and transport systems of the proximal tubular apical membrane surface. No evidence for any such concerted and dynamic properties of microvilli has yet been gathered.

Biochemical studies have shed light on the identities and functional properties of some of the proteins which contribute to the interfibrillar cross bridges observed in transmission electron micrographic profiles of microvilli. Howe and Mooseker identified a protein of molecular weight 110 kDa that participates in cross-linking the filaments of intestinal microvilli to the plasma membrane.[70] This protein exhibits a high affinity for the calcium-binding protein calmodulin, which participates in the transduction of a number of calcium-regulated phenomena.[70] Of further interest was the fact that the 110 kDa protein manifests a myosin-like Mg-ATPase activity.[71] Addition of ATP to intact microvilli results in solubilization of the 110 kDa protein, and disruption of the cross-links between the actin filaments and the microvillar membrane.[72,73] Thus, attachment of the plasma membrane to the thin filaments may be regulated by ATP and calcium. The degree to which this putative capacity for structural modulation plays a role in microvillar function has yet to be clarified. Subsequent molecular analysis revealed that the brush border 110 kDa protein belongs to the myosin I family of unconventional myosin molecules.[74,75] Unlike skeletal muscle myosin (which is assigned to the myosin II classification), brush border myosin I molecules possess a single globular head group, and do not form bipolar filaments.[71,72,76,77] Members of the myosin I family, including brush border myosin (myosin Ia), have been found to associate with the membranes of intracellular vesicles, prompting the hypothesis that these motor proteins serve to propel vesicles through the cytoplasm along actin filament tracks.[78,79] Co-localization studies have demonstrated that brush border myosin I and the microtubule-dependent motor protein dynein can be found together on the membranes of post-Golgi vesicles.[80] This observation has inspired the hypothesis that apically-directed vesicles depart the Golgi along microtubule tracks powered by the action of dynein. Upon their arrival at the actin-rich terminal web, they switch engines and are carried the rest of the way to the brush border by myosin I.[81] While brush border myosin I is abundantly expressed in intestinal epithelial cells, it may be present at lower levels in the renal proximal tubule.[82] Since the myosin I family is large and diverse, however, it is extremely likely that an as-yet-unidentified member of this class subserves similar structural and mechanical functions in the epithelial cells of the kidney.[83,84]

Another protein that apparently participates in the organization of the microvillus has a molecular weight of 95 kDa, and has been dubbed villin.[85] Villin belongs to a large family of actin-binding proteins.[86] Prominent in its structure is a pair of sequence domains that appear to be involved in associations with f-actin. The presence of this tandem repeat justifies the contention that villin mediates the bundling of actin fibers. It is interesting to note that villin is a calcium-binding protein, and that interaction with calcium alters its behavior in the presence of actin filaments.[87] In experiments carried out with purified villin in solution, it has been found that this protein bundles actin filaments when the free calcium concentration is less than 1 μM. When the calcium concentration rises to 10 μM, villin severs actin filaments into short protofilaments. At intermediate calcium concentrations, villin binds to actin filaments at their growing ends, forming a cap that prevents further elongation. Due to the dynamic nature of the microfilament polymer, this capping results in the formation of shortened filaments. It is not known whether these calcium-dependent activities of villin are manifest *in vivo*. If villin does indeed sever or shorten actin filaments within the living cell, it would seem likely that perturbations which produce elevations of intracellular calcium concentrations may lead to structurally significant alterations in the organization of the microvillar scaffolding. During embryonic development, villin is expressed throughout

the cytoplasm of epithelial cells prior to the elevation of a brush border.[88] At later stages, villin becomes localized to the cytosolic surface of the apical membrane, and is subsequently incorporated into forming microvilli. This behavior has led to the suggestion that the localization of villin to the apical surface is a watershed event in the biogenesis of microvilli. Thus, the formation of inter-filamentous bridges, presumably mediated by villin, may be a critical first step in the organization of the microvillar infrastructure. Supporting this model are the results of experiments in which Caco-2 intestinal epithelial cells were stably transfected with a vector encoding antisense villin mRNA.[89] The consequent reduction in villin expression resulted in a loss of the brush border and mis-sorting of a subset of apical microvillar proteins. It must be noted, however, that results from gene knockout experiments argue against an obligate role for villin in microvillus formation.[90] Mice whose villin genes have been disrupted, and which produce no villin protein, are able nonetheless to generate morphologically and apparently physiologically normal brush borders. Presumably, other components of the microvillar infrastructure can shoulder the cross-linking and organizational duties normally performed by villin. Such functional redundancy is typical of biological systems endowed with architecture as esthetically elegant and complex as that which graces the microvillus.

While villin is limited in its distribution to those cell types endowed with brush borders, another actin-bundling component of the microvillus is present in numerous structures. Plastin-1, which is also known as fimbrin, is a 68 kDa polypeptide associated with the interfilamentous cross bridges that can also be detected in hair cell stereocilia and in ruffled borders.[91] Plastin-1 is clearly a multivalent actin-binding protein, and participates in the cross-linking of the microvillar actin filament array. Structural studies suggest that the cross-linking activity of plastin-1 constitutes the principal means through which the parallel actin filaments are interconnected in microvilli,[92] and the length and organization of brush borders are abnormal in plastin-1 knockout mice.[93] A third bundling protein, known as espin, also participates in the organization of the microvillar actin filaments.[94] While microvilli appear to form normally in the absence of espin,[95] espin overexpression leads to microvillar lengthening[96] by exerting subtle effects on the relative rates of actin filament polymerization and depolymerization. Simultaneous knockout of plastin-1, villin, and espin produces animals whose brush borders are short, and characterized by reduced numbers of disorganized actin filaments and mislocalized myosin. Interestingly, localization of enzymes that are normally concentrated in microvilli is markedly compromised in epithelial cells from these animals, suggesting that the organization of the overlying plasma membrane is dependent upon the structural integrity of the microvillar actin bundle.[97]

Several other polypeptides, associated with the microvillus core and the terminal web, have also been identified. Among the most interesting and important of these is ezrin, a member of the ezrin−radixin−moesin family of proteins.[98] The C-terminal tails of these polypeptides bind to actin filaments, while their N-termini interact with proteins in the membrane. A number of proteins involved in the generation or regulation of intracellular second messengers associate in macromolecular complexes with ezrin−radixin−moesin family members, suggesting that in addition to functioning as linkers these proteins may also act as scaffolding for the assembly of components involved in signal transduction. Knockout of ezrin expression results in shortened and poorly formed brush border microvilli, and perturbations in the organization of the terminal web.[99] In addition, ezrin participates in forming complex molecular scaffolds that regulate and stabilize the expression of solute transport proteins in the apical membranes of renal epithelial cells.[100]

The terminal web mentioned above consists of three morphologically distinguishable domains. In addition to the cytoskeletal fibers that receive the rootlets of the microvilli, fibers that arise from desmosomes and the *zonula adherens* contribute to this meshwork. The desmosomal fibers consist primarily of 10 nm intermediate filaments composed of keratins.[15] At the level of the *zonula adherens*, the cell is ringed by a complex of randomly polarized actin filaments which also contains myosin and tropomyosin[67] (Figure 1.2). *In vitro* experiments have demonstrated that this ring has the capacity to contract circumferentially.[101] This capacity has led to the idea that contraction of the *zonula adherens* ring might contribute to the alterations in tight junctional permeability which have been observed in several epithelial systems in response to certain second messengers and osmotic stress, as described earlier.[20] Thus, activation of sodium-coupled glucose uptake in cultured intestinal epithelial cells has been shown to induce a decrease in transepithelial resistance. This effect is dependent upon the activity of myosin light chain kinase.[51,52] It is thought that by shortening in a "purse-string" fashion, these filaments might actually draw neighboring cells away from one another, and thus modify the structure and permeability of the occluding junctions. The relevance of this model to the functioning of renal epithelia has yet to be established.

The anisotropy and structural complexity that characterize the filamentous core of the microvillus apparently also extend to its overlying plasma membrane. The proteins embedded in, and associated with, the plasmalemma of the proximal tubule brush border are not uniformly distributed over its surface, but rather

are restricted to specific subdomains. This lateral segregation is epitomized by the behavior of two transmembrane polypeptides, maltase and gp330. The 300 kDa enzyme maltase is distributed over the entire surface of the microvilli themselves, but is absent from the intermicrovillar membrane regions.[102,103] In contrast, the heavily glycosylated gp330 (also known as megalin) is restricted in its distribution to these intermicrovillar regions. The restriction of megalin to the intermicrovillar regions appears to be mediated by its interactions with protein components of the endocytic machinery. Ultrastructural examination of the intermicrovillar regions reveals the presence of coated pits. The cytosolic surface of the plasma membrane in these domains is coated with an electron dense material that biochemical and immunoelectron microscopic studies have demonstrated to be clathrin.[103] The presence in these intermicrovillar pits of morphologic and compositional features associated with the process of endocytosis has led investigators to believe that this domain mediates the retrieval of large peptides and proteins from the proximal tubular fluid. The proximal tubular epithelial cells are responsible for capturing and degrading any proteins that pass through the glomerular filtration barrier.[58] This function is apparently served by the profusion of coated pits and vesicles that decorate the surfaces of membranes at the microvillar base. Megalin is a member of the LDL receptor family and, together with cubulin, serves as a receptor that binds to and mediates the uptake of filtered proteins and peptides. Megalin knockout mice exhibit low molecular weight proteinuria, establishing the critical role for megalin as the proximal tubule's pre-eminent scavenger.

Finally, it is worth noting that most or all of the epithelial cells of the nephron are endowed with a single primary cilium (Figure 1.2). This non-motile cilium possesses a ring of nine microtubules, but lacks the central pair of microtubules found in motile cilia. This primary cilium appears to serve sensory functions. Bending the primary cilium, in response to flow or mechanical stimuli, induces calcium signaling in renal epithelial cells. Furthermore, the functional integrity of the primary cilium appears to be a prerequisite for the maintenance of normal renal tubular architecture. A number of cystic diseases of the kidney are attributable to mutations in genes encoding proteins found in cilia.[104–108] Similarly, mice in which expression of ciliary proteins has been disrupted develop cysts. The mechanisms through which loss of the cilium's mechanosensory functions leads to cystic transformation remain to be established.

The Basolateral Plasma Membrane

The rigid subservience of structure to function so elegantly exemplified by the apical microvillar membrane also extends to the basolateral surface of the epithelial plasma membrane. As was mentioned above, the basolateral membrane possesses the ion pumps that power the transepithelial resorption of solutes and water. The resorptive capacity of a given cell type is thus largely dependent on the quantity of ion pumps embedded within its basolateral membrane. This parameter appears, in turn, to be roughly proportional to the surface area encompassed by this membrane domain.[8] Consequently, renal epithelial cells that participate in resorption of large quantities of ions and fluid (such as those of the proximal tubule), as well as cells that carry out resorption of ions against steep concentration gradients (such as those of the thick ascending limb of the loop of Henle), are endowed with basolateral plasma membranes whose surface areas are amplified through massively redundant infoldings.

As was detailed in the discussion of the apical membrane, the lateral distribution of proteins within the plane of the basolateral membrane is not uniform. This fact is most dramatically illustrated by epithelial cell types that lack the deeply invaginated basolateral infoldings discussed above. Studies have demonstrated that the Na^+/K^+-ATPase is concentrated in subdomains of the basolateral membranes of small intestinal epithelial cells.[109] The sodium pump is essentially restricted to the lateral membranes of these cells, and is absent from the basal surfaces that rest on the basement membrane. Dislodging these cells from the underlying basement membrane produces a redistribution of the sodium pump throughout the entire basolateral surface. These results suggest that the sodium pump is either actively or passively prevented from entering the basal domain of the plasma membrane, in some manner that is dependent on an intact interaction with the basement membrane. The meshwork of cytoskeletal elements associated with those sites at which the epithelial cell is anchored to the basement membrane may be too dense to allow membrane proteins such as the sodium pump to penetrate. Conversely, cytoskeletal restraints whose integrity requires cell attachment to the basement membrane might retain the sodium pump within the lateral subdomains. In each of these scenarios, the cytoskeleton plays an important role in determining the subcellular distribution of a transmembrane protein. Research over the years has made it quite clear that the cytoskeleton plays a critical role in defining polarized domains, and in determining aspects of their protein compositions.[110–125]

The Basement Membrane

The basement membrane, while not strictly part of the epithelium, is such an essential contributor to epithelial function that it cannot be excluded from any comprehensive description of the renal epithelium. The basement

membrane is a thin layer of secreted and assembled extracellular matrix that underlies all epithelia and endothelia in the body, and also surrounds skeletal muscle fibers and peripheral nerves.[126] In the past, the terms basement membrane and basal lamina were used inconsistently to describe morphological features of this layer, but there is no longer sufficient reason to distinguish these terms from each other, and they may be used interchangeably.[12] In the kidney, the tubular basement membrane is comparable to that found under other epithelia in the body, while that of the glomerulus is more complex and unusual.[127–129] In the glomerulus, the basement membrane is synthesized from proteins secreted by both podocytes and the closely apposed endothelium, resulting in a double-thick layer of matrix proteins that is an essential part of the glomerular blood filter. Diseases affecting the glomerular basement membrane often lead to compromise of the filter and proteinuria. Detailed discussion of this barrier and its specialized and distinctive composition is beyond the scope of our overall discussion of the biology of the renal epithelium, and will not be pursued in this chapter.

Basement membranes are visible by transmission electron microscopy of glutaraldehyde-fixed and heavy metal stained thin sections of epithelia, and classically appear as an electron dense layer (*lamina densa*) separated from an electron lucid (*lamina lucida*) layer adjacent to the basal epithelial surface.[12] While these morphological features were originally believed to have a structural basis, there is now evidence that they may be fixation artifacts. All basement membranes are composed of a common set of protein components which include laminins, type IV collagen, heparan sulfate proteoglycans, and nidogen, although the specific types of these can vary depending on both developmental stage and tissue, as well as accompanying pathology.[126] The most important component is probably laminin, because of its role in both assembly of the basement membrane and signaling.[130] Laminins consist of large (~400–800 kDa) heterotrimeric secreted glycoproteins. In mammals, five α-, three β-, and three γ-subunits have been identified in at least 15 different heterotrimeric complexes. Prototypical laminins are cross-shaped molecules in which the short arms of the cross are contributed by the amino-termini of each subunit, and the stem by a coiled-coil made up of the carboxy-terminal halves of each subunit.[130] Typically, the amino-termini of each subunit consist of a globular LN or polymer domain that is involved in basement membrane assembly. The carboxy-terminus of the α-subunit is folded into a series of five globular domains (G1–5) that are essential for binding to the cell surface. Laminins are named according to their subunit composition, such that LM-511, the most common laminin in the kidney, is composed of the α5-, β1-, and γ1-subunits.[131] Like all collagens, collagen IV is a trimeric molecule composed of combinations of various type IV α-subunits that fold into an elongated triple helix.[126] In contrast with fibrillar collagens such as collagen I, type IV collagen does not form bundles, because of the persistence of carboxy-terminal noncollagenous domains (NC1) and interruptions in the collagen repeats within the triple-helix forming regions that render the molecule more flexible. The most common types of proteoglycans found in the basement membrane are perlecan and agrin.[126] Each is a complex molecule that contains a variety of structural motifs resembling those found in laminins, in addition to substantial negatively-charged heparan sulfate polysaccharides. Nidogen (also called entactin) is a relatively small basement membrane protein that acts primarily to link laminin and collagen IV in the assembled structure. In addition to the core components of laminin, collagen IV, and proteoglycans, a variety of other minor components may also be present under particular, poorly-defined conditions, including extracellular matrix proteins normally considered to be primarily components of the interstitial matrix, such as fibronectin.

Basement membranes initially form during embryogenesis, and are then remodeled during development.[132,133] In addition, *de novo* basement membrane assembly may occur in adults following injuries that interrupt basement membrane continuity. Assembly is believed to occur through a mass-action process driven primarily by laminin polymerization.[126,130,134] Laminin molecules secreted by epithelial cells bind to receptors on the basal cell surface until the density of bound molecules permits formation of heterotrimeric complexes of α, β, and γ amino-terminal LN domains contributed by three different laminin molecules. The resulting structure is a polymerized network of molecules closely associated with the basal surface. Subsequently, collagen IV intercalates into this primary network to form a secondary network created by head-to-tail interactions between collagen IV molecules. The two networks are then linked through nidogen interactions between laminin and collagen, and other molecules, including notably proteoglycans, fill the spaces within the interlocked laminin and collagen networks.[126,130,134]

During pathological processes such as renal cyst formation and recovery from ischemic injury to the tubular epithelium, there is evidence that the atypical laminin isoform LM-332 is expressed.[135–138] This laminin consists of the α3-, β3-, and γ2-subunits, with both the α3- and γ2-subunits lacking amino-terminal LN domains, precluding the molecule from participating in typical network formation. The specific function of LM-332 in these pathological situations is unknown, but one hypothesis is that it interacts with prototypical laminins, such as LM-511, to terminate or even disrupt normal basement membrane assembly, facilitating remodeling of the basement membrane, and possibly

signaling the epithelium to differentiate into a more plastic state suitable for injury repair.[139]

The basement membrane interacts with epithelial cells primarily by binding to the integrin family of extracellular matrix receptors. Integrins are a superfamily of cell adhesion receptors found in nearly all cells.[140] Each integrin consists of a heterodimer of α- and β-subunits, both of which are transmembrane glycoproteins. A total of 18 α- and 8 β-subunits are known in mammals, resulting in at least 24 heterodimers.[140] Although integrins are known primarily as receptors for extracellular matrix proteins, they may also participate in cell−cell adhesion.[141] Epithelial cells of the kidney and other organs typically express an array of integrins, including multiple forms with the β1-subunit, such as α2β1 and α3β1, as well as integrins with the β3-, β5-, and β6-subunits in combination with αV[142] (A. Manninen, personal communication). Many, if not all, epithelial cells also express integrin α6β4.[140,142] The β4-subunit is uniquely found in epithelial cells and, unlike most other epithelial integrins, interacts on the cytoplasmic side with cytokeratins, rather than the actin cytoskeleton. Integrin α2β1 is a collagen receptor, while α3β1 and α6β4 are receptors for multiple isoforms of laminin.[140] The various αV-containing integrins are receptors for ligands containing the binding sequence arginine−glycine−aspartate (RGD), such as fibronectin and vitronectin.[140] They may also play a role in activation of transforming growth factor β (TGFβ), which is important in epithelial repair and other processes.[143] The MDCK cell line, for example, expresses α2β1, α3β1, α6β4, and several αV-containing integrins, with α3β1 and α6β4 mediating adhesion to different laminins, and with αVβ3 (and possibly other αV integrins) activating TGFβ to turn on specific laminin expression during wound-healing.[143,144] In the kidney tubule, the complement of integrins expressed varies along the nephron, as does the expression of their extracellular matrix ligands, underlining their involvement not only in cell adhesion, but also in differentiation.[142]

In adherent cells, most integrins facilitate adhesion through dynamic interactions with the actin cytoskeleton.[145−148] Linkage to actin is mediated by adapter protein complexes that bind to integrin cytoplasmic tails and then to actin. Proteins found in these complexes include talin, which binds directly to integrins and activates their adhesive properties, paxillin, α-actinin, and vinculin.[145−148] Studies of migrating cells suggest that initial adhesive interactions occur through small "focal complexes" that form on leading lamellipodia and are linked to branched actin through the action of the Rac1, a small GTPase of the rho family. As the cell moves over these contacts, they mature into larger "focal adhesions" that associate with robust actin stress fibers (at least in culture) controlled by another GTPase RhoA and its effectors.[145−149] While the general elements of this model have been somewhat validated in epithelial cells during wound healing, the status of focal complexes and focal adhesions in mature polarized epithelia of the kidney and elsewhere remain, for the most part, unexplored. As mentioned previously, α6β4 is a novel integrin, in that it is epithelial-specific and is capable of assembling adhesion complexes that interact with the cytokeratin cytoskeleton.[140] In normal skin, α6β4 is an essential part of hemidesmosomes.[150] These are large protein complexes containing a second transmembrane protein BP180 in addition to α6β4, as well as the cytoplasmic proteins BP230 and plectin that interact with cytokeratin filaments. The type of hemidesmosome found in the skin (type I) is visible as a dense plaque on the cytoplasmic surface of the basal plasma membrane under the electron microscope.[151] In the kidney such structures have not been reported. However, it is possible that a less developed type of hemidesmosome that is not apparent ultrastructurally (type II) is present in the kidney, although this has not been examined.[151]

In addition to their role in mechanical adhesion, focal complexes and focal adhesions are also platforms for signaling.[145−149] A variety of kinases including, notably, focal adhesion kinase (FAK) and members of the src family of tyrosine kinases, associate with integrin adhesion complexes and are activated by binding to the extracellular matrix. Subsequent signals then activate downstream serine/threonine kinases, such as integrin-linked kinase (ILK), and MAP kinases, such as ERK, to regulate a diverse range of processes including proliferation, migration, and apoptosis. Indeed, at least 180 different cytoskeletal, adapter, and signaling proteins are known to be associated with integrin adhesion complexes, depending on the cell type and circumstances.[149]

In addition to integrins, other membrane proteins are involved in epithelial cell adhesion to the extracellular matrix, including dystroglycan, a laminin receptor, and possibly a membrane-bound form of the Lutheran antigen.[129,130] There is evidence that glycolipids may also serve as transient laminin receptors.[152,153] While it is not proven that any of these receptors play a direct role in epithelial polarization, they may act indirectly by affecting assembly of the basal lamina.[152,153]

BIOGENESIS OF EPITHELIAL POLARITY

In the kidney, polarization of epithelial cells occur under two different circumstances: early development of the tubular epithelium; and repair of an existing epithelium following injury. In mammals, formation of the renal tubular epithelium is initiated by induction of the metanephric mesenchyme by the invading ureteric bud.[154] Following induction, cells of the mesenchyme

form aggregates known as condensates, and these subsequently differentiate into polarized epithelial cells facing a central lumen. Extension of this lumen and further, more specialized, differentiation of epithelial cells eventually forms the nephron. In the case of injury by, for example, nephrotoxic substances or ischemia, the existing polarized tubular epithelium is disrupted in spots.[155,156] Cells at the periphery of these damaged areas then convert from relatively sessile cells polarized along an apical-to-basal axis to flatter, more migratory cells that now have front–rear rather than apical–basal polarity and the capacity to proliferate, enabling them to fill gaps in the epithelium. Once continuity has been achieved, apical–basal polarity is restored.[155,156] While front–rear and apical–basal polarization would seem to be quite distinctive, there is evidence that many of the important molecules and signals are shared. Indeed, as we are now beginning to understand, even front–rear polarization during injury repair is a close mechanistic cousin of apical–basal polarization.[157]

In the following sections, our current understanding of the mechanism of epithelial polarization will be described, after a brief introduction to the predominant experimental system used to study these processes.

In Vitro Systems

The kidney's complicated architecture and cellular heterogeneity renders it a poor substrate for studies designed to examine dynamic cell biological processes. Over the past four decades, the vast majority of research into the mechanisms through which epithelia generate and maintain their polarized phenotype has made use of several continuous lines of cultured epithelial cells. These cell lines retain many of the differentiated properties of their respective parent tissues *in vitro*. Thus, LLC-PK1 cells resemble the proximal tubule (although their precise origin is uncertain).[158] Similarly, Caco-2, HT-29, and T84 cells behave like their progenitors, the colonocytes of the large intestine.[158] Most importantly for this discussion, they manifest in culture the biochemical and morphologic features of the polarized state. Perhaps the best characterized and most heavily used of these culture models is the Madin–Darby canine kidney (MDCK) cell line (Figure 1.3). MDCK cells were originally derived from normal dog kidney in 1959, and grown in culture as a partially transformed line; that is, MDCK cells grow immortally as a monolayer and will not form tumors in nude mice.[159,160] Although their precise point of origin along the nephron is not entirely clear, their physiological and morphological properties suggest that they derive from cells of the thick ascending limb, distal tubule or collecting tubule.[161]

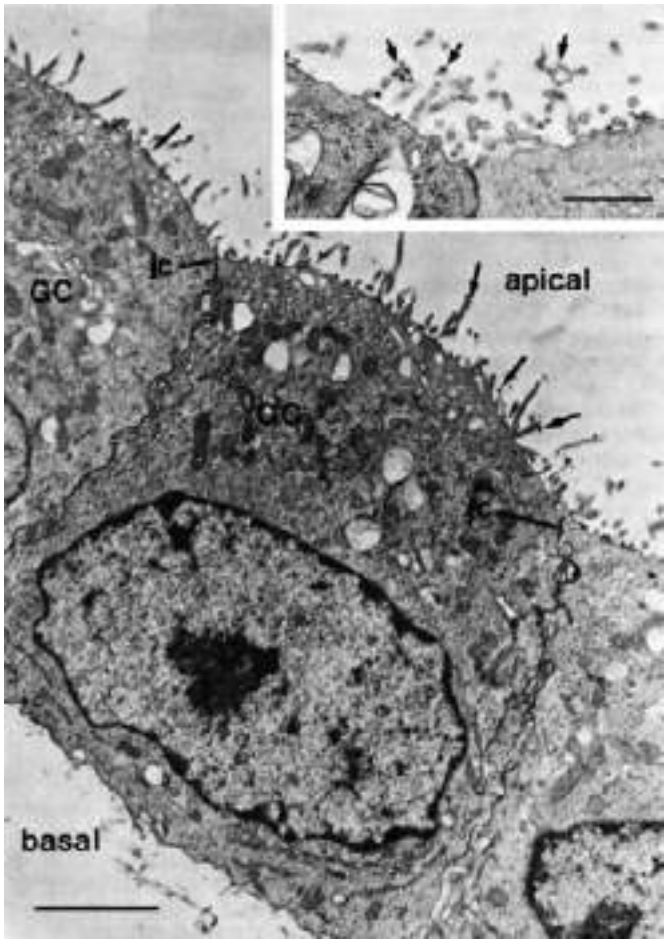

FIGURE 1.3 **Influenza virus buds from the apical surface of polarized MDCK cells.** MDCK cells were grown on a hydrated collagen gel, infected with influenza virus for 6 hours, and prepared for electron microscopy. The arrows denote mature virions which assemble at, and bud from, the apical surface. No virus particles are detected at the basal or lateral surfaces. Bar represents 3.0 μm (inset bar represents 1.0 μm) (GC: Golgi complex; jc: junctional complex). *(Reprinted with permission ref. [1].)*

The first clues to the polarized nature of the MDCK cell line came from the direct observation of these cells' capacity for vectorial transport. When grown on impermeable substrata, MDCK cells form domes (also called blisters or hemicysts).[162] Physiological studies have demonstrated that domes develop as a result of the transepithelial transport of solutes from the apical media to the basolateral surface.[163] Water that passively follows these solutes results in the generation of the fluid-filled blisters. It is fair to say that domes arise in regions where the cells have literally pumped themselves up off the dish. In keeping with this dramatic propensity for unidirectional solute movement, each MDCK cell manifests a polarized distribution of ion transport proteins, including several routes for sodium entry into its apical membrane, and approximately one million molecules of the

Na^+/K^+-ATPase in its basolateral plasmalemma.[164] The popularity of MDCK cells for polarity research developed out of the seminal observations of Rodriguez-Boulan and Sabatini in 1978.[165] In studies of enveloped virus budding from infected MDCK cells, these investigators found that influenza virus assembles at, and buds from, the apical cell surface (Figure 1.3). Of even greater significance was the demonstration that the spike glycoproteins which populate the membranes of these viruses accumulate preferentially at the cell surface from which budding is to occur.[166] Thus, the influenza hemagglutinin (HA) protein is predominantly on the apical surface early in infection. Similarly, the G protein of vesicular stomatitis virus (VSV) is almost exclusively basolateral in infected cells. The viral proteins provided investigators with the first experimentally manipulatable system for the study of membrane protein sorting. A large number of studies have subsequently elucidated the sorting of many endogenous MDCK cell proteins, as well as exogenous proteins expressed from vectors. This system remains the most thoroughly investigated paradigm and, as will be detailed below, has yielded important insights into the nature of pathways and signals that participate in membrane protein targeting and the overall biogenesis of epithelial polarity.

More recently, investigators have endeavored to develop new cell lines to study particular aspects of renal cell biology.[167–170] For example, immortalization genes from human papillomavirus or a hybrid between adenovirus and SV40 have been used to create permanent cell lines from human proximal tubule cells. These lines are of particular interest because of the proclivity of the proximal tubule to suffer injury following ischemic insult. The cell lines retain some differentiated characteristics of the proximal tubule, including expression of brush border markers and sodium dependent/phlorizin-sensitive sugar transport.[169,170] Cultures of cell lines derived in this fashion are not, however, always able to stably maintain the uniform morphology of a simple epithelium, limiting their usefulness for studies of epithelial polarity. More promising results have been obtained using cell lines derived from mice constitutively expressing immortalization factors as transgenes. Among these is the BUMPT-306 line derived from the mouse proximal tubule.[167,168] While certainly not perfect, this line does grow as a simple epithelium, and has the added advantage of providing an *in vitro* correlate to *in vivo* mouse experiments.

The study of epithelial polarization using cell lines has been facilitated by culturing cells in configurations that more closely resemble *in vivo* conditions (Figure 1.4 and 1.5). For example, many varieties of epithelial cells can be grown on permeable filter supports.[171,172] Originally, these were designed to mimic the Ussing chamber used for physiological studies, but later turned out to also be very useful for biochemical and morphological experiments. In their most common commercially-available configuration, these supports are composed of polycarbonate filters with pore sizes typically in the range of 0.4 μm that form the bottom cup. The cup is then suspended in a plastic well containing culture medium, and medium is also added to the inner compartment of the cup (Figure 1.4). Cells are plated on the upper surface of the filter. When a confluent monolayer is formed, it effectively creates a barrier between media compartments. The medium in the interior of the cup bathes the epithelial apical surface, whereas the basolateral surface communicates with the exterior media compartment through the pores of the filter (Figure 1.4). As epithelial cells in the kidney and other organs would normally receive most of their nutrition from the basolateral (serosal) surface, permeable supports are, in a sense, a more natural growth environment than impermeable tissue culture plastic or glass. Indeed, there is some evidence that epithelial cells are more polarized in filter cultures than on solid substrata.[173] Furthermore, the use of filters for the culture of epithelial cells permits investigators simultaneous and independent access to the apical and basolateral plasmalemma surfaces.[174–176] This useful capacity has been extensively exploited in the experiments described in the protein sorting section of this chapter.

In addition to permeable supports, a number of investigators also culture renal and other epithelial cell lines embedded in a gel of collagen type I or other

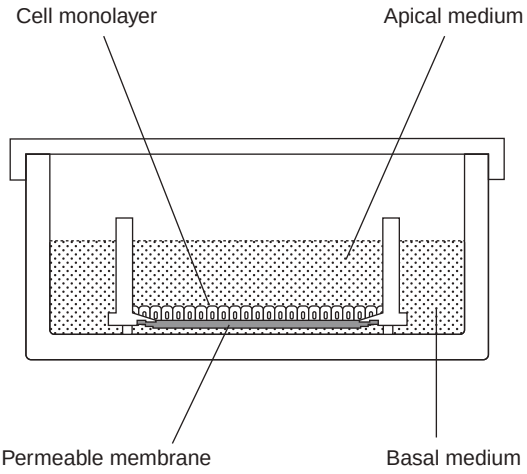

FIGURE 1.4 **Epithelial monolayers can be grown on permeable filter supports.** As depicted in the diagram, a porous filter, composed of cellulose actetate or polycarbonate, forms the bottom of a cylindrical cup. Epithelial cells are plated on top of the filter, and the cup is placed in a well filled with media. When the cells become confluent, the resultant monolayer forms a barrier between the media bathing the apical surface and the media in communication with the basolateral surface. This system thus provides investigators with simultaneous and independent access to both plasmalemmal domains.

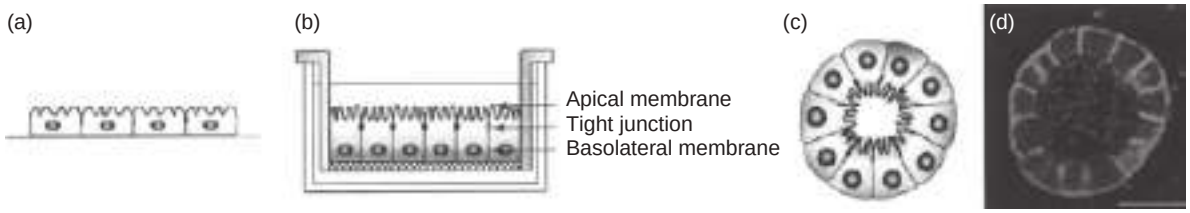

FIGURE 1.5 **Two- and three-dimensional cultures of polarized epithelial cells.** Epithelial cell lines may be grown on conventional impermeable substrata such as plastic or glass (a), or on permeable supports (b). In both cases, the provision of a flat, two-dimensional surface may provide spatial signals that normally would be generated by the cells themselves *in vivo*. In this regard, three-dimensional culture of cells in collagen gels, where a polarized cyst develops over 7 to 10 days (c), may more accurately represent the *in vivo* environment. In (d), an MDCK cell cyst is fluorescently labeled with antibodies to β-catenin to highlight the basolateral surface. *Reprinted with permission from ref. [178].)*

extracellular matrix molecules (Figure 1.5). These are called three-dimensional (3D) cultures, to distinguish them from more common two-dimensional (2D) cultures on either solid or permeable surfaces.[177,178] As with permeable supports, the idea behind 3D cultures is that placing the epithelial cell in an environment in which it is surrounded by extracellular matrix similar to that of the interstitium more closely resembles the *in vivo* environment. While that conclusion is subject to debate, there is no doubt that certain epithelial phenotypes are more readily expressed in 3D than in 2D cultures.[177,178] Nevertheless, these phenotypes are often slow to develop, frequently taking 7–10 days, and may occur asynchronously; this, and the inaccessibility of the cultures, somewhat limits their usefulness for biochemical studies. With the advent of high resolution confocal fluorescence microscopy and the wide array of fluorescent proteins and probes, the impact of this limitation is lessened. In the case of MDCK cells, individual suspended cells develop into polarized cysts or, when stimulated with certain growth factors, tubules. As will be described below, use of 3D cultures has led to important fundamental observations about epithelial cell polarization.[177,178] As a final note on the experimental use of 2D and 3D culture modalities, it is important to point out that formation of polarized cysts in 3D may be most closely analogous to the formation of the primordial kidney epithelium from condensed metanephric mesenchyme during development. In contrast, *in vitro* polarization of kidney epithelial cells in 2D cultures is more akin to the repair of existing kidney tubular epithelia following injury, a scenario that requires the spreading, migration, and proliferation of cells on a pre-existing surface to re-establish a contiguous epithelium.

Polarization Mechanisms: Spatial Cues from Cell Adhesion

It is now understood that not only epithelial cells but, indeed, all cell types are capable of polarizing in response to signals from the environment.[3,4,154,157,179,180] Migrating cells of all types, for example, are polarized in the direction of migration in response to chemotactic or haptotactic gradients and even dividing cells can polarize through unequal division of their cytoplasm upon cytokinesis.[157,181] Epithelial cells are unique, in that their polar organization is stable over time and the apical–basal axis of polarity exhibited by each cell in the epithelium is parallel to the axes of its neighbors. These features permit epithelial cells to form an asymmetrically organized, semipermeable surface that defines the borders of tissues in complex organisms, and separates the inside of the body from the outside environment, while helping to create and maintain distinctly different milieus on each side.[182] The mechanism of epithelial cell polarization depends on specific spatial cues that cause the assembly and asymmetric reorganization of the intrinsic polarization machinery. The spatial cues are adhesive interactions between neighboring cells and the extracellular matrix, while the intrinsic machinery consists of primarily three polarity complexes called Par, Scribble, and Crumbs.[157,182] If the pattern of cell adhesion is asymmetric, then the response of the cell is asymmetric, and a polar phenotype results (Figure 1.6). This section will describe the specific nature of the cell–cell and cell–extracellular matrix adhesive interactions. The mechanisms by which adhesion is translated by the intrinsic polarization machinery into a polarized epithelial cell with distinct apical and basolateral plasma membrane domains will be presented in subsequent sections.

As mentioned previously, polarization of kidney epithelial cells occurs during initial differentiation of the primordial tubular epithelium from condensed mesenchyme, and after disruption of an existing mature epithelium following injury. These two situations are somewhat mimicked *in vitro* by, respectively, 3D culture and 2D culture of renal epithelial cell lines. It is important to recognize that the pattern of spatial cues provided by adhesive interactions is different in these two situations. In the developing kidney epithelium, cell–cell interactions in the condensed

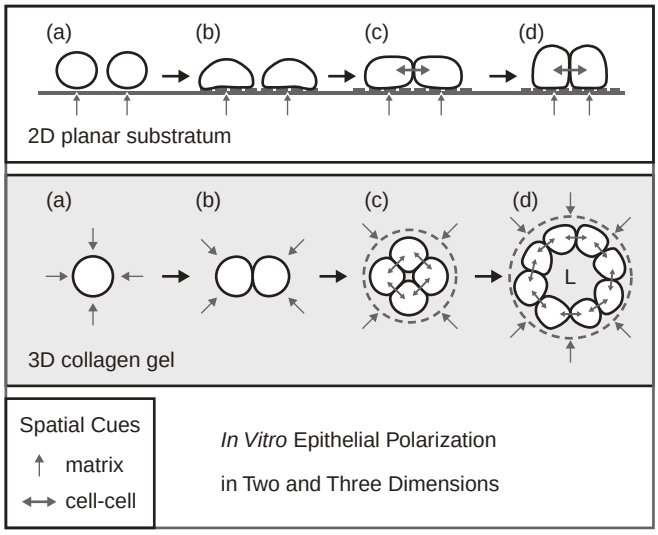

FIGURE 1.6 **Geometry of spatial cues in two-dimensional and three-dimensional culture of epithelial cells.** In two-dimensional culture (top) an asymmetric spatial cue is given by substratum adhesion as soon as contact occurs between the cell and the culture surface. A second spatial cue orthogonal to the first occurs when cell–cell contacts are initiated. In three-dimensional culture (bottom), the initial spatial cue impinging on single cells suspended in the collagen gel is isotropic. As soon as cell division takes place, an asymmetry is set up in which both the spatial cue from the collagen (and other secreted extracellular matrix proteins) and from cell–cell adhesion are asymmetric. The combination of asymmetric cues is required for full apical–basal polarization of epithelial cells.

mesenchyme are believed to precede meaningful cell matrix interactions[154] (Figure 1.7). These condensates are spatially differentiated: cells at the peripheries of the condensates have both a "free" plasma membrane domain facing the outside of the condensates and the undifferentiated mesenchyme, and an "attached" plasma membrane domain in contact with other cells of the condensate. Following this rudimentary polarization, the adherent mesenchymal cells in the condensate become more polarized, eventually forming a lumen and reorganizing into a simple epithelium attached to a basement membrane.[154,183] Similarly, in 3D collagen gel cultures of MDCK cells, individual cells are initially suspended in the gel. Spatial cues from collagen adhesion at this point are isotrophic rather than asymmetric, in that any signals impinging on the cell are unbiased with regard to direction (Figure 1.6). As soon as that cell divides, an asymmetric spatial cue is elicited from the resulting cell–cell adhesion, because the cells remain attached. This situation persists through subsequent divisions until at some point a basement membrane is formed, and the individual cells create a lumen.[178] In contrast, in a wounded epithelium and in 2D culture of epithelial cell lines, the persistent spatial cue from the extracellular matrix substratum is asymmetric, and then an additional although qualitatively different asymmetric spatial cue develops as cell–cell adhesion is restored[139,157] (Figure 1.6). The take-home message from this discussion is that epithelial cells utilize both cell–cell and cell–extracellular matrix interactions as asymmetric spatial cues to polarize. The order in which these cues are provided to the cell may yield qualitatively different results but, in the end, both are required for full apical–basal polarization.

The hierachical relationship between cell–cell and cell–substratum interactions in epithelial cell polarization is illustrated best by a description of early experiments utilizing the MDCK cell line. MDCK cells cultured in suspension as individual cells lack polarized plasma membrane domains.[118,184] Upon attachment to a substratum in 2D culture, apical proteins are restricted to the free or apical surface, while basolateral proteins are distributed over the entire plasma membrane. This situation persists as the cell density increases and initial cell–cell contacts form until, as the cells reach confluency to form a true epithelium, basolateral proteins also become completely polarized.[118,185]

The relative roles of cell–cell and cell–substratum interactions can also be dissected by culturing MDCK cells in medium containing reduced amounts of calcium.[120,186,187] If cells are cultured on collagen-coated surfaces in medium with less than 5 μM calcium, they attach to the substratum but formation of cell–cell contacts mediated by the calcium-dependent adhesion protein E-cadherin is inhibited.[120,186,187] Cells assume a rounded morphology with no appreciable lateral membrane. In this situation, an immature apical surface forms. Microvilli are decreased in number, and expression of apical proteins on the cell surface, although reduced in quantity, remains polarized to the free surface.[186] Basolateral proteins, in contrast, are not polarized in cells cultured in medium containing low calcium concentrations. However, when the calcium concentration is raised to normal values (1.8 mM), then cell–cell contacts rapidly form and basolateral proteins polarize.[186]

The culturing of MDCK cells as multicellular aggregates in suspension also permits the relative effects of cell–cell and cell–substratum interactions to be independently evaluated. Under these conditions, which are different from the 3D culture described previously because the cells are surrounded only by culture medium, aggregated cells gradually form cysts with small central lumina.[184] In the absence of recognizable cell–substratum contact, both apical and basolateral polarization occurs, with the apical surface facing the outside of the cell aggregate. At this time, the tight junctional protein ZO-1 is found distributed over the entire lateral membrane, where cell–cell contacts occur. As the lumen forms, the cells secrete and deposit type IV collagen and laminin into the lumen.[184] Interaction with

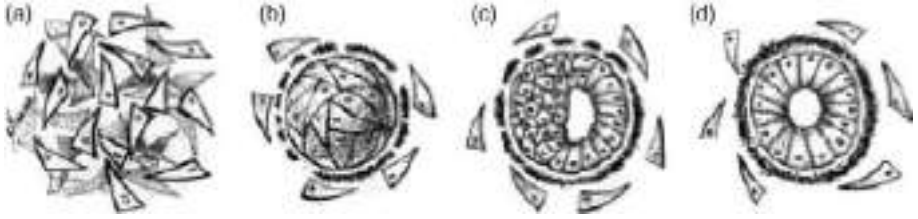

FIGURE 1.7 **Development of the kidney epithelium from induced mesenchyme.** The kidney epithelium develops *in vivo* following induction of the metanephric mesenchyme by the ureteric bud. The initial stages of differentiation from mesenchymal to epithelial cells may also be followed *in vitro* by organ culture. In this schematic view, induced mesenchymal cells are initially randomly oriented and show little cell–cell adhesion (a); Some mesenchymal cells adhere closely to each other and begin to produce a basement membrane at the periphery of the condensate (b); The cells of the condensate begin to reorganize into an epithelium and form a lumen as the basement membrane becomes more extensive (c); Finally, formation of the pretubular renal vesicle consisting of a polarized epithelium is complete, (d). *Redrawn with permission from ref. [154].*

this interior extracellular matrix then triggers redistribution of ZO-1 to the point of intersection between the apical and lateral membrane.[184] Thus, as in the reduced calcium experiments, cell–cell and cell–substratum interactions have somewhat independent but complementary effects on cell polarization.

The adherens junction provides the spatial cue from cell–cell interactions leading to polarization of epithelial cells. One of the most important components of the adherens junction is E-cadherin, the calcium-dependent homophilic cell adhesion molecule discussed previously. Suppression of E-cadherin expression by small-interfering RNAs prevents polarization, clearly implicating it in the polarization process.[188] However, other cell–cell adhesion proteins such as nectins and JAMs may be important as well. Nectins are transmembrane adhesion molecules containing immunoglobulin-like extracellular domains.[189] When epithelial cells transition from a migratory phenotype, as they exhibit during wound healing, nectins may be one of the earliest molecules in nascent cell–cell adhesions. Homophylic interaction of nectins between neighboring cells activates a variety of signaling pathways, among which are those involving the small GTPases Cdc42 and Rac1.[189,190] This, in turn, leads to reorganization of the cortical actin cytoskeleton and, consequently, facilitates the formation and stabilization of E-cadherin-mediated contacts, creating the mature adherens junction.[189] During this process, both nectins and JAMs may initiate the asymmetric activation of the intrinsic polarization machinery. Nectins and JAMs bind Par3, an element of the Par polarization complex (see below).[189,191,192] As the adherens junction matures, other polarization complexes bind and specification of the apical and basolateral plasma membrane domains occurs, with the dividing line located just at the adherens and tight junctions, collectively referred to as the apical junctional complex. At the same time, a complex of proteins known as the exocyst is also assembled at this location.[157,191,192] The exocyst is a kind of tethering complex designed to capture transport vesicles carrying newly synthesized membrane proteins. Delivery of these proteins to this region of the plasma membrane then facilitates the development of the apical and basolateral surfaces.[193,194]

It is likely that the spatial cue emanating from cell–substratum adhesive interactions originates from integrin-mediated cell interactions with the basement membrane protein laminin. In the developing kidney, conversion of condensed mesenchyme into a polarized epithelium is dependent on laminin.[154,195,196] The laminin α1-subunit and integrin $\alpha 6\beta 1$, a laminin receptor, are first detected in the induced mesenchyme following condensation.[129,154,195,196] Laminin localizes to the periphery of the condensate, suggesting that the crude polarization caused by condensation leads to polarized laminin secretion to the periphery. In organ culture antibodies against laminin α1 or the integrin α6-subunit block formation of a polarized epithelium from condensed mesenchyme, suggesting that their involvement in epithelial differentiation is critical.[154,196,197]

Results from a variety of other experimental systems generally support the conclusion that laminins and their integrin receptors play a role in epithelial polarization. Mutations in either integrin or laminin subunits lead to disruption of epithelial differentiation and polarization in the nematode *Caenorhabditis elegans*, and the fruit fly *Drosophila melanogaster*.[132] Expression of laminin in the early mouse embyro generally coincides with development of epithelial tissues. In embryoid bodies derived from cultures of aggregated embryonic stem (ES) cells, an LM-111 containing basement membrane forms between the endoderm and the polarizing inner cell mass cells. When ES cells deleted of both laminin γ1 alleles are aggregated into embryoid bodies, the inner cell mass forms, but does not polarize.[132] Laminin has also been implicated in the polarization of MDCK cells. When MDCK cells are cultured in 3D collagen gels for 7–10 days, they form polarized cysts with the apical surface facing the

lumen, and the basal surface facing the extracellular matrix. Under these conditions, the cells secrete LM-511 and form a discrete layer closely associated with the basal surface, resembling an assembled basement membrane.[198,199] When MDCK cells are treated either with a function-blocking anti-β1 integrin antibody or express dominant-negative Rac1 during cyst formation, the laminin layer does not form properly, although laminin is secreted, and the cells display an inverted and somewhat disorganized polarity with apical antigens expressed on surfaces facing the extracellular matrix.[198,199] Addition of excess exogenous LM-111 to the collagen gel partially rescues both basement membrane assembly and correct polarization in cells expressing dominant-negative Rac1, possibly by driving laminin assembly adjacent to the basal plasma membrane.[198,199] Inverted polarization of the cyst caused by anti-β1 integrin can also be rescued by expression of constitutively-active Rac1.[198,199] These experiments suggest that a "serpentine" signaling pathway exists, leading from ligation of a β1 integrin outside the cell, to Rac1 activation inside the cell, to laminin assembly outside the cell, and finally to polarization. It is important to emphasize that the perturbations that lead to inverted polarity do not seem to affect the segregation of apical and basolateral proteins in individual cells, but instead affect the orientation of apical–basal axes in the cyst. It is unclear how intracellular signaling events can cause laminin assembly. Recent findings have implicated the polarization signaling molecule Par1b and dystroglycan, a non-integrin laminin receptor, in effecting laminin assembly, but the mechanisms are not apparent.[200,201]

Polarization Mechanisms: The Intrinsic Polarization Machinery

In epithelial cells, the intrinsic polarization machinery has traditionally been separated into three so-called polarity protein complexes that function collectively to control the formation of apical and basolateral domains of the plasma membrane.[191,192] Many of the components of the polarity complexes were initially identified in mutant screens in *Caenorhabditis elegans* and *Drosophila melanogaster*, but homologs that function in an essentially identical manner have also been identified in mammals. The first, and perhaps most important, polarity complex generally associated with apical surface determination is the Par complex composed of Par3, Par6, atypical protein kinase C (aPKC), and the small-GTPase Cdc42 (Figure 1.8). A second apical complex is the Crumbs complex, containing in mammals the transmembrane protein Crumbs (Crb3 in the kidney) associated with Lin-7 (PALS1), and PALS1-associated tight junction protein (PATJ). The final complex, which is located on the lateral surface in polarized epithelia, is the Scribble complex composed of Scribble (SCRIB), discs large (Dlg), and lethal giant larvae (Lgl).[191,192] In the case of the Par and Crumbs complex, physical interactions between the components have been demonstrated, while interactions of Scribble complex components have been implied by genetic experiments. In addition to these polarity complexes, other proteins are involved in regulating apical–basal polarization in mammals or lower organisms including, in particular, Par1b and LKB1 (Par4). In the core polarity protein complexes, only aPKC and Cdc42 have enzymatic activities: the former a serine/threonine kinase; and the latter a GTPase-mediated molecular switch, while the others are largely scaffolds with a myriad of binding domains, including on many PDZ domains, that facilitate association with the apical junctional complex of the polarized cell.[191,192]

The mechanisms by which these complexes function to help establish and maintain apical–basal polarity is often described as a process of mutual antagonism or inhibition that creates and maintains a particular balance between the amounts of distinct apical and basolateral plasma membranes, with the "front line" of this battle being the apical junctional complex[191,192] (Figure 1.8). While the concept of mutual antagonism is not inaccurate, how this translates into intuitively comprehensible mechanisms has, until recently, not been obvious. Studies in *Drosophila* have highlighted the critical role of Par3 (Bazooka or Baz in *Drosophila*) and have, to some extent, called into question the idea of distinct, somewhat independently functioning polarization protein complexes.[191] A compelling model proposes that initiation of polarization commences when Par3 (Baz) associates with the region of cell–cell adhesion that will become the adherens junction, prior to the concentration of DE-cadherin (the *Drosophila* version of E-cadherin) in that location. Association is facilitated by phosphoinositides. Once the adherens junction forms, then Par3 binds Par6 and aPKC, and Cdc42 is activated. Activation of aPKC then leads to phosphorylation of Par3, as well as Crb and Lgl, following the delivery of Crb to the plasma membrane through vesicles. The phosphorylation of Par3 on serine 980 by aPKC weakens the interaction between Par3 and aPKC, as well as the interaction between Par3 and the Crb complex protein PALS1 (Lin-7, Stardust or Sdt in *Drosophila*). These changes permit formation of the apical complex Crb–PALS1–PATJ, while interactions between Crb and Par6 prevent association of Par3 with the forming apical surface. At the same time, Par1-mediated phosphorylation of Par3 creates binding sites for the scaffold 14-3-3, and the subsequent Par3-14-3-3 interaction further inhibits the association of Par3 with Par6/aPKC. Since Par1 is localized to the lateral surface, this prevents Par3 from assembling on the lateral surface.

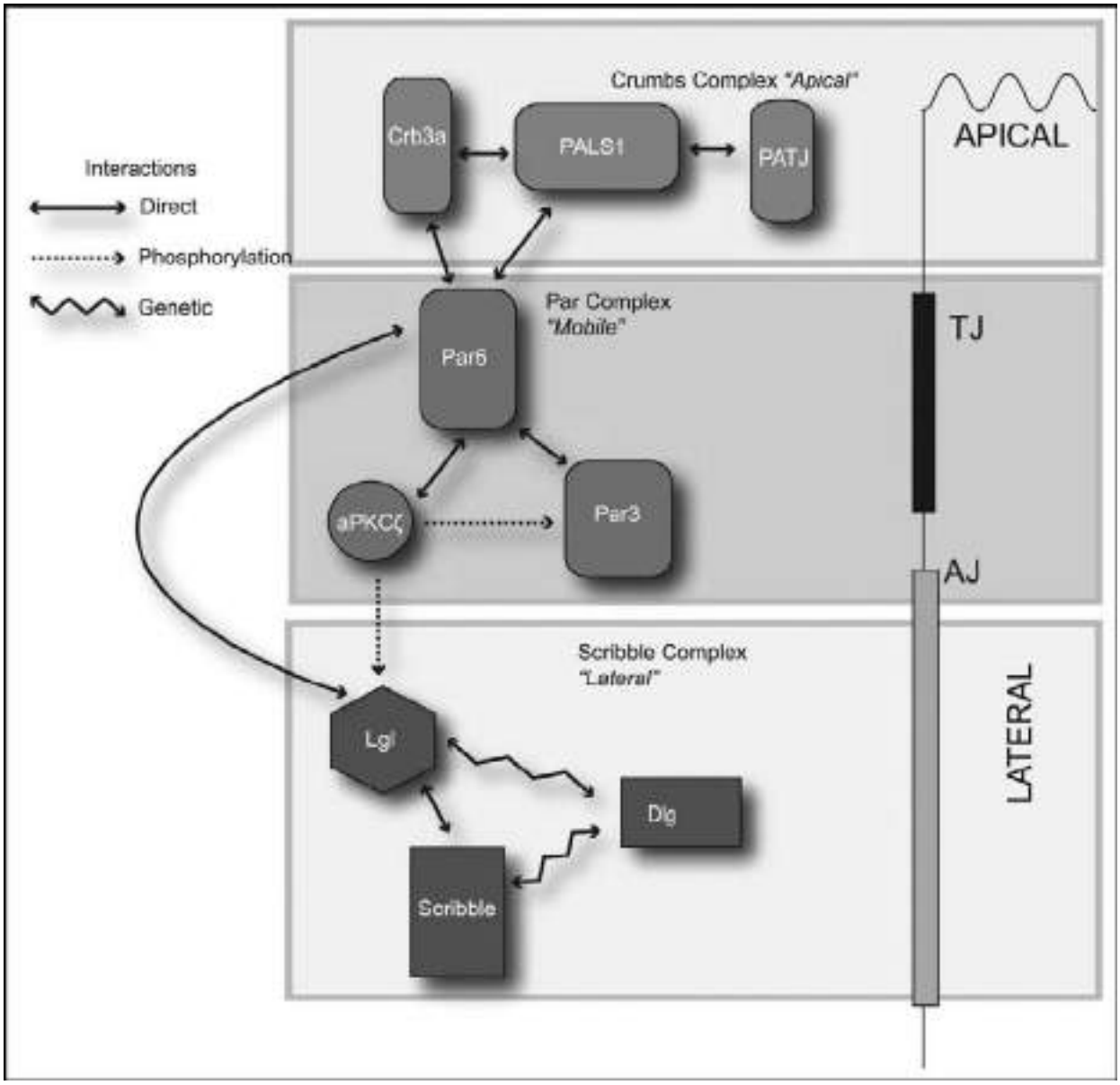

FIGURE 1.8 **Distribution of polarity complexes in polarized epithelial cells.** Solid lines indicate demonstrated physical interactions between components, while jagged lines indicate genetic interactions established from studies of invertebrate epithelial cells. *(Reprinted with permission from Laprise, J. and Margolis, B. (2011). AJP Renal Physiology **300**, F589–F601.)*

Lgl is also phosphorylated by aPKC, which prevents its apical localization.[191] With Dlg and Scrib, it then contributes to maintaining the identity of the lateral membrane in a manner that is poorly understood.

In all likelihood this scenario, derived primarily from experiments on *Drosophila*, is also valid in renal epithelial cells. Studies in MDCK cells, in particular, have illuminated a number of steps and, in some instances, provided additional critical details. As mentioned previously, nascent cell–cell contacts may be initiated by nectins and JAMs prior to the coalescence, stabilization, and assembly of the adherens junction nucleated by E-cadherin and its associated proteins.[189,191,192] Nectins and JAM, which bind Par3, may serve to localize Par3 to the forming junction. In addition to its roles in facilitating the assembly of the other polarization complexes as described earlier, Par3 binds phosphoinositides in the membrane, as well as the phosphoinositide phosphatase PTEN (phosphatase and tensin homolog).[191,192] This phosphatase converts phosphatidylinositol (3,4,5)P_3 (PIP3) on the inner leaflet of the membrane to phosphatidylinositol (4,5)P_2 (PIP2). The latter lipid then facilitates the development of the apical surface by binding annexin2, which then

recruits Cdc42, leading to the cascade of events involving aPKC described earlier.[202] The importance of the conversion of PIP3 to PIP2 in the formation of the apical surface was highlighted dramatically when exogenous PIP2 was added to the basolateral pole of mature MDCK cell cysts in 3D culture.[202] Incorporation of PIP2 into the basolateral plasma membrane led to gradual extension of the apical surface to the basal pole with collapse of the lumen.

The description of the polarization process so far has focused only on events initiated by cell–cell adhesion. However, as was described in the previous section, adhesion of epithelial cells to the basement membrane is also a key part of polarization, functioning particularly to orient the apical–basal axis in a coordinated fashion in neighboring cells. How basement membrane adhesion and, particularly, adhesion to laminin does this is not clear, but it likely involves the microtubule cytoskeleton (Figure 1.2). In individual MDCK cells adherent to a substratum in 2D culture, the organization of microtubules resembles that in other nonepithelial adherent cells, in that microtubule growth is initiated from a juxtanuclear centrosome or microtubular organizing center, and extends radially towards the cell surface.[203–205] Once cell–cell adhesion is initiated, the microtubule organizing activity begins to disperse to the cell periphery and, as the cell polarizes, it relocalizes diffusely to the apical surface.[203–205] In response to this, microtubules reassemble along the apical–basal axis with the plus (growing) ends pointing basally. Networks of microtubules also form roughly parallel to the basal and apical surfaces[203–205] (Figure 1.2). Reorganization of the microtubules depends on a family of GTPases known as septins, which provide directionality to the process,[206,207] while stabilization and anchoring depend on the plekstrin homology-like domain family A protein LL5, microtubule plus-end tracking proteins, and the APC (adenomatous polyposis coli) tumor suppressor.[208–211] LL5 anchors microtubule plus ends to the basal plasma membrane by associating with integrin-mediated cell adhesions to laminin.[208] Furthermore, the polarity protein Par1b, which has been implicated in assembly of the laminin network in the basement membrane, is also important in the formation of the apical surface in 3D cysts, reportedly through a mechanism that depends on signaling from the extracellular matrix.[212] Thus, there appears to be a signaling network linking laminin assembly and microtubule reorganization to formation of the apical surface in the correct location. How these microtubules mechanistically contribute to polarization is not clear, but it is known that they provide tracks for vesicle transport that are necessary for formation of the apical lumen through its population with specific proteins, a process facilitated by septins.[121,122,125]

Ultimately, cooperation of extrinsic spatial cues and the intrinsic polarization machinery creates a polarized cellular infrastructure composed of adhesive interactions, a spatially-differentiated cytoskeleton, and asymmetrically disposed signaling complexes. Completion of polarization, and its maintenance during cell and tissue function, then depends on the targeting of specific membrane proteins to the apical and basolateral plasma membrane domains. How this is accomplished is the subject of the following section.

Sorting Pathways

One of the first, and perhaps most easily addressed, questions presented by the phenomenon of epithelial polarity relates to where, within the cell, sorting occurs. The membrane proteins that populate the apical and basolateral plasmalemmal domains are all synthesized in association with the membranous elements of the rough endoplasmic reticulum (RER).[213] It has further been shown that after their co-translational insertion into the membranes of the RER, apically- and basolaterally-directed proteins share the same cisternae of the Golgi complex as they transit the secretory pathway en route to their respective sites of ultimate functional residence.[214,215] Immunoelectron microscopic studies performed on MDCK cells doubly infected with the VSV and influenza viruses revealed, through double labeling, that the influenza HA protein and the VSV G protein could be co-localized throughout the cisternae of the Golgi complex.[215]

This observation was confirmed and extended through a series of elegant biochemical studies. It had previously been shown that when cells are incubated at 20°C newly synthesized membrane proteins accumulate in the trans-most cisterna of the Golgi complex.[216,217] Elevating the temperature to 37°C relieves this block, and allows the proteins to proceed to the cell surface.[218] By examining the nature of the complex N-linked glycosylation associated with the VSV G protein, it was demonstrated that sialic acid residues are added in the 20°C compartment.[214] These investigators took advantage of the fact that in addition to the HA protein the membrane of the influenza virus contains a neuraminidase in their efforts to determine whether segregation of the apically directed influenza proteins from the basolaterally targeted VSV G protein occurs before or after the 20°C block compartment. They found that in singly infected cells incubated at 20°C, the VSV G protein became heavily sialylated. In contrast to this, when cells which had been doubly infected with both the VSV and influenza viruses were incubated at 20°C, little if any sialic acid could be detected on the newly synthesized VSV G protein.

These results demonstrate that as late as the 20°C block compartment, which corresponds to the trans-most cisterna of the Golgi complex, the newly synthesized apical neuraminidase and basolateral VSV G protein are still intermingled and capable of physical interaction. The segregation of these two classes of proteins from one another must, therefore, occur at or after this subcellular locus. It is interesting to note that immunoelectron microscopic studies of endocrine cells reveal that proteins destined for packaging in secretory granules are separated from those bound for constitutive delivery to the cell surface in the trans-most cisterna of the Golgi complex.[219–221] Observations such as these have prompted investigators to speculate that this compartment, which is referred to as the Trans Golgi Network (TGN), might be the site of several intracellular sorting events.[222] More recently, it has been shown that sorting may occur as well at the level of the recycling endosome. Loading endosomes with HRP-conjugated transferrin, and subsequently disrupting endosome function through the deposition of peroxidase reaction product, prevents the surface delivery of a subset of newly synthesized basolateral membrane proteins.[223] While the delivery of the VSV G protein to basolateral plasma membrane is prevented by this ablation of the recycling endosome, the delivery of the newly synthesized Na^+/K^+-ATPase to the basolateral surface is unaffected by this maneuver.[224] Thus, it would appear that proteins can pursue more than one route from the TGN to the basolateral membrane domain.

Three epithelial sorting pathways can be imagined (Figure 1.9).[1,2,158] In the direct model, sorting would take place prior to cell surface delivery. Segregation of basolateral from apical proteins would be completed intracellularly, and proteins would never appear, even transiently, in the inappropriate membrane domain. The random sorting scheme dictates that no separation of apical from basolateral proteins occurs prior to arrival at the cell surface. Following their insertion into the plasmalemma, proteins that find themselves in the wrong surface domain would be removed by endocytosis, and either transcytosed to the proper surface[225] or degraded. Finally, the indirect paradigm predicts that all newly synthesized plasmalemmal proteins initially appear together, either at the apical or basolateral membrane. The proteins for which this delivery is correct would be retained in that membrane domain, while those which had been mis-delivered would be internalized and transcytosed to their sites of ultimate functional residence.

These three models, although perhaps somewhat simplistic, are valuable for the relative ease with which they can be experimentally distinguished. Over the past two decades a great deal of effort has been invested in identifying which of these routes is, in fact, operational. The rather surprising answer appears to indicate that the sorting pathway pursued varies among different cell types, and even among different proteins within the same cell type.

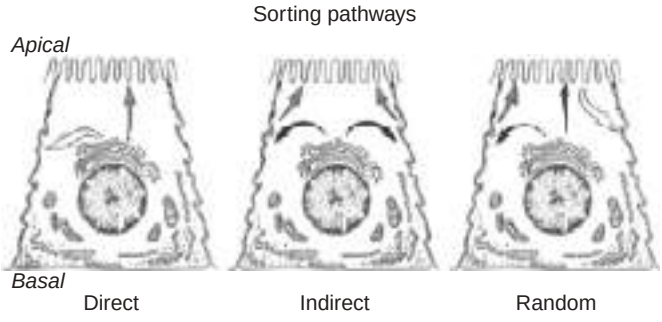

FIGURE 1.9 **Three potential pathways for the sorting of membrane proteins in polarized epithelial cells.** In the vectorial sorting scheme, apical and basolateral membrane proteins are separated from one another intracellularly and prior to plasmalemmal delivery (left). The indirect, or obligate, misdelivery model predicts that all newly synthesized plasma membrane proteins are carried together to a common cell surface domain. Proteins destined for the opposite surface are then internalized and transported to their appropriate destinations (middle). Finally, random sorting is defined by a complete lack of intracellular segregation. Apical and basolateral proteins are delivered without preference to both surfaces, and are subsequently redistributed by endocytosis and transcellular transport (right). Clear arrows represent vesicles carrying only basolateral proteins; hatched arrows denote vesicles carrying only apical proteins; and black arrows indicate vesicles carrying intermixed apical and basolateral membrane proteins. *Reprinted with permission from ref. [1].*

Technical Approaches

Much of the early research into the nature of epithelial sorting pathways was carried out on MDCK cells that had been infected with the VSV or influenza viruses. The infected cells produced massive quantities of viral proteins, and retained their polarized distribution throughout at least the initial stages of the infection. These properties greatly facilitated the detection of cohorts of newly synthesized membrane proteins in the pulse chase protocols generally employed to monitor the polarity of cell surface delivery. Pulse labeling experiments demonstrated that the VSV G protein was not accessible to apically added antibodies at any point during its post-synthetic processing.[226] In the case of the influenza HA protein, the converse was true. Proteases[174] or antibody probes[227] added to the media compartment bathing the basolateral surfaces of MDCK cells grown on filters could not cleave or interact with this polypeptide during its journey to the apical cell surface. From these results, it was concluded that the direct model of sorting applied for at least these two proteins in MDCK cells.

Other labeling tools have also been brought to bear on the study of sorting pathways. The N-hydroxysuccinimidyl (NHS) derivative of biotin is a membrane impermeant molecule that will covalently combine with the ε-amino groups of exposed lysine residues.[228] Proteins thus modified are substrates for precipitation or detection with avidin-conjugated secondary reagents. These tools can be used to follow the fate of large numbers of membrane proteins that have been exposed at one or other cell surface to the NHS biotin compound. Using such a protocol, it has been demonstrated that several MDCK cell apical and basolateral membrane proteins are directly targeted to their appropriate membrane domains.[229,230]

Advances in the development of genetically encodable probes have also permitted sorting pathways to be visualized directly. By creating chimeras that incorporate photoactivatable versions of the green fluorescent protein (GFP), the trafficking of newly synthesized proteins of interest can be observed in intact cells in real-time.[231] Alternatively, the SNAP tag similarly permits newly synthesized cohorts of proteins to be observed in pulse chase protocols. The 20 kDa SNAP-Tag is a modified version of the DNA repair protein 0^6-alkylguanine-DNA alkyltransferase, which cleaves para-substituted benzyl guanines (BGs) by covalently transferring the substituted benzyl group to its active thiol.[232] The resulting thioether bond irreversibly prevents the reacted SNAP-Tag from participating in any further labeling reactions. Fluorescent BG derivatives allow for the labeling and detection of SNAP-Tagged fusion proteins in either live or fixed cells.[232,233] Through the combination of a "pre-pulse" blocking step with non-fluorescent BG, followed by selective labeling of newly synthesized protein with fluorescent BG, it is possible to follow a cohort of protein as it is synthesized and trafficked.[224]

Sodium Pump Targeting

Further support for the direct pathway paradigm in MDCK cells came from studies on the sorting of the endogenous Na^+/K^+-ATPase.[175] Filter grown MDCK cells which had been pulse-labeled with [35S]-methionine were exposed to the N-azidobenzoyl (NAB) derivative of ouabain at either their apical or basolateral surfaces during the course of a 90 minute chase. NAB-ouabain will bind to catalytically active sodium pumps with high affinity and, following UV photolysis, will become covalently incorporated into the protein backbone of the Na^+/K^+-ATPase α-subunit.[234–236] By analyzing immunoprecipitates prepared from these cells using an anti-ouabain antibody, it was possible to demonstrate that no sodium pump in a state competent to bind ouabain ever appears at the apical surface. Subsequent studies using a SNAP-tagged version of the Na^+/K^+-ATPase expressed in the same MDCK cell line recapitulated the finding that the newly synthesized pump trafficks directly to the basolateral surface in these cells.[224]

Another investigation of sodium pump sorting in a different clonal line of MDCK cells made use of the NHS biotin surface-labeling technique, and arrived at a conclusion diametrically opposed to the one described above. The results of this study indicated that the Na^+/K^+-ATPase is randomly delivered to the apical and basolateral plasmalemmal surfaces.[237] The authors further suggested that stabilizing interactions with cytoskeletal elements which underly the basolateral, but not the apical, cell surface[112,114,119] result in a much longer residence time for pump inserted into the basolateral domain. These studies are thus consistent with a model in which sodium pump is not sorted intracellularly, but instead achieves its basolateral distribution through a mechanism based on random delivery followed by differential stabilization.

The apparent discrepancy among these studies appears to be attributable to differences in the pathways and processes through which these closely related cell lines achieve the polarized distribution of the Na^+/K^+-ATPase. While one line targets the pump directly to its basolateral destination, the other delivers it randomly and depends upon cytoskeletal interactions to stabilize only the basolateral pool.[238,239] Clearly, therefore, while cytoskeletal interactions may be sufficient to localize the Na^+/K^+-ATPase to the basolateral surface, they are not the sole mechanism involved in producing the sodium pump's anisotropic distribution. Instead, they may act as a failsafe mechanism to back up and reinforce the initial biosynthetic sorting of the Na^+/K^+-ATPase, to ensure that its polarized distribution is attained and maintained.

The preceding discussion suggests that the direct scheme cannot be applied to all epithelia or even to all MDCK cell clones. An alternative system has been shown to apply to the liver, for example. Cell fractionation studies performed on liver by Bartles et al. reveal that several apical membrane proteins appear in the fraction corresponding to the hepatocyte basolateral plasma membrane prior to being delivered to the apical surface.[240] This route has been especially well-documented for the polymeric immunoglobulin receptor (pIgR) expressed by hepatocytes. This 120 kDa polypeptide serves to carry dimeric IgA from the blood to the lumena of the bile cannaliculi. During its biosynthesis, the pIgR is transported directly from the TGN to the basolateral cell surface where it is available to bind dimeric IgA.[241,242] Independent of any interaction with IgA the receptor becomes phosphorylated in the basolateral plasmalemma, and the phosphorylated form is internalized and carried by a transcytotic vesicle to the apical, or canalicular, surface.[243] Following its insertion

into the apical plasma membrane the ectodomain of the pIgR is cleaved and released into the bile as an 80 kDa protein referred to as secretory component.[241,242] Association with secretory component helps to protect the bound IgA from intestinal proteases. Coupled with other results,[240] the behavior of pIgR in hepatocytes supports the contention that apical membrane proteins arrive at their site of ultimate functional residence via obligate mis-delivery to the basolateral domain. This paradigm may not apply to all apical proteins in hepatocytes. Studies of the trafficking of apical members of the multidrug resistance (MDR) family of transport proteins indicate that these polytopic membrane proteins do not make an appearance at the basolateral surface en route to the apical membrane.[244,245] Thus, within a single polarized cell type multiple trafficking routes can be employed to target different proteins to the same place.

A combination of the direct and indirect paradigms seems to be involved in membrane protein delivery in cultured intestinal cells. The Caco-2 line of human colon carcinoma cells can be grown on filters and subjected to the NHS-biotin labeling protocol described above. Such experiments reveal that the basolateral protein followed is vectorially targeted.[246] Analysis of the apical polypeptides produced a somewhat more complicated picture. A fraction of these proteins appeared to transit through the basolateral plasmalemma prior to their apical delivery. The remainder of the apical proteins studied in this sampling were sorted intracellularly and inserted directly at the apical domain. Related and somewhat more complicated results have been gathered from studies on the biogenesis of brush border hydrolases by colonocytes *in situ*.[110,247,248]

To complete this already confusing picture it is necessary to return to a discussion of targeting studies in MDCK cells. A cDNA encoding the pIgR has been expressed by transfection in this cell line. Remarkably, the sorting pathway pursued by this protein in the cultured renal epithelium is apparently identical to the rather baroque scheme that characterizes its route in hepatocytes.[249] From the TGN, the pIgR travels to the basolateral surface from which it is internalized and subsequently transcytosed to the apical pole or recycled to the basolateral side. These observations demonstrate that an obligate mis-delivery pathway is either created or simply revealed in MDCK cells expressing the pIgR. Results from studies employing real-time imaging to follow the surface delivery of a class of newly synthesized apical proteins support the possibility that this indirect pathway does, in fact, exist constitutively in MDCK cells. As discussed in greater detail in the section on sorting signals, proteins whose attachments to the membrane are mediated by covalent linkage to glycosylphosphotidyl inositol (GPI) lipids tend to accumulate in the apical domains of most varieties of polarized epithelial cells. A study that employed live cell imaging to track the sorting of GPI-linked proteins found that these proteins were delivered to the basolateral surface, after which they were endocytosed and carried to the apical plasmalemma.[250] It is worth noting, however, that subsequent studies found that several GPI-linked proteins were delivered directly to the apical membrane in MDCK cells, without making any detectable transient appearance at the basolateral surface.[251]

This apparent diversity of sorting pathways is perhaps not as surprising as it first appears. The relative flow of membranous vesicles from the Golgi complex to the two plasmalemmal surfaces in different epithelial cell types is likely to reflect a cell's biologic mission, as well as the nature of the environment in which it functions. It appears, for example, that although hepatocytes produce copious quantities of secretory proteins, none are released directly into the bile.[252] It has been proposed that newly synthesized membrane proteins depart the Golgi in the same transport vesicles that carry proteins destined for constitutive secretion.[158,252] Were this the case, then cells which do not produce a secretory content targeted for one or another membrane domain may also lack a direct traffic of membrane vesicles directed from the Golgi to that domain. The full complement of plasmalemmal proteins might thus be forced by default to share the same carrier out of the Golgi, and to be sorted by transcytosis subsequent to cell surface delivery. Some hepatic apical membrane proteins may transit through the basolateral surface, because there is very little non-stop cargo traveling from the TGN to the apical domain in this particular cell type. The apparent multiplicity of sorting pathways available to different proteins within the same cell type may reflect specializations relevant to these proteins' functions. Diversity may also arise from the nature of the signals and mechanisms that mediate these proteins' polarized distribution. The potential contribution of this latter influence will be referred to again in sections to follow. The lack of a single answer or unifying solution to the problem of sorting pathways is a theme that carries through the entire study of epithelial polarity. A number of equally effective mechanisms appear to have evolved for segregating membrane proteins into distinct domains. It remains to be determined how these differing approaches benefit their respective tissues and contribute to the maintenance of their unique functions.

Regulation of Renal Transport Protein Function by Endocytosis and Recycling

The delivery of a protein to its site of functional residence in a domain of the plasma membrane does not

end that protein's involvement with the cellular sorting machinery. Cell surface proteins are subject to endocytic internalization, after which their fate is determined through processes that are mechanistically closely related to those that mediate biosynthetic sorting. Following their delivery to endosomes, endocytically internalized proteins can be recycled, meaning that they are returned to the same domain of the plasma membrane. Alternatively, they can be carried by transcytosis to the opposite plasma membrane domain. Finally, they can be targeted for degradation in the lysosome. The cellular machinery and molecular signals that govern these post-endocytic sorting processes appear to closely resemble those that mediate biosynthetic sorting.

From the perspective of the renal tubular epithelial cell, perhaps the most important implication of post-endocytic sorting relates to its role in the regulation of ion transport protein activity. The activities of a number of critically important transport proteins are controlled by regulated membrane insertion and endocytotic events.[253] Included on this list are the aquaporin 2 water channel (AQP2),[254] the ROMK potassium channel,[255] and the ENaC sodium channel of collecting duct principal cells[256]; the V-type proton ATPase of collecting duct intercalated cells[257]; the Na,Cl co-transporter (NCC) of the distal convoluted tubule[258]; the Na phosphate co-transporter (NaPi),[100] the Na proton exchanger (NHE3),[259] and the Na^+/K^+-ATPase of the proximal convoluted tubule.[260] These regulated trafficking events are precipitated by a variety of hormonal and physical stimuli, and involve the participation of a diverse collection of signaling cascades and trafficking proteins. While their details will be explored in far greater individual detail in the chapters that relate to each of the specific tubule segments and relevant transport systems, it is worth noting that these regulated trafficking processes exploit many of the biosynthetic sorting signals and components of the cellular trafficking machinery that are discussed in the following sections.

Sorting Signals

Rodriguez-Boulan and Sabatini's 1978 observation that viral spike glycoproteins are targeted to opposite domains of polarized epithelial cells[165,166] gave rise to the hypothesis that sorting signals – that is, the information required to direct a protein or proteins to a given subcellular location – might be wholly contained within the structure of the sorted proteins themselves. Evidence in favor of this contention has come from studies examining the distribution of viral membrane proteins expressed by transfection (rather than infection) in polarized cultured cells. A number of investigators have shown that the influenza HA protein, the VSV G protein, and related viral spike glycoproteins are sorted correctly in the absence of any other proteins encoded by viral genomes.[261–264] It is apparent, therefore, that all of the addressing information necessary to produce the polarized distributions of these polypeptides must be embodied within the proteins themselves. It has further been shown that this information is almost certainly associated with the protein backbone, rather than with any post-translational modification. Cells whose capacity to add asparagine-linked sugar residues has been impaired, either through mutation or via treatment with tunicamycin,[265,266] are nonetheless able to correctly target the viral spike proteins. Observations such as these have sparked an intensive search for the actual molecular information that specifies localization, and for the machinery that acts upon this information. It must be stated at the outset, however, that despite the rather confident and declarative tone of this section's heading the identification and characterization of epithelial sorting signals and mechanisms is far from complete.

Several distinct classes of signals have been found to specify basolateral sorting.[267] Perhaps the best characterized of these are short motifs that contain tyrosine residues and resemble or overlap with sequences involved in endocytosis. Work from a number of groups has suggested that sequences in the cytosolic tail of membrane proteins determine the rates at which these proteins are internalized. The presence of a tyrosine residue appears to be a critical determinant of the efficacy of an endocytosis signal.[268] The rapid endocytosis of both the LDL receptor and the transferrin receptor, for example, is dependent upon the presence of short, tyrosine-containing sequences in these proteins' cytoplasmic tails. Mutation of this tyrosine residue to any other amino acid vastly reduces the rates at which both of these proteins are internalized. The apically sorted influenza HA protein is normally endocytosed extremely slowly. Addition of a tyrosine residue to the cytosolic tail of the influenza HA protein causes it to behave like the LDL receptor or transferin receptor with respect to endocytosis – that is, it is rapidly internalized and recycled.[269] When this altered form of the HA protein is expressed in MDCK cells it is detected predominantly at the basolateral plasma membrane.[270] It would appear, therefore, that a signal that is permissive for endocytosis is also competent to mediate basolateral accumulation.

Studies of the VSV G protein reveal that its basolateral sorting is also driven by a tyrosine-containing motif.[271,272] Uptake measurements suggest, however, that the VSV G protein is internalized relatively slowly, suggesting that its tyrosine-based motif confers basolateral targeting, but not rapid endocytosis. Mutagenesis studies of the tyrosine-modified influenza HA protein, as well as several other basolateral

membrane proteins, indicate that while internalization signals and basolateral sorting signals can share the same critical tyrosine residues, they are not identical.[273] Altering residues near the tyrosine can produce apically sorted influenza HA protein that is rapidly endocytosed, and basolateral HA protein that is internalized only slowly. Thus, basolateral and endocytosis signals can overlap, sharing one or more residues, but are clearly distinguishable from one another. Presumably, therefore, they must be interpreted by non-identical cellular machinery.

Data pointing to a similar conclusion have been gathered for Fc receptors.[274] One of the Fc receptor isoforms includes a di-leucine sequence in its cytoplasmic tail. This sequence has been shown to function as an endocytosis signal, and it also appears to confer basolateral targeting when the protein is expressed in polarized cells. Once again, alteration of residues flanking the di-leucine motif demonstrates that the sequence requirements for basolateral sorting are distinct from those that specify internalization.[275,276]

Tyrosine-containing basolateral sorting signals that are entirely distinct from recognizable endocytosis motifs have also been detected. The LDL receptor depends upon a basolateral sorting signal that bears no sequence resemblance to any known internalization motif.[276,277] Although this motif includes a tyrosine residue, mutation of that tyrosine to phenylalanine still permits basolateral localization. A distinct tyrosine-containing motif appears to mediate the internalization of the LDL receptor.[278] In the absence of the primary basolateral signal, this endocytosis motif can mediate a basolateral sorting function. Once again, however, with the exception of the tyrosine residue, the amino acids that contribute to the basolateral and endocytic aspects of this signal are distinct from one another.

Several basolateral sorting signals unrelated to tyrosine residues have also been reported. The well-characterized tyrosine-based endocytosis motif of the transferrin receptor is completely distinct from this protein's basolateral targeting signal, which resides in a different portion of the cytoplasmic tail. The peptide processing enzyme furin cycles between the trans-Golgi network and the basolateral plasmalemma. Its trafficking to the basolateral surface appears to be driven by residues that are associated with a casein kinase II phosphorylation site.[279,280] The invariant chain of the major histocompatibility class II complex is sorted to the basolateral membrane by virtue of the dihydrophobic sequence Met−Leu.[281] Once again, endocytic internalization of this molecule is conferred by a similar dihydrophobic sequence, Leu−Ile, which is present at another position on the cytoplasmic tail. All of the basolateral sorting motifs discussed thus far function in the context of membrane proteins that span the bilayer once. As will be discussed below, a distinct cadre of molecular sequences appears to mediate the targeting of many ion transporters and other multispanning membrane proteins.

The list of identified basolateral sorting signals is considerably more extensive than the inventory of characterized apical membrane protein sorting signals. Perhaps the best studied member of this latter roster is not, in fact, a protein-based signal at all, but is instead constituted entirely of phospholipid. Glycophospholipid (or GPI)-linked proteins are synthesized as transmembrane polypeptides that are co-translationally inserted into the membrane of the RER.[282] While still associated with the ER, the GPI-linked protein's ectodomain is proteolytically removed and transferred to a preassembled structure composed of a complex glycan tethered to the membrane through its attachment to a molecule of phospholipid (frequently phosphotidylinositol). Previous work has shown that in polarized epithelial cells, most of the GPI-linked proteins reside in the apical plasmalemma.[230,283] Interestingly, the apical surface also plays host to most of the cell's complement of glycolipid.[284] Investigators prepared a construct in which the VSV G ectodomain was wedded to the transmembrane tail of Thy-1, which carries a signal for glycophospholipidation.[285] The resultant GPI-linked G protein is sorted to the apical membrane. The results of these and related experiments have generally been interpreted to indicate that a strong apical sorting signal is embodied in some component of the GPI linkage itself. The transmembrane domains of several single-spanning apical membrane proteins appear to carry information important for apical targeting. The transmembrane domains of the influenza virus neuraminidase and HA proteins, for example, are sufficient to mediate sorting to the apical surface when they are included in constructs expressed by transfection in MDCK cells.[286] As will be discussed below, the same mechanisms that are thought to be involved in recognizing the GPI tail as an apical sorting motif may also interpret signals embedded in transmembrane domains. Furthermore, transmembrane domain sorting signals may be important not only in the localization of single spanning membrane proteins, but may also determine the distributions of polytopic ion pumps such as the Na^+/K^+- and H^+/K^+-ATPases (see below). It should also be noted that the extracytoplasmic or ecto domains of several apical proteins appear to incorporate directional signals. Roth et al. have shown that the ectodomain of the influenza HA protein is sufficient to specify apical targeting.[287] When a cDNA construct encoding an anchor-minus form of the HA protein, which lacks both the cytosolic and transmembrane segments, is expressed in polarized cells it is secreted exclusively into the apical medium compartment. This is also true well for the polymeric immunoglobulin receptor.[288] These results suggest

that a signal involved in apical sorting resides in the lumenal portion of the HA molecule, and that this signal remains interpretable when it is presented as a soluble protein or in association with portions of a basolateral membrane polypeptide. Finally, N-linked sugar groups, which are also present on the extracytoplasmic domains of membrane proteins, can in some circumstances contribute apical sorting information.[289] It is logical to conclude from this discussion that machinery necessary to read and interpret this putative ectodomain apical sorting information must be exposed at the lumenal surface of the organellar compartments involved in the segregation and targeting of newly synthesized membrane proteins.

As discussed above in the section on sorting pathways, not all of the plasma membrane proteins expressed by polarized epithelial cells pursue a direct course to their sites of ultimate functional residence. The polymeric immunoglobulin receptor (pIgR) for example, when examined in its native liver[241,242,290] or in transfected MDCK cells,[249] travels first to the basolateral surface and subsequently to the apical pole. A number of studies have examined the contributions that various portions of the pIgR molecule may make to this complicated sorting behavior. Anchor-minus ectodomain constructs of the pIgR are secreted apically from transfected MDCK cells.[288] Furthermore, deletion of the pIgR cytosolic tail results in a membrane protein that travels directly to the apical surface without ever appearing at the basolateral side.[291] These observations have led to the suggestion that the ectodomain of the pIgR receptor contains an apical sorting signal, and that this protein's cytosolic tail embodies information that is required for its initial appearance at the basolateral plasma membrane. Extensive mutational analysis reveals that a trio of amino acids in the sequence His, Arg, Val is primarily responsible for the vectorial targeting of the newly synthesized pIgR protein to the basolateral plasmalemma. This motif constitutes yet another addition to the growing collection of distinct amino acid sequences that can encode basolateral sorting.[292,293]

During its tenure at the basolateral membrane, the pIgR's cytosolic tail becomes phosphorylated on a serine residue. The phosphorylation event occurs both in liver[243] and in transfected MDCK cells.[294] Intriguing experiments demonstrated that the addition of this phosphate group acts as a switch that allows the apical sorting signal to predominate, and results in the protein's transcytosis to the apical side. Site directed mutagenesis has been performed on the cDNA encoding the pIgR in order to convert the serine of interest into either an alanine or an aspartate residue.[294] When expressed in MDCK cells, the wild-type, as well as the two mutant forms, are all initially targeted to the basolateral surface, and all three undergo endocytosis and recycling at similar rates. Interestingly, however, while the wild-type receptor undergoes fairly rapid transcytosis, the alanine form remains largely associated with the basolateral plasma membrane. In contrast, the aspartate form is transcytosed at a rate that exceeds that characteristic of the non-mutant form. These observations suggest that the negative charge associated with the phosphate and aspartate residues permits or activates the incorporation of the pIgR into transcytotic vesicles, and thus initiates the protein's delivery to the apical surface. The mechanism through which this signal is detected and interpreted remains unclear.

The recognition and segregation of pIgR destined for transcytosis probably occurs in an endosome following internalization from the basolateral surface. The second sorting event involved in the targeting of the pIgR is thus almost certainly completed at a subcellular location distinct from the TGN. This behavior suggests that, once again, the sorting of apical from basolateral proteins need not occur exclusively on the exocytic pathway. The endosome or an endosome-related compartment appears competent to sense and act upon the sorting signals that are necessary for the pIgR's apical localization. It remains to be determined whether signals detected in the endosome correspond to the same ectodomain-associated information that mediates the apical secretion of an anchor-minus form of the pIgR. The segregation of this secretory form to the apical pathway almost certainly occurs during its passage through the Golgi, and is not likely to involve elements of the endocytic apparatus.

Most ion transport proteins and receptors span the membrane several times, and many are composed of multiple subunits. Their intricate structures complicate the search for sorting signals and increase the likelihood that multiple independent or hierarchical signals might be present. This is clearly the case for the gastric H,K-ATPase. Acid secretion in the stomach is mediated by the gastric H^+/K^+-ATPase. This dimeric ion pump is stored within an intracellular population of membranous vesicles, known as tubulovesicular elements (TVEs), in gastric parietal cells. Stimulation of acid secretion by secretagogues induces the TVEs to fuse with the parietal cell apical plasma membrane, resulting in the formation of deeply invaginated secretory canaliculi rich in H^+/K^+-ATPase. The cessation of acid secretion involves the retrieval of the H^+/K^+-ATPase from the cell surface, and the regeneration of the TVE storage compartment.[295] Both the α- and β-subunits of the H^+/K^+-ATPase belong to the large P-type ATPase gene family.[296] Their closest cousins in this collection are the corresponding α- and β-subunits of the Na^+/K^+-ATPase. Interestingly, while the H^+/K^+-ATPase functions at the apical surface of gastric parietal

epithelial cells, the Na^+/K^+-ATPase is restricted in its distribution to the basolateral plasmalemma, in this and most other epithelial cell types.[297] The homology relating these ATPases has permitted the creation of chimeric ion pumps, whose subunits are composed of complementary portions of the H^+/K^+- and Na^+/K^+-ATPase α- and β-polypeptides. By expressing these constructs in cultured polarized epithelial cells it has been possible to determine the molecular domains of the ion pump subunit proteins that are responsible for their sorting. Through this analysis it has become clear that both the α- and β-subunit polypeptides of the H^+/K^+-ATPase contain molecular signals which can contribute to the targeting of the holo-enzyme.[298–300] Expression of a large number of progressively more refined α-subunit chimeras reveals that an eight amino acid sequence within the α-subunit of the H^+/K^+-ATPase is sufficient to specify apical sorting.[300] This domain is predicted to reside within a transmembrane helix, thus suggesting that protein–lipid or protein–protein interactions within the plane of the membrane are responsible for pump sorting.

The β-subunit of the H^+/K^+-ATPase contains a tyrosine-based sorting signal that functions to internalize the pump complex from the surface of the gastric parietal cell, and return it to an intracellular regulated storage compartment.[301] This internalization is responsible for the cessation of gastric acid secretion following the removal of secretagogue stimulation. This was demonstrated by generating a transgenic mouse which expresses an H^+/K^+-ATPase β-subunit lacking this endocytosis signal.[301] These animals are unable to reinternalize H^+/K^+-ATPase from the apical surfaces of their gastric parietal cells. Consequently, they produce elevated gastric acid secretion during the interdigestive period. Mice carrying the mutant β-subunit develop gastritis and gastric ulcerations, with histologic features that are essentially identical to those found in human disease. Examination of renal potassium clearance in these animals reveals that the same β-subunit sorting signal regulates active potassium resorption in the collecting tubule.[302]

Several studies have begun to define other signals employed in the polarized sorting of polytopic membrane proteins. Recently, for example, a novel motif has been identified in the cytoplasmic tail of the seven-membrane-span receptor rhodopsin that mediates this protein's apical sorting when it is expressed in MDCK cells.[303] Another member of the seven transmembrane G protein-coupled receptor family, the P2Y2 receptor, manifests an apical sorting signal in one of its extracellular loops.[304] Furthermore, studies of neurotransmitter re-uptake systems have demonstrated that the four members of the highly homologous GABA transporter gene family are differentially sorted in epithelial cells and in neurons.[305,306] The GAT-1 and GAT-3 isoforms, which are restricted to axons when expressed endogenously or by transfection in neurons, are sorted to the apical membranes of epithelial cells. The GAT-2 and betaine transporters, which are 50–67% identical to GAT-1 and GAT-3, behave as basolateral proteins in epithelia, and are restricted to dendrites when expressed in neurons. Production of chimeric and deletion constructs have permitted the identification of very short amino acid sequences at the extreme C-terminal tails of these transporters which manifest targeting information. The nature of these sequences suggests that they may interact with polypeptides containing PDZ-type protein–protein interaction domains, raising the possibility that this association may play a direct role in the sorting of ion transport proteins.[307] A similar PDZ-dependent mechanism also appears to mediate the apical trafficking of CFTR.[308–311] The basolateral isoform of the Na,K,2Cl co-transporter, NKCC1, has recently been shown to be targeted to the basolateral surface by virtue of a di-leucine motif in its cytoplasmic C-terminal tail. The renal isoform of this protein, NKCC2, depends for its apical localization on a two non-contiguous stretch of amino acids that appear to collaborate to form a conformation-dependent signal in the context of the fully folded transporter's C-terminal domain. The mechanism through which this non-contiguous conformational determinant is recognized by the cellular sorting machinery has yet to be determined.[312]

Cell Type-Specific Sorting: Patterns

The message encoded within a membrane protein's sorting signal is dependent not only upon its own specific biochemical composition, but also upon the cellular context in which it is expressed. Several examples of membrane proteins that are differentially targeted in distinct epithelial cell types have been documented. The vacuolar H^+-ATPase, for example, accumulates at the apical surfaces of α-type intercalated cells, but at the basolateral plasmalemmas of β-type intercalated cells in the renal collecting duct.[313] Similarly, the Na^+/K^+-ATPase is basolateral in most epithelia, but behaves as an apical protein in cells derived from the neural crest, such as choroid plexus and retinal pigment epithelium.[314,315] Targeting of particular proteins or classes of proteins can also vary as a function of the differentiation states of epithelial cells. For example, the sorting of well-characterized polarity markers expressed in *Drosophila* via germ line transformation was followed in the developing *Drosophila* embryo. Human placental alkaline phosphatase (PLAP) is a glycosylphosphatidyl inositol (GPI)-linked protein that accumulates at the apical membranes of mammalian epithelial cells. A chimeric construct composed of the

transmembrane and cytosolic portions of the vesicular stomatitis virus (VSV) G protein coupled to the ectodomain of PLAP has been found to behave as a basolateral protein when expressed in the MDCK cell system.[285] The subcellular distributions of these proteins were examined in the epithelial tissues of transgenic *Drosophila* embryos which expressed these proteins under the control of a heat shock promoter.[316] In the surface ectoderm both PLAP and PLAPG were restricted to the basolateral membranes throughout development. Internal epithelia derived from the surface ectoderm accumulated PLAP at their apical surfaces, while PLAPG retained its basolateral distribution. The redistribution of PLAP from the basolateral to the apical plasma membrane was found to be coincident with the invagination of the surface epithelium to form internal structures, suggesting that the sorting pathways which function in the epithelium of the *Drosophila* embryo are developmentally regulated.

In light of both the multiplicity of sorting signals presented in the preceding section, and the apparent potential for heterogeneity in their interpretation discussed above, it is natural to wonder whether any logic or consistency governs nature's solution to the deceptively simple problem of apportioning proteins among two separate membrane domains. Upon further reflection, however, the complexity and degeneracy of the "sorting code" can be seen as a tremendous virtue. Two different epithelial cell types may need to target a given membrane protein to opposite surfaces of their respective plasma membranes in order to fulfill their unique physiologic functions. These same functions may also require, however, that other membrane proteins occupy the same surface distributions in both cellular contexts. Thus, while the sodium pump occupies the apical membranes of the cells of the choroid plexus and the basolateral membranes of renal epithelial cells, receptors for basement membrane components are present at the basolateral surfaces of both cell types. If only a single class of basolateral sorting signal and a single class of apical sorting signal existed, then it would not be possible for a cell to selectively alter the distribution of one set of plasmalemmal proteins, without simultaneously altering the distributions of the entire population of the plasma membrane. In order to target the sodium pump to the apical surface, choroid plexus epithelial cells would be forced to target basement membrane receptors there as well. This would obviously constitute a wasteful compromise. In order to endow each epithelial cell type with the capacity to select individualized complements of proteins for its apical and basolateral domains, a dizzying multitude of sorting signals has evolved. Cells can thus customize the distributions of proteins among their plasmalemmal domains, without the constraints that would be imposed by a limited number of sorting signals. According to this interpretation, sorting signals do not specify a specific destination such as apical or basolateral. Instead, they specify classes of proteins whose members are always sorted together. The membrane domain to which any one of these classes is sorted will depend upon the cellular context in which it is expressed, and will be determined by the idiosyncratic array of sorting machinery and pathways present in each individual epithelial cell type.

Sorting: Mechanisms

Extensive progress has been made in illuminating the mechanisms through which the sorting signals discussed above exert their effects and ensure the polarized delivery of newly synthesized plasma membrane proteins. The strong evidence for the existence of sorting signals leads quite naturally to the postulate that sorting receptors must exist that are capable both of recognizing these signals, and of transducing their messages to the relevant cellular machinery. Such receptors have, in fact, been demonstrated in the case of lysosomal enzyme sorting. Targeting of a newly synthesized hydrolase to the lysosome is mediated by the interaction between the enzyme's mannose-6-phosphate (man-6-p) recognition marker, and one of two receptors which bind man-6-p bearing ligands in the Golgi and mediate their segregation to pre-lysosomal endosomes.[317] Binding of newly synthesized lysosomal enzymes to the man-6-p receptors is pH-dependent. At the relatively neutral pH of the Golgi ligands are tightly bound, whereas in the acid environment of the pre-lysosomal endosome they are rapidly released. No such well-characterized receptor systems have yet emerged to explain the sorting behavior of secretory and membrane proteins in polarized cells. While sorting receptors for secretory proteins remain to be identified definitively, some progress has been made in understanding how such receptors might function. Lysosomotropic amines, such as NH_4Cl and chloroquine, elevate the lumenal pH of acidic organelles.[318] The resulting neutralization of acidic compartments can have profound effects on sorting. In the case of lysosomal enzyme targeting, addition of NH_4Cl raises the pH of the pre-lysosomal endosome, and thus prevents the acid-dependent unbinding of newly synthesized hydrolases from the man-6-p receptor.[317] In the continued presence of the drug, the Golgi becomes depleted of receptors available to complex with free ligand. Newly synthesized enzymes bearing the man-6-p recognition marker are thus secreted constitutively and by default. Experiments on cultured polarized epithelial cells suggest that a similar pH-dependent mechanism may function in the sorting of basolateral secretory proteins.[176]

Laminin and heparan sulfate proteoglycan are constituents of epithelial basement membranes.[130,319] Studies of MDCK cells grown on permeable filter supports revealed that both of these proteins are normally secreted predominantly into the basolateral medium compartment.[176] When secretion from cells treated with NH_4Cl was monitored, it was found that both proteins were released into both media compartments in roughly equal proportions. Removal of the drug reversed this effect and restored normal basolateral secretion. As mentioned above, studies have demonstrated that the secretory default pathway for MDCK cells – that is the route pursued by soluble proteins which lack any means of interacting with the cellular sorting machinery – is apical and basolateral.[176,261,320] It appears, therefore, that targeting of these two basolateral secretory proteins requires the participation of an intracellular acidic compartment. Elevation of the lumenal pH of this compartment reversibly blocks laminin and HSPG sorting, and results in their apical and basolateral default secretion.

Although the nature of the dependence of this sorting event on acidic compartments remains unknown, it is interesting to speculate that a mechanism similar to that which functions in lysosomal enzyme sorting may also be involved in routing basolateral secretory proteins. In such a model, binding or unbinding of laminin and HSPG from a sorting receptor would require the participation of an acidic organellar pH. Confirmation of this hypothesis will await the identification of such a pH-dependent binding protein with affinity for these and other basolaterally targeted proteins.[321] Finally, it is worth noting that the basolateral sorting of the Na^+/K^+-ATPase, and the apical sorting of the influenza HA protein and a complex of secretory polypeptides, occurs normally in the presence and absence of NH_4C1.[175,176,322] It would appear, therefore, that different mechanisms are brought to bear in ushering different classes of proteins to their sites of ultimate functional residence.

Tyrosine-Based Motifs and Adaptors

Recent studies suggest that several different classes of soluble proteins may regulate the subcellular distributions of proteins bearing tyrosine-based signals. Perhaps the best understood of these are the adaptins.[323] The adaptins comprise a group of peripheral membrane proteins that mediate the interaction between transmembrane proteins and the clathrin skeletons of coated pits and vesicles. Adaptins recognize and bind to tyrosine-containing coated pit localization sequences and link the proteins bearing these motifs to the clathrin coat.[323–327] Adaptins can thus be considered to be among the most proximal elements of the endocytic sorting machinery – they recognize polypeptides endowed with endocytosis signals and ensure that they are incorporated into the specified internalization pathway. Distinct classes of adaptins function in the segregation of proteins into the coated structures associated with the trans-Golgi network, and into cell surface coated pits.[230] While AP2 adaptors mediate internalization of proteins from the cell surface, AP1 adaptor complexes participate in trafficking proteins out of the TGN. The μ-subunits of adaptor complexes appear to be responsible for interacting with tyrosine-based motifs.[325] Two isoforms of μ-subunits are found in AP1 complexes. The μ1a protein is ubiquitously expressed, and is found in both polarized and nonpolar cell types. The μ1b protein is instead found in only a subset of polarized cell types.[328] Proteins bearing tyrosine-based motifs are basolaterally sorted in MDCK cells, but accumulate apically in LLC-PK cells.[329] It was noted that MDCK cells express μ1b, whereas this protein is absent from LLC-PK cells. Remarkably, expression of μ1b in LLC-PK cells at least partially "normalizes" their sorting properties, so that many (but not all) membrane proteins containing tyrosine-based signals are directed to the basolateral surface.[330] Thus, μ1b constitutes perhaps the best characterized component of the sorting machinery. It is clearly capable of recognizing a class of sorting signals and acting upon the instructions that they convey. Consistent with the idea that clathrin adaptors play an important role in the sorting of at least some basolateral proteins, it has been demonstrated that knockdown of clathrin expression in cultured renal epithelial cells perturbs basolateral, but not apical, protein delivery.[331]

It is interesting to note that recent studies demonstrate that different proteins bind to and interpret the messages encoded by tyrosine-based and di-leucine endocytosis motifs. Overexpression of tyrosine-motif containing proteins can inhibit the endocytosis of other proteins carrying a similar endocytosis signal, presumably by competing for limited quantities of the adaptor proteins that cluster proteins bearing these signals into clathrin-coated pits. This intervention does not affect, however, the internalization of proteins endowed with di-leucine motifs, indicating that they must be recognized and interpreted by a different class of polypeptides.[332] It appears that the β-subunits of adaptor complexes interact with di-leucine motifs.[333] Finally, a very different type of protein has been shown to interact with a tyrosine-based proline-rich sequence in the C-terminal tails of epithelial sodium channel (ENaC) subunits. The Nedd-4 protein possesses a ubiquitin ligase domain, and through its interaction with the ENaC tails may lead to these channels' downregulation through degradation.[334]

The association of basolateral membrane proteins, such as the Na^+/K^+-ATPase with elements of the subcortical cytoskeleton,[112,119] has led to the speculation

that this interaction may play a role in targeting. Evidence in support of this proposition was found in the studies, described above, which suggested that, at least in one MDCK cell clone, the Na^+/K^+-ATPase may be delivered in equal proportions to the apical and basolateral surface.[237] Apically delivered material may be rapidly degraded, whereas basolateral sodium pump would be stabilized through interaction with the cytoskeleton and consequently would turn over very slowly. The pump's polarized distribution would thus be the product of differential susceptibility to degradation, rather than sorting at the level of the Golgi. The degree to which stabilization through interaction with the cytoskeleton contributes to the polarized distribution of the sodium pump or any other proteins remains to be established.

Glycosphingolipid-Rich Membrane Domains

The observation that all of the glycolipids and GPI-linked proteins associated with epithelial cells tend to be found in the apical plasmalemmal domain led to the proposal that lipids may play a role in membrane protein sorting.[335] Since glycolipids and GPI-linked proteins are only associated with the outer leaflet of the plasma membrane, these molecules will be exposed at the lumenal face of the organelles of the biosynthetic pathway. Any sorting machinery that interacts with glycolipids, therefore, must do so either at the lumenal surface or within the plane of the membrane itself. These constraints have suggested to some investigators the possibility that lipid–lipid interactions are sufficient to segregate apically directed glycolipids and GPI-linked proteins into distinct patches during their residence in the Golgi. These self-assembled patches could then serve as the nuclei from which apically directed vesicles would bud. The biophysical properties of these patches might be involved in ensnaring other apically directed proteins, as well as the components necessary to appropriately target the resultant transit vesicle.[336] While evidence of lipid patches exists in both *in vitro* and *in vivo* systems,[284,337] their precise role in the sorting process remains to be elucidated. Independent of its applicability, however, this model is extremely interesting. It is a useful reminder that forces other than simple receptor–ligand interactions are likely to be involved in generating and maintaining the anisotropic protein distributions that define the polarized state.

As noted above, several proteins are targeted to the apical membrane by virtue of signals embedded within their transmembrane domains. The fact that the amino acid residues of a transmembrane domain may be in direct contact with lipid molecules suggests the possibility that they may mediate apical sorting through interactions with glycosphingolipid-rich membrane domains. According to this hypothesis, the composition of its transmembrane domain may permit a protein to partition into glycosphingolipid rich patches, and thus to become concentrated in a region of the membrane that will give rise to an apically directed transport vesicle. GPI-linked proteins which have become associated with glycosphingolipid-rich membrane domains are insoluble in 1% TritonX-100 at 4°C. When a cell lysate prepared in this fashion is fractionated on a sucrose gradient, insoluble proteins are found near the top of the gradient, whereas soluble proteins remain in the heavier fractions.[337] Interestingly, the transmembrane domain of the apical protein influenza neuraminidase carries apical sorting information, and also enables the protein to incorporate into insoluble material.

PDZ Domain-containing Proteins

As discussed above, the C-terminus of GABA transporter GAT-3 appears to be important for its apical localization in MDCK cells.[307] The final residues of this C-terminal tail, threonine, histidine, and phenylalanine (THF), are reminiscent of the sequences present at the extreme C-terminal tails of proteins known to associate with members of the membrane-associated guanylate kinase (MAGUK) family. The MAGUK proteins incorporate one or more copies of the PDZ domain, which is named for three of the proteins in which the sequence homology defining this protein–protein interaction motif were first identified; PSD-95/SAP90, Dlg, and ZO-1. Interactions between the PDZ domain of a MAGUK protein and the extreme cytoplasmic tail of an integral membrane polypeptide appear to be important in organizing the surface distributions of intrinsic membrane proteins.[338,339]

Observations obtained from a number of experimental systems provide further evidence for the involvement of PDZ domain-containing polypeptides in epithelial membrane protein sorting.[340] The LET-23 receptor tyrosine kinase is localized to the basolateral cell surfaces of vulvar epithelial cells in *C. elegans*. Genetic studies reveal that at least three proteins contribute to the generation or maintenance of this distribution. Mutation of the lin2, lin7 or lin10 genes leads to loss of LET-23 basolateral polarity. Each of the proteins encoded by these genes includes one or more PDZ domains. A mutation in the *Drosophila* discs lost protein, which contains multiple PDZ domains, also leads to the mis-localization of several apical and basolateral proteins in the epithelial structures of affected embryos.[341] It would appear, therefore, that PDZ domain-containing proteins may play a direct role in the polarized sorting of at least some membrane proteins or may be required for the generation or definition of polarized domains. These observations may be especially relevant to physiologic function of polarized renal epithelial cells, since a number of important ion

transport proteins, including CFTR and NHE3, appear to interact with cytoplasmic proteins containing PDZ domains.[342–344] It seems likely that these interactions may play a role in establishing these proteins distributions, and hence in determining their capacity to participate in vectorial ion transport.

Finally, it is important to note that once proteins have been sorted into the vesicles that will carry them to the appropriate cell surface domain, these vesicles themselves need to be targeted appropriately. Presumably, the vesicular membranes include proteins that ensure that the vesicles will interact and fuse with only the proper domain of the epithelial plasmalemma. This recognition machinery is likely to include components of the membrane fusion machinery, such as vesicular SNARE (soluble NSF attachment receptor) proteins.[345] SNARE proteins present in both vesicular and target membranes form complexes that appear to be necessary for most normal cellular fusion processes. The extent to which different members of the SNARE family impart specificity to intracellular vesicular fusion events remains to be established.[346–348] Interestingly, however, a component of the machinery involved in vesicular targeting in yeast was identified in mammalian cells.[349] This Sec 6/8 "exocyst" complex appears to play a role specifically in the fusion of basolaterally-directed, but not apically-directed, post-Golgi carrier vesicles in epithelial cells.[350] It is likely that the number of "destination-specific" vesicular and plasma membrane proteins important for directing vesicular traffic in polarized cells will continue to grow.

Epithelial Cell Polarity and Renal Disease

Because kidney function is dependent on the polarity of tubular epithelial cells, any condition that compromises this polarity will lead to renal failure.[351,352] In general, this may occur through neoplastic processes, cell injury due to ischemia or nephrotoxicity, or through inherited genetic effects.[179,351] Each of these may affect the tubular epithelial cells, their surrounding environment including the basal lamina and interstitial compartment, or both.

Carcinogenesis

During neoplastic growth it can be appreciated on the basis of morphology alone that the changes in cell and tissue organization wrought by tumorigenesis are likely to affect cell polarity.[179] Model studies confirm this suspicion. When MDCK cells, which are not normally tumorigenic, are oncogenically transformed by introduction of the v-Ki-*ras* oncogene, they are converted from a simple epithelium to a multilayer, with great heterogeneity in overall cell morphology.[179] Ultrastructural examination of these cells suggests that apical–basal polarity is severely compromised. Microvilli are diminished from the cells at the top layer, and organization of the cytoplasm is scrambled. Golgi complexes and centrosomes, which normally reside in an apical supranuclear location, are now randomly positioned.[179] Despite this apparent high degree of disorganization, immunocytochemical localization of specific antigens and physiological measurements suggests that polarity is not totally disrupted. Basolateral proteins, including Na^+/K^+-ATPase and the cell-adhesion molecule E-cadherin, are restricted to regions of cell–cell contact, as in normal polarized MDCK cells. Apical proteins, on the other hand, are randomly localized to the free surface of the multilayered epithelia, as well as to areas of cell–cell contact in cells throughout the multilayer. The tight junctional antigen ZO-1 is found typically at the point where the free and adherent surfaces of the uppermost cell layer meet, as well as at a number of sites within the multilayer.[179] The latter may be intercellular lumina or canaliculi connected to the upper surface. This localization probably reflects the presence of functional tight junctions, because the multilayer is both electrically tight and impermeant to inulin.

It is interesting to note that recent studies demonstrate that proteins encoded by tumor suppressor genes may function as key regulators of polarity. Mutations in the von Hippel–Lindau tumor suppressor gene can lead to renal cell carcinoma. While the primary function of the von Hippel–Lindau gene product (VHL) relates to the negative regulation of the activity of the hypoxia inducible factor (HIF) transcription factor, the VHL protein also appears to participate in the formation or stabilization of intercellular adhesive junctions.[353] Mutations in the gene encoding the LKB1 protein kinase are responsible for Peutz–Jaeger syndrome, an inherited form of tumor susceptibility associated with the development of numerous hamartomas. Epithelial cells expressing LKB1 that is constitutively activated are able to form polarized domains in the absence of cell–cell and cell–substratum contact.[354] Thus, proteins that participate in epithelial polarization may function as tumor suppressors by virtue of their capacity to control the growth and morphogenesis of the cells in which they are expressed.

Ischemic Injury

Other alterations in cell polarity may come about through the effect of renal ischemia on the tubular epithelium.[355–358] Ischemic episodes of less than 1 hour often do not lead to tubular necrosis but may, nevertheless, cause diminished sodium and water uptake by the proximal tubule.[359] Such brief ischemia compromises the polarity of tubular cells, resulting in

the redistribution of a fraction of the Na^+/K^+-ATPase from the basolateral domain to the apical domain, preventing net sodium uptake by the tubule.[359,360] At the same time, leucine aminopeptidase moves from the apical to the basolateral domain, and also becomes intracellular, presumably through endocytosis. At later times, Na^+/K^+-ATPase and leucine aminopeptidase are randomly distributed on the plasma membrane of tubular epithelial cells, remaining attached to the basement membrane or exfoliated into the lumenal space. The mechanism leading to this loss of polarity is not known. It is possible that ischemia, which is known to affect mitochondria and other organelles and to possibly alter the permeability of the plasma membrane, may result in increased cytoplasmic calcium concentrations.[355,358] This, in turn, could disrupt elements of the cytoskeleton, perhaps affecting the maintenance of polarity. These may represent disruption or perturbation of the cortical actin cytoskeleton. In fact, *in vitro* studies with renal epithelial cell lines demonstrate that ATP depletion causes disassembly of the cytoskeleton and redistribution of actin from its normal locations in the cell cortex, terminal web, and microvilli to perinuclear cytoplasmic aggregates.[361,362] In addition, energy depletion can lead to the endocytic internalization and proteolytic cleavage of cell adhesion molecules such as E-cadherin.[363,364] Such alterations might affect transduction of spatial signals from the extracellular matrix to the polarization machinery along the lines previously discussed.

During reperfusion following renal ischemia, tubular epithelial cells detach from the basement membrane and accumulate in the lumen. It has been postulated that ischemia-induced depolarization of integrins from basal to apical domains of the plasma membrane contributes not only to cell detachment, but also to cell aggregation and tubular obstruction. According to this hypothesis, at early times post-ischemia, redistribution of integrins would loosen attachment of cells from the basal lamina, allowing some of them to detach.[365–367] Released cells would then aggregate and adhere to remaining tubular epithelial cells via their integrins. These would either bind directly to each other by homotypic interactions or associate through bridging matrix molecules. Collections of such aggregates would obstruct the tubules, causing oliguria and destruction of renal tissue.[365–367] In support of this hypothesis, integrins were observed to redistribute apically in oxidatively injured epithelial cell lines.[365] Even more compelling was the observation that infusion of RGD peptides, which block some integrin–matrix interactions, appeared to ameliorate the effects of ischemia-induced by clamping of the renal artery.[367,368] More recent *in vivo* findings utilizing a rat model of renal ischemia do not, however, support this hypothesis, at least with regard to β1 integrins.[156] Soon after reperfusion, β1 integrins redistributed from a strictly basal to basolateral location in cells of the S3 segment of the proximal tubule, but did not appear on the apical plasma membrane at this time.[156] Surprisingly, β1 integrins could not be detected by immunofluorescence in cells released from the basal lamina into the tubular lumen, precluding the possibility that they were mediating either cell aggregation or attachment of exfoliated cells to the residual tubular epithelium. Apical β1 integrins only appeared at later times post-ischemia, as cells lost polarity in the process of regeneration.[156]

Genetic Diseases of Proximal Tubule Apical Endocytosis: Dent's Disease and the Oculo Cerebral Renal Syndrome of Lowe

It is interesting to note that at least two genetic diseases with overlapping constellations of symptoms lead to perturbations of the proximal tubule's megalin-mediated scavenging activity that normally prevents the urinary loss of low molecular weight filtered proteins. Dent's disease is caused by inactivating mutations in the gene encoding the ClC5 protein, which functions as a chloride:proton exchanger in the membranes of proximal tubule epithelial cell endosomes.[369,370] ClC5 activity leads to the accumulation of chloride ions in these endosomes, which appears to be required for steps in the internalization or recycling of the proximal tubule endocytic machinery. The Oculo Cerebral Renal Syndrome of Lowe is caused by mutations in an inositol lipid phosphatase that participates in controlling the inventory of inositol phospholipids in subcellular membranes.[371] These inositol phospholipids help to establish the compartmental identity of subcellular membranes, and to facilitate the assembly of trafficking machinery on their cytosolic surfaces. While the precise mechanisms through which intra-endosomal chloride concentrations and intramembranous inositol phospholipid levels participate in the process of megalin endocytosis remain to be elucidated, it is clear that both of these parameters collaborate in generating or maintaining the proximal tubule epithelial cell's unusual active apical endocytic machinery.

Polycystic Kidney Disease

The progressive formation of renal cysts, which characterizes autosomal dominant polycystic kidney disease (ADPKD), has also been suggested to occur as a result of polarity defects. ADPKD is the most common potentially lethal dominant genetic human disease. Approximately 85% of all cases are linked to mutations in the PKDl gene, with another 10% linked to PKD2.[108,372] While the specific functions of the proteins encoded by these genes are the focus of intense study, the behavior of cyst

epithelial cells *in situ* and in culture is consistent with a role for the PKD proteins in directing epithelial differentiation. Whereas renal tubular epithelial cells normally mediate fluid and electrolyte absorption, cyst epithelial cells carry out net secretion.[373,374] It has been suggested that the proximal cause of renal cyst formation in polycystic kidney disease may be the mis-targeting of Na^+/K^+-ATPase to the apical plasmalemma.

According to this model, the presence of sodium pump at the apical surface leads to active apical ion secretion and the accumulation of lumenal cyst fluid.[375,376] Other studies suggest that mis-localization of Na^+/K^+-ATPase cannot be the primary driving force for cyst fluid accumulation. When examined in cyst cells in culture or *in situ*, the Na^+/K^+-ATPase was found to be exclusively basolateral.[377] Instead, the secretion appears to be driven by intracellular chloride accumulation via a basolateral $Na^+/K/^+2Cl^-$ co-transporter and apical chloride exit through the CFTR protein.[377] A similar mechanism is responsible for fluid secretion by the poorly differentiated epithelial cells lining the crypts of the small intestine. As these crypt cells migrate up the intestinal villus they mature functionally, metamorphosing from secretory into resorptive epithelial cells.[378] It has been suggested that the secretory phenotype is characteristic of immature epithelial cells, while more highly developed epithelial cells acquire the capacity to absorb fluid and electrolytes.[379] The physiologic similarities relating cyst and crypt epithelial cells has prompted the hypothesis that loss of appropriate PKD function results in the dedifferentiation of mature resorptive renal tubular epithelial cells into more primitive secretory cells. The precise mechanisms through the PKDl and PKD2 mutations produce the dramatic pathology associated with ADPKD, and the potential role of epithelial differentiation and sorting pathways, remain to be determined.

Acknowledgments

K. S. Matlin and M. J. Caplan acknowledge support for the research in their laboratories through grants from the National Institutes of Health. They would also like to thank Aki Manninen for permitting the use of unpublished material, Jonathan Bowen and Elias T. Spoliotis for the images in Figure 1.2, and Ms. Ruth Crawford for assistance with the references.

References

[1] Caplan MJ, Matlin KS. Sorting of membrane and secretory proteins in polarized epithelial cells. In: Matlin KS, Valentich JD, editors. Functional epithelial cells in culture. New York: Alan R. Liss; 1989. p. 71–127.
[2] Matlin KS. The sorting of proteins to the plasma membrane in epithelial cells. J Cell Biol 1986;103:2565–8.
[3] Nelson WJ. Adaptation of core mechanisms to generate cell polarity. Nature 2003;422:766–74.
[4] Rodriguez-Boulan E, Nelson WJ. Morphogenesis of the polarized epithelial cell phenotype. Science 1989;245:718–25.
[5] Duffield A, Caplan MJ, Muth TR. Protein trafficking in polarized cells. Int Rev Cell Mol Biol 2008;270:145–79.
[6] Muth TR, Caplan MJ. Transport protein trafficking in polarized cells. Annu Rev Cell Dev Biol 2003;19:333–66.
[7] Koeppen BM, Giebisch G. Mineralcorticoid regulation of sodium and potassium transport by the cortical collecting duct. In: Graves JS, editor. Regulation and development of membrane transport processes. New York: John Wiley and Sons; 1985. p. 89–104.
[8] O'Neil RG. Adrenal steroid regulation of potassium transport. In: Giebisch GH, editor. Current topics in membranes and transport: potassium transport: physiology and pathophysiology. New York: Academic Press; 1987. p. 185–206.
[9] Schultz SG. Cellular models of epithelial ion transport. In: Andreoli TE, Hoffman JF, Fanestil DD, Schultz SG, editors. Physiology of membrane disorders. New York: Plenum Press; 1986. p. 519–34.
[10] Sweadner KJ, Goldin SM. Active transport of sodium and potassium ions: mechanism, function, and regulation. N Engl J Med 1980;302:777–83.
[11] Palmer LG, Frindt G. Amiloride-sensitive Na channels from the apical membrane of the rat cortical collecting tubule. Proc Natl Acad Sci USA 1986;83:2767–70.
[12] Fawcett DW. Bloom and Fawcett: a textbook of histology. Philadelphia: W.B. Saunders; 1986.
[13] Farquhar MG, Palade GE. Junctional complexes in various epithelia. J Cell Biol 1963;17:375–412.
[14] Schwarz MA, Owaribe K, Kartenbeck J, Franke WW. Desmosomes and hemidesmosomes: constitutive molecular components. Annu Rev Cell Biol 1990;6:461–91.
[15] Franke WW, Winter S, Grund C, Schmid E, Schiller DL, et al. Isolation and characterization of desmosome-associated tonofilaments from rat intestinal brush border. J Cell Biol 1981;90:116–27.
[16] Ben-Ze'ev A, Geiger B. Differential molecular interactions of beta-catenin and plakoglobin in adhesion, signaling and cancer. Curr Opin Cell Biol 1998;10:629–39.
[17] Simon AM. Gap junctions: more roles and new structural data. Trends Cell Biol 1999;9:169–70.
[18] Simon AM, Goodenough DA. Diverse functions of vertebrate gap junctions. Trends Cell Biol 1998;8:477–83.
[19] Fromter E, Diamond J. Route of passive ion permeation in epithelia. Nat New Biol 1972;235:9–13.
[20] Madara JL, Hecht G. Tight (occluding) junctions in cultured (and native) epithelial cells. In: Matlin KS, Valentich JD, editors. Functional epithelial cells in culture. New York: Alan R. Liss; 1989. p. 131–64.
[21] Shen L, Weber CR, Raleigh DR, Yu D, Turner JR. Tight junction pore and leak pathways: a dynamic duo. Annu Rev Physiol 2011;73:283–309.
[22] Anderson JM, Van Itallie CM. Physiology and function of the tight junction. Cold Spring Harb Perspect Biol 2009;1:a002584.
[23] Cereijido M, Ponce A, Gonzalez-Mariscal L. Tight junctions and apical/basolateral polarity. J Membr Biol 1989;110:1–9.
[24] Gonzalez-Mariscal L, Chavez de Ramirez B, Cereijido M. Tight junction formation in cultured epithelial cells (MDCK). J Membr Biol 1985;86:113–25.
[25] Hartsock A, Nelson WJ. Adherens and tight junctions: Structure, function and connections to the actin cytoskeleton. Biochim Biophys Acta 2008;1778:660–9.
[26] Schneeberger EE, Lynch RD. The tight junction: a multifunctional complex. Am J Physiol Cell Physiol 2004;286:C1213–28.
[27] Stevenson BR, Anderson JM, Bullivant S. The epithelial tight junction: Structure, function and preliminary biochemical characterization. Mol Cell Biochem 1988;83:129–45.

[28] Stevenson BR, Keon BH. The tight junction: morphology to molecules. Annu Rev Cell Dev Biol 1998;14:89–109.
[29] Denker BM, Sabath E. The biology of epithelial cell tight junctions in the kidney. J Am Soc Nephrol 2011;22:622–5.
[30] Hendler RW. Biological membrane ultrastructure. Physiol Rev 1971;51:66–97.
[31] Dragsten PR, Blumenthal R, Handler JS. Membrane asymmetry in epithelia: is the tight junction a barrier to diffusion in the plasma membrane? Nature 1981;294:718–22.
[32] van Meer G, Simons K. The function of tight junctions in maintaining differences in lipid composition between the apical and the basolateral cell surface domains of MDCK cells. EMBO J 1986;5:1455–64.
[33] van Meer G, Gumbiner B, Simons K. The tight junction does not allow lipid molecules to diffuse from one epithelial cell to the next. Nature 1986;322:639–41.
[34] Staehelin LA. Further observations on the fine structure of freeze-cleaved tight junctions. J Cell Sci 1973;13:763–86.
[35] Claude P, Goodenough DA. Fracture faces of zonulae occludentes from "tight" and "leaky" epithelia. J Cell Biol 1973;58:390–400.
[36] Stevenson BR, Siliciano JD, Mooseker MS, Goodenough DA. Identification of ZO-1: a high molecular weight polypeptide associated with the tight junction (zonula occludens) in a variety of epithelia. J Cell Biol 1986;103:755–66.
[37] Fanning AS, Van Itallie C, Anderson JM. Zonula occludens (ZO)-1 and -2 regulate apical cell structure and the zonula adherens cytoskeleton in polarized epithelia. Mol Biol Cell 2011;23(4):577–90.
[38] Angelow S, Ahlstrom R, Yu ASL. Biology of claudins. AJP: Renal Physiol 2008;295:F867–76.
[39] Balkovetz DF. Claudins at the gate: Determinants of renal epithelial tight junction paracellular permeability. Am J Physiol Renal Physiol 2006;290:F572–9.
[40] Colegio OR, Van Itallie CM, McCrea HJ, Rahner C, Anderson JM. Claudins create charge-selective channels in the paracellular pathway between epithelial cells. Am J Physiol Cell Physiol 2002;283:C142–7.
[41] Furuse M, Tsukita S. Claudins in occluding junctions of humans and flies. Trends Cell Biol 2006;16:181–8.
[42] Morita K, Furuse M, Fujimoto K, Tsukita S. Claudin multigene family encoding four-transmembrane domain protein components of tight junction strands. Proc Natl Acad Sci USA 1999;96:511–6.
[43] Van Itallie CM, Anderson JM. Claudins and epithelial paracellular transport. Annu Rev Physiol 2006;68:403–29.
[44] Furuse M. Molecular basis of the core structure of tight junctions. Cold Spring Harb Perspect Biol 2010;2:a002907-a.
[45] Furuse M, Sasaki H, Fujimoto K, Tsukita S. A single gene product, claudin-1 or -2, reconstitutes tight junction strands and recruits occludin in fibroblasts. J Cell Biol 1998;143:391–401.
[46] Furuse M, Furuse K, Sasaki H, Tsukita S. Conversion of zonulae occludentes from tight to leaky strand type by introducing claudin-2 into Madin–Darby canine kidney I cells. J Cell Biol 2001;153:263–72.
[47] Kiuchi-Saishin Y, Gotoh S, Furuse M, Takasuga A, Tano Y, et al. Differential expression patterns of claudins, tight junction membrane proteins, in mouse nephron segments. J Am Soc Nephrol JASN 2002;13:875–86.
[48] Haskins J, Gu L, Wittchen ES, Hibbard J, Stevenson BR. ZO-3, a novel member of the MAGUK protein family found at the tight junction, interacts with ZO-1 and occludin. J Cell Biol 1998;141:199–208.
[49] Jesaitis LA, Goodenough DA. Molecular characterization and tissue distribution of ZO-2, a tight junction protein homologous to ZO-1 and the *Drosophila* discs-large tumor suppressor protein. J Cell Biol 1994;124:949–61.
[50] Marchiando AM, Graham WV, Turner JR. Epithelial barriers in homeostasis and disease. Annu Rev Pathol 2010;5:119–44 Mechanisms of Disease
[51] Hecht G, Pestic L, Nikcevic G, Koutsouris A, et al. Expression of the catalytic domain of myosin light chain kinase increases paracellular permeability. Am J Physiol 1996;271: C1678–84.
[52] Turner JR, Rill BK, Carlson SL, Carnes D, Kerner R, Mrsny RJ, et al. Physiological regulation of epithelial tight junctions is associated with myosin light-chain phosphorylation. Am J Physiol 1997;273:C1378–85.
[53] Yap AS, Brieher WM, Gumbiner BM. Molecular and functional analysis of cadherin-based adherens junctions. Annu Rev Cell Dev Biol 1997;13:119–46.
[54] Nelson WJ. Regulation of cell–cell adhesion by the cadherin–catenin complex. Biochem Soc Trans 2008;36:149–55.
[55] Barth AI, Nathke IS, Nelson WJ. Cadherins, catenins and APC protein: interplay between cytoskeletal complexes and signaling pathways. Curr Opin Cell Biol 1997;9:683–90.
[56] Gumbiner B, Lowenkopf T, Apatira D. Identification of a 160-kDa polypeptide that binds to the tight junction protein ZO-1. Proc Natl Acad Sci USA 1991;88:3460–4.
[57] Griffith LD, Bulger RE, Trump BF. Fine structure and staining of mucosubstances on "intercalated cells" from the rat distal convoluted tubule and collecting duct. Anat Rec 1968;160:643–62.
[58] Maunsbach AB. Cellular mechanisms of tubular protein transport. Int Rev Physiol 1976;11:145–67.
[59] Welling LW, Welling DJ. Surface areas of brush border and lateral cell walls in the rabbit proximal nephron. Kidney Int 1975;8:343–8.
[60] Mandel LJ, Balaban RS. Stoichiometry and coupling of active transport to oxidative metabolism in epithelial tissues. Am J Physiol 1981;240:F357–71.
[61] Mooseker MS. Organization, chemistry, and assembly of the cytoskeletal apparatus of the intestinal brush border. Annu Rev Cell Biol 1985;1:209–41.
[62] Brown JW, McKnight CJ. Molecular model of the microvillar cytoskeleton and organization of the brush border. PLoS One 2010;5:e9406.
[63] McConnell RE, Benesh AE, Mao S, Tabb DL, Tyska MJ. Proteomic analysis of the enterocyte brush border. Am J Physiol Gastrointest Liver Physiol 2011;300:G914–26.
[64] Rodman JS, Mooseker M, Farquhar MG. Cytoskeletal proteins of the rat kidney proximal tubule brush border. Eur J Cell Biol 1986;42:319–27.
[65] Bretscher A, Weber K. Localization of actin and microfilament-associated proteins in the microvilli and terminal web of the intestinal brush border by immunofluorescence microscopy. J Cell Biol 1978;79:839–45.
[66] Glenney Jr. JR, Glenney P. Fodrin is the general spectrin-like protein found in most cells whereas spectrin and the TW protein have a restricted distribution. Cell 1983;34:503–12.
[67] Drenckhahn D, Groschel-Stewart U. Localization of myosin, actin, and tropomyosin in rat intestinal epithelium: immunohistochemical studies at the light and electron microscope levels. J Cell Biol 1980;86:475–82.
[68] Hirokawa N, Keller III TC, Chasan R, Mooseker MS. Mechanism of brush border contractility studied by the quick-freeze, deep-etch method. J Cell Biol 1983;96:1325–36.
[69] Mooseker MS. Brush border motility. Microvillar contraction in triton-treated brush borders isolated from intestinal epithelium. J Cell Biol 1976;71:417–33.
[70] Hayden SM, Wolenski JS, Mooseker MS. Binding of brush border myosin I to phospholipid vesicles. J Cell Biol 1990;111:443–51.

[71] Mooseker MS, Coleman TR. The 110-kD protein-calmodulin complex of the intestinal microvillus (brush border myosin I) is a mechanoenzyme. J Cell Biol 1989;108:2395–400.
[72] Coluccio LM, Bretscher A. Reassociation of microvillar core proteins: making a microvillar core *in vitro*. J Cell Biol 1989;108:495–502.
[73] Matsudaira PT, Burgess DR. Identification and organization of the components in the isolated microvillus cytoskeleton. J Cell Biol 1979;83:667–73.
[74] Garcia A, Coudrier E, Carboni J, Anderson J, Vanderkerkhove J, Mooseker M, et al. Partial deduced sequence of the 110-kD-calmodulin complex of the avian intestinal microvillus shows that this mechanoenzyme is a member of the myosin I family. J Cell Biol 1989;109:2895–903.
[75] Hoshimaru M, Nakanishi S. Identification of a new type of mammalian myosin heavy chain by molecular cloning. Overlap of its mRNA with preprotachykinin B mRNA. J Biol Chem 1987;262:14625–32.
[76] Cheney RE, Mooseker MS. Unconventional myosins. Curr Opin Cell Biol 1992;4:27–35.
[77] Mooseker MS, Cheney RE. Unconventional myosins. Annu Rev Cell Dev Biol 1995;11:633–75.
[78] Drenckhahn D, Dermietzel R. Organization of the actin filament cytoskeleton in the intestinal brush border: a quantitative and qualitative immunoelectron microscope study. J Cell Biol 1988;107:1037–48.
[79] McConnell RE, Tyska MJ. Leveraging the membrane – cytoskeleton interface with myosin-1. Trends Cell Biol 2010;20:418–26.
[80] Fath KR, Burgess DR. Golgi-derived vesicles from developing epithelial cells bind actin filaments and possess myosin-I as a cytoplasmically oriented peripheral membrane protein. J Cell Biol 1993;120:117–27.
[81] Fath KR, Trimbur GM, Burgess DR. Molecular motors are differentially distributed on Golgi membranes from polarized epithelial cells. J Cell Biol 1994;126:661–75.
[82] Barylko B, Wagner MC, Reizes O, Albanesi JP. Purification and characterization of a mammalian myosin I. Proc Natl Acad Sci USA 1992;89:490–4.
[83] Coudrier E, Kerjaschki D, Louvard D. Cytoskeleton organization and submembranous interactions in intestinal and renal brush borders. Kidney Int 1988;34:309–20.
[84] Coluccio LM. Identification of the microvillar 110-kDa calmodulin complex (myosin-1) in kidney. Eur J Cell Biol 1991;56:286–94.
[85] Bretscher A, Weber K. Villin: the major microfilament-associated protein of the intestinal microvillus. Proc Natl Acad Sci USA 1979;76:2321–5.
[86] Arpin M, Pringault E, Finidori J, Garcia A, Jeltsch JM, Vanderkerckhove J, et al. Sequence of human villin: a large duplicated domain homologous with other actin-severing proteins and a unique small carboxy-terminal domain related to villin specificity. J Cell Biol 1988;107:1759–66.
[87] Matsudaira PT, Burgess DR. Partial reconstruction of the microvillus core bundle: characterization of villin as a Ca^{++}-dependent, actin-bundling/depolymerizing protein. J Cell Biol 1982;92:648–56.
[88] Robine S, Huet C, Moll R, Sahuquillo-Merino C, Coudrieri E, Zweibaum A, et al. Can villin be used to identify malignant and undifferentiated normal digestive epithelial cells? Proc Natl Acad Sci USA 1985;82:8488–92.
[89] Costa de Beauregard MA, Pringault E, Robine S, Louvard D. Suppression of villin expression by antisense RNA impairs brush border assembly in polarized epithelial intestinal cells. EMBO J 1995;14:409–21.
[90] Pinson KI, Dunbar L, Samuelson L, Gumucio DL. Targeted disruption of the mouse villin gene does not impair the morphogenesis of microvilli. Dev Dyn 1998;211:109–21.
[91] Bretscher A, Weber K. Fimbrin, a new microfilament-associated protein present in microvilli and other cell surface structures. J Cell Biol 1980;86:335–40.
[92] Volkmann N, DeRosier D, Matsudaira P, Hanein D. An atomic model of actin filaments cross-linked by fimbrin and its implications for bundle assembly and function. J Cell Biol 2001;153:947–56.
[93] Grimm-Gunter EM, Revenu C, Ramos S, Hurbain I, Smyth N, Ferrary E, et al. Plastin 1 binds to keratin and is required for terminal web assembly in the intestinal epithelium. Mol Biol Cell 2009;20:2549–62.
[94] Bartles JR, Zheng L, Li A, Wierda A, Chen B. Small espin: a third actin-bundling protein and potential forked protein ortholog in brush border microvilli. J Cell Biol 1998;143:107–19.
[95] Zheng L, Sekerkova G, Vranich K, Tilney LG, Mugnaini E, et al. The deaf jerker mouse has a mutation in the gene encoding the espin actin-bundling proteins of hair cell stereocilia and lacks espins. Cell 2000;102:377–85.
[96] Loomis PA, Zheng L, Sekerkova G, Changyaleket B, Mugnaini E, et al. Espin cross-links cause the elongation of microvillus-type parallel actin bundles *in vivo*. J Cell Biol 2003;163:1045–55.
[97] Revenu C, Ubelmann F, Hurbain I, El-Marjou F, Dingli F, Loew D, et al. A new role for the architecture of microvillus actin bundles in apical retention of membrane proteins. Miol Biol Cell 2011;23(2):324–36.
[98] Bretscher A, Reczek D, Berryman M. Ezrin: a protein requiring conformational activation to link microfilaments to the plasma membrane in the assembly of cell surface structures. J Cell Sci 1997;110(Pt 24):3011–8.
[99] Saotome I, Curto M, McClatchey AI. Ezrin is essential for epithelial organization and villus morphogenesis in the developing intestine. Dev Cell 2004;6:855–64.
[100] Bacic D, Wagner CA, Hernando N, Kaissling B, Biber J, et al. Novel aspects in regulated expression of the renal type IIa Na/Pi-cotransporter. Kidney Int Suppl 2004;:S5–12.
[101] Burgess DR. Reactivation of intestinal epithelial cell brush border motility: ATP-dependent contraction via a terminal web contractile ring. J Cell Biol 1982;95:853–63.
[102] Kerjaschki D, Noronha-Blob L, Sacktor B, Farquhar MG. Microdomains of distinctive glycoprotein composition in the kidney proximal tubule brush border. J Cell Biol 1984;98:1505–13.
[103] Rodman JS, Seidman L, Farquhar MG. The membrane composition of coated pits, microvilli, endosomes, and lysosomes is distinctive in the rat kidney proximal tubule cell. J Cell Biol 1986;102:77–87.
[104] Lina F, Satlinb LM. Polycystic kidney disease: the cilium as a common pathway in cystogenesis. Curr Opin Pediatr 2004;16:171–6.
[105] Yoder BK, Mulroy S, Eustace H, Boucher C, Sandford R. Molecular pathogenesis of autosomal dominant polycystic kidney disease. Expert Rev Mol Med 2006;8:1–22.
[106] Mollet G, Silbermann F, Delous M, Salomon R, Antignac C, et al. Characterization of the nephrocystin/nephrocystin-4 complex and subcellular localization of nephrocystin-4 to primary cilia and centrosomes. Hum Mol Genet 2005;14:645–56.
[107] Lin F, Hiesberger T, Cordes K, Sinclair AM, Goldstein LS, Somlo S, et al. Kidney-specific inactivation of the KIF3A subunit of kinesin-II inhibits renal ciliogenesis and produces polycystic kidney disease. Proc Natl Acad Sci USA 2003;100:5286–91.
[108] Takiar V, Caplan MJ. Polycystic kidney disease: pathogenesis and potential therapies. Biochim Biophys Acta 2011;1812:1337–43.

[109] Amerongen HM, Mack JA, Wilson JM, Neutra MR. Membrane domains of intestinal epithelial cells: Distribution of Na^{+}/K^{+}-ATPase and the membrane skeleton in adult rat intestine during fetal development and after epithelial isolation. J Cell Biol 1989;109:2129–38.

[110] Achler C, Filmer D, Merte C, Drenckhahn D. Role of microtubules in polarized delivery of apical membrane proteins to the brush border of the intestinal epithelium. J Cell Biol 1989;109:179–89.

[111] McNeill H, Ozawa M, Kemler R, Nelson WJ. Novel function of the cell adhesion molecule uvomorulin as an inducer of cell surface polarity. Cell 1990;62:309–16.

[112] Morrow JS, Cianci CD, Ardito T, Mann AS, Kashgarian M. Ankyrin links fodrin to the alpha subunit of Na,K-ATPase in Madin–Darby canine kidney cells and in intact renal tubule cells. J Cell Biol 1989;108:455–65.

[113] Nelson WJ. Development and maintenance of epithelial polarity: a role for the submembranous cytoskeleton. In: Matlin KS, Valentich JD, editors. Functional epithelial cells in culture. New York: Alan R. Liss; 1989. p. 3–42.

[114] Nelson WJ, Hammerton RW. A membrane-cytoskeletal complex containing Na^{+}/K^{+}-ATPase, ankyrin, and fodrin in Madin–Darby canine kidney (MDCK) cells: implications for the biogenesis of epithelial cell polarity. J Cell Biol 1989;108:893–902.

[115] Nelson WJ, Hammerton RW, McNeill H. Role of the membrane-cytoskeleton in the spatial organization of the Na,K-ATPase in polarized epithelial cells. Soc Gen Physiol Ser 1991;46:77–87.

[116] Nelson WJ, Hammerton RW, Wang AZ, Shore EM. Involvement of the membrane-cytoskeleton in development of epithelial cell polarity. Semin Cell Biol 1990;1:359–71.

[117] Nelson WJ, Shore EM, Wang AZ, Hammerton RW. Identification of a membrane-cytoskeletal complex containing the cell adhesion molecule uvomorulin (E-cadherin), ankyrin, and fodrin in Madin–Darby canine kidney epithelial cells. J Cell Biol 1990;110:349–57.

[118] Nelson WJ, Veshnock PJ. Dynamics of membrane-skeleton (fodrin) organization during development of polarity in Madin–Darby canine kidney epithelial cells. J Cell Biol 1986;103:1751–65.

[119] Nelson WJ, Veshnock PJ. Ankyrin binding to (Na^{++} K^{+}) ATPase and implications for the organization of membrane domains in polarized cells. Nature 1987;328:533–6.

[120] Nelson WJ, Veshnock PJ. Modulation of fodrin (membrane skeleton) stability by cell–cell contact in Madin–Darby canine kidney epithelial cells. J Cell Biol 1987;104:1527–37.

[121] Parczyk K, Haase W, Kondor-Koch C. Microtubules are involved in the secretion of proteins at the apical cell surface of the polarized epithelial cell, Madin–Darby canine kidney. J Biol Chem 1989;264:16837–46.

[122] Rindler MJ, Ivanov IE, Sabatini DD. Microtubule-acting drugs lead to the nonpolarized delivery of the influenza hemagglutinin to the cell surface of polarized Madin–Darby canine kidney cells. J Cell Biol 1987;104:231–41.

[123] Salas PJ, Vega-Salas DE, Hochman J, Rodriguez-Boulan E, Edidin M. Selective anchoring in the specific plasma membrane domain: a role in epithelial cell polarity. J Cell Biol 1988;107:2363–76.

[124] Grindstaff KK, Bacallao RL, Nelson WJ. Apiconuclear organization of microtubules does not specify protein delivery from the trans-Golgi network to different membrane domains in polarized epithelial cells. Mol Biol Cell 1998;9:685–99.

[125] Spiliotis ET, Hunt SJ, Hu Q, Kinoshita M, Nelson WJ. Epithelial polarity requires septin coupling of vesicle transport to polyglutamylated microtubules. J Cell Biol 2008;180:295–303.

[126] Yurchenco PD. Basement membranes: cell scaffoldings and signaling platforms. Cold Spring Harb Perspect Biol 2011;3: a004911-a.

[127] Miner JH. Organogenesis of the kidney glomerulus: focus on the glomerular basement membrane. Organogenesis 2011;7:75–82.

[128] Aumailley M. Structure and supramolecular organization of basement membranes. Kidney Int Suppl 1995;49:S4–7.

[129] Miner JH. Renal basement membrane components. Kidney Int 1999;56:2016–24.

[130] Miner JH, Yurchenco PD. Laminin functions in tissue morphogenesis. Annu Rev Cell Dev Biol 2004;20:255–84.

[131] Aumailley M, Bruckner-Tuderman L, Carter W, et al. A simplified laminin nomenclature. Matrix Biol 2005;24:326–32.

[132] Li S, Edgar D, Fassler R, Wadsworth W, Yurchenco PD. The role of laminin in embryonic cell polarization and tissue organization. Dev Cell 2003;4:613–24.

[133] Yurchenco PD, Patton BL. Developmental and pathogenic mechanisms of basement membrane assembly. Curr Pharm Des 2009;15:1277–94.

[134] Yurchenco P, Cheng Y. Laminin self-assembly: a three-arm interaction hypothesis for the formation of a network in basement membranes. Contrib Nephrol 1994;107:47–56.

[135] Joly D, Berissi S, Bertrand A, Strehl L, Patey N, et al. Laminin 5 regulates polycystic kidney cell proliferation and cyst formation. J Biol Chem 2006;281:29181–9.

[136] Joly D, Morel V, Hummel A, Ruello A, Nusbaum P, Patey N, et al. β4 integrin and laminin 5 are aberrantly expressed in polycystic kidney disease. Am J Pathol 2003;163:1791–800.

[137] Shannon MB, Patton BL, Harvey SJ, Miner JH. A hypomorphic mutation in the mouse laminin alpha5 gene causes polycystic kidney disease. J Am Soc Nephrol 2006;17:1913–22.

[138] Zuk A, Matlin KS. Induction of a laminin isoform and alpha (3)beta(1)-integrin in renal ischemic injury and repair *in vivo*. Am J Physiol Renal Physiol 2002;283:F971–84.

[139] Greciano PG, Moyano JV, Buschmann MM, Tang J, Lu Y, Rudnicki J, et al. Laminin 511 partners with laminin 332 to mediate directional migration of Madin–Darby canine kidney (MDCK) epithelial cells. Mol Biol Cell 2012;24:121–36.

[140] Hynes RO. Integrins: bidirectional, allosteric signaling machines. Cell 2002;110:673–87.

[141] Hemler ME. VLA proteins in the integrin family: structures, functions, and their role on leukocytes. Annu Rev Immunol 1990;8:365–400.

[142] Kreidberg JA, Symons JM. Integrins in kidney development, function, and disease. Am J Physiol Renal Physiol 2000;279: F233–42.

[143] Moyano JV, Greciano PG, Buschmann MM, Koch M, Matlin KS. Autocrine transforming growth factor-{beta}1 activation mediated by integrin {alpha}V{beta}3 regulates transcriptional expression of laminin-332 in Madin–Darby canine kidney epithelial cells. Mol Biol Cell 2010;21:3654–68.

[144] Schoenenberger CA, Zuk A, Zinkl GM, Kendall D, Matlin KS. Integrin expression and localization in normal MDCK cells and transformed MDCK cells lacking apical polarity. J Cell Sci 1994;107(Pt 2):527–41.

[145] Geiger B, Bershadsky A. Assembly and mechanosensory function of focal contacts. Curr Opin Cell Biol 2001;13:584–92.

[146] Zamir E, Geiger B. Components of cell–matrix adhesions. J Cell Sci 2001;114:3577–9.

[147] Zamir E, Geiger B. Molecular complexity and dynamics of cell–matrix adhesions. J Cell Sci 2001;114:3583–90.

[148] Zamir E, Katz BZ, Aota S, Yamada KM, Geiger B, et al. Molecular diversity of cell-matrix adhesions. J Cell Sci 1999;112(Pt 11):1655–69.

[149] Geiger B, Yamada KM. Molecular architecture and function of matrix adhesions. Cold Spring Harb Perspect Biol 2011;3: pii: a005033.
[150] Tsurata D, Hashimoto T, Hamill K, Jones JCR. Hemidesmosomes and focal contact proteins: functions and cross-talk in keratinocytes, bullous diseases and wound healing. J Derm Sci 2011;62:1–7.
[151] Zhang H, Labouesse M. The making of hemidesmosome structures *in vivo*. Dev Dyn 2010;239:1465–76.
[152] Li S, Liquari P, McKee KK, Harrison D, Patel R, Lee S, et al. Laminin-sulfatide binding initiates basement membrane assembly and enables receptor signaling in Schwann cells and fibroblasts. J Cell Biol 2005;169:179–89.
[153] Zinkl GM, Zuk A, van der Bijl P, van Meer G, Matlin KS. An antiglycolipid antibody inhibits Madin–Darby canine kidney cell adhesion to laminin and interferes with basolateral polarization and tight junction formation. J Cell Biol 1996;133:695–708.
[154] Ekblom P. Developmentally regulated conversion of mesenchyme to epithelium. FASEB J 1989;3:2141–50.
[155] Molitoris B, Wilson P, Schrier R, Simon FR. Ischemia induces partial loss of surface membrane polarity and accumulation of putative calcium ionophores. J Clin Invest 1985;76(6):2097–105.
[156] Zuk A, Bonventre JV, Brown D, Matlin KS. Polarity, integrin, and extracellular matrix dynamics in the postischemic rat kidney. Am J Physiol 1998;275:C711–31.
[157] Nelson WJ. Remodeling epithelial cell organization: transitions between front–rear and apical–basal polarity. Cold Spring Harb Perspect Biol 2009;1:a000513.
[158] Simons K, Fuller SD. Cell surface polarity in epithelia. Annu Rev Cell Biol 1985;1:243–88.
[159] Gausch CR, Hard WL, Smith TF. Characterization of an established line of canine kidney cells (MDCK). Proc Soc Exp Biol Med 1966;122:931–5.
[160] Madin SH, Darby NB. In: American type culture collection catalogue of strains II. Rockville, Maryland: American Type Culture Collection; 1975.
[161] Herzlinger DA, Easton TG, Ojakian GK. The MDCK epithelial cell line expresses a cell surface antigen of the kidney distal tubule. J Cell Biol 1982;93:269–77.
[162] Leighton J, Brada Z, Estes LW, Justh G. Secretory activity and oncogenicity of a cell line (MDCK) derived from canine kidney. Science 1969;163:472–3.
[163] Abaza NA, Leighton J, Schultz SG. Effects of ouabain on the function and structure of a cell line (MDCK) derived from canine kidney. I. Light microscopic observations of monolayer growth. In Vitro 1974;10:72–183.
[164] Cereijido M, Ehrenfeld J, Fernandez-Castelo S, Meza I. Fluxes, junctions, and blisters in cultured monolayers of epithelioid cells (MDCK). Ann NY Acad Sci 1981;372:422–41.
[165] Rodriguez Boulan E, Sabatini DD. Asymmetric budding of viruses in epithelial monlayers: a model system for study of epithelial polarity. Proc Natl Acad Sci USA 1978;75:5071–5.
[166] Rodriguez Boulan E, Pendergast M. Polarized distribution of viral envelope proteins in the plasma membrane of infected epithelial cells. Cell 1980;20:45–54.
[167] Jat PS, Noble MD, Ataliotis P, Tanaka Y, Yannoutsos N, Larsen L, et al. Direct derivation of conditionally immortal cell lines from an H-2Kb-tsA58 transgenic mouse. Proc Natl Acad Sci USA 1991;88:5096–100.
[168] Geng H, Lan R, Wang G, Siddiqi AR, Naski MC, Brooks AI, et al. Inhibition of autoregulated TGFbeta signaling simultaneously enhances proliferation and differentiation of kidney epithelium and promotes repair following renal ischemia. Am J Pathol 2009;174:1291–308.
[169] Racusen LC, Monteil C, Sgrignoli A, Lucskay M, Marouillat S, Rhim JG, Morin JP. Cell lines with extended *in vitro* growth potential from human renal proximal tubule: characterization, response to inducers, and comparison with established cell lines. J Lab Clin Med 1997;129:318–29.
[170] Ryan MJ, Johnson G, Kirk J, Fuerstenberg SM, Zager RA, et al. HK-2: an immortalized proximal tubule epithelial cell line from normal adult human kidney. Kidney Int 1994;45:48–57.
[171] Handler JS, Preston AS, Steele RE. Factors affecting the differentiation of epithelial transport and responsiveness to hormones. Fed Proc 1984;43:2221–4.
[172] Misfeldt DS, Hamamoto ST, Pitelka DR. Transepithelial transport in cell culture. Proc Natl Acad Sci USA 1976;73:1212–6.
[173] Fuller SD, Simons K. Transferrin receptor polarity and recycling accuracy in "tight" and "leaky" strains of Madin–Darby canine kidney cells. J Cell Biol 1986;103:1767–79.
[174] Matlin KS, Simons K. Sorting of an apical plasma membrane glycoprotein occurs before it reaches the cell surface in cultured epithelial cells. J Cell Biol 1984;99:2131–9.
[175] Caplan MJ, Anderson HC, Palade GE, Jamieson JD. Intracellular sorting and polarized cell surface delivery of (Na^+,K^+)ATPase, an endogenous component of MDCK cell basolateral plasma membranes. Cell 1986;46:623–31.
[176] Caplan MJ, Stow JL, Newman AP, Madri J, Anderson HC, Farquhar MG, et al. Dependence on pH of polarized sorting of secreted proteins. Nature 1987;329:632–5.
[177] O'Brien LE, Zegers MM, Mostov KE. Opinion: building epithelial architecture: Insights from three-dimensional culture models. Nat Rev Mol Cell Biol 2002;3:531–7.
[178] Zegers MM, O'Brien LE, Yu W, Datta A, Mostov KE. Epithelial polarity and tubulogenesis *in vitro*. Trends Cell Biol 2003;13:169–76.
[179] Schoenenberger CA, Matlin KS. Cell polarity and epithelial oncogenesis. Trends Cell Biol 1991;1:87–92.
[180] Yeaman C, Grindstaff KK, Nelson WJ. New perspectives on mechanisms involved in generating epithelial cell polarity. Physiol Rev 1999;79:73–98.
[181] Macara IG, Mili S. Polarity and differential inheritance: Universal attributes of life? Cell 2008;135:801–12.
[182] Bryant DM, Mostov KE. From cells to organs: building polarized tissue. Nat Rev Mol Cell Biol 2008;9:887–901.
[183] Lelongt B, Ronco P. Role of extracellular matrix in kidney development and repair. Pediatr Nephrol 2003;18:731–42.
[184] Wang AZ, Ojakian GK, Nelson WJ. Steps in the morphogenesis of a polarized epithelium. II. Disassembly and assembly of plasma membrane domains during reversal of epithelial cell polarity in multicellular epithelial (MDCK) cysts. J Cell Sci 1990;95(Pt 1):153–65.
[185] Balcarova-Stander J, Pfeiffer SE, Fuller SD, Simons K. Development of cell surface polarity in the epithelial Madin–Darby canine kidney (MDCK) cell line. EMBO J 1984;3:2687–94.
[186] Vega-Salas DE, Salas PJ, Gundersen D, Rodriguez-Boulan E. Formation of the apical pole of epithelial (Madin–Darby canine kidney) cells: polarity of an apical protein is independent of tight junctions while segregation of a basolateral marker requires cell–cell interactions. J Cell Biol 1987;104:905–16.
[187] Vega-Salas DE, Salas PJ, Rodriguez-Boulan E. Modulation of the expression of an apical plasma membrane protein of Madin-Darby canine kidney epithelial cells: cell–cell interactions control the appearance of a novel intracellular storage compartment. J Cell Biol 1987;104:1249–59.
[188] Capaldo CT, Macara IG. Depletion of E-cadherin disrupts establishment but not maintenance of cell junctions in

Madin–Darby canine kidney epithelial cells. Mol Biol Cell 2007;18:189–200.
[189] Takai Y, Miyoshi J, Ikeda W, Ogita H. Nectins and nectin-like molecules: roles in contact inhibition of cell movement and proliferation. Nat Rev Mol Cell Biol 2008;9:603–15.
[190] Ehrlich J, Hansen M, Nelson W. Spatio-temporal regulation of rac1 localization and lamellipodia dynamics during epithelial cell–cell adhesion. Dev Cell 2002;3:259–70.
[191] Laprise P, Tepass U. Novel insights into epithelial polarity proteins in *Drosophila*. Trends Cell Biol 2011;21:401–8.
[192] Pieczynski J, Margolis B. Protein complexes that control renal epithelial polarity. AJP: Renal Physiology 2011;300:F589–601.
[193] Bryant D, Datta A, Rodriguez-Fraticelli A, Peranen J, Martin-Belmonte F, et al. A molecular network for de novo generation of the apical surface and lumen. Nat Cell Biol 2010;12 (11):1035–45 advance online publication:
[194] Macara IG, Spang A. Closing the GAP between polarity and vesicle transport. Cell 2006;125:419–21.
[195] Ekblom P. Formation of basement membranes in the embryonic kidney: an immunohistological study. J Cell Biol 1981;91(1):1–10.
[196] Klein G, Langegger M, Timpl R, Ekblom P. Role of laminin a chain in the development of epithelial cell polarity. Cell 1988;55:331–41.
[197] Sorokin L, Sonnenberg A, Aumailley M, Timpl R, Ekblom P. Recognition of the laminin E8 cell-binding site by an integrin possessing the alpha 6 subunit is essential for epithelial polarization in developing kidney tubules. J Cell Biol 1990;111:1265–73.
[198] O'Brien LE, Jou TS, Pollack AL, Zhang Q, Hansen SH, Yurchenco P, et al. Rac1 orientates epithelial apical polarity through effects on basolateral laminin assembly. Nat Cell Biol 2001;3:831–8.
[199] Yu W, Datta A, Leroy P, O'Brien LE, Mak G, Jou TS, et al. Beta1-integrin orients epithelial polarity via Rac1 and laminin. Mol Biol Cell 2005;16:433–45.
[200] Cohen D, Fernandez D, Lázaro-Diéguez F, Müsch A. The serine/threonine kinase Par1b regulates epithelial lumen polarity via IRSp53-mediated cell–ECM signaling. J Cell Biol 2011;192:525–40.
[201] Masuda-Hirata M, Suzuki A, Amano Y, Yamashita K, Ide M, Yamanaka T, et al. Intracellular polarity protein PAR-1 regulates extracellular laminin assembly by regulating the dystroglycan complex. Genes Cells 2009;14:835–50.
[202] Martin-Belmonte F, Gassama A, Datta A, Yu W, Rescher U, Gerke V, et al. PTEN-mediated apical segregation of phosphoinositides controls epithelial morphogenesis through Cdc42. Cell 2007;128:383–97.
[203] Bacallao R, Antony C, Dotti C, Karsenti E, Stelzer EH, et al. The subcellular organization of Madin–Darby canine kidney cells during the formation of a polarized epithelium. J Cell Biol 1989;109:2817–32.
[204] Bre MH, Kreis TE, Karsenti E. Control of microtubule nucleation and stability in Madin–Darby canine kidney cells: the occurrence of noncentrosomal, stable detyrosinated microtubules. J Cell Biol 1987;105:1283–96.
[205] Bre MH, Pepperkok R, Hill AM, Levilliers N, Ansorge W, Stelzer EH, et al. Regulation of microtubule dynamics and nucleation during polarization in MDCK II cells. J Cell Biol 1990;111:3013–21.
[206] Bowen JR, Hwang D, Bai X, Roy D, Spiliotis ET. Septin GTPases spatially guide microtubule organization and plus end dynamics in polarizing epithelia. J Cell Biol 2011;194:187–97.
[207] Spiliotis ET, Gladfelter AS. Spatial Guidance of cell asymmetry: septin GTPases show the way. Traffic (Copenhagen, Denmark) 2012;13(2):195–203.
[208] Hotta A, Kawakatsu T, Nakatani T, Sato T, Matsui C, et al. Laminin-based cell adhesion anchors microtubule plus ends to the epithelial cell basal cortex through LL5α/β. J Cell Biol 2010;189:901–17.
[209] Mogensen MM, Tucker JB, Mackie JB, Prescott AR, Nathke IS. The adenomatous polyposis coli protein unambiguously localizes to microtubule plus ends and is involved in establishing parallel arrays of microtubule bundles in highly polarized epithelial cells. J Cell Biol 2002;157:1041–8.
[210] Reilein A, Nelson WJ. APC is a component of an organizing template for cortical microtubule networks. Nat Cell Biol 2005;7:463–73.
[211] Reilein A, Yamada S, Nelson WJ. Self-organization of an acentrosomal microtubule network at the basal cortex of polarized epithelial cells. J Cell Biol 2005;171:845–55.
[212] Cohen D, Brennwald PJ, Rodriguez-Boulan E, Müsch A. Mammalian PAR-1 determines epithelial lumen polarity by organizing the microtubule cytoskeleton. J Cell Biol 2004;164:717–27.
[213] Walter P, Lingappa VR. Mechanism of protein translocation across the endoplasmic reticulum membrane. Annu Rev Cell Biol 1986;2:499–516.
[214] Fuller SD, Bravo R, Simons K. An enzymatic assay reveals that proteins destined for the apical or basolateral domains of an epithelial cell line share the same late Golgi compartments. EMBO J 1985;4:297–307.
[215] Rindler MJ, Ivanov IE, Plesken H, Rodriguez-Boulan E, Sabatini DD. Viral glycoproteins destined for apical or basolateral plasma membrane domains traverse the same Golgi apparatus during their intracellular transport in doubly infected Madin–Darby canine kidney cells. J Cell Biol 1984;98:1304–19.
[216] Matlin KS, Simons K. Reduced temperature prevents transfer of a membrane glycoprotein to the cell surface but does not prevent terminal glycosylation. Cell 1983;34:233–43.
[217] Saraste J, Kuismanen E. Pre- and post-Golgi vacuoles operate in the transport of Semliki Forest virus membrane glycoproteins to the cell surface. Cell 1984;38:535–49.
[218] Griffiths G, Pfeiffer S, Simons K, Matlin K. Exit of newly synthesized membrane proteins from the trans cisterna of the Golgi complex to the plasma membrane. J Cell Biol 1985;101:949–64.
[219] Orci L, Ravazzola M, Amherdt M, Perrelet A, Powell SK, Quinn DL, et al. The trans-most cisternae of the Golgi complex: a compartment for sorting of secretory and plasma membrane proteins. Cell 1987;51:1039–51.
[220] Tooze J, Tooze SA, Fuller SD. Sorting of progeny coronavirus from condensed secretory proteins at the exit from the trans-Golgi network of AtT20 cells. J Cell Biol 1987;105:1215–26.
[221] Tooze SA, Huttner WB. Cell-free protein sorting to the regulated and constitutive secretory pathways. Cell 1990;60:837–47.
[222] Griffiths G, Simons K. The trans Golgi network: sorting at the exit site of the Golgi complex. Science 1986;234:438–43.
[223] Ang AL, Taguchi T, Francis S, Folsch H, Murrells LJ, Pypaert M, et al. Recycling endosomes can serve as intermediates during transport from the Golgi to the plasma membrane of MDCK cells. J Cell Biol 2004;167:531–43.
[224] Farr GA, Hull M, Mellman I, Caplan MJ. Membrane proteins follow multiple pathways to the basolateral cell surface in polarized epithelial cells. J Cell Biol 2009;186:269–82.
[225] Matlin K, Bainton DF, Pesonen M, Louvard D, Genty N, et al. Transepithelial transport of a viral membrane glycoprotein implanted into the apical plasma membrane of Madin–Darby canine kidney cells. I. Morphological evidence. J Cell Biol 1983;97:627–37.
[226] Pfeiffer S, Fuller SD, Simons K. Intracellular sorting and basolateral appearance of the G protein of vesicular stomatitis

virus in Madin–Darby canine kidney cells. J Cell Biol 1985;101:470–6.
[227] Misek DE, Bard E, Rodriguez-Boulan E. Biogenesis of epithelial cell polarity: intracellular sorting and vectorial exocytosis of an apical plasma membrane glycoprotein. Cell 1984;39:537–46.
[228] Sargiacomo M, Lisanti M, Graeve L, Le Bivic A, Rodriguez-Boulan E. Integral and peripheral protein composition of the apical and basolateral membrane domains in MDCK cells. J Membr Biol 1989;107:277–86.
[229] Le Bivic A, Sambuy Y, Mostov K, Rodriguez-Boulan E. Vectorial targeting of an endogenous apical membrane sialoglycoprotein and uvomorulin in MDCK cells. J Cell Biol 1990;110:1533–9.
[230] Lisanti MP, Le Bivic A, Saltiel AR, Rodriguez-Boulan E. Preferred apical distribution of glycosyl-phosphatidylinositol (GPI) anchored proteins: a highly conserved feature of the polarized epithelial cell phenotype. J Membr Biol 1990;113:155–67.
[231] Patterson GH, Lippincott-Schwartz J. A photoactivatable GFP for selective photolabeling of proteins and cells. Science 2002;297:1873–7.
[232] Keppler A, Kindermann M, Gendreizig S, Pick H, Vogel H, et al. Labeling of fusion proteins of O6-alkylguanine-DNA alkyltransferase with small molecules *in vivo* and *in vitro*. Methods 2004;32:437–44.
[233] Keppler A, Arrivoli C, Sironi L, Ellenberg J. Fluorophores for live cell imaging of AGT fusion proteins across the visible spectrum. Biotechniques 2006;41:167–70 72, 74-75
[234] Caplan MJ, Forbush III B, Palade GE, Jamieson JD. Biosynthesis of the Na,K-ATPase in Madin–Darby canine kidney cells. Activation and cell surface delivery. J Biol Chem 1990;265:3528–34.
[235] Forbush III B, Hoffman JF. Evidence that ouabain binds to the same large polypeptide chain of dimeric Na,K-ATPase that is phosphorylated from Pi. Biochemistry 1979;18:2308–15.
[236] Forbush III B, Kaplan JH, Hoffman JF. Characterization of a new photoaffinity derivative of ouabain: labeling of the large polypeptide and of a proteolipid component of the Na, K-ATPase. Biochemistry 1978;17:3667–76.
[237] Hammerton RW, Krzeminski KA, Mays RW, Ryan TA, Wollner DA, et al. Mechanism for regulating cell surface distribution of Na^+,$K(^+)$-ATPase in polarized epithelial cells. Science 1991;254:847–50.
[238] Mays RW, Siemers KA, Fritz BA, Lowe AW, van Meer G, et al. Hierarchy of mechanisms involved in generating Na/K-ATPase polarity in MDCK epithelial cells. J Cell Biol 1995;130:1105–15.
[239] Gottardi CJ, Caplan MJ. Delivery of Na^+,K^+)-ATPase in polarized epithelial cells. Science 1993;260:552–4. Author reply 4-6.
[240] Bartles JR, Feracci HM, Stieger B, Hubbard AL. Biogenesis of the rat hepatocyte plasma membrane *in vivo*: comparison of the pathways taken by apical and basolateral proteins using subcellular fractionation. J Cell Biol 1987;105:1241–51.
[241] Hoppe CA, Connolly TP, Hubbard AL. Transcellular transport of polymeric IgA in the rat hepatocyte: biochemical and morphological characterization of the transport pathway. J Cell Biol 1985;101:2113–23.
[242] Sztul ES, Howell KE, Palade GE. Biogenesis of the polymeric IgA receptor in rat hepatocytes. II. Localization of its intracellular forms by cell fractionation studies. J Cell Biol 1985;100:1255–61.
[243] Larkin JM, Sztul ES, Palade GE. Phosphorylation of the rat hepatic polymeric IgA receptor. Proc Natl Acad Sci USA 1986;83:4759–63.
[244] Kipp H, Arias IM. Trafficking of canalicular ABC transporters in hepatocytes. Annu Rev Physiol 2002;64:595–608.
[245] Wakabayashi Y, Lippincott-Schwartz J, Arias IM. Intracellular trafficking of bile salt export pump (ABCB11) in polarized hepatic cells: constitutive cycling between the canalicular membrane and rab11-positive endosomes. Mol Biol Cell 2004;15:3485–96.
[246] Matter K, Brauchbar M, Bucher K, Hauri HP. Sorting of endogenous plasma membrane proteins occurs from two sites in cultured human intestinal epithelial cells (Caco-2). Cell 1990;60:429–37.
[247] Hauri HP, Quaroni A, Isselbacher KJ. Biogenesis of intestinal plasma membrane: posttranslational route and cleavage of sucrase-isomaltase. Proc Natl Acad Sci USA 1979;76:5183–6.
[248] Massey D, Feracci H, Gorvel JP, Rigal A, Soulie JM, et al. Evidence for the transit of aminopeptidase N through the basolateral membrane before it reaches the brush border of enterocytes. J Membr Biol 1987;96:19–25.
[249] Mostov KE, Deitcher DL. Polymeric immunoglobulin receptor expressed in MDCK cells transcytoses IgA. Cell 1986;46:613–21.
[250] Polishchuk R, Di Pentima A, Lippincott-Schwartz J. Delivery of raft-associated, GPI-anchored proteins to the apical surface of polarized MDCK cells by a transcytotic pathway. Nat Cell Biol 2004;6:297–307.
[251] Paladino S, Pocard T, Catino MA, Zurzolo C. GPI-anchored proteins are directly targeted to the apical surface in fully polarized MDCK cells. J Cell Biol 2006;172:1023–34.
[252] Hubbard AL, Stieger B, Bartles JR. Biogenesis of endogenous plasma membrane proteins in epithelial cells. Annu Rev Physiol 1989;51:755–70.
[253] Welling PA, Weisz OA. Sorting it out in endosomes: an emerging concept in renal epithelial cell transport regulation. Physiology (Bethesda) 2010;25:280–92.
[254] Lencer WI, Verkman AS, Arnaout MA, Ausiello DA, Brown D. Endocytic vesicles from renal papilla which retrieve the vasopressin-sensitive water channel do not contain a functional H^+ ATPase. J Cell Biol 1990;111:379–89.
[255] Fang L, Garuti R, Kim BY, Wade JB, Welling PA. The ARH adaptor protein regulates endocytosis of the ROMK potassium secretory channel in mouse kidney. J Clin Invest 2009;119:3278–89.
[256] Butterworth MB, Edinger RS, Frizzell RA, Johnson JP. Regulation of the epithelial sodium channel by membrane trafficking. Am J Physiol Renal Physiol 2009;296:F10–24.
[257] Schwartz GJ, Al-Awqati Q. Regulation of transepithelial H^+ transport by exocytosis and endocytosis. Annu Rev Physiol 1986;48:153–61.
[258] Mount DB. Regulated endocytosis of NCC. Am J Physiol Renal Physiol 2010;299:F297–9.
[259] Hu MC, Fan L, Crowder LA, Karim-Jimenez Z, Murer H, et al. Dopamine acutely stimulates Na^+/H^+ exchanger (NHE3) endocytosis via clathrin-coated vesicles: dependence on protein kinase A-mediated NHE3 phosphorylation. J Biol Chem 2001;276:26906–15.
[260] Pedemonte CH, Efendiev R, Bertorello AM. Inhibition of Na, K-ATPase by dopamine in proximal tubule epithelial cells. Semin Nephrol 2005;25:322–7.
[261] Gottlieb TA, Beaudry G, Rizzolo L, Colman A, Rindler M, Adesnik M, et al. Secretion of endogenous and exogenous proteins from polarized MDCK cell monolayers. Proc Natl Acad Sci USA 1986;83:2100–4.
[262] Jones LV, Compans RW, Davis AR, Bos TJ, Nayak DP. Surface expression of influenza virus neuraminidase, an amino-terminally anchored viral membrane glycoprotein, in polarized epithelial cells. Mol Cell Biol 1985;5:2181–9.
[263] Roth MG, Compans RW, Giusti L, Davis AR, Nayak DP, Gething MJ, et al. Influenza virus hemagglutinin expression is

polarized in cells infected with recombinant SV40 viruses carrying cloned hemagglutinin DNA. Cell 1983;33:435–43.
[264] Stephens EB, Compans RW, Earl P, Moss B. Surface expression of viral glycoproteins is polarized in epithelial cells infected with recombinant vaccinia viral vectors. EMBO J 1986;5:237–45.
[265] Green RF, Meiss HK, Rodriguez-Boulan E. Glycosylation does not determine segregation of viral envelope proteins in the plasma membrane of epithelial cells. J Cell Biol 1981;89:230–9.
[266] Roth MG, Fitzpatrick JP, Compans RW. Polarity of influenza and vesicular stomatitis virus maturation in MDCK cells: lack of a requirement for glycosylation of viral glycoproteins. Proc Natl Acad Sci USA 1979;76:6430–4.
[267] Carmosino M, Valenti G, Caplan M, Svelto M. Polarized traffic towards the cell surface: how to find the route. Biol Cell 2010;102:75–91.
[268] Davis CG, Lehrman MA, Russell DW, Anderson RG, Brown MS, et al. The J.D. mutation in familial hypercholesterolemia: amino acid substitution in cytoplasmic domain impedes internalization of LDL receptors. Cell 1986;45:15–24.
[269] Lazarovits J, Roth M. A single amino acid change in the cytoplasmic domain allows the influenza virus hemagglutinin to be endocytosed through coated pits. Cell 1988;53:743–52.
[270] Brewer CB, Roth MG. A single amino acid change in the cytoplasmic domain alters the polarized delivery of influenza virus hemagglutinin. J Cell Biol 1991;114:413–21.
[271] Thomas DC, Brewer CB, Roth MG. Vesicular stomatitis virus glycoprotein contains a dominant cytoplasmic basolateral sorting signal critically dependent upon a tyrosine. J Biol Chem 1993;268:3313–20.
[272] Thomas DC, Roth MG. The basolateral targeting signal in the cytoplasmic domain of glycoprotein G from vesicular stomatitis virus resembles a variety of intracellular targeting motifs related by primary sequence but having diverse targeting activities. J Biol Chem 1994;269:15732–9.
[273] Lin S, Naim HY, Roth MG. Tyrosine-dependent basolateral sorting signals are distinct from tyrosine-dependent internalization signals. J Biol Chem 1997;272:26300–5.
[274] Hunziker W, Mellman I. Expression of macrophage-lymphocyte Fc receptors in Madin–Darby canine kidney cells: polarity and transcytosis differ for isoforms with or without coated pit localization domains. J Cell Biol 1989;109:3291–302.
[275] Hunziker W, Fumey C. A di-leucine motif mediates endocytosis and basolateral sorting of macrophage IgG Fc receptors in MDCK cells. EMBO J 1994;13:2963–9.
[276] Matter K, Yamamoto EM, Mellman I. Structural requirements and sequence motifs for polarized sorting and endocytosis of LDL and Fc receptors in MDCK cells. J Cell Biol 1994;126:991–1004.
[277] Hunziker W, Harter C, Matter K, Mellman I. Basolateral sorting in MDCK cells requires a distinct cytoplasmic domain determinant. Cell 1991;66:907–20.
[278] Matter K, Hunziker W, Mellman I. Basolateral sorting of LDL receptor in MDCK cells: the cytoplasmic domain contains two tyrosine-dependent targeting determinants. Cell 1992;71:741–53.
[279] Jones BG, Thomas L, Molloy SS, Thulin CD, Fry MD, Walsh KA, et al. Intracellular trafficking of furin is modulated by the phosphorylation state of a casein kinase II site in its cytoplasmic tail. EMBO J 1995;14:5869–83.
[280] Simmen T, Nobile M, Bonifacino JS, Hunziker W. Basolateral sorting of furin in MDCK cells requires a phenylalanine-isoleucine motif together with an acidic amino acid cluster. Mol Cell Biol 1999;19:3136–44.
[281] Odorizzi G, Trowbridge IS. Structural requirements for major histocompatibility complex class II invariant chain trafficking in polarized Madin–Darby canine kidney cells. J Biol Chem 1997;272:11757–62.
[282] Cross GA. Eukaryotic protein modification and membrane attachment via phosphatidylinositol. Cell 1987;48:179–81.
[283] Lisanti MP, Caras IW, Davitz MA, Rodriguez-Boulan E. A glycophospholipid membrane anchor acts as an apical targeting signal in polarized epithelial cells. J Cell Biol 1989;109:2145–56.
[284] van Meer G. Polarity and polarized transport of membrane lipids in cultured epithelium. In: Matlin KS, Valentich JD, editors. Functional epithelial cells in culture. New York: Alan R. Liss; 1989. p. 43–69.
[285] Brown DA, Crise B, Rose JK. Mechanism of membrane anchoring affects polarized expression of two proteins in MDCK cells. Science 1989;245(4925):1499–501.
[286] Kundu A, Avalos RT, Sanderson CM, Nayak DP. Transmembrane domain of influenza virus neuraminidase, a type II protein, possesses an apical sorting signal in polarized MDCK cells. J Virol 1996;70:6508–15.
[287] Roth MG, Gundersen D, Patil N, Rodriguez-Boulan E. The large external domain is sufficient for the correct sorting of secreted or chimeric influenza virus hemagglutinins in polarized monkey kidney cells. J Cell Biol 1987;104:769–82.
[288] Mostov KE, Breitfeld P, Harris JM. An anchor-minus form of the polymeric immunoglobulin receptor is secreted predominantly apically in Madin–Darby canine kidney cells. J Cell Biol 1987;105:2031–6.
[289] Scheiffele P, Peranen J, Simons K. N-glycans as apical sorting signals in epithelial cells. Nature 1995;378:96–8.
[290] Mostov KE, Simister NE. Transcytosis. Cell 1985;43:389–90.
[291] Mostov KE, de Bruyn Kops A, Deitcher DL. Deletion of the cytoplasmic domain of the polymeric immunoglobulin receptor prevents basolateral localization and endocytosis. Cell 1986;47:359–64.
[292] Aroeti B, Kosen PA, Kuntz ID, Cohen FE, Mostov KE. Mutational and secondary structural analysis of the basolateral sorting signal of the polymeric immunoglobulin receptor. J Cell Biol 1993;123:1149–60.
[293] Reich V, Mostov K, Aroeti B. The basolateral sorting signal of the polymeric immunoglobulin receptor contains two functional domains. J Cell Sci 1996;109(Pt 8):2133–9.
[294] Casanova JE, Breitfeld PP, Ross SA, Mostov KE. Phosphorylation of the polymeric immunoglobulin receptor required for its efficient transcytosis. Science 1990;248:742–5.
[295] Wolosin JM, Forte JG. Stimulation of oxyntic cell triggers K^+ and Cl^- conductances in apical H^+–K^+-ATPase membrane. Am J Physiol 1984;246:C537–45.
[296] Hersey SJ, Sachs G. Gastric acid secretion. Physiol Rev 1995;75:155–89.
[297] Dunbar LA, Caplan MJ. Ion pumps in polarized cells: Sorting and regulation of the Na^+, K^+- and H^+, K^+-ATPases. J Biol Chem 2001;276:29617–20.
[298] Gottardi CJ, Caplan MJ. An ion-transporting ATPase encodes multiple apical localization signals. J Cell Biol 1993;121:283–93.
[299] Muth TR, Gottardi CJ, Roush DL, Caplan MJ. A basolateral sorting signal is encoded in the alpha-subunit of Na-K-ATPase. Am J Physiol 1998;274:C688–96.
[300] Dunbar LA, Aronson P, Caplan MJ. A transmembrane segment determines the steady-state localization of an ion-transporting adenosine triphosphatase. J Cell Biol 2000;148:769–78.
[301] Courtois-Coutry N, Roush D, Rajendran V, McCarthy JB, Geibel J, Kashgarian M, et al. A tyrosine-based signal targets

H/K-ATPase to a regulated compartment and is required for the cessation of gastric acid secretion. Cell 1997;90:501–10.
[302] Wang T, Courtois-Coutry N, Giebisch G, Caplan MJ. A tyrosine-based signal regulates H-K-ATPase-mediated potassium reabsorption in the kidney. Am J Physiol 1998;275:F818–26.
[303] Chuang JZ, Sung CH. The cytoplasmic tail of rhodopsin acts as a novel apical sorting signal in polarized MDCK cells. J Cell Biol 1998;142:1245–56.
[304] Qi AD, Wolff SC, Nicholas RA. The apical targeting signal of the P2Y2 receptor is located in its first extracellular loop. J Biol Chem 2005;280:29169–75.
[305] Ahn J, Mundigl O, Muth TR, Rudnick G, Caplan MJ. Polarized expression of GABA transporters in Madin–Darby canine kidney cells and cultured hippocampal neurons. J Biol Chem 1996;271:6917–24.
[306] Pietrini G, Suh YJ, Edelmann L, Rudnick G, Caplan MJ. The axonal gamma-aminobutyric acid transporter GAT-1 is sorted to the apical membranes of polarized epithelial cells. J Biol Chem 1994;269:4668–74.
[307] Muth TR, Ahn J, Caplan MJ. Identification of sorting determinants in the C-terminal cytoplasmic tails of the gamma-aminobutyric acid transporters GAT-2 and GAT-3. J Biol Chem 1998;273:25616–27.
[308] Cheng J, Moyer BD, Milewski M, Loffing J, Ikeda M, et al. A Golgi-associated PDZ domain protein modulates cystic fibrosis transmembrane regulator plasma membrane expression. J Biol Chem 2002;277:3520–9.
[309] Milewski MI, Mickle JE, Forrest JK, Stafford DM, Moyer BD, Cheng J, et al. PDZ-binding motif is essential but not sufficient to localize the C terminus of CFTR to the apical membrane. J Cell Sci 2001;114:719–26.
[310] Moyer BD, Denton J, Karlson KH, Reynolds D, Wang S, Mickle JE, et al. PDZ-interacting domain in CFTR is an apical membrane polarization signal. J Clin Invest 1999;104:1353–61.
[311] Moyer BD, Duhaime M, Shaw C, Denton J, Reynolds D, et al. The PDZ-interacting domain of cystic fibrosis transmembrane conductance regulator is required for functional expression in the apical plasma membrane. J Biol Chem 2000;275:27069–74.
[312] Carmosino M, Gimenez I, Caplan M, Forbush B. Exon loss accounts for differential sorting of Na-K-Cl cotransporters in polarized epithelial cells. Mol Biol Cell 2008;19:4341–51.
[313] Al-Awqati Q. Plasticity in epithelial polarity of renal intercalated cells: Targeting of the H(+)-ATPase and band 3. Am J Physiol 1996;270:C1571–80.
[314] Alper SL, Stuart-Tilley A, Simmons CF, Brown D, Drenckhahn D. The fodrin-ankyrin cytoskeleton of choroid plexus preferentially colocalizes with apical Na^+K^+)-ATPase rather than with basolateral anion exchanger AE2. J Clin Invest 1994;93:1430–8.
[315] Gundersen D, Orlowski J, Rodriguez-Boulan E. Apical polarity of Na,K-ATPase in retinal pigment epithelium is linked to a reversal of the ankyrin-fodrin submembrane cytoskeleton. J Cell Biol 1991;112:863–72.
[316] Shiel MJ, Caplan MJ. Developmental regulation of membrane protein sorting in *Drosophila* embryos. Am J Physiol 1995;269: C207–16.
[317] Kornfeld S. Trafficking of lysosomal enzymes. FASEB J 1987;1:462–8.
[318] Maxfield FR. Weak bases and ionophores rapidly and reversibly raise the pH of endocytic vesicles in cultured mouse fibroblasts. J Cell Biol 1982;95:676–81.
[319] Martin GR, Timpl R. Laminin and other basement membrane components. Annu Rev Cell Biol 1987;3:57–85.
[320] Kondor-Koch C, Bravo R, Fuller SD, Cutler D, Garoff H. Exocytotic pathways exist to both the apical and the basolateral cell surface of the polarized epithelial cell MDCK. Cell 1985;43:297–306.
[321] Chung KN, Walter P, Aponte GW, Moore HP. Molecular sorting in the secretory pathway. Science 1989;243:192–7.
[322] Matlin KS. Ammonium chloride slows transport of the influenza virus hemagglutinin but does not cause mis-sorting in a polarized epithelial cell line. J Biol Chem 1986;261:15172–8.
[323] Pearse BM, Robinson MS. Clathrin, adaptors, and sorting. Annu Rev Cell Biol 1990;6:151–71.
[324] Beltzer JP, Spiess M. *In vitro* binding of the asialoglycoprotein receptor to the beta adaptin of plasma membrane coated vesicles. EMBO J 1991;10:3735–42.
[325] Ohno H, Stewart J, Fournier MC, Bosshart H, Rhee I, Miyatake S, et al. Interaction of tyrosine-based sorting signals with clathrin-associated proteins. Science 1995;269:1872–5.
[326] Pearse BM. Receptors compete for adaptors found in plasma membrane coated pits. EMBO J 1988;7:3331–6.
[327] Pearse BM. Assembly of the mannose-6-phosphate receptor into reconstituted clathrin coats. EMBO J 1985;4:2457–60.
[328] Ohno H, Tomemori T, Nakatsu F, Okazaki Y, Aguilar RC, Foelsch H, et al. MulB a novel adaptor medium chain expressed in polarized epithelial cells. FEBS Lett 1999;449: 215–20.
[329] Roush DL, Gottardi CJ, Naim HY, Roth MG, Caplan MJ. Tyrosine-based membrane protein sorting signals are differentially interpreted by polarized Madin–Darby canine kidney and LLC-PK1 epithelial cells. J Biol Chem 1998;273:26862–9.
[330] Folsch H, Ohno H, Bonifacino JS, Mellman I. A novel clathrin adaptor complex mediates basolateral targeting in polarized epithelial cells. Cell 1999;99:189–98.
[331] Deborde S, Perret E, Gravotta D, Deora A, Salvarezza S, Schreiner R, et al. Clathrin is a key regulator of basolateral polarity. Nature 2008;452:719–23.
[332] Marks MS, Woodruff L, Ohno H, Bonifacino JS. Protein targeting by tyrosine- and di-leucine-based signals: evidence for distinct saturable components. J Cell Biol 1996;135: 341–54.
[333] Rapoport I, Chen YC, Cupers P, Shoelson SE, Kirchhausen T. Dileucine-based sorting signals bind to the beta chain of AP-1 at a site distinct and regulated differently from the tyrosine-based motif-binding site. EMBO J 1998;17:2148–55.
[334] Staub O, Dho S, Henry P, Correa J, Ishikawa T, McGlade J, et al. domains of Nedd4 bind to the proline-rich PY motifs in the epithelial Na^+ channel deleted in Liddle's syndrome. EMBO J 1996;15:2371–80.
[335] Simons K, Wandinger-Ness A. Polarized sorting in epithelia. Cell 1990;62:207–10.
[336] Skibbens JE, Roth MG, Matlin KS. Differential extractability of influenza virus hemagglutinin during intracellular transport in polarized epithelial cells and nonpolar fibroblasts. J Cell Biol 1989;108:821–32.
[337] Arreaza G, Melkonian KA, LaFevre-Bernt M, Brown DA. Triton X-100-resistant membrane complexes from cultured kidney epithelial cells contain the Src family protein tyrosine kinase p62yes. J Biol Chem 1994;269:19123–7.
[338] Fanning AS, Anderson JM. PDZ domains and the formation of protein networks at the plasma membrane. Curr Top Microbiol Immunol 1998;228:209–33.
[339] Songyang Z, Fanning AS, Fu C, Xu J, Marfartia SM, Chishti AH, et al. Recognition of unique carboxyl-terminal motifs by distinct PDZ domains. Science 1997;275:73–7.
[340] Kim SK. Polarized signaling: basolateral receptor localization in epithelial cells by PDZ-containing proteins. Curr Opin Cell Biol 1997;9:853–9.

[341] Bhat MA, Izaddoost S, Lu Y, Cho KO, Choi KW, et al. Discs Lost, a novel multi-PDZ domain protein, establishes and maintains epithelial polarity. Cell 1999;96:833–45.
[342] Hall RA, Ostedgaard LS, Premont RT, Blitzer JT, Rahman N, Welsh MJ, et al. C-terminal motif found in the beta2-adrenergic receptor, P2Y1 receptor and cystic fibrosis transmembrane conductance regulator determines binding to the $Na^{+/}H^{+}$ exchanger regulatory factor family of PDZ proteins. Proc Natl Acad Sci USA 1998;95:8496–501.
[343] Short DB, Trotter KW, Reczek D, Kreda SM, Bretscher A, Boucher RC, et al. An apical PDZ protein anchors the cystic fibrosis transmembrane conductance regulator to the cytoskeleton. J Biol Chem 1998;273:19797–801.
[344] Wang S, Raab RW, Schatz PJ, Guggino WB, Li M. Peptide binding consensus of the NHE-RF-PDZ1 domain matches the C-terminal sequence of cystic fibrosis transmembrane conductance regulator (CFTR). FEBS Lett 1998;427:103–8.
[345] Ferro-Novick S, Jahn R. Vesicle fusion from yeast to man. Nature 1994;370:191–3.
[346] Ikonen E, Tagaya M, Ullrich O, Montecucco C, Simons K. Different requirements for NSF, SNAP, and Rab proteins in apical and basolateral transport in MDCK cells. Cell 1995;81: 571–80.
[347] Inoue T, Nielsen S, Mandon B, Terris J, Kishore BK, et al. SNAP-23 in rat kidney: colocalization with aquaporin-2 in collecting duct vesicles. Am J Physiol 1998;275:F752–60.
[348] Low SH, Chapin SJ, Wimmer C, Whiteheart SW, Komuves LJ, Mostov KE, et al. The SNARE machinery is involved in apical plasma membrane trafficking in MDCK cells. J Cell Biol 1998;141:1503–13.
[349] Guo W, Roth D, Walch-Solimena C, Novick P. The exocyst is an effector for Sec4p, targeting secretory vesicles to sites of exocytosis. EMBO J 1999;18:1071–80.
[350] Grindstaff KK, Yeaman C, Anandasabapathy N, Hsu SC, Rodriguez-Boulan E, Scheller RH, et al. Sec6/8 complex is recruited to cell–cell contacts and specifies transport vesicle delivery to the basal-lateral membrane in epithelial cells. Cell 1998;93:731–40.
[351] Fish EM, Molitoris BA. Alterations in epithelial polarity and the pathogenesis of disease states. N Engl J Med 1994;330:1580–8.
[352] Stein M, Wandinger-Ness A, Roitbak T. Altered trafficking and epithelial cell polarity in disease. Trends Cell Biol 2002;12:374–81.
[353] Calzada MJ, Esteban MA, Feijoo-Cuaresma M, Castellanos MC, Naranjo-Suarez S, Temes E, et al. von Hippel-Lindau tumor suppressor protein regulates the assembly of intercellular junctions in renal cancer cells through hypoxia-inducible factor-independent mechanisms. Cancer Res 2006;66:1553–60.
[354] Baas AF, Kuipers J, van der Wel NN, Batlle E, Koerten HK, Peters PJ, et al. Complete polarization of single intestinal epithelial cells upon activation of LKB1 by STRAD. Cell 2004;116:457–66.
[355] Edelstein CL, Ling H, Schrier RW. The nature of renal cell injury. Kidney Int 1997;51:1341–51.
[356] Oliver J. Correlations of structure and function and mechanisms of recovery in acute tubular necrosis. Am J Med 1953;15:535–57.
[357] Oliver J, Mac DM, Tracy A. The pathogenesis of acute renal failure associated with traumatic and toxic injury; renal ischemia, nephrotoxic damage and the ischemic episode. J Clin Invest 1951;30:1307–439.
[358] Thadhani R, Pascual M, Bonventre JV. Acute renal failure. N Engl J Med 1996;334:1448–60.
[359] Molitoris BA, Chan LK, Shapiro JI, Conger JD, Falk SA. Loss of epithelial polarity: a novel hypothesis for reduced proximal tubule Na^{+} transport following ischemic injury. J Membr Biol 1989;107:119–27.
[360] Spiegel DM, Wilson PD, Molitoris BA. Epithelial polarity following ischemia: a requirement for normal cell function. Am J Physiol 1989;256:F430–6.
[361] Bacallao R, Garfinkel A, Monke S, Zampighi G, Mandel LJ. ATP depletion: a novel method to study junctional properties in epithelial tissues. I. Rearrangement of the actin cytoskeleton. J Cell Sci 1994;107(Pt 12):3301–13.
[362] Golenhofen N, Doctor RB, Bacallao R, Mandel LJ. Actin and villin compartmentation during ATP depletion and recovery in renal cultured cells. Kidney Int 1995;48:1837–45.
[363] Mandel LJ, Doctor RB, Bacallao R. ATP depletion: a novel method to study junctional properties in epithelial tissues. II. Internalization of Na^{+},$K(^{+})$-ATPase and E-cadherin. J Cell Sci 1994;107(Pt 12):3315–24.
[364] Bush KT, Tsukamoto T, Nigam SK. Selective degradation of E-cadherin and dissolution of E-cadherin-catenin complexes in epithelial ischemia. Am J Physiol Renal Physiol 2000;278:F847–52.
[365] Gailit J, Colflesh D, Rabiner I, Simone J, Goligorsky MS. Redistribution and dysfunction of integrins in cultured renal epithelial cells exposed to oxidative stress. Am J Physiol 1993;264:F149–57.
[366] Goligorsky MS, Lieberthal W, Racusen L, Simon EE. Integrin receptors in renal tubular epithelium: new insights into pathophysiology of acute renal failure. Am J Physiol 1993;264:F1–8.
[367] Noiri E, Romanov V, Czerwinski G, Gailit J, DiBona GF, Som P, et al. Adhesion molecules and tubular obstruction in acute renal failure. Ren Fail 1996;18:513–5.
[368] Noiri E, Gailit J, Sheth D, Magazine H, Gurrath M, Muller G, et al. Cyclic RGD peptides ameliorate ischemic acute renal failure in rats. Kidney Int 1994;46:1050–8.
[369] Piwon N, Gunther W, Schwake M, Bosl MR, Jentsch TJ. ClC-5 Cl-channel disruption impairs endocytosis in a mouse model for Dent's disease. Nature 2000;408:369–73.
[370] Novarino G, Weinert S, Rickheit G, Jentsch TJ. Endosomal chloride-proton exchange rather than chloride conductance is crucial for renal endocytosis. Science 2010;328:1398–401.
[371] McCrea HJ, De Camilli P. Mutations in phosphoinositide metabolizing enzymes and human disease. Physiology (Bethesda) 2009;24:8–16.
[372] Chapin HC, Caplan MJ. The cell biology of polycystic kidney disease. J Cell Biol 2010;191:701–10.
[373] Grantham JJ. 1992 Homer Smith Award. Fluid secretion, cellular proliferation, and the pathogenesis of renal epithelial cysts. J Am Soc Nephrol 1993;3:1841–57.
[374] Sullivan LP, Wallace DP, Grantham JJ. Epithelial transport in polycystic kidney disease. Physiol Rev 1998;78:1165–91.
[375] Avner ED, Sweeney Jr. WE, Nelson WJ. Abnormal sodium pump distribution during renal tubulogenesis in congenital murine polycystic kidney disease. Proc Natl Acad Sci USA 1992;89:7447–51.
[376] Wilson PD, Sherwood AC, Palla K, Du J, Watson R, et al. Reversed polarity of $Na(^{+})$-$K(^{+})$-ATPase: mislocation to apical plasma membranes in polycystic kidney disease epithelia. Am J Physiol 1991;260:F420–30.
[377] Brill SR, Ross KE, Davidow CJ, Ye M, Grantham JJ, et al. Immunolocalization of ion transport proteins in human autosomal dominant polycystic kidney epithelial cells. Proc Natl Acad Sci USA 1996;93:10206–11.
[378] Freeman TC. Parallel patterns of cell-specific gene expression during enterocyte differentiation and maturation in the small intestine of the rabbit. Differentiation 1995;59:179–92.
[379] Sullivan LP, Grantham JJ. Mechanisms of fluid secretion by polycystic epithelia. Kidney Int 1996;49:1586–91.

This page intentionally left blank

CHAPTER

2

Mechanisms of Ion Transport across Cell Membranes

Luis Reuss and Guillermo A. Altenberg

Department of Cell Physiology and Molecular Biophysics, and Center for Membrane Protein Research, Texas Tech University Health Sciences Center, Lubbock, Texas, TX, USA

INTRODUCTION

Ion transport by cell membranes serves two important purposes in pluricellular organisms, the maintenance of the volume and composition of the intracellular fluid, and the preservation and regulation of the volume and composition of the extracellular fluid. The first process involves fluxes between the cell interior and its surrounding medium ("homocellular" transport[91]), whereas the second one occurs because of transport across epithelial and endothelial cell layers (transcellular or "heterocellular" transport[91]). In addition, ion transport across intracellular membranes, which surround the nucleus and cytoplasmic organelles, is essential to generate and maintain ion concentration gradients between those organelles and the cytosol.

Needless to say, the narrowly regulated volume and ionic composition – inorganic cations (Na^+, K^+, H^+, Ca^{2+}, Mg^{2+}) and anions (Cl^-, phosphate, bicarbonate) – of the intracellular fluid is essential for cell survival, and for the cell's normal functions. A similar argument can be made for the extracellular fluid compartments, that is, whole body balances of water and the ions listed above are essential for the survival, growth, and development of the organism.

Our main focus in this chapter will be on the molecular mechanisms of ion transport by the plasma membranes of cells. The cell membrane is a phospholipid bilayer doped with abundant proteins. This structure is both a barrier between the cytoplasm and the extracellular fluid, and the pathway for ion and water transport between the two compartments. For most ions, the lipid bilayer is the barrier and membrane transport proteins are the pathway for these fluxes.

The Cell Interior and Extracellular Fluid Have Different Ionic Compositions

A crucial property of living cells is their capacity to maintain an internal (intracellular or cytosolic) composition different from that of the surrounding (extracellular) medium. As with all other ionic solutions, the cytosol and the extracellular fluid obey the principle of macroscopic (or bulk) electroneutrality, that is, the sum of cationic and anionic charges are the same in each compartment. As discussed below, there is a microscopic deviation from this principle at the membrane surfaces when there is a difference in electrical potential across the membrane, but the actual differences between anion and cation concentrations are extremely small.

The maintenance of ionic asymmetry between intracellular and extracellular compartments is based on the existence of the cell membrane (or plasma membrane), which separates the cell interior from its surroundings. As shown schematically in Figure 2.1, the membrane is a phospholipid bilayer, with high protein content. Membrane proteins can span the phospholipid bilayer (integral proteins, some of which span the membrane and are known as transmembrane proteins) or can be associated with the membrane surface (peripheral proteins). Transmembrane proteins perform many functions, including translocation of ions, nonelectrolytes, and water across the membrane (transport function, the main theme of this chapter); sensing and early transduction of extracellular events (signaling function); attachment to components of the cytoskeleton, the extracellular matrix or adjacent cells (adhesion function).

Seldin and Giebisch's The Kidney, Fifth Edition.
DOI: http://dx.doi.org/10.1016/B978-0-12-381462-3.00002-1

© 2013 Elsevier Inc. All rights reserved.

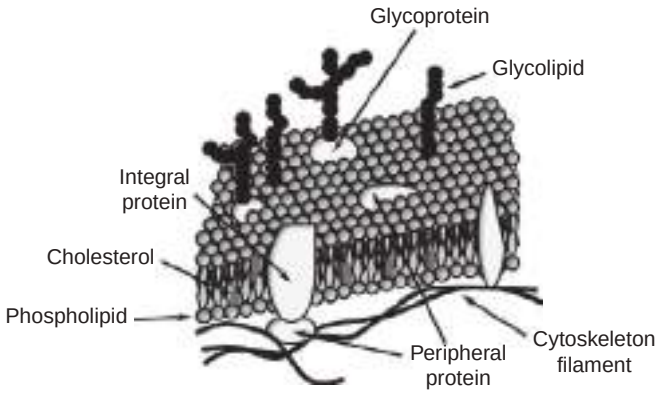

FIGURE 2.1 **Structure of the plasma membrane.** This two-dimensional representation of the plasma membrane is based on the fluid-mosaic model[95,96] modified according to recent observations.[30,59,71,94,112] The membrane is a lipid bilayer that contains integral and peripheral membrane proteins. The bilayer is largely made of phospholipids that have polar heads and hydrophobic tails. The hydrophobic tails face each other, while the polar head groups face the adjacent aqueous solutions (extracellular fluid and cytosol). In addition, the membrane contains glycolipids and cholesterol. The phospholipid compositions of the two leaflets differ; e.g., phosphatidyl inositol is more abundant in the inner leaflet. Additionally, certain areas of the membrane form *lipid rafts* (see text). A small fraction of the membrane surface area is occupied by either strongly-bound proteins (integral membrane proteins), some crossing the membrane one or more times (transmembrane proteins) or loosely attached (peripheral) membrane proteins. Membrane proteins can be glycosylated or have other post-translational modifications (not shown). Some membrane proteins are attached to components of the cytoskeleton or the exoskeleton, directly or via other proteins. Integral membrane proteins can associate forming oligomers, as well as macromolecular complexes.

Two properties of the cell membrane are needed to generate and maintain the intracellular ion composition essential for life: the barrier function and the transport function. This distinction is didactically convenient, although both functions are clearly linked. By the barrier function, the cell membrane prevents the flux of certain molecules; by the transport function, it translocates certain molecules. These two functions bring about a steady-state in which cell volume and composition are kept constant and appropriate for cell survival. Relative to the extracellular fluid, some substances are maintained at high concentrations (e.g., K^+ and ATP), whereas others are maintained at low concentrations (e.g., Ca^{2+} and Cl^-) inside the cell.

The cell interior is not homogeneous, but is rather a complex medium including a highly structured cytoplasm (cytosol and cytoskeleton) and numerous organelles. The latter are separated from the cytosol by their membranes. Exchanges between each organelle and the cytosol occur by mechanisms similar to those present in the plasma membrane. In this chapter, we will not address organelle membrane function.

The Plasma Membrane: Structure Related to Function

The plasma membrane, which is 3–8 nm thick, is largely formed by phospholipids, organized in a bilayer, and proteins. The main phospholipids are phosphatidylcholine and phosphatidylethanolamine, with lower levels of phosphatidylinositol, phosphatidylserine, and phosphatidylglycerol, and sterols (cholesterol, ergosterol, zymosterol).[6,63] The precise proportions vary among cells. Hydrophobic or amphipathic proteins are essential components of biological membranes. In most membranes, the w/w protein: lipid ratio is *ca.* 1, and therefore a membrane protein of *ca.* 40 kDa is surrounded by 50–55 lipid molecules.

Experimental work during the last two or three decades has ruled out the "fluid-mosaic" (Singer and Nicolson) model of membrane structure.[95,96] In this model, biological membranes are considered two-dimensional viscous phospholipid bilayers in which integral membrane proteins are randomly distributed and free to rotate and diffuse laterally. A main objection is the demonstration of asymmetry in the lipid composition of the membrane.[71] The current view is that the plasma membrane is a highly-organized and asymmetric structure composed of lipids and proteins.[30] There are lateral differences in lipid composition within a monolayer; sphingolipids, sterols, and phosphatidylcholine predominate on the extracellular leaflet, whereas the cytoplasmic leaflet is enriched in phosphatidylinositol, phosphatidylethanolamine, phosphatidylserine, and phosphatidic acid, which results in a negative charge that facilitates binding of peripheral and transmembrane proteins.[71] In addition, many membrane proteins cluster with others in microdomains, in which the lipid composition may differ from that of the bulk bilayer. These clusters are maintained by intramembrane lipid–lipid, protein–protein, and protein–lipid interactions, as well as interactions with intracellular molecules (cytoskeletal proteins) and extracellular components (extracellular matrix proteins and membrane proteins of adjacent cells). It is clear that the two monolayers also differ in composition. Lipid rafts are microdomains in the submicron range in which cholesterol and sphingolipids are enriched in the external leaflet, and cholesterol and phospholipids with saturated fatty acids in the internal leaflet of the plasma membrane. The surrounding bilayer is abundant in unsaturated fatty acids and contains more fluid than that in the raft.[59] Lipid rafts exclude certain proteins and organize others in specific oligomeric structures.[94] Rapid changes in composition and location in the membrane are essential for the role that lipid rafts play in signaling processes (e.g., receptor tyrosine kinases).

Phospholipids in the plasma membrane are not just a barrier and a "solvent" for membrane proteins, but play important roles in signaling processes. Inositol-1,4,5-triphosphate, diacylglycerol, and phosphatidylinositol-3,4,5-triphosphate (derived from phosphatidylinositol) are good examples.[9,72,73] Phosphatidylinositol 4,5-bisphosphate (PIP_2) exerts regulatory effects on a number of ion channels and other transport proteins. Its effects can be stimulatory or inhibitory and appear to require PIP_2 binding.[49,102] Other signaling molecules originating from plasma membrane phospholipids are arachidonic and docosahexaenoic acids, which are generated from phosphatidylethanolamine, phosphatidylcholine, and phosphatidylinositol by the action of phospholipase A_2. Certainly, being a dielectric is not the only function of the phospholipid moiety of the cell membrane.

This new notion of the structure of the plasma membrane[112] is based on results of biophysical studies, including fluorescence recovery after photo-bleaching, single-particle tracking techniques, optical trapping by laser tweezers, and fluorescence correlation spectroscopy. These methods, applied to cell membranes, have yielded quantitative dynamic information on the distribution, mobility, and compartmentalization of membrane proteins.[112] Biochemical, molecular, and physiological studies indicate that membrane transport proteins are not randomly distributed, but that they undergo homo- and hetero-associations,[59] and that these associations may have functional significance. A case in point is the proposed proximity between plasma membrane Ca^{2+} channels and Ca^{2+}-sensitive proteins, including Ca^{2+}-activated channels: Ca^{2+} entry results in a large, but highly localized, increase in intracellular [Ca^{2+}], because of effective cytosolic buffering, and thus its signaling effects may be quite local.[70]

In summary, the current view of the structure of the plasma membrane is that of a compartmentalized two-dimensional structure, mosaic-like, with less fluidity than proposed by the Singer–Nicolson model. The phospholipids have signaling functions in addition to previously recognized ones. The mobility of membrane proteins may be restricted by the structure of the lipid domain, interactions with cytoskeletal proteins or other cytoplasmic components, and/or homo- and hetero-associations with other integral membrane proteins. Future studies of membrane transport proteins along these lines are likely to reveal important aspects of their function and regulation in health and disease (see Chapter 14).

The Plasma Membrane is Selectively Permeable

The barrier and transport functions of the plasma membrane are determined by its composition, mostly regarding lipids and integral transmembrane proteins (for membrane structure, see references [59,95,96] and [112]; for a review of membrane proteins, see [103]). When the membrane is *permeable* to a specific molecule, then that molecule can cross the membrane. *Permeability* (cm s^{-1}) is a property of a specific membrane for a specific molecule. The amount of substance that crosses the membrane per unit of time and membrane area is the *flux*. Using radioactive techniques, unidirectional fluxes can be measured (e.g., in case of a cell, influx and efflux); the *net flux* is the difference between the two unidirectional fluxes. A finite net flux denotes the presence of either a net driving force across the membrane or an active process.

Permeation of a specific molecule can take place through the lipid phase (i.e., *solubility diffusion*) and/or through membrane proteins (i.e., *mediated transport*). Solubility diffusion always results in equilibrating transport, dissipating differences in concentration or electrochemical potential (see the section "Diffusion and Electrodiffusion," below). In contrast, mediated transport can either dissipate or generate differences in chemical or electrochemical potentials across the membrane. An example of mediated transport is the operation of the sodium pump, the Na^+,K^+-ATPase.

The lipid phase of the plasma membrane is hydrophobic, and therefore has high permeability for lipophilic molecules and low permeability for hydrophilic molecules. Thus, a protein-free phospholipid membrane has a high permeability for nonpolar small molecules such as O_2 and CO_2, a much lower permeability for uncharged small polar substances such as water, urea, and glycerol, and an extremely low permeability for ions and larger uncharged polar molecules, such as glucose. Most molecules are measurably permeable across plasma membranes. However, the diffusive permeability coefficients range over several orders of magnitude. It is thought that hydrophilic molecules permeate the membrane bilayer to some extent, because the thermal motion of the phospholipid molecules causes transient kinks in the bilayer structure.

Transport proteins can be classified in four groups, namely pores, channels, carriers (also referred to as transporters), and pumps (see next section). The expression of some transport proteins can be specific to tissue, cell, and sometimes membrane domain. Others are expressed in most, if not all, cell membranes. The functional significance of transport proteins is apparent in two realms. Some are primarily related to the establishment and maintenance of cellular composition (intracellular "homeostasis"), such as the Na^+,K^+-ATPase and K^+ channels in most animal cells. Others are primarily related to specific cell functions, such as excitability (e.g., the tetrodotoxin-sensitive, voltage-activated Na^+ channel in nerve and muscle), and transepithelial Na^+ transport (e.g., the

amiloride-sensitive, voltage-insensitive Na^+ channel in the apical membrane of certain epithelial cells).

A *pore* is an aqueous communication between both sides of the membrane, accessible to both sides at all times – that is, it is always "open" (permeable). A *channel* is also an aqueous communication between the two sides of the membrane, but it opens and closes stochastically by changes in conformation called *gating*; when open, a channel is accessible from both sides of the membrane, when closed, it is impermeable. A *carrier* is a membrane transport protein whose permeation pathway is not simultaneously accessible to both sides of the membrane, but to one side at a time; changes in conformation change the orientation of the carrier, moving the transported ion to the other side; an appropriate simplified description is that a carrier has two gates and they are never open at the same time. Finally, a *pump* has the properties of a carrier, but in addition it is coupled to a metabolic energy source, in most cases hydrolysis of ATP.

MECHANISMS OF ION TRANSPORT

Ion Transport can be Active or Passive

The definitions of active and passive transport are thermodynamic. Passive transport occurs in the direction expected for the existing driving force, which in the case of ions involves the chemical gradient (given by the difference in concentration between the two sides of the membrane) and the electrical gradient (given by the transmembrane electrical potential difference or membrane voltage). In other words, passive transport is energetically downhill. In contrast, active transport takes place in the absence of or against the prevailing electrochemical gradient. In other words, active transport is energetically uphill, and therefore requires an energy input. Depending on the origin of this energy, one can distinguish two types of active transport.

Primary active transport is characterized by the direct use of metabolic energy, supplied by light, redox potential or ATP hydrolysis. In most cases of plasma membrane primary active transport in eukaryotic organisms, the energy is provided by the hydrolysis of ATP, a process catalyzed by the same molecule that performs the transport. Hence, in this case the transporter is also an ATP hydrolase (ATPase). Transporters responsible for primary active transport are referred to as pumps. In plasma membranes of most animal cells there can be expression of one or more of four ion-transporting ATPases. These are the Na^+,K^+-ATPase, H^+-ATPase, H^+,K^+-ATPase, and Ca^{2+}-ATPase.

Secondary active transport is characterized by the indirect use of metabolic energy. The energy stored in the electrochemical gradient of one substrate is utilized to transport actively another species (ion or molecule). In animal cells, including those from epithelia, secondary active transport is most frequently linked to Na^+ transport. The Na^+,K^+-ATPase establishes an electrochemical potential gradient for Na^+ across the plasma membrane, which includes chemical (high extracellular and low intracellular [Na^+]) and electrical components (cell electrically negative to the extracellular compartment), both contributing to a net driving force favoring Na^+ entry into the cell. This gradient is then utilized by carriers to actively transport other substrates, by coupling their translocation to that of Na^+ at the molecular level.

Depending on the directions of the fluxes, there are two kinds of secondary active transport: One is *co-transport* (or *symport*) in which the substrates move in the same direction, such as downhill for Na^+ and uphill for the co-transported substrate (e.g., Na^+-glucose co-transport). The other one is *countertransport* (also *antiport* or *exchange*), in which the fluxes are in opposite directions (e.g., $Na^+ - H^+$ exchange). In most instances, secondary active transport involves only two species (Na^+ and another substrate), but in some cases there are three: an example is the Na^+-K^+-$2Cl^-$ co-transporter, an electroneutral symporter that is expressed principally in epithelial cells. This transporter accounts for uphill Cl^- uptake, a step necessary for Cl^- absorption (e.g., in the apical membrane of cells of the thick ascending limb of the loop of Henle) or Cl^- secretion (e.g., in the basolateral membrane of crypt cells in the intestine and epithelial cells in the airway). For quantitative analyses of membrane transport processes, see Läuger,[64] Macey and Moura,[67] and Stein.[99]

Active and Passive Transport Processes can be Evaluated by Considering Direction of Electrochemical Potential Difference (Driving Force)

As stated above, passive transport is energetically downhill, driven by the pre-existing driving force; this force depends on the chemical or electrochemical gradient, for uncharged and charged solutes, respectively. Under isothermal conditions the driving force encompasses differences in concentration, electrical potential, and/or pressure across the membrane. Under these conditions, the electrochemical potential difference ($\Delta\overline{\mu}_j$) for the jth ion is given by Eq. (2.1):

$$\Delta\overline{\mu}_j = z_j V_m F + RTln\left(\frac{C_j^i}{C_j^o}\right) + \Delta P\overline{V}_j \qquad (2.1)$$

where z is the valence, V_m is the membrane voltage, F is the Faraday constant, R is the gas constant, T is the absolute temperature, C is the concentration, i and o refer to

the two sides of the membrane (inside and outside, respectively), ΔP is the transmembrane hydrostatic pressure difference, and $\overline{V}_j$ is the ion's partial molar volume. The electrochemical potential has the three components defined above, given by the three terms on the right side of the equation. Across animal cell membranes, steady-state hydrostatic or osmotic pressure differences are small or nil (see Chapter 4), and therefore the third term of Eq. (2.1) is eliminated, yielding:

$$\Delta\overline{\mu}_j = z_j V_m F + RTln\left(\frac{C_j^i}{C_j^o}\right) \tag{2.2}$$

This equation is used to evaluate the driving force for ion transport under isobaric conditions. In the case of nonelectrolytes, $z = 0$ and the first term of Eq. (2.2) can also be eliminated, yielding:

$$\Delta\mu_j = RTln\left(\frac{C_j^i}{C_j^o}\right) \tag{2.3}$$

where $\Delta\mu_j$ denotes the chemical potential difference. This equation describes the driving force for nonelectrolyte transport.

From Eq. (2.2) (under isobaric and isothermal conditions), Ussing[111] derived the flux-ratio equation, a fundamental expression which provides a thermodynamic test for active or passive transport:

$$J_{in}/J_{out} = (C_i/C_o)\exp(zV_mF/RT) \tag{2.4}$$

where J is flux (the subscripts denote influx and efflux, respectively). The test proceeds as follows: the ratio of unidirectional fluxes (J_{in}/J_{out}) is determined experimentally, and the driving forces are measured; if the ratio deviates from the prediction given by Eq. (2.4), which evaluates the passive driving forces, then active transport is suspected. Deviations from the flux-ratio equation can also result from the presence of exchange diffusion and single-file diffusion, as discussed by Schultz.[90]

Pathways and Mechanisms of Passive Transport

Passive transport can be *via* the lipid bilayer (solubility diffusion) or *via* transmembrane proteins (mediated). Solubility diffusion is a permeation process that involves the movement of a molecule dissolved in the aqueous solution bathing one side of the membrane into the lipid phase of the membrane, then across the membrane, and then from the membrane lipid into the solution bathing the opposite side. Clearly, two processes are involved. The first one ("solubility") governs the fluxes at the solution–membrane interface, and depends on the relative solubility of the molecule in lipid and water, which can be quantified by the oil–water partition coefficient, β, a coefficient equal to the ratio of the molecule's steady-state concentrations in lipid and water. The second process ("diffusion") governs the solute translocation within the membrane lipid, which depends largely on the mass and shape of solute molecules. The lipid solubility of the molecule is the main factor determining its permeability via the lipid moiety of the membrane.

Mediated transport is the mode of transmembrane transport of substances with very low solubility in phospholipids, that is, charged and polar substances. The transport proteins provide a hydrophilic path across the membrane, through which the solute permeates or a narrow pore in which amino acid charges replace the water molecules surrounding the ion or polar molecule in free solution.

Diffusion and Electrodiffusion

Diffusion and electrodiffusion are the main processes of passive solute transport across homogeneous phases (e.g., lipid membranes or aqueous pores) by independent motion of the solute molecules. Diffusion applies to uncharged particles and electrodiffusion to ions. Although diffusion does not strictly apply to ion transport, its analysis is simpler and helps in understanding electrodiffusion.

Diffusion of a solute in aqueous solution is the result of the random thermal motion of solute molecules. In the absence of convection, if there are differences in concentration between different sectors of the solution, then random solute motion will tend to make its distribution homogeneous (equilibrating transport). All solute particles move randomly at uniform average velocities, dependent on the solution temperature. Hence, more particles will tend to move from regions of high concentration to sectors of low concentration than in the opposite direction, simply because there are more particles per unit volume in the high concentration regions. In other words, differences in concentration cause unequal unidirectional fluxes in a regime of diffusion because of differences in the number of particles flowing in each direction per unit of time, not because of different velocities of individual particles flowing in one direction or the other. In diffusion, the molecules move independently of each other and of other particles present in the solution, that is, there is no flux coupling. This is the *independence principle*.

Diffusion of a nonelectrolyte in solution is described by Fick's first law[34]:

$$J_s = -D_s\frac{dC_s}{dx} \tag{2.5}$$

where J_s is the solute flux (moles $cm^2\,sec^{-1}$), D_s is the solute diffusion coefficient ($cm^2\,sec^{-1}$) and dC_s/d_x is the concentration gradient. The negative sign denotes the direction of the flux.

Fick's second law of diffusion[34] considers the time course of the process:

$$\frac{dC}{dt} = D_s \frac{d^2C_s}{dx^2} \tag{2.6}$$

where dC/dt is the rate of change in solute concentration, and x denotes distance.

The average time required by diffusing particles to cover a given distance is inversely proportional to the diffusion coefficient, and directly proportional to the square of the traveled distance. Einstein approximated the second law of diffusion with $\lambda = (D_s t)^{1/2}$, where λ is the traveled distance in the x-axis. The dependence of t on the square of the distance makes diffusion a very slow transport process for long distances. For a typical $D_s = 10^{-5}$ cm^2 sec^{-1}, it takes 1 millisecond for the solute to diffuse 1 μm, but it takes 1000 seconds (*ca.* 16.7 minutes) to diffuse 1 mm. Convective flow (see Chapter 9) is a much more effective mass transport mechanism for long distances.

Now we consider a thin lipid membrane of thickness δ_m separating two aqueous compartments (Figure 2.2). The solutions on both sides are well stirred, so that the solute concentrations are homogeneous in both. Inserting the solute partition coefficient (β_s) in Eq. (2.5) (β_s denotes lipid solubility relative to water solubility), we obtain the following expression for the solute flux:

$$J_s = -\frac{D_s \beta_s}{\delta_m} \Delta C_s \tag{2.7}$$

where ΔC_s is the solute concentration difference between the two solutions. Defining the solute permeability (P_s) as $P_s = D_s\, \beta_s\, / \Delta_m$, Eq. (2.7) reduces to:

$$J_s = -P_s \Delta C_s \tag{2.8}$$

The diffusive permeability coefficient of the membrane relates the flux to the driving force and denotes the ease with which the membrane permits mass transfer of a particular species. Its units are cm s^{-1}, those of velocity. In the simple case of a nonelectrolyte, under isothermal and isobaric conditions, the permeability (P) of solute s is given by a rearrangement of Eq. (2.8): $P_s = J_s/\Delta C_s$. This is the phenomenological, experimentally determined permeability, calculated by dividing the steady-state solute flux by the difference between the solute concentrations of well-stirred bathing solutions. The other definition of diffusive permeability is mechanistic, and considers the factors involved in solubility diffusion, D_s, β_s, and δ_m, as described above.

The preceding discussion considers the specific case of solubility diffusion, but the phenomenological definition of permeability can be applied in principle to any transport mechanism. Of course, its interpretation varies. An important case is that of the permeation of certain hydrophilic nonelectrolytes through aqueous pores in the membrane. If the lipid bilayer is impermeable to the solute, then diffusive transport is entirely via the pores. The permeable area of this membrane (S_p) is only a fraction of the total membrane area, given (for 1 cm^2 of membrane) by $S_p = n\pi r^2$, where n is the density of homogeneous pores of radius r. The partition coefficient is unity (the solute is dissolved in water both inside and outside of the pore), and is hence eliminated from the equation:

$$P_s = n\pi r^2 D_s / L \tag{2.9}$$

where L is the pore length (nearly equivalent to membrane thickness).

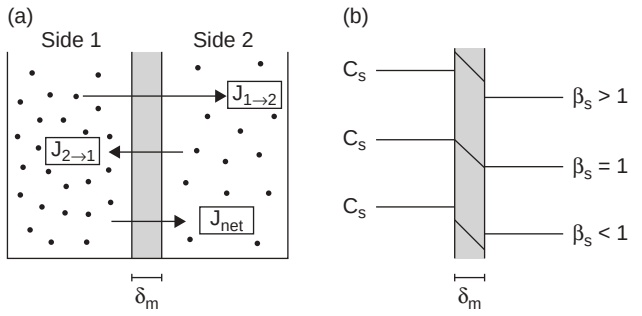

FIGURE 2.2 **Diffusion across a membrane.** (a) A membrane separates two aqueous solutions (1 and 2). The dots represent molecules of a solute to which the membrane is permeable; the solute concentration (C_s) is greater in solution 1. Solute molecules move randomly in each solution and collide with the membrane with a probability proportional to the concentration. Solutes collide, dissolve in, and diffuse across the membrane. The unidirectional fluxes ($J_{1\rightarrow2}$ and $J_{2\rightarrow1}$) are proportional to the solute concentrations in sides 1 and 2, respectively; the net flux (J_{net}) is proportional to the concentration difference. The concentration difference does not accelerate the molecules, and hence it is not a force, although it is usually referred to as the *chemical driving force*. Diffusion is a passive, equilibrating transport, i.e., net transport ceases when the concentrations on both sides of the membrane are equal. (b) Lines denote solute concentration profiles in the solutions and the membrane depending on the partition coefficient (β_s). When $\beta_s = 1$, solute concentration in the membrane boundaries are identical to those in the adjacent solutions; concentrations in the membrane are greater or smaller than those in the adjacent solution if β_s is greater or smaller than unity, respectively. The membrane thickness is denoted by δ_m.

Electrodiffusion

Electrodiffusion is the main mechanism of passive transport of ions in homogeneous media, that is, bulk aqueous solution or relatively large water-filled pores. Electrodiffusive transmembrane ion transport is a mediated transport process, but it is better discussed with diffusion for continuity. In large-diameter pores, electrodiffusion theory explains ion permeation very well. In ion channels, which have smaller diameter and are highly selective, there are significant interactions between the

ions and the permeation pathway. For this reason, simple electrodiffusion theory is not entirely applicable to ion channels, but is nevertheless a useful approximation. For ion transport across a membrane, two factors determine the flux: the chemical potential difference (difference in concentration across the membrane) and the electrical potential difference (membrane voltage). The net ion flux (J_i) is given by the Nernst–Planck equation (see [50]). If a constant electrical field is assumed in the membrane and other assumptions are made, the Nernst–Planck equation can be solved, yielding the Goldman–Hodgkin–Katz (GHK) equation[41,51]:

$$J_i = -P_i \frac{z_i V_m F}{RT}\left[\frac{C_i^o - C_i^i \exp(V_m F/RT)}{1-\exp(V_m F/RT)}\right] \qquad (2.10)$$

where R, T, z, and F have their usual meanings, P is permeability, V_m is membrane voltage, C is concentration, the subscript i denotes the ith ion, and the superscripts i and o denote the two sides of the membrane.

Under zero current conditions, the GHK flux equation yields the membrane voltage as a function of the permeabilities and concentrations of all permeant ions. For the case of three monovalent permeant ions (Na^+, K^+, and Cl^-), the equation (GHK voltage equation) is:

$$V_m = -\frac{RT}{F}\ln\frac{P_{Na}[Na^+]_i + P_K[K^+]_i + P_{Cl}[Cl^-]_o}{P_{Na}[Na^+]_o + P_K[K^+]_o + P_{Cl}[Cl^-]_i} \qquad (2.11)$$

where the brackets denote concentrations. Note that if the fraction including permeability coefficients and ion concentrations is inverted, then the sign of the right side of the equation is also inverted. We prefer the notation given here, because it gives the intracellular potential minus the extracellular potential, the convention used in electrophysiology. This also applies to the Nernst equation below.

Note that if only one ion is permeable, e.g., if P_{Na} and P_{Cl} are 0 in Eq. (2.11), then the membrane voltage becomes equal to the equilibrium potential for that ion, in this example K^+. The equilibrium potential is given by the Nernst equation[81]:

$$V_m = -\frac{RT}{F}\ln\frac{[K^+]_i}{[K^+]_o} \qquad (2.12)$$

Under these conditions, the two compartments separated by the membrane are at a *steady-state* (the amounts of K^+ on each side remain constant with time), but also at *equilibrium*, which means that the net driving force for K^+ is zero, and hence the unidirectional fluxes are equal (Figure 2.3). In the case of cells, one frequently observes a steady-state K^+ distribution without equilibrium; the net efflux through channels is exactly balanced by influx via the Na^+,K^+-ATPase.

Another interesting point is that the Nernst equation indicates that if only one ion is permeable, then the membrane voltage is determined by the concentration ratio for that ion, not its absolute concentrations. In addition, the membrane voltage is independent of the absolute value of the ion permeability. As shown by the GHK voltage equation, in the case of a membrane permeable to more than one ion, the membrane voltage depends on the absolute concentrations and permeability coefficients of all permeant ions. The Nernst equation can be derived more directly from the definitions of electrochemical potential (Eq. (2.1)) and equilibrium ($\Delta\overline{\mu}_i = 0$).

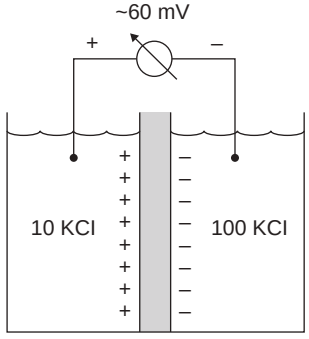

FIGURE 2.3 **Electrochemical equilibrium.** A membrane permeable to K^+ and impermeable to Cl^- separates two KCl solutions of 10 mM and 100 mM concentrations, respectively. Because of the difference in concentrations, there is a chemical driving force for K^+ and Cl^- fluxes from right to left. While the impermeant Cl^- cannot move, the permeant K^+ moves across the membrane, and in doing so creates a difference in electrical potential across the membrane. The membrane becomes electrically charged by a tiny excess of K^+ on the left, and a tiny excess of Cl^- on the right. This difference in electrical potential (the *transmembrane voltage*) opposes further K^+ flux, and a state is reached at which the chemical driving force and the electrical driving force for K^+ movement are equal and opposite. This condition, described by the Nernst equation (Eq. (2.12)), denotes electrochemical equilibrium.

The essential points concerning electrodiffusion are that ion fluxes across membranes are determined by both permeability and driving force, and that the driving force has chemical and electrical components. Hence, these three elements must be known to predict the direction and magnitude of the flux. For example, knowledge of the K^+ concentrations inside and outside a cell is insufficient to decide whether the ion is at equilibrium across the membrane or whether there is a passive driving force inwardly or outwardly directed. To establish this simple point, it is necessary to know the membrane voltage. However, knowledge of the electrochemical gradient is insufficient to predict the magnitude of the K^+ flux expected for this gradient; the K^+ permeability of the membrane must also be known.

Mediated Transport

This expression means that translocation across the membrane is not via the lipid bilayer, but via membrane

transport proteins: pores, channels, carriers or pumps. Mediated transport is the process by which ions and polar nonelectrolytes undergo passive transport across the cell membrane. Hence, this mechanism is complementary to that provided by solubility diffusion, in that it is specialized for hydrophilic solutes, whereas solubility diffusion is more effective for lipophilic solutes. For certain solutes, both mechanisms may operate. Even for solutes with very low permeability across the phospholipid moiety of the membrane, a significant contribution of the diffusive flux may exist because of the large fractional area covered by phospholipids, in particular if there is also a low level of expression of the relevant transporters.

In mediated transport, specialized proteins spanning the membrane provide an aqueous environment that allows for the transmembrane flux of particles that are virtually insoluble in phospholipids. Recent advances have permitted the molecular identification of many of these proteins, as well as the genes that encode them. In addition to providing an aqueous environment for solute translocation, these molecules may undergo conformational changes during or related to the substrate translocation. The transport proteins underlying mediated transport can be classified in four groups: pores; channels; carriers; and pumps.

Thermodynamics of Mediated Passive Transport

Pores, channels, and carriers are membrane transport proteins that can only perform *overall* passive transport, meaning that the total energy employed in the transport is equal to or less than the energy available in the electrochemical gradients (see "Secondary Active Transport" section below). Carriers and channels do not use a metabolic energy supply for solute translocation. Some channels are activated by ATP binding and hydrolysis, but once they become permeable, ion translocation is passive and does not use metabolic energy. Some carriers are able to transport more than one solute in the same cycle. In this case, the energy stored in the electrochemical gradient for one of these solutes (accessory) can be employed for uphill transport of another (principal) solute, a process known as secondary active transport. Nevertheless, the total energy change is dissipative, that is, the energy stored in the accessory solute's electrochemical gradient is always greater than that used to actively transport the principal solute.

Kinetics of Mediated Passive Transport

The dependence of the transport rates on solute concentration are different in solubility diffusion and carrier-mediated transport. As shown in Figure 2.4, in diffusion the flux increases linearly with the concentration, whereas in carrier-mediated transport it saturates. This is explained because transport occurs via a finite number of carrier molecules that can also operate at a finite rate. The simplest case of carrier-mediated transport can be described by the Michaelis–Menten equation; the two kinetic parameters are the maximum flux (J_{max}) and K_m, the concentration at which the flux is half-maximal (see Figure 2.4):

$$J_s = -\frac{C_s J_{\max}}{C_s + K_m} \tag{2.13}$$

where J_s is the solute flux, and C_s is its concentration. For a detailed description of this, and more complex kinetic processes, see Segel.[92]

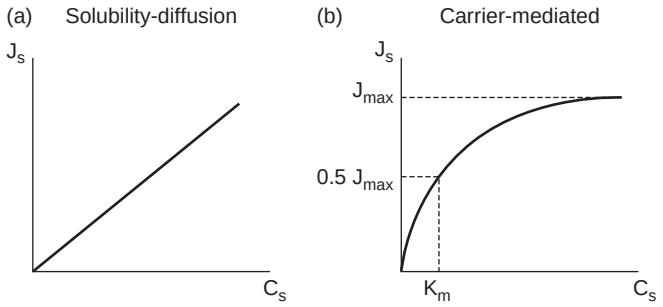

FIGURE 2.4 **Kinetics of diffusion and carrier-mediated transport.** Both graphs depict solute flux (J_s) as a function of solute concentration (C_s). In (a), the mechanism of translocation across the membrane is diffusion, which does not involve chemical reactions between solute and membrane. In (b), the mechanism of translocation is mediated (i.e., it involves a transport protein in the membrane). In (a), the flux is linear with the concentration, whereas in (b) it saturates, because of occupation of a finite number of sites by a solute that moves at a finite velocity. In the simplest case, the relationship in (b) is described by the Michaelis–Menten equation (Eq. (2.13)).

Modes of Coupled Transport

Coupled transport denotes the linked translocation of two or more species (ions and/or molecules) through a barrier. One can distinguish two coupling modes. *Molecular* coupling denotes carrier- or pump-mediated transport of more than one species by the same molecule. Examples shown in Figure 2.5a are the Na^+ and glucose fluxes via the Na^+-glucose co-transporter, and the Na^+ and K^+ fluxes via the Na^+K^+-ATPase. In addition, there is *thermodynamic* coupling. In this case, the fluxes of two or more species occur through different molecules, but are related to each other by electrochemical driving forces. For example, transepithelial Na^+ transport via cell membranes (apical membrane Na^+ channel in series with basolateral membrane Na^+ pump) can produce a transepithelial electrical potential difference responsible for a passive Cl^- flux via the intercellular (junctional) pathway. In this instance, the

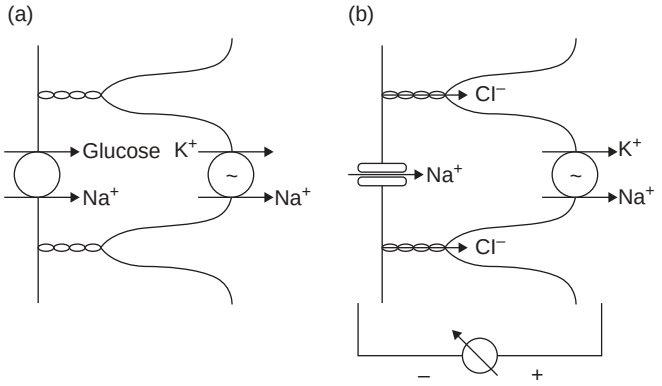

FIGURE 2.5 **Modes of coupled transport.** (a) Molecular coupling: glucose-absorbing epithelial cell (e.g., renal proximal tubule). Two cases of molecular coupling are depicted: the Na^+-glucose symporter (SGLT) at the apical membrane, and the Na^+,K^+-ATPase at the basolateral membrane. In both instances, the transport of two substrates occurs obligatorily in the same transport molecule. (b) Thermodynamic coupling: the epithelial cell depicted absorbs Na^+ by an electrogenic process that generates a lumen-negative transepithelial voltage. This voltage drives a paracellular, electrodiffusive Cl^- flux. The Na^+ and Cl^- fluxes occur via different pathways, and are linked by the driving force, not by binding to the same molecule.

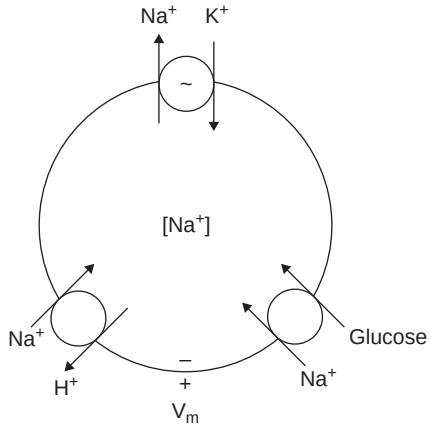

FIGURE 2.6 **Active transport.** The diagram represents a cell expressing three membrane transporters. Top: Primary-active transport of Na^+ and K^+ via the Na^+,K^+-ATPase. The energy for active transport is provided by the hydrolysis of ATP. The flux coupling is $3Na^+$:$2\,K^+$ per ATP molecule hydrolyzed. Bottom: Two mechanisms of secondary active transport. In both cases, the Na^+ electrochemical gradient (oriented inwards) is the driving force for the uphill movement of the other solute (glucose or H^+). On the right, Na^+-glucose co-transport via SGLT, the stoichiometry (Na^+:glucose) is 1:1 (SGLT2) or 2:1 (SGLT1). On the left, Na^+–H^+ exchange via NHE; the stoichiometry is 1:1. Note that the Na^+ driving forces operative in the two cases are different. Since Na^+–H^+ exchange is electroneutral, the driving force depends only on the difference in Na^+ concentrations. Since Na^+-glucose co-transport is electrogenic the driving force involves both the Na^+ chemical gradient and the membrane voltage. For a quantitative analysis, see text.

coupling is not obligatory (if the potential difference is abolished, Cl^- transport ceases while Na^+ transport continues), and does not involve the Na^+ transport molecules. Instead, it corresponds to the parallel operation of two transporters linked by a driving force (Figure 2.5b). This apparently simple point has been a source of confusion in the transport literature (in particular of epithelial cells), where on occasion it has been incorrectly implied that all coupling is molecular.

Pathways and Mechanisms of Active Transport

Primary Active Transport

Primary active transport occurs in the absence of or against the existing electrochemical gradient, and is powered by metabolic energy, such as that originated by the exergonic hydrolysis of ATP (Figure 2.6). Ion pumps are the only molecules capable of performing primary active transport. Most ion pumps of interest to us are transport ATPases, bifunctional molecules that hydrolyze ATP and perform the translocation of the substrate against the prevailing electrochemical gradient. The Na^+,K^+-ATPase[85], Na^+-K^+ pump or Na^+ pump, was the first enzyme demonstrated to be an active ion transporter (reviewed in[97,98]). It is likely that the energy-consuming steps are the conformational changes of the pump protein required for the substrate translocation, that is, for making the substrate first inaccessible to the *cis* side, and then accessible to the *trans* side of the membrane.

Secondary Active Transport

Secondary active transport is characterized by the indirect use of metabolic energy. The electrochemical gradient drives a downhill substrate flux, and part of this energy is utilized for the uphill flux of another substrate (Figure 2.6). The coupling between the two fluxes occurs in the same transport protein, and therefore there is molecular coupling.

In animal cells, secondary active transport is most frequently linked to Na^+ transport. The Na^+,K^+-ATPase establishes an electrochemical potential gradient for Na^+ across the plasma membrane, which includes a chemical (higher extracellular [Na^+]) and an electrical component (cell electrically negative to the extracellular compartment), both contributing to a net driving force (electrochemical gradient) favoring Na^+ entry into the cell. This energy is utilized to transport other substrates by coupling translocation to that of Na^+ at the molecular level.

Depending on the directions of the fluxes, there are two kinds of secondary active transport: *co-transport* (or *symport*), in which the substrates move in the same direction, such as downhill for Na^+ and uphill for the co-transported substrate (e.g., glucose); and *counter-transport* (also *antiport* or *exchange*) in which the fluxes are in opposite directions. Secondary active transport

may involve two substrates (Na^+ and another substrate) or more (e.g., the Na^+-K^+-$2Cl^-$ co-transporter). Sodium-glucose co-transport was the first secondary active transport mechanism studied experimentally, giving rise to the *Na^+ gradient hypothesis*.[16]

Transport by Na^+-glucose co-transporters and Na^+-Ca^{2+} exchangers is electrogenic, that is, there is net translocation of charge across the membrane in each cycle. The concentration ratios (intracellular/extracellular) for glucose and Ca^{2+}, respectively, depend on both the Na^+ concentration ratio and the membrane voltage (V_m). The equation describing the maximum substrate concentration ratio that can be obtained by co-transport is:

$$\frac{S_i}{S_o} = \left[\frac{A_o}{A_i}\right]^n \exp\left(\frac{-nzFV_m}{RT}\right) \tag{2.14}$$

where S is the main substrate (glucose), A is the accessory substrate (Na^+), the subscripts i and o denote intra- and extracellular concentrations, respectively, n is the transport stoichiometry (number of A molecules/number of S molecules), z is the valence of the translocated species per cycle ($z = zA + zS$), V_m is the membrane voltage, and R, T, and F have their usual meanings. Changing to decimal power notation and inserting appropriate values for the constants, the exponent becomes $\sim nzV_m/60$. Hence, in the case of glucose transport via SGLT1 ($n = 2$), for $V_m = -60$ mV and Na^+ concentration ratio is 10, the maximum glucose concentration ratio (cell/lumen) is 10^4.

A similar equation describes the minimum concentration ratio of main substrate that can be achieved by an antiport:

$$\frac{S_i}{S_o} = \left[\frac{A_o}{A_i}\right]^n \exp\left(\frac{-nzFV_m}{RT}\right) \tag{2.15}$$

where the symbols are the same as for Eq. (2.14). The difference is that the concentration ratios for A are inverted in these equations, denoting that in one case S and A are transported in the same direction, and in the other case they are transported in opposite directions. For the example of Na^+–Ca^{2+} exchange with $V_m = -60$ mV and Na^+ concentration ratio is 10, the minimum Ca^{2+} concentration ratio (cell/extracellular) is 10^{-6} for $n = 4$, the most likely stoichiometry.

ION TRANSPORT PROTEINS

Ion transport proteins are best classified in four groups: pores; channels; carriers (also called *transporters*); and pumps. Ion pores and channels are integral membrane proteins that when "open" communicate the aqueous solutions adjacent to the membrane, and permit ion flux in a direction determined by the electrochemical gradient. The permeant ion interacts little with the pore or channel, and thus the number of ions translocated per unit time (turnover number) is very high, typically 10^6–10^8 s^{-1}. Whereas pores are always open (ion conductive), ion channels undergo "gating," transitions between open (conductive) and closed (nonconductive) states. The part of the protein thought to move or change conformation during the gating is called the *gate*. Gating can be elicited by physical factors (changes in membrane voltage or mechanical stretch) or chemical factors (such as neurotransmitters or second messengers).

Carriers are also integral membrane proteins. In contrast with channels, the function of carrier proteins involves a chemical interaction with the transported ion, namely ion binding, which elicits conformational changes in the carrier, eventually resulting in the translocation of the ion across the membrane. Because of these interactions between the carrier and the transported ion, the transport rate is much slower than that of channels, typically 10^2–10^4 s^{-1}. The net ion flux through carriers is also determined by the electrochemical gradient, as in channels, but in a more complex fashion, because certain carriers can transport several ions in the same cycle.

Pumps are similar to carriers in that there are ion binding and conformational changes that cause ion translocation, but differ in that their function is coupled to a metabolic energy source, such as ATP hydrolysis. Pumps have low turnover numbers, similar to those of carriers.

Many ion transport proteins associate with so-called adapter proteins that appear to have two roles: to determine the subcellular location of the transport protein; and to facilitate its interaction with signal transduction components, including receptors, second messenger producing enzymes, and protein kinases. These adapter proteins often contain a specific protein–protein interaction domain called the *PDZ domain*.[82] Adapter proteins therefore contribute to the formation of macromolecular complexes of which ion transport proteins are important components.

During the last decade, atomic-resolution structures have been obtained by X-ray crystallography for a number of prototypical transport proteins, including bacterial pores,[21,89] prokaryotic ion channels,[26,28] the lac-permease of *Escherichia coli* carrier,[1,2] the mammalian sarcoplasmic-reticulum Ca^{2+} pump,[107,108] and several ATP-binding cassette (ABC) proteins.[4,19,53,113] These studies have provided detailed insight into the mechanism of the function of these specific transport proteins, as well as a framework in which to analyze other proteins. An example is the modeling of the cystic fibrosis transmembrane conductance regulator (CFTR) channel, based on the structure of other ABC proteins.[78]

As summarized in an excellent recent review,[74] the first atomic-resolution structure of an integral membrane protein, the reaction center from photosynthetic bacteria, was reported in 1985.[20] At that time there were 268 entries in the Protein Data Bank (PDB). In 2010, the PDB contained almost 60,000 entries, with about 700 of these being membrane proteins, and 80% of these belonging to the all-alpha type (i.e., the transmembrane regions are α helices, instead of the β sheets found in prokaryotic membrane proteins). Only *ca.* 250 of these structures are considered unique.[114]

An essential property of membrane proteins involved in ion transport is their selectivity, i.e., their capacity to "distinguish" between similar ions. This requires the ion pathway to have specific binding sites. In ion selective channels, the ion is at least partially dehydrated, with the binding sites providing favorable interactions, i.e., "replacing" the water molecules surrounding the ion in free solution. Selectivity results from a more favorable interaction of the site with one type of ion than another.[42] Ion-binding sites in transport proteins are formed by amino acid residues that provide charges of the opposite sign, with a size that specifically accommodates the ion. These sites have been identified in several crystal structures of transport proteins.[42] Small molecules selective for monovalent cations have been synthesized by changing the size of the cavity.[23,42]

Pores

Pores are wide conduits across biological membranes that are permanently open; they do not gate (Figure 2.7a). The best studied examples are those formed by bacterial porins, but they are also present in mitochondria (porins) and lymphocytes (perforin, a secretory product). It is also possible that most aquaporins are pores (see Chapters 4 and 41).

Bacterial pores formed by the transmembrane proteins called *porins* are radically different from animal membrane proteins, in that the transmembrane domains, instead of being α helices, are β sheets. For discussions of porin structures, see Delcour[21] and Schulz.[89]

Channels

Like pores, channels have the property of being accessible to both sides of the membrane at the same time, but this occurs only part of the time. Channels open and close stochastically. Gating may be determined by physical or chemical processes (see below), both requiring a sensing mechanism. In the open channel there is ion permeation with a characteristic selectivity for one or more ion species. Channels also have typical conductance (related to ion permeability),

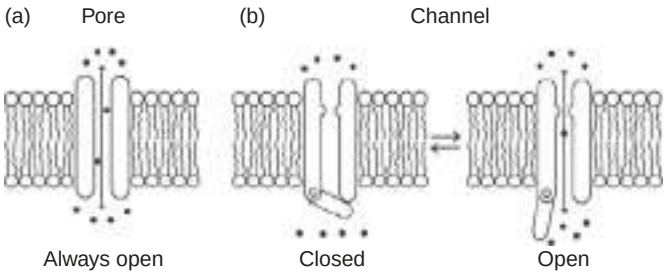

FIGURE 2.7 **Pores and channels.** (a) A pore is a transmembrane protein that forms an aqueous conduit across the membrane that is always accessible from both sides and never closed. Pores are generally of large diameter, and thus permit passive transport of small ions as well as larger hydrophilic solutes, driven by the electrochemical gradient across the membrane. (b) A channel is also a transmembrane protein that forms an aqueous conduit across the membrane. However, in contrast with a pore, it can have at least two conformations, closed and open. The change in conformation is depicted in the figure by a swiveling portion of the molecule, the gate. Gating is the process by which the channels open and close. When the channel is open, it is permeable (conductive), and its interior is accessible to both sides. When the channel is closed, it is impermeable. Channels are generally of smaller radius than pores, and exhibit varying degrees of ion selectivity. As in the case of pores, ion fluxes through channels are driven by the electrochemical gradient across the membrane.

physiological regulation, and inhibitor pattern. Hence, the functional "fingerprint" of a channel includes gating, sensing mechanism, conductance, selectivity, regulation, and pharmacological inhibition.

In channels, the main transport-related conformational change is the gating between open and closed states (Figure 2.7b). The gate is the portion of the channel protein that "moves" to cause channel opening and closure. When the channel is closed, it is impermeable, that is, nonconductive. When it is open, it is permeable or conductive, and allows ion fluxes, with a net flux that can also be expressed as the current carried by the ions. The flux, and hence the current, are determined by the permeability of the channel and the driving force, that is, the electrochemical gradient for the permeant ion. The channel persists in the open state for a given time and allows ion permeation without additional conformational changes during the opening. Hence, one conformational change (gating) allows for transport of a large number of ions, with no additional chemical modification of the protein. The open channel constitutes a water-filled conduit that spans the lipid bilayer communicating the two solutions separated by the membrane. The interior of the open channel is accessible from both solutions at the same time. The large number of ions that cross a channel per unit of time causes a measurable electrical current, allowing investigators to measure single channel events, net ion movements across individual molecules, either *in situ*, using the patch-clamp technique[88] or reconstituting purified channels and incorporating them

in artificial planar bilayers.[75] The two channel conformations, open and closed, underlie the discrete levels observed in current records.

The total current (which denotes ion flux) via a population of channels of one kind in a membrane is given by:

$$I = N \cdot P_o \cdot g \cdot (V_m - E_i) \tag{2.16}$$

where I is the current, N is the number of functional channels in the membrane, P_o is the channel open probability (time open/total time), g is the single channel conductance (the reciprocal of resistance), V_m is the membrane voltage, and E_i is the permeant ion's equilibrium potential. Note that the term $g\ (V_m - E_i)$ denotes i, the single channel current. Equation (2.16) encompasses all mechanisms of channel function regulation: number of copies in the membrane; open probability (gating); conductance; and electrochemical driving force. The ion flux and the ion current through are related by the Faraday constant and the ion valence.

Whereas carriers can be uniporters, symporters or antiporters, channels can only be uniporters. There can be ion–ion interactions in channels, such as single file diffusion,[36,50] but molecular flux coupling, such as observed in carriers, does not occur. As is the case of carriers, channels exhibit substrate selectivity, typical pharmacological inhibition, and transport saturation, although the latter is more evident in carriers.

Plasma membrane ion channels are classified based on their selectivity. The most studied can be selective for K^+, Na^+, Ca^{2+}, H^+, Cl^-, cation or anions, or may be nonselective. Certain channels are highly selective for specific ions, whereas others discriminate less among different ions. The bases of selectivity are ion size and charge. It has been well-established that the Na^+, K^+, and Ca^{2+} channels of excitable membranes, as well as the epithelial Na^+ channel, K^+ channels, and Cl^- channels, are highly selective, where permeability ratios between two ions of the same charge and similar size can be 100 or more. As explained in more detail below, the structural basis of high selectivity channels is a very narrow region in the pore, called the *selectivity filter*, in which the dehydrated permeant ion is coordinated by dipoles in the protein.[69] Other ion channels are less selective. For example, gap junction channels, which communicate between adjacent cells, have cation–anion permeability ratios ranging from about 1 to 10, values similar to those of tight junctions of leaky (high permeability) epithelia. These channels are wider, the ions permeate in the hydrated state, and the cation–anion selectivity is probably governed by fixed charges facing the pore.

K^+-Selective Channels

All known K^+ channels belong to a single protein family, characterized by the highly conserved K^+ channel signature sequence,[48] which forms the selectivity filter. K^+ channels display high selectivity and high conduction rates. X-ray crystallographic studies performed in recent years have revealed the atomic structures of several K^+ channels. Roderick MacKinnon was awarded the 2003 Nobel Prize for Chemistry for this work. In this section, we summarize the current understanding of K^+ channel selectivity and conduction derived from structural studies. For a discussion of the gating process, see MacKinnon.[69]

The K^+ channel is formed by four subunits arranged around a central pore.[24,120] Each subunit consists of two transmembrane α helices (inner and outer, relative to the pore), and the pore helix, which is tilted and penetrates only half of the membrane thickness. Near the center of the membrane the pore forms a water-filled cavity that contains a hydrated K^+.[120] As shown in Figure 2.8, the selectivity filter, formed by the signature-sequence amino acids, is located between the central cavity and the extracellular solution. The filter consists of four layers of carbonyl oxygen atoms and a layer of threonine hydroxyl oxygen atoms, creating four K^+-binding sites (numbered one to four starting from the extracellular side). Thus, each dehydrated K^+ is surrounded by eight oxygen atoms, four "above" and four "below." The selectivity filter thus mimics the arrangement of the K^+ hydration shell, in which a single K^+ is surrounded on average by eight water molecules. The K^+ ions are "transferred" by diffusion from water to the selectivity filter, the hydration energy being compensated for by the binding energy in the filter. Sodium ions do not enter the selectivity filter,[119,120] because the selectivity filter binding energy cannot compensate for the Na^+ higher hydration energy. The small distances between the four K^+-binding sites cause electrostatic repulsion, so only two sites (one and three or two and four) are thought to be occupied at a time.[77] The electrostatic repulsion tends to balance the binding forces, thus ensuring a high turnover number.[69]

K^+ channels are present in the plasma membranes of virtually all cells. Their principal functions are generation of the resting membrane potential of the cell (inside negative), and performance of transepithelial K^+ transport, principally in renal and intestine epithelia. In addition, K^+ channels are involved in cell volume regulation, in the regulation of insulin secretion by pancreatic β-cells, and probably in cell growth and differentiation, although the latter functions remain controversial.

Na^+-Selective Channels

There are two broad classes of Na^+ channels: depolarization-activated Na^+ channels expressed in neurons and other excitable cells and the ENaC/degenerin ion family, which includes the epithelial Na^+ channel

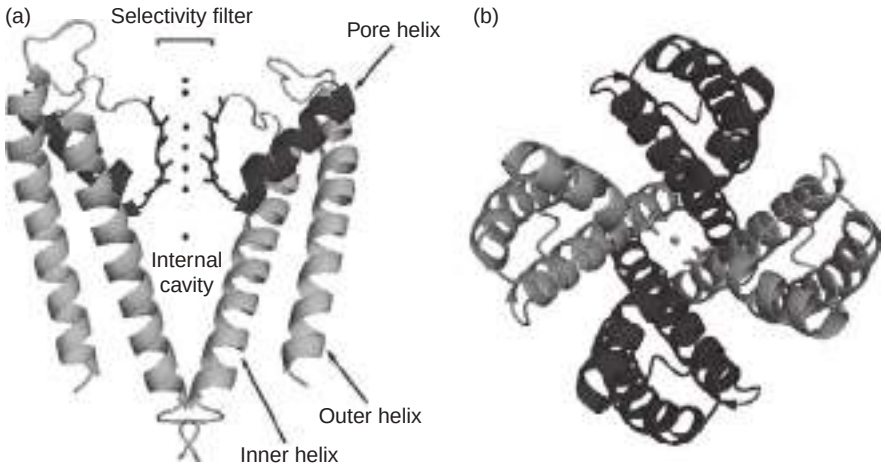

FIGURE 2.8 **Structure of a potassium channel.** (a) Side view of the KcsA channel showing only two subunits for simplicity. Two TM2 helices (pore helices) are shown in darker gray. The oxygens from backbone carbonyl groups at the selectivity filter coordinate K^+ (black circles) at four sites. There are two additional binding sites on the extracellular side (ions in transition), and one ion trapped in the internal cavity, presumably stabilized by the electrical dipole of the pore helices. (b) Tetrameric structure of the channel viewed from the extracellular side. The inner helices form the pore, with the narrowest part corresponding to the activation gate. Each subunit is shown in a tone different from that of the neighboring subunits (built with PyMol).

(ENaC). Other family members are proteins involved in mechanoreception and neuronal degeneration. ENaC is expressed in the apical (luminal) membrane of principal cells of the collecting duct, and in epithelial cells of colon and airway epithelium. ENaC has slow kinetics, low conductance, and a high open probability. Its function is to absorb Na^+ across the apical membrane of the epithelial cells; the Na^+ is then pumped out of the cell by the Na^+,K^+-ATPase expressed in the basolateral membrane. Mammalian ENaC is a heterotrimer (α-, β-, and γ-subunits with high structural homology[12]). All three subunits are thought to contribute to the formation of the pore, but no crystal structure is available.[100]

Cl^- Selective Channels

The largest family of Cl^- channels is the ClC family, with nine members in mammals. ClC channels participate in cell excitability, maintenance of the resting potential, Cl^- transport in certain epithelial cells, Cl^- and H^+ transport in intracellular vesicles, and cell volume regulation. ClC genes, expressed in both prokaryotes and eukaryotes, encode both Cl^- channels and Cl^-/H^+ antiporters.[27,60] In mammals, the channels (ClC-1, ClC-2, ClC-Ka, and ClC-Kb) are expressed in the plasma membrane, whereas the antiporters (ClC-3, 4, -5, -6, and -7) are expressed in endosomal/lysosomal membranes. This is an interesting case in which members of a family of ion transport proteins include channels and carriers.[60,76]

The structure of a bacterial ClC protein[28,29] shows a double-barrel channel: homodimer with each monomer containing a pore. Each subunit has 17 transmembrane helices and Cl^- in the channel is coordinated by residues from several helices, including a highly-conserved Lys. In the membrane, ClC proteins form two hourglass-like funnels that meet in a narrow constriction near the middle of the bilayer, the anion selectivity filter.[29] Some mammalian isoforms of ClC proteins require α- and β-subunits for function.[60] The cystic fibrosis transmembrane conductance regulator (CFTR) is a Cl^- channel expressed in Cl^--secreting epithelial cells; it does not belong to the ClC family, but is a member of the ABC superfamily. ABC proteins can be either channels or pumps. CFTR is expressed in the apical membranes of airway, small intestine, pancreatic duct, biliary tree, and vas deferens epithelia. It consists of two homologous halves, each formed by six transmembrane helices followed by a nucleotide-binding domain (NBD). The two halves are joined by the regulatory or R domain, a large hydrophilic sequence located in the cytoplasm. The function of CFTR is Cl^- secretion across the apical membrane, which is the primary event for salt and water secretion by the epithelia listed above. CFTR gating is a complex process involving phosphorylation of the R domain by protein kinase A, ATP binding to the NBDs, their dimerization, and ATP hydrolysis.[15] CFTR also appears to regulate other Cl^- channels, as well as Na^+ and K^+ channels, by unclear mechanisms. CFTR is expressed in all segments of the renal tubule, but its functional role in the normal kidney is not clear; also, cystic fibrosis patients have no discernible renal phenotype.[22] In polycystic kidney disease, CFTR is abundantly expressed in the apical membranes of the cysts cells, and plays an essential role in Cl^- secretion, which drives fluid secretion and cyst growth[11] (Chapter 81).

A third group of Cl^- channels are Ca^{2+}-activated (Ca^{2+}-activated Cl^- channels or CaCCs). They are involved in epithelial absorption and secretion, muscle contraction, neuronal excitability, sensory transduction, cell volume regulation, and other cell functions. Several protein types have been proposed to account for CaCC currents, but very recent studies by three groups have provided solid evidence that TMEM16A (also named anoctamin-1 or ANO1) has functional characteristics consistent with CaCCs. Site-specific mutations alter channel properties, suggesting that TMEM16A is at least part of the channel. Expression of TMEM16B also results in CaCC functions, but with different biophysical properties than those associated with TMEM16A. The function(s) of other TMEM16 proteins remain unknown. TMEM16A and the nine other members of the family have a similar topology and secondary structure, with eight transmembrane helices and intracellular N- and C-termini. This protein family has been long-studied by developmental and cancer biologists. Some family members are upregulated in tumors and loss-of-function of others is conducive to defects in development (see [39] and [45] for reviews).

For a detailed discussion of ion channels, see Chapter 8. In addition, excellent treatments of ion channels in general can be found in the book by Hille,[50] and the review articles by Catterall[13] and Dawson.[18] There are also several excellent recent reviews on ion channel structure–function relationships,[24,25,42,68,69] and on ion channels in renal epithelial cells.[14,46,52,56,60] Chapters 8, 30, 31, 47, and 63 cover renal ion channels.

Carriers

Carriers are transporters that perform transmembrane translocation of solute (and perhaps water; see Chapter 4) by a sequential process thought to involve three basic steps. First, binding of the transported substrate to the carrier facing one side of the membrane; second, change in conformation of the carrier, with translocation of the substrate (and the binding site) to the opposite side of the membrane; and third, release of the substrate. It is thought that access to the binding site from either bathing solution is by diffusion (or electrodiffusion) in pore-like regions of the carrier molecule.[61] Hence, two such steps could be added to the simplified scheme above.

In carriers, there is a state in which the binding site and the substrate are inaccessible from either side of the membrane.[62] The existence of this state, called *occlusion*, is one of many arguments supporting the idea of conformational change in carrier function. Carriers behave like enzymes, in that the substrate binds to the protein; however, instead of chemical transformation of the substrate, the carrier performs its translocation. Carriers contain substrate-binding domains accessible from one side of the membrane at a time. In contrast with channels, they never form a conduit that communicates the two bathing solutions, i.e., the binding site is never accessible from both sides of the membrane. Instead, carriers undergo conformational changes that alter the "sidedness" of the substrate-binding site; the substrate binds on one side, the conformation of the carrier protein changes, the substrate is occluded, the binding site is translocated (with substrate) to the other side of the membrane, and the substrate is then released. In comparison with a channel, which has one gate, a carrier may be considered to have two gates, as illustrated in Figure 2.9.

The notion of a carrier protein as a "ferryboat" binding the substrate at a membrane–solution interface and carrying it to the other side, where the solute is released to the other solution, is inconsistent with current knowledge of the biochemistry and molecular biology of carriers. Nevertheless, kinetic schemes based on the ferryboat model remain very useful to explain carrier function at a phenomenological level.

Substrate transport by carriers is inherently slow, because each substrate molecule (or group of molecules in cases of coupled transport; see below) must undergo an independent binding reaction, followed by the conformational change of the carrier molecule. This explains the low turnover number of carriers, similar to typical rates of enzyme catalysis of 10^2–10^3 per second.[99]

Most carriers have exquisite substrate selectivity (e.g., the glucose carrier GLUT1 transports D-glucose, but not L-glucose) and can also exhibit quite specific pharmacological inhibition. At low substrate concentration, the substrate flux increases linearly with the concentration, and can be confused with simple diffusion, but at high substrate concentration it saturates, as expected from occupancy of a limited number of slowly turning binding sites. The low turnover number, high substrate selectivity and saturation of carriers, and to some extent the mechanisms of pharmacological inhibition, also support the notions of substrate binding and conformational change during the transport cycle.

Carrier-mediated transport can be classified in three types depending on the number of substrates and the transport directions (Figure 2.10). When the carrier transports only one substrate, the process is called *facilitated diffusion* or *uniport*; the carrier is a uniporter. Other carriers transport two or more substrates. When all substrates are transported in the same direction, the process is called *co-transport* or *symport*; the carrier is a *co-transporter* or *symporter*. When there is substrate transport in opposite directions, the process is called

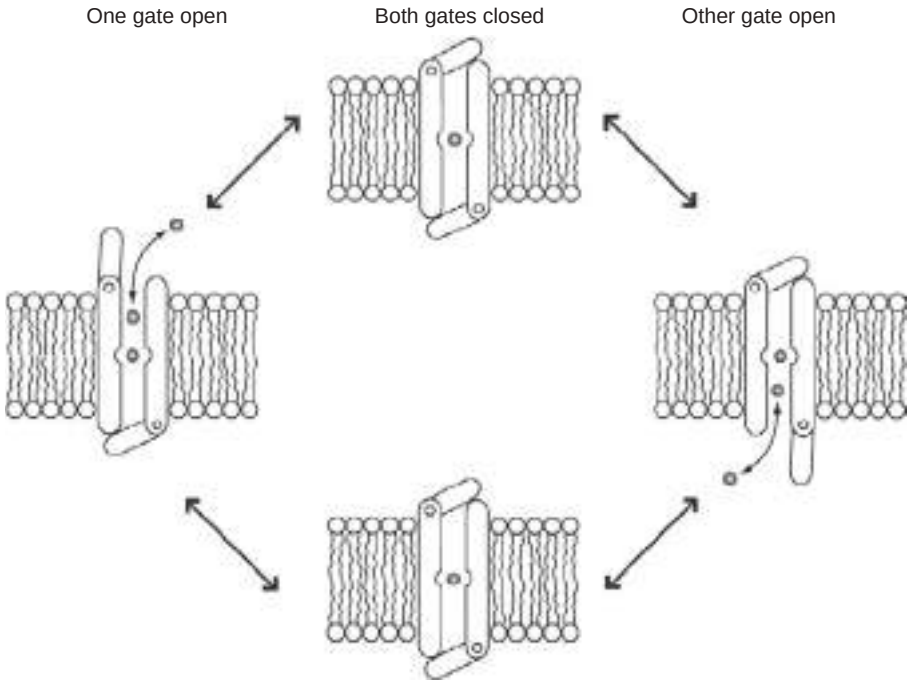

FIGURE 2.9 **Carriers.** A carrier can be understood as a membrane transport protein with two gates and one or more binding sites for the substrate. The figure depicts the transport stages for a uniporter, the simplest kind of carrier molecule. From left to right: the substrate binds to the carrier at a site available to only one side of the membrane (first gate open, second gate closed); this closes the second gate and the substrate is occluded (both gates closed); the second gate opens and the binding site and the substrate become accessible to the other side of the membrane, and the substrate is then released. The transport process is passive. The unidirectional and net fluxes are determined by the chemical or electrochemical potential difference, for uncharged and charged substrates, respectively (*modified with permission from ref. [37]).*

exchange or *antiport*; the carrier is an *exchanger* or *antiporter*. Uniporters, like channels, can only perform passive transport. The overall transport via a symporter or an antiporter is downhill. There is always passive translocation of at least one substrate, and there can be secondary active translocation of one or more additional substrates, using the energy stored in another substrate's chemical or electrochemical gradient. For example, in the case of two substrates, all the energy employed in uphill translocation of one species derives from the passive transport of the other one, so that no metabolic energy is directly used.

The largest family of secondary active transporters is the major facilitator superfamily (MFS).[87] MFS proteins are expressed from bacteria to vertebrates. They range from 400 to 600 amino acids in size, have 12 transmembrane helices, and N- and C-termini are located on the cytoplasmic side. These proteins transport numerous substrates, and may be uniporters, symporters or antiporters. The atomic structures of four bacterial members of the MFS have been solved: the H^+-lactose co-transporter (LacY) or lac-permease,[2] the P_I/glycerol-3-phosphate antiporter (GlpT),[58] the multidrug-resistance antiporter EmrD,[117] and the fucose permease FucP.[17] In all structures the transmembrane helices form two domains, N- and C-termini (each consisting of a six-helix bundle) with a pseudo two-fold symmetry. A large cavity open to the cytoplasm and closed to the periplasm is present in the LacY and GlpT structures, suggesting that the crystals correspond to the inward facing conformation.[2,58] The structure of the FucP shows an outward open amphipathic cavity.[17]

Of great importance for mammalian physiology in general and renal physiology in particular are the solute sodium symporters (SSS), a subset of the MFS. These constitute a large family of proteins that co-transport Na^+ with a variety of solutes, including sugars, amino acids, inorganic acids, and vitamins.[115] They are expressed in the kidney and other transport organs. The crystal structure of a bacterial Na^+-galactose symporter was solved in 2008.[32] As predicted from earlier studies, it has 14 transmembrane helices, extracellular N- and C-termini, and a structural core formed by two clusters of five helices each, with opposite orientations. This structure is similar to that of lac-permease,[2] suggesting a common structure for sugar co-transporters. The galactose-binding site is central, and is separated from the adjacent solutions by hydrophobic amino acid residues; the Na^+-binding site could not be identified in the crystal structure.[32] Another

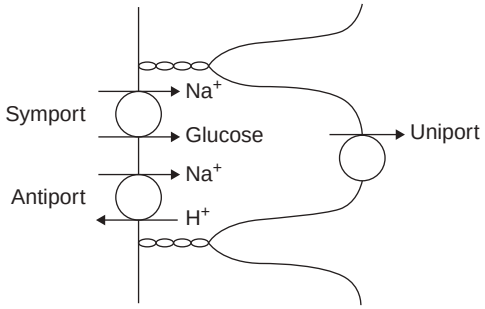

FIGURE 2.10 **Types of carrier-mediated transport.** The figure depicts an epithelial cell (e.g., renal proximal tubule) expressing different kinds of carriers, classified according to the number of substrates and the directions of the net fluxes. *Uniporter* is a carrier that transports only one substrate in a complete cycle; the process is known as facilitated diffusion or uniport, and is always passive. Shown in the figure is a glucose uniporter at the basolateral membrane. *Symporter* is a carrier that transports at least two substrates in the same direction in each cycle. The process is known as co-transport or symport; the overall transport process is downhill, but the electrochemical gradient of one substrate can be used to transport the other one actively (a form of secondary active transport). Shown in the figure is a Na^+-glucose symporter at the apical membrane. *Antiporter* is a carrier that transports at least two substrates in opposite directions in each cycle. The process is known as countertransport, exchange or antiport; the overall transport process is downhill, but again the electrochemical gradient of one substrate can be used to translocate the other one actively (secondary active transport). Shown in the figure is a Na^{++}/H^+ antiporter at the apical membrane. See also Figure 2.6.

symporter, LeuT (leucine and Na^+)[116] clearly shows leucine and Na^+ bound to a deep region of the protein (Figure 2.11). The Na^+ ions are fully dehydrated and surrounded by six oxygen atoms in one site and by five in the other. These studies represent impressive progress in a few years, but considerably more work will be needed to fully understand the function of these proteins at the atomic level.

Specific aspects of carrier-mediated transport are covered in Chapters 32, 53, 54, 55, and 73. The reader is also referred to LeFevre,[66] Schultz,[90] and Stein[99] for quantitative treatments of carrier-mediated transport. Some specific carriers are well covered in recent reviews by Abramson et al.,[1] Hediger et al.,[47] Tanner,[104] and Zachos et al.[118]

Pumps

Ion pumps are discussed in Chapter 3. Other reviews of ion pumps are Apell,[5] Brini and Carafoli,[10] Facciotti et al.,[31] Fambrough and Inesi,[33] Finbow and Harrison,[35] Horisberger,[54,55] Läuger,[65] Pedersen,[83] Sachs and Munson[85] and Toyoshima.[106]

Ion pumps can be classified according to the source of metabolic energy. Pumps in general can be driven by light, redox potential or ATP hydrolysis. Animal cell plasma membrane ATPases belong to the P type, which is characterized by the formation of a phosphorylated intermediary (Na^+,K^+-, H^+,K^+-, and Ca^{2+}-ATPase) (Figure 2.12) or to the V type (vacuolar H^+-ATPase). In intracellular membranes, there is expression of the vacuolar-type H^+ pump, as well as F-type (or F_{1-} or F_{0-} type) ATPases, the ATP synthase expressed in the inner mitochondrial membrane. ATP synthases are also expressed in purple bacteria and in green plants. Their function can be outlined as follows. Multimeric protein complexes (respiratory chain complex in mitochondria, bacteriorhodopsin in purple bacteria, photosynthetic reaction center in chloroplasts) generate an H^+ electrochemical gradient from the redox potential of NADPH (mitochondria) or light energy (others). The transmembrane H^+ electrochemical gradient is then used by ATP synthases to synthesize ATP from ADP and P_i. Hence, the function of these proteins is to synthesize ATP, dissipating the ion gradient in the process. However, they are reversible, and under appropriate conditions they will hydrolyze ATP and generate an electrochemical ion gradient. Similarly, the Na^+,K^+-ATPase normally hydrolyzes ATP to transport actively Na^+ out of the cell and K^+ into the cell, but under certain experimental conditions it can operate in a reverse mode, that is, downhill ion fluxes (Na^+ into the cell and K^+ out of the cell) coupled to the synthesis of ATP.

The ion pumps present in plasma membranes of epithelial cells are the Na^+,K^+-ATPase, Ca^{2+}-ATPase, H^+-ATPase, and H^+,K^+-ATPase. Other pumps have been suggested to exist in these tissues, but they are either unique to certain epithelia or controversial. The molecular structures of these pumps have been identified, and significant progress has been made in understanding their function, but much work remains to be done in this area. Ion occlusion is a well-known stage during the pump cycle.[40] As is the case with carrier function, occlusion denotes that the conformational change necessary for transport does change the accessibility of the substrate-binding sites to the solutions bathing the membrane.

The Na^+,K^+-, H^+,K^+-, and Ca^{2+}-ATPase are all of the P type, which is characterized by the phosphorylation of an aspartic acid residue (in the sequence DKTG) during the pump catalytic cycle. The Na^+,K^+-ATPase is a ubiquitous pump in epithelial cells. In each cycle, one ATP molecule is hydrolyzed, three Na^+ are transported from the cytoplasm to the interstitial fluid, and two K^+ are transported in the opposite direction. In each cycle there is thus a net transfer of charge across the membrane (one net positive charge is extruded), and hence the pump is electrogenic, tending to hyperpolarize the cell. Its turnover number is in the range of values for carriers less than $10^2\ s^{-1}$. The catalytic cycle of P-type ATPases is shown in Figure 2.12.

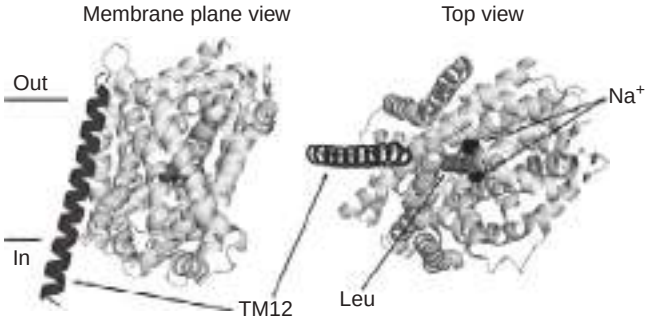

FIGURE 2.11 **Structure of a symporter.** Side (left) and extracellular (right) views of the LeuT, a prokaryotic Leu-Na^+ symporter that belongs to the neurotransmitter sodium symporter family. One protomer of the dimer in the crystal structure is shown. Transmembrane helix 12 is shown in darker gray. Leu and Na^+ bound deep into the structure core are shown in darker gray and black, respectively (built with PyMol from PDB 2A65).

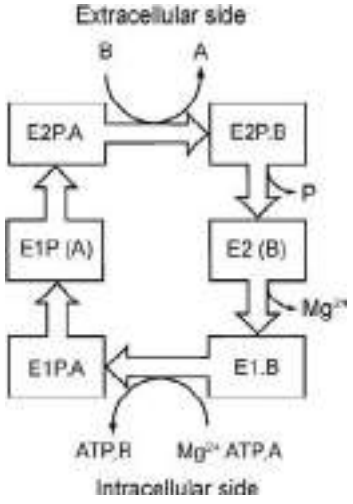

FIGURE 2.12 Catalytic cycle for P-type ATPases modeled as countertransport pumps exchanging Na^+ (*A*) for K^+ (*B*), Ca^{2+} (*A*) for H^+ (*B*) or H^+ (*A*) for K^+ (*B*) (Na^+,K^+-, Ca^{2+}-, and H^+,K^+-ATPase, respectively) (E1: conformation with ion-binding sites accessible from cytoplasm; E2: conformation with ion-binding sites accessible from the extracellular face; E(A) or E(B): ion "occluded" in the protein) (*modified with permission from ref. [85]).*

The Na^+,K^+-ATPase is expressed in virtually all vertebrate epithelial cells, where it is usually targeted to the basolateral membrane. In two cases, the choroid plexus and the retinal pigment epithelium, the pump is targeted to the apical membrane and epithelial cell polarity is inverted *vis-à-vis* other tissues. The pump consists of α- and β-subunits in a 1:1 stoichiometry (likely α2:β2). The α-subunit is responsible for both ion transport and ATPase activity, and contains the binding sites for Na^+, K^+, and ouabain, a specific inhibitor, as well as the phosphorylation site. The β-subunit, previously thought to be just involved in assembly and delivery of the pump, has in addition an important role in K^+ binding.[93] The α-subunit has three isoforms (apparent molecular mass 120 kDa) and the β-subunit has two isoforms, with apparent molecular mass of 50 kDa. Pump isoforms are tissue-specific, change during organ development, and exhibit different pharmacological properties. The Na^+,K^+ pump was first crystallized in 2007,[79] and a higher resolution structure was obtained in 2009.[93] At this time, our understanding of the structure−function relationships is less than that for the sarcoplasmic reticulum Ca^{2+} pump (see below). The regulation of the activity of the Na^+,K^+ pump is complex, and an important regulatory mechanism in the kidney is the increase in Na^+ pump expression in principal cells of the collecting duct under the action of mineralocorticoids. These hormones stimulate of Na^+ entry via ENaC, which results in an increase in intracellular Na^+ concentration that appears to mediate the stimulation of pump expression.

The plasma membrane Ca^{2+} pump (PMCA pump) actively exports Ca^{2+} from the cell, exchanging it for H^+ (the stoichiometry appears to be 1 Ca^{2+} out:2 H^+ in:1 ATP molecule hydrolyzed). The pump is 120−140 kDa, with ten transmembrane helices and three substantial intracellular domains. The crystal structure of the Ca^{2+} pump from sarcoplasmic/endoplasmic reticulum (SERCA pump) was solved a decade ago.[107] It has two Ca^{2+}-binding sites from which the ions are extruded, with a stoichiometry of 2 Ca^{2+} per ATP hydrolyzed, different from that of the PMCA pump. The PMCA pump has high affinity for intracellular Ca^{2+}, in the submicromolar range. The conformational change elicited by ATP hydrolysis is thought to make the Ca^{2+} sites face the extracellular space and the affinity decrease, causing Ca^{2+} release. The function of the PMCA pump is to help maintain a low intracellular Ca^{2+} concentration. It is a high affinity, low capacity system. The PMCA pump is stimulated by calmodulin and 1,25-dihydroxyvitamin D (for a review, see [10]).

The H^+/K^+-ATPase is expressed in gastric epithelial cells (gastric isoform), colonocytes (colonic isoform), and renal collecting ducts (both isoforms). As with the Na^+,K^+-ATPase and the Ca^{2+}-ATPases, the H^+/K^+-ATPase consists of α- and β-subunits. The α-subunits of the two isoforms, are very similar in amino acid sequence to the α-subunit of the Na^+,K^+-ATPase. The function of the renal H^+/K^+-ATPase is acid secretion and K^+ reabsorption

In the last decade, crystal structures have been obtained for the Ca^{2+} pump from sarcoplasmic reticulum,[107,109,110] the plasma membrane Na^+,K^+-ATPase[79,80,93] and the plant plasma membrane H^+-ATPase.[83] Although the Ca^{2+}-ATPase from rabbit

skeletal muscle sarcoplasmic reticulum (SERCA1a) is not a plasma membrane protein, it is currently the better known P-type ion transporting ATPase. The mass of SERCA1a is 110 kDa, it has 10 transmembrane helices (M1−M10), three cytoplasmic domains (A [actuator or anchor]; N [nucleotide-binding]; and P [phosphorylation]), and small SR-lumen loops. SERCA1a transports, against the electrochemical gradient across the SR membrane, two Ca^{2+} per ATP hydrolyzed, reducing [Ca^{2+}] in the cytosol, and accumulating it in the SR lumen. Two or three H^+ are exchanged for the Ca^{2+} in each cycle. As is the case with other P-ATPases, primary active ion transport results from a conformational change of the pump (from E1 to E2). In E1, the Ca^{2+} ions bind with high affinity and face the cytoplasm; in E2, the affinity is low and Ca^{2+} ions face the SR lumen. The Ca^{2+} translocation would take place between E1P and E2P, two states of the phosphorylated pump. Similar states exist in the operation of the Na^+,K^+-ATPase (see Chapter 3).

The first determination of the structure of SERCA1 by X-ray crystallography in 2000[107] was followed by over 20 structures in different states that essentially cover the reaction cycle, making it the best characterized P-type ion-translocating ATPase.[106] The atomic structure, represented in Figure 2.13,[107,108] revealed that transmembrane helices 4, 5, and 6 contain the amino acid residues that bind the two Ca^{2+} ions transported per cycle. These results, combined with molecular dynamics simulations[101] have provided detailed information about the binding sites and the conformational changes underlying ion pumping.[105,106] Differences between several structures revealed that SERCA1 Ca^{2+} binding and dissociation elicit large conformational changes in the transmembrane domains, mechanically linked to similar changes in the cytoplasmic domains. Homology modeling suggests that the cation-binding sites of the Ca^{2+}- and Na^+,K^+-ATPases are virtually the same.[84] A critical movement of transmembrane helix 4 causes the release of a cation (Ca^{2+} or Na^+) and the binding of the other cation (H^+ or K^+) at a displaced position with respect to the membrane, thus preventing competition between the cations.

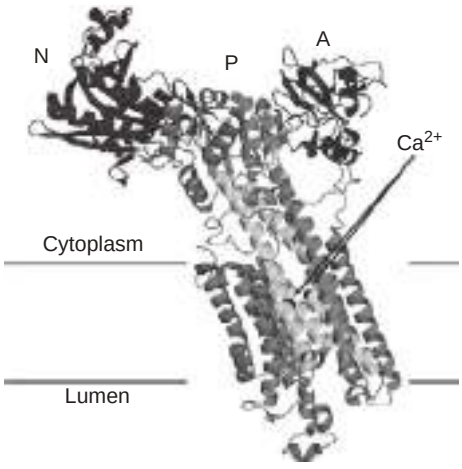

FIGURE 2.13 **Structure of a pump.** Side view of the Ca^{2+}-ATPase in the E1•2Ca^{2+} state. The cytoplasmic nucleotide binding (N) and actuator (A) domains are shown in darker gray. The A domain is part of the mechanism that controls Ca^{2+} binding and release. The cytoplasmic P domain is also labeled. This domain contains the phosphorylation residue Asn^{351} and several P-type ATPase critical residues, including the Mg^{2+} coordination residue Asp^{703}. Transmembrane helices 4−6, which contribute residues to the binding of Ca^{2+}, are shown in lighter gray. The two Ca^{2+} are shown as black balls (built with PyMol from PDB 1SU4).

Similarities and Differences between Ion Transport Proteins

The recent progress in genomics and structural biology of membrane proteins (*ca.* 700 crystal structures, of which 250 are unique[114]), combined with increasing sophistication of biochemical and biophysical studies has began to clarify the essential similarities and differences between these proteins. We wish to make several important points in this closing section. First, there are big differences between ion channels, on the one hand, and carriers and pumps, on the other, and the differences in function are explained by the differences in structure. Second, there are families in which individuals can be either channels or carriers, or either channels or pumps, suggesting something akin to a "common ancestor." Third, there is at least one instance in which pharmacological intervention can transform a pump into a channel. We discuss briefly these three points.

1. *Channels versus carriers and pumps.* The crucial functional difference between channels, on the one hand, and carriers or pumps, on the other, is in the turnover numbers: channels conduct ions rapidly (10^6−10^8 s^{-1}), whereas carriers and pumps are much slower (10^2−10^4 s^{-1}). This difference is related to the relatively slow conformational changes that accompany solute flux in carriers and pumps, while in open channels no conformational changes occur during transport. In addition, there is a difference in access of the transported ion(s) to the critical site. As we saw in the structures of K^+ and Cl^- channels, the narrow region of the permeation pathway (selectivity filter) is short relative to the thickness of the membrane, facilitating rapid conduction. In K^+ channels, in addition, the four binding sites in single file cause repulsion between adjacent ions, also facilitating rapid conduction. In contrast, in carriers (such as LeuT) and pumps (such as the Ca^{2+}-ATPase) the ion-binding sites are located deep inside the protein, with no

unobstructed pathway to the adjacent aqueous solutions. This feature limits the speed of ion transport, but permits occlusion, i.e., the ion pathway is never simultaneously open to both sides of the membrane. These arguments are lucidly presented by Gouaux and MacKinnon.[42]

2. *Functionally different transport proteins present in the same family.* The ClC proteins appear to be an intermediate class of ion transport proteins in between channels and carriers. Their structure is channel-like, with vestibules in series with a short selectivity filter with capacity to contain several ions. Functionally, some ClC proteins are indeed channels, whereas others are antiporters in which the Cl^- flux is coupled to flux of H^+ in the opposite direction.[3,76] A somewhat similar situation holds for the case of ABC proteins, which in most instances are pumps (ATPases), but at least one member (CFTR) is an ion channel. There is no crystal structure of CFTR yet, but from the primary and secondary structures one would not predict that the protein is a channel. It has been recently proposed that both CFTR and ClC-O are Cl^- channels evolved from transporters.[15]
3. *A pump can be transformed into a channel.* The marine toxin palitoxin (PTX) is a ~3000 Da molecule that consists of a chain of over 100 carbons with a complex variety of organic side groups. The mechanism of the toxic effect of PTX is to convert the Na^+,K^+-ATPase from a cation pump into a nonselective cation channel that dissipates the Na^+ and K^+ gradients between the cell and the extracellular fluid. This could be explained if the effect of PTX were to open the two gates necessary for the normal operation of the pump, thus revealing the ion translocation pathway. PTX was shown to interact with the pump in excised membrane patches, this interaction was dependent of the presence of ATP on the inside of the membrane, and was modulated by extracellular K^+, indicating that the PTX-dependent channel function shares properties of the native pump.[7,8] In other studies, the permeation pathway was mapped using the technique known as cysteine-scanning mutagenesis, in which the accessibility of amino acid sites to small hydrophilic thiol reagents is assessed after mutating those sites to Cys. Residues in transmembrane helices 4, 5, and 6 became accessible by exposure to PTX,[43,44,57] consistent with the structural studies described above.

We have presented three arguments that support the notion that ion channels, carriers, and pumps share a basic molecular architecture (see [37] and [38]). In sum, and as illustrated in Figure 2.14, the simplest ion transport protein would be a pore (no gate), followed by a pore with one gate (channel), a pore with two gates (carrier), and finally a pore with two gates coupled to a metabolic-energy source (pump). As more structures of membrane transport proteins become available the "missing links" might be identified.

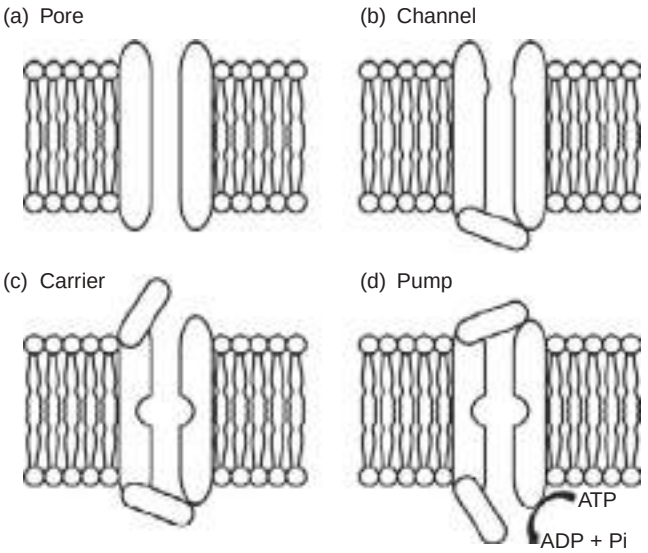

FIGURE 2.14 **A simplified view of structure–function correlations in ion transport proteins.** (a) Pore, the simplest ion transport protein, is a transmembrane aqueous conduit with no gates, accessible to both sides of the membrane at all times (always open). (b) Channel, a pore with a gate whose position determines whether the channel is open or closed. The open channel is accessible to both sides of the membrane. (c) Carrier, a transmembrane protein with two gates that are never open at the same time. Thus, the carrier interior may be accessible to only one side of the membrane; when both gates are closed the substrate is occluded (inaccessible to either side). (d) Pump, a carrier that is directly coupled to a metabolic energy source, e.g., hydrolysis of ATP.

References

[1] Abramson J, Iwata S, Kaback HR. Lactose permease as a paradigm for membrane transport proteins. Mol Membr Biol 2004;21:227–36.
[2] Abramson J, Smirnova I, Kasho V, Verner G, Kaback HR, Iwata S. Structure and mechanism of the lactose permease of *Escherichia coli*. Science 2003;301:610–5.
[3] Accardi A, Miller C. Secondary active transport mediated by a prokaryotic homologue of ClC Cl^- channels. Nature 2004;427:803–7.
[4] Aller P, Garnier N, Genest M. Transmembrane helix packing of ErB/Neu receptor in membrane environment: a molecular dynamics study. J Biomol Struct Dyn 2006;24:209–28.
[5] Apell HJ. How do P-type ATPases transport ions? Bioelectrochemistry 2004;63:149–56.
[6] Arnold WN. Yeast cell envelopes: biochemistry, biophysics, and ultrastructure. Boca Raton, FL: CRC Press; 1981.
[7] Artigas P, Gadsby DC. Na^+/K^+ pump ligands modulate gating of palytoxin-induced ion channels. Proc Natl Acad Sci USA 2003;100:501–5.

[8] Artigas P, Gadsby DC. Large diameter of palytoxin-induced Na^+/K^+ pump channels and modulation of palytoxin interaction by Na^+K^+ pump ligands. J Gen Physiol 2004;123:357–76.
[9] Behnia R, Munro S. Organelle identity and the signposts for membrane traffic. Nature 2005;438:597–604.
[10] Brini M, Carafoli E. Calcium pumps in health and disease. Physiol Rev 2009;89:1341–78.
[11] Calvet JP, Grantham JJ. The genetics and physiology of polycystic kidney disease. Semin Nephrol 2001;21:107–23.
[12] Canessa CM, Horisberger JD, Rossier BC. Epithelial sodium channel related to proteins involved in neurodegeneration. Nature 1993;361:467–70.
[13] Catterall WA. Structure and function of voltage-gated ion channels. In: Schultz SG, Andreoli TE, Brown AM, Fambrough DM, Hoffman JF, Welsh MJ, editors. Molecular biology of membrane transport disorders. New York: Plenum Press; 1996. p. 129–45.
[14] Chen TY. Structure and function of ClC channels. Annu Rev Physiol 2005;67:809–39.
[15] Chen TY, Hwang TC. CLC-0 and CFTR: chloride channels evolved from transporters. Physiol Rev 2008;88:351–87.
[16] Crane RK. Intestinal absorption of sugars. Physiol Rev 1960;40:789–825.
[17] Dang S, Sun L, Huang Y, Lu F, Liu Y, Gong H, et al. Structure of fucose transporter in an outward-open confrontation. Nature 2010;467:734–8.
[18] Dawson DC. Permeability and conductance in ion channels: a primer. In: Schultz SG, Andreoli TE, Brown AM, Fambrough DM, Hoffman JF, Welsh MJ, editors. Molecular biology of membrane transport disorders. New York: Plenum Press; 1996. p. 87–110.
[19] Dawson RJ, Locher KP. Structure of a bacterial multidrug ABC transporter. Nature 2006;443:180–5.
[20] Deisenhofer J, Epp O, Miki K, Huber R, Michel H. Structure of the protein subunits in the photosynthetic reaction centre of Rhodopseudomonas viridis at 3 Å resolution. Nature 1985;318:618–24.
[21] Delcour AH. Solute uptake through general porins. Front Biosci 2003;8:d1055–71.
[22] Devuyst O, Guggino WB. Chloride channels in the kidney: lessons learned from knockout animals. Am J Physiol Renal Physiol 2002;283:F1176–91.
[23] Dietrich B. Coordination chemistry of alkali and alkaline-earth cations with macrocyclic ligands. J Chem Educ 1985;62:954–8.
[24] Doyle DA. Molecular insights into ion channel function. Mol Membr Biol 2004;21:221–5.
[25] Doyle DA. Structural changes during ion channel gating. Trends Neurosci 2004;27:298–302.
[26] Doyle DA, Morais Cabral J, Pfuetzner RA, Kuo A, Gulbis JM, Cohen SL, et al. The structure of the potassium channel: molecular basis of K^+ conduction and selectivity. Science 1998;280:69–77.
[27] Duran C, Thompson CH, Xiao Q, Hartzell HC. Chloride channels: often enigmatic, rarely predictable. Annu Rev Physiol 2010;72:95–121.
[28] Dutzler R, Campbell EB, Cadene M, Chait BT, MacKinnon R. X-ray structure of a ClC chloride channel at 3.0 Å reveals the molecular basis of anion selectivity. Nature 2002;415:287–94.
[29] Dutzler R, Campbell EB, MacKinnon R. Gating the selectivity filter in ClC chloride channels. Science 2003;300:108–12.
[30] Engelman DM. Membranes are more mosaic than fluid. Nature 2005;438:578–80.
[31] Facciotti MT, Rouhani-Manshadi S, Glaeser RM. Energy transduction in transmembrane ion pumps. Trends Biochem Sci 2004;29:445–51.
[32] Faham S, Watanabe A, Besserer GM, Cascio D, Specht A, Hirayama BA, et al. The crystal structure of sodium galactose transporter reveals mechanistic insights into Na^+/sugar symport. Science 2008;321:810–4.
[33] Fambrough DM, Inesi G. Cation transport ATPases. In: Schultz SG, Andreoli TE, Brown AM, Fambrough DM, Hoffman JF, Welsh MJ, editors. Molecular biology of membrane transport diseases. New York: Plenum Press; 1996. p. 223–41.
[34] Fick A. Ueber diffusion. Ann Phys Chem 1855;94:59–86.
[35] Finbow ME, Harrison MA. The vacuolar H^+-ATPase: a universal proton pump of eukaryotes. Biochem J 1997;324:697–712.
[36] Finkelstein A, Rosenberg PA. Single-file transport: implications for ion and water movement through gramidicin a channels. In: Stevens CF, Tsien RW, editors. Membrane transport processes. New York: Raven Press; 1979. p. 73–88.
[37] Gadsby DC. Ion transport: spot the difference. Nature 2004;427:795–7.
[38] Gadsby DC. Ion channels versus ion pumps: the principal difference, in principle. Nat Rev Mol Cell Biol 2009;10:344–52.
[39] Galietta LJ. The TMEM16 protein family: a new class of chloride channels? Biophys J 2009;97:3047–53.
[40] Glynn IM, Hoffman JF. Nucleotide requirements for sodium–sodium exchange catalysed by the sodium pump in human red cells. J Physiol 1971;218:239–56.
[41] Goldman DE. Potential, impedance, and rectification in membranes. J Gen Physiol 1943;27:37–60.
[42] Gouaux E, Mackinnon R. Principles of selective ion transport in channels and pumps. Science 2005;310:1461–5.
[43] Guennoun S, Horisberger JD. Structure of the 5th transmembrane segment of the Na, K-ATPase a subunit: a cysteine-scanning mutagenesis study. FEBS Lett 2000;482:144–8.
[44] Guennoun S, Horisberger JD. Cysteine scanning mutagenesis study of the 6th transmembrane segment of the Na, K-ATPase a subunit: a cysteine-scanning mutagenesis study. FEBS Lett 2002;513:277–88.
[45] Hartzell HC, Yu K, Xiao Q, Chien LT, Qu Z. Anoctamin/TMEM16 family members are Ca^{2+}-activated Cl^- channels. J Physiol 2009;587:2127–39.
[46] Hebert SC, Desir G, Giebisch G, Wang W. Molecular diversity and regulation of renal potassium channels. Physiol Rev 2005;85:319–71.
[47] Hediger MA, Romero MF, Peng JB, Rolfs A, Takanaga H, Bruford EA. The ABCs of solute carriers: physiological, pathological and therapeutic implications of human membrane transport proteins. Pflügers Arch 2004;447:465–8.
[48] Heginbotham L, Lu Z, Abramson T, MacKinnon R. Mutations in the K^+ channel signature sequence. Biophys J 1994;66:1061–7.
[49] Hilgemann DW, Feng S, Nasuhoglu C. The complex and intriguing lives of PIP_2 with ion channels and transporters. Science-STKE 2001;111:1–8.
[50] Hille B. Ionic channels of excitable membranes. 3rd ed. Sunderland: Sinauer; 2001.
[51] Hodgkin AL, Katz B. The effect of sodium ions on the electrical activity of the giant axon of the squid. *J Physiol* (*London*) 1949;108:37–77.
[52] Hoenderop JG, Nilius B, Bindels RJ. Calcium absorption across epithelia. Physiol Rev 2005;85:373–422.
[53] Hollenstein K, Dawson R, Locher K. Structure and mechanism of ABC transporter proteins. Curr Opin Struct Biol 2007;17:412–8.
[54] Horisberger JD. The Na, K-ATPase: structure-function relationship. Boca Raton, FL: CRC Press; 1994. p. 1–20.
[55] Horisberger JD. Recent insights into the structure and mechanism of the sodium pump. *Physiology* (*Bethesda*) 2004;19:377–87.
[56] Horisberger JD, Chraibi A. Epithelial sodium channel: a ligand-gated channel? Nephron Physiol 2004;96:37–41.

[57] Horisberger JD, Kharoubi-Hess S, Guennoun S, Michielin O. The fourth transmembrane segment of the Na, K-ATPase a subunit: a systematic mutagenesis study. J Biol Chem 2004;279:29542–50.
[58] Huang Y, Lemieux MJ, Song J, Auer M, Wang DN. Structure and mechanism of the glycerol-3-phosphate transporter from *Escherichia coli*. Science 2003;301:616–20.
[59] Jacobson K, Dietrich C. Looking at lipid rafts? Trends Cell Biol 1999;9:87–91.
[60] Jentsch TJ. CLC chloride channels and transporters: from genes to protein structure, pathology and physiology. Crit Rev Biochem Mol Biol 2008;43:3–36.
[61] Krämer R. Functional principles of solute transport systems: concepts and perspectives. Biochim Biophys Acta 1994;1185:1–34.
[62] Krarup T, Jensen BS, Hoffmann EK. Occlusion of K^+ in the Na^+/K^+2Cl^- co-transporter of Ehrlich ascites tumor cells. Biochim Biophys Acta 1996;1284:97–108.
[63] Kurtzman CP, Fell JW. The yeasts: a Taxonomic study. 4th ed. Amsterdam; New York: Elsevier; 1998.
[64] Läuger P. Dynamics of ion transport systems in membranes. Physiol Rev 1987;67:1296–331.
[65] Läuger P. Electrogenic ion pumps. Sunderland: Sinauer; 1991.
[66] LeFevre PG, Bronner F, Kleinzeller A. The present state of the carrier hypothesis. Curr Top Membr Transport 1975;7:109–251.
[67] Macey RI, Moura TF. Basic principles of transport. In: Hoffman JF, Jamieson JD, editors. Handbook of physiology. Section 14: cell physiology. New York: Oxford University Press; 1997. p. 181–260.
[68] MacKinnon R. Nobel Lecture. Potassium channels and the atomic basis of selective ion conduction. Biosci Rep 2004;24:75–100.
[69] MacKinnon R. Potassium channels. FEBS Lett 2003;555:62–5.
[70] Macrez N, Mironneau J. Local $Ca^{2=}$ signals in cellular signaling. Curr Mol Med 2004;4:263–75.
[71] McIntosh TJ, Simon SA. Roles of bilayer material properties in function and distribution of membrane proteins. Annu Rev Biophys Biomol Struct 2006;35:177–98.
[72] McLaughlin S, Murray D. Plasma membrane phosphoinositide organization by protein electrostatics. Nature 2005;438:605–11.
[73] McLaughlin S, Wang J, Gambhir A, Murray D. PIP(2) and proteins: Interactions, organization, and information flow. Annu Rev Biophys Biomol Struct 2002;31:151–75.
[74] McLuskey K, Roszak AW, Zhu Y, Isaacs NW. Crystal structures of all-alpha type membrane proteins. Eur Biophys J 2010;39:723–55.
[75] Miller C. Ion Channel Reconstitution. New York: Plenum Press; 1986.
[76] Miller C. ClC chloride channels viewed through a transporter lens. Nature 2006;440:484–9.
[77] Morais-Cabral JH, Zhou Y, MacKinnon R. Energetic optimization of ion conduction rate by the K^+ selectivity filter. Nature 2001;414:37–42.
[78] Mornon J, Lehn P, Callebaut I. Molecular models of the open and closed states of the whole human CFTR protein. Cell Mol Life Sci 2009;66:3469–86.
[79] Morth JP, Pedersen BP, Toustrup-Jensen MS, Sørensen TL, Petersen J, Andersen JP, et al. Crystal structure of the sodium-potassium pump. Nature 2007;450:1043–9.
[80] Morth JP, Pedersen BP, Buch-Pedersen MJ, Andersen JP, Vilsen B, Palmgren MG, et al. A structural overview of the plasma membrane Na^+, K^+-ATPase and H^+-ATPase ion pumps. Nature Rev Mol Cell Biol 2011;12:60–70.
[81] Nernst W. Zur Kinetik der in Lösung befindlichen Körper: theorie der diffusion. Z Phys Chem 1888;2:613–37.
[82] Noury C, Grant SGN, Borg JP. PDZ domain proteins: plug and play!. Science-STKE 2003;179:1–12.
[83] Pedersen BP, Buch-Pedersen MJ, Morth JP, Palmgren MG, Nissen P. Crystal structure of the plasma membrane proton pump. Nature 2007;450:1111–4.
[84] Ogawa H, Toyoshima C. Homology modeling of the cation binding sites of the Na^+,K^+-ATPase. Proc Natl Acad Sci USA 2002;99:15977–82.
[85] Sachs G, Munson K. Mammalian phosphorylating ion motive ATPases. Curr Opin Cell Biol 1991;3:685–94.
[86] Sachs G, Shin JM, Bamberg K, Prinz C. Gastric acid secretion: the H,K-ATPase and ulcer disease. In: Schultz SG, Andreoli TE, Brown AM, Fambrough DM, Hoffman JF, Welsh MJ, editors. Molecular biology of membrane transport disorders. New York: Plenum Press; 1996. p. 469–84.
[87] Saier Jr. MH. A functional-phylogenetic classification system for transmembrane solute transporters. Microbiol Mol Biol Rev 2000;64:354–411.
[88] Sakmann B, Neher E. Single-channel recording. New York: Plenum Press; 1995.
[89] Schulz GE. The structure of bacterial outer membrane proteins. Biochim Biophys Acta 2002;1565:308–17.
[90] Schultz SG. Basic principles of membrane transport. Cambridge: Cambridge University Press; 1980.
[91] Schultz SG. Homocellular regulatory mechanisms in sodium-transporting epithelia: avoidance of extinction by "flush-through. Am J Physiol 1981;241:F579–90.
[92] Segel IH. Enzyme kinetics: behavior and analysis of rapid equilibrium and steady-state enzyme systems. New York: John Wiley & Sons, Inc.; 1975.
[93] Shinoda T, Ogawa H, Cornelius F, Toyoshima C. Crystal structure of the sodium-potassium pump at 2.4 Å resolution. Nature 2009;459:446–50.
[94] Simons K, Toomre D. Lipid rafts and signal transduction. Nat Rev Mol Cell Biol 2000;1:31–9.
[95] Singer SJ. The structure and function of membranes: a personal memoir. J Membr Biol 1992;129:3–12.
[96] Singer SJ, Nicolson GL. The fluid mosaic model of the structure of cell membranes. Science 1972;175:720–31.
[97] Skou JC. The Na-K pump. Methods Enzymol 1988;156:1–25.
[98] Skou JC, Esmann M. The Na,K-ATPase. J Bioenerg Biomembr 1992;24:249–61.
[99] Stein WD. Channels, carriers, and pumps. An introduction to membrane transport. San Diego, CA: Academic Press; 1990.
[100] Stockand JD, Staruschenko A, Pochynyuk O, Botth RE, Silverthorn DU. Insight toward epithelial Na channel mechanism revealed by the acid-sensing ion channel 1 structure. IUBMB Life 2008;60:620–8.
[101] Sugita Y, Miyashita N, Yoda T, Ikeguchi M. Structural changes in the cytoplasmic domain of phospholamban by phosphorylation at Ser16: a molecular dynamics study. Biochemistry 2006;45:11752–61.
[102] Suh BC, Hille B. PIP2 is a necessary cofactor for ion channel function: how and why? Annu Rev Biophys 2008;37:175–95.
[103] Tanford C, Reynolds JA. Membrane structure/proteins. In: Hoffman JF, Jamieson JD, editors. Handbook of physiology. Section 14: cell physiology. New York: Oxford University Press; 1997. p. 59–74.
[104] Tanner MJ. The structure and function of band 3 (AE1): recent developments. Mol Membr Biol 1997;14:155–65.
[105] Toyoshima C. Structural aspects of ion pumping by Ca^{2+}-ATPase of sarcoplasmic reticulum. Arch Biochem Biophys 2008;476:3–11.
[106] Toyoshima C. How Ca^{2+}-ATPase pumps ions across the sarcoplasmic reticulum membrane. Biochim Biophys Acta 2009;1793:941–6.

[107] Toyoshima C, Nakasake M, Nomura H, Ogawa H. Crystal structure of the calcium pump of sarcoplasmic reticulum at 2.6 Å resolution. Nature 2000;405:647–55.
[108] Toyoshima C, Nomura H. Structural changes in the calcium pump accompanying dissociation of calcium. Nature 2002;418:605–11.
[109] Toyoshima C, Nomura H, Sugita Y. Crystal structures of Ca^{2+}-ATPase in various physiological states. Ann NY Acad Sci 2003;986:1–8.
[110] Toyoshima C, Nomura H, Sugita Y. Structural basis of ion pumping by Ca^{2+}-ATPase of sarcoplasmic reticulum. FEBS Lett 2003;555:106–10.
[111] Ussing HH. Transport of ions across cellular membranes. Physiol Rev 1949;29:127–55.
[112] Vereb G, Szöllösi J, Matkó J, Nagy P, Farkas T, Vigh L, et al. Dynamic, yet structured: the cell membrane three decades after the Singer–Nicolson model. Proc Natl Acad Sci USA 2003;100:8053–8.
[113] Ward A, Reyes CL, Yu J, Roth CB, Chang G. Flexibility in the ABC transporter MsbA: alternating access with a twist. Proc Natl Acad Sci USA 2007;104:19005–10.
[114] White S. Membrane proteins of known structure. 2010; http://blanco.biomol.uci.edu/Membrane_Proteins_xtal.html.
[115] Wright EM, Loo DD, Hirayama BA, Turk E. Surprising versatility of Na^+-glucose co-transporters: SLC5. Physiology 2004;19:370–6.
[116] Yamashita A, Singh SK, Kawate T, Jin Y, Gouaux E. Crystal structure of a bacterial homologue of Na^+/Cl^--dependent neurotransmitter transporters. Nature 2005;437:215–23.
[117] Yin Y, He X, Szewczyk P, Nguyen T, Chang G. Structure of the multidrug transporter EmrD from *Escherichia coli*. Science 2006;312:741–4.
[118] Zachos NC, Tse M, Donowitz M. Molecular physiology of intestinal Na^+/H^+ exchange. Annu Rev Physiol 2005;67:411–43.
[119] Zhou Y, MacKinnon R. The occupancy of ions in the K^+ selectivity filter: charge balance and coupling of ion binding to a protein conformational change underlie high conduction rates. J Mol Biol 2003;333:965–75.
[120] Zhou Y, Morais-Cabral JH, Kaufman A, MacKinnon R. Chemistry of ion coordination and hydration revealed by a K^+ channel-Fab complex at 2.0 Å resolution. Nature 2001;414:43–8.

CHAPTER

3

Renal Ion-Translocating ATPases

Dominique Eladari[1], *Udo Hasler*[2] *and Eric Féraille*[2]

[1]INSERM U872, Centre de Recherche des Cordeliers, Paris, France

[2]Department of Cell Physiology and Metabolism and Service of Nephrology, University Medical Center, Geneva, Switzerland

Active transport of solutes across membranes against their concentration or electrochemical gradients requires energy. For ion-motive ATPases (F-type, V-type, and P-type), this process is an exchange between energy contained in the electrochemical gradient and chemical energy provided by ATP hydrolysis. F-type ATPases or ATP synthases are responsible for the generation of ATP using energy of the proton gradient created by the respiratory chain in mitochondria or photosynthetic complexes in chloroplasts. V-type ATPases acidify vesicles by transporting protons from the cytoplasm to the lumen of intracellular organelles (endosomes, lysosomes, vacuoles, . . .). V-ATPases are also present in the plasma membrane of some epithelial cells. Despite sharing a common general architecture and a large number of subunits, F- and V-ATPases usually work in opposite directions. P-type ATPases (also called E1-, E2-ATPases) form a third group of ion-motive ATPases that perform unidirectional or exchange transport of monovalent (H^+, Na^+, K^+) or divalent (Ca^{2+}, Cu^{2+}, Mg^{2+}, . . .) cations.

P-ATPASES

While some members of the P-ATPase family are probably active as a single polypeptide, the functional unit of others consists of several subunits. The major subunit (α- or catalytic subunit for multimeric P-ATPases) consists of a series of hairpins formed by pairs of transmembrane segments linked by short extracellular loops. Two large intracellular loops make the connection between the first, second, and third hairpins. The largest cytoplasmic loop contains the ATP-binding domain and the phosphorylation site. Transient phosphorylation of this aspartate residue occurring during the transport cycle is a hallmark of P-ATPases (Figure 3.1).

STRUCTURE AND FUNCTION OF Ca^{2+}-ATPASES (SERCA AND PMCA)

SERCA is found in intracellular organelles related to the endoplasmic reticulum, such as the sarcoplasmic reticulum of cardiac and skeletal muscle cells. Three differently expressed genes have been identified: SERCA1 in fast-twitch skeletal muscle; SERCA2 in slow-twitch skeletal muscle, heart, and smooth muscle; and SERCA3 in blood, endothelial, and epithelial tissue. SERCA mediates uptake of Ca^{2+} from the cytoplasm into the sarcoplasmic reticulum following calcium release from intracellular stores. It therefore acts as a terminator signal in excitation–contraction coupling processes in muscle, and plays a key role in excitation–secretion coupling in neurons and other secretory cells. Extensive structure–function studies have been performed with SERCA and a high resolution (2.6 Å) structure of this protein was obtained.[1]

PMCA is expressed at the plasma membrane, where it extrudes Ca^{2+} out of the cell. Four PMCA genes are known, with multiple splicing variants for each gene, resulting in the existence of about 20 isoforms. PMCA1 and PMCA4 are ubiquitous, while PMCA2 and PMCA3 are restricted to neurons, brain, muscle, and kidney. PMCA plays an important role in tubular reabsorption of calcium.[1] The long C-terminal intracellular domain maintains PMCA in an inactive state by interacting with the catalytic site. A rise of cytosolic Ca^{2+} concentration increases Ca^{2+}–calmodulin-binding, allowing calmodulin to interact with the PMCA C-terminal domain. This releases PMCA autoinhibition, activating the pump.

Seldin and Giebisch's The Kidney, Fifth Edition.
DOI: http://dx.doi.org/10.1016/B978-0-12-381462-3.00003-3

© 2013 Elsevier Inc. All rights reserved.

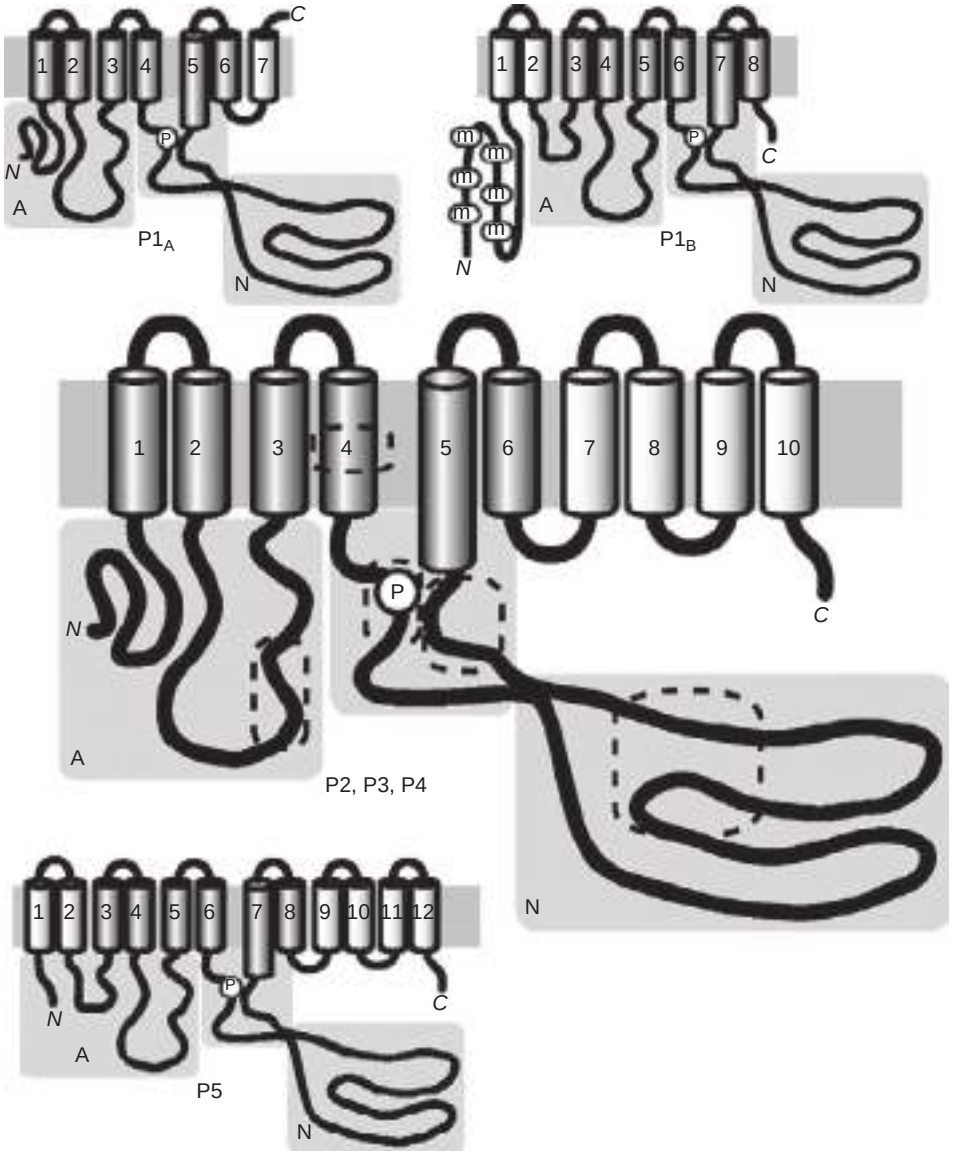

FIGURE 3.1 **General structure and conserved motifs of P-ATPases.** The four schemes show the general architecture of the main catalytic subunit of the large group of P-ATPases. The large scheme in the center corresponds to the common general structure of P2, P3, and P4 subfamilies. The two smaller schemes at the top illustrate the structure of bacterial KDP-B potassium transport ATPase ($P1_A$ subfamily, left) and the universal metal ion transport ATPases ($P1_B$ subfamily, right) in which the large N-terminal domain contains a number (usually 6) of cysteine-rich metal-binding domains (m). The small scheme at the bottom left illustrates the putative structure of P5-ATPase. The six transmembrane segments that are common to all P-ATPase together with the two major intracellular domains form the core of the ion translocation engine, and are shaded in a darker gray. The positions of highly conserved motives common to all P-ATPases are encircled by a dashed line. The cytoplasmic part of the protein is divided into three A, P, and N main functional domains according to Toyoshima et al.[396]. The circled P indicates the location of the phosphorylation site. The N- and C-termini are indicated by italicized *N* and *C*.

Conversely, calcium extrusion decreases cytosolic Ca^{2+} concentration, and consequently its association with calmodulin. Calmodulin release from PMCA increases PMCA auto-inhibition. Regulatory inhibition of SERCA is mediated by the small associated protein phospholamban, which plays a role equivalent to that of the PMCA C-terminal domain. Phosphorylation of phospholamban by protein kinase C releases SERCA inhibition.[1]

STRUCTURE OF Na,K-ATPASE AND H,K-ATPASE

Na,K- and H,K-ATPases are heteromeric proteins consisting of an α-subunit and a smaller glycosylated β-subunit. Na,K-ATPase hydrolytic activity, cation transport activity, and ouabain-binding properties were demonstrated by co-expression of α- and β-subunits in

several expression systems (mammalian cells, *Xenopus* oocytes, baculovirus-infected insect cells, and yeast). Na- (or H-) and K-activated ATPase and cation transport activities (i.e., uphill cation transport driven by ATP hydrolysis) characteristic of Na,K- or H,K-ATPases have been demonstrated only in the presence of both α- and β-subunits. Expression of the α-subunit alone in insect cells[2] resulted in Mg^2-dependent ATPase activity that was not specifically activated by Na^+ and K^+. The exact stoichiometry of the minimal functional unit is still a matter of debate. However, Na,K-ATPase activity is associated with solublized α−β protomers,[3] and cross-linking experiments did not show evidence for a close interaction between α-subunits.[4] A third subunit, the γ-subunit, can be associated with the α−β complex (see below).

Catalytic α-Subunit

Structure

Na,K- and H,K-ATPase α-subunit peptides range in length from about 1000 to 1040 amino acids. Their primary structure is characterized by a first group of four transmembrane segments, followed by a large cytoplasmic loop, and a second group of six transmembrane segments (Figure 3.1). Crystal structures of pig[5] and shark[6] Na,K-ATPase at 3.5 and 2.4 Å resolutions, respectively, confirmed that the α-subunit has three cytoplasmic domains and 10 transmembrane helices, designated *M1* to *M10*. Two-thirds of its mass is contained in the large cytoplasmic domain, while one-third spans the lipid bilayer. Of the total mass, only a small part is extracellular.[6] Sequence homology between Na,K- and H,K-ATPases is high enough to safely predict H,K-ATPase structure, at least for the general architecture of this molecule, and for large domains where homology is highest.

Isoforms

Six different α-subunit genes have been identified in mammals: α1-4 isoforms of the Na,K-ATPase α-subunit; gastric H,K-ATPase α-subunit (αHKg); and colonic H,K-ATPase α-subunit (αHKc). Related isoforms have been identified in birds and amphibians. Na,K-ATPase sequences from *Caenorhabditis elegans* or *Drosophila melanogaster* do not show close similarity with any mammalian isoform. This suggests that the divergence between Na,K- and H,K-ATPase α-subunits precedes the divergence between mammals, amphibians and birds, and has occurred early in vertebrate evolution.

All Na,K-ATPase isoforms primarily maintain Na^+ and K^+ gradients across the cell membrane. The large inward electrochemical gradient for Na^+ is in turn used by numerous secondary active transport systems for various "housekeeping" functions: maintenance of intracellular pH via Na−H exchangers; extrusion of calcium via Na−Ca exchanger; control of cell volume via Na−K−2Cl symport and other coupled transport systems; and import of amino acids, nucleotides, and other nutrients or osmolytes through various Na^+-coupled co-transport systems. The outward electrochemical gradient for K^+ is responsible for the intracellular negative membrane potential, because K^+ flows out of the cell through K^+ selective channels that are active in most cells. In addition to these general functions, Na^+ and K^+ gradients across cell membranes are essential for specialized functions, such as the generation and propagation of action potentials in excitable cells, neurotransmitter uptake, and transcellular transport of solutes and water by epithelial cells.

The α1 isoform is the most ubiquitous and abundant α isoform, and is responsible for the maintenance of whole-cell Na^+ and K^+ gradients necessary for housekeeping functions. Because of its abundance (it is the only α isoform present in many epithelial cells, including renal cells) it provides the driving force for solute and water transepithelial transport. The α2 isoform is found in skeletal and heart muscle, and in the nervous system (neurons and glial cells). The α3 isoform is essentially neuronal, but is also found in blood cells and macrophages. The α4 isoform is mostly expressed in testes, and plays a critical role in sperm motility.[7]

αHKg is abundantly expressed in parietal cells of the gastric gland, where it plays a central role in proton secretion. Under resting conditions, it is mainly located in an intracellular tubulo−vesicular network that fuses with the apical membrane of parietal cells in response to stimuli, allowing the H,K-pump to secrete protons into the gastric gland lumen in exchange for potassium. αHKc is mainly expressed in the (rat) distal colon, but also in the kidney, uterus, and, to a lesser extent, in the heart.[8]

β-Subunit

Isoforms

As stated above, the β-subunit is an essential constituent of functional Na,K-ATPase and H,K-ATPase. Five different genes encoding similar proteins are known in mammalian genomes: β1; β2; β3; βHK; and βm ("m" emphasizes its predominant expression in skeletal muscle). β1, β2, and β3 are clearly Na,K-ATPase β-subunit isoforms, while βHK is co-expressed with gastric H,K-ATPase. Although usually described as ubiquitous, β1 appears to be absent, or at best is only a minor component, in several tissues such as liver and red blood cells. The β2 isoform was initially identified in glial cells, but is also present in other cell types, including neurons, blood cells, and epithelial cells. The β3 isoform, initially identified in nervous systems, is also widely distributed, being most abundant in testes, liver, and lungs and less so in skeletal

muscle and kidney. Despite sharing sufficient sequence similarity to be classified in the same family, βm does not associate with any known mammalian α-subunit.[9]

Structure and α−β Interaction

β-subunit peptides range in length from 288 to 315 amino acids, and show a lower degree of homology (about 30%−40% identity between isoforms) than α isoforms. Crystal structures of Na,K-ATPase obtained at resolutions of 3.5 Å[5] and 2.4 Å[6] have lent detailed insight into β-subunit structure. These studies, together with experimental evidence, show that the β-subunit is a type II membrane protein consisting of a single transmembrane segment, a ∼35-amino acid N-terminal domain, and a large extracellular domain containing two to seven glycosylation sites, depending on the isoform, and six cysteine residues that form three disulfide bridges (Figure 3.1).

Experimental modeling and analysis of Na,K-ATPase crystal structures has revealed complex interactions between α- and β-subunits. The transmembrane helix of the β-subunit forms several hydrogen bonds and numerous contacts with *M7* and *M10* transmembrane helices of the α-subunit, primarily via clusters of aromatic residues. At the extracellular side of the β-subunit, a stretch of amino acids adjacent to its transmembrane domain interacts with the α*M7/M8* extracellular loop that contains a consensus sequence SYGQ.[6] Further downstream, Lys250 of the β-subunit forms a salt bridge with Glu899, located in the α*M7/M8* extracellular loop.[6]

Except for gastric αHK and βHK, which are most abundantly expressed in a single cell type (parietal cells of gastric glands), there is no obvious common pattern of distribution between α isoforms and β isoforms that would define preferential physiological associations. Indeed, some cells even express as many as three α isoforms and at least two β isoforms. Unless formation of specific complexes is favored or repressed by unknown mechanisms, numerous combinations are possible, as suggested by studies using artificial expression systems. β1 is abundantly expressed in tissues in which α1 predominates, such as the kidney, strongly suggesting that α1β1 represents the predominant isozyme in these tissues. The nature of the β-subunit associated with αHKc is also a matter of debate, since all β isoforms are able to associate with αHKc, depending on the expression system used.

Functional Role

The functional interaction between α- and β-subunits has been studied and reviewed in detail.[9] By acting as a molecular chaperone, the β-subunit plays a critical role in the maturation of the α-subunit. Indeed, the α-subunit reaches a mature and functional conformation, ready to be translocated from the endoplasmic reticulum to the plasma membrane, only when associated with a β-subunit.

The β-subunit contributes to intrinsic transport properties of the whole enzyme in several expression systems by influencing its apparent K^+ and Na^+ affinities. Biochemical analysis and crystallization of Na,K-ATPase has lent some mechanistic insight as to how this is achieved. By interacting with the *M7* transmembrane domain of the α-subunit, Tyr40 and Tyr44 of the β-subunit transmembrane helix help confer intrinsic transport properties of the Na,K-ATPase enzyme, as suggested by a mutagenic study.[10] Unwinding of *M7* via hydrogen bonding of Tyr44 with Gly855 appears to be of central importance to K^+ binding. The role of the β-subunit ectodomain in modulating cation transport is further illustrated by the complex interactions between this domain and the α*M7/M8* extracellular loop.

The role of the β-subunit in cell−cell adhesion will be discussed in the section "New Physiological Functions of Na,K-ATPase."

FXYD Proteins

Isoforms

FXYD proteins are a third component of Na,K-ATPase. There are seven isoforms in mammals, ranging from 61 to 95 amino acids in length, except for FXYD5, which consists of 178 amino acids due to an N-terminal extension. Most FXYD proteins are small type 1 membrane proteins containing an extracellular N-terminus. This family of proteins is so named since all members contain a FXYD (Phe-X-Tyr-Asp) sequence located immediately downstream of the transmembrane segment. All members also contain two conserved glycine residues in the transmembrane domain, as well as a serine residue located further downstream. As with α and β isoforms, the tissue distribution of FXYD proteins is isoform-specific.[11] FXYD1 (phospholemman) is predominately expressed in heart and skeletal muscle and, to a lesser extent, in brain, FXYD2 (γ-subunit) in kidney, FXYD3 (MAT-8) in stomach and colon, FXYD4 (CHIF) in kidney and distal colon, FXYD5 (RIC) in kidney, intestine and lung, and FXYD6 and FXYD7 in brain. In the kidney FXYD2 is mostly expressed in proximal tubule and thick ascending limb of Henle, while FXYD4 is exclusively found in the collecting duct where its expression increases from cortical to medullary portions.[12]

Function and Interaction with α- and β-Subunits

FXYD proteins were first thought to be regulators of ion channels or even to act as ion channels themselves. It has now been demonstrated that FXYD proteins interact

with Na,K-ATPase. Contrary to the β-subunit, most FXYD proteins do not associate with H,K-ATPase and do not appear to act as a molecular chaperone. Rather, they regulate Na,K-ATPase functional properties. As recently reviewed,[9] analysis of FXYD-deficient mice and *in vitro* modulation of Na,K-ATPase activity by different FXYD proteins has shown that FXYD1−4, 6, and 7 all decrease Na,K-ATPase apparent affinity for Na^+ and/or K^+, with the exception of FXYD4 which has been shown to decrease apparent affinity for K^+ but increase that for Na^+. FXYD5 does not appear to influence Na,K-ATPase affinity for either Na^+ or K^+, but enhances maximal transport activity. By modulating Na,K-ATPase activity, FXYD proteins play important physiological roles, each isoform playing a different role depending on its tissue-specific distribution. For instance, FXYD1 influences myocardial contractility by modulating Na,K-ATPase activity and calcium handling, as demonstrated in FXYD1-deficient mice that display depressed cardiac contractile function and increased cardiac mass.[13] FXYD6, the only FXYD isoform expressed in the inner ear, may play an auditory and vestibular role by contributing to endolymph ionic compostion, whose production depends on Na,K-ATPase activity.[14] Reflecting altered expression levels in various types of cancer, FXYD3 may be implicated in the control of cell differentiation, proliferation, and/or apoptosis through regulation of Na,K-ATPase activity.[15] Finally, the renal tubule segment-specific distribution of FXYD2 and FXYD4 may explain, at least in part, the higher apparent Na^+ affinity of collecting duct Na,K-ATPase as compared to that of more proximal nephron segments.[16,17]

Crystallization of the Na,K-ATPase holoenzyme[5,6] has deciphered FXYD structure, and revealed how it interacts with α- and β-subunits, providing some insight into how it modulates Na,K-ATPase activity. This notably involves interaction between the transmembrane domain of FXYD proteins, particularly Gly34, with the α*M9* transmembrane domain. Hydrogen bonds between Cys31 and αGlu960 may additionally play a structural role important for FXYD functional regulation. The FXYD motif helps confer β conformational structure. This is partly achieved via Phe12, which anchors this segment to the β-subunit, and Tyr14, which forms a cluster of aromatic residues with Tyr69 of the β-subunit and Trp987 of the α*M9/M10* extracellular loop.

PROPERTIES OF Na,K-ATPase AND H,K-ATPASE

Ion Transport

Under physiological conditions, Na,K-ATPase exchanges three intracellular Na^+ for two extracellular K^+ at the expense of one ATP during each cycle, generating an outward current of one net charge per cycle. The outward current generated by the Na,K-pump tends to hyperpolarize the cell membrane to a few millivolts under steady-state conditions. The majority of the 50 to 80 mV resting-membrane potential is due to flow of K through K channels, which relies on Na,K-pump activity, since high intracellular K^+ concentration is maintained by the Na,K-pump. The apparent affinities for Na^+ and K^+ are dependent on experimental conditions, but under physiological conditions intracellular Na^+ activates the Na,K-pump with a $K^1/_2$ of 10 to 20 mM and a Hill coefficient between 2 and 3. Extracellular K^+ has a $K^1/_2$ of about 1 mM, with a Hill coefficient between 1 and 2.

Despite extensive studies, the difference in transport properties between Na,K-ATPase α isoforms has not been entirely resolved. Initial studies performed in native tissues indicated that α2/α3 isoforms have a higher affinity for Na^+. More recent studies comparing isoforms in the same artificial expression system revealed that α2 has a slightly lower (about 20 mM), and α3 a much lower (30−70 mM), affinity for Na.[18] However, other factors, such as the type of associated β-subunit and FXYD protein, also modulate Na,K-ATPase transport properties (see above).

The mechanism of cation translocation by Na,K-ATPase can be summarized as follows (Figure 3.2). Na,K-ATPase exists under two main conformations, E1 and E2, and transport activity is performed via a cycle in which the protein is transiently phosphorylated, and alternately adopts E1 or E2 conformations. These two conformations differ in their apparent affinities for Na^+ and K^+. The E1 conformation has high affinity sites for Na^+ exposed at the intracellular side of the membrane, while the E2 conformation has high affinity sites for K^+ exposed at the extracellular side of the membrane. Three Na^+ and two K^+ ions are alternately bound to the enzyme and then "occluded," that is, tightly bound inside the protein. This model is compatible with the reported structure of the major conformations of SERCA, and the E2-P conformation of Na,K-ATPase.[6,19]

Non-electrogenic transport is achieved by gastric H,K-ATPase, indicating that a symmetrical number of H^+ and K^+ ions are translocated across the membrane during each cycle. Transport stoichiometry depends on pH. Under conditions of high or near neutral pH, the stoichiometry is 2H,2K^+-1ATP, and shifts to 1H,1K^+-1ATP under physiological conditions, i.e., conditions of very low extracellular pH.[20] The transport properties of colonic H,K-ATPase and its close relatives (human ATP1AL1 and toad *Bufo marinus* bladder H,K-pump) are not yet completely defined. Artificial systems have demonstrated an inward transport of K^+, and an

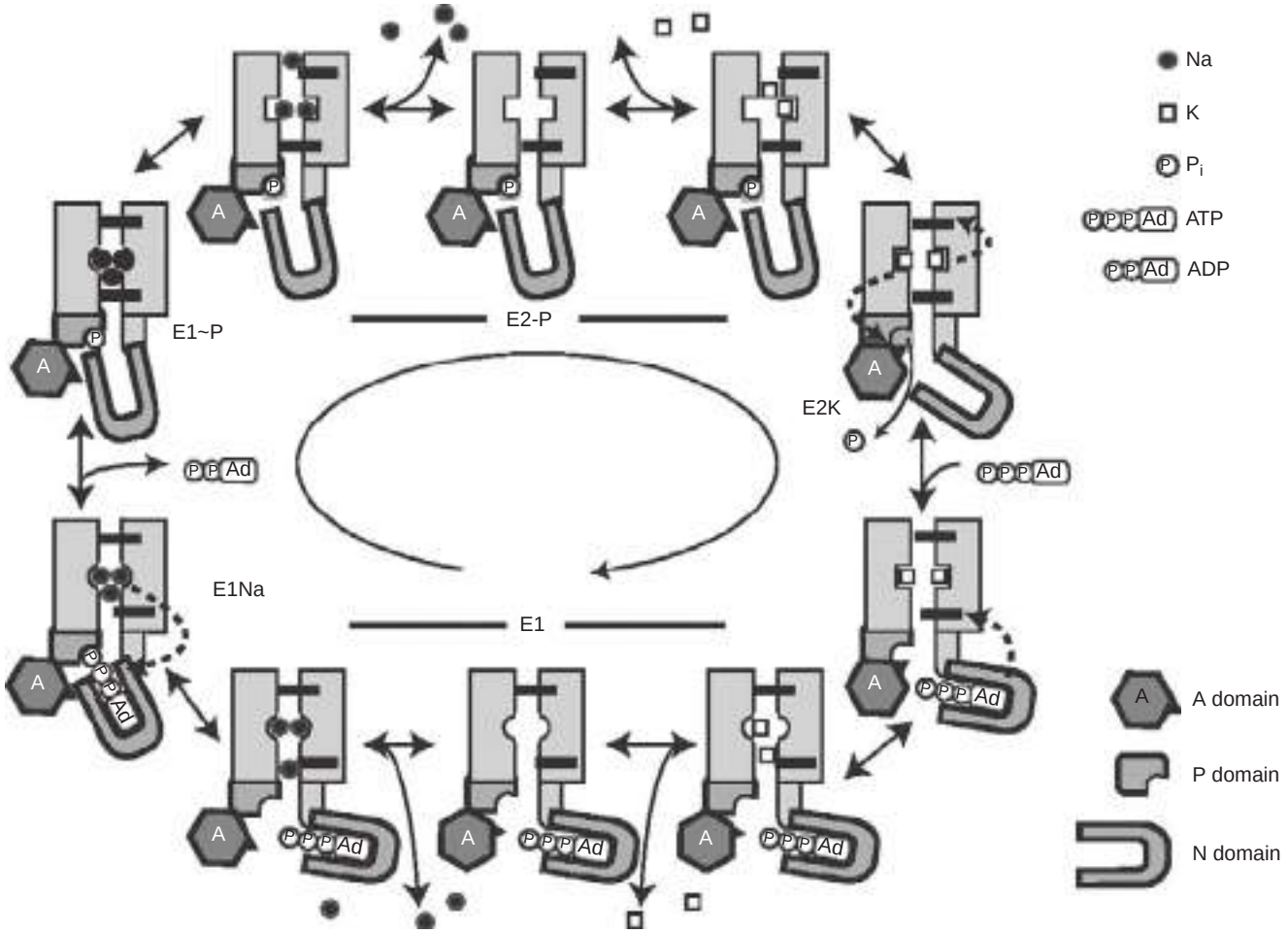

FIGURE 3.2 The Na,K-ATPase transport cycle. This cartoon illustrates the principle of the "alternating access" transport model of Na,K-ATPase. Na^+ ions are indicated by small, filled circles, and K^+ ions by small, open squares. Starting from the E^+ conformation where ATP is present at its binding site, three Na^+ ions enter from the intracellular site through an open, internal gate and reach their occlusion site (E1Na state). Na^+ binding induces (dotted arrow) movement of the N domain, resulting in positioning of the γ phosphate close to the phosphorylation site, phosphorylation of the α-subunit via transfer of the γ phosphate to Asp351, release of ADP and closure of the internal gate which results in the occlusion of the three Na^+ in the E1P state. The conformational change to the E2-P state that follows results in the opening of the extracellular gate, and a structural change of the cation-binding site, resulting in a large decrease of their affinity for Na^+ and an increase of their affinity for K^+. This leads to release of Na^+ to the extracellular side and loading of two K^+. K^+ binding has two major consequences (dotted arrows): first, the external gate closes, resulting in K^+ occlusion; and second, D_{351} (E2K state) is dephosphorylated. This latter event is catalyzed by a conserved motif (TGES, small black triangle) of the A domain that is brought in contact with the phosphorylation site via rotation of this domain. The N domain also moves, allowing it to be accessible (with a low affinity) to ATP. Binding of ATP then results in opening of the intracellular gate (back to the E1 conformation), and allows release of K^+ ions to the intracellular side. This last step can also occur in the absence of ATP, but at a much reduced rate.

outward transport of H^+.[21] However, data obtained in heterologous expression systems have suggested that these enzymes may exchange Na^+ for K^+.[22]

Pharmacology

A group of natural compounds known as "cardiac steroids," so named because they contain a steroid nucleus attached to a lactone ring and are used for treatment of congestive heart failure, are potent Na,K-ATPase inhibitors. In addition, one or several endogenously related compounds may also act as hormonal agents that participate in regulating Na,K-ATPase activity.

Cardiac steroid interaction with Na,K-ATPase, particularly ouabain, has been extensively studied. Differences of ouabain affinity between Na,K-ATPase isoforms, together with mutagenesis studies[23] and recently obtained crystal structures of ouabain bound to Na,K-ATPase,[5] all show that ouabain binds to a deep cavity formed by the transmembrane helices *M1*, *M2*, *M4*, *M5*, and *M6* at the proximity of the K^+-binding site. The slow kinetics of ouabain binding may be associated with partial unwinding of the *M4* helix.

Large differences in ouabain sensitivity occur among animal species. The α1 isoform is ouabain-resistant in rat, mouse, and toad *Bufo marinus*, but is sensitive in human, rabbit, sheep, and *Xenopus*.[23] The α2 and α3 isoforms are more sensitive than the α1 isoform in "resistant" species.[7] However, in humans, little difference of equilibrium binding is found among α1, α2, and α3 isoforms, except for a slightly higher K_I for α2. However, the α2 isoform also exhibits a faster ouabain association and dissociation rate constant than α1 and α3.[24] The "resistant" phenotype of some species is linked to charged amino acids in the first extracellular loop between *M1* and *M2*.[23] The presence of endogenous circulating inhibitors of Na,K-ATPase ("endo-ouabain") is well-demonstrated. However, their precise chemical nature needs to be clarified, their controlled synthesis and release better understood, and their specific effects more precisely described, before the hypothesis of controlled Na,K-ATPase activity by such circulating hormones can be considered as fully established.[25]

Gastric H,K-ATPase is insensitive to ouabain,[20] as demonstrated by an absence of detectable effects at millimolar concentrations of ouabain. On the other hand, non-gastric H,K-ATPases, expressed in *Xenopus* oocytes, show some sensitivity to ouabain and exhibit inhibitory constants (K_I) between 10 and 100 mM.[8] Two types of gastric H,K-pump inhibitors are known. SCH-28080 is a reversible inhibitor that competes with extracellular K^+, while substituted benzimidazole compounds irreversibly inhibit gastric H,K-ATPase by forming a covalent (disulfide) bond between the sulfonamide form of the compound (produced in very acid pH) and the thiol group of a cysteine residue exposed at the cell surface.[20]

Genetics

Gene inactivation studies have shown that Na,K-ATPase is essential for life. Absence of Na,K-ATPase α1 expression is embryonically lethal, even though $\alpha1^{-/-}$ embryos develop beyond the blastocyst stage.[26] In contrast, $\alpha2^{-/-}$ animals are born alive but die soon after birth, most likely as the result of dysfunctional neuronal circuits involved in controlled respiration.[27] α1 or α2 gene inactivation in heterozygous animal tissues leads mostly to disturbances of cardiac phenotype, supporting an important role for the α2 isoform in intracellular calcium homeostasis.[28,29] Only two human genetic diseases are known to be related to mutations of Na,K-ATPase α isoforms. A familial form of hemiplegic migraine has been associated with mutations in the α2 gene that abolish or greatly reduce enzyme activity[30,31] (OMIM #602481). Rapid onset dystonia parkinsonism has been associated with an inactivating mutation of the α3 gene[32] (OMIM #128235). In both cases, the mode of inheritance is dominant, suggesting that the disease is due to a haploinsufficiency of α2 and α3 isoforms, respectively. A dominant form of familial hypomagnesemia has been associated with a mutation in the FXYD2 gene.[33]

REGULATION OF Na,K-ATPASE

Obviously, the activity of an enzyme of such paramount importance for so many cellular and organ functions must be tightly regulated. Physiological regulation of Na,K-ATPase activity is complex and occurs at several levels. First, the activity of Na,K-ATPase depends on its three substrates, Na^+, K^+, and ATP. Second, for short-term regulation, the activity of Na,K-ATPase present at the cell surface can be regulated by post-translational modifications, such as phosphorylation. Third, Na,K-ATPase density at the cell surface is controlled by its rate of synthesis, at both transcriptional and post-transcriptional levels, by its degradation, and by its distribution between the cell surface and intracellular pools. Finally, there is some evidence that protein−protein interactions further regulate Na,K-ATPase activity and abundance.

Substrates

Interaction of intracellular Mg-ATP with Na,K-ATPase is complex and involves high- and low-affinity sites. Since intracellular ATP concentration is usually largely above $K_{1/2}$ values, ATP is not considered a physiological limiting factor for Na,K-ATPase activity. However, under pathological conditions, such as ischemia/hypoxia, ATP may become rate limiting. Similarly, since normal concentrations of extracellular K^+ (3.5−4.5 mM) are above $K_{1/2}$ values, physiological variations are not expected to influence Na,K-ATPase activity, although decreased activity could occur under conditions of severe hypokalemia. In contrast, intracellular Na^+ concentration is below, or close to, $K_{1/2}$ values. Considering the steep concentration−activity relationship, with a Hill coefficient between 2 and 3, a low concentration of intracellular Na^+ implies that Na,K-ATPase operates far from its maximal rate under physiological conditions. It follows that small variations in intracellular Na^+ are immediately followed by parallel variations in Na,K-ATPase activity, in order to maintain a constant intracellular Na^+ concentration.

Intracellular Na^+ and extracellular K^+ concentrations can also have a long-term effect on Na,K-pump density. The influence of extracellular K^+ on α2

expression was demonstrated in skeletal muscle.[34] Under conditions of hypokalemia, α2 is downregulated, allowing release of K^+ from large intracellular pools in muscle and fine regulation of K^+ homeostasis in small extracellular pools. Similarly, intracellular Na^+ modulates Na,K-ATPase expression (see "Na,K-ATPase and the Kidney").

Post-Translational Modifications

Na,K-ATPase α-subunits can be phosphorylated by several protein kinases. PKA phosphorylates a serine residue (S_{943})[35,36] located in a short intracellular loop that links the *M8* and *M9* segments, conserved in all Na,K-ATPase and H,K-ATPase isoforms. However, the functional relevance of this PKA site has been questioned, because it should be poorly accessible under native conformational states,[37] and because its mutation did not alter the effect of PKA on Na,K-ATPase activity in renal epithelial cells.[38] Activation of PKC also results in Na,K-ATPase α-subunit phosphorylation. A conserved, non-conventional PKC phosphorylation site, S_{16}, located in the intracellular N-terminal domain of the α1-subunit,[36,39] as well as two species-specific PKC sites (S_{23} in rat α1, and T_{15} in *Bufo marinus* α1) have been identified. α2- and α3-subunits are poor substrates for PKC or are not phosphorylated at all.[40] PKC phosphorylation of the α-subunit may regulate both apparent Na^+ affinity and cell surface expression of the enzyme.[41–43] More recently, tyrosine phosphorylation of α1 at Y_{10} in response to insulin,[44,45] and also at Y_{260} in response to ouabain,[46] has been described. Similarly, tyrosine phosphorylation of α2 was reported, although the phosphorylation site has not been mapped.[45] Tyrosine phosphorylation of Na,K-ATPase is functionally associated with both an increase of apparent Na^+ affinity and an increase of the enzyme's cell surface expression.[44,45] Finally, phosphorylation of α1 by ERK has been shown *in vitro* and in response to insulin in skeletal muscle. This ERK-dependent phosphorylation is associated with stimulation of Na,K-ATPase activity via increased cell surface expression.[43]

Synthesis and Degradation

Since αβ-subunit stoichiometry is inflexible, controlled synthesis of both subunits is expected to participate in regulating Na,K-ATPase activity. Hormonal control by glucocorticoids, mineralocorticoids, and thyroid hormones has been demonstrated. Thyroid hormones have been shown to regulate the synthesis of both subunits, but the mechanism of this regulation is complex and differs between organs.[47] For instance, glucocorticoids stimulate the transcription of mostly β-subunit mRNA in lungs, even though expression of both α and β protein is increased, indicative of complex transcriptional and post-transcriptional control.[48,49] Regulation of Na,K-ATPase by mineralocorticoids will be discussed later in the section "Na,K-ATPase in the Kidney."

In addition to the rate of synthesis of its subunits, Na,K-ATPase abundance is dependent on its degradation rate. Recent experimental evidence obtained by pulse-chase experiments in lung alveolar[50] and renal (E. Feraille, unpublished results) epithelial cells indicates that the half-life of plasma membrane Na,K-ATPase is approximately 4 hours, while that of newly synthesized α-subunits is approximately 6 hours. Therefore, in contrast to current belief, Na,K-ATPase half-life is relatively short in epithelial cells. The majority of Na,K-ATPase is degraded by lysosomes, and ubiquitination of its α-subunit may participate in this process.[50] Regulation of Na,K-ATPase degradation in response to variations of transepithelial sodium transport will be discussed later in the section "Na,K-ATPase in the Kidney."

Membrane Trafficking

An increasing amount of experimental evidence indicates that plasma membrane Na,K-ATPase expression is controlled via regulated membrane trafficking. Regulated Na,K-ATPase endocytosis was first demonstrated in response to dopamine by atypical PKC-ζ in rat proximal tubule cells.[51] This will be discussed later in the section "Na,K-ATPase in the Kidney." The role of PKC-ζ in Na,K-ATPase endocytosis has been confirmed in alveolar lung cells in response to hypoxia.[52] Downregulation of plasma membrane Na,K-ATPase has also been demonstrated in response to ouabain in renal epithelial cells (LLCPK1 cells),[52] and to AMPK activation in response to CO_2 in lung alveolar cells.[53] Moreover, direct interaction of the Na-K-ATPase α-subunit with arrestins and spinophilin modulates its endocytotic rate in COS-7 cells.[54] It remains to be determined whether internalized Na,K-ATPase units are degraded or recycled back to the plasma membrane.

Rapid recruitment of Na,K-ATPase to the plasma membrane has first been demonstrated in response to insulin in skeletal muscle[55] and following an increase of intracellular sodium concentration in renal collecting ducts.[56] This latter event will be discussed in the section "Na,K-ATPase in the Kidney." Increased cell surface expression of Na,K-ATPase was subsequently demonstrated in response to aldosterone in renal collecting duct cells,[57] and to increased cAMP levels in both renal[58] and lung epithelial cells.[59] This process is sensitive to brefeldin A,[58] suggesting that a latent pool of Na,K-ATPase units is recruited from the trans-Golgi network. In addition, activation of PKC-β in proximal tubule cells[51] and PKC-δ–εδ in lung alveolar cells[60] increases Na,K-ATPase plasma membrane expression. Exocytosis of Na,K-ATPase is dependent on RhoA,[61]

kinesin,[62] and myosin-Va[63] in lung alveolar cells. The amount of active Na,K-ATPase units at the cell surface is therefore highly regulated via both endocytotic and exocytotic processes.

Interaction with the Cytoskeleton

Na-K-ATPase interacts both directly and indirectly with the membrane cytoskeleton in several ways. Na,K-ATPase binds directly to ankyrin, which itself links Na,K-ATPase to spectrin (fodrin) and consequently to the basolateral cytoskeleton.[64,65] Ankyrin-spectrin interaction is thought to participate in specific targeting of Na-K-ATPase to the basolateral membrane of epithelial cells. Na-K-ATPase activity may also be modulated via its association with ankyrin.[66]

Na,K-ATPase and actin filaments display a complex relationship that is not fully understood. Actin filaments may directly modulate Na,K-ATPase activity[67] or indirectly control Na,K-ATPase plasma membrane expression via adducins which control actin polymerization.[68] Mutant α-adducin associated with hypertension in rats and humans was shown to decrease constitutive Na,K-ATPase endocytosis, and thereby increase the number of active Na,K-ATPase units at the cell surface.[68] Direct activation of Na,K-ATPase activity by adducin was also demonstrated.[66] In addition, Na,K-ATPase directly binds to cofilin, which modulates actin filament polymerization.[69] Na,K-ATPase basolateral targeting and modulation of its activity appears additionally to depend on its interaction with multiple cytoskeletal elements.

NEW PHYSIOLOGICAL FUNCTIONS OF Na,K-ATPASE

In addition to its well-known function, i.e., Na^+ and K^+ membrane translocation, Na,K-ATPase modulates a variety of cellular processes involved in cell growth, differentiation, and intercellular adhesion.

Cell Signaling by Na,K-ATPase

Since the pioneering work of Askari et al. which demonstrated that ouabain induces early response genes involved in cardiac hypertrophy in a Ca^{2+}-dependent manner,[70] a large body of experimental evidence collectively indicates that Na,K-ATPase behaves as a signaling platform in both mesenchymal and epithelial cells. Activation of Src and Epidermal Growth Factor (EGF) receptor tyrosine kinases, and downstream activation of MAP kinases (ERK) by ouabain at concentrations that do not alter intracellular Na^+ concentration was demonstrated in cardiac myocytes and in LLC-PK1 renal epithelial cells.[71] Ouabain induces dissociation and activation of Src from Na,K-ATPase,[72] and subsequent transactivation of EGF receptor. This ouabain-induced signaling depends on a pool of non-functional Na,K-ATPase specifically located in caveola.[73–75] In addition to ERK activation, ouabain induces calcium oscillations via close association of phospholipase C and IP3 receptors in cell signaling microdomains.[76,77] However, these ouabain-dependent signaling events remain to be demonstrated in native tissues, and their physiological relevance is not yet established.

Role of Na,K-ATPase in Cell Adhesion

An increasing amount of experimental evidence indicates that the Na,K-ATPase β1-subunit plays a direct role in homotypic cell−cell adhesion.[78] This cell−cell adhesion function is negatively correlated with the level of complexity of β glycosylation.[79] Moreover, the transcription factor Snail, which plays a key role in epithelial-to-mesenchymal transition processes observed in poorly differentiated carcinoma cells, represses Na,K-ATPase β1-subunit transcription.[80] In addition to a direct inhibition of cell motility via increased cell−cell adhesion, Na,K-ATPase may also modulate cell migration via its interaction with the PI3-kinase p85 regulatory subunit.[81] This adhesive function of Na,K-ATPase may play important roles in organogenesis and carcinoma invasiveness.

Na,K-ATPase also modulates tight junction dynamics and permeability in cultured renal epithelial cells.[82] Indeed, both ouabain and low extracellular K^+, which inhibit Na,K-ATPase and increase intracellular Na^+, prevent tight junction recovery in calcium switch experiments performed on MDCK cells.[83] This effect is dependent on inhibition of RhoA GTPase activity by high intracellular Na^+. In addition, ouabain at concentrations that do not alter transcellular K^+ transport increases tight junction permeability via activation of Src and ERK.[84] The physiological relevance of these findings remains to be demonstrated.

Na,K-ATPASE IN THE KIDNEY

Tubular epithelial cells are characterized by their functional polarity. Na,K-ATPase is exclusively located in the basolateral membrane, the infoldings of which are closely surrounded by mitochondria which provide a constant supply of ATP. The Na^+ gradient generated by Na,K-ATPase between intra- and extracellular compartments is mainly dissipated across the apical membrane. A net reabsorption of Na^+ results from this architectural organization, and the main role of Na,K-ATPase in the kidney is to energize Na^+ reabsorption. In humans, kidneys reabsorb over 500 g of

sodium per day, and utilize over 2 kg of ATP to fuel Na,K-ATPase. Although renal Na,K-ATPase also energizes secondary active transport of other solutes, its main function is related to Na^+ transport.

Measurements in microdissected segments of the mammalian renal tubule indicate that Na,K-ATPase activity is high in the thick ascending limb of Henle's loop (TAL) and the distal convoluted tubule (DCT), intermediate in the proximal tubule (PT) and the collecting duct (CD), and very low in the thin segments of Henle's loop. This distribution profile of Na,K-ATPase activity is correlated with transtubular Na^+ reabsorption capacity in various nephron segments.[85] In PT and CD, Na,K-ATPase activity declines from the kidney cortex toward the outer and inner medulla.[48] This distribution profile is confirmed by immunocytochemistry on kidney sections and by quantification of the number of pumps by ^{3}H-ouabain binding or by Western blotting of α1- and β1-subunits. Immunohistochemistry on kidney sections indicate that Na,K-ATPase expression in the collecting duct is much higher in principal than in intercalated cells. In contrast, quantification of Na,K-ATPase mRNA along the rat nephron does not confirm this axial heterogenic distribution, at least for α- and β-subunits (A. Doucet, personnal communication). This suggests the presence of segment-specific control mechanisms for Na,K-ATPase translation and/or degradation.

Regulation of Na,K-ATPase in Proximal Tubule

Na,K-ATPase activity must be tightly controlled, since the PT reabsorbs the bulk of filtrated sodium (more than 60%). Na,K-ATPase is regulated by hormones, neurotransmitters, and para/autocrine factors acting via synergistic or antagonistic signaling pathways, and one should keep in mind that the final effect, i.e., stimulation of inhibition of Na,K-ATPase activity, is not the result of activation of a single signaling pathway, but rather of a highly complex integrated response. Modulation of Na,K-ATPase cell surface expression and its affinity for Na^+ are the most important mechanisms of regulation identified in PT.

Control of Na,K-ATPase by Insulin

Stimulation of Na,K-ATPase by insulin in the PT most likely participates in stimulation of Na^+ reabsorption in this nephron segment.[86] Indeed, in isolated rat PT, insulin stimulates Na,K-ATPase transport activity in the presence of physiological concentrations of intracellular Na^+, not by changing V_{max} values, but by increasing apparent Na^+ affinity.[87] Experiments performed in isolated rat PT and in cultured OK cells (a cellular model of PT) strongly suggest that stimulation of Na,K-ATPase activity relies on phosphorylation of the α-subunit at Y_{10}.[44] However, the causal relationship between tyrosine phosphorylation of Na,K-ATPase and increased Na^+ affinity remains to be directly demonstrated. Insulin also reduces the inhibitory effect of dopamine on Na,K-ATPase (see next section),[88] and this may also participate in its overall stimulatory effect.

Control of Na,K-ATPase by Dopamine and Parathormone

Dopamine is produced from L-dopa by PT, and its synthesis is increased by high sodium intake, making it a putative local modulator of sodium and fluid handling. Dopamine decreases fluid and sodium reabsorption *in vitro* in microperfused rabbit PT.[89] Accordingly, dopamine decreases Na,K-ATPase V_{max} values in rat PT,[90] as well as in OK cells.[42] Although dopamine also increases Na,K-ATPase apparent affinity for Na^+ in the PT,[90] the overall resulting effect in intact cells is Na,K-ATPase inhibition.[42] This inhibition results from activation of both dopamine DA_1- and DA_2-like receptors,[91] and is mediated by PKCζ.[51]

Within minutes, dopamine induces Na,K-ATPase endocytosis from the plasma membrane to intracellular compartments. Decreased Na,K-ATPase expression at the basolateral membrane of rat PT is associated with a sequential increase of Na,K-ATPase abundance in clathrin-coated pits (1 minute), early endosomes (2.5 minutes), and late endosomes (5 minutes).[92] Results obtained in OK cells strongly suggest that the inhibitory effect of dopamine is dependent on PKC-mediated phosphorylation of the Na,K-ATPase α-subunit on S_{23}.[42,93] Following endocytosis, the α-subunit is dephosphorylated in late endosome compartments[42] (Figure 3.3).

Dopamine-induced endocytosis of Na,K-ATPase is also associated with activation of phosphatidylinositol 3-kinase (PI3K), an enzyme critical for membrane trafficking.[94] However, dopamine-induced activation of PI3K is not secondary to its phosphorylation. Rather, S_{23} phosphorylation of the Na,K-ATPase α-subunit serves as an anchor signal for the sequential recruitment of 14-3-3 protein[95] and PI3K[96] to the membrane. Activation of PI3K in turn generates local production of phosphatidylinositol 3-phosphate, which allows binding of Na,K-ATPase with adaptor protein-2 (AP2), recruitment of clathrin, and endocytosis of Na,K-ATPase.[97] Concomitantly, dopamine activates protein phosphatase 2A which in turn dephosphorylates dynamin 2, thus allowing Na,K-ATPase recruitment at the plasma membrane.[98]

Parathormone (PTH) inhibits fluid and solute transport by PT,[99] at least in part via inhibition of Na,K-ATPase activity, as first demonstrated in PT suspensions.[100] This inhibitory effect relies partly on generation of arachidic acid metabolites via the cytochrome P450 pathway.[101] Na,K-ATPase endocytosis in response to PTH has been observed both *in vitro*, in OK

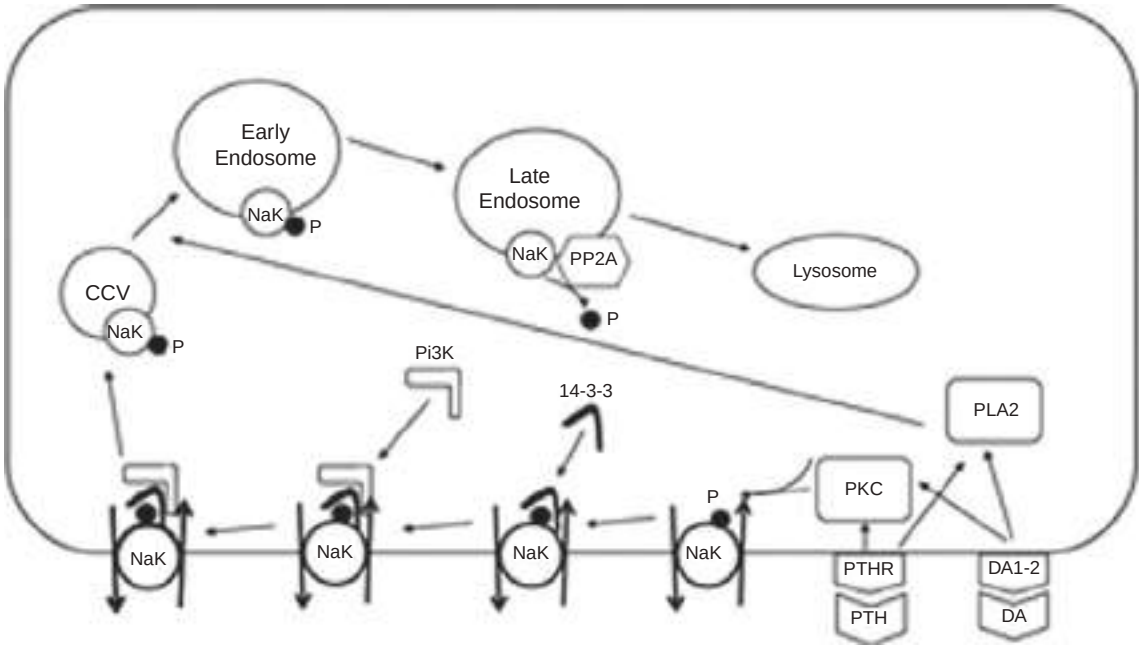

FIGURE 3.3 **Regulation of Na,K-ATPase by dopamine and parathormone (PTH) in proximal tubule.** After dopamine or PTH bind to their cognate receptor, PKC is activated leading to phosphorylation of the Na,K-ATPase α-subunit on S23, followed by binding of 14-3-3 protein and p85 subunit of the Pi3-kinase. This cascade of events leads to Na,K-ATPase endocytosis via clathrin coated vesicles (CVV). Na,K-ATPase is then dephosphorylated in endosomes by PP2A and degraded in lysosomes. Phospholipase A2 (PLA2) activation modulates Na,K-ATPase internalization.

cells,[102] and *in vivo* after infusion of PTH in normal rats,[103] and may account for the inhibitory effect of this hormone. Studies performed in the OK cell model have shown that PTH-induced endocytosis of Na,K-ATPase is ERK-dependent, requires S_{16} phosphorylation of the α-subunit and the scaffolding protein NHERF1.[102,104]

Endocytotic removal of active Na,K-ATPase from the plasma membrane therefore constitutes a major regulatory mechanism of fluid and sodium reabsorption by the PT.

Angiotensin II Exerts a Biphasic Effect on Na,K-ATPase

Angiotensin II (ANG II) controls PT Na^+ reabsorption from both luminal and basolateral sides. High concentrations of ANG II can be found in the PT lumen with respect to plasma circulating concentrations,[105] suggesting that the majority of luminal ANG II originates from local synthesis. Indeed, PT cells express angiotensinogen,[106] renin,[107] and angiotensin converting enzyme.[108] Only a very small fraction of ANG II is excreted in the urine, since it is almost entirely reabsorbed and degraded by PT.[109] ANG II exerts a biphasic effect. Low levels of ANG II (12^{-12} to 10^{-10} M) stimulate, while high levels of ANG II (10^{-9} to 10^{-7} M) inhibit, fluid and solute reabsorption *in vivo* in microperfused rat PT.[110] ANG II also modulates Na,K-ATPase activity in a biphasic manner in isolated PT.[111] At low concentrations, ANG II enhances Na,K-ATPase activity via an increase in its apparent Na^+ affinity.[112] The mechanism by which high levels of ANG II inhibit Na,K-ATPase activity remains to be determined.

Regulation of Na,K-ATPase in Thick Ascending Limb of Henle's Loop

The TAL reabsorbs close to 15% of the filtered Na^+ load and is impermeable to water. As a result, fluid delivered to the distal convoluted tubule is hypotonic, NaCl concentration levels being close to 50 mM. Na^+ enters the luminal side of the cell via a furosemide-sensitive Na-K-2Cl-co-transporter (BSC1 or NKCC2), and Cl^- leaves the cell via Cl^--channels and K-Cl co-transporters. K^+ is recycled back to the lumen via inwardly rectifying and voltage-insensitive K^+-channels expressed at the apical membrane. Conductive diffusion of Cl^- and K^+ depolarizes the basolateral membrane and hyperpolarizes the apical membrane, respectively. The combination of both diffusion potentials generates positive transepithelial voltage which provides the driving force for paracellular cation reabsorption.

Micropuncture and *in vitro* microperfusion experiments show that cAMP analogs and hormones coupled to adenylyl cyclase activation enhance NaCl reabsorption in the TAL.[48] Stimulation of Na^+ reabsorption by the cAMP signaling pathway is at least in

part mediated by stimulation of Na,K-ATPase activity. This stimulatory effect is observed at V_{max} values, and requires sufficient amounts of oxygen and metabolic substrates. Indeed, when metabolic supply is limiting, an increase of cellular cAMP content actually inhibits Na,K-ATPase activity via generation of arachidonic acid metabolites that in turn is dependent on the cytochrome P450 pathway. Na,K-ATPase stimulation by cAMP is correlated with increased phosphorylation levels of the Na,K-ATPase α-subunit.[113] It remains to be determined whether this effect results from phosphorylation of the α-subunit by PKA or by another kinase.

The stimulatory effect of the cAMP/PKA signaling pathway is subject to negative modulation by numerous signaling pathways, including protein Gαi activation by prostaglandins,[114] cGMP generation in response to nitric oxide[115] and natriuretic peptides,[116] and PKC stimulation in response to angiotensin II,[117] bradykinin,[118] and extracellular Ca^{2+} via activation of the extracellular Ca^{2+} receptor.[119]

Control of Na,K-ATPase in Collecting Duct

Mammalian connecting tubules (CNT) and CD (cortical collecting duct: CCD, outer medullary collecting duct: OMCD, inner medullary collecting duct: IMCD) are the main sites for the fine-tuning of sodium reabsorption, crucial for the adjustment of daily urinary sodium excretion to dietary intake. In these renal tubule segments, apical sodium entry is primarily mediated by amiloride-sensitive sodium channels (ENaC),[48] and accessorily mediated by a recently identified sodium-dependent chloride/bicarbonate exchanger, SLC4A8.[120] ENaC was long thought to be the principal player for sodium transport, Na,K-ATPase activity being adapted secondarily to changes of intracellular Na^+ concentration, itself brought about by changes in ENaC activity. However, it is now clearly established that regulation of sodium transport results from the coordinated regulation of both ENaC and Na,K-ATPase.

Aldosterone Induces a Biphasic Stimulation of Na,K-ATPase

Na,K-ATPase activity (V_{max} values) is decreased by ~70% in collecting ducts[121] within 4–5 days of adrenalectomy, but is increased following administration of supraphysiological doses of mineralocorticoid. This latter effect appears after a 24-hour latency, and culminates after approximately 6 days.[85] Administration of aldosterone to adrenalectomized animals[122] or *in vitro* addition of aldosterone to renal tubules isolated from adrenalectomized animals[123] also increases Na,K-ATPase activity (V_{max} values) in the CD, but this effect is much more rapid than in adrenal-intact animals since it is observed after only an hour, and is maximal after only 2–3 hours. These data indicate that low levels of CCD Na,K-ATPase activity and plasma aldosterone concentration is associated with a fast stimulatory response.[124]

Short-term (2–6 hour) aldosterone challenge increases both the activity and cell surface expression of Na,K-ATPase via recruitment of a latent pool of pumps, as shown both in CD isolated from adrenalectomized rats, and in cultured $mpkCCD_{C14}$ cells, a model of CCD principal cells[57] (Figure 3.4). Although cell fractionation and cell-surface labeling studies suggest that a latent pool of Na,K-ATPase is intracellular,[58,92] its exact localization has not yet been established. Short-term stimulation of Na,K-ATPase activity occurs independently of ENaC and apical sodium entry, but does depends on *de novo* transcription and translation.[57] Experiments performed on *Xenopus* oocytes demonstrated that serum and glucocorticoid-regulated kinase-1 (SGK1), an early aldosterone-inducible gene, increased Na,K-ATPase activity and cell surface expression.[125] This suggests that aldosterone-induced recruitment of latent Na,K-ATPase units may be mediated by SGK1. Early recruitment of latent Na,K-ATPase is followed by transcriptional stimulation and synthesis of Na,K-ATPase α1- and β1-subunits.[126] In summary, after a latency period of 1 hour, aldosterone stimulates Na,K-ATPase activity in a biphasic manner. First via recruitment of an inactive Na,K-ATPase reservoir to the cell surface, and then by increased synthesis of Na,K-ATPase subunits.

Vasopressin Stimulates Na,K-ATPase

Vasopressin (AVP) is coupled to adenylyl cyclase via V_2 receptors, and stimulates the cAMP/PKA signaling pathway in CD principal cells. The major role of AVP in CD is to stimulate water reabsorption by increasing water permeability of the apical membrane of principal cells. However, *in vitro* microperfusion studies have shown that AVP also stimulates Na^+ reabsorption and K^+ secretion along the CD.[48] This effect of AVP on urinary Na^+ excretion has recently been confirmed in humans.[127]

Na,K-ATPase stimulation is a prerequisite for increased Na^+ reabsorption, but initial studies reported an inhibitory effect of AVP and cAMP analogs on Na,K-ATPase activity in isolated rat CCD.[128] Results from our laboratory indicate that an arachidonic acid-dependent inhibitory pathway is induced by metabolic stress related to *ex vivo* experimental conditions.[113] Indeed, in both well-oxygenated, isolated rat CCDs, and cultured $mpkCCD_{Cl4}$ cells, cAMP analogs induced a two-fold stimulation of Na,K-ATPase activity.[58,129] This stimulatory effect is rapid (5 min), and is associated with a proportional increase of Na,K-ATPase cell surface

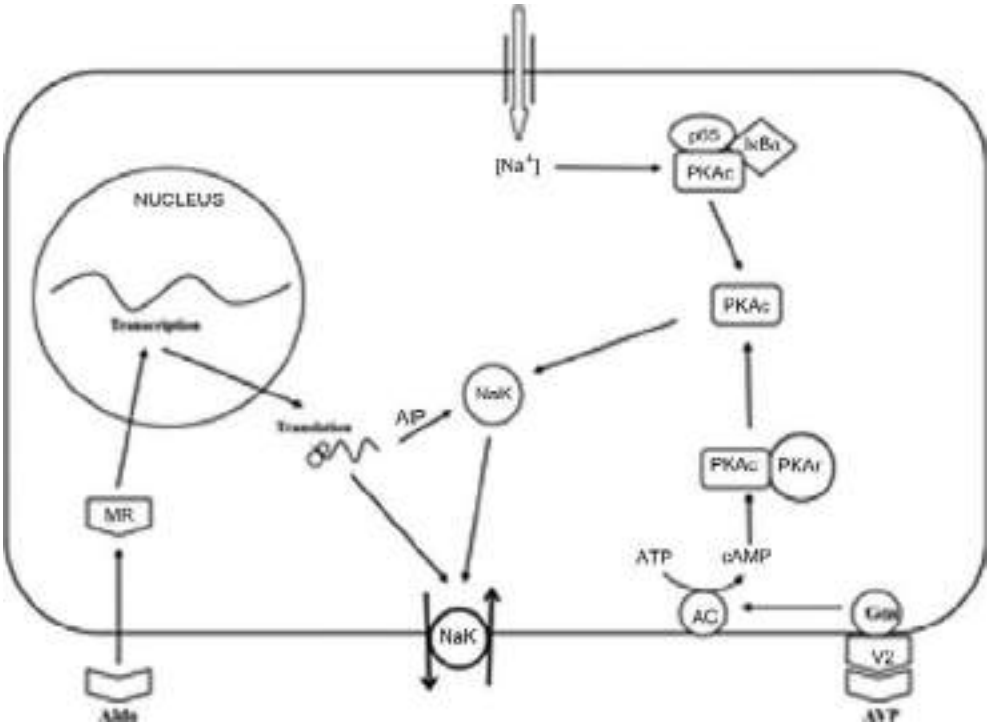

FIGURE 3.4 **Regulation of Na,K-ATPase by aldosterone, vasopressin, and Na^+ in the collecting duct.** Binding of aldosterone to the mineralocorticoid receptor leads to its translocation to the nucleus. This first increases the expression of early aldosterone-induced proteins (AIP), and then induces late expression of Na,K-ATPase. AIP leads to the recruitment of inactive intracellular Na,K pumps to the plasma membrane. Binding of vasopressin to its V_2 receptor induces cAMP synthesis, leading to dissociation of the PKA catalytic subunit (PKAc) from its regulatory subunit (PKAr). An increase of intracellular Na^+ leads to the dissociation of a protein complex containing p65 NF-κB, IκBα and PKAc. Free PKAc participates in the recruitment of inactive intracellular Na,K pumps to the plasma membrane.

expression in the absence of a change in whole-cell Na,K-ATPase abundance in a PKA-dependent manner[38,129] (Figure 3.4). Identification of a cAMP-responsive Na,K-ATPase pool and its relation to an aldosterone controlled reservoir remains to be determined.

Na,K-ATPase Expression is Regulated by Sodium Availability

Acute (hour) increases of intracellular Na^+ in CD not only activate Na,K-ATPase activity via a substrate effect, but also rapidly increase V_{max} values and the number of active Na,K-ATPase units present at the cell surface.[56] This rapid stimulation occurs independently of protein synthesis, suggesting that pre-existing Na,K-ATPase units present in a latent pool are recruited to the cell surface (see above). The effect of intracellular Na^+ is mediated by cAMP-independent PKA activation[130] that itself results from dissociation of a complex consisting of NF-κB, IκBα and the catalytic PKA subunit.[131] This indicates that the pro-inflammatory NF-κB pathway may be part of a Na^+ sensing mechanism that mediates cross-talk between apical Na^+ entry and basolateral Na^+ exit (Figure 3.4). Recent experimental evidence indicates that a sustained increase of apical Na^+ entry also increases Na,K-ATPase expression via inhibition of Na,K-ATPase endocytosis and degradation (E. Feraille, personal communication). Such modulation of Na,K-ATPase activity by Na^+ load may be involved, to some extent at least, in diuretic resistance. Accordingly, chronic administration of the loop diuretic furosemide stimulates CD Na,K-ATPase activity independently of variations of circulating aldosterone.[132]

Induction of Na,K-ATPase is Associated with Sodium Retention in Nephrotic Syndrome and Liver Cirrhosis

Interstitial edema is a cardinal clinical manifestation in nephrotic syndrome. It is secondary to the accumulation of sodium in the extracellular compartment following imbalanced dietary sodium intake and urinary sodium output, and also results from alterations of fluid transfer across the capillary endothelial barrier. Mechanisms behind sodium retention have been extensively investigated using a rat model of puromycin aminonucleoside (PAN)-induced nephrotic syndrome. Both *in vivo* and *in vitro* studies demonstrated that the CCD is the main site of increased Na^+ reabsorption in

PAN nephrotic rats.[133,134] Na,K-ATPase hydrolytic and transport activities are increased two-fold in CCD of PAN nephrotic rats.[135] Increased Na,K-ATPase stimulation, which culminates at day 6 following PAN administration, parallels decreased urinary sodium excretion and development of a positive sodium balance.[136] Moreover, a linear inverse correlation between urinary sodium excretion and CD Na,K-ATPase activity is observed in three different experimental models of nephrotic syndrome.[136] Stimulation of Na,K-ATPase activity is paralleled by increased abundance of α and β Na,K-ATPase mRNA and basolateral protein expression.[129] Sodium retention and induction of Na,K-ATPase activity in CCD are independent of variations of circulating aldosterone.[135,137]

Interstitial edema and ascites are frequently observed in liver cirrhosis. The mechanism governing sodium retention in liver cirrhosis is under debate; however, dysregulation of CD Na,K-ATPase activity may play a key role. Indeed, in the bile duct ligation model Na,K-ATPase activity is specifically increased in mouse CCD independently of variations of circulating glucocorticoids or aldosterone.[138]

In summary, increased Na,K-ATPase activity in the CCD participates in sodium retention in both experimental nephrotic syndrome and liver cirrhosis, and may therefore play a key role in the pathogenesis of edematous diseases.

The previous paragraphs collectively outline the complexity of Na,K-ATPase regulation in the kidney. They demonstrate that: (1) hormonal triggering of intracellular signaling pathways can rapidly alter Na,K-ATPase V_{max} values and/or modulate the pump's affinity for Na^+; (2) these changes are true regulatory mechanisms that occur independently of changes in apical Na^+ entry; and (3) they are generally accompanied by a concomitant regulation of apical Na^+ entry. Thus, despite repetitive and rapid changes of Na^+ reabsorption, whole-body sodium balance and intracellular Na^+ homeostasis are maintained, at least in part, by short-term regulation of Na,K-ATPase activity. Finally, alterations of Na,K-ATPase activity are relevant to the pathophysiology of edematous diseases.

H,K-ATPASES IN KIDNEY

Kidney H,K-ATPase was first described following the discovery that it participates in primary active K^+ reabsorption, a process characterized by H,K-ATPase-like activity in the mammalian distal nephron.[139] Gastric and colonic H,K-ATPase α-subunits were subsequently cloned and mRNAs encoding these two ATPases were shown to be expressed in the kidney. We will discuss the specific inference of gastric and colonic H,K-ATPases in the kidney. Special attention will be paid to studies performed in K^+-replete and K^+-depleted animals in consideration of gastric and colonic H,K-ATPases, respectively. Indeed, kidney expression of αHKc is very low or even absent in K^+-replete animals, whereas it is markedly induced in response to K^+ depletion.

Gastric H,K-ATPase

Gastric H,K-ATPase activity, referred to as type I K-ATPase activity, was first detected as a Na^+-independent, K^+-activated ATPase activity in CD isolated from several mammalian species administered a standard diet.[139] Type I K-ATPase activity is ouabain-insensitive, and is inhibited by omeprazole and Sch 28080. This pharmacological profile fits well with that reported for gastric mucosa K-ATPase and gastric H,K-ATPase expressed in artificial systems. Moreover, Type I K-ATPase is not detected in CD of αHKg knockout mice,[21] thus demonstrating that gastric H,K-ATPase is responsible for type I K-ATPase activity. Most studies have detected moderate levels of αHKg mRNA and protein in rat and mouse CD,[140] while βHKg mRNA has been detected in rat and rabbit CD and CNT.[22] However, HKg-subunit expression remains to be demonstrated in human kidney. *In situ* hybridization, immunochemistry, and functional studies indicate that αHKg is mostly (if not exclusively) expressed in both α- and β-intercalated cells.[140]

In vitro microperfusion studies performed on rats have shown that HCO_3^- reabsorption is inhibited by luminal (but not peritubular) addition of Sch 28080 to OMCD, but not to CCD. However, peritubular addition of Sch 28080 reduces HCO_3^- secretion induced by *in vivo* CD alkalosis. These results suggest the involvement of apical H,K-ATPase in OMCD α-intercalated cells, and in the basolateral membrane of CCD β-intercalated cells, at least during metabolic alkalosis.[141] The functional role of CD H,K-ATPase has been more extensively studied in normal rabbits. *In vitro* microperfusion studies performed in rabbit OMCD indicate that HCO_3^- reabsorption is markedly reduced by luminal addition of Sch 28080 and by removal of luminal K^+.[140] An Sch 28080-sensitive, K^+-dependent mechanism of H^+ extrusion has been demonstrated in CCD α- and β-intercalated cells by measuring their pH recovery following intracellular acidification.[142] However, the contribution of H,K-ATPase to K^+ reabsorption under normal conditions may be minimal, since most K^+ that enters the cytoplasm via H,K-ATPase is recycled back to the lumen via apical K^+-channels.[143]

Transgenic mice expressing βHKg containing a mutant endocytosis signal display H,K-ATPase that is constitutively expressed at the apical membrane of

stomach parietal cells. This is accompanied by gastric acid hypersecretion.[144] These animals also display constitutively active renal K^+ reabsorption,[145] suggesting that gastric H,K-ATPase participates in K^+ reabsorption in mouse kidney, at least when overexpressed at the apical membrane. In contrast, transgenic mice deficient in αHKg do not display altered H^+ and K^+ renal handling.[146] Indeed, the rate of CCD K^+-dependent proton secretion is similar between wild-type and αHKg-deficient mice.[147] However, K^+-dependent H^+ secretion is sensitive to Sch 28080 in wild-type mice, whereas it is insensitive to Sch 28080 in αHKg-deficient mice.[147] This suggests that αHKg deficiency is functionally compensated by expression of another, yet unidentified, K^+-dependent H transporter.

Altogether, these studies indicate that gastric H,K-ATPase expressed in CD intercalated cells of normal rat, rabbit, and mouse kidney participates mostly in urinary acidification and/or HCO_3^- reabsorption. Its contribution to a K^+-reabsorption process is weak, except when artificially overexpressed.

Only a few studies evaluated how gastric H,K-ATPase adapts to disorders of acid−base balance. On the one hand, type I K-ATPase activity is increased in rat CCD and OMCD during hypercapnia-induced respiratory acidosis, whereas it is reduced by hypocapnia. On the other hand, chronic metabolic acidosis increases H,K-ATPase-mediated H^+ secretion by rabbit CCD that may rely on increased transcription of αHKg during the first hours of acid challenge, and thereafter on post-transcriptional mechanisms.[140,148] In contrast to acidosis, K^+ depletion increases neither type I K-ATPase activity, nor αHKg expression.[140] Post-transcriptional control of gastric H,K-ATPase in rat collecting ducts is demonstrated by the *in vitro* stimulatory effects of calcitonin and isoproterenol on type I K-ATPase,[149] two hormones that stimulate proton secretion and reabsorption in α- and β-intercalated cells, respectively. Stimulation of type I K-ATPase by calcitonin in α-intercalated cells is mediated by activation of ERK, by a cAMP-dependent and protein kinase A-independent mechanism, via the guanine-nucleotide exchange factor Epac 1.[150] Stimulation of type I K-ATPase by isoproterenol in β-intercalated cells is also secondary to ERK activation, occurring rather through PKA-dependent activation of the Ras/Raf1 pathway.[151]

Colonic H,K-ATPase

Type III K-ATPase activity sensitive to both Sch 28080 ($IC_{50} \approx 1\ \mu M$) and ouabain ($IC_{50} \approx 20\ \mu M$) is detected in CD of K^+-depleted, but not normal, rats.[152] Type III K-ATPase activity is absent in CD of K^+-depleted αHKc-deficient mice.[21] In the kidney of normal rats, αHKc mRNA is expressed at low levels along the entire distal nephron, from medullary thick ascending limb of Henle's loop to IMCD.[153] αHKc mRNA and protein expression levels are much higher in K^+-depleted rats than in normal rats.[140,153] Immunohistochemistry studies performed on normal rats revealed that labeling of OMCD principal cells at the apical membrane is markedly increased in K^+-depleted rats,[154] but that curiously K^+ depletion does not induce labeling of CCD principal cells, even though CCD from K^+-depleted rats display increased mRNA expression[153] and increased type III K-ATPase activity.[152] In normal rabbits, αHKc was detected at the apical pole of principal cells and intercalated cells in CNT and CD.[155] In transgenic mice expressing EGFP under the control of the αHKc promoter, EGFP is specifically expressed in CD principal cells.[156] Altogether, these studies demonstrate that αHKc is specifically expressed at the apical pole of CD principal cells, and that this expression is markedly increased in response to K^+ depletion. The site-specific localization of αHKc in principal cells is consistent with the functional localization of type III K-ATPase.[149]

Potassium depletion is a condition in which CD reabsorbs, rather than secretes, K^+. Because of its expression at the apical pole of principal cells, colonic H,K-ATPase was proposed to be the motor for K^+ reabsorption in the collecting duct that occurs during K^+-depletion. *In vitro* microperfusion studies provided the first evidence for H,K-ATPase-dependent reabsorption of K^+ and HCO_3^- in OMCD from K^+-deprived rabbits.[140] Sch 28080-sensitive K^+ reabsorption also occurs in distal tubules, accessible by *in vivo* micropuncture, in K^+-depleted rats, but not in normal rats.[157] In addition, part of HCO_3^- reabsorption is inhibited by both ouabain and Sch 28080 in IMCD of K^+-depleted rats.[158] Surprisingly, αHKc-deficient mice do not display any renal phenotype, even when fed a K^+-depleted diet.[159] This indicates that an alternative transport mechanism functionally compensates for colonic H,K-ATPase deficiency.

Expression of colonic H,K-ATPase in the kidney is markedly increased by dietary K^+ restriction.[140] Because chronic dietary K^+ restriction induces metabolic alkalosis, and reduces plasma aldosterone levels, the role of both of these factors in regulating CD H,K-ATPase expression was investigated. In CD of rats clamped either in the absence of circulating aldosterone or under physiological or high levels of circulating aldosterone, K^+ depletion increased H,K-ATPase activity to similar extents, regardless of aldosterone concentration.[160] In addition, neither adrenalectomy nor a Na^+-depleted diet, which increases endogenous aldosterone levels, altered αHKc mRNA expression in the rat kidney medulla.[154] Thus, aldosterone does not control H,K-ATPase expression in the CD.

Similarly, increased expression of αHKc mRNA in the kidney during K^+ depletion most likely is not related to alkalosis, since it is observed in the absence of a significant change in plasma acid–base parameters.[161]

While changes in plasma acid–base status do not alter αHKc transcription, an increase of pCO_2 results in increased H,K-ATPase-mediated potassium and bicarbonate reabsorption in the CCD of K^+-depleted rabbits,[162] demonstrating post-transcriptional regulation of colonic H,K-ATPase during acidosis. Post-transcriptional regulation of colonic H,K-ATPase also occurs in the CCD of K^+-depleted rats in response to vasopressin, which increases type III ATPase activity in a PKA-dependent manner.[149] In the long-term, cAMP also controls the expression of αHKc by binding to cAMP-responsive elements present in the αHKc promoter.[163]

In conclusion, gastric H,K-ATPase is expressed in intercalated cells of the distal nephron where, along with other systems, it participates in proton transport and helps regulate acid–base balance. Colonic H,K-ATPase is also expressed in the distal nephron, but in principal cells where it energizes potassium reabsorption, especially under conditions of dietary K^+ restriction. Neither ATPase appears to be essential for animal survival or even for the continued maintenance of acid–base and potassium balance, at least under experimental conditions studied so far. Compensatory transport systems are able to palliate the genetic absence of gastric and colonic H,K-ATPase in the kidney. Such compensatory mechanisms need to be characterized, and it remains to be determined whether their activity relies on as yet unidentified ATPases.

V-ATPase

The vacuolar H^+-ATPases (V-ATPases) are among the most broadly expressed enzymes that convert the chemical energy of ATP breakdown into electric and chemical gradients. V-ATPases share a lot of structural similarities with mitochondrial F-ATPases, probably because both complexes have subunits that arise from common ancestors.[164–167] However, F-ATPases differ from V-ATPases, in that their expression is restricted to organelles that arise from bacterial endosymbiosis such as mitochondria (or chloroplast in plants), where they serve to generate ATP at the expense of the proton motive force (pmf), whereas V-ATPases use the energy produced by ATP breakdown to pump protons across membranes. The pmf and membrane potential difference ($\Delta\psi$) that result from the primary active transport of H^+ are then used to energize a large number of secondary active transporters. V-ATPases are found in virtually all eukaryotic cell types in endomembranes of intracellular organelles from the secretory pathway. In addition, in higher organisms V-ATPases can be found at the plasma membrane of highly specialized cells, such as the epithelial cells of the kidney, the male reproductive tract, the inner ear, and in osteoclasts. Because of this broad pattern of expression, V-ATPases play a critical role in a large number of different functions.[168] Plasma membrane V-ATPases are important for biological processes that require acidification of the extracellular space, such as bicarbonate reclamation from the urinary fluid, bone resorption, and sperm maturation, while acidification by intracellular V-ATPases of vesicles or endosomes is critical for normal endocytosis, intracellular trafficking, polypeptide processing, neurotransmitter uptake, accumulation and secretion, and for breakdown of macromolecules.

STRUCTURE AND MECHANISM OF ACTION OF V-ATPASES

Like F-ATPases, V-ATPases are integral macromolecular complexes with up to 14 different subunits. The molecular structure and the function of V-ATPases have received considerable attention, and have been the subject of excellent reviews.[168–171] V-ATPases are divided in two principal functional domains, V0, the transmembrane domain (240 kDa) that mediates the transfer of protons across the membrane and V1, the catalytic domain (900 kDa) that binds and hydrolyzes ATP. The V1 domain is always facing the cytoplasm; hence, when located in the plasma membrane, the pump always mediates extrusion of protons out of the cell, and when present in intracelullar membranes, it mediates acidification of the organelles. The V0 domain represents the proton transporting pore, and is formed by a ring of at least 6 subunits. For example, in mammals, several subunit c assembles with single subunit c″, d, and e in a channel-like structure with the a subunit.[172] The V1 domain comprises at least eight different subunits (A–H), and is divided into the "catalytic unit" which binds and hydrolyzes ATP, and the "stalk" which links the hydrolytic unit to the integral V0 domain.

Studies of the prokaryotic V-Na^+-ATPase of *Enterococcus hirae*[173,174] have reached the conclusion that V-ATPase might function following the model of rotational catalysis initially proposed for F-ATPases[175,176]: the central core of the V1 stalk, consisting of subunits D and F, and the proteolipid ring of c-subunits of the V0 domain rotate, driven by the hydrolysis of ATP, while the remaining subunits of the pump are static. One proton enters the machinery through an inner hemi-channel opened at the cytosolic surface of subunit a, and reaches the binding site of one of the c-subunits in the central ring[174]; the proton is then moved by the complete rotation of the ring

towards the opening of a second hemi-channel, also in the a-subunit, but open on the outer space, where it can unbind. Recently, experiments in which movements of the V1 complex of bacteriae were visualized with fluorescent actin filaments have confirmed that rotational catalysis does exist *in vivo*.[177,178] Bafilomycin and concanamycin A, which are specific inhibitors of the pump, both bind to subunit c.[179,180]

Isoforms

Multiple homologs and splice variants of the different V-ATPase subunits have been identified.[181,182] In mammals particularly, multiple variants exist for the B-, C-, E-, and G-subunits of the V1 catalytic domain, and for the a-, d-, and e-subunits of the V0 integral domain. Some of these homologs or variants, such as B2, C1, E1, G1, a1, d1, e1, have a very broad distribution, while other variants have a very restricted expression pattern. Some subunits also exhibit variable expression during development.[183] Hence, the timing and tissue specificity of V-ATPase expression, as well as the functional diversity of the pump, are thought to stem from combinations of V-ATPase subunit variants, and mutations of genes encoding for different variants of the same V-ATPase subunit can result in very different phenotypes. Furthermore, the existence of highly specific combinations of variants in one cell type or for a particular function raises the exciting possibility of developing targeted pharmacological strategies directed at one specific combination. An extended nomenclature assembly of a unique combination of the different genes and splice variants of V-ATPase subunits has been recently proposed.[182] Importantly, this work included a wide scan of published studies and sequence databases in order to provide the scientific community with the most complete catalog of function, tissue-specificity, and subcellular localization known to date for the different molecular forms of V-ATPase subunits.

Renal Isoforms of the V-ATPase

All the different subunits are necessary for the proper assembly, expression, and function of the pump, and the kidney expresses all the ubiquitous variants of V-ATPase subunits. In addition, among the different subunits with more restricted expression (for review see [184]), some variants such as B1,[185,186] C2,[187] G3,[188,189] a4,[190–192] d2,[193] and e2,[194] although not strictly "specific," are especially enriched in the kidney. In particular, the a4-subunit is expressed all along the nephron, while the B1-subunit is markedly enriched in the intercalated cells of the collecting system. The exact reason for the presence of these tissue-specific isoforms is not yet clear. It is possible that these isoforms have specific targeting or assembly motives required in a given cell type to drive the expression of the pump in a particular subcellular domain. For example, the B1-subunit differs from the B2-subunit by the presence of a COOH-terminal "DTAL" motif typical of a PDZ-interacting domain that is required for molecular interactions with the PDZ protein NHERF-1. Moreover, NHERF-1 is specifically expressed at the basolateral pole of β- but not α-intercalated cells, which raises the possibility that molecular interactions between the B1-subunit and NHERF-1 are required for the characteristic basolateral targeting of the V-ATPase in this particular cell type.[195,196] It is also possible that specific variants of the different subunits allow assembly with regulatory elements. For example, the actin cytoskeleton[197,198] or the glycolytic enzyme aldolase B[199,200] have been demonstrated to interact with the B-subunit of the V1 integral domain, and these interactions are believed to be critical for proper pump trafficking, assembly, and regulation.[201,202] An interaction between the a4-subunit and the enzyme phospho-fructokinase 1 has also been shown to be necessary for coupling the catalytic activity of the pump with its transport activity.[203] Nevertheless, the observation that inactivating mutations or disruption of genes encoding for kidney specific subunits, such as the a4- or B1-subunit, lead to a defect in proton secretion by α-Ics and to distal tubular acidosis[204–207] indicates that these tissue-specific subunits are critical for the proper functioning of the pump in the kidney. Indeed, even though under certain circumstances, such as targeted disruption of the B1-subunit in mouse, the B2-subunit can substitute partly for the B1-subunit, it cannot fully compensate for its loss.[208,209]

Multiple Functions of the V-ATPASE in the Kidney

Expression in the Kidney

The role of V-ATPase in urine acidification was first described in turtle bladder epithelium, whose characteristics are close to those of the mammalian collecting duct. In this system, H^+ secretion was shown to be an active, sodium-independent[210] process coupled to oxidative metabolism.[211,212] Final proof of a role for V-ATPase came from a very elegant study showing that reversal of H^+ fluxes induced ATP synthesis.[213] V-ATPase was subsequently purified and characterized in microsomal fractions isolated from these cells.[214] The bovine renal medulla exhibits the same V-ATPases as turtle bladder epithelium.[215] A number of subsequent studies detected the presence of V-ATPases, in both the apical plasma membrane and membranes of organelles, in almost all mammalian renal epithelial cells,

including the brush border membrane of the proximal tubule,[186,216–222] and the apical membranes of the thick ascending limb[186,216,217] and distal convoluted tubule.[186,216,217] In the collecting duct, V-ATPase is present in the apical membrane and cytoplasm of α-intercalated cells and in the basolateral membrane of β-intercalated cells; low expression levels have also been reported in principal cells.[186,216,223]

Bicarbonate Absorption

Along the nephron, the role of plasma membrane V-ATPases is to excrete protons from cells into the outer space. Hence, except for β-intercalated cells in which the pump is expressed basolaterally, the pump secretes protons into the urinary fluid. Urine acidification is the primary mechanism of renal bicarbonate absorption and acid excretion, and is therefore critical for acid–base regulation. To avoid leaking bicarbonate into urine, the kidney has to reclaim virtually all the bicarbonate filtered at the glomerulus (~4300 mmol/day). Bicarbonate absorption is achieved in the proximal tubule, the ascending limb of the loop of Henle, and to lesser extent in the distal convoluted tubule. In general, protons secreted into the urinary fluid can combine with bicarbonate ions also present therein to yield carbonic acid (H_2CO_3), which is quickly dehydrated into CO_2 and H_2O by a luminal carbonic anhydrase. CO_2 diffuses back from the urinary fluid into epithelial cells down its concentration gradient. Within the cell, it is then rehydrated by a cytosolic carbonic anhydrase, and the resulting bicarbonate ion exits the cell at the basolateral side via an electrogenic Na-HCO_3 co-transporter in the proximal tubule or a Cl^-/HCO_3^- exchanger in the TAL. Functional studies have shown that the main mechanism of proton secretion that drives bicarbonate absorption is Na^+/H^+ exchange,[224–226] a secondary active transport process is energized by the inward Na^+ gradient generated by the basolateral Na^+/K^+-ATPase. Molecular studies have demonstrated that this process depends on NHE3[227–229] and a Na^+-dependent amiloride-insensitive transporter[230] in the proximal tubule, and on NHE2 in the distal convoluted tubule.[228,231,232] However, a number of functional studies have also revealed the presence of bafilomycin A1-sensitive, ATP-dependent H^+ secretion that accounts for at least ~20% of proton secretion in the proximal tubule,[224–227,233,234] and that correlates with V-ATPase immunodetection in this nephron segment (see above). Moreover, pump activity appears to be stimulated by acidosis[235] or by angiotensin II[218,236] suggesting that the pump may participate significantly in bicarbonate reclamation by the proximal tubule.

Approximatively 10% of the bicarbonate filtered at the glomerulus is absorbed by the thick ascending limb of Henle's loop. As in the proximal tubule, the primary mechanism of bicarbonate absorption in the TAL is the Na^+/H^+ exchanger NHE3. Active secretion of protons with pharmacological characteristics of V-ATPases has also been detected in the TAL,[237–239] and immunoreactivity to different subunits of the pump has been shown in the apical membrane of TAL cells.[186,216,217] Even though these observations suggest that the pump might play a significant role in bicarbonate transport in the TAL, direct examination of bicarbonate transport in isolated, microperfused TAL demonstrated that all bicarbonate absorption by the TAL is sodium-dependent and sensitive to amiloride, which indicates that Na^+/H^+ exchange accounts for virtually all bicarbonate transport.[240] Thus, the role of the V-ATPase in the TAL remains unclear.

Role of the V-ATPase in Intercalated Cells

The second process that the kidney uses to keep blood bicarbonate constant is the excretion of the daily acid load generated by protein catabolism (~1 mmol/kg/j). This is achieved in the collecting system, which includes the late distal convoluted tubule, the connecting tubule, the cortical collecting duct and the medullary collecting duct. All these segments are characterized by the presence of intercalated cells (ICs), a subpopulation expressing the proton pump and characterized by the presence of the B1-subunit. At least two different sub-types of intercalated cells have been identified: the "canonical" form of type α IC secretes H^+ through the apical vacuolar H^+-ATPase and reabsorbs HCO_3^- via the basolateral $Cl^-/HCO3^-$ exchanger AE1, whereas the "canonical" form of type β IC has the opposite polarity and function.[223,241,242] There is some evidence for at least one other subtype of intercalated cells, called non-α non-β, which express both the proton pump and a $Cl^-/HCO3^-$ exchanger at the apical membrane.[242] The function of this third type remains unclear. For simplicity, the term β-IC is used in this review to refer to both canonical β and non-α non-β ICs.

Type α-intercalated cells secrete acid into a urinary fluid virtually devoid of bicarbonate, because of bicarbonate absorption in the upstream nephron segments. A fraction of protons remain free in urine and decrease urine pH. However, the amount of protons that can be freely eliminated in solution is very limited, because urine volume has to remain small and because at urine pH values below 4.4, the transepithelial gradient of H^+ overcomes the capabilities of the V-ATPase and proton secretion stops. Thus, a majority of protons secreted in the collecting system are instead titrated by urine buffers that can be weak bases (e.g., in humans, mostly creatinine and HPO_4^-) yielding titrable acids or the strong base NH_3 yielding the ammonium ion (NH_4^+). Since the different products resulting from these reactions cannot diffuse

back across the collecting system epithelium, this titration serves to trap and eliminate protons in urine. In addition, because at an acidic urine pH ammonia (NH_3) is transformed into ammonium NH_4^+, the action of V-ATPase is also crucial to maintain a concentration gradient of NH_3 across the collecting duct epithelium, and V-ATPase can be viewed as the energizer of ammonium secretion.[243] Protons secreted by the V-ATPase into urine are generated, together with bicarbonate ions from CO_2 and H_2O within intercalated cells. Proton secretion is functionally coupled to basolateral bicarbonate extrusion through the Cl^-/HCO_3^- exchanger AE1, because in the absence of bicarbonate exit, accumulation of bicarbonate into the cell would limit proton secretion. Thus, the bicarbonate that has been "generated" from proton secretion by intercalated cells replaces the bicarbonate that has been consumed when buffering the metabolically produced protons.

Type β ICs have the opposite polarity of α ICs.[223,241,242] They mediate bicarbonate secretion and generate protons. They are therefore adapted to excrete bases in response to metabolic alkalosis. In intercalated cells, V-ATPase is expressed both at the plasma membrane and in intracellular vesicles that can be recruited rapidly by exocytosis when increased pump activity is required.[244] Moreover, intercalated cells are also able to reverse the polarity of the pump's expression. Induction of metabolic acidosis or alkalosis produces a profound change in the population distribution of these different cell types, with acidosis shifting the distribution towards type α with apical ATPases, and alkalosis increasing the number of canonical β-cells at the expense of α-cells. The observation that this shift from one cell type to the other occurs while the total number of ICs remains constant was interpreted as evidence that ICs can convert from one phenotype to the other.[245] Since this seminal observation, compelling evidence has shown that this interconversion can occur *in vitro* or in isolated tubules, and that it requires secretion by intercalated cells of the matrix protein hensin, and activation of a complex signaling pathway that involves integrin b1.[246–249]

The contribution of β-intercalated cells to renal NaCl balance and blood pressure regulation is an emerging aspect of intercalated cell function.[250] Studies of a mouse model with disruption of the apical Cl^-/HCO_3^- exchanger pendrin demonstrated that β ICs are the main pathway for chloride absorption across the collecting duct epithelium,[251] and disruption of pendrin impairs renal ability to conserve NaCl.[251] Conversely, disruption of Cl^- absorption by β ICs protects against mineralocorticoid-induced hypertension.[252] It has also been recently demonstrated that coupling of the sodium-independent Cl^-/HCO_3^- exchanger pendrin with the sodium-driven Cl^-/HCO_3^- exchanger NDCBE (SLC4A8) mediates thiazide-sensitive NaCl absorption.[120] Importantly, as indicated above, Cl^-/HCO_3^- exchange in intercalated cells is tightly coupled to proton transport mediated by V-ATPases. Whether the V-ATPase energizes chloride transport and thereby participates in renal NaCl handling has not yet been determined. However, it was recently shown that bafilomycin, a specific V-ATPase blocker, inhibits angiotensin II-stimulated Cl^- absorption,[253] which suggests that V-ATPases may energize part of the NaCl absorption in the distal nephron. It is noteworthy that some patients with dRTA exhibit a salt- and potassium-loosing nephropathy. Even though these features can be explained by the frequent association of dRTA with nephrocalcinosis and interstitial nephritis, the exact involvement of V-ATPase dysfunction in these disorders has not yet been directly evaluated.

Role of the V-ATPase in Endocytosis in Renal Epithelial Cells

As indicated above, V-ATPase is not exclusively present in the plasma membrane of renal cells. As in all other eukaryotic cells, V-ATPase is abundantly expressed in the membrane of intracellular organelles. In intracellular membranes, the V1 catalytic domain is located in the cytosol and therefore the pump drives the transport of protons from the cytosol into the organelles. Many cellular processes, such as endo- or exocytosis, catalytic activity into lysosomes, neurotransmitter uptake into synaptic vesicles or release from secretory granules, receptor recycling, and sorting of proteins from the golgi apparatus, are critically dependent upon proper V-ATPase activity.[168,254]

In the kidney, much attention has been paid to the link between V-ATPase-dependent acidification of endosomes and endo-exocytosis. Receptor-dependent or -independent endocytosis of filtered molecules or of apical membrane proteins is an important function achieved by proximal tubule cells. Impairment of this function leads to low molecular weight proteinuria, which is one of the most prominent features of Dent's disease,[255] a rare condition characterized by a Fanconi-like syndrome associated with nephrolithiasis or nephrocalcinosis, caused by mutations in the chloride transporter CLC5.[256–259] Because proton transport by the V-ATPase is electrogenic, intracellular organelle acidification is accompanied by the development of an inside-positive potential difference. In the absence of an electrical shunt, this membrane voltage would represent a self-limiting factor for proton pump activity. In most cells, this shunt is achieved by a chloride conductance activated by voltage. Since CLC5 co-localizes with the V-ATPase in apical

endosomes,[260] it has been proposed that inactivating mutations of CLC5 inhibit endocytosis, because they prevent endosome acidification.[261–263] This paradigm, however, has been challenged by studies showing that CLC5 is not a Cl^- channel, but is rather an electrogenic Cl^-/H^+ antiporter,[264] and more recently that mutations that switch CLC5 function from Cl^-/H^+ exchange to Cl^- conductive transport are able to restore endosomal acidification, but impair endocytosis.[265] The latter study also suggests that endosomal V-ATPases control endocytosis by energizing chloride accumulation into intracellular organelles, rather than by promoting intravesicular acidification. How intravesicular chloride controls endocytosis, however, remains unsettled.

References

[1] Brini M, Carafoli E. Calcium pumps in health and disease. Physiol Rev 2009;89(4):1341–78.

[2] Blanco G, DeTomaso AW, Koster J, Xie ZJ, Mercer RW. The alpha-subunit of the Na,K-ATPase has catalytic activity independent of the beta-subunit. J Biol Chem 1994;269(38):23420–5.

[3] Ward DG, Cavieres JD. Solubilized alpha beta Na,K-ATPase remains protomeric during turnover yet shows apparent negative cooperativity toward ATP. Proc Natl Acad Sci USA 1993;90(11):5332–6.

[4] Martin DW, Sachs JR. Cross-linking of the erythrocyte Na^+,K^+-ATPase. Chemical cross-linkers induce alpha-subunit-band 3 heterodimers and do not induce alpha-subunit homodimers. J Biol Chem 1992;267(33):23922–9.

[5] Morth JP, Pedersen BP, Toustrup-Jensen MS, Sørensen TL, Petersen J, Andersen JP, et al. Crystal structure of the sodium-potassium pump. Nature 2007;450(7172):1043–9.

[6] Shinoda T, Ogawa H, Cornelius F, Toyoshima C. Crystal structure of the sodium-potassium pump at 2.4 Å resolution. Nature 2009;459(7245):446–50.

[7] Blanco G, Mercer RW. Isozymes of the Na-K-ATPase: heterogeneity in structure, diversity in function. Am J Physiol 1998;275(5 Pt 2):F633–50.

[8] DuBose Jr. TD, Gitomer J, Codina J. H^+,K^+-ATPase. Curr Opin Nephrol Hypertens 1999;8(5):597–602.

[9] Geering K. Functional roles of Na,K-ATPase subunits. Curr Opin Nephrol Hypertens 2008;17(5):526–32.

[10] Hasler U, Crambert G, Horisberger JD, Geering K. Structural and functional features of the transmembrane domain of the Na,K-ATPase beta subunit revealed by tryptophan scanning. J Biol Chem 2001;276(19):16356–64.

[11] Geering K. FXYD proteins: new regulators of Na-K-ATPase. Am J Physiol Renal Physiol 2006;290(2):F241–50.

[12] Capurro C, Coutry N, Bonvalet JP, Escoubet B, Garty H, Farman N. Cellular localization and regulation of CHIF in kidney and colon. Am J Physiol 1996;271(3 Pt 1):C753–62.

[13] Shattock MJ. Phospholemman: its role in normal cardiac physiology and potential as a druggable target in disease. Curr Opin Pharmacol 2009;9(2):160–6.

[14] Delprat B, Schaer D, Roy S, Wang J, Puel JL, Geering K. FXYD6 is a novel regulator of Na,K-ATPase expressed in the inner ear. J Biol Chem 2007;282(10):7450–6.

[15] Bibert S, Aebischer D, Desgranges F, Roy S, Schaer D, Kharoubi-Hess S, et al. A link between FXYD3 (Mat-8)-mediated Na,K-ATPase regulation and differentiation of Caco-2 intestinal epithelial cells. Mol Biol Cell 2009;20(4):1132–40.

[16] Barlet-Bas C, Cheval L, Khadouri C, Marsy S, Doucet A. Difference in the Na affinity of Na + -K + -ATPase along the rabbit nephron: modulation by K. Am J Physiol 1990;259(2 Pt 2):F246–50.

[17] Feraille E, Vogt B, Rousselot M, Barlet-Bas C, Cheval L, Doucet A, et al. Mechanism of enhanced Na-K-ATPase activity in cortical collecting duct from rats with nephrotic syndrome. J Clin Invest 1993;91(4):1295–300.

[18] Munzer JS, Daly SE, Jewell-Motz EA, Lingrel JB, Blostein R. Tissue- and isoform-specific kinetic behavior of the Na,K-ATPase. J Biol Chem 1994;269(24):16668–76.

[19] Toyoshima C, Inesi G. Structural basis of ion pumping by Ca^{2+}-ATPase of the sarcoplasmic reticulum. Annu Rev Biochem 2004;73:269–92.

[20] Rabon EC, Reuben MA. The mechanism and structure of the gastric H,K-ATPase. Annu Rev Physiol 1990;52:321–44.

[21] Dherbecourt O, Cheval L, Bloch-Faure M, Meneton P, Doucet A. Molecular identification of Sch28080-sensitive K-ATPase activities in the mouse kidney. Pflugers Arch 2006;451(6):769–75.

[22] Campbell-Thompson ML, Verlander JW, Curran KA, Campbell WG, Cain BD, Wingo CS, et al. *In situ* hybridization of H-K-ATPase beta-subunit mRNA in rat and rabbit kidney. Am J Physiol 1995;269(3 Pt 2):F345–54.

[23] Lingrel JB, Van Huysse J, O'Brien W, Jewell-Motz E, Askew R, Schultheis P. Structure–function studies of the Na,K-ATPase. Kidney Int Suppl 1994;44:S32–9.

[24] Crambert G, Hasler U, Beggah AT, Yu C, Modyanov NN, Horisberger JD, et al. Transport and pharmacological properties of nine different human Na, K-ATPase isozymes. J Biol Chem 2000;275(3):1976–86.

[25] Lingrel JB. The physiological significance of the cardiotonic steroid/ouabain-binding site of the Na,K-ATPase. Annu Rev Physiol 2010;72:395–412.

[26] Barcroft LC, Moseley AE, Lingrel JB, Watson AJ. Deletion of the Na/K-ATPase alpha1-subunit gene (Atp1a1) does not prevent cavitation of the preimplantation mouse embryo. Mech Dev 2004;121(5):417–26.

[27] Moseley AE, Lieske SP, Wetzel RK, James PF, He S, Shelly DA, et al. The Na,K-ATPase alpha 2 isoform is expressed in neurons, and its absence disrupts neuronal activity in newborn mice. J Biol Chem 2003;278(7):5317–24.

[28] Shelly DA, He S, Moseley A, Weber C, Stegemeyer M, Lynch RM, et al. Na^+ pump alpha 2-isoform specifically couples to contractility in vascular smooth muscle: evidence from gene-targeted neonatal mice. Am J Physiol Cell Physiol 2004;286(4):C813–20.

[29] Moseley AE, Huddleson JP, Bohanan CS, James PF, Lorenz JN, Aronow BJ, et al. Genetic profiling reveals global changes in multiple biological pathways in the hearts of Na, K-ATPase alpha 1 isoform haploinsufficient mice. Cell Physiol Biochem 2005;15(1-4):145–58.

[30] De Fusco M, Marconi R, Silvestri L, Atorino L, Rampoldi L, Morgante L, et al. Haploinsufficiency of ATP1A2 encoding the Na^+/K^+ pump alpha2 subunit associated with familial hemiplegic migraine type 2. Nat Genet 2003;33(2):192–6.

[31] Capendeguy O, Horisberger JD. Functional effects of Na^+,K^+-ATPase gene mutations linked to familial hemiplegic migraine. Neuromolecular Med 2004;6(2-3):105–16.

[32] de Carvalho Aguiar P, Sweadner KJ, Penniston JT, Zaremba J, Liu L, Caton M, et al. Mutations in the Na^+/K^+-ATPase alpha3 gene ATP1A3 are associated with rapid-onset dystonia parkinsonism. Neuron 2004;43(2):169–75.

[33] Meij IC, Koenderink JB, van Bokhoven H, Assink KF, Groenestege WT, de Pont JJ, et al. Dominant isolated renal magnesium loss is caused by misrouting of the Na^+,K^+-ATPase gamma-subunit. Nat Genet 2000;26(3):265–6.

[34] Thompson CB, McDonough AA. Skeletal muscle Na,K-ATPase alpha and beta subunit protein levels respond to hypokalemic challenge with isoform and muscle type specificity. J Biol Chem 1996;271(51):32653–8.

[35] Fisone G, Cheng SX, Nairn AC, Czernik AJ, Hemmings Jr. HC, Höög JO, et al. Identification of the phosphorylation site for cAMP-dependent protein kinase on Na^+,K^+-ATPase and effects of site-directed mutagenesis. J Biol Chem 1994;269 (12):9368–73.

[36] Beguin P, Beggah AT, Chibalin AV, Burgener-Kairuz P, Jaisser F, Matthews PM, et al. Phosphorylation of the Na,K-ATPase alpha-subunit by protein kinase A and C *in vitro* and in intact cells. Identification of a novel motif for PKC-mediated phosphorylation. J Biol Chem 1994;269(39):24437–45.

[37] Sweadner KJ, Feschenko MS. Predicted location and limited accessibility of protein kinase A phosphorylation site on Na-K-ATPase. Am J Physiol Cell Physiol 2001;280(4):C1017–26.

[38] Mordasini D, Bustamante M, Rousselot M, Martin PY, Hasler U, Feraille E. Stimulation of Na^+ transport by AVP is independent of PKA phosphorylation of the Na-K-ATPase in collecting duct principal cells. Am J Physiol Renal Physiol 2005;289(5): F1031–9.

[39] Logvinenko NS, Dulubova I, Fedosova N, Larsson SH, Nairn AC, Esmann M, et al. Phosphorylation by protein kinase C of serine-23 of the alpha-1 subunit of rat Na^+,K^+-ATPase affects its conformational equilibrium. Proc Natl Acad Sci U S A 1996;93 (17):9132–7.

[40] Beguin P, Peitsch MC, Geering K. alpha 1 but not alpha 2 or alpha 3 isoforms of Na,K-ATPase are efficiently phosphorylated in a novel protein kinase C motif. Biochemistry 1996;35 (45):14098–108.

[41] Feraille E, Beguin P, Carranza ML, Gonin S, Rousselot M, Martin PY, et al. Is phosphorylation of the alpha1 subunit at Ser-16 involved in the control of Na,K-ATPase activity by phorbol ester-activated protein kinase C? Mol Biol Cell 2000;11(1):39–50.

[42] Chibalin AV, Ogimoto G, Pedemonte CH, Pressley TA, Katz AI, Feraille E, et al. Dopamine-induced endocytosis of Na^+,K^+-ATPase is initiated by phosphorylation of Ser-18 in the rat alpha subunit and is responsible for the decreased activity in epithelial cells. J Biol Chem 1999;274(4):1920–7.

[43] Efendiev R, Bertorello AM, Pressley TA, Rousselot M, Feraille E, et al. Simultaneous phosphorylation of Ser11 and Ser18 in the alpha-subunit promotes the recruitment of Na^+, K^+-ATPase molecules to the plasma membrane. Biochemistry 2000;39(32):9884–92.

[44] Feraille E, Carranza ML, Gonin S, Beguin P, Pedemonte C, Rousselot M, et al. Insulin-induced stimulation of Na^+,K^+-ATPase activity in kidney proximal tubule cells depends on phosphorylation of the alpha-subunit at Tyr-10. Mol Biol Cell 1999;10(9):2847–59.

[45] Chibalin AV, Kovalenko MV, Ryder JW, Feraille E, Wallberg-Henriksson H, Zierath JR. Insulin- and glucose-induced phosphorylation of the Na^+,K^+-adenosine triphosphatase alpha-subunits in rat skeletal muscle. Endocrinology 2001;142(8): 3474–82.

[46] Holthouser KA, Mandal A, Merchant ML, Schelling JR, Delamere NA, Valdes Jr. RR, et al. Ouabain stimulates Na-K-ATPase through a sodium/hydrogen exchanger-1 (NHE-1)-dependent mechanism in human kidney proximal tubule cells. Am J Physiol Renal Physiol 2010;299(1):F77–90.

[47] Otulakowski G, O'Brodovich H. Thyroid hormone and Na^+-K^+-ATPase: more than simple transcription. Am J Physiol Lung Cell Mol Physiol 2007;292(1):L4–5.

[48] Feraille E, Doucet A. Sodium-potassium-adenosinetriphosphatase-dependent sodium transport in the kidney: hormonal control. Physiol Rev 2001;81(1):345–418.

[49] Clausen T. Na^+-K^+ pump regulation and skeletal muscle contractility. Physiol Rev 2003;83(4):1269–324.

[50] Lecuona E, Sun H, Vohwinkel C, Ciechanover A, Sznajder JI. Ubiquitination participates in the lysosomal degradation of Na, K-ATPase in steady-state conditions. Am J Respir Cell Mol Biol 2009;41(6):671–9.

[51] Efendiev R, Bertorello AM, Pedemonte CH. PKC-beta and PKC-zeta mediate opposing effects on proximal tubule Na + , K + -ATPase activity. FEBS Lett 1999;456(1):45–8.

[52] Liu J, Kesiry R, Periyasamy SM, Malhotra D, Xie Z, Shapiro JI. Ouabain induces endocytosis of plasmalemmal Na/K-ATPase in LLC-PK1 cells by a clathrin-dependent mechanism. Kidney Int 2004;66(1):227–41.

[53] Vadasz I, Dada LA, Briva A, Trejo HE, Welch LC, Chen J, et al. AMP-activated protein kinase regulates CO_2-induced alveolar epithelial dysfunction in rats and human cells by promoting Na,K-ATPase endocytosis. J Clin Invest 2008;118 (2):752–62.

[54] Kimura T, Allen PB, Nairn AC, Caplan MJ. Arrestins and spinophilin competitively regulate Na^+,K^+-ATPase trafficking through association with a large cytoplasmic loop of the Na^+, K^+-ATPase. Mol Biol Cell 2007;18(11):4508–18.

[55] Hundal HS, Marette A, Mitsumoto Y, Ramlal T, Blostein R, Klip A. Insulin induces translocation of the alpha 2 and beta 1 subunits of the Na^+/K^+-ATPase from intracellular compartments to the plasma membrane in mammalian skeletal muscle. J Biol Chem 1992;267(8):5040–3.

[56] Barlet-Bas C, Khadouri C, Marsy S, Doucet A. Enhanced intracellular sodium concentration in kidney cells recruits a latent pool of Na-K-ATPase whose size is modulated by corticosteroids. J Biol Chem 1990;265(14):7799–803.

[57] Summa V, Mordasini D, Roger F, Bens M, Martin PY, Vandewalle A, et al. Short term effect of aldosterone on Na,K-ATPase cell surface expression in kidney collecting duct cells. J Biol Chem 2001;276(50):47087–93.

[58] Gonin S, Deschenes G, Roger F, Bens M, Martin PY, Carpentier JL, et al. Cyclic AMP increases cell surface expression of functional Na,K-ATPase units in mammalian cortical collecting duct principal cells. Mol Biol Cell 2001;12(2):255–64.

[59] Bertorello AM, Ridge KM, Chibalin AV, Katz AI, Sznajder JI. Isoproterenol increases Na^+-K^+-ATPase activity by membrane insertion of alpha-subunits in lung alveolar cells. Am J Physiol 1999;276(1 Pt 1):L20–7.

[60] Ridgem K, Dada M, Lecuona L, Bertorello E, Katz AM, Mochly-Rosen AI, et al. J. L. Dopamine-induced exocytosis of Na,K-ATPase is dependent on activation of protein kinase C-epsilon and -delta. Mol Biol Cell 2002;13(4):1381–9.

[61] Lecuona E, Ridge K, Pesce L, Batlle D, Sznajder JI. The GTP-binding protein RhoA mediates Na,K-ATPase exocytosis in alveolar epithelial cells. Mol Biol Cell 2003;14(9):3888–97.

[62] Trejo HE, Lecuona E, Grillo D, Szleifer I, Nekrasova OE, Gelfand VI, et al. Role of kinesin light chain-2 of kinesin-1 in the traffic of Na,K-ATPase-containing vesicles in alveolar epithelial cells. FASEB J 2010;24(2):374–82.

[63] Lecuona E, Minin A, Trejo HE, Chen J, Comellas AP, Sun H, et al. Myosin-Va restrains the trafficking of Na^+/K^+-ATPase-containing vesicles in alveolar epithelial cells. J Cell Sci 2009;122(21):3915–22.

[64] Devarajan P, Scaramuzzino DA, Morrow JS. Ankyrin binds to two distinct cytoplasmic domains of Na,K-ATPase alpha subunit. Proc Natl Acad Sci USA 1994;91(8):2965–9.
[65] Nelson WJ, Hammerton RW. A membrane-cytoskeletal complex containing Na^+,K^+-ATPase, ankyrin, and fodrin in Madin–Darby canine kidney (MDCK) cells: implications for the biogenesis of epithelial cell polarity. J Cell Biol 1989;108(3): 893–902.
[66] Ferrandi M, Salardi S, Tripodi G, Barassi P, Rivera R, Manunta P, et al. Evidence for an interaction between adducin and Na^+-K^+-ATPase: relation to genetic hypertension. Am J Physiol 1999;277(4 Pt 2):H1338–49.
[67] Cantiello HF. Actin filaments stimulate the Na^+-K^+-ATPase. Am J Physiol 1995;269(5 Pt 2):F637–43.
[68] Torielli. L, Tivodar. S, Montella RC, Iacone R, Padoani G, Tarsini P, et al. a-adducin mutations increase Na/K pump activity in renal cells by affecting onstitutive endocytosis: implications for tubular Na reabsorption. Am J Physiol Renal Physiol 2008;295(2):F478–87.
[69] Lee K, Jung J, Kim M, Guidotti G. Interaction of the alpha subunit of Na,K-ATPase with cofilin. Biochem J 2001;353(Pt 2): 377–85.
[70] Peng M, Huang L, Xie Z, Huang WH, Askari A. Partial inhibition of Na^+/K^+-ATPase by ouabain induces the Ca^{2+}-dependent expressions of early-response genes in cardiac myocytes. J Biol Chem 1996;271(17):10372–8.
[71] Haas M, Wang H, Tian J, Xie Z. Src-mediated inter-receptor cross-talk between the Na^+/K^+-ATPase and the epidermal growth factor receptor relays the signal from ouabain to mitogen-activated protein kinases. J Biol Chem 2002;277 (21):18694–702.
[72] Tian J, Cai T, Yuan Z, Wang H, Liu L, Haas M, et al. Binding of Src to Na^+/K^+-ATPase forms a functional signaling complex. Mol Biol Cell 2006;17(1):317–26.
[73] Liang M, Tian J, Liu L, Pierre S, Liu J, Shapiro J, et al. Identification of a pool of non-pumping Na/K-ATPase. J Biol Chem 2007;282(14):10585–93.
[74] Cai T, Wang H, Chen Y, Lui L, Gunning WT, Quintas LE, et al. Regulation of caveolin-1 membrane trafficking by the Na/K-ATPase. J Cell Biol 2008;182(6):1153–69.
[75] Tian J, Li X, Liang M, Liu L, Xie JX, Ye Q, et al. Changes in sodium pump expression dictate the effects of ouabain on cell growth. J Biol Chem 2009;284(22):14921–9.
[76] Yuan Z, Cai T, Tian J, Ivanov AV, Giovannucci DR, Xie Z. Na/K-ATPase tethers phospholipase C and IP3 receptor into a calcium-regulatory complex. Mol Biol Cell 2005;16(9):4034–45.
[77] Miyakawa-Naito A, Uhlen P, Lal M, Aizman O, Mikoshiba K, Brismar H, et al. Cell signaling microdomain with Na,K-ATPase and inositol 1,4,5-trisphosphate receptor generates calcium oscillations. J Biol Chem 2003;278(50):50355–61.
[78] Padilla-Benavides T, Roldan ML, Larre I, Flores-Benitez D, Villegas-Sepulveda N, Contreras RG, et al. The polarized distribution of Na^+,K^+-ATPase: role of the interaction between b subunits. Mol Biol Cell 2010;21(13):2217–25.
[79] Liu X, Spicarova Z, Rydholm S, Li J, Brismar H, Aperia A. Ankyrin B modulates the function of Na,K-ATPase/inositol 1,4,5-trisphosphate receptor signaling microdomain. J Biol Chem 2008;283(17):11461–8.
[80] Espineda CE, Chang JH, Twiss J, Rajasekaran SA, Rajasekaran AK. Repression of Na,K-ATPase beta1-subunit by the transcription factor snail in carcinoma. Mol Biol Cell 2004;15(3):1364–73.
[81] Barwe SP, Anilkumar G, Moon SY, Zheng Y, Whitelegge JP, Rajasekaran SA, et al. Novel role for Na,K-ATPase in phosphatidylinositol 3-kinase signaling and suppression of cell motility. Mol Biol Cell 2005;16(3):1082–94.
[82] Rajasekaran AK, Rajasekaran SA. Role of Na-K-ATPase in the assembly of tight junctions. Am J Physiol Renal Physiol 2003;285(3):F388–96.
[83] Rajasekaran SA, Palmer LG, Moon SY, Peralta Soler A, Apodaca GL, Harper JF, et al. Na,K-ATPase activity is required for formation of tight junctions, desmosomes, and induction of polarity in epithelial cells. Mol Biol Cell 2001;12(12):3717–32.
[84] Mays RW, Siemers KA, Fritz BA, Lowe AW, van Meer G, Nelson WJ. Hierarchy of mechanisms involved in generating Na/K-ATPase polarity in MDCK epithelial cells. J Cell Biol 1995;130(5):1105–15.
[85] Garg LC, Knepper MA, Burg MB. Mineralocorticoid effects on Na-K-ATPase in individual nephron segments. Am J Physiol 1981;240(6):F536–44.
[86] Baum M. Insulin stimulates volume absorption in the rabbit proximal convoluted tubule. J Clin Invest 1987;79(4):1104–9.
[87] Feraille E, Carranza ML, Rousselot M, Favre H. Insulin enhances sodium sensitivity of Na-K-ATPase in isolated rat proximal convoluted tubule. Am J Physiol 1994;267(1 Pt 2): F55–62.
[88] Banday AA, Asghar M, Hussain T, Lokhandwala MF. Dopamine-mediated inhibition of renal Na,K-ATPase is reduced by insulin. Hypertension 2003;41(6):1353–8.
[89] Baum M, Quigley R. Inhibition of proximal convoluted tubule transport by dopamine. Kidney Int 1998;54(5):1593–600.
[90] Aperia A, Bertorello A, Seri I. Dopamine causes inhibition of Na^+-K^+-ATPase activity in rat proximal convoluted tubule segments. Am J Physiol 1987;252(1 Pt 2):F39–45.
[91] Bertorello A, Aperia A. Inhibition of proximal tubule Na^+-K^+-ATPase activity requires simultaneous activation of DA1 and DA2 receptors. Am J Physiol 1990;259(6 Pt 2):F924–8.
[92] Chibalin AV, Katz AI, Berggren PO, Bertorello AM. Receptor-mediated inhibition of renal Na^+-K^+-ATPase is associated with endocytosis of its alpha- and beta-subunits. Am J Physiol 1997;273(5 Pt 1):C1458–65.
[93] Chibalin AV, Pedemonte CH, Katz AI, Feraille E, Berggren PO, Bertorello AM. Phosphorylation of the catalyic alpha-subunit constitutes a triggering signal for Na^+,K^+-ATPase endocytosis. J Biol Chem 1998;273(15):8814–9.
[94] Chibalin AV, Zierath JR, Katz AI, Berggren PO, Bertorello AM. Phosphatidylinositol 3-kinase-mediated endocytosis of renal Na + , K + -ATPase alpha subunit in response to dopamine. Mol Biol Cell 1998;9(5):1209–20.
[95] Efendiev R, Chen Z, Krmar RT, Uhles S, Katz AI, Pedemonte CH, et al. The 14-3-3 protein translates the Na^+, K^+-ATPase a1-subunit phosphorylation signal into binding and activation of phosphoinositide 3-kinase during endocytosis. J Biol Chem 2005;280(16):16272–7.
[96] Yudowski GA, Efendiev R, Pedemonte CH, Katz AI, Berggren PO, Bertorello AM. Phosphoinositide-3 kinase binds to a proline-rich motif in the Na^+, K^+-ATPase alpha subunit and regulates its trafficking. Proc Natl Acad Sci U S A 2000;97 (12):6556–61.
[97] Ogimoto G, Yudowski GA, Barker CJ, Kohler M, Katz AI, Feraille E, et al. G protein-coupled receptors regulate Na^+,K^+-ATPase activity and endocytosis by modulating the recruitment of adaptor protein 2 and clathrin. Proc Natl Acad Sci USA 2000;97(7):3242–7.
[98] Efendiev R, Yudowski GA, Zwiller J, Leibiger B, Katz AI, Berggren PO, et al. Relevance of dopamine signals anchoring dynamin-2 to the plasma membrane during Na^+,K^+-ATPase endocytosis. J Biol Chem 2002;277(46):44108–14.
[99] Bank N, Aynediian HS. A micropuncture study of the effect of parathyroid hormone on renal bicarbonate reabsorption. J Clin Invest 1976;58(2):336–44.

[100] Ribeiro CP, Mandel LJ. Parathyroid hormone inhibits proximal tubule Na^+-K^+-ATPase activity. Am J Physiol 1992;262(2 Pt 2): F209–16.

[101] Derrickson BH, Mandel LJ. Parathyroid hormone inhibits Na^+-K^+-ATPase through Gq/G11 and the calcium-independent phospholipase A2. Am J Physiol 1997;272(6 Pt 2): F781–8.

[102] Khundmiri SJ, Bertorello AM, Delamere NA, Lederer ED. Clathrin-mediated endocytosis of Na^+,K^+-ATPase in response to parathyroid hormone requires ERK-dependent phosphorylation of Ser-11 within the alpha1-subunit. J Biol Chem 2004;279(17):17418–27.

[103] Zhang Y, Norian JM, Magyar CE, Holstein-Rathlou NH, Mircheff AK, McDonough AA. *In vivo* PTH provokes apical NHE3 and NaPi2 redistribution and Na-K-ATPase inhibition. Am J Physiol 1999;276(5 Pt 2):F711–9.

[104] Lederer ED, Khundmiri SJ, Weinman EJ. Role of NHERF-1 in regulation of the activity of Na-K ATPase and sodium-phosphate co-transport in epithelial cells. J Am Soc Nephrol 2003;14 (7):1711–9.

[105] Navar LG, Harrison-Bernard LM, Imig JD, Wang CT, Cervenka L, Mitchell KD. Intrarenal angiotensin II generation and renal effects of AT1 receptor blockade. J Am Soc Nephrol 1999;10(Suppl 12):S266–72.

[106] He P, Klein J, Yun CC. Activation of Na^+/H^+ exchanger NHE3 by angiotensin II is mediated by inositol 1,4,5-triphosphate (IP3) receptor-binding protein released with IP3 (IRBIT) and Ca^{2+}/calmodulin-dependent protein kinase II. J Biol Chem 2010;285(36):27869–78.

[107] Moe OW, Ujiie K, Star RA, Miller RT, Widell J, Alpern RJ, et al. Renin expression in renal proximal tubule. J Clin Invest 1993;91(3):774–9.

[108] Bruneval P, Hinglais N, Alhenc-Gelas F, Tricottet V, Corvol P, Menard J, et al. Angiotensin I converting enzyme in human intestine and kidney. Ultrastructural immunohistochemical localization. Histochemistry 1986;85(1):73–80.

[109] Peterson DR, Oparil S, Flouret G, Carone FA. Handling of angiotensin II and oxytocin by renal tubular segments perfused *in vitro*. Am J Physiol 1977;232(4):F319–24.

[110] Harris PJ, Young JA. Dose-dependent stimulation and inhibition of proximal tubular sodium reabsorption by angiotensin II in the rat kidney. Pflugers Arch 1977;367(3):295–7.

[111] Bharatula M, Hussain T, Lokhandwala MF. Angiotensin II AT1 receptor/signaling mechanisms in the biphasic effect of the peptide on proximal tubular Na^+,K^+-ATPase. Clin Exp Hypertens 1998;20(4):465–80.

[112] Aperia A, Holtback U, Syren ML, Svensson LB, Fryckstedt J, Greengard P. Activation/deactivation of renal Na^+,K^+-ATPase: a final common pathway for regulation of natriuresis. FASEB J 1994;8(6):436–9.

[113] Kiroytcheva M, Cheval L, Carranza ML, Martin PY, Favre H, Doucet A, et al. Effect of cAMP on the activity and the phosphorylation of Na^+,K^+-ATPase in rat thick ascending limb of Henle. Kidney Int 1999;55(5):1819–31.

[114] Stokes JB. Effect of prostaglandin E2 on chloride transport across the rabbit thick ascending limb of Henle. Selective inhibitions of the medullary portion. J Clin Invest 1979;64 (2):495–502.

[115] Plato CF, Stoos BA, Wang D, Garvin JL. Endogenous nitric oxide inhibits chloride transport in the thick ascending limb. Am J Physiol 1999;276(1 Pt 2):F159–63.

[116] Nonoguchi H, Tomita K, Marumo F. Effects of atrial natriuretic peptide and vasopressin on chloride transport in long- and short-looped medullary thick ascending limbs. J Clin Invest 1992;90(2):349–57.

[117] Lerolle N, Bourgeois S, Leviel F, Lebrun G, Paillard M, Houillier P. Angiotensin II inhibits NaCl absorption in the rat medullary thick ascending limb. Am J Physiol Renal Physiol 2004;287(3):F404–10.

[118] Grider JS, Falcone JC, Kilpatrick EL, Ott CE, Jackson BA. P450 arachidonate metabolites mediate bradykinin-dependent inhibition of NaCl transport in the rat thick ascending limb. Can J Physiol Pharmacol 1997;75(2):91–6.

[119] De Jesus Ferreira MC, Bailly C. Extracellular Ca^{2+} decreases chloride reabsorption in rat CTAL by inhibiting cAMP pathway. Am J Physiol 1998;275(2 Pt 2):F198–203.

[120] Leviel F, Hubner CA, Houillier P, Morla L, El Moghrabi S, Brideau G, et al. The Na^+-dependent chloride-bicarbonate exchanger SLC4A8 mediates an electroneutral Na^+ reabsorption process in the renal cortical collecting ducts of mice. J Clin Invest 2010;120(5):1627–35.

[121] Doucet A, Katz AI. Short-term effect of aldosterone on Na-K-ATPase in single nephron segments. Am J Physiol 1981;241(3): F273–8.

[122] El Mernissi G, Doucet A. Short-term effect of aldosterone on renal sodium transport and tubular Na-K-ATPase in the rat. Pflugers Arch 1983;399(2):139–46.

[123] Rayson BM, Lowther SO. Steroid regulation of Na^+-K^+-ATPase: differential sensitivities along the nephron. Am J Physiol 1984;246(5 Pt 2):F656–62.

[124] Hayhurst RA, O'Neil RG. Time-dependent actions of aldosterone and amiloride on Na^+-K^+-ATPase of cortical collecting duct. Am J Physiol 1988;254(5 Pt 2):F689–96.

[125] Zecevic M, Heitzmann D, Camargo SM, Verrey F. SGK1 increases Na,K-ATPase cell-surface expression and function in *Xenopus laevis* oocytes. Pflugers Arch 2004;448(1):29–35.

[126] Verrey F, Kraehenbuhl JP, Rossier BC. Aldosterone induces a rapid increase in the rate of Na,K-ATPase gene transcription in cultured kidney cells. Mol Endocrinol 1989;3 (9):1369–76.

[127] Bankir L, Fernandes S, Bardoux P, Bouby N, Bichet DG. Vasopressin-V2 receptor stimulation reduces sodium excretion in healthy humans. J Am Soc Nephrol 2005;16(7):1920–8.

[128] Satoh T, Cohen HT, Katz AI. Intracellular signaling in the regulation of renal Na-K-ATPase. I. Role of cyclic AMP and phospholipase A2. J Clin Invest 1992;89(5):1496–500.

[129] Deschenes G, Gonin S, Zolty E, Cheval L, Rousselot M, Martin PY, et al. Increased synthesis and avp unresponsiveness of Na, K-ATPase in collecting duct from nephrotic rats. J Am Soc Nephrol 2001;12(11):2241–52.

[130] Vinciguerra M, Deschenes G, Hasler U, Mordasini D, Rousselot M, Doucet A, et al. Intracellular Na^+ controls cell surface expression of Na,K-ATPase via a cAMP-independent PKA pathway in mammalian kidney collecting duct cells. Mol Biol Cell 2003;14(7):2677–88.

[131] Vinciguerra M, Hasler U, Mordasini D, Roussel M, Capovilla M, Ogier-Dennis E, et al. Cytokines and sodium induce protein kinase A-dependent cell-surface Na,K-ATPase recruitment via dissociation of NF-kappaB/IkappaB/protein kinase A catalytic subunit complex in collecting duct principal cells. J Am Soc Nephrol 2005;16(9):2576–85.

[132] Buffin-Meyer B, Younes-Ibrahim M, El Mernissi G, Cheval L, Marsy S, Grima M, et al. Differential regulation of collecting duct Na^+,K^+-ATPase and K^+ excretion by furosemide and piretanide: role of bradykinin. J Am Soc Nephrol 2004;15 (4):876–84.

[133] Ichikawa I, Rennke HG, Hoyer JR, Badr KF, Schor N, Troy JL, et al. Role for intrarenal mechanisms in the impaired salt excretion of experimental nephrotic syndrome. J Clin Invest 1983;71(1):91–103.

[134] Deschenes G, Wittner M, Stefano A, Jounier S, Doucet A. Collecting duct is a site of sodium retention in PAN nephrosis: a rationale for amiloride therapy. J Am Soc Nephrol 2001;12 (3):598–601.

[135] Vogt B, Favre H. Na^+,K^+-ATPase activity and hormones in single nephron segments from nephrotic rats. *Clin Sci* (*Lond*) 1991;80(6):599–604.

[136] Deschenes G, Doucet A. Collecting duct (Na^+/K^+)-ATPase activity is correlated with urinary sodium excretion in rat nephrotic syndromes. J Am Soc Nephrol 2000;11(4):604–15.

[137] Lourdel S, Loffing J, Favre G, Paulais M, Nissant A, Fakitsas P, et al. Hyperaldosteronemia and activation of the epithelial sodium channel are not required for sodium retention in puromycin-induced nephrosis. J Am Soc Nephrol 2005;16 (12):3642–50.

[138] Ackermann D, Mordasini D, Cheval L, Imbert-Teboul M, Vogt B, Doucet A. Sodium retention and ascites formation in a cholestatic mice model: role of aldosterone and mineralocorticoid receptor? Hepatology 2007;46(1):173–9.

[139] Doucet A. H^+,K^+-ATPASE in the kidney: localization and function in the nephron. Exp Nephrol 1997;5(4):271–6.

[140] Gumz ML, Lynch IJ, Greenlee MM, Cain BD, Wingo CS. The renal H^+-K^+-ATPases: physiology, regulation, and structure. Am J Physiol Renal Physiol 2010;298(1):F12–21.

[141] Gifford JD, Rome L, Galla JH. H^+-K^+-ATPase activity in rat collecting duct segments. Am J Physiol 1992;262(4 Pt 2):F692–5.

[142] Silver RB, Frindt G. Functional identification of H-K-ATPase in intercalated cells of cortical collecting tubule. Am J Physiol 1993;264(2 Pt 2):F259–66.

[143] Armitage FE, Wingo CS. Luminal acidification in K-replete OMCDi: contributions of H-K-ATPase and bafilomycin-A1-sensitive H-ATPase. Am J Physiol 1994;267(3 Pt 2):F450–8.

[144] Courtois-Coutry N, Roush D, Rajendran V, McCarthy JB, Geibel J, Kashgarian M, et al. A tyrosine-based signal targets H/K-ATPase to a regulated compartment and is required for the cessation of gastric acid secretion. Cell 1997;90(3):501–10.

[145] Wang T, Courtois-Coutry N, Giebisch G, Caplan MJ. A tyrosine-based signal regulates H-K-ATPase-mediated potassium reabsorption in the kidney. Am J Physiol 1998;275(5 Pt 2): F818–26.

[146] Spicer Z, Miller ML, Andringa A, Riddle TM, Duffy JJ, Doetschman T, et al. Stomachs of mice lacking the gastric H,K-ATPase alpha-subunit have achlorhydria, abnormal parietal cells, and ciliated metaplasia. J Biol Chem 2000;275(28):21555–65.

[147] Petrovic S, Spicer Z, Greeley T, Shull GE, Soleimani M. Novel Schering and ouabain-insensitive potassium-dependent proton secretion in the mouse cortical collecting duct. Am J Physiol Renal Physiol 2002;282(1):F133–43.

[148] Silver RB, Soleimani M. H^+-K^+-ATPases: regulation and role in pathophysiological states. Am J Physiol 1999;276(6 Pt 2): F799–811.

[149] Laroche-Joubert N, Marsy S, Doucet A. Cellular origin and hormonal regulation of K^+-ATPase activities sensitive to Sch-28080 in rat collecting duct. Am J Physiol Renal Physiol 2000;279(6):F1053–9.

[150] Laroche-Joubert N, Marsy S, Michelet S, Imbert-Teboul M, Doucet A. Protein kinase A-independent activation of ERK and H,K-ATPase by cAMP in native kidney cells: role of Epac I. J Biol Chem 2002;277(21):18598–604.

[151] Laroche-Joubert N, Marsy S, Luriau S, Imbert-Teboul M, Doucet A. Mechanism of activation of ERK and H-K-ATPase by isoproterenol in rat cortical collecting duct. Am J Physiol Renal Physiol 2003;284(5):F948–54.

[152] Buffin-Meyer B, Younes-Ibrahim M, Barlet-Bas C, Cheval L, Marsy S, Doucet A. K depletion modifies the properties of Sch-28080-sensitive K-ATPase in rat collecting duct. Am J Physiol 1997;272(1 Pt 2):F124–31.

[153] Marsy S, Elalouf JM, Doucet A. Quantitative RT-PCR analysis of mRNAs encoding a colonic putative H, K-ATPase alpha subunit along the rat nephron: effect of K^+ depletion. Pflugers Arch 1996;432(3):494–500.

[154] Sangan P, Rajendran VM, Mann AS, Kashgarian M, Binder HJ. Regulation of colonic H-K-ATPase in large intestine and kidney by dietary Na depletion and dietary K depletion. Am J Physiol 1997;272(2 Pt 1):C685–96.

[155] Verlander JW, Moudy RM, Campbell WG, Cain BD, Wingo CS. Immunohistochemical localization of H-K-ATPase alpha (2c)-subunit in rabbit kidney. Am J Physiol Renal Physiol 2001;281(2):F357–65.

[156] Zhang W, Xia X, Zou L, Xu X, LeSage GD, Kone BC. *In vivo* expression profile of a H^+-K^+-ATPase alpha2-subunit promoter-reporter transgene. Am J Physiol Renal Physiol 2004;286 (6):F1171–7.

[157] Okusa MD, Unwin RJ, Velazquez H, Giebisch G, Wright FS. Active potassium absorption by the renal distal tubule. Am J Physiol 1992;262(3 Pt 2):F488–93.

[158] Wall SM, Mehta P, DuBose Jr. TD. Dietary K^+ restriction upregulates total and Sch-28080-sensitive bicarbonate absorption in rat tIMCD. Am J Physiol 1998;275(4 Pt 2):F543–9.

[159] Meneton P, Schultheis PJ, Greeb J, Nieman ML, Liu LH, Clarke LL, et al. Increased sensitivity to K^+ deprivation in colonic H,K-ATPase-deficient mice. J Clin Invest 1998;101 (3):536–42.

[160] Eiam-Ong S, Kurtzman NA, Sabatini S. Regulation of collecting tubule adenosine triphosphatases by aldosterone and potassium. J Clin Invest 1993;91(6):2385–92.

[161] DuBose Jr. TD, Codina J, Burges A, Pressley TA. Regulation of H^+-K^+-ATPase expression in kidney. Am J Physiol 1995;269(4 Pt 2):F500–7.

[162] Zhou X, Nakamura S, Xia SL, Wingo CS. Increased $CO(_2)$ stimulates K/Rb reabsorption mediated by H-K-ATPase in CCD of potassium-restricted rabbit. Am J Physiol Renal Physiol 2001;281(2):F366–73.

[163] Xu X, Zhang W, Kone BC. CREB trans-activates the murine H^+-K^+-ATPase a2-subunit gene. Am J Physiol Cell Physiol 2004;287(4):C903–11.

[164] Gogarten JP, Kibak H, Dittrich P, Taiz L, Bowman BJ, Manolson MF, et al. Evolution of the vacuolar H^+-ATPase: implications for the origin of eukaryotes. Proc Natl Acad Sci USA 1989;86(17):6661–5.

[165] Bowman EJ, Tenney K, Bowman BJ. Isolation of genes encoding the *Neurospora* vacuolar ATPase. Analysis of vma-1 encoding the 67-kDa subunit reveals homology to other ATPases. J Biol Chem 1988;263(28):13994–4001.

[166] Bowman BJ, Allen R, Wechser MA, Bowman EJ. Isolation of genes encoding the *Neurospora* vacuolar ATPase. Analysis of vma-2 encoding the 57-kDa polypeptide and comparison to vma-1. J Biol Chem 1988;263(28):14002–7.

[167] Mandel M, Moriyama Y, Hulmes JD, Pan YC, Nelson H, Nelson N. cDNA sequence encoding the 16-kDa proteolipid of chromaffin granules implies gene duplication in the evolution of H^+-ATPases. Proc Natl Acad Sci U S A 1988;85(15):5521–4.

[168] Nishi T, Forgac M. The vacuolar H^+-ATPases: Nature's most versatile proton pumps. Nat Rev Mol Cell Biol 2002;3(2):94–103.

[169] Forgac M. Vacuolar ATPases: rotary proton pumps in physiology and pathophysiology. Nat Rev Mol Cell Biol 2007;8 (11):917–29.

[170] Beyenbach KW, Wieczorek H. The V-type H^+-ATPase: molecular structure and function, physiological roles and regulation. J Exp Biol 2006;209(Pt 4):577–89.

[171] Nelson N, Harvey WR. Vacuolar and plasma membrane proton-adenosinetriphosphatases. Physiol Rev 1999;79(2):361–85.
[172] Wang Y, Cipriano DJ, Forgac M. Arrangement of subunits in the proteolipid ring of the V-ATPase. J Biol Chem 2007;282 (47):34058–65.
[173] Murata T, Yamato I, Kakinuma Y, Leslie AG, Walker JE. Structure of the rotor of the V-Type Na^+-ATPase from *Enterococcus hirae*. Science 2005;308(5722):654–9.
[174] Murata T, Yamato I, Kakinuma Y, Shirouzo M, Walker JE, Yokoyama S, et al. Ion binding and selectivity of the rotor ring of the Na^+-transporting V-ATPase. Proc Natl Acad Sci USA 2008;105(25):8607–12.
[175] Noji H, Yasuda R, Yoshida M, Kinosita Jr. K. Direct observation of the rotation of F1-ATPase. Nature 1997;386 (6622):299–302.
[176] Junge W, Sielaff H, Engelbrecht S. Torque generation and elastic power transmission in the rotary F(O)F(1)-ATPase. Nature 2009;459(7245):364–70.
[177] Yokoyama K, Nakano M, Imamura H, Yoshida M, Tamakoshi M. Rotation of the proteolipid ring in the V-ATPase. J Biol Chem 2003;278(27):24255–8.
[178] Imamura H, Nakano M, Noji H, Muniyuki E, Ohkuma S, Yoshida M, et al. Evidence for rotation of V1-ATPase. Proc Natl Acad Sci USA 2003;100(5):2312–5.
[179] Bowman EJ, Siebers A, Altendorf K. Bafilomycins: a class of inhibitors of membrane ATPases from microorganisms, animal cells, and plant cells. Proc Natl Acad Sci USA 1988;85 (21):7972–6.
[180] Bowman BJ, Bowman EJ. Mutations in subunit C of the vacuolar ATPase confer resistance to bafilomycin and identify a conserved antibiotic binding site. J Biol Chem 2002;277 (6):3965–72.
[181] Smith AN, Lovering RC, Futai M, Takeda J, Brown D, Karet FE. Revised nomenclature for mammalian vacuolar-type H^+-ATPase subunit genes. Mol Cell 2003;12(4):801–3.
[182] Miranda KC, Karet FE, Brown D. An extended nomenclature for mammalian V-ATPase subunit genes and splice variants. PLoS One 2010;5(3):e9531.
[183] Jouret F, Auzanneau C, Debaix H, Wada GH, Pretto C, Marbaix E, et al. Ubiquitous and kidney-specific subunits of vacuolar H^+-ATPase are differentially expressed during nephrogenesis. J Am Soc Nephrol 2005;16(11):3235–46.
[184] Wagner CA, Finberg KE, Breton S, Marshansky V, Brown D, Geibel JP. Renal vacuolar H^+-ATPase. Physiol Rev 2004;84 (4):1263–314.
[185] Finberg KE, Wagner CA, Stehberger PA, Geibel JP, Lifton RP. Molecular cloning and characterization of Atp6v1b1, the murine vacuolar H^+-ATPase B1-subunit. Gene 2003;318:25–34.
[186] Nelson RD, Guo XL, Masood K, Brown D, Kalkbrenner M, Gluck S. Selectively amplified expression of an isoform of the vacuolar H^+-ATPase 56-kilodalton subunit in renal intercalated cells. Proc Natl Acad Sci USA 1992;89(8):3541–5.
[187] Sun-Wada GH, Murata Y, Namba M, Yamamoto A, Wada Y, Futai M. Mouse proton pump ATPase C subunit isoforms (C2-a and C2-b) specifically expressed in kidney and lung. J Biol Chem 2003;278(45):44843–51.
[188] Smith AN, Borthwick KJ, Karet FE. Molecular cloning and characterization of novel tissue-specific isoforms of the human vacuolar H^+-ATPase C, G and d subunits, and their evaluation in autosomal recessive distal renal tubular acidosis. Gene 2002;297(1-2):169–77.
[189] Sun-Wada GH, Yoshimizu T, Imai-Senga Y, Wada Y, Futai M. Diversity of mouse proton-translocating ATPase: presence of multiple isoforms of the C, d and G subunits. Gene 2003;302 (1-2):147–53.
[190] Schulz N, Dave MH, Stehberger PA, Chau T, Wagner CA. Differential localization of vacuolar H^+-ATPases containing a1, a2, a3, or a4 (ATP6V0A1-4) subunit isoforms along the nephron. Cell Physiol Biochem 2007;20(1-4):109–20.
[191] Kawasaki-Nishi S, Yamaguchi A, Forgac M, Nishi T. Tissue specific expression of the splice variants of the mouse vacuolar proton-translocating ATPase a4 subunit. Biochem Biophys Res Commun 2007;364(4):1032–6.
[192] Smith AN, Finberg KE, Wagner CA, Lifton RP, Devonald MA, Su Y, et al. Molecular cloning and characterization of Atp6n1b: a novel fourth murine vacuolar H^+-ATPase a-subunit gene. J Biol Chem 2001;276(45):42382–8.
[193] Smith AN, Jouret F, Bord S, Borthwick KJ, Al-Lamki RS, Wagner CA, et al. Vacuolar H^+-ATPase d2 subunit: molecular characterization, developmental regulation, and localization to specialized proton pumps in kidney and bone. J Am Soc Nephrol 2005;16(5):1245–56.
[194] Blake-Palmer KG, Su Y, Smith AN, Karet FE. Molecular cloning and characterization of a novel form of the human vacuolar H^+-ATPase e-subunit: an essential proton pump component. Gene 2007;393(1-2):94–100.
[195] Pushkin A, Abuladze N, Newman D, Muronets V, Sassani P, Tatischev S, et al. The COOH termini of NBC3 and the 56-kDa H + -ATPase subunit are PDZ motifs involved in their interaction. Am J Physiol Cell Physiol 2003;284(3):C667–73.
[196] Breton S, Wiederhold T, Marshansky V, Nsumu NN, Ramesh V, Broiwn D. The B1 subunit of the H^+ATPase is a PDZ domain-binding protein. Colocalization with NHE-RF in renal B-intercalated cells. J Biol Chem 2000;275(24):18219–24.
[197] Chen SH, Bubb MR, Yarmola EG, Zuo J, Jiang J, Lee BS, et al. Vacuolar H^+-ATPase binding to microfilaments: regulation in response to phosphatidylinositol 3-kinase activity and detailed characterization of the actin-binding site in subunit B. J Biol Chem 2004;279(9):7988–98.
[198] Holliday LS, Lu M, Lee BS, Nelson RD, Solivan S, Zhang L, et al. The amino-terminal domain of the B subunit of vacuolar H^+-ATPase contains a filamentous actin binding site. J Biol Chem 2000;275(41):32331–7.
[199] Lu M, Ammar D, Ives H, Albrecht F, Gluck SL. Physical interaction between aldolase and vacuolar H^+-ATPase is essential for the assembly and activity of the proton pump. J Biol Chem 2007;282(34):24495–503.
[200] Lu M, Holliday LS, Zhang L, Dunn Jr. WA, Gluck SL. Interaction between aldolase and vacuolar H^+-ATPase: evidence for direct coupling of glycolysis to the ATP-hydrolyzing proton pump. J Biol Chem 2001;276(32):30407–13.
[201] Beaulieu V, Da Silva N, Pastor-Soler N, Brown CR, Smith PJ, Brown D, et al. Modulation of the actin cytoskeleton via gelsolin regulates vacuolar H^+-ATPase recycling. J Biol Chem 2005;280(9):8452–63.
[202] Lu M, Sautin YY, Holliday LS, Gluck SL. The glycolytic enzyme aldolase mediates assembly, expression, and activity of vacuolar H^+-ATPase. J Biol Chem 2004;279(10):8732–9.
[203] Su Y, Blake-Palmer KG, Sorrell S, Javid B, Bowers K, Zhou A, et al. Human H^+ATPase a4 subunit mutations causing renal tubular acidosis reveal a role for interaction with phosphofructokinase-1. Am J Physiol Renal Physiol 2008;295(4):F950–8.
[204] Karet FE, Finberg KE, Nelson RD, Nayir A, Mocan H, Sanjad SA, et al. Mutations in the gene encoding B1 subunit of H^+-ATPase cause renal tubular acidosis with sensorineural deafness. Nat Genet 1999;21(1):84–90.
[205] Finberg KE, Wagner CA, Bailey MA, Paunescu TG, Breton S, Brown D, et al. The B1-subunit of the H^+-ATPase is required for maximal urinary acidification. Proc Natl Acad Sci USA 2005;102(38):13616–21.

[206] Stover EH, Borthwick KJ, Bavalia C, Eady N, Fritz DM, Rungroj N, et al. Novel ATP6V1B1 and ATP6V0A4 mutations in autosomal recessive distal renal tubular acidosis with new evidence for hearing loss. J Med Genet 2002;39(11):796–803.

[207] Smith AN, Skaug J, Choate KA, Navir A, Bakkaloglu A, Ozen S, et al. Mutations in ATP6N1B, encoding a new kidney vacuolar proton pump 116-kD subunit, cause recessive distal renal tubular acidosis with preserved hearing. Nat Genet 2000;26 (1):71–5.

[208] Da Silva N, Shum WW, El-Annan J, Paunescu TG, McKee M, Smith PJ, et al. Relocalization of the V-ATPase B2 subunit to the apical membrane of epididymal clear cells of mice deficient in the B1 subunit. Am J Physiol Cell Physiol 2007;293(1): C199–210.

[209] Paunescu TG, Russo LM, Da Silva N, Kovacikova J, Mohebbi N, Van Hoek AN, et al. Compensatory membrane expression of the V-ATPase B2 subunit isoform in renal medullary intercalated cells of B1-deficient mice. Am J Physiol Renal Physiol 2007;293(6):F1915–26.

[210] Al-Awqati Q, Norby LH, Mueller A, Steinmetz PR. Characteristics of stimulation of H^+ transport by aldosterone in turtle urinary bladder. J Clin Invest 1976;58(2):351–8.

[211] Beauwens R, Al-Awqati Q. Active H^+ transport in the turtle urinary bladder. Coupling of transport to glucose oxidation. J Gen Physiol 1976;68(4):421–39.

[212] Al-awqati Q, Mueller A, Steinmetz PR. Transport of H^+ against electrochemical gradients in turtle urinary bladder. Am J Physiol 1977;233(6):F502–8.

[213] Dixon TE, Al-Awqati Q. Urinary acidification in turtle bladder is due to a reversible proton-translocating ATPase. Proc Natl Acad Sci USA 1979;76(7):3135–8.

[214] Gluck S, Kelly S, Al-Awqati Q. The proton translocating ATPase responsible for urinary acidification. J Biol Chem 1982;257(16):9230–3.

[215] Gluck S, Al-Awqati Q. An electrogenic proton-translocating adenosine triphosphatase from bovine kidney medulla. J Clin Invest 1984;73(6):1704–10.

[216] Brown D, Hirsch S, Gluck S. Localization of a proton-pumping ATPase in rat kidney. J Clin Invest 1988;82(6):2114–26.

[217] Paunescu TG, Da Silva N, Marshansky V, McKee M, Breton S, Brown D. Expression of the 56-kDa B2 subunit isoform of the vacuolar H^+-ATPase in proton-secreting cells of the kidney and epididymis. Am J Physiol Cell Physiol 2004;287(1): C149–62.

[218] Wagner CA, Giebisch G, Lang F, Geibel JP. Angiotensin II stimulates vesicular H^+-ATPase in rat proximal tubular cells. Proc Natl Acad Sci U S A 1998;95(16):9665–8.

[219] Sabolic I, Haase W, Burckhardt G. ATP-dependent H^+ pump in membrane vesicles from rat kidney cortex. Am J Physiol 1985;248(6 Pt 2):F835–44.

[220] Sabolic I, Burckhardt G. Characteristics of the proton pump in rat renal cortical endocytotic vesicles. Am J Physiol 1986;250(5 Pt 2):F817–26.

[221] Jehmlich K, Sablotni J, Simon BJ, Burckhardt G. Biochemical aspects of H^+-ATPase in renal proximal tubules: inhibition by N,N′-dicyclohexylcarbodiimide, N-ethylmaleimide, and bafilomycin. Kidney Int Suppl 1991;33:S64–70.

[222] Hilden SA, Johns CA, Madias NE. $Cl^(-)$-dependent ATP-driven H^+ transport in rabbit renal cortical endosomes. Am J Physiol 1988;255(5 Pt 2):F885–97.

[223] Alper SL, Natale J, Gluck S, Lodish HF, Brown D. Subtypes of intercalated cells in rat kidney collecting duct defined by antibodies against erythroid band 3 and renal vacuolar H^+-ATPase. Proc Natl Acad Sci USA 1989;86(14):5429–33.

[224] Fleser A, Marshansky V, Duplain M, Noel J, Hoang A, Teledor A, et al. Cross-talk between the Na^+-K^+-ATPase and the H^+-ATPase in proximal tubules in suspension. Ren Physiol Biochem 1995;18(3):140–52.

[225] Kurtz I. Apical Na^+/H^+ antiporter and glycolysis-dependent H^+-ATPase regulate intracellular pH in the rabbit S3 proximal tubule. J Clin Invest 1987;80(4):928–35.

[226] Preisig PA, Ives HE, Cragoe Jr. EJ, Alpern RJ. Rector FC, Jr. Role of the Na^+/H^+ antiporter in rat proximal tubule bicarbonate absorption. J Clin Invest 1987;80(4):970–8.

[227] Wang T, Yang CL, Abbiati T, Schultheis PJ, Schull GE, Giebisch G, et al. Mechanism of proximal tubule bicarbonate absorption in NHE3 null mice. Am J Physiol 1999;277(2 Pt 2): F298–302.

[228] Wang T, Hropot M, Aronson PS, Giebisch G. Role of NHE isoforms in mediating bicarbonate reabsorption along the nephron. Am J Physiol Renal Physiol 2001;281(6):F1117–22.

[229] Schultheis PJ, Clarke LL, Meneton P, Miller ML, Soleimani M, Gawenis LR, et al. Renal and intestinal absorptive defects in mice lacking the NHE3 Na^+/H^+ exchanger. Nat Genet 1998;19 (3):282–5.

[230] Choi JY, Shah M, Lee MG, Schultheis PJ, Schull GE, Muallem S, et al. Novel amiloride-sensitive sodium-dependent proton secretion in the mouse proximal convoluted tubule. J Clin Invest 2000;105(8):1141–6.

[231] Bailey MA, Giebisch G, Abbiati T, Aronson PS, Gawenis LR, Schull GE, et al. NHE2-mediated bicarbonate reabsorption in the distal tubule of NHE3 null mice. J Physiol 2004;561(Pt 3):765–75.

[232] Chambrey R, Warnock DG, Podevin RA, Bruneval P, Mandet C, Belair MF, et al. Immunolocalization of the Na^+/H^+ exchanger isoform NHE2 in rat kidney. Am J Physiol 1998;275 (3 Pt 2):F379–86.

[233] Zimolo Z, Montrose MH, Murer H. H^+ extrusion by an apical vacuolar-type H^+-ATPase in rat renal proximal tubules. J Membr Biol 1992;126(1):19–26.

[234] Malnic G, Geibel JP. Cell pH and $H(^+)$ secretion by S3 segment of mammalian kidney: role of H^+-ATPase and Cl^-. J Membr Biol 2000;178(2):115–25.

[235] Chambrey R, Paillard M, Podevin RA. Enzymatic and functional evidence for adaptation of the vacuolar H^+-ATPase in proximal tubule apical membranes from rats with chronic metabolic acidosis. J Biol Chem 1994;269(5):3243–50.

[236] Carraro-Lacroix LR, Malnic G. Signaling pathways involved with the stimulatory effect of angiotensin II on vacuolar H^+-ATPase in proximal tubule cells. Pflugers Arch 2006;452 (6):728–36.

[237] Froissart M, Borensztein P, Houillier P, Leviel F, Poggioli J, Marty E, et al. Plasma membrane Na^+-H^+ antiporter and H^+-ATPase in the medullary thick ascending limb of rat kidney. Am J Physiol 1992;262(4 Pt 1):C963–70.

[238] Khadouri C, Marsy S, Barlet-Bas C, Cheval L, Doucet A. Effect of metabolic acidosis and alkalosis on NEM-sensitive ATPase in rat nephron segments. Am J Physiol 1992;262(4 Pt 2): F583–90.

[239] Sabatini S, Laski ME, Kurtzman NA. NEM-sensitive ATPase activity in rat nephron: effect of metabolic acidosis and alkalosis. Am J Physiol 1990;258(2 Pt 2):F297–304.

[240] Good DW, Watts III BA. Functional roles of apical membrane Na^+/H^+ exchange in rat medullary thick ascending limb. Am J Physiol 1996;270(4 Pt 2):F691–9.

[241] Brown D, Hirsch S, Gluck S. An H^+-ATPasein opposite plasma membrane domains in kidney epithelial cell subpopulations. Nature 1988;331(6157):622–4.

[242] Teng-umnuay P, Verlander JW, Yuan W, Tisher CC, Madsen KM. Identification of distinct subpopulations of intercalated cells in the mouse collecting duct. J Am Soc Nephrol 1996;7 (2):260–74.

[243] Star RA, Kurtz I, Mejia R, Burg MB, Knepper MA. Disequilibrium pH and ammonia transport in isolated perfused cortical collecting ducts. Am J Physiol 1987;253(6 Pt 2):F1232–42.

[244] Schwartz GJ, Al-Awqati Q. Carbon dioxide causes exocytosis of vesicles containing H^+ pumps in isolated perfused proximal and collecting tubules. J Clin Invest 1985;75(5):1638–44.

[245] Schwartz GJ, Barasch J, Al-Awqati Q. Plasticity of functional epithelial polarity. Nature 1985;318(6044):368–71.

[246] Takito J, Hikita C, Al-Awqati Q. Hensin, a new collecting duct protein involved in the *in vitro* plasticity of intercalated cell polarity. J Clin Invest 1996;98(10):2324–31.

[247] van Adelsberg J, Edwards JC, Takito J, Kiss B, al-Awqati Q. An induced extracellular matrix protein reverses the polarity of band 3 in intercalated epithelial cells. Cell 1994;76 (6):1053–61.

[248] Schwartz GJ, Tsuruoka S, Vijayakumar S, Petrovic S, Mian A, Al-Awgati Q. Acid incubation reverses the polarity of intercalated cell transporters, an effect mediated by hensin. J Clin Invest 2002;109(1):89–99.

[249] Vijayakumar S, Erdjument-Bromage H, Tempst P, Al-Awqati Q. Role of integrins in the assembly and function of hensin in intercalated cells. J Am Soc Nephrol 2008;19(6):1079–91.

[250] Eladari D, Chambrey R, Frische S, Vallet M, Edwards A. Pendrin as a regulator of ECF and blood pressure. Curr Opin Nephrol Hypertens 2009;18(4):356–62.

[251] Wall SM, Kim YH, Stanley L, Glapion DM, Everett LA, Green ED, et al. NaCl restriction upregulates renal Slc26a4 through subcellular redistribution: role in Cl^- conservation. Hypertension 2004;44(6):982–7.

[252] Verlander JW, Hassell KA, Royaux IE, Glapion DM, Wang ME, Everett LA, et al. Deoxycorticosterone upregulates PDS (Slc26a4) in mouse kidney: role of pendrin in mineralocorticoid-induced hypertension. Hypertension 2003;42(3):356–62.

[253] Pech V, Kim YH, Weinstein AM, Everett LA, Pham TD, Wall SM. Angiotensin II increases chloride absorption in the cortical collecting duct in mice through a pendrin-dependent mechanism. Am J Physiol Renal Physiol 2007;292(3):F914–20.

[254] Marshansky V, Futai M. The V-type H^+-ATPase in vesicular trafficking: targeting, regulation and function. Curr Opin Cell Biol 2008;20(4):415–26.

[255] Wrong OM, Norden AG, Feest TG. Dent's disease: a familial proximal renal tubular syndrome with low-molecular-weight proteinuria, hypercalciuria, nephrocalcinosis, metabolic bone disease, progressive renal failure and a marked male predominance. QJM 1994;87(8):473–93.

[256] Pook MA, Wrong O, Wooding C, Norden AG, Feest TG. and Thakker, R. V. Dent's disease, a renal Fanconi syndrome with nephrocalcinosis and kidney stones, is associated with a microdeletion involving DXS255 and maps to Xp11.22. Hum Mol Genet 1993;2(12):2129–34.

[257] Fisher SE, van Bakel I, Lloyd SE, Pearce SH, Thakker RV, Craig IW. Cloning and characterization of CLCN5, the human kidney chloride channel gene implicated in Dent disease (an X-linked hereditary nephrolithiasis). Genomics 1995;29 (3):598–606.

[258] Lloyd SE, Pearce SH, Gunther W, Kawaguchi H, Igarashi T, Jentsch TJ, et al. Idiopathic low molecular weight proteinuria associated with hypercalciuric nephrocalcinosis in Japanese children is due to mutations of the renal chloride channel (CLCN5). J Clin Invest 1997;99(5):967–74.

[259] Lloyd SE, Pearce SH, Fisher SE, Steinmeyer K, Schwappach B, Scheinman SJ, et al. A common molecular basis for three inherited kidney stone diseases. Nature 1996;379 (6564):445–9.

[260] Gunther W, Luchow A, Cluzeaud F, Vandewalle A, Jentsch TJ. ClC-5, the chloride channel mutated in Dent's disease, colocalizes with the proton pump in endocytotically active kidney cells. Proc Natl Acad Sci USA 1998;95(14):8075–80.

[261] Piwon N, Gunther W, Schwake M, Bosl MR, Jentsch TJ. ClC-5 Cl^--channel disruption impairs endocytosis in a mouse model for Dent's disease. Nature 2000;408(6810):369–73.

[262] Gunther W, Piwon N, Jentsch TJ. The ClC-5 chloride channel knock-out mouse – an animal model for Dent's disease. Pflugers Arch 2003;445(4):456–62.

[263] Hara-Chikuma M, Wang Y, Guggino SE, Guggino WB, Verkman AS. Impaired acidification in early endosomes of ClC-5 deficient proximal tubule. Biochem Biophys Res Commun 2005;329(3):941–6.

[264] Scheel O, Zdebik AA, Lourdel S, Jentsch TJ. Voltage-dependent electrogenic chloride/proton exchange by endosomal CLC proteins. Nature 2005;436(7049):424–7.

[265] Novarino G, Weinert S, Rickheit G, Jentsch TJ. Endosomal chloride-proton exchange rather than chloride conductance is crucial for renal endocytosis. Science 2010;328(5984):1398–401.

This page intentionally left blank

CHAPTER

4

Mechanisms of Water Transport Across Cell Membranes and Epithelia

Guillermo A. Altenberg and Luis Reuss

Department of Cell Physiology and Molecular Biophysics, and Center for Membrane Protein Research, Texas Tech University Health Sciences Center, Lubbock, Texas, TX, USA

INTRODUCTION

The main purpose of this chapter is to review the basic aspects of water transport mechanisms across cell membranes and epithelia. In the first section we will discuss biophysical principles and definitions, with the aim of providing a theoretical framework useful for the analysis of experimental observations. In the second section, we will address general issues pertaining to water transport across cell membranes, focusing on intracellular water, and the pathways and mechanism for osmotic water flow. In the third section, we will discuss water transport by epithelia, focusing on pathways and mechanisms, in particular the role of solute–solvent coupling. We intend this chapter to serve as both an overview and an introduction to chapters covering specific aspects of water transport (Chapters 5, 9, 41, 42, 43). The three sections of the chapter are to a certain extent independent from each other, and can be studied separately.

The field of water transport across biological membranes has made a recent major transition with the discovery and characterization of the aquaporins. Aquaporins are integral membrane proteins, most of which are highly specific water pores expressed in plants and animals from bacteria to humans. The discovery of the aquaporins confirmed a long-held prediction for the existence of these pores, emanating from biophysical studies in red blood cells[110] and renal proximal tubules.[165]

BASIC PRINCIPLES

This section is largely based on the excellent water transport treaty by Finkelstein.[34] Other sources are House,[62] Reuss and Cotton,[123] Dawson,[26] Hallows and Knauf,[50] and Macey and Moura.[91] Derivations of the equations can be found in Finkelstein's book.[34] Deliberately, this section has been kept simple, and qualitative explanations have been superimposed on a succinct quantitative analysis.

The main mechanism of *net water transport* in animal cells is osmosis, that is, net water flow driven by differences in water chemical potential, in turn dependent on differences in solute concentrations. Concerning water flow across a cell membrane, an important issue is whether water moves through the phospholipid bilayer and/or through specialized water-conducting pores. The mechanisms involved in water permeation via these two pathways constitute the main content of this first section. Hence, we start with osmosis.

Osmotic Equilibrium is a Balance of Osmotic and Hydrostatic Forces

The principle of *osmotic equilibrium* can be illustrated by considering a simple system, that is, a semipermeable membrane separating two aqueous phases: pure water and a solution that contains a nondissociating solute (Figure 4.1). The membrane is permeable to

Seldin and Giebisch's The Kidney, Fifth Edition.
DOI: http://dx.doi.org/10.1016/B978-0-12-381462-3.00004-5

© 2013 Elsevier Inc. All rights reserved.

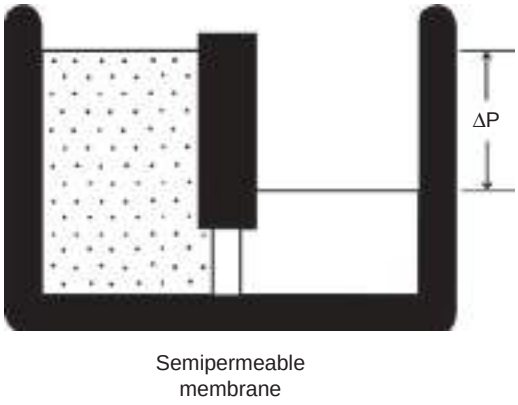

FIGURE 4.1 **Osmotic equilibrium.** A semipermeable membrane (clear section of middle partition) separates two aqueous compartments: a solution containing impermeable solute (left) and pure water (right). If the heights of both compartments are initially equal, then water will flow from right to left until equilibrium is established. At equilibrium, the water flow across the membrane is zero, and is described by Eq. (4.1), that is, ΔP and $\Delta\pi$ cancel each other.

water and impermeable to the solute (hence the term *semipermeable*). At thermodynamic equilibrium, the net water flow across the membrane is zero. (In the case of water, flow can be expressed in molar terms [moles of water per unit area and unit time] or volume terms [volume of water per unit area and unit time]. For conversion to volume flow, the molar flow must be multiplied by $\overline{V}_w$ [partial molar volume, a constant equal to 18 cm^3/mole].) The equilibrium of net flows is the result of the equality of two forces: an osmotic force favoring water flow into the solution; and an opposing hydrostatic force resulting, for instance, from the difference in height of the fluid compartments generated by the osmotic water flow. For dilute solutions, osmotic equilibrium is approximately described by Van't Hoff's law[149]:

$$\Delta P = \pi = RTC_s \tag{4.1}$$

where ΔP (atm) is the hydrostatic pressure difference between the two compartments ($P' - P''$), R (cm^3 atm mol^{-1} K^{-1}) and T [K] are the gas constant and the absolute temperature, respectively, C_s (mol cm^{-3}) is the molar concentration of the solute, and π (atm) is the *osmotic pressure* of the solution. The latter is conveniently defined as the hydrostatic pressure in the solution compartment (relative to the pressure in the water compartment) needed to abolish water flow across the membrane.

When the semipermeable membrane separates two solutions, equilibrium is described by a slightly different equation: $\Delta P = \Delta\pi = RT\Delta C_s$, where $\Delta\pi$ is the difference in osmotic pressure ($\pi' - \pi''$) and ΔC_s is the solute concentration difference ($C_s' - C_s''$).

The osmotic pressure depends on the molar concentration (C_s) and on the degree of dissociation of the solute, that is, the number of particles that each molecule yields in solution (n). Ideally, the osmolality of a solution, in osmol/kg of water, is given by $Osm = nC_s$, where C_s is in mol l^{-1}. However, the effect of solute on the activity of the solvent is generally nonideal, that is, it may depend on the nature of the solute. The correction term for this effect is the osmotic coefficient, φ_s, where the subscript denotes the solute. For physiological concentration ranges, the osmotic coefficient is closer to unity than the activity coefficient, but it can be significantly greater than 1 for macromolecules.[50] For the sake of simplicity, the osmotic coefficient will be neglected in this discussion.

A 1 Osm solution at room temperature exerts an osmotic pressure of about 24.6 atm, which is equivalent to about 18,700 mm Hg. In a mammal, a 1% change in extracellular fluid osmolality (< 3 mosmol/kg) is equivalent, as a driving force for water flow, to a hydrostatic pressure of 56 mm Hg. In animal cells, changes in osmolality cause large water fluxes across the plasma membrane, whereas hydrostatic pressure changes do not. Osmolality is a measure of concentration of particles, not of osmotic pressure, but it is frequently used to denote the latter.

The generation of ΔP in the presence of impermeant solute on one side can be explained[96] on the basis of changes in the water chemical potential (μ_w), which is given by:

$$\mu_w = \mu_w^o + RT \ln X_w + P\overline{V}_w \tag{4.2}$$

where μ_w^o is the standard chemical potential, X_w is the water mole fraction (moles of water/[moles of water + moles of solute]), and $\overline{V}_w$ is the partial molar volume of water. A solute addition to one side (at constant total volume) reduces the water chemical potential in that side (μ_w') because the water is "diluted" by the solute (and X_w falls). The difference in water chemical potential thus generated ($\Delta\mu_w' = \mu_w' - \mu_w''$) is the "driving force" for water flow toward the side of higher osmolality (and lower μ_w). If both compartments are open and of appropriate dimensions, then a ΔP will result from changes in height (Figure 4.1). If a compartment is closed, then its pressure will change in proportion to the water flux, with a proportionality constant dependent on compliance of the compartment.

Osmotic Water Flows Across Lipid and Porous Membranes have Different Properties

Near equilibrium, the volume flow is linearly related to the driving force:

$$J_v = L_p\,(\Delta P - \Delta\pi) \tag{4.3}$$

where J_v is the volume flow (volume area^{-1} time^{-1}), L_p is the *hydraulic permeability coefficient* of the membrane, and ΔP and $\Delta\pi$ are the differences in hydrostatic and osmotic pressure, respectively. The L_p can be expressed in cm sec^{-1} (osmol/kg)$^{-1}$. In most cases, a *filtration* (P_f) or *osmotic permeability coefficient* (P_{os}; $P_f = P_{os}$) is used instead of L_p. The P_{os} (cm sec^{-1}) is related to L_p by $P_{os} = L_p RT/\overline{V}_w$.

The above discussion underscores the fact that ΔP and $\Delta\pi$ are equivalent as "driving forces" in causing osmotic water flow. The mechanism of this equivalence can be understood if one considers the nature of the membrane and the mechanism of osmotic water transport, as explained below.

Osmotic Water Flow Across Lipid Membranes

Osmotic water flow across lipid membranes occurs by *solubility diffusion*. Water molecules move from one aqueous solution into the lipid and then into the other solution by independent, random motion. When $\Delta P = \Delta\pi$ (0 net driving force) there are two diffusive water fluxes of equal magnitude and opposite direction, with no net water flow across the membrane. In the presence of a net driving force ($\Delta P - \Delta\pi \neq 0$), a net flux arises. To examine the mechanism of water flow, let us consider the effects of ΔC_s and ΔP on the water chemical potential in the two compartments.

A net diffusive water flow requires a difference in water chemical potential across the membrane. In a homogeneous membrane, a steady flux denotes a constant chemical potential gradient throughout the membrane thickness. If there is a difference in osmotic pressure between the two solutions, then the water mole fractions (and therefore the water concentrations) at the two sides, *just inside* the membrane must differ. It is commonly assumed that water transport across the membrane–solution interface is faster than water diffusion in the membrane itself. It follows that the water chemical potential just inside the membrane is very close to that in the adjacent layer of solution; therefore, water is near equilibrium across the interfaces. Finally, since μ_w is inversely related to C_s, a gradient of water concentration must exist across the membrane. This intramembrane gradient is the direct consequence of the differences in impermeant solute concentrations in the adjacent aqueous phases.

When $\Delta\pi = 0$, but $\Delta P \neq 0$, the chemical potentials of water in the two solutions differ (see Eq. (4.2)). If $P' > P''$, then the water flux from side $'$ is greater than that from side $''$, creating an intramembrane gradient of water concentration and chemical potential.

The osmotic water permeability coefficient of a lipid membrane is given by:

$$P_{os} = \frac{D_w^m \beta_w \overline{V}_w}{\delta_m \overline{V}_{oil}} \tag{4.4}$$

where D_w^m is the diffusion coefficient of water in the membrane, β_w is the partition coefficient of water in the membrane (oil/water), δ_w is the thickness of the membrane, and $\overline{V}_{oil}$ is the partial molar volume of the membrane lipid.

Osmotic Water Flow Across a Porous Membrane

Let us consider a membrane made of a rigid, water-impermeable material. The pore density (number of pores per unit area) is n. Each pore is a water-filled cylinder of length L and radius r, and cannot be penetrated by the solute. The mechanism of water flow in this situation depends mostly on the pore radius. In large pores there is viscous water flow that can be described by Newtonian mechanics. In pores of molecular dimensions there is no appropriate theoretical treatment, but if the pores are so small that there is single file water transport (i.e., water molecules in the pore cannot slip past each other), then there is a surprisingly simple solution.

LARGE PORES

In large pores water flow driven by a hydrostatic pressure is described by Poiseuille's law, which was derived for water flow in thin capillaries:

$$J_v = n\frac{(\Pi) r^4}{8L\eta}\Delta P \tag{4.5}$$

where η is the water viscosity and π denotes 3.1415 ... (do not confuse with π, the osmotic pressure). This law is valid for steady-state flow and neglects pore access effects. Under these conditions, the pressure gradient along the pore (dP/dL) has a constant value (Figure 4.2a). From Eq. (4.4) and the definition of P_{os}, the P_{os} for a membrane containing large homogeneous cylindrical pores is $n(\pi)r^4 RT/8L\eta\, V_w$.

If the only driving force is osmotic, then the mechanism of water flow involves the development of a hydrostatic pressure gradient within the pore. Initially, the water concentrations in the pore and in the water-filled compartment are the same, but at the other interface the solution has lower water concentration than the pore. If water transport across the membrane interfaces is faster than within the membrane, then the water chemical potentials just inside the pore are equal to those in the adjacent solutions. At the pore end facing the water compartment there is no difference in hydrostatic pressure, but at the end facing the solution

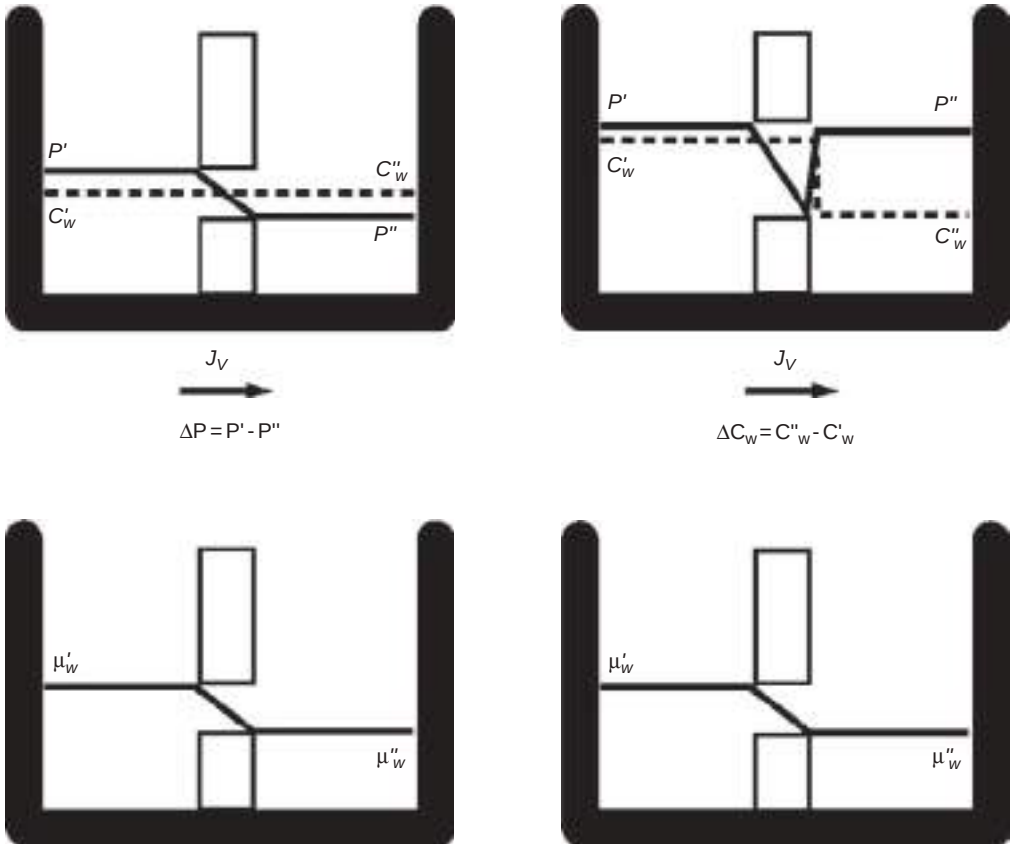

FIGURE 4.2 **Water flow across a porous membrane.** Top left: Driving force is a hydrostatic-pressure difference ($P' - P''$), continuous line. Same water concentrations on both sides ($C'_w - C''_w$), segmented line. Top right: Driving force is a difference in osmotic pressure. Same hydrostatic pressure on both sides, but the water concentrations differ. Bottom: The steady-state water chemical potential gradients (μ_w, proportional to the sum of hydrostatic and osmotic pressure) are the same for both conditions. *(Modified with permission from Reuss, L. (2000). General principles of water transport*. In *"The Kidney: Physiology and Pathophysiology," 321–340, Seldin, D. W. and Giebisch, G. (eds.). Raven Press, New York.)*

compartment the pressure inside the pore falls, because the lower water concentration in the solution elicits a water efflux from the pore. If $\Delta\mu_w$ is zero across the opening, then the difference in water concentration between solution and pore is exactly balanced by a drop in the pore pressure.[96] In the steady-state, the pressure gradient in the pore is constant (Figure 4.2, top right).

The analysis presented above holds for pores of r equal to or greater than 15 nm.[12] For pores smaller than 15 nm, several corrections have been attempted, but the underlying assumptions are questionable.[34] Regardless of the lack of a satisfactory theory, it has been suggested that Poiseuille's law is a reasonable approximation for water diffusion and convection in small pores.[86]

SINGLE-FILE PORE

The P_{os} of a single-file pore is given by[34,35]:

$$P_{os} = n\frac{\overline{v}_w kTN}{\gamma L^2} \tag{4.6}$$

where $\overline{v}_w$ is the volume of a water molecule, k is the Boltzmann constant (gas constant/molecule, equal to R/N_A where N_A is Avogadro's number), N is the number of water molecules inside the pore, and γ is the friction coefficient per water molecule. Assuming that the water densities in the pore and in the bulk solution are equal, and recalling that $kT/\gamma = D_w$:

$$P_{os} = n\frac{(\Pi)r^2 D_w}{L} \tag{4.7}$$

which is the result expected for osmotic water flow through a single-file pore if it can be described as a diffusive flux.

Comparison of Diffusion and Osmotic Permeability Coefficients Reveals Whether Water Permeates Lipid Bilayer or Pores

Now we consider a membrane exposed to solutions of identical composition, except that water is partially replaced with tracer water at a concentration C_w (Figure 4.3). There are no other differences in composition or pressure between the two compartments.

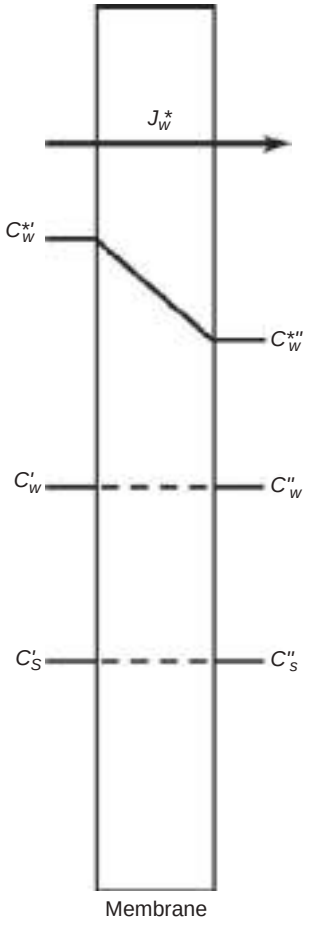

FIGURE 4.3 **Tracer water diffusion across a lipid membrane separating solutions of identical compositions ($C_w' - C_w''$, $= C_s' - C_s''$, $= 0$, as shown by the two lines at the bottom).** At the steady-state (constant flux, J_w^*), the tracer concentration gradient in the membrane (second line from top) is also constant. Arbitrarily, the oil/water partition coefficient (β) of tracer water is 1.0. If β were smaller, the tracer water concentrations inside the membrane would be less than in the respective solutions. *(Modified with permission from Reuss, L. (2000). General principles of water transport.* In *"The Kidney: Physiology and Pathophysiology," 321–340, Seldin, D. W. and Giebisch, G. (eds.). Raven Press, New York.)*

Both contain solutions of infinite volume and ideally mixed (C_w at the membrane surface $= C_w$ in the bulk solution). The tracer water flux is given by:

$$J_w^* = P_{dw}\Delta C_w^* \tag{4.8}$$

where P_{dw} is the diffusive water permeability coefficient and ΔC_w^* is the difference in concentration of tracer water ($C_w^{*\prime} - C_w^{*\prime\prime}$). In the case of a lipid membrane, the tracer–water flux is by solubility diffusion; hence:

$$P_{dw} = \frac{D_w^m \beta_w \overline{V}_w}{\partial_m \overline{V}_{oil}} \tag{4.9}$$

This expression is identical to that for P_f (or P_{os}) for a lipid membrane (Eq. (4.7)). Therefore, for a lipid membrane, $P_{os} = P_{dw}$.

The case of a porous membrane is discussed below.

Porous Membrane

If the pores obey Poiseuille's law, the diffusive water flux *via* the pores is:

$$J_w^* = \frac{n(\Pi)r^2 D_w}{L}\Delta C_w^* \tag{4.10}$$

where the pore cross-sectional area $[n(\Pi)r^2]$ is available for water diffusion and is the water self-diffusion coefficient (tracer water traverses the membrane via the aqueous pores). P_{dw} is $n(\Pi)r^2 D_w/L$. Hence, the ratio between and for a porous membrane is:

$$P_{os}/P_{dw} = \frac{RT}{8\eta D_w \overline{V}_w} r^2 + 1 \tag{4.11}$$

where the second term on the right ($=1$) denotes the diffusive water flow via the pores. The equivalent pore radius can be estimated from experimental values using Eq. (4.11); at 25°C, the value of $[RT/(8\eta D_w \overline{V}_w)]$ is 8.04×10^{-14} cm^{-2}.

For single file pores, the diffusive water flux is $J_w = nP_{dw}\Delta n^*$, where Δn^* is the tracer-water concentration difference (molecules per unit volume). P_{dw} is given by:

$$P_{dw} = \frac{n\overline{v}_w kT}{dL^2} \tag{4.12}$$

and the ratio P_{os}/P_{dw}, from Eqs. (4.6) and (4.12), equals the number of water molecules in the pore: $P_{os}/P_{dw} = N$.

Water movement in single file pores is not independent of the movement of neighboring water molecules: for a tracer molecule to cross the pore, other water molecules must also cross.

Unstirred Layers are a Major Source of Artifacts in Water Permeability Measurements

Unstirred layers are static layers of fluid at membrane–solution interfaces, that is, they are not mixed by convection. Unstirred-layer solute concentrations are entirely determined by diffusion, can differ from that of the bulk solutions, and are position dependent. Unstirred layers introduce errors in the experimental determination of P_{dw} and P_{os}. These errors can lead to incorrect conclusions about the existence of aqueous pores. For an excellent treatment of unstirred layers, see Barry and Diamond.[11]

Unstirred-Layer Effects on Measurement of P_{dw}

In the system illustrated in Figure 4.4, tracer water encounters three barriers to diffusion between the two

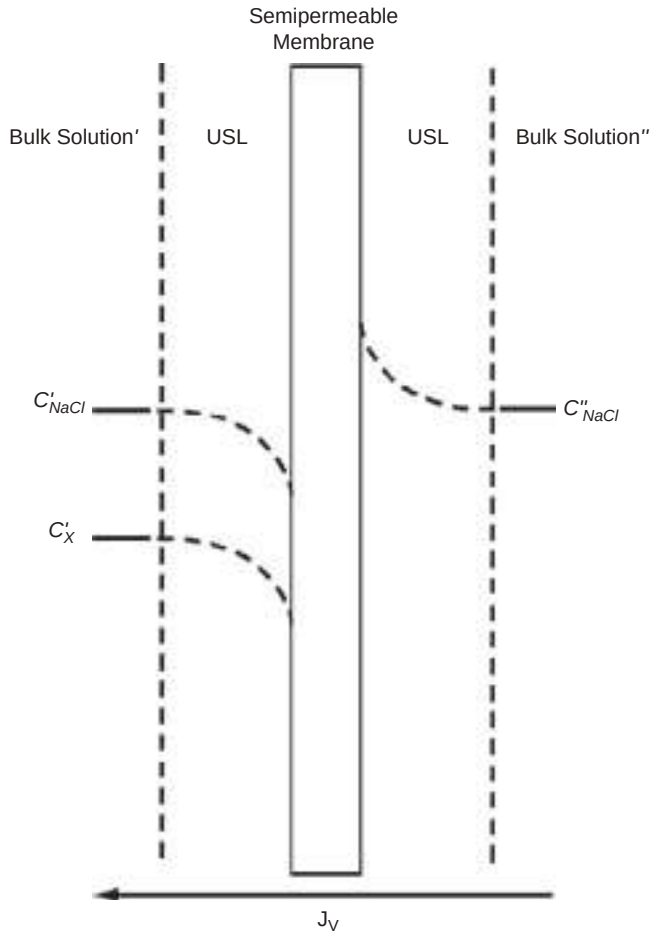

FIGURE 4.4 Unstirred-layer effects on the measurement of P_{os}, C_{NaCl} and C_x, concentrations of NaCl and the osmotic solute, respectively. Both are assumed impermeant for simplicity. The osmotic water flow ($J_w = J_v$) "dilutes" both solutes on the hyperosmotic side (solution′) and "concentrates" the NaCl on the hyposmotic side (solution″). The net result is a reduction in the concentration gradient of the osmotic solute (reduced ΔC_x), and the creation of an opposing ΔC_{NaCl} at the membrane boundaries. Hence, the driving force for J_v is diminished. *(Modified with permission from Reuss, L. (2000). General principles of water transport.* In *"The Kidney: Physiology and Pathophysiology," 321–340, Seldin, D. W. and Giebisch, G. (eds.). Raven Press, New York.)*

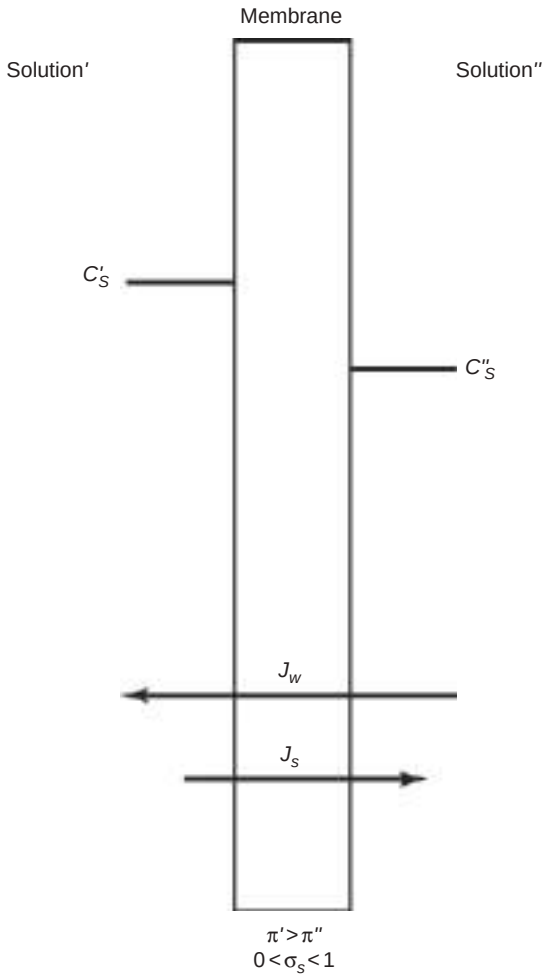

FIGURE 4.5 Volume flow (J_v) between solutions containing different concentrations of a permeant solute ($0 < \sigma_s < 1$). C_s is the solute concentration. J_v is the difference between the net water flow (J_w) to the left, and the net solute flow (J_s) to the right (i.e., $J_v = J_w - J_s$). *(Modified with permission from Reuss, L. (2000). General principles of water transport.* In *"The Kidney: Physiology and Pathophysiology," 321–340, Seldin, D. W. and Giebisch, G. (eds.). Raven Press, New York.)*

solutions, namely the membrane and the two unstirred layers (of width Δ_1 and Δ_2, respectively). These three barriers are in series. The *observed* (experimentally determined) diffusive water permeability of the system differs from the true diffusive water permeability of the membrane (P_{dw}) according to:

$$\frac{1}{P^o_{dw}} = \frac{1}{P_{dw}} + \frac{1}{D_w/\delta_1} + \frac{1}{D_w/\delta_2} \qquad (4.13)$$

where P^o_{dw} is the observed value. Inasmuch as D_w has a finite value, P_{dw} and P^o_{dw} are equal only when $\delta_1 = \delta_2 = 0$. For typical permeability and unstirred-layer thickness values, P_{dw} can be easily underestimated by 50% or more.

Unstirred-Layer Effects on the Measurement of P_{os}

In the experiment depicted in Figure 4.5, a semipermeable membrane separates equal NaCl solutions; then, a second solute is added to one side ($C'_s > C''_s$, eliciting osmotic water flow. The NaCl concentration in the unstirred layers changes because of the water flow, rising in the right side and falling in the left side, relative to the bulk solution concentrations. The added solute qualitatively behaves like the NaCl present on the same side. Water flow tends to accentuate the changes described, whereas solute diffusion in the solution has the opposite effect. At the steady-state, the effects of osmotic water flow and solute diffusion balance each other and the unstirred-layer

concentration profiles remain constant. At the surface of the membrane:

$$C_m = C_b \exp(\pm v\delta/D_s) \quad (4.14)$$

where the sign of the exponent is (−) for the left ("diluted") side and (+) for the right ("concentrated") side, and denote solute concentrations (membrane surface and bulk solution, respectively), v is the water flow velocity (normal to the membrane), and D_s is the solute diffusion coefficient in water.

The ratio between P^o_{os} (observed value) and P_{os} (true value) is $-v\Delta/D_s$, that is, the magnitude of the error in estimating P_{os} is directly proportional to v and inversely proportional to D_s. In planar membranes, for small v (low water flux and flow velocity) the exponential term approaches 1. In folded membranes, where there can be water "funneling" (microvilli, lateral intercellular spaces), v can be much larger than in a planar membrane and can be seriously underestimated.[11]

The above analysis is limited to the effect of J_v on impermeant solute concentration. If permeant solutes are present as well, they must be considered, making the analysis more complex.[11]

Solute Reflection Coefficients Denote Effective Osmolality of a Solution vis-à-vis a Membrane

The situation is more complicated than the preceding analysis if the solute is permeant (Figure 4.6). In this case, J_v will be described by:

$$J_v = L_p(\Delta P - \sigma_s \Delta\pi) \quad (4.15)$$

where σ_s is the reflection coefficient of the solute. If $\sigma_s < 1$, then J_v will be less than if the same osmotic gradient is elicited with an impermeable solute. The value of σ_s is specific for each combination of membrane and solute, and depends on both permeabilities and partial molar volumes of water and solute (see below). In general, the value of σ_s varies between 0 (solute as permeable as water) and 1 (solute impermeable).

Lipid Membrane

It can be shown that the solute reflection coefficient of a lipid membrane is[34]:

$$\sigma_s = 1 - \frac{P_{ds}\overline{V}_s}{P_{dw}\overline{V}_w} \quad (4.16)$$

As expected, $\sigma_s = 1$ when $P_{ds} = 0$, $\sigma_s = 0$ when $P_{ds}\overline{V}_s = P_{dw}\overline{V}_w$, and $\sigma_s < 0$ when $P_{ds}\overline{V}_s > P_{dw}\overline{V}_w$. In other words, σ_s depends on the solute permeability and partial molar volume compared with those of water. If the products are the same for solute and water, then the reflection coefficient is zero: solute addition to one side causes no transmembrane volume flow because the water flux toward the solute is of the same magnitude as the solute flux in the opposite direction. A solute with a negative σ_s will elicit a net volume flow in the opposite direction to the water flow ("negative osmosis").[34]

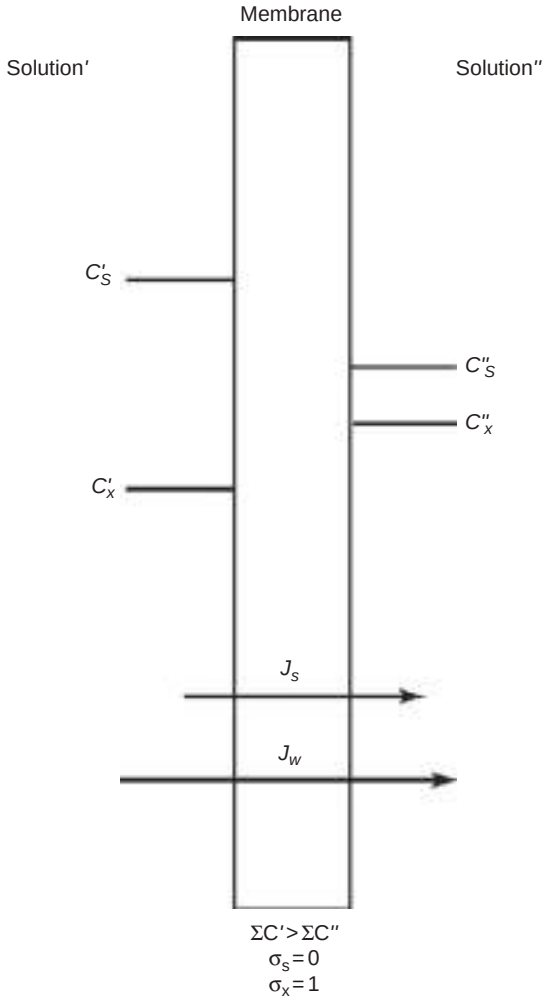

FIGURE 4.6 **Volume flow (J_v) between isosmotic solutions ($\sum C' = \sum C''$).** Solutes s and x gradients are of the same magnitude and opposite direction. Since the reflection coefficients differ, the effective osmolalities also differ, and there is a net J_v toward the side containing impermeant solute (i.e., $J_v = J_w + J_s$). *(Modified with permission from Reuss, L. (2000). General principles of water transport.* In *"The Kidney: Physiology and Pathophysiology," 321–340, Seldin, D. W. and Giebisch, G. (eds.). Raven Press, New York.)*

Porous Membrane

For a quantitative analysis of this complicated problem, see Anderson and Malone[3] and Finkelstein.[34] For large pores and solute particles larger than water particles, the solute is excluded from the periphery of the pore, that is, from a region slightly wider than the solute radius. In the pore axis, C_s is maximum (equal to

the concentration in the bulk solution) and C_w is less than at the pore periphery (where the solute is excluded). This generates a radial water concentration gradient within the pore. At equilibrium, this gradient is balanced by a fall in hydrostatic pressure in the periphery of the pore. In addition, there is a solute concentration gradient along the pore length, because of the transmembrane difference in C_s. These two gradients combine to generate a longitudinal hydrostatic pressure gradient along the pore's periphery, which causes water flow toward the high concentration side. The thickness of the ring subjected to this regime is directly proportional to the molecular size of the solute. When the solute is so large that it cannot enter the pore, J_v is maximum and $\sigma_s = 1$. When the solute has the same size as water, its distribution within the pore is identical to that of water, no pressure gradient develops, the water and solute net fluxes are purely diffusive and of equal magnitude and opposite direction, and $J_v = 0$. When the solute is smaller than water, J_v is greater than J_w, and J_v is in the same direction as J_s. Water is largely excluded from the periphery of the pore, and the pore hydrostatic pressure gradient is opposite to that generated by the impermeant solute.

We consider now the case of single file pores; the solution is dilute enough so that the number of solute molecules inside a pore can be only 0 or 1. Two pore populations will exist at any given time: pores containing water only, through which there is water flow toward the high-C_s side, and pores containing solute, in which solute and water are transported toward the low-C_s side by single file diffusion. When both water and solute permeation are single file, σ_s is[34,87]:

$$\sigma_s = 1 - \frac{P_{ds}\overline{V}_p^s}{P_{dw}\overline{V}_p} \tag{4.17}$$

where $\overline{V}_p$ denotes pore molar volume, solute-containing (superscript s) and solute-free (no superscript). Compare with Eq. (4.16).

In a system with more than one solute there can be net water and/or volume flows between solutions with the same total solute concentrations (and osmolalities). This will occur if the specific C_s values on the two sides of the membrane and the reflection coefficients differ. As shown in Figure 4.6, if , $\Delta C_s = -\Delta C_x$, $\sigma_s = 0$, and $\sigma_x = 1$, then there will be a net volume flow towards the right, although the solutions have equal total osmolalities. If the hydrostatic pressures are the same on both sides, then $J_v = L_p RT\ (\sigma_x \Delta C_x - \sigma_s \Delta C_s)$. Expressions such as σRTC denote "effective osmolality," in contrast with the "total osmolality" given by RTC. Effective osmolality is also referred to as *tonicity*. In epithelia, active transepithelial solute transport can generate asymmetries in the composition of the adjacent solutions. These asymmetries may in principle drive net water transport without differences in the total osmolalities of the bulk solutions, because of differences in the solute reflection coefficients.

Solvent Drag Can Account for Uphill Solute Transport

When there is net water flow (filtration and/or osmosis) across a porous membrane and a pore-permeant solute is present, there is a solute flux in the same direction as the water flow. This flux reflects water–solute frictional interaction within the pores. In the case of large pores, if $C'_s = C''_s$, and J_v is elicited by a hydrostatic pressure gradient or an asymmetrical addition of impermeant solute, the solute flux due to solvent drag is given by:

$$J_s = J_v C_s\ (1 - \sigma_s) \tag{4.18}$$

Uphill solute transport (i.e., transport in the absence of or against the prevailing electrochemical gradient) can be demonstrated, which is always in the same direction as the water flow. The energy is provided by the water flow, and conveyed to the solute by frictional interaction.

Demonstration of solvent drag is, in principle, a clear-cut argument for the existence of solute permeable water pores in membranes. However, many such demonstrations have been proven to be experimental artifacts. If there are unstirred layers, J_v will produce changes in solute concentrations at the membrane–solution interfaces; if the membrane is permeable to the solute, then a diffusive solute flux will occur (see Eq. (4.14)). This phenomenon is called "pseudo-solvent drag".[11] Putative demonstrations of pore-mediated water transport based on the observation of "solvent drag" must consider this possibility.

WATER TRANSPORT ACROSS THE CELL MEMBRANE

In this section we will first address some general issues pertinent to intracellular water, and then discuss in some detail the pathways and mechanisms for water transport across the cell membrane. Cell volume regulation is the subject of Chapter 5, and will not be addressed here.

Intracellular Water Behaves Similar to Water in Free Solution

The best direct assessment of the state of intracellular water was obtained from nuclear magnetic resonance (NMR) studies, which indicate that only a small fraction of cell water (< 5%) behaves as if it were

immobilized.[137] However, indirect arguments suggest that this may be an underestimate.[50] A related issue is whether the cytosol is a near-ideal aqueous solution or a gel, as suggested by numerous observations.[85] If this is the case, its higher viscosity may have a strong effect on enzyme catalysis rates.[100] In any event, the behavior of water fluxes in cells supports the idea that most of the intracellular water behaves as water in dilute solutions.

The Osmotic Behavior of Cells is not Ideal

Consider a cell at steady-state (constant volume) in suspension; then, the external concentration of an impermeant solute (and hence the external osmolality) are suddenly changed. If the cell is permeable to water, then water will flow until its osmolality becomes equal to the new medium osmolality. Numerically, $V_0 \cdot \pi_0 = V_t \cdot \pi_t$, where V is cell water volume and π is total solute concentration (or osmolality), and the subscripts 0 and t denote steady-state values before and after the solution change. The above equation assumes that there is no change in the amount of cell solute between 0 and t, and defines the ideal ("osmometric") behavior of cells. However, not all cells behave ideally. Non-ideal behavior can result from loss or gain of solute between times 0 and t (e.g., some cell solutes are permeable) or from changes in the osmotic coefficient of intracellular solute(s) secondary to the water flux. This appears to be the case in red blood cells, because of concentration dependence of the osmotic coefficient of hemoglobin. This and other issues relevant to non-ideal osmotic behavior of cells have been discussed by Hallows and Knauf.[50]

Another important point in quantifying cell volume changes in response to alterations in extracellular osmolality is the fact that although most of the cell volume is solvent water ("osmotically sensitive"), a fraction is nonsolvent volume (also referred to as "solids"). If one considers this factor, then the above equation becomes:

$$(V_0 - b)\pi'_0 = (V_t - b)\pi'_t \qquad (4.19)$$

where b is the nonsolvent volume. This is a modified form of the Boyle–Van't Hoff equation, and is very useful to interpret changes in cell volume. The plot of Eq. (4.19) is shown in Figure 4.7.

In experimental osmotic studies, the behavior of cells or membrane vesicles may not be linear, for the reasons given above. For instance, if the amount of cell solute changes during the experiment, then the slope will not be a constant.

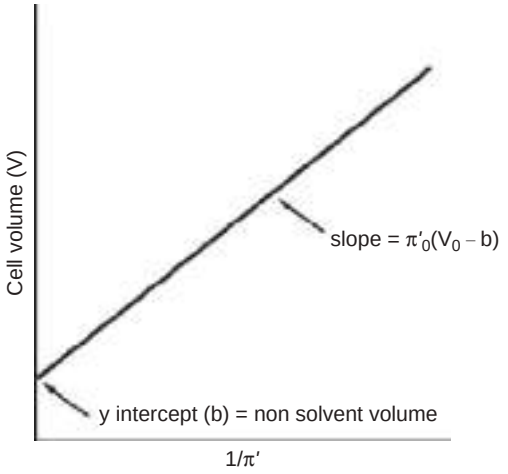

FIGURE 4.7 **Boyle–Van't Hoff plot for a theoretical cell.** The equation plotted is $V = (1/\pi')[\pi'_0(V_0 - b)] + b$ (see Eq. (4.19)). The y-axis intercept is b, the nonsolvent volume, and the slope is $[\pi'_0(V_0 - b)]$, that is, the amount of water-dissolved solutes in the cell. *(Copyright 1994 by CRC Press, Inc. From Hallows, K. R. and Knauf, P. A. (1994) "Principles of Cell Volume Regulation." CRC Press, Boca Raton FL. Reproduced with permission of Routledge/Taylor & Francis Group, LLC.)*

Net Water Transport Across Membranes of Animal Cells is Osmotic

In plant cells, which have rigid walls, the intracellular hydrostatic pressure can vary over a considerable range. In animal cells, which have compliant plasma membranes, hydrostatic pressure differences are small. In contrast, small differences in concentration of impermeable or low permeability solutes across the cell membrane can result in sizable water flows by osmotic mechanisms. The water flow under these conditions can be via the phospholipid bilayer (solubility diffusion), driven by the difference in water chemical potential across the membrane or via pores driven by a hydrostatic pressure gradient inside the pore. This pressure gradient is caused by the difference between the water chemical potentials inside the pore and in the external solution (see Figure 4.2). It is generally assumed that under steady-state conditions *in vivo*, the osmolalities of the intracellular and extracellular compartments are equal. There is some experimental evidence supporting this,[94] but based on rather indirect estimations of intracellular osmolality. Also, it has been argued that, in order to balance a 1 mosmol/kg difference in osmolality (cell higher), the cell hydrostatic pressure would have to be ~19 mm Hg higher than the extracellular pressure, something that a soft-tissue cell membrane is extremely unlikely to support.[93] However, mechanical support of the cell membrane by the cytoskeleton and/or the exoskeleton may allow for the maintenance of transmembrane hydrostatic

pressure gradients.[50] This issue is unresolved, but it is unlikely that in the steady-state large gradients of osmotic or hydrostatic pressure exist across plasma membranes.

Quantitative treatment of water transport across the plasma membrane usually involves another assumption, namely that the cytoplasm behaves as a free solution, similar to the interstitial fluid. However, it is far more likely that the cytoplasm is a gel, as discussed above.[85] This problem is also unresolved.

The fact that animal cells lack rigid walls and do not develop sizeable transmembrane hydrostatic pressure differences determines that the only means to maintain or regulate cell volume is to change the cell content of osmotically-active solutes. This is the main theme of the next section.

Cell Volume is Determined by the Amount of Cell Solute and the Extracellular Osmolality

With the questionable exception of water co-transport (see below), net water transport between intracellular and extracellular compartments is the result of differences in effective osmotic pressure between these compartments. The effective osmotic pressure, in turn, is proportional to the total number of particles in solution, and their reflection coefficients. Hence, at the same total osmotic pressure, impermeant particles are more effective than permeant particles in generating water flow toward the side in which they are contained. This can be demonstrated experimentally by exposing cells to solutions of identical osmolalities, but different tonicities, by using solutes having different permeabilities. Depending on the relative permeabilities of the plasma membrane to water and the solute, cell volume can remain constant, increase or decrease. This phenomenon can be explained by the effect of the solute reflection coefficient on osmotic water flow.

A solution is defined as isotonic (with the cell interior) when exposure of cells to this solution results in no change in cell volume; hypertonic and hypotonic solutions elicit decreases and increases in cell volume, respectively. Therefore, a hypertonic solution has a greater effective osmolality, and a hypotonic solution a lower effective osmolality, than the isotonic solution. Because of the role of the solute reflection coefficient in determining the effective osmolality (see above), the terms hypertonic and hypotonic are not equivalent to hyperosmotic or hyposmotic; the latter expressions denote the total osmolality of the solutions, disregarding the reflection coefficients. The osmolalities of biological fluids are largely determined by their total salt concentrations, because low molecular weight salts are the solutes at highest concentrations, expressed as number of particles relative to water mass. Hence, the extracellular fluid osmolality is largely determined by Na^+ salts (mainly sodium chloride and sodium bicarbonate), and the intracellular osmolality is mostly determined by K^+ salts.

Under most physiological and pathophysiological conditions, the intracellular and extracellular compartments can be treated as two closed compartments separated by a semipermeable membrane (i.e., a membrane permeable to water and impermeable to the solute). This simplification is valid because, in the short-term, solute gains or losses by the whole system and solute fluxes between the compartments are slow relative to potential water fluxes. It follows that: (1) the amount of solute in each compartment can be considered constant; and (2) the steady-state osmolalities of both compartments must be equal. Therefore, the amount of cell water is inextricably related to the amount of cell solute and to the extracellular osmolarity:

$$V_w^c = \frac{S^c}{Osm_{ec}} \tag{4.20}$$

where V_w^c is the cell water volume (L), S^c is the amount of cell solute (mosmol), and Osm_{ec} is the extracellular osmolarity (mosm/L).

It follows from Eq. (4.20) that cell volume can change by two mechanisms, namely changes in the amount of cell solute or in the extracellular osmolality. From a homeostasis point of view, if pure water is added to the extracellular compartment, reducing its tonicity, then part of the water will flow across the cell membrane into the intracellular compartment, until the osmolalities are again equal. If pure water is lost from the extracellular compartment, then water will flow from the intracellular compartment until the osmolalities become equal. In contrast, if isotonic solution is added to or lost from the extracellular compartment, there will be no water flow across the cell membrane, because no osmotic pressure difference has been established, and in the body the ensuing changes in hydrostatic pressure will be very small. This analysis is rather qualitative; knowledge or assumption of the initial conditions allows for a highly quantitative analysis, essential for understanding the pathogenesis and planning the treatment of water and electrolyte disorders.

Water Permeability of the Plasma Membrane Varies Considerably Among Cell Types

Cell membranes are endowed with highly variable osmotic water permeability coefficients, ranging from practically zero (apical membrane of thick-ascending loop of Henle cells) to 400–600 $\mu m\ s^{-1}$ in red blood cells and renal proximal tubules. Most

nonepithelial cells display quite high osmotic water permeabilities. The best-studied case is that of the mammalian red blood cell, whose P_{os} is in the range of 50−400 μm s^{-1}.[39] In artificial lipid bilayers, P_{os} ranges from <1 to <100 μm s^{-1}, depending on the lipid composition. Bilayers of higher fluidity are more permeable to water, and increased bilayer cholesterol content decreases bilayer water permeability. Recent studies have shown that certain biological membranes that are highly water permeable contain water-selective pores (aquaporins).

The structural bases for the extremely low P_{os} of some cell membranes were recently discovered; others remain unknown. As detailed in Chapter 2, lipid rafts in membranes are microdomains rich in cholesterol and sphingolipids in the external leaflet and cholesterol and phospholipids with saturated fatty acids in the internal leaflet of the membrane. The surrounding bilayer is abundant in unsaturated fatty acids, and considerably more fluid than that in the raft.[71] Membrane rafts have low fluidity, and hence a low diffusional water permeability. Addition of cholesterol to liposomes formed by phosphatidylcholine produces a major decrease in water permeability.[6,7,116] In liposomes formed by mixtures of phosphatidylcholine, cholesterol, and sphingomyelin, which contain lipid microdomains similar to membrane lipid rafts, water permeability is significantly lower than that expected based on the lysis tension.[116]

Apical membranes of certain tight epithelia have an extremely low permeability to water. A case in point is the apical membrane of the urothelium, that is, the epithelium that lines the renal calices, pelvis, ureters, urinary bladder, and urethra. The apical membranes of the epithelial cells of the urothelium are covered by rigid plaques consisting of hexagonal arrays of particles.[14,57,156] The plaques contain four transmembrane domain proteins named uroplakins, of which there are four isoforms.[88,170,172] It has been suggested that uroplakins could influence the passive permeability of the apical membrane of the urothelium,[56] but evidence was lacking until the permeabilities of normal mice urinary bladders were compared to those of uroplakinIII (UPIII)-knockout mice.[64] The normal mouse bladder has high transepithelial electrical resistance, and low water permeability. The bladders from UPIII-knockout mice maintained the high transepithelial resistance, but their water permeability was 20-fold higher than in controls. These results strongly suggest that the low permeability of the tight junctions and the apical membrane to ions are preserved in the knockout mice, whereas the water permeability of the apical membrane is increased. This is the first instance in which expression of a transmembrane protein has been shown to decrease the permeability of a biological membrane. It has been speculated that the uroplakin crystals limit plasma membrane lipid mobility, reducing fluctuations in acyl chains, decreasing water permeability through the bilayer.[73,169] However, the UPIII-knockout mice urinary bladders display significant anatomical alterations, including the presence of small hyperplastic superficial cells,[63] and therefore other mechanisms for the decrease in water permeability cannot be ruled out.

The thick ascending limb of the loop of Henle also has an extremely low permeability to water[126] necessary for the operation of the urine concentration mechanism (see Chapter 43). The biophysical reasons for this low permeability are not entirely clear. Certainly there is no expression of water pores (AQP) in the apical membrane (see Chapter 41), and its surface area is small relative to that of the basolateral membrane,[126] but whether the composition of the membrane has a role is yet to be determined.

Pathways for Water Transport Across Cell Membranes

As explained above, water transport across biological membranes can be across the lipid phase of the membrane (solubility diffusion) or across membrane proteins. The mammalian aquaporin family consists of 13 members that form water pores and are expressed in the plasma membranes of numerous cell types. Their important role in water transport across cell membranes is unquestionable. It has also been suggested that other transport proteins may transport water, in addition to their substrates. Such suggestions have been made for both ion channels and carriers. We will discuss first aquaporins and then these membrane proteins in the context of water transport across cell membranes. The accepted water transport pathways across the cell membrane are illustrated in Figure 4.8.

Water Pores Determine High Cell-Membrane Water Permeability

The existence of water pores was first deduced from biophysical studies (reviewed in Macey[90] and Verkman[150]), and then elegantly confirmed by biochemical, molecular-biological, and structural studies (reviewed in Agre[1] and King et al.[75]). Over the years, several criteria were developed to ascertain the presence of water pores in membranes. The principal ones are discussed below.

HIGH P_{os}/P_d

If the membrane contains pores, then osmotic water flow does not occur via a diffusion-like mechanism, which obeys the independence principle. Instead, it

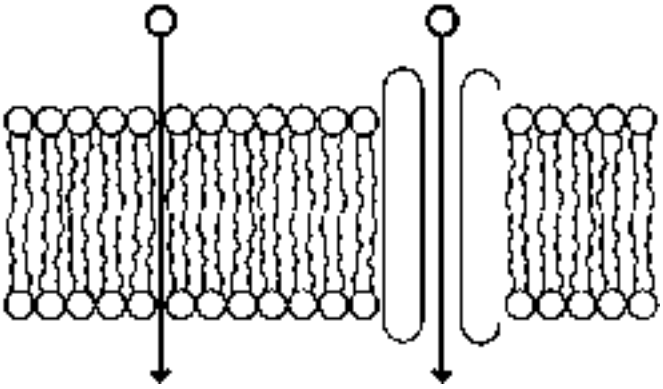

FIGURE 4.8 **Water transport pathways across plasma membranes.** Left arrow: Solubility diffusion across the phospholipid bilayer. The water permeability is directly proportional to the fluidity of the membrane. Right arrow: Permeation via pores. The water flux obeys Pouiseuille's Law in wide pores, and occurs by single-file diffusion in narrow pores such as those of aquaporins.

involves some form of interaction between water molecules, either Poiseuille-like (viscous) flow in thin capillaries or single file transport. As discussed previously, in both cases the flow of individual water molecules depends on the flow of other water molecules. It follows that the value of P_{os}/P_d is significantly greater than unity (the ratio is proportional to the square of the pore radius in case of viscous flow, and equal to the number of water molecules contained in the case of single file transport). However, unstirred-layer effects can cause a disproportionately large underestimation of P_d relative to P_{os}, with the end result of an artifactually large ratio. This error can be prevented by measuring the unstirred-layer equivalent thickness, and making appropriate corrections for P_{os} and P_d.[34] In conclusion, a correctly obtained $P_{os}/P_d > 1$ is strong evidence for water transport via pores. The value of P_{os}/P_d can denote either the pore radius or the number of water molecules in the pore. Resolving this issue requires additional experimental work, such as permeation studies with solutes of varying sizes to estimate the pore radius.

LOW ARRHENIUS ACTIVATION ENERGY

The activation energies (E_a) for water permeation via aqueous pores and for water self-diffusion are about the same (<5 kcal mol^{-1}), that is, much lower than the E_a for water permeation by solubility diffusion across a lipid membrane (<12 kcal mol^{-1}). This can be established by measuring the water permeability at different temperatures.

SENSITIVITY TO Hg

Water transport via proteinaceous pores is inhibited by $HgCl_2$ and organic mercurial compounds, an effect suggestive of a critical SH group in the protein underlying the pore function.[91,92] This was corroborated when the protein was identified.[113] The mercury sensitivity of water transport is conferred by a specific cysteine residue (Cys189 in human AQP1),[138] located ~8 Å above the NPA region.[59]

FLUX INTERACTIONS

In the case of large pores with finite solute permeability, there are frictional interactions between water and solutes (see above), with the end result of solvent drag and/or electrokinetic phenomena. Although this has been demonstrated for some membrane pores, it does not seem to take place with aquaporins, the water-selective pores in animal cell membranes. This suggests that these pores are impermeable to most solutes, and hence too narrow for solvent drag or electrokinetic phenomena.

Among cell membranes from epithelia, the best studied from a water-pore viewpoint is the apical membrane of the mammalian renal proximal tubule, where the above criteria have been clearly satisfied.[167] Water pores have been identified in numerous organs and cell types, and in the renal proximal tubule they are constitutively active; in contrast, in the collecting duct under resting conditions they exist in a cytoplasmic vesicular pool, and are inserted in the apical membrane after stimulation by vasopressin.[15,16]

Cell Membrane Water Pores are Aquaporins

The existence of water pores on cell membranes was demonstrated in red blood cells and renal tubules by the biophysical approaches described above (for reviews see Macey[90] and Verkman[150]). The pores were identified by the discovery of the red cell membrane protein first named CHIP28,[29,113] and now aquaporin 1 (AQP1). When expressed in amphibian oocytes or purified and reconstituted in liposomes, AQP1 forms Hg^{2+}-sensitive water pores with low activation energy, and no ion conductance (reviewed in Agre,[2] Engel et al.,[33] Heymann,[55] King et al.[75]). Later studies have shown three important facts: (1) AQPs are expressed in plant and animal cells, in both simple and complex organisms; (2) AQPs are expressed in the plasma and intracellular membranes of most cells, not just red cells and renal epithelial cells; and (3) there are 13 AQP isoforms in mammals, which have unique cellular and subcellular distributions.[43,70,75,151] Aquaporins are present in most cell types in the body, and there is reason to suspect that they are the predominant pathway for water transport across cell membranes.[75] In this section, we will discuss aquaporins largely from a molecular point of view. Aquaporins in the kidney are treated in Chapter 41, and aquaporins in other organs by King et al.[75] For excellent recent

reviews on AQPs, see Agre[1] and King et al.,[75] as well as more recent ones.[43,70,78,95,109,151,152,157] Peter Agre received the 2003 Nobel Prize in Chemistry for his work on aquaporins.

Based on their permeability properties, primary sequence, and gene structure, mammalian AQPs have been classified into three groups: Class 1, 2, and 3. Class 1 AQPs are permeated only by water (isoforms 0, 1, 2, 4, 5, 6, 8); class 2 AQPs, also known as aquaglyceroporins (isoforms 3, 7, 9, 10), are permeated by both water and small organic solutes such as glycerol; whereas class 3 AQPs are of unknown or unclear permeability properties (isoforms 11 and 12). AQPs in cell membranes are tetramers, with one subunit N-glycosylated.[72,135] Each monomer is ~30 kD, and contains a narrow aqueous pore surrounded by α helices. AQP monomers display N- and C-termini on the same side of the membrane (intracellular for plasma membrane AQPs), and the primary and tertiary structures clearly show an inverted symmetric pattern, each formed by three bilayer-spanning α helices. In each repeat, the loops B and E (C-terminal to the transmembrane helices 2 and 5), which contain the highly conserved signature motif Asn-Pro-Ala (NPA), form short hydrophobic α helices that reach halfway through the membrane from opposite sides to end facing each other. The overall fold has been described as an hourglass consisting of the two hemipores that face each other, with wider bases and a narrow area in the membrane center, lined by the two NPA-containing loops, which contribute to the pore selectivity.[65,75,113] The hourglass model was proposed from sequence analysis,[72] and has been confirmed by cryoelectron microscopy and X-ray crystallography studies.[37,41,60,103,119,142,158,159] A schema of this structure is shown in Figure 4.9.

The class 3 AQPs, AQP11, and AQP12, are located in intracellular compartments, and are closer to the SIP plant family (Small basic Intrinsic Proteins), displaying less than 20% homology with other members of the mammalian AQP family.[95] In AQP11 and AQP12, the highly-conserved NPA motif in the AQP N-terminal half is substituted with the sequences NPC and NPT, respectively, but they still have a conserved C-terminal half NPA motif.[69] The function of AQP11 is unknown, and that of AQP12 is unclear, without evidence for water permeability in frog-oocyte studies, but displaying water permeability when reconstituted in liposomes.[69,70]

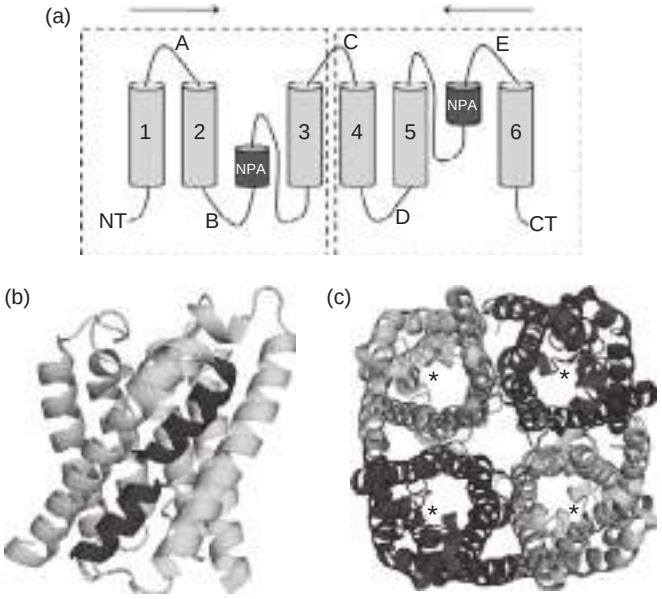

FIGURE 4.9 Membrane topology and structure of aquaporin 1 (AQP1). (a) Predicted secondary structure. AQP1 consists of two repeats of three transmembrane helices (1, 2, and 3; 4, 5, and 6). Amino and carboxy termini are on the cytoplasmic side. Loops B and E contain the Asn-Pro-Ala motifs (NPA) that form part of the water pore and are important to determine selectivity. Loop E contains Cys189, responsible for Hg^{2+} sensitivity. (b) Monomer structure (side view, ribbon representation). Transmembrane helices are shown in the same tone, whereas loops B and E, which contain the NPA sequences that meet approximately halfway into the membrane, are shown in a darker tone. (c) Tetramer structure (view from top). The monomers are functional *per se*, but AQP1 assembles into tetramers. Each monomer is shown in a tone different from that of the neighboring subunits. Asterisks denote the approximate location of the water pore in each subunit. Built with PyMol from PDB 1J4N.

Mechanism of Water Permeation in AQPs

The high selectivity of AQPs such as AQP1 for water – excluding even proton permeation – is consistent with the minimum width of the pore (2.8 Å), which limits the size of permeant molecules. The dipole moments of the two half-helices that contain the NPA motifs are oriented on the center of the hydrophilic pore, creating an electrostatic barrier to H^+ movement, and inducing a complementary alignment of the water molecules' dipole moments as they pass the signature motif.[8,9,27,28,65,66,160] Interaction of the water molecules inside the pore with the NPA motifs dipoles prevents formation of hydrogen bonds between adjacent water molecules. In other words, similar to what happens to K^+ permeating K^+-selective channels, the water molecules in the AQP1 pore lose contact with other molecules. One could say that the water becomes "dehydrated," and permeates in single file. The lack of hydrogen bonding of water molecules inside the pore prevents proton conduction via "water wires".[142,144]

Water selectivity arises at a constriction located ~8 Å extracellular to the NPA region, the aromatic/arginine region (ar/R), which contains a conserved arginine.[65,66,160] The ar/R region acts as a selectivity filter that limits permeation based on size and hydrophobicity.[65] This region is wider and more hydrophobic in aquaglyceroporins, allowing permeation of small

TABLE 4.1 Permeability Characteristics and Predominant Distribution for Known Mammalian Aquaporins

Isoform	Permeability	Tissue Distribution	Subcellular Distribution[a]
AQP0	Water (low)	Lens	Plasma membrane
AQP1	Water (high)[b]	Red blood cell; kidney; lung; vascular endothelium; brain; eye	Plasma membrane
AQP2	Water (high)	Kidney; vas deferens	Apical membrane; intracellular
AQP3	Water (high); glycerol (high); urea (moderate)	Kidney; skin; lung; eye; colon	Basolateral membrane
AQP4	Water (high)[b]	Brain; muscle; kidney; lung; stomach; small intestine	Basolateral membrane
AQP5	Water (high)[b]	Salivary gland; lacrimal gland; sweat gland; lung; cornea	Apical membrane
AQP6	Water (low); anions ($NO_3^- > Cl^-$	Kidney	Plasma membrane; intracellular
AQP7	Water (high); glycerol (high); urea (high); metalloids[d]	Adipose tissue; kidney; testis	Plasma membrane
AQP8	Water (high)[c]	Testis; kidney; liver; pancreas; small intestine; colon	Plasma membrane; intracellular
AQP9	Water (low); glycerol (high); urea (high); metalloids	Liver; leukocytes; brain; testis	Plasma membrane
AQP10	Water (low); glycerol (high); urea (high)	Small intestine	Intracellular
AQP11	Water?	Testis; kidney; brain; heart; thymus; intestine; liver	Intracellular
AQP12	?	Pancreas	Intracellular

[a] *Aquaporins that are present primarily in either the apical or basolateral membrane are noted as residing in one of these membranes, whereas homologs that are present in both of these membranes are described as having a plasma membrane distribution.*
[b] *These AQPs may be permeable to gases such as CO_2, O_2, NH_3, and/or NO.*
[c] *AQP8 might be permeated by water and urea.*
[d] *The transported species are most likely the undissociated arsenite and antimonite trioxides $As(OH)_3$ and $Sb(OH)_3$.*

solutes such as glycerol.[65] In members of the AQP family such as the *Escherichia coli* GlpF channel, sequence tuning of the selectivity filter region allows permeation of small uncharged solutes.[65] In the case of GlpF, the minimum diameter of the pore is ~3.8 Å, allowing passage of glycerol. Both polarity and diameter of the selectivity filter are essential to determine the permeability properties of AQPs.[65,160]

Certain Aquaporins are Permeable to Solutes and Perhaps to Physiologic Gases

As shown in Table 4.1, five of the eleven AQP isoforms have been shown to display solute permeability, in addition to water permeability. It has also been claimed that AQP1 has ion-channel activity when stimulated by cGMP, but this is unclear at this time (see below). Class II AQPs (aquaglyceroporins, isoforms 3, 7, 9, and 10) are permeable to small, neutral, hydrophilic solutes. Of these, urea is critical for renal function (see Chapter 43). Recent observations also point to permeability to the trivalent metalloids arsenite, As(III), and antimonite, Sb(III) through aquaglyceroporins.[5] As(III) and Sb(III) are protonated at physiological pH, with the main species in solution being the undissociated trioxides of a molecular volume slightly smaller than that of glycerol, which may explain permeation through the aquaglyceroporins.[5,114]

From the point of view of permeability properties, AQP6 differs from other AQPs in that it displays low water permeability, and behaves as an anion channel selective for anions such as nitrate over Cl^-.[67,68] Lowering pH and reaction with Hg^{2+}, a known blocker of water permeation through AQPs, increase anion conductance.[67,68,109] AQP6 has been traditionally considered an intracellular AQP present in intracellular vesicles of α-intercalated cells of the renal collecting ducts,[68,70,109] but it has been more recently identified in other tissues, including the apical membrane of parotid acinar cells, where it seems to contribute to the anionic conductance of the membrane.[67]

A very interesting issue is whether AQPs are permeable to gases, in particular CO_2 and NH_3.[21,65,104,106] It was reported that AQP1 expression in *Xenopus* oocytes elicits an almost twofold, Hg^{2+}-sensitive increase in plasma membrane CO_2 permeability,[21,106] and an even larger effect (also Hg^{2+}-sensitive) was

obtained in *E. coli* membrane vesicles expressing AQP1.[112] Other aquaporins may also be permeable to gases.[104] However, the CO_2 permeabilities of red blood cells and alveolar epithelium of mice in which *Aqp1* was deleted were found to be no different from those of wild type mice.[171] The differences between these sets of studies remain unresolved (see [22,153]).

Regulation of AQP-Mediated Water Permeability

In principle, the water permeability of a cell membrane via AQP depends on the number of functional pores (N per cell or membrane surface area), the single-pore water permeability, and the pore open probability (the fraction of the time that it is water permeable). Changes in N have been clearly demonstrated to regulate AQP-mediated water permeability. The most striking example of this mechanism is the effect of vasopressin on the insertion of AQP2 in the luminal membrane of the cortical collecting duct (see Chapter 42). As discussed below, certain solutes decrease the water permeability of AQP pores, but there is no definitive evidence for a regulatory role of pore "gating" in the sense that this expression is used in ion channel function (see Chapters 2 and 8). However, there is some evidence for regulation of aquaporin opening through phosphorylation.[49,51,95,101,145]

The permeability of several AQP isoforms is modulated by the composition of the extracellular solution. The water permeability of AQP0 expressed in *Xenopus* oocytes was reported to be increased by lowering external pH and $[Ca^{2+}]$.[107] Both effects depend on the pore residue His40.[44] In another study, the water permeability of AQP3, also expressed in oocytes, was found to be reduced by external acidification, whereas AQP0, AQP1, AQP2, AQP4, and AQP5 were found to be pH-insensitive,[177] in contrast with the study quoted above. In oocytes or LLC-PK1 cells expressing heterologous AQP4, PKC agonists were reported to reduce cell membrane water permeability,[50,173] an effect abolished by deletion of Ser180.[173] However, when purified AQP4 was reconstituted in liposomes, its phosphorylation by PKC did not affect the water permeability (quoted in King et al.[75]). Finally, *Xenopus* oocytes expressing AQP1 develop an ion current after injection of cGMP, whereas this agent had no effect on oocytes expressing AQP5.[4] Further, the effect is dependent on specific charged residues in the C-terminal domain of AQP1.[13] It is not clear, however, that the pathways for water permeation and ion fluxes are the same: when the experiment was carried out with AQP1 reconstituted in planar bilayers, an organic mercurial compound inhibited water permeability, but not cGMP-induced ion conductance.[133] Further, the ratio of ion permeability to water permeability was extremely small, suggesting that only a minute fraction of AQP1 molecules would form cGMP-activated ion channels.[133] Calmodulin binds to AQP0 and AQ6 (acidification-induced anion channel AQP), in a calcium dependent manner, and it inhibits AQP0 permeability.[107,115,118,127] The mechanism of the decrease in water permeability and functional role of the interactions of Ca^{2+}−calmodulin with AQPs have not been established. In conclusion, contrary to statements in the literature, there is no evidence that the AQP water pore is gated, that is, opens and closes stochastically as an ion channel. The available information is consistent with modulatory effects, such as by H^+ or divalent cations that could simply block the water permeation pathway. It is also clear that the finding that expression of a membrane protein results in water and ion permeability does not mean that they occur through the same pathway.

Other Membrane Proteins May Contribute to Water Transport

Water permeation through narrow ion channels has been studied by molecular-dynamics simulations based in the atomic structure of the KcsA channel[129] (see also Chapter 2). In the narrow part of the pore (selectivity filter), K^+ is transported in single file; two adjacent ions are separated by a water molecule; therefore, the molar flux ratio (K^+/water) is unity. For "near-isosmotic" water transport, the flux of 1 ion has to be coupled to that of 157 water molecules. Therefore, direct coupling between ion and water transport in narrow ion channels contributes only a minute fraction of the water flux expected to be produced by the changes in the osmolality of the solutions adjacent to the membrane that are produced by the ion flux.

One would expect that wider ion channels, in which the ions permeate in a hydrated state, would result in larger water fluxes coupled to the ion flow, and perhaps also in water permeation in the absence of a net ion flux. Although there is no direct evidence for this, it was recently shown that blocking the volume-regulated anion channel (VRAC) decreased significantly the water permeability of endothelial cells.[108] This result suggests that these channels constitute a significant pathway for osmotic water flow in these cells.

Do Co-Transporters Perform Active Water Transport?

Experiments in the choroid plexus epithelium of *Necturus maculosus*[174,175] and retinal pigment epithelium of frog[176] suggested that water transport and solute transport (KCl and lactate, respectively) are directly coupled. Under energetically favorable conditions, water would move uphill in the direction of the net ion flux and by the same pathway, implying

molecular coupling (in the carrier molecule) between the solute and water fluxes. If this is correct, then the water is co-transported, that is, transported uphill by a secondary active mechanism. Several co-transporters have been suggested to perform this function when expressed in *Xenopus* oocytes: Na^+-glucose,[84,97,98] Na^+-glutamate,[89] Na^+-dicarboxylate,[99] and others.[80,175] The rate of water transport via these carriers would range between 40 and 600 molecules per cycle. The water/solute coupling ratio in the case of the human Na^+-glucose co-transporter[98] indicates that the transported fluid would be hyperosmotic, instead of near-isosmotic. Hence, near-isosmolality could result from the parallel operation of transcellular osmosis (see [175] for a recent review). The critical experimental result supporting the water co-transport hypothesis is that solute transport via a co-transporter is associated with a water flux much larger than that observed with a similar solute flux via ion channels,[83] an argument that would rule out the alternative explanation that the co-transporter-mediated solute flux increases the osmolality in the plane adjacent to the membrane, and that the resultant generated osmotic gradient is responsible for water flux across the plasma membrane,[79,80] and not necessarily the co-transporter itself. A careful study of water fluxes in *Xenopus* oocytes expressing heterologous proteins, including Na^+-glucose co-transporters, glucose transporters or the K^+-channel ROMK2, permitted another group to relate solute accumulation in the oocytes to water flow. Their conclusion is that the glucose accumulation quantitatively accounts for the water flux by simple osmosis, and therefore that there would be no need to postulate water co-transport.[20,42] A critical factor in the solute accumulation in these studies is the intracellular solute diffusion coefficient, which in the oocytes is about one-fifth of that in free solution.[19,20]

Summary and Conclusions

In conclusion, the osmotic behavior of cells is not ideal because of the presence of cell solids; water transport across the cell membrane occurs by osmosis; and the determinants of cell volume are the intracellular solute content and the extracellular osmolality. Water permeation across the plasma membrane occurs via AQP pores and/or the phospholipid bilayer. Other pathways contribute at most a small fraction of the water flow.

WATER TRANSPORT IN EPITHELIA

Two modalities of transepithelial water transport occur in renal tubules *in situ*: (1) net transport between isosmotic (or near-isosmotic) fluids (e.g., water reabsorption in the proximal tubule); and (2) net transport in the direction of a pre-existing osmotic gradient (e.g., water reabsorption in the collecting duct). Although other mechanisms have been proposed, the dominant view is that water transport is passive and driven by osmotic forces. Pinocytosis has also been suggested, but is considered highly unlikely.[167] Solute−water co-transport, discussed in the previous section, is also unlikely given recent experimental results.[42] Electro-osmosis[132] and mechano-osmosis[130] have also been proposed, largely on the basis of neglecting the presence of unstirred layers in theoretical or experimental analyses. The reader interested in these hypotheses should consult additional references.[32,36,82,102,130,132,167]

Characteristics of Transepithelial Water Transport

The main consequence of water transport across cell membranes of epithelial cells is to contribute to transepithelial transport, that is, fluid absorption or secretion. In addition, similar to most other cells, epithelial cells are endowed with mechanisms of maintenance and regulation of their own volume. Physiologic regulation of transepithelial transport may involve changes in solute transport rate at one of the two cell membranes. This causes an instantaneous imbalance between the transport rates of apical and basolateral membranes, and therefore a change in cell solute and water content. In most epithelial cells, there is a rapid readjustment of the transport rate by a complex process called intermembrane "cross-talk"[134,135] (see Chapter 2).

Epithelia Have Very Different Water Permeabilities

Epithelia differ widely in their osmotic water permeabilities (Table 4.2). From the points of view of magnitude and regulation of their osmotic permeability coefficient, epithelia can be classified in the following three groups:

1. *High constitutive osmotic water permeability.* In these epithelia the P_{os} is permanently high. This group includes most leaky epithelia (epithelia with high ionic paracellular permeability relative to the transcellular permeability), such as renal proximal tubule, descending limb of the loop of Henle, small intestine, gallbladder, and choroid plexus. The high value of P_{os} is in large part (or exclusively) attributable to high permeabilities of both cell membranes (apical and basolateral). The cell membranes express water pores, so that water is likely to permeate by both solubility diffusion (via the lipid bilayer) and osmosis (via the pores).

TABLE 4.2 Osmotic Water Permeability of Epithelial Cell Membranes

Epithelium	Apical	Basolateral	Transepithelial	Reference
ADH-INSENSITIVE				
Rabbit PST	4500	5000	4280	18
Necturus gallbladder	640	460	350	23
Rabbit/rat TALH	–	–	0–20[a]	117
ADH-SENSITIVE				
Rabbit CCD				
(−) ADH	70	450	–	141
(+) ADH	310	490	–	
Rabbit IMCD				38
(−) ADH	70	480	–	
(+) ADH	260	390	–	

P_f values are rounded and expressed in $\mu m\ s^{-1}$, without correction for membrane folding factors; that is, they are referred to an "idealized" epithelial surface. For P_f values considering membrane folding, see Tripathi and Boulpaep.[146]

[a]*Range of several studies.*

ADH: antidiuretic hormone (vasopressin); PST: proximal straight tubule; TALH: thick ascending limb of loop of Henle; CCD: cortical collecting duct; IMCD: inner medullary collecting duct.

It is also possible that part of the water flow is intercellular (or paracellular), as discussed below.

2. *Low constitutive osmotic water permeability.* In mammals the only epithelia with this property are the ascending limb of the loop of Henle and urinary tract epithelia. The P_{os} is extremely low and insensitive to hormonal action (vasopressin). Both the apical membranes and the junctional complexes are low permeability barriers. In the thick ascending loop of Henle, the basolateral membrane has a high water permeability, so that changes in peritubular fluid osmolality result in rapid cell volume changes, whereas changes in luminal (apical) solution osmolality are ineffective.[54,143] The transepithelial P_{os} is low, although there is a high junctional ionic permeability. This lack of correlation between permeability to ions and water is not unexpected. As discussed in the context of cell membrane water permeability, ion channels permeate little water, and their expression level is quite low, so they do not increase P_{os} by a large amount. The molecular explanations for the low P_{os} of the apical membranes and junctions of the ascending limb of loop of Henle cells are unknown. In the case of urinary tract epithelia, there appears to be a major role of apical membrane uroplakins (see previous discussion and Hu et al.[64]).
3. *Variable (regulated) water permeability.* The renal collecting duct and the anuran urinary bladder and epidermis have low baseline P_{os} values, which are elevated when plasma osmolality rises by a mechanism involving secretion of antidiuretic hormone (vasopressin) by the neurohypophysis. Vasopressin binds to the basolateral V2 receptor, and activates a signaling mechanism that involves an increase in intracellular cAMP, resulting in insertion and then retrieval of preformed water pores in the apical membrane by exocytosis and endocytosis, respectively. The cytoplasmic pool of pores is contained in subapical tubulovesicles.[16,38,52,53,150,154,155]

Two Types of Transepithelial Water Transport

It is not difficult to understand the mechanisms of water reabsorption in either the cortical or the medullary collecting duct (CCD and MCD, respectively) under the influence of vasopressin. The tubule fluid at the end of the distal tubule is hyposmotic to plasma (and to the renal cortex interstitial fluid). Hence, if the CCD is water permeable, then water will be reabsorbed down the osmotic gradient. A similar situation occurs in the MCD, where the entering lumen fluid is at most isosmotic to plasma and the osmolality of the surrounding interstitial fluid ranges in humans, from 300 mosmol/kg at the cortico-medullary junction to 1200 mosmol/kg at the papilla (Chapter 43). In the frog epidermis, water reabsorption occurs from the pond (osmolality <10) to the frog's extracellular fluid (200–250 mosmol/kg). Thus, in these three epithelia there is a pre-existing osmotic force, and whether water is absorbed or not depends on the P_{os} of the apical membrane of the epithelial cells. As discussed previously, P_{os} at this membrane is regulated by insertion and retrieval of AQP2 water pores in response to changes in extracellular osmolality, a process mediated by secretion of vasopressin (see also Chapters 42 and 43).

In the renal proximal tubule, small intestine, gallbladder, and other epithelia, the fluids bathing the epithelium are usually isosmotic or near-isosmotic, and transepithelial water transport can take place in the absence of a measurable driving force between the bulk solutions. Further, early experimental observations showed that water absorption can occur against the transepithelial osmotic gradient, that is, from the concentrated to the diluted solution.[25] This occurs both in small intestine and renal proximal tubule, and unquestionably demonstrates uphill water transport (see Whittembury and Hill[166] and Whittembury and Reuss[167] for detailed discussions). Of course, this does

not necessarily mean that there is a "water pump" (primary or secondary active water transporter) in the system. Studies in small intestine epithelium revealed that uphill water absorption occurs only together with net solute absorption and in the same direction, suggesting some form of "coupling" between water and solute fluxes.[25,161,162,163] Over the next 50 years, these puzzling observations elicited a great deal of experimental and theoretical work, which resulted in successive proposals to explain: (1) water transport between isosmotic bulk solutions; (2) uphill water transport; and (3) the nature of the coupling between solute and water flow.

Solute–Solvent Coupling

Passive mechanisms may exist that would couple salt to water absorption or secretion. Intuitively, active salt absorption by an epithelium (see Chapter 2) will create, at both apical and basolateral membranes, differences in the concentration of salt, with the side from which the salt is transported becoming "dilute" and the side toward which the salt is transported becoming "concentrated." The magnitude of the concentration changes in the fluids adjacent to the epithelial cells will depend on whether they are mixed (by convection) with the bulk solutions, and on the rates of solute diffusion into or away from these areas. Clearly, changes in concentration must be created inside the cell, in the surfaces immediately adjacent to the membranes, where the cytosol is not well mixed and the diffusion rates are much smaller than in free solution. In addition, in the extracellular surfaces adjacent to the cell membranes the solutions are not well mixed with the bulk, for two reasons: the existence of unstirred layers (see above); and the existence of anatomic restricted spaces in which good mixing cannot occur. In the case of the basolateral cell membrane of an epithelium, the histology indicates that there cannot be good mixing with the extracellular solution because of the complex architecture of the lateral intercellular spaces, the basal membrane infoldings, and the presence of the basement membrane, which is a barrier for hydraulic flow. At the apical membrane surface, fluid mixing is easier, but is also not ideal if there are microvilli. Hence, in a fluid absorbing epithelium at the steady-state one would expect a solute concentration profile in which there are salt concentration gradients across the apical membrane, with the lumen fluid diluted with respect to the cell interior, and across the basolateral membrane, with the cell diluted with respect to the extracellular solution.

The central points in this analysis of solute–solvent coupling in epithelia will be two. First, the functional anatomy of epithelia determines the existence of compartments (i.e., spaces that are "unstirred"); in these spaces osmotic coupling occurs, explaining the relationship (coupling) between salt and water transport. Second, the water permeability of the cell membranes is so high that the osmotic gradients required for near-isosmotic coupling are very small, and detectable only under rather artificial experimental conditions. This view is not universally accepted. As we discuss the details below, we will point out criticisms and alternative explanations.

Three-Compartment Models Define the Problem

An epithelial monolayer and the surrounding fluid compartments can be modeled as a three-compartment system with two barriers. The essence of these models is that the specific properties of the barriers and the compartments can account for solute–water flux coupling and explain apparently active water transport. Two proposals were developed based on this idea, namely the three-compartment model of Curran and MacIntosh[24] and the standing-gradient hypothesis of Diamond and Bossert.[31]

In the three-compartment model, illustrated in Figure 4.10, water transport occurs from the *cis* solution (A) to the *trans* solution (B), against the osmotic pressure difference between these two solutions [C_s (B) > C_s (A)]. The *cis* solution and *trans* solution are separated from the middle compartment (M) by barriers with different properties, semipermeable and porous, respectively. Active salt transport into an unstirred intraepithelial compartment renders it hyperosmotic to the *cis* solution (hyperosmotic middle compartment). Water then flows from A to M by osmosis (the membrane is semipermeable) and, as the hydrostatic pressure rises in M, solution flows from the M into B by bulk flow (the membrane is porous). The equivalent of this system in an absorptive epithelium would be as follows: the semipermeable membrane is constituted by the two cell membrane domains (apical and basolateral) in series, and the porous membrane by the distal end of the lateral intercellular spaces and the basement membrane, also in series. Compartment A is the lumen, compartment B the basolateral (interstitial) solution, and compartment M the lateral intercellular space. Water can be transported uphill (against the osmotic gradient between A and B) only while the middle compartment is hyperosmotic to the *cis* compartment. In addition, for this model to operate the absorbed fluid must be hyperosmotic to the *cis* solution. Experimental studies showed that the emerging fluid is virtually isosmotic with the *cis* solution,[30] requiring revision of the above theory. This resulted in the formulation of the standing-gradient hypothesis, explained below.

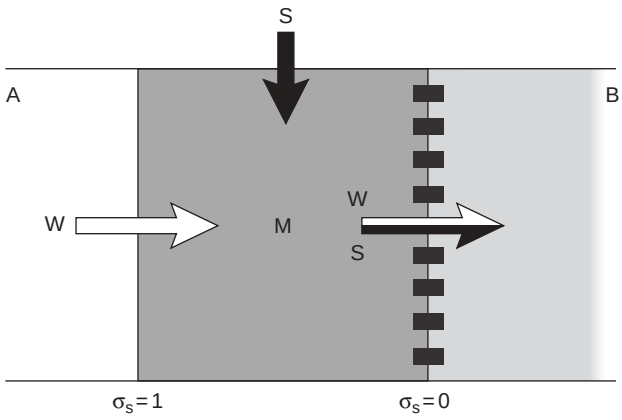

FIGURE 4.10 **Three-compartment model of Curran and MacIntosh.**[18] Solute entry (s, solid arrow) into the middle compartment (compartment M) causes osmotic *water* flow (w, open arrow) from compartment A to compartment M. The elevation of the hydrostatic pressure in compartment M causes *solution* flow from compartment M into compartment B (w/s open/solid arrow). Hence, there is water flux from A to B, although $C_s(B) > C_s(A)$. Darker tones in the compartment denote higher solute concentrations. See text.

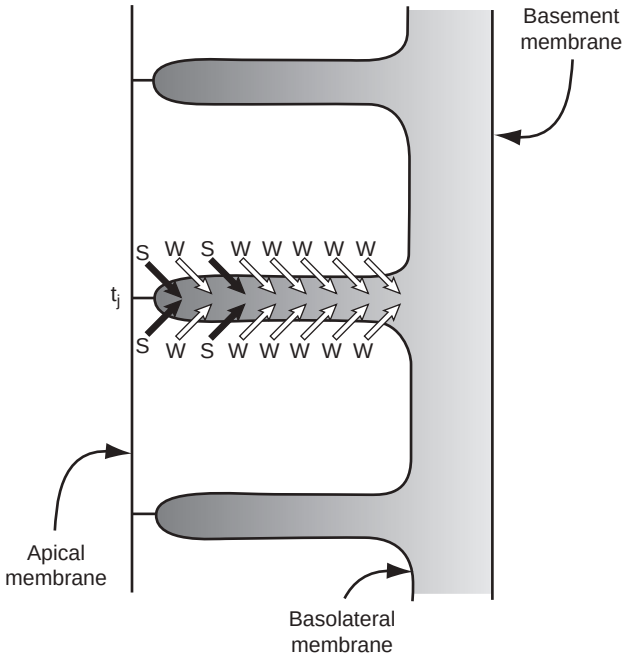

FIGURE 4.11 **Standing-gradient hypothesis of Diamond and Bossert.**[23] Solute transport (s, solid arrows) into the channel (lateral intercellular space) causes a local increase in osmolality; water flows osmotically across the bounding membranes (w, open arrows), "diluting" the solution in the channel. Transport toward the open end is by bulk flow and diffusion. See text.

Standing-Gradient Hypothesis Explains Near-Isosmotic Fluid Transport, but is Difficult to Reconcile with Current Experimental Knowledge

The standing-gradient hypothesis of Diamond and Bossert[31] is depicted in Figure 4.11. It is based on the following definitions and assumptions: (1) the lateral intercellular space is the hyperosmotic middle compartment; (2) the junctional complexes are impermeable to both solute and water; (3) solute transport from the cell to the *trans* solution takes place across the lateral membranes near the apical poles of the cells; (4) in contrast, secondary (osmotic) water flow occurs across the entire lateral membrane; (5) the lateral intercellular space solution is unstirred; (6) solute diffusion along the length of the lateral intercellular spaces is restricted by their geometry (the spaces are long and narrow). Under these conditions, the solution of the complicated mathematical model describing the system yields a continuously decreasing osmolality from the apical (blind) to the basolateral (open) end of the space. Also, the emerging solution is more likely to be near-isosmotic when the following conditions hold: long and narrow spaces, small solute diffusion coefficient, and high cell membrane P_{os} relative to the solute transport rate.

Direct and indirect observations demonstrated that some of the above assumptions are not correct. (1) In many instances the junctions have high permeability to ions[40,61,164,168] and perhaps to water.[165,167] (2) The Na^+, K^+-ATPase is distributed homogeneously in the lateral cell membrane,[99] not restricted to the apical region. (3) Both morphometric studies and electrophysiological computations yield short times for lateral space solute diffusion,[58,74,131,158,162] making longitudinal concentration gradients unlikely. (4) Realistic calculations based on geometry predict that the transported fluid must be hyperosmotic,[131] because the spaces are not sufficiently long and narrow. (5) The hypothesis predicted sizable hyperosmolality in the lateral intercellular spaces, but this was based on the early estimations of transepithelial P_{os}, which were in error due to unstirred-layer artifacts.[11,62] (6) Measurements of transepithelial voltage changes elicited by changes in solution osmolality revealed that the lateral intercellular spaces are in virtual osmotic equilibrium with the cell.[124,125]

An important point in this discussion is that for a constant fluid transport rate, the magnitude of the osmotic gradient and of the hyperosmolality of the transported fluid is inversely proportional to the effective P_{os} of the osmotic barriers. In fact, many of the above problems were solved with the development of methods to measure the osmotic water permeability of the cell membranes of leaky epithelia, which were demonstrated to be very large. On these bases, some of the above notions must be discarded, because they

were based on incorrect experimental data and a simpler mechanism of transepithelial water transport has emerged.

Near-Isosmotic Fluid Transport Model Solves the Difficulties of Three-Compartment Models

Measurements of P_{os} in high water permeability membranes give values ranging from 100 to 400 $\mu m\ s^{-1}$, that is, 10- to 100-fold greater than early estimates.[167] Hence, instead of a needed osmolality difference of about 20 mosmol kg^{-1}, as predicted from the standing-gradient hypothesis, a very small difference in osmolality, of only 1–2 mosmol kg^{-1}, quantitatively accounts for the measured water transport rates.[23,111,167] As explained previously, the primary event in transepithelial water transport is active salt transport. Inasmuch as solute is removed from the *cis* side and added to the *trans* side, there must be a decrease in *cis* fluid and an increase in *trans* fluid osmolality in the immediate vicinity of the respective membranes, as well as opposite changes in osmolality at the intracellular surface of the two membranes: an increase at the apical membrane and a decrease at the basolateral membrane. The magnitude of these changes will depend on the transport rate and geometry of the systems, and can be generally expected to be quite small. Measurements in fluid samples from isolated, perfused renal tubules reveal small differences, supporting this view.[10,46] In conclusion, recent studies support the notion that so-called isosmotic transepithelial water transport is not truly isosmotic, but near-isosmotic. Further, the osmotic driving forces required to account for water transport are quite small, and hence difficult to determine *in situ*, and substantial hyperosmotic compartments or sizable longitudinal standing gradients probably do not exist[121,141,167] (see Figure 4.12).

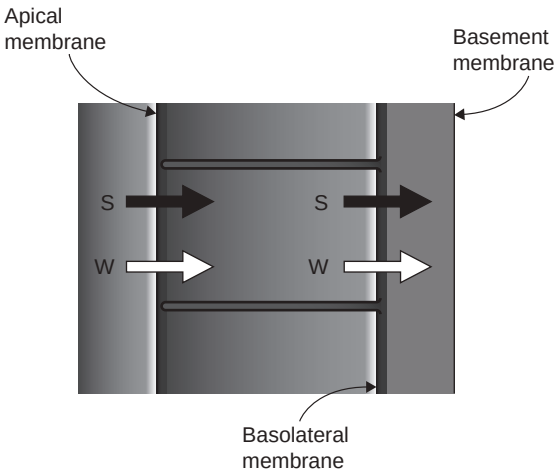

FIGURE 4.12 **Near-isosmotic transport model.** Because of the high osmotic water permeability of the cell membranes, the differences in solution osmolality needed to account for fluid transport are small, probably localized at epithelium–solution interfaces. Salt transport causes dilution of solution on *cis* side and concentration of the solution on *trans* side at the two cell membranes. In the case of fluid absorption, at the apical membrane the intracellular solution is hyperosmotic to the lumen solution; at the basolateral membrane, the intracellular solution is hyposmotic to the extracellular solution. These small differences in osmolality, denoted in the figure by shades of gray (hyperosmotic solution being darker), cause osmotic water flow into the cell across the apical membrane and out of the cell across the basolateral membrane. The magnitude of the paracellular water flow is uncertain. Because of the high surface area of the lateral membranes, and the small volume of the lateral intercellular spaces, the space osmolality is "clamped" by the cell osmolality, making longitudinal osmotic gradients in the spaces small at most.

Solute Recirculation in the Paracellular Pathway in Theory Explains Truly Isosmotic Transepithelial Fluid Transport

Truly isosmotic transepithelial water transport[147,148] may occur, in theory, if there is solute recirculation across the epithelium. In other words, it is argued that an epithelium cannot perform transepithelial truly isosmotic transport if it is bathed by identical solutions on both sides, and there are no differences in electrical potential or hydrostatic pressure, unless part of the transported solute recirculates to the solution of origin. In frog skin glands, there is transcellular Cl^- secretion (secondary active uptake at the basolateral membrane, channel-mediated downhill Cl^- extrusion across the apical membrane) and paracellular Na^+ secretion (driven by the lumen-negative transepithelial voltage generated by Cl^- transport). As such, this transport mechanism would cause secretion of a hyperosmotic fluid, but it was proposed that this fluid can become truly isosmotic. Larsen and co-workers[81,82] developed an interesting mathematical model for solute recirculation in the epithelium of the small intestine. The essential points are as follows: the primary transport event is active Na^+ transport across the lateral cell membrane (by the Na^+,K^+-ATPase). Water follows osmotically across the lateral cell membranes and the tight junctions. With appropriate geometric and transport parameters, the solution in the lateral intercellular spaces would be hyperosmotic by a small amount. The transported fluid would become isosmotic by uptake (recirculation) of salt across the basal membrane, via Na^+-K^+-$2Cl^-$ co-transport. This model has been criticized[140] on two main grounds: the use of experimental measurements of the Cs^+ flux ratio to assess transcellular and paracellular Na^+ fluxes, and the energetic cost of recirculation, namely the fact that about half of the pump work would be wasted. However, both sides agree that the model is amenable to further experimental testing.[81,140]

In Certain Epithelia Asymmetries in Solute Composition Play Significant Roles

It is possible that factors other than the total osmolalities of the solutions on either side of the epithelium contribute to transepithelial water transport. Three possibilities should be considered (see Whittembury and Hill[166] for a more detailed discussion). First is a colloid-osmotic force: transepithelial differences in protein concentration can result in colloid-osmotic pressure differences that can be significant in the case of epithelia with high permeability to water and small solutes. In the renal proximal tubule, this factor accounts for a small portion of water reabsorption.[48] Second is a difference in the effective osmolalities of the solutions: if the epithelium is exposed to solutions containing solutes of different reflection coefficients, then there could be transepithelial effective osmolality gradients, even if the solutions have the same total osmolality. Under the conditions described there will be osmotic water flow toward the side containing the higher concentration of low permeability (high reflection coefficient) solutes.[47] This has been proposed to occur in the late renal proximal tubule because of reabsorption of organic solutes such as glucose, and preferential reabsorption of HCO_3^-. Both have been claimed to have higher reflection coefficients than Cl^-. However, the notion of low reflection coefficients in epithelial cells has been disputed, and attributed to errors caused by uncorrected unstirred-layer effects.[154] Third are hydrostatic pressure differences: under most conditions, these differences are small and hence do not contribute significantly to water flow.

Pathways for Transepithelial Water Transport are also Controversial

Is water transport transcellular and/or paracellular? Epithelial transport pathways can be in series or in parallel. The cells consist of pathways in series (apical membrane, cytoplasm, and basolateral membrane), as does the intercellular (paracellular) pathway (junction in series with lateral intercellular space). In turn, the transcellular pathway and the paracellular pathway are in parallel with each other. A major problem in the phenomenological description of transepithelial transport has been to ascertain the portions of ion and water fluxes occurring across each pathway. In the case of ions, it has been clearly shown that in some epithelia most passive permeation is paracellular (leaky epithelia); whereas in others most passive permeation is transcellular (tight epithelia) (see Reuss[123] for a review). In the case of water, there is convincing experimental evidence demonstrating transcellular transport, but paracellular transport is controversial.[122]

Transcellular Osmotic Water Transport is Supported by High Cell-Membrane P_{os}

In high water permeability epithelia (mammalian renal proximal tubule, *Necturus* gallbladder), apical and basolateral membrane P_{os} values range from <500 to $5000\ \mu m\ s^{-1}$ (renal tubule [17,18,19,45,167]; gallbladder [23,111]). In both membrane domains, there can be considerable "amplification," by the presence of microvilli at the apical membrane and infoldings at the basolateral membrane. Hence, the P_{os} values expressed per unit surface area of membrane are much smaller than those relative to the idealized geometry of the tissue. Regardless of this, the water permeability of these epithelia is high, and attributable to the expression of water pores.

Paracellular Osmotic Water Transport is Supported by Indirect Arguments

The paracellular P_{os} can be estimated in principle from the transepithelial and cell membrane P_{os}. Given that the transcellular and paracellular pathways are in parallel:

$$P_{os}^t = P_{os}^c + P_{os}^p \tag{4.21}$$

where P_{os} denotes osmotic permeability, and the superscripts t, c, and p refer to transepithelial, cellular, and paracellular pathways, respectively. In the proximal tubule, P_{os}^t appears to be significantly higher than P_{os}^c, suggesting that P_{os}^p is sizable.[167] The problems with these calculations are the errors involved in the measurements of transepithelial and cell membrane P_{os} values.

Paracellular water transport is also supported by quantitative assessments of the effect of organomercurial compounds, presumed to be specific pore blockers, on P_{os}^t and P_{os}^c. An agent such as pCMBS inhibits P_f^c by more than 90%, but P_{os}^t is reduced by only 50%, which strongly suggests a finite parallel water permeation pathway.[167] These calculations imply a single site of action of pCMBS and other effects are, in principle, possible.

Another argument suggesting paracellular water flow is the observation of solvent drag and electrokinetic phenomena. If osmotic water flow takes place across large pores, which are also permeable to solute, then there will be a frictional interaction between water and solute, and the water flow will cause a solute flow in the same direction. This solute flux can occur in the absence of a favorable solute electrochemical gradient between the solutions. It is usually demonstrated using hydrophilic nonelectrolytes (e.g., small sugars such as mannitol); the mannitol and water fluxes correlate linearly, as predicted by Eq. (4.18). Results suggesting solvent drag have been reported for several epithelia.[167] The simplest electrokinetic

phenomenon to study is the streaming potential produced when, in the absence of a favorable electrochemical gradient, the solute is a permeant ion that flows in the same direction as water. Streaming potentials are generated if the water permeation pathway is ion-selective, that is, more permeable to that ion than to the counterion. The observation of this phenomenon has been interpreted as supportive of solute–water coupling in the paracellular pathway (reviewed in Tripathi and Boulpaep[146]).

The main problem with experiments purporting to demonstrate solvent drag or streaming potentials is the complication introduced by unstirred layers. Water transport in such a system causes changes in solute concentrations next to the membrane surfaces, raising the concentration on the *cis* side and lowering it on the *trans* side. Therefore, even if the concentrations of a given solute are the same in the bulk solution, there will be a concentration gradient at the membrane surfaces (unstirred-layer polarization), which explains the apparent solvent drag (pseudo-solvent drag). Pseudo-streaming potentials can be similarly caused by ion concentration changes elicited by the water flux. It is possible to distinguish true from apparent streaming potentials by comparing the time courses of the transepithelial voltage changes caused by the addition of nonelectrolyte or by a unilateral ionic substitution.[120,124,125] This criterion could help confirm or rule out the legitimacy of claimed true streaming potentials.

One recent approach to assess the role of the paracellular pathway in water permeation has been the use of genetic manipulation of claudins in mice and culture cells. Tight junctions are composed of several membrane proteins, including occludin and claudins.[77,136] Claudin-2 is frequently located at tight junctions of leaky epithelia that display high fluid transport rates, and seems to be responsible for the cation selectivity of the paracellular pathway in these tissues.[77,105] Recent studies have shown that expression of claudin-2 in an MDCK cell line increases water permeability,[128] and that the proximal tubules of mice deficient in claudin-2 display increased paracellular electrical resistance with loss of cation selectivity.[105] The decrease in net fluid transport in the claudin-2-deficient mice parallels the decreases in NaCl reabsorption, and cannot be unambiguously ascribed to a primary decrease in water permeability.[105,128]

In sum, the cellular pathway is certain to contribute to transepithelial osmotic water transport, and there are suggestions of a significant paracellular contribution. However, the latter is based on indirect evidence, and is questionable because of possible unstirred-layer artifacts. This problem will be definitively solved only by direct measurements of transcellular and paracellular water flows, which is a daunting task. Recent elegant fluorescence microscopy studies[76] suggest that there is no significant water flow across tight junctions of MDCK monolayers, relative to the transcellular flow. However, in these experiments the rate of transepithelial water flux was much smaller than observed in native epithelia. Sachar-Hill and Hill[130] have argued, on the basis of analyses of hydrophilic probe and water fluxes, that the paracellular water flux of several epithelia is quite high. However, the problem of unstirred layers was neglected in their analysis. Additional studies using genetic manipulations, in combination with sophisticated imaging studies, may shed light into the long-standing issue of the physiological role of water permeation through the paracellular pathway.

Summary and Conclusions

Water transport in leaky epithelia occurs in the same direction as solute transport and in near-isosmotic proportions. The available experimental evidence supports the view that the coupling between solute and water transport is not molecular, but thermodynamic, that is, osmotic. Solute transport by pumps, carriers, and/or channels elicits differences in solute concentration at the membrane surfaces, with a decrease in concentration on the *cis* side and an increase on the *trans* side. The establishment of osmotic gradients is favored because of the architecture of epithelia, which contain compartments that do not mix well with the surrounding fluids. The magnitude of the osmotic gradients is small and difficult to measure, but sufficient to account for the measured rates of fluid transport. Osmotic water flow takes place predominantly across the cell membranes, via both AQP pores and the phospholipid bilayer, with a small or nil contribution of other proteins. It is possible that part of the water flow is paracellular via the tight junctions, but this is likely to be relatively small.

References

[1] Agre P. Aquaporin water channels (Nobel Lecture). Angew Chem Int Ed Engl 2004;43:4278–90.
[2] Agre P, Preston GM, Smith BL, Jung JS, Raina S, Moon C, et al. The archetypal molecular water channel. Am J Physiol 1993;265: F463–76.
[3] Anderson JL, Malone DM. Mechanism of osmotic flow in porous membranes. Biophys J 1974;14:957–82.
[4] Anthony TL, Brooks HL, Boassa D, Leonov S, Yanochko GM, Regan JW, et al. Cloned human aquaporin-1 is a cyclic GMP-gated ion channel. Mol Pharm 2000;57:576–88.
[5] Bhattacharjee H, Rosen BP, Mukhopadhyay R. Aquaglyceroporins and metalloid transport: implications in human diseases. Handb Exp Pharmacol 2009;190:309–25.

[6] Blok MC, Van Deenen LL, De Gier J. The effect of cholesterol incorporation on the temperature dependence of water permeation through liposomal membranes prepared from phosphatidylcholines. Biochim Biophys Acta 1977;464:509–18.
[7] Bloom M, Evans E, Mouritsen OG. Physical properties of the fluid lipid-bilayer component of cell membranes: aperspective. Q Rev Biophys 1991;24:293–397.
[8] Burykin A, Warshel A. What really prevents proton transport through aquaporin? Charge self-energy versus proton wire proposals. Biophys J 2003;85:3696–706.
[9] Burykin A, Warshel A. On the origin of the electrostatic barrier for proton transport in aquaporin. FEBS Lett 2004;570: 41–6.
[10] Barfuss DW, Schafer JA. Hyperosmolarity of absorbate from isolated rabbit proximal tubules. Am J Physiol 1984;247:F130–9.
[11] Barry PH, Diamond JM. Effects of unstirred layers on membrane phenomena. Physiol Rev 1984;64:763–873.
[12] Bean CP. The physics of porous membranes—neutral pores. In: Eisenman G, editor. Membranes I. Macroscopic systems and models. New York: Dekker; 1972. p. 1–54.
[13] Boassa D, Yool AJ. Single amino acids in the carboxyl terminal domain of aquaporin-1 contribute to cGMP-dependent ion channel activation. BMC Physiol 2003;3:12.
[14] Brisson A, Wade RH. Three-dimensional structure of luminal plasma membrane protein from urinary bladder. J Mol Biol 1983;166:21–36.
[15] Brown D. Membrane recycling and epithelial cell function. Am J Physiol 1989;256:F1–12.
[16] Brown D. Structural–functional features of vasopressin-induced water flow in the kidney collecting duct. Semin Nephrol 1991;11:478–501.
[17] Carpi-Medina P, González E, Whittembury G. Cell osmotic water permeability of isolated rabbit proximal convoluted tubules. Am J Physiol 1984;244:F554–63.
[18] Carpi-Medina P, Whittembury G. Comparison of transcellular and transepithelial water osmotic permeabilities in the isolated proximal straight tubule of the rabbit kidney. Pflügers Arch 1988;412:66–74.
[19] Charron F, Lapointe JY. Slow ionic diffusion in oocytes and the water co-transport hypothesis. FASEB J 2005;19:A1156.
[20] Charron FM, Blanchard MG, Lapointe JY. Intracellular hypertonicity is responsible for water flux associated with Na^+/glucose co-transport. Biophys J 2006;90:3546–54.
[21] Cooper GJ, Boron WF. Effect of PCMBS on CO_2 permeability of *Xenopus* oocytes expressing aquaporin-1 or its C189S mutant. Am J Physiol 1998;275:C1481–6.
[22] Cooper GJ, Zhou Y, Bouyer P, Grichtchenko II, Boron WF. Transport of volatile solutes through AQP1. J Physiol 2002;542: 17–29.
[23] Cotton CU, Weinstein AM, Reuss L. Osmotic water permeability of *Necturus* gallbladder. J Gen Physiol 1989;93:649–79.
[24] Curran PF, MacIntosh JR. A model system for biological water transport. *Nature* (Lond) 1962;193:347–8.
[25] Curran PF, Solomon AK. Ion and water fluxes in the ileum of rats. J Gen Physiol 1957;41:143–68.
[26] Dawson DC. Water transport. In: Seldin DW, Giebisch G, editors. The Kidney: physiology and pathophysiology. New York: Raven Press; 1992. p. 301–16.
[27] de Groot BL, Frigato T, Helms V, Grubmüller H. The mechanism of proton exclusion in the aquaporin-1 water channel. J Mol Biol 2003;333:279–93.
[28] de Groot BL, Grubmüller H. The dynamics and energetics of water permeation and proton exclusion in aquaporins. Curr Opin Struct Biol 2005;15:176–83.
[29] Denker BM, Smith BL, Kuhajda FP, Agre P. Identification, purification, and partial characterization of a novel M_r 28,000 integral membrane protein from erythrocytes and renal tubule. J Biol Chem 1988;263:14634–5642.
[30] Diamond JM. The mechanism of water transport by the gallbladder. J Physiol (Lond) 1962;161:503–27.
[31] Diamond JM, Bossert WH. Standing-gradient osmotic flow: a mechanism for coupling of water and solute transport in epithelia. J Gen Physiol 1967;50:2061–83.
[32] Diecke FP, Ma L, Iserovich P, Fischbarg J. Corneal endothelium transports fluid in the absence of net solute transport. Biochim Biophys Acta 2007;1768:2043–8.
[33] Engel A, Walz T, Agre P. The aquaporin family of membrane water channels. Curr Opin Struct Biol 1994;4:545–53.
[34] Finkelstein A. Water movement through lipid bilayers, pores and plasma membranes: theory and reality. New York: John Wiley & Sons; 1986.
[35] Finkelstein A, Rosenberg PA. Single-file transport: implications for ion and water movements through gramicidin a channels. In: Stevens CF, Tsien RW, editors. Membrane transport processes, vol. 3. Copenhagen: Munksgaard; 1979. p. 107–19.
[36] Fischbarg J. Fluid transport across leaky epithelia: central role of the tightjunction and supporting role of aquaporins. Physiol Rev 2010;90:1271–90.
[37] Fischer G, Kosinska-Eriksson U, Aponte-Santamaría C, Palmgren M, Geijer C, Hedfalk K, et al. Crystal structure of a yeast aquaporin at 1.15 angstrom reveals a novel gating mechanism. PLoS Biol 2009;7:e1000130.
[38] Flamion B, Spring KR. Water permeability of apical and basolateral cell membranes of rat inner medullary collecting duct. Am J Physiol 1990;259:F986–99.
[39] Forster RE. The transport of water in erythrocytes. In: Bronner F, Kleinzeller, editors. Current topics in membranes and transport, vol. 2. New York: Academic Press; 1971. p. 41–98.
[40] Frömter E. The route of passive ion movement through the epithelium of *Necturus* gallbladder. J Membr Biol 1972;8: 259–301.
[41] Fu D, Libson A, Miercke LJ, Weitzman C, Nollert P, Krucinski J, et al. Structure of a glycerol-conducting channel and the basis for its selectivity. Science 2000;290:481–6.
[42] Gagnon MP, Bissonnette P, Deslandes LM, Wallendorff B, Lapointe JY. Glucose accumulation can account for the initial water flux triggered by Na^+/glucose co-transport. Biophys J 2004;86:125–33.
[43] Gomes D, Agasse A, Thiébaud P, Delrot S, Gerós H, Chaumont F. Aquaporins are multifunctional water and solute transporters highly divergent in living organisms. Biochim Biophys Acta 2009;1788:1213–28.
[44] Gonen T, Sliz P, Kistler J, Cheng Y, Walz T. Aquaporin-0 membrane junctions reveal the structure of a closed water pore. Nature 2004;429:193–7.
[45] González E, Carpi-Medina P, Whittembury G. Cell osmotic water permeability of isolated rabbit proximal straight tubules. Am J Physiol 1982;242:F321–30.
[46] Green R, Giebisch G. Luminal hypotonicity: a driving force for fluid absorption from the proximal tubule. Am J Physiol 1984;246:F167–74.
[47] Green R, Giebisch G. Reflection coefficients and water permeability in rat proximal tubule. Am J Physiol 1989;257: F658–68.
[48] Green R, Windhager EE, Giebisch G. Protein osmotic pressure effects on proximal tubule fluid movement in the rat. Am J Physiol 1974;226:267–76.
[49] Hachez C, Chaumont F. Aquaporins: a family of highly regulated multifunctional channels. Adv Exp Med Biol 2010;679: 1–17.
[50] Hallows KR, Knauf PA. Principles of cell volume regulation. In: Strange K, editor. Cellular and molecular physiology

of cell volume regulation. Boca Raton, FL: CRC Press; 1994. p. 3–29.
[51] Han H, Wax MB, Patil RV. Regulation of aquaporin-4 water channels by phorbol ester-dependent protein phosphorylation. J Biol Chem 1998;273:6001–4.
[52] Handler JS. Antidiuretic hormone moves membranes. Am J Physiol 1988;255:F375–82.
[53] Harris HW, Handler JS. The role of membrane turnover in the water permeability response to antidiuretic hormone. J Membr Biol 1988;103:207–16.
[54] Hebert SC. Hypertonic cell volume regulation in mouse thick limbs. I. ADH dependency and nephron heterogeneity. Am J Physiol 1986;250:C907–19.
[55] Heymann JB, Agre P, Engel A. Progress on the structure and function of aquaporin 1. J Struct Biol 1998;121:191–206.
[56] Hicks RM. The mammalian urinary bladder: an accommodating organ. Biol Rev Camb Philos Soc 1975;50:215–46.
[57] Hicks RM, Ketterer B. Hexagonal lattice of subunits in the thick luminal membrane of the rat urinary bladder. Nature 1969;224: 1304–5.
[58] Hill AE. Solute–solvent coupling in epithelia: a critical examination of the standing-gradient osmotic flow theory. Proc R Soc Lond Biol 1975;190:99–114.
[59] Hirano Y, Okimoto N, Kadohira I, Suematsu M, Yasuoka K, Yasui M. Molecular mechanisms of how mercury inhibits water permeation through aquaporin-1: understanding by molecular dynamics simulation. Biophys J 2010;98:1512–9.
[60] Ho JD, Yeh R, Sandstrom A, Chorny I, Harries WE, Robbins RA, et al. Crystal structure of human aquaporin 4 at 1.8 A and its mechanism of conductance. Proc Natl Acad Sci USA 2009;106: 7437–742.
[61] Hoshi T, Sakai F. A comparison of the electrical resistances of the surface cell membrane and cellular wall in the proximal tubule of the newt kidney. Jpn J Physiol 1967;17: 627–37.
[62] House CR. Water transport in cells and tissues. London: Arnold; 1974.
[63] Hu P, Deng FM, Liang FX, Hu CM, Auerbach AB, Shapiro E, et al. Ablation of uroplakin III gene results in small urothelial plaques, urothelial leakage, and vesicoureteral reflux. J Cell Biol 2000;151:961–72.
[64] Hu P, Meyers S, Liang FX, Deng FM, Kachar B, Zeidel ML, et al. Role of membrane proteins in permeability barrier function: uroplakin ablation elevates urothelial permeability. Am J Physiol Renal Physiol 2002;283:F1200–1207.
[65] Hub JS, de Groot BL. Mechanism of selectivity in aquaporins and aquaglyceroporins. Proc Natl Acad Sci USA 2008;105: 1198–203.
[66] Hub JS, Grubmüller H, de Groot BL. Dynamics and energetics of permeation through aquaporins. What do we learn from molecular dynamics simulations? Handb Exp Pharmacol 2009;190: 57–76.
[67] Ichikawa H, Shibukawa Y, Sahara Y, Tsumura M, Qi B, Satoh K, et al. Electrophysiological properties of AQP6 in mouse parotid acinar cells. J Med Invest 2009;56:347–9.
[68] Ikeda M, Beitz E, Kozono D, Guggino WB, Agre P, Yasui M. Characterization of aquaporin-6 as a nitrate channel in mammalian cells. Requirement of pore-lining residue threonine 63. J Biol Chem 2002;277:39873–9.
[69] Ishibashi K. New members of mammalian aquaporins: AQP10-AQP12. Handb Exp Pharmacol 2009;190:251–62.
[70] Ishibashi K, Hara S, Kondo S. Aquaporin water channels in mammals. Clin Exp Nephrol 2009;13:107–17.
[71] Jacobson K, Dietrich C. Looking at lipid rafts? Trends Cell Biol 1999;9:87–91.
[72] Jung JS, Preston GM, Smith BL, Guggino WB, Agre P. Molecular structure of the water channel through aquaporin CHIP: the tetrameric-hourglass model. J Biol Chem 1994;269: 14648–54.
[73] Khandelwal P, Abraham SN, Apodaca G. Cell biology and physiology of the uroepithelium. Am J Physiol Renal Physiol 2009;297:F1477–501.
[74] King-Hele JA. Approximate analytical solutions for water and solute flow in intercellular spaces with a leaky tight junction. J Theor Biol 1979;80:451–65.
[75] King LS, Kozono D, Agre P. From structure to disease: the evolving tale of aquaporin biology. Nat Rev Mol Cell Biol 2004;5:687–98.
[76] Kovbasnjuk O, Leader JP, Weinstein AM, Spring KR. Water does not flow across the tight junctions of MDCK cell epithelium. Proc Natl Acad Sci USA 1998;95:6520–6.
[77] Krause G, Winkler L, Mueller SL, Haseloff RF, Piontek J, Blasig IE. Structure and function of claudins. Biochim Biophys Acta 2008;1778:631–45.
[78] Kwon TH, Nielsen J, Møller HB, Fenton RA, Nielsen S, Frøkiaer J. Aquaporins in the kidney. Handb Exp Pharmacol 2009; 190:95–132.
[79] Lapointe Jy Gagnon M, Poirier S, Bissonnette P. The presence of local osmotic gradients can account for the water flux driven by the Na^+–glucose co-transporter. J Physiol 2002;542:61–2.
[80] Lapointe JY, Gagnon MP, Gagnon DG, Bissonnette P. Controversy regarding the secondary active water transport hypothesis. Biochem Cell Biol 2002;80:525–33.
[81] Larsen EH, Sørensen JB, Sørensen JN. Analysis of the sodium recirculation theory of solute-coupled water transport in small intestine. J Physiol 2002;542:33–50.
[82] Larsen EH, Willumsen NJ, Møbjerg N, Sørensen JN. The lateral intercellular space as osmotic coupling compartment in isotonic transport. Acta Physiol (Oxf) 2009;195:171–86.
[83] Loo DD, Wright EM, Zeuthen T. Water pumps. J Physiol 2002;542:53–60.
[84] Loo DD, Zeuthen T, Chandy G, Wright EM. Co-transport of water by the Na^+/glucose co-transporter. Proc Natl Acad Sci USA 1996;93:13367–70.
[85] Lechène C. Cellular volume and cytoplasmic gel. Biol Cell 1985;55:177–80.
[86] Levitt DG. Kinetics of diffusion and convection in 3-X pores. Exact solution by computer simulation. Biophys J 1973;13: 186–206.
[87] Levitt DG. A new theory of transport for cell membrane pores. I. General theory and application to red cell. Biochim Biophys Acta 1974;373:115–31.
[88] Lin JH, Wu XR, Kreibich G, Sun TT. Precursor sequence, processing, and urothelium-specific expression of a major 15-kDa protein subunit of asymmetric unit membrane. J Biol Chem 1994;269:1775–84.
[89] MacAulay N, Gether U, Klaerke DA, Zeuthen T. Water transport by the human Na^+coupled glutamate co-transporter expressed in *Xenopus* oocytes. J Physiol 2001;530:367–78.
[90] Macey RI. Transport of water and urea in red blood cells. Am J Physiol 1984;246:C195–203.
[91] Macey RI, Farmer REI. Inhibition of water and solute permeability in human red cells. Biochim Biophys Acta 1970;211: 104–6.
[92] Macey RI, Moura TF. Basic principles of transport. In: Hoffman JD, Jamieson JD, editors. Handbook of Physiology. New York: Oxford University Press; 1997. p. 181–259.
[93] Macknight ADC. Principles of cell volume regulation. Renal Physiol Biochem 1988;11:114–48.

[94] Maffly RH, Leaf A. The potential of water in mammalian tissues. J Gen Physiol 1959;42:1257–75.
[95] Maurel C, Verdoucq L, Luu DT, Santoni V. Plant aquaporins: membrane channels with multiple integrated functions. Annu Rev Plant Biol 2008;59:595–624.
[96] Mauro A. The role of negative pressure in osmotic equilibrium and osmotic flow. In: Ussing HH, Bindslev N, Lassen NA, Sten-Knudsen O, editors. Water transport across epithelia. Barriers, gradients and mechanisms. Copenhagen: Munksgaard; 1981. p. 107–19.
[97] Meinild A-K, Klaerke D, Loo DDF, Wright EM, Zeuthen T. The human Na^+/glucose co-transporter is a molecular water pump. J Physiol 1998;508:15–21.
[98] Meinild AK, Loo DD, Pajor AM, Zeuthen T, Wright EM. Water transport by the renal Na^+-dicarboxylate co-transporter. Am J Physiol Renal Physiol 2000;278:F777–83.
[99] Mills JW, DiBona DR. Distribution of Na^+ pump sites in the frog gallbladder. *Nature* (Lond) 1978;271:273–5.
[100] Minton AP, Colclasure GC, Parker JC. Model for the role of macromolecular crowding in regulation of cellular volume. Proc Natl Acad Sci USA 1992;89:10504–6.
[101] Moeller HB, Olesen ET, Fenton RA. Invited review- regulation of the water channel Aquaporin-2 by post-translational modifications. Am J Physiol Renal Physiol 2011;300:F1062–73.
[102] Montalbetti N, Fischbarg J. Frequency spectrum of transepithelial potential difference reveals transport-related oscillations. Biophys J 2009;97:1530–7.
[103] Murata K, Mitsuoka K, Hirai T, Walz T, Agre P, Heymann JB, et al. Structural determinants of water permeation through aquaporin-1. Nature 2000;407:599–605.
[104] Musa-Aziz R, Chen LM, Pelletier MF, Boron WF. Relative CO2/NH3 selectivities of AQP1, AQP4, AQP5, AmtB, and RhAG. Proc Natl Acad Sci USA 2009;106:5406–11.
[105] Muto S, Hata M, Taniguchi J, Tsuruoka S, Moriwaki K, Saitou M, et al. Claudin-2-deficient mice are defective in the leaky and cation-selective paracellular permeability properties of renal proximal tubules. Proc Natl Acad Sci USA 2010;107: 8011–6.
[106] Nakhoul NL, Davis BA, Romero MF, Boron WF. Effect of expressing the water channel aquaporin-1 on the CO_2 permeability of *Xenopus* oocytes. Am J Physiol 1988;45: C543–8.
[107] Nemeth-Cahalan KL, Hall JE. pH and calcium regulate the water permeability of aquaporin 0. J Biol Chem 2000;275: 6777–82.
[108] Nilius B. Is the volume-regulated anion channel VRAC a "water-permeable" channel? Neurochem Res 2004;29:3–8.
[109] Noda Y, Sohara E, Ohta E, Sasaki S. Aquaporins in kidney pathophysiology. Nat Rev Nephrol 2010;6:168–78.
[110] Paganelli CV, Solomon AK. The rate of exchange of tritiated water across the human red cell membrane. J Gen Physiol 1957;41:259–77.
[111] Persson BE, Spring KR. Gallbladder epithelial cell hydraulic water permeability and volume regulation. J Gen Physiol 1982;79:481–505.
[112] Prasad GV, Coury LA, Fin F, Zeidel ML. Reconstituted aquaporin 1 water channels transport CO_2 across membranes. J Biol Chem 1998;273:33123–6.
[113] Preston GM, Agre P. Isolation of the cDNA for erythrocyte integral membrane protein of 28 kilodaltons: member of an ancient channel family. Proc Natl Acad Sci USA 1991;88: 11110–4.
[114] Porquet A, Filella M. Structural evidence of the similarity of $Sb(OH)_3$ and $As(OH)_3$ with glycerol: Implications for their uptake. Chem Res Toxicol 2007;20:1269–76.
[115] Rabaud NE, Song L, Wang Y, Agre P, Yasui M, Carbrey JM. Aquaporin 6 binds calmodulin in a calcium-dependent manner. Biochem Biophys Res Commun 2009;383:54–7.
[116] Rawicz W, Smith BA, McIntosh TJ, Simon SA, Evans E. Elasticity, strength, and water permeability of bilayers that contain raft microdomain-forming lipids. Biophys J 2008;94: 4725–36.
[117] Reeves WB, Andreoli E. Sodium chloride transport in the loop of Henle. In: Seldin DW, Giebisch G, editors. The Kidney: physiology and pathophysiology. New York: Raven Press; 1992. p. 1975–2001.
[118] Reichow SL, Gonen T. Noncanonical binding of calmodulin to aquaporin-0: implications for channel regulation. Structure 2008;16:1389–98.
[119] Ren G, Reddy VS, Cheng A, Melnyk P, Mitra AK. Visualization of a water-selective pore by electron crystallography in vitreous ice. Proc Natl Acad Sci USA 2001;98:1398–403.
[120] Reuss L. Pathways for osmotic water transport in gallbladder epithelium. In: Ussing HH, Fischbarg J, Sten-Knudsen O, Larsen EH, Willumsen NJ, editors. Isotonic transport in leaky epithelia. Copenhagen: Munksgaard; 1993. p. 181–200. Alfred Benzon Symposium 34.
[121] Reuss L. Epithelial transport. In: Hoffman JE, Jamieson, editors. Handbook of physiology: cell physiology. New York: Oxford University Press; 1997. p. 309–38.
[122] Reuss L, Hirst BH. Water transport controversies-an overview. J Physiol 2002;542:1–2.
[123] Reuss L, Cotton CU. Isosmotic fluid transport across epithelia. Contemp Nephrol 1988;4:1–37.
[124] Reuss L, Simon B, Cotton CU. Pseudo-streaming potentials in *Necturus* gallbladder epithelium. II. The mechanism is a junctional diffusion potential. J Gen Physiol 1992;99:317–38.
[125] Reuss L, Simon B, Xi Z. Pseudo-streaming potentials in *Necturus* gallbladder epithelium. I. Paracellular origin of the transepithelial voltage changes. J Gen Physiol 1992;99: 297–316.
[126] Rivers R, Blanchard A, Eladari D, Leviel F, Paillard M, Podevin RA, et al. Water and solute permeabilities of medullary thick ascending limb apical and basolateral membranes. Am J Physiol 1998;274:F453–62.
[127] Rose KM, Wang Z, Magrath GN, Hazard ES, Hildebrandt JD, Schey KL. Aquaporin 0-calmodulin interaction and the effect of aquaporin 0 phosphorylation. Biochemistry 2008;47: 339–47.
[128] Rosenthal R, Milatz S, Krug SM, Oelrich B, Schulzke JD, Amasheh S, et al. Claudin-2, a component of the tight junction, forms a paracellular water channel. J Cell Sci 2010;123: 1913–21.
[129] Roux B, Schulten K. Computational studies of membrane channels. *Structure* (Camb) 2004;12:1343–51.
[130] Sachar-Hill B, Hill AE. Paracellular fluid transport by epithelia. Int Rev Cytol 2002;215:319–50.
[131] Sackin H, Boulpaep EL. Models for coupling of salt and water transport. Proximal tubular reabsorption in *Necturus* kidney. J Gen Physiol 1975;66:671–733.
[132] Sánchez JM, Li Y, Rubanshkin A, Iserovich P, Wen Q, Ruberti JW, et al. Evidence for a central role for electro-osmosis in fluid transport by corneal endothelium. J Membr Biol 2002;187: 37–50.
[133] Saparov SM, Kozono D, Rothe U, Agre P, Pohl P. Water and ion permeation of aquaporin-1 in planar lipid bilayers. J Biol Chem 2001;276:31515–20.
[134] Schultz SG. Homocellular regulatory mechanisms in sodium-transporting epithelia: avoidance of extinction by "flush-through." Am J Physiol 1981;241:F579–90.

[135] Schultz SG, Hudson RL. Biology of sodium-absorbing epithelial cells: dawning of a new era. In: Schultz SG, Field M, Frizzell RA, editors. Handbook of physiology. The gastrointestinal system. New York: Oxford University Press; 1991. p. 45–81.
[136] Shen L, Weber CR, Raleigh DR, Yu D, Turner JR. Tight junction pore and leak pathways: a dynamic duo. Annu Rev Physiol 2011;73:283–309.
[137] Shporer M, Civan MM. Structuring of water and immobilization of ions within the intracellular fluids: the contribution of NMR spectroscopy. Curr Topics Membr Trans 1977;9:1–69.
[138] Smith BL, Agre P. Erythrocyte M_r 28,000 transmembrane protein exists as a multisubunit oligomer similar to channel proteins. J Biol Chem 1991;266:6407–15.
[139] Spring KR. Routes and mechanism of fluid transport by epithelia. Annu Rev Physiol 1998;60:105–19.
[140] Spring KR. Solute recirculation. J Physiol 2002;542:51.
[141] Strange K, Spring KR. Cell membrane permeability of rabbit cortical collecting duct. J Membr Biol 1987;96:27–43.
[142] Sui H, Han BG, Lee JK, Walian P, Jap BK. Structural basis of water-specific transport through the AQP1 water channel. Nature 2001;414:872–8.
[143] Sun AM, Saltzbert SN, Kikeri D, Hebert SC. Mechanisms of cell volume regulation by the mouse medullary thick ascending limb of Henle. Kidney Int 1990;38:1019–29.
[144] Tajkhorshid E, Nollert P, Jensen MO, Miercke LJ, O'Connell J, Stroud RM, et al. Control of the selectivity of the aquaporin water channel family by global orientational tuning. Science 2002;296:525–30.
[145] Törnroth-Horsefield S, Hedfalk K, Fischer G, Lindkvist-Petersson K, Neutze R. Structural insights into eukaryotic aquaporin regulation. FEBS Lett 2010;584:2580.
[146] Tripathi S, Boulpaep EL. Mechanisms of water transport by epithelial cells. Q J Exp Physiol 1989;74:385–417.
[147] Ussing HH, Eskesen K. Mechanism of isotonic water transport in glands. Acta Physiol Scand 1989;136:443–54.
[148] Ussing HH, Lind F, Larsen EH. Ion secretion and isotonic transport in frog skin glands. J Memb Biol 1996;152:101–10.
[149] vant'Hoff JH. Die Rolle des osmotischen Druckes in der Analogie zwischen Lösungen und Gasen. Z Physik Chemie 1887;1:481–93.
[150] Verkman AS. Mechanisms and regulation of water permeability in renal epithelia. Am J Physiol 1989;257:C837–50.
[151] Verkman AS. Aquaporins: translating bench research to human disease. J Exp Biol 2009;212:1707–15.
[152] Verkman AS. Knock-out models reveal new aquaporin functions. Handb Exp Pharmacol 2009;190:359–81.
[153] Verkman AS. Does aquaporin-1 pass gas? An opposing view. J Physiol 2002;542:31.
[154] Verkman AS, van Hoek AN, Ma T, Frigeri A, Skach WR, Mitra A, et al. Water transport across mammalian cell membranes. Am J Physiol 1996;270:C12–30.
[155] Wade JB. Role of membrane traffic in the water and Na^+ responses to vasopressin. Semin Nephrol 1994;14: 322–32.
[156] Walz T, Haner M, Wu XR, Henn C, Engel A, Sun TT, et al. Towards the molecular architecture of the asymmetric unit membrane of the mammalian urinary bladder epithelium: a closed "twisted ribbon" structure. J Mol Biol 1995;248: 887–900.
[157] Walz T, Fujiyoshi Y, Engel A. The AQP structure and functional implications. Handb Exp Pharmacol 2009;190: 31–56.
[158] Walz T, Hirai T, Murata K, Heymann JB, Mitsuoka K, Fujiyoshi Y, et al. The three-dimensional structure of aquaporin-1. Nature 1997;387:624–6.
[159] Walz T, Smith BL, Agre P, Engel A. The 3-D structure of human erythrocyte aquaporin CHIP. EMBO J 1994;13:2985–93.
[160] Wang Y, Tajkhorshid E. Molecular mechanisms of conduction and selectivity in aquaporin water channels. J Nutr 2007;137:1509S–15S.
[161] Weinstein AM, Stephenson JL. Electrolyte transport across a simple epithelium. Steady-state and transient analysis. Biophys J 1979;27:165–86.
[162] Weinstein AM, Stephenson JL. Coupled water transport in standing gradient models of the lateral intercellular space. Biophys J 1981;35:167–91.
[163] Weinstein AM, Stephenson JL. Models of coupled salt and water transport across leaky epithelia. J Membr Biol 1981;60:1–20.
[164] Whittembury G, Rawlins FA. Evidence of a paracellular pathway for ion flow in the kidney proximal tubule: electron microscopic demonstration of lanthanum precipitate in the tight junction. Pflügers Arch 1971;330:302–9.
[165] Whittembury G, Carpi-Medina P, Gonzalez E, Linares H. Effect of parachloromercuribenzene sulfonic acid and temperature on cell water osmotic permeability of proximal straight tubules. Biochim Biophys Acta 1984;775:365–73.
[166] Whittembury G, Hill A. Coupled transport of water and solute across epithelia. In: Seldin DW, Giebisch G, editors. The Kidney: physiology and pathophysiology. New York: Raven Press; 2000. p. 341–62.
[167] Whittembury G, Reuss L. Mechanisms of coupling of solute and solvent transport in epithelia. In: Seldin DW, Giebisch G, editors. The Kidney: physiology and pathophysiology. New York: Raven Press; 1992. p. 317–60.
[168] Windhager EE, Boulpaep EL, Giebisch G. Electrophysiological studies in single nephrons. In: Schreiner GE, editor. Proceedings of the third international congress on nephrology. New York: Karger; 1967. p. 35–47.
[169] Wu XR, Kong XP, Pellicer A, Kreibich G, Sun TT. Uroplakins in urothelial biology, function, and disease. Kidney Int 2009;75:1153–65.
[170] Wu XR, Manabe M, Yu J, Sun TT. Large scale purification and immunolocalization of bovine uroplakins I, II, and III. Molecular markers of urothelial differentiation. J Biol Chem 1990;265:19170–9.
[171] Yang B, Fukuda N, van Hoek A, Matthay MA, Ma T, Verkman AS. Carbon dioxide permeability of aquaporin-1 measured in erthrocytes and lung of aquaporin-1 null mice and in reconstituted liposomes. J Biol Chem 2000;275: 2686–92.
[172] Yu J, Manabe M, Wu XR, Xu C, Surya B, Sun TT, et al. A 27-kD protein associated with the asymmetric unit membrane of mammalian urothelium. J Cell Biol 1990;111: 1207–16.
[173] Zelenina M, Zelenin S, Bondar AA, Brismar H, Aperia A. Water permeability of aquaporin-4 is decreased by protein kinase C and dopamine. Am J Physiol 2002;283: F309–18.
[174] Zeuthen T. Co-transport of K^+, Cl^- and H_2O by membrane proteins from choroid plexus Epithelium of *Necturus maculosus*. *J Physiol* (Lond) 1994;478:203–19.
[175] Zeuthen T. Water-transporting proteins. J Membr Biol 2010;234:57–73.
[176] Zeuthen T, Hamann S, La Cour M. Co-transport of H^1, a lactate and H_2O by membrane proteins in retinal pigment epithelium of bullfrog. J Physiol 1996;497:3–17.
[177] Zeuthen T, Klaerke DA. Transport of water and glycerol in aquaporin 3 is gated by H^1. J Biol Chem 1999;274: 21631–6.

CHAPTER

5

Cell Volume Control

Florian Lang

Department of Physiology, University of Tübingen, Tübingen, Germany

Cells must avoid gross alterations of volume in order to survive. Obviously, excessive cell swelling will jeopardize the integrity of the cell membrane, and both cell swelling and cell shrinkage will interfere with cytoskeletal architecture. Moreover, cellular function critically depends on the hydration of cytosolic proteins. Proteins and protein-bound water occupy a large portion of the cell interior (macromolecular crowding), leaving only a small fraction of cellular volume to free water.[1–6] Abstraction or addition of only a few percentage points of cellular water thus has profound effects on protein function and cellular performance.

In most mammalian cells, the plasma membrane is highly permeable to water,[7,8] a property in large part due to virtually ubiquitous expression of water channels in the cell membrane.[9–11] In theory, driving forces for movement of water include hydrostatic and osmotic pressure gradients. However, the cell membrane is too fragile to withstand significant hydrostatic pressure gradients, and if extension of the cell is not prevented by extracellular constraints the movement of water is governed almost exclusively by osmotic gradients.[12–15] Thus, to avoid swelling or shrinkage, a cell has to achieve osmotic equilibrium across the cell membrane (Figure 5.1). At excessive intracellular osmolarity, water will enter following its osmotic gradient, and the cell will swell. Conversely, at excessive extracellular osmolarity, water will leave, and the cell will shrink. As outlined in this chapter a wide variety of factors modify intra- or extracellular osmolarity, and thus challenge osmotic equilibrium across the cell membrane.

For maintenance of volume constancy, cells employ a number of mechanisms, including metabolism and altered transport across the cell membrane. These mechanisms may also participate in the regulation of cell function. Hormones and mediators may influence cell volume regulatory mechanisms, and thus manipulate cell volume. Alterations of cell volume will in turn modify other cell volume-sensitive functions. The interplay among cell volume regulatory mechanisms, cell hydration, and cell function does not only contribute to physiological regulation of cellular function, but also participates in the pathophysiology of a wide variety of diseases.

In this chapter a description of cell volume regulatory mechanisms will be followed by a synopsis of factors challenging cell volume constancy, and a discussion on the impact of cell volume regulatory mechanisms on the physiology and pathophysiology of cellular function. Due to space constraints, many excellent original papers on cell volume regulation could not be cited, and the reader is referred to reviews instead. For more detailed analysis of the pertinent original literature, the reader is encouraged to consult previous reviews on cell volume regulation.[16–41]

CELL VOLUME REGULATORY MECHANISMS

Cell volume constancy is challenged by alterations of extracellular osmolarity, by intracellular metabolic generation of osmotically active solutes and by transport across the cell membrane.[31] To counteract those challenges, cells employ a variety of cell volume regulatory mechanisms.[32] Following cell swelling, these mechanisms decrease intracellular osmolarity and cell volume, thus accomplishing regulatory cell volume decrease (RVD). Upon cell shrinkage the mechanisms increase intracellular osmolarity and cell volume, thereby accomplishing regulatory cell volume increase (RVI). Upon slow changes of extracellular osmolarity, the volume regulatory mechanisms may be fast

Seldin and Giebisch's The Kidney, Fifth Edition.
DOI: http://dx.doi.org/10.1016/B978-0-12-381462-3.00005-7

© 2013 Elsevier Inc. All rights reserved.

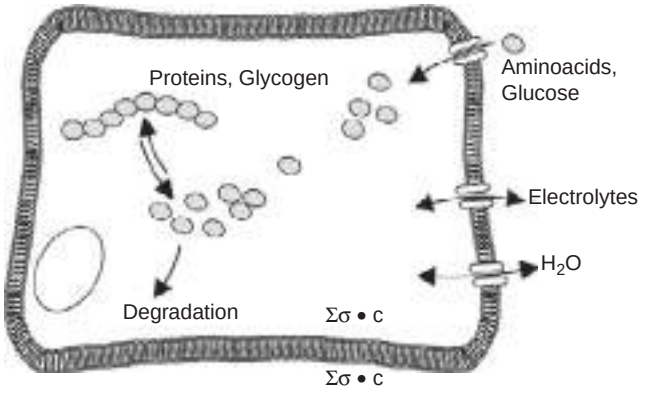

FIGURE 5.1 **Determinants of cell volume.** Water moves according to osmotic gradients across the cell membranes, that is, differences between intracellular and extracellular $\sum\sigma.c$, where σ is the reflection coefficient and c the concentration of each solute on either side. Even at constant extracellular $\sum\sigma.c$, an osmotic gradient is generated by transport of osmotically active solutes across the cell membrane and by metabolic generation or disposal of intracellular solutes.

enough to prevent significant alterations of cell volume, leading to isovolumetric volume regulation.[42]

The most powerful mechanisms of cell volume regulation are ion transporters in the cell membrane.[32] As outlined below, uneven ion composition of intracellular and extracellular fluid is one prerequisite for the establishment of osmotic equilibrium across the cell membrane. Furthermore, several ion transport systems in the cell membrane are modified upon alterations of cell volume. Following cell swelling they mediate cellular ion release; upon cell shrinkage they allow cellular ion accumulation to re-establish osmotic equilibrium across the cell membrane.

However, the use of ions in cellular osmoregulation is limited, since high inorganic ion concentrations interfere with the stability of proteins.[43] Beyond that, altered ion gradients across the cell membrane interfere with the function of gradient-driven transporters. For instance, an increase of intracellular Na^+ activity decreases the chemical gradient for Na^+ across the cell membrane, and reduces the driving force for Ca^{2+} extrusion via the Na^+/Ca^{2+} exchanger, which increases intracellular Ca^{2+} activity. To avoid excessive alterations of intracellular ion concentration, cells also utilize organic osmolytes for osmoregulation.[20,21,44] Moreover, cells adapt a variety of metabolic functions, and thus modify the cellular generation or disposal of osmotically active organic substances.

It should be pointed out that a single cell does not usually employ all cell volume regulatory mechanisms described in the following text. In most cases, it is not clear why a given cell selects a certain set of ion transporters and osmolytes without using other mechanisms. Presumably, the large repertoire of cell volume regulatory transporters and osmolytes available enables any given cell to regulate its volume with relatively little impairment of its particular function.

Cell Volume Regulatory Ion Transport

To counterbalance the intracellular osmolarity due to osmotically active organic solutes, such as amino acids and carbohydrates, cell volume regulatory mechanisms need to maintain intracellular concentrations of inorganic ions below extracellular ion concentrations. In addition, cell volume regulatory ion transport systems are employed to counteract alterations of cell volume by appropriate transport of ions across the cell membrane.

Ions in Cell Volume Maintenance

To compensate for the cellular accumulation of organic solutes, cells maintain a low intracellular Cl^- concentration.[31] In most cells, Cl^- may move across the cell membrane through Cl^- channels. Cl^- movement through those channels is governed by the cell's negative potential across the cell membrane, which is built up by asymmetric cation gradients[8]: the cells extrude Na^+ in exchange for K^+ by the Na^+/K^+-ATPase. The cell membrane is, on average, less permeable to Na^+ than to K^+. K^+ tends to leave the cell through K^+ channels following its chemical gradient. The exit of K^+ generates a cell-negative potential difference across the cell membrane, and thus establishes the driving force for the exit of anions such as Cl^-. At a cell membrane potential of some -18 mV, for instance, Cl^- is in equilibrium at a chemical gradient of 1:2. Accordingly, at an extracellular Cl^- concentration of 110 mmol/L, the intracellular Cl^- concentration is in electrochemical equilibrium at 55 mmol/L. In theory, such a Cl^- distribution would allow the excess accumulation of 55 mmol/L of organic solutes. In most cells the potential difference across the cell membrane is higher (more negative) than -18 mV, and intracellular Cl^- is even lower than 55 mmol/L.

As long as the cell membrane is perfectly impermeable to Na^+, cell membrane potential, cytosolic Cl^- concentration, and cell volume could be maintained constant without continued expenditure of energy. Maintenance of the asymmetric cation distribution requires, however, that any Na^+ entering the cell is subsequently extruded by Na^+/K^+-ATPase, an ATP-consuming process.

Ion Release Following Cell Swelling

Ion transport is not only crucial for the establishment of osmotic equilibrium across the cell membrane, but accomplishes rapid correction of any osmotic imbalance across the cell membrane. Following cell swelling, cells must release ions to decrease their osmolarity. Most cells release ions by activation of K^+ channels and/or anion channels (Figure 5.2). Cell volume regulation requires the operation of both ion channel types, since neither K^+ nor anions can leave the cells without the respective counterion. Several cell volume regulatory ion channels have been identified at the molecular level, including the K^+ channels Kv1.3,[45] Kv1.5,[46] Kv4.2, 3,[47] IsK or KCNE1/Q1,4,5,[26,48–51] TWIK1,[52] TASK2/KCNK5,[53] TREK1/KCNK2,[26] TRAAK/KCNK4,[26] intermediate or MaxiK (Kca),[26,54] and the anion channels ClC-2,[55–59] ClC-3,[60,61] phospholemman,[62] and bestrophins.[63] The role of other ion channels in cell volume regulation, such as I_{Cln},[64–66] P-glycoprotein (MDR) ,[67–70] and CFTR,[71,72] has been a matter of controversy. Clearly, many different ion channels are likely to contribute to cell volume regulation in various tissues, and the molecular identity of some of those channels is still elusive. Some anion channels not only allow the exit of Cl^-, but also of HCO_3^-, organic anions, and noncharged osmolytes.[73–80]

Swelling of some cells activates unspecific cation channels, including some transient receptor potential (TRP) channels.[15,32,81–87] Since the electrochemical gradient favors entry rather than exit of cations, these channels cannot directly serve cell volume regulation. Instead, the channels allow the entry of Ca^{2+}, which in turn activates Ca^{2+}-sensitive K^+ channels and/or Cl^- channels.

Besides ion channels, the most important mechanism contributing to regulatory cell volume decrease is KCl co-transport by one of the four members of the KCC family,[88,89,90–94] which allows coupled cellular release of both ions.

Some cells release cellular KCl via parallel activation of K^+–H^+ exchange and Cl^-–HCO_3^- exchange.[95,96] The H^+ and HCO_3^- thus taken up in exchange for KCl react via H_2CO_3 to produce CO_2, which can easily leave the cell again.

Water efflux during volume regulatory decrease could be fully accomplished by existing water channels. Nevertheless, aquaporins participate in cell volume regulation by modifying the activity of ion channels.[9]

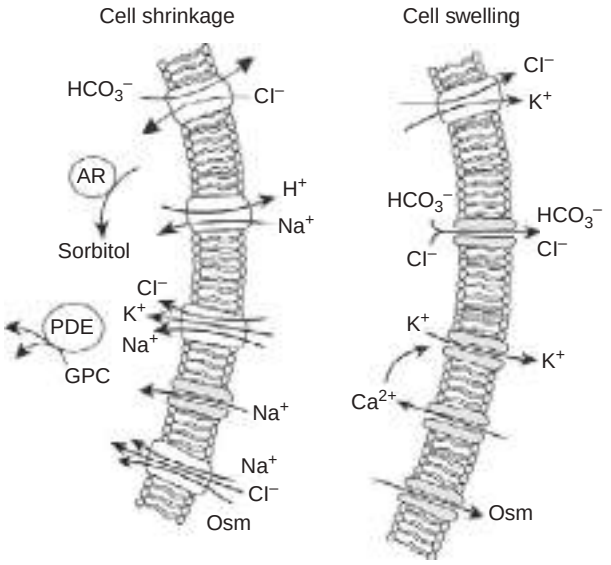

FIGURE 5.2 **Most widely employed mechanisms of regulatory cell volume regulation.** Left: Mechanisms of regulatory cell volume decrease. Cell swelling leads to activation of KCl co-transport, anion channels, K^+ channels, cation channels, and channels releasing organic osmolytes such as sorbitol, inositol, taurine, and betaine. The cation channels do not directly serve cell volume regulatory decrease, but rather increase of cytosolic Ca^+ activity that triggers activation of Ca^{2+} sensitive K^+ channels. Right: Mechanisms of cell volume increase. Cell shrinkage leads to parallel activation of Na^+/H^+ exchanger and Cl^-/HCO_3^- exchanger, $Na^+K^+2Cl^-$ co-transport, Na^+ channels, and Na^+-coupled accumulation of inositol, taurine, and betaine. Furthermore, cell shrinkage leads to cellular accumulation of glycerophosphorylcholine by inhibition of phosphodiesterase (PDE), and of sorbitol by activation of aldosereducase (AR).

Ion Uptake upon Cell Shrinkage

Cell shrinkage activates the Na^+–K^+–$2Cl^-$ co-transporters NKCC1, and NKCC2,[97–100] and/or the Na^+/H^+ exchangers NHE1,[101] NHE2[102] or NHE4[103] parallel to the $Cl^-HCO_3^-$ exchanger AE1.[36,104,105] The parallel activation of Na^+/H^+ exchangers and Cl^-/HCO_3^- exchangers leads to uptake of NaCl, while the H^+ and HCO_3^- lost in exchange for NaCl are replenished in the cell from CO_2 via H_2CO_3 (Figure 5.2). The epithelial Na^+/H^+ exchanger NHE3 is inhibited by cell shrinkage.[106] The Na^+ ions accumulated by either Na^+–K^+–$2Cl^-$ co-transport or Na^+H^+ exchange are extruded by Na^+K^+-ATPase in exchange for K^+. Accordingly, the transporters eventually lead to cellular KCl uptake.

Several cells activate Na^+ channels or unspecific cation channels following cell shrinkage.[107–112] The channels may include some members of the transient receptor potential (TRP) channel family or ENaC.[113–116,181] The resulting depolarization drives Cl^- into the cell, so that the net effect is cellular accumulation of NaCl. Other cells inhibit K^+ and/or Cl^- channels to avoid cellular ion loss.[32]

Osmolytes

The most important osmolytes are polyols such as sorbitol and myoinositol, methylamines such as betaine and glycerophosphorylcholine, as well as amino acids including taurine.[3,21,28,41,44,117,118] In contrast to inorganic ions, organic osmolytes do not destabilize proteins, but rather stabilize them. They counteract the destabilizing effects of inorganic ions, some organic ions (e.g., spermidine), and urea.[3,18] The stabilizing potency of the diverse organic osmolytes is not identical. The destabilizing effects of urea are counteracted most efficiently by betaine and glycerophosphorylcholine, and less efficiently by myoinositol.[18] The stabilizing effects of osmolytes may protect proteins against excessive ion concentrations, as well as against heat shock, freezing, desiccation, and presumably radiation.[119–123]

Osmolyte Accumulation by Metabolism

Sorbitol is generated from glucose under the catalytic action of aldose reductase.[124–126] Stimulation of the transcription rate of the aldose reductase during osmotic cell shrinkage leads to cellular accumulation of sorbitol. The expression of the protein takes many hours, and the appropriate increase of sorbitol concentration requires hours to days.[127]

Glycerophosphorylcholine (GPC) is produced from phosphatidylcholine under the catalytic action of a phospholipase A_2, which is distinct from the arachidonyl selective enzyme.[21,128] GPC is degraded by a phosphodiesterase to glycerol-phosphate and choline. Inhibition of the phosphodiesterase during cell shrinkage leads to cellular accumulation of GPC.[129]

Osmolyte Accumulation by Transport

Myoinositol (inositol),[28,130–133] betaine[134–136] and taurine[137] are taken up by specific Na^+-coupled transporters SMIT (inositol), BGT (betaine), and NCT (taurine), respectively. The carriers accumulate Na^+, the respective organic osmolyte, and in the case of BGT and NCT, Cl^- as well. Movement of excess positive charge by the carriers depolarizes the cell membrane, thus favoring entry of Cl^- via anion channels. The transporters thus mediate uptake of NaCl parallel to organic osmolytes. The transcription rate of the transporters and the cellular accumulation of the respective osmolytes are stimulated by osmotic cell shrinkage. Expression of the transporters is slow, and full adaptation requires hours to days. Moreover, volume regulation by activation of transport systems depends on the availability of osmolytes in the extracellular fluid.

Analogous to osmolytes, some amino acids are accumulated by cell volume-sensitive, Na^+-coupled transport.[138–140] In addition, amino acids could be generated by autophagic proteolysis, as discussed in the next section.

Osmolyte Release

Cell swelling stimulates the rapid release of GPC,[27,141] sorbitol,[142–144] inositol,[27,145] betaine,[27,145] and taurine.[77,146–150] The mechanisms mediating osmolyte release are still poorly understood. Clearly, several mechanisms are simultaneously operative. At least some of the release mechanisms are thought to be anion channels. As shown for taurine,[147] the osmolyte release could be triggered by oxidative stress.

Metabolic Pathways Sensitive to Cell Volume

Alterations of cell volume influence a variety of metabolic pathways. The effects of cell volume on metabolism are accomplished in part by activation and inhibition, and in part by altered expression of enzymes.[31]

Protein and Glycogen Metabolism

Cell shrinkage stimulates the breakdown of proteins to amino acids, and of glycogen to glucosephosphate.[24,151–154] Moreover, cell shrinkage inhibits protein and glycogen synthesis.[153,154] The sum of amino acids generated during proteolysis is osmotically more active than the osmolarity of the respective protein. Thus, net formation of macromolecules decreases, and net degradation of macromolecules enhances, cellular osmolarity. Cell swelling stimulates protein and glycogen synthesis, and inhibits proteolysis and glycogenolysis, thus decreasing the intracellular concentration of amino acids and glucosephosphate.

Glucose and Amino Acid Metabolism

In addition to affecting protein and glycogen metabolism, alterations of cell volume influence several pathways of glucose and amino acid metabolism.[154] Cell swelling inhibits glucose uptake and glycolysis, stimulates flux through the pentose phosphate pathway, and favors lipogenesis from glucose, effects reversed by cell shrinkage.[154–156] Transcription of phosphoenolpyruvate carboxykinase, a key enzyme for gluconeogenesis, is decreased by cell swelling. Cell swelling stimulates glycine and alanine oxidation and glutamine breakdown, as well as formation of NH_4^+ and urea from amino acids; these effects are reversed by cell shrinkage.[154]

Oxidative Metabolism

The stimulation of flux through the pentose phosphate pathway during cell swelling enhances NADPH production, which favors the formation of glutathione (GSH).[154,156] Cell shrinkage decreases NADPH production and GSH formation. Accordingly, cell swelling increases and cell shrinkage decreases cellular resistance to oxidative stress. On the other hand, cell swelling stimulates, and cell shrinkage decreases, the activity of NADPH-oxidase, thus modulating cellular O_2^- formation.[157,158] Accordingly, leukocyte oxidative burst, and thus immune response, is blunted by the high osmolarity of kidney medulla.[159,160]

Other Metabolic Pathways

Cell swelling stimulates ketoisocaproate oxidation, acetyl CoA carboxylase, and lipogenesis, and inhibits carnitine palmitoyltransferase I. It decreases cytosolic ATP and phosphocreatine concentrations, and increases respiration. Cell swelling stimulates RNA and DNA synthesis. All of these effects are reversed by cell shrinkage.[31]

Cell Volume-Sensitive Genes

Cell volume influences the transcription of a wide variety of genes,[31,44,117,161] leading to differential expression of a wide variety of proteins.[162,163] Transcription factors involved include AP1, c-FOS, cJUN, tonicity-response enhancer binding protein TONEBP, serum response factor (SRF), and myocardin related transcription factor.[26,161] Many of the cell volume-regulated genes are related to cell volume regulation. Accordingly, cell shrinkage stimulates expression of enzymes or transporters engaged in cellular formation or accumulation of osmolytes, such as aldose reductase, and the Na^+-coupled transporters for betaine (BGT), taurine (NCT), myoinositol (SMIT), and amino acids, as well as Na^+,K^+,$2Cl^-$ co-transport (see above). Moreover, cell shrinkage upregulates the expression of the ATPase α1-subunit.[164]

The products of other genes may be involved in the signaling of cell volume regulatory mechanisms, such as the kinases ERK1, ERK2, and JNK-1, which are expressed during cell swelling[165] or the serum and glucocorticoid inducible kinase SGK1[166,167] and cyclooxygenase-2,[168] which are preferably expressed in shrunken cells.[31]

Heat shock proteins serve to stabilize proteins, and their expression in shrunken cells may counteract the destabilizing effects of accumulated ions.[169–173] Several genes expressed in response to altered cell volume do not have obvious roles in cell volume regulation. Cell swelling stimulates the expression of the cytoskeletal elements β-actin and tubulin, the immediate early genes c-jun and c-fos, the enzyme ornithine decarboxylase, and the cytokine TNF-α.[165,174,175]

Cell shrinkage stimulates the expression of the channels CIC-K1, the transporter P-glycoprotein, the immediate early genes Egr-1 and c-fos, the GTPase inhibitor α1-chimaerin, the CDβ antigen, the enzymes phosphoenolpyruvate carboxykinase (PEPCK), arginine succinate lyase, tyrosine aminotransferase, tyrosine hydroxylase, dopamine β-hydroxylase, matrix metalloproteinase 9, tissue plasminogen activator, as well as matrix proteins including biglycan and laminin B_2.[31] Cell shrinkage stimulates both expression and release of ADH, which serves to eliminate water and thus increase extracellular osmolarity.[176]

The mechanisms mediating the altered gene expression are beginning to be understood. The promoter region of the genes encoding aldose reductase, BGT, TAUT, and SGK1 have been ascribed to contain osmolarity responsive (ORE), tonicity responsive (TonE) or cell volume-responsive (CVE) elements, which are required for osmolarity or cell volume-sensitive expression of the respective genes.[125,177,178] TonE has been shown to bind a tonicity-responsive element-binding protein (TonEBP) for stimulation of expression.[179–186] TonEBP is regulated by ataxia teleangiectasia-mutated (ATM) kinase.[181]

Signaling of Cell Volume Regulation

The stimulation of effectors of cell volume regulation requires that alterations of cell volume or osmolarity are perceived and trigger a signaling cascade, eventually leading to stimulation of cell volume regulatory mechanisms.

Little is known about sensors of cell size and hydration. Circumstantial evidence points to the ability of cells to determine cellular protein content or macromolecular crowding.[187] It has been speculated that macromolecular crowding directly or indirectly regulates kinases which in turn influence the activity of cell volume regulatory KCl and $Na^+-K^+-2Cl^-$ co-transport (see below).[31] Alternatively, alterations of ionic strength or the concentration of individual ions such as Cl^- modify volume regulatory mechanisms.[26] Moreover, alterations of cell size are thought to impose stretch on the cytoskeleton and/or cell membrane or change the curvature of the cell membrane,[188–190] again leading directly or indirectly to activation of cell volume regulatory mechanisms.[31,191,192] Cell swelling leads to unfolding of the cell membrane and, if this does not suffice, to endomembrane insertion. Alterations of cell volume could be further sensed by

cytokine[193] and Ca^{2+} sensing receptors,[194] as well as by integrins.[26]

A multitude of signaling pathways link the alterations of cell volume and cell volume regulatory mechanisms. The respective signaling varies considerably between different cells or a given cell in different functional states.

Intracellular Ca^{2+}

Cell swelling increases intracellular Ca^{2+} activity in many, but not all, cells. Ca^{2+} enters through Ca^{2+} channels in the plasma membrane, and/or is released from intracellular stores triggered by 1,4,5-inositol-trisphosphate. The channels involved include nonselective Ca^{2+} channels, Ca^{2+} permeable members of the TRP (transient receptor potential) channel family, such as TRPV4, and L-type voltage gated Ca^{2+} channels.[41,113,195,196] Ca^{2+} in turn activates some cell volume regulatory K^+ channels and Cl^- channels.[197–199] In addition to its involvement in regulatory cell volume decrease, intracellular Ca^{2+} may mediate some of the functional consequences of cell shrinkage.

Cytoskeleton

Alterations of cell volume modify the architecture of the cytoskeleton and the expression of cytoskeletal proteins.[200–204] Cell shinkage increases and cell swelling decreases actin polymerization. Both microtubules[200] and actin filaments[201] have been implicated in cell volume regulation. In several cells, disruption of actin filaments and/or the microtubule network have been shown to interfere with cell volume regulation.[31]

Protein Phosphorylation

Cell swelling and cell shrinkage have both been shown to modify the phosphorylation of a variety of proteins. Kinases reported to be activated during cell swelling include tyrosine kinases,[205–209] protein kinase-C,[210,211] phosphoinositide (PI) 3 kinase,[212] Jun-kinase, and extracellular signal-regulated kinases ERK-1 and ERK-2,[165,208,213–219] as well as focal adhesion kinase ($p121^{FAK}$).[212] Activation of PI3 kinase leads to stimulation of protein kinase B (Akt), and serum and glucocorticoid inducible kinase isoforms, which modify a wide variety of carriers and channels.[220] Expression of SGK1 is, however, downregulated by cell swelling, and thus SGK1 dependent signaling is disrupted.[220] In Jurkat lymphocytes, cell swelling leads to activation of the src-like kinase lck,[56] which in turn activates the cell volume regulatory Cl^- channel ORCC.[206]

Osmotic cell shrinkage stimulates WNK (with no lysine kinase) 1 and 4, which in turn activate Ste-20-related proline alanine rich kinase (SPAK) and oxidative stress responsive kinase (OSR1).[222–224] SPAK and OSR1 activate the Na^+-K^+-$2Cl^-$ co-transporters NKCC1 and NKCC2.[222,223,225] Conversely, WNK4 inhibits KCl co-transporters.[226] WNK1 activates SGK1, which in turn inhibits WNK4.[227,228] Osmotic cell shrinkage further triggers several MAP (mitogen-activated protein) kinase cascades, and activates SAPK, p38 kinase, myosin light-chain-kinase (MLCK), Jun kinase (JNK), p21-activated kinases PAKs Rho kinase, LIM kinase, and casein kinase.[193,229–239] MLCK may modulate the cytoskeleton, and thus cell volume regulatory ion transport. Moreover, the kinase cascades lead to activation of transcription factors governing expression of cell volume-regulated genes.[31] Hyperosmolarity activates the tyrosine kinase Fyn-dependent phosphorylation of caveolin,[240] which in turn inhibits volume-sensitive Cl^- channels.[241]

Phosphatidylinositol 4,5,-Bisphosphate

Cell swelling decreases and cell shrinkage increases the formation of phosphatidylinositol 4,5 bisphosphate ($PtdIns(4,5)P_2$)[242] by the phosphatidylinositol 4-phosphate 5-kinase beta isoform (PIP5KIbeta).[243] Among other effects, $PtdIns(4,5)P_2$ stimulates the transient receptor potential channel TRPV1, Na^+/H^+ exchanger NHE1, the Na^+/Ca^{2+} exchanger NCX, and the Na^+ channel ENaC, and inhibits the transient receptor potential channel TRPC6.[26,244] $PtdIns(4,5)P_2$ may further foster actin polymerization by inhibiting the monomer-binding protein profilin, the severing protein cofilin, the capping protein gelsolin, as well as the Wiskott–Aldrich syndrome protein (WASP).[26,245]

Phospholipase A_2 and Eicosanoids

Cell swelling activates phospholipase A_2 and subsequently stimulates the formation of the 15-lipoxygenase product hepoxilin A_3, and the 5-lipoxygenase product leukotriene LTD_4.[246] Phospholipase A2 is phosphorylated by casein kinases CK1 and CK2, protein kinase A, protein kinase C, and mitogen activated kinases.[247–249] In some cells the eicosanoids generated following ativation of phospholipase A_2 stimulate cell volume regulatory K^+,Cl^- channels, and/or taurine release.[246] Enhanced formation of leukotrienes parallels decreased formation of PGE_2, with subsequent decrease of Na^+ channel activity.[246,250] Conversely, osmotic cell shrinkage may stimulate formation of PGE_2, with subsequent activation of PGE_2-sensitive Na^+ channels.[251] In other cells PGE_2 may activate volume regulatory K^+ channels.[252] In erythrocytes, activation of phospholipase A_2 by hyperosmotic shock leads to release of platelet-activating factor PAF, which in turn activates a sphingomyelinase, thus stimulating ceramide formation.[253]

pH of Acidic Cellular Compartments

In all cells studied thus far, swelling alkalinizes and cell shrinkage acidifies acidic cellular compartments, presumably including endosomes, lysosomes, and secretory granules.[31,254] This effect is apparently mediated by the microtubules, since it is abolished by disruption of the microtubule network. The alkalinization of the acidic cellular compartments may contribute to the antiproteolytic action of cell swelling, since the pH optimum of lysosomal proteases is in the acidic range, and lysosomal alkalinization has indeed been shown to inhibit proteolysis.[255]

Others

Several G-proteins have been implicated in cell volume regulation including Rho, Rac, and Ras.[26,256,257] Hyperosmotic cell shrinkage further activates ezrin/radixin/moesin (ERM) proteins, which in turn mitigate the shrinkage-induced activation of NHE1, augment Rho activity, and presumably modify actin architecture.[258] Cell swelling may trigger release of ATP, which in turn leads to autocrine stimulation of purinergic receptors with the respective activation of cell volume regulatory ion channels.[259]

CHALLENGES AND FUNCTIONS AFFECTING CELL VOLUME

A wide variety of factors alters extracellular and/or intracellular osmolarity, and thus challenges cell volume constancy. Due to the exquisite sensitivity of cell function to even minor alterations of cell volume, those factors may modify a multitude of physiological functions and participate in several pathophysiological conditions.

Alterations of Extracellular Fluid Osmolarity and Composition

In mammals, most cells are usually bathed in well-controlled extracellular fluid. However, both extracellular osmolarity and composition could vary to an extent, challenging cell volume regulation.

Osmolarity

Excessive alterations of extracellular osmolarity are only encountered in kidney medulla, where extracellular osmolarity may approach 1400 mosmol/L in humans (see Chapter 40). Renal medullary cells are exposed to this excessive extracellular osmolarity during antidiuresis, and have to cope with rapid changes of extracellular osmolarity during transition from antidiuresis to diuresis. Blood cells passing the kidney medulla experience high medullary osmolarity and subsequent return to isoosmolarity within seconds (see Chapter 40).

During intestinal absorption, intestinal cells are exposed to anisosmotic luminal fluid, and liver cells to minor alterations of portal blood osmolarity. Other tissues are exposed to anisotonic extracellular fluid during deranged regulation of extracellular osmolarity (see Chapters 41 and 42). As Na^+ salts (mainly NaCl) contribute normally more than 90% to extracellular osmolarity, hypernatremia is necessarily paralleled by an increase in extracellular osmolarity (see Chapter 42). During hypernatremia, cells defend themselves against increased extracellular osmolarity by triggering regulatory cell volume increase involving cellular accumulation of osmolytes. Owing to cell volume regulation, cell volume may become normal despite enhanced extracellular osmolarity. Rapid correction of chronically enhanced osmolarity may then lead to deleterious cell swelling, since the organic osmolytes accumulated during hyperosmolarity cannot be rapidly released. The most serious consequence is cerebral edema.

Hyponatremia cannot be equated with hypoosmolarity, but may occur in isoosmolar or even hyperosmolar states, as in hyperglycemia of uncontrolled diabetes mellitus and ethanol poisoning (see Chapter 44). When hyponatremia reflects a decreased extracellular osmolarity, the cells must undergo regulatory cell volume decrease to escape cell swelling. Among other mechanisms, cells release organic osmolytes. Upon rapid correction of hyponatremia, cells are unable to rapidly accumulate the osmolytes, and the iatrogenic cell shrinkage may prove more harmful than the untreated hypoosmolarity.

Hypoosmolar hyponatremia is observed following burns, pancreatitis, and crush syndrome, which are generally paralleled by cell shrinkage.[24] In those conditions, the primary event may be cell shrinkage leading to ADH release with subsequent renal water retention and to cellular catabolism with enhanced release of organic solutes to the extracellular fluid.

Extracellular K^+ Concentration

The potential difference across the cell membrane is maintained by K^+ flux through K^+ channels, which in turn depends on the electrochemical driving force for K^+. An increase of extracellular K^+ concentration decreases the chemical gradient for K^+ ions, impedes K^+ efflux, depolarizes the cell membrane, and thus favors Cl^- entry into the cell. The cellular accumulation of KCl eventually leads to cell swelling. Conversely, a decrease of extracellular K^+ may lead to cell shrinkage secondary to cellular loss of KCl.[31]

H^+ and HCO_3^- Concentration

On increase of extracellular HCO_3^- concentration, cellular HCO_3^- release through anion channels and Na^+–HCO_3^- co-transport is blunted or even reversed, and the decreased efflux of negative charge hyperpolarizes the cell membrane, and thus decreases the electrochemical gradient for K^+ efflux. As a result, the cell may swell due to accumulation of K^+ and HCO_3^-.[260]

An increasing extracellular pH favors cellular H^+ elimination through the Na^+/H^+ exchanger, and the resulting cellular Na^+ accumulation may lead to cell swelling.[261] During hyperkapnea, cellular CO_2 dissociates to form H^+, which is subsequently extruded by the Na^+/H^+ exchanger. Again, cellular Na^+ accumulation is paralleled by cell swelling. Due to sensitivity of the Na^+/H^+ exchanger to intracellular pH, cellular acidification favors cell swelling, whereas cellular alkalinization has the opposite effect.[262]

Organic Acids

Some organic anions, such as acetate, lactate, and proprionate, may enter cells as unionized acids. Intracellular dissociation of the acids then leads to intracellular acidification, stimulation of Na^+/H^+ exchange, accumulation of Na^+ and organic anions, and subsequent cell swelling.[31] Isotonic replacement of Cl^- with impermeant gluconate, on the other hand, leads to cell shrinkage due to cellular loss of Cl^-.[31]

Urea, Drugs, and Toxins

Urea readily passes cell membranes, and does not usually create osmotic gradients across them. On the other hand, it has been shown that urea destabilizes proteins, and thus shifts the cell volume regulatory set point towards smaller cell volumes. Through activation of some cell volume regulatory mechanisms, such as KCl co-transport, urea shrinks cells, as shown for erythrocytes, hepatocytes, renal cells, and vascular smooth muscle cells.[31]

Beyond these mechanisms, cell volume is influenced by a wide variety of drugs and toxins, interfering with cell volume regulatory mechanisms.[31] For instance, inhibition of K^+ channels leads to cell swelling, and inhibition of Na^+–K^+2Cl^- co-transport and/or Na^+/H^+ exchanger leads to cell shrinkage.

Functional States Affecting Cell Volume Control

Even at normal extracellular osmolarity and composition, osmotic gradients across the cell membrane could arise from unbalanced transport across the cell membrane, and from intracellular generation or disposal of osmotically active solutes. Cellular conditions and functions affecting intracellular osmolarity thus impact on cell volume control (Figure 5.3).

Energy Depletion

Impairment of Na^+/K^+-ATPase function, such as during pharmacological inhibition, energy depletion or decrease of ambient temperature, eventually leads to cell swelling due to cellular Na^+ accumulation, dissipation of the K^+ gradient, depolarization, and subsequent accumulation of Cl^-.[31] In some cells, the

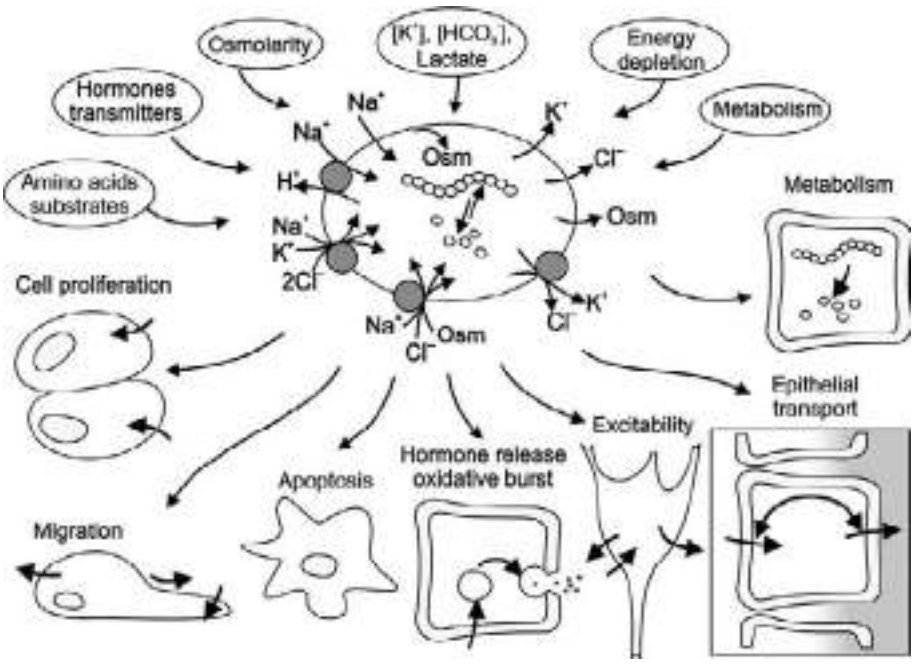

FIGURE 5.3 **Synopsis of challenges of cell volume constancy and functional significance of cell volume regulatory mechanisms.** Cell volume is altered by concentrative uptake of amino acids and additional substrates, alterations of ion transport by hormones and transmitters, changes of extracellular osmolarity, alterations of extracellular K^+, HCO_3^- and organic acid concentrations, energy depletion, and metabolic generation or disposal of osmolarity. Altered cell volume, as well as cell volume regulatory transport and metabolism, participate in the regulation of cell proliferation, migration, apoptosis, hormone release and oxidative burst, neuromuscular excitability, epithelial transport, and metabolism.

swelling is preceded by transient cell shrinkage.[263,264,265] The increase of intracellular Na^+ concentration reverses the driving force for the Na^+/Ca^{2+} exchanger; the increase of intracellular Ca^{2+} activity in turn leads to activation of Ca^{2+}-sensitive K^+ channels and/or Cl^- channels, as well as contraction of cytoskeletal elements.

Transport

Most epithelial cells are faced with large transcellular fluxes of osmotically active substances (see Chapter 2). To cope with transcellular transport, the cells have to coordinate the various transport systems at the apical and basolateral cell membranes. In both reabsorbing and secreting epithelia, cell volume participates in the coupling of those transport processes.

In proximal renal tubules[266] and intestine[267] for instance, Na^+-coupled transport of substrates such as amino acids or glucose across the luminal cell membrane leads to cellular accumulation of Na^+ and substrate. Moreover, the entry of excess positive charge leads to depolarization, impeding the exit of Cl^- and HCO_3^-, thus favoring cell swelling. In Na^+ reabsorbing epithelia, such as renal collecting duct and colon, entry of Na^+ via Na^+ channels similarly challenges cell volume constancy. Limitation of cell swelling during stimulated Na^+ transport requires the operation of cell volume regulatory mechanisms, including activation of K^+ channels, which in turn maintain the electrical driving force for Na^+ entry into the cell.[266,267] Activation of Cl^- and/or K^+ channels in several Cl^- secreting epithelia is paralleled by decrease of intracellular Cl^- activity and cell shrinkage, which in turn stimulate $Na^+-K^+-2Cl^-$ co-transport and/or Na^+H^+ exchanger with Cl^-/HCO_3^- exchanger.[268–271]

The influence of Na^+-coupled transport on cell volume is not limited to epithelial cells. In several epithelial and nonepithelial cells, concentrated uptake of substrates such as amino acids, glucose, taurine, and taurocholate increases cell volume.[31]

Deranged transport participates in disordered function of erythrocytes in sickle cell disease. In this disorder, a point mutation of hemoglobin (HbS) favors polymerization of desoxyhemoglobin, dramatically decreasing erythrocyte deformability and increasing blood viscosity.[272] The depolymerization of hemoglobin is critically dependent on cell volume. Cell shrinkage due to enhanced ambient osmolarity, activation of KCl co-transport by urea or activation of Ca^{2+}-sensitive K^+ channels by a rise in intracellular Ca^{2+} activity potentiates polymerization of HbS. The high osmolarity and urea concentration in kidney medulla thus contribute to the particular vulnerability of this tissue to ischemia in sickle cell anemia. Cell shrinkage and subsequent triggering of erythrocyte cell membrane scrambling (see below) presumably participate in accelerated erythrocyte turnover in various anemic conditions.[273]

Influence of Hormones and Transmitters on Cell Volume

A wide variety of hormones and other mediators have been shown to alter cell volume.[31] Insulin swells liver cells by activation of both Na^+/H^+ exchange and $Na^+-K^+2Cl^-$ co-transport, and glucagon shrinks hepatocytes, presumably by activation of ion channels.[274] The effect of insulin depends partially on the cell volume regulated serum and glucocorticoid inducible kinase SGK1.[275] The effect of the hormones on cell volume accounts for several of their metabolic effects (Figure 5.4). Notably, the swelling effect of insulin accounts for its antiproteolytic effect, and the shrinking effect of glucagon accounts for its proteolytic effect.[276,277]

Virtually all known growth factors increase cell volume by stimulation of Na^+/H^+ exchange, and in some cases by $Na^+K^+2Cl^-$ co-transport. As amplified below, an increase of cell volume appears to be required for cell proliferation.[35]

Several excitatory neurotransmitters, such as glutamate, activate Na^+ channels or nonselective cation channels, the entry of Na^+ and depolarization then favor cell swelling.[278–280] Other neurotransmitters, such as GABA, activate K^+ channels and/or anion channels, and thus induce cell shrinkage.[281]

Mediators and hormones regulating epithelial transport, such as ADH, adrenaline or acetylcholine, may either swell or shrink epithelial cells, depending on their effect on ion transport.[31] Stimulation of Na^+/H^+ exchange, $Na^+-K^+2Cl^-$ co-transport or Na^+ channels tends to swell epithelial cells, whereas prevailing stimulation of Cl^- and/or K^+ channels shrinks epithelial cells. Cell volume may in turn affect hormone and transmitter release. In a variety of cells, swelling stimulates and cell shrinkage inhibits the release of hormones.[282]

Neuromuscular Excitability

Cell volume could affect neuronal excitability by affecting ionic gradients, ion channel activity or cell volume regulatory release of neurotransmitters.[31] Dehydration enhances the neuronal expression of SGK1, which in turn regulates channels and transporters relevant for neuroexcitability.[283] Moreover, glial cell swelling may impede glial cell function.[284] In liver insufficiency, for instance, formation of urea is impaired, leading to accumulation of NH_3. NH_3 enters the brain and is taken up by glial cells, which then stimulates cellular formation and accumulation of glutamine, resulting eventually in glial cell swelling.[285,286] To counteract swelling, glial cells release inositol,

a mechanism, however, limited by the availability of inositol.[287,288] Inhibition of glutamine synthase has indeed been shown to protect against hepatic encephalopathy.[289]

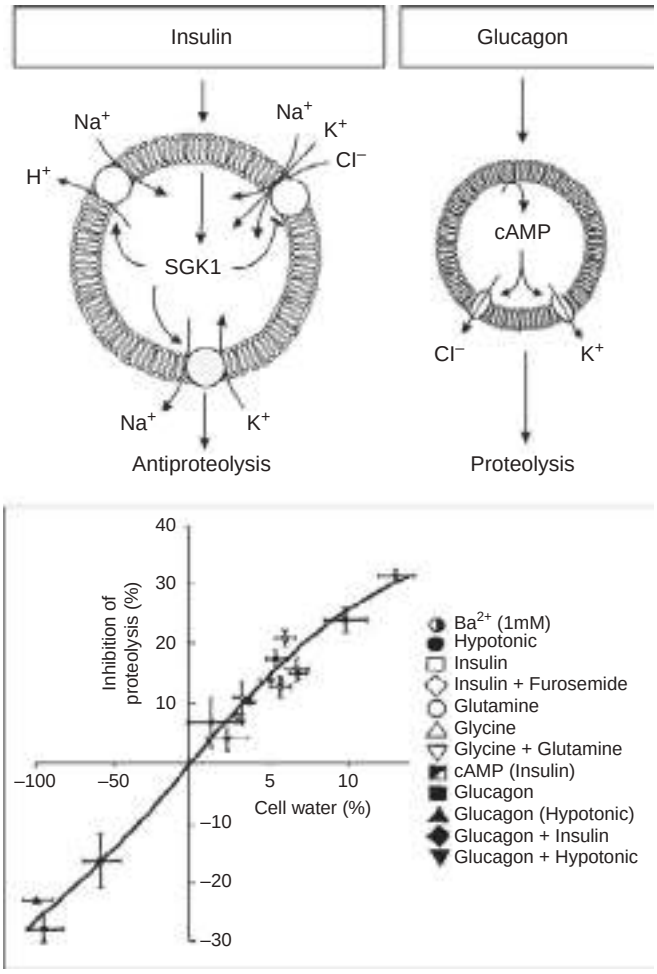

FIGURE 5.4 **Cell volume in the regulation of metabolism by hormones.** Insulin swells cells by KCl uptake via activation of Na^+/H^+ exchange, $Na^+–K^+–2Cl^-$ co-transport, and Na^+/K^+-ATPase. Glucagon shrinks cells by activation of K^+ and anion channels. The cell volume changes participate in the signaling of hormone action. Cell swelling stimulates protein synthesis, and cell shrinkage stimulates proteolysis. The diagram at the bottom illustrates the correlation between inhibition of proteolysis and hydration of hepatocytes. Cell swelling was induced by inhibition of K^+ channels (Ba^{2+}) decrease of extracellular osmolarity (hypotonic), insulin ± $Na^+–K^+2Cl^-$ co-transport inhibitor furosemide or concentrative uptake of amino acids (glutamine ± glycine). Cell swelling was counteracted or shrinkage accomplished by (additional) application of glucagon or cyclic AMP. The cell volume changes fully account for the effect of both hormones on proteolysis, and contribute to the other effects on macromolecule metabolism such as protein synthesis, as well as glycogen formation and breakdown *(modified from ref. [22]).*

Metabolism

Any reaction resulting in an increase of osmotically active solutes, such as degradation of proteins to amino acids, glycogen to glucose phosphate or triglycerides to glycerol and fatty acids, is expected to create intracellular osmolarity.[31] The degradation of the substrates to CO_2 and H_2O then decreases intracellular osmolarity.

Enhanced glycolysis, as it occurs during forced exercise for instance, leads to cellular accumulation of lactate and H^+, subsequent activation of Na^+/H^+ exchanger, and cell swelling.[290] Metabolic pathways may influence cell volume indirectly through alteration of transport across the cell membrane. A decrease of cellular ATP could activate ATP-sensitive K^+ channels, and thus shrink susceptible cells.[31] Similarly, cellular formation of peroxides may shrink cells through activation of K^+ channels, as shown for hepatocytes, pancreatic β-cells, and vascular smooth muscle cells.[31] In endothelial cells, peroxides inhibit $Na^+–K^+2Cl^-$ co-transport, an effect similarly expected to shrink the cells.[291] On the other hand, oxidation leads to inhibition of n-type K^+ channels in lymphocytes and IsK K^+ channels in a variety of tissues, effects that tend to favor cell swelling.[31]

In several hypercatabolic states, such as burns, acute pancreatitis, severe injury, and liver carcinoma, a decrease of muscle cell volume is observed that correlates with urea excretion, an indicator of protein degradation.[24] Since cell shrinkage is known to stimulate proteolysis, this correlation points to a causal role of altered cell volume in these hypercatabolic states. Conversely, hypercatabolism can be reversed by glutamine, which is known to swell cells by Na^+-coupled cellular accumulation.[24]

Diabetic ketoacidosis may be paralleled by cell swelling due to cellular accumulation of organic acids and enhanced Na^+/H^+ exchange activity in response to cellular acidosis.[221,261,292–294] Furthermore, the excessive glucose concentrations of hyperglycemia stimulate cellular formation and accumulation of sorbitol through aldose reductase.[17] As an attempt to counteract swelling, cells decrease other osmolytes such as myoinositol, an effect that can be reversed by inhibition of aldose reductase with sorbinil.[295–297] On the other hand, hyperglycemia is paralleled by hyperosmolarity, and intriguing evidence has been gathered pointing to cell shrinkage in hyperosmolar diabetes mellitus, which increases cellular Ca^{2+} concentration, and thus induces cell injury.[298,299] Obviously, more experimental information is needed to clarify the role of cell volume changes in the pathophysiology of diabetic complications.

In uremia, extracellular osmolarity is usually enhanced due to accumulation of urea, which interferes with protein stability and thus cell volume regulation (see previous discussion). The high urea concentrations in uremia stimulate the formation of methylamines, which counteract the perturbing effect of urea.[300] Rapid alterations in urea concentration such as during dialysis presumably do not allow full adjustment of osmolyte concentration, and are thus expected to disturb the balance of stabilizing osmolytes and destabilizing urea.[301] Alterations of cell volume may participate in the progression of renal failure: TGF-β1 has been postulated to accelerate renal fibrosis by inhibition of proteolysis and stimulation of protein synthesis, which both lead to enhanced deposition of matrix proteins.[299,302]

Cell Proliferation

Mitogenic factors are known to stimulate Na^+/H^+ exchange and $Na^+-K^+2Cl^-$ co-transport.[35] As shown in ras oncogene-expressing cells, activation of those carriers leads to a shift of the set point for cell volume regulation toward greater volumes (Figure 5.5). In addition, activation of Na^+/H^+ exchange leads to cellular alkalinization. Apparently, the increase of cell volume is one of the prerequisites for cell proliferation, which is impeded by pharmacological inhibition of Na^+/H^+ exchange and $Na^+-K^+2Cl^-$ co-transport, as well as osmotic cell shrinkage.[31,303] Cell volume changes parallel transition through the cell cycle,[304] and cell proliferation requires further timely activation of volume-sensitive Ca^{2+} channels, K^+ channels, and Cl^- channels.[305–307] Moreover, cell proliferation is substantially influenced by the cell volume-sensitive SGK1.[308]

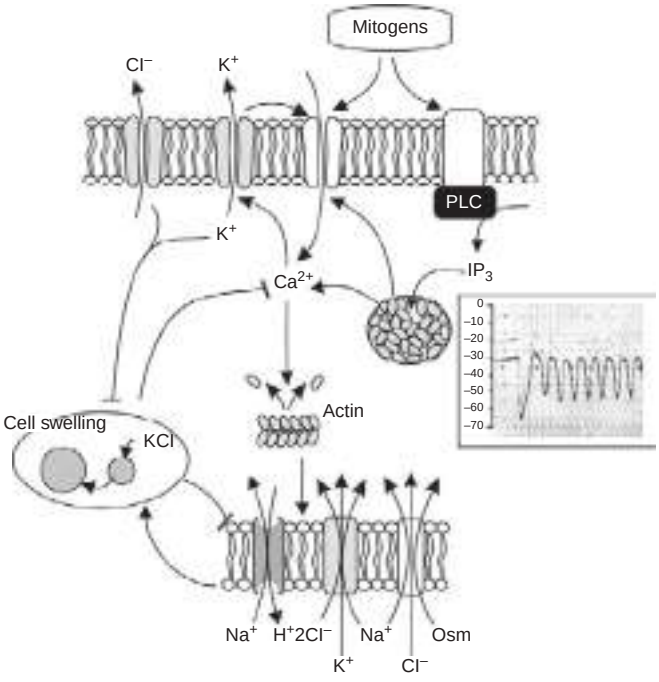

FIGURE 5.5 **Cell volume regulatory transport in regulation of cell proliferation.** The case of Ras oncogene expressing cells. Application of mitogenic factors in cells overexpressing Ras oncogene triggers intracellular Ca^+ release and Ca^+ entry, leading to oscillations of cytosolic Ca^+ activity and cell membrane potential (insert). Increased cytosolic Ca^{2+} activity stimulates Ca^{2+}-sensitive K^+ channels and triggers initial cell shrinkage. Ca^{2+} further leads to depolymerization of the microfilaments, which disinhibits the Na^+/H^+ exchanger and $Na^+-K^+-2Cl^-$ co-transporter. The activation of these carriers eventually leads to cell swelling, a prerequisite for cell proliferation *(from ref. [31])*.

Migration

Locomotion of cells requires alteration of cell shape, and thus of cytoskeletal architecture. At the leading edge actin filaments are polymerized, and at the rear they are depolymerized.[309,310] The movement of cells is paralleled by movement of water that is driven by osmotic gradients. Na^+/H^+ exchange and $Na^+-K^+2Cl^-$ co-transport drive water entry at the leading edge, and the activity of K^+ channels and anion channels drive water extrusion at the rear.[31,311–314] The respective water movement is facilitated by water channels.[315] Activation of cell volume regulatory mechanisms during migration is similar to that of cell proliferation (Figure 5.6). However, the elements are polarized, and cells undergo cell volume regulatory increase at the leading edge, and cell volume regulatory decrease at the rear.[31]

Apoptotic Cell Death

Cell shrinkage is one of the hallmarks of apoptotic cell death, and marked osmotic cell shrinkage ($>30\%$) has been shown to trigger this type of cell death.[193] Apoptotic cell shrinkage requires the participation of cell volume regulatory mechanisms (Figure 5.6). Apoptotic death of Jurkat T-lymphocytes following CD95 triggering is indeed paralleled by inhibition of the Na^+/H^+ exchanger, as well as activation of the anion channel ORCC and osmolyte release.[316] The release of ions, and subsequent cell shrinkage, are apparently a prerequisite for induction of apoptosis.[317–319] On the other hand, at an early stage of CD95 triggering, the cell volume-regulatory K^+ channel Kv1.3 is inhibited, and a moderate decrease of cell volume ($<30\%$) has been shown to blunt receptor (CD95)-triggered apoptotic cell death.[320] The cellular mechanisms triggered by moderate osmotic cell shrinkage apparently interfere with the signaling of the CD95 receptor, such as cellular O_2^--formation.

The triggering of cell death by hyperosmotic shock has been attributed to upregulation or clustering and subsequent activation of apoptosis-inducing receptors,

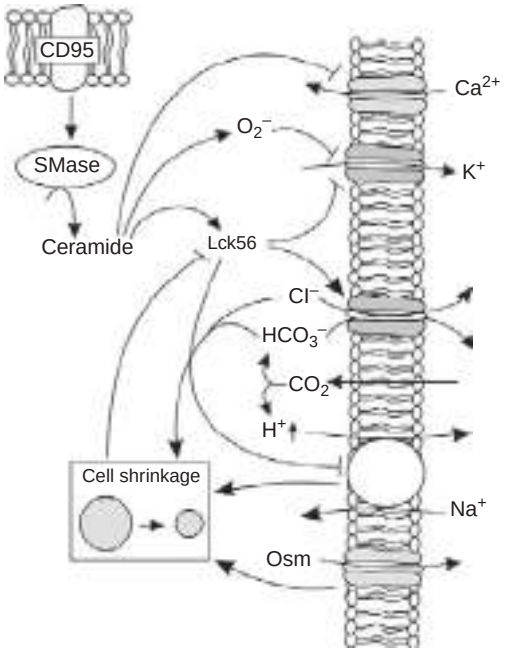

FIGURE 5.6 **Cell volume regulatory ion transport during CD95-induced apoptosis of lymphocytes.** CD95-induced apoptosis of Jurkat T-lymphocytes is paralleled by inhibition of the Na^+/H^+ exchanger, as well as activation of the anion channel ORCC and osmolyte release. The altered transport leads eventually to cytosolic acidification and cell shrinkage. Initially, CD95 stimulation leads to inhibition of the cell volume regulatory K^+ channel Kv1.3, thus preventing early cell shrinkage. At a later stage (not shown), additional activation of K^+ channels leads to apoptotic cell shrinkage. *(From Lang, F., Lepple-Wienhues, A., Paulmichi, M., Szabo, I., Siemen, D. and Gulbins, E. (1998). Ion channels, cell volume, and apoptotic cell death. Cell Physiol. Biochem. 8(6), 285–292.)*

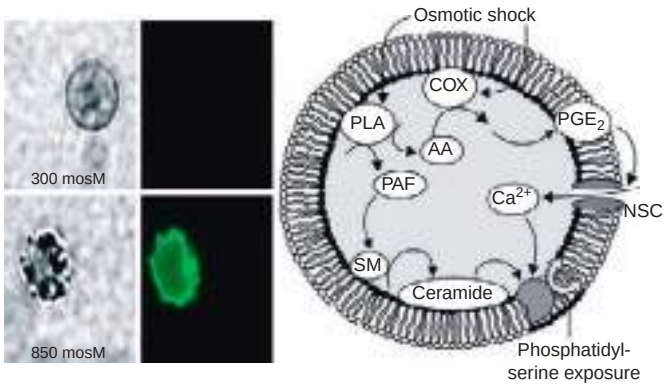

FIGURE 5.7 **Stimulation of erythrocyte death by osmotic cell shrinkage.** Osmotic shock activates a phospholipase A_2 leading to formation of platelet activating factor (PAF) on the one hand, and of arachidonic acid on the other. PAF stimulates a sphingomyelinase leading to formation of ceramide; arachidonic acid is converted by cyclooxygenase (COX) to PGE2 which activates a Ca and Na permeable cation channel. Ca entering through the cation channels activates a scramblase, leading to phosphatidylserine exposure at the cell surface (left), a typical feature of apoptotic cells. Ceramide sensitizes the scramblase for Ca, and thus contributes to the activation of this enzyme *(from ref. [273])*.

such as CD95 or TNFα-receptor[193,321–323] or to formation of their ligands, such as TNFα.[324] Beyond that, cell shrinkage could trigger cell death more directly, by activating a signaling cascade of rac, p38 kinase, p53, and subsequent upregulation of pro-apoptotic proteins Bax/Bid.[325] Conversely, osmotic shrinkage may downregulate signaling supporting cell survival, such as the PI3 kinase pathway leading to protein kinase B-dependent phosphorylation, and thus inactivation of Bad.[236] In erythrocytes, hyperosmotic shock stimulates a phospholipase A_2 with subsequent formation of PGE_2[251] and PAF.[253] PGE_2 stimulates a cation channel, allowing the entry of Ca^{2+} and subsequent triggering of Ca^{2+}-sensitive cell membrane scrambling.[251] PAF stimulates a sphingomyelinase that leads to formation of ceramide, which sensitizes the erythrocyte for the scrambling effect of Ca^{2+}.[253] Cell membrane scrambling leads to breakdown of phosphatidylserine asymmetry and exposure of phosphatidylserine at the outer surface of the cell membrane, a typical feature of apoptotic cells (Figure 5.7).

Necrotic Cell Death

As pointed out above, energy depletion impairs the function of the Na^+/K^+-ATPase, dissipates the Na^+ and K^+ gradients, depolarizes the cell membrane, and leads to cellular accumulation of Cl^-.[31] During ischemia, the cell membrane is further depolarized by increasing extracellular K^+ concentrations. Cellular Na^+ and Cl^- accumulation eventually lead to cell swelling. Moreover, the excessive formation and reduced clearance of lactate during ischemia induces cellular acidosis and enhanced Na^+/H^+ exchange activity, compounding cell swelling. In the brain, the depolarization triggers the release of glutamate, which activates unspecific cation channels and thus induces further cell swelling.[31]

References

[1] Brown GC. Total cell protein concentration as an evolutionary constraint on the metabolic control distribution in cells. J Theor Biol 1991;153:195–203.
[2] Fulton AB. How crowded is the cytoplasm? Cell 1982;30:345–7.
[3] Garner MM, Burg MB. Macromolecular crowding and confinement in cells exposed to hypertonicity. Am J Physiol 1994;266: C877–92.
[4] Minton AP. Excluded volume as a determinant of macromolecular structure and reactivity. Biopolymers 1981;20:2093–120.
[5] Minton AP. Macromolecular crowding and molecular recognition. J Mol Recognit 1993;6:211–4.

[6] Parker JC. In defense of cell volume? Am J Physiol 1993;265: C1191–200.
[7] Colombe BW, Macey RI. Effects of calcium on potassium and water transport in human erythrocyte ghosts. Biochim Biophys Acta 1974;363:226–39.
[8] Macknight AD. Principles of cell volume regulation. Ren Physiol Biochem 1988;11:114–41.
[9] Galizia L. Flamenco MP, Rivarola V, Capurro C, Ford P. Role of AQP2 in activation of calcium entry by hypotonicity: implications in cell volume regulation. Am J Physiol Renal Physiol 2008;294:F582–90.
[10] King LS, Kozono D, Agre P. From structure to disease: the evolving tale of aquaporin biology. Nat Rev Mol Cell Biol 2004;5:687–98.
[11] Liu X, Bandyopadhyay BC, Nakamoto T, Singh B, Liedtke W, Melvin JE, et al. A role for AQP5 in activation of TRPV4 by hypotonicity: concerted involvement of AQP5 and TRPV4 in regulation of cell volume recovery. J. Biol. Chem. 2006;281:15485–95.
[12] Graf J, Haddad P, Haeussinger D, Lang F. Cell volume regulation in liver. Ren Physiol Biochem 1988;11:202–20.
[13] Guharay F, Sachs F. Stretch-activated single ion channel currents in tissue-cultured embryonic chick skeletal muscle. J Physiol 1984;352:685–701.
[14] Kelly SM, Macklem PT. Direct measurement of intracellular pressure. Am J Physiol 1991;260:C652–7.
[15] Sackin H. Stretch-activated ion channels. In: Strange K, editor. Cellular and Molecular Physiology of Cell Volume Regulation. Boca Raton, FL: CRC Press; 1994. p. 215–40.
[16] Burg MB. Molecular basis of osmotic regulation. Am J Physiol 1995;268:F983–96.
[17] Burg MB, Kador PF. Sorbitol, osmoregulation, and the complications of diabetes. J Clin Invest 1988;81:635–40.
[18] Burg MB, Kwon ED, Peters EM. Glycerophosphocholine and betaine counteract the effect of urea on pyruvate kinase. Kidney Int Suppl 1996;57:S100–4.
[19] De Mello WC. Renin angiotensin system as a regulator of cell volume. Implications to myocardial ischemia. Curr Cardiol Rev 2009;5:65–8.
[20] Fisher SK, Heacock AM, Keep RF, Foster DJ. Receptor regulation of osmolyte homeostasis in neural cells. J. Physiol. 2010;288 (Pt 18):3355–64.
[21] Garcia-Perez A, Burg MB. Renal medullary organic osmolytes. Physiol Rev 1991;71:1081–115.
[22] Haussinger D, Lang F. Cell volume: a "second messenger" in the regulation of metabolism by amono acids and hormones. Cell Physiol Biochem 1991;1:121–30.
[23] Haussinger D. Osmosensing and osmosignaling in the liver. Wien Med Wochenschr 2008;158:549–52.
[24] Haussinger D, Roth E, Lang F, Gerok W. Cellular hydration state: an important determinant of protein catabolism in health and disease. Lancet 1993;341:1330–2.
[25] Hoffmann EK, Dunham PB. Membrane mechanisms and intracellular signalling in cell volume regulation. Int Rev Cytol 1995;161:173–262.
[26] Hoffmann EK, Lambert IH, Pedersen SF. Physiology of cell volume regulation in vertebrates. Physiol Rev 2009;89:193–277.
[27] Kinne RK, Czekay RP, Grunewald JM, Mooren FC, Kinne-Saffran E. Hypotonicity-evoked release of organic osmolytes from distal renal cells: systems, signals, and sidedness. Ren Physiol Biochem 1993;16:66–78.
[28] Kwon HM, Handler JS. Cell volume regulated transporters of compatible osmolytes. Curr Opin Cell Biol 1995;7:465–71.
[29] Lang F. Cell Volume Regulation. Contributions to Nephrology ed. Basel: Karger; 1998.
[30] Lang F. Mechanisms and significance of cell volume regulation. J Am Coll Nutr 2007;26:613S–23S.
[31] Lang F, Busch GL, Ritter M, Völkl H, Waldegger S, Gulbins E, et al. Functional significance of cell volume regulatory mechanisms. Physiol Rev 1998;78:247–306.
[32] Lang F, Busch GL, Volkl H. The diversity of volume regulatory mechanisms. Cell Physiol Biochem 1998;8:1–45.
[33] McManus ML, Churchwell KB, Strange K. Regulation of cell volume in health and disease. N Engl J Med 1995;333:1260–6.
[34] Pasantes-Morales H, Cruz-Rangel S. Brain volume regulation: osmolytes and aquaporin perspectives. Neuroscience 2010;168:871–84.
[35] Ritter M, Woell E. Modification of cellular ion transport by the ha-ras oncogene: steps towards malignant transformation. Cell Physiol Biochem 1996;6:245–70.
[36] Ritter M, Fuerst J, Woll E, Chwatal S, Gschwentner M, Lang F, et al. $Na(^+)/H(^+)$exchangers: linking osmotic dysequilibrium to modified cell function. Cell Physiol Biochem 2001;11:1–18.
[37] Schliess F, Reinehr R, Haussinger D. Osmosensing and signaling in the regulation of mammalian cell function. FEBS J 2007;274:5799–803.
[38] Strange K. Cellular and Molecular Physiology of Cell Volume Regulation. Boca Raton, FL: CRC Press; 1994.
[39] Strange K. Cellular volume homeostasis. Adv Physiol Educ 2004;28:155–9.
[40] Usher-Smith JA, Huang CL, Fraser JA. Control of cell volume in skeletal muscle. Biol Rev Camb Philos Soc 2009;84:143–59.
[41] Wehner F, Olsen H, Tinel H, Kinne-Saffran E, Kinne RK. Cell volume regulation: osmolytes, osmolyte transport, and signal transduction. Rev Physiol Biochem Pharmacol 2003;148:1–80.
[42] Lohr JW, Grantham JJ. Isovolumetric regulation of isolated S2 proximal tubules in anisotonic media. J Clin Invest 1986;78:1165–72.
[43] Minton AP. Influence of macromolecular crowding on intracellular association reactions: Possible role in volume regulation. In: Strange K, editor. Cellular and Molecular Physiology of Cell Volume Regulation. Boca Raton, FL: CRC Press; 1994. p. 181–90.
[44] Burg MB, Kwon ED, Kultz D. Osmotic regulation of gene expression. FASEB J 1996;10:1598–606.
[45] Deutsch C, Chen LQ. Heterologous expression of specific K^+ channels in T lymphocytes: functional consequences for volume regulation. Proc Natl Acad Sci USA 1993;90:10036–40.
[46] Felipe A, Snyders DJ, Deal KK, Tamkun MM. Influence of cloned voltage-gated K^+ channel expression on alanine transport, Rb^+ uptake, and cell volume. Am J Physiol 1993;265: C1230–8.
[47] Wang GL, Wang GX, Yamamoto S, Ye L, Baxter H, Hume JR, et al. Molecular mechanisms of regulation of fast-inactivating voltage-dependent transient outward K^+ current in mouse heart by cell volume changes. J Physiol 2005;568:423–43.
[48] Busch AE, Maylie J. MinK channels: a minimal channel protein with a maximal impact. Cell Physiol Biochem 1993;3:270–6.
[49] Busch AE, Varnum M, Adelman JP, North RA. Hypotonic solution increases the slowly activating potassium current IsK expressed in *Xenopus* oocytes. Biochem Biophys Res Commun 1992;184:804–10.
[50] Byfield FJ, Aranda-Espinoza H, Romanenko VG, Rothblat GH, Levitan I. Cholesterol depletion increases membrane stiffness of aortic endothelial cells. Biophys J 2004;87:3336–43.
[51] vanTol BL, Missan S, Crack J, Moser S, Baldridge WH, Linsdell P, et al. Contribution of KCNQ1 to the regulatory volume decrease in the human mammary epithelial cell line MCF-7. Am J Physiol Cell Physiol 2007;293:C1010–9.
[52] Decressac S, Franco M, Bendahhou S, Warth R, Knauer S, Barhanin J, et al. ARF6-dependent interaction of the TWIK1 K^+

channel with EFA6, a GDP/GTP exchange factor for ARF6. EMBO Rep 2004;5:1171–5.
[53] Barriere H, Belfodil R, Rubera I, Tauc M, Lesage F, Poujeol C, et al. Role of TASK2 potassium channels regarding volume regulation in primary cultures of mouse proximal tubules. J Gen Physiol 2003;122:177–90.
[54] Wang SX, Ikeda M, Guggino WB. The cytoplasmic tail of large conductance, voltage- and Ca^{2+}-activated K^+ (MaxiK) channel is necessary for its cell surface expression. J Biol Chem 2003;278:2713–22.
[55] Grunder S, Thiemann A, Pusch M, Jentsch TJ. Regions involved in the opening of CIC-2 chloride channel by voltage and cell volume. Nature 1992;360:759–62.
[56] Jentsch TJ. Molecular physiology of anion channels. Curr Opin Cell Biol 1994;6:600–6.
[57] Jentsch TJ. Chloride channels: a molecular perspective. Curr Opin Neurobiol 1996;6:303–10.
[58] Lorenz C, Pusch M, Jentsch TJ. Heteromultimeric CLC chloride channels with novel properties. Proc Natl Acad Sci USA 1996;93:13362–6.
[59] Thiemann A, Grunder S, Pusch M, Jentsch TJ. A chloride channel widely expressed in epithelial and non-epithelial cells. Nature 1992;356:57–60.
[60] Jin NG, Kim JK, Yang DK, Cho SJ, Kim JM, Koh EJ, et al. Fundamental role of ClC-3 in volume-sensitive Cl^- channel function and cell volume regulation in AGS cells. Am J Physiol Gastrointest Liver Physiol 2003;285:G938–48.
[61] McCloskey DT, Doherty L, Dai YP, Miller L, Hume JR, Yamboliev IA. Hypotonic activation of short ClC3 isoform is modulated by direct interaction between its cytosolic C-terminal tail and subcortical actin filaments. J Biol Chem 2007;282:16871–7.
[62] Nilius B, Eggermont J, Voets T, Buyse G, Manolopoulos V, Droogmans G. Properties of volume-regulated anion channels in mammalian cells. Prog Biophys Mol Biol 1997;68:69–119.
[63] Chien LT, Hartzell HC. *Drosophila* bestrophins are dually regulated by calcium and cell volume (Abstract). J Gen Physiol 2007;130:21A–2A.
[64] Buyse G, de Greef C, Raeymaekers L, Droogmans G, Nilius B, Eggermont J. The ubiquitously expressed pICln protein forms homomeric complexes *in vitro*. Biochem Biophys Res Commun 1996;218:822–7.
[65] Paulmichl M, Li Y, Wickman K, Ackerman M, Peralta E, Clapham D. New mammalian chloride channel identified by expression cloning. Nature 1992;356:238–41.
[66] Ritter M, Ravasio A, Jakab M, Chwatal S, Furst J, Laich A, et al. Cell swelling stimulates cytosol to membrane transposition of ICln. J Biol Chem 2003;278:50163–74.
[67] Hardy SP, Goodfellow HR, Valverde MA, Gill DR, Sepulveda V, Higgins CF. Protein kinase C-mediated phosphorylation of the human multidrug resistance P-glycoprotein regulates cell volume-activated chloride channels. EMBO J 1995;14:68–75.
[68] Higgins CF. Volume-activated chloride currents associated with the multidrug resistance P-glycoprotein. J Physiol 1995;482:31S–6S.
[69] Jirsch J, Deeley RG, Cole SP, Stewart AJ, Fedida D. Inwardly rectifying K^+ channels and volume-regulated anion channels in multidrug-resistant small cell lung cancer cells. Cancer Res 1993;53:4156–60.
[70] Jirsch JD, Loe DW, Cole SP, Deeley RG, Fedida D. ATP is not required for anion current activated by cell swelling in multidrug-resistant lung cancer cells. Am J Physiol 1994;267: C688–99.
[71] Cho WK, Siegrist VJ, Zinzow W. Impaired regulatory volume decrease in freshly isolated cholangiocytes from cystic fibrosis mice: implications for cystic fibrosis transmembrane conductance regulator effect on potassium conductance. J Biol Chem 2004;279:14610–8.
[72] Valverde MA, Vazquez E, Munoz FJ, Nobles M, Delaney SJ, Wainwright BJ, et al. Murine CFTR channel and its role in regulatory volume decrease of small intestine crypts. Cell Physiol Biochem 2000;10:321–8.
[73] Chan HC, Fu WO, Chung YW, Huang SJ, Chan PS, Wong PY. Swelling-induced anion and cation conductances in human epididymal cells. J Physiol 1994;478(Pt 3):449–60.
[74] Jackson PS, Strange K. Volume-sensitive anion channels mediate swelling-activated inositol and taurine efflux. Am J Physiol 1993;265:C1489–500.
[75] Junankar PR, Kirk K. Organic osmolyte channels: a comparative view. Cell Physiol Biochem 2000;10:355–60.
[76] Kinne RK, Tinel H, Kipp H, Kinne-Saffran E. Regulation of sorbitol efflux in different renal medullary cells: similarities and diversities. Cell Physiol Biochem 2000;10:371–8.
[77] Kirk K, Ellory JC, Young JD. Transport of organic substrates via a volume-activated channel. J Biol Chem 1992;267:23475–8.
[78] Okada SF, O'Neal WK, Huang P, Nicholas RA, Ostrowski LE, Craigen WJ, et al. Voltage-dependent anion channel-1 (VDAC-1) contributes to ATP release and cell volume regulation in murine cells. J Gen Physiol 2004;124:513–26.
[79] Roy G, Banderali U. Channels for ions and amino acids in kidney cultured cells (MDCK) during volume regulation. J Exp Zool 1994;268:121–6.
[80] Strange K, Jackson PS. Swelling-activated organic osmolyte efflux: a new role for anion channels. Kidney Int 1995;48:994–1003.
[81] Nilius B, Owsianik G, Voets T, Peters JA. Transient receptor potential cation channels in disease. Physiol Rev 2007;87:165–217.
[82] Numata T, Shimizu T, Okada Y. Direct mechano-stress sensitivity of TRPM7 channel. Cell Physiol Biochem 2007;19:1–8.
[83] Numata T, Shimizu T, Okada Y. TRPM7 is a stretch- and swelling-activated cation channel involved in volume regulation in human epithelial cells. Am J Physiol Cell Physiol 2007;292: C460–7.
[84] Pedersen SF, Nilius B. Transient receptor potential channels in mechanosensing and cell volume regulation. Methods Enzymol 2007;428:183–207.
[85] Plettenberg S, Weiss EC, Lemor R, Wehner F. Subunits alpha, beta and gamma of the epithelial Na^+ channel (ENaC) are functionally related to the hypertonicity-induced cation channel (HICC) in rat hepatocytes. Pflugers Arch 2008;455:1089–95.
[86] Ross SB, Fuller CM, Bubien JK, Benos DJ. Amiloride-sensitive Na^+ channels contribute to regulatory volume increases in human glioma cells. Am J Physiol Cell Physiol 2007;293: C1181–5.
[87] Sachs F. Mechanical transduction by membrane ion channels: a mini review. Mol Cell Biochem 1991;104:57–60.
[88] Adragna NC, Lauf PK. K–Cl co-transport function and its potential contribution to cardiovascular disease. Pathophysiology 2007;14:135–46.
[89] Boettger T, Rust MB, Maier H, Seidenbecher T, Schweizer M, Keating DJ, et al. Loss of K–Cl co-transporter KCC3 causes deafness, neurodegeneration and reduced seizure threshold. EMBO J 2003;22:5422–34.
[90] Lauf PK. K:Cl co-transport: emerging molecular aspects of a ouabain-resistant, volume-responsive transport system in red blood cells. Ren Physiol Biochem 1988;11:248–59.
[91] Lauf PK, Adragna NC. K-Cl co-transport: properties and molecular mechanism. Cell Physiol Biochem 2000;10:341–54.

[92] Lauf PK, Erdmann A, Adragna NC. K-Cl co-transport, pH, and role of Mg in volume-clamped low-K sheep erythrocytes: three equilibrium states. Am J Physiol 1994;266:C95–103.
[93] Perry PB, O'Neill WC. Swelling-activated K fluxes in vascular endothelial cells: volume regulation via K-Cl co-transport and K channels. Am J Physiol 1993;265:C763–9.
[94] Thornhill WB, Laris PC. KCl loss and cell shrinkage in the Ehrlich ascites tumor cell induced by hypotonic media, 2-deoxyglucose and propranolol. Biochim Biophys Acta 1984;773:207–18.
[95] Bonanno JA. $K(^{+})-H^{+}$ exchange, a fundamental cell acidifier in corneal epithelium. Am J Physiol 1991;260:C618–25.
[96] Cala PM. Volume regulation by *Amphiuma* red blood cells: strategies for identifying alkali metal/H^{+} transport. Fed Proc 1985;44:2500–7.
[97] Dunham PB, Jessen F, Hoffmann EK. Inhibition of Na-K-C1 co-transport in Ehrlich ascites cells by antiserum against purified proteins of the co-transporter. Proc Natl Acad Sci USA 1990;87:6828–32.
[98] Gamba G. Molecular physiology and pathophysiology of electroneutral cation-chloride co-transporters. Physiol Rev 2005;85:423–93.
[99] Geck P, Pfeiffer B. $Na^{+} + K^{+} + 2Cl^{-}$ co-transport in animal cells: its role in volume regulation. Ann NY Acad Sci 1985;456:166–82.
[100] Hebert SC, Mount DB, Gamba G. Molecular physiology of cation-coupled Cl^{-} co-transport: the SLC12 family. Pflugers Arch 2004;447:580–93.
[101] Wakabayashi S, Shigekawa M, Pouyssegur J. Molecular physiology of vertebrate Na^{+}/H^{+} exchangers. Physiol Rev 1997;77:51–74.
[102] Demaurex N, Grinstein S. Na + /H + antiport: modulation by ATP and role in cell volume regulation. J Exp Biol 1994;196:389–404.
[103] Bookstein C, Musch MW, DePaoli A, Xie Y, Villereal M, Rao MC, et al. A unique sodium-hydrogen exchange isoform (NHE-4) of the inner medulla of the rat kidney is induced by hyperosmolarity. J Biol Chem 1994;269:29704–9.
[104] Barone S, Amlal H, Xu J, Kujala M, Kere J, Petrovic S, et al. Differential regulation of basolateral Cl^{-}. J Am Soc Nephrol 2004;15:2002–11.
[105] Grinstein S, Clarke CA, Rothstein A. Activation of Na^{+}/H^{+} exchange in lymphocytes by osmotically induced volume changes and by cytoplasmic acidification. J Gen Physiol 1983;82:619–38.
[106] Good DW, Di Mari JF, Watts III BA. Hyposmolality stimulates $Na(^{+})/H(^{+})$ exchange and $HCO(3)(^{-})$ absorption in thick ascending limb via PI 3-kinase. Am J Physiol Cell Physiol 2000;279:C1443–54.
[107] Cabado AG, Vieytes MR, Botana LM. Effect of ion composition on the changes in membrane potential induced with several stimuli in rat mast cells. J Cell Physiol 1994;158:309–16.
[108] Chan HC, Nelson DJ. Chloride-dependent cation conductance activated during cellular shrinkage. Science 1992;257:669–71.
[109] Lang F, Lang KS, Wieder T, Myssina S, Birka C, Lang PA, et al. Cation channels, cell volume and the death of an erythrocyte. Pflugers Arch 2003;447:121–5.
[110] Volk T, Fromter E, Korbmacher C. Hypertonicity activates nonselective cation channels in mouse cortical collecting duct cells. Proc Natl Acad Sci USA 1995;92:8478–82.
[111] Wehner F, Bohmer C, Heinzinger H, van den BF, Tinel H. The hypertonicity-induced $Na(^{+})$ conductance of rat hepatocytes: physiological significance and molecular correlate. Cell Physiol Biochem 2000;10:335–40.
[112] Wehner F, Sauer H, Kinne RK. Hypertonic stress increases the Na^{+} conductance of rat hepatocytes in primary culture. J Gen Physiol 1995;105:507–35.
[113] Christensen AP, Corey DP. TRP channels in mechanosensation: direct or indirect activation? Nat Rev Neurosci 2007;8:510–21.
[114] Gottlieb P, Folgering J, Maroto R, Raso A, Wood TG, Kurosky A, et al. Revisiting TRPC1 and TRPC6 mechanosensitivity. Pflugers Arch 2008;455:1097–103.
[115] Liedtke W. Transient receptor potential vanilloid channels functioning in transduction of osmotic stimuli. J Endocrinol 2006;191:515–23.
[116] Wehner F. Cell volume-regulated cation channels. Contrib Nephrol 2006;152:25–53.
[117] Burg MB, Ferraris JD, Dmitrieva NI. Cellular response to hyperosmotic stresses. Physiol Rev 2007;87:1441–74.
[118] Pasantes-Morales H, Franco R, Torres-Marquez ME, Hernandez-Fonseca K, Ortega A. Amino acid osmolytes in regulatory volume decrease and isovolumetric regulation in brain cells: contribution and mechanisms. Cell Physiol Biochem 2000;10:361–70.
[119] Back JF, Oakenfull D, Smith MB. Increased thermal stability of proteins in the presence of sugars and polyols. Biochemistry 1979;18:5191–6.
[120] Carpenter JF, Crowe JH. The mechanism of cryoprotection of proteins by solutes. Cryobiology 1988;25:244–55.
[121] Santoro MM, Liu Y, Khan SM, Hou LX, Bolen DW. Increased thermal stability of proteins in the presence of naturally occurring osmolytes. Biochemistry 1992;31:5278–83.
[122] Storey KB, Storey JM. Freeze tolerance in animals. Physiol Rev 1988;68:27–84.
[123] Taneja S, Ahmad F. Increased thermal stability of proteins in the presence of amino acids. Biochem J 1994;303(Pt 1):147–53.
[124] Bedford JJ, Bagnasco SM, Kador PF, Harris Jr. HW, Burg MB. Characterization and purification of a mammalian osmoregulatory protein, aldose reductase, induced in renal medullary cells by high extracellular NaCl. J Biol Chem 1987;262:14255–9.
[125] Ferraris JD, Williams CK, Martin BM, Burg MB, Garcia-Perez A. Cloning, genomic organization, and osmotic response of the aldose reductase gene. Proc Natl Acad Sci USA 1994;91:10742–6.
[126] Garcia-Perez A, Martin B, Murphy HR, Uchida S, Murer H, Cowley Jr. BD, et al. Molecular cloning of cDNA coding for kidney aldose reductase. Regulation of specific mRNA accumulation by NaCl-mediated osmotic stress. J Biol Chem 1989;264:16815–21.
[127] Garcia-Perez A, Ferraris JD. Aldose reductase gene expression and osmoregulation in mammalian renal cells. In: Strange K, editor. Cellular and Molecular Physiology of Cell Volume Regulation. Boca Raton, FL: CRC Press; 1994. p. 373–82.
[128] Garcia-Perez A, Burg MB. Role of organic osmolytes in adaptation of renal cells to high osmolality. J Membr Biol 1991;119:1–13.
[129] Ullrich KJ. Glycerylphosphorylcholinumsatz und Glycerylphosphorylcholindiesterase in der Säugetier-Niere. Biochem Z 1959;331:98–102.
[130] Berry GT, Mallee JJ, Kwon HM, Rim JS, Mulla WR, Muenke M, et al. The human osmoregulatory Na^{+}/myo-inositol co-transporter gene (SLC5A3): molecular cloning and localization to chromosome 21. Genomics 1995;25:507–13.
[131] Hammerman MR, Sacktor B, Daughaday WH. Myo-inositol transport in renal brush border vesicles and its inhibition by D-glucose. Am J Physiol 1980;239:F113–20.

[132] Kwon HM, Yamauchi A, Uchida S, Preston AS, Garcia-Perez A, Burg MB, et al. Cloning of the cDNa for a Na^+/myo-inositol cotransporter, a hypertonicity stress protein. J Biol Chem 1992;267:6297–301.

[133] Yamauchi A, Sugiura T, Ito T, Miyai A, Horio M, Imai E, et al. Na^+/myo-inositol transport is regulated by basolateral tonicity in Madin–Darby canine kidney cells. J Clin Invest 1996;97:263–7.

[134] Burnham CE, Buerk B, Schmidt C, Bucuvalas JC. A liver-specific isoform of the betaine/GABA transporter in the rat: cDNA sequence and organ distribution. Biochim Biophys Acta 1996;1284:4–8.

[135] Takenaka M, Bagnasco SM, Preston AS, Uchida S, Yamauchi A, Kwon HM, et al. The canine betaine gamma-amino-n-butyric acid transporter gene: diverse mRNA isoforms are regulated by hypertonicity and are expressed in a tissue-specific manner. Proc Natl Acad Sci USA 1995;92:1072–6.

[136] Yamauchi A, Kwon HM, Uchida S, Preston AS, Handler JS. Myo-inositol and betaine transporters regulated by tonicity are basolateral in MDCK cells. Am J Physiol 1991;261:F197–202.

[137] Uchida S, Kwon HM, Yamauchi A, Preston AS, Marumo F, Handler JS. Molecular cloning of the cDNA for an MDCK cell $Na(^+)$- and $Cl(^-)$-dependent taurine transporter that is regulated by hypertonicity. Proc Natl Acad Sci USA 1992;89:8230–4.

[138] Chen JG, Klus LR, Steenbergen DK, Kempson SA. Hypertonic upregulation of amino acid transport system A in vascular smooth muscle cells. Am J Physiol 1994;267:C529–36.

[139] Soler C, Felipe A, Casado FJ, McGivan JD, Pastor-Anglada M. Hyperosmolarity leads to an increase in derepressed system A activity in the renal epithelial cell line NBL-1. Biochem J 1993;289(Pt 3):653–8.

[140] Yamauchi A, Miyai A, Yokoyama K, Itoh T, Kamada T, Ueda N, et al. Response to osmotic stimuli in mesangial cells: role of system A transporter. Am J Physiol 1994;267:C1493–500.

[141] Kinne RK. The role of organic osmolytes in osmoregulation: from bacteria to mammals. J Exp Zool 1993;265:346–55.

[142] Bagnasco SM, Murphy HR, Bedford JJ, Burg MB. Osmoregulation by slow changes in aldose reductase and rapid changes in sorbitol flux. Am J Physiol 1988;254: C788–92.

[143] Garty H, Furlong TJ, Ellis DE, Spring KR. Sorbitol permease: an apical membrane transporter in cultured renal papillary epithelial cells. Am J Physiol 1991;260:F650–6.

[144] Wiesinger H, Thiess U, Hamprecht B. Sorbitol pathway activity and utilization of polyols in astroglia-rich primary cultures. Glia 1990;3:277–82.

[145] Furlong TJ, Moriyama T, Spring KR. Activation of osmolyte efflux from cultured renal papillary epithelial cells. J Membr Biol 1991;123:269–77.

[146] Boese SH, Wehner F, Kinne RK. Taurine permeation through swelling-activated anion conductance in rat IMCD cells in primary culture. Am J Physiol 1996;271:F498–507.

[147] Friis MB, Vorum KG, Lambert IH. Volume-sensitive NADPH oxidase activity and taurine efflux in NIH3T3 mouse fibroblasts. Am J Physiol Cell Physiol 2008;294:C1552–65.

[148] Lambert IH. Activation and inactivation of the volume-sensitive taurine leak pathway in NIH3T3 fibroblasts and Ehrlich Lettre ascites cells. Am J Physiol Cell Physiol 2007;293: C390–400.

[149] Lambert IH, Hoffmann EK. Regulation of taurine transport in Ehrlich ascites tumor cells. J Membr Biol 1993;131:67–79.

[150] Sanchez-Olea R, Morales-Mulia M, Moran J, Pasantes-Morales H. Inhibition by polyunsaturated fatty acids of cell volume regulation and osmolyte fluxes in astrocytes. Am J Physiol 1995;269:C96–102.

[151] Berneis K, Ninnis R, Haussinger D, Keller U. Effects of hyper- and hypoosmolality on whole body protein and glucose kinetics in humans. Am J Physiol 1999;276:E188–95.

[152] Hallbrucker C, vom DS, Lang F, Haussinger D. Control of hepatic proteolysis by amino acids. The role of cell volume. Eur J Biochem 1991;197:717–24.

[153] Haussinger D, Lang F, Bauers K, Gerok W. Control of hepatic nitrogen metabolism and glutathione release by cell volume regulatory mechanisms. Eur J Biochem 1990;193:891–8.

[154] Haussinger D, Lang F, Gerok W. Regulation of cell function by the cellular hydration state. Am J Physiol 1994;267: E343–55.

[155] Gual P, Gonzalez T, Gremeaux T, Marchand-Brustel Y, Tanti JF. Osmotic regulation of cellular glucose uptake. Methods Enzymol 2007;428:343–54.

[156] Saha N, Stoll B, Lang F, Haussinger D. Effect of anisotonic cell-volume modulation on glutathione-S-conjugate release, t-butylhydroperoxide metabolism and the pentose-phosphate shunt in perfused rat liver. Eur J Biochem 1992;209:437–44.

[157] Haussinger D, Gorg B. Interaction of oxidative stress, astrocyte swelling and cerebral ammonia toxicity. Curr Opin Clin Nutr Metab Care 2010;13:87–92.

[158] Lambert IH. Reactive oxygen species regulate swelling-induced taurine efflux in NIH3T3 mouse fibroblasts. J Membr Biol 2003;192:19–32.

[159] Iyer SS, Pearson DW, Nauseef WM, Clark RA. Evidence for a readily dissociable complex of p47phox and p67phox in cytosol of unstimulated human neutrophils. J Biol Chem 1994;269:22405–11.

[160] Kataoka S, Fujita Y. [Basal experiments of active oxygen generation in urinary polymorphonuclear leukocytes]. Nippon Hinyokika Gakkai Zasshi 1991;82:16–23.

[161] Ferraris JD, Burg MB. Tonicity-regulated gene expression. Methods Enzymol 2007;428:279–96.

[162] Chen Y, Schnetz MP, Irarrazabal CE, Shen RF, Williams CK, Burg MB, et al. Proteomic identification of proteins associated with the osmoregulatory transcription factor TonEBP/OREBP: functional effects of Hsp90 and PARP-1. Am J Physiol Renal Physiol 2007;292:F981–92.

[163] Valkova N, Kultz D. Constitutive and inducible stress proteins dominate the proteome of the murine inner medullary collecting duct-3 (mIMCD3) cell line. Biochim Biophys Acta 2006;1764:1007–20.

[164] Ferrer-Martinez A, Casado FJ, Felipe A, Pastor-Anglada M. Regulation of Na^+,$K(^+)$-ATPase and the $Na^+/K^+/Cl^-$ cotransporter in the renal epithelial cell line NBL-1 under osmotic stress. Biochem J 1996;319(Pt 2):337–42.

[165] Sadoshima J, Qiu Z, Morgan JP, Izumo S. Tyrosine kinase activation is an immediate and essential step in hypotonic cell swelling-induced ERK activation and c-fos gene expression in cardiac myocytes. EMBO J 1996;15:5535–46.

[166] Firestone GL, Giampaolo JR, O'Keeffe BA. Stimulus-dependent regulation of the serum and glucocorticoid inducible protein kinase (Sgk) transcription, subcellular localization and enzymatic activity. Cell Physiol Biochem 2003;13:1–12.

[167] Waldegger S, Barth P, Raber G, Lang F. Cloning and characterization of a putative human serine/threonine protein kinase transcriptionally modified during anisotonic and isotonic alterations of cell volume. Proc Natl Acad Sci USA 1997;94:4440–5.

[168] Zhang F, Warskulat U, Wettstein M, Schreiber R, Henninger HP, Decker K, et al. Hyperosmolarity stimulates prostaglandin synthesis and cyclooxygenase-2 expression in activated rat liver macrophages. Biochem J 1995;312(Pt 1):135–43.

[169] Alfieri R, Petronini PG, Urbani S, Borghetti AF. Activation of heat-shock transcription factor 1 by hypertonic shock in 3T3 cells. Biochem J 1996;319(Pt 2):601–6.
[170] Beck FX, Grunbein R, Lugmayr K, Neuhofer W. Heat shock proteins and the cellular response to osmotic stress. Cell Physiol Biochem 2000;10:303–6.
[171] Cohen DM, Wasserman JC, Gullans SR. Immediate early gene and HSP70 expression in hyperosmotic stress in MDCK cells. Am J Physiol 1991;261:C594–601.
[172] Sheikh-Hamad D, Garcia-Perez A, Ferraris JD, Peters EM, Burg MB. Induction of gene expression by heat shock versus osmotic stress. Am J Physiol 1994;267:F28–34.
[173] Tanaka K, Jay G, Isselbacher KJ. Expression of heat-shock and glucose-regulated genes: differential effects of glucose starvation and hypertonicity. Biochim Biophys Acta 1988;950:138–46.
[174] Finkenzeller G, Newsome W, Lang F, Haussinger D. Increase of c-jun mRNA upon hypo-osmotic cell swelling of rat hepatoma cells. FEBS Lett 1994;340:163–6.
[175] Zhang F, Warskulat U, Haussinger D. Modulation of tumor necrosis factor-alpha release by anisoosmolarity and betaine in rat liver macrophages (Küpffer cells). FEBS Lett 1996;391:293–6.
[176] Murphy D, Carter D. Vasopressin gene expression in the rodent hypothalamus: transcriptional and posttranscriptional responses to physiological stimulation. Mol Endocrinol 1990;4:1051–9.
[177] Ferraris JD, Williams CK, Jung KY. Bedford JJ, Burg MB, Garcia-Perez A. ORE, a eukaryotic minimal essential osmotic response element. The aldose reductase gene in hyperosmotic stress. J Biol Chem 1996;271:18318–21.
[178] Ruepp B, Bohren KM, Gabbay KH. Characterization of the osmotic response element of the human aldose reductase gene promoter. Proc Natl Acad Sci USA 1996;93:8624–9.
[179] Ferraris JD, Williams CK, Persaud P, Zhang Z, Chen Y, Burg MB. Activity of the TonEBP/OREBP transactivation domain varies directly with extracellular NaCl concentration. Proc Natl Acad Sci USA 2002;99:739–44.
[180] Go WY, Liu X, Roti MA, Liu F, Ho SN. NFAT5/TonEBP mutant mice define osmotic stress as a critical feature of the lymphoid microenvironment. Proc Natl Acad Sci USA 2004;101:10673–8.
[181] Irarrazabal CE, Liu JC, Burg MB, Ferraris JD. ATM a DNA damage-inducible kinase, contributes to activation by high NaCl of the transcription factor TonEBP/OREBP. Proc Natl Acad Sci USA 2004;101:8809–14.
[182] Ito T, Fujio Y, Hirata M, Takatani T, Matsuda T, Muraoka S, et al. Expression of taurine transporter is regulated through the TonE (tonicity-responsive element)/TonEBP (TonE-binding protein) pathway and contributes to cytoprotection in HepG2 cells. Biochem J 2004;382:177–82.
[183] Lam AK, Ko BC, Tam S, Morris R, Yang JY, Chung SK, et al. Osmotic response element-binding protein (OREBP) is an essential regulator of the urine concentrating mechanism. J Biol Chem 2004;279:48048–54.
[184] Lee SD, Colla E, Sheen MR, Na KY, Kwon HM. Multiple domains of TonEBP cooperate to stimulate transcription in response to hypertonicity. J Biol Chem 2003;278:47571–7.
[185] Lopez-Rodriguez C, Antos CL, Shelton JM, Richardson JA, Lin F, Novobrantseva TI, et al. Loss of NFAT5 results in renal atrophy and lack of tonicity-responsive gene expression. Proc Natl Acad Sci USA 2004;101:2392–7.
[186] Stroud JC, Lopez-Rodriguez C, Rao A, Chen L. Structure of a TonEBP-DNA complex reveals DNA encircled by a transcription factor. Nat Struct Biol 2002;9:90–4.
[187] Burg MB. Macromolecular crowding as a cell volume sensor. Cell Physiol Biochem 2000;10:251–6.
[188] Alexander RT, Malevanets A, Durkan AM, Kocinsky HS, Aronson PS, Orlowski J, et al. Membrane curvature alters the activation kinetics of the epithelial Na^+/H^+ exchanger, NHE3. J Biol Chem 2007;282:7376–84.
[189] Asaoka Y, Yoshida K, Sasaki Y, Nishizuka Y. Potential role of phospholipase A2 in HL-60 cell differentiation to macrophages induced by protein kinase C activation. Proc Natl Acad Sci USA 1993;90:4917–21.
[190] Maingret F, Patel AJ, Lesage F, Lazdunski M, Honore E. Lysophospholipids open the two-pore domain mechano-gated $K(^+)$ channels TREK-1 and TRAAK. J Biol Chem 2000;275:10128–33.
[191] Hamill OP, Martinac B. Molecular basis of mechanotransduction in living cells. Physiol Rev 2001;81:685–740.
[192] Ingber DE. Tensegrity: the architectural basis of cellular mechanotransduction. Annu Rev Physiol 1997;59:575–99.
[193] Rosette C, Karin M. Ultraviolet light and osmotic stress: activation of the JNK cascade through multiple growth factor and cytokine receptors. Science 1996;274:1194–7.
[194] Fiol DF, Kultz D. Osmotic stress sensing and signaling in fishes. FEBS J 2007;274:5790–8.
[195] Cohen DM. TRPV4 and the mammalian kidney. Pflugers Arch 2005;451:168–75.
[196] O'Neil RG, Heller S. The mechanosensitive nature of TRPV channels. Pflugers Arch 2005;451:193–203.
[197] Chen B, Nicol G, Cho WK. Role of calcium in volume-activated chloride currents in a mouse cholangiocyte cell line. J Membr Biol 2007;215:1–13.
[198] McCarty NA, O'Neil RG. Calcium signaling in cell volume regulation. Physiol Rev 1992;72:1037–61.
[199] Tinel H, Kinne-Saffran E, Kinne RK. Calcium signalling during RVD of kidney cells. Cell Physiol Biochem 2000;10:297–302.
[200] Cornet M, Lambert IH, Hoffmann EK. Relation between cytoskeleton, hypo-osmotic treatment and volume regulation in Ehrlich ascites tumor cells. J Membr Biol 1993;131:55–66.
[201] Haussinger D, Stoll B, vom Dahl S, Theodoropoulos PA, Markogiannakis E, Gravanis A, et al. Effect of hepatocyte swelling on microtubule stability and tubulin mRNA levels. Biochem Cell Biol 1994;72:12–9.
[202] Papakonstanti EA, Vardaki EA, Stournaras C. Actin cytoskeleton: a signaling sensor in cell volume regulation. Cell Physiol Biochem 2000;10:257–64.
[203] Szaszi K, Grinstein S, Orlowski J, Kapus A. Regulation of the epithelial $Na(^+)$ /$H(^+)$ exchanger isoform by the cytoskeleton. Cell Physiol Biochem 2000;10:265–72.
[204] Tamma G, Procino G, Svelto M, Valenti G. Hypotonicity causes actin reorganization and recruitment of the actin-binding ERM protein moesin in membrane protrusions in collecting duct principal cells. Am J Physiol Cell Physiol 2007;292:C1476–84.
[205] Feranchak AP, Kilic G, Wojtaszek PA, Qadri I, Fitz JG. Volume-sensitive tyrosine kinases regulate liver cell volume through effects on vesicular trafficking and membrane Na^+ permeability. J Biol Chem 2003;278:44632–8.
[206] Lepple-Wienhues A, Szabo I, Laun T, Kaba NK, Gulbins E, Lang F. The tyrosine kinase p56lck mediates activation of swelling-induced chloride channels in lymphocytes. J Cell Biol 1998;141:281–6.
[207] Nilius B, Eggermont J, Droogmans G. The endothelial volume-regulated anion channel, VRAC. Cell Physiol Biochem 2000;10:313–20.
[208] Tilly BC, van den BN, Tertoolen LG, Edixhoven MJ, de Jonge HR. Protein tyrosine phosphorylation is involved in osmoregulation of ionic conductances. J Biol Chem 1993;268:19919–22.
[209] van der Wijk T, Tomassen SF, de Jonge HR, Tilly BC. Signalling mechanisms involved in volume regulation of intestinal epithelial cells. Cell Physiol Biochem 2000;10:289–96.

[210] Richter EA, Cleland PJ, Rattigan S, Clark MG. Contraction-associated translocation of protein kinase C in rat skeletal muscle. FEBS Lett 1987;217:232–6.
[211] Rosales OR, Sumpio BE. Changes in cyclic strain increase inositol trisphosphate and diacylglycerol in endothelial cells. Am J Physiol 1992;262:C956–62.
[212] Tilly BC, Edixhoven MJ, Tertoolen LG, Morii N, Saitoh Y, Narumiya S, et al. Activation of the osmo-sensitive chloride conductance involves P21rho and is accompanied by a transient reorganization of the F-actin cytoskeleton. Mol Biol Cell 1996;7:1419–27.
[213] Agius L, Peak M, Beresford G, al Habori M, Thomas TH. The role of ion content and cell volume in insulin action. Biochem Soc Trans 1994;22:516–22.
[214] Belsey MJ, Davies AR, Witchel HJ, Kozlowski RZ. Inhibition of ERK and JNK decreases both osmosensitive taurine release and cell proliferation in glioma cells. Neurochem Res 2007;32:1940–9.
[215] Galcheva-Gargova Z, Derijard B, Wu IH, Davis RJ. An osmosensing signal transduction pathway in mammalian cells. Science 1994;265:806–8.
[216] Han J, Lee JD, Bibbs L, Ulevitch RJ. A MAP kinase targeted by endotoxin and hyperosmolarity in mammalian cells. Science 1994;265:808–11.
[217] Itoh T, Yamauchi A, Imai E, Ueda N, Kamada T. Phosphatase toward MAP kinase is regulated by osmolarity in Madin–Darby canine kidney (MDCK) cells. FEBS Lett 1995;373:123–6.
[218] Noe B, Schliess F, Wettstein M, Heinrich S, Haussinger D. Regulation of taurocholate excretion by a hypo-osmolarity-activated signal transduction pathway in rat liver. Gastroenterology 1996;110:858–65.
[219] Schliess F, Sinning R, Fischer R, Schmalenbach C, Haussinger D. Calcium-dependent activation of Erk-1 and Erk-2 after hypo-osmotic astrocyte swelling. Biochem J 1996;320(Pt 1): 167–71.
[220] Lang F, Bohmer C, Palmada M, Seebohm G, Strutz-Seebohm N, Vallon V. (Patho)physiological significance of the serum- and glucocorticoid-inducible kinase isoforms. Physiol Rev 2006;86:1151–78.
[221] Clements Jr. RS, Blumenthal SA, Morrison AD, Winegrad AI. Increased cerebrospinal-fluid pressure during treatment of diabetic ketosis. Lancet 1971;2:671–5.
[222] Gagnon KB, England R, Delpire E. Characterization of SPAK and OSR1, regulatory kinases of the Na-K-2Cl co-transporter. Mol Cell Biol 2006;26:689–98.
[223] Gagnon KB, England R, Delpire E. A single binding motif is required for SPAK activation of the Na-K-2Cl co-transporter. Cell Physiol Biochem 2007;20:131–42.
[224] Zagorska A, Pozo-Guisado E, Boudeau J, Vitari AC, Rafiqi FH, Thastrup J, et al. Regulation of activity and localization of the WNK1 protein kinase by hyperosmotic stress. J Cell Biol 2007;176:89–100.
[225] Delpire E. KBSPAK Gagnon and OSR1: STE20 kinases involved in the regulation of ion homoeostasis and volume control in mammalian cells. Biochem J 2008;409:321–31.
[226] Garzon-Muvdi T, Pacheco-Alvarez D, Gagnon KB, Vazquez N, Ponce-Coria J, Moreno E, et al. WNK4 kinase is a negative regulator of K^+-Cl^- co-transporters. Am J Physiol Renal Physiol 2007;292:F1197–207.
[227] Peng JB, Warnock DG. WNK4-mediated regulation of renal ion transport proteins. Am J Physiol Renal Physiol 2007;293: F961–73.
[228] Ring AM, Leng Q, Rinehart J, Wilson FH, Kahle KT, Hebert SC, et al. An SGK1 site in WNK4 regulates Na^+ channel and K^+ channel activity and has implications for aldosterone signaling and K^+ homeostasis. Proc Natl Acad Sci USA 2007;104:4025–9.
[229] Bode JG, Gatsios P, Ludwig S, Rapp UR, Haussinger D, Heinrich PC, et al. The mitogen-activated protein (MAP) kinase p38 and its upstream activator MAP kinase kinase 6 are involved in the activation of signal transducer and activator of transcription by hyperosmolarity. J Biol Chem 1999;274:30222–7.
[230] Feranchak AP, Berl T, Capasso J, Wojtaszek PA, Han J, Fitz JG. p38 MAP kinase modulates liver cell volume through inhibition of membrane Na^+ permeability. J Clin Invest 2001;108:1495–504.
[231] Haussinger D, Schliess F, Dombrowski F, vom Dahl S. Involvement of p38MAPK in the regulation of proteolysis by liver cell hydration. Gastroenterology 1999;116:921–35.
[232] Hilder TL, Malone MH, Johnson GL. Hyperosmotic induction of mitogen-activated protein kinase scaffolding. Methods Enzymol 2007;428:297–312.
[233] Hoffmann EK. Intracellular signalling involved in volume regulatory decrease. Cell Physiol Biochem 2000;10:273–88.
[234] Jacobsen JH, Clement CA, Friis MB, Lambert IH. Casein kinase 2 regulates the active uptake of the organic osmolyte taurine in NIH3T3 mouse fibroblasts. Pflugers Arch 2008;457:327–37.
[235] Moriguchi T, Kawasaki H, Matsuda S, Gotoh Y, Nishida E. Evidence for multiple activators for stress-activated protein kinase/c-Jun amino-terminal kinases. Existence of novel activators. J Biol Chem 1995;270:12969–72.
[236] Nielsen MB, Christensen ST, Hoffmann EK. Effects of osmotic stress on the activity of MAPKs and PDGFR-beta-mediated signal transduction in NIH-3T3 fibroblasts. Am J Physiol Cell Physiol 2008;294:C1046–55.
[237] Pan Z, Capo-Aponte JE, Zhang F, Wang Z, Pokorny KS, Reinach PS. Differential dependence of regulatory volume decrease behavior in rabbit corneal epithelial cells on MAPK superfamily activation. Exp Eye Res 2007;84:978–90.
[238] Pedersen SF, Darborg BV, Rentsch ML, Rasmussen M. Regulation of mitogen-activated protein kinase pathways by the plasma membrane Na^+/H^+ exchanger, NHE1. Arch Biochem Biophys 2007;462:195–201.
[239] Strange K, Denton J, Nehrke K. Ste20-type kinases: evolutionarily conserved regulators of ion transport and cell volume. *Physiology* (Bethesda) 2006;21:61–8.
[240] Sanguinetti AR, Cao H, Corley MC. Fyn is required for oxidative- and hyperosmotic-stress-induced tyrosine phosphorylation of caveolin-1. Biochem J 2003;376:159–68.
[241] Trouet D, Carton I, Hermans D, Droogmans G, Nilius B, Eggermont J. Inhibition of VRAC by c-Src tyrosine kinase targeted to caveolae is mediated by the Src homology domains. Am J Physiol Cell Physiol 2001;281:C248–56.
[242] Nielsen DK, Jensen AK, Harbak H, Christensen SC, Simonsen LO. Cell content of phosphatidylinositol (4,5)bisphosphate in Ehrlich mouse ascites tumour cells in response to cell volume perturbations in anisotonic and in isosmotic media. J Physiol 2007;582:1027–36.
[243] Yamamoto M, Chen MZ, Wang YJ, Sun HQ, Wei Y, Martinez M, et al. Hypertonic stress increases phosphatidylinositol 4,5-bisphosphate levels by activating PIP5KIbeta. J Biol Chem 2006;281:32630–8.
[244] Gamper N, Shapiro MS. Target-specific PIP (2) signalling: how might it work? J Physiol 2007;582:967–75.
[245] Janmey PA, Lindberg U. Cytoskeletal regulation: rich in lipids. Nat Rev Mol Cell Biol 2004;5:658–66.
[246] Lambert IH. Eicosanoids and cell volume regulation. In: Strange K, editor. Cellular and Molecular Physiology of

Cell Volume Regulation. Boca Raton, FL: CRC Press; 1994. p. 179–98.

[247] Meyer MC, McHowat J. Calcium-independent phospholipase A2-catalyzed plasmalogen hydrolysis in hypoxic human coronary artery endothelial cells. Am J Physiol Cell Physiol 2007;292:C251–8.

[248] Steer SA, Wirsig KC, Creer MH, Ford DA, McHowat J. Regulation of membrane-associated iPLA2 activity by a novel PKC isoform in ventricular myocytes. Am J Physiol Cell Physiol 2002;283:C1621–6.

[249] Tay HK, Melendez AJ. Fcgamma RI-triggered generation of arachidonic acid and eicosanoids requires iPLA2 but not cPLA2 in human monocytic cells. J Biol Chem 2004;279:22505–13.

[250] Lambert IH, Hoffmann EK, Christensen P. Role of prostaglandins and leukotrienes in volume regulation by Ehrlich ascites tumor cells. J Membr Biol 1987;98:247–56.

[251] Lang PA, Kempe DS, Myssina S, Tanneur VBC, Laufer S, Lang F, et al. PGE2 in the regulation of programmed erythrocyte death. Cell Death Diff 2005;12(5):415–28.

[252] Civan MM, Coca-Prados M, Peterson-Yantorno K. Pathways signaling the regulatory volume decrease of cultured nonpigmented ciliary epithelial cells. Invest Ophthalmol Vis Sci 1994;35:2876–86.

[253] Lang PA, Kempe DS, Tanneur V, Eisele K, Klarl BA, Myssina S, et al. Stimulation of erythrocyte ceramide formation by platelet activating factor. J. Cell Science 2005;118(Pt 6):1233–43.

[254] Busch GL, Lang HJ, Lang F. Studies on the mechanism of swelling-induced lysosomal alkalinization in vascular smooth muscle cells. Pflugers Arch 1996;431:690–6.

[255] Busch GL, Schreiber R, Dartsch PC, Volkl H, vom DS, Haussinger D, et al. Involvement of microtubules in the link between cell volume and pH of acidic cellular compartments in rat and human hepatocytes. Proc Natl Acad Sci USA 1994;91:9165–9.

[256] Malek AM, Xu C, Kim ES, Alper SL. Hypertonicity triggers RhoA-dependent assembly of myosin-containing striated polygonal actin networks in endothelial cells. Am J Physiol Cell Physiol 2007;292:C1645–59.

[257] Schneider L, Klausen TK, Stock C, Mally S, Christensen ST, Pedersen SF, et al. H-ras transformation sensitizes volume-activated anion channels and increases migratory activity of NIH3T3 fibroblasts. Pflugers Arch 2008;455:1055–62.

[258] Rasmussen M, Alexander RT, Darborg BV, Mobjerg N, Hoffmann EK, Kapus A, et al. Osmotic cell shrinkage activates ezrin/radixin/moesin (ERM) proteins: activation mechanisms and physiological implications. Am J Physiol Cell Physiol 2008;294:C197–212.

[259] Pedersen S, Pedersen SF, Nilius B, Lambert IH, Hoffmann EK. Mechanical stress induces release of ATP from Ehrlich ascites tumor cells. Biochim Biophys Acta 1999;1416:271–84.

[260] Poronnik P, Schumann SY, Cook DI. HCO3($^-$)-dependent ACh-activated Na^+ influx in sheep parotid secretory end-pieces. Pflugers Arch 1995;429:852–8.

[261] Van der Meulen JA, Klip A, Grinstein S. Possible mechanism for cerebral oedema in diabetic ketoacidosis. Lancet 1987;2:306–8.

[262] Saltin B, Sjogaard G, Strange S, Juel C. Redistribution of K^+ in the human body during muscular exercise: Its role to maintain whole body homeostasis. In: Shirak KYMK, editor. Man in Stressful Environments: Thermal and Work Physiology. Springfield, IL: Thomas; 1987. p. 247–67.

[263] Chacon E, Reece JM, Nieminen AL, Zahrebelski G, Herman B, Lemasters JJ. Distribution of electrical potential, pH, free Ca^{2+}, and volume inside cultured adult rabbit cardiac myocytes during chemical hypoxia: a multiparameter digitized confocal microscopic study. Biophys J 1994;66:942–52.

[264] Faff-Michalak L, Reichenbach A, Dettmer D, Kellner K, Albrecht J. K($^+$)-, hypoosmolarity-, and NH4($^+$)-induced taurine release from cultured rabbit Muller cells: role of Na^+ and Cl^- ions and relation to cell volume changes. Glia 1994;10:114–20.

[265] Smith TW, Rasmusson RL, Lobaugh LA, Lieberman M. Na^+/K^+ pump inhibition induces cell shrinkage in cultured chick cardiac myocytes. Basic Res Cardiol 1993;88:411–20.

[266] Lang F, Rehwald W. Potassium channels in renal epithelial transport regulation. Physiol Rev 1992;72:1–32.

[267] Schultz SG. Homocellular regulatory mechanisms in sodium-transporting epithelia: avoidance of extinction by "flush-through.". Am J Physiol 1981;241:F579–90.

[268] Foskett JK, Wong MM, Sue AQ, Robertson MA. Isosmotic modulation of cell volume and intracellular ion activities during stimulation of single exocrine cells. J Exp Zool 1994;268:104–10.

[269] Hoffmann EK, Ussing HH. Membrane mechanisms in volume regulation in vertebrate cells and epithelia. In: Giebisch GH, Schafer JA, Ussing HH, Kristensen P, editors. Membrane Transport in Biology. Heidelberg: Springer-Verlag; 1992. p. 317–99.

[270] Manganel M, Turner RJ. Agonist-induced activation of Na^+/H^+ exchange in rat parotid acinar cells is dependent on calcium but not on protein kinase C. J Biol Chem 1990;265:4284–9.

[271] Manganel M, Turner RJ. Rapid secretagogue-induced activation of Na^+H^+ exchange in rat parotid acinar cells. Possible interrelationship between volume regulation and stimulus-secretion coupling. J Biol Chem 1991;266:10182–8.

[272] Joiner CH. Cation transport and volume regulation in sickle red blood cells. Am J Physiol 1993;264:C251–70.

[273] Lang KS, Lang PA, Bauer C, Duranton C, Wieder T, Huber SM, et al. Mechanisms of suicidal erythrocyte death. Cell Physiol Biochem 2005;15:195–202.

[274] Lang F, Busch G, Völkl H, Häussinger D. Cell volume: a second message in regulation of cellular function. News Physiol Sci 1995;10:18–22.

[275] Boini KM, Graf D, Kuhl D, Haussinger D, Lang F. SGK1 dependence of insulin induced hypokalemia. Pflugers Arch 2009;457:955–61.

[276] Schliess F, Haussinger D. Cell volume and insulin signaling. Int Rev Cytol 2003;225:187–228.

[277] Schliess F, Reissmann R, Reinehr R, vom DS, Haussinger D. Involvement of integrins and Src in insulin signaling toward autophagic proteolysis in rat liver. J Biol Chem 2004;279:21294–301.

[278] Choi DW, Rothman SM. The role of glutamate neurotoxicity in hypoxic-ischemic neuronal death. Annu Rev Neurosci 1990;13:171–82.

[279] Polischuk TM, Andrew RD. Real-time imaging of intrinsic optical signals during early excitotoxicity evoked by domoic acid in the rat hippocampal slice. Can J Physiol Pharmacol 1996;74:712–22.

[280] Saransaari P, Oja SS. Excitatory amino acids evoke taurine release from cerebral cortex slices from adult and developing mice. Neuroscience 1991;45:451–9.

[281] Ballanyi K, Grafe P. Cell volume regulation in the nervous system. Ren Physiol Biochem 1988;11:142–57.

[282] Strbak V, Greer MA. Regulation of hormone secretion by acute cell volume changes: Ca($^{2+}$)-independent hormone secretion. Cell Physiol Biochem 2000;10:393–402.

[283] Bohmer C, Philippin M, Rajamanickam J, Mack A, Broer S, Palmada M, et al. Stimulation of the EAAT4 glutamate transporter by SGK protein kinase isoforms and PKB. Biochem Biophys Res Commun 2004;324:1242–8.
[284] Kimelberg HK. Current concepts of brain edema. Review of laboratory investigations. J Neurosurg 1995;83:1051–9.
[285] Cordoba J, Gottstein J, Blei AT. Glutamine, myo-inositol, and organic brain osmolytes after portocaval anastomosis in the rat: implications for ammonia-induced brain edema. Hepatology 1996;24:919–23.
[286] Norenberg MD, Bender AS. Astrocyte swelling in liver failure: role of glutamine and benzodiazepines. *Acta Neurochir Suppl* (Wien) 1994;60:24–7.
[287] Haussinger D, Laubenberger J, vom Dahl S, Ernst T, Bayer S, Langer M, et al. Proton magnetic resonance spectroscopy studies on human brain myo-inositol in hypo-osmolarity and hepatic encephalopathy. Gastroenterology 1994;107:1475–80.
[288] Kreis R, Ross BD, Farrow NA, Ackerman Z. Metabolic disorders of the brain in chronic hepatic encephalopathy detected with H-1 MR spectroscopy. Radiology 1992;182:19–27.
[289] Hawkins RA, Jessy J, Mans AM, De Joseph MR. Effect of reducing brain glutamine synthesis on metabolic symptoms of hepatic encephalopathy. J Neurochem 1993;60:1000–6.
[290] Sakai H, Kakinoki B, Diener M, Takeguchi N. Endogenous arachidonic acid inhibits hypotonically-activated Cl^- channels in isolated rat hepatocytes. Jpn J Physiol 1996;46:311–8.
[291] Elliott SJ, Schilling WP. Oxidant stress alters Na^+ pump and $Na(^+)$-$K(^+)$-Cl^- co-transporter activities in vascular endothelial cells. Am J Physiol 1992;263:H96–102.
[292] Brizzolara A, Barbieri MP, Adezati L, Viviani GL. Water distribution in insulin-dependent diabetes mellitus in various states of metabolic control. Eur J Endocrinol 1996;135:609–15.
[293] Krane EJ, Rockoff MA, Wallman JK, Wolfsdorf JI. Subclinical brain swelling in children during treatment of diabetic ketoacidosis. N Engl J Med 1985;312:1147–51.
[294] Young E, Bradley RF. Cerebral edema with irreversible coma in severe diabetic ketoacidosis. N Engl J Med 1967;276:665–9.
[295] Edmands S, Yancey PH. Effects on rat renal osmolytes of extended treatment with an aldose reductase inhibitor. Comp Biochem Physiol C 1992;103:499–502.
[296] Finegold D, Lattimer SA, Nolle S, Bernstein M, Greene DA. Polyol pathway activity and myo-inositol metabolism. A suggested relationship in the pathogenesis of diabetic neuropathy. Diabetes 1983;32:988–92.
[297] Tomlinson DR, Stevens EJ, Diemel LT. Aldose reductase inhibitors and their potential for the treatment of diabetic complications. Trends Pharmacol Sci 1994;15:293–7.
[298] Demerdash TM, Seyrek N, Smogorzewski M, Marcinkowski W, Nasser-Moadelli S, Massry SG. Pathways through which glucose induces a rise in $[Ca^{2+}]i$ of polymorphonuclear leukocytes of rats. Kidney Int 1996;50:2032–40.
[299] Lang F, Klingel K, Wagner CA, Stegen C, Warntges S, Friedrich B, et al. Deranged transcriptional regulation of cell-volume-sensitive kinase hSGK in diabetic nephropathy. Proc Natl Acad Sci USA 2000;97:8157–62.
[300] Lee JA, Lee HA, Sadler PJ. Uraemia: is urea more important than we think? Lancet 1991;338:1438–40.
[301] Friedrich B, Alexander D, Aicher WK, Duszenko M, Schaub T, Passlick-Deetjen J, et al. Influence of standard haemodialysis on transcription of human serum and glucocorticoid inducible kinase SGK1 and taurine transporter TAUT in blood leukocytes. Nephrology Dialysis Transplantation 2005;20(4): 768–74.
[302] Ling H, Vamvakas S, Busch G, Dammrich J, Schramm L, Lang F, et al. Suppressing role of transforming growth factor-beta 1 on cathepsin activity in cultured kidney tubule cells. Am J Physiol 1995;269:F911–7.
[303] Chiang Y, Chou CY, Hsu KF, Huang YF, Shen MR. EGF upregulates Na^+/H^+ exchanger NHE1 by post-translational regulation that is important for cervical cancer cell invasiveness. J Cell Physiol 2008;214:810–9.
[304] Habela CW, Sontheimer H. Cytoplasmic volume condensation is an integral part of mitosis. Cell Cycle 2007;6:1613–20.
[305] Chen LX, Zhu LY, Jacob TJ, Wang LW. Roles of volume-activated Cl^- currents and regulatory volume decrease in the cell cycle and proliferation in nasopharyngeal carcinoma cells. Cell Prolif 2007;40:253–67.
[306] Klausen TK, Bergdahl A, Hougaard C, Christophersen P, Pedersen SF, Hoffmann EK. Cell cycle-dependent activity of the volume- and Ca^{2+}-activated anion currents in Ehrlich lettre ascites cells. J Cell Physiol 2007;210:831–42.
[307] Lang F, Foller M, Lang K, Lang P, Ritter M, Vereninov A, et al. Cell volume regulatory ion channels in cell proliferation and cell death. Methods Enzymol 2007;428:209–25.
[308] Lang F, Perrotti N, Stournaras C. Colorectal carcinoma cells: regulation of survival and growth by SGK1. Int. J. Biochem. Cell Biol. 2010;42(10):1571–5.
[309] Jakab M, Ritter M. Cell volume regulatory ion transport in the regulation of cell migration. Contrib Nephrol 2006;152: 161–80.
[310] Stossel TP. On the crawling of animal cells. Science 1993;260:1086–94.
[311] Mao J, Wang L, Fan A, Wang J, Xu B, Jacob TJ, et al. Blockage of volume-activated chloride channels inhibits migration of nasopharyngeal carcinoma cells. Cell Physiol Biochem 2007;19:249–58.
[312] McFerrin MB, Sontheimer H. A role for ion channels in glioma cell invasion. Neuron Glia Biol 2006;2:39–49.
[313] Schwab A. Function and spatial distribution of ion channels and transporters in cell migration. Am J Physiol Renal Physiol 2001;280:F739–47.
[314] Schwab A, Nechyporuk-Zloy V, Fabian A, Stock C. Cells move when ions and water flow. Pflugers Arch 2007;453:421–32.
[315] Papadopoulos MC, Saadoun S, Verkman AS. Aquaporins and cell migration. Pflugers Arch 2008;456:693–700.
[316] Lang F, Gulbins E, Szabo I, Lepple-Wienhues A, Huber SM, Duranton C, et al. Cell volume and the regulation of apoptotic cell death. J Mol Recognit 2004;17:473–80.
[317] Bortner CD, Cidlowski JA. Caspase independent/dependent regulation of $K(^+)$, cell shrinkage, and mitochondrial membrane potential during lymphocyte apoptosis. J Biol Chem 1999;274:21953–62.
[318] Bortner CD, Hughes Jr. FM, Cidlowski JA. A primary role for K^+ and Na^+ efflux in the activation of apoptosis. J Biol Chem 1997;272:32436–42.
[319] Maeno E, Ishizaki Y, Kanaseki T, Hazama A, Okada Y. Normotonic cell shrinkage because of disordered volume regulation is an early prerequisite to apoptosis. Proc Natl Acad Sci USA 2000;97:9487–92.
[320] Gulbins E, Welsch J, Lepple-Wienhuis A, Heinle H, Lang F. Inhibition of Fas-induced apoptotic cell death by osmotic cell shrinkage. Biochem Biophys Res Commun 1997;236: 517–21.
[321] Reinehr R, Becker S, Hongen A, Haussinger D. The Src family kinase Yes triggers hyperosmotic activation of the epidermal

growth factor receptor and CD95. J Biol Chem 2004;279:23977–87.

[322] Reinehr R, Gorg B, Hongen A, Haussinger D. CD95-tyrosine nitration inhibits hyperosmotic and CD95 ligand-induced CD95 activation in rat hepatocytes. J Biol Chem 2004;279: 10364–73.

[323] Reinehr R, Haussinger D. Hyperosmotic activation of the CD95 system. Methods Enzymol 2007;428:145–60.

[324] Lang KS, Fillon S, Schneider D, Rammensee HG, Lang F. Stimulation of TNF alpha expression by hyperosmotic stress. Pflugers Arch 2002;443:798–803.

[325] Reinehr R, Schliess F, Haussinger D. Hyperosmolarity and CD95L trigger CD95/EGF receptor association and tyrosine phosphorylation of CD95 as prerequisites for CD95 membrane trafficking and DISC formation. FASEB J 2003;17: 731–3.

This page intentionally left blank

CHAPTER

6

Solute Transport, Energy Consumption, and Production in the Kidney

Takashi Sekine[1] *and Hitoshi Endou*[2]

[1]Department of Pediatrics, Toho University School of Medicine, Ohashi Hospital, Tokyo, Japan
[2]Department of Pharmacology and Toxicology, Kyorin University School of Medicine, Tokyo, Japan

INTRODUCTION

The kidney must reabsorb more than 99% of approximately 180 liters of water and 25,000 mmoles of Na^+ daily. To do this, the kidney consumes a large amount of energy. Although the kidney is only 0.5% of the total body weight, it utilizes approximately 7% of the oxygen consumed by the body.[1] In fact, the kidney is the second only to the heart in terms of the rate of energy consumption.[1] In this chapter, first we describe the energy consuming and production processes in the kidney. Second, the mechanisms of mutual relationships between energy consumption and production will be described. Significant advances have been made with regard to this issue, and AMPK (AMP-activated kinase) is considered to be the central for the regulation of energy consuming processes. Finally, we also refer to the pathophysiological states in which renal energy production is inhibited.

ENERGY CONSUMPTION

Na Transport and Energy Consumption in the Kidney

Na^+ Transport and O_2 Consumption

The energy utilized in the kidney is primarily required for the active reabsorption of Na^+ from the glomerular filtrate. This seems rational considering that the amount of Na^+ reabsorbed by the kidney is much higher than that of HCO_3^- (4,000 mmole/day), Ca^{2+} (210 mmole/day), other electrolytes, and organic substances. The active Na^+ transport also energizes the reabsorption of water and other solutes by the osmotic gradient generated by Na^+ transport, and by the electrochemical gradient of Na^+ across the plasma membrane.

The data shown in Figures 6.1 and 6.2 indicate another important point. Extrapolation of the regression line to the Y ordinate indicates the basal oxygen consumption (Figure 6.1). This value is identical to the energy used for cellular functions other than Na^+ transport, and was estimated to be between 3 to 18%,[2] while other studies indicated a higher value for this basal O_2 consumption in the kidney.

With regard to energy production, the kidney generates approximately 95% of the ATP produced via aerobic mechanism,[3] while in some nephron segments anaerobic metabolism also occurs efficiently. This is reasonable because of the highly efficient ATP production by mitochondrial oxidative phosphorylation compared to anaerobic glycolysis. Thirty-six moles of ATP are generated by the mitochondrial oxidative phosphorylation of one mole of glucose, whereas only two moles of ATP are produced via glycolysis in the absence of O_2. Thus, historically, the relationship between Na transport and O_2 consumption (QO_2) in renal tissues has been extensively investigated.

Several investigators have examined Na^+/O_2 stoichiometry in the kidney.[4–6] Thurau demonstrated a linear relationship between Na^+ transport and QO_2 with a ratio of 28 Na^+/O_2 in the whole dog kidney[6] (Figure 6.1). This stoichiometry is equal to a ratio of 4.6 for Na^+/ATP, which indicates more efficient transport in the kidney compared to that in the frog skin and toad bladder. The discrepancy has been studied by many investigators and is attributed to the following.[7]

Seldin and Giebisch's The Kidney, Fifth Edition.
DOI: http://dx.doi.org/10.1016/B978-0-12-381462-3.00006-9

© 2013 Elsevier Inc. All rights reserved.

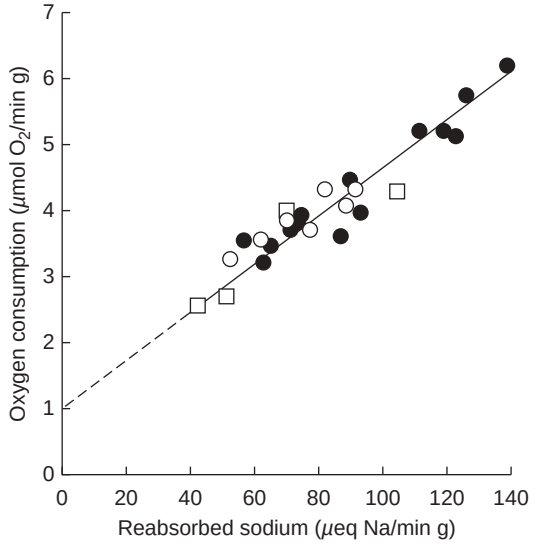

FIGURE 6.1 Oxygen consumption as a function of net sodium reabsorption in whole dog kidneys. *(Adapted from [6] with permission.)*

First, there are alternative pathways for Na^+ transport in the nephron. In the leaky epithelia, such as proximal tubule (PT), paracellular Na^+ transport occurs, while only transepithelial transport is possible in the tight epithelia in cortical collecting duct (CCD) cells. Second, coupling of Na^+ transport to that of other solutes occurs, such as bicarbonate transport in PT, and Na^+-K^+-$2Cl^-$ transport via NKCC2 in the thick ascending limb of Henle (TAL). These two mechanisms produce more efficient Na^+ transport in certain nephron segments compared to that observed in frog skin and toad bladder, where only cellular transport of Na^+ driven by Na^+,K^+-ATPase occurs. The different Na^+/O_2/ATP stoichiometry among individual nephron segments will be described below.

Heterogeneity in Na^+ Transport Efficiency among Nephron Segments

Proximal Tubule

In the PT, the Na^+/QO_2 was reported to be 24 to 30, corresponding to a Na^+/ATP ratio of 4 to 5. In the early portion of the PT (S1), preferential absorption of bicarbonate occurs,[8] resulting in a rise in the luminal Cl^- concentration, defined as axial anionic asymmetry.[9,10] In the basolateral membrane of proximal tubular cells, a Na^+-bicarbonate co-transporter (NBC) extrudes Na^+ with HCO_3^-[11] with a stoichiometry of 1: 2∼3.[12] The electrochemical gradient of HCO_3^- across the plasma membrane in the PT cells, which is generated by the coordinated function of carbonic anhydrase and H^+-ATPase or Na^+-H^+ exchanger, drives Na^+ efflux via NBC. Because PT is more permeable to Cl^- than to HCO_3^-, a driving force develops for isotonic fluid transport. It was suggested that 30%[13] to 50%[14] of Na^+ transport in the PT is passive, and not directly related to ATP consumption. In addition, in the early part of the PT, glucose, amino acids, and phosphate are actively reabsorbed by the Na^+-co-transport mechanism, thereby rapidly reducing their concentration in the lumen. This luminal hypotonicity also contributes to the solvent drag which involves Na^+. Thus, in the PT, more than 3 Na^+ could be transported via the hydrolysis of one mole of ATP.

Thick Ascending Limb of Henle

In the TAL, the most efficient sodium transport occurs, with the Na^+-K^+-$2Cl^-$ co-transporter (NKCC2) playing an important role. The transport by NKCC2 is electrically neutral, and the K^+ reabsorbed by NKCC2 in the TAL is leaked back into the tubular lumen via the ROMK channel in the apical membrane. This K^+ leakage results in a positive electrical potential difference in the lumen, which drives paracellular transport of Na^+ from the lumen to the plasma (Figure 6.3). Although no direct measurement has been made of the Na^+/O_2/ATP stoichiometry in the TAL, the results obtained in the rectal gland[15] and tracheal epithelium[16] indicated that the Na^+/ATP ratio could theoretically be up to 6 in the TAL.

CCD

In the CCD, the efficiency of Na^+ transport is the lowest among the nephron segments. In this segment, the junction between the epithelia is very tight, and paracellular transport is minimal. In addition, Na^+ entry from the luminal side into CCD cells is mediated only by ENaC, which is not associated with any coupled transport other than that of Na^+. Thus, the Na^+: ATP ratio in the CCD is estimated to be 3.

Energy Cost of Primary Active Transport

The cellular transport of electrolytes and organic substances is classified into three types, namely, primary active, secondary active, and tertiary active transport. Primary active transport refers to that which directly utilizes ATP hydrolysis energy to accomplish transepithelial transport. The primary active transporter in the plasma membrane of mammalian cells is further subdivided into three subtypes, i.e., P-type-ATPase, V-type-ATPase, and ABC transporter. The secondary active transporters utilize the Na^+ gradient across the plasma membrane generated by the Na^+,K^+-ATPase. Na^+-coupled co-transporters (e.g., Na^+-glucose co-transporter, Na^+-amino acid co-transporter) transport substrates with Na^+ in the same direction, while Na^+-exchangers (e.g., NHE: the Na^+-H^+ exchanger) transport substrate

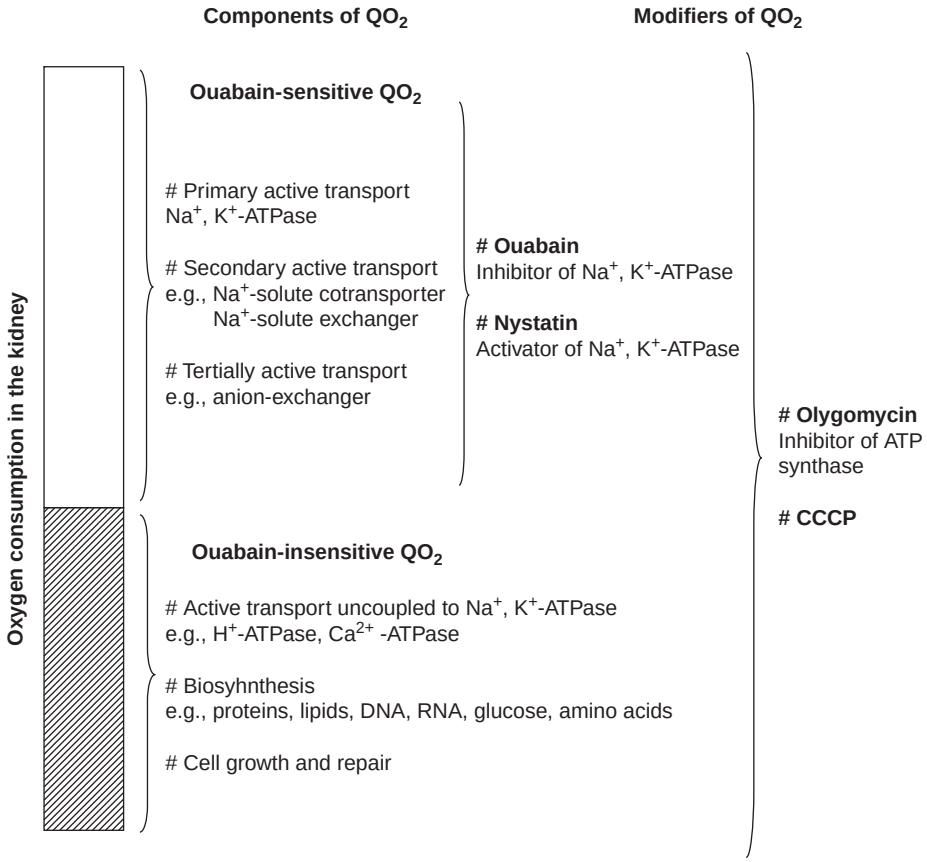

FIGURE 6.2 **Cellular components of oxygen consumption (QO_2).** Cellular QO_2 is divided primarily into two components. The first is ouabain-sensitive QO_2, which is identical to the sum of Na^+,K^+-ATPase, secondary active and tertiary active transport coupled to the Na^+ gradient. The other is an ouabain-insensitive portion, which is related to transport processes uncoupled to Na^+,K^+-ATPase (e.g., H^+-ATPase and Ca^{2+}-ATPase) and catabolic processes (e.g., biosynthesis and cell growth and repair). Ouabain-sensitive QO_2 is markedly different among nephron segments. In the PCT, 60% of QO_2 is ouabain-sensitive, whereas in OMCD, only 8% of QO_2 is ouabain-sensitive. These differences reflect the activities of Na^+,K^+-ATPase among nephron segments.

and Na^+ in opposite directions. In addition, there exist the tertiary active transporters. One example of this is the anion exchangers (AE: Cl^-/HCO_3^- exchanger). The proton gradient generated by the coordinated function of Na^+,K^+-ATPase (primary active transporter) and NHE (secondary active transporter) is used as the driving force for the exchange of Cl^- and HCO_3^- by AE (tertiary active transporter).

The energy cost for secondary and tertiary active transport processes is attributed to the active transport via Na^+,K^+-ATPase, which alone is accompanied by hydrolysis of ATP. Primary active transporters other than Na^+,K^+-ATPase are also related to the energy consumption processes in the kidney. In general, the expression level of ATPases along the nephron segments correlates well with the transport activity of each solute.

P-type-ATPases

P-type-ATPases (Figure 6.4), including Na^+,K^+-ATPase, H^+,K^+-ATPase, and Ca^{2+}-ATPase, share several common features: (1) they possess a seven amino acid motif with aspartate to which ATP binds; (2) they are transiently phosphorylated during the cation transport cycle (the term P-type derives from this transient phosphorylation); and (3) they catalyze cation transport between E_1 and E_2 conformations (P-type-ATPase was previously called E_1-E_2-ATPase). The transport activity of P-type-ATPases is commonly inhibited by vanadate.

Na^+,K^+-ATPase

Na^+,K^+-ATPase extrudes 3 Na^+ and takes up 2 K^+ across the plasma membranes through the hydrolysis of one ATP molecule in the presence of Mg^{2+}. Na^+,K^+-ATPase generates an inwardly-directed Na^+ gradient and inside a negative electrical gradient. Na^+,K^+-ATPase accounts for approximately half of the total Na^+ reabsorption in the kidney.[17]

Na^+,K^+-ATPase is a heterodimeric integral membrane protein, with a minimal composition of α- and

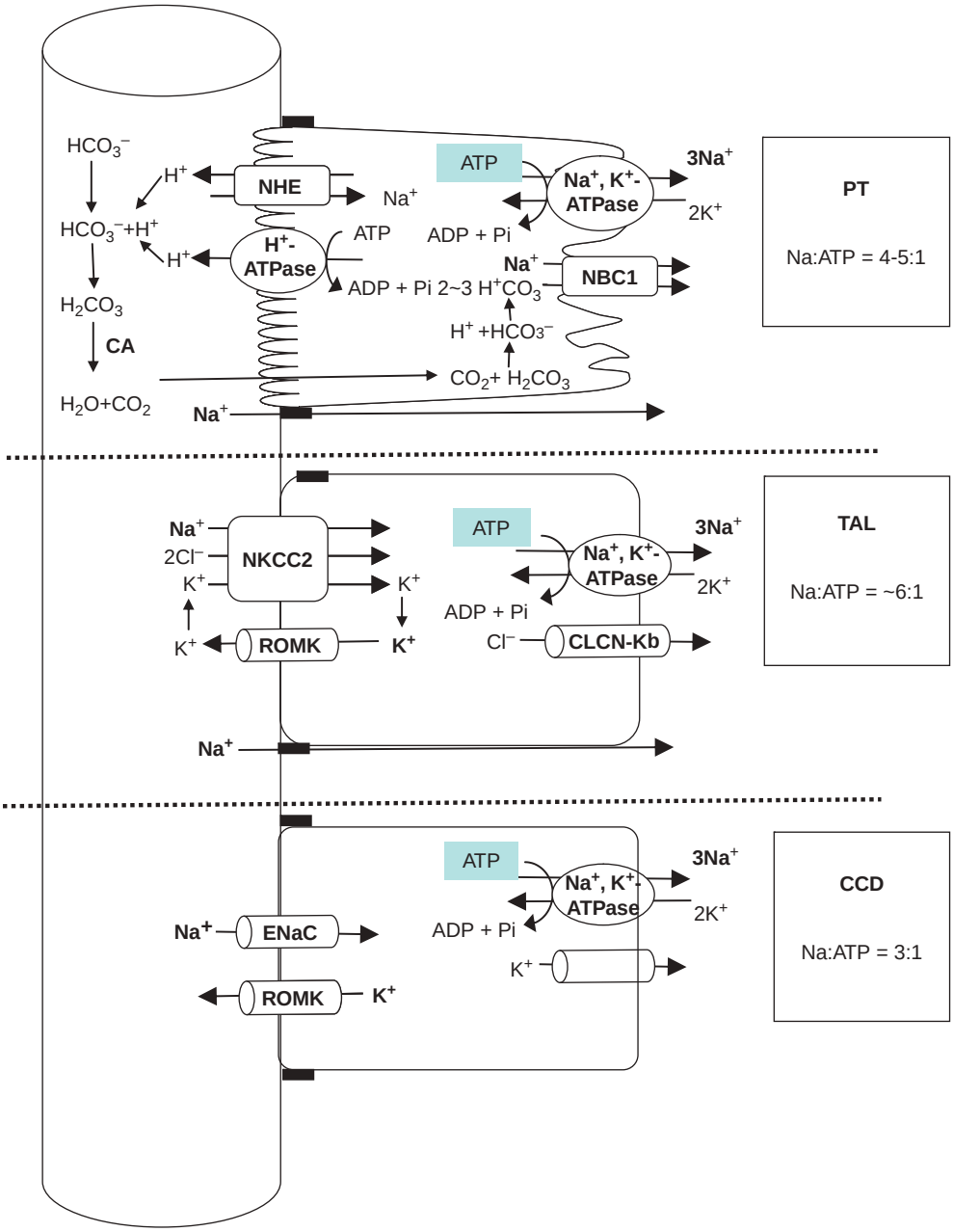

FIGURE 6.3 Heterogeneity of Na^+ transport/O_2/ATP along nephron segments.

β-subunits. The α-subunit possesses ten membrane-spanning domains with a molecular mass of approximately 100 kDa. The β-subunit is a glycosylated type II membrane protein with a molecular weight of approximately 55 kDa.[18] In mammalian genomes, four α-subunits and at least three β-subunits of Na^+,K^+-ATPase have been identified.[19,20] In addition, a γ-subunit, a member of the FXYD family of type II transmembrane proteins, constitutes an Na^+,K^+-ATPase.[21] In the kidney, two γ-subunit isoforms are expressed.[19,20] The combination of each isoform comprises a number of Na^+,K^+-ATPase isozymes that are expressed in a tissue- and cell-specific manner to evolve distinct properties to respond to cellular requirements.[19] In the kidney, α1β1 is predominantly expressed.[20,22,23]

The α-subunit is the catalytic subunit of the Na^+, K^+-ATPase, and α1, α2, and α3 isoforms differ in their affinities for ATP, Na^+ and K^+.[24] β-subunits are suggested to facilitate the correct membrane integration and packing of the α-subunit, and β-subunits also participate in the determination of the intrinsic transport properties of Na^+,K^+-ATPase.[25] The γ-subunit was

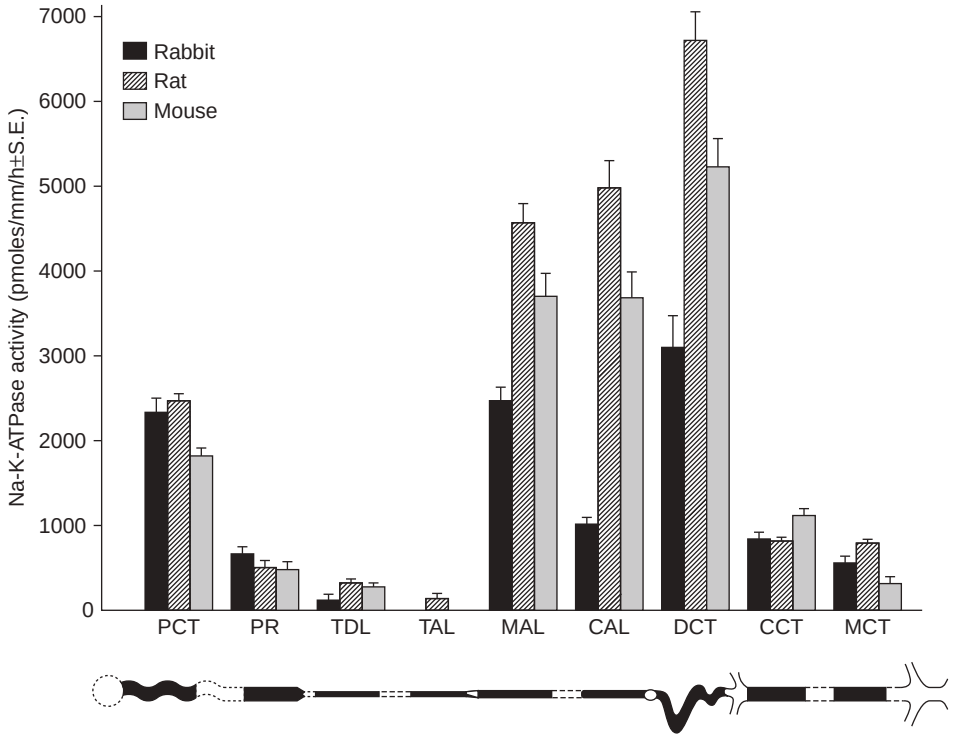

FIGURE 6.4 Na^+,K^+-ATPase activity in individual nephron segments measured using hydrolysis activity. *(Adapted from [34] with permission.)*

shown to be a specific regulator of renal $\alpha1\beta1$ isozymes.[26] A putative dominant-negative mutation in the gene encoding the γ-subunit (FXYD2) which leads to defective routing of the protein in a family with dominant renal hypomagnesaemia indicates the physiological importance of the γ-subunit.[27] The overall structure of the α-subunit of Na^+,K^+-ATPase determined by electron crystallography using two-dimensional crystals is similar to the X-ray structure of Ca^{2+}-ATPase.[28,29]

The pump activity of Na^+,K^+-ATPase has been investigated using direct measurement of hydrolysis activity, and axial heterogeneity in the nephron segments was demonstrated[30–34] (Figure 6.4). Na^+,K^+-ATPase hydrolysis activity was high in the TAL, distal convoluted tubule (DCT), and proximal convoluted tubule (PCT), and low in the pars recta (PST) and collecting tubule (CT).[30–34] Ouabain binding studies show the highest density of Na^+,K^+-ATPase (20–30 fmol/mm length of tubule) in the DCT and the MTAL, intermediate density (10 fmol/ mm) in the PCT and connecting tubule (CNT), and lowest density (2–7 fmol/mm) in the PST, CTAL, and CT.[35] The pump activity was proportional to the number of catalytic units. $\alpha1\beta1$ has a maximum turnover rate of 7,700/min.[36] The measurement of Na^+,K^+-ATPase hydrolytic activity at V_{max}, and initial rates of ouabain-sensitive Rb uptake indicated that in intact cells the pump works at approximately 20–30% of its V_{max}.[37] Western blotting analysis,[38,39] RT-PCR using microdissected nephron segments,[39] *in situ* hybridization,[23,40] and immunohistochemical analysis[41–43] demonstrated similar intranephron heterogenetic localization of Na^+,K^+-ATPase consistent with those observed in the studies on pump activity.

Regulation of Na^+,K^+-ATPase by dexamethasone,[44] deoxycorticosterone,[45] intracellular Na concentration,[46] cAMP,[47] potassium depletion,[48] aldosterone and vasopressin[49,50] was demonstrated. Many of these modulations influence the cell surface expression of Na^+,K^+-ATPase,[49,50] while MEK1/2 inhibitors changed the intrinsic activity rather than cell surface expression.[51]

Ca^{2+}-ATPase

Renal calcium transport is comprised of two processes: a paracellular, passive process that predominates in most nephron segments; and a transcellular, energy-dependent step in the DCT. Transcellular calcium transport involves: (1) entry into the DCT cell via a Ca^{2+} channel (ECaC) across the luminal membrane; (2) intracellular Ca movement facilitated by the presence of the vitamin D-dependent calcium-binding protein (calbindin D); and (3) extrusion by the Ca^{2+}-ATPase located at the basolateral membrane.[52]

The extrusion of Ca^{2+}, the final step in the transcellular transport of Ca^{2+}, is mediated by the plasma membrane Ca^{2+}-ATPase (PMCA), which is a P-type-ATPase.

PMCA is a monomeric protein consisting of approximately 1,220 amino acids with a molecular mass of 140 kDa.[53,54] The sequence contains the calmodulin-binding domain, and two domains resembling calmodulin, one of which may play a role in the binding of Ca^{2+}.[54] There are at least four isoforms of PMCA, and isoforms 1 and 4 are more widely distributed than 2 and 3.[55–57] The activity of renal PMCA showed two saturable components: a high-affinity component with a Km of 33 μM ATP, and a low-affinity component with a Km of 0.63 mM ATP.[58] PMCA is regulated by calmodulin,[55] estrogen and dihydrotestosterone,[59] protein kinase C or A,[55] extracellular ATP,[60] and pathophysiologic states such as hypercalciuria.[61] RT-PCR,[62,63] immunohistochemical analysis,[64] and Western blot analysis[53] demonstrated high expression of PMCA in the DCT. PMCA was also detected in Madin–Darby canine kidney (MDCK) cells.[65] Doucet and co-workers examined sodium azide-insensitive plasma membrane Ca^{2+}-ATPase activity. The Ca^{2+}-ATPase was maximally activated by Ca^{2+} concentrations with an apparent Km of 0.3–0.4 μM. Ca^{2+}-ATPase activity was found in all segments of the nephron: activity was highest in the DCT and CCT, intermediate in the PCT and MTAL, and lowest in the PST, CTAL and MCT.[66]

In addition to PMCA, there exists another distinct Ca^{2+}-ATPase, the sarco/endoplasmic reticulum Ca^{2+}-ATPase (SERCA), which also belongs to the P-type-ATPase. The SERCA family includes three gene products, SERCA1 (ATP2A1), SERCA2 (ATP2A2), and SERCA 3 (ATP2A3),[67] which function in the removal of free cytosolic Ca^{2+} into the sarco/endoplasmic reticulum. Although thapsigarigin is known to be a specific inhibitor of the endoplasmic reticulum Ca^{2+}-pump,[68] no study has been reported on the relative energy consumption rate of SERCA in the kidney.

H^+,K^+-ATPase

H^+,K^+-ATPase was originally characterized in a study of gastric mucosa. The gastric H^+,K^+-ATPase is located in the apical membrane of stomach parietal cells, and mediates electroneutral exchange of K^+ and H^+. Gastric H^+,K^+-ATPase activity is independent of extracellular sodium, and is inhibited by vanadate.[69]

Molecular cloning identified two types of H^+,K^+-ATPase: gastric and colonic type H^+,K^+-ATPase. H^+,K^+-ATPase is comprised of α- and β-subunits. The catalytic α-subunit of gastric H^+,K^+-ATPase shows structural similarity to that of Na^+,K^+-ATPase, and the greatest homology occurs in the phosphorylation site region, and domains presumably involved in nucleotide binding and energy transduction.[70] The α-subunit of colonic H^+,K^+-ATPase exhibits 63% amino acid identity to that of the gastric H^+,K^+-ATPase.[71] The β-subunit of H^+,K^+-ATPase shows 41% amino acid sequence identity to the β2-subunit of Na^+,K^+-ATPase in the rat.[72]

In the kidney, the existence of both gastric H^+,K^+-ATPase[70] and colonic H^+,K^+-ATPase[71] was demonstrated. Gastric H^+,K^+-ATPase is expressed constitutively along the length of the collecting duct, is responsible for H^+ secretion and K^+ reabsorption under normal conditions, and may be stimulated with acid–base perturbations and/or K^+ depletion.[73] The level of expression of colonic H^+,K^+-ATPase is much lower in the kidney than in the distal colon.[71]

Using *in vitro* microperfusion, Wingo and colleagues provided evidence of the existence of omeprazole-sensitive acidification and a K^+-absorptive mechanism in OMCD in rabbits.[74] By enzymatic analysis, Doucet[75] and Garg[76] quantified the K^+-stimulated, Na-insensitive ATPase activity in the nephron segments. K^+-stimulated ATPase activity was identified in the CNT, CCT, and MCT, although the activities were very low compared to those of other P-type-ATPases in the kidney.[76] The renal K^+-ATPase had a high affinity for K^+ (Km of approximately $0.2 \sim 0.4$ mM) and was inhibited by vanadate, omeprazole, and SCH 28080, specific inhibitors of gastric H^+,K^+-ATPase, but was insensitive to ouabain.[75,76] A correlation between the magnitude of enzymatic activity and the percentage of intercalated cells in a given segment suggested that K^+-ATPase activity originates in intercalated cells.[75]

Immunohistochemical analysis revealed H^+,K^+-ATPase in intercalated cells in the CCD and OMCD. In all segments studied, except for the CCD, the percentage of H^+,K^+-ATPase-immunoreactive cells corresponded to the percentage of intercalated cells.[77] The RT-PCR technique demonstrated the gastric H^+,K^+-ATPase α-subunit in the CCD and IMCD, and a specific hybridization signal for the gastric H^+,K^+-ATPase α-subunit cDNA was demonstrated.[78] The colonic H^+,K^+-ATPase α-subunit is specifically expressed in the CCD and OMCD in K^+-depleted rats.[79] An increase in the H^+,K^+-ATPase activity,[75] and enhanced expression of gastric H^+,K^+-ATPase α-subunit[80] and colonic H^+,K^+-ATPase[73] in K^+ depletion, suggests the physiological adaptation of renal H^+,K^+-ATPase.

V-type ATPases

V-type (vacuolar) ATPases represent the second family of ATP-dependent ion pumps. Vacuolar H^+-ATPase is primarily responsible for the acidification of intracellular compartments such as endosomes, lysosomes, Golgi apparatus, and clathrin-coated vesicles.

H^+-ATPase is also expressed in the plasma membrane, and functions in acid–base transport in epithelia. In the kidney, vacuolar H^+-ATPase mediates H^+ secretion, mainly in the PT and CCD.[81,82]

H^+-ATPase is a multi-subunit complex composed of two functional domains.[83,84] The V(1) domain is a 570 kDa peripheral complex composed of eight subunits of molecular mass 73–14 kDa (subunits A–H) that is responsible for ATP hydrolysis. The V(o) domain is a 260 kDa integral complex composed of five subunits of molecular mass 100–17 kDa (subunits a, d, c, c′, and c″) that is responsible for proton translocation.

H^+-ATPase is insensitive to vanadate or ouabain, but inhibited by bafilomycin A, N,N′-dicyclohexylcarbodiimide (DCCD: Ki = 50 μM) and N-ethylmaleimide (NEM: Ki = 20 μM). Physiological experiments indicated the existence of H^+-ATPase in the PT. DCCD caused a fall in CO_2 absorption by 15% under eucapnia, and by 30% during acute hypercapnia in the PT.[85] In other experiments, the S_3 segment was shown to possess plasma membrane H^+-ATPase activity.[86]

The relative contribution of H^+-ATPase to ATP consumption by the kidney was examined by Noel et al. In dog proximal tubules incubated under control conditions, 81% of the respiration was directly related to oligomycin-sensitive ATP synthesis, and 29% of this amount was inhibited by bafilomycin A. In rabbit and hamster PT, the bafilomycin-sensitive ATP requirement involves only 5 and 10%, respectively, of the total ATP turnover. Thus, the metabolic cost of H^+-ATPase in PT varies significantly among species.[87]

Ait-Mohamed et al. examined the localization of NEM-sensitive ATPase in all the segments of the rat nephron; its activity was highest in the PCT; intermediate in the PST, TAL and CCT; and lowest in the OMCD.[88] Immunocytochemical analysis demonstrated localization of rat H^+-ATPase in the PCT, the initial part of the thin descending limb, TAL, DCT, and CT[89] consistent with the aforementioned H^+-ATPase activity.

Garg and co-workers examined the effect of acid-base balance[90–92] and aldosterone[93] on NEM-sensitive ATPase activity, and demonstrated the modulation of NEM-sensitive ATPase activity by metabolic acidosis and administration of aldosterone, and these effects were observed mainly in the CT.

The significance of H^+-ATPase in final urinary acidification along the collecting system has been confirmed by hereditary defects in H^+-ATPase. Mutations in the gene encoding the B1-subunit of H^+-ATPase cause distal renal tubular acidosis with sensorineural deafness, and defects in the 116 kDa subunit ATP6N1B cause recessive distal renal tubular acidosis with preserved hearing.[94–96]

ABC Superfamily

The third subgroup of primary active transporters is the ABC (ATP-binding cassette) transporter family. The prototype ABC transporter is the P-glycoprotein (P-gp) encoded by the MDR gene. P-gp was originally isolated as a drug extrusion pump in cancer cells which confers multiresistance to antineoplastic drugs.[97,98] Later, P-gp was also shown to be expressed in normal tissues such as the kidney, intestine, and brain capillary cells, where it acts as a functional barrier to xenobiotics by extruding them from the tissues. Then, a subfamily of ABC transporters, the MRP (multidrug-resistance-associated protein) family, was identified, and the number of its isoforms is expanding rapidly.[99]

The common molecular structure of ABC transporters is as follows; they possess two transmembrane (TM) domains, each with six TM segments and two nucleotide-binding domains, both of which can hydrolyze ATP.[100] The stoichiometry of two ATPs hydrolyzed per molecule of drug transported was proposed.[97]

Although the molecular properties of the members of ABC transporters, such as tissue distribution and substrate selectivity, have been extensively characterized, their significance in energy consumption in the kidney remains to be investigated, and to date no information is available.

Comparison of Ion Transporting ATPase Activities and QO_2 along the Nephron

In the upper panel of Figure 6.5 a comparison of the ion transporting ATPase activities is shown. In the lower part, relative distribution of QO_2 along the nephron segments is depicted.

METABOLIC BASIS IN THE KIDNEY

Energy Production Pathway in the Kidney

ATP synthesis in the kidney is mainly performed by mitochondrial oxidative phosphorylation, and a variety of energy fuels, such as glucose, fatty acids, and ketone bodies, are metabolized. Anaerobic glycolysis also occurs in certain nephron segments. Because of its heterogeneity in structural and functional properties, metabolic pathways and preferred substrates are distinct among the nephron. In this section, metabolic basis in the kidney and individual nephron segments are described.

Mitochondrial Oxidative Phosphorylation

Mitochondrial oxidative phosphorylation (Figures 6.6, 6.7) is comprised of the following three steps: (1)

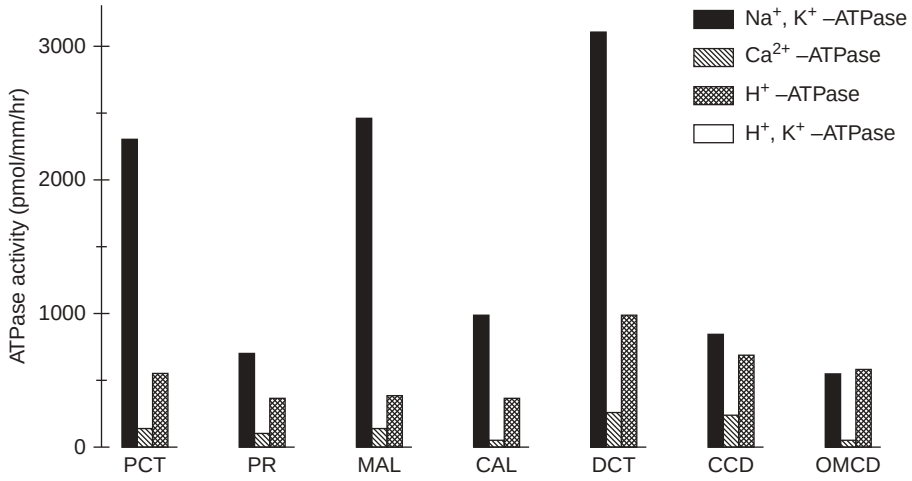

FIGURE 6.5 Comparison of ATPase activities employed from representative studies. *(Upper part adapted from [101] with permission; lower part from [102] with permission.)*

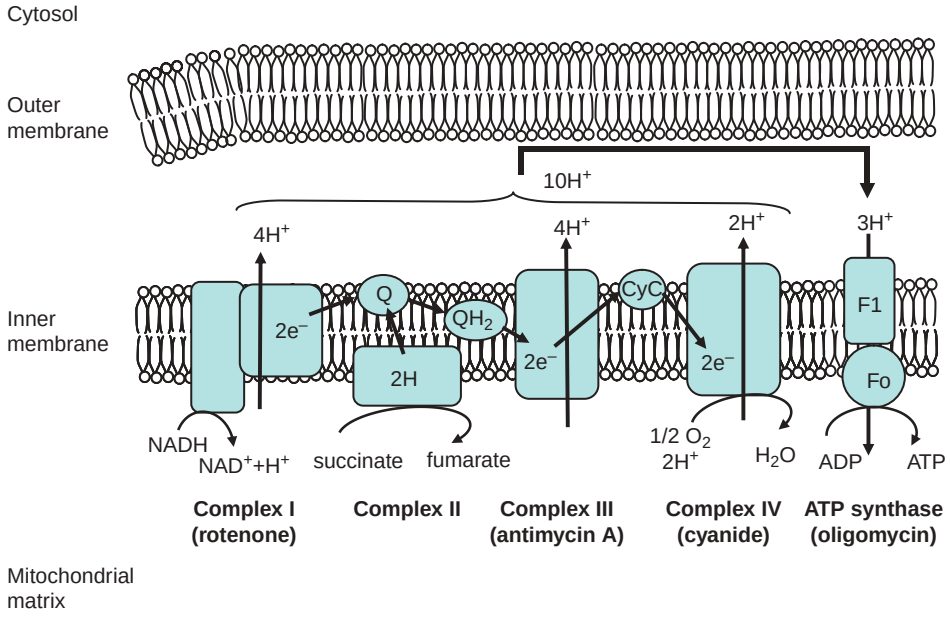

FIGURE 6.6 **Schematic representation of mitochondrial oxidative phosphorylation.** In the inner membrane of the mitochondria, four large multimeric membrane proteins complexes (complex I, II, III, and IV) catalyze electron transfer and proton extrusion. Two relatively small mobile proteins (Q and CytC) also mediate electron transport. Finally, ATP synthase produces ATP using the electrochemical gradient generated across the inner membrane of the mitochondria. Rotenone, antimycin A, cyanide, and oligomycin are representative inhibitors for the complexes I, III and IV, and ATP synthase, respectively.

production of reduced equivalents, i.e., NADH and $FADH_2$, mostly by the TCA cycle in the matrix of mitochondria; (2) electron transfer via the mitochondrial respiratory chain in the inner membrane of mitochondria, associated with proton extrusion across the inner membrane of mitochondria; and (3) ATP production by F_0F_1-ATPase using the proton gradient generated[103] (Figures 6.6 and 6.7). The mitochondrial respiratory chain catalyzes electron transfer via four large multimeric integral membrane protein complexes (complex I to IV), ATP synthase (alternatively called complex V), and two relatively small hydrophobic proteins, i.e., ubiquinone (Q: Coenzyme Q) and cytochrome c.

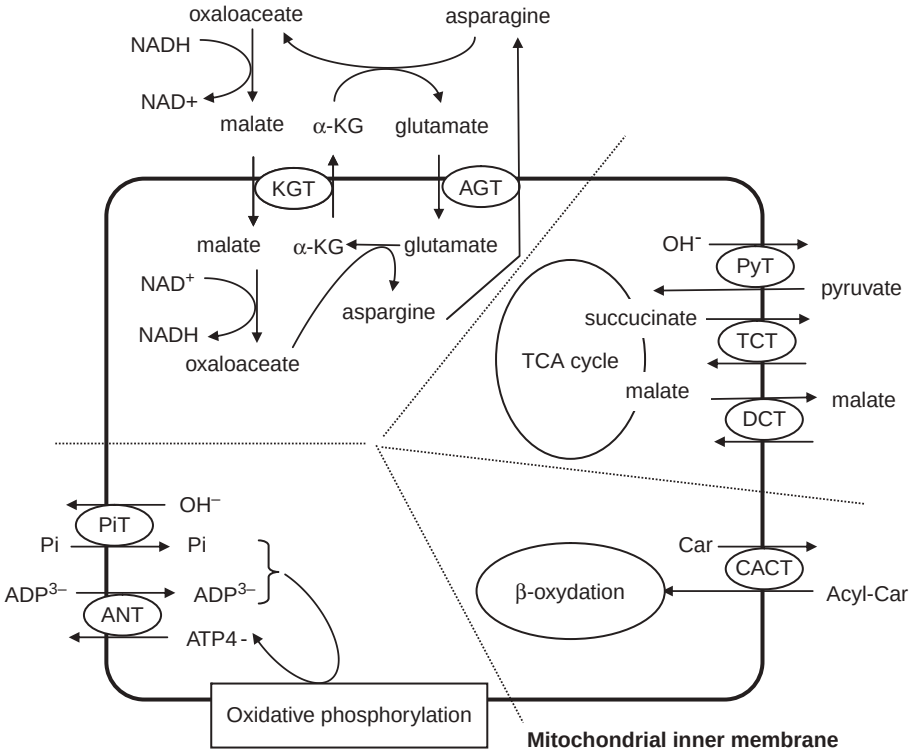

FIGURE 6.7 **Mitochondrial solute transporters located in mitochondrial inner membrane.** These transporters are divided into four groups from the functional viewpoints. The lower left part indicates the interchange of ADP, Pi, and ATP between the inner membrane by ANT and PiT. The left upper part indicates the malate-asparagine shuttle transporting the reducing potential from the cytosol to the matrix. The right upper part indicates the transport of substrates of the TCA cycle. The right lower part indicates the acyl-CoA transport to the mitochondrial matrix. Acyl-CoA is used for β-oxidation. In this figure, the ornithine transport system is not depicted.

Tricarboxylic Acid Cycle

The tricarboxylic acid (TCA) (Figure 6.8) cycle is present in all mammalian cells, except those lacking mitochondria such as mature red blood cells. The TCA cycle oxidizes acetyl CoA derived from carbohydrates, fatty acids, amino acids, and ketone bodies, and produces NADH and $FADH_2$. In addition, the TCA cycle provides intermediates that are utilized for the formation of glucose, lipids, and amino acids. Thus, the TCA cycle is central for metabolism, and is regulated to meet a variety of cellular metabolic demands.

Le Hir et al. assayed three TCA cycle enzymes, i.e., oxoglutarate dehydrogenase, citrate synthase and isocitrate dehydrogenase, in dissected rat nephron segments. The activities of the enzymes were higher in distal segments (TAL and DCT) than in the PT. The distal versus proximal ratios of activities were about 1.5, 2.5, and 2 for oxoglutarate dehydrogenase, citrate synthase, and isocitrate dehydrogenase, respectively. Oxoglutarate dehydrogenase showed the lowest activity along the entire nephron segments, and appeared to catalyze the rate-limiting step of the TCA cycle.[104] Marver et al. determined citrate synthase levels in isolated rabbit nephron segments. The order of relative citrate synthase activities in normal rabbit nephron segments (per kg of dry tissue) was as follows: DCT > PCT > CTAL > CCD > PST. The activity in CCD was regulated by aldosterone.[105]

β-Oxidation of Fatty Acids

Fatty acid is a major energy fuel in the kidney. β-Oxidation of short-, medium- and long- chain fatty acids (Figure 6.8) occurs in mitochondria, and that of very long-chain fatty acids in peroxisomes. The 3-hydroxyacyl-CoA dehydrogenase activity, which mainly represents the mitochondrial β-oxidation pathway, is similarly distributed in all cortical proximal and distal segments, and is much lower in glomeruli and collecting ducts. The peroxisomal fatty acyl-CoA oxidase is restricted to the PT, with a capacity comparable to that in liver cells.[106]

Ketone Body Metabolism

The kidney, as well as the muscle and brain, utilizes ketone bodies as metabolic fuel, while the liver cells do not. Acetoacetate and β-hydroxybutyrate are converted to acetyl CoA in the mitochondrial matrix. In this process, three enzymes, i.e., D-3-hydroxybutyrate

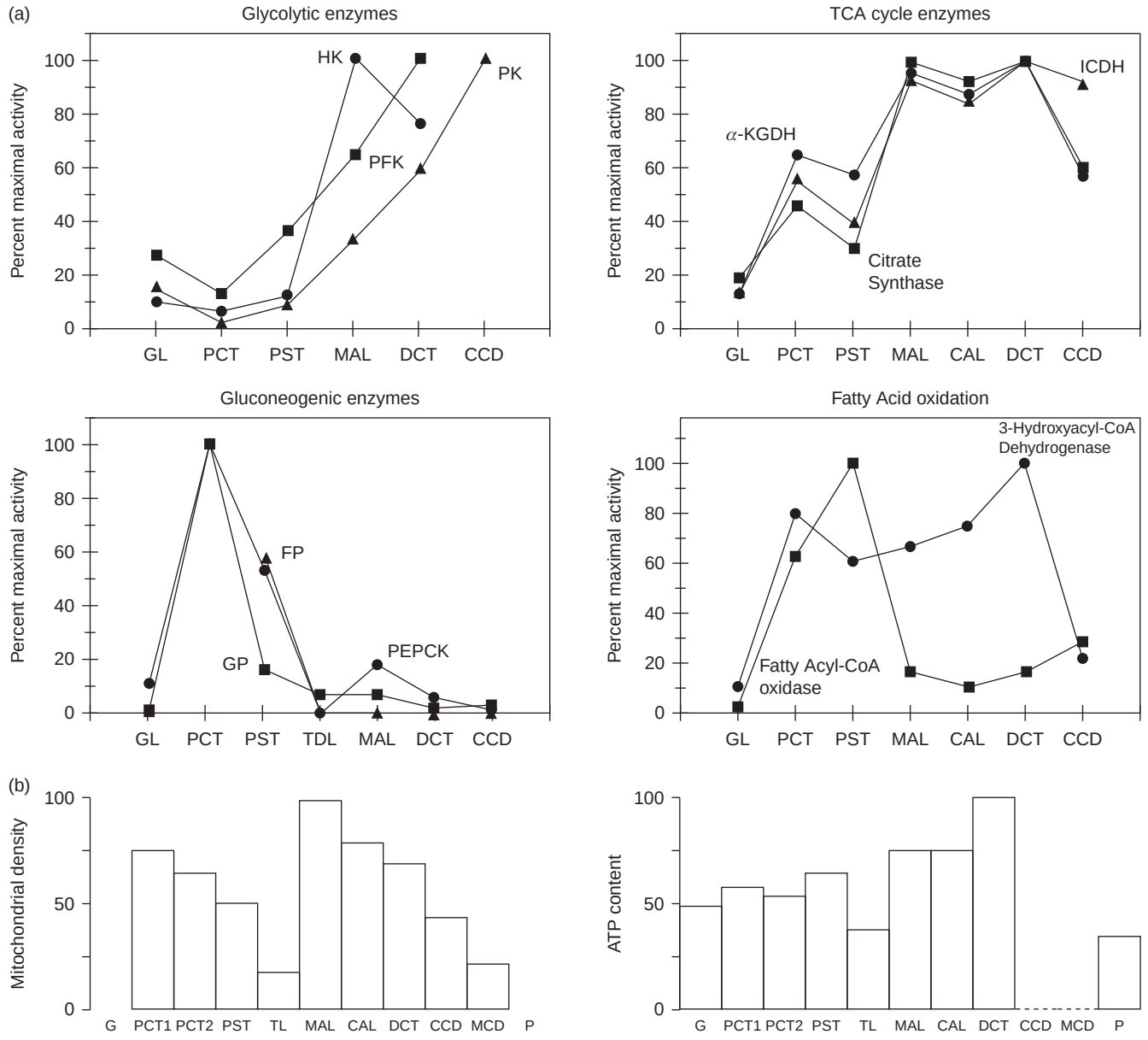

FIGURE 6.8 **(a) Distribution of enzymes involved in four major metabolic pathways:** TCA cycle, β-oxidation of fatty acids, glycolysis and gluconeogenesis. *(Adapted from [101] with permission.)* (b) Mitochondrial density distribution and ATP content along nephron segments. *(Adapted from [3] with permission.)*

dehydrogenase, 3-ketoacyl CoA transferase (3-oxoacid CoA- transferase), and acetoacetyl CoA thiorase, are involved.

Guder and co-workers measured 3-oxoacid CoA-transferase, and D-3-hydroxybutyrate dehydrogenase in mouse nephron. The activities of these enzymes were high in TAL and DCT, but decreased to nearly 20% in the CCD. In the PCT and PST, the 3-oxoacid CoA-transferase activity was almost equal, while the 3-hydroxybutyrate dehydrogenase activity was five-fold higher in PST than in PCT. In glomeruli and thin descending limbs of Henle's loop, the enzymatic activities were markedly low. These results indicate that 3-hydroxybutyrate and acetoacetate can be metabolized in all of the mouse nephron segments with different capacities. The enzymatic activity for ketone body oxidation mirrors the distribution of mitochondria along the nephron segment.[107]

Glycolysis

The role of glycolysis (Figure 6.8) as a metabolic pathway is different among cells and the state of oxygen supply. In the kidney, glycolysis occurs primarily from glucose, since the storage of glycogen is

minimal.[108] The hexokinase activity in single microdissected rabbit nephron segments was the lowest in the PCT, and increased along the nephron segments. It was the highest activity in the CNT.[109] The activities of phosphofructokinase and pyruvate kinase in the rat nephron were ten-fold higher in the distal nephron than in the proximal portion.[110] Thus, the glycolytic activity in the kidney is mostly distributed along the distal part of the nephron. Lactate production from glucose, with and without antimycin A, was investigated in the rat nephron.[111] PT produced no lactate, and the distal segments all produced lactate. Antimycin A, an inhibitor of mitochondrial oxidation, increased lactate production significantly in all of the distal segments. The increase was the largest in the MTAL (1400%), cortical (798%), and outer medullary collecting ducts (357%). Increments were smaller in CTAL (98%) and DCT (98%), and were the lowest in the IMCD (28%). Thus, anaerobic glycolysis is important, particularly in the distal segments of the nephron.

Gluconeogenesis

The capacity of the kidney to conduct gluconeogenesis (Figure 6.8) was demonstrated more than 50 years ago. Actually, the glucose synthesis rate of the kidney is higher than that of the liver when they are compared using the same tissue amount.[112] The release of glucose by the kidney has been reported to account for ~20% of all glucose released into the circulation in postabsorptive healthy humans.[113] Sustained hypoglycemia enhances the renal extraction of circulating precursors for gluconeogenesis, and stimulates renal glucose production, which may represent an important additional component of the body's defense mechanism against hypoglycemia in humans.[114,115]

Among the nephron segments, the PT is the only site where net glucose synthesis occurs.[101,116] The gluconeogenic enzyme PEPCK was exclusively found in the PT, and the PST exhibited 50% of the enzyme activity in the PCT.[109] All other renal structures exhibited only negligible PEPCK activity.[109] Thus, the activities of glycolysis and gluconeogenesis are a mirror image. Meyer et al. demonstrated that lactate is the most important precursor in renal gluconeogenesis, which exceeded the sum of renal gluconeogenesis from glycerol, glutamine, and alanine.[113] Gluconeogenesis from these substrates accounts for ~90% of renal glucose release.

Kondou et al. demonstrated that renal gluconeogenesis is stimulated by short-term ischemia.[117] They suggested that such stimulating gluconeogenesis supplies an energy fuel for further regeneration in nephron segments other than the PT.

There are several studies indicating a reciprocal relationship between Na^+ transport and gluconeogenesis.

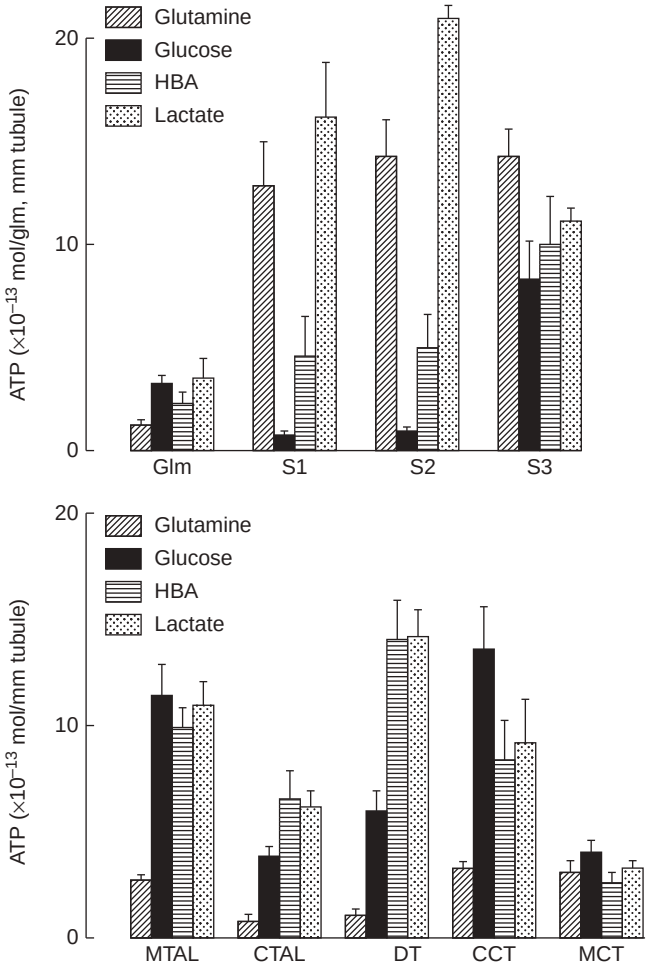

FIGURE 6.9 ATP content in nephron segments in the presence of several metabolic substrates. *(Adapted from [127] with permission.)*

The inhibition of Na^+,K^+-ATPase by ouabain stimulated gluconeogenesis.[118–120] In contrast, the stimulation of Na^+,K^+-ATPase by nystatin and monesin inhibited gluconeogenesis.[119,121] Silva et al. suggested that under certain circumstances, gluconeogenesis competes with Na^+ reabsorption in an intact kidney.[122,123]

Metabolic Parameters along Nephron Segments

As described, aerobic and anaerobic metabolisms are different among the nephron segments (Figure 6.8). This difference is in good accord with the distribution of mitochondria along the nephron. Pfaller and colleagues investigated the density of mitochondrial volume (mitochondrial volume per unit volume of cytoplasm) by stereoscopic analysis, and demonstrated PCT (33%), PST (22%), thin limb (6–8%), MTAL (44%), DCT (33%), CCD (20%), and MCD (10%)[124,125] (Figure 6.8).

Intracellular ATP contents in various nephron segments were measured by several investigators.[111,126,127] Uchida and Endou demonstrated that the cellular ATP

(a)

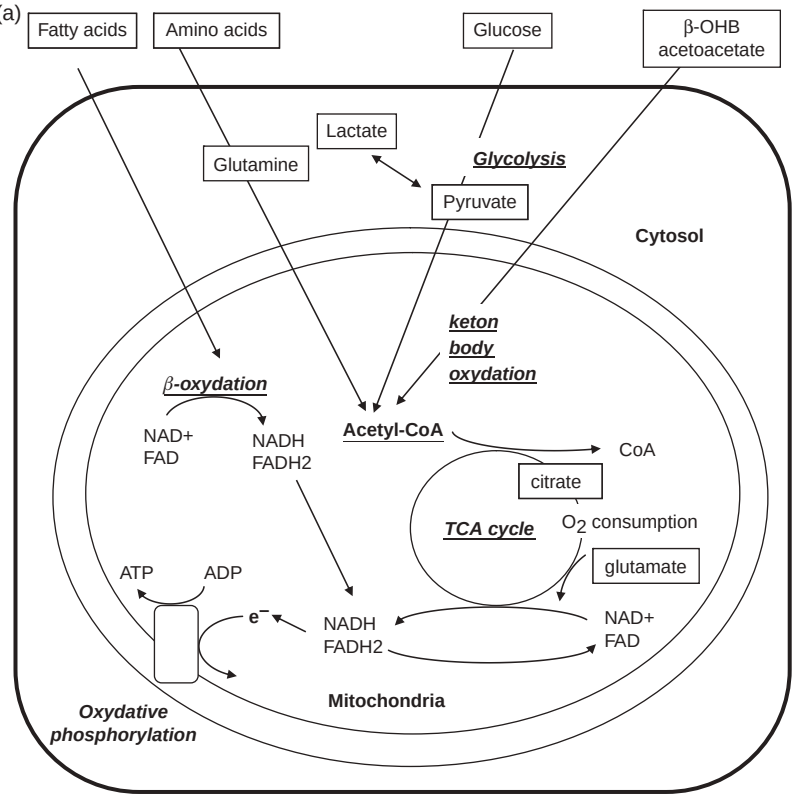

(b)

	Preferred substrates	
PT	Lactate glutamine citrate fatty acids	Glutamine pyruvate acetate ketone bodies
TAL	Glucose fatty acids acetate	Lactate ketone bodies
DCT	Glucose β-OHB	Lactate
CCD	Glucose pyruvate β-OHB	Lactate fatty acids
OMCD	Glucose glutamine	Lactate β-OHB
IMCD	Glucose	Lactate

FIGURE 6.10 **Metabolic pathways and substrates used to fuel renal transport.** (a) Boxed substances are typical substrates used in nephron segments. (b) Substrate preference of each nephron segment.

content is largely dependent on the exogenous substrates available (Figure 6.9).When appropriate exogenous substrates are present, the cellular ATP content is high in the PT, MTAL DT, and CCD, whereas it is low in glomerulus, CTAL, and MCD.

Preference of Metabolic Substrates in Nephron Segments (Figure 6.10a,b)

Substrate Preference Along the Nephron Segments

Ever since Gyoergy et al. identified differences in metabolisms between the renal cortex and medulla in 1928,[128] numerous studies identified different metabolic profiles along the nephron. In the previous section, the activities of metabolic enzymes in the nephron were described. However, preferred substrates for each segment do not always correlate well with the distribution of specific enzymes. The substrate preference in a specific nephron segment depends on several factors other than the enzymatic activities, such as the cellular uptake systems for substrates, oxygen supply, hormonal stimuli, and the demand for metabolic end products.

Knowledge of the preferred substrates for each segment has accumulated, especially from studies using microdissected nephrons. The determination of $^{14}CO_2$ production from distinct labeled substrates, in conjunction with the effects of the substrate on cellular ATP level, QO_2, redox state (NADH fluorescence), and active ion transports provide evidence that a variety of metabolic fuels, such as lactate, glucose, pyruvate, fatty acids, ketone bodies, amino acids, and TCA cycle intermediates energize cellular metabolism.

In this section, we briefly summarize the data on the substrate preference in each nephron segment.

Proximal Tubule (PT)

Numerous studies examined the metabolic profiles of the PT, and consistently indicated that the PT metabolizes a variety of substrates, such as fatty acids, ketone bodies, lactate, pyruvate, glutamine, glutamate, and TCA cycle intermediates. One notable exception is glucose: the PT, especially proximal convoluted tubule (PCT), poorly metabolizes glucose.

Glucose: PT poorly metabolizes glucose, and there is a difference in the utilization of glucose between PCT and the proximal straight tubule (PST). $^{14}CO_2$ production from glucose in the PT was low,[129–131] and glucose was poorly converted to lactate under both aerobic and anaerobic conditions.[111] Uchida and

Endou measured cellular ATP contents in mouse nephron segments in the presence of several exogenous substrates. When only glucose was supplied to the PT, the cellular ATP content significantly decreased in the S1 and S2 segments, while it was sustained in the S3 segment (PST).[127] A study using rabbit PCT or PST suspensions demonstrated a similar metabolic profile for glucose: the addition of glucose to the rabbit PCT did not increase QO_2, whereas that to the rabbit PST increased it by 57%.[130] The differences in glucose utilization do not correlate with the distribution of glycolytic enzymes between the PCT and PST,[132] suggesting that a metabolic regulation mechanism other than that by glycolytic enzymes may determine the ability of each segment to utilize glucose. It should be noted that the gluconeogenic activity is high in the PT.

Fatty acids: Short-chain fatty acids are important fuels in the PT. Balaban and Mandel examined the effects of various short-chain fatty acids, carboxylic acids, and amino acids on NADH fluorescence and QO_2 in the rabbit PT.[133] The short-chain fatty acids (butyrate, valerate, and heptanoate) were the most effective in increasing NADH fluorescence and QO_2, followed by the carboxylic acids and amino acids. Butyrate supported mitochondrial respiration to a greater degree than lactate, glucose, and alanine when the Na^+,K^+-ATPase activity was maximally stimulated by nystatin.[134] Butyrate was also shown to enhance the volume regulation of the isolated nonperfused PST under hypoosmotic conditions by activating Na^+ Cl^- transport.[135] Ruegg et al. demonstrated that PT exhibits maximal QO_2 and ATP content when incubated in culture medium with 2 mM heptanoate.[130] In contrast, palmitate oxidation occurs minimally in the PCT.[129] Thus, short-chain fatty acids are one of the best substrates, especially when active sodium transport is stimulated.

TCA cycle intermediates: The PCT demonstrated marked $^{14}CO_2$ production from labeled succinate, 2-oxoglutarate, glutamate, glutamine, and malate (approximately 10 to 45 pmoles/mm/hr), and moderate $^{14}CO_2$ production from citrate (approximately 3 pmoles/ml/hr).[129] Gullans et al. demonstrated that succinate stimulates gluconeogenesis, and the hyperpolarization of the plasma membrane potential, and promotes intracellular K^+ without altering Na^+,K^+-ATPase activity.[136] Since TCA cycle intermediates are highly hydrophilic substances, cellular metabolisms of TCA cycle intermediates require specific transporters in the plasma membrane. The sodium-dicarboxylate co-transporters, NaDCs encoded by the *SLC13* family, are expressed mainly in both the luminal and basolateral membrane of the PT.[137–140]

Ketone bodies: Guder et al. reported that ketone bodies, i.e., acetoacetate and β-hydroxybutyrate, are presumably the most preferred substrate as kidney fuel.[141] In a study using kidney slices, acetoacetate was estimated to support up to 80% of renal energy demands.[131] β-hydroxybutyrate supported ATP levels to the same extent as lactate and glutamine in isolated mouse S3, while S1 and S2 had a low capacity to metabolize β-hydroxybutyrate. These results correlate with the high enzyme activities for ketone bodies such as 3-hydroxybutylate dehydrogenase in this segment.[101]

Lactate: Lactate is also a preferred substrate for the PT. Goldstein et al. investigated the extraction of substrates from the blood by the rat kidney in normal, acidotic, and diabetic ketoacidotic conditions, and demonstrated that lactate accounts for 78% of the total amount of substrates extracted in normal control rats.[142] Exogenous lactate maintained the cellular ATP content in the mouse PT.[127] However, Kline et al. indicated that a negligible amount of $^{14}CO_2$ was released from the labeled lactate as well as glucose in the rat PCT.[129]

Thus, the proximal tubule metabolizes a wide range of substrates. This seems to be, at least in part, due to the existence of cellular transport systems for various substrates in the PT. PT cells possess Na-dependent transport systems for most of the nutrients across the luminal membrane. Nutrient transporters also exist in the basolateral membrane of the PT. Recent molecular studies have revealed the exclusive distribution of these transporters in the PT.

In the rat PT, preferred substrates are ketone bodies, short-chain fatty acids, lactate, and TCA cycle intermediates. However, there are species differences: the rabbit PT has a limited capacity to oxidize ketone bodies.[133]

The PT normally conducts transport work at 50 to 60% of its maximal respiratory capacity, and has significant amounts of endogenous fuels, probably neutral lipids, which support about half of the energy in the absence of exogenous substrates. Metabolism of endogenous fuel is suppressed when there is an adequate supply of exogenous substrates. The preferred substrates differ under different physiological conditions.[142]

Thin Descending Limb of the Loop of Henle (TDL)

The data available regarding the metabolic profile of the TDL is insufficient. The mitochondrial density of this segment is low, and its oxidative metabolism is limited. Jung and Endou measured the cellular ATP content in the rat short loop of TDL (SDL) and the rat long loop of TDL (LDL) in the presence of alanine, glucose, glutamine, β-HBA, lactate, and pyruvate.[143] They demonstrated that the substrate preference in SDL is pyruvate = glucose > glutamine = lactate = β-HBA

> alanine, and that in the LDL is pyruvate- = glucose = glutamine > alanine = β-HBA = lactate. They also demonstrated that ATP is depleted when the TDL is incubated in the absence of exogenous substrate, indicating a limited store of endogenous fuels in this segment.

Cortical Thick Ascending Limb of the Loop of Henle (CTAL)

In the TAL, the rate of Na^+ transport and QO_2 are high, and the mitochondria are enriched, suggesting there is active oxidative metabolism in this segment. Klein et al. measured $^{14}CO_2$ production from ^{14}C-labeled substrates in the rat MTAL and CTAL.[129] MTAL and CTAL oxidized glucose, 2-oxoglutarate, lactate, glutamate, and glutamine, but not malate, succinate, and citrate. Palmitate oxidation occurred in MTAL and CTAL.[129] Lactate production from glucose in the rat nephron indicated that the distal segments produce a significant amount of lactate from glucose, and under anaerobic conditions (with antimycin A), lactate production increased significantly in all of the distal segments. The increase was the largest in the MTAL (1400%), CCD (798%), and OMCD (357%), whereas increments were smaller in CTAL (98%) and DCT (98%), and were the lowest in the IMCD (28%).[111] Thus, CTAL possesses modest anaerobic glycolysis capacity. The ATP content in the mouse CTAL is maintained in the presence of glucose, β-OHB or lactate, but not with glutamine.[127]

Wittner et al. investigated the substrate preference by measuring the short circuit current (Isc) in the isolated rabbit CTAL perfused *in vitro*.[144] They further examined which sides, i.e., luminal or basolateral, substrates were taken up from. Isc rapidly decreased to 50% after 3 minutes and to 27% after 10 minutes without any exogenous substrates, indicating that Na^+ transport is strictly related to the presence of substrates in CTAL segments.[144] When substrates were added from the luminal side, only butyrate sustained Isc, while all other substrates tested (pyruvate, acetate, β-OHB, D-glucose, and L-lactate) showed a marked decrease in Isc. When the substrates were added from the basolateral side, D-glucose, D-mannose, butyrate, β-OHB, acetoacetate, L-lactate, acetate, and pyruvate sustained the Isc, but citrate, α-ketoglutarate, succinate, glutamate, glutamine, propionate, caprylate, and oleate did not. This study clearly indicates that the cellular uptake system is an important determinant in the substrate metabolisms in the CTAL. In the CTAL, most substrates, except for butyrate, are taken up by basolateral nutrient transporters. In fact, cytochalasin B and phloretin, inhibitors of the facilitated glucose transporter (GLUTs), inhibited the sustained Isc by glucose.[144]

Regarding fatty acids, the CTAL possesses mitochondrial β-oxidation activity (3-hydroxyacyl-CoA dehydrogenase),[106] and $^{14}CO_2$ is produced from palmitate,[129] while oleate (C-18) does not sustain Isc in the CTAL.[144] Taken together, glucose, lactate, pyruvate, ketone bodies, and fatty acids are the preferred exogenous substrates for the CTAL.

Medullary Thick Ascending Limb of the Loop of Henle (MTAL)

Chamberlin and Mandel measured QO_2 in MTAL suspensions.[145] In the absence of exogenous substrates, the control QO_2 decreased only by 15%. Torikai et al. demonstrate a similar result in the rat MTAL.[146] These results indicate that endogenous substrates support most of the energy required for the MTAL under normal conditions. However, nystatin-stimulated QO_2 was inhibited 36% in the absence of exogenous substrates, indicating that the oxidation of endogenous substrates cannot meet the ATP demand when Na^+ transport is fully stimulated. They also investigated the role of endogenous substrates in the MTAL. The inhibitors of fatty acid, carbohydrate or amino acid metabolisms further inhibited QO_2, revealing that endogenous fatty acids, glycogen, and amino acids (or proteins) contribute to energy production in the MTAL. The addition of fatty acids or acetoacetate increased QO_2 in 10 mM glucose, indicating that the MTAL oxidizes exogenous fatty acids and ketones in addition to glucose. In the MTAL, organic acids failed to enhance QO_2, possibly due to the absence of transport systems for organic acids. The rat MTAL generated $^{14}CO_2$ from glucose, lactate, palmitate, glutamate, glutamine, and α-ketoglutarate. $^{14}CO_2$ from succinate, citrate, and malate was minimal. Glucose, β-hydroxybutyrate, and lactate maintained the intracellular ATP content, whereas the effect of glutamine on the ATP content was partial.[127] The tight coupling of Na transport and QO_2 was demonstrated in the MTAL. Furosemide inhibited oxygen consumption by 43%, and ouabain inhibited it by 42%[147]; 50% of the oxygen consumption of the MTAL cells is related to the transport of Na^+ and Cl^-.[148]

In the MTAL, anaerobic glycolysis is also an important energy source.[149] Ten mimutes of anoxia led to only a 15% decrease in potassium content in the rabbit MTAL, and an anaerobic metabolism maintained 73% of cellular ATP during 10 minutes of anoxia. The exposure of anoxic tubules to iodoacetate produced a 57% decrease in ATP level, and a 33% decrease in potassium content. Lactate production was remarkably enhanced in MTAL (1400%) under anaerobic conditions with antimycin A.[111]

Distal Convoluted Tubule (DCT)

Although studies have examined the metabolic and transport properties in DCT, such as the mitochondrial density, Na^+,K^+-ATPase activity, and enzymatic activities, data regarding its substrate preference is limited. The ATP content of the DCT was maximal in the presence of β-OHB or lactate, and somewhat lower in the presence of glucose. Glutamine did not increase the ATP content in the DCT.[127] The lactate production rates from glucose under aerobic conditions were comparable to that observed in the CTAL, whereas under anoxic conditions, the glycolytic lactate production rate was increased two-fold as observed in CTAL.[111] These results indicate that DCT utilizes both oxidative metabolisms and anaerobic glycolysis.

Cortical Collecting Duct (CCD)

Torikai demonstrated that substrate deprivation for 30 minutes does not change the cellular ATP content in the rat CCD and OMCD. However, a marked decrease in the PT and medullary TDL, and a slight decrease in CTAL and MTAL were observed, suggesting that CCD and OMCD possess sufficient amount of endogenous fuels.[146] Hering-Smith et al. demonstrated the dependence of CCD on oxidative metabolisms in the Na^+ reabsorption and bicarbonate transport in the rabbit CCD.[150] There was no significant glycolysis or any difference in substrate-dependence of solute transport in the CCD. Na^+ reabsorption was optimally supported by a mixture of basolateral metabolic substrates (glucose, acetate, and fatty acid), whereas bicarbonate secretion was fully supported by either glucose or acetate. This result indicates that principal cells and intercalated cells differ not only in their morphology and function, but also in their metabolism. Alanine was not effective in the CCD. Nonaka and Stokes examined the effects of substrates on Na^+ transport in the rabbit CCD, and concluded that the majority of the energetic support of Na^+ transport appears to come from an oxidative metabolism. Glucose supports transport better than the other substrates tested, and lactate, pyruvate and some organic acids also provide near maximal support.[151]

The CCD synthesized modest amounts of lactate from glucose under aerobic conditions, which increased eight times under anaerobic conditions.[111] The addition of glucose, β-hydroxybutyrate or lactate, but not glutamine, restored the cellular ATP content, and glucose was the best substrate in CCD for maintaining the ATP level.[127] Natke showed that the rabbit nonperfused CCD regulates the cellular volume against extracellular hypertonic solution when exogenous butyrate is available,[152] although rat CCD possesses a relatively low enzymatic activity for β-oxidation.

Outer Medullary Collecting Duct (OMCD)

The OMCD cells play an important role in the final acidification of urine, which is mediated by apical H^+-ATPase.[89] The OMCD has a relatively low QO_2, which is inhibited only by 8% by ouabaine.[153] Several studies indicated the importance of anaerobic glycolysis in this segment. The ATP content in the OMCD did not significantly change with the addition of antimycin A.[146] Lactate production from glucose was significantly increased in the outer medullary collecting ducts by 357% under anaerobic conditions.[111] Under aerobic conditions, the ATP content was supported equally well by glucose, glutamine, lactate or β-hydroxybutyrate. Thus, glucose appears to be a preferred substrate for this segment, particularly under hypoxic or anoxic conditions, but other alternative substrates, such as glutamine, lactate or β-hydroxybutyrate, can be metabolized under aerobic conditions. The uptake of glucose by the OMCD, as well as that by the TAL cells, is mainly through a facilitated basolateral diffusion.[154] Studies of H^+ transport[155] and ATP content[127] also indicated the existence of a significant amount of endogenous fuel, most likely glycogen in the OMCD.

Inner Medullary Collecting Duct (IMCD)

Substrate metabolism in IMCD cells has not been sufficiently analyzed. QO_2 in IMCD is lower than that in other nephron segments.[156–158] Glycolysis under aerobic and anaerobic conditions was examined by several investigators. Addition of glucose to IMCD cells stimulates both QO_2 and lactate production, indicating that glucose can be readily metabolized to both CO_2 and lactate under aerobic conditions.[111,156,157,159] Lactate production in the IMCD under aerobic conditions was three- to five-fold greater than that in other nephron segments in the outer medulla, such as the TAL or OMCD.[111]

To evaluate the relative contributions of aerobic and anaerobic metabolism in the IMCD, the effects of specific inhibitors of mitochondrial oxidative phosphorylation and glycolysis were examined. Stokes et al. examined metabolism in rat renal papillary collecting duct cells, i.e., IMCD cells.[157] In the presence of rotenone, glycolysis increased by 56% and maintained the cellular ATP level at 65% of the control. Without any exogenous substrates, IMCD respiration was normal, and had a nearly normal ATP content, but lactate production was markedly decreased. At normal PO_2 and in the presence of D-glucose, the IMCD cells showed a substantial amount of aerobic glycolysis, although their mitochondrial respiration was not rate-limiting. In the absence of glucose, the cells acquired the majority of their energy from an endogenous substrate.[157]

Kone and co-workers showed that the addition of glucose to IMCD cells results in the accumulation of 12% more intracellular K^+, even in the presence of lactate and glutamine.[159] The data indicates that glucose is a preferred substrate in IMCD.

COUPLING OF TRANSPORT AND METABOLISM IN THE KIDNEY

As described in the section "Energy Consumption," Na transport and QO_2 show a linear relationship in the kidney. The nature of the cellular mechanism linking active transport to energy production is a fundamental physiological question. Alterations in the rate of active transport cause changes in the mitochondrial state and/or concentrations of adenine nucleotides in epithelia.[7] Conversely, the cellular respiration rate and/or ATP concentration affects active transport. This section focuses on the coupling mechanism of transport and energy production in the kidney.

The Effect of Active Transport on Metabolism

Whittam Model: Intracellular Signaling Between Transport and Energy Production

Whittam and co-workers primarily proposed a simple model indicating the coupling of active transport and mitochondrial respiration[160,161](Figure 6.11). In this model, the rate of active cation transport is a pacemaker for cellular respiration in the renal cells: increased ATP hydrolysis and elevated cytosolic levels of ADP and Pi by Na^+,K^+-ATPase activity would activate mitochondrial oxidative phosphorylation and oxygen consumption. Conversely, decreased Na^+,K^+-ATPase activity would induce the opposite result (Figure 6.11).

The validity of this model has been examined by: (1) direct measurement of ATP, ADP, Pi; and/or (2) monitoring of the mitochondrial redox state, in various states of transport. Early investigations into the intracellular nucleotide concentration failed to detect a change in the intracellular ATP levels.[162,163] This was probably due to the rapid ATP turnover in the renal cortex; the half-life of ATP in the anoxic state was estimated to be as low as 3.3 seconds.[164] Balaban and co-workers measured the cellular ATP/ADP concentrations and the QO_2 of a rabbit cortical tubule suspension under ideally designed conditions. They demonstrated that: (1) ouabain caused a 54% inhibition of QO_2 and a 30% increase in the ATP/ADP ratio; and (2) the addition of K^+ (5 mM) to K^+-depleted tubules caused an initial 127% stimulation of QO_2, followed by a new steady-state QO_2 50% above the control, and a 47% decrease in the cellular ATP/ADP ratio.[165]

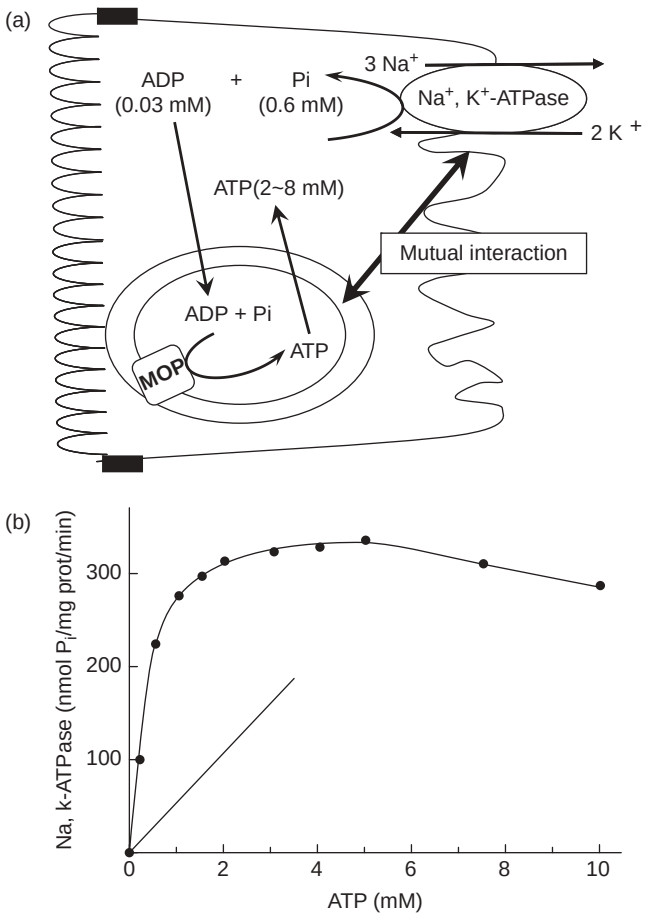

FIGURE 6.11 **Schematic representation of Whittam model, and dependence of Na^+,K^+-ATPase activity on ATP concentration.** (a) Schematic representation of Whittam model, MOP: mitochondrial oxidative phosphorylation; (b) Dependence of Na^+,K^+-ATPase activity of proximal tubule membranes (solid line) and that of intact proximal tubules (dashed line) on ATP concentration. *(Adapted from [3] with permission.)*

The monitoring of the redox state by optical measurements also demonstrated appropriate "mitochondrial state of transition." Stimulation of Na^+,K^+-ATPase activity stimulated QO_2 and decreased NADH fluorescence (in whole kidney and proximal tubules). Inhibition of Na^+,K^+-ATPase with ouabain decreased QO_2 and increased NADH. Addition of rotenone to proximal tubules decreased QO_2, and ATP content net fluid transport with increase of NADH fluorescence.[165]

Regulation of Mitochondrial Respiration

The precise mechanism by which the rate of mitochondrial oxidative phosphorylation is regulated is of major interest in the field. There is much evidence suggesting the importance of cytosolic ADP concentration. Chance and Williams first proposed that the availability

of ADP determines the mitochondrial respiration rate.[166–168] The respiratory state of mitochondria was classified into five states according to the supply of ADP, Pi, substrates, and O_2.[7,166] The addition of ADP to the mitochondria with a sufficient amount of substrates and O_2 induces the maximal rate of respiration, called "state 3 (active)" respiration. When all of the ADP is phosphorylated to ATP, QO_2 and ATP production decrease (the phase called "state 4 resting" respiration). The ratio of QO_2 in state 3 and state 4 is termed the "*respiratory control index*." This change in respiration was also demonstrated in proximal tubules permeabilized to ADP by digitonin, in which QO_2 was stimulated by four- to five-fold by the addition of ADP.[169] Nevertheless, the predominant parameter, (e.g., only [ADP] itself, [ATP]/[ADP] ratio or [ATP]/[ADP][Pi] ratio), should be determined by further studies using mitochondria, and two conflicting hypotheses on mitochondrial phosphorylation have been proposed.

The first hypothesis indicated that the [ATP]/[ADP] ratio is the rate-limiting step in oxidative phosphorylation.[170] This hypothesis is founded on kinetic considerations of adenine nucleotide translocase. Addition of atractyloside, an inhibitor of ATP/ADP translocase, caused inhibition of ADP influx into the mitochondrial matrix and oxidative respiration.[171] However, the data from intact tissues with high oxidative phosphorylation capacities, i.e., heart, brain, and kidney, indicated that the cytosolic concentration of ADP and Pi do not change significantly with work.[172]

The second hypothesis, called the "near-equilibrium theory," stated that oxidative phosphorylation is dependent on the phosphorylation potential.[173,174] This hypothesis suggested that oxidative phosphorylation is regulated thermodynamically by four factors: (1) [ATP]/[ADP][Pi] ratio; (2) intramitochondrial [NAD^+]/[NADH] ratio; (3) respiratory chain components, especially cytochrome c oxidase; and (4) oxygen concentration. This theory was partially correct, however, oxidative phosphorylation is not always close to equilibrium, at least in isolated mitochondria.[175]

Furthermore, both of these hypotheses should be re-evaluated by the determination of the cytosolic concentration of ATP, ADP, and Pi by nuclear magnetic resonance (NMR) spectroscopy. NMR spectroscopy is a method by which the radiofrequency signal of specific molecules (P, N, C, and H) in a strong magnetic field can be recorded and quantified. There are particular features of this technology which can be applied to the measurement of biological events as follows: (1) the ability to define the chemical nature of phosphorus-containing molecules and follow their transition in time; (2) completely nondestructive and repeated determination is possible; (3) rapid determination over a few seconds; and (4) wide application from isolated mitochondria to intact kidney *in vivo*.[176,177] Freeman and colleagues quantified inorganic phosphate (Pi) and high-energy phosphates in the isolated, functioning perfused rat kidney. Compared with enzymatic analysis, 100% of ATP, but only 25% of ADP and 27% of Pi were visible by NMR spectroscopy,[178] indicating that a large proportion of both ADP and Pi are bound to proteins in the intact kidney. The data obtained by NMR spectroscopy, in conjunction with biochemical assays, estimated the free concentration of cytosolic ADP as approximately 30 μM[178,179] and Pi as 0.6 mM.[178] As a consequence, the [ATP]/[ADP][Pi] ratio (phosphorylation potential) and [ATP]/[ADP] ratio should be at least one order of magnitude higher than previously estimated values.

There are several other theories on the regulation of mitochondrial respiration. One claimed that the interplay of all aspects of oxidative phosphorylation affects respiration control.[180] Another new hypothesis implies the regulation of respiration and ATP synthesis via allosteric modification of respiratory chain complexes, in particular of cytochrome c oxidase by metabolites, cofactors, ions, hormones, and the membrane potential.[181,182] At the moment, there seems no simple answer to the question "what controls respiration?" The answer varies with: (1) the size of the system examined (mitochondria, cells or organs); (2) the conditions (rate of ATP use, level of hormonal stimulation); and (3) the particular organ examined.[175]

The Effect of Metabolism on Active Transport

Intracellular ATP and Cation Transport

The intracellular ATP content was reported 2∼8 mM,[165,183–187] and the Km value of α-subunits for ATP was estimated to be 0.1 to 0.4 mM.[188] Therefore, Na^+,K^+-ATPase should be saturated for ATP under physiological conditions. However, intact renal cells normally function at almost half of their maximal respiratory capacity.[189] Harris measured cellular QO_2 during stimulation and inhibition of the Na^+,K^+-ATPase in mitochondria released from the rabbit renal tubules by digitonin shock. In the presence of NADH-linked substrates and fats, isolated renal cells respired at 50 to 60% of the maximum occurring in state 3 respiration, and addition of ouabain resulted in a decline in respiration to 25 to 30%. Stimulation of Na^+,K^+-ATPase by nystatin resulted in increased respiration with increased oxygen consumption.[134] Gullans and colleagues demonstrated that partial inhibition of oxidative metabolism with rotenone caused proportional reduction in QO_2, ATP content, and absorption rates of fluid and phosphate.[190] The effect of inhibition of oxidative metabolism on transport systems was also

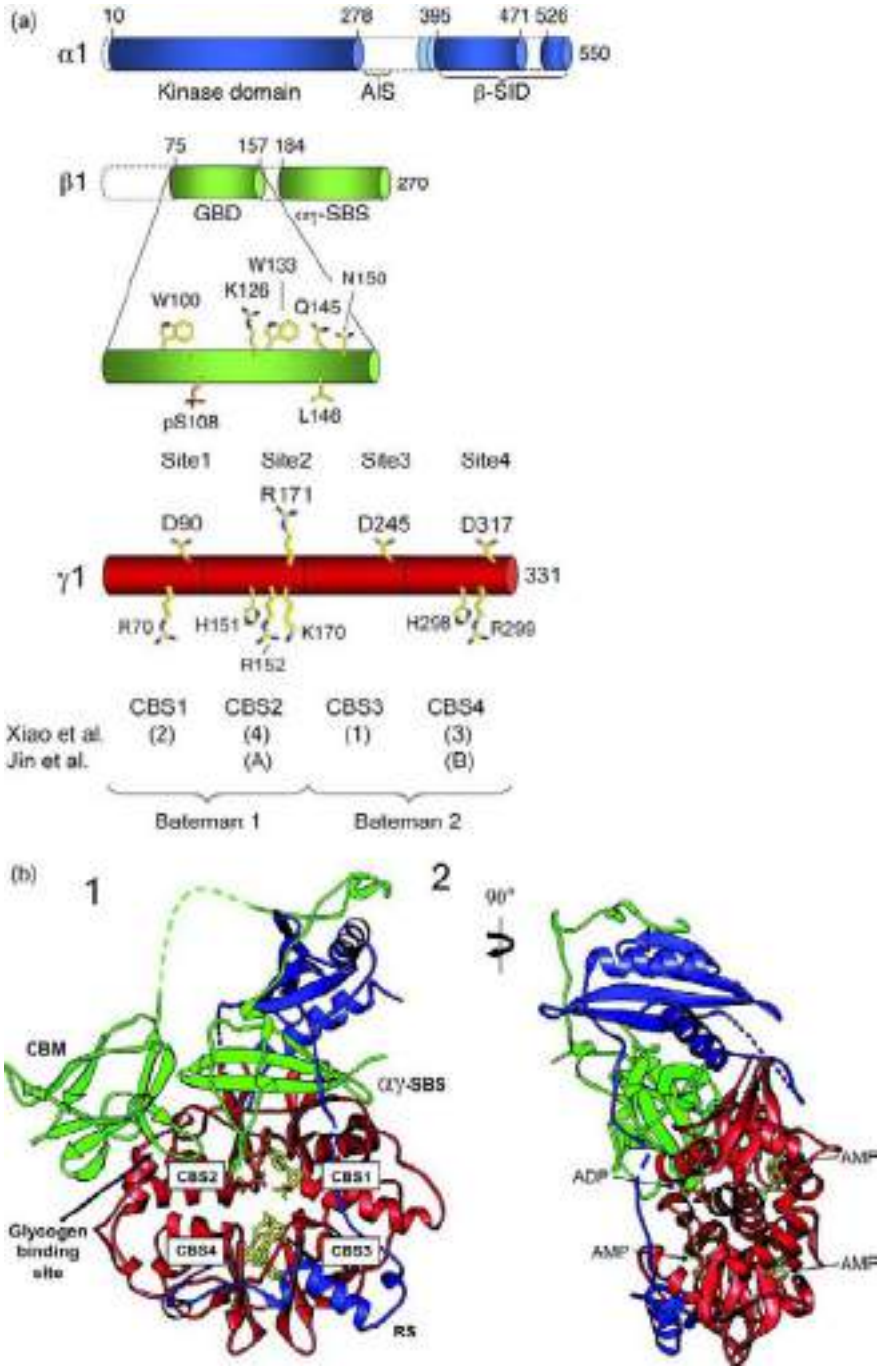

FIGURE 6.12 **Structure and function of AMPK.** (a) AMPK subunit composition. Details are described in the text. (b) Tertiary structure of AMPK. *(Adapted from [195] with permission).*

demonstrated using arsenate, which uncouples oxidative phosphorylation.[191]

This inconsistency was explained through a study by Soltoff and Mandel. In the membrane fraction of the PT, Na^+,K^+-ATPase hydrolytic activity showed saturated kinetics with a Km value of 0.4 mM for ATP. In contrast, Na^+,K^+-ATPase activity was demonstrated to have a linear, nonsaturating dependence on the ATP concentration in the intact proximal cells (Figure 6.11).[186] The authors speculated that unknown cytosolic factors in the intact renal cell, such as local concentration of ADP, Pi, and Mg in the vicinity of Na^+,K^+-ATPase may be different, which might account for the discrepancy between the two

measurements. In contrast to Na^+,K^+-ATPase, decreased concentration of cytosolic ATP does not significantly alter the Ca^{2+}-ATPase activity, probably due to its relatively high affinity for ATP.[192]

AMPK-Activated Protein Kinase (AMPK): A Regulator of Energy Consumption and Generation

For the last decade, numerous experimental data have indicated the significant role of AMP-activated kinase (AMPK) in the regulation of the energy consuming and producing process in the living cells. AMPK appears to be the molecular entity which Whittam had proposed as "the pacemaker of respiration." AMPK has been extensively analyzed in the regulation of metabolism of carbohydrate, lipid, protein, and other cellular functions, such as cell polarity and growth; several studies have demonstrated its critical roles in solute transport in the kidney. In this section, we will review AMPK, and thereafter describe its role in the kidney.

AMP-Activated Protein Kinase (AMPK)

The AMP-activated protein kinase is an evolutionarily conserved heterotrimeric kinase acting as an ultrasensitive cellular energy sensor.[193–195] AMPK is activated by increased levels of cytoplasmic AMP, and controls various energy-dependent cellular processes. Recent studies have shown that the activities of membrane proteins, such as epithelial Na^+ channel (ENaC), Na^+-K^+-$2Cl^-$ co-transporter (NKCC2), cystic fibrosis transmembrane conductance regulator (CFTR), and vacuolar H^+-ATPase, are regulated by AMPK.[193] This evidence strongly suggests that energy sensing by AMPK would be a physiologically relevant mechanism by which renal tubular cells maintain tight coupling between energy metabolism and tubular transport.[193] AMPK appears to be the molecule which couples cellular respiration and solute transport proposed by Whittam and colleagues (Figure 6.11). In this section the biological basis of AMPK is briefly reviewed, and the current information on AMPK in solute transport in the kidney will be described.

Discovery of AMPK as an Ultrasensitive Cellular Energy Sensor

In 1980, Yeh et al. demonstrated that the rate of phosphorylation and inactivation of rat liver acetyl-CoA carboxylase (ACC) was stimulated by AMP and inhibited by high levels of ATP[196]. In 1988, Munday and colleagues demonstrated that the enzyme formerly called acetyl-CoA carboxylase kinase-3 (ACC kinase-3) reduces the maximum velocity of ACC, and they proposed the name of AMP-activated protein kinase for ACC kinase-3.[197] Mammalian AMPK was first purified and sequenced by two groups from porcine or rat liver.[198,199] Subsequent studies revealed that AMPK acts to balance energy status by stimulating pathways leading to ATP synthesis and inhibiting those leading to ATP consumption.

One of the best characterized pathways and substrates regulated by AMPK is 3-hydroxy-3-methylglutaryl (HMG)-CoA reductase, the rate-limiting enzyme for cholesterol synthesis.[195] Other than enzymatic activities, diverse biological processes have been reported to be regulated by AMPK, such as cellular nutrient uptake, protein synthesis, gene transcription, inflammation, autophagy, cellular polarity, and nitric oxide synthesis.[195] In addition to these metabolic processes, recent studies have indicated that solute transport is also regulated by AMPK.[193]

Structure and Regulation of AMPK

Mammalian AMPK is a heterotrimeric protein that comprises of two α-subunits, two regulatory β-subunits, and three regulatory γ-subunits allowing for the generation of 12 different heterotrimeric complexes[193,195,200] (Figure 6.13). γ-Subunits have several spliced variants.[193] The AMPK α1- and α2-subunits are approximately 550 residue proteins, and comprise an N-terminal kinase domain, followed by an auto-inhibitory sequence (AIS), and a β-subunit interacting domain. Phosphorylation at Thr^{271} in the α-subunit kinase domain is essential for activation of AMPK, and significantly increases its kinase activity.[201] β-Subunits have a carbohydrate-binding domain (CBM) in their central region, which binds glycogen and regulates AMPK activity. The C-terminus of β-subunits is necessary for the formation of αβγ AMPK heteromer. γ-Subunits possess the binding sites for AMP, which is the key process for the regulation of AMPK activity. In the c-terminus of γ-subunits, there are four cystathione-β-synthase (CBS) domains, and two CBS domains form one Bateman domain which bind AMP or ATP.[202] The Bateman domain has higher affinity for AMP than ATP, and the Kd for ATP is 3.3-fold higher than that for AMP.[202] The activity of AMPK is regulated by the concentration of AMP and an increase in the AMP/ATP ratio. As AMP levels rise, there is a resulting AMP binding to the Bateman domain of the regulatory γ-subunit.[202]

When ATP is utilized and its intacellular level decreased, cellular concentrations of AMP increase drastically, which leads to activation of AMPK, and activated AMPK regulates the energy homeostasis by

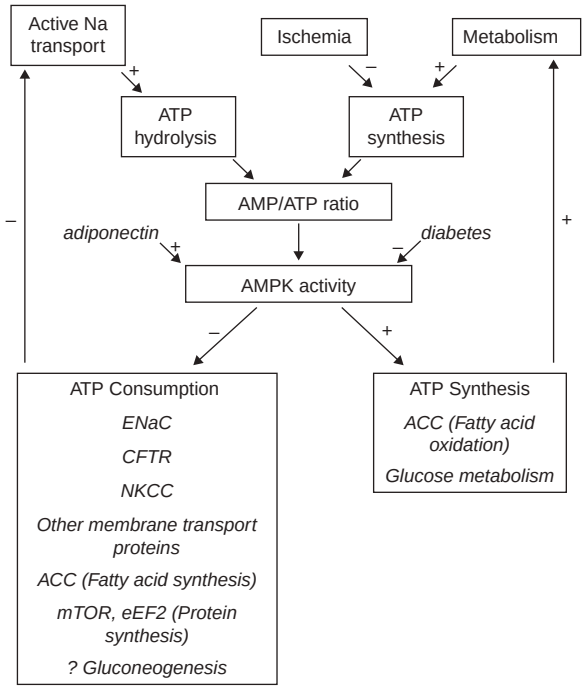

FIGURE 6.13 **Proposed role for AMPK.** Deduced role of AMPK in the kidney. Catabolic pathway requiring ATP hydrolysis (primarily sodium transport) and metabolic pathways leading to ATP synthesis (primarily fatty acid and glucose oxidation) are depicted. (*Adapted from [193] with permission.*)

stimulating energy production and minimizing energy consumption. AMPK activity is regulated by three mechanisms.[194] First, AMP allosterically activates AMPK complex in mammalian cells.[194] Second, AMP binding to the Betaman domain of the γ-subunit activates phosphorylation of Thr^{271} by upstream AMPK kinases. The third is that AMP binding to AMPK significantly reduces the dephosphorylation of Thr^{172} by 2Cα dephosphorylation phosphatase.[200] These three mechanisms make AMPK very sensitive to energy status, i.e., changes of cellular AMP and ATP concentration.

So far, three physiological kinases upstream of AMPK have been identified, namely LKB1, CaMKKβ (Ca^{2+}/calmodulin-dependent protein kinase kinase β), and TAK1 (a member of the mitogen-activated protein kinase kinase family).[200]

Expression of AMPK in the Kidney and Localization along the Nephron Segment

Expression of the AMPK catalytic α-subunit and its enzymatic activity was examined in various tissues.[203] In the rat, mRNA of the α1-subunit of AMPK was ubiquitously expressed among tissues including heart, brain, spleen, lung, liver skeletal muscle, and kidney, whereas the α2-subunit is strongly expressed in the heart, liver, and skeletal muscle, but its expression was comparatively weak in the brain, lung and kidney. Expression of α1- and α2-subunit protein showed similar patterns to those of mRNA: mRNA of the α2-subunit in the kidney was very weak. In terms of kinase activity, AMPK activity was highest in the kidney, followed by liver, lung, heart, and brain. Taken together, the kidney possesses very high AMPK activity, and its main α-subunit is α1.

Localization of AMPK subunits along the nephron segments has been investigated in the rat.[204,205] Immunoprecipitation and Western blot of protein lysates from whole rat kidney showed that the α1 catalytic subunit is expressed in the kidney, associated with the β2- and either γ1- or γ2-subunits. Phospho-Thr^{172} AMPK ($pThr^{172}$) was expressed on the apical surface of the cortical thick ascending limb of the loop of Henle, including the macula densa, and some parts of the distal convoluted tubule. α1-$pThr^{172}$ AMPK was also expressed on the basolateral surface of the cortical and medullary collecting ducts, as well as some portions of the distal convoluted tubules.[204] In another study, AMPK catalytic α2-subunits were expressed in the isolated distal tubule.[205] There seems some species difference as to which isoform(s) of each subunit are predominantly expressed in the nephron segment.[193] At the moment, there is limited information on the expression of AMPK isoforms in the kidney. Further studies are required to elucidate the significance of AMPK in the kidney, because there are remarkable differences in the metabolic profile among the nephron segments, as described in this chapter.

Regulation of Solute Transport by AMPK

Recently, regulation of renal solute transport by AMPK has been examined in several important transport and channel proteins. Low sodium and low chloride conditions activate AMPK in the murine macula densa cells indicating a potential role of AMPK in salt homeostasis in the body.[204] As is been expected, AMPK regulates the solute transport in accordance with the energy status in the kidney cells.

NA^+,K^+-ATPASE

Considering the relationship between the cellular energy status and solute transport activity, Na^+,K^+-ATPase is the membrane protein whose regulation by AMPK should first be elucidated in the kidney. So far, no definite information on this relationship in the kidney has been reported, while it was examined in the

lung cells. Woollhead and colleagues examined the effect of AMPK on Na^+,K^+-ATPase using H441 lung cells.[206,207] H441 human lung epithelial cells express α1 and α2 catalytic subunits of AMPK, and additional activators of AMPK, phenformin and 5-aminoimidazole-4-carboxamide-1-beta-D-ribofuranoside (AICAR), to H441 cells increased AMPK activity in a dose-dependent fashion. Both agents significantly decreased basal ion transport (measured as short circuit current) across H441 monolayers by approximately 50% compared with that of controls. Phenformin and AICAR significantly reduced amiloride-sensitive transepithelial Na^+ transport compared with controls. This was a result of both decreased Na^+, K^+-ATPase activity and amiloride-sensitive apical Na^+ conductance.

Vadász et al. examined the mechanisms regulating CO_2-induced Na^+,K^+-ATPase endocytosis in alveolar epithelial cells (AECs).[208] They showed that elevated CO_2 levels are sensed by AECs, and that AMPK mediates CO_2-induced Na^+,K^+-ATPase endocytosis. Elevated CO_2 levels caused a rapid activation of AMPK in AECs. Activation of AMPK was mediated by a CO_2-triggered increase in intracellular Ca^{2+} concentration and Ca^{2+}/calmodulin-dependent kinase kinase-β (CaMKK-β). Chelating intracellular Ca^{2+} or abrogating CaMKK-β function prevented the CO_2-induced AMPK activation in AECs. Activation of AMPK or overexpression of constitutively active AMPK was sufficient to activate PKC-zeta and promote Na^+,K^+-ATPase endocytosis. Inhibition or downregulation of AMPK using dominant-negative AMPK-α1 prevented CO_2-induced Na^+,K^+-ATPase endocytosis.

The Epithelial Na^+ Channel (ENaC)

Oocytes microinjected with mouse ENaC (mENaC) with either active AMPK protein or an AMPK activator inhibited mENaC currents relative to controls, as measured by two-electrode voltage-clamp studies.[209] In addition, pharmacological AMPK activation or overexpression of an activating AMPK mutant in mpkCCD (c14) cells inhibited amiloride-sensitive short circuit currents via ENaC. However, AMPK did not bind ENaC or phosphorylate ENaC *in vitro*.[209] Furthermore, they demonstrated that AMPK promotes ENaC-Nedd4-2 interaction, thereby inhibiting ENaC by increasing Nedd4-2-dependent ENaC retrieval from the plasma membrane. The results indicated that AMPK-dependent ENaC inhibition is mediated through a decrease in the number of active channels at the plasma membrane, presumably due to enhanced Nedd4-2-dependent ENaC endocytosis. This regulation of ENaC by AMPK was confirmed by AMPK α1-KO mice.[210] Almaça et al. demonstrated AMPK-α1 KO mice showed enhanced electrogenic Na^+ absorption, and that AMPK uses the ubiquitin ligase Nedd4-2 to inhibit ENaC by increasing ubiquitination and endocytosis of ENaC, leading to the enhanced expression of ENaC detected in the colon, airways, and kidney of AMPK-α1 KO mice.

Bhalla et al. examined the effects of AMPK activation on ENaC currents in *Xenopus* oocytes co-expressing ENaC and wild-type (WT) or mutant forms of Nedd4-2. ENaC inhibition by AMPK was blocked in oocytes expressing either a dominant-negative or constitutively active Nedd4-2 mutant, suggesting that AMPK-dependent modulation of Nedd4-2 function is involved.[211] Moreover, cellular AMPK activation significantly enhanced the interaction of the β-EnaC-subunit with Nedd4-2, as measured by co-immunoprecipitation assays in HEK-293 cells.

Na^+-K^+-2Cl^- Co-transporter 2 (NKCC2)

It has been known that renal-specific NKCC2 (Na^+-K^+-2Cl^- co-transporter 2) is regulated by changes in phosphorylation state, however, the phosphorylation sites and kinases responsible have not been fully elucidated. Fraser et al. demonstrated a physical association between AMPK and the N-terminal cytoplasmic domain of NKCC2 by immunoprecipitation experiments.[212] Activation of AMPK in the mouse macula densa-derived 1 cell line resulted in an increase in Ser126 phosphorylation of NKCC *in situ*, suggesting that AMPK may phosphorylate NKCC2 *in vivo*. When exogenously expressed in *Xenopus laevis* oocytes, S126A mutated NKCC showed a marked reduction in co-transporter activity. Thus, Ser^{126} in the N-terminus of NKCC2 was identified as a novel activating phosphorylation site by AMPK.

The Vacuolar H^+-ATPase (V-ATPase)

V-ATPase subcellular localization in intercalated cells by PKA and AMPK was examined in rat kidney tissue slices *ex vivo*.[213] Immunofluorescence labeling of kidney slices revealed that the PKA activator induced V-ATPase apical membrane accumulation in collecting duct intercalated cells. Pre-incubation of kidney slices with an AMPK activator blocked V-ATPase apical membrane accumulation induced by PKA activator, suggesting that AMPK antagonizes cAMP/PKA effects on V-ATPase distribution.

The Cystic Fibrosis Transmembrane Conductance Regulator (CFTR)

The cystic fibrosis transmembrane conductance regulator is an ATP-gated Cl^- channel that regulates other epithelial transport proteins. Using a yeast two-hybrid

screening technique, the α1- and α2-subunit of AMPK was identified as a novel interacting protein. AMPK phosphorylated full-length CFTR *in vitro*, and AMPK co-expression with CFTR in *Xenopus* oocytes inhibited cAMP-activated CFTR whole-cell Cl^- conductance by approximately 35–50%.[214]

Other Transport Proteins and Channels Regulated by AMPK

Other than the above-mentioned transporters and channels, several membrane proteins have been reported to be regulated by AMPK. These include a Na^+-coupled glucose carrier SGLT1[215] and an ATP-sensitive K^+ (K_{ATP}) channel.[216]

Other Factors Linking Transport and Cellular Metabolism

ATP-Sensitive Cation Channels

ATP-sensitive K^+-channels (K^+-ATP channels), the activity of which are inhibited by micromolar to millimolar concentrations of ATP, contribute to the potassium balance by coupling cellular metabolism with K^+ transport.[217–219] Tsuchiya of the Welling laboratory identified K^+-ATP channel activity at the basolateral membrane in the PT, which is a major determinant of the macroscopic K conductance.[220] The open probability of K^+-ATP channel determined by the intracellular ATP concentration altered the extent of K recycling: a decrease in intracellular ATP by stimulation of Na^+, K^+-ATPase activity increased the macroscopic K conductance, and intracellular ATP loading uncoupled the response. Wang and Giebisch demonstrated the effect of ATP on the small-conductance potassium channel in the apical membrane of CCD using the patch-clamp technique.[221] A dual effect of ATP was observed: low concentrations of ATP (0.05–0.1 mM) restored channel activity in the presence of cAMP-dependent PKA, while high concentrations of ATP (1 mM) and ADP (1.2 mM) blocked it completely. The dual effect of ATP was explained by assuming: (1) ATP-dependent PKA-mediated phosphorylation of the potassium channel under physiological conditions; and (2) direct inhibitory action of high concentrations of ATP on the channel activity. ATP-sensitive K^+ channels, the open probability of which was downregulated by ATP concentrations greater than 0.1 mmol/l, were also identified in the TAL.[222] These studies indicate that ATP acts as a coupling modulator between cellular metabolism and K^+-ATP channel activity, and regulates the transepithelial transport of K^+. Tsuboi and co-workers investigated the molecular effect of ATP on a Kir6.2, a K^+-ATP channel. ATP inhibits the channel activity by binding to a specific site formed by the N- and C-termini of the pore-forming subunit. The structural changes associated with the interaction of ATP with Kir6.2 were as follows: (1) the interaction between the N- and C-terminal domains was altered; (2) both intra-subunit and intersubunit interactions were probably involved; (3) ligand binding and not channel gating was affected; and (4) these effects occurred in intact cells when subplasmalemmal ATP concentrations changed in the millimolar range.[223]

The regulation of cation transport by intracellular ATP was also identified in a stretch-activated nonselective cation channel in the basolateral membrane of the PT.[224] This cation channel is primarily regulated by stretching (membrane deformation), depolarization, and hypotonic swelling. In addition, intracellular ATP reversibly blocks this cation channel (Ki approximately 0.48 mM). Thus, this cation channel activity is coupled to the metabolic state of the cell, particularly when intracellular ATP is depleted, as occurs during increased transepithelial transport or ischemia.

Purinergic Receptors

ATP and its metabolites, ADP, UTP, and UDP, act as extracellular signaling molecules via purinergic P2 receptors.[225–227] ATP is readily released from epithelial cells across their luminal membrane when the cells are damaged by ischemia or the toxic effects of exogenous compounds. ATP released from the cells is metabolized by ecto-nucleotidases, and thereby acts on the epithelial cells as paracrine and autocrine regulators. Mammalian P2 receptors are subdivided into P2Y (G-protein-coupled) and P2X (ligand-gated channels). In the kidneys, P2 receptors are expressed both in the basolateral and luminal membranes, and induce a variety of biological effects. In the distal nephron, luminal nucleotides inhibit Ca^{2+} and Na^+ absorption and K^+ secretion via the $P2Y_2$ receptor. In steroid-sensitive cells, luminal ATP/UTP inhibits epithelial Na^+ channel-mediated Na^+ absorption. Adenosine generated by ecto-nucleotidases may introduce further effects on ion transport, often opposite to those caused by ATP. Bailey demonstrated that activation of the $P2Y_1$ receptor impairs acidification in the PT through inhibiting the reabsorption of bicarbonate.[228] As well as having effects on solute transport, P2 receptors also modulate cellular metabolism. Cha and Endou demonstrated that renal gluconeogenesis was increased via P2Y stimulation.[229] The suggested functions of luminal P2 receptors include: (1) an epithelial "secretory" defense; (2) the regulation of cell volume when transcellular solute transport is out of balance; and (3) autocrine/paracrine regulators mediating cellular protection and regeneration after ischemic cell damage.[225]

Nephrons are also equipped with adenosine/P1 receptors, which have been further subdivided into

four subtypes, A1, A2A, A2B, and A3, all of which couple to G-proteins.[226] Adenosine is produced by biochemical reactions, and by the extracellular cAMP-adenosine pathway, in which cAMP effluxed from cells is converted to adenosine by the serial actions of ecto-phosphodiesterase and ecto-5′-nucleotidase.[230] Adenosine modulates Na^+,K^+-ATPase via A1 and A2 adenosine receptors.[231]

Nitric oxide (NO)

In the kidney, nitric oxide participates in several regulatory processes, including those for the glomerular and medullary hemodynamics, the tubuloglomerular feedback, renin release, and the extracellular fluid volume.[232,233] NO is formed from L-arginine by NO synthases (NOSs), a family of related enzymes encoded by separate unlinked genes. Three isoforms of NOS, i.e., nNOS (or NOS I), eNOS (or NOS III), and iNOS (or NOS III) were shown to be expressed in the kidney with distinct localization.[232,234] NO affects transporters and channels, such as Na^+,K^+-ATPase, NHE3, NKCC2, H^+-ATPase, and K^+-channels, in a segment-specific manner.[233] For examples, NO inhibited Na^+,K^+-ATPase in PT cells, while it did not change Na^+,K^+-ATPase activity in the TAL and CCD.[233] NO also affects mitochondrial QO_2. Granger and Lehninger initially observed an inhibition of mitochondrial electron transport in a murine cell line exposed to endotoxin-stimulated macrophages,[235] and subsequently NO was suggested to mediate this phenomenon.[236] NO inhibits QO_2,[237] and conversely nitro-L-arginine, a NO synthesis inhibitor, increases QO_2.[238] The inhibitory effect of NO on QO_2 appears to occur reversibly through the direct inhibition of the mitochondrial electron transport chain.[239,240] Adler et al. investigated the effects of renal NO production on QO_2 using eNOS KO mice.[241] Basal QO_2 in the renal cortex was higher in eNOS KO mice than in the heterozygous control mice. NO production stimulated by bradykinin or ramiprilat decreased QO_2 to a lesser extent in eNOS KO mice than in the control mice. These results indicate that NO production via eNOS regulates the renal QO_2. Laycock and colleagues indicated that NO plays a role in maintaining a balance between QO_2 and sodium reabsorption in the dog.[242] The administration of nitro-L-arginine decreased sodium reabsorption, and increased renal QO_2.

PATHOPHYSIOLOGICAL STATES IN ENERGY PRODUCTION IN THE KIDNEY

Pathophysiological states, in which energy production is inhibited, lead to significant alterations in renal function. In this final section, we focus on these pathophysiological states.

Mitochondrial Cytopathies

Mitochondrial cytopathies are metabolic diseases caused by mutations in nuclear DNA or mitochondrial DNA encoding the proteins involved in the mitochondrial oxidative chain. These genetic lesions alter mitochondrial oxidative phosphorylation, with a reduction in energy produced for cell activity.[243] The manifestation of mitochondrial cytopathies occurs in tissues where energy requirement is high, such as skeletal muscle and brain. Given the high energy utilization in the kidney, it is not surprising that mitochondrial cytopathies cause dysfunction of renal transport, and various renal involvements in mitochondrial diseases have been reported.

In most cases of Fanconi syndrome, a generalized dysfunction of proximal tubular cells results in glucosuria, aminoaciduria, and phosphaturia.[244–249] In patients manifesting Fanconi syndrome, defects in complex IV (CCO) activities are most commonly detected.[247] Bartter syndrome,[250] acute renal failure,[251] chronic renal failure,[252] and chronic tubulointerstitial nephritis[253,254] were also reported. The renal tubule in patients with mitochondrial disease may be susceptible to renal hypoxic injury and acute renal failure. In the renal tissues of patients with mitochondrial cytopathies, giant and degenerated mitochondria are observed by electron microscopy.[255,256] Glomerular involvement was occasionally reported.[245,257–261]

Renal Ischemia

Ischemia-induced renal dysfunction involves multifactorial events, and there are two effects regarding tubular damage due to ischemia: effects that occur during ischemia; and those occurring during reperfusion (reoxygenation), although these two factors are not always separable.[262] If the ischemic damage is severe, tubular cells undergo necrosis and/or apoptosis.

Necrosis is characterized by the progressive loss of cytoplasmic membrane integrity, rapid influx of Na^+, Ca^{2+}, and water due to the disturbance of several ATP-dependent ion channels, which results in cytoplasmic swelling, the disruption of the actin cytoskeleton, nuclear pyknosis, and eventual collapse of the cells.[263,264] Necrosis is considered to be mediated by ATP depletion,[265] the redistribution of Na^+,K^+-ATPase,[266] an increase in free cytosolic Ca^{2+},[267] reactive oxygen species generation,[268] and activation of several enzymes, such as proteases, phospholipases,

and endonucleases. Apoptosis is a highly coordinated process mediated by active intrinsic mechanism or extrinsic factors.[264]

Both apoptosis and necrosis occur simultaneously in acute renal failure (ARF),[269] and the relative contribution of the two mechanisms depends on the severity of the injury and the cell type.[270] Lieberthal et al. investigated the effect of graded ATP depletion ranging from 2 to 70% of control levels induced by either antimycin or 2-deoxyglucose in mouse PT cells.[271] The cells subjected to ATP depletion to less than 15% of the control level developed necrosis uniformly. In contrast, the cells subjected to ATP depletion to between 25 and 70% of control levels developed apoptosis. A narrow range of ATP depletion exists (15 to 25% of control level), representing a threshold that determines whether cells die by necrosis or apoptosis. The degree of cellular GTP depletion plays also a crucial role in determining the mode of cell death.[272]

ATP Depletion during Acute Ischemia and its Consequence

After one minute of ischemia, whole kidney ATP content decreased by 70%,[273] and after 10 minutes renal ischemia ATP levels fall quickly to less than 10% of control values.[274] During ischemia, tubular cells should maintain ATP content by anaerobic metabolisms, and the vulnerability of each nephron segment depends partly on the glycolytic properties. The S3 (PST) segment of the PT is extremely susceptible to ischemic injury, because of its low glycolytic capacity, and severe ATP depletion leads to necrotic cell death in this segment. In the rabbit PT, hypoxia (1% O_2) induced lactate production, whereas anoxia (0% O_2) failed to stimulate glycolysis. The addition of ouabain during rotenone treatment reduced lactate production by 50%, indicating that glycolytic ATP can be used to fuel the Na^+,K^+-ATPase when mitochondrial ATP production is inhibited. In addition, this study suggested that mitochondrial inhibition is not obligatorily linked to the activation of glycolysis.[275]

Weinberg and colleagues investigated anaerobic metabolism other than glycolysis in the PT during ischemia.[276,277] A severe mitochondrial energy deficit in the PT subjected to hypoxia/reoxygenation was prevented, and reversed by supplementation with α-ketoglutarate (α-KG) and aspartate. The anaerobic metabolism of α-KG and aspartate generated ATP, and maintained the mitochondrial membrane potential. Malate and fumarate were also effective singly or in combination with α-KG, while succinate showed a protective effect only during reoxygenation. In other studies, Weinberg and co-workers further demonstrated that the events upstream of complex I are important for the energetic deficit in the PT during hypoxia.[278]

The TAL possesses a relatively greater glycolytic capacity than the PT, and is less vulnerable to ischemic injury.[279,280] In a suspension of rabbit MTAL under anoxic conditions, anaerobic metabolism maintained 73% of cellular ATP during 10 minutes of anoxia, and exposure of anoxic tubules to iodoacetate, an inhibitor of glycolysis, resulted in a 57% decline in ATP levels, indicating that glycolysis is an important pathway in supplying energy during anaerobiosis in MTAL.[149] The cellular damage of the TAL by ischemia is influenced by cellular transport. The TAL develops a specific structural lesion during perfusion of the isolated rat kidney. The fraction of the TAL showing severe damage was reduced by furosemide, but not by acetazolamide, and the lesion was also eliminated by perfusion with ouabain or by preventing glomerular filtration.[281]

Mitochondrial Injury during Reperfusion

It is known that cell death following ischemia-reperfusion is closely related to functional changes in the mitochondria. Liu et al. revealed that apoptotic programmed death is associated with the release of cytochrome c (cyt c) due to caspase (cysteinyl aspartate-specific proteinase) activity.[282] Cyt c release is dependent on the site and the type of mitochondrial injury. Isolated mouse PT was subjected to mitochondrial oxidative phosphorylation inhibitors, rotenone and antimycin A or hypoxia. Antimycin A caused a significantly higher level of cyt c release from the PT than rotenone or hypoxia.[283] The efflux of cyt c and other apoptosis-related compounds, such as apotosis-inducing factor (AIF) and pro-caspases-2, -3, and -9, is mediated by the disrupted mitochondrial membrane or MPT (mitochondrial permeability transition).[284] Although the precise molecular mechanism of MPT remains to be elucidated, MPT occurs by a multiprotein channel composed of a voltage-dependent anion channel (VDAC), which comprises a nonselective channel for any substances with a molecular mass less than 15 kDa,[285] and adenine nucleotide translocase (ANT).

ATP depletion causes an increase in cellular free Ca^{2+},[286,287,288] and this phenomenon causes mitochondrial injury and apoptosis in renal tubular cells. Tanaka and colleagues demonstrated that voltage-dependent Ca^{2+} channels are involved in cellular and mitochondrial accumulation of Ca^{2+} due to ATP depletion.[289]

Chronic Ischemia

Recently, accumulating evidence has emphasized the effects of chronic hypoxia on renal structure and function.[290] In the advanced stage of renal dysfunction with tubulointerstitial damage, peritubular capillaries

are lost, and the development of interstitial fibrosis decreases oxygen diffusion to tubules. As a consequence, nephron segments are exposed to chronic hypoxia, and this in turn exacerbates renal insufficiency. Diffuse cortical hypoxia was demonstrated in the puromycin aminonucleoside-induced nephrotic syndrome and focal and segmental hypoxia in a remnant kidney model.[291]

When cells are exposed to hypoxia, the activation of hypoxia-inducible factor-1 (HIF-1) occurs, which is a primary defensive mechanism against hypoxia.[292,293] HIF-1 transcriptionally regulates many factors associated with hypoxia, such as the increased expression of VDGF,[294] erythropoietin,[295] a glucose transporter (Glut-1),[296] and PGK,[297] thereby chronic hypoxia alters the cellular transport and metabolism via HIF-1 activation. It is suggested that the induction of the HIF signal, which adapts the renal cells to hypoxia, may be a therapeutic option against the development of renal dysfunction.

Nephrotoxicants

Several nephrotoxic drugs, such as certain cephalosporins,[298] tacrolimus and sirolimus,[299] cadmium metallothionein,[300] probenecid,[301] prednisolone and azathioprine,[302] and cyclosporine A,[303] were shown to impair mitochondria and cellular metabolism. Ochratoxin A, a mycotoxin, also inhibits mitochondrial oxidative phosphorylation in the PT.[304] In contrast, enalapril and losartan attenuate mitochondrial dysfunction.[305]

A Novel Technology Analyzing Renal Blood Oxygenation

Recently, a novel technique called the Blood Oxygen Level-Dependent (BOLD) MRI method has been applied to renal physiology. The BOLD MRI method measures blood deoxyhemoglobin, and indirectly estimates intrarenal oxygenation in a noninvasive fashion, allowing sequential measurements in humans as well as animals in response to a variety of physiological or pharmacological stimuli with high reproducibility.[306,307] The effects of diuretics on renal oxygenation were investigated using the BOLD method. Furosemide, but not acetazolamide, increased medullary oxygenation by inhibiting active transport and QO_2 in the medullary thick ascending limb, consistent with their separate sites of action in the nephron.[308] The effect of furosemide on medullary oxygenation was absent or slight in an elderly human population.[309] Moreover, the BOLD method was applied to changes in intrarenal oxygenation in a variety of pathophysiological states, such as an acute reduction in RBF,[310] the diabetic state,[311] and the administration of NO synthase inhibitor.[312] BOLD-contrast imaging appears to predict the tissue at risk from ischemia by revealing information on the balance between tubular workload and delivery of oxygen.[311] Refined methods with improved visualization and more precise quantification have been developed.[313]

CONCLUSIONS

Most of the energy produced in the kidney is primarily utilized for the active reabsorption of Na^+, which further drives the cellular and paracellular transport of water and solutes. Renal metabolism for energy production is regulated by transport activity, and conversely, transport is affected by the cellular energy status. The intracellular adenine nucleotide level is an important regulatory factor for metabolism and transport; however, the interactions of these two processes are diverse and complex. For the last decade, AMPK was identified as the critical molecule for the regulator of cell metabolisms in various cells. Although the current information on its importance in the kidney is not abundant, emerging evidence has demonstrated its significance in the kidney, especially in energy metabolism in several solute transports. Other regulators, such as ATP-sensitive cation channels, NO, and purinergic receptors, should play some roles. Futher studies are required to elucidate the fine regulatory mechanisms for renal transport and cellular metabolisms. A novel methodology, BOLD MRI, will provide some progress in this field.

From pathophysiological viewpoints, the susceptibility of the kidney to ischemia and agents affecting energy production are critical clinical issues. Not only the role of acute ischemia, but also that of chronic ischemia in the kidney is now beginning to be a novel research subject.

References

[1] Valtin H. Renal function: mechanisms preserving fluid and solute balance in health. 2nd ed. Boston: Little, Brown; 1983.
[2] Cohen JJ, Kamm DE. Renal metabolism: relation to renal function. In: Brenner BM, Rector FC, editors. The kidney. Philadelphia: Saunders; 1976.
[3] Soltoff S. ATP and the regulation of renal cell function. Annu Rev Physiol 1986;48:9–31.
[4] Deetjen P. Measurement of metabolism during renal work. Int J Biochem 1980;12:243–4.
[5] Kiil F, Aukland K, Refsum HE. Renal sodium transport and oxygen consumption. Am J Physiol 1961;201:511–6.
[6] Thurau K. Renal Na-reabsorption and O_2-uptake in dogs during hypoxia and hydrochlorothiazide infusion. Proc Soc Exp Biol Med 1961;106:714–7.

[7] Mandel LJ, Balaban RS. Stoichiometry and coupling of active transport to oxidative metabolism in epithelial tissues. Am J Physiol 1981;240:F357–371.
[8] Gottschalk CW, Mylle M. Micropuncture study of the mammalian urinary concentrating mechanism: evidence for the countercurrent hypothesis. Am J Physiol 1959;196:927–36.
[9] Andreoli TE, Schafer JA. Effective luminal hypotonicity: the driving force for isotonic proximal tubular fluid absorption. Am J Physiol 1979;236:F89–96.
[10] Schafer JA, Patlak CS, Andreoli TE. Fluid absorption and active and passive ion flows in the rabbit superficial pars recta. Am J Physiol 1977;233:F154–167.
[11] Soleimani M, Burnham CE. Na + :HCO(3-) co-transporters (NBC): cloning and characterization. J Membr Biol 2001;183:71–84.
[12] Gross E, Hawkins K, Pushkin A, Sassani P, Dukkipati R, Abuladze N, et al. Phosphorylation of Ser(982) in the sodium bicarbonate co-transporter KNBC1 shifts the HCO(3)(−): Na (+) stoichiometry from 3: 1 to 2: 1 in murine proximal tubule cells. J Physiol 2001;537:659–65.
[13] Kiil F, Sejersted OM, Steen PA. Energetics and specificity of transcellular NaCl transport in the dog kidney. Int J Biochem 1980;12:245–50.
[14] Fromter E, Rumrich G, Ullrich KJ. Phenomenologic description of Na^+, Cl^- and HCO_3^- absorption from proximal tubules of rat kidney. Pflugers Arch 1973;343:189–220.
[15] Silva P, Myers MA. Stoichiometry of sodium chloride transport by rectal gland of *Squalus acanthias*. Am J Physiol 1986;250: F516–519.
[16] Welsh MJ. Energetics of chloride secretion in canine tracheal epithelium. comparison of the metabolic cost of chloride transport with the metabolic cost of sodium transport. J Clin Invest 1984;74:262–8.
[17] Ross B, Leaf A, Silva P, Epstein FH. Na-K-ATPase in sodium transport by the perfused rat kidney. Am J Physiol 1974;226:624–9.
[18] Kaplan JH. Biochemistry of Na,K-ATPase. Annu Rev Biochem 2002;71:511–35.
[19] Blanco G, Mercer RW. Isozymes of the Na-K-ATPase: heterogeneity in structure, diversity in function. Am J Physiol 1998;275: F633–650.
[20] Jorgensen PL. Aspects of gene structure and functional regulation of the isozymes of Na,K-ATPase. *Cell Mol Biol* (Noisy-legrand) 2001;47:231–8.
[21] Sweadner KJ, Rael E. The FXYD gene family of small ion transport regulators or channels: cDNA sequence, protein signature sequence, and expression. Genomics 2000;68:41–56.
[22] Barlet-Bas C, Arystarkhova E, Cheval L, Marsy S, Sweadner K, Modyanov N, et al. Are there several isoforms of Na,K-ATPase alpha subunit in the rabbit kidney? J Biol Chem 1993;268:11512–5.
[23] Farman N, Corthesy-Theulaz I, Bonvalet JP, Rossier BC. Localization of alpha-isoforms of Na(+)-K(+)-ATPase in rat kidney by *in situ* hybridization. Am J Physio 1991;260: C468–474.
[24] Segall L, Daly SE, Blostein R. Mechanistic basis for kinetic differences between the rat Alpha 1, Alpha 2, and Alpha 3 isoforms of the Na,K-ATPase. J Biol Chem 2001;276:31535–41.
[25] Geering K. The functional role of beta subunits in oligomeric P-type ATPases. J Bioenerg Biomembr 2001;33:425–38.
[26] Geering K, Beguin P, Garty H, Karlisch S, Füzesi M, Horisberger JD, et al. FXYD proteins: new tissue- and isoform-specific regulators of Na,K-ATPase. Ann N Y Acad Sci 2003;986:388–94.
[27] Meij IC, Koenderink JB, van Bokhoven H, Assink KF, Groenestege WT, de Pont JJ, et al. Dominant isolated renal magnesium loss is caused by misrouting of the Na(+),K (+)-ATPase gamma-subunit. Nat Genet 2000;26:265–6.
[28] Hebert H, Purhonen P, Thomsen K, Vorum H, Maunsbach AB. Renal Na,K-ATPase structure from cryo-electron microscopy of two-dimensional crystals. Ann NY Acad Sci 2003;986:9–16.
[29] Jorgensen PL, Hakansson KO, Karlish SJ. Structure and mechanism of Na,K-ATPase: functional sites and their interactions. Annu Rev Physiol 2003;65:817–49.
[30] Doucet A. Function and control of Na-K-ATPase in single nephron segments of the mammalian kidney. Kidney Int 1988;34:749–60.
[31] Doucet A, Morel F, Katz AI. Microdetermination of Na-K-ATPase in single tubules: its application for the localization of physiologic processes in the nephron. Int J Biochem 1980;12:47–52.
[32] Garg LC, Knepper MA, Burg MB. Mineralocorticoid effects on Na-K-ATPase in individual nephron segments. Am J Physiol 1981;240:F536–544.
[33] Katz AI. Distribution and function of classes of ATPases along the nephron. Kidney Int 1986;29:21–31.
[34] Katz AI, Doucet A, Morel F. Na-K-ATPase activity along the rabbit, rat, and mouse nephron. Am J Physiol 1979;237: F114–120.
[35] El Mernissi G, Doucet A. Quantitation of [3h]ouabain binding and turnover of Na-K-ATPase along the rabbit nephron. Am J Physiol 1984;247:F158–167.
[36] Jorgensen PL. Structure, function and regulation of Na,K-ATPase in the kidney. Kidney Int 1986;29:10–20.
[37] Cheval L, Doucet A. Measurement of Na-K-ATPase-mediated rubidium influx in single segments of rat nephron. Am J Physiol 1990;259:F111–121.
[38] McDonough AA, Magyar CE, Komatsu Y. Expression of Na (+)-K(+)-ATPase alpha- and beta-subunits along rat nephron: isoform specificity and response to hypokalemia. Am J Physiol 1994;267:C901–908.
[39] Tumlin JA, Hoban CA, Medford RM, Sands JM. Expression of Na-K-ATPase alpha- and beta-subunit mRNA and protein isoforms in the rat nephron. Am J Physiol 1994;266:F240–245.
[40] Ahn KY, Madsen KM, Tisher CC, Kone BC. Differential expression and cellular distribution of mRNAs encoding alpha- and beta-isoforms of $Na(^+)$-$K(^+)$-ATPase in rat kidney. Am J Physiol 1993;265:F792–801.
[41] Kashgarian M, Biemesderfer D, Caplan M, Forbush III B. Monoclonal antibody to Na,K-ATPase: immunocytochemical localization along nephron segments. Kidney Int 1985;28:899–913.
[42] Piepenhagen PA, Peters LL, Lux SE, Nelson WJ. Differential expression of Na(+)-K(+)-ATPase, ankyrin, fodrin, and e-cadherin along the kidney nephron. Am J Physiol 1995;269: C1417–1432.
[43] Wetzel RK, Sweadner KJ. Immunocytochemical localization of Na-K-ATPase alpha- and gamma-subunits in rat kidney. Am J Physiol Renal Physiol 2001;281:F531–545.
[44] Doucet A, Hus-Citharel A, Morel F. *In vitro* stimulation of Na-K-ATPase in rat thick ascending limb by dexamethasone. Am J Physiol 1986;251:F851–857.
[45] Terada Y, Knepper MA. Na^+-K^+-ATPase activities in renal tubule segments of rat inner medulla. Am J Physiol 1989;256: F218–223.
[46] Vinciguerra M, Deschenes G, Hasler U, Mordasini D, Rousselot M, Doucet A, et al. Intracellular Na^+ controls cell surface expression of Na,K-ATPase via a camp-independent PKA

pathway in mammalian kidney collecting duct cells. Mol Biol Cell 2003;14:2677–88.
[47] Kiroytcheva M, Cheval L, Carranza ML, Martin PY, Favre H, Doucet A, et al. Effect of Camp on the activity and the phosphorylation of Na^+,K(+)-ATPase in rat thick ascending limb of Henle. Kidney Int 1999;55:1819–31.
[48] Buffin-Meyer B, Verbavatz JM, Cheval L, Marsy S, Younes-Ibrahim M, Le Moal C, et al. Regulation of Na+, K(+)-ATPase in the rat outer medullary collecting duct during potassium depletion. J Am Soc Nephrol 1998;9:538–50.
[49] Feraille E, Doucet A. Sodium-potassium-adenosinetriphosphatase-dependent sodium transport in the kidney: hormonal control. Physiol Rev 2001;81:345–418.
[50] Feraille E, Mordasini D, Gonin S, Deschênes G, Vinciguerra M, Doucet A, et al. Mechanism of control of Na,K-ATpase in principal cells of the mammalian collecting duct. Ann NY Acad Sci 2003;986:570–8.
[51] Michlig S, Mercier A, Doucet A, Schild L, Horisberger JD, Rossier BC, et al. ERK1/2 controls Na,K-ATPase activity and transepithelial sodium transport in the principal cell of the cortical collecting duct of the mouse kidney. J Biol Chem 2004;279:51002–12.
[52] Bronner F. Renal calcium transport: mechanisms and regulation–an overview. Am J Physiol 1989;257:F707–711.
[53] Magyar CE, White KE, Rojas R, Apodaca G, Friedman PA. Plasma membrane Ca^{2+}-ATPase and NCX1 Na^+/Ca^{2+} exchanger expression in distal convoluted tubule cells. Am J Physiol Renal Physiol 2002;283:F29–40.
[54] Verma AK, Filoteo AG, Stanford DR, Wieben ED, Penniston JD, Strehler EE, et al. Complete primary structure of a human plasma membrane Ca^{2+} pump. J Biol Chem 1988;263:14152–9.
[55] Penniston JT, Enyedi A. Modulation of the plasma membrane Ca^{2+} pump. J Membr Biol 1998;165:101–9.
[56] Stauffer TP, Guerini D, Carafoli E. Tissue distribution of the four gene products of the plasma membrane Ca^{2+} pump. A study using specific antibodies. J Biol Chem 1995;270:12184–90.
[57] Stauffer TP, Hilfiker H, Carafoli E, Strehler EE. Quantitative analysis of alternative splicing options of human plasma membrane calcium pump genes. J Biol Chem 1993;268:25993–6003.
[58] Brunette MG, Mailloux J, Chan M, Ramachandran C. Characterization of the high and low affinity components of the renal Ca2(+)-Mg2+ ATPase. Can J Physiol Pharmacol 1990;68:718–26.
[59] Dick IM, Liu J, Glendenning P, Prince RL. Estrogen and androgen regulation of plasma membrane calcium pump activity in immortalized distal tubule kidney cells. Mol Cell Endocrinol 2003;212:11–8.
[60] Qi Z, Murase K, Obata S, Sokabe M. Extracellular ATP-dependent activation of plasma membrane Ca(2+) pump in HEK-293 cells. Br J Pharmacol 2000;131:370–4.
[61] Caride AJ, Chini EN, Penniston JT, Dousa TP. Selective decrease of mRNAs encoding plasma membrane calcium pump isoforms 2 and 3 in rat kidney. Kidney Int 1999;56:1818–25.
[62] Caride AJ, Chini EN, Homma S, Penniston JT, Dousa TP. mRNA encoding four isoforms of the plasma membrane calcium pump and their variants in rat kidney and nephron segments. J Lab Clin Med 1998;132:149–56.
[63] Magosci M, Yamaki M, Penniston JT, Dousa TP. Localization of mRNAs coding for isozymes of plasma membrane $Ca^{(2+)}$-ATPase pump in rat kidney. Am J Physiol 1992;263:F7–14.
[64] Loffing J, Loffing-Cueni D, Valderrabano V, Kläusli L, Hebert SC, Rossier BC, et al. Distribution of transcellular calcium and sodium transport pathways along mouse distal nephron. Am J Physiol Renal Physiol 2001;281:F1021–1027.
[65] Kip SN, Strehler EE. Characterization of PMCA isoforms and their contribution to transcellular Ca^{2+} flux in MDCK cells. Am J Physiol Renal Physiol 2003;284:F122–132.
[66] Doucet A, Katz AI. High-affinity Ca-Mg-ATPase along the rabbit nephron. Am J Physiol 1982;242:F346–352.
[67] Martin V, Bredoux R, Corvazier E, Van Gorp R, Kovacs T, Gelebart P, et al. Three novel sarco/endoplasmic reticulum Ca^{2+}-ATPase (SERCA) 3 isoforms. Expression, regulation, and function of the membranes of the SERCA3 family. J Biol Chem 2002;277:24442–52.
[68] Thastrup O, Cullen PJ, Drobak BK, Hanley MR, Dawson AP. Thapsigargin, a tumor promoter, discharges intracellular Ca^{2+} stores by specific inhibition of the endoplasmic reticulum Ca2(+)-ATPase. Proc Natl Acad Sci USA 1990;87:2466–70.
[69] Doucet AH. K(+)-ATPase in the kidney: localization and function in the nephron. Exp Nephrol 1997;5:271–6.
[70] Shull GE, Lingrel JB. Molecular cloning of the rat stomach (H^+ + K^+)-ATPase. J Biol Chem 1986;261:16788–91.
[71] Crowson MS, Shull GE. Isolation and characterization of a cDNA encoding the putative distal colon H^+,K(+)-Atpase. Similarity of deduced amino acid sequence to gastric H^+,K(+)-ATPase and Na^+,K(+)-ATPase and mRNA expression in distal colon, kidney, and uterus. J Biol Chem 1992;267:13740–8.
[72] Canfield VA, Okamoto CT, Chow D, Dorfman J, Gros P, Forte JG, et al. Cloning of the H,K-ATPase beta subunit. Tissue-specific expression, chromosomal assignment, and relationship to Na,K-ATPase beta subunits. J Biol Chem 1990;265:19878–84.
[73] Silver RB, Soleimani H. H^+-K^+-ATPases: regulation and role in pathophysiological states. Am J Physiol 1999;276:F799–811.
[74] Wingo CS. Active proton secretion and potassium absorption in the rabbit outer medullary collecting duct. Functional evidence for proton-potassium-activated adenosine triphosphatase. J Clin Invest 1989;84:361–5.
[75] Doucet A, Marsy S. Characterization of K-ATPase activity in distal nephron: stimulation by potassium depletion. Am J Physiol 1987;253:F418–423.
[76] Garg LC, Narang N. Ouabain-insensitive K-adenosine triphosphatase in distal nephron segments of the rabbit. J Clin Invest 1988;81:1204–8.
[77] Wingo CS, Madsen KM, Smolka A, Tisher CC. H-K-ATPase immunoreactivity in cortical and outer medullary collecting duct. Kidney Int 1990;38:985–90.
[78] Ahn KY, Kone BC. Expression and cellular localization of mRNA encoding the "gastric" isoform of $H(^+)$-$K(^+)$-ATPase alpha-subunit in rat kidney. Am J Physiol 1995;268:F99–109.
[79] Marsy S, Elalouf JM, Doucet A. Quantitative Rt-Pcr analysis of mRNAs encoding a colonic putative H, K-ATPase alpha subunit along the rat nephron: effect of K^+ depletion. Pflugers Arch 1996;432:494–500.
[80] Ahn KY, Turner PB, Madsen KM, Kone BC. Effects of chronic hypokalemia on renal expression of the "gastric" $H(^+)$-$K(^+)$-ATPase alpha-subunit gene. Am J Physiol 1996;270:F557–566.
[81] Gluck SL, Underhill DM, Iyori M, Holliday LS, Kostrominova TY, Lee BS. Physiology and biochemistry of the kidney vacuolar H^+-ATPase. Annu Rev Physiol 1996;58:427–45.
[82] Wagner CA, Finberg KE, Breton S, Marshansky V, Brown D, Geibel JP. Renal vacuolar H^+-ATPase. Physiol Rev 2004;84:1263–314.
[83] Forgac M. Structure, mechanism and regulation of the clathrin-coated vesicle and yeast vacuolar H(+)-ATPases. J Exp Biol 2000;203:71–80.
[84] Gruber G. Introduction: a close look at the vacuolar ATPase. J Bioenerg Biomembr 2003;35:277–80.

[85] Bank N, Aynedjian HS, Mutz BF. Evidence for a DCCD-sensitive component of proximal bicarbonate reabsorption. Am J Physiol 1985;249:F636–644.
[86] Kurtz I. Apical Na^+/H^+ antiporter and glycolysis-dependent H^+-ATPase regulate intracellular Ph in the rabbit S3 proximal tubule. J Clin Invest 1987;80:928–35.
[87] Noel J, Vinay P, Tejedor A, Fleser A, Laprade R. Metabolic cost of bafilomycin-sensitive H^+ pump in intact dog, rabbit, and hamster proximal tubules. Am J Physiol 1993;264: F655–661.
[88] Ait-Mohamed AK, Marsy S, Barlet C, Khadouri C, Doucet A. Characterization of N-ethylmaleimide-sensitive proton pump in the rat kidney. Localization along the nephron. J Biol Chem 1986;261:12526–33.
[89] Brown D, Hirsch S, Gluck S. Localization of a proton-pumping ATPase in rat kidney. J Clin Invest 1988;82:2114–26.
[90] Garg LC, Narang N. Changes in H-ATPase activity in the distal nephron segments of the rat during metabolic acidosis and alkalosis. Contrib Nephrol 1991;92:39–45.
[91] Garg LC, Narang N. Decrease in N-ethylmaleimide-sensitive ATPase activity in collecting duct by metabolic alkalosis. Can J Physiol Pharmacol 1990;68:1119–23.
[92] Garg LC, Narang N. Stimulation of an N-ethylmaleimide-sensitive ATPase in the collecting duct segments of the rat nephron by metabolic acidosis. Can J Physiol Pharmacol 1985;63:1291–6.
[93] Garg LC, Narang N. Effects of aldosterone on Nem–sensitive ATPase in rabbit nephron segments. Kidney Int 1988;34:13–7.
[94] Karet FE, Finberg KE, Nelson RD, Nayir A, Mocan H, Sanjad SA, et al. Mutations in the gene encoding B1 subunit of H^+-ATPase cause renal tubular acidosis with sensorineural deafness. Nat Genet 1999;21:84–90.
[95] Smith AN, Skaug J, Choate KA, Nayir A, Bakkaloglu A, Ozen S, et al. Mutations in ATP6N1B, encoding a new kidney vacuolar proton pump 116-Kd subunit, cause recessive distal renal tubular acidosis with preserved hearing. Nat Genet 2000;26:71–5.
[96] Stover EH, Borthwick KJ, Bavalia C, Eady N, Fritz DM, Rungroj N, et al. Novel ATP6V1B1 and ATP6V0A4 mutations in autosomal recessive distal renal tubular acidosis with new evidence for hearing loss. J Med Genet 2002;39:796–803.
[97] Ambudkar SV, Kimchi-Sarfaty C, Sauna ZE, Gottesman MM. P-glycoprotein: from genomics to mechanism. Oncogene 2003;22:7468–85.
[98] Gottesman MM, Fojo T, Bates SE. Multidrug resistance in cancer: role of ATP-dependent transporters. Nat Rev Cancer 2002;2:48–58.
[99] Haimeur A, Conseil G, Deeley RG, Cole SP. The MRP-related and BCRP/ABCG2 multidrug resistance proteins: biology, substrate specificity and regulation. Curr Drug Metab 2004;5:21–53.
[100] Hrycyna CA, Ramachandra M, Ambudkar SV, Ko YH, Pedersen PL, Pastan I, et al. Mechanism of action of human P-glycoprotein ATPase activity. Photochemical cleavage during a catalytic transition state using orthovanadate reveals cross-talk between the two ATP sites. J Biol Chem 1998;273:16631–4.
[101] Gullans SR, Mandel LJ. In: Seldin, Giebisch G, editors. The kidney: physiology & pathophysiology. 3rd ed Williams & Wilkins; 2000.
[102] Kone BC, The metabolic basis of solute transport. Brenner BM, editor. The Kidney; 2004.
[103] Hatefi Y. The mitochondrial electron transport and oxidative phosphorylation system. Annu Rev Biochem 1985;54:1015–69.
[104] Le Hir M, Dubach UC. Activities of enzymes of the tricarboxylic acid cycle in segments of the rat nephron. Pflugers Arch 1982;395:239–43.
[105] Marver D, Schwartz MJ. Identification of mineralocorticoid target sites in the isolated rabbit cortical nephron. Proc Natl Acad Sci USA 1980;77:3672–6.
[106] Le Hir M, Dubach UC. Peroxisomal and mitochondrial beta-oxidation in the rat kidney: distribution of fatty acyl-coenzyme a oxidase and 3-hydroxyacyl-coenzyme a dehydrogenase activities along the nephron. J Histochem Cytochem 1982;30:441–4.
[107] Guder WG, Purschel S, Wirthensohn G. Renal ketone body metabolism. Distribution of 3-Oxoacid Coa-Transferase and 3-hydroxybutyrate dehydrogenase along the mouse nephron. Hoppe Seylers Z Physiol Chem 1983;364:1727–37.
[108] Schlender KK. Regulation of renal glycogen synthase. interconversion of two forms *in vitro*. Biochim Biophys Acta 1973;297:384–98.
[109] Vandewalle A, Wirthensohn G, Heidrich HG, Guder WG. Distribution of hexokinase and phosphoenolpyruvate carboxykinase along the rabbit nephron. Am J Physiol 1981;240: F492–500.
[110] Schmid H, Mall A, Scholz M, Schmidt U. Unchanged glycolytic capacity in rat kidney under conditions of stimulated gluconeogenesis. Determination of phosphofructokinase and pyruvate kinase in microdissected nephron segments of fasted and acidotic animals. Hoppe Seylers Z Physiol Chem 1980;361:819–27.
[111] Bagnasco S, Good D, Balaban R, Burg M. Lactate production in isolated segments of the rat nephron. Am J Physiol 1985;248:F522–526.
[112] Krebs HA. Renal gluconeogenesis. Adv Enzyme Regul 1963;17:385–400.
[113] Meyer C, Stumvoll M, Dostou J, Welle S, Haymond M, Gerich J. Renal substrate exchange and gluconeogenesis in normal postabsorptive humans. Am J Physiol Endocrinol Metab 2002;282:E428–434.
[114] Cersosimo E, Garlick P, Ferretti J. Renal glucose production during insulin-induced hypoglycemia in humans. Diabetes 1999;48:261–6.
[115] Cersosimo E, Garlick P, Ferretti J. Renal substrate metabolism and gluconeogenesis during hypoglycemia in humans. Diabetes 2000;49:1186–93.
[116] Maleque A, Endou H, Koseki C, Sakai F. Nephron heterogeneity: gluconeogenesis from pyruvate in rabbit nephron. FEBS Lett 1980;116:154–6.
[117] Kondou I, Nakada J, Hishinuma H, Masuda F, Machida T, Endou H. Alterations of gluconeogenesis by ischemic renal injury in rats. Ren Fail 1992;14:479–83.
[118] Friedrichs D, Schoner W. Stimulation of renal gluconeogenesis by inhibition of the sodium pump. Biochim Biophys Acta 1973;304:142–60.
[119] Gullans SR, Brazy PC, Dennis VW, Mandel LJ. Interactions between gluconeogenesis and sodium transport in rabbit proximal tubule. Am J Physiol 1984;246:F859–869.
[120] Nagami GT, Lee P. Effect of luminal perfusion on glucose production by isolated proximal tubules. Am J Physiol 1989;256: F120–127.
[121] Veiga JA, Carpenter CA, Saggerson ED. Effect of the Na^+ ionophore monensin on basal and noradrenaline stimulated gluconeogenesis in rat renal tubule fragments. FEBS Lett 1981;134:183–4.
[122] Silva P, Hallac R, Spokes K, Epstein FH. Relationship among gluconeogenesis, QO_2, and Na^+ transport in the perfused rat kidney. Am J Physiol 1982;242:F508–513.

[123] Silva P, Ross B, Spokes K. Competition between sodium reabsorption and gluconeogenesis in kidneys of steroid-treated rats. Am J Physiol 1980;238:F290–295.
[124] Pfaller W. Structure function correlation on rat kidney. Quantitative correlation of structure and function in the normal and injured rat kidney. Adv Anat Embryol Cell Biol 1982;70:1–106.
[125] Pfaller W, Rittinger M. Quantitative morphology of the rat kidney. Int J Biochem 1980;12:17–22.
[126] Burch HB, Choi S, Dence CN, Alvey TR, Cole BR, Lowry OH. Metabolic effects of large fructose loads in different parts of the rat nephron. J Biol Chem 1980;255:8239–44.
[127] Uchida S, Endou H. Substrate specificity to maintain cellular ATP along the mouse nephron. Am J Physiol 1988;255: F977–983.
[128] Gyoergy P, Keller W, Brehme TH. Nierestoffwechsel und nierenentwicklung. Biochem Zeitschr 1928;200:356–66.
[129] Klein KL, Wang MS, Torikai S, Davidson WD, Kurokaqwa K. Substrate oxidation by isolated single nephron segments of the rat. Kidney Int 1981;20:29–35.
[130] Ruegg CE, Mandel LJ. Bulk isolation of renal Pct and Pst. Ii. Differential responses to anoxia or hypoxia. Am J Physiol 1990;259:F176–185.
[131] Weidemann MJ, Krebs HA. The fuel of respiration of rat kidney cortex. Biochem J 1969;112:149–66.
[132] Guder WG, Ross BD. Enzyme distribution along the nephron. Kidney Int 1984;26:101–11.
[133] Balaban RS, Mandel LJ. Metabolic substrate utilization by rabbit proximal tubule. An NADH fluorescence study. Am J Physiol 1988;254:F407–416.
[134] Harris SI, Balaban RS, Barrett L, Mandel LJ. Mitochondrial respiratory capacity and Na^+- and K^+-dependent adenosine triphosphatase-mediated ion transport in the intact renal cell. J Biol Chem 1981;256:10319–28.
[135] Rome L, Grantham J, Savin V, Lohr J, Lechene C. Proximal tubule volume regulation in hyperosmotic media: intracellular K^+, Na^+, and Cl. Am J Physiol 1989;257:C1093–1100.
[136] Gullans SR, Harris SI, Mandel LJ. Glucose-dependent respiration in suspensions of rabbit cortical tubules. J Membr Biol 1984;78:257–62.
[137] Markovich D, Murer H. The Slc13 gene family of sodium sulphate/carboxylate co-transporters. Pflugers Arch 2004;447:594–602.
[138] Pajor AM. Sodium-coupled transporters for Krebs Cycle intermediates. Annu Rev Physiol 1999;61:663–82.
[139] Sekine T, Cha SH, Hosoyamada M, Kanai Y, Watanabe N, Furuta Y, et al. Cloning, functional characterization, and localization of a rat renal Na^+-dicarboxylate transporter. Am J Physiol 1998;275:F298–305.
[140] Unwin RJ, Capasso G, Shirley DG. An overview of divalent cation and citrate handling by the kidney. Nephron Physiol 2004;98:p15–20.
[141] Guder WG, Wagner S, Wirthensohn G. Metabolic fuels along the nephron: pathways and intracellular mechanisms of interaction. Kidney Int 1986;29:41–5.
[142] Goldstein L. Renal substrate utilization in normal and acidotic rats. Am J Physiol 1987;253:F351–357.
[143] Jung KY, Endou H. Cellular adenosine triphosphate production and consumption in the descending thin limb of Henle's loop in the rat. Ren Physiol Biochem 1990;13:248–58.
[144] Wittner M, Weidtke C, Schlatter E, di Stefano A, Greger R. Substrate utilization in the isolated perfused cortical thick ascending limb of rabbit nephron. Pflugers Arch 1984;402:52–62.
[145] Chamberlin ME, Mandel LJ. Substrate support of medullary thick ascending limb oxygen consumption. Am J Physiol 1986;251:F758–763.
[146] Torikai S. Dependency of microdissected nephron segments upon oxidative phosphorylation and exogenous substrates: a relationship between tubular anatomical location in the kidney and metabolic activity. *Clin Sci* (Lond) 1989;77: 287–95.
[147] Chamberlin ME, LeFurgey A, Mandel LJ. Suspension of medullary thick ascending limb tubules from the rabbit kidney. *Am J Physiol* 1984;247:F955–964.
[148] Eveloff J, Bayerdorffer E, Silva P, Kinne R. Sodium-chloride transport in the thick ascending limb of Henle's loop. Oxygen consumption studies in isolated cells. Pflugers Arch 1981;389:263–70.
[149] Chamberlin ME, Mandel LJ. Na^+-K^+-ATPase activity in medullary thick ascending limb during short-term anoxia. Am J Physiol 1987;252:F838–843.
[150] Hering-Smith KS, Hamm LL. Metabolic support of collecting duct transport. Kidney Int 1998;53:408–15.
[151] Nonaka T, Stokes JB. Metabolic support of Na^+ transport by the rabbit CCD: analysis of the use of equivalent current. Kidney Int 1994;45:743–52.
[152] Natke Jr. E. Cell volume regulation of rabbit cortical collecting tubule in anisotonic media. Am J Physiol 1990;258: F1657–1665.
[153] Zeidel ML, Seifter JL, Lear S, Brenner BM, Silva P. Atrial peptides inhibit oxygen consumption in kidney medullary collecting duct cells. Am J Physiol 1986;251:F379–383.
[154] Vinay P, Senecal J, Noel J, Chirinian C, Vinay MC, Ammann H, et al. Basolateral glucose transport in distal segments of the dog nephron. Can J Physiol Pharmacol 1991;69:964–77.
[155] Zeidel ML, Silva P, Seifter JL. Intracellular pH regulation in rabbit renal medullary collecting duct cells. Role of chloride-bicarbonate exchange. J Clin Invest 1986;77:1682–8.
[156] Grunewald RW, Kinne RK. Sugar transport in isolated rat kidney papillary collecting duct cells. Pflugers Arch 1988;413:32–7.
[157] Stokes JB, Grupp C, Kinne RK. Purification of rat papillary collecting duct cells: functional and metabolic assessment. Am J Physiol 1987;253:F251–262.
[158] Zeidel ML. Hormonal regulation of inner medullary collecting duct sodium transport. Am J Physiol 1993;265:F159–173.
[159] Kone BC, Kikeri D, Zeidel ML, Gullans SR. Cellular pathways of potassium transport in renal inner medullary collecting duct. Am J Physiol 1989;256:C823–830.
[160] Blond DM, Whittam R. The regulation of kidney respiration by sodium and potassium ions. Biochem J 1964;92:158–67.
[161] Whittam R. Active cation transport as a pace-maker of respiration. Nature 1961;191:603–4.
[162] Rea C, Segal S. ATP content of rat kidney cortex slices: relation to alpha-aminoisobutyric acid uptake. Kidney Int 1972;2:101–6.
[163] Urbaitis BK, Kessler RH. Actions of inhibitor compounds on adenine nucleotides of renal cortex and sodium excretion. Am J Physiol 1971;220:1116–23.
[164] Needleman P, Passonneau JV, Lowry OH. Distribution of glucose and related metabolites in rat kidney. Am J Physiol 1968;215:655–9.
[165] Balaban RS, Mandel LJ, Soltoff SP, Storey JM. Coupling of active ion transport and aerobic respiratory rate in isolated renal tubules. Proc Natl Acad Sci USA 1980;77:447–51.
[166] Chance BG, Williams R. The respiratory chain and oxidative phosphorylation. Adv Enzymol Relat Subj Biochem 1956;17:65–134.

[167] Jacobus WE, Moreadith RW, Vandegaer KM. Mitochondrial respiratory control. evidence against the regulation of respiration by extramitochondrial phosphorylation potentials or by [Atp]/[Adp] Ratios. J Biol Chem 1982;257:2397–402.
[168] Lardy HA, Wellman H. Oxidative phosphorylations: role of inorganic phosphate and acceptor systems in control of metabolic rates. J Biol Chem 1952;195:215–24.
[169] Harris SI, Balaban RS, Mandel LJ. Oxygen consumption and cellular ion transport: evidence for adenosine triphosphate to O_2 ratio near 6 in intact cell. Science 1980;208:1148–50.
[170] Slater EC, Rosing J, Mol A. The phosphorylation potential generated by respiring mitochondria. Biochim Biophys Acta 1973;292:534–53.
[171] Lemasters JJ, Sowers AE. Phosphate dependence and atractyloside inhibition of mitochondrial oxidative phosphorylation. The ADP-ATP carrier is rate-limiting. J Biol Chem 1979;254:1248–51.
[172] Balaban RS. Regulation of oxidative phosphorylation in the mammalian cell. Am J Physiol 1990;258:C377–389.
[173] Erecinska M, Wilson DF. Regulation of cellular energy metabolism. J Membr Biol 1982;70:1–14.
[174] Erecinska M, Wilson DF, Nishiki K. Homeostatic regulation of cellular energy metabolism: experimental characterization *in vivo* and fit to a model. Am J Physiol 1978;234: C82–89.
[175] Brown GC. Control of respiration and ATP synthesis in mammalian mitochondria and cells. Biochem J 1992;284(Pt 1): 1–13.
[176] Foxall PJ, Nicholson JK. Nuclear magnetic resonance spectroscopy: a non-invasive probe of kidney metabolism and function. *Exp Nephrol* 1998;6 1998;:409–14.
[177] Wong GG, Ross BD. Application of phosphorus nuclear magnetic resonance to problems of renal physiology and metabolism. Miner Electrolyte Metab 1983;9:282–9.
[178] Freeman D, Bartlett S, Radda G, Ross B. Energetics of sodium transport in the kidney. Saturation transfer 31P-NMR. Biochim Biophys Acta 1983;762:325–36.
[179] Veech RL, Lawson JW, Cornell NW, Krebs HA. Cytosolic phosphorylation potential. J Biol Chem 1979;254:6538–47.
[180] Brand MD, Murphy MP. Control of electron flux through the respiratory chain in mitochondria and cells. Biol Rev Camb Philos Soc 1987;62:141–93.
[181] Kadenbach B. Intrinsic and extrinsic uncoupling of oxidative phosphorylation. Biochim Biophys Acta 2003;1604:77–94.
[182] Kadenbach B. Regulation of respiration and ATP synthesis in higher organisms: hypothesis. J Bioenerg Biomembr 1986;18:39–54.
[183] Akerboom TP, Bookelman H, Tager JM. Control of ATP transport across the mitochondrial membrane in isolated rat-liver cells. FEBS Lett 1977;74:50–4.
[184] Pfaller W, Guder WG, Gstraunthaler G, Kotanko P, Jehart I, Pürschel S. Compartmentation of ATP within renal proximal tubular cells. Biochim Biophys Acta 1984;805:152–7.
[185] Schwenke WD, Soboll S, Seitz HJ, Sies H. Mitochondrial and cytosolic ATP/ADP ratios in rat liver *in vivo*. Biochem J 1981;200:405–8.
[186] Soltoff SP, Mandel LJ. Active ion transport in the renal proximal tubule. III. The ATP dependence of the Na pump. J Gen Physiol 1984;84:643–62.
[187] Urbaitis BK, Kessler RH. Concentration of adenine nucleotide compounds in renal cortex and medulla. Nephron 1969;6:217–34.
[188] Daly SE, Lane LK, Blostein R. Functional consequences of amino-terminal diversity of the catalytic subunit of the Na,K-ATPase. J Biol Chem 1994;269:23944–8.
[189] Mandel LJ. Primary active sodium transport, oxygen consumption, and ATP: coupling and regulation. Kidney Int 1986;29:3–9.
[190] Gullans SR, Brazy PC, Soltoff SP, Dennis VW, Mandel LJ. Metabolic inhibitors: effects on metabolism and transport in the proximal tubule. Am J Physiol 1982;243:F133–140.
[191] Brazy PC, Balaban RS, Gullans SR, Mandel LJ, Dennis VW. Inhibition of renal metabolism. relative effects of arsenate on sodium, phosphate, and glucose transport by the rabbit proximal tubule. J Clin Invest 1980;66:1211–21.
[192] Goligorsky MS, Hruska KA. Hormonal modulation of cytoplasmic calcium concentration in renal tubular epithelium. Miner Electrolyte Metab 1988;14:58–70.
[193] Hallows K, Mount P, Pastor-Soler N, Power DA. Role of the energy sensor AMP-activated protein kinase in renal physiology and disease. Am J Physiol Renal Physiol 2010;298: F1067–1077.
[194] Kahn B, Alquier T, Carling D, Hardie DG. AMP-activated protein kinase: ancient energy gauge provides clues to modern understanding of metabolism. Cell Metab 2005;1:15–25.
[195] Steinberg G, Kemp B. AMPK in health and disease. Physiol Rev 2009;89:1025–78.
[196] Yehm L, Lee K, Kim K. Regulation of rat liver acetyl-coa carboxylase. regulation of phosphorylation and inactivation of acetyl-coa carboxylase by the adenylate energy charge. J Biol Chem 1980;255:2308–14.
[197] Munday M, Campbell D, Carling D, Hardie DG. Identification by amino acid sequencing of three major regulatory phosphorylation sites on rat acetyl-CoA carboxylase. Eur J Biochem 1988;175:331–8.
[198] Carling D, Aguan K, Woods A, Verhoeven AJ, Beri RK, Brennan CH, et al. Mammalian AMP-activated protein kinase is homologous to yeast and plant protein kinases involved in the regulation of carbon metabolism. J Biol Chem 1994;269:11442–8.
[199] Mitchelhill K, Stapleton D, Gao G, House C, Michell B, Katsis F, et al. Mammalian AMP-activated protein kinase shares structural and functional homology with the catalytic domain of yeast SNF1 protein kinase. J Biol Chem 1994;269:2361–4.
[200] Sanders M, Grondin P, Hegarty B, Snowden MA, Carling D. Investigating the mechanism for AMP activation of the AMP-activated protein kinase cascade. Biochem J 2007;403:139–48.
[201] Hawley S, Selbert M, Goldstein E, Edelman AM, Carling D, Hardie DG. 5′-AMP activates the AMP-activated protein kinase cascade, and Ca^{2+}/calmodulin activates the calmodulin-dependent protein kinase I cascade, via three independent mechanisms. J Biol Chem 1995;270:27186–91.
[202] Scott J, Hawley S, Green K, Anis M, Stewart G, Scullion GA, et al. CBS domains form energy-sensing modules whose binding of adenosine ligands is disrupted by disease mutations. J Clin Invest 2004;113:182–4.
[203] Stapleton D, Mitchelhill K, Gao G, Widmer J, Michell BJ, Teh T, et al. Mammalian AMP-activated protein kinase subfamily. J Biol Chem 1996;271:611–4.
[204] Fraser S, Mount P, Hill R, Levidiotis V, Katsis F, Stapleton D, et al. Regulation of the energy sensor AMP-activated protein kinase in the kidney by dietary salt intake and osmolality. Am J Physiol Renal Physiol 2005;288:F578–586.
[205] Cammisotto P, Londono I, Gingras D, Bendayan M. Control of glycogen synthase through ADIPOR1-AMPK pathway in renal distal tubules of normal and diabetic rats. Am J Physiol Renal Physiol 2008;294:F881–889.
[206] Woollhead A, Scott J, Hardie D, Baines DL. Phenformin and 5-aminoimidazole-4-carboxamide-1-beta-D-ribofuranoside (Aicar) activation of amp-activated protein kinase inhibits

transepithelial Na^+ transport across H441 lung cells. J Physiol 2005;566:781–92.

[207] Woollhead A, Sivagnanasundaram J, Kalsi K, Pucovsky V, Pellatt LJ, Scott JW, et al. Pharmacological activators of amp-activated protein kinase have different effects on Na + transport processes across human lung epithelial cells. Br J Pharmacol 2007;151:1204–15.

[208] Vadász I, Dada L, Briva A, Trejo HE, Welch LC, Chen J, et al. AMP-activated protein kinase regulates CO_2-induced alveolar epithelial dysfunction in rats and human cells by promoting Na,K-ATPase endocytosis. J Clin Invest 2008;118:752–62.

[209] Carattino M, Edinger R, Grieser H, Wise R, Neumann D, Schlattner U, et al. Epithelial sodium channel inhibition by AMP-activated protein kinase in oocytes and polarized renal epithelial cells. J Biol Chem 2005;280:17608–16.

[210] Almaça J, Kongsuphol P, Hieke B, Ousingsawat J, Viollet B, Schreiber R, et al. AMPK controls epithelial Na(+) channels through Nedd4-2 and causes an epithelial phenotype when mutated. Pflugers Arch 2009;458:713–21.

[211] Bhalla V, Oyster N, Fitch A, Wijngaarden MA, Neumann D, Schlattner U, et al. AMP-activated kinase inhibits the epithelial Na + channel through functional regulation of the ubiquitin ligase Nedd4-2. J Biol Chem 2006;281:26159–69.

[212] Fraser S, Gimenez I, Cook N, Jennings I, Katerelos M, Katsis F, et al. Regulation of the renal-specific Na^+-K^+-$2Cl^-$ co-transporter NKCC2 by amp-activated protein kinase (AMPK). Biochem J 2007;405:85–93.

[213] Gong F, Alzamora R, Smolak C, Li H, Naveed S, Neumann D, et al. Vacuolar H^+-ATPase apical accumulation in kidney intercalated cells is regulated by PKA and AMP-activated protein kinase. Am J Physiol Renal Physiol 2010; epub ahead of print.

[214] Hallows K, Raghuram V, Kemp B, Witters LA, Foskett JK. Inhibition of cystic fibrosis transmembrane conductance regulator by novel interaction with the metabolic sensor AMP-activated protein kinase. J Clin Invest 2000;105:1711–21.

[215] Sopjani M, Bhavsar S, Fraser S, Kemp BE, Föller M, Lang F. Regulation of Na^+-coupled glucose carrier SGLT1 by AMP-activated protein kinase. Mol Membr Biol 2010;27:137–44.

[216] Sukhodub A, Jovanović S, Du Q, Budas G, Clelland AK, Shen M, et al. AMP-activated protein kinase mediates preconditioning in cardiomyocytes by regulating activity and trafficking of sarcolemmal ATP-sensitive K(+) channels. J Cell Physiol 2007;210:224–36.

[217] Hebert SC, Desir G, Giebisch G, Wang W. Molecular diversity and regulation of renal potassium channels. Physiol Rev 2005;85:319–71.

[218] Misler S, Giebisch G. ATP-sensitive potassium channels in physiology, pathophysiology, and pharmacology. Curr Opin Nephrol Hypertens 1992;1:21–33.

[219] Wang W. Renal potassium channels: recent developments. Curr Opin Nephrol Hypertens 2004;13:549–55.

[220] Tsuchiya K, Wang W, Giebisch G, Welling PA. ATP is a coupling modulator of parallel Na,K-ATPase-K-channel activity in the renal proximal tubule. Proc Natl Acad Sci USA 1992;89:6418–22.

[221] Wang W, Giebisch G. Dual effect of adenosine triphosphate on the apical small conductance K^+ channel of the rat cortical collecting duct. J Gen Physiol 1991;98:35–61.

[222] Bleich M, Schlatter E, Greger R. The luminal K^+ channel of the thick ascending limb of Henle's loop. Pflugers Arch 1990;415:449–60.

[223] Tsuboi T, Lippiat JD, Ashcroft FM, Rutter GA. ATP-dependent interaction of the cytosolic domains of the inwardly rectifying K^+ channel KIR6.2 revealed by fluorescence resonance energy transfer. Proc Natl Acad Sci USA 2004;101:76–81.

[224] Hurwitz CG, Hu VY, Segal AS. A mechanogated nonselective cation channel in proximal tubule that is ATP sensitive. Am J Physiol Renal Physiol 2002;283:F93–104.

[225] Leipziger J. Control of epithelial transport via luminal P2 receptors. Am J Physiol Renal Physiol 2003;284:F419–432.

[226] Ralevic V, Burnstock G. Receptors for purines and pyrimidines. Pharmacol Rev 1998;50:413–92.

[227] Unwin RJ, Bailey MA, Burnstock G. Purinergic signaling along the renal tubule: the current state of play. News Physiol Sci 2003;18:237–41.

[228] Bailey MA. Inhibition of bicarbonate reabsorption in the rat proximal tubule by activation of luminal P2y1 receptors. Am J Physiol Renal Physiol 2004;287:F789–796.

[229] Cha SH, Jung KY, Endou H. Effect of P2y-purinoceptor stimulation on renal gluconeogenesis in rats. Biochem Biophys Res Commun 1995;211:454–61.

[230] Jackson EK, Raghvendra DK. The extracellular cyclic AMP-adenosine pathway in renal physiology. Annu Rev Physiol 2004;66:571–99.

[231] Wengert M, Berto Jr. C, Kaufman J, Leão-Ferreira LR, Paes-de-Carvalho R, Lopes AG, et al. Stimulation of the proximal tubule Na^+-ATPase activity by adenosine A(2a) receptor. Int J Biochem Cell Biol 2005;37:155–65.

[232] Kone BC. Nitric oxide in renal health and disease. Am J Kidney Dis 1997;30:311–33.

[233] Ortiz PA, Garvin JL. Role of nitric oxide in the regulation of nephron transport. Am J Physiol Renal Physiol 2002;282: F777–784.

[234] Terada Y, Tomita K, Nonoguchi H, Marumo F. Polymerase chain reaction localization of constitutive nitric oxide synthase and soluble guanylate cyclase messenger RNAs in microdissected rat nephron segments. J Clin Invest 1992;90:659–65.

[235] Granger DL, Lehninger AL. Sites of inhibition of mitochondrial electron transport in macrophage-injured neoplastic cells. J Cell Biol 1982;95:527–35.

[236] Stuehr DJ, Nathan CF. Nitric oxide. A macrophage product responsible for cytostasis and respiratory inhibition in tumor target cells. J Exp Med 1989;169:1543–55.

[237] Shen W, Hintze TH, Wolin MS. Nitric oxide. An important signaling mechanism between vascular endothelium and parenchymal cells in the regulation of oxygen consumption. Circulation 1995;92:3505–12.

[238] Shen W, Xu X, Ochoa M, Zhao G, Wolin MS, Hintze TH. Role of nitric oxide in the regulation of oxygen consumption in conscious dogs. Circ Res 1994;75:1086–95.

[239] Brown GC. Nitric oxide regulates mitochondrial respiration and cell functions by inhibiting cytochrome oxidase. FEBS Lett 1995;369:136–9.

[240] Brown GC, Cooper CE. Nanmolar concentrations of nitric oxide reversibly inhibit synaptosomal respiration by competing with oxygen at cytochrome oxidase. FEBS Lett 1994;356:295–8.

[241] Adler S, Huang H, Loke KE, Xu X, Tada H, Laumas A, et al. Endothelial nitric oxide synthase plays an essential role in regulation of renal oxygen consumption by NO. Am J Physio l Renal Physiol 2001;280:F838–843.

[242] Laycock SK, Vogel T, Forfia PR, Tuzman J, Xu X, Ochoa M, et al. Role of nitric oxide in the control of renal oxygen consumption and the regulation of chemical work in the kidney. Circ Res 1998;82:1263–71.

[243] Buemi M, Allegra A, Rotig A, Gubler MC, Aloisi C, Corica F, et al. Renal failure from mitochondrial cytopathies. Nephron 1997;76:249–53.

[244] Kuwertz-Broking E, Koch HG, Marquardt T, Rossi R, Helmchen U, Müller-Höcker J, et al. Renal Fanconi syndrome: first sign of partial respiratory chain complex IV deficiency. Pediatr Nephrol 2000;14:495–8.
[245] Mochizuki H, Joh K, Kawame H, Imadachi A, Nozaki H, Ohashi T, et al. Mitochondrial encephalomyopathies preceded by De-Toni-Debre-Fanconi syndrome or focal segmental glomerulosclerosis. Clin Nephrol 1996;46:347–52.
[246] Niaudet P. Mitochondrial disorders and the kidney. Arch Dis Child 1998;78:387–90.
[247] Niaudet P, Rotig A. Renal involvement in mitochondrial cytopathies. Pediatr Nephrol 1996;10:368–73.
[248] Rotig A. Renal disease and mitochondrial genetics. J Nephrol 2003;16:286–92.
[249] Wang LC, Lee WT, Tsai WY, Tsau YK, Shen YZ. Mitochondrial cytopathy combined with Fanconi's syndrome. Pediatr Neurol 2000;22:403–6.
[250] Goto Y, Itami N, Kajii N, Tochimaru H, Endo M, Horai S. Renal tubular involvement mimicking bartter syndrome in a patient with Kearns–Sayre syndrome. J Pediatr 1990;116:904–10.
[251] Hsieh F, Gohh R, Dworkin L. Acute renal failure and the Melas syndrome, a mitochondrial encephalomyopathy. J Am Soc Nephrol 1996;7:647–52.
[252] Yanagihara C, Oyama A, Tanaka M, Nakaji K, Nishimura Y. An autopsy case of mitochondrial encephalomyopathy with lactic acidosis and stroke-like episodes syndrome with chronic renal failure. Intern Med 2001;40:662–5.
[253] Rotig A, Goutieres F, Niaudet P, Rustin P, Chretien D, Guest G, et al. Deletion of mitochondrial DNA in patient with chronic tubulointerstitial nephritis. J Pediatr 1995;126:597–601.
[254] Szabolcs MJ, Seigle R, Shanske S, Bonilla E, DiMauro S, D'Agati V. Mitochondrial DNA deletion: a cause of chronic tubulointerstitial nephropathy. Kidney Int 1994;45:1388–96.
[255] Gilbert RD, Emms M. Pearson's syndrome presenting with Fanconi syndrome. Ultrastruct Pathol 1996;20:473–5.
[256] Zsurka G, Ormos J, Ivanyi B, Turi S, Endreffy E, Magyari M, et al. Mitochondrial mutation as a probable causative factor in familial progressive tubulointerstitial nephritis. Hum Genet 1997;99:484–7.
[257] Cheong HI, Chae JH, Kim JS, Park HW, Ha IS, Hwang YS, et al. Hereditary glomerulopathy associated with a mitochondrial tRNA(Leu) gene mutation. Pediatr Nephrol 1999;13:477–80.
[258] Doleris LM, Hill GS, Chedin P, Nochy D, Bellanne-Chantelot C, Hanslik T, et al. Focal segmental glomerulosclerosis associated with mitochondrial cytopathy. zz 2000;58:1851–8.
[259] Jansen JJ, Maassen JA, van der Woude FJ, Lemmink HA, van den Ouweland JM, t' Hart LM, et al. Mutation in mitochondrial tRNA(Leu(UUR)) gene associated with progressive kidney disease. J Am Soc Nephrol 1997;8:1118–24.
[260] Kurogouchi F, Oguchi T, Mawatari E, Yamaura S, Hora K, Takei M, et al. A case of mitochondrial cytopathy with a typical point mutation for Melas, presenting with severe focal-segmental glomerulosclerosis as main clinical manifestation. Am J Nephrol 1998;18:551–6.
[261] Scaglia F, Vogel H, Hawkins EP, Vladutiu GD, Liu LL, Wong LJ. Novel homoplasmic mutation in the mitochondrial tRNA Tyr gene associated with atypical mitochondrial cytopathy presenting with focal segmental glomerulosclerosis. Am J Med Genet A 2003;123:172–8.
[262] Dickman KG, Jacobs WR, Mandel LJ. Renal metabolism and acute renal failure. Pediatr Nephrol 1987;1:359–66.
[263] Barros LF, Hermosilla T, Castro J. Necrotic volume increase and the early physiology of necrosis. Comp Biochem Physiol A Mol Integr Physiol 2001;130:401–9.
[264] Padanilam BJ. Cell death induced by acute renal injury: a perspective on the contributions of apoptosis and necrosis. Am J Physiol Renal Physiol 2003;284:F608–627.
[265] Lieberthal W, Nigam SK. Acute renal failure. I. Relative importance of proximal vs. distal tubular injury. Am J Physiol 1998;275:F623–631.
[266] Molitoris BA. Na(+)-K(+)-ATPase that redistributes to apical membrane during ATP depletion remains functional. Am J Physiol 1993;265:F693–697.
[267] Edelstein CL, Ling H, Schrier RW. The nature of renal cell injury. Kidney Int 1997;51:1341–51.
[268] Thadhani R, Pascual M, Bonventre JV. Acute renal failure. N Engl J Med 1996;334:1448–60.
[269] De Broe ME. Apoptosis in acute renal failure. Nephrol Dial Transplant 2001;16(Suppl 6):23–6.
[270] Lieberthal W, Levine JS. Mechanisms of apoptosis and its potential role in renal tubular epithelial cell injury. Am J Physiol 1996;271:F477–488.
[271] Lieberthal W, Menza SA, Levine JS. Graded ATP depletion can cause necrosis or apoptosis of cultured mouse proximal tubular cells. Am J Physiol 1998;274:F315–327.
[272] Lieberthal W, Koh JS, Levine JS. Necrosis and apoptosis in acute renal failure. Semin Nephrol 1998;18:505–18.
[273] Hems DA, Brosnan JT. Effects of ischaemia on content of metabolites in rat liver and kidney *in vivo*. Biochem J 1970;120:105–11.
[274] Siegel NJ, Avison MJ, Reilly HF, Alger JR, Schulman RG. Enhanced recovery of renal Atp with postischemic infusion of ATP-MgCl2 determined by 31P-NMR. Am J Physiol 1983;245: F530–534.
[275] Dickman KG, Mandel LJ. Differential effects of respiratory inhibitors on glycolysis in proximal tubules. Am J Physiol 1990;258:F1608–1615.
[276] Weinberg JM, Venkatachalam MA, Roeser NF, Nissim I. Mitochondrial dysfunction during hypoxia/reoxygenation and its correction by anaerobic metabolism of citric acid cycle intermediates. Proc Natl Acad Sci USA 2000;97:2826–31.
[277] Weinberg JM, Venkatachalam MA, Roeser NF, Saikumar P, Dong Z, Senter RA, et al. Anaerobic and aerobic pathways for salvage of proximal tubules from hypoxia-induced mitochondrial injury. Am J Physiol Renal Physiol 2000;279: F927–943.
[278] Feldkamp T, Kribben A, Roeser NF, Senter RA, Kemner S, Venkatachalam MA, et al. Preservation of complex i function during hypoxia-reoxygenation-induced mitochondrial injury in proximal tubules. Am J Physiol Renal Physiol 2004;286: F749–759.
[279] Bonventre JV. Mechanisms of ischemic acute renal failure. Kidney Int 1993;43:1160–78.
[280] Bonventre JV, Weinberg JM. Recent advances in the pathophysiology of ischemic acute renal failure. J Am Soc Nephrol 2003;14:2199–210.
[281] Brezis M, Rosen S, Silva P, Epstein FH. Transport activity modifies thick ascending limb damage in the isolated perfused kidney. Kidney Int 1984;25:65–72.
[282] Liu X, Kim CN, Yang J, Jemmerson R, Wang X. Induction of apoptotic program in cell-free extracts: requirement for dATP and cytochrome c. Cell 1996;86:147–57.
[283] Zager RA, Johnson AC, Hanson SY. Proximal tubular cytochrome C efflux: determinant, and potential marker, of mitochondrial injury. Kidney Int 2004;65:2123–34.
[284] Kowaltowski AJ, Castilho RF, Vercesi AE. Mitochondrial permeability transition and oxidative stress. FEBS Lett 2001;495:12–5.

[285] Tatton WG, Olanow CW. Apoptosis in neurodegenerative diseases: the role of mitochondria. Biochim Biophys Acta 1999;1410:195–213.
[286] McCoy CE, Selvaggio AM, Alexander EA, Schwartz JH. Adenosine triphosphate depletion induces a rise in cytosolic free calcium in canine renal epithelial cells. J Clin Invest 1988;82:1326–32.
[287] Snowdowne KW, Freudenrich CC, Borle AB. The effects of anoxia on cytosolic free calcium, calcium fluxes, and cellular ATP levels in cultured kidney cells. J Biol Chem 1985;260:11619–26.
[288] Weinberg JM, Davis JA, Trivedi B. Calcium compartmentation in isolated renal tubules in suspension. Biochem Med Metab Biol 1988;39:234–45.
[289] Tanaka T, Nangaku M, Miyata T, Inagi R, Ohse T, Ingelfinger JR, et al. Blockade of calcium influx through L-type calcium channels attenuates mitochondrial injury and apoptosis in hypoxic renal tubular cells. J Am Soc Nephrol 2004;15:2320–33.
[290] Eckardt K, Rosenberger C, Jürgensen J, Wiesener MS. Role of hypoxia in the pathogenesis of renal disease. Blood Purif 2003;21:253–7.
[291] Tanaka T, Miyata T, Inagi R, Fujita T, Nangaku M. Hypoxia in renal disease with proteinuria and/or glomerular hypertension. Am J Pathol 2004;165:1979–92.
[292] Maxwell P. HIF-1: an oxygen response system with special relevance to the kidney. J Am Soc Nephrol 2003;14:2712–22.
[293] Manotham K, Tanaka T, Ohse T, Kojima I, Miyata T, Inagi R, et al. A biologic role of HIF-1 in the renal medulla. Kidney Int 2005;67:1428–39.
[294] Bernaudin M, Tang Y, Reilly M, Petit E, Sharp FR. Brain genomic response following hypoxia and re-oxygenation in the neonatal rat. Identification of genes that might contribute to hypoxia-induced ischemic tolerance. J Biol Chem 2002;277:39728–38.
[295] Bernaudin M, Marti HH, Roussel S, Divoux D, Nouvelot A, MacKenzie ET, et al. A potential role for erythropoietin in focal permanent cerebral ischemia in mice. J Cereb Blood Flow Metab 1999;19:643–51.
[296] Ebert BL, Firth JD, Ratcliffe PJ. Hypoxia and mitochondrial inhibitors regulate expression of glucose transporter-1 via distinct cis-acting sequences. J Biol Chem 1995;270:29083–9.
[297] Rodriguez H, Drouin R, Holmquist GP, Akman SA. A hot spot for hydrogen peroxide-induced damage in the human hypoxia-inducible factor 1 binding site of the PGK 1 gene. Arch Biochem Biophys 1997;338:207–12.
[298] Tune BM, Hsu CY. Toxicity of cephalosporins to fatty acid metabolism in rabbit renal cortical mitochondria. Biochem Pharmacol 1995;49:727–34.
[299] Simon N, Morin C, Urien S, Tillement JP, Bruquerolle B. Tacrolimus and sirolimus decrease oxidative phosphorylation of isolated rat kidney mitochondria. Br J Pharmacol 2003;138:369–76.
[300] Tang W, Shaikh ZA. Renal cortical mitochondrial dysfunction upon cadmium metallothionein administration to Sprague-Dawley rats. J Toxicol Environ Health A 2001;63:221–35.
[301] Masereeuw R, van Pelt AP, van Os SH, Willems PH, Smits P, Russel FG. Probenecid interferes with renal oxidative metabolism: a potential pitfall in its use as an inhibitor of drug transport. Br J Pharmacol 2000;131:57–62.
[302] Simon N, Zini R, Morin C, Bree F, Tillement JP. Prednisolone and azathioprine worsen the cyclosporine A-induced oxidative phosphorylation decrease of kidney mitochondria. Life Sci 1997;61:659–66.
[303] Justo P, Lorz C, Sanz A, Egido J, Ortiz A. Intracellular mechanisms of cyclosporin A-induced tubular cell apoptosis. J Am Soc Nephrol 2003;14:3072–80.
[304] Jung KY, Endou H. Nephrotoxicity assessment by measuring cellular ATP Content. II. Intranephron site of ochratoxin a nephrotoxicity. Toxicol Appl Pharmacol 1989;100: 383–90.
[305] de Cavanagh EM, Piotrkowski B, Basso N, Stella I, Inserra F, Ferder L, et al. Enalapril and losartan attenuate mitochondrial dysfunction in aged rats. Faseb J 2003;17:1096–8.
[306] Li LP, Storey P, Pierchala L, Li W, Polzin J, Prasad P. Evaluation of the reproducibility of intrarenal R2* and Deltar2* measurements following administration of furosemide and during waterload. J Magn Reson Imaging 2004;19:610–6.
[307] Prasad PV, Priatna A. Functional imaging of the kidneys with Fast MRI techniques. Eur J Radiol 1999;29:133–48.
[308] Prasad PV, Edelman RR, Epstein FH. Noninvasive evaluation of intrarenal oxygenation with BOLD MRI. Circulation 1996;94:3271–5.
[309] Epstein FH, Prasad P. Effects of furosemide on medullary oxygenation in younger and older subjects. Kidney Int 2000;57:2080–3.
[310] Juillard L, Lerman LO, Kruger DG, Haas JA, Rucker BC, Polzin JA, et al. Blood oxygen level-dependent measurement of acute intra-renal ischemia. Kidney Int 2004;65:944–50.
[311] Ries M, Basseau F, Tyndal B, Jones R, Deminière C, Catargi B, et al. Renal diffusion and BOLD MRI in experimental diabetic nephropathy. Blood oxygen level-dependent. J Magn Reson Imaging 2003;17:104–13.
[312] Li L, Storey P, Kim D, Prasad P. Kidneys in hypertensive rats show reduced response to nitric oxide synthase inhibition as evaluated by BOLD MRI. J Magn Reson Imaging 2003;17:671–5.
[313] Zuo CS, Rofsky NM, Mahallati H, Yu J, Zhang M, Gilbert S, et al. Visualization and quantification of renal R2* changes during water diuresis. J Magn Reson Imaging 2003;17:676–82.

This page intentionally left blank

CHAPTER

7

Electrophysiological Analysis of Transepithelial Transport

Henry Sackin[1] *and Lawrence G. Palmer*[2]

[1]Department of Physiology & Biophysics, Rosalind Franklin University/The Chicago Medical School, North Chicago, IL, USA

[2]Department of Physiology & Biophysics, Weill Medical College of Cornell University, New York City, NY, USA

INTRODUCTION

In this chapter we discuss electrophysiological approaches to the study of renal function. The purpose is to provide an overview of the available techniques, with particular emphasis on what can be learned using the latest methods. However, the chapter is neither a technical manual nor a comprehensive review of the literature. For this, we refer the reader to other sections of the book which deal with specific nephron segments and transport mechanisms. Finally, we will not derive mathematical equations from first principles. Those equations that are essential to the text are provided in the main body of the chapter, while the more detailed formulae are described in the appendices.

We have arbitrarily divided the field of epithelial electrophysiology into three major sections. The first describes measurements of transepithelial electrical properties. The second section focuses on the use of intracellular microelectrodes to discriminate apical and basolateral membrane properties. The final section deals with the technique of patch clamping to investigate the functional characteristics of individual ion channels, and in some cases their molecular identification.

The interpretation of electrical signals from epithelia is complicated by the geometry of the tissues. At least three structures within an epithelium contribute to its electrical properties: the apical plasma membrane; the basolateral plasma membrane; and the paracellular pathway. The individual cell membrane properties will, in turn, be determined by various conductive pathways, including those of passive or dissipative pathways, through which ions flow driven by their own electrochemical potential differences, and active transport, which can use metabolic energy to drive ions against these potential differences. The paracellular pathway, in turn, consists of the tight junctions connecting the epithelial cells and the lateral interspaces between the cells.

The electrical properties of this complex structure can be most easily understood in terms of equivalent circuits. A comprehensive equivalent circuit of a generic reabsorbing epithelium is illustrated in Figure 7.1. Electrolyte diffusion across the apical membrane can be separated into its constituent ionic pathways, as shown by the expanded view of the apical membrane in Figure 7.1. Each ionic pathway is associated with an electromotive force (EMF) or battery representing the chemical potential for each ion. Electrogenic carriers such as the Na-glucose co-transporter can also be represented by an additional resistor (R_{glu}) and EMF (E_{glu}) in parallel with the diffusional elements. All of the batteries and resistors can be lumped respectively into a single apical EMF (E_{ap}) and a single resistance R_{ap} as shown in the center diagram. The basal membrane has a similar set of elements: R_b and E_b which represent a dissipative ion pathway in parallel with an active transport pathway, represented by a resistor (R_{ap}) and an EMF (E_p). Thus:

$$E_x = -\frac{RT}{z_i F} Ln \frac{[X_1]}{[X_2]} \tag{7.1}$$

where $[X_1]$ and $[X_2]$ are the concentrations of ion X on the two sides of the membrane, and z_i is the charge on the

Seldin and Giebisch's The Kidney, Fifth Edition.
DOI: http://dx.doi.org/10.1016/B978-0-12-381462-3.00007-0

© 2013 Elsevier Inc. All rights reserved.

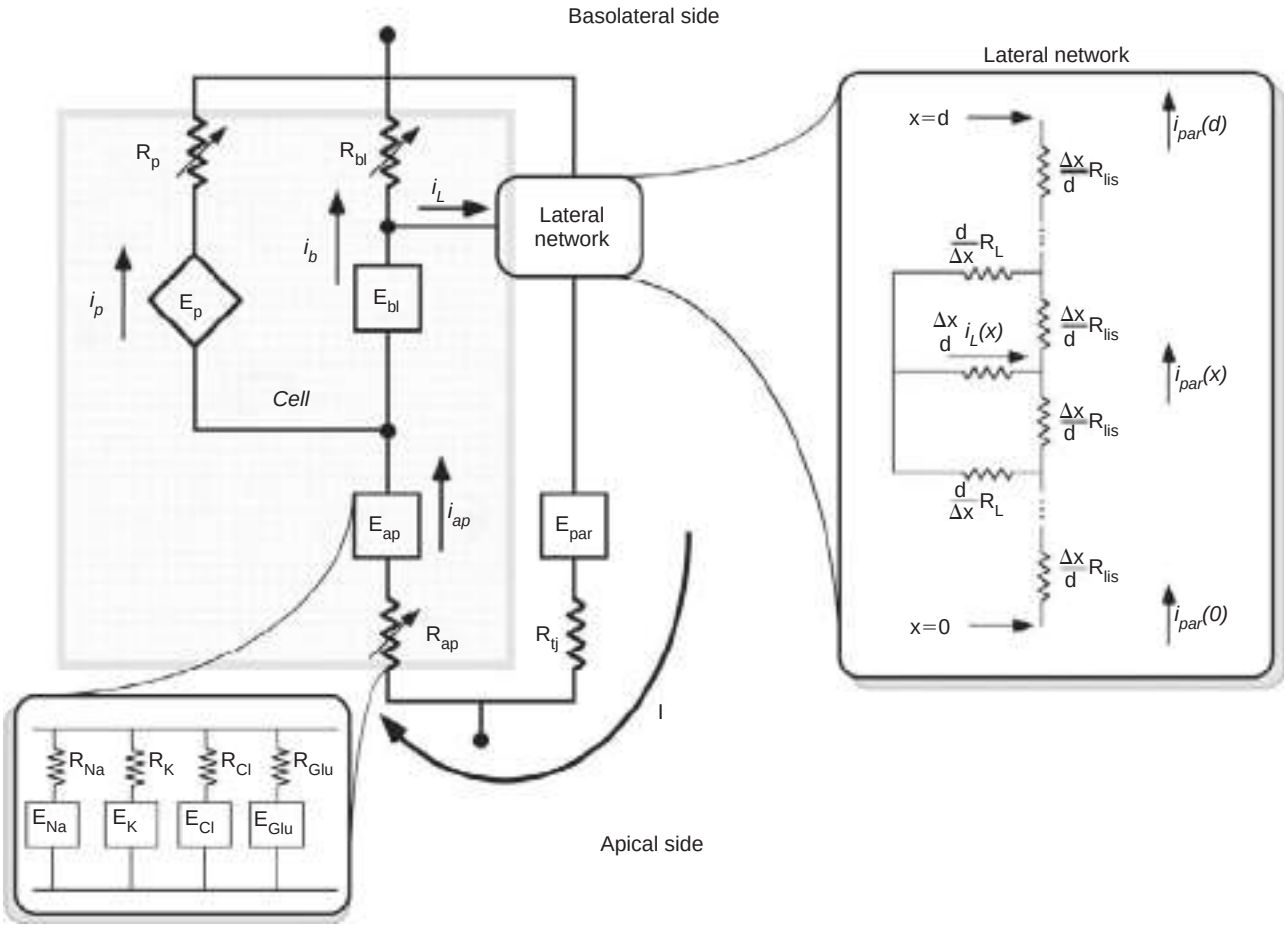

FIGURE 7.1 **Electrical equivalent circuit for a general epithelium.** Each membrane or barrier is associated with an electromotive force (**E**) that represents the weighted average of the ionic diffusion potentials at that barrier. Electrogenic carriers (such as the apical Na-glucose co-transporter) and electrogenic pumps (such as the basolateral Na,K-ATPase) can also be formally represented by a series resistor and an associated EMF. The lateral network takes into account the nonzero electrical resistance of the lateral intercellular spaces.

ion. The weighting factor for each ion is the transference number, t_x, which expresses the fraction of membrane conductance that is attributable to that particular ion:

$$t_x = \frac{g_x}{g_{tot}} \tag{7.2}$$

where g represents the conductance of the individual ion pathways and g_{tot} is the total ionic conductance of the membrane. In most cases g_{tot} will simply be the sum of the Na, K, and Cl conductances of the barrier. Hence, the total EMF can be generally expressed by the equation:

$$\begin{aligned} E &= t_{Na}E_{Na} + t_K E_K + t_{Cl}E_{Cl} \\ &= -\frac{RT}{F} \sum_{x=Na,K,Cl} \frac{t_x}{z_x} Ln \frac{[X_1]}{[X_2]} \end{aligned} \tag{7.3}$$

The overall goal of classical electrophysiology, described in the first two sections of this chapter, is to evaluate the different elements of this equivalent circuit, to quantify the various resistances and EMFs, and to describe the extent to which they change during regulation. To this end, it has often been desirable to use reductions of the main equivalent circuit of Figure 7.1, and to work under conditions in which these reduced circuits are applicable. Such simplifications are discussed in more detail in the sections entitled, "Transepithelial Measurements" and "Intracellular Measurements." Finally, the section entitled, "Measurements of Individual Ion Channels" describes application of the patch clamp technique to epithelia, and permits a description of ion transport in more molecular terms.

The rationale for representing the pump by a resistance and an EMF is discussed further in the section entitled "Intracellular Measurements." Briefly, the E_p represents the maximum amount of energy that the pump derives from splitting ATP or, alternatively, the maximum electrochemical potential difference against which the pump can operate. The pump pathway

must also include a non-zero internal resistance. The magnitude of this internal resistance is determined by the actual current–voltage relation for the membrane bound Na-K-ATPase. To maintain generality, all membrane resistances are shown as variable resistors to include the possibility of intrinsic or extrinsic regulation of ion channels.

Although the paracellular pathway is not a membrane barrier, it can also be modeled by resistive (R_{tj}) and electromotive elements (E_{par}). A lateral network (indicated to the right of the main circuit) is also included in the model. This network takes into consideration the finite resistance of fluid in the lateral spaces. This aspect of the circuit becomes important for calculation of individual membrane resistances from voltage deflection experiments (see Section entitled "Intracellular Measurements").

TRANSEPITHELIAL MEASUREMENTS

Measurements of transepithelial electrical properties are by far the simplest to perform, and the most difficult to interpret. They are easy to carry out because they are non-invasive; only extracellular electrodes are employed. They are difficult to interpret because the parameters which can be measured reflect, in most cases, a combination of many of the circuit elements shown in Figure 7.1. In this chapter we will describe how transepithelial techniques are used to measure three basic parameters that characterize an epithelium: transepithelial voltage; transepithelial resistance; and short-circuit current. We will then discuss a number of special extracellular approaches which have been employed to gain additional insights into epithelial properties.

Measurement of Transepithelial Voltage

Methods of measuring transepithelial voltage (V_{te}) are conceptually simple. In principle, the potential difference between two electrodes placed on either side of the epithelium is simply determined with an appropriate electrometer. With flat epithelia that can be mounted in Ussing chambers, the transepithelial electrodes are placed in the two bathing compartments.[1] In cylindrical epithelia such as the renal nephron, classical measurements of transepithelial potential have been performed *in vivo* using micropuncture techniques. In this technique, a pipette filled with electrolyte is introduced into the lumen of the tubule, and voltage is measured relative to another electrode placed in a capillary. Here, the presumption is that the voltage reflects the properties of the impaled tubule, and is not greatly influenced by those of neighboring segments. Under most conditions this should be a reasonable assumption. For a lumen of 10 μm diameter and an isoosmotic saline solution with a resistivity of around 60 Ω•cm, the axial resistance of the tubule will be about 8×10^7 Ω/cm. This is much larger than the value of the transepithelial resistance of around 100 Ω•cm^2 (Table 7.1), which for the same 10 μm lumen is equivalent to 3×10^4 Ω/cm. Thus, each part of the nephron will be effectively electrically isolated from other parts of the high resistance of the luminal pathway. If the nephron segment can be isolated and perfused *in vitro*, the perfusion and/or collection pipette can be used to monitor the intraluminal voltage with respect to the bath potential. This is illustrated in Figure 7.2.

Measurement of Transepithelial Resistance

For measurements of transepithelial resistance (R_{te}), current must be injected across the epithelium to perturb V_{te}. This is most easily accomplished when the epithelium can be mounted in Ussing chambers, where current flow and voltage changes are assumed to be uniform in the plane of the tissue. Resistance can then be computed from Ohms law as the ratio of the change in V_{te} to the amount of current passed:

$$R_{te} = \frac{\Delta V_{te}}{\Delta I} \tag{7.4}$$

Epithelia can be studied in open-circuited or voltage-clamped conditions. In open circuit the tissue is allowed to maintain its spontaneous transepithelial voltage. In this case the resistance is determined from the change in voltage produced by passing a known amount of current. Under voltage-clamp conditions a current is passed across the epithelium to maintain the transepithelial voltage at a predetermined level. In the case where this level is zero, so that the transepithelial voltage is abolished, it is called the "short-circuited" state. If the epithelium is voltage-clamped, resistance is determined from the change in current produced by a controlled voltage step. In open-circuited tubular epithelia, transepithelial current flow is not constant along the length of the tubule. In this case, cable analysis must be used to estimate the transepithelial resistance (see below).

Measurement of Transepithelial Resistance in Open Circuited Renal Tubules

The measurement of overall transepithelial resistance, R_{te}, in renal tubules under open circuit conditions is best carried out with a double-barreled perfusion pipette system similar to the one illustrated in Figure 7.2. In this technique, the tubule is cannulated at both the perfusion and collection ends. The

TABLE 7.1 Transepithelial Properties of Renal Epithelia

Tissue	V_{te} (mV)	R_{te} (Ωcm^2)	R_{par} (Ωcm^2)	P_{Na}/P_{Cl}	Reference
Amphibians					
Proximal tubule (*Ambystoma*)	−10	70	70	0.25	4
Diluting segment (*Amphiuma*, frog)	+10	290	306	4 to 5	135
Collecting duct (*Amphiuma*)	−24	160	200	0.84	136
Urinary bladder (Toad)	−94	8,900	50,000	–	22
Mammals					
Proximal tubule (rabbit)	−2 to +2	5	5		13
TALH[a] (rabbit)	+3 to +10	10 to 35	10 to 50	2 to 4	12
CCD[a] (rabbit)	0 to −60	110	160	0.8	137
OMCD[a] (rabbit)	−2 to −11	233			138
IMCD[a] (rabbit)	−2 to 0	73			139
Urinary bladder (rabbit)	−20 to −75	13,000 to 23,000	>78,000	–	140

[a]*TALH, thick ascending limb of Henle's loop; CCD, cortical collecting duct; OMCD, outer medullary collecting duct; IMCD, inner medullary collecting duct.*

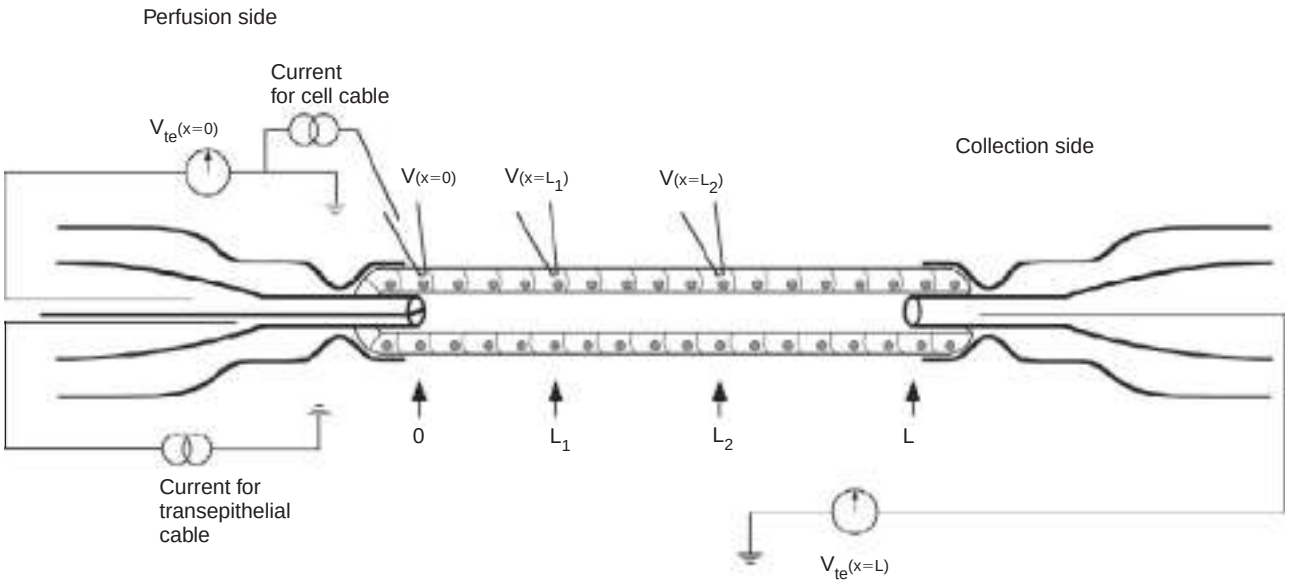

FIGURE 7.2 **Experimental apparatus for determining electrophysiological properties of renal epithelia.** The segment of isolated renal tubule is held at both ends by constriction pipettes. The tubule perfusion pipette is fabricated from "theta" glass and has separate pathways for both current injection and transepithelial measurement, $V_{te}(x = 0)$. The transepithelial potential, $V_{te}(x = L)$, can also be determined at the collection side of the tubule. For determination of cell membrane resistance, current is passed into the cell layer via the microelectrode at location $x = 0$ and the resultant voltage deflections are measured by intracellular microelectrodes at locations $x = 0$, L_1, and L_2.

double-barreled perfusion pipette, fabricated from *theta* glass[2–4] creates separate pathways for current flow and voltage recording. An alternative technique uses the same single-barreled pipette for both current injection and voltage measurement. This is not nearly as accurate as the double-barreled technique, because the voltage deflection arising from the internal resistance of the perfusion pipette must be nulled with a bridge circuit. The microelectrodes in Figure 7.2 are for evaluation of individual cell membrane resistances. This will be discussed in the section entitled, "Intracellular Measurements."

A thin fluid-exchange tubing (not shown) can be inserted into one barrel of the perfusion pipette of Figure 7.2 to permit rapid exchange of the perfusion solution while measuring the transepithelial potential $V_{te}(x=0)$. Current is passed from a chlorided silver wire glued into the other barrel of the pipette. The transepithelial length constant of the tubule λ_{te} is determined from the voltage deflections at the perfusion, $\Delta V_{te}(x=0)$, and collection, $\Delta V_{te}(x=L)$, sides of the tubule, resulting from a transepithelial current pulse, I_{te}, through the current side of the perfusion pipette. For a doubly cannulated, isolated tubule of length L, λ_{te} is given by Eq. (7.5) from Sackin and Boulpaep[5]:

$$\frac{L}{\lambda_{te}} = cosh^{-1}\left[\frac{\Delta V_{te}(x=0)}{\Delta V_{te}(x=L)}\right] \tag{7.5}$$

The transepithelial resistance R_{te} in Ωcm^2 is given by Eq. (7.6):

$$R_{te} = 2\sqrt{\pi \lambda_{te}^3 R_{in} R_i}\sqrt{tanh(L/\lambda_{te})} \tag{7.6}$$

In the above equation, R_{in} is the input resistance measured in ohms (Ω). It is operationally defined as the voltage deflection at the perfusion end $\Delta V_{te}(x=0)$ divided by the total injected current I_{te}. Typical injected currents for proximal tubules are 100 nA pulses of 1 to 5 seconds duration. Ideally, none of the current injected into the lumen from the perfusion pipette enters the compressed region of tubule within the holding pipette, which presumably acts like an electrical insulator when compared to the relatively low resistance of the tubule. However, artifacts may still arise from current leaks at either the perfusion or collection ends of the tubule. These can be detected by a "mismatch" between the calculated electrical radius (r_e) of the tubule and its measured optical radius (r_o).

$$r_e = \frac{2\,R_i \lambda_{te}^2}{R_{te}} \tag{7.7}$$

Use of a double-barreled perfusion pipette (Figure 7.2) eliminates much of the uncertainty in R_{in}. Double-barreled perfusion pipettes have the additional advantage that R_{te} can be measured during changes in the perfusion solution. This is practically impossible with a single-barreled perfusion pipette, because the bridge circuit is unstable during solution changes. Finally, the term R_i (Ω•cm) is the volume resistivity of the perfusion solution, as measured with a standard conductivity meter.

Measurement of Transepithelial Resistance in Voltage Clamped Renal Tubules

There have been a number of early attempts to elucidate the electrical properties of renal tubules using voltage clamp techniques similar to those originally developed for flat epithelia. The basis of these methods is to isolate a segment of tubule (usually with oil droplets) that is short enough to permit a uniform current distribution across the epithelium. To accomplish this, metallic axial electrodes are directly inserted into the lumen of the tubule.[6] These axial electrodes can also be used for AC impedance analysis.[7,50] However, one important problem with metal electrodes is the release of ions into a restricted space during continuous current flow.

An alternative technique employs segments of isolated, perfused tubules that have been shortened to such an extent that the current distribution within the lumen is virtually homogeneous.[8] In this case R_{te} is essentially determined from the input resistance according to Eq. (7.8):

$$R_{te} = 2\pi r_o L \cdot R_i \tag{7.8}$$

where r_o is the optical radius, and R_{te} has units of Ω•cm^2.

Typical Results

Measurements of V_{te} and R_{te} in some representative epithelia are shown in Table 7.1. The range of both these parameters is large, with values of V_{te} ranging from ± 2 mV in the proximal tubule to as much as -60 to -80 mV in the CCT. R_{te} values vary from less than 10 Ωcm^2 in proximal tubule to more than 5000 Ωcm^2 in urinary bladder. Despite the range of values observed, the transepithelial voltages in all cases reflect two factors: the conductance of the epithelium to the major ions and the active transport of ions. In general, a high value of V_{te} indicates that active transport is taking place across a high resistance epithelium, whereas low values of V_{te} can reflect either a low R_{te} or a low rate of active transport.

Traditionally, epithelia have been divided into the categories "tight" and "leaky," according to their transepithelial resistances. In leaky epithelia the low value of R_{te} is thought to largely reflect the low resistance of the tight junctions which constitute the major electrical resistance of the paracellular pathway between the epithelial cells.[9] In tight epithelia the tight junctional resistance, and therefore the transepithelial resistance, is much higher. However, the resistance above which an epithelium is considered "tight" is not precisely defined.[10] Even though the amphibian proximal tubule and the mammalian collecting duct have similar absolute values of paracellular resistance, the proximal tubule is considered a leaky epithelium, whereas the collecting duct is usually referred to as "tight." Thus, a better definition of a leaky epithelium is one in which the paracellular resistance is low relative to that of the cell membranes. For example, in Table 7.1 it can be

seen that in leaky proximal tubules R_{te} is virtually equal to R_{par}, which is small compared to the parallel transcellular resistance R_c. In tight epithelia R_{par} is significantly larger than R_{te}. This implies that R_{par} is of the same order of magnitude as R_c or even much larger in the case of the urinary bladder. Another feature of a tight epithelium is its ability to separate two fluid compartments with very different ion compositions. High resistance tight junctions slow the "backleak" of ions and other solutes down their concentration gradients. Thus, in a tight epithelium it is harder to dissipate the ion gradients established by active transport processes.

Interpretation of Measurements of V_{te} and R_{te}

As discussed above, transepithelial measurements of voltage and resistance are difficult to interpret because they lump together information from many different electrical pathways arranged in parallel. To analyze such data, it is often useful to use a simplified equivalent electrical circuit.

The terms R_c and E_c represent the resistance and electromotive forces across the transcellular pathway, whereas R_{ti} and E_{par} are respectively the resistance and electromotive forces across the paracellular pathway. If the potential differences V_{te}, E_c, and E_{par} are all defined with respect to the bath or serosal side, the overall measured transepithelial values R_{te} and V_{te} are related to this circuit by Eqs (7.9) and (7.10):

$$R_{te} = \frac{R_{tj}R_c}{R_{tj} + R_c} \tag{7.9}$$

$$V_{te} = \frac{E_cR_{tj} + E_{par}R_c}{R_{tj} + R_c} \tag{7.10}$$

The dissection of the measured parameters into the appropriate contributions from cellular and paracellular pathways can sometimes be accomplished by using maneuvers that affect only one of the pathways or cause one pathway to dominate the other. Some of these perturbations and special conditions will be discussed below.

Contribution of Active Transport to V_{te}

The major effect of the pump is to establish transmembrane ionic gradients, i.e., to keep cell Na low and cell K high. As was first pointed out by Koefoed-Johnsen and Ussing in their classic paper of 1958,[11] the permeability properties of the apical and basolateral membranes of the frog skin are quite different. Since the apical membrane is selectively permeable to Na, and the driving force for this ion is inward, the entry of Na will tend to make the cell voltage positive with respect to the mucosal solution. Conversely, the basolateral membrane is selectively permeable to K. This ion will tend to flow out of the cell, making the cell voltage negative with respect to that of the serosal fluid. The EMFs E_{ap} ($=RT/F\ \Delta\ln$[Na]) and E_{bl} ($=RT/F\ \Delta\ln$[K]) will be in the same direction with respect to the epithelium and the transepithelial EMF, and hence V_{te}, will reflect their sum (Figure 7.4).

Although the Na-K-ATPase is ultimately responsible for the transepithelial potential in many Na-reabsorptive epithelia, the magnitude of V_{te} does not correlate with the magnitude of active transport when different tissues are compared. In general, the effect of active ion transport will be shunted by the paracellular resistance. This shunting is least in the tight epithelia such as frog skin and toad urinary bladder, where V_{te} can be over 100 mV. In leaky epithelia such as the proximal tubule the shunting is considerable, and the values of V_{te} are much lower.

In leaky epithelia, E_{par} will be much smaller than E_c (Figure 7.3), since ion gradients across the tight junction are relatively small. In tight epithelia where ion gradients can be significant, $R_{tj} > R_c$ so that the term $E_{par}R_c$ will be small compared to E_cR_{tj}, and Eq. (7.10) becomes:

$$V_{te} = \frac{E_c}{1 + R_c/R_{tj}} \tag{7.11}$$

The implication of Eq. (7.11) is that if $R_{tj} >> R_c$, V_{te} will approach E_c, a quantity which is limited by the EMF of the Na-pump. In general, V_{te} will be reduced according to the ratio R_c/R_{tj}. The contribution of active transport to cell membrane potential is discussed in the section entitled, "Estimation of renal Na,K pump current and electrogenic potential."

The mammalian TALH, and its amphibian counterpart the diluting segment, have lumen-positive V_{te} despite the fact that they are also Na-reabsorbing epithelia (Table 7.1, Figure 7.4). This turns out to be the exception that proves the rule. As discussed in detail by Greger,[12] Na does not enter the TALH cell through a conductive mechanism, as in the frog skin and other epithelia, but through an

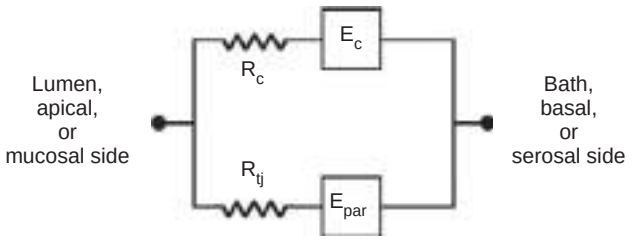

FIGURE 7.3 **Simplified equivalent electrical circuit for an epithelium.**

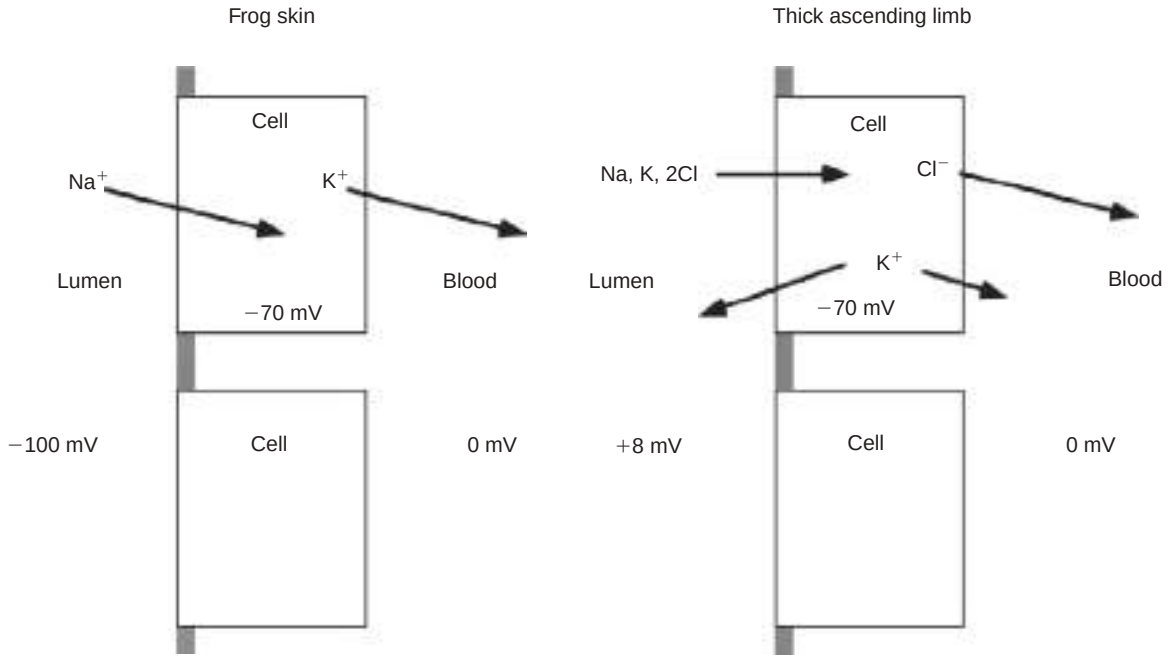

FIGURE 7.4 **Contribution of transcellular potentials to the transepithelial potential.** On the left is a tight epithelium such as the frog skin or cortical collecting duct (CCD). Influx of Na across the apical membrane and efflux of K across the basolateral membrane create a lumen-negative voltage which is not significantly shunted because of the high tight-junctional resistance. Consequently, most of the transepithelial potential arises from diffusion potentials for Na and K that are established across the cell membranes by active transport, and by the different ion-selectivities of the apical and basolateral membranes. The figure on the right is a model of a TALH cell. Here Na entry across the luminal membrane is electrically silent. The dominant electrodiffusive ion movements are K efflux across both apical and basolateral membranes, and Cl efflux across the basolateral membrane. The basolateral Cl conductance makes the cell less negative relative to interstitial fluid versus luminal fluid.

electrically neutral co-transport system along with K and Cl. Thus, Na entry does not contribute to a lumen-negative voltage, and in fact the membrane is more permeable to K than to Na. Furthermore, the basolateral membrane has a rather high permeability to Cl. This makes the lumped EMF E_{ap} less negative than E_{bl}, and the potential difference between the cell and the blood side is less negative than the potential difference between the cell and the lumen. Hence, the mechanism for the lumen-positive potential in the TALH is accounted for by the different permeability properties of the two membranes, just as in the frog skin.

Contribution of Diffusion Potentials to V_{te}

Paracellular diffusion potentials can contribute significantly to the overall transepithelial potential, especially when V_{te} is small. For example, in the mammalian proximal tubule the early portion of the segment has a lumen-negative V_{te} *in vivo*, which is thought to reflect active Na reabsorption. Farther down the nephron, however, the lumen becomes positive with respect to the blood. Preferential luminal reabsorption of HCO_3^- relative to Cl^- establishes opposing gradients for Cl^- and HCO_3^- across the tight junction (Figure 7.5). This results in a lumen-positive potential since Cl^- diffuses more rapidly across the junctions than HCO_3^-.[13]

Diffusion potentials may also contribute to the normal lumen-positive V_{te} in the mammalian TALH (Table 7.1). In this segment NaCl is reabsorbed but water is not, leading to a dilution of the luminal fluid. Since the tight junctions of the mammalian TALH are cation-selective, Na diffuses back more rapidly than the Cl, contributing to a lumen-positive diffusion potential[12] (Figure 7.5).

Contribution of Circulating Current to V_{te}

The different equivalent EMFs at the apical and basolateral sides of the cell produce a circulating current (I) which traverses both cell membranes in series, and returns via the paracellular shunt (Figure 7.1). The magnitude of this current depends on the relative resistances of paracellular versus cell pathways, as well as the active transport rate for the particular epithelium.[14,15] For example, in renal proximal tubules, the low shunt resistance (compared to transcellular resistance) characterizes this nephron segment as a leaky epithelia with large circulating current.[13,16] On the other hand, tight epithelia like the urinary bladder or the frog skin have shunt resistances comparable to or larger

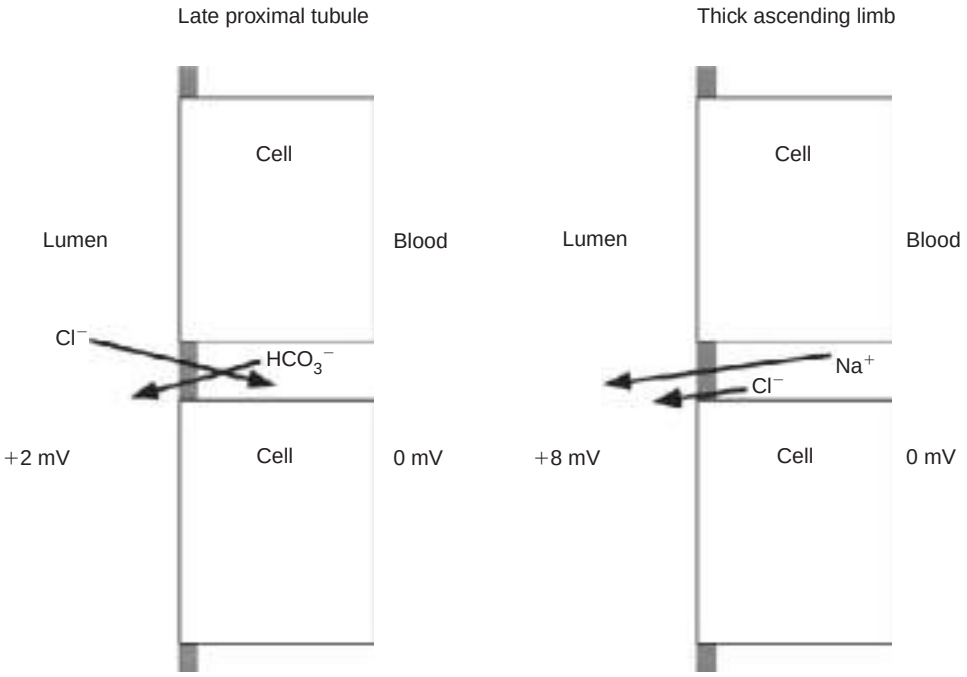

FIGURE 7.5 **Contribution of paracellular potentials to the transepithelial potential.** The figure on the left corresponds to the late proximal tubule. Preferential reabsorption of HCO_3^- in the early proximal tubule produces opposite gradients for Cl^- and HCO_3^- across the tight junction of late proximal tubule. Since the junctions are more permeable to Cl^- than to HCO_3^-, a lumen-positive diffusion potential develops. The paracellular contribution in the TALH is illustrated on the right. Here, reabsorption of NaCl across the water-impermeable epithelium results in an accumulation of NaCl within the interspaces between the cells, producing a similar gradient for both Na^+ and Cl^- across the tight junction. Since the junctions in this epithelium are more permeable to Na^+ than to Cl^-, a lumen-positive diffusion potential develops.

than the transcellular resistance, so that the circulating current is small in comparison with proximal tubule.[17]

The effect of circulating current on renal transepithelial potentials can be understood qualitatively by considering the electrical profiles depicted in Figure 7.6. In this figure, the serosal or blood side of the epithelium is considered at ground and the voltage at any point is displayed as a function of distance from mucosa to serosa. For the sake of simplicity, we have assumed that the apical membrane is primarily selective to sodium, the basolateral membrane is primarily selective to potassium, and the interior of the cell is isopotential. Therefore, in the absence of circulating current, there is a "staircase" voltage profile through the epithelium determined by the respective diffusion potentials across the mucosal (or apical) membrane and across the serosal (or basolateral) membrane (Figure 7.6a). Under these conditions the measured V_{te} (mucosa minus serosa) would actually be more negative than the basolateral cell membrane potential (E_K).

In most epithelia the diffusion potential steps of Figure 7.6a would be modified by the effect of circulating current (I) across the resistance of the mucosal and serosal barriers. Specifically, the mucosal to cell step will be raised by an amount: $I \bullet R_{ap}$ due to the circulating current crossing the mucosal membrane resistance (Figure 7.6b). The same current crossing the basolateral side of the cell will decrease the size of the cell-to-serosal step by $I \bullet R^*_{bl}$, where R^*_{bl} is the effective basolateral resistance. The final values of V_{te} and V_{bl} can be calculated by considering the complete equivalent circuit (Appendix 7.1).

In most epithelia, the resistance of the apical membrane is larger than the resistance of the basolateral membrane, and the effect of the circulating current is to transform the staircase potential (Figure 7.6a) into a "well-type" potential (Figure 7.6c), where the intracellular region is the most negative space and V_{te} is directly dependent on the magnitude of the current and the tightness of the epithelial cell layer. In some tight epithelia (*Necturus* urinary bladder) with high paracellular resistance and low circulating current, the "staircase" potential profile is still maintained despite "IR drops" at both membranes.[18]

Short-Circuit Current

It is also possible to measure transepithelial currents while controlling the transepithelial voltage. A special case of this voltage-clamp approach is the short-circuit current technique[1] in which V_{te} is maintained at zero.

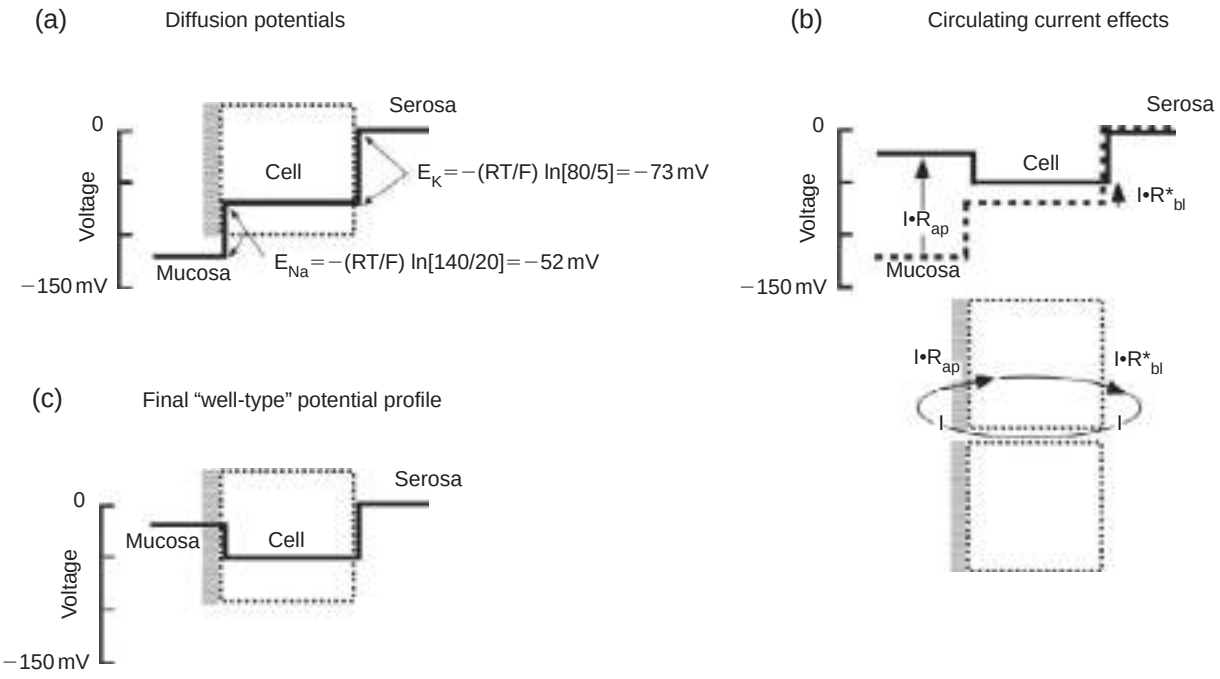

FIGURE 7.6 **Electrical potential profiles across a simple epithelium.** (a) In the absence of circulating currents, the electrical potential from serosal to mucosal sides would be largely determined by the Na diffusion potential at the apical membrane, and the K diffusion potential at the serosal membrane. (b) Circulating currents that arise from a net (open-circuit) EMF produce additional voltage drops across both the apical membrane ($=I \bullet R_{ap}$) and across the basolateral membrane ($=I \bullet R_{bl}$). (c) This changes the "staircase" potential profile to a "well-type" potential, where the cell is more negative than either the mucosal or serosal sides.

If the solutions on both sides of the epithelium are identical, there is no net movement of ions through the paracellular spaces, since both electrical and chemical driving forces are reduced to zero. The current across the tissue, which must also pass through the external circuit and can thus be readily measured, results only from active transport processes (defined as those which take place against an electrochemical activity gradient). Thus this current (called the short-circuit current), will equal the sum of all active ion transport processes.

The particular ion being actively transported can be identified rigorously by measuring net fluxes at the same time as the short circuit current. For some cases, such as the frog skin and toad bladder,[19,20] the short-circuit current can be accounted for by the active transport of only one ion species, namely Na (Table 7.2). In general, the short-circuit current will represent the sum of the net transport of Na, K, H, Cl, and HCO_3. Another way to identify actively transported ions is to eliminate them from the bathing media and measure the resulting effects on short-circuit current. This approach is often experimentally much simpler, but it is less rigorous since the apical and basolateral solutions will not be identical. Furthermore, changing the external environment of the tissue can lead to secondary changes in cell composition and volume. In any case, once the transported species have been identified, the technique becomes a very convenient way to analyze the regulation of the active transport systems.

TABLE 7.2 Equivalence of Net Na + Fluxes and Short-Circuit Current in Model Epithelia, Transepithelial fluxes ($nEq/cm^2/min$)

Type of Epithelium	Mucosal to Serosal	Serosal to Mucosal	Net	Short-circuit Current
Frog skin	24.6	1.5	23.1	23.6
Toad urinary bladder	35.7	9.5	26.2	26.8

Data are from [1] for frog skin and from [19] for toad bladder.

An important limitation of the short-circuit current technique is that it often requires unphysiological conditions. For example, short-circuiting high resistance epithelia like frog skin will reduce the normally large V_{te} to values near zero. This will necessarily affect the transmembrane voltage of one or both cell membranes, which may in turn affect the ionic conductances of those membranes.

The short-circuit technique also involves bathing the apical side of the tissue with a solution that has an electrolyte composition close to that of the blood. This is a highly unphysiological condition for many tight epithelia like the frog skin, which is normally in contact with pond water, and the toad bladder, which is

normally in contact with dilute urine. Another important problem with short-circuit experiments is that short-circuited tissues do not have to maintain the electroneutrality of the transported species. For example, in Na-transporting epithelia, such as the frog skin, Na ions can be reabsorbed only if another cation (e.g., K, H) is secreted or if an anion (Cl) is also reabsorbed. Under physiological conditions these other ionic pathways can be rate-limiting for Na reabsorption.

Finally, the uniform current distribution required by the short-circuit technique has largely restricted its use to flat epithelia which can be mounted in Ussing chambers. However, in some cases it has been possible to voltage-clamp large-diameter amphibian tubules.[21] Attempts have also been made to circumvent these technical problems by defining an "equivalent short-circuit current" for renal epithelia. In this method, the current at $V_{te} = 0$ is estimated by dividing the spontaneous value of V_{te} by the transepithelial resistance R_{te}. This approach assumes that R_{te} is constant; i.e., that the current voltage relation of the epithelium is linear. Even when this condition is satisfied, it is not always possible to attribute the equivalent short-circuit current to specific ion species, since net fluxes of the ions must be measured under true short-circuited conditions.

Technical Problems

For epithelia that can be studied as flat sheets *in vitro*, the major technical problem with transepithelial measurements is avoiding edge damage to the tissues, particularly when these tissues are mounted in Ussing chambers.[22,23] On the other hand, for renal micropuncture experiments performed *in situ*, the major technical problem is localization of the microelectrode tip within the tubular lumen.[13]

The most important general problem in the measurement of transepithelial resistance is the choice of the magnitude and duration of the applied perturbations. Currents (or voltage changes) which are too large can result in changes in the electrical properties of the membranes due to voltage-dependent ion conductances. Perturbations which are either too large or too long can lead to redistribution of ions across the cell membranes, which can also alter electrical properties. For example, in toad urinary bladder modest changes in V_{te} in the order of 10 mV under voltage-clamp conditions can result in time-dependent changes in the tissue resistance.[24] On the other hand, if perturbations are too small they are difficult to measure accurately, and if they are applied for too short a time the capacitative, as well as the resistive, properties of the epithelium will affect the response. There are no generally accepted rules for determining the size and duration of the perturbations.

Estimation of Membrane Parameters from Transepithelial Measurements

Measurement of transepithelial electrical properties does not, in general, give any direct, quantitative information about the circuit elements of greatest interest, namely the conductances of individual membranes to specific ions. As emphasized throughout this section, R_{te} is a lumped parameter determined by R_{ap}, R_b, R_{tj}, and in some cases R_{lis} (see Figure 7.1). V_{te} is determined by all the R_s and EMFs in the circuit. Clearly, measuring two parameters is insufficient to determine seven or eight unknowns.

However, in some cases it has been possible to either use conditions which simplify the equivalent circuit or to use experimental perturbations that selectively change only one electrical parameter. These methods have provided a good deal of information about epithelial properties from purely transepithelial measurements. Some examples are given below.

Paracellular Resistance and Selectivity

When the paracellular (tight junction) resistance is low compared to the transcellular resistance, the transepithelial resistance is dominated by the resistance of the paracellular pathway. This happens in a leaky epithelium like the proximal tubule. This condition can also be produced in some tight epithelia by blocking the major conductive pathways at the apical membrane. The most frequently used blockers are amiloride, for the Na conductance, and Ba, for the K conductance. In both of these cases the paracellular resistance can then be estimated from transepithelial measurements (Table 7.1), although intracellular recordings are usually required to prove that the transcellular resistance is high.

The ion selectivity of the paracellular pathway can also be evaluated under these circumstances. This involves measurement of the transference numbers for various ions across the tight junction (see Eq. (7.12)). The most important ions in this case are Na and Cl, and their transference numbers can be estimated by reducing the concentration of NaCl on one side of the junction by diluting one of the bathing solutions. If the transcellular resistance is sufficiently high (i.e., $R_{ap} >> R_{tj}$, see Eq. (A2.3) in Appendix 2) and is unaffected by the dilution, the measured change in V_{te} will approximately reflect the change in E_{par} where:

$$\Delta E_{par} = -\frac{RT}{F}(t_{Na} - t_{Cl}) Ln \frac{[NaCl]_1}{[NaCl]_2} \qquad (7.12)$$

If sodium and chloride are the only conducting ions in the external solutions, the absolute transference numbers can be calculated from Eq. (7.12) and the requirement that $t_{Na} + t_{Cl} = 1$. Some measurements of

paracellular selectivity in renal epithelia are listed in Table 7.1. This parameter is of considerable physiological interest. The results range from a significant selectivity for anions (Cl) over cations (Na) in the amphibian proximal tubule, to a cation selectivity in the thick ascending limb of Henle's loop or its counterpart, the diluting segment, in the amphibian kidney. If ions moved through the tight junctions as if they were in free solution, a permeability ratio P_{Na}/P_{Cl} of 0.8 would be expected. The variations in selectivity result from differences in the expression of specific members of the tight-junction proteins claudins.[25]

Membrane Selectivity

If the paracellular or tight junction resistance is much greater than the transcellular resistance, it is possible to determine the ion selectivity of the individual cell membranes. Specifically, if R_{tj} is very large compared to $R_{ap} + R_{bl}$, there will be negligible current through either the paracellular pathway or the cell pathway under open-circuit conditions. Under these conditions, the circuit of Figure 7.1 predicts that changes in E_{ap} will parallel changes in V_{ap} which, in turn, can be estimated from the measured changes in transepithelial potential ΔV_{te} (see Equations (A1.8) and (A1.11)–(A1.13) of Appendix 7.1). Such a situation was studied by Koefoed-Johnsen and Ussing[11] in their classic paper on the frog skin, where pre-treatment of the skins with low concentrations of Cu^{+2} produced very high values of R_{te} and V_{te}.

This permits evaluation of individual membrane selectivities from transepithelial measurements alone if the concentration of just one ion on one side of the epithelium is replaced with an impermeant species, and the conditions associated with Eq. (A1.13) (Appendix 7.1) are satisfied. If this is the case and Na is partially replaced on the apical side, then:

$$\Delta V_{te} = \Delta E_{ap} = -\frac{RT}{F} t_{Na} Ln \frac{[Na]_{ap}^{exp}}{[Na]_{ap}^{con}} \quad for\ R_{tj} >> R_{ap} + R_{bl}^{*} \tag{7.13}$$

where the change in potential is measured as experimental minus control. $[Na]^{exp}$ and $[Na]^{con}$ represent the concentrations of Na under experimental and control conditions, i.e., after and before the solution change.

Koefoed-Johnsen and Ussing[11] found that changes in mucosal Na produced changes in V_{te} close to those which would be expected if $t_{Na} = 1$. From this they inferred that the apical membrane was primarily conductive to Na ions. Similarly, changes in serosal K concentration produced changes consistent with the idea that the basolateral membrane conducted only K. The elegant conclusions of this study depended upon the rather unusual conditions achieved, namely a very high paracellular resistance and the absence of other "leak" pathways due to other cell types. Except for the case of the urinary bladder, such conditions are difficult to achieve in renal epithelia where paracellular pathways are usually leakier than in the frog skin.

Selectivity of the epithelial basolateral membrane has also been studied by using pore-forming polyene antibiotics to reduce apical membrane resistance[26] so that V_{te} becomes a reasonable estimate of the basolateral potential V_{bl} (see Equation A1.16 of Appendix 7.1). For example, in the turtle colon, Germann et al.[27] were able to characterize two different conductances for K across the basolateral membrane using the amphotericin-B permeabilized epithelium. This approach has also been used mostly in flat epithelia rather than renal tubules.

Impedance Analysis

Impedance analysis permits estimation of the electrical properties of individual membranes using transepithelial measurements.[28] In principle, transepithelial impedance can be measured from the time-course of the response to any electrical perturbation. In practice, it is usually obtained either under "current-clamp" conditions, using sine wave current perturbations at different frequencies or under voltage-clamp conditions by applying voltage perturbations. Since the apical and basolateral membranes will each have an associated complex impedance that depends on frequency, it is possible to distinguish contributions from the two membranes if they have very different time constants ($\tau = RC$, where R is the resistance and C the capacitance).

Typically four parameters (consisting of the amplitudes and time-constants of the two membrane components) are measured to fit a circuit with five parameters (resistance and capacitance of apical and basolateral membranes and the paracellular resistance). To fully solve the system one model parameter (e.g., the paracellular resistance) usually must be determined independently.

Impedance analysis has also been used to derive detailed information about the paracellular pathway, including the distribution of resistance across tight junctions and along intercellular spaces. In this regard, it has been used to estimate individual resistances and capacitances of the apical and basolateral membranes of flat epithelial sheets obtained from frog skin, amphibian and mammalian urinary bladder, colon, and cultured epithelial cells.[29–32] The elegance of the technique is that it is non-invasive, yielding information about individual membranes without the need for intracellular probes or electrodes. Because of the

requirement of uniform currents or voltage fields, its application to renal tubules has been very limited.[7,33]

CONCLUSIONS

Many important epithelial properties can be determined from transepithelial measurements alone. In fact, the original Koefoed-Johnsen/Ussing model for Na transport by the frog skin was based entirely on transepithelial electrical and flux measurements, and the ingenious use of special simplifying conditions. Thus, a number of important physical and thermodynamic properties of epithelia are still estimated from transepithelial measurements, particularly in renal tissues. These include the magnitude and selectivity of the paracellular shunt pathway, the ion selectivity of cell membranes (qualitatively in most instances), and the currents and EMF's associated with active transepithelial transport. On the other hand, the quantitative description of membrane properties requires detailed intracellular measurements to specifically characterize the apical and basolateral membrane components, as well as the contribution of the paracellular pathway. These measurements will be discussed in the next section.

INTRACELLULAR MEASUREMENTS

Intracellular measurements with voltage-sensitive and ion-sensitive microelectrodes permit a more detailed evaluation of individual membrane parameters than transepithelial measurements. This has been essential to our understanding of ion transport in epithelia. Three important membrane characteristics that are amenable to study with intracellular techniques are: (1) ionic selectivity; (2) membrane conductance; and (3) estimation of pump current. Although there are significant differences in the methodology of these measurements depending on the particular tissue involved, much of the underlying theory is similar in both flat epithelia and renal tubules. The emphasis of this section will be on describing the simplest and most straightforward methods for evaluation of single-membrane parameters with emphasis on renal epithelia, although much of the theory is applicable to flat epithelia as well.

Cell Membrane Potentials in Epithelia

An epithelium is a sheet of polarized cells joined together to function as a selective barrier between two compartments. Epithelia not only structurally define two compartments, but also maintain the composition of those compartments via the specific transport of electrolytes, non-electrolytes, and water. The electrical voltage measured across either the apical or basolateral membrane of an epithelium is the sum of the ionic diffusion potentials across the membrane, and the voltage drops arising from current flow across the resistance of that membrane. This current flow (depicted by the thick arrow in Figure 7.1) arises in part from the differences in membrane ionic diffusion potentials and the sum of epithelial barrier electrical resistances (Appendix 7.1).

In practice, cell membrane potentials are determined by impaling the cell with fine tipped glass microelectrodes, filled with a highly conductive electrolyte solution (1 M or 3 M KCl). Uniform filling is often accomplished by starting with glass tubing that contains a thin glass filament, allowing solution to flow smoothly from the back to the tip of the finished electrode. The microelectrode is then mounted on a stable micromanipulator. Given the elasticity of most cell membranes, impalement usually requires a rapid forward movement of the tip that can be accomplished either mechanically or with piezoelectric headstage. Sometimes a high frequency alternating current is briefly applied to the tip to permit entry into the cell with minimum damage.

A major technical problem with microelectrode measurements is the damage to the cell that may be produced by impalement. For a discussion of this topic see Higgins et al.[18] and Nelson et al..[34] Cell damage can be minimized by utilizing epithelia with large cells (e.g., *Necturus*; *Amphiuma*), and by recording from the basolateral rather than the apical membrane. This will result in less electrical shunting of the membrane potential, since in many cases the basolateral membrane has a much lower resistance than the apical membrane and an additional leak conductance at the basal side will have a smaller overall effect.[18] Furthermore, epithelia like the proximal tubule, whose cells are electrically coupled, are less sensitive to impalement artifacts, since the effective cell membrane area is larger. Finally, the use of very fine-tipped micropipettes can minimize membrane damage during intracellular measurements. However, such pipettes are more likely to produce artifacts due to changes in the liquid-junction potentials ("tip potentials") when the tip enters the cytoplasm.

Use of microelectrodes to measure cell potential may result in KCl leakage into the cell. Although these tips are extremely small ($< 0.2\ \mu m$), the use of concentrated KCl in the electrode to minimize liquid junction potentials can lead to KCl influx into the cell, alterations in cell composition, and cell swelling.[34] Thus, the choice of a filling solution is a trade-off between a concentrated KCl solution, which yields low tip potentials

but possible KCl leakage, versus a low salt pipette solution, which results in higher tip potentials but less salt leakage into the cytoplasm.

Intracellular potential can also be measured with relatively large diameter patch-clamp pipettes. In a "whole-cell clamp" experiment, a high resistance seal is formed between the pipette and the cell membrane. This permits direct electrical contact between the recording electrode and the cell interior with negligible impalement damage. If the amplifier is used in the voltage-clamp mode, the holding potential that reduces the membrane current to zero becomes a good measure of the cell potential. One disadvantage of using the whole-cell clamp to measure cell potential is that the cell is dialyzed with the pipette solution.[35] The exchange of vital cell constituents with the pipette solution may alter the intracellular ion composition, as well as change the normal cell membrane permeabilities through the loss of regulatory factors. The latter effect can be minimized by using the "perforated-patch" technique, in which the patch is permeabilized by the addition of pore-forming substances such as nystatin to the pipette solution.[36]

Evaluation of Individual Membrane Resistances from an Equivalent Circuit Analysis

The simplest technique for determining individual cell membrane resistance is to measure intracellular and transepithelial potential during an experimental maneuver that produces only a single perturbation in the parameters of the equivalent circuit. These techniques have been particularly useful in mammalian proximal tubules where multiple microelectrode impalements are difficult or in nephron segments that are not electrically coupled.

When only one microelectrode is used, the circuit of Figure 7.1 must be simplified to permit an indirect evaluation of the cell membrane resistances. This type of reduction is illustrated in Figure 7.7, and is permissible when most of the paracellular resistance is contributed by the tight junction resistance (i.e., when $R_{par} \approx R_{tj}$), which is equivalent to the assumption that R_{tj} is $>>$ lateral interspace resistance ($=R_{lis}$). This is particularly appropriate for mammalian proximal tubule, where basal interdigitations of adjacent cells greatly reduce the lateral space resistance, and most of the paracellular resistance is contributed by the tight junction resistance.

The circuit of Figure 7.7a can be further reduced to the simpler form of Figure 7.7b by defining an effective basolateral EMF (E^*_{bl}) and an effective basolateral resistance (R^*_{bl}), as described in Appendix 7.1. Although the electromotive forces or EMFs (E_{ap}, E_{bl}, E_{par}) in the circuit cannot be measured directly, the potential differences across each barrier can be measured with intracellular or transepithelial electrodes. These are defined as transepithelial potential (lumen-bath) $= V_{te}$, apical cell membrane potential (lumen-cell) $= V_{ap}$, and basolateral potential (cell-bath) $= V_{bl}$.

An important consequence of the circulating epithelial current in Figure 7.7 is that alterations in any of the electrical parameters on one side of the cell will produce changes in the measured electrical potentials on the contralateral side. This actually provides an indirect method for evaluating those resistances that remain constant during a change in loop current, I. Individual cell membrane resistances R^*_{bl} and R_{ap} can be evaluated by any experimental maneuver that changes only the parameters at one membrane. For example, rapid addition of amiloride or glucose to the apical solution presumably alters only the resistance and/or the EMF of the apical membrane by blocking Na channels or stimulating Na-glucose co-transport, respectively.

Amiloride causes a hyperpolarization of V_{bl} by both increasing the measured apical resistance (R_{ap}) and decreasing the contribution of the Na gradient to the value of E_{ap} (see Appendix 7.1, Eq. (A1.7)). On the other hand, addition of glucose to the luminal solution depolarizes V_{bl} by stimulating Na-glucose co-transport, which effectively increases both the apical Na conductance and the relative contribution of the Na gradient to the apical diffusion potential. Since the primary effect of both amiloride and glucose occurs at the apical membrane, the ratio of basolateral to apical resistance is directly related to the measured ratio of basolateral to transepithelial voltage deflections according to Eq. (7.14), which applies for addition of either apical-side amiloride or apical-side glucose:

$$\frac{R^*_{bl}}{R_{tj}} = -\frac{\Delta V_{bl}}{\Delta V_{te}} = \beta \tag{7.14}$$

This equation implicitly assumes that neither glucose nor amiloride affect the paracellular pathway, and that the potential measurements can be performed before any changes in cell composition have occurred that would affect E_{ap}, E_{bl}, and R_{bl}.

Similarly, measurement of the ratio of apical to transepithelial potential change following addition of barium to the basolateral solution permits estimation of the apical membrane resistance via Eq. (7.15):

$$\frac{R_{ap}}{R_{tj}} = -\frac{\Delta V_{ap}}{\Delta V_{te}} = \frac{\Delta V_{bl}}{\Delta V_{te}} - 1 = \alpha \tag{7.15}$$

Again, it has been assumed that basolateral application of barium has no effect on the paracellular pathway, and that the measurement can be performed rapidly enough to avoid changes in cell composition.

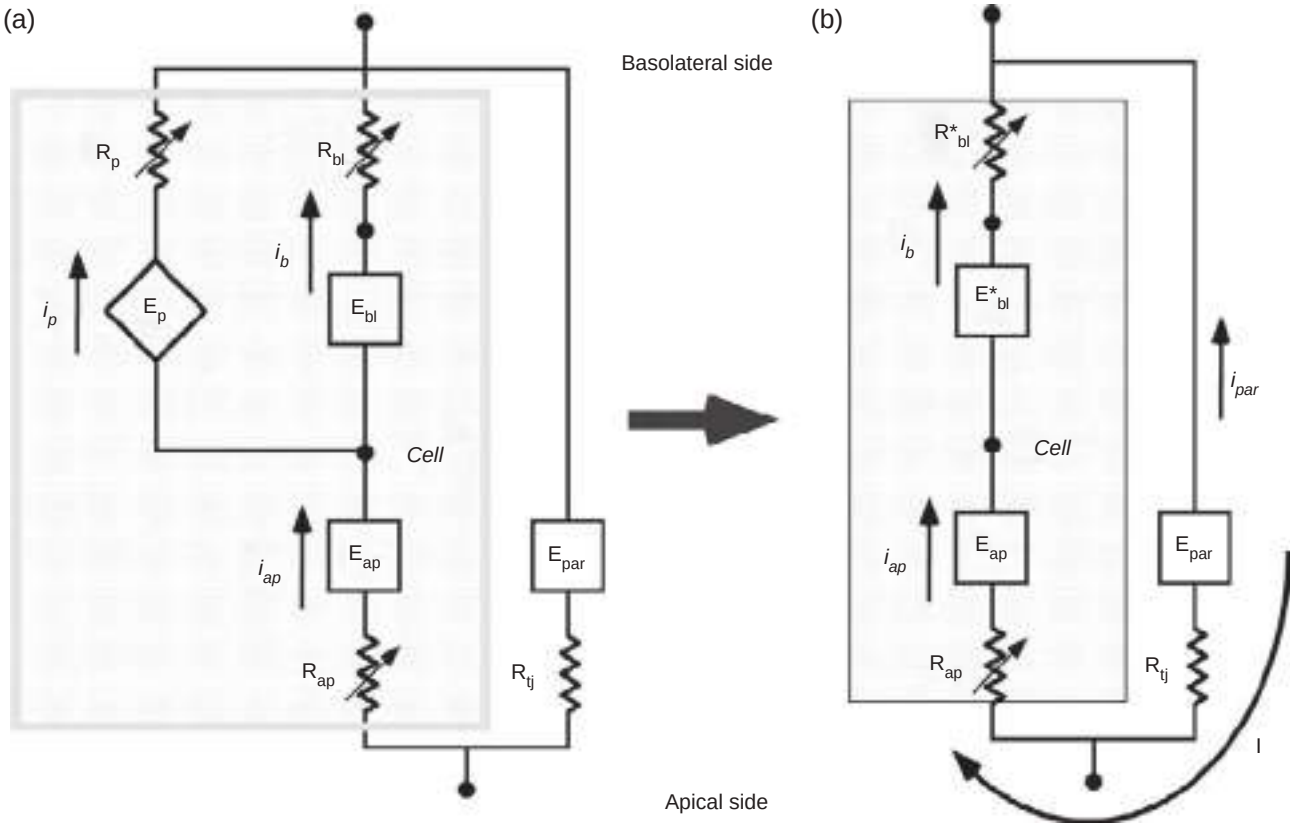

FIGURE 7.7 (a) Reduced form of the general equivalent circuit, where the lateral resistive network has been neglected because most of the paracellular resistance is assumed to reside at the tight junction (i.e., $R_{tj} >> R_{lis}$). This situation applies in a number of epithelia and greatly simplifies the equivalent circuit. (b) Reduced circuit in which the parallel diffusive and active transport paths across the basolateral membrane have been combined into an effective basolateral EMF (E^*_{bl}) and an effective basolateral resistance (R^*_{bl}). "I" denotes direction of positive net circulating current under open-circuit conditions.

Finally, in cases where it is feasible to make changes on only one side of the epithelium, the voltage divider ratio can be used instead of either Eq. (7.14) or Eq. (7.15). When current is injected into the tubule lumen via the perfusion pipette, a certain fraction of that current will cross the apical and basolateral cell membrane in series, producing voltage deflections ΔV_{ap} and ΔV_{bl}. If the lateral and basal resistances of Figure 7.1 are combined into a single effective resistance R^*_{bl} (defined in Appendix 7.1, Eq. (A1.4)) the ratio of apical to basolateral resistance during transepithelial injection of current is given by Eq. (7.16):

$$\gamma = \frac{R_{ap}}{R^*_{bl}} = \frac{\Delta V_{ap}}{\Delta V_{bl}} = \frac{\Delta V_{te}}{\Delta V_{bl}} - 1 \tag{7.16}$$

The term "γ" is sometimes referred to as the voltage divider ratio. An alternative to Eq. (7.16) is to define the "fractional resistance" of either the apical (fR_{ap}) or basolateral membranes (fR_{bl}), according to Eqs. (7.17a), (7.17b):

$$fR_{ap} = \frac{R_{ap}}{R_{ap} + R^*_{bl}} = 1 - \frac{\Delta V_{bl}}{\Delta V_{te}} \tag{7.17a}$$

$$fR^*_{bl} = \frac{R^*_{bl}}{R_{ap} + R^*_{bl}} = \frac{\Delta V_{bl}}{\Delta V_{te}} \tag{7.17b}$$

Since γ, α, β, and R_{te} are all measured quantities, the individual resistances: R^*_{bl}, R_{ap}, R_{tj}, can be evaluated by using any three of the four equations Eqs. (7.14), (7.15), (7.16), and Eq. (A1.5).

An example of these methods is illustrated by the experiment depicted in Figure 7.8.[37] In this experiment, changes in transepithelial (V_{te}) and basolateral potential (V_{bl}) are shown during addition of 1 mM barium to the bath (Figure 7.8a), followed by addition of 8 mM glucose to the lumen (Figure 7.8b). The superimposed smaller deflections are due to periodic current injection for evaluating "γ" from Eq. (7.16).

In both these experiments, ΔV_{bl} and ΔV_{te} were taken as the initial changes in voltage resulting from a particular maneuver. For example, in the barium experiment, only changes in V_{bl} and R^*_{bl} were presumed to occur, and ΔV_{bl} was taken as the difference between the baseline V_{bl} and the V_{bl} at the inflection point (asterisk). The origin of the slow secondary depolarization of V_{bl} in Figure 7.8a is not known.

The above methods have been used to determine individual cell membrane resistance in mammalian proximal tubule. Some of these results are summarized in Table 7.3. Although there are some differences in the absolute values of cell resistances, there is general agreement that in proximal tubule the resistance of the cellular pathway is between 20 and 30 times higher than the resistance of the shunt pathway. This factor is even higher in amphibian proximal tubule.

Determination of individual membrane parameters from Eqs. (7.14)–(7.16) involves certain practical problems. These methods require measurement of ΔV_{te} and ΔV_{bl} in the same tubule at the same axial distance along its length. As indicated in Figure 7.8, the small magnitude of the change in transepithelial potential renders the two ratios α and β in Eqs. (7.14) and (7.15) particularly susceptible to errors in ΔV_{te}. Measurements of ΔV_{te} obtained by advancing a microelectrode into the lumen are unreliable, because damage to the epithelium can produce artificially low values of ΔV_{te}. Since transepithelial potential is measured only at the perfusion or collection ends of the tubule, the value of ΔV_{te} must be calculated from the electrotonic voltage spread along the tubule using a terminated cable analysis (see section entitled, "Transepithelial Measurements").

Evaluation of Individual Membrane Resistances Using Multiple Intracellular Recordings

In the relatively large cells of amphibian proximal tubule (30 μm diameter), direct electrical measurement of cell membrane resistance is possible. Exploiting the property of electrical coupling between adjacent proximal cells,[16] it is possible to pass current from an intracellular microelectrode through an annular syncytium, with an outer specific resistance of R^*_{bl} and an inner specific resistance of R_{ap}. This cannot be done in nephron segments like the collecting duct, where adjacent cells are not electrically coupled.[38]

The use of cellular cable analysis to evaluate the individual resistances R^*_{bl}, R_{ap}, and R_{tj} still depends on the definition of transepithelial resistance (Eq. (A1.5)) and the "voltage-divider" ratio (Eq. (7.16)) that were discussed in the section entitled, "Cell Membrane Potentials in Epithelia." However, instead of relying on the ratio $\Delta V_{bl}/\Delta V_{te}$, obtained during application of barium or amiloride, the parallel resistance of the cell layer (R_z) is computed directly from the electrotonic voltage spread along the double core cable, where R_z is defined by Eq. (7.18).

$$1/R_z = 1/R_{ap} + 1/R^*_{bl} \tag{7.18}$$

In practice, R_z is evaluated by injecting current I_o into the cell layer at x = 0 via a microelectrode and measuring the voltage deflection ΔV_x at two or more locations "x," downstream from the injection site. The arrangement of microelectrodes is illustrated in Figure 7.2. If x is at least twice the diameter of the tubule, the electrotonic voltage spread along the cable will be given by Eq. (7.19), where λ_c is the cellular length constant of the tubule[5]:

$$Ln[\Delta V_x] = Ln\left[\frac{R_z I_o}{4\pi r \lambda_c}\right] - \frac{1}{\lambda_c}x \tag{7.19}$$

The best fit for the two unknown parameters λ_c and R_z is determined by evaluating Eq. (7.19) at a number of locations along the tubule. The radius of the tubule, r_o, is measured with an optical micrometer. Combining Eqs. (7.16), (7.18), (7.19), and (A1.5), the individual membrane resistances R_{ap}, R^*_{bl}, and R_{tj} are uniquely determined by the two parameters R_z, γ, and the measured value of R_{te} according to Eqs. (7.20)–(7.22):

$$R_{ap} = R_z[1 + \gamma] \tag{7.20}$$

$$R^*_{bl} = R_z\left[1 + \frac{1}{\gamma}\right] \tag{7.21}$$

$$R_{ti} = \frac{R_{te}[R^*_{bl} + R_{ap}]}{R_{ap} + R^*_{bl} - R_{te}} \tag{7.22}$$

The transepithelial resistance of the tubule, R_{te}, is determined by passing current and measuring voltage through a doubled-barreled perfusion pipette according to the methods described in the section entitled, "Transepithelial Measurements" and Figure 7.2.

In amphibian proximal tubule, most measurements of individual cell resistances have been performed using a cellular cable analysis with two or more intracellular microelectrodes. On the other hand in mammalian tubules, the method of relative voltage deflections (Eqs. (7.14) and (7.15)) have been used exclusively. However, in *Ambystoma* proximal tubule, a direct comparison of the two methods has been made under similar conditions. These results are summarized in the first two rows of Table 7.4. As indicated, the absolute values of resistance are quite close considering the propagation of errors that occur with both types of measurements. The remaining rows of Table 7.4 summarize additional resistance measurements in amphibian renal epithelia.

As with the mammalian proximal tubule, the ratio of shunt to cell resistance clearly establishes the amphibian proximal tubule as a "leaky" epithelium. In contrast, the *Necturus* urinary bladder (a "tight" epithelium) possesses a shunt resistance that is several times larger than the cell resistance pathway. Neither the diluting segment nor the collecting tubule of the *Amphiuma* fall neatly into the "tight" or "leaky" category, since both of these segments have cellular

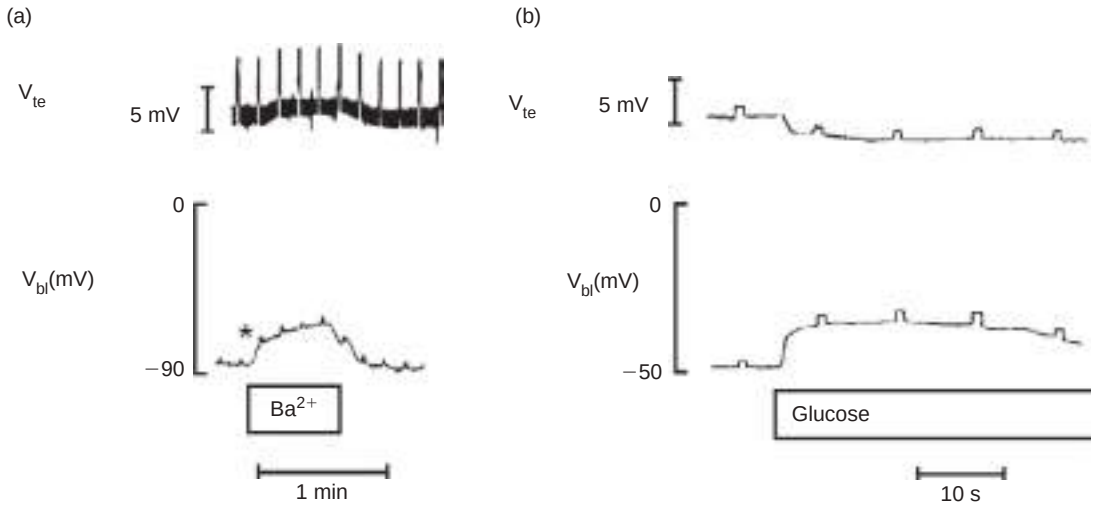

FIGURE 7.8 **Effect of barium and glucose on membrane voltages in rabbit proximal convoluted tubule (from [37]).** (a) Reversible depolarization of both the transepithelial (V_{te}) and the basolateral membrane potential (V_{bl}) produced by addition of barium to the basolateral side of isolated proximal tubules. (b) Simultaneous depolarization of the transepithelial (V_{te}), and hyperpolarization of the basolateral membrane potential (V_{bl}) produced by addition of glucose to the apical side of isolated proximal tubules. In both panels the superimposed periodic voltage deflections were produced by current pulses injected through the perfusion pipette.

TABLE 7.3 Cell Membrane Resistances in Mammalian Tubules (Ωcm^2 Epithelium)

Segment	Apical Resistance	Basolateral Resistance	Shunt Resistance	Method	Species	Reference
PCT	238	68	16	Apical glucose Basal Ba^{21} Voltage divider	Rabbit (PCT)	37
PCT	118	39	8	Apical glucose Voltage divider	Rabbit (PCT)	141
PCT	255	92	5	Apical glucose Voltage divider	Rat	142
TALH	88	47	47	Apical high K^+, Ba^{2+} Voltage divider	Rabbit	41
TALH	57	21	37	Apical Ba^{2+} Voltage divider	Mouse	12
CCD	149	123	166	Apical Ba^{2+} Voltage divider	Rabbit	143
CCD	57	80	230	Apical amiloride, Ba^{2+} + Voltage divider	Rabbit	144
OMCD	707	176	393	Apical glucose Voltage divider	Rabbit	138,145
Urinary bladder	3700 to 154,000	5000 to 10,300	6500 to 38,000	Apical amiloride Voltage divider Cell cable	Rabbit	146

Adapted from ref. [145]. TALH, thick ascending limb of Henle's loop; CCD, cortical collecting duct; OMCD, outer medullary collecting duct; PCT, proximal convoluted tubule.

and paracellular resistances that are in the same order of magnitude. Interestingly, both the diluting segment and collecting duct have higher shunt resistances and lower cellular resistances than the corresponding membrane of the proximal tubule. Mammalian collecting ducts and diluting segments also have higher shunt resistances than mammalian proximal tubules, although differences in cell resistance are less dramatic along the mammalian nephron.

The resistances quoted for the *Amphiuma* diluting segment in Table 7.4 assumed a single cell type throughout the cable analysis.[39] This greatly simplified the calculation of membrane resistance. Unfortunately, subsequent experiments indicated that this nephron segment actually consists of two different cell types with dissimilar conductive properties.[40] One cell type has a high basal K and Cl conductance (HBC), whereas the other cell type (LBC) has a low basolateral conductance for both ions.[40] There is also some evidence that mammalian TALH may exhibit a certain amount of cell heterogeneity as well.[41] Since it is unlikely that different cell types in the same nephron segment are directly coupled to each other, a unique value of cell membrane resistance cannot be determined from cable analysis on these nephron segments unless all recordings are made from the same cell type.

The cellular cable equations (Eqs. (7.18) and (7.19)) were originally derived for *in situ* proximal tubules, in which the cables are effectively infinite in length.[16] However, they should be reasonably valid for isolated perfused tubules as long as the voltage recording microelectrodes are several tubule diameters from either end of the tubule. Under these conditions the electrotonic voltage spread would be effectively the same as for an infinite cable. The problem of "cross-talk" or interactions between the transepithelial and cellular cables has been suggested as a source of error in these measurements.[42] The complication of cable−cable interactions would only be significant if current injected into the cell layer leaks into the lumen and then re-enters the cell layer at the some point downstream. A thorough analysis by Guggino et al.[16] for *Necturus* proximal tubule suggests that cross-talk will be negligible if intracellular voltage deflections ΔV_x are recorded at locations $x > \lambda_c$.

Evaluation of cell membrane resistance via Eqs. (7.14)−(7.16) is only as accurate as the equivalent circuit of Figure 7.7. An important aspect of this electrical model is the assumption that the tight junction constitutes the principal resistance of the paracellular pathway, or $R_{par} \approx R_{tj}$. This is probably true in tight epithelia like the urinary bladder, where the lateral intercellular space has a negligible resistance compared to that of the tight junction. However, the low transepithelial resistance of the proximal tubule raises the possibility that the resistivity of free solution in the lateral space contributes significantly to overall shunt resistance. In this case, evaluation of the divider ratio is complicated by the lateral resistive network shown in Figure 7.1. Current flow through a distributed network of this kind will cause the measured value of $\Delta V_{ap}/\Delta V_{bl}$ to *underestimate* the actual value of R_{ap}/R^*_{bl} by an amount that depends on the ratio of lateral space resistance, R_{lis}, to paracellular resistance R_{par} (see Figure 7.9).

As illustrated in Figure 7.9, the larger the contribution of the fluid-filled interspace to the total paracellular resistance (i.e., the larger the ratio R_{lis}/R_{par}), the more the measured voltage ratio will underestimate the actual resistance ratio, γ. In epithelia where the paracellular resistance is essentially determined by the resistance of the tight junction and $R_{lis}/R_{par} < 0.01$, the resistance ratio (γ) will be correctly given by Eq. (7.16). On the other hand, if the lateral interspace is long and narrow and constitutes a non-negligible electrical resistance, R_{par} will be related to R_{te} according to a complicated function (see Eqs. (31−40)) of reference[6] with $R_3 = R_{par}$). As can be seen in the figure, significant deviations from Eq. (7.16) occur even if R_{lis} is as little as 10% of R_{par}. A detailed analysis regarding the effect of lateral resistive networks on measurement of cell membrane resistance has also been presented by Weber and Frömter.[43]

Determination of individual cell membrane resistances involves a number of technical difficulties. In addition to those indicated above, positioning of the intracellular electrodes is particularly tedious. If the first cell voltage electrode is within one cell length constant of the cell current electrode there may be significant cross-talk between cell and luminal cables. If the second cell voltage electrode is too far from the current injection electrode, the size of the deflection will be immeasurably small. Use of a third voltage recording electrode gives a better definition of the electrotonic voltage spread, but is often impractical. If sequential voltage impalements are used, the first recording should be made at the farthest distance from the current electrode. In this manner, intracellular recording at $x = L_1$ will be insignificantly affected by cell damage at $x = L_2$, as long as $L_2 > L_1$, and the current electrode is maintained at $x = 0$ (see Figure 7.2).

A significant source of error in cellular cable measurements arises from voltage-dependent membrane conductances. These can result from asymmetry of the electrolyte composition on the two sides of the membrane ("Goldman rectification"). Furthermore, patch-clamp experiments have indicated that a number of renal channels are voltage-gated. The specific magnitude and type of gating varies with each nephron segment. Since the current injections used for determination of cell membrane resistance often

TABLE 7.4 Cell Membrane Resistances in Amphibian Tubules (Ωcm^2 Epithelium)

Segment	Apical Resistance	Basolateral Resistance	Shunt Resistance	Method	Species	Reference
Proximal tubule	2509	683	71	Apical glucose Basal barium Voltage divider	*Ambystoma*	37
Proximal tubule	2305	591	53	2 electrode Cable analysis	*Ambystoma*	5,147
Proximal tubule	6957	2399	267	2 electrode Cable analysis	*Necturus*	16
Proximal tubule	2700	1900	—	2 electrode Cable analysis	Frog	148
Proximal tubule	1350	2100	166	2 electrode Cable analysis	*Triturus*	149
Dilute segment[a]	550	219	306	2 electrode Cable analysis	*Amphiuma*	39
Collecting tubule	154	192[b]	454	Voltage clamp Voltage divider	*Amphiuma*	53,150
Urinary bladder	9000–65,000	1000–7000	100,000	Apical amiloride Voltage divider	*Necturus*	151

[a]*These measurements assumed that the Amphiuma diluting segment has only one cell type.*
[b]*The basolateral conductance of this segment is strongly inward rectifying and quoted value applies only at a membrane potential of −60 mV.*

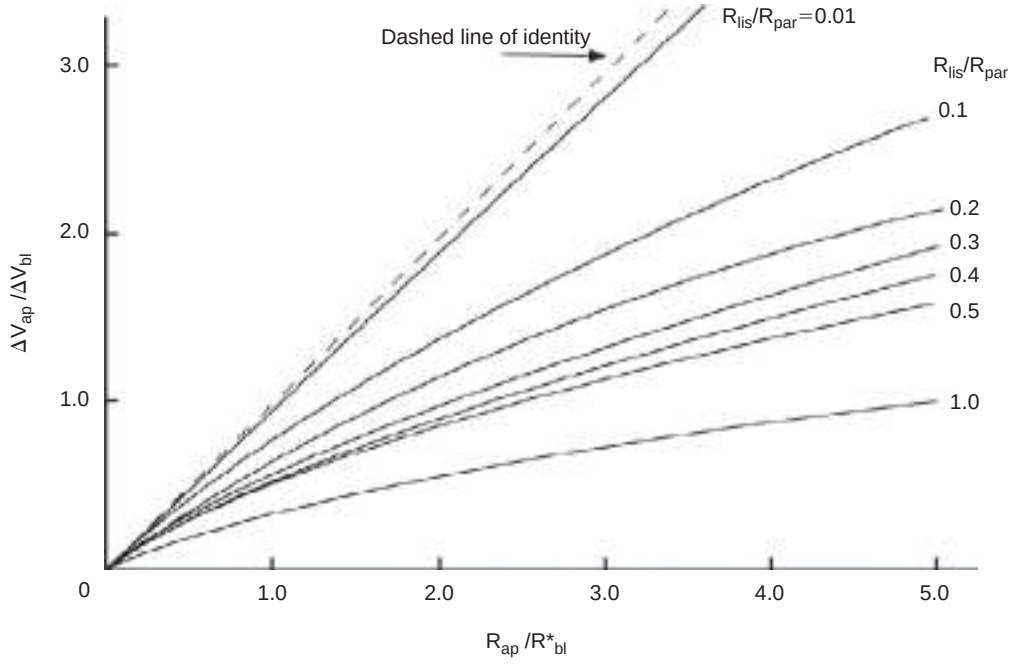

FIGURE 7.9 **Relationship between the measured voltage divider ratio ($\Delta V_{ap}/\Delta V_{bl}$) and the actual ratio of apical to basolateral resistance (R_{ap}/R_{bl}) at different values of fractional interspace resistance (R_{lis}/R_{par}).** Negligible values of R_{lis} result in the voltage divider ratio being a good measure of R_{ap}/R_{bl} (line of identity). In epithelia where R_{lis} is a significant fraction of the paracellular resistance, the voltage divider ratio is not a good measure of the apical to basal resistance ratio.[179]

produce 10 to 15 mV voltage deflections across the basolateral membrane, the conductance could be affected by the process of measurement. One solution to this difficulty has been to take the average value of ΔV_{bl} determined from both positive and negative going currents.

Evaluation of Ion Selectivities from Ion Substitution Experiments

One of the most important membrane properties that can be determined from electrophysiological measurements is membrane selectivity. The basic equation that defines the transference number of the membrane for ion x is obtained by rearranging Eq. (7.3) to yield Eq. (7.23) below:

$$t_x = -\frac{\Delta E}{\frac{RT}{z_x F} Ln\left[\frac{[X^{expt}]}{[X^{con}]}\right]} \tag{7.23}$$

Eq. (7.23) can then be used to evaluate the ion selectivity of the individual epithelial membranes from changes in the total EMF ΔE (expt − control) produced by replacement of a specific *apical* ion X by an impermeant ion. In Eq. (7.23), X^{expt} and X^{con} respectively refer to the extracellular ion concentration of the apical solution under experimental (expt) or control (con) conditions. If ΔE is produced by a change in *basolateral* composition, the transference numbers would be calculated from the negative of Eq. (7.23). As indicated in Figure 7.7b, the circulating current, I, prevents a simple equivalence between the measured change in potential difference (ΔV) and the actual change in the EMF of the membrane (ΔE). The effects of circular current flow on the actual changes in EMF resulting from ion substitution, ΔE, are described in detail in Appendix 7.2. These equations are essential for evaluating membrane selectivities from ion substitution experiments.

The partial conductance of the membrane for any ion "x" (G_x) can be determined from the transference number for the membrane and the total ionic conductance of that membrane (G_{tot}), according to Eq. (7.24):

$$G_x = t_x \cdot G_{tot} \tag{7.24}$$

There is no simple relation between the partial ionic *conductance* and the *permeability* of the membrane to a particular ion. However, it is possible to develop a general relation between the conductance and the permeability of a particular ion (X). This is given by Eq. (7.25), where $\langle X \rangle$ is a weighted average of the concentrations of X on both sides of the membrane. Its value depends on the particular assumptions about ion permeation across the membrane.

$$G_x \approx P_x \frac{z^2 F^2}{RT} \langle X \rangle \tag{7.25}$$

In the constant field assumption, $\langle X \rangle$ is a complicated function of both the membrane potential and the ion concentrations on both sides of the membrane. Explicit forms of Eq. (7.25) are discussed in Appendix 7.3. However, if the membrane is assumed to be permeant to only three ions: Na, K, and Cl, the permeability ratios P_{Na}/P_K and P_{Cl}/P_K can be evaluated from a two parameter fit to the general form of the Goldman–Hodgkin–Katz equation.[44] This procedure has not been used extensively for renal epithelia because of uncertainties in a simultaneous evaluation of P_{Na}/P_K and P_{Cl}/P_K.

On the other hand, if the membrane is primarily selective to two rather than three ions, a closed form expression can be obtained for the permeability ratio:

$$\frac{P_K}{P_{Na}} = \frac{[Na]_o - [Na]_i \exp\left(\frac{E_{rev}}{RT/F}\right)}{[K]_i \exp\left(\frac{E_{rev}}{RT/F}\right) - [K]_o} \tag{7.26}$$

In Eq. (7.26) the term, E_{rev}, is the potential difference, inside (i) minus outside (o), associated with zero current across the membrane. The principle disadvantage of Eq. (7.26) for kidney tubules is that determination of E_{rev} requires voltage-clamping the individual cell membranes of the epithelium. So far this has really only been accomplished for the *Amphiuma* collecting tubule.[21]

Since the specific conductance of a membrane for ion X is generally a function of the concentration of that ion (Eq. (7.25)), the values of t_x obtained from Eq. (7.23) only apply to the concentration range over which the ion replacement is actually performed. Consequently, any determination of normal transference numbers requires that the ionic replacement: $X^{con} - X^{expt}$ be as small as possible, but still produce a measurable ΔE. On the other hand, the permeability ratio of Eq. (7.26) should (in theory) be less dependent on external ion concentrations.

Estimation of Renal Na-K Pump Current and Electrogenic Potential

The 3Na/2K stoichiometry and electrogenic nature of the Na/K pump has been demonstrated in a number of non-epithelial tissues.[45,46] Most studies on red cells,[47,48] squid axon,[49] and Purkinje fibers[50] indicate a fairly consistent Na/K coupling ratio of 3/2 for the Na-K-ATPase. This electrogenicity not only causes the pump to contribute to total membrane potential, but also requires that the pump itself be dependent on membrane potential.

Mullins and Noda[51] and Ascher (cited in [52]) have derived an expression for the electrogenic contribution to the membrane potential of nerve and muscle cells which predicts a steady-state contribution of no larger than about 11 mV. This theory depends on the observation that electroneutrality conditions on symmetric cells require that there be no net macroscopic current under open-circuit, steady-state conditions. The estimate of 11 mV maximal electrogenic hyperpolarization also depends on the assumption that the membrane permeabilities are voltage independent, which is somewhat of an approximation, even for nonexcitable tissues.

In epithelial tissues, where current circulates around a cellular and paracellular path (see Figure 7.7), the electrogenic contribution to the membrane potential may be larger than in symmetric cells, but it is also more difficult to quantify. Early estimates of pump current and electrogenic potential in epithelial tissues were determined by comparing the observed change in basolateral potential ΔV_{bl} to the potential changes predicted from the measured ion gradients and electrical resistances, during rapid return of K to the basolateral solution[5] or application of cardiac glycosides.[21,53] These experiments clearly demonstrated net transfer of charge by the pump, but uncertainty about the potassium concentration in unstirred layers outside the cell made it difficult to determine pump stoichiometry from these types of experiments.

In general, the calculation of the electrogenic potential in epithelial tissues requires explicit knowledge of both membrane and pump resistances, which may themselves be a function of pump activity (see Appendix 7.4). This significantly complicates the situation, and the electrogenicity of the pump is better characterized by evaluating its I–V relation than by evaluating its contribution to the open-circuit potential.

Since electrogenicity requires that pump current be sensitive to membrane potential, the I–V relation for the pump must intersect the voltage axis at some reversal potential E_p. The reversal potential of the pump should correspond to the membrane potential against which the pump can no longer translocate a net charge (i.e., 3Na for 2 K). The value of E_p can be calculated from Eq. (7.27) using estimates of the free energy of ATP hydrolysis (E_{ATP}) and the concentration work involved in moving "m" sodium ions (mE_{Na}) and "n" potassium ions (nE_K) per molecule of ATP split.[54]

$$E_p = EMF_{pump} = \frac{E_{ATP} + mE_{Na} - nE_K}{m - n} \tag{7.27}$$

where E_{ATP} is the free energy of ATP hydrolysis (about −600 mV for m − n = 1, from ref [14]), and E_{Na}, E_K, are respectively the Na and K Nernst potentials across the membrane. For amphibian tubules, E_{Na} is about 55 mV and E_K is about −80 mV at room temperature. According to Eq. (7.27), the predicted value of E_p is about −275 mV for a net translocation of one (m − n) positive charge. This value of E_p corresponds to the reversal potential of the current–voltage relation for the pump.

The existence of a pump reversal potential defined by Eq. (7.27) provides no information about the sensitivity of pump current to membrane voltage. This sensitivity is determined by the specific shape of the current–voltage (I–V) relation of the pump. For example, if the pump I–V relation exhibits a low angle slope in the region of normal membrane potential, the pump would be best represented as a (Norton equivalent) constant current source. On the other hand, if the I–V relation is linear between zero voltage and the pump reversal potential, the pump would be best represented as a (Thevenin equivalent) constant voltage source (Figures 7.1 and 7.7). Four examples of I–V relations for the Na,K-ATPase are illustrated in Figure 7.10.

These pump, current–voltage relations were determined by measuring either the strophanthidin (a, c) or the ouabain (b, d)-sensitive currents at different voltages. Figure 7.10a and 7.10b are I–V relations from symmetric cell preparations, whereas Figure 7.10c and 7.10d were measured in renal epithelia. In both isolated guinea-pig ventricular myocytes[55] and *Xenopus* oocytes,[56] pump current is linearly dependent on membrane voltage with a reversal potential of at least −150 mV. Saturation of current, with decreasing slope, was only evident at positive membrane potentials.

On the other hand, voltage-clamp studies in amphibian (*Amphiuma*) collecting tubules[21] indicate a curvilinear I–V relation (Figure 7.10c), which would imply that (in this tissue) the Na,K pump behaves as a constant current source at normal membrane potentials (− 20 mV to −75 mV). Differences in the I–V curves of Figures 7.10a, 7.10b, and 7.10c may indicate true distinctions between Na pumps of different preparations or may simply reflect differences in experimental technique. The final I–V relation (Figure 7.10d)[57] indicates that the pump current in the mammalian CCD, like that of symmetric cells, is sensitive to voltage in the physiological range.

The variability in the shape of the I–V relations for the Na,K-ATPase (Figure 7.10) implies some uncertainty as to whether the Na pump of a particular tissue behaves more like a constant current or a constant voltage source. Nonetheless, we have chosen to represent the Na pump in the equivalent circuits of Figures 7.1 and 7.7 as a voltage source (E_p) in series with an internal resistance (R_p), because this is a somewhat more general form than a constant-current source.

CONCLUSIONS

With the use of microelectrodes to record intracellular voltages and voltage changes, it has been possible to characterize renal epithelia according to the equivalent circuit in Figure 7.1. Overall conductances of apical and basolateral membranes can be computed, and the contribution of various ions to these conductances can be estimated. Our understanding of the major nephron segments at this level is fairly secure. In the next section we discuss how measurements at the single-channel level have yielded a more detailed description of renal ion transport processes.

Patch-Clamp and Single-Channel Analysis

Defining a Channel

The ability to measure currents through individual ion channels in small "patches" of biological membranes has, over the course of the last 25 years, increased enormously the type of information that can be gleaned about ion channels and the details of our knowledge of how these transport proteins work. With this technique we can find out how many different types of channels there are in a membrane, and how many of each type is present, without the need for specific pharmacological agents. It is possible to determine what gene produces a given membrane conductance by comparing the properties of the channels in that membrane with those of the gene product when it is heterologously expressed in another cells type. In other cases a gene can be specifically deleted using genetic techniques, and the disappearance of a channel type from the membrane can be followed. The patch-clamp technique can also be very useful to determine what agents or second messengers directly or indirectly regulate ion channels.

An ion channel is defined in physical terms as a membrane protein which forms a continuous pathway for the diffusion of an ion from one side of the membrane to the other. In contrast to active transporters, the direction of movement of the ion is determined by the electrochemical energy difference across the membrane. Unlike more complex "carriers" (including facilitated transporters and co- and countertransporters) a conformation change in the channel protein is not required for the translocation of the ions. This permits ions to move quite quickly through the channels. While co-transporters or exchangers generally have maximal turnover rates of about 10^5/sec, and metabolically driven pumps are even slower, channels can achieve rates of 10^8/sec or more through individual units.[58]

Most channels exhibit gating; they switch between distinct open and closed states, producing abrupt transitions in current under voltage-clamp conditions. Patch-clamp recording can generally resolve currents of around 10^6/sec or 0.15 pA. Thus, the ability to see an individual transport unit using the patch-clamp is a reasonably good operating definition of a channel. Although the appearance of current transitions is a good operational definition of channel activity, this is actually too restrictive since some channels may have a low turnover rate. Nevertheless the definition is a useful one, and most channels that we know about have currents large enough – at least under optimal conditions – to be seen by patch-clamp.

Most biologically important channels will also have a density high enough to be observed frequently. For a moderate membrane conductance of 1 mS/cm^2, a single channel conductance of 40 pS and an open probability of 0.5, the density of channels will be 5×10^7/cm^2 or 0.5/μm^2. If a patch contains 5 μm^2 it will have on the average 2 to 3 channels. This simple calculation illustrates that a patch pipette of average diameter will usually contain at least one channel, making this technique a highly efficient method for studying the characteristics of individual ion channels.

High resolution patch-clamp recording was developed in the early 1980s by Neher, Sackmann, and colleagues.[35] The patch methodology consists of four major configurations, three of which can be used to study single channels. As illustrated in Figure 7.11, the cell-attached patch consists simply of forming a seal on the surface of a cell, and studying the resulting piece of membrane *in situ*. This is obviously the most physiological condition. The same patch can be excised from the cell membrane, forming an inside-out patch in which the cytoplasmic surface of the membrane now faces the bathing medium. This is useful for studying the effects of second messengers and other cytoplasmic components which can be added back to the medium to test for their ability to regulate the channels. A cell-attached patch can also be broken with suction, to form a whole-cell voltage-clamp. This is a very convenient method for studying the total current from the entire cell membrane. It is usually not possible to resolve single-channel events in this configuration, although noise analysis of whole-cell recordings can give information about single-channel properties (see below). Finally, withdrawing the pipette from the cell under the whole-cell condition often gives rise to the outside-out configuration, in which a new patch is formed with the former extracellular surface of the membrane facing the bath. This can be used to study the effects of hormones, drugs, and other ligands which interact with the external face of the channel.

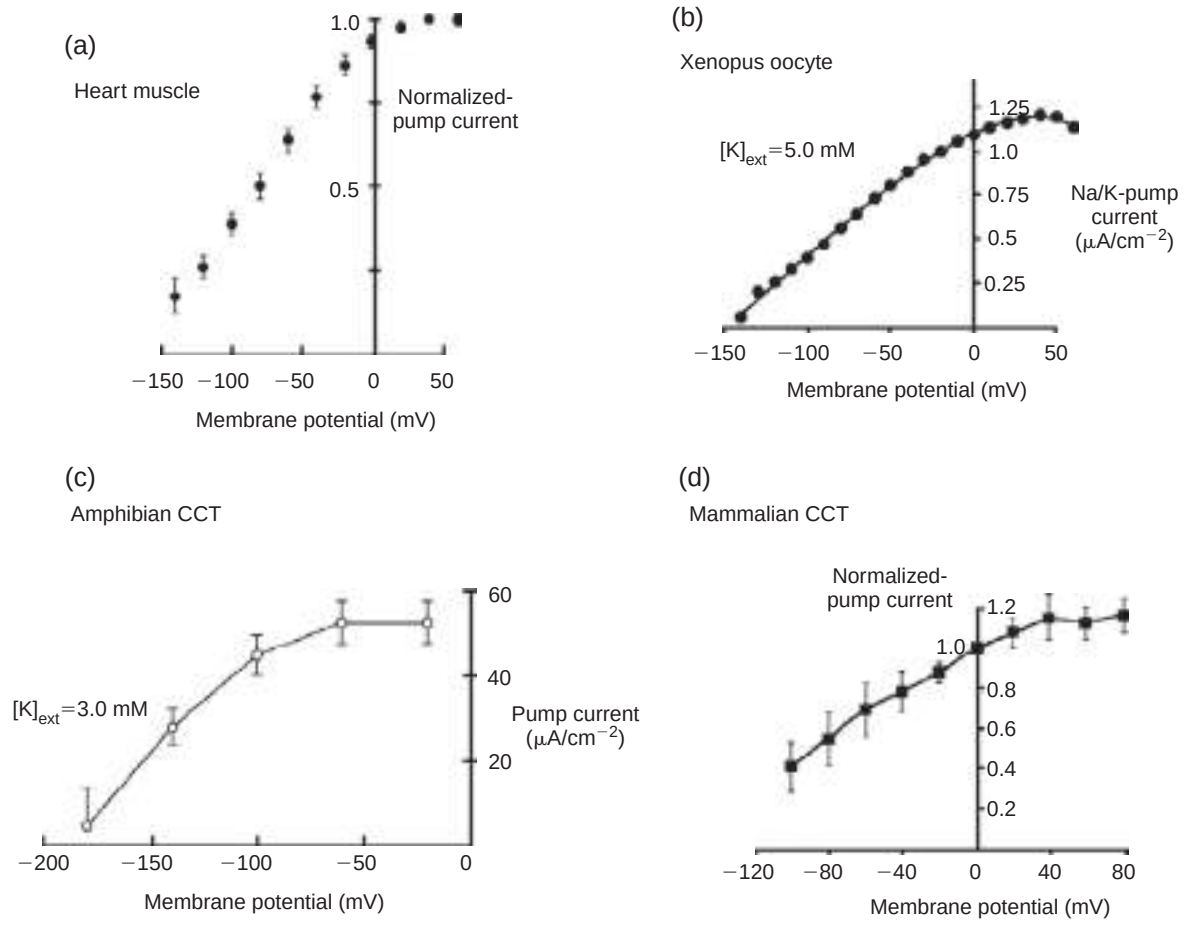

FIGURE 7.10 (a) Current-voltage relation of the cardiac Na-K-ATPase as determined from the strophanthidin-sensitive pump current in a whole-cell recording from a single isolated ventricular myocyte. Dissipative current pathways were blocked with Cs, Cd, TEA, and Ba (from [55]). (b) Current-voltage relation for the Na/K pump of *Xenopus* oocytes, bathed in a 90 mM Na, 5 mM K solution. Pump current was determined as the difference between current measured at 5 mM external K and current measured in K-free solutions (from [180]). (c) Current-voltage relation of the basolateral Na pump of *Amphiuma* collecting tubule as determined from the strophanthidin-sensitive current in short segments of voltage-clamped tubules (from [150]). (d) Current-voltage relation of the rat principal cell Na-K-ATPase. Ouabain-sensitive currents were normalized to their values at zero mV (from [57]).

PARAMETERS MEASURED ON SINGLE CHANNELS

Single-Channel Current

The simplest measure of channel electrical activity is the single-channel current (Figure 7.12). This is the change in current under voltage-clamp conditions which occurs when a channel opens or closes. It is generally quite reproducible for a given set of conditions, but varies with ion concentration, temperature, and voltage. It is common to characterize channels by their single-channel conductance. This is defined as the slope of the current versus the voltage relationship. For some channels this conductance is roughly independent of voltage. Many others, however, have highly non-linear current-voltage relationships. In the latter case, the voltage at which the conductance was measured must always be specified.

Normally, the lowest single channel conductance that can be reliably measured is in the neighborhood of 1 pS. This would correspond to measuring a 0.1 pA current at an electrical driving force of 100 mV. Most channels can conduct much larger currents; an upper limit of about 33 pA has been estimated from limitations of diffusion rates.[58] Eukaryotes have channels with conductances up to about 400 pS.

Some channels have more than one conducting state. Usually the largest one is chosen as the characteristic conductance, and smaller ones are referred to as "subconductance" states. Presumably these reflect different conformations of the channel protein. In one special case of the Cl channel CLC-0, the channel has two conductance states, with one being precisely half of the

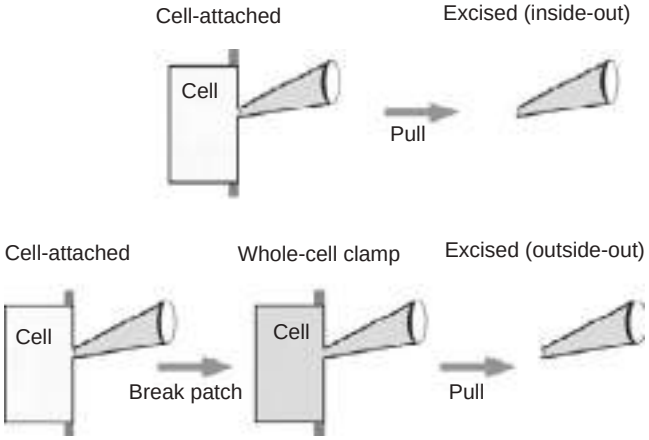

FIGURE 7.11 **Schematic of the patch-clamp technique, applied to the apical membrane of an epithelium.** Patch-clamping the basolateral membrane involves a similar procedure. In a cell-attached recording, the cell retains its original composition. Formation of a (conventional) whole-cell clamp causes most of the cell contents to be replaced by pipette solution. Withdrawal of the pipette from the whole-cell configuration often produces an excised, outside-out patch.

other.[59] The interpretation of these results was that two identical conducting pores are linked together such that they can close either separately or together. The "full" conductance state represents both pores conducting simultaneously, and the "sub" conductance state reflects the opening of just one of them. In general, the structural basis of subconductance states – which can have any fraction of the full conductance – is not well-understood.

Channel Selectivity

In addition to conductance, the ionic selectivity of the channel can also be determined from single-channel i-V plots under appropriate conditions. As in the case of macroscopic currents discussed in the last section, the selectivity of an individual ion channel can be defined and measured in different ways. Inside-out and outside-out patches are particularly well suited for measurements of permeability ratios, since the ions on both sides of the membrane can be set to known concentrations.

The ionic transference numbers for a channel can be evaluated using the same relationships discussed previously (see Eq. (7.23)). However, instead of perturbing the concentration of an ion across the membrane, it is simpler in a patch-clamp experiment to change the transmembrane voltage (see Eq. (7.26)). The reversal potential (E_{rev}) is then defined as the voltage at which current flow through the channel changes direction. Measurement of E_{rev} is easiest to interpret in excised patches, where ionic concentrations can be precisely controlled. For measurement of cation versus anion selectivity, dilution conditions are normally used, with a single salt at different concentrations (S1 and S2) on both sides of the membrane. For the case of a monovalent salt:

$$E_{rev} = (t_+ - t_-)\frac{RT}{F} Ln\ \frac{S_1}{S_2} \tag{7.28}$$

where t_+ and t_- are the transference numbers for ion movement through the individual pore, and S_1 and S_2 are the salt concentrations on either side of the membrane. This is equivalent to Eq. (7.12). Thus, if a channel has perfect selectivity for cations (or for anions) the reversal potential will shift by 59 mV for a 10-fold concentration gradient (at 25°C).

The permeability ratio is a common measure of the selectivity among ions of the same charge. In general, the permeability ratio can be computed from a constant-field equation similar to Eq. (7.26). This equation reduces to a particularly simple and useful form under bi-ionic conditions, with two different salts at the same concentration on either side of the membrane (e.g., NaCl and KCl for an exclusively cation-selective channel):

$$E_{rev} = \frac{RT}{F} Ln\ \frac{P_x}{P_y} \tag{7.29}$$

where P_x and P_y represent the permeabilities of the two ions x and y. A selectivity (permeability ratio) of 10 will give rise to a reversal potential of 59 mV at 25°C. Notice that Eq. (7.29) does not involve the actual salt concentration, as long as the concentration of salt X on one side is the same as the concentration of salt Y on the other side.

The relative permeability of a channel to different ions can be measured in cell-attached patches, even when the intracellular ion composition is not precisely known, from changes in the single-channel reversal potential associated with different patch pipette solutions. When the highly selective renal K channel, ROMK2, is expressed in K-depolarized *Xenopus* oocytes, the single-channel (cell-attached) i-V curve intersects the origin at a reversal potential of zero (solid line, Figure 7.13). When the same experiment is performed with Rb (rather than K) in the patch pipette, the single channel i-V relation becomes less steep, and the reversal potential shifts in a negative direction by 14 mV (dashed line, Figure 7.13). Using Eq. (7.29), this change in reversal potential implies a permeability ratio, $P_{Rb}/P_K = 0.63$ for ROMK2, expressed in *Xenopus* oocytes.

Ionic selectivity can also be estimated from single-channel conductance ratios determined under different ionic conditions. These can be compared with selectivity ratios derived from the permeability ratios described above. In general, the conductance ratio will

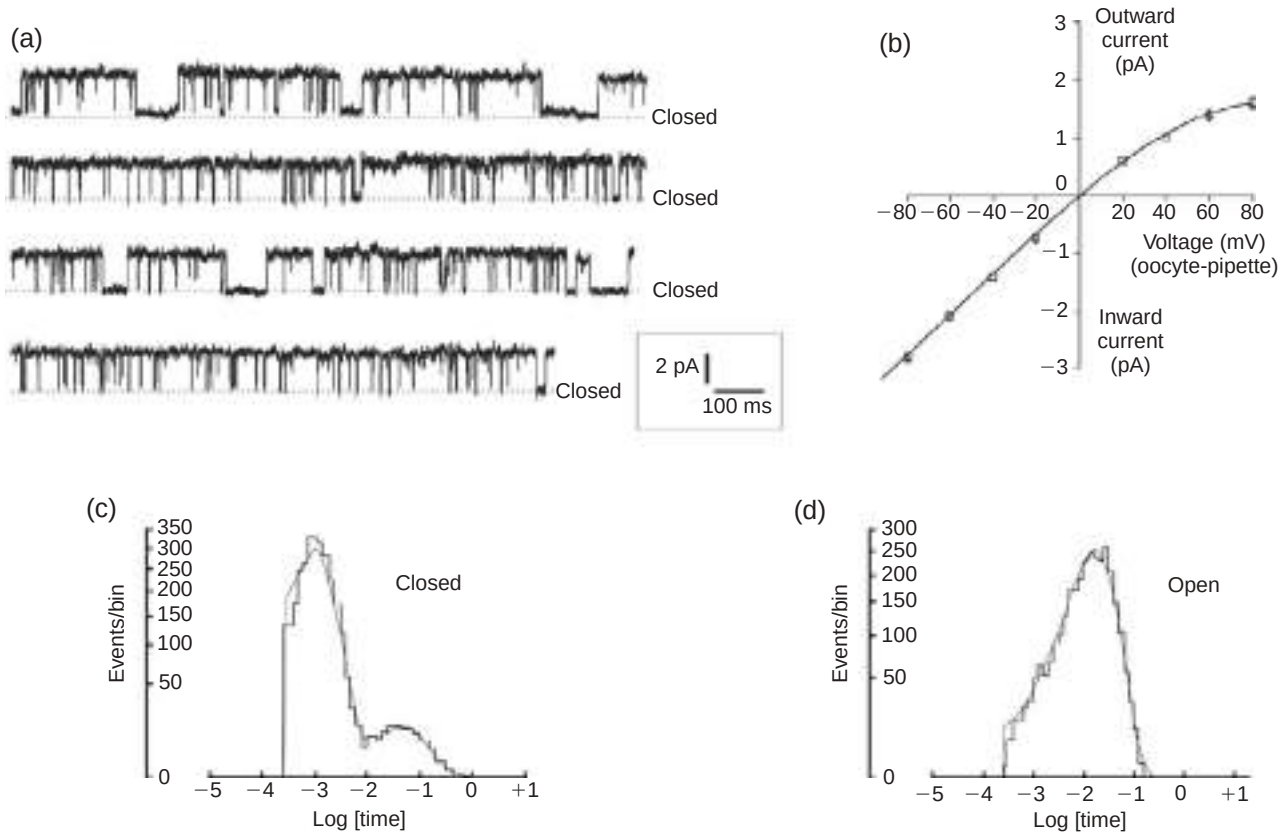

FIGURE 7.12 **Example of single-channel current records and associated analysis.** ROMK2 was expressed in *Xenopus* oocytes, and currents were recorded from a single channel in a cell-attached patch. The oocyte membrane potential was reduced close to zero by 100 mM KCl in the bath. The patch pipette also contained 100 mM KCl. Neither divalent ions nor specific chelating agents like EDTA were added to the pipette. (a) Currents recorded with the membrane potential clamped at −80 mV (cytoplasm relative to pipette). Upward deflections from the closed state correspond to inward K currents. (b) Current voltage relation for ROMK2, constructed by recording currents at different (clamped) membrane potentials. (c) Closed time distribution at −80 mV, showing two discrete closed states with time constants of 1.2 msec and 47 msec. (d) Open time distribution at −80 mV, with mean open time of 19 msec (from [60]).

differ from the permeability ratio, derived from reversal potentials and Eq. (7.29). For example, using the data of Figure 7.13, the ratio of inward Rb conductance to inward K conductances is $g_{Rb}/g_K = 0.36$. This differs significantly from the permeability ratio, $P_{Rb}/P_K = 0.63$ determined from reversal potentials. The discrepancy is even larger when the selectivity of K versus NH_4 is considered. Here the shift in reversal potential implies $P_{NH4}/P_K = 0.1$. However, the conductance to NH_4 at large negative potentials is equal to or higher than that to K at voltages driving inward currents, giving $g_{NH4}/g_K \geq 1$.[60,61] Discrepancies of this kind may indicate an interaction between the permeant ions and the channel. Rb may bind tightly a particular site within the pore, thus passing slowly through the channel. However, this binding will displace K from the channel, also reducing K conductance. The permeability ratio will reflect the relative affinity of the binding site for the two ions. Conversely, NH_4 may bind less tightly than K within the conduction pathway.

Open Probability

A second fundamental parameter of an ion channel that can be measured directly using single-channel recording is the open probability (P_o) or the fraction of time the channel spends in the open state. If there is only a single channel in the patch, P_o is determined by dividing the amount of time spent in the open state by the total recording time. P_o can also be measured in patches with more than one channel, provided that the number of channels (N) is known. This requires identification of the states with all channels open and with all channels closed, as discussed below.

A useful measure of overall channel activity in multichannel patches is the mean number of open channels, defined by Eq. (7.30):

$$NP_o = \sum_{n=1}^{N} nP_n \qquad (7.30)$$

where P_n equals (the dwell time with n channels open)/(total time); and N is the total number of

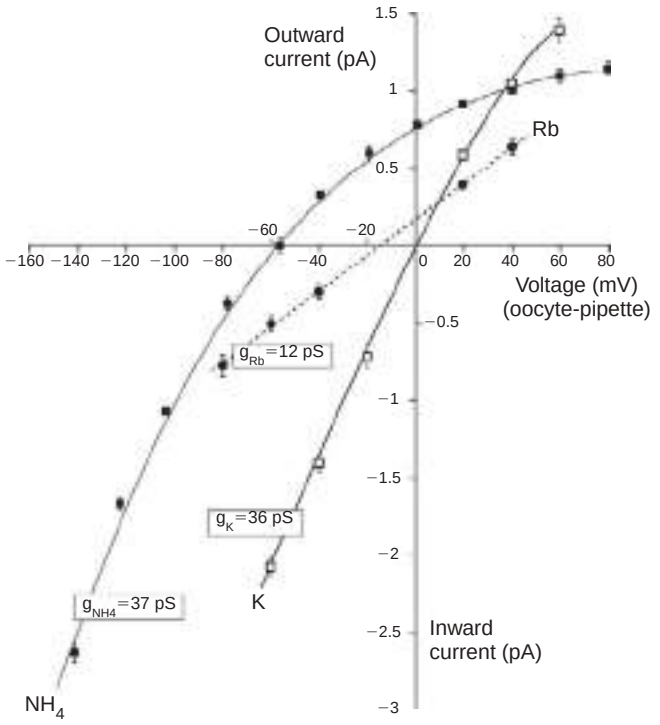

FIGURE 7.13 **Differences between relative conductances and relative permeabilities.** When R_b replaces K as the permeating cation of ROMK2, there is a shift in both the reversal potential (x intercept) and single-channel conductance (slope) of the i-V relation. The Rb/K permeability ratio calculated from the change in reversal potential was 0.63, which is significantly larger than the Rb/K conductance ratio of 0.36 determined from the inward slopes of the i-V curves. Similarly, the NH_4/K permeability ratio calculated from the change in reversal potential was 0.12, compared to a NH_4/K inward conductance ratio of unity (from [60]).

channels in the patch. Single-channel open probability (P_o) can be readily determined from Eq. (7.30), if the number (N) of channels in the patch is known. One caveat is that channels whose kinetics are very slow relative to the recording time may not be counted by Eq. (7.30).

An alternative method for estimating open probability is to compare the total macroscopic current (I) resulting from N channels to the single channel current (i), using Eq. (7.31), assuming that the number of channel proteins (N^*) can be measured independently. Under these conditions, the open probability would be given by (P^*_o):

$$P^*_o = I/N^*i \tag{7.31}$$

In *Xenopus* oocytes expressing ENaC channels, P^*_o was estimated to be 0.05 with Eq. (7.31) (Table 7.5). This is an order of magnitude lower than the P_o of about 0.5 that was determined by conventional electrical methods.[62] Presumably, this difference reflects a large number of silent channels, which are electrically invisible and therefore do not contribute to patch-clamp determinations of P_o. Equations (7.30) and (7.31) yield comparable estimates of P_o only for the special case where all channels in the membrane are active during the electrical measurements.

NUMBER OF CHANNELS

The number of channels in a patch (N) divided by the area of the patch will reflect, on average, the density of channels in the membrane. In principle, N can be observed. In practice, not all the possible current levels will be visited during the lifetime of the recording. This is particularly problematic when the P_o of the channels is either very low or very high. Sometimes this difficulty can be mitigated by maximally activating or deactivating channels at the end of a recording by applying voltage or chemical regulators.

If the properties of all channels are identical and are independent of each other, then the percentage of time spent in each state (e.g., 1 channel open, 2 channels open, etc.) should follow the binomial distribution. Fitting the measured distribution of times with a binomial function can then be used to estimate channel number.[63] This method is less biased than that of counting current levels, as the latter will always be an underestimate. However, the assumption that channels have identical kinetics is probably not always valid.

In some cases the kinetics of the channels can be used to estimate N. If all channels have a high P_o such that the state with all channels open is clearly defined, and a reproducible mean open time t_{open} (see below), then the mean time that an ensemble of N channels will stay in the all-open state will be t_{open}/N. Thus, N can be estimated even if the current level with all channels closed is never directly identified.[64] A similar procedure can be used on channels with a low P_o if the mean closed time is reproducible. This procedure works only if the channels have a single open (or closed) state (see below).

The area of patches is also difficult to quantify precisely. When the membrane patch can be seen in the light microscope, it often appears to be drawn a considerable distance into the patch-clamp pipette by the process of seal formation.[65,66] A typical patch geometry might correspond to a membrane area of about 5 μm^2. Areas estimated from electrical capacitance measurements varied from about 1 μm^2 to over 15 μm^2.[65] The area will depend on both the size of the micropipette and the cell type. Perhaps the surest way of estimating single-channel density is to combine single-channel measurements with a macroscopic measurement. For example, the number of Na channels in the apical membrane of the rat CCD has been estimated from the whole-cell, amiloride-sensitive conductance, and the

TABLE 7.5 Open Probability of Na Channels Expressed in *Xenopus* Oocytes[a]

Direct measurement: $P_o = 0.42$	Patch-clamp
Macroscopic current: I = 0.94 μA (100 mV)	TEVC
Single-channel current: i = 0.60 (− 100 mV)	Patch-clamp
Channel number $N^* = 1.7 \times 10^8$/cell	Ab binding (assume 4 subunits/channel)
Open probability: $P_o^* = I/N^*i = 0.04$	

[a]*Data from* [62].

TABLE 7.6 Computation of Na-Channel Density in Rat[a]

Macroscopic conductance: $I_{Na} = 510$ pA/cell ($V_m = -100$ mV)	Whole-cell clamp
Apical membrane area: A = 185 μm^2/cell	Morphological studies
Single channel conductance: $i_{Na} = 0.81$ pA ($V_m = -100$ mV)	Patch-clamp
Open probability: $P_o = 0.5$	Patch-clamp
Channel density $N = I_{Na}/[A \cdot i_{Na} \cdot P_o]$	
$N = 1260$/cell = 6.8 μm^2	

[a]*Data from* [152–154].

average single-channel conductance and open probability measured under similar conditions (Table 7.6).

OPEN AND CLOSED TIMES

All channels that open and close can be characterized, not only by the percent time in the open state (P_o), but also by the mean times spent in these states or, equivalently, the rates of transition between them. The mean lifetimes of the open and closed states can range from less than 1 msec to more than 1 second. The lifetimes of a given state are presumed to be exponentially distributed, similar to those of radioactive isotopes. The transition rates can be estimated by plotting the number of open (or closed) events of a given duration as a function of that duration.

In the simplest kinetic scheme, a channel that has just one open and one closed state can be diagrammed as follows:

This will result in open- and closed-time histograms which are monotonically decreasing functions of interval length, and which can be fitted by a single exponential decay curve.

In practice, the kinetic parameters of a particular channel are usually estimated by fitting the open and closed dwell time distributions with multiple exponential components. In this regard, it has proved most useful to generate event histograms with a logarithmic time axis and a square root transformation of the ordinate.[67] This greatly simplifies interpretation and fitting of distributions that contain multiple exponential components. Examples of two such fitted distributions are shown in Figure 7.12c and Figure 7.12d, respectively, for the closed and open times of single ROMK2 channels expressed in *Xenopus* oocytes. In this type of representation, the peaks of each of the skewed, bell-shaped curves correspond to time constants for the open and closed states of the channel.

Even after the number and duration of closed and open states have been determined, the exact kinetic scheme for the channel may still be ambiguous. Both of the models depicted below are consistent with two closed states and one open state. The first model corresponds to transitions between a single open state and a long-lived closed state (closed 2) that can only be reached by passage through a short-lived closed state (closed 1). In the second model, both the short and long-lived closed states are accessible from the open state. Even with this modest degree of complexity these two patterns cannot readily be distinguished, and the rate constants among the states cannot always be unequivocally derived.

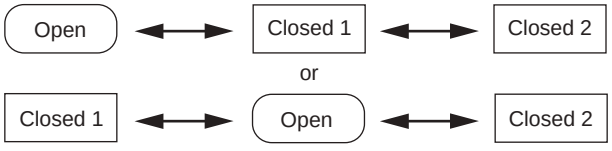

Channels can have multiple open states as well as multiple closed states. In Ca-activated BK channels, for example, models with 50 different states are required to portray channel kinetics.[68] As the number of possible open and closed states increases, the difficulty of the analysis increases as well, making it difficult to assign values to individual rate constants or to distinguish alternative kinetic schemes.

The situation can be even more complicated if the channel exhibits bursts of activity that are themselves part of a larger pattern of activity. This behavior requires even more states. Alternatively, a kinetic scheme based on fractals has been proposed[69] on the basis that a burst within a burst pattern will continue to be observed as the time domain over which

measurements are made becomes smaller or larger. The relative merits of fractal models as opposed to the more conventional discrete-state models are discussed in detail elsewhere.[70–72] Although the fractal approach is mathematically elegant, it is rarely used in practice since discrete-state models more closely correspond to the simple physical picture of a channel protein having several alternative conformations. It emphasizes, however, that the kinetic models are based on measurable time scales determined by technical limitations. Events of <0.1 msec duration are difficult to resolve with current instrumentation. On the other side of the spectrum, it is difficult to record a sufficient number of events of duration >10 sec to analyze accurately.

In some cases multiple gating "modes" have been distinguished from different kinetic states.[73,74] Here a channel will shift abruptly from one pattern of gating to another. This can be thought of as preserving the same open and closed states, but changing the rate constants for moving from one state to another. In some cases, changes in gating mode could reflect a chemical modification of a channel, such as a change in the phosphorylation state. However, reversible mode switches have also been observed with channels reconstituted into planar lipid bilayers.[75] In these cases the modes must be intrinsic to the channel proteins themselves.

Channel Pharmacology

Another defining characteristic of a channel type is its response to pharmacological agents, usually those which block the channel. If a specific blocker can be identified, it is also quite useful to compare single-channel data with macroscopic currents, similar to what was shown above for estimation of channel density. Amiloride is a commonly used blocker for epithelial Na channels, whereas Ba, TEA or Cs, block K channels. The dihydropyridines and certain divalent cations such as Cd^{+2} block Ca-selective channels, disulfonic stilbenes as well as a variety of organic anions block Cl channels, and gadolinium inhibits stretch-activated cation channels. A variety of naturally produced toxins work by blocking ion channels; most are directed against voltage-gated channels in excitable epithelia. However, tertiapin, a component of honey-bee venom, is a potent and fairly selective blocker of the renal K channel ROMK.[76,77] In addition, high-throughput screening has been used to identify novel inhibiters of specific ion channels. This approach has identified small-molecule blockers of ROMK channels that may be useful for *in vivo* or clinical applications.[78]

Channel blockers can affect either the open probability of the channel or its (apparent) single-channel conductance. The effect depends on the rates of association and dissociation of the blocker with the channel. In particular, if the off-rate is *slow* relative to the bandwidth of the recording device and the duration of the spontaneous open and closed states, the blocking action will be revealed as a new long-lived closed state. Block of the maxi-K channel by Ba^{+2} on the cytoplasmic side is an example of this type of interaction (Figure 7.14a). On the other hand, if the blocking action is *fast* relative to the bandwidth, it will show up as a decrease in the apparent single-channel conductance. Block of the maxi-K channel by extracellular TEA is a good example (Figure 7.14b).

Often the on-rates for blocking ions are diffusion-limited, i.e., very roughly in the range of $10^8\ sec^{-1}\ M^{-1}$. In this case, the rates of unblocking are inversely related to the affinities of block. For blockers with affinities in the nM range, the off-rate will be 10^{-1}/sec. This is a slow block, with a mean lifetime of the blocked state of 10 sec. For blockers with affinities in the μM range the mean lifetime could be 10 msec, corresponding to an intermediate blocking speed in which the blocking events are readily observed in patch-clamp recordings. For blockers with affinities in the mM range, the mean lifetime of the closed state would be 10 μsec, too fast to be resolved under most conditions.

There are at least two basic mechanisms of block, regardless of the blocking kinetics. In one, the blocker enters the pore part way, and sticks there by binding to a site within the pore. This type of block is usually voltage-dependent, particularly if the blocker is charged, since the transmembrane electric field will tend to either pull it into the pore or push it out. Voltage dependence may also arise if the blocker displaces permeant ions from the electric field. Examples of this type of block include those of Mg^{+2} and polyamines in inward-rectifier channels,[79] Ba^{+2} on several types of K channels,[80] and amiloride on the epithelial Na channel.[81] Another type of block involves an allosteric interaction with the channel protein. This changes the conformation of the protein to one in which the pore is closed or stabilizing a spontaneously occurring closed conformation. A well-studied example of this type of block is that of dihydropyridines on voltage-dependent Ca-channels.[73] The second type of block may be voltage-independent. However, a voltage-dependence could arise if the conformational change involves a movement of charge on the channel protein with respect to the electric field across the membrane.

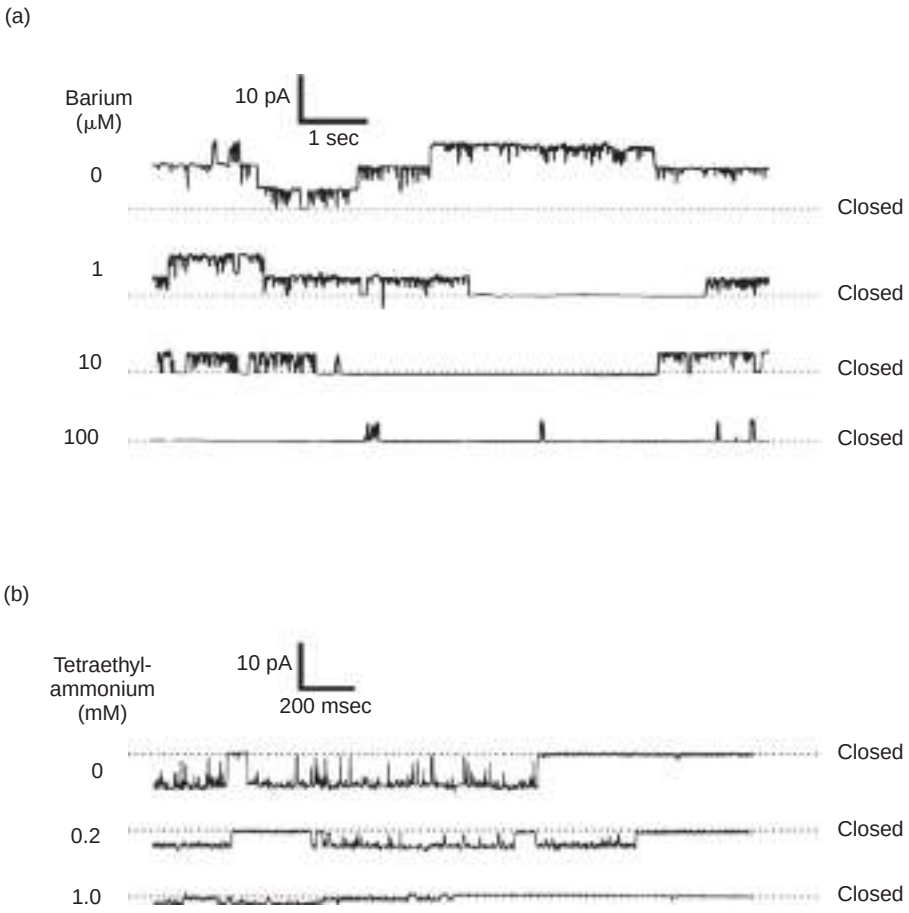

FIGURE 7.14 Comparison of (a) block of maxi-K channels by a slow blocker, Ba, which is effective at micromolar concentrations and reduces the open probability, with (b) block by tetraethyl ammonium, which is effective at mM concentrations and reduces the apparent single channel conductance (from [181]).

APPLICATION TO EPITHELIA

One of the major difficulties in the application of the patch-clamp technique to renal epithelia has been gaining access to the plasma membranes. Different methods have been used for both apical and basolateral membranes.

Apical Membranes

One successful approach to gaining access to the apical membrane is to split the tubules mechanically and flatten them onto their basolateral surfaces.[82,83] The use of a transparent, non-toxic, molluscan adhesive (Cell-Tak, Becton-Dickinson, Bedford, MA) has greatly improved attachment of the basement membrane to the bottom of the chamber and increased the stability of the patch-clamp recording.[82,84] An example of a split, flattened proximal tubule from *Necturus maculosus* is shown in Figure 7.15. Absence of staining with Trypan blue, except around the edge of the tissue, indicates viability of most of the hexagonal cells. Gigaohm seals can be formed on the apical surface of this preparation (shadow of a patch pipette can be seen near the center of the field). Although splitting individual nephron segments works best in large, amphibian tubules,[82,84–86] it has also been successfully used in mammalian CCD and TALH.[83,87,88]

A second approach to patch-clamping the apical surface of renal tubules has been to insert a micropipette into the open lumen of a perfused tubule.[89] This has the advantage of maintaining the tubule in the perfused state, and theoretically permits independent control of the solution on both sides of the tubule. However, this technique significantly increases the complexity of the patch-clamp procedure and decreases cell visibility, making it difficult or impossible to be absolutely sure which cell type is actually being studied within a given nephron segment.

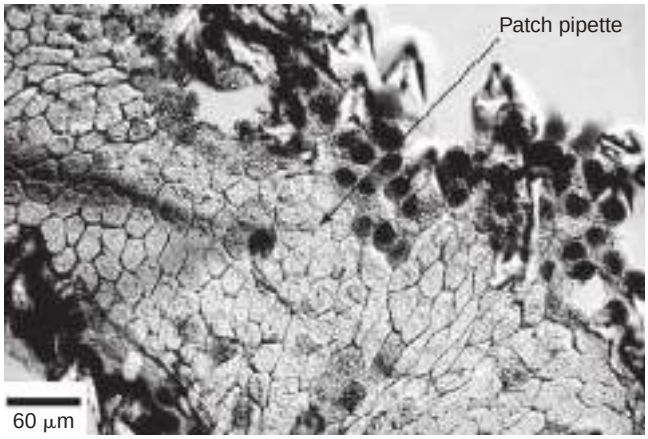

FIGURE 7.15 **Light micrograph of split-open *Necturus* proximal tubule (apical side up), viewed from below with modulation contrast optics.** The tissue was attached with Cell-Tak. Nuclei of damaged cells at the periphery are readily identified by their uptake of Trypan blue. Undamaged cells are approximately hexagonal in shape and exhibit well-defined boundaries with a diagonal diameter of about 30 μm. The tip and shadow of a patch pipette are visible at the left of the figure.

Another technique that preserves the separation of apical and basolateral solutions entails the eversion of the entire tubule, which can then be perfused with the luminal surface on the outside.[90–92] This approach has the advantage of maintaining the integrity of the entire tubule, but is technically demanding.

Finally, renal cells can be studied in culture, taking advantage of the tendency of epithelial cells to attach to a suitable substrate with their basolateral side down, leaving the apical membranes facing up and accessible for patch-clamping. Both continuous cell lines[93–95] and primary cultures of renal tubules[34,84,86,96–98] have been used. A problem with this approach is the difficulty of preserving the properties of the original cells in culture. One cell line which does appear to closely resemble native epithelial cells from the distal nephron is the A6 line from *Xenopus* kidney.[99] This has been a particularly useful preparation for studying epithelial Na channels.[93,100–102] A mammalian cell line that also preserves a distal nephron phenotype and has been used for patch-clamp is the mouse line mpkCCDc14.[95,103]

Basolateral Membranes

Basolateral channels are difficult to study because the basal surface is covered with a basement membrane that must be removed to allow access to the plasma membrane. With isolated amphibian tubules it has been possible to gain access to the basolateral membrane by manually removing a small segment of basement membrane.[84,104] This process has also been applied to the mammalian collecting tubule.[105] However, most patch-clamp studies on mammalian basolateral membranes have used pre-treatment of the tubules with a collagenase solution to remove enough of the basement membrane to permit formation of a high resistance patch-clamp seal.[105–109]

In an effort to circumvent the possible problems associated with enzymatic digestion, the lateral cell membranes of mammalian nephron segments have been patch-clamped either on the open end of a perfused tubule[89] or by mechanically removing an adjacent cell in an otherwise intact epithelium. The latter method was used to study basolateral channels on the lateral membrane of principal cells of rat CCD.[110] Here, a suction pipette is used to remove an entire intercalated cell from a split-open rat collecting tubule. This exposes a clean, lateral surface of an adjacent principal cell on which a high resistance seal can be formed with a standard patch pipette (Figure 7.16).

Isolated Cells

Another way of gaining access to either the apical or basolateral cell membranes is to use isolated, polarized cells, derived by a brief collagenase or trypsin treatment of the epithelium. This weakens the basement membrane sufficiently so that individual, undamaged cells can be obtained by moderate mechanical agitation. A number of studies have been carried out using isolated cell preparations of proximal tubules, since these cells often retain their polarity for extended periods.[111–115] Detailed cytochemical studies on isolated cells of this type have confirmed the stability of markers normally associated with either the apical or basolateral membranes of intact epithelia.[115] An example of an isolated amphibian proximal tubule cell is illustrated in Figure 7.16.[112,115] These cells maintain their polarity by assuming a bi-spherical,

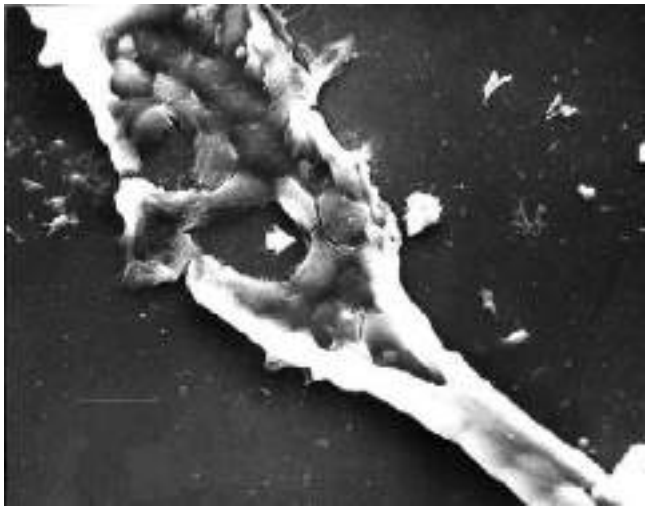

FIGURE 7.16 **Scanning electron micrograph of split open CCD.** Arrow shows lateral membrane of a principal cell. The intercalated cell adjacent to the principal cell was removed by mechanical suction, leaving the principal cell intact (from [110]).

minimum energy configuration. In this picture the apical surface, with brush border, is clearly visible as the smaller hemisphere, whereas the larger spherical surface consists of basolateral membrane.

NOISE ANALYSIS

Noise or fluctuation analysis provides an alternative approach to obtaining information at the level of single channels. In this technique the mean current level, as well as the variations about the mean, is used to infer single-channel properties. The principle behind the measurement is that random openings and closures of channels within a population will give rise to appreciable fluctuations in the overall number of open channels. The amplitudes of the fluctuations depend on the number channels, their open probability, and the single-channel current (see below). For a given mean current level, the fluctuations will be larger for a small number of channels (with large single-channel currents) than for a large number of channels (with smaller single-channel currents), since opening or closing one channel will produce a larger change in the mean current. A major disadvantage of this approach versus that of patch-clamp is that the single-channel events are not observed directly, but need to be extracted from the data using kinetic models, Fourier transforms, and curve fitting. A second drawback is that information on variations in channel behavior may be lost, and only the mean properties of an ensemble of the channels are obtained. This loss of information can sometimes be a blessing in disguise, particularly when the overall performance of the whole population of channels needs to be assessed, by focusing attention on the quantitatively important aspects of channel function. Another advantage is that the sampling of channel properties is not biased by those of a few "good" patches which may be easy to analyze, but are not necessarily representative. A third advantage of noise analysis over direct recording of single-channel events is that it can resolve smaller single-channel currents. For example, the inward-rectifier K channel Kir7.1 has a single-channel conductance of $\sim$50 fS estimated from noise analysis.[116] Single-channel openings and closings associated with this conductance would be impossible to see using patch-clamp recordings.

Like single-channel recordings, noise analysis depends on abrupt changes in currents which occur when channels open or close, giving rise to fluctuations. Although it is possible to analyze noise due to spontaneous opening and closing, in practice most uses of noise analysis in epithelia have made use of blocker-induced noise in which the fluctuations are promoted by addition of blocking ions to the medium. This has two advantages. First, if the blockers interact with the channel through a first-order process, the kinetic scheme is particularly simple:

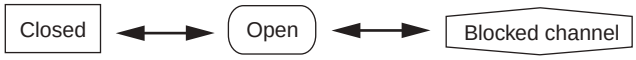

In the frequency domain, such a scheme predicts fluctuations which follow the form of a simple Lorentzian equation[117]:

$$S = S_o/[1 + (f/f_c)^2] \quad (7.32)$$

Where S is the power associated with a given frequency f, S_o is the plateau power approached at low frequencies, and f_c is a constant called the corner frequency, and is the frequency at which the power is reduced to half that of the plateau (Figure 7.17). Furthermore, f_c is determined by the kinetics of the blocking interaction:

$$2\pi f_c = [B]k_{on} + k_{off} \quad (7.33)$$

where [B] is the blocker concentration, and k_{on} and k_{off} are the on and off rate constants, respectively for the blocking reaction.

A second advantage of studying blocker-induced noise is that both the blocker and its concentration can be chosen to optimize the frequency of the fluctuations. This is important because technical problems can often limit the frequencies over which the noise can be reliably measured. For example, although amiloride-induced noise was originally used to study properties of epithelial Na channels,[117] recordings could be improved by using a lower affinity analog which produced fluctuations at higher frequencies.[118]

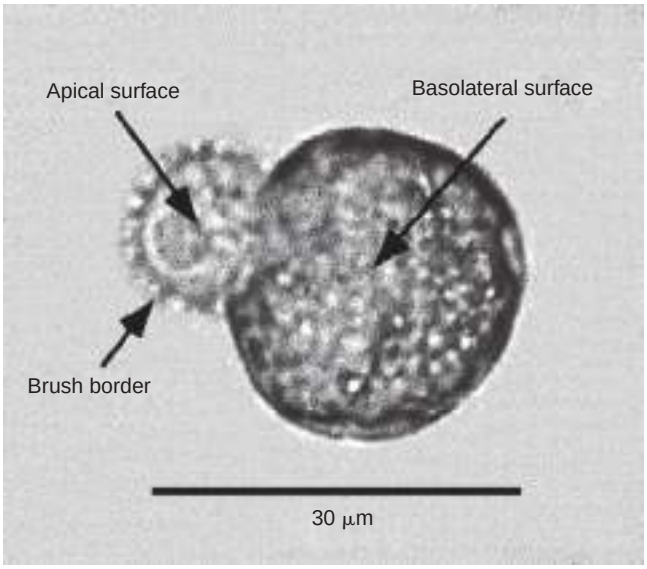

FIGURE 7.17 Isolated *Necturus* proximal tubule cell. The cell is bi-spherical in shape and about 30 microns in diameter. Evidence of a brush border is apparent on the smaller apical sphere. The larger spherical side of the cell consists of basolateral membrane. Isolated amphibian proximal tubule cells retain their polarity much longer than mammalian isolated epithelial cells. Patch-clamp recordings from both apical and basal surfaces indicate channel types similar to those found in native tubules.

The simplest piece of information that can be extracted from the noise analysis is the single-channel current[117]:

$$i = S_o 2\pi f_c / 4IF_B \tag{7.34}$$

Where F_B represents the fraction of blocked channels and I is the total (mean) current through the ensemble of channels measured in the presence of the blocker. F_B can be determined from the ratio of k_{on}/k_{off}, noting that $F_B = 1/(1 + k_{off}/k_{on}\bullet[B])$. F_B can also be estimated from the macroscopic dose-response curve (Figure 7.18a), although this may give different results if the blocker increases the number of channels contributing to the noise. The quantity N_o (=mean number of open + blocked channels) can be calculated from:

$$N_o = I/[i(1 - F_B)] \tag{7.35}$$

In general, N_o will be smaller than the total number of active channels N, since closed channels are not included. Helman and colleagues have made use of this discrepancy, and the finding that N_o increases as the concentration of blocker is increased, to assess P_o, the open probability of unblocked channels. This was analyzed in terms of a three-state model [118]:

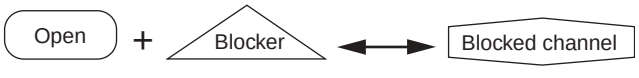

Assuming that closed channels cannot be blocked, the number of open + blocked channels is increased by the blocker through the principal of mass action.

A second approach to estimate P_o is to measure the fluctuations associated with the spontaneous opening and closing.[119] Again a simple model is assumed:

In which the variance (σ^2) of the current is given by[58]:

$$\sigma^2 = Ni^2P_o(1 - P_o) = I(1 - P_o)i \tag{7.36}$$

Therefore, the three measurements of blocker-induced noise, mean current, and variance in the absence of blocker can be used to estimate the three variables i, N, and P_o.

Most noise analysis studies have used flat epithelia in which the transepithelial voltage is clamped. Both native tissues[44,117,120,121] and cultured cells[118,122] have been successfully studied. In these instances blockers have been added to the apical side of the epithelia to measure properties of Na channels (using amiloride or its analogs as blockers) or K channels (using Ba^{+2}). More recently, fluctuation analysis has been applied to whole-cell recordings of renal epithelia, particularly the CCD, where the cells are not electrically coupled to each other.[38] Na channel fluctuations similar to those of flat epithelial can be measured in this way.[119] Another application involved characterization of basolateral K channels which, as described above, are difficult to study directly.[123] Similar techniques were also used to examine cell-attached patches in which channel density was too high to resolve single-channel events directly.[124]

Molecular Identification of Channels

Detailed information about channel properties obtained from patch-clamp analysis can, in some cases, be used to establish the molecular identity of the channels. Ideally this identification is corroborated using biochemical and genetic techniques. Table 7.7 provides a list of such channels for the mammalian nephron.

ROMK (Kir1.1), the apical K^+ channel of the TAL and CNT/CCD, provides a good example of this process. The channel was observed characterized in both of these segments[125,126] before the cDNA encoding it was cloned.[127] Subsequent detailed comparison of the biophysical properties of the native and cloned channels made it highly likely that the two were identical.[61] This was supported by immunocytochemical evidence demonstrating expression of the channel protein in the luminal membrane of the appropriate segments of the rat kidney.[128–130] Finally, genetic deletion of ROMK

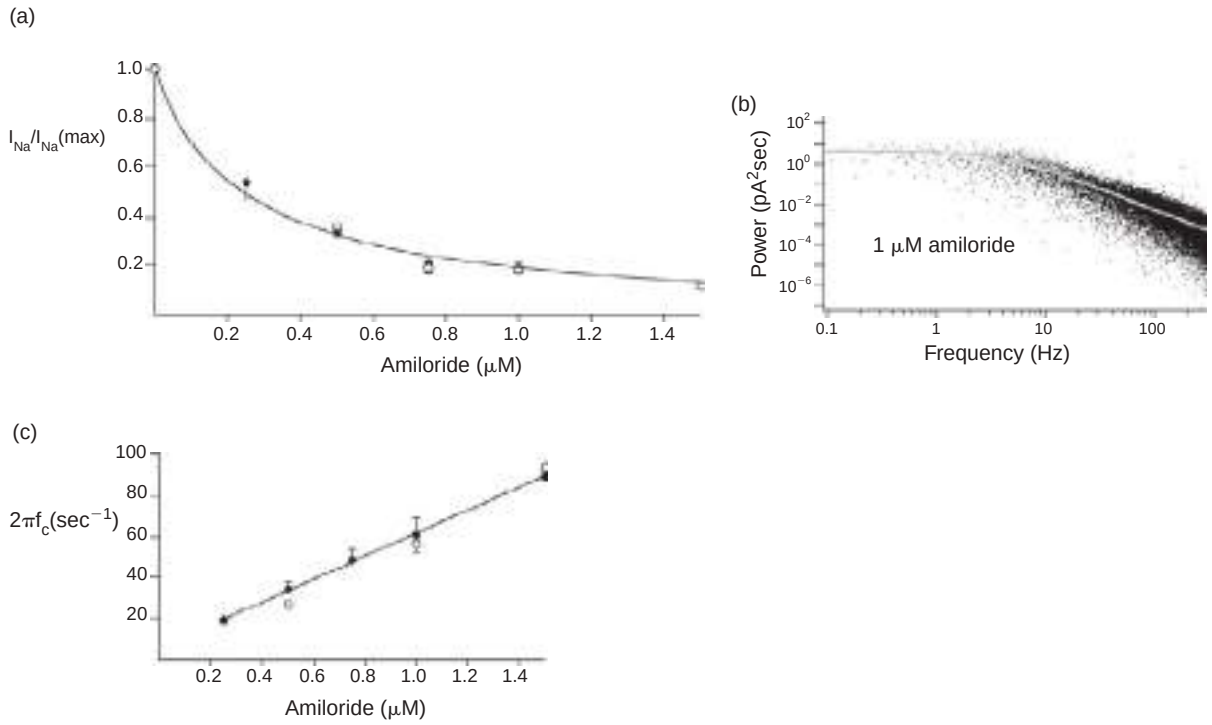

FIGURE 7.18 Noise analysis of whole-cell currents in a principal cell of the mouse CCD. The power density spectrum was obtained with 1 μM amiloride in the bath. The line represents a fit to a Lorentzian function with So = 3.06 pA^2 sec and f_c = 3.8 Hz (from [119]).

in the mouse led to the disappearance of the channels from the apical membranes of both the CCD and TALH.[131]

Although few channels have been examined as fully as ROMK, the list of fully and partially identified conductances is growing. In some cases, the genetic identification cited in Table 7.7 entails the analysis of phenotypes of human mutations such Bartter's[132] and SESAME/EAST[133,134] syndromes rather than a knock-out line. This is a less direct approach, but one that increases the pathophysiological relevance of the channel.

CONCLUSIONS

The patch-clamp approach has made it possible to study renal ion channels one molecule at a time. Insights into ion transport mechanisms that have emerged from these studies have greatly expanded the information that was previously available from equivalent circuit analysis. Although single-channel measurements provide details about how ion *channels* work, they do not provide complete information about how an *epithelium* works. Achieving this goal requires measurements of transepithelial, intracellular, and single channel properties.

APPENDIX 1. THE BASIC EQUATIONS FOR THE GENERAL EQUIVALENT CIRCUIT

The lateral resistive network in the circuit of Figure 7.1 makes it difficult to obtain a closed form solution for the electrical parameters of interest. However, if the lateral network is neglected, Figure 7.1 reduces to the simpler circuit of Figure 7.7a, which can be evaluated as follows.

Since the pump and diffusional EMFs are in parallel, the effective electromotive force of the cellular pathway is the sum of the individual EMFs weighted by their relative conductances:

$$E_{bl}^{*} = \frac{R_{bl}}{R_p + R_{bl}} E_p + \frac{R_p}{R_p + R_{bl}} E_{bl} \qquad \text{(A1.1)}$$

where E_p is the reversal potential of the pump and E_{bl} is the total ionic diffusion potential across the basolateral membrane, as given either by the mosaic membrane equation (Eq. (A1.2)) or the constant field equation (Eq. (A1.3)):

$$E_{bl} = -\frac{RT}{F}\left[t_{Na} Ln \frac{[Na]_c}{[Na]_b} + t_K Ln \frac{[K]_c}{[K]_b} + t_{Cl} Ln \frac{[Cl]_b}{[Cl]_c}\right] \qquad \text{(A1.2)}$$

TABLE 7.7 Molecular Identification of Ion Channels in Renal Tubules

Channel			Identification	
		Function	Protein	Genetic
PROXIMAL TUBULE				
Basolateral	K: K_{ATP} (Kir6?)	106, 107, 109, 155	–	–
TALH				
Apical	K: Kir1.1 (ROMK)	126	128, 130, 156	131
Basolateral	Cl: CLCK1(A)/2(B)	108, 157	158-160	132, 161
DCT				
Basolateral	K: Kir4.1/5.1	162	163, 164	133, 134
	Cl: CLCK2(B)	165, 166	159	–
CNT/CD PRINCIPAL CELL				
Apical	Na: ENaC	87, 167	168, 169	170
	K: Kir1.1 (ROMK)	125, 171	128, 130, 156	131
	K: mSlo (BK)	83, 172	–	–
Basolateral	K: Kir4.1/5.1	173	173	–
	K: Kir4.1	110, 123	173	–
	Cl: CLCK2(B)	174	159	–
CNT/CD INTERCALATED CELL				
Apical	K: mSlo (BK)	175, 176	177	–
Basolateral	Cl: CLCK2(B)	174, 178	158, 159	–

$$E_{bl} = -\frac{RT}{F} Ln \frac{P_{Na}[Na]_c + P_K[K]_c + P_{Cl}[Cl]_b}{P_{Na}[Na]_b + P_K[K]_b + P_{Cl}[Cl]_c} \quad \text{(A1.3)}$$

The effective basolateral resistance R^*_{bl} is the parallel sum of pump resistance (R_p) and the passive resistive elements of the membrane (R_{bl}):

$$R^*_{bl} = \frac{R_p \cdot R_{bl}}{R_p + R_{bl}} \quad \text{(A1.4)}$$

Transepithelial resistance (R_{te}) is a function of the other resistances in the network as defined by:

$$\frac{1}{R_{te}} = \frac{1}{R_{tj}} + \frac{1}{R_{ap} + R^*_{bl}} \quad \text{(A1.5)}$$

Considering the circuit of Figure 7.7b, the total circulating current (I) can be calculated from the total EMF of the circuit divided by the total resistance according to the equation:

$$I = \frac{-E^*_{bl} - E_{ap} + E_{par}}{R^*_{bl} + R_{ap} + R_{tj}} \quad \text{where } E^*_{bl} \text{ and } E_{ap} < 0 \quad \text{(A1.6)}$$

Under these conditions, the measured basolateral potential will be given by:

$$V_{bl} = E^*_{bl} + I \cdot R^*_{bl} = \frac{E^*_{bl}(R_{ap} + R_{tj}) + R^*_{bl}(E_{par} - E_{ap})}{R^*_{bl} + R_{ap} + R_{tj}} \quad \text{(A1.7)}$$

The measured apical membrane potential will be given by:

$$V_{ap} = E_{ap} + I \cdot R_{ap} = \frac{E_{ap}(R^*_{bl} + R_{tj}) + R_{ap}(E_{par} - E^*_{bl})}{R^*_{bl} + R_{ap} + R_{tj}} \quad \text{(A1.8)}$$

and the measured transepithelial potential will be given by:

$$V_{te} = E_{par} - I \cdot R_{par} = \frac{E_{par}(R_{ap} + R^*_{bl}) + R_{tj}(E_{ap} + E^*_{bl})}{R^*_{bl} + R_{ap} + R_{tj}} \quad \text{(A1.9)}$$

Equations (A1.7)–(A1.9) can be evaluated for the limiting cases of very tight and very leaky epithelia. In the case where the cell (rather than the interspace) is the primary conductive pathway:

$$Lim\ V_{bl} = E^*_{bl} \qquad \text{for } R_{tj} >> R_{ap} + R^*_{bl} \text{ (very tight epithelium)} \quad \text{(A1.10)}$$

and:

$$Lim\ V_{ap} = E_{ap} \qquad \text{for } R_{tj} >> R_{ap} + R^*_{bl} \text{ (very tight epithelium)} \quad \text{(A1.11)}$$

If perturbations are confined to the apical membrane, the additional limiting case is sometimes useful when only transepithelial measurements can be performed:

$$Lim\ \ \Delta V_{ap} = \Delta E_{ap} = \Delta V_{te} \qquad \text{for } R_{tj} >> R_{ap} + R^*_{bl} \quad \text{(very tight epithelium)} \tag{A1.12}$$

since:

$$Lim\ \ V_{te} = E_{ap} + E^*_{bl} \qquad \text{for } R_{tj} >> R_{ap} + R^*_{bl} \quad \text{(very tight epithelium)} \tag{A1.13}$$

At the other extreme, if the paracellular pathway has a much higher conductance than the cellular pathway:

$$Lim\ \ V_{te} = E_{par} \qquad \text{for } R_{ap} + R^*_{bl} >> R_{tj} \quad \text{(very leaky epithelium)} \tag{A1.14}$$

Finally, two other limiting cases of the general circuit equations permit determination of cell membrane properties from transepithelial measurements under special conditions. First, application of a high K solution to the serosal side of an epithelium having a predominantly K selective basolateral membrane reduces both R^*_{bl} and E^*_{bl} to values close to zero. Under these conditions, Eqs. (A1.8) and (A1.9) imply the following simple relation between V_{ap} and V_{te}.

$$V_{ap} = V_{te} = \frac{R_{tj}}{R_{ap} + R_{tj}} E_{ap} + \frac{R_{ap}}{R_{ap} + R_{tj}} E_{par} \tag{A1.15}$$

(K depolarized tissue)

Second, protocols that involve selective permeabilization of the apical membrane reduce both R_{ap} and E_{ap} to values near zero, and Eqs. (A1.7) and (A1.9) imply a simple relation between V_{bl} and V_{te}:

$$V_{bl} = V_{te} = \frac{R_{tj}}{R^*_{bl} + R_{tj}} E^*_{bl} + \frac{R^*_{bl}}{R^*_{bl} + R_{tj}} E_{par} \tag{A1.16}$$

(permeabilized apical membrane)

APPENDIX 2. RELATION BETWEEN THE REAL CHANGE IN EMF AND THE MEASURED CHANGE IN POTENTIAL

Circular current flow in polarized epithelial cells produces important discrepancies between the real change in EMF at a particular barrier, ΔE, and the change in voltage, ΔV, that can actually be measured with electrodes (see Figure 7.7). In order to evaluate individual ion selectivities, some assumption must be made about the equivalent circuit of the epithelium. In the simple model of Figure 7.7a, luminal replacement of Na, K or Cl with an impermeant ion will produce changes in the measured basolateral ΔV_{bl} and transepithelial potentials ΔV_{te} that are related to the change in apical membrane EMF according to:

$$\Delta E_{ap} = \Delta V_{te} - \Delta V_{bl}\left[1 + \frac{R_{ap}}{R_p} + \frac{R_{ap}}{R_{bl}}\right] \tag{A2.1}$$

where R_{ap}, R_{bl}, and R_p respectively refer to the apical membrane resistance, the lumped basolateral membrane resistance, and the intrinsic resistance of the basolateral Na-K pump. In Eqs. (A2.1)–(A2.3), it is assumed that the external ion replacements are performed rapidly enough so that the resistance ratios (R_{ap}/R_p, R_{ap}/R_{bl}) are constant, and the ion composition of the cell is essentially unchanged. The equations were derived by noting that the total current entering the cell across the apical membrane must equal the total current leaving the cell across the basolateral membrane.

Basolateral replacement of Na, K or Cl with an impermeant ion yields an analogous expression for the relation between the change in basolateral EMF and the measured potentials ΔV:

$$\Delta E_{bl} = \Delta V_{bl}\left[1 + \frac{R_{bl}}{R_p} + \frac{R_{bl}}{R_{ap}}\right] - \frac{R_{bl}}{R_{ap}}\Delta V_{te} \tag{A2.2}$$

Finally, the paracellular EMF would be given by Eq. (A2.3) for experiments involving basolateral replacement of Na, K or Cl by an impermeant ion.

$$\Delta E_{par} = \Delta V_{te}\left[1 + \frac{R_{tj}}{R_{ap}}\right] - \frac{R_{tj}}{R_{ap}}\Delta V_{bl} \tag{A2.3}$$

Equations (A2.1)–(A2.3) would be used together with Eq. (7.23) of the text to evaluate the ionic transference numbers of the apical, basolateral, and paracellular barriers.

APPENDIX 3. EQUATIONS FOR PARTIAL IONIC CONDUCTANCE

Specific expressions for the partial conductance G_x can be obtained by differentiating the Goldman–Hodgkin–Katz flux equation with respect to voltage:

$$G_x = \frac{\partial I_x}{\partial V} = \frac{\partial}{\partial V}\left\{P_x \frac{z^2F^2}{RT} V \cdot \left[\frac{[X]_o - [X]_i e^{zFV/RT}}{(1 - e^{zFV/RT})}\right]\right\} \tag{A3.1}$$

In the limiting case of zero membrane potential, the complicated form of Eq. (A3.1) reduces to the

arithmetic average of the concentrations on both sides of the membrane. This equation does not depend on the ion being distributed near its electrochemical equilibrium:

$$G_x \approx P_x \frac{z^2F^2}{RT}\frac{1}{2}(X_o + X_i) \tag{A3.2}$$

At large negative membrane potentials, positive ions will be driven from outside to inside, and the limiting conductance will be:

$$G_x \approx P_x \frac{z^2F^2}{RT} X_o \tag{A3.3}$$

Conversely, at large positive potentials, negative ions will be driven from inside to outside, and the limiting conductance will be:

$$G_x \approx P_x \frac{z^2F^2}{RT} X_i \tag{A3.4}$$

Although the above relations reduce the complicated general equation (Eq. (A3.1)) to a manageable form, neither the assumption of zero membrane potential (Eq. (A3.2)) nor the assumption of very large membrane potentials (Eqs. (A3.3), (A3.4)) are terribly physiological.

For ions like K and Cl, which are often distributed close to their electrochemical equilibrium, it is possible to simplify the algebraic form of the 'X' term in Eq. (7.25) of the text. Under these conditions, the conductance would be given by the equation:

$$G_x \approx P_x \frac{z_x^2F^2}{RT}\left(\frac{[X]_i[X]_o}{[X]_o - [X]_i}\right)\mathrm{Ln}\frac{[X]_o}{[X]_i} \tag{A3.5}$$

If more than one ion (X and Y) is distributed close to equilibrium across the membrane, the ratios of transference numbers, conductances and permeabilities are given by the equation:

$$\frac{t_x}{t_y} = \frac{G_x}{G_y} \approx \frac{P_x}{P_y}\cdot\frac{[X]_o}{[Y]_i} = \frac{P_x}{P_y}\cdot\frac{[X]_i}{[Y]_o} \tag{A3.6}$$

APPENDIX 4. CONTRIBUTION OF THE ELECTROGENIC Na-K PUMP TO THE MEMBRANE POTENTIAL

The contribution of the Na-K pump to the cell membrane potential of epithelial tissues is different than its contribution to the membrane potential of symmetric cells. The existence of circulating currents in the open-circuited state places a different set of constraints on the magnitude of the cell potential. This can be derived from the reduced equivalent circuit of Figure 7.7b. In this circuit, the electrogenic and diffusive ion pathways are combined into an effective EMF of the basolateral membrane (E^*_{bl}), and an effective basolateral resistance (R^*_{bl}). These lumped quantities are directly related to the individual parameters of the pump and the basolateral diffusion potential according to standard equations of linear circuit theory:

$$R^*_{bl} = \frac{R_{bl}\cdot R_p}{R_{bl} + R_p} \tag{A4.1}$$

$$E^*_{bl} = \frac{R_{bl}}{R_{bl} + R_p}E_p + \frac{R_p}{R_{bl} + R_p}E_{bl} \tag{A4.2}$$

If the circulating currents of Figure 7.7b are also considered, the measured membrane potential (V_{bl}) can be described by Eq. (A4.3), which indicates the specific contribution of the electrogenic pump (E_p), the ionic diffusion potential (E_{bl}), and the apical and paracellular diffusion potentials (E_{ap}, E_{par}).

$$\begin{aligned} V_{bl} = {} & f\left[\frac{R_{bl}}{R_{bl} + R_p}\right]E_p \\ & + f\left[\frac{R_p}{R_{bl} + R_p}\right]E_{bl} + g\left[E_{par} - E_{ap}\right] \end{aligned} \tag{A4.3}$$

where the factors "f" and "g" arise from the circulating current "I" in the model of Figure 7.7b:

$$f = \frac{R_{ap} + R_{tj}}{R^*_{bl} + R_{ap} + R_{tj}} \tag{A4.4}$$

$$g = \frac{R^*_{bl}}{R^*_{bl} + R_{ap} + R_{tj}} \tag{A4.5}$$

Equations (A4.3)–(A4.5) are the general equations for the relative contributions of the electrogenic pump (denoted by E_p), ionic diffusion (denoted by E_{bl}), and circulating current (denoted by $E_{par} - E_{ap}$) to the observed basolateral membrane potential (V_{bl}). As indicated by Eq. (A4.3), the membrane potential depends critically on the relative magnitude of the pump resistance (R_p) versus the diffusion resistance of the membrane R_{bl}.

The term R^*_{bl} can be determined from cable analysis (as described in the text). This value can then be used to calculate R_{bl} from Eq. (A4.1), assuming that the internal resistance of the pump (R_p) can be estimated from its I–V relation (see Figure 7.10).

If the internal pump resistance (R_p) is high compared to the ionic resistance (R_{bl}), the ratio $R_{bl}/(R_{bl} + R_p)$ will be low, and the measured membrane potential V_{bl} (given by Eq. (A4.3)) will be dominated by the diffusional EMF term involving E_{bl}. Conversely, if the

internal pump resistance is low, V_{bl} will be dominated by the pump term involving E_p.

References

[1] Ussing HH, Zerahn K. Active transport of sodium as the source of electric current in the short-circuited isolated frog skin. Acta Physiol Scand 1951;23:110–27.

[2] Greger R. Cation selectivity of the isolated perfused cortical thick ascending limb of Henle's loop of rabbit kidney. Pflügers Arch 1981;390:30–7.

[3] Hebert SC, Andreoli TE. Control of NaCl transport in the thick ascending limb. Am J Physiol 1984;246:F745–56.

[4] Sackin H, Boulpaep EL. Isolated perfused salamander proximal tubule: methods, electrophysiology, and transport. Am J Physiol 1981;241:F39–52.

[5] Sackin H, Boulpaep EL. Rheogenic transport in the renal proximal tubule. J Gen Physiol 1983;82:819–51.

[6] Spring K. Insertion of an axial electrode into renal proximal tubule. Yale J Biol Med 1972;45:426.

[7] Hegel U, Boulpaep EL. Studies of electrical impedence of kidney proximal tubular epithelium in *Necturus*. Abstr 6th Intern Congr Nephr 1975;45.

[8] Horisberger J-D, Giebisch G. Voltage dependence of the basolateral membrane conductance in the *Amphiuma* collecting tubule. J Membr Biol 1988;105:257–63.

[9] Frömter E. The route of passive ion movement through the epithelium of *Necturus* gallbladder. J Membr Biol 1972;8:259–301.

[10] Frömter E, Diamond JM. Route of passive ion permeation in epithelia. Nature New Biol 1972;235:9–13.

[11] Koefoed-Johnsen V, Ussing HH. On the nature of the frog skin potential. Acta Physiol Scand 1958;42:298–308.

[12] Greger R. Ion transport mechanisms in thick ascending limb of Henle's loop of mammalian nephron. Physiol Rev 1985;65:760–97.

[13] Frömter E. Viewing the kidney through microelectrodes. Am J Physiol 1984;247:F695–705.

[14] Boulpaep E. Electrical phenomena in the nephron. Kidney Int 1976;9:88–102.

[15] Boulpaep EL, Sackin H. Equivalent electrical circuit analysis and rheogenic pumps in epithelia. Federation Proc 1979;38:2030–6.

[16] Guggino WB, Windhager EE, Boulpaep EL, Giebisch G. Cellular and paracellular resistances of the *Necturus* proximal tubule. J Membrane Biol 1982;67:143–54.

[17] Wills NK, Eaton D, Lewis SA, Ifshin M. Current-voltage relationship of the basolateral membrane of a tight epithelium. Biochim Biophys Acta 1979;555:519–23.

[18] Higgins JT, Gebler B, Frömter E. Electrical properties of amphibian urinary bladder epithelia II. The cell potential profile in *Necturus* maculosus. Pflügers Arch 1977;371:87–97.

[19] Leaf A, Anderson J, Page LB. Active sodium transport by the isolated toad bladder. J Gen Physiol 1958;41:657–68.

[20] Ussing HH, Windhager EE. Nature of shunt path and active sodium transport path through frog skin epithelium. Acta Physiol Scand 1964;61:484–504.

[21] Horisberger J-D, Giebisch G. Na/K pump currents in the *Amphiuma* collecting tubule. J Gen Physiol 1989;94:493–510.

[22] Erlij D. Basic electrical properties of tight epithelia determined with a simple method. Pflügers Archiv 1976;364:91–3.

[23] Helman SI, Miller DA. *In vitro* techniques for avoiding edge damage in studies of the frog skin. Science 1971;173:146–8.

[24] Weinstein FC, Rosowski JJ, Peterson K, Delalic Z, Civan MM. Relationship of transient electrical properties to active sodium transport by toad urinary bladder. J Membrane Biol 1980; 52:25–35.

[25] Van Itallie CM, Anderson JM. Claudins and epithelial paracellular transport. Annu Rev Physiol 2006;68:403–29.

[26] Lewis SA, Eaton DC, Clausen C, Diamond JM. Nystatin as a probe for investigating the electrical properties of a tight epithelum. J Gen Physiol 1977;70:427–40.

[27] Germann WJ, Lowy ME, Ernst SA, Dawson DC. Differentiation of two distinct K conductances in the basolateral membrane of turtle colon. J Gen Physiol 1986;88:237–51.

[28] Clausen C, Wills NK. Impedance analysis in epithelia. In: Schultz SG, editor. Ion Transport by Epithelia: Recent Advances. New York: Raven Press; 1981. p. 79–92.

[29] Awayda M, Van Driessche W, Helman SI. Frequency-dependent capacitance of the apical membrane of frog skin: Dielectric relaxation processes. Biophysical Journal 1999;76:219–32.

[30] Clausen C, Lewis SA, Diamond JM. Impedance analysis of a tight epithelium using a distributed resistance model. Biophys J 1979;26:291–317.

[31] Van-Driessche W, Erlij D. Cyclic AMP increases electrical capacitance of apical membrane of toad urinary bladder. Arch Int Physiol Biochim Biophys 1991;99(6):409–11.

[32] Wills NK, Purcell RK, Clausen C. Na^+ transport and impedance properties of cultured renal (A6 and 2F3) epithelia. J Membr Biol 1992;125(3):273–85.

[33] Spring KR. Current-induced voltage transients in *Necturus* proximal tubule. J Membr Biol 1973;13:299–322.

[34] Nelson DJ, Ehrenfeld J, Lindemann B. Volume changes and potential artifacts of epithelial cells of frog skin following impalement with microelectrodes filled with 3M KCl. J Membrane Biol 1978;40(Special Issue):91–119.

[35] Hamill OP, Marty A, Neher E, Sakmann B, Sigworth FJ. Improved patch clamp techniques for high resolution current recording from cells and cell-free membrane patches. Pflügers Arch 1981;391:85–100.

[36] Horn R, Marty A. Muscarinic activation of ionic currents measured by a new whole-cell recording method. J Gen Physiol 1988;92(2):145–59.

[37] Bello-Reuss E. Cell membrane and paracellular resistances in isolated renal proximal tubules from rabbit and *Ambystoma*. J Physiol 1986;370:25–38.

[38] Frindt G, Sackin H, Palmer LG. Whole-cell currents in rat cortical collecting tubule: Low-Na diet increases amiloride-sensitive conductance. Am J Physiol 1990;258:F562–7.

[39] Oberleithner H, Guggino W, Giebisch G. Resistance properties of the diluting segment of *Amphiuma* kidney: influence of K adaptation. J Membr Biol 1985;88:139–47.

[40] Guggino WB. Functional heterogeneity in the early distal tubule of the *Amphiuma* kidney: evidence for two modes of Cl and K transport across the basolateral cell membrane. Am J Physiol 1986;250:F430–40.

[41] Greger R, Schlatter E. Properties of the lumen membrane of the cortical thick ascending limb of Henle's loop of rabbit kidney: a model for secondary active chloride transport. Pflügers Arch 1983;396:315–24.

[42] Anagnostopoulos T, Velu E. Electrical resistance of cell membranes in *Necturus* kidney. Pflügers Arch 1974;346:327–39.

[43] Weber GH, Frömter E. Influence of lateral intercellular spaces on current propagation in tubular epithelia as estimated by a multi-cable model. Pflügers Arch 1988;411:153–9.

[44] Wills NK, Alles WP, Sandle GI, Binder HJ. Apical membrane properties and amiloride binding kinetics of the human descending colon. Am J Physiol 1984;247:G749–57.

[45] DeWeer P. Electrogenic pumps: theoretical and practical considerations. In: Blaustein M, Lieberman M, editors. Electrogenic transport: Fundamental Principles and Physiological Implications. New York: Raven Press; 1984.

[46] Glynn IM. The electrogenic sodium pump. In: Blaustein MP, Lieberman M, editors. Electrogenic Transport: Fundamental Principles and Physiological Implications, 38. New York: Raven Press; 1984. p. 33–48.
[47] Garrahan PJ, Glynn IM. The stoichiometry of the sodium pump. J Physiol (Lond) 1967;192:217–35.
[48] Post RL, Jolly PC. The linkage of sodium, potassium and ammonium active transport across the human erthrocyte membrane. Biochim Biophys Acta 1957;25:118–28.
[49] Rakowski RF, Gadsby DC, DeWeer P. Stoichiometry and voltage dependence of the sodium pump in voltage-clamped, internally dialyzed squid giant axon. J Gen Physiol 1989;93:903–41.
[50] Eisner DA, Lederer WJ, Vaughan-Jones RD. The dependence of sodium pumping and tension on intracellular sodium activity in voltage-clamped sheep Purkinje fibres. J Physiol (Lond) 1981;317:163–87.
[51] Mullins LJ, Noda K. The influence of sodium-free solutions on the membrane potential of frog muscle fibers. J Gen Physiol 1963;47:117–39.
[52] Thomas RC. Electrogenic sodium pump in nerve and muscle cells. Physiol Rev 1972;52:563–94.
[53] Horisberger JD, Giebisch G. Voltage dependence of the basolateral membrane conductance in the *Amphiuma* collecting tubule. J Membrane Biol 1988;105:257–63.
[54] DeWeer P. Cellular sodium–potassium transport. In: Seldin DW, Giebisch G, editors. The Kidney: Physiology and Pathophysiology. New York: Raven Press; 1985.
[55] Gadsby D, Nakao M. The steady-state current-voltage relationship of the Na/K pump in guinea pig ventricular myocytes. J Gen Physiol 1989;94:511–37.
[56] Rakowski. Charge movement by the Na/K pump in *Xenopus* oocytes. J Gen Physiol 1993;101:117–44.
[57] Palmer LG, Antonian L, Frindt G. Regulation of the Na-K pump of the rat cortical collecting tubule by aldosterone. J Gen Physiol 1993;102(1):43–57.
[58] Hille B. Ionic channels of excitable membranes. *3rd ed*. Sunderland, Massachusetts: Sinauer Associates; 2001.
[59] Miller C. Open-state substructure of single chloride channels from *Torpedo* electroplax. Phil Trans R Soc Lond B 1982;299:401–11.
[60] Chepilko S, Zhou H, Sackin H, Palmer LG. Permeation and gating properties of a cloned renal K^+ channel. Am J Physiol 1995;268:C389–401.
[61] Palmer LG, Choe H, Frindt G. Is the secretory K channel in the rat CCT ROMK? Am J Physiol 1997;273:F404–10.
[62] Firsov D, Schild L, Gautschi I, Merillat AM, Schneeberger E, Rossier BC. Cell surface expression of the epithelial Na channel and a mutant causing Liddle syndrome: a quantitative approach. Proc Natl Acad Sci USA 1996;93(26):15370–5.
[63] Palmer LG, Frindt G. Conductance and gating of epithelial Na channels from rat cortical collecting tubule. Effects of Na and Li. J Gen Physiol 1988;92:121–38.
[64] Palmer LG, Frindt G. Regulation of apical K channels in rat cortical collecting tubule during changes in dietary K intake. Am J Physiol 1999;277:F805–12.
[65] Sakmann B, Neher E. Single-Channel Recording. 2nd ed. New York: Plenum Press; 1995.
[66] Sokabe M, Sachs F. The structure and dynamics of patch-clamped membranes: a study using differential interference contrast light microscopy. J Cell Biol 1990;111:599–606.
[67] Sigworth FJ, Sine SM. Data transformations for improved display and fitting of single-channel dwell time histograms. Biophys J 1987;52:1047–54.
[68] Cox DH, Aldrich RW. Role of the beta1 subunit in large-conductance Ca^{2+}-activated K^+ channel gating energetics. Mechanisms of enhanced Ca^{2+} sensitivity. J Gen Physiol 2000;116:411–32.
[69] Liebovitz LS, Fischbarg J, Koniarek JP. Ion channel kinetics: a model based on fractal scaling rather than multistate Markov processes. Math Biosci 1987;84:37–68.
[70] Korn SJ, Horn R. Statistical discrimination of fractal and Markov models of single-channel gating. Biophys J 1988;54:871–7.
[71] McManus OB, Weiss DS, Spivak CE, Blatz AL, Magleby KL. Fractal models are inadequate for the kintics of four different ion channels. Biophys J 1988;45:859–70.
[72] Millhauser GL, Salpeter EE, Oswald RE. Diffusion models of ion-channel gating and the origin of power-law distributions from single channel recordings. Proc Natl Acad Sci 1988;85:1503–7.
[73] Hess P, Lansman JB, Tsien RW. Different modes of Ca channel gating behaviour favored by dihydropyridine Ca agonists and antagonists. Nature 1984;311:538–44.
[74] Horn R, Vandenbert C, Lange K. Statistical analysis of single sodium channels. Effects of N-bromoacetamide. Biophys J 1984;45:323–35.
[75] O'Connell A.M. *Modal gating behavior of batrachotoxin-modified sodium channels* [Ph.D. thesis], Cornell University Medical College; 1992.
[76] Jin W, Klem AM, Lewis JH, Lu Z. Mechanisms of inward-rectifier K^+ channel inhibition by tertiapin-Q. Biochemistry 1999;38:14294–301.
[77] Jin W, Lu Z. A novel high-affinity inhibitor for inward-rectifier K^+ channels. Biochemistry 1998;37:13291–9.
[78] Lewis LM, Bhave G, Chauder BA, Banerjee S, Lornsen KA, Redha R, et al. High-throughput screening reveals a small-molecule inhibitor of the renal outer medullary potassium channel and Kir7.1. Mol Pharmacol 2009;76(5): 1094–103.
[79] Lopatin AN, Makhina EN, Nichols CG. The mechanism of inward rectification of potassium channels: "Long-pore plugging" by cytoplasmic polyamines. J Gen Physiol 1995;106:923–56.
[80] Latorre R, Miller C. Conduction and selectivity in potassium channels. J Membr Biol 1983;71:11–30.
[81] Palmer LG. Voltage-dependent block by amiloride and other monovalent cations of apical Na channels in the toad urinary bladder. J Membrane Biol 1984;80:153–65.
[82] Filipovic D, Sackin H. A calcium-permeable stretch-activated cation channel in renal proximal tubule. Am J Physiol 1991;260: F119–29.
[83] Hunter M, Lopes AG, Boulpaep E, Giebisch G. Single channel recordings of calcium-activated potassium channels in the apical membrane of rabbit cortical collecting tubule. Proc Natl Acad Sci USA 1984;81:4237–9.
[84] Sackin H, Palmer LG. Basolateral potassium channels in renal proximal tubule. Am J Physiol 1987;253:F476–87.
[85] Sackin H. Stretch-activated potassium channel in renal proximal tubule. Am J Physiol 1987;253:F1253–62.
[86] Sackin H. A stretch-activated K^+ channel sensitive to cell volume. Proc Natl Acad Sci USA 1989;86:1731–5.
[87] Palmer LG, Frindt G. Amiloride-sensitive Na channels from the apical membrane of the rat cortical collecting tubule. Proc Natl Acad Sci U S A 1986;83:2767–70.
[88] Wang W, White S, Geibel J, Giebisch G. A potassium channel in the apical membrane of rabbit thick ascending limb of Henle's loop. Am J Physiol 1990;258:F244–53.
[89] Gögelein H, Greger R. Single channel recordings from basolateral and apical membranes of renal proximal tubules. Pflügers Archiv 1984;401:424–6.

[90] Engbretson BG, Beyenbach KW, Stoner LC. The everted renal tubule: a methodology for direct assessment of apical membrane function. Am J Physiol 1988;255:F1276–80.
[91] Stoner LC, Engbretson BG, Viggiano SC, Benos DJ, Smith PR. Amiloride-sensitive apical membrane sodium channels of everted *Ambystoma* collecting tubule. J Membr Biol 1995;144 (2):147–56.
[92] Stoner LC, Morley GE. Effect of basolateral or apical hyposmolarity on apical maxi K channels of everted rat collecting tubule. Am J Physiol 1995;268(4 Pt 2):F569–580.
[93] Hamilton KL, Eaton DC. Single-channel recordings from amiloride-sensitive epithelial sodium channel. Am J Physiol 1985;249:C200–7.
[94] Lang F, Friedrich F, Paulmilch M, Schobersberger W, Jungwirth A, Ritter M, et al. Ion channels in Madin–Darby canine kidney cells. Renal Physiol Biochem 1990;13:82–93.
[95] Staruschenko A, Pochynyuk O, Vandewalle A, Bugaj V, Stockand JD. Acute regulation of the epithelial Na^+ channel by phosphatidylinositide 3-OH kinase signaling in native collecting duct principal cells. J Am Soc Nephrol 2007;18 (6):1652–61.
[96] Gitter AH, Beyenbach KW. Christine C, Gross P, Minuth WW, Frömter E. High conductance K^+ channel in apical membranes of principal cells cultured from rabbit renal cortical collecting duct anlagen. Pflügers Arch 1987;408:282–90.
[97] Light DB, McCann FV, Keller TM, Stanton BA. Amiloride-sensitive cation channel in apical membrane of inner medullary collecting duct. Am J Physiol 1988;255:F278–86.
[98] Ling BN, Hinton CF, Eaton DC. Amiloride-sensitive sodium channels in rabbit cortical collecting tubule primary cultures. Am J Physiol 1991;261:F933–44.
[99] Handler JS, Perkins FM, Johnson JP. Hormone effects on transport in cultured epithelia with high electrical resistance. Am J Physiol 1981;240:C103–5.
[100] Ma HP, Li L, Zhou ZH, Eaton DC, Warnock DG. ATP masks stretch activation of epithelial sodium channels in A6 distal nephron cells. Am J Physiol 2002;282:F501–5.
[101] Marunaka Y, Eaton DC. Effects of vasopressin and cAMP on single amiloride-blockable Na channels. Am J Physiol 1991;260:C1071–84.
[102] Ohara A, Matsunaga H, Eaton DC. G protein activation inhibits amiloride-blockable highly selective sodium channels in A6 cells. Am J Physiol 1993;.
[103] Duong Van Huyen J, Bens M, Vandewalle A. Differential effects of aldosterone and vasopressin on chloride fluxes in transimmortalized mouse cortical collecting duct cells. J Membr Biol 1998;164(1):79–90.
[104] Kawahara K, Hunter M, Giebisch G. Potassium channels in *Necturus* proximal tubule. Am J Physiol 1987;253:F488–94.
[105] Sansom SC, La BQ, Carosi SL. Double-barrelled choride channels of collecting duct basolateral membrane. Am J Physiol 1990;259:F46–52.
[106] Hurst AM, Beck J, Laprade R, Lapointe J-Y. Na pump inhibition downregulates an ATP-sensitive K channel in rabbit proximal tubule. Am J Physiol 1993;264:F760–4.
[107] Parent L, Cardinal J, Sauvé R. Single-channel analysis of a K channel at basolateral membrane of rabbit proximal convoluted tubule. Am J Physiol 1988;254:F105–13.
[108] Paulais M, Teulon J. cAMP-activated chloride channel in the basolateral membrane of the thick ascending limb of the mouse kidney. J Membr Biol 1990;113(3):253–60.
[109] Tsuchiya K, Wang W, Giebisch G, Welling PA. ATP is a coupling modulator of parallel Na/K ATPase K channel activity in the renal proximal tubule. Proc Natl Acad Sci USA 1992;89:6418–22.
[110] Wang W-H, McNicholas CM, Segal AS, Giebisch G. A novel approach allows identification of K channels in the lateral membrane of rat CCD. Am J Physiol 1994;266:F813–22.
[111] Cemerikic D, Sackin H. Substrate activation of mechanosensitive, whole cell currents in renal proximal tubule. Am J Physiol 1993;264:F707–14.
[112] Filipovic D, Sackin H. Stretch- and volume-activated channels in isolated tubule cells. Am J Physiol 1992;262:F857–70.
[113] Kawahara K. A stretch-activated K^+ channel in the basolateral membrane of *Xenopus* kidney proximal tubule cells. Pflügers Arch 1990;415:624–9.
[114] Robson L, Hunter M. Volume regulatory responses in frog isolated proximal tubules. Pflügers Arch 1994;428:60–8.
[115] Segal A, Boulpaep EL, Maunsbach AB. A novel preparation of dissociated renal proximal tubule cells that maintain epithelial polarity in suspension. Am J Physiol (Cell) 1996;270: C1843–63.
[116] Krapininsky G, Medina I, Eng L, Krapivinsky L, Yang Y, Clapham D. A novel inward rectifier K^+ channel with unique pore properties. Neuron 1998;20:995–1005.
[117] Lindemann B, Van Driessche W. Sodium specific membrane channels of frog skin are pores: Current fluctuations reveal high turnover. Science 1977;195:292–4.
[118] Helman SI, Baxendale LM. Blocker-related changes of channel density. Analysis of a three-state model for apical Na channels of frog skin. J Gen Physiol 1990;95:647–78.
[119] Dahlmann A, Pradervand S, Hummler E, Rossier BC, Frindt G, Palmer LG. Mineralocorticoid regulation of epithelial Na^+ channels is maintained in a mouse model of Liddle's syndrome. Am J Physiol 2003;285:F310–8.
[120] Li H-Y, Palmer LG, Edelman IS, Lindemann B. The role of Na-channel density in the natriferic response of the toad urinary bladder to an antidiuretic hormone. J Membr Biol 1982; 64:77–89.
[121] Van Driessche W, Zeiske W. Ba^{2+}-induced conductance fluctuations of spontaneously fluctuating K^+ channels in the apical membrane of frog skin (*Rana temporaria*). J Membr Biol 1980;56:31–42.
[122] Blazer-Yost BL, Helman SI. The amiloride-sensitive epithelial Na^+ channel: Binding sites and channel densities. Am J Physiol 1997;272(3):C761–9.
[123] Gray DA, Frindt G, Zhang YY, Palmer LG. Basolateral K^+ conductance in principal cells of rat CCD. Am J Physiol Renal Physiol 2005;288(3):F493–504.
[124] Frindt G, Silver RB, Windhager EE, Palmer LG. Feedback regulation of Na channels in rat CCT. III. Response to cAMP. Am J Physiol 1995;268:F480–9.
[125] Frindt G, Palmer LG. Low-conductance K channels in apical membrane of rat cortical collecting tubule. Am J Physiol 1989;256:F143–51.
[126] Wang W, White S, Geibel J, Giebisch G. A potassium channel in the apical membrane of rabbit thick ascending limb of Henle's loop. Am J Physiol 1990;258:F244–53.
[127] Ho KH, Nichols CG, Lederer WJ, Lytton J, Vassilev PM, Kanazirska MV, et al. Cloning and expression of an inwardly rectifying ATP-regulated potassium channel. Nature 1993;362:31–7.
[128] Kohda Y, Ding W, Phan E, Housini I, Wang J, Star RA, et al. Localization of the ROMK potassium channel to the apical membrane of distal nephron in rat kidney. Kidney Int 1998;54:1214–23.
[129] Mennitt PA, Wade JB, Ecelbarger CA, Palmer LG, Frindt G. Localization of ROMK channels in the rat kidney. J Am Soc Nephrol 1997;8:1823–30.
[130] Xu JZ, Hall AE, Peterson LN, Bienkowski MJ, Eesalu TB, Hebert SC. Localization of the ROMK protein on apical

membranes of rat kidney nephron segments. Am J Physiol 1997;273:F739–48.
[131] Lu M, Wang T, Yan Q, Yang X, Dong K, Knepper MA, et al. Absence of small conductance K^+ channel (SK) activity in apical membranes of thick ascending limb and cortical collecting duct in ROMK (Barrter's) knockout mice. J Biol Chem 2002;277:37881–7.
[132] Simon DB, Bindra RS, Mansfield TA, Nelson-Williams C, Mendonca E, Stone R, et al. Mutations in the chloride channel gene, CLCNKB, cause Bartter's syndrome type III. Nat Genet 1997;17(2):171–8.
[133] Bockenhauer D, Feather S, Stanescu HC, Bandulik S, Zdebik AA, Reichold M, et al. Epilepsy, ataxia, sensorineural deafness, tubulopathy, and KCNJ10 mutations. N Engl J Med 2009;360(19):1960–70.
[134] Scholl UI, Choi M, Liu T, Ramaekers VT, Hausler MG, Grimmer J, et al. Seizures, sensorineural deafness, ataxia, mental retardation, and electrolyte imbalance (SeSAME syndrome) caused by mutations in KCNJ10. Proc Natl Acad Sci USA 2009;106(14):5842–7.
[135] Guggino WB, Oberleithner H, Giebisch G. The amphibian diluting segment. Am J Physiol 1988;254:F615–27.
[136] Hunter M, Horisberger J-D, Stanton BA, Giebisch G. The collecting tubule of *Amphiuma* I. Electrophysiological characterization. Am J Physiol 1987;253:1263–72.
[137] Koeppen BM, Biagi BA, Giebisch G. Intracellular microelectrode characteriation of the rabbit cortical collecting duct. Am J Physiol 1983;244:F35–47.
[138] Koeppen BM. Conductive properties of the rabbit outer medullary collecting duct: Outer stripe. Am J Physiol 1986;250: F70–6.
[139] Stanton BA. Characterization of apical and basolateral membrane conductances of rat inner medullary collecting duct. Am J Physiol 1989;256:F862–8.
[140] Lewis SA, Diamond JM. Na^+ transport by rabbit urinary bladder, a tight epithelium. J Membrane Biol 1976;28:1–40.
[141] Lapointe JY, Laprade R. Cardinal J. Transepithelial and cell membrane electrical resistances of the rabbit proximal convoluted tubule. Am J Physiol 1984;247:F637–49.
[142] Frömter E. Electrophysiological analysis of rat renal sugar and amino acid transport. I. Basic phenomena. Pflügers Arch 1982;393:179–89.
[143] O'Neil RG, Sansom SC. Electrophysiological properties of cellular and paracellular conductive pathways of the rabbit cortical collecting duct. J Membr Biol 1984;82:281–95.
[144] Koeppen B, Giebisch G. Cellular electrophysiology of potassium transport in the mammalian cortical collecting tubule. Pflügers Arch 1985;405(Suppl 1):S143–6.
[145] Koeppen B. Electrophysiology of ion transport in renal tubule epithelia. Semin Nephrol 1987;7:37–47.
[146] Lewis SA, Eaton DC, Diamond JM. The mechanism of Na^+ transport by rabbit urinary bladder. J Memb Biol 1976;28:41–70.
[147] Maunsbach AB, Boulpaep EL. Quantitative ultrastructure and functional correlates in proximal tubules of *Ambystoma* and *Necturus*. Am J Physiol 1984;246:F710–24.
[148] Messner G, Wang W, Paulmichl M, Oberleithner H, Lang F. Ouabain decreases apparent potassium-conductance in proximal tubules of the amphibian kidney. Pflügers Arch 1985;404:131–7.
[149] Hoshi T, Kawahara K, Yokoyama R, Suenga K. Change in membrane resistances of renal proximal tubule induced by cotransport of sodium and organic solutes. In: Takacs L, editor. Adv Physiol. Sci (Kidney and Body Fluids), 11. Budapest: Pergamon Press and Akademiai Kiado; 1981.
[150] Horisberger JD, Giebisch G. Intracellular Na and K activities and membrane conductances in the collecting tubule of *Amphiuma*. J Gen Physiol 1988;92:643–65.
[151] Frömter E, Gebler B. Electrical properties of amphibian urinary bladder epithelia III. The cell membrane resistances and the effect of amiloride. Pflügers Arch 1977; 371:99–108.
[152] Frindt G, Masilamani S, Knepper MA, Palmer LG. Activation of epithelial Na channels during short-term Na deprivation. Am J Physiol 2001;280:F112–8.
[153] Pácha J, Frindt G, Antonian L, Silver R, Palmer LG. Regulation of Na channels of the rat cortical collecting tubule by aldosterone. J Gen Physiol 1993;102:25–42.
[154] Palmer LG, Sackin H, Frindt G. Regulation of Na channels by luminal Na in rat cortical collecting tubule. J Physiol (London) 1998;509:151–62.
[155] Gögelein H, Greger R. Properties of single K channels in the basolateral membrane of rabbit proximal straight tubules. Pflügers Archiv 1987;410:288–95.
[156] Mennitt PA, Frindt G, Silver RB, Palmer. Potassium restriction downregulates ROMK expression in rat kidney. Am J. Physiol (Renal) 2000;278:F916–24.
[157] Reeves WB, Winters CJ, Filipovic DM, Andreoli TE. Cl^- channels in basolateral renal medullary vesicles. IX. Channels from mouse MTAL cell patches and medullary vesicles. Am J Physiol 1995;269(5 Pt 2):F621–627.
[158] Estevez R, Boettger T, Stein V, Birkenhager R, Otto E, Hildebrandt F, et al. Barttin is a Cl^- channel beta-subunit crucial for renal Cl^- reabsorption and inner ear K^+ secretion. Nature 2001;414(6863):558–61.
[159] Kobayashi K, Uchida S, Mizutani S, Sasaki S, Marumo F. Intrarenal and cellular localization of CLC-K2 protein in the mouse kidney. J Am Soc Nephrol 2001;12(7):1327–34.
[160] Vandewalle A, Cluzeaud F, Bens M, Kieferle S, Steinmeyer K, Jentsch TJ. Localization and induction by dehydration of ClC-K chloride channels in the rat kidney. Am J Physiol 1997;272(5 Pt 2):F678–688.
[161] Zimniak L, Winters CJ, Reeves WB, Andreoli TE. Cl^- channels in basolateral renal medullary vesicles XI. rbClC-Ka cDNA encodes basolateral MTAL Cl^- channels. Am J Physiol 1996;270(6 Pt 2):F1066–1072.
[162] Lourdel S, Paulais M, Cluzeaud F, Bens M, Tanemoto M, Kurachi Y, et al. An inward rectifier K(+) channel at the basolateral membrane of the mouse distal convoluted tubule: similarities with Kir4-Kir5.1 heteromeric channels. J Physiol 2002;538(Pt 2):391–404.
[163] Ito M, Inanobe A, Horio Y, Hibino H, Isomoto S, Ito H, et al. Immunolocalization of an inwardly rectifying K^+ channel, K (AB)-2 (Kir4.1), in the basolateral membrane of renal distal tubular epithelia. FEBS Lett 1996;388(1):11–5.
[164] Tucker SJ, Imbrici P, Salvatore L, D'Adamo MC, Pessia M. pH dependence of the inwardly rectifying potassium channel, Kir5.1, and localization in renal tubular epithelia. J Biol Chem 2000;275(22):16404–7.
[165] Lourdel S, Paulais M, Marvao P, Nissant A, Teulon J. A chloride channel at the basolateral membrane of the distal-convoluted tubule: a candidate ClC-K channel. J Gen Physiol 2003;121(4):287–300.
[166] Nissant A, Lourdel S, Baillet S, Paulais M, Marvao P, Teulon J, et al. Heterogeneous distribution of chloride channels along the distal convoluted tubule probed by single-cell RT-PCR and patch clamp. Am J Physiol Renal Physiol 2004;287(6): F1233–1243.
[167] Frindt G, Palmer LG. Na channels in the rat connecting tubule. Am J Physiol 2004;286:F669–74.

[168] Duc C, Farman N, Canessa C, Bonvalet J-P, Rossier B. Cell-specific expression of epithelial sodium channel α, β and γ subunits in aldosterone-responsive epithelia from the rat: localization by *in situ* hybridization and immunocytochemistry. J Cell Biol 1994;127:1907–21.

[169] Loffing J, Pietri L, Aregger F, Bloch-Faure M, Ziegler U, Meneton P, et al. Differential subcellular localization of ENaC subunits in mouse kidney in response to high- and low-Na diets. Am J Physiol Renal Physiol 2000;279(2):F252–258.

[170] Rubera I, Loffing J, Palmer LG, Frindt G, Fowler-Jaeger N, Sauter D, et al. Collecting duct specific gene inactivation of αENaC in the mouse kidney does not impair sodium and potassium balance. J Clin Invest 2003;112:554–65.

[171] Wang W, Schwab A, Giebisch G. Regulation of small conductance K channel in apical membrane of rat cortical collecting tubule. Am J Physiol 1990;259:F494–502.

[172] Bailey MA, Cantone A, Yan Q, MacGregor GG, Leng Q, Amorim JB, et al. Maxi-K channels contribute to urinary potassium excretion in the ROMK-deficient mouse model of Type II Bartter's syndrome and in adaptation to a high-K diet. Kidney Int 2006;70(1):51–9.

[173] Lachheb S, Cluzeaud F, Bens M, Genete M, Hibino H, Lourdel S, et al. Kir4.1/Kir5.1 channel forms the major K^+ channel in the basolateral membrane of mouse renal collecting duct principal cells. Am J Physiol Renal Physiol 2008;294(6):F1398–1407.

[174] Palmer LG, Frindt G. Cl^- channels of the distal nephron. Am J Physiol Renal Physiol 2006;:.

[175] Pácha J, Frindt G, Sackin H, Palmer LG. Apical maxi K channels in intercalated cells of CCT. Am J Physiol 1991;261: F696–705.

[176] Palmer LG, Frindt G. High-conductance K channels in intercalated cells of the rat distal nephron. Am J Physiol Renal Physiol 2007;292(3):F966–973.

[177] Najjar F, Zhou H, Morimoto T, Bruns JB, Li HS, Liu W, et al. Dietary K^+ regulates apical membrane expression of maxi-K channels in rabbit cortical collecting duct. Am J Physiol Renal Physiol 2005;289(4):F922–932.

[178] Nissant A, Paulais M, Lachheb S, Lourdel S, Teulon J. Similar chloride channels in the connecting tubule and cortical collecting duct of the mouse kidney. Am J Physiol Renal Physiol 2006;290(6):F1421–1429.

[179] Boulpaep EL, Sackin H. Electrical analysis of intraepithelial barriers. Curr Top Membr Transp 1980;13:169–97.

[180] Rakowski RF, Vasilets LA, LaTona J, Schwarz W. A negative slope in the current-voltage relationship of the Na/K pump in *Xenopus* oocytes produced by reduction of external [K]. J Membr Biol 1991;121:177–87.

[181] Frindt G, Palmer LG. Ca-activated K channels in apical membrane of mammalian CCT, and their role in K secretion. Am J Physiol 1987;252:F458–67.

CHAPTER

8

Renal Ion Channels, Electrophysiology of Transport, and Channelopathies

James D. Stockand

Department of Physiology, University of Texas Health Science Center, San Antonio, TX, USA

The purposes of this chapter are to explain what an ion channel is and how it works, provide an overview of the contribution ion channel proteins make to renal transport, and suggest how changes in the structure and biophysical properties of renal ion channels cause disease. Emphasis is placed on recent information gained from the latest techniques. This chapter is neither a technical manual nor a comprehensive review. Its goal, rather, is to demonstrate how appreciation of renal physiology is expanded by considering the structure and biophysical properties of ion channels. Important equations are provided only in their simplest forms to demonstrate how the understanding of channel biophysics informs us about the role played by these proteins in the kidney. The goals of this chapter necessitate coverage of a wide subject matter. Several topics are introduced here in brief but are covered in more depth in other chapters of this book and elsewhere.[1,2,3] This chapter is about how we move from understanding channel biophysics and structure to understanding how changes in them cause disease.

Ion channels are central to renal transport. A diverse group of ion channels, including Ca^{2+}, Cl^{-}, K^{+}, Mg^{2+}, Na^{+}, and non-selective cation channels, are expressed along the length of the renal tubule and collecting duct system. Figure 8.1 and Table 8.1 report the expression profile for ion channels in the kidney at sites where their functions have been firmly established. Channels act as selective and regulated gateways, conducting ions down electrochemical gradients via restrictive diffusion. This enables channel proteins to serve as physical conduits for the movement of ions across epithelial cell membranes. In addition to functioning as gateways during transport, channel activity sets the electrical and chemical forces driving the movement of ions and coupled molecules, such as water and glucose, through and between renal epithelial cells. As such, the activities of renal ion channels often serve as the final arbiters of the electrolyte content of urine and plasma. This is true for Ca^{2+}, K^{+}, Mg^{2+}, and Na^{+}. Ion channels in the kidney, consequently, are targets for hormones and pharmacological agents to affect plasma ion content and volume. Aberrant regulation of renal ion channels or dysfunction of these proteins, moreover, cause kidney disease with compromised tubule transport. For instance, renal Mg^{2+} excretion is fine-tuned in the early distal convoluted tubule (DCT). Inactivating mutations in the Mg^{2+}-selective transient receptor potential (TRP) channel, TRPM6, causes hypomagnesemia with secondary hypocalcemia (HSH). This is a familial form of an autosomal recessive renal Mg^{2+}- and Ca^{2+}-wasting tubulopathy that ultimately leads to neurological damage and dysfunction.[4,5,6,7,8,9] Figure 8.2 shows models of epithelial cells in different segments of the nephron, and emphasizes the location of transport proteins and ion channels.

Renal ion channels also play important roles in cell signaling. They set membrane potential that modulates intracellular signaling. They also allow access to the ions involved in cell signaling, as typified by Ca^{2+}. Involvement of renal channels in cell signaling is highlighted by the role played by TRPC6 channels in podocytes of Bowman's capsule. Here, gain-of-function mutations in TRPC6 facilitate Ca^{2+} entry, leading to prolonged changes in the dynamics of Ca^{2+} signaling ultimately causing a familial form of focal segmental glomerulosclerosis (FSGS[10,11,12,13]).

Over the last few decades, the application of contemporary molecular genetics and gene knockout technology to cell biology and physiological questions

Seldin and Giebisch's The Kidney, Fifth Edition.
DOI: http://dx.doi.org/10.1016/B978-0-12-381462-3.00008-2

© 2013 Elsevier Inc. All rights reserved.

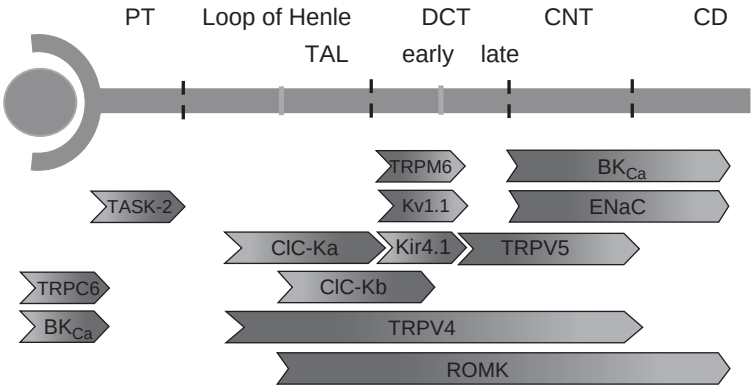

FIGURE 8.1 Functional expression of ion channels in the nephron. Expression in the apical membrane is indicated by a darker to lighter gray scale. Expression in the basolateral membrane is indicated by a lighter to darker gray scale.

has revealed much about the roles played by renal ion channels, and the diseases caused by their dysfunction. An improvement in electrophysiological methods has allowed the detailed study of single ion channel proteins. Furthermore, the resolution of the crystal structures for several different channels has contributed greatly to determining the mechanisms by which channels gate and are regulated, facilitating our understanding at the atomic level of structure–function relations in these proteins. This allows the rationalization of how mutations in the genes encoding renal channels and channel regulators lead to disease, and how agents used in the clinic to modulate renal channel activity exert their pharmacological actions. For instance, it is recognized now that the renal phenotype resulting from decreased activity of the luminal Na^+,K^+,Cl^--co-transporter (NKCC2) in the thick ascending limb (TAL) shares many common features with those arising from inactivation of the luminal renal outer medullary K^+ (ROMK) channel responsible for K^+ recycling across the apical membrane of TAL epithelial cells and serosal ClC-Kb channels responsible for Cl^- exit from these cells, in that they all cause Bartter syndrome (BS) with hallmark NaCl wasting and compromised urine-concentrating ability.[14,15,16,17,18] Smilar salt- and water-wasting stems from the inhibition of NKCC2 in the TAL by furosemide and bumetenide loop diuretics. Both are important clinical tools used in the treatment of high blood pressure and heart failure.

As stated above, this chapter applies understanding of channel biophysics to the understanding of physiology, focusing on the role played by channels in renal transport, and rationalizes how compromises in channel properties cause channelopathies and tubulopathy. Important concepts are reinforced with specific examples. To facilitate discussion, a general appreciation of the structure and functional properties of the renal epithelium to include routes of transport, types of transport proteins common to epithelial cell membranes and forces driving transport are first developed. These are covered in greater detail in Chapters 1 and 2. What an ion channel is, and the biophysical explanation and atomic origins of gating, selectivity, and permeation are also addressed. Again, this material has some overlap with that presented in Chapter 7. The rich understanding of renal ion channels that has emerged over the last two decades makes it reasonable to describe briefly the roles played by these channels in transport and disease, and to discuss how the biophysical properties of renal channels determine their function in the kidney (see also Chapters 30, 31, 47, 62 and 80). The number of crystal structures now available for different types of channels makes it feasible to include a brief review of channel structure, and to discuss how this determines channel properties. Examples then can be examined where known changes in the biophysical properties of specific renal channels cause tubulopathies.

STRUCTURE–FUNCTION OF TUBULE EPITHELIUM

The renal tubule is a single epithelial cell thick. It is linear with ultrafiltrate and pro-urine separated from interstitial fluid by epithelial cells coupled together with tight junctions to form the epithelium. Fluid flows down the tubule in one direction from Bowman's space to the collecting duct system, ultimately into the ureter. Fluid flows down the tubule driven by hydrostatic pressure renewed by constant filtration at the glomerulus.

The Tubule is a Barrier

The structure of the tubule provides a barrier function separating fluid compartments; pro-urine from interstitial fluid. The electrical properties of the tubule and transport across the tubule can be understood in terms of equivalent circuits, such that ions cross a resistive barrier driven by electrochemical forces

TABLE 8.1 Renal Ion Channels with Recognized Function

Channel	Alternative Names	Expression	Gene Pore/ Accessory	Chromosome Location	Function	References
CALCIUM						
TRPC3	TRP3	podocyte + CD (ubiquitous)	*TRPC3*	4, 123.02-123.09	Receptor operated Ca^{2+} entry pathway in podocytes.	10, 11, 12
TRPC6	FSGS2, TRP6	podocyte + CD	*TRPC6*	11, 101.32-101.45	Receptor operated Ca^{2+} entry pathway in podocytes; role in CD less clear but may be involved in mechanosensation.	10, 11, 12
TRPP2	PCL, PKD2L, PKDL	TAL + DCT	*PKD2L1*	10, 102.04-102.08	See chapter 80	
TRPV4	OTRPC4, TRP12 VRL-2, VROAC,	AtL + TAL + DCT + CNT	*TRPV4*	12, 108.71-108.76	Molecular osmoreceptor.	12
TRPV5	ECaC1, CAT2, OTRPC3	late DCT + CNT	*TRPV5*	7, 142.32-142.34	Apical entry pathway for Ca^{2+} in the late DCT.	84, 85, 12, 49
CHLORIDE						
ClC-Ka[a]	ClC-K1	AtL, TAL	*CLCNKA* + *BSND (Barttin)*	1, 16.22-16.23 1, 55.24-55.25	Basolateral Cl^- exit pathway.	79, 59, 71, 60
ClC-Kb[a]	ClC-K2	TAL + early DCT	*CLCNKB* + *BSND (Barttin)*	1, 16.24-16.26 1, 55.24-55.25	Basolateral Cl^- exit pathway.	79, 59, 71, 60
POTASSIUM						
BK_{Ca}	maxi K^+, Slo	podocytes, CNT + CCD	α, *KCNMα1* + $\beta1$, *KCNMβ1*, $\beta4$, *KCNMβ4*	10, 78.31-79.07 5, 169.74-169.75 12, 69.05-69.11	Stabilizes membrane potential in podocytes to facilitate Ca^{2+} entry via TRPC6; flow-sensitive K^+ secretion in the distal nephron.	10, 11, 12
Kir4.1[a]	BIRK-10, KCNJ13-PEN, Kir1.2	DCT + CNT	*KCNJ10*	1, 158.27-158.31	Allows basolateral K^+ recycling facilitating Mg^{2+} reabsorption via TRPM6/TRPM7.	96, 92, 97, 98
Kv1.1	HUK1, RBK1, AEMK, HBK1, MK1	DCT	*KCNA1*	12, 4.89-4.9	Hyperpolarizes the luminal membrane to facilitate Mg^{2+} influx thru TRPM6/TRPM7.	20, 92
ROMK1	ROMK, $K_{ir}1.1$	TAL + DCT + CNT + CD	*KCNJ1*	11, 128.21-128.24	Apical K^+ recycling in the TAL; aldosterone and plasma K^+-sensitive K^+ secretion from principal cells in the CNT + CD	14, 23, 31, 33
TASK-2[a]	$K_{2P}5.1$	PT	*KCNK5*	6, 39.26-39.31	Functions as a hyperpolarizing influence to maintain favorable conditions across the basolateral membrane for electrogenic HCO_3^- reabsorption.	80, 99
MAGNESIUM						
TRPM6	CHAK2, HMGX, HSH, HOMG	early DCT	*TRPM6*	9, 76.53-76.69	Apcial entry pathway for Mg^{2+} in the early DCT.	10, 20, 12, 24, 9
TRPM7	CHAK1, TRP-PLIK	ubiquitous	*TRPM7*	15, 48.64-48.77	Apical entry pathway for Mg^{2+} in the early DCT.	10, 20, 12, 24, 9
SODIUM						
ENaC		CNT + CCD	α, *SCNN1A* β, *SCNN1B* γ, *SCNN1C*	12, 6.33-6.35 16, 23.22-23.3 16, 23.1-23.14	Apical entry pathway for Na^+ in CNT and CD principal cells.	41, 83

[a]*Expressed in the basolateral membrane.*

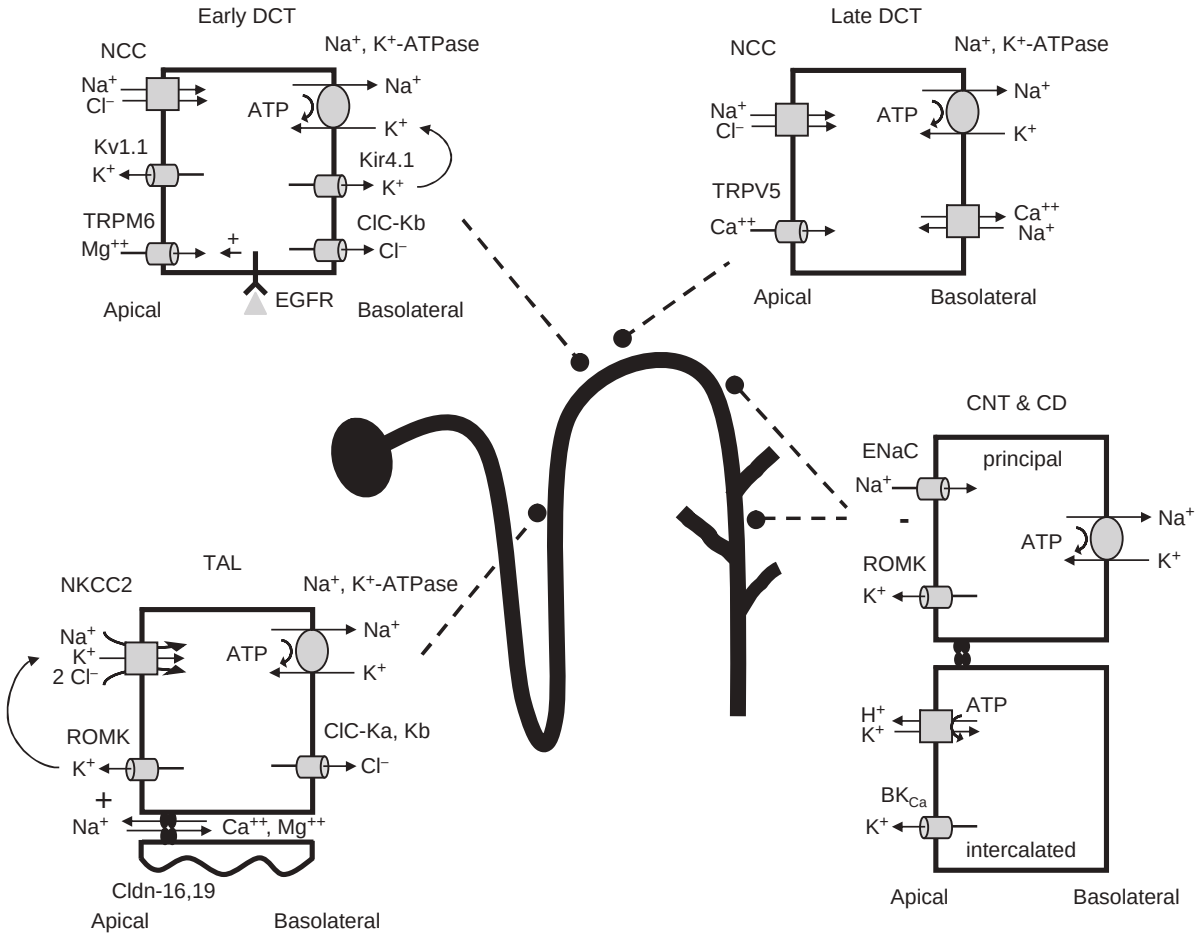

FIGURE 8.2 **Models of renal epithelial cells lining the tubule emphasizing the location of transport proteins and ion channels.**

through conductive pathways. Figure 8.3 shows a simplified equivalent circuit representing tubule epithelium. In this regard, ion channels and tight junctions serve as conductive pathways across epithelial cell membranes and the epithelial barrier, respectively, with voltage and concentration gradients existing across these membranes and the barrier. Because channels, which are gated, make a significant contribution to membrane resistance, epithelial cell membranes are best described as variable resistors. Accordingly, channels affect the resistance of the epithelial cell membrane and electrochemical driving forces across these membranes and the epithelium.

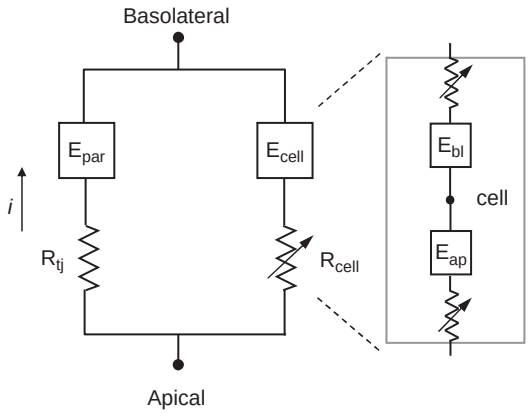

FIGURE 8.3 **Tubule epithelium can be represented by an equivalent circuit.** (Abbreviations: ap: apical; bl: basolateral; par: paracellular; tj: tight junction.)

Routes of Transport across the Tubule

Two different routes of transit from one fluid compartment to the other exist across the renal epithelial barrier. Movement through the epithelial cell is termed transcellular, and between epithelial cells across tight junctions is termed paracellular. Transcellular movement, as depicted in the simple equivalent circuit shown in Figure 8.3, includes crossing both the apical and basolateral membranes. Channels facilitate the crossing of these membranes by ions. Tight junctions serve a similar function for paracellular movement

across the epithelium. Tight junctions, like channels, are selectively permeable. Nothing to date, though, suggests that tight junctions act in a gated manner; rather, they function as doorways of fixed resistance that are selective in what they let pass. Diffusion through tight junctions is passive, driven by electrochemical gradients.

Epithelial Cells are Polarized

Tubule epithelial cells, and thus the tubule epithelium, are polarized with distinct membranes facing the pro-urine, the apical membrane, and the interstitial fluid, the basolateral membrane. These distinct membranes have different protein profiles, including the expression of ion channels. The net result is that each cell membrane has different capability, selectivity, and capacity for moving ions and other molecules. This, combined with the barrier function of the epithelium, provides epithelial cells with the ability to transport in a directional manner. This process is often termed vectoral transport.

Types of Transport and Transporters

Epithelial transport and specific transport proteins are covered in more detail in Chapters 1 and 2. In brief, transport across an epithelial cell can be divided into those that do not require a protein, and those that are protein-mediated. The former is termed simple diffusion and is passive, being dependent on the concentration gradient and surface area. If a molecule is capable of permeating the cell membrane, it will cross according to its chemical gradient. Molecules that move using this form of transport are exclusively small and non-polar, and are capable of crossing a lipid bilayer. Simple diffusion cannot be saturated and is not regulated. The movement of NH_3 in parts of the tubule is a good example of this form of transport. Mediated transport, in contrast, is capable of being saturated, and is dependent on the presence of specific proteins. Moreover, it often is regulated by cell signaling. Figure 8.4 shows models representative of the different classes of transport proteins common to renal epithelial cells. Forces driving protein-mediated transport are discussed in more detail below, but they can include the concentration difference of the molecule to be transported across the membrane or barrier, electrical potential differences, and the activity of transport proteins.

Facilitative diffusion, similar to simple diffusion, is passive, allowing molecules to move down concentration gradients. Facilitative transporters translocate molecules across membranes. An example of a facilitative transport protein in the kidney is the proximal tubule glucose transporter, GLUT2.

Ion channels allow restrictive diffusion, a unique form of passive transport. Channels form selective pores in the membrane, allowing ions to cross the membrane through permeation rather than being translocated across the membrane. Restrictive diffusion through ion channels is driven by electrochemical gradients.

The two remaining types of transport proteins allow active transport: the active movement of molecules against gradients. This type of transport is directly, in the case of primary active transport, and indirectly, in the case of secondary active transport, tied to the consumption of energy. Primary active transporters require ATP to transport molecules against their concentration gradients. As discussed below, this ultimately energizes all transport across the renal tubule. The Na^+,K^+-ATPase is a notable primary active transporter in the tubule and

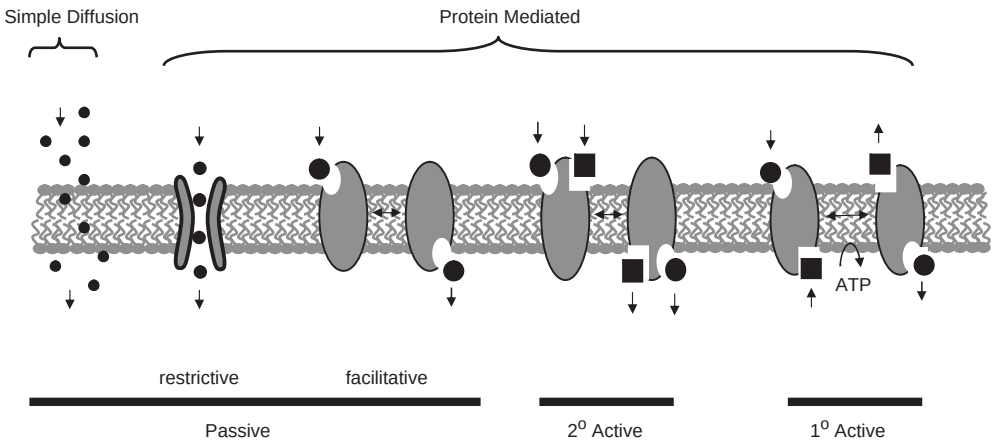

FIGURE 8.4 **Representative models of the different types of renal transport proteins.**

collecting duct system. Secondary active transporters use gradients established by primary active transporters. They couple the movement of one molecule against its gradient to the movement of another molecule down its gradient. NKCC2 in the TAL and the thiazide-sensitive Na^+,Cl^--co-transporter (NCC) in the DCT are prominent secondary active transporters in the kidney. The latter couples the inward movement of Cl^- into the cell against its gradient to the inward movement of Na^+ into the cell with its gradient. Thus, Na^+ entering the cell downhill on this transporter pulls Cl^- uphill with it.

Forces Driving Transport across the Tubule: The Importance of Disequilibrium

Filtration at the glomerulus, as discussed in Chapter 21, is governed by Starling forces. The difference in hydrostatic pressure between plasma in the glomerular capillary and ultrafiltrate in Bowman's space, the beginning of the tubule, drives filtration. The difference in oncotic pressure between these fluids impedes filtration. The net result of filtration is that ultrafiltrate entering the renal tubule is similar in content to plasma minus blood cells and proteins. Electrolytes or other small molecules, therefore, have little gradient initially to cross the epithelial barrier, leaving pro-urine for interstitial fluid or *vice versa*. The activity of the Na^+,K^+-ATPase pump localized to the basolateral membrane of all tubule epithelial cells changes this by providing the motivation, ultimately, for all transport. This protein consumes ATP to generate disequilibrium for Na^+ and K^+ across cell membranes. Because epithelial cell membranes are effective at separating fluid compartments, this disequilibrium can be maintained and converted into voltage differences and differences in ion concentrations by the activities of ion channels, other transport proteins, and the capacitive nature of cell membranes. Similarly, because epithelial cells, coupled together by tight junctions, effectively separate fluid compartments, disequilibrium across the tubule epithelium is maintained. Urine flowing in only one direction down the tubule also helps maintain disequilibrium, by moving processed fluid too quickly for equilibrium to be reached. Ion channels and other transport proteins tap these electrochemical gradients to transport molecules across the epithelium. Thus, disequilibrium enables modification of urine by tubule epithelial cells. Renal transport ultimately, then, is the movement of molecules through channels and other transporters, tending towards an equilibrium that is kept beyond reach by the continuous activity of the Na^+,K^+-ATPase.

The Tubule Epithelium has Emergent Properties

The importance of the structure of the epithelial barrier and state of disequilibrium maintained across this barrier to transport is apparent when considering the similar Ca^{2+}- and Mg^{2+}-wasting phenotypes arising from inactivation in the TAL of NKCC2, ROMK, claudin-16, and claudin-19.[19,20,21,22,23,24] Dysfunction of claudin-16 and -19 cause familial hypomagnesemia, with hypercalciuria and nephrocalcinosis (FHHNC[25,26,27,28]). These claudins are critical components of the tight junction in the TAL, where they provide cation-selectivity, allowing Na^+ back-flux into tubular fluid more rapidly than Cl^-, contributing to a lumen-positive diffusion potential. The lumen-positive potential that results from the combination of this Na^+ back-flux with apical K^+ recycling mediated by the coordinated activities of luminal ROMK channels and NKCC2 drives paracellular Mg^{2+} and Ca^{2+} transport. Claudin dysfunction, like dysfunction of ROMK or NKCC2, then compromises the electrochemical gradient responsible for divalent cation reabsorption in the TAL. This illustrates that a break in function of any of several components of the whole leads to the same disease. This is an important concept: epithelial cells and epithelial barriers have emergent properties that are dependent on the proper functioning of each component part, including ion channels.

Urine Flows down the Tubule

An additional point important to recognize about renal transport is that urine flows in the tubule in one direction; what happens upstream affects transport downstream. This is so because the modification of urine in upstream segments determines the constituents of urine in downstream segments. For instance, inhibition of NKCC2 in the TAL by loop diuretics, in addition to compromising urine-concentrating ability by destroying the axial corticomedullary hyperosmotic gradient, also leads to an increase in K^+ secretion at the collecting duct (CD), and ultimately to K^+ excretion by the kidney. This is due to increased urine flow and Na^+ delivery to the CD. Increased urine delivery to the CD promotes flow-induced K^+ secretion by BK_{Ca} channels, which are activated by mechanical stimuli.[29,30] Increased Na^+ delivery drives increased Na^+ reabsorption via the epithelial Na^+ channel (ENaC) across principal cells of the CD, due to a change in the electrochemical gradient for Na^+ across the apical membrane. This increase in Na^+ reabsorption in turn affects the electrochemical gradient across the apical membrane, driving additional K^+ secretion through ROMK channels.[31,32] For the same reasons, any inactivating mutation in a TAL transport protein

involved in NaCl reabsorption, including NKCC2, ClC-Kb, and ROMK channels, causes the renal K^+ wasting associated with Bartter syndrome.[15,16,17,18] Moreover, disease resulting from inactivation of NCC and the ClC chloride channel beta subunit barttin, and diuretics such as thiazide inhibitors of the NCC co-transporter that decrease NaCl reabsorption in the DCT, also cause renal K^+ wasting by this common mechanism.

Transport does not Happen in a "Vacuum"

Another concept emerging from the above discussion is that the transport of one type of ion through renal ion channels influences the movement of different ions through other distinct channels. This coupling is a manifestation of ion channel activity influencing electrochemical driving forces. An example of this, as discussed above, is the electrogenic Na^+ reabsorption via ENaC influencing ROMK-mediated K^+ secretion in the CD. This will be touched upon again in more detail below. Similarly, as mentioned earlier, Mg^{2+} and Ca^{2+} reabsorption in the TAL are positively coupled to NaCl reabsorption with K^+ recycling across the luminal membrane via ROMK channels and paracellular Na^+-back flux via claudin proteins, setting the electrochemical driving forces moving these divalent cations.[21,22,26,31,33]

ION CHANNELS: BIOPHYSICAL PROPERTIES

An ion channel is an integral membrane protein or protein complex that forms a continuous conductive pore through a membrane. The pore spans the entirety of the membrane with the conduction pathway perpendicular to the plane of the lipid bilayer. The mouths of an ion channel pore are in contact with the aqueous solutions on both sides of the bilayer. As ions enter the permeation pathway of a channel pore and reach the selectivity-filter, they become partially dehydrated, moving through the channel only after losing surrounding water molecules. Binding sites within the pore then mimic solvation by water as ions permeate across the membrane through the channel.

Channel pores are selective and gated. The basis of selectivity is usually a defined sequence of residues at the narrowest part of the pore. Residues in the selectivity-filter are highly conserved across a channel family, and generally across a class of channels. Most, if not all, K^+-selective channels, for instance, share the common signature selectivity sequence TXGYG.[32,34,35,36] Moreover, all known

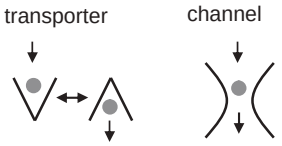

FIGURE 8.5 **Simplified modes of transport used by transporters versus ion channels.** Translocation of molecules across the membrane by transporters entails relatively large changes in conformation compared to ion permeation across the membrane through ion channels.

K^+ channels with this selectivity-filter use a common mechanism of permeation to conduct K^+ through the pore, as discussed in greater detail below.

Ion Channels Provide a Unique Form of Passive Diffusion

As emphasized in the simplified forms of transport shown in Figure 8.5, ion channels differ from other transport proteins, in that they form a physical hole through the membrane. No other type of transport protein does this. Rather, the molecule to be translocated by transport proteins other than ion channels interacts with a binding site on one face of the protein, but does not actually move across the membrane until a change in conformation takes place where the initial entry site closes as the exit site opens to allow the bound molecule to be released and egress out across the opposite face of the protein from which it entered. Ion channels also contain binding sites for permeant ions. Ions transiently bind to these sites during permeation, with the electrochemical gradient driving the direction of transport. In conjunction with properties of the pore and charge repulsion between permeant ions, this gradient determines the magnitude of ion flow.[36,37,38] Because channels are pores that allow ions to permeate through the membrane, they facilitate crossing of the membrane with relatively little change in overall conformation. Transporters, in comparison, typically require greater relative changes in conformation to translocate molecules across the membrane. The result is that single-channel proteins move a far greater number of molecules per unit of time (10^7 to 10^8 ions/second) compared to any other single-transport protein.

Recording Ion Channel Activity with Patch-Clamp Electrophysiology

When open, a channel conducts the movement of ions across the cell membrane. This manifests as a decrease in resistance the membrane has to the permeant ion. Current through an ion channel is dependent on the electrochemical driving force, whether

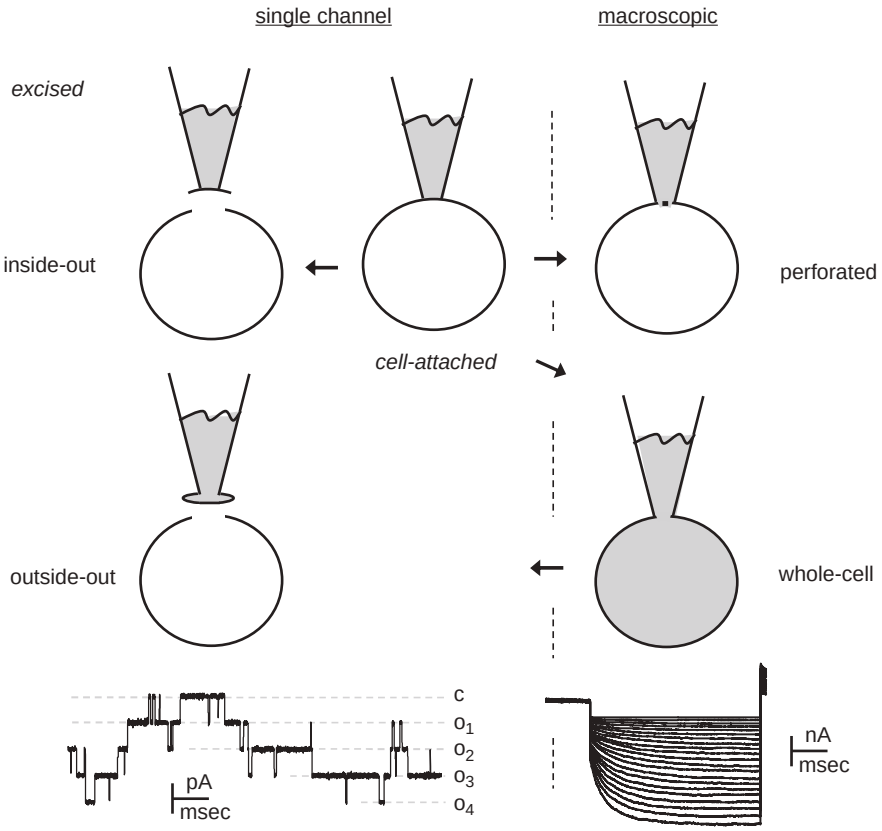

FIGURE 8.6 **Patch-clamp configurations.** This illustration depicts the five different seal configurations available for patch-clamp analysis: three are amenable to single channel recording, cell-attached, excised inside-out and excised outside-out; and two for macroscopic current recording, perforated and whole-cell. In this figure, the cell is represented as a circle and the recording pipette as a V. Gray shading defines continuity between the solution in the recording pipette and intracellular solution. Arrows represent transition steps during seal formation taken to establish the distinct types of seals. Shown below are representative current data from configurations with single channel (left) and macroscopic (right) resolutions. Closed (C) and open (O) states are noted in the single channel trace. *(Data from J.D. Stockand or published previously in ref. [39].)*

the channel is open or closed and the selectivity of the channel, and how well a certain ion moves through, or rather permeates through, the conduction pathway. The activity and biophysical properties of ion channels can be assayed in experiments with electrophysiological tools, including sharp electrodes and two-electrode voltage clamping. The most sophisticated tool used to probe the biophysical properties of channels is patch-clamp electrophysiology. Erwin Neher and Bert Sakmann were awarded the Nobel Prize in Physiology or Medicine in 1991, in part for this development.[3] Patch-clamp electrophysiology enables the study of both macroscopic and single-channel currents. It has a high degree of precision and fidelity, allowing the resolution of the activity of a single protein in real-time. Figure 8.6 shows the different patch configurations available for the study of ion channels, and sample data from experiments investigating the single-channel properties of wild-type ENaC (left) and macroscopic currents from a mutant form of ENaC (right) that activates upon hyperpolarization due to the voltage-dependent block of the pore by intracellular Na^+.[39]

Adaptation of Ohm's Law to Biological Systems: Explaining Current Carried by Ion Channels

Current flow in an electrical circuit obeys Ohm's Law which, when reordered, states $I = gE$, where current (I) equals the product of the conductance (g) and voltage difference (E) across the conductor, which in biological systems is an ion channel protein. This simple formula was adapted to $I_x = g_x\ (E-E_x)$ by Hodgkin and Huxley, in their seminal electrophysiological studies (as explained by Hille and Cole in their books[2,40]) to fit biological reality better where current through an ion channel crosses a capacitive membrane that separates fluid compartments of different ionic activities. The gradient across the membrane acts like a battery represented by an equivalent circuit with an

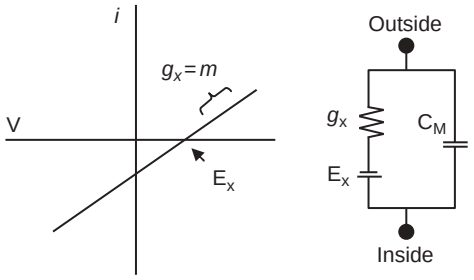

FIGURE 8.7 **An idealized I–V relation and equivalent circuit describing a channel obeying Ohm's Law.** Conductance (g) is equal to the slope of the I–V line. E_x is the reversal potential, and C_M is membrane capacitance.

electromotive force, E_x, in series with a channel resistor, g_x. This conductive branch is in parallel with the capacitor representing the membrane. In this modified equation, E remains voltage across the membrane, and the net driving force on ion X is now $E - E_x$. Thus, current in biological systems is driven by an electrochemical gradient rather than by voltage alone.

Figure 8.7 shows a graphical representation of an idealized current–voltage relation for an equivalent circuit describing an open ion channel obeying this modified Ohm's Law. When voltage, E, is equal to E_x, no net current flows through the channel. When $E < E_x$, current flows into the cell. If this represents a cation channel, for instance ENaC, and extracellular $[Na^+]$ is greater than intracellular $[Na^+]$, as is the normal case in physiological systems, this inward current flow would be carried by Na^+ entering the cell through ENaC. This represents the normal conditions under which ENaC functions in CD principal cells, allowing Na^+ to enter the cell across the apical membrane during electrogenic Na^+ reabsorption.[41,42] The typical concentration of ions in urine and intracellular fluid combined with the activities of K^+ channels in the apical and basolateral membranes set the potential (E) across the apical membrane lower than E_{Na}. This facilitates Na^+ influx through ENaC. In contrast, when $E > E_x$ current flows outwards, Na^+ exits the cell. This explains the consequences of the electrochemical gradient driving Na^+ through ENaC. Sodium movement through ENaC across the membrane, in turn, influences electrochemical gradients. If no other parameter changed, Na^+ moving through ENaC would dissipate the $E - E_{Na}$ difference, eventually arriving at equilibrium where E and E_{Na} are equalized. Restated, net flux through a channel occurs only as long as the system is out of electrochemical equilibrium. This is where the Na^+,K^+-ATPase and separation of fluid compartments with different ionic activities by cell membranes come into play. They enable epithelial cells to remain out of equilibrium.

The Nernst Equation

In the above description, E_x is the equilibrium potential (or reversal potential) for ion X, a state where the tendency for further change vanishes, and all existing forces on X are in balance. This would be where voltage across the membrane containing the channel permeable to ion X equals the diffusion potential developed by the ionic gradient for ion X across this membrane. Mathematically, as noted above, this is where $E = E_x$. Equilibrium potentials are easily measured in the laboratory with electrophysiology. Moreover, they can be calculated empirically using a formula developed by Nernst in 1888.[40,43] This led to the equilibrium potential sometimes being referred to as the Nernst potential. The Nernst equation states $E_x = (RT/zF)\ln([X]_o/[X]_i)$, where R and F are physical constants having the usual meanings of Universal Gas constant and Faraday's constant, T is temperature in kelvin, z accounts for the charge and valence of ion X, ln indicates natural logarithm, and $[X]_o$ and $[X]_i$ are the concentrations of ion X outside and inside the cell, respectively. Accordingly, the equilibrium potential falls to zero in the absence of a gradient, reverses signs as the direction of the gradient is reversed (e.g., that for Na^+ compared to K^+) and as the charge of the ion is reversed, for example Na^+ versus Cl^-. Equilibrium potentials across cell membranes for ions common to physiological solutions are $\sim$130, $-$98 and 67 mV, respectively, for Ca^{2+}, K^+, and Na^+ [2]. The equilibrium potential for Cl^- is more variable, because $[Cl^-]_i$ varies more widely with cell type, but it usually is close to the resting membrane potential of the cell, often being slightly above or below that level. Calculating equilibrium potential across tubular epithelial cell membranes is complicated by the luminal and serosal membranes facing different solutions. The apical membrane may have a different equilibrium potential for Na^+ as compared to that across the basolateral membrane, because the concentration of this ion in urine may be greater or less than that of plasma, depending on Na^+ and water transport along the length of the nephron.

The Goldman–Hodgkin–Katz Voltage Equation

Work performed by Hodgkin, Huxley, and Goldman and others led to the realization that cell membrane potential reflects the equilibrium potentials of all permeant ions at a given time, and that this can be mathematically represented.[2,40] When calculating membrane potential (E_{mem}), the magnitude of ion movement through any given class of channel, for example K^+ versus Na^+ channels, is accounted for by using weighted averages of each ion's equilibrium potential. These weighted averages convey the relative

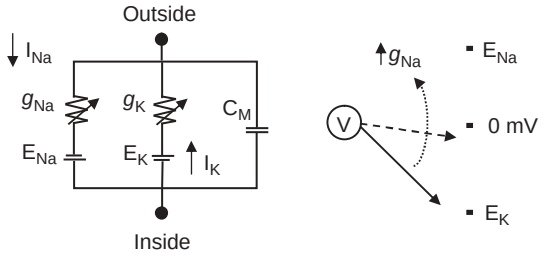

FIGURE 8.8 **A simplified equivalent circuit of a cell containing Na^+ and K^+ channels contributing to membrane potential.** Shown to the right is the change in membrane potential resulting from activation of Na^+ channels.

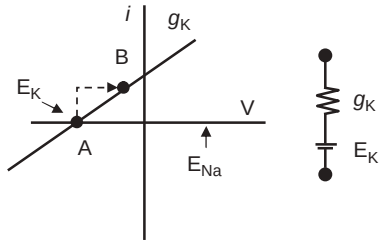

FIGURE 8.9 **Changes in membrane potential influence current through open channels.** Shown are an idealized I–V relation (left), and associated equivalent circuit (right) for a K^+ channel. Movement from point A to B notes the effect on current through this channel as the membrane becomes depolarized in response to the activation of Na^+ channels.

permeability (P_x) of each ion to total ion permeability (P_{tot}). By using the simplified condition of only considering flux of monovalent cations through channels, which is not too distant from reality, the Goldman–Hodgkin–Katz (GHK) equation is $E_{mem} = (P_K/P_{tot})E_K + (P_{Na}/P_{tot})E_{Na}$. Figure 8.8 shows an equivalent circuit representing the cell membrane and individual ionic conductances contributing to this membrane potential. Because K^+ channel activity predominates at rest with P_K approaching P_{tot}, membrane potential is closest to E_K. An increase in the activity of Na^+ channels, which increases the relative permeability of this ion, causes the membrane to become more depolarized, as represented by the volt meter in Figure 8.8 moving E_{mem} towards E_{Na} as ENaC becomes active.

What do Ohm's Law, the Nernst Equation, and the GHK Equation Tell us About Transport?

Reconsidering now Figure 8.7 and the scenario described earlier, inward Na^+ flow through ENaC depolarizes the apical membrane, moving E_{mem} towards E_{Na}. Because the ionic gradient for K^+ across the apical membrane is the reverse of that for Na^+, depolarizing the apical membrane would move E_{mem} further away from E_K, driving more K^+ out of the cell through apical K^+ channels, for instance, through ROMK channels in the apical membrane of principal cells.[32] Figure 8.9 shows an idealized current–voltage relation for an open K^+ channel, and notes the influence of membrane depolarization (moving from A to B) on K^+ current through this channel as the apical membrane is depolarized by Na^+ reabsorption through ENaC, activated perhaps by the addition of aldosterone. There is greater outward K^+ current and greater K^+ secretion. The idealized graphs of cumulative K^+ secretion, membrane voltage, and relative K^+ and Na^+ permeability shown in Figure 8.10 expand on this concept. Basolateral leak K^+ channels, which provide the majority of ion permeability at rest, sets E_{mem} of CD principal

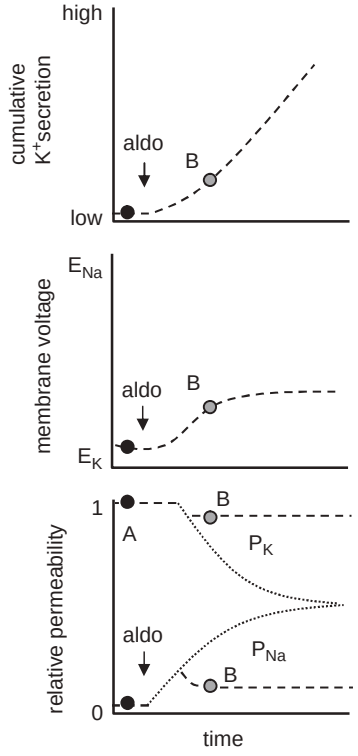

FIGURE 8.10 **Activation of ENaC depolarizes the apical membrane driving K^+ secretion through ROMK.** Shown are idealized graphs representing changes in K^+ secretion (top); apical membrane potential (middle); and relative permeability (bottom) as ENaC becomes activated by aldosterone to drive K secretion through ROMK, moving from point A to point B.

cells to near E_K. There is little electrochemical force, therefore, for K^+ to exit the cell through ROMK under these conditions. This resting condition is time A, with little K^+ secretion across the apical membrane. The introduction of aldosterone to the system activates ENaC, increasing the relative permeability of Na^+ and allowing this ion to enter the cell down its electrochemical gradient. This begins to depolarize the apical membrane, as E_{mem} moves towards E_{Na}. As E_{mem} moves

towards E_{Na}, K^+ exits the cell at an increased rate across apical ROMK channels. This is time B.

Another consequence of ENaC opening is that the relative permeability of K^+ begins to fall as that of Na^+ rises; however, as K^+ exits the cell through ROMK, a new steady-state is reached where membrane potential has increased, and P_{Na} and P_K have stabilized with constant K^+ secretion. Neither the K^+ nor Na^+ concentration gradients change substantially across the apical membrane, due to the constant activity of the Na^+,K^+-ATPase pump. These gradients are also protected by the constant flow of urine, bringing Na^+ to the cell and washing away K^+ that has been secreted through ROMK. This scenario is simplified compared to the real-life situation, but it shows how the equations described above can be used to understand the role played by renal ion channels better. This simplified description, moreover, reveals the mechanistic underpinnings of why K^+ secretion from CD principal cells is tied in a positive manner to Na^+ reabsorption by these cells, as initially raised in earlier sections. In addition, it explains why diuretics, such as amiloride and triemterene, which block ENaC, also have K^+-sparing action.[41,44] They retard the development of the normal electrochemical driving forces favoring K^+ secretion from the CD, because they block the entry of Na^+ across the apical membrane necessary to drive K^+ from the cell. Because the CD is the final site along the nephron where urinary $[K^+]$ is fine-tuned, decreased secretion here leads to K^+ retention in plasma.

Channels are Selective

Ion channels need to be selective to perform their role of converting chemical disequilibrium into electrical signals. In epithelial cells, moreover, they need to be selective to facilitate vectoral transport. The chemistry of selectivity (often called the selectivity sequence), for a channel can also be empirically determined using the GHK Voltage Equation discussed above. The extended equation is $E_{rev} = (RT/F)\ \ln\ \{(P_K[K]_o + P_{Na}[Na]_o + P_{Cl}[Cl]_i)/(P_K[K]_i + P_{Na}[Na]_i + P_{Cl}[Cl]_o)\}$.[2] This equation allows one to calculate permeability ratios by measuring reversal potential, but it does not allow the determination of absolute permeabilities. Bi-ionic conditions, where only one permeant ion is presented to either side of the -channel, are the simplest when testing selectivity. Under such conditions, the equation reduces to $E_{rev} = (RT/zF)\ \ln\ \{(P_x[X]_o)/(P_y[Y]_i)\}$. Figure 8.11 shows predicted results from a hypothetical excised inside-out patch-clamp experiment with bi-ionic conditions used to determine that the channel within the patched membrane is selective for Na^+ over K^+. With Na^+ in

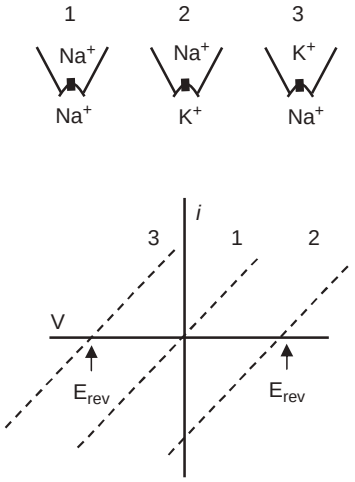

FIGURE 8.11 **A channel's selectivity sequence can be experimentally determined by quantifying how different ionic gradients influence reversal potential.** Shown at top are three different experimental conditions with distinct Na^+ and K^+ concentrations in the bath and pipette solutions for an excised inside-out patch containing an ion channel. Below is the predicted I–V relation for a Na^+ channel in this patched membrane under the three conditions.

the bath and recording pipette, there is no gradient across the membrane, and reversal potential is 0 mV (condition 1). Next, when the bath contains K^+ as the sole cation, condition 2, the reversal potential moves to E_{Na}, which is $\sim$70 mV. Similarly, when the cations in the pipette and bath are reversed, the equilibrium potential again moves to E_{Na}, which is ~ -70 mV with condition 3.

What provides a channel with selectivity? In the simplest sense, it is how capable binding sites within the pore are at coordinating an ion permeating through the pore. If we view a channel pore as a tunnel with consecutive constrictions followed by recesses, as shown in Figure 8.12a, then the selectivity-filter is the tightest constriction. A pore can also be understood by considering thermodynamics. As shown in Figure 8.12b, there would be energy wells followed by energy barriers along the length of the pore. The selectivity-filter then is the greatest barrier that a permeant ion must cross to move through the channel. Using equivalent circuits to describe ion channels, as shown in Figure 8.12c, a change in selectivity would be observed as a change in the electromotive force driving current across the channel upon ion substitution.

The physical basis of selectivity is set by the selectivity-filter defining an internal diameter within the pore, which prohibits molecules larger than this diameter from crossing. This represents the idea that ion channel pores are sieves, selecting on size. With such a description, a selectivity-filter that passes large ions, presumably, would also pass smaller ions, but clearly this is not the case. There are, obviously, other

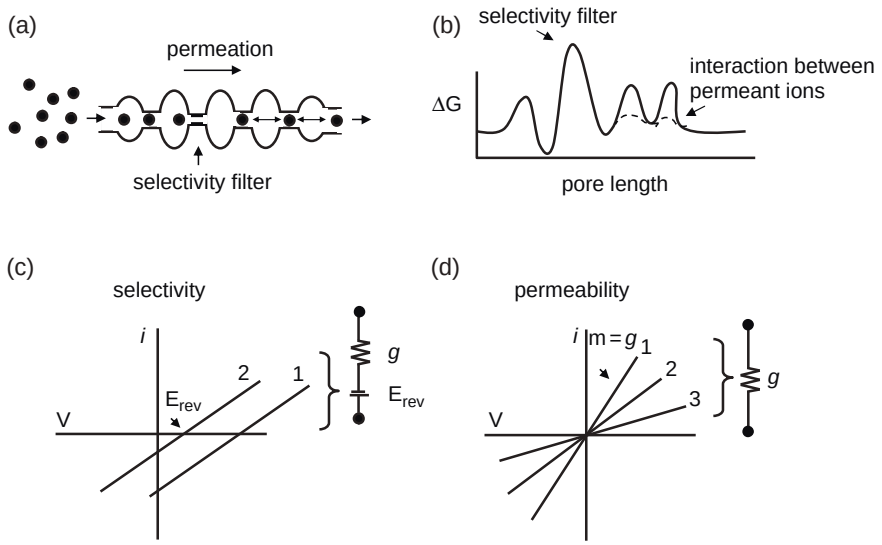

FIGURE 8.12 **Selectivity and permeation.** Shown in (a) is an illustration of a channel pore acting as a filter selecting on size. Ions permeating through the channel pore are shown as black balls. Shown in (b) is a representation of a channel pore as understood by thermodynamics. The I–V relation and equivalent circuit shown in (c) emphasize that selectivity is calculated experimentally by measuring changes in reversal potential resulting from changes in ionic gradients. The I–V relation and equivalent circuit shown in (d) emphasize that permeation is measured in experiments by calculating conductance in the presence of different permeant ions. The two-headed arrows in (a) indicate charge repulsion between permeant ions within the pore. The dashed lines in (b) show decreases in energy barriers along the pore and also indicate the effects of charge repulsion on permeation.

factors contributing to selectivity. Ions move through channel-selectivity filters only after they shed their layer of surrounding water.[35,36,37,45,46] So, it is the dehydrated diameter of an ion, and its ability to shed surrounding water molecules, that are important when moving through a selectivity-filter. Moreover, selectivity-filters also select on the basis of charge: side chains of amino acids defining or near the selectivity-filter present as a charge barrier. The side chains and backbone carbons of residues within or near the selectivity-filter also form transient bonds with the permeant ion and, thus, there is a chemical component to selectivity. Selectivity, then, is a culmination of several factors, including size and charge, and the ability to shed solvating water molecules and interact with residues at or near the selectivity-filter. The precision of selectivity among ion channels varies widely from ENaC having a $P_{Na}/P_K > 100$ being at the highly selective end of the spectrum, to some TRP channels with $P_{Na}/P_K \approx 1$ being at the other end of the spectrum of non-selective channels.[11,47,48,49]

It is easiest to view selectivity as fixed and immutable. However, this is not exactly the case. Channel selectivity can be influenced by experimental conditions, and even the presence or absence of permeant ions in the pore.[50,51] Moreover, the selectivity-filter can be involved in channel gating, as it is in ROMK and ClC channels.[32,52,53,54,55] Gating is discussed in more detail below.

Ions Permeate Through Channels

Selectivity and permeation are related, but they are not exactly the same thing. Selectivity, as emphasized in Figures 8.12a and 8.12b, is set by the physical properties of ion-binding sites within the pore, and how well they coordinate permeant ions when bound. Permeation refers to how fast or rather how many ions move through the pore per unit of time, and speaks of how well an ion surmounts energy barriers within the pore. Stated another way, selectivity can be viewed as a filter with certain physical properties, and permeation is how well molecules cross this filter. Experimentally, as shown in Figure 8.12d, permeation is measured as conductance, where a channel passing a more permeant ion has a higher conductance relative to when it passes a less permeant ion. Ions permeate through the narrowest portions of a channel pore in a single-file manner.[34,35,36,45,56] One then might expect a channel that is less selective to have a higher conductance compared to a highly selective channel. In general, this rule is only loosely obeyed. The reasons for this are discussed below. One might also expect that the ion for which a channel is most selective would permeate through the channel best. This is most often the case, but it is not absolute.

Permeation is a result of how easily an ion surmounts every energy barrier within the pore, as well as interactions between permeant ions with each other

when occupying the pore. Ions occupying the pore can exert a pushing effect on each other, impeding and propelling progression depending on the relative order of these ions within the pore and opposing energy barriers each ion is facing. Repulsion between ions within a pore is indicated in Figures 8.12a and 8.12b with two-headed arrows and decreases in the size of energy barriers, respectively. Such repulsion contributes to highly selective channels passing large numbers of ions per second. For instance, charge repulsion between the Cl^- ions occupying the pore of ClC channels makes a significant contribution to the conductance of these channels.[53,57] In addition, most channels have large aqueous vestibules lined by polar residues at the extracellular and intracellular mouths of their pores.[36,37,45,46,58] The vestibules act as reservoirs concentrating the permeant ion, increasing conductance.

The pores of ClC and ENaC channels contain three binding sites for permeant ions.[37,52,55,58] In ENaC, sites immediately adjacent likely are not occupied simultaneously, due to charge repulsion between permeant ions within the pore. This is also the case for K^+ channels, such as Kv and Kir, which use a single-file mode of multiple ion permeation with four pause/binding sites within the pore.[35,36,45,56] As illustrated in Figure 8.13, only two sites are occupied at any one time, with the occupied pairs always separated by an empty site filled with water.[35,36,45,56]

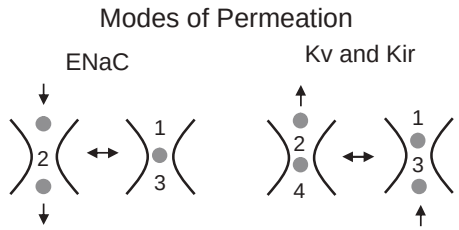

FIGURE 8.13 **Modes of permeation.** Shown here are representative modes of ion (represented by gray balls) permeation through ENaC (left); and Kv and Kir (right) channels. Ions permeate through channel pores in a single-file manner with several ions occupying different binding/pause sites along the length of the pore at any one time. However, charge repulsion often precludes neighboring sites from being occupied by permeant ions simultaneously. Such mechanisms of permeation allow highly selective channels to have large conductance.

Channels Gate

Channels transition between closed and open states as they gate.[2,3] By definition, no current flows through a closed channel. Upon opening, current flows through the channel obeying $i = g_x(E-E_x)$. The open current level of a single channel then is a determinant of its conductance, which is measured by taking the slope of i−V curves for single-channel currents captured with a voltage-clamp recording (see Figure 8.12d). Current flow through a channel, as shown in Figure 8.14, is an all-or-nothing event: with no change in driving force, the channel transitions from closed to open and back again, always the same as defined by a normally distributed Gaussian curve unitary step in single-channel current.

Channels gate in a stochastic manner: a new and random pattern of openings is observed for each trial period.[2] The stochastic nature of gating makes it possible to describe gating in terms of probabilities, where the sum of the probability of a channel being in either the open (P_o) or closed (P_c) state is equal to 1. Channel open probability is calculated from single-channel activity (NP_o) defined as $NP_o = \sum(t_1 + 2t_2 + \ldots\ nt_n)$, where N and P_o are the number of channels in a patch and the mean P_o of these channels, and t_n is the fractional open time spent at each of the observed current levels. P_o is calculated by dividing NP_o by the number of active channels (N) within a patch, as defined by all-point amplitude histograms. Another common way of representing this is:

$$NP_o = \sum_{i=0}^{N_A} \frac{it_i}{T}$$

where T is the total recording time, N_A is the observable number of current levels corresponding to channel number as established with all-point histograms, i is the number of channels open, and t_i is the time during which i channels are open. P_o can be calculated as above, by dividing NP_o by the channel number.

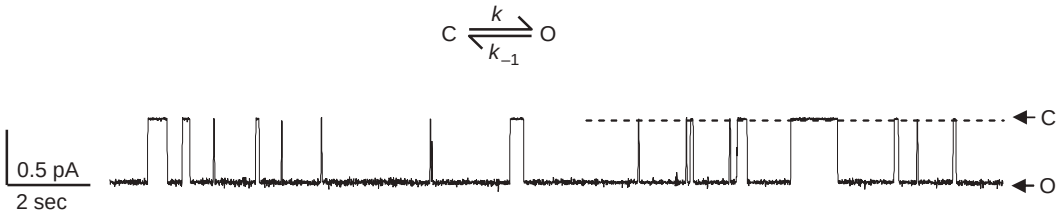

FIGURE 8.14 **Channels gate in a stochastic manner.** Shown here is a typical single-channel current trace for ENaC in an excised outside-out patch containing a single channel. Open and closed states are indicated with O and C, respectively. Shown above is a kinetic scheme describing gating. At a fixed driving force, the channel opening is always to the same unitary current level, and gating is stochastic.

Macroscopic channel current is related to unitary current by $I = iNP_o$, where i is unitary single-channel current at a given voltage. Similarly, macroscopic conductance is $G = gNP_o$. This provides another means for estimating NP_o from experimental data where NP_o can be estimated as I/i. This latter estimation is often used in experiments where N cannot be fixed with certainty, but i can be or when N and I (and i) are measured independently of each other.

All channels have inherent gating activity: with time, they transition between open and closed states in a random manner driven by thermal energy. So, all channels have at least one gate. The physical nature of a channel gate, though, may be different among different kinds of channels. Moreover, channels often have more than one distinct gate. This seems to be the rule rather than the exception. For example, ClC channels are double-barreled channels containing two proto-pores, each having an independent gate .[53,57,59,60] Both proto-pores, moreover, are also covered by a common gate. For the channel to be open, both the gate of the proto-pore and the common gate must be open. Similarly, Kir channels, such as ROMK, have fast and slow gating, showing the effects of at least two different gates.[32,34,35,45,56]

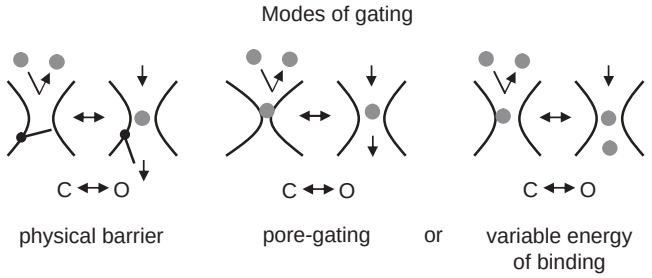

FIGURE 8.15 **Two different general types of gates are known to exist in channels.** Illustrated are the two different types of channel gates identified to date. The left shows a representation of a physical barrier functioning as a gate where the barrier is a side chain, residue or domain of the channel (represented by a black line connected to a small black circle on the wall of the pore) that occludes the pore in the closed state. The regulated common gate and slow gate in ClC and Kir channels, respectively, are this type of gate. The middle and right illustrations represent two different understandings of a pore-gate where the pore collapses around a permeant ion (middle) or the permeant ion sticks to a binding site within the pore (right) to occlude the pore in the closed state. Fast gating of Kir channels and fast gating of proto-pores in ClC channels represent gating of this type. Closed-to-open transitions are shown below, and movement of the permeant ion (gray ball) through the pore is indicated by arrows.

Types of Gates

We typically think of a channel gate as a domain or residue that occludes or covers the pore in a dynamic manner. This may be the case for gates in many types of channels typified by the regulated gate in Kv channels, the slow-gate in Kir, and the common gate in ClC channels.[37,52,61] The crystal structures of many ion channels have recently advanced the understanding of gates. As depicted in Figure 8.15, at least two types of gates are now known to exist. Several channels contain both types of gates, as typified by the fast and slow gates in Kir channels.[32] These two types of gates share some properties, such as they both prevent further permeation of the conductance pathway, but also have important differences albeit sometimes subtle. In addition to a physical gating particle that may obstruct the pore, collapse of the pore around a permeant ion prohibiting further permeation has also been identified as a means of gating.[32,35,36] During pore-gating, the channel is open when the pore is open, and closed when the pore is collapsed. So, there is no true gate with a pore-gating mechanism, rather the physical diameter of the pore is the gate.

In the pore-gating model, the selectivity-filter or another portion of the pore is the working part. This is the case for the fast gating seen in the ROMK channel, where K^+ occupancy of the pore has a profound influence on the structure of the selectivity-filter.[32] Fast gating is characterized by the rapid transition between the open and shortest-lived closed states. The role of pore-gating and the selectivity-filter in this fast-gating process was noticed because the rate of entering the shortest-lived closed state varies as a function of K^+ concentration, and is proportional to current amplitude.[50,51,62–64] The crystal structures of bacterial Kir channels, sharing structure with ROMK as discussed below, provides additional support for this mechanism, showing how a pore may collapse around a permeant ion to gate the channel. A similar relation between extracellular Cl^- and gating of ClC channels has also been noticed.[65–68] This has led to speculation that the proto-pores of ClC channels may also use a pore-gating mechanism. This is supported by the crystal structure of ClC channels.[37,46,53,57]

An alternative to mechanical collapse of the pore/selectivity-filter around the permeant ion to explain pore-gating is a variable energy-of-binding model. Simply put, in some instances, such as that during the shortest-lived closed state of ROMK channels, K^+ may be bound so tightly to the pore that it briefly plugs the permeation pathway.[63] This latter mechanism shares similarities with a traditional gate, in that it is a manifestation of a particle physically clogging the pore to prevent further permeation, but here the gating particle is also the permeant ion rather than a distinct part of the channel. It is different from a pore-collapse mechanism, in that the pore remains in an open state

in the variable energy-of-binding model, merely being clogged. Both the mechanical pore collapse and variable energy-of-binding modes of gating result from interactions between the ion permeating the pore and pore residues.

Regulation of Gating

The inherent activities of gates can be influenced by factors that change the kinetics and equilibrium between the closed and open states. This change can be reversible or irreversible. Only the former is involved in the dynamic regulation of channel activity. The latter permanently changes the gating state. Factors that influence gating assume many forms. They can be extracellular and intracellular ligands that bind the channel, for instance Ca^{2+} binding to calcium bowls and RCK domains in the intracellular portions of BK_{Ca} channels.[69,70] They can be enzymes, for instance kinases and proteases, which chemically modify channels or change channel structure. For instance, ROMK is activated and maintained in a high-P_o state by PKA phosphorylation, and inhibited by intracellular acidification.[32] Voltage also can influence the gating of some channels. This represents a special case as discussed below in the section titled "Some Channels Rectify." Channel oligomerization and association with accessory subunits can also influence gating. Barttin plays such a role for ClC-Ka and ClC-Kb channels.[71] As shown in Figure 8.16, the presence of barttin reverses the voltage-dependence of the rat ClC-Ka ortholog, ClC-K1, switching it from being activated by membrane depolarization to being activated by membrane hyperpolarization. Such regulation of gating allows ClC-Ka and ClC-Kb channels to be active under physiological conditions, facilitating NaCl reabsorption in both the TAL and DCT.[72,73]

Many factors that influence gating to change P_o work through an allosteric mechanism, using a binding or effector site that is away from the pore. With such a mechanism, the effector molecule or influence of voltage affects an allosteric site where the free energy of interaction at this site is translated into a change in conformation that alters gating kinetics, equilibrium or both. As discussed further below, channel subunits in the Kv channel family have a core structure containing six transmembrane domains with an extracellular pore-forming loop between S5 and S6. In these channels, S4 is the voltage-sensor. This transmembrane domain contains conserved positive charged residues that sense voltage and move the S4 domain in response to a voltage-change across the membrane. In this sense, S4 is a molecular voltmeter. Movement of S4 is conveyed to the gate to change its position. BK_{Ca} channels contain intracellular Ca^{2+}-binding sites that also act as allosteric regulators of gating.[69,70] Occupancy of these sites by Ca^{2+} increases P_o by making it more likely that the channel will be in an open state.

Pore-gates, like those in ClC channels, can also be influenced by modulators to change gating. For instance, ClC channels are also voltage-dependent (see Figure 8.16). Because of the nature of the gate in these channels, regulation of ClC gating by voltage, though, is not allosteric. Rather, voltage directly influences the interaction of Cl^- with residues in the pore.[37,46,61]

The Consequences of Regulation of Gating

Regulation of gating determines how active a channel is, and the magnitude of the current through the channel. For instance, the regulation of gating, as noted above, enables ClC channels to be active under physiological conditions. Because gating can be regulated, channels act as variable resistors in equivalent circuits: their mode of gating can change, which causes P_o to be able to be changed in a dynamic manner. Recall that $I = iNP_o$ and $G = gNP_o$. In experiments quantifying macroscopic current, like the idealized results shown in

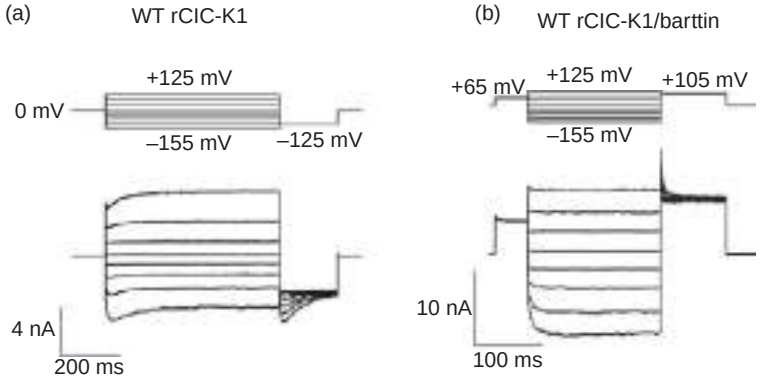

FIGURE 8.16 The regulatory subunit, barttin, reverses the voltage-dependence of ClC-K channels, allowing them to be active under physiological conditions. (*Adapted from Figure 1 in* [72].) Voltage-step protocols and representative current responses for cells expressing rat ClC-K1 alone (a) or together with barttin (b).

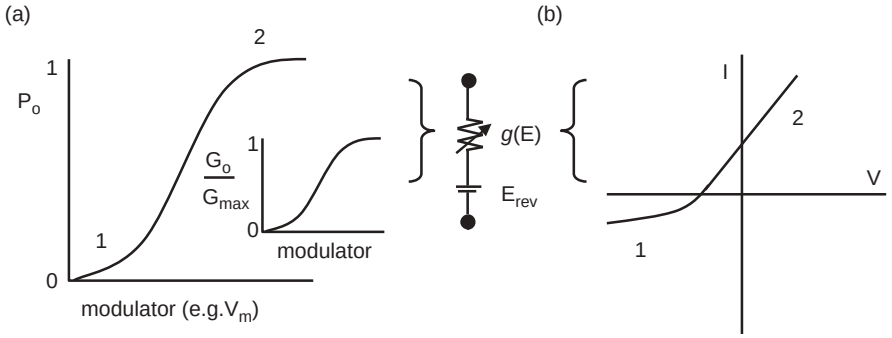

FIGURE 8.17 Changes in gating influence channel activity. The idealized graph in (a) shows P_o as a function of the effects of a modulator of gating, which changes the resistance of the channel shown in the idealized equivalent circuit shown to the right. (The inset in (a) shows the effects of a gating modulator on channel conductance.) The I–V relation in (b) shows the effects of the gating modulator changing P_o on macroscopic current, with point 1 being when the channel has low P_o and point 2 when P_o is approaching 1.

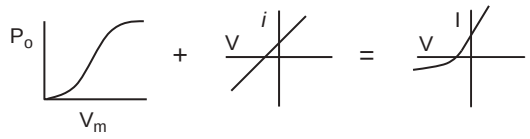

FIGURE 8.18 A channel's macroscopic I–V relation is a determinant of the effects of gating modulators on P_o and its single-channel *i*–V relation.

Figure 8.17, conductance changes as P_o changes, as a result of effectors influencing gating. The importance of this to physiology is clear when considering that voltage-dependent activation of BK_{Ca} channels enables them to conduct more current at depolarizing potentials, which in turn prevents further membrane depolarization by driving the membrane potential toward E_K. As noted previously, feedback activation of BK_{Ca} channels is critical to nearby TRPC6 channels functioning as Ca^{2+} entry pathways in podocytes.[11]

Some Channels Rectify

Rectification is when the macroscopic I–V relation of a channel deviates from strictly obeying Ohm's Law.[2] A macroscopic I–V relation, as detailed in Figure 8.18, is the sum of the single-channel i–V relation, and effects of gating modulators on channel P_o. Our discussion of ion channels has been simplified, in that we have presumed that they all rigorously follow Ohm's Law. This is not actually the case. As the concentration gradient of the permeant ion across the membrane increases, and as the concentration of the permeant ion approaches 0, all channels show some degree of rectification. This is referred to as Goldman rectification, and is a manifestation of the asymmetrical distribution of permeant ions across the membrane.[2] As such, it can be described by the GHK current equation. Further discussion of this, though, is beyond the scope of our discourse. Rectification that is of relevance here is that caused by voltage-dependent gating, because it can influence (as discussed immediately above) how active a channel is under physiological conditions.

Modulation of gating by voltage represents a special case. In this case, voltage has two affects. It influences P_o and the unitary current i of the channel. As such, macroscopic I–V relations for voltage-gated channels show rectification. Channels that rectify exhibit greater conductance at either positive or negative potentials applied across the membrane, meaning that they facilitate the movement of ions in a particular direction (into the cell or out of the cell). Macroscopic I–V relations for such channels are illustrated in Figures 8.17 and 8.18. The voltage-dependence of gating is routinely described with a Boltzmann function where $P_o = 1/[1 + e^{-V-V1/2zF/RT}]$.[2] All symbols in this equation have their usual meaning as described in previous sections, and $V_{½}$ is the voltage at which P_o is 0.5 or, if used to describe macroscopic conductance, the voltage at which conductance is half of the maximum. In most cases, when fitting the voltage-dependence of macroscopic conductance, G is normalized to maximum conductance (G_{max}), giving $G = G_{max}/[1 + e^{-V-V1/2zF/RT}]$. Fitting with a Boltzmann function provides two important pieces of information describing the effects of voltage on gating. It provides the voltage at which half the channels are open, telling us about the threshold for activation by voltage. It also describes the degree to which a channel responds to voltage. This is the slope of the fit, and informs us about the range over which the channel responds to voltage and how tightly channel gating is linked to changes in voltage: a steeper slope indicates a tighter association.

Modeling Channel Gating

Gating of an ion channel is akin to an enzyme transitioning between an unbound and substrate-bound active state, with rate constants determining the state

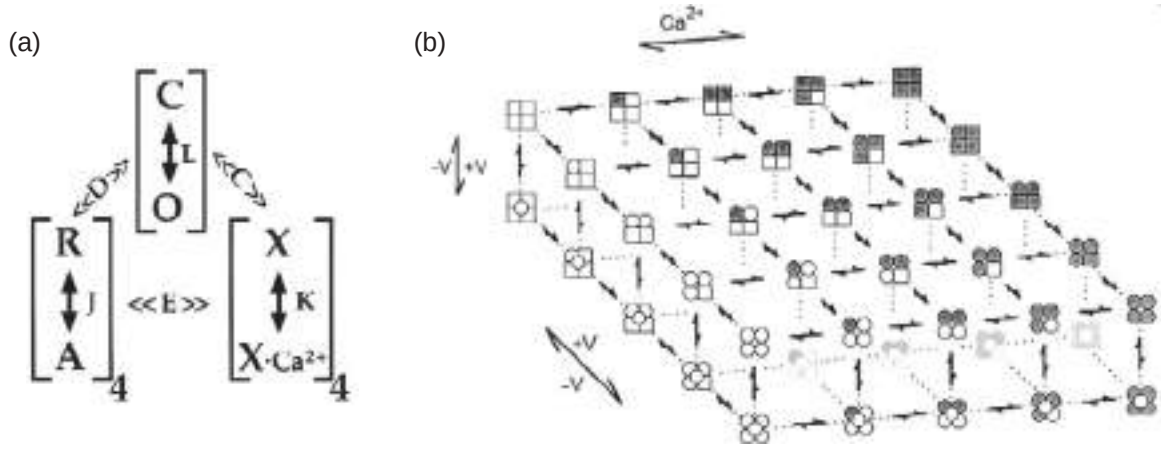

FIGURE 8.19 Channel gating can be described with kinetic models and state diagrams. The kinetic model (a) and state diagram (b) describing BK_{Ca} channel gating are from [69] and [70], respectively. The gating mechanism involves an allosteric interaction between channel opening (C−O) and voltage sensor activation (R−A). L is the C−O equilibrium constant when all voltage sensors are in the resting (R) state. J is the R−A equilibrium constant when channels are closed. D is the allosteric interaction factor where the C−O equilibrium constant increases D-fold for each voltage sensor activated, and the R−A equilibrium constant increases D-fold when the channel opens. Subscripts for closed and open states denote 0−4 activated voltage sensors of the tetrameric channel. The Ca^{2+}-binding transition (X−XCa) for each subunit has an equilibrium constant $K = [Ca^{2+}]/K_D$ when channels are closed and voltage sensors are not activated. Allosteric interactions of Ca^{2+}-binding with channel opening and voltage sensor activation are determined by the allosteric factors C and E, respectively. In the state diagram, a change in subunit conformation is indicated by the square-to-circle transition. The effects of voltage and Ca^{2+} are noted on the axes, with Ca^{2+}-binding indicated with gray shading. The open channel state is noted by a white circle in the center of the tetramer.

occupied. This allows gating to be viewed as a biochemical reaction, where standard analysis of reaction rates and kinetics can be used to describe the gating process. The simplest mode of gating is one containing forward and backward transitions between a single closed and open state. Such a gating scheme with associated kinetic constants is shown above the current trace in Figure 8.14.

Kinetic models and state diagrams have explained much about how factors influence gating. As we learn more about the biophysical properties of channels, these models have been becoming more complex, but also they are better at explaining the features and caveats of how channels transition and gate. Figure 8.19 shows a kinetic model and state diagram explaining the effects of voltage and Ca^{2+} on BK_{Ca} channel gating. Both models assume allosteric interaction between the voltage-sensor and Ca^{2+}-binding site(s) with the channel gate. When expanded, these models contain at least 50 different states. The kinetic model originated from the investigation of macroscopic currents under extreme conditions used to isolate specific effects of voltage and Ca^{2+} away from intrinsic gating events.[69] The state diagram was derived from single-channel data, including the analysis of single-channel gating kinetics.[70] These models have common features, and do a good job of predicting the voltage- and Ca^{2+}-dependence of BK_{Ca}-channel gating over a range of $[Ca^{2+}]$ and voltages, justifying their continued use for explaining BK_{Ca}-channel activity and regulation.

Such models have important ramifications for how we think about renal ion channels and understand their role in physiology. BK_{Ca} channels are critical to protecting membrane potential in podocytes during TRPC6-mediated Ca^{2+} influx, and are involved in K^+ secretion from the CD.[10,11,12] A detailed understanding of how BK_{Ca} channels gate in response to voltage and Ca^{2+} then is critical to appreciating these processes.

Pore Block

Although not a true change in gating in that the gate is not affected, a block of the pore by a factor other than the permeant ion or gating particle may also alter single-channel and macroscopic currents. For instance, the blocking of the ENaC pore by amiloride decreases the mean P_o these channels have with channels spending briefer periods in the open state.[47,48,74,75] In experiments, this appears as frequent transitions between the open and open-blocked state, with the latter appearing as a closed state. Block of a pore can also be voltage-sensitive if the blocker interacts with the blocking site in a voltage-dependent manner. For instance, rectification of Kir channels results from voltage-dependent block of the pore by Mg^{2+} and polyamines. This appears as an effect on gating.[43,76,77] Because such factors influence P_o and the time channels spend in the open state, their actions can also be assessed with standard kinetic analysis and measurements of voltage-dependence.

FUNCTION OF RENAL ION CHANNELS

Interpreting experimental results from a biophysical perspective, as developed above, has been instrumental in defining the roles of many channels in the kidney. In the next section, expression patterns are discussed in terms of where function has been established with some degree of certainty from experimental results (see Figures 8.1 and 8.2 and Table 8.1). Two channel proteins in the ClC transporter/channel family are expressed in the kidney: ClC-Ka in the basolateral membrane of ascending thin limb (ATL) and TAL cells, and CLC-Kb in the basolateral membrane of TAL and DCT cells.[60,78,79] Barttin, a regulatory subunit obligatory for ClC-Ka and ClC-Kb activity, is expressed along with these channel proteins in the nephron.[71,72,73] K^+ channels from at least four different families are functionally expressed in the kidney. The inward rectifiers Kir1.1 and 4.1 are expressed in the apical membranes of TAL, DCT, CNT and CD, and the basolateral membrane of DCT cells, respectively.[20] BK_{Ca} channels are expressed in podocytes and the apical membranes of CD cells.[11,19,29,30,31,33] Proximal tubule epithelial cells express the TWIK-related acid-sensitive K^+-2 (TASK-2) channel, a member of the two-pore K^+ channel family, in their basolateral membranes.[80] Kv1.1 is expressed in the luminal membrane of DCT cells.[20] A single type of Na^+ channel, ENaC, is expressed in the kidney in the apical membrane of CD principal cells.[41,81,82,83] Several members of the TRP channel family are expressed in the kidney. TRPC6 is expressed in podocytes.[11,13] The nonselective TRPV4 channel is expressed in the apical membranes of cells lining the water-impermeable segments of the tubule, including the ATL, TAL, and DCT.[12] TRPP2 is expressed in the apical membranes of TAL and DCT cells, as well as in other segments of the nephron.[12] Inactivating mutations in the gene encoding this channel protein cause autosomal dominant polycystic kidney disease. Coverage of this area of research is broad and beyond the scope of the current chapter. Chapter 80 discusses polycystic kidney disease, and TRPP2. The Mg^{2+}-selective TRPM6 channel is expressed in the apical membrane of early DCT cells.[9,10,19,20] The epithelial Ca^{2+} channel, TRPV5, is expressed in the apical membrane of late DCT and CNT cells.[49,84,85,86]

CLC (CLCN) Channels and Barttin (BSND)

The ClC proteins are members of a large family of Cl^- transport proteins that serve diverse functions (Chapter 31).[59,60] These proteins are widely expressed in every animal and most, if not all, bacteria. The ClC family is divided into two branches depending on function; three if sequence identity is the discriminator. Members of one branch (two if using identity) function as electrogenic anti-porters, moving $2Cl^-$ and H^+ in opposite directions in a secondary-active manner. This branch is likely to be the older for most, if not all, ClC proteins identified in bacteria belong to it. The younger branch contains proteins that have lost their need for H^+ to move Cl^- in a coupled manner, and now function as voltage-gated ion channels with anions moving through the ClC channel pore via restrictive diffusion.

ClC-Ka and ClC-Kb proteins form anion channels selective for Cl^- with similar biophysical properties. ClC-Ka and ClC-Kb have overlapping, but not identical, function in the kidney. This was revealed by the different tubulopathies arising from the inactivation of ClC-Ka (diabetes insipidus) versus ClC-Kb (Bartter's syndrome type III), and the realization that inactivation of barttin (BS type IV with sensorineural deafness) recapitulates the entirety of the phenotype resulting from loss of both ClC channels.[14,18,71,87] In the TAL, ClC-Ka and ClC-Kb serve as basolateral exit pathways for Cl^- brought into the cell along with Na^+ and K^+ by apical NKCC2. ClC-Kb, but not ClC-Ka, serves a similar function in the DCT, with the caveat that Cl^- enters these cells along with Na^+ across the apical membrane on NCC. Because ClC-Kb functions as a basolateral Cl^- exit gateway in both the TAL and DCT, inactivating mutations in this gene sometimes can appear to result in a mixed Bartter–Gitleman's phenotype.[14,18,88] Moreover, because both ClC-Ka and ClC-Kb are expressed in the TAL, the phenotype resulting from inactivation of ClC-Kb is not as severe as that seen with inactivation of barttin (BS type IV) or NKCC2 (BS type I).

Barttin, as indicated above, is required for ClC-Ka and ClC-Kb activity, making mutations in this accessory subunit also capable of causing disease.[72,73] The effect of barttin on ClC-K channels is complex and not fully-understood. What is clear is that ClC-K channels are the only members of the ClC family not to contain the critical E166 gating moiety at the extracellular mouth of the pore. Rather, these channels have a Val residue here.[46,57,61,72] This may contribute in part to why these channels are not functional in the absence of barttin, for this gating moiety enables other ClC channels to sense and respond to voltage with activation. Mutagenesis studies have shown that the transmembrane core of barttin is necessary and sufficient to promote ClC-K trafficking to the plasma membrane, a short cytoplasmic segment following the second transmembrane domain modifies the unitary conductance of ClC-K channels, and the entire COOH-terminal cytoplasmic domain is

involved in affecting channel P_o.[73] The biophysical mechanism whereby barttin affects ClC-K channel P_o involves locking the common gate covering the two proto-pores open: in the presence of barttin, ClC-Ka and ClC-Kb channels can reach full activity with their proto-pore gates primarily modulating P_o.[72] The physiological importance of this is clear. Without barttin, there is no ClC-K channel activity, concomitant K^+ recycling across the apical membrane of TAL cells or dependent NaCl reabsorption, resulting in the compromise of the axial corticomedullary hypertonic gradient necessary to concentrate urine.

KCNA (Kv) Channels

The Kv1.1 channel is expressed in the luminal membrane of DCT cells.[20] Kv1.1 is best known as the first cloned mammalian fast delayed rectifier channel belonging to the Shaker subfamily, named so because flies lacking the Shaker channel shake their legs while under ether anesthesia.[89,90,91] There is little difference between the intracellular and extracellular concentrations of ionized Mg^{2+} in the renal tubule. The electrochemical force driving cell entry of Mg^{2+} as a consequence is mostly a result of the apical membrane being hyperpolarized. Kv1.1 is K^+-selective and voltage-gated, rapidly activating upon membrane depolarization. Activation of Kv1.1 stabilizes the potential across the luminal membrane hyperpolarized near E_K. This function makes Kv1.1 well-qualified to facilitate Mg^{2+} reabsorption in the DCT. Inactivation of Kv1.1 leads to autosomal dominant hypomagnesaemia resulting from decreases in Mg^{2+} reabsorption in the DCT.[20,92]

KCNM (BK_{Ca}) Channels

BK_{Ca} channels are expressed in both podocytes and the apical membrane of CD epithelial cells. In podocytes, BK_{Ca} channels co-localize with TRPC6 channels, where they serve in a feedback capacity to facilitate and fine-tune receptor-operated Ca^{2+} influx mediated by TRPC6.[11] The Ca^{2+} and voltage-sensitivity of BK_{Ca} channels, as well as their selectivity and the influence that activating these channels have on membrane potential, makes them well-suited for such a task. This function, though, is not definitive; rather it is extrapolated from co-localization with TRPC6, and the biophysical properties of BK_{Ca} and TRPC6 channels. It has not been determined yet whether BK_{Ca} channel mutation causes any type of proteinuric glomerulopathy akin to the FSGS arising from the mutation of TRPC6.[13]

BK_{Ca} channels are also expressed in the apical membrane of CD epithelial cells. Here, they function as one of two discrete apical exit gateways for K^+ secretion in the distal nephron.[23,29,31,33] ROMK, as discussed below, serves a similar function in the parallel secretory pathway. Although both pathways mediating K^+ secretion in the distal nephron coexist and provide some redundancy and protection, they do not have a complete overlap of function. The ability of BK_{Ca} channels to respond to mechanical stimuli with changes in gating and P_o makes them particularly well-suited to mediate flow-induced K^+ secretion.[29,30] In comparison, ROMK activity is not sensitive to flow. Decreases in K^+ excretion in electrolyte-balance studies during states of high K^+ intake in animals with compromised BK_{Ca} channel activity resulting from gene deletion of the critical β1 regulatory subunit recapitulate findings testing the actions of BK_{Ca} channel blockers on K^+ secretion in isolated perfused tubules.[93]

KCNJ (Kir) Channels

ROMK (Kir1.1) is the founding member of the inward-rectifying K^+ channel family.[94] Inward-rectifying K^+ channels exhibit a non-linear I−V relation characterized by a larger inward current than outward current. ROMK, though, is only weakly inwardly rectified. ROMK is active at physiological potentials with electrochemical gradient, rectification, and other regulatory factors fine-tuning the amount of outward current carried by this channel. Under normal conditions, activated ROMK is well-suited for K^+ secretion, having a P_o approaching 0.9.

ROMK channels serve a dual role in the kidney. In the TAL, ROMK channels provide the majority of apical membrane K^+ conductance. This activity enables K^+ recycling across the apical membrane, to facilitate NaCl entry along with K^+ on the NKCC2 driving NaCl reabsorption by this segment of the tubule and, ultimately, creation of the axial corticomedullary hyperosmotic gradient necessary for concentrating urine.[31,32,33] This function of ROMK was revealed upon discovery of the genetic basis of Bartter syndrome.

ROMK is also an essential component of one of two parallel K^+ secretory pathways in the CNT and CD.[31,32,33,95] As discussed above, BK_{Ca} channels replace ROMK in the ROMK-independent K^+ secretory pathway. This explains how K^+-wasting can happen in BS type II, even in the absence of ROMK. In the same way, upregulation of ROMK channels preserves K^+ secretion in BK_{Ca} channel knockout mice. It has been speculated that this redundancy is a protective mechanism to ensure high-capacity K^+ excretion to guard against fatal hyperkalemia.[32]

Kir4.1 is another member of the inward rectifier family of K^+ channels expressed in the kidney.[92,96,97,98] Compared to ROMK, less is known about the function of this channel in the kidney, but emerging evidence supports that it acts as an important basolateral K^+ exit pathway in DCT cells. Potassium exiting through this channel contributes to the extracellular pool of K^+ immediately available to serosal Na^+,K^+-ATPases. This is necessary for Mg^{2+} reabsorption in the DCT, because Mg^{2+} entry across the apical membrane is intimately tied to membrane potential and NaCl reabsorption where maximal Na^+,K^+-ATPase activity is required to maintain the electrochemical gradients driving Mg^{2+} across the luminal membrane. Proper Kir4.1 function in the DCT is critical, in that the loss of this channel's function causes disease, SeSAME, with notable renal Mg^{2+}-wasting.[92,96,97,98] Clearly, the unique biophysical properties this channel provides to the basolateral membrane of DCT cells cannot be compensated for by the presence of other K^+ channels.

KCNK (K_{2P}) Channels

TASK-2 is a member of the alkaline-activated TALK sub-family within the larger two-pore K^+ channel family.[80] TASK-2 is expressed in the basolateral membrane of PT epithelial cells. As revealed in TASK-2 $-/-$ mice, this channel functions as an alkali-activated counterbalance to the depolarizing influence of the electrogenic Na^+,3-HCO_3^--co-transporter also in the basolateral membrane of PT cells.[80,99] Outward K^+ conductance through TASK-2 counteracts the depolarizing effects of this co-transporter by hyperpolarizing membrane potential back towards E_K. This function makes TASK-2 a key component of a positive feedback pathway maximizing HCO_3^- reabsorption in the PT. Loss of TASK-2 function causes metabolic acidosis, as expected but also modestly increases Na^+ and water excretion by the kidney.[99,100] These effects on pH and renal salt and water handling are akin to those seen with diuretic inhibitors of carbonic anydrase, which promote a weak diuresis by decreasing bulk fluid reabsorption in the PT due to decreased $NaHCO_3^-$ reabsorption. Although the role of TASK-2 in the mouse is clear, it remains to be determined whether mutations in this channel account for familial forms of proximal renal tubule acidosis in humans.

SCNN (ENaC) Channels

ENaC is a member of the ENaC/Degenerin channel family.[101–103] Acid-sensing ion channels (ASIC) are also in this family. ENaC/Deg channels are widely distributed in epithelial and nervous tissues. These channels are Na^+- or non-selective cation channels. Some of the non-selective ENaC/Deg channels also conduct Ca^{2+}. ENaC, which is highly selective for Na^+, though, does not.[41,83,104,141] The activity of ENaC in the CNT and CD is limiting for electrogenic transcellular Na^+ reabsorption here.[41,82,83] This reabsorption fine-tunes urine and plasma Na^+ content. Consequently, ENaC is a physiologically important target for hormones that control blood pressure through feedback regulation of systemic Na^+ and water levels, including those in the renin–angiotensin–aldosterone system. As such, ENaC mutation resulting in gain- and loss-of-function cause improper Na^+ retention and excretion, respectively, leading to increases and decreases in blood pressure.[83,106,107] The prior is Liddle's syndrome, and the latter is pseudohypoaldosteronism (PHA) type-I. Because the electrochemical gradients driving Na^+ reabsorption and K^+ secretion across the apical membrane of CD principal cells are intimately tied to each other, factors that change ENaC activity, including the steroid hormone aldosterone, also affect renal K^+ excretion.

TRP Channels

The TRP protein family is a diverse group of cation channels that participate in a wide range of physiological processes. The mono- and divalent cation conductance of TRP channels enables them to influence both membrane potential and intracellular Ca^{2+} signaling, allowing them to function as important signal transduction switches and gateways for Ca^{2+} and Mg^{2+} entry into the cell during transcellular transport. Mammalian TRP proteins are organized into six subfamilies based on sequence identity. These are C (Canonical, TRPC1-TRPC7 with TRPC2 being a pseudogene in humans), V (Vanilloid, TRPV1-TRPV6), M (Melastatin, TRPM1-TRPM8), A (Ankyrin, TRPA1), P (Polycystin, TRPP1-TRPP3), and ML (Mucolipin, TRPML1-TRPML3).

TRPC6

TRPC6 is a non-selective cation channel with finite Ca^{2+} permeability.[10–12] This channel is expressed in the foot processes of podocytes of Bowman's capsule in the vicinity of the slit diaphragm, as well as in the cell body and major processes of these cells. TRPC6, possibly oligomerized with TRPC3, functions as a receptor-operated Ca^{2+} entry channel in podocytes, where activation leads to cell entry of Ca^{2+} capable of modulating a host of secondary cascades. TRPC6 is only Ca^{2+} permeable under hyperpolarizing conditions. During depolarization Ca^{2+} binds to an

inhibitory site within the pore. Binding to this site results in the block of the pore, with a dependent decrease in P_o and inward rectification of macroscopic TRPC6 currents.[108,109,110] Pore block of TRPC6 by a permeant ion is accurately described by a standard single binding site, two-barrier pore model, where the binding site has a two-fold higher affinity for Ca^{2+} than it does for monovalent cations.[108] Consequently, binding to the inhibitory site impedes Ca^{2+} permeation, causing a relative increase in permeation of monovalent cations. The result is that, in the presence of membrane depolarization, TRPC6 converts from a Ca^{2+} entry channel that affects cell signaling to a channel that depolarizes the membrane. BK_{Ca} channels colocalize with TRPC6 channels in the foot processes and other major structures of podocytes.[11] This suggests a tight relation between the function of these channels with TRPC6 allowing Ca^{2+} to enter the cell, which in turn activates nearby BK_{Ca} channels to facilitate or fine-tune further Ca^{2+} entry through TRPC6 channels. Gain-of-function mutations in TRPC6, leading to increased activity and plasma membrane expression, cause familial forms of FSGS.[10,11,12,13] Mutation of other proteins in the podocyte, including nephron and podocin, that interact with TRPC6 also cause FSGS-like proteinuric glomerulopathies.[10,11] Similarly, the mutation of PLC-ε, an important regulator of DAG-sensitive TRPC6 channel activity, causes an FSGS-like disease.[10]

TRPM6

TRPM6 functions as a Mg^{2+}-selective channel in the apical membrane of early DCT cells.[4,19,20,24] TRPM6 may possibly oligomerize with the more widely-expressed TRPM7 to perform this function. Nevertheless, it is clear that TRPM6 brings a unique component to the channel for inactivating mutations in the gene encoding TRPM6 leading to HSH and, thus, TRPM7 does not fully recapitulate the properties of TRPM6.[4,10,12,19,20,24] Macroscopic current through channels containing TRPM6 is both outwardly and inwardly rectified, and activated by deceases in intracellular Mg^{2+}. This activation serves as a feedback mechanism favoring Mg^{2+} reabsorption. In addition to inactivating mutations in TRPM6, mutations in the genes encoding regulators of this channel cause hypomagnesemia.

Inactivation of the gene encoding pro-epidermal growth factor (EGF), for instance, causes isolated autosomal-recessive hypomagnesemia.[9,10,19,20,24] EGF is a magnesiotropic factor that controls the expression of TRPM6 in the apical membrane of DCT cells. Cetuximab, which is an inactivating monoclonal antibody inhibitor of the EGF receptor used in the treatment of colorectal cancer, causes pronounced renal Mg^{2+}-wasting, also resulting from decreased TRPM6 expression, an acquired form of isolated renal hypomagnesemia.[20,111,112] Magnesium reabsorption via TRPM6 is dependent on NaCl reabsorption and membrane potential in the DCT mediated by the coordinated activities of the apical membrane thiazide-sensitive NCC co-transporter and basolateral Na^+,K^+-ATPase. Mutation of the *FXYD2* gene, which encodes the γb splice variant of the Na^+,K^+-ATPase γ-subunit expressed in this segment of the tubule, causes isolated dominant hypomagnesemia.[9,19,20] Similarly, one component of the complex renal salt-wasting phenotype arising from the inactivation of NCC (Gitleman's syndrome) is Mg^{2+}-wasting.[9,12,19,20,88]

TRPV4

TRPV4 was originally described as an osmotically-responsive monovalent cation-selective cation channel/current with the different names of OTRPC4, VR-OAC, TRP12, and VRL-2.[12] This channel is activated by hypotonic stimuli, resulting in an increase in $[Ca^{2+}]_i$. Increases in Ca^{2+} are secondary to membrane depolarization, rather than Ca^{2+} flux through the channel. TRPV4 is expressed in the water-impermeable segments of the nephron and circumventricular nuclei of the CNS, which governs vasopressin release. The osmotic sensitivity of this channel and its expression in the part of the CNS controlling AVP release led to the idea that TRPV4 contributes to the sensing of osmotic stress and plasma osmolarity. Such a function is supported by findings that AVP release is dysregulated in TRPV4 knockout mice.[113,114] The expression pattern of this channel in the kidney is also consistent with it acting as a cellular-level osmoreceptor that enables epithelial cells to adapt and respond to changes in osmolarity with a change in NaCl transport. Again, findings in the knockout animal are consistent with this.[114,115]

TRPV5

The activity of TRPV5 is voltage- and Ca^{2+}-dependent. This channel is active at physiological potentials and $[Ca^{2+}]_i$ concentrations, but quickly inactivates in response to feedback regulation from intracellular Ca^{2+}.[12,49,84,85] TRPV5 is permeable to Ca^{2+}, and is selective for this divalent cation over monovalent cations. The relative permeability of Ca^{2+} versus Na^+ for channels containing TRPV5 is greater than 100. This is fairly unique for TRP channels, with TRPV6 being the only other TRP channel to share this preference for Ca^{2+}. The selectivity and activity of TRPV5 allows it to function as the apical gateway for Ca^{2+} entry into late DCT and CNT epithelial cells. As such, TRPV5 activity is rate-limiting for Ca^{2+} reabsorption in the nephron beyond the Loop of Henle, where urine and plasma $[Ca^{2+}]$ are fine-tuned. Inactivating mutations of TRPV5 or proteins that regulate the activity

of this channel, such as Klotho, cause hypercalcuria and renal Ca^{2+}-wasting in mice.[12,49,84] It has not been established yet if mutations in human TRPV5 cause a similar renal phenotype.

ION CHANNEL STRUCTURE

Ion channels are multimeric, made of component subunits. There are two general types of channel subunits: those that form the pore, termed pore-forming or α-subunits, and those that do not directly contribute to the pore, but rather modify the properties of the channel proper or pore-forming subunits; these routinely are labeled accessory or β-subunits, but also have been called auxiliary and regulatory subunits. Pore-forming subunits must span the lipid bilayer to create the conductive pore. As depicted in the idealized models of the different subunits making renal channels shown in Figure 8.20, pore-forming subunits contain two or more membrane-spanning domains. Many, but not all, accessory subunits are also integral membrane proteins. (These are not represented in Figure 8.20.) The presence or absence of an accessory subunit has significant consequence to the biophysical and physiological function of a channel. For instance, the activities and properties of the human ClC channels, ClC-Ka and ClC-Kb, are greatly changed by interaction with their β-subunit, barttin.[71,72,73]

Families of pore-forming channel subunits are comprised of homologous proteins that share amino acid identity. The degree of similarity determines how much overlapping function members within a family have. The consequence of a channel family being composed of homologous subunits is that they often differentially assemble into homomeric and heteromeric channels containing a single type of subunit or one with many different but related subunits. The biophysical ramifications of this ability to assemble differentially are profound, leading to differences in channel gating, expression, and regulation to name just a few. This greatly broadens the functional range of channels within the same family. It also can impact the ability to use redundancy to circumvent pathological consequences when one subunit is compromised. Moreover, it can confound the understanding of the specific role played by a particular channel protein within a channel family.

Pore-forming subunits oligomerize into one of three general quaternary structures, as represented in Figure 8.20. ClC family members dimerize into channels containing two subunits, with each subunit encompassing an independent pore.[53,57,116] Most often, as is the case for the renal ClC-Ka and ClC-Kb channels, these dimers are made of identical subunits,

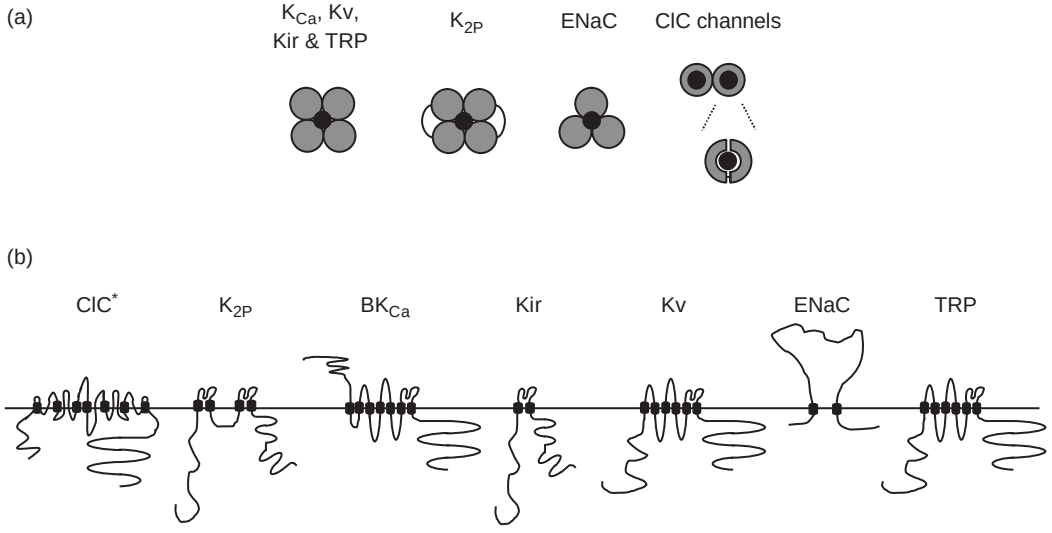

FIGURE 8.20 **Channel structure.** The idealized illustrations in (a) indicate how renal ion channel subunits assemble to form pores. Subunits are indicated by gray circles or half circles with black lines representing the connection between the two subdomains within each monomer of dimeric K_{2P} and ClC channels. The position of the pore is represented by a black circle. Views are parallel to the plane of the membrane. The idealized illustrations in (b) represent the topology of pore-forming subunits of renal ion channels. These views are perpendicular to the plane of the membrane, which is represented by a solid black horizontal line. Transmembrane domains are represented by small black barrels. Extracellular and cytoplasmic portions of these channel subunits are shown above and below the line representing the plasma membrane, respectively, and only loosely correspond to the real structure of these domains. It is difficult to represent the structure of ClC subunits faithfully using such a diagram, as many intra-membrane helices in this channel do not fully span the membrane. Refer to Figures 8.21 and 8.23 for a better understanding of the secondary and tertiary structure of transmembrane helices in ClC channel subunits.

being homodimers. ENaC is an obligatory heterotrimeric channel containing one α-, β-, and γ-subunit surrounding a central pore.[117,118] (The Greek letters referring to the subunits in ENaC are not indicative of whether they contribute to formation of the pore or not for they all do; rather, they reflect the order of cloning.) In comparison, K^+-channel subunits and TRP subunits assemble into tetramers with identical or like subunits forming homotetramic and heterotetramic channels with a central pore. K_{2P} channels are a slight variation on this theme. These channels are homodimers, with each component subunit containing two pore-forming domains that contribute to a central pore that has four-fold symmetry.[119] Thus, K_{2P} subunits oligomerize into a channel with structure that is reminiscent of that formed by Kir channel subunits. Because good structural information exists for ClC, ENaC, and Kir channels or channels closely related to them, discussion in the next section focuses on these channels as representative of the three types of general structure renal channels assume.

The Architecture of ClC Channels

Every ClC protein, including both transporters and channels, shares a conserved molecular architecture consisting of a complex transmembrane transport domain and soluble regulatory domain. Representative crystal structures for both domains are available: the transmembrane domains of two bacteria ClC homologs, ClC-ec1 and ClC-st1, and a cyanobacterial ClC protein, ClC-sy1, and the regulatory domains of three eukaryote family members, ClC-0, ClC-Ka, and ClC-5.[53,57,116,120–122] ClC channels are unique for ion channel proteins, probably reflecting their evolutionary roots as transporters, in that many of their intramembrane helices are of unequal size not completely crossing the membrane. This places several intramembrane helices of ClC proteins at acute angles, rather than right angles as is more common for channels, to the plane of the lipid bilayer. This is clear in the crystal structure for ClC-ec1 shown in Figure 8.21.[52]

Also clear in this structure is that the assembled ClC channel is a homodimer containing two similar

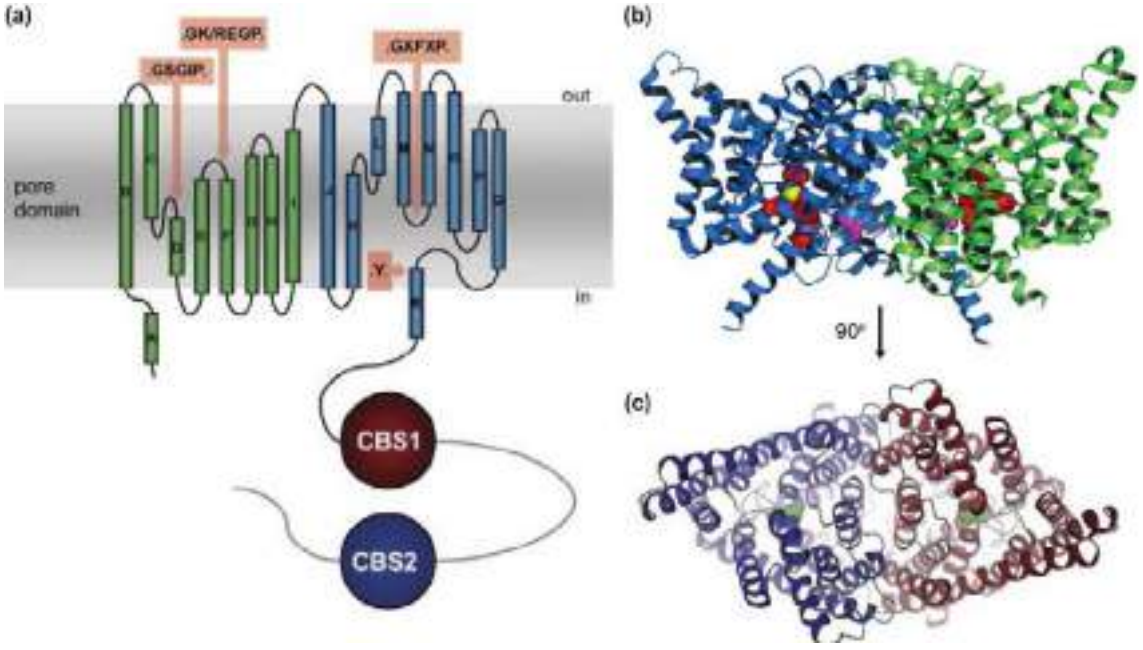

FIGURE 8.21 **Topology and structure of ClC proteins.** (a) *(Figure from [52].)* Schematic representation of ClC channel proteins with topology inferred from the known structure of the bacterial homolog ClC-ec1. The 18 α-helices in these proteins are labeled A–R. The two similar halves within the transmembrane domain (α-helices B–I and J–Q), which have anti-parallel orientation, are colored in green and cyan, respectively. The sequence and position of conserved residues that contribute to the Cl^- selectivity filter are noted with arrows and peach highlighting. The two cytoplasmic CBS domains are shown as red and blue spheres. (b) *(Figure from [79].)* Crystal structure of the *Salmonella enterica* serovar *typhimurium* ClC protein viewed parallel to the plane of the lipid bilayer. One subunit of the dimeric protein is shown in blue and the other green. Cl^- ions in the pore are shown as yellow spheres. Residues comprising the selectivity filter (S106, E1148, and Y445) are shown as red spheres. (c) *(Figure from [52].)* Structure of the *Escherichia coli* ClC protein, ClC-ec1, viewed from the extracellular side. The two subunits of the homodimer are colored red and blue, with ions in the selectivity filter of each subunit represented as green spheres. See color section at the back of the book.

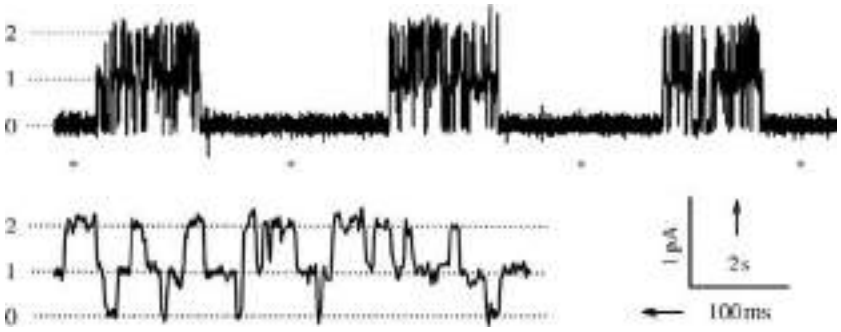

FIGURE 8.22 **ClC subunits form double-barreled Cl^- channels.** *(Figure from [61].)* Shown here is a representative single-channel current trace of a ClC-0 channel. Slow gating by the common gate is noted by asterisks. Fast gating of the proto-pore gates occurs between slow-gate closures: conductance level 0, both pores closed; conductance level 1, one pore closed, one pore open; conductance level 2, both pores open. Below is part of the current trace shown with an expanded timescale.

monomers, each having two topologically related halves, which span the membrane in opposite directions in an antiparallel arrangement. Despite their similarity in structure, the two antiparallel halves of each monomer share only weak conservation at the 1° amino acid sequence level. The two monomers within the channel are structurally related by an axis of two-fold symmetry perpendicular to the membrane plane. When viewed looking down on the plane of the extracellular leaflet of the membrane, the two monomers appear triangular, with a subunit interface at the bases of these triangles. A pore is completely contained within the center of each triangular subunit. That the assembled ClC homodimeric channel contains two independent pores with separate but identical ion permeation pathways has led to these channels being referred to as double-barreled channels. This is consistent with early electrophysiological work on the ClC-0 channel predicting this double-barreled architecture.[52,61,79] Each pore, sometimes termed proto-pore, has its own gate that functions independently gating in a fast manner. Both pores also are covered by a common gate that gates, in comparison, slower. These types of gating are clear in the representative single-channel current trace of homodimeric ClC-0 shown in Figure 8.22. In comparison to this fully assembled channel, the limiting functional unit of a ClC pore, as recently proven by Jayaram and colleagues using a molecularly "designed" ClC-ec1 protein mutating it from a transporter to channel, is a monomer containing the two antiparallel halves capable of conducting Cl^- through a single pore.[123] Experiments on this designed ClC-ec1 channel, moreover, addressed the line separating ClC channels from ClC transporters: it was shown to be thin, involving replacement of only two amino acids. Although the limiting functional unit is a monomer, binding sites critical to regulation of gating, for instance that for Ca^{2+}, are formed at the interface between the two monomers of the homodimer.[124]

The Cl^- Permeation Pathway in ClC Channels: The Molecular Basis of Selectivity

All known ClC channel subunits use a conserved permeation pathway through the protein and common binding sites to conduct Cl^-.[37,46] This vestigal pathway is also present and used in ClC anti-porters to translocate Cl^-. The permeation pathway for anions was unexpectedly revealed by the presence of Cl^- ions bound within each pore in the first crystal structures of bacterial ClC transporters.[53,57] As recognized now from this early work, and reflected in the ribbon structures shown in Figure 8.23, the permeation pathway contains three Cl^--binding sites: an external binding site, S_{ext}; a central binding site, S_{cen}; and an internal binding site, S_{int}. The external binding site can be occupied by Cl^- or the side chain of a conserved Glu residue, E148 in bacterial ClC homologs.[46,52,79] This observation generated many of the initial hypotheses regarding the molecular basis of fast gating in ClC channels. This will be addressed further below.

Formation of a complete permeation pathway containing a selectivity-filter with three Cl^--binding sites, as depicted in Figure 8.23, is possible because the two structurally related antiparallel halves of a monomer are arranged in opposite directions, giving rise to a pseudo two-fold axis of symmetry in the center of the membrane. This makes it possible to bring together loops at the end of helices from different parts of the structure to form the pore in the center of the triangular monomer. Moreover, in this arrangement, the positive ends of the helix dipole point toward the ions entering the pore and stabilize them by electrostatic interactions. Interestingly, nature seems to have conserved this means of pore formation, because an antiparallel architecture also forms the pore of the unrelated aquaporins.[125,126]

Although scattered across the entire subunit, the signature sequences defining the three Cl^--binding sites, as noted in Figure 8.21, are conserved throughout all ClC proteins.[46–52] This speaks to the functional importance of conserving key residues at critical sites in the three-dimensional structure of the protein. The pore of ClC channels is hourglass in shape, bound by aqueous vestibules on the extracellular and intracellular end narrowing in the middle at the selectivity-filter. The intracellular Cl^--binding site is located at the interface between the intracellular vestibule and

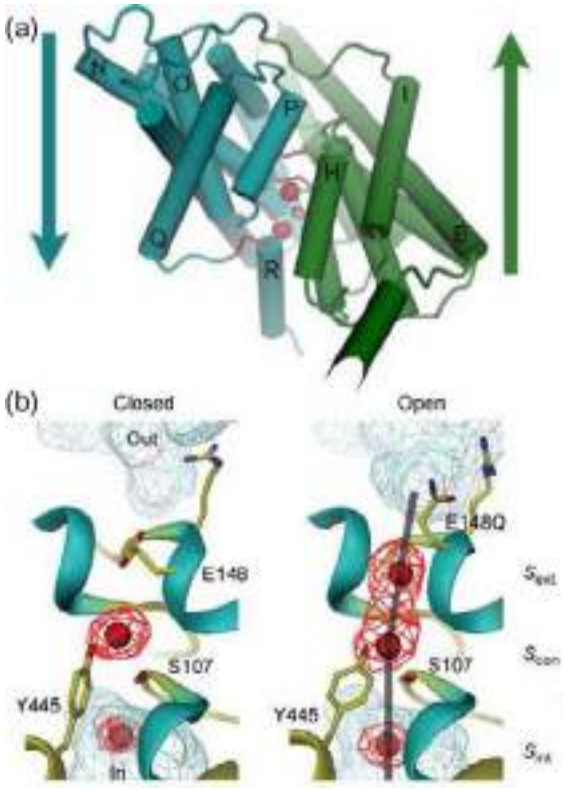

FIGURE 8.23 **The selectivity filter of ClC channels.** (a) *(Figure from [52].)* View of an EcClC monomer parallel to the plane of the membrane. The two anti-parallel halves of the monomer are colored blue and green. Their orientation in the membrane is indicated by arrows and helices are labeled. Ions in the pore are shown as red spheres. Regions of the protein contributing to the selectivity filter are colored red. (b) *(Figure from [55].)* The selectivity filter of wild-type EcClC (closed) and the EcClC mutant E148Q (open) viewed parallel to the plane of the lipid bilayer. The protein backbone is shown as a ribbon with NH_2-terminal ends of α-helices colored cyan. Selected residues are shown as sticks. Ions in the pore are represented as red spheres. The contoured (at 6σ) Br^- anomalous difference density is shown superimposed (red). Aqueous cavities from the extracellular (out) and intracellular (in) solutions are shown as cyan mesh. Ion-binding sites in the pore are labeled. See color section at the back of the book.

selectivity-filter. The Cl^- ion occupying S_{int} is only partly desolvated, and still hydrated where it is exposed to the aqueous environment of the vestibule. The desolvated surface of this Cl^- ion is coordinated by backbone amide groups on the loop preceding the D helix. The Cl^- ion at S_{cen} has completely shed its water shell, and is now coordinated by partial positive charges from backbone amide nitrogen groups in residues preceding the N helix. In addition, key interactions are made here with selectivity-filter side chain hydroxyls of S107 in the conserved GSGIP sequence and of Y445 located at the beginning of the R helix. When S_{ext} is occupied by E148, not only is the pore physically blocked by the residue side-chain, but a negative charge is also placed within 4 Å of the Cl^- ion occupying S_{cen}. This provides two alternatives to explain gating: a physical occlusion of the pore and a repulsion mechanism involving pore-gating. When the channel is conducting, E148 has moved from S_{ext}, opening this binding site to the Cl^- ion. Supporting this are findings showing that, upon substituting E148 with either an Ala or a Gln, a Cl^- ion is bound to this site coordinated by free backbone amide NH groups of residues in the NH_2-termini of the N and F helices.[37,46,57]

ClC Channel Gating

The gating of ClC channels is complex and incompletely understood. More is understood about the mechanisms underpinning fast gating of proto-pores, as compared to gating by the common gate. Gating of both the fast and common gates is inextricably linked to ion permeation.[37,61,127] In addition to being modulated by extracellular $[Cl^-]$ where increases in $[Cl^-]_{ex}$ increase P_o, fast gating (and also slow gating) is modulated in a positive manner by depolarizing voltages and decreases in pH.[61,67,128,129] Dependence on pH is thought to be a remnant from its days as a transporter. Compelling evidence has emerged that E148 mediates the effects of pH on the fast gate. There is a real possibility also, as supported by experimental evidence, that the effects of voltage on the fast gate are felt by the permeant Cl^- ion and/or modulatory H^+.[61,130] This likely arises from the fact that proto-pores use some form of a pore-gating mechanism, with the interaction between the permeant ion and permeation pathway doing the "gating." Working in combination with this is the charged side chain of E148, which also may be sensitive to voltage or even extracellular $[Cl^-]$ and pH in a voltage-dependent manner.

An important point to note is that ClC-Ka and ClC-Kb do not have a Glu at the position corresponding to 148, which is 166 in ClC-Kb, but rather have a Val at this site, yet both channels show fast gating.[46,79,131] This suggests that, while E148 and the corresponding Glu residues in other ClC channels may be involved in gating, it is not functioning in isolation. In addition, ClC-K1 channels are voltage-sensitive where interaction with the accessory subunit barttin reverses the voltage-activation profile (see Figure 8.16[72,73]). Chimeras of ClC-K1 and ClC-Kb retain this barttin-dependent switch in voltage-sensitivity, suggesting that ClC-Kb channels are also voltage-sensitive in the absence of barttin and E148. The importance of E148 to gating in most ClC channels, though, is not trivial for mutation of the homologous residues in ClC-0, ClC-1, and ClC-2 to neutral residues abolishes voltage-dependent gating.[57,132,133]

The Architecture of ENaC/Deg Channels

The three-dimensional structure of ENaC awaits elucidation, but much can be inferred with a degree of certainty from the known structure of chicken ASIC1.[58,117] As discussed below, we can make predictions about the selectivity-filter and permeation pathway of ENaC and how the channel gates, which are supported by electrophysiology studies.[104,105,134–136]

Subunits forming ENaC/Deg channels share a common topology, which is shown in Figure 8.24, containing a large extracellular domain with much secondary structure bound by two transmembrane (TM) domains, TM1 and TM2, with intracellular NH_2- and COOH-termini.[58,117] As noted above, ENaC is an obligatory heterotrimer containing one α-, one β-, and one γ-subunit contributing to a central pore.[118] These orthologs are encoded by different genes.[101,102] The relative order of subunits within ENaC has yet to be determined. Oligomerized ENaC likely appears as a "chalice," similar to that shown in Figure 8.25, with extracellular domains forming the cup, the transmembrane domains the stem, and intracellular domains the base.[117,137] In comparison to K^+ channels, the ENaC/Deg pore and selectivity-filter, as defined by the cASIC1 crystal, are not made of P-loops diving back into the membrane, but rather are formed by the TM2 domains of the three component subunits as they run in a linear manner through the membrane. The pore as defined by TM2 domains is "hourglass" in shape, with wide extracellular and intracellular facing vestibules and a narrowing in the middle. The extracellular mouth of the pore is coupled to the extracellular domain by short linker sequences in the wrist of the channel. TM1 domains lie just outside TM2 domains within the same subunit as they run the length of the pore sheltering TM2 residues, with TM1 making most of the contact with the lipid bilayer. There are extensive interactions between residues in the adjacent TM1 and TM2 helices within the same subunit, and also between TM domains in neighboring subunits.

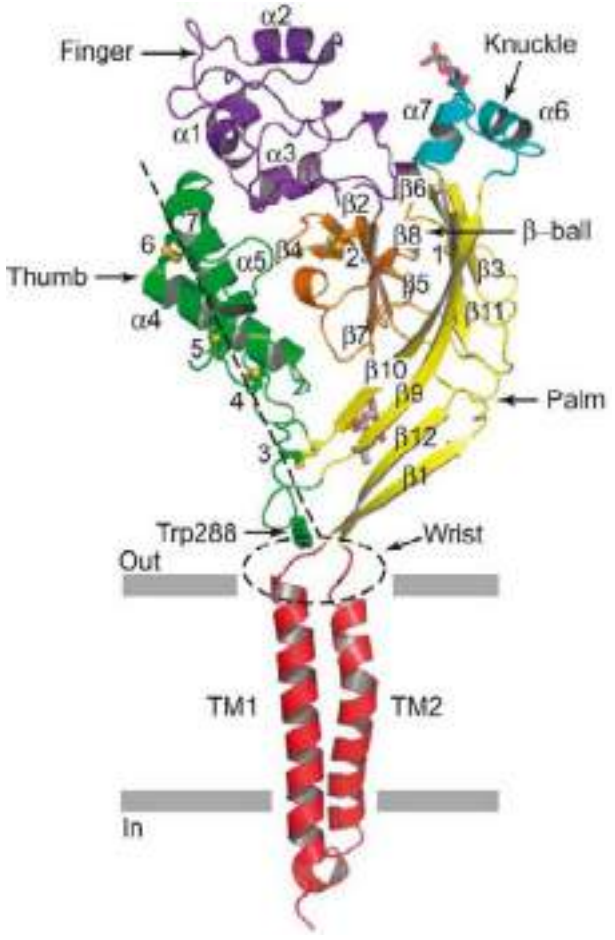

FIGURE 8.24 **The topology of ENaC/Deg channel subunits.** *(Figure from [117].)* This cartoon shows the topology of a monomer within the homotrimeric cASIC1 channel, as defined by the crystal structure. The view is perpendicular to the plane of the membrane. Transmembrane helices (TM1 and TM2) are shown in red. Location of intra-subunit disulphide bridges are labelled 1–7. See color section at the back of the book.

The Permeation Pathway in ENaC/Deg Channels: Selectivity and Ion-Binding Sites

Similar to cASIC1, the ENaC pore likely has pseudo three-fold symmetry around the central axis of the pore, perpendicular to the plane of the lipid bilayer. Ions enter the extracellular mouth of the pore proper through a large vestibule that has profound negative electrostatic potential where the lower half of this molecular "basket" sits within the membrane plane. The negative electrostatic potential of the vestibule allows it to act as a cation reservoir, concentrating cations around the mouth of the pore, contributing to robust channel conductance.[58] The bottom of this vestibule in cASIC1 is defined by D433 corresponding to N530 in γ-ENaC, which when substituted as discussed below causes disease.[58,138] D433 has been proposed to contribute to the desensitization gate in cASIC1 in response to H^+.[58] The cytoplasmic mouth of the pore, similarly, is bound by a large vestibule, shaped like an inverted cone. This vestibule is lined by residues with negatively charged side chains, again possibly allowing the vestibule to act as a cation reservoir. Substitution leading to charge neutralization of these negatively charged residues in ENaC eliminates conductance through the channel.[136]

Figure 8.26 shows the three-dimensional structure of cASIC1, including the radius of a possible conduction pathway along the three-fold axis. The cASIC1 pore, and likely that in ENaC, contains three Na^+-

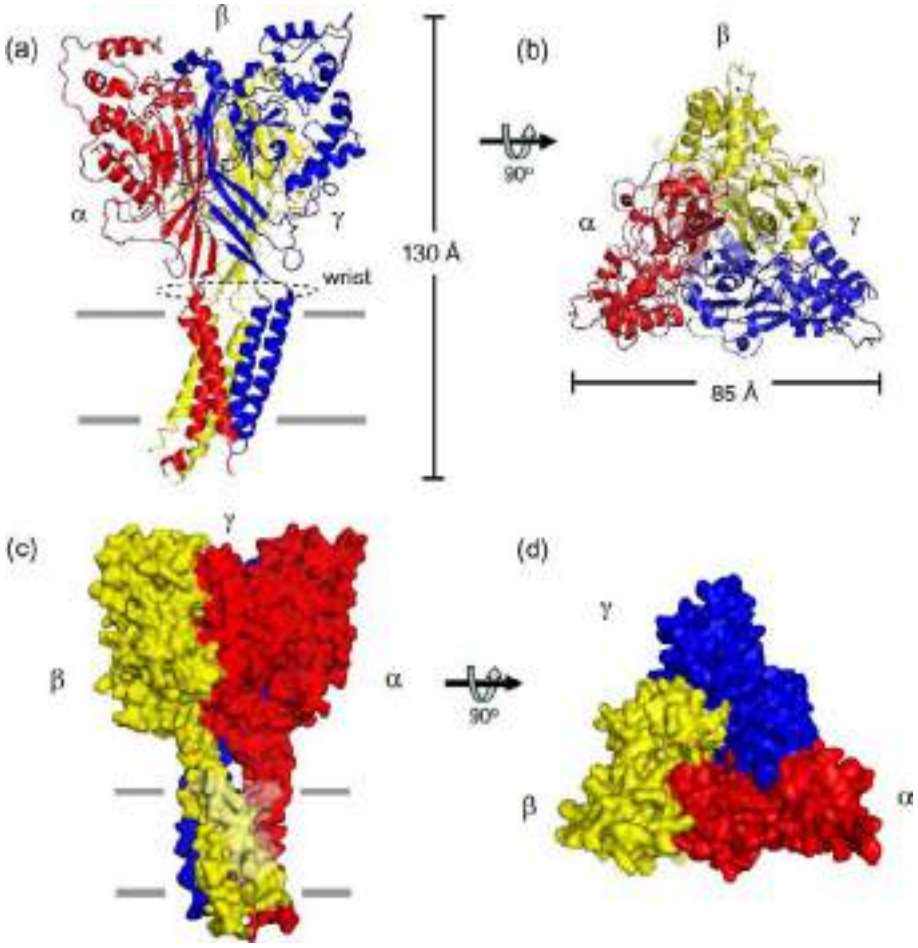

FIGURE 8.25 **Predicted structure of ENaC.** *(Figure adapted from Figure 3 in [137].)* View of the predicted ribbon and space-filled structure of heterotrimeric ENaC perpendicular (a and c) and parallel (b and d), from the extracellular side, to the molecular three-fold axis. ENaC subunits, α- (red), β- (yellow), and γ- (blue), modeled using the 2QTS structural coordinates for the A, B, and C subunits of the cASIC1 homotrimer.[117]

binding sites that are occupied during permeation. Adjacent sites are unlikely to be occupied at the same time due to charge repulsion (see Figure 8.15[58]). In open cASIC1, main chain carbonyl oxygen atoms from the symmetry-related G436, G439, and G443 residues coordinate Na^+ permeating through the pore. As shown in Figure 8.27, permeant ions are bound by six ligands arranged in a trigonal antiprism geometry arising from the three ligands on the upper triangular plane being staggered in comparison to those in the lower triangular plane. This geometry provides the appropriate number of partial negative charges for coordination of a Na^+ ion, while perfectly accommodating the underlying molecular symmetry of the trimeric channel.

Several of the coordinating Gly residues in cASIC1 are replaced by Ser residues in ENaC subunits (see Figure 8.27a). ENaC is about 10-fold more selective for Na^+ than ASIC.[47,48,58,139] Although Gly and Ser are structurally similar, the latter is larger, containing an extra carbon and hydroxyl moiety. Thus, Ser occupies a larger volume. Perhaps this larger volume introduces a steric constraint that allows better accommodation of Na^+ in the permeation pathway over other cations. This awaits experimental testing. Nevertheless, the geometry and atomic volumes of the pore in cASIC1 suggest that Na^+ sheds its hydration shell to permeate through the channel. Electrophysiology findings for ENaC support this. Mutations in and near the ENaC selectivity-filter reduce both the Na^+ conductance and Na^+ to K^+ selectivity, possibly because of a perturbation of precise channel-ion hydration geometry.[104,105,140]

The trigonal antiprism coordination of Na^+ in the pore of ENaC/Deg channels, as exemplified by cASIC1, has been proposed to be the archetypal molecular basis of permeation through cation-selective ion channels containing three component subunits.[58] The crystal structure of the P2X4 channel, which also was recently solved, agrees with this position.[58,141] The P2X4 channel is cation-selective, and has 2°, 3°, and 4° structures similar to those in ENaC/Deg channels, but little 1° amino acid sequence identity. Yet, both use identical modes and means of permeation and coordination of permeant ions. The ideal ion-to-ligand distance in the trigonal antiprism arrangement in

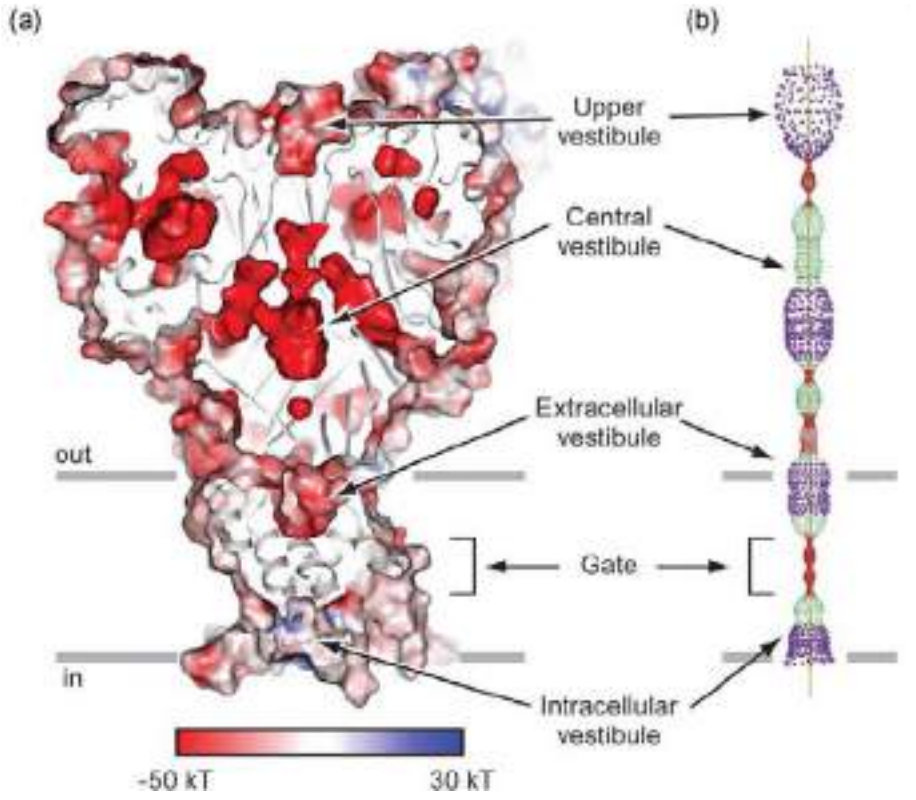

FIGURE 8.26 **The structure of ASIC.** *(Figure from [58].)* (a) An electrostatic potential surface and cartoon representation of cASIC1 viewed along the molecular three-fold axis of symmetry. Color is based on electrostatic potential, ranging from −50 kT (red) to +30 kT (blue). White is 0 kT. (b) Illustration of the radius of possible pathways along the three-fold axis of cASIC1 where red <1.4 Å <green <2.3 Å< purple. See color section at the back of the book.

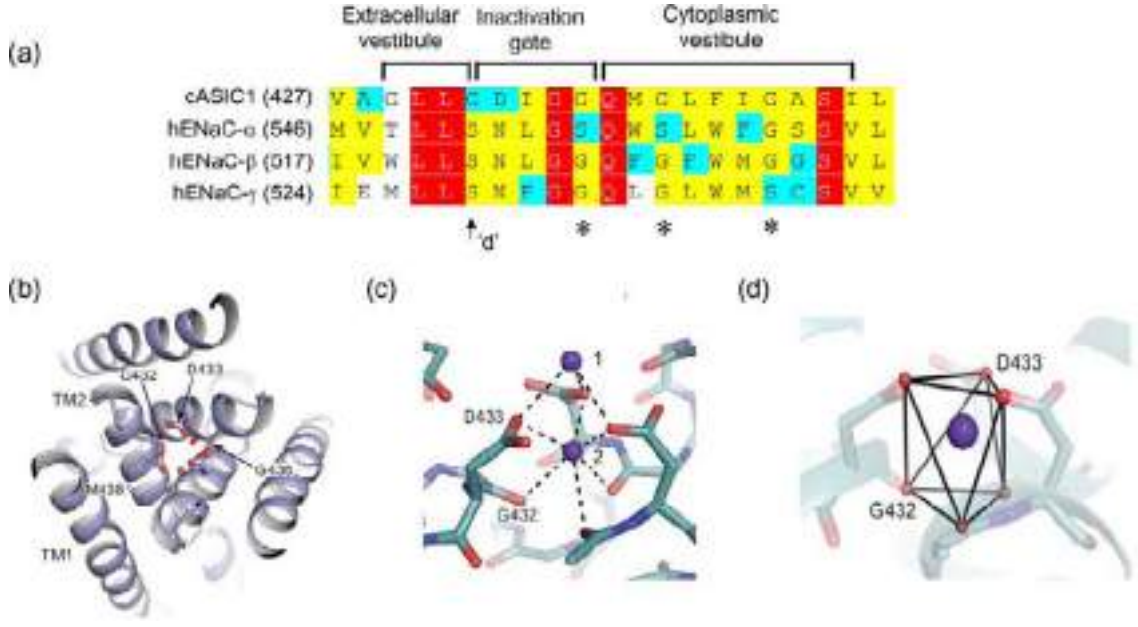

FIGURE 8.27 **The pore of ENaC/Deg channels.** *(Figures adapted from Figures 4 and 5 in [58].)* (a) Sequence alignment of pore lining residues in TM2 of cASIC1 and human ENaC subunits. Identity indicated with red, conservative substitutions yellow, and similarity light-blue coloring. Asterisks indicate residues thought to contribute to binding sites within the permeation pathway of the pore. "d" indicates the degenrin site.[144,145] (b) View of the cASIC pore from the extracellular side of the membrane, with the position of selected side chain residues shown. (c) Key interactions between Cs^+ ions, shown as purple balls, in the cASIC1 pore with main chain and side chain oxygen atoms of Gly 432 and Asp 433, respectively. (d) Trigonal antiprism coordination of a Cs^+ ion in the cASIC1 pore by the symmetry related Gly 432 carbonyl and Asp 433 carboxyl oxygens in the three momomers. Oxygen atoms are shown as red spheres. See color section at the back of the book.

ENaC/Deg channels, where six partial-charge ligands coordinate cation binding, is stereochemically analogous to the eight-fold square antiprism coordination of larger K^+ ions in K^+ channels containing four subunits.[36,58] In both ENaC/Deg and K^+ channels, the symmetry of the pore and number of subunits contributing to the pore are matched to the optimal coordination requirements of the permeant ion.[142,143] Moreover, although the linear pore of ENaC/Deg channels lined by the three TM2 domains of component subunits differs in general construction from the pore of K^+ channels, which is formed by the four-component P-loops dipping back into the membrane, the basic chemistry and physical tenets underpinning the coordination of permeant ions within these pores are conserved. This speaks to conservation by nature of a workable blueprint.

The Gate in ENaC/Deg Channels

Compared to ASIC channels, which activate and inactivate in response to H^+ binding to an extracellular allosteric site, ENaC is held to gate in a constitutive manner, with gating modulated by regulatory factors.[41,58,81,117] In cASIC1, a constriction formed by the crossing of TM2 domains at D433 occludes the pore acting as an inactivation gate. The channel is thought to open by TM domains untwisting around the central axis of the pore perpendicular to the plane of the lipid bilayer, partially uncrossing TM2 domains and relieving obstruction of the pore by the inactivation gate. The *degenerin* mutation that constitutively activates ENaC/Deg channels by locking them in long-lived open states is at 432 in cASIC1, one position upstream of the crossing site of TM2 domains.[144,145] Placement of an amino acid larger than Gly at this site sterically clashes with symmetry-related TM2 domains, providing a mechanism whereby mutations at the *degenerin* site perturb gating.

It is interesting that Asn residues, as clear in the alignment shown in Figure 8.27, occupy the positions in ENaC subunits homologous to D433 in cASIC1. This appears to be a signature feature of ENaC, as most other non-ENaC subunits in the ENaC/Deg family have Asp at this position. Moreover, it is likely to be of biophysical importance, for Asn is the uncharged derivative of Asp. This may explain why ENaC constitutively gates and does not inactivate. In ENaC, TM2 crossing at this Asn, for instance, may not be as stable as that in cASIC1 and, thus, transient or it may not obstruct the pore. In addition to an inactivation gate, the crystal structure of cASIC1 suggested that ENaC/Deg channels use a pore-gating mechanism.[58] This possibly explains constitutive gating of ENaC.

The Architecture of K^+ Channels and TRP Channels: ROMK as a Representative

Subunits that form K^+ channels have either two, four, six or six-plus-one transmembrane domains, as typified by Kir-, K_{2P}-, Kv-, and BK_{Ca}-subunits, respectively (see Figure 8.20). Whereas at first glance the apparently different 2° and 3° structures of these subunits may suggest that they assemble into channels of different 4° structure, the fact is they do not, but rather all form channels having a similar core structure surrounding a central pore with four-fold symmetry .[35,36,45,56,146,147] The canonical K^+ channel pore is formed by transmembrane domains and the P-loop, as defined by the two transmembrane domains of Kir channels. The crystal structures of the bacterial KvAP, MthK, KirBac1.1, KirBac3.1, and KcsA channels (and chimeras of KcsA-Kv1.3 and Kir3.1-prokaryotic Kir channel) show slight variations of a common K^+ channel pore, informing on the molecular basis of selectivity, permeation, and gating.[35,36,45,56,146,147] Segments defining this core pore structure are repeated as a pair in the four transmembrane domains of K_{2P} channels. This explains why these channel subunits form a dimeric channel with a central pore that has four-fold symmetry.[80] Moreover, this core pore-forming structure is retained in Kv and BK_{Ca} channels as the S5-P-loop-S6 domains.[2] BK_{Ca} channels mirror the general structure of Kv channels, with the exception that they have one additional transmembrane domain placing their NH_2-terminus outside the cell. TRP channels are also thought to assume this basic structure, often being modeled on the six transmembrane Kv channel.[2,119] The formal structure of TRP channels, however, awaits crystallization studies.

To facilitate discussion of the molecular basis of selectivity, permeation, and gating of the common K^+ channel pore, we focus on ROMK. The reason for this is that the ROMK channel is made of subunits having two transmembrane domains containing all the components comprising the core K^+ channel pore and a regulated gate.

The ROMK Channel Pore: Selectivity and Permeation

Welling and Ho,[32] in a recent review article, reported a compelling atomic model for ROMK based on known Kir channel structures, including regions defined in the crystal structures of the bacterial KirBac1.1 channel, a chimeric Kir3.1-prokaryotic Kir channel, the pore region of the mammalian GIRK1 channel, and the cytoplasmic domains of Kir2.1 and Kir3.1.[35,56,146,147] This model is shown in Figure 8.28.[32] ROMK contains the canonical transmembrane pore common to all K^+ channels, but also a unique central

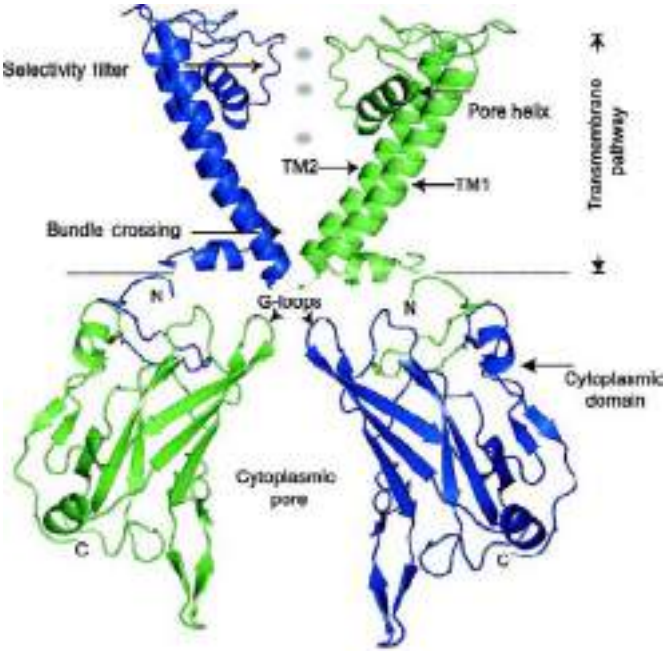

FIGURE 8.28 **Predicted structure of ROMK.** *(Figure from [32].)* An atomic model of ROMK was developed from known K_{ir} channel structures and an iterative optimization algorithm. Shown are two subunits, one green and the other blue, of the tetrameric channel.

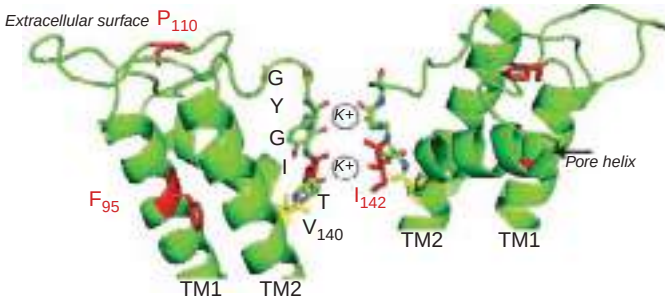

FIGURE 8.29 **The selectivity filter of ROMK.** *(Figure from [32].)* Backbone carbonyl oxygens of selectivity-filter residues T_{141}IGYG point into the pore, mimicking the hydration shell of potassium. Rapid conformational movement of $T_{141}I_{142}$ likely underpins fast gating in ROMK. Residues in red are mutated in Bartter's syndrome type II. See color section at the back of the book.

cavity contained by a large cytoplasmic domain, which is characteristic of Kir channels.[148,149]

The four component subunits of ROMK assemble around a central pore that has four-fold symmetry. The helices of TM2 domains span the membrane at a tilt, narrowing at the intracellular base of the pore. The four TM2 helices of the component subunits frame the pore as it spans the membrane, with TM1 domains running along but outside TM2 domains of the same subunit. The narrowest part of the open conduction pathway is defined by P-loops of the four subunits. These P-loops are linker regions that connect TM1 to TM2 and contain short helical domains that dip back into the mouth of the pore. The symmetry related linkers contain the conserved K^+-selectivity sequence, T[V/I]GYG.[35,36,45,56,146] This motif adopts a strand conformation, as depicted in Figure 8.29, where the NH_2-terminal end is deepest in the pore and COOH-terminal end at the mouth of the pore. The backbone carbonyl oxygen of these T[V/I]GYG residues projects into the central axis of the open pore. Similar to all K^+ channels, the carbonyl oxygen of residues in this selectivity sequence from each symmetry-related subunit form four equally spaced K^+-binding sites in the pore. Four oxygen atoms at the top and bottom of each binding site cage a K^+ ion with eight-fold square antiprism coordination. Such coordination is similar to the way water molecules surround K^+ ions in solution.[36,142,143] This mimicry of water solvation at the selectivity-filter creates an energetically favorable means for K^+ to diffuse into binding sites as they shed their surrounding water shell. Because the volume and ion coordination of these binding sites do not accommodate smaller ions in a dehydrated state, like Na^+, this molecular structure provides high-fidelity K^+-selectivity.

The sequential arrangement of the four equally spaced K^+-binding sites in the linear ROMK pore facilitates a single-file multiple-ion conduction mechanism in agreement with findings from early biophysical measurements.[150–152] As revealed in the crystal structure of the KcsA channel, K^+ ions are simultaneously absorbed to two binding sites at a time, with an empty site positioned between the two occupied sites due to electrostatic charge repulsion between permeant ions.[36,45,151,152] Conduction by K^+ channels then, as depicted in Figure 8.13, is the rapid jumping of K^+ ions in a pair-wise manner from one to the other paired-binding sites within the pore. Such movement involves several rounds of dehydration and rehydration, as the K^+ ion moves into the pore and is absorbed and released from each binding site, and as it exits the pore. The energetics of this sequential dehydration and rehydration as counterbalanced by electrochemical driving forces and electrostatic repulsion between ions within the pore sets conductance. Such a structure enables K^+ ions to move through the pore with high-throughput, but yet with remarkable selectivity.[151,153]

Molecular Basis of Rectification in ROMK Channels

A unique feature of ROMK and other inward rectifier K^+ channels, as their name suggests, is that they have larger inward currents compared to outward currents.[32] The molecular basis of this rectification

involves a pore-block mechanism, where Mg^{2+} and polyamines enter the pore at depolarizing voltages through the intracellular mouth of the channel.[76,77] Once in the pore, Mg^{2+} and polyamines interact with a binding site near the selectivity-filter, plugging the pore. This gives rise to inward rectification, which actually is a decrease in P_o as a function of a voltage-dependent block of the pore where channel P_o is higher at hyperpolarizing potentials compared to depolarizing potentials, allowing greater inward as compared to outward current flow. The degree of rectification is different between distinct members of the Kir channel family, depending on subtle differences in the binding sites for blocking Mg^{2+} and polyamines. ROMK only marginally rectifies. This rectification phenotype is largely a factor of N171 in the pore lining TM2 domain of ROMK or its equivalent in other Kir channels. This is supported by the observation that the N171D substitution in ROMK produces strong rectification. The reverse mutation, D172N, in the strong inward-rectifying Kir2.1 channel weakens rectification, making it more akin to that of ROMK.[154] Figure 8.30 reports the relative position of N171 in ROMK showing that its side chain projects into the aqueous environment of the pore, a position consistent with it being involved in an intra-pore binding site for large blocking cations like Mg^{2+} and polyamines.

Molecular Basis of ROMK Gating

ROMK channels have, at least, two different types of gates. The fast gating of ROMK, as discussed above, involves a pore-gating mechanism. Potassium in the pore of ROMK has profound influence on the structure of the selectivity-filter and pore-binding sites.[151,152] As K^+ binds to a particular position in the selectivity-filter of ROMK (as seen in Figure 8.29), the energetics of binding to this site cause a conformational change at T141-I142, briefly shuttling the channel into a nonconducting conformation.[50,51] An alternative to this physical mechanism, as mentioned above, is a chemical mechanism where the pore does not change conformation but rather K^+ binding affects the energy of binding where the permeant ion is briefly stuck and is unable to move along the pore.[63]

In addition to using a pore-gating mechanism for fast gating, ROMK channels also use a distinct type of gating mechanism that is slower and is regulated. As shown in Figure 8.30, the side chain of L179 in the TM2 domain of ROMK subunits projects into the mouth of the pore and obstructs permeation. It is widely held that regulated K^+ channel opening involves the movement of the pore helixes (TM2) away from the bundle-crossings (with TM1) at the intracellular base of the pore, with extracellular G167 and G176 or their equivalents acting as flexible "hinges" allowing this opening pivot. This movement carries the putative L179 gate at the base of TM2 away from the pore, physically removing this obstruction. Replacement of L179 with small or charged residues stabilizes the open state, just as would be predicted if this residue acts as a regulated gate to obstruct the conduction pathway during the closed state.[155,156] Moreover, such a gating movement is consistent with the differences identified in the crystal structure "snap-shots" of KirBac3.1 in the open and closed state.[35] Figure 8.31 shows these structures. The Y132 gating residue in KirBac3.1 corresponds to L179 in ROMK.

The regulated gate is actually a larger structure involving complex interactions between residues in TM2 and TM1, where an ε-nitrogen of K80 in TM1 forms a hydrogen bond with the backbone carbonyl oxygen of A177 to control the energetics of gating as performed by L179. Such a gating structure provides the molecular basis for regulation, with information arising from conformational changes in intracellular domains translated to the gate via K80. K80 sits at the base of TM1 at the bundle-crossing, which is positioned immediately above the G-loops of the cytoplasmic domains. The idea is that allosteric sites in the

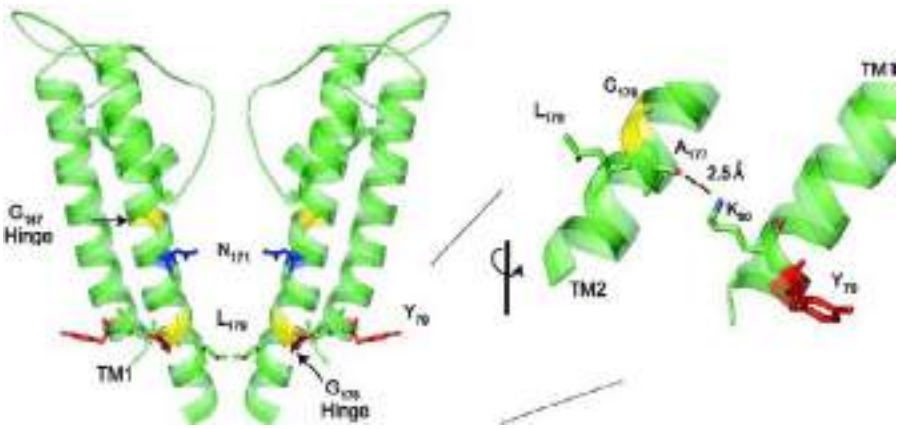

FIGURE 8.30 **The molecular determinants of regulated gating and rectification of ROMK.** *(Figure from [32].)* ROMK gating is thought to involve the twisting of membrane helices pulling L179, the putative gate, out of the pore. Hydrogen bonds between K80 at the base of TM1, and A177, in TM2 stabilizes the gate. Y79 is mutated in Bartter's syndrome. The side chain of N171 projects into the pore and is a key determinant of inward rectification.

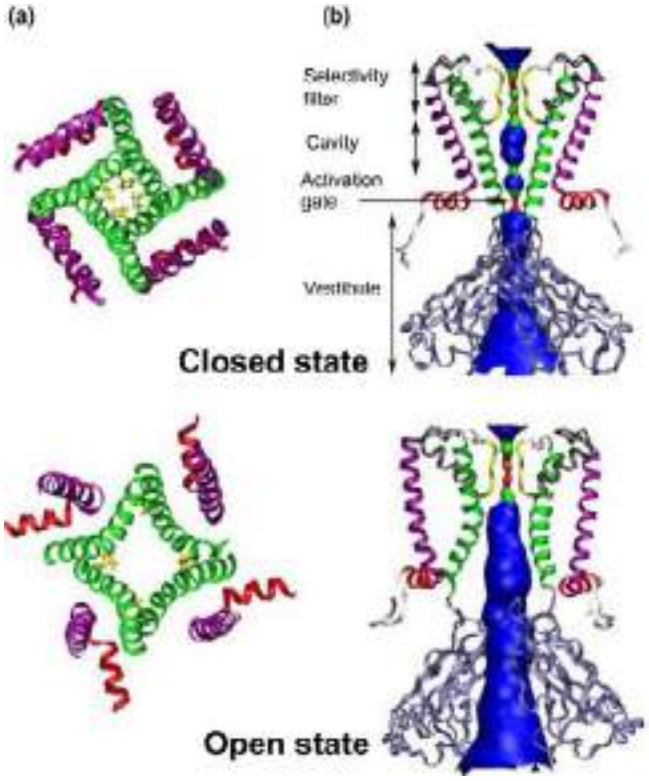

FIGURE 8.31 **"Snap-shots" of KirBac3.1 in the closed and open state.** *(Figure from [35].)* (a) View of the transmembrane section of KirBac from the extracellular side of the membrane in a closed (top) and open (bottom) conformation. Helices are shown as ribbons with outer helices, purple; inner helices, green; and the slide helices, red. The activation gate is displayed as yellow sticks. (b) Two monomers of the closed (top) and open (bottom) channel are shown superimposed on a representation of the diameter of the central ion conduction pathway. Structural elements are colored as in (a). Red coloring in the central conduction pathway indicates that there is not enough space to allow a water molecule to pass; green shows where one or two water molecules could fit; and blue where many water molecules can fit. See color section at the back of the book.

intracellular portion of the channel communicate to the gate through the G-loop positioned just below the intracellular mouth of the pore, although this remains an open question.[32]

The cytoplasmic domains of ROMK assemble just below the canonical transmembrane pore to form a long water-filled cavity extending the length of the conduction pathway. The characteristics of secondary structures and position of side chains of residues lining this water-filled cavity are consistent with it being a pathway for permeation. For instance, this intracellular pore is lined by residues that provide an electrostatic environment favorable for efficient K^+ transport and cation-blocker binding.[157] In addition, there is a high degree of concordance between residues contributing to the electrostatic field, favoring transport and binding with residues known from mutagenesis studies to affect cation block and single-channel conductance.[43] Moreover, studies on the chimeric ROMK-Kir2.1 channel, in addition to other mutagenesis studies, revealed that residues lining the inner wall of this intracellular pore, with N259 in ROMK playing the most significant role, directly influence single-channel conductance. This effect is independent of structures in the transmembrane selectivity-filter, suggesting that the symmetry related cytoplasmic domains provide additional energy barriers to the flow of K^+ through the channel.[157–159] The putative gate for this intracellular pore is thought to be at the narrowing created by the four G-loops as they coalesce just below the mouth of the membrane-spanning pore. This gate is believed to create a flexible diffusion barrier between the cytoplasmic and transmembrane pores. Supporting this are findings that mutations in this region of Kir2.1 and Kir3.1 alter channel gating and inward rectification.[160]

TUBULOPATHIES RESULTING FROM CHANGES IN CHANNEL BIOPHYSICAL PROPERTIES

The majority of channelopathies, including those causing tubulopathy, result from loss of expression or changes in the expression level of functional channels at the membrane. These are not covered here. Less common are channelopathies resulting from mutations that affect the biophysical properties of an ion channel. The latter are informative about residues and structures critical to function. Such mutations, as listed in Table 8.2, are a focus of this discussion.

ClC-Kb: Barrter Syndrome Type III

Mutations in the gene *CLCNKB* encoding the ClC-Kb Cl^- channel cause Bartter syndrome type III, characterized by hypokalaemic metabolic alkalosis, renal salt-wasting, and hyper-reninaemic hyperaldosteronism.[14,18,161] The root cause of BS type III is abberant transport in the TAL and DCT, stemming from pathological changes in membrane voltage and diffusion potentials resulting from loss of the basolateral exit pathway for Cl^-. Although several missense mutations resulting in amino acid substitutions in ClC-Kb are known to cause BS type III, the effects of these mutations on the biophysical properties of this channel are largely unexplored. The R351W Bartter mutation in ClC-Kb is an exception.[162]

Homodimeric ClC-Ka and ClC-Kb channels contain extracellular regulatory Ca^{2+}- and H^+-binding sites at inter-subunit interfaces.[124] Increases in extracellular $[Ca^{2+}]$ and extracellular alkalinization increase ClC-K

TABLE 8.2 Renal Channelopathies Caused by Changes in Biophysical Properties

Channel	Disease Causing Mutation[a]	Result	Disease	References
ENaC	G37S in β-ENaC	Decreased activity due to voltage-dependent block of the pore by a permeant ion.	PHA-I	174, 134
	S562P in α-ENaC	Likely to affect ENaC selectivity or permeation.	PHA-I	107, 181
	N530S in γ-ENaC	Likely to lock the channel in a high P_o state.	Liddle's syndrome	138
ROMK	Y79H, A177T	Disrupts the regulated gating-structure at the bundle-crossing in ROMK.	BS-II	15, 189
	T332*fs*	Disrupts domains involved in sensing or conveying pH-dependent effects to the regulated gate.	BS-II	195, 148, 185, 186
	A306T	Disrupts the gate in the cytosolic domain of the channel.	BS-II	15
	C49Y, I51T, A214V and L220F[b]	Disrupts PIP_2-regulation of gating.	BS-II	15, 194, 186
	S219R and S313C	Disrupts PKA phosphorylation sites essential for modulating the effects of gating factors.	BS-II	194, 186
	R311Q/W[b]	Disrupts a critical salt bridge.	BS-II	15, 194
	I142T	Disrupts K^+ selectivity filter sequence decreasing K^+ conductance.	BS-II	185
	A198T, Y314C and V315G[b]	Decreased activity due to entering a long closed/inactive state.	BS-II	198, 185, 15
	W99C, A103V, P110L and N124K	Loss-of-function with dominant negative effect.	BS-II	185
	T71M, F95S, A156V and R324L	Loss-of-function where the molecular mechanism is undefined, but channels make it to the membrane in some systems.	BS-II	15
ClC-Kb	R351W	Decreases activation by extracellular Ca^{2+} and alkaline pH.	BS-III	162
	A77T, L139P, A204, S297R, S337F, A349D, H357Q, R438C, R438H, R438L and R538P	Loss-of-function where the molecular mechanism, as yet, is undefined.	BS-III	161, 165, 166
	K560M and S573Y	Substitutions within the first CBS domain of ClC-Kb possibly affecting regulation of gating.	BS-III	79, 161
	P124L and Y432H	Substitution near a Cl^- binding site within the permeation pathway possibly affecting permeabiton, gating or selectivity.	BS-III	46, 79, 161, 165, 166
Barttin	R8L, R8W and G10S	Inactivating mutants in BSND causing loss of function of membrane ClC-Ka and ClC-Kb channels.	BS-IV	71, 173, 73
	G47R	Decreased interaction with ClC-K channels leading to a milder decrease in function and a milder phenotype.	BS-IV	71, 173
TRPM6	P1017R	Decreases activity of membrane resident TRPM6/TRPM7 channels.	HSH	4

[a]*Positions noted for human sequences.*
[b]*These mutations may also be involved in coupling to/from PKA phosphorylation sites or the state of phosphorylation — fs = frameshift.*

channel activity: Ca^{2+} binding is stimulatory, whereas H^+ binding is inhibitory.

The R351W substitution in ClC-Kb abolishes sensitivity to extracellular [Ca^{2+}], and markedly reduces activation by alkaline pH.[162] The consequence of these changes in biophysical properties is that mutant ClC-Kb is less active under physiological conditions. The mechanism whereby mutation of R351 affects Ca^{2+}- and pH-regulated gating has not been determined. R351 is positioned at the COOH-terminal end of the linker coupling helices K and L. This positions the residue near the extracellular surface of the

channel. Perhaps R351 plays a role in coupling Ca^{2+}- and H^+-binding to the channel gate or it is an essential component of an allosteric regulatory binding site, or integral to the structure of the gate itself. The importance of this position to ClC channel function is underscored by the fact that mutations in this region of ClC-1, for instance F413C and A415V corresponding to two and four positions downstream from R351 in ClC-Kb, cause myotonia.[163,164]

In addition to R351W, a host of other point mutations, as listed in Table 8.2, decrease ClC-Kb channel activity to cause BS type III.[161,165] As yet, no experimental information is avaliable about how these Bartter mutations cause ClC-Kb dysfunction. There is circumstantial evidence, though, that some may affect the biophysical properties of the channel, for they involve nonconservative substitutions of residues highly conserved across paralogs and orthologs. For instance, L139 is conserved in most ClC proteins across species ranging from *C. elegans* to man, and S297 and S337 are conserved in all mammalian ClC-K channels. The P124L substitution changes a conserved residue in the first Cl^--binding site in the permeation pathway, predicting a change in conductance, selectivity or even gating, considering ClC channels use a pore-gating mechanism.[55,161,166] The S123P mutation in this region of the ClC-0 channel, that corresponds to three residues upstream of P124 in ClC-Kb, increases nitrate permeability.[167] Moreover, covalent modification by sulfhydryl reagents of a P126C mutant in ClC-0, which corresponds to P124 in ClC-Kb, markedly reduces P_o.[168] The Y432H mutation, similarly, is four positions downstream of residues forming the third Cl^--binding site, suggesting that it may also impact permeation. Additional support comes from the fact that several Bartter mutations in ClC-Kb occupy the same sites or are near residues in ClC-1 that when mutated, cause myotonia. For instance, the A349D mutation in ClC-Kb is two positions downstream of the F413C, and homologous with the A415V myotonia causing mutations.[161,163,164] The Bartter mutation H357Q is one position upstream of the myotonia mutation I424M. Futher investigation of these Bartter mutations is of importance, moreover, for they cause disease with varying degrees of severity, and several of them, as typified by mutation of R438 and the P124L substituion, appear in unrelated families of different ethnic origin in different geographical locations.[161,165]

The cytoplasmic COOH-terminal domains of all mammalian ClC proteins contain two interacting cystathionine-β-synthase CBS domains that form intrasubunit dimers.[121,122] CBS domains regulate ClC channel gating. For instance, ATP binding is coordinated at the CBS1/CBS2 interface, as shown in the ClC-5 crystal structure,[169] and ATP is known to modulate gating of ClC-1 and ClC-2 channels.[170,171,172] The Bartter mutations K560M and S573Y substitutions in ClC-Kb are within the first CBS domain, predicting that they may influence regulated gating.[121]

Barttin: Bartter Syndrome Type IV

Barttin is an obligatory accessory subunit for human ClC-K channel activity.[71] Inactivating mutations in barttin cause corresponding loss of ClC-K channel function, leading to BS type IV.[18,71,173] This form of Bartter syndrome has the hallmark renal salt-wasting phenotype, but also a sensorineural deafness phenotype. The reason for the additional phenotype in BS type IV is that, similar to their roles in renal epithelial cells, ClC-K channels also serve as Cl^- exit pathways in strial marginal cells.[87] Barttin is required for this activity, which in turn is required for active K^+ secretion into endolymph. In the ear, loss of ClC-Ka or ClC-Kb individually can be compensated for by the presence of the other protein; however, the loss of both channel proteins or of barttin cannot be.[87] Compensation also explains why loss of ClC-Kb, but not ClC-Ka, causes BS type III without accompanying deafness.[14,87] Although ROMK mediates apical K^+ secretion in TAL epithelial cells, KCNQ1 oligomerized with KCNE1 mediates apical K^+ secretion in marginal cells.[87] This explains why BS type II, which results from loss-of-function of ROMK, as discussed below, is not associated with deafness.

Several missense mutations causing substitutions in barttin change the biophysical properties of ClC-K channels to cause disease. The Bartter mutations R8L, R8W, and G10S in barttin eliminate ClC-Ka and ClC-Kb function, as shown in Figure 8.32, but they do not prevent channel insertion into the membrane (not shown[71,173]). This identifies changes in either channel gating or permeation as the disease-causing defects. It is not clear yet which of these two alternatives is correct. However, investigation of chimeric hClC1-ClC-Kb channels, as shown in Figure 8.33, revealed that these mutations influence voltage-dependent activation, with channels containing mutant barttin having less activity at hyperpolarizing potentials. This is most consistent with an effect on gating.

The Bartter's mutation G47R in barttin produces a mild renal phenotype.[71,173] The G47 residue is at the intracellular COOH-terminus of the second transmembrane domain of barttin. This position, and the fact that barttin containing the G47R substitution interacts less effectively with ClC-Kb, suggests that association of the accessory subunit with the pore-forming subunit is compromised in some manner. Such interpretation is consistent with the recent finding that the

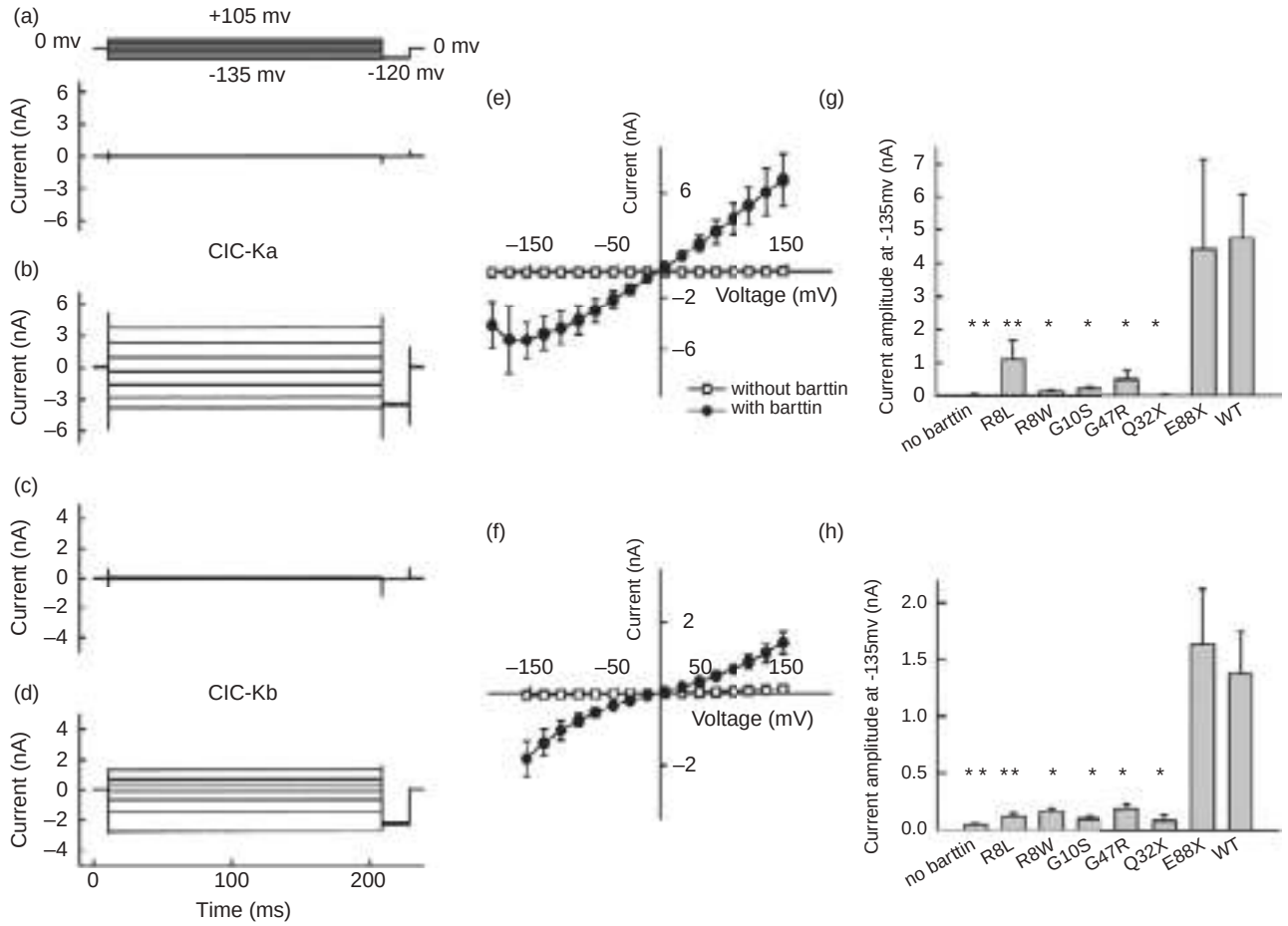

FIGURE 8.32 **Some disease-causing mutations in barttin decrease ClC-Ka and ClC-Kb channel activity.** *(Figure from[173].)* (a)–(d) Representative macroscopic ClC-Ka ((a) and (b)) and ClC-Kb ((c) and (d)) currents with ((b) and (d)) and without ((a) and (c)) barttin. Corresponding I–V relations for ClC-Ka and ClC-Kb with and without barttin are shown in (e) and (f), respectively. Steady-state currents at −135 mV for ClC-Ka and ClC-Kb expressed with wild-type and barttin containing Bartter mutations are shown in g and h, respectively.

transmembrane core of barttin is necessary and sufficient to promote ClC-K channel trafficking.[73] Moreover, the fact that the G47R phenotype is milder compared to that seen with complete loss or inactivation of barttin demonstrates that the physiological effects of barttin can be titrated, indicating that there is some finite threshold at which the loss of barttin activity causes disease.

ENaC

ENaC activity, as mentioned above, is the final arbiter of renal Na^+ reabsorption setting urinary and plasma $[Na^+]$[82,83,106]. This function makes ENaC an important end-effector of feedback systems controlling blood pressure. As such, ENaC activity is a critical determinant of blood pressure in all mammals, including humans. Loss- and gain-of-function mutations in ENaC and modulators of this channel then cause a host of diseases having pathological changes in renal Na^+ handling and blood pressure.

PHA-I: Loss of ENaC Function

Pseudohypoaldosteronism is a group of rare genetic diseases presenting with hallmark hyperkalemia and renal Na^+ wasting in the presence of high aldosterone.[107,174] Renal Na^+ wasting is a consequence of decreased Na^+ reabsorption in the CNT and CD. Such a phenotype represents end-organ resistance, identifying ENaC or cellular regulators of this channel as dysfunctional.

Compared to ROMK, less is known about the structure of the cytoplasmic portions of ENaC. Therefore, we do not have precise structural information to guide the interpretation of recent electrophysiology findings relevant to PHA. The missense mutation, G37S, in human β-ENaC nonetheless causes PHA type-I.[134,174] This Gly residue is in an absolutely conserved HG motif located in the intracellular NH_2-terminal portions of all

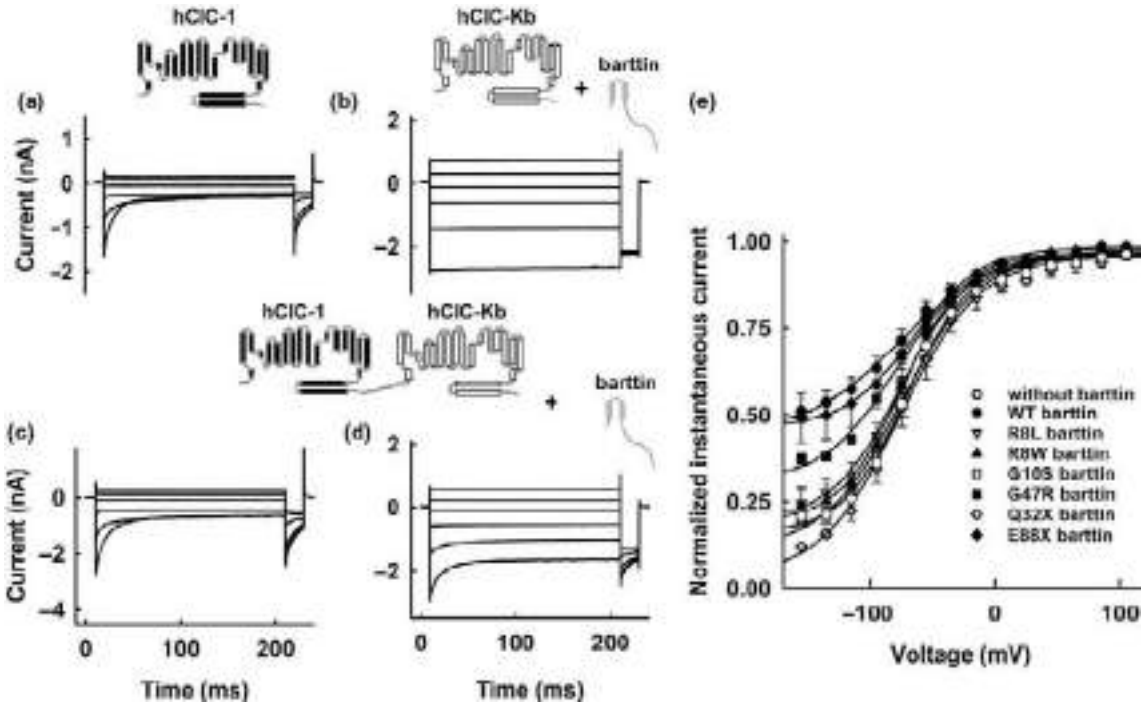

FIGURE 8.33 **Some disease-causing mutations in barttin affect ClC-K channel gating.** *(Figure from [173].)* (a)–(d) Representative macroscopic currents from human ClC-1 alone (a), ClC-Kb with barttin (b), and concatameric hClC-1-ClC-Kb without barttin (c), and with barttin (d). (e) Normalized instantaneous macroscopic currents as a function of voltage for hClC-1-ClC-Kb concatamers alone and together with wild-type and mutant barttin. The action of voltage on normalized current indicates that these mutations in barttin affect ClC-K channel gating.

ENaC/Deg subunits. The HG motif is required for normal gating.[134,135,174] The molecular mechanism whereby the HG motif influences the gate is unknown, but in the primary sequence of ENaC, the motif is in the NH_2-terminal cytoplasmic domain just preceding TM1. As shown by the results in Figure 8.34 from whole-cell and outside-out single-channel patch-clamp experiments probing the effects on gating, substituting either the H or G residue decreases P_o to where ENaC is not active under physiological conditions.[175] Decreases in P_o, as supported by results shown in Figure 8.35, arise from the voltage-dependent block of the pore by the permeant ion where the block is from the intracellular side and relieved by hyperpolarization.[39] A possible explanation for this is that ENaC gates through a pore-gating mechanism, and mutation of the HG motif destabilizes the pore to where Na^+ sometimes sticks to a binding site in the permeation pathway or the pore collapses around a Na^+ ion moving through the pore. More study is needed to determine if this is the case, but the crystal structure of cASIC1 is consistent with ENaC/Deg channels using a pore-gating mechanism.[58] Moreover, the biophysical consequences of substituting a Trp residue (W112 in α-mENaC) at the base of TM1 mimic the effects of substituting HG motif residues.[39] Like the HG motif, this Trp is conserved in all ENaC/Deg subunits. It is unknown at this time if mutation of this key Trp also causes PHA-I.

Many ion channels contain similar interfacial Trp residues at the intracellular bases of transmembrane domains.[176–178] Such Trp residues often modulate gating. In cASIC1, the side chain of the homologous Trp at the base of TM1 projects into the aqueous environment of the pore.[58] Interestingly, M_2 proton channels also contain a critical Trp residue at the intracellular base of the transmembrane domain lining the pore. The side chain of this Trp, akin to that in ENaC/Deg channels, projects into the aqueous mouth of the pore. Through Pi-bond interactions with a nearby His, the critical Trp in a M_2 proton channel stabilizes the gating state.[176,179,180] Perhaps the homologous Trp in ENaC interacting with the His in the HG motif serves a similar function. This possibility seems to reconcile the parallel findings that substitution of the HG motif and interfacial Trp residues cause identical changes in ENaC biophysical properties. Although further research is required to clarify the structure–function relation between the conserved HG motif and interfacial Trp in ENaC if there is any, it is clear that a pathological consequence of mutating the HG motif is that ENaC gating becomes voltage-dependent, with P_o being extremely low at physiological voltages.

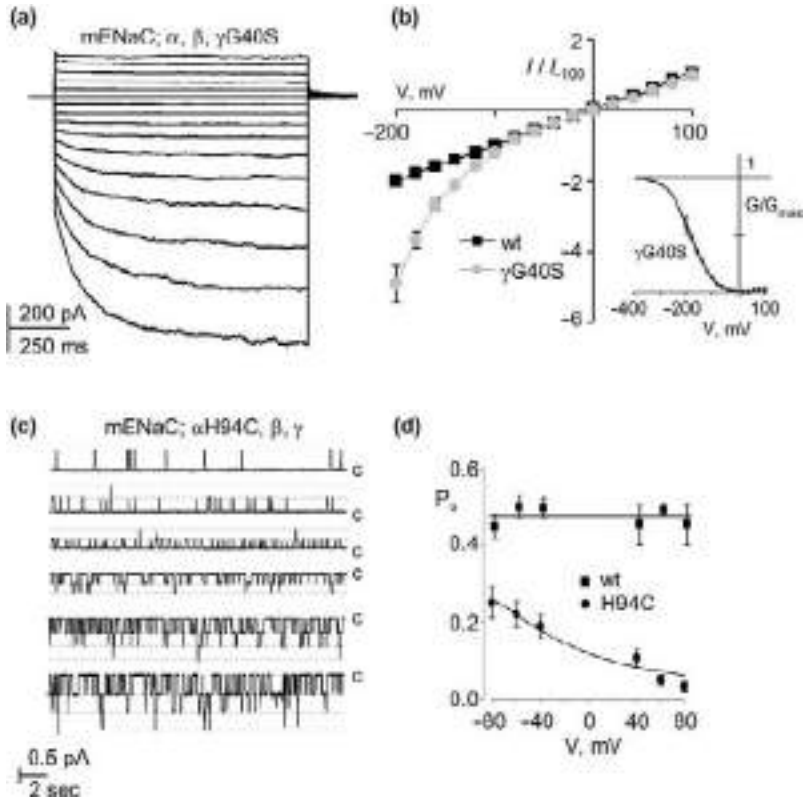

FIGURE 8.34 **Some disease-causing PHA-I mutations in ENaC affect channel gating.** *(Figure from [175].)* (a) Representative macroscopic Na^+ currents for a mouse ENaC channel containing the γG40S PHA-I mutation. (b) Macroscopic current-voltage (*I*−V) relations for CHO cells expressing wild-type (black lines) and mutant mENaC (gray lines) containing the γG40S mutation. For presentation, current normalized to current at −100 mV. The inset shows the G−V relation for mutant ENaC. (c) Representative single channel current traces for mouse ENaC harboring a αH94C substitution in outside-out patches stepped from 80 mV to −80 mV. Inward Na^+ current is downwards and closed states noted with (c). (d) Plot showing ENaC open probability (P_o) as a function of voltage for wild-type (black squares) and mutant mENaC containing αH94C. Data fit with a Boltzman function.

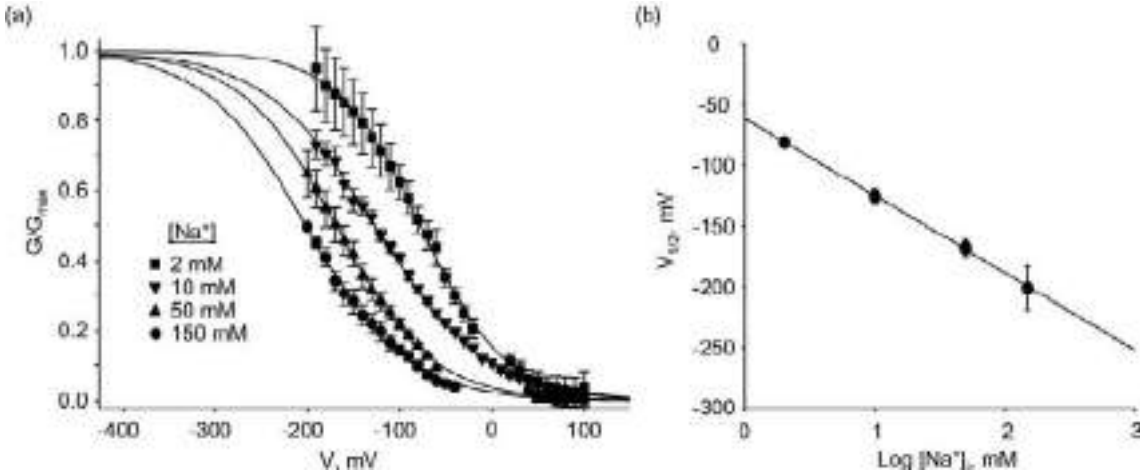

FIGURE 8.35 **Intracellular Na^+ can block mutant ENaC in a voltage-dependent manner to decrease macroscopic conductance.** *(Figure from [39].)* (a) Summary G−V curves for steady-state currents from mutant ENaC, containing the αW112C mutation, acquired in symmetrical 150, 50, 10, and 2 mm $[Na^+]$. (b) Summary graph showing the voltage resulting in half-maximal activity at steady-state, as established from G−V curves, for mutant ENaC as a function of $[Na^+]_i$.

Decreased ENaC P_o, then, is the biophysical cause of this form of PHA-I.

A missense mutation, S562P, in α-ENaC also causes familial PHA-I.[181] S562 occupies the third position in the selectivity-filter, GSS, sequence.[104,105,136] Little electrophysiology information is available for this mutant, but understanding that channel function is determined by its structural and biophysical properties makes it reasonable to predict that the S562P substitution disrupts permeation, resulting in a disease-causing loss-of-function.

Liddle's Syndrome: Gain of ENaC Function

Gain-of-function mutations in ENaC cause an inheritable form of hypertension, Liddle's syndrome, marked by high blood pressure in the presence of low plasma renin and aldosterone, and uncontrolled Na^+ reabsorption in the distal nephron.[106] This also represents end-organ resistance, where ENaC activity is inappropriately high in the presence of low aldosterone. Amiloride, an inhibitor of ENaC, reverses the high blood pressure and renal phenotype of Liddle's syndrome. The majority of mutations in ENaC that cause Liddle's syndrome retard retrieval of the channel from the apical membrane of CNT and CD principal cells.[182–184] An exception to this common mechanism is the Liddle mutation N530S in γ-ENaC, which increases channel activity but not membrane expression level.[138] Detailed biophysical experiments have yet to be performed on this mutant. Its position in the channel when considering the three-dimensional structure of cASIC1,[58] and previous findings from the study of the activating *Degenerin* mutation in *C. elegans* homologs,[144,145] though, are informative. N530 is one position downstream of the *Deg* position in the primary structure of ENaC (see Figure 8.27). This places it at the extracellular apex of the TM2 pore-lining transmembrane domain. This region of ENaC/Deg channels is thought to be important for ion permeation and gating. It is widely held that the *Deg* mutation locks open ENaC/Deg channels, because it occupies such a position. Perhaps the N530S Liddle mutation does the same thing in ENaC. ENaC locked in an open state would maximize Na^+ reabsorption in the distal nephron, moving it beyond the control of feedback regulation, explaining the salt-sensitive hypertension in this form of Liddle's syndrome even in the presence of low aldosterone. Supporting such a role are findings that covalent modification by sulfhydryl reagents of a N530C mutant in γ-ENaC and modification of Cys substitutions of the corresponding residues in α- and β-subunits increase activity of ENaC within the membrane.[140] In fact, this region of ENaC is particularly sensitive to alteration. Modification of cysteines substituted for residues throughout this region consistently affect channel activity.[105,136,140]

ROMK: Bartter Syndrome Type II

A constellation of mutations in *KCNJ1* leading to loss-of-function of ROMK causes BS type II.[14,15,23,185,186] Several of these mutations, as listed in Table 8.2, affect channel gating and conductance. It is possible, with our current understanding of ROMK structure and biophysical properties, to rationalize how these Bartter mutations affect channel function to change physiology and cause disease. Bartter mutations in ROMK that change biophysical properties can be placed into several groups. First are those that immediately disturb the gate based around the interaction of K80 at the intracellular base of TM1 with A177 at the intracellular base of TM2 as it couples to the putative L179 gate. This structure is held to be the regulated gate responsive to pH, PKA phosphorylation, and PIP_2-binding.[32] The remaining types of Bartter mutations that change the biophysical properties of ROMK interrupt regions in cytoplasmic domains to affect gating. They include those that disrupt PIP_2 binding sites, critical PKA phosphorylation sites, domains important for a response to pH, and inter- and intra-subunit salt-bridges required for normal structure. In addition to these are Bartter mutations that affect a distinct gate in the cytosolic portion of the channel, and one that affects a key residue in the selectivity-filter.

Mutation of the Regulated Gating Structure at the Bundle-Crossing

A hallmark feature of ROMK, as emphasized in Figure 8.36, is its sensitivity to intracellular pH, where P_o

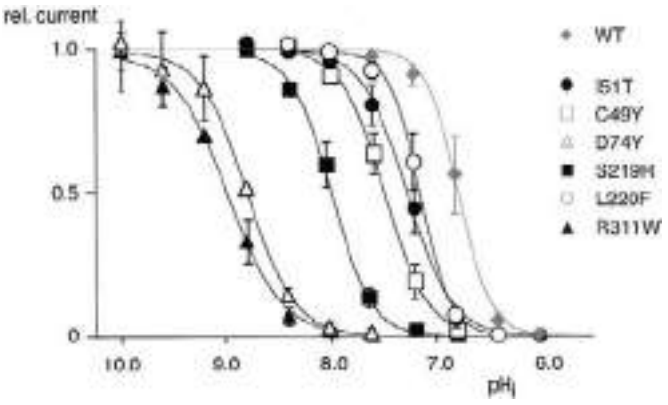

FIGURE 8.36 **ROMK gates in a pH-dependent manner with some Bartter mutations changing the apparent pK_a of activation.** *(Figure from [194].)* Current-pH_i relations are shown for wild-type ROMK and channels containing Bartter mutations.

increases as a function of increasing pH_i with intracellular acidification inducing a long-lived closed-state.[187,188] Residues and domains in ROMK involved in sensing pH are yet to be identified. Nevertheless, sensitivity to pH is routinely measured using titration experiments plotting relative current as a function of pH, and fitting the data with a modified Hill equation, such as $I/I_{max} = 1/(1 + ([H^+]/K_a)^{nH})$, where K_a is the half-maximal inhibitory proton concentration and n_H is the Hill coefficient.[148] As noted above, the influence of pH on gating is manifested by the regulated L179-gate coupled to A177 and K80.[32,148] The A177T Bartter mutation disrupts this interaction, and causes a marked alkaline-shift in the pH sensitivity of ROMK gating effectively turning the channel off at physiological pH_i.[15,189] The biophysical and physiological consequences are that, although the driving force remains for K^+ efflux across the apical membrane of TAL cells through ROMK, it cannot be harnessed, with the result that NKCC2 cannot run at full capacity. This compromises NaCl reabsorption in the loop of Henle, and breaks down the axial corticomedullary hyperosmotic gradient, causing a pathological decrease in the ability to concentrate urine. Substitution of K80 with residues unable to form an H-bond with A177, in addition, alters gating in a similar manner.[190] Additional support for this mechanism of pathology is the finding that the Bartter mutation Y79H also disrupts regulated gating.[15] The side chain of Y79 projects into the lipid bilayer, possibly stabilizing the interaction of K80 with A177 and ultimately the L179 gate. Interestingly, mutations in comparable residues in the Kir6.2 K_{ATP} channel alter ATP-dependent gating, and cause neonatal diabetes.[191] Such results summate to suggest that the energetics of regulated K^+ channel opening are strongly influenced by H-bonds formed between residues at the base of TM1 and TM2, and between interactions of residues in TM1 with the inner leaflet. Disruption of this gating structure, then, is one cause of ROMK channel dysfunction in BS type II.

Mutation Leading to Loss of pH-Sensitivity

ROMK gates in a high P_o state at normal intracellular pH_i, with a pK_a near neutral pH making the channel especially susceptible to pathological changes in pH_i. Interestingly, the pK_a for activation of ROMK is under physiological control, and can be dynamically changed by PIP_2 binding and PKA phosphorylation of the channel.[192,193] Bartter mutations disrupting the normal regulation of pK_a shift the pH_i of activation.[194] Moreover, a Bartter mutation causing a frameshift at T332 interrupts pH-dependent gating, moving the apparent pK_a at which ROMK opens markedly in the alkaline direction outside the physiological range.[148,186,185] The biophysical consequence of this is that the channel enters long-closed states for prolonged periods of time, greatly decreasing K^+ exit across the apical membrane. The structural basis for this effect remains to be determined, but clearly, this mutation involves changes in the intracellular domains of ROMK likely resulting in destruction or uncoupling of allosteric sites from the regulated gate.

Mutation of the Intracellular Gating Structure

The narrowing at the apex of the cytoplasmic pore of ROMK where G-loops coalesce is also involved in gating.[32] The Bartter mutation A306T disrupts K^+ conductance by ROMK.[15] This residue is located in the G-loop, possibly affecting the intracellular gate. Underscoring the importance of this intracellular resistance barrier to channel structure and function are findings that disease (Andersen–Tawil syndrome)-causing mutations in other Kir channels cluster in G-loops.[196,197] The Y314C, V315G, and A198T Bartter mutations, as discussed below, may also affect gating that involves the interactions of intracellular domains of the channel with the bundle-crossing.[15,185,198]

Mutation of the PIP_2-Binding Site

Phosphoinositide 4,5-*bis*phosphate (PIP_2) is an important physiological regulator of Kir channel gating, including ROMK, which it stabilizes in a high P_o state.[32,199,200,201] A comprehensive investigation of ROMK mutants and mutants of its homolog, Kir2.1, combined with the study of Kir1.1-Kir2.1 chimeric channel proteins, identified several basic amino acids corresponding to R48, K181, K184, K186, R188, R217, K218, and R311 in ROMK that are required for PIP_2-dependent gating.[201–203] Substitution that neutralizes these charged residues reduces channel activity. That the side chains of these residues carry a positive charge is consistent with them contributing to a *bona fide* allosteric PIP_2-binding site. This was reinforced by findings that a portion of ROMK containing four of these basic residues (aa. 183–221) has the capacity in solution to bind PIP_2.[204] Although these four basic residues are in a portion of Kir for which structure has not been resolved, their position in the linear sequence suggests that they reside at the apex of the cytoplasmic domains near the intracellular face of the lipid bilayer.[32] Moreover, modeling clusters R48, R217, and R218 at the top of the cytoplasmic domain where they are predicted to face the inner lipid leaflet. Considering findings from functional studies and lipid-binding studies, this position is consistent with these residues having the capacity to interact in a direct manner with membrane phospholipids. That ROMK and other Kir channels contain a PIP_2-binding site capable of signaling to a gate becomes important

when recognizing that a group of Bartter mutations, C49Y, I51T, A214V, and L220F, disrupt PIP_2-dependent gating.[15,186,194] In three-dimensional ROMK models, all of these residues cluster on the membrane-facing surface of the cytoplasmic domain near the putative PIP_2-binding pocket, suggesting that they modulate binding to this site or transduction of information from this site to the gate. Importantly, similar observations made for Kir2.1, which when dysfunctional causes the familial Andersen–Tawil form of long QT syndrome, have been interpreted to indicate that the disruption of PIP_2-binding underlies many Kir channelopathies.[200,201,205]

Mutation of Salt-Bridges Critical to Structure

The cytoplasmic domain of ROMK is stabilized by inter- (R311–E302) and intrasubunit (R41–E318) salt-bridges. Compromise of these bridges uncouples ligand binding in cytoplasmic domains from the regulated gate.[15,194] This is underscored by the dramatic alkaline-shift in apparent pK_a of activation for ROMK containing the R311W or R311Q Bartter mutation. A shift in pK_a leads to these channels being in a prolonged closed state at physiological pH_i.

Mutation of PKA Phosphorylation Sites

Similar to the secretory channel in native tissue, ROMK in heterologous expression systems is also responsive to PKA phosphorylation.[206,207] In concert with physiological pH_i and PIP_2 levels, PKA phosphorylation sets ROMK to a high P_o state.[32] Biochemical studies identified three discrete PKA phosphorylation sites in the cytoplasmic NH_2- and COOH-termini of ROMK: S44, S219, and S313.[208,209,210] Each of these must be phosphorylated for full channel function. The site in the NH_2-terminus is an absolute requirement for expression at the membrane. Those in the COOH-terminus are necessary for the high P_o state, modulating regulated-gating in response to pH, PIP_2, and ATP.[192,211] These latter two phosphorylation sites are strategically positioned in the channel to modulate the effects of regulators of gating. S219 is positioned between a PIP_2-binding site, the G-loop, and an intersubunit (E311–E302) salt-bridge. In comparison, S313 is sandwiched between an intrasubunit (R41–E318) and intersubunit (E311–E302) salt-bridge. Such positions provide a structural explanation for how phosphorylation may be involved in the functional coupling of gating factors. As such, phosphorylation of S219 and S313 provoke an acidic shift in the apparent pK_a activating ROMK at physiological pH_i.[192] The Bartter mutations S219R and S313C remove these critical phosphorylation sites; consequently, ROMK containing these mutations has decreased activity, being in a low P_o state under physiological conditions.[186,194] Two other Bartter mutations, Y314C and V315G, are one and two positions downstream of the critical Ser at 313.[198] It is not clear yet, but the Bartter mutations L220F and R311W may also influence the phosphorylation state or be involved in coupling PIP_2 binding and PKA phosphorylation. These are reasonable expansions on the possibility that the L220F mutation impacts PIP_2 binding and R311W is critical to salt-bridge formation, and is also possibly involved in PIP_2 binding as discussed above.

Mutation of a Selectivity-Filter Residue

ROMK channels, similar to all K^+ channels, contain the signature K^+-selectivity sequence T[V/I]GYG in the P-loop linking TM1 to TM2 (see Figure 8.29). The Bartter mutation I142T substitutes the critical second residue in this selectivity sequence, disrupting K^+ permeation significantly and decreasing conductance.[15] I142 is also involved in pore-gating of ROMK channels, as discussed above.[50,51] Therefore, this mutation may also affect gating. Regardless, as a result of this mutation, the ability to reabsorb NaCl in the TAL is compromised, destroying the axial corticomedullary hyperosmotic gradient necessary to concentrate urine.

Loss-of-Function Mutations with Undefined Mechanism

There are several other mutations in ROMK that also possibly change the channel's biophysical properties to cause disease. For instance, the Bartter mutations W99C, A103V, P110L, and N124K act in a dominant negative manner. When co-expressed with wild-type subunits, these mutant subunits decrease channel activity.[185] This is consistent with channels containing both wild-type and mutant subunits making it to the membrane, but having abnormal biophysical properties. Similarly, ROMK channels containing the T71M, F95S, A156V, and R324L Bartter mutations also traffic in a normal manner to the plasma membrane in some expression systems, but have decreased activity.[15] Again, this points to a change in biophysical properties as the disease-causing mechanism.

TRPM6: Hypomagnesemia with Secondary Hypocalcemia

Genetic studies in patients with hereditary HSH identified disease-causing mutations in TRPM6.[9,10,19,20,24] The missense substitution, P1017R, in TRPM6 is one such mutation.[4,10] Although a crystal structure for TRP channels is currently not available, it is accepted that these channels contain six transmembrane domains and assume a tetrameric structure similar to voltage-gated K^+ channels, with extracellular P-loops diving into the

membrane to form the pore. Using the structural coordinates of the KvAP channel to model the putative S5-S6 segment of TRPM6, including the putative P-loop, places P1017 in the predicted pore region of the channel.[4,212] A recent study by Chubanov and colleagues showed that co-expression of wild-type TRPM6 with TRPM7 significantly increases current through the channel.[4] In contrast, co-expression of TRPM6 containing the P1017R mutation with wild-type TRPM7 suppresses channel activity. Consistent with this dominant-negative effect, co-expression of TRPM7 containing a homologous P-to-R mutation decreases wild-type TRPM6 activity. This action is restricted to changes in the biophysical properties of the channel, for the P1017R mutation has no effect on channel assembly or trafficking. These results strongly suggest that the P1017R mutation affects either permeation through the channel or channel gating to decrease activity. Decreases in TRPM6 channel activity would reduce Mg^{2+} reabsorption by the kidney, leading to the disease phenotype.

Acknowledgments

I thank Drs. John Johnson (Dept. Physiology, UTHSCSA), Kishore Kamaraju (Dept. Physiology, UTHSCSA), Volodymyr Kucher (Dept. Physiology, UTHSCSA), Steve Sansom (Dept. Cellular and Integrative Physiology, UNMC), and Bin Wang (Dept. Physiology, UTHSCSA) for critically reading this chapter.

References

[1] Ashcroft FM. Ion channels and disease. Oxford: Academic Press; 2000.
[2] Hille B. Ion channels of excitable membranes. Sinauer Associates, Inc; 2001.
[3] Sackin H, Nanazashvili M, Palmer LG, Krambis M, Walters DE. Structural locus of the pH gate in the Kir1.1 inward rectifier channel. Biophys J 2005;88:2597–606.
[4] Chubanov V, Schlingmann KP, Waring J, Heinzinger J, Kaske S, Waldegger S, et al. Hypomagnesemia with secondary hypocalcemia due to a missense mutation in the putative pore-forming region of TRPM6. J Biol Chem 2007;282:7656–67.
[5] Schlingmann KP, Konrad M, Jeck N, Waldegger P, Reinalter SC, Holder M, et al. Salt wasting and deafness resulting from mutations in two chloride channels. N Engl J Med 2004;350:1314–9.
[6] Tseng PY, Bennetts B, Chen TY. Cytoplasmic ATP inhibition of CLC-1 is enhanced by low pH. J Gen Physiol 2007;130:217–21.
[7] Waldegger S, Jentsch TJ. Functional and structural analysis of ClC-K chloride channels involved in renal disease. J Biol Chem 2000;275:24527–33.
[8] Walder RY, Landau D, Meyer P, Shalev H, Tsolia M, Borochowitz Z, et al. Mutation of TRPM6 causes familial hypomagnesemia with secondary hypocalcemia. Nat Genet 2002;31:171–4.
[9] Woda CB, Bragin A, Kleyman TR, Satlin LM. Flow-dependent K^+ secretion in the cortical collecting duct is mediated by a maxi-K channel. Am J Physiol Renal Physiol 2001;280:F786–93.
[10] Dietrich A, Chubanov V, Gudermann T. Renal TRPathies. J Am Soc Nephrol 2010;21:736–44.
[11] Dryer SE, Reiser J. TRPC6 channels and their binding partners in podocytes: role in glomerular filtration and pathophysiology. Am J Physiol Renal Physiol 2010;299:F689–701.
[12] Hsu YJ, Hoenderop JG, Bindels RJ. TRP channels in kidney disease. Biochim Biophys Acta 2007;1772:928–36.
[13] Williamson IM, Alvis SJ, East JM, Lee AG. The potassium channel KcsA and its interaction with the lipid bilayer. Cell Mol Life Sci 2003;60:1581–90.
[14] Hebert SC. Bartter syndrome. Curr Opin Nephrol Hypertens 2003;12:527–32.
[15] Pegan S, Arrabit C, Zhou W, Kwiatkowski W, Collins A, Slesinger PA, et al. Cytoplasmic domain structures of Kir2.1 and Kir3.1 show sites for modulating gating and rectification. Nat Neurosci 2005;8:279–87.
[16] Pochynyuk O, Kucher V, Boiko N, Mironova E, Staruschenko A, Karpushev AV, et al. Intrinsic voltage dependence of the epithelial Na^+ channel is masked by a conserved transmembrane domain tryptophan. J Biol Chem 2009;284:25512–21.
[17] Schlanger LE, Kleyman TR, Ling BN. K^+-sparing diuretic actions of trimethoprim: inhibition of Na^+ channels in A6 distal nephron cells. Kidney Int 1994;45:1070–6.
[18] Schwalbe RA, Bianchi L, Accili EA, Brown AM. Functional consequences of ROMK mutants linked to antenatal Bartter's syndrome and implications for treatment. Hum Mol Genet 1998;7:975–80.
[19] Dimke H, Hoenderop JG, Bindels RJ. Hereditary tubular transport disorders: implications for renal handling of Ca^{2+} and Mg^{2+}. Clin Sci (Lond) 2010;118:1–18.
[20] Glaudemans B, Knoers NV, Hoenderop JG, Bindels RJ. New molecular players facilitating Mg(2+) reabsorption in the distal convoluted tubule. Kidney Int 2010;77:17–22.
[21] Hou J, Goodenough DA. Claudin-16 and claudin-19 function in the thick ascending limb. Curr Opin Nephrol Hypertens 2010;19:483–8.
[22] Hou J, Renigunta A, Konrad M, Gomes AS, Schneeberger EE, Paul DL, et al. Claudin-16 and claudin-19 interact and form a cation-selective tight junction complex. J Clin Invest 2008;118:619–28.
[23] Landau D. Potassium-related inherited tubulopathies. Cell Mol Life Sci 2006;63:1962–8.
[24] Voets T, Nilius B, Hoefs S, van der Kemp AW, Droogmans G, Bindels RJ, et al. TRPM6 forms the Mg^{2+} influx channel involved in intestinal and renal Mg^{2+} absorption. J Biol Chem 2004;279:19–25.
[25] Hou J, Renigunta A, Gomes AS, Hou M, Paul DL, Waldegger S, et al. Claudin-16 and claudin-19 interaction is required for their assembly into tight junctions and for renal reabsorption of magnesium. Proc Natl Acad Sci USA 2009;106:15350–5.
[26] Konrad M, Hou J, Weber S, Dotsch J, Kari JA, Seeman T, et al. CLDN16 genotype predicts renal decline in familial hypomagnesemia with hypercalciuria and nephrocalcinosis. J Am Soc Nephrol 2008;19:171–81.
[27] Konrad M, Schaller A, Seelow D, Pandey AV, Waldegger S, Lesslauer A, et al. Mutations in the tight-junction gene claudin 19 (CLDN19) are associated with renal magnesium wasting, renal failure, and severe ocular involvement. Am J Hum Genet 2006;79:949–57.
[28] Simon DB, Bindra RS, Mansfield TA, Nelson-Williams C, Mendonca E, Stone R, et al. Mutations in the chloride channel gene, CLCNKB, cause Bartter's syndrome type III. Nat Genet 1997;17:171–8.
[29] Richard EA, Miller C. Steady-state coupling of ion-channel conformations to a transmembrane ion gradient. Science 1990;247:1208–10.

[30] Winn MP, Conlon PJ, Lynn KL, Farrington MK, Creazzo T, Hawkins AF, et al. A mutation in the TRPC6 cation channel causes familial focal segmental glomerulosclerosis. Science 2005;308:1801–4.
[31] Murata K, Mitsuoka K, Hirai T, Walz T, Agre P, Heymann JB, et al. Structural determinants of water permeation through aquaporin-1. Nature 2000;407:599–605.
[32] Warth R, Barriere H, Meneton P, Bloch M, Thomas J, Tauc M, et al. Proximal renal tubular acidosis in TASK2 K^+ channel-deficient mice reveals a mechanism for stabilizing bicarbonate transport. Proc Natl Acad Sci USA 2004;101:8215–20.
[33] Wang W, Giebisch G. Dual modulation of renal ATP-sensitive K^+ channel by protein kinases A and C. Proc Natl Acad Sci USA 1991;88:9722–5.
[34] Boiteux C, Kraszewski S, Ramseyer C, Girardet C. Ion conductance vs. pore gating and selectivity in KcsA channel: modeling achievements and perspectives. J Mol Model 2007;13:699–713.
[35] Kuo A, Domene C, Johnson LN, Doyle DA, Venien-Bryan C. Two different conformational states of the KirBac3.1 potassium channel revealed by electron crystallography. Structure 2005;13:1463–72.
[36] Zhang YY, Robertson JL, Gray DA, Palmer LG. Carboxy-terminal determinants of conductance in inward-rectifier K channels. J Gen Physiol 2004;124:729–39.
[37] Dutzler R. Structural basis for ion conduction and gating in ClC chloride channels. FEBS Lett 2004;564:229–33.
[38] Krapivinsky G, Gordon EA, Wickman K, Velimirovic B, Krapivinsky L, Clapham DE. The G-protein-gated atrial K^+ channel IKACh is a heteromultimer of two inwardly rectifying K(+)-channel proteins. Nature 1995;374:135–41.
[39] Pluznick JL, Wei P, Grimm PR, Sansom SC. BK-{beta}1 subunit: immunolocalization in the mammalian connecting tubule and its role in the kaliuretic response to volume expansion. Am J Physiol Renal Physiol 2005;288:F846–54.
[40] Cole KS. Membranes, ions and impulses: a chapter of classical biophysics. Berkely: University of California Press; 1968.
[41] Kellenberger S, Schild L. Epithelial sodium channel/degenerin family of ion channels: a variety of functions for a shared structure. Physiol Rev 2002;82:735–67.
[42] Nishida M, MacKinnon R. Structural basis of inward rectification: cytoplasmic pore of the G protein-gated inward rectifier GIRK1 at 1.8 Å resolution. Cell 2002;111:957–65.
[43] Kurata HT, Marton LJ, Nichols CG. The polyamine binding site in inward rectifier K^+ channels. J Gen Physiol 2006;127:467–80.
[44] Schild L. The epithelial sodium channel and the control of sodium balance. Biochim Biophys Acta 2010;1802:1159–65.
[45] Doyle DA, Morais CJ, Pfuetzner RA, Kuo A, Gulbis JM, Cohen SL, et al. The structure of the potassium channel: molecular basis of K^+ conduction and selectivity. Science 1998;280:69–77.
[46] Dutzler R. The structural basis of ClC chloride channel function. Trends Neurosci 2004;27:315–20.
[47] Hamilton KL, Eaton DC. Single-channel recordings from two types of amiloride-sensitive epithelial Na^+ channels. Membr Biochem 1986;6:149–71.
[48] Hinton CF, Eaton DC. Expression of amiloride-blockable sodium channels in *Xenopus* oocytes. Am J Physiol 1989;257(Pt 1):C825–829.
[49] McNicholas CM, Wang W, Ho K, Hebert SC, Giebisch G. Regulation of ROMK1 K^+ channel activity involves phosphorylation processes. Proc Natl Acad Sci USA 1994;91:8077–81.
[50] Berneche S, Roux B. A gate in the selectivity filter of potassium channels. Structure 2005;13:591–600.
[51] Domene C, Klein ML, Branduardi D, Gervasio FL, Parrinello M. Conformational changes and gating at the selectivity filter of potassium channels. J Am Chem Soc 2008;130:9474–80.
[52] Dutzler R. A structural perspective on ClC channel and transporter function. FEBS Lett 2007;581:2839–44.
[53] Dutzler R, Campbell EB, Cadene M, Chait BT, MacKinnon R. X-ray structure of a ClC chloride channel at 3.0 Å reveals the molecular basis of anion selectivity. Nature 2002;415:287–94.
[54] Hierholzer K, and Lange S. Kidney and urinary tract Physiology. 1995.
[55] Lobet S, Dutzler R. Ion-binding properties of the ClC chloride selectivity filter. EMBO J 2006;25:24–33.
[56] Kuo A, Gulbis JM, Antcliff JF, Rahman T, Lowe ED, Zimmer J, et al. Crystal structure of the potassium channel KirBac1.1 in the closed state. Science 2003;300:1922–6.
[57] Dutzler R, Campbell EB, MacKinnon R. Gating the selectivity filter in ClC chloride channels. Science 2003;300:108–12.
[58] Gonzales EB, Kawate T, Gouaux E. Pore architecture and ion sites in acid-sensing ion channels and P2X receptors. Nature 2009;460:599–604.
[59] Dutzler R. The ClC family of chloride channels and transporters. Curr Opin Struct Biol 2006;16:439–46.
[60] Jentsch TJ, Neagoe I, Scheel O. CLC chloride channels and transporters. Curr Opin Neurobiol 2005;15:319–25.
[61] Lisal J, Maduke M. Review. Proton-coupled gating in chloride channels. Philos Trans R Soc Lond B Biol Sci 2009;364:181–7.
[62] Choe H, Palmer LG, Sackin H. Structural determinants of gating in inward-rectifier K^+ channels. Biophys J 1999;76:1988–2003.
[63] Choe H, Sackin H, Palmer LG. Permeation and gating of an inwardly rectifying potassium channel. Evidence for a variable energy well. J Gen Physiol 1998;112:433–46.
[64] Choe H, Sackin H, Palmer LG. Gating properties of inward-rectifier potassium channels: effects of permeant ions. J Membr Biol 2001;184:81–9.
[65] Pusch M. Myotonia caused by mutations in the muscle chloride channel gene CLCN1. Hum Mutat 2002;19:423–34.
[66] Pusch M. Structural insights into chloride and proton-mediated gating of CLC chloride channels. Biochemistry 2004;43:1135–44.
[67] Pusch M, Ludewig U, Jentsch TJ. Temperature dependence of fast and slow gating relaxations of ClC-0 chloride channels. J Gen Physiol 1997;109:105–16.
[68] Rychkov GY, Pusch M, Astill DS, Roberts ML, Jentsch TJ, Bretag AH. Concentration and pH dependence of skeletal muscle chloride channel ClC-1. J Physiol 1996;497(Pt 2):423–35.
[69] Horrigan FT, Aldrich RW. Coupling between voltage sensor activation, Ca^{2+} binding and channel opening in large conductance (BK) potassium channels. J Gen Physiol 2002;120:267–305.
[70] Rohacs T, Chen J, Prestwich GD, Logothetis DE. Distinct specificities of inwardly rectifying K(+) channels for phosphoinositides. J Biol Chem 1999;274:36065–72.
[71] Estevez R, Boettger T, Stein V, Birkenhager R, Otto E, Hildebrandt F, et al. Barttin is a Cl^- channel beta-subunit crucial for renal Cl^- reabsorption and inner ear K^+ secretion. Nature 2001;414:558–61.
[72] Fischer M, Janssen AG, Fahlke C. Barttin activates ClC-K channel function by modulating gating. J Am Soc Nephrol 2010;21:1281–9.
[73] Schnell JR, Chou JJ. Structure and mechanism of the M2 proton channel of influenza A virus. Nature 2008;451:591–5.
[74] Palmer LG. Epithelial Na channels: function and diversity. Annu Rev Physiol 1992;54:51–6.
[75] Palmer LG, Andersen OS. Interactions of amiloride and small monovalent cations with the epithelial sodium channel. Inferences about the nature of the channel pore. Biophys J 1989;55:779–87.

[76] Lopatin AN, Nichols CG. Internal Na^+ and Mg^{2+} blockade of DRK1 (Kv2.1) potassium channels expressed in *Xenopus* oocytes. Inward rectification of a delayed rectifier. J Gen Physiol 1994;103:203–16.
[77] Lu Z, MacKinnon R. Electrostatic tuning of Mg^{2+} affinity in an inward-rectifier K^+ channel. Nature 1994;371:243–6.
[78] Accardi A, Picollo A. CLC channels and transporters: proteins with borderline personalities. Biochim Biophys Acta 2010;1798:1457–64.
[79] Duran C, Thompson CH, Xiao Q, Hartzell HC. Chloride channels: often enigmatic, rarely predictable. Annu Rev Physiol 2010;72:95–121.
[80] Bayliss DA, Barrett PQ. Emerging roles for two-pore-domain potassium channels and their potential therapeutic impact. Trends Pharmacol Sci 2008;29:566–75.
[81] Benos DJ, Stanton BA. Functional domains within the degenerin/epithelial sodium channel (Deg/ENaC) superfamily of ion channels. J Physiol (Lond) 1999;520(Pt 3):631–44.
[82] Loffing J, Korbmacher C. Regulated sodium transport in the renal connecting tubule (CNT) via the epithelial sodium channel (ENaC). Pflugers Arch 2009;458:111–35.
[83] Sakmann B, Neher E. Single-Channel recording. New York: Plenum Press; 1983.
[84] Boros S, Bindels RJ, Hoenderop JG. Active Ca(2 +) reabsorption in the connecting tubule. Pflugers Arch 2009;458:99–109.
[85] de GT, Bindels RJ, Hoenderop JG. TRPV5: an ingeniously controlled calcium channel. Kidney Int 2008;74:1241–6.
[86] Dimke H, Hoenderop JG, Bindels RJ. Molecular basis of epithelial Ca^{2+} and Mg^{2+} transport: insights from the TRP channel family. J. Physiol. 2011;589(Pt 7):1535–42.
[87] Lang F, Vallon V, Knipper M, Wangemann P. Functional significance of channels and transporters expressed in the inner ear and kidney. Am J Physiol Cell Physiol 2007;293: C1187–208.
[88] Knoers NV, Levtchenko EN. Gitelman syndrome. Orphanet J Rare Dis 2008;3:22.
[89] Gan L, Kaczmarek LK. When, where, and how much? Expression of the Kv3.1 potassium channel in high-frequency firing neurons. J Neurobiol 1998;37:69–79.
[90] Kamb A, Iverson LE, Tanouye MA. Molecular characterization of Shaker, a *Drosophila* gene that encodes a potassium channel. Cell 1987;50:405–13.
[91] Tejpar S, Piessevaux H, Claes K, Piront P, Hoenderop JG, Verslype C, et al. Magnesium wasting associated with epidermal-growth-factor receptor-targeting antibodies in colorectal cancer: a prospective study. Lancet Oncol 2007;8:387–94.
[92] Glaudemans B, van der WJ, Scola RH, Lorenzoni PJ, Heister A, van der Kemp AW, et al. A missense mutation in the Kv1.1 voltage-gated potassium channel-encoding gene KCNA1 is linked to human autosomal dominant hypomagnesemia. J Clin Invest 2009;119:936–42.
[93] Plaster NM, Tawil R, Tristani-Firouzi M, Canun S, Bendahhou S, Tsunoda A, et al. Mutations in Kir2.1 cause the developmental and episodic electrical phenotypes of Andersen's syndrome. Cell 2001;105:511–9.
[94] Ho K, Nichols CG, Lederer WJ, Lytton J, Vassilev PM, Kanazirska MV, et al. Cloning and expression of an inwardly rectifying ATP-regulated potassium channel. Nature 1993;362:31–8.
[95] Wang WH, Giebisch G. Regulation of potassium (K) handling in the renal collecting duct. Pflugers Arch 2009;458:157–68.
[96] Bockenhauer D, Feather S, Stanescu HC, Bandulik S, Zdebik AA, Reichold M, et al. Epilepsy, ataxia, sensorineural deafness, tubulopathy, and KCNJ10 mutations. N Engl J Med 2009;360:1960–70.
[97] Scholl U, Hebeisen S, Janssen AG, Muller-Newen G, Alekov A, Fahlke C. Barttin modulates trafficking and function of ClC-K channels. Proc Natl Acad Sci USA 2006;103:11411–6.
[98] Tempel BL, Papazian DM, Schwarz TL, Jan YN, Jan LY. Sequence of a probable potassium channel component encoded at Shaker locus of *Drosophila*. Science 1987;237:770–5.
[99] Wang WH, Yue P, Sun P, Lin DH. Regulation and function of potassium channels in aldosterone-sensitive distal nephron. Curr. Opin. Nephrol. Hypertens. 2010;19(5):463–70.
[100] Rychkov GY, Pusch M, Roberts ML, Jentsch TJ, Bretag AH. Permeation and block of the skeletal muscle chloride channel, ClC-1, by foreign anions. J Gen Physiol 1998;111:653–65.
[101] Canessa CM, Horisberger JD, Rossier BC. Epithelial sodium channel related to proteins involved in neurodegeneration. Nature 1993;361:467–70.
[102] Canessa CM, Schild L, Buell G, Thorens B, Gautschi I, Horisberger JD, et al. Amiloride-sensitive epithelial Na channel is made of three homologous subunits. Nature 1994;367:463–7.
[103] Lingueglia E, Voilley N, Waldmann R, Lazdunski M, Barbry P. Expression cloning of an epithelial amiloride-sensitive Na^+ channel. A new channel type with homologies to Caenorhabditis elegans degenerins. FEBS Lett 1993;318:95–9.
[104] Kellenberger S, Gautschi I, Schild L. A single point mutation in the pore region of the epithelial Na^+ channel changes ion selectivity by modifying molecular sieving. Proc Natl Acad Sci USA 1999;96:4170–5.
[105] Kellenberger S, Hoffmann-Pochon N, Gautschi I, Schneeberger E, Schild L. On the molecular basis of ion permeation in the epithelial Na^+ channel. J Gen Physiol 1999;114:13–30.
[106] Lifton RP, Gharavi AG, Geller DS. Molecular mechanisms of human hypertension. Cell 2001;104:545–56.
[107] Rieg T, Vallon V, Sausbier M, Sausbier U, Kaissling B, Ruth P, et al. The role of the BK channel in potassium homeostasis and flow-induced renal potassium excretion. Kidney Int 2007;72:566–73.
[108] Estacion M, Sinkins WG, Jones SW, Applegate MA, Schilling WP. Human TRPC6 expressed in HEK 293 cells forms non-selective cation channels with limited Ca^{2+} permeability. J Physiol 2006;572:359–77.
[109] Inoue R, Okada T, Onoue H, Hara Y, Shimizu S, Naitoh S, et al. The transient receptor potential protein homologue TRP6 is the essential component of vascular alpha(1)-adrenoceptor-activated Ca(2 +)-permeable cation channel. Circ Res 2001;88:325–32.
[110] Sheng S, McNulty KA, Harvey JM, Kleyman TR. Second transmembrane domains of ENaC subunits contribute to ion permeation and selectivity. J Biol Chem 2001;276:44091–8.
[111] Scholl UI, Choi M, Liu T, Ramaekers VT, Hausler MG, Grimmer J, et al. Seizures, sensorineural deafness, ataxia, mental retardation, and electrolyte imbalance (SeSAME syndrome) caused by mutations in KCNJ10. Proc Natl Acad Sci USA 2009;106:5842–7.
[112] Tang Y, Zaitseva F, Lamb RA, Pinto LH. The gate of the influenza virus M2 proton channel is formed by a single tryptophan residue. J Biol Chem 2002;277:39880–6.
[113] Liedtke W, Choe Y, Marti-Renom MA, Bell AM, Denis CS, Sali A, et al. Vanilloid receptor-related osmotically activated channel (VR-OAC), a candidate vertebrate osmoreceptor. Cell 2000;103:525–35.
[114] Liedtke W, Friedman JM. Abnormal osmotic regulation in trpv4 − / − mice. Proc Natl Acad Sci USA 2003;100:13698–703.
[115] Meyer S, Savaresi S, Forster IC, Dutzler R. Nucleotide recognition by the cytoplasmic domain of the human chloride transporter ClC-5. Nat Struct Mol Biol 2007;14:60–7.

[116] Jayaram H, Robertson JL, Wu F, Williams C, Miller C. Structure of a slow CLC Cl/H + antiporter from a cyanobacterium. Biochemistry 2011;50:788–94.
[117] Jasti J, Furukawa H, Gonzales EB, Gouaux E. Structure of acid-sensing ion channel 1 at 1.9 Å resolution and low pH. Nature 2007;449:316–23.
[118] Snyder PM, Price MP, McDonald FJ, Adams CM, Volk KA, Zeiher BG, et al. Mechanism by which Liddle's syndrome mutations increase activity of a human epithelial Na^+ channel. Cell 1995;83:969–78.
[119] Kollewe A, Lau AY, Sullivan A, Roux B, Goldstein SA. A structural model for K2P potassium channels based on 23 pairs of interacting sites and continuum electrostatics. J Gen Physiol 2009;134:53–68.
[120] Alioth S, Meyer S, Dutzler R, Pervushin K. The cytoplasmic domain of the chloride channel ClC-0: structural and dynamic characterization of flexible regions. J Mol Biol 2007;369:1163–9.
[121] MacKinnon R. Nobel Lecture. Potassium channels and the atomic basis of selective ion conduction. Biosci Rep 2004;24:75–100.
[122] Mensenkamp AR, Hoenderop JG, Bindels RJ. TRPV5, the gateway to Ca^{2+} homeostasis. Handb Exp Pharmacol 2007;:207–20.
[123] Jayaram H, Accardi A, Wu F, Williams C, Miller C. Ion permeation through a Cl^--selective channel designed from a CLC Cl^-/H^+ exchanger. Proc Natl Acad Sci USA 2008;105:11194–9.
[124] Gradogna A, Babini E, Picollo A, Pusch M. A regulatory calcium-binding site at the subunit interface of CLC-K kidney chloride channels. J Gen Physiol 2010;136:311–23.
[125] Mizuno A, Matsumoto N, Imai M, Suzuki M. Impaired osmotic sensation in mice lacking TRPV4. Am J Physiol Cell Physiol 2003;285:C96–101.
[126] Waldmann R, Champigny G, Voilley N, Lauritzen I, Lazdunski M. The mammalian degenerin MDEG, an amiloride-sensitive cation channel activated by mutations causing neurodegeneration in *Caenorhabditis elegans*. J Biol Chem 1996;271:10433–6.
[127] Rapedius M, Haider S, Browne KF, Shang L, Sansom MS, Baukrowitz T, et al. Structural and functional analysis of the putative pH sensor in the Kir1.1 (ROMK) potassium channel. EMBO Rep 2006;7:611–6.
[128] Chen TY, Miller C. Nonequilibrium gating and voltage dependence of the ClC-0 Cl^- channel. J Gen Physiol 1996;108:237–50.
[129] Hanke W, Miller C. Single chloride channels from *Torpedo electroplax*. Activation by protons. J Gen Physiol 1983;82:25–45.
[130] Roux B, MacKinnon R. The cavity and pore helices in the KcsA K^+ channel: electrostatic stabilization of monovalent cations. Science 1999;285:100–2.
[131] Capaldi RA. Membrane proteins. New York, New York: Marcel Dekker Inc; 1995.
[132] Fahlke C, Yu HT, Beck CL, Rhodes TH, George Jr. AL. Pore-forming segments in voltage-gated chloride channels. Nature 1997;390:529–32.
[133] Thompson DA, Feather S, Stanescu HC, Freudenthal B, Zdebik AA, Warth R, et al. Altered electroretinograms in patients with KCNJ10 mutations and EAST syndrome. J. Physiol. 2011;589(Pt 7):1681–9.
[134] Grunder S, Firsov D, Chang SS, Jaeger NF, Gautschi I, Schild L, et al. A mutation causing pseudohypoaldosteronism type 1 identifies a conserved glycine that is involved in the gating of the epithelial sodium channel. EMBO J 1997;16:899–907.
[135] Grunder S, Jaeger NF, Gautschi I, Schild L, Rossier BC. Identification of a highly conserved sequence at the N-terminus of the epithelial Na^+ channel alpha subunit involved in gating. Pflugers Arch 1999;438:709–15.
[136] Seyberth HW. An improved terminology and classification of Bartter-like syndromes. Nat Clin Pract Nephrol 2008;4:560–7.
[137] Staub O, Dho S, Henry P, Correa J, Ishikawa T, McGlade J, et al. domains of Nedd4 bind to the proline-rich PY motifs in the epithelial Na^+ channel deleted in Liddle's syndrome. EMBO J 1996;15:2371–80.
[138] Hiltunen TP, Hannila-Handelberg T, Petajaniemi N, Kantola I, Tikkanen I, Virtamo J, et al. Liddle's syndrome associated with a point mutation in the extracellular domain of the epithelial sodium channel gamma subunit. J Hypertens 2002;20:2383–90.
[139] Yu Y, Xu C, Pan X, Ren H, Wang W, Meng X, et al. Identification and functional analysis of novel mutations of the CLCNKB gene in Chinese patients with classic Bartter syndrome. Clin Genet 2010;77:155–62.
[140] Simon DB, Lu Y, Choate KA, Velazquez H, Al-Sabban E, Praga M, et al. Paracellin-1, a renal tight junction protein required for paracellular Mg^{2+} resorption. Science 1999;285:103–6.
[141] Kawate T, Michel JC, Birdsong WT, Gouaux E. Crystal structure of the ATP-gated P2X(4) ion channel in the closed state. Nature 2009;460:592–8.
[142] Harding MM. Metal-ligand geometry relevant to proteins and in proteins: sodium and potassium. Acta Crystallogr D Biol Crystallogr 2002;58:872–4.
[143] Harding MM. The architecture of metal coordination groups in proteins. Acta Crystallogr D Biol Crystallogr 2004;60:849–59.
[144] Goodman MB, Ernstrom GG, Chelur DS, O'Hagan R, Yao CA, Chalfie M. MEC-2 regulates *C. elegans* DEG/ENaC channels needed for mechanosensation. Nature 2002;415:1039–42.
[145] Walder RY, Shalev H, Brennan TM, Carmi R, Elbedour K, Scott DA, et al. Familial hypomagnesemia maps to chromosome 9q, not to the X chromosome: genetic linkage mapping and analysis of a balanced translocation breakpoint. Hum Mol Genet 1997;6:1491–7.
[146] Nanazashvili M, Li H, Palmer LG, Walters DE, Sackin H. Moving the pH gate of the Kir1.1 inward rectifier channel. Channels (Austin) 2007;1:21–8.
[147] Nishida M, Cadene M, Chait BT, MacKinnon R. Crystal structure of a Kir3.1-prokaryotic Kir channel chimera. EMBO J 2007;26:4005–15.
[148] Flagg TP, Yoo D, Sciortino CM, Tate M, Romero MF, Welling PA. Molecular mechanism of a COOH-terminal gating determinant in the ROMK channel revealed by a Bartter's disease mutation. J Physiol 2002;544:351–62.
[149] Stouffer AL, Acharya R, Salom D, Levine AS, Di CL, Soto CS, et al. Structural basis for the function and inhibition of an influenza virus proton channel. Nature 2008;451:596–9.
[150] Lu Z, MacKinnon R. A conductance maximum observed in an inward-rectifier potassium channel. J Gen Physiol 1994;104:477–86.
[151] Macgregor GG, Xu JZ, McNicholas CM, Giebisch G, Hebert SC. Partially active channels produced by PKA site mutation of the cloned renal K^+ channel, ROMK2 (kir1.2). Am J Physiol 1998;275:F415–22.
[152] Rothberg BS, Magleby KL. Voltage and Ca^{2+} activation of single large-conductance Ca^{2+}-activated K^+ channels described by a two-tiered allosteric gating mechanism. J Gen Physiol 2000;116:75–99.
[153] Berneche S, Roux B. Energetics of ion conduction through the K^+ channel. Nature 2001;414:73–7.
[154] Welling PA, Ho K. A comprehensive guide to the ROMK potassium channel: form and function in health and disease. Am J Physiol Renal Physiol 2009;297:F849–63.
[155] Muto S. Potassium transport in the mammalian collecting duct. Physiol Rev 2001;81:85–116.

[156] Sachs F, Qin F. Gated, ion-selective channels observed with patch pipettes in the absence of membranes: novel properties of a gigaseal. Biophys J 1993;65:1101–7.
[157] Riepe FG, van Bemmelen MX, Cachat F, Plendl H, Gautschi I, Krone N, et al. Revealing a subclinical salt-losing phenotype in heterozygous carriers of the novel S562P mutation in the alpha subunit of the epithelial sodium channel. Clin Endocrinol (Oxf) 2009;70:252–8.
[158] Choe H, Sackin H, Palmer LG. Permeation properties of inward-rectifier potassium channels and their molecular determinants. J Gen Physiol 2000;115:391–404.
[159] Zhang P, Canessa CM. Single-channel properties of recombinant acid-sensitive ion channels formed by the subunits ASIC2 and ASIC3 from dorsal root ganglion neurons expressed in *Xenopus* oocytes. J Gen Physiol 2001;117:563–72.
[160] Pegan S, Arrabit C, Slesinger PA, Choe S. Andersen's syndrome mutation effects on the structure and assembly of the cytoplasmic domains of Kir2.1. Biochemistry 2006;45:8599–606.
[161] Konrad M, Vollmer M, Lemmink HH, van den Heuvel LP, Jeck N, Vargas-Poussou R, et al. Mutations in the chloride channel gene CLCNKB as a cause of classic Bartter syndrome. J Am Soc Nephrol 2000;11:1449–59.
[162] Yoo D, Kim BY, Campo C, Nance L, King A, Maouyo D, et al. Cell surface expression of the ROMK (Kir 1.1) channel is regulated by the aldosterone-induced kinase, SGK-1, and protein kinase A. J Biol Chem 2003;278:23066–75.
[163] Kubisch C, Schmidt-Rose T, Fontaine B, Bretag AH, Jentsch TJ. ClC-1 chloride channel mutations in myotonia congenita: variable penetrance of mutations shifting the voltage dependence. Hum Mol Genet 1998;7:1753–60.
[164] Pressler CA, Heinzinger J, Jeck N, Waldegger P, Pechmann U, Reinalter S, et al. Late-onset manifestation of antenatal Bartter syndrome as a result of residual function of the mutated renal Na^+-K^+-$2Cl^-$ co-transporter. J Am Soc Nephrol 2006;17:2136–42.
[165] Shi J, Mori E, Mori Y, Mori M, Li J, Ito Y, et al. Multiple regulation by calcium of murine homologues of transient receptor potential proteins TRPC6 and TRPC7 expressed in HEK293 cells. J Physiol 2004;561:415–32.
[166] Wagner CA. Disorders of renal magnesium handling explain renal magnesium transport. J Nephrol 2007;20:507–10.
[167] Bergsdorf EY, Zdebik AA, Jentsch TJ. Residues important for nitrate/proton coupling in plant and mammalian CLC transporters. J Biol Chem 2009;284:11184–93.
[168] Engh AM, Maduke M. Cysteine accessibility in ClC-0 supports conservation of the ClC intracellular vestibule. J Gen Physiol 2005;125:601–17.
[169] Meyer S, Dutzler R. Crystal structure of the cytoplasmic domain of the chloride channel ClC-0. Structure 2006;14:299–307.
[170] Bennetts B, Rychkov GY, Ng HL, Morton CJ, Stapleton D, Parker MW, et al. Cytoplasmic ATP-sensing domains regulate gating of skeletal muscle ClC-1 chloride channels. J Biol Chem 2005;280:32452–8.
[171] Traverso S, Elia L, Pusch M. Gating competence of constitutively open CLC-0 mutants revealed by the interaction with a small organic Inhibitor. J Gen Physiol 2003;122:295–306.
[172] Zhou Y, Morais-Cabral JH, Kaufman A, MacKinnon R. Chemistry of ion coordination and hydration revealed by a K^+ channel-Fab complex at 2.0 Å resolution. Nature 2001;414:43–8.
[173] Janssen AG, Scholl U, Domeyer C, Nothmann D, Leinenweber A, Fahlke C. Disease-causing dysfunctions of barttin in Bartter syndrome type IV. J Am Soc Nephrol 2009;20:145–53.
[174] Chang SS, Grunder S, Hanukoglu A, Rosler A, Mathew PM, Hanukoglu I, et al. Mutations in subunits of the epithelial sodium channel causes salt wasting with hyperkalaemic acidosis, pseudohypoaldosteronism type 1. Nature Genet 1996;12:248–53.
[175] Kucher V, Boiko N, Pochynyuk O, Stockand JD. Voltage-dependent gating underlies loss of ENaC function in pseudohypoaldosteronis type 1. Biophys. J. 2011;100(8):1930–9.
[176] Tammaro P, Flanagan SE, Zadek B, Srinivasan S, Woodhead H, Hameed S, et al. Kir6.2 mutation causing severe functional effects *in vitro* produces neonatal diabetes without the expected neurological complications. Diabetologia 2008;51:802–10.
[177] Wible BA, Taglialatela M, Ficker E, Brown AM. Gating of inwardly rectifying K^+ channels localized to a single negatively charged residue. Nature 1994;371:246–9.
[178] Xu ZC, Yang Y, Hebert SC. Phosphorylation of the ATP-sensitive, inwardly rectifying K^+ channel, ROMK, by cyclic AMP-dependent protein kinase. J Biol Chem 1996;271: 9313–9.
[179] Schlingmann KP, Weber S, Peters M, Niemann NL, Vitzthum H, Klingel K, et al. Hypomagnesemia with secondary hypocalcemia is caused by mutations in TRPM6, a new member of the TRPM gene family. Nat Genet 2002;31:166–70.
[180] Stockand JD, Staruschenko A, Pochynyuk O, Booth RE, Silverthorn DU. Insight toward epithelial Na^+ channel mechanism revealed by the acid-sensing ion channel 1 structure. IUBMB Life 2008;60:620–8.
[181] Riepe FG. Clinical and molecular features of type 1 pseudohypoaldosteronism. Horm Res 2009;72:1–9.
[182] Goulet CC, Volk KA, Adams CM, Prince LS, Stokes JB, Snyder PM. Inhibition of the epithelial Na^+ channel by interaction of Nedd4 with a PY motif deleted in Liddle's syndrome. J Biol Chem 1998;273:30012–7.
[183] Snyder PM, Olson DR, Bucher DB. A pore segment in DEG/ENaC Na(+) channels. J Biol Chem 1999;274:28484–90.
[184] Staruschenko A, Adams E, Booth RE, Stockand JD. Epithelial Na^+ channel subunit stoichiometry. Biophys J 2005;88:3966–75.
[185] Jeck N, Derst C, Wischmeyer E, Ott H, Weber S, Rudin C, et al. Functional heterogeneity of ROMK mutations linked to hyperprostaglandin E syndrome. Kidney Int 2001;59: 1803–11.
[186] Schulte U, Hahn H, Konrad M, Jeck N, Derst C, Wild K, et al. pH gating of ROMK (K(ir)1.1) channels: control by an Arg-Lys-Arg triad disrupted in antenatal Bartter syndrome. Proc Natl Acad Sci USA 1999;96:15298–303.
[187] Choe H, Zhou H, Palmer LG, Sackin H. A conserved cytoplasmic region of ROMK modulates pH sensitivity, conductance, and gating. Am J Physiol 1997;273:F516–29.
[188] Markovic S, Dutzler R. The structure of the cytoplasmic domain of the chloride channel ClC-Ka reveals a conserved interaction interface. Structure 2007;15:715–25.
[189] Rapedius M, Fowler PW, Shang L, Sansom MS, Tucker SJ, Baukrowitz T. H bonding at the helix-bundle crossing controls gating in Kir potassium channels. Neuron 2007;55:602–14.
[190] Pusch M, Ludewig U, Rehfeldt A, Jentsch TJ. Gating of the voltage-dependent chloride channel CIC-O by the permeant anion. Nature 1995;373:527–31.
[191] Hattersley AT, Ashcroft FM. Activating mutations in Kir6.2 and neonatal diabetes: new clinical syndromes, new scientific insights, and new therapy. Diabetes 2005;54:2503–13.
[192] Leipziger J, Macgregor GG, Cooper GJ, Xu J, Hebert SC, Giebisch G. PKA site mutations of ROMK2 channels shift the pH dependence to more alkaline values. Am J Physiol Renal Physiol 2000;279:F919–26.
[193] Leung YM, Zeng WZ, Liou HH, Solaro CR, Huang CL. Phosphatidylinositol 4,5-bisphosphate and intracellular pH

regulate the ROMK1 potassium channel via separate but interrelated mechanisms. J Biol Chem 2000;275:10182–9.
[194] Schrag D, Chung KY, Flombaum C, Saltz L. Cetuximab therapy and symptomatic hypomagnesemia. J Natl Cancer Inst 2005;97:1221–4.
[195] Flagg TP, Tate M, Merot J, Welling PA. A mutation linked with Bartter's syndrome locks Kir 1.1a (ROMK1) channels in a closed state. J Gen Physiol 1999;114:685–700.
[196] Ma D, Tang XD, Rogers TB, Welling PA. An Andersen–Tawil syndrome mutation in Kir2.1 (V302M) alters the G-loop cytoplasmic K^+ conduction pathway 1. J Biol Chem 2007;282:5781–9.
[197] Palmer LG, Frindt G. Amiloride-sensitive Na channels from the apical membrane of the rat cortical collecting tubule. Proc Natl Acad Sci USA 1986;83:2767–70.
[198] Fallen K, Banerjee S, Sheehan J, Addison D, Lewis LM, Meiler J, et al. The Kir channel immunoglobulin domain is essential for Kir1.1 (ROMK) thermodynamic stability, trafficking and gating. Channels (Austin) 2009;3:57–68.
[199] Cheng WW, D'Avanzo N, Doyle DA, Nichols CG. Dual-mode phospholipid regulation of human inward rectifying potassium channels. Biophys J 2011;100:620–8.
[200] D'Avanzo N, Cheng WW, Doyle DA, Nichols CG. Direct and specific activation of human inward rectifier K^+ channels by membrane phosphatidylinositol 4,5-bisphosphate. J Biol Chem 2010;285:37129–32.
[201] Lopes C, Zhang H, Rohacs T, Jin T, Logothetis D. Alterations in conserved Kir channel-PIP2 interactions underlie channelopathies. Neuron 2002;34:933–44.
[202] Robertson JL, Palmer LG, Roux B. Long-pore electrostatics in inward-rectifier potassium channels. J Gen Physiol 2008;132:613–32.
[203] Rohacs T, Lopes C, Jin T, Ramdya P, Molnar Z, Logothetis D. Specificity of activation by phosphoinositides determines lipid regulation of Kir channels. PNAS 2003;100:745–50.
[204] Peters M, Ermert S, Jeck N, Derst C, Pechmann U, Weber S, et al. Classification and rescue of ROMK mutations underlying hyperprostaglandin E syndrome/antenatal Bartter syndrome. Kidney Int 2003;64:923–32.
[205] McNicholas CM, Macgregor GG, Islas LD, Yang Y, Hebert SC, Giebisch G. pH-dependent modulation of the cloned renal K^+ channel, ROMK. Am J Physiol 1998;275:F972–81.
[206] Walz T, Hirai T, Murata K, Heymann JB, Mitsuoka K, Fujiyoshi Y, et al. The three-dimensional structure of aquaporin-1. Nature 1997;387:624–7.
[207] MacGregor G, Dong K, Vanoye C, Tang L, Giebisch G, Hebert S. Nucleotides and phospholipids compete for binding to the C terminus of K-ATP channels. PNAS 2002;99:2726–31.
[208] Xi Q, Hoenderop JG, Bindels RJ. Regulation of magnesium reabsorption in DCT. Pflugers Arch 2009;458:89–98.
[209] Yau WM, Wimley WC, Gawrisch K, White SH. The preference of tryptophan for membrane interfaces. Biochemistry 1998;37:14713–8.
[210] Liou HH, Zhou SS, Huang CL. Regulation of ROMK1 channel by protein kinase A via a phosphatidylinositol 4,5-bisphosphate-dependent mechanism. Proc Natl Acad Sci USA 1999;96:5820–5.
[211] Jiang Y, Lee A, Chen J, Ruta V, Cadene M, Chait BT, et al. X-ray structure of a voltage-dependent K^+ channel. Nature 2003;423:33–41.
[212] Zifarelli G, Pusch M. The muscle chloride channel ClC-1 is not directly regulated by intracellular ATP. J Gen Physiol 2008;131:109–16.

CHAPTER

9

Microvascular Permeability and the Exchange of Water and Solutes Across Microvascular Walls

C. Charles Michel

Department of Bioengineering, Imperial College, London, UK

INTRODUCTION

Exchange through microvascular walls is both the initial and the final step of transport of materials by the circulation. In most tissues, microvascular exchange is a passive process, driven by differences in hydrostatic pressure and solute concentration between the circulating plasma and the interstitial fluid that flank microvessel walls. Lipophilic molecules and small water-soluble molecules and ions can exchange rapidly in most vascular beds, but microvascular walls are a barrier to macromolecules, severely impeding their exchange. The consequent differences in macromolecular concentration across microvascular walls are responsible for differences in osmotic pressure, which were identified over a century ago to play an essential role in the balance of fluid between the circulating blood and the tissues.[121]

Although small hydrophilic molecules can exchange rapidly between the blood and the tissues, it is wrong to assume that microvascular walls are no barrier to them. The rate at which changes of concentration of a solute in the blood can be reflected as changes in interstitial fluid (ISF) concentration depends both on the blood flow to the capillary beds, and on the permeability of the capillary walls to the solute. It is often assumed that for small molecules only blood flow is important, but once flow has exceeded a certain minimum range of values, the rate of equilibration of blood and ISF becomes limited by permeability.

Microvascular exchange and microvascular permeability are sometimes regarded as synonymous but this in incorrect and it is important to distinguish between them. Microvascular permeability to a substance is the conductivity of the microvessel wall and the permeability coefficients which describe permeability in functional terms are determined by the structure and properties of the pathways through which its molecules traverse the vessel wall. Microvascular exchange rates and net transport through microvascular walls for a particular substance are determined by microvascular permeability to that substance and also by the value and direction of net fluid flow through the vessel wall and by differences in concentration of the substance between plasma and ISF. The difference between microvascular exchange and microvascular permeability is important when interpreting methods that claim to demonstrate changes in permeability. Many of these methods involve the measurement of changes in net transport of macromolecules between blood and tissues, without controlling the transcapillary differences in hydrostatic pressure and macromolecular concentration. We shall consider the potential errors later in this chapter.

First, we consider microvascular permeability, and then microvascular exchange. Not included in this chapter is a consideration of transport through the walls of microvessels of the central nervous system. The low permeabilities of these vessels and the specialized transport mechanisms for certain solutes constituting the

Seldin and Giebisch's The Kidney, Fifth Edition.
DOI: http://dx.doi.org/10.1016/B978-0-12-381462-3.00009-4

© 2013 Elsevier Inc. All rights reserved.

blood–brain barrier are atypical of other microvessels, and resemble those of tight epithelia.

MICROVASCULAR PERMEABILITY

Microvascular Ultrastructure

Capillary walls consist of a single layer of flattened endothelial cells, the endothelia, and these cells constitute the barrier between the blood and the ISF. Electron microscopy has revealed that endothelial cells in different tissues are of two distinct types: "continuous" and "fenestrated" (Figure 9.1). Continuous endothelium is found in microvessels of skin, muscle, lung, and connective tissues. Here, the endothelial cells are joined together by tight junctions to form a continuous layer surrounded by a continuous basement membrane. The plasmalemmal membranes of the continuous endothelia retain their integrity; even in areas where the cells are flattened, reducing their thickness to less than 0.1 μm, the distinct luminal and abluminal membranes are separated by a thin layer of cytoplasm.

Fenestrated endothelium is found in microvessels associated with secretory and absorptive epithelia, e.g., the capillaries of the intestinal mucosae, glomerular, and peri-tubular capillaries of the kidney. The walls of fenestrated microvessels are also made of a single continuous layer of endothelial cells joined by tight junctions and surrounded by a continuous basement membrane, but in these vessels attenuated areas of cells appear to be penetrated by circular openings 40 to 70 nm in diameter. These are the fenestrae (or fenestrations), and in most cases the fenestrations are closed by a thin electron-dense diaphragm, which appears to be arranged as a series of broad spokes with central "hub"[14] (Figure 9.2).

Covering the luminal surface of endothelial cells is a layer of glycoprotein called the glycocalyx or endocapillary layer (ECL). First identified by Luft in 1966[68] using ruthenium red staining, its importance has only come to be widely appreciated in the past 15 years. Although both continuous and fenestrated endothelia have been found to contain the various inclusions common to most cells (e.g., mitochondria, rough and smooth endoplasmic reticulum) the dominating ultrastructural feature seen in transmission electron micrographs is the large number of small endoplasmic vesicles (Figure 9.3). The majority of vesicles are arranged in fused clusters that communicate with each other and with flask like pits on either the luminal or abluminal surfaces of the cells called the caveolae

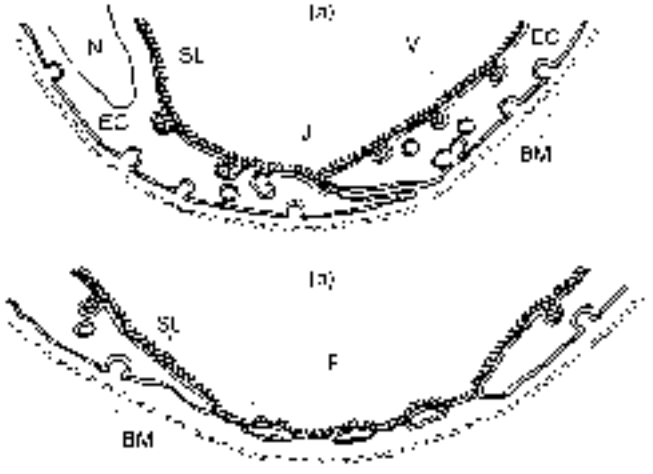

FIGURE 9.1 **Diagrams showing the ultrastuctural features of microvascular walls in transverse section: (a) Vessel with continuous endothelium; (b) Vessel with fenestrated endothelium**. The basement membrane (BM) forms a continuous layer around the outside of both vessel types and the luminal surfaces of both endothelia are covered with a negatively charged glycocalyx (SL) (EC: endothelial cell; J: junction; F: fenestration (fenestra); N: endothelial cell nucleus).

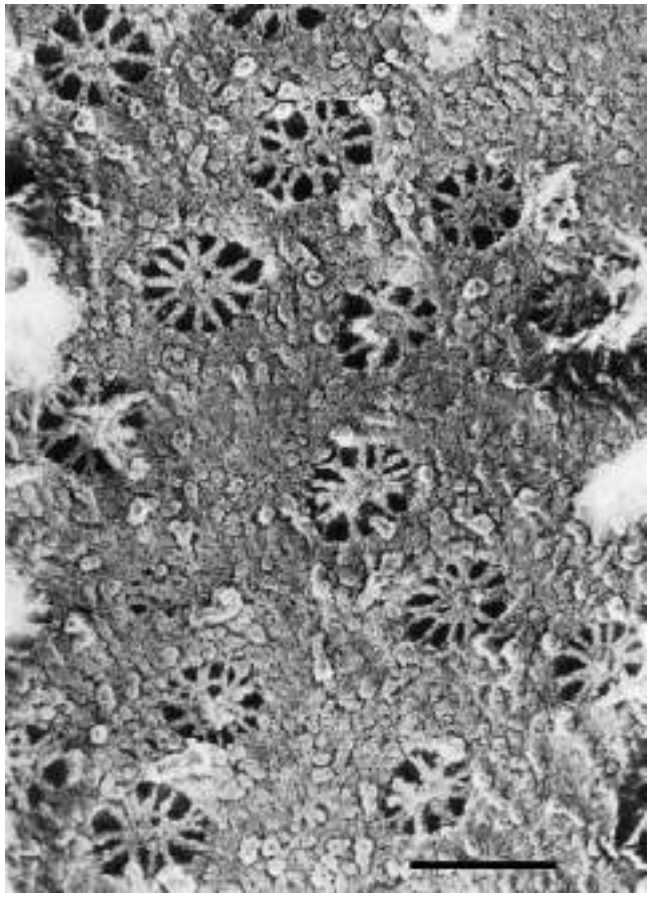

FIGURE 9.2 ***En face* view of fenestrated endothelium of peritubular capillary of the kidney in a rapid freeze deep etch preparation**. Scale bar = 0.1 μm. *(From ref. [14].)*

FIGURE 9.3 **Electron micrograph of microvascular endothelium of frog.** There are three mitochondria in the central part of the cell and large numbers of plasmalemmel vesicles. Scale bar = 0.2 μm. *(Electron micrograph by H.Moffitt.)*

intracellulares. Chains of fused vesicles forming channels that pass through endothelial cells[119] appear to be relatively rare occurrences in unstimulated endothelium, but are a feature of endothelium activated by certain mediators.[34,35]

The intercellular clefts of continuous endothelia, the fenestrae of fenestrated endothelia, and the small vesicles have all been implicated as pathways through the endothelia as a result of experiments using electron-dense tracers. Controversy surrounded the interpretation of many of these experiments, but progress has been made over the past 20 years as physiological evidence clarified their interpretation. For this reason, the ultrastructural basis of permeability is considered after we have defined the permeability coefficients by considering the principles of passive transport and have discussed their values in different endothelia to different types of molecules.

Passive Transport and Permeability Coefficients of Porous Membranes

The mechanisms of transport are convection and diffusion. Convection is equivalent to bulk flow of solutions and the solutes within them. Thus, if a solution flows from a reservoir A at a high pressure to a second reservoir, B, at a lower pressure, there is bulk flow of the solution and transport of the solutes by convection. If J_V ml sec^{-1} is the rate at which the solution flows from A to B, it is proportional to the difference in hydrostatic pressure, ΔP, between A and B as follows:

$$J_V = K\Delta P \tag{9.1}$$

where K is the conductance of the system between A and B.

If A and B are separated by a porous membrane, K is proportional to the area of the membrane, A_m, through which fluid can flow. Thus:

$$J_V = L_P A_m \Delta P$$

and

$$L_P = (J_V / A_m \Delta P) \tag{9.2}$$

where L_P is the hydraulic conductivity or hydraulic permeability of the membrane. L_P is one of several membrane permeability coefficients. It describes the ease with which fluid flows through a unit area of membrane when driven by a unit difference in pressure. It can be thought of as describing the frictional interactions between the membrane molecules and the molecules of the solution (principally water), and like the other permeability coefficients its value depends on the structure of the membrane. If small water-filled pores penetrate the membrane, L_P is proportional to the number of pores per unit area of membrane, to the fluid viscosity, and to a function of the dimensions of the pores. This function depends on the size and shape of the pores and the nature of flow through them.

Equation (9.2) describes the flow of a solution through a membrane only if the solute molecules can pass through the membrane as easily as the water molecules. If movement of solute is hindered to a greater extent than the water, filtration of the solution leads to the development of a solute concentration difference across the membrane as water enters compartment B faster than solute. The difference in solute concentration gives rise to a difference in osmotic pressure which opposes filtration of the solution across the membrane. The force driving solution through the membrane is no longer just ΔP, but ΔP minus the effective osmotic pressure between the solutions in A and B. The magnitude of this osmotic pressure difference is related not only to the concentration difference itself, but also to the degree to which the membrane hinders the movement of solute relative to water. This is described by a second membrane coefficient, σ_d, referred to as the osmotic reflection coefficient. If the channels in the membrane are permeable to water but not solute molecules, filtration of a solution of this solute through the membrane will separate the solute from the water, with pure water leaving the membrane and concentration of the solution upstream. Since all

the solute molecules are reflected at the membrane, σ_d has a value of 1.0. The osmotic pressure exerted by differences in its concentration across this particular membrane should be close to that calculated from Van't Hoff's law, i.e., $\Delta\Pi = RT\Delta C$, depending on the "ideality" of the solution. If, alternatively the solute molecules are able to pass through the membrane as easily as the water molecules, σ_d has a value of 0, as none of the solute molecules are reflected. If the solute passes the membrane more easily than water, σ_d has a negative value. If only a fraction of the solute molecules are "reflected" during ultrafiltration of the solution, σ_d has a value between zero and one.

Only those molecules that are reflected at the membrane during ultrafiltration can exert an osmotic pressure across it. Thus, the osmotic pressure difference, $\Delta\Pi$, is related to the concentration difference, ΔC, through the universal gas constant, R, and the absolute temperature, T:

$$\Delta\Pi = \sigma_d\, RT\Delta C$$

and

$$\sigma_d = \frac{\Delta\Pi}{RT\Delta C} \tag{9.3}$$

At microvascular walls, macromolecules such as plasma proteins have high values of σ_d and σ_f (0.8–0.999), whereas small ions (e.g., Na^+, K^+, Cl^-) and small hydrophilic molecules (e.g., glucose, lactic acid, amino acids, urea) have values of σ less than 0.2 in most vessels.

Net fluid flow through microvascular walls carries dissolved solutes by convection. The rate of solute transport by convection from A to B depends on J_V, and also upon the value of σ for the particular solute at the membrane. If σ has a value of zero, then J_S is equal to $J_V C$ (in moles per second), where C is the solute concentration in the solution (in moles per ml), i.e., the solution flowing out of the membrane into B has the same concentration as that entering the membrane from A. If, however, σ has a value between zero and one, then the solution emerging from the membrane into B will have a lower solute concentration than that entering the membrane at A. Convective transport of solute through the membrane is now described by the relation:

$$J_S = J_V(1 - \sigma_f)C \tag{9.4}$$

where C now refers to the concentration entering the membrane from A. Note that in Eq. (9.4) σ is written as σ_f, whereas in describing the effective osmotic pressure σ is written as σ_d. For "an ideal solute" $\sigma_f = \sigma_d$, but solutions of macromolecules deviate from "ideal" behavior and σ_d is often measurably greater than σ_f. Rearrangement of Eq. (9.3) provides a definition of σ_f:

$$\sigma_f = 1 - \frac{J_S}{J_V C} \tag{9.5}$$

If the only pathway for both water and solutes through the membrane is a population of equally sized channels, σ_d and σ_f are determined only by the ratio of the dimensions of the solute molecules to those of the channels, and are independent of the number of channels per unit area of membrane.

A second mechanism of transport through porous membranes is diffusion. This is most important for the transport of small molecules across microvascular walls. In contrast to the stately progression of molecules by convection, diffusion results from the random jostling of all molecules in a solution that represents their thermal energy. Diffusion is a mixing process, and where there are differences in concentration in a solution diffusion is responsible for the spontaneous net transport of solute from regions of high to regions of low concentration. On a macroscopic scale, Fick's first law of diffusion describes net transport of solute by diffusion:

$$J_S = DA\left(\frac{-dC}{dx}\right) \tag{9.6}$$

where D is the diffusion coefficient of the solute in the solution, A is the area through which diffusion occurs, and the derivative $(-dC/dx)$ is the concentration gradient of solute down which diffusion occurs. The negative sign of the derivative is to indicate that diffusion occurs from a region of high concentration (low value of x) to a region of lower concentration (higher value of x), i.e., the diffusion of a solute is directed down its concentration gradient.

Diffusion coefficients of solutes in aqueous solutions reflect the ability of solute molecules to slip past adjacent molecules of water. They are measured and defined in terms of net movements of solute under conditions in which there is no overall movement of the solution. Thus, diffusion in solution is a displacement process whereby the displacement of a solute molecule in one direction is accompanied by the displacement of an equal volume of water in the opposite direction. Because the rate at which displacement occurs is dependent on the thermal energy of the solution, the diffusion coefficient is directly proportional to temperature. It is also inversely proportional to the frictional interactions between the solute and water molecules.

When diffusion of a solute occurs through a thin porous membrane, the diffusional permeability of the membrane to the solute, P_d, is defined in terms

of the net solute flux, J_S, the solute concentration difference across the membrane, ΔC, and the membrane area, A_m, under conditions where there is no volume flow through the membrane. Thus:

$$P_d = \left(\frac{J_S}{A_m \Delta C}\right)_{J_V=0} \tag{9.7}$$

P_d has units of velocity (cm sec^{-1}), and like L_P and σ_f, it has meaning in terms of the interactions between the solute molecules, the molecules of the membrane, and the water within the membrane. Such interactions depend critically upon the ultrastructure of the pathways for solute and water through the membrane, particularly when the width of the pathways is comparable to the diameter of the diffusing molecules.

Diffusional permeability coefficients are defined under conditions where there is no net volume flow through the membrane. In measuring P_d of microvascular walls, it is often convenient to use radioactive isotopes or fluorescent tracers, because their fluxes can be detected when their concentration differences are in the micromolar range. Larger differences in concentration may set up significant differences in osmotic pressure, which may complicate the estimation of P_d by giving rise to net fluid flows in the opposite direction to those of the diffusing molecules.

Permeability to Lipophilic Solutes

Solutes that can dissolve to a significant extent in lipids have high cell membrane permeabilities, and very high microvascular permeabilities. It is assumed that these molecules diffuse directly through the entire microvascular wall. This group of solutes includes gas molecules, including O_2 and CO_2, as well as N_2, the inert gases, and molecules of general anesthetics, although recent evidence suggests CO_2 and NH_3 may cross membranes additionally through specialized channels.[15]

So rapidly can small lipophilic solutes cross microvascular walls that, under physiological conditions, their transport between the blood and the tissues is always limited by their rate of delivery or clearance by blood flow through the microcirculation, and it has been impossible to estimate their microvascular permeability coefficients with accuracy with values for some greater than 10^{-2} cm.sec^{-1}.

Microvascular permeability to lipophilic molecules is, however, sensitive to temperature. Renkin[101] showed that antipyrene, which is fat-soluble at body temperature, could exert substantial osmotic pressures across the walls of capillaries in cat hind limbs when the tissue was cooled to 15°C, but not when the tissue was at 37°C. A similar phenomenon has been demonstrated by Curry[25] in single mesenteric capillaries.

Permeability Coefficients to Small Hydrophilic Molecules

Microvascular permeability to macromolecules is usually considered separately from permeability to hydrophilic molecules smaller than serum albumin, as different mechanisms of transport appear to be involved. Evidence for this emerged in 1956 from studies on the passage of a range of dextran polymers between plasma and lymph.[45] Some of the original data are shown in Figure 9.4, where it is seen that the steady-state concentrations of the smaller dextrans in the lymph draining hind limb tissues of anesthetized dogs relative to the plasma levels fall rapidly as their molecular radii increase up to 4–5 nm; for the larger molecules the decline of lymph concentration with molecular size is so small as to appear barely significant in these data.

This two-component relation between P_d and molecular diameter is seen in nearly all microvascular beds, suggesting that small molecules use different mechanisms or pathways to cross microvascular walls from those used by macromolecules.[78,108,123]

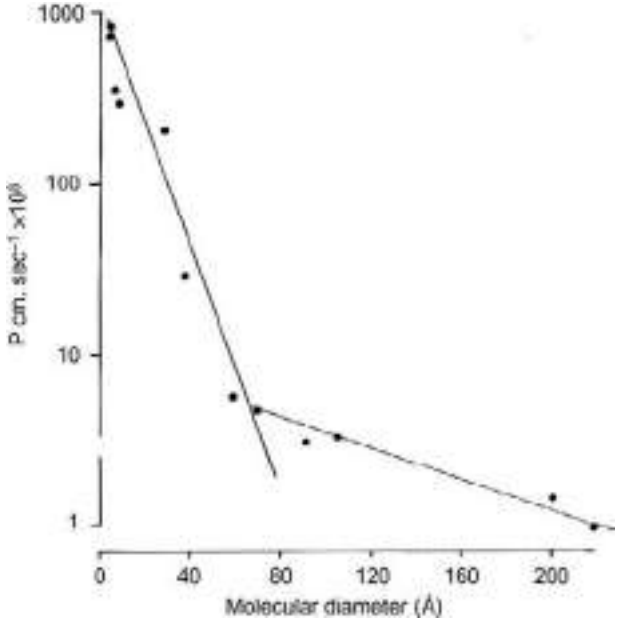

FIGURE 9.4 **Relations between permeability (P) of dog hind limb microvessels to hydrophilic solutes and the molecular diameter of the solutes.** The endothelium of these vessels is continuous and P has been calculated assuming they have a surface area for exchange of 7000 cm^2 $100g^{-1}$ of tissue. Note that P, which has been plotted on a logarithmic scale, declines sharply as molecular diameter increases up to 70 Å (7 nm), which is approximately the diameter of serum albumin. A less steep relation is seen for larger molecules. *(From ref. [78]. With permission)*

Permeability Coefficients to Small Hydrophilic Molecules

In Figure 9.5, the values of P_d measured in microvascular beds of skeletal muscle and single mesenteric microvessels to some small water soluble solutes have been plotted against solute molecular radius. In mesenteric capillaries, values for P_d to the smallest molecules and ions (e.g., Na^+, K^+, urea) are ten times greater than values of P_d for the same solutes in muscle capillaries. To make the comparison easier, both the P_d values and values for molecular radius are shown on logarithmic scales. The decline of P_d with molecular radius for both types of microvessel is much greater than the decline of diffusion coefficient (D) for the same molecules in open aqueous solution. The more rapid decline of P_d can be accounted for if molecules were diffusing through water-filled channels whose widths were comparable to their own diameters.[94] The smooth curves, which have been fitted to the data, converge as molecular radius increases. If the channels were cylindrical pores, the convergence implies that the radii of the pores is very similar in mesenteric and muscle capillaries, but there are ten times more pores penetrating per unit area of the walls of mesenteric capillaries than of muscle capillaries. The value of molecular radius at which the curves intersect provides an estimate of the pore radius – in this case between 3.5 and 4 nm.

This pattern of declining P_d to small hydrophilic solutes with increasing molecular diameter is seen in all microvessels where it has been sought, and curves based on the theory of diffusion through pores of radii between 3.5 nm–5 nm can be fitted to these data.

The values of P_d to a particular small hydrophilic solute (e.g., Na^+, K^+, sucrose, and inulin) in different microvascular beds correlate with the values of hydraulic permeability (L_P). This is shown in Figure 9.6, where each point represents the mean value of L_P plotted against the mean value of P_d to Na^+ or K^+ in the same microvessel or microvascular bed, different points representing values for vessels in different tissues. The data have been plotted on logarithmic scales so that values covering two orders of magnitude can be compared. The slope that has been drawn through the points has been given a value of unity, to indicate that direct proportionality is a reasonable description of the relationship. The correlation is strong circumstantial evidence for believing that the same pathways through the endothelium serve both for the rapid exchange of small hydrophilic solutes, and for most net fluid movements. Furthermore, because Na^+ ions are likely to follow an extracellular route, it seems likely that this shared pathway is extracellular. This line of reasoning is greatly strengthened by the demonstration of similar linear correlations between L_P and P_d values for other extracellular solutes, such as sucrose and inulin[81] in different microvascular beds.

Although the exchange of small hydrophilic molecules occurs through the same channels that account for most of L_P, some water may also cross microvascular walls of continuous endothelium by channels not available to solutes. This additional route has been

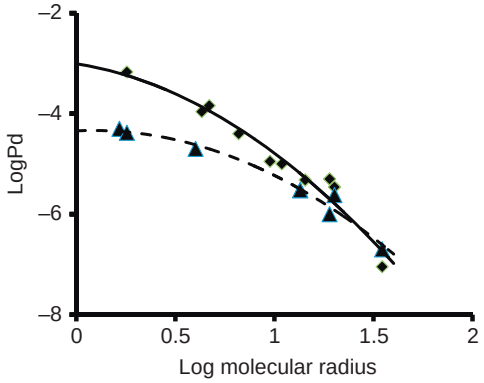

FIGURE 9.5 **Relations between the logarithms of P_d and molecular radius for small to intermediate sized hydrophilic solutes in capillaries of frog mesentery (filled circles) and cat skeletal muscle (filled triangles).** Data for frog obtained from measurements made in single perfused microvessels *in situ*. Data from cat based on measurements on perfused vascular bed. Both types of vessel have continuous endothelium. Note whereas P_d for the smallest solutes is 10 times greater in mesentery than in muscle (1 $\log_{10}$ unit = 10 ×), values for P_d converge as molecular size increases.

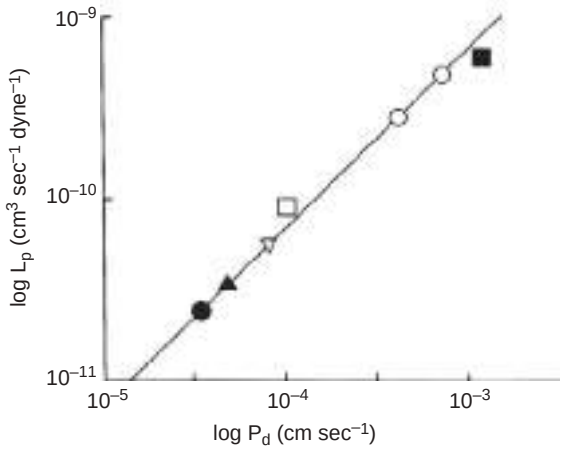

FIGURE 9.6 **Variations in L_P and P_d to small ions (Na^+ and K^+) in different microvascular beds.** The scales are logarithmic to include values covering two orders of magnitude, and the line has a slope of 1.0, indicating direct proportionality. Each point represents the value for L_P and P_d for one vascular bed; where several values of P_d are available the largest has been used to minimize errors resulting from flow-limited transport. ○, frog mesentery; ∇, frog muscle; ●, mammalian skeletal muscle; ϒ, mammalian heart muscle; ▲, dog lung; ■, cat salivary gland. *(From ref. [74]. With permission)*

identified by Pallone et al.[92] as channels formed by the membrane protein aquaporin-1, AQP-1.[6] The first real evidence for a "water only" pathway was indicated by Yudilevich and Alvarez from measurements of the rates of diffusion of triated water and Na^+ through dog heart capillaries. From measurements of σ to small hydrophilic solutes, Curry and colleagues[29] estimated that in single perfused capillaries between 5 and 10% of the pathways responsible for L_P were available only to water, and not to small solutes. More recently, Turner and Pallone[126] have shown that "water only" channels account for a similar proportion of the L_P of descending vasa recta of rat kidney. It is worth emphasizing that although fluid movements through AQP-1 channels of the descending vasa recta are of physiological importance, the channels contribute no more than 5 to 10% to the total L_P of these vessels. Although it has been suggested that AQP-1 channels might contribute to as much as 30% of the L_P of skeletal muscle capillaries,[137] the strong correlation between P_d and L_P shown in Figure 9.6 indicates that the contribution of AQP-1 channels to the L_P of most exchange vessels is small.

Although absolute values of L_P and P_d to small hydrophilic solutes vary greatly from one microvascular bed to another, the reflection coefficient to large molecules are remarkably similar in different vessels when the tissues are undamaged (or unstimulated). This is shown in Figure 9.7, where the mean values of σ to serum albumin have been plotted against the mean value of L_P for various tissues. Whereas L_P varies over three orders of magnitude, σ to albumin is usually in the range of 0.8 to 1.0. There is no trend in the relation between $\sigma_{albumin}$ and L_P. Vessels with high values of L_P have mean values of $\sigma_{albumin}$ that are as high, if not higher, than in vessels with low values of L_P. This means that the channels or pores that are largely responsible for the L_P of vessels in different tissues all restrict the passage of albumin to a similar extent. Thus, both the variations of P_d with molecular size and the variations in $\sigma_{albumin}$ and L_P in different capillary beds lead to the same conclusion: individual channels for exchange of water and small hydrophilic solutes are similar in different capillary types, but the density of these channels in vessel walls varies considerably.

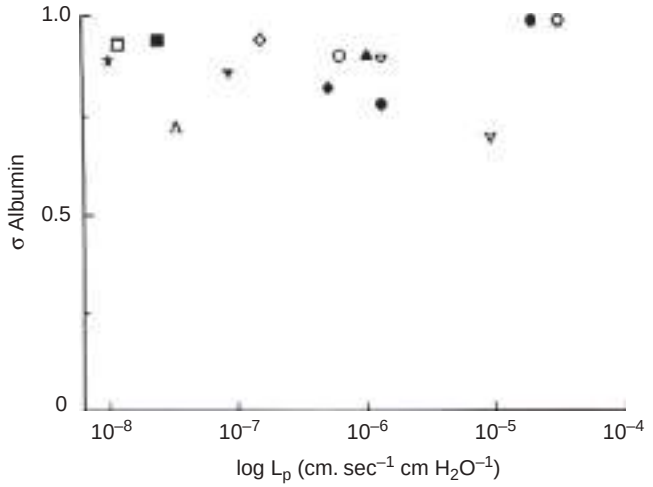

FIGURE 9.7 **Relation between the reflection coefficient to serum albumin (σ) and the L_P in different microvascular beds.** Each point represents a mean value for one vascular bed: * dog paw; □ dog skeletal muscle; ■ rat skeletal muscle; △ dog lung; ▼ rabbit heart muscle; rat mesentery; □ frog mesentery; ○ cat vary gland; ▲ rat descending vasa recta; ◒ cat small intestine; ● rabbit synovium; ▽ rat ascending vasa recta; ◍ dog renal glomerulus; ○ rat renal glomerulus. *(With permission from ref. [74].)*

Permeability Coefficients to Macromolecules

Apart from the sinusoids of the liver and spleen, microvascular walls have high reflection coefficients and low permeabilities to macromolecules. These permeability properties are essential if the circulating blood is to be retained within the vascular system. Although their permeabilities are low, macromolecules do cross the walls of all microvessels at slow but finite rates. Table 9.1 compares estimates of σ and P_d made from the transport of macromolecules between blood and lymph in the dog paw and the cat intestine.[106] Although it is possible that the values given in this table are actually overestimates of the permeability coefficient of macromolecules, there are three important points to note here. First, the values of P_d for serum albumin are more than 3000 times less than the permeabilities of the same vessels to Na^+ and urea. The diffusion coefficient of albumin in aqueous solutions is only 20 times less than those of Na^+ and urea. This means that the diffusion of albumin molecules through microvascular walls is hindered 150 times more than the diffusion of Na^+ ions or urea molecules. Second, compared with the changes seen for small molecules, there is a relatively small decrease in P_d and rise in σ with increases in molecular size. The third point is the similarity of the values of P_d to the same macromolecule at the predominantly continuous endothelium of the dog paw capillaries, and also at the predominantly fenestrated endothelium of vessels in the small intestine. The values of L_P and P_d to small hydrophilic solutes in these two microvascular beds differ by nearly two orders of magnitude. This would seem to be further evidence supporting the belief that the transport pathways through microvascular walls are different for macromolecules from those responsible for water small hydrophilic solutes.

TABLE 9.1 Reflection Coefficients (σ) and Permeability Coefficients (P_d) to Macromolecules of Selected Molecular Radii (a_{ES}, nm) in Microvascular Beds of Dog Paw and Cat Ileum

		Dog Paw		Cat Ileum	
Molecule	a_{ES} (nm)	σ	$P_d \times 10^8$ (cm sec^{-1})	σ	$P_d \times 10^8$ (cm sec^{-1})
Serum albumin	3.55	0.89	1.0–4.7	0.9	3.0
Transferrin	4.3	0.89	6.3	–	–
Haptoglobin	4.6	0.91	3.1	–	1.4
Immunoglobulin	5.6	0.91	3.3	0.95	–
Fibrinogen	10.0	0.94	1.6	0.98	0.7

Renkin, E. M. (1988). Transport pathways and processes. In "Endothelial Cell Biology," 51–68, Simionescu, N., and Simionescu, M., (eds.) Plenum Publishing, New York.[104]

It is possible that some of the values for P_d in Table 9.1 are overestimates and those for σ are underestimates because, in calculating vascular permeability coefficients from plasma to lymph transport, it is assumed that a steady-state has been established between the newly formed filtrate surrounding the microvessels and the ISF entering the lymph. Simple calculations suggest that in some tissues the time taken to reach a steady-state after a change in microvascular filtration rate can be many hours.[78] This can be understood by considering the events that follow an increase in microvascular filtration. A rise in filtration rate is accompanied by a rise in lymph flow and a fall in the concentrations of macromolecules in the newly formed interstitial fluid. It may, however, take several hours before the lymph has the same composition as this new filtrate, and if the lymph is sampled prematurely its concentration of macromolecules will be greater than that in the ultrafiltrate. The lymph flow, however, may reach its new steady-state level before the lymph concentration of macromolecules, and if flux of macromolecules is estimated from values for the product of lymph flow and lymph concentration of macromolecules at this stage, its value will exceed the real rate of transport into the tissue. Not only is macromolecular transport overestimated, but the mean concentration differences across the microvascular walls are also underestimated.[107]

Since 1990, much work has been conducted on the passage of macromolecules through monolayers of culture endothelial cells. In many of these studies, changes in permeability to macromolecules have been investigated, and relative rather than absolute values of permeability coefficients have been reported. In most but not all studies, absolute values for P_d of monolayers of cultured endothelial cells to albumin lie in the range of 10^{-6} cm sec^{-1}, about 100 times greater than the values of P_d to albumin at microvascular walls *in situ*.[9] In a few laboratories, values in the range of 10^{-7} to 10^{-6} cm sec^{-1} have been reported, but even these values are at the very high end of the range found in microvessel walls *in vivo*. The reasons for this difference are not understood at present. Although studies on cultured endothelial cells have provided essential information of intracellular processes, conclusions from them relating to macromolecular permeability should be viewed with caution.

Like smaller hydrophilic molecules, the microvascular permeability coefficients to macromolecules decrease as molecular size increases, although the decline is considerably less steep. Molecular charge is also more important as molecular size increases. Evidence for the charge-selective nature of ultrafiltration in the renal glomerular capillaries is well-known, but in other microvessels, charge selectivity has been investigated in less detail. Areekul[8] first provided evidence for charge selectivity in systemic capillaries. Working on the isolated perfused rabbit ear, he showed that σ_d to sulfated dextran (which is negatively charged) was always greater than σ_d to neutral dextran of the same molecular weight. Work on single perfused capillaries[2] and on microvascular beds in rat hind limbs also supported the view of microvascular walls as a negatively-charged barrier.

This picture was temporarily confused by studies on the transport of charged macromolecules between plasma and lymph. Negatively-charged macromolecules appeared more rapidly in the lymph and at higher concentration than positively-charged molecules, suggesting a positively-charged barrier. It was then appreciated that the large number of fixed anionic sites in the interstitium (see [49]) would reduce the volume of distribution of the negatively-charged molecules relative to cationic or neutral molecules of the same molecular size. Parker and co-workers[95] showed that the greater volume of distribution of neutral and cationic molecules increased the time for these molecules to reach a steady-state concentration in the ISF. This delay accounted for the apparently more rapid transport of the anionic molecules, a conclusion reinforced by the recent study of

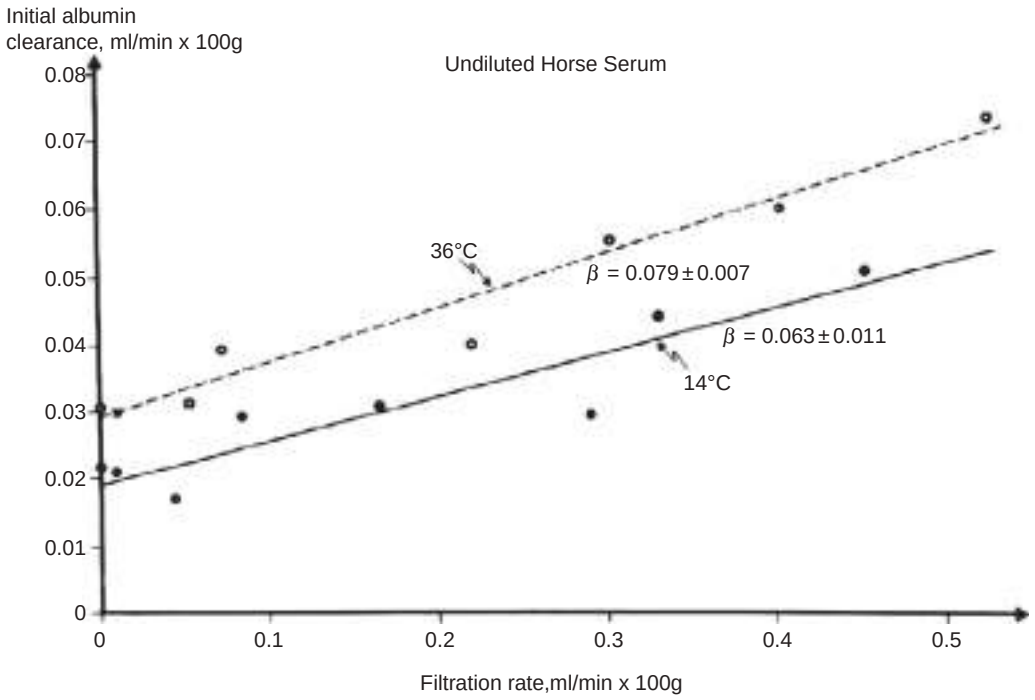

FIGURE 9.8 **The clearance of serum albumin from perfusate into tissues of rat skeletal muscle at different filtration rates in experiments conducted at 36°C and 13–15°C.** β is the slope of the relation. *(From ref. [107]. With permission.)*

Gyenge and her co-workers[49] on albumin distribution in skin and muscle tissue. With this point clarified, the evidence once again supports the concept of a negatively-charged barrier at microvascular walls hindering the transport of negatively-charged macromolecules greater than 3.0 nm in diameter.

The decline of P_d (and an increase in σ) with an increase in molecular size led to the suggestion that macromolecules cross the endothelium through a system of large pores with radii in the range of 20–40 nm. These pores would be few in number compared with the small pores that act as a pathway for small hydrophilic solutes.[45] Calculations suggest that individual capillaries in skeletal muscle may have an average of only three large pores[81] and with the usual variation between microvessels this indicates that many vessels will have no large pores at all. In a comprehensive review, Taylor and Granger[123] showed that microvascular permeability to macromolecules in different tissues could be described by transport through a population of small pores (radii 3.5–5 nm) and a set of large pores (15–30 nm radii). If large pores do exist, then transport of macromolecules through them will be largely convective, sensitive to microvascular pressure, and increase with fluid filtration rate. Experiments by Rippe and his colleagues[109] showed that this is the case for the transport of labelled albumin from capillaries in skeletal muscle of an isolated perfused rat limb preparation. Defining the clearance of tracer from the blood into the tissue as the rate of its accumulation divided by the perfusate concentration, they not only showed that clearance of albumin increased linearly with fluid filtration into the tissues, but also that cooling the tissue from 36° to 14°C reduced albumin clearance by only 40%. This was similar to the reduction of the apparent hydraulic permeability of the microvessels. The results of this classic experiment are shown in Figure 9.8. A 40% reduction in L_P would be expected because the filtrate flow through the water-filled channels through the vessel walls is inversely proportional to fluid viscosity, and the viscosity of water at 36°C is approximately 60% of that at 14°C. Because albumin transported is proportional to filtration rate and is reduced in parallel to J_V as the viscosity of water is increased, Rippe and his colleagues[109] concluded that albumin is transport through water-filled channels in the microvascular walls. Figure 9.8 shows that the clearance of albumin from plasma to tissue is significant when fluid filtration is zero. Rippe and his colleagues[109] accounted for this by pointing out that, because the hydrostatic pressure difference across microvascular walls is greater than zero under these conditions, there would still be fluid filtration through the large pores, and consequent transport of albumin because σ_d to plasma proteins here is low. This filtration through the large pores

would not be detected in whole tissue, because it would be balanced by an equal and opposite uptake of fluid through the "small pores" where σ_d to plasma proteins is high. As we shall see, the steady uptake of fluid from tissues into capillary blood may peter out and become a low level of filtration in tissues such as muscle.

Ultrastructural Basis of Permeability

Small Hydrophilic Solutes and Water

If the molecular sieving properties of microvascular endothelia are determined by pores or channels of similar dimensions, one might expect to find common structural features in all endothelia that are more frequent in the more permeable vessels. Unfortunately, electron micrographs of endothelia do not reveal an obvious structure that might fill this role.

The endothelia of the vessels with the four highest values of L_P in Figure 9.9 are fenestrated, while those with the seven lowest L_P values are continuous. In some others (e.g., small intestine) values of L_P and σ represent those of a microvascular bed where there are both fenestrated and non-fenestrated vessels. In a quantitative analysis of permeability of fenestrated vessels, Levick and Smaje[66] found that variations in L_P and P_d to small hydrophilic solutes in fenestrated vessels can be correlated with the number of fenestrations per unit area of endothelium. From their analysis they estimated the mean hydraulic conductance per unit increment of area for fenestrations in a variety of microvascular beds as $0.38\,\mu m.sec^{-1}$ $mmHg^{-1}$ (2.8×10^{-5} $cm.sec^{-1}$ cmH_2O^{-1}). This means that the addition of a single fenestration (diameter = 60 nm) to one μm^2 of the endothelium of a skeletal muscle microvessel increases the L_P of that area approximately 2.6 times. Although fenestrations appear as large pores passing through the endothelium, the fenestrations themselves are much too large to account for molecular sieving and their high reflection coefficients to macromolecules. Molecular sieving is now thought to be achieved by the endothelial glycocalyx, with significant contributions to the hydraulic resistance from the fenestral diaphragms and the basement membrane.

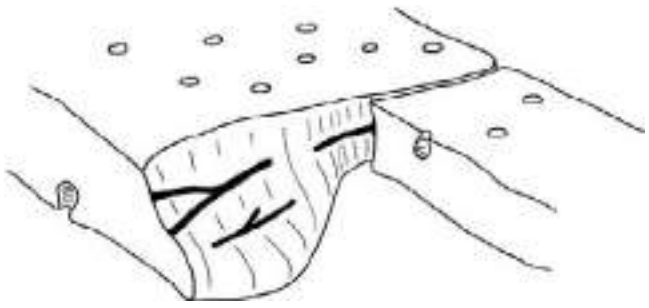

FIGURE 9.9 **Diagram of the ultra-structure of an intercellular cleft based on reconstructions from serial ultrathin sections (A&M).** Part of the cell in the foreground has been removed to expose the interior of the cleft showing the junctional strands (heavy lines), which correspond to points of close apposition between the cells (tight junctions) in single sections. Lanthanum ions cannot diffuse through the junctional strands, but pass through breaks in the strands. Because there is usually only one continuous strand in the junctions of mesenteric microvessels, each break provides a direct pathway through the cleft.

The luminal glycocalyx was proposed by Curry and Michel[30] as the structure responsible for molecular sieving in microvessels with continuous endothelia. Its wide acceptance came after direct observations of the exclusion of macromolecules from the luminal surface of living microvessels had been demonstrated 16 years later by Vink and Duling.[129] Whereas variations in L_P of fenestrated vessels results from variations in the number of fenestrae per unit area of vessel wall, the variations in L_P and P_d to small hydrophilic molecules in vessels with continuous endothelia appears to correlate with the numbers of breaks and complexity of the junctional strands of the intercellular clefts. Although evidence for this concept was available in 1978 from the work of Wissig and Williams,[136] progress was hindered by the beliefs that: (1) the molecular sieve consisted of pores or narrow openings in the tight junction strands; and (2) that the breaks forming a pathway through the junctional strands were too few in number to account for permeability to water and small hydrophilic solutes. Thus, Bundgaard[19] reconstructed the intercellular clefts of rat heart capillaries from ultrathin serial sections and confirmed the presence of a tortuous pathway through the cleft, but rejected this as the route taken by water and small hydrophilic solutes on the grounds that the dimensions of the openings through the junctional strands were too great to filter plasma proteins, and the number of breaks per unit length of junction were too few to account for water and small solute permeabilities.

The question was clarified by Adamson and Michel.[4] Working on frog mesenteric capillaries *in situ*, they perfused single capillaries briefly with solutions containing lanthanum ions, before the tissues were fixed for electron microscopy. Micrographs of serial sections of the walls of the perfused vessels demonstrated that lanthanum ions were only able to pass through the intercellular clefts at breaks in the junctional strands. In a second series of experiments, they measured L_P in individual capillaries *in situ* before fixing the tissue for electron microscopy (EM). The three-dimensional structures of the intercellular clefts of that capillary were then reconstructed from long runs of ultrathin sections of the vessel. Although the breaks only represented 3–10% of the length of the strands, Adamson and Michel[4] used a mathematical

model of Parker and colleagues to show that this was more than sufficient to account for permeabilities that were three times greater than those they had measured. The mathematical model provided a rigorous argument for believing that a small break in the junctional strands has a much greater effect upon L_P than its size might suggest. The pressure gradient driving fluid flow through the intercellular cleft is steepest across the tiny distance through the break in the strand, and is much greater than that calculated for the entire cleft. More detailed mathematical models have been developed by Weinbaum and his colleagues[38,55,133] and more recently, Adamson et al.[3] have shown that the fine structure of the tight junction in intercellular clefts of rat mesenteric venules is very similar to that seen in frog vessels.

The L_P of mesenteric vessels is approximately three times greater than the L_P of heart muscle capillaries, which is approximately three times greater than the L_P of capillaries in skeletal muscle. These differences in permeability appear to correlate with the complexity of the pathway through the tight junction in these different types of capillary. This is illustrated in Figure 9.10 for pathways through the intercellular clefts of mesenteric, cardiac, and skeletal muscle capillaries. It seems most probable that the wide variations in permeability to fluid and small hydrophilic solutes that is found in microvessels with continuous endothelium are determined by the complexity of the tight junctional architecture within the intercellular clefts.

As mentioned earlier, the glycocalyx on the luminal surface of the endothelium that covers the entrances to intercellular clefts and fenestrae is now considered to be the barrier to macromolecules. When this was first proposed[30] there was indirect evidence to support it, and more evidence of this kind accumulated during the 1980s.[81] In 1990, Adamson[1] showed that the L_P of single vessels was doubled by brief perfusions of pronase that disrupt the glycocalyx without having any other detectable effects on endothelial ultrastructure

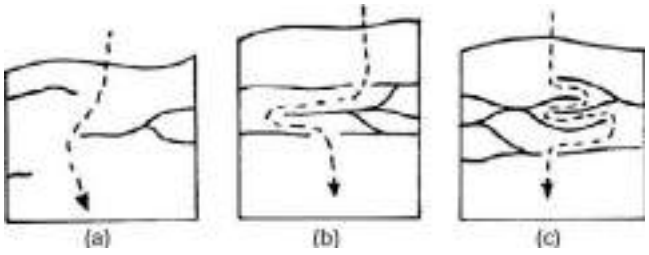

FIGURE 9.10 **Variations in the complexity of arrangement of junctional strands in intercellular clefts of microvessels with different hydraulic permeabilities.** The dashed lines with arrows indicate potential pathways through the breaks in the strands. (a) Mesenteric capillary (based on [4] and [5]); (b) Cardiac muscle capillary (based on [19]); (c) Skeletal muscle capillary (based on [136]).

when electron micrographs of the same vessels were inspected. General recognition of the concept of the glycocalyx barrier resulted from some remarkable *in vivo* observations of Vink, Duling, and their colleagues.[52,128,129] Using confocal microscopy to visualize capillaries in rat cremaster muscle, these authors observed that FITC dextrans were excluded from the endothelial cell membranes by a distance of 0.5 μm. The exclusion layer was diminished or even abolished by prolonged exposure to UV light and after perfusion with hyaluronidase. Observations of this kind continue to bolster the view of the glycocalyx as a barrier.

Direct evidence for how its structure acts as a molecular filter comes from the analysis of electron micrographs of glycocalyx.[9,120] Examining very differently prepared specimens, including some made by the rapid freeze-deep etch technique in the absence of chemical fixatives, Squire et al.[120] have concluded that the glycocalyx may be regarded as a regular cubic lattice with side length of 20 nm and a cubic internal space of side length 8 nm (see Figure 9.11). Since serum albumin molecules have diameter of 7−7.2 nm, the dimensions of this internal space are consistent with the glycocalyx acting as the molecular filter in microvascular walls. The initial observations were all made on the glycocalyx of continuous endothelia of the frog, but more recent work has revealed very similar structural features to the glycocalyx covering both continuous and fenestrated endothelia, including that over fenestrae in mammalian microvessels in a wide range of tissues.[9]

In summary, the main permeability pathways through microvascular walls to water and small hydrophilic solutes are located in the fenestrations of fenestrated endothelium, and through the intercellular clefts in vessels with continuous endothelium. In both types of endothelia, the molecular filter that forms the barrier to macromolecules at most microvascular walls is in the luminal glycocalyx of the endothelial cells.

Macromolecules

Just how macromolecules cross the walls of small blood vessels remains a controversial subject. Two apparently conflicting hypotheses emerged from very different lines of evidence more than 40 years ago, and the question of which is more correct has not been finally resolved. As summarized earlier, a purely functional approach has led to the proposal that microvascular walls were penetrated by a small number of "large pores" (30−80 nm in diameter) through which macromolecules pass from plasma to interstitial fluid (ISF).[45] The large pores are estimated to occur so infrequently that their contribution to the P_d of small hydrophilic solutes would be negligible, although they might make a 5 to 10% contribution to L_P. The large pores, however, would be entirely responsible for the permeability of

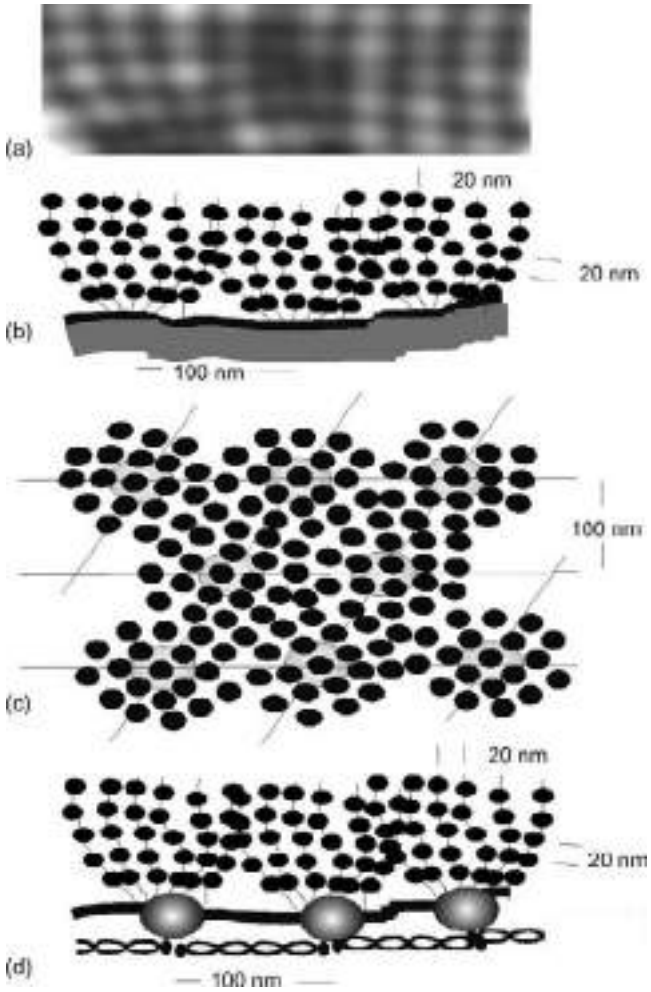

FIGURE 9.11 Models of glycocalyx based on image analysis of electron micrographs. (a) An autocorrelation function of the glycocalyx indicating the underlying regularity of structure with a periodicity of approximately 20 nm both parallel and perpendicular to the cell membrane. (b) A molecular interpretation of (a). It consists of clusters of fibrous strands projecting perpendicular to the luminal cell membrane with periodicity along the strand provided by equally spaced globular proteins. It is suggested that adjacent clusters are separated by approximately 100 nm (consistent with a longer range periodicity) where they linked to the cortical cytoskeleton of the cell. Figures 9.11(c) and (d) show luminal surface and saggital views of the proposed structure. *(From ref. [118].)*

macromolecules, and transport through them would be largely by convection.

The alternative arises from electron microscopy, and proposes that macromolecules cross endothelial cells by transcytosis via the small vesicles.[17,18] After their injection into the blood, electron-dense macromolecules have been found labeling caveolae and small vesicles of the endothelia. Initially it was suggested that the vesicles acted as ferries, equilibrating with plasma when they opened as caveolae at the luminal surface, then budding off as small vesicles to travel across the cell where they fused with the abluminal surface of the endothelium and equilibrated with the ISF. In the absence of evidence for active transport of macromolecules through microvascular walls, it was suggested that equal fluxes of vesicles occurred in opposite directions across the cells, and the vesicles moved as a result of Brownian motion.[22] The size dependence of macromolecular permeability arises in vesicular transport from volume exclusion of the macromolecules by the walls of the vesicles.[103] The exclusion effect is considerably enhanced if the caveolae and small vesicles are lined with glycocalyx.[67,118]

A detailed examination of the labeling of vesicles with ferritin molecules led to a more complicated model, in which neighboring vesicles periodically fused transiently for long enough for their contents to equilibrate.[23] It was also shown that cooling the tissue inhibited the labeling of vesicles with ferritin.[24] This fusion–fission hypothesis was consistent with the detailed structural analysis showing the vesicles to be arranged in fused clusters communicating with caveolae at either the luminal or the abluminal cell membranes.[20,36] One extreme form of the fusion–fission hypothesis is for the joined vesicles to form channels through the endothelium. Evidence for such vesicular channels has been reported,[119] and these could act as large pores.

Direct evidence for transport by vesicles through normal endothelium has been reported by Wagner and Chen,[130] who demonstrated caveolae emptying terbium label at the abluminal endothelial surface at points distant from intercellular clefts. The demonstration of membrane binding sites for transferrin,[56] insulin,[59] ceruloplasmin,[122] and albumin[42] on endothelia suggested that the vesicle pathway might be involved in receptor mediated transport. A series of papers by Schnitzer and colleagues[113–117] seemed to bolster the idea of vesicular shuttling or fusion–fission as an important mechanism of macromolecular transport through endothelium. The cholesterol scavenger, filipin, removes caveolae in cultured endothelial cells and in rat lung microvessels, and was also reported to reduce the clearance of albumin from perfusate to tissue in the isolated perfused rat lung.[113] It was also reported that N-ethylmaleimide (NEM), which inhibits fusion processes of vesicles and vacuoles in yeast, in synaptic vesicles, and in transport vesicles operating between the Golgi stacks and the endoplasmic reticulum, inhibited transendothelial transport of macromolecules in microvessels of mouse heart and rat lung.[114] Schnitzer and colleagues[117] have reported that endothelial caveolae from rat lung capillaries can bud away from their anchorage in the presence of GTP and extracts of cytosol. Critical studies by Rippe and his colleagues, however, have cast serious doubt on the relevance of these findings to

macromolecular permeability.[21,111] They found that both filipin and NEM increased albumin transport in the isolated perfused rat lung. NEM was found to reduce σ to albumin. Reducing the tissue temperature from 35° to 22°C, however, lowered both albumin clearance and L_PS in rough proportion to increased water viscosity. NEM also increased both albumin clearance and L_PS in the microcirculation of rat muscle,[21] and increased precapillary vascular resistance in both rat lung and rat muscle. The authors suggested that increased resistance would reduce microvascular perfusion, and this could account for the earlier studies where NEM appeared to reduce albumin clearance. Rippe and colleagues have recently reviewed the controversy,[110] and provided further less direct evidence against endothelial transcytosis of macromolecules from studies of peritoneal dialysis.[112]

Rippe's arguments for convective transport of macromolecules via large pores are convincing. At present it seems that whereas there is strong evidence favoring convective transport of macromolecules (i.e., the large pore hypothesis), evidence that transcytosis makes a significant contribution to transendothelial transport of macromolecules is lacking. It is possible that the caveolae/small vesicle system is important for the transport of specific molecules. The blood−tissue transport of insulin, for example, appears to be anomalous for a protein of its size,[53] and is more consistent with receptor-mediated transport.[59] As mentioned already, the large pores carrying most macromolecules could be trans-endothelial channels formed by the fusion of vesicles. At normal tissue temperatures they might be continually forming and re-forming, accounting for the progressive labeling of the vesicle system with tracer macromolecules. On cooling the tissues, the open channels would remain open, but no new channels would form, consistent with both the effects of cooling on albumin transport, and the reduced vesicle labeling reported by electron microscopists.

The question of whether macromolecules are transported mainly by convection through large pores in the walls of microvessels in normal healthy tissue has implications for our understanding of fluid exchange between the blood and the tissues.

THE EXCHANGE OF FLUID AND SOLUTES BY CONVECTION AND DIFFUSION THROUGH MICROVASCULAR WALLS

Coupling of Fluid and Solute Transport during Ultrafiltration

In most tissues, ISF is formed by the ultrafiltration of plasma, a process that is driven by the greater hydrostatic pressure inside the microvessels than in the surrounding tissues. As fluid begins to be filtered through the vessel walls, its composition is determined by the rates at which the different plasma solutes can move with the filtrate by convection and diffusion. If one considers the transport of a solute past a point at a distance x cm along a pathway within the microvascular wall, and of cross-sectional area, A, the net flux of solute, J_S, can be described by adding together the contributions of convection and diffusion. Thus from Eqs. (9.4)−(9.6):

Total transport = Convective transport + Diffusive transport

$$J_S = J_V(1-\sigma_f)C + D'A(-dC/dx) \tag{9.8}$$

where C is the solute concentration of the solute at x, D' is solute diffusion coefficient, and $(-)$ is the direction of the concentration gradient (from plasma to ISF). The first term on the right hand side of Eq. (9.8) is the convective component of transport, and the second term is the diffusive component. The concentration gradient that is responsible for net transport by diffusion is equal to the solute concentration difference between the plasma and the ISF, divided by the length of the pathway through the wall only when fluid filtration is zero and there is no convection of solute. When net fluid movements are present they distort the concentration gradients in the channels within the vessel walls. Once a steady-state is established so the solute flux, J_S, is the same at all points along the diffusion pathway (i.e., the rate of solute entry equals the rate of its exit from the channels), then the extent of the distortion can be inferred by integrating Eq. (9.8). This leads to a form of the Patlak expression[96] which here relates J_S through an area of vessel wall, A_m, to the plasma concentration of solute, C_p, and the concentration emerging from the vessel walls into the peri-capillary ISF, C_i :

$$\frac{J_S}{A_m} = \frac{J_V}{A_m}(1-\sigma_f)\frac{(C_p - C_i e^{-Pe})}{(1-e^{-Pe})} \tag{9.9}$$

where

$$Pe = \frac{J_V(1-\sigma_f)}{P_d A_m}$$

Pe is a dimensionless number, called the Péclet number, which expresses the ratio of solute velocities by convection and diffusion, P_d being the diffusional permeability coefficient. Curry[26] has recast Eq. (9.9) in a form that allows the convective and diffusive components of transport to be recognized:

$$\frac{J_S}{A_m} = \frac{J_V}{A_m}(1-\sigma_f)C_p + P_d(C_p - C_i)\left(\frac{Pe}{e^{Pe}-1}\right) \tag{9.10}$$

Equation (9.10) is analogous to Eq. (9.8), with the first term on the right-hand-side describing convective transport, and the second term describing diffusion. The expression $Pe/(e^{Pe} - 1)$ describes the effects of solute convection upon the mean concentration gradient within the diffusion pathway by convective flow in the same direction as net diffusion.

Earlier it was noted that ultrafiltration through microvascular walls is driven by the hydrostatic pressure difference, ΔP, between the plasma inside the vessels and the surrounding ISF. If, initially, all the solutes were at the same concentration in plasma and ISF, the filtration rate per unit area of vessel wall (J_V) is $L_P A_m \Delta P$, as in Eq. (9.2). The process of ultrafiltration, however, soon leads to differences in solute concentration between the plasma and the newly formed ISF, as a consequence of the differences in σ and the Péclet numbers of the different solutes. These concentration differences give rise to osmotic pressure differences that oppose ΔP. In this way, the rate of fluid filtration per unit area of vessel wall becomes the product of L_P and the difference between ΔP and the sum of all the osmotic pressures opposing it. Thus:

$$\frac{J_V}{A} = L_P\left(\Delta P - \sum_n \sigma_{d_n}\Delta\Pi_n\right) \tag{9.11}$$

where $\sigma_{dn}\Delta\Pi_n$ is the effective osmotic pressure set up across the vessel wall by the n^{th} solute.

Equation (9.9) can be used to calculate the contribution of different plasma solutes to the osmotic term in Eq. (9.11). When the filtration rate is steady, C_i becomes equal to the ratio of the rate of solute transport to the filtration rate i.e., $C_i = J_S/J_V$. Combining this relation with Eq. (9.9) leads to the following expressions for C_i and $\Delta C = C_p - C_i$:

$$C_i = \frac{J_S}{J_V} = C_P\frac{(1-\sigma_f)}{(1-\sigma_f e^{-Pe})} \tag{9.12}$$

and:

$$\Delta C = C_p - C_i = C_p\sigma_f\frac{(1-e^{-Pe})}{(1-\sigma_f e^{-Pe})} \tag{9.13}$$

Differences in concentration (and hence differences in osmotic pressure) can only be sustained for those solutes that have low permeabilities. If permeability is high, concentration gradients are dissipated by diffusion, and for differences of concentration and osmotic pressure to be maintained both reflection coefficient and Péclet number of the solute must be high. The implication of this is that when Pe is zero (e.g., when $J_V = 0$) the concentration differences will dissipate, even for those solutes that have very low permeabilities.[75]

The message of Eq. (9.13) can be appreciated by evaluating Pe for urea and serum albumin during slow filtration (at a rate of 2×10^{-7}cm^{-2}sec^{-1}) through the walls of skeletal muscle capillaries.[75] For urea, P_d is 2.7×10^{-5} cm sec^{-1} and σ is 0.1, so that Pe is 0.0074; for serum albumin with P_d at 10^{-8} cm sec^{-1} and σ at 0.95, Pe is 1. Thus, C_i would be more than 99.9% C_p for urea, and ΔC is therefore 0.1% C_p, so that urea makes a negligible contribution to $\sigma_{ds}\Delta\Pi$ (about 0.1 cmH_2O). For serum albumin, however, C_i is only 7.6% of C_p and ΔC is 92.4% C_p accounting for the major contribution of albumin to $\sigma_{ds}\Delta\Pi$ (about 19 cmH_2O). Similar calculations can be made for microvessels in most other tissues (the exception being those of the brain), and it is therefore the osmotic pressure of the macromolecules that constitute the osmotic pressure difference that acts as a break on fluid filtration and holds the plasma in the vascular system. The osmotic pressure of the macromolecules of plasma and other body fluids is often referred to as the *oncotic pressure*.

Equations (9.12) and (9.13) indicate the close coupling between microvascular fluid exchange and microvascular solute permeability. The concentration of plasma proteins in the ISF (and hence the ISF oncotic pressure) is almost an inverse function of ultrafiltration rate. This relation is of considerable significance in interpreting microvascular fluid exchange, and its consequences are discussed further below.

Fluid Movements through Microvascular Walls

General Approximation: Starling Forces

The principle that fluid is held in the vascular system by a balance of hydrostatic and oncotic pressures across capillary walls was recognized over a century ago by Ernest Starling.[121] Since then it has been demonstrated to apply in a large number of vascular beds in different animals, including humans, using a variety of techniques. It remains the basis for understanding fluid exchange between the blood and the tissues.[65,77,79,81,83]

For most purposes, Eq. (9.11) can be written in a simplified form, in which the effective osmotic pressure term becomes the effective oncotic pressure difference across microvascular walls, $\sigma_m(\Pi_c - \Pi_i)$, i.e.:

$$\frac{J_V}{A} = L_P(\Delta P - \sigma_m\Delta\Pi) = L_P[(P_c - P_i) - \sigma_m(\Pi_c - \Pi_i)] \tag{9.14}$$

The reflection coefficient, σ_m, refers to the mean (or effective) reflection coefficient of microvascular walls to macromolecules and the pressures, P_c, P_i, Π_c, and Π_i are often referred to as the *Starling pressures*.

Equation (9.14) is a clear statement of Starling's principle of fluid movement between the plasma and the ISF. Under suitable experimental conditions it is possible to compare fluid movements through microvascular walls when ΔP is varied as $\Delta\Pi$ is held constant. This has been achieved most unambiguously in single perfused microvessels (e.g., Figure 9.12). Essentially similar results have been obtained by less direct methods in perfused vascular beds[93]; see [79] for review).

Experiments such as that shown in Figure 9.12 reveal several general features of the permeability of microvascular walls.[74] The linearity of the relation between fluid flux and pressure suggests that the pathways conducting fluid through the vessel walls are not stretched or deformed over this range of pressures. If the channels were stretched and widened, their conductivity, L_P, would be raised and this would be seen as an increase in the slope of the relation between J_V/A and ΔP (which is L_P) with increasing pressure. Furthermore, the value of L_P is the same during fluid absorption (negative values of J_V/A) as it is during filtration, indicating that there is no significant rectification of flow within the conducting channels. (With less careful experimental design, however, rectification of flow may appear to occur.) A third feature of importance is the effect of changing the concentration of macromolecules in the perfusate. The consequent change in oncotic pressure results in a parallel shift of the relation between J_V/A and fluid pressure. The magnitude of the displacement is equivalent to 70% of the perfusate oncotic pressure, as measured in a membrane osmometer. This indicates that σ_d is greater than or at least equal to 0.7 in this vessel. Overall, the experiment reveals that the permeability coefficients L_P and σ_m, can be regarded as independent of the Starling forces. Although permeability can be modulated, a background of constant permeability provides a basis to discuss fluid movements that occur physiologically as a result of changes in the Starling pressures.

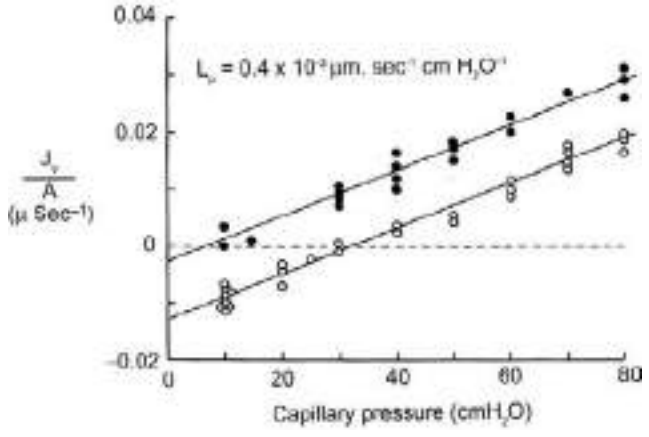

FIGURE 9.12 **Relation between net fluid movement per unit area of microvascular wall (JV/A) and capillary pressure in a single frog mesenteric capillary perfused with Ringer's solution containing high (o) and low (●) concentrations of serum albumin.** Positive values of JV/A indicate fluid filtration from vessel to tissue and negative values show movement from tissue into vessel. *(From ref. [72]. With permission.)*

Changes in Microvascular Pressure

Although textbooks so often say that P_c has a mean value that approximates to plasma oncotic pressure, this is true only for systemic microvessels of small mammals, and for systemic pressures at heart level in larger mammals. In the pulmonary microcirculation of all mammals investigated, mean P_c is more often closer to a third of the value of plasma oncotic pressure. In larger mammals, such as humans, mean P_c varies with the vertical height between the vessel and the heart. When a human subject lies horizontally, mean P_c in most systemic microcirculations may approximate to plasma oncotic pressure, but as soon as the subject sits or stands, P_c in vessels below the heart increases, and that in vessels above the heart decreases. The changes in P_c above and below the heart are not symmetrical; the decrease in P_c in vessels in the upper parts of the body is checked as the local venous pressure falls below atmospheric and the veins collapse. Measurements of P_c in skin suggest that once this happens, P_c becomes independent of position.[60] Below the heart, arterial and venous pressures increase in proportion to their vertical distance beneath the heart providing the subject remains still, and mean P_c in the feet also increases but to a lesser extent than arterial and venous pressures (see Figure 9.13). Movements of the legs increase venous return from the feet, reducing the local venous pressures and P_c.

The smaller increase in P_c than arterial and venous pressure in tissues below heart level (see Figure 9.13) suggests how P_c may be regulated. For blood to flow through a vascular bed there must be a lower pressure in the veins than in the capillaries, and in the capillaries than in the arteries. The fall in pressure from arteries to capillaries, $P_a - P_c$, is the product of the blood flow from arteries to capillaries, and the resistance of the vessels between them (i.e., the pre-capillary resistance, r_a). Similarly, the fall in pressure between the capillaries to the veins, $P_c - P_v$, is the product of the blood flow and the post-capillary resistance, r_v. Providing the blood flows into and out of the circulation are equal, P_c can be related to P_a and P_v through r_a and r_v:

$$\frac{(P_a - P_a)}{(P_c - P_v)} = \frac{r_a}{r_v}$$

which can be rearranged in the form derived by Pappenheimer and Soto-Rivera[93]:

$$P_c = \frac{P_a + P_v(r_a/r_v)}{1 + r_a/r_v} \qquad (9.15)$$

Equation (9.15) reveals how the value of P_c between P_a and P_v is determined by the ratio of r_a/r_v, and since local blood flow is regulated in most vascular beds by alterations in r_a, it also suggests how P_c might be regulated. Even if P_a and P_v remain constant, arteriolar vasodilatation, which reduces r_a/r_v, increases P_c and enhances fluid filtration. Arteriolar vasoconstriction, which increases r_a/r_v, reduces P_c consequently promoting fluid absorption from the tissues. A sudden loss of a substantial volume of blood (e.g., by hemorrhage or blood donation) is followed by intensive vasoconstriction, increasing r_a/r_v and leading to a shift of fluid from ISF to plasma (largely in skin and muscle). It is seen as a fall in hematocrit, and is usually complete within 30 minutes of the cessation of bleeding.[91]

In most tissues a local increase in P_v is associated with constriction of the local arterioles, increasing r_a/r_v and tending to minimize the increase in P_c. This phenomenon has been called the veno-arteriolar response, and appears to be a local response dependent on the presence, but not the central connections, of the sympathetic nerves.[51] It is largely responsible for the smaller increase in P_c than either P_a or P_v in the skin of the human foot as the subject moves from a supine to a standing position (Figure 9.13). Although P_c has to remain above P_v, it approaches P_v very closely when the subject is standing still. As soon as the subject moves, P_v falls. With an efficient muscle pump acting on the veins in the leg, P_v may be reduced from 120 to 130 cmH_2O when the person is standing still, to less than 30 cmH_2O in within a few seconds of starting to walk, and P_c presumably is reduced.

Landis[61] argued that P_c was the most variable of the Starling pressures in human subjects, drawing attention to the large changes in its value that followed changes in posture. P_c is also the one Starling pressure that can be regulated quickly in parallel with the local blood flow, inducing fluid shifts between the circulation and the ISF that appear to improve the chances of the organism's survival.

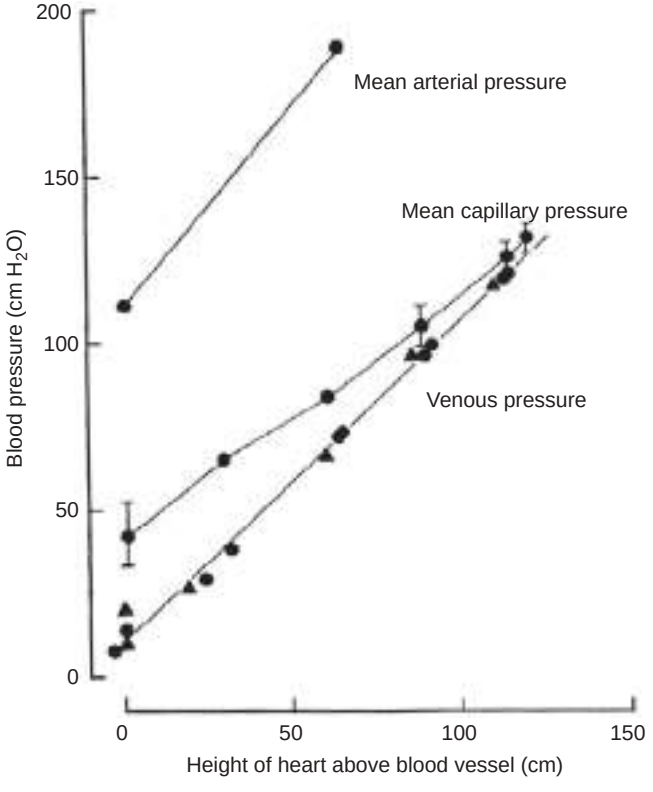

FIGURE 9.13 **Relation between the local blood pressure in the feet and the height of the heart above the feet in two normal subjects in supine, sitting, and standing positions.** Mean values for capillary pressure were based on direct measurements (by micropuncture) of capillary loops in the nail fold of the great toe. *(From ref. [62]. With permission.)*

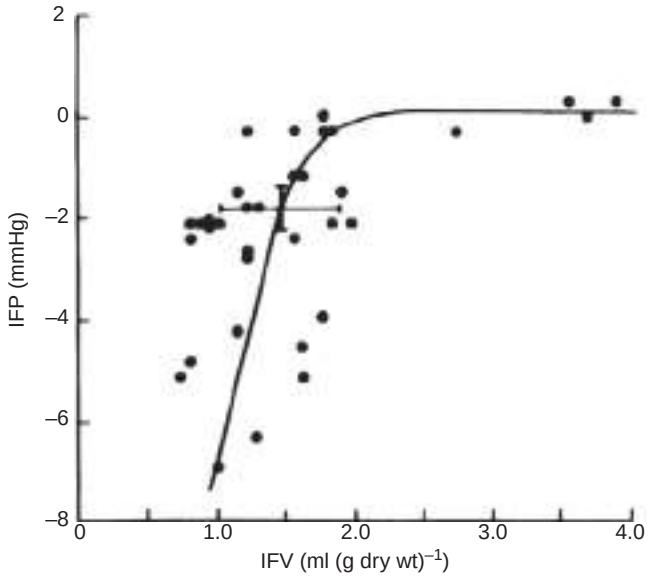

FIGURE 9.14 **The effects of changes in interstitial fluid volume (IFV) upon the interstitial fluid pressure (IFP) in cat skin.** Mean and standard deviations represent control values. IFV was varied by intravenous infusion of saline or by peritoneal dialysis. *(From ref. [131]. With permission.)*

Plasma Oncotic Pressure

Although reduced levels of circulating plasma proteins may be associated with edema, the steady-state relations between edema formation and plasma protein concentration are complicated by adjustments of microvascular pressures, and of ISF hydrostatic and oncotic pressures.[90] There is evidence to suggest that the oncotic pressure difference may be adjusted by atrial natriuretic peptide regulating the transport of proteins from plasma to ISF.[31,127]

In normal healthy subjects, oncotic pressure of the arterial plasma may be regarded as constant in the short-term. The plasma oncotic pressure, however, may increase considerably as blood flows through the microcirculation under conditions where the filtration rate becomes a significant fraction of the plasma flow. In most microvascular beds, L_P is too low for this to be significant, but it does occur in the renal glomerular capillaries, where L_P is very high,[16] and in the microcirculation of the feet of human subjects during prolonged standing or sitting, where P_c is high and plasma flow is very low.[40,87,89] In the glomerular capillaries it underlies the dependence of glomerular filtration rate upon renal blood flow (see Chapter on Glomerular Filtration).

Interstitial Hydrostatic Pressure

Before 1963, P_i was believed to approximate to atmospheric pressure in non-edematous tissues and steady fluid filtration, which expanded ISF volume, was thought to increase P_i proportionately. In this way, the increase in P_i would reduce the difference in hydrostatic pressure across microvascular walls, and so limit the rate of filtration protecting the tissues from edema.

The pioneering work of Guyton and colleagues showed that P_i of subcutaneous tissues and many others was 4 to 7 mmHg below atmospheric pressure.[46,47,48] After much controversy, sub-atmospheric or negative values for P_i in non-edematous tissues have been confirmed using a series of different techniques. There is some variation from tissue to tissue, most negative values being found in the lung and positive values being found in the kidney with the subcutaneous tissues of many mammals being in the range of -0.5 to -2.0 mmHg.[10,99]

At an early stage in his investigations, Guyton[47] showed that expansion of the ISF by filtration from the microvasculature quickly raised P_i to atmospheric pressure. Further expansion of the ISF volume, however, was accompanied by little change of P_i in most tissues. These relations between P_i and ISF volume have been extended and confirmed by others (see Figure 9.14 and [134]). Whereas there have been minor differences in some of the absolute values reported by different investigators, the general picture of a steep relation between P_i and ISF volume (low interstitial compliance) at normal and at low ISF volumes, and a flat relation between P_i and ISF volume (high compliance) when ISF volume is slightly expanded and P_i has risen to atmospheric pressure, has been widely confirmed (see Figure 9.14). The renal interstitium appears to be an exception to this general pattern. In the kidney, P_i is $+4$ to $+6$ mmHg, and increases and decreases linearly with ISF volume.[41] It has been argued that, in the kidney, P_i does fulfill the role of limiting the expansion of ISF volume, and promotes the uptake of fluid and solutes (including macromolecules) by the microcirculation.[10,69,70] For a more detailed discussion of the role of P_i in trans-capillary fluid exchange the reader is referred to the recent review of Reed and Rubin.[100]

Interstitial Oncotic Pressure

Measurements of ISF oncotic pressure are usually global values for a particular tissue. The values of importance for microvascular fluid exchange, however, are those for the newly formed ISF in contact with the abluminal surface of the ultrafilter within walls of the microvessels. Here, we have to be guided by theory. Equations (9.12) and (9.13) argue that if microvascular permeability of a solute is finite, the concentration of that solute in the ISF ultimately depends on its permeability and the rate of fluid filtration through the microvascular walls. If the Péclet number is zero (net filtration = 0), the concentration of a protein such as serum albumin in the interstitial fluid, C_i, will rise until it equals its plasma concentration. In the presence of net filtration from plasma to ISF, the concentration of plasma protein in the newly formed ISF will fall, reaching a plateau when C_i approximates to $C_p(1 - \sigma_f)$, as shown in the upper panel of Figure 9.15. The effective osmotic pressure difference exerted by albumin (and other large plasma protein molecules) across microvascular walls ($\sigma\Delta\Pi$) under conditions of steady fluid filtration varies with the filtration rate. This variation is shown in the lower panel of Figure 9.15. It can be estimated as follows:

$$\sigma\Delta\Pi = \sigma(\Pi_c - \Pi_i) = \sigma_d RT(\gamma_c C_c - \gamma_i C_i) \qquad (9.16)$$

The symbols γ_c and γ_i are the osmotic coefficients of albumin at its concentrations in capillary plasma and ISF. If they are approximated by a single value γ, Eq. (9.16) can be developed using Eq. (9.13)[75]:

$$\sigma_d\Delta\Pi = \sigma_d RT\gamma(C_c - C_i) = \sigma_d\sigma_f RTC_c\left(\frac{1 - e^{-Pe}}{1 - \sigma_f e^{-Pe}}\right) \qquad (9.17)$$

Equation (9.17) provides an explicit statement of the effective osmotic pressure difference exerted by a plasma protein across microvascular walls in terms of the filtration rate and through the Péclet number, the permeability coefficients P_d and σ_f of the vessel walls to the protein. Increases in J_V increase Pe and as e^{-Pe} approaches zero, $\sigma_d \Delta\Pi$ approaches a limit of $\sigma_d\sigma_f\ \Pi_c$, or approximately $\sigma^2\Pi_c$.

Both P_i and π_i change[75] with fluid filtration rate, and since they themselves influence J_V, after a step change in P_c, an initial change of J_V is likely to be followed by a further changes as P_i and Π_i adjust to their new steady-state values. Thus, we should expect there to be differences between the initial transient changes in J_V and the steady-state values, and we shall consider these differences next.

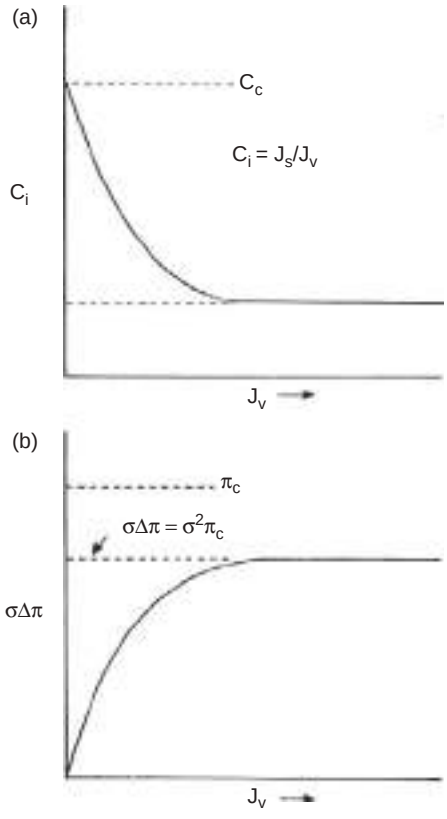

FIGURE 9.15 (a) Steady-state relations between the concentration of proteins (C_i) in capillary ultrafiltrate and the capillary filtration rate, J_V. The limiting value of C_i is $C_c(1 - \sigma)$ where C_c is the concentration of protein in the capillary. (b) Steady-state relations between the effective oncotic pressure across the walls of the microvessel ($\sigma\Delta\Pi$) consequent to changes in C_i and J_V. The oncotic pressure of the plasma, Π_c, is indicated as is the maximum value of $\sigma\Delta\Pi$. *(From [77]. With permission.)*

Transient and Steady-State Fluid Movements through Microvascular Walls

Figure 9.16 shows the results of an experiment on a single mesenteric capillary perfused with a Ringer solution containing serum albumin and the macromolecule Ficoll 70.[84] Both the immediate (transient) and steady-state values of fluid filtration were measured following step changes in capillary pressure. The transient changes (open circles) were measured after the vessel had been perfused at high pressure (35–50 cmH_2O) for several minutes, and then the pressure lowered to a predetermined value. The steady-state measurements (solid circles) were made after the vessel had been perfused for several minutes at that pressure, and preliminary measurement suggested a steady-state had been achieved. The transient values of J_V/A are related to P_c in the same linear fashion predicted by the standard Starling equation (Eq. (9.14)), and as shown by a similar experiment in Figure 9.12. This is the expected relation between ΔP and J_V/A when ΔP is varied and $\sigma_d\ \Delta\Pi$ remains constant. The steady-state measurements (solid circles) can be described by a non-linear (hockey stick) curve which can be predicted using Eq. (9.17) to calculate $\sigma_d\ \Delta\Pi$.

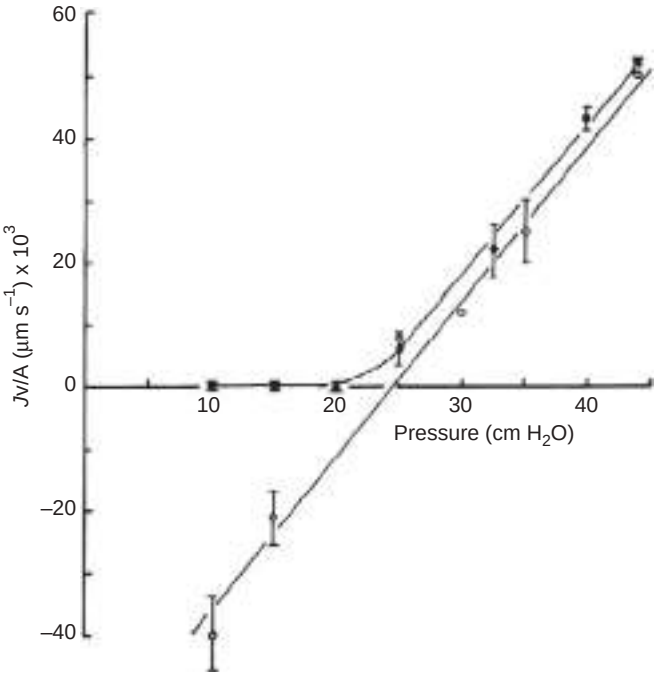

FIGURE 9.16 **The relations between fluid filtration and absorption (J_V/A) and microvascular pressure in a single frog mesenteric microvessel under transient (o) and steady-state (●) conditions.** Perfusate oncotic pressure was 32 cmH_2O. The oncotic pressure difference was the same at all values of J_V/A under transient conditions, but varied with J_V/A in the steady-state in the way indicated in Figure 9.15b. Note that absorption of fluid from the tissues is seen only under transient conditions. *(From ref. [82]. With permission.)*

Here, Π_c is constant, but Π_i varies with J_V, which changes *Pe*.

When P_c is greater than the effective osmotic pressure opposing filtration, both transient and steady-state values lie close together, and the linear portion of the steady-state relation at these higher values of ΔP has a slope of L_P, and is described by the following expression:

$$\frac{J_V}{A} = L_P(\Delta P - \sigma_m^2 \Pi_c) \tag{9.18}$$

At low values of P_c the transient and steady-state values of J_V/A deviate considerably with no fluid uptake from the tissue occurring under steady-state conditions. Not only are these results consistent with the theoretical picture, but analysis of the steady-state data also allows estimates to be made for both σ_m and P_d (the macromolecular permeability), which agree quantitatively with other determinations.[84] One surprising observation made during the measurement of the steady-state relations on single mesenteric capillaries was the relatively short time (2–5 minutes) required for a new steady-state to be established after capillary pressure had been changed.[84] This drew attention to the importance of the value of Π_i in the small volume of ISF in contact microvessel, and the relative lack of importance of the value of Π_i for the ISF of the entire tissue.

Figure 9.17 summarizes the transient and steady-state changes in fluid filtration and absorption in a microvessel of constant permeability, perfused at a rate sufficient to keep the plasma oncotic pressure constant. The dashed lines are drawn with a slope = L_P for the vessel. The solid line indicates the steady-state relations between J_V/A and ΔP. If P_c initially has a value, A, which is less than the plasma oncotic pressure, and remains constant for long enough for a steady-state to be established (at point T), a subsequent increase in P_c from A to B leads to a rapid increase in filtration (T→W). J_V then attenuates (to X), as Π_i is reduced and P_i increases. If P_c is then returned to A, fluid uptake from the tissues occurs (X→S), and the rate of absorption diminishes as Π_i increases returning J_V to its initial level of T.

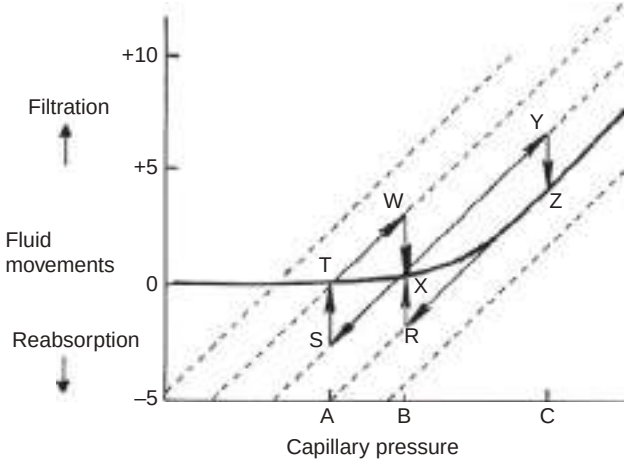

FIGURE 9.17 **Transient and steady-state relations between fluid movements and microvascular (capillary) pressure.** The dashed lines have slopes equal to L_P. The arrowed straight lines show transient changes in fluid movements with changes in pressure. The OTXZ (heavy line) represents the steady-state relation between J_V/A and capillary pressure. *(From ref. [81]. With permission.)*

In the pulmonary microcirculation, mean values of P_c are usually well below Π_c, and fluid movements fluctuate around a point half-way along the flat part of the steady-state relationship. Small changes in P_c lead to changes in filtration or absorption that are rapidly checked as a new steady-state is established. So long as $P_c - P_i$ is greater than $\Pi_c - \Pi_i$, there is a low level of fluid filtration into the tissues that is balanced by lymph drainage.

The steady-state analysis predicts that when the exchange vessels are finitely permeable to macromolecules, and there is no source of ISF other than the ultrafiltrate from these vessels, fluid absorption from the tissues is transient, and low levels of fluid filtration from blood to the tissues maintain the differences in oncotic pressures between the plasma and the ISF. The sustained levels of fluid filtration are matched by lymphatic drainage from the tissue, so that ISF volume remains approximately constant. Providing that the time-averaged mean P_c in most tissues approximates to the plasma oncotic pressure, this picture is consistent with blood–tissue fluid balance. It is not consistent, however, with the popular representation of the Starling Principle, which depicts fluid being filtered into the tissues from the arterial end of a capillary and absorbed from the tissues at its venous end. Quite apart from the lack of evidence for this picture, the steady-state analysis predicts that rising concentrations of macromolecules around the venular regions of the vessel would bring absorption to a halt. The experimental and theoretical arguments against this textbook picture of the filtering-absorbing capillary have been forcefully expressed in a series of publications by Levick.[62,63]

Steady-State Fluid Uptake into Microvessels Associated with Absorptive Epithelia

Continuous uptake of fluid into the microcirculation does occur in tissues such as intestinal mucosa, the post-glomerular capillaries of the renal cortex, and the ascending vasa recta of the renal medulla. Here, however, the bulk of the ISF is not formed by filtration from the capillaries, but by the secretion of

protein free fluid from the adjacent epithelia. In intestinal mucosa and in renal cortex, the large fluid uptake from the ISF into the blood capillaries is accompanied by a very much smaller flow of ISF into the lymphatics.[43,44] Although only a fraction of the fluid is absorbed from the ISF, the lymph flow is sufficient to clear proteins and keep their ISF concentrations low.

The renal medulla, however, has no lymphatics and special mechanisms appear to operate here. The continuous addition of protein free fluid into the medullary ISF is matched by the uptake of fluid into the ascending vasa recta (AVR). The AVR have relatively low σ to plasma proteins (0.7 to albumin). This allows the absorbed fluid to carry protein from the ISF into the blood. The uptake of labeled proteins from medullary ISF into the blood has been demonstrated directly,[125] and estimates of P_c, P_i, Π_c, and Π_i in and around the AVR indicate that these favor fluid uptake.[70] Theoretical studies have supported this "bootstrap" mechanism, whereby plasma proteins are carried up their own concentration gradient by the osmotic flow that arises from that same gradient.[70,131,138] In addition, unusual structural features of the ascending vasa recta, and the low compliance of the renal interstitium, ensure that fluid uptake is maintained even if Π_i increases. The low compliance means that P_i is high, and rises if ISF volume expands to levels that may equal or even exceed the pressure in the ascending vasa recta. When this occurs the vessels do not collapse as there are fine projections from their endothelial cells, which are inserted into the basal laminae of neighboring vessels and tubules, holding them open.[69] Because L_P of these fenestrated vessels is very high, an increment of P_i over P_c of only 1.0 to 2.5 cm H_2O is sufficient to account for the clearance of all fluid entering the medullary ISF from the loops of Henle and collecting ducts.[69] A more detailed discussion of the special features of the extra-glomerular renal microcirculation is given elsewhere in this volume.

Starling Pressures and Local Lymph Flow

In most tissues, ISF volume is maintained by a low level of filtration from the microcirculation being matched by an equal efflux of fluid from the tissue in the lymph. From this, one would anticipate that the magnitude of the lymph flow from a tissue could be estimated from the mean Starling pressures, the L_P, and the exchange surface area of the microcirculation. In an incisive review, Levick[62] pointed out that where the mean Starling pressures have been measured, they predict much greater filtration rates than the lymph flow and the lymph protein concentration would indicate. From 15 sets of data, he estimated P_0, the net pressure opposing filtration from the following relation:

$$P_0 = \sigma_m(\Pi_c - \Pi_i) + P_i \tag{9.19}$$

When values of P_0 are compared with direct measurements of pressure in post-capillary venules, P_{Vc}, it is found that P_{Vc} is nearly always greater than P_0, and in several cases P_{Vc} exceeds P_0 by 5 to 10 mmHg (Table 9.2). Net driving pressures for filtration of this magnitude would be expected to result in high lymph flows, but in most of the tissues concerned (e.g., subcutaneous tissue, muscle, and mesentery), the basal lymph flows are so low that they are difficult to measure.

To account for these discrepancies, Levick[62] suggested that vasomotion, the spontaneous contraction and relaxation of arteriolar smooth muscle, might be responsible for large variations in P_c, and that P_c measurements tended to be made in vessels where there was brisk flow and a higher than average P_c. The few direct estimates of P_c during vasomotion, however, suggest that the fluctuations are relatively small.

An alternative hypothesis was put forward by Michel[79] and Weinbaum.[132] Independently, they both realized that if the filtrate leaving the "small pores" was uncontaminated by fluid containing the higher concentration of macromolecules, the effective $\sigma\Delta\Pi$ opposing filtration may approximate to that across the small pores. This would be considerably greater than that calculated from global values of Π_i, and would increase the force opposing filtration (P_0), reducing filtration rates to levels consistent with basal rates of lymph flow. The significant deviations between P_0 and P_{Vc} reported by Levick[62] are found in microvessels with continuous endothelium, where the small pores are the interstices of the glycocalyx lying above the intercellular clefts. The downstream side of the

TABLE 9.2 Starling Pressures in Muscle, Mesentery, and Subcutaneous Tissues at Heart Level

Species and Tissue	Π_c	Π_i	P_i	P_o	P_c	$P_c - P_o$
Dog, skeletal muscle	26.0	11.0	−2.0	13.0	12–20	−1 + 7
Cat, mesentery	19.1	6.1	0	13.0	23.5	10.5
Human, chest subcutis	26.8	15.6	−1.5	9.7	>15.0	>5.3

P_o is calculated from Eq. (9.17) assuming that $\sigma = 1$ and thus is an overestimate. P_c is based on direct measurements in venules or venular capillaries, and is therefore an underestimate of mean P_c. The difference ($P_c - P_o$) is consequently the minimum difference based on available data. From Levick, J. R. (1991). Capillary filtration–absorption balance reconsidered in light of dynamic extravascular factors. *Exp. Physiol.* **76**, 825–85.[60]

microvascular ultrafilter is therefore the abluminal surface of the glycocalyx, which is separated from the ISF immediately outside the microvessel by the intercellular cleft with its tortuous pathway through the tight junctions. The pathway for macromolecules (the large pores) is either through the endothelial cell vesicles (via channels or by a fission–fusion mechanism) or by the very occasional leaky intercellular cleft. For the high protein concentration of this large pore filtrate to mix with that emerging from the small pores, protein molecules would have to diffuse back through the intercellular clefts to the site of ultrafiltration at the glycocalyx. Although this pathway is short, diffusion has to occur against the flow of fluid from the vessel lumen. The velocity of this filtrate is increased ten-fold or more as it passes through the breaks in the tight junctions. Rough calculations[79] and a detailed mathematical model[55] both indicate that, even with filtration rates driven by pressure differences across the glycocalyx as small as 1–2 cm H_2O, the fluid velocity through the breaks in the tight junctions impose a major barrier to the diffusion of proteins through the clefts in the luminal direction. These levels of filtration, nevertheless, are consistent with basal rates of lymph flow.

The hypothesis has been examined experimentally in single frog mesenteric capillaries[54] and in rat mesenteric venules.[3] In these studies, it was found that even when the interstitial concentration of serum albumin in contact with the outside wall of a vessel was the same as that in the perfusate, fluid movements through the vessel wall were opposed by oncotic pressures much greater than those estimated from global values of Π_i. The authors concluded that these observations were consistent with the oncotic pressures opposing fluid filtration from continuous (non-fenestrated) capillaries are developed across the glycocalyx, and that global values of Π_i do not determine fluid exchange directly. Some of their data are shown in Figure 9.18.

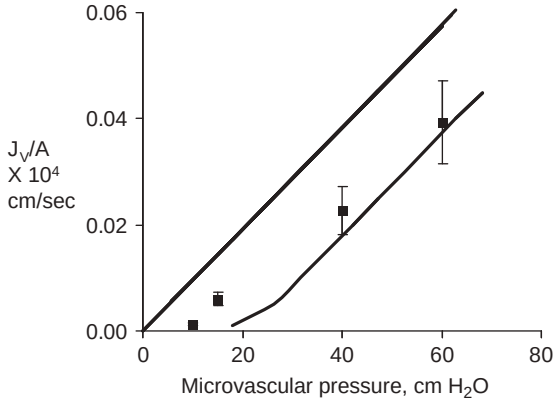

FIGURE 9.18 **Steady-state relations between microvascular filtration (J_V/A) and pressure in rat microvessels when the interstitial oncotic pressure is varied by superfusion.** The vessel is perfused with a 5% serum albumin solution (Π_c = 21.25 cmH_2O). The points are mean values from four experiments in which the ISF concentration of albumin in contact with the outside of the vessel was equal to the perfusate concentration. The curve on the left is the relation predicted when the interstitial concentration of albumin in contact with vessel is the same as the perfusate concentration; that on the right shows the relations when no albumin is added to the superfusate. Note that at high P_c, J_V/A has values comparable with those expected with no albumin present outside the vessel. Only at low J_V/A, when P_c is less than Π_c, does Π_i appear to influence the steady-state. *(From ref. [3].)*

Transient and steady-state fluid exchange and their relations to local lymph flow have been reviewed recently by Levick and Michel.[64]

Microvascular Blood Flow and Solute Transport

The rate of delivery of molecules, and the rate of their clearance to and from a tissue, depends on both microvascular blood flow and microvascular permeability. Where permeability is very high, transport depends on blood flow alone and is said to be "flow limited." Where solute permeability is low, increasing blood flow increases transport to a progressively smaller extent, and when further increases in blood flow no longer increase transport, transport is said to be "*diffusion limited*" or "*permeability limited*." Renkin set out the general principles of blood–tissue exchange in a series of papers between 1955 and 1970.[101,102,104,105] Figure 9.19 is taken from Renkin's work, to illustrate *flow limited* transport of antipyrene and *permeability limited* transport of urea between the microcirculation of skeletal muscle tissue. Both solutes are usually considered to have high permeabilities, but it is seen that as flow increases, the transport of urea becomes independent of flow. This maximum level of transport is determined by the product of P_d to urea and the surface area of the exchange vessels. Antipyrene is lipid soluble and has a much higher permeability than urea. Its transport remains proportional to flow over the range investigated.

Insight into the relations between blood flow and solute transport can be gained by considering the plasma or blood concentrations of a diffusible solute as it flows along an exchange vessel. If the Péclet number for the solute is low (as it is for most small solutes), its unidirectional transport through the vessel wall from a small volume of plasma, ΔV, flowing along the vessel is proportional to the product of its concentration, C, in that volume and its permeability, P_d (Figure 9.20). It is also proportional to the surface area, ΔS, with which ΔV makes contact as it flows along the vessel.

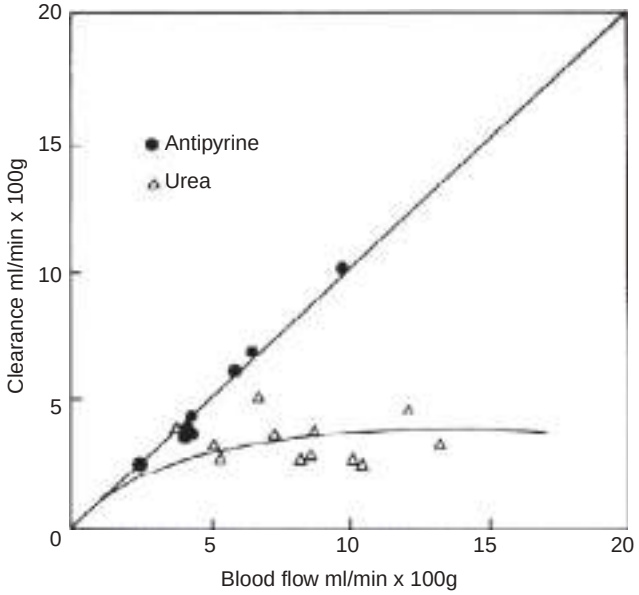

FIGURE 9.19 **Relations between blood−tissue clearance and blood flow for a small lipid soluble solute (antipyrene) and a small hydrophilic solute (urea) in skeletal muscle.** Whereas the clearance of antipyrene is limited only by blood flow over the range of flows investigated, clearance of urea is limited by its microvascular permeability, and is independent of flow when this exceeds 5 ml min − 1 100 g − 1 tissue. *(Re-plotted from ref. [102]. With permission.)*

FIGURE 9.20 **Model illustrating the principles of diffusion and flow in microvascular exchange.** Exchange of solute is considered to occur from a small volume as it flows along a cylindrical microvessel.

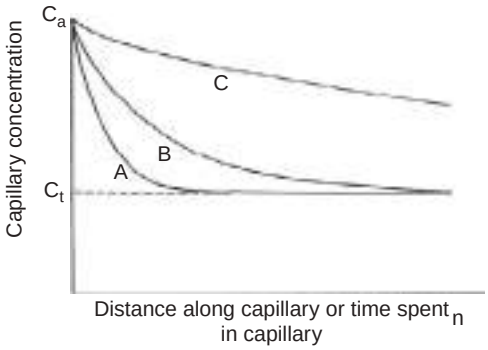

FIGURE 9.21 **Decrease in plasma concentration of three solutes as they equilibrate with the tissues during their passage along a microvessel.** The vessel is more permeable to A than to B, and more permeable to B than to C. Because equilibration is achieved for A and B before the blood leaves the vessel, net transport for these substances can only be increased by increasing the flow (cf. curve for antipyrene in Figure 9.20). Substance C does not equilibrate, and its transport is said to be permeability- or diffusion-limited (cf. with curve for urea in Figure 9.20). *(From ref. [71]. With permission.)*

The changes in C resulting from unidirectional loss of solute from ΔV are given by the following equation:

$$-\Delta V\frac{dC}{dt} = P_d \Delta A.C \tag{9.20}$$

For a cylindrical vessel, the ratio of $\Delta A/\Delta V$ is constant and is equal to the ratio of surface area to volume for the entire vessel, A/V. Thus:

$$C_{(t)} = C_0 \exp\left(\frac{-P_d A.t}{V}\right) \tag{9.21}$$

where $C_0 = C$ at time = 0, that is the concentration of solute at the point of entry to the vessel, and this would usually be the arterial concentration, C_a. When $t = \tau$, the transit time through the vessel, $C = C_v$, the venous concentration of the solute. Furthermore, V/τ is equivalent to the flow through the vessel, F, so that Eq. (9.19) can be rewritten as:

$$C_V = C_a e^{-P_d A/F} \tag{9.22}$$

The net transport of solute from blood to tissue is equal to J_S:

$$J_S = F(C_a - C_v) = FC_a(1 - e^{-P_d A/F}) \tag{9.23}$$

Since the clearance of solute from blood to tissue is J_S/C_a, clearance becomes:

$$Clearance = F(1 - e^{-P_d A/F}) \tag{9.24}$$

Renkin used expressions such as Eq. (9.24) to describe data such as those shown in Figure 9.19.

Equation (9.21) can be used to give additional insight into the nature of flow-limited and permeability limited transport. In Figure 9.21, Eq. (9.21) has been used to calculate the changes in concentration that occur in a bolus of blood flowing along a single vessel. The three curves represent the concentrations for three solutes that have different values of P_d. It is assumed that the flow is constant, so that distance and time are directly proportional to one another. The three curves start from the same value of C_a and finish at three different points, the venous concentrations. From Eq. (9.23), the net transport of solute from blood to tissue, J_S, for each solute is $F(C_a - C_v)$. F varies inversely with τ so that if F is doubled, τ is halved. Because solute A reaches its end capillary concentration before it has spent half its residence

time in the vessel, doubling F will not change $(C_a - C_v)$. Doubling F will therefore double J_S and the relation between clearance and blood flow is linear so that transport is flow-limited over this range of flows, and will resemble that for antipyrene in Figure 9.19. By contrast, for solute C, halving τ almost halves $(C_a - C_v)$, so that the product, F $(C_a - C_v)$ remains almost constant as flow is increased. Transport is now "permeability-limited," and the relation between clearance and flow resembles that shown for urea at high blood flows in Figure 9.19. In theory, the transport of all solutes is limited by permeability if blood flow is high enough. In practice, the permeability of microvascular walls to some substances is so high that transport is always flow-limited.

Although so far we have discussed only solute transport from blood to tissue, equivalent expressions describe the clearance of substances from tissues to blood, so long as the barrier to diffusion through microvascular walls is greater than the resistance to diffusion through the tissues. The latter is certainly not true when the clearance of highly diffusible lipid soluble solutes is being considered. For these molecules, transport between blood and tissues is determined more by the gradients of their concentration in the tissues.

The Renkin expressions (e.g., Eqs. (9.22) and (9.24)) have provided the basis of understanding blood tissue exchange, but Renkin himself has drawn attention to their limitations.[105] Considerations of heterogeneity of microvascular flow and permeability in different vessels in a microvascular bed have led to sophisticated models for the analysis of blood tissue exchange in intact tissues.[13,105] These models may well have to be revised in the light of observations on the relations between flow and transport of small hydrophilic solutes in single capillaries *in situ*. Indications that P_d may itself vary with flow have been confirmed, and greatly extended in a series of measurements on single microvessels of frogs and rats.[57,58,86] The increase in P_d with flow can be inhibited in rat vessels with NO-synthase blockers, and by procedures that raise intracellular cAMP levels. The effects of flow P_d are largest for small ions and hydrophilic molecules. They appear to involve a pathway more selective than the traditional small pores, and therefore make little contribution to fluid exchange.[86]

The implications of these findings for blood−tissue transport in the intact animal have yet to be assessed, but it could mean that increases in P_dA that, in the past, have been interpreted as the consequence of increases in A, are the result of changes in P_d, and a common set of control mechanisms regulate the permeability and the perfusion of the microcirculation.

Increased Microvascular Permeability

Over 50 years ago Majno and Palade[71] demonstrated that the classical mediators of acute inflammation (e.g., histamine, serotonin) increased vascular permeability by inducing openings in the endothelia of the post-capillary venules. The openings were believed to lie between the endothelial cells, and Majno[72] suggested that they were formed by the contraction of adjacent endothelial cells away from each other. This view, however, was controversial, and continues to be so.[5]

Two groups working in the mid-1990s, reconstructed openings in endothelium from electron micrographs of ultrathin serial sections of venules exposed to a range of mediators to increase their permeability. Whereas with some stimuli (e.g., substance P and PAF), the openings were predominantly paracellular with other stimuli (e.g., VEGF and A23187), they passed through the body of one cell close to the intercellular cleft, but clearly separate from it.[35,88] It seems that transcellular openings may be derived from vesicles or vacuoles in the endothelium.[88] Dvorak and her colleagues identified fused clusters of vesicles and vacuoles, the vacuolar-vesicular organelles (VVOs) in the highly permeable vessels of tumors as transcellular pathways.[33] Subsequent work revealed that VVOs were present in normal (healthy) vessels, but did not form a pathway for macromolecules until the tissues were stimulated by mediators, when they develop into transcellular openings.[34]

Considerable progress has been made unraveling the signaling events that follow the binding of an agonist with its receptor on the venular endothelial cell and the appearance of openings in the vessel wall.[27,28] From studies both in cultured endothelial cells and in intact vessels, it is clear that the early stages of signaling involve a steep rise in the intracellular activity of free Ca^{2+}. The agonist molecules, such as histamine and ATP, bind to endothelial cell membrane receptors linked to G-proteins, which then activate phospholipases (particularly β and γ isoforms of phospholipase-C) that release inositol tri-phosphate (IP_3) and di-acyl glyceric acid (DAG) from the membrane lipids. IP_3 releases Ca^{2+} from the intracellular Ca^{2+} stores, and this in turn leads to the opening of Ca^{2+} channels in the cell membrane so that the Ca^{2+} activity of the cytosol is rapidly raised by the combined influx of Ca^{2+} from both the stores and ISF (for review see [28]). Agonists such as VEGF bind to a tyrosine kinase receptor that phophorylates PLC-γ, and activate a DAG signal that opens membrane Ca^{2+} channels directly.[11,97] With VEGF, the rise in cytostolic Ca^{2+} is achieved entirely by influx from the ISF, and is independent of its release from the intracellular Ca^{2+} stores.

The sequence of events that follows the rise of cytostolic Ca^{2+} activity remains less clear, and this is particularly true of the final stages when the endothelial openings are formed. Several different studies have shown that, in intact venules, there is cascade involving NO and cGMP downstream from the initial peak of intracellular Ca^{2+} activity.[12,27] The effects of PAF and VEGF on permeability are prevented or greatly attenuated if the enzymes of the NO-synthase − cGMP cascade are blocked.[50,135] The details of other events are continually changing as new investigations are published, and the reader is referred to a recent review of Curry and Adamson,[28] and other contributors to the same issue of *Cardiovascular Research*.

Measuring Increases in Vascular Permeability

To assess the role of different molecules in signaling or in the mechanics of increased permeability, it is necessary to have trustworthy methods for measuring permeability. Earlier we have seen that the permeability coefficients, L_P, σ, and P_d provide quantitative estimates of the permeability properties of microvascular walls. Figure 9.22 shows the results of an experiment on a single rat venule where values of J_V/A were measured at two different microvascular pressures before and after exposure to histamine.[82] From this experiment, the values of L_P and σ can be estimated and interpreted in terms of endothelial openings forming and closing.

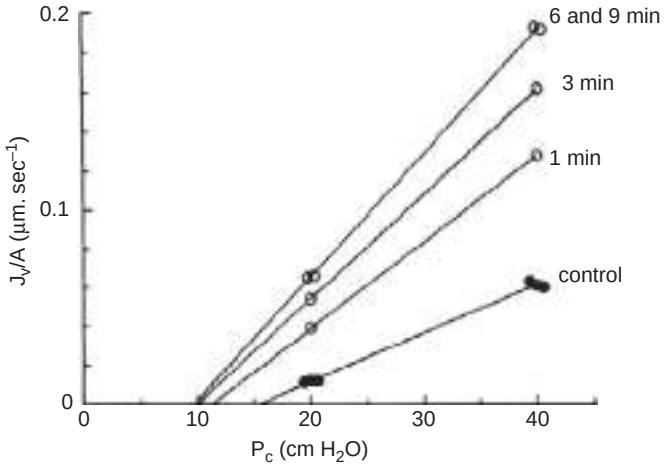

FIGURE 9.22 **Relations between fluid filtration (J_V/A) and microvascular pressure (P_c) before and following addition of histamine to the solution washing a single venule in rat mesentery.** Note how the slope of the relation between J_V/A and P_c (L_P) increases rapidly and the intercept with the P_c axis ($\sigma\Delta\Pi$) falls over the first 6min of exposure to histamine. *(From ref. [80].)*

While this practice of measuring permeability coefficients to chart increases in vascular permeability is used by some investigators, and provides reliable information, the great majority of reports of increased permeability are based on estimates of the rates of transport of macromolecules through endothelia. In the latter case the results should be viewed critically until the reader is satisfied that changes in permeability really have been demonstrated. In this final section, we discuss how results from two frequently used assays of changes in permeability can be easily misinterpreted.

A comparison of the rates of labeled serum albumin transport through monolayers of cultured endothelium *in vitro* in the absence and presence of various concentrations of a potential mediator are frequenty used to assay the latter's potency in increasing permeability. The most important question to ask of these studies is the absolute value of the permeability of the monolayer under control conditions. This is often unavailable, as authors have expressed their results as relative increases in permeability. The reason for questioning these assays is that most published control values of P_d for endothelial monolayers to serum albumin are high[7] ($>10^{-6}$ cm.sec^{-1}). This leads one to suspect that endothelial monolayers form leaky barriers to macromolecules. Strengthening this criticism is the finding that thrombin, which increases permeability of endothelial monolayers by inducing large openings between the cells, has no effects on unstimulated microvascular endothelium *in vivo*.[1] Thrombin will increase permeability in microvessels that are already in a pre-inflammatory state.[32]

Other studies compare transport rates of labeled macromolecules into tissues *in vivo*. Many of these derive from the method described by Miles and Miles[85] in 1952. Here, labeled protein is injected into the circulation of an experimental animal (rat, mouse, guinea pig or rabbit) in which a relatively large area of its dorsal skin has been shaved. Small volumes of varying concentrations of a potential mediator, suitably diluted in physiological salt solution, are injected into the skin. To act as a control, a similar volume of the physiological salt solution containing no mediator is also injected. If the potential mediator does increase vascular permeability to macromolecules, label will accumulate in the area where the injections have been made, and these are then compared with the accumulation of label at the control site over the same period. Initially the labels used were blue dyes that bound to plasma proteins, and the degree of accumulation was estimated from the mean diameter of blue area around the injection site. Later, the technique was made more quantitative by extracting the dye from the tissue or by using radioactive agents. A further refinement was

measurement of the plasma concentration of labeled macromolecule during the period that it was accumulating in the tissue. From these data it was possible to estimate the clearance of label from the plasma in the test and control areas.

Although methods such as these are very widely used, the belief that changes in the flux of macromolecules from blood to tissues reflect changes in permeability quantitatively is only valid when all other factors determining the flux rate are constant. It is apparent from Eq. (9.10) that net transport has a convective component, and while an increase in L_P and a fall in σ might both be responsible for increasing J_V, the increase will only be proportional to the permeability change if $P_c - P_i$ is unchanged. Many of the molecules that increase permeability also cause vasodilatation of the arterioles, so that by reducing r_a/r_v they will also raise P_c (see Eq. (9.15)). A vasodilator might also open previously unperfused microvessels, increasing the area available for exchange in Eq. (9.10). In these ways, changes in local blood flow compromise the quantitative relation between changes in net macromolecular flux from blood to tissue and changes in permeability, and mean that permeability assays based macromolecular leakage can only be used as qualitative guides of changes in permeability unless additional evidence is available. Sometimes molecules that are vasodilators and have no action on vascular permeability are erroneously reported as amplifying or potentiating increased permeability. This error was exposed in experiments by Williams and Peck,[135] who showed that the effects of prostaglandins E_1 and E_2 in enhancing protein leakage in inflammation were due to its action as a vasodilator. Not only did the effectiveness of the prostaglandins to enhance protein leakage correlate with their potency as vasodilators, but similar enhancement of protein leakage could be produced by other vasodilators not associated with inflammation. Finally, it is worth emphasizing that if σ to a macromolecule is high in non-stimulated endothelium, quite a modest fall in its value can have a large effect on the convective transport to that macromolecule. For example, if under control conditions σ to serum albumin at the wall of a venule is 0.98, and after exposure to a possible mediator σ falls to 0.80 (a reduction of σ of less than 20%), the convective component of albumin transport increases ten-fold in the presence of the mediator, even if P_c and L_P (and hence J_V) are unchanged. This is because the convective component is proportional to $(1 - \sigma)$, which increases from 0.02 to 0.2.

In conclusion, large changes in the net flux of macromolecules from blood to tissues usually indicate increased vascular permeability, but information obtained in this way is qualitative and should be treated as such unless strict control of J_V has been maintained. If one wants to measure changes in vascular permeability one should measure the changes in the permeability coefficients, for these are the functional measures of the properties of the endothelial barrier.

References

[1] Adamson RH. Permeability of frog mesenteric capillaries after partial pronase digestion of the endothelial glycocalyx. J Physiol 1990;428:1–13.

[2] Adamson RH, Huxley VH, Curry FE. Single capillary permeability to proteins having similar size but different charge. Am J Physiol 1988;254:H304–12.

[3] Adamson RH, Lenz JF, Zhang X, Adamson GN, Weinbaum S, Curry FE. Oncotic pressures opposing filtration across non-fenestrated rat microvessels. J Physiol 2004;557:889–907.

[4] Adamson RH, Michel CC. Pathways through the intercellular clefts of frog mesenteric capillaries (Appendix by Parker KH, Phillips CG, Wang W) J Physiol 1993;466:303–27.

[5] Adamson RH, Zeng M, Adamson GN, Lenz JF, Curry FE. PAF- and bradykinin-induced hyperpermeability of rat venules is independent of actin myosin contraction. Am J Physiol 2003;285:H406–17.

[6] Agre P, Brown D, Nielsen S. Aquaporin water channels: unanswered questions and unresolved controversies. Curr Opin Cell Biol 1995;7(472):483.

[7] Albelda SM, Sampson PM, Haselton FR, McNiff JM, Meuller SM, Williams SK, et al. Permeability characteristics of cultured endothelial cell monolayers. J Appl Physiol 1988;64:308–22.

[8] Areekul S. Reflection coefficients of neutral and sulphate-substituted dextran molecules in capillaries of the isolated perfused ear. Acta Societatis Medicorum Uppsaliensis 1969;74:129–38.

[9] Arkill KP, Knupp C, Michel CC, Neal CR, Qvortrup K, Rostgaard J, et al. Similar endothelial glycocalyx structures in microvessels from a range of mammalian tissues: evidence for a common filtering mechanism. Biophysical Journal 2011;101:1046–56.

[10] Aukland K, Bogufsky RT, Renkin EM. Renal cortical interstitium and fluid absorption by peritubular capillaries. Am J Physiol 1994;266:F175–84.

[11] Bates DO. Vascular endothelial growth factors and vascular permeability. Cardiovasc Res 2010;87:262–71.

[12] Bates DO, Curry FE. Vascular endothelial growth factor increases microvascular permeability via Ca^{2+}-dependent pathway. Am J Physiol 1997;273:H687–94.

[13] Bass L. Flow dependence of first-order uptake of substances by heterogeneous perfused organs. J Theor Biol 1980;86:365–76.

[14] Bearer EL, Orci L. Endothelial fenestral diaphragms: a quick freeze, deep etch study. J Cell Biol 1985;100:418–28.

[15] Boron WF. Sharpey-Schafer Lecture: gas Channels. Exp. Physiol. 2010;95:1107–30.

[16] Brenner BM, Baylis C, Deen WM. Transport of molecules across renal glomerular capillaries. Physiol Rev 1976;56:502–34.

[17] Bruns RR, Palade GE. Studies on blood capillaries. I. General organization of blood capillaries in muscle. J Cell Biol 1968;37 (2):244–76.

[18] Bruns RR, Palade GE. Studies on blood capillaries. II. Transport of ferritin molecules across the wall of muscle capillaries. J Cell Biol 1968;37(2):277–99.

[19] Bundgaard M. The three dimensional organization of tight junctions in a capillary endothelium as revealed by serial section electron microscopy. J Ultrastruct Res 1984;88:1–17.

[20] Bundgaard M, Frokjaer-Jensen J, Crone C. Endothelial plasmalemmal vesicles as elements in a system of branching invaginations from the cell surface. Proc Natl Acad Sci 1979;76:6439–42.
[21] Carlsson O, Rosengren B-I, Rippe B. Transcytosis inhibitor N-ethylmaleimide increases microvascular permeability in rat muscle. Am J Physiol 2001;281:H1728–33.
[22] Casley-Smith JR. The Brownian movements of pinocytotic vesicles. J Microscopy 1963;82:257.
[23] Clough G, Michel CC. The role of vesicles in the transport of ferritin across frog endothelium. J Physiol 1981;315:127–42.
[24] Clough G, Michel CC. The effects of temperature on ferritin transport by endothelial cell vesicles in capillaries of frog mesentery. Int J Microcirc Clin Exp 1982;1:29–39.
[25] Curry FE. Antipyrine and aminopyrine permeability of individually perfused frog capillaries. Am J Physiol 1981;240: H597–605.
[26] Curry FE. Mechanics and thermodynamics of transcapillary exchange Sec 2 In: Renkin EM, Michel CC, editors. Handbook of Physiology, vol IV. Washington DC: American Physiological Society; 1984. p. 309–74.
[27] Curry FE. Modulation of venular microvessel permeability by calcium influx into endothelial cells. FASEB J 1992;6:2456–66.
[28] Curry FE, Adamson RH. Vascular permeability modulation at the cell. Microvessel, or whole organ level: Towards closing gaps in our knowledge. Cardiovasc Res 2010;87:218–29.
[29] Curry FE, Mason JC, Michel CC. Osmotic reflection coefficients of capillary walls to low molecular weight hydrophilic solutes measured in single perfused capillaries of the frog mesentery. J Physiol 1976;261:319–36.
[30] Curry FE, Michel CC. A fiber matrix model of capillary permeability. Microvasc Res 1980;20:96–9.
[31] Curry FE, Rygh CB, Karlsen T, Wiig H, Adamson RH, Clark JF, et al. Atrial natriuretic peptide modulation of albumin clearance and contrast agent permeability in mouse skeletal muscle and skin: Role in regulation of plasma volume. J Physiol 2010;588:325–39.
[32] Curry FE, Zeng M, Adamson RH. Thrombin increases permeability only in venules exposed in inflammatory conditions. Am J Physiol 2003;285:H2446–53.
[33] Dvorak AM, Kohn S, Morgan ES, Fox P, Nagy JA, Dvorak HF. The vesiculo-vacuolar organelle (VVO): A distinct endothelial cell structure that provides a transcellular pathway for macromolecular extravasation. J Leukoc Biol 1996;59:100–15.
[34] Feng D, Nagy JA, Hipp J, Dvorak HF, Dvorak AM. Vesiculovacuolar organelles and the regulation of venule permeability to macromolecules by vascular permeability factor, histamine and serotonin. J Exp Med 1996;183:1981–6.
[35] Feng D, Nagy JA, Hipp J, Pine K, Dvorak HF, Dvorak AM. Reinterpretation of endothelial cell gaps induced by vasoactive mediators in guinea pig, mouse and rat: Many are transcellular pores. J Physiol 1997;504:747–61.
[36] Frøkjaer-Jensen J. Three dimensional organization of plasmalemmal vesicles in endothelial cell: An analysis based on serial sectioning of frog mesenteric capillaries. J Ultrastruct Res 1980;73:9–20.
[37] Fu BM, Weinbaum S, Tsay RY, Curry FE. A junction-orifice-fiber entrance layer model for capillary permeability: application to frog mesenteric capillaries. J Biomechan Eng 1994;116:502–13.
[38] Gamble J, Christ F, Gartside IB. The effect of passive tilting on microvascular parameters in the human calf: a strain gauge plethysmographic study. J Physiol 1997;498:541–52.
[39] Garcia-Estan J, Roman RJ. Role of interstitial hydrostatic pressure in the pressure diuresis response. Am J Physiol 1989;256: F63–70.
[40] Ghitescu L, Fixman M, Simionescu M, Simionescu N. Specific binding sites for albumin restricted to plasmalemmal vesicles of continuous capillary endothelium: receptor mediated transcytosis. J Cell Biol 1986;102:1304–11.
[41] Gore R, Bohlen HG. Microvascular pressures in rat intestinal smooth muscle and mucosal villi. Am J Physiol 1978;233: H685–93.
[42] Granger DN, Kvietys PR, Premen AJ. Microcirculation of the intestinal mucosa section 6, The Gastrointestinal System In: Schultz SG, Woods JD, editors. Handbook of Physiology, vol 1. Bethesda MD: American Physiological Society; 1989. p. 1405–74
[43] Grotte G. Passage of dextran molecules across the blood–lymph barrier. Acta Chir Scand Suppl 1956;211:1–84.
[44] Guyton AC. A concept of negative interstitial pressure based on pressures in implanted perforated capsules. Circ Res 1963;12:399–415.
[45] Guyton AC. Interstitial fluid pressure. II: pressure volumes curves of the interstitial space. Circ Res 1965;16:452–60.
[46] Guyton AC, Granger HJ, Taylor AE. Interstitial fluid pressure. Physiol Rev 1971;51:527–63.
[47] Gyenge CC, Tenstad O, Wiig H. *In vivo* determination of steric and electrostatic exclusion of albumin in rat skin and skeletal muscle. J Physiol 2003;552:907–16.
[48] He P, Zeng M, Curry FE. cGMP modulates basal and activated microvascular permeability independently of $[Ca^{2+}]_i$. Am J Physiol 1998;274:H1865–74.
[49] Henriksen O. Local sympathetic reflex mechanism in regulation of blood flow in human subcutaneous adipose tissue. Acta Physiol Scand 1977;(Suppl. 450):7–48.
[50] Henry CBS, Duling BR. Permeation of the luminal capillary glycocalyx is determined by hyaluronan. Am J Physiol 1999;277: H508–14.
[51] Holmang A, Björntorp P, Rippe B. Tissue uptake of insulin and inulin in red and white skeletal muscle *in vivo*. Am J Physiol 1992;263:H1170–6.
[52] Hu X, Adamson RH, Lui B, Curry FE, Weinbaum S. Starling forces that oppose filtration after tissue oncotic pressure is increased. Am J Physiol 2000;279:H1724–36.
[53] Hu X, Weinbaum S. A new view of Starling's hypothesis at the microstructural level. Microvasc Res 1999;58:281–304.
[54] Jeffries W, Brandon M, Hunt S, Williams AF, Gatter KC, Mason DY. Transferrin receptor on endothelium of brain capillaries. Nature 1984;312:162–3.
[55] Kajimura M, Head SD, Michel CC. The effects of flow on the transport of potassium ions through the walls of single perfused frog mesenteric capillaries. J Physiol 1998;511:707–18.
[56] Kajimura M, Michel CC. Flow modulates the transport of K^+ through the walls of single perfused mesenteric venules in anaesthetized rats. J Physiol 1999;521:665–7.
[57] King G, Johnson S. Receptor mediated transport of insulin across endothelial cells. Science 1985;227:1583–6.
[58] Landis EM. Micro-injection studies of capillary blood pressure in human skin. Heart 1930;15:209–28.
[59] Landis EM. Capillary pressure and capillary permeability. Physiol Rev 1934;14:404–81.
[60] Levick JR. Capillary filtration-absorption balance reconsidered in the light of extravascular factors. Exp Physiol 1991;76:825–57.
[61] Levick JR. An introduction to cardiovascular physiology. Fifth edition London: Hodder Arnold; 2010:170-198 [Chapter 11].
[62] Levick JR, Michel CC. The effects of position and skin temperature on the capillary pressure in the fingers and toes. J Physiol 1978;274:97–109.
[63] Levick JR, Michel CC. Microvascular fluid exchange and revised Starling principle. Cardiovasc Res 2010;87:198–210.

[64] Levick JR, Smaje LH. An analysis of the permeability of a fenestra. Microvasc Res 1987;33:233–56.
[65] Loudon MF, Michel CC, White IF. The labeling of vesicles on frog endothelial cells with ferritin. J Physiol 1979;296:97–112.
[66] Luft JH. Fine structure of the capillary and endo-capillary layer as revealed by ruthenium red. Fed Proc 1966;25:1773–83.
[67] Macphee PJ, Michel CC. Sub-atmospheric closing pressures in individual microvessels of rats and frogs. J Physiol 1995;486:183–7.
[68] Macphee PJ, Michel CC. Fluid uptake from the renal medulla into the ascending vasa recta of anaesthetized rats. J Physiol 1995;487:169–83.
[69] Majno G, Palade GE. Studies on inflammation. I. The effects of histamine and serotonin on vascular permeability. An electron microscopic study. J Biophy Biochem Cytol 1961;11:571–605.
[70] Majno G, Shea S, Leventhal M. Endothelial contraction induced by histamine type mediators. An electron microscopic study. J Cell Biol 1969;42:647–72.
[71] Michel CC. Flows across the capillary wall. In: Bergel DH, editor. *Cardiovascular fluid dynamics 2*. New York: Academic Press; 1972. p. 241–98.
[72] Michel CC. The flow of water through the capillary wall. In: Ussing HH, Bindslev N, Lassen NA, et al., editors. *Water transport across epithelia*. Copenhagen: Munksgaard; 1981. p. 268–79.
[73] Michel CC. Fluid movements through capillary walls Section 2, Microcirculation In: Renkin EM, Michel CC, editors. *Handbook of Physiology*, vol 4. Bethesda MD: American Physiological Society; 1984. p. 375–409.
[74] Michel CC. Review lecture: capillary permeability and how it may change. J Physiol 1988;404:1–29.
[75] Michel CC. One hundred years of Starling's hypothesis. News in Physiol Sci 1996;11:229–37.
[76] Michel CC. Transport of macromolecules through microvascular walls. Cardiovasc Res 1996;32:644–53.
[77] Michel CC. Starling: the formulation of his hypothesis of microvascular fluid exchange and its significance after 100 years. Exp Physiol 1997;82:1–30.
[78] Michel CC, Clough GF. Capillary permeability and transvascular fluid balance. In: Sleight P, Vann Jones J, editors. Scientific foundations of cardiology. London: Heineman; 1983. p. 25–30.
[79] Michel CC, Curry FE. Microvascular permeability. Physiol Rev 1999;79:703–61.
[80] Michel CC, Kendall S. Differing effects of histamine and serotonin on microvascular permeability in anaesthetized rats. J Physiol 1997;501:657–62.
[81] Michel CC, Moyses C. The measurement of fluid filtration in human limbs. In: Tooke JE, Smaje LH, editors. Clinical investigation of the microcirculation. Boston: Martinus Nijhoff; 1986.
[82] Michel CC, Phillips ME. Steady-state filtration at different capillary pressures in perfused frog mesenteric capillaries. J Physiol 1987;:421–35.
[83] Miles AA, Miles EM. Vascular reactions to histamine, histamine liberator and leukotaxine in skin of guinea pigs. J Physiol 1952;118:228–57.
[84] Montermini D, Winlove CP, Michel CC. Effects of perfusion rate on permeability of frog and rat microvessels to sodium fluorescein. J Physiol 2002;543:959–75.
[85] Moyses C, Cederholm-Williams SA, Michel CC. Haemoconcentration and accumulation of white cells in the feet during venous stasis. Int J Microcirc Clin Exp 1987;5:311–20.
[86] Neal CR, Michel CC. Transcellular gaps in microvascular walls of frog and rat when permeability is increased by perfusion with the ionophore A23187. J Physiol 1995;488:427–37.
[87] Noddeland H, Aukland K, Nicolaysen G. Plasma colloid osmotic pressure in venous blood from the human foot in orthostasis. Acta Physiol Scand 1981;113:447–54.
[88] Noddeland H, Riisnes SM, Fadnes HO. Interstitial fluid colloid osmotic pressure and hydrostatic pressure in subcutaneous tissue of patients with nephritic syndrome. Scand J Clin Lab Invest 1982;42:139–46.
[89] Öberg B. Effects of cardiovascular reflexes on net capillary fluid transfer. Acta Physiol Scand 1964;62(Suppl):229.
[90] Pallone TL, Kishore BK, Nielsen S, Agre P, Knepper MA. Evidence that aquaporin-1 mediates NaCl induced water flux across the descending vasa recta. Am J Physiol 1997;272:F587–96.
[91] Pappenheimer JR, Soto-Rivera A. Effective osmotic pressure of the plasma proteins and other quantities associated with the capillary circulation in the hind limbs of cats and dogs. Am J Physiol 1948;152:471–91.
[92] Pappenheimer JR, Renkin EM, Borrero LM. Filtration, diffusion and molecular sieving through peripheral capillary membranes. A contribution to the pore theory of capillary permeability. Am J Physiol 1951;167:13–46.
[93] Parker JC, Gilchrist S, Cartledge JT. Plasma-lymph exchange and interstitial distribution volumes of charged macromolecules in the lung. Am J Physiol 1985;59:1128–36.
[94] Patlak CS, Goldstein DA, Hoffman JF. The flow of solute and solvent across a two-membrane system. J Theoret Biol 1963;5:426–42.
[95] Pocock TM, Foster RR, Bates DO. Evidence for a role for TRPC channels in VEGF-mediated increased vascular permeability *in vivo*. Am J Physiol 2004;286:H1015–26.
[96] Reed RK. Transcapillary albumin extravasation in rat skin and muscle: Effect of increased venous pressure. Acta Physiol Scand 1988;134:375–82.
[97] Reed RK. Interstitial fluid pressure. In: Reed RK, McHale NG, Bert JL, et al., editors. *Interstitium, connective tissue and lymphatics*. London: Portland Press; 1995. p. 85–100.
[98] Reed RK, Rubin K. Transcapillary exchange: role and importance of the interstitial fluid pressure and extracellular matrix. Cardiovasc Res 2010;87:211–7.
[99] Renkin EM. Capillary permeability to lipid soluble molecules. Am J Physiol 1952;168:538–45.
[100] Renkin EM. Transport of potassium-42 from blood to tissue in isolated mammalian skeletal muscle. Am J Physiol 1959;197:125–1210.
[101] Renkin EM. Transport of large molecules across capillary walls. Physiologist 1964;7:13–28.
[102] Renkin EM. Blood flow and transcapillary exchange in skeletal and cardiac muscle. In: Marchetti G, Taccardi B, editors. International symposium on coronary circulation. Basel: Karger; 1967. p. 18–30.
[103] Renkin EM. Control of microcirculation and blood tissue exchange. In: Renkin EM, Michel CC, editors. Handbook of physiology. the cardiovascular system. microcirculation, vol IV. Washington DC: American Physiological Society; 1984: 627–87.
[104] Renkin EM. Transport pathways and processes. In: Simionescu N, Simionescu M, editors. *Endothelial cell biology*. New York: Plenum Publishing; 1988.
[105] Renkin EM, Tucker VL. Measurements of microvascular transport parameters of macromolecules in tissues and organs of intact animals. Microcirculation 1998;5:139–52.
[106] Rippe B, Haraldsson B. Transport of macromolecules across microvascular walls: two pore theory. Physiol Rev 1994;74:163–219.
[107] Rippe B, Kamiya A, Folkow B. Transcapillary passage of albumin, effects of tissue cooling and of increases in filtration and plasma colloid osmotic pressure. Acta Physiol Scand 1979;105:171–87.

[108] Rippe B, Rosengren B-I, Carlsson O, Venturoli D. Transendothelial transport: the vesicle controversy. J Vasc Res 2002;39:375–90.
[109] Rippe B, Taylor AE. NEM and filipin increase albumin transport in lung microvessels. Am J Physiol 2001;280:H34–41.
[110] Rosengren B-I, Rippe A, Rippe C, Venturoli D, Swärd K, Rippe B. Transvascular protein transport in mice lacking caveolae. Am J Physiol 2006;291:H1371–7.
[111] Schnitzer J, Oh P, Pinney E, Allard J. Filipin sensitive caveolae-mediated transport in endothelium: reduced transcytosis, scavenger endocytosis and capillary permeability of select macromolecules. J Cell Biol 1994;127:1217–32.
[112] Schnitzer J, Allard J, Oh P. NEM inhibits transcytosis, endocytosis and capillary permeability: Implication of caveolae fusion in endothelia. Am J Physiol 1995;37:H48–55.
[113] Schnitzer J, Oh P, Jacobson BS, Dvorak AM. Caveolae from luminal plasmalemma of rat lung endothelium: Microdomains enriched in caveolin, Ca^{2+}-ATPase and IP3 receptor. Proc Natl Acad Sci USA 1995;92:1759–63.
[114] Schnitzer J, Lui J, Oh P. Endothelial caveolae have the molecular transport machinery for vesicle budding, docking and fusion including VAMP, NSF, SNAP, annexins and GTPases. J Biol Chem 1995;270:14399–404.
[115] Schnitzer J, Oh P, McIntosh DP. Role of GTP hydrolysis in fission of caveolae directly from plasma membranes. Science 1996;274:239–42.
[116] Shirahama T, Cohen AS. The role of mucopolysaccharides in vesicle architecture and endothelial transport. J Cell Biol 1972;52:198–205.
[117] Simionescu N, Simionescu M, Palade GE. Permeability of muscle capillaries to small hemepeptides. J Cell Biol 1975;64:586–607.
[118] Squire JM, Chew M, Nneji G, Neal C, Barry J, Michel C. Quasi-periodic substructure in the microvessel endothelial glycocalyx: a possible explanation for molecular filtering? J Struct Biol 2001;136:239–55.
[119] Starling EH. On the absorption of fluids from connective tissue spaces. J Physiol 1896;19:312–26.
[120] Tavassoli M, Kishimoto T, Kataoka M. Liver endothelium mediates the hepatocyte's uptake of ceruloplasmin. J Cell Biol 1986;102:1298–303.
[121] Taylor AE, Granger DN. Exchange of macromolecules across the microcirculation. In: Renkin EM, Michel CC, editors. Handbook of physiology. microcirculation, vol IV. Washington: American Physiological Society; 1984. p. 467–520.
[122] Tenstad O, Heyeraas KJ, Wiig H, Aukland K. Drainage of plasma proteins from the renal medullary interstitium in rats. J Physiol 2001;:533–9.
[123] Turner MR, Pallone TL. Hydraulic and diffusional permeabilities of isolated outer medullary descending vasa recta from the rat. Am J Physiol 1997;272:H392–400.
[124] Tucker VL, Simanok KE, Renkin EM. Tissue specific effects of physiological ANP infusion on blood tissue albumin transport. Am J Physiol 1992;63:R945–53.
[125] Van Haaren PMA, VanBavel E, Vink H, Spaan JAE. Localization of the permeability barrier to solutes in isolated arteries by confocal microscopy. Am J Physiol 2003;285: H2848–56.
[126] Vink H, Duling BR. Identification of distinct luminal domains for macromolecules, erythrocytes and leukocytes within mammalian capillaries. Circ Res 1996;79:581–9.
[127] Wagner RC, Chen SC. Transcapillary transport of solute by the endothelial vesicular system: Evidence from serial section analysis. Microvasc Res 1991;42:139–50.
[128] Wang W, Michel CC. Modeling exchange of plasma proteins between microcirculation and interstitium of renal medulla. Am J Physiol 2000;279:F334–44.
[129] Weinbaum S. Distinguished lecture. Models to solve the mysteries in biomechanics at a cellular level. A new view of fiber matrix layers. Ann Biomed Eng 1998;26:627–43.
[130] Weinbaum S, Tsay R, Curry FE. A three-dimensional junction-pore matrix model for capillary permeability. Microvasc Res 1992;44:85–111.
[131] Wiig H, Reed RK. Interstitial compliance and transcapillary pressures in cat skin and skeletal muscle. Am J Physiol 1985;248:H666–73.
[132] Williams TJ, Peck MJ. Role of prostaglandin-mediated vasodilatation in inflammation. Nature 1977;270:530–2.
[133] Wissig S, Williams MC. The permeability of muscle capillaries to microperoxidase. J Cell Biol 1978;76:341–59.
[134] Wolf MB, Watson PD. Measurement of osmotic reflection coefficient for small molecules in cat hind limbs. Am J Physiol 1989;256:H282–90.
[135] Wu HM, Huang Q, Yuan Y, Granger HJ. VEGF induces NO-dependent hyperpermeability in coronary venules. Am J Physiol 1996;271:H2735–9.
[136] Yuan Y, Granger HJ, Zawieja DC, Chilian WM. Flow modulates coronary venular permeability by a nitric oxide related mechanism. *Am J Physiol* 1992; 263 1992;:H641–6.
[137] Yudilevich DL, Alvarez OA. Water, sodium and thiourea transcapillary diffusion in the dog heart. Am J Physiol 1967;213:308–14.
[138] Zhang W, Edwards A. Transport of plasma proteins across vasa recta in the renal medulla. Am J Physiol 2001;281: F478–92.

CHAPTER

10

External Balance of Electrolytes and Acids and Alkali

Man S. Oh

State University of New York, Downstate Medical Center, Brooklyn, NY, USA

This chapter will cover discussions on principles of external balance for electrolytes, and for acids and bases. The first section will deal with discussions on principles of electrolyte balance in general, and the second section discusses the acid–base balance.

PRINCIPLES OF ELECTROLYTE BALANCE

Introduction

Prolonged imbalance between input and output of most quantifiable elements in a living organism is incompatible with life. The duration of imbalance varies, but eventually balance must be restored for maintenance of survival. This rule applies to all quantifiable elements *in vivo* as well as *in vitro*. Red cell destruction equals red cell production. Oxygen uptake equals oxygen utilization. Sodium intake must equal sodium output, and water input must match water loss. Yet transient discrepancies occur regularly in living organisms, but balance is ultimately achieved. The same rule applies to the balance of any quantifiable elements in nature. The duration of imbalance is usually quite short in living organisms, because protracted imbalance results in death. However, not limited by survival, the duration of imbalance in nature could be more protracted.

The main aim of this chapter is to describe the underlying principles for eventual restoration of balance in nature, and then to extrapolate these principles to the understanding of human physiology, particularly the principles of fluid and electrolyte balance.

WHY IS BALANCE ALWAYS RESTORED?

The underlying mechanism that allows eventual restoration of balance is perfect and foolproof. As an example, the kidney is a central player in the restoration and achievement of fluid and electrolyte balance in living organisms, but the smartness of the kidney is not the reason for perfect balance. The kidney merely accelerates the process by utilizing a principle ubiquitous in nature, but it does not determine its ultimate outcome. The most crucial element of the control system that restores ultimate balance is that a discrepancy between intake and output inevitably leads to a change in total content of the element in the system, and the uncorrected imbalance is cumulative. When input is greater than output the content increases, and the continued imbalance keeps increasing the content. When output is greater than input the content decreases, and the continuing imbalance keeps decreasing the content. In a system with a limited capacity, a change in content of a substance alters its concentration; this invariably affects output, and sometimes also input. The key points here are: (1) an uncorrected balance invariably leads to a change in content; (2) a change in content leads to a change in concentration; (3) an altered concentration affects output or input; and (4) these effects are cumulative.

IS THE CAPACITY OF ANY SYSTEM ALWAYS LIMITED?

Is the capacity of any system always limited? The answer is yes. We often say: the sky has no limit. Yet

Seldin and Giebisch's The Kidney, Fifth Edition.
DOI: http://dx.doi.org/10.1016/B978-0-12-381462-3.00010-0

© 2013 Elsevier Inc. All rights reserved.

there is a limit even to the capacity of atmospheric air volume. The apparent air volume is about 4.08×10^{21} liters. (The apparent air volume is calculated considering that air is denser at sea level, and density declines progressively with rising altitude until there are no more air molecules. Thus, the apparent air volume is the theoretical volume that would be required if all the gases in the air were contained at the same concentrations as those at sea level at a pressure of 760 mmHg when the 1 mole of gas is contained in 22.4 liters.)

In recent years, the rising CO_2 concentration of the atmosphere and its impact on global warming is the source of a great deal of public concern. The rising CO_2 concentration implies that the amount of CO_2 added to the atmosphere is more than the amount eliminated from the atmosphere. However, the discrepancy will not and cannot remain permanent, because the CO_2 concentration in the atmosphere has a positive influence on the rate of its removal from the atmosphere. The main source of CO_2 addition to the air is the burning of fossil fuels (oil, gas, and coal). The total amount of CO_2 added is about 30 billion tons per year.[1] This amount added to the air volume of 4.08×10^{21} liters would increase atmospheric CO_2 concentration by about 3.74 ppm per year. Currently, the actual rise in CO_2 concentration is about 2 ppm per year. The difference, 1.74 ppm, is absorbed by the oceans, mostly by direct diffusion and some by diffusion into rain water entering the ocean. In the ocean, CO_2 is in equilibrium with bicarbonate and carbonate.[2] As the atmospheric CO_2 concentration increases, the amount entering the ocean would increase progressively. Since the industrial revolution, the atmospheric CO_2 level has been rising rapidly, because the rate of CO_2 addition has been increasing rapidly with the progressively greater consumption of fossil fuel worldwide. Once the rate of fossil fuel consumption stops increasing further, the rate of CO_2 removal will eventually equal the rate of CO_2 addition. Of course, it is quite likely that at the time of new balance, the earth could be much warmer and the ocean much more acidic, with major ecological changes. Nevertheless, imbalance does not last forever, because imbalance always leads to a new balance.

Many substances in the human body utilize the same principles to reach a state of balance. For example, if creatinine production is doubled in the absence of any change in GFR, serum creatinine would exactly double, at which point the renal excretion of creatinine would also double. At this point a new balance is reached between production and excretion. For some substances, a new balance is accelerated by physiological control mechanisms. For example, if sodium intake is doubled, renal sodium excretion will also double, but doubling of renal sodium excretion does not require doubling of serum sodium or total body sodium content, only a slight increase in sodium content of the body, because of the excellent renal regulation of sodium balance. By the same token, a reduction in sodium intake to 1/10 of the usual amount does not require sodium content of the body to decrease to 1/10 of normal when the balance is restored.

In the human body, the capacity for most substances is quite limited, and daily variations for most electrolytes are quite large in relation to total body content. Furthermore, there is a limit to which the organism can tolerate a deviation in the content of these substances. Therefore, survival of the organism demands the existence of certain physiological mechanisms to accelerate the compensation processes, to prevent a deviation from occurring to a lethal level.

Following is the sequence of events in the control system: a certain amount of an element is contained in a compartment, if input of the element into the compartment exceeds its output, the content will increase. The higher content influences the control mechanisms to reduce input or to increase output. As long as the discrepancy remains, the content will keep increasing, because the consequence of discrepancy is cumulative; the higher the content, the greater the effect on input or output. A cumulative change stops only when input equals output. When input is less than output, the opposite sequence of events restores the balance (Figure 10.1).

Restoration of salt balance will be used as an example. A person in a state of sodium balance has been ingesting 10 g of salt per day, and excreting 10 g of salt per day. Now, assume that a diuretic is given to this person. On the first day of diuretic therapy, salt output is 20 g per day, with net loss of 10 g of salt. The next day, although the diuretic dosage remains unchanged, salt excretion has to be less, for example, 15 g a day, because the reduction in effective vascular volume caused by the previous day's salt loss has activated salt-retaining mechanisms, and has reduced salt losing hormones. Still, the overall result is an additional negative balance of 5 g of salt. Although the negative balance is less on the second day, the cumulative loss (15 g) is greater on the second day than on the first, and the effective vascular volume is even lower on the second day than the first. The lower effective volume reduces salt output further to 12 g per day on the third day, with an additional negative balance of 2 g. The overall cumulative loss is now 17 g, resulting in a further decrease in effective vascular volume. As long as the salt output remains greater than salt intake, cumulative salt loss becomes larger and larger, albeit less steeply than before. Cumulative salt loss stops only when salt output equals salt intake. Indefinite net salt loss is theoretically impossible, because continued salt loss will ultimately cause such severe volume depletion that the

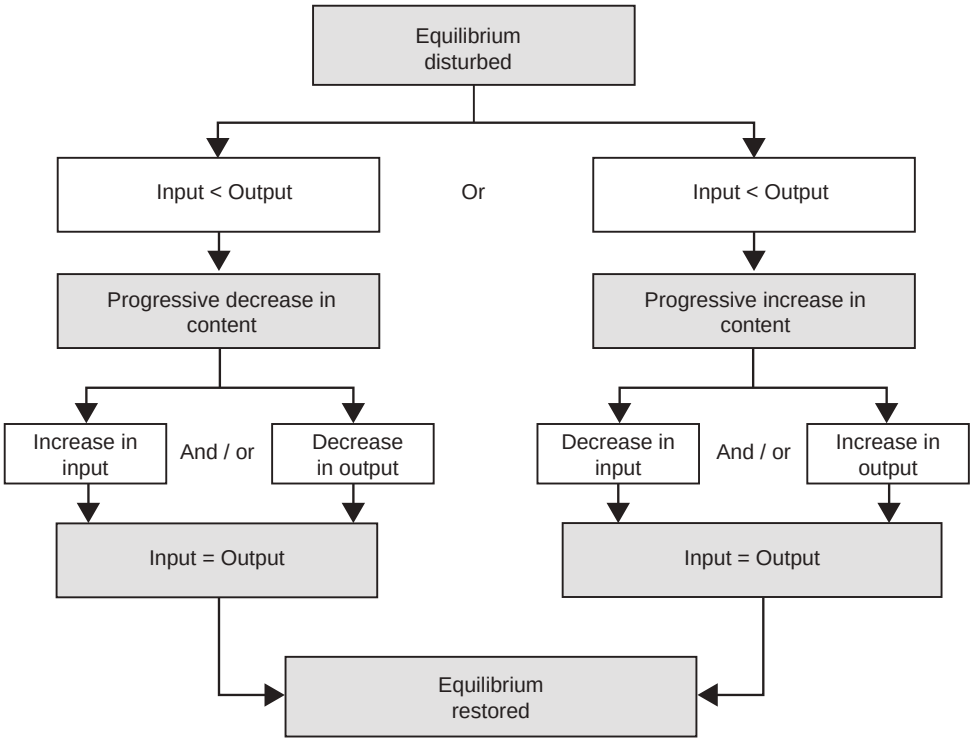

FIGURE 10.1 **Mechanisms by which balance is restored.**

person will become hypotensive, and salt excretion would stop completely. Of course, long before reaching such an extreme state, renal excretion of salt would decrease to a level equaling intake.

In the example given, what causes restoration of balance is not the smartness of the kidney or the cleverness of humoral mechanisms, but the principle of balance restoration, which is ubiquitous in nature. For example, sodium balance in a person on chronic diuretic therapy would still be restored in the absence of aldosterone, in which case the person could be quite sick with dehydration when balance is attained.

The same control mechanism explains why urinary excretion of potassium does not remain greater than intake in patients with primary hyperaldosteronism. With increased aldosterone, K output will initially exceed K intake. The resulting negative K balance causes hypokalemia, which in turn reduces urine K excretion. As long as K excretion exceeds K intake, serum K will decrease progressively until K excretion equals K intake. Occasionally, a patient dies of a cardiac arrhythmia before balance is attained. In the vast majority of cases, balance is achieved before the patient dies.

SPEED OF BALANCE RESTORATION

In a living organism, the speed of restoration of balance is teleologically determined. If an organism can tolerate protracted imbalance of a particular element without death or severe disability, balance need not be restored promptly. If quick restoration of balance is vital for survival, a mechanism for rapid restoration of balance is necessarily acquired in the process of evolution. Thus, the acceptable duration of discrepancy or alternatively speed with which restoration of balance is achieved, depends on the importance of maintaining the content of an element within a narrow range, in order to prevent the demise or serious disability of the organism. Four main factors influence the speed of balance restoration (Table 10.1).

For example, an adult of average size has about 40 liters of total body water, and daily intake and output of water is about 2 liters. Obviously, water output exceeding water intake by one liter a day would lead to fatal dehydration in 10 days to two weeks. Conversely, water intake exceeding water output by the same magnitude would lead to water intoxication and death. An opposite example is calcium balance. The total body calcium content of an average adult man is about 1,200,000 mg (60,000 mEq), and net daily external flux is about 150 mg (7.5 mEq). A daily negative balance of calcium of 100 mg for one year would reduce total body calcium by mere 36,500 mg; 3% of total body calcium content. Obviously, a negative calcium balance of such a magnitude, even for a protracted period, is not incompatible with life. Indeed, during the period of development of osteoporosis,

TABLE 10.1 Factors Influencing the Speed of Balance Restoration

1. Magnitude of flux.
2. Basal store.
3. Capacity for additional storage.
4. The physiological limit for deviation of the body content.

a substantial negative balance of calcium for 10 years or longer is a common occurrence. Similarly, a positive caloric balance of 500 calories a day for a year will result in a total positive balance of 182,500 calories ($500 \times 365 = 182{,}500$). This amount would result in an increase in adipose tissue weight of about 50 lbs, an undesirable situation, but with no immediate effect on survival.

A large storage capacity does not guarantee a protracted imbalance. A quantitative analysis must be applied before that conclusion is reached. Once it was widely accepted that a large store of alkali of the bone was responsible for the maintenance of stable serum bicarbonate concentrations in chronic renal failure, despite a substantial daily positive balance of acid.[3,4] However, this conclusion was reached without quantitative analysis. The bone content of alkali is indeed very large, but it is not sufficiently large to provide 19 mEq of alkali per day for six years in chronic renal failure. Since the total content of acid in the bone is about 25,000 mEq, a quick calculation would indicate that at a rate of consumption at 19 mEq per day, the entire bone content of alkali would be gone in about 3.6 years. Clearly, uremic patients with metabolic acidosis are in states of good or near acid–base balance, i.e., acid production equals acid excretion.

The cumulative net loss of a substance from the body cannot exceed the total amount of that substance contained in the body (Table 10.2). For example, one can conclude with certainty that a person who has total body sodium content of 3500 mEq could not have been in daily negative balance of sodium by 10 mEq per day for one year, since the total loss of 3650 mEq ($10 \times 365 = 3650$) would exceed the total body store of sodium. Even before exceeding the total body content, one cannot exceed a physiological limit of deficit for the substance. For example, potassium loss in excess of a third of the body store (3000 mEq) is usually fatal. Hence, you would reject a claim that a patient with Conn's tumor has been losing 20 mEq of potassium daily for three months, since loss of such an amount ($20 \times 30 \times 3 = 1800$ mEq) would certainly be lethal. In contrast, the body can tolerate a greater fraction of sodium loss. A person who loses half of the body's sodium would be gravely ill, but still alive.

While the total stored amount sets the absolute upper limit on losses, the amount that can be gained depends on the additional storage capacity, which varies widely with electrolytes. In the case of sodium, the storage capacity for additional Na^+ in the body is enormous. In certain edema-forming states, the Na^+ content may increase by 300% of the basal amount. Caloric balance is another example. In a normally-built adult, the total stored in fat and protein is about 130,000 calories. At the caloric consumption rate of 1200 calories per day, about 50% of the stored calories would be consumed in 55 days. In contrast, a person can gain as much as 500 lbs of fat, which are equal to 4,500,000 calories, about 35 times the normal caloric storage.

TABLE 10.2 Major Elements of Human Body: Total Body Content, Daily Turnover Rate, and Days Required for 50% Turnover

Body Elements	Total Body Content	Usual Daily Turnover	Days for 50% Turnover
Na	3500 mEq	4%	12
K	3000 mEq	2.3%	22
Ca	60,000 mEq	0.01%	2700
Mg	2000 mEq	0.5%	100
P	18,000 mmol	0.17%	290
Water	40 L	5%	10
Alkali	28,000 mEq	0.2%	250
Calories	130,000 kcal	1.5%	33
Creatinine	400 mg	400%	0.12
Urea-N	4000 mg	250%	0.2

MECHANISM OF BALANCE RESTORATION

All control mechanisms are activated by the introduction of a new influence into a system that causes imbalance between input and output of an element, and this leads to an alteration in a parameter of the element in the system. In biological systems, parameters that are most often disturbed are concentrations of elements in the plasma. Other disturbed parameters include pressure, volume, temperature, and body weight. Alterations in a parameter affect either input or output, which in turn affects the parameter directly or indirectly. Examples of an element that is directly responsible for a change in a parameter are balance of potassium (element) affecting plasma potassium concentration (parameter), and balance of magnesium (element) affecting the plasma magnesium

concentration (parameter). Examples of an element that is indirectly responsible for a change in parameter include the balance of sodium (element) affecting the effective vascular volume (parameter), and the balance of calories (element) affecting body weight (parameter).

The effectiveness of the compensation mechanism determines the degree of deviation of a parameter from the baseline value when the balance is restored. A poor compensation mechanism restores balance with the parameter greatly deviated from the baseline value. An example of a poor compensation mechanism is a change in plasma urea concentration with a change in the rate of urea production. When urea production doubles, the renal excretion will eventually also double and equal the increased production rate. However, at equilibrium the plasma urea concentration will be twice the baseline value. An example of a good compensation mechanism is a change in a sodium content of the body in response to a change in sodium intake. When salt intake is doubled, renal excretion of salt will eventually double; at this point the total body sodium content would be very slightly greater than the baseline value.

MODELS OF EXTERNAL BALANCE

The pattern of restoration of new balance for control of various elements in the human body is broadly classified into three models. The main source of input for most electrolytes in our body is oral intake and the main output the renal excretion, with some additional output through the GI tract.

Model A

This model is depicted in Figure 10.2 as a cylinder filled with water. Water enters from a faucet into the cylinder, and leaves through a hole at the bottom. The height of the water column depends on water input and water output, and water output in turn depends on the size of the hole at the bottom and the hydrostatic pressure. The hydrostatic pressure in turn depends on the height of water column. Under these conditions, only two factors can change the height of the water column permanently; the rate of water input and the size of the hole. If the rate of water input is doubled while the size of the outlet hole is kept constant, water output will also double when the balance is restored.

With the same size outlet hole, doubling of water output would require doubling of hydrostatic pressure, which in turn requires doubling of the water column height. Before balance is restored, the water column height rises, because water input exceeds water output. The rise in the water column height gradually increases the hydrostatic pressure, and therefore the water output. Hence the discrepancy between the water input and the water output gradually lessens. However, as long as water input remains greater than water output, the water level will keep rising, and the rise will stop only when the water output equals the water input; this occurs when the water column height is exactly doubled.

Conversely, decreasing the size of the outlet hole to double the resistance to water flow, with an unchanged rate in the water input, would initially reduce the water output to half. The ensuing imbalance between the water output and the water input would cause a rise in the water column height. A higher hydrostatic pressure resulting from the rise in the water column would allow more water to come out through a narrower hole. Thus, in this example, doubling of the water column height will restore the water output to the baseline value.

The main characteristic of this type of compensation is that the alteration in content or concentration caused by a disturbance is directly or inversely proportionate to the magnitude of the alteration in input or output function. For example, if the input of a substance is doubled, the content or concentration of the substance will be doubled when balance is restored. If input is increased three-fold, the content or concentration will be tripled. Similarly, if the output function is halved, the content or concentration will be doubled when balance is restored. If the output function is reduced to one tenth of the baseline, the content or concentration will be increased ten-fold when balance is restored.

Many substances in the body follow this pattern of compensation mechanism in order to achieve a new balance. When a substance follows this pattern of compensation, the body must have a high degree of tolerance for a large deviation in the body content or concentration for the substance. For example, if creatinine clearance diminishes to half of the baseline value with an unchanged creatinine production rate, serum creatinine concentration will double in order to achieve the same rate. Similarly, if creatinine production is reduced to half of the baseline value with the same renal creatinine clearance, serum creatinine concentration will be half of the original value. Likewise, if urea production is doubled, with unchanged kidney function, serum urea concentration is doubled when balance is restored.

Model B

In this model, the cylinder has a wedge-shaped slit on its side instead of a hole at the bottom (Figure 10.3). Water enters the cylinder from a faucet, and leaves through the slit. As in model A, water output depends on the height of the water column. But, because of the

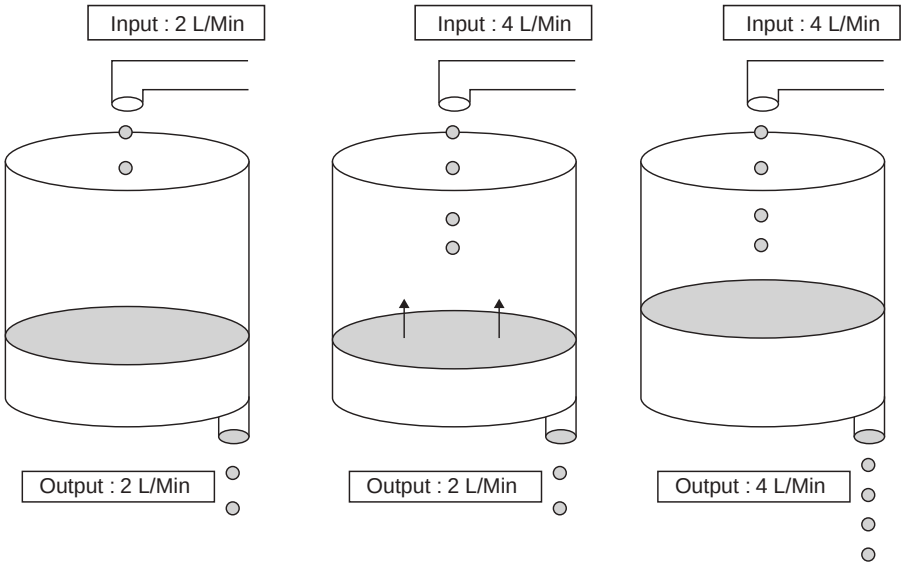

FIGURE 10.2 **Model A.** The input and output determines the balance, but the output changes in proportion to the height of the water column. When the water input doubles while the size of the output hole remains unchanged, the only way for the output to increase to the same level as the input is to double the height of the water column. At this point, a new balance is struck between input and output. For example, if creatinine production doubled while creatinine clearance remained unchanged, serum creatinine concentration will be doubled when a new balance is achieved between creatinine production and creatinine excretion

wedge shaped slit, the effect of a rise in water level on water output is exponential. Therefore, when water intake doubles, doubling of water output does not require doubling of the water column height. Depending on the shape of the slit, the water level may rise only slightly before a new balance is restored. In other words, an increase in water output in response to a change in the height of water column is magnified in this system. Furthermore, unlike model A, when the water level drops below the lowest part of the slit, water output stops altogether.

The regulation of the body content or plasma concentration of most electrolytes and other essential body elements utilizes this type of compensation. For example, when potassium intake is increased five-fold, plasma potassium concentration does not increase five-fold when balance is restored. In the presence of normal renal function and normal aldosterone response, plasma potassium concentration will increase only slightly. Likewise, a five-fold increase in sodium intake causes only a slight increase in body sodium content or plasma sodium concentration; when sodium intake is greatly reduced, the body sodium content decreases only slightly before renal sodium excretion ceases.

Model C

The pattern of water excretion in model C (Figure 10.4) is similar to model A, but in this model two cylinders, one big (A) and the other small (B), are connected at the bottom. Water enters only into cylinder A, but once it enters, it equilibrates with cylinder B. Ordinarily, because cylinder A has a bigger hole than cylinder B, the water output is determined primarily by the size of hole A. However, as the size of hole A decreases, the role of hole B increases. When water input is doubled, the height of the water column will have to be doubled in order to permit establishment of a new steady-state. On the other hand, when the resistance to flow through hole A is doubled, the height of the water column will be less than doubled when balance is restored, provided that the size of hole B is unchanged.

When the excretion rate through hole A decreases, the excretion through hole B becomes more important. The regulation of plasma concentration of uric acid follows the pattern in model C. Uric acid is cleared by the kidney, and is also cleared metabolically by colonic bacteria. The renal clearance of uric acid is normally about 8 liters per day, and the colonic clearance is about 4 liters per day. Thus, 2/3 of the uric acid produced is cleared by the kidney and 1/3 by the colon.[5] If the plasma concentration of uric acid is 5 mg/dl (50 mg/L), renal excretion of uric acid would be 400 mg per day (uric acid clearance of 8 liters per day), and the amount cleared by the colonic bacteria would be 200 mg, with a total uric acid removal rate of 600 mg per day. If chronic renal disease reduces the renal clearance of uric acid to 4 L a day (half of normal), total uric acid clearance would now be 8 liters

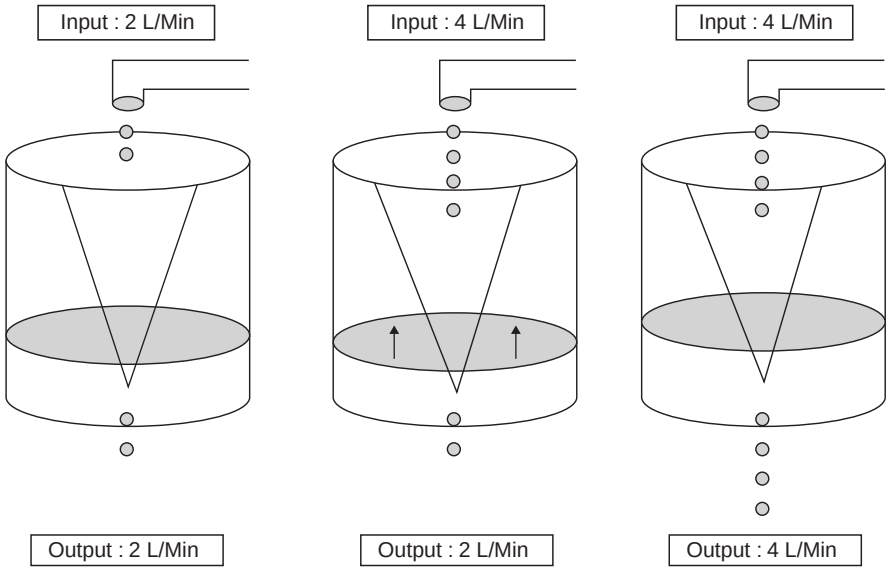

FIGURE 10.3 **Model B.** As in model A, input and output determines the balance, and output depends on the height of water column. However, unlike model A, a change in water output by the change in the height of water column is magnified. When the height of water column increases slightly, water output increases greatly, and a decrease in its height reduces water output markedly. Furthermore, when the height of the water column decreases below a certain level, output ceases completely. Thus, doubling of input from 2 liters per minute to 4 liters per minute requires increases in water level only slightly before output also increased to 4 liters a minute.

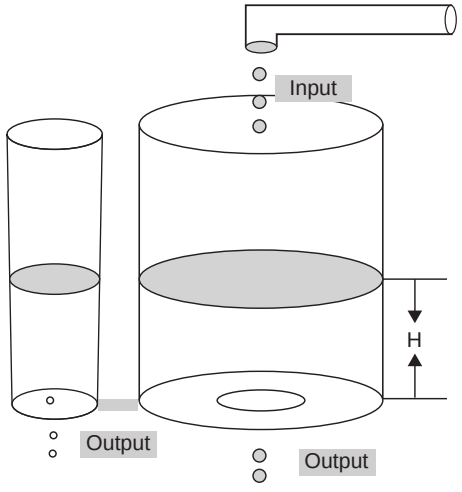

FIGURE 10.4 **Model C.** Two compartments A and B are connected to each other, and each has an outlet hole. Water output from both compartments depends on the height of water column. Because hole A is much larger than hole B, the bulk of water output occurs through hole A. When hole A becomes smaller, output through hole B plays a greater role in water output.

per day, if the colonic clearance remained unchanged at 4 liters per day. If the rate of production remained the same (600 mg/day), plasma uric acid concentration would not double to 10 mg/dl, but would increase to 7.5 mg/dl, because total body uric acid clearance would be 8 liters per day (4 + 4 = 8 liters); at this concentration, the total amount of uric acid cleared would be 600 mg/day (75 mg/L × 8 L/day = 600 mg/day).

The regulation of plasma creatinine concentration follows the same type of compensation as shown in model C. Normally, creatinine is cleared mainly by the kidney, with a daily clearance of about 180 liters, but the colonic bacteria also remove a small amount of creatinine, providing about 3 liters of creatinine clearance per day.[6] Thus, normally the colonic clearance, which constitutes less than 2% of the total creatinine clearance, has little impact on the plasma concentration of creatinine. However, in the presence of advanced renal failure, which does not diminish the colonic clearance of creatinine, it could have a substantial impact on plasma concentration of creatinine. For example, in a person who has 5 ml/min of renal creatinine clearance (7.2 liters per day), 3 liters of colonic clearance would now represent about 30% of the total creatinine clearance. For these reasons, the rate of rise in serum creatinine in advanced renal failure is not exactly inversely proportionate to the reduction in renal clearance of creatinine.

INFINITE GAIN CONTROL MECHANISM

The ultimate aim of all compensation mechanisms is restoration of balance between input and output, after balance is disturbed by introduction of an abnormality. In most instances restoration of balance is possible only when the abnormality persists. For example, increased renal excretion of potassium by primary hyperaldosteronism will result in imbalance between input and

output, with output exceeding input. Development of hypokalemia is needed for output to decrease to match input, and hypokalemia is the price that must paid in order to restore balance. Similarly, an increase salt intake would result in chronic volume expansion, in order for salt excretion to increase to equal the increased intake. The infinite gain control mechanism, to be discussed below, is unique in that the abnormality is corrected completely when a balance is restored.

This principle is well illustrated in Figure 10.5. In this model system, water enters the tank from a faucet at the top, and leaves the tank through a hole at the bottom. The input is independently regulated, but the water output depends on two factors, the size of the outlet hole and the hydrostatic pressure. The hydrostatic pressure in turn depends on the water level, which is determined by the balance between the water input and water output. At equilibrium, the water input is equal to the water output. What would happen if the capacity of the tank is suddenly altered at this point by, for example, placing a brick in the tank, without a change in the water input or the size of outlet hole (i.e., output function)? Initially, the water level would rise and hydrostatic pressure at the bottom of the tank would be increased. The higher pressure with the same size outlet hole would cause the output of water to exceed water input. The consequent imbalance between the input and output would cause a gradual decline in the water level. But, as long as the water level is higher, even slightly, than the baseline value, the water output will exceed the water input. Only when the water level decreases to the original level, will the water input equal the water output. A sudden increase in the capacity of the tank, for example by creating a pouch on the tank, would cause an imbalance between the water input and the water output because of the initial reduction in the water level and the hydrostatic pressure, but the discrepancy would be only transient. At equilibrium, the water level will return to the original level.

This type of compensation mechanism is ubiquitous in various physiological and pathological states in the human body, but the importance of this mechanism was first recognized by Guyton, who presented the concept in his discussion of the regulation of arterial blood pressure.[7–10] He boldly predicted that in the absence of an altered function of renal excretion of salt, no abnormality will sustain hypertension chronically. This prediction was made on the basis of the observation that the arterial blood pressure is normally a powerful regulator of renal salt excretion, and that a minute increase in blood pressure results in a large increase in salt excretion, and salt excretion in excess of salt intake will continue until the blood pressure returns to normal[9].

Suppose hypertension develops as a result of increased systemic vascular resistance, while the responsiveness of the kidney to changes in blood pressure to influence salt output (i.e., renal function curve in response to blood pressure) remains unchanged; the higher the pressure, the higher the renal salt output. Increased salt output caused by a higher blood pressure in the absence of commensurate increase in salt intake would lead to a negative salt balance. The negative salt balance would reduce effective vascular volume, circulating blood volume, and eventually cardiac output. A lower cardiac output will reduce blood pressure to a lower level, but as long as the blood pressure is still higher than the baseline, salt output will remain greater than the basal salt output. The salt output in excess of salt intake progressively reduces the salt content of the body. Only when blood pressure returns to the original value will the renal salt output return to the baseline value. At this point, balance is restored between salt intake and salt output, and the abnormality in blood pressure is completely dissipated.

In Guyton's use, the term "gain" is defined as the fraction of abnormality that has been corrected divided by the fraction yet to be corrected.[8] For example, if an abnormality causes an increase in blood pressure, and a control system brings it back halfway to the original value, the feedback gain is one ($0.5/0.5 = 1$). Gain is zero if a control system does not correct at all ($0/1 = 0$). Gain is infinite if the abnormality is almost all corrected completely with virtually nothing left to be corrected, because division of a number with an infinitely small number results in an infinitely large number.

What is the reason why an abnormality disappears completely in the infinite gain control mechanism, but not in other control mechanisms? The main difference is in the nature of the influence that causes disturbances in the system. When the disturbance affects either input or responsiveness of the system to change in a parameter for the output (i.e., output function), the abnormality will not be corrected completely, and the compensation mechanism does not involve the infinite gain control mechanism. On the other hand, when the disturbance introduced is not one of these two kinds, the compensation mechanism is an infinite gain control mechanism.

COMMON MISCONCEPTIONS AND NEW INSIGHTS

A series of topics discussed in the following section deals with widespread misconceptions regarding principles related to restoration of balance states.

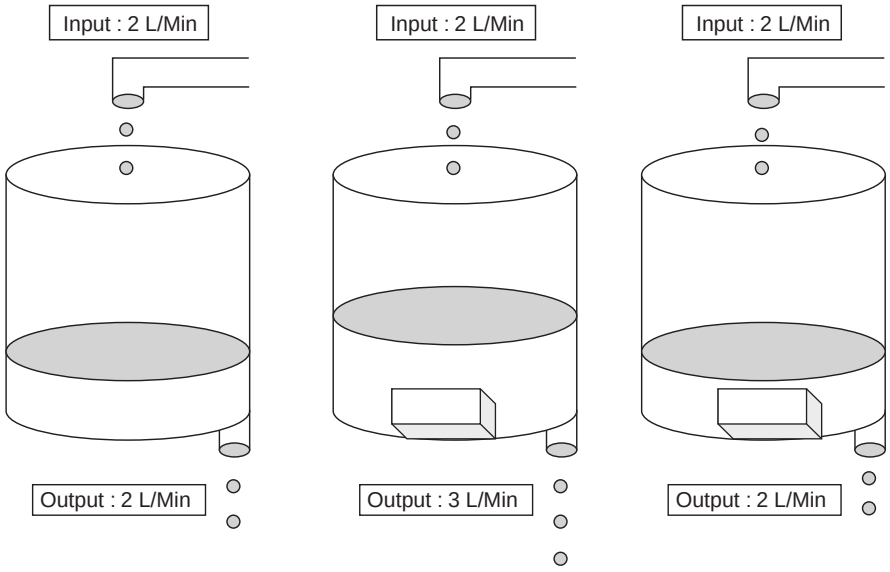

FIGURE 10.5 **An example of infinite gain control mechanism.** Water input and water output determine the balance, but water output is determined by the size of the hole at the bottom and the height of the water column. If water input and the size of the hole at the bottom remain unchanged, any change in the capacity of the tank will alter the height of water column only temporarily. For example, putting a brick into the tank reduces the capacity of the tank. This will increase the water column height only transiently. A higher level of water column with the same size of outlet hole will increase water output. Water output in excess of water input gradually decreases the height of the water column. Only when the height of the water column returns to the original level, is a balance restored between input and output.

There is no Set Point for Renal Salt Excretion

Hollenberg, citing the earlier writing on the same subject by Straus and colleagues[11] proposed a hypothesis for the existence of a set point for the regulation of body sodium content by the kidney. The set point is defined in his writings as the level of sodium content in the body that the kidney tries to maintain as the normal and desirable level. Henceforth, this hypothesis will be called the *set point hypothesis*. The evidence for the set point hypothesis follows.

First, when sodium intake is suddenly reduced, the rate of decrease in urine sodium excretion is exponential. The authors of the hypothesis consider the exponential decline thermodynamically unsound. If the decline were in response to progressive volume depletion, the authors argued, the decline should be accelerating, not declining exponentially. Second, when patients in sodium balance on a low sodium diet (10 mEq/day) were given a small amount of extra sodium (e.g., 30 mEq), the extra sodium was promptly excreted. It is further argued that if the patient had been volume depleted at the time, he should not have excreted the extra sodium. Finally, when a patient who was volume depleted by chronic diuretic therapy was given sodium, no sodium diuresis occurred until the body sodium content was brought back to the level that was achieved on zero sodium intake.

On the basis of these observations, the set point for renal sodium excretion was defined as the amount of sodium in the body when the subject is in balance on a salt-free diet. Accordingly, most humans are in a state of sodium excess, and hence the unloading of excess sodium diminishes the stimulus for sodium diuresis, producing an exponential decrease in renal sodium excretion. It was further argued that the absence of a set point would lead to chaos, and a control system without a reference point is unimaginable. The possibility of a set point being higher or lower than the level defined above was dismissed; the exponential decrease in sodium excretion on a salt-free diet is considered to be evidence against a higher set point, whereas the absence of sodium diuresis upon salt administration in patients pretreated with a diuretic was thought to be evidence against the existence of a lower set point. The set point hypothesis has been debated in the public forum previously[12,13] - but the uniqueness of the current argument against the hypothesis is that it is advanced by the use of counter examples (three counter examples follow).

1. When water intake is suddenly stopped after a period of normal water intake, the pattern of urine water output follows the same pattern as the renal salt output after sudden curtailment of salt intake. With increasing water deficit on a zero water intake, urine output declines exponentially, not accelerating, despite progressive water deficit and progressive activation of the water-conserving mechanism. Clearly, the water content of the body

on zero water intake cannot be the desirable water content.

2. When a patient is on a potassium-free diet, urinary excretion of potassium declines exponentially, not accelerating, despite a progressive increase in potassium deficit. Again, no one would argue that the potassium content of the body on zero potassium intake is the desirable body potassium content.
3. The arterial pCO_2 declines exponentially with increasing severity of metabolic acidosis, despite metabolic acidosis becoming more and more severe.

These counter examples indicate that the finding that urinary sodium declines exponentially neither supports nor argues against the existence of a set point, as previously defined. When sodium intake is stopped, urine sodium decreases progressively because effective vascular volume declines progressively, and as a result sodium reabsorption mechanisms in the kidney are activated progressively. Whether the body sodium content at usual sodium intake is normal or excessive is not a question that can be decided by the pattern of renal sodium excretion, just as we cannot decide the normal plasma potassium concentration by the pattern of renal potassium output in response to a change in potassium intake.

In an attempt to define a normal value in the set point hypothesis, a special meaning has been attached to the pattern of renal sodium excretion. However, normalcy of any physiological values must ultimately be decided by their relation to morbidity and mortality. Given the well-known effects of the body salt content on blood pressure, it may be more advantageous to have a salt content that is achieved on a near salt-free diet than the content attained on the current usual salt intake. The fact that the body's sodium content attained on a near salt free diet is more advantageous to human health is, in my opinion, pure chance, but may have contributed to the set point hypothesis. At different times in human history, a slight excess in sodium content might have been beneficial to survival, when salt was not readily available in many parts of the world and salt loss was a common occurrence from gastroenteritis and sweating. This scenario seems more plausible when one realizes that the main adverse effect of excess salt content in the body is increase in blood pressure, and hypertension was not the main cause of death when the average lifespan was 30 to 40 years. Normally, urine sodium excretion decreases when effective vascular volume declines. Thus, the relationship between effective vascular volume and renal sodium excretion can be summed up in one sentence: the lower the effective vascular volume, the lower the renal sodium output, and the higher the effective vascular volume, the higher the renal sodium output.

As explained in model B (Figure 10.3), the relationship between renal sodium excretion and effective vascular volume is not continuous; below a certain level of effective vascular volume, renal sodium output virtually disappears, and this happens before any overt signs of clinical dehydration. When effective vascular volume decreases further, renal sodium excretion cannot decrease further because renal sodium excretion cannot be a negative number, even though the sodium retaining mechanisms are even more activated. Administration of sodium in such a state would not cause sodium diuresis until effective vascular volume increases to a higher level. The proponent of the set point hypothesis asks the question: "if a subject is volume depleted on 10 mEq per day sodium diet, why would he excrete the administered sodium?" The simple answer would be "because he is less volume depleted now."

It is the central core of the set point hypothesis that the kidney stops excreting sodium at the set point, i.e., the salt content attained at near zero sodium intake, in order to preserve the most desirable value of body sodium content. However, that is not the consistent behavior of the kidney. Urine output never becomes zero until the kidney is completely shut off, despite progressive water deficit and clear clinical evidence of dehydration. Likewise, renal potassium output does not cease on a zero potassium intake, despite clinically evident hypokalemia.[14]

Renal Salt Output Does Not Exceed Salt Intake in Salt Losing Nephropathy

An often-cited diagnostic criterion for salt losing nephropathy is urine sodium excretion in excess of sodium intake.[15] This is obviously impossible on a chronic basis, just as chronic diuretic therapy cannot produce persistent net sodium loss. Salt intake must equal salt output in the long run, but transient imbalance often occurs. Salt output exceeds intake while volume depletion develops, but the reverse occurs when volume depletion is being corrected. If a patient with salt-losing nephropathy who had been on a high-salt diet reduces salt intake because of an illness, the patient will develop volume depletion, and during this period urine salt output exceeds salt intake, and hence a negative salt balance occurs. On the other hand, when the same patient resumes his usual salt intake or receives intravenous fluid, salt balance will be positive during the period of recovery. The diagnosis of salt losing nephropathy requires documentation of inappropriate urinary salt excretion in the presence of volume depletion.

Mechanism of Low Urea Nitrogen Concentration in Liver Disease

It is often stated that serum urea nitrogen level is very low in chronic liver disease because urea is produced in the liver, and the diseased liver cannot produce urea at the normal rate.[16] It is obvious that a low serum urea concentration without increased urea clearance must be due to reduced production, but impaired liver function is not the reason for reduced production. Once ingested protein is broken down to individual amino acids, and is absorbed into the bloodstream, it has three metabolic pathways: (1) metabolism to urea to be excreted in urine; (2) metabolism to non-urea nitrogen compounds to be excreted in urine; and (3) protein synthesis. Patients with chronic liver disease are not in a state of net protein synthesis, i.e., an anabolic state. Major non-urea nitrogen compounds normally excreted in urine include ammonia, amino acids, creatinine, and uric acid, and urinary excretion of these compounds is not increased in chronic liver disease. One might suggest that nitrogen could accumulate as ammonia in the blood as metabolic conversion of ammonia to urea is impaired in liver disease. In severe liver disease, ammonia concentration in plasma is indeed increased, but the total amount of nitrogen that can accumulate in the body in the form of ammonia without fatal consequences is extremely small. The concentrations of ammonia in plasma are expressed in micrograms per dl, whereas those of urea are in milligrams per dl. Accumulation of only 10% of ingested nitrogen as ammonia instead of its conversion to urea would lead to fatal hyper-ammonemia within hours.

The only logical explanation for low urea production, therefore, is reduced protein intake. Chronic alcoholics often have persistently low protein ingestion, and they have low plasma urea nitrogen. However, any normal person ingesting a low protein diet will also have low urea nitrogen production, and therefore low plasma urea nitrogen. A strict vegetarian often has a low urea nitrogen concentration, for these reasons. When a patient with a liver disease has a G-I hemorrhage, serum urea nitrogen concentration rises promptly, indicating that the diseased liver can produce urea rapidly when substrate is available. If a person with severe liver disease ingests a normal amount of protein, urea production will be normal, but plasma ammonia will be higher.

It is a general rule that an impaired metabolic pathway does not reduce the output of its metabolic product unless there is another pathway to which the precursor of the product can be shunted. In the absence of another pathway, at equilibrium the concentration of the precursor will be increased, and the rate of output of the metabolic product will return to the baseline. The situation is analogous to the quantity of creatinine excretion in chronic renal failure. When the kidney function is impaired, the amount of creatinine excreted in the urine does not decrease, as long as creatinine production remains unchanged. The amount excreted will decrease at the onset of renal failure, but at equilibrium it will return to baseline. One does not measure the rate of urinary creatinine excretion as a means of determining renal function; one looks at serum creatinine concentration instead. Likewise, the rate of production of urea by the liver does not offer any clue to the level of liver function, but serum ammonia level does.

Sodium Intake and Sodium Balance are Poor Predictors of Effective Vascular Volume

The assessment of effective vascular volume by urinary sodium excretion is a widely used and useful clinical tool. Most physicians, however, believe that knowledge of both sodium intake and urine sodium output provides a better clue to the status of effective vascular volume. The following example explains why this reasoning is flawed.

Question: Two subjects, A and B, have been admitted to the hospital with unknown status of their effective vascular volume. Subject A is given a diet containing 100 mEq of sodium per day, and subject B gets a sodium intake of 20 mEq a day. In the next 24 hours, subject A excretes 60 mEq of sodium per day, and subject B excretes 40 mEq of sodium per day. On the basis of this information, which subject do you believe has a higher effective vascular volume? You should assume that neither subject has any renal or hormonal disorder that would affect renal sodium excretion.

Answer and discussion: The most common answer is that A has a lower effective vascular volume than B. The reasoning for the answer: person A is in positive sodium balance because the "smart kidney," sensing volume depletion, retains sodium, whereas person B is in negative sodium balance because the "smart kidney," sensing the volume expansion, compels him to excrete the excess sodium. It is true that the balance data indicates that A is in a state of sodium retention and B in a state of sodium loss. However, sodium retention need not indicate the presence of volume depletion, and sodium loss not does prove the state of expanded volume. The following examples will make these points obvious.

A person in salt balance while ingesting 100 mEq of sodium per day suddenly increased sodium intake to 200 mEq per day. Salt excretion will eventually increase to the same level as intake, but not on the

first day. If adjustment in salt excretion matched intake immediately, there would be no retention of sodium, and there would be no harmful effect of a high salt intake. Instead, there would be some sodium retention. On the first day he may excrete only 150 mEq, causing net retention of 50 mEq of sodium. The positive sodium balance in this instance is due to increased intake, not to reduced excretion. Furthermore, a positive sodium balance increases the effective vascular volume to a higher level than the previous day, and the higher effective vascular volume is indeed the reason for the greater urinary sodium excretion. Clearly, positive sodium balance does not necessarily mean low effective vascular volume.

In another example, a patient with intractable heart failure is ingesting 50 mEq of sodium per day and excretes only 10 mEq per day. He is retaining sodium avidly, and hence the term renal sodium retention would be appropriate in this setting, as positive sodium balance in this instance is due to low effective vascular volume. Frustrated by relentless sodium retention, the physician prescribes a salt-free diet, and urine sodium drops further to 5 mEq per day. At this point, however, his overall sodium balance is −5 mEq per day. Can we say, then, that his effective vascular volume is no longer diminished, since he is no longer retaining sodium?

Sodium intake itself has no direct effect on renal sodium output. Any influence of sodium intake on renal sodium output is always mediated through effective vascular volume, because balance between sodium intake and sodium output influences effective vascular volume. If we think of renal sodium output in terms of model B (Figure 10.3), the height of the water column represents effective vascular volume. Just as the only factor that influences water output in model B is the height of water column, the only factor that influences renal sodium excretion directly is effective vascular volume. The higher the effective vascular volume, the higher is the urine sodium; the lower the effective vascular volume, the lower is the urine sodium. Once this relationship is understood, the question regarding subjects A and B is easy; subject A has higher effective vascular volume, because he is excreting more sodium in urine than subject B.

The reason for the widespread belief that sodium intake and output is a better predictor of effective vascular volume is likely to be due to the misuse of the term renal sodium retention. The train of logic goes as follows. First, sodium intake in excess of sodium output represents sodium retention. Second, sodium retention in most clinical situations is due to reduced renal excretion of sodium. Third, reduced renal excretion of sodium is most often due to low effective vascular volume. Fourth, therefore sodium retention is most often due to low effective vascular volume. Finally, any sodium retention, i.e., positive sodium balance, signifies low effective vascular volume. Although the fatal error in reasoning is in the final step, the major mistake occurred in the thinking that sodium retention is always due to reduced renal sodium output, instead of thinking that it is *usually* due to reduced renal sodium output.[17]

Does Overflow Mechanism Explain Ascites Formation?

The overflow theory of ascites formation states that an important mechanism of sodium retention in ascites formation in cirrhosis of the liver is primary renal sodium retention due to a diseased liver. The argument is based on the data from drug-induced cirrhosis of the liver in dogs, which developed ascites and salt retention in the absence of signs of reduced effective vascular volume, such as elevated PRA and plasma aldosterone concentration. On the basis of these observations, the authors of the study concluded that renal sodium retention could not have been a response to volume depletion caused by loss of fluid to the peritoneal cavity (i.e., under-filling), and therefore renal salt retention was a primary event that led to increased effective vascular volume resulting in the ascites formation (i.e., overflow).[18,19] Two major errors were made in this line of thinking.

The first error is the assumption that the proof of salt retention (i.e., positive salt balance) due to the under-filling mechanism requires the presence of overt volume depletion. The following example will demonstrate how effective vascular volume could remain "normal" during the period of positive salt balance by an under-filling mechanism. Assume that a person, who has been in salt balance while ingesting 15 g of salt a day and excreting 15 g a day, develops chronic diarrhea and loses 5 g of salt in the stool daily. The net GI absorption of salt after subtracting the amount lost in the stool would then be 10 g per day, and he would excrete 10 g of salt in the urine per day. His effective vascular volume during diarrhea will be lower than it was before the start of diarrhea, but not lower than that of a person ingesting only 10 g of salt per day without diarrhea. Likewise, if a person ingesting 15 g of salt per day develops ascites slowly, and sequesters 5 g of salt daily in the peritoneal space, his effective vascular volume would not be lower than a person who ingests 10 g of salt a day without development of ascites. In both cases, ingestion of 15 g of salt, in the absence of abnormal salt loss, would have resulted in excretion of 15 g of salt. With ascites formation or diarrhea, the kidney excretes 10 g instead of 15 g, because the effective vascular volume is slightly lower than in

a person without ascites formation or diarrhea. In both cases, the reduction in renal sodium output clearly was in response to "under-filling," even though there would be no discernible volume depletion. In both examples, effective vascular volume was maintained sufficiently high to allow renal excretion of 10 g of salt a day. If plasma renin activity were measured during the period of sodium retention in these examples, it would have been normal. The absence of apparent volume depletion in any edema-forming conditions does not prove that the kidney did not retain sodium in response to a volume stimulus.

The second error is the failure to recognize that the infinite gain control mechanism operates in ascites formation by the under-filling mechanism. If the salt intake and the function curve for renal salt output remain unchanged, effective vascular volume would return to the baseline when steady-state is achieved. The sequence of events would be as follows. Ascites formation by the transudation of fluid from the vascular space into the peritoneal cavity would reduce effective vascular volume, which reduces renal salt output. The normal salt intake with reduced renal salt output causes salt retention, which would tend to increase effective vascular volume. However, as long as effective vascular volume remains lower than the baseline value, renal salt output will remain lower than the baseline, and the positive salt balance will continue. Only when effective vascular volume returns to the baseline, will renal salt output return to the baseline, and the salt retention will stop. Thus, at equilibrium, effective vascular volume in any patient with ascites would be normal, unless he is treated with a low-salt diet or a diuretic.

Main Mechanism of Nephrotic Edema: Low Oncotic Pressure versus Primary Renal Salt Retention

It has been suggested that primary renal salt retention plays a more important role in the formation of nephrotic edema than low oncotic pressure which would cause secondary renal salt retention.[20] This belief is based on the observation that in untreated subjects with nephrotic syndrome, plasma renin activity is often reduced. The reasoning goes this way: if low oncotic pressure is the primary cause of edema formation, transudation of fluid from the vascular space into the interstitial space would reduce effective vascular volume, which is expected to increase plasma renin activity; the suppressed plasma renin activity, therefore, is the evidence for primacy of primary salt retention in the pathogenesis of nephrotic edema.

The flaw of this reasoning lies in the faulty assumption that edema due to low oncotic pressure must be accompanied by low effective vascular volume. The truth is that nephrotic edema entirely due to low oncotic pressure would not maintain low effective vascular volume, unless the patient is treated with salt restriction or a diuretic. The compensation mechanism against a low effective vascular volume in such situations would be the infinite gain control mechanism.

Imagine a patient in a third world country develops nephrotic syndrome. The patient is not treated with a diuretic, and he does not know the value of a low-salt diet in treating edema. He continues to ingest a diet that contains the usual amount of salt. Yet almost invariably, his renal salt output returns to the baseline and salt retention stops. Otherwise, the patient will develop relentless sodium retention and progressive edema, and will die in a relatively short period with massive edema. Since a slight reduction in effective vascular volume diminishes renal sodium excretion to virtually zero, restoration of renal sodium excretion to a usual normal value is proof that effective vascular volume has been restored to normal. Plasma renin activity at this point would be normal.

If a patient now develops a renal disease that results in primary renal salt retention, edema will be worse and effective vascular volume will be greater than the usual value, which would cause suppression of plasma renin activity. When the natriuretic effect of the increased effective vascular volume is sufficient to counterbalance the sodium retaining effect of the renal disease, renal sodium output will increase further to achieve a new balance. At this point, edema will not progress any further. The presence of suppressed plasma renin activity in a patient with nephrotic syndrome is a strong indication for the presence of primary renal sodium retention, but it does not prove that low oncotic pressure is not the main cause of edema formation. Indeed, primary renal Na retention alone, e.g., acute glomerulonephritis, rarely causes as severe edema as a non-nephrotic cause of low oncotic pressure, such as severe protein malnutrition.

CLINICAL APPLICATION OF EXTERNAL BALANCE

A serious topic discussed below utilizes the principles of external balance to explain physiological concepts and clinical manifestations of certain disorders of fluid and electrolyte balance.

Determinants of Sodium Delivery to the Cortical Collecting Duct and Renal K Excretion

According to the principles outlined at the beginning of this chapter, in the steady-state, sodium output

is equal to sodium intake, including all salt-retaining and salt-wasting conditions, such as hyperaldosteronism and hypoaldosteronism. One might therefore conclude that sodium delivery to the cortical collecting duct cannot remain chronically abnormal unless intake is altered. However, the principles discussed in earlier sections predict that total sodium output will eventually equal intake; it does not predict that sodium delivery to any particular nephron site cannot remain chronically altered.

In the steady-state, a patient receiving chronic diuretic therapy or one with primary hyperaldosteronism will excrete the same amount of sodium as before the abnormalities developed, if the intake remains the same. In both states, however, a greater amount of sodium would be reabsorbed at the collecting duct because of the increased aldosterone effect, but the amount excreted in the final urine cannot be more or less than the intake. To satisfy both conditions, sodium delivery to the collecting duct at the time of balance restoration must be increased in hyperaldosteronism, and decreased in hypoaldosteronism. Primary hyperaldosteronism will be used as an example to explain this.

The initial abnormality in primary hyperaldosteronism is increased salt reabsorption, mainly at the cortical collecting duct, resulting in reduced salt output. The consequent positive salt balance increases effective vascular volume, which inhibits the proximal tubular salt reabsorption, resulting in increased delivery of salt to the cortical collecting duct. With the increased delivery of salt, the amount of salt that escapes into the urine is more now than at the beginning, but still less than intake because of increased salt reabsorption in the collecting duct. As long as urinary excretion of salt is less than intake, net positive salt retention continues, causing further increase in effective vascular volume. A higher effective vascular volume further inhibits proximal tubular salt reabsorption, causing even greater increase in the distal delivery of salt. The process will continue, with progressive increase in effective vascular volume and further increase in salt excretion. Only when excretion of salt is equal to intake will positive salt balance stop. At equilibrium, salt output equals salt intake, but the quantity of salt delivered to the collecting duct remains increased.

In the case of therapy with a loop diuretic or a thiazide diuretic, initially salt delivery to the collecting duct would be greatly increased; during this period salt balance will be negative. The ensuing volume depletion activates salt-retaining mechanisms at the proximal tubule, and also stimulates aldosterone secretion causing increased reabsorption of salt in the cortical collecting duct. One might predict that in a steady-state, sodium delivery to the collecting duct would be normalized as the two opposing effects cancel out each other's effect. However, as long as the increased aldosterone secretion caused by volume depletion increases reabsorption of Na in the cortical collecting duct, Na delivery to the collecting duct must remain increased, in order to have a normal amount of Na excretion in the final urine. In other words, the combined effect of increased proximal Na reabsorption and decreased Na reabsorption by the diuretics would be chronic increase in Na delivery to the cortical collecting duct. Normal delivery of sodium accompanied by increased reabsorption of sodium at the cortical collecting duct would result in reduced excretion of sodium in the final urine; this is impossible.

For the same reasons, sodium delivery to the cortical collecting duct remains reduced chronically in states of hypoaldosteronism, such as Addison's disease. Because the Na reabsorption at the cortical collecting duct is reduced, the only way to have the same normal amount of Na excretion in the final urine is to have reduced delivery of Na to the collecting duct.

Two most important factors that influence renal K excretion are the amount of Na delivery to the cortical collecting duct and aldosterone concentration. Most clinical states that cause increased renal excretion of K are accompanied by increased Na delivery and increased aldosterone, whereas conditions characterized by reduced renal K excretion are accompanied by reduced Na delivery and a low plasma aldosterone or an impaired aldosterone effect. Renal K excretion is unaffected when these two factors are altered in opposite directions. In a high-salt diet sodium delivery to the cortical collecting duct is increased, but aldosterone secretion is reduced, resulting in a normal K excretion. A salt restriction reduces sodium delivery to the cortical collecting duct, but the aldosterone secretion is increased, resulting in a normal K excretion (Table 10.3).

Enigma of Pendred Syndrome

Pendred syndrome is a genetic disorder characterized by goiter and sensorineural hearing loss, responsible for about 7.5% of congenital hearing loss. The disease is named after Vaughan Pendred, an English physician who first described the condition in 1896.[21] The mechanism of the disease is a defect in an anion exchanger pendrin, which is located in the inner ear, thyroid gland, and the cortical collecting duct. The exchanger, located on the luminal membrane of beta-intercalated cells, appears to play an important role in the reabsorption of chloride, and therefore indirectly of sodium.[22]

Despite the common belief that chloride reabsorption in the collecting tubule duct depends mainly on

TABLE 10.3 Na Delivery to Cortical Collecting Duct (CCD) and Aldosterone Affecting Urine K

Clinical States	Na Delivery to CCD	Aldosterone Effect	Urine K Excretion
Hyperaldosteronism	Increased	Increased	Increased
Diuretics	Increased	Increased	Increased
Hypoaldosteronism	Decreased	Decreased	Decreased
K sparing diuretics	Decreased	Decreased	Decreased
Pendred syndrome	Decreased	Increased	Normal
High-salt diet	Increased	Decreased	Normal
Low-salt diet	Decreased	Increased	Normal

the paracellular chloride channel, supportive evidence is not very strong. For example, in severe volume depletion states, urine chloride concentration is as low as 2 mEq/L.[23] The Nernst Equation would predict that such a low chloride concentration, to be explained entirely by a passive mechanism through the paracellular pathway, would require the transepithelial voltage of over 100 mV. The highest transepithelial voltage observed in states of high aldosterone effect is about 60 mV. It is likely that other mechanisms exist for reabsorption of chloride in the cortical collecting duct, and the most likely one is pendrin-mediated chloride reabsorption.[22] If pendrin were such an important transporter for reabsorption of chloride in the cortical collecting duct, why isn't a pendrin defect associated with any electrolyte abnormality? Indeed, the apparent absence of electrolyte abnormalities is one of the reasons why Pendred syndrome, well-known among specialists of ENT, is not widely appreciated among nephrologists.

The most common and apparent electrolyte abnormality associated with impaired renal salt transport is hypokalemia, but Pendred syndrome is not known to be associated with hypokalemia. The following is the likely scenario. A pendrin defect would reduce the overall reabsorption of NaCl in the cortical collecting duct, and the ensuing volume depletion would stimulate renin and hence aldosterone. However, unlike defects in salt transport caused by impaired salt reabsorption in the distal convoluted tubule (Gitelman's syndrome) or the thick ascending limb of Henle (Bartter's syndrome), both of which are characterized by increased salt delivery to the cortical collecting duct, the delivery of salt to the cortical collecting duct in Pendred syndrome would be reduced. That is because the site of defect in salt transport is the cortical collecting duct itself. According to the principle of external balance, in the long run salt intake must equal salt output, no matter what and where defects in renal salt transport may be. Thus, a patient with Pendred syndrome would be excreting the normal amount of salt in the final urine. The excretion of the normal amount of salt and the reduced salt reabsorption at the cortical collecting duct is possible if the amount delivered to the cortical collecting duct is reduced. The end result is that patients with Pendred syndrome would have hyperaldosteronism, but reduced delivery of salt to the collecting duct. There has been no measurement of plasma aldosterone in patients with Pendred syndrome, but effective vascular volume is likely to be reduced and plasma aldosterone is likely to be increased. As supportive evidence, in a study of 21 patients with Pendred syndrome, not a single subject was shown to have hypertension.[24]

Is it possible that salt reabsorption at the cortical collecting duct is not reduced in Pendred syndrome because of the two opposite influences, a high aldosterone state increasing salt reabsorption and a defective pendrin impairing salt reabsorption? That is unlikely because reduced salt delivery with normal salt reabsorption at the cortical collecting duct would mean reduced salt excretion. Remember that in a steady-state final urine sodium excretion is always normal. Is it possible that salt delivery to the cortical collecting duct is normalized in a steady-state? Again, it is unlikely, because normal salt delivery would mean normal effective vascular volume, and then aldosterone secretion cannot be increased. In the end, in a steady-state in Pendred syndrome, there must be some volume depletion accompanied by hyperaldosteronism. At equilibrium renal K excretion in Pendred syndrome would be normal, because two main regulators of renal K excretion are altered in opposite directions; aldosterone is increased and Na delivery to the cortical collecting duct is reduced. The situation would be analogous to a person on a low-salt diet, in which aldosterone is increased but sodium delivery is reduced (Table 10.3). Thus, the patient with Pendred syndrome would be normotensive (low normal blood pressure) and normokalemic, and have no apparent electrolyte abnormalities.

In a recent case report,[25] a patient with Pendred syndrome treated with a thiazide diuretic developed severe hypokalemia (serum K 2.2 mEq/L) and signs of profound volume depletion. The likely explanation for severe potassium depletion is that the patient has impaired salt transport in both the distal convoluted tubule and collecting duct. Severe renal K-wasting occurred because sodium delivery to the cortical collecting duct was increased by a thiazide diuretic in the setting of high aldosterone. In another report, a patient with Pendred syndrome developed life-threatening

metabolic alkalosis during intercurrent illnesses, indicating the importance in chloride reabsorption.[26]

Hypoxemia is necessary to restore balance between oxygen supply and oxygen demand

While the principle of external balance is most useful in explaining homeostatic mechanisms of fluid and electrolyte balance, the same principle applies to restoration of balances in other homeostatic mechanisms. The following example illustrates the mechanism by which a patient with severe lung disease can maintain the normal supply of oxygen necessary to sustain life.

The basal oxygen consumption of a person with advanced lung disease is no less, perhaps slightly greater because of the increased work of breathing, than that of a healthy individual. This means that the diseased lung somehow takes up a normal amount of oxygen. How does this happen? Here is the explanation. A normal person who has alveolar ventilation of 4 liters a minute needs an uptake of 200 ml of oxygen per minute at the basal state. The oxygen content of one liter of inspired air at an atmospheric pO_2 of 150 mmHg is 200 ml, and the oxygen content the expired air is about 150 ml per liter with the pO_2 at 110 mmHg. With an alveolar−arterial pO_2 gradient of 10 mmHg, the arterial pO_2 would be about 100 mmHg. This means that each liter of ventilated air has resulted in uptake of 50 ml of oxygen or total of 200 ml of oxygen by 4 liters of alveolar ventilation. When alveolar ventilation is reduced to 2 liters per minute, how is it possible to extract the same 200 ml of oxygen? A quick calculation will indicate that, in order to extract the same 200 ml of oxygen, each of 2 liters of alveolar ventilation must result in an uptake of 100 ml of oxygen. Since the inspired air has still the same oxygen content at pO_2 150 mmHg, the expired air must have a pO_2 of 70 mmHg. This requires alveolar pO_2 to decrease to 70 mmHg. Since arterial pO_2 is about 10 mmHg lower, it must decrease to 60 mmHg. In other words, hypoxemia is a necessary condition for restoring oxygen uptake to normal.

How does the body know to reduce the arterial pO_2 precisely to the right level to restore oxygen balance? The body does not know, but the general principle of external balance allows automatic restoration of balance. Let us suppose that alveolar ventilation drops to half that of normal. Initially there will be a discrepancy between the body's demand for oxygen and oxygen supply. The reduced supply in the face of unchanged demand will decrease arterial pO_2. A lower arterial pO_2 means a lower alveolar pO_2, which permits greater uptake of oxygen for a given volume of alveolar ventilation. As long as oxygen uptake is less than oxygen demand, arterial pO_2 will keep decreasing, with further reduction in alveolar pO_2. Only when the alveolar pO_2 decreases sufficiently to allow oxygen uptake to meet oxygen demand, is a new balance achieved between oxygen demand and oxygen uptake.

Will this mechanism of external balance restore oxygen uptake at any severity of lung disease? The answer is no. What would happen if the alveolar ventilation decreased to 1 liter per minute? In order to have an uptake of 200 ml of oxygen by 1 liter of alveolar ventilation, each liter now extracts the entire oxygen content of the inspired air, since the total content of oxygen at pO_2 of 150 mmHg is 200 ml. This would mean that alveolar pO_2 must be 0 mmHg, clearly an impossible situation, since arterial pO2, always lower than alveolar pO2, must be a negative number. Long before the alveolar pO_2 drops to 0 mmHg, the person will die of severe hypoxia.

Mechanism of Volume Expansion in SIADH

Ample evidence exists that patients with SIADH with chronic hyponatremia are volume expanded. Evidence for expanded volume includes low plasma creatinine, low plasma urea, and low plasma uric acid,[27,28] all caused by increased renal clearances. However, persistence of chronic volume expansion in SIADH would seem paradoxical. In the absence of disorders that cause primary renal Na retention, such as renal diseases and primary hyperaldosteronism, would the normal kidney not promptly eliminate the excess Na until the volume is restored to normal?

The explanation for the persistence of volume expansion in SIADH lies in the antinatriuretic effect of hyponatremia.[29,30] The sequence of events is as follows. Initially, water retention causes hyponatremia and volume expansion. Volume expansion causes sodium diuresis, resulting in further reduction in serum sodium. But as serum sodium declines, the antinatriuretic effect of hyponatremia opposes the natriuretic effect of volume expansion. When these two opposing effects are equal, renal Na excretion returns to the baseline value, and a new balance is established, with renal Na excretion equaling salt intake. In other words, when renal Na excretion returns to the baseline, the effective vascular volume must be expanded.

Mechanism of Volume Depletion in Chronic Hypernatremia

In the presence of normal renal function, chronic hypernatremia is always accompanied by reduced effective vascular volume, and the degree of reduction in effective vascular volume is proportionate to the level of serum sodium.[31,32] Exceptions are chronic hypernatremia in renal failure or hypernatremia that develops as a result of chronic administration of

a large amount of sodium. Even in the latter condition, the effective vascular volume would be lower with high serum sodium than with normal serum sodium for the same amount of sodium administered. Although some authors postulate that the effective vascular volume is normal in essential hypernatremia,[31] this rule applies to all hypernatremic states including essential hypernatremia. The following analysis will elaborate on the mechanism.

As hyponatremia is antinatriuretic, hypernatremia is natriuretic.[33,34] For this reason, renal sodium excretion would be increased in normovolemic hypernatremia, as long as the kidney function is normal. Increased renal sodium excretion with the usual intake of sodium would reduce effective vascular volume. Volume depletion would reduce renal sodium excretion and oppose the natriuretic effect of hypernatremia. As long as renal sodium excretion exceeds sodium intake, volume depletion will become progressively greater. Only when volume depletion is sufficiently great to exactly oppose the natriuretic effect of hypernatremia, does renal sodium excretion return to the baseline, equaling the intake. At this point, a new sodium balance is struck between sodium intake and output, but at the expense of volume depletion. Since the natriuretic effect of hypernatremia is proportionate to the degree of hypernatremia, the magnitude of volume depletion needed to counterbalance the natriuretic effect of hypernatremia must also be proportionately great, to match the degree of hypernatremia when the new sodium balance is achieved. In other words, the more severe the hypernatremia, the greater is the volume depletion in a steady-state.

It has been suggested that patients with essential hypernatremia are euvolemic, because hypernatremia in this condition is a result of the resetting of the osmostat.[31] Resetting means that the osmostat is regulated normally, but at higher than usual serum sodium concentrations. More recent evidence indicates that essential hypernatremia is caused by defects in the osmoreceptors, not the resetting.[35] However, regardless of its pathogenetic mechanism, chronic volume depletion is inevitable in essential hypernatremia if renal function is normal. Mild volume depletion can escape detection even by careful physical examination. For example, a small amount of a diuretic, e.g., 50 mg hydrochlorothiazide, can reduce effective vascular volume sufficiently for the kidney to sense a reduction in volume, and thereby reduce clearances of urea, creatinine, and uric acid. Yet a careful physical examination by an astute physician will not detect signs of dehydration without the help of laboratory tests, e.g., a higher serum urate. Indeed, it has been shown that most patients with essential hypernatremia have laboratory evidence of volume depletion when the data are carefully analyzed.[32]

EXTERNAL BALANCE OF PROTONS

Determination of external balance of most univalent ions such as sodium, potassium, and chloride is straightforward; intestinal absorption is complete and they are eventually eliminated from the body since none is metabolized. Balance of polyvalent inorganic ions such as calcium, magnesium and phosphate is more complicated, because of incomplete intestinal absorption. External balance of acids and bases is even more complicated than that of polyvalent ions, because of uncertainties in their intestinal absorption and variations in their metabolism after absorption.

In the steady-state, hydrogen ions enter the body through ingestion of acid or are created endogenously through metabolism. The pH of food offers little guidance to its character as a donor of acid or alkali. Most fruit juices have low pH because of the organic acids in them, but overall they are contributors of alkali, because organic acid is metabolized to CO_2, while organic anions are metabolized to bicarbonate. Sulfur-containing amino acids are mostly metabolized to produce sulfuric acid, but not all sulfur is metabolized to sulfuric acid.

Under steady-state conditions, net acid production must equal net acid excretion, and the traditional view of the external balance of acid–base has been as follows. Acids are produced from three main sources: sulfuric acid derived from the metabolism of sulfur-containing amino acids; incompletely metabolized organic acids; and acid (or alkali) from the diet absorbed in the intestine.[36–38] Acids are excreted either in the form of ammonium or titratable acid, while a small amount of alkali is lost in the urine as bicarbonate. Hence, the total acid excretion measured as the sum of urine ammonium and titratable acid minus bicarbonate is called net acid excretion. However, this traditional view of the acid–base balance must be re-evaluated in light of conceptual uncertainties of this approach, and methodological limitations in the measurement of parameters of acid–base balance by conventional techniques.[38] The following discussion will shed some light on these uncertainties and limitations.

MEASUREMENT OF NET ACID EXCRETION

The concept of titratable acid is straightforward. The pH of urine following glomerular ultrafiltration is the same as that of plasma, but decreases progressively with addition of H^+ by tubular secretion. Most of the secreted H^+ is buffered by HCO_3^-, and this represents indirect reabsorption of HCO_3^-. As urine pH falls

further with tubular secretion of H^+, other urinary buffers are titrated to retard a fall in urine pH. Addition of alkali to the urine until its pH is the same as that of the plasma measures the titratable acid. This back-titration of urine releases all the H^+ titrated by non-bicarbonate buffers except those in the form of NH_4^+, which is not titrated because of its high pK (9.2), and therefore is measured separately.

However, the measurement of titratable acid, ammonium, and bicarbonate does not accurately reflect net acid excretion by the kidney, for the following reasons. First, there is a technical problem with the measurement of titratable acid.[39] Addition of alkali to the urine causes partial precipitation of some urine calcium with HPO_4^{2-}. Selective depletion of HPO_4^{2-} causes conversion of $H_2PO_4^-$ to HPO_4^{2-} with liberation of protons, leading to overestimation of titratable acid. Furthermore, titration of urine to the plasma pH results in titration of 1/64th of urinary ammonium (calculated with the pKa of ammonium of 9.2), resulting in further overestimation of titratable acid; this error is usually negligible, but would be substantial when urine contains a large amount of ammonium.

A potentially more serious source of error is the presence of buffers other than ammonium that are not titrated when urine pH is increased to 7.4.[40] The original assumption that ammonium is the only urinary buffer that escapes titration during the measurement of titratable acid has not been fully proven. Normal urine contains various amines such as ethanolamine, phosphoethanolamine, methylamine, and dimethylamine. Urinary excretion of these substances would represent acid excretion, as does the excretion of ammonium. However, titration of urine to pH 7.4 would not detect the presence of such substances. The individual urine concentration of each of these substances appears to be quite low individually, but the amount might be substantial collectively.

SOURCES OF ACID

Sulfuric Acid

The metabolism of sulfur-containing amino acids produces sulfuric acid:

$$RN - S \rightarrow CO_2 + UREA + H_2SO_4.$$

The resulting H_2SO_4 is buffered by the body alkali, mainly HCO_3^-. Previously it was assumed that virtually all urinary sulfates originate from sulfur-containing amino acids. However, this assumption is wrong, since soft drinks regularly contain sulfate as a preservative, and persons consuming large quantities of soft drinks could acquire a substantial amount of sulfate. In one such study, the average amount of urinary sulfate originating from soft drinks was estimated to be 15 mEq/day.[41] Furthermore, the metabolism of sulfur-containing amino acids does not always result in production of sulfuric acid,[42,43] because some of the sulfur is excreted in a neutral form, such as cystine, taurine or sulfate conjugate.[44–46] Each mmol of sulfur metabolized to H_2SO_4 produces 2 mEq of protons in the following reaction:

$$H_2SO_4 \rightarrow SO_4^= + 2H^+$$

On the other hand, the sulfate conjugation reaction consumes a proton; the result is net production of only 1 mEq of proton for each mole of sulfur oxidized when the final product is sulfate conjugate.

$$R - OH + SO_4^= + H^+ \rightarrow R - O - SO_3^-$$

Sulfate conjugation reaction is an important detoxification mechanism, and the reactions are regulated by various enzymes, such as phenol sulfotransferase.[44–46] The rate of sulfate conjugation reaction seems to depend, in part, on the availability of inorganic sulfate. For these reasons, the fraction of sulfur contained in amino acids that is oxidized to sulfuric acid might vary with individuals, and also with the amount of protein intake. In one study, urinary sulfate recovered following ingestion of methionine was shown to be 85–90% of the sulfur content of the ingested amino acid.[43] On the other hand, urinary excretion of sulfate esters is shown to be as much as 17% of total urinary sulfur excretion,[47] and the amount might be higher in certain situations such as renal insufficiency, in which plasma sulfate concentrations are much higher.[48,49] Another common pathway for sulfate conjugation is the formation of sulfated glycosaminoglycans, such as chondroitin sulfate and heparin (Table 10.4).

The sulfur content of proteins of different food sources varies greatly, and depends on the content of methionine and cysteine.[50] For example, the sulfur content of human milk protein is only half of that of most cereal proteins. The sulfur content of beef is less than that of pork or lamb. In general, with the exception of grains, proteins of vegetable origin have lower sulfur content than proteins from animal sources.[50] The rate of excretion of sulfate in patients on CAPD was shown to be much less than in normal subjects,[48] suggesting the possibility that a greater fraction of sulfur is excreted as sulfate conjugate and other organic sulfur compounds.

In conclusion, the proper method for determining the contribution of sulfur-containing amino acids to the endogenous acid production would require the measurement of sulfate, sulfate esters, and neutral

sulfur in the urine. In addition, the dietary intake of sulfate from soft drinks must be known.[41]

Organic Acid

Production of organic acid results in consumption of HCO_3^- in the reaction:

$$RH + HCO_3^- \rightarrow R^- + H_2CO_3$$

If the organic anion is retained in the body, and subsequently metabolized to HCO_3^-, there is no net loss of alkali. When the organic anion is not metabolized, is not metabolizable (e.g., urate) or escapes metabolism because it is excreted in the urine (e.g., citrate), this represents a net loss of alkali. The nature of many of these organic anions excreted in the urine is not known,[51–53] and therefore total organic acid production cannot be determined by measuring individual components. Instead, they are measured collectively by titration of urine. However, the titration method used most widely, the van Slyke and Palmer method,[54] contains many potential sources of error, some of which result in underestimation and some in overestimation.[55,56]

When a metabolizable organic anion cannot be excreted because of renal failure, it is eventually metabolized. Hence, renal function is an important consideration in the overall contribution of organic acids to total acid production. In the absence of renal excretion, only non-metabolizable organic acids would accumulate. It is not known what fraction of organic acids normally excreted in urine is metabolizable. To the extent that metabolizable organic anions are not excreted, patients in renal failure would have reduced net acid production, as shown in patients treated with maintenance hemodialysis.[57] On the other hand, net organic acid production is greatly increased during hemodialysis procedures, as a large quantity of organic anions are lost into the dialysate during dialysis.[57]

Net organic acid production is also regulated by the blood pH.[58–60] The regulation of net production of organic acids occurs in two ways. One way is the regulation of its production, which is pH-dependent; acidic systemic pH decreases production of both ketoacids and lactic acid, while alkaline pH promotes their production.[60] Another mechanism is regulation of their renal excretion. This effect is mediated mainly by the proximal tubular cell pH. An acidic pH of the proximal tubular cell increases reabsorption of organic anions, and thereby reduces urinary excretion, while an alkaline pH has the opposite effect.[58] Usually the proximal cell pH parallels the blood pH, but sometimes the two are dissociated. In proximal (type II) renal tubular acidosis (RTA) and type IV RTA, the systemic pH is low, but the proximal tubular cell pH is not, and hence organic anion excretion remains normal. On the other hand, in K^+ depletion, the tubular cell pH tends to be low (as H^+ enters the cell in exchange for K^+), and therefore organic anion loss is reduced, contributing to the pathogenesis of metabolic alkalosis.

TABLE 10.4 Major Sulfated Glycosaminoglycan in Human Body

Chondroitin sulfate
Keratan sulfate
Dermatan sulfate
Heparin sulfate
Heparan sulfate

Phosphoric Acid

Phosphate is ingested as inorganic phosphate and organic phosphate. Phosphates in milk and other dairy products are mostly inorganic. Inorganic phosphates in food usually exist at neutral pH, and hence their influence on the acid–base balance depends mainly on the absorption of phosphate relative to its accompanying cation, calcium and magnesium.[61] To the extent that phosphate absorption exceeds calcium absorption, it will add acid to the body.

Organic phosphates are ingested in food as components of intracellular organic compounds. These include creatine phosphate, ATP, ADP, AMP, cyclic AMP, phospholipids in the cell membrane and intracellular organelles, nucleic acids in DNA and RNA, and phosphoproteins. Their eventual fate either as acid or alkali depends on the number of non-metabolizable cations that balance the phosphate anions. If the total number of non-metabolizable cations in mEq is equal to 1.8 times the number of phosphate in mM, the compound is neutral upon complete metabolism. This prediction is based on the fact the average balance of phosphate at pH 7.4 is 1.8. When the number is greater than 1.8 times phosphate, the compound is an alkali, and when it is less than 1.8, it would be an acid. For example, each molecule of ATP has three molecules of phosphate (which has 5.4 negative charge equivalents when metabolized completely) balanced by four cationic charges, two of which are usually provided by magnesium. Hence, metabolic breakdown of each mole of ATP to adenosine and phosphate results in production of 1.4 mEq of acid. Likewise, metabolism of ADP (3 cationic charges against anionic charges of 3.6 P) and cyclic AMP (1 cationic charge against anionic charges of 1.8 P) produce acid, while breakdown of AMP (2 cationic charges against 1.8 P) would produce alkali (Table 10.5).

Conversion of ATP to ADP during exercise therefore represents an acid releasing process, as the net acid value of 1.4 (ATP) is reduced to the net acid value of 0.6 (ADP). Conversely, conversion of ADP to ATP represents an alkali releasing process. On the other

hand, breakdown of creatine-P to creatine and phosphate represents an alkali releasing process by a slight extent, as it consumes 0.2 mEq of proton for each mmol of creatine-P broken down.

It must be realized, however, that these calculations are based on the mean valence of phosphate of 1.8, which is the value at pH of 7.4. The value will change at different pH values. For example, at the usual pH of the cell, 7.1, the mean valence of phosphate is 1.67, and at a pH of 6.8, the mean phosphate valence is 1.5. Thus, at pH 6.8 (the likely muscle cell pH during exercise), metabolism of each mole of ATP would yield 0.5 mole of acid and that of ADP would result in zero acid production; the conversion of one mole of ATP to ADP would produce 0.5 mole of acid.

Metabolism of phospholipids and nucleic acids in DNA and RNA produces acid, whereas metabolism of phosphoproteins and creatine phosphate produces alkali (Table 10.5). The type of phosphate in the diet is a factor determining the magnitude of intestinal absorption. Phosphate present in phytic acid is poorly absorbable, because the human body lacks the enzyme phytase.[62] However, its GI absoption is greatly increased when phytic acid is broken down by bacterial phytase in the colon.

Another way of determining the fate of phosphate as a generator of acid or alkali is to examine the number of ester bonds. Phosphate has a total of three anionic charges when it is fully dissociated. As phosphate forms an ester bond with an organic substance, the number of anionic charges is reduced, and hence the requirement for the number of non-metabolizable cations such as potassium to balance the anion is also reduced. Thus, when phosphate forms two ester bonds (di-ester bonds) it has only one anionic charge remaining to be balanced by a cation. Phosphates in ATP, ADP, nucleic acids in the DNA and RNA, and phospholipids all form di-ester bonds. This explains why metabolism of AMP results in production of alkali, whereas metabolism of cyclic AMP and cyclic GMP (both are di-esters) result in production of acid. In the case of ATP, first two phosphates form di-ester bonds, and the third phosphate has a mono-ester bond. When phosphate contains tri-ester bonds, it has no metabolizable alkali, and its acid content is equal to the molal content of phosphate $\times$ 1.8.

The effect of phosphate in the diet on acid–base balance depends on the extent of GI absorption. The fraction of phosphate absorbed depends greatly on the type of cation that accompanies phosphate. When phosphate is ingested from the usual diet, about 2/3 is absorbed because food contains calcium, and calcium binds phosphate to form brushite ($CaHPO_4$), which is rapidly precipitated and excreted in stools. On the other hand, phosphate ingested as Na or K phosphate is nearly completely absorbed along with sodium and potassium, as long as the amount ingested does not exceed the capacity of the sodium–phosphate transporter.[63–65] When a large amount of sodium phosphate is ingested, the excess amount causes diarrhea. In summary, the contribution of phosphate to net acid production cannot be determined from dietary intake or urinary excretion of phosphate, but is included as part of net GI alkali absorption, which will be discussed separately later in this chapter.

TABLE 10.5 Alkali Value of Phosphate Compounds after Complete Breakdown to Inorganic Phosphate at pH 7.4

ATP^{4-}: 3 P and 4 negative charges: $4 - (3 \times 1.8) = -1.4$ (net acid)
ADP^{3-}: 2 P and 3 negative charges: $3 - (2 \times 1.8) = -0.6$ (net acid)
AMP^{2-}: 1 P and 2 negative charges: $2 - (1 \times 1.8) = 0.2$ (net alkali)
GMP^{2-}: 1 P and 2 negative charges: $2 - (1 \times 1.8) = 0.2$ (net alkali)
Cyclic AMP^{-}: 1 P and 1 negative charge: $1 - (1 \times 1.8) = -0.8$ (net acid)
Cyclic GMP^{-}: 1 P and 1 negative charge: $1 - (1 \times 1.8) = -0.8$ (net acid)
Creatine-P^{2-}: 1 P and 2 negative charges: $2 - (1 \times 1.8) = 0.2$ (net alkali)
DNA: 1 P and 1 negative charge: $1 - (1 \times 1.8) = -0.8$ (net acid).
RNA: 1 P and 1 negative charge: $1 - (1 \times 1.8) = -0.8$ (net acid)

Conversion of Creatine-P to ATP

During anaerobic metabolism, creatine-P is converted to ATP, which results in the generation of one mole of alkali for each mole of such conversion. The actual chemical reaction that occurs can be summarized as follows: creatine-P + ADP + $H^+ \rightarrow$ ATP + creatine. In other words, conversion of creatine-P to creatine with the simultaneous conversion of ADP to ATP results in the consumption of a proton. This reaction can also be summarized this way. Each molecule of creatine-P has two negative charges, each molecule of ADP has three negative charges, but ATP has four negative charges. Hence, one anionic charge must be buffered by the consumption of H^+. In other words, transfer of P from creatine-P to ADP to form ATP is a hydrogen ion-consuming process. If these reactions occurred at pH 6.8, conversion of 1 mmol of ADP to ATP would lead to production of 0.5 mmol of alkali, and the metabolism of creatine-P to creatine and phosphate would result in the additional production of 0.5 mmol of alkali. A hypothesis has been proposed to explain hyperkalemia during vigorous exercise as a response to the initial increase in intracellular pH caused by these reactions. According to this hypothesis, at the start of vigorous muscle exercise, a fall in ATP concentration causes a conversion of creatine-P in the muscle to ATP, and this is accompanied by an

increase in intracellular pH.[66] There are several flaws to this hypothesis, for many reasons.

First, the actual gain in alkali by these reactions is much less, because the overall reaction assumes gain of ATP at the expense of creatine-P. However, if the primary driving force of the reaction is low ATP, there must be net conversion of ATP to ADP, which is an acid-producing process. Second, the authors assumed that creatine-P exists as a trivalent anion, resulting in overestimation of alkali production upon conversion of creatine-P to creatine and phosphate. Finally, the consumption of creatine-P and ADP to produce creatine and ATP during vigorous exercise is not mediated by low ATP, but by low intracellular pH.[67] There is very little change in ATP concentration in the early stages of muscular exercise, but a huge decrease in pH during vigorous exercise. The initial intracellular shift of hydrogen ion during the early stages of exercise may be due to an extracellular shift of K, which in turn is caused by repeated depolarization of muscle cells during exercise. This, indeed, has been the traditional explanation for exercise-induced hyperkalemia.[68]

Amino acids

Proteins are potential sources of acid, based mainly on their sulfur content, which has already been discussed. Acidity or alkalinity of proteins also depends on the relative content of basic and acidic amino acids. Metabolism of cationic amino acids, arginine and lysine, produces acid:

$$\text{Arginine}^{+}\text{Cl}^{-} \rightarrow \text{urea} + CO_2 + \text{HCl}.$$

On the other hand, metabolism of aspartic acid and glutamic acid results in production of alkali:

$$\text{Na}^{+}\text{glutamate}^{-} + H_2CO_3 \rightarrow NaHCO_3 + CO_2 + \text{urea}.$$

However, the net content of acid and base of proteins cannot simply be determined from the total amounts of basic amino acids relative to the total content of acidic amino acids. We can understand this from plasma albumin. The total number of glutamate and aspartate in a molecule of albumin is 99, and the total number of arginine and lysine is 81, and the net excess of acidic amino acid over basic amino acid would be 18. The molecular weight of albumin is 66,5000 Da, and at a plasma concentration of albumin of 4 g/dL, the concentration of albumin in molarity is about 0.6 mmol/L. If each mole contains 18 negative charges, the net negative charge would be 10.8 mmol/L. In addition, albumin also contains 16 histidine molecules, and some of these will be in a cationic form, and therefore net negative charge should be less than 10.8 mmol/L. The actual measured net negative charge of albumin is about 12 mmol/L,[69] and the greater net negative charges may be explained by the reaction of cationic amino acids with various organic compounds. For example, N-acetylation and glycosylation of amino acids would reduce cationic charges and increase net anionic charges. Furthermore, some of the cationic charges of the amino groups of lysine are no longer cationic at pH 7.4.

The imidazole group of histidine is present in either of two forms: neutral or cationic. Metabolism of the cationic histidine results in the production of acid, whereas metabolism of neutral histidine has no effect on acid balance. The ratio of the neutral histidine to cationic histidine depends on the pK of the imidazole group in the molecule, and the pH of the solution in which histidine is dissolved. The pK of histidine varies widely between 5 and 8, depending on the nature of the molecule with which histidine is associated.[70] The pK is 6. 1 in histidine, but carnosine, a dipeptide composed of beta-alanine and histidine, an important intracellular buffer in the muscle of many vertebrates, has a pK of 6.83.[71] When histidine is part of a protein molecule or peptide molecule, its pK depends on the adjacent amino acid. Next to an acidic group, the pK of histidine rises, and next to a basic group, the pK decreases. Each of 16 histidine molecules in albumin has different pK values because of the differing influences of neighboring amino acids.[72]

The histidine content of hemoglobin is particularly high (38 per molecule of hemoglobin), this fact and a very high concentration of hemoglobin (about 7 times that of plasma albumin) explain the excellent buffering capacity of hemoglobin.[73] Oxygenation of hemoglobin at the lung reduces the pK of the imidazole group, i.e., it becomes a stronger acid. The acid reacts with bicarbonate to create more CO_2, which is eliminated by ventilation.

Even in the case of the basic and acidic amino acids, their eventual acidity or alkalinity depends on the nature of the counter-ions balancing the respective amino or carboxyl groups; when these groups are balanced by non-combustible ions such as Na^+, K^+, Cl^- or phosphate, their metabolism results in a net gain of acid or alkali. If the counter-ions are organic ions, the metabolism of the amino acid does not result in a net gain of acid or alkali. In most foods the total number of non-metabolizable cations exceeds that of non-metabolizable anions,[74] and therefore, apart from the contribution of sulfuric acid production, their metabolism would produce alkali.

Organic Acids in Meat

A substantial amount of organic anions, especially lactate, has been found in meat, and it has been

suggested that in the overall calculation of dietary net acid production a role for lactic acid be included.[75] However, most of lactate present in meat is produced after the death of the animal. Initially, lactic acid is formed and reacts with cellular alkali. When meat is digested and absorbed, during the process of lactate metabolism, exactly the same amount of protons is consumed as were released during the production of lactic acid. In the end, the net alkali or acid content of the body is unaffected by the production of lactic acid. By analogy, addition of acetic acid in the form of vinegar to food would produce acetate, but would not alter the net acid or alkali value of the food. As long as the content of non-combustible cations and anions remains the same, the net acid or alkali of meat would not change.

GI ABSORPTION OF ACIDS AND ALKALI

The normal diet contains large quantities of alkali, potential alkali, acids, and potential acids, but their ultimate impact on the body's acid–base balance depends primarily on their absorption. The pattern of absorption depends not only on the nature of the substance, but also on its interaction with other chemicals, both endogenous and exogenous.[76,77] In general, the amount absorbed is nearly equal to the amount ingested, if the substance is soluble and is readily absorbed. The examples include $NaHCO_3$, Na^+ citrate, K^+ citrate, and NH_4Cl. An insoluble substance such as $CaCO_3$ must react with gastric acid or acid in food to become soluble and absorbable. In some cases, only the anionic part is absorbable (e.g., Cl^- in cholestyramine chloride); in other cases, only the cationic part (e.g., Na^+ sodium polystyrene sulfonate) is absorbable. The overall effects of these substances on the body's acid–base balance are complex, and are often unrelated to the acidity or alkalinity of the substance. The following section describes two major categories of chemical substances, and the effects of their ingestion on acid–base balance.

Ingestion of a Poorly- or Non-Absorbable Cation Accompanied by an Absorbable Anion

Intravenous $CaCl_2$ is neutral, but ingested $CaCl_2$ is an acidifying agent. When ingested, virtually all of the Cl^-, but only a fraction of the Ca^{2+}, is absorbed. The excess Ca^{2+} remaining in the gut is excreted in the stool after combining with $CO_3^=$, organic anions or $HPO_4^=$. The type of anionic exchange determines the effect on acid–base balance. Typically, ingested $CaCl_2$ reacts with $NaHCO_3$:

$$CaCl_2 + 2NaHCO_3 \rightarrow 2NaCl + CaCO_3 + H_2CO_3$$

NaCl is absorbed and the insoluble $CaCO_3$ is excreted in the stool, resulting in net loss of $NaHCO_3$. Thus, the net effect of oral ingestion of $CaCl_2$ that results in formation and fecal excretion of $CaCO_3$ is loss of two moles of alkali for each mole of Ca ingested. On the other hand, when $CaCl_2$ reacts with Na_2HPO_4, NaCl is absorbed and $CaHPO_4$ is excreted in the stool:

$$CaCl_2 + Na_2HPO_4 \rightarrow 2NaCl + CaHPO_4$$

The loss of one mole of Na_2HPO_4 changes the ratio of Na_2HPO_4/NaH_2PO_4 from 4:1 to 3:1. In order to re-establish the ratio of Na_2HPO_4/NaH_2PO_4 at 4:1, 0.2 mole of NaH_2PO_4 must be converted to 0.2 mole of Na_2HPO_4, which would release of 0.2 mole of H^+. The new ratio would be 3.2 $(3 + 0.2)/0.8$ $(1 - 0.2)$, the same 4:1 ratio. Thus, the net effect is the gain of 0.2 mole of acid for each mole of $CaCl_2$ ingested. $CaCl_2$, if absorbed, would have no effect on the acid–base balance.

Since $SO_4^=$ is more readily absorbed than Mg^{2+}, the overall effect of $MgSO_4$ ingestion would be similar to that of ingestion of $CaCl_2$. Similarly, $FeSO_4$ could result in a net gain of acid, to the extent that more SO_4^{2-} than Fe^{2+} is absorbed.

When a person ingests salts consisting of a non-absorbable or poorly absorbable cation, accompanied by an absorbable and metabolizable anion, for example, $CaCO_3$, $Al(OH)_3$, Ca acetate, and Ca citrate, the amount of alkali gained depends on the absorption of anions, either with the accompanying cations or in exchange for non-metabolizable anions, such as phosphate. Absorption of $CaCO_3$ is facilitated when it reacts with HCl in the stomach or acid in food, because $CaCO_3$ is poorly soluble. The reaction in the stomach will be:

$$CaCO_3 + 2HCl \rightarrow CaCl_2 + H_2CO_3.$$

The fate of $CaCl_2$ formed will be the same as that of $CaCl_2$ ingested. Absorption of Ca as $CaCO_3$ or $CaCl_2$ represents a gain of alkali. Absorption of $CO_3^=$ in exchange for $HPO_4^=$ also represents a gain of alkali. Loss of $CaCO_3$ in the stool has no effect on the acid–base balance. Ingestion of organic salts of calcium, such as calcium citrate, calcium lactate, calcium gluconate, and calcium acetate also result in a similar gain of alkali. As with calcium carbonate, alkali gain occurs when these organic anions are absorbed either with calcium or in exchange with phosphate. The overall alkalinizing effect of various calcium antacids depends more on the ability of calcium to bind phosphate than on the absorption of calcium, because the amount of Ca^{2+} absorbed is usually much less than

the amount bound to phosphate to be excreted in the stool. The phosphate-binding ability depends in part on availability of soluble calcium.[78] This might explain why the amount of phosphate bound by calcium when calcium is ingested as $CaCl_2$ is comparable to that bound by aluminum ingested as $Al(OH)_3$,[79] whereas calcium carbonate salt removes only half as much phosphate for the same amount of calcium, because of its poor solubility. Despite poor absorption of aluminum, net gain of alkali is greater with $Al(OH)_3$ than with $CaCO_3$, because aluminum is a more effective binder of phosphate than calcium.[80]

Anion exchange resins are other examples of non-reabsorbable cations accompanied by absorbable anions.[79] As with calcium salts, they have either an acidifying or alkalinizing effect, depending on whether the accompanying anion is metabolizable or not. When the counter-ion is non-metabolizable, such as chloride (e.g., cholestyramine), its absorption in exchange for organic anions, carbonate or bicarbonate represent loss of alkali. When chloride is exchanged for phosphate, it represents 0.2 mEq of alkali loss for each mmol of phosphate lost as HPO_4. When the counter-ion is metabolizable (e.g., acetate), a net gain of alkali occurs when the metabolizable anion is absorbed in exchange for chloride or phosphate. An exchange of a metabolizable anion with organic anions, carbonate or bicarbonate is a neutral process (Table 10.6).

TABLE 10.6 Effect on Acid–Base Balance of Anion Exchange Resins (AER), Depending on its Accompanying Anion and Type of Anion in the Gut to be Exchanged

- Resin with metabolizable anion, exchanged for non-metabolizable anion: Gain of alkali
- Resin with metabolizable anion, exchanged for metabolizable anion: Neutral
- Resin with non-metabolizable anion, exchanged for metabolizable anion: Gain of Acid
- Resin with non-metabolizable anion, exchange for non-metabolizable anion: Neutral

Ingestion of a Poorly- or Non-Absorbable Anion Accompanied by an Absorbable Cation

An example is ingestion of Na^+ or K^+ phosphate. Intestinal absorption of Na^+ and K^+ is nearly complete as long as the accompanying anion can also be readily absorbed. Absorption of phosphate, on the other hand, is limited for two reasons. First, absorption of phosphate is achieved by sodium–phosphate co-transporters,[63–65] which have a limited capacity. When the intake of phosphate is in excess of the transporter capacity, unabsorbed phosphate is excreted in the stool. This explains why an excessive amount of sodium phosphate causes diarrhea. Second, some of the ingested phosphate can form an insoluble complex with calcium, which is precipitated and excreted in the stool. Na^+ or K^+ will then be balanced by the anion that is left behind, and the precipitated calcium will be absorbed. If the anion that is absorbed with sodium or potassium is an organic anion or carbonate, the result will be net gain of alkali:

$$Na_2HPO_4 + CaCO_3 \rightarrow Na_2CO_3 \text{ (absorbed after conversion to } NaHCO_3) + CaPO_4 \text{ (excreted in stool)}$$

Ingestion of a Cation-Exchange Resin Results in Net Gain of Alkali by a Similar Mechanism

The unabsorbable polyanion in a cation exchange resin is usually sulfonate attached to a polystyrene skeleton balanced by an exchangeable and absorbable cation, e.g., Na^+ in sodium polystyrene sulfonate (Kayexalate). When Na^+ exchanges for K^+, it has no effect on acid–base balance. An exchange of Na^+ for NH_4^+ or H^+ results in gain of alkali. When it exchanges with Ca^{2+}, the net effect is also gain of alkali, because normally the bulk of Ca^{2+} excreted in the stool is insoluble calcium carbonate, which represents loss of alkali.[80,81] When Ca^{2+} in calcium carbonate is exchanged for Na^+ in sodium polystyrene sulfonate (PSS), Na_2CO_3 is formed and then absorbed; at physiological pH, Na_2CO_3 will react with H_2CO_3, and two molecules of $NaHCO_3$ will form, and then be absorbed. This effect is more pronounced when the resin is administered with calcium salts,[80,81] aluminum salts or magnesium salts. Exchange between Na^+ and Al^{3+} or between Na^+ and Mg^{2+} results in formation of NaOH or Na^+ carbonate, which is readily absorbable directly or indirectly.

$$Na_2 - PSS + CaCO_3 \rightarrow Ca - PSS \text{ (excreted in stool)} + Na_2CO_3 \text{ (absorbed after conversion to } NaHCO_3).$$

If sodium polystyrene sulfonate (PSS) is ingested along with $Al(OH)_3$, the following reaction will occur:

$$Na_3 - PSS + Al(OH)_3 \rightarrow Al - PSS \text{ (excreted in stool)} + 3NaOH \text{ (absorbed after conversion to } 3NaHCO_3).$$

Calculation of Net Alkali in a Complex System

Ingestion of, for example, 20 mmol of K^+ citrate, which is completely absorbable and metabolized to $KHCO_3$ in the body, would result in net gain of

20 mEq of alkali. Ingestion of 10 mmol of arginine Cl would result in net gain of 10 mEq of acid. If a food contained both, the net gain of alkali would be 10 mEq. The food contains numerous chemicals, and their absorption depends not only on the type of chemicals ingested, but also on interactions with gastric acid and other chemicals in simultaneously ingested food or drugs. Thus, prediction of the effect of food ingestion on acid–base balance is nearly impossible. Measurements are made, instead, by analyzing net alkali content of food and feces. The difference between these two represents net alkali absorbed.

Net alkali content of food and feces is estimated by the electrolyte balance technique, i.e., the sum of non-combustible cations ($Na^+ + K^+ + Ca^{2+} + Mg^{2+}$) minus the sum of non-combustible anions ($Cl^- + 1.8$ P).[36] The assumption here is that when non-metabolizable cations are accompanied by metabolizable anions, the subsequent absorption and metabolism of their anions would result in gain of alkali, and that ingestion and absorption of non-metabolizable anions accompanied by metabolizable cations would lead to gain of acid. Hence, the difference between the two represents a net gain of alkali or acid. The concentrations of all of the electrolytes are expressed in mEq, except phosphate, which is expressed in mmol and then multiplied by the factor 1.8, the average valence of phosphate at pH 7.4. The pH of food or feces is not a determinant in the calculation of valency of phosphate, since that pH is relevant only in reference to blood pH.

For the calculation of net alkali content of food and feces, the only non-metabolizable ions presumed to be present are Na^+, K^+, Ca^{2+}, Mg^{2+}, Cl^-, and P, because no other ions in food are present in significant amounts. Urinary excretion of sulfate is substantial, but it is assumed to originate almost exclusively from sulfur-containing amino acids, and is measured separately.[43] This assumption does not appear valid any longer, because of ingestion of inorganic sulfates that are contained in substantial amounts in soft drinks. According to one estimate, an average amount of sulfate ingested per day in USA is about 15 mEq/day.[41] Thus, the presence of inorganic sulfate in the diet would lead to the estimation of a falsely increased amount of net GI alkali content. On the other hand, the inclusion of sulfate that originates from inorganic sulfate in soft drinks in the calculation of endogenous acid production would falsely increase its estimation. Thus, these two errors would cancel each other out.

Some organic anions found in food, e.g., tartarate, are poorly metabolized by the human body, and such anions would also result in a falsely increased estimation of net GI alkali absorption. On the other hand, all organic anions excreted in the urine estimated by the titration method are assumed to originate from organic acids produced in the body, and this assumption results in a falsely increased measurement of organic acid generation by the presence of substances such as tartarate in urine. These two errors would cancel each other out. Furthermore, it has been shown that the bulk of ingested tartarate in humans is actually metabolized by colonic bacteria, and only about 14% of ingested tartarate appear in urine unchanged.[82] Choline is an example of an incompletely metabolizable cation, but choline is also mostly metabolized by colonic bacteria.[83]

The measurement of GI absorption of alkali by the analysis of food and feces is difficult and prone to inaccuracies for obvious technical reasons. Measurements can be made only in inpatient settings with controlled diet, and consequently no study has measured net GI absorption of alkali on a normal diet in an outpatient setting. In a simplified technique, net GI absorption of alkali is estimated as urinary non-combustible cations minus urinary non-combustible anions:[84]

$$\text{Net GI Alkali absorption} = \text{Urine}\,(Na^+ + K^+ + Ca^{2+} + Mg^{2+}) - \text{Urine}\,(Cl^- + P \times 1.8).$$

The method is based on the assumption that the difference between the amounts of non-combustible cations and non-combustible anions absorbed from the gut equal the difference between the amounts excreted in the urine under stable conditions. The validity of this assumption is supported by empirical, as well as theoretical, evidence. Theoretically, the amount of non-metabolizable ions absorbed must equal the amount excreted, for the following reasons. The total extracellular content of divalent ions is small (about 45 mEq of Ca^{2+}, 30 mEq of Mg^{2+}, and 30 mEq of P), and their daily net flux with bone is negligible.[38] Hence, the amount of divalent ions excreted in the urine must be quite close to the amount absorbed from the GI tract. For univalent ions, Na^+, K^+, and Cl^-, their GI absorption is nearly complete. Consequently, the amount excreted in the urine would closely reflect the amount absorbed from the GI tract in states of acid–base balance. In a non-steady-state with a net gain of acid by the kidney, there would be excess excretion of Na and K. In a non-steady-state with a net gain of alkali by the kidney, there would be excess excretion of Cl.

Empirically, the measurement of net alkali absorption from the GI tract measured by the analysis of diet and stool showed near perfect correlation with the measurement made by urine electrolytes.[84] The amount

of net alkali absorbed on a usual diet by the latter technique is about 30 mEq/day.[38]

BONE BUFFERING IN METABOLIC ACIDOSIS

Bone Buffering in Chronic Metabolic Acidosis

It was once widely believed that bone was very important in maintaining stable serum HCO_3^- in chronic renal acidosis. Studies have shown that patients with chronic renal acidosis are able to maintain a stable serum HCO_3^-, despite retention of 12–19 mEq of acid daily, with the average duration of acidosis of six years. Because bone is known to have a large alkali reserve, the maintenance of a stable serum HCO_3^- in such settings has been attributed to the sustained release of alkali from bone.[3,4]

However, there has been little direct evidence for substantial bone buffering of acids in chronic acidosis of such long duration. The best evidence against a substantial role of bone in chronic renal acidosis is the lack of significant calciuria.[85] Addition of alkali to the body from Ca^{2+} release by bone occurs only when Ca^{2+} is excreted in urine. Re-deposition of Ca^{2+} salts in tissues or excretion in the stool as alkaline Ca^{2+} salts would reclaim alkali released from bone.[86] If the released calcium is lost in the stool as $CaCO_3$, it would actually result in net loss of alkali. Each mmol of Ca hydroxyapatite releases 10 mmol of Ca and 9.2 mEq of alkali. Loss of 10 mmols of calcium as calcium carbonate excreted in the stool removes 20 mmols of alkali from the body. Hence, the net alkali loss would be 10.8 mmols. If calcium from bone is released as $CaCO_3$, and excreted in the stool as $CaCO_3$, there will be no loss or gain of alkali. Release of calcium from hydroxy apatite with subsequent deposition as hydroxy apatite represents no gain or loss of alkali.

Furthermore, the total amount of alkali reserve in bone is insufficient to account for the buffering of acid for such a protracted period. Assuming total bone content of Ca^{2+} at 60,000 mEq, the total alkali content of bone is estimated to be about 25,000 mEq. At the rate of 19 mEq of acid buffering per day, the bone alkali store would be exhausted in 3.6 years.[38,87]

Bone Buffering in Acute Metabolic Acidosis

It is also widely believed that bone plays an important role in buffering in super-acute acidosis, but the available evidence is not convincing. Fraley and Adler showed that rats and dogs with total thyroparathyroidectomy developed a much more severe metabolic acidosis than those with intact organs.[88] The authors concluded that without intact parathyroid glands, non-extracellular buffers were responsible for titrating only 3 and 22% of the administered acid in rats and dogs, respectively. They concluded that the difference in buffering capacity was due to a difference in bone buffering. Arruda et al. concurred with Fraley and Adler that PTH significantly affected the overall buffering,[89] but the data of Madias et al. did not show any difference in buffering capacity.[90] Buffering of acid by bone could occur in three different ways: (1) release of cations such as Na^+, K^+, Ca^{2+}, and Mg^{2+} accompanied by carbonate, hydroxide or phosphate; (2) exchange of bone carbonate for extracellular phosphate; and (3) deposition of extracellular non-metabolizable anion such as Cl^- along with an H^+.

The third mechanism has not been shown to exist. For the first mechanism to operate, a cation must be released from bone. Mg^{2+} does not participate in acid buffering of bone. Release of bone K^+ cannot play a quantitatively significant role, because the entire bone content of K^+ in adult humans is a mere 20 mEq.[91] Evidence for Na^+ release from bone exists in acute metabolic acidosis, but the magnitude is a not very substantial. Bettice and Gamble showed that the bone content of exchangeable Na^+ decreased by about 5% in 5 hours following acute acid loading in dogs.[92] The bone Na^+ content is about 1200 mEq, and about 40% of this, 480 mEq, is exchangeable. Thus, 5% of 480 mEq represents a mere 24 mEq ($480 \times 0.05 = 24$). In conclusion, it seems highly improbable that bone contributes substantially to the buffering in super-acute metabolic acidosis (acidosis within a few hours).

Release of Ca^{2+} from bone is an important mechanism of bone buffering in acute metabolic acidosis. Urinary excretion of Ca^{2+} can increase by 80 mEq per day. If the entire amount came from Ca^{2+} carbonate, that amount of calcium release would release 80 mEq of alkali. If the same amount of Ca^{2+} originated from hydroxyapatite, alkali released is 36.8 mEq. Increased excretion of Ca^{2+} in metabolic acidosis reaches a maximal value a few days after the start of acid load.[93]

The likely explanation for the appearance of impaired buffering in animals with thyroparathyroidectomy is tissue under-perfusion due to circulatory shock. Since the blood flow to the muscle in humans is only about 700 ml per minute, it is obvious that buffering by skeletal muscle would not be complete in 30 minutes in a resting state. Reduced blood flow by circulatory shock would further delay the buffering by both intra- and extracellular fluid of the muscle, and could have given the impression that cell buffering was virtually absent in this setting.

In conclusion, bone is quantitatively an unimportant source of alkali in chronic metabolic acidosis of several years' duration. In acute acidosis, contribution of bone to acid buffering could be substantial, but its contribution in super-acute acidosis (that of several hours duration) appears negligible.

References

[1] Pearson PN, Palmer MR. Atmospheric carbon dioxide concentrations over the past 60 million years. Nature 2000;406:695–9.

[2] Canadell JG, Le Quéré C, Raupach MR, Field CB, Buetenhuis ET, Ciais P, et al. Contributions to accelerating atmospheric CO_2 growth from economic activity, carbon intensity, and efficiency of natural sinks. Proc Natl Acad Sci 2007;104:18866–70.

[3] Lemann Jr J, Litzow JR, Lennon EJ. The effects of chronic acid loads in normal man: further evidence for the participation of bone mineral in the defense against chronic metabolic acidosis. J Clin Invest 1966;45:1608–14.

[4] Goodman AD, Lemann Jr J, Lennon EJ, Relman AS. Production, excretion and net balance of fixed acid in patients with renal acidosis. J Clin Invest 1965;44:495–506.

[5] Vaziri ND, Freel RW, Hatch M. Effect of chronic experimental renal insufficiency on urate metabolism. J Am Soc Nephrol 1995;6:1313–7.

[6] Costello JF, Smith M, Stolarski C, Sadovnic MJ. Extrarenal clearance of oxalate increases with progression of renal failure in the rat. J Am Soc Nephrol 1992;3:1098–104.

[7] Guyton A. Control of blood pressure. Am J Med 1972;52:484–92.

[8] Guyton AC, Hall JE, Lohmeier TE, Jackson TE, Kastner PR. Blood pressure regulation: basic concepts. Fed Proc 1981;4:2252–6.

[9] Guyton AC. Abnormal renal function and autoregulation in essential hypertension. Hypertension 1991;18(Suppl. 3):49–53.

[10] Guyton AC. The surprising kidney-fluid mechanism for pressure control: its infinite gain!. Hypertension 1990;16:725–30.

[11] Hollenberg NK. Set point for sodium homeostasis: surfeit, deficit and their implications. Kidney Int 1980;17:423–9.

[12] Walser M. Phenomenological analysis of sodium and potassium homeostasis. Kidney Int 1985;217:837–41.

[13] Bonventre JV, Leaf A. Sodium homeostasis: steady states without a set point. Kidney Int 1982;21:880–3.

[14] Squires RD, Huth EJ. Experimental potassium depletion in normal human subjects. Relation of ion intake to the renal conservation of potassium. J Clin Invest 1959;38:1134–48.

[15] Uribarri J, Oh MS, Carroll HJ. Salt-losing nephropathy. Clinical presentation and mechanisms. Am J Nephrol 1983;3:193–8.

[16] Lum G, Leal-Khouri S. Significance of low serum urea nitrogen concentrations. Clin Chem 1989;35:639–40.

[17] Oh MS, Carroll HJ. Salt output in relation to salt intake vs. salt output alone: which is a better predictor of effective vascular volume? Nephron 1992;61:7–9.

[18] Levy M, Wexler MJ. Renal sodium retention and ascites formation in dogs with experimental cirrhosis but with portal hypertension or increased splanchnic vascular capacity. J Lab Clin Med 1978;91:520.

[19] Cardenas A, Arroyo V. Mechanisms of water and sodium retention in cirrhosis and the pathogenesis of ascites. Best Pract Res Clin Endocrinol Metab 2003;17:607–22.

[20] Dorhout EJ, Roos JC, Boer P, Yoe EH, Simatupang TA. Observations on edema formation in the nephrotic syndrome in adults with minimal lesions. Am J Med 1979;67:378–84.

[21] Pendred V. Deaf-mutism and goitre. Lancet 1896;2:532.

[22] Eladari D, Chambrey R, Frische S, Vallet M, Edwards A. Pendrin as a regulator of ECF and blood pressure. Curr Opin Nephrol Hypertens 2009;18:356–62.

[23] Kamel KS, Magner PO, Ethier JH, Halperin ML. Urine electrolytes in the assessment of extracellular fluid volume contraction. Am J Nephrol 1989;9:344–7.

[24] Madeo AC, Manichaikul A, Pryor SP, Griffith AJ. Do mutations of the Pendred syndrome gene, SLC26A4, confer resistance to asthma and hypertension? J Med Genet 2009;46:405–6.

[25] Bigozzi M, Bianchi B. Profound hypokalemia and hypochloremic metabolic alkalosis during thiazide therapy in a child with Pendred syndrome. Clin Nephrol 2008;69:450–3.

[26] Kandasamy N, Fugazzola L, Evans M, Chatterjee K, Karret F. Life-threatening metabolic alkalosis in Pendred syndrome. Eur J Endocrinol 2011;165:167–70.

[27] Decaux G, Genette F, Mokel J. Hyponatremia in the syndrome of inappropriate ADH secretion. Ann Intern Med 1980;93: 716–22.

[28] Jaenike JR, Waterhouse C. The renal response to sustained administration of water and vasopressin in man. J Clin Endocrinol Metab 1961;21:231.

[29] Boonjaren S, Stein J, Baehler R, Osgood RW, Hsueh W, Cohen S, et al. Effect of plasma sodium concentration on diluting segment sodium reabsorption. Kidney Int 1974;5:1.

[30] Schrier RW, Fein FL, McNeil TS, Cirksena WJ. Influence of interstitial fluid volume expansion and plasma sodium concentration on the natriuresis response to volume expansion in dogs. Clin Sci 1969;36:371.

[31] Oh MS, Carroll HJ. Essential hypernatremia: is there such a thing? Nephron 1994;67:144–7.

[32] Alford FP, Scoggins BA, Wharton C. Symptomatic essential hypernatremia. Am J Med 1973;54:359.

[33] Kamm DE, Levinsky NG. Inhibition of renal tubular sodium reabsorption by hypernatremia. J Clin Invest 1965;44:1144.

[34] Bresler EH, Nielson KT, Miller III MC, Stoud MR. Renal tubular reabsorptive response to hypernatremia. Am J Physiol 1976;231:642.

[35] Robertson GL, Aycinena P, Zerbe RL. Neurogenic disorders of osmoregulation. Am J Med 1982;72:339–53.

[36] Relman AS, Lennon EJ, Lemann Jr. J. Endogenous production of fixed acid and the measurement of the net balance of acid in normal subjects. J Clin Invest 1961;40:1621–30.

[37] Lennon EJ, Lemann Jr J, Litzow JR. The effects of diet and stool composition on the net external acid balance of normal subjects. J Clin Invest 1966;45:1601–7.

[38] Oh MS, Carroll HJ. Whole body acid-base balance. In: Berlyne G, editor. The kidney today. Selected topics in renal science. Contrib Nephrol 1992;100:89–104

[39] Lemann Jr J, Lennon EJ, Brock J. A potential error in the measurement of urinary titratable acid. J Lab Clin Med 1966;67:906–13.

[40] Oh MS, Kim MJ, Tan C, et al. Untitrated titratable acid in urine. *Proc Am Soc Nephrol* 1992;3:328.

[41] Magee EA, Curno R, Edmond LM, Cummings JH. Contribution of dietary protein and inorganic sulfur to urinary sulfate toward a biomarker of inorganic sulfur intake. Am J Clin Nutr 2004;80:137–42.

[42] Lemann Jr J, Relman AS. The relation of sulfur metabolism to acid–base balance and electrolyte excretion: the effects of DL-methionine in normal man. J Clin Invest 1959;38:2215–23.

[43] Hunt JN. The influence of dietary sulphur on the urinary output of acid in man. Clin Sci 1956;15:119–34.

[44] Banoglu E. Current status of the cytosolic sulfotransferases in the metabolic activation of promutagens and procarcinogens. Curr Drug Metab 2000;1:1–30.

[45] Kauffman FC. Sulfonation in pharmacology and toxicology. Drug Metab Rev 2004;36:823–43.

[46] Glatt H. Sulfotransferases in the bioactivation of xenobiotics. Chem Biol Interact 2000;1(129):141–70.

[47] Baldetorp L, Martensson J. Urinary excretion of inorganic sulfate, ester sulfate, total sulfur and taurine in cancer patients. Acta Med Scand 1980;208:293–5.
[48] Uribarri J, Buquing J, Oh MS. Acid–base balance in chronic peritoneal dialysis patients. Kidney Int 1995;47:269–73.
[49] Uribarri J, Zia M, Mahmood J, Marcus RA, Oh MS. Acid production in chronic hemodialysis patients. J Am Soc Nephrol 1998;9:114–20.
[50] Lenter C. Ed. Composition of foods. In Geigy Scientific Tables. vol. 1. Units of measurement, body fluids, composition of the body, nutrition. Basel, Switzerland: Ciba-Geigy Ltd, Basel; 1981 p. 241–66
[51] Chalmers RA, Healy MJ, Lawson AM, Hart JT, Watts RW. Urinary organic acids in man. III. Quantitative ranges and patterns of excretion in a normal population. Clin Chem 1976;22:1292–8.
[52] Chalmers RA, Healy MJ, Lawson AM, Watts RW. Urinary organic acids in man. II. Effects of individual variation and diet on the urinary excretion of acidic metabolites. Clin Chem 1976;22:1288–91.
[53] Lawson AM, Chalmers RA, Watts RW. Urinary organic acids in man. I. Normal patterns. Clin Chem 1976;22:1283–7.
[54] Van Slyke DD, Palmer WW. Studies of acidosis. XVI. Titration of organic acids in urine. J Biol Chem 1920;41:567–9.
[55] Oh MS, Rakesh V, Carroll HJ. A new method for measurement of organic anions in urine. Proc Amer Soc Nephrol 1993;:38 Boston
[56] Dawson J, Dempsey E, Bartter F, Leaf A, Albright F. Evidence for the presence of an amphoteric electrolyte in the urine of patients with "renal tubular acidosis.". Metabolism 1953;2:225–37.
[57] Uribarri J, Douyon H, Oh MS. A re-evaluation of the urinary parameters of acid production and excretion in patients with chronic renal acidosis. Kidney Int 1995;47:624–7.
[58] Kaufman AM, Brod-Miller C, Kahn T. Role of citrate excretion in acid–base balance in diuretic-induced alkalosis in the rat. Am J Physiol 1985;248:F796–803.
[59] Brown JC, Packer RK, Knepper MA. Role of organic anions in renal response to dietary acid and base loads. Am J Physiol 1989;257:F170–176.
[60] Hood VL, Tannen RL. Protection of acid-base balance by pH regulation of acid production. N Engl J Med 1998;339:819–26.
[61] Lennon EJ, Lemann Jr J, Relman AS. The effects of phosphoproteins on acid balance in normal subjects. J Clin Invest 1962;41:637–45.
[62] Hubert W, Lopez HW, Coudray C, et al. Mineral utilization in rats. J Clin Nutri 1998;128:1192–8.
[63] Quamme GA, Shapiro RJ. Membrane controls of epithelial phosphate transport. Can J Physiol Pharmacol 1987;65:275–86.
[64] Murer H, Forster I, Biber J. The sodium phosphate cotransporter family SLC34. Pflugers Arch 2004;447:763–7.
[65] Murer H, Hernando N, Forster L, Biber J. Molecular mechanisms in proximal tubular and small intestinal phosphate reabsorption. Mol Membr Biol 2001;18:3–11.
[66] Wasserman K, Stringer WW, Caserburi R. The mechanism of exercise hyperkalemia: an alternative hypothesis. J Appl Physiol 1997;8:631–43.
[67] Sahlin K, Harris RC, Hultman E. Creatine kinase equilibrium and lactate compared with muscle pH in tissue obtained after isometric exercise. Biochem J 1975;152:173–80.
[68] Lindinger JI, McKelvie RS, Heigenhauser JF. $K.^{+}$ and Lac^{-} distribution in humans during exercise during and after high intensity exercise. J Appl Physiol 1995;78:765–77.
[69] Watson PD. Modeling the effects of proteins on pH in plasma. J Appl Physiol 1999;86:1421–7.
[70] Hochachka PW, Somero GN. Biochemical adaptations. Princeton, New Jersey: Princeton University Press; 1984. p. 337–48
[71] Bate-Smith EC. The buffering of muscle in rigor: protein, phosphate and carnosine. J Physiol 1938;92:336–43.
[72] Figge J, Mydosh T, Fencl V. Serum protein and acid–base equilibria: a follow-up. J Lab Clin Med 1992;120:713–9.
[73] Riggs A. The amino acid composition of some mammalian hemoglobins. J Biol Chem 1963;238:2983–7.
[74] Halperin ML, Jungas RL. Metabolic production and renal disposal of hydrogen ions. Kidney Int 1983;24:709–13.
[75] Berlyne GM, Adler AJ, Barth RH. Perspectives on acid–base balance in advanced chronic renal failure. In: Berlyne G, editor. The kidney today. Selected topics in renal science. Contrib Nephrol 1992;100:105–17
[76] de Strihou C, van Y. Importance of endogenous acid production in the regulation of acid–base equilibrium: the role of the digestive tract. Adv Nephrol 1980;9:367–85.
[77] Lennon EJ, Lemann Jr J, Litzow JR. The effects of diet and stool composition on the net external acid balance of normal subjects. J Clin Invest 1966;45:1601–7.
[78] Sheikh MS, Maguire JA, Emmett M, Santa Ana CA, Nicar MJ, Schiller LR, et al. Reduction of dietary phosphorus absorption by phosphorus binders. a theoretical, *in vitro*, and *in vivo* study. J Clin Invest 1989;83:66–73.
[79] Hurst PE, Morrison RB, Timoneer J, Metcalfe-Gibson A, Wrong O. The effect of oral anion exchange resins on faecal anions. Comparison with calcium salts and aluminium hydroxide. Clin Sci 1963;24:187–200.
[80] Schroeder ET. Alkalosis resulting from combined administration of a "nonsystemic" antacid and a cation-exchange resin. Gastroenterology 1969;56:868–74.
[81] Madias NE, Levey AS. Metabolic alkalosis due to absorption of "nonabsorbable" antacids. Am J Med 1983;74:155–8.
[82] Chadwick VS, Vince A, Killingley M, Wrong OM. The metabolism of tartrate in man and the rat. Clin Sci Mol Med 1978;54:273–81.
[83] De La Huerga J, Gyorgy P, Waldstein D, Katz R, Popper H. The effects of antimicrobial agents upon choline degradation in the intestinal tract. J Clin Invest 1953;32:1117–20.
[84] Oh MS, Carroll HJ. A new method for the measurement of net GI absorption of alkali. Kidney Int 1989;36:915–7.
[85] Litzow JR, Lemann Jr J, Lennon EJ. The effect of treatment of acidosis on calcium balance in patients with chronic azotemic renal disease. J Clin Invest 1967;46:280–6.
[86] Contiguglia SR, Alfrey AC, Miller NL, Runnells DE, Le Geros RZ. Nature of soft tissue calcification in uremia. Kidney Int 1973;4:229–35.
[87] Oh MS. Irrelevance of bone buffering to acid–base homeostasis in chronic metabolic acidosis. Nephron 1991;59:7–10.
[88] Fraley DS, Adler S. An extrarenal role for parathyroid hormone in the disposal of acute acid loads in rats and dogs. J Clin Invest 1979;63:985–97.
[89] Arruda JA, Alla V, Rubinstein H, Cruz-Soto M, Sabatini S, Battle DC, et al. Metabolic and hormonal factors influencing extrarenal buffering of an acute acid load. Miner Electrolyte Metab 1982;:36–43.
[90] Madias NE, Johns CA, Homer SM. Independence of the acute acid-buffering response from endogenous parathyroid hormone. Am J Physiol 1982;243:F141–149.
[91] Pellegrino ED, Biltz RM. The composition of human bone in uremia. Observations on the reservoir functions of bone and demonstration of a labile fraction of bone carbonate. Medicine (Baltimore) 1965;44:397–418.
[92] Bettice JA, Gamble Jr. JL. Skeletal buffering of acute metabolic acidosis. Am J Physiol 1975;229:1618–24.
[93] Leman J, John R, Litzow JR, Lennon EJ. Studies of the mechanism by which chronic metabolic acidosis augments urinary calcium excretion in man. J Clin Invest 1967;46:1318–28.

This page intentionally left blank

CHAPTER

11

Renal Cilia Structure, Function, and Physiology

Jay N. Pieczynski and Bradley K. Yoder

Department of Cell Biology, University of Alabama at Birmingham, Birmingham, AL, USA

INTRODUCTION

The first descriptions of the cilium are generally attributed to Leeuwenhoek (as translated in [1]). Cilia were thought to be analogous to the flagellum used by single cell organisms for motility. It soon became obvious that motile cilia also have a function in multiple human tissues; motile cilia found in the respiratory track are involved in clearance of mucus and debris, cerebral spinal fluid movement is assisted by motile cilia on ependymal cells lining the brain ventricles, and flagella function to propel sperm through the reproductive tract for fertilization. In fact, the first human disease associated with cilia dysfunction was Primary Ciliary Dyskinesia ("primary" here referring to the fact that impaired movement of cilia was the cause of the disease (PCD)[2,3]). These patients suffer from chronic rhinitis, bronchiectasis, infertility, and abnormal left–right body axis specification caused by defects in cilia motility.

Most cell types in the mammalian body do not have motile cilia; they possess a single immotile cilium (referred to as the *primary cilium*). The functional importance of the primary cilium remained enigmatic, and the primary cilium was often considered vestigial. It wasn't until the mid-1990s and early 2000s that a number of essential observations were made linking the primary cilium to disease phenotypes, largely through studies in model organisms. One of the initial breakthroughs came from a large-scale insertional mutagenesis project conducted on mice in the laboratory of Dr. Rick Woychik at the Oak Ridge National Laboratories. This screen resulted in the identification of the Oak Ridge Polycystic Kidney (*orpk*) mouse,[4] a genetic model for autosomal recessive polycystic kidney disease (ARPKD, OMIM# 263200). *orpk* mutants have multi-organ defects, including cystic lesions in the kidney, liver, and pancreas, hydrocephalus, anosmia, retinal degeneration, skin and hair abnormalities, brain malformation, and skeletal defects.[5] Many of the phenotypes observed in the *orpk* mutants have also been reported in human disorders caused by mutations in proteins associated with the cilium (Table 11.1). These disorders are collectively referred to as "*ciliopathies*," and the *orpk* mutant mouse has become an important mammalian model system for studying ciliary dysfunction and disease. The transgene insertion in *orpk* mutant mice caused a hypomorphic mutation in a gene called "*Tg737*" that encodes the protein Polaris.[4,6,7] Polaris localizes to the cilium, and in the *orpk* mutants both motile and primary cilia were stunted and malformed, although the function of the protein remained unknown.[8]

Another major advance came from the proteomic analysis of flagella isolated from the green alga *Chlamydomonas reinhardt*.[9] This study identified several components of the intraflagellar transport (IFT) particle that included intraflagellar protein 88 (*Ift88*), the homolog of Polaris in *Chlamydomonas*.[10] IFT is an evolutionarily conserved transport system that mediates bidirectional movement of proteins between the base and tip of the cilia/flagella, and is essential for the construction and maintenance of cilia/flagella (Figure 11.1; Table 11.2; see section "Intraflagellar Transport (IFT) and IFT Motors").[11] In agreement with a role in IFT, further studies in *Caenorhabditis elegans* (*C. elegans*) on OSM-5, the IFT88/Polaris homolog, revealed that mutations disrupting this protein also cause severe defects in cilia assembly.[12]

Seldin and Giebisch's The Kidney, Fifth Edition.
DOI: http://dx.doi.org/10.1016/B978-0-12-381462-3.00011-2

© 2013 Elsevier Inc. All rights reserved.

TABLE 11.1 Ciliopathy Genes that Cause Known Renal Phenotypes[a]

Gene Name	Gene Location	Protein Name	Aliases	Overlapping Loci	Associated Ciliopathies	Protein Characteristics	Subcellular Localization
BBS1	11q13.2	BBS1	BBS2L2		BBS	BBSome component	Basal body; cilium
BBS2	16q12.2	BBS2	–		BBS	BBSome component	Basal body; cilium
ARL6	3q11.2	Arl6	–		BBS	GTPase	Basal body; cilium
BBS4	15q24.1	BBS4	–		BBS	BBSome component	Basal body; cilium
BBS5	2q31.1	BBS5	–		BBS	BBSome component	Basal body; cilium
MKKS	20p12.2	BBS6	–		BBS	Chaperonin-like	Basal body
BBS7	4q27	BBS7	BBS2L1, FLJ10715		BBS	BBSome component	Basal body; cilium
TTC8	14q31.3	BBS8	–		BBS	BBSome component	Basal body; cilium
PTHB1	7p14.3	BBS9	–		BBS	BBSome component	Basal body; cilium
BBS10	12q21.2	BBS10	–		BBS	Chaperonin-like	Basal body
TRIM32	9q33.1	BBS11	HT2A		BBS	E3 ubiquitin ligase motif; RING zinc finger	Cytosol; nucleus
BBS12	4q27	BBS12	FLJ35630		BBS	Chaperonin-like	Basal body
WDPCP	2p15	BBS15	Fritz		BBS	WD40 domains	Cytosol
INPP5E	9q34.3	INPP5E	CORS1, MORMS		JBTS	Inositol polyphosphate-5-phosphatase	Cilium
AHI1	6q23.3	AHI1	Jouberin		JBTS	SH3 domain; W40 repeats; coiled-coil domain	Cilium
ARL13B	3q11.1	ARL13B	ARL2L1		JBTS	GTPase	Basal body; cilium
ACLS	15q26.1	Klf7	KIF7, Costal2		JBTS	Kinesin-family protein	Cilium
TCTN1	12q24.11	Tectonic	TECT-1, Tectonic 1		JBTS, MKS?	Transmembrane domain	Transition zone
MKS1	17q22	MKS1	MKS	BBS13	MKS, BBS	B9 domain	Transition zone
TMEM216	11q12.2	MKS2	JBTSB, CORS2	JBTS2	MKS, JBTS	Transmembrane domain	Transition zone
TMEM67	8q22.1	MKS3	Meckelin	JBTS6, NPHP11	MKS, JBTS, NPHP	7-pass transmembrane domain protein	Transition zone
CEP290	12q21.32	Cep290	–	NPHP6, BBS14, JBTS5, SLSN6	MKS, BBS, NPHP, JBTS, SLSN	Coiled-coil domains/ bipartite NLS	Basal body/ centrosome
RPGR1P1L	16q12.2	MKS5	NPHP8	NPHP8, JBTS7	MKS, NPHP, JBTS	C2 domains, coiled-coil domains, bipartite NLS	Transition zone
CC2D2A	4p15.32	MKS6	–	JBTS9	MKS, JBTS	C2 domains, coiled-coil domains	Transition zone
TCTN2	12q24.31	Tectonic-2			MKS	Transmembrane domain	Transition zone
B9D1	17p11.2	B9D1			MKS	B9 domain	Transition zone
B9D2	19q13.2	B9D2			MKS	B9 domain	Transition zone
NPHP1	2q13	NPHP1		JBTS4, SLSN1	NPHP, JBTS, SLSN	SH3 domain/coiled-coil domain	Transition zone, adherens junctions
INVS	9q31.1	Inversin	NPHP2		NPHP	IQ calmodulin-binding domain/ankyrin repeats	Inversin domain, cilium

(*Continued*)

TABLE 11.1 (*Continued*)

Gene Name	Gene Location	Protein Name	Aliases	Overlapping Loci	Associated Ciliopathies	Protein Characteristics	Subcellular Localization
NPHP3	3q22.1	NPHP3	Nephrocystin-3, NPH3	MKS7, SLSN3	NPHP, MKS, SLSN	IQ calmodulin-binding domain	Cilium
NPHP4	1p36.31	NPHP4	Nephroretinin	SLSN4	NPHP, SLSN	SH3 domain	Transition zone, adherens junctions
IQCB1	3q13.33	NPHP5	PIQ	SLSN5	NPHP, SLSN	IQ calmodulin-binding domain	Inversin domain, cilium
GLIS2	15p13.3	Glis2	–		NPHP	Kruppel-like zinc finger	Cilium
NEK8	17q11.2	Nek8	NPHP9, JCK		NPHP	NIMA kinase	Inversin domain, cilium
SDCCAG8	1q43	SDCCAG8	NPHP10, CCCAP	SLSN7	NPHP, SLSN	Coiled-coil domains, colon cancer auto-antigen	Basal body/ centrosome
XPNPEP3	22q13.2	NPHP-1L	APP3		NPHP	Peptidase	Mitochondria
ATD	15q13	ATD1	ATD		ATD	Unknown	Cilium?
IFT80	3q25.33	IFT80	WDR56		ATD	IFT-B complex, WD40 domains	Cilium
DYNC2H1	11q22.3	Dync2H1	DHC2, DHC1B		ATD	Cytoplasmic dyenin component	Cilium, cytosol
TTC21B	2q24.3	IFT139	THM1	JBTS11, NPHP12	ATD, NPHP, JBTS	IFT-A complex, TPR repeats	Cilium
IFT122	3q21.3–q22.1	IFT122	WDR10		CED	IFT-A complex, WD40 domains	Cilium
WDR35	2p24.1	IFT121	TULP4, Naofen		CED	IFT-A complex, WD40 domains	Cilium
IFT43	14q24.3	IFT43	–		CED	IFT-A complex	Cilium
OFD1	Xp22.2	Ofd1	–	JBTS10	OFD, JBTS	Coiled-coil domains	Basal body/ centrosome
ALSM1	2p13.1	ALSM	ALSS		ALMS	Trafficking protein?	Cytosol
ATXN10	22q13.31	Ataxin 10	E46L, SCA10		MKS?	ATTCT repeats	Perinuclear

[a]*Genes are categorized by ciliopathy based on Online Mendelian Inheritance in Man (OMIM, http://www.ncbi.nlm.nih.gov/omim) entries at time of writing.*

Thus, the function IFT88 is highly conserved across diverse species.

One of the most significant breakthroughs connecting cilia dysfunction to human diseases came from studies in *C. elegans* by Barr et al. They conducted a genetic screen to identify genes involved in male mating behavior and uncovered mutations in *lov-1* and *pkd-2*, the homologs of human polycystin-1 (PC-1) and polycystin-2 (PC-2), respectively.[13] Importantly, mutations in these two genes cause human autosomal dominant polycystic kidney disease (ADPKD OMIM# 601313, # 173910); a disorder that affects nearly 1 in 1000 individuals and is a leading cause of end-stage renal disease. In *C. elegans*, both *lov-1* and *pkd-2* proteins localize to the cilium of male sensory neurons.[14] Subsequently, the mammalian proteins were also localized in the cilium of renal epithelium[15,16] leading to a paradigm shift in the understanding of the possible mechanisms involved in human PKD. Multiple cystic kidney disease genes in mice, rats, and humans have now been identified and in nearly every case, the affected proteins encoded by these genes are associated with the cilium (reviewed in [17–20]).

These initial observations in model systems ushered in a renewed interest into the functions and clinical importance of the primary cilium. Even though research into the role of primary cilia has now extended to almost every tissue in the body, the involvement of the cilium in the kidney has garnered particular focus. In part this may reflect the morbidity and mortality associated with PKD, as well as the high incidence of PKD.

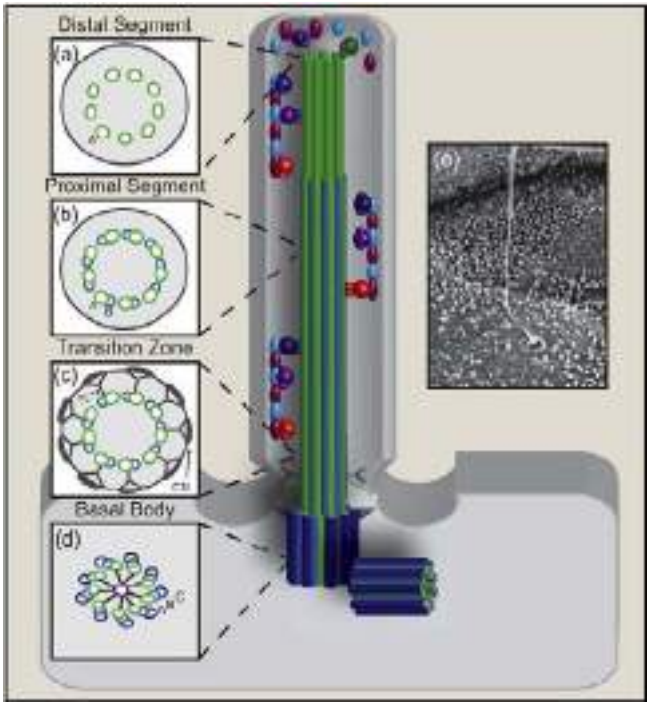

FIGURE 11.1 **Ultrastructure of the primary cilium**. A microtubule-based axoneme nucleates from the basal body and extends the length of the cilium. IFT-A (maroon) and IFT-B (light blue) complexes form IFT-A/B particle trains and travel along the axoneme via IFT with their associated cargoes. Anterograde IFT (left side of axoneme) occurs via Kinesin-2 (dark blue) and Kif-17 (purple) motor proteins. IFT-A/B particle trains are disassembled and reassembled at the ciliary tip. Retrograde IFT (right side of the axomene) removes IFT-A/B particles and associated proteins from the cilium via the cytoplasmic dynein-1 retrograde motor protein (red). Insets (a–d) illustrate cross-sections of ciliary microtubule structure. (a) Distal segment with 9 + 0 "A" axonemal microtuble singlets; (b) Proximal segment with 9 + 0 "A/B" axonemal doublets; (c) transition zone with Y-links (YL) and ciliary necklace (CN) respectively; (d) basal body with "A/B/C" microtubule triplets; (e) scanning electron micrograph of the primary cilium. *(Image adapted from Alvaro, D. et al. (2008).* Am. J. Pathol. *Feb;* ***172****(2), 321–332, with permission.)*

CILIA ULTRASTRUCTURE AND COMPONENTS

The primary cilium on renal epithelial cells is a small, membranous, hair-like extension protruding from the surface of the cell into the lumen of the nephron tubule. This simple description, however, disguises the high level of complexity that is necessary for the cilium to function as an intricate signaling and sensory organelle (Figure 11.1). Below the membranous covering of the cilium lies a precisely ordered series of axoneme microtubules. At the base of the cilium, the axoneme microtubules are anchored to the cell and cell membrane by a series of specialized structural components including transition fibers, the transition zone, ciliary necklace, and a modified centriole termed the *basal body*. These structures are further defined below.

Centrosomes and Basal Bodies

Centrosomes are comprised of a pair of centrioles, an older mother centriole and a daughter centriole, surrounded by a proteinaceous matrix. Mother–daughter centrioles are aligned orthogonally, with the mother centriole aligned towards the cell surface. The mother centriole becomes the basal body, which acts as a microtubule-organizing center (MTOC) for axonemal nucleation at the base of the extending cilium. Basal bodies are comprised of a nine-ring helix of triplet microtubules that contain γ-tubulin, in addition to α- and β-tubulins (Figure 11.1d). Axoneme microtubule polymerization is initiated by nucleation of γ-tubulin-containing microtubules of the basal body.

In addition to their microtubule cores, basal bodies are also comprised of numerous associated proteinaceous appendages that facilitate ciliogenesis. Although the basal body appears symmetrical, the distribution of centriolar appendages gives the basal body asymmetry with respect to its proximal–distal axis. The basal foot (also called sub-distal appendages) and the transition fibers (also called distal appendages) extend from the more distal end of the basal body. The formation of transition fibers on the basal body is a distinct process from that of ciliogenesis, yet it has been demonstrated that transition fibers are necessary for cilia to form.[21,22] Transition fibers appear necessary for tethering the basal body to the membrane (see section "Transition Fibers" and [23]), thus establishing the basis for cilia anchorage.

The proteinaceous matrix surrounding the basal body is termed the *pericentriolar material* and contains centriolar components. Although the pericentriolar material does not form the structure of the centriole/basal body, these proteins are necessary for centriolar organization and control of mitosis. Puncta of proteins surrounding centrioles (centriolar satellites) will often be dynamically associated with the centrosome depending on cell cycle stage.[24]

Ciliary Axoneme

The core of both motile and primary cilium is an organized microtubule-based axoneme extending from the basal body. Axonemal microtubules have (+) ends, localized at the ciliary tip, and (−) ends anchored to the basal body. These microtubules serve as tracks for molecular motor protein transport of cargo along the cilium (Table 11.2 and see section "Intraflagellar Transport (IFT) and IFT Motors").

TABLE 11.2 Intraflagellar Transport (IFT) Complex Proteins and Motors (Known Disease Genes are Annotated)

IFTA-Complex	IFTB-Complex	IFT Anterograde Motors	IFT Retrograde Motors
IFT43*	IFT20	KIF3A	Cytoplasmic dynenin2^
IFT121*	IFT22	KIF3B	
IFT122*	IFT25	KAP3	
IFT139^	IFT27		
IFT140	IFT46		
IFT144	IFT52		
	IFT54		
	IFT57		
	IFT70		
	IFT74		
	IFT80^		
	IFT81		
	IFT88		
	IFT172		

*Mutated in CED.
^Mutated in ATD.

Axonemal microtubules are arranged in a ring of nine doublets (Figure 11.1b). Cryo-electron tomography imaging of cilia axoneme microtubles by Sui and Downing[25] illustrate that each doublet is comprised of a larger A-tubule, and a smaller incomplete B-tubule. Both A and B tubules of the axoneme microtubles are comprised of α- and β-tubulin protofilaments similar to the cytoplasmic microtubules. The axonemal microtubule doublet may either extend the entire length of the cilium or terminate into a mircotubule singlet that continues into the distal cilium (Figure 11.1a). Most motile forms of cilia also contain additional structures used in generating motility. These include a central pair of microtubules, in addition to their nine-ring doublet, radial spokes, inner and outer dynein arms, and nexin links.[26] The incorporation of a central pair of microtubles in motile cilia is referred to as a *9 + 2 arrangement*. However, not all 9 + 2 cilia are motile, as revealed by olfactory sensory neuron cilia. Immotile primary cilia, such as those found in renal epithelia, lack the central microtubule pair and many of the motility components.[27] Lack of a central microtubule pair is referred to as a *9 + 0 axonemal* microtubule arrangement (Figure 11.1).

The Transition Zone

The cilium is not a simple extension of the cell membrane or cytosol, but rather it has a distinct complement of proteins necessary for its construction, signaling, and sensory functions. The specialization is established by structures located at the base of the cilium that function to separate the ciliary compartment from the rest of the cell.

At the proximal end of the cilium nearest the basal body, the cilia membrane is closely associated with the axoneme microtubules. This region is known as the *transition zone*. Ultrastructurally, the transition zone (Figure 11.1c) is comprised of a radial array of Y-shaped links, with the bottom of the "Y" attaching to each axonemal microtubule doublet and top of the "Y" likely forming attachments with the nearby cilia membrane.[28] The molecular composition of the Y-links are unknown, however, centrosomal protein 290 (CEP290)[29] and the protein p210[30] were shown to localize to the distal end of the basal body in the area of the transition zone Y-links in *Chlamydomonas*. The transition zone appears to be an important domain, as many proteins associated with Meckel-Gruber Syndrome (MKS, OMIM# 249000) and Nephronophthisis (NPHP, OMIM# 256100) function as part of genetically and biochemically interacting complexes that also localize in this region.[31,32] In *C. elegans*, mutations disrupting the interactions between the transition zone proteins involved in NPHP and MKS cause the loss of Y-links, detachment of the ciliary membrane from the axoneme, abnormalities in regulating protein entry into the cilium, and defects in cilia positioning, orientation, and assembly.[32] It is not currently known whether the MKS and NPHP proteins are a direct component of the Y-links or whether the loss of the Y-links in *nphp* and *mks* mutants is a secondary consequence.

The Ciliary Necklace

At the position where the Y-links attach to the inside of the ciliary membrane, the outside of the membrane is decorated with electron-dense proteinaceous nodules.[28] These decorations are collectively referred to as the "*ciliary necklace*" (Figure 11.1d; denoted "CN"). When observed by electron microscopy, the ciliary necklace appears to restrict around the axoneme, and somewhat resemble tight junctions in epithelial cells. As such, the ciliary necklace, along with the Y-links, may function as a barrier machinery that is selective for ciliary transmembrane and membrane associated proteins. The composition of the ciliary necklace remains to be defined, and the mechanisms by which this region may function as ciliary barrier is a major focus of ongoing studies.

Transition Fibers

Through electron microscopy studies, it is apparent that there are electron-dense fiber-like structures

extending from the distal end of the basal body that tether the basal body to the base of the ciliary membrane.[23] These structures are known as transition fibers (Figure 11.1). Nine transition zone fibers extend at an angle from the distal tip of the basal body and connect with membrane creating an elaborate pinwheel-like conformation.[23] Space filling models reconstructed from electron micrographs suggest that the space between transition fibers could accommodate particles up to 60 nm,[23] suggesting that this region could act as part of a ciliary gating or barrier mechanism preventing soluble cytosolic protein from entering the cilia. It has therefore been hypothesized that there must be other, active mechanisms for ciliary entry that are localized to this region.[33] Data obtained from studies in *C. elegans* suggest that the transition fibers are docking sites for the IFT particles (see section "Cilia Transport and Trafficking"), and that the transition fibers function in loading and unloading of ciliary cargo onto the IFT particles for transport.[34] Relatively few transition fiber proteins have been identified. One candidate is Cep164, which localizes in the region of the transition fibers and is necessary for ciliogenesis.[21]

Cilia Membrane

The cilium has a distinct composition with regards to both protein and lipid content.[35,36] Identifying the composition of the primary cilia in mammalian cells has been technically challenging, as the surface area of the cilia membrane comprises a small fraction of the total cell membrane. Initial analyses indicate that the cilia membrane contains a high concentration of sterols relative to phosphinostitides when compared to plasma membrane.[37] The high levels of sterols in cilia have led some to speculate that cilia are enriched in lipid rafts, which also have high sterol content. In fact, several ciliary and cystic kidney disease proteins, such as cystin, associate with lipid raft components, and inhibiting this association can impair their transport to the cilium.[38]

Information regarding the protein composition of the cilium has been obtained through proteomic and genetic studies in model systems, as well as comparing the genomes of ciliated and non-ciliated organisms.[39] Although proteomic analysis has been performed on motile cilia and photoreceptor cilia isolated from mammalian cells, currently the most complete information regarding the protein composition of the cilium/flagellum come from *Chlamydomonas*.[40] This is in part due to the ease with which deflagellation can be induced in this organism, allowing for purification and proteomic analyses.

Proteomic data revealed that the cilium contains a large number of transmembrane and membrane associated proteins that in many cases are not found in other regions of the cell. These proteins must be specifically targeted to the cilium (see section "Cilia Transport and Trafficking"). The localization of proteins in the cilia membrane is necessary for normal cilia mediated sensory functions and signaling activities (see section "Cilia Signaling in the Nephron"). This has important implications in common renal disorders, since transmembrane proteins, such as PC-1 and PC-2[15,16] localize in the cilium (see Chapter 81 for a detailed description). Other cystic kidney disease transmembrane proteins found in the cilium include fibrocystin/polyductin, and the Meckel–Gruber syndrome proteins 2[41] and 3[42] (MKS2 and MKS3 respectively) that localize to the transition zone region (see section "Transition Fibers").

CILIA TRANSPORT AND TRAFFICKING

For the cilium to function as a sensory and signaling center, it requires the specific targeting and transport of proteins into and out of the cilium. Although the mechanism of ciliary targeting and protein transport remain poorly understood, great advances have come from seminal studies in model organisms and human ciliopathy patients. We now know many of the core components of the cilia trafficking machinery. Machinery involved in cilia trafficking include the microtubule motor driven intraflagellar transport (IFT) proteins originally defined in *Chlamydomonas*, and the BBSome, a complex of proteins disrupted in Bardet–Biedl syndrome (BBS, OMIM# 209900), that function in cilia membrane protein trafficking and vesicular transport. It has become evident that ciliary trafficking machinery often utilizes canonical endocytic pathways involving the Rab-family of proteins (reviewed in [43]). Understanding how ciliary trafficking falls into conventional trafficking modules is the focus of many ongoing studies.

Intraflagellar Transport (IFT) and IFT Motors

The axoneme provides the cilium structure, and also serves an important role in building the organelle and trafficking proteins through the cilium. Axonemal microtubules are used for trafficking components in both anterograde (toward the cilia tip) and retrograde (toward the basal body) directions in a process known as *intraflagellar transport* (IFT).[11] Coordinated, bidirectional IFT movement is localized between the outer doublet microtubules and the ciliary membrane.

IFT is required to build and maintain the primary cilium through the movement of two interacting

macromolecule complexes, IFT-A and IFT-B (summarized in Table 11.2 and reviewed in [44,45]). IFT-A and IFT-B interact to form a large IFT-A/B particle chain that moves together in both anterograde and retrograde IFT. It has been documented that mutations in IFT complex proteins can cause human ciliopathies. Both Jeune Asphixiating Thoracic Dystrophy (ATD, OMIM# 208500) and Sensenbrenner syndrome (CED, OMIM# 218330) are caused by mutations in IFT genes (Tables 11.1 and 11.2, and see sections "Jeune Asphyxiating Thoracic Dystrophy (ATD)" and "Sensenbrenner Syndrome (Cranionectodermal Dysplasia, CED)." In general, the mutations in IFT proteins identified in human patients are thus far hypomorphic, suggesting that complete loss of IFT function is not viable.

In addition to the proteins that make up IFT complexes A and B proper, there is emerging evidence for IFT associated proteins that are important for ciliary protein trafficking and ciliary function. For example, IFT20 is associated with trafficking of proteins from the Golgi to the cilia base.[46] Also, IFT27 (Rabl4) and IFTA-2 (Rabl5) are both Rab-like proteins that associate with the IFT-A/B complex.[47,48] The function of these proteins is poorly understood; however, in the absence of *Rabl5* in *C. elegans*, cilia regulated signaling pathways are affected even though *Rabl5* is not required for ciliogenesis.[48] Thus, the current hypothesis is that *Rabls5* and other IFT associated proteins may function to connect specific cargo with the IFT complex or in more subtle regulation of cilia signaling and sensory activities.

Specific motor proteins mediate IFT bidirectional movement in the cilium (Table 11.2). Kinesin-2 associates with the IFT-A/B complex to move the IFT particle in the anterograde direction toward the cilia distal segment.[49,50] A second kinesin, Kif17, specifically associates with the IFT-B complex, and appears to function largely in movement of the IFT-A/B particle along the distal segment of the cilium.[51] The retrograde motor, cytoplasmic dynein-2, mediates movement of the IFT-A/B particle with its associated cargo in the retrograde direction toward the basal body.[52] It should be noted that most of the data concerning motor-microtubule specificity is largely based on studies using homologs of cilia motor proteins in *C. elegans* and *Chlamydomonas*.

IFT builds and maintains its primary cilium by shuttling tubulin subunits to the growing (+) end of the axoneme microtubules at the ciliary tip by anterograde IFT, while cilia microtubles are cleared from the cilia by retrograde IFT. This can be demonstrated both *in vivo* and *in vitro*, where mutations in Kinesin-2 proteins (anterograde motor) lead to the absence of cilia,[53,54] while mutations in cytoplasmic dynein-2 (retrograde motor) lead to bulbous, stumpy cilia caused by an accumulation of IFT particles and other ciliary proteins.[52,55–57]

Mechanisms of Cilia Protein Entry

The correct function of the primary cilium is dependent on the localization or enrichment of receptors, channels, and effectors in this specialized compartment. As such, the mechanisms restricting or facilitating protein entry into the cilium remain an area of intense research.

A ciliary barrier or gate, which is likely found at the base of the cilium, could function to restrict entry of non-ciliary proteins and/or impair exit of proteins from the cilium. As indicated above, one of the current models is that the transition zone, transition fibers, and ciliary necklace constitute the barrier machinery (Figure 11.1). Evidence supporting a diffusion barrier at the base of the cilium comes from studies using a glycosylphosphatidylinositol-anchored fluorescent protein that is targeted to the apical plasma membrane.[36] This protein diffuses rapidly across the apical surface, but is restricted from the cilium and a region around the base of the cilium called the *periciliary membrane domain*. Similarly, other membrane proteins localized to the apical plasma membrane are not found in the cilium.

Although there is evidence for a cilia barrier, there are also data indicating that cilia access may in part be determined by protein size and governed by diffusion. GFP is a 27 kDal protein that rapidly equilibrates between the cilium and cytosol. However, larger proteins do not accumulate freely in the cilium, and are dependent on IFT. This has led to the hypothesis that the ciliary barrier may be analogous to nuclear pore complex. Passage through the nuclear pore involves the association of a protein containing a nuclear localization signal (NLS) binding to an importin-family protein for movement into the nucleus catalyzed by Ran GTPase activity. Intriguingly, importin-β2 has been localized to the basal body/transition zone in cultured cells, and knockdown of importin-β2 inhibits cilia localization of retinitis pigmentosa 2.[58] Likewise, Ran is found in the cilium, and experiments using mutated Ran have shown that ciliary entry is mediated through a Ran-GTP gradient.[59] The question remains as to whether there are specific cilia localization signals (CLS) similar to the putative NLS sequence. Indeed, NLS-like sequences have been reported in cilia proteins, such the kinesin KIF17, and disruption of this NLS motif inhibits Kif17 cilia localization.[59] A sequence, V-x-P, necessary for ciliary localization[60] has also been identified in the transmembrane proteins

PC-2 and CNGB1b, and in several G-protein coupled receptors (SSTR3, 5HT6, DRD1, Rhodopsin, and MCHR1); however, the mechanism by which this motif targets these proteins to the cilium is variable, and is most likely protein-specific. Most other cilia transmembrane proteins do not have this signature, indicating there is no universal sequence directing proteins into the cilium.

An alternate hypothesis for ciliary enrichment was proposed by Hu et al. and involves inhibition of lateral diffusion. Ciliary proteins were highly mobile within the cilium, but there was limited exchange between the plasma membrane and the cilium. These data suggest a barrier-impeded diffusion. Hu et al. demonstrated that septin-2 is located around the base of the cilium, and may function as this barrier.[61] Septins were originally identified as a family of guanosine triphosphatases with diffusion barrier function. Knockdown of septin-2 in embryonic fibroblasts and renal epithelium resulted in a marked increase in diffusion and exchange between cell and ciliary membranes, defects in ciliogenesis, and inhibition of cilia dependent signaling (e.g., Sonic Hedgehog (Shh) pathway, see section "Renal Cilia and Hedgehog Signaling").[61] Thus, one possible mechanism is that ciliary transmembrane proteins are continually transported into the cilium and accumulate there as a consequence of slow outward diffusion.

Recently, another model for ciliary membrane protein entry was proposed from the laboratory of Ira Mellman.[62] Francis et al. analyzed gp135/podocalyxin, which is a transmembrane protein localized to the apical surface of renal epithelial cells that is also restricted from the cilium and the periciliary membrane region around the cilia base. gp135 is anchored to the cortical actin cytoskeleton through its PDZ domain. When this motif was disrupted, gp135 was now present ectopically in the cilium. Conversely, proteins that normally enter the cilia could be inhibited from doing so if the gp135 PDZ domain was incorporated into the protein. These data suggested that ciliary exclusion was dependent on attachment of membrane proteins to the cytoskeletal network, rather than the presence of a diffusion barrier. This model is hard to reconcile with the septin-2 data from Hu et al.,[61] the evidence for the BBSome in cilia membrane trafficking of specific GPCRs (see section "Ciliary Targeting and the BBSome" and [60,63,64]), and the presence of multiple membrane proteins that are freely diffusible and have not been detected in the cilium.[36] Further, lipid content in the cilium has been reported to be distinct from that of cell membrane (reviewed in [65]). In the absence of a barrier, one would expect an equilibration between the two compartments.

Vesicular Trafficking of Transmembrane Proteins to the Cilium

Transmembrane proteins destined for the cilia are dependent on the activity of Rab-GTPases. One of the initial Rabs shown to be involved in ciliary targeting was Rab8. Inhibition of Rab8 leads to accumulation of vesicles at the base of the cilium, while Rab8 constitutive activation causes elongated cilia.[66] Rab8 utilizes the ciliary localized exocyst complex and activity from its guanine nucleotide exchange factor (GEF) Rabin8 to dock and fuse vesicles at the cilia base. Although the process of targeting transmembrane proteins to the ciliary base is still being fully deduced, one of the most widely accepted models involves polarized exocytosis through a Rab11-associated trafficking pathway. Through this pathway, transmembrane proteins are shuttled from a Rab11 positive compartment to a Rab8 positive vesicle, dependent on Rab11 activation of Rabin8. Transmembrane proteins in these Rab8 positive vesicles are then transported to the cilia base, and inserted directly into the periciliary membrane domain.[67,68] Importantly, although some vesicular structures have been reported in olfactory and chondrocyte cilia,[69,70] vesicles are not commonly seen in most other cilia or flagella. These data indicate that if polarized exocytosis occurs, the fusion of the vesicles with the cilia membrane likely occurs at the base. In support of this are ultrastructural studies showing numerous vesicles containing putative ciliary-targeted proteins located around the base of cilia and flagella actively fusing with the membrane.[71,72] How these proteins then get across a ciliary barrier, if it exists, is unknown.

It is also possible that the initial targeting of ciliary transmembrane proteins is to the plasma membrane. The ciliary protein would then translocate into the cilium by either lateral diffusion or through an endocytic pathway. This is best understood in the case of Smoothened (Smo), the transmembrane effector protein of the Sonic hedgehog-signaling pathway (Shh). In response to Shh stimulation, Smo translocates from the cell membrane into the cilium. This translocation is not inhibited by expression of a dominant negative form of dynamin,[73] a GTPase required for scission of vesicles during endocytosis in eukaryotic cells. Thus, the data indicate that at least in this case, ciliary targeting is likely mediated through lateral diffusion, and does not require endocytosis of vesicles from the plasma membrane.

Ciliary Targeting and the BBSome

The BBSome is a protein complex involved in trafficking of specific cilia membrane proteins.[64,66]

Mutations affecting this complex of proteins cause Bardet–Biedl Syndrome (BBS). BBS is a rare human ciliopathy characterized by obesity, sensory defects, and cystic kidney disease (see section "Bardet-Biedl Syndrom (BBS)). The assembled BBSome shares structural similarities with the COP/clatherin family of coat proteins, suggesting the BBSome functions as a coat for ciliary cargos. The BBSome coat associates with the GTPase Arl6 (also known as BBS3) when Arl6 is in its GTP–bound, active state. The BBSome/Arl6 complex recognizes the ciliary localization sequence (CLS) in proteins such as SSTR3, and then escorts the protein into the cilium. The BBSome may also function for removal of proteins from the cilium. This is evidenced by the abnormal accumulation of specific transmembrane proteins in the cilium of *bbs* mutant mice.[63]

CILIOGENESIS

Cilia are complex structures that require continual maintenance[74] and must be dissembled and subsequently reassembled at the beginning and end of each cell cycle. The process of building a cilium (ciliogenesis) requires the coordination of centriolar modification/maturation to form a basal body, the motor driven process of IFT to build the cilia axoneme, and carefully timed transcriptional events. These processes are synchronized with cell cycle progression, as cilia are assembled on quiescent cells.[75] Likewise, during mitosis the centrioles must be released from their position below the cilia, and migrate to opposite spindle poles for proper cell division. Ciliogenesis can also be regulated by other factors, such as cell confluence, fluid flow, mechanical stimuli, and injury.[76]

Transcriptional Control of Ciliogenesis

Cilia are extremely dynamic structures that grow and reabsorb depending on physiological conditions. Ciliogenesis is in part regulated through transcriptional control. This is demonstrated in *Chlamydomonas*, where experimentally induced deflagellation results in a large increase in the expression of flagellar genes, including the IFT proteins.[39,40,72,77–79] In addition, in *C. elegans* and mammalian systems, transcription factors of the RFX (regulatory factor X) family have been shown to coordinately control expression of several IFT genes through a motif called the X-box located in their promoters.[80] This process is evolutionarily conserved, and was first reported in *C. elegans.* The RFX transcription factor DAF-19 was needed for expression of several IFT proteins, as well as a few proteins known to be involved in human syndromes with cystic kidney disease phenotypes.[81,82] This includes transition zone proteins such as the NPHP genes *nphp-1* and *nphp-4*, and the MKS genes *mks-1*, *b9d1*(*mksr1*), and *b9d2*(*mksr2*), as well as multiple BBS genes including *bbs-1*, *bbs-2*, *bbs-5*, *bbs-8*, and *bbs-9* (reviewed in [83]).

Cilia and the Cell Cycle

The basal body (see section "Centrosomes and Basal Bodies") is generated from the centrioles that are also components of mitotic machinery. Therefore, cell division, cell differentiation, and ciliogenesis are inherently linked. As cells exit mitosis, ciliogenesis is initiated in the G_1 or G_0 phase of the cell cycle. This can be modeled *in vitro*, as cells will become increasingly ciliated as they reach confluence. Additionally, ciliogenesis can be induced precociously in subconfluent cells when cultured in serum-free medium. These data indicate that cilia formation and mitosis are intertwined, and has led to the proposal that the presence of the cilium may act as a G_0 checkpoint and thus as a tumor suppressor.[84] In addition, rapid or aberrantly dividing cells, such as some tumor cells, frequently do not have a cilium.[85,86] Despite this connection, increased tumor rates are uncommon in human ciliopathy patients or mouse cilia mutants. An exception to this was recently shown in the skin of cilia mutant mouse models in tumors associated with Shh signaling, where cilia have a direct role in pathway regulation.[87]

As cells re-enter the cell cycle, cilia begin to be dismantled. This usually occurs by the G2 phase. Deconstruction of the cilium can occur by either cilia severing or resorbtion.[75] These mechanism(s) regulating deciliation are still poorly understood. Work from *Chlamydomonas* suggests that katanin, a microtubule-severing protein, cleaves microtubules at the junction between the axoneme and the basal body to facilitate cilia release.[88] In *Chlamydomonas*, the kinase activity of Nek8 (NPHP9) is required for deflagellation.[89] In mammalian systems, HEF1 (human enhancer of filamentation 1) in association with Aurora A kinase and the tubule deacetylase (HDAC6) reduce axoneme microtubule stability and induce deciliation.[90]

Cilia Extension

At the initiation of ciliogenesis, the centriole migrates towards the cell surface and proteins required for ciliogenesis, including the IFT proteins, begin to aggregate at a *preciliary patch*. There appear to be at least two mechanisms in which cilia initially form. The first method requires the formation of a ciliary vesicle (CV),[91] a Golgi-derived structure that forms at the distal tip of the mother centriole. As the CV-

mother centriole nears the cell surface, the cilium axoneme extends into the CV. The CV fuses with the plasma membrane, allowing the cilium to extend from the cell surface and emerge into the extracellular space. As a consequence, the basal body and the cilium remain in a small depression in the cell called the *ciliary pocket*.[92,93] The functional importance of the pocket is not certain, but it closely resembles the flagella pocket present in some protists. In these organisms, the pocket serves as a critical sight for vesicular trafficking and endo- and exocytic activity. In the second method, the cell forgoes forming a CV, and the centrosome complex migrates to the cell surface. It is at the cell surface that the mother centriole recruits materials to begin forming the cilia from plasma membrane components.

Post Ciliogenesis Growth Control

Cilia length is an actively controlled process, and is important for normal function (reviewed in [44]). In motile cilia, the increase in cilia length alters beating frequency and pattern, and thus disrupts fluid movement. In primary cilia, it is less clear how changes in length may influence many of the signaling activities. Normal control of cilia length is important, as both excessively short or elongated cilia in the kidney have been shown to cause cysts.[94–97]

Cilia length control is best understood from studies in *Chlamydomonas*, where genetic mutants have been isolated that produce either short or long flagella. Several genes involved in this process have been identified and encode kinases, such as cyclin-dependant kinase,[98] and a mitogen-activated protein kinase (MAPK) member.[99] The homologs for these proteins are present in mammals, suggesting evolutionarily conserved pathways; however, the targets of the kinases are not known.

One of the initial functions assigned to primary cilia in the kidney and several other tissues is that of a mechanosensor (see section "Renal Cilia and Mechanosensation"). Thus, cilia length could greatly influence the response or sensitivity of the cell to mechanical stimuli. As in some ciliated protists, mammalian cells are also able to modulate cilia length. Recent studies have revealed that decreased Ca^{2+} or increased levels of cAMP can cause a marked increase in cilia length.[100,101] This length increase is in part dependent on protein kinase A (PKA), and is associated with increased rate of anterograde IFT. Shear stress across the surface of many cell types is able to reduce cilia length. This was also shown to decrease cAMP levels. Importantly, this adaptive response to shear stress was not observed in cells that lack the polycystins.[102] Thus, it has been proposed that dynamic regulation of cilia length is an important regulatory process that controls sensitivity to extracellular stimuli, and that in PKD this has been disconnected.

In addition, cilia length in the kidney, pancreas, and other tissues can be influenced by injury.[103,104] Since renal injury causes rapid cyst formation in the inducible adult cilia mutant mice but not their controls,[105,106] it is tempting to speculate that the cilium may have a function in regulating a pathway involved in a tissue repair process.

Other studies have revealed that cilia length can be influenced by changes in the actin and microtubule cytoskeleton. In a genomic screen for modulators of cilia length, Gleeson and colleagues identified numerous genes required for ciliogenesis, as well as for the maintenance of cilia length.[107] Among these were genes involved in actin dynamics and organization. This included ARP3, a protein necessary for actin polymerization at filament branches, that when knocked-down caused cilia elongation. This effect was further demonstrated using the actin polymerization inhibitor cytochalasin D. These effects on actin are believed to interrupt vesicular docking and stabilization of the pericilary membrane domain at the ciliary base. Further, Sharma et al. demonstrated that actin disruption leads to a concurrent increase in the levels of soluble tubulin that can now be incorporated into the elongating ciliary axoneme. This cilia elongation was inhibited by pretreatment with the microtubule-stabilizing drug paclitaxel.[101] This phenomenon is further supported by data showing that low levels of nocodazole, a microtubule-depolymerizing agent, could recapitulate the effects observed with actin destabilization.

CILIA SIGNALING IN THE NEPHRON

The spectrum of processes regulated by the renal cilium is not fully known. There are a large number of receptors and channels that have now been localized or enriched in the cilium.[15,60,102,108–110] For several of these proteins, their localization in the cilium has great importance to their function. In many cases, loss of ciliary signaling leads to the formation of renal cysts. Therefore, much of our understanding of cilia signaling in the kidney comes from the study of cystic kidney disease models. This section discusses some of the major signaling pathways involved in renal development and physiology in which the cilium is required for efficient signal transduction, and how disruption of these signals results in cyst formation.

Renal Cilia and Mechanosensation

Data indicating that renal cilium function as a mechanosensor came from studies in Ken Spring's laboratory.[111–113] Fluid-flow induced deflection of the cilium causes a transient increase in cytosolic calcium (Figure 11.2). Furthermore, studies by Liu et al.[114] demonstrated that in perfused tubules from the *orpk* mutants, where cilia are severely truncated, this calcium signal is abrogated. The proteins involved in this signal are believed to be polycystin-1 (PC-1) and polycystin-2 (PC-2), both of which localize to the primary cilium. PC-2 is a transient receptor potential (TRP)-like cation channel known to mediate calcium signals. PC-1, which binds to PC-2, is suspected to be a regulator of the channel. Mutations in PC-1 or PC-2 disrupt this calcium signal, even in the presence of a fully formed cilium.[102] This led to a model of cystogenesis where the loss of a cilia-mediated mechanical signal was a driving force responsible for the development of renal cysts.

Recently, data from inducible cilia and *PKD1* mutant mice have raised concern about the cilia mechanosensory model of cyst formation.[106] Disruption of *IFT88* or *PKD1* using conditional alleles and tamoxifen inducible Cre-deletor lines revealed that cilia dysfunction induced prior to postnatal day 12 (P12) caused a rapid onset of the cystic kidney phenotype.[115–117] However, cyst formation is very protracted if induction of cilia loss occurred after P12. It is difficult to reconcile how cyst development could be delayed in the adult induced cilia mutants if cysts arose due simply to the loss of a mechanosensory signal.

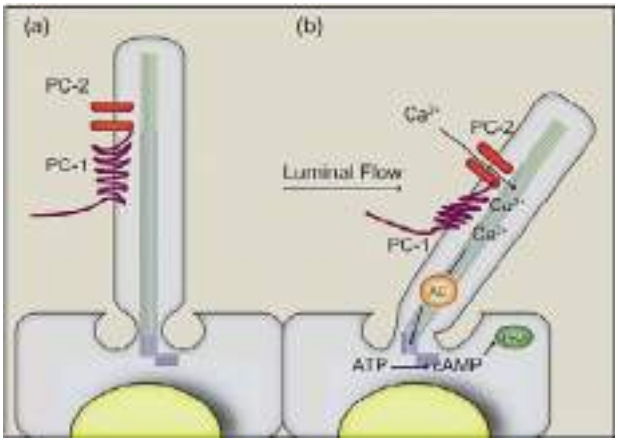

FIGURE 11.2 **Cilia and mechanosensation.** In low flow conditions (a), the TRP-like cation channel, polycystin-2 (PC-2, red) localizes to the cilium and is regulated by polcysitin-1 (PC-1, maroon). Under flow conditions (b), deflection of the primary results in an opening of the PC-2 channel, allowing Ca^{2+} ions to enter the cell, and increasing cytosolic Ca^{2+} levels. As a result of increased Ca^{2+} concentration, adenylyl cyclase (AC, orange) becomes activated, converts free ATP to cAMP, and cAMP activates protein kinase A (PKA) which phosphorylates multiple downstream targets. See color section at the end of the book.

Renal Cilia and Jak/STAT Signaling

The loss of the mechanosensory-based increase in transient cellular Ca^{2+} levels alone is not enough to induce the formation of renal cysts, as revealed by the large delay in cyst formation observed when cilia dysfunction is induced in adult mice. Recently, it has been demonstrated that in addition to regulating PC-2 channel activity, PC-1 also plays a role in transducing a flow-induced signal in the renal cilium through either the Jak/STAT pathway or mTOR signaling (see section "Renal Cilia and mTOR"). PC-1 activates the STAT-family of transcription factors via dual mechanisms (Figure 11.3a,b),[118] depending on the proteolytic processing and nuclear translocation of the PC-1 C-terminal tail (PC-1 CTT).[119,120] In a direct activation pathway, PC-1 resides in the cilium and is able to bind the Jak2 kinase.[118] When luminal flow is lost, Jak2 kinase phosphorylates and activates STAT3, which translocates to the nucleus (Figure 11.3b). Importantly, this process requires the PC-1 CTT to remain membrane-bound to activate STAT3.[118] Also, when fluid flow is lost in the nephron and PC1 is cleaved to release the PC-1 CTT, the PC-1 CTT can bind and activate both P100 and STAT6, which can be found in the cilium or at the basal body (Figure 11.3a).[120] This complex then enters the nucleus to influence gene expression. Alternatively, the PC-1-CTT has been shown to translocate directly into the nucleus, where it enhances the activity of cytokine activated STAT1 and/or STAT3.[118]

The Jak/STAT pathway is canonically described in the human immune response, driving differentiation and proliferation in response to cytokines. So what is the function of the Jak/Stat pathway in the cilium, and how does this relate to cyst growth? Under loss of flow conditions, such as injury, obstruction or cyst formation, the kidney undergoes an inflammatory response, which includes an increase in cytokine levels,[121,122] and infiltration of macrophages.[123–125] The increased cytokine levels trigger the upregulation of the Jak/STAT pathway in the cilium, possibly through association of PC-1 acting as a pseudo-cytokine receptor for Jak2 kinase.[118] This in turn begins the Jak/STAT signaling cascade, where the PC-1 CTT is eventually cleaved and enters the nucleus leading to proliferation. Indeed, high levels of nuclear PC-1 CTT have been observed in the metanephric mesenchyme, developing tubules,[119] and in cyst lining cells[120] where proliferation levels are high.

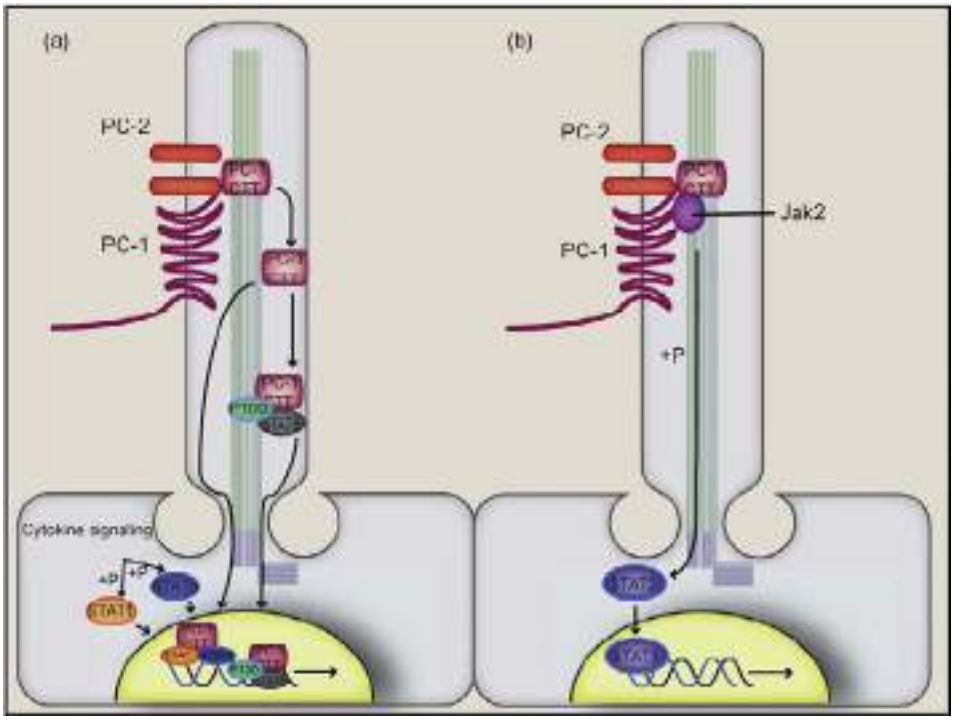

FIGURE 11.3 **Cilia and Jak/STAT signaling.** (a) When luminal flow is lost, the polycystin-1 C-terminal tail (PC-1 CTT, maroon) is cleaved and regulates the nuclear localization and activity of STAT6 (gray) and p100 (green). The PC1-CTT may also translocate into the nucleus to enhance activity of nuclear STAT1 (orange) and STAT3 (blue). (b) Membrane-associated polycystin-1 also directly interacts with Jak2 kinase (purple) to activate STAT3 under low flow conditions. See color section at the end of the book.

Further evidence to support the model of inflammation-based cyst growth has been demonstrated by monitoring macrophage infiltration in renal ischemic injury. The macrophage infiltrate found in ischemic reperfusion injury mice are pro-proliferation instead of pro-inflammatory.[124] Furthermore, Karihaloo and colleagues demonstrated that depleting macrophages in *PKD1* mutant mice lowered cystic growth significantly.[123] Continued work on the contribution of the immune response is needed to fully understand the role of Jak/STAT- and cilia-regulated signaling in the kidney.

Renal Cilia and Non-Canonical Wnt/Planar Cell Polarity (PCP) Signaling

Non-canonical Wnt signaling (Figure 11.4b) is best known for regulating planar cell polarity (PCP). PCP is the ability of cells to position and orient themselves along the plane of the tissue (Figure 11.5). This is accomplished by modulating the cytoskeleton via the Rho-kinase family, positioning of basal bodies, and the asymmetric distribution of proteins to establish cell orientation. Evidence from model organisms demonstrates a role for cilia in controlling the PCP response, most likely due to the close association of the cilium with the basal body and cell cytoskeleton. Morpholino knockdown of cilia or BBS genes in zebrafish give defects in body axis elongation typical of altered convergent extension during gastrulation.[126] Similarly, *bbs* and *ift88* mutant mice have inner ear abnormalities typical of PCP defects.[126,127] Collectively, these findings led to a model where cilia function to modulate the strength and spatial activity of the non-canonical Wnt pathway.

In the developing kidney, PCP likely has a role in controlling orientated cell division, and for convergent extension like movements that occur in the early developing nephron.[128] Therefore, loss of cilia-regulated oriented cell division could cause defects in development of the nephron, and lead to cyst formation. Using mouse and rat models of PKD, Fischer et al. demonstrated that the orientation of the mitotic spindle became randomized in cystic animals, rather than being parallel to the nephron lumen as seen in the control kidneys (Figure 11.5[129]). Similarly, the cystic kidney phenotype observed in conditional cilia mutant mice or mice with mutations in PCP genes, such as the proto-cadherin Fat4, are associated with misorientated cell division.[130–134] The above data suggested that parallel divisions to the long axis of the nephron would drive nephron elongation, whereas division perpendicular to the long axis would result in tubule diameter expansion and eventual cyst development. One proposed model was that cilia function in establishing the position of the mitotic spindle through a mechanical signal, such as fluid flow. Loss of the signal resulting from cilia dysfunction would then alter orientation of cell division and eventually lead to cyst formation.

The connection between changes in orientation of cell division and cyst formation must be considered

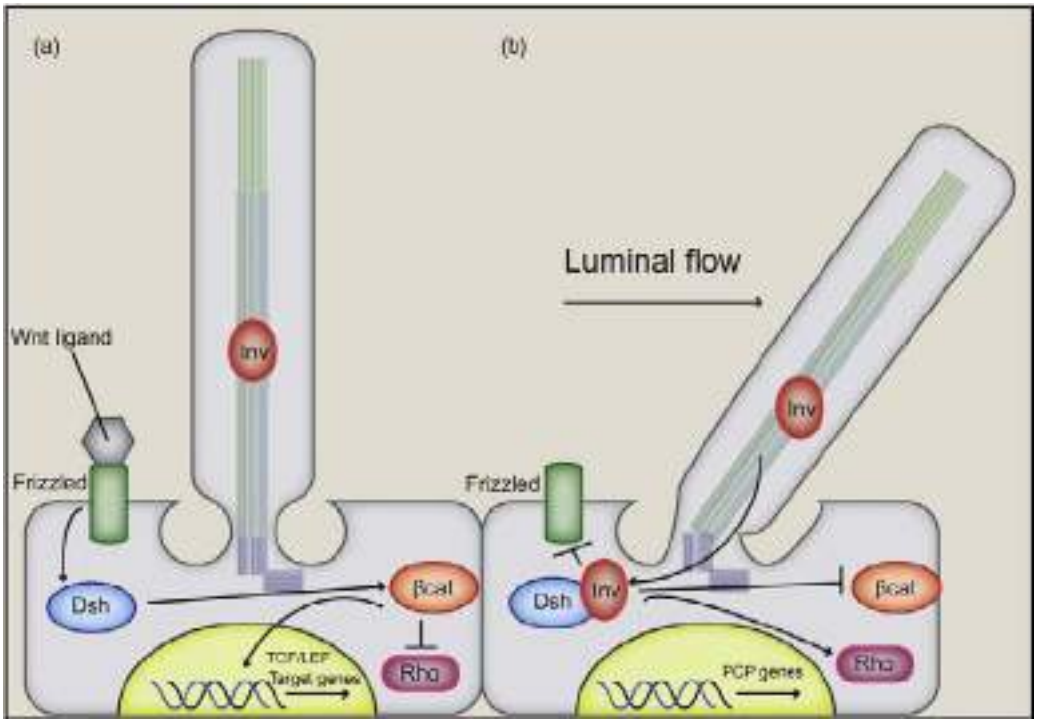

FIGURE 11.4 **Wnt signaling in the cilium.** In the canonical Wnt pathway (a), Wnt ligands (gray) bind the Frizzled receptor (green). Frizzled activates Disheveled (Dsh, blue) which in turn activates β-catenin (βcat, orange). βcat translocates to the nucleus (yellow), resulting in transcription of TCF/LEF target genes. (b) In the presence of fluid flow, cilia bending causes Inversin/NPHP2 (Inv, red) to translocate from the cilium to inhibit Dsh activation of the non-canonical Wnt pathway. Without Dsh activation, βcat is not activated and degraded. Rho-family kinases and PCP genes then become activated. See color section at the end of the book.

in the context of proliferation rate in the developing tubule. As noted in "Renal Cilia and Mechanosensation" there is a dramatic shift in the rate of cyst progression in mouse cilia mutant kidneys after day P12–13.[115–117] Importantly, in mice there is a dramatic drop in proliferation that occurs in a wild-type kidney as part of its maturation process around P12. Thus, it has been proposed that a combination of a highly proliferative environment, along with misoriented cell division that occurs in cilia or PCP mutants, leads to rapid cyst formation. The possible effect of proliferation on cyst initiation and progression was further analyzed using renal injury models. Through either ischemia reperfusion or nephrotoxin induced injury in the adult induced cilia mutants, several groups have shown that insult and subsequent proliferation induced by the repair process reinitiates a program of rapid cyst development, similar to that seen in the young (≤P12) cilia mutants.[105,135,136] This injury model data must be viewed with caution, as the injury also causes significant inflammation, apoptosis, and dedifferentiation of the nephron segments as a part of the repair process. The contribution of these factors to the rate of cyst formation after injury is not known, and could also contribute to cystogenic mechanisms.

The connection between cilia, cyst development, and oriented cell division was recently brought into question as a result of analysis in the *pkhd1* mutants. *PKHD1* mutations in humans cause ARPKD. In the *pkhd1* mouse mutants the orientation of cell division in the nephron was abnormal, yet they do not develop renal cysts.[137] These data indicate that changes in orientation of cell division are not sufficient to cause cystic disease.

Renal Cilia and Canonical Wnt Signaling

In the canonical Wnt pathway, a Wnt ligand binds to and activates a Frizzled-family receptor that stabilizes β-catenin (Figure 11.4a). β-catenin then translocates into the nucleus, where it combines with TCF/LEF to activate transcription of target genes. One of the initial studies establishing a cilia-Wnt connection came from analysis of *nephrocystin-2* (NPHP2, *Inv*) a gene disrupted in human patients with NPHP (see [138] and section "Nephronophthisis (NPHP)"). NPHP2 localizes to cilia and antagonizes Disheveled, a Wnt pathway component regulating β-catenin stability. NPHP2 expression was able to inhibit the ability of Disheveled to activate Wnt signaling. Simmons et al. have demonstrated a link

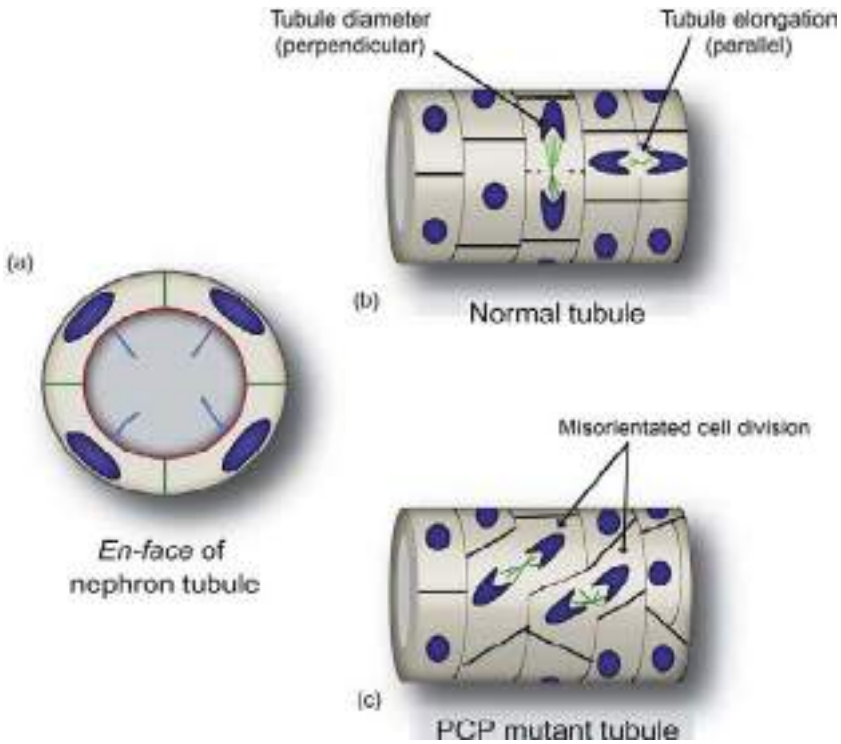

FIGURE 11.5 **Cilia influence planar cell polarity (PCP).** (a) Cilia (light blue) extend from the apical surface (red) into the lumen of the nephron tubule. Under normal conditions (b) cilia may modulate signals controlling cell division, either parallel to the long axis of the tubule to increase tubular length or perpendicular to the long axis of the tubule to increase tubule diameter. In some cilia mutants, a PCP-like pathway is disrupted (c) and cell division becomes random and disorientated with respect to the axis of the tubule. See color section at the end of the book.

between fluid flow through the renal tubules and a switch between canonical and non-canonical Wnt signaling pathways.[139] In this process, NPHP2 modulates the balance between the two different Wnt signaling pathways. Additionally, knockdown studies of the BBS genes lead to an increase in canonical Wnt response, and also inhibited non-canonical Wnts from repressing the canonical response in cultured cells.[140] Furthermore, genetic mutations in the IFT genes *kif3a*, *ift88* or *ahi1*, a cilia gene involved in Joubert Syndrome (JBTS, OMIM# 21330), caused an increase in canonical Wnt activity *in vivo*.[141,142] *Ahi1* mutant mice have vermis-midline fusion defects, and these defects could be partially restored by the canonical Wnt agonist lithium chloride.[142]

In contrast, several studies have argued against any direct role for cilia in Wnt signaling (see [143]). This is supported by the lack of clear canonical phenotypes in most tissues of cilia mutant mice, and in zebrafish maternal zygotic mutants in the *ift88* (*oval*) gene. These studies also analyzed Wnt signaling in mutant fibroblasts, and in direct contrast to the previous data did not find changes in Wnt signaling.[144]

Renal Cilia and mTOR

The renal cilium has also been shown to be a regulator of the mammalian target of Rapamycin (mTOR). mTOR integrates multiple upstream signals to regulate cell processes such as translation, cell growth, proliferation, and protein synthesis. In several of the cystic kidney disease mouse models the mTOR pathway is aberrantly activated.[145–147] Intriguingly, mTOR activation was also shown to be downstream of PC-1 proteolytic processing in the cilium (Figure 11.6a). Dere et al. demonstrated that the C-terminal tail of PC-1 undergoes cleavage in the absence of flow. This regulates the localization of tuberous sclerosis complex 2 (TSC2) to the cell membrane. Importantly, TSC2 is an inhibitor of mTOR, and TSC2 inhibitor activity is controlled by its membrane localization.[148] Therefore, in the absence of PC-1, the PC-1 tail does not undergo processing, which in turn affects the ability of TSC2 membrane association and inhibition of mTOR signaling.

Additional studies indicated that renal cells without a cilium were markedly larger than cells with a cilium when placed in fluid flow conditions. This was also associated with changes in activity of the mTOR pathway. The effect of flow on cell size could be inhibited by treating cells with Rapamycin or inactivating Raptor, a key component of the mTOR pathway.[146] Surprisingly, this fluid flow/cell-size correlation was not dependent on calcium signal mediated by PC-2 or PC-1 cleavage, but rather the tumor suppressor kinase LKB1. LKB1 localizes to the cilium, and has increased activity in response to flow conditions (Figure 11.6b). LKB1 inhibits the mTOR pathway through AMP-

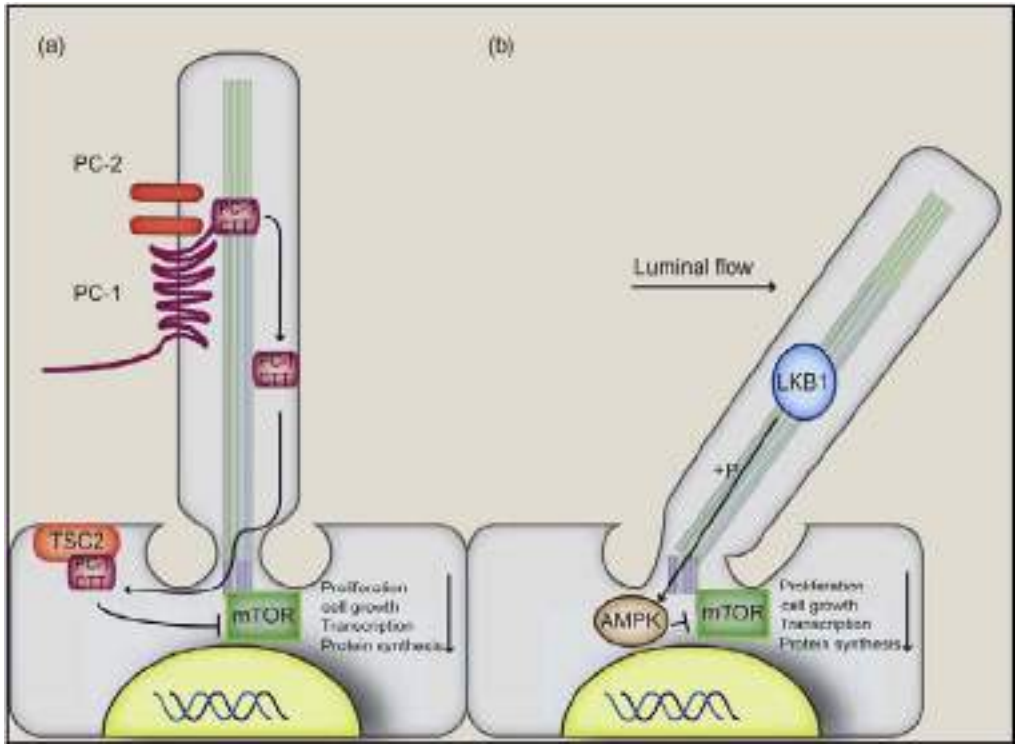

FIGURE 11.6 **Cilia and mTOR signaling under no flow and flow conditions.** Under static conditions (a), TSC2 (orange) is associated with the plasma membrane and functions to inhibit mTOR (green) signaling. The polycystin-1 C-terminal tail (PC-1 CTT, maroon) undergoes proteolytic cleavage by an unknown mechanism. The PC-1 CTT leaves the cilium, binds TSC2, and retains it at the plasma membrane, thus enhancing the ability of TSC2 to inhibit mTOR signaling. Under flow conditions (b), the ciliary kinase LKB1 (blue) phosphorylates and activates AMP-activated protein kinase (AMPK, tan). AMPK in turn phosphorylates and restrains mTOR activity. See color section at the end of the book.

activated protein kinase (AMPK). Thus, the cell size decrease induced by flow appeared to be regulated by cilia deflection that promotes LKB1 activity to phosphorylate AMPK at the basal body to restrain mTOR signaling.

Another connection between mTOR and the renal cilium was reported by Bell et al., using the adult induced cilia mutant mouse model and unilateral nephrectomy.[145] In contrast to the renal damage and the complex repair process that occurs in the ischemia reperfusion/nephrotoxin injury model, unilateral nephrectomy predominantly leads to a hypertrophic signal in the remaining kidney. In control mice, nephrectomy caused normal activation of mTOR, and produced appropriate structural and functional hypertrophy in the absence of cyst formation. In contrast, in cilia mutant mice there was an exaggerated and prolonged activation of mTOR, increased renal hypertrophy, and accelerated cystogenesis.

The increase in mTOR activity reported in multiple cystic kidney diseases, and its disregulation in cilia mutants, suggested that mTOR inhibition was a potential common site for therapeutic intervention. This was demonstrated in several cystic kidney mouse models where Rapamycin treatment was shown to be a potent inhibitor of cyst formation.[149,150] However, initial clinical trials of mTOR inhibitors in human PKD patients have not been overly encouraging (see [149] for a summary of results).

Renal Cilia and Vasopressin Signaling

Vasopressin (ADH) is the major hormone responsible for regulating water homeostasis throughout the body. The vasopressin type-2 receptor (V2R) localizes to the primary renal cilium (Figure 11.7), in addition to its normal basolateral localization in renal collecting duct epithelia. *In vitro* assays confirmed that V2R in the cilium is a functional G-protein coupled receptor (GPCR) activating G_s.[109] The G_s subunit in turn activates adenyl cylclase (AC) in the presence of ADH. AC initiates the conversion of ATP to cAMP, and cAMP ultimately activates protein kinase-A (PKA). PKA is responsible for the phosphorylation of the water channel Aquaporin-2 (AQP2).[151] The phosphorylation of AQP2 by PKA causes trafficking of the AQP2 to the apical (luminal) surface to facilitate water

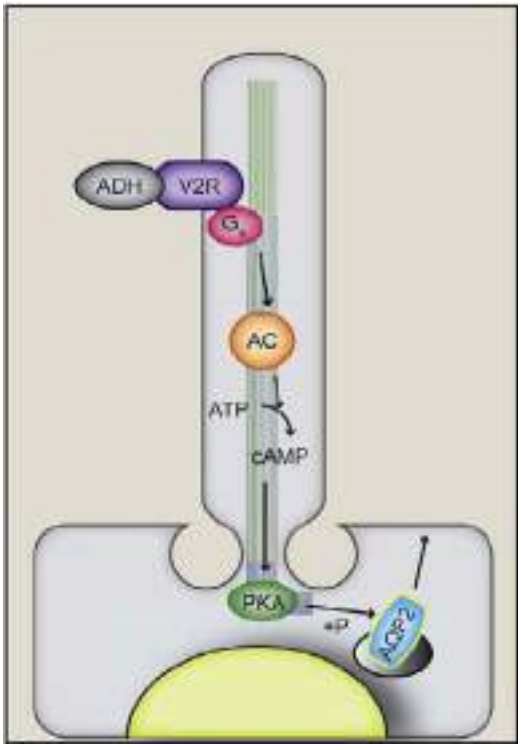

FIGURE 11.7 **Proposed mechanism for the cilium in vasopressin (ADH) signaling.** Luminal ADH signaling is believed to utilize the primary renal cilium. Luminal vasopressin receptor (V2R, purple) localizes to the primary cilium and binds ADH (gray). Binding of ADH triggers the canonical-ADH signaling pathway where G_s activates adenylyl cyclase (AC, orange), causing an increase in cellular cAMP levels. cAMP activates PKA which phosphorylates internalized aquaporin-2 (AQP2, blue), and causes AQP2 trafficking to the apical membrane and water uptake by the renal epithelium.

uptake and ultimately produce more concentrated urine. As a consequence of V2R signaling and corresponding downstream activation of cAMP, *AQP2* gene transcription is increased to further enhance cellular response to dehydration.

Interestingly, mice with cilia dysfunction often have defects in urine concentrating ability that may be associated with altered V2R activity.[152] Also, nearly all cystic kidney mutant mice and human cystic patients have marked elevation of intracellular cAMP levels (reviewed in [153]). The most recent therapeutic strategies have targeted these elevated levels of cAMP using V2R antagonists.[110,154,155] In mouse models, this approach has been remarkably successful in correcting the cystic phenotype,[110] and clinical trials in human patients are currently underway.[156]

Renal Cilia and Hedgehog Signaling

During development, the Hedgehog (Hh) signaling pathway is necessary for the establishment of body pattern, cell and tissue differentiation, proliferation, and growth. Components of the Hh signaling cascade localize to, and function in, the primary cilium (Figure 11.8). Defects in Hh signaling cause severe developmental malformations in many systems, including but not limited to the brain, skeleton, and renal system, and in adults altered Hh signaling contributes to basal cell carcinoma and other tumors. Hh signaling defects have not been directly implicated in the formation of renal cysts, although hydronephrosis and other renal abnormalities are present in mice where Hh signaling is disrupted. Regulation of the Hh pathway is very complex (see [157] for a recent in-depth review). Briefly, in the absence of an Hh ligand, the receptor Patched1 (PTCH1) localizes to the primary cilium. PTCH1 functions to inhibit a second transmembrane protein Smoothened (Smo). Binding of an Hh ligand to PTCH1 in the cilium induces its translocation out of the cilium, while Smo becomes enriched in the ciliary compartment. Additional components of the Hh pathway have also been reported in the cilium, including the Gli transcription factors (Gli1-3), Suppressor of Fussed (SuFu), and the kinesins Kif7/Kif27. When Smo is activated, which appears to require the cilium,[158] it induces the pathway leading to the activation of the Gli proteins. The activated Gli transcription factors enter the nucleus and induce expression of the downstream target genes. In the absence of the Hh ligand, the Gli proteins (Gli3 in particular) are proteolytically processed to a smaller Gli3 repressor (Gli3R) to keep the pathway off. The processing of the Gli proteins into their repressor forms, as well as the initial activating step are both dependent on the presence of the cilium.[159,160] Thus, in the absence of the cilium neither the Gli activator nor repressor proteins are formed, leading to a deregulated pathway.

Multiple Hh signaling components are expressed in the developing and adult kidney. Sonic Hedgehog (Shh) is expressed in the embryonic distal epithelium of the ureter and medulary collecting ducts, and mutations in Shh cause renal aplasia.[161] This in turn influences nephron number[162] and renal patterning[163] during continued development. *Glis2* (NPHP7), a Gli-like protein, transduces an Hh signal in the kidney, and *Glis2* mutant mice have severe renal fibrosis and renal atrophy.[164] Multiple syndromes associated with Hh signaling defects have been identified in humans, and in several cases these syndromes are associated with renal malformation. For example, Pallister–Hall syndrome (PHS) is caused by a mutation in the DNA binding domain of Gli3R, and causes renal dysplasia, hypoplasia, hydroureter, and hydronephrosis (see,[165] and reviewed in [166]). These data suggest an important role for Hh signaling and the primary renal cilium during normal kidney development.

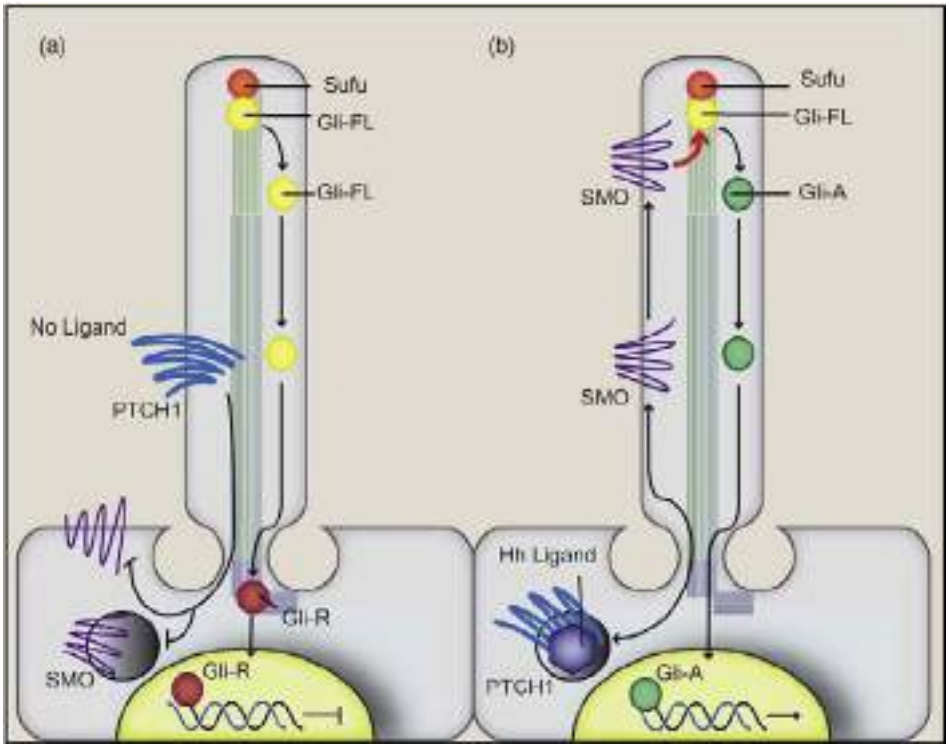

FIGURE 11.8 **Cilia and hedgehog signaling.** In the absence of Hh ligand (a), ciliary Patched-1 (PTCH1, blue) inhibits Smoothened (SMO, purple). Without SMO activation, Supressor of Fused (Sufu, orange) is in association with full-length Gli (Gli-FL, yellow) at the ciliary tip, where SuFu protects Gli-GL from degradation. In an unknown mechanism, Gli-FL is processed to Gli-repressor (Gli-R, red). Gli-R enters the nucleus and silences transcription of Gli-target genes. In the presence of Hh ligand (b), PTCH1 no longer inhibits SMO. PTCH1 translocates from the cilium to the cytosol and SMO enters the cilium. Ciliary SMO activates Gli-FL (red arrow) at the ciliary tip converting Gli-FL to activated Gli (Gli-A, green). Gli-A then translocates out of the cilium and enters the nucleus to transcribe Gli-target genes. See color section at the end of the book.

MODEL SYSTEMS FOR THE STUDY OF CILIOGENESIS AND CILIA DISEASE

Cilia are ancient organelles that have high levels of evolutionary conservation from invertebrates to humans. This high degree of conservation has allowed for the extensive use of model systems to identify molecular mechanisms of ciliogenesis, and has facilitated the analysis of how cilia function as specialized signaling centers. Despite the fact that many of these model systems do not have organs analogous to mammals, they have contributed enormously to the identification of novel ciliopathy genes and the characterization of disease causing alleles. In this section, we discuss some common model systems to study cilia/flagella, and provide a brief description of how these models are contributing to our understanding of cilia function and cystic kidney disease.

Chlamydomonas reinhardtii

Chlamydomonas reinhardtii are single-celled, fresh water, biflagellate alga (Figure 11.9a). One of the most significant contributions to our understanding of cilia biology from *Chlamydomonas* was the initial description of the intraflagellar transport (IFT) system.[11] The ease with which flagella can be isolated from *Chlamydomonas* then led to the isolation of the IFT complex, the identification of individual IFT protein components, and subsequently to the characterization of the entire flagella proteome. Work by Pazour et al. revealed that one of the IFT proteins in *Chlamydomonas* was the homolog of a gene identified in the Oak Ridge Polycystic Kidney (*orpk*) disease mouse model,[10] and is one of the seminal studies establishing the ciliary hypothesis of cystic kidney disease. Importantly, many of the proteins involved in human ciliopathies are present in the proteome of the *Chlamydomonas* flagella. This database of flagella/cilia proteins (http://labs.umassmed.edu/chlamyfp/) continues to be a major resource available to basic and clinical scientists to prioritize candidate genes involved in human disorders thought to be related to ciliary dysfunction.

Caenorhabditis elegans

C. elegans is a transparent soil nematode that provides a powerful genetic model for analysis of the cilium (Figure 11.9b). Unlike mammalian systems, where most cell types contain a cilium, *C. elegans* only have cilia on a subset of sensory neurons. Several of these cilia extend through small pores in the worm cuticle and are exposed to the environment, where they mediate sensory activities involved in chemotaxis and repulsion. These cilia also allow males to locate hermaphrodites and detect the vulva during mating,

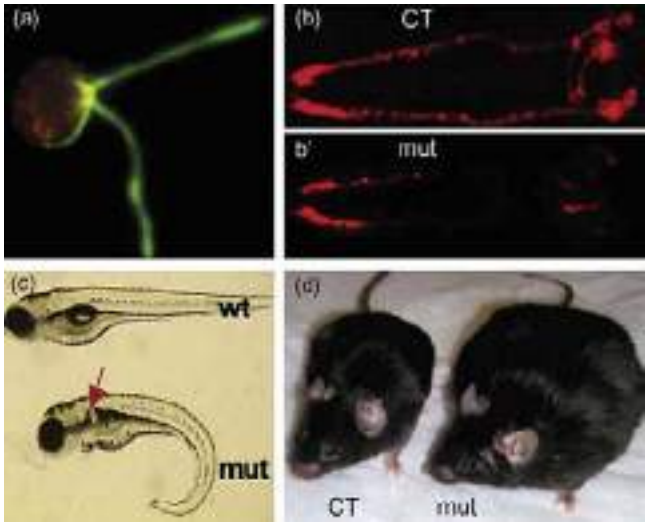

FIGURE 11.9 **Model systems to study cilia structure and function.** (a). *Chlamydomonas reinhardtii* expressing acetylated tubulin (green) in the flagella and IFT72/74 (red) in the cell body and basal bodies. (Adapted from Pedersen et al. (2005). *Curr Biol*. Feb 8; **15**(3), 262–266. With permission.) (b) Dye filling of Control (CT) and (b′) cilia double mutant (mut) *Caenorhabditis elegans*. Note the dye-filling defective (dyf) phenotype of the mutant strain. (Image: J. Pieczynski, unpublished.) (c) Wild-type (top) and *seahorse* mutant *Dario reno* (zebrafish). The *seahorse* gene product, Lrrc6l, modulates Wnt and non-canonical Wnt signaling in zebrafish, and when mutated results in a cystic pronephros phenotype (red arrow). (Image adapted with permission from Kishimoto et al. (2008). *Dev. Cell* Jun; **14**(6), 954–961.) (d) Control (CT, left) and BBS mutant (mut, right) mice (*Mus musculus*). Note the obesity phenotype found in BBS mutants. *(Image from Sharma et al. (2008). Curr. Top. Dev. Biol. **85**, 371–427, with permission.)*

and to assess food status and population density. Exposed sensory cilia able absorb fluorescent based dyes and worms with cilia abnormalities are often dye-filling defective (*Dyf*). Thus, *C. elegans* provides easily quantifiable traits to probe behavioral defects and structural phenotypes associated with cilia genes.

Even though *C. elegans* does not have the equivalent of the mammalian kidney, this model system has been responsible for another of the initial breakthroughs connecting cilia to cystic kidney disease. This came from a genetic screen by Barr et al. looking for mutations that cause male mating defects. Two of the mutations identified were in the gene *lov-1* (Location Of Vulva defective) and *pkd*-2, which are the homolog of human PC-1 and PC-2.[13] *lov-1* and *pkd-2* were placed genetically in the same signaling pathway in *C. elegans*, and the localization of these proteins in the cilium was first reported in this model.[14]

Recently the *Dyf* phenotype has been utilized as a means to analyze genetic interactions between mutations in ciliopathy genes associated with cystic kidney phenotypes.[32] Ciliopathies (see "The Human Renal Ciliopathies") such as NPHP, MKS, and BBS are recessive disorders; however, in many human patients mutations are found in only one copy of the gene. This raises questions regarding genetic causality, especially in the case of polymorphisms resulting in missense changes in the protein. This led to the hypothesis that phenotype in ciliopathy patients can be influenced by the overall mutational load in the cilia proteome.[167] *C. elegans* is providing an important system to explore this hypothesis. Single homozygous mutations in any of the known *nphp* or *mks* genes in *C. elegans* does not cause major cilia structural defects and have only minor changes in cilia signaling activity. However, combining mutations between an *nphp* and *mks* genes caused a near complete *Dyf* phenotype. This synthetic *Dyf* phenotype in *nphp;mks* double mutant worms is amiable to chemical mutagenesis screens that will lead to the identification of mutations in genetic loci that interact with either an *nphp* or *mks* mutation (Masyukova and Yoder, in prep).

Another area in which *C. elegans* is providing important insights is in assessing the pathogenic potential of missense mutations that were identified in human ciliopathy patients. This is becoming a major issue as a consequence of NextGen sequencing efforts that have uncovered a large number of missense changes in suspected ciliopathy patients. The contribution of these polymorphisms to disease pathogenesis requires functional assessment. Since *C. elegans* has easily quantifiable phenotypes associated with cilia dysfunction, these phenotypes can be used to assay the pathogenic outcome of these mutations. This has recently been demonstrated for heterozygous missense changes identified in NPHP4 in human NPHP patients.[168] Several of these missense changes altered NPHP4 protein localization/function, enhanced phenotypes in the presence of other ciliopathy gene mutations, and disrupted cilia mediated signaling, and thus are likely to have pathogenic effects.

Danio rerio

Danio rerio, (zebrafish) has become one of the primary vertebrate model systems for analyzing cilia and cilia related diseases (Figure 11.9c). A large number of mutations affecting cilia proteins have now been identified in zebrafish. Unlike *C. elegans* and *Chlamydomonas*, zebrafish contains most of the same basic organ systems as the human body. Thus, these cilia mutants develop many of the same multi-organ phenotypes as observed in human ciliopathy patients, such as hydrocephalus, retinal degeneration, left–right body axis defects, and cystic kidney disease. This is true particularly in the zebrafish kidney, which contains a highly simplified pronephros consisting of a

central glomerulus connected to two pronephric ducts that extend along the body empting through the cloaca. This pronephric tubule consists of epithelial cells with multiple motile cilia and single cilia. The function of these cilia and the consequences of their dysfunction have been well-characterized by Iain Drummond and co-workers.[169] The presence of similar multiciliated cells is not observed in the normal mammalian kidney; however, they have been reported in human diseased kidneys, as well as in distended renal tubules from the *pkhd1*$^{-/-}$ mutant rat.[170] The formation of these motile multiciliated cells in mammals is associated with the induction of the transcription factor FoxJ1 in response to tissue damage.[171]

Zebrafish has become a primary model system for analysis of cilia, in part due to the ease of genetic manipulation and the ability to conduct live, *in vivo* imaging in embryos or high-resolution analysis in fixed tissue. Cilia can easily be visualized with fluorescent tagged proteins using transgenic lines that allow cilia orientation and beat to be evaluated through high-speed video microscopy. Additionally, one of the major uses of the zebrafish model is the ability to conduct morpholino (MO) antisense oligonucleotide knockdown studies utilizing high-throughput approaches. This permits rapid analysis of gene function, and the analysis of the pathogenic effect of missense mutations associated with ciliopathy patients. These studies are done utilizing MO knockdowns to disrupt the function of the endogenous gene, followed by assessing whether expression of the human gene containing the specific missense mutation is able to rescue the ciliary phenotypes. Using these techniques, Nicolas Katsanis and co-workers have demonstrated genetic interactions between ciliopathy genes involved in BBS and assessed mutational load on disease presentation.[172] These studies have also demonstrated a connection between cilia and regulation of canonical and non-canonical Wnt signaling (see sections "Renal Cilia and Jak/STAT Signaling" and "Renal Cilia and Non-Canonical Wnt/Planar Cell Polarity (PCP) Signaling") during convergent extension movements and body axis elongation that may involve the planar cell polarity pathway (reviewed in [173]).

Mus musculus

The mouse (Figure 11.9d) has played a seminal role as the *in vivo* model to assess ciliopathy phenotypes, and was a key factor establishing the initial connection between cilia dysfunction and renal cystic disorders (reviewed in [5]). As described earlier in this chapter, this came from the *orpk* mutant mouse that had a hypmorphic mutation in the *IFT88* gene.[4,174] The *orpk* mouse develops cystic kidney disease, along with other ciliopathy phenotypes including biliary and pancreatic duct cysts, hepatic and pancreatic fibrosis, hydrocephlalus, skeletal patterning and osteogenic abnormalities, retinal degeneration, anosmia, along with skin, hair, and other ectodermal defects.[5] Left–right body axis defects were subsequently observed in mice with null mutations in *IFT88*[6] and *pkd2* mutant mice.[175] The numerous conditional alleles generated in cilia related genes, along with specificity of Cre-deletor lines, are now providing the means to assess cilia function in different developmental stages, specific tissues, and in defined cell types.

THE HUMAN RENAL CILIOPATHIES

The renal ciliopathies are a complex group of oligogenic disorders that now include Polycystic Kidney Disease (PKD, OMIM# 173900, described in Chapter 81), Nephronophthisis (NPHP, OMIM# 256100), Joubert Syndrome (JBTS, OMIM# 21330), Meckel–Gruber Syndrome (MKS, OMIM# 249000), Bardet–Biedl Syndrome (BBS, OMIM# 209900), Alstrom syndrome (ALMS, OMIM# 203800), Orofaciodigital Syndrome Type 1 (OFD1, OMIM# 311200), Jeune Asphyxiating Thoracic Dystrophy (ATD, OMIM# 208500), and Sensenbrenner Syndrome (Cranioectodermal Dysplasia, CED, OMIM# 218330). The phenotypes associated with the ciliopathies can include renal, hepatic, and pancreatic cysts (Figure 11.10a), mental retardation, obesity (Figure 11.10b), neural tube closure and patterning abnormalities, oculomotor apraxia, polydactyly and other skeletal malformations (Figure 11.10c), retinal degeneration, hypotonia, ataxia and cereberellar hypoplasia (Figure 11.10d), hydrocephalus, and cardiovascular defects. Other ciliopathies such as Leber Congenital Amaurosis (LCA, OMIM# 611755) or Senior–Loken syndrome (SLSN, OMIM# 266900), represent variations of the above syndromes (including renal phenotypes) and are not discussed below.

More than 45 human renal ciliopathy disease genes have been identified (Table 11.1); however, in most patients the underlying genetic defect remains unknown. The pace with which ciliopathy mutations are being identified is increasing rapidly due to advances in whole genome sequencing and the availability of cilia/flagella proteome databases. Surprisingly, ciliopathy syndromes share loci (Figure 11.11) despite having very distinct clinical presentations. It is thought that these disorders represent a spectrum of related phenotypes, determined in part by the gene affected and the nature of the mutation. For example, missense mutations may lead to non-lethal ciliopathies, such as NPHP or SLSN, while truncating mutations or null deletions in the same gene cause the lethal MKS. This genotype–phenotype

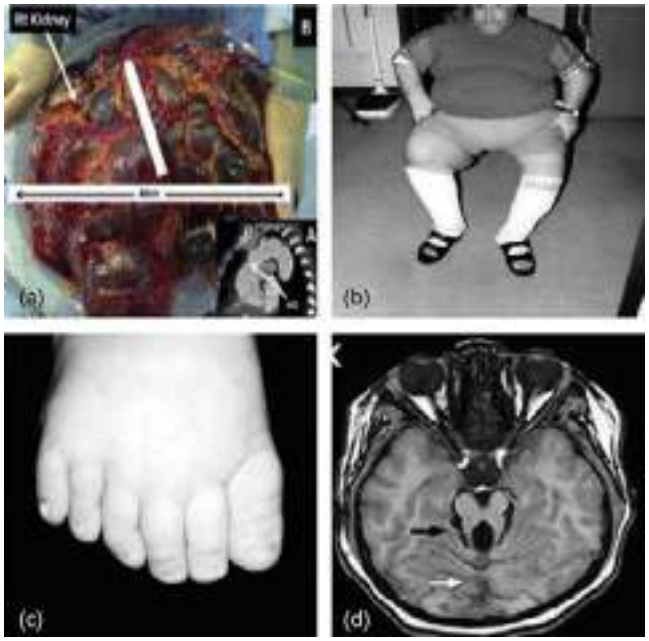

FIGURE 11.10 **Common phenotypes associated with cilia dysfunction.** (a) Cystic kidneys are a common phenotype to many ciliopathies. *(Image adapted from Menon et al. (2011). Ann. Thorac. Surg. Mar; 91 (3), 919–920. With permission.)* (b) Obese BBS patient. *(Image adapted from Iannello et al. (2002). Obes. Rev. May; 3(2), 123–135. With permission.)* (c) Polydactyly associated with in an intra-familiar BBS patient. *(Image adapted from Riise et al. (1997). Br. J. Ophthalmol. May; 81(5), 378–385. With permission.)* (d) Molar tooth malforma- tion (MTM) found in the cerebral vermis of a JBTS patient. *(Image adapted from Gunay-Aygunetal. (2009). J. Pediatr. Sep; 155(3), 386–392, with permission.)*

correlation, however, has not held up in many ciliopathy patients, leading to the possibility that strong genetic interactions or modifier effects will ultimately determine a phenotype based on the combination of different ciliopathy mutations in the patient's background (reviewed in [167]). The contribution that mutational load has on disease phenotypes will be addressed in the near future through next-generation sequencing of ciliopathy patients, the identification of the full complement of ciliopathy genes, and the generation of informative animal models.

Polycystic Kidney Disease (PKD)

PKD is one of the most common and widely studied ciliopathies. Nearly 1 in 1000 individuals are afflicted with PKD. Most forms of PKD result from mutations in three genes. Autosomal dominant PKD (ADPKD) is caused by mutations in either *PKD1* or *PKD2*, which code for the proteins PC-1 and PC-2 respectively. Autosomal recessive PKD (ARPKD) results from mutations in *PKHD1*, the gene for fibrocystin/polyductin. PC-1, PC-2, and fibrocystin/polyductin localize in the cilium, and have been shown to be involved in the cilia mechanosory signal (see section "Renal Cilia and Mechanosensation").

Nephronophthisis (NPHP)

NPHP is an autosomal recessive cystic kidney disease associated with mutations in at least 13 loci (*NPHP1-12* and *NPHP1L*; Table 11.1 and Figure 11.11). The most frequent mutation occurs in the gene NPHP1 (20%) with mutations in the other known genes (NPHP2-NPHP12, and NPHP1L) accounting for approximately 3% of the cases.[176] In most patients (~70%), the causative mutation is still unknown.

NPHP is the leading cause of heritable end-stage renal failure (ESRF) in children and adolescents, and depending of the genetic mutation,[177] ESRF occurs in infantile, juvenile or adolescent life. All NPHP cases involve renal defects, but approximately 15% of NPHP patients also experience extra-renal phenotypes including mental retardation, retinal degeneration (characterized as SLSN; Figure 11.11), brainstem malformation, situs inversus, cerebellar vermis aplasia (JBTS, see section "Joubert Syndrome (JBTS)"), oculomotor apraxia (Cogan Syndrome), and hepatic and pancreatic fibrosis. Unlike cysts associated with PKD, renal cysts in NPHP patients are located in the corticomedullary junction of the kidney, and the kidney remains normal size or even reduced in size.[178,179]

NPHP proteins localize to the transition zone, centrosome or in some cases cell–cell junctions, where they may have scaffolding functions (reviewed extensively in [20]). Physical interactions link NPHP proteins into functional complexes[31] with several other ciliopathy diseases proteins, such as TCTN1 (Tectonic, see section "Joubert Syndrome (JBTS)"), MKS5, and B9D1 (see section "Meckel-Gruber Syndrome (MKS)"). In general, mutations in NPHP proteins do not cause ciliogenesis defects, and the phenotype in human NPHP patients is thought to be due to abnormal cilia mediated signaling or sensory function. However, stunted cilia were reported in some NPHP shRNA knockdown studies.[180] Also, in *nphp4* mutant mice there is retinal degeneration and male sterility due to photoreceptor cilia defects and loss of sperm flagella, although no cysts are evident in the kidney.[181] Mutations in either *nphp*2 or *nphp3* cause more severe instances of NPHP, often associated with extra-renal developmental phenotypes (situs inversus, cardiac ventricular septal defects), and are involved in modulating Wnt signaling (see sections "Renal Cilia and Jak/STAT Signaling" and "Renal Cilia and Non-Canonical Wnt/Planar Cell Polarity (PCP) Signaling" and [139]). For a comprehensive review of NPHP the reader is referred to Wolf and Hildebrandt.[20]

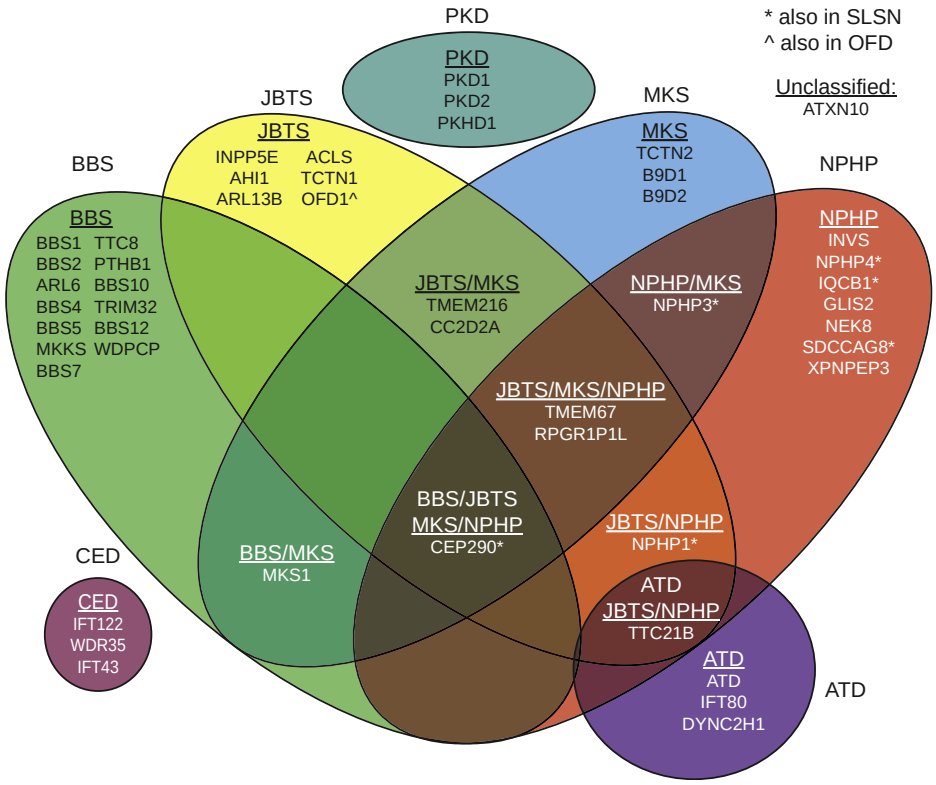

FIGURE 11.11 **Overlapping genes of ciliopathies.** A four-way Venn diagram showing the overlapping causative genes behind renal ciliopathies, creating a spectrum of disease phenotypes that include the kidney but may extend to other organs.

Joubert Syndrome (JBTS)

JBTS is a highly variable disorder with renal phenotypes similar to juvenile NPHP patients (i.e., as small cysts at the cortico-medullary junction and a potential delay in ESRF). Additional phenotypes include vermis hypoplasia, polydactyly, mental retardation, ataxia, retinal degeneration, hypotonia, abnormal breathing pattern, and oculomotor apraxia. The presence of distinct defects in the cerebellar vermis gives JBTS an indicative Molar Tooth Malformation (MTM) that can be clearly distinguished via MRI. There is significant overlap of genetic loci between JBTS patients and those loci associated with other ciliopathies (Table 11.1, Figure 11.11), perhaps explaining why JBTS displays such heterogeneous phenotypes. For this reason, JBTS is often categorized as Joubert Syndrome Related Disorders or JSRD.

There are currently 13 identified JBTS loci (Table 11.1), with *INPP5E* (JBTS1), *AHI1* (JBTS3), *ARL13B* (JBTS8), and *TCTN1* (JBTS13) being identified solely in JBTS. INPP5E is involved in regulating phosphatidyl inostitol signaling,[182] furthering the hypothesis that the primary cilium function as complex signaling centers. Consistent with signaling in cilia, ARL13B (JBTS8) is a Ras-family GTPase localized to the cilia that causes Shh mutant-like phenotypes and lethality when mutated in mice.[183,184] AHI1 interacts with Rab8[185] and with NPHP1,[186] demonstrating a physical linkage between NPHP and JBTS proteins, and possibly explaining the similarity of phenotypes between the syndromes. Likewise, TCTN1 is a transmembrane protein with physical interactions to NPHP and MKS proteins.[31] *TCTN1* mutant mice also have Hh signaling defects[187] consistent with a role for JBTS proteins in cilia signaling.

Meckel–Gruber Syndrome (MKS)

MKS is a prenatal lethal ciliopathy that displays severe developmental defects, including occipital encephalocole, postaxial polydactyly, and cystic kidneys. Other common traits include CNS malformation, underdeveloped genitals, oral/facial abnormalities, and hepatic cysts. There are 10 identified MKS loci that include both cytosolic and tramsmembrane proteins (Table 11.1). A comprehensive review of MKS can be found in .[188]

Many of the known the MKS proteins share similar C2 (MKS5 and MKS6) and B9 (MKS1, B9D1, and B9D2) domains thought to mediate calcium-dependent lipid binding. In *C. elegans*, the B9/C2 domain proteins form a complex (MKS complex) at the transition zone. This complex was shown to genetically interact with several genes encoding NPHP proteins to regulate cilia formation, positioning, and cilia protein composition.[189]

Since these MKS proteins co-localize in the transition zone, it has been hypothesized that they are components of the ciliary necklace and Y-links (see section "The Transition Zone"). MKS2, MKS3, and Tectonic-2 (TCTN2) all contain transmembrane domains, suggesting they may be the anchors that connect the cilia membrane to the microtubule axoneme. This hypothesis is strengthened by data on Cep290 (MKS4) in *Chlamydomonas* showing that it localizes to the Y-links in the transition zone, and that in its absence the Y-links are disrupted.[29]

Bardet–Biedl Syndrome (BBS)

BBS is a ciliopathy with extensive pleiotropy. Phenotypes include hypertension, mental retardation, obesity, retinopathy, hypogonadism, polydactyly, anosmia, and renal malformations. Renal phenotypes of BBS vary, and can include the formation of renal cysts, urine acidification, and reduced filtration rate with difficulties concentrating urine being the most common phenotype.[190,191] Renal mass, localization of cysts, and tubule size can vary widely between BBS patients. It has been demonstrated that ESRD often occurs in BBS patients, and is a significant contributing factor towards mortality. For a comprehensive review of BBS the reader is referred to Zaghloul et al.[192]

BBS has been linked to at least 15 identified genetic loci (Table 11.1). BBS1, BBS2, BBS4, BBS5, BBS7, BBS8, and BBS9 are components of a complex called the BBSome. The BBSome has important functions in regulating cilia membrane composition, possibly as coat proteins on vesicular structures, and for the transport of specific transmembrane proteins into or out of the cilium[64,66] (see section "Ciliary Targeting and the BBSome").

Interestingly, a comparative histological analysis of the renal phenotypes between *bbs2* and *bbs4* null mice showed that although these two genes code for components of the BBSome, they produce different BBS associated renal phenotypes.[193] Differences in renal phenotypes between *bbs2* and *bbs4* mice argue that BBS proteins may have tissue specific functions that contribute to pleiotropy of the disease.[193] Other BBS proteins such as BBS6, BBS10, and BBS12 are not components of the BBSome, and are believed to have chaperone activity facilitating the formation of the BBSome complex.[194] *In vitro* analysis of BBS6, BBS10, and BBS12 knockdown cell lines suggests that these BBS proteins are essential for ciliogenesis, and that dilute urine found in BBS patients could be attributed to the inability to target V2R to the cilium.[152]

Alstrom Syndrome (ALMS)

ALMS is a rare ciliopathy highly related to BBS, with the main distinguishing feature being later onset of symptoms than typically found in BBS patients. There is currently one identified ALMS locus. The majority of mutations in *ALMS1* result in severe truncations of the protein, however the protein still appears to maintain partial function. Interestingly, mutant mouse models of *ALMS* have no cilia structural defects, yet *in vitro* knockdown studies show defects in ciliogenesis.[195]

Orofaciodigital Syndrome Type 1 (OFD1)

OFD1 is a ciliopathy affecting the development of the craniofacial region, central nervous system, and limbs, in the form of postaxial polydactyl. In a few cases of OFD1, patients presented cystic kidneys. The OFD1 protein is expressed in the metanephric mesenchyme during development,[196] and localizes to the basal body[24] where it is required for ciliogenesis.[197] Ablation of the *OFD1* gene in the kidney in mice results in renal cyst formation, and cells lining these cysts fail to form cilia.[147] The cystic phenotype in *OFD1* animals was further associated with an upregulation of the mTOR pathway (see section "Renal Cilia and Canonical Wnt Signaling"), suggesting a mechanism of cyst growth.[147]

Jeune Asphyxiating Thoracic Dystrophy (ATD)

ATD is a ciliopathy classified in the category of autosomal recessive chondrodysplasias. Commonly associated bone defects in ATD include a shortening of long bones, polydactyly, and constriction of the thoracic rib cage. Approximately 30% of documented ATD patients also display renal phenotypes consistent with the loss or dysfunction of cilia.[198] Causative genes of ATD include *IFT80*,[199] *DYNC2H1*,[200] and *TTC21B* (*IFT139*).[201] Importantly, ATD represents one of the first human ciliopathies with identified mutations in IFT genes. These mutations are largely hypomorphic, thus potentially explaining the phenotypic variability found in ATD patients. The identity of genes mutated in ATD suggests that ATD is related to defects in retrograde IFT. Evidence that mutations in *TTC21B* and *DYNC2H1* cause defects in Hh signaling, possibly related to the inability to translocate Hh components (see section "Renal Cilia and Hedgehog Signaling") from the cilia,[57,199,202] are consistent with this hypothesis. Recently, an ATD patient with a *TTC21B* mutation and associated NPHP was uncovered.[201] This study demonstrated genetic interactions between *TTC21B*

and other ciliopathy genes, and further extends the hypothesis of the oligogenic nature of ciliopathies.

Sensenbrenner Syndrome (Cranionectodermal Dysplasia, CED)

CED is a ciliopathy highly related to ATD, with craniosynostosis being the distinguishing feature in CED.[202] Patients may also develop renal phenotypes similar to NPHP. As with ATD, CED represents a ciliopathy with mutations in IFT genes. All currently known CED loci are IFT-A components: *IFT43*,[203] *IFT122*,[204] and *WDR35* (*TULP4*/*IFT121*),[202] and are likely hypomorphic mutations. At the cellular level, CED appears to be correlated with Shh signaling (see section "Renal Cilia and Hedgehog Signaling") defects that arise from improper IFT[203,204] similar to ATD.

CONCLUDING REMARKS

The primary cilium is an evolutionarily conserved organelle, in terms of structure and its capacity to act as a complex signaling and sensory center for the cell. In the past 15–20 years, there have been remarkable advances in our understanding of the role of primary cilium in signaling and development. This is due, in large part, to the multiple model systems available to study the relationship between cilia structure and function. Importantly, since the initial publication of the *orpk* mouse model, the kidney has remained at the forefront of cilia related research. Much of our understanding of cilia biology is due to the use of renal cystic disease models that clearly demonstrate the developmental consequences of cilia dysfunction. Current advances in sequencing, proteomics, microscopy, and molecular genetics will only serve to further our understanding of cilia biology in the kidney and beyond.

References

[1] Dobell C, Leeuwenhoek Av. Antony van Leeuwenhoek and his "Little animals;" being some account of the father of protozoology & bacteriology and his multifarious discoveries in these disciplines. New York: Russell & Russell; 1958.

[2] Kartagener M. Zur pathogenese der Bronchiectasien. I Mitteilung: Bronchiectasien bei situs viscerum inversus. Betr Klin Tuberk 1933;83:498–501.

[3] Siewert A. Uber einem fall von Bronchiectasie bei einem patienten mit situs inversusviscerum. Berliner klinische Wochenschrift 1904;41:139–41.

[4] Moyer JH, Lee-Tischler MJ, Kwon HY, Schrick JJ, Avner ED, Sweeney WE, et al. Candidate gene associated with a mutation causing recessive polycystic kidney disease in mice. Science 1994;264(5163):1329–33.

[5] Lehman JM, Michaud EJ, Schoeb TR, Aydin-Son Y, Miller M, Yoder BK. The oak ridge polycystic Kidney mouse: modeling ciliopathies of mice and men. Dev Dyn 2008;237(8):1960–71.

[6] Murcia NS, Richards WG, Yoder BK, Mucenski ML, Dunlap JR, Woychik RP. The oak ridge polycystic Kidney (orpk) disease gene is required for left–right axis determination. Development 2000;127(11):2347–55.

[7] Taulman PD, Haycraft CJ, Balkovetz DF, Yoder BK. Polaris, a protein involved in left–right axis patterning, localizes to basal bodies and cilia. Mol Biol Cell 2001;12(3):589–99.

[8] Yoder BK, Tousson A, Millican L, Wu JH, Bugg Jr. CE, Schafer JA, et al. Polaris, a protein disrupted in orpk mutant mice, is required for assembly of renal cilium. Am J Physiol Renal Physiol 2002;282(3):F541–552.

[9] Cole DG, Diener DR, Himelblau AL, Beech PL, Fuster JC, Rosenbaum JL. *Chlamydomonas* kinesin-II-dependent intraflagellar transport (IFT): IFT particles contain proteins required for ciliary assembly in *Caenorhabditis elegans* sensory neurons. J Cell Biol 1998;141(4):993–1008.

[10] Pazour GJ, Dickert BL, Vucica Y, Seeley ES, Rosenbaum JL, Witman GB, et al. *Chlamydomonas* IFT88 and its mouse homologue, polycystic kidney disease gene tg737, are required for assembly of cilia and flagella. J Cell Biol 2000;151(3): 709–18.

[11] Kozminski KG, Johnson KA, Forscher P, Rosenbaum JL. A motility in the eukaryotic flagellum unrelated to flagellar beating. Proc Natl Acad Sci USA 1993;90(12):5519–23.

[12] Haycraft CJ, Swoboda P, Taulman PD, Thomas JH, Yoder BK. The *C. elegans* homolog of the murine cystic kidney disease gene Tg737 functions in a ciliogenic pathway and is disrupted in osm-5 mutant worms. Development 2001;128(9):1493–505.

[13] Barr MM, Sternberg PW. A polycystic kidney-disease gene homologue required for male mating behaviour in *C. elegans*. Nature 1999;401(6751):386–9.

[14] Barr MM, DeModena J, Braun D, Nguyen CQ, Hall DH, Sternberg PW. The *Caenorhabditis elegans* autosomal dominant polycystic kidney disease gene homologs lov-1 and pkd-2 act in the same pathway. Curr Biol 2001;11(17):1341–6.

[15] Pazour GJ, San Agustin JT, Follit JA, Rosenbaum JL, Witman GB. Polycystin-2 localizes to kidney cilia and the ciliary level is elevated in orpk mice with polycystic kidney disease. Curr Biol 2002;12(11):R378–380.

[16] Yoder BK, Hou X, Guay-Woodford LM. The polycystic kidney disease proteins, polycystin-1, polycystin-2, polaris, and cystin, are co-localized in renal cilia. J Am Soc Nephrol 2002;13(10): 2508–16.

[17] Badano JL, Mitsuma N, Beales PL, Katsanis N. The ciliopathies: an emerging class of human genetic disorders. Annu Rev Genomics Hum Genet 2006;7:125–48.

[18] Brancati F, Dallapiccola B, Valente EM. Joubert syndrome and related disorders. Orphanet J Rare Dis 2010;5:20.

[19] Sharma N, Berbari NF, Yoder BK. Ciliary dysfunction in developmental abnormalities and diseases. Curr Top Dev Biol 2008;85:371–427.

[20] Wolf MT, Hildebrandt F. Nephronophthisis. Pediatr Nephrol Feb 2011;26(2):181–94.

[21] Graser S, Stierhof YD, Lavoie SB, Gassner OS, Lamla S, Le Clech M, et al. Cep164, a novel centriole appendage protein required for primary cilium formation. J Cell Biol 2007;179(2): 321–30.

[22] Ishikawa H, Kubo A, Tsukita S. Odf2-deficient mother centrioles lack distal/subdistal appendages and the ability to generate primary cilia. Nat Cell Biol 2005;7(5):517–24.

[23] Anderson RG. The three-dimensional structure of the basal body from the rhesus monkey oviduct. J Cell Biol. 1972;54(2): 246–65.

[24] Lopes CA, Prosser SL, Romio L, Hirst RA, O'Callaghan C, Woolf AS, et al. Centriolar satellites are assembly points for proteins implicated in human ciliopathies, including oral-facial-digital syndrome 1. J Cell Sci. 2011;124(Pt 4):600–12.
[25] Sui H, Downing KH. Molecular architecture of axonemal microtubule doublets revealed by cryo-electron tomography. Nature 2006;442(7101):475–8.
[26] Sanchez T, Welch D, Nicastro D, Dogic Z. Cilia-like beating of active microtubule bundles. Science 2011;333(6041):456–9.
[27] Andrews PM, Porter KR. A scanning electron microscopic study of the nephron. Am J Anat 1974;140(1):81–115.
[28] Gilula NB, Satir P. The ciliary necklace. A ciliary membrane specialization. J Cell Biol 1972;53(2):494–509.
[29] Craige B, Tsao CC, Diener DR, Hou Y, Lechtreck KF, Rosenbaum JL, et al. CEP290 tethers flagellar transition zone microtubules to the membrane and regulates flagellar protein content. J Cell Biol 2010;190(5):927–40.
[30] Lechtreck KF, Teltenkotter A, Grunow A. A 210 kDa protein is located in a membrane-microtubule linker at the distal end of mature and nascent basal bodies. J Cell Sci 1999;112(Pt 11): 1633–44.
[31] Sang L, Miller JJ, Corbit KC, Giles RH, Brauer MJ, Otto EA, et al. Mapping the NPHP-JBTS-MKS protein network reveals ciliopathy disease genes and pathways. Cell 2011;145(4): 513–28.
[32] Williams CL, Li C, Kida K, Inglis PN, Mohan S, Semenec L, et al. MKS and NPHP modules cooperate to establish basal body/transition zone membrane associations and ciliary gate function during ciliogenesis. J Cell Biol 2011;192(6):1023–41.
[33] Satir P, Christensen ST. Overview of structure and function of mammalian cilia. Annu Rev Physiol 2007;69:377–400.
[34] Deane JA, Cole DG, Seeley ES, Diener DR, Rosenbaum JL. Localization of intraflagellar transport protein IFT52 identifies basal body transitional fibers as the docking site for IFT particles. Curr Biol 2001;11(20):1586–90.
[35] Janich P, Corbeil D. GM1 and GM3 gangliosides highlight distinct lipid microdomains within the apical domain of epithelial cells. FEBS Lett 2007;581(9):1783–7.
[36] Vieira OV, Gaus K, Verkade P, Fullekrug J, Vaz WL, Simons K. FAPP2, cilium formation, and compartmentalization of the apical membrane in polarized Madin–Darby canine kidney (MDCK) cells. Proc Natl Acad Sci USA 2006;103(49):18556–61.
[37] Montesano R. Inhomogeneous distribution of filipin-sterol complexes in the ciliary membrane of rat tracheal epithelium. Am J Anat. 1979;156(1):139–45.
[38] Tao B, Bu S, Yang Z, Siroky B, Kappes JC, Kispert A, et al. Cystin localizes to primary cilia via membrane microdomains and a targeting motif. J Am Soc Nephrol 2009;20(12):2570–80.
[39] Li JB, Gerdes JM, Haycraft CJ, Fan Y, Teslovich TM, May-Simera H, et al. Comparative genomics identifies a flagellar and basal body proteome that includes the BBS5 human disease gene. Cell 2004;117(4):541–52.
[40] Pazour GJ, Agrin N, Leszyk J, Witman GB. Proteomic analysis of a eukaryotic cilium. J Cell Biol 2005;170(1):103–13.
[41] Valente EM, Logan CV, Mougou-Zerelli S, Lee JH, Silhavy JL, Brancati F, et al. Mutations in TMEM216 perturb ciliogenesis and cause Joubert, Meckel and related syndromes. Nat Genet 2010;42(7):619–25.
[42] Smith UM, Consugar M, Tee LJ, McKee BM, Maina EN, Whelan S, et al. The transmembrane protein meckelin (MKS3) is mutated in Meckel–Gruber syndrome and the wpk rat. Nat Genet 2006;38(2):191–6.
[43] Lim YS, Chua CE, Tang BL. Rabs and other small GTPases in ciliary transport. Biol Cell 2011;103(5):209–21.
[44] Ishikawa H, Marshall WF. Ciliogenesis: building the cell's antenna. Nat Rev Mol Cell Biol. 2011;12(4):222–34.
[45] Silverman MA, Leroux MR. Intraflagellar transport and the generation of dynamic, structurally and functionally diverse cilia. Trends Cell Biol 2009;19(7):306–16.
[46] Follit JA, Tuft RA, Fogarty KE, Pazour GJ. The intraflagellar transport protein IFT20 is associated with the Golgi complex and is required for cilia assembly. Mol Biol Cell. 2006;17(9): 3781–92.
[47] Qin H, Wang Z, Diener D, Rosenbaum J. Intraflagellar transport protein 27 is a small G protein involved in cell-cycle control. Curr Biol 2007;17(3):193–202.
[48] Schafer JC, Winkelbauer ME, Williams CL, Haycraft CJ, Desmond RA, Yoder BK. IFTA-2 is a conserved cilia protein involved in pathways regulating longevity and dauer formation in *Caenorhabditis elegans*. J Cell Sci 2006;119(Pt 19):4088–100.
[49] Ou G, Blacque OE, Snow JJ, Leroux MR, Scholey JM. Functional coordination of intraflagellar transport motors. Nature 2005;436 (7050):583–7.
[50] Pan X, Ou G, Civelekoglu-Scholey G, Blacque OE, Endres NF, Tao L, et al. Mechanism of transport of IFT particles in *C. elegans* cilia by the concerted action of kinesin-II and OSM-3 motors. J Cell Biol 2006;174(7):1035–45.
[51] Snow JJ, Ou G, Gunnarson AL, Walker MR, Zhou HM, Brust-Mascher I, et al. Two anterograde intraflagellar transport motors cooperate to build sensory cilia on *C. elegans* neurons. Nat Cell Biol. 2004;6(11):1109–13.
[52] Pazour GJ, Wilkerson CG, Witman GB. A dynein light chain is essential for the retrograde particle movement of intraflagellar transport (IFT). J Cell Biol 1998;141(4):979–92.
[53] Kozminski KG, Beech PL, Rosenbaum JL. The *Chlamydomonas* kinesin-like protein FLA10 is involved in motility associated with the flagellar membrane. J Cell Biol 1995;131(6 Pt 1): 1517–27.
[54] Lin F, Hiesberger T, Cordes K, Sinclair AM, Goldstein LS, Somlo S, et al. Kidney-specific inactivation of the KIF3A subunit of kinesin-II inhibits renal ciliogenesis and produces polycystic kidney disease. Proc Natl Acad Sci USA 2003;100(9): 5286–91.
[55] Pazour GJ, Dickert BL, Witman GB. The DHC1b (DHC2) isoform of cytoplasmic dynein is required for flagellar assembly. J Cell Biol 1999;144(3):473–81.
[56] Schafer JC, Haycraft CJ, Thomas JH, Yoder BK, Swoboda P. XBX-1 encodes a dynein light intermediate chain required for retrograde intraflagellar transport and cilia assembly in *Caenorhabditis elegans*. Mol Biol Cell 2003;14(5):2057–70.
[57] Tran PV, Haycraft CJ, Besschetnova TY, Turbe-Doan A, Stottmann RW, Herron BJ, et al. THM1 negatively modulates mouse sonic hedgehog signal transduction and affects retrograde intraflagellar transport in cilia. Nat Genet 2008;40(4): 403–10.
[58] Hurd TW, Fan S, Margolis BL. Localization of retinitis pigmentosa 2 to cilia is regulated by Importin beta2. J Cell Sci 2011;124 (Pt 5):718–26.
[59] Dishinger JF, Kee HL, Jenkins PM, Fan S, Hurd TW, Hammond JW, et al. Ciliary entry of the kinesin-2 motor KIF17 is regulated by importin-beta2 and RanGTP. Nat Cell Biol 2010;12(7): 703–10.
[60] Berbari NF, Johnson AD, Lewis JS, Askwith CC, Mykytyn K. Identification of ciliary localization sequences within the third intracellular loop of G protein-coupled receptors. Mol Biol Cell. 2008;19(4):1540–7.
[61] Hu Q, Milenkovic L, Jin H, Scott MP, Nachury MV, Spiliotis ET, et al. A septin diffusion barrier at the base of the primary

cilium maintains ciliary membrane protein distribution. Science 2010;329(5990):436–9.
[62] Francis SS, Sfakianos J, Lo B, Mellman I. A hierarchy of signals regulates entry of membrane proteins into the ciliary membrane domain in epithelial cells. J Cell Biol 2011;193(1): 219–33.
[63] Domire JS, Green JA, Lee KG, Johnson AD, Askwith CC, Mykytyn K. Dopamine receptor 1 localizes to neuronal cilia in a dynamic process that requires the Bardet–Biedl syndrome proteins. Cell Mol Life Sci 2011;68(17):2951–60.
[64] Jin H, White SR, Shida T, Schulz S, Aguiar M, Gygi SP, et al. The conserved Bardet–Biedl syndrome proteins assemble a coat that traffics membrane proteins to cilia. Cell 2010;141(7): 1208–19.
[65] Emmer BT, Maric D, Engman DM. Molecular mechanisms of protein and lipid targeting to ciliary membranes. J Cell Sci 2010;123(Pt 4):529–36.
[66] Nachury MV, Loktev AV, Zhang Q, Westlake CJ, Peranen J, Merdes A, et al. A core complex of BBS proteins cooperates with the GTPase Rab8 to promote ciliary membrane biogenesis. Cell 2007;129(6):1201–13.
[67] Knodler A, Feng S, Zhang J, Zhang X, Das A, Peranen J, et al. Coordination of Rab8 and Rab11 in primary ciliogenesis. Proc Natl Acad Sci USA 2010;107(14):6346–51.
[68] Westlake CJ, Baye LM, Nachury MV, Wright KJ, Ervin KE, Phu L, et al. Primary cilia membrane assembly is initiated by Rab11 and transport protein particle II (TRAPPII) complex-dependent trafficking of Rabin8 to the centrosome. Proc Natl Acad Sci USA 2011;108(7):2759–64.
[69] Poole CA, Flint MH, Beaumont BW. Analysis of the morphology and function of primary cilia in connective tissues: a cellular cybernetic probe? Cell Motil 1985;5(3):175–93.
[70] Reese TS. Olfactory cilia in the frog. J Cell Biol 1965;25(2): 209–30.
[71] Baldari CT, Rosenbaum J. Intraflagellar transport: It's not just for cilia anymore. Curr Opin Cell Biol 2010;22(1):75–80.
[72] Perrone CA, Tritschler D, Taulman P, Bower R, Yoder BK, Porter ME. A novel dynein light intermediate chain colocalizes with the retrograde motor for intraflagellar transport at sites of axoneme assembly in *chlamydomonas* and mammalian cells. Mol Biol Cell 2003;14(5):2041–56.
[73] Milenkovic L, Scott MP, Rohatgi R. Lateral transport of Smoothened from the plasma membrane to the membrane of the cilium. J Cell Biol 2009;187(3):365–74.
[74] Berbari NF, O'Connor AK, Haycraft CJ, Yoder BK. The primary cilium as a complex signaling center. Curr Biol 2009;19(13): R526–535.
[75] Quarmby LM, Parker JD. Cilia and the cell cycle? J Cell Biol 2005;169(5):707–10.
[76] Jain R, Pan J, Driscoll JA, Wisner JW, Huang T, Gunsten SP, et al. Temporal relationship between primary and motile ciliogenesis in airway epithelial cells. Am J Respir Cell Mol Biol 2010;43(6): 731–9.
[77] Lefebvre PA, Silflow CD, Wieben ED, Rosenbaum JL. Increased levels of mRNAs for tubulin and other flagellar proteins after amputation or shortening of *Chlamydomonas* flagella. Cell 1980;20(2):469–77.
[78] Remillard SP, Witman GB. Synthesis, transport, and utilization of specific flagellar proteins during flagellar regeneration in *Chlamydomonas*. J Cell Biol 1982;93(3):615–31.
[79] Stolc V, Samanta MP, Tongprasit W, Marshall WF. Genome-wide transcriptional analysis of flagellar regeneration in *Chlamydomonas reinhardtii* identifies orthologs of ciliary disease genes. Proc Natl Acad Sci USA 2005;102(10):3703–7.
[80] Efimenko E, Bubb K, Mak HY, Holzman T, Leroux MR, Ruvkun G, et al. Analysis of xbx genes in *C. elegans*. Development 2005;132(8):1923–34.
[81] Swoboda P, Adler HT, Thomas JH. The RFX-type transcription factor DAF-19 regulates sensory neuron cilium formation in *C. elegans*. Mol Cell. 2000;5(3):411–21.
[82] Winkelbauer ME, Schafer JC, Haycraft CJ, Swoboda P, Yoder BK. The *C. elegans* homologs of nephrocystin-1 and nephrocystin-4 are cilia transition zone proteins involved in chemosensory perception. J Cell Sci 2005;118(Pt 23):5575–87.
[83] Thomas J, Morle L, Soulavie F, Laurencon A, Sagnol S, Durand B. Transcriptional control of genes involved in ciliogenesis: a first step in making cilia. Biol Cell 2010;102(9):499–513.
[84] Michaud EJ, Yoder BK. The primary cilium in cell signaling and cancer. Cancer Res. 2006;66(13):6463–7.
[85] Kobayashi T, Dynlacht BD. Regulating the transition from centriole to basal body. J Cell Biol 2011;193(3):435–44.
[86] Seeley ES, Carriere C, Goetze T, Longnecker DS, Korc M. Pancreatic cancer and precursor pancreatic intraepithelial neoplasia lesions are devoid of primary cilia. Cancer Res 2009;69(2): 422–30.
[87] Wong SY, Seol AD, So PL, Ermilov AN, Bichakjian CK, Epstein Jr. EH, et al. Primary cilia can both mediate and suppress Hedgehog pathway-dependent tumorigenesis. Nat Med 2009;15(9):1055–61.
[88] Rasi MQ, Parker JD, Feldman JL, Marshall WF, Quarmby LM. Katanin knockdown supports a role for microtubule severing in release of basal bodies before mitosis in *Chlamydomonas*. Mol Biol Cell 2009;20(1):379–88.
[89] Mahjoub MR, Qasim Rasi M, Quarmby LMA. NIMA-related kinase, Fa2p, localizes to a novel site in the proximal cilia of *Chlamydomonas* and mouse kidney cells. Mol Biol Cell 2004; 15(11):5172–86.
[90] Pugacheva EN, Jablonski SA, Hartman TR, Henske EP, Golemis EA. HEF1-dependent Aurora A activation induces disassembly of the primary cilium. Cell 2007;129(7):1351–63.
[91] Sorokin S. Centrioles and the formation of rudimentary cilia by fibroblasts and smooth muscle cells. J Cell Biol 1962;15:363–77.
[92] Ghossoub R, Molla-Herman A, Bastin P, Benmerah A. The ciliary pocket: a once-forgotten membrane domain at the base of cilia. Biol Cell 2011;103(3):131–44.
[93] Molla-Herman A, Ghossoub R, Blisnick T, Meunier A, Serres C, Silbermann F, et al. The ciliary pocket: an endocytic membrane domain at the base of primary and motile cilia. J Cell Sci 2010;123(Pt 10):1785–95.
[94] Bonnet CS, Aldred M, von Ruhland C, Harris R, Sandford R, Cheadle JP. Defects in cell polarity underlie TSC and ADPKD-associated cystogenesis. Hum Mol Genet 2009;18(12):2166–76.
[95] DiBella LM, Park A, Sun Z. Zebrafish Tsc1 reveals functional interactions between the cilium and the TOR pathway. Hum Mol Genet 2009;18(4):595–606.
[96] Smith LA, Bukanov NO, Husson H, Russo RJ, Barry TC, Taylor AL, et al. Development of polycystic kidney disease in juvenile cystic kidney mice: insights into pathogenesis, ciliary abnormalities, and common features with human disease. J Am Soc Nephrol 2006;17(10):2821–31.
[97] Tammachote R, Hommerding CJ, Sinders RM, Miller CA, Czarnecki PG, Leightner AC, et al. Ciliary and centrosomal defects associated with mutation and depletion of the Meckel syndrome genes MKS1 and MKS3. Hum Mol Genet 2009;18(17): 3311–23.
[98] Tam LW, Wilson NF, Lefebvre PAA. CDK-related kinase regulates the length and assembly of flagella in *Chlamydomonas*. J Cell Biol 2007;176(6):819–29.

[99] Berman SA, Wilson NF, Haas NA, Lefebvre PA. A novel MAP kinase regulates flagellar length in *Chlamydomonas*. Curr Biol 2003;13(13):1145–9.
[100] Besschetnova TY, Kolpakova-Hart E, Guan Y, Zhou J, Olsen BR, Shah JV. Identification of signaling pathways regulating primary cilium length and flow-mediated adaptation. Curr Biol 2010;20(2):182–7.
[101] Sharma N, Kosan ZA, Stallworth JE, Berbari NF, Yoder BK. Soluble levels of cytosolic tubulin regulate ciliary length control. Mol Biol Cell 2011;22(6):806–16.
[102] Nauli SM, Alenghat FJ, Luo Y, Williams E, Vassilev P, Li X, et al. Polycystins 1 and 2 mediate mechanosensation in the primary cilium of kidney cells. Nat Genet 2003;33(2):129–37.
[103] Verghese E, Ricardo SD, Weidenfeld R, Zhuang J, Hill PA, Langham RG, et al. Renal primary cilia lengthen after acute tubular necrosis. J Am Soc Nephrol 2009;20(10):2147–53.
[104] Verghese E, Weidenfeld R, Bertram JF, Ricardo SD, Deane JA. Renal cilia display length alterations following tubular injury and are present early in epithelial repair. Nephrol Dial Transplant 2008;23(3):834–41.
[105] Patel V, Li L, Cobo-Stark P, Shao X, Somlo S, Lin F, et al. Acute kidney injury and aberrant planar cell polarity induce cyst formation in mice lacking renal cilia. Hum Mol Genet 2008;17(11):1578–90.
[106] Takakura A, Contrino L, Zhou X, Bonventre JV, Sun Y, Humphreys BD, et al. Renal injury is a third hit promoting rapid development of adult polycystic kidney disease. Hum Mol Genet 2009;18(14):2523–31.
[107] Kim J, Lee JE, Heynen-Genel S, Suyama E, Ono K, Lee K, et al. Functional genomic screen for modulators of ciliogenesis and cilium length. Nature 2010;464(7291):1048–51.
[108] Berbari NF, Lewis JS, Bishop GA, Askwith CC, Mykytyn K. Bardet–Biedl syndrome proteins are required for the localization of G protein-coupled receptors to primary cilia. Proc Natl Acad Sci USA 2008;105(11):4242–6.
[109] Raychowdhury MK, Ramos AJ, Zhang P, McLaughin M, Dai XQ, Chen XZ, et al. Vasopressin receptor-mediated functional signaling pathway in primary cilia of renal epithelial cells. Am J Physiol Renal Physiol 2009;296(1):F87–97.
[110] Wang X, Wu Y, Ward CJ, Harris PC, Torres VE. Vasopressin directly regulates cyst growth in polycystic kidney disease. J Am Soc Nephrol 2008;19(1):102–8.
[111] Praetorius HA, Frokiaer J, Nielsen S, Spring KR. Bending the primary cilium opens Ca^{2+}-sensitive intermediate-conductance K^+ channels in MDCK cells. J Membr Biol 2003;191(3):193–200.
[112] Praetorius HA, Spring KR. Removal of the MDCK cell primary cilium abolishes flow sensing. J Membr Biol 2003;191(1):69–76.
[113] Praetorius HA, Spring KR. The renal cell primary cilium functions as a flow sensor. Curr Opin Nephrol Hypertens 2003;12(5):517–20.
[114] Liu W. Mechanoregulation of intracellular Ca^{2+} concentration is attenuated in collecting duct of monocilium-impaired orpk mice. Am J Physiol Renal Physiol 2005;289(5):F978–988.
[115] Davenport JR, Watts AJ, Roper VC, Croyle MJ, van Groen T, Wyss JM, et al. Disruption of intraflagellar transport in adult mice leads to obesity and slow-onset cystic kidney disease. Curr Biol 2007;17(18):1586–94.
[116] Lantinga-van Leeuwen IS, Leonhard WN, van der Wal A, Breuning MH, de Heer E, Peters DJ. Kidney-specific inactivation of the Pkd1 gene induces rapid cyst formation in developing kidneys and a slow onset of disease in adult mice. Hum Mol Genet 2007;16(24):3188–96.
[117] Piontek K, Menezes LF, Garcia-Gonzalez MA, Huso DL, Germino GG. A critical developmental switch defines the kinetics of kidney cyst formation after loss of Pkd1. Nat Med 2007;13(12):1490–5.
[118] Talbot JJ, Shillingford JM, Vasanth S, Doerr N, Mukherjee S, Kinter MT, et al. Polycystin-1 regulates STAT activity by a dual mechanism. Proc Natl Acad Sci USA 2011;108(19):7985–90.
[119] Chauvet V, Tian X, Husson H, Grimm DH, Wang T, Hiesberger T, et al. Mechanical stimuli induce cleavage and nuclear translocation of the polycystin-1 C terminus. J Clin Invest 2004;114(10):1433–43.
[120] Low SH, Vasanth S, Larson CH, Mukherjee S, Sharma N, Kinter MT, et al. STAT6, and P100 function in a pathway that transduces ciliary mechanosensation and is activated in polycystic kidney disease. Dev Cell 2006;10(1):57–69.
[121] Gardner Jr. KD, Burnside JS, Elzinga LW, Locksley RM. Cytokines in fluids from polycystic kidneys. Kidney Int 1991;39(4):718–24.
[122] Mrug M, Zhou J, Woo Y, Cui X, Szalai AJ, Novak J, et al. Overexpression of innate immune response genes in a model of recessive polycystic kidney disease. Kidney Int 2008;73(1):63–76.
[123] Karihaloo A, Koraishy F, Huen SC, Lee Y, Merrick D, Caplan MJ, et al. Macrophages promote cyst growth in polycystic kidney disease. J Am Soc Nephrol 2011;22(10):1809–14.
[124] Lee S, Huen S, Nishio H, Nishio S, Lee HK, Choi BS, et al. Distinct macrophage phenotypes contribute to kidney injury and repair. J Am Soc Nephrol 2011;22(2):317–26.
[125] Zhou J, Ouyang X, Cui X, Schoeb TR, Smythies LE, Johnson MR, et al. Renal CD14 expression correlates with the progression of cystic kidney disease. Kidney Int 2010;78(6):550–60.
[126] Ross AJ, May-Simera H, Eichers ER, Kai M, Hill J. Disruption of Bardet–Biedl syndrome ciliary proteins perturbs planar cell polarity in vertebrates. Nat Genet 2005;37(10):1135–40.
[127] Jones C, Roper VC, Foucher I, Qian D, Banizs B, Petit C, et al. Ciliary proteins link basal body polarization to planar cell polarity regulation. Nat Genet 2008;40(1):69–77.
[128] Karner CM, Chirumamilla R, Aoki S, Igarashi P, Wallingford JB, Carroll TJ. Wnt9b signaling regulates planar cell polarity and kidney tubule morphogenesis. Nat Genet 2009;41(7):793–9.
[129] Fischer E, Legue E, Doyen A, Nato F, Nicolas JF, Torres V, et al. Defective planar cell polarity in polycystic kidney disease. Nat Genet 2006;38(1):21–3.
[130] Delaval B, Bright A, Lawson ND, Doxsey S. The cilia protein IFT88 is required for spindle orientation in mitosis. Nat Cell Biol 2011;13(4):461–8.
[131] Jonassen JA, San Agustin J, Follit JA, Pazour GJ. Deletion of IFT20 in the mouse kidney causes misorientation of the mitotic spindle and cystic kidney disease. J Cell Biol 2008;183(3):377–84.
[132] Rawls AS, Guinto JB, Wolff T. The cadherins fat and dachsous regulate dorsal/ventral signaling in the *Drosophila* eye. Curr Biol 2002;12(12):1021–6.
[133] Saburi S, Hester I, Fischer E, Pontoglio M, Eremina V, Gessler M, et al. Loss of Fat4 disrupts PCP signaling and oriented cell division and leads to cystic kidney disease. Nat Genet 2008;40(8):1010–5.
[134] Yang CH, Axelrod JD, Simon MA. Regulation of Frizzled by fat-like cadherins during planar polarity signaling in the *Drosophila* compound eye. Cell 2002;108(5):675–88.
[135] Happe H, Leonhard WN, van der Wal A, van de Water B, Lantinga-van Leeuwen IS, Breuning MH, et al. Toxic tubular injury in kidneys from Pkd1-deletion mice accelerates cystogenesis accompanied by dysregulated planar cell polarity

and canonical Wnt signaling pathways. Hum Mol Genet 2009;18(14):2532–42.
[136] Verdeguer F, Le Corre S, Fischer E, Callens C, Garbay S, Doyen A, et al. A mitotic transcriptional switch in polycystic kidney disease. Nat Med 2010;16(1):106–10.
[137] Nishio S, Tian X, Gallagher AR, Yu Z, Patel V, Igarashi P, et al. Loss of oriented cell division does not initiate cyst formation. J Am Soc Nephrol 2010;21(2):295–302.
[138] Otto EA, Schermer B, Obara T, O'Toole JF, Hiller KS, Mueller AM, et al. Mutations in INVS encoding inversin cause nephronophthisis type 2, linking renal cystic disease to the function of primary cilia and left–right axis determination. Nat Genet 2003;34(4):413–20.
[139] Simons M, Gloy J, Ganner A, Bullerkotte A, Bashkurov M, Kronig C, et al. Inversin, the gene product mutated in nephronophthisis type II, functions as a molecular switch between Wnt signaling pathways. Nat Genet 2005;37(5): 537–43.
[140] Wiens CJ, Tong Y, Esmail MA, Oh E, Gerdes JM, Wang J, et al. Bardet–Biedl syndrome-associated small GTPase ARL6 (BBS3) functions at or near the ciliary gate and modulates Wnt signaling. J Biol Chem 2010;285(21):16218–30.
[141] Corbit KC, Shyer AE, Dowdle WE, Gaulden J, Singla V, Chen MH, et al. Kif3a constrains beta-catenin-dependent Wnt signalling through dual ciliary and non-ciliary mechanisms. Nat Cell Biol 2008;10(1):70–6.
[142] Lancaster MA, Gopal DJ, Kim J, Saleem SN, Silhavy JL, Louie CM, et al. Defective Wnt-dependent cerebellar midline fusion in a mouse model of Joubert syndrome. Nat Med 2011;17(6): 726–31.
[143] Sugiyama N, Tsukiyama T, Yamaguchi TP, Yokoyama T. The canonical Wnt signaling pathway is not involved in renal cyst development in the kidneys of inv mutant mice. Kidney Int 2011;79(9):957–65.
[144] Ocbina PJ, Tuson M, Anderson KV. Primary cilia are not required for normal canonical Wnt signaling in the mouse embryo. PLoS One 2009;4(8):e6839.
[145] Bell PD, Fitzgibbon W, Sas K, Stenbit AE, Amria M, Houston A, et al. Loss of primary cilia upregulates renal hypertrophic signaling and promotes cystogenesis. J Am Soc Nephrol 2011;22(5):839–48.
[146] Boehlke C, Kotsis F, Patel V, Braeg S, Voelker H, Bredt S, et al. Primary cilia regulate mTORC1 activity and cell size through Lkb1. Nat Cell Biol 2010;12(11):1115–22.
[147] Zullo A, Iaconis D, Barra A, Cantone A, Messaddeq N, Capasso G, et al. Kidney-specific inactivation of Ofd1 leads to renal cystic disease associated with upregulation of the mTOR pathway. Hum Mol Genet 2010;19(14):2792–803.
[148] Dere R, Wilson PD, Sandford RN, Walker CL. Carboxy terminal tail of polycystin-1 regulates localization of TSC2 to repress mTOR. PLoS One 2010;5(2):e9239.
[149] Huber TB, Walz G, Kuehn EW. mTOR and rapamycin in the kidney: signaling and therapeutic implications beyond immunosuppression. Kidney Int 2011;79(5):502–11.
[150] Shillingford JM, Piontek KB, Germino GG, Weimbs T. Rapamycin ameliorates PKD resulting from conditional inactivation of Pkd1. J Am Soc Nephrol 2010;21(3):489–97.
[151] Nishimoto G, Zelenina M, Li D, Yasui M, Aperia A, Nielsen S, et al. Arginine vasopressin stimulates phosphorylation of aquaporin-2 in rat renal tissue. Am J Physiol 1999;276(2 Pt 2): F254–259.
[152] Marion V, Schlicht D, Mockel A, Caillard S, Imhoff O, Stoetzel C, et al. Bardet–Biedl syndrome highlights the major role of the primary cilium in efficient water reabsorption. Kidney Int 2011;79(9):1013–25.
[153] Calvet JP. Strategies to inhibit cyst formation in ADPKD. Clin J Am Soc Nephrol 2008;3(4):1205–11.
[154] Chen NX, Moe SM, Eggleston-Gulyas T, Chen X, Hoffmeyer WD, Bacallao RL, et al. Calcimimetics inhibit renal pathology in rodent nephronophthisis. Kidney Int 2011;80(6):612–9.
[155] Torres VE. Role of vasopressin antagonists. Clin J Am Soc Nephrol 2008;3(4):1212–8.
[156] Patel V, Chowdhury R, Igarashi P. Advances in the pathogenesis and treatment of polycystic kidney disease. Curr Opin Nephrol Hypertens 2009;18(2):99–106.
[157] Ingham PW, Nakano Y, Seger C. Mechanisms and functions of Hedgehog signalling across the metazoa. Nat Rev Genet 2011;12(6):393–406.
[158] Corbit KC, Aanstad P, Singla V, Norman AR, Stainier DY, Reiter JF. Vertebrate smoothened functions at the primary cilium. Nature 2005;437(7061):1018–21.
[159] Haycraft CJ, Banizs B, Aydin-Son Y, Zhang Q, Michaud EJ, Yoder BK. Gli2 and Gli3 localize to cilia and require the intraflagellar transport protein polaris for processing and function. PLoS Genet 2005;1(4):e53.
[160] Huangfu D, Anderson KV. Cilia and Hedgehog responsiveness in the mouse. Proc Natl Acad Sci USA 2005;102(32): 11325–30.
[161] Yu J, Carroll TJ, McMahon AP. Sonic hedgehog regulates proliferation and differentiation of mesenchymal cells in the mouse metanephric kidney. Development 2002;129(22): 5301–12.
[162] Hu MC, Mo R, Bhella S, Wilson CW, Chuang PT, Hui CC, et al. GLI3-dependent transcriptional repression of Gli1, Gli2 and kidney patterning genes disrupts renal morphogenesis. Development 2006;133(3):569–78.
[163] Cain JE, Islam E, Haxho F, Chen L, Bridgewater D, Nieuwenhuis E, et al. GLI3 repressor controls nephron number via regulation of Wnt11 and Ret in ureteric tip cells. PLoS One 2009;4(10):e7313.
[164] Attanasio M, Uhlenhaut NH, Sousa VH, O'Toole JF, Otto E, Anlag K, et al. Loss of GLIS2 causes nephronophthisis in humans and mice by increased apoptosis and fibrosis. Nat Genet 2007;39(8):1018–24.
[165] Cain JE, Islam E, Haxho F, Blake J, Rosenblum ND. GLI3 repressor controls functional development of the mouse ureter. J Clin Invest 2011;121(3):1199–206.
[166] Cain JE, Rosenblum ND. Control of mammalian kidney development by the Hedgehog signaling pathway. Pediatr Nephrol 2011;26(9):1365–71.
[167] Zaghloul NA, Katsanis N. Functional modules, mutational load and human genetic disease. Trends Genet 2010;26(4): 168–76.
[168] Masyukova SV, Winkelbauer ME, Williams CL, Pieczynski JN, Yoder BK. Assessing the pathogenic potential of human Nephronophthisis disease-associated NPHP-4 missense mutations in *C. elegans*. Hum Mol Genet 2011;20(15):2942–54.
[169] Drummond IA. Kidney development and disease in the zebrafish. J Am Soc Nephrol 2005;16(2):299–304.
[170] Woollard JR, Punyashtiti R, Richardson S, Masyuk TV, Whelan S, Huang BQ, et al. A mouse model of autosomal recessive polycystic kidney disease with biliary duct and proximal tubule dilatation. Kidney Int 2007;72(3):328–36.
[171] Hellman NE, Liu Y, Merkel E, Austin C, Le Corre S, Beier DR, et al. The zebrafish foxj1a transcription factor regulates cilia function in response to injury and epithelial stretch. Proc Natl Acad Sci USA 2010;107(43):18499–504.
[172] Zaghloul NA, Liu Y, Gerdes JM, Gascue C, Oh EC, Leitch CC, et al. Functional analyses of variants reveal a significant role for dominant negative and common alleles in oligogenic

Bardet–Biedl syndrome. Proc Natl Acad Sci USA 2010;107 (23):10602–7.
[173] Wallingford JB, Mitchell B. Strange as it may seem: the many links between Wnt signaling, planar cell polarity, and cilia. Genes Dev 2011;25(3):201–13.
[174] Yoder BK, Richards WG, Sweeney WE, Wilkinson JE, Avener ED, Woychik RP. Insertional mutagenesis and molecular analysis of a new gene associated with polycystic kidney disease. Proc Assoc Am Physicians 1995;107(3):314–23.
[175] Bataille S, Demoulin N, Devuyst O, Audrezet MP, Dahan K, Godin M, et al. Association of PKD2 (Polycystin 2) mutations with left–right laterality defects. Am J Kidney Dis 2011;58(3): 456–60.
[176] Hildebrandt F, Otto E, Rensing C, Nothwang HG, Vollmer M, Adolphs J, et al. A novel gene encoding an SH3 domain protein is mutated in nephronophthisis type 1. Nat Genet 1997;17(2): 149–53.
[177] Hildebrandt F, Otto E. Cilia and centrosomes: a unifying pathogenic concept for cystic kidney disease? Nat Rev Genet 2005;6(12):928–40.
[178] Waldherr R, Lennert T, Weber HP, Fodisch HJ, Scharer K. The nephronophthisis complex. A clinicopathologic study in children. Virchows Arch A Pathol Anat Histol 1982;394(3):235–54.
[179] Zollinger HU, Mihatsch MJ, Edefonti A, Gaboardi F, Imbasciati E, Lennert T. Nephronophthisis (medullary cystic disease of the kidney). A study using electron microscopy, immunofluorescence, and a review of the morphological findings. Helv Paediatr Acta 1980;35(6):509–30.
[180] Delous M, Hellman NE, Gaude HM, Silbermann F, Le Bivic A, Salomon R, et al. Nephrocystin-1 and nephrocystin-4 are required for epithelial morphogenesis and associate with PALS1/PATJ and Par6. Hum Mol Genet 2009;18(24):4711–23.
[181] Won J, Marin de Evsikova C, Smith RS, Hicks WL, Edwards MM, Longo-Guess C, et al. NPHP4 is necessary for normal photoreceptor ribbon synapse maintenance and outer segment formation, and for sperm development. Hum Mol Genet 2011;20(3):482–96.
[182] Bielas SL, Silhavy JL, Brancati F, Kisseleva MV, Al-Gazali L, Sztriha L, et al. Mutations in INPP5E, encoding inositol polyphosphate-5-phosphatase E, link phosphatidyl inositol signaling to the ciliopathies. Nat Genet 2009;41(9):1032–6.
[183] Caspary T, Larkins CE, Anderson KV. The graded response to Sonic Hedgehog depends on cilia architecture. Dev Cell 2007; 12(5):767–78.
[184] Horner VL, Caspary T. Disrupted dorsal neural tube BMP signaling in the cilia mutant Arl13b hnn stems from abnormal Shh signaling. Dev Biol 2011;355(1):43–54.
[185] Hsiao YC, Tong ZJ, Westfall JE, Ault JG, Page-McCaw PS, Ferland RJ. Ahi1, whose human ortholog is mutated in Joubert syndrome, is required for Rab8a localization, ciliogenesis and vesicle trafficking. Hum Mol Genet 2009;18(20):3926–41.
[186] Eley L, Gabrielides C, Adams M, Johnson CA, Hildebrandt F, Sayer JA. Jouberin localizes to collecting ducts and interacts with nephrocystin-1. Kidney Int 2008;74(9):1139–49.
[187] Reiter JF, Skarnes WC. Tectonic, a novel regulator of the Hedgehog pathway required for both activation and inhibition. Genes Dev 2006;20(1):22–7.
[188] Alexiev BA, Lin X, Sun CC, Brenner DS. Meckel–Gruber syndrome: pathologic manifestations, minimal diagnostic criteria, and differential diagnosis. Arch Pathol Lab Med 2006;130(8): 1236–8.
[189] Williams CL, Winkelbauer ME, Schafer JC, Michaud EJ, Yoder BK. Functional redundancy of the B9 proteins and nephrocystins in *Caenorhabditis elegans* ciliogenesis. Mol Biol Cell 2008;19(5):2154–68.
[190] Fralick RA, Leichter HE, Sheth KJ. Early diagnosis of Bardet–Biedl syndrome. Pediatr Nephrol 1990;4(3):264–5.
[191] Harnett JD, Green JS, Cramer BC, Johnson G, Chafe L, McManamon P, et al. The spectrum of renal disease in Laurence–Moon–Biedl syndrome. N Engl J Med 1988;319(10): 615–8.
[192] Zaghloul NA, Katsanis N. Mechanistic insights into Bardet–Biedl syndrome, a model ciliopathy. J Clin Invest 2009;119(3):428–37.
[193] Guo DF, Beyer AM, Yang B, Nishimura DY, Sheffield VC, Rahmouni K. Inactivation of Bardet–Biedl syndrome genes causes kidney defects. Am J Physiol Renal Physiol 2011;300(2): F574–580.
[194] Seo S, Baye LM, Schulz NP, Beck JS, Zhang Q, Slusarski DC, et al. BBS10, and BBS12 form a complex with CCT/TRiC family chaperonins and mediate BBSome assembly. Proc Natl Acad Sci USA 2010;107(4):1488–93.
[195] Li G, Vega R, Nelms K, Gekakis N, Goodnow C, McNamara P, et al. A role for Alstrom syndrome protein, alms1, in kidney ciliogenesis and cellular quiescence. PLoS Genet 2007;3(1):e8.
[196] Romio L, Wright V, Price K, Winyard PJ, Donnai D, Porteous ME, et al. OFD1, the gene mutated in oral–facial–digital syndrome type 1, is expressed in the metanephros and in human embryonic renal mesenchymal cells. J Am Soc Nephrol 2003;14(3):680–9.
[197] Singla V, Romaguera-Ros M, Garcia-Verdugo JM, Reiter JF. Ofd1, a human disease gene, regulates the length and distal structure of centrioles. Dev Cell 2010;18(3):410–24.
[198] Keppler-Noreuil KM, Adam MP, Welch J, Muilenburg A, Willing MC. Clinical insights gained from eight new cases and review of reported cases with Jeune syndrome (asphyxiating thoracic dystrophy). Am J Med Genet A 2011;155A(5): 1021–32.
[199] Rix S, Calmont A, Scambler PJ, Beales PL. An Ift80 mouse model of short rib polydactyly syndromes shows defects in hedgehog signalling without loss or malformation of cilia. Hum Mol Genet 2011;20(7):1306–14.
[200] Dagoneau N, Goulet M, Genevieve D, Sznajer Y, Martinovic J, Smithson S, et al. DYNC2H1 mutations cause asphyxiating thoracic dystrophy and short rib-polydactyly syndrome, type III. Am J Hum Genet 2009;84(5):706–11.
[201] Davis EE, Zhang Q, Liu Q, Diplas BH, Davey LM, Hartley J, et al. TTC21B contributes both causal and modifying alleles across the ciliopathy spectrum. Nat Genet 2011;43(3):189–96.
[202] Gilissen C, Arts HH, Hoischen A, Spruijt L, Mans DA, Arts P, et al. Exome sequencing identifies WDR35 variants involved in Sensenbrenner syndrome. Am J Hum Genet 2010;87(3): 418–23.
[203] Arts HH, Bongers EM, Mans DA, van Beersum SE, Oud MM, Bolat E, et al. C14ORF179 encoding IFT43 is mutated in Sensenbrenner syndrome. J Med Genet 2011;48(6):390–5.
[204] Walczak-Sztulpa J, Eggenschwiler J, Osborn D, Brown DA, Emma F, Klingenberg C, et al. Cranioectodermal dysplasia, sensenbrenner syndrome, is a ciliopathy caused by mutations in the IFT122 gene. Am J Hum Genet 2010;86(6):949–56.

CHAPTER

12

Intercellular Junctions

Alan S. L. Yu[1], *Fiona Hanner*[2,3] *and János Peti-Peterdi*[2,3]

[1]Division of Nephrology, and Hypertension, and The Kidney Institute, University of Kansas Medical Center, Kansas City, KS, USA

[2]Department of Physiology and Biophysics, University of Southern California Keck School of Medicine, Los Angeles, CA, USA

[3]Zilkha Neurogenetic Institute, University of Southern California Keck School of Medicine, Los Angeles, CA, USA

TIGHT JUNCTIONS

Structure

General Structure

The tight junction is the most apical component of the junctional complex (Figure 12.1). It is located at the boundary between the apical and lateral membranes, and encircles the cells to form a continuous belt-like attachment. By transmission electron microscopy, it appears morphologically as a series of appositions or "kisses" between the lateral membranes of adjacent cells (Figure 12.2a). The outer leaflet of the lipid bilayers approach each other so closely that they appear to be fused. In the technique of freeze-fracture electron microscopy, the hydrophobic phospholipid interior of the lipid bilayer is cleaved, allowing the tight junctions to be visualized within the plane of the lateral membrane. By this means, tight junctions appear as a series of continuous, anastomosing intramembranous strands on the protoplasmic or P-face, with complementary grooves on the exoplasmic or E-face (Figure 12.5). It is believed that these strands associate in pairs from neighboring cells and obliterate the intercellular space, thus accounting for the kissing points seen by transmission electron microscopy (Figure 12.2b).

Early models of the tight junction posited that it was composed purely of lipid organized into inverted cylindrical micelles, that constituted the tight junction strands.[2,3] There now exist three lines of evidence that refute this. First, tight junction strands were found to be resistant to deoxycholate, an ionic detergent that should solubilize lipids.[4] Second, the lipid model predicts that the outer leaflets of the bilayers of adjacent cells are continuous, yet no transfer of glycolipid or a fluorescent probe could be demonstrated.[5–7] Finally, the discovery of integral membrane proteins within the tight junction now supports a model in which tight junction strands are composed of proteins embedded in the lipid membrane (see below).

Regional Differences in Structure

The structure of the tight junction varies considerably in different regions of the kidney. This is summarized briefly below. For further details, the reader is referred to comprehensive surveys by Orci, Brown, and colleagues.[8,9]

GLOMERULUS

The parietal epithelium of Bowman's capsule is constituted of squamous cells whose extensions overlap obliquely (Figure 12.3). Their tight junctions consist of networks of two to four anastomosing strands with many discontinuities.[10,11] The mature visceral epithelial cell (podocyte) forms a specialized intercellular junction, the slit diaphragm (Chapter 23). Short elements of incomplete tight junctions can sometimes also be seen between the foot processes of adjacent podocytes. True tight junctions do form between immature podocytes in the fetal glomerulus and are of uncertain functional significance.[12,13] These disappear during development, but can reappear during nephrotic states, coincident with effacement of the foot processes and obliteration of the slit pore[14–16] (Figure 12.4).

Seldin and Giebisch's The Kidney, Fifth Edition.
DOI: http://dx.doi.org/10.1016/B978-0-12-381462-3.00012-4

© 2013 Elsevier Inc. All rights reserved.

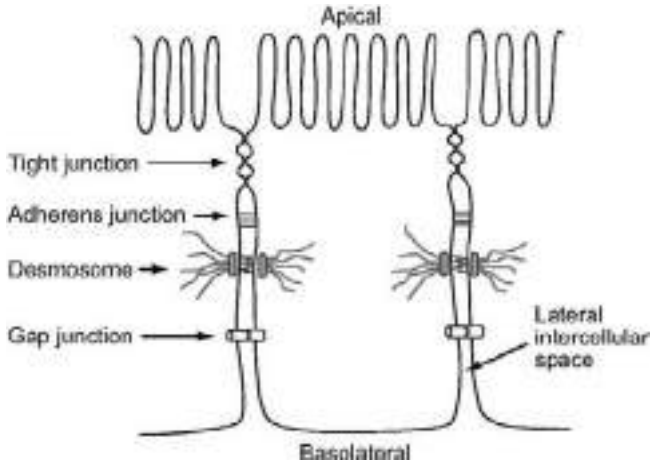

FIGURE 12.1 **Organization of the junctional complex in a typical monolayer of epithelial cells.**

RENAL TUBULE

Tight junctions are found between the epithelial cells of all tubules, but they vary considerably in their morphology in different tubule segments (Figure 12.5 and Table 12.1). In general, the more proximal segments tend to have simpler junctions, with fewer strands and more discontinuities, correlating with a leaky paracellular pathway, as judged by transepithelial resistance (TER). By contrast, more distal segments tend to have greater numbers of strands, with more continuity and complex anastomosing patterns, loosely correlating with higher TER. Indeed, Claude proposed a model in which TER is dependent primarily on strand number.[17] However, as discussed below, we now know that the TER is also highly dependent on the composition of the tight junction.

Physiological Functions

Gate Function

The gate function refers to the ability to regulate the paracellular permeability. This determines the rate of passive diffusion of extracellular solutes and water between the apical and basolateral aqueous compartments. Early studies, using extracellular macromolecules and lanthanum as electron-dense markers, clearly established the tight junction as the site of the paracellular gate.[1,18,19]

In epithelia that mediate active, uphill transcellular transport, such as the collecting duct of the kidney, this gate must act predominantly as a barrier to prevent backleak of solute gradients that have been generated. To do so, these so-called "tight" epithelia must have very low paracellular permeability and conductance (typical transepithelial resistances (TER) range from 1−2 k′Ω.cm^2 for the renal collecting duct[20] to ~8 k′Ω.cm^2 for amphibian skin[21]).

In contrast, in epithelia that mediate bulk transport of solutes via the paracellular pathway, the gate is predominantly open. For example, in the late proximal tubule of the kidney about one-third of NaCl reabsorption occurs by the paracellular route,[22] and in the thick ascending limb of Henle, Ca^{2+} and Mg^{2+} are exclusively reabsorbed via the paracellular pathway.[23] Characterization of the properties of leaky epithelia have indicated that there must be paracellular aqueous pores.[24,25] Fromter and Diamond were the first to prove that the paracellular leak is physically located at the intercellular junction.[26] Thus, the tight junction is not always a complete barrier, but must also have pores that pass through it.

Fence Function

In epithelia, the lipid and protein components of the plasma membrane are separated into distinct apical and basolateral domains at the tight junction, and this polarity is critical for functions such as vectorial transport. Apical−basolateral polarity is initially established by the Par/aPKC, Crumbs, and Scribble complexes,[27,28] while the tight junction is primarily responsible for maintenance of this polarity. Specifically, the tight junction behaves like a fence, preventing diffusion within the plane of the lipid bilayer. Interestingly, markers that are confined to the exocytoplasmic leaflet cannot pass across the tight junction, but markers that can flip-flop across the bilayer freely diffuse across it,[6,29] suggesting that the fence is located in the exocytoplasmic half of the plasma membrane. Several manipulations can dissociate the barrier and fence functions of the tight junction. Transient ATP depletion[30,31] and depolymerization of the cortical actin network[32] disrupt the paracellular barrier while preserving fence function. This suggests that the fence function of the tight junction is mechanistically independent of its gate function.

Biochemical Composition

The first tight junction-associated protein to be identified was ZO-1, in 1986.[33] Since then, it has become clear that the tight junction is actually a complex of many different proteins. These fall into one of four categories: transmembrane proteins; scaffolding proteins; signaling molecules; and transcriptional regulators. These molecules are associated, through multiple protein−protein interactions, with the scaffolding proteins serving to anchor the complex to the cortical actin cytoskeleton. Table 12.2 lists the known molecules in each category. Here, we focus solely on the transmembrane proteins. These are important because their transmembrane domains traverse the lipid bilayer, while their extracellular domains protrude into the paracellular space. Thus, tight junction membrane proteins are the leading candidates to mediate both gate and fence functions.

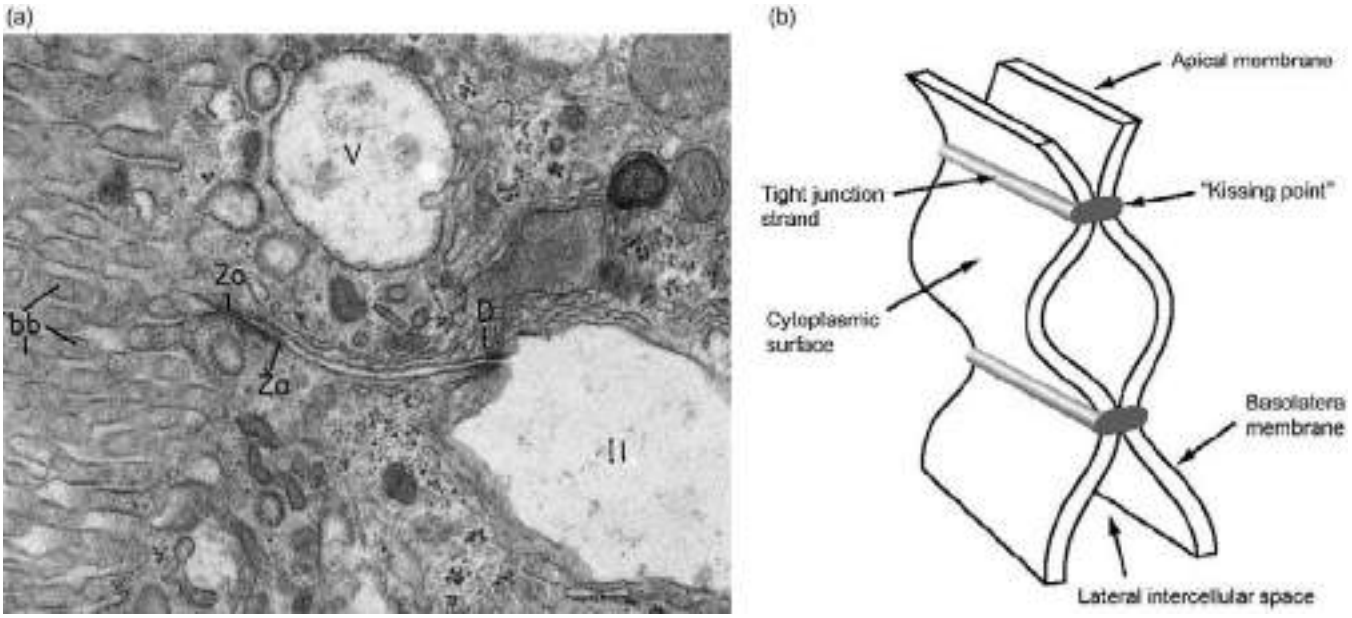

FIGURE 12.2 **Structure of the tight junction.** (a) Transmission electron micrograph of the junctional complex in the epithelium of the rat proximal convoluted tubule (Zo: zonula occludens (tight junction); Za: zonula adherens (adherens junction); D: desmosome; bb: brush border; Il: lateral intercellular space). (b) Three-dimensional depiction of the tight junction. Tight junction strands of neighboring cells associate in a pairwise manner at points where the lateral membranes are closely apposed, obliterating the intercellular space ("kissing points"). *(©The Rockefeller University Press.* The Journal of Cell Biology, *(1963).* ***17****, 375–412.*[1]*)*

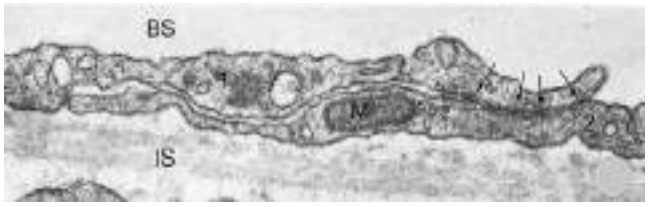

FIGURE 12.3 **Section through Bowman's capsule of rat kidney showing two adjacent parietal epithelial cells (labeled 1 and 2).** The cells are flat, so that their extensions overlap obliquely to form the tight junction. Arrows indicate points of close apposition between their lateral membranes (BS: Bowman's space; IS: interstitial space; Mi: mitochondrion; × 40,000). *(Reproduced with permission from Taugner et al. (1976).* Cell Tissue Res. ***172****(4), 431–446.*[10]*)*

Occludin

Occludin was the first integral tight junction membrane protein to be identified.[34] It has four transmembrane domains with intracellular N- and C-termini. Occludin is ubiquitously expressed in epithelial cells, localizing predominantly at bicellular junctions (junctions where two cells meet). Its role is poorly understood. Overexpression of a C-terminally truncated occludin protein increases TER, but paradoxically increases mannitol flux, and also disrupts tight junction fence function.[35,36] However, after knockdown or knockout of occludin, cells can still form normally appearing tight junction strands.[37,38] In fibroblasts that do not have tight junctions, occludin cannot reform tight junction networks, but it does co-polymerize into strands with claudin-1.[39] Knockdown of occludin in MDCK cells causes only a slight increase in permeability to small inorganic and organic cations.[38] Interestingly, occludin null mice have assorted unexplained abnormalities, including retarded postnatal growth, male sterility, and chronic inflammation and epithelial hyperplasia in the gastric mucosa.[40] Importantly, though, epithelial barrier function is normal in these mice.[41] Thus, occludin is neither necessary nor sufficient to form tight junction strands and perform barrier, pore or fence functions. However, occludin can incorporate into claudin-based strands, in which case dominant-negative occludin constructs are presumably able to disrupt normal tight junction function.

Tricellulin

Tricellulin is a homolog of occludin that is localized to tricellular junctions (junctions at the confluence of three cells.[42] It is clearly important for barrier function, because knockdown of tricellulin increases paracellular conductance and permeability to uncharged macromolecules,[42] and its overexpression reduces macromolecular permeability.[43] Mutations in tricellulin cause a form of non-syndromic hereditary deafness, indicating that it plays a critical role in inner ear function,[44] but its role in the kidney has not been explored.

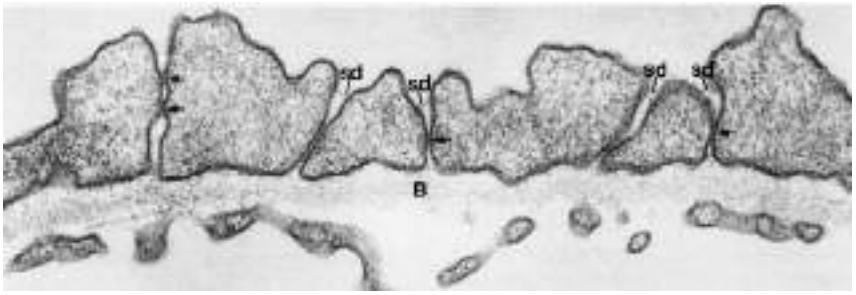

FIGURE 12.4 **Morphologic changes in glomerular podocytes in the puromycin aminonucleoside nephrotic rat kidney.** The membranes of the foot processes appear to come into close apposition or to be fused (arrows), forming tight junction-like structures between neighboring processes. The slit diaphragms (sd), which are normally located above the basement membrane (B), are found above the newly formed junctions between the podocytes (× 74,000). *(Reprinted from* Am. J. Pathol. *(1992),* ***141****, 805–816.*[226] *With permission from the American Society for Investigative Pathology.)*

Claudins

Claudins were discovered by Tsukita and colleagues.[45] They are members of a multigene family of ~20–24 kDa tight junction proteins with four predicted transmembrane segments and two extracellular domains (see refs [46–48] for several recent reviews). When expressed in claudin-deficient cells such as fibroblasts, claudins can form tight junction-like networks of strands, indicating that they polymerize in *cis* (within the same cell membrane), and can mediate intercellular adhesion, indicating the ability to interact in *trans* (across two lateral membranes of adjacent cells).[39,49] Thus, claudins have all the properties expected for a structural component of the paracellular barrier. In 1999, Lifton's group identified the culprit gene mutated in familial hypercalciuric hypomagnesemia, an inherited disorder thought to be due to failure of paracellular reabsorption of divalent cations in the thick ascending limb of the renal tubule. This gene, which was initially named paracellin, turned out to be a claudin (claudin-16),[50] and its involvement in this disease strongly suggested that claudins play a role in regulating paracellular transport. This is now supported by numerous studies demonstrating that overexpressing or ablating expression of various claudin isoforms in cultured cell lines or in mice affects both the degree of paracellular permeability, and its selectivity (reviewed in ref [51]). Moreover, Colegio et al. have convincingly shown that the net charge on residues in the first extracellular domain of claudins determines the charge selectivity of paracellular conductance.[52,53] This suggests fairly strongly that the first extracellular domain of claudins actually forms the lining of the paracellular pore. The permeability properties of different claudin isoforms, as inferred from *in vitro* overexpression and knockdown studies, are summarized in Table 12.3.

FUNCTIONAL DOMAINS OF CLAUDIN

The functions of several of the domains within the claudin protein have been determined (Figure 12.6). The first extracellular loop of claudin forms the lining of the paracellular pore. Chimera studies have shown that exchanging the first extracellular loop between different claudin isoforms confers different pore selectivity characteristics.[53] Furthermore, point mutations that reverse the charge on residues in the first extracellular loop alter the charge selectivity of the paracellular pore, as would be expected if this domain faced the pore lumen.[52] In claudin-2, a cation-selective pore, this loop specifically contains an aspartate residue (Asp-65) that acts as a Na^+-binding site.[54] Several other residues in this domain have also been mapped by cysteine-scanning mutagenesis.[55]

The second extracellular loop of claudin is postulated to participate in *trans*-intermolecular interactions, acting as the adhesion receptor between neighboring cells. This is based on the finding that mutations of selected residues in the second extracellular loop of claudin-5 abolish its ability to concentrate at cell contact sites when expressed in HEK cells.[56]

Claudins all have a long cytoplasmic C-terminal tail that appears to be involved in protein trafficking and degradation. Deletion of this tail in claudin-5 and -6 leads to accumulation of the protein in the cytoplasm.[57,58] This domain also affects protein stability, since swapping it between different claudins confers different protein half-lives.[59] The terminal dipeptide motif in claudins (tyrosine-valine in the majority) binds to PDZ domains on the scaffolding proteins, ZO-1, 2, and 3,[60] and MUPP1.[61,62] However, deletion of this motif does not seem to affect normal trafficking of claudins to the tight junction.[57,63]

The cytoplasmic C-terminal tail in all claudin isoforms also contains multiple potential

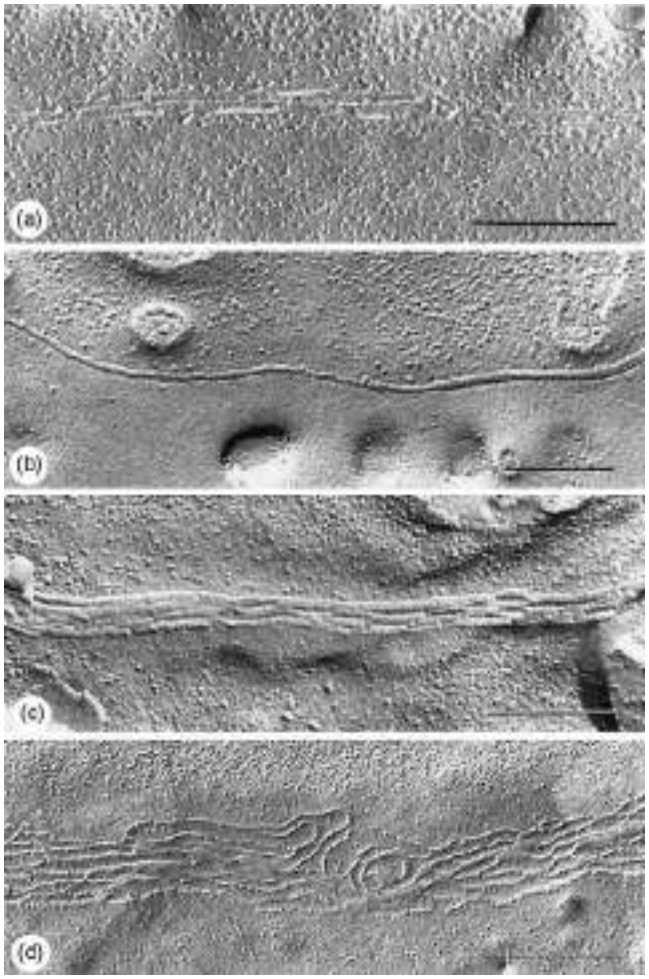

FIGURE 12.5 **Freeze-fracture morphology of tight junctions on the P-faces of four regions of the urinary tubule.** The tight junctions of the proximal convoluted tubule (a) are characterized by fibrils that are often ill-defined and discontinuous. In the ascending thin limb of Henle (b), the tight junctions usually appear as one continuous strand or two closely apposed strands that are covered with fragments of E-face from the adjacent cell, giving the impression of a single, thick strand. In the distal tubule (c), the junctions are composed of several parallel elements. In the collecting duct (d), the tight junctions are the most complex in the entire urinary tubule, and are formed of multiple, branching fibrils (a–c: bar = 0.25 μm; d: bar = 0.5 μm). *(Reproduced with permission from Orci et al. (1981).* Int. Rev. Cytol. *73, 183–242.*[9]*)*

TABLE 12.1 Morphology of the Tight Junctions Compared with Transepithelial Resistance in Different Nephron Segments of the Rat Renal Tubule[a]

Tubular segment	Transepithelial resistance ($\Omega.cm^2$)[b]	Number of junctional strands (typical range)
Proximal	5–7	1–2
Thin descending limb of Henle	700[c]	1
Thick ascending limb of Henle	10–35	5–6[d]
Distal convoluted tubule	350	
Collecting duct	867	8–9

[a]*Table adapted with permission from Pricam et al.*[158]
[b]*Values from references.*[218–222]
[c]*Values measured in the rabbit.*
[d]*Values from both thick ascending limb and distal convoluted tubule.*

TABLE 12.2 Composition of the Tight Junction Protein Complex

Transmembrane proteins	Scaffolding proteins	Signaling proteins	Transcriptional regulators
Occludin	ZO-1, 2, 3	aPKC	ZONAB
Claudins	Par-3, 6	GEF-H1	Symplekin
Tricellulin	Pals1	Gαi-2, αo, α12	AP-1
MarvelD3	PATJ	Rab13, 3B	
JAM	MUPP1	c-Yes	
CAR	MAGI-2, 3	WNK3, 4	
	JACOP/ paracinguilin	CDK4	
	Cingulin		
	AF-6		

phosphorylation sites for a variety of protein kinases (see ref [64] for a comprehensive review). The most common outcome of phosphorylation by protein kinases in this domain is increased assembly at the tight junction,[65,66] but there are examples of phosphorylation leading to decreased assembly at the tight junction,[67] and also to changes in paracellular permeability.[68–70]

Finally, all claudins have two pairs of conserved cysteines immediately following the second and fourth transmembrane domains. In claudin-14, these have been shown to be palmitoylated, and this seems to be required for efficient localization to the tight junction.[71]

Physiology of the Tight Junction in Different Nephron Segments

Different nephron segments exhibit different tight junction permeability characteristics that are important for their specific function. These paracellular permeability characteristics are likely a function both of the general structure of the tight junction (discussed above), and of the properties of the specific claudin isoforms expressed in that segment. The nephron

TABLE 12.3 Putative Ion Permeability Characteristics of Claudin Isoforms[a]

Pore-forming claudins[b]	Refs	Barrier-forming claudins	Refs
Cation-selective pore		**Cation barrier**	
Claudin-2	54,86,87	Claudin-1	36,74
Claudin-10b	90	Claudin-3	114
Claudin-16	109–111	Claudin-4[c]	115,125
Anion-selective pore		Claudin-5	223
Claudin-4[c]	125	Claudin-6[d]	93
Claudin-10a	90	Claudin-8	116,224
Claudin-11[c]	88	Claudin-9[d]	93
Claudin-17	108	Claudin-11[c]	88
		Claudin-14	117
		Claudin-18	118
		Anion barrier	
		Claudin-15	52,88
		Claudin-19[e]	112

[a]*Based on in vitro overexpression or knockdown studies in cultured cell lines. We assume that permeability and selectivity are properties intrinsic to individual claudin isoforms, and ignore the possible confounding effect of heteromeric interactions between isoforms. Claudin-7 is omitted because conflicting data exist suggesting that it is either a Cl-barrier[124,225] or a Na-barrier/Cl-pore.[125]*
[b]*Pore-forming claudins refer to those that predominantly decrease TER or increase solute permeability, while barrier-forming claudins refer to those that predominantly increase TER or decrease solute permeability. The distinction is somewhat arbitrary, since most claudins probably have some finite permeability to most solutes, and the observable phenotype is highly dependent on the properties of the host cell line.[87,222]*
[c]*Acts as a Na barrier in MDCK II cells, but as a Cl pore in LLC-PK1 cells.*
[d]*Net flux studies suggest that claudin-6 and -9 may also act as Cl-barriers.[93]*
[e]*Conflicting data also exists suggesting claudin-19 can act as a Na barrier.[105]*

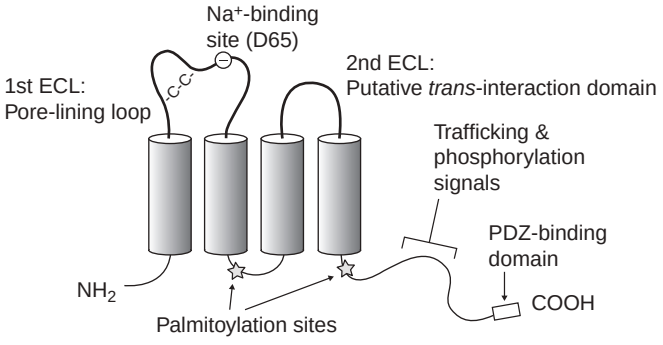

FIGURE 12.6 **Functional domains that have been mapped in claudins.** The Na^+-binding site at D65 has been demonstrated in claudin-2 (ECL: extracellular loop).

segment localization of different claudin isoforms is summarized in Figure 12.7.

Bowman's Capsule

The function of the parietal epithelium of Bowman's capsule is poorly understood, but one might assume that it needs to act primarily as a barrier to contain the glomerular filtrate, and direct flow into the proximal tubule. The tight junction of parietal epithelial squamous cells is unique among cells of the nephron in expressing claudin-1,[72,73] an isoform that has been shown to act as a barrier to ion conductance, and to permeation of 4–40 kDa dextran.[36,74] Claudin-2, a cation- and water-permeable claudin isoform predominantly expressed in the proximal tubule (see below), has also been reported to be expressed in the parietal epithelium.[72,73] However, it is well-known that the parietal epithelium at the urinary pole is constituted of columnar cells that are distinct from the squamous parietal epithelial cells, and morphologically and functionally resemble proximal tubule cells.[75,76] These columnar cells can cover a substantial surface area of Bowman's capsule, for example, one-third of it in male mice, and it is probably just these cells that express claudin-2 (see, for example, Fig. 3A in ref [77]).

Ohse recently showed that the parietal epithelium in mice functions as a barrier to macromolecules, as detected with 3 kDa dextran and 45 kDa ovalbumin as tracers.[78] After experimental induction of glomerulonephritis, this barrier is disrupted and the macromolecule tracers can be observed leaking into the space between the parietal epithelium and the underlying basement membrane of Bowman's capsule, as well as the extraglomerular space.

Proximal Tubule

The primary role of the proximal tubule is bulk reclamation of solutes that evade the glomerular filter, such as Na, K, Ca, Cl, HCO_3, phosphate, glucose, and water. Since the free concentration of these solutes in the glomerular filtrate is similar to that of the peritubular fluid, relatively little energy expenditure should be needed to transport them across the epithelium. To achieve this sort of energy efficiency, the proximal tubule uses a two-step process. In the first step, ATP consumed by the Na-K-ATPase is used to generate a transmembrane Na gradient that drives secondary and tertiary active transcellular reabsorption of Na and other solutes. The stoichiometry of the Na-K-ATPase dictates that the hydrolysis of each ATP molecule in this step should be coupled to the direct transport of three Na ions. In the second step, the transepithelial electrochemical gradients generated by transcellular transport then provide the driving force for passive diffusion of solutes across the paracellular pathway. Measurements of whole kidney oxygen consumption have been used to estimate that five Na ions are transported per ATP molecule,[79,80] demonstrating that paracellular transport greatly enhances the metabolic efficiency of the proximal tubule.

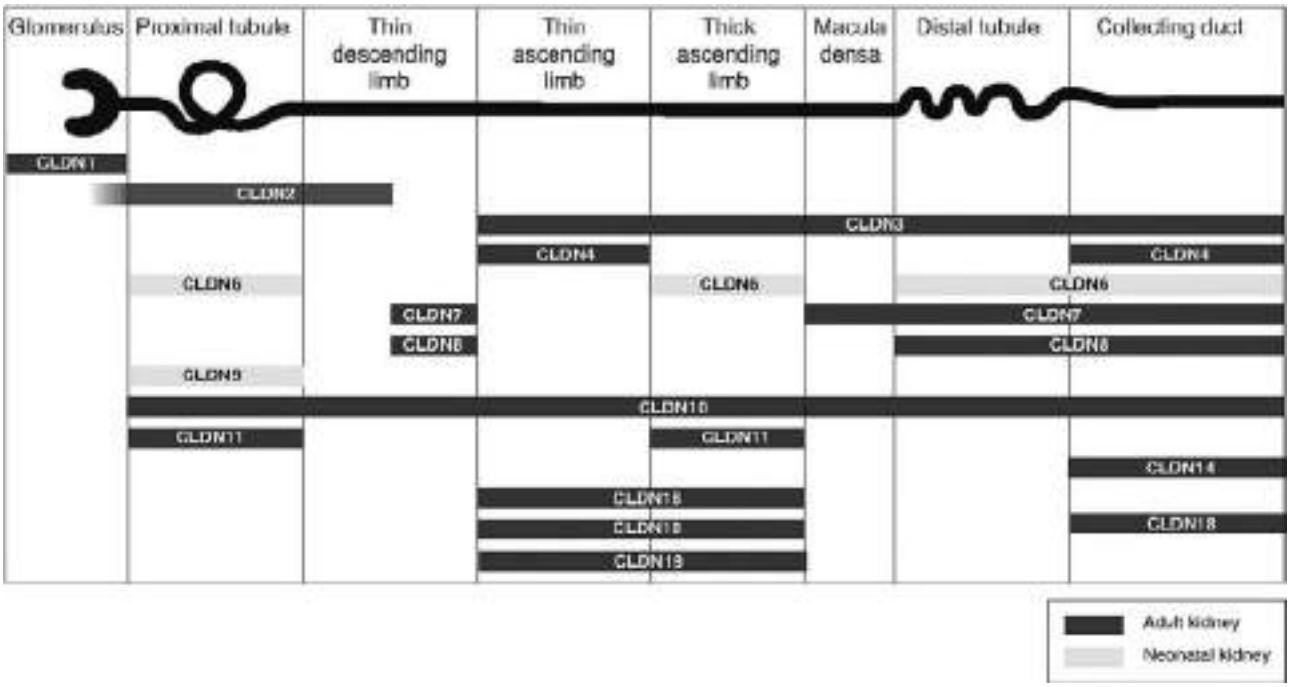

FIGURE 12.7 **Localization of claudin proteins in rodent kidney.** Localization data were collated from the following studies: claudins 1, 3, and 4,[72] claudin-2,[77] claudin-6,[92] claudins 7 and 8,[227] claudin-9,[92] claudin-10,[90] claudin-14,[108] claudin-16,[106] claudin-17,[85] claudin-18,[107] and claudin-19.[105,106] Macula densa claudin expression is from our own unpublished results. Tubule expression of claudins 6 and 9 are only found in neonatal kidney.[92] Localization of claudins in human kidney are essentially identical,[50,228] except that claudin-1 is found in collecting duct and distal tubule, claudin-10 is not found in the distal nephron, and claudin-14 is reportedly in the distal convoluted tubule.[228] Many of these claudins have not been rigorously examined in all nephron segments so the data shown are not comprehensive. Claudins 5 and 15 are confined to endothelial cells of the vasculature and glomeruli,[72] and so are not shown. Claudins 12, 18 and 20–24 have not yet been examined. *(Figure modified from Angelow, S. and Yu, A. S. (2007). Claudins and paracellular transport: an update. Curr. Opin. Nephrol. Hypertens.* ***16****, 459–464. Copyright Lippincott, Williams & Wilkins, 2007.)*

NaCL REABSORPTION

The underlying mechanism for paracellular NaCl reabsorption in the proximal tubule was first proposed by Rector.[22,81] In this model, transcellular Na reabsorption in the early proximal convoluted tubule is coupled primarily to reabsorption of most of the organic solutes and significant amounts of bicarbonate, and followed by isosmotic reabsorption of water. This leads to a luminal fluid that is high in chloride, but low in bicarbonate. The late proximal tubule has a very high passive permeability (presumably due to the paracellular pathway) both to Na and to Cl, but much less so to HCO_3.[82–84] Thus, Cl is reabsorbed paracellularly, driven by its concentration gradient. This in turn generates a lumen-positive electrical potential which then drives concomitant reabsorption of Na.

The claudin isoforms that are known to be expressed in the proximal tubule are claudin-2, -10, and -17.[72,77,85] Claudin-2 behaves *in vitro* as a cation-selective paracellular pore.[54,86–88] Knockout of claudin-2 in mice led to an approximately two-fold reduction in transepithelial conductance, P_{Na}/P_{Cl}, and passive flux of Na, Cl, and water in perfused S2 segments, and an exaggerated natriuretic response to a NaCl challenge.[89] Thus, claudin-2 seems to be the primary route for paracellular Na reabsorption. Claudin-10 exists in two splice variants that differ in their first extracellular domain, and hence charge selectivity.[90] Claudin-10a behaves as a Cl-selective pore, while claudin-10b is Na-selective. The 10a splice variant is uniquely expressed in the kidney, and by *in situ* hybridization appears to be predominantly in the cortex, although tubule localization could not be ascertained. Studies of claudin-17 overexpression in MDCK-C7 cells and knockdown in LLC-PK1 cells indicate that it functions as a Cl pore.[85] Thus, either claudin-10a or -17 could potentially mediate paracellular Cl reabsorption in the proximal tubule.

The neonate proximal tubule has a lower chloride permeability than the adult, which may predispose it to salt-wasting and dehydration.[91] Claudins 6 and 9 are predominantly expressed in the neonatal proximal tubule,[92] but the published functional data are somewhat conflicting as to whether they primarily act as Cl-barriers (which would be consistent with the tubule physiology) or Na-barriers.[93]

WATER REABSORPTION

A substantial amount of water is reabsorbed in the proximal tubule. It is now clear that the majority of water transport is transcellular and mediated by aquaporins. Nevertheless, knockout of AQP1 in mice only reduces proximal tubule water transport by 80%, suggesting that an alternative pathway for water transport exists and is either active under normal conditions or is upregulated to compensate for loss of AQP1.[94] Weinstein has argued that the low reflection coefficient for NaCl ($\sim$0.7)[95] suggests the existence of a paracellular shunt pathway for water.[96] However, Preisig and Berry measured the permeability of the proximal tubule to mannitol and sucrose and, assuming that they were only transported paracellularly, modeled the pore size with the Renkin equation to predict the paracellular water permeability and concluded that it was $<$2% of transepithelial water permeability.[97] Moreover, Spring measured water flow in the lateral intercellular spaces of MDCK cells (admittedly not necessarily a proximal tubule model cell line) by an optical technique, and concluded that water transport in these cells was entirely transcellular.[98] Thus, the existence of paracellular water reabsorption in the proximal tubule has been quite controversial. Recently, Rosenthal et al. reported that transfection of claudin-2 increases transepithelial osmotic water permeability.[99] Interestingly, they found that when they imposed a transepithelial Na^+ concentration gradient, not only was Na^+ transported vectorially, but water flowed in the same direction, suggesting that Na^+ and water movement are in some way "coupled," and therefore that they probably flow through the same pore.

REABSORPTION OF OTHER CATIONS

A substantial proportion of the filtered load of K, Ca, and Mg are reabsorbed in the proximal tubule, largely by the paracellular pathway. The driving force in each case is probably both an increased concentration of the cation in the lumen due to water reabsorption, and the lumen-positive voltage in the mid-to-late proximal tubule. Claudin-2 is permeable to both K and Ca (Mg has not been tested),[54] and therefore likely mediates their reabsorption by diffusion down their electrochemical gradients.

Thick Ascending Limb of Henle

The thick ascending limb of Henle is a quantitatively important site for paracellular reabsorption of the divalent cations, Ca and Mg.[100] In addition, some of the Na reabsorbed in this nephron segment is also thought to occur paracellularly, thus enhancing the metabolic efficiency of transcellular Na reabsorption, just as in the proximal tubule. The driving force for paracellular reabsorption of each of these cations is a lumen-positive electrical potential difference. This voltage is generated by two distinct and additive mechanisms: (1) transcellular reabsorption of NaCl through the apical Na-K-2Cl co-transporter and basolateral Na-K-ATPase and ClC-K chloride transporter occurs concomitantly with apical recycling of K through the apical K channel, ROMK, giving rise to a net movement of positive charge apically; this generates a 3–9 mV lumen-positive transepithelial potential difference[101]; (2) because the paracellular pathway of the thick ascending limb is highly cation-selective ($P_{Na}/P_{Cl} = 2–6$),[101,102] accumulation of a high concentration of reabsorbed NaCl basolaterally generates a diffusion potential, adding another 10–15 mV to the transepithelial voltage.[103] The paracellular pathway of the thick ascending limb is well adapted for this purpose. It is characterized by a low TER (11–34 $\Omega.cm^2$),[104] high selectivity for Na over Cl, and high permeability to divalent cations.[23]

The thick ascending limb is known to express claudins 3, 10, 11, 14, 16, 18, and 19.[50,72,90,105–108] Claudin-16 (also known as paracellin) and claudin-19 are of particular interest, because mutations in these genes cause familial hypercalciuric hypomagnesemia with nephrocalcinosis (FHHNC), an autosomal recessive disorder characterized by renal Ca and Mg wasting.[50,106] There are two prevailing hypotheses as to the physiological role of claudins 16 and 19. The first hypothesis, initially suggested by Simon et al.,[50] is that they are divalent cation-permeable paracellular pore proteins. In this model, Ca and Mg normally diffuse through these claudins, driven by the lumen-positive potential, but in FHHNC this pathway is abolished. Consistent with this, Ikari et al. found that overexpression of claudin-16 increased Ca permeability, and that this could be competitively inhibited by Mg, while TER was paradoxically increased.[109] Similarly, Kausalya et al. found that claudin-16 increased Mg permeability, but did not affect P_{Na}/P_{Cl}.[110] The second hypothesis is that claudin-16 and -19 together form a pore that is highly selective for Na over Cl, and therefore facilitates the component of the lumen-positive potential generated by the NaCl concentration gradient (component (2) above). In other words, claudin-16 and -19 are involved in creating the driving force for Ca and Mg reabsorption, rather than being part of the permeation pathway. This second hypothesis is supported predominantly by the work of Hou, Goodenough, and colleagues. In their hands, claudin-16 acts like a cation pore that is not selective between monovalent and divalent cations,[111] and claudin-19 acts like an anion barrier.[112] Hou et al. showed that the two isoforms physically interact with each other, and have additive effects to increase P_{Na}/P_{Cl} when co-expressed

together.[112] Indeed, knockdown of both isoforms in mice recapitulated the main features of FHHNC, and was associated with decreased P_{Na}/P_{Cl} as measured in isolated, perfused thick ascending limbs.[107,113]

Claudin-14 appears to act as a negative regulator that binds to claudin-16 to reduce the PNa/PCl of this complex.[108] Importantly, claudin-14 expression is upregulated in response to high extracellular calcium or a high-calcium diet, which stimulate the Ca-sensing receptor in the thick ascending limb and thereby downregulate two micro-RNAs that normally suppress claudin-14 expression. This provides an elegant homeostatic mechanism to increase renal calcium excretion in the setting of calcium excess. The role of the other claudins in this segment is not known at this time.

Aldosterone-Sensitive Distal Nephron

The aldosterone-sensitive distal nephron (ASDN) encompasses the distal convoluted tubule, connecting segment, and collecting duct. This is the last section of the nephron, and is responsible for fine-tuning urinary composition. The remaining excess Na in the tubular fluid has to be reabsorbed here, and K and H^+ secreted. These are active, highly energy-consuming processes, because they need to drive transport uphill against steep electrochemical gradients, utilizing transcellular pathways. Transtubular concentration gradients for Na, K, and H^+ (lumen:blood) of 1:3, 20:1, and 1000:1, respectively, are often achieved by the end of the collecting duct. Thus, the major role of the tight junction in the ASDN is to act as a very tight paracellular cation barrier to prevent dissipation of these transtubular cation gradients. Consistent with this, the ASDN (or at least the collecting duct) expresses five claudins that function primarily as cation barriers: claudins 3, 4, 8, 14, and 18.[114–118] For claudin-8 and -18, the ability to act as a barrier to acid permeation has also been demonstrated.[118,119]

In the connecting segment and collecting duct, Na is reabsorbed primarily electrogenically through epithelial Na channels (ENaC), as distinct from the distal convoluted tubule, which mediates electroneutral, NaCl reabsorption. Thus, Cl in the connecting segment and collecting duct must be reabsorbed either through an independent transcellular pathway (e.g., via the Na-driven Cl-bicarbonate exchanger and pendrin in β-intercalated cells[120,121]) or paracellularly. Consistent with a role in paracellular Cl transport, the cortical collecting duct has been shown to have a substantial paracellular permeability to Cl.[122] A recent study suggests that this paracellular Cl permeability may be mediated by claudin-4 and -8, perhaps interacting with each other to form a heteromeric pore.[123]

Claudin-7 is expressed in the ASDN. When overexpressed in LLC-PK cells, it appeared to reduce Cl permeability (i.e., acted as a Cl barrier).[124] However, knockdown of its expression paradoxically also decreased Cl permeability, suggesting that claudin-7 might normally behave as a Cl pore, and might be responsible for the paracellular Cl conductance in the ASDN.[125] Importantly, mice that had claudin-7 knocked-out by gene targeting exhibited severe renal salt-wasting, hypovolemia, and acute renal failure,[126] which is consistent with a role for claudin-7 in ASDN Cl reabsorption.

REGULATION BY ALDOSTERONE AND WNK KINASES

NaCl reabsorption in the ASDN is stimulated by mineralocorticoids. This is achieved in part by stimulating transcellular Na transport. In addition, aldosterone and other mineralocorticoids regulate paracellular permeability. For example, mineralocorticoids reduce Na permeability in the inner medullary collecting duct.[127–129] This would serve to limit paracellular back-leak of Na, and thereby enhance the efficiency of Na reabsorption. Mineralocorticoids have also been shown to reduce paracellular Cl permeability in the collecting duct,[129,130] but the physiological significance of this is less clear. Interestingly, Le Moellic et al. found that in a rat cortical collecting duct cell line, very brief (<1 hour) aldosterone exposure actually increased paracellular anion permeability.[69] This correlated temporally with phosphorylation of claudin-4 at a threonine residue, although a causal relationship was not established.

NaCl reabsorption in the ASDN is also regulated by WNK1 and WNK4. These are protein kinases that, when mutated, cause pseudohypoaldosteronism, type II (PHAII), a genetic disorder characterized by salt-sensitive hypertension and hyperkalemia.[131] The normal physiological function of the WNKs is quite controversial, but it is clear that PHAII mutations in WNK4 lead to enhanced NaCl reabsorption in the ASDN. This is partly transcellular and mediated by stimulation of the thiazide-sensitive NaCl co-transporter, NCC.[132,133] However, there is also evidence that WNK4 regulates paracellular Cl permeability. WNK4 is localized to the tight junction *in vivo*.[131] When overexpressed in cell lines, WNK4 (particularly the PHAII mutant) stimulates paracellular Cl conductance.[68,70,134] The exact mechanism is unclear. There is evidence both for[68,70] and against[135] direct phosphorylation by WNK4 of several claudin isoforms, including claudins 4 and 7, that are normally expressed in the ASDN.

Tight Junction Dysfunction in Ischemic Acute Kidney Injury

Ischemic injury to the kidney causes reversible disruption of renal tubule epithelial barrier function and

polarity. Renal ischemia or ATP depletion in humans, animal models, and cultured cells cause disruption of the tight junction,[30,136] with internalization of occludin, ZO-1 and -2, and cingulin.[137,138] Similar findings have been demonstrated in renal allografts with post-ischemic injury.[139] One consequence of this is loss of the epithelial barrier and backleak of filtrate into the interstitium,[139,140] which can partly explain the oliguria seen in severe acute kidney injury. Renal ischemia also impairs tight junction fence function, and disrupts epithelial polarity, including mislocalization of the Na-K-ATPase,[141,142] which would be predicted to impair transcellular tubular Na reabsorption. This probably contributes to the inappropriately elevated fractional excretion of Na (F_ENa) commonly observed clinically in ATN, and may also stimulate tubuloglomerular feedback, and thereby contribute to the reduction in GFR.

GAP JUNCTIONS AND CONNEXIN HEMICHANNELS

Structure and Biochemical Composition

Gap junctions are non-selective channels located in the plasma membranes of adjacent cells, and are critical to intercellular communication in most cell types. Functionally, they serve to couple non-excitable cells by allowing the passage of small molecules (less than 1 kDa in size), such as inorganic ions and secondary messengers, between the two cells.[143] Gap junction channels exhibit open and closed configurations, and this gating can be regulated by intracellular molecule concentration, mechanical stress, metabolic inhibition, and transjunctional voltage.[144–146]

Each half of the gap junction, known as a connexon, is composed of six transmembrane proteins from the connexin (Cx) family. There are 21 known human Cx isoforms, all of which present the same topology: intracellular N- and C-termini; four transmembrane domains; two extracellular loops with three cysteine residues; and a single intracellular loop. The N-terminus and position of the cysteine residues are conserved. Variability among the Cx isoforms is found in the intracellular loop and C-terminus. Consequently, these regions appear to be responsible for differences that exist in charge and size discrimination among isoforms.[143] Two styles of nomenclature identifying these isoforms are used. Cxs are most commonly identified by their molecular weight in kiloDaltons (e.g., Cx45), which presents a problem when discussing Cx expression in different species, as molecular weight of the same isoform can vary. Alternatively, Cx isoforms are sorted by class (alpha, beta, gamma), and assigned a number (e.g., Gja1).[147] For simplicity, we will adhere to the first naming convention throughout the chapter.

Connexons may be composed of a single isoform (homomeric) or a mix of Cxs (heteromeric), and their trafficking can occur by two pathways. The first involves formation of the connexon at the endoplasmic reticulum, with trafficking through the Golgi apparatus to the plasma membrane. Alternatively, Cx proteins may bypass the Golgi, and form the hexamer once in the plasma membrane. In either case, the transmembrane domains appear to be involved in the oligomerization process. Within the plasma membrane, connexons tend to group together to form a gap junction plaque. The plaque is a highly dynamic body, with gap junction protein half-life in the order of 2–5 hours. This allows for rapid regulation of the composition of Cxs within the plaque in response to cellular demands.[143] Docking of the connexons in adjacent cells creates the intercellular channel, and connexons of different Cx isoforms can couple to form heterotypic gap junctions. Since different Cx isoforms exhibit variation in terms of gating, regulation, and interaction, the modular and combinatorial nature of gap junctions allows a diversity of function within one type of channel.[148,149]

Beyond the typical intercellular gap junction structure, there is evidence that Cxs can regulate intercellular communication without directly coupling cells. Uncoupled connexons form transmembrane pores known as hemichannels, and these Cx hemichannels serve as a conduit between the intra- and extracellular environments, facilitating the transport of signaling molecules such as ATP.[150,151] They are gated, since a constitutively open channel would be lethal to the cell, and are regulated by the same factors as gap junctions.[146,152] Cx hemichannels are thought to conduct intercellular communication via calcium wave propagation. In this model, mechanical or chemical stimulation triggers the opening of Cx hemichannels in a cell which allows ATP to passively move through the hemichannel into the extracellular environment. The newly released ATP binds to purinergic receptors on local cells, triggering an increase in intracellular calcium levels in these cells, thereby propagating the calcium signal. The functionality of Cx hemichannels, however, remains controversial and it is difficult to prove their existence with certainty.[151]

Gap junctions play a vital role in many cellular processes in nearly every cell type in the body, facilitating normal development, physiology, and apoptosis. Consequently, Cx mutations are associated with pathophysiological conditions including Charcot Marie Tooth disease, congenital deafness, and the skin disease erythrokeratoderma variabilis.[147] Outside of hereditary conditions, complex diseases including diabetes and hypertension have been linked to changes in the expression of Cxs.[153–155]

Renal Localization

Renal intercellular channels were first identified in afferent arteriole vascular smooth muscle cells (VSMC) in the 1970s.[156] Electron microscopy images later provided evidence of gap junction channels in the renal tubules, as well as in the renal vasculature.[157,158] Specification of the Cx isoforms that made up renal gap junctions came later, with mRNA expression studies.[159–164] Localization of Cx proteins in the kidney has been limited by the availability of specific antibodies, and by variation among species. As a result, different studies present divergent results. More recently, the development of Cx knockout and reporter mouse models have provided new insight into the expression of Cxs within the nephron, as well as suggesting their significance in renal physiology.[165–170] Table 12.4 summarizes the renal localization of connexin isoforms.

Vasculature

The renal vasculature expresses Cxs37, 40, 43, and 45, which are found in all vascular systems.[159,166,171,172] Within vessels, gap junction coupling occurs between endothelial cells, between the smooth muscle cells, and at the myoendothelial junctions. Cx expression is best defined in endothelial cells. In rodents, Cx40 is abundantly expressed in the afferent arteriole endothelium, with lower levels of Cx37 and 43 also detected.[159,164,173] In the endothelial cells of the efferent arteriole, Cx37 is expressed in rat, while mice express Cx43.[172,173] Beyond the juxtaglomerular apparatus (JGA), all three isoforms are expressed in the vasa recta and vascular bundles.[173] Cx43 is also expressed in the peritubular capillaries and renal veins.[171,173]

The identity of the vascular smooth muscle Cx(s) is less clear. Cx37 was detected in the VSMCs of murine arcuate and interlobular arteries,[173] but not in rats.[159,174] Likewise, one study found evidence of Cx43 in the preglomular media,[161] but later reports have failed to confirm this.[159,164,174] Cx45, which is commonly expressed in smooth muscle cells in other vascular systems,[175] appears to exhibit the same characteristic localization in the kidney. Several studies have shown Cx45 expression in VSMCs of the interlobular, afferent, and efferent arterioles, both by immunohistochemistry and reporter gene mouse methods.[166,171,176] A lack of Cx40 expression in renal VSMCs has been shown in all studies.[159,164,173]

Glomerulus and Juxtaglomerular Apparatus

Both the glomerulus and juxtaglomerular apparatus (JGA) express gap junction proteins abundantly. Podocytes, endothelial cells, mesangial cells, and the renin-producing JG cells are all characterized by gap

TABLE 12.4 Summary of the Localization of Connexin Isoforms in the Kidney

Cx	Renal Localization	Cell Type	Species
26	Proximal tubule*	Epithelial	Mouse
30	Distal nephron	Epithelial	Rat
	Cortical CD, CNT	Intercalated	Mouse, rabbit, rat
30.3	ATL	Epithelial	Mouse, rabbit, rat
	Cortical CD	Intercalated	Mouse, rabbit, rat
32	Proximal tubule*	Epithelial	Mouse
37	Arcuate artery; IA*	VSMC	Mouse
	RA; AA, EA	Endothelial	Mouse, rat
	Vasa recta	Pericytes	Rat
	Vascular bundles	Endothelial	Mouse
	JGA*	Granular, mesangial	Mouse, rat
	Proximal tubule, TAL, DCT	Epithelial	Mouse, rat
	CNT, CD	Principal > Intercalated	Mouse, rat
40	RA; Arcuate artery; IA; AA	Endothelial	Mouse, rat
	Vasa recta	Endothelial	Rat
	Vascular bundles	Endothelial	Mouse
	Glomerulus	Endothelial*, mesangial	Mouse
	JGA	Endothelial*, granular, mesangial	Mouse, rat
43	RA, AA, EA	Endothelial, VSMC*	Mouse, rat
	Peritubular capillaries	Endothelial	Mouse
	Vascular bundles, vasa recta	Endothelial	Rat
	Renal veins	Endothelial	Mouse
	Glomerulus	Podocytes	Human
	Proximal tubule	Epithelial	Human
	Inner medullary CD*	Epithelial	Rat
45	IA, AA, EA	VSMC	Mouse
	Glomerulus	Mesangial, podocytes	Mouse
	JGA	Granular*, mesangial	Mouse

*indicates conflicting localization data; > indicates stronger than. (Table modified with permission from Hanner, F., Sorensen, C. M., Holstein-Rathlou, N. H. and Peti-Peterdi, J. (2010). Connexins and the kidney. Am. J. Physiol. Regul. Integr. Comp. Physiol. 298, R1143–1155. Copyright American Physiological Society).
ATL: Ascending thin limb of the loop of Henle; AA: afferent arteriole; CD: Collecting duct; CNT: connecting tubule; DCT: Distal convoluted tubule; EA: efferent arteriole; IA: interlobular artery. JGA: juxtaglomerular apparatus; RA: renal artery; TAL: thick ascending limb of the loop of Henle; VSMC: vascular smooth muscle cell.

junction coupling. In addition, the different cell types that constitute the JGA appear to be interconnected by gap junctions. The macula densa cells, however, are exclusive of gap junctions.[157,177] Again, Cx isoform localization has been primarily determined by antibody-based localization techniques, and as a result many studies present differing data. In podocytes, Cx43 is primarily expressed, although Cx45 has been detected in these cells as well.[178] Glomerular endothelial cells showed expression of Cx40 in one study,[164] but another report was unable to reproduce this finding.[173] Cx40 is, however, prominently expressed in the intra- and extraglomerular mesangium, as well as the renin-producing JG cells.[159,171–173] Cx37 follows a similar, if weaker, pattern of expression as Cx40. Expression in the intraglomerular mesangium is limited to the vascular pole, and lower levels of Cx37 staining are found in the extraglomerular mesangium and JG cells.[172,173] The glomerulus also appears to be positive for Cx45, and studies using reporter gene mouse models indicated Cx45 expression was localized to the mesangial cells. These studies also showed Cx45-positive cells expressing renin, leading to the conclusion that the JG cells express Cx45 alongside Cx40.[166] This study conflicts with antibody-based approaches, where Cx45 labeling is only evident in JG cells during embryogenesis.[171] Finally, the endothelial cells of the afferent and efferent arterioles closest to the glomerulus lack any Cx protein expression or structural evidence of gap junction coupling.[164]

Tubules

Despite the recognition of gap junction channels in the proximal tubules,[179] attempts to localize Cx isoforms along the nephron present a complex picture, with different techniques and species again producing varying expression patterns. In the proximal tubules, Cxs26, 37, and 43 have been detected in epithelial cells; however, proximal tubule Cx expression appears weak at best.[180,181] The distal tubules present much stronger levels of gap junction protein expression, but lack any signs of gap junction coupling by freeze-fracture microscopy.[182] While no Cx isoforms have been found in the descending limb of the loop of Henle, the ascending portion expresses Cxs30 and 30.3 in the apical membrane of the thin limb, and Cx37 in the basolateral membrane of the thick limb.[170,180,183] Continuing the pattern seen in Henle's loop Cx30, 30.3, and 37 are expressed along the connecting segment and collecting duct, and are similarly localized to the apical or basolateral membranes. Both Cx30 and Cx30.3 were detected in the intercalated, but not the principal, cells of connecting segment and cortical collecting duct.[170,180,183] The absence of gap junction coupling between epithelial cells, as well as their subcellular localization to apical or basolateral membranes, suggests these Cx proteins may form hemichannels in this region of the nephron. This hypothesis appears to be supported by a study of primary proximal tubular cells that expressed Cx43 and demonstrated hemichannel activity.[182]

Physiological Function in the Kidney

As is the case with the localization of renal connexins, the physiological significance of gap junction proteins in the kidney is still emerging, and current research does not always present a consistent story. To study the functional roles of gap junction proteins in the kidney, both specific methods and non-specific inhibitors are used. In the latter category are chemical gap junction uncouplers and blockers, such as heptanol and carbenoxolone, that inhibit channel activity without regard to their component proteins.[184–186] More specific approaches focus on the Cx isoforms involved, and include the use of knockout mice and gap mimetic peptides.[187–190] These peptides mimic the extracellular loop sequence of Cx isoforms and block gap junction channels through an unknown mechanism.

Vascular Conduction and Myoendothelial Communication

One key area where gap junction coupling influences renal vascular physiology is in the propagation of a vasomotor response, either dilatory or constrictive, along vessels in response to local stimulation. In rat preglomerular arteries and vasa recta, vascular conducted responses are inhibited by the gap junction uncouplers carbenoxolone and 18α-glycyrrhetinic acid.[185,186] Interestingly, vasodilation and vasoconstriction responses appear to involve gap junctions via independent mechanisms. Studies with Cx40 knockout mice and Cx40 mimetic peptides both demonstrated an inhibitory effect of Cx40 loss on vasodilation in mesenteric arteries.[188,190] Conversely, Cx37, but not Cx40, knockout mice have reduced vasoconstriction responses.[190]

Vasomotor stimulation may also spread between the endothelium and the smooth muscle cells of renal vessels via myoendothelial gap junctions. Vasodilation of smooth muscle occurs in response to the hyperpolarization of endothelial cells, and this response can be inhibited by non-specific gap junction blockers in rabbit renal arteries.[184] A similar effect was observed with Cx40 and Cx43 mimetic peptides; however, the inhibition appears to be dependent on the agonist used.[187,189]

Tubuloglomerular Feedback and Renin Secretion

The JGA regulates renal hemodynamics through the mechanism of tubuloglomerular feedback (TGF),

whereby variations in tubular fluid flow and composition in the cortical thick ascending limb are detected by the macula densa cells, and trigger changes in afferent arteriole diameter and renin secretion in response (see also Chapter 24). The TGF mechanism involves a calcium wave (Figure 12.8) which propagates through the JGA.[191] The regulation of calcium signaling by Cxs is well-established in other systems,[143] and given the extensive gap junction coupling in the JGA it appears that this calcium wave is similarly controlled. The gap junction uncoupler 18α-glycyrrhetinic acid and heptanol inhibit the spread of calcium in the JGA in response to an increase in flow.[191] Two possible pathways explain how gap junction proteins coordinate calcium signaling in the JGA. Calcium may spread in coupled cells directly via intercellular gap junction communication. Alternatively, the calcium wave may propagate indirectly via purinergic signaling. In this model, increased intracellular calcium triggers the opening of Cx hemichannels and the release of ATP/UTP to the extracellular environment, which subsequently binds purinergic receptors on neighboring cells, increasing intracellular $[Ca^{2+}]$.[192] Several observations point to the latter mechanism. Removal of direct contact between cells did not inhibit calcium signaling, and stimulation of cells led to the release of ATP, as measured by a biosensor cell technique. The use of purinergic receptor blockers and ATP scavengers also inhibited the JGA calcium wave.[191,193] Both Cx40 and Cx45 appear to function in the JGA calcium wave. Cx40 siRNA reduced calcium signaling in glomerular endothelial cells, while VSMCs isolated from a conditional Cx45 knockout mouse model or treated with a Cx45 gap mimetic peptide showed reduced propagation speed.[166,193]

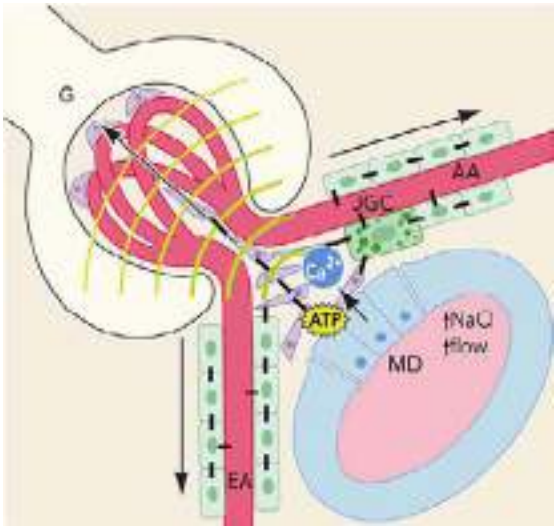

FIGURE 12.8 **Role of gap junctions in the juxtaglomerular apparatus.** Components of the TGF calcium wave include ATP release from macula densa (MD) cells in response to elevations in tubular NaCl and/or flow rate, and paracrine, purinergic calcium signaling. Extracellular ATP-induced elevations in mesangial, vascular smooth muscle (VSMC), and renin-producing juxtaglomerular cell (JGC) $[Ca^{2+}]_i$ are then propagated via gap junctions to distant cells of the afferent arteriole (AA), efferent arteriole (EA), and glomerulus (G) away from the MD region, causing cell contractions. All cell types of the JGA are abundant in gap junctions (−), except for the cells of the MD. Vascular endothelial cells in the AA, EA, and G are also connected with each other and JGCs and VSMCs via gap junctions, and are involved in the calcium wave of TGF. *(Figure modified from Peti-Peterdi, J., Toma, I., Sipos, A. and Vargas, S. L. (2009). Multiphoton imaging of renal regulatory mechanisms. Physiology (Bethesda)* ***24****, 88–96. Copyright American Physiological Society.)*

Renin secretion regulation and control of systemic blood pressure also require gap junction protein expression. Cx40 knockout mice have high blood pressure and high plasma renin, due primarily to the lack of negative feedback control of renin secretion by blood pressure and angiotensin II. Regulation of renin by beta adrenergic receptor stimulation and dietary salt is not affected.[194,195] These mice also show aberrant expression of renin in the preglomerular interstitium, extraglomerular mesangium, and glomerular tuft, while the afferent arteriole VSMCs are entirely devoid of renin. Cx45-deficient mice, which lack Cx45 in afferent and efferent VSMCs, renin-producing granular cells, and mesangium have a similar phenotype as the Cx40 knockout mouse.[166] Replacement of Cx40 by Cx45 (Cx40KI45) results in a reduction of blood pressure and the return of renin regulation. Normal renin cell recruitment in response to a low-salt diet is not restored.[176] These results indicate that cell−cell communication via Cx channels is critical to renin secretion, and that specifically Cx40 is required for renin expression. Cx37 knockout mice have normal renin regulation, while Cx43 knockout models are lethal. Replacement of Cx43 by Cx32 (Cx43KI32) resulted in reduced plasma renin content, loss of renin regulation, and *de novo* renin expression in endothelial cells.[196] An endothelial-specific Cx43 knockout model, however, does not show any changes to renin secretion.[197]

Tubule Function

The role of Cxs in tubular function remains largely unclear despite the expression of Cx proteins along the nephron and gap junction coupling in the proximal tubules. The expression of Cxs 30 and 37 is regulated by dietary salt, with high salt increasing Cx30 expression at the apical membrane of medullary collecting ducts, and low salt increasing cortical expression of Cx37, presumably along basolateral membranes.[180,183] It is hypothesized that Cx hemichannels regulate epithelial transport along the nephron via purinergic signaling (Figure 12.9). Activation of P2 purinergic receptors in the nephron is known to regulate renal transporters, modulating sodium, potassium, and

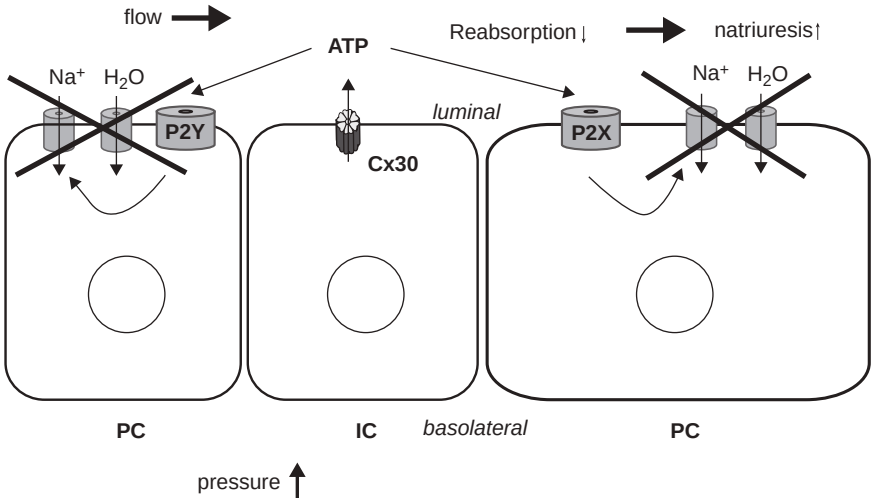

FIGURE 12.9 **Schematic illustration of mechanically induced, Cx30 hemichannel-mediated ATP release into the tubular lumen in the cortical collecting duct (CCD), and its paracrine effects on salt and water reabsorption, natriuresis, and diuresis.** Increases in intra-renal pressure and/or tubular flow rate that accompany blood pressure elevations result in the opening of Cx30 hemichannels at the luminal membrane of CCD intercalated cells (IC), and the release of ATP. Stimulation of luminal purinergic receptors (mainly P_2Y_2) in adjacent principal cells (PC) results in the inhibition of salt and water reabsorption, and increased natriuresis and diuresis. This inhibitory mechanism is absent in $Cx30^{-/-}$ mice, resulting in a salt retention phenotype. *(Reproduced with permission from Sipos et al. (2009). J. Am. Soc. Nephrol. **20**(8), 1724–1732.[10])*

water reabsorption.[198–200] The close proximity of ectonucleotidases and purinergic receptors in the tubular lumen implies local release of ATP.[199,201] Supporting this hypothesis is recent data which shows that Cx30 knockout mice have an impaired pressure natriuresis response, and that at the cellular level, isolated cortical collecting ducts from these mice release less ATP in response to stimulation than their wild-type counterparts. Based on these findings, the study presented a model suggesting a mechanism by which Cx30 plays a role in pressure natriuresis. Increased pressure/flow in the collecting ducts induces the opening of Cx30 hemichannels, allowing ATP to enter the local extracellular environment and bind local P2 receptors. Activation of these receptors inhibits salt and water reabsorption, resulting in homeostasis.[167]

Roles in Renal Pathology

In the kidney, the role that Cxs plays in pathology is relatively unknown and mostly hypothetical. Human mutations in gap junction genes are linked to a variety of diseases, with altered expression of Cxs leading to the pathophysiology observed. Moreover, primary diseases can result in changes to the levels and localization of gap junction proteins. Global genetic knockouts of several Cx genes are embryonically lethal, indicating their importance during development.[147] Despite the widespread expression of gap junctions in the kidney, mutations in Cx genes have only minor effects on renal organogenesis.[202] As described above, Cx40 knockout mice show defects in JGA renin localization, but this is only apparent after birth.[168]

In adult mutant mice, the predominantly observed renal pathology is hypertension. Genetic loss of Cx40 or Cx45 in the kidney leads to high blood pressure in mice, as does the use of gap mimetic peptides in rats.[166,172,194,195] Knockin mice in which the coding region of Cx43 is replaced by that of Cx32 (Cx43KI32) have a protective phenotype, failing to develop renin-dependent hypertension in response to clipping one renal artery (two-kidney, one-clip model).[196] As detailed in the previous section, it appears that the effect on systemic blood pressure is due to the loss of gap junction communication, preventing renin–angiotensin system signaling. There is no known effect of primary hypertension on renal Cx expression in rats or mice. In humans, a variant in the Cx40 promoter that results in lower gene activity is associated with increased risk of high blood pressure, but it is unclear what mechanism drives this correlation.[203]

An increase in vascular intercellular communication and changes in renal Cx expression are also associated with diabetes.[204,205] In diabetic mice, endothelial cells express Cx40 in place of Cx37, and Cx43 is expressed in renin-producing cells *de novo*. The link between Cx expression and diabetes appears to be the nitric oxide (NO) pathway. Diabetes is associated with increased NO availability, and when diabetes was induced in endothelial nitric oxide synthase (eNOS) knockout mice, no changes in Cx expression were observed. Overexpression of eNOS caused changes in renal Cx expression which mimic the pattern seen in diabetes.[173]

ADHERENS JUNCTIONS AND DESMOSOMES

The adherens junction and desmosome are considered together here, because they share a similar function—to maintain the physical association between cells—and similar arrangements of their molecular components. These junctions are found in all epithelia, and there is little about them that is unique to the kidney, so we summarize here the general features of adherens junctions and desmosomes, and refer the reader to several recent reviews for more in-depth discussions.[206,207]

Structure and Localization of the Adherens Junction

The adherens junction in epithelia spans the lateral plasma membranes of adjacent cells at a distance of 10–20 nm, and forms a continuous belt around the circumference of each cell (the "zonula adherens")[206] (Figure 12.2a). The calcium-dependent component is formed by a classical (Type I) cadherin (such as E-cadherin or N-cadherin), a transmembrane protein whose extracellular domain undergoes homophilic adhesion in the presence of calcium, and whose cytoplasmic domain binds to p120-catenin and either β- or γ-catenin (plakoglobin) (Figure 12.10a). These catenins in turn associate with a number of other cytosolic proteins (e.g., α-catenin), some of which are responsible for anchoring the adherens junction to the actin cytoskeleton. In addition, there is a calcium-independent component to the adherens junction, which is formed by members of the nectin family of transmembrane proteins. Nectins, like cadherins, interact via their extracellular domains, although preferentially in a heterotypic manner. Their cytoplasmic terminal has a PDZ-binding motif that associates with afadin (AF6), which can either bind actin directly or indirectly via α-catenin and its partners.

As alluded to in the introduction to this chapter, the mature glomerular slit diaphragm expresses several adherens junction proteins,[208] including P-cadherin, FAT,[209] α-, β-, and γ-catenin, and so it has been proposed to represent a modified adherens junction.[208] In the adult renal tubule, there is differential localization of classical cadherins. The proximal tubule predominantly expresses N-cadherin; the thick ascending limb, distal tubule, and collecting duct predominantly express E-cadherin; and Bowman's capsule and the thin limbs of Henle express both isoforms.[210–212] However, the functional significance of this is unknown. In contrast, the cytoplasmic catenins are ubiquitously expressed in all tubule segments.[213]

Structure and Localization of Desmosomes

Desmosomes are specialized anchoring junctions that serve as tethers for cytoplasmic intermediate filaments.[207] While they are particularly important for maintaining the integrity of tissues subject to mechanical stress, such as the epidermis and myocardium, they are also present in all epithelia and are thought to play roles in tissue morphogenesis. Desmosomes appear as

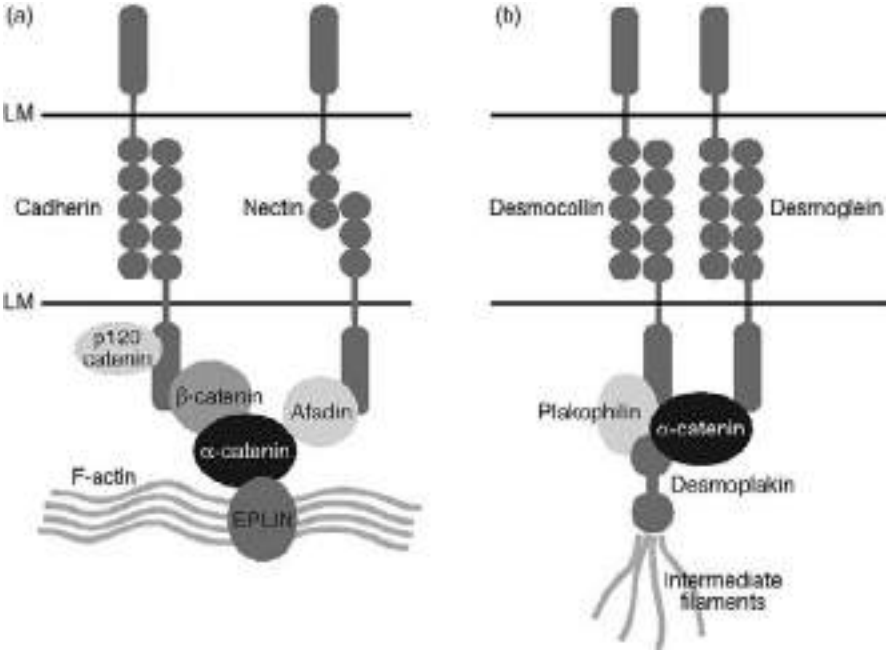

FIGURE 12.10 **Molecular components of the adherens junction (a) and desmosome (b).** LM: lateral plasma membrane.

pairs of dense, disc-shaped plaques on opposing lateral membranes of adjacent cells (Figure 12.2a). The desmosomal cadherins, desmoglein and desmocollin, mediate cell–cell adhesion via their extracellular domains (Figure 12.10b). The armadillo proteins, plakoglobin/γ-catenin, and plakophilin act as adaptor proteins that link the cytoplasmic domain of the desmosomal cadherins to desmoplakin, which in turn links the desmosomal plaque to the intermediate filament cytoskeleton.

In mice, desmoplakin and plakoglobin are expressed at highest levels in the distal tubule, connecting tubule, and collecting duct,[211] whereas in humans, plakoglobin, like other catenins, is expressed along the entire nephron.[213]

Adherens and Desmosomal Junctions in Kidney Disease

In ischemic acute kidney injury, as discussed earlier, there is disruption of the tight junction. This is also associated with degradation of E-cadherin, and dissolution of the adherens junction complex.[139,214] Polycystin-1, the product of the gene PKD1 that is mutated in autosomal dominant polycystic kidney disease (ADPKD), is localized to adherens junctions and desmosomes in renal epithelia, and participates in cell–cell adhesion.[215] In ADPKD, both adherens and desmosomal junctions are abnormal in morphology.[216] Most of the cysts are of distal tubule origin, yet they lack E-cadherin at the adherens junction, and N-cadherin is expressed in its place.[217]

References

[1] Farquhar MG, Palade GE. Junctional complexes in various epithelia. J Cell Biol 1963;17:375–412.
[2] Kachar B, Reese TS. Evidence for the lipidic nature of tight junction strands. Nature 1982;296(5856):464–6.
[3] Pinto da Silva P, Kachar B. On tight-junction structure. Cell 1982;28(3):441–50.
[4] Stevenson BR, Goodenough DA. Zonulae occludentes in junctional complex-enriched fractions from mouse liver: preliminary morphological and biochemical characterization. J Cell Biol 1984;98(4):1209–21.
[5] van Meer G, Gumbiner B, Simons K. The tight junction does not allow lipid molecules to diffuse from one epithelial cell to the next. Nature 1986;322(6080):639–41.
[6] van Meer G, Simons K. The function of tight junctions in maintaining differences in lipid composition between the apical and the basolateral cell surface domains of MDCK cells. EMBO J 1986;5(7):1455–64.
[7] Nichols GE, Borgman CA, Young Jr. WW. On tight junction structure: Forssman glycolipid does not flow between MDCK cells in an intact epithelial monolayer. Biochem Biophys Res Commun 1986;138(3):1163–9.
[8] Brown D, Orci L. Junctional complexes and cell polarity in the urinary tubule. J Electron Microsc Tech 1988;9(2):145–70.
[9] Orci L, Humbert F, Brown D, Perrelet A. Membrane ultrastructure in urinary tubules. Int Rev Cytol 1981;73:183–242.
[10] Taugner R, Boll U, Zahn P, Forssmann WG. Cell junctions in the epithelium of Bowman's capsule. Cell Tissue Res 1976;172(4):431–46.
[11] Kuhn K, Reale E, Wermbter G. The glomeruli of the human and the rat kidney studied by freeze-fracturing. Cell Tissue Res 1975;160(2):177–91.
[12] Humbert F, Montesano R, Perrelet A, Orci L. Junctions in developing human and rat kidney: a freeze-fracture study. J Ultrastruct Res 1976;56(2):202–14.
[13] Reeves W, Caulfield JP, Farquhar MG. Differentiation of epithelial foot processes and filtration slits: sequential appearance of occluding junctions, epithelial polyanion, and slit membranes in developing glomeruli. Lab Invest 1978;39(2):90–100.
[14] Caulfield JP, Reid JJ, Farquhar MG. Alterations of the glomerular epithelium in acute aminonucleoside nephrosis. Evidence for formation of occluding junctions and epithelial cell detachment. Lab Invest 1976;34(1):43–59.
[15] Ryan GB, Leventhal M, Karnovsky MJ. A freeze-fracture study of the junctions between glomerular epithelial cells in aminonucleoside nephrosis. Lab Invest 1975;32(3):397–403.
[16] Pricam C, Humbert F, Perrelet A, Amherdt M, Orci L. Intercellular junctions in podocytes of the nephrotic glomerulus as seen with freeze-fracture. Lab Invest 1975;33(3):209–18.
[17] Claude P. Morphological factors influencing transepithelial permeability: a model for the resistance of the zonula occludens. J Membr Biol 1978;39:219–32.
[18] Kaye GI, Pappas GD. Studies on the cornea. I. The fine structure of the rabbit cornea and the uptake and transport of colloidal particles by the cornea *in vivo*. J Cell Biol 1962;12:457–79.
[19] Martinez-Palomo A, Erlij D, Bracho H. Localization of permeability barriers in the frog skin epithelium. J Cell Biol 1971;50(2):277–87.
[20] Rau WS, Fromter E. Electrical properties of the medullary collecting ducts of the golden hamster kidney. II. The transepithelial resistance. Pflugers Arch 1974;351(2):113–31.
[21] Isaacson LC. Resolution of parameters in the equivalent electrical circuit of the sodium transport mechanism across toad skin. J Membr Biol 1977;30(4):301–17.
[22] Rector Jr FC, Martinez-Maldonado M, Brunner FP, Seldin DW. Evidence for passive reabsorption of NaCl in proximal tubule of rat kidney. J Clin Invest 1966;45:1060–70.
[23] Bourdeau JE, Burg MB. Voltage dependence of calcium transport in the thick ascending limb of Henle's loop. Am J Physiol 1979;236:F357–64.
[24] Barry PH, Diamond JM, Wright EM. The mechanism of cation permeation in the rabbit gallbladder: dilution potentials and biionic potentials. J Membr Biol 1971;4:358–94.
[25] Wright EM, Barry PH, Diamond JM. The mechanism of cation permeation in the rabbit gallbladder: conductances, the current–voltage relation, the concentration dependence of anion–cation discrimination, and the calcium competition effect. J Membr Biol 1971;4:331–57.
[26] Fromter E, Diamond J. Route of passive ion permeation in epithelia. Nat New Biol 1972;235(53):9–13.
[27] Wang Q, Margolis B. Apical junctional complexes and cell polarity. Kidney Int 2007;72(12):1448–58.
[28] Goldstein B, Macara IG. The PAR proteins: fundamental players in animal cell polarization. Dev Cell 2007;13(5):609–22.
[29] Dragsten PR, Blumenthal R, Handler JS. Membrane asymmetry in epithelia: Is the tight junction a barrier to diffusion in the plasma membrane? Nature 1981;294(5843):718–22.
[30] Bacallao R, Garfinkel A, Monke S, Zampighi G, Mandel LJ. ATP depletion: a novel method to study junctional properties

in epithelial tissues. I. Rearrangement of the actin cytoskeleton. J Cell Sci 1994;107(Pt 12):3301–13.
[31] Mandel LJ, Bacallao R, Zampighi G. Uncoupling of the molecular "fence" and paracellular "gate" functions in epithelial tight junctions. Nature 1993;361(6412):552–5.
[32] Takakuwa R, Kokai Y, Kojima T, Akatsuta T, Tobioka H, Sawada N, et al. Uncoupling of gate and fence functions of MDCK cells by the actin-depolymerizing reagent mycalolide B. Exp Cell Res 2000;257(2):238–44.
[33] Stevenson BR, Siliciano JD, Mooseker MS, Goodenough DA. Identification of ZO-1: a high molecular weight polypeptide associated with the tight junction (zonula occludens) in a variety of epithelia. J Cell Biol 1986;103(3):755–66.
[34] Furuse M, Hirase T, Itoh M, Nagafuchi A, Yonemura S, Tsukita S, et al. Occludin: a novel integral membrane protein localizing at tight junctions [see comments]. J Cell Biol 1993;123(6 Pt 2):1777–88.
[35] Balda MS, Whitney JA, Flores C, Gonzalez S, Cereijido M, Matter K. Functional dissociation of paracellular permeability and transepithelial electrical resistance and disruption of the apical–basolateral intramembrane diffusion barrier by expression of a mutant tight junction membrane protein. J Cell Biol 1996;134(4):1031–49.
[36] McCarthy KM, Francis SA, McCormack JM, Lai J, Rogers RA, Skare IB, et al. Inducible expression of claudin-1-myc but not occludin-VSV-G results in aberrant tight junction strand formation in MDCK cells. J Cell Sci 2000;113:3387–98.
[37] Saitou M, Fujimoto K, Doi Y, Itoh M, Fujimoto T, Furuse M, et al. Occludin-deficient embryonic stem cells can differentiate into polarized epithelial cells bearing tight junctions. J Cell Biol 1998;141(2):397–408.
[38] Yu AS, McCarthy KM, Francis SA, McCormack JM, Lai J, Rogers RA, et al. Knockdown of occludin expression leads to diverse phenotypic alterations in epithelial cells. Am J Physiol Cell Physiol 2005;288(6):C1231–1241.
[39] Furuse M, Sasaki H, Fujimoto K, Tsukita S. A single gene product, claudin-1 or -2, reconstitutes tight junction strands and recruits occludin in fibroblasts. J Cell Biol 1998;143(2):391–401.
[40] Saitou M, Furuse M, Sasaki H, Schulzke JD, Fromm M, Takano H, et al. Complex phenotype of mice lacking occludin, a component of tight junction strands. Mol Biol Cell 2000;11(12):4131–42.
[41] Schulzke JD, Gitter AH, Mankertz J, Speigel S, Siedler U, Amashe S, et al. Epithelial transport and barrier function in occludin-deficient mice. Biochim Biophys Acta 2005;1669 (1):34–42.
[42] Ikenouchi J, Furuse M, Furuse K, Sasaki H, Tsukita S. Tricellulin constitutes a novel barrier at tricellular contacts of epithelial cells. J Cell Biol 2005;171(6):939–45.
[43] Krug SM, Amasheh S, Richter JF, Milatz S, Gunzel D, Westphal JK, et al. Tricellulin forms a barrier to macromolecules in tricellular tight junctions without affecting ion permeability. Mol Biol Cell 2009;20(16):3713–24.
[44] Riazuddin S, Ahmed ZM, Fanning AS, Lagzeil A, Kitajiri S, Ramzan K, et al. Tricellulin is a tight-junction protein necessary for hearing. Am J Hum Genet 2006;79(6):1040–51.
[45] Furuse M, Fujita K, Hiiragi T, Fujimoto K, Tsukita S. Claudin-1 and -2: novel integral membrane proteins localizing at tight junctions with no sequence similarity to occludin. J Cell Biol 1998;141(7):1539–50.
[46] Furuse M, Tsukita S. Claudins in occluding junctions of humans and flies. Trends Cell Biol 2006;16(4):181–8.
[47] Van Itallie CM, Anderson JM. Claudins and epithelial paracellular transport. Annu Rev Physiol 2006;68:403–29.
[48] Angelow S, Ahlstrom R, Yu AS. Biology of claudins. Am J Physiol Renal Physiol 2008;295(4):F867–876.
[49] Kubota K, Furuse M, Sasaki H, Sonoda N, Fujita K, Nagafuchi A, et al. Ca(2 +)-independent cell-adhesion activity of claudins, a family of integral membrane proteins localized at tight junctions. Curr Biol 1999;9(18):1035–8.
[50] Simon DB, Lu Y, Choate KA, Velazquez H, El-Sabban E, Praga M, et al. Paracellin-1, a renal tight junction protein required for paracellular Mg^{2+} resorption. Science 1999;285:103–6.
[51] Van Itallie CM, Anderson JM. Claudins and epithelial paracellular transport. Annu Rev Physiol 2005.
[52] Colegio OR, Van Itallie CM, McCrea HJ, Rahner C, Anderson JM. Claudins create charge-selective channels in the paracellular pathway between epithelial cells. Am J Physiol Cell Physiol 2002;283(1):C142–147.
[53] Colegio OR, Van Itallie C, Rahner C, Anderson JM. Claudin extracellular domains determine paracellular charge selectivity and resistance but not tight junction fibril architecture. Am J Physiol Cell Physiol 2003;284(6):C1346–1354.
[54] Yu AS, Cheng MH, Angelow S, Gunzel D, Kanzawa SA, Schneeberger EE, et al. Molecular basis for cation selectivity in claudin-2-based paracellular pores: identification of an electrostatic interaction site. J Gen Physiol 2009;133(1):111–27.
[55] Angelow S, Yu AS. Structure–function studies of claudin extracellular domains by cysteine-scanning mutagenesis. J Biol Chem 2009;284(42):29205–17.
[56] Piontek J, Winkler L, Wolburg H, Muller SL, Zuleger N, Piehl C, et al. Formation of tight junction: determinants of homophilic interaction between classic claudins. Faseb J 2008;22(1):146–58.
[57] Ruffer C, Gerke V. The C-terminal cytoplasmic tail of claudins 1 and 5 but not its PDZ-binding motif is required for apical localization at epithelial and endothelial tight junctions. Eur J Cell Biol 2004;83(4):135–44.
[58] Arabzadeh A, Troy TC, Turksen K. Role of the Cldn6 cytoplasmic tail domain in membrane targeting and epidermal differentiation *in vivo*. Mol Cell Biol 2006;26(15):5876–87.
[59] Van Itallie CM, Colegio OR, Anderson JM. The cytoplasmic tails of claudins can influence tight junction barrier properties through effects on protein stability. J Membr Biol 2004;199(1):29–38.
[60] Itoh M, Furuse M, Morita K, Kubota K, Saitou M, Tsukita S. Direct binding of three tight junction-associated MAGUKs, ZO-1, ZO-2, and ZO-3, with the COOH termini of claudins. J Cell Biol 1999;147(6):1351–63.
[61] Hamazaki Y, Itoh M, Sasaki H, Furuse M, Tsukita S. Multi-PDZ domain protein 1 (MUPP1) is concentrated at tight junctions through its possible interaction with claudin-1 and junctional adhesion molecule. J Biol Chem 2002;277(1):455–61.
[62] Jeansonne B, Lu Q, Goodenough DA, Chen YH. Claudin-8 interacts with multi-PDZ domain protein 1 (MUPP1) and reduces paracellular conductance in epithelial cells. Cell Mol Biol (Noisy-le-grand) 2003;49(1):13–21.
[63] Kobayashi J, Inai T, Shibata Y. Formation of tight junction strands by expression of claudin-1 mutants in their ZO-1 binding site in MDCK cells. Histochem Cell Biol 2002;117(1):29–39.
[64] González-Mariscal L, Garay E, Quirós M. Regulation of claudins by post-translational modifications and cell signaling cascades. In: Yu AS, editor. Claudins, vol 65. Philadelphia, PA: Elsevier; 2010. p. 113–50.
[65] Ishizaki T, Chiba H, Kojima T, Fujibe M, Soma T, Miyajima H, et al. Cyclic AMP induces phosphorylation of claudin-5 immunoprecipitates and expression of claudin-5 gene in blood–brain-barrier endothelial cells via protein kinase A-dependent and -independent pathways. Exp Cell Res 2003;290(2):275–88.

[66] Ikari A, Matsumoto S, Harada H, Takagi K, Hayashi H, Suzuki Y, et al. Phosphorylation of paracellin-1 at Ser217 by protein kinase A is essential for localization in tight junctions. J Cell Sci 2006;119(Pt 9):1781–9.
[67] Tanaka M, Kamata R, Sakai R. EphA2 phosphorylates the cytoplasmic tail of Claudin-4 and mediates paracellular permeability. J Biol Chem 2005;280(51):42375–82.
[68] Yamauchi K, Rai T, Kobayashi K, Sohara E, Suzuki T, Itoh T, et al. Disease-causing mutant WNK4 increases paracellular chloride permeability and phosphorylates claudins. Proc Natl Acad Sci USA 2004;101(13):4690–4.
[69] Le Moellic C, Boulkroun S, Gonzalez-Nunez D, Dublineau I, Cluzead F, Fay M, et al. Aldosterone and tight junctions: modulation of claudin-4 phosphorylation in renal collecting duct cells. Am J Physiol Cell Physiol 2005;289(6): C1513–1521.
[70] Tatum R, Zhang Y, Lu Q, Kim K, Jeansonne BG, Chen YH. WNK4 phosphorylates ser(206) of claudin-7 and promotes paracellular Cl(−) permeability. FEBS Lett 2007;581 (20):3887–91.
[71] Van Itallie CM, Gambling TM, Carson JL, Anderson JM. Palmitoylation of claudins is required for efficient tight-junction localization. J Cell Sci 2005;118(Pt 7):1427–36.
[72] Kiuchi-Saishin Y, Gotoh S, Furuse M, Takasuga A, Tano Y, Tsukita S. Differential expression patterns of claudins, tight junction membrane proteins, in mouse nephron segments. J Am Soc Nephrol 2002;13(4):875–86.
[73] Ohse T, Pippin JW, Vaughan MR, Brinkkoetter PT, Krofft RD, Shankland SJ. Establishment of conditionally immortalized mouse glomerular parietal epithelial cells in culture. J Am Soc Nephrol 2008;19(10):1879–90.
[74] Inai T, Kobayashi J, Shibata Y. Claudin-1 contributes to the epithelial barrier function in MDCK cells. Eur J Cell Biol 1999;78(12):849–55.
[75] Crabtree C. Sex differences in the structure of Bowman's capsule in the mouse. Science 1940;91(2360):299.
[76] Dietert SC. The columnar cells occurring in the parietal layer of Bowman's capsule. Cellular fine structure and protein transport. J Cell Biol 1967;35(2):435–44.
[77] Enck AH, Berger UV, Yu AS. Claudin-2 is selectively expressed in proximal nephron in mouse kidney. Am J Physiol Renal Physiol 2001;281(5):F966–974.
[78] Ohse T, Chang AM, Pippin JW, Jarad G, Hudkins KL, Alpers CE, et al. A new function for parietal epithelial cells: a second glomerular barrier. Am J Physiol Renal Physiol 2009;297(6):F1566–1574.
[79] Torelli G, Milla E, Faelli A, Costantini S. Energy requirement for sodium reabsorption in the *in vivo* rabbit kidney. Am J Physiol 1966;211(3):576–80.
[80] Knox FG, Fleming JS, Rennie DW. Effects of osmotic diuresis on sodium reabsorption and oxygen consumption of kidney. Am J Physiol 1966;210(4):751–9.
[81] Berry CA, Rector Jr. FC. Mechanism of proximal NaCl reabsorption in the proximal tubule of the mammalian kidney. Semin Nephrol 1991;11(2):86–97.
[82] Kokko JP, Burg MB, Orloff J. Characteristics of NaCl and water transport in the renal proximal tubule. J Clin Invest 1971;50(1):69–76.
[83] Schafer JA, Troutman SL, Andreoli TE. Volume reabsorption, transepithelial potential differences, and ionic permeability properties in mammalian superficial proximal straight tubules. J Gen Physiol 1974;64(5):582–607.
[84] Neumann KH, Rector Jr. FC. Mechanism of NaCl and water reabsorption in the proximal convoluted tubule of rat kidney. J Clin Invest 1976;58(5):1110–1.
[85] Krug SM, Gunzel D, Conrad MP, et al. Claudin-17 forms tight junction channels with distinct anion selectivity. Cell Mol Life Sci 2012;69(20):2765–78.
[86] Furuse M, Furuse K, Sasaki H, Tsukita S. Conversion of zonulae occludentes from tight to leaky strand type by introducing claudin-2 into Madin–Darby canine kidney I cells. J Cell Biol 2001;153(2):263–72.
[87] Amasheh S, Meiri N, Gitter AH, Schoneberg T, Mankertz J, Schulzke JD, et al. Claudin-2 expression induces cation-selective channels in tight junctions of epithelial cells. J Cell Sci 2002;115(Pt 24):4969–76.
[88] Van Itallie C, Fanning AS, Anderson JM. Reversal of charge selectivity in cation or anion selective epithelial lines by expression of different claudins. Am J Physiol Cell Physiol 2003;286:F1078–1084.
[89] Muto S, Hata M, Taniguchi J, Tsururoka S, Moriwaki K, Saitou M, et al. Claudin-2-deficient mice are defective in the leaky and cation-selective paracellular permeability properties of renal proximal tubules. Proc Natl Acad Sci USA 2010;107(17):8011–6.
[90] Van Itallie CM, Rogan S, Yu AS, Seminario-Vidal L, Holmes J, Anderson JM. Two splice variants of claudin-10 in the kidney create paracellular pores with different ion selectivities. Am J Physiol Renal Physiol 2006;291:F1288–1299.
[91] Quigley R, Baum M. Developmental changes in rabbit proximal straight tubule paracellular permeability. Am J Physiol Renal Physiol 2002;283(3):F525–531.
[92] Abuazza G, Becker A, Williams SS, Chakravarty S, Truong HT, Lin F, et al. Claudins 6, 9, and 13 are developmentally expressed renal tight junction proteins. Am J Physiol Renal Physiol 2006;291(6):F1132–1141.
[93] Sas D, Hu M, Moe OW, Baum M. Effect of claudins 6 and 9 on paracellular permeability in MDCK II cells. Am J Physiol Regul Integr Comp Physiol 2008;295(5):R1713–1719.
[94] Schnermann J, Chou CL, Ma T, Traynor T, Knepper MA, Verkman AS. Defective proximal tubular fluid reabsorption in transgenic aquaporin-1 null mice. Proc Natl Acad Sci USA 1998;95(16):9660–4.
[95] Ullrich KJ, Rumrich G, Schmidt-Nielsen B. Reflection coefficient of different nonelectrolytes in the proximal convolution of the rat kidney. Federation Proc 1967;26:375.
[96] Weinstein AM. Transport by epithelia with compliant lateral intercellular spaces: asymmetric oncotic effects across the rat proximal tubule. Am J Physiol 1984;247(5 Pt 2):F848–862.
[97] Preisig PA, Berry CA. Evidence for transcellular osmotic water flow in rat proximal tubules. Am J Physiol 1985;249(1 Pt 2): F124–131.
[98] Kovbasnjuk O, Leader JP, Weinstein AM, Spring KR. Water does not flow across the tight junctions of MDCK cell epithelium. Proc Natl Acad Sci USA 1998;95(11):6526–30.
[99] Rosenthal R, Milatz S, Krug SM. et al. The tight junction protein claudin-2 forms a paracellular water channel. (Abstr); New Orleans 2009 [Paper presented at: Experimental Biology Annual Meeting].
[100] Gunzel D, Yu AS. Function and regulation of claudins in the thick ascending limb of Henle. Pflugers Arch 2009;458 (1):77–88.
[101] Burg MB, Green N. Function of the thick ascending limb of Henle's loop. Am J Physiol 1973;224(3):659–68.
[102] Greger R. Cation selectivity of the isolated perfused cortical thick ascending limb of Henle's loop of rabbit kidney. Pflugers Arch 1981;390(1):30–7.
[103] Greger R. Chloride reabsorption in the rabbit cortical thick ascending limb of the loop of Henle. A sodium dependent process. Pflugers Arch 1981;390(1):38–43.

[104] Burg M, Good D. Sodium chloride coupled transport in mammalian nephrons. Annu Rev Physiol 1983;45:533–47.
[105] Angelow S, El-Husseini R, Kanzawa SA, Yu AS. Renal localization and function of the tight junction protein, claudin-19. Am J Physiol Renal Physiol 2007;293(1):F166–177.
[106] Konrad M, Schaller A, Seelow D, et al. Mutations in the tight-junction gene claudin 19 (CLDN19) are associated with renal magnesium wasting, renal failure, and severe ocular involvement. Am J Hum Genet 2006;79(5):949–57.
[107] Hou J, Renigunta A, Gomes AS, Hou M, Paul DL, Waldegger S, et al. Claudin-16 and claudin-19 interaction is required for their assembly into tight junctions and for renal reabsorption of magnesium. Proc Natl Acad Sci USA 2009;106(36):15350–5.
[108] Gong Y, Renigunta V, Himmerkus N, et al. Claudin-14 regulates renal Ca(++) transport in response to CaSR signalling via a novel microRNA pathway. The EMBO journal. 2012;31 (8):1999–2012.
[109] Ikari A, Hirai N, Shiroma M, Harada H, Sakai H, Hayashi H, et al. Association of paracellin-1 with ZO-1 augments the reabsorption of divalent cations in renal epithelial cells. J Biol Chem 2004;279(52):54826–32.
[110] Kausalya PJ, Amasheh S, Gunzel D, Wurps H, Muller D, Fromm M, et al. Disease-associated mutations affect intracellular traffic and paracellular Mg^{2+} transport function of Claudin-16. J Clin Invest 2006;116(4):878–91.
[111] Hou J, Paul DL, Goodenough DA. Paracellin-1 and the modulation of ion selectivity of tight junctions. J Cell Sci 2005;118(Pt 21):5109–18.
[112] Hou J, Renigunta A, Konrad M, Gomes AS, Schneeberger EE, Paul DL, et al. Claudin-16 and claudin-19 interact and form a cation-selective tight junction complex. J Clin Invest 2008;118 (2):619–28.
[113] Hou J, Shan Q, Wang T, Gomes AS, Yan Q, Paul DL, et al. Transgenic RNAi depletion of claudin-16 and the renal handling of magnesium. J Biol Chem 2007;282 (23):17114–22.
[114] Milatz S, Krug SM, Rosenthal R, Gunzel D, Muller D, Schulzke JD, et al. Claudin-3 acts as a sealing component of the tight junction for ions of either charge and uncharged solutes. Biochim Biophys Acta 2010;1798(11):2048–57.
[115] Van Itallie C, Rahner C, Anderson JM. Regulated expression of claudin-4 decreases paracellular conductance through a selective decrease in sodium permeability. J Clin Invest 2001;107(10):1319–27.
[116] Yu AS, Enck AH, Lencer WI, Schneeberger EE. Claudin-8 expression in MDCK cells augments the paracellular barrier to cation permeation. J Biol Chem 2003;278:17350–9.
[117] Ben-Yosef T, Belyantseva IA, Saunders TL, et al. Claudin 14 knockout mice, a model for autosomal recessive deafness DFNB29, are deaf due to cochlear hair cell degeneration. Hum Mol Genet 2003;12(16):2049–61.
[118] Jovov B, Van Itallie CM, Shaheen NJ, Carson JL, Gambling TM, Anderson JM, et al. Claudin-18: a dominant tight junction protein in Barrett's esophagus and likely contributor to its acid resistance. Am J Physiol Gastrointest Liver Physiol 2007;293(6): G1106–1113.
[119] Angelow S, Kim KJ, Yu AS. Claudin-8 modulates paracellular permeability to acidic and basic ions in MDCK II cells. J Physiol 2006;571:15–26.
[120] Pech V, Kim YH, Weinstein AM, Everett LA, Pham TD, Wall SM. Angiotensin II increases chloride absorption in the cortical collecting duct in mice through a pendrin-dependent mechanism. Am J Physiol Renal Physiol 2007;292(3): F914–920.
[121] Leviel F, Hubner CA, Houillier P, et al. The Na^+-dependent chloride-bicarbonate exchanger SLC4A8 mediates an electroneutral Na^+ reabsorption process in the renal cortical collecting ducts of mice. J Clin Invest 2010;120 (5):1627–35.
[122] Sansom SC, Weinman EJ, O'Neil RG. Microelectrode assessment of chloride-conductive properties of cortical collecting duct. Am J Physiol 1984;247(2 Pt 2):F291–302.
[123] Hou J, Renigunta A, Yang J, Waldegger S. Claudin-4 forms paracellular chloride channel in the kidney and requires claudin-8 for tight junction localization. Proc Natl Acad Sci USA 2010;107(42):18010–5.
[124] Alexandre MD, Lu Q, Chen YH. Overexpression of claudin-7 decreases the paracellular Cl^- conductance and increases the paracellular Na^+ conductance in LLC-PK1 cells. J Cell Sci 2005;118:2683–93.
[125] Hou J, Gomes AS, Paul DL, Goodenough DA. Study of claudin function by RNA interference. J Biol Chem 2006;281 (47):36117–23.
[126] Tatum R, Zhang Y, Salleng K, Lu Z, Lin JJ, Lu Q, et al. Renal salt wasting and chronic dehydration in claudin-7-deficient mice. Am J Physiol Renal Physiol 2010;298(1): F24–34.
[127] Uhlich E, Baldamus CA, Ullrich KJ. [Effect of aldosterone on sodium transport in the collecting ducts of the mammalian kidney]. Pflugers Arch 1969;308(2):111–26.
[128] Uhlich E, Halbach R, Ullrich KJ. [Influence of aldosterone on 24Na-efflux in collecting ducts of rats]. Pflugers Arch 1970;320 (3):261–4.
[129] Sands JM, Nonoguchi H, Knepper MA. Hormone effects on NaCl permeability of rat inner medullary collecting duct. Am J Physiol 1988;255(3 Pt 2):F421–428.
[130] O'Neil RG, Helman SI. Transport characteristics of renal collecting tubules: influences of DOCA and diet. Am J Physiol 1977;233(6):F544–558.
[131] Wilson FH, Disse-Nicodeme S, Choate KA, et al. Human hypertension caused by mutations in WNK kinases. Science 2001;293(5532):1107–12.
[132] Wilson FH, Kahle KT, Sabath E, Lalioti MD, Rapson AK, Hoover RS, et al. Molecular pathogenesis of inherited hypertension with hyperkalemia: The Na-Cl co-transporter is inhibited by wild-type but not mutant WNK4. Proc Natl Acad Sci USA 2003;100(2):680–4.
[133] Yang CL, Angell J, Mitchell R, Ellison DH. WNK kinases regulate thiazide-sensitive Na-Cl co-transport. J Clin Invest 2003;111(7):1039–45.
[134] Kahle KT, Macgregor GG, Wilson FH, et al. Paracellular Cl^- permeability is regulated by WNK4 kinase: insight into normal physiology and hypertension. Proc Natl Acad Sci USA 2004;101(41):14877–82.
[135] Vitari AC, Deak M, Morrice NA, Alessi DR. The WNK1 and WNK4 protein kinases that are mutated in Gordon's hypertension syndrome phosphorylate and activate SPAK and OSR1 protein kinases. Biochem J 2005;391(Pt 1):17–24.
[136] Molitoris BA, Falk SA, Dahl RH. Ischemia-induced loss of epithelial polarity. Role of the tight junction. J Clin Invest 1989;84 (4):1334–9.
[137] Gopalakrishnan S, Raman N, Atkinson SJ, Marrs JA. Rho GTPase signaling regulates tight junction assembly and protects tight junctions during ATP depletion. Am J Physiol 1998;275(3 Pt 1):C798–809.
[138] Tsukamoto T, Nigam SK. Tight junction proteins form large complexes and associate with the cytoskeleton in an ATP depletion model for reversible junction assembly. J Biol Chem 1997;272(26):16133–9.

[139] Kwon O, Nelson WJ, Sibley R, Huie P, Scandling JD, Dafoe D, et al. Backleak, tight junctions, and cell–cell adhesion in post-ischemic injury to the renal allograft. J Clin Invest 1998;101 (10):2054–64.
[140] Moran SM, Myers BD. Pathophysiology of protracted acute renal failure in man. J Clin Invest 1985;76(4):1440–8.
[141] Mandel LJ, Doctor RB, Bacallao R. ATP depletion: a novel method to study junctional properties in epithelial tissues. II. Internalization of Na + ,K(+)-ATPase and E-cadherin. J Cell Sci 1994;107(Pt 12):3315–24.
[142] Kwon O, Corrigan G, Myers BD, Sibley R, Scandling JD, Dafoe D, et al. Sodium reabsorption and distribution of $Na^{+/}K^{+}$-ATPase during postischemic injury to the renal allograft. Kidney Int 1999;55(3):963–75.
[143] Evans WH, Martin PE. Gap junctions: structure and function (Review). Mol Membr Biol 2002;19(2):121–36.
[144] Bao L, Sachs F, Dahl G. Connexins are mechanosensitive. Am J Physiol Cell Physiol 2004;287(5):C1389–1395.
[145] Qu Y, Dahl G. Function of the voltage gate of gap junction channels: selective exclusion of molecules. Proc Natl Acad Sci USA 2002;99(2):697–702.
[146] Contreras JE, Sanchez HA, Eugenin EA, Speidel D, Theis M, Willecke K, et al. Metabolic inhibition induces opening of unapposed connexin 43 gap junction hemichannels and reduces gap junctional communication in cortical astrocytes in culture. Proc Natl Acad Sci USA 2002;99(1):495–500.
[147] Willecke K, Eiberger J, Degen J, Eckardt D, Romualdi A, Güldenagel M, et al. Structural and functional diversity of connexin genes in the mouse and human genome. Biol Chem 2002;383(5):725–37.
[148] Rackauskas M, Kreuzberg MM, Pranevicius M, Willecke K, Verselis VK, Bukauskas FF. Gating properties of heterotypic gap junction channels formed of connexins 40, 43, and 45. Biophys J 2007;92(6):1952–65.
[149] Bukauskas FF, Angele AB, Verselis VK, Bennett MV. Coupling asymmetry of heterotypic connexin 45/connexin 43-EGFP gap junctions: properties of fast and slow gating mechanisms. Proc Natl Acad Sci USA 2002;99(10):7113–8.
[150] Ebihara L. New roles for connexons. News Physiol Sci 2003;18:100–3.
[151] Spray DC, Ye ZC, Ransom BR. Functional connexin "hemichannels:" a critical appraisal. Glia 2006;54(7):758–73.
[152] Paul DL, Ebihara L, Takemoto LJ, Swenson KI, Goodenough DA. Connexin46, a novel lens gap junction protein, induces voltage-gated currents in nonjunctional plasma membrane of *Xenopus* oocytes. J Cell Biol 1991;115(4):1077–89.
[153] Figueroa XF, Duling BR. Gap junctions in the control of vascular function. Antioxid Redox Signal 2009;11(2):251–66.
[154] Hamelin R, Allagnat F, Haefliger JA, Meda P. Connexins diabetes and the metabolic syndrome. Curr Protein Pept Sci 2009;10(1):18–29.
[155] Haefliger JA, Demotz S, Braissant O, Suter E, Waeber B, Nicod P, et al. Connexins 40 and 43 are differentially regulated within the kidneys of rats with renovascular hypertension. Kidney Int 2001;60(1):190–201.
[156] Biava C, West M. Fine structure of normal human juxtaglomerular cells. I. General structure and intercellular relationships. Am J Pathol 1966;49(4):679–721.
[157] Taugner R, Schiller A, Kaissling B, Kriz W. Gap junctional coupling between the JGA and the glomerular tuft. Cell Tissue Res 1978;186(2):279–85.
[158] Pricam C, Humbert F, Perrelet A, Orci L. A freeze-etch study of the tight junctions of the rat kidney tubules. Lab Invest 1974;30(3):286–91.
[159] Arensbak B, Mikkelsen HB, Gustafsson F, Christensen T, Holstein-Rathlou NH. Expression of connexin 37, 40, and 43 mRNA and protein in renal preglomerular arterioles. Histochem Cell Biol 2001;115(6):479–87.
[160] Guo R, Liu L, Barajas L. RT-PCR study of the distribution of connexin 43 mRNA in the glomerulus and renal tubular segments. Am J Physiol 1998;275(2 Pt 2):R439–447.
[161] Barajas L, Liu L, Tucker M. Localization of connexin43 in rat kidney. Kidney Int 1994;46(3):621–6.
[162] Haefliger JA, Bruzzone R, Jenkins NA, Gilbert DJ, Copeland NG, Paul DL. Four novel members of the connexin family of gap junction proteins. Molecular cloning, expression, and chromosome mapping. J Biol Chem 1992;267(3):2057–64.
[163] Hillis GS, Duthie LA, Mlynski R, McKay NG, Mistry S, Macleod AM, et al. The expression of connexin 43 in human kidney and cultured renal cells. Nephron 1997;75(4):458–63.
[164] Hwan Seul K, Beyer EC. Heterogeneous localization of connexin40 in the renal vasculature. Microvasc Res 2000;59 (1):140–8.
[165] de Wit C, Roos F, Bolz SS, Kirchoff S, Krüger O, Willecke K, et al. Impaired conduction of vasodilation along arterioles in connexin40-deficient mice. Circ Res 2000;86(6):649–55.
[166] Hanner F, von Maltzahn J, Maxeiner S, Toma I, Sipos A, Krüger O, et al. Connexin45 is expressed in the juxtaglomerular apparatus and is involved in the regulation of renin secretion and blood pressure. Am J Physiol Regul Integr Comp Physiol 2008;295(2):R371–380.
[167] Sipos A, Vargas SL, Toma I, Hanner F, Willecke K, Peti-Peterdi J. Connexin 30 deficiency impairs renal tubular ATP release and pressure natriuresis. J Am Soc Nephrol 2009;20 (8):1724–32.
[168] Kurtz L, Schweda F, de Wit C, Kriz W, Witzgall R, Warth R, et al. Lack of connexin 40 causes displacement of renin-producing cells from afferent arterioles to the extraglomerular mesangium. J Am Soc Nephrol 2007;18(4):1103–11.
[169] Kruger O, Maxeiner S, Kim JS, van Rijen HV, de Bakker JM, Eckhardt D, et al. Cardiac morphogenetic defects and conduction abnormalities in mice homozygously deficient for connexin40 and heterozygously deficient for connexin45. J Mol Cell Cardiol 2006;41(5):787–97.
[170] Hanner F, Schnichels M, Zheng-Fischhofer Q, Yang LE, Toma I, Willecke K, et al. Connexin 30.3 is expressed in the kidney but not regulated by dietary salt or high blood pressure. Cell Commun Adhes 2008;15(1):219–30.
[171] Kurtz L, Janssen-Bienhold U, Kurtz A, Wagner C. Connexin expression in renin-producing cells. J Am Soc Nephrol 2009;20 (3):506–12.
[172] Takenaka T, Inoue T, Kanno Y, Okada H, Meaney KR, Hill CE, et al. Expression and role of connexins in the rat renal vasculature. Kidney Int 2008;73(4):415–22.
[173] Zhang J, Hill CE. Differential connexin expression in preglomerular and postglomerular vasculature: accentuation during diabetes. Kidney Int 2005;68(3):1171–85.
[174] Gustafsson F, Mikkelsen HB, Arensbak B, Thuneberg L, Neve S, Jensen LJ, et al. Expression of connexin 37, 40 and 43 in rat mesenteric arterioles and resistance arteries. Histochem Cell Biol 2003;119(2):139–48.
[175] Rummery NM, Hill CE. Vascular gap junctions and implications for hypertension. Clin Exp Pharmacol Physiol 2004;31 (10):659–67.
[176] Schweda F, Kurtz L, de Wit C, Janssen-Bienhold U, Kurtz A, Wagner C. Substitution of connexin40 with connexin45 prevents hyperreninemia and attenuates hypertension. Kidney Int 2009;75(5):482–9.

[177] Taugner R, Kirchheim H, Forssmann WG. Myoendothelial contacts in glomerular arterioles and in renal interlobular arteries of rat, mouse and *Tupaia belangeri*. Cell Tissue Res 1984;235(2):319–25.

[178] Sawai K, Mukoyama M, Mori K, et al. Redistribution of connexin43 expression in glomerular podocytes predicts poor renal prognosis in patients with type 2 diabetes and overt nephropathy. Nephrol Dial Transplant 2006;21 (9):2472–7.

[179] Kuhn K, Reale E. Junctional complexes of the tubular cells in the human kidney as revealed with freeze-fracture. Cell Tissue Res 1975;160(2):193–205.

[180] Stoessel A, Himmerkus N, Bleich M, Bachmann S, Theilig F. Connexin 37 is localized in renal epithelia and responds to changes in dietary salt intake. Am J Physiol Renal Physiol 2010;298(1):F216–223.

[181] Butterweck A, Gergs U, Elfgang C, Willecke K, Traub O. Immunochemical characterization of the gap junction protein connexin45 in mouse kidney and transfected human HeLa cells. J Membr Biol 1994;141(3):247–56.

[182] Vergara L, Bao X, Bello-Reuss E, Reuss L. Do connexin 43 gap-junctional hemichannels activate and cause cell damage during ATP depletion of renal-tubule cells? Acta Physiol Scand 2003;179(1):33–8.

[183] McCulloch F, Chambrey R, Eladari D, Peti-Peterdi J. Localization of connexin 30 in the luminal membrane of cells in the distal nephron. Am J Physiol Renal Physiol 2005;289(6): F1304–1312.

[184] Kagota S, Yamaguchi Y, Nakamura K, Kunitomo M. Characterization of nitric oxide- and prostaglandin-independent relaxation in response to acetylcholine in rabbit renal artery. Clin Exp Pharmacol Physiol 1999;26 (10):790–6.

[185] Sorensen CM, Salomonsson M, Braunstein TH, Nielsen MS, Holstein-Rathlou NH. Connexin mimetic peptides fail to inhibit vascular conducted calcium responses in renal arterioles. Am J Physiol Regul Integr Comp Physiol 2008;295(3): R840–847.

[186] Zhang Q, Cao C, Mangano M, Zhang Z, Silldorf EP, Lee-Kwon W, et al. Descending vasa recta endothelium is an electrical syncytium. Am J Physiol Regul Integr Comp Physiol 2006;291(6):R1688–1699.

[187] De Vriese AS, Van de Voorde J, Lameire NH. Effects of connexin-mimetic peptides on nitric oxide synthase- and cyclooxygenase-independent renal vasodilation. Kidney Int 2002;61 (1):177–85.

[188] de Wit C, Roos F, Bolz SS, Pohl U. Lack of vascular connexin 40 is associated with hypertension and irregular arteriolar vasomotion. Physiol Genomics 2003;13(2):169–77.

[189] Karagiannis J, Rand M, Li CG. Role of gap junctions in endothelium-derived hyperpolarizing factor-mediated vasodilatation in rat renal artery. Acta Pharmacol Sin 2004;25 (8):1031–7.

[190] McKinnon RL, Lidington D, Bolon M, Ouellette Y, Kidder GM, Tyml K. Reduced arteriolar conducted vasoconstriction in septic mouse cremaster muscle is mediated by nNOS-derived NO. Cardiovasc Res 2006;69(1):236–44.

[191] Peti-Peterdi J. Calcium wave of tubuloglomerular feedback. Am J Physiol Renal Physiol 2006;291(2):F473–480.

[192] Cotrina ML, Lin JH, Alves-Rodrigues A, Liu S, Li J, Azmi-Ghadimi H, et al. Connexins regulate calcium signaling by controlling ATP release. Proc Natl Acad Sci USA 1998;95 (26):15735–40.

[193] Toma I, Kang JJ, Sipos A, Vargas S, Bansal E, Hanner F, et al. Succinate receptor GPR91 provides a direct link between high glucose levels and renin release in murine and rabbit kidney. J Clin Invest 2008;118(7):2526–34.

[194] Krattinger N, Capponi A, Mazzolai L, Aubert JF, Caille D, Nicod P, et al. Connexin40 regulates renin production and blood pressure. Kidney Int 2007;72(7):814–22.

[195] Wagner C, de Wit C, Kurtz L, Grunberger C, Kurtz A, Schweda F. Connexin40 is essential for the pressure control of renin synthesis and secretion. Circ Res 2007;100 (4):556–63.

[196] Haefliger JA, Krattinger N, Martin D, Pedrazzini T, Capponi A, Döring B, et al. Connexin43-dependent mechanism modulates renin secretion and hypertension. J Clin Invest 2006;116 (2):405–13.

[197] Liao Y, Day KH, Damon DN, Duling BR. Endothelial cell-specific knockout of connexin 43 causes hypotension and bradycardia in mice. Proc Natl Acad Sci USA 2001;98 (17):9989–94.

[198] Schwiebert EM, Kishore BK. Extracellular nucleotide signaling along the renal epithelium. Am J Physiol Renal Physiol 2001;280(6):F945–963.

[199] Vallon V. P2 receptors in the regulation of renal transport mechanisms. Am J Physiol Renal Physiol 2008;294(1):F10–27.

[200] Praetorius HA, Leipziger J. Intrarenal purinergic signaling in the control of renal tubular transport. Annu Rev Physiol 2010;72:377–93.

[201] Le Hir M, Kaissling B. Distribution and regulation of renal ecto-5′-nucleotidase: implications for physiological functions of adenosine. Am J Physiol 1993;264(3 Pt 2):F377–387.

[202] Willecke K, Kirchhoff S, Plum A, Temme A, Thonnissen E, Ott T. Biological functions of connexin genes revealed by human genetic defects, dominant negative approaches and targeted deletions in the mouse. Novartis Found Symp 1999;219:76–88 discussion 88-96

[203] Firouzi M, Kok B, Spiering W, et al. Polymorphisms in human connexin40 gene promoter are associated with increased risk of hypertension in men. J Hypertens 2006;24(2):325–30.

[204] Kuroki T, Inoguchi T, Umeda F, Ueda F, Nawata H. High glucose induces alteration of gap junction permeability and phosphorylation of connexin-43 in cultured aortic smooth muscle cells. Diabetes 1998;47(6):931–6.

[205] Inoguchi T, Ueda F, Umeda F, Yamashita T, Nawata H. Inhibition of intercellular communication via gap junction in cultured aortic endothelial cells by elevated glucose and phorbol ester. Biochem Biophys Res Commun 1995;208(2):492–7.

[206] Meng W, Takeichi M. Adherens junction: molecular architecture and regulation. Cold Spring Harb Perspect Biol 2009;1(6): a002899.

[207] Huber O. Structure and function of desmosomal proteins and their role in development and disease. Cell Mol Life Sci 2003;60(9):1872–90.

[208] Reiser J, Kriz W, Kretzler M, Mundel P. The glomerular slit diaphragm is a modified adherens junction. J Am Soc Nephrol 2000;11(1):1–8.

[209] Inoue T, Yaoita E, Kurihara H, et al. FAT is a component of glomerular slit diaphragms. Kidney Int 2001;59(3):1003–12.

[210] Nouwen EJ, Dauwe S, van der Biest I, De Broe ME. Stage- and segment-specific expression of cell-adhesion molecules N-CAM, A-CAM, and L-CAM in the kidney. Kidney Int 1993;44(1):147–58.

[211] Piepenhagen PA, Peters LL, Lux SE, Nelson WJ. Differential expression of Na(+)-K(+)-ATPase, ankyrin, fodrin, and E-cadherin along the kidney nephron. Am J Physiol 1995;269(6 Pt 1):C1417–1432.

[212] Tani T, Laitinen L, Kangas L, Lehto VP, Virtanen I. Expression of E- and N-cadherin in renal cell carcinomas, in renal cell

carcinoma cell lines *in vitro* and in their xenografts. Int J Cancer 1995;64(6):407–14.

[213] Kwon O, Myers BD, Sibley R, Dafoe D, Alfrey E, Nelson WJ. Distribution of cell membrane-associated proteins along the human nephron. J Histochem Cytochem 1998;46(12):1423–34.

[214] Bush KT, Tsukamoto T, Nigam SK. Selective degradation of E-cadherin and dissolution of E-cadherin- catenin complexes in epithelial ischemia. Am J Physiol Renal Physiol 2000;278(5): F847–852.

[215] Streets AJ, Newby LJ, O'Hare MJ, Bukanov NO, Ibraghimov-Beskrovnaya O, Ong AC. Functional analysis of PKD1 transgenic lines reveals a direct role for polycystin-1 in mediating cell-cell adhesion. J Am Soc Nephrol 2003;14(7):1804–15.

[216] Russo RJ, Husson H, Joly D, Bukanov NO, Patey N, Knebelmann B, et al. Impaired formation of desmosomal junctions in ADPKD epithelia. Histochem Cell Biol 2005;124 (6):487–97.

[217] Roitbak T, Ward CJ, Harris PC, Bacallao R, Ness SA, Wandinger-Ness A. A polycystin-1 multiprotein complex is disrupted in polycystic kidney disease cells. Mol Biol Cell 2004;15(3):1334–46.

[218] Abramow M, Orci L. On the "tightness" of the rabbit descending limb of the loop of Henle: physiological and morphological evidence. Int J Biochem 1980;12(1-2):23–7.

[219] Hegel U, Fromter E, Wick T. [Transmural electrical resistance of the proximal convoluted rat kidney tubule]. Pflugers Arch Gesamte Physiol Menschen Tiere 1967;294(4):274–90.

[220] Greger R. Ion transport mechanisms in thick ascending limb of Henle's loop of mammalian nephron. Physiol Rev 1985;65 (3):760–97.

[221] Malnic G, Giebisch G. Some electrical properties of distal tubular epithelium in the rat. Am J Physiol 1972;223 (4):797–808.

[222] Helman SI, Grantham JJ, Burg MB. Effect of vasopressin on electrical resistance of renal cortical collecting tubules. Am J Physiol 1971;220(6):1825–32.

[223] Wen H, Watry DD, Marcondes MC, Fox HS. Selective decrease in paracellular conductance of tight junctions: role of the first extracellular domain of claudin-5. Mol Cell Biol 2004;24 (19):8408–17.

[224] Angelow S, Schneeberger EE, Yu AS. Claudin-8 expression in renal epithelial cells augments the paracellular barrier by replacing endogenous claudin-2. J Membr Biol 2007;215(2-3):147–59.

[225] Alexandre MD, Jeansonne BG, Renegar RH, Tatum R, Chen YH. The first extracellular domain of claudin-7 affects paracellular Cl^- permeability. Biochem Biophys Res Commun 2007;357 (1):87–91.

[226] Kurihara H, Anderson JM, Kerjaschki D, Farquhar MG. The altered glomerular filtration slits seen in puromycin aminonucleoside nephrosis and protamine sulfate-treated rats contain the tight junction protein ZO-1. Am J Pathol 1992;141 (4):805–16.

[227] Li WY, Huey CL, Yu AS. Expression of claudin-7 and -8 along the mouse nephron. Am J Physiol Renal Physiol 2004;286(6): F1063–1071.

[228] Kirk A, Campbell S, Bass P, Mason J, Collins J. Differential expression of claudin tight junction proteins in the human cortical nephron. *Nephrol Dial Transplant* 2010;25(7):2107–19.

CHAPTER

13

Principles of Cell Signaling

Lloyd Cantley

Yale University School of Medicine, New Haven, CT, USA

INTRODUCTION

The successful transition from single cells to complex multicellular organisms has required the development of mechanisms for cells to communicate with each other, so as to act in concert during processes such as nutrient acquisition, motility, and defense. The most fundamental of these are cell–cell junctions that serve as structural organizers, but also provide information that individual cells can utilize to orient themselves in relation to the remainder of the organism. In larger species that contain multiple organs and cell types, the need to communicate information over long distances has led to the development of diffusible factors that are secreted by one cell and travel to distant cells. These factors can be delivered locally, via the circulation (e.g., hormones and cytokines) or via the nervous system (e.g., neurotransmitters), and are recognized by the appropriate cell surface receptor on the recipient cell. The complex nature of the numerous signals presented to the cell at any given point in time has led to the development of an intricate array of receptor-activated intracellular second messengers that, by undergoing a coordinated series of interactions and enzymatic alterations, can transduce the information presented on the cell surface to effector molecules that mediate the appropriate cellular response.

The kidney serves to protect the internal milieu of higher organisms from perturbations due to the accumulation of metabolic products, as well as those resulting from fluctuations in the intake or loss of water and various salts. To regulate this intricate function, the body must continuously monitor the composition and quantity of the extracellular fluid, and then signal the nephron to appropriately regulate glomerular filtration and tubular cell function in response to changes in these parameters. Regulation of these exquisitely precise events requires that the cells of the kidney are able to respond to signals emanating from distant sites, and then efficiently communicate in an intercellular and intracellular manner to coordinate the response. This chapter will provide an overview of several of the most common receptors and intracellular second messenger pathways that are utilized in this process.

CELL SURFACE RECEPTORS

In the best studied pathway of cell signaling, a first messenger is secreted by one group of cells and travels either to distant cells (endocrine factors) or to local cells (autocrine or paracrine factors), where it binds to a specific receptor. The first messengers in these classic pathways are generally either proteins (growth factors, cytokines), catecholamines (epinephrine, dopamine) or steroids (mineralocorticoids, sex hormones), although receptors have been identified for multiple circulating factors including lipids (e.g., lysophosphatidic acid), ions (e.g., calcium), eicosanoids (e.g., prostaglandin E_2), sugars (e.g., glucose), nucleosides (e.g., ATP), and gases (e.g., nitric oxide). Most of these receptors are located on the cell surface and have an extracellular region (domain) that recognizes and binds to the specific ligand. This ligand-binding domain is connected via one or more transmembrane segments to the intracellular (cytosolic) domain that undergoes a change in conformation or activity in response to ligand binding, and thus initiates the activation and/or modification of intracellular second messengers. In contrast to these cell surface receptors, steroid receptors, which are discussed later in this chapter, are typically located in the cytoplasm. The lipophilic steroid ligands are capable of crossing the cell membrane and binding the receptor, which then initiates signaling events by translocating into the nucleus where the ligand–receptor complex can regulate gene transcription.

Seldin and Giebisch's The Kidney, Fifth Edition.
DOI: http://dx.doi.org/10.1016/B978-0-12-381462-3.00013-6

© 2013 Elsevier Inc. All rights reserved.

Based on their structure, the type of ligand that they bind, and the principle second messengers that are activated, classical cell surface receptors can be grouped into G-protein coupled receptors, receptor tyrosine kinases (RTKs), serine/threonine kinase receptors, and receptor-like phosphatases. However, it has become increasingly clear that other surface proteins serve as signaling initiators to transduce information about the environment surrounding the cell. Thus, cell−cell and cell−matrix adhesion molecules initiate signaling cascades that regulate cell shape, differentiation, proliferation, and survival. The following section will provide a brief overview of these various signaling initiators, focused on those presently considered to be important in regulating normal renal development and maintaining adult kidney homeostasis.

G-Protein Coupled Receptors

The receptor sub-type that is responsible for mediating the signaling responses of the greatest number of ligands in the kidney is probably the G-protein-coupled receptor (GPCR). GPCRs make up the largest family of cell surface receptors, with over 800 members predicted from the sequence of the human genome (reviewed in [1]) (Figure 13.1). GPCRs are transmembrane proteins with their amino terminus on the cell exterior, seven transmembrane α helical segments, and the carboxyl terminus in the cell interior. This arrangement results in three extracellular loops and three intracellular loops joining the transmembrane segments. They bind to extracellular ligands such as epinephrine, dopamine, angiotensin II, adenosine, vasopressin, calcium, and parathyroid hormone, and mediate their intracellular actions.

The extracellular loops serve as the primary binding site for the specific GPCR ligand, with the amino terminus also contributing to the binding site for some ligands. The intracellular loops, most critically the 5−6 loop, serve as the binding site for the principal GPCR intracellular effectors, the heterotrimeric G-proteins. These small GDP/GTP-binding protein complexes are made up of α-, β-, and γ-subunits, with the α-subunit serving as the GDP/GTP-binding site, and the βγ-subunits acting both as regulators of α-subunit localization, and independently as intracellular signaling effectors. The existence of multiple different α-, β-, and γ-subunits allows for hundreds of potential combinations of heterotrimeric G-proteins, and thus imparts specificity of response to the individual GPCR and its ligand.

In the absence of receptor activation, the α-subunit is bound to GDP, and associates with the βγ-subunits at the membrane. However, following ligand binding to the extracellular surface of the GPCR, a conformational change of the receptor results in disassociation of GDP, and binding of GTP to the α-subunit. The binding of GTP stimulates disassociation of the α-subunit from the βγ-subunits and the receptor. The GTP-loaded α-subunit can then associate with its intermediary effectors (such as adenylyl cyclase and phospholipase), while the βγ-subunits can associate with and regulate independent effectors, such as ion channels and the β adrenergic receptor kinase (βARK) (reviewed in [2,3]).

The protein products of the 16 mammalian genes encoding Gα-subunits have been grouped into four classes, the $G_{s\alpha}$ (stimulatory for adenylyl cyclase), $G_{i\alpha}$ (inhibitory for adenylyl cyclase), $G_{q/11\alpha}$ (regulators of phospholipase Cβ (PLCβ)), and $G_{12\alpha}$ (regulators of RhoGEF). Binding of the appropriate GTP-loaded Gα-subunit to its primary effector results in the

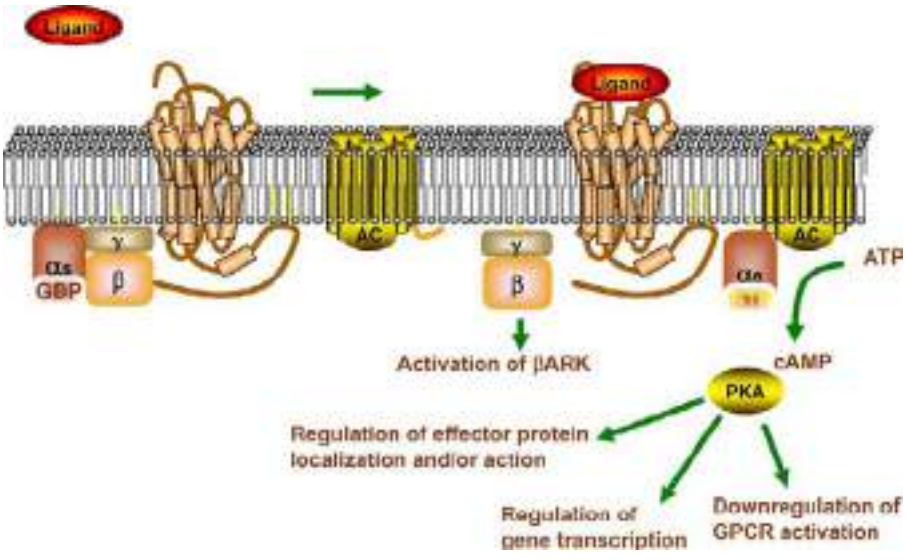

FIGURE 13.1 GPCR signaling through adenylate cyclase. Binding of the extracellular ligand to the GPCR results in the exchange of GTP for GDP on Gα, and its disassociation from the αβγ heterotrimer. βγ can then associate with and activate downstream effectors such as the β-adregeneric receptor kinase (BARK), while the GTP-loaded α-subunit can bind and regulate effectors including adenylate cyclase (AC). In the example shown, Gsα activates AC to convert ATP to cAMP, and thus stimulates downstream PKA signaling.

activation or inhibition of effector function; for example, adenylyl cyclase catalyzes the cyclation of ATP to form 3′,5′-cyclic AMP (cAMP), an intracellular second messenger that can bind and activate downstream signaling proteins such as protein kinase A (PKA). This reaction is activated by GTP-$G_{s\alpha}$ binding to adenylyl cyclase and inhibited by GTP-$G_{i\alpha}$ binding. In addition, $\beta\gamma$ binding to adenylyl cyclase can augment its activation by GTP-$G_{s\alpha}$.

An important concept in all forms of signal transduction is the ability of the cell to carefully control the location, amplitude, and duration of the signal. Signal amplification is the process whereby the cell can regulate the amplitude of the signal. For example, a single GPCR can generate between tens and hundreds of GTP-coupled $G\alpha$-subunits, which can subsequently bind to and activate similar numbers of adenylyl cyclase enzymes, which in turn generate multiple copies of cAMP. The number and availability of the intracellular effector enzymes and substrates thus determines the level of signal amplification following the activation of relatively few receptors on the cell surface.

Just as important as signal amplification is the ability of the cell to downregulate the signaling pathway once the desired response has been initiated. For GPCRs, this occurs in several ways. First, the α-subunit is itself a GTPase, meaning that it hydrolyzes GTP to form GDP and inorganic phosphate. This hydrolysis occurs spontaneously following GTP binding to $G\alpha$, but can be augmented by the association of specific RGS proteins (regulators of G-protein signaling) with the GDP/$G\alpha$ complex, as this interaction stabilizes the inactivated state. Once the $G\alpha$-subunit is in the GDP-bound state, it can associate again with the $\beta\gamma$-subunit to regenerate the inactive heterotrimeric G-protein.

In addition, many GPCRs are themselves inactivated by a process called homologous desensitization. As has been noted above, the $\beta\gamma$-subunits can associate with the cytosolic protein βARK. βARK, also known as GRK2, is a member of the G-protein-coupled receptor kinases (GRKs) that, following association with $G_{\beta\gamma}$, phosphorylate the intracellular loops and/or C terminus of ligand-associated GPCRs on serine and/or threonine residues. This phosphorylation results in the association of β-arrestin with the receptor, mediating the uncoupling of the ligand−receptor complex from the heterotrimeric G-proteins, and thus diminishing its activity. Binding of β-arrestin has also been shown to target the receptor−ligand complexes to clathrin-coated pits on the cell surface, followed by internalization and either lysosomal degradation or recycling of the inactivated receptor to the cell surface.[4]

The downstream GPCR effector adenylyl cyclase is also subject to phosphorylation-dependent inhibition. As noted above, activated adenylyl cyclase catalyzes the formation of cAMP, which in turn associates with and activates PKA. This enzyme, an intracellular serine/threonine kinase, has multiple phosphorylation substrates within the cell. Phosphorylation of these substrates can regulate their activity, cellular localization, and/or their interaction with other proteins. One phosphorylation substrate is adenylyl cyclase itself, resulting in inhibition of cAMP production. A second substrate is the GPCR. In a process known as heterologous desensitization, activation of PKA by a non-GPCR signal can result in phosphorylation of the GPCR and subsequent inhibition of ligand-mediated GPCR activation.[5]

Receptors for Dopamine and AVP are GPCRs that Regulate Adenylyl Cyclase

A prototypic family of GPCRs in the kidney is the dopamine receptors. There are five dopamine receptors presently described (D_1−D_5), and they are further sub-classified into D_1-like (D_1 and D_5) or D_2-like (D_2−D_4). The D_1-like receptors are associated with $G_{s\alpha}$, and therefore activate adenylyl cyclase, whereas the D_2-like receptors inhibit adenylyl cyclase activity (reviewed in [6,7]). In the kidney, D_1-like and D_2-like receptors are expressed throughout the tubules. The net effect of activating these receptors is the induction of a salt and water diuresis, although by different mechanisms in the different tubular segments. Dopamine-mediated activation of D_1 receptors in the proximal tubule results in activation of adenylyl cyclase, leading to cAMP-dependent inhibition of the activity of NHE-3, NaPi-2, and the Na,K-ATPase, thus inhibiting proximal sodium reabsorption. In contrast, activation of the D_2-like receptor D_4 in the cortical collecting duct leads to a water diuresis by preventing vasopressin-stimulated adenylyl cyclase activation. Dopamine receptors also mediate renal vasodilation, and appear to regulate renin secretion. Due to these effects, defects in dopamine receptor function in mice are associated with salt retention, vasoconstriction, and increased blood pressure.[8−10]

Arginine vasopressin (AVP, also known as antidiuretic hormone (ADH)) binds to three GPCRs, the $G_{q/11\alpha}$-linked V1a and V1b receptors, and the $G_{s\alpha}$-linked V2 receptor. V1 receptors are located on several cell types, including smooth muscle cells of blood vessels, where they mediate the vasoconstrictive ("pressor") response of vasopressin, while V2 receptors are located on epithelial cells in the collecting duct and mediate water reabsorption. Binding of vasopressin to the V2 receptor stimulates adenylyl cyclase-mediated cAMP production, which in turn causes insertion of vesicles containing the water channel aquaporin-2 into the apical membrane of collecting

duct cells. By inhibiting adenylyl cyclase activation in these cells, dopamine can partially counteract this water-reabsorptive effect of vasopressin.

GPCRs Can also Signal through Phospholipase C and MAPK

An example of a GPCR that is coupled to PLCβ signaling is the type 1 receptor for angiotensin II ($AT_{1A}R$). Angiotensin II is the eight amino acid peptide product of the angiotensin converting enzyme (ACE)-mediated cleavage of angiotensin I. Angiotensin II is capable of binding to and activating two distinct G-protein coupled receptors, the type 1 receptor (AT_1R) and the type 2 receptor (AT_2R). The predominant actions of angiotensin in the kidney and adrenal gland are mediated by the AT_1R, including vasoconstriction, smooth muscle hypertrophy, sodium retention, and aldosterone secretion. Most data presently support the idea that the AT_2R receptor acts as an antagonist to AT_1R signaling,[11] although exactly how the AT_2R signals has been much less apparent. The topology of the AT_2R is consistent with a seven transmembrane G-protein coupled receptor, yet it has been controversial as to whether AT_2R in fact signals via traditional G-proteins. There have been several reports that AT_2R can signal via $G_{i\alpha}$, although this has not been universally accepted (reviewed in [12]). Other groups have suggested that AT_2R signaling is pertussis-toxin insensitive (i.e., not dependent on $G_{i\alpha}$), and is instead mediated by production of cyclic GMP.[13] It remains unclear whether the generation of cGMP is a direct result of AT_2R activation or is mediated in an autocrine/paracrine fashion by AT_2R-stimulated bradykinin production.[14]

The AT_1R is in the $G_{q/11\alpha}$ family of GPCRs, meaning that binding of angiotensin II to the receptor stimulates GTP-loading of $G_{q\alpha}$ which in turn associates with and activates phospholipase Cβ (PLCβ) (Figure 13.2). The active form of PLCβ mediates the hydrolysis of phosphotidylinositol 4,5 bisphosphate ($PI_{4,5}P_2$) in the membrane to produce diacylglycerol (DAG) and inositol trisphosphate (IP_3). IP_3 is hydrophilic and enters the cytoplasm where it activates the IP_3 receptor on the surface of the endoplasmic reticulum, thereby stimulating calcium release from internal stores. The simultaneous production of DAG at the membrane, and local release of stored calcium, leads to the recruitment and activation of the classic, calcium-dependent protein kinases C (PKCs). Activation of PKC appears to be required for angiotensin II-mediated renal efferent arteriole vasoconstriction,[15] Na,K-ATPase recruitment to the membrane in proximal tubule cells (resulting in increased proximal sodium reabsorption),[16,17] and stimulation of aldosterone secretion by adrenal zona glomerulosa cells.[18]

In addition to activation of PLCβ, a second signaling pathway that is activated by the AT_1R is the mitogen activated protein kinase (MAPK) pathway. As mentioned earlier, phosphorylation of GPCRs by βARK results in the recruitment of β-arrestin to the receptor complex, and subsequent receptor internalization. β-arrestin has been found to act as a binding scaffold for the core components of the MAPK pathway, including Raf, MEK, and ERK (see "Intracellular Signaling Pathways," below; reviewed in [19]), resulting in the activation of this pathway that mediates cell growth and proliferation.[20–22] This scaffolding function of β-arrestin appears to be both cell type and receptor specific, and can mediate activation of additional intracellular signaling pathways, including the phosphoinositide 3-kinase (PI 3-K) pathway that will be discussed later in this chapter.[23] Activation of these signaling pathways appears to play an important role during kidney development, since newborn mice null for the type I angiotensin receptor or in which angiotensin signaling has been inhibited, have significant renal developmental abnormalities, including renal arterial hypertrophy and papillary atrophy.[24,25]

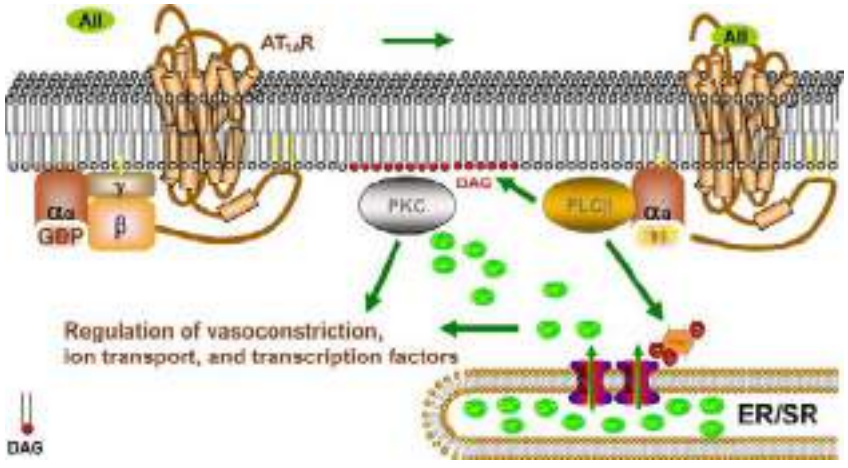

FIGURE 13.2 **Signaling by the angiotensin II (AII) receptor.** Binding of AII results in GTP-loading of the associated Gqα-subunit of the αβγ heterotrimer, which in turn activates phospholipase C β (PLCβ). Activated PLCβ stimulates the hydrolysis of $PI_{4,5}P_2$ in the membrane to form IP3 and diacylglycerol (DAG). IP3 can then bind to its receptor on the endoplasmic or sarcoplasmic reticulum, activating calcium release. The increase in cytosolic calcium can stimulate multiple cellular responses, including activation of PKC (which associates with DAG at the membrane), influx of extracellular calcium via channels at the cell surface, and contraction via actin–myosin coupling.

A second means by which GPCRs can activate MAPK signaling was discovered when the levels of β-arrestin were depleted using RNA interference (RNAi). Under these conditions, angiotensin II was still able to activate MAPK, although to a lesser degree. These experiments uncovered a β-arrestin-independent pathway of angiotensin II-dependent MAPK stimulation that occurs via activation of a second cell surface receptor, a process known as receptor transactivation. As noted above, stimulation of $G_{q\alpha}$ by the $AT_{1A}R$ leads to activation of PKC. PKC, in addition to regulating processes such as ion transport, can activate a cell surface protein called heparin-binding epidermal growth factor (HB-EGF). HB-EGF is one of the ligands for a separate cell surface receptor, the epidermal growth factor receptor (EGFR), and binding of HB-EGF to the EGFR results in the stimulation of multiple signaling events, including MAPK activation (see "Intracellular Signaling Pathways").[18]

Localization and Timing of Pathway Activation Promotes Diverse Cell type Specific Responses

These two independent pathways for activating MAPK signaling provide an example of how scaffolding proteins can compartmentalize signaling within the cell. The β-arrestin-mediated ERK activation is sustained for several hours and occurs in the cytoplasm, whereas the $G_{q\alpha}$/PKC-dependent ERK activation appears to be more transient and primarily within the nucleus. This ability to localize activated ERK in different cellular compartments allows the cell to differentially regulate specific effector proteins, and thus direct distinct cellular outcomes. In the heart, for example, AT_1R-mediated $G_{q\alpha}$/PKC-dependent transactivation of the EGFR, and ultimately MAPK nuclear signaling, is believed to at least partially mediate angiotensin-stimulated cardiac hypertrophy.[26,27]

Many GPCRs can activate multiple Gα-subunits, depending on cellular location and availability. For example, the parathyroid hormone (PTH) receptor can potentially activate $G_{s\alpha}$ (thus activating adenylate cyclase and PKA), $G_{q\alpha}$ (activating PLCβ and PKC), and G_i (inhibiting adenylate cyclase). PTH is an 84 amino acid peptide hormone secreted by the parathyroid gland that acts on bone to increase calcium and phosphate release into the circulation, as well as on the proximal and distal tubules of the kidney to inhibit phosphate reabsorption and stimulate calcium reabsorption, respectively. PTH is proteolytically processed to generate multiple fragments which can bind to and activate the PTH receptor, a class B GPCR (defined by the six conserved cysteine residues that form disulfide bonds in the large extracellular amino terminal domain).[28] Expression of a mutant form of the receptor that selectively fails to activate $G_{q\alpha}$-dependent PLCβ signaling in mice results in abnormalities in bone ossification without a change in serum calcium.[29] The normal serum calcium in these animals suggests that renal tubular calcium handling in these mice is dependent on $G_{s\alpha}$- or G_i-regulated adenylate cyclase signaling, while bone ossification appears to require $G_{q\alpha}$-PLCβ signaling. In support of this hypothesis, complete loss of PTH receptor signaling results in hypocalcemia in addition to bone abnormalities.[30,31] In humans, this is recapitulated by an autosomal recessive mutation in the receptor in patients with Blomstrand chondrodysplasia, a lethal disorder characterized by excessive bone maturation and mineralization.[32]

As noted previously, receptor internalization mediated by β-arrestin is frequently a means by which GPCR are uncoupled from their ligands and signaling is downregulated. For example, PTH related protein (PTHrP) can bind and activate the PTH receptor, leading to GTP-loading of $G_{s\alpha}$ and a transient increase in cAMP followed by receptor desensitization. In contrast, PTH receptor ligands such as PTH_{1-34} (the first 34 amino acids of PTH) can induce a more sustained increase in adenylyl cyclase activation and cAMP levels, leading to systemic responses such as increased vitamin D hydroxylation and higher serum calcium levels. Investigation into the mechanism of this difference has demonstrated that binding of PTH_{1-34} to the PTH receptor leads to internalization of the active receptor−ligand complex in endosomes that also contain adenylyl cyclase, leading to sustained signaling from this intracellular site.[33] These structures, referred to as signaling endosomes, have been shown to mediate signaling via multiple receptor types in addition to GPCR, and to regulate complex cellular responses such as migration, differentiation, and asymmetric division.[34,35]

Kinase Receptors

A second class of transmembrane receptors is the kinase receptors. These proteins typically contain an extracellular ligand-binding domain at the amino terminus, a single membrane-spanning domain, and an intracellular carboxy terminus that includes the kinase domain. In most cases, binding of the ligand to the receptor results in homodimerization of two receptor molecules, bringing the intracellular kinase domains into close proximity where they phosphorylate substrate residues on the adjacent receptor. This phosphorylation step generates binding sites for the recruitment of intracellular signaling molecules, as well as further activating the kinase domain so that non-receptor substrates recruited to the complex can also be phosphorylated.

Tyrosine Kinase Receptors

The largest class of kinase receptors is the tyrosine kinase receptors, also known as receptor tyrosine kinases (RTKs) (Figure 13.3). These molecules frequently serve as receptors for extracellular growth factors, circulating proteins that stimulate cell growth and division. Examples of ligand–receptor combinations in this family include epidermal growth factor (EGF) and its receptors ErbB1 (or EGFR) and ErbB2; platelet-derived growth factor (PDGF) and the PDGF receptor; insulin and the insulin receptor; and vascular endothelial growth factor and its major receptors VEGFR1 and VEGFR2 (also called Flt1 and Flk1).

Once the growth factor has bound to and activated the receptor, newly phosphorylated tyrosine residues on the intracellular carboxy terminus of the receptor serve as binding sites for cytosolic or membrane-associated proteins that contain phosphotyrosine-binding domains. The best characterized of these domains are the src-homology 2 (SH2) domains that share characteristic features first described in the phosphotyrosine-binding region of the cytosolic tyrosine kinase Src. SH2 domains are approximately 100 amino acids in length, and provide specificity of interaction in two ways. First, the interaction of the binding pocket of the SH2 domain and the tyrosine residue is only stabilized when the tyrosine residue is phosphorylated. Second, the amino acids immediately flanking the phosphorylated tyrosine residue determine which SH2 domain interaction is preferred. For example, the SH2 domain on the p85 adaptor protein, α-subunit of the lipid enzyme phosphoinositide 3-kinase (PI 3-K, see "Intracellular Signaling Pathways," below), strongly prefers to bind to phosphotyrosine with a methionine residue at the +3 position.[36]

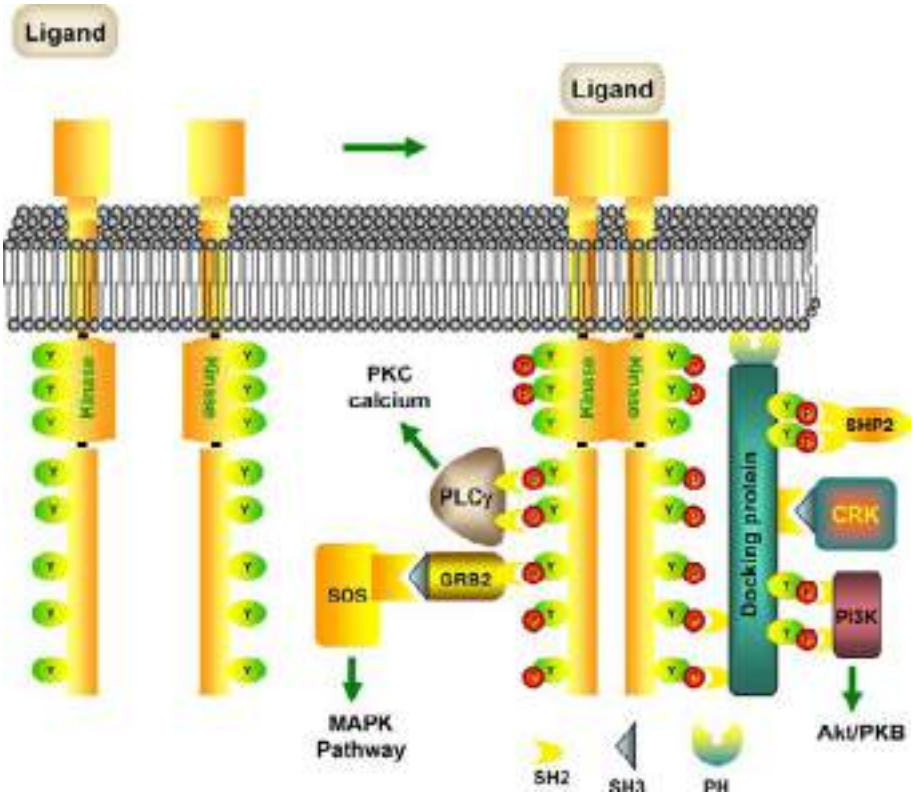

FIGURE 13.3 **Schematic view of a receptor tyrosine kinase (RTK).** In the inactive state, the receptor is primarily in the monomeric form. Following binding of the extracellular ligand, the receptor dimerizes, bringing the kinase domains in close proximity where they cross-phosphorylate each other. This enhances the kinase activity and leads to phosphorylation of tyrosine residues outside of the kinase domain, which in turn become binding sites for proteins that contain SH2 domains. In this manner, downstream signaling pathways can be regulated by recruitment to the receptor. This recruitment can occur via direct association of the effector protein with the receptor (as is the case for phospholipase Cγ (PLCγ)), via association with small adaptor proteins such as Grb2 (as is the case for the guanine exchange factor Sos) or via association with a larger docking protein such as Gab1 or Nck that mediates the association of multiple proteins with the receptor (as can be seen with the phosphoinositide 3-kinase (PI 3K) or the tyrosine phosphatase SHP2). Some docking proteins are additionally stabilized at the membrane via lipid binding domains, such as the pleckstrin homology (PH) domain on Gab1. In addition to SH2 domain interactions, multiple other protein–protein interactions occur and regulate the recruitment of proteins into the complex, including interactions between SH3 domains and proline-rich regions in interacting partners. In this manner, multiple signaling effectors are brought into close proximity where they can interact with each other, be phosphorylated or dephosphorylated (thereby altering their activity or interacting partners) or regulate processes at the cell membrane.

Thus, receptors containing the sequence pTyr-X-X-Met (where X can be almost any amino acid) specifically recruit and activate the PI 3-K.

In the kidney, tyrosine kinase receptors have been implicated in controlling development, mediating hypertrophy, regulating the balance between repair and fibrosis after injury, and promoting the growth of renal carcinomas. During development, glial derived neurotrophic factor (Gdnf) is made by the embryonic metanephric mesenchyme and activates the c-Ret tyrosine kinase receptor that is expressed on the epithelial cells of the adjacent Wolffian duct. The activation of Ret is somewhat unusual, since Gdnf does not directly bind to Ret, but rather binds to a third membrane protein, Gfrα, that mediates dimerization of Ret in response to association with Gdnf (reviewed in [37]). Activation of Ret in this manner results in the activation of multiple intracellular signaling pathways, including the Erk-MAPK pathway, the PI 3-K pathway, members of the Src family of non-receptor tyrosine kinases, and phospholipase Cγ (PLCγ). Activation of the MAPK and Src pathways (see "Intracellular Signaling Pathways") have been found to be critical for the outgrowth and branching of the ureteric bud from the Wolffian duct, the first step in the formation of the metanephric kidney.[38]

Signaling by several other tyrosine kinase receptors has been implicated in kidney development, including the fibroblast growth factor (FGF) receptors, hepatocyte growth factor receptor (Met), and the epidermal growth factor receptor.[39,40] FGF signaling is a complex process that includes 18 known ligands and 4 distinct tyrosine kinase receptors (FGFR1-4) (reviewed in [41]). Like many receptor ligands, FGFs are secreted glycoproteins that are concentrated in proximity to their cell surface receptor by binding to heparan sulfate proteoglycans on the cell and/or nearby matrix components. The interaction between FGFs and their receptors can be further regulated by cell- or tissue-specific expression of FGF co-receptors such as Klotho.[42] Intracellular signaling by the FGFR is regulated in part by the cytosolic adaptor protein FGFR substrate 2 (FRS2), which is phosphorylated by the FGFR kinase domain, leading to the recruitment and activation of downstream MAPK and PI 3-K signaling. In the developing kidney, FGF7 and FGF10, signaling via the IIIb isoform of FGFR2,[43] have been shown to be critical for normal branching and extension of the collecting system,[44] while FGF8 appears to be required for nephrogenesis by the adjacent metanephric mesenchyme.[45]

Many growth factor receptors are expressed in the mature kidney, and are believed to be critical for maintenance of normal tubule architecture and for regulating the cellular response to injury. Renal tubular epithelial cells express EGF receptors as well as Met, the receptor for hepatocyte growth factor (HGF). These tyrosine kinase receptors directly bind their respective ligands via their extracellular amino terminal domains, followed by homodimerization and activation of intracellular signaling. A major mediator of the intracellular signaling mediated by EGF and HGF is the Gab1 docking protein, which functions in a manner similar to that of FRS2 for the FGFR.[46] Recruitment of Gab1 to Met or the EGFR results in its phosphorylation on multiple tyrosine residues and subsequent association with p85, PLCγ, Grb2, a second adaptor protein known as Crk, and the protein tyrosine phosphatase SHP2.[47] Following acute kidney injury, the level of HGF increases in the kidney, resulting in activation of Met, mediating MAPK, PI 3-K, and PLC signaling.[48,49] These pathways in turn are believed to be important for inhibition of apoptosis (the PI 3-K pathway), and stimulation of cell migration and proliferation during the repair process (PI 3-K, MAPK, and PLC pathways).[50–52]

Serine-Threonine Kinase Receptors

A second group of transmembrane kinase receptors are the serine-threonine kinase receptors. Like the non-receptor kinases PKA and PKC, these receptors catalyze the phosphorylation of serine or threonine residues in their substrate molecules. Perhaps the best studied of these receptors in the kidney is the receptor for transforming growth factor β (TGFβ), a member of the TGFβ superfamily of secreted factors that also includes the bone morphogenic proteins (BMPs) and activin.[53] TGFβ-like proteins signal into the cell via a heterotetrameric complex comprised of two subclasses of serine-threonine kinase receptors, the type I receptor and the type II receptor.[54] Like the tyrosine kinase receptors, these proteins have an extracellular ligand recognition domain, a single transmembrane spanning domain, and an intracellular kinase domain. The different TGFβ-like ligands utilize distinct type I and II receptor combinations. For example, TGFβ1-3 signals via the combination of the type II receptor TβR-II and the type I receptors activin receptor-like kinase 1 (ALK-1) or ALK-5,[55,56] while BMPs signal through the type II receptors ActR-II or BMPR-II and the type I receptors ALK-2, ALK-3 or ALK-6.[57]

TGFβ receptor signaling begins when the ligand binds to the extracellular domain of its cognate type II receptor (Figure 13.4). The kinase domain of type II receptors is constitutively active, and binding to the extracellular ligand results in the recruitment of the appropriate type I receptor to the complex, where it is phosphorylated and activated by the type II receptor. In this manner, the TGFβ1-dependent association of ALK-5 with TβR-II allows the constitutively active TβR-II to phosphorylate ALK-5 and activate its intracellular

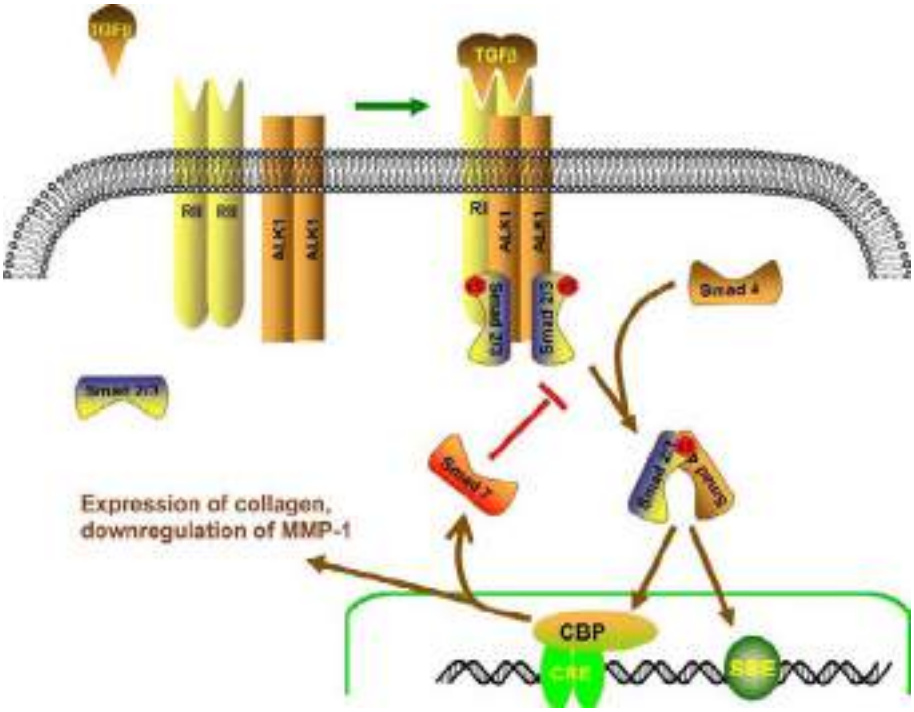

FIGURE 13.4 **Signaling by the TGFβ family of serine-threonine kinase receptors.** Binding of the TGF ligand to the constitutively active type II receptor results in association of RII with the appropriate type I receptor (in this case ALK-1), which is phosphorylated and activated. The activated type I receptor can then phosphorylate the appropriate Smad protein, which then disassociates from the receptor complex, associates with Smad 4, and translocates into the nucleus. In the nucleus the Smad complex can regulate RNA transcription by binding directly to the appropriate DNA Smad-binding elements (SBE) or by binding to and regulating transcriptional regulators such as the cAMP response element (CRE) binding protein (CBP). One of the DNA targets induced by Smad activation is the inhibitory Smad, Smad7. Increased expression of Smad7 inhibits further TβR signaling, providing negative feedback to prevent sustained activation of the pathway.

serine-threonine kinase domain. The specificity of signaling by TGFβ family members is further regulated by the presence in many cells of the accessory receptors betaglycan and endoglin. These transmembrane proteins lack intracellular kinase domains, and appear to regulate the affinity of TGFβ proteins for the various type II receptors, as well as modifying intracellular signaling by the ligand–receptor complex.[58,59]

As opposed to tyrosine kinase receptors that signal primarily via recruitment of SH2 domain containing proteins to activate pathways such as MAPK and PI 3-K, TGFβ receptors signal primarily via a distinct signaling pathway, the Smad proteins. Smads are small cytoplasmic proteins that contain a DNA-binding domain and a TβR-I/Smad4-interacting domain. Based on their structure and function, Smads have been divided into three groups, the receptor activated Smads (Smad1, 2, 3, 5, 8), a regulatory Smad (Smad4), and the inhibitory Smads (Smad6, 7). Upon activation of TβR-I, the appropriate receptor activated Smads (e.g., Smad2 and 3 for ALK-5) are phosphorylated on regulatory serine residues in the TβR-I/Smad4 interacting domain, resulting in their disassociation from the receptor and association with Smad4. This Smad2–Smad4 complex then translocates to the nucleus, where the Smad DNA-binding domain can mediate direct association with Smad-binding elements (SBE) in the DNA of the promotor region of target genes, as well as association with other transcriptional regulators.

One of the transcriptional targets that is regulated by Smad2–4 signaling is another member of the Smad family, Smad7. Smad7 is an inhibitory Smad that can bind to TβR-I, and prevent Smad2 or Smad3 from associating and being activated. In this manner, TGFβ stimulation of Smad7 transcription provides a negative feedback loop that acts to prevent sustained Smad2 and Smad3 activation by the TGFβ receptor.[60]

TGFβ Signaling in the Kidney

Studies in mice that have undergone genetic inactivation of various TGFβ family members demonstrate that Bmp2 and Bmp4 have important roles in normal kidney development (reviewed in [57]). In the mouse embryo, Bmp4 is expressed in the metanephric mesenchyme surrounding the Wolffian duct and adjacent to the ureteric bud (the epithelial structure that will branch to form the entire collecting system of the kidney), while Bmp2 is expressed in the condensing mesenchyme at the tips of the ureteric bud (the region that will differentiate into the glomerulus and proximal portions of the nephron through the connecting segment). The Bmp receptors Alk3 and Alk6 are expressed on the invading urteric bud itself.[61] While complete loss of Bmp2 or Bmp4 results in embryonic lethality prior to kidney development,[62] mice that are heterozygous for loss of Bmp4 expression exhibit multiple defects in the collecting system of the kidney, including doubling of the collecting system, hydroureter, and dysplastic kidneys,[61] and Bmp2 heterozygotes demonstrate exaggerated uretic bud branching.[63]

Thus, it appears that Bmps normally act to inhibit ureteric bud outgrowth and branching during development.

In addition to their role in kidney development, TGFβ proteins have been shown to play a major role in regulating fibrotic responses of the adult kidney by both increasing new matrix deposition and inhibiting matrix degradation.[53,64] *In vitro* studies have shown that TGFβ-dependent Smad3–Smad4 nuclear signaling can induce the expression of multiple collagen isoforms, along with their cellular binding partner β1 integrin,[65–67] and activated Smad3 has been found to mediate decreased transcription of the gene for matrix metalloproteinase-1 (*MMP-1*)[68]. In support of an important role for the TGFβ-Smad signaling pathway in the development and progression of renal fibrosis *in vivo*, genetic overexpression of TGFβ in the rat has been shown to induce glomerulosclerosis due to increased extracellular matrix deposition,[69] while mice lacking Smad3 demonstrate less fibrosis following ureteral obstruction.[70]

Receptor-Like Phosphatases

Much attention has been focused in the field of signal transduction on the role of substrate phosphorylation by receptor kinases in regulating protein–protein interactions or altering the activity of effector proteins. However, a second class of proteins, the phosphatases, is emerging as equally important signaling regulators in determining cellular responses. Similar to kinases, phosphatases can be grouped into transmembrane receptor-like phosphatases and intracellular (cytosolic) phosphatases (to be discussed below). The receptor-like phosphatases that have been identified to date are protein tyrosine phosphatases (PTPs) with an extracellular domain, single transmembrane spanning segment, and intracellular phosphatase domain.

The first receptor-like PTP to be cloned and sequenced was the neutrophil antigen CD45. This protein was found to be necessary for both T-cell development and T-cell activation following engagement of the T-cell receptor (reviewed in [71]). Although there has been no activating ligand identified for CD45, binding to extracellular galectin-1 inhibits CD45 phosphatase activity, resulting in T-cell death.[72] Several intracellular substrates for CD45 have been identified, including members of the Src and JAK kinase families. One critical substrate of CD45 in T-cell signaling is the cytosolic tyrosine kinase Lck[73](Figure 13.5). Lck, like the related tyrosine kinase Src, is normally maintained in the inactive state by the association of phosphotyrosine 505 near the carboxy terminus with its own SH2 domain closer to the amino terminus of the protein.[74] This interaction results in folding of Lck, and thereby prevents the intervening tyrosine kinase domain from recognizing or phosphorylating its substrates. Dephosphorylation of phosphotyrosine 505 by CD45 following antigen presentation by a nearby dendritic cell allows Lck to unfold, and activates the kinase domain.[75] The resultant phosphorylation of the ζ-chain of the T-cell receptor by activated Lck is necessary for recruitment of a second cytosolic tyrosine kinase, ZAP70, to the complex, and subsequent T-cell activation.[76] The administration of monoclonal antibodies that prevent activation of CD45 has been shown to markedly diminish the occurrence of acute rejection in a rodent model of kidney transplantation.[77]

In contrast to CD45, the receptor-like protein tyrosine phosphatase PTPζ/β is expressed on epithelial cells, and has been found to bind to several putative extracellular ligands, including contactin, neural cell adhesion molecule (NCAM), and pleiotrophin.[78,79] Rather than activating PTPζ/β, as is typical of most ligand–receptor interactions, the association of pleiotrophin with PTPζ/β inhibits the phosphatase activity of PTPζ/β.[80] In the kidney, pleiotrophin has been shown to markedly increase branching by the explanted ureteric bud, and thus is believed to play a significant role in determining the number of nephrons that form during kidney development.[81] One substrate for PTPζ/β is the cytosolic protein Git1,[82] a multifunctional adaptor protein that can regulate the signaling pathways that control actin cytoskeletal rearrangement.[83] Dephosphorylation of Git1 by PTPζ/β is therefore proposed to play an important role in the regulation of cell adhesion and migration, as well as cytosolic vesicle trafficking.[84]

Receptors Activated by Proteolytic Cleavage

The previously described receptors bind to their respective ligands and then signal into the cell via activation of substrate protein phosphorylation or dephosphorylation, thus regulating cytosolic signaling pathways that in turn mediate the activation or inhibition of downstream effectors. In contrast, cleavage-activated receptors such as Notch signal directly to the nucleus to regulate gene transcriptional events. Notch is a cell surface protein that contains an extracellular ligand-binding domain, a single transmembrane spanning segment, and an intracellular domain capable of binding and activating nuclear transcriptional factors (reviewed in [85]). The classic Notch ligands, Jagged and Delta, are also transmembrane proteins that contain extracellular EGF-like repeats and a unique domain for binding Notch. When Jagged on one cell engages Notch on an adjacent cell, a cleavage

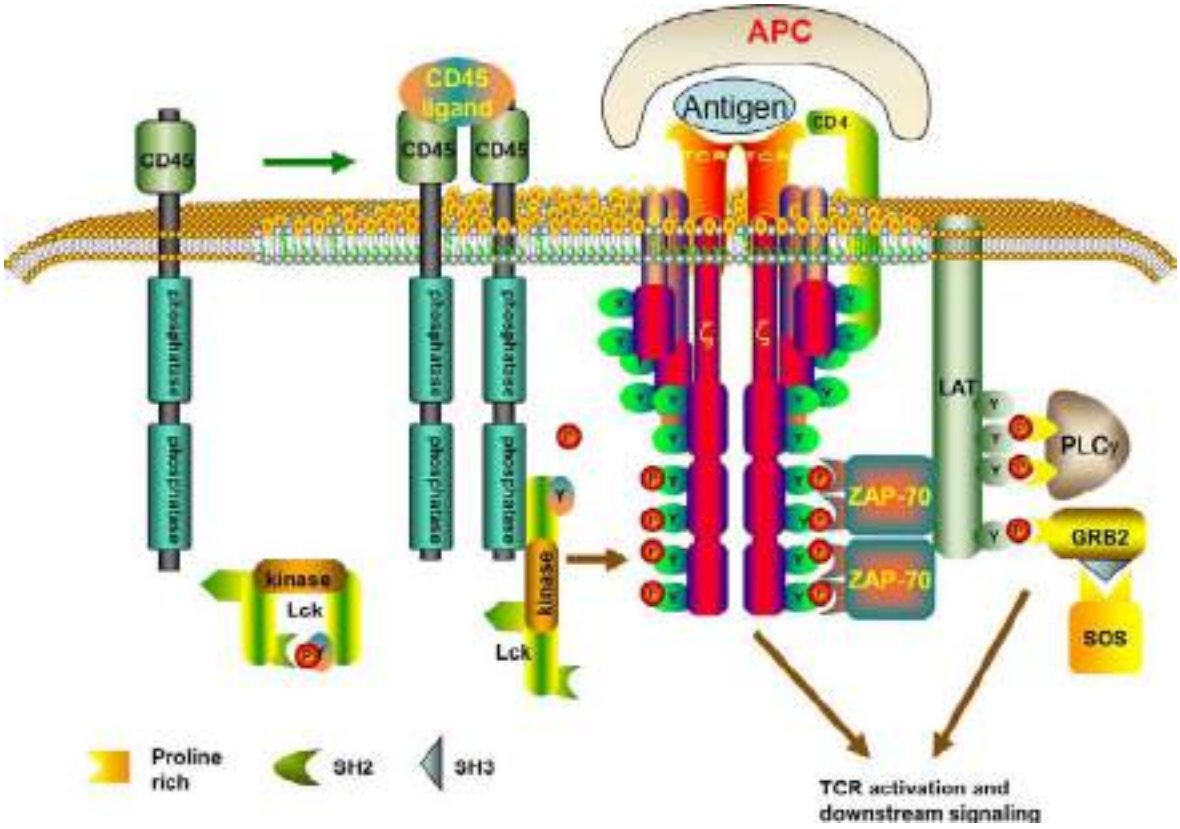

FIGURE 13.5 **Signaling by the CD45 receptor phosphatase.** CD45 is a single membrane spanning receptor phosphatase that is activated by an unknown extracellular ligand. Ligand binding activates the intracellular phosphatase domains, possibly by clustering of the receptors, which dephosphorylate the carboxy terminal tyrosine residue on the cytosolic non-receptor tyrosine kinase Lck. This allows a conformational change in Lck that exposes the kinase domain and facilitates phosphorylation of the ζ chain of the multimeric T-cell receptor. In conjunction with antigen presentation by an antigen presenting cell (APC) to the extracellular domain of the TCR, Lck phosphorylation of the TCR results in recruitment of a second tyrosine kinase, Zap70, to the complex via binding of the Zap70 SH2 domains to the phosphorylated receptor. Zap70 recruitment and activation are required for normal TCR activation, and for phosphorylation of the adaptor protein, Linker for Activation of T cells (LAT). LAT in turn serves as the site for recruitment of multiple signaling pathways involved in the T-cell immune response, including PLCγ (for activation of PKC and calcium signaling) and Grb2-Sos (for MAPK signaling).

site is exposed on the extracellular side of Notch near the membrane, and Notch is cleaved by a member of the A Disintegrin And Metalloproteinase (ADAM) family of proteases.[86] The remaining transmembrane/intracellular portion of Notch then becomes a target for further cleavage by presenilin (a member of the γ-secretase complex) at a conserved site in the intramembranous domain of Notch.[87] Cumulatively, this process is termed regulated intramembranous proteolysis (RIP) (Figure 13.6).

This final cleavage event releases the cytosolic domain of Notch (called the Notch intracellular domain (NICD)) that translocates to the nucleus where it can directly bind and regulate transcription factors. In mammals, Notch controls transcriptional regulation by interacting with the DNA-binding protein CSL (also called RBP-J), which in turn regulates transcriptional expression of members of the Hairy and Enhancer of Split (HES), and Hairy-Related Transcription factor (HRT) family of transcription factors. These nuclear proteins control the expression of genes that are critical for regulating normal development.

In the kidney, activation of Notch signaling has been implicated in the specification of the proximal tubule and glomerular podocytes during development.[88,89] The cleaved form of Notch is present in the developing S-shaped body that ultimately differentiates into the nephron, and inhibition of γ-secretase in organ culture leads to the loss of the proximal nephron, even though the distal nephron still develops and fuses to the collecting duct.[90] Genetic interruption of Notch expression has revealed that nuclear signaling by Notch2, rather than Notch1, is required for this proximal specification.[91] In the mature kidney, Notch expression is normally downregulated. However, in disease states such as diabetic nephropathy, re-expression of Notch can activate the transcription of cell cycle genes, leading to increased cell proliferation and ultimately exaggerated fibrosis.[92]

More recently, it has become clear that receptor activation by regulated cleavage plays a role in

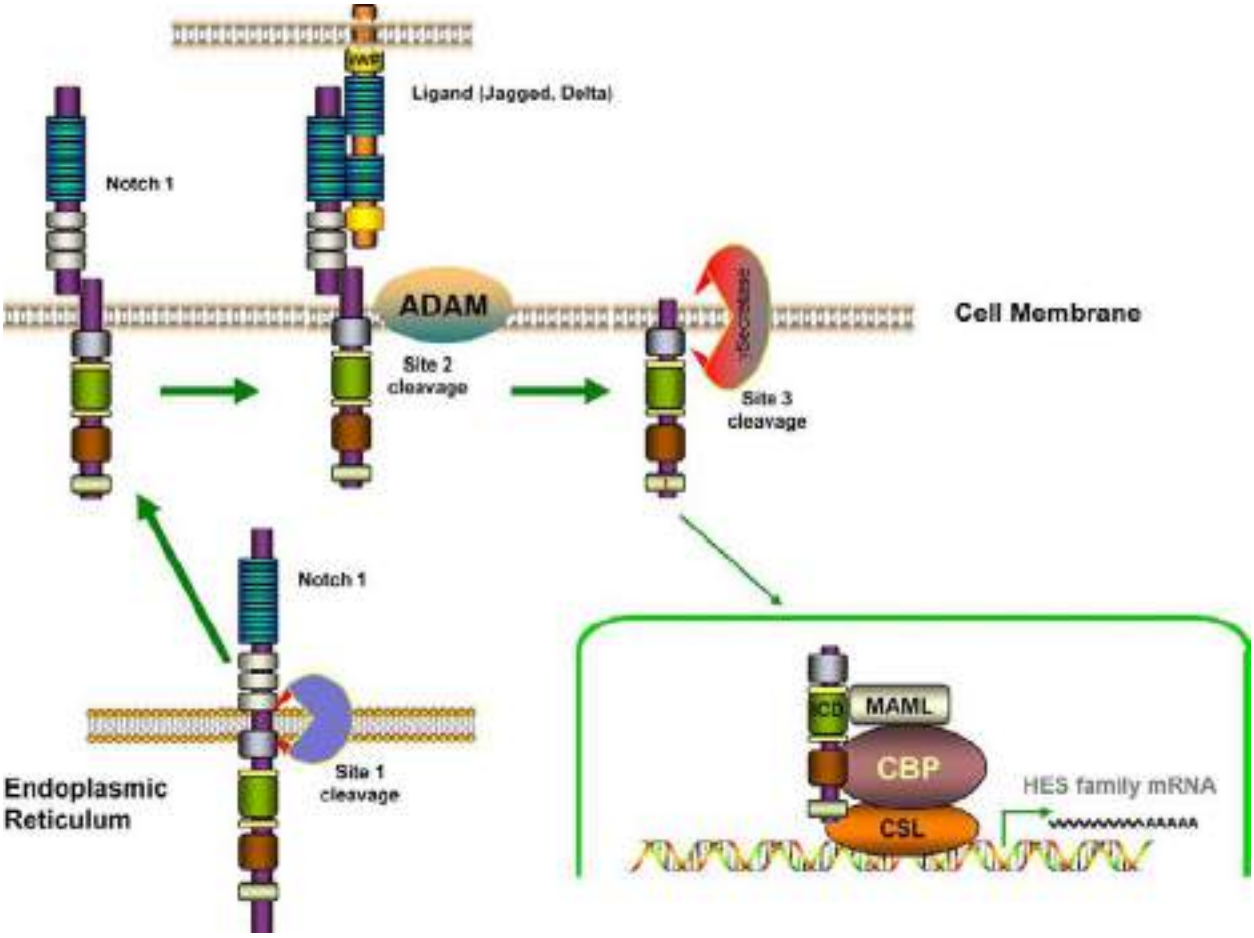

FIGURE 13.6 **Notch signaling as an example of regulated intramembranous proteolysis (RIP).** It is believed that Notch is proteolytically processed in the ER (site 1 cleavage), and expressed on the cell surface as a disulfide-linked dimer of the extracellular domain and the transmembrane-intracellular domain. Binding of the extracellular domain to a Notch ligand (such as Jagged-1) on an adjacent cell exposes a juxtamembrane cleavage site (site 2) for a member of the ADAM family of extracellular proteases. This second cleavage allows the γ-secretase complex (containing presenilin) to cleave the remaining carboxy-terminus at a site within the membrane (site 3 cleavage), releasing the intracellular domain (ICD) which translocates to the nucleus. In the nucleus, the ICD of Notch can bind to members of the CSL family of transcriptional repressors, and in the presence of CSL-binding protein (CBP) and mastermind like protein-1 (MAML), activate transcription of the HES family of genes.

signaling by other cell surface proteins. For example, the γ-secretase complex has been shown to cleave the EGF tyrosine kinase receptor ErbB4 and the adherens junction protein E-cadherin.[93] In the case of ErbB4, this cleavage event is required for the normal proapoptotic effects of receptor activation, arguing that some cell outcomes previously ascribed to activation of tyrosine kinase cascades may in fact be due to receptor cleavage, and subsequent direct regulation of nuclear transcriptional events.[94] While the nuclear targets of some of these cleaved receptors remain to be determined, the likely importance of this pathway in normal cell signaling is emphasized by the finding that the HGF receptor c-Met undergoes a similar cleavage event that regulates cell survival signaling.[95]

Recently recognized targets of regulated intramembrane proteolysis in the kidney include the proximal tubule scavenger receptor megalin, as well as polycystin-1. In the proximal tubule, megalin can undergo ligand-dependent γ-secretase mediated cleavage,[96] leading to release of the megalin intracellular domain that in turn downregulates mRNA expression for both megalin itself and the Na^+/H^+ exchanger 3 (NHE3).[97] Polycystin-1, the protein product of the PKD1 gene that is defective in the majority of patients with autosomal dominant polycystic kidney disease (ADPKD), has also been shown to undergo RIP, releasing an intracellular carboxy-terminal tail (CTT) that is believed to traffic to the nucleus, where it can regulate gene expression.[98,99] γ-Secretase-mediated cleavage of polycystin-1 to generate the CTT appears to be dependent on the presence of polycystin-2, as well as mechanical stimuli such as those that might occur with urinary flow.[100]

Receptors that Signal Cell Location

One of the most important roles of cell signaling is to organize when a given cell should undergo differentiation toward a highly specialized function (such as the increase in sodium transporters in the brush border of a proximal tubule cell in response to angiotensin II signals mediated by volume depletion[101]) or should revert to more basic processes such as cell division and migration (e.g., during development of the embryonic kidney or recovery of the adult kidney from acute kidney injury). While these widely divergent responses are primarily mediated by receptor–ligand interactions such as those mentioned above, cells also have surface proteins that provide important clues regarding cell location and density, and thus establish their level of differentiation, polarity, and responsiveness to outside signals.

Cell–Matrix Interactions can Signal Cell Location

The cells of the nephron reside on a complex basement membrane that provides specific clues regarding cell location. In the glomerulus this structure is highly specialized to not only support epithelial cell attachment (the podocyte), but also endothelial cell attachment, and to serve as a significant component of the glomerular filtration barrier. The basement membrane of the kidney has been shown to be composed of multiple matrix proteins, including collagen, laminin, perlecan, nidogen, nephronectin, and entactin. The specific isoforms and relative contributions of these proteins vary during the course of renal development, as well as along the length of the adult nephron (reviewed in [102]). These matrix proteins interact with members of a large family of specific cell surface receptors, the heterodimeric α/β integrins.

In the kidney, $\alpha_1\beta_1$, $\alpha_2\beta_1$, $\alpha_3\beta_1$, $\alpha_6\beta_4$, $\alpha_8\beta_1$, and $\alpha_V\beta_3$ have been found to be highly expressed in developing and/or adult renal tubular cells (reviewed in [103]). The binding of the heterodimeric integrin complex to its matrix ligand in the basement membrane ($\alpha_1\beta_1$ integrin and type IV collagen, for example) results in clustering of the integrins on the basal surface of the cell at contact sites known as focal contacts or adhesions, and the concomitant accumulation of a large group of intracellular signaling proteins at these sites known as the focal adhesion complex. This complex typically includes the focal adhesion scaffolding proteins paxillin and HEF1, the non-receptor kinases Src, PI 3-K, integrin-linked kinase (ILK) and focal adhesion kinase (FAK), the small G-protein regulated signaling proteins PIX and PAK, and actin-binding proteins such as vinculin, talin, and actopaxin (reviewed in [104,105]). Signaling through this complex can occur in a traditional "outside-in" manner, in which integrin binding to matrix results in formation and activation of the signaling complex or in an "inside-out" manner, in which signals from other sites, such as activated growth factor receptors, can regulate the affinity of the integrin complex for its matrix ligand, for example during growth factor-stimulated cell adhesion and/or migration.

Signals emanating from focal adhesions provide critical clues regarding cell location, establishment of cell polarity, regulation of cell proliferation, and determination of cell differentiation. The recruitment of actin-binding proteins into the focal adhesion complex provides important clues for cell polarity, while the regulation of small G-proteins such as Rac and Cdc42 is critical for regulating cell differentiation and directed migration.[106] Focal adhesion signaling through Src, FAK, and the P I3-K are required to normally activate the ERK MAPK pathway in response to proliferative growth factor stimuli, and thus promote entry into the cell cycle and subsequent cell proliferation.[107] In the event that cell–matrix adhesion is lost, such as can occur in proximal tubule cells following ischemic renal injury, growth factor signaling is muted, the cells enter cell cycle arrest and eventually undergo anoikis (programmed cell death induced by cell detachment) due to activation of the JNK MAPK pathway (see "Intracellular Signaling Pathways").[108]

The importance of providing the right matrix environment for normal kidney development and function has been demonstrated in mice lacking specific matrix proteins and/or integrin receptors. For example, failure to express laminin-10 results in severe abnormalities in glomerular development, as does loss of expression of the laminin-10 receptor $\alpha_3\beta_1$ integrin,[109,110] while loss of β1 integrin severely impairs branching of the ureteric bud.[111] In contrast, mice lacking integrin α_1 expression demonstrate normal kidney development,[112] but have increased fibrosis after glomerular injury, due to an increase in reactive oxygen species (ROS) generation[113] (Figure 13.7).

Cell–Cell Interactions such as Adherens Junctions and Gap Junctions can Signal Cell Density and allow Cells to act in Concert

A second means by which cells obtain clues about their immediate environment is via cell–cell interactions. Of the many types of cell–cell interactions, at least three, adherens junctions, tight junctions, and the gap junctions, play important roles in cell signaling. Adherens junctions form at the lateral border of adjacent cells due to the intercellular interactions of cadherins, a family of cell type specific transmembrane proteins (reviewed in [114]). There are multiple cadherin family members, including the classic epithelial cell member E-cadherin, the endothelial cell cadherin VE-cadherin, and the renal tubule associated cadherin Ksp-cadherin.[115] The extracellular portion of cadherins

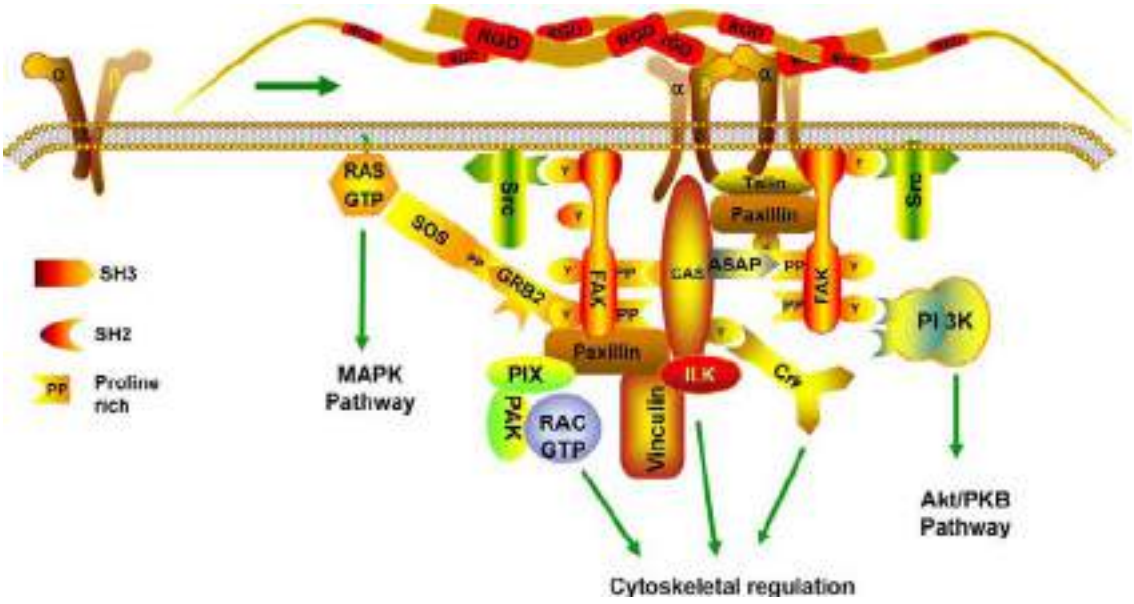

FIGURE 13.7 **Integrin signaling at the cell–matrix interface.** The αβ integrin heterodimers on the cell surface bind to specific sequences in the subcellular matrix (RGD domains in collagen for example), triggering a conformational change in the integrin, and the subsequent recruitment of a large number of cytosolic and membrane-associated proteins (the focal adhesion complex). These proteins include the adaptor and scaffolding proteins p130Cas, Paxillin, Crk, and Grb2. These adaptor proteins in turn mediate the interaction of large numbers of signaling proteins, including tyrosine kinases such as Src, which can phosphorylate and activate other proteins in the complex (including the EGF receptor), and FAK, which activates turnover of the focal adhesion so that cells can migrate. The formation of this complex also activates cell survival and proliferation signals, including the PI 3-kinase and MAPK pathways, and regulators of the actin cytoskeleton such as vinculin, talin, integrin-linked kinase (ILK), and Rac.

contains five repeat sequences (known as EC repeats), that can interact in a homophilic, calcium-dependent manner with the EC repeats present on cadherins in adjacent cells. This interaction is important for providing cell sorting signals during tissue development.[116]

The intracellular domain of the cadherins associates with a group of cytoplasmic proteins known as the catenins. One of these proteins, β-catenin, has a dual role in the cell. It directly binds to cadherins, and thus participates in the formation of cell–cell junctions, but it can also disassociate from adherens junctions and translocate to the nucleus, where it regulates signaling events involved in cell differentiation and proliferation. Originally it was believed that the direct interaction of cadherins with β-catenin created a stable binding site for the actin-binding protein α-catenin, thus generating a static site for lateral attachment of the actin cytoskeleton. However, more recent studies have demonstrated that this protein complex is a dynamic structure that can support actin filament rearrangement during the movement of cells, while maintaining cell–cell junctional integrity.[117]

β-Catenin Signaling can Regulate Cell Differentiation and Proliferation

As noted, β-catenin can leave the adherens junction and enter the nucleus, where it acts as a transcriptional regulator by binding to the TCF/Lef transcriptional complex.[118] Genes that are induced downstream of β-catenin typically lead to increased cell proliferation and regulation of differentiation, events that are important during normal development, but that are typically downregulated in the adult.[119] This transcriptional activity of β-catenin is tightly regulated by controlling the free cytosolic pool of β-catenin that is available for translocation into the nucleus. In the adult renal tubule, the extensive array of intercellular adherens junctions that forms in the confluent monolayer of epithelial cells results in sequestration of the majority of β-catenin with cadherin. To further ensure that free β-catenin levels remain low in the cytosol, a serine-threonine kinase, glycogen synthase kinase-3β (GSK-3β), phosphorylates cytosolic β-catenin and targets it for degradation by the proteosomal pathway.[120] GSK-3β is associated with the adenomatous polyposis coli (APC) protein, and mutations in this complex that prevent β-catenin phosphorylation and degradation lead to increased nuclear β-catenin signaling, cell proliferation, and subsequent tumor formation.[121]

During organ development, and following some types of organ injury, β-catenin nuclear signaling is activated by destabilization of adherens junctions (thereby releasing β-catenin into the cytoplasm) and coincident inhibition of GSK-3β kinase activity.

The classic developmental regulator that has been found to activate β-catenin signaling in this manner is the growth factor Wnt and its receptor Frizzled (Fz)[122] (Figure 13.8). Frizzled is a member of the GPCR family of seven membrane spanning cell surface receptors, and has been proposed to signal, at least in part, by activation of heterotrimeric G-proteins.[123] However, in the canonical Wnt signaling pathway, binding of Wnt to Fz leads to the GSK-3β-dependent phosphorylation of a second membrane spanning protein, the Low-density lipoprotein Receptor-related Proteins 5 and/or 6 (LRP5/6), which in turn mediate the recruitment/activation of the cytosolic protein dishevelled (Dsh).[124] This complex appears to inhibit GSK-3β-dependent phosphorylation of β-catenin and other substrates in the cytosol by sequestering GSK-3β into multivesicular endosomes, thus preventing β-catenin degradation.[125,126]

During kidney development, Wnt4 and Wnt9b, acting at least in part via activation of β-catenin, have been shown to be required for both maintenance of the nephron progenitor pool and normal differentiation of these progenitor cells to form the nephron, suggesting that careful titration of the level of activation of canonical Wnt signaling is critical during mesenchymal-to-epithelial differentiation.[127–129] In addition, multiple Wnts are upregulated following kidney injury, where they appear to play a role in normal repair, as well as in the promotion of fibrosis.[130,131]

Podocyte Slit Diaphragms are Highly Specialized Tight Junctions that Signal to the Cytoskeleton

Tight junctions are cell–cell junctions that are typically located at the interface of the apical and basolateral membranes of epithelial cells, where they serve to regulate the composition of the fluid that moves between cells into the interstitial space. In glomerular podocytes, tight junctions have evolved into elaborate structures that support the extensive interdigitation of adjacent cells along the glomerular basement membrane, and thus constitute a critical component of the glomerular filtration barrier. These cell–cell junctions are termed slit diaphragms, and form when Ig-like domains in the extracellular portion of the transmembrane proteins nephrin and Neph1 form homotypic and heterotypic interactions with nephrin/Neph1 molecules in the adjacent podocyte.[132] Dynamic regulation of these interactions is critical for maintaining the integrity of the slit diaphragm, which is achieved by signaling from the slit diaphragm to the actin cytoskeleton (reviewed in [133,134]). This signaling involves phosphorylation of the intracellular domain of nephrin by the Src-family kinase Fyn, followed by recruitment of a signaling complex including the adaptor proteins Nck1/2, Grb2, and p85, which in turn mediate recruitment/activation of cytoskeletal regulatory proteins including WASP, Pak, and Rac that regulate actin polymerization/depolymerization in the foot process. Mutations that alter nephrin/NEPH interactions lead to disruption of this intracellular signaling complex, destabilization of the actin cytoskeleton and foot process retraction/fusion.

Gap Junctions Promote Rapid Signaling Between Groups of Cells

A second type of cell–cell interaction that is important for cell signaling is the gap junction. These junctions are formed by the alignment of hemichannels on the lateral borders of two adjacent cells to establish a direct cytoplasmic link between the cells, thus allowing the rapid movement of small molecules and electrical charge through multiple cells within a specified region of the organ.[135] Gap junctions are primarily composed of a family of proteins known as connexins, and have traditionally been studied for their ability to rapidly transmit contraction signals through muscles. Investigation of gap junction function within the kidney has demonstrated that mesangial cells contain large numbers of gap junctions comprised of connexin 43 (Cx43), and that these are critical for mediating intercellular calcium-dependent coordinated mesangial contraction.[136] In addition, tubular epithelial cells maintain intercellular gap junctions that can be regulated by growth factors, as well as by ischemic injury,[137,138] although the precise role of these channels in normal tubule function is presently not well-understood.

The Cilia as a Signaling Structure

Many cells of the body, including renal epithelial cells, have a surface structure known as the primary cilium. Cilia are elongated membrane protrusions that surround a central core of microtubules arising from a microtubule organizing center known as the basal body (reviewed in [139,140]). Cells that express cilia with a microtubular arrangement of 9 + 2 (9 microtubule doublets arranged in a cylinder around a core of 2 microtubule singlets), such as those lining the trachea, are motile and can act to facilitate directional movement of fluid (reviewed in [141]). In other cells, such as those lining the renal tubules, cilia have a 9 + 0 arrangement, are non-motile, and were previously believed to be rudimentary structures. However, the finding that genetic mutations that interrupt cilia formation can result in cystic kidney diseases in rodents,[142,143] along with the recent discovery that the two predominant gene products known to cause human autosomal dominant polycystic kidney disease, polycystin-1 (Pc-1) and polycystin-2 (Pc-2), localize to cilia, has resulted in intense investigations into the role of non-motile cilia as renal epithelial mechanosensors.[143,144]

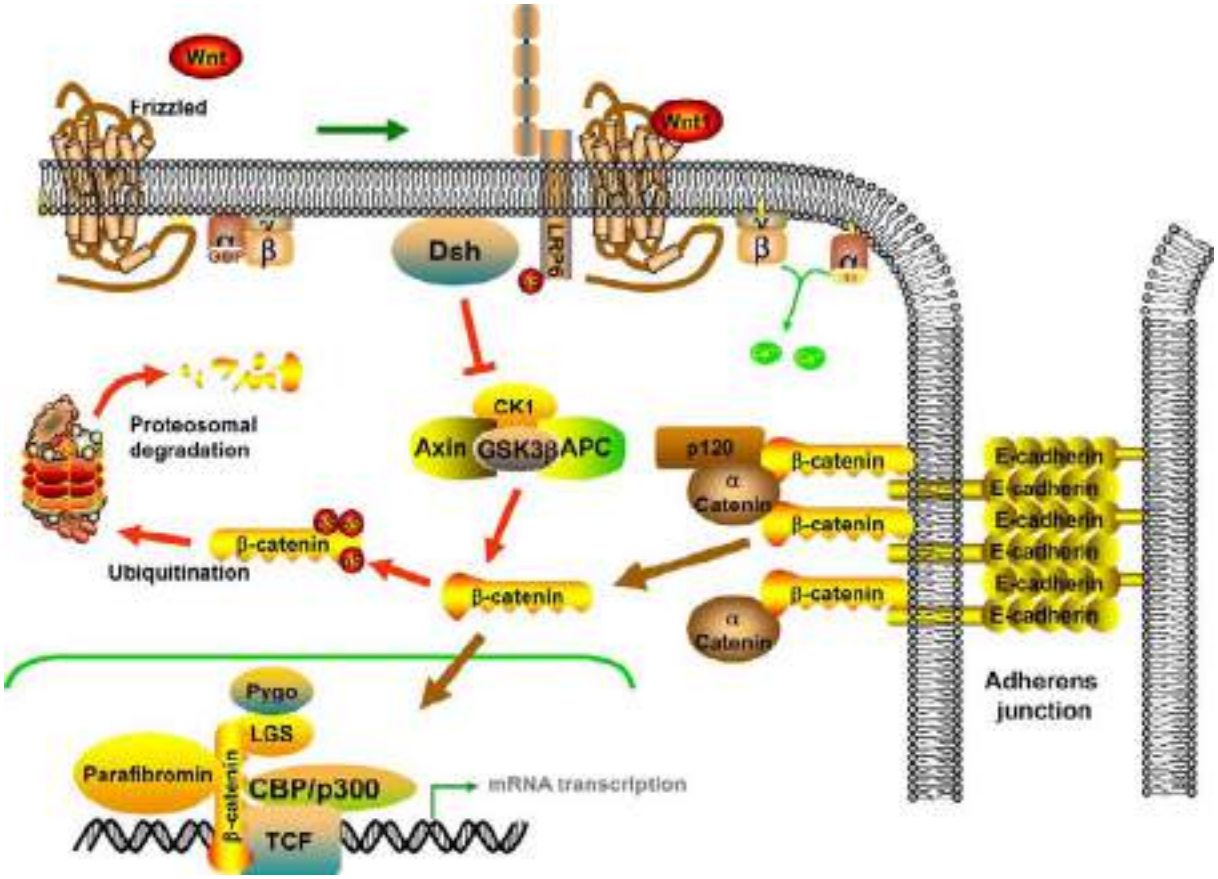

FIGURE 13.8 **Wnt/β-catenin signaling.** Formation of stable cell−cell adherens junctions in mature epithelia occurs due to the lateral interactions of cadherins on adjacent cells. This results in the formation of an intracellular complex of proteins comprised of β-catenin, α-catenin, and p120. α-Catenin can interact with the actin cytoskeleton and the adherens junction complex in a dynamic manner, and thus serve as a nidus for actin cytoskeletal arrangement along the lateral border of the cell. β-catenin can either be sequestered in the adherens junction or released into the cytosol where it is capable of translocating to the nucleus and activating the transcription of multiple genes involved in cell proliferation and dedifferentiation. In mature, non-proliferating cells, free cytosolic β-catenin is rapidly degraded, because phosphorylation by GSK-3β targets β-catenin for ubiquitination and degradation in the proteosome. GSK-3β is found in a complex that includes the regulatory/targeting proteins axin and APC. The kinase activity of GSK-3β can be inhibited following activation of several growth factor receptors. In the best studied pathway, stimulation of the Wnt receptor Frizzled leads to phosphorylation of the membrane spanning protein Lrp6, which in turn activates the Dishevelled (Dsh)-dependent sequestration and inhibition of GSK-3β. The resultant increase in free cytosolic β-catenin leads to its nuclear translocation, where it serves as a scaffold for the association of a complex of proteins that bind and activate RNA polymerase II, leading to gene transcription. There is data supporting a second signaling pathway downstream of Frizzled in which GTP-loading of the Gαi-subunit of the heterotrimeric G-protein results in release of the βγ-subunit, which in turn activates phosphoinositide hydrolysis and downstream calcium release.

These studies have demonstrated that Pc-2 acts as a cation channel, and that regulation of this channel activity can be mediated by its interaction with Pc-1.[145−147] *In vitro* studies have demonstrated that Pc-1 and Pc-2 co-localize on the primary cilium of the apical cell membrane in renal epithelial cells, and that physiological levels of fluid shear stress, such as that created by urine flow in the renal tubule, may be sufficient to stimulate cilia-dependent Pc-1/Pc-2-mediated calcium signaling.[143,148,149] It is presently hypothesized that failure of this signaling pathway can result in abnormalities in both the rate and organization of cell proliferation, and thus can lead to cyst formation.[150]

INTRACELLULAR SIGNALING PATHWAYS

As is clear from the preceding section, activation of cell surface receptors results in the regulation of multiple intracellular signaling pathways. Although numerous studies from the past decade have emphasized the vast amount of cross-talk between the proteins involved in these pathways, it remains useful to identify core signaling cascades that can transduce signals from the receptor to effector proteins that mediate specific cellular responses. Several of these signaling cascades, including the heterotrimeric G-protein-adenylate cyclase-cAMP-PKA pathway, the TGFβ-Smad pathway,

and the Wnt-Fz-Dsh-Gsk3β-β-catenin pathways, have been described in some detail in the section "Cell Surface Receptors." This section will focus on several other signaling cascades that are believed to be fundamental regulators of cell survival and function in the kidney, including the PLC-Ca-PKC pathway, the MAPK pathway, and the PI 3-kinase pathway.

The Phospholipase C Pathway Regulates Intracellular Calcium Release and Activates PKC Signaling

Phospholipase C (PLC) is an enzyme that catalyzes the hydrolysis of the membrane lipid phosphoinositide 4,5 bisphosphate ($PI_{4,5}P_2$) to generate diacylglycerol (DAG) in the membrane and release inositol trisphosphate (IP_3) into the cytoplasm (reviewed in [151]). DAG provides a binding site to recruit protein kinase C (PKC) to the membrane, while IP_3 binds to its receptor on the endoplasmic reticulum that mediates the intracellular release of stored calcium. Thus, activation of PLC regulates both PKC-dependent and calcium-dependent intracellular signaling.

In mammals, there are four known families of phospholipases C, PLCβ, PLCγ, PLCδ, and PLCε. While all four groups share the catalytic X and Y lipase domains, the regulatory domains are widely divergent, allowing activation by distinct upstream receptors. For example, PLCβ is activated following stimulation of certain GPCRs, because it has a carboxy terminal domain that recognizes and binds GTP-loaded $G_{q\alpha}$, as well as the free βγ heterodimer[152,153] (see section "G-protein coupled receptors"). Activation of PLCδ and PLCε are less well-understood, although each appears to be mediated by interaction with small GTP-binding proteins. PLCδ can be activated by associating with the GTPase Ral, whereas PLCε has a Ras-binding domain and can be activated by associating with GTP-loaded Ras.[154–157]

In contrast, PLCγ family members lack the Gα- and βγ-binding regions, but instead encode two SH2 domains and one SH3 domain that mediate their recruitment and activation by receptor tyrosine kinases (RTKs) such as the PDGF receptor, vascular endothelial growth factor (VEGF) receptor, and HGF receptor.[158] Interestingly, PLCγ can also be phosphorylated and activated by non-receptor protein tyrosine kinases, such as Src family members. In this manner, PLCγ can be secondarily activated in immune cells downstream of T-cell receptor activation (see Figure 13.5), as well as following activation of certain GPCRs, such as the angiotensin II receptor.[159]

For PLC to hydrolyze $PI_{4,5}P_2$, it must be recruited to the membrane. Members of both the PLCβ and PLCγ families have pleckstrin homology (PH) domains at their amino termini that promote membrane association by binding to select membrane phospholipids, such as $PI_{4,5}P_2$ and $PI_{3,4,5}P_3$.[160] PLCβ family members are further stabilized at the membrane because their PH domain can also interact with the membrane bound βγ G-protein heterodimer, while the SH2 domains of PLCγ proteins enhance membrane association by mediating recruitment to cell surface receptors. In this manner, PLC is recruited to specific sites at the membrane in the vicinity of the activating receptor, allowing the cell to selectively upregulate DAG and IP_3 production in that area.

PLC-dependent generation of DAG provides a membrane binding site for recruitment and activation of several members of the protein kinase C (PKC) family of non-receptor serine-threonine kinases (Figure 13.9). PKCs are a large group of proteins that are subdivided into the conventional PKCs, novel PKCs, and atypical PKCs. The conventional PKCs (PKCα, PKCβ, PKCγ) are activated in a calcium-dependent fashion following recruitment to the cell membrane by binding to DAG and phospholipids such as phosphatidylserine (PS). The novel PKCs (PKCδ, PKCε, PKCη, and PKCθ) are also recruited to the membrane by binding to DAG and membrane phospholipids, but do not require calcium for activation. The atypical PKCs (PKCλ, PKCζ, PKCμ, and PKCι) lack both the DAG and calcium binding sites, and instead appear to be associated with the membrane and activated solely via their association with membrane phospholipids (reviewed in [161]). In addition to PS, it has been found that the 3-phosphorylated lipid products of the PI 3-K (such as $PI_{3,4}P_2$ and $PI_{3,4,5}P_3$) can bind and activate both novel and atypical PKCs.[162]

Once activated, PKCs have multiple potential phosphorylation targets in the cell. The determination of which targets are phosphorylated is dependent on cell type, the isoform of PKC that is activated, and targeting proteins that specify subcellular localization of the activated PKC. Proteins that are not phosphorylation substrates of PKC, but serve only to target specific PKCs to select sites in the cell, are collectively termed RACKs (receptors of activated C kinase). For example, the cell polarity proteins Par3 and Par6 associate with atypical PKCs, such as PKCζ, and specifically target them to epithelial tight junctions on renal tubular cells.[163] In this location, PKCζ has been shown to regulate both tight junction assembly and disassembly, although the exact phosphorylation targets of PKCζ have yet to be identified.[164,165]

Recent studies have demonstrated that PKC localization to the basolateral membrane can regulate Na,K-ATPase activity in the renal tubule as well. Several phosphorylation sites for classical PKCs (such as PKCα) have been identified in the amino terminus of the Na,K-ATPase α-subunit, and phosphorylation of

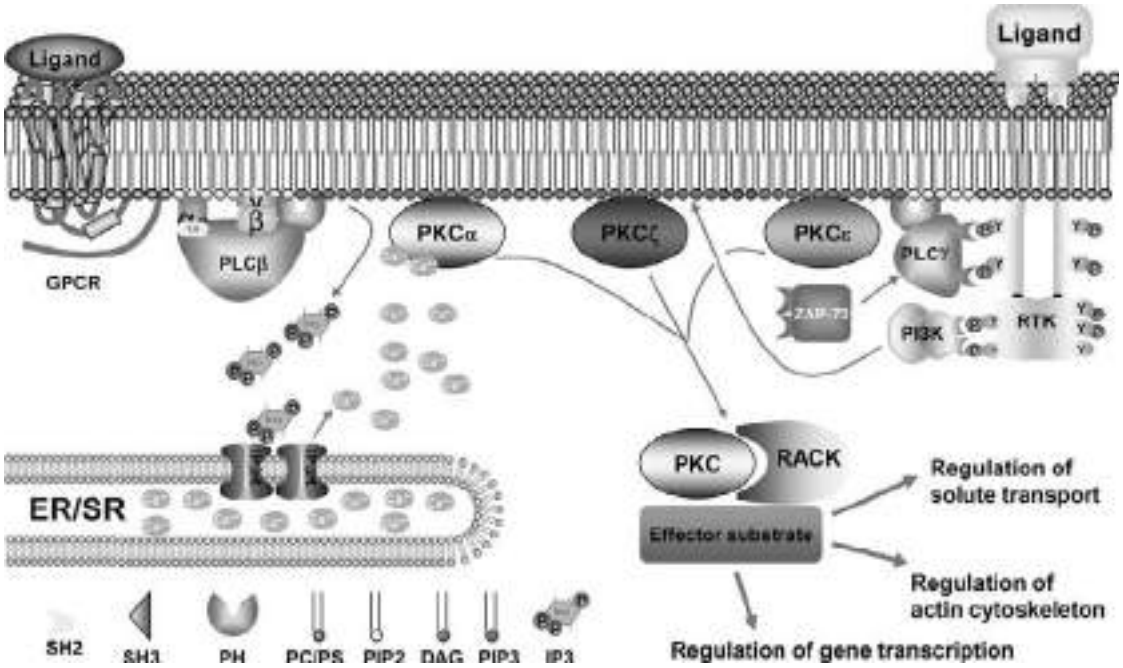

FIGURE 13.9 **Phospholipase C-protein kinase C signaling.** Activation of GPCRs coupled to Gαq can recruit PLCβ to the membrane and activate its phospholipase activity via interactions with the GTP-loaded α-subunit, as well as the free βγ-subunit. PLCγ is classically activated via binding of its SH2 domains to phosphotyrosine residues on RTKs, although PLCγ can also be activated by the non-receptor tyrosine kinase Zap-70. Both PLCβ and PLCγ are stabilized at the membrane via their lipid-binding PH domain, where they hydrolyze PI4,5P2 (PIP2) to generate DAG and IP3. DAG serves as a binding site at the membrane for both conventional PKCs (such as PKCα) and novel PKCs (such as PKCε). While novel PKCs are activated as a consequence of this membrane recruitment, conventional PKCs also require calcium-binding for full activation. This calcium signal comes from IP3-mediated calcium release from intracellular stores. A third family of PKCs, the atypical PKCs such as PKCζ, lack the DAG-binding domain, and are recruited to the membrane and activated by binding to phosphatidyl serine (PS) as well as the lipid product of the PI3K, $PI_{3,4,5}P_3$ (PIP3). Specificity of signaling for this diverse family of serine-threonine kinases is provided by association with receptors of activated C kinase (RACKs) which target the activated PKC isoform to the correct effector protein (such as the α-subunit of the Na,K-ATPase in renal tubular cells).

these sites appears to increase cellular sodium pump activity by increasing membrane localization of the enzyme.[166,167] Interestingly, activation of PKC downstream of the D_1-type dopamine receptors appears to have the opposite effect, inhibiting sodium pump activity as part of the overall effect of the D_1 receptor in inhibiting tubular sodium reabsorption.[168] Exploration of this response has demonstrated that novel PKCs such as PKCθ and PKCε are likely to mediate this Na,K-ATPase inhibitory effect.[169] It is unknown whether these PKCs phosphorylate different sites on the sodium pump than PKCα or act indirectly via phosphorylation of intermediate proteins such as the sodium hydrogen regulatory factor Nherf-1.[170]

Another group of PKC regulatory targets are transcription factors. PKC isoforms such as PKCδ, PKCε, and PKCθ have been found to regulate the activity of multiple transcription factors, including NF-κB (involved in immune and inflammatory responses), signal transducers and activators of transcription (STATs, regulators of inflammatory responses, cell proliferation, and differentiation), and Jun N-terminal kinase (JNK, involved in cell stress response and survival) (reviewed in [171]). By acting upstream of JNK as well as the Raf-MEK-ERK pathway (see below), PKC isoforms can cooperate to mediate increased activity of the immediate early response genes Jun and Fos.[172]

An interesting example of convergence of PKC with other signaling pathways is seen during the activation of T-cells. The rise in intracellular calcium following T-cell stimulation results in the activation of calmodulin and binding of the calcium−calmodulin complex to the non-receptor serine-threonine phosphatase calcineurin (also known as protein phosphatase 2B or PP2B). Activated calcineurin dephosphorylates and activates the nuclear translocation of another protein, nuclear factor of activated T-cells or NFAT (reviewed in [173,174]). While originally described in T-cells, NFATs are expressed in multiple cell types and control the expression of genes such as Il-2, GM-CSF, interferon-γ, TNFα, and Cox2 that regulate processes as diverse as T- and B-cell proliferation in response to antigen stimulation, cardiac myocyte differentiation and hypertrophy, and sodium channel expression (reviewed in [175,176]).

However, the DNA-binding sites of many of these gene targets contain nearby AP-1 promoter sites, and are only upregulated in an efficient manner following the concerted actions of NFAT and the AP-1 binding elements Jun and Fos. Thus, concerted activation of PKC (to activate Jun and Fos) and calcineurin (to activate NFAT) leads to maximal gene expression and cellular response. The importance of calcineurin in mediating immune cell activation has led to the extensive use of calcineurin inhibitors, such as cyclosporine and tacrolimus, for the prevention of transplant rejection.

The Mitogen Activated Protein Kinase (MAPK) Pathway Regulates Cell Survival, Proliferation, and Morphology

The MAPK pathway provides an excellent example of the way in which different extracellular signals can converge on the regulation of a single intracellular signaling pathway, and demonstrates how targeting of that pathway to specific sites in the cell via scaffolding proteins can determine which effector proteins are regulated, and what cell responses are affected. As the name implies, this protein cascade was originally identified based on its activation downstream of pro-proliferative growth factors such as insulin and EGF.[177] In the classic MAPK cascade, binding of the growth factor to its receptor tyrosine kinase (RTK) initiates a series of protein−protein interactions that ultimately result in activation of the cytosolic serine-threonine kinase ERK, which can phosphorylate and regulate diverse effector substrates including transcription factors in the nucleus, focal adhesion proteins at the cell surface, and contractile proteins in the cytosol.[178−180]

The core proteins of this classic MAPK cascade are three kinases, Raf, MEK, and ERK. Raf-1 (also called MEK kinase (MEKK) or MAPK kinase kinase (MAPKKK)) is a serine-threonine kinase that phosphorylates and activates two closely related MEK isoforms, MEK1 and 2. MEK1/2 are dual specificity (tyrosine as well as serine/threonine) kinases that phosphorylate ERK1 and 2 on a highly conserved amino acid motif, Thr-Glu-Tyr, contained in the activation loop of the protein.[181] The efficient activation of ERK in this cascade requires that the three proteins (Raf, MEK, and ERK) are brought into close proximity on a single scaffolding protein. Present studies indicate that several different proteins can serve this scaffolding function, including β-arrestin, IQGAP, kinase suppressor of Ras (KSR), and paxillin.[20,182−184] The location of the scaffolding protein and the regulation of Raf/MEK/ERK association determines which effector proteins are likely to be regulated (reviewed in [185]).

The core module of Raf, MEK, and ERK can be activated following binding of receptor tyrosine kinases to their extracellular ligands. The initial step in RTK-mediated MAPK activation is the recruitment of the GRB2 adaptor protein to the tyrosine phosphorylated receptor. GRB2 is a small molecule that is composed of one SH2 domain and two SH3 domains.[186] As noted previously, proteins containing SH2 domains interact with other proteins that contain phosphorylated tyrosine residues flanked by the appropriate amino acids. The GRB2 SH2 domain preferentially binds to phosphotyrosine residues with an asparagine at the +2 position, such as tyrosine 1096 in the activated c-Ret receptor (pYANW) or tyrosine 1356 in activated c-Met (pYVNV). In contrast, SH3 domains typically mediate constitutive association with short proline-rich sequences in target proteins. The guanine nucleotide exchange factor (GEF) Sos contains such a sequence, and associates with the GRB2 SH3 domain in a constitutive fashion. Sos acts as a GEF for the membrane-associated small GTP-binding protein Ras.[187]

Ras is structurally similar to the α-subunit of the αβγ heterotrimer that associates with GPCRs. However, Ras is activated by non-GPCR GEFs such as Sos and, in the GTP-bound state, associates with and activates Raf rather than adenylyl cylase. This activation step appears to involve the Ras-dependent dephosphorylation of Raf by PP2A, a non-receptor protein phosphatase.[188] Thus, RTK activation results in recruitment of the GRB2-Sos complex to the membrane where it mediates GTP-loading of Ras, and activation of the Raf-MEK-ERK signaling pathway (Figure 13.10).

In addition to this classic model of GRB2-Sos-Ras-dependent MAPK activation mediated by RTKs, several alternative mechanisms of MAPK pathway activation have now been elucidated. For example, as described in the section "G-protein coupled receptors," the recruitment of β-arrestin to activated GPCRs can result in β-arrestin-dependent scaffolding of Raf, MEK, and ERK, and thus can facilitate ERK activation (reviewed in [189]). Another pathway of MAPK activation is that of PKC-mediated Raf activation. As noted previously, PKCs are activated downstream of GPCRs, RTKs, and non-receptor kinases (such as the PI 3-K) by associating with DAG and/or phospholipids at the cell membrane. Once activated, one of the PKC phosphorylation targets is Raf,[190] leading to Raf activation and the downstream activation of MEK and ERK, even in the absence of GTP-loaded Ras.[191]

ERK Activation is Regulated by the Cross-Talk of Multiple Signaling Pathways

Classically, activated ERK has been shown to regulate gene transcription factors involved in promoting cell survival and inducing cell proliferation. Careful

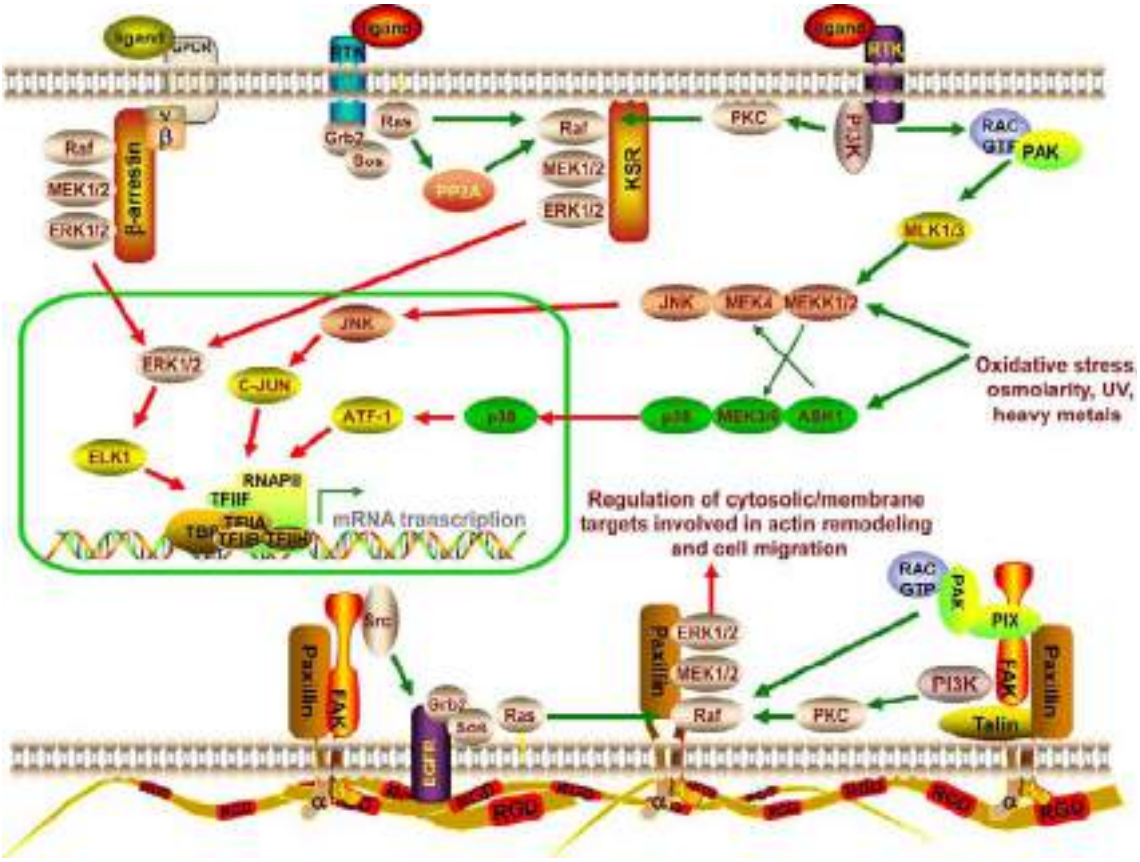

FIGURE 13.10 **MAPK signaling.** The prototypic MAPK pathway involves the growth factor stimulated activation of the small G-protein Ras at the membrane, followed by Ras binding and activation of the serine-threonine kinase Raf (a MAPK kinase kinase or MAPKKK). This process involves dephosphorylation of Raf at an inhibitory site by the serine-threonine phosphatase PP2A. In addition, Raf can be activated by PKC-dependent phosphorylation or by recruitment to the GPCR scaffolding protein β-arrestin. The MAPK pathway can also be activated in a growth factor-independent fashion via focal adhesion signaling when cells attach to the basement membrane. Activation of Raf results in phosphorylation and activation of the downstream kinases MEK and ERK. Depending on the site of ERK activation, it can translocate to the nucleus where it phosphorylates and activates transcription factors such as Elk1 or it can remain in the cytoplasm where it phosphorylates and regulates proteins involved in actin cytoskeletal rearrangement and cell migration, such as Myosin Light Chain Kinase (MLCK) and paxillin. Two other MAPK pathways present in most cells are the stress-activated protein kinases (SAPK) p38 and JNK. Multiple factors have been shown to activate p38 and JNK, including oxidative or osmolar stress, heavy metals, cytokines, and growth factors such as EGF and TGFβ. These stimuli induce the activation of a group of MAPKKKs including apoptosis signal-regulating kinase 1 (ASK1) and MEKK1/2. Activation of the MAPKKK results in phosphorylation of the appropriate dual specificity MAPKK (MEK) such as MEK3, MEK4, and MEK6, which in turn phosphorylate and activate JNK and p38. Small G-proteins such as Rac and Cdc42 can also activate the p38 and JNK pathways via binding and activating intermediate kinases such as the Mixed Lineage Kinase (MLK) family of serine-threonine kinases. There is considerable cross-talk between these pathways, resulting in simultaneous activation of JNK and p38 under many conditions. Like ERK, activated JNK and p38 translocate into the nucleus, where they phosphorylate regulatory transcription factors such as c-Jun, ATF-1, Elk-1, and Sap1. These in turn regulate the RNA polymerase transcription initiation complex to activate the transcription of multiple genes including pro-survival and pro-apoptotic factors, matrix proteins, heat shock factors, etc.

control of these events is fundamental to normal organ physiology, so it is not surprising that ERK activation is regulated by a complex series of signals derived from extracellular stimuli, such as growth factors and cell–matrix interactions. It has long been known that adherent cells, such as endothelial cells and epithelial cells, can proliferate when attached to the proper basement membrane, but undergo anoikis when they lose their attachment. This type of cell death is common in detached tubular epithelial cells following acute renal injury, and it is believed that the loss of anoikis contributes to the metastatic spread of tumor cells.[192–194] As described earlier, the sites of cell attachment to the basement membrane, focal adhesions, provide the nidus for the aggregation of multiple signaling proteins on the cytosolic face of the attachment. Among the many proteins involved in this complex are the MAPK scaffolding protein paxillin, the Rac-activated protein p21 associated kinase (PAK), the EGF receptor, and the non-receptor tyrosine kinases Src and FAK.

Attachment of the cell to a subcellular matrix can activate MAPK signaling, even in the absence of extracellular growth factor or cytokine stimulation. One mechanism for this activation is that attachment-dependent activation of FAK results in the recruitment and activation of the PI 3-kinase, which leads to the local production of $PI_{3,4,5}P_3$. As noted earlier, $PI_{3,4,5}P_3$ binds and activates PKC, which in turn can phosphorylate and activate Raf.[195] Furthermore, the EGF receptor localizes to focal adhesions in adherent cells, and can be phosphorylated and transactivated by the non-receptor tyrosine kinase Src even in the absence of extracellular EGF, thus mediating ERK activation via the classical Grb2-Sos-Ras pathway. In addition to the ability of focal adhesions to directly activate MAPK signaling, these signaling structures are also required for growth factors to efficiently stimulate MAPK signaling.[196] Although the mechanism of this is not entirely understood, recent studies suggest that activation of the focal adhesion associated serine-threonine kinase PAK leads to phosphorylation of Raf that is required for the efficient activation of Raf by GTP-Ras.[197] Thus, focal adhesions serve as sites to directly activate ERK, as well as supporting ERK activation downstream of proliferative stimuli.

ERK Regulates both Nuclear and Cytosolic Protein Actions

Translocation of activated ERK to the nucleus has been found to signal both pro-proliferative and anti-apoptotic responses. In the nucleus, ERK phosphorylates and activates transcription factors such as Elk-1 and RUNX2, which in turn regulate the mRNA expression of the cell cycle proteins cyclin D1 and $p21^{WAF1}$,[198–200] (reviewed in [201]). Furthermore, ERK activation can downregulate the expression of pro-apoptotic proteins such as Bim1, a process that is believed to be critical for ERK-dependent inhibition of anoikis.[202] These effects of ERK depend on both the amplitude and the duration of ERK activation. For example, transient high level ERK activation in renal tubular cells treated with the growth factor HGF results in activation of focal complex signaling and Rac-dependent cell migration, but does not result in significant cell proliferation.[183] In contrast, sustained low level ERK activation appears to be required for cell cycle entry (leading to proliferation) and the anti-apoptotic effects of ERK.[203–205] For this reason, the degree of ERK activation is tightly regulated by a series of phosphorylation and dephosphorylation steps at the level of Raf.[188]

Activation of ERK can also lead to the phosphorylation of substrate proteins in the cytoplasm. ERK has been shown to phosphorylate and activate myosin light chain kinase (MLCK), resulting in stimulation of cell motility.[180] In addition, ERK activation at focal adhesions in renal epithelial cells can mediate phosphorylation of paxillin, and subsequent FAK and PI 3-K activation.[52] This process plays a regulatory role in the local activation of another family of small GTP-binding proteins, Rho, Rac, and Cdc42. These proteins are regulators of actin cytoskeletal remodeling, and by binding to their respective effector proteins (such as the Rho-kinase for Rho), mediate the cytoskeletal changes required for cell spreading, lamellipodia formation, and migration (reviewed in [206]). Besides activation downstream of ERK and the PI 3-K, focal adhesion signaling can also activate Rho family members by stimulating the guanine nucleotide exchange factors Vav and/or PIX (reviewed in [207]). In the kidney, regulated activation of Rac and Rho are fundamental for the morphogenic changes involved in developmental tubulogenesis,[208] and Rho activation appears to be required for angiotensin II-dependent regulation of glomerular arteriolar tone.[209]

In addition to the classic ERK MAPK pathway, two other well-conserved MAPK pathways, the JNK and p38 pathways, have been extensively studied and found to play important roles in regulating cell survival (reviewed in [210,211]). Similar to the ERK pathway, p38 and JNK signaling are mediated by a core complex of three proteins, including a MEK kinase which phosphorylates a MEK family member (MEK3 or 6 in the p38 pathway, MEK4 or 7 in the JNK pathway), which in turn phosphorylates the effector kinase p38 or JNK, respectively. Activated p38 or JNK can then translocate to the nucleus, where they phosphorylate and regulate transcription factors such as ATF-1, ATF-2, c-Jun, and STAT-3.

Activation of the p38 and JNK signaling cascades occurs in response to cell stress signals, including UV irradiation, ischemia, and hypoxia, as well as following cytokine stimulation (IL-1 and TNFα) and certain growth factors (EGF, TGFβ).[212,213] Based on *in vitro* studies demonstrating increased extracellular matrix production following p38 activation, it has been proposed that p38 may play an important role in the development of renal fibrosis following injury (reviewed in [214]). In support of this, *in vivo* studies using p38 inhibitors in rodents have demonstrated that activation of p38 stimulates the progressive renal tubular fibrosis seen in models of chronic ureteral obstruction.[215] Similarly, mice that overexpress TGFβ exhibit p38-dependent glomerular podocyte apoptosis, an early component of the progression to glomerulosclerosis,[213] and p38 activation may be required for the development of proteinuria following acute glomerular injury.[216] Activation of the ERK, p38, and JNK pathways occurs during the oxidative stress of renal ischemia/reperfusion. Under these conditions, JNK activation appears to mediate the tubular cell apoptotic response, while ERK activation can be protective.[217–219]

The Phosphoinositide 3-Kinase Pathway Regulates Diverse Events Including Glucose Metabolism, Cell Migration, Cell Survival, and Proliferation

Another major intracellular signaling pathway is regulated by a lipid kinase known as the phosphoinositide 3-kinase (PI 3-K).[220] This enzyme is composed of two subunits, the p85 adapter protein and the p110 catalytic-subunit. Recruitment of the p85/p110 complex to the membrane occurs when p85 binds via its SH2 domains to tyrosine phosphorylated receptors (such as the PDGF receptor) or docking proteins (such as the EGF receptor associated protein Gab1 or the insulin receptor associated protein IRS-1). The p110 enzymatic-subunit is activated by this translocation and phosphorylates target lipids, such as $PI_{4,5}P_2$ (PIP2), to form the 3-phosphorylated derivative $PI_{3,4,5}P_3$ (PIP3). PIP3 then serves as a membrane-binding site for multiple proteins that contain lipid-binding domains, such as the pleckstrin homology (PH) domain, the PTB domain, and FYVE domains (reviewed in [221]).

As described previously, several PKC family members are recruited to the membrane and activated by binding to PIP3, as are the docking protein DOCK180 and the guanine nucleotide exchange factor Vav.[222,223] However, the best described targets of PIP3 are the PH-domain containing proteins 3-phosphoinositide dependent kinase-1 (PDK1) and its major substrate enzyme Akt (also known as protein kinase B (PKB)). The generation of PIP3 at the membrane results in recruitment and activation of PDK1, which in turn phosphorylates and activates Akt.[224] In addition to Akt, activated PDK1 can phosphorylate and activate IKK, the upstream regulator of NF-κB, as well as the p70 and p90 ribosomal S6 kinases, and several PKC isoforms.[225,226]

Akt is a serine-threonine kinase that regulates multiple intracellular events, including protein ubiquitination/degradation, glucose metabolism, nitric oxide generation, cell survival, and cell proliferation. To regulate these disparate processes, Akt associates with and phosphorylates multiple cytosolic protein targets (reviewed in [227]). One of these targets is the constitutively active cytosolic enzyme glycogen synthase kinase-3β (GSK-3β), described earlier for its role as a regulator of β-catenin ubiquitination and degradation downstream of the Wnt signaling pathway.[228,229] Phosphorylation of serine 9 at the N-terminus of GSK-3β by Akt causes the kinase domain of GSK-3β to recognize this region as a pseudosubstrate, leading to autoinhibition of the GSK-3β kinase activity and an increase in free cytosolic β-catenin levels.[230,231] β-catenin can then translocate into the nucleus, where it regulates the transcriptional expression of genes involved in stimulating cell proliferation and dedifferentiation. In addition to β-catenin, GSK-3β has also been shown to phosphorylate several other cellular substrates that regulate cell proliferation as well as cell survival. For example, GSK-3β can enter the nucleus where it phosphorylates the cell cycle protein cyclin D1, thus targeting it for rapid degradation.[232] In addition, phosphorylation of translation initiation factor eIF2B by GSK-3β inhibits protein translation, leading to initiation of apoptosis and ultimately cell death.[233] Thus, activation of the PI 3-K/Akt pathway by inhibiting GSK-3β results in increased cyclin D1 levels and eIF2B activation, promoting entry into the cell cycle and preventing apoptotis.

Besides these indirect effects of Akt in preventing cell apoptosis, Akt activation directly inhibits apoptotic responses by phosphorylating and inhibiting the pro-apoptotic factors BAD and caspase 9, as well as the forkhead transcription factor FKHRL1.[234] In addition, Akt activation can stimulate protein synthesis and cell growth via its effects on mTOR, the mammalian target of rapamycin (reviewed in [235]). mTOR is a serine-threonine kinase that phosphorylates and activates the ribosomal protein translation initiators S6 kinase and 4EBP, leading to increased protein translation and promoting cell growth and division. Rapamycin, by inhibiting mTOR, prevents protein translation and inhibits cell division, leading to its use to suppress tumor growth, and as an immune suppressant (due to inhibition of T- and B-cell expansion).

The kinase activity of mTOR is activated by binding to the small GTP-binding protein Rheb. Like Ras, Rac, and Gα, Rheb is active when in the GTP-bound state, and inactive when in the GDP-bound state. Conversion of GTP-Rheb to GDP-Rheb is mediated by a GTPase complex made up of two proteins, tuberin and hammartin. The GTPase activity of these proteins, which are mutated in many patients with tuberous sclerosis, is in turn negatively regulated by phosphorylation of tuberin by activated Akt.[236] In this manner, activation of Akt downstream of the PI 3-K results in stabilization of Rheb in the GTP-bound state, thereby activating mTOR and accelerating cell growth and division (Figure 13.11).

In addition to its fundamental role in regulating cell survival and proliferation, another major physiologic process regulated by the PI 3-K/Akt pathway is insulin-dependent glucose metabolism (reviewed in [237]). Binding of insulin to its receptor tyrosine kinase results in the tyrosine phosphorylation of a docking protein, insulin receptor substrate (IRS-1), which in turn activates multiple intracellular signaling pathways including the PI 3-K. Activation of the PI 3-K has been shown to regulate insulin-dependent glucose uptake, glycogen synthesis, and lipolysis. Glucose uptake is

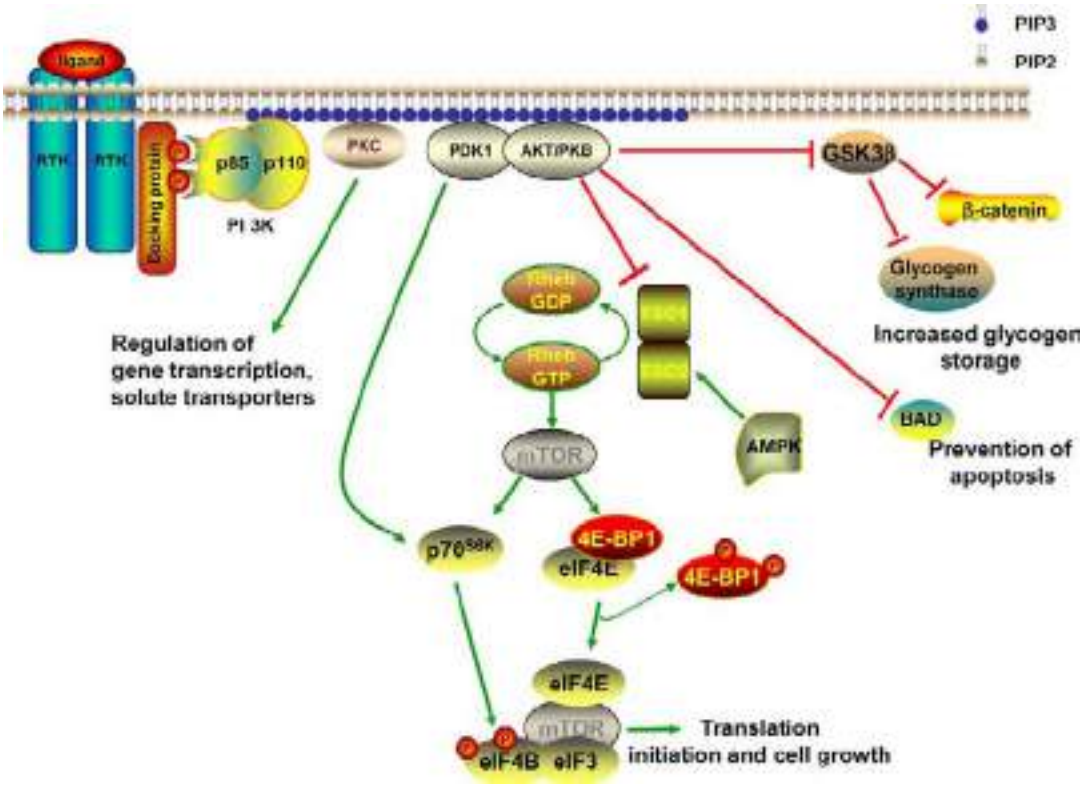

FIGURE 13.11 **Signaling through the PI 3-kinase/Akt pathway.** The activation of growth factor receptors results in the recruitment of the p85/p110 PI 3-kinase heterodimer to the membrane via binding of the SH2 domains of p85 to phosphotyrosine residues on the receptor or an associated docking protein such as IRS-1. Activation of the lipid kinase activity of p110 occurs, resulting in generation of $PI_{3,4,5}P_3$ (PIP3) at the inner leaflet of the membrane. PIP3 serves as a binding site for proteins that contain lipid-binding domains, including several PKC family members, docking proteins, and the serine-threonine kinase phosphoinositide-dependent kinase (PDK1). PDK1 has several targets in the cell, including the protein translation activator p70 S6kinase and the cytosolic serine-threonine kinase protein kinase B (PKB), also known as Akt. Akt phosphorylates multiple substrates in the cell (typically resulting in inhibition of their action) that promote cell growth and survival. Thus, phosphorylation of the tuberosis sclerosis complex (TSC1 and TSC2) inhibits their GTPase activity, leading to accumulation of GTP Rheb and activation of mTOR. mTOR in turn activates p70 S6kinase and phosphorylates 4E-BP, resulting in its disassociation from eukaryotic initiation factor 4E (eIF4E), and cumulatively stimulating increased protein translation. During times of ATP depletion and AMP accumulation, mTOR activity is inhibited by the AMP activated kinase AMPK. AMPK phosphorylates and activates the TSC complex, thus converting GTP Rheb to GDP Rheb and inactivating mTOR. Activated Akt also phosphorylates and inhibits pro-apoptotic factors such as BAD and caspase 9, and inhibits degradation of intracellular proteins, such as glycogen synthase, by phosphorylating and inhibiting GSK-3β.

mediated by the transport protein GLUT4. In the absence of insulin, GLUT4 is located in intracellular vesicles, but fuses with the plasma membrane following insulin stimulation. This translocation of GLUT4-containing vesicles to the membrane is mediated by $PI_{3,4,5}P_3$-dependent activation of both PKCζ and Akt (reviewed in [238]).

Once glucose enters the cell, it is rapidly sequestered by conversion into glycogen via the actions of the enzyme glycogen synthase. In quiescent cells, the constitutively active form of GSK-3β normally phosphorylates glycogen synthase, keeping it in the inactive state. By stimulating the PI 3-kinase, insulin can increase Akt activation, thereby inhibiting GSK-3β activity and increasing glycogen synthase-dependent incorporation of glucose into glycogen.[239]

EXAMPLES OF SIGNALING EFFECTORS IN THE KIDNEY

The extraordinarily complex interactions that initiate, regulate, and terminate intracellular second messenger pathways, such as those described above, ultimately lead to the change in location, function or amount of effector proteins that actually mediate the cellular response to the initial signal. These effector proteins regulate fundamental cellular events such as division, programmed cell death, migration, and differentiation that are required for the development, maintenance, and repair of all tissues. In the kidney, signaling pathways are also critical for the precise regulation of glomerular filtration and for alteration of tubular cell channel function in response to changes in

the internal milieu. While more detailed descriptions of these regulatory events are presented in the appropriate chapters of this book, examples of several specific effector proteins are presented here in order to provide general paradigms of the ways in which signaling pathways can regulate effector protein function in the kidney.

Angiotensin II Signaling in Glomerular Vascular Smooth Muscle

Maintenance of GFR in the face of falling renal perfusion is achieved by the independent regulation of afferent and efferent vascular tone, which is in part determined by the arteriolar smooth muscle response to locally produced angiotensin II. In the efferent arteriole of the glomerulus, stimulation of smooth muscle contraction by angiotensin II requires the coordinated regulation of both myosin light chain kinase (MLCK) and myosin light chain phosphatase (MLCP, reviewed in [240,241]). Activation of the AT1 receptor on the efferent arteriole results in activation of $G_{\alpha q}$ and the downstream second messenger PLCβ. As noted previously, the hydrolysis of PIP2 by PLCβ results in the formation of DAG and the release of IP_3. In smooth muscle cells, IP3 binds to its receptor on the sarcoplasmic reticulum, stimulating intracellular calcium release, which in turn activates calcium entry from outside the cell. The resultant rise in intracellular calcium leads to calmodulin-dependent activation of MLCK, which in turn phosphorylates and activates the regulatory light chain of smooth muscle myosin II, leading to actin−myosin coupling and muscle contraction.

The phosphorylation sites on myosin II are targets for subsequent dephosphorylation by MLCP (also known as myosin phosphatase). In concert with its activation of MLCK, activation of the AT1 receptor stimulates two pathways that lead to inhibition of MLCP (reviewed in [242]). First, the formation of DAG in the membrane, coupled with the rise in intracellular calcium, leads to recruitment and activation of both conventional and novel PKCs. One of the phosphorylation targets of activated PKC in the smooth muscle cell is CPI-17, and in the phosphorylated state CPI-17 associates with and inhibits MLCP via binding to the PP1Cδ catalytic-subunit.

A second group of proteins phosphorylated by PKC are the matrix metalloproteinases.[243] These proteins are involved in cleaving and shedding cell surface proteins, including the cell attached growth factor HB-EGF. Shedding of HB-EGF leads to activation of the EGF receptor, with stimulation of downstream signaling including the PI 3-kinase. This process of GPCR-dependent activation of a nearby growth factor receptor is termed transactivation. In smooth muscle cells, one target of the activated PI 3-kinase is a Rho GEF named leukemia-associated Rho guanine nucleotide exchange factor (LARG).[244] Activation of LARG converts Rho to the GTP-bound state, mediating its association with Rho kinase. This activation of Rho kinase can inhibit MLCP activity, both by direct phosphorylation of MLCP at an inhibitory site, and via phosphorylation of CPI-17 in conjunction with PKC. By simultaneously increasing the phosphorylation of the light chain of myosin II via activation of MLCK and inhibiting its dephosphorylation via inactivation of MLCP, angiotensin II can greatly augment myosin II coupling with actin and subsequent smooth muscle contraction. In addition to stimulating smooth muscle contraction, sustained angiotensin II-dependent increases in intracellular calcium can lead to calmodulin−calcineurin interactions and subsequent activation of NFAT, which in turn activates the transcription of genes involved in promoting muscle cell hypertrophy (reviewed in [245]) (Figure 13.12).

Regulation of Ion Transport Channels

The regulation of GFR by controlling afferent and efferent vascular tone must be coordinated with appropriate changes in solute reabsorption along the nephron. Typically this regulation occurs in one of three ways: regulation of the amount of the transporter in the cell; regulation of the location of the transporter; or regulation of the active state of the transporter at the membrane. In most cases, more than one of these regulatory steps is utilized, allowing both short- and long-term regulation of transporter function.

Sodium Reabsorption in the Collecting Duct can be Regulated by Controlling Cellular Levels of ENaC

The epithelial sodium channel ENaC is expressed on the apical membrane of principal cells of the collecting duct. Regulation of ENaC function is one of the major ways in which the kidney controls the amount of sodium that is excreted in the urine each day. ENaC is comprised of three subunits that are synthesized in the ER and then transported to the Golgi for proteolytic cleavage and activation, followed by trafficking to the apical membrane. ENaC channels present in the membrane can then be internalized where they are either degraded or maintained in a submembranous pool available for rapid recycling back to the membrane. The principal factors that regulate the synthesis, location, and degradation of ENaC are aldosterone and, to a lesser degree, AVP.

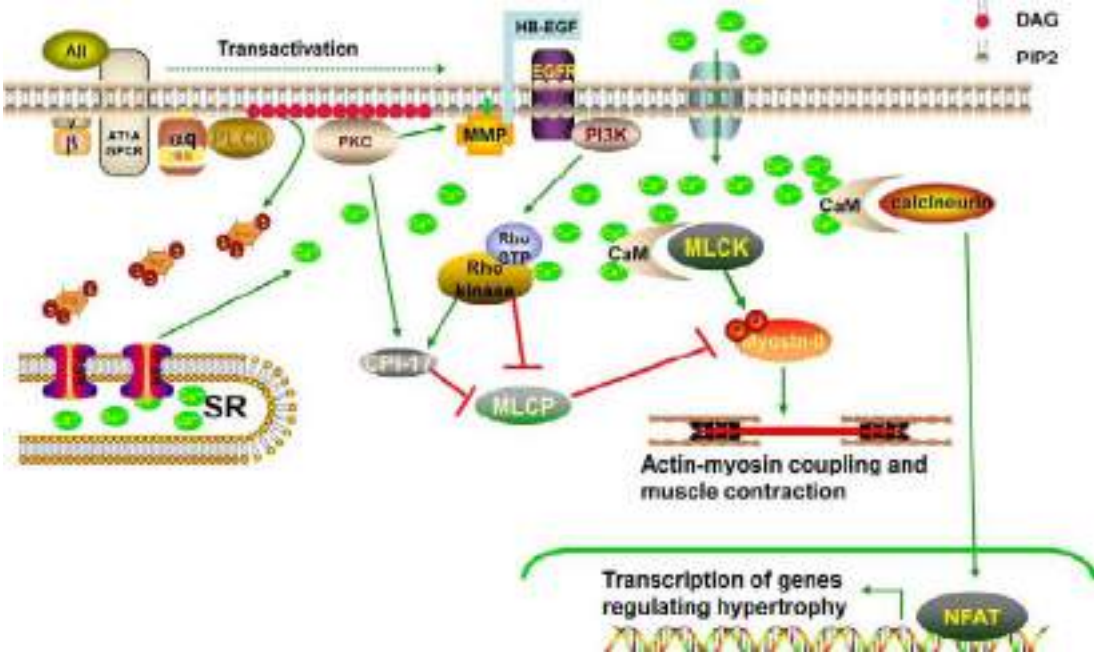

FIGURE 13.12 **Angiotensin II regulation of vascular smooth muscle contraction.** Binding of angiotensin II to the AT1A receptor results in activation of PLCβ, and subsequent generation of IP3 and DAG. DAG production at the membrane can mediate the recruitment and activation of PKC, while IP3 binding to the IP3 receptor in the sarcoplasmic reticulum stimulates calcium release. Angiotensin II may also stimulate extracellular calcium entry via cell surface calcium channels. Binding of the calcium to calmodulin (CaM) results in calmodulin-dependent activation of myosin light chain kinase (MLCK), which phosphorylates myosin II to initiate actin–myosin contraction. Myosin II is dephosphorylated by myosin light chain phosphatase (MLCP) to end the contraction. However, during the period immediately after AT1A stimulation, myosin II phosphorylation is maximized, because MLCP is inhibited by PKC-dependent phosphorylation of the MLCP inhibitory binding protein CPI-17. In addition, GPCR activation can stimulate transactivation of nearby growth factor receptors (such as the EGFR) which in turn can activate the PI 3-K. One mechanism of transactivation is the PKC-dependent activation of matrix metalloproteinases (MMP) which cause shedding of the cell attached protein HB-EGF, which binds and activates the EGFR. The resultant PI 3-K activation mediates GTP loading of the small G-protein Rho, and subsequent activation of Rho kinase. Rho kinase can directly phosphorylate MLCP at an inhibitory site, and can phosphorylate CPI-17 and thus increase its inhibitory effect on MLCP. Sustained contractile stimuli result in the calmodulin-dependent activation of calcineurin. Calcineurin is a phosphatase that binds to and dephosphorylates the nuclear factor of activated T-cells (NFAT), resulting in NFAT-dependent transcriptional regulation of genes involved in smooth muscle cell hypertrophy.

Steroid Hormones such as Aldosterone Bind to Cytoplasmic Receptors and Regulate Nuclear Transcription Events

Aldosterone is a steroid hormone that binds to and activates the mineralocorticoid receptor (MR), which is present in the principal cell, but also in other cell types including intestinal epithelial cells, neuronal cells, and cardiac myocytes. The MR is a member of the steroid/thyroid family of ligand-inducible transcription factors that includes the vitamin D receptor, glucocorticoid receptor, thyroid receptor, and retinoic acid receptor (reviewed in [246]). Unlike the transmembrane receptors discussed in the section "Cell Surface Receptors," these receptors reside in the cytoplasm. The ligand, such as thyroid hormone or aldosterone, can cross the cell membrane, bind the cytosolic receptor, and then translocate as a ligand–receptor complex into the nucleus and bind to specific DNA sequences known as steroid response elements (SRE). In the case of aldosterone, these regulatory sequences are found in the promoter regions of target genes such as *SCNN1A* (the ENaC α-subunit gene) and *SGK-1* (encodes SGK, serum, and glucocorticoid-induced kinase).

In the principal cell, the β- and γ-subunits of ENaC are produced in excess, but do not traffic efficiently to the cell surface until the α-subunit is made (reviewed in [247]). The increase in ENaC α-subunit protein expression that occurs following stimulation with aldosterone leads to ER assembly of αβγ in a complex with the predicted stoichiometry of 2α:β:γ, and its subsequent proteolytic activation in the Golgi. In this manner, aldosterone directly increases the total number of active ENaC transporters available in the cell, leading to an increase in sodium reabsorptive capacity.

A second way in which aldosterone can increase the number of ENaC channels available to reabsorb sodium is by inhibiting ENaC degradation. This is mediated by the transcriptional regulation of SGK expression.[248] SGK is a serine-threonine kinase that phosphorylates and inactivates Nedd4-2, a ubiquitin–protein ligase that can

associate with ENaC and stimulate its internalization and degradation[249] (Figure 13.13). By increasing SGK expression, aldosterone inhibits Nedd4-2-mediated ENaC degradation, and thereby increases the amount of ENaC present on the cell surface. Mutations in ENaC that prevent its association with Nedd4-2 lead to sustained increases in sodium reabsorption due to increased ENaC expression, resulting in the progressive hypertension seen in Liddle's syndrome.[250]

Regulation of Water Reabsorption in the Collecting Duct is Achieved by Trafficking of Aquaporin-2.

The regulation of channel amount by altering rates of synthesis and/or degradation is a relatively slow process that typically takes hours to days to accomplish, and is believed to be most relevant in the adaptive responses to long-standing volume depletion or volume excess. In contrast, regulation of channel location provides a way to rapidly alter channel function in the cell. Aquaporins, transmembrane channels that provide a conduit for water movement across cell membranes, are one of many proteins that can be regulated in this fashion. In the kidney, aquaporin-2 (AQP2) is expressed in cells of the collecting duct, and its ability to mediate water movement is regulated by AVP (reviewed in [251]). In contrast, AQP1 (present in the proximal tubule and thin descending limb[252]) and AQP3 (present on the basolateral side of collecting duct cells[253]) are relatively insensitive to AVP.

In the absence of AVP, AQP2 is present primarily in submembranous vesicles in the collecting duct. Stimulation of V2 receptors by AVP results in the fusion of these vesicles with the apical membrane of the collecting duct cell. Mutations in either the V2

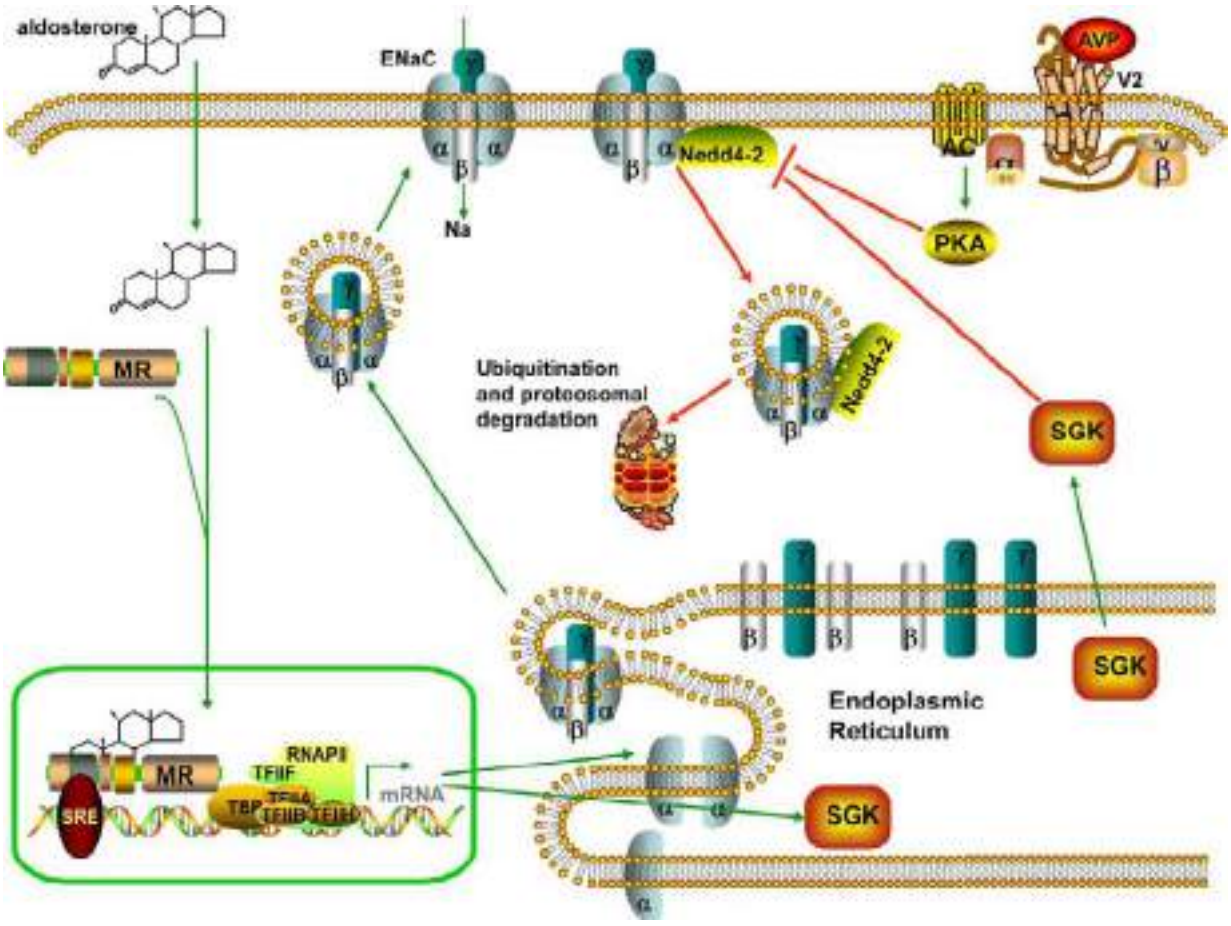

FIGURE 13.13 **Regulation of ENaC.** Aldosterone is a steroid hormone that can cross the cell membrane and bind to the mineralocorticoid receptor (MR) in the cell cytoplasm. The aldosterone–MR complex translocates into the nucleus, where it binds to steroid response elements in genes such as *SCNN1A* encoding the α-subunit of ENaC and *SGK-1* encoding a cytosolic serine threonine kinase. Synthesis of the α-subunit of ENaC promotes formation of the complete ENaC multimer in the ER and its translocation to the cell surface. At the membrane, the ubiquitin ligase Nedd4-2 can bind to ENaC, targeting it for internalization and proteosomal degradation. Nedd4-2 function is inhibited following phosphorylation by SGK, further increasing ENaC expression at the cell membrane, and therefore sodium reabsorptive capacity. Vasopressin (AVP), acting through the V2 GPCR, can also increase collecting duct sodium reabsorption. V2 activation leads to cAMP production and subsequent PKA activation. Like SGK, PKA can phosphorylate and inhibit Nedd4-2.

receptor or AQP2 itself result in nephrogenic diabetes insipidus, due to the failure of the collecting duct to increase water reabsorption in response to AVP. The translocation of AQP2 vesicles to the cell membrane is dependent on AVP-stimulated production of cAMP, and the subsequent activation of PKA. Activated PKA is targeted to AQP2-containing vesicles via association with A kinase anchoring proteins (AKAPs). AKAPs comprise a large family of proteins that localize activated PKA to specific sites within the cell, thus providing specificity and compartmentalization of PKA signaling. AKAP18δ, PKA, and AQP2 can be co-purified from vesicles isolated from the cytosol of inner medullary collecting duct cells, suggesting that this AKAP may be important for facilitating the recruitment of PKA to AQP2-containing vesicles.[254]

Activated PKA directly phosphorylates serine 256 in the carboxy terminus of AQP2, stimulating membrane translocation of the AQP2-containing vesicles.[255] How phosphorylation of serine-256 in AQP2 mediates vesicle fusion with the membrane is not yet fully-understood (reviewed in [256]). Based on present studies, it appears that membrane targeting involves the actin cytoskeletal-dependent association of SNARE proteins (such as syntaxin-3 and -4) on the AQP2-containing vesicles with SNAP23 at the cell membrane.[257,258]

The vesicles that mediate AQP2 translocation to the membrane also carry signals for downregulation of the pathway. Recently it has been found that these vesicles contain cAMP-specific phosphodiesterase-4D (PDE4D), an enzyme that can degrade cAMP, leading to inactivation of PKA.[259] In the presence of the AKAP18δ scaffold, PKA can phosphorylate and activate PDE4D, leading to decreased cAMP, loss of PKA activation, and prevention of AQP2 phosphorylation and translocation. In addition, the serine-threonine phosphatase PP2B is present in these vesicles, and is capable of dephosphorylating AQP2, thereby potentially inhibiting channel translocation.[260]

AQP2 function can be regulated by mechanisms in addition to membrane trafficking. In the setting of continuous stimulation by AVP, total cellular levels of AQP2 message and protein increase, demonstrating that AVP can induce transcription of the AQP2 gene. *In vitro* experiments have suggested that this is due to transcriptional activation of AQP2 mRNA expression via a cyclic AMP response element (CRE) in the AQP2 promotor.[261] Activation of multiple intracellular serine-threonine kinases, including PKA, can stimulate phosphorylation and activation of the CRE-binding protein (CREB), which in turn binds CRE and activates transcription of the appropriate target gene, in this case AQP2. Sustained exposure to hypertonicity can also increase AQP2 mRNA expression in cultured collecting duct cells, independent of AVP-mediated PKA activation.[262]

In addition to its ability to regulate AQP2-mediated water absorption, AVP has been shown to regulate ENaC-mediated salt absorption (see Figure 13.13). Nedd4-2, the ubiquitin ligase that is inactivated by SGK-mediated phosphorylation, can be phosphorylated at the same sites by AVP-activated PKA, leading to inhibition of the Nedd4-2/ENaC association and increased ENaC protein stability.[263] In addition, the cAMP-stimulated activation of PKA by AVP can promote the translocation of ENaC from a pool of internalized channels to the membrane, similar to its effects on AQP2.[264,265] The increase in ENaC surface expression resulting from these signaling events is believed to partially mediate the observed increase in sodium reabsorption following AVP treatment[266] (reviewed in [267]).

Transporters such as ROMK can be Regulated by Changes in their Active State

A third way in which transporters can be regulated is via alteration of the active state of the protein. For membrane channels this typically means a change in the open probability (P_o) of the channel (the time that the channel spends in the open configuration). ROMK (also known as Kir1.1) is an apical membrane potassium channel in thick ascending limb cells and principal cells that is required for potassium recycling in the TAL, and potassium secretion in the collecting duct (reviewed in [268]). One of the major determinants of P_o for ROMK is the concentration of PIP_2 in the membrane in the vicinity of the channel, an effect that appears to be due to an extensive series of interactions between the basic amino acids in the carboxy terminus of ROMK and the negatively charged head groups of the membrane phospholipids (reviewed in [269]). PIP_2 is produced by lipid kinases such as the $PI(4)P_5$ kinase, and degraded by phospholipases such as PLA_2 and PLC (reviewed in [270,271]). Thus, it is speculated that signals that enhance PIP_2 production or inhibit its degradation will increase ROMK activity at the membrane, whereas pathways that reduce PIP_2 levels, such as activation of PKC, will inhibit its activity.

Alterations in the P_o for ROMK have also been found to be due to direct phosphorylation of the channel by PKA (reviewed in [269]). *In vitro* studies have demonstrated three PKA phosphorylation sites in ROMK, and phosphorylation of two of those sites (serine 219 and 313) causes an increase in P_o for the channel, without changing the number of channels at the membrane. As with other PKA effectors, the presence of the appropriate AKAP is required to target activated PKA to ROMK at the membrane. Although the precise mechanism by which PKA phosphorylation regulates P_o in ROMK has yet to be determined, it appears that at least part of the effect is due to an increased affinity of ROMK for PIP_2, thus reducing the concentration of PIP_2 needed to

support the channel in the open state.[272] Based on these studies, it is presently believed that the AVP-stimulated increase in thick ascending limb potassium recycling is due to V2-dependent activation of PKA, and subsequent phosphorylation and activation of ROMK.[273]

Similar to the regulation of aquaporin-2 and ENaC, ROMK can also be regulated by altering channel location or synthesis. Several kinases have been implicated in regulating the trafficking of ROMK, including PKA, SGK, and a recently described kinase WNK (with no K (lysine)). As noted above, there are three PKA phosphorylation sites on ROMK. While two of the sites directly regulate channel open probability, phosphorylation of the third residue (serine 44) increases the number of channels present on the cell membrane. In addition to PKA, SGK can phosphorylate ROMK on serine 44 and increase channel activity in the oocyte expression system.[274] This appears to occur in concert with a scaffolding protein, NHERF2, which increases trafficking of ROMK to the membrane via its interaction with the carboxy terminal PDZ-binding motif.[275] Thus, the increased expression of SGK following aldosterone stimulation can lead to sustained increases in ROMK-dependent potassium excretion via increased numbers of channels on the cell membrane.

Recently, another family of serine/threonine kinases, the WNKs, have been found to play an important role in regulating the activity of diverse ion channels in the kidney (reviewed in [276]). To date there have been four WNK kinases described in humans, all sharing the unusual substitution of a cysteine residue for the more typical lysine in β strand 3 of the kinase domain.[277] Of these four, WNK1, WNK3, and WNK4 have been directly implicated in regulation of tubular ion transport, including the sodium-potassium-chloride co-transporter in the TAL (NKCC2), the sodium-chloride co-transporter in the distal convoluted tubule (NCC), ROMK, EnaC, and the tight junctional proteins claudin1-4 that regulate paracellular chloride flux,([278–280] reviewed in [281]). Mutations of WNK1 and WNK4 have been shown to cause pseudohypoaldosteronism II (PHAII), a syndrome consisting of hypertension with increased sodium reabsorption and hyperkalemia.[282]

The mechanisms by which WNKs regulate ROMK and NCC depend on distinct aspects of WNK function. Mutations in WNK1 and WNK4 that cause PHAII result in decreased ROMK at the membrane, and therefore hyperkalemia due to decreased K secretion.[280,283] It has been shown that ROMK associates with a complex including WNK1, WNK4, and the scaffolding protein intersectin, and that intersectin is required for the endocytosis of ROMK in clathrin-coated vesicles.[284] The formation of this complex is independent of WNK kinase activity, and instead requires the association of proline-rich regions of WNK1 and WNK4 with the SH3 domain of intersectin. Mutations in WNK4 that cause PHAII appear to increase the association of the ROMK−WNK1−WNK4 complex with intersectin, thereby augmenting ROMK internalization and impairing potassium secretion.[285]

WNK kinases regulate sodium uptake by determining both the surface availability and activation state of NCC. This process is complex and not yet fully elucidated, but appears to involve a balance between WNK4-dependent degradation of NCC and WNK1-dependent activation of NCC that is present on the cell surface (reviewed in [276]). In the presence of active WNK4, newly synthesized NCC is targeted via sortilin for lysosomal degradation rather than cell surface expression, thus reducing the pool of NCC available for sodium transport.[286,287] In contrast, WNK1 and WNK3 activate the sodium transport function of NCC that is on the cell surface by phosphorylating the intracellular kinase SPAK, which then phosphorylates and activates NCC. A second phosphorylation target of WNK3 is WNK4 itself, resulting in inhibition of the WNK4-mediated NCC degradation, and thus increasing NCC surface expression. Mutations in WNK4 that cause PHAII result in increased sodium reabsorption at least in part due to increased NCC on the cell surface.[288]

References

[1] Miura S, Saku K, Karnik SS. Molecular analysis of the structure and function of the angiotensin II type 1 receptor. Hypertens Res 2003;26:937.

[2] Malbon CC. G proteins in development. Nat Rev Mol Cell Biol 2005;6:689.

[3] Strock J, Diverse-Pierluissi MA. Ca^{2+} channels as integrators of G protein-mediated signaling in neurons. Mol Pharmacol 2004;66:1071.

[4] Krasel C, Bunemann M, Lorenz K, Lohse MJ. Beta-arrestin binding to the beta2-adrenergic receptor requires both receptor phosphorylation and receptor activation. J Biol Chem 2005;280:9528.

[5] Tran TM, Friedman J, Quniabi E, Baameur F, Moore RH, Clark RB. Characterization of agonist stimulation of cAMP-dependent protein kinase and G protein-coupled receptor kinase phosphorylation of the beta2-adrenergic receptor using phosphoserine-specific antibodies. Mol Pharmacol 2004;65:196.

[6] Jose PA, Eisner GM, Felder RA. Renal dopamine and sodium homeostasis. Curr Hypertens Rep 2000;2:174.

[7] Beaulieu JM, Gainetdinov RR. The physiology, signaling, and pharmacology of dopamine receptors. Pharmacol Rev 2011;63:182.

[8] Jose PA, Eisner GM, Felder RA. Role of dopamine receptors in the kidney in the regulation of blood pressure. Curr Opin Nephrol Hypertens 2002;11:87.

[9] Yang Z, Sibley DR, Jose PA. D5 dopamine receptor knockout mice and hypertension. J Recept Signal Transduct Res 2004;24:149.

[10] Banday AA, Lokhandwala MF. Dopamine receptors and hypertension. Curr Hypertens Rep 2008;10:268.

[11] Carey RM. Update on the role of the AT2 receptor. Curr Opin Nephrol Hypertens 2005;14:67.
[12] Porrello ER, Delbridge LM, Thomas WG. The angiotensin II type 2 (AT2) receptor: an enigmatic seven transmembrane receptor. Front Biosci 2009;14:958.
[13] Siragy HM, Carey RM. The subtype-2 (AT2) angiotensin receptor regulates renal cyclic guanosine 3′, 5′-monophosphate and AT1 receptor-mediated prostaglandin E2 production in conscious rats. J Clin Invest 1996;97:1978.
[14] Tsutsumi Y, Matsubara H, Masaki H, Kurihara H, Murusawa S, Takai S, et al. Angiotensin II type 2 receptor overexpression activates the vascular kinin system and causes vasodilation. J Clin Invest 1999;104:925.
[15] Nagahama T, Hayashi K, Ozawa Y, Takenaka T, Saruta T. Role of protein kinase C in angiotensin II-induced constriction of renal microvessels. Kidney Int 2000;57:215.
[16] Rangel LB, Caruso-Neves C, Lara LS, Lopes AG. Angiotensin II stimulates renal proximal tubule Na(+)-ATPase activity through the activation of protein kinase C. Biochim Biophys Acta 2002;1564:310.
[17] Efendiev R, Budu CE, Cinelli AR, Bertorello AM, Pedemonte CH. Intracellular Na^+ regulates dopamine and angiotensin II receptors availability at the plasma membrane and their cellular responses in renal epithelia. J Biol Chem 2003;278:28719.
[18] Foster RH. Reciprocal influences between the signalling pathways regulating proliferation and steroidogenesis in adrenal glomerulosa cells. J Mol Endocrinol 2004;32:893.
[19] DeFea KA. Beta-arrestins as regulators of signal termination and transduction: how do they determine what to scaffold? Cell Signal 2011;23:621.
[20] Wei H, Ahn S, Shenoy SK, Karnik SS, Hunyady L, Luttrell MM, et al. Independent beta-arrestin 2 and G protein-mediated pathways for angiotensin II activation of extracellular signal-regulated kinases 1 and 2. Proc Natl Acad Sci USA 2003;100:10782.
[21] Kim J, Ahn S, Ren XR, Whalen EJ, Reiter E, Wei H, et al. Functional antagonism of different G protein-coupled receptor kinases for beta-arrestin-mediated angiotensin II receptor signaling. Proc Natl Acad Sci USA 2005;102:1442.
[22] Meng D, Lynch MJ, Huston E, Beyermann M, Eichorst J, Adams DR, et al. MEK1 binds directly to betaarrestin1, influencing both its phosphorylation by ERK and the timing of its isoprenaline-stimulated internalization. J Biol Chem 2009;284:11425.
[23] Reiter E, Ahn S, Shukla AK, Lefkowitz RJ. Molecular mechanism of β-arrestin-biased agonism at seven-transmembrane receptors. Annu Rev Pharmacol Toxicol 2012;52:179–97.
[24] Tsuchida S, Matsusaka T, Chen X, Okubo S, Nijmura F, Nishimura H, et al. Murine double nullizygotes of the angiotensin type 1A and 1B receptor genes duplicate severe abnormal phenotypes of angiotensinogen nullizygotes. J Clin Invest 1998;101:755.
[25] Chen Y, Lasaitiene D, Friberg P. The renin–angiotensin system in kidney development. Acta Physiol Scand 2004;181:529.
[26] Eguchi S, Numaguchi K, Iwasaki H, Matsumoto T, Yamakawa T, Utsunomiya H, et al. Calcium-dependent epidermal growth factor receptor transactivation mediates the angiotensin II-induced mitogen-activated protein kinase activation in vascular smooth muscle cells. J Biol Chem 1998;273:8890.
[27] Thomas WG, Brandenburger Y, Autelitano DJ, Pham T, Qian H, Hannan RD. Adenoviral-directed expression of the type 1A angiotensin receptor promotes cardiomyocyte hypertrophy via transactivation of the epidermal growth factor receptor. Circ Res 2002;90:135.
[28] Gensure RC, Gardella TJ, Juppner H. Parathyroid hormone and parathyroid hormone-related peptide, and their receptors. Biochem Biophys Res Commun 2005;328:666.
[29] Guo J, Chung UI, Kondo H, Bringhurst FR, Kronenberg HM. The PTH/PTHrP receptor can delay chondrocyte hypertrophy *in vivo* without activating phospholipase C. Dev Cell 2002;3:183.
[30] Kovacs CS, Lanske B, Hunzelman JL, Guo J, Karaplis AC, Kronenberg HM. Parathyroid hormone-related peptide (PTHrP) regulates fetal-placental calcium transport through a receptor distinct from the PTH/PTHrP receptor. Proc Natl Acad Sci USA 1996;93:15233.
[31] Lanske B, Karaplis AC, Lee K, Luz A, Vortkamp A, Pirro A, et al. PTH/PTHrP receptor in early development and Indian hedgehog-regulated bone growth. Science 1996;273:663.
[32] Jobert AS, Zhang P, Couvineau A, Bonaventure J, Roume J, Le Merrer M, et al. Absence of functional receptors for parathyroid hormone and parathyroid hormone-related peptide in Blomstrand chondrodysplasia. J Clin Invest 1998;102:34–40.
[33] Ferrandon S, Feinstein TN, Castro M, Wang B, Bouley R, Potts JT, et al. Sustained cyclic AMP production by parathyroid hormone receptor endocytosis. Nat Chem Biol 2009;5:734–42.
[34] Miaczynska M, Bar-Sagi D. Signaling endosomes: seeing is believing. Curr Opin Cell Biol 2010;22:535.
[35] Schiefermeier N, Teis D, Huber LA. Endosomal signaling and cell migration. Curr Opin Cell Biol 2011.
[36] Songyang Z, Blechner S, Hoagland N, Hoekstra MF, Piwinica-Worms H, cantley LC. Use of an oriented peptide library to determine the optimal substrates of protein kinases. Curr Biol 1994;4:973–82.
[37] Sariola H, Saarma M. Novel functions and signalling pathways for GDNF. J Cell Sci 2003;116:3855.
[38] Degl'Innocenti D, Arighi E, Popsueva A, Sangregorio R, Alberti L, Rizzetti MG, et al. Differential requirement of Tyr1062 multidocking site by RET isoforms to promote neural cell scattering and epithelial cell branching. Oncogene 2004;23:7297–309.
[39] Bates CM. Role of fibroblast growth factor receptor signaling in kidney development. Pediatr Nephrol 2007;22:343.
[40] Ishibe S, Karihaloo A, Ma H, Zhang J, Marlier A, Mitobe M, et al. Met and the epidermal growth factor receptor act cooperatively to regulate final nephron number and maintain collecting duct morphology. Development 2009;136:337–45.
[41] Turner N, Grose R. Fibroblast growth factor signalling: from development to cancer. Nat Rev Cancer 2010;10:116.
[42] Kurosu H, Kuro OM. The Klotho gene family as a regulator of endocrine fibroblast growth factors. Mol Cell Endocrinol 2009;299:72.
[43] Revest JM, Spencer-Dene B, Kerr K, De Moerlooze L, Rosewall I, Dickson C. Fibroblast growth factor receptor 2-IIIb acts upstream of Shh and Fgf4 and is required for limb bud maintenance but not for the induction of Fgf8, Fgf10, Msx1, or Bmp4. Dev Biol 2001;231:47–62.
[44] Qiao J, Uzzo R, Obara-Ishihara T, Degenstein L, Fuchs E, Herzlinger D. FGF-7 modulates ureteric bud growth and nephron number in the developing kidney. Development 1999;126:547–54.
[45] Grieshammer U, Cebrián C, Ilagan R, Meyers E, Herzlinger D, Martin GR. FGF8 is required for cell survival at distinct stages of nephrogenesis and for regulation of gene expression in nascent nephrons. Development 2005;132:3847–57.
[46] Holgado-Madruga M, Emlet DR, Moscatello DK, Godwin AK, Wong AJ. A Grb2-associated docking protein in EGF- and insulin-receptor signalling. Nature 1996;379:560.
[47] Weidner KM, Di Cesare S, Sacks M, Brinkmann V, Behrens J, Birchmeier W. Interaction between Gab1 and the c-Met receptor tyrosine kinase is responsible for epithelial morphogenesis. Nature 1996;384:173–6.
[48] Ishibashi K, Sasaki S, Sakamoto H, Hoshino Y, Nakamura T, Marumo F. Expressions of receptor gene for hepatocyte growth

factor in kidney after unilateral nephrectomy and renal injury. Biochem Biophys Res Commun 1992;187:1454–9.
[49] Joannidis M, Spokes K, Nakamura T, Faletto D, Cantley LG. Regional expression of hepatocyte growth factor/c-met in experimental renal hypertrophy and hyperplasia. Am J Physiol 1994;267:F231.
[50] Miller SB, Martin DR, Kissane J, Hammerman MR. Hepatocyte growth factor accelerates recovery from acute ischemic renal injury in rats. Am J Physiol 1994;266:F129.
[51] Maroun CR, Naujokas MA, Holgado-Madruga M, Wong AJ, Park M. The tyrosine phosphatase SHP-2 is required for sustained activation of extracellular signal-regulated kinase and epithelial morphogenesis downstream from the met receptor tyrosine kinase. Mol Cell Biol 2000;20:8513.
[52] Ishibe S, Joly D, Liu ZX, Cantley LG. Paxillin serves as an ERK-regulated scaffold for coordinating FAK and Rac activation in epithelial morphogenesis. Mol Cell 2004;16:257.
[53] Wang W, Koka V, Lan HY. Transforming growth factor-beta and Smad signalling in kidney diseases. Nephrology (Carlton) 2005;10:48.
[54] Luo K, Lodish HF. Signaling by chimeric erythropoietin-TGF-beta receptors: homodimerization of the cytoplasmic domain of the type I TGF-beta receptor and heterodimerization with the type II receptor are both required for intracellular signal transduction. Embo J 1996;15:4485.
[55] Oh SP, Seki T, Goss KA, Imamura T, Yi Y, Donahoe PK, et al. Activin receptor-like kinase 1 modulates transforming growth factor-beta 1 signaling in the regulation of angiogenesis. Proc Natl Acad Sci USA 2000;97:2626–31.
[56] Schnaper HW, Hayashida T, Hubchak SC, Poncelet AC. TGF-beta signal transduction and mesangial cell fibrogenesis. Am J Physiol Renal Physiol 2003;284:F243.
[57] Cain JE, Hartwig S, Bertram JF, Rosenblum ND. Bone morphogenetic protein signaling in the developing kidney: present and future. Differentiation 2008;76:831.
[58] Sankar S, Mahooti-Brooks N, Centrella M, McCarthy TL, Madri JA. Expression of transforming growth factor type III receptor in vascular endothelial cells increases their responsiveness to transforming growth factor beta 2. J Biol Chem 1995;270:13567.
[59] Letamendia A, Lastres P, Botella LM, Raab U, Langa C, Velasco B, et al. Role of endoglin in cellular responses to transforming growth factor-beta. A comparative study with betaglycan. J Biol Chem 1998;273:33011–9.
[60] Nakao A, Afrahkte M, Moren A, Nakayama T, Christian JL, Heuchel R, et al. Identification of Smad7, a TGFbeta-inducible antagonist of TGF-beta signalling. Nature 1997;389:631–5.
[61] Miyazaki Y, Oshima K, Fogo A, Hogan BL, Ichikawa I. Bone morphogenetic protein 4 regulates the budding site and elongation of the mouse ureter. J Clin Invest 2000;105:863.
[62] Lawson KA, Dunn NR, Roelen BA, Zeinstra LM, Davis AM, Wright CV, et al. Bmp4 is required for the generation of primordial germ cells in the mouse embryo. Genes Dev 1999;13:424–36.
[63] Hartwig S, Hu MC, Cella C, Pisicone T, Filmus J, Rosenblum ND. Glypican-3 modulates inhibitory Bmp2-Smad signaling to control renal development *in vivo*. Mech Dev 2005;122:928–38.
[64] Border WA, Noble NA. TGF-beta in kidney fibrosis: a target for gene therapy. Kidney Int 1997;51:1388.
[65] Verrecchia F, Chu ML, Mauviel A. Identification of novel TGF-beta/Smad gene targets in dermal fibroblasts using a combined cDNA microarray/promoter transactivation approach. J Biol Chem 2001;276:17058.
[66] Basu RK, Hubchak S, Hayashida T, Runyan CE, Schumacker PT, Schnaper HW. Interdependence of HIF-1alpha and TGF-beta/Smad3 signaling in normoxic and hypoxic renal epithelial cell collagen expression. Am J Physiol Renal Physiol 2011;300: F898–905.
[67] Yeh YC, Wei WC, Wang YK, Lin SDC, Sung JM, Tang MJ. Transforming growth factor-{beta}1 induces Smad3-dependent {beta}1 integrin gene expression in epithelial-to-mesenchymal transition during chronic tubulointerstitial fibrosis. Am J Pathol 2010;177:1743–54.
[68] Hall MC, Young DA, Waters JG, Rowan AD, Chantry A, Edwards DR, et al. The comparative role of activator protein 1 and Smad factors in the regulation of Timp-1 and MMP-1 gene expression by transforming growth factor-beta 1. J Biol Chem 2003;278:10304–13.
[69] Isaka Y, Fujiwara Y, Ueda N, Kaneda Y, Kamada T, Imai E. Glomerulosclerosis induced by *in vivo* transfection of transforming growth factor-beta or platelet-derived growth factor gene into the rat kidney. J Clin Invest 1993;92:2597–601.
[70] Sato M, Muragaki Y, Saika S, Roberts AB, Ooshima A. Targeted disruption of TGF-beta1/Smad3 signaling protects against renal tubulointerstitial fibrosis induced by unilateral ureteral obstruction. J Clin Invest 2003;112:1486.
[71] Saunders AE, Johnson P. Modulation of immune cell signalling by the leukocyte common tyrosine phosphatase, CD45. Cell Signal 2010;22:339.
[72] Earl LA, Bi S, Baum LG. N- and O-glycans modulate galectin-1 binding, CD45 signaling, and T cell death. J Biol Chem 2010;285:2232.
[73] Grigorian A, Torossian S, Demetriou M. T-cell growth, cell surface organization, and the galectin-glycoprotein lattice. Immunol Rev 2009;230:232.
[74] Yamaguchi H, Hendrickson WA. Structural basis for activation of human lymphocyte kinase Lck upon tyrosine phosphorylation. Nature 1996;384:484.
[75] Mustelin T, Coggeshall KM, Altman A. Rapid activation of the T-cell tyrosine protein kinase pp56lck by the CD45 phosphotyrosine phosphatase. Proc Natl Acad Sci USA 1989;86:6302.
[76] Iwashima M, Irving BA, van Oers NS, Chan AC, Weiss A. Sequential interactions of the TCR with two distinct cytoplasmic tyrosine kinases. Science 1994;263:1136.
[77] Lazarovits AI, Poppema S, Zhang Z, Khandaker M, Le Feuvre CE, Singhal SK, et al. Prevention and reversal of renal allograft rejection by antibody against CD45RB. Nature 1996;380:717–20.
[78] Peles E, Nativ M, Campbell PL, Sakuri T, Martinez R, Lev S, et al. The carbonic anhydrase domain of receptor tyrosine phosphatase beta is a functional ligand for the axonal cell recognition molecule contactin. Cell 1995;82:251–60.
[79] Maeda N, Nishiwaki T, Shintani T, Hamanaka H, Noda M. 6B4 proteoglycan/phosphacan, an extracellular variant of receptor-like protein-tyrosine phosphatase zeta/RPTPbeta, binds pleiotrophin/heparin-binding growth-associated molecule (HB-GAM). J Biol Chem 1996;271:21446.
[80] Meng K, Rodriguez-Pena A, Dimitrov T, Chen W, Yamin M, Noda M, et al. Pleiotrophin signals increased tyrosine phosphorylation of beta beta-catenin through inactivation of the intrinsic catalytic activity of the receptor-type protein tyrosine phosphatase beta/zeta. Proc Natl Acad Sci USA 2000;97:2603–8.
[81] Sakurai H, Bush KT, Nigam SK. Identification of pleiotrophin as a mesenchymal factor involved in ureteric bud branching morphogenesis. Development 2001;128:3283.
[82] Kawachi H, Fujikawa A, Maeda N, Noda M. Identification of GIT1/Cat-1 as a substrate molecule of protein tyrosine phosphatase zeta /beta by the yeast substrate-trapping system. Proc Natl Acad Sci USA 2001;98:6593.
[83] Manabe R, Kovalenko M, Webb DJ, Horwitz AR. GIT1 functions in a motile, multi-molecular signaling complex that

regulates protrusive activity and cell migration. J Cell Sci 2002;115:1497.
[84] Fujikawa A, et al. Mice deficient in protein tyrosine phosphatase receptor type Z are resistant to gastric ulcer induction by VacA of *Helicobacter pylori*. Nat Genet 2003;33:375.
[85] Andersson ER, Sandberg R, Lendahl U. Notch signaling: simplicity in design, versatility in function. Development 2011;138:3593.
[86] Brou C, Logeat F, Gupta N, Bessia C, LeBail O, Doedens JR, et al. A novel proteolytic cleavage involved in Notch signaling: the role of the disintegrin-metalloprotease TACE. Mol Cell 2000;5:207–16.
[87] De Strooper B, et al. A presenilin-1-dependent gamma-secretase-like protease mediates release of Notch intracellular domain. Nature 1999;398:518–22.
[88] Cheng HT, Kopan R. The role of Notch signaling in specification of podocyte and proximal tubules within the developing mouse kidney. Kidney Int 2005;68:1951.
[89] Kopan R, Cheng HT, Surendran K. Molecular insights into segmentation along the proximal–distal axis of the nephron. J Am Soc Nephrol 2007;18:2014.
[90] Cheng HT, Miner JH, Lin M, Tansey MG, Roth. K, Kopan R. Gamma-secretase activity is dispensable for mesenchyme-to-epithelium transition but required for podocyte and proximal tubule formation in developing mouse kidney. Development 2003;130:5031–42.
[91] Cheng HT, Kim M, Valerius MT, Surendran K, Schuster-Gossler K, Gossler A, et al. Notch2, but not Notch1, is required for proximal fate acquisition in the mammalian nephron. Development 2007;134:801–11.
[92] Bielesz B, Sirin Y, Si H, Niranjan T, Gruenwald A, Ahn S, et al. Epithelial Notch signaling regulates interstitial fibrosis development in the kidneys of mice and humans. J Clin Invest 2010;120:4040–54.
[93] Ni CY, Murphy MP, Golde TE, Carpenter G. gamma-Secretase cleavage and nuclear localization of ErbB-4 receptor tyrosine kinase. Science 2001;294:2179.
[94] Vidal GA, Naresh A, Marrero L, Jones FE. Presenilin-dependent gamma-secretase processing regulates multiple ERBB4/HER4 activities. J Biol Chem 2005;280:19777.
[95] Tulasne D, et al. Proapoptotic function of the MET tyrosine kinase receptor through caspase cleavage. Mol Cell Biol 2004;24:10328.
[96] Zou Z, Chung B, Nguyen T, Mentone S, Thomson B, Beimesderfer D. Linking receptor-mediated endocytosis and cell signaling: evidence for regulated intramembrane proteolysis of megalin in proximal tubule. J Biol Chem 2004;279:34302–10.
[97] Li Y, Cong R, Biemesderfer D. The COOH terminus of megalin regulates gene expression in opossum kidney proximal tubule cells. Am J Physiol Cell Physiol 2008;295:C529.
[98] Chauvet V, et al. Mechanical stimuli induce cleavage and nuclear translocation of the polycystin-1 C terminus. J Clin Invest 2004;114:1433.
[99] Low SH, Vansanth S, Larson CH, Mukherjee S, Sharma N, Kinter MT, et al. Polycystin-1, STAT6, and P100 function in a pathway that transduces ciliary mechanosensation and is activated in polycystic kidney disease. Dev Cell 2006;10:57–69.
[100] Bertuccio CA, Chapin HC, Cai Y, Mistry K, Chauvet V, Somlo S, et al. Polycystin-1 C-terminal cleavage is modulated by polycystin-2 expression. J Biol Chem 2009;284:21011–26.
[101] Kwon TH, Nielsen J, Kim YH, Knepper MA, Frokaier J, Nielsen S. Regulation of sodium transporters in the thick ascending limb of rat kidney: response to angiotensin II. Am J Physiol Renal Physiol 2003;285:F152–165.
[102] Miner JH. Renal basement membrane components. Kidney Int 1999;56:2016.
[103] Pozzi A, Zent R. Integrins: sensors of extracellular matrix and modulators of cell function. Nephron Exp Nephrol 2003;94:e77.
[104] Turner CE. Paxillin and focal adhesion signalling. Nat Cell Biol 2000;2:E231.
[105] Zheng M, McKeown-Longo PJ. Regulation of HEF1 expression and phosphorylation by TGF-beta 1 and cell adhesion. J Biol Chem 2002;277:39599.
[106] Cox EA, Sastry SK, Huttenlocher A. Integrin-mediated adhesion regulates cell polarity and membrane protrusion through the Rho family of GTPases. Mol Biol Cell 2001;12:265.
[107] Schwartz MA, Assoian RK. Integrins and cell proliferation: regulation of cyclin-dependent kinases via cytoplasmic signaling pathways. J Cell Sci 2001;114:2553.
[108] Frisch SM, Vuori K, Kelaita D, Sicks S. A role for Jun-N-terminal kinase in anoikis; suppression by bcl-2 and crmA. J Cell Biol 1996;135:1377.
[109] Miner JH, Li C. Defective glomerulogenesis in the absence of laminin alpha5 demonstrates a developmental role for the kidney glomerular basement membrane. Dev Biol 2000;217:278.
[110] Kreidberg JA, Donovan MJ, Goldstein SL, Rennke H, Shepherd K, Jones RC, et al. Alpha 3 beta 1 integrin has a crucial role in kidney and lung organogenesis. Development 1996;122:3537–47.
[111] Zhang X, et al. beta1 integrin is necessary for ureteric bud branching morphogenesis and maintenance of collecting duct structural integrity. Development 2009;136:3357.
[112] Gardner H, Kreidberg J, Koteliansky V, Jaenisch R. Deletion of integrin alpha 1 by homologous recombination permits normal murine development but gives rise to a specific deficit in cell adhesion. Dev Biol 1996;175:301.
[113] Chen X, Moeckel G, Morrow JD, Cosgrove D, Harris RC, Fogo AB, et al. Lack of integrin alpha1beta1 leads to severe glomerulosclerosis after glomerular injury. Am J Pathol 2004;165:617–30.
[114] Gumbiner BM. Regulation of cadherin-mediated adhesion in morphogenesis. Nat Rev Mol Cell Biol 2005;6:622.
[115] Thomson RB, Igarashi P, Biemesderfer D, Kim R, Abu-Alfa A, Soleimani M, et al. Isolation and cDNA cloning of Ksp-cadherin, a novel kidney-specific member of the cadherin multigene family. J Biol Chem 1995;270:17594–601.
[116] Steinberg MS, Takeichi M. Experimental specification of cell sorting, tissue spreading, and specific spatial patterning by quantitative differences in cadherin expression. Proc Natl Acad Sci USA 1994;91:206.
[117] Drees F, Pokutta S, Yamada S, Nelson WJ, Weis WI. Alpha-catenin is a molecular switch that binds E-cadherin-beta-catenin and regulates actin-filament assembly. Cell 2005;123:903.
[118] Molenaar M, et al. XTcf-3 transcription factor mediates beta-catenin-induced axis formation in *Xenopus* embryos. Cell 1996;86:391.
[119] Nelson WJ, Nusse R. Convergence of Wnt, beta-catenin, and cadherin pathways. Science 2004;136:3357.
[120] Fagotto F, Guger K, Gumbiner BM. Induction of the primary dorsalizing center in *Xenopus* by the Wnt/GSK/beta-catenin signaling pathway, but not by Vg1, Activin or Noggin. Development 1997;124:453.
[121] Korinek V, Barker N, Morin PJ, van Wichen D, de Weger R, Kinzler KW, et al. Constitutive transcriptional activation by a beta-catenin-Tcf complex in APC−/− colon carcinoma. Science 1997;275:1784–7.
[122] Wodarz A, Nusse R. Mechanisms of Wnt signaling in development. Annu Rev Cell Dev Biol 1998;14:59.

[123] Slusarski DC, Corces VG, Moon RT. Interaction of Wnt and a Frizzled homologue triggers G-protein-linked phosphatidylinositol signalling. Nature 1997;390:410.
[124] Zeng X, Tamai K, Doble B, Li S, Huang H, Habas R, et al. A dual-kinase mechanism for Wnt co-receptor phosphorylation and activation. Nature 2005;438:873–7.
[125] Wallingford JB, Habas R. The developmental biology of Dishevelled: an enigmatic protein governing cell fate and cell polarity. Development 2005;132:4421.
[126] Taelman VF, et al. Wnt signaling requires sequestration of glycogen synthase kinase 3 inside multivesicular endosomes. Cell 2010;143:1136.
[127] Kuure S, Popsueva A, Jakobson M, Sainio K, Sariola H. Glycogen synthase kinase-3 inactivation and stabilization of beta-catenin induce nephron differentiation in isolated mouse and rat kidney mesenchymes. J Am Soc Nephrol 2007;18:1130.
[128] Park JS, Valerius MT, McMahon AP. Wnt/beta-catenin signaling regulates nephron induction during mouse kidney development. Development 2007;134:2533.
[129] Schmidt-Ott KM, Barasch J. WNT/beta-catenin signaling in nephron progenitors and their epithelial progeny. Kidney Int 2008;74:1004.
[130] Lin SL, et al. Macrophage Wnt7b is critical for kidney repair and regeneration. Proc Natl Acad Sci USA 2010;107:4194.
[131] He W, Dai C, Li Y, Zeng G, Monga SP, Liu Y. Wnt/beta-catenin signaling promotes renal interstitial fibrosis. J Am Soc Nephrol 2009;20:765–76.
[132] Patrakka J, Tryggvason K. Nephrin: a unique structural and signaling protein of the kidney filter. Trends Mol Med 2007;13:396.
[133] Machuca E, Benoit G, Antignac C. Genetics of nephrotic syndrome: connecting molecular genetics to podocyte physiology. Hum Mol Genet 2009;18:R185.
[134] Schermer B, Benzing T. Lipid–protein interactions along the slit diaphragm of podocytes. J Am Soc Nephrology: JASN 2009;20:473.
[135] Li H, Liu TF, Lazrak A, Peracchia C, Goldberg GS, Lampe PD, et al. Properties and regulation of gap junctional hemichannels in the plasma membranes of cultured cells. J Cell Biol 1996;134:1019–30.
[136] Yao J, Morioka T, Li B, Oite T. Coordination of mesangial cell contraction by gap junction-mediated intercellular Ca(2 +) wave. J Am Soc Nephrol 2002;13:2018.
[137] Vikhamar G, Rivedal E, Mollerup S, Sanner T. Role of Cx43 phosphorylation and MAP kinase activation in EGF induced enhancement of cell communication in human kidney epithelial cells. Cell Adhes Commun 1998;5:451.
[138] Vergara L, Bao X, Cooper M, Bello-Reuss E, Reuss L. Gap-junctional hemichannels are activated by ATP depletion in human renal proximal tubule cells. J Membr Biol 2003;196:173.
[139] Davenport JR, Yoder BK. An incredible decade for the primary cilium: a look at a once-forgotten organelle. Am J Physiol Renal Physiol 2005;289:F1159.
[140] Praetorius HA, Spring KR. A physiological view of the primary cilium. Annu Rev Physiol 2005;67:515.
[141] Afzelius BA. Cilia-related diseases. J Pathol 2004;204:470.
[142] Taulman PD, Haycraft CJ, Balkovetz DF, Yoder BK. Polaris, a protein involved in left–right axis patterning, localizes to basal bodies and cilia. Mol Biol Cell 2001;12:589.
[143] Yoder BK, Hou X, Guay-Woodford LM. The polycystic kidney disease proteins, polycystin-1, polycystin-2, polaris, and cystin, are co-localized in renal cilia. J Am Soc Nephrol 2002;13:2508.
[144] Nauli SM, Zhou J. Polycystins and mechanosensation in renal and nodal cilia. Bioessays 2004;26:844.
[145] Cai Y, et al. Identification and characterization of polycystin-2, the PKD2 gene product. J Biol Chem 1999;274:28557.
[146] Hanaoka K, et al. Co-assembly of polycystin-1 and -2 produces unique cation-permeable currents. Nature 2000;408:990.
[147] Gonzalez-Perrett S, et al. Polycystin-2, the protein mutated in autosomal dominant polycystic kidney disease (ADPKD), is a Ca^{2+}-permeable nonselective cation channel. Proc Natl Acad Sci USA 2001;98:1182.
[148] Nauli SM, et al. Polycystins 1 and 2 mediate mechanosensation in the primary cilium of kidney cells. Nat Genet 2003;33:129.
[149] Liu W, Murcia NS, Duan Y, Weinbaum S, Yoder BK, Schweibert E, et al. Mechanoregulation of intracellular Ca2 + concentration is attenuated in collecting duct of monocilium-impaired orpk mice. Am J Physiol Renal Physiol 2005;289: F978–988.
[150] Gallagher AR, Germino GG, Somlo S. Molecular advances in autosomal dominant polycystic kidney disease. Adv Chronic Kidney Dis 2010;17:118.
[151] Rhee SG. Regulation of phosphoinositide-specific phospholipase C. Annu Rev Biochem 2001;70:281.
[152] Park D, Jhon DY, Lee CW, Ryu SH, Rhee SG. Removal of the carboxyl-terminal region of phospholipase C-beta 1 by calpain abolishes activation by G alpha q. J Biol Chem 1993;268:3710.
[153] Park D, Jhon DY, Lee CW, Lee KH, Rhee SG. Activation of phospholipase C isozymes by G protein beta gamma-subunits. J Biol Chem 1993;268:4573.
[154] Sidhu RS, Clough RR, Bhullar RP. Regulation of phospholipase C-delta1 through direct interactions with the small GTPase Ral and calmodulin. J Biol Chem 2005;280:21933.
[155] Allen V, Swigart P, Cheung R, Cockcroft S, Katan M. Regulation of inositol lipid-specific phospholipase cdelta by changes in Ca^{2+} ion concentrations. Biochem J 1997;327:545.
[156] Kelley GG, Reks SE, Ondrako JM, Smrcka AV. Phospholipase C (epsilon): a novel Ras effector. Embo J 2001;20:743.
[157] Bunney TD, Katan M. Phospholipase C epsilon: linking second messengers and small GTPases. Trends Cell Biol 2006;16:640.
[158] Van Lint J, Ni Y, Valius M, Merlevede W, Vandenheede JR. Platelet-derived growth factor stimulates protein kinase D through the activation of phospholipase Cgamma and protein kinase C. J Biol Chem 1998;273:7038.
[159] Haendeler J, et al. GIT1 mediates Src-dependent activation of phospholipase Cgamma by angiotensin II and epidermal growth factor. J Biol Chem 2003;278:49936.
[160] Bae YS, Cantley LG, Chen CS, Kim SR, Kwon KS, Rhee SG. Activation of phospholipase C-gamma by phosphatidylinositol 3,4,5-trisphosphate. J Biol Chem 1998;273:4465–9.
[161] Ron D, Kazanietz MG. New insights into the regulation of protein kinase C and novel phorbol ester receptors. Faseb J 1999;13:1658.
[162] Toker A, Meyer M, Reddy KK, Falck JR, Aneja R, Aneja S, et al. Activation of protein kinase C family members by the novel polyphosphoinositides PtdIns-3,4-P2 and PtdIns-3,4,5-P3. J Biol Chem 1994;269:32358–67.
[163] Joberty G, Petersen C, Gao L, Macara IG. The cell-polarity protein Par6 links Par3 and atypical protein kinase C to Cdc42. Nat Cell Biol 2000;2:531.
[164] Gao L, Joberty G, Macara IG. Assembly of epithelial tight junctions is negatively regulated by Par6. Curr Biol 2002;12:221.
[165] Togawa A, Sfakianos J, Ishibe S, Suzuki S, Fujigaki Y, Kitagawa M, et al. Hepatocyte Growth Factor stimulated cell scattering requires ERK and Cdc42-dependent tight junction disassembly. Biochem Biophys Res Commun 2010;400:271–7.

[166] Pedemonte CH, Pressley TA, Lokhandwala MF, Cinelli AR. Regulation of Na,K-ATPase transport activity by protein kinase C. J Membr Biol 1997;155:219.
[167] Efendiev R, Bertorello AM, Pressley TA, Rousselot M, Feraille E, Pedemonte CH. Simultaneous phosphorylation of Ser11 and Ser18 in the alpha-subunit promotes the recruitment of Na(+),K(+)-ATPase molecules to the plasma membrane. Biochemistry 2000;39:9884–92.
[168] Gomes P, Soares-da-Silva P. Role of cAMP-PKA-PLC signaling cascade on dopamine-induced PKC-mediated inhibition of renal Na(+)-K(+)-ATPase activity. Am J Physiol Renal Physiol 2002;282:F1084.
[169] Yao LP, Li XX, Yu PY, Xu J, Ascio LD, Jose PA. Dopamine D1 receptor and protein kinase C isoforms in spontaneously hypertensive rats. Hypertension 1998;32:1049–53.
[170] Salyer S, Lesousky N, Weinman EJ, Clark BJ, Lederer ED, Khundmiri SJ. Dopamine regulation of Na^+-K^+-ATPase requires the PDZ-2 domain of sodium hydrogen regulatory factor-1 (NHERF-1) in opossum kidney cells. Am J Physiol Cell Physiol 2011;300:C425–434.
[171] Steinberg SF. Distinctive activation mechanisms and functions for protein kinase Cdelta. Biochem J 2004;384:449.
[172] Soh JW, Lee EH, Prywes R, Weinstein IB. Novel roles of specific isoforms of protein kinase C in activation of the c-fos serum response element. Mol Cell Biol 1999;19:1313.
[173] Isakov N, Altman A. Protein kinase C(theta) in T cell activation. Annu Rev Immunol 2002;20:761.
[174] Schulz RA, Yutzey KE. Calcineurin signaling and NFAT activation in cardiovascular and skeletal muscle development. Dev Biol 2004;266:1.
[175] Macian F, Lopez-Rodriguez C, Rao A. Partners in transcription: NFAT and AP-1. Oncogene 2001;20:2476.
[176] Kobayashi H, Shiraishi S, Yanagita T, Yokoo H, Yamamoto R, Minami S, et al. Regulation of voltage-dependent sodium channel expression in adrenal chromaffin cells: Iinvolvement of multiple calcium signaling pathways. Ann NY Acad Sci 2002;971:127–34.
[177] Boulton TG, Yancopoulos GD, Gregory JS, Slaughter C, Moomaw C, Hsu J, et al. An insulin-stimulated protein kinase similar to yeast kinases involved in cell cycle control. Science 1990;249:64–7.
[178] Whitmarsh AJ, Shore P, Sharrocks AD, Davis RJ. Integration of MAP kinase signal transduction pathways at the serum response element. Science 1995;269:403.
[179] Liu ZX, Yu CF, Nickel C, Thomas S, Cantley LG. Hepatocyte growth factor induces ERK-dependent paxillin phosphorylation and regulates paxillin-focal adhesion kinase association. J Biol Chem 2002;277:10452.
[180] Klemke RL, Cai S, Giannini AL, Gallagher PJ, de Lanerolle P, Cheresh DA. Regulation of cell motility by mitogen-activated protein kinase. J Cell Biol 1997;137:481–92.
[181] Crews CM, Alessandrini A, Erikson RL. The primary structure of MEK, a protein kinase that phosphorylates the ERK gene product. Science 1992;258:478.
[182] Nguyen A, et al. Kinase suppressor of Ras (KSR) is a scaffold which facilitates mitogen-activated protein kinase activation in vivo. Mol Cell Biol 2002;22:3035.
[183] Ishibe S, Joly D, Zhu X, Cantley LG. Phosphorylation-dependent paxillin-ERK association mediates hepatocyte growth factor-stimulated epithelial morphogenesis. Mol Cell 2003;12:1275.
[184] Roy M, Li Z, Sacks DB. IQGAP1 is a scaffold for mitogen-activated protein kinase signaling. Mol Cell Biol 2005;25:7940.
[185] Kolch W. Coordinating ERK/MAPK signalling through scaffolds and inhibitors. Nat Rev Mol Cell Biol 2005;6:827.
[186] Lowenstein EJ, et al. The SH2 and SH3 domain-containing protein GRB2 links receptor tyrosine kinases to ras signaling. Cell 1992;70:431.
[187] Bonfini L, Karlovich CA, Dasgupta C, Banerjee U. The Son of sevenless gene product: a putative activator of Ras. Science 1992;255:603.
[188] Dougherty MK, et al. Regulation of Raf-1 by direct feedback phosphorylation. Mol Cell 2005;17:215.
[189] Kovacs JJ, Hara MR, Davenport CL, Kim J, Lefkowitz RJ. Arrestin development: emerging roles for beta-arrestins in developmental signaling pathways. Developmental Cell 2009;17:443.
[190] Siegel JN, Klausner RD, Rapp UR, Samelson LE. T cell antigen receptor engagement stimulates c-raf phosphorylation and induces c-raf-associated kinase activity via a protein kinase C-dependent pathway. J Biol Chem 1990;265:18472.
[191] Kolch W, Hiedecker G, Kochs G, Hummel R, Vahidi H, Mischak H, et al. Protein kinase C alpha activates RAF-1 by direct phosphorylation. Nature 1993;364:249–52.
[192] Racusen LC, Fivush BA, Li YL, Slatnik I, Solez K. Dissociation of tubular cell detachment and tubular cell death in clinical and experimental "acute tubular necrosis.". Lab Invest 1991;64:546.
[193] Park MY, Lee RH, Lee SH, Jung JS. Apoptosis induced by inhibition of contact with extracellular matrix in mouse collecting duct cells. Nephron 1999;83:341.
[194] Nony PA, Schnellmann RG. Mechanisms of renal cell repair and regeneration after acute renal failure. J Pharmacol Exp Ther 2003;304:905.
[195] Subauste MC, Pertz O, Adamson ED, Turner CE, Junger S, Hahn KM. Vinculin modulation of paxillin-FAK interactions regulates ERK to control survival and motility. J Cell Biol 2004;165:371–81.
[196] Aplin AE, Juliano RL. Integrin and cytoskeletal regulation of growth factor signaling to the MAP kinase pathway. J Cell Sci 1999;112(**Pt 5**):695.
[197] Edin ML, Juliano RL. Raf-1 serine 338 phosphorylation plays a key role in adhesion-dependent activation of extracellular signal-regulated kinase by epidermal growth factor. Mol Cell Biol 2005;25:4466.
[198] Gille H, Kortenjaan M, Thomae O, Moomaw C, Slaughter C, Cobb MH, et al. ERK phosphorylation potentiates Elk-1-mediated ternary complex formation and transactivation. Embo J 1995;14:951–62.
[199] Talarmin H, et al. The mitogen-activated protein kinase kinase/extracellular signal-regulated kinase cascade activation is a key signalling pathway involved in the regulation of G(1) phase progression in proliferating hepatocytes. Mol Cell Biol 1999;19:6003.
[200] Qiao M, Shapiro P, Kumar R, Passaniti A. Insulin-like growth factor-1 regulates endogenous RUNX2 activity in endothelial cells through a phosphatidylinositol 3-kinase/ERK-dependent and Akt-independent signaling pathway. J Biol Chem 2004;279:42709.
[201] Roovers K, Assoian RK. Integrating the MAP kinase signal into the G1 phase cell cycle machinery. Bioessays 2000;22:818.
[202] Reginato MJ, Mills KR, Paulus JK, Lynch DK, Sjroi DC, Debnath J, et al. Integrins and EGFR coordinately regulate the pro-apoptotic protein Bim to prevent anoikis. Nat Cell Biol 2003;5:733–40.
[203] Marshall CJ. Specificity of receptor tyrosine kinase signaling: transient versus sustained extracellular signal-regulated kinase activation. Cell 1995;80:179.
[204] Thrane EV, Schwarze PE, Thoresen GH, Lag M, Refsnes M. Persistent versus transient map kinase (ERK) activation in the

proliferation of lung epithelial type 2 cells. Exp Lung Res 2001;27:387.
[205] Collins NL, Reginato MG, Paulus JK, Sgroi DC, Labaer J, Brugge JS. G1/S cell cycle arrest provides anoikis resistance through Erk-mediated Bim suppression. Mol Cell Biol 2005;25:5282–91.
[206] Heasman SJ, Ridley AJ. Mammalian Rho GTPases: new insights into their functions from *in vivo* studies. Nat Rev Mol Cell Biol 2008;9:690.
[207] DeMali KA, Wennerberg K, Burridge K. Integrin signaling to the actin cytoskeleton. Curr Opin Cell Biol 2003;15:572.
[208] Rogers KK, Jou TS, Guo W, Lipschutz JH. The Rho family of small GTPases is involved in epithelial cystogenesis and tubulogenesis. Kidney Int 2003;63:1632.
[209] Nakamura A, Hayashi K, Ozawa Y, Fujiwara K, Okubo K, Kanda T, et al. Vessel- and vasoconstrictor-dependent role of rho/rho-kinase in renal microvascular tone. J Vasc Res 2003;40:244–51.
[210] Zarubin T, Han J. Activation and signaling of the p38 MAP kinase pathway. Cell Res 2005;15:11.
[211] Roux PP, Blenis J. ERK and p38 MAPK-activated protein kinases: a family of protein kinases with diverse biological functions. Microbiol Mol Biol Rev 2004;68:320.
[212] Chen Z, et al. MAP kinases. Chem Rev 2001;101:2449.
[213] Schiffer M, Bitzer M, Roberts IS, Koop JB, ten Dijke P, Mundel P, et al. Apoptosis in podocytes induced by TGF-beta and Smad7. J Clin Invest 2001;108:807–16.
[214] Ma FY, Sachchithananthan M, Flanc RS, Nikolic-Paterson DJ. Mitogen activated protein kinases in renal fibrosis. Front Biosci (Schol Ed) 2009;1:171.
[215] Stambe C, Atkins RC, Tesch GH, Masaki T, Schreiner GF, Nikolic-Paterson DJ. The role of p38alpha mitogen-activated protein kinase activation in renal fibrosis. J Am Soc Nephrol 2004;15:370–9.
[216] Koshikawa M, et al. Role of p38 mitogen-activated protein kinase activation in podocyte injury and proteinuria in experimental Nephrotic syndrome. J Am Soc Nephrol 2005;16:2690.
[217] Park KM, Kramers C, Vayssier-Taussat M, Chen A, Bonventre JV. Prevention of kidney ischemia/reperfusion-induced functional injury, MAPK and MAPK kinase activation, and inflammation by remote transient ureteral obstruction. J Biol Chem 2002;277:2040.
[218] Hung CC, Ichimura T, Stevens JL, Bonventre JV. Protection of renal epithelial cells against oxidative injury by endoplasmic reticulum stress preconditioning is mediated by ERK1/2 activation. J Biol Chem 2003;278:29317.
[219] Arany I, Megyesi JK, Kaneto H, Tanaka S, Safirstein RL. Activation of ERK or inhibition of JNK ameliorates $H(_2)O(_2)$ cytotoxicity in mouse renal proximal tubule cells. Kidney Int 2004;65:1231.
[220] Auger KR, Serunian LA, Soltoff SP, Libby P, Cantley LC. PDGF-dependent tyrosine phosphorylation stimulates production of novel polyphosphoinositides in intact cells. Cell 1989;57:167.
[221] Balla T. Inositol-lipid binding motifs: signal integrators through protein–lipid and protein–protein interactions. J Cell Sci 2005;118:2093.
[222] Kobayashi S, Shirai T, Kiyokawa E, Mochizuki N, Matsuda M, Fukui Y. Membrane recruitment of DOCK180 by binding to PtdIns(3,4,5)P3. Biochem J 2001;354:73–8.
[223] Palmby TR, Abe K, Der CJ. Critical role of the pleckstrin homology and cysteine-rich domains in Vav signaling and transforming activity. J Biol Chem 2002;277:39350.
[224] Andjelkovic M, Maira SM, Cron P, Parker PJ, Hemmings BA. Domain swapping used to investigate the mechanism of protein kinase B regulation by 3-phosphoinositide-dependent protein kinase 1 and Ser473 kinase. Mol Cell Biol 1999;19:5061.
[225] Alessi DR, Kozlowski MT, Weng QP, Morrice N, Avruch J. 3-Phosphoinositide-dependent protein kinase 1 (PDK1) phosphorylates and activates the p70 S6 kinase *in vivo* and *in vitro*. Curr Biol 1998;8:69.
[226] Tanaka H, Fujita N, Tsuruo T. 3-Phosphoinositide-dependent protein kinase-1-mediated IkappaB kinase beta (IkkB) phosphorylation activates NF-kappaB signaling. J Biol Chem 2005;280:40965.
[227] Woodgett JR. Recent advances in the protein kinase B signaling pathway. Curr Opin Cell Biol 2005;17:150.
[228] Cross DA, Alessi DR, Cohen P, Andjelkovich M, Hemmings BA. Inhibition of glycogen synthase kinase-3 by insulin mediated by protein kinase B. Nature 1995;378:785.
[229] Rubinfeld B, Albert I, Porfiri E, Fiol C, Munemitsu S, Polakis P. Binding of GSK3beta to the APC-beta-catenin complex and regulation of complex assembly. Science 1996;272:1023–6.
[230] Ilouz R, Pietrokovski S, Eisenstein M, Eldar-Finkelman H. New insights into the autoinhibition mechanism of glycogen synthase kinase-3beta. J Mol Biol 2008;383:999.
[231] Ishibe S, Haydu JE, Togawa A, Marlier A, Cantley LG. Cell confluence regulates hepatocyte growth factor-stimulated cell morphogenesis in a beta-catenin-dependent manner. Mol Cell Biol 2006;26:9232.
[232] Diehl JA, Cheng M, Roussel MF, Sherr CJ. Glycogen synthase kinase-3beta regulates cyclin D1 proteolysis and subcellular localization. Genes Dev 1998;12:3499.
[233] Pap M, Cooper GM. Role of translation initiation factor 2B in control of cell survival by the phosphatidylinositol 3-kinase/Akt/glycogen synthase kinase 3beta signaling pathway. Mol Cell Biol 2002;22:578.
[234] Brunet A, Bonni A, Zigmond MJ, Lin MZ, Juo P, Hu LS, et al. Akt promotes cell survival by phosphorylating and inhibiting a Forkhead transcription factor. Cell 1999;96:857–68.
[235] Fingar DC, Blenis J. Target of rapamycin (TOR): an integrator of nutrient and growth factor signals and coordinator of cell growth and cell cycle progression. Oncogene 2004;23:3151.
[236] Manning BD, Cantley LC. United at last: the tuberous sclerosis complex gene products connect the phosphoinositide 3-kinase/Akt pathway to mammalian target of rapamycin (mTOR) signalling. Biochem Soc Trans 2003;31:573.
[237] Katso R, Okkenhaug K, Ahmadi K, White S, Timms J, Waterfield MD. Cellular function of phosphoinositide 3-kinases: implications for development, homeostasis, and cancer. Annu Rev Cell Dev Biol 2001;17:615–75.
[238] Ishiki M, Klip A. Minireview: recent developments in the regulation of glucose transporter-4 traffic: new signals, locations, and partners. Endocrinology 2005;146:5071.
[239] Summers SA, Kao AW, Kohn AD, Backus GS, Roth RA, Pessin JE, et al. The role of glycogen synthase kinase 3beta in insulin-stimulated glucose metabolism. J Biol Chem 1999;274:17934–40.
[240] Kanaide H, Ichiki T, Nishimura J, Hirano K. Cellular mechanism of vasoconstriction induced by angiotensin II: it remains to be determined. Circ Res 2003;93:1015.
[241] Woodsome TP, Polzin A, Kitazawa K, Eto M, Kitazawa T. Agonist- and depolarization-induced signals for myosin light chain phosphorylation and force generation of cultured vascular smooth muscle cells. J Cell Sci 2006;119:1769.
[242] Ito M, Nakano T, Erdodi F, Hartshorne DJ. Myosin phosphatase: structure, regulation and function. Mol Cell Biochem 2004;259:197.

[243] Flannery PJ, Spurney RF. Transactivation of the epidermal growth factor receptor by angiotensin II in glomerular podocytes. Nephron Exp Nephrol 2006;103:e109.
[244] Ying Z, Jin L, Palmer T, Webb RC. Angiotensin II up-regulates leukemia-associated rho guanine nucleotide exchange factor (LARG), a RGS domain containing RhoGEF, in vascular smooth muscle cells. Mol Pharmacol 2005;14:14.
[245] Im SH, Rao A. Activation and deactivation of gene expression by Ca^{2+}/calcineurin-NFAT-mediated signaling. Mol Cells 2004;18:1.
[246] Rogerson FM, Brennan FE, Fuller PJ. Mineralocorticoid receptor binding, structure and function. Mol Cell Endocrinol 2004;217:203.
[247] Snyder PM. Minireview: regulation of epithelial Na^+ channel trafficking. Endocrinology 2005;146:5079.
[248] Naray-Fejes-Toth A, Fejes-Toth G. The sgk, an aldosterone-induced gene in mineralocorticoid target cells, regulates the epithelial sodium channel. Kidney Int 2000;57:1290.
[249] Snyder PM, Olson DR, Thomas BC. Serum and glucocorticoid-regulated kinase modulates Nedd4-2-mediated inhibition of the epithelial Na^+ channel. J Biol Chem 2002;277:5.
[250] Hansson JH, et al. Hypertension caused by a truncated epithelial sodium channel gamma-subunit: genetic heterogeneity of Liddle syndrome. Nat Genet 1995;11:76.
[251] Valenti G, Procino G, Tamma G, Carmosino M, Svelto M. Minireview: aquaporin 2 trafficking. Endocrinology 2005;146:5063.
[252] Sabolic I, Valenti G, Verbavatz JM, Van Hoek AN, Verkman AS, Ausiello DA, et al. Localization of the CHIP28 water channel in rat kidney. Am J Physiol 1992;263:C1225–1233.
[253] Ishibashi K, et al. Molecular cloning and expression of a member of the aquaporin family with permeability to glycerol and urea in addition to water expressed at the basolateral membrane of kidney collecting duct cells. Proc Natl Acad Sci USA 1994;91:6269.
[254] Henn V, et al. Identification of a novel A-kinase anchoring protein 18 isoform and evidence for its role in the vasopressin-induced aquaporin-2 shuttle in renal principal cells. J Biol Chem 2004;279:26654.
[255] Kuwahara M, Fushimi K, Terada Y, Bai L, Marumo F, Sasaki S. cAMP-dependent phosphorylation stimulates water permeability of aquaporin-collecting duct water channel protein expressed in *Xenopus* oocytes. J Biol Chem 1995;270:10384–7.
[256] Nedvetsky PI, Tamma G, Beulshausen S, Valenti G, Rosenthal W, Klussmann E. Regulation of aquaporin-2 trafficking. Handb Exp Pharmacol 2009;190:133–57.
[257] Gouraud S, et al. Functional involvement of VAMP/synaptobrevin-2 in cAMP-stimulated aquaporin 2 translocation in renal collecting duct cells. J Cell Sci 2002;115:3667–74.
[258] Mistry AC, Mallick R, Klein JD, Weimbs T, Sands JM, Frölich O. Syntaxin specificity of aquaporins in the inner medullary collecting duct. Am J Physiol Renal Physiol 2009;297:F292–300.
[259] Stefan E, et al. Compartmentalization of cAMP-dependent signaling by phosphodiesterase-4D is involved in the regulation of vasopressin-mediated water reabsorption in renal principal cells. J Am Soc Nephrol: JASN 2007;18:199.
[260] Jo I, Ward DT, Baum MA, Scott JD, Coghlan VM, Hammond TG, et al. AQP2 is a substrate for endogenous PP2B activity within an inner medullary AKAP-signaling complex. Am J Physiol Renal Physiol 2001;281:F958–965.
[261] Yasui M, Zelenin SM, Celsi G, Aperia A. Adenylate cyclase-coupled vasopressin receptor activates AQP2 promoter via a dual effect on CRE and AP1 elements. Am J Physiol 1997;272:F443.
[262] Hasler U, Vinciguerra M, Vandewalle A, Martin PY, Feraille E. Dual effects of hypertonicity on aquaporin-2 expression in cultured renal collecting duct principal cells. J Am Soc Nephrol 2005;16:1571.
[263] Snyder PM, Olson DR, Kabra R, Zhou R, Steines JC. cAMP and serum and glucocorticoid-inducible kinase (SGK) regulate the epithelial Na(+) channel through convergent phosphorylation of Nedd4-2. J Biol Chem 2004;279:45753.
[264] Snyder PM. Liddle's syndrome mutations disrupt cAMP-mediated translocation of the epithelial Na(+) channel to the cell surface. J Clin Invest 2000;105:45.
[265] Butterworth MB, Edinger RS, Johnson JP, Frizzell RA. Acute ENaC stimulation by cAMP in a kidney cell line is mediated by exocytic insertion from a recycling channel pool. J Gen Physiol 2005;125:81.
[266] Schnizler M, Mastroberardino L, Reifarth F, Weber WM, Verrey F, Clauss W. cAMP sensitivity conferred to the epithelial Na^+ channel by alpha-subunit cloned from guinea-pig colon. Pflugers Arch 2000;439:579–87.
[267] Stockand JD. Vasopressin regulation of renal sodium excretion. Kidney international 2010;78:849.
[268] Welling PA, Ho K. A comprehensive guide to the ROMK potassium channel: form and function in health and disease. Am J Physiol Renal Physiol 2009;297:F849.
[269] Hebert SC, Desir G, Giebisch G, Wang W. Molecular diversity and regulation of renal potassium channels. Physiol Rev 2005;85:319.
[270] Heath CM, Stahl PD, Barbieri MA. Lipid kinases play crucial and multiple roles in membrane trafficking and signaling. Histol Histopathol 2003;18:989.
[271] Doughman RL, Firestone AJ, Anderson RA. Phosphatidylinositol phosphate kinases put PI4,5P(2) in its place. J Membr Biol 2003;194:77.
[272] Liou HH, Zhou SS, Huang CL. Regulation of ROMK1 channel by protein kinase A via a phosphatidylinositol 4,5-bisphosphate-dependent mechanism. Proc Natl Acad Sci USA 1999;96:5820.
[273] Reeves WB, McDonald GA, Mehta P, Andreoli TE. Activation of K^+ channels in renal medullary vesicles by cAMP-dependent protein kinase. J Membr Biol 1989;109:65.
[274] Yoo D, Kim BY, Campo C, Nance L, King A, Mauoyo D, et al. Cell surface expression of the ROMK (Kir 1.1) channel is regulated by the aldosterone-induced kinase, SGK-1, and protein kinase A. J Biol Chem 2003;278:23066–75.
[275] Yoo D, Flagg TP, Ohlson O, Raghuram V, Foskett JK, Welling PA. Assembly and trafficking of a multiprotein ROMK (Kir 1.1) channel complex by PDZ interactions. J Biol Chem 2004;279:6863–73.
[276] Hoorn EJ, Nelson JH, McCormick JA, Ellison DH. The WNK kinase network regulating sodium, potassium, and blood pressure. J Am Soc Nephrol: JASN 2011;22:605.
[277] Verissimo F, Jordan P. WNK kinases, a novel protein kinase subfamily in multi-cellular organisms. Oncogene 2001;20:5562.
[278] Leng Q, Kahle KT, Rinehart J, MacGregor GG, Wilson FH, Canessa CM, et al. WNK3, a kinase related to genes mutated in hereditary hypertension with hyperkalemia, regulates the K^+ channel ROMK1 (Kir1.1). J Physiol 2005;15:15.
[279] Rinehart J, et al. WNK3 kinase is a positive regulator of NKCC2 and NCC, renal cation-Cl^- cotransporters required for normal blood pressure homeostasis. Proc Natl Acad Sci USA 2005;102:16777.
[280] Lazrak A, Liu Z, Huang CL. Antagonistic regulation of ROMK by long and kidney-specific WNK1 isoforms. Proc Natl Acad Sci USA 2006;103:1615.
[281] Kahle KT, Wilson FH, Lifton RP. Regulation of diverse ion transport pathways by WNK4 kinase: a novel molecular switch. Trends Endocrinol Metab 2005;16:98.

[282] Wilson FH, et al. Human hypertension caused by mutations in WNK kinases. Science 2001;293:1107.

[283] Kahle KT, Gimenez I, Hassan H, Wilson FH, Wong RD, Forbush B, et al. WNK4 regulates apical and basolateral Cl^- flux in extrarenal epithelia. Proc Natl Acad Sci USA 2004;101:2064–9.

[284] Huang CL, Yang SS, Lin SH. Mechanism of regulation of renal ion transport by WNK kinases. Curr Opin Nephrol Hypertens 2008;17:519.

[285] He G, Wang HR, Huang SK, Huang CL. Intersectin links WNK kinases to endocytosis of ROMK1. J Clin Invest 2007;117:1078.

[286] Subramanya AR, Liu J, Ellison DH, Wade JB, Welling PA. WNK4 diverts the thiazide-sensitive NaCl cotransporter to the lysosome and stimulates AP-3 interaction. J Biol Chem 2009;284:18471.

[287] Zhou B, Zhuang J, Gu D, Wang H, Cebotaru L, Guggino WB, et al. WNK4 enhances the degradation of NCC through a sortilin-mediated lysosomal pathway. J Am Soc Nephrol:JASN 2010;21:82–92.

[288] Lalioti MD, et al. Wnk4 controls blood pressure and potassium homeostasis via regulation of mass and activity of the distal convoluted tubule. Nat Genet 2006;38:1124.

This page intentionally left blank

CHAPTER

14

Scaffolding Proteins in Transport Regulation

Paul A. Welling

Department of Physiology, University of Maryland School of Medicine, Baltimore, MD, USA

PDZ-PROTEINS

PDZ domains (also known as DHR domains or GLGF repeats) are ~90 amino acid, protein−protein interaction modules that bind short amino-acid motifs (4−5 residues) generally found at the extreme COOH-terminus of target proteins.[1] More rarely, PDZ domains recognize internal sequences that mimic the COOH-terminal binding motif.[2,3] The term PDZ is derived from the names of the three proteins that the structure was originally identified from (PSD 95, a post synaptic density protein), Dlg (Dropsophila Disc large tumor suppressor), and ZO-1 (zona occludens, the tight junction protein). Since its discovery as a region of sequence homology in these few proteins,[4] the PDZ domain has become recognized as one of the most common interaction modules. The human genome contains over 250 PDZ domains in nearly 100 human proteins. The structure is evolutionarily conserved, emerging largely in metazoans, perhaps to accommodate the increased signaling needs of multicellular organisms.[5]

PDZ domain containing proteins usually possess multiple protein−protein recognition modules. Because the domains act independently and allow concurrent recruitment of different binding targets, PDZ proteins function as molecular scaffolds. Indeed, PDZ proteins facilitate multi-protein complex formation, and organize expression of target proteins on specific membrane domains for a wide range of physiological processes. A growing body of work has strongly implicated PDZ proteins in targeting and clustering various receptors, channels, transporters, and signal transduction elements at specific plasma membrane domains in different cell types, including neurons,[6] muscle,[7] and the visual system.[8] PDZ proteins play especially important roles in epithelial transport processes.

CLASSES OF PDZ DOMAINS

PDZ domains have been traditionally divided into three different classes, categorized by the nature of their ligands.[1] The different ligand classes are distinguished by differences in the binding residues found at the extreme COOH of target proteins (Figure 14.1). Type I domains recognize the sequence, X-S/T-X-Φ* (where X = any amino acid; Φ = hydrophobic amino acid; * = COOH terminus). Type II domains bind to ligands with the sequence X-Φ-X-Φ*. Type III domains interact with X-D/E-X-Φ* sequences.[9,10] Binding specificity within each domain class can be conferred by the variant (X) residues, as well as residues outside the canonical binding motif, especially at the -3 and -4 positions (where 0 position is the C-terminal residue). Moreover, a few PDZ domains do not fall into any of these specific classes.[5]

Based on large-scale proteomic analysis of PDZ-ligand interactions, it has been suggested the traditional three-class definition be extended to include 16 distinct binding classes.[11] Such a classification has been proposed to predict specific interaction partners of known PDZ domains with greater fidelity than the traditional scheme.

STRUCTURAL BASIS FOR PDZ INTERACTION

In recent years, the structures of over 20 different PDZ domains have been solved at atomic resolution. Like many protein−protein recognition modules, PDZ domains are small globular structures. Comprised of six β-strands (βA-βF) and two alpha helices (αA and

Seldin and Giebisch's The Kidney, Fifth Edition.
DOI: http://dx.doi.org/10.1016/B978-0-12-381462-3.00014-8

© 2013 Elsevier Inc. All rights reserved.

(a)

	(X–P$_{-2}$–X – P$_0$)
Type I	X–S/T–X–Φ–COOH
Type II	X–Φ–X–Φ–COOH
Type III	X–D/E–X–Φ–COOH

(b)

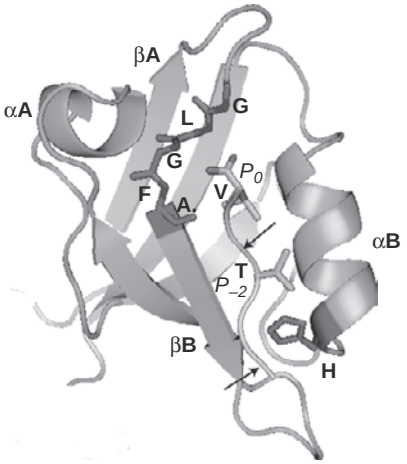

FIGURE 14.1 **PDZ-binding classes and structures.** (a) PDZ-binding motifs of the three different PDZ ligand classes are shown (X: any amino acid; Φ: hydrophobic amino acid). Residues in PDZ ligands are conventionally numbered from the final amino acid at the extreme COOH terminus, the so-called P0 position. (b) Structure of a type I PDZ domain with its ligand (third PDZ domain of PSD-95 is shown (PDB,1BFE) Doyle). The conserved GLGF motif in βA-βB linker provides a cradle of main chain amides for interaction with the terminal carboxylate group of the P0 residue. A hydrophobic pocket accommodates the hydrophobic P0 side chain. The first residue of the αB helix, a conserved histidine, forms hydrogen bonds with the P-2 threonine residue in the target protein.

αB), PDZ domains fold into a six stranded beta sandwich[12,13] (Figure 14.1). The peptide ligand inserts into a binding cleft, created by the βB strand and the αB helix, effectively forming an additional antiparallel beta strand. An extensive network of hydrogen bonds and hydrophobic interactions stabilizes binding of the peptide. For instance, the conserved glycine-leucine-glycine-phenylalanine-alanine (GLGF) motif contained within a βA-βB linker provides a cradle of main chain amides, and confers recognition of the terminal carboxylate group of the peptide.[13] A hydrophobic pocket accommodates the hydrophobic COOH-terminal residue, thereby accounting for preferential interaction with proteins ending with a hydrophobic residue (the so-called P0 position).

Binding specificity among the different binding classes is determined partly by an interaction between the P-2 residue of the target protein and the first residue of the PDZ domain αB-helix.[13] In Class I PDZ domains, a conserved histidine residue forms hydrogen bonds with the invariant P-2 serine or threonine residue in the target protein. In class II PDZ domains, this position of the PDZ domain and the P-2 residue of the target protein are usually occupied by a hydrophobic amino acid.[14]

Binding specificity within each domain class is also observed. At least three factors account for this. First, unique residues within or adjacent to the peptide-binding groove in the PDZ domain can interact with the target at sites other than the P-2 and P0 residues.[13,15–17] For example, the side chain of the P-1 target protein residue usually points away from the invariant interaction surface but, in some cases, it can bond with residues that are distinct to a particular PDZ domain.[15,17] Likewise, the P-3 side chain can make contact with unique residues in the interaction groove. Sites proximal to the archetypal, four amino acid-binding motif can also interact with regions outside the canonical-binding site, and thereby also contribute to binding specificity and affinity.[17,18] Second, because interacting residues in PDZ domains can undergo large ligand-dependent conformational changes,[19,20] variations in binding pocket flexibility may contribute to binding specificity. Such a mechanism has been proposed to explain the different binding specificity of the two highly homologous PDZ domains in NHERF1.[21] Finally, genome-wide analysis of PDZ domain binding suggests that PDZ domain selectivity is also achieved by the cellular and subcellular context of the interaction, and this may actually play a more important role than inherent binding specificity.[22]

REGULATION OF PDZ BINDING

PDZ interactions can be dynamically regulated to control the composition and stoichiometry of different multimeric complexes. Phosphorylation of the binding target is the most common mechanism. This is explained by the fact the P-2 serine or threonine in canonical type I PDZ targets can be a substrate for phosphorylation. In these cases, phosphorylation of the residue creates an energetically unfavorable PDZ ligand. For example, phosphorylation of the COOH-terminal site in the Kir 2.3 channel by Protein Kinase A inhibits its interaction with the synaptic PDZ protein, PSD-95,[23] to regulate the channel.[24] Likewise, phosphorylation of the P-2 serine in the β2 adrenergic receptor uncouples the receptor from the NHERF1 PDZ protein, and disrupts receptor recycling in the post-endocytic pathway.[25]

Phosphorylation of sites within PDZ proteins is emerging as an additional mechanism for modulating PDZ binding. Evidence for this was first provided by observations that the interaction of a PDZ protein, NHERF1 (see below), with CFTR is negatively

regulated by phosphorylation of a residue in the second PDZ domain.[26] Phosphorylation of sites in or near the first PDZ domain of NHERF1 also disrupt interaction with the Na-phosphate co-transporter, Npt2a.[27–29] Phosphorylation of sites that are involved in PDZ–PDZ protein oligomerization has also been observed.[30] This is believed to modulate the extent to which some PDZ proteins can form higher order scaffolding complexes.[31,32]

Finally, switching interactions with different PDZ proteins can differently regulate the activity and localization of target proteins. This occurs when the target has the capacity to bind to several PDZ proteins that have different properties. For example, TIP-1, a protein that consists of a single PDZ domain and lacks other protein–protein interaction modules, binds to certain target proteins to antagonize the scaffolding functions of canonical PDZ proteins.[33]

POLARIZED EXPRESSION OF PDZ PROTEINS IN EPITHELIAL CELLS

A number of PDZ proteins are preferentially expressed at polarized membrane domains or within critical sorting compartments (Figure 14.2), where they perform retention/sorting operations and organize local signaling complexes at polarized locales.[34] Examples of PDZ proteins that predominately reside at the basolateral membrane of certain intestinal and renal epithelia include syntrophin[35] (see "Dystrophin-Associated Protein Complex," below), Lin-7[36,37] (see "Lin-7/CASK/SAP97," below), the ErbB interacting protein, ERBIN,[38] and certain members of the membrane associated guanylate kinase family of PDZ proteins, such as CASK,[39] PSD-93,[40] and SAP97 (aka Discs large homolog 1[41]). Other PDZ proteins, including the sodium hydrogen exchange regulator factors (see "NHERF, "below), Shank2E,[42] and PSD-95,[40] are chiefly expressed on or near the apical membrane. Some PDZ proteins, such as zonula occludens, PALS1 (Stardust), and PATJ (Disc lost),[43] play important roles in the generation and maintenance of the tight junction.[44] Still others, like CAL, which is primarily located in the Golgi[45] or SNX27,[46] and syntenin,[47,48] which are found in endosomes, reside in biosynthetic or endocytotic sorting compartments.

A PDZ-binding motif can serve as a polarized sorting[49] or retention signal.[50] One of the first examples evolved from studies with the GABA transporters or GATs[51]; deletion of the PDZ-binding motif from the apical isoform GAT-3 caused the transporter to localize randomly to both apical and basolateral membranes.[52] Basolateral membrane expression of several membrane proteins has also been found to require a PDZ-binding motif. For instance ERBB receptors, which play crucial roles in morphogenesis and oncogenesis, interact with a basolateral PDZ protein, called ERBIN, and require a PDZ-binding motif for basolateral membrane expression.[38] ERBIN is targeted to the basolateral membrane by its leucine-rich repeat domain.[53] Efficient basolateral membrane expression of a number of transporters that interact with the basolateral PDZ protein Lin-7 also require an intact PDZ-binding site (see below).

MAGUKS, THE ARCHETYPAL PDZ SCAFFOLDS

Members of the MAGUK (membrane associated guanylate kinase) family of PDZ proteins are the archetypal PDZ scaffolds. MAGUK proteins are equipped to assemble large molecular complexes, having one to three PDZ domains, a SRC homology 3 domain (SH3), and a catalytically inactive guanylate kinase-like (GK) domain. In addition to the PDZ domains, the GK and the SH3 domains function as independent protein–protein interaction modules; GK domains recruit scaffold adaptor molecules called guanylate kinase-associated proteins or GKAPs,[54] while SH3 domains have been shown to coordinate interaction with at least one non-

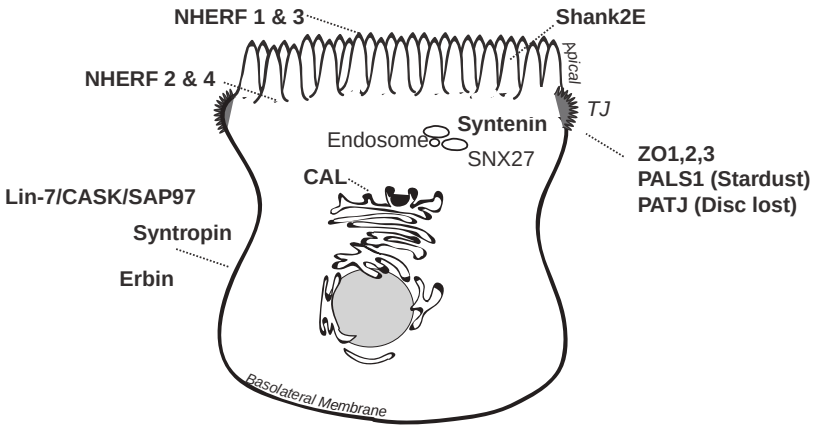

FIGURE 14.2 **Major PDZ proteins in epithelial cells.** PDZ domain containing proteins differentially localize to epithelial cell brush borders, subapical domains, endosomes, tight junctions, and basolateral membranes.

receptor tyrosine kinase.[55] The SH3 and GK domains can also interact with one another, forming a composite SH3–GK structure[56,57] that acts as an additional intermolecular protein–protein interaction domain with a binding specificity that is distinct from either SH3 or GK domains.[58]

The PSD-95 family, encoded by four genes (PSD-95/SAP90, PSD-93/Chapsyn-110, SAP102, and SAP97), exemplifies MAGUK proteins. Two of these, PSD-93[40] and SAP97 (see below), are expressed in renal epithelial cells. However, the best characterized member, PSD-95, is largely expressed in excitable tissues, and plays central roles in maintaining and modulating the strength and structure of glutamatergic synapses.[59] Generally, its properties and functions are likely to be applicable to the other MAGUKs, including those expressed in the kidney.

Like many scaffolds, PSD-95 not only contains multiple protein–protein interaction modules, it also assembles into multimers, creating an extended platform for efficient scaffolding.[60,61] These qualities, combined with palmitoylation-dependent membrane tethering and synaptic localization signals,[62] make PSD-95 ideally designed to cluster ion channels, receptors, trafficking proteins, and signal transduction machinery at the post-synaptic membrane. In doing so, PSD-95 influences trafficking, endocytosis, and activities of target proteins at the synapse.[59] Organizing local signaling complexes is one of the most important clustering functions of PSD-95. For example, the PDZ domains in PSD-95 independently interact with the calcium/calmodulin-activated nitric oxide synthase, nNOS, and NMDA (N-methyl-D-aspartate) receptors to form a ternary complex.[63,64] The organization is thought to be important for regulated synthesis of nitric oxide. Because NMDA receptors are permeable to calcium, the physical linkage of nNOS with the excitatory receptors is believed to allow nitric oxide production to be efficiently coupled to receptor activation, calcium influx, and local changes in intracellular calcium.[65] Significantly, disruption of NMDAR interaction with PSD-95 dissociates the receptors from downstream neurotoxic signaling, without blocking synaptic activity or calcium influx.[66]

Local signaling complexes that control the production of NOS in the kidney have been proposed.[67] One may involve PSD-93, the predominate MAGUK in renal epithelial cells.[40] Similar to PSD-95, PSD-93 associates with the plasmalemma via palmitoylation-dependent tethering signals,[68] where it recruits and clusters various target proteins, including nNOS.[69] In the kidney, PSD-93 is largely expressed along the basolateral membrane of the thick ascending limb, macula densa cells and the distal nephron.[40] In the macula densa, PSD-93 colocalizes with the pool of nNOS that is associated with intracellular vesicles and the basolateral membrane.[40] It remains to be tested if PSD-93 interaction with nNOS in the macula densa coordinates regulated NO production in the manner that is observed with PSD-95 at the excitatory synapse.

FORM AND FUNCTION OF PDZ PROTEIN FAMILIES IN THE KIDNEY

Apical Membrane PDZ Protein Complexes

NHERF

The Na/H exchange regulator factor PDZ proteins, NHERF, are highly expressed in the kidney and small intestine where they act as molecular scaffolds, associating with a number of transporters, channels, signaling proteins, transcription factors, and receptors to regulate apical membrane transport processes.[70,71] There is a family of four related NHERF proteins encoded by separate genes[72,73] (Figure 14.3). Originally known by many names, a unifying nomenclature has been proposed,[72,73] designating the genes as NHERF-1[74,75] (also known as Ezrin Binding Protein-50, EBP-50[76]); NHERF-2 (also known as NHE-3 kinase A (E3KARP)[77]); tyrosine kinase activator-1 (TKA) and sex-determining region of the Y chromosome (SRY-1)-interacting protein[78]; NHERF-3 (also called PDZK1,[79] Cap70,[80] DiPHOR or NaPi-Cap1[81]); and NHERF-4 (also called IKEPP,[82] DIPHOR-2, and NaPi-Cap 2[81]). Each member of the NHERF family of proteins is believed to play important roles in the regulation of transport processes within the proximal tubule, as well as other sites along the nephron, acting by three different but not mutually exclusive mechanisms. Present evidence indicates that the NHERFs function to: (1) organize local signaling complexes; (2) control apical membrane trafficking; and (3) couple apical membrane transport proteins with other PDZ-binding targets. In this way, NHERFs modulate transporter activity and/or apical abundance of transporters, channels, and receptors. Importantly, each NHERF isoform appears to have unique regulatory properties that are manifested in cell-specific manners.[83] Studies in NHERF isoform knockout-mice have begun to clarify their different physiologic roles in the renal proximal tubule, small intestine, and other epithelia.

Like other scaffolding proteins, the functions of the NHERFs are made possible by the presence of their multiple protein–protein interaction domains. NHERF-1 and NHERF-2 contain two PDZ domains and a COOH-terminal Ezrin/Radixin/Mosein/Merlin (ERM)-binding domain. The latter coordinates interaction with the ERM family of actin binding and A-kinase anchoring proteins to direct linkage with the actin cytoskeleton[84] and signal transduction machinery.[85] By contrast, NHERF-3 and

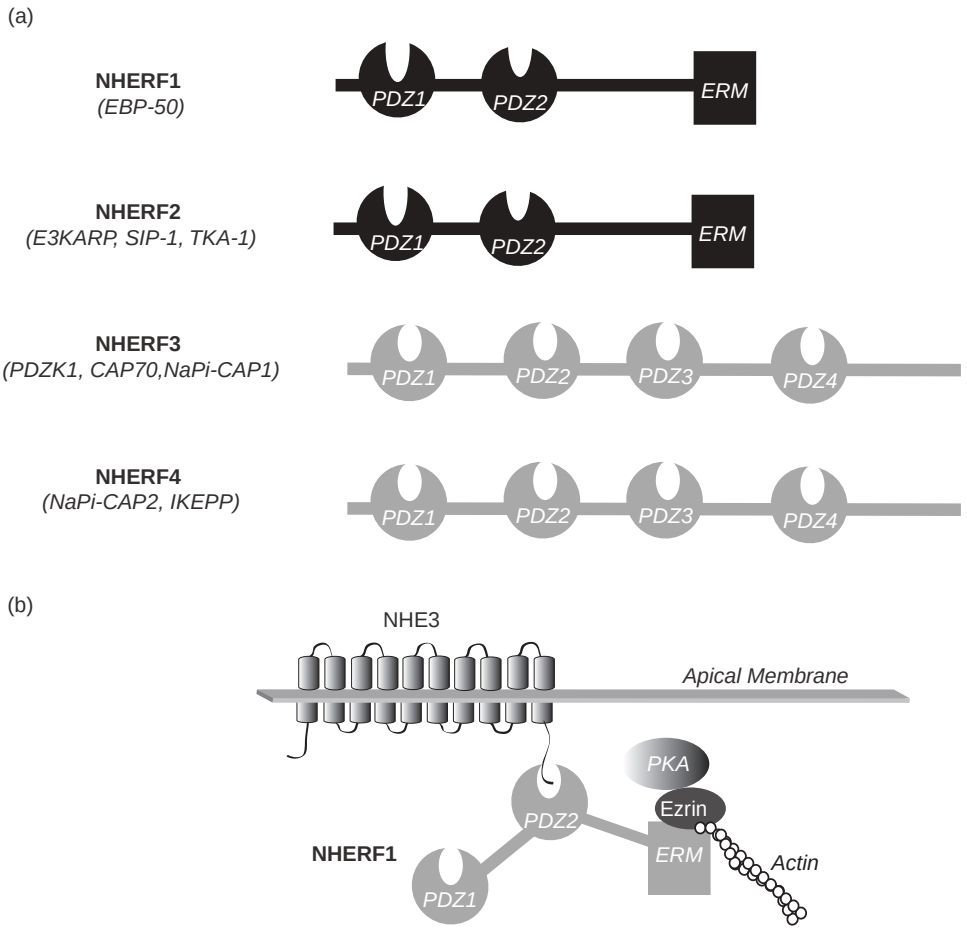

FIGURE 14.3 **NHERF.** (a) Domain architecture of NHERF family members. NHERF 1 and NHERF 2 contain two PDZ domains and an ERM-binding domain. NHERF 3 and NHERF 4 contain four PDZ domains, but no ERM-binding domain. (b) The protein−protein interaction modules in NHERF1 allow it to assemble multi-protein complexes, consisting of PDZ-binding targets (such as NHE3, shown), ezrin, and PKA.

NHERF-4 contain four PDZ domains, but no ERM domain (Figure 14.3).

NHERF proteins can also interact with one another, forming higher order protein networks. Indeed, NHERF1 and NHERF2 associate as homodimers and heterodimers.[30,86−88] Interestingly, oligomerization of NHERF-1, but not NHERF-2, is highly regulated by association with other proteins and by phosphorylation.[30] NHERF3 has been reported to interact with NHERF1 and NHERF2 to form an extensive heteromeric complex.[87] Interaction between NHERF1 and NHERF3 and ezrin is corroborative, providing a mechanism to regulate formation of a ternary scaffolding complex that contributes to the organization microvilli.[31,89,90]

NHERF in Epithelial Transport

A growing body of evidence indicates each NHERF isoform has individual and specialized activities in the kidney. It some cases, specific roles of several NHERF proteins may converge and act cooperatively to regulate target proteins. Here we review the state of knowledge about each NHERF isoform.

NHERF1 was originally discovered as a co-factor necessary for cAMP-kinase dependent phosphorylation and inhibition of NHE3, a brush border Na^+/H^+ exchanger.[74,75] Biochemical studies and work in heterologous expression systems established a likely mechanism whereby NHERF1 organizes a local PKA signaling complex, using its PDZ domains and the ERM-binding domain (Figure 14.3b). The second PDZ domain of NHERF1 directly interacts with NHE3,[91] while the ERM-binding domain simultaneously engages ezrin.[92] By acting as an A-kinase anchor protein (AKAP, see below),[85] ezrin recruits the regulatory subunit of PKA II[92] to the NHERF1 complex. Consequently, NHERF1 juxtaposes PKA with NHE3 for efficient phosphorylation of the transporter and

inhibition of Na^+/H^+ exchange. Consistent with the model, removal of the ERM-binding domain in NHERF1 disrupts formation of NHERF1−ezrin signal complex and attenuates the inhibitory effect of cAMP on NHE3 activity.[93] EPAC (the exchange protein directly activated by cAMP) also participates in the NHERF1-dependent inhibitory response in the proximal tubule, but it is not presently understood how NHERF couples EPAC to NHE3.[94]

Direct evidence that the NHERF1 signal complex is required for phospho-regulation of NHE3 has been provided by studies in NHERF1 gene knockout mice.[95] In this model, activation of PKA fails to phosphorylate and inhibit NHE3 activity in the proximal tubule.[96] The response appears to be specific to NHERF1 removal, in that other proximal tubule NHERF isoforms are not affected by NHERF1 gene ablation. Moreover, the inhibitory effect of PKA can be completely restored in NHERF1-null proximal tubule cells upon adenoviral-mediated delivery of wild-type NHERF1.[97]

The PKA coupling function of NHERF1 is believed to be widespread, with a body of work indicating that the NHERF1 can act as a nexus of signaling complex assembly for efficient phosphorylation and regulation of a variety of transporters, channels, and receptors (reviewed in [98]). For example, NHERF1 (as well as NHERF2[99]) binds to CFTR[100,101] through a PDZ interaction to potentiate PKA phosphorylation-dependent CFTR Cl(−) currents[102] in an ezrin-AKAP dependent manner.

Simultaneous PDZ-dependent recruitment of G-protein coupled receptors by NHERF proteins can further focus local signaling around NHE3 and other transport proteins.[71] For instance, studies in heterologous systems reveal that NHERF binds to the β2-adrenergic receptor (BAR2) by means of a PDZ domain-mediated interaction to recruit NHE3 and the receptor into a local signaling complex for efficient receptor-mediated regulation of sodium−hydrogen exchange. Removal of the PDZ interaction motif in the BAR2 disrupts receptor interaction with NHERF1, and markedly reduces β2-adenergic receptor-mediated regulation of NHE3 without altering activation of adenylyl cyclase.[103] Likewise, NHERF1 facilitates the assembly of a complex containing the β2-adenergic receptor, ezrin, PKA, and CFTR at the apical membrane of epithelial cells for compartmentalized and specific signaling of the channel.[104] Other examples have recently been extensively reviewed.[71]

The tandem PDZ domains in NHERF1 also provide a structural framework to link PDZ-binding transport proteins with PDZ-binding signal transduction machinery. Indeed, several different kinases,[105,106] phospholipase C isoforms,[107] and the receptor for activated C kinase, RACK,[108] have been identified as NHERF1 PDZ-binding targets. Characterization of consensus binding sequences of isolated NHERF-1 PDZ domains by phage-display, affinity selection techniques revealed that the two PDZ domains have different ligand-binding specificities, with distinct preferences for residues at the 0, −1 and −3 positions of type I PDZ ligands.[101] Thus, NHERF1 has a biochemical capacity to tether different PDZ-binding targets together. In addition, because NHERF1 interacts with itself and links with the actin cytoskeleton, formation of an extended network of NHERF1 molecules may join different PDZ-interacting proteins to the same locale. Such a mechanism has been proposed to explain NHERF1-dependent coupling of phospholipase C with the TRP4 channel.[107]

In some cases, the PDZ domains in NHERF1 can support simultaneous interaction of two identical proteins. The best-characterized example is CFTR, which interacts with both PDZ domains in NHERF1, albeit with different binding affinities.[109] In this case, NHERF1 has been reported to induce a high open probability conformation of CFTR by cross-linking the C-terminal tails of a CFTR dimer. Because CFTR binds to the two PDZ domains with different kinetics and affinities, channel gating is profoundly sensitive to alterations in NHERF1 abundance. Moreover, the composition and stoichiometry of NHERF-CFTR interactions can be dynamically regulated. Phosphorylation of NHERF1 has been found to specifically disrupt CFTR interaction with the second PDZ domain, uncoupling the tethered C-terminal tails and inducing a low open-probability conformation.[26] A similar PDZ-dependent cross-linking mechanism has been described with NHERF3.[80]

NHERF1-Dependent Apical Membrane Trafficking

In addition to co-localizing key components of signal transduction pathways, NHERF1 can also regulate cell surface expression and localization of some of its binding targets. It appears to function by controlling trafficking operations in the post-endocytic recycling pathway,[25,110] as well as by anchoring target proteins on the plasma membrane,[100,111] likely by interactions with the cytoskeleton.

Regulation of the Na-dependent phosphate transporter, Npt2a, in the proximal tubule provides a salient example. It is well-known that factors which regulate proximal tubule Pi reabsorption and Pi homeostasis do so by altering the density of Npt2a at the apical membrane. NHERF1 plays an important role in this process. Indeed, NHERF1 gene ablation causes diminished expression of Npt2a at the apical membrane and renal phosphate-wasting.[95] In the NHERF1 knockout model, the Npt2a transporter is misrouted into a subapical, intracellular compartment,[95,112] indicative of a trafficking defect.

Studies in model systems have begun to cast light on the underlying mechanism. Npt2a binds to the first PDZ domain of NHERF1 via a type 1 interaction, requiring the last three amino acids of the co-transporter.[81] These residues are also necessary for efficient apical expression of Npt2a,[111,113,114] suggesting that apical targeting and/or anchoring is specified by direct NHERF1 interaction. Apical localization of the co-transporter can be blocked by ectopic expression of truncated NHERF1 proteins, which contain the first PDZ domain and are able to interact with the transporter, but lack the ERM-binding domain. Thus, it is likely that NHERF1 coordinates localization of the co-transporter by tethering Npt2a with the actin cytoskeleton through the ERM-binding domain.[111]

Exciting recent studies reveal that PTH induced internalization and lysosomal degradation of Npt2a in the proximal tubule are coincident with phosphorylation of NHERF1, and disruption of Npt2a/NHERF1 interaction.[115] These observations strongly suggest that Npt2a−NHERF1 interactions are physiologically regulated to control Npt2a apical surface density for maintenance of calcium and phosphate metabolism. Recent live-cell imaging studies indicate NHERF1 regulates apical expression of Npt2a by a brush border retention mechanism.[116,117] A similar process controls the localization of the PTH receptor.[118] In other proteins, such as CFTR[110] and certain G-protein coupled receptors,[25,119] NHERF1 maintains surface expression by driving recycling to the cell surface after internalization.

Although NHERF1 effectively anchors NHE3 and Npt2a within the microvilli by directly interacting with the transporters and engaging the underlying microvillar cytoskeleton, the transporters have different fates in the renal proximal tubule when they disassociate from NHERF1. In NHERF1 knockout mice, localization of NHE3 is maintained within the microvilli, but Npt2a is targeted to the lysosome. By contrast, when interaction with NHERF1 become severed by physiological signaling processes (e.g., PTH-dependent), a myosin VI driven translocation process moves NHE3 and Npt2a out of the microvilli.[120–123] Because NHE3 selectively assimilates with lipid rafts, the translocated NHE3 molecules are effectively excluded from clathrin-coated pits and consequently are retained at the base of the microvilli.[121] By contrast, Npt2a transporters do not partition into rafts, and are free to be internalized once its ties with the microvillar anchor are broken.

Direct phosphorylation of NHERF1 is emerging as an important mechanism for negatively regulating PDZ-dependent binding interactions in the proximal tubule. Two residues, threonine 95 and serine 77, within the first PDZ domain are phosphorylated in response to PTH and dopamine treatment in the renal proximal tubule. This decreases the binding affinity for the Npt2a transporter, and likely contributes to the hormonal suppression of renal phosphate transport.[27–29] Additional phosphorylation-dependent mechanisms have been reported to control binding at the second PDZ domain in ways that are important for regulating microvilli assembly.[31]

NHERF2

NHERF2 appears to have different functions than NHERF1 in the kidney,[72,124] even though the two PDZ proteins share a common domain structure and NHERF2 is equally effective as NHERF1 in mediating cAMP inhibition of NHE3 in heterologous systems.[77] Unlike NHERF1, which is exclusively expressed in the human, rat, and mouse proximal tubule, expression of NHERF2 in the proximal tubule is species-specific. Found only in the mouse proximal tubule, NHERF2 predominantly localizes to a subapical, intermicrovillar compartment that is distinct from NHERF1 in the brush border.[125] Importantly, NHERF2 does not support phosphorylation-dependent inhibition of NHE3 or apical localization of Npt2a in the NHERF1 knockout model, indicating that NHERF2 does not share physiologically redundant functions with NHERF1 in the proximal tubule.[124]

The functions of NHERF2 are, in fact, better understood at sites outside the proximal tubule. In the kidney, NHERF2 is predominately expressed in the glomerulus, vas recta, and the collecting duct.[126] Physiologically important PDZ-binding partners have been identified in each of these locales. In the glomerulus, NHERF2 interacts with podocalyxin, possibly functioning to retain podocalyxin at the apical surface of the podocyte and provide a mechanism for linking this important surface sialomucin to the actin cytoskeleton.[127] NHERF2 associates with the TRPC4 channel in the descending vasa recta, where it has been suggested to control Ca^{2+} signaling[128] in a similar way that the INAD PDZ protein controls TRP in the *Drosophila* eye.[129] In the collecting duct, NHERF2 co-localizes and interacts with the ROMK channel. Studies in heterologous expression systems indicate that NHERF2 couples accessory proteins and signal transduction machinery to ROMK for efficient channel regulation and trafficking.[130]

The PDZ-binding specificity of NHERF2 also undoubtedly contributes to its unique functions as compared to NHERF1. While NHERF2 shares many of the same PDZ-binding partners as NHERF1, with nearly 60 having been identified,[70] it also interacts with several proteins that NHERF1 does not react with. These include alpha-actinin-4[131]; cGMP kinase I and II[132]; a putative Cl/HCO_3 exchanger downregulated in adenoma[133]; podocalyxin[127]; human Y-linked

testis determining gene-binding factor[78]; serum glucocorticoid stimulated kinase, SGK-1[134]; and transcriptional co-activation with PDZ-binding motif, TAZ.[135]

By organizing these unique partners into protein complexes, NHERF2 can affect functions that are distinct from NHERF1. NHERF isoform-specific regulation of NHE3 in heterologous systems provides an excellent illustration. NHERF2 uniquely confers Ca^{2+}-dependent inhibition on NHE3[136] by scaffolding the exchanger to PKCα and alpha-actinin-4.[72] NHERF1 does not support this activity, presumably because it is not capable of interacting with alpha-actinin-4. Likewise, by acting as a unique protein kinase G-anchoring protein, NHERF2 specifically confers cGMP inhibition on NHE3.[83,132] Finally, activation of NHE3 by dexamethasone requires NHERF2 rather than NHERF1.[134] In this case, the first PDZ domain of NHERF2 uniquely recruits the serum- and glucocorticoid-induced protein kinase, SGK1, into a complex with NHE3 to phosphorylate and enhance exchanger activity. Such a mechanism has been suggested to offer an explanation for glucocorticoid stimulation of sodium absorption in ileum, proximal colon, and renal proximal tubule.[134]

NHERF2-dependent scaffolding of SGK1 may also play an important role in the collecting duct for the regulation of the potassium secretory channel, ROMK.[137,138] It has been reported that NHERF2 can synergize with SGK1 to augment cell surface expression of ROMK in oocyte expression experiments.[138] Biochemical studies indicate that NHERF2 has the capacity to recruit ROMK and SGK-1 into a ternary complex by preferentially binding to the channel with the first PDZ domain,[130] while simultaneously recruiting the kinase by preferred interaction with the second PDZ domain.[134] Formation of such a complex would allow efficient phosphorylation of a residue that is required for delivery of the channel to the cell surface. Indeed, SGK1 directly phosphorylates serine 44[137] in ROMK1, creating a forward trafficking signal[139] that overrides an endoplasmic reticulum localization signal.[140,139] Together the observations suggest a potential molecular mechanism for the regulation of ROMK density by dietary potassium, whereby the NHERF2 scaffold juxtaposes the SGK-1 with ROMK for efficient phosphorylation-dependent trafficking to the apical membrane.

NHERF3

NHERF3 was first discovered as PDZK1, a PDZ domain-containing protein that is upregulated in carcinomas, and abundantly expressed in the proximal tubule brush border.[79,87,141] Significantly, the four PDZ domains of NHERF3 support interaction with many proximal tubule apical membrane transporter proteins, including Npt2a, the solute carrier SLC17A1 (NaPi-I), NHE3, the organic cation transporter (OCTN1), chloride-formate exchanger (CFEX), and the urate-anion exchanger (URAT1),[87] as well as a protein kinase A anchoring protein, D-AKAP2.[142] Based on these observations and findings that NHERF1 can interact with NHERF3, it has been suggested that NHERF3 and NHERF1 may form an extended scaffolding network in brush borders of proximal tubular cells for the regulation of transport.

Although the NHERF3-NHERF1 scaffolding network concept is an attractive hypothesis, it should be pointed out that targeted disruption of the NHERF3 gene by homologous recombination does not[143] cause global alterations in the expression or localization of most of its interacting transport proteins in the proximal tubule.[144,145] Instead, the major effects of NHERF3 gene disruption presently appear to be very specific, confined only to two interacting proteins. A selective reduction in the abundance and functional activity of the chloride-formate exchanger, CFEX, at the proximal tubule brush border is observed in NHERF3-null animals.[145] Physiologic stimulation of the NaPi-IIc isoform by dietary phosphate restriction is also impaired in NHERF3-null animals. A minor role of NHERF3 in Npt2a regulation can be provoked by physiological perturbations; while NHERF3 null animals on a normal or low phosphate diet do not exhibit alterations in Npt2a abundance or function, high dietary phosphate unmasks a modest attenuation of Npt2a levels at the proximal tubule brush border.[146] Differences in affinities of the NaPi-II isoforms for NHERF1(Npt2a) and NHERF3 (Npt2c) have been proposed to account for this behavior.[147]

NHERF4

This member of the NHERF family was originally identified in independent screens for PDZ-binding partners of the Npt2a transporter[81] and the receptor guanylyl cyclase.[82] First dubbed as NaPi Cap-2 or IKEPP (Intestinal and Kidney-Enriched PDZ Protein), it was subsequently reclassified as NHERF4 based on sequence homology modeling.[73] In the proximal tubule where it is abundantly expressed, NHERF4 localizes to a subapical region, like NHERF2, that is distinct from the brush border and NHERF1.[81] Little is known about the function of NHERF4 except that it inhibits heat stable toxin induced cGMP synthesis,[82] by a mechanism suggested to involve PDZ-dependent recruitment of inhibitory factors.[73] Roles in regulating the TRPV5 and TRPV6 calcium channels have also been described.[203] Based on its structural similarities with other NHERF forms and the site of expression in the kidney,[73] it seems likely that NHERF4 also modulates apical membrane transport and cell signaling in the proximal tubule.

Shank (SH3 Domain and Ankyrin Repeating Proteins, A.K.A Proline-Rich Synapse-Associated Protein-1/Cortactin-Binding Protein 1 (ProSAP1/CortBP1))

In addition to the established role as master scaffolds at the postsynaptic density,[148] members of the Shank (SH3 domain and ankyrin repeating proteins) family of proteins play roles as apical membrane-associated scaffolds in epithelial cells. The three known Shank genes (Shank1, Shank2, and Shank3) are expressed in a tissue-specific manner. Shank 1 is almost exclusively expressed in the brain, products of the Shank2 gene are found in brain, kidney, and liver, whereas Shank 3 is most abundantly expressed in the heart.[149] The prototypical Shank, Shank1, is a relatively large protein (> 200 KDa) containing multiple ankyrin repeats,[150] a SH3 domain, a PDZ domain, and a long proline repeat domain. A self-oligomerization domain, called a sterile alpha motif (SAM), assembles the scaffolds into head-to-tail helical sheets, forming an extensive Shank network for protein complex assembly.[151] In neurons, Shank forms a polymeric structure with another protein, Homer, to serve as a platform for assembling postsynaptic density proteins.[152] Multiple splice variants of each gene have been identified that contain different combinations of protein−protein interaction domains (Figure 14.4). For example, Shank2E, a form that is predominantly expressed in epithelial cells,[42] contains ankyrin repeats whereas the Shank2 splice form found in the brain does not.

Extensive studies in the brain provide models for Shank function in epithelial cells. It is well-established that Shank family members localize to the postsynaptic density of excitatory synapses, where they act as master scaffolds along with Homer and PSD-95.[148] Here, the Shanks physically couple the two major receptor complexes, N-methyl-d-aspartate receptors (NMDAR) and metabotropic glutamate receptors (mGluR), and recruit associated signaling proteins. They do so by concurrently engaging two different adaptors through distinct protein−protein interaction domains. The Shank PDZ domain associates with the GUK-associated protein, GKAP which, in turn, interacts with the PSD-95 complex, containing NMDA receptors.[148] At the same time, the proline rich domain of Shank interacts with another adaptor protein, Homer, to link with metabotropic glutamate receptors. Proline rich domains often serve as binding sites for SH3 (SrC homology), WW (conserved two-tryptophan domain), and EVH1 domains (enabled/vasodilator-stimulated phosphoprotein homology 1).[153] A single EVH1 domain in Homer directly interacts with a PPXXF motif in the Shank proline-rich domain, as well as with similar proline motifs in group 1 mGluR and other proteins, such as the IP3 receptor.[154] Because Homer proteins self-associate in a head-to-tail fashion, two EVH1 domains per dimer are available to bridge Shank with group 1 mGluRs. Consequently, Shank cross-links Homer and PSD-95 complexes in the PSD, presumably to couple signaling transduction pathways emanating from NMDAR and mGluR. Disruption in this synaptic scaffolding mechanism may be responsible for human disease, as mutations in SPAK2 have been associated with autism and mental retardation.[155]

More recently, Shank2 forms have been implicated in the modulation of apical membrane transport

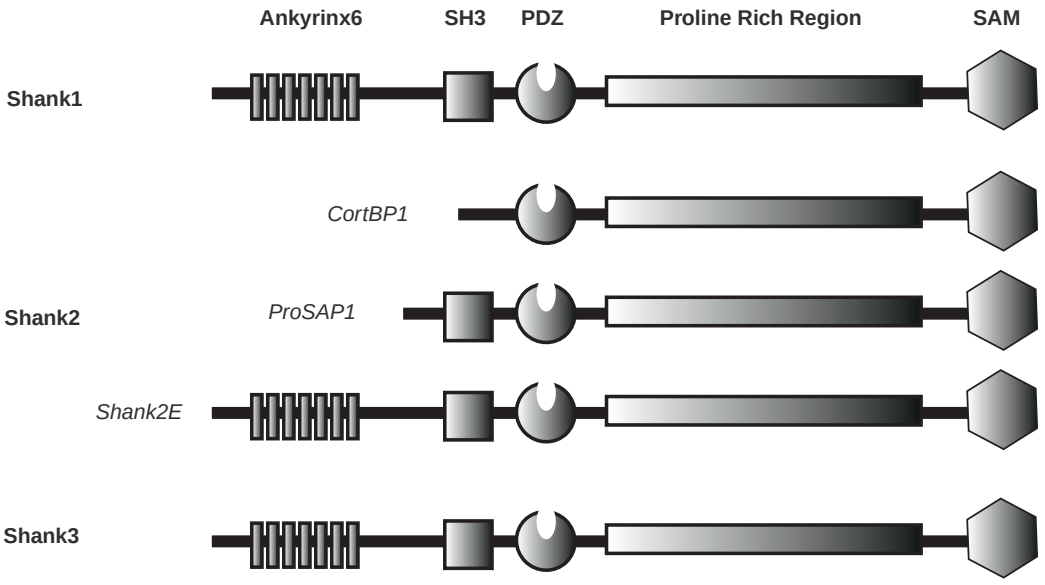

FIGURE 14.4 **Shank family members.** Domain architectures of Shank1, 2, 3, and Shank2 splice variants are shown. The major epithelial form, Shank2E, contains six ankyrin repeats, a SH3 domain, a PDZ domain, a proline rich domain, and a self-oligomerization region called a SAM domain.

processes. In the kidney, Shank2E is concentrated at the apical membrane of proximal tubule cells were it interacts with NHE3 and Npt2a, similar to NHERF1. Present evidence indicates that Shank2 and NHERF may control the activity of these transport proteins in divergent manners. Studies with NHE3 in heterologous expression systems, for example, revealed that Shank2 positively regulates NHE3 membrane expression and blunts the cAMP-dependent inhibition of NHE3, in part by antagonizing the action of NHERF1. Likewise, in pancreatic duct cells, Shank2E associates with CFTR at the apical membrane and inhibits Cl channel activity,[156] contrasting the positive effects of NHERF1 and NHERF2 on CFTR (see above). Shank2 also positively regulates NHE3 by recruiting BetaPix, a guanine nucleotide exchange factor for the Rho-GTPase.[157] Because retention and targeting of NHE3 in the apical microvilli depends on the sustained activity of Rho-GTPases,[158] the interaction between NHE3 and the Shank2-BetaPix complex may allow NHE3 trafficking to be linked to the maintenance of the microvilliar actin cytoskeleton.

Shank2E appears to regulate Npt2a in a different manner than NHERF1. In the proximal tubule, increased extracellular Pi triggers internalization and degradation of Shank2E and Npt2a in parallel, but has no effect on NHERF1 localization or abundance.[159] Combined with observations that regulated endocytosis of Npt2a is associated with disruption of Npt2a/NHERF1 interaction at the brush border,[115] one might speculate that internalization of Npt2a involves a NHERF1-to-Shank2E interaction switch. Importantly, Shank redistributes with Npt2a during regulated endocytosis,[160] and interacts with dynamin II, a GTPase that is critical for endocytic vesicle formation, via proline-rich domain interaction.[161] Thus, Shank2E is especially poised to facilitate Npt2a endocytosis and/or lysosomal trafficking, in contrast to the apparent membrane-retention and/or recycling function of NHERF1. The molecular mechanisms underlying the function of Shank2E in the proximal tubule remain to be firmly established, however. It will be interesting to learn if the activities of Shank2E in the kidney depend on scaffold adaptors, such as Homer and GKAP, as has been shown in excitatory synapses.

BASOLATERAL MEMBRANE PDZ PROTEIN COMPLEXES

The Lin-7/CASK/PSD-97 System

Lin-7 and CASK (Lin-2) are components of an evolutionarily conserved basolateral membrane scaffolding complex, important for polarized targeting and controlling cell surface density of their PDZ-binding partners. They were discovered along with another PDZ protein, Lin-10 (Lin, from abnormal cell lineage), in a genetic screen for components of the LET-23 receptor tyrosine kinase signaling pathway in *C. Elegans* vulva progenitor cells (VPC).[162] These molecules form a tripartite protein complex in VPC that interacts with a receptor tyrosine kinase, LET-23, to coordinate receptor expression on the basolateral membrane.[162–164] Importantly, null mutations in Lin-7, Lin-2 or Lin-10 cause the Let-23 receptor to become mislocalized to the apical membrane, and consequently disrupt LET-23 signaling and VPC development.

Orthologs of the *C. elegans* PDZ protein complex have been identified in mammalian tissues (Lin-7 = mLin7/Veli/MALS; Lin-2 = CASK; Lin-10 = Mint-1/X11).[37,165–167] In the mammalian kidney, a partially conserved complex, consisting of mLin-7 and CASK but not Lin-10,[19] localizes to the basolateral membrane[36,37] where it coordinates polarized expression of mLin-7-binding partners (Figure 14.5). It has been implicated in basolateral expression of the epithelial GABA transporter, BGT-1,[168] the strong inward-rectifying potassium channels, Kir 2.X,[167,169,170] the EGF-like receptor, ErbB-2/Her2,[171] and the insulin receptor substrate, p53.[172] Present evidence suggests that the mLin-7/CASK complex may offer a general mechanism for polarized expression of basolateral membrane proteins containing Type I PDZ-binding motifs.

Lin-7 acts as the upstream scaffolding molecule. It binds directly to target molecules through a Type I PDZ interaction while simultaneously engaging CASK via another protein−protein interaction module,[37,173] called a L27 domain (from Lin-2, Lin-7).[174] L27 domains, which present a number of related PDZ proteins (see PALS, below), are helical bundle structures[175,176] that mediate heterotypic assembly, important for polymerization of different scaffolds. In fact, basolateral membrane localization of Lin-7 and its PDZ-binding partners is afforded by the L27 domain and CASK interaction.[37,177,178]

CASK associates with the basolateral membrane through a web of interactions to function as the master basolateral membrane attachment factor. As a member of the MAGUK family (see above), CASK contains multiple protein−protein interactions sites, allowing it to simultaneously bind to Lin-7, extracellular matrix receptors, adhesion molecules, the actin cytoskeleton 4.1-binding proteins,[39] and another MAGUK protein, SAP-97.[173] The mLin-7 and SAP-97 L27 domains separately assemble with two L27 domains of CASK, possibly as a dimer of L27 heterodimers,[175,176] to form a mLin-7/SAP97/CASK complex.[170,173] By linking extracellular matrix receptors and the cytoskeleton, the Lin-7/CASK/SAP97 complex has the capacity to act as a stable anchor to retain Lin-7 interacting proteins on the basolateral membrane.

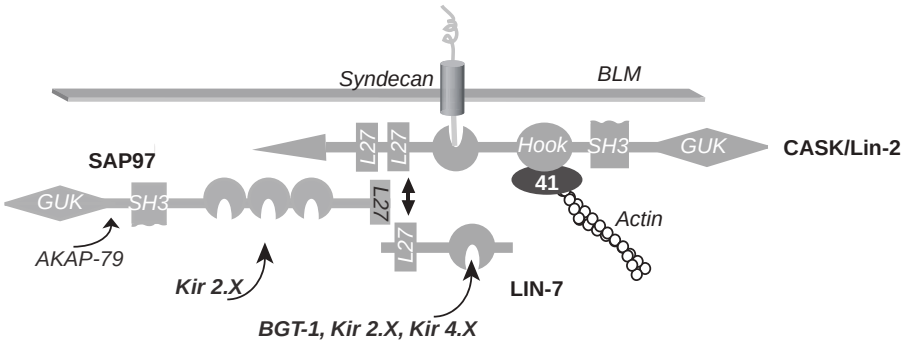

FIGURE 14.5 **Lin-7/CASK/SAP-97 complex at the basolateral membrane (BLM).** Lin-7 recruits PDZ-binding targets, such as the BGT-1 transporter and the inwardly rectifying potassium channels, Kir 2.X and Kir 4.X, to the basolateral membrane by interacting with CASK through a L27 domain interaction. CASK acts as the master anchor; it not only interacts with Lin-7, it also binds to extracellular matrix receptors, such as syndecan, through a type II PDZ interaction, while simultaneously engaging the actin cytoskeleton through a hook domain interaction with 4.1 proteins. CASK also recruits SAP-97 to the basolateral membrane through an L27 interaction. SAP-97 has the capacity to recruit PDZ-binding targets, as well as proteins that interact with the guanylate kinase (GK) and SH3 domains, such as AKAP-79.

The mammalian counterpart of Lin-10 is actually encoded by a family of proteins called the Mints or X11s.[179] Although all three members of the Mint family share C-terminal PDZ and PTB domains, only Mint-1 contains a CASK interaction domain.[165] In neuronal tissues and the heart, which express the complete Lin-7/CASK/Mint-1 complex, Mint-1 has been suggested to provide an additional membrane trafficking function. Mint-1 interacts with microtubule motors, and has been reported to transport N-methyl-D-aspartate (NMDA)-type receptor vesicles along microtubules.[180] In addition, Mint-1 interacts with Munc-18 docking machinery.[165,166,181] Importantly, mammalian epithelial cells do not express Mint-1. In its absence, the Lin-2/CASK system loses the obvious link to microtubule-mediated trafficking and fusion, suggesting that Lin-7/CASK plays a major role in retention rather than directed-delivery in renal epithelia.

Consistent with this notion, present evidence indicates that Lin-7/CASK primarily functions to retain target proteins at the basolateral membrane of mammalian epithelia. For example, Perego et al. found that removing the PDZ ligand in BGT-1 disrupted Lin-7 association in MCDK cells and dramatically increased the internalization of the transporter from the plasmalemma.[168] The retention function of Lin-7 depends on its L27 domain, which directs interaction with a cognate L27 domain in CASK.[170,177] In this way, Lin-7 acts as a PDZ-to-L27 adapter, mediating indirect association of its PDZ-binding target proteins with the larger basolateral membrane scaffold, CASK.

Although Lin-7 primarily operates as a component of a basolateral membrane retention machine in mammalian epithelial cells, it should be pointed out that disruption of Lin-7 interactions can produce a wide range of mis-localization phenotypes, depending on the Lin-7-binding partner and the types of sorting signals embedded within them. For instance, mutant BGT transporters, lacking their PDZ-binding motif, are predominately localized on the basolateral membrane. In this case, BGT-1 transporters are presumably directed to the basolateral membrane by non-PDZ-dependent sorting signals.[182] On the other hand, mutant Kir2.3 channels, lacking the PDZ-binding motif, are largely directed to an endosomal compartment, rather than the basolateral membrane,[167,177] consistent with strong endosomal targeting signals. An apical-missorting phenotype is produced by removing the PDZ-binding site from a chimeric LET-23/nerve growth factor receptor protein.[183] In this case, Lin-7 interaction may stabilize the receptor on the basolateral membrane or limit post-endocytic trafficking in such a way that it prevents transcytosis to the apical membrane.

At present, it is not known if the Lin-7/CASK/SAP97 scaffold also participates in signal complex localization and organization at the basal membrane in the way that has been described for the NHERF proteins at the apical membrane. SAP97 has been shown to recruit AKAP proteins to related PDZ protein complexes in neurons,[58] and the *Drosophila* CASK ortholog protein, Camguk, functionally modulates Ether-a-go-go potassium channels by a phosphorylation-dependent mechanism.[184] Interestingly, CASK contains an unusual CAM-kinase like domain, which can phosophorylate interacting proteins at the synapse.[185] However, it remains to be established if similar mechanisms are in place at the basolateral membrane of renal epithelial cells, which express the Lin-7/CASK/SAP97 complex.

Lin 7 Isoforms (Veli/MALS) and PALS (Partners of Lin7) in the Kidney

Three different Lin-7 isoforms, encoded by separate genes, have been identified. In mammalian systems,

these are often called Veli/MALS 1,2,3 (Vertebrate Lin-7 or Mammalian Lin Seven). Each of the MALS/Veli isoforms are expressed in the kidney, but each are differentially localized along the nephron.[36] MALS/Veli 1 is predominately expressed in the glomerulus, thick ascending limb of Henle's loop (TAL), and the distal convoluted tubule (DCT). MALS/Veli 2 is exclusively expressed in the vasa recta. MALS/Veli 3 is largely located in the proximal tubule, DCT, and collecting duct. The subcellular localization of MALS/Veli proteins can vary, depending on the isoform and the cell type. In contrast to the predominate basolateral location of MALS/Veli 1 in the TAL and DCT and MALS/Veli 3 in the DCT, MALS/Veli 1 is found diffusely throughout the cytosol of intercalated cells. In the collecting duct, MALS/Veli 3 is chiefly located on the basal membrane. Collectively, these results suggest that different MALS/Veli isoforms may carry out cell type-specific functions. MALS/Veli 1 and 2 isoforms in the thick ascending limb and distal segments appear to have the most significant capacity for a basolateral membrane targeting mechanism. MAL3/Veli 3 has been implicated in generation of polarity in the proximal tubule.[186]

The disparate subcellular localization patterns of MALS/Veli isoforms are likely to arise from at least two different factors. First, differences in the primary structures provide reason to suspect that the MALS/Velis may have specific binding preferences. In contrast to the nearly identical PDZ domains amongst the MALS/Veli isoforms, the extreme NH_2- and COOH-termini are highly divergent. Most importantly, the region believed to direct MALS/Veli subcellular localization, the L27 interaction module, exhibits only 57% amino acid identity between isoforms, raising the possibility that different isoforms preferentially bind to different L27 domain proteins. Second, cell-specific expression of Lin-7-binding partners may account for differences in isoform localization in different nephron segments and cell-types. A group of CASK-like MAUGK proteins, called PALS (Partners of Lin-7), that contain L27 hetero-oligomerization domains, have been identified as potential partners of Lin-7.[187] The different PALS might substitute for CASK under certain circumstances, forming MALS/Veli complexes with different subcellular locations and disparate functions. For instance, PALS1 targets Lin-7 to the tight junction,[188] in contrast to the basolateral membrane location of the CASK/Lin-7 complex.

Dystrophin-Associated Protein Complex

The dystrophin-associated protein complex (DPC) is a transmembrane scaffolding machine that is expressed in a variety of tissues. Extensive studies in skeletal muscle revealed the DPC serves structural and signaling functions.[189] In epithelia, the DPC localizes to the basolateral membrane (Figure 14.6), where it is organized in a manner similar to the skeletal muscle complex, functioning to compartmentalize and tether signaling and transport proteins.

In the sarcolemma, the DPC is nucleated by dystrophin, a flexible rod-like cytoplasmic protein containing multiple spectrin-like repeats. Dystrophin directly interacts with the transmembrane protein, β-dystroglycan, via a C-terminal cysteine-rich region, and connects the complex to lammin through α-dystroglycan (Figure 14.6). Because dystrophin also binds actin, it effectively links the extracellular matrix with the cytoskeleton, offering an architecture that protects the sarcolemma from shearing forces of contraction. This point is underscored by the link to disease. Specific mutations in the X-linked dystrophin have been identified that disrupt dystrophin and consequently destabilize DGC elements at the sarcolemma, producing Duchenne muscular dystrophy, the milder Becker muscular dystrophy, and X-linked dilated cardiomyopathy (reviewed in [189]).

Dystrophin also interacts with the scaffolding molecules dystrobrevin, and three isoforms of syntrophin (α1, β1 and β2), to organize local signaling complexes in muscle. The syntrophrins contain several protein−protein interaction domains, including two pleckstrin homology domains and a PDZ domain. The PDZ domains recruit a variety of proteins to the DPC, including voltage-gated sodium channels[190,191] and nNOS.[2] α-Dystrobrevin directly interacts with dystrophin via coiled-coil domains, while simultaneously binding to the syntrophins through an independent binding site.[192]

The basolateral membrane associated DRC in renal epithelial cells exhibits the same basic design as in skeletal muscle, but differs somewhat in molecular composition.[193,194] An autosomal homolog of dystrophin, called utrophin, along with less abundant C-terminal dystrophin isoforms, Dp71 and Dp140,[189] takes the place of the longer muscle-specific dystrophin in renal epithelia. In addition, differential expression of dystrobrevin and three syntrophin isoforms along the nephron give rise to nephron segment-specific DPCs with distinct molecular properties.[193] In the connecting segment and the cortical collecting duct where the DPC is especially enriched, the DPC includes utrophin, β1-/β2 syntrophin, dystrobrevin, and β-dystroglycan.[193]

Like dystrophin in muscle, utrophin directly interacts with the actin cytoskeleton in epithelial cells,[195] while associating with laminin in the extracellular matrix via the basolateral dystroglycans[196] (Figure 14.6). Thus,

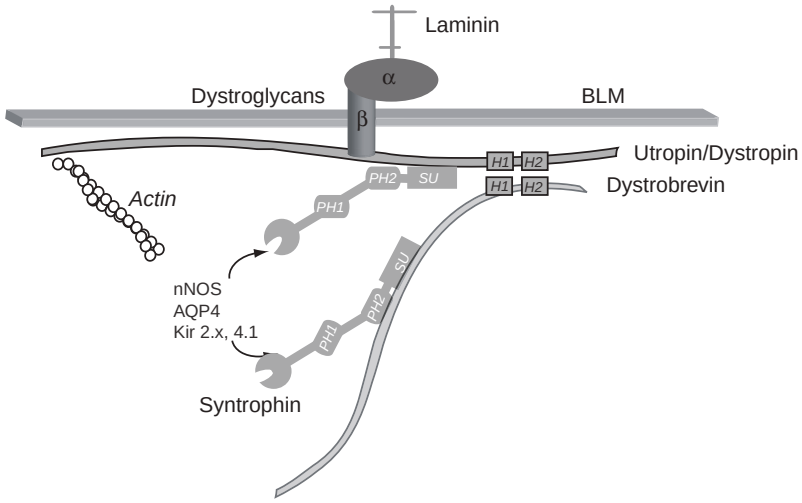

FIGURE 14.6 **The dystrophin-associated protein complex (DPC) at the basolateral membrane.** The PDZ protein, syntrophin, is recruited to the basolateral membrane via its interaction with utropin and possibly dystrobrevin, requiring one of its pleckstrin homology (PH2) domains and the syntrophin unique (SU) domain. This leaves the syntrophin PDZ domain free to recruit basolateral membrane proteins, such as the AQP4 water channel, potassium channels, Kir 2.X and Kir 4.X, as well as nNOS. Utropin/dystropin interacts with actin via N-terminal spectrin repeats, with β-dystroglycan via a C-terminal cysteine-rich region and with dystrobrevin via coiled-coiled domains (H1, H2).

utrophrin is poised to provide a secure anchoring point for polarized expression of syntrophin. Consistent with this notion, it has been reported that basolateral membrane localization of β2-syntrophin depends on its utrophin-binding activity, requiring one of its pleckstrin homology domains and the syntrophin unique (SU) domain.[35] Moreover, utrophin knockout mice exhibit a selective reduction of β2-syntrophin at renal epithelial basolateral membrane domains.[193] Syntrophins also interact with dystrobrevin via the PH and SU domains, allowing recruitment of additional syntrophin molecules to the same DPC.[197]

Importantly, the association of syntrophin with dystrobrevin, utrophin, and the basolateral membrane occurs independently of the syntrophin PDZ domain.[35] This leaves the Type I PDZ domain free to interact with proteins containing a syntrophin PDZ recognition motif. Basolateral membrane proteins, such as the inward rectifying channel proteins Kir 2.X[169] and Kir 4.X,[198] the AQP4 water channel,[199] as well as nNOS, have been shown to interact with the syntrophin PDZ-binding domain. At present, the functional relevance of these interactions in the kidney is not well-understood.

Several clues about the roles of transport protein interaction with syntrophin and the DPC are provided by studies in other tissues. In astrocytes, for example, α-syntrophin is required for the polarized expression of AQP4[199] and Kir 4.1[198] at end-feet membranes adjacent to blood vessels for efficient water and potassium siphoning.[200,201] It will be interesting to learn if genetic ablation of β2 syntrophin, the prevalent form in the kidney, has similar effects on AQP4 in the proximal straight tubule[202] and Kir 4.1 in the distal nephron.[203]

Utrophin knockout animals have been generated.[204] Unfortunately, expression of the shorter C-terminal dystrophin forms in the kidney compensate for the utrophin ablation, making it difficult to precisely define the functional role of the renal DPC by a genetic approach. Double utrophin/dystrophin knockout mice exhibit a fragile phenotype with complete disintegration of the DPC and premature death.[193] It will be important to determine how much of the phenotype can be attributed to impaired kidney function.

AKAP

AKAPs (A-kinase anchoring proteins) are a diverse group of molecules that function as cell signaling scaffolds. Specifically, AKAPs organize and juxtapose protein kinase A (PKA) with specific substrates and other signaling machinery at specific cellular locales. In doing so, AKAP proteins can precisely control where and when second-messengers will act on select cellular effectors. Since the first discovery of an AKAP, a microtubule anchoring protein that binds to the regulatory subunit of PKA with high affinity,[205] nearly 50 AKAP proteins have been identified. Many of them control phosphorylation of channels, receptors, and membrane transport proteins.[206] Several are suspected of modulating renal tubule transport processes.

COMMON PROPERTIES OF AKAP PROTEINS

AKAP proteins are structurally diverse, related only by general signaling functions and three common properties. First, classification as an AKAP protein requires the presence of a PKA-anchoring domain. Second, AKAPs contain cellular localization signals that provide a means to spatially organize second-messenger cascades at specific subcellular compartments. Third, AKAPs possess other protein−protein interaction domains, which specify interaction with select effectors and/or other signaling molecules. While all AKAPs have these common properties, they each have distinct targeting signals and different scaffolding

motifs. Consequently, they have specialized functions, modulating distinct intracellular signaling events.

AKAPs bind PKA by means of a small anchoring domain, comprised of a short (13–18 amino acid), amphipathic α-helix. NMR solution structures reveal that the hydrophobic side of the amphipathic helix makes numerous hydrophobic contacts within a hydrophobic surface of a four-helix bundle formed by the N-terminal domains of the PKA regulatory subunit homodimer.[208–210] Consequently, the AKAP–PKA interaction occurs with relatively high affinity (~1–10 nM). While most AKAPs interact with the RII isotypes of the PKA regulatory subunit, several AKAPs have been identified, D-AKAP1[211] and D-AKAP2,[211] which can interact with both RI and RII forms. Sphingosine kinase interacting protein (SKIP), an AKAP that is enriched in the inner mitochondrial membrane, exclusively interacts with RI.[212] Importantly, AKAP function can be disrupted by exogenous expression of a peptide mimic of the amphipathic helix.[213] Regulatory subunit isotype specific competitors have been developed.[214]

Specialized targeting sequences on anchoring proteins compartmentalize different AKAPs to distinct subcellular compartments, including plasma membrane microdomains, intracellular vesicles, nuclei, mitochondria, microtubules, and the actin cytoskeleton.[215] Certain AKAPs contain polarized trafficking signals that direct asymmetric localization in epithelial cells. AKAP2 (AKAP-KL), for example, is compartmentalized on the apical membrane[216] by its PDZ-binding motif, which specifies interaction with NHERF3.[81] Similarly ezrin, a low RII affinity AKAP, localizes to the apical membrane through a protein–protein recognition domain that directs interaction with NHERF1.[217] In many cases, different splice products of the same AKAP gene can be differentially targeted to different compartments. Splice forms of the AKAP18 gene, for instance, are expressed on opposite plasma membrane domains in epithelial cells; AKAP18-α is targeted to basolateral membranes, whereas AKAP18-β localizes to the apical membrane. In this case, a unique 23 amino acid insert in AKAP18-β acts as an apical membrane targeting determinant.[218]

As multivalent scaffolds, AKAPs can juxtapose the right combination of enzymes with their substrates. Consequently, AKAPs not only synchronize signal transduction processes, but they can also orchestrate signal termination events. The archetypal example is provided by the AKAP75/150 family, which influences the phosphorylation state of several different channels and transporters, including the Npt2a co-transporter,[219] L-type calcium channels,[220] M-type potassium channels,[221] and AMPA-type glutatamate receptors.[222,223] AKAP75 not only contains a binding site for PKA, it also directly interacts with PKC and the calcium-calmodulin-dependent phosphatase, PP2B (calcineurin).[224,225] Consequently, the same AKAP scaffold can coordinate signal transduction processes by phosphorylation as well as dephosphorylation. Thus, AKAPs can influence the balance of signal transduction and termination by differentially tethering different signaling components and effectors.[226]

Function of AKAPS in Kidney Transport Processes

AKAP-Dependent AQP2 Water Channel Shuttling

A critical role for AKAPs in water channel trafficking is strongly suggested by observations that cAMP-dependent AQP2 translocation to the cell surface can be inhibited with a synthetic peptide mimic of the AKAP amphipathic helix, which prevents binding of AKAPs to the PKA RII subunit.[227] Several different AKAPs appear to be associated with endosomal structures containing AQP2. Biochemical characterization of inner medullary collecting duct (IMCD) heavy endosomes, containing AQP2, revealed the presence of an associated multiprotein-signaling complex, composed of a 90 kD AKAP, PKA, and protein phosphatase 2a.[228] While the precise molecular identity of the 90 kD AKAP is still not certain, a smaller anchoring protein, AKAP18-δ, was subsequently discovered.[229] In the kidney, AKAP18-δ is mainly expressed in IMCD principal cells, where it appears to be confined to intracellular vesicles containing AQP2 and PKA. Observations that vasopressin recruits AKAP18-δ with AQP2 to the plasma membrane suggest that this AKAP is specifically involved in the PKA phosphorylation-dependent AQP2 translocation process. Reminiscent of the multifactoral roles of AKAP75 (see above), the AKAP-signaling complex in IMCD endosomes also contains PP2B[228] and phosphodiesterases.[230] Thus, the endosomal AKAPs in the collecting duct are also likely to participate in maintaining AQP2 in a quiescent dephosphorylated conformation in water diuresis.

AKAPs in the Proximal Tubule Apical Membrane Scaffolding Complex

Two different AKAPs, D-AKAP2 and AKPA79, have been implicated in the modulation of proximal tubule sodium phosphate transport. AKAP2 has been shown to interact with a PDZ scaffolding protein, NHERF3, at the apical membrane where it has been suggested to play an important role in the parathyroid hormone (PTH)-mediated regulation of Npt2a, involving PKA compartmentalization.[142] In a proximal tubule model, OK cells, PTH-dependent regulation of Npt2a can be uncoupled with a synthetic peptide mimic of

the AKAP amphipathic helix, indicating that an AKAP is required for PKA-dependent modulation of Npt2a regulation. In this system, AKAP79 was shown to associate with the Npt2a transporter, PKA, and the parathyroid hormone receptor.[219] Because AKAP 79 also has the capacity to interact with PDZ proteins in neuronal systems,[58] it may interact with the Npt2a co-transporter and the PTH receptor through its interaction with the apical NHERF complex.

AKAP Control of the Potassium Secretory Channel ROMK (Kir 1.1)

Studies of the renal potassium secretory channel, ROMK, in heterologous expression systems have suggested a potential role for AKAPs in the physiological regulation of potassium secretion. Because open channel gating and cell surface expression of the ROMK require direct phosphorylation by PKA[231,232] and other kinases,[137] a critical role of an AKAP has been an attractive idea. In fact, it has been reported that maximal activation of ROMK in *Xenopus* oocytes by forskolin and/or 8-bromo-cAMP-dependent kinase requires co-expression of an AKAP.[233] High basal phosphorylation of the channel in this expression system makes the effects of AKAPs modest. Nevertheless, the response appears to be AKAP specific, being dependent on AKAP-75 but not AKAP18, AKAP-2 (KL).[234] AKAP-75 is not expressed with ROMK in the thick ascending limb or collecting duct, however, so the AKAP in the kidney that interacts with ROMK still remains to be determined. Given observations that ROMK interacts with NHERF1 and 2 (see above), the ERM proteins[85] are obvious AKAP candidates.

CONCLUSION

Exciting discoveries in recent years have cast light onto the molecular mechanisms of epithelial transport modulation. The discovery of proteins that bring together physiologically appropriate assemblages of cell signaling and trafficking proteins with transport molecules for efficient regulation has been especially insightful. The molecular identities and functions of many of these scaffolding molecules in the kidney have now begun to come into focus. Still, there is much more to be learned. For example, observations that some transport proteins such as NHE1, the housekeeping sodium-hydrogen exchanger,[207] NHE3,[235] and the Na/K ATPase,[236,237] might twilight as scaffolding proteins is emerging as an intriguing possibility that we certainly will hear more about in the future. Also, with the application of powerful new tools in cell biology, genomics, and proteomics, it is likely that more scaffolding candidates will be identified. As they are, it will be important not only to continue probing into the mechanistic basis of function in model systems, but also to rigorously explore how these fascinating molecules work in their native cellular environments.

References

[1] Songyang Z, Fanning AS, Fu C, Xu J, Marfatia SM, Chishti AH, et al. Recognition of unique carboxyl-terminal motifs by distinct PDZ domains. Science 1997;275:73–7.

[2] Hillier BJ, Christopherson KS, Prehoda KE, Bredt DS, Lim WA. Unexpected modes of PDZ domain scaffolding revealed by structure of nNOS-syntrophin complex. Science 1999;284:812–85.

[3] Harris BZ, Hillier BJ, Lim WA. Energetic determinants of internal motif recognition by PDZ domains. Biochim Biophys Acta 2001;40:5530–921.

[4] Cho KO, Hunt CA, Kennedy MB. The rat brain postsynaptic density fraction contains a homolog of the *Drosophila* discs-large tumor suppressor protein. Neuron 1992;9:929–42.

[5] Harris BZ, Lim WA. Mechanism and role of PDZ domains in signaling complex assembly. J Cell Sci 2001;114:3219–31.

[6] Sheng M, Sala C. PDZ domains and the organization of supramolecular complexes. Annual Review of Neuroscience 2001;24:1–29.

[7] Adams ME, Mueller HA, Froehner SC. *In vivo* requirement of the alpha-syntrophin PDZ domain for the sarcolemmal localization of nNOS and aquaporin-4. J Cell Biol 2001;155:113–22.

[8] Xu XZ, Choudhury A, Li X, Montell C. Coordination of an array of signaling proteins through homo- and heteromeric interactions between PDZ domains and target proteins. J Cell Biol 1998;142:545–55.

[9] Borrell-Pages M, Fernandez-Larrea J, Borroto A, Rojo F, Baselga J, Arribas J. The carboxy-terminal cysteine of the tetraspanin L6 antigen is required for its interaction with SITAC, a novel PDZ protein. Mol Biol Cell 2000;11:4217–425.

[10] Maximov A, Sudhof TC, Bezprozvanny I. Association of neuronal calcium channels with modular adaptor proteins. J Biol Chem 1999;274:24453–6.

[11] Tonikian R, Zhang Y, Sazinsky SL, Currell B, Yeh JH, Reva B, et al. A specificity map for the PDZ domain family. PLoS Biol 2008;6: e239.

[12] Cabral JH, Petosa C, Sutcliffe MJ, Raza S, Byron O, Poy F, et al. Crystal structure of a PDZ domain. Nature 1996;382:649–52.

[13] Doyle DA, Lee A, Lewis J, Kim E, Sheng M, MacKinnon R. Crystal structures of a complexed and peptide-free membrane protein-binding domain: Molecular basis of peptide recognition by PDZ. Cell 1996;85:1067–76.

[14] Daniels DL, Cohen AR, Anderson JM, Brunger AT. Crystal structure of the hCASK PDZ domain reveals the structural basis of class II PDZ domain target recognition. Nat Struct Biol 1998;5:317–25.

[15] Karthikeyan S, Leung T, Ladias JA. Structural basis of the Na^+/H^+ exchanger regulatory factor PDZ1 interaction with the carboxyl-terminal region of the cystic fibrosis transmembrane conductance regulator. J Biol Chem 2001;276:11966–9683.

[16] Tochio H, Zhang Q, Mandal P, Li M, Zhang M. Solution structure of the extended neuronal nitric oxide synthase PDZ domain complexed with an associated peptide. Nat Struct Biol 1999;6:417–21.

[17] Zhang Y, Yeh S, Appleton BA, Held HA, Kausalya PJ, Phua DC, et al. Convergent and divergent ligand specificity among PDZ domains of the LAP and zonula occludens (ZO) families. J Biol Chem 2006;281:22299–311.

[18] Birrane G, Chung J, Ladias JA. Novel mode of ligand recognition by the Erbin PDZ domain. J Biol Chem 2003;278:1399–402.
[19] Elkins JM, Gileadi C, Shrestha L, Phillips C, Wang J, Muniz JR, et al. Unusual binding interactions in PDZ domain crystal structures help explain binding mechanisms. Protein Sci 2010;19:731–41.
[20] Karthikeyan S, Leung T, Ladias JA. Structural determinants of the Na^+/H^+ exchanger regulatory factor interaction with the beta 2 adrenergic and platelet-derived growth factor receptors. J Biol Chem 2002;277:18973–8.
[21] Ladias JA. Structural insights into the CFTR-NHERF interaction. J Mol Biol 2003;192:79–88.
[22] te Velthuis AJ, Sakalis PA, Fowler DA, Bagowski CP. Genome-wide analysis of PDZ domain binding reveals inherent functional overlap within the PDZ interaction network. PLoS One 2011;6:e16047.
[23] Cohen NA, Brenman JE, Snyder SH, Bredt DS. Binding of the inward rectifier K channel Kir2.3 to PSD-95 is regulated by protein kinase A phosphorylation. Neuron 1996;17:759–67.
[24] Horio Y, Hibino H, Inanobe A, Yamada M, Ishii M, Tada Y, et al. Clustering and enhanced activity of an inwardly rectifying potassium channel, Kir4.1, by an anchoring protein, PSD-95/SAP90. J Biol Chem 1997;272:12885–8.
[25] Cao TT, Deacon HW, Reczek D, Bretscher A, von Zastrow M. A kinase-regulated PDZ-domain interaction controls endocytic sorting of the beta2-adrenergic receptor. Nature 1999;401:286–90.
[26] Raghuram V, Hormuth H, Foskett JK. A kinase-regulated mechanism controls CFTR channel gating by disrupting bivalent PDZ domain interactions. Proc Natl Acad Sci USA 2003;100:9620–5.
[27] Voltz JW, Brush M, Sikes S, Steplock D, Weinman EJ, Shenolikar S. Phosphorylation of PDZ1 domain attenuates NHERF-1 binding to cellular targets. J Biol Chem 2007;282:33879–87.
[28] Weinman EJ, Biswas RS, Peng G, Shen L, Turner CL, E Xiaofei, et al. Parathyroid hormone inhibits renal phosphate transport by phosphorylation of serine 77 of sodium-hydrogen exchanger regulatory factor-1. J Clin Invest 2007;117:3412–20.
[29] Weinman EJ, Steplock D, Zhang Y, Biswas R, Bloch RJ, Shenolikar S. Cooperativity between the phosphorylation of Thr95 and Ser77 of NHERF-1 in the hormonal regulation of renal phosphate transport. J Biol Chem 2010;285:25134–8.
[30] Lau AG, Hall RA. Oligomerization of NHERF-1 and NHERF-2 PDZ domains: Differential regulation by association with receptor carboxyl-termini and by phosphorylation. Biochemistry 2001;40:8572–80.
[31] Garbett D, LaLonde DP, Bretscher A. The scaffolding protein EBP50 regulates microvillar assembly in a phosphorylation-dependent manner. J Cell Biol 2010;191:397–413.
[32] Li J, Poulikakos PI, Dai Z, Testa JR, Callaway DJ, Bu Z. Protein kinase C phosphorylation disrupts Na^+/H^+ exchanger regulatory factor 1 autoinhibition and promotes cystic fibrosis transmembrane conductance regulator macromolecular assembly. J Biol Chem 2007;282:27086–99.
[33] Alewine C, Olsen O, Wade JB, Welling PA. TIP-1 has PDZ scaffold antagonist activity. Mol Biol Cell 2006;17:4200–11.
[34] Campo C, Mason A, Maouyo D, Olsen O, Yoo D, Welling PA. Molecular mechanisms of membrane polarity in renal epithelial cells. Rev Physiol Biochem Pharmacol 2005;153:47–99.
[35] Kachinsky AM, Froehner SC, Milgram SL. A PDZ-containing scaffold related to the dystrophin complex at the basolateral membrane of epithelial cells. J Cell Biol 1999;145:391–402.
[36] Olsen O, Wade JB, Morin N, Bredt DS, Welling PA. Differential localization of mammalian Lin-7 (MALS/Veli) PDZ proteins in the kidney. Am J Physiol Renal Physiol 2005;288:F345–352.
[37] Straight SW, Karnak D, Borg JP, Kamberov E, Dare H, Margolis B, et al. mLin-7 is localized to the basolateral surface of renal epithelia via its NH(2) terminus. Am J Physiol Renal Physiol 2000;278:F464–75.
[38] Borg JP, Marchetto S, Le Bivic A, Ollendorff V, Jaulin-Bastard F, Saito H, et al. ERBIN: A basolateral PDZ protein that interacts with the mammalian ERBB2/HER2 receptor. Nat Cell Biol 2000;2:407–14.
[39] Cohen AR, Woods DF, Marfatia SM, Walther Z, Chishti AH, Anderson JM, et al. Human CASK/LIN-2 binds syndecan-2 and protein 4.1 and localizes to the basolateral membrane of epithelial cells [published erratum appears in J Cell Biol 1998 Aug 24;142(4): following 1156]. J Cell Biol 1998;142:129–38.
[40] Tojo A, Bredt DS, Wilcox CS. Distribution of postsynaptic density proteins in rat kidney: relationship to neuronal nitric oxide synthase. Kidney Int 1999;55:1384–94.
[41] Wu H, Reuver SM, Kuhlendahl S, Chung WJ, Garner CC. Subcellular targeting and cytoskeletal attachment of SAP97 to the epithelial lateral membrane. J Cell Sci 1998;111:2365–76.
[42] McWilliams RR, Gidey E, Fouassier L, Weed SA. and Doctor RB. Characterization of an ankyrin repeat-containing Shank2 isoform (Shank2E) in liver epithelial cells. Biochem J 2004;380:181–91.
[43] Roh MH, Margolis B. Composition and function of PDZ protein complexes during cell polarization. Am J Physiol Renal Physiol 2003;285:F377–387.
[44] Pieczynski J, Margolis B. Protein complexes that control renal epithelial polarity. Am J Physiol Renal Physiol 2011;300:F589–601.
[45] Cheng J, Moyer BD, Milewski M, Loffing J, Ikeda M, Mickle JE, et al. Golgi-associated PDZ domain protein modulates cystic fibrosis transmembrane regulator plasma membrane expression. J Biol Chem 2002;277:3520–9.
[46] Joubert L, Hanson B, Barthet G, Sebben M, Claeysen S, Hong W, et al. New sorting nexin (SNX27) and NHERF specifically interact with the 5-HT4a receptor splice variant: Roles in receptor targeting. J Cell Sci 2004;117:5367–79.
[47] Fialka I, Steinlein P, Ahorn H, Bock G, Burbelo PD, Haberfellner M, et al. Identification of syntenin as a protein of the apical early endocytic compartment in Madin-Darby canine kidney cells. J Biol Chem 1999;274:26233–9.
[48] Simonsen A, Gaullier JM, D'Arrigo A, Stenmark H. The Rab5 effector EEA1 interacts directly with syntaxin-6. J Biol Chem 1999;274:28857–60.
[49] Maday S, Anderson E, Chang HC, Shorter J, Satoh A, Sfakianos J, et al. PDZ-binding motif controls basolateral targeting of syndecan-1 along the biosynthetic pathway in polarized epithelial cells. Traffic 2008;9:1915–24.
[50] Straight SW, Pieczynski JN, Whiteman EL, Liu CJ, Margolis B. Mammalian lin-7 stabilizes polarity protein complexes. J Biol Chem 2006;281:37738–47.
[51] Ahn J, Mundigl O, Muth TR, Rudnick G, Caplan MJ. Polarized expression of GABA transporters in Madin-Darby canine kidney cells and cultured hippocampal neurons. J Biol Chem 1996;271:6917–24.
[52] Muth TR, Ahn J, Caplan MJ. Identification of sorting determinants in the C-terminal cytoplasmic tails of the gamma-aminobutyric acid transporters GAT-2 and GAT-3. J Biol Chem 1998;273:25616–27.
[53] Legouis R, Jaulin-Bastard F, Schott S, Navarro C, Borg JP, Labouesse M. Basolateral targeting by leucine-rich repeat domains in epithelial cells. EMBO Rep 2003;4:1096–102.
[54] Kim E, Naisbitt S, Hsueh YP, Rao A, Rothschild A, Craig AM, et al. GKAP, a novel synaptic protein that interacts with the guanylate kinase-like domain of the PSD-95/SAP90 family of channel clustering molecules. J Cell Biol 1997;136:669–78.

[55] Seabold GK, Burette A, Lim IA, Weinberg RJ, Hell JW. Interaction of the tyrosine kinase Pyk2 with the N-methyl-D-aspartate receptor complex via the Src homology 3 domains of PSD-95 and SAP102. J Biol Chem 2003;278:15040–8.

[56] McGee AW, Dakoji SR, Olsen O, Bredt DS, Lim WA, Prehoda KE. Structure of the SH3-guanylate kinase module from PSD-95 suggests a mechanism for regulated assembly of MAGUK scaffolding proteins. Mol Cell 2001;8:1291–301.

[57] Tavares GA, Panepucci EH, Brunger AT. Structural characterization of the intramolecular interaction between the SH3 and guanylate kinase domains of PSD-95. Mol Cell 2001;8:1313–25.

[58] Colledge M, Dean RA, Scott GK, Langeberg LK, Huganir RL, Scott JD. Targeting of PKA to glutamate receptors through a MAGUK-AKAP complex. Neuron 2000;27:107–19.

[59] Kim E, Sheng M. PDZ domain proteins of synapses. Nat Rev Neurosci 2004;5:771–81.

[60] Christopherson KS, Sweeney NT, Craven SE, Kang R, El-Husseini AD, Bredt DS. Lipid- and protein-mediated multimerization of PSD-95: Implications for receptor clustering and assembly of synaptic protein networks. J Cell Sci 2003;116:3213–9.

[61] Hsueh YP, Kim E, Sheng M. Disulfide-linked head-to-head multimerization in the mechanism of ion channel clustering by PSD-95. Neuron 1997;18:803–14.

[62] El-Husseini AE, Craven SE, Chetkovich DM, Firestein BL, Schnell E, Aoki C, et al. Dual palmitoylation of PSD-95 mediates its vesiculotubular sorting, postsynaptic targeting, and ion channel clustering. J Cell Biol 2000;148:159–72.

[63] Brenman JE, Chao DS, Gee SH, McGee AW, Craven SE, Santillano DR, et al. Interaction of nitric oxide synthase with the postsynaptic density protein PSD-95 and alpha-1 syntrophin mediated by PDZ motifs. Cell 1996;84:757–67.

[64] Christopherson KS, Hillier BJ, Lim WA, Bredt DS. PSD-95 assembles a ternary complex with the N-methyl-D-aspartic acid receptor and a bivalent neuronal NO synthase PDZ domain. J Biol Chem 1999;274:27467–73.

[65] McGee AW, Bredt DS. Assembly and plasticity of the glutamatergic postsynaptic specialization. Curr Opin Neurobiol 2003;13:111–8.

[66] Aarts M, Liu Y, Liu L, Besshoh S, Arundine M, Gurd JW, et al. Treatment of ischemic brain damage by perturbing NMDA receptor- PSD-95 protein interactions. Science 2002;298:846–50.

[67] Kone BC, Kuncewicz T, Zhang W, Yu ZY. Protein interactions with nitric oxide synthases: controlling the right time, the right place, and the right amount of nitric oxide. Am J Physiol Renal Physiol 2003;285:F178–190.

[68] El-Husseini AE, Topinka JR, Lehrer-Graiwer JE, Firestein BL, Craven SE, Aoki C, et al. Ion channel clustering by membrane-associated guanylate kinases. Differential regulation by N-terminal lipid and metal binding motifs. J Biol Chem 2000;275:23904–10.

[69] Brenman JE, Christopherson KS, Craven SE, McGee AW, Bredt DS. Cloning and characterization of postsynaptic density 93, a nitric oxide synthase interacting protein. J Neurosci 1996;16:7407–15.

[70] Shenolikar S, Weinman EJ. NHERF: Targeting and trafficking membrane proteins. Am J Physiol Renal Physiol 2001;280:F389–95.

[71] Weinman EJ, Hall RA, Friedman PA, Liu-Chen LY, Shenolikar S. The association of NHERF adaptor proteins with G protein-coupled receptors and receptor tyrosine kinases. Annu Rev Physiol 2006;68:491–505.

[72] Donowitz M, Cha B, Zachos NC, Brett CL, Sharma A, Tse CM, et al. NHERF family and NHE3 regulation. J Physiol 2005;567:3–11.

[73] Thelin WR, Hodson CA, Milgram SL. Beyond the brush border: NHERF4 blazes new NHERF turf. J Physiol 2005;567:13–9.

[74] Weinman EJ, Steplock D, Shenolikar S. CAMP-mediated inhibition of the renal brush border membrane Na^+-H^+ exchanger requires a dissociable phosphoprotein cofactor. J Clin Invest 1993;92:1781–6.

[75] Weinman EJ, Steplock D, Wang Y, Shenolikar S. Characterization of a protein cofactor that mediates protein kinase a regulation of the renal brush border membrane Na ($^+$)-H^+ exchanger. J Clin Invest 1995;95:2143–219.

[76] Reczek D, Berryman M, Bretscher A. Identification of EBP50: A PDZ-containing phosphoprotein that associates with members of the ezrin-radixin-moesin family. J Cell Biol 1997;139:169–79.

[77] Yun CH, Oh S, Zizak M, Steplock D, Tsao S, Tse CM, et al. cAMP-mediated inhibition of the epithelial brush border Na^+/H^+ exchanger, NHE3, requires an associated regulatory protein. Proc Natl Acad Sci USA 1997;94:3010–5.

[78] Poulat F, Barbara PS, Desclozeaux M, Soullier S, Moniot B, Bonneaud N, et al. The human testis determining factor SRY binds a nuclear factor containing PDZ protein interaction domains. J Biol Chem 1997;272:7167–72.

[79] Kocher O, Comella N, Gilchrist A, Pal R, Tognazzi K, Brown LF, et al. PDZK1, a novel PDZ domain-containing protein up-regulated in carcinomas and mapped to chromosome 1q21, interacts with cMOAT (MRP2), the multidrug resistance-associated protein. Lab Invest 1999;79:1161–70.

[80] Wang S, Yue H, Derin RB, Guggino WB, Li M. Accessory protein facilitated CFTR-CFTR interaction, a molecular mechanism to potentiate the chloride channel activity. Cell 2001;103:169–79.

[81] Gisler SM, Stagljar I, Traebert M, Bacic D, Biber J, Murer H. Interaction of the type IIa Na/Pi co-transporter with PDZ proteins. J Biol Chem 2001;276:9206–913.

[82] Scott RO, Thelin WR, Milgram SL. A novel PDZ protein regulates the activity of guanylyl cyclase C, the heat-stable enterotoxin receptor. J Biol Chem 2002;277:22934–41.

[83] Sarker R, Valkhoff VE, Zachos NC, Lin R, Cha B, Chen TE, et al. NHERF1 and NHERF2 are necessary for multiple but usually separate aspects of basal and acute regulation of NHE3 activity. Am J Physiol Cell Physiol 2011;300:C771–782.

[84] Bretscher A, Edwards K, Fehon RG. ERM proteins and merlin: Integrators at the cell cortex. Nat Rev Mol Cell Biol 2002;3:586–99.

[85] Dransfield DT, Bradford AJ, Smith J, Martin M, Roy C, Mangeat PH, et al. Ezrin is a cyclic AMP-dependent protein kinase anchoring protein. EMBO J 1997;16:35–43.

[86] Fouassier L, Yun CC, Fitz JG, Doctor RB. Evidence for ezrin-radixin-moesin-binding phosphoprotein 50 (EBP50) self-association through PDZ-PDZ interactions. J Biol Chem 2000;275:25039–45.

[87] Gisler SM, Pribanic S, Bacic D, Forrer P, Gantenbein A, Sabourin LA, et al. PDZK1: I. A major scaffolder in brush borders of proximal tubular cells. Kidney Int 2003;64:1733–45.

[88] Shenolikar S, Minkoff CM, Steplock DA, Evangelista C, Liu M, Weinman EJ. N-terminal PDZ domain is required for NHERF dimerization. FEBS Lett 2001;489:233–6.

[89] LaLonde DP, Bretscher A. The scaffold protein PDZK1 undergoes a head-to-tail intramolecular association that negatively regulates its interaction with EBP50. Biochemistry 2009;48:2261–71.

[90] LaLonde DP, Garbett D, Bretscher A. A regulated complex of the scaffolding proteins PDZK1 and EBP50 with ezrin contribute to microvillar organization. Mol Biol Cell 2010;21:1519–29.

[91] Weinman EJ, Wang Y, Wang F, Greer C, Steplock D, Shenolikar SA. C-terminal PDZ motif in NHE3 binds NHERF-1 and enhances cAMP inhibition of sodium–hydrogen exchange. Biochemistry 2003;42:12662–8.

[92] Lamprecht G, Weinman EJ, Yun CH. The role of NHERF and E3KARP in the cAMP-mediated inhibition of NHE3. J Biol Chem 1998;273:29972–8.

[93] Weinman EJ, Steplock D, Wade JB, Shenolikar S. Ezrin binding domain-deficient NHERF attenuates cAMP-mediated inhibition of $Na^{(+)}/H^{(+)}$ exchange in OK cells. Am J Physiol Renal Physiol 2001;281:F374–380.

[94] Murtazina R, Kovbasnjuk O, Zachos NC, Li X, Chen Y, Hubbard A, et al. Tissue-specific regulation of sodium/proton exchanger isoform 3 activity in $Na^{(+)}/H^{(+)}$ exchanger regulatory factor 1 (NHERF1) null mice. cAMP inhibition is differentially dependent on NHERF1 and exchange protein directly activated by cAMP in ileum versus proximal tubule. J Biol Chem 2007;282:25141–51.

[95] Shenolikar S, Voltz JW, Minkoff CM, Wade JB, Weinman EJ. Targeted disruption of the mouse NHERF-1 gene promotes internalization of proximal tubule sodium-phosphate co-transporter type IIa and renal phosphate wasting. Proc Natl Acad Sci USA 2002;99:11470–5.

[96] Weinman EJ, Steplock D, Shenolikar S. NHERF-1 uniquely transduces the cAMP signals that inhibit sodium–hydrogen exchange in mouse renal apical membranes. FEBS Lett 2003;536:141–4.

[97] Cunningham R, Steplock D, Wang F, Huang H, X E, Shenolikar S, et al. Defective parathyroid hormone regulation of NHE3 activity and phosphate adaptation in cultured NHERF-$1^{-/-}$ renal proximal tubule cells. J Biol Chem 2004;279:37815–21.

[98] Weinman EJ. New functions for the NHERF family of proteins. J Clin Invest 2001;108:185–6.

[99] Hall RA, Ostedgaard LS, Premont RT, Blitzer JT, Rahman N, Welsh MJ, et al. C-terminal motif found in the beta2-adrenergic receptor, P2Y1 receptor and cystic fibrosis transmembrane conductance regulator determines binding to the Na^+/H^+ exchanger regulatory factor family of PDZ proteins. Proc Natl Acad Sci USA 1998;95:8496–501.

[100] Short DB, Trotter KW, Reczek D, Kreda SM, Bretscher A, Boucher RC, et al. An apical PDZ protein anchors the cystic fibrosis transmembrane conductance regulator to the cytoskeleton. J Biol Chem 1998;273:19797–801.

[101] Wang S, Raab RW, Schatz PJ, Guggino WB, Li M. Peptide binding Consensus of the NHE-RF-PDZ1 doamin matches the C-terminal sequence of CFTR. FEBS Letters 1998;427:103–8.

[102] Sun F, Hug MJ, Lewarchik CM, Yun CH, Bradbury NA, Frizzell RA. E3KARP mediates the association of ezrin and protein kinase A with the cystic fibrosis transmembrane conductance regulator in airway cells. J Biol Chem 2002;275:29539–46.

[103] Hall RA, Premont RT, Chow CW, Blitzer JT, Pitcher JA, Claing A, et al. The beta2-adrenergic receptor interacts with the Na^+/H^+-exchanger regulatory factor to control Na^+/H^+ exchange. Nature 1998;392:626–30.

[104] Naren AP, Cobb B, Li C, Roy K, Nelson D, Heda GD, et al. A macromolecular complex of beta 2 adrenergic receptor, CFTR, and ezrin/radixin/moesin-binding phosphoprotein 50 is regulated by PKA. Proc Natl Acad Sci USA 2003;100:342–6.

[105] Hall RA, Spurney RF, Premont RT, Rahman N, Blitzer JT, Pitcher JA, et al. G protein-coupled receptor kinase 6A phosphorylates the $Na^{(+)}/H^{(+)}$ exchanger regulatory factor via a PDZ domain-mediated interaction. J Biol Chem 1999;274:24328–34.

[106] Mohler PJ, Kreda SM, Boucher RC, Sudol M, Stutts MJ, Milgram SL. Yes-associated protein 65 localizes p62(c-Yes) to the apical compartment of airway epithelia by association with EBP50. J Cell Biol 1999;147:879–90.

[107] Tang Y, Tang J, Chen Z, Trost C, Flockerzi V, Li M, et al. Association of mammalian trp4 and phospholipase C isozymes with a PDZ domain-containing protein, NHER. J Biol Chem 2000;275:37559–64.

[108] Liedtke CM, Yun CH, Kyle N, Wang D. Protein kinase C epsilon-dependent regulation of cystic fibrosis transmembrane regulator involves binding to a receptor for activated C kinase (RACK1) and RACK1 binding to Na^+/H^+ exchange regulatory factor. J Biol Chem 2002;277:22925–33.

[109] Raghuram V, Mak DD, Foskett JK. Regulation of cystic fibrosis transmembrane conductance regulator single-channel gating by bivalent PDZ-domain-mediated interaction. Proc Natl Acad Sci USA 2001;98:1300–5.

[110] Swiatecka-Urban A, Duhaime M, Coutermarsh B, Karlson KH, Collawn J, Milewski M, et al. PDZ domain interaction controls the endocytic recycling of the cystic fibrosis transmembrane conductance regulator. J Biol Chem 2002;277:40099–105.

[111] Hernando N, Deliot N, Gisler SM, Lederer E, Weinman EJ, Biber J, et al. PDZ-domain interactions and apical expression of type IIa Na/P(i) co-transporters. Proc Natl Acad Sci USA 2002;99:11957–62.

[112] Weinman EJ, Boddeti A, Cunningham R, Akom M, Wang F, Wang Y, et al. NHERF-1 is required for renal adaptation to a low-phosphate diet. Am J Physiol Renal Physiol 2003;285: F1225–32.

[113] Hernando N, Karim-Jimenez Z, Biber J, Murer H. Molecular determinants for apical expression and regulatory membrane retrieval of the type IIa Na/Pi co-transporter. Pflug Archiv - Eur J Physiol 2001;60:431–45.

[114] Karim-Jimenez Z, Hernando N, Biber J, Murer H. Molecular determinants for apical expression of the renal type IIa Na^+/Pi-co-transporter. Pflug Archiv - Eur J Physiol 2001;442:782–90.

[115] Deliot N, Hernando N, Horst-Liu Z, Gisler SM, Capuano P, Wagner CA, et al. Parathyroid hormone treatment induces dissociation of type IIa Na^+-P(i) co-transporter-Na^+/H^+ exchanger regulatory factor-1 complexes. Am J Physiol Cell Physiol 2005;289:C159–167.

[116] Weinman EJ, Steplock D, Cha B, Kovbasnjuk O, Frost NA, Cunningham R, et al. PTH transiently increases the percent mobile fraction of Npt2a in OK cells as determined by FRAP. Am J Physiol Renal Physiol 2009;297:F1560–1565.

[117] Weinman EJ, Steplock D, Shenolikar S, Blanpied TA. Dynamics of PTH-induced disassembly of Npt2a/NHERF-1 complexes in living OK cells. Am J Physiol Renal Physiol 2011;300:F231–235.

[118] Wang B, Bisello A, Yang Y, Romero GG, Friedman PA. NHERF1 regulates parathyroid hormone receptor membrane retention without affecting recycling. J Biol Chem 2007;282:36214–22.

[119] Sneddon WB, Syme CA, Bisello A, Magyar CE, Rochdi MD, Parent JL, et al. Activation-independent parathyroid hormone receptor internalization is regulated by NHERF1 (EBP50). J Biol Chem 2003;278:43787–96.

[120] Blaine J, Okamura K, Giral H, Breusegem S, Caldas Y, Millard A, et al. PTH-induced internalization of apical membrane NaPi2a: role of actin and myosin VI. Am J Physiol Cell Physiol 2009;297:C1339–1346.

[121] Riquier AD, Lee DH, McDonough AA. Renal NHE3 and NaPi2 partition into distinct membrane domains. Am J Physiol Cell Physiol 2009;296:C900–910.

[122] Riquier-Brison AD, Leong PK, Pihakaski-Maunsbach K, McDonough AA. Angiotensin II stimulates trafficking of NHE3, NaPi2, and associated proteins into the proximal tubule microvilli. Am J Physiol Renal Physiol 2010;298: F177–186.

[123] Yang LE, Maunsbach AB, Leong PK, McDonough AA. Redistribution of myosin VI from top to base of proximal tubule microvilli during acute hypertension. J Am Soc Nephrol 2005;16:2890–6.

[124] Weinman EJ, Cunningham R, Wade JB, Shenolikar S. The role of NHERF-1 in the regulation of renal proximal tubule sodium-hydrogen exchanger 3 and sodium-dependent phosphate co-transporter 2a. J Physiol 2005;567:27–32.

[125] Wade JB, Liu J, Coleman RA, Cunningham R, Steplock DA, Lee-Kwon W, et al. Localization and interaction of NHERF isoforms in the renal proximal tubule of the mouse. Am J Physiol Cell Physiol 2003;285:C1494–1503.

[126] Wade JB, Welling PA, Donowitz M, Shenolikar S, Weinman EJ. Differential renal distribution of NHERF isoforms and their colocalization with NHE3, ezrin, and ROMK. Am J Physiol Cell Physiol 2001;280:C192–8.

[127] Li Y, Li J, Straight SW, Kershaw DB. PDZ domain-mediated interaction of rabbit podocalyxin and $Na^{(+)}/H^{(+)}$ exchange regulatory factor-2. Am J Physiol Renal Physiol 2004;282: F1129–39.

[128] Lee-Kwon W, Wade JB, Zhang Z, Pallone TL, Weinman EJ. Expression of TRPC4 channel protein that interacts with NHERF-2 in rat descending vasa recta. Am J Physiol Cell Physiol 2005;288:C942–949.

[129] Montell C. TRP trapped in fly signaling web. Curr Opin Neurobiol 1998;8:389–97.

[130] Yoo D, Flagg TP, Olsen O, Raghuram V, Foskett JK, Welling PA. Assembly and trafficking of a multiprotein ROMK (Kir 1.1) channel complex by PDZ interactions. J Biol Chem 2004;279:6863–73.

[131] Kim JH, Lee-Kwon W, Park JB, Ryu SH, Yun CH, Donowitz M. $Ca^{(2+)}$-dependent inhibition of Na^+/H^+ exchanger 3 (NHE3) requires an NHE3-E3KARP-alpha-actinin-4 complex for oligomerization and endocytosis. J Biol Chem 2002;277:23714–24.

[132] Cha B, Kim JH, Hut H, Hogema BM, Nadarja J, Zizak M, et al. cGMP inhibition of Na^+/H^+ antiporter 3 (NHE3) requires PDZ domain adapter NHERF2, a broad specificity protein kinase G-anchoring protein. J Biol Chem 2005;280:16642–50.

[133] Lamprecht G, Heil A, Baisch S, Lin-Wu E, Yun CC, Kalbacher H, et al. The down regulated in adenoma (dra) gene product binds to the second PDZ domain of the NHE3 kinase A regulatory protein (E3KARP), potentially linking intestinal Cl^-/HCO_3^- exchange to Na^+/H^+ exchange. Biochemistry 2002;41:12336–42.

[134] Yun CC, Chen Y, Lang F. Glucocorticoid activation of $Na^{(+)}/H^{(+)}$ exchanger isoform 3 revisited. The roles of SGK1 and NHERF2. J Biol Chem 2002;277:7676–783.

[135] Kanai F, Marignani PA, Sarbassova D, Yagi R, Hall RA, Donowitz M, et al. TAZ: a novel transcriptional co-activator regulated by interactions with 14-3-3 and PDZ domain proteins. Embo J 2000;19:6778–91.

[136] Lee-Kwon W, Kim JH, Choi JW, Kawano K, Cha B, Dartt DA, et al. Ca^{2+}-dependent inhibition of NHE3 requires PKC alpha which binds to E3KARP to decrease surface NHE3 containing plasma membrane complexes. Am J Physiol Cell Physiol 2003;285:C1527–1536.

[137] Yoo D, Kim BY, Campo C, Nance L, King A, Maouyo D, et al. Cell surface expression of the ROMK (Kir 1.1) channel is regulated by the aldosterone-induced kinase, SGK-1, and protein kinase A. J Biol Chem 2003;278:23066–75.

[138] Yun CC, Palmada M, Embark HM, Fedorenko O, Feng Y, Henke G, et al. The serum and glucocorticoid-inducible kinase SGK1 and the $Na^{(+)}/H^{(+)}$ exchange regulating factor NHERF2 synergize to stimulate the renal outer medullary $K^{(+)}$ channel ROMK1. J Am Soc Nephrol 2002;13:2823–30.

[139] Yoo D, Fang L, Mason A, Kim BY, Welling PA. A phosphorylation-dependent export structure in ROMK (Kir 1.1) channel overrides an endoplasmic reticulum localization signal. J Biol Chem 2005;280:35281–9.

[140] O'Connell AD, Leng Q, Dong K, MacGregor GG, Giebisch G, Hebert SC. Phosphorylation-regulated endoplasmic reticulum retention signal in the renal outer-medullary K^+ channel (ROMK). Proc Natl Acad Sci USA 2005;102:9954–9.

[141] Kocher O, Comella N, Tognazzi K, Brown LF. Identification and partial characterization of PDZK1: A novel protein containing PDZ interaction domains. Lab Invest 1998;78:117–25.

[142] Gisler SM, Madjdpour C, Bacic D, Pribanic S, Taylor SS, Biber J, et al. PDZK1: II. An anchoring site for the PKA-binding protein D-AKAP2 in renal proximal tubular cells. Kidney Int 2003;64:1746–54.

[143] van de Graaf SF, Hoenderop JG, van der Kemp AW, Gisler SM, Bindels RJ. Interaction of the epithelial Ca^{2+} channels TRPV5 and TRPV6 with the intestine- and kidney-enriched PDZ protein NHERF4. Pflugers Arch 2006;452:407–17.

[144] Kocher O, Pal R, Roberts M, Cirovic C, Gilchrist A. Targeted disruption of the PDZK1 gene by homologous recombination. Mol Cell Biol 2003;23:1175–80.

[145] Thomson RB, Wang T, Thomson BR, Tarrats L, Girardi A, Mentone S, et al. Role of PDZK1 in membrane expression of renal brush border ion exchangers. Proc Natl Acad Sci USA 2005;102:13331–6.

[146] Capuano P, Bacic D, Stange G, Hernando N, Kaissling B, Pal R, et al. Expression and regulation of the renal Na/phosphate co-transporter NaPi-IIa in a mouse model deficient for the PDZ protein PDZK1. Pflugers Arch 2005;449:392–402.

[147] Lanzano L, Lei T, Okamura K, Giral H, Caldas Y, Masihzadeh O, et al. Differential modulation of the molecular dynamics of the type IIa and IIc sodium phosphate co-transporters by parathyroid hormone. Am J Physiol Cell Physiol 2011;301:C850–861.

[148] Sheng M, Kim E. The Shank family of scaffold proteins. J Cell Sci 2000;113(Pt 11):1851–6.

[149] Lim S, Naisbitt S, Yoon J, Hwang JI, Suh PG, Sheng M, et al. Characterization of the Shank family of synaptic proteins. Multiple genes, alternative splicing, and differential expression in brain and development. J Biol Chem 1999;274:29510–8.

[150] Mosavi LK, Cammett TJ, Desrosiers DC, Peng ZY. The ankyrin repeat as molecular architecture for protein recognition. Protein Sci 2004;13:1435–48.

[151] Baron MK, Boeckers TM, Vaida B, Faham S, Gingery M, Sawaya MR, et al. An architectural framework that may lie at the core of the postsynaptic density. Science 2006;311:531–5.

[152] Hayashi MK, Tang C, Verpelli C, Narayanan R, Stearns MH, Xu RM, et al. The postsynaptic density proteins Homer and Shank form a polymeric network structure. Cell 2009;137:159–71.

[153] Kay BK, Williamson MP, Sudol M. The importance of being proline: The interaction of proline-rich motifs in signaling proteins with their cognate domains. FASEB Journal 2000;14:231–41.

[154] Xiao B, Tu JC, Worley PF. Homer: a link between neural activity and glutamate receptor function. Curr Opin Neurobiol, 10. 2000.

[155] Berkel S, Marshall CR, Weiss B, Howe J, Roeth R, Moog U, et al. Mutations in the SHANK2 synaptic scaffolding gene in autism spectrum disorder and mental retardation. Nat Genet 2010;42:489–91.

[156] Kim JY, Han W, Namkung W, Lee JH, Kim KH, Shin H, et al. Inhibitory regulation of cystic fibrosis transmembrane conductance regulator anion-transporting activities by Shank2. J Biol Chem 2004;279:10389–96.

[157] Lee JS, Lee YM, Kim JY, Park HW, Grinstein S, Orlowski J, et al. BetaPix up-regulates Na^+/H^+ exchanger 3 through a Shank2-mediated protein−protein interaction. J Biol Chem 2010;285:8104−13.

[158] Alexander RT, Furuya W, Szaszi K, Orlowski J, Grinstein S. Rho GTPases dictate the mobility of the Na/H exchanger NHE3 in epithelia: Role in apical retention and targeting. Proc Natl Acad Sci USA 2005;102:12253−8.

[159] McWilliams RR, Breusegem SY, Brodsky KF, Kim E, Levi M, Doctor RB. Shank2E binds NaP(i) co-transporter at the apical membrane of proximal tubule cells. Am J Physiol Cell Physiol 2005;289:C1042−1051.

[160] Dobrinskikh E, Giral H, Caldas YA, Levi M, Doctor RB. Shank2 redistributes with NaPilla during regulated endocytosis. Am J Physiol Cell Physiol 2010;299:C1324−1334.

[161] Okamoto PM, Gamby C, Wells D, Fallon J, Vallee RB. Dynamin isoform-specific interaction with the shank/ProSAP scaffolding proteins of the postsynaptic density and actin cytoskeleton. J Biol Chem 2001;276:48458−65.

[162] Kaech SM, Whitfield CW, Kim SK. The LIN-2/LIN-7/LIN-10 complex mediates basolateral membrane localization of the *C. elegans* EGF receptor LET-23 in vulval epithelial cells. Cell 1998;94:761−71.

[163] Rongo C, Whitfield CW, Rodal A, Kim SK, Kaplan JM. LIN-10 is a shared component of the polarized protein localization pathways in neurons and epithelia. Cell 1998;94:751−9.

[164] Simske JS, Kaech SM, Harp SA, Kim SK. LET-23 receptor localization by the cell junction protein LIN-7 during *C. elegans* vulval induction. Cell 1996;85:195−204.

[165] Borg JP, Straight SW, Kaech SM, de Taddeo-Borg M, Kroon DE, Karnak D, et al. Identification of an evolutionarily conserved heterotrimeric protein complex involved in protein targeting. J Biol Chem 1998;273:31633−6.

[166] Butz S, Okamoto M, Sudhof TC. A tripartite protein complex with the potential to couple synaptic vesicle exocytosis to cell adhesion in brain. Cell 1998;94:773−82.

[167] Olsen O, Liu H, Wade JB, Merot J, Welling PA. Basolateral membrane expression of the Kir 2.3 channel is coordinated by PDZ interaction with Lin-7/CASK complex. Am J Physiol Cell Physiol 2002;282:C183−95.

[168] Perego C, Vanoni C, Villa A, Longhi R, Kaech SM, Frohli E, et al. PDZ-mediated interactions retain the epithelial GABA transporter on the basolateral surface of polarized epithelial cells. EMBO J 1999;18:2384−93.

[169] Leonoudakis D, Conti LR, Anderson S, Radeke CM, McGuire LM, Adams ME, et al. Protein trafficking and anchoring complexes revealed by proteomic analysis of inward rectifier potassium channel (Kir2.x)-associated proteins. J Biol Chem 2004;279:22331−46.

[170] Leonoudakis D, Conti LR, Radeke CM, McGuire LM, Vandenberg CA. A multiprotein trafficking complex composed of SAP97, CASK, Veli, and Mint1 is associated with inward rectifier Kir2 potassium channels. J Biol Chem 2004;279:19051−63.

[171] Shelly M, Mosesson Y, Citri A, Lavi S, Zwang Y, Melamed-Book N, et al. Polar expression of ErbB-2/HER2 in epithelia. Bimodal regulation by Lin-7. 2003;5: 475−86.

[172] Massari S, Perego C, Padovano V, D'Amico A, Raimondi A, Francolini M, et al. LIN7 mediates the recruitment of IRSp53 to tight junctions. Traffic 2009;10:246−57.

[173] Lee S, Fan S, Makarova O, Straight S, Margolis B. A novel and conserved protein−protein interaction domain of mammalian Lin-2/CASK binds and recruits SAP97 to the lateral surface of epithelia. Mol Cell Biol 2002;22:1778−91.

[174] Doerks T, Bork P, Kamberov E, Makarova O, Muecke S, Margolis B. L27, a novel heterodimerization domain in receptor targeting proteins Lin-2 and Lin-7. Trends Biochem Sci 2000;25:317−38.

[175] Feng W, Long JF, Fan JS, Suetake T, Zhang M. The tetrameric L27 domain complex as an organization platform for supramolecular assemblies. Nat Struct Mol Biol 2004;11:475−80.

[176] Li Y, Karnak D, Demeler B, Margolis B, Lavie A. Structural basis for L27 domain-mediated assembly of signaling and cell polarity complexes. Embo J 2004;23:2723−33.

[177] Alewine C, Kim BY, Hegde V, Welling PA. Lin-7 targets the Kir 2.3 channel on the basolateral membrane via a L27 domain interaction with CASK. Am J Physiol Cell Physiol 2007;293: C1733−1741.

[178] Lozovatsky L, Abayasekara N, Piawah S, Walther Z. CASK deletion in intestinal epithelia causes mislocalization of LIN7C and the DLG1/Scrib polarity complex without affecting cell polarity. Mol Biol Cell 2009;20:4489−99.

[179] Okamoto M, Sudhof TC. Mints, Munc18-interacting proteins in synaptic vesicle exocytosis. J Biol Chem 1997;272:31459−64.

[180] Setou M, Nakagawa T, Seog DH, Hirokawa N. Kinesin superfamily motor protein KIF17 and mLin-10 in NMDA receptor-containing vesicle transport. Science 2000;288:1796−802.

[181] Hata Y, Slaughter CA, Sudhof TC. Synaptic vesicle fusion complex contains unc-18 homologue bound to syntaxin. Nature 1993;366:347−51.

[182] Perego C, Bulbarelli A, Longhi R, Caimi M, Villa A, Caplan MJ. Sorting of two polytopic proteins, the gamma-aminobutyric acid and betaine transporters, in polarized epithelial cells. J Biol Chem 1997;272:6584−92.

[183] Straight SW, Chen L, Karnak D, Margolis B. Interaction with mLin-7 alters the targeting of endocytosed transmembrane proteins in mammalian epithelial cells. Mol Biol Cell 2001;12:1329−40.

[184] Marble DD, Hegle AP, Snyder 2nd ED, Dimitratos S, Bryant PJ, Wilson GF. Camguk/CASK enhances Ether-a-go-go potassium current by a phosphorylation-dependent mechanism. J Neurosci 2005;25:4898−907.

[185] Mukherjee K, Sharma M, Urlaub H, Bourenkov GP, Jahn R, Sudhof TC, et al. CASK functions as an Mg^{2+}-independent neurexin kinase. Cell 2008;133:328−39.

[186] Olsen O, Funke L, Long JF, Fukata M, Kazuta T, Trinidad JC, et al. Renal defects associated with improper polarization of the CRB and DLG polarity complexes in MALS-3 knockout mice. J Cell Biol 2007;179:151−64.

[187] Kamberov E, Makarova O, Roh M, Liu A, Karnak D, Straight S, et al. Molecular cloning and characterization of Pals, proteins associated with mLin-7. J Biol Chem 2000;275:11425−31.

[188] Roh MH, Makarova O, Liu CJ, Shin K, Lee S, Laurinec S, et al. The Maguk protein, Pals1, functions as an adapter, linking mammalian homologues of Crumbs and Discs Lost. J Cell Biol 2002;157:161−72.

[189] Lapidos KA, Kakkar R, McNally EM. The dystrophin glycoprotein complex: Signaling strength and integrity for the sarcolemma. Circ Res 2004;94:1023−31.

[190] Gee SH, Madhavan R, Levinson SR, Caldwell JH, Sealock R, Froehner SC. Interaction of muscle and brain sodium channels with multiple members of the syntrophin family of dystrophin-associated proteins. J Neurosci 1998;18:128−37.

[191] Schultz J, Hoffmuller U, Krause G, Ashurst J, Macias MJ, Schmieder P, et al. Specific interactions between the syntrophin PDZ domain and voltage-gated sodium channels. Nat Struct Biol 1998;5:19−24.

[192] Grady RM, Grange RW, Lau KS, Maimone MM, Nichol MC, et al. Role for alpha-dystrobrevin in the pathogenesis of dystrophin-dependent muscular dystrophies. Nat Cell Biol 1999;1:215–20.

[193] Haenggi T, Schaub MC, Fritschy JM. Molecular heterogeneity of the dystrophin-associated protein complex in the mouse kidney nephron: differential alterations in the absence of utrophin and dystrophin. Cell Tissue Res 2005;319:299–313.

[194] Loh NY, Newey SE, Davies KE, Blake DJ. Assembly of multiple dystrobrevin-containing complexes in the kidney. J Cell Sci 2000;113(Pt 15):2715–24.

[195] Keep NH, Winder SJ, Moores CA, Walke S, Norwood FL, Kendrick-Jones J. Crystal structure of the actin-binding region of utrophin reveals a head-to-tail dimer. Structure 1999;7:1539–46.

[196] James M, Nuttall A, Ilsley JL, Ottersbach K, Tinsley JM, Sudol M, et al. Adhesion-dependent tyrosine phosphorylation of (beta)-dystroglycan regulates its interaction with utrophin. J Cell Sci 2000;113(Pt 10):1717–26.

[197] Newey SE, Benson MA, Ponting CP, Davies KE, Blake DJ. Alternative splicing of dystrobrevin regulates the stoichiometry of syntrophin binding to the dystrophin protein complex. Curr Biol 2000;10:1295–8.

[198] Connors NC, Adams ME, Froehner SC, Kofuji P. The potassium channel Kir4.1 associates with the dystrophin–glycoprotein complex via alpha-syntrophin in glia. J Biol Chem 2004;279:28387–92.

[199] Neely JD, Amiry-Moghaddam M, Ottersen OP, Froehner SC, Agre P, Adams ME. Syntrophin-dependent expression and localization of Aquaporin-4 water channel protein. Proc Natl Acad Sci USA 2001;98:14108–13.

[200] Amiry-Moghaddam M, Otsuka T, Hurn PD, Traystman RJ, Haug FM, Froehner SC, et al. An alpha-syntrophin-dependent pool of AQP4 in astroglial end-feet confers bidirectional water flow between blood and brain. Proc Natl Acad Sci USA 2003;100:2106–11.

[201] Amiry-Moghaddam M, Williamson A, Palomba M, Eid T, de Lanerolle NC, Nagelhus EA, et al. Delayed K^+ clearance associated with aquaporin-4 mislocalization: Phenotypic defects in brains of alpha-syntrophin-null mice. Proc Natl Acad Sci USA 2003;100:13615–20.

[202] Nielsen S, Frokiaer J, Marples D, Kwon TH, Agre P, Knepper MA. Aquaporins in the kidney: From molecules to medicine. Physiol Rev 2002;82:205–44.

[203] Ito M, Inanobe A, Horio Y, Hibino H, Isomoto S, Ito H, et al. Immunolocalization of an inwardly rectifying K^+ channel, K (AB)-2 (Kir4.1), in the basolateral membrane of renal distal tubular epithelia. FEBS Letters 1996;388:11–5.

[204] Deconinck AE, Potter AC, Tinsley JM, Wood SJ, Vater R, Young C, et al. Postsynaptic abnormalities at the neuromuscular junctions of utrophin-deficient mice. J Cell Biol 1997;136:883–94.

[205] Lohmann SM, DeCamilli P, Einig I, Walter U. High-affinity binding of the regulatory subunit (RII) of cAMP-dependent protein kinase to microtubule-associated and other cellular proteins. Proc Natl Acad Sci USA 1984;81:6723–7.

[206] Fraser ID, Scott JD. Modulation of ion channels: a "current" view of AKAPs. Neuron 1999;23:423–6.

[207] Baumgartner M, Patel H, Barber DL. $Na(^+)/H(^+)$ exchanger NHE1 as plasma membrane scaffold in the assembly of signaling complexes. Am J Physiol Cell Physiol 2004;287:C844–850.

[208] Banky P, Newlon MG, Roy M, Garrod S, Taylor SS, Jennings PA. Isoform-specific differences between the type Ialpha and IIalpha cyclic AMP-dependent protein kinase anchoring domains revealed by solution NMR. J Biol Chem 2000;275:35146–52.

[209] Newlon MG, Roy M, Morikis D, Carr DW, Westphal R, Scott JD, et al. A novel mechanism of PKA anchoring revealed by solution structures of anchoring complexes. Embo J 2001;20:1651–62.

[210] Newlon MG, Roy M, Morikis D, Hausken ZE, Coghlan V, Scott JD, et al. The molecular basis for protein kinase A anchoring revealed by solution NMR. Nat Struct Biol 1999;6:222–7.

[211] Huang LJ, Wang L, Ma Y, Durick K, Perkins G, Deerinck TJ, et al. NH2-Terminal targeting motifs direct dual specificity A-kinase-anchoring protein 1 (D-AKAP1) to either mitochondria or endoplasmic reticulum. J Cell Biol 1999;145:951–9.

[212] Means CK, Lygren B, Langeberg LK, Jain A, Dixon RE, Vega AL, et al. An entirely specific type I A-kinase anchoring protein that can sequester two molecules of protein kinase A at mitochondria. Proc Natl Acad Sci USA 2011;108:E1227–1235.

[213] Alto NM, Soderling SH, Hoshi N, Langeberg LK, Fayos R, Jennings PA, et al. Bioinformatic design of A-kinase anchoring protein-in silico: A potent and selective peptide antagonist of type II protein kinase A anchoring. Proc Natl Acad Sci USA 2003;100:4445–50.

[214] Burns-Hamuro LL, Ma Y, Kammerer S, Reineke U, Self C, Cook C, et al. Designing isoform-specific peptide disruptors of protein kinase A localization. Proc Natl Acad Sci USA 2003;100:4072–7.

[215] Wong W, Scott JD. AKAP signalling complexes: Focal points in space and time. Nat Rev Mol Cell Biol 2004;5:959–70.

[216] Dong F, Feldmesser M, Casadevall A, Rubin CS. Molecular characterization of a cDNA that encodes six isoforms of a novel murine A kinase anchor protein. J Biol Chem 1998;273:6533–41.

[217] Morales FC, Takahashi Y, Kreimann EL, Georgescu MM. Ezrin-radixin-moesin (ERM)-binding phosphoprotein 50 organizes ERM proteins at the apical membrane of polarized epithelia. Proc Natl Acad Sci USA 2004;101:17705–10.

[218] Trotter KW, Fraser ID, Scott GK, Stutts MJ, Scott JD, Milgram SL. Alternative splicing regulates the subcellular localization of A-kinase anchoring protein 18 isoforms. J Cell Biol 1999;147:1481–92.

[219] Khundmiri SJ, Rane MJ, Lederer ED. Parathyroid hormone regulation of type II sodium-phosphate co-transporters is dependent on an A kinase anchoring protein. J Biol Chem 2003;278:10134–41.

[220] Gao T, Yatani A, Dell'Acqua ML, Sako H, Green SA, Dascal N, et al. cAMP-dependent regulation of cardiac L-type Ca^{2+} channels requires membrane targeting of PKA and phosphorylation of channel subunits. Neuron 1997;19:185–96.

[221] Hoshi N, Zhang JS, Omaki M, Takeuchi T, Yokoyama S, Wanaverbecq N, et al. AKAP150 signaling complex promotes suppression of the M-current by muscarinic agonists. Nat Neurosci 2003;6:564–71.

[222] Carr DW, Stofko-Hahn RE, Fraser ID, Bishop SM, Acott TS, Brennan RG, et al. Interaction of the regulatory subunit (RII) of cAMP-dependent protein kinase with RII-anchoring proteins occurs through an amphipathic helix binding motif. J Biol Chem 1991;266:14188–92.

[223] Rosenmund C, Carr DW, Bergeson SE, Nilaver G, Scott JD, Westbrook GL. Anchoring of protein kinase A is required for modulation of AMPA/kainate receptors on hippocampal neurons. Nature 1994;368:853–6.

[224] Coghlan VM, Perrino BA, Howard M, Langeberg LK, Hicks JB, Gallatin WM, et al. Association of protein kinase A

and protein phosphatase 2B with a common anchoring protein. Science 1995;267:108–11.

[225] Klauck TM, Faux MC, Labudda K, Langeberg LK, Jaken S, Scott JD. Coordination of three signaling enzymes by AKAP79, a mammalian scaffold protein. Science 1996;271:1589–92.

[226] Hoshi N, Langeberg LK, Scott JD. Distinct enzyme combinations in AKAP signalling complexes permit functional diversity. Nat Cell Biol 2005;7:1066–73.

[227] Klussmann E, Maric K, Wiesner B, Beyermann M, Rosenthal W. Protein kinase A anchoring proteins are required for vasopressin-mediated translocation of aquaporin-2 into cell membranes of renal principal cells. J Biol Chem 1999;274:4934–8.

[228] Jo I, Ward DT, Baum MA, Scott JD, Coghlan VM, Hammond TG, et al. AQP2 is a substrate for endogenous PP2B activity within an inner medullary AKAP-signaling complex. Am J Physiol Renal Physiol 2001;281:F958–965.

[229] Henn V, Edemir B, Stefan E, Wiesner B, Lorenz D, Theilig F, et al. Identification of a novel A-kinase anchoring protein 18 isoform and evidence for its role in the vasopressin-induced aquaporin-2 shuttle in renal principal cells. J Biol Chem 2004;279:26654–65.

[230] McSorley T, Stefan E, Henn V, Wiesner B, Baillie GS, Houslay MD, et al. Spatial organisation of AKAP18 and PDE4 isoforms in renal collecting duct principal cells. Eur J Cell Biol 2006;85:673–8.

[231] MacGregor GG, Xu JZ, McNicholas CM, Giebisch G, Hebert SC. Partially active channels produced by PKA site mutation of the cloned renal K^+ channel, ROMK2 (kir1.2). Am J Physiol 1998;275:F415–22.

[232] Xu ZC, Yang Y, Hebert SC. Phosphorylation of the ATP-sensitive, inwardly rectifying K^+ channel, ROMK, by cyclic AMP-dependent protein kinase. J Biol Chem 1996;271:9313–9.

[233] Ali S, Chen X, Lu M, Xu JZ, Lerea KM, Hebert SC, et al. The A kinase anchoring protein is required for mediating the effect of protein kinase A on ROMK1 channels. Proc Natl Acad Sci USA 1998;95:10274–1028.

[234] Ali S, Wei Y, Lerea KM, Becker L, Rubin CS, Wang W. PKA-induced stimulation of ROMK1 channel activity is governed by both tethering and non-tethering domains of an A kinase anchor protein. Cell Physiol Biochem 2001;11:135–42.

[235] Donowitz M, Mohan S, Zhu CX, Chen TE, Lin R, Cha B, et al. NHE3 regulatory complexes. J Exp Biol 2009;212:1638–46.

[236] Xie Z. Molecular mechanisms of Na/K-ATPase-mediated signal transduction. Ann NY Acad Sci 2003;986:497–503.

[237] Yuan Z, Cai T, Tian J, Ivanov AV, Giovannucci DR, Xie Z. Na/K-ATPase tethers phospholipase C and IP3 receptor into a calcium-regulatory complex. Mol Biol Cell 2005;16:4034–45.

CHAPTER

15

The Renin–Angiotensin System

Thu H. Le[1], *Steven D. Crowley*[2], *Susan B. Gurley*[2] *and Thomas M. Coffman*[2,3]

[1]Division of Nephrology, Department of Medicine, University of Virginia, Charlottesville, VA, USA
[2]Division of Nephrology, Department of Medicine, Duke University and Durham VA Medical Centers, Durham, North Carolina, USA
[3]Cardiovascular and Metabolic Disorders Research Program, Duke-NUS, Singapore

Highly conserved through phylogeny, the renin–angiotensin system (RAS) is an essential regulator of blood pressure and fluid balance. This biological system is a multi-enzymatic cascade in which angiotensinogen, its major substrate, is processed in a two-step reaction by renin- and angiotensin-converting enzyme (ACE), resulting in the sequential generation of angiotensin I and angiotensin II. Along with its importance in maintaining normal circulatory homeostasis, abnormal activation of the RAS can contribute to the development of hypertension and target organ damage.

The importance of the RAS in clinical medicine is highlighted by two sets of observations. First are associations between polymorphisms of genes encoding RAS components and cardiovascular disease.[1–6] Second, and perhaps more compelling, is the impressive efficacy of pharmacological agents that inhibit the synthesis or activity of angiotensin II. For example, angiotensin converting enzyme (ACE) inhibitors are very effective and well-tolerated anti-hypertensive agents.[7] Along with their ability to lower blood pressure, these agents also effectively prevent or ameliorate morbidity and mortality associated with cardiovascular diseases. In this regard, large clinical trials have demonstrated that ACE inhibitors improve survival in patients with congestive heart failure,[8,9] and in patients with risk factors for coronary artery disease.[10] They also slow the progression of a variety of kidney diseases, including diabetic nephropathy.[11] Angiotensin receptor blockers (ARBs), which block AT_1 receptors, are similarly effective for treating these disorders.[12–14] The purpose of this chapter is to provide an overview of the major physiological features of the RAS, focusing on its role in the kidney.

THE COMPONENTS OF THE RENIN–ANGIOTENSIN SYSTEM

Renin

The aspartyl protease renin was first isolated from the kidney by Tigerstedt more than a century ago. Renin is synthesized as a precursor protein, pro-renin, containing an additional 43 amino acids at the N-terminus that block the enzyme's active site.[15] Active renin is generated by removal of this N-terminal peptide fragment, presumably by proteases in the juxtaglomerular cells of the kidney. Whether intact pro-renin has a distinct physiological role remains to be determined; however, there is accumulating evidence suggesting specific contributions of the pro-renin molecule in some normal and disease states.[16–19]

Active renin specifically cleaves the 10 amino acids from the N-terminus of angiotensinogen to form angiotensin I. A substantial excess of angiotensinogen is present in serum, and ACE is ubiquitous in the endothelium and plasma.[20] Accordingly, in the bloodstream, the amount of renin is the rate-limiting step determining the level of angiotensin II, and thus the activity of the system. The primary source of renin in the circulation is the kidney, where its expression and secretion are tightly regulated at the juxtaglomerular apparatus by two distinct mechanisms: a renal baroreceptor[21,22] and sodium chloride delivery to the macula densa.[23–25] Through these sensing mechanisms, levels of renin in plasma can be incrementally titrated in response to changes in blood pressure and salt balance. These regulatory principles provide a basis for many of the physiological characteristics of the RAS, and regulation of renin release in the kidney will be discussed in detail below.

Seldin and Giebisch's The Kidney, Fifth Edition.
DOI: http://dx.doi.org/10.1016/B978-0-12-381462-3.00015-X

© 2013 Elsevier Inc. All rights reserved.

In addition to its protease activity, renin may also bind specifically to other proteins or putative receptors.[19,26–28] This binding may induce physiologically significant intracellular signaling.[27] It has been suggested that the mannose-6-phosphate receptor (M6P-R), also known as insulin-like growth factor II receptor, binds renin and pro-renin, leading to internalization and degradation.[26] Nguyen et al. reported cloning a receptor from human kidney expression library that binds renin and pro-renin specifically and with high affinity, termed the (pro)renin receptor (PRR). Binding of PRR causes a conformational change of renin that leads to increased renin catalytic activity. Similarly, binding of PRR to pro-renin causes a conformational change, resulting in an ezymatically active pro-renin without the requirement for cleavage of the pro-segment. Furthermore, binding of renin to this receptor induces a rapid and sustained activation of ERK1/ERK2, without affecting concentrations of calcium or cAMP.[27] It has been suggested that it may mediate angiotensin II-independent effects of renin, and might also indicate a functional role of pro-renin.[29] Although the physiological significance of PRR remains unclear, recent studies suggest PRR may have a role in blood pressure regulation. Transgenic rats overexpressing human PRR selectively in vascular smooth muscle cells display elevated blood pressure and heart rate.[30,31] In addition, human PRR gene polymorphism has been shown to be associated with ambulatory blood pressure in Japanese men.[32] PRR may also play a role in development. Deletion of PRR in mice results in early embryonic lethality.[33] In a family with X-linked mental retardation and epilepsy, linkage analysis identified an exonic splice enhancer in the PRR gene as the only mutation, and this resulted in the loss of the capacity of renin to phosphorylate ERK1/2.[34]

The pro-renin receptor appears to have other functions independent of the renin–angiotensin system. For example, it is found as part of a complex required for the normal function of V-ATPase in several cell lineages, including cardiac myocytes.[35] The pro-renin receptor acts as an adaptor between the Wnt receptor and V-ATPase in a Wnt/β-catenin signaling complex required for normal CNS development.[36] Thus, deletion of the pro-renin receptor gene causes a lethal phenotype at a very early embryonic stage, which contrasts significantly with the phenotype of renin knockouts,[37] indicating important functions of the receptor that are independent of its actions in the RAS. Two groups have recently described studies of mouse lines in which the pro-renin receptor was deleted specifically from podocytes. In both cases, there was a similar, dramatic phenotype characterized by disruption of the glomerular filtration barrier, with marked proteinuria and abnormal podocyte structure, perhaps due to dysregulated autophagy.[38,39] Thus, while this molecule appears to play a critical role in the kidney, much remains to be learned about its functions in normal kidney physiology and disease, including the extent to which these functions are influenced by renin or pro-renin binding.

Angiotensinogen

Angiotensinogen, the substrate for renin, is the source of all angiotensin peptides. Angiotensinogen in the circulation is derived primarily from synthesis in the liver. In humans, plasma concentrations of angiotensinogen are typically near the Km for renin,[40] so that changes in plasma concentration may influence the rate of angiotensin I generation at any given level of renin. In human hypertensive siblings, Jeunemaitre et al.[2] showed that a specific variant of the human angiotensinogen gene, M235T, was linked to hypertension, and was also associated with a modestly elevated plasma angiotensinogen concentration, about 120% of normal. They proposed that this variant of the *AGT* gene leads to an increase in plasma angiotensinogen levels and thereby eventually to increased blood pressure. However, because amino acid 235 is in a non-conserved portion of the angiotensinogen protein and variation of this amino acid does not affect protein stability, a mechanism to explain the physiological consequences of the mutation was not clear. An apparent explanation came later, when the M235T variant was found to be in linkage disequilibrium with another variant in the 5′ untranslated region of the *AGT* gene.[41] This second variant, a single nucleotide substitution in the promoter of the *AGT* gene, was associated with increased transcriptional activity of the gene.[41] Higher levels of *AGT* mRNA were found in patients carrying the variant allele.[41] The causal capacity of alterations in plasma angiotensinogen level to affect blood pressure was demonstrated in studies of mice engineered to carry from 0 to 4 copies of the *AGT* gene.[42] In these animals, there was a positive correlation between the number of *AGT* gene copies, plasma levels of angiotensinogen, and blood pressure.

In addition to its synthesis by the liver, angiotensinogen is also produced by other tissues including the brain, the immune system, and the kidney.[43] In the kidney, synthesis of angiotensinogen in proximal tubules has been well-documented,[44] and proximal tubule synthesis may be regulated in part by the end-product, angiotensin II.[45] Along with angiotensinogen, the kidney expresses all of the other components of the RAS. Accordingly, it has been suggested that regulation and functioning of autonomous "tissue" renin–angiotensin systems in the kidney, as well as

other organs, may contribute to the physiological functions of the system, especially in disease states.[46] This hypothesis has been used to explain additional complexity of the system, whereby the apparent activity of the RAS is not reflected by measured plasma levels of it major components. For example, in the broad population of patients with hypertension, diabetes, and cardiovascular disease, pharmacological antagonists of the RAS lower blood pressure and prevent end-organ damage, even in the absence of overt elevation of plasma renin levels. However, the precise nature and physiological contributions of these tissue systems has been difficult to define experimentally.

Angiotensin Converting Enzyme

Angiotensin converting enzyme (ACE) is a carboxypeptidase that generates the vasoactive peptide angiotensin II by cleaving two amino acids from the c-terminus of the inactive precursor angiotensin I.[47] There are two distinct forms of ACE, somatic and testicular, both generated by alternative splicing of a single gene.[48–50] Somatic ACE is expressed as an ectoenzyme on the surface of endothelial cells throughout the body, and is particularly abundant in lung, intestine, choroid plexus, placenta, and on brush border membranes in the kidney. A soluble form of ACE that circulates in plasma is formed by enzymatic cleavage of tissue-bound ACE at its transmembrane domain.[51] As with other components of the RAS, molecular variants of *ACE* have been proposed as candidate genes in hypertension, cardiovascular, and kidney diseases.[52] Insertion (I) and deletion (D) polymorphisms of the human *ACE* gene are common, and have been associated with altered levels of ACE in plasma.[53,54] In some cohorts, but not others, these *ACE* gene variants have been linked to differing susceptibilities to hypertension, cardiovascular, and renal diseases.[52,55]

In addition to angiotensin I, other biologically active peptides are substrates for ACE. Perhaps the most important of these is bradykinin.[56] ACE degrades bradykinin into an inactive peptide, representing a significant biological pathway for bradykinin metabolism *in vivo*[57]; in older literature, ACE was referred to as kininase II. Since bradykinin has vasodilator and natriuretic properties,[56] it has been suggested that one mechanism of blood pressure reduction with ACE inhibition is blockade of this kininase activity. This was clearly demonstrated by Brown and associates, who showed that the anti-hypertensive efficacy of ACE inhibitors is attenuated by simultaneous administration of a bradykinin receptor antagonist.[58]

Using genome-based strategies, homologs of ACE have been identified.[59–61] One of these, ACE2, exhibits more than 40% identity at the protein level with the catalytic domain of ACE.[59,60] Similar to ACE, ACE2 is expressed on the surface of certain endothelial cell populations. However, compared to the ubiquitous distribution of ACE, the expression pattern of ACE2 is more limited, with most abundant expression in kidney followed by heart and testis.[59,60] Their substrate specificities also differ; ACE2 hydrolyzes angiotensin II with high efficiency, but has much lower activity against angiotensin I.[59,62] Hydrolysis of angiotensin II by ACE2 generates another peptide with putative biological actions: angiotensin 1-7.[62] Accumulating evidence indicates that this peptide causes vasodilation, natriuresis, and may promote reduced blood pressures[63] via the Mas receptor.[64] It has been further suggested that ACE2 may be a major pathway for synthesis of angiotensin 1-7.[65] Thus, the functions of ACE2 may be determined by its distinct actions to metabolize angiotensin II and to generate angiotensin 1-7.

Although the precise physiological role of ACE2 is not clear, it was originally identified and cloned from a cDNA library prepared from ventricular tissue of a patient with heart failure.[59] Initial studies in ACE2-deficient mice have suggested a role for ACE2 in cardiac function[364,365] and in blood pressure regulation.[66] More recent work by many groups has demonstrated roles for ACE2 in renal diseases, such as diabetic and non-diabetic kidney disease,[67–70] and hypertension[67,71,72] in both experimental models and human cohorts.

A third member of the ACE gene family, collectrin, was identified as a gene that is upregulated in the subtotal nephrectomy model of chronic kidney disease.[73] Collectrin is highly homologous to the transmembrane portion of ACE2, but lacks the carboxypeptidase domain.[61] Its physiological functions are emerging[74,75] and appear to regulate amino acid transport by the kidney.

Angiotensin Receptors

The biological actions of angiotensin II are mediated by cell surface receptors that belong to the large family of 7 transmembrane receptors.[7,76] The angiotensin receptors can be divided into two pharmacological classes, type 1 (AT_1) and type 2 (AT_2), based on their different affinities for various non-peptide antagonists (Figure 15.1). Studies using these antagonists suggested that most of the classically recognized functions of the RAS are mediated by AT_1 receptors.[76] Gene targeting studies have confirmed these conclusions.[77]

AT_1 receptors from a number of species have been cloned[78–80] and two subtypes, designated AT_{1A} and

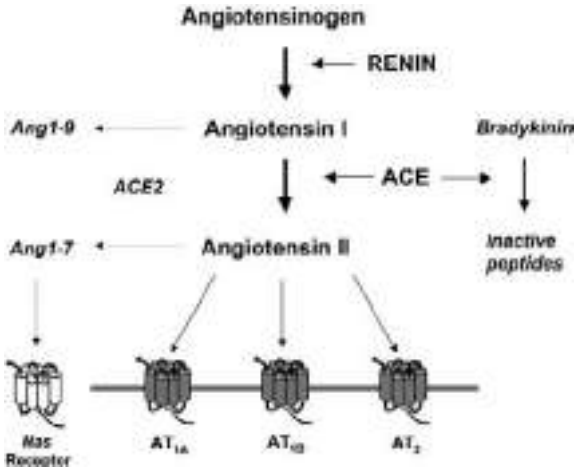

FIGURE 15.1 Angiotensinogen is cleaved by renin to form angiotensin I, which is then cleaved by angiotensin-converting enzyme (ACE) to form angiontesin II, the major effector molecule of the RAS. The biological effects of angiotensin II are mediated by the G-protein-coupled seven-transmembrane cell surface receptors AT1 and AT2. Angiotensin II is hydrolyzed by angiotensin-converting enzyme 2 (ACE2), a homologue of ACE. This hydrolysis results in the generation of the angiotensin 1–7 peptide, the actions of which are mediated by the *Mas* receptor. After: *Le, TH and Coffman TM. Targeting genes in the renin-angiotensin system. Current Opinion in Nephrology and Hypertension 2008, 17:57-63. Lippincott Williams & Wilkins.*

AT_{1B}, have been identified in rat[81–83] and mouse.[84] In the classical view, AT_1 receptors signal through $G_{\alpha q}$-linked signaling pathways involving phospholipase C, IP3, and increases in intracellular calcium.[85] However, the AT_1 receptor has also been linked to JAK/STAT activation,[86] as well as β-arrestin-dependent pathways linked to ERK activation.[87–89] In addition, recent studies have shown that the AT1 receptor has the capacity to transactivate the EGF receptor, which may be independent of ligand.[90,91] This pathway may contribute to chronic kidney injury.[92]

The murine AT_1 receptors are products of separate genes and share substantial sequence homology.[83,93,94] AT_{1A} receptors predominate in most organs, except the adrenal gland and regions of the CNS, where AT_{1B} expression may be more prominent.[93,95,96] A single report has suggested that AT_{1B} receptors might also exist in man,[97] but this has not been confirmed in the unpublished work of several independent groups, and the consensus view is that there is no human counterpart to the murine AT_{1B} receptor. Thus, the AT_{1A} receptor is considered the closest murine homolog to the single human AT_1 receptor.

The binding signatures of the AT_{1A} and AT_{1B} receptors are virtually identical,[98] and it was difficult to discriminate their *in vivo* functions pharmacologically. Experiments using gene targeting have provided insights into the discrete functions of the two AT_1 receptor genes.[99,100] Although the AT_{1B} receptor has a unique role to mediate thirst responses in the CNS,[101] AT_{1A} receptors have the predominant role in determining the level of blood pressure,[102–104] and in mediating vasoconstrictor responses.[99,102] The phenotype of markedly reduced blood pressures and profound sodium sensitivity in mice lacking the AT_{1A} receptor[102,105] underscores its importance in blood pressure control.

Pharmacological and genetic studies have confirmed that virtually all of the classically recognized functions of the RAS are mediated by AT_1 receptors. Until recently, little was known about the physiological role of AT_2 receptors. AT_2 receptors are found in abundance during fetal development,[106,107] but their expression generally falls after birth. However, persistent AT_2 receptor expression can be detected in several adult tissues including the kidney, adrenal gland and the brain, and absolute levels of AT_2 receptor expression may be modulated by angiotensin II and certain growth factors.[108] AT_2 receptors appear to signal by coupling to $G_{\alpha i2}$ and $G_{\alpha i3}$ proteins.[109] Using site-directed mutagenesis, the intermediate portion of the third intracellular loop of the AT_2 receptor was found to be necessary for normal receptor signaling.[110,111] Moreover, it has been suggested that activation of AT_2 receptors stimulates bradykinin, nitric oxide, and guanosine cyclic 3′,5′-monophosphate (cGMP),[112,113] and these pathways may mediate actions of the receptor to promote natriuresis and blood pressure lowering. Finally, there is also evidence to support HETEs as second messengers for AT_2 receptors in the kidney, leading to ERK1/2 phosphorylation.[114]

Targeted disruption of the mouse *Agtr2* gene did not cause a dramatically abnormal phenotype. These animals clearly manifest increased sensitivity to the pressor actions of angiotensin II.[115,116] One of the AT_2 deficient lines manifested increased baseline blood pressure and heart rate.[115] Interestingly, behavioral changes were also observed in AT_2-deficient mice. They had decreased spontaneous movements and rearing activity,[115,116] and impaired drinking response to water deprivation.[116] Transgenic mice that overexpress the AT_2 receptor gene under control of a cardiac-specific promoter have decreased sensitivity to AT_1-mediated pressor and chronotropic actions.[117] Moreover, the pressor actions of angiotensin II are significantly attenuated in these transgenic mice. This attenuation was completely reversed following pretreatment with a specific AT_2 receptor antagonist. Taken together, these data suggest that a primary function of the AT_2 receptor may be to negatively modulate the actions of the AT_1 receptor. Along similar lines, the recently described non-peptide agonist, compound 21, has been used to uncover additional functions of the AT_2 receptor, which appear quite diverse. Studies with this agonist regarding blood pressure have been

variable, but it appears to have minimal effect on blood pressure in normal situations; the potential to affect blood pressure in disease states may be different.[118]

Aldosterone

Aldosterone is a steroid hormone synthesized in the zona glomerulosa (ZG) of the adrenal gland. The two dominant regulators of aldosterone synthesis and release are angiotensin II and the level of serum potassium.[119] The RAS-dependent component of aldosterone regulation is triggered by binding of angiotensin II to AT_1 receptors in the ZG.[119] Stimulation of aldosterone release by angiotensin II contributes to enhanced sodium reabsorption and anti-natriuresis. Independently of angiotensin II, hyperkalemia can control the release of aldosterone through a process that involves the membrane depolarization of ZG cells.[120,121] In addition, adrenocorticotropic hormone (ACTH) can stimulate aldosterone via its G-protein coupled receptor.[121] Elevations in ACTH influence aldosterone production only during short-term stress, as this response is attenuated with persistent exposure to ACTH. In contrast, angiotensin II and potassium can both exert a chronic, sustained stimulation of aldosterone generation by the zona glomerulosa.[122]

The classically recognized effects of aldosterone to influence sodium handling in the distal nephron are mediated by aldosterone binding to the mineralocorticoid receptor (MR). The MR is a 107 kD protein that acts as a transcription factor to regulate gene expression in target tissues. The molecular mechanisms used by the MR to drive epithelial sodium channel (ENaC) function in the collecting tubule have been reviewed recently.[123] Cortisol actually exhibits a higher affinity for the mineralocorticoid receptor than aldosterone, but locally expressed 11ß-hydroxysteroid dehydrogenase type 2 "protects" the MR by converting cortisol to cortisone, which does not activate the MR.[124] The binding of aldosterone to the MR in the principal cell of the collecting tubule epithelium induces transcription of the α-subunit, the multimeric coupling of the α-, β-, and γ-subunits of the EnaC, and the translocation of the ENaC complex to the luminal surface of the tubule.[125,126] Aldosterone-induced expression of the αENaC-subunit, in particular, follows a diurnal variation pattern that depends on the circadian transcription factor Period1.[127]

Aldosterone stimulates ENaC transcription and activity largely through the upregulation of serum- and glucocorticoid-regulated kinase 1 (sgk1).[128–130] At the transcriptional level, Sgk1 phosphorylates ALL1-fused gene from chromosome 9 (Af9), which in turn blocks the repressor effects of the histone H3 Lys79 methyltransferase disruptor of telomeric silencing alternative splice variant a (Dot1a) on αENaC gene transcription.[131] At the post-translational level, Sgk1 phosphorylates Nedd4-2, causing ENaC proteins to remain in the apical membrane of the principal cell.[132,133] Once inserted into the luminal membrane of the principal cell, ENaC permits cellular uptake of intraluminal sodium, generating an electronegative potential in the distal tubular lumen which favors secretion of potassium from the principal cell into the urinary filtrate via the renal outer medullary potassium channel (ROMK). Sgk1 may also phosphorylate ROMK, similarly increasing its apical density, further facilitating the kaliuresis induced by aldosterone.[134] In addition, aldosterone appears to directly increase ROMK expression.[135] Finally, aldosterone modulates sodium transport in the distal nephron independently of ENaC by enhancing expression and activity of the thiazide-sensitive Na-Cl co-transporter (NCC). Sgk-1 mediates this effect by phosphorylating serine/threonine kinase with-no-lysine 4 (WNK4), thereby diminishing the inhibitory effects of WNK4 on NCC activity.[136] Through these pathways, the MR regulates sodium and potassium transport within the mineralocorticoid-responsive segments of the distal nephron.

Recent human phenotyping studies and animal studies using gene-targeting strategies have confirmed the contribution of the MR to tubular function and salt balance. For example, in humans with a mutation leading to a constitutively active MR, early onset hypertension develops,[137] whereas heterozygosity for an inactivating mutation of the MR leads to salt-wasting, hypotension, metabolic acidosis, and hyperkalemia.[138] Mice genetically deficient for the MR similarly develop severe salt-wasting that leads to neonatal death,[139] whereas mice with genetic deletion of the MR restricted to the principal cell waste salt and lose body weight only when exposed to a low-sodium diet,[140] suggesting that at baseline the late distal convoluted tubule and early connecting tubule may be able to compensate for a lack of ENaC activity in the distal nephron. Alternatively, the discrepancy in phenotypes between the global and conditional knockout mice may be due to discrete functions of aldosterone to modulate solute transport in the proximal tubule[141,142] and/or medullary thick ascending limb.[143] Mutations that activate the ENaC may cause hypertension,[144–146] whereas global inactivation of the subunits of the ENaC in mice causes sodium-wasting, potassium retention, and early mortality, and in humans pseudohypoaldosteronism type 1 with severe salt-wasting.[147] In contrast, inactivation of the α-ENaC gene only in the collecting duct does not impair sodium and potassium balance,[148] again indicating that the regulation by aldosterone of ENaC in the latter regions of

the distal convoluted tubule and/or the connecting tubule may also contribute to sodium and fluid homeostasis.[149]

In addition to its physiologic effects on renal solute handling, aldosterone has the capacity to mediate direct cellular injury in the kidney.[150] In this regard, pathologic functions of aldosterone in non-tubular renal compartments become increasingly relevant. For example, aldosterone impairs vascular reactivity by diminishing expression of glucose-6-phosphate in the endothelium[151] and mediates direct vascular injury via a placental growth factor-dependent pathway.[152] In mesangial cells, aldosterone activates sgk-1, NF-kB, and MAP kinases, leading to cellular proliferation, generation of oxidative stress, and connective tissue growth factor expression.[153–155] Emerging evidence suggest aldosterone may also promote oxidative stress and apoptosis directly within podocytes.[156,157] Consistent with these pathologic effects of aldosterone in several cell lineages of the kidney glomerulus, human studies have now demonstrated a role for aldosterone blockade in ameliorating the progression of proteinuric kidney disease.[158]

Integrated Actions of the RAS in the Kidney

The important role of the kidney in regulation of blood pressure has been long recognized,[159] and the relationship between alterations in systemic blood pressure and changes in renal sodium excretion is well-documented.[160] For example, an elevation in perfusion pressure in the renal artery results in a rapid increase in sodium and water excretion by the kidney, so-called "pressure natriuresis".[160] Based on such observations, Guyton and co-workers suggested that whenever arterial pressure is elevated, activation of this pressure-natriuresis mechanism will cause sufficient excretion of sodium and water to return systemic pressures to normal.[161] They further hypothesized that the substantial capacity for sodium excretion by the kidney provides a compensatory system of virtually infinite gain to oppose processes, including increases in peripheral vascular resistance, which would tend to increase blood pressure. It follows that defects in renal excretory function would therefore be a pre-requisite for sustaining a chronic increase in intra-arterial pressure.

The RAS has potent actions to modulate pressure-natriuresis relationships in the kidney[162,163] and these actions shape the characteristics of RAS-dependent blood pressure regulation in normal physiology and in disease states. For example, as depicted in Figure 15.2, chronic infusion of angiotensin II causes a shift of the pressure natriuresis curve to the right, suggesting that when the RAS is activated, higher pressures are required to excrete an equivalent sodium load[164] (Figure 15.2). Conversely, administration of ACE inhibitors or ARBs shifts the curve to the left, meaning that natriuresis is facilitated at lower levels of blood pressure (Figure 15.2). The basic features of endogenous control of the RAS are consistent with these homeostatic functions. As shown in Figure 15.2, the system is activated at low levels of salt intake, stimulating renal sodium reabsorption and conservation of body fluid volumes and blood pressure. In contrast, with high sodium intake, the system is suppressed, facilitating natriuresis.

REGULATION OF RENIN

As discussed above, the concentration of renin in plasma is the rate-limiting step in the production of angiotensin II. Accordingly, the activity of the RAS in the circulation is largely determined by the factors that regulate renin. The kidney is the major source of renin, where its generation and secretion are primarily controlled by renal perfusion pressure and by the luminal delivery of sodium chloride to the macula densa in the distal nephron. The major features of these regulatory processes are described in the sections that follow.

Sources of Renin

The major source of renin in the circulation is the kidney. Following bilateral nephrectomy, plasma levels of renin and angiotensin II fall precipitously.[165] In the kidney, the location of renin-expressing cells varies from development through adulthood, and in response to homeostatic challenges. During embryonic development, renin-expressing cells are found in the undifferentiated metanephric mesenchyme.[166] In the fetal kidney, these cells are present in the large intrarenal arteries, glomeruli, and interstitium.[166] In the adult kidney, renin expression is primarily restricted to granular cells which are modified smooth muscle cells within the juxtaglomerular apparatus (JGA). The JGA is located in the region where the afferent arteriole enters the glomerulus.[167,168] As shown in Figure 15.3, the JGA is a highly organized structure composed of three distinct anatomical parts: granular cells, the macula densa, and the extraglomerular mesangial cells.[169] The macula densa is a specialized tubular area that marks the transition from the ascending loop of Henle to the distal tubule lying in direct contact with the vascular pole of the glomerulus from which it originated.[169] By light microscopy, the unique characteristics of the macula densa epithelial cells can be discerned by their narrow, columnar shape and apparent

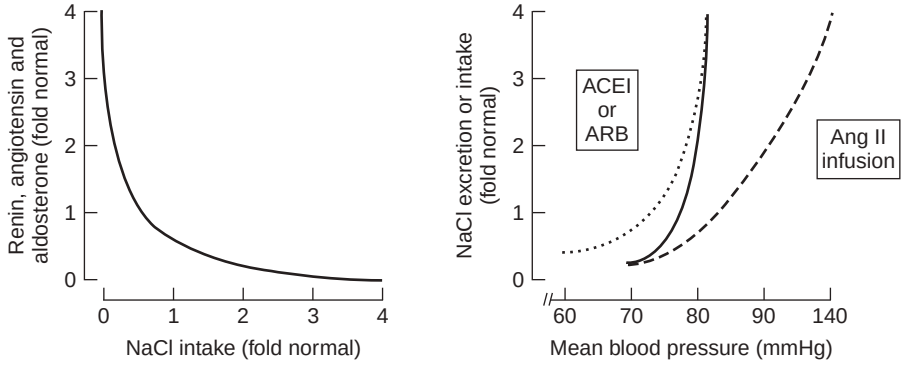
Renin, angiotensin and aldosterone (fold normal)
NaCl intake (fold normal)
NaCl excretion or intake (fold normal)
ACEI or ARB
Ang II infusion
Mean blood pressure (mmHg)

FIGURE 15.2 Chronic infusion of angiotensin II causes a shift of the pressure natriuresis curve to the right. Conversely, administration of ACE inhibitors or ARBs shifts the curve to the left. After: *Guyton, AC et al. In: Hypertension, Pathophysiology, Diagnosis and Management. Laragh, JH and Brenner, BM (Eds). Raven Press, NY (Publ). pp 1311-1326, 1995.*

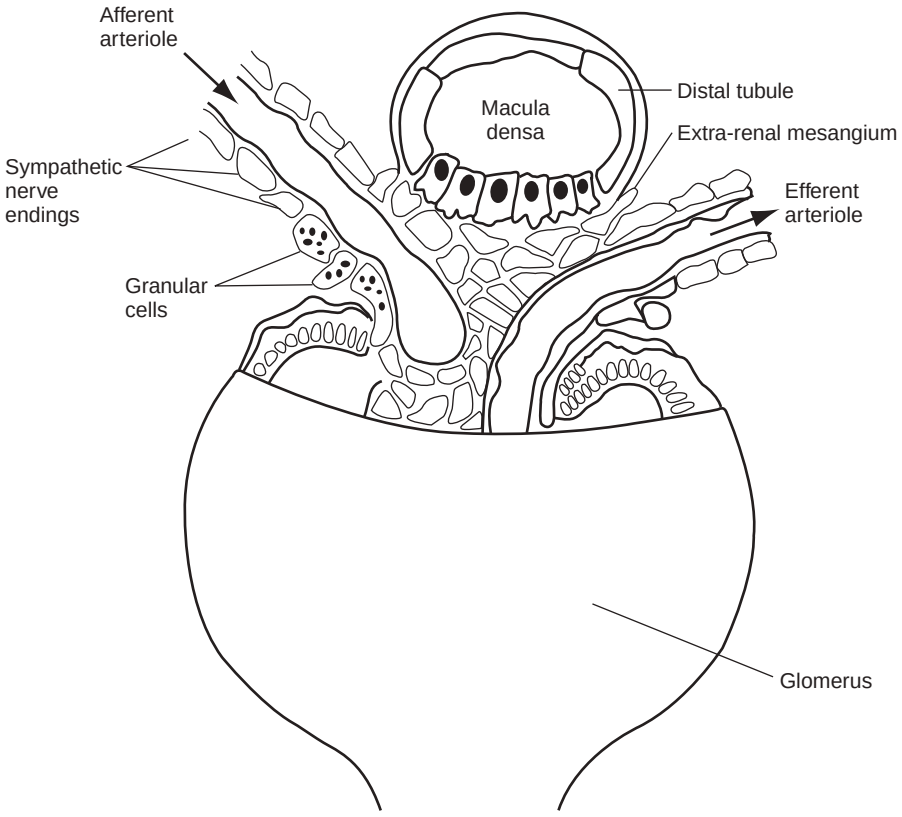

FIGURE 15.3 The juxtaglomerular apparatus (JGA). Integration of the regulated secretion of renin is carried out at the JGA. There are three major pathways regulating the secretion of renin by granular cells at the JGA: the baroreceptor, the macula densa mechanism, and direct stimulation by the sympathetic nervous system. The renal baroreceptor monitors renal perfusion pressure and signals an increase in renin when renal perfusion pressure falls. In the macula densa mechanism, macula densa cells sense the decrease in chloride ions in the filtrate in the distal tubule, thereby stimulating release of renin. Increased activity of renal sympathetic nerves directly stimulates renin release via activation of adrenergic receptors. Sympathetic innervation also modulates both the baroreceptor and macula densa mechanisms. After: *Francois H and Coffman TM. Prostanoids and blood pressure: which way is up? J Clin Invest. 2004; 114(6):757-759. American Society for Clinical Investigation.*

accumulation of nuclei, distinguishing them from cells in the adjacent parts of the distal tubule.[167] By electron microscopy, the basement membrane of the macula densa appears to be fused with the vacular component, and continuous with the basement membranes surrounding the granular and agranular cells in the extraglomerular mesangium.[167] As described below, the macula densa acts as a sensor of chloride concentration in the distal tubule, providing signals that are important for control of renin.[169] The anatomical organization of the JGA facilitates the regulation of renin secretion in response to critical environmental cues.

Although JG cells are clearly the primary source of renin in the adult kidney, studies by Gomez and associates suggest that renin-expressing cells are not terminally differentiated, but can be recruited during periods of homeostatic pertubations such as dehydration and hypotension. For example, in angiotensinogen-deficient mice, renin is expressed extensively along the entire length of the afferent arteriole and intrarenal arteries.[170] Similarly, in mice subjected to a low-sodium diet combined with captopril treatment, renin-expressing cells can be found throughout the length of the afferent arteriole, in the glomerular and

extraglomerular messangium, and in the glomerular capsule.[170] Studies by Lalouel and associates suggest that renin is also present in the connecting tubule, at least in the mouse kidney. Moreover, their studies indicate that renin expression in the connecting tubule may be regulated by sodium intake.[171] Although its physiological role is unclear, it has been suggested that renin expressed in the distal nephron may contribute to regulation of angiotensin peptide concentrations in the tubular lumen.

Expression of renin outside the kidney has also been documented. Levi and associates have recently shown that mast cells express renin mRNA and contain large quantities of renin protein, apparently within the secretory granules.[172] Mast cell-derived renin can efficiently convert angiotensinogen to angiotensin I after mast cell degranulation.[172] Moreover, release of renin by cardiac mast cells can be triggered by ischemia, producing pathophysiologic consequences such as release of norepinephrine and generation of cardiac arrhythmias.[173] Taken together, this work has suggested that resident mast cells in the heart and perhaps other organs, upon appropriate stimulation, are capable of generating ample quantities of renin to activate the RAS locally, and thereby affect organ function. Furthermore, it appears the factors controlling renin release from mast cells will be quite different from those that regulate JG cells, and are likely to involve signals associated with inflammation and injury.[174] Nonetheless, it remains to be determined whether this alternative pathway for RAS activation plays any major role in physiology or disease pathogenesis.

Baroreceptor Regulation of Renin Release

The baroreceptor theory was developed to explain observations that renin secretion is directly stimulated by reduced renal perfusion. This theory was first developed in the context of experimental observations that granularity of the JG cells was inversely correlated with the magnitude of renal perfusion pressure.[175] Since then, numerous studies have shown that renin secretion is inversely related to renal perfusion pressure or pulse amplitude.[21,176–179] This relationship is preserved in denervated kidneys[180,181] and in isolated perfused kidneys with a non-functioning macula densa mechanism.[182–184] Thus, the baroreceptor is an independent mechanism for controlling renin, residing within the kidney and clearly separate from regulation by the sympathetic nervous system.[179] In renovascular hypertension, the baroreceptor is the primary mechanism for stimulating renin release. In the presence of a critical stenosis of the renal artery, renal perfusion pressure drops, stimulating renin and generating hypertension.[185]

While the independent nature of the baroreceptor mechanism and its localization to the kidney has been clearly established, identification of its precise nature has been elusive. Various models have been proposed to explain the mechanism for pressure sensing and consequent signal transduction, including direct stretch of the JG cells due to transmural pressure across the afferent arteriole[22,186] or indirect pathways involving secondary release of autocoids.[187] Some of these candidate soluble factors include nitric oxide[188–190] and prostanoids,[191,192] which are stimulatory or endothelins, which are inhibitory.[193]

Gene-targeting in the mouse has been utilized to examine the role of some of these mediators in the baroreceptor response. In one study, genetic deletion of endothelial nitric oxide synthase (eNOS) had no effect on renin release in response to change in renal perfusion pressure, suggesting that eNOS-derived nitric oxide is not a mediator of the baroreceptor–renin coupling.[194] On the other hand, the absence of the IP receptor, the single known receptor for PGI_2 (prostacyclin), conferred substantial resistance to hypertension and hyperreninemia after unilateral renal artery stenosis.[195] This suggests an absolute requirement for PGI_2 in triggering renin release after baroreceptor activation. A number of questions remain concerning the mechanism and cell lineages controlling synthesis of key mediators such as prostacyclin, and the cellular targets for these mediators affecting renin release.[196]

Over the past 40 years, much deliberation has been rendered regarding the existence and location of a baroreceptor for renin release. The mechanism by which renal perfusion pressure regulates renin secretion remains poorly understood. However, this mechanism appears to be dependent on extracellular calcium concentration. Kurtz and colleagues demonstrated that when the extracellular level of calcium is lowered, the inhibitory effect of renal perfusion pressure on renin release is abolished.[197] A potential mediator in this process may involve connexin proteins that form gap junctions between JG cells and adjacent endothelial cells. Disruption of connexin40 (Cx40) in the mouse, either through gene deletion or point mutation, results in hyperreninemia and hypertension, and loss of pressure control of renin release[198,366-368]; similar to the effect observed with the lowering of extracellular calcium concentration.[197] Other connexin proteins have been demonstrated to also play a role in renin release. Connexin45, another gap junction protein, can replace the function of connexin40, since genetic substitution of the coding region of connexin40 by connexin45 resulted in the attenuation of hypertension and near normalization of the pressure control of renin secretion.[200] Replacement of connexin43 by connexin32 in

the mouse resulted in decreased renin levels that did not change in response to a high-salt diet and protection from hypertension induced by a 2-kidney-1clip model.[201] A consensus remains to be established regarding whether connexin proteins (and which one (s)), are indeed the elusive baroreceptor, but the evidence suggests that connexins play an essential role in the regulation of renin release in response to change in perfusion pressure. Future studies are required to determine whether these connexins interact in coordination with other mediators mentioned above in the baroreceptor response.

Macula Densa Mechanism for Renin Regulation

The second major pathway for physiological regulation of renin is the so-called macula densa mechanism, whereby cells at the macula densa sense a reduction in chloride ions in the filtrate of the distal tubule, triggering renin release.[25] In this circumstance, release of renin and the consequent generation of angiotensin II are believed to serve as a mechanism for enhancing renal sodium reabsorption in states of fluid volume depletion. The anatomical association of the macula densa with the JG cells stimulated the first speculation by Goormaghtigh of its physiological function.[202] As mentioned above, the macula densa is made up of specialized epithelial cells at the terminal portion of the thick ascending limb. Their basolateral membrane is in contact with glomerular mesangial cells which, in turn, are contiguous with granular cells in the JGA.[24] The role of the macula densa in renin regulation was initially hypothesized by Vander in 1967,[169] and there is now general consensus that this mechanism provides a control of renin secretion that is directly determined by sodium chloride delivery to the distal nephron.[203,204] Moreover, several studies indicate that chloride flux through the Na-K-2Cl transporter (NKCC2) regulates the signaling pathways linked to renin secretion.[205,206] Increased chloride delivery to the MD inhibits, whereas reduced chloride delivery stimulates, renin release.[23,197,207]

In addition to the well-studied NKCC2 transporter, the Na^+/H^+ exchanger isoform 2 (NHE2) expressed on the apical surface of the macula densa also plays a role in renin release, perhaps through its effect on macula densa cell volume. A recent study by Peti-Peterdi and colleagues demonstrated that NHE2-deficient mice have significant mechanisms responsible for increased renin levels which are macula-densa specific,[208] since these mice have been characterized to have normal blood pressure.[209]

Several candidate signaling pathways linking distal tubule solute concentration to control of renin have been proposed. These include adenosine, nitric oxide, and prostanoids.[210] The most compelling current evidence suggests that MD stimulation of renin involves activation of cyclo-oxygenase (COX)-2[211] constitutively expressed at high levels in the macula densa, generating the prostanoid PGE_2.[212,213] PGE_2 then activates an EP receptor on granular cells in the JGA to stimulate renin release.[214] The EP4 receptor is likely the major EP receptor that mediates the actions of PGE2 in this process. Facemire et al. demonstrated that EP4 receptor-deficient mice display a ~70% reduction in renal renin expression and plasma renin concentration compared to wild-type mice after treatment with furosemide.[215] In contrast, deletion of EP2 receptors in the mice has no effect on renin stimulation by furosemide. Interestingly, this study also suggested that the source of PGE2 in this pathway is not dependent on microsomal PGE synthases 1 and 2 (mPGES1, mPGES2). The capacity for prostaglandins to directly stimulate renin secretion has been long recognized.[216,217] Moreover, studies using specific inhibitors and COX-2 deficient mice have clearly demonstrated the importance of COX-2 in the macula densa pathway.[218,219] In addition, the activity of various components of this system has been demonstrated in the isolated perfused macula densa segments[220] and JG cell lines.[221] However, at least one study[195] has failed to confirm a non-redundant role for individual EP receptors for PGE_2 in furosemide-stimulated renin release *in vivo*.

Initial evidence suggesting a role for adenosine in MD signaling came from studies using the selective A1AR antagonist 8-cyclopentyl-1,3-dipropylxanthine. The major effect of the inhibitor was to attenuate the actions of increasing luminal NaCl concentrations to inhibit renin release.[222] Later studies using A1AR-deficient mice confirmed that the role of adenosine is primarily restricted to the arm mediating inhibition of renin release. In A1AR-deficient mice, renin-inhibitory actions of enhanced sodium chloride delivery to the macula densa are blocked, whereas stimulation of renin secretion caused by reduced sodium chloride transport at the macula densa is unaffected.[223]

Macula densa cells express high levels of neuronal nitric oxide synthase (nNOS).[224,225] The role of NO in regulation of renin was first tested using nonselective inhibitors of nitric oxide synthesis, which attenuated renin release stimulated by reduced luminal sodium chloride concentrations.[226,227] The specific roles of the individual NOS isoforms have been examined using mice with targeted deletion of nNOS or eNOS. In these studies, activation of the macula densa pathway was achieved by administration of NKCC2 blocking loop diuretics *in vivo* and in isolated perfused mouse kidneys. Deficiency of either nNOS or eNOS alone did not significantly affect macula densa-dependent renin secretion,[228] while nonspecific NOS blockade attenuated renin stimulation by loop diuretics. This suggests that nitric oxide plays a permissive, rather than a

primary, role in the macula densa control of renin release.[228]

Short Loop Feedback: Regulation of Renin by Angiotensin II

Angiotensin II also contributes to the regulatory pathways for renin and may control its own synthesis by activating AT_1 receptors, highly expressed at the JGA, thereby suppressing renin release.[229,230] Evidence supporting the existence of this so-called short-loop feedback mechanism includes studies in the isolated perfused kidney, where infusion of angiotensin II suppresses renin release.[179] Administration of ACE inhibitors and angiotensin receptor blockers increases renin mRNA expression and causes JGA hypertrophy.[231] Similarly, mice lacking AT_{1A} receptors also develop marked JGA hypertrophy.[103,230] However, in *Agtr1a*$^{-/-}$ chimeric mice,[103] and in kidney cross-transplantation experiments,[232] JGA hypertrophy correlated with blood pressure, but not with the absence of AT_1 receptors at the JGA, indicating a significant role for baroreceptor mechanisms in this response. Nonetheless, a role for the short-loop feedback mechanism to alter the sensitivity of baroreceptor or MD mechanisms would be consistent with current data.

Role of Sympathetic Nerve Activity

The capacity for sympathetic nerve activation to stimulate renin has been long recognized. For example, β-adrenoceptors are abundant in the JGA of kidneys from various species.[233] Furthermore, numerous studies have demonstrated that β-adrenergic agonists stimulate renin release.[234] Chronic renal nerve activation also stimulates renin,[235,236] along with its affects to modulate renal blood flow and tubular function. In experiments controlling for these factors, a clear relationship between increasing renal sympathetic nerve activity and renin secretion is maintained.[237,238] However, as discussed above, renal denervation does not abolish the capacity of the baroreceptor[181,239] or macula densa mechanisms to stimulate renin.[182–184] Accordingly, it appears likely that β-sympathetic tone has a modulatory, rather than primary, role in regulation of renin. Recently, a randomized controlled clinical trial demonstrated that renal sympathetic denervation is more effective than medical management alone in patients with resistant hypertension.[240] The original report did not mention any measurement of renin, but it will be of significant interest to determine the effect of the procedure on plasma renin levels in patients who did or did not have a significant reduction in blood pressure.

Regulation of Cellular Release of Renin

At the JGA, renin is stored in cytoplasmic granules within granular cells. In response to activating stimuli, renin is released into the circulation by exocytosis. This process of renin secretion is carried out by fusion events between the secretory granules and cell membrane of afferent arterioles.[241] Furthermore, the extent of secretory activity or exocytosis can be assessed using electrophysiological techniques that directly measure cell membrane capacitance of single mouse JG cells.[242] The control mechanisms for renin, described above, act by triggering this exocytotic pathway. Compared to the relative wealth of available information about physiological regulation of renin, much less is known about the precise intracellular pathways involved in renin secretion, and how these mechanisms are controlled in the granular cell. The general consensus is that the environmental signals regulating renin act through a limited number of intracellular second messengers, including calcium and cyclic AMP.[214,243]

The cyclic AMP pathway appears to be the major trigger for cellular release of renin. In a variety of experimental models, maneuvers causing an elevation of intracellular concentrations of cyclic AMP cause rapid stimulation of renin secretion.[243,244] In this regard, most of the documented secretagogues for renin, including PGE_2, PGI_2, dopamine, and β-adrenoreceptor, act via 7 transmembrane receptors linked to G_s-proteins that increase cyclic AMP levels in JG cells.[244] The specific biochemical pathways by which cyclic AMP acts to stimulate renin secretion are unclear, but likely involve protein kinase A, since inhibition of protein kinase A attenuates the stimulatory effect of β-adrenoreceptors on renin secretion.[190]

By contrast, increases in intracellular calcium levels may inhibit renin release. For example, experimental maneuvers that reduce intracellular calcium concentration stimulate renin release.[243] Moreover, several mediators with putative actions to inhibit renin release, such as angiotensin II, α-receptor agonists, vasopressin, and endothelins, have receptors that couple to G_q-proteins, and activation of these receptors by ligand increases intracellular calcium concentrations in JG cells.[214,243] The inhibitory effect of calcium on renin release appears to be mediated by protein kinase C, since stimulation of protein kinase C inhibits renin secretion,[245–247] whereas blockade of protein kinase C attenuates the inhibitory effect on renin secretion.[245–247] There is also evidence that the effects of calcium on renin release are mediated in part by a calmodulin-dependent process, since inhibition of calmodulin activity stimulates renin secretion.[248,249] Antagonistic interactions between the cyclic AMP and intracellular

calcium may ultimately determine the final consequences of extracellular signals on renin release.[243,250]

Regulation of Renin Gene Expression

The steady-state activity of the RAS is generally reflected by renin mRNA levels in the kidney. During chronic stimulation of the RAS, for example, upregulation of renin gene expression is required to sustain over time the enhanced release of renin protein by the JGA. Understanding of tissue-specific control of renin gene expression has been complicated by the difficulty of developing tractable cell culture preparations derived from JG cells. Thus, transgenic mice have been used extensively to assess *in vivo* regulation of renin gene expression.[251,252] Using this approach, minimal segments of the human renin gene sufficient to recapitulate temporal- and cell-specific patterns of gene expression have been identified.[251,252]

There is strong sequence conservation of 5′ proximal promoter regions between the renin genes of the human, rat, and mouse.[253] This region contains a cyclic AMP (cAMP) response element (CRE),[254–256] which is required for cAMP stimulation of transcription.[254,257] In addition, there are at least seven transcription factor-binding sites within the proximal promoter, including a binding site for HOX proteins that play critical roles in specifying positional information along embryonic axes.[253] The renin promoter is relatively weak in isolation,[254,257,258] but is strengthened up to 80-fold by a distal enhancer element.[259,260] This enhancer contains at least eleven transcription factor-binding sites responsive to a variety of signal transduction pathways.[261] Inhibitory factors, including endothelin-1, angiotensin II, mechanical stretch, and inflammatory cytokines, may act through target sequences within the enhancer.[261]

Post-transcriptional mechanisms also play a key role in determining steady-state renin mRNA levels. cAMP appears to be a critical mediator in this process. For example, in cell systems, cAMP has only a modest effect in inducing renin gene transcription of the renin gene, but nonetheless it causes marked induction of renin mRNA levels.[262] This augmentation is associated with enhanced stability of renin mRNA.[263] cAMP also increases levels of RNA-binding proteins targeting the 3′UTR of the human renin gene,[264] suggesting a potential mechanism for its effects to promote renin mRNA stability.

Control of Renal Hemodynamics by the RAS

Angiotensin II, acting via its AT_1 receptor, is a potent vasoconstrictor. Stimulation of AT_1 receptors in vascular smooth muscle cells initiates a signaling cascade including increased intracellular calcium concentration and alterations in cytoskeleton, inducing contraction with consequent increases in vascular resistance.[265] Studies in mice deficient in both the AT_{1A} and AT_{1B} receptor isoforms have confirmed the importance of AT_1 receptors in this response.[102,100] The pressor response to acute angiotensin II infusion is completely abolished in these double-knockout animals[100]; whereas response to another pressor agent, epinephrine, is not affected. These vasoconstrictor actions of angiotensin II play a central role in maintaining circulatory homeostasis in a number of tissues, including the kidney. In the kidney, the hemodynamic actions of angiotensin II impact renal blood flow, glomerular filtration rate, excretion of salt and water, and progression of renal damage in disease states.

Glomerular Microcirculation

The coordinated regulation of resistances in the afferent and efferent arterioles plays a critical role in determining and maintaining the glomerular filtration rate (GFR). The RAS has potent effects on glomerular hemodynamics. Angiotensin II causes constriction of both the afferent and efferent arterioles. However, the effect of high levels of angiotensin II is to induce a more profound constriction of the efferent arteriole.[266–268] The reasons for this disproportionate effect of angiotensin II on the efferent arteriole are not clear, but may include differences in levels of AT_1 receptor expression,[269] modulating actions of vasodilators such as prostaglandins and nitric oxide on preglomerular vessels[270,271] or differences in calcium responses to angiotensin II in the afferent versus efferent arterioles.[272–274] In mice, the AT_{1A} and AT_{1B} receptor isoforms have distinct actions in the glomerular circulation. Both AT_{1A} and AT_{1B} receptors contribute to the afferent arteriolar response to angiotensin II, whereas the efferent arteriolar response is mediated exclusively by AT_{1A} receptors.[275]

The overall effect of angiotensin II on glomerular hemodyamics is a predominant increase in post-glomerular resistance, resulting in an increase in glomerular hydrostatic pressure. These actions serve to protect GFR in states of intravascular volume depletion. Because angiotensin II also simultaneously reduces renal blood flow, there will be a coincident increase in filtration fraction, and a decrease in peritubular capillary pressure[276] promoting an increase in sodium reabsorption in the proximal tubule.[277,278] The importance of angiotensin II in maintaining GFR when renal perfusion is threatened is illustrated by the effect of ACE inhibitors in patients with critical bilateral renal artery stenosis or critical stenosis in the renal artery of a single functioning kidney. When blood pressures in such patients are reduced to equivalent levels with

a non-specific vasodilator, such as nitroprusside, compared to an ACE inhibitor, the ACE inhibitor causes a much more marked deterioration in GFR.[279,280]

The glomerular hemodynamic responses to angiotensin II may be modified significantly by other circulating factors. For example, the vasoconstrictor actions of angiotensin II may be substantially augmented in the presence of elevated adenosine levels.[281–285] This can occur in pathologic states including malignant hypertension, renal artery stenosis, and in some experimental models of renal ischemia.[286–288] When both angiotensin II and adenosine are present at high concentrations, there is a dramatic increase in preglomerular resistance that does not occur with either agent alone. Other mediators, such as prostanoids[289] and nitric oxide, may also modulate the actions of angiotensin II in the glomerular microcirculation, particularly in disease states such as diabetes.[290] In angiotensin II-induced hypertension, for example, nitric oxide attenuates afferent arteriolar constriction.[291]

In kidney disease, abnormal activation of the RAS and coincident increases in glomerular hydrostatic pressure have been suggested to contribute to progressive renal injury.[292,293] For example, in the remnant kidney model of chronic kidney disease, post-glomerular resistances are increased, and this is associated with increased glomerular hydrostatic pressures.[294,295] This abnormal glomerular hemodynamic pattern is reversed with RAS blockade. These observations formed the basis of the rationale for using ACE inhibitors or angiotensin receptor blockers in chronic kidney diseases. Reduction of glomerular hemodynamic pressure may be a key mechanism explaining the renoprotective effects of these agents in diseases such as diabetic nephropathy.[11,13,14]

Renal Medullary Circulation

Along with its effects on the glomerular circulation angiotensin II, acting through AT_1 receptors, has important regulatory functions in the renal circulation in general. In the mouse, regulation of renal blood flow by angiotensin II is primarily mediated by AT_{1A} receptors.[296] Moreover, effects of AT_1 receptors to modulate blood flow in the medulla significantly impact the kidney's excretory capacity for sodium.[297] In this regard, it has been suggested that regulation of medullary blood flow by angiotensin II represents a critical pathway for modulating the pressure-natriuresis response discussed earlier in the chapter.[161,276] Thus, regulation of medullary blood flow by the RAS is likely to be a key pathway used by the kidney to maintain blood pressure homeostasis.

The mechanisms controlling medullary blood flow in the kidney are complex. As in the glomerulus, vasodilator effects of mediators such as nitric oxide and prostanoids act to counterbalance the actions of angiotensin II. For example, a subpressor dose of angiotensin II, which by itself has a negligible effect on the medullary circulation, significantly reduces medullary blood flow when combined with the NO inhibitor L-NAME.[298] Cortical blood flow is unaffected in this circumstance. Nitric oxide also protects medullary blood flow during chronic infusion of angiotensin II.[299] In the outer medulla, angiotensin II stimulates NO production by tubular epithelium, potentially as a compensatory mechanism, and this may be an example of "tubulo-vascular cross-talk," whereby the effects of angiotensin II on tubular epithelium may modify its vasoconstrictor actions.[300] Similarly, renal prostaglandins also appear to modulate pressure natriuresis by altering renal medullary hemodynamics.[301] These hemodynamic changes from the inhibition of prostaglandin production lead to increased chloride reabsorption in the loop of Henle and collecting duct.[302,303]

Alterations in the balance of angiotensin II and NO in the medulla may have significant consequences on systemic blood pressure regulation. For example, angiotensin II-stimulated NO production is impaired in Dahl-sensitive hypertensive rats,[263,304,305] and attenuated generation of NO in kidneys of these animals is associated with reduced medullary blood flow.[306,307] Furthermore, delivery of L-NAME directly into the renal medulla of Dahl salt-sensitive rats reverses the hypertensive actions of angiotensin II,[305] as does intravenous infusion of L-arginine.[308]

RENAL EPITHELIAL ACTIONS OF THE RAS

Along with its hemodynamic actions, angiotensin II may modulate fluid and solute excretion through two distinct pathways: (1) an indirect pathway involving stimulation of aldosterone release from the adrenal gland; and (2) through direct effects of AT_1 receptors expressed by renal epithelia.[162]

In the adrenal cortex, activation of AT_1 receptors stimulates the release of aldosterone[119] which in turn promotes sodium reabsorption by binding to mineralocorticoid receptors in the mineralocorticoid-responsive segments of the distal nephron.[125] The biology of the aldosterone system is described elsewhere, and historically was thought to be the major effector system used by the RAS to control renal sodium handling.[123] Direct actions of angiotensin II in the kidney were defined later using isolated perfused tubules[309–314] and micropuncture studies.[315–318] Using these approaches, renal epithelial responses to angiotensin II were documented in several nephron segments. However, it has been

difficult, in the intact animal, to separate the effects of AT_1 receptors in renal epithelium from other renal and systemic effects of angiotenson II, and to determine their contribution to integrated control of blood pressure. Nonetheless, recent studies using renal cross-transplantation and regional genetic deletion clearly indicate significant, non-redundant contributions of AT_1 receptors within the kidney to determining the level of blood pressure.[232,319] Activation of AT_1 receptors in the nephron can have physiologic or pathophysiologic effects depending on the clinical context. For example, stimulation of AT_1 receptors in the proximal tubules helps to prevent circulatory collapse at baseline by promoting sodium retention,[319] whereas the accumulated stimulation of AT_1 receptors on tubular cells that occurs over the span of a normal lifetime downregulates pro-survival genes including sirtuin 3, such that AT_1 receptor deficiency is associated with enhanced longevity in mice.[320] In the next section, we will provide an overview of tubular actions of the RAS.

Tubular Effects of Angiotensin II

Proximal Tubule

Direct actions of angiotensin II in the proximal tubule are perhaps the best characterized. These actions were first implied in whole animal studies,[321–323] and then were specifically defined using *in vitro* perfused proximal tubules[313] and micropuncture studies.[317] Taken together, these studies suggest that angiotensin II, acting through AT_1 receptors on the basolateral surface of proximal tubules, promotes sodium reabsorption by coordinately stimulating the sodium-proton anti-porter on the luminal membrane along with the sodium-potassium-ATPase on the basolateral surface.[310,313,317] These actions result in enhanced basolateral sodium bicarbonate flux.[310] In addition, although angiotensin II is thought to regulate renal water handling primarily through actions in the collecting tubule (discussed below), data are emerging to suggest that AT_1 receptor activation also modulates proximal tubular expression of the aquaporin 1 channel, heretofore considered to be constitutively expressed.[324]

The capacity for proximal tubular actions of the RAS to influence blood pressure was first demonstrated in elegant experiments by Sigmund and associates.[325] In these studies, isolated co-expression of human renin and angiotensinogen in the proximal tubule caused hypertension without any detectable increase in circulating angiotensin II levels. In more recent work from this group, overexpression of the type AT_1 receptor in the proximal tubule raised baseline blood pressure levels.[326] Inversely, Gurley and colleagues showed that deletion of AT_1 receptors selectively from the proximal tubular epithelium using a Cre/loxp approach reduces the baseline level of blood pressure by diminishing fluid reabsorption from the proximal tubule, and protects from angiotensin II-induced hypertension by mitigating sodium reabsorption.[319] These studies also illustrated that angiotensin II regulates the abundance of key apical membrane sodium transporters, as AT_1 receptor deletion in the proximal tubule allowed the downregulation of the NHE3 exchanger and the NaPi2 co-transporter, thereby facilitating hypertension-induced natriuresis.[319] Complementary studies in a rat model demonstrated that angotensin II directs these transporters to redistribute within the luminal membrane microvilli of the proximal tubular cell to promote sodium and water reabsorption.[327]

AT_1 receptors are also present on the luminal brush border of the proximal tubular epithelium.[328–330] Moreover, angiotensin II is secreted into, and endocytosed from, the proximal tubular lumen where its levels may not correlate with plasma angiotensin II levels.[331–333] It has been suggested that control of angiotensin II generation in this luminal compartment might provide separate regulation of epithelial function that is independent of the systemic RAS.[334] Moreover, activation of AT_1 receptors on the luminal membrane of the proximal tubular cell can promote sodium reabsorption, in part through a G_i-protein-mediated reduction in cyclic AMP.[313,317,333] There is some evidence for an independent regulation of luminal concentrations of angiotensin II. For example, although both whole kidney and proximal tubular angiotensin II levels are elevated in response to reduced renal perfusion,[335] angiotensin II levels in proximal tubular fluid are not suppressed with acute volume expansion, and may even increase in this setting.[335,336]

The net effect of angiotensin II on bicarbonate handling in the proximal tubule appears to be neutral. Coordinating with its stimulation of the apical membrane sodium-proton exchanger, angiotensin II enhances the activity of the sodium-bicarbonate co-transporter on the basolateral surface of the early proximal tubule.[310,313] As such, angiotensin II acts as a potent stimulus for proximal acidification, coupled to reclamation of bicarbonate from the early proximal tubule.[310,337,338] Nevertheless, the resulting reduction in delivery of bicarbonate to the late proximal tubule leads to less bicarbonate reabsorption in that segment. Moreover, at higher concentrations, angiotensin II paradoxically inhibits sodium-bicarbonate transporter activity,[339] such that overall the bicarbonate concentration in the urinary filtrate reaching the distal convoluted tubule is not altered by angiotensin II stimulation.[340] Thus, the contribution of the RAS to acid–base regulation is primarily mediated by aldosterone in the distal nephron.[341–345]

Loop of Henle

Compared to the proximal tubule, the functions of angiotensin II in the medullary thick ascending limb (MTAL) are not as well-characterized. AT_1 receptors are expressed on both the luminal and basolateral membranes of the MTAL epithelium.[346,347] *In vitro* studies addressing the role of angiotensin II in MTAL ion transport suggest that cellular responses may differ, depending on the local concentrations of angiotensin II.[348,349] At lower concentrations of angiotensin II, inhibition of the sodium-potassium-chloride co-transporter (NKCC2) may be seen,[348,349] whereas stimulation of NKCC2 can be seen at higher concentrations.[348] *In vivo* microperfusion experiments have also demonstrated physiological consequences of angiotensin II in the MTAL, including increased bicarbonate transport out of the urinary filtrate.[350] This heightened bicarbonate flux is likely due to an increase in sodium–hydrogen exchange, as has been observed in the proximal tubule, suggesting that angiotensin II increases sodium reabsorption from the MTAL. These data are consistent with the finding that *in vivo* administration of angiotensin II leads to heightened expression of both the NHE3 sodium-hydrogen exchanger and NKCC2 in the MTAL.[351]

Distal Nephron

SOLUTE TRANSPORT

Although angiotensin II indirectly influences distal and collecting tubular function through the generation of aldosterone, more recent studies have demonstrated that angiotensin II also has direct effects in modulating ion flux along the distal nephron. As in other nephron segments, all the elements of the RAS are present along the distal nephron, and relatively high concentrations of angiotensin II can be detected in the tubular fluid of these segments.[171,330,332] Angiotensin II, acting via AT_1 receptors, stimulates sodium–hydrogen exchange in the cortical and outer medullary collecting tubule by increasing the density of the vacuolar sodium-hydrogen-ATPase in the apical membrane of the type A intercalated cell, which in turn leads to an increase in bicarbonate reabsorption.[315,316,352,353] On the apical membrane of the principal cells in the cortical collecting duct (CCD), luminal angiotensin II stimulates amiloride-sensitive sodium transport by increasing activity of the epithelial sodium channel (ENaC) through an AT_1 receptor-dependent mechanism.[312,318] Furthermore, activation of AT_1 receptors on the basolateral membrane of CCD cells stimulates the activity of potassium channels via a nitric oxide-dependent pathway.[354] As the distal nephron ultimately determines urine flow and composition, actions of angiotensin II to modulate sodium handling at this site may impact blood pressure homeostasis.[164,312]

WATER HANDLING

Recent studies suggest a role for the RAS in the control of urinary concentrating mechanisms and free water handling. For example, the complete absence of angiotensinogen, ACE or AT_{1A}/AT_{1B} receptors in mice is associated with atrophy of the renal papilla and a marked urinary concentrating defect.[230,355,356] Mice lacking AT_{1A} receptors are also unable to generate maximally concentrated urine, despite having apparently normal renal papillae.[357] These animals generate vasopressin normally in response to water restriction, but are resistant to dDAVP.[357] Administration of an AT_1 receptor-antagonist to wild-type mice, and even selective deletion of AT_1 receptors from the collecting duct using a Cre/loxp approach, recapitulates this urinary concentrating defect.[357,358] Similarly, AT_1 receptor blockade also blunts the maximal urine concentrating capacity in DDAVP-challenged rats, and this effect is associated with reduced expression of aquaporins-1 and -2.[359] In the medullary collecting duct, angiotensin II upregulates gene expression for the V_2 vasopressin receptor, and the expression and apical membrane targeting of the aquaporin-2 channel.[360–363] These effects are mediated through a protein kinase A-dependent pathway.[360] Thus, direct effects of angiotensin II on expression of water channels and perhaps vasopressin receptors may contribute to its actions on renal water handling.

References

[1] Tiret L, Bonnardeaux A, Poirier O, Ricard S, Marques-Vidal P, Evans A, et al. Synergistic effects of angiotensin converting enzyme and angiotensin II type I receptor polymorphisms on risk of myocardial infarction. Lancet 1994;344:910–3.

[2] Jeunemaitre X, Soubrier F, Kotelevtsev YV, Lifton RP, Williams CS, Charru A, et al. Molecular basis of human hypertension: role of angiotensinogen. Cell 1992;71(1):169–80.

[3] Bonnardeaux A, Davies E, Jeunemaitre X, Féry I, Charru A, Clauser E, et al. Angiotensin II type 1 receptor gene polymorphisms in human essential hypertension. Hypertension 1994;24:63–9.

[4] Benetos A, Gautier S, Ricard S, Topouchian J, Asmar R, Poirier O, et al. Angiotensin-converting enzyme inhibitors: influence of angiotensin-converting enzyme and angiotensin II type 1 receptor gene polymorphisms on aortic stiffness in normotensive and hypertensive patients. Circulation 1996;94:698–703.

[5] Wang J, Staessen J. Genetic polymorphisms in the renin–angiotensin system: relevance for susceptibility to cardiovascular disease. Eur J Pharmacol 2000;410:289–302.

[6] Yoshida H, Kon V, Ichikawa I. Polymorphisms of the renin–angiotensin system genes in progressive renal diseases. Kidney Int 1996;50:732–44.

[7] Husain A, Drugs Graham R. Enzymes and Receptors of the Renin-Angiotensin System: Celebrating a Century of Discovery. Sidney: Harwood Academic; 2000.
[8] Investigators TS. Effect of enalapril on survival in patients with reduced left ventricular ejection fractions and congestive heart failure. The SOLVD Investigators. N Engl J Med 1991;325:293–302.
[9] Investigators TS. Effect of enalapril on mortality and the development of heart failure in asymptomatic patients with reduced left ventricular ejection fractions. The SOLVD Investigators. N Engl J Med 1992;327:725–7.
[10] Yusuf S, Sleight P, Pogue J, Bosch J, Davies R, Dagenais G. Effects of an angiotensin-converting-enzyme inhibitor, ramipril, on cardiovascular events in high-risk patients. The Heart Outcomes Prevention Evaluation Study Investigators. N Engl J Med 2000;342(3):145–53.
[11] Lewis EJ, Hunsicker LG, Bain RP, Rohde RD. The effect of angiotensin-converting-enzyme inhibition on diabetic nephropathy. The Collaborative Study Group. N Engl J Med 1993;329 (20):1456–62.
[12] Dahlof B, Devereux RB, Kjeldsen SE, Julius S, Beevers G, de Faire U, et al. Cardiovascular morbidity and mortality in the Losartan Intervention For Endpoint reduction in hypertension study (LIFE): a randomised trial against atenolol. Lancet 2002;359(9311):995–1003.
[13] Lewis EJ, Hunsicker LG, Clarke WR, Berl T, Pohl MA, Lewis JB, et al. Renoprotective effect of the angiotensin-receptor antagonist irbesartan in patients with nephropathy due to type 2 diabetes. N Engl J Med 2001;345(12):851–60.
[14] Brenner BM, Cooper ME, de Zeeuw D, Keane WF, Mitch WE, Parving HH, et al. Effects of losartan on renal and cardiovascular outcomes in patients with type 2 diabetes and nephropathy. N Engl J Med 2001;345(12):861–9.
[15] Danser AH, Deinum J. Renin, pro-renin and the putative (pro) renin receptor. Hypertension 2005;46(5):1069–76.
[16] Luetscher JA, Kraemer FB, Wilson DM, Schwartz HC, Bryer-Ash M. Increased plasma inactive renin in diabetes mellitus. A marker of microvascular complications. N Engl J Med 1985;312(22):1412–7.
[17] Deinum J, Ronn B, Mathiesen E, Derkx FH, Hop WC, Schalekamp MA. Increase in serum pro-renin precedes onset of microalbuminuria in patients with insulin-dependent diabetes mellitus. Diabetologia 1999;42(8):1006–10.
[18] Veniant M, Menard J, Bruneval P, Morley S, Gonzales MF, Mullins J. Vascular damage without hypertension in transgenic rats expressing pro-renin exclusively in the liver. J Clin Invest 1996;98(9):1966–70.
[19] Peters J, Farrenkopf R, Clausmeyer S, Zimmer J, Kantachuvesiri S, Sharp MG, et al. Functional significance of pro-renin internalization in the rat heart. Circ Res 2002;90(10):1135–41.
[20] Peach MJ. Renin–angiotensin system: Biochemistry and mechanisms of action. Physiol Rev 1977;57(2):313–70.
[21] Bock HA, Hermle M, Brunner FP, Thiel G. Pressure dependent modulation of renin release in isolated perfused glomeruli. Kidney Int 1992;41(2):275–80.
[22] Carey RM, McGrath HE, Pentz ES, Gomez RA, Barrett PQ. Biomechanical coupling in renin-releasing cells. J Clin Invest 1997;100(6):1566–74.
[23] Lorenz JN, Weihprecht H, Schnermann J, Skott O, Briggs JP. Renin release from isolated juxtaglomerular apparatus depends on macula densa chloride transport. Am J Physiol 1991;260(4 Pt 2):F486–493.
[24] Bell PD, Lapointe JY, Sabirov R, Hayashi S, Peti-Peterdi J, Manabe K, et al. Macula densa cell signaling involves ATP release through a maxi anion channel. Proc Natl Acad Sci USA 2003;100(7):4322–7.
[25] Lorenz JN, Weihprecht H, He XR, Skott O, Briggs JP, Schnermann J. Effects of adenosine and angiotensin on macula densa-stimulated renin secretion. Am J Physiol 1993;265(2 Pt 2): F187–194.
[26] Admiraal PJ, van Kesteren CA, Danser AH, Derkx FH, Sluiter W, Schalekamp MA. Uptake and proteolytic activation of pro-renin by cultured human endothelial cells. J Hypertens 1999;17(5):621–9.
[27] Nguyen G, Delarue F, Burckle C, Bouzhir L, Giller T, Sraer JD. Pivotal role of the renin/pro-renin receptor in angiotensin II production and cellular responses to renin. J Clin Invest 2002;109(11):1417–27.
[28] van Kesteren CA, Danser AH, Derkx FH, Dekkers DH, Lamers JM, Saxena PR, et al. Mannose 6-phosphate receptor–mediated internalization and activation of pro-renin by cardiac cells. Hypertension 1997;30(6):1389–96.
[29] Nguyen G. Renin/pro-renin receptors. Kidney Int 2006;69 (9):1503–6.
[30] Burckle C, Bader M. Pro-renin and its ancient receptor. Hypertension 2006;48(4):549–51.
[31] Burckle CA, Jan Danser AH, Muller DN, Garrelds IM, Gasc JM, Popova E, et al. Elevated blood pressure and heart rate in human renin receptor transgenic rats. Hypertension 2006;47 (3):552–6.
[32] Hirose T, Hashimoto M, Totsune K, Metoki H, Asayama K, Kikuya M, et al. Association of (pro)renin receptor gene polymorphism with blood pressure in Japanese men: the Ohasama study. Am J Hypertens 2009;22(3):294–9.
[33] Nguyen G, Muller DN. The biology of the (pro)renin receptor. J Am Soc Nephrol 2010;21(1):18–23.
[34] Ramser J, Abidi FE, Burckle CA, Lenski C, Toriello H, Wen G, et al. A unique exonic splice enhancer mutation in a family with X-linked mental retardation and epilepsy points to a novel role of the renin receptor. Hum Mol Genet 2005;14(8):1019–27.
[35] Kinouchi K, Ichihara A, Sano M, Sun-Wada GH, Wada Y, Kurauchi-Mito A, et al. The (pro)renin receptor/ATP6AP2 is essential for vacuolar H^+-ATPase assembly in murine cardiomyocytes. *Circ Res* 2010;107(1):30–4.
[36] Cruciat CM, Ohkawara B, Acebron SP, Karaulanov E, Reinhard C, Ingelfinger D, et al. Requirement of pro-renin receptor and vacuolar H^+-ATPase-mediated acidification for Wnt signaling. *Science* 2010;327(5964):459–63.
[37] Yanai K, Saito T, Kakinuma Y, Kon Y, Hirota K, Taniguchi-Yanai K, et al. Renin-dependent cardiovascular functions and renin-independent blood–brain barrier functions revealed by renin-deficient mice. J Biol Chem 2000;275(1):5–8.
[38] Oshima Y, Kinouchi K, Ichihara A, Sakoda M, Kurauchi-Mito A, Bokuda K, et al. Pro-renin receptor is essential for normal podocyte structure and function. *J Am Soc Nephrol* 2011;22 (12):2203–12.
[39] Riediger F, Quack I, Qadri F, Hartleben B, Park JK, Potthoff SA, et al. Pro-renin receptor is essential for podocyte autophagy and survival. *J Am Soc Nephrol* 2011;22(12):2193–202.
[40] Gould AB, Green D. Kinetics of the human renin and human substrate reaction. Cardiovasc Res 1971;5(1):86–9.
[41] Inoue I, Nakajima T, Williams CS, Quackenbush J, Puryear R, Powers M, et al. A nucleotide substitution in the promoter of human angiotensinogen is associated with essential hypertension and affects basal transcription *in vitro*. J Clin Invest 1997;99 (7):1786–97.
[42] Kim HS, Krege JH, Kluckman KD, Hagaman JR, Hodgin JB, Best CF, et al. Genetic control of blood pressure and the

angiotensinogen locus. Proc Natl Acad Sci USA 1995;92 (7):2735–9.
[43] Dickson ME, Sigmund CD. Genetic basis of hypertension: revisiting angiotensinogen. Hypertension 2006;48(1):14–20.
[44] Ingelfinger JR, Zuo WM, Fon EA, Ellison KE, Dzau VJ. *In situ* hybridization evidence for angiotensinogen messenger RNA in the rat proximal tubule. An hypothesis for the intrarenal renin angiotensin system. J Clin Invest 1990;85(2):417–23.
[45] Kobori H, Harrison-Bernard LM, Navar LG. Expression of angiotensinogen mRNA and protein in angiotensin II-dependent hypertension. J Am Soc Nephrol 2001;12(3):431–9.
[46] Dzau VJ, Ellison KE, Brody T, Ingelfinger J, Pratt RE. A comparative study of the distributions of renin and angiotensinogen messenger ribonucleic acids in rat and mouse tissues. Endocrinology 1987;120(6):2334–8.
[47] Corvol P, Williams TA, Soubrier F. Peptidyl dipeptidase A: Angiotensin I-converting enzyme. Methods Enzymol 1995;248:283–305.
[48] Ehlers MR, Fox EA, Strydom DJ, Riordan JF. Molecular cloning of human testicular angiotensin-converting enzyme: the testis isozyme is identical to the C-terminal half of endothelial angiotensin-converting enzyme. Proc Natl Acad Sci USA 1989;86 (20):7741–5.
[49] Hubert C, Houot AM, Corvol P, Soubrier F. Structure of the angiotensin I-converting enzyme gene. Two alternate promoters correspond to evolutionary steps of a duplicated gene. J Biol Chem 1991;266(23):15377–83.
[50] Langford KG, Shai SY, Howard TE, Kovac MJ, Overbeek PA, Bernstein KE. Transgenic mice demonstrate a testis-specific promoter for angiotensin-converting enzyme. J Biol Chem 1991;266 (24):15559–62.
[51] Beldent V, Michaud A, Wei L, Chauvet MT, Corvol P. Proteolytic release of human angiotensin-converting enzyme. Localization of the cleavage site. J Biol Chem 1993;268 (35):26428–34.
[52] Sayed-Tabatabaei FA, Oostra BA, Isaacs A, van Duijn CM, Witteman JC. ACE polymorphisms. Circ Res 2006;98(9):1123–33.
[53] Rigat B, Hubert C, Alhenc-Gelas F, Cambien F, Corvol P, Soubrier F. An insertion/deletion polymorphism in the angiotensin I-converting enzyme gene accounting for half the variance of serum enzyme levels. J Clin Invest 1990;86(4):1343–6.
[54] Villard E, Tiret L, Visvikis S, Rakotovao R, Cambien F, Soubrier F. Identification of new polymorphisms of the angiotensin I-converting enzyme (ACE) gene, and study of their relationship to plasma ACE levels by two-QTL segregation-linkage analysis. Am J Hum Genet 1996;58(6):1268–78.
[55] Takahashi N, Smithies O. Human genetics, animal models and computer simulations for studying hypertension. Trends Genet 2004;20(3):136–45.
[56] Margolius HS. Kallikreins and kinins. Molecular characteristics and cellular and tissue responses. Diabetes 1996;45(Suppl 1): S14–19.
[57] Campbell DJ, Alexiou T, Xiao HD, Fuchs S, McKinley MJ, Corvol P, et al. Effect of reduced angiotensin-converting enzyme gene expression and angiotensin-converting enzyme inhibition on angiotensin and bradykinin peptide levels in mice. Hypertension 2004;43(4):854–9.
[58] Gainer JV, Morrow JD, Loveland A, King DJ, Brown NJ. Effect of bradykinin-receptor blockade on the response to angiotensin-converting-enzyme inhibitor in normotensive and hypertensive subjects. N Engl J Med 1998;339(18):1285–92.
[59] Donoghue M, Hsieh F, Baronas E, Godbout K, Gosselin M, Stagliano N, et al. A novel angiotensin-converting enzyme-related carboxypeptidase (ACE2) converts angiotensin I to angiotensin 1-9. Circ Res 2000;87(5):E1–9.
[60] Tipnis SR, Hooper NM, Hyde R, Karran E, Christie G, Turner AJ. A human homolog of angiotensin-converting enzyme. Cloning and functional expression as a captopril-insensitive carboxypeptidase. J Biol Chem 2000;275(43):33238–43.
[61] Zhang H, Wada J, Hida K, Tsuchiyama Y, Hiragushiet K, Shikata K, et al. Collectrin, a collecting duct-specific transmembrane glycoprotein, is a novel homolog of ACE2 and is developmentally regulated in embryonic kidneys. J Biol Chem 2001;276(20):17132–9.
[62] Vickers C, Hales P, Kaushik V, Dick L, Gavin J, Tang J, et al. Hydrolysis of biological peptides by human angiotensin-converting enzyme-related carboxypeptidase. J Biol Chem 2002;277 (17):14838–43.
[63] Ferrario C, Brosnihan K, Diz D, Jaiswal N, Khosla MC, Milsted A, et al. Angiotensin-(1-7): a new hormone of the angiotensin system. Hypertension 1991;18: [III-126-133]
[64] Santos RA, Simoes e Silva AC, Maric C, Silva DM, Machado RP, de Buhr I, et al. Angiotensin-(1-7) is an endogenous ligand for the G protein-coupled receptor Mas. Proc Natl Acad Sci USA 2003;100(14):8258–63.
[65] Ferrario CM, Trask AJ, Jessup JA. Advances in biochemical and functional roles of angiotensin-converting enzyme 2 and angiotensin-(1-7) in regulation of cardiovascular function. Am J Physiol Heart Circ Physiol 2005;289(6):H2281–2290.
[66] Gurley SB, Allred A, Le TH, Griffiths R, Mao L, Philip N, et al. Altered blood pressure responses and normal cardiac phenotype in ACE2-null mice. J Clin Invest 2006;116 (8):2218–25.
[67] Oudit GY, Herzenberg AM, Kassiri Z, Wong D, Reich H, Khokha R, et al. Loss of angiotensin-converting enzyme-2 leads to the late development of angiotensin II-dependent glomerulosclerosis. Am J Pathol 2006;168(6):1808–20.
[68] Oudit GY, Liu GC, Zhong J, Basu R, Chow FL, Zhou J, et al. Human recombinant ACE2 reduces the progression of diabetic nephropathy. *Diabetes* 2009;59(2):529–38.
[69] Wong DW, Oudit GY, Reich H, Kassiri Z, Zhou J, Liu QC, et al. Loss of angiotensin-converting enzyme-2 (Ace2) accelerates diabetic kidney injury. Am J Pathol 2007;171(2):438–51.
[70] Wysocki J, Ye M, Soler MJ, Gurley SB, Xiao HD, Bernstein KE, et al. ACE and ACE2 activity in diabetic mice. Diabetes 2006;55 (7):2132–9.
[71] Gurley SB, Coffman TM. Angiotensin-converting enzyme 2 gene targeting studies in mice: mixed messages. Exp Physiol 2008;93(5):538–42.
[72] Zhong J, Guo D, Chen CB, Wang W, Schuster M, Loibner H, et al. Prevention of angiotensin II-mediated renal oxidative stress, inflammation, and fibrosis by angiotensin-converting enzyme 2. *Hypertension* 2010;57(2):314–22.
[73] Zhang H, Wada J, Kanwar YS, Tsuchiyama Y, Hiragushi K, Hida K, et al. Screening for genes upregulated in 5/6 nephrectomized mouse kidney. Kidney Int 1999;56(2):549–58.
[74] Malakauskas SM, Quan H, Fields TA, McCall SJ, Yu MJ, Kourany WM, et al. Aminoaciduria and altered renal expression of luminal amino acid transporters in mice lacking novel gene collectrin. Am J Physiol Renal Physiol 2007;292(2): F533–544.
[75] Danilczyk U, Sarao R, Remy C, Benabbas C, Stange G, Richter A, et al. Essential role for collectrin in renal amino acid transport. Nature 2006;444(7122):1088–91.
[76] Timmermans PB, Wong PC, Chiu AT, Herblin WF, Benfield P, Carini DJ, et al. Angiotensin II receptors and angiotensin II receptor antagonists. Pharmacol Rev 1993;45(2):205–51.
[77] Tharaux P-L, Coffman TM. Transgenic mice as a tool to study the renin–angiotensin system. Contrib Nephrol 2001;135:72–91.

[78] Murphy TJ, Alexander RW, Griendling KK, Runge MS, Bernstein KE. Isolation of a cDNA encoding the vascular type-1 angiotensin II receptor. Nature 1991;351(6323):233–6.
[79] Sasaki K, Yamano Y, Bardhan S, Iwai N, Murray JJ, Hasegawa M, et al. Cloning and expression of a complementary DNA encoding a bovine adrenal angiotensin II type-1 receptor. Nature 1991;351(6323):230–3.
[80] Inagami T, Iwai N, Sasaki K, Yamamo Y, Bardhan S, Chaki S, et al. Cloning, expression and regulation of angiotensin II receptors. J Hypertens 1992;10(8):713–6.
[81] Sandberg K, Ji H, Clark AJ, Shapira H, Catt KJ. Cloning and expression of a novel angiotensin II receptor subtype. J Biol Chem 1992;267(14):9455–8.
[82] Iwai N, Inagami T. Identification of two subtypes in the rat type I angiotensin receptor. FEBS Letts 1992;298:257–60.
[83] Kakar S, Riel K, Neill J. Differential expression of angiotensin II receptor subtype mRNAs (AT-1A and AT-1B) in the brain. Biochem Biophys Res Comm 1992;185:688–92.
[84] Sasamura H, Hein L, Krieger JE, Pratt RE, Kobilka BK, Dzau VJ. Cloning, characterization, and expression of two angiotensin receptor (AT-1) isoforms from the mouse genome. Biochem Biophys Res Commun 1992;185(1):253–9.
[85] de Gasparo M, Catt KJ, Inagami T, Wright JW, Unger T. International union of pharmacology. XXIII. The angiotensin II receptors. Pharmacol Rev 2000;52(3):415–72.
[86] Marrero M, Schieffer B, Paxton W, Heerdt L, Berk BC, Delafontaine P, et al. Direct stimulation of Jak/STAT pathway by the angiotensin II AT_1 receptor. Nature 1995;375:247–50.
[87] Rakesh K,, Yoo B,, Kim IM,, Salazar N,, Kim KS,, Rockman HA. beta-Arrestin-biased agonism of the angiotensin receptor induced by mechanical stress. *Sci Signal*.3(125):ra46.
[88] Shenoy SK, Lefkowitz RJ. Angiotensin II-stimulated signaling through G proteins and beta-arrestin. Sci STKE 2005;(311): cm14.
[89] Ahn D, Ge Y, Stricklett PK, Gill P, Taylor D, Hughes AK, et al. Collecting duct-specific knockout of endothelin-1 causes hypertension and sodium retention. J Clin Invest 2004;114 (4):504–11.
[90] Yasuda N,, Akazawa H,, Ito K,, Shimizu I,, Kudo-Sakamoto Y,, Yabumoto C,, et al. Agonist-independent constitutive activity of angiotensin II receptor promotes cardiac remodeling in mice. *Hypertension*. March;59(3):627-633.
[91] Eguchi S, Numaguchi K, Iwasaki H, Matsumoto T, Yamakawa T, Utsunomiya H, et al. Calcium-dependent epidermal growth factor receptor transactivation mediates the angiotensin II-induced mitogen-activated protein kinase activation in vascular smooth muscle cells. J Biol Chem 1998;273(15):8890–6.
[92] Lautrette A, Li S, Alili R, Sunnarborg SW, Burtin M, Lee DC, et al. Angiotensin II and EGF receptor cross-talk in chronic kidney diseases: a new therapeutic approach. Nat Med 2005;11(8):867–74.
[93] Burson JM, Aguilera G, Gross KW, Sigmund CD. Differential expression of angiotensin receptor 1A and 1B in mouse. Am J Physiol 1994;267(2 Pt 1):E260–267.
[94] Iwai N, Inagami T, Ohmichi N, Nakamura Y, Saeki Y, Kinoshita M. Differential regulation of rat AT1a and AT1b receptor mRNA. Biochem Biophys Res Commun 1992;188 (1):298–303.
[95] Gasc JM, Shanmugam S, Sibony M, Corvol P. Tissue-specific expression of type 1 angiotensin II receptor subtypes. An *in situ* hybridization study. Hypertension 1994;24(5):531–7.
[96] Llorens-Cortes C, Greenberg B, Huang H, Corvol P. Tissular expression and regulation of type 1 angiotensin II receptor subtypes by quantitative reverse transcriptase-polymerase chain reaction analysis. Hypertension 1994;24(5):538–48.
[97] Konishi H, Kuroda S, Inada Y, Fujisawa Y. Novel subtype of human angiotensin II type 1 receptor: cDNA cloning and expression. Biochem Biophys Res Commun 1994;199 (2):467–74.
[98] Chiu A, Dunscomb J, McCall D, Benfield P, Baubonis W, Sauer B. Characterization of angiotensin AT1A receptor isoform by it ligand binding signature. Regul Pept 1993;44:141–7.
[99] Oliverio MI, Best CF, Kim HS, Arendshorst WJ, Smithies O, Coffman TM. Angiotensin II responses in AT1A receptor-deficient mice: a role for AT1B receptors in blood pressure regulation. Am J Physiol 1997;272(4 Pt 2):F515–520.
[100] Oliverio MI, Kim HS, Ito M, Le T, Audoly L, Best CF, et al. Reduced growth, abnormal kidney structure, and type 2 (AT2) angiotensin receptor-mediated blood pressure regulation in mice lacking both AT1A and AT1B receptors for angiotensin II. Proc Natl Acad Sci USA 1998;95(26):15496–501.
[101] Davisson RL, Oliverio MI, Coffman TM, Sigmund CD. Divergent functions of angiotensin II receptor isoforms in the brain. J Clin Invest 2000;106(1):103–6.
[102] Ito M, Oliverio MI, Mannon PJ, Best CF, Maeda N, Smithies O, et al. Regulation of blood pressure by the type 1A angiotensin II receptor gene. Proc Natl Acad Sci USA 1995;92 (8):3521–5.
[103] Matsusaka T, Nishimura H, Utsunomiya H, Kakuchi J, Nijmura F, Inagami T, et al. Chimeric mice carrying "regional" targeted deletion of the angiotensin type 1A receptor gene. Evidence against the role for local angiotensin in the *in vivo* feedback regulation of renin synthesis in juxtaglomerular cells. J Clin Invest 1996;98(8):1867–77.
[104] Sugaya T, Nishimatsu S, Tanimoto K, Takimoto E, Yamagishi T, Imamura K, et al. Angiotensin II type 1a receptor-deficient mice with hypotension and hyperreninemia. J Biol Chem 1995;270 (32):18719–22.
[105] Oliverio MI, Best CF, Smithies O, Coffman TM. Regulation of sodium balance and blood pressure by the AT(1A) receptor for angiotensin II. Hypertension 2000;35(2):550–4.
[106] Grady E, Sechi L, Griffn C, Schambelan M, Kalinyak J. Expression of AT2 receptors in the developing rat fetus. J Clin Invest 1991;88:921–33.
[107] Millan M, Carvallo P, Izumi S-I, Zemel S, Catt K, Aguilera G. Novel sites of expression of functional angiotensin II receptors in the late gestation fetus. Science 1989;244:1340–2.
[108] Ichiki T, Kambayashi Y, Inagami T. Multiple growth factors modulate mRNA expression of angiotensin II type-2 receptor in R3T3 cells. Circ Res 1995;77(6):1070–6.
[109] Berry C, Touyz R, Dominiczak AF, Webb RC, Johns DG. Angiotensin receptors: Signaling, vascular pathophysiology, and interactions with ceramide. Am J Physiol Heart Circ Physiol 2001;281(6):H2337–2365.
[110] Hayashida W, Horiuchi M, Dzau VJ. Intracellular third loop domain of angiotensin II type-2 receptor. Role in mediating signal transduction and cellular function. J Biol Chem 1996;271 (36):21985–92.
[111] Lehtonen JY, Daviet L, Nahmias C, Horiuchi M, Dzau VJ. Analysis of functional domains of angiotensin II type 2 receptor involved in apoptosis. Mol Endocrinol 1999;13(7):1051–60.
[112] Carey RM, Wang ZQ, Siragy HM. Role of the angiotensin type 2 receptor in the regulation of blood pressure and renal function. Hypertension 2000;35(1 Pt 2):155–63.
[113] Siragy HM, Carey RM. The subtype-2 (AT2) angiotensin receptor regulates renal cyclic guanosine 3′,5′-monophosphate and AT1 receptor-mediated prostaglandin E2 production in conscious rats. J Clin Invest 1996;97(8):1978–82.
[114] Dulin NO, Alexander LD, Harwalkar S, Falck JR, Douglas JG. Phospholipase A2-mediated activation of mitogen-activated

protein kinase by angiotensin II. Proc Natl Acad Sci USA 1998;95(14):8098–102.
[115] Hein L, Barsh GS, Pratt RE, Dzau VJ, Kobilka BK. Behavioural and cardiovascular effects of disrupting the angiotensin II type-2 receptor in mice. Nature 1995;377(6551):744–7.
[116] Ichiki T, Labosky PA, Shiota C, Okuyama S, Imagawa Y, Fogo A, et al. Effects on blood pressure and exploratory behaviour of mice lacking angiotensin II type-2 receptor. Nature 1995;377(6551):748–50.
[117] Masaki H, Kurihara T, Yamaki A, Inomata N, Nozawa Y, Mori Y, et al. Cardiac-specific overexpression of angiotensin II AT2 receptor causes attenuated response to AT1 receptor-mediated pressor and chronotropic effects. J Clin Invest 1998;101(3):527–35.
[118] Steckelings UM, Larhed M, Hallberg A, Widdop RE, Jones ES, Wallinder C, et al. Non-peptide AT2-receptor agonists. *Curr Opin Pharmacol* 2011;11(2):187–92.
[119] Aguilera G. Role of angiotensin II receptor subtypes on the regulation of aldosterone secretion in the adrenal glomerulosa zone in the rat. Mol Cell Endocrinol 1992;90(1):53–60.
[120] Okubo S, Niimura F, Nishimura H, Takemoto F, Fogo A, Matsusaka T, et al. Angiotensin-independent mechanism for aldosterone synthesis during chronic extracellular fluid volume depletion. J Clin Invest 1997;99(5):855–60.
[121] Quinn SJ, Williams GH. Regulation of aldosterone secretion. Annu Rev Physiol 1988;50:409–26.
[122] Aguilera G. Factors controlling steroid biosynthesis in the zona glomerulosa of the adrenal. J Steroid Biochem Mol Biol 1993;45(1-3):147–51.
[123] Fuller PJ, Young MJ. Mechanisms of mineralocorticoid action. Hypertension 2005;46(6):1227–35.
[124] Rogerson FM, Fuller PJ. Mineralocorticoid action. Steroids 2000;65(2):61–73.
[125] Masilamani S, Kim GH, Mitchell C, Wade JB, Knepper MA. Aldosterone-mediated regulation of ENaC alpha, beta, and gamma subunit proteins in rat kidney. J Clin Invest 1999;104 (7):R19–23.
[126] Asher C, Wald H, Rossier BC, Garty H. Aldosterone-induced increase in the abundance of Na^+ channel subunits. Am J Physiol 1996;271(2 Pt 1):C605–611.
[127] Gumz ML, Stow LR, Lynch IJ, Greenlee MM, Rudin A, Cain BD, et al. The circadian clock protein Period 1 regulates expression of the renal epithelial sodium channel in mice. J Clin Invest 2009;119(8):2423–34.
[128] Naray-Fejes-Toth A. Sgk: a new player (star?) in the early action of aldosterone. News Physiol Sci 1999;14:274–5.
[129] Brennan FE, Fuller PJ. Rapid upregulation of serum and glucocorticoid-regulated kinase (sgk) gene expression by corticosteroids *in vivo*. Mol Cell Endocrinol 2000;166(2):129–36.
[130] Bhargava A, Fullerton MJ, Myles K, Purdy TM, Funder JW, Pearce D, et al. The serum- and glucocorticoid-induced kinase is a physiological mediator of aldosterone action. Endocrinology 2001;142(4):1587–94.
[131] Zhang W, Xia X, Reisenauer MR, Rieg T, Lang F, Kuhl D, et al. Aldosterone-induced Sgk1 relieves Dot1a-Af9-mediated transcriptional repression of epithelial Na^+ channel alpha. J Clin Invest 2007;117(3):773–83.
[132] McCormick JA, Bhalla V, Pao AC, Pearce D. SGK1: a rapid aldosterone-induced regulator of renal sodium reabsorption. Physiology (Bethesda) 2005;20:134–9.
[133] Vallon V, Wulff P, Huang DY, Loffing J, Völkl H, Kuhl D, et al. Role of Sgk1 in salt and potassium homeostasis. Am J Physiol Regul Integr Comp Physiol 2005;288(1):R4–10.
[134] Yoo D, Kim BY, Campo C, Nance L, King A, Maouyo D, et al. Cell surface expression of the ROMK (Kir 1.1) channel is regulated by the aldosterone-induced kinase, SGK-1, and protein kinase A. J Biol Chem 2003;278(25):23066–75.
[135] Beesley AH, Hornby D, White SJ. Regulation of distal nephron K^+ channels (ROMK) mRNA expression by aldosterone in rat kidney. J Physiol 1998;509(Pt 3):629–34.
[136] Rozansky DJ. Cornwall T, Subramanya AR, Rogers S, Yang YF, David LL, Zhu X, Yang CL, Ellison DH. Aldosterone mediates activation of the thiazide-sensitive Na-Cl co-transporter through an SGK1 and WNK4 signaling pathway. J Clin Invest 2009;119(9):2601–12.
[137] Geller DS, Farhi A, Pinkerton N, Fradley M, Moritz M, Spitzer A, et al. Activating mineralocorticoid receptor mutation in hypertension exacerbated by pregnancy. Science 2000;289(5476):119–23.
[138] Geller DS, Rodriguez-Soriano J, Vallo Boado A, Schifter S, Bayer M, Chang SS, et al. Mutations in the mineralocorticoid receptor gene cause autosomal dominant pseudohypoaldosteronism type I. Nat Genet 1998;19(3):279–81.
[139] Berger S, Bleich M, Schmid W, Cole TJ, Peters J, Watanabe H, et al. Mineralocorticoid receptor knockout mice: Pathophysiology of Na^+ metabolism. PNAS 1998;95(16):9424–9.
[140] Ronzaud C, Loffing J, Bleich M, Gretz N, Grone HJ, Schutz G, et al. Impairment of sodium balance in mice deficient in renal principal cell mineralocorticoid receptor. J Am Soc Nephrol 2007;18(6):1679–87.
[141] Pergher PS, Leite-Dellova D, de Mello-Aires M. Direct action of aldosterone on bicarbonate reabsorption in *in vivo* cortical proximal tubule. Am J Physiol Renal Physiol 2009;296(5): F1185–1193.
[142] Leite-Dellova DC, Oliveira-Souza M, Malnic G, Mello-Aires M. Genomic and nongenomic dose-dependent biphasic effect of aldosterone on Na^+/H^+ exchanger in proximal S3 segment: role of cytosolic calcium. Am J Physiol Renal Physiol 2008;295 (5):F1342–1352.
[143] Watts 3rd BA, George T, Good DW. Aldosterone inhibits apical NHE3 and HCO_3^- absorption via a nongenomic ERK-dependent pathway in medullary thick ascending limb. Am J Physiol Renal Physiol 2006;291(5):F1005–1013.
[144] Lifton R. Genetic determinants of human hypertension. PNAS 1995;92(19):8545–51.
[145] Firsov D, Schild L, Gautschi I, Merillat A-M, Schneeberger E, Rossier Bernard C. Cell surface expression of the epithelial Na channel and a mutant causing Liddle syndrome: a quantitative approach. PNAS 1996;93(26):15370–5.
[146] Tamura H, Schild L, Enomoto N, Matsui N, Marumo F, Rossier BC. Liddle disease caused by a missense mutation of beta subunit of the epithelial sodium channel gene. J Clin Invest 1996;97(7):1780–4.
[147] Rossier BC, Pradervand S, Schild L, Hummler E. Epithelial sodium channel and the control of sodium balance: interaction between genetic and environmental factors. Annu Rev Physiol 2002;64:877–97.
[148] Rubera I, Loffing J, Palmer LG, Frindt G, Fowler-Jaeger N, Sauter D, et al. Collecting duct-specific gene inactivation of alphaENaC in the mouse kidney does not impair sodium and potassium balance. J Clin Invest 2003;112(4):554–65.
[149] Biner HL, Arpin-Bott MP, Loffing J, Wang X, Knepper M, Hebert SC, et al. Human cortical distal nephron: distribution of electrolyte and water transport pathways. J Am Soc Nephrol 2002;13(4):836–47.
[150] Greene EL, Kren S, Hostetter TH. Role of aldosterone in the remnant kidney model in the rat. J Clin Invest 1996;98 (4):1063–8.
[151] Leopold JA, Dam A, Maron BA, Scribner AW, Liao R, Handy DE, et al. Aldosterone impairs vascular reactivity by

decreasing glucose-6-phosphate dehydrogenase activity. Nat Med 2007;13(2):189–97.
[152] Jaffe IZ, Newfell BG, Aronovitz M, Mohammad NN, McGraw AP, Perreault RE, et al. Placental growth factor mediates aldosterone-dependent vascular injury in mice. J Clin Invest 2010;120(11):3891–900.
[153] Terada Y, Kobayashi T, Kuwana H, Tanaka H, Inoshita S, Kuwahara M, et al. Aldosterone stimulates proliferation of mesangial cells by activating mitogen-activated protein kinase 1/2, cyclin D1, and cyclin A. J Am Soc Nephrol 2005;16(8):2296–305.
[154] Miyata K, Rahman M, Shokoji T, Nagai Y, Zhang GX, Sun GP, et al. Aldosterone stimulates reactive oxygen species production through activation of NADPH oxidase in rat mesangial cells. J Am Soc Nephrol 2005;16(10):2906–12.
[155] Terada Y, Kuwana H, Kobayashi T, Okado T, Suzuki N, Yoshimoto T, et al. Aldosterone-stimulated SGK1 activity mediates profibrotic signaling in the mesangium. J Am Soc Nephrol 2008;19(2):298–309.
[156] Shibata S, Nagase M, Yoshida S, Kawachi H, Fujita T. Podocyte as the target for aldosterone: roles of oxidative stress and Sgk1. Hypertension 2007;49(2):355–64.
[157] Lee SH, Yoo TH, Nam BY, Kim DK, Li JJ, Jung DS, et al. Activation of local aldosterone system within podocytes is involved in apoptosis under diabetic conditions. Am J Physiol Renal Physiol 2009;297(5):F1381–1390.
[158] Chrysostomou A, Pedagogos E, MacGregor L, Becker GJ. Double-blind, placebo-controlled study on the effect of the aldosterone receptor antagonist spironolactone in patients who have persistent proteinuria and are on long-term angiotensin-converting enzyme inhibitor therapy, with or without an angiotensin II receptor blocker. Clin J Am Soc Nephrol 2006;1(2):256–62.
[159] Cowley Jr. AW, Roman RJ. The role of the kidney in hypertension. Jama 1996;275(20):1581–9.
[160] Aperia AC, Broberger CG, Soderlund S. Relationship between renal artery perfusion pressure and tubular sodium reabsorption. Am J Physiol 1971;220(5):1205–12.
[161] Guyton AC, Coleman TG, Cowley Jr. AV, Scheel KW, Manning Jr. RD, Norman Jr. RA. Arterial pressure regulation. Overriding dominance of the kidneys in long-term regulation and in hypertension. Am J Med 1972;52(5):584–94.
[162] Hall JE, Brands MW, Henegar JR. Angiotensin II and long-term arterial pressure regulation: the overriding dominance of the kidney. J Am Soc Nephrol 1999;10(Suppl 12):S258–265.
[163] Hall JE, Granger JP. Adenosine alters glomerular filtration control by angiotensin II. Am J Physiol 1986;250(5 Pt 2): F917–923.
[164] Hall JE. Control of sodium excretion by angiotensin II: Intrarenal mechanisms and blood pressure regulation. Am J Physiol 1986;250(6 Pt 2):R960–972.
[165] Campbell DJ. Extrarenal renin and blood pressure regulation. An alternative viewpoint. Am J Hypertens 1989;2(4):266–75.
[166] Sequeira Lopez ML, Pentz ES, Robert B, Abrahamson DR, Gomez RA. Embryonic origin and lineage of juxtaglomerular cells. Am J Physiol Renal Physiol 2001;281(2):F345–356.
[167] Barajas L. Anatomy of the juxtaglomerular apparatus. Am J Physiol 1979;237(5):F333–343.
[168] Taugner C, Poulsen K, Hackenthal E, Taugner R. Immunocytochemical localization of renin in mouse kidney. Histochemistry 1979;62(1):19–27.
[169] Vander AJ. Control of renin release. Physiological Review 1967;47(3):359–82.
[170] Sequeira Lopez ML, Gomez RA. The role of angiotensin II in kidney embryogenesis and kidney abnormalities. Curr Opin Nephrol Hypertens 2004;13(1):117–22.
[171] Rohrwasser A, Morgan T, Dillon HF, Zhao L, Callaway CW, Hillas E, et al. Elements of a paracrine tubular renin-angiotensin system along the entire nephron. Hypertension 1999;34 (6):1265–74.
[172] Silver RB, Reid AC, Mackins CJ, Askwith T, Schaefer U, Herzlinger D, et al. Mast cells: a unique source of renin. Proc Natl Acad Sci USA 2004;101(37):13607–12.
[173] Mackins CJ, Kano S, Seyedi N, Schafer U, Reid AC, Machida T, et al. Cardiac mast cell-derived renin promotes local angiotensin formation, norepinephrine release, and arrhythmias in ischemia/reperfusion. J Clin Invest 2006;116 (4):1063–70.
[174] Le TH, Coffman TM. A new cardiac MASTer switch for the renin–angiotensin system. J Clin Invest 2006;116(4):866–9.
[175] Tobian L, Tomboulian A, Janecek J. The effect of high perfusion pressures on the granulation of juxtaglomerular cells in an isolated kidney. J Clin Invest 1959;38(4):605–10.
[176] Skinner SL, McCubbin JW, Page IH. Control of renin secretion. Circ Res 1964;15:64–76.
[177] Kirchheim H, Ehmke H, Persson P. Physiology of the renal baroreceptor mechanism of renin release and its role in congestive heart failure. Am J Cardiol 1988;62(8):68E–71E.
[178] Nobiling R, Munter K, Buhrle CP, Hackenthal E. Influence of pulsatile perfusion upon renin release from the isolated perfused rat kidney. Pflugers Arch 1990;415(6):713–7.
[179] Hackenthal E, Paul M, Ganten D, Taugner R. Morphology, physiology, and molecular biology of renin secretion. Physiol Rev 1990;70(4):1067–116.
[180] Blaine EH, Davis JO, Witty RT. Renin release after hemorrhage and after suprarenal aortic constriction in dogs without sodium delivery to the macula densa. Circ Res 1970;27 (6):1081–9.
[181] Blaine EH, Davis JO, Prewitt RL. Evidence for a renal vascular receptor in control of renin secretion. Am J Physiol 1971;220 (6):1593–7.
[182] Fray JC. Stretch receptor model for renin release with evidence from perfused rat kidney. Am J Physiol 1976;231(3):936–44.
[183] Hofbauer KG, Zschiedrich H, Hackenthal E, Gross F. Function of the renin–angtiotensin system in the isolated perfused rat kidney. Circ Res 1974;:I193–202.
[184] Tokumori Y, Kurahashi A, Murakami J, Mokuda GO, Ikeda T, Takeda A, et al. Biphasic renin release from perfused rat kidney. Horm Metab Res 1983;15(6):310–1.
[185] Romero JC, Feldstein AE, Rodriguez-Porcel MG, Cases-Amenos A. New insights into the pathophysiology of renovascular hypertension. Mayo Clin Proc 1997;72(3):251–60.
[186] Fray JC. Regulation of renin secretion by calcium and chemiosmotic forces: (Patho) physiological considerations. Biochim Biophys Acta 1991;1097(4):243–62.
[187] Osborn JL, Kopp UC, Thames MD, DiBona GF. Interactions among renal nerves, prostaglandins, and renal arterial pressure in the regulation of renin release. Am J Physiol 1984;247(5 Pt 2):F706–713.
[188] Knoblich PR, Freeman RH, Villarreal D. Pressure-dependent renin release during chronic blockade of nitric oxide synthase. Hypertension 1996;28(5):738–42.
[189] Persson PB, Baumann JE, Ehmke H, Hackenthal E, Kirchheim HR, Nafz B. Endothelium-derived NO stimulates pressure-dependent renin release in conscious dogs. Am J Physiol 1993;264(6 Pt 2):F943–947.
[190] Kurtz A, Wagner C. Role of nitric oxide in the control of renin secretion. Am J Physiol 1998;275(6 Pt 2):F849–862.
[191] Data JL, Gerber JG, Crump WJ, Frolich JC, Hollifield JW, Nies AS. The prostaglandin system. A role in canine baroreceptor control of renin release. Circ Res 1978;42(4):454–8.

[192] Gerber JG, Keller RT, Nies AS. Prostaglandins and renin release: the effect of PGI2, PGE2, and 13,14-dihydro PGE2 on the baroreceptor mechanism of renin release in the dog. Circ Res 1979;44(6):796–9.

[193] Munter K, Hackenthal E. The effects of endothelin on renovascular resistance and renin release. J Hypertens Suppl 1989;7(6): S276–277.

[194] Beierwaltes WH, Potter DL, Shesely EG. Renal baroreceptor-stimulated renin in the eNOS knockout mouse. Am J Physiol Renal Physiol 2002;282(1):F59–64.

[195] Fujino T, Nakagawa N, Yuhki K, Hara A, Yamada T, Takayama K, et al. Decreased susceptibility to renovascular hypertension in mice lacking the prostaglandin I2 receptor IP. J Clin Invest 2004;114(6):805–12.

[196] Francois H, Coffman TM. Prostanoids and blood pressure: which way is up? J Clin Invest 2004;114(6):757–9.

[197] Scholz H, Gotz KH, Hamann M, Kurtz A. Differential effects of extracellular anions on renin secretion from isolated perfused rat kidneys. Am J Physiol 1994;267(6 Pt 2):F1076–1081.

[198] Krattinger N, Capponi A, Mazzolai L, Aubert JF, Caille D, Nicod P, et al. Connexin40 regulates renin production and blood pressure. Kidney Int 2007;72(7):814–22.

[199] Wagner C, de Wit C, Kurtz L, Grunberger C, Kurtz A, Schweda F. Connexin40 is essential for the pressure control of renin synthesis and secretion. Circ Res 2007;100(4):556–63.

[200] Schweda F, Kurtz L, de Wit C, Janssen-Bienhold U, Kurtz A, Wagner C. Substitution of connexin40 with connexin45 prevents hyperreninemia and attenuates hypertension. Kidney Int 2009;75(5):482–9.

[201] Haefliger JA, Krattinger N, Martin D, Pedrazzini T, Capponi A, Doring B, et al. Connexin43-dependent mechanism modulates renin secretion and hypertension. J Clin Invest 2006;116 (2):405–13.

[202] Goormaghtigh N. Fact in favor of an endocrine function of the renal arterioles. *J. Pathol Bacteriol* 1945;57:392–404.

[203] Thurau K, Schnermann J, Nagel W, Horster M, Wahl M. Composition of tubular fluid in the macula densa segment as a factor regulating the function of the juxtaglomerular apparatus. Circ Res 1967;21((1):Suppl 2):79–90.

[204] Skott O, Briggs JP. Direct demonstration of macula densa-mediated renin secretion. Science 1987;237(4822):1618–20.

[205] Schlatter E, Salomonsson M, Persson AE, Greger R. Macula densa cells sense luminal NaCl concentration via furosemide sensitive $Na^+2Cl^-K^+$ co-transport. Pflugers Arch 1989;414 (3):286–90.

[206] Martinez-Maldonado M, Gely R, Tapia E, Benabe JE. Role of macula densa in diuretics-induced renin release. Hypertension 1990;16(3):261–8.

[207] Kotchen TA, Galla JH, Luke RG. Failure of $NaHCO_3$ and $KHCO_3$ to inhibit renin in the rat. Am J Physiol 1976;231 (4):1050–6.

[208] Hanner F, Chambrey R, Bourgeois S, Meer E, Mucsi I, Rosivall L, et al. Increased renal renin content in mice lacking the Na^+/H^+ exchanger NHE2. Am J Physiol Renal Physiol 2008;294(4):F937–944.

[209] Ledoussal C, Lorenz JN, Nieman ML, Soleimani M, Schultheis PJ, Shull GE. Renal salt wasting in mice lacking NHE3 Na^+/H^+ exchanger but not in mice lacking NHE2. Am J Physiol Renal Physiol 2001;281(4):F718–727.

[210] Churchill PC, Churchill MC. A1 and A2 adenosine receptor activation inhibits and stimulates renin secretion of rat renal cortical slices. J Pharmacol Exp Ther 1985;232(3):589–94.

[211] Harris RC, Breyer MD. Physiological regulation of cyclooxygenase-2 in the kidney. Am J Physiol Renal Physiol 2001;281 (1):F1–11.

[212] Schweda F, Klar J, Narumiya S, Nusing RM, Kurtz A. Stimulation of renin release by prostaglandin E2 is mediated by EP2 and EP4 receptors in mouse kidneys. Am J Physiol Renal Physiol 2004;287(3):F427–433.

[213] Schnermann J, Homer W. Smith Award lecture. The juxtaglomerular apparatus: from anatomical peculiarity to physiological relevance. J Am Soc Nephrol 2003;14(6):1681–94.

[214] Schweda F, Kurtz A. Cellular mechanism of renin release. Acta Physiol Scand 2004;181(4):383–90.

[215] Facemire CS, Nguyen M, Jania L, Beierwaltes WH, Kim HS, Koller BH, et al. A major role for the EP4 receptor in regulation of renin. Am J Physiol Renal Physiol 2011;301(5): F1035–1041.

[216] Beierwaltes WH, Schryver S, Sanders E, Strand J, Romero JC. Renin release selectively stimulated by prostaglandin I2 in isolated rat glomeruli. Am J Physiol 1982;243(3):F276–283.

[217] Webber PC, Larsson C, Anggard E, Hamberg M, Corey EJ, Nicolaou KC, et al. Stimulation of renin release from rabbit renal cortex by arachidonic acid and prostaglandin endoperoxides. Circ Res 1976;39(6):868–74.

[218] Harding P, Sigmon DH, Alfie ME, Huang PL, Fishman MC, Beierwaltes WH, et al. Cyclooxygenase-2 mediates increased renal renin content induced by low-sodium diet. Hypertension 1997;29(1 Pt 2):297–302.

[219] Cheng H, Harris R. Angiotensin converting enzyme inhibitor-mediated increases in renal renin expression are not seen in cyclooxygenase-2 knockout mice. J Am Soc Nephrol 1999;10:343A.

[220] Peti-Peterdi J, Komlosi P, Fuson AL, Guan Y, Schneider A, Qi Z, et al. Luminal NaCl delivery regulates basolateral PGE2 release from macula densa cells. J Clin Invest 2003;112(1):76–82.

[221] Yang T, Endo Y, Huang YG, Smart A, Briggs JP, Schnermann J. Renin expression in COX-2-knockout mice on normal or low-salt diets. Am J Physiol Renal Physiol 2000;279(5): F819–825.

[222] Weihprecht H, Lorenz JN, Schnermann J, Skott O, Briggs JP. Effect of adenosine1-receptor blockade on renin release from rabbit isolated perfused juxtaglomerular apparatus. J Clin Invest 1990;85(5):1622–8.

[223] Kim SM, Mizel D, Huang YG, Briggs JP, Schnermann J. Adenosine as a mediator of macula densa-dependent inhibition of renin secretion. Am J Physiol Renal Physiol 2006;290(5): F1016–1023.

[224] Mundel P, Bachmann S, Bader M, Fischer A, Kummer W, Mayer B, et al. Expression of nitric oxide synthase in kidney macula densa cells. Kidney Int 1992;42(4):1017–9.

[225] Wilcox CS, Welch WJ. Macula densa nitric oxide synthase: expression, regulation, and function. Kidney Int Suppl 1998;67:S53–57.

[226] He XR, Greenberg SG, Briggs JP, Schnermann JB. Effect of nitric oxide on renin secretion. II. Studies in the perfused juxtaglomerular apparatus. Am J Physiol 1995;268(5 Pt 2): F953–959.

[227] Tharaux PL, Dussaule JC, Pauti MD, Vassitch Y, Ardaillou R, Chatziantoniou C. Activation of renin synthesis is dependent on intact nitric oxide production. Kidney Int 1997;51 (6):1780–7.

[228] Castrop H, Schweda F, Mizel D, Huang Y, Briggs J, Kurtz A, et al. Permissive role of nitric oxide in macula densa control of renin secretion. Am J Physiol Renal Physiol 2004;286(5): F848–857.

[229] Shricker K, Holmer S, Kramer BK, Riegger GA, Kurtz A. The role of angiotensin II in the feedback control of renin gene expression. Pflugers Arch 1997;434(2):166–72.

[230] Oliverio MI, Madsen K, Best CF, Ito M, Maeda N, Smithies O, et al. Renal growth and development in mice lacking AT1A receptors for angiotensin II. Am J Physiol 1998;274(1 Pt 2): F43–50.
[231] Gomez RA, Chevalier RL, Everett AD, Elwood JP, Peach MJ, Lynch KR, et al. Recruitment of renin gene-expressing cells in adult rat kidneys. Am J Physiol 1990;259(4 Pt 2):F660–665.
[232] Crowley SD, Gurley SB, Oliverio MI, Pazmino AK, Griffiths R, Flannery PJ, et al. Distinct roles for the kidney and systemic tissues in blood pressure regulation by the renin–angiotensin system. J Clin Invest 2005;115(4):1092–9.
[233] Lew R, Summers RJ. The distribution of beta-adrenoceptors in dog kidney: an autoradiographic analysis. Eur J Pharmacol 1987;140(1):1–11.
[234] Keeton TK, Campbell WB. The pharmacologic alteration of renin release. Pharmacol Rev 1980;32(2):81–227.
[235] Holdaas H, DiBona GF, Kiil F. Effect of low-level renal nerve stimulation on renin release from nonfiltering kidneys. Am J Physiol 1981;241(2):F156–161.
[236] Holdaas H, Langard O, Eide I, Kiil F. Mechanism of renin release during renal nerve stimulation in dogs. Scand J Clin Lab Invest 1981;41(7):617–25.
[237] DiBona GF. Neural regulation of renal tubular sodium reabsorption and renin secretion. Fed Proc 1985;44(13):2816–22.
[238] Kirchheim HR, Gross R, Hackenberg HM, Hackenthal E, Huber J. Autoregulation of renin release and its modification by renal sympathetic nerves in conscious dogs. Kidney Inst 1981;20:152.
[239] Blaine EH, Davis JO. Evidence for a renal vascular mechanism in renin release: new observations with graded stimulation by aortic constriction. Circ Res 1971;28((5):Suppl 2):118–26.
[240] Esler MD, Krum H, Sobotka PA, Schlaich MP, Schmieder RE, Bohm M. Renal sympathetic denervation in patients with treatment-resistant hypertension (The Symplicity HTN-2 Trial): a randomised controlled trial. *Lancet* 2010;376 (9756):1903–9.
[241] Friis UG, Jensen BL, Hansen PB, Andreasen D, Skott O. Exocytosis and endocytosis in juxtaglomerular cells. Acta Physiol Scand 2000;168(1):95–9.
[242] Friis UG, Jensen BL, Aas JK, Skott O. Direct demonstration of exocytosis and endocytosis in single mouse juxtaglomerular cells. Circ Res 1999;84(8):929–36.
[243] Churchill PC. Second messengers in renin secretion. Am J Physiol Renal Physiol 1985;249(2):F175–184.
[244] Kurtz A, Wagner C. Cellular control of renin secretion. J Exp Biol 1999;202(Pt 3):219–25.
[245] Kurtz A, Pfeilschifter J, Hutter A, Buhrle C, Nobiling R, Taugner R, et al. Role of protein kinase C in inhibition of renin release caused by vasoconstrictors. Am J Physiol 1986;250(4 Pt 1):C563–571.
[246] Churchill MC, Churchill PC. 12-0-Tetradecanoylphorbol 13-acetate inhibits renin secretion of rat renal cortical slices. Journal of Hypertension 1984;2(1):25–8.
[247] Churchill PC, Rossi NF, Churchill MC, Ellis VR. Effect of melittin on renin and prostaglandin E2 release from rat renal cortical slices. J Physiol 1990;428:233–41.
[248] Park CS, Honeyman TW, Chung ES, Lee JS, Sigmon DH, Fray JC. Involvement of calmodulin in mediating inhibitory action of intracellular Ca^{2+} on renin secretion. Am J Physiol 1986;251 (6 Pt 2):F1055–1062.
[249] Della Bruna R, Pinet F, Corvol P, Kurtz A. Calmodulin antagonists stimulate renin secretion and inhibit renin synthesis *in vitro*. Am J Physiol 1992;262(3 Pt 2):F397–402.
[250] Rasmussen H, Barrett PQ. Calcium messenger system: an integrated view. Physiol Rev 1984;64(3):938–84.
[251] Sigmund CD, Jones CA, Kane CM, Wu C, Lang JA, Gross KW. Regulated tissue- and cell-specific expression of the human renin gene in transgenic mice. Circ Res 1992;70 (5):1070–9.
[252] Fukamizu A, Hatae T, Kon Y, Sugimura M, Hasegawa T, Yokoyama M, et al. Human renin in transgenic mouse kidney is localized to juxtaglomerular cells. Biochem J 1991;278(Pt 2):601–3.
[253] Pan L, Wang Y, Jones CA, Glenn ST, Baumann H, Gross KW. Enhancer-dependent inhibition of mouse renin transcription by inflammatory cytokines. Am J Physiol Renal Physiol 2005;288(1):F117–124.
[254] Borensztein P, Germain S, Fuchs S, Philippe J, Corvol P, Pinet F. cis-Regulatory elements and trans-acting factors directing basal and cAMP-stimulated human renin gene expression in chorionic cells. Circ Res 1994;74(5):764–73.
[255] Smith DL, Morris BJ, Do YS, Law RE, Shaw KJ, Hseuh WA. Identification of cyclic AMP response element in the human renin gene. Biochem Biophys Res Commun 1994;200 (1):320–9.
[256] Paul M, Burt DW, Krieger JE, Nakamura N, Dzau VJ. Tissue specificity of renin promoter activity and regulation in mice. Am J Physiol 1992;262(5 Pt 1):E644–650.
[257] Morris BJ, Smith DL, Law RE, Do YS, Shaw KJ, Hsueh WA. Function of human renin proximal promoter DNA. Kidney Int 1994;46(6):1516–21.
[258] Ying L, Morris BJ, Sigmund CD. Transactivation of the human renin promoter by the cyclic AMP/protein kinase A pathway is mediated by both cAMP-responsive element binding protein-1 (CREB)-dependent and CREB-independent mechanisms in Calu-6 cells. J Biol Chem 1997;272(4):2412–20.
[259] Petrovic N, Black TA, Fabian JR, Kane C, Jones CA, Loudon JA, et al. Role of proximal promoter elements in regulation of renin gene transcription. J Biol Chem 1996;271(37):22499–505.
[260] Germain S, Bonnet F, Philippe J, Fuchs S, Corvol P, Pinet F. A novel distal enhancer confers chorionic expression on the human renin gene. J Biol Chem 1998;273(39):25292–300.
[261] Pan L, Gross KW. Transcriptional regulation of renin: an update. Hypertension 2005;45(1):3–8.
[262] Lang JA, Ying LH, Morris BJ, Sigmund CD. Transcriptional and posttranscriptional mechanisms regulate human renin gene expression in Calu-6 cells. Am J Physiol 1996;271(1 Pt 2): F94–100.
[263] Chen M, Schnermann J, Smart AM, Brosius FC, Killen PD, Briggs JP. Cyclic AMP selectively increases renin mRNA stability in cultured juxtaglomerular granular cells. J Biol Chem 1993;268(32):24138–44.
[264] Morris BJ, Adams DJ, Beveridge DJ, van der Weyden L, Mangs H, Leedman PJ. cAMP controls human renin mRNA stability via specific RNA-binding proteins. Acta Physiol Scand 2004;181(4):369–73.
[265] Griendling KK, Ushio-Fukai M, Lassegue B, Alexander RW. Angiotensin II signaling in vascular smooth muscle. New concepts. Hypertension 1997;29(1 Pt 2):366–73.
[266] Blantz RC, Konnen KS, Tucker BJ. Angiotensin II effects upon the glomerular microcirculation and ultrafiltration coefficient of the rat. J Clin Invest 1976;57(2):419–34.
[267] Dworkin LD, Ichikawa I, Brenner BM. Hormonal modulation of glomerular function. Am J Physiol 1983;244(2):F95–104.
[268] Navar LG, Inscho EW, Majid SA, Imig JD, Harrison-Bernard LM, Mitchell KD. Paracrine regulation of the renal microcirculation. Physiol Rev 1996;76(2):425–536.
[269] Mendelsohn F, Dunbar M, Allen A, Chou S, Millan M, Aguilera G. Angiotensin II receptors in the kidney. Fed Proc 1986;45:1420–5.

[270] Ito S, Johnson CS, Carretero OA. Modulation of angiotensin II-induced vasoconstriction by endothelium-derived relaxing factor in the isolated microperfused rabbit afferent arteriole. J Clin Invest 1991;87(5):1656–63.
[271] Olsen ME, Hall JE, Montani JP, Cornell JE. Interaction between renal prostaglandins and angiotensin II in controlling glomerular filtration in the dog. Clin Sci (Lond) 1987;72(4):429–36.
[272] Fleming JT, Parekh N, Steinhausen M. Calcium antagonists preferentially dilate preglomerular vessels of hydronephrotic kidney. Am J Physiol 1987;253(6 Pt 2):F1157–1163.
[273] Carmines PK, Morrison TK, Navar LG. Angiotensin II effects on microvascular diameters of *in vitro* blood-perfused juxtamedullary nephrons. Am J Physiol 1986;251(4 Pt 2): F610–618.
[274] Carmines PK, Navar LG. Disparate effects of Ca channel blockade on afferent and efferent arteriolar responses to ANG II. Am J Physiol 1989;256(6 Pt 2):F1015–1020.
[275] Harrison-Bernard LM, Monjure CJ, Bivona BJ. Efferent arterioles exclusively express the subtype 1A angiotensin receptor: functional insights from genetic mouse models. Am J Physiol Renal Physiol 2006;290(5):F1177–1186.
[276] Cowley AW, Roman RJ, Fenoy FJ, Mattson DL. Effect of renal medullary circulation on arterial pressure. J Hypertens Suppl 1992;10(7):S187–193.
[277] Earley LE, Friedler RM. Changes in renal blood flow and possibly the intrarenal distribution of blood during the natriuresis accompanying saline loading in the dog. J Clin Invest 1965;44:929–41.
[278] Earley LE, Friedler RM. The effects of combined renal vasodilatation and pressor agents on renal hemodynamics and the tubular reabsorption of sodium. J Clin Invest 1966;45 (4):542–51.
[279] Hricik DE. Captopril-induced renal insufficiency and the role of sodium balance. Ann Intern Med 1985;103(2):222–3.
[280] Textor SC, Tarazi RC, Novick AC, Bravo EL, Fouad FM. Regulation of renal hemodynamics and glomerular filtration in patients with renovascular hypertension during converting enzyme inhibition with captopril. Am J Med 1984;76 (5B):29–37.
[281] Miller WL, Thomas RA, Berne RM, Rubio R. Adenosine production in the ischemic kidney. Circ Res 1978;43(3):390–7.
[282] Haddy FJ, Scott JB. Metabolically linked vasoactive chemicals in local regulation of blood flow. Physiol Rev 1968;48 (4):688–707.
[283] Spielman WS, Thompson CI. A proposed role for adenosine in the regulation of renal hemodynamics and renin release. Am J Physiol 1982;242(5):F423–435.
[284] Woodcock EA, Loxley R, Leung E, Johnston CI. Demonstration of RA-adenosine receptors in rat renal papillae. Biochem Biophys Res Commun 1984;121(2):434–40.
[285] Miyamoto M, Yagil Y, Larson T, Robertson C, Jamison RL. Effects of intrarenal adenosine on renal function and medullary blood flow in the rat. Am J Physiol 1988;255(6 Pt 2): F1230–1234.
[286] Mason J. The pathophysiology of ischaemic acute renal failure. A new hypothesis about the initiation phase. Ren Physiol 1986;9(3):129–47.
[287] Osswald H, Schmitz HJ, Kemper R. Tissue content of adenosine, inosine and hypoxanthine in the rat kidney after ischemia and postischemic recirculation. Pflugers Arch 1977;371(1-2):45–9.
[288] Yagil Y, Miyamoto M, Jamison RL. Inner medullary blood flow in postischemic acute renal failure in the rat. Am J Physiol 1989;256(3 Pt 2):F456–461.
[289] Purdy KE, Arendshorst WJ. Prostaglandins buffer ANG II-mediated increases in cytosolic calcium in preglomerular VSMC. Am J Physiol 1999;277(6 Pt 2):F850–858.
[290] Jaimes EA, Hua P, Tian RX, Raij L. Human glomerular endothelium: interplay among glucose, free fatty acids, angiotensin II, and oxidative stress. *Am J Physiol Renal Physiol* 2010;298(1): F125–132.
[291] Ichihara A, Imig JD, Inscho EW, Navar LG. Interactive nitric oxide-angiotensin II influences on renal microcirculation in angiotensin II-induced hypertension. Hypertension 1998;31 (6):1255–60.
[292] Zatz R, Dunn B, Anderson S, Rennke H, Brenner B. Prevention of diabetic glomerulopathy by pharmacological amelioration of glomerular capillary hypertension. J Clin Invest 1986;77:1925–30.
[293] Meyer TW, Anderson S, Rennke HG, Brenner BM. Reversing glomerular hypertension stabilizes established glomerular injury. Kidney Int 1987;31(3):752–9.
[294] Anderson S, Meyer T, Rennke H, Brenner B. Control of glomerular hypertension limits renal injury in rats with reduced renal mass. J Clin Invest 1985;76:612–9.
[295] Simons JL, Provoost AP, De Keijzer MH, Anderson S, Rennke HG, Brenner BM. Pathogenesis of glomerular injury in the fawn-hooded rat: effect of unilateral nephrectomy. J Am Soc Nephrol 1993;4(6):1362–70.
[296] Ruan X, Oliverio MI, Coffman TM, Arendshorst WJ. Renal vascular reactivity in mice: AngII-induced vasoconstriction in AT1A receptor null mice. J Am Soc Nephrol 1999;10 (12):2620–30.
[297] Faubert PF, Chou SY, Porush JG. Regulation of papillary plasma flow by angiotensin II. Kidney Int 1987;32 (4):472–8.
[298] Zou AP, Wu F, Cowley Jr. AW. Protective effect of angiotensin II-induced increase in nitric oxide in the renal medullary circulation. Hypertension 1998;31(1 Pt 2):271–6.
[299] Szentivanyi Jr. M, Maeda CY, Cowley Jr. AW. Local renal medullary L-NAME infusion enhances the effect of long-term angiotensin II treatment. Hypertension 1999;33(1 Pt 2):440–5.
[300] Dickhout JG, Mori T, Cowley Jr. AW. Tubulovascular nitric oxide crosstalk: buffering of angiotensin II-induced medullary vasoconstriction. Circ Res 2002;91(6):487–93.
[301] Roman RJ, Lianos E. Influence of prostaglandins on papillary blood flow and pressure-natriuretic response. Hypertension 1990;15(1):29–35.
[302] Roman RJ, Kauker ML. Renal effect of prostaglandin synthetase inhibition in rats: Micropuncture studies. Am J Physiol 1978;235(2):F111–118.
[303] Higashihara E, Stokes JB, Kokko JP, Campbell WB, DuBose Jr. TD. Cortical and papillary micropuncture examination of chloride transport in segments of the rat kidney during inhibition of prostaglandin production. Possible role for prostaglandins in the chloruresis of acute volume expansion. J Clin Invest 1979;64(5):1277–87.
[304] Chen PY, Sanders PW. L-arginine abrogates salt-sensitive hypertension in Dahl/Rapp rats. J Clin Invest 1991; 88(5):1559–67.
[305] Szentivanyi Jr. M, Zou AP, Mattson DL, Soares P, Moreno C, Roman RJ, et al. Renal medullary nitric oxide deficit of Dahl S rats enhances hypertensive actions of angiotensin II. Am J Physiol Regul Integr Comp Physiol 2002;283(1):R266–272.
[306] He H, Kimura S, Fujisawa Y, Tomohiro A, Kiyomoto K, Aki Y, et al. Dietary L-arginine supplementation normalizes regional blood flow in Dahl-Iwai salt-sensitive rats. Am J Hypertens 1997;10(5 Pt 2):89S–93S.

[307] Hu L, Manning Jr. RD. Role of nitric oxide in regulation of long-term pressure-natriuresis relationship in Dahl rats. Am J Physiol 1995;268(6 Pt 2):H2375–2383.
[308] Rajapakse NW, Mattson DL. Role of L-arginine uptake mechanisms in renal blood flow responses to angiotensin II in rats. Acta Physiol (Oxf) 2011;203(3):391–400.
[309] Weiner I, New A, Milton A, Tisher C. Regulation of luminal alkalinization and acidification in the cortical collecting duct by angiotensin II. Am J Physiol 1995;38:F730–8.
[310] Geibel J, Giebisch G, Boron WF. Angiotensin II stimulates both $Na(^{+})$-H^{+} exchange and Na^{+}/HCO_3^{-} co-transport in the rabbit proximal tubule. Proc Natl Acad Sci USA 1990;87 (20):7917–20.
[311] Komlosi P, Fuson A, Fintha A, Peti-Peterdi J, Rosivall L, Warnock DG, et al. Angiotensin I conversion to angiotensin II stimulates cortical collecting duct sodium transport. Hypertension 2003;42:195–9.
[312] Peti-Peterdi J, Warnock DG, Bell PD. Angiotensin II directly stimulates ENaC activity in the cortical collecting duct via AT (1) receptors. J Am Soc Nephrol 2002;13(5):1131–5.
[313] Schuster VL, Kokko JP, Jacobson HR. Angiotensin II directly stimulates sodium transport in rabbit proximal convoluted tubules. J Clin Invest 1984;73(2):507–15.
[314] Tojo A, Tisher CC, Madsen KM. Angiotensin II regulates H $(^{+})$-ATPase activity in rat cortical collecting duct. Am J Physiol 1994;267(6 Pt 2):F1045–1051.
[315] Barreto-Chaves ML, Mello-Aires M. Effect of luminal angiotensin II and ANP on early and late cortical distal tubule HCO_3^{-} reabsorption. Am J Physiol 1996;271(5 Pt 2):F977–984.
[316] Levine DZ, Iacovitti M, Buckman S, Burns KD. Role of angiotensin II in dietary modulation of rat late distal tubule bicarbonate flux *in vivo*. J Clin Invest 1996;97(1):120–5.
[317] Cogan MG. Angiotensin II: a powerful controller of sodium transport in the early proximal tubule. Hypertension 1990;15 (5):451–8.
[318] Wang T, Giebisch G. Effects of angiotensin II on electrolyte transport in the early and late distal tubule in rat kidney. Am J Physiol 1996;271(1 Pt 2):F143–149.
[319] Gurley SB, Riquier-Brison AD, Schnermann J, Sparks MA, Allen AM, Haase VH, et al. AT1A angiotensin receptors in the renal proximal tubule regulate blood pressure. Cell Metab 2011;13(4):469–75.
[320] Benigni A, Corna D, Zoja C, Sonzogni A, Latini R, Salio M, et al. Disruption of the Ang II type 1 receptor promotes longevity in mice. J Clin Invest 2009;119(3):524–30.
[321] Olsen ME, Hall JE, Montani JP, Guyton AC, Langford HG, Cornell JE. Mechanisms of angiotensin II natriuresis and antinatriuresis. Am J Physiol 1985;249(2 Pt 2):F299–307.
[322] Hall JE, Guyton AC, Smith Jr MJ, Coleman TG. Blood pressure and renal function during chronic changes in sodium intake: role of angiotensin. Am J Physiol Renal Physiol 1980;239(3): F271–280.
[323] Hall JE, Guyton AC, Jackson TE, Coleman TG, Lohmeier TE, Trippodo NC. Control of glomerular filtration rate by renin–angiotensin system. Am J Physiol 1977;233(5):F366–372.
[324] Bouley R, Palomino Z, Tang SS, Nunes P, Kobori H, Lu HA, et al. Angiotensin II and hypertonicity modulate proximal tubular aquaporin 1 expression. Am J Physiol Renal Physiol 2009;297(6):F1575–1586.
[325] Davisson R, Ding Y, Stec D, Catterall J, Sigmund C. Novel mechanism of hypertension revealed by cell-specific targeting of human angiotensinogen in transgenic mice. Physiol Genomics 1999;1:3–9.
[326] Li H, Weatherford ET, Davis DR, Keen HL, Grobe JL, Daugherty A, et al. Renal proximal tubule angiotensin AT1A receptors regulate blood pressure. Am J Physiol Regul Integr Comp Physiol 2011;301(4):R1067–1077.
[327] Riquier-Brison AD, Leong PK, Pihakaski-Maunsbach K, McDonough AA. Angiotensin II stimulates trafficking of NHE3, NaPi2, and associated proteins into the proximal tubule microvilli. Am J Physiol Renal Physiol 2010;298(1): F177–186.
[328] Brown GP, Douglas JG. Angiotensin II binding sites on isolated rat renal brush border membranes. Endocrinology 1982;111(6):1830–6.
[329] Brown GP, Douglas JG. Angiotensin II-binding sites in rat and primate isolated renal tubular basolateral membranes. Endocrinology 1983;112(6):2007–14.
[330] Harrison-Bernard LM, Navar LG, Ho MM, Vinson GP, el-Dahr SS. Immunohistochemical localization of ANG II AT1 receptor in adult rat kidney using a monoclonal antibody. Am J Physiol 1997;273(1 Pt 2):F170–177.
[331] Braam B, Mitchell KD, Fox J, Navar LG. Proximal tubular secretion of angiotensin II in rats. Am J Physiol 1993;264(5 Pt 2):F891–898.
[332] Navar LG, Lewis L, Hymel A, Braam B, Mitchell KD. Tubular fluid concentrations and kidney contents of angiotensins I and II in anesthetized rats. J Am Soc Nephrol 1994;5(4):1153–8.
[333] Li XC, Hopfer U, Zhuo JL. AT1 receptor-mediated uptake of angiotensin II and NHE-3 expression in proximal tubule cells through a microtubule-dependent endocytic pathway. Am J Physiol Renal Physiol 2009;297(5):F1342–1352.
[334] Quan A, Baum M. Endogenous production of angiotensin II modulates rat proximal tubule transport. J Clin Invest 1996;97 (12):2878–82.
[335] Boer WH, Braam B, Fransen R, Boer P, Koomans HA. Effects of reduced renal perfusion pressure and acute volume expansion on proximal tubule and whole kidney angiotensin II content in the rat. Kidney Int 1997;51(1):44–9.
[336] Thomson SC, Deng A, Wead L, Richter K, Blantz RC, Vallon V. An unexpected role for angiotensin II in the link between dietary salt and proximal reabsorption. J Clin Invest 2006;116 (4):1110–6.
[337] Liu FY, Cogan MG. Angiotensin II: a potent regulator of acidification in the rat early proximal convoluted tubule. J Clin Invest 1987;80(1):272–5.
[338] Liu FY, Cogan MG. Angiotensin II stimulation of hydrogen ion secretion in the rat early proximal tubule. Modes of action, mechanism, and kinetics. J Clin Invest 1988;82(2):601–7.
[339] Li Y, Yamada H, Kita Y, Kunimi M, Horita S, Suzuki M, et al. Roles of ERK and cPLA2 in the angiotensin II-mediated biphasic regulation of Na^{+}-$HCO_3(^{-})$ transport. J Am Soc Nephrol 2008;19(2):252–9.
[340] Liu FY, Cogan MG. Role of angiotensin II in glomerulotubular balance. Am J Physiol 1990;259(1 Pt 2):F72–79.
[341] Stone DK, Seldin DW, Kokko JP, Jacobson HR. Mineralocorticoid modulation of rabbit medullary collecting duct acidification. A sodium-independent effect. J Clin Invest 1983;72(1):77–83.
[342] Weiner ID, Hamm LL. Regulation of intracellular pH in the rabbit cortical collecting tubule. J Clin Invest 1990;85(1):274–81.
[343] Hays SR. Mineralocorticoid modulation of apical and basolateral membrane $H^{+}/OH^{-}/HCO_3^{-}$ transport processes in the rabbit inner stripe of outer medullary collecting duct. J Clin Invest 1992;90(1):180–7.
[344] Harrington JT, Hulter HN, Cohen JJ, Madias NE. Mineralocorticoid-stimulated renal acidification: the critical role of dietary sodium. Kidney Int 1986;30(1):43–8.
[345] Batlle DC. Segmental characterization of defects in collecting tubule acidification. Kidney Int 1986;30(4):546–54.

[346] Paxton WG, Runge M, Horaist C, Cohen C, Alexander RW, Bernstein KE. Immunohistochemical localization of rat angiotensin II AT1 receptor. Am J Physiol 1993;264(6 Pt 2): F989–995.

[347] Poumarat JS, Houillier P, Rismondo C, Rogues B, Lazar G, Paillard M, et al. The luminal membrane of rat thick limb expresses AT1 receptor and aminopeptidase activities. Kidney Int 2002;62(2):434–45.

[348] Amlal H, LeGoff C, Vernimmen C, Soleimani M, Paillard M, Bichara M. ANG II controls $Na(^{+})$-K^{+}(NH_4^{+})-$2Cl^{-}$ co-transport via 20-HETE and PKC in medullary thick ascending limb. Am J Physiol 1998;274(4 Pt 1):C1047–1056.

[349] Lerolle N, Bourgeois S, Leviel F, Lebrun G, Paillard M, Houillier P. Angiotensin II inhibits NaCl absorption in the rat medullary thick ascending limb. Am J Physiol Renal Physiol 2004;287(3):F404–410.

[350] Capasso G, Unwin R, Ciani F, De Santo NG, De Tommaso G, Russo F, et al. Bicarbonate transport along the loop of Henle. II. Effects of acid–base, dietary, and neurohumoral determinants. J Clin Invest 1994;94(2):830–8.

[351] Kwon TH, Nielsen J, Kim YH, Knepper MA, Frokiaer J, Nielsen S. Regulation of sodium transporters in the thick ascending limb of rat kidney: response to angiotensin II. Am J Physiol Renal Physiol 2003;285(1):F152–165.

[352] Rothenberger F, Velic A, Stehberger PA, Kovacikova J, Wagner CA. Angiotensin II stimulates vacuolar H^{+}-ATPase activity in renal acid-secretory intercalated cells from the outer medullary collecting duct. J Am Soc Nephrol 2007;18 (7):2085–93.

[353] Pech V, Zheng W, Pham TD, Verlander JW, Wall SM. Angiotensin II activates H^{+}-ATPase in type A intercalated cells. J Am Soc Nephrol 2008;19(1):84–91.

[354] Wei Y, Wang W. Angiotensin II stimulates basolateral K channels in rat cortical collecting ducts. Am J Physiol Renal Physiol 2003;284(1):F175–181.

[355] Esther C, Howard T, Marino E, Goddard J, Capecchi M, Bernstein K. Mice lacking angiotensin converting enzyme have low blood pressure, renal pathology, and reduced male fertility. Lab Invest 1996;74:953–65.

[356] Kihara M,, Umemura S,, Sumida Y,, Yokoyama M,, Yabana M,, Nyui N,, et al. Genetic deficiency of angiotensinogen produces an impaired urine concentrating ability in mice. 1998;53(3):548.

[357] Oliverio MI, Delnomdedieu M, Best CF, Li P, Morris M, Callahan MF, et al. Abnormal water metabolism in mice lacking the type 1A receptor for ANG II. Am J Physiol Renal Physiol 2000;278(1):F75–82.

[358] Sparks MA, Parsons KK, Stegbauer J, Gurley SB, Vivekanandan-Giri A, Fortner CN, et al. Angiotensin II type 1A receptors in vascular smooth muscle cells do not influence aortic remodeling in hypertension. *Hypertension* 2011;57(3):577–85.

[359] Kwon T-H, Nielsen J, Knepper MA, Frokiaer J, Nielsen S. Angiotensin II AT1 receptor blockade decreases vasopressin-induced water reabsorption and AQP2 levels in NaCl- restricted rats. Am J Physiol Renal Physiol 2005;288(4):F673–684.

[360] Wong NL, Tsui JK. Angiotensin II upregulates the expression of vasopressin V2 mRNA in the inner medullary collecting duct of the rat. Metabolism 2003;52(3):290–5.

[361] Wang W, Li C, Summer S, Falk S, Schrier RW. Interaction between vasopressin and angiotensin II *in vivo* and *in vitro*: effect on aquaporins and urine concentration. Am J Physiol Renal Physiol 2010;299(3):F577–584.

[362] Li C, Wang W, Rivard CJ, Lanaspa MA, Summer S, Schrier RW. Molecular mechanisms of angiotensin II stimulation on aquaporin-2 expression and trafficking. Am J Physiol Renal Physiol 2011;300(5):F1255–1261.

[363] Stegbauer J, Gurley SB, Sparks MA, Woznowski M, Kohan DE, Yan M, et al. AT1 receptors in the collecting duct directly modulate the concentration of urine. *J Am Soc Nephrol* 2011;22 (12):2237–46.

[364] Crackower MA, Sarao R, Oudit GY, et al. Angiotensin-converting enzyme 2 is an essential regulator of heart function. Nature 2002;417(6891):822–8.

[365] Yamamoto K, Ohishi M, Katsuya T, et al. Deletion of angiotensin-converting enzyme 2 accelerates pressure overload-induced cardiac dysfunction by increasing local angiotensin II. Hypertension 2006;47(4):718–26.

[366] Krattinger N, Capponi A, Mazzolai L, et al. Connexin40 regulates renin production and blood pressure. Kidney Int 2007;72 (7):814–22.

[367] Lubkemeier I, Machura K, Kurtz L, et al. The connexin 40 A96S mutation causes renin-dependent hypertension. J Am Soc Nephrol 2011;22(6):1031–40.

[368] Wagner C, de Wit C, Kurtz L, Grunberger C, Kurtz A, Schweda F. Connexin40 is essential for the pressure control of renin synthesis and secretion. Circ Res 2007;100(4):556–63.

CHAPTER

16

Neural Control of Renal Function

Edward J. Johns[1] *and Ulla C. Kopp*[2]

[1]Department of Physiology, University College Cork, Cork, Republic of Ireland
[2]Departments of Internal Medicine & Pharmacology, University of Iowa Carver College of Medicine, Iowa City, IA, USA

RENAL SYMPATHETIC NERVES

Introduction

One of the first observations of a potential neural control of kidney function was made by Claude Bernard in the middle of the 19th century, who reported a unilateral diuresis following section of the greater splanchnic nerve of the anesthetized dog.[17] However, the critical role of the sympathetic nervous system in the control of renal function was long questioned due to the views of Homer Smith,[244] who regarded the renal innervation to be of little importance in determining the function of the kidney. It was not until the 1960s that the innervation of the kidney and its regulation of renal function came under detailed scrutiny. Over the following three-to-four decades a wealth of information has been generated and concepts developed which have provided the foundation for how the renal sympathetic nerves regulate all aspects of vascular, tubular, and secretory functions of the kidney, both normally and in pathophysiological states of cardiovascular diseases. A number of major reviews have brought together the most significant pieces of information about the renal sympathetic nerves over this period.[51,52,58,189] This knowledge is now being translated into therapeutic approaches in man, particularly in relation to hypertension, heart failure, and renal disease.[53,234] The recent reports by Esler and co-workers[76,172,173,234] that bilateral renal denervation in patients with resistant hypertension resulted in a profound and sustained (≥2 years) reduction in blood pressure reinforces the important contribution of the autonomic control of the kidney in determining cardiovascular homeostasis and how it may be involved in pathophysiological states. These findings are set to reinforce the drive to gain knowledge of both the efferent and afferent innervations of the kidney, and to stimulate the development of further therapeutic avenues to modulate the neural control of the kidney.

NEUROANATOMY, PHARMACOLOGY, AND PHYSIOLOGY

Extrinsic Innervation

The efferent innervation of the kidney comprises pre-ganglionic fibers which arise from spinal segments T_{11}–L_3, and traverse to both pre-vertebral (thoraco-lumbar sympathetic chain) and para-vertebral ganglia (aortico-renal, splanchnic, coeliac, superior mesenteric ganglia) which give rise to the post-ganglionic fibers. There is great species variation in the overall contribution from the various ganglia, for example, with 80% arising from the ipsilateral para-vertebral ganglia (T_{11}–L_2) in the rat and hamster, but only 50% for the cat and monkey (T_{11}–L_3).[58] Figure 16.1 gives a brief outline of these different neural pathways. Tracer studies with horseradish peroxidase and herpes virus have been used to demonstrate the neural pathways for the sympathetic innervation. The pre-ganglionic sympathetic nerve fibers in the rat are primarily located in the intermediolateral column of the spinal cord, from T_9–T_{13}, suggesting that they descend three to four segments before exiting the spinal column at T_{11}–L_3. A number of nuclei within the central nervous system project to these intermediolateral areas of the spinal cord, including the raphe nuclei, rostral

Seldin and Giebisch's The Kidney, Fifth Edition.
DOI: http://dx.doi.org/10.1016/B978-0-12-381462-3.00016-1

© 2013 Elsevier Inc. All rights reserved.

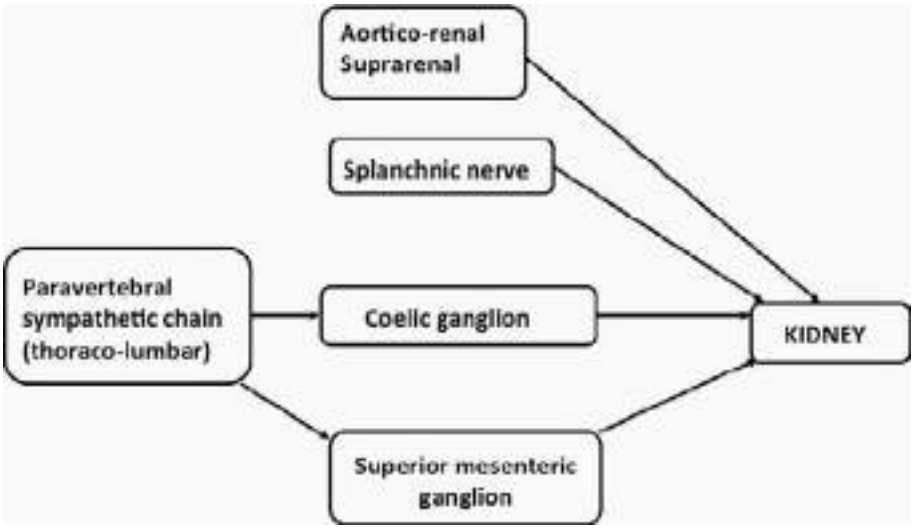

FIGURE 16.1 **This shows the main ganglia providing the sympathetic post-ganglionic fibers which innervate the kidney.**

venterolateral medulla, an A5 group, and the paraventricular hypothalamic nucleus.[42] Together, there is a view that descending projections from the supra-spinal systems are the primary regulators of sympathetic outflow to the kidney.

There has been a continuing evaluation of the size and type of nerves forming the efferent innervation of the kidney. Analyses performed in the rabbit utilizing electron microscopy have demonstrated two types of nerve fibers with different diameters in the renal cortex,[49,183] suggesting that different functionalities may exist within these different nerve populations. Detailed counts of fiber number and diameter in the rat[67,233] have found that the majority of the fibers are unmyelinated (96%) with the remainder being myelinated. The average diameter of the unmyelinated fibers was approximately 1.3 μm, and while DiBona and colleagues[67] reported a bimodal distribution, this was not observed in the report of Sato and co-workers.[233] More recently, Fazan and colleagues[81] investigated the situation in the mouse and found that, although the nerve fibers had a similar mean diameter, 0.76 ± 0.02 μm, compared to the rat, the distribution was clearly unimodal. Together, these observations provide no consistent support for the argument that different nerve fibers are directed towards the innervation of specific cell types (vascular, epithelial or granular) in order to control selected functions.

Intrinsic Innervation

The sympathetic nerves generally traverse from the ganglia, running alongside the renal artery, and enter the hilus of the kidney where they begin to divide, with smaller nerve bundles approximately following the major divisions of the blood vessels. The sympathetic nerves begin to divide into smaller bundles which penetrate and form a network throughout the cortical and juxta-medullary areas. Early studies by Barajas and co-workers[9,10] demonstrated discrete neuro-effector junctions present at the afferent and efferent arterioles, the granular cells of the juxtaglomerular apparatus, the proximal and distal tubules, and the thick limb of the ascending limb of the loop of Henle. This group of investigators, utilizing electron microscopy, went on to show that the sympathetic nerves were typical autonomic fibers having varacosities associated with the neuro-effector junctions that contained dense cored vesicles. Using a tritiated noradrenaline radiographic approach they[9,10] clearly showed the presence of noradrenaline, and although there was a suggestion that acetylcholine esterase was present, there was no indication that the fibers were cholinergic. Later, more detailed studies indicated that there was a variation in the number of neuro-effector junctions along the nephron, with the greatest number being at the proximal tubule, fewer at the thick ascending limb of the loop of Henle, and the smallest number at the distal tubules and collecting duct.[58] Interestingly, when calculated as the density of neuro-effector junctions per unit length, the density was found to be greatest in the thick ascending limb of the loop of Henle and progressively less in the distal and proximal tubules.[9,10] There is also a regional variation, with the innervation being greatest along the cortico-medullary border and becoming less in the outer cortex and deeper regions of the medulla. This regional variation in innervation density is paralleled in both the vascular and tubular structures. Figure 16.2 illustrates the cell types where neuro-effector junctions have been described and the functions they may regulate.

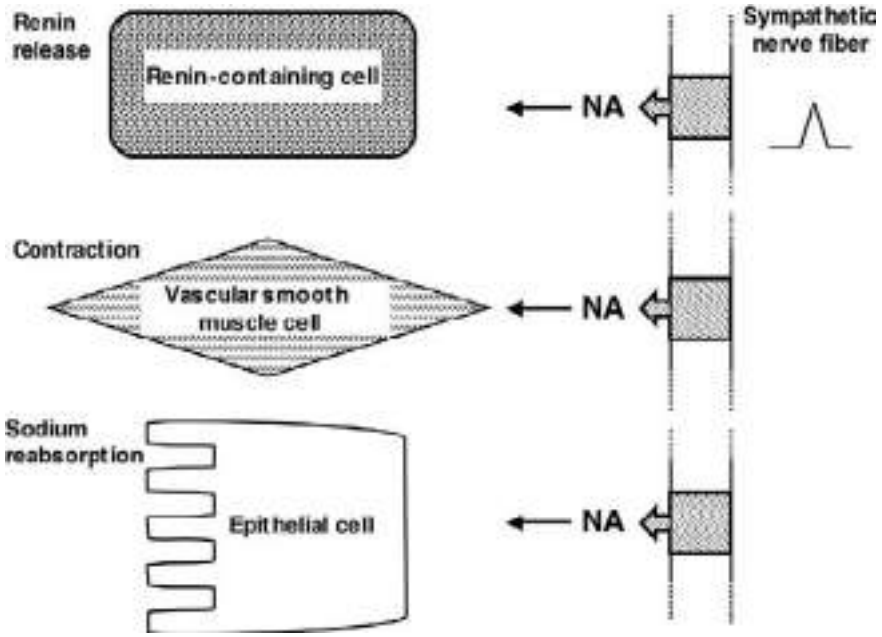

FIGURE 16.2 **Neuro-effector junctions are formed at the renin-containing cells, the vascular smooth muscle cells (interlobular arteries, afferent, and efferent arterioles) and the epithelial cells of the proximal tubule, thick ascending limb of the loop of Henle, and the distal tubule.** Noradrenaline (NA) is contained in granules within varicosities which are exocytosed following passage of an action potential.

Pharmacology

Neurotransmitters

A large body of evidence from biochemical and pharmacological studies indicates that the primary neurotransmitter arising from the sympathetic innervation is noradrenaline. Functional studies have shown that renal denervation, in the initial stages, is associated with a marked decrease in noradrenaline content of some 95%,[58] while activation of the renal sympathetic nerves results in an elevation in noradrenaline production or spillover into the renal venous blood.[75,76] The role of dopamine and potential dopaminergic nerve-mediated influences remains unclear, as all adrenergic nerve varicosities contain dopamine as an intermediary in noradrenaline biosynthesis, but there is little evidence that dopamine acts as a neurotransmitter[58] in the neural regulation of either renal hemodynamic function, renin release or fluid reabsorption.

Adrenoceptors

Multiple types of adrenoceptors are present within the kidney mediating the actions of noradrenaline released from the nerve varicosities, and a range of α_1- and α_2-adrenoceptors subtypes exist along the renal vasculature and nephrons. At a functional level, stimulation of the α-adrenoceptors causes a vasoconstriction of vascular smooth muscle and reabsorption of fluid at tubular epithelial cells. Stimulation of β-adrenoceptors increases renin release at the juxtaglomerular granular cells. A number of molecular biological and cloning investigations have defined α_1-adrenoceptors into α_{1A}-, α_{1B}-, and α_{1D}-subtypes, α_2-adrenoceptors into α_{2A}-, α_{2B}-, and α_{2C}-subtypes, and β-adrenoceptors as β_1-, β_2-, and β_3-subtypes, all of which are G-protein coupled receptors comprising a superfamily of membrane proteins that signal the actions of adrenaline and noradrenaline.[251] The α_1-adrenoceptors utilize a range of signaling pathways including activation of phospholipases A and C, mobilization of intracellular calcium stores, as well as opening of voltage-dependent and independent calcium channels[225] which results in a rapid vascular smooth muscle contraction. Interestingly, noradrenaline binding to α_1-adrenoceptors also activates the MAP kinase pathways which, in the longer term, are responsible for regulating growth and hypertrophy of the vascular smooth muscle.[263] There are reports that α_{1A}- and α_{1B}-adrenoceptors are present to a similar degree in the cortex and outer stripe of the medulla, while in the inner stripe of the medulla the α_{1B}-adrenoceptor subtype appears to predominate.[83] However, in terms of hemodynamic functionality, α_{1A}-adrenoceptors are more effective than the α_{1B}-adrenoceptor subtypes in causing renal vasoconstriction.

α-Adrenoceptors are also present on the epithelial cells of the nephron, where they modulate fluid reabsorption. There is evidence, at least in the proximal tubule, that α_1-adrenoceptor stimulation engages both the phospholipase C and MAP kinase[264] pathways, but these signal to different end-points, that is to the sodium/hydrogen exchanger, isoforms-1 (NHE1) and isoform-3 (NHE3), respectively.[179] At the more distal sections of the nephron, the distal tubule and collecting duct, α_2-adrenoceptors are the primary subtype, and in this segment their activation results in a decrease in cAMP which blunts the action of other factors signaling through this pathway. A key example is AVP,[223] which stimulates both water reabsorption

and ENaC insertion in this region where these actions are blunted by α_2-adrenoceptor agonists.[8] β_1-adrenoceptors are found primarily on the granular renin-containing cells of the afferent arteriole, and their activation stimulates adenylyl cyclase which increases intracellular levels of cAMP. The β_2-adrenoceptors found on the tubules, primarily collecting duct, also utilize cAMP production as the signaling molecule, but their function at this site has not been resolved.

PHYSIOLOGY

Activation of the various signaling pathways via ligand binding to the adrenoceptors increases fluid reabsorption at the level of the proximal tubule. In the proximal tubule, the catecholamines stimulate Na/K-ATPase at the basolateral membrane,[4] resulting in increased sodium reabsorption from the tubular lumen across the apical membrane. There is evidence from micropuncture studies,[212] as well as *in vitro* studies,[180] that the sodium−hydrogen exchanger is activated, particularly isoform 3 (NHE3), the isoform primarily responsible for the regulation of sodium entry into the epithelial cells at the proximal tubule.[179,180] The NHE3 protein in the proximal tubule appears to be present in the microvillae, either incorporated into the plasma membrane[273] where it is likely to be active or internally in the subapical vesicles, where it is considered to be inactive in terms of a transporting protein. The mechanisms involved in the translocation of the NHE3 from the plasma membrane into the subapical vesicles are complex[197] and require the interaction of a number of proteins (NHERF1, myosin VI, ezrin, raft, non-raft, and myosin). McDonough[197] has recently reviewed the evidence showing that when blood pressure is elevated acutely[273] or when the sympathetic nervous system is reflexly activated there is increased movement of NHE3 into the subapical compartment where the transporter is inactive. McDonough and co-workers have put forward the concept that translocation of the NHE3 into the subapical regions is a key element whereby sodium reabsorption may be regulated by catecholamines, both in the short-term as well as over a longer timeframe, thereby contributing to cardiovascular homeostasis.[197,198]

Autocrine and Paracrine Influences on Neurotransmission

The interstitium of the kidney contains a complex milieu of hormones and factors which may vary across the cortex and medulla, but can determine the level of functions of all cell types, vascular smooth muscle, renin containing, and epithelial cells. There are modulator influences at the neuro-effector junction which can come into play and influence the amount of noradrenaline released in response to depolarization caused by the passage of an action potential. An outline of potential interactions with various agents is illustrated in Figure 16.3.

Adrenoceptors

At an early stage it was recognized that pre-synaptic α_2-adrenoceptors were able to act in an auto-inhibitory fashion, whereby when activated by noradenaline released into the neuro-effector junction, they decreased neurotransmitter release caused by subsequent depolarizations. There is evidence that this situation pertains at the kidney. α_2-adrenoceptors are present in the kidney,[18,19] and their blockade enhances noradrenaline release and renal nerve induced vasoconstriction in the dog.[113] In the rabbit[109] blockade of α_2-adrenoceptors peripherally has little effect on renal nerve-induced vasoconstrictions, but potentiates the renal nerve-mediated antidiuresis and antinatriuresis.

Angiotensin II

A second important neuro-modulator is angiotensin II, which is present in the renal interstitium at high levels in conditions of increased endogenous angiotensin II production.[122,211,243] Activation of pre-synaptic AT-1 receptors facilitates the release of noradrenaline. This was first reported by Boke and Malik[21] using the isolated perfused rat kidney. They found that renal nerve-induced catacholamine release into the renal vein was facilitated when angiotensin II was added to the perfusate. At a functional level, studies in the anaesthetized rat using both direct and reflex activation of the renal nerves, at levels which had little or no effect on renal hemodynamics, caused decreases in fluid excretion which were blocked in the presence of an angiotensin-converting enzyme inhibitor,[102] and restored following administration of exogenous angiotensin II.[129] Similar observations were reported by Veelken and colleagues[258] in the conscious rat, where administration of the AT1-receptor antagonist ZD 7155 blunted the renal nerve-dependent antidiuresis and antinatriuresis in response to an air-jet stress test. Together, these findings support the view that at both renal vascular and epithelial cell neuro-effector junctions occupation of pre-synaptic AT1 receptors enhances neurotransmission. It would seem that these receptors are fully occupied, even at low endogenous levels of angiotensin II[256,258] and under normal conditions the facilitation is maximal but when production is prevented, then neurotransmission will be blunted. There may be other interactions at the post-synaptic membranes of the epithelial cells. Quan and colleagues[228,229] demonstrated that the ability of angiotensin II

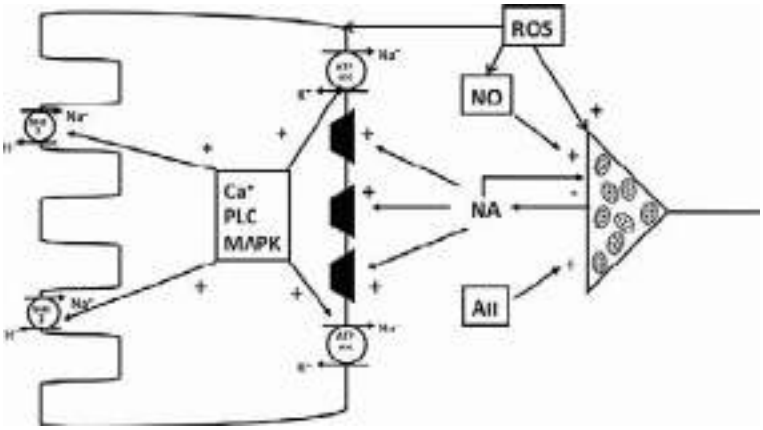

FIGURE 16.3 **Noradrenaline (NA) acts on the epithelial cells to activate phospholipase C, increases intracellular calcium (Ca^+) which initiates MAP kinase signaling pathways stimulating both the apical sodium–hydrogen exchanger isoform 3 (NHE3) and the basolateral sodium/potassium-ATPase.** Noradrenaline exerts an auto-inhibitory feedback action on further release (−) while nitric oxide (NO) and angiotensin II (AII) exert an action (+) to increase the amount of noradrenaline release on passage of each action potential. Reactive oxygen species (ROS) appear to directly facilitate noradrenaline release and indirectly to modulate the action of NO.

to stimulate proximal tubule fluid reabsorption was blunted following acute renal denervation, but augmented if the renal sympathetic nerves were stimulated at low levels not affecting filtration rate. A comparable interaction was reported by Abdulla and co-workers,[1,2] who found that the renal vasoconstriction caused by close renal arterial infusion of angiotensin II was blunted following acute renal denervation. Thus, these observations demonstrate that angiotensin II has modulatory activities at the neuro-effector junction, both pre-synaptically and post-synaptically, which determine the effectiveness of the neural control of renin release, fluid reabsorption, and vascular tone in the kidney.

Nitric Oxide

A third potentially important factor determining noradrenaline release, and hence its impact on functional end-points, is nitric oxide (NO). All isoforms of nitric oxide synthase (NOS), endothelial (eNOS), neuronal (nNOS), and inducible (iNOS) are present in the kidney. eNOS has been found along the vasculature and glomerular capillaries,[7,194] nNOS is present in the renal nerves,[156,181] at low concentrations along the tubules[24] and high concentrations in the macula densa,[7] while iNOS is expressed constitutively in the medulla.[142] It is possible that in the environment of the neuro-effector junction, NO may have both pre-synaptic and post-synaptic actions, and this probably contributes to the conflicting findings which have been reported. Thus, in the anaesthetized dog, the low level renal nerve stimulated noradrenaline output was enhanced following NOS inhibition and suppressed in the presence of an NO donor, consistent with an inhibitory pre-synaptic action.[71,188] In contrast in the rat, NOS blockade suppressed renal nerve mediated noradrenaline output and neurally induced renal vasoconstriction.[253,259] In terms of the influence of NO on renal nerve stimulated increases in sodium reabsorption, there is a lack of consistency. It is evident that NOS inhibition increases, and exogenous NO decreases, proximal tubule fluid reabsorption,[72,213] suggesting an inhibitory action of NO on reabsorptive processes. Importantly, this action of NO is only evident if the renal nerves are intact.[266] In an apparent conflict with these studies are the findings that renal nerve-induced increases in fluid reabsorption are prevented by NOS blockade, consistent with a facilitating action of NO.[268] In attempting to clarify these differing reports, it is possible that NO could act in two ways, directly within the post-synaptic cell, either vasculature or epithelial cells, where it may blunt the neurally controlled cell function, or indirectly by facilitating neurotransmitter release. The differing balances between these two sites of action may simply reflect how the NO generating systems may be activated by the various experimental conditions of the investigations.

Reactive Oxygen Species

The generation of cellular energy results in the production of reactive oxygen species which comprise radicals that can damage both nuclear and cytoplasmic proteins and phospholipids. A raised output of reactive oxygen species is recognized as a state of oxidative stress that is associated with a range of metabolic and cardiovascular diseases. Reactive oxygen species comprise superoxide anions, H_2O_2, and other reactive radicals which are able to influence both neurotransmission and the responsiveness of the target cells to the neurotransmitter. The actions of the reactive oxygen species may be either direct or indirect, as a consequence of their ability to reduce the bioavailability of NO. There are reports that systemic infusion of tempol, a synthetic diffusible superoxide dismutase mimetic which scavenges superoxide anions,[239,272] reduced blood pressure and renal sympathetic nerve activity to the same extent before and following NOS blockade. These findings would be compatible with the argument that in states of oxidative stress, for example hypertension, increased production of superoxide anions could enhance the activity of the sympathetic nervous system, and hence the level at

which it influences kidney function. The enzymes NAD(P)H and superoxide dismutase are present in both the cortex and medulla of the kidney,[133] with the level of the latter being somewhat higher in the medulla. This group[133] demonstrated that oxidative stress increased the activity of NAD(P)H, but not superoxide dismutase, in the cortex but not the medulla. This would suggest that in renal oxidative stress whereas superoxide anion generation would increase, the level of scavenging would remain unaltered, implying greater activity of the reactive oxygen species. This is important in terms of renal sympathetic nerve activity, as Shokoji et al.[239] demonstrated that direct application of tempol or DETC, a blocker of superoxide dismutase, directly onto renal sympathetic nerve fibers decreased and increased nerve traffic, respectively. These findings imply that oxidative stress in the kidney can itself alter the level of reactive oxygen species in the local environment, which may directly affect the level of renal sympathetic nerve activity and renal nerve-dependent function.

CONTROL OF THE RENAL CIRCULATION

Activation of Renal Sympathetic Nerves

The earliest studies by Cohnheim and Roy[38] using a renal plethysmograph, demonstrated that renal volume was decreased following asphyxia or when the cut ends of the renal nerves were stimulated. Indeed, these early plethysmographic studies also identified the spinal origin of the vasoconstrictor fibers. The advent of the modern flowmeters to measure renal blood flow dynamically allowed studies in anaesthetized dogs, cats, rabbits, and rats[58] which convincingly demonstrated that direct electrical stimulation of the renal nerves caused frequency related reductions in renal blood flow. Furthermore, reflex activation of the renal sympathetic nerves, either as a consequence of activation of the baroreceptor reflex by reduction in carotid sinus pressure[54,69] or activation of the somatosensory system[45,255] resulted in a renal nerve-mediated reduction in renal blood flow. Together, these reports indicate that renal nerves cause contraction of the vascular smooth muscle of the resistance vessels, thereby reducing blood flow. While the innervation of the afferent arteriole would cause a reduction in renal blood flow because it is the major resistance bed within the kidney, the impact and relative importance of a neurally induced vasoconstriction at the efferent arteriole is less clear cut in terms of its overall contribution to the reduction in renal blood flow. Luff and co-workers[49,183] were able to identify at the ultrastructural level two types of fibers in the rabbit that were differentially distributed, one type solely innervating the afferent arteriole and a second type evenly distributed to both afferent and efferent arterioles, which they argued enabled an independent regulation of the two resistance vasculatures. However, an alternative view is that because of the differing wall thicknesses and lengths of the afferent and efferent arterioles, even if both vessels constricted to a similar degree, the efferent arteriolar constriction would have a greater impact on glomerular filtration pressure,[48,50] and hence filtration rate.

A number of studies have reported a disparity in the magnitudes of the reduction in renal blood flow and glomerular filtration rate produced by renal nerve stimulation. Studies in the anaesthetized rabbit,[108] cat,[131] and rat[102] demonstrated that modest neurally induced reductions in renal blood flow (of 15–20%) were accompanied by either no change or a small 2–5% reduction in glomerular filtration. However, if angiotensin II activity was reduced by converting enzyme inhibitors, angiotensin II type 1 (AT-1) receptor blocking drugs or β-adrenoceptor antagonists, the neural impact on glomerular filtration rate became greater, with the magnitude of reductions in glomerular filtration rate becoming roughly proportionate with renal blood flow.[128] These reports gave rise to the important concept that the renal nerves, indirectly via locally produced angiotensin II acting at the efferent arteriole, could ensure that over a modest range of variation in renal blood flow, the glomerular filtration rate, and hence filtered load presented to the nephrons, was maintained at a relatively constant level.

Renal Denervation

An important question is whether under basal, unstressed conditions the renal sympathetic nerves have a tonic influence on basal blood flow through the kidney. The reasons for this uncertainty reside in the manner of the experimental studies, whether anaesthetized or conscious preparations were used, the degree of surgical stress and type of anaesthesia used, and, to a degree, the species under study. Thus, in a number of reports in the anaesthetized rat, there was very little change in renal blood flow following acute renal denervation.[58] However, in these studies there was often a relatively long period of time between basal measurements, the surgical manipulation and denervation of the kidney, and the post-surgery measurements, with the result that it was difficult to determine whether changes had taken place. In an attempt to resolve this issue, Kompanowska-Jezierska and colleagues[141] inserted an electro-cautery wire around the bulk of the nerves, and instantaneous denervation occurred when

a current was passed to destroy the neural tissue. Under these conditions, it was found that over the first 10 to 20 minutes an increase of some 20% in blood perfusing the outer cortex occurred when measured by laser Doppler flowmetry, suggesting there was sufficient activity within the renal nerves to decrease basal renal blood flow. This view was to a degree supported by the conscious rabbit reports of Malpas and co-workers,[190] who found that seven days after renal denervation, renal blood flow was some 55% to 65% higher in the denervated compared to the innervated kidney, the large difference most likely indicative of greater basal sympathetic outflow in the rabbit.

The studies of Miki and co-workers[277] using the conscious rat showed that while basal renal blood flow in the groups of animals with either intact or denervated kidneys could not be distinguished, an increase in renal sympathetic nerve activity during grooming and movement caused a proportionate decrease in blood flow to the intact kidneys of some 15%, whereas that to the denervated kidneys tended to increase in line with blood pressure. The relationship between renal blood flow and stress-induced activation of the sympathetic nervous system was the basis of the study undertaken by Brod and co-workers.[25] They demonstrated in man that, in the unstressed state, administration of an adrenergic blocking drug, dibenamine, had no effect on para aminohippurate (PAH) clearance (effective renal plasma flow), but if the patients were tense, anxious, and stressed, the dibenamine administration was associated with a rise in PAH clearance compatible with the view that there was a tonic renal nerve-induced reduction in renal blood flow. Thus, the degree of tonic influence of the renal sympathetic nerves on basal hemodynamics is dependent on the level of stress impinging on the subjects, and in the normal conscious state the renal sympathetic nerves have relatively little impact.

Neural Regulation of Intra-Renal Hemodynamics

Measurement of Intra-Renal Hemodynamics

The measurement of blood flow through the cortical and medullary regions of the kidney is difficult and fraught with technical limitations. Videomicroscopic techniques have been used to evaluate blood flow through single vasa recta vessels.[41] The limitation of many techniques used such as the Rhubidium-86 methodology is single estimations from one kidney,[107] the H_2-washout method is the accuracy of curve fitting of the data,[5,6] and the trapping of labeled microspheres in glomerular is only two to three measurements per kidney.[37] More recently, there has been greater use of laser-Doppler technology, which allows continuous measurements of blood perfusion through the cortex and medulla of the same kidney. The limitations of this technique are that the values recorded are not flow, but are a flux measurement derived from the product of the velocity as well as the number of red cells moving through the volume of tissue illuminated by the laser. Consequently, the values arising from this technique represent qualitative rather than quantitative evaluations of blood flow.

Activation of the Renal Nerves

There have been a series of investigations addressing how and whether the renal sympathetic nerves may differentially regulate blood flow through the cortex and medulla. Early studies in this area applying the H_2-washout approach in the anaesthetized dog[5,6] indicated that adrenergically-mediated decreases in flow were of comparable magnitude in both cortical and medullary regions. Similar findings were reported using the Rhubidium-86 methodology,[107] in that stimulation of the renal sympathetic nerves caused equivalent decreases in flow through both cortex and medulla. By contrast in later reports, Rudenstam et al.[231] used laser-Doppler flowmetry in the rat and observed a relative resistance of medullary perfusion to decrease in response to renal sympathetic nerve stimulation. Evans and co-workers,[74,97,177] using the same technique in the anaesthetized rabbit, demonstrated smaller reductions of the perfusion in the medulla than in the cortex or total renal blood flow. Further studies in rabbits[96] showed that the magnitude of reduction was similar across the medullary region, irrespective of the depth at which measurements were made (inner or outer medulla). This, to a degree, contrasts with the findings in the anaesthetized rat,[259] where the inner medullary perfusion was less responsive than the outer medullary area to renal nerve stimulation. The reasons underlying the differences reported in the sensitivity of the two vascular regions (cortex versus medulla) to adrenergic stimulation are unclear, but they may reside in the differing characteristics of the afferent and efferent arterioles (which may also vary between outer and inner cortical regions), possible variations in innervation density, species variation or the mix of paracrine and autocrine factors residing in the interstitium in these different regions. The potential interactions of all these factors have been considered in detail in recent reviews.[78,79]

CONTROL OF RENAL TUBULAR SOLUTE AND WATER TRANSPORT

Renal Denervation

Claude Bernard[17] first noted that section of the splanchnic nerve of the anaesthetized dog caused an

increase in urine flow. Questions arising from this finding were whether the raised fluid excretion was due indirectly to an increase in glomerular filtration rate, whether it was the result of a direct action on the tubular reabsorptive processes of the epithelial cells or a combination of these mechanisms. This problem was addressed by Bonjour and co-workers[22] using the anaesthetized dog, who convincingly demonstrated that the elevated urine flow and sodium excretion subsequent to the section of the renal sympathetic nerves was independent of any changes in glomerular filtration rate. They concluded that the raised fluid excretion reflected a direct influence of the nerves on tubular function. Thereafter, this view was supported by a series of reports using micropuncture techniques which directly examined reabsorptive rates along accessible segments of the nephron. Bello-Reuss and colleagues[14,15] observed in the anaesthetized rat that section of the splanchnic nerves had a minimal effect on single nephron glomerular filtration rate, but was associated with significant decreases in both absolute and fractional sodium and water reabsorption at the proximal tubule. These conclusions were supported by other investigators at that time, using comparable techniques to directly measure tubular function.[252,267,268]

Renal Nerve Stimulation

The removal of the influence of the renal sympathetic nerves represents only one way of illustrating their action, and to fully appreciate their influence a corresponding series of studies were necessary in which the renal nerves were activated. In a ground-breaking study, LaGrange and co-workers,[175] using the anaesthetized dog, found that direct electrical stimulation of the nerves at levels that were sub-threshold for changing either renal blood flow or glomerular filtration rate, caused a 30–40% fall in water and sodium excretion, which was interpreted as a direct action of the renal nerves on tubular fluid reabsorption. A similar situation was found to exist in the rabbit[108] and rat,[132] in that electrical stimulation of the renal nerves at levels subthreshold for decreasing renal blood flow, decreased both urine flow and sodium excretion. These observations were supported by micropuncture studies which more directly evaluated the tubular actions of the nerves. These studies[16] demonstrated that the absolute and fractional sodium and water reabsorption of the proximal tubule was increased by low frequency direct electrical stimulation of the renal nerves which was without effect on single nephron filtration rate. Moreover, DiBona and Sawin[62] found in the anaesthetized rat that low frequency stimulation of the renal nerves, at rates which did not alter renal blood flow or glomerular filtration rate, also increased fluid reabsorption at the thick limb of the ascending loop of Henle.

Thus, there is a large body of information which substantiates the view that the renal sympathetic nerves, when activated at low rates which have minimal effects on renal hemodynamics, have a direct action on the transport processes of the epithelial cells of the proximal tubule and the thick ascending limb of the loop of Henle. The situation regarding the distal tubule and the collecting duct has not been investigated in depth, primarily because of the technical hurdles required to evaluate reabsorption in these segments *in vivo*. Interestingly, Bankir and colleagues[8] have reviewed evidence for the concept that activation of vasopressin V2 receptors along the collecting duct not only increases water abstraction, but also activates epithelial sodium channels (ENaC) in the principal cells of this nephron segment. The EnaC-mediated antinatriuresis takes place in association with V2-induced increases in cAMP, and occurs at high plasma levels of vasopressin typically seen in pathophysiological states. The possibility arises that activation of α_2-adrenoceptors along this nephron segment,[222,223] which are known to suppress cAMP, could interact with vasopressin to determine the level not only of water retention, but also of the sodium due to ENaC insertion. The relationship between vasopressin and adrenoceptor activation at this nephron segment remains a source of investigation.

NEURAL CONTROL OF RENIN RELEASE

Renin Containing Cells

Renin Production

The granular cells of the juxtaglomerular apparatus contain renin. These cells are found in the afferent arterioles at increasing density as the vessel approaches the glomerulus.[98] The origin of these cells has been examined in a study by Sequeira-Lopez et al.[236] using single cell PCR and double immunostaining combined with lineage markers. By transplanting embryonic kidneys between genetically lineage marked mice containing cells for renin, smooth muscle, and endothelial cells with wild-type mice, they showed two distinct populations of cells expressing either renin or smooth muscle cell markers, but never both in the same cell. During the course of maturation, the renin cell began to express the smooth muscle cell markers, suggesting that renin cells could progress into smooth muscle cells and, if required, back into renin cells. Importantly, it appears that the transformation the other way round cannot happen, that is, the smooth muscle cells do not transform into renin cells.[220,236] The situation seems to be that when demand for renin is high, for example as a consequence of

reduced renal perfusion pressure or following a low dietary sodium intake, some smooth muscles will transform back into renin producing cells. Expression of the renin gene generates a specific mRNA which translates into a large protein, pre-pro-renin, which then undergoes processing to generate pro-renin.[98] The pro-renin then undergoes one of two fates, it can be secreted constitutively in an unchanged form, which represents "inactive" renin or it is incorporated into the secretory granules, where it undergoes further modification into mature renin. The secretion of renin occurs when exocytosis of the granules is stimulated. The exocytosis of the granular cells is regulated by two main intracellular signaling molecules, cAMP which stimulates renin release and intracellular calcium ion concentration (Ca^{2+}) which inhibits renin secretion.

Renin Cell Electrophysiology

The membrane potential of the granular cells is determined by a variety of ion channels influenced by cAMP and Ca^{2+}. Large conductance calcium-sensitive voltage-activated channels (BKa) are opened by increased intracellular cAMP, resulting in hyperpolarization. L-type voltage-dependent calcium channels ($Ca_v1.2$) which inhibit cAMP-mediated exocytosis.[85,86] The normal physiological process is one where the cAMP stimulation of renin granule exocytosis is protected against activation of L-type calcium channel by the hyperpolarization that results from the cAMP induced opening of the BKa. In this way, renin secretion can occur in a regulated manner independent of intracellular Ca^{2+}. These relationships and interactions are illustrated in Figure 16.4.

There are three primary intracellular signaling pathways which interact to determine the rate of renin secretion: cAMP; cGMP; and cytosolic calcium. Good evidence exists[13] that cAMP is the key signaling molecule. In mice with deletion of the G-protein $G_{s\alpha}$ in juxtaglomerular cells,[30] plasma renin is low and the mice are unresponsive to stimuli such as β_1-adrenoceptor stimulation which utilize cAMP. On the other hand in intact mice, challenges that stimulate adenyl cyclase or suppress phosphodiesterase enzymes result in increased renin release. The role of intracellular calcium in the regulation of renin secretion is only now becoming clear.[235] Angiotensin II-, endothelin-, and ADH- receptor-mediated increases in intracellular calcium suppress the exocytosis of the renin granules. Indeed, the intracellular calcium levels are inversely proportional to those of cAMP, that is, as intracellular calcium decreases there is an increase in cAMP and renin release, and *vice versa*.[98,221] It would seem that adenylyl cyclase isoforms 5/6 are inhibited by increased intracellular calcium, thereby determining the rate of cAMP generation. Taken together, the scenario put forward[235] is that cAMP is the primary intracellular signaling molecule eliciting renin release, and this occurs through activation of β_1-adrenoceptors. The other factors and mechanisms, which exert their actions via changes in calcium entry into the granular cells and therefore the activity of adenyl cyclase 5/6, will serve to modulate the sensitivity of the cAMP-dependent pathways for renin secretion.

Activation of the Renal Nerves

The stimulation of renal secretion and the exocytosis of the granules are regulated through three main routes, the renal baroreceptor mechanism, the macula densa and the renal sympathetic nerves. Many of the early investigations utilized either electrical stimulation or reflex activation of the renal sympathetic nerves, and showed that plasma renin activity or renin

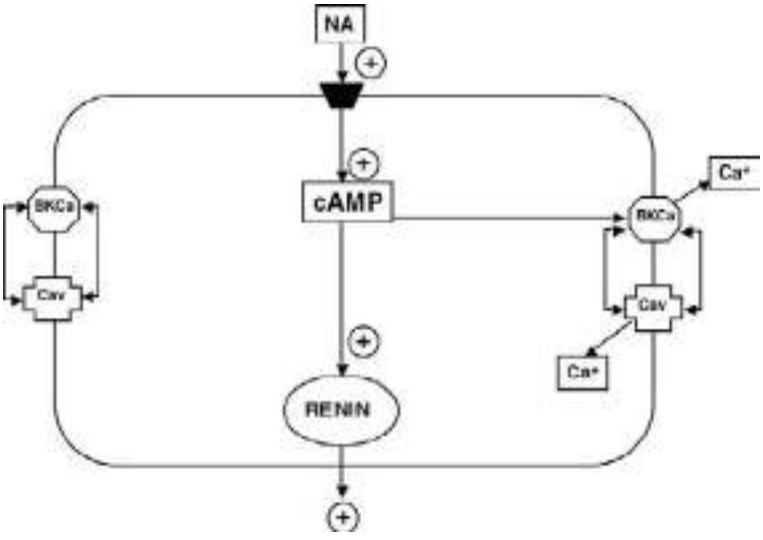

FIGURE 16.4 **Noradrenaline-adrenoceptor on a renin-containing cell to increase (NA) stimulates intracellular cAMP which then initiates exocytosis of renin-containing granules, releasing renin.** At the same time, cAMP acts at the BKCa channel to cause a hyperpolarization which to a degree suppresses the CaV channel offsetting calcium entry, an effect tending to inhibit renin secretion.

secretion was increased[58,143] which could be prevented by administration of β-adrenoceptor antagonists. Often interpretation of these findings was complicated by the concomitant reductions in renal blood flow and glomerular filtration rate which could have also contributed to the rise in renin release. The reports by Kopp et al.[143] and Osborn et al.[215] demonstrated that electrical stimulation of the renal sympathetic nerves at low frequencies producing no or small decreases in renal blood flow resulted in increases in renin release that were prevented by administration of a β_1-adrenoceptor antagonist in anesthetized dogs. This view of renin release from the granular cells being due to a direct action of neurally released noradrenaline has been supported by comparable observations in the rabbit and rat, as well as man.[128,269]

It is now clear that the neurally-induced renin release is associated with a rise in renal renin mRNA. This effect becomes measurable at relatively high levels of renal nerve stimulation over an extended period of time, of approximately an hour, causing large increases in plasma renin activity.[207] Interestingly, a number of reports have indicated that cAMP stimulates renin gene expression by binding to an enhancer region upstream of the gene,[218,240] as well as increasing the stability of renin mRNA.[221,242,261] The mechanisms involve cAMP-dependent phosphorylation mediated by ERK kinases.[98] Thus, the nerve-mediated increase in cAMP may act in several ways, first to cause an immediate release of renin as a result of exocytosis of the granules; second to increase renin gene expression; and third to cause a stabilization and prolongation of the action of renin mRNA, all actions to ensure that sufficient renin is available and stores are replenished.

Neural and Non-Neural Interactions and Renin Release

A number of early observations gave rise to the concept that a background level of renal nerve activity was necessary to allow the differing renin releasing mechanisms to operate normally. It was the initial studies of Stella et al.[248] in the anaesthetized cat that demonstrated that increased renin secretion as a result of reductions in renal perfusion pressure or renal blood flow were blunted in the denervated compared to the innervated kidneys. Furthermore, Johns[130] demonstrated that during reflex activation of the sympathetic nervous system following reduction of perfusion pressure at the carotid sinus, the magnitude of renin release when renal perfusion pressure was reduced was greater in the innervated than denervated kidneys. These findings were extended by Holdaas et al.[114] and Osborn et al.[216] using the anaesthetized dog, who found that furosemide-induced renin release was enhanced when the renal sympathetic nerves were intact compared to that obtained when the kidneys were denervated. Indeed, Kopp and DiBona[160] clearly demonstrated in the dog that the relationship between the magnitude of renin released in response to a particular level of electrical stimulation of the renal nerves was dependent on the prevailing level of renal perfusion pressure. The mechanisms involved at the cellular level remain undefined.

INTEGRATION OF RENAL NERVE ACTIVITY AND FUNCTION

Recruitment of Functionalities

An important consideration after having defined the exact mechanisms by which the renal nerves exert their influence on the different end-points of kidney function, renin release, fluid reabsorption, and renal hemodynamics, is the relationship between the recruitment of these functionalities under normal conditions. At low levels of renal nerve stimulation, which is subthreshold for changing fluid reabsorption and renal hemodynamics, there is an increase in renin secretion. At somewhat higher levels of renal nerve activation, but again sub-threshold for impacting on renal hemodynamics, not only are there larger increases in renin secretion, but there is also an antidiuresis and antinatriuresis which has been demonstrated in the anaesthetized dog, rabbit, and rat.[58] It is clear that the renal nerve-induced sodium and water retention under these conditions reflects a direct action on proximal tubule reabsorptive processes, as described in micropuncture studies using the anaesthetized rat.[16,266,267] At high levels of renal nerve stimulation, the raised renin release and fluid retention is enhanced, but is now accompanied by a reduction in renal blood flow and, depending on the actual level of stimulation, a decrease in glomerular filtration rate.[58] Indeed, this progressive recruitment of renal functionalities has been shown to occur in man in an elegant study by Wurzner et al.[269] who used lower body negative pressure (LBNP) to reflexly activate the sympathetic nervous system. They found that as LBNP was progressively reduced, there were associated proportionate increases in plasma noradrenaline and plasma renin activity, while sodium excretion was only reduced at the lowest LBNP used. During these challenges neither renal blood flow nor glomerular filtration rate were changed. The way in which these functionalities are recruited is illustrated in Figure 16.5.

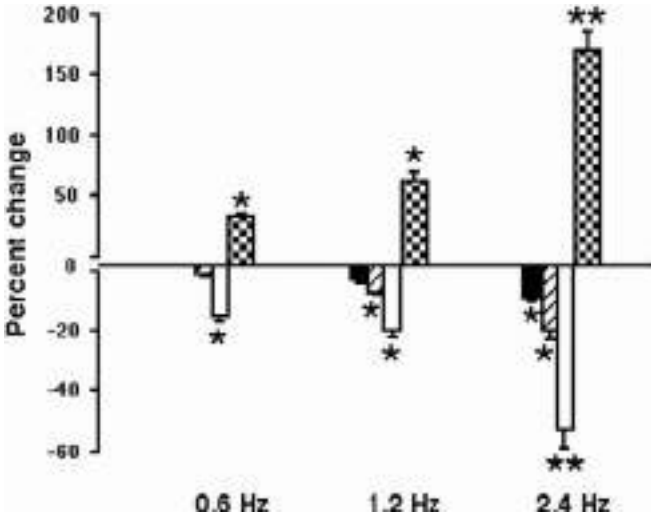

FIGURE 16.5 **At the lowest level of renal nerve stimulation (0.6 Hz), there are significant increases in plasma renin activity (stippled bars) and decreases in sodium excretion (open bars), but no effect on either renal blood flow (hatched bars) or glomerular filtration rate (filled bars).** As the frequency of stimulation is increased there are larger increases in all variables, particularly the decreases in renal hemodynamics which become significant. Importantly the frequency–response relationships are much steeper for plasma renin activity and sodium excretion than for renal blood flow or glomerular filtration rate. *(Modified from ref. [109].)*

There are two important considerations which arise from this pattern of responses. At low levels of renal sympathetic nerve activity, the major impact will be on renin release and sodium and water reabsorption. At these low levels of activity there will only be small increases in circulating renin (50–70%) and reductions in sodium excretion of some 20–40%. However, if these effects persist over a long timeframe, they could have a profound impact on extracellular fluid volume, and thereby on the level at which blood pressure is set. Again, it is worth reiterating that these renin releasing and sodium retaining responses can occur with little evidence of major reductions in renal hemodynamics.

By contrast, when renal sympathetic nerve activity is raised to higher levels by major stressors (for example emotional challenges, severe exercise), then blood flow through the kidney will be markedly reduced. However, it is important to emphasize that these are short acting events, and therefore they are likely to have only minor influences on overall cardiovascular homeostasis.

Patterns of Electrical Stimulation of the Renal Nerves

Patterns of Efferent Activity

The concepts of how the renal nerves influence kidney function have been based largely on experiments in which the sympathetic nerves to the kidney have been dissected out, placed on electrodes, and stimulated using square wave pulses of defined width and voltage at increasing frequencies and constant current delivery. It has been recognized that this pattern of stimulation bears no relation to that passing down the nerves naturally to reach the kidney. Indeed, multifiber nerve recordings have shown the signal to be composed of a bursting nature where larger or smaller numbers of fibers fire together in a coordinated or disparate fashion, with the result that complex patterns are generated. The issue is whether the effectiveness or impact of the nerves on one or more functions might be different if they were stimulated in a way more representative of that occurring under natural conditions.

Lacroix et al.[176] and Nilsson et al.,[210] using isolated mesenteric and nasal vessels, demonstrated that larger sympathetically-mediated vasoconstrictions were produced using high frequency bursts of impulses compared to the delivery of the same number of impulses as a continuous train. This was to a degree reinforced by the observations of Hardebo,[103] who found that the high frequency bursting pattern caused a greater release of noradrenaline from cerebral vessels than that achieved with the same number of impulses delivered as a continuous stream. Thus, the amount of neurotransmitter released can be influenced by the exact pattern of stimulation used.

Electrical Activation with Frequency Enriched Stimuli

HEMODYNAMICS AND FUNCTION

The question therefore arises as to whether the effectiveness or impact of the renal sympathetic nerves could be influenced by the pattern of the stimulation parameters. This was investigated by DiBona and Sawin[66] in the anaesthetized rat using a complex computer generated stimulus pattern basically of a sine wave, within which was embedded a randomly generated white noise signal. The patterned stimulus was designed to approximate that which the kidney might normally be expected to receive. The authors used two levels of intensities, one impacting on renal hemodynamics and one at a lower level which only influenced excretory function. Importantly, they showed that for the same integrated voltage applied to the nerves, the magnitude of reduction in renal blood flow was greater with the sinusoidal patterned stimulus than with the square wave stimulus at all frequencies tested. This data is presented in Figure 16.6, where there is a clear shift of the frequency–response curve to the left with the sinusoidal stimuli compared to the square wave stimuli. In a similar way, application of sub-threshold stimuli for changing renal hemodynamics had no effect

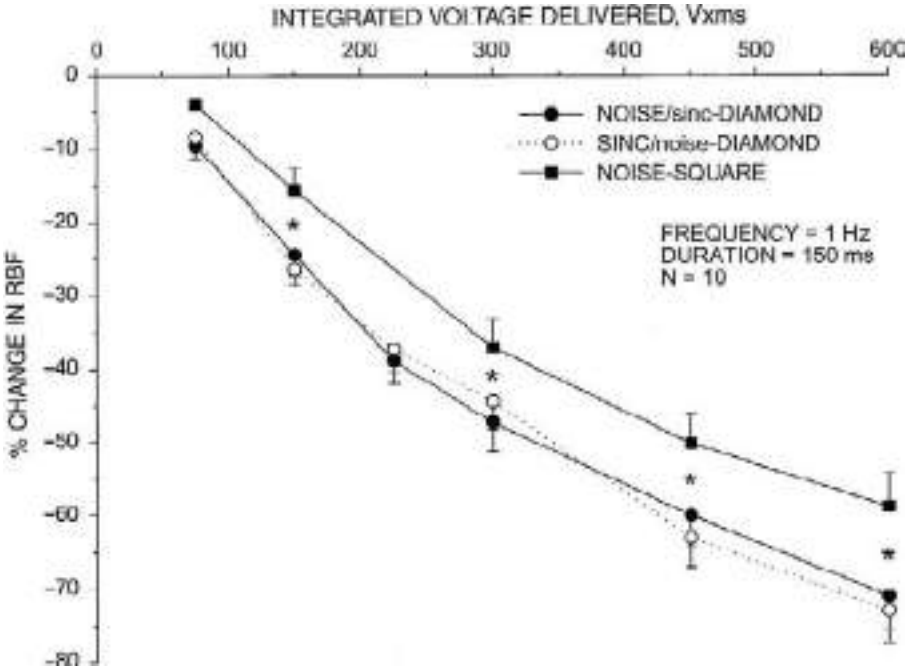

FIGURE 16.6 This figure *(taken from* ref. *[66] with permission)* demonstrates that delivery of an electrical stimulus as a square wave pulse (NOISE-SQUARE) is less efficient in decreasing renal blood flow (RBF) at every integrated voltage step compared with stimuli delivered as a sinusoidal wave containing either noise (NOISE/SINC-DIAMOND) or fixed frequency within the sinusoidal wave (SINC/NOISE-DIAMOND).

on sodium excretion if delivered in a square wave form, but did cause an antidiuresis and antinatriuresis at the same integrated voltage if the sinusoidal signal was used, and this is illustrated in Figure 16.7. Thus, together these reports serve to emphasize that the way in which the neural signals are delivered into the kidney can determine the impact on end-organ function.

HEMODYNAMICS

Malpas and colleagues,[95,191,192] using the anaesthetized rabbit, investigated whether the bursting pattern of naturally occurring renal nerve activity could in any way determine the dynamic regulation of renal blood flow. Utilizing a similar patterned stimulus, i.e., a sine wave of varying voltage within which square wave pulses were embedded, as against steady square wave pulses, they showed that the frequency of the sine wave could determine the degree of reduction in renal blood flow, even though the total current delivered was the same.[191] The authors proposed that the low frequency pulses in renal sympathetic nerve activity were likely to result in an enhanced dynamic gain to allow the renal blood flow to respond rapidly to normal everyday variations in blood pressure. Interestingly, this hypothesis was not supported by an investigation in the rat[63] in which the renal nerves were similarly stimulated with sine wave modulation with embedded high frequency pulses. These investigators found that there were reductions in renal blood flow with superimposed low frequency oscillations, but that the magnitude of these vasoconstrictor responses were not altered when basal tone was increased by exogenous administration of noradrenaline or angiotensin II. The reasons why there is a disparity between these reports are unclear, but may reflect a fundamental difference in the regulation of the renal vasculature in the rabbit versus the rat.

Analysis of Renal Nerve Activity

The central mechanisms involved in the generation, regulation, and analysis of the sympathetic outflow have been reviewed in detail by Malpas.[189] It has become possible to resolve the frequency and amplitude components, phase relationships, and coherence between renal sympathetic nerve activity, renal blood flow, and blood pressure. These techniques have been applied to gain insight into how low levels of renal sympathetic nerve activity may influence renal function. It is evident that renal sympathetic nerve activity is at a level which tonically reduces renal blood flow, at least, in the rabbit.[96,190] Moreover, following power spectral analysis of the renal blood flow signal it has become apparent that at a spectral frequency range above 0.6 Hz in the renal sympathetic nerve signal, the nerves exert a tonic vasoconstrictor action on the renal vasculature.[191] However, the lower frequency power spectral peaks, below 0.6 Hz, cause slow cycles of vasoconstriction and vasodilation which, it has been argued, may enhance the responsiveness of the vasculature to other stimuli to allow renal blood flow and glomerular filtration rate to dynamically adapt to ensure constancy of filtered load, and hence fluid processing by the nephron.[192] Indeed, it has been emphasized that this role of the renal nerves is integral to the maintenance of cardiovascular homeostasis.[12]

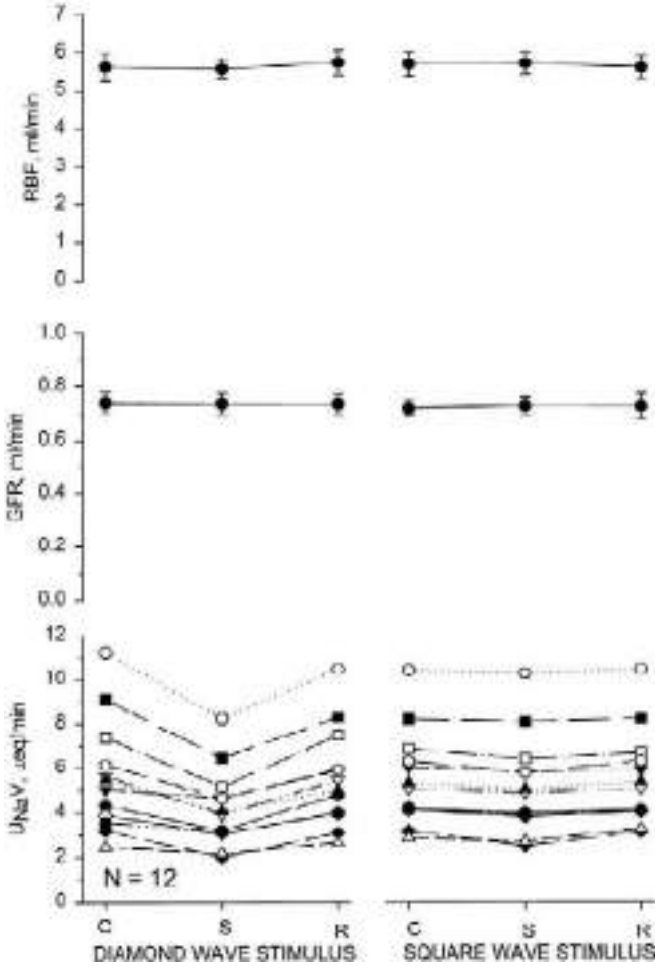

FIGURE 16.7 **Electrical stimulation of the renal sympathetic nerves with the diamond wave stimulus, which had no effect on either renal blood flow (RBF) or glomerular filtration rate, (GFR) significantly decreased sodium excretive (UNAV), whereas delivery of the same integrated voltage as a square wave stimulus was without effect on any of the measured variables.** *(Taken with permission from ref. [66].)*

The situation in the rat appears somewhat different, as many reports[58] demonstrate that under basal conditions the renal sympathetic nerves have a much smaller, if any, influence on basal renal blood flow. DiBona and Sawin[61,65] evaluated the transfer function gain between blood pressure and renal blood flow under a variety of conditions where renal sympathetic nerve activity was removed or enhanced. There was a characteristic pattern to the transfer function gain under basal conditions. The transfer function gain decreased below zero over the frequency range 0.02 and 0.06 Hz, which was taken to represent a slower tubuloglomerular feedback mechanism of autoregulation, and increased above zero with a plateau region over the higher frequency range 0.1 to 0.2 Hz, which was taken to reflect the myogenic component of autoregulation. They found that acute denervation had little impact on the overall pattern of transfer function gain over the whole frequency range.[61] In contrast, in two pathophysiological states, congestive heart failure and in the spontaneously hypertensive rat where basal renal sympathetic nerve activity is elevated, transfer function gain was suppressed over both these frequency ranges, but was relatively normalized following acute renal denervation.[63] The authors concluded that in the rats with elevated renal nerve activity, the coupling between blood pressure and renal blood flow was overridden such that autoregulation of renal blood flow was impaired. These authors went on to show that this effect was mediated via angiotensin II, as blockade of angiotensin AT1 receptors with losartan depressed the transfer function gain in rats fed on low or normal dietary sodium intake, but not a high dietary sodium intake.[59,63] Indeed, the outcome of these studies indicated that the renin–angiotensin system enhanced the tubuloglomerular feedback component of autoregulation, but not the myogenic component, and that the elevated angiotensin II increased the efficiency of transfer of the neural signal to control the renal vasculature.

Reflex Regulation of the Renal Nerves

Activity within the renal sympathetic nerves represents an integration of a number of sensory inputs arising from different regions of the body by the central nervous system. Malpas has recently reviewed the central mechanisms regulating sympathetic outflow to the periphery, including that to the kidney.[189] The changing output of renal sympathetic nerve activity represents a means by which renal functionalities, that is, renin release, sodium reabsorption, and renal hemodynamics are regulated at an appropriate level. The different sensory systems sending information into the central nervous system are shown in Figure 16.8.

Cardiovascular Baroreceptors

HIGH PRESSURE BARORECEPTORS

A number of early studies demonstrated that the high pressure baroreceptors in the carotid sinuses exerted an important influence on the neural regulation of the kidney. Studies undertaken in anaesthetized and conscious dogs in which carotid sinus pressure was reduced mechanically[94,278] or as a consequence of periods of head up tilt[54,201,202] increased renal nerve activity, renin secretion, and caused a renal nerve-dependent antidiuresis and antinatriuresis with relatively little change in renal hemodynamics. This means that during everyday activity, the baroreflex control of blood pressure will impact on kidney function; renin

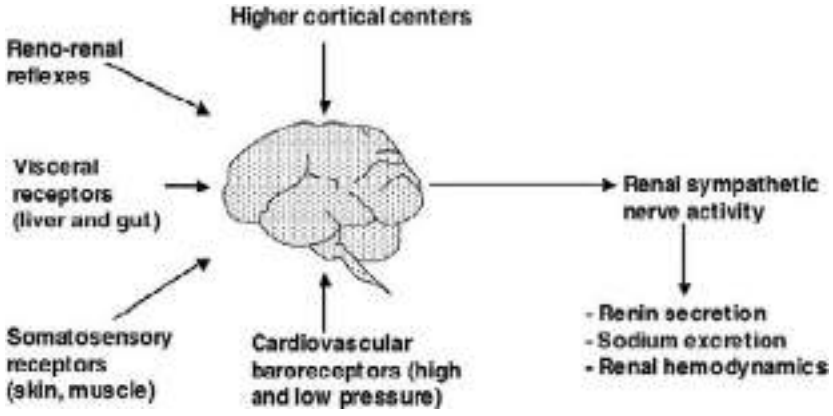

FIGURE 16.8 **The figure summarizes the input from different sensory system which are integrated by the central nervous system to determine the degree of renal sympathetic nerve activity to regulate renin secretion, sodium excretion and renal hemodynamics.**

release and sodium and water retention to a greater degree than vasomotor tone. However, what has become evident from the conscious rat studies of Miki and colleagues, is that the baroreflex control of renal sympathetic nerve activity is shifted towards a higher blood pressure as muscle activity increases, for example during grooming and exercise on a treadmill.[204,206,277]

LOW PRESSURE BARORECEPTORS

The low pressure baroreceptors are contained in the cardiopulmonary areas, and are mechanosensitive nerves embedded in the atria and great veins (superior and inferior venae cavae and pulmonary vein) which respond to stretch. Activation of these sensory nerves by inflation of balloons in the left atria results in a reflex decrease in renal sympathetic nerve activity associated with a rise in water and sodium excretion.[90,178] While many of these studies were undertaken in anaesthetized preparations, DiBona and Sawin[68] demonstrated in the conscious rat that volume expansion decreased and volume depletion increased renal sympathetic nerve activity. These observations correlated with a key report by Miki et al.[201] in the conscious dog showing that head-out total body water immersion, a maneuver that shifts fluid into the more central compartments of the cardiovascular system, caused a reflex renal sympatho-inhibition associated with a diuresis and natriuresis. The cardiopulmonary receptors were demonstrated to be essential in this reflex, as following chronic cardiac denervation both the renal sympatho-inhibition and excretory responses were markedly blunted when these dogs were subjected to the water immersion challenge.[202]

Somatosensory System

There are mechanosensory nerve fibers in the joints and tendons, chemosensitive nerves within the muscle tissue itself depolarized by metabolites.[127,128] The skin contains nociceptors and thermoreceptors. Each of these classes of sensory nerves sends important afferent information into the central nervous system to be integrated. At the level of the kidney, an early study by Thames and Abboud[255] demonstrated that sciatic nerve stimulation caused profound reductions in renal blood flow. In the anaesthetized rat, electrical stimulation of the brachial nerves, application of capsaicin subcutaneously to depolarize afferent nerve endings or inhalation of noxious fumes[45,46,279] caused increases in renal sympathetic nerve activity and a renal nerve-mediated antidiuresis and antinatriuresis with little change in renal hemodynamics. Interestingly, the magnitude of the renal sympathetic nerve activity responses is under tonic inhibitory control by the cardiopulmonary receptors, as suggested by studies showing that activation of the cardiopulmonary receptors blunts the sympatho-excitatory and antinatriuretic responses to capsaisin-induced activation of the afferent nerves.[279] These studies illustrate the point that the somatosensory system does provide an important input to the brain, but its impact is modulated by input from the cardiovascular baroreceptors.

Visceral System

Less well-studied, but nonetheless important, are the chemo- and mechano sensory nerves in the visceral system. In early studies, Weaver and co-workers[262] demonstrated that activation of chemosensitive nerve fibers in the small intestine of the cat, by bradykinin, caused a reflex activation of the renal sympathetic nerves. Furthermore, they demonstrated that the effectiveness of this sensory input from the gut was under a tonic inhibitory influence from both the low and high pressure cardiovascular baroreceptor.

Chemo- and mechanosensory nerves are also present within the liver, where they modulate renal sympathetic nerve activity and renal nerve mediated fluid excretion.[110,111,171,205] A reduction in plasma sodium concentration in the hepatic portal vein, but not hepatic artery, resulted in increased adrenaline secretion, indicative of a sympatho-excitation, which was blocked by

denervation of the hepatic portal vein.[110,111] Moreover, infusion of a hypertonic solution in the hepatic portal vein[205] caused a renal sympatho-inhibition and a renal nerve-dependent increase in sodium and water excretion. Taken together, these observations lay the foundation of important reflexes whereby food and fluid absorption from the gut initiates an appropriate neural regulation of kidney function to ensure that sodium and water homeostasis is maintained.

The spleen has also been found to be a source of sensory information which can modulate renal sympathetic nerve activity and its functional end-points. Hamza and Kaufman[99–101] reported that an increase in splenic venous pressure resulted in small rises in blood pressure and reductions in renal blood flow, with the latter being prevented following surgical section of the renal sympathetic nerves. It can be speculated that this relationship becomes important in portal hypertension and liver cirrhosis in eliciting a reflex renal sympatho-excitation which will contribute to the sodium retention associated with these disease states.

Higher Cortical Centers

The role of psychological stress in regulating renal sympathetic nerve outflow and renal function is less clear-cut and far more difficult to study. Nonetheless, chronically instrumented rats have been used and subjected to a range of challenges to engage the higher cortical centers. An arousal stimulus of an air jet stress has been found to reflexly increase renal sympathetic nerve activity along with a renal nerve-dependent antinatriuresis and antidiuresis.[64,258] However, studies to determine potential control by the cardiovascular baroreceptors of physiological stresses have been difficult to achieve in conscious studies. Nonetheless, the recent observations of Miki and his group have revealed a number of important findings. First, it was apparent that renal sympathetic nerve activity was lower during rapid eye movement sleep than in non-rapid eye movement sleep and became higher as the level of physical activity rose, from quiet awake to grooming.[277] At the same time, there was an adaptation of the baroreflex to function over a higher blood pressure range as the activity of the animal increased.[277] Second, during treadmill exercise,[204] there was an increased sensitivity of the baroreflex relationship, which they interpreted as important in buffering the raised blood pressure under conditions of increased muscular activity. This group has also evaluated the cardiovascular changes induced during "freezing" behavior, when conscious rats are exposed to a high level of white noise.[203,276] Under these conditions, there was a minimal change in blood pressure, but heart rate decreased while renal sympathetic nerve activity increased, and lumbar sympathetic nerve activity did not change. The alterations in renal sympathetic nerve activity and heart rate during the freezing behavior were largely prevented by prior sino-aortic denervation, which indicated their important contribution to this pattern of responses. Thus, the cardiovascular and sympathetically-mediated responses during the freezing behavior prepare the animal for an active response to the threatening situation. Taken together, it is apparent that in all these different behavioral states central command exerts an important differential regulatory influence on the baroreflex control of sympathetic outflow to many organs, including that to the kidney.

Reflex Control of Selective Functions

Attention has been focused on whether the renal innervation could selectively regulate either renal hemodynamics or tubular fluid reabsorption or renin secretion. The findings of Luff et al. in the rabbit[183] and DiBona and Sawin in the rat[67] demonstrated that two types of structurally different nerve fibers exist within the nerve bundles and within the kidney itself. Evidence has been produced in the rabbit, where glomerular capillary pressure was measured as an indirect estimate of pre- and post-glomerular resistances.[48–50] Using an angiotensin II clamp, to remove any confounding influences of changes in endogeneous angiotensin II levels, a hypoxic challenge increased glomerular filtration pressure. The authors' interpreted these observations as reflecting a selective neural regulation post-glomerular vascular resistance, possibly via one of the subtypes of nerve fiber, independent of the renin–angiotensin system.

DiBona and colleagues[51,67] using the rat analyzed the strength-duration relationship during direct electrical renal nerve stimulation in relation to renal blood flow, urine flow, and sodium excretion. They found a higher stimulation threshold for the nerve fibers involved in regulating renal blood flow than for those involved in regulating fluid excretion. Moreover, activity in single sympathetic fibers innervating the kidney could be selectively modified by different reflexes. Thus, stimulation of arterial baroreceptors, central chemoreceptors, and thermoreceptors activated a large proportion (88%) of spontaneously active fibers, whereas thermoreceptors only increased the firing rate of those fibers which had no spontaneous activity. In a different series of studies, examining patterns of renal sympathetic nerve activity by evaluating the peaks of activity and time between peaks, DiBona and co-workers were able to show that although somatosensory (pinch) and heat stimuli resulted in similar increases in total renal sympathetic nerve activity, it was only the heat stimulus that caused a decrease in renal blood flow. The authors took these responses to indicate that two different stimuli could result in a distinctly

different control of sympathetic outflow regulating renal hemodynamics.

It would seem that there is a small, but persuasive, body of evidence for the view that there may be a degree of selectivity of functional control in the neural control of the kidney. There is a need for more investigation of this particular topic.

Central Nervous System

Central Processing

The processing of this sensory information within the central nervous system to generate an appropriate level of sympathetic outflow, not only to the kidney but to other organs, is complex and attention has been directed towards the cardiovascular baroreceptors which exert a major influence on autonomic control.[44] The sensory information from both the high and low pressure baroreceptors pass to the nucleus tractus solitarius (NTS) for initial processing, and subsequently via multiple pathways to the caudal and rostral ventrolateral medulla (CVLM and RVLM) where a complex interaction takes place before the pre-ganglionic fibers are stimulated. The way in which the major sensory inputs feed into these pathways is illustrated and summarized in Figure 16.9.

The situation regarding the somatosensory and visceral systems and their inputs to the areas regulating the autonomic nervous system are much less defined. The somatosensory system appears to have a direct input at three levels, NTS, CVLM, and RVLM,[42] but the actions exerted at each of these sites, whether excitatory or inhibitory, and the neurotransmitters involved, have not been resolved.

There is now a body of evidence that autonomic control is organized in a patterned manner. Micro-injection of glutamate onto the RVLM elicited an increase in cardiac, splenic, and renal sympathetic nerve activities that were very different in magnitude.[195,196] In conscious rat studies there is a relatively low degree of autonomic control of lumbar sympathetic nerve activity during treadmill exercise or in the freezing behavior,[203,204,276] whereas there are large dynamic responses in renal sympathetic nerve activity. There is also a clear differential control of cardiac and renal sympathetic outflow in the conscious sheep. Thus, following an infusion of hypertonic saline icv, renal sympathetic nerve activity markedly decreased, whereas cardiac sympathetic nerve activity did not change.[195] By contrast, in a model of pacing-induced heart failure, there was a large elevation in cardiac sympathetic, but not renal sympathetic, nerve activity. It was also reported in conscious rats[275] that icv infusion of angiotensin II reduced renal, but not lumbar, sympathetic nerve activity. A fuller analysis of the evidence has been presented by Malpas[189] in a recent review. The exact way in which information from each sensory system is integrated to provide an appropriate output of renal sympathetic nerve activity and neural control of renal function in order to ensure cardiovascular homeostasis remains to be explored.

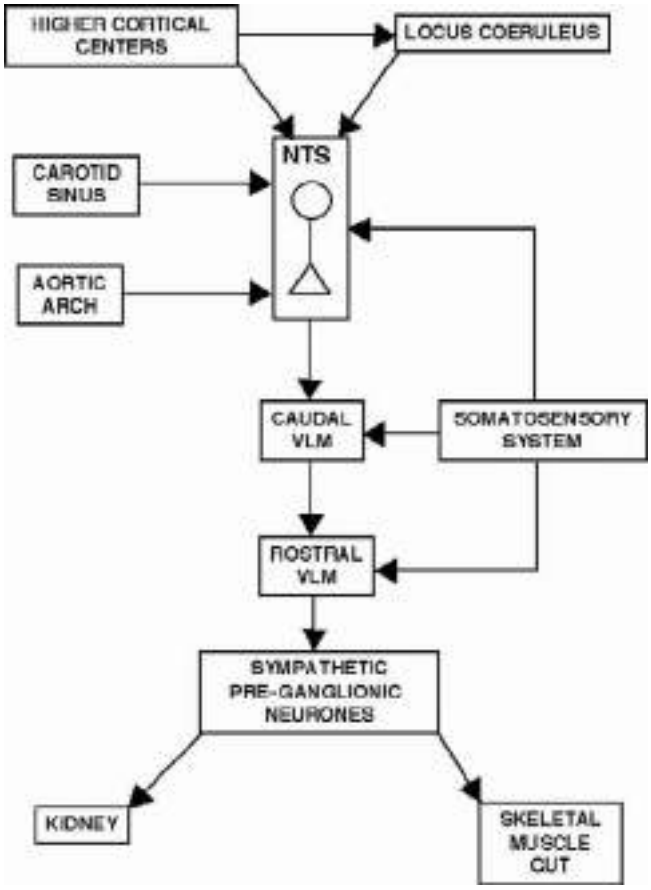

FIGURE 16.9 **This illustration indicates how input from the baroreceptors, somatosensory system, and higher cortical centers act at the nucleus tractus solitarus (NTS), which feeds into the caudal and rostal venterolateral medulla (CVLM and RVLM).** This determines the level of excitability of pre-ganglionic neurones and thereby sympathetic outflow to the kidney and other vascular beds.

Brain Angiotensin II

ANGIOTENSIN II AND AUTONOMIC PATHWAYS

There is accumulating evidence that the renin–angiotensin system and angiotensin II can influence the reflex responses in sympathetic nerve activity generated by the central nervous system. This can arise in two ways, either via circulating angiotensin II or by means of angiotensin II generated locally within the brain at specific nuclei. Moreover, angiotensin II receptors have been demonstrated in many regions of the brain, and particularly at those nuclei involved with cardiovascular control.[3] It is now accepted that in the

areas of the circumventricular organs the blood–brain barrier is leaky,[200] enabling angiotensin II to act on nuclei within this region which have been shown to contain a high density of angiotensin II receptors. At these sites the peptide is able to influence fluid balance; it stimulates drinking, induces ADH release, and causes increased sodium reabsorption and renin release.[199] The second route whereby angiotensin II may influence autonomic control is that generated within the brain itself, as all components of the renin–angiotensin system are present, that is renin, angiotensinogen, converting enzyme, and angiotensin II receptors.[265] It is also necessary to emphasize that immunocytochemical, *in situ* hybridization studies, and mRNA measurements of angiotensin II receptors and angiotensinogen have shown them to be present or their genes expressed at those nuclei involved with autonomic control, that is the NTS, RVLM, and CVLM, and the paraventricular nucleus (PVN),[199] as well as those other nuclei of the subfornical organ and the area postrema which are most likely subject to the action of circulating angiotensin II. Neurophysiological studies have shown that local administration of angiotensin II onto the NTS and RVLM is excitatory and produces a sympathetically-mediated pressor response, but when applied to the CVLM it causes a sympatho-inhibition[43,105]; thus, angiotensin II may have different actions and consequences depending on its site of production and action.

BRAIN ANGIOTENSIN II AND NEURAL CONTROL OF THE KIDNEY

The functional role played by angiotensin II within the brain in modulating autonomic control, both normally and in pathophysiological states, is only now being elucidated. There are now a number of reports showing that the baroreflex control of renal sympathetic nerve activity was suppressed by angiotensin II in conscious normotensive Wistar rats,[120] and enhanced in the spontaneously hypertensive rat (SHR).[117,174] In terms of the somatosensory reflex, angiotensin II within the central nervous system is important, in that losartan given icv blocked the renal nerve-mediated antinatriuresis and antidiuresis resulting from nociceptor stimulation[118] and angiotensin II icv restored the renal nerve-dependent functional responses[119] which could be correlated with marked changes in the pattern with which energy was distributed within the renal nerve signal.[127,279] The central issue which arises is to understand which factors could affect the level of angiotensin II within the central nervous system which would then impact on the degree of autonomic control exerted peripherally and particularly at the kidney. Indeed, it is important to distinguish between acute bolus administration of angiotensin II administered systemically and the application of the peptide as an icv infusion which may be associated with increases in blood pressure and a renal sympatho-excitation.

The level of dietary sodium intake can modulate this very important link between the autonomic control of the cardiovascular system and brain angiotensin II. An early report by Huang and Leenen[117] demonstrated that raised levels of dietary sodium intake in normotensive rats from four to eight weeks-of-age, led to an increase in baroreflex gain associated with a resetting to a higher pressure for renal nerve activity, but not for heart rate. The importance of dietary sodium intake during development has been reinforced by the studies of Osborn and his group,[27,214] who showed that in rats fed a high-salt diet from four to eight weeks-of-age, low dose infusion of angiotensin II into the brain (icv) over five days caused a sustained increase in blood pressure associated with a renal nerve-dependent antinatriuresis. This was not observed in rats fed a normal or low-salt diet. Further evidence for this role of the renal sympathetic nerves was reported by Houghton and co-workers[115,116] who found that a bolus injection of angiotensin II icv had vasopressor and renal sympatho-excitatory actions, the magnitudes of which were enhanced in rats fed a high-sodium diet over the period of growth and development that was in part mediated by vasopressin release both systemically and within the spinal cord.

This influence of dietary sodium intake on the contribution of angiotensin II in the brain on central pathways regulating renal sympathetic nerve activity has received some attention. DiBona and co-workers[56,57] using rats subjected to a low, normal or high dietary sodium intake for two weeks, microinjected an AT-1 receptor antagonist onto the RVLM, and observed a decreased blood pressure and a shift in the baroreflex gain curve for renal nerve activity to a lower pressure in the animals fed a low-sodium diet, but not in those animals fed the normal or high-sodium intakes. Furthermore, it was evident that administration of an AT-1 receptor antagonist to the RVLM blunted the increases in blood pressure, heart rate, and renal sympathetic nerve activity produced by bicuculline, a GABA receptor antagonist, injected onto the PVN. Importantly, the renal sympathetic nerve responses to the bicuculline administration into the PVN were enhanced in the rats subjected to the low-sodium diet, but blunted in those fed the high salt intake.[55]

Together, these findings highlight the importance of the brain renin–angiotensin system and the significance of angiotensin II in determining the sensitivity of neural pathways regulating sympathetic outflow to the kidney. They also emphasize how alterations in dietary sodium intake may impact on these neural control pathways, which may reset kidney function to a level which could predispose the individual to a hypertensive state.

Neural Regulation of the Kidney in Man

Knowledge of the sympathetic nerve control of the kidney in experimental animals under normal physiological conditions is now extensive in relation to the regulation of renal hemodynamics, renin secretion, and tubular sodium reabsorption. Indeed, although not touched upon in this chapter, there is an extensive body of work in relation to the role of the renal sympathetic nerves in pathophysiological states.[53,58,124,189] However, knowledge of the importance and significance of the renal sympathetic nerves in man remains a relatively unexplored area, although their contribution to cardiovascular and renal diseases is increasingly recognized and alluded to above in different sections. The most striking demonstration of their importance in man has come in a report by Krum et al.,[172,173] who utilized an angioplasty catheter inserted into the renal arteries with a probe at the tip which emitted radiofrequencies with sufficient intensity to disrupt the renal nerves passing alongside the renal artery. In a group of patients with hypertension that was resistant to conventional drug based therapy, bilateral ablation of the renal nerves in this way resulted in a reduction in systolic blood pressure of some 30 mmHg which was maintained for at least 24 months after the manoeuvre. Currently, these initial observations are being further investigated in randomized multicenter trials. DiBona and Esler[53] have emphasized that the knowledge gained from the experimental studies is now being successfully translated into therapeutic approaches, and that the role of the renal sympathetic nerves in heart failure, renal failure, and metabolic diseases of diabetes and obesity will now be explored.

AFFERENT RENAL SENSORY NERVES

Introduction

Not much focus has previously been placed on the afferent sensory innervation of the kidney and its physiological importance in the cardiovascular regulation compared to the efferent renal sympathetic innervation of the kidney. However, recent studies in man showing long-term depressor effects following renal nerve ablation which reduces both efferent and afferent renal nerve activity have highlighted a possible role for the afferent renal nerves in hypertension.[53] As will be discussed in more detail below, in healthy animals activation of the afferent renal sensory nerves elicits an inhibitory renorenal reflex response consisting of increases in afferent renal nerve activity, the nerve signals going from the kidney to the neuraxis, causing decreases in efferent renal sympathetic nerve activity which in turn result in a natriuresis (Figure 16.10). Available evidence would suggest that in many pathological conditions the nature of the renorenal reflexes is switched from being of an inhibitory to an excitatory nature (*vide infra*).

NEUROANATOMY

In the kidney, the majority of the afferent renal nerves containing substance P and calcitonin gene-related peptide (CGRP) are located in the renal pelvic wall,[147,156,182] where their circumferential orientation make them ideally suitable for sensing stretch (Figure 16.11). The majority of the renal sensory nerves are unmyelinated.[139]

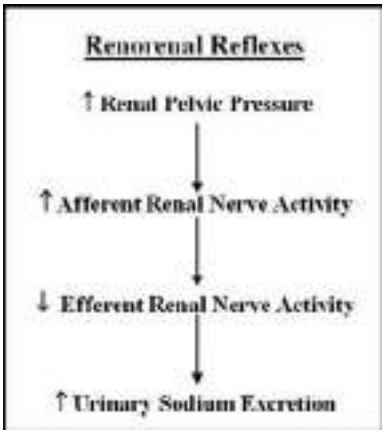
Renorenal Reflexes
↑ Renal Pelvic Pressure
↑ Afferent Renal Nerve Activity
↓ Efferent Renal Nerve Activity
↑ Urinary Sodium Excretion

FIGURE 16.10 **Increasing renal pelvic pressure ≥3 mmHg stretches the renal pelvic wall, leading to activation of the afferent renal mechanosensory nerves.** The increase in afferent renal nerve activity leads to decreases in efferent renal nerve activity, which in turn increases urinary sodium excretion, i.e., a renorenal reflex mechanism.

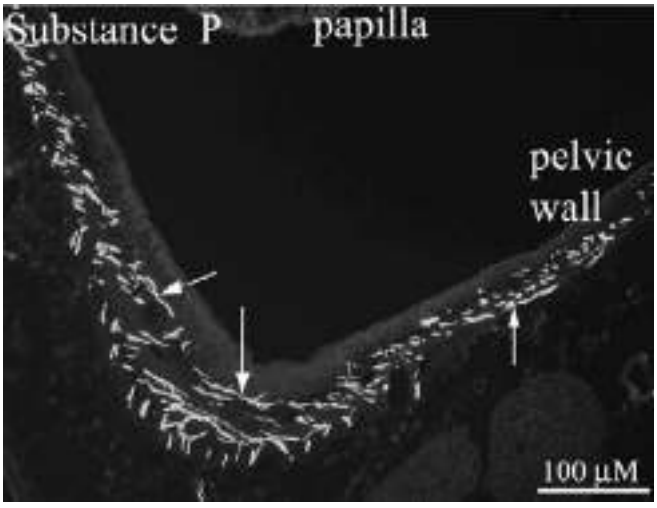

FIGURE 16.11 **In the kidney, the majority of the substance P containing nerve fibers (arrows) is located in the muscular layer of the renal pelvic wall.**

Depending on the species, the cell bodies of the afferent renal nerves are located in ipsilateral dorsal root ganglia (DRG) from T_6-L_4, with predominance in $T_{12}-L_3$.[58] Viral tracing studies combined with dorsal rhizotomy (DRX) at $T_{10}-T_{13}$ have provided evidence for the afferent renal nerves projecting from the DRG to the ipsilateral dorsal horn mainly in Laminae I, III–V,[36] where they synapse with interneurons projecting to sites within the central nervous system which are associated with cardiovascular regulation, including nucleus tractus solitarius, rostral ventrolateral medulla, subfornical organ, and paraventricular nucleus of hypothalamus.[247] There is also evidence for a monosynaptic projection of the afferent renal nerves to areas within the brainstem.[270]

Stimulation of the afferent renal nerves may activate spinal and supraspinal pathways.[29,35,138,241] Electrical stimulation of the afferent renal nerves results in widespread decreases in efferent renal sympathetic nerve activity, including renal, cervical, and cardiac nerves, in association with decreases in arterial pressure.[232] A majority of the neurons in the ventral lateral medulla that decrease their activity in response to afferent renal nerve stimulation also respond to stimulation of the central portion of the aortic nerves, with a decrease in efferent renal sympathetic nerve activity.[232] These neurons are also responsive to inputs from the carotid sinus nerves.[254] In addition, activation of the afferent renal nerves alters the activity of vasopressin and oxytocin neurons in the paraventricular nucleus of hypothalamus in rats,[35] resulting in increases in arterial pressure and plasma vasopressin and oxytocin concentrations. These effects are abolished by prior denervation of the stimulated kidney.

The convergence of the afferent signals from the renal and carotid sinus nerves on neurons in several brain areas involved in cardiovascular control[26,82,247] provides an anatomical basis for possible interactions among the afferent signals deriving from various organs, including the kidney.

Two classes of renal sensory nerves have been identified neurophysiologically: renal mechanosensory nerves responding to stretch of the renal pelvic wall; and renal chemosensory nerves responding to renal ischemia and/or changes in the chemical environment of the renal interstitium. The electrophysiology of the renal sensory nerves has previously been reviewed extensively.[58,249] Isotonic saline volume expansion results in a differential activation of renal mechano- and chemosensitive nerves.[33] Whereas volume expansion increased the activity of mechanosensitive nerves, it decreased the activity of the chemosensitive nerves, type R2 chemoreceptors. Stretch is associated with an increase in muscle spindle cell membrane sodium permeability, resulting in an inward flux of sodium and depolarization.[121,217] The afferent renal nerve activity responses to increased renal pelvic pressure are reduced by renal pelvic administration of amiloride and lidocaine,[165,169] agents known to reduce sodium influx by different mechanisms. Conversely, inhibition of Na^+-K^+-ATPase by ouabain increases the afferent renal nerve activity response to increased renal pelvic pressure.[170] These studies suggest that changes in intracellular sodium concentration may modulate the responsiveness of renal pelvic mechanosensitive nerves.

RENORENAL REFLEXES

The identification of a reflex originating in one kidney and affecting contralateral renal function was first demonstrated in the early 1980s. In healthy normotensive animals, the afferent renal nerves were activated by increases in renal pelvic pressure of a magnitude ≥ 3 mmHg, commonly seen during high urine flow rate,[33,88,151] suggesting that the afferent renal nerves were tonically active in conditions of high-sodium diet and/or volume expansion. Supporting this argument were studies in anesthetized volume expanded rats showing that increases in ipsilateral urinary sodium excretion produced by total, i.e., efferent plus afferent, unilateral renal denervation were accompanied by decreases in contralateral urinary sodium excretion. The contralateral antinatriuresis was caused by increases in contralateral efferent renal sympathetic nerve activity; this is called a renorenal reflex response[39,60] (Figure 16.12). Because unilateral renal denervation results in an ipsilateral diuresis and natriuresis, total (ipsilateral plus contralateral) urine flow rate and urinary sodium excretion are unchanged. Thus, the afferent renal nerves exert tonic inhibitory effects on contralateral efferent renal sympathetic nerve activity.

Selective Afferent Renal Denervation: Dorsal Rhizotomy

The overall importance of the natriuretic inhibitory renorenal reflexes can be evaluated by selective bilateral afferent renal denervation produced by dorsal rhizotomy (DRX) at T_9-L_1. Cutting the dorsal roots from T_9-L_1 interrupts the afferent renal neural input to the central nervous system.[70] Both DRX and sham-DRX rats are able to establish external sodium balance on both a normal dietary sodium intake and a four-fold higher dietary sodium intake. However, this is achieved at markedly different levels of arterial pressure.[150] On a normal or low-sodium diet, the levels of mean arterial pressure are similar in DRX and sham-DRX rats.[126,150] However, the process of achieving external sodium balance while consuming an increased dietary sodium intake resulted in a mean arterial pressure in DRX rats

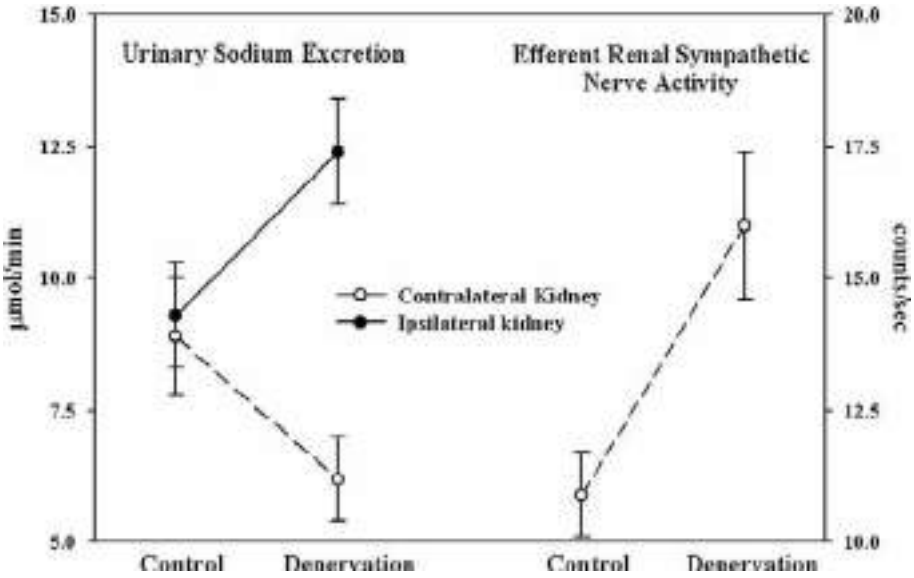

FIGURE 16.12 **In normotensive healthy rats, denervation of one kidney (ipsilateral kidney) results in increases in ipsilateral urinary sodium excretion, and decreases in contralateral urinary sodium excretion.** The decreases in contralateral urinary sodium excretion are the result of increases in contralateral efferent renal sympathetic nerve activity, i.e., the afferent renal nerves exert a tonic inhibition of sympathetic nerve activity to the contralateral kidney. *(Modified from ref. [58].)*

that was some 30 mmHg greater than that in sham-DRX rats[150] (Figure 16.13). These findings support the view that the afferent renal nerves are tonically active in high-sodium dietary conditions.[151] Thus, the afferent renal nerves are essential for achieving sodium balance during increased dietary sodium intake. Rats lacking intact afferent renal innervation can only achieve sodium balance at the cost of increased mean arterial pressure. Thus, afferent renal denervation leads to salt-sensitive hypertension. Among the mechanisms contributing to the development of salt-sensitive hypertension in DRX rats are increased efferent renal sympathetic nerve activity and increased responsiveness of efferent renal sympathetic nerves to various sympathetic stimuli due, at least in part, to impairment of the arterial baroreflex function.[164]

Wang and co-workers have presented evidence for salt-sensitive hypertension in rats neonatally treated with capsaicin to destroy the sensory innervation of all organs.[260] The salt-sensitive hypertension in DRX rats would suggest that the lack of intact afferent renal innervation in the capsaicin treated rats may contribute to the increased arterial pressure in these rats when fed a high-sodium diet.

Activation of Renal Mechanosensory Nerves: Physiological Conditions

The inhibitory nature of the afferent renal nerves in healthy normal rats has been further demonstrated in studies examining the functional responses to activation of the afferent renal nerves. The renal mechanosensory nerves respond to stretch of the smooth muscle layer in which many of the sensory nerves are embedded. Studies in cats showed that the increased urine flow rate produced by volume expansion resulted in parallel increases in renal pelvic pressure and afferent renal nerve activity.[88] Importantly, the activation threshold of the mechanosensory nerves was <5 mmHg above baseline pelvic pressure, suggesting that the renal pelvic mechanosensory nerves are activated by increases in renal pelvic pressure within the physiological range and below that required for sensation of pain. Studies to examine the mechanisms involved in the activation of the renal sensory nerves in the absence of changes in the renal circulation utilized a fluid-filled ureteral catheter elevated to different levels above the kidney. These studies, performed in rats, showed that graded increases in renal pelvic pressure resulted in graded increases in afferent renal nerve activity, with the activation threshold being between 3 to 5 mmHg,[170] i.e., a similar activation threshold as that produced by volume expansion. The increase in afferent renal nerve activity produced bilateral decreases in efferent renal sympathetic nerve activity and increases in urinary sodium excretion[166,169,187] (Figure 16.10). Ipsilateral renal denervation blocks the increases in urinary sodium excretion, demonstrating that stimulation of renal mechanosensory nerves activates an inhibitory bilateral renorenal reflex mechanism. The afferent renal nerves are not responsive to NaCl concentrations within the physiological range, as shown by lack of increases in afferent renal nerve activity in response to renal pelvic perfusion with NaCl at <900 mM.[170]

The natriuretic nature of the renorenal reflexes would suggest that this reflex mechanism contributes to total body sodium and fluid volume balance by assisting in the excretion of sodium and water. In this case, it would be expected that this reflex mechanism would be enhanced or upregulated during conditions

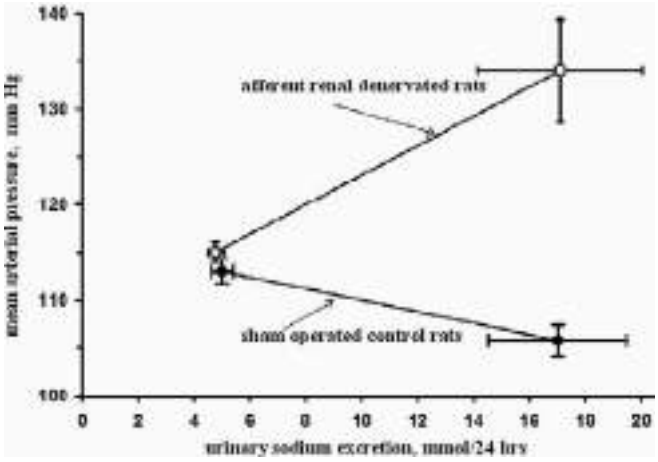

FIGURE 16.13 **Recording mean arterial pressure in conscious rats fed either normal or high-sodium diet for three weeks following dorsal rhizotomy at T_9-L_1 to remove the afferent renal innervation showed markedly elevated mean arterial pressure in the afferent renal denervated rats fed a high-sodium diet compared to the sham-operated litter mates.** Mean arterial pressure was similar in the two groups of rats fed normal sodium diet. Thus, afferent renal denervated rats are characterized by salt-sensitive hypertension. *(Modified from references [53,152]).*

of sodium and volume-loading. Indeed, studies examining the responsiveness of the renal mechanosensory nerves in rats fed various sodium diets showed that, in comparison to low-sodium dietary intake, high-sodium dietary intake enhances the renorenal reflex responses.[151] At every level of renal pelvic pressure, the increases in both afferent renal nerve activity and urinary sodium excretion were greater in rats fed high-sodium diet compared to rats fed low-sodium diet (Figure 16.14). Importantly, in rats fed high-sodium diet, the threshold of activation of the renal mechanosensory nerves was 2–3 mmHg, suggesting that the afferent renal nerves are tonically active in high-sodium dietary conditions.

Interaction between Efferent and Afferent Renal Nerve Activity

Not only is the renal pelvic wall innervated by afferent sensory nerves, but it is also innervated by efferent sympathetic nerves which are in close contact with the sensory nerves in the renal pelvic wall[157] (Figure 16.15). These findings provide anatomical support for a functional interaction between the efferent and afferent renal nerves. As discussed above in normotensive rats, activation of the afferent renal sensory nerves leads to decreases in efferent renal sympathetic nerve activity and natriuresis, an inhibitory renorenal reflex response.[166] However, not only do increases in afferent renal nerve activity decrease efferent renal sympathetic nerve activity, but increases in efferent renal sympathetic nerve activity increase afferent renal nerve activity[157,163,158] (Figure 16.16). The increased afferent renal nerve activity will, in turn, decrease efferent renal sympathetic nerve activity via activation of the renorenal reflexes, a negative feedback mechanism, to maintain low-level efferent renal sympathetic nerve activity (Figure 16.17). Similar to the responsiveness of the renal mechanosensory nerves being modulated by dietary sodium, the interaction between efferent renal sympathetic nerve activity and afferent renal nerve activity is also modulated by dietary sodium. Reflex increases in efferent renal sympathetic nerve activity results in much larger increases in afferent renal nerve activity in rats fed high-sodium diet than in rats fed low-sodium diet (Figure 16.14).

Thus, in high-sodium dietary conditions, the enhanced afferent renal nerve activity responses to increases in efferent renal sympathetic nerve activity and/or increases in renal pelvic pressure would lead to enhanced inhibitory renorenal reflex control of efferent renal sympathetic nerve activity to minimize sodium retention. Conversely, in low-sodium dietary conditions, the suppressed afferent renal nerve activity responses to increases in efferent renal sympathetic nerve activity and/or increases in renal pelvic pressure would result in little or no inhibition of efferent renal sympathetic nerve activity, which eventually would lead to sodium retention. It is important to note that these are physiologically appropriate responses to changes in dietary sodium in the overall goal of maintaining sodium balance.

Mechanisms Involved in Activation of Renal Mechanosensory Nerves

SUBSTANCE P

Substance P is produced in the neural cell bodies in the dorsal root ganglia and transported along the afferent nerves towards the peripheral nerve endings, where it is stored in vesicles and released in response to various stimuli. The presence of substance P-containing sensory nerves in the renal pelvic wall[156] (Figure 16.11) suggested a role for this neuropeptide in the activation of the renal sensory nerves. Single unit recordings of afferent renal nerve activity showed that the same single nerve fiber could be activated by increases in renal pelvic pressure and substance P administered directly into the renal pelvic area, suggesting an important role for substance P in the inhibitory renorenal reflex responses to increased renal pelvic pressure.[185] Substance P is released from the renal pelvic sensory nerves by a calcium (Ca^{2+})-dependent mechanism requiring influx of Ca_i^{2+} via N-type Ca_i^{2+} channels in response to prostaglandin E_2 (PGE_2),[146] a known activator of sensory neurons.[31,112,257]

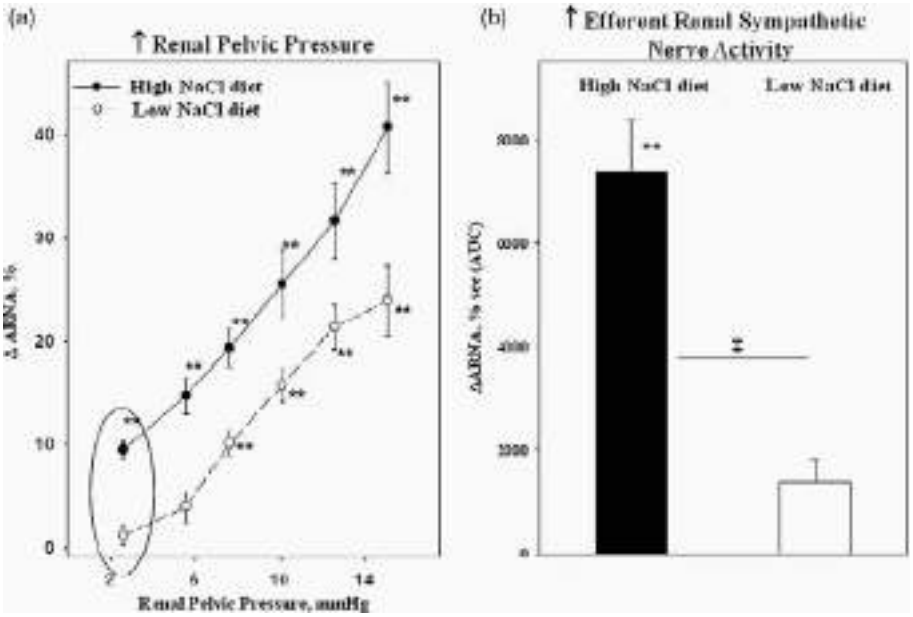

FIGURE 16.14 **High-sodium diet enhances the afferent renal nerve activity (ARNA) responses to increases in renal pelvic pressure (a) and reflex increases in efferent renal sympathetic nerve activity produced by thermal cutaneous stimulation (b).** The activation threshold for the renal mechanosensory nerves is 2–3 mmHg in rats fed high-sodium diet suggesting that the afferent renal nerves are tonically active in high-sodium dietary conditions. *(Modified from references [151,158].)*

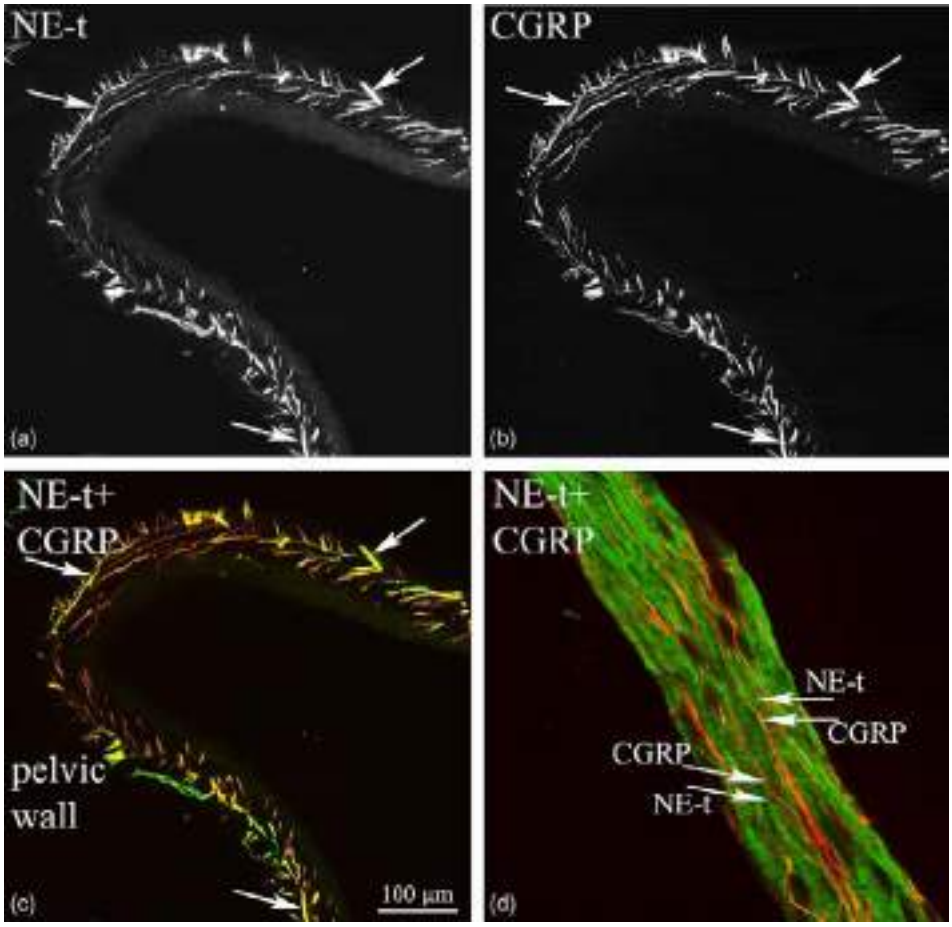

FIGURE 16.15 **Applying antibodies against the norepinephrine transporter (NE-t) and the neuropeptide calcitonin gene-related peptide (CGRP) to kidney tissue to identify sympathetic and sensory nerve fibers, respectively (arrows) showed that the sympathetic nerves in the renal pelvic wall (a); are in close contact with the sensory nerves (b); as indicated by the color yellow (c).** Higher magnification showed that the sympathetic and sensory nerves are separate fibers in close contact in the same nerve bundle (d). *(Modified from reference [157].)*

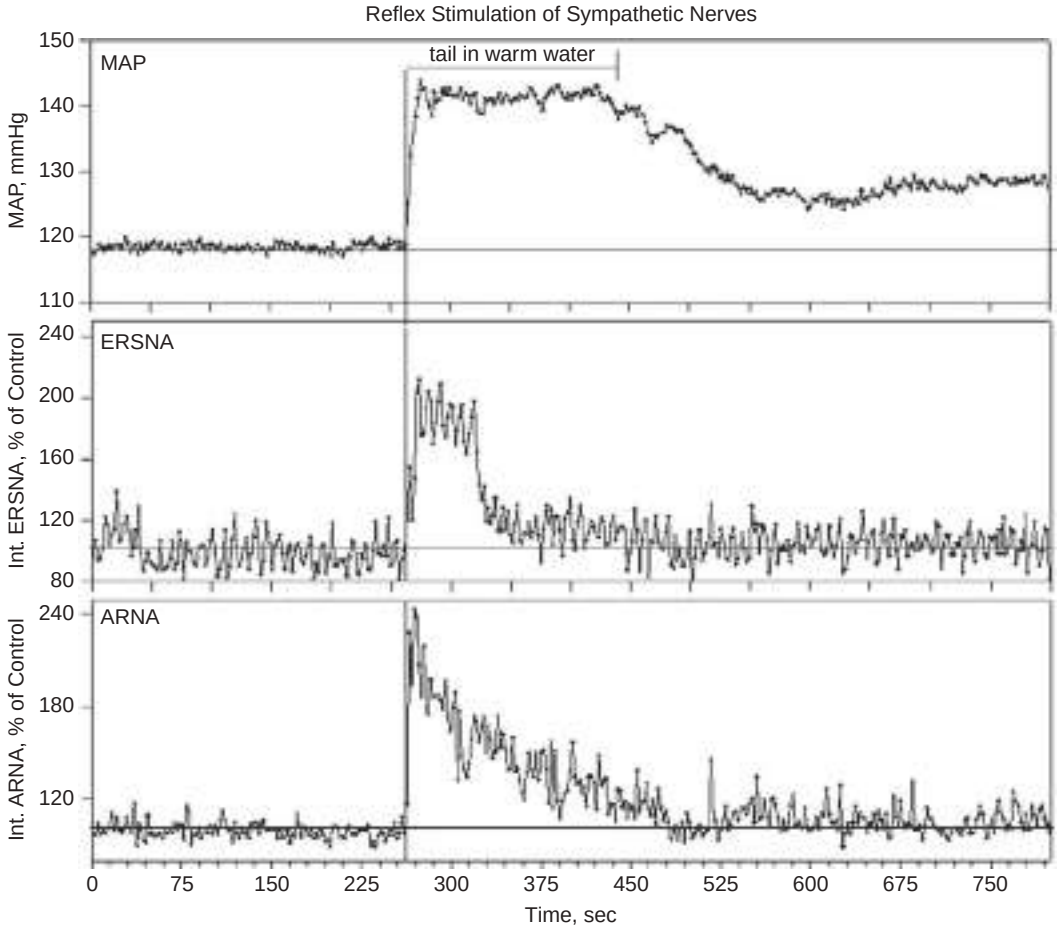

FIGURE 16.16 **Thermal cutaneous stimulation by placing the rat's tail in 47°C water results in a general increase in sympathetic nerve activity, as indicated by the increases in mean arterial pressure (MAP) and efferent renal sympathetic nerve activity (ERSNA).** The increases in ERSNA produced the increases in afferent renal nerve activity (ARNA), see text for further details. *(Modified from reference [157].)*

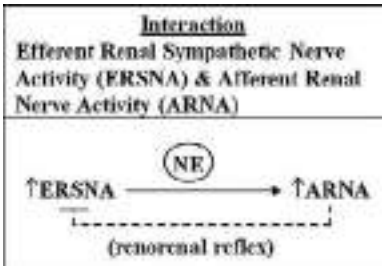

FIGURE 16.17 **There is a reciprocal interaction between efferent renal sympathetic nerve activity (ERSNA) and afferent renal nerve activity (ARNA).** Increases in ERSNA increase ARNA, the increase in ARNA would in turn decrease ERSNA via activation of the inhibitory renorenal reflexes in the overall goal of maintaining low ERSNA to minimize sodium retention. Norepinephrine (NE) is involved in the ERSNA-induced increase in ARNA.

Functional support for a role of substance P in the activation of renal pelvic sensory nerves is derived from *in vivo* studies showing that activation of renal mechanosensory nerves results in renal pelvic release of substance P.[155,161,162] Renal pelvic administration of substance P receptor antagonists abolishes the renorenal reflex responses to increased renal pelvic pressure.[167]

On the other hand, the role of CGRP in the activation of renal sensory nerves is unclear. Although CGRP is colocalized with substance P in the majority of the sensory nerves in the renal pelvic wall and released in response to stimuli that also release substance P,[154,156] blocking CGRP receptors does not reduce the responsiveness of the afferent renal nerves to various stimuli. Rather, available evidence would indicate that CGRP plays a role in delaying the catabolism of substance P, thereby prolonging the effects of neurally released substance P.[92,93]

There is considerable evidence for the transient receptor potential vanilloid type 1 (TRPV1) channels in the renal pelvic wall which, upon activation, elicits a similar inhibitory renorenal reflex response as activation of renal mechanosensory nerves. The TRPV1 channels are nonselective cation channels that can be activated by capsaicin, resiniferatoxin, noxious heat or a low pH. In the kidney,

activation of the TRPV1 channels by capsaicin or a capsaicin analog activates renal mechanosensory nerves resulting in increases in substance P release, afferent renal nerve activity, and a contralateral natriuresis. The physiological importance of the TRPV1 channels is currently not known, although it has been proposed that they serve as an integral part of the mechanosensory nerve complex.[84,280]

PROSTAGLANDIN E_2 (PGE_2)

There is considerable evidence for prostaglandins (PGs) enhancing the responsiveness of various sensory nerve fibers.[208,219] The kidney, especially the renal medulla, is an active PG-producing tissue.[23] A role for PGs in renal sensory receptor activation by reduced renal perfusion pressure was demonstrated by the finding that PG synthesis inhibition reduced the afferent renal nerve activity and reflex pressor responses to reduction in renal blood flow.[11,80]

Stretching the renal pelvic wall leads to activation of protein kinase C (PKC) via activation of bradykinin 2 (B2) receptors (*vide infra*) and induction of cyclooxygenase-2 (COX-2) mRNA in the renal pelvic wall, with a resultant increase in renal pelvic release of PGE_2[146,147,154,162] (Figure 16.18). PGE receptors have been classified into four general subtypes, EP1, EP2, EP3, and EP4, based on cloning and pharmacological interventions.[20] Immunohistochemical studies together with functional studies have provided evidence for a role of EP4 receptors in the activation of renal pelvic mechanosensory nerves.[147] It is well-established that PGE_2 activates the cAMP-protein kinase A (PKA) transduction cascade in DRG neurons, leading to depolarization of the cell membrane and a release of substance P and CGRP.[73,209,245] Using various activators and inhibitors of cAMP and PKA it was shown that PGE_2 increased the release of substance P and stimulated renal mechanosensory nerves by activating the cAMP/PKA transduction cascade in renal pelvic tissue.[154]

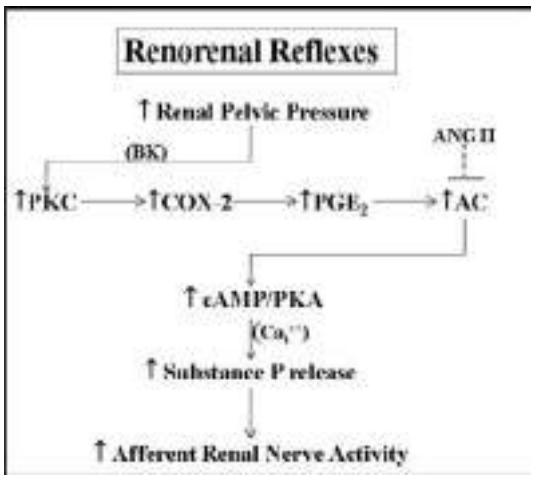

FIGURE 16.18 **Mechanisms involved in the activation of renal mechanosensory nerves. Stretching the renal pelvic wall by increasing renal pelvic pressure activates bradykinin (BK) 2 receptors, leading to activation of protein kinase C (PKC) and induction of cycloxygenase-2 (COX-2) with a resultant increase in renal pelvic release of PGE_2.** PGE_2 activates EP4 receptors on/close to the renal sensory nerves which leads to activation of adenylyl cyclase (AC)/cAMP/protein kinase A (PKA) transduction pathway, resulting in a calcium-dependent release of substance P and increases in afferent renal nerve activity. In conditions of increased endogenous angiotensin (ANG) II activity, e.g., low-sodium diet, the responsiveness of the renal mechanosensory nerves is suppressed due to ANG II reducing the PGE_2-mediated activation of AC by a pertussis toxin sensitive mechanism. *(Data derived from references [146,147,151,154,162].)*

ANGIOTENSIN II

In normal rats, low-sodium diet reduces the responsiveness of renal mechanosensory nerves,[151] i.e., similar to the well-known reduced responsiveness of carotid baroreceptors in healthy low-sodium diet rats.[57,117] The reduced afferent renal nerve activity response to increased renal pelvic pressure in low-sodium diet rats was associated with impaired PGE_2-mediated release of substance P from the isolated renal pelvic wall preparation. These data suggested that the reduced responsiveness of the renal sensory nerves was, at least in part, due to a mechanism at the peripheral sensory nerve endings.

A low-sodium diet is characterized by increased activity of the renin–angiotensin system.[56–58] Angiotensin II present in the renal pelvic wall is modulated by dietary sodium.[149] Renal pelvic administration of angiotensin II reduces, and renal pelvic administration of the AT1 receptor antagonist losartan enhances, the PGE_2-mediated release of substance P and activation of renal mechanosensory nerves.[151] Because the effects of losartan on the PGE_2-mediated release of substance P were observed in response to acute administration of losartan to an isolated renal pelvic wall preparation, these data suggest that endogenous angiotensin II exerts its inhibitory effect on renal mechanosensory nerves by a mechanism at the peripheral renal sensory nerve endings. Further studies showed that endogenous angiotensin II in the renal pelvic tissue reduces the responsiveness of the renal sensory nerves by suppressing the PGE_2-mediated activation of cAMP by a pertussis toxin sensitive mechanism[149] (Figure 16.18).

ALPHA-ADRENOCEPTORS

The increases in afferent renal nerve activity produced by reflex increases in efferent renal sympathetic nerve activity are reduced by renal pelvic administration of prazosin, an α_1-adrenoceptor antagonist, and enhanced by rauwolscine, an α_2-adrenoceptor antagonist[157] in rats fed normal-sodium diet, demonstrating that changes in

efferent renal sympathetic nerve activity modulate afferent renal nerve activity by the release of norepinephrine (Figure 16.17). The presence of α_1-adrenoceptors on the renal sensory nerves modulating their activation was demonstrated in an isolated renal pelvic wall preparation. These studies showed that norepinephrine resulted in a release of substance P that was blocked by prazosin and dependent on intact renal PG synthesis. Prazosin reduced the norepinephrine-induced release of PGE_2. Taken together these findings suggest that increases in efferent renal sympathetic nerve activity increases the release of norepinephrine which activates α_1-adrenoceptors on or close to the renal sensory nerves, resulting in increases in PGE_2 synthesis leading to release of substance P and increases in afferent renal nerve activity.

Similar to the responsiveness of the renal mechanosensory nerves being modulated by dietary sodium, the interaction between efferent renal sympathetic nerve activity and afferent renal nerve activity is also modulated by dietary sodium. Examining the mechanisms involved in the reduced responsiveness of the renal sensory nerves to increases in efferent renal sympathetic nerve activity in rats fed low-sodium diet it became clear that renal pelvic administration of losartan alone failed to enhance the efferent renal sympathetic nerve activity-induced increase in afferent renal nerve activity or the norepinephrine-induced increase in substance P. These findings suggested that the impaired responsiveness of the renal sensory nerves to increases in efferent renal sympathetic nerve activity may involve additional mechanisms upstream of PGE_2. Because activation of renal pelvic α_2-adrenoceptors reduces the activation of renal sensory nerves in rats fed normal-sodium diet,[157] one of the mechanisms contributing to the suppressed responsiveness of the renal sensory nerves in low-sodium diet rats likely involved increased activation of renal α_2-adrenoceptors. The involvement of α_2-adrenoceptors in the central nervous system in the cardiovascular regulation has long been known.[224,226] Of the three subtypes of α_2-adrenoceptors, the $\alpha^2{}_A$- and $\alpha^2{}_C$-adrenoceptors are expressed on primary afferent neurons in the spinal cord and DRG.[237,238] Whether α_{2B}-adrenoceptors are also expressed on DRG is not clear.[34,91,238] In the kidney, α_{2A}- and α_{2C}-adrenoceptors are localized on or close to sensory nerve fibers in the renal pelvic wall[158] (Figure 16.19). A role for increased activation of these receptors in the suppressed responsiveness of the renal sensory nerves to increases in efferent renal sympathetic nerve activity was subsequently shown by studies which showed that a combination of losartan plus rauwolscine enhanced the responsiveness of the renal sensory nerves to norepinephrine towards that seen in high-sodium diet rats.[158] Importantly, rauwolscine has no effect in rats fed a high-sodium diet.

Taken together in low-sodium dietary conditions, increased activation of α_2-adrenoceptors together with increased endogenous angiotensin II activity suppress the norepinephrine-mediated activation of the renal sensory nerves. The consequence is decreased PG synthesis and reduced PGE_2-mediated activation of the adenylyl cyclase/cAMP/PKA transduction pathway, leading to little or no increase in substance P release, and afferent renal nerve activity, and thereby no inhibition of efferent renal sympathetic nerve activity. In high-sodium dietary conditions, the enhanced norepinephrine-mediated activation of renal sensory nerves is due, at least in part, to little or no activation of renal α_2-adrenoceptors and very low endogenous angiotensin II opposing the norepinephrine-mediated increase in afferent renal nerve activity which will eventually lead to renorenal reflex decreases in efferent renal sympathetic nerve activity (Figure 16.20).

BRADYKININ

Among the various mechanisms involved in the release of substance P and activation of renal mechanosensory nerves is bradykinin (*vide supra*). Bradykinin is a well-known activator of sensory nerve fibers.[89] Bradykinin receptors have been localized on sensory nerve fibers[250] and in the lamina propria of the tissue lining the pelvis.[193] Bradykinin increases afferent renal nerve activity when administered into the renal pelvis in association with an increased renal pelvic release of PGE_2 and substance P, and a contralateral natriuresis. B2 receptor antagonists block the renorenal reflex responses to either bradykinin *per se* or increases in renal pelvic pressure.[161,162] Interestingly, the responses to bradykinin are dependent on the route of administration. In contrast to the inhibitory reflex response elicited by renal pelvic administration of bradykinin,[161,162] administration of bradykinin into the renal artery (i.r.a.) elicits an excitatory reflex which includes activation of neurosecretory vasopressin cells in the supraoptic nucleus,[47] increases in plasma ADH concentration, and increased arterial pressure and vascular resistance in most circulatory beds.[246] The sympatho-excitatory effects of i.r.a. bradykinin were due to activation of afferent renal nerves since they were abolished by denervation of the infused kidney. This reflex has been suggested to be of importance during renal ischemia, which is likely to be associated with increased release of bradykinin.

These findings suggest that bradykinin activates different reflex pathways, one excitatory and one inhibitory, when administered into the renal artery and pelvis, respectively. The physiological or pathophysiological significance of these different reflexes is currently not known.

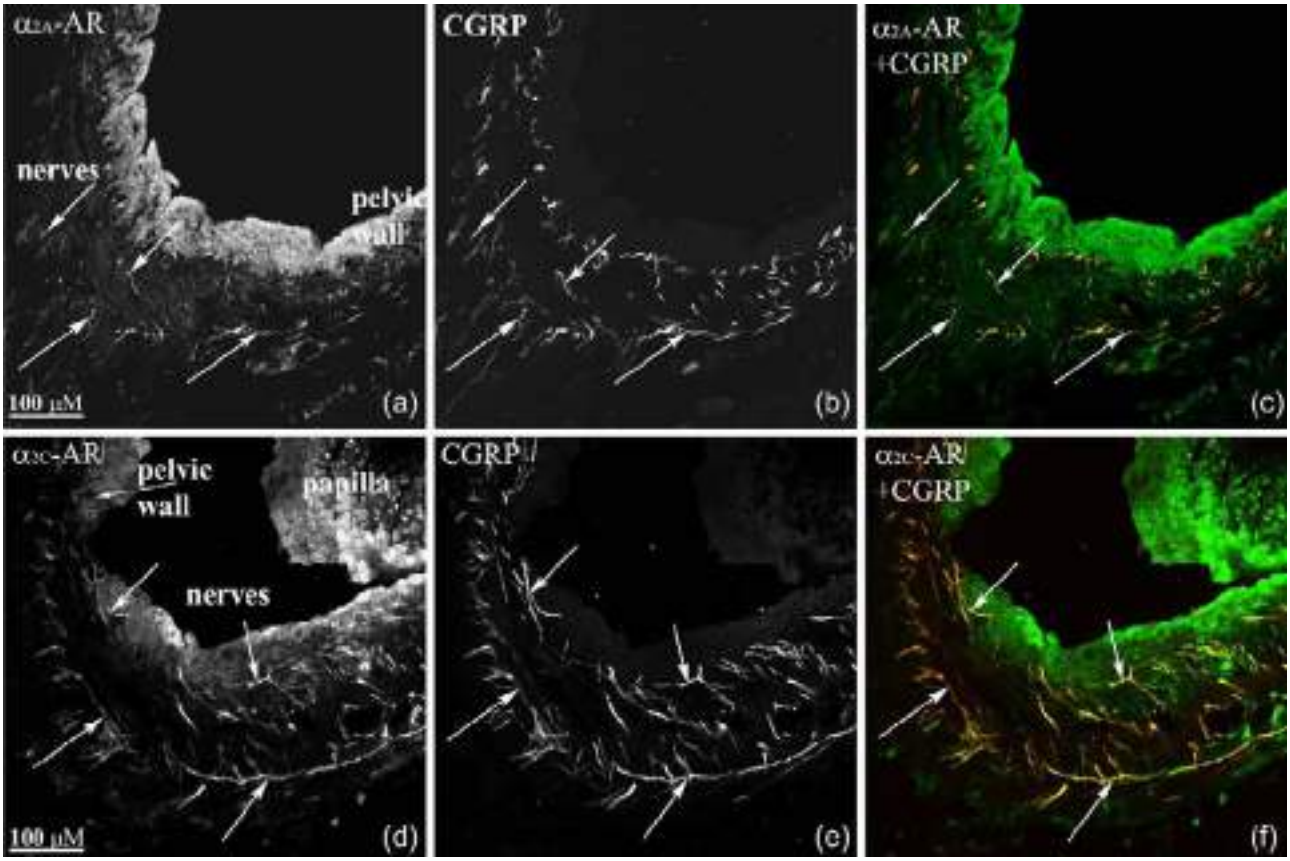

FIGURE 16.19 **Applying antibodies against α_{2A}-adrenoceptors (AR) (a) and α_{2C}-(AR) (d) labels nerve fibers (arrows) in the renal pelvic wall that are also labeled with an antibody against CGRP, a marker for sensory nerve fibers (b,e) as shown by the color yellow in (c) and (f).** *(Reference [158].)*

ENDOTHELIN

Endothelin is abundantly expressed throughout the body, including the brain and the kidney.[106] Endothelin exerts its effects by activating two G-protein coupled receptors, endothelin-A (ETA) and endothelin-B (ETB) receptors.[230] Both ETA and ETB receptors are localized in the renal pelvic wall, the ETA receptors on smooth muscle cells and the ETB receptors on or close to the afferent renal sensory nerves,[163] suggesting a role for endothelin in modulating the activation of afferent renal sensory nerves. Studies examining the role of endothelin in the activation of afferent renal sensory nerves by increased renal pelvic pressure or reflex increases in efferent renal sympathetic nerve activity suggested an important role for endothelin in modulating the responsiveness of the renal sensory nerves. The nature of the endothelin-induced activation of the afferent renal sensory nerves is dependent on dietary sodium intake.[163] In low-sodium dietary conditions, activation of ETA-receptors contributes to the suppressed responsiveness of the renal sensory nerves, whereas in high-sodium dietary conditions activation of ETB-receptors plays a major role in the enhanced responsiveness of the renal sensory nerves. These findings are of interest in view of the well-documented hypertension in ETB-receptor deficient rats and mice fed high-sodium diets.[87,227] Together, these studies may suggest that impairment of the inhibitory renorenal reflexes contributes to the salt-sensitive hypertension in conditions of renal ETB-receptor deficiency. Further support for this hypothesis is derived from studies in rats treated neonatally with capsaicin to destroy all sensory nerves.[274] These rats develop salt-sensitive hypertension which is reduced by ETA receptor antagonists in a similar fashion to that seen in ETB receptor deficient rats.[87,227]

The similar effects of an ETA-receptor antagonist and an AT1-receptor antagonist in low-sodium diet rats to restore the suppressed activation of renal sensory nerves towards that seen in rats fed normal-sodium diet[151,163] suggested an interaction between angiotensin II and endothelin. Comparing the effects of inhibitors of ETA-receptors and AT-1 receptors on the responses to activation of the renal mechanosensory nerves showed that ETA receptors play an important contributory role to the angiotensin II-induced

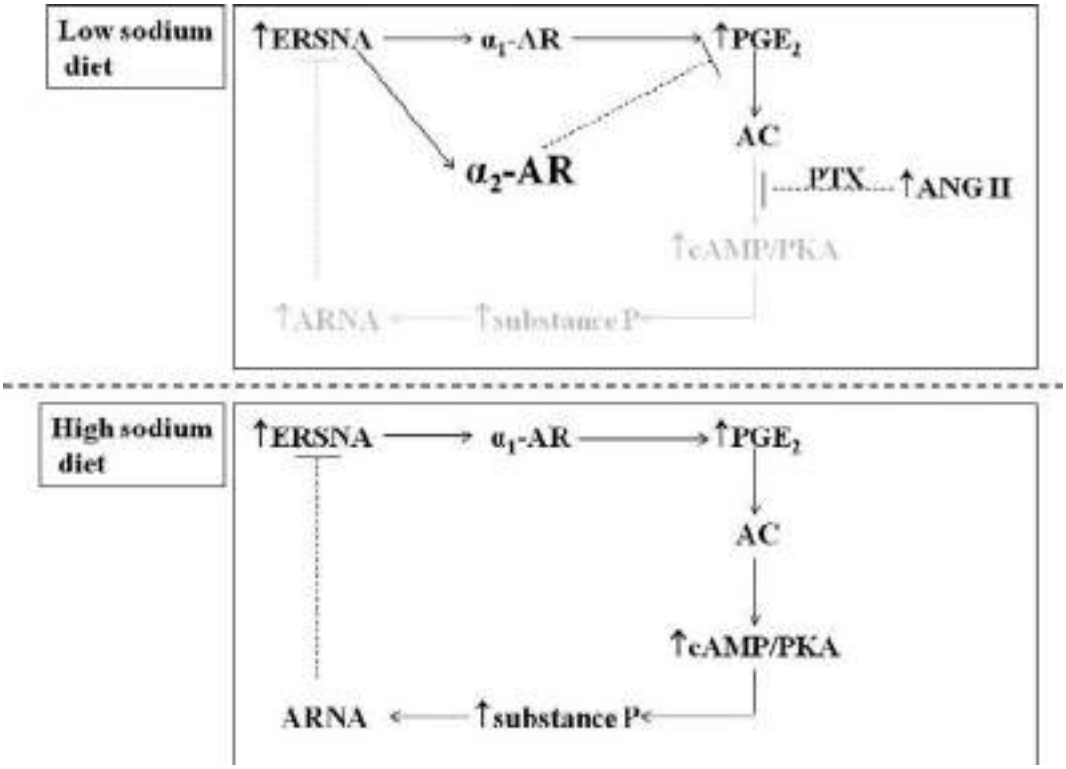

FIGURE 16.20 **In low-sodium dietary conditions, increased activation of α_2-adrenoceptor (AR) together with increased endogenous angiotensin (ANG) II activity suppresses the norepinephrine-mediated activation of the renal sensory nerves by decreasing PG synthesis, leading to reduced PGE_2-mediated activation of adenylyl/cAMP/PKA transduction pathway resulting in little or no increase in substance P release and increase in afferent renal nerve activity, and thereby no inhibition of efferent renal sympathetic nerve activity (ERSNA).** In high-sodium dietary conditions, the enhanced norepinephrine-mediated activation of renal sensory nerves is due, at least in part, to little or no activation of renal α_2-AR and very low endogenous ANG II activity opposing the norepinephrine-mediated increase in PGE_2 synthesis, substance P release, and increase in afferent renal nerve activity, leading to renorenal reflex decreases in ERSNA. Modulation of the interaction between efferent and afferent renal nerve activity is an appropriate physiological response to changes in dietary sodium intake in the overall goal of maintaining water and sodium balance.

suppression of the responsiveness of the afferent renal mechanosensory nerves[148] in low-sodium diet rats. These findings are supported by the considerable evidence showing that angiotensin II increases the expression of preproendothelin-1 mRNA in various tissues, including the kidney and urinary bladder,[123] increases endothelin-1 protein expression and secretion in vascular smooth muscle cells, cardiomyocytes and mesangial cells,[125,140,271] and increases ETA expression in cardiomyocytes.[125]

Activation of Renal Mechanosensory Nerves: Pathohysiological Conditions

Impairment of the Inhibitory Renorenal Reflexes in Various Diseases

Activation of the renal mechanosensory nerves is impaired in various pathological conditions of increased efferent renal sympathetic nerve activity and sodium retention, including congestive heart failure, spontaneous hypertension, diabetes type I, ischemia-induced acute renal failure, obstructive nephropathy, cirrhosis, and chronic hypoxia.[32,33,145,152,153,159,168,185–187] Impairment of the inhibitory renorenal reflexes in pathological conditions would aggravate and/or contribute to further increases in efferent renal sympathetic nerve activity and sodium retention. Many of these pathological conditions are characterized by increased angiotensin II activity. Importantly, renal pelvic administration of an AT-1 receptor antagonist has been shown to markedly improve the responsiveness of the renal mechanosensory nerves in rats with congestive heart failure, hypertension, and diabetes type I.[145,153,159] The marked enhancement of the renorenal reflex mechanism produced by AT1 receptor antagonists may contribute to the well-known beneficial effects of inhibiting the renin–angiotensin system in heart failure and hypertension.

In addition to the impaired responsiveness of the renal mechanosensory nerves in spontaneous hypertensive rats, the interaction between efferent renal sympathetic nerve activity and afferent renal nerve

activity is also impaired. The impaired interaction between efferent renal sympathetic nerve activity and afferent renal nerve activity is related to increased activation of renal pelvic α_2-adrenoceptors, in addition to increased activation of AT-1 receptors,[152] i.e., similar mechanisms as those contributing to the suppressed responsiveness of the renal sensory nerves in low-sodium diet rats.

Excitatory Reflexes Originating in Injured/Diseased Kidneys

The depressor effects of (T_9–L_1)DRX observed in rats with one-kidney, one-clip hypertension,[137] 5/6 nephrectomy,[28] and in rats exposed to i.v. infusion of cyclosporine[184] would appear to contradict the notion of the afferent renal nerves exerting a tonic inhibitory effect on efferent renal sympathetic nerve activity. However, it is likely that different mechanisms are involved in the activation of renal sensory nerves in normal and diseased kidneys. Whereas in normal kidneys activation of renal sensory nerves elicits inhibitory renorenal reflexes (*vide supra*), in diseased kidneys when the inhibitory renorenal reflexes are impaired, activation of renal sensory nerves may result in excitatory reflexes. Studies in 2-kidney 1-clip rats would support this notion. The responsiveness of the renal mechanosensory nerves in the clipped ischemic kidney is impaired.[144] Interestingly, renal denervation of the clipped kidney increased urinary sodium excretion from both the clipped and the contralateral non-clipped kidney, which is in contrast to the findings in normal healthy rats in which unilateral renal denervation decreases contralateral urinary sodium excretion.[39,60] In 2-kidney 1-clip rats, the contralateral natriuretic response was associated with decreases in contralateral efferent renal sympathetic nerve activity, suggesting that the balance between inhibitory and excitatory reflexes originating in the kidney was shifted from mainly being of an inhibitory nature to being of an excitatory nature in ischemic kidneys.[144] Thus, these data suggest that the afferent renal nerves in the ischemic kidney exert an excitatory influence on the sympathetic nervous system, in contrast to the inhibitory reflexes originating from normal healthy kidneys.[39,60] Further support for excitatory reflexes originating in an ischemic kidney derives from long-term blood pressure recordings in conscious rats following the onset of hypertension in 2-kidney 1-clip hypertension rats. Whereas renal denervation of the clipped kidney (six weeks after renal artery clipping) reduced arterial pressure almost to the same level as removing the clip from the renal artery, denervation of the contralateral non-clipped kidney had no effect on arterial pressure.[136] Further studies suggested an important role for adenosine in the excitatory reflexes originating in the ischemic kidneys. Intrarenal administration of adenosine deaminase reduced arterial pressure in 1-kidney 1-clip hypertensive rats, but had no effect in healthy normal rats.[134] Also, administration of adenosine into one renal artery resulted in increases in contralateral efferent renal sympathetic nerve activity and arterial pressure which were abolished by renal denervation of the infused kidney in healthy dogs.[135] Taken together, these studies suggest that excitatory reflexes originating in ischemic kidneys involve adenosine activating chemosensitive afferent renal nerves.

Further evidence for excitatory reflexes originating in diseased/injured kidneys is derived from studies in humans and rats with renal failure. Comparing arterial blood pressure and muscle sympathetic nerve activity in hemodialysis patients with and without their native diseased kidneys intact showed markedly reduced arterial pressure and muscle sympathetic nerve activity in patients with bilateral nephrectomy compared with patients who had their kidneys intact.[40] These findings were subsequently confirmed and extended in studies comparing arterial pressure and muscle sympathetic nerve activity in patients with kidney transplants, with and without their native kidneys intact.[104] None of the patients were uremic, thus they all had well-functioning renal grafts. However, muscle sympathetic nerve activity was increased in all patients versus healthy controls, except in the patients in which bilateral nephrectomy had been performed. In a subgroup of transplant patients, muscle sympathetic nerve activity was measured before and after the second kidney was removed, and was found to be reduced following removal of the second diseased kidney. Thus, these studies provide strong evidence for the diseased kidneys exerting an excitatory effect on sympathetic nerve activity. Studies in rats with chronic renal failure would support the notion that excitatory effects exerted by the diseased kidneys are related to activation of the afferent renal nerves in the diseased/injured kidney.[28] These rat studies showed that chronic renal failure increased arterial pressure and norepinephrine turnover in posterior hypothalamus and locus coeruleus. Importantly, prior dorsal rhizotomy to remove the afferent renal innervation prevented the increases in arterial pressure and norepinephrine turnover in the various brain regions.

Thus, local renal injury may result in sympathoexcitatory reflexes involving afferent renal nerves, central cardiovascular regulatory areas, and efferent systemic and renal sympathetic nerve activity, eventually leading to hypertension.

The notion of excitatory reflexes originating in diseased/injured kidney may provide an explanation to the marked prolonged decrease in arterial pressure in drug-resistant hypertensive patients following the one-time renal denervation procedure.[53,77,173] The reduction in arterial pressure following renal denervation is

associated with reduction in whole body norepinephrine spillover and reduction in muscle sympathetic nerve activity, indicative of removal of excitatory reflexes originating in the kidneys.

SUMMARY

The efferent renal sympathetic and afferent renal nerves constitute a significant control system for the physiological regulation of renal function. Efferent renal sympathetic nerve activity is governed by a centrally-based reflex control system which responds to diverse peripheral and central afferent inputs. The kidney is densely innervated by sympathetic nerves, including the renal vasculature, the nephron, the juxtaglomerular cells, and the renal pelvic wall, enabling the renal nerves to contribute to one of the major tasks of the kidney, the homeostatic regulation of body fluid volume.

Activation of the afferent renal nerves located in the renal pelvic wall leads to decreases in efferent renal sympathetic nerve activity and increases in urinary sodium excretion, a renorenal reflex response. Changes in efferent renal sympathetic nerve activity modulate the responsiveness of the renal sensory nerves. Increases in efferent renal sympathetic nerve activity increase afferent renal nerve activity. The increased afferent renal nerve activity will, in turn, decrease efferent renal sympathetic nerve activity via activation of the renorenal reflexes, a negative feedback mechanism, to maintain low-level efferent renal sympathetic nerve activity. Thus, there is an interaction between efferent renal sympathetic nerve activity and afferent renal nerve activity in the renal neural control of body fluid and sodium homeostasis wherein activation of the afferent renal nerves buffers the antinatriuretic effects of increases in efferent renal sympathetic nerve activity. This is most clearly evident in conditions of high-sodium dietary intake, when the afferent renal nerves are tonically active to suppress efferent renal sympathetic nerve activity to minimize sodium retention. Conversely, in low-sodium dietary conditions when increased efferent renal sympathetic nerve activity is essential for maintaining sodium balance, the activity of the afferent renal nerves are suppressed.

In pathophysiological sodium-retaining states, efferent renal sympathetic nerve activity is inappropriately increased in the presence of sodium retention. It has long been known that impairment of the aortic and arterial baroreflexes contributes to the inappropriately increased efferent renal sympathetic nerve activity in these pathological conditions. What has previously been overlooked is an impairment of reflexes originating in the kidneys, *per se*. However, there is now convincing evidence that impairment of the inhibitory renorenal reflexes contributes to the increased efferent renal sympathetic nerve activity and sodium retention prevalent in hypertension and various disease models of sodium retention. In conditions of renal injury/disease, available data would suggest that there is a shift from inhibitory to excitatory renorenal reflexes which would contribute to the increased efferent renal sympathetic nerve activity, leading to increased sodium retention and arterial pressure prevalent in these pathophysiological conditions.

Acknowledgments

The work performed in the authors' laboratories was supported by the National Institutes of Health, Heart, Lung and Blood Institute, RO1 HL66068, and by research grants from the Department of Veterans Affairs and the American Heart Association (Kopp), The British Heart Foundation (Johns), Wellcome Trust (Johns), Health Research Board (Johns), and Science Foundation Ireland (Johns).

References

[1] Abdulla MH, Sattar MA, Abdul Hye Khan M, Abdullah NA, Johns EJ. Influence of sympathetic and AT(1)-receptor blockade on angiotensin II and adrenergic agonists-induced renal vasoconstrictions in spontaneously hypertensive rats. Acta Physiol 2008;195:397–404.

[2] Abdulla MH, Sattar MA, Khan MA, Abdullah NA, Johns EJ. Influence of sympathetic and AT-receptor blockade on angiotensin II and adrenergic agonist-induced renal vasoconstrictions in spontaneously hypertensive rats. Acta Physiol (Oxf) 2009;195:397–404.

[3] Allen AM, Moeller I, Jenkins TA, Zhuo J, Aldred GP, Chai SY, et al. Angiotensin receptors in the nervous system. Brain Res Bull 1998;47:17–28.

[4] Aperia A, Ibarra F, Svensson LB, Klee C, Greengard P. Calcineurin mediates alpha-adrenergic stimulation of Na^+, K^+-ATPase activity in renal tubule cells. Proc Natl Acad Sci USA 1992;89:7394–7.

[5] Aukland K. Hydrogen polarography in measurement of local blood flow; theoretical and empirical basis. Acta Neurol Scand Suppl 1965;14:42–5.

[6] Aukland K, Bower BF. Berliner RW. Measurement of local blood flow with hydrogen gas. Circ Res 1964;14:164–87.

[7] Bachmann S, Bosse HM, Mundel P. Topography of nitric oxide synthesis by localizing constitutive NO synthases in mammalian kidney. Am J Physiol 1995;268:F885–898.

[8] Bankir L, Bichet DG, Bouby N. Vasopressin V2 receptors, ENaC, and sodium reabsorption: a risk factor for hypertension? Am J Physiol 2010;299:F917–928.

[9] Barajas L, Liu L, Powers K. Anatomy of the renal innervation: intrarenal aspects and ganglia of origin. Can J Physiol Pharmacol 1992;70:735–49.

[10] Barajas L, Powers K, Wang P. Innervation of the renal cortical tubules: a quantitative study. Am J Physiol 1984;247:F50–60.

[11] Barber JD, Moss NG. Reduced renal perfusion pressure causes prostaglandin-dependent excitation of R2 chemoreceptors in rats. Am J Physiol 1990;259:R1243–9.

[12] Barrett CJ, Navakatikyan MA, Malpas SC. Long-term control of renal blood flow: what is the role of the renal nerves? Am J Physiol 2001;280:R1534–1545.

[13] Beierwaltes WH. The role of calcium in the regulation of renin secretion. Am J Physiol 2010;298:F1–11.

[14] Bello-Reuss E, Colindres RE, Pastoriza-Munoz E, Mueller RA, Gottschalk CW. Effects of acute unilateral renal denervation in the rat. J Clin Invest 1975;56:208–17.
[15] Bello-Reuss E, Pastoriza-Munoz E, Colindres RE. Acute unilateral renal denervation in rats with extracellular volume expansion. Am J Physiol 1977;232:F26–32.
[16] Bello-Reuss E, Trevino DL, Gottschalk CW. Effect of renal sympathetic nerve stimulation on proximal water and sodium reabsorption. J Clin Invest 1976;57:1104–7.
[17] Bernard C. Lecons sur les Proprietes Physiologique et les Alterations Pathoogique des Liquides de l'Organisme. Paris: Bailleère et Fils 1859;2:170–1.
[18] Bohmann C, Schollmeyer P, Rump LC. Alpha 2-autoreceptor subclassification in rat isolated kidney by use of short trains of electrical stimulation. Br J Pharmacol 1993;108:262–8.
[19] Bohmann C, Schollmeyer P, Rump LC. Effects of imidazolines on noradrenaline release in rat isolated kidney. Naunyn Schmiedebergs Arch Pharmacol 1994;349:118–24.
[20] Boie Y, Stocco R, Sawyer N, Slipetz DM, Ungrin MD, Neuschafer-Rube F, et al. Molecular cloning and characterization of the four rat prostaglandin E2 prostanoid receptor subtypes. Eur J Pharmacol 1997;340:227–41.
[21] Boke T, Malik KU. Enhancement by locally generated angiotensin II of release of the adrenergic transmitter in the isolated rat kidney. J Pharmacol Exp Ther 1983;226:900–7.
[22] Bonjour JP, Churchill PC, Malvin RL. Change of tubular reabsorption of sodium and water after renal denervation in the dog. J Physiol 1969;204:571–82.
[23] Bonvalet JP, Pradelles P, Farman N. Segmental synthesis and actions of prostaglandins along the nephron. Am J Physiol 1987;253:F377–87.
[24] Bosse HM, Bohm R, Resch S, Bachmann S. Parallel regulation of constitutive NO synthase and renin at JGA of rat kidney under various stimuli. Am J Physiol 1995;269:F793–805.
[25] Brod J. [Regulation of renal function.]. Chekh Fiziol 1952;1:274–300.
[26] Calaresu FR, Ciriello J. Renal afferent nerves affect discharge rate of medullary and hypothalamic single units in the cat. J Auton Nerv Syst 1981;3:311–20.
[27] Camara AK, Osborn JL. AT1 receptors mediate chronic central nervous system AII hypertension in rats fed high sodium chloride diet from weaning. J Auton Nerv Syst 1998;72:16–23.
[28] Campese VM, Kogosov E. Renal afferent denervation prevents hypertension in rats with chronic renal failure. Hypertension 1995;25:878–82.
[29] Caverson MM, Ciriello J. Effect of stimulation of afferent renal nerves on plasma levels of vasopressin. Am J Physiol 1987;252: R801–7.
[30] Chen L, Kim SM, Oppermann M, Faulhaber-Walter R, Huang Y, Mizel D, et al. Regulation of renin in mice with Cre recombinase-mediated deletion of G protein Gsalpha in juxtaglomerular cells. Am J Physiol 2007;292:F27–37.
[31] Chen HI, Chapleau MW, McDowell TS, Abboud FM. Prostaglandins contribute to activation of baroreceptors in rabbits. Possible paracrine influence of endothelium. Circ Res 1990;67:1394–404.
[32] Chien CT, Chien HF, Cheng YJ, Chen CF, Hsu SM. Renal afferent signaling diuretic response is impaired in streptozotocin-induced diabetic rats. Kidney Int 2000;57:203–14.
[33] Chien CT, Fu TC, Wu MS, Chen CF. Attenuated response of renal mechanoreceptors to volume expansion in chronically hypoxic rats. Am J Physiol 1997;273:F712–7.
[34] Cho HJ, Kim DS, Lee NH, Kim JK, Lee KM, Han KS, et al. Changes in the alpha 2-adrenergic receptor subtypes gene expression in rat dorsal root ganglion in an experimental model of neuropathic pain. Neuroreport 1997;8:3119–22.
[35] Ciriello J. Afferent renal inputs to paraventricular nucleus vasopressin and oxytocin neurosecretory neurons. Am J Physiol 1998;275:R1745–54.
[36] Ciriello J, Calaresu FR. Central projections of afferent renal fibers in the rat an antegrade transport study of horseradish peroxidase. J Auton Nerv Syst 1983;8:273–85.
[37] Clausen G, Tyssebotn I, Kirkebo A, Ofjord ES, Aukland K. Distribution of blood flow in the dog kidney. III. Local uptake of 10 mum and 15 mum microspheres during renal vasodilation and constriction. Acta Physiol Scand 1981;113:471–9.
[38] Cohnhein J, Roy S. Untersuchungen uber die Zirkulation in den Nieren. Virchows Arch Path Anat Physiol 1883;93:424–57.
[39] Colindres RE, Spielman WS, Moss NG, Harrington WW, Gottschalk CW. Functional evidence for renorenal reflexes in the rat. Am J Physiol 1980;239:F265–70.
[40] Converse Jr RL, Jacobsen TN, Toto RD, Jost CM, Cosentino F, Fouad-Tarazi F, et al. Sympathetic overactivity in patients with chronic renal failure. N Engl J Med 1992;327:1912–8.
[41] Cupples WA, Marsh DJ. Autoregulation of blood flow in renal medulla of the rat: no role for angiotensin II. Can J Physiol Pharmacol 1988;66:833–6.
[42] Dampney RA. Functional organization of central pathways regulating the cardiovascular system. Physiol Rev 1994;74:323–64.
[43] Dampney RA, Fontes MA, Hirooka Y, Horiuchi J, Potts PD, Tagawa T. Role of angiotensin II receptors in the regulation of vasomotor neurons in the ventrolateral medulla. Clin Exp Pharmacol Physiol 2002;29:467–72.
[44] Dampney RA, Horiuchi J, Tagawa T, Fontes MA, Potts PD, Polson JW. Medullary and supramedullary mechanisms regulating sympathetic vasomotor tone. Acta Physiol Scand 2003;177:209–18.
[45] Davis G, Johns EJ. Effect of somatic nerve stimulation on the kidney in intact, vagotomized and carotid sinus-denervated rats. J Physiol 1991;432:573–84.
[46] Davis G, Johns EJ. Somatosensory regulation of renal function in the stroke-prone spontaneously hypertensive rat. J Physiol 1994;481(Pt 3):753–9.
[47] Day TA, Ciriello J. Effects of renal receptor activation on neurosecretory vasopressin cells. Am J Physiol 1987;253:R234–41.
[48] Denton KM, Fennessy PA, Alcorn D, Anderson WP. Morphometric analysis of the actions of angiotensin II on renal arterioles and glomeruli. Am J Physiol 1992;262:F367–372.
[49] Denton KM, Luff SE, Shweta A, Anderson WP. Differential neural control of glomerular ultrafiltration. Clin Exp Pharmacol Physiol 2004;31:380–6.
[50] Denton KM, Shweta A, Flower RL, Anderson WP. Predominant postglomerular vascular resistance response to reflex renal sympathetic nerve activation during ANG II clamp in rabbits. Am J Physiol 2004;287:R780–786.
[51] DiBona GF. Nervous kidney. Interaction between renal sympathetic nerves and the renin–angiotensin system in the control of renal function. Hypertension 2000;36:1083–8.
[52] DiBona GF. Peripheral and central interactions between the renin–angiotensin system and the renal sympathetic nerves in control of renal function. Ann N Y Acad Sci 2001;940:395–406.
[53] DiBona GF, Esler M. Translational medicine: the antihypertensive effect of renal denervation. Am J Physiol 2010;298: R245–253.
[54] DiBona GF, Johns EJ. A study of the role of renal nerves in the renal responses to 60 degree head-up tilt in the anaesthetized dog. J Physiol 1980;299:117–26.
[55] DiBona GF, Jones SY. Effect of dietary sodium intake on the responses to bicuculline in the paraventricular nucleus of rats. Hypertension 2001;38:192–7.

[56] DiBona GF, Jones SY. Sodium intake influences hemodynamic and neural responses to angiotensin receptor blockade in rostral ventrolateral medulla. Hypertension 2001;37:1114–23.
[57] DiBona GF, Jones SY, Sawin LL. Effect of endogenous angiotensin II on renal nerve activity and its arterial baroreflex regulation. Am J Physiol 1996;271:R361–367.
[58] DiBona GF, Kopp UC. Neural control of renal function. Physiol Rev 1997;77:75–197.
[59] Dibona GF, Sawin LL. Effect of endogenous angiotensin II on the frequency response of the renal vasculature. Am J Physiol 2004;287:F1171–1178.
[60] DiBona GF, Rios LL. Renal nerves in compensatory renal response to contralateral renal denervation. Am J Physiol 1980;238:F26–30.
[61] DiBona GF, Sawin LL. Effect of renal denervation on dynamic autoregulation of renal blood flow. Am J Physiol 2004;286: F1209–1218.
[62] DiBona GF, Sawin LL. Effect of renal nerve stimulation on NaCl and H_2O transport in Henle's loop of the rat. Am J Physiol 1982;243:F576–580.
[63] DiBona GF, Sawin LL. Effect of renal nerve stimulation on responsiveness of the rat renal vasculature. Am J Physiol 2002;283:F1056–1065.
[64] DiBona GF, Sawin LL. Exaggerated natriuresis in experimental hypertension. Proc Soc Exp Biol Med 1986;182:43–51.
[65] DiBona GF, Sawin LL. Frequency response of the renal vasculature in congestive heart failure. Circulation 2003;107:2159–64.
[66] Dibona GF, Sawin LL. Functional significance of the pattern of renal sympathetic nerve activation. Am J Physiol 1999;277: R346–353.
[67] DiBona GF, Sawin LL. Renal hemodynamic effects of activation of specific renal sympathetic nerve fiber groups. Am J Physiol 1999;276:R539–549.
[68] DiBona GF, Sawin LL. Renal nerve activity in conscious rats during volume expansion and depletion. Am J Physiol 1985;248:F15–23.
[69] DiBona GF, Zambraski EJ, Aguilera AJ, Kaloyanides GJ. Neurogenic control of renal tubular sodium reabsorption in the dog: a brief review and preliminary report concerning possible humoral mediation. Circ Res 1977;40:I127–130.
[70] Donovan MK, Wyss JM, Winternitz SR. Localization of renal sensory neurons using the fluorescent dye technique. Brain Res 1983;259:119–22.
[71] Egi Y, Matsumura Y, Murata S, Umekawa T, Hisaki K, Takaoka M, et al. The effects of NG-nitro-L-arginine, a nitric oxide synthase inhibitor, on norepinephrine overflow and antidiuresis induced by stimulation of renal nerves in anesthetized dogs. J Pharmacol Exp Ther 1994;269:529–35.
[72] Eitle E, Hiranyachattada S, Wang H, Harris PJ. Inhibition of proximal tubular fluid absorption by nitric oxide and atrial natriuretic peptide in rat kidney. Am J Physiol 1998;274: C1075–1080.
[73] England S, Bevan S, Docherty RJ. PGE2 modulates the tetrodotoxin-resistant sodium current in neonatal rat dorsal root ganglion neurones via the cyclic AMP-protein kinase A cascade. J Physiol 1996;495(Pt 2):429–40.
[74] Eppel GA, Malpas SC, Denton KM, Evans RG. Neural control of renal medullary perfusion. Clin Exp Pharmacol Physiol 2004;31:387–96.
[75] Esler M. The sympathetic system and hypertension. Am J Hypertens 2000;13:99S–105S.
[76] Esler M, Rumantir M, Kaye D, Jennings G, Hastings J, Socratous F, et al. Sympathetic nerve biology in essential hypertension. Clin Exp Pharmacol Physiol 2001;28:986–9.
[77] Esler MD, Krum H, Sobotka PA, Schlaich MP, Schmieder RE, Bohm M. Renal sympathetic denervation in patients with treatment-resistant hypertension (The Symplicity HTN-2 Trial): a randomised controlled trial. Lancet 2010;376:1903–9.
[78] Evans RG, Eppel GA, Anderson WP, Denton KM. Mechanisms underlying the differential control of blood flow in the renal medulla and cortex. J Hypertension 2004;22:1439–51.
[79] Evans RG, Head GA, Eppel GA, Burke SL, Rajapakse NW. Angiotensin II and neurohumoral control of the renal medullary circulation. Clin Exp Pharmacol Physiol 2010;37:e58–69.
[80] Faber JE. Role of prostaglandins and kinins in the renal pressor reflex. Hypertension 1987;10:522–32.
[81] Fazan VP, Ma X, Chapleau MW, Barreira AA. Qualitative and quantitative morphology of renal nerves in C57BL/6J mice. Anat Rec 2002;268:399–404.
[82] Felder RB. Excitatory and inhibitory interactions among renal and cardiovascular afferent nerves in dorsomedial medulla. Am J Physiol 1986;250:R580–8.
[83] Feng F, Pettinger WA, Abel PW, Jeffries WB. Regional distribution of alpha 1-adrenoceptor subtypes in rat kidney. J Pharmacol Exp Ther 1991;258:263–8.
[84] Feng N-H, Lee H-H, Shiang J-C, Ma M-C. Transient receptor potential vanilloid type 1 channels act as mechanoreceptors and cause substance P release and sensory activation in rat kidneys. Am J Physiol 2008;294:F316–25.
[85] Friis UG, Jensen BL, Sethi S, Andreasen D, Hansen PB, Skott O. Control of renin secretion from rat juxtaglomerular cells by cAMP-specific phosphodiesterases. Circ Res 2002;90:996–1003.
[86] Friis UG, Jorgensen F, Andreasen D, Jensen BL, Skott O. Membrane potential and cation channels in rat juxtaglomerular cells. Acta Physiol Scand 2004;181:391–6.
[87] Gariepy CE, Ohuchi T, Williams C, Richardson JA, Yanagisawa M. Salt-sensitive hypertension in endothelin-B receptor-deficient rats. J Clin Invest 2000;105:925–33.
[88] Genovesi S, Pieruzzi F, Wijnmaalen P, Centonza L, Golin R, Zanchetti A, et al. Renal afferents signaling diuretic activity in the cat. Circ Res 1993;73:906–13.
[89] Geppetti P. Sensory neuropeptide release by bradykinin: mechanisms and pathophysiological implications. Regul Pept 1993;47:1–23.
[90] Gilmore JP, Echtenkamp S, Wesley CR, Zucker IH. Atrial receptor modulation of renal nerve activity in the nonhuman primate. Am J Physiol 1982;242:F592–598.
[91] Gold MS, Dastmalchi S, Levine JD. Alpha 2 adrenergic receptor subtypes in rat dorsal root and superior cervical ganglion neurons. Pain 1997;69:179–90.
[92] Gontijo RJ, Kopp UC. Renal sensory receptor activation by calcitonin gene-related peptide. Hypertension 1994;23(Part 2):1063–7.
[93] Gontijo JR, Smith LA, Kopp UC. CGRP activates renal pelvic substance P receptors by retarding substance P metabolism. Hypertension 1999;33:493–8.
[94] Gross R, Ruffmann K, Kirchheim H. The separate and combined influences of common carotid occlusion and nonhypotensive hemorrhage on kidney blood flow. Pflügers Arch 1979;379:81–8.
[95] Guild SJ, Austin PC, Navakatikyan M, Ringwood JV, Malpas SC. Dynamic relationship between sympathetic nerve activity and renal blood flow: a frequency domain approach. Am J Physiol 2001;281:R206–212.
[96] Guild SJ, Barrett CJ, Evans RG, Malpas SC. Interactions between neural and hormonal mediators of renal vascular tone in anaesthetized rabbits. Exp Physiol 2003;88:229–41.
[97] Guild SJ, Eppel GA, Malpas SC, Rajapakse NW, Stewart A, Evans RG. Regional responsiveness of renal perfusion to activation of the renal nerves. Am J Physiol 2002;283: R1177–1186.

[98] Hackenthal E, Paul M, Ganten D, Taugner R. Morphology, physiology, and molecular biology of renin secretion. Physiol Rev 1990;70:1067–116.
[99] Hamza SM, Kaufman S. Effect of mesenteric vascular congestion on reflex control of renal blood flow. Am J Physiol 2007;293:R1917–1922.
[100] Hamza SM, Kaufman S. Role of spleen in integrated control of splanchnic vascular tone: physiology and pathophysiology. Can J Physiol Pharmacol 2009;87:1–7.
[101] Hamza SM, Kaufman S. Splenorenal reflex modulates renal blood flow in the rat. J Physiol 2004;558:277–82.
[102] Handa RK, Johns EJ. Interaction of the renin–angiotensin system and the renal nerves in the regulation of rat kidney function. J Physiol 1985;369:311–21.
[103] Hardebo JE. Influence of impulse pattern on noradrenaline release from sympathetic nerves in cerebral and some peripheral vessels. Acta Physiol Scand 1992;144:333–9.
[104] Hausberg M, Kosch M, Harmelink P, Barenbrock M, Hohage H, Kisters K, et al. Sympathetic nerve activity in end-stage renal disease. Circulation 2002;106:1974–9.
[105] Head GA. Role of AT1 receptors in the central control of sympathetic vasomotor function. Clin Exp Pharmacol Physiol Suppl 1996;3:S93–98.
[106] Hemsen A, Lundberg JM. Presence of endothelin-1 and endothelin-3 in peripheral tissues and central nervous system of pig. Reg Peptides 1991;36:71–83.
[107] Hermansson K, Kallskog O, Wolgast M. Effect of renal nerve stimulation on the activity of the tubuloglomerular feedback mechanism. Acta Physiol Scand 1984;120:381–5.
[108] Hesse IF, Johns EJ. The effect of graded renal nerve stimulation on renal function in the anaesthetized rabbit. Comp Biochem Physiol A 1984;79:409–14.
[109] Hesse IF, Johns EJ. The subtype of alpha-adrenoceptor involved in the neural control of renal tubular sodium reabsorption in the rabbit. J Physiol 1984;352:527–38.
[110] Hevener AL, Bergman RN, Donovan CM. Hypoglycemic detection does not occur in the hepatic artery or liver: findings consistent with a portal vein glucosensor locus. Diabetes 2001;50:399–403.
[111] Hevener AL, Bergman RN, Donovan CM. Portal vein afferents are critical for the sympathoadrenal response to hypoglycemia. Diabetes 2000;49:8–12.
[112] Hintze TH, Kaley G. Ventricular receptors activated following myocardial prostaglandin synthesis initiate reflex hypotension, reduction in heart rate, and redistribution of cardiac output in the dog. Circ Res 1984;54:239–47.
[113] Hisa H, Araki S, Tomura Y, Hayashi Y, Satoh S. Effects of alpha adrenoceptor blockade on renal nerve stimulation-induced norepinephrine release and vasoconstriction in the dog kidney. J Pharmacol Exp Ther 1989;248:752–7.
[114] Holdaas H, DiBona GF, Kiil F. Effect of low-level renal nerve stimulation on renin release from nonfiltering kidneys. Am J Physiol 1981;241:F156–161.
[115] Houghton BL, Huang C, Johns EJ. Influence of dietary sodium on the blood pressure and renal sympathetic nerve activity responses to intracerebroventricular angiotensin II and angiotensin III in anaesthetized rats. Exp Physiol 2010;95:282–95.
[116] Houghton BL, Johns EJ. The pressor and renal sympathetic nerve responses to vascular and spinal V1 receptor activation after manipulation of dietary sodium intake. J Hypertens 2011.
[117] Huang BS, Leenen FH. Dietary Na and baroreflex modulation of blood pressure and RSNA in normotensive vs. spontaneously hypertensive rats. Am J Physiol 1994;266:H496–502.
[118] Huang C, Johns EJ. Role of ANG II in mediating somatosensory-induced renal nerve-dependent antinatriuresis in the rat. Am J Physiol 1998;275:R194–202.
[119] Huang C, Johns EJ. Role of brain angiotensin II in the somatosensory induced antinatriuresis in the anaesthetized rat. Clin Exp Pharmacol Physiol 2000;27:191–6.
[120] Huang C, Yoshimoto M, Miki K, Johns EJ. The contribution of brain angiotensin II to the baroreflex regulation of renal sympathetic nerve activity in conscious normotensive and hypertensive rats. J Physiol 2006;574:597–604.
[121] Hunt CC, Wilkinson RS, Fukami Y. Ionic basis of the receptor potential in primary endings of mammalian muscle spindles. J Gen Physiol 1978;71:683–98.
[122] Ichihara A, Kobori H, Nishiyama A, Navar LG. Renal renin–angiotensin system. Contrib Nephrol 2004;143:117–30.
[123] Imai T, Hirata Y, Emori T, Yanagisawa M, Masaki T, Marumo F. Induction of endothelin-1 gene by angiotensin and vasopressin in endothelial cells. Hypertension 1992;19:753–7.
[124] Ishii M, Ikeda T, Takagi M, Sugimoto T, Atarashi K, Igari T, et al. Elevated plasma catecholamines in hypertensives with primary glomerular diseases. Hypertension 1983;5:545–51.
[125] Ito H, Hirata Y, Adachi S, Tanaka M, Tsujino M, Koike A, et al. Endothelin-1 is an autocrine/paracrine factor in the mechanism of angiotensin II-induced hypertrophy in cultured rat cardiomyocytes. J Clin Invest 1993;92:398–403.
[126] Janssen BJ, Struijker Boudier HA, Smits JF. Role of afferent renal nerves in renal adaptation to sodium restriction in uninephrectomized rats. Acta Physiol Scand 1994;151:395–402.
[127] Johns EJ. The autonomic nervous system and pressure-natriuresis in cardiovascular–renal interactions in response to salt. Clin Auton Res 2002;12:256–63.
[128] Johns EJ. Role of angiotensin II and the sympathetic nervous system in the control of renal function. J Hypertension 1989;7:695–701.
[129] Johns EJ. The role of angiotensin II in the antidiuresis and antinatriuresis induced by stimulation of the sympathetic nerves to the rat kidney. J Auton Pharmacol 1987;7:205–14.
[130] Johns EJ. Role of the renal nerves in modulating renin release during pressure reduction at the feline kidney. Clin Sci (Lond) 1985;69:185–95.
[131] Johns EJ, Lewis BA, Singer B. The sodium-retaining effect of renal nerve activity in the cat: role of angiotensin formation. Clin Sci Mol Med 1976;51:93–102.
[132] Johns EJ, Manitius J. An investigation into the neural regulation of calcium excretion by the rat kidney. J Physiol 1987;383:745–55.
[133] Johns EJ, O'Shaughnessy B, O'Neill S, Lane B, Healy V. Impact of elevated dietary sodium intake on NAD(P)H oxidase and SOD in the cortex and medulla of the rat kidney. Am J Physiol 2010;299:R234–240.
[134] Katholi RE, McCann WP, Woods WT. Intrarenal adenosine produces hypertension via renal nerves in the one-kidney, one-clip rat. Hypertension 1985;7(Pt 2):I88–93.
[135] Katholi RE, Whitlow PL, Hageman GR, Woods WT. Intrarenal adenosine produces hypertension by activating the sympathetic nervous system via the renal nerves in the dog. J Hypertension 1984;2:349–59.
[136] Katholi RE, Whitlow PL, Winternitz SR, Oparil S. Importance of the renal nerves in established two-kidney, one-clip Goldblatt hypertension. Hypertension 1982;4(suppl II):II-166–74.
[137] Katholi RE, Woods WT. Afferent renal nerves and hypertension. Clin Exp Hypertens A 1987;9(Suppl 1):211–26.
[138] Knuepfer MM, Akeyson EW, Schramm LP. Spinal projections of renal afferent nerves in the rat. Brain Res 1988;446:17–25.

[139] Knuepfer M, Schramm LP. The conduction velocities and spinal projections of single renal afferent fibers in the rat. Brain Res 1987;435:167–73.
[140] Kohno M, Horio T, Ikeda M, Yokokawa K, Fukui T, Yasanari K, et al. Angiotensin II stimulates endothelin-1 secretion in cultured rat mesangial cells. Kid Int 1992;42:860–6.
[141] Kompanowska-Jezierska E, Walkowska A, Johns EJ, Sadowski J. Early effects of renal denervation in the anaesthetised rat: natriuresis and increased cortical blood flow. J Physiol 2001;531:527–34.
[142] Kone BC, Baylis C. Biosynthesis and homeostatic roles of nitric oxide in the normal kidney. Am J Physiol 1997;272:F561–578.
[143] Kopp U, Aurell M, Nilsson IM, Ablad B. The role of beta-1-adrenoceptors in the renin release response to graded renal sympathetic nerve stimulation. Pflugers Arch 1980;387:107–13.
[144] Kopp UC, Buckley-Bleiler RL. Impaired renorenal reflexes in two-kidney, one-clip hypertensive rats. Hypertension 1989;14:445–52.
[145] Kopp UC, Cicha MZ. Impaired substance P release from renal sensory nerves in SHR involves a pertussis toxin-sensitive mechanism. Am J Physiol 2004;286:R326–33.
[146] Kopp UC, Cicha MZ. PGE_2 increases substance P release from pelvis sensory nerves via activation of N-type calcium channels. Am J Physiol 1999;276:R1241–8.
[147] Kopp UC, Cicha MZ, Nakamura K, Nusing RM, Smith LA, Hökfelt T. Activation of EP4 receptors contributes to prostaglandin E2-mediated stimulation of renal sensory nerves. Am J Physiol 2004;287:F1269–82.
[148] Kopp UC, Cicha MZ, Smith LA. Activation of endothelin-A receptors contributes to angiotensin-induced suppression of renal sensory nerve activation. Hypertension 2007;49:141–7.
[149] Kopp UC, Cicha MZ, Smith LA. Angiotensin blocks substance P release from renal sensory nerves by inhibiting PGE_2-mediated activation of cAMP. Am J Physiol 2003;285:F472–83.
[150] Kopp UC, Cicha MZ, Smith LA. Dietary sodium loading increases arterial pressure in afferent renal-denervated rats. Hypertension 2003;42:968–73.
[151] Kopp UC, Cicha MZ, Smith LA. Endogenous angiotensin modulates PGE_2-mediated release of substance P from renal mechanosensory nerve fibers. Am J Physiol 2002;282:R19–30.
[152] Kopp UC, Cicha MZ, Smith LA. Impaired interaction between efferent and afferent renal nerve activity in SHR involves increased activation of α_2-adrenoceptors. Hypertension 2011;57(part 2):640–7.
[153] Kopp UC, Cicha MZ, Smith LA. Impaired responsiveness of renal mechanosensory nerves in heart failure: role of endogenous angiotensin. Am J Physiol 2003;284:R116–24.
[154] Kopp UC, Cicha MZ, Smith LA. PGE_2 increases release of substance P from renal sensory nerves by activating the cAMP-PKA transduction cascade. Am J Physiol 2002;282:R1618–27.
[155] Kopp UC, Cicha MZ, Smith LA, Haeggstrom JZ, Samuelsson B, Hokfelt T. Cyclooxygenase-2 involved in stimulation of renal mechanosensitive neurons. Hypertension 2000;35:373–8.
[156] Kopp UC, Cicha MZ, Smith LA, Hokfelt T. Nitric oxide modulates renal sensory nerve fibers by mechanisms related to substance P receptor activation. Am J Physiol 2001;281: R279–90.
[157] Kopp UC, Cicha MZ, Smith LA, Mulder J, Hökfelt T. Renal sympathetic nerve activity modulates afferent renal nerve activity by PGE2-dependent activation of alpha1- and alpha2-adrenoceptors on renal sensory nerve fibers. Am J Physiol 2007;293:R1561–1572.
[158] Kopp UC, Cicha MZ, Smith LA, Ruohonen S, Scheinin M, Fritz N, et al. Dietary sodium modulates the interaction between efferent and afferent renal nerve activity by altering activation of α2-adrenoceptors on renal sensory nerves. Am. J. Physiol 2011;300:R298–310.
[159] Kopp UC, Cicha MZ, Yorek MA. Impaired responsiveness of renal sensory nerves in streptozotocin-treated rats and obese Zucker diabetic fatty rats: role of angiotensin. Am J Physiol 2008;294:R858–66.
[160] Kopp UC, DiBona GF. Interaction between neural and non-neural mechanisms controlling renin secretion rate. Am J Physiol 1984;246:F620–626.
[161] Kopp UC, Farley DM, Cicha MZ, Smith LA. Activation of renal mechanosensitive neurons involves bradykinin, protein kinase C, PGE2, and substance P. Am J Physiol 2000;278: R937–46.
[162] Kopp UC, Farley DM, Smith LA. Bradykinin-mediated activation of renal sensory neurons due to prostaglandin-dependent release of substance P. Am J Physiol 1997;272:R2009–16.
[163] Kopp UC, Grisk O, Cicha MZ, Smith A, Steinbach A, Schlüter T, et al. Dietary sodium modulates the interaction between efferent renal sympathetic nerve activity and afferent renal nerve activity: role of endothelin. Am J Physiol 2009;297:R337–51.
[164] Kopp UC, Jones SY, DiBona GF. Afferent renal denervation impairs baroreflex control of efferent renal sympathetic nerve activity. Am J Physiol 2008;295:R1882–90.
[165] Kopp UC, Matsushita K, Sigmund RD, Smith LA, Watanabe S, Stokes JB. Amiloride-sensitive Na^+ channels in pelvic uroepithelium involved in renal sensory receptor activation. Am J Physiol 1998;275:R1780–92.
[166] Kopp UC, Olson LA, DiBona GF. Renorenal reflex responses to mechano- and chemoreceptor stimulation in the dog and rat. Am J Physiol 1984;246:F67–77.
[167] Kopp UC, Smith LA. Effects of the substance P receptor antagonist CP-96,345 on renal sensory receptor activation. Am J Physiol 1993;264:R647–53.
[168] Kopp UC, Smith LA, DiBona GF. Impaired renorenal reflexes in spontaneously hypertensive rats. Hypertension 1987;9:69–75.
[169] Kopp UC, Smith LA, DiBona GF. Renorenal reflexes: neural components of ipsilateral and contralateral renal responses. Am J Physiol 1985;249:F507–17.
[170] Kopp UC, Smith LA, Pence AL. Na^+-K^+-ATPase inhibition sensitizes renal mechanoreceptors activated by increases in renal pelvic pressure. Am J Physiol 1994;267:R1109–17.
[171] Kostreva DR, Castaner A, Kampine JP. Reflex effects of hepatic baroreceptors on renal and cardiac sympathetic nerve activity. Am J Physiol 1980;238:R390–394.
[172] Krum H, Schlaich M, Whitbourn R, Sobotka PA, Sadowski J, Bartus K, et al. Catheter-based renal sympathetic denervation for resistant hypertension: a multicentre safety and proof-of-principle cohort study. Lancet 2009;373:1275–81.
[173] Krum H, Barman N, Schlaich M, Sobotka P, Esler M, Mahfoud F, et al. (Simplicity HTN-1 Investigators). Catheter-based renal sympathetic denervation for resistant hypertension: durability of blood pressure reduction out to 24 months. Hypertension 2011;57:911–7.
[174] Kumagai H, Averill DB, Ferrario CM. Renal nerve activity in rats with spontaneous hypertension: effect of converting enzyme inhibitor. Am J Physiol 1992;263:R109–115.
[175] La Grange RG, Sloop CH, Schmid HE. Selective stimulation of renal nerves in the anesthetized dog. Effect on renin release during controlled changes in renal hemodynamics. Circ Res 1973;33:704–12.
[176] Lacroix JS, Stjarne P, Anggard A, Lundberg JM. Sympathetic vascular control of the pig nasal mucosa: (I). Increased resistance and capacitance vessel responses upon stimulation with irregular bursts compared to continuous impulses. Acta Physiol Scand 1988;132:83–90.

[177] Leonard BL, Evans RG, Navakatikyan MA, Malpas SC. Differential neural control of intrarenal blood flow. Am J Physiol 2000;279:R907–916.
[178] Linden RJ, Mary DA, Weatherill D. The nature of the atrial receptors responsible for a reflex decrease in activity in renal nerves in the dog. J Physiol 1980;300:31–40.
[179] Liu F, Gesek FA. alpha(1)-Adrenergic receptors activate NHE1 and NHE3 through distinct signaling pathways in epithelial cells. Am J Physiol 2001;280:F415–425.
[180] Liu F, Nesbitt T, Drezner MK, Friedman PA, Gesek FA. Proximal nephron Na^+/H^+ exchange is regulated by $alpha_{1A}$- and $alpha_{1B}$-adrenergic receptor subtypes. Mol Pharmacol 1997;52:1010–8.
[181] Liu GL, Liu L, Barajas L. Development of NOS-containing neuronal somata in the rat kidney. J Auton Nerv Syst 1996;58:81–8.
[182] Liu L, Barajas L. The rat renal nerves during development. Anat Embryol (Berl) 1993;188:345–61.
[183] Luff SE, Hengstberger SG, McLachlan EM, Anderson WP. Two types of sympathetic axon innervating the juxtaglomerular arterioles of the rabbit and rat kidney differ structurally from those supplying other arteries. J Neurocytol 1991;20:781–95.
[184] Lyson T, McMullan DM, Ermel LD, Morgan BJ, Victor RG. Mechanism of cyclosporine-induced sympathetic activation and acute hypertension in rats. Hypertension 1994;23:667–75.
[185] Ma MC, Huang HS, Chen CF. Impaired renal sensory responses after unilateral urseteral obstruction in the rat. J Am Soc Nephrol 2002;13:1008–16.
[186] Ma MC, Huang HS, Chien CT, Wu MS, Chen CF. Temporal decrease in renal sensory responses in rats after chronic ligation of the bile duct. Am J Physiol 2002;283:F164–72.
[187] Ma MC, Huang HS, Wu MS, Chien CT, Chen CF. Impaired renal sensory responses after renal ischemia in the rat. J Am Soc Nephrol 2002;13:1872–83.
[188] Maekawa H, Matsumura Y, Matsuo G, Morimoto S. Effect of sodium nitroprusside on norepinephrine overflow and antidiuresis induced by stimulation of renal nerves in anesthetized dogs. J Cardiovasc Pharmacol 1996;27:211–7.
[189] Malpas SC. Sympathetic nervous system overactivity and its role in the development of cardiovascular disease. Physiol Rev 2010;90:513–57.
[190] Malpas SC, Evans RG. Do different levels and patterns of sympathetic activation all provoke renal vasoconstriction? J Auton Nerv Syst 1998;69:72–82.
[191] Malpas SC, Hore TA, Navakatikyan M, Lukoshkova EV, Nguang SK, Austin PC. Resonance in the renal vasculature evoked by activation of the sympathetic nerves. Am J Physiol 1999;276:R1311–1319.
[192] Malpas SC, Leonard BL. Neural regulation of renal blood flow: a re-examination. Clin Exp Pharmacol Physiol 2000;27:956–64.
[193] Manning DC, Snyder SH. Bradykinin receptors localized by quantitative autoradiography in kidney, ureter, and bladder. Am J Physiol 1989;256:F909–15.
[194] Mattson DL, Wu F. Nitric oxide synthase activity and isoforms in rat renal vasculature. Hypertension 2000;35:337–41.
[195] May CN, Frithiof R, Hood SG, McAllen RM, McKinley MJ, Ramchandra R. Specific control of sympathetic nerve activity to the mammalian heart and kidney. Exp Physiol 2010;95:34–40.
[196] McAllen RM, May CN. Differential drives from rostral ventrolateral medullary neurons to three identified sympathetic outflows. Am J Physiol 1994;267:R935–944.
[197] McDonough AA. Mechanisms of proximal tubule sodium transport regulation that link extracellular fluid volume and blood pressure. Am J Physiol 2010;298:R851–861.
[198] McDonough AA, Leong PK, Yang LE. Mechanisms of pressure natriuresis: how blood pressure regulates renal sodium transport. Ann NY Acad Sci 2003;986:669–77.
[199] McKinley MJ, Albiston AL, Allen AM, Mathai ML, May CN, McAllen RM, et al. The brain renin–angiotensin system: location and physiological roles. Int J Biochem Cell Biol 2003;35:901–18.
[200] McKinley MJ, Pennington GL, Oldfield BJ. Anteroventral wall of the third ventricle and dorsal lamina terminalis: headquarters for control of body fluid homeostasis? Clin Exp Pharmacol Physiol 1996;23:271–81.
[201] Miki K, Hayashida Y, Sagawa S, Shiraki K. Renal sympathetic nerve activity and natriuresis during water immersion in conscious dogs. Am J Physiol 1989;256:R299–305.
[202] Miki K, Hayashida Y, Shiraki K. Role of cardiac-renal neural reflex in regulating sodium excretion during water immersion in conscious dogs. J Physiol 2002;545:305–12.
[203] Miki K, Yoshimoto M. Role of differential changes in sympathetic nerve activity in the preparatory adjustments of cardiovascular functions during freezing behaviour in rats. Exp Physiol 2010;95:56–60.
[204] Miki K, Yoshimoto M, Tanimizu M. Acute shifts of baroreflex control of renal sympathetic nerve activity induced by treadmill exercise in rats. J Physiol 2003;548:313–22.
[205] Morita H, Nishida Y, Hosomi H. Neural control of urinary sodium excretion during hypertonic NaCl load in conscious rabbits: role of renal and hepatic nerves and baroreceptors. J Auton Nerv Syst 1991;34:157–69.
[206] Nagura S, Sakagami T, Kakiichi A, Yoshimoto M, Miki K. Acute shifts in baroreflex control of renal sympathetic nerve activity induced by REM sleep and grooming in rats. J Physiol 2004;558:975–83.
[207] Nakamura A, Johns EJ. Effect of renal nerves on expression of renin and angiotensinogen genes in rat kidneys. Am J Physiol 1994;266:E230–241.
[208] Nicol GD, Cui M. Enhancement by prostaglandin E_2 of bradykinin activation of embryonic rat sensory neurones. J Physiol 1994;480(Pt 3):485–92.
[209] Nicol GD, Klingberg DK, Vasko MR. Prostaglandin E_2 increases calcium conductance and stimulates release of substance P in avian sensory neurons. J Neurosci 1992;12:1917–27.
[210] Nilsson H, Ljung B, Sjoblom N, Wallin BG. The influence of the sympathetic impulse pattern on contractile responses of rat mesenteric arteries and veins. Acta Physiol Scand 1985;123:303–9.
[211] Nishiyama A, Seth DM, Navar LG. Angiotensin II type 1 receptor-mediated augmentation of renal interstitial fluid angiotensin II in angiotensin II-induced hypertension. J Hypertension 2003;21:1897–903.
[212] Nord EP, Howard MJ, Hafezi A, Moradeshagi P, Vaystub S, Insel PA. Alpha 2 adrenergic agonists stimulate Na^+-H^+ antiport activity in the rabbit renal proximal tubule. J Clin Invest 1987;80:1755–62.
[213] Ortiz PA, Garvin JL. Role of nitric oxide in the regulation of nephron transport. Am J Physiol 2002;282:F777–784.
[214] Osborn JL, Camara AK. Renal neurogenic mediation of intracerebroventricular angiotensin II hypertension in rats raised on high sodium chloride diet. Hypertension 1997;30:331–6.
[215] Osborn JL, DiBona GF, Thames MD. Beta-1 receptor mediation of renin secretion elicited by low-frequency renal nerve stimulation. J Pharmacol Exp Ther 1981;216:265–9.
[216] Osborn JL, Thames MD, DiBona GF. Role of macula densa in renal nerve modulation of renin secretion. Am J Physiol 1982;242:R367–371.
[217] Ottoson D, Shepherd GM. Transducer characteristics of the muscle spindle as revealed by its receptor potential. Acta Physiol Scand 1971;82:545–54.

[218] Pan L, Black TA, Shi Q, Jones CA, Petrovic N, Loudon J, et al. Critical roles of a cyclic AMP responsive element and an E-box in regulation of mouse renin gene expression. J Biol Chem 2001;276:45530–8.
[219] Pateromichelakis S, Rood JP. Prostaglandin E1-induced sensitization of A delta moderate pressure mechanoreceptors. Brain Res 1982;232:89–96.
[220] Persson PB. Renin: origin, secretion and synthesis. J Physiol 2003;552:667–71.
[221] Persson PB, Skalweit A, Thiele BJ. Controlling the release and production of renin. Acta Physiol Scand 2004;181:375–81.
[222] Pettinger WA, Smyth DD, Umemura S. Renal alpha 2-adrenoceptors, their locations and effects on sodium excretion. J Cardiovasc Pharmacol 1985;7(Suppl 8):S24–27.
[223] Pettinger WA, Umemura S, Smyth DD, Jeffries WB. Renal alpha 2-adrenoceptors and the adenylate cyclase-cAMP system: biochemical and physiological interactions. Am J Physiol 1987;252:F199–208.
[224] Philipp M, Brede M, Hein L. Physiological significance of α_2-adrenergic receptor subtype diversity: one receptor is not enough. Am J Physiol 2002;283:R287–95.
[225] Piascik MT, Perez DM. Alpha1-adrenergic receptors: new insights and directions. J Pharmacol Exp Ther 2001;298:403–10.
[226] Pohjanoksa K, Jansson CC, Luomala K, Marjamäki A, Savola JM, Scheinin M. α_2-adrenoceptor regulation of adenylyl cyclase in CHO cells: dependence on receptor density, receptor subtype and current activity of adenylyl cyclase. Eur J Pharmacol 1997;335:53–63.
[227] Pollock DM, Pollock JS. Evidence for endothelin involvement in the response to high salt. Am J Physiol 2001;281:F144–50.
[228] Quan A, Baum M. Renal nerve stimulation augments effect of intraluminal angiotensin II on proximal tubule transport. Am J Physiol 2002;282:F1043–1048.
[229] Quan A, Baum M. The renal nerve is required for regulation of proximal tubule transport by intraluminally produced ANG II. Am J Physiol 2001;280:F524–529.
[230] Rubanyi GM, Polokoff MA. Endothelins: molecular biology, biochemistry, pharmacology, physiology and pathophysiology. Pharmacol Rev 1994;46:325–415.
[231] Rudenstam J, Bergstrom G, Taghipour K, Gothberg G, Karlstrom G. Efferent renal sympathetic nerve stimulation *in vivo*. Effects on regional renal haemodynamics in the Wistar rat, studied by laser-Doppler technique. Acta Physiol Scand 1995;154:387–94.
[232] Saeki Y, Terui N, Kumada M. Physiological characterization of the renal-sympathetic reflex in rabbits. Jap J Physiol 1988;38:251–66.
[233] Sato KL, do Carmo JM, Fazan VP. Ultrastructural anatomy of the renal nerves in rats. Brain Res 2006;1119:94–100.
[234] Schlaich MP, Krum H, Esler MD. New therapeutic approaches to resistant hypertension. Curr Hypertension Rep 2010;12:296–302.
[235] Schweda F, Friis U, Wagner C, Skott O, Kurtz A. Renin release. Physiology (Bethesda) 2007;22:310–9.
[236] Sequeira Lopez ML, Pentz ES, Robert B, Abrahamson DR, Gomez RA. Embryonic origin and lineage of juxtaglomerular cells. Am J Physiol 2001;281:F345–356.
[237] Shi TS, Winzer-Serhan U, Leslie F, Hökfelt T. Distribution and regulation of α_2-adrenoceptors in rat dorsal root ganglia. Pain 2000;84:319–30.
[238] Shi TS, Winzer-Serhan U, Leslie F, Hökfelt T. Distribution of α_2-adrenoceptor mRNAs in the rat lumbar spinal cord in normal and axotomized rats. NeuroReport 1999;10:2835–9.
[239] Shokoji T, Fujisawa Y, Kimura S, Rahman M, Kiyomoto H, Matsubara K, et al. Effects of local administrations of tempol and diethyldithio-carbamic on peripheral nerve activity. Hypertension 2004;44:236–43.
[240] Sigmund CD, Jones CA, Fabian JR, Mullins JJ, Gross KW. Tissue and cell specific expression of a renin promoter-reporter gene construct in transgenic mice. Biochem Biophys Res Commun 1990;170:344–50.
[241] Simon JK, Ciriello J. Contribution of afferent renal nerves to the metabolic activity of central structures involved in the control of the circulation. Can J Physiol Pharmacol 1989;67:1130–9.
[242] Sinn PL, Sigmund CD. Human renin mRNA stability is increased in response to cAMP in Calu-6 cells. Hypertension 1999;33:900–5.
[243] Siragy HM, Howell NL, Ragsdale NV, Carey RM. Renal interstitial fluid angiotensin. Modulation by anesthesia, epinephrine, sodium depletion, and renin inhibition. Hypertension 1995;25:1021–4.
[244] Smith H. The kidney: Structure and Function in Health and Disease. New York: Oxford University Press; 1951.
[245] Smith JA, Davis CL, Burgess GM. Prostaglandin E_2-induced sensitization of bradykinin-evoked responses in rat dorsal root ganglion neurons is mediated by cAMP-dependent protein kinase A. Eur J Neurosci 2000;12:3250–8.
[246] Smits JF, Brody MJ. Activation of afferent renal nerves by intrarenal bradykinin in conscious rats. Am J Physiol 1984;247: R1003–8.
[247] Solano-Flores LP, Rosa-Arellano MP, Ciriello J. Fos induction in central structures after afferent renal stimulation. Brain Res 1997;753:102–19.
[248] Stella A, Calaresu F, Zanchetti A. Neural factors contributing to renin release during reduction in renal perfusion pressure and blood flow in cats. Clin Sci Mol Med 1976;51:453–61.
[249] Stella A, Zanchetti A. Functional role of renal afferents. Physiol Rev 1991;71:659–82.
[250] Steranka LR, Manning DC, DeHaas CJ, Ferkany JW, Borosky SA, Connor JR, et al. Bradykinin as a pain mediator: receptors are localized to sensory neurons, and antagonists have analgesic actions. Proc Natl Acad Sci USA 1988;85:3245–9.
[251] Summers RJ, Broxton N, Hutchinson DS, Evans BA. The Janus faces of adrenoceptors: factors controlling the coupling of adrenoceptors to multiple signal transduction pathways. Clin Exp Pharmacol Physiol 2004;31:822–7.
[252] Szenasi G, Bencsath P, Takacs L. Proximal tubular transport and urinary excretion of sodium after renal denervation in sodium depleted rats. Pflugers Arch 1985;403:146–50.
[253] Tanioka H, Nakamura K, Fujimura S, Yoshida M, Suzuki-Kusaba M, Hisa H, et al. Facilitatory role of NO in neural norepinephrine release in the rat kidney. Am J Physiol 2002;282: R1436–1442.
[254] Terui N, Saeki Y, Kumuda M. Barosensory neurons in the ventrolateral medulla in rabbits and their responses to various afferent inputs from peripheral and central sources. Jap J Physiol 1986;36:1141–64.
[255] Thames MD, Abboud FM. Interaction of somatic and cardiopulmonary receptors in control of renal circulation. Am J Physiol 1979;237:H560–565.
[256] Tobian L, MacNeill D, Johnson MA, Ganguli MC, Iwai J. Potassium protects against renal tubule lesions in NaCl-fed hypertensive Dahl S rats. Trans Assoc Am Physicians 1983;96:417–25.
[257] Vasko MR, Campbell WB, Waite KJ. Prostaglandin E2 enhances bradykinin-stimulated release of neuropeptides from rat sensory neurons in culture. J Neurosci 1994;14:4987–97.
[258] Veelken R, Hilgers KF, Stetter A, Siebert HG, Schmieder RE, Mann JF. Nerve-mediated antidiuresis and antinatriuresis after

air-jet stress is modulated by angiotensin II. Hypertension 1996;28:825–32.
[259] Walkowska A, Badzynska B, Kompanowska-Jezierska E, Johns EJ, Sadowski J. Effects of renal nerve stimulation on intrarenal blood flow in rats with intact or inactivated NO synthases. Acta Physiol Scand 2005;183:99–105.
[260] Wang DH, Li J, Qiu J. Salt-sensitive hypertension induced by sensory denervation: introduction of a new model. Hypertension 1998;32:649–53.
[261] Wang J, Rose JC. Developmental changes in renal renin mRNA half-life and responses to stimulation in fetal lambs. Am J Physiol 1999;277:R1130–1135.
[262] Weaver LC, Genovesi S, Stella A, Zanchetti A. Neural, hemodynamic, and renal responses to stimulation of intestinal receptors. Am J Physiol 1987;253:H1167–1176.
[263] Widmann C, Gibson S, Jarpe MB, Johnson GL. Mitogen-activated protein kinase: conservation of a three-kinase module from yeast to human. Physiol Rev 1999;79:143–80.
[264] Williams NG, Zhong H, Minneman KP. Differential coupling of alpha1-, alpha2-, and beta-adrenergic receptors to mitogen-activated protein kinase pathways and differentiation in transfected PC12 cells. J Biol Chem 1998;273:24624–32.
[265] Wright JW, Harding JW. Important role for angiotensin III and IV in the brain renin–angiotensin system. Brain Res Brain Res Rev 1997;25:96–124.
[266] Wu XC, Harris PJ, Johns EJ. Nitric oxide and renal nerve-mediated proximal tubular reabsorption in normotensive and hypertensive rats. Am J Physiol 1999;277:F560–566.
[267] Wu XC, Johns EJ. Interactions between nitric oxide and superoxide on the neural regulation of proximal fluid reabsorption in hypertensive rats. Exp Physiol 2004;89:255–61.
[268] Wu XC, Johns EJ. Nitric oxide modulation of neurally induced proximal tubular fluid reabsorption in the rat. Hypertension 2002;39:790–3.
[269] Wurzner G, Chiolero A, Maillard M, Nussberger J, Hayoz D, Brunner HR, et al. Renal and neurohormonal responses to increasing levels of lower body negative pressure in men. Kidney Int 2001;60:1469–76.
[270] Wyss JM, Donovan K. A direct projection from the kidney to the brainstem. Brain Res 1984;298:130–4.
[271] Xia Y, Karmazyn M. Obligatory role for endogenous endothelin in mediating the hypertrophic effects of phenylephrine and angiotensin II in neonatal rat ventricular myocytes: evidence for two distinct mechanisms for endothelin regulation. J Pharmacol Exp Ther 2004;310:43–51.
[272] Xu H, Fink GD, Galligan JJ. Tempol lowers blood pressure and sympathetic nerve activity but not vascular O_2^- in DOCA-salt rats. Hypertension 2004;43:329–34.
[273] Yang L, Leong PK, Chen JO, Patel N, Hamm-Alvarez SF, McDonough AA. Acute hypertension provokes internalization of proximal tubule NHE3 without inhibition of transport activity. Am J Physiol 2002;282:F730–740.
[274] Ye DZ, Wang DH. Function and regulation of endothelin-1 and its receptors in salt sensitive hypertension induced by sensory nerve degeneration. Hypertension 2002;39:673–8.
[275] Yoshimoto M, Miki K, Fink GD, King A, Osborn JW. Chronic angiotensin II infusion causes differential responses in regional sympathetic nerve activity in rats. Hypertension 2010;55:644–51.
[276] Yoshimoto M, Nagata K, Miki K. Differential control of renal and lumbar sympathetic nerve activity during freezing behavior in conscious rats. Am J Physiol 2010;299:R1114–1120.
[277] Yoshimoto M, Sakagami T, Nagura S, Miki K. Relationship between renal sympathetic nerve activity and renal blood flow during natural behavior in rats. Am J Physiol 2004;286:R881–887.
[278] Zambraski EJ, Dibona GF, Kaloyanides GJ. Effect of sympathetic blocking agents on the antinatriuresis of reflex renal nerve stimulation. J Pharmacol Exp Ther 1976;198:464–72.
[279] Zhang T, Johns EJ. Somatosensory influences on renal sympathetic nerve activity in anesthetized Wistar and hypertensive rats. Am J Physiol 1997;272:R982–990.
[280] Zhu Y, Wang Y, Wang DH. Diuresis and natriuresis caused by activation of VR1-positive sensory nerves in renal pelvis of rats. Hypertension 2005;46:992–7.

CHAPTER

17

Eicosanoids and Renal Function

Matthew D. Breyer[1], *Raymond C Harris*[2] *and Richard M. Breyer*[2]

[1]Biotechnology Discovery Research Eli Lilly and Company Indianapolis, IN, USA

[2]Division of Nephrology, Department of Medicine, Vanderbilt University, Nashville, TN, USA

Perhaps nothing underscores the special relationship between the kidney and the eicosanoids better than the profound clinical effects non-steroidal anti-inflammatory drugs (NSAIDS) have on kidney function. NSAIDs are widely used to treat pain and inflammatory diseases, and work by blocking the enzymatic synthesis of prostaglandins, a type of eicosanoid, from arachidonic acid. However, chronic NSAID use is often complicated by major side effects, including renal sodium retention, resulting in edema, hypertension, and congestive heart failure.[1,2] Conversely, in the sodium depleted state, NSAIDs can reduce renal blood flow, glomerular filtration rate, and cause acute renal failure.[3–5] These observations underscore the critical role cyclooxygenase-derived arachidonic acid metabolites play in maintaining normal kidney function – particularly in the setting of physiological stress.

CELLULAR ORIGIN OF EICOSANOIDS

Eicosanoids are a family of biologically active, oxygenated metabolites derived from arachidonic acid (AA). AA is comprised of 20 carbon atoms configured as a polyunsaturated fatty acid chain with four double bonds (C20:4). Mammals lack the enzymatic machinery to synthesize AA *de novo*, instead it must be formed from dietary linoleic acid (C18:2) by addition of two carbons and further desaturation.[6,7] Essential fatty acid (EFA) deficiency occurs in the absence of dietary linoleic and other fatty acid AA precursors, depleting the hormone-responsive pool of AA metabolite products.[8,9] Of the approximate 10 gm of linoleic acid ingested per day, only about 1 mg/day is eliminated as end products of AA metabolism.[10–12] Following its formation, AA is esterified into cell membrane phospholipids, principally at the 2 position of the phosphatidylinositol fraction (i.e., sn-2 esterified AA). This source comprises the major hormone-sensitive pool of AA that is susceptible to release by phospholipases.

Phospholipase-Mediated Arachidonic Acid Release

Multiple stimuli lead to release of membrane-phospholipid esterified AA via activation of cellular phospholipases, principally phospholipase A2s (PLA_2).[13,14] This cleavage step is rate-limiting in the production of arachidonate metabolites. Activation of phospholipase C or PLD, on the other hand, releases AA via the sequential action of the phospholipase C-mediated production of diacylglycerol (DAG), with subsequent release of AA from DAG by DAG lipase.[15] The physiological significance of AA release by these other phospholipases remains uncertain since, at least in the setting of inflammation, phospholipase A_2 action appears to be essential for the generation of biologically active AA metabolites.[16] Cellular levels of free arachidonic acid available for eicosanoid production are primarily controlled by phospholipase A2 (PLA2).[16–18] So far, more than 30 enzymes with PLA_2 activity have been identified, and have been classified into four groups: secretory PLA_2 (sPLA2); cytosolic PLA2 (cPLA2); calcium-independent PLA2 (iPLA2); and PAF acetylhydrolases (PAF-AH).[14,19] The activity of cPLA2 is regulated by diverse cell membrane receptors, including the EGF receptor, and transmembrane guanine-nucleotide protein coupled (GPCRs) including adrenergic receptors, angiotensin II receptors, and purinergic receptors.[20–25] These receptors activate guanine nucleotide-binding (G) proteins, leading to PLA_2-mediated release of AA from membrane phospholipids.[20,26,27] Alternatively, these receptors may

Seldin and Giebisch's The Kidney, Fifth Edition.
DOI: http://dx.doi.org/10.1016/B978-0-12-381462-3.00017-3

© 2013 Elsevier Inc. All rights reserved.

activate cPLA$_2$ via mitogen-activated protein kinases (MAPK), protein kinase C (PKC), and Ca^{2+}-calmodulin-dependent kinases.

Ambient physical conditions in the kidney including hypoxia, oxidative stress, and mechanical stretch can also activate PLA$_2$ activity.[28–32] Dysregulated renal PLA$_2$ activity with attendant change in AA release results in altered substrate availability for the production of downstream metabolic products. This activation is believed to contribute to pathologic processes including acute kidney injury, diabetic nephropathy, and inflammatory glomerulonephritis.[33–35] Some snake and bee venoms are imbued with high levels of secretory PLA$_2$ activity and, in part through this activity, can induce acute renal failure[36,37]. A role for secretory PLA$_2$ in the pathogenesis of acute ischemic-reperfusion renal injury has also been supported by studies showing that sPLA$_2$ neutralizing antibodies protect rats from this form of injury.[36,38]

Phospholipase A2 Receptors

Recently, an important role for a transmembrane cell surface secretory PLA$_2$ receptor (PLA$_2$R) has been recognized in the pathogenesis of human idiopathic membranous nephropathy.[39] Auto-antibodies to PLA$_2$R are detected in ~70% of cases of human idiopathic membranous nephropathy.[39] The antigen appears to be selectively expressed in podocytes[39]; however, the mechanism by which the auto-antibodies induce proteinuria and how these auto-antibodies arise remains to be determined. PLA$_2$R is a type I transmembrane receptor and one of four mammalian members of the mannose-receptor family.[40] PLA$_2$R was initially identified as a binding protein for secreted phospholipase A$_2$ (PLA$_2$) that now has been expanded to a PLA$_2$R family that exhibit different affinities for the secreted PLA$_2$.[41] New studies suggest these receptors could play additional transmembrane signaling roles, and may promote terminal cell differentiation and mitotic arrest.[42]

Arachidonic Acid Metabolism

Following its release from membrane phospholipids, AA is usually rapidly re-esterified into the membrane or avidly bound by intracellular proteins, becoming unavailable for further metabolism. Should AA escape re-esterification and protein binding, it may be metabolized through one of three major enzymatic transformations, the common result of which is the incorporation of oxygen atoms at various sites of the fatty acid backbone, with accompanying changes in its molecular structure (such as ring formation). This results in the formation of biologically active molecules, collectively referred to as "eicosanoids." The specific nature of the products generated is a function of the initial stimuli for AA release, as well as the metabolic enzymes available, as determined by the cell type involved.[43,44]

Enyzmes capable of mediating AA metabolism through all three known pathways are present in the kidney, including cyclooxygenases 1 and 2, lipoxygenases, and cytochrome P450s (Figure 17.1). Cyclooxygenase (COX, also called Prostaglandin H2 synthase or PGHS)-mediated AA metabolism comprises the first committed step in the formation of prostaglandins (PGs), prostacyclin, and thromboxane.[45] The lipoxygenase pathway mediates the formation of mono-, di-, and trihydroxyeicosatetraenoic acids (HETEs), leukotrienes (LTs), and lipoxins (LXs),[46,47] and the cytochrome P450-dependent oxygenation of AA mediates the formation of epoxyeicosatrienoic acids (EETs), their corresponding diols, HETEs, and monooxygenated AA derivatives.[48–50] Fish oil diets, rich in *n-3* polyunsaturated fatty acids (*n-3* fatty acids are those in which the double bond is three carbons from the terminal, i.e., *n* carbon, that is furthest from the carboxy-group atom, AA is thus an n-6 fatty acid) interfere with metabolism via all three pathways by competing with AA oxygenation, resulting in the formation of biologically inactive end-products.[51,52] Interference with the production of pro-inflammatory lipids has been hypothesized to underlie the beneficial effects of fish-oil in IgA nephropathy, membranous nephropathy, and other cardiovascular diseases.[7,53,54]

CYCLOOXYGENASE DERIVED PROSTANOIDS

Prostanoids, including the prostaglandins PGE$_2$, PGF$_{2\alpha}$, and PGD$_2$, as well as the non-prostaglandin molecules thromboxane A$_2$ (TxA2) and prostacyclin (PGI$_2$), are derived from arachidonic acid via its dioxygenation by cyclooxygenases 1 and 2 (COX1 and COX2).[52] Cyclooxygenases exist as homodimers that are physically associated with, but do not pass through, the intracellular endoplasmic reticular membrane.[55–57] Cyclooxygenases mediate a two-step reaction, initially converting free arachidonic acid to the unstable intermediate PGG$_2$ via a *bis*-oxygenase activity. PGG$_2$ is converted to PGH$_2$ via the peroxidase activity of COX.[52,58–63] PGH$_2$ is subsequently metabolized to more stable primary biologically active prostanoids PGE$_2$, PGF$_{2\alpha}$, PGD$_2$, PGI$_2$, and TxA$_2$ by distinct enzymatic prostanoid synthases. These prostanoids exit the cell through uncharacterized mechanisms, where they exert paracrine or autocrine activity on specific and distinct cell surface G-protein coupled receptor(s).[64,65] There is also less definitive evidence that prostanoids may provide physiologically relevant

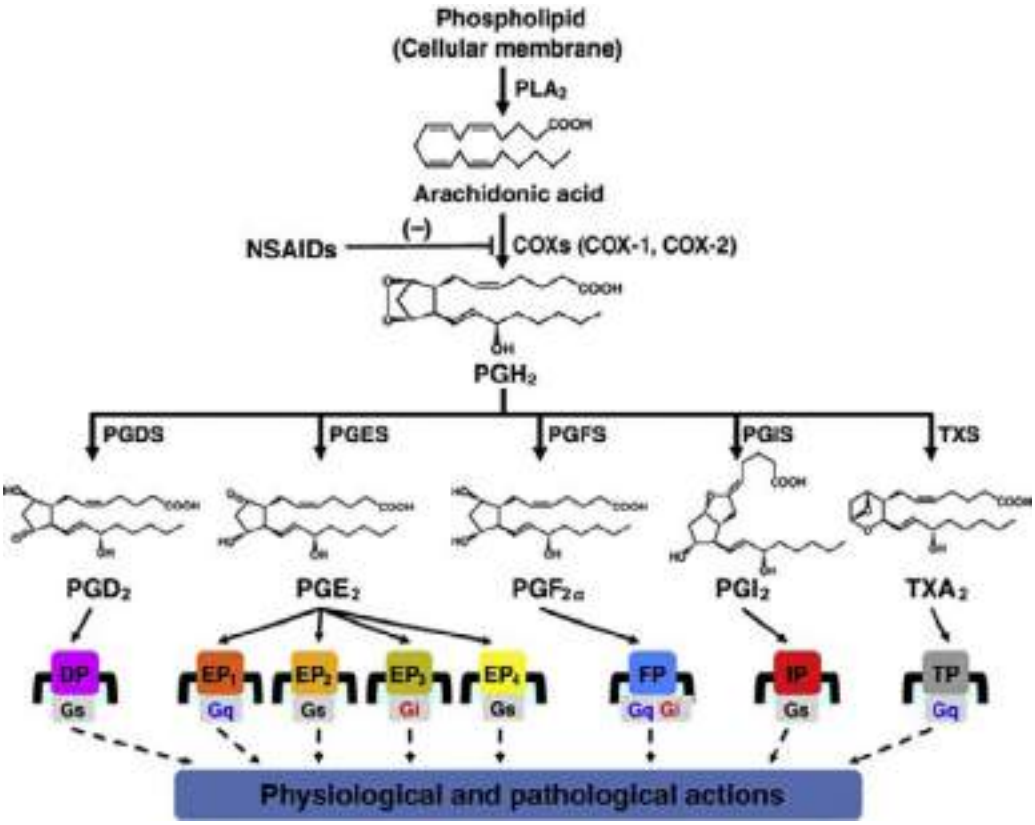

FIGURE 17.1 **Prostaglandin synthesis and the family of G-protein coupled receptors that mediate their functional effects.** *(With permission from Yuhki et al. [348].)*

ligands for nuclear hormone receptors, including peroxisome proliferator activated receptors.[66–68]

Two isoforms of COX have been identified, designated COX1 and COX2.[69–71] Based on transcriptional elements in its 5′ upstream sequence, COX1 is believed to serve a constitutive housekeeping role, responsible for maintaining basic physiological function such as cytoprotection of the gastric mucosa, and control of platelet aggregation.[72,73] Conversely, COX2 upstream promoter region has NF-κB, NFAT, and its expression is potently induced by inflammatory mediators and mitogens, consistent with its role in pathophysiologic processes including angiogenesis, inflammation, and tumorigenesis.[74–77]

The major phenotype of COX2 knockout mice is renal dysgenesis,[78–80] underscoring the special role COX2 plays in the kidney. This defect is characterized by a structurally normal medulla, but hypotrophic renal cortical development with small glomerular size,[79] due to a defect occurring relatively late in parturition.[79] The mechanism is undetermined, but may be related to the particular expression pattern of COX2 in the kidney since normally it is focally expressed adjacent to the glomerulus in the macula densa and the surrounding thick ascending limb cells.[81–83] As in other organs, the housekeeping gene is COX1, which is also constitutively expressed at high levels in the kidney but in cellular compartments distinct from COX2, especially in the collecting duct and glomerular parietal epithelium.[84,85] Low levels of COX1 are also detected in medullary interstitial cells,[81,86,87] but these cells are also uniquely characterized by high endogenous levels of COX2.[81,88,89]

Clinical pharmacologic studies are also consistent with a critical role of COX2 for maintaining cardiovascular homeostasis and normal renal function.[90–92] Indeed, most of the clinically observed side effects associated with the use of non-selective NSAIDs, including edema, hypertension, increased congestive heart failure, hyperkalemia, and acute renal failure, have also been observed with COX2 selective inhibitors.[3] COX2-dependent PGE_2 production is inversely related to luminal chloride concentration delivered to the macula densa,[93] so that in volume depleted states high PGE_2 production rates may exert a vasodilator effect on the afferent arteriole, contributing to maintenance of glomerular blood flow. Impairment of renal function is presumed due to loss of specific prostanoids, derived from the metabolism of the common cyclooxygenase product PGH_2.

Prostanoid Function

Once formed, the COX-derived arachidonate metabolite PGH_2 is further metabolized by prostanoid synthases into at least five primary biologically active prostanoids. Prostanoid synthases include PGE_2 synthase (PGES), prostacyclin synthase (PGIS), PGD synthase (PGDS), PGF synthase (PGFS), and thromboxane synthase, responsible for PGE2, PGI2, PGD2, PGF2α, and TxA2 biosynthesis respectively.[77,94,95]

Most prostanoids are short lived, being highly susceptible to enzymatic inactivation, thereby limiting their effect to the immediate vicinity of their synthesis. The paracrine and autocrine biologic effects of COX-derived prostanoids are diverse and complex, depending on which prostanoid is produced and which receptor is available.[96,97] Thus, the effects of prostanoids on kidney function rely on distinct enzymatic machinery that couples phospholipase and COX to specific prostanoid synthase in specific cells, yielding a specific prostanoid which acts locally through specific G-protein coupled receptors, exerting its particular effect.[96]

At steady-state PGE_2 is the most abundant prostanoid in the mouse kidney, followed by PGI_2, $PGF_{2\alpha}$, and TxA_2.[98] Under basal conditions, both COX1 and COX2 pathways are responsible for the biosynthesis of these prostanoids.[98] Similarly, PGE2 is the most abundant prostanoid in human urine, and under basal, non-stressed conditions is produced by both COX1 and COX.[99,100] In contrast, COX2 primarily contributes to angiotensin II-induced PGE_2 and PGI2 generation in the kidney,[98] and under conditions of low-sodium diet in humans.[101] The intrarenal cellular sites where COX1 and COX2 prostanoids are synthesized remain to be fully defined.

Following their synthesis, these prostanoids become available to exert their biological effects via a diverse family of membrane spanning G-protein coupled prostanoid receptors. These include the DP, EP, FP, IP, and TP receptors, each of which is selectively activated by a specific ligand – PGD_2, PGE_2, $PGF_{2\alpha}$, PGI_2 or TXA_2, respectively.[97,102] PGE2 receptors, designated EP receptors, are unique in that they are encoded by four distinct genes encoding the proteins for EP1, EP2, EP3, and EP4 receptors.[102,103] Each prostanoid receptor activates a distinct G-protein coupled signaling pathway. The IP, DP1, EP2, and EP4 receptors are coupled to the stimulatory G-protein (Gs) and signal by increasing intracellular cAMP levels, whereas the TP, FP, and EP1 receptors induce calcium mobilization.[96,97] The FP, DP2, and EP3 receptors can couple to an inhibitory G-protein (Gi) and reduce cAMP synthesis.[97,102,104]

Restricted cellular expression of prostanoid receptors provides an important mechanism by which a COX-derived prostanoid can exert differential actions in physiological and pathophysiological processes. In the kidney the EP receptors map to distinct segments of the nephron.[96,105] Similarly, all four EP receptors have been described in major inflammatory cells including T-lymphocytes, B-lymphocytes, macrophage, and mast cells[106]; however, whether these receptors are simultaneously expressed in individual cells is uncertain. It has been proposed that activation of different receptors on different cells at different stages of inflammation may account for the pro- or anti-inflammatory action of PGE_2.[107,108]

Prostaglandin E2

PGE_2 is synthesized by at least three forms of PGE synthases, including microsomal PGE synthase 1 (mPGES1), microsomal PGE synthase 2 (mPGES2), and cytosolic PGE synthase (cPGES1).[109–111] The two membrane associated PGE_2 synthases are 33 kDa and 16 kDa enzymes designated mPGES1 and mPGES2, respectively. Microsomal PGES1 displays a higher catalytic activity relative to other PGE synthases and, like COX2, its expression can be induced by cytokines and inflammatory stimuli.[109] In contrast, the expression of cPGES and mPGES2 do not seem to be inducible and may play housekeeping functions.

Genetic disruption confirms that mPGES1$^{-/-}$ mice exhibit a marked reduction in inflammatory responses compared with mPGES1$^{+/+}$ mice,[112] and indicates that mPGES1 is critical for the induction of inflammatory fever.[113] It has been proposed that mPGES1 couples primarily to the inducible COX2 in inflammatory cells.[114] In contrast, intrarenal expression of mPGES1 maps to cells of the collecting duct that primarily express COX1 with lower expression in medullary interstitial cells and macula densa that express COX2[84,115–117] (Figure 17.2). Thus, in the kidney mPGE1 co-localizes with both cyclooxygenase 1 and 2.

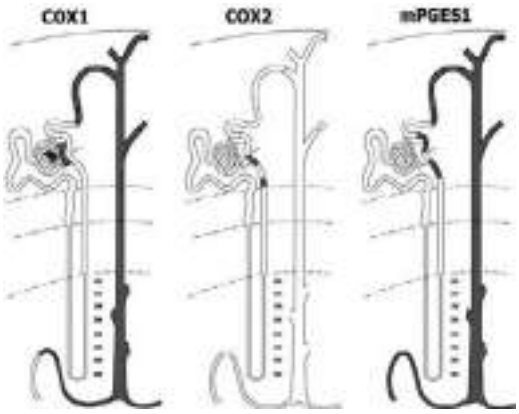

FIGURE 17.2 **Expression of COX1, COX2, and microsomal prostaglandin E synthase 1 in the kidney.** *(With permission from ref. [84].)*

The renal phenotype of the mPGE1 knockout mouse is relatively subtle, and is characterized by increased blood pressure sensitivity to high-sodium diet and mineralocorticoids, as well as increased vascular reactivity to angiotensin-II,[118,119] although not all investigators have seen these effects.[120] These results are consistent with a role for mPGES1-derived PGE_2 in buffering physiologic stresses that tend to increase blood pressure. Notably, the kidneys of mPGES1$^{-/-}$ mice are normal and do not exhibit the renal dysgenesis observed in COX2$^{-/-}$ mice.[78,80] Nor do these mice exhibit perinatal death from patent ductus arteriosus observed with the prostaglandin EP4 receptor knockout mouse,[121] suggesting other sources of PGE2 production are sufficient to provide adequate receptor activation. These sources could include cPGES and mPGES2.[122] Both cPGES and mPGES2 are expressed in the kidney[123]; however, their intrarenal role(s) have not yet been elucidated. In addition, several cytosolic glutathione-S-transferases have the capacity to convert PGH_2 to PGE_2; however, their physiologic role in this process remains uncertain.[122]

E-Prostanoid Receptors

All four E-Prostanoid receptors (EP receptors) are expressed in the kidney (Figure 17.3). Each exhibits a distinct mRNA expression profile along the nephron. The EP4 receptor predominates in the glomerulus, while the EP3 and EP1 receptors are primarily detected in the thick limb and collecting duct.[105,124] The EP2 receptor is expressed at lower levels in the renal vaculature and stroma.[125,126] Each receptor plays a distinct role in these regions, mediating many of the well-defined physiologic actions of PGE_2 that have been identified over the past several decades.

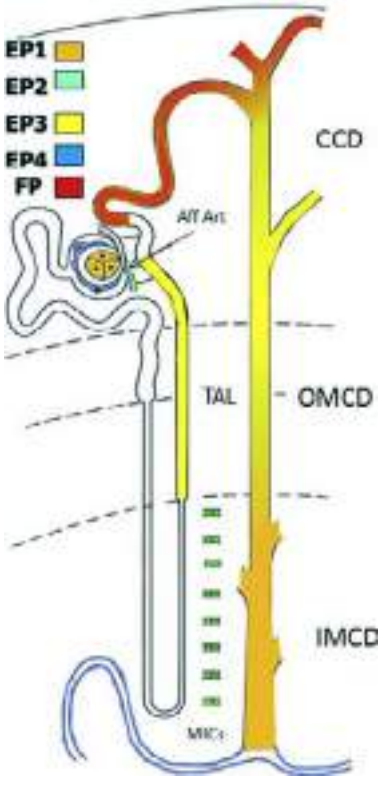

FIGURE 17.3 **Distribution of EP1, 2, 3, 4, and FP receptors in the kidney.**

EP_1 Receptor

The EP1 receptor was originally identified pharmacologically via its smooth muscle constrictor activity in guinea pig ileum, and its unique profile of response to a series of prostanoid analogs.[127–130] The EP1 receptor cDNA has been cloned from numerous species, including human, dog, mouse, rat, and rabbit.[131–135] The human EP1 receptor cDNA encodes a 402 amino acid polypeptide with a predicted molecular mass of 41,858 kDa.[131] This receptor signals via a mechanism linked to increased cell Ca^{2+}, and is accompanied by modest increases in IP_3 generation.

Studies of EP1 receptors have taken advantage of several relatively selective antagonists that block their activation, including SC-19220, SC-53122,[136,137] and ONO-8130.[138–141] A significant impetus behind the development of clinically active EP1 receptor antagonists derives from evidence that the EP_1 receptor plays an important role in prostaglandin-mediated pain,[140,142,143] and that EP1 receptor antagonists have EP1 properties.[136,137,139,144,145] These antagonists provide useful tools to study EP_1 receptor physiology *in vivo*.

The EP1 receptor is highly expressed in the kidney, where it primarily localizes to the collecting duct with an increasing mRNA expression gradient from the cortical to the medullary collecting duct.[105,132,146] In the collecting duct, activation of the EP1 receptor inhibits Na^+ and water reabsorption via a Ca^{2+}-coupled mechanism.[132] These results suggest that renal EP_1 receptor activation contributes to PGE_2-dependent natriuresis by inhibiting Na^+ transport in the collecting duct. Despite this *in vitro* demonstration, these natriuretic effects have been difficult to demonstrate *in vivo*.[132,143]

Genetic disruption of the EP1 receptor does not lead to a significant impairment of sodium excretion; however, EP1 knockout mice do exhibit increased renin and aldosterone levels, consistent with maintenance of normotension at the expense of activation of the renin–angiotensin system.[132,143] EP1 receptor knockout mice not only exhibit reduced blood pressure on normal chow, but also impaired pressor response to angiotensin II.[145] These studies identified EP1 mRNA expression in small resistance vessels of mice including the afferent arterioles of the glomerulus, and are

consistent with more recent studies suggesting Ang II-stimulated vasoconstriction may in part be mediated by activation of vascular EP1 receptors.[147] EP1 receptors have also been identified in glomerular mesangial cells, where they may contribute to mesangial contraction. Inhibition of the EP1 receptor slows the progression of mesangial expansion in experimental models of diabetic nephropathy.[139] EP1 receptor knockout mice are resistant to the pressor effects of angiotensin II, and EP1 receptor antagonists can also block the Ang II pressor activity.[145,147–149] It is instructive to consider the role of PGE_2 as a vasoconstrictor through its actions on the EP1 receptor, as opposed to its classically characterized role as a vasodilator/vasodepressor. This underscores the capacity of PGE_2 to serve as a physiological buffer of blood pressure, either in support or reduction of blood pressure (see below).

EP_2 Receptors

In contrast to the smooth muscle constrictor activity of the EP1 receptor, the EP2 receptor was originally defined by its relaxant activity in smooth muscle.[128] The human EP_2 receptor cDNA encodes a 358 amino acid polypeptide, which signals through increased cAMP and is selectively activated by butaprost.[150] The EP_2 receptor may be distinguished from the EP_4 receptor, the other major cAMP stimulating and vasorelaxant EP receptor, by its selective activation by butaprost and relative insensitivity to the EP_4 agonist PGE_1-OH.[150] Literature prior to 1995 may be confusing regarding the EP_2receptor, because before the human EP_2 receptor was cloned, the previously cloned EP_4 receptor was classified as the EP_2 receptor.[150,151]

The physiological processes mediated by the EP2 receptor include important roles in reproduction and blood pressure regulation. The precise tissue distribution of the EP_2 receptor has only been characterized by Northern blot analysis of mRNA distribution. This reveals a major mRNA species of ~3.1 kb that is most abundant in the uterus, lung, and spleen, exhibiting only low levels of expression in the kidney.[135,150,152] EP2 knockout mice exhibit a fertility defect and the development of hypertension on a high NaCl diet (these latter effects are significantly influenced by the genetic background of the mouse strain).[153,154] In the kidney, despite incomplete histological characterization, a preponderance of functional and mRNA expression evidence suggests the EP2 receptor is expressed in stromal cells of the kidney, including renal medullary interstitial cells,[125] vascular pericytes along the vasa recta,[126,155,156] and glomerular arterioles where it contributes to afferent arteriolar dilation (Figure 17.4).[126,157] Evidence suggests that deletion of the EP2 receptor in renal medullary interstitial cells,[158] combined with the absence of its systemic vasodilator activity, contributes to salt-sensitive hypertension in the EP2 knockout mouse.

EP_3 Receptor

In smooth muscle the EP_3 receptor generally acts as a constrictor.[159,160] This receptor is unique, in that at least seven alternatively spliced variants defined by unique COOH-terminal cytoplasmic tails exist in humans alone, and over 22 unique variants have been observed in rats, rabbits, mice, cows, and humans.[161–164] These splice variants encode proteins of a predicted molecular mass between 40 and 45 kDa.[161–164] All the EP_3 splice variants bind PGE_2 and the EP_3 specific prostanoid analogs with similar affinity, and inhibit cAMP generation via a pertussis toxin-sensitive G_i-coupled mechanism; however, additional signaling mechanisms may be differentially activated by the different COOH-terminal tails.[165]

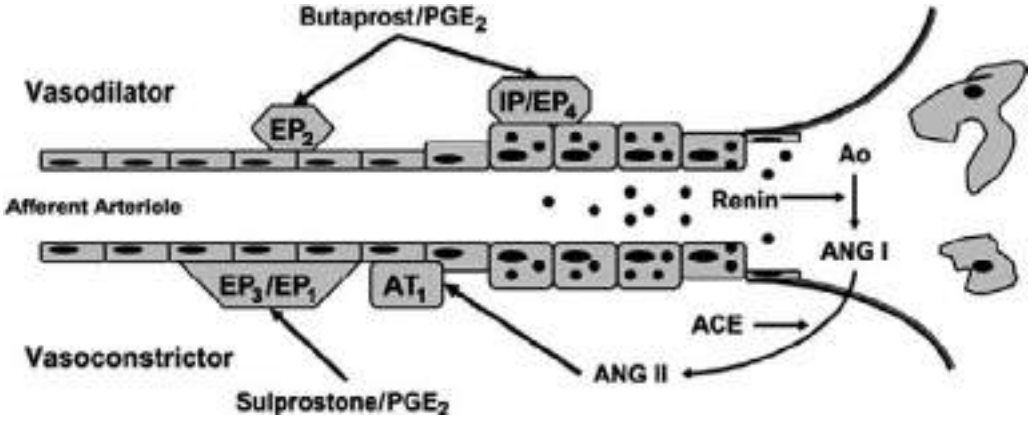

FIGURE 17.4 **Schematic of prostanoid receptor action at the afferent arteriole including EP1, EP2, EP3, EP4, and IP receptors.** *(From ref. [157], with permission from Am J. Physiol.)*

Mice with targeted deletion of the EP_3 receptor exhibit an impaired febrile response to lipopolysaccaride and PGE_2, suggesting that the EP_3 receptor antagonists could be effective antipyretic agents.[166] In the kidney the EP_3 receptor is highly expressed in the cortical and outer medullary collecting duct, where it antagonizes vasopressin-stimulated water absorption via pertussis toxin-sensitive inhibition of cAMP generation.[167,168] Despite relatively high levels of EP_3 receptor in the kidney collecting duct, mice with targeted disruption of this receptor only display a subtle alteration with altered urinary concentrating ability in mice treated with NSAIDs.[169] These findings raise the possibility that prostaglandin receptors other than the EP_3 receptor exert overlapping effects that also (such as the EP1 and FP receptor) modulate the urinary concentration and dilution by this segment of the nephron.

EP_4 Receptor

The EP_4 receptor can be distinguished from the EP_1 and EP_3 receptors by its insensitivity to sulprostone, and from EP_2 receptors by its insensitivity to butaprost and relatively selective activation by PGE_1-OH.[129,150,170,171] The human EP_4 receptor cDNA encodes a 488 amino acid polypeptide with a predicted molecular mass of ~53 kDa.[171] Like the EP_2 receptor, EP_4 signals through increased cAMP, but may also engage other signaling mechanisms including PI3K activation.[172,173] EP_4 receptor mRNA is relatively highly expressed compared with the EP_2 receptor and widely distributed, with a major species of ~3.8 kb detected by Northern analysis in thymus, ileum, lung, spleen, adrenal gland, and kidney.[133,174,175] In contrast to other EP receptor knockouts, EP4 receptor knockout mice exhibit a profound perinatal lethal phenotype due to impaired closure of the ductus arteriosus,[121,176] consistent with its robust expression in this vessel.

In the kidney, EP4 receptor mRNA is predominantly expressed in the glomerulus[105,124,126] where it modulates glomerular hemodynamics through opposing direct vasodilator activity,[157,177] and an indirect vasoconstrictor activity via stimulation of renin release (Figure 17.4).[178] The ability of PGE_2 to increase renin release is well-established[178–181] and of clinical relevance, since NSAID blockade of prostaglandin synthesis can be associated with hyporeninemic hypoaldosteronism,[182] and COX2 inhibitors can block the hyper-reninemia associated with volume depletion or Bartter's syndrome.[101,183,184] Accumulating evidence supports a role for COX2-mediated PGE_2 production, and subsequent activation of juxtaglomerular EP4 receptor in mediating renin release.[93,181] As mPGES-specific inhibitors and EP4 receptor antagonists become increasingly available it will be important to determine the relative contribution of PGE2-dependent renin release versus prostacyclin-dependent effects (see below).

In volume depletion,[185] congestive heart failure,[186] and shock, intrarenal PGE_2 production helps maintain glomerular perfusion via afferent arteriolar vasodilator EP2 receptors[157] (Figure 17.4), while simultaneously maintaining systemic blood pressure by stimulating renin release through EP4 receptors.[187,188] Genetic deletion of the EP4 receptor or EP4 inhibitors impairs renin release in mice following furosemide-induced volume depletion.[181] Inhibition of PGE_2 synthesis using NSAIDs or COX2 inhibition in these settings can actually drop blood pressure by inhibiting renin release,[189] and lead to acute renal failure due to decreased glomerular perfusion.[190–192]

The EP4 receptor is also abundant in glomerular podocytes.[124,193,194] In podocytes EP4 receptor activation may impair their ability to withstand mechanical stress, since podocyte selective overexpression of EP4 receptors accelerates renal injury in a mouse renal ablation model of kidney disease.[195]

Other roles for the EP4 receptor in controlling blood pressure have been suggested, including the ability to stimulate aldosterone release from zona glomerulosa cells.[196] It remains to be determined whether the adrenal EP4 receptor plays any role in hyperkalemia and hyporeninemic hypoaldosteronism associated with NSAID blockade of prostaglandin synthesis[182,197,198] or whether this is primarily due to hyporeninemia.[199] Important vasodilator effects of EP_4 receptor activation in venous and arterial beds have been described.[130,200] Roles for EP4 receptors in immune cell activation and osteoblast function have also been reported.[201–203]

Prostaglandin F Synthesis

$PGF_{2\alpha}$ may derive either directly from PGH_2 via a PGF synthase[204] or via a NADPH-dependent 9 ketoreductase, which converts PGE_2 into $PGF_{2\alpha}$. This enzymatic activity is typically cytosolic,[204] and may be detected in homogenates from renal cortex, medulla or papilla.[204,205] Another more obscure pathway for PGF formation is by the action of a PGD_2 ketoreductase, yielding a stereoisomer of $PGF_{2\alpha}$, 9α,11ß-PGF_2 (11epi-$PGF_{2\alpha}$).[204] This reaction, and conversion of PGD_2 into the biologically active metabolite (9α,11β-$PGF_{2\alpha}$) has been documented *in vivo*.[206] This $PGF_{2\alpha}$ isomer can also ligate and activate the FP receptor.[207] The physiologically relevant enzymes responsible for $PGF_{2\alpha}$ formation in the kidney remain incompletely characterized.

Prostaglandin 9-Ketoreductase (PG9KR) and $PGF_{2\alpha}$ Synthesis

Prostaglandin F synthase activity may be mediated via several distinct, and incompletely defined, enzymes. One major synthetic pathway appears to occur via a member of the aldo-ketoreductase 1C family.[208] Renal PGE_2 9-ketoreductase also exhibits 20α-hydroxyl-steroid reductase activity that may be involved in steroid metabolism.[204] PG9KR activity appears to be particularly robust in suspensions from the thick ascending limb of Henle (TALH).

Interestingly, some studies suggest activity of a 9-ketoreductase may be modulated by salt intake and the angiotensin AT2 receptor.[209] This activity may play a role in the development of salt-sensitive hypertension.[210] AT2 receptor knockout mice exhibit salt-sensitive hypertension associated with increased PGE_2 production and reduced production of $PGF_{2\alpha}$,[209] consistent with decreased 9-ketoreductase activity. Other studies suggest increased dietary potassium intake may also enhance the activity of conversion from PGE_2 to $PGF_{2\alpha}$.[211] The intrarenal sites of expression of this enzymatic activity remain to be characterized.

F-Prostanoid Receptors

Once formed, $PGF_{2\alpha}$ is available to interact with the intrarenal FP receptors. The human FP receptor mRNA is predicted to encode 359 amino acid residues with a molecular mass of ~40 kDa.[212] In fibroblasts and smooth muscle the FP receptor signals through increased cellular calcium, and its activation is associated with muscle contraction.[213–215] The FP receptor is highly expressed in the ovarian corpus luteum, and mice lacking the FP receptor exhibit a major reproductive defect due to failure of partuition because of impaired reduction of progesterone at term.[216] FP receptor antagonists have been developed, and their use proposed as a means of delaying pre-term delivery.[217,218] The FP receptor is highly expressed in the ocular ciliary body and FP selective agonists including travaprost, latanoprost, and bimatoprost are in use for clinical treatment of glaucoma d.[214,219] In the kidney, the FP receptor is highly expressed in the distal convoluted tubule, connecting tubule, and cortical collecting duct, where it inhibits vasopressin-stimulated renal water transport[104,220] consistent with recent studies that the FP receptor knockout mice exhibit mild polyuria and polydipsia.[221] Interestingly, in the rabbit cortical collecting duct epithelium the FP receptor appears to signal through a pertussis toxin-sensitive G_i-coupled mechanism, rather than the classical Ca^{2+}-coupled signaling mechanism observed in smooth muscle cells.[104] Vascular expression of FP receptor in pre-glomerular arterioles and other resistance vessels has also been demonstrated, and studies in FP receptor knockout mice show they are relatively hypotensive.[221] These studies also provide evidence that renal JGA FP receptor activation directly stimulates renin release.[221]

Prostaglandin D_2 is derived from PGH_2 via the action of specific enzymes designated PGD synthases. Two major enzymes are capable of transforming PGH_2 to PGD_2 – a lipocalin type PGD synthase and a hematopoietic type PGDS.[222,223] RT-PCR showed that L-PGDS is strongly expressed in kidney cortex and outer medulla, including in nearly all segments of the nephron,[224] while H-PGDS mRNA is only detected in microdissected outer medullary collecting duct.[224]

Lipocalin PGD synthase (L-PGDS) is a multifunctional molecule, and on addition to prostaglandin H2 it binds a variety of small lipophilic molecules including bilirubin and biliverdin.[225] Mice lacking the lipocalin D synthase gene exhibit pain sensation.[226] LPGDS-mediated PGD2 synthesis also appears to play an important role in the sleep/wake cycle,[225] but its role in renal PGD2 synthesis has not been studied. Urinary levels of L-PGDS, also known as beta-trace protein, have been increasingly studied as a biomarker of acute and chronic renal injury.[227–230] LPDGS knockout mice appear to be more susceptible to diabetic nephropathy.[231]

PGD_2 is the major prostanoid released from mast cells following challenge with IgE, and this synthesis appears to be mediated by the hematopoietic form of PGDS.[223,232,233] The precise role of hematopoietic PGDS in the kidney remains uncertain, as does the significance of its reported localization in the outer medullary collecting duct.[224]

D-Prostanoid Receptors

Once synthesized, PGD_2 is available to interact with either the DP1 or DP2 (originally identified as CRTH2) receptors or undergo further metabolism to a PGF_2-like compound that can interact with the FP receptor (see above). The human DP1 receptor is a cAMP-coupled GPCR with a predicted molecular mass similar to other prostanoid receptors (~40 kDa).[234,235] It exhibits a relatively selective tissue distribution, with particularly high expression in retina and small intestine, where it appears to be highly expressed in mucus secreting goblet cells.[235] The DP2 receptor is a GPCR that is also activated by PGD2, but it is unrelated in sequence to the classic prostanoid receptor family, being more closely related to members of the *N*-formyl peptide receptor (FPR) subfamily.[236,237] DP2 is selectively expressed in Th2 cells, cytotoxic T-cells,

eosinophils, and basophils. DP and DP2 receptors are intimately involved in the immune allergic response.[236,238] Neither DP1 receptors nor DP2 receptors appear to be highly expressed in the kidney, and while infusion of a DP1 selective agonist lowers blood pressure these effects appear to be primarily due to peripheral vasodilation and not by directly affecting renal blood flow.[239]

Prostacyclin (PGI_2)

The biological effects of prostacyclin are numerous and include nocioception, anti-thrombosis, and vasodilator actions, which have been targeted therapeutically to treat pulmonary hypertension.[240] Prostacyclin (PGI_2) is derived from the enzymatic conversion of PGH_2 via prostacyclin synthase (PGIS) to PGI_2. The PGIS cDNA is comprised of a 1500 bp open reading frame that encodes a 500 amino acid protein of approximately 56 kDa.[241] Northern blot analysis shows prostacyclin synthase mRNA is widely expressed in human tissues and is particularly abundant in ovary, heart, skeletal muscle, lung, and prostate. PGI synthase expression exhibits segmental expression in the kidney, especially in kidney inner medulla tubules and interstitial cells.[224,242]

PGI_2 synthase-null mice exhibit a profound renal phenotype with nephrosclerosis and areas of renal infarction.[243] PGI_2 levels in the plasma, kidneys, and lungs were reduced, documenting the role of this enzyme as an *in vivo* source of PGI_2. Blood pressure and blood urea nitrogen and creatinine in the PGIS knockout mice were significantly increased, and renal pathological findings included surface irregularity, fibrosis, cysts, arterial sclerosis, and hypertrophy of vessel walls. Thickening of the thoracic aortic media and adventitia were observed in aged PGIS-null mice.[243] Interestingly, this is a phenotype different from that reported for the IP receptor knockout mouse,[244] which failed to exhibit abnormal kidney morphology. These differences suggests the presence of additional IP receptor independent PGI_2 activated signaling pathways – possibly through nuclear receptors such as PPARdelta.[245,246] Regardless, these findings demonstrate the importance of PGI_2 in the maintenance of blood vessels and to the kidney.

IP Receptor

The IP receptor mRNA is highly expressed in the afferent arteriole, where it may combine with the effects of EP2 and EP4 receptors to dilate renal arterioles and stimulate renin release.[247,248] IP receptor deficient mice exhibit reduced renin and are resistant to the development of hypertension following unilateral renal artery stenosis, consistent with an impaired IP receptor-mediated renin release.[249] COX2-derived prostacyclin from the endothelium also appears to serve an atheroprotective role in mice, and its loss could contribute to the cardiovascular risks associated with the use of COX2 inhibitors.[250] Conversely, thromboxane receptors may counteract the effects of these protective effects of prostacyclin and accelerate atherosclerotic lesions, as well as increasing vascular resistance.

Thromboxane A2

Thromboxane A_2 (TxA_2) is produced from PGH_2 by thromboxane synthase (TxAS), a microsomal protein of 533 amino acids with a predicted molecular weight of ~60 kDa. The human gene is located on chromosome 7q, and the enzyme exhibits homology to the cytochrome P450s and is now classified as CYP5A1.[251] TxAS mRNA is highly expressed in hematopoietic cells, including platelets, macrophages, and leukocytes, as well as thymus, kidney, lung, spleen, prostate, and placenta.[252,253] Immunolocalization of TxA synthase demonstrates high expression in the dendritic cells of the interstitium, with lower expression in glomerular podocytes of human kidney.[254] In the kidney, thromboxane synthase is mainly detected in the glomeruli.[224] TxA_2 synthase expression is regulated by dietary salt intake.[255] Furthermore, experimental use of ridogrel, a specific thromboxane synthase inhibitor, reduced blood pressure in spontaneously hypertensive rats.[256] The clinical use of TxA_2 synthase inhibitors is complicated by the fact that its endoperoxide precursors (PGG_2/PGH_2) are also capable of activating its downstream target, the TP receptor,[257] so thromboxane receptor antagonists would be expected to more definitively interfere with this pathway.

TP Receptor

The thromboxane receptor (TP) was the first member of the prostanoid receptor family cloned.[258] This GPCR has a predicted molecular mass ~37.5 kDa, and is highly expressed in platelets and vascular tissue where its activation increases intracellular calcium.[258] In the kidney TP receptor mRNA is predominantly expressed in the glomerulus and vascular tissue,[224,259] where it contributes to vasoconstrictor activity following Ang II infusion[260] and following renal injury.[261–263]

Prostaglandin Transport

One of the major areas of uncertainty in eicosanoid research is precisely how prostanoids, synthesized inside the cell, transit the cell membrane to become available to interact with cell surface receptors.

Recent studies have identified several transmembrane proteins capable of facilitated transport of prostaglandins across cell membranes.[264] Schuster's group identified a lactate/PGE_2 exchanger they designated prostaglandin transporter or PGT.[265] The importance of PGT in mediating the *in vivo* effects of PGE_2 has been substantially bolstered by studies showing genetic disruption of the PGT gene is associated with perinatal death due to persistence of a patent ductus arteriosus[266] recapitulating the phenotype of the EP4 receptor knockout.[121,176] Although this prostaglandin transporter appears poised primarily to provide a PGE2 re-uptake mechanism, it is notable that the transporter is expressed in renal cells that are major sites of prostaglandin synthesis,[267] rather than those renal cells involved in PGE_2 inactivation.[264] These findings are consistent with the possibility that PGT plays an important role in directing vectorial PGE_2 release. Nevertheless, it seems unlikely that this protein comprises the pathway mediating PGE_2 release. More recent evidence supports a role for the multi-drug resistance protein 4 (MRP4) as a potential PGE_2 efflux mechanism.[268] MRP4 knockout mice exhibit low levels of circulating PGE_2 and reduced inflammatory pain,[269] consistent with a role in PGE2 extrusion.

Prostaglandins and the Pathogenesis of Kidney Disease

Renal Inflammation

Increased glomerular COX1 or COX2 expression has been reported in patients with nephritis, and in animal models of nephritis.[270,271] Glomerular expression of COX2 is upregulated in patients with active lupus nephritis and in lupus nephritis animal models.[270,272] COX2 inhibition has shown beneficial effects on passive Heymann nephritis (PHN), a model of membranous nephropathy.[273] Cell culture studies show that thromboxane A2 contributes to complement-induced cytotoxicity of glomerular epithelial cells.[273] In contrast, in anti-Thy1.1 glomerulonephritis model, an animal model of mesangioproliferative glomerulonephritis (MPGN) that is characterized by endothelial injury, COX2 inhibition is associated with increased mesangiolysis, albuminuria, and delayed recovery from glomerular injury.[274] Further studies suggest that healing of injured glomerular capillary endothelium in this model may depend on COX2-derived prostanoids, and COX2 inhibition may lead to impaired capillary endothelium healing.[274] The role of COX-derived prostanoids in autoimmune and inflammatory disease has been well-documented.[275,276] COX2 expression and prostanoid biosynthesis can be induced in macrophages and dendritic cells by inflammatory agents, such as LPS, IL-1ß, and interferon.[74,75] PGDS expression or activity has been described in dendritic cells, macrophage, eosinophil, neutrophil, and mast cells.[106] Prostanoids, particularly PGE2 and PGI2, have been shown to enhance inflammatory reactions.[106] Conversely prostanoids also exert anti-inflammatory effects. The pro- or anti-inflammatory effect of prostanoids is dependent on specific prostanoid, receptor subtype, cell population, and context of activation.[106] Additional studies are required to define the precise roles of prostanoids in different forms of glomerulonephritis.

Renal COX-Derived Prostanoids and Diabetic Nephropathy

Diabetic nephropathy is characterized by microalbuminuria, glomerular hypertrophy, mesangial expansion with glomerular basement membrane thickening, arteriolar hyalinosis, and global glomerular sclerosis, which ultimately lead to the progression to proteinuria and renal failure.[277,278] Supra-normal GFR (hyperfiltration) typifies the early stages of diabetic nephropathy.[279–282] Studies in diabetic humans and streptozotocin (STZ)-induced type I diabetic rats show increased renal PGE2, PGI2, and TxB2 levels.[282–285] COX2 expression is increased in the thick ascending limb and macula densa in diabetic humans and rodents.[286–288] Selective COX2 inhibition reduces glomerular hyperfiltration in streptozotocin-induced diabetic rats, consistent with COX2-derived prostanoids increasing renal blood flow in the diabetic kidney.[288] The identity of the specific COX2-derived prostanoids and their cognate receptors involved in pathogenesis of diabetic hyperfiltration has not been completely characterized. EP1 receptor antagonist treatment ameliorates renal and glomerular hypertrophy, and decreases mesangial expansion.[139] A thromboxane receptor (TP) antagonist has also been reported to attenuate proteinuria and ameliorate histological changes of diabetic nephropathy in diabetic apolipoprotein E-deficient mice.[289] It has not been determined whether similar beneficial effects might be observed in human diabetic nephropathy.

Prostaglandins and Progression of Kidney Disease

COX-derived prostanoids may also modify renal function and glomerular damage in non-diabetic chronic renal disease.[290,291] After subtotal renal ablation, renal cortical COX2 expression is increased, predominantly in the macula densa and surrounding cTAL.[291,292] Selective COX2 inhibition decreases proteinuria and inhibits the development of glomerular

sclerosis.[291,292] These studies are consistent with a role of COX2-derived prostanoids in the pathogenesis of structural and functional deterioration of kidney in chronic kidney disease.

LIPOXYGENASE DERIVED EICOSANOIDS: 5-, 12-, AND 15-HETES AND LEUKOTRIENES

Arachidonic acid may be metabolized to form leukotrienes and hydroxyeicosatetraenoic acids (HETEs) by a family of enzymes designated lipoxygenases[293,294] (Figure 17.5). Leukotriene arachidonic acid metabolites play a major role in inflammatory disease, especially asthma and other inflammatory pulmonary diseases where cysteinyl leukotriene receptor antagonists have found a place as a standard of care.[295,296] In contrast to the prostaglandins, it has been difficult to demonstrate a major role for leukotrienes in the normal kidney.

Lipoxygenases (LOX) are comprised of non-heme iron containing enzymes that insert molecular oxygen into polyunsaturated fatty acids such as arachidonic acid and linoleic acid.[294,297] Six functional human lipoxygenases have been cloned: 5-lipoxygenase (gene name: ALOX5); platelet-type 12-lipoxygenase (gene name: ALOX12); 12/15-lipoxygenase (leukocyte-type 12-LO for mice, 15-LO type 1 for human, gene name: ALOX15); epidermal-type 12-lipoxgenase (gene name: ALOXE3); 12(R)-lipoxygenase (gene name: ALOX12B); and 15-lipoxygenase type 2 (gene name: ALOX15B, 8-lipoxygenase in mice).[293,297]

5-Lipoxygenase is the key enzyme in leukotriene biosynthesis.[293,296,297] In the presence of 5-LO-activating protein (FLAP)[298] 5-lipoxygenase catalyzes the generation of leukotriene A4 (LTA4). LTA4, in turn, is converted by LTA4 hydrolase to LTB4, capable of activating LTB4 receptors. LTB4 is a potent chemotactic substance, and increases polymorphonuclear leukocytes (PMN) aggregation and adhesion to the endothelium.[299,300] Alternatively, LTA4 can be converted to cysteinyl (cys) leukotrienes (LTC4, LTD4, and LTE4) through leukotriene C4 synthase.[297] LTC4 and LTD4 contract vascular smooth muscle cells and increase vascular permeability.[301–304] These leukotrienes are usually released locally by leukocytes. Mice with 5-LO gene disruption exhibit a reduced inflammatory reaction,[305–307] supporting the pro-inflammatory action of 5-LO-derived metabolites. Recently, increased expression of leukotriene C4 synthase and formation of cysteinyl-leukotrienes have been reported in human abdominal aortic aneurysm.[308]

As might be predicted from its expression in inflammatory cells, 5-LO-derived products appear to play an important role in glomerular immune injury.[309–311] 5-LO mRNA and 5-LOX-activating protein (FLAP) mRNA are detected in the glomeruli and vasa recta.[312] Both leukotriene receptor B4 and the cysteinyl leukotriene receptor type 1 are selectively expressed in the

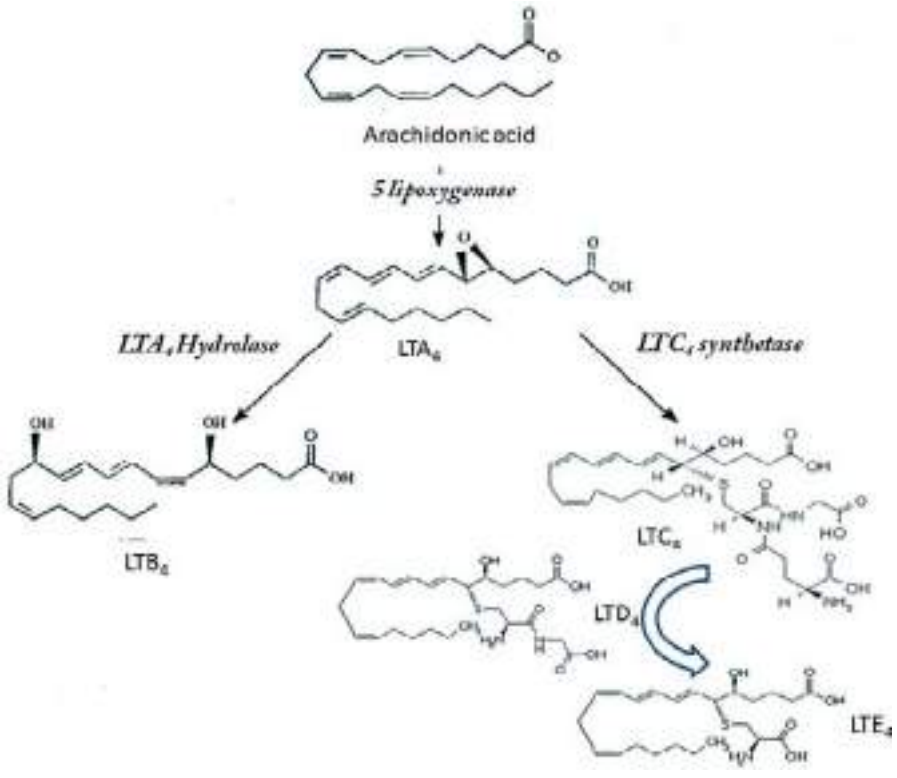

FIGURE 17.5 **Leukotriene synthetic pathway.**

glomerulus,[312] suggesting 5-LO products are involved in glomerular function. Glomerular synthesis of LTB4 and LTC4/LTD4 is markedly enhanced in both human disease and experimental glomerular immune injury.[313–315] LTD4 may contribute to the reduction of GFR in the acute phase of injury by virtue of its potent vasoconstrictor action and contraction of mesangial cells.[314] LTD4 may also increase intraglomerular pressure, contributing to proteinuria.[315] LTB4, a potent promoter of PMN attraction, participates in glomerular damage by amplifying PMN-dependent mechanisms of injury.[314]

The biological functions of the other members of the lipoxygenase family are more obscure. The 12-LO, catalyzes the formation of oxidized lipids 12(S)-hydroxyeicosatetraenoic acid [12(S)-HETE]. Human 15-LO type 1 shares high homology with rodent leukocyte-type 12-LO; both can mediate the formation of 12(S)-HETE and 15(S)-HETE from arachidonic acid, and are thus classified as 12/15-LO.[293,297,316] Some evidence suggests that 12(S)-HETE and 15(S)-HETE play important roles in systemic homeostasis and renal–cardiovascular pathology[317,318]; however, specific receptors for these products have not yet been identified. A recent study implicates ALOX15 as playing a role in bone mineralization.[319] 12/15-Lipoxygenase products also appear to be involved in the pathogenesis of atherosclerosis.[320]

12/15-Lipoxygenase-derived products may contribute to the pathogenesis of diabetic complications, including diabetic nephropathy.[321,322] 12/15-LO is detected in renal microvessels, glomeruli, and mesangial cells.[312,323,324] 12/15-LO levels are increased in the glomeruli of experimental diabetic animals.[321,325] The 12/15 LO pathway has been shown to be a critical mediator of TGFβ and angiotensin II (ANG II)-induced mesangial cell hypertrophy and extracellular matrix accumulation.[322,326,327] These studies also suggest that ANG II-induced mesangial cell hypertrophy and extracellular matrix synthesis in cultured rat mesangial cells can be blocked by an LO inhibitor or targeted 12/15 LO gene deletion.

CYTOCHROME P450 MONOOXYGENASE-DERIVED EICOSANOIDS: 20-HETE AND EETS

Free arachidonic acid can also be metabolized by the cytochrome P450 monooxygenases (CYP450) to produce hydroxy- and epoxy-arachidonic acid derivatives.[328,329] The major CYP450-catalyzed reactions in most tissues are mediated by epoxygenase and ω-hydroxylase activities of the CYP450 family, which are responsible for biosynthesis of epoxyeicosatrienoic acids (EETs) and 20-hydroxyeicosatetraenoic acid (20-HETE), respectively[328,329](Figure 17.6). These metabolites have been shown to possess biological activity, but the mechanisms mediating these biological effects remain obscure since specific receptors have not been identified.[48,330,331]

Members of the P450 *CYP2C*, and *2J* subfamilies have been identified as functionally relevant epoxygenases, while members of 4A and 4F are ω-hydroxylases, respectively.[48,331–333] 20-HETE is a potent vasoconstrictor.[334–336] EETs are produced in the vascular endothelium, and are potent vasodilators.[337,338] EETs are also produced in tubules, including the proximal tubule and collecting ducts in the rodent kidney.[335,339] EETs have been shown to inhibit ENaC activity,[339,340] which may contribute to their natriuretic effect. EETs have also been shown to mediate the natriuretic effect of angiotensin II.[339,341] Studies of knockout mice have supported a role for CYP450 metabolism in the regulation of blood pressure, but the mechanisms of these effects remain incompletely understood. Genetic disruption of CYP2J8 was associated with hypertension in females, but it is uncertain whether this effect is related to its arachidonate epoxygenase activity in mice or an effect on estrogen metabolism.[342] Genetic disruption of cyp4a10 and 4a14 are also associated with hypertension,[343,344] adding to uncertainty regarding the distinct roles of epoxygenase and ω-hydroxylase activity of arachidonic acid in regulating vascular tone and blood pressure.

Role of Renal CYP450-Derived Arachidonate Metabolites in Renal Damage

Increased EET formation has been reported in the kidney of rats with liver cirrhosis. While it is well-documented that renal vasoconstriction leading to impaired renal function occurs during cirrhosis, this result suggests increased EET synthesis may be a homeostatic response to help preserve renal perfusion.[345] Reduced CYP arachidonate hydroxyglase activity and 20-HETE levels have been reported in the kidney following ischemia and reperfusion. Reduced CYP4A protein expression and enzyme activity in ischemia/reperfusion was suggested as an adaptive mechanism to preserve renal vasculature from excessive vasoconstriction.[346] Other studies suggest that the CYP hydroxylase-derived product 20-HETE plays an important role in the maintenance of the glomerular protein permeability barrier.[347] An *in vitro* glomerular albumin permeability study using isolated rat glomeruli shows that puromycin aminonucleoside (PAN) significantly increases glomerular albumin permeability.[347] 20-HETE treatment blocks PAN-induced increase in albumin permeability.[347]

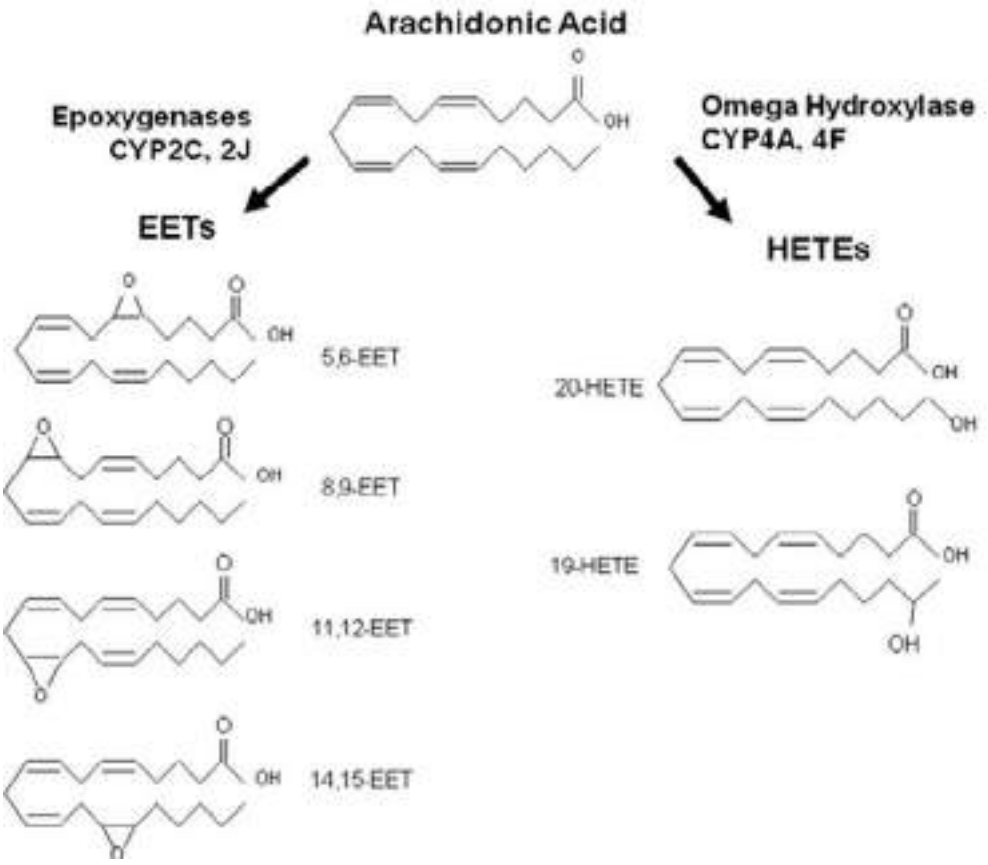

FIGURE 17.6 **Products of cytochrome P450-mediated metabolism of arachidonic acid.**

SUMMARY

Eicosanoids exert diverse and sometimes self-opposing functions. The specific effect of each eicosanoid depends on sequential enzymatic machinery in a specific cell, yielding a specific eicosanoid, exerting its distinct function. The biosynthesis of each eicosanoid is regulated at multiple levels from phospholipase A2 that catalyzes the release of arachidonic acid to specific enzymes that catalyze the formation of bioactive eicosanoids. Arachidonate-derived eicosanoids including prostanoids, leukotrienes, 12/15-HETEs, EETs, and HETEs, and sphingomyelin-derived ceramide play important roles in maintaining normal renal function. They are also involved in the pathophysiology of diabetic nephropathy, and inflammatory or toxic glomerular injury. Those signaling pathways should provide a fruitful area to identify targets for intervention in the pharmacologic treatment of renal disease.

References

[1] Page J, Henry D. Consumption of NSAIDs and the development of congestive heart failure in elderly patients: an underrecognized public health problem. Arch Intern Med 2000;160:777–84.

[2] White WB. Cardiovascular risk, hypertension, and NSAIDs. Curr Rheumatol Rep 2007;9:36–43.

[3] Breyer MD, Harris RC. Cyclooxygenase 2 and the kidney. Curr Opin Nephrol Hypertens 2001;10:89–98.

[4] Eras J, Perazella MA. NSAIDs and the kidney revisited: are selective cyclooxygenase-2 inhibitors safe? Am J Med Sci 2001; 321:181–90.

[5] Winkelmayer WC, Waikar SS, Mogun H, Solomon DH. Nonselective and cyclooxygenase-2-selective NSAIDs and acute kidney injury. Am J Med 2008;121:1092–8.

[6] Hansen AE, Burr GO. Essential fatty acids and human nutrition. J Am Med Assoc 1946;132:855–9.

[7] De Caterina R. n-3 Fatty acids in cardiovascular disease. N Engl J Med 2011;364:2439–50.

[8] Burr GO, Burr MM. Nutrition classics from The Journal of Biological Chemistry 82:345-67, 192[9] A new deficiency disease produced by the rigid exclusion of fat from the diet. Nutr Rev 1973;31:248–9.

[9] Lands WE. The biosynthesis and metabolism of prostaglandins. Annu Rev Physiol 1979;41:633–52.

[10] Dunham EW, Balasingam M, Privett OS, Nickell EC. Effects of essential fatty acid deficiency on prostaglandin synthesis and fatty acid composition in rat renal medulla. Lipids 1978;13:892–7.

[11] Moussa M, Garcia J, Ghisolfi J, Periquet B, Thouvenot JP. Dietary essential fatty acid deficiency differentially affects tissues of rats. J Nutr 1996;126:3040–5.

[12] Soares AF, Santiago RC, Alessio ML, Descomps B, de Castro-Chaves C. Biochemical, functional, and histochemical effects of

essential fatty acid deficiency in rat kidney. Lipids 2005; 40:1125–33.
[13] Boyanovsky BB, Webb NR. Biology of secretory phospholipase A2. Cardiovasc Drugs Ther 2009;23:61–72.
[14] Burke JE, Dennis EA. Phospholipase A2 structure/function, mechanism, and signaling. J Lipid Res 2009;50:S237–42.
[15] Boulven I, Palmier B, Robin P, Vacher M, Harbon S, Leiber D. Platelet-derived growth factor stimulates phospholipase C-gamma 1, extracellular signal-regulated kinase, and arachidonic acid release in rat myometrial cells: contribution to cyclic 3′,5′-adenosine monophosphate production and effect on cell proliferation. Biol Reprod 2001;65:496–506.
[16] Fujishima H, Sanchez Mejia RO, Bingham III CO, Lam BK, Sapirstein A, Bonventre JV, et al. Cytosolic phospholipase A2 is essential for both the immediate and the delayed phases of eicosanoid generation in mouse bone marrow-derived mast cells. Proc Natl Acad Sci USA 1999;96:4803–7.
[17] Samad TA, Moore KA, Sapirstein A, Billet S, Allchorne A, Poole S, et al. Interleukin-1beta-mediated induction of Cox-2 in the CNS contributes to inflammatory pain hypersensitivity. Nature 2001;410:471–5.
[18] Sapirstein A, Bonventre JV. Specific physiological roles of cytosolic phospholipase A(2) as defined by gene knockouts. Biochim Biophys Acta 2000;1488:139–48.
[19] Kudo I, Murakami M. Phospholipase A2 enzymes. Prostag Oth Lipid M 2002;68-69:3–58.
[20] Mangat H, Peterson LN, Burns KD. Hypercalcemia stimulates expression of intrarenal phospholipase A2 and prostaglandin H synthase-2 in rats. Role of angiotensin II AT1 receptors. J Clin Invest 1997;100:1941–50.
[21] Pavoine C, Behforouz N, Gauthier C, Le Gouvello S, Roudot-Thoraval F, Martin CR, et al. beta2-Adrenergic signaling in human heart: shift from the cyclic AMP to the arachidonic acid pathway. Mol Pharmacol 2003;64:1117–25.
[22] Xing M, Insel PA. Protein kinase C-dependent activation of cytosolic phospholipase A2 and mitogen-activated protein kinase by alpha 1-adrenergic receptors in Madin–Darby canine kidney cells. J Clin Invest 1996;97:1302–10.
[23] Jiao H, Cui XL, Torti M, Chang CH, Alexander LD, Lapetina EG, et al. Arachidonic acid mediates angiotensin II effects on p21ras in renal proximal tubular cells via the tyrosine kinase-Shc-Grb2-Sos pathway. Proc Natl Acad Sci USA 1998; 95:7417–21.
[24] Marin Castano ME, Schanstra JP, Hirtz C, Pesquero JB, Pecher C, Girolami JP, et al. B2 kinin receptor upregulation by cAMP is associated with BK-induced PGE2 production in rat mesangial cells. Am J Physiol 1998;274:F532–40.
[25] Murakami M, Kambe T, Shimbara S, Kudo I. Functional coupling between various phospholipase A2s and cyclooxygenases in immediate and delayed prostanoid biosynthetic pathways. J Biol Chem 1999;274:3103–15.
[26] Jacobs LS, Douglas JG. Angiotensin II type 2 receptor subtype mediates phospholipase A2-dependent signaling in rabbit proximal tubular epithelial cells. Hypertension 1996;28:663–8.
[27] Slivka SR, Insel PA. Alpha 1-adrenergic receptor-mediated phosphoinositide hydrolysis and prostaglandin E2 formation in Madin–Darby canine kidney cells. Possible parallel activation of phospholipase C and phospholipase A2. J Biol Chem 1987; 262:4200–7.
[28] Choi KH, Edelstein CL, Gengaro P, Schrier RW, Nemenoff RA. Hypoxia induces changes in phospholipase A2 in rat proximal tubules: evidence for multiple forms. Am J Physiol 1995;269: F846–53.
[29] Osada-Oka M, Takahashi M, Akiba S, Sato T. Involvement of Ca^{2+}-independent phospholipase A2 in the translocation of hypoxia-inducible factor-1alpha to the nucleus under hypoxic conditions. Eur J Pharmacol 2006;549:58–62.
[30] Petry C, Huwiler A, Eberhardt W, Kaszkin M, Pfeilschifter J. Hypoxia increases group IIA phospholipase A(2) expression under inflammatory conditions in rat renal mesangial cells. J Am Soc Nephrol 2005;16:2897–905.
[31] Goto S, Nakamura H, Morooka H, Terao Y, Shibata O, Sumikawa K. Role of reactive oxygen in phospholipase A2 activation by ischemia/reperfusion of the rat kidney. J Anesth 1999;13:90–3.
[32] Alexander LD, Alagarsamy S, Douglas JG. Cyclic stretch-induced cPLA2 mediates ERK 1/2 signaling in rabbit proximal tubule cells. Kidney Int 2004;65:551–63.
[33] Bonventre JV. The 85-kD cytosolic phospholipase A2 knockout mouse: a new tool for physiology and cell biology. J Am Soc Nephrol 1999;10:404–12.
[34] DeRubertis FR, Craven PA. Eicosanoids in the pathogenesis of the functional and structural alterations of the kidney in diabetes. Am J Kidney Dis 1993;22:727–35.
[35] Beck S, Beck G, Ostendorf T, Floege J, Lambeau G, Nevalainen T, et al. Upregulation of group IB secreted phospholipase A(2) and its M-type receptor in rat ANTI-THY-1 glomerulonephritis. Kidney Int 2006;70:1251–60.
[36] Zager RA, Schimpf BA, Gmur DJ, Burke TJ. Phospholipase A2 activity can protect renal tubules from oxygen deprivation injury. Proc Natl Acad Sci USA 1993;90:8297–301.
[37] dos Reis MA, Costa RS, Coimbra TM, Teixeira VP. Acute renal failure in experimental envenomation with Africanized bee venom. Ren Fail 1998;20:39–51.
[38] Takasaki J, Kawauchi Y, Urasaki T, Tanaka H, Usuda S, Masuho Y. Antibodies against type II phospholipase A2 prevent renal injury due to ischemia and reperfusion in rats. FEBS Lett 1998;440:377–81.
[39] Beck Jr. LH, Bonegio RG, Lambeau G, Beck DM, Powell DW, Cummins TD, et al. M-type phospholipase A2 receptor as target antigen in idiopathic membranous nephropathy. N Engl J Med 2009;361:11–21.
[40] Lambeau G, Lazdunski M. Receptors for a growing family of secreted phospholipases A2. Trends Pharmacol Sci 1999; 20:162–70.
[41] Rouault M, Le Calvez C, Boilard E, Surrel F, Singer A, Ghomashchi F, et al. Recombinant production and properties of binding of the full set of mouse secreted phospholipases A2 to the mouse M-type receptor. Biochemistry 2007;46: 1647–62.
[42] Augert A, Payre C, de Launoit Y, Gil J, Lambeau G, Bernard D. The M-type receptor PLA2R regulates senescence through the p53 pathway. EMBO Rep 2009;10:271–7.
[43] Fitzpatrick FA, Soberman R. Regulated formation of eicosanoids. J Clin Invest 2001;107:1347–51.
[44] FitzGerald GA, Loll P. COX in a crystal ball: current status and future promise of prostaglandin research. J Clin Invest 2001; 107:1335–7.
[45] Smith WL, DeWitt DL, Garavito RM. Cyclooxygenases: structural, cellular, and molecular biology. Annu Rev Biochem 2000; 69:145–82.
[46] Funk CD. Prostaglandins and leukotrienes: advances in eicosanoid biology. Science 2001;294:1871–5.
[47] Murphy RC, Gijon MA. Biosynthesis and metabolism of leukotrienes. Biochem J 2007;405:379–95.
[48] Capdevila JH. Regulation of ion transport and blood pressure by cytochrome p450 monooxygenases. Curr Opin Nephrol Hypertens 2007;16:465–70.
[49] Fleming I. Epoxyeicosatrienoic acids, cell signaling and angiogenesis. Prostaglandins Other Lipid Mediat 2007;82:60–7.

[50] Zeldin DC. Epoxygenase pathways of arachidonic acid metabolism. J Biol Chem 2001;276:36059–62.
[51] Hansen RA, Ogilvie GK, Davenport DJ, Gross KL, Walton JA, Richardson KL, et al. Duration of effects of dietary fish oil supplementation on serum eicosapentaenoic acid and docosahexaenoic acid concentrations in dogs. Am J Vet Res 1998; 59:864–8.
[52] Smith WL. Nutritionally essential fatty acids and biologically indispensable cyclooxygenases. Trends Biochem Sci 2008;33: 27–37.
[53] De Caterina R, Caprioli R, Giannessi D, Sicari R, Galli C, Lazzerini G, et al. n-3 Fatty acids reduce proteinuria in patients with chronic glomerular disease. Kidney Int 1993;44:843–50.
[54] Grande JP, Donadio Jr. JV. Dietary fish oil supplementation in IgA nephropathy: a therapy in search of a mechanism? Nutrition 1998;14:240–2.
[55] Garavito MR, Malkowski MG, DeWitt DL. The structures of prostaglandin endoperoxide H synthases-1 and -2. Prostag Oth Lipid M 2002;68-69:129–52.
[56] Kiefer JR, Pawlitz JL, Moreland KT, Stegeman RA, Hood WF, Gierse JK, et al. Structural insights into the stereochemistry of the cyclooxygenase reaction. Nature 2000;405:97–101.
[57] Picot D, Loll PJ, Garavito RM. The X-ray crystal structure of the membrane protein prostaglandin H2 synthase-1. Nature 1994; 367:243–9.
[58] Yuan C, Sidhu RS, Kuklev DV, Kado Y, Wada M, Song I, et al. Cyclooxygenase allosterism, fatty acid-mediated cross-talk between monomers of cyclooxygenase homodimers. J Biol Chem 2009;284:10046–55.
[59] Yuan C, Rieke CJ, Rimon G, Wingerd BA, Smith WL. Partnering between monomers of cyclooxygenase-2 homodimers. PNAS 2006;103:6142–7.
[60] Mbonye UR, Wada M, Rieke CJ, Tang HY, Dewitt DL, Smith WL. The 19-amino acid cassette of cyclooxygenase-2 mediates entry of the protein into the endoplasmic reticulum-associated degradation system. J Biol Chem 2006;281:35770–8.
[61] Sidhu, R. S., Lee, J. Y., Yuan, C., and Smith, W. L. Comparison of cyclooxygenase-1 crystal structures: cross-talk between monomers comprising cyclooxygenase-1 homodimers. *Biochemistry* 49:7069–7079.
[62] Rimon, G., Sidhu, R. S., Lauver, D. A., Lee, J. Y., Sharma, N. P., Yuan, C., et al. Coxibs interfere with the action of aspirin by binding tightly to one monomer of cyclooxygenase-1. *Proc Natl Acad Sci USA* 107:28–33.
[63] Dong L, Vecchio AJ, Sharma NP, Jurban BJ, Malkowski MG, Smith WL. Human cyclooxygenase-2 is a sequence homodimer that functions as a conformational heterodimer. J Biol Chem 2011;286:19035–46.
[64] Kobayashi T, Narumiya S. Function of prostanoid receptors: studies on knockout mice. Prostaglandins Other Lipid Mediat 2002;68-69:557–73.
[65] Narumiya S, Sugimoto Y, Ushikubi F. Prostanoid receptors: structures, properties, and functions. Physiol Rev 1999;79:1193–226.
[66] Kliewer S, Lenhard J, Wilson T, Patel I, Morris D, Lehmann J. A prostaglandin J_2 metabolite binds peroxisome proliferator-activated receptor gamma and promotes adipocyte differentiation. Cell 1995;83:813–9.
[67] Narumiya S, Ohno K, Fujiwara M, Fukushima M. Site and mechanism of growth inhibition by prostaglandins. II. Temperature-dependent transfer of a cyclopentenone prostaglandin to nuclei. J Pharmacol Exp Ther 1986;239:506–11.
[68] Reginato MJ, Krakow SL, Bailey ST, Lazar MA. Prostaglandins promote and block adipogenesis through opposing effects on peroxisome proliferator-activated receptor gamma. J Biol Chem 1998;273:1855–8.
[69] Hla T, Neilson K. Human cyclooxygenase-2 cDNA. Proc Natl Acad Sci USA 1992;89:7384–8.
[70] Kujubu DA, Fletcher BS, Varnum BC, Lim RW, Herschman HR. TIS10, a phorbol ester tumor promoter-inducible mRNA from Swiss 3T3 cells, encodes a novel prostaglandin synthase/cyclooxygenase homologue. J Biol Chem 1991;266:12866–72.
[71] Kujubu DA, Herschman HR. Dexamethasone inhibits mitogen induction of the TIS10 prostaglandin synthase/cyclooxygenase gene. J Biol Chem 1992;267:7991–4.
[72] Tanabe T, Tohnai N. Cyclooxygenase isozymes and their gene structures and expression. Prostaglandins Other Lipid Mediat 2002;68-69:95–114.
[73] Cheng Y, Wang M, Yu Y, Lawson J, Funk CD, Fitzgerald GA. Cyclooxygenases, microsomal prostaglandin E synthase-1, and cardiovascular function. J Clin Invest 2006;116:1391–9.
[74] Hla T, Bishop-Bailey D, Liu CH, Schaefers HJ, Trifan OC. Cyclooxygenase-1 and -2 isoenzymes. Int J Biochem Cell Biol 1999;31:551–7.
[75] Herschman HR. Prostaglandin synthase 2. Bba-Lipid Lipid Metab 1996;1299:125–40.
[76] Smith WL. Prostanoid biosynthesis and mechanisms of action. Am J Physiol 1992;263:F181–91.
[77] Smith WL, Langenbach R. Why there are two cyclooxygenase isozymes? J Clin Invest 2001;107:1491–5.
[78] Dinchuk JE, Car BD, Focht RJ, Johnston JJ, Jaffee BD, Covington MB, et al. Renal abnormalities and an altered inflammatory response in mice lacking cyclooxygenase II. Nature 1995;378:406–9.
[79] Komhoff M, Wang JL, Cheng HF, Langenbach R, McKanna JA, Harris RC, et al. Cyclooxygenase-2-selective inhibitors impair glomerulogenesis and renal cortical development. Kidney Int 2000;57:414–22.
[80] Morham SG, Langenbach R, Loftin CD, Tiano HF, Vouloumanos N, Jennette JC, et al. Prostaglandin synthase 2 gene disruption causes severe renal pathology in the mouse. Cell 1995;83:473–82.
[81] Harris RC, McKanna JA, Akai Y, Jacobson HR, Dubois RN, Breyer MD. Cyclooxygenase-2 is associated with the macula densa of rat kidney and increases with salt restriction. J Clin Invest 1994;94:2504–10.
[82] Komhoff M, Jeck ND, Seyberth HW, Grone HJ, Nusing RM, Breyer MD. Cyclooxygenase-2 expression is associated with the renal macula densa of patients with Bartter-like syndrome. Kidney Int 2000;58:2420–4.
[83] Vio CP, An SJ, Cespedes C, McGiff JC, Ferreri NR. Induction of cyclooxygenase-2 in thick ascending limb cells by adrenalectomy. J Am Soc Nephrol 2001;12:649–58.
[84] Campean V, Theilig F, Paliege A, Breyer M, Bachmann S. Key enzymes for renal prostaglandin synthesis: site-specific expression in rodent kidney (rat, mouse). Am J Physiol Renal Physiol 2003;285:F19–32.
[85] Smith WL, Bell TG. Immunohistochemical localization of the prostaglandin-forming cyclooxygenase in renal cortex. Am J Physiol 1978;235:F451–7.
[86] Yang T, Singh I, Pham H, Sun D, Smart A, Schnermann JB, et al. Regulation of cyclooxygenase expression in the kidney by dietary salt intake. Am J Physiol 1998;274:F481–9.
[87] Castrop H, Schweda F, Schumacher K, Wolf K, Kurtz A. Role of renocortical cyclooxygenase-2 for renal vascular resistance and macula densa control of renin secretion. J Am Soc Nephrol 2001;12:867–74.
[88] Guan Y, Chang M, Cho W, Zhang Y, Redha R, Davis L, et al. Cloning, expression, and regulation of rabbit cyclooxygenase-2 in renal medullary interstitial cells. Am J Physiol 1997;273: F18–26.

[89] Hao CM, Komhoff M, Guan Y, Redha R, Breyer MD. Selective targeting of cyclooxygenase-2 reveals its role in renal medullary interstitial cell survival. Am J Physiol 1999; 277:F352–9.
[90] Bresalier RS, Sandler RS, Quan H, Bolognese JA, Oxenius B, Horgan K, et al. Cardiovascular events associated with rofecoxib in a colorectal adenoma chemoprevention trial. N Engl J Med 2005;352:1092–102.
[91] Zewde T, Mattson DL. Inhibition of cyclooxygenase-2 in the rat renal medulla leads to sodium-sensitive hypertension. Hypertension 2004;44:424–8.
[92] Zhang MZ, Yao B, Cheng HF, Wang SW, Inagami T, Harris RC. Renal cortical cyclooxygenase 2 expression is differentially regulated by angiotensin II AT(1) and AT(2) receptors. Proc Natl Acad Sci USA 2006;103:16045–50.
[93] Peti-Peterdi J, Komlosi P, Fuson AL, Guan Y, Schneider A, Qi Z, et al. Luminal NaCl delivery regulates basolateral PGE2 release from macula densa cells. J Clin Invest 2003;112:76–82.
[94] Helliwell RJ, Adams LF, Mitchell MD. Prostaglandin synthases: recent developments and a novel hypothesis. Prostaglandins Leukot Essent Fatty Acids 2004;70:101–13.
[95] Urade Y, Watanabe K, Hayaishi O. Prostaglandin D, E, and F synthases. J Lipid Mediat Cell Signal 1995;12:257–73.
[96] Breyer MD, Breyer RM. Prostaglandin E receptors and the kidney. Am J Physiol Renal Physiol 2000;279:F12–23.
[97] Narumiya S, FitzGerald GA. Genetic and pharmacological analysis of prostanoid receptor function. J Clin Invest 2001; 108:25–30.
[98] Qi Z, Cai H, Morrow JD, Breyer MD. Differentiation of cyclooxygenase 1- and 2-derived prostanoids in mouse kidney and aorta. Hypertension 2006;48:323–8.
[99] Murphey LJ, Williams MK, Sanchez SC, Byrne LM, Csiki I, Oates JA, et al. Quantification of the major urinary metabolite of PGE2 by a liquid chromatographic/mass spectrometric assay: Determination of cyclooxygenase-specific PGE2 synthesis in healthy humans and those with lung cancer. Anal Biochem 2004;334:266–75.
[100] Whelton A, Schulman G, Wallemark C, Drower EJ, Isakson PC, Verburg KM, et al. Effects of celecoxib and naproxen on renal function in the elderly. Arch Intern Med 2000; 160:1465–70.
[101] Kammerl MC, Nusing RM, Schweda F, Endemann D, Stubanus M, Kees F, et al. Low sodium and furosemide-induced stimulation of the renin system in man is mediated by cyclooxygenase 2. Clin Pharmacol Ther 2001;70:468–74.
[102] Breyer RM, Kennedy CR, Zhang Y, Breyer MD. Structure–function analyses of eicosanoid receptors. Physiologic and therapeutic implications. Ann NY Acad Sci 2000;905:221–31.
[103] Sugimoto Y, Narumiya S. Prostaglandin E receptors. J Biol Chem 2007;282:11613–7.
[104] Hebert RL, Carmosino M, Saito O, Yang G, Jackson CM, Qi Z, et al. Characterization of a rabbit PGF2alpha (FP) receptor exhibiting Gi-restricted signaling and that inhibits water absorption in renal collecting duct. J Biol Chem 2005;280: 35028–37.
[105] Breyer MD, Davis L, Jacobson HR, Breyer RM. Differential localization of prostaglandin E receptor subtypes in human kidney. Am J Physiol 1996;270:F912–8.
[106] Tilley SL, Coffman TM, Koller BH. Mixed messages: modulation of inflammation and immune responses by prostaglandins and thromboxanes. J Clin Invest 2001;108:15–23.
[107] Cronstein BN, Weissmann G. Targets for antiinflammatory drugs. Annu Rev Pharmacol Toxicol 1995;35:449–62.
[108] Honda T, Tokura Y, Miyachi Y, Kabashima K. Prostanoid receptors as possible targets for anti-allergic drugs: recent advances in prostanoids on allergy and immunology. Curr Drug Targets 2010;11:1605–13.
[109] Jakobsson PJ, Thoren S, Morgenstern R, Samuelsson B. Identification of human prostaglandin E synthase: a microsomal, glutathione-dependent, inducible enzyme, constituting a potential novel drug target. Proc Natl Acad Sci USA 1999; 96:7220–5.
[110] Tanioka T, Nakatani Y, Semmyo N, Murakami M, Kudo I. Molecular identification of cytosolic prostaglandin E2 synthase that is functionally coupled with cyclooxygenase-1 in immediate prostaglandin E2 biosynthesis. J Biol Chem 2000;275: 32775–82.
[111] Tanikawa N, Ohmiya Y, Ohkubo H, Hashimoto K, Kangawa K, Kojima M, et al. Identification and characterization of a novel type of membrane-associated prostaglandin E synthase. Biochem Biophys Res Commun 2002;291:884–9.
[112] Trebino CE, Stock JL, Gibbons CP, Naiman BM, Wachtmann TS, Umland JP, et al. Impaired inflammatory and pain responses in mice lacking an inducible prostaglandin E synthase. Proc Natl Acad Sci USA 2003;100:9044–9.
[113] Engblom D, Saha S, Engstrom L, Westman M, Audoly LP, Jakobsson P -J, et al. Microsomal prostaglandin E synthase-1 is the central switch during immune-induced pyresis. Nat Neurosci 2003;6:1137–8.
[114] Uematsu S, Matsumoto M, Takeda K, Akira S. Lipopolysaccharide-dependent prostaglandin E(2) production is regulated by the glutathione-dependent prostaglandin E(2) synthase gene induced by the Toll-like receptor 4/MyD88/NF-IL6 pathway. J Immunol 2002;168:5811–6.
[115] Schneider A, Zhang Y, Zhang M, Lu WJ, Rao R, Fan X, et al. Membrane-associated PGE synthase-1 (mPGES-1) is coexpressed with both COX-1 and COX-2 in the kidney. Kidney Int 2004;65:1205–13.
[116] Guan Y, Zhang Y, Schneider A, Riendeau D, Mancini JA, Davis L, et al. Urogenital distribution of a mouse membrane-associated prostaglandin E(2) synthase. Am J Physiol Renal Physiol 2001;281:F1173–7.
[117] Ouellet M, Falgueyret JP, Hien Ear P, Pen A, Mancini JA, Riendeau D, et al. Purification and characterization of recombinant microsomal prostaglandin E synthase-1. Protein Expr Purif 2002;26:489–95.
[118] Jia Z, Aoyagi T, Yang T. mPGES-1 protects against DOCA-salt hypertension via inhibition of oxidative stress or stimulation of NO/cGMP. Hypertension 2010;55:539–46.
[119] Jia Z, Guo X, Zhang H, Wang MH, Dong Z, Yang T. Microsomal prostaglandin synthase-1-derived prostaglandin E2 protects against angiotensin II-induced hypertension via inhibition of oxidative stress. Hypertension 2008;52:952–9.
[120] Francois H, Facemire C, Kumar A, Audoly L, Koller B, Coffman T. Role of microsomal prostaglandin E synthase 1 in the kidney. J Am Soc Nephrol 2007;18:1466–75.
[121] Nguyen M, Camenisch T, Snouwaert JN, Hicks E, Coffman TM, Anderson PA, et al. The prostaglandin receptor EP4 triggers remodelling of the cardiovascular system at birth. Nature 1997;390:78–81.
[122] Murakami M, Nakatani Y, Tanioka T, Kudo I. Prostaglandin E synthase. Prostaglandins Other Lipid Mediat 2002;68-69: 383–99.
[123] Zhang Y, Schneider A, Rao R, Lu WJ, Fan X, Davis L, et al. Genomic structure and genitourinary expression of mouse cytosolic prostaglandin E(2) synthase gene. Biochim Biophys Acta 2003;1634:15–23.
[124] Breyer RM, Davis LS, Nian C, Redha R, Stillman B, Jacobson HR, et al. Cloning and expression of the rabbit prostaglandin EP4 receptor. Am J Physiol 1996;270:F485–93.

[125] Guan Y, Stillman BA, Zhang Y, Schneider A, Saito O, Davis LS, et al. Cloning and expression of the rabbit prostaglandin EP2 receptor. BMC Pharmacol 2002;2:14.
[126] Jensen BL, Stubbe J, Hansen PB, Andreasen D, Skott O. Localization of prostaglandin E(2) EP2 and EP4 receptors in the rat kidney. Am J Physiol Renal Physiol 2001;280:F1001–9.
[127] Sheldrick R, Coleman R, Lumley P. Iloprost-A potent EP1- and IP- receptor agonist. Br J Pharmacol 1987;: xxx: 334p
[128] Coleman RA, Kennedy I, Humphrey PPA, Bunce K, Lumley P. Prostanoids and their Receptors. In: Emmet JC, editor. Comprehensive Medicinal Chemistry. Oxford: Pergammon Press; 1990. p. 643–714.
[129] Coleman RA, Smith WL, Narumiya S. VIII. International union of pharmacology classification of prostanoid receptors: properties, distribution, and structure of the receptors and their subtypes. Pharmacol Rev 1994;46:205–29.
[130] Lawrence RA, Jones RL, Wilson NH. Characterization of receptors involved in the direct and indirect actions of prostaglandins E and I on the guinea-pig ileum. Br J Pharmacol 1992;105:271–8.
[131] Funk C, Furchi L, FitzGerald G, Grygorczyk R, Rochette C, Bayne MA, et al. Cloning and expression of a cDNA for the human prostaglandin E receptor EP_1 subtype. J Biol Chem 1993;268:26767–72.
[132] Guan Y, Zhang Y, Breyer RM, Fowler B, Davis L, Hebert RL, et al. Prostaglandin E2 inhibits renal collecting duct Na^+ absorption by activating the EP1 receptor. J Clin Invest 1998;102:194–201.
[133] Hibbs TA, Lu B, Smock SL, Vestergaard P, Pan LC, Owen TA. Molecular cloning and characterization of the canine prostaglandin E receptor EP2 subtype. Prostaglandins Other Lipid Mediat 1999;57:133–47.
[134] Watabe A, Sugimoto Y, Honda A, Irie A, Namba T, Negishi M, et al. Cloning and expression of cDNA for a mouse EP1 subtype of prostaglandin E receptor. J Biol Chem 1993;268: 20175–8.
[135] Boie Y, Stocco R, Sawyer N, Slipetz DM, Ungrin MD, Neuschafer-Rube F, et al. Molecular cloning and characterization of the four rat prostaglandin E2 prostanoid receptor subtypes. Eur J Pharmacol 1997;340:227–41.
[136] Hallinan EA, Hagen TJ, Tsymbalov S, Husa RK, Lee AC, Stapelfeld A, et al. Aminoacetyl moiety as a potential surrogate for diacylhydrazine group of SC-51089, a potent PGE2 antagonist, and its analogs. J Med Chem 1996;39:609–13.
[137] Hallinan EA, Hagen TJ, Tsymbalov S, Stapelfeld A, Savage MA. 2,4-Disubstituted oxazoles and thiazoles as latent pharmacophores for diacylhydrazine of SC-51089, a potent PGE2 antagonist. Bioorg Med Chem 2001;9:1–6.
[138] Hall A, Atkinson S, Brown SH, Chessell IP, Chowdhury A, Giblin GM, et al. Discovery of novel, non-acidic 1,5-biaryl pyrrole EP1 receptor antagonists. Bioorg Med Chem Lett 2007;17: 1200–5.
[139] Makino H, Tanaka I, Mukoyama M, Sugawara A, Mori K, Muro S, et al. Prevention of diabetic nephropathy in rats by prostaglandin E receptor EP1-selective antagonist. J Am Soc Nephrol 2002;13:1757–65.
[140] Miki T, Matsunami M, Nakamura S, Okada H, Matsuya H, Kawabata A. ONO-8130, a selective prostanoid EP1 receptor antagonist, relieves bladder pain in mice with cyclophosphamide-induced cystitis. Pain 2011;152:1373–81.
[141] Naganawa A, Matsui T, Ima M, Saito T, Murota M, Aratani Y, et al. Further optimization of sulfonamide analogs as EP1 receptor antagonists: synthesis and evaluation of bioisosteres for the carboxylic acid group. Bioorg Med Chem 2006;14: 7121–37.
[142] Johansson T, Narumiya S, Zeilhofer HU. Contribution of peripheral versus central EP1 prostaglandin receptors to inflammatory pain. Neurosci Lett 2011;495:98–101.
[143] Stock JL, Shinjo K, Burkhardt J, Roach M, Taniguchi K, Ishikawa T, et al. The prostaglandin E2 EP1 receptor mediates pain perception and regulates blood pressure. J Clin Invest 2001;107:325–31.
[144] Biswas S, Bhattacherjee P, Paterson CA, Maruyama T, Narumiya S. Modulation of ocular inflammatory responses by EP1 receptors in mice. Exp Eye Res 2007;84:39–43.
[145] Guan Y, Zhang Y, Wu J, Qi Z, Yang G, Dou D, et al. Antihypertensive effects of selective prostaglandin E2 receptor subtype 1 targeting. J Clin Invest 2007;117:2496–505.
[146] Sugimoto Y, Namba T, Shigemoto R, Negishi M, Ichikawa A, Narumiya S. Distinct cellular localization of mRNAs for three subtypes of prostaglandin E receptor in kidney. Am J Physiol 1994;266:F823–8.
[147] Capone C, Faraco G, Anrather J, Zhou P, Iadecola C. Cyclooxygenase 1-derived prostaglandin E2 and EP1 receptors are required for the cerebrovascular dysfunction induced by angiotensin II. Hypertension 2010;55:911–7.
[148] Pena-Silva RA, Heistad DD. EP1c times for angiotensin: EP1 receptors facilitate angiotensin II-induced vascular dysfunction. Hypertension 2010;55:846–8.
[149] Rutkai I, Feher A, Erdei N, Henrion D, Papp Z, Edes I, et al. Activation of prostaglandin E2 EP1 receptor increases arteriolar tone and blood pressure in mice with type 2 diabetes. Cardiovascular Research 2009;83:148–54.
[150] Regan JW, Bailey TJ, Pepperl DJ, Pierce KL, Bogardus AM, Donello JE, et al. Cloning of a novel human prostaglandin receptor with characteristics of the pharmacologically defined EP2 subtype. Mol Pharmacol 1994;46:213–20.
[151] Nishigaki N, Negishi M, Honda A, Sugimoto Y, Namba T, Narumiya S, et al. Identification of prostaglandin E receptor 'EP2 cloned from mastocytoma cells as EP4 subtype. FEBS Letters 1995;364:339–41.
[152] Katsuyama M, Nishigaki N, Sugimoto Y, Morimoto K, Negishi M, Narumiya S, et al. The mouse prostaglandin E receptor EP2 subtype: cloning, expression, and Northern blot analysis. FEBS Lett 1995;372:151–6.
[153] Kennedy CR, Zhang Y, Brandon S, Guan Y, Coffee K, Funk CD, et al. Salt-sensitive hypertension and reduced fertility in mice lacking the prostaglandin EP2 receptor. Nat Med 1999;5: 217–20.
[154] Tilley SL, Audoly LP, Hicks EH, Kim HS, Flannery PJ, Coffman TM, et al. Reproductive failure and reduced blood pressure in mice lacking the EP2 prostaglandin E2 receptor. J Clin Invest 1999;103:1539–45.
[155] Pallone T. Vasoconstriction of outer medullary vasa recta by angiotensin II is modulated by prostaglandin E2. Am J Physiol 1994;266:F850–7.
[156] Pallone TL, Silldorff EP. Pericyte regulation of renal medullary blood flow. Exp Nephrol 2001;9:165–70.
[157] Imig JD, Breyer MD, Breyer RM. Contribution of prostaglandin EP(2) receptors to renal microvascular reactivity in mice. Am J Physiol Renal Physiol 2002;283:F415–22.
[158] Chen J, Zhao M, He W, Milne GL, Howard JR, Morrow J, et al. Increased dietary NaCl induces renal medullary PGE2 production and natriuresis via the EP2 receptor. Am J Physiol Renal Physiol 2008;295:F818–25.
[159] Savage MA, Moummi C, Karabatsos PJ, Lanthorn TH. SC-46275: a potent and highly selective agonist at the EP3 receptor. Prostaglandins Leukot Essent Fatty Acids 1993;49:939–43.
[160] van Rodijnen WF, Korstjens IJ, Legerstee N, Ter Wee PM, Tangelder GJ. Direct vasoconstrictor effect of prostaglandin E2

on renal interlobular arteries: role of the EP3 receptor. Am J Physiol Renal Physiol 2007;292:F1094–101.
[161] Breyer RM, Emeson RB, Tarng JL, Breyer MD, Davis LS, Abromson RM, et al. Alternative splicing generates multiple isoforms of a rabbit prostaglandin E2 receptor. J Biol Chem 1994;269:6163–9.
[162] Irie A, Segi E, Sugimoto Y, Ichikawa A, Negishi M. Mouse prostaglandin E receptor EP3 subtype mediates calcium signals via Gi in cDNA-transfected Chinese hamster ovary cells. Biochem Biophys Res Commun 1994;204:303–9.
[163] Pierce KL, Regan JW. Prostanoid receptor heterogeneity through alternative mRNA splicing. Life Sci 1998;62:1479–83.
[164] Schmid A, Thierauch KH, Schleuning WD, Dinter H. Splice variants of the human EP3 receptor for prostaglandin E2. Eur J Biochem 1995;228:23–30.
[165] Namba T, Sugimoto Y, Negishi M, Irie A, Ushikubi F, Kakizuka A, et al. Alternative splicing of C-terminal tail of prostaglandin E receptor subtype EP3 determines G-protein specificity. Nature 1993;365:166–70.
[166] Ushikubi F, Segi E, Sugimoto Y, Murata T, Matsuoka T, Kobayashi T, et al. Impaired febrile response in mice lacking the prostaglandin E receptor subtype EP3. Nature 1998;395: 281–4.
[167] Hébert, R, Jacobson, H, Breyer, M. PGE2 inhibits AVP induced water flow in cortical collecting ducts by protein kinase C activation. Am J Physiol 1990;259:F318–5.
[168] Sonnenburg, WK, Zhu, J, Smith, WL. A prostglandin E receptor coupled to a pertussis toxin-sensitive guanine nucleotide regulatory protein in rabbit cortical collecting tubule cells. J Biol Chem 1990;265:8479–83.
[169] Fleming E, Athirakul K, Oliverio M, Key M, Goulet J, Koller B, et al. Urinary concentrating function in mice lacking the EP3 receptors for prostaglandin E2. Am J Physiol 1998;275:F955–61.
[170] Abramovitz M, Adam M, Boie Y, Carriere M, Denis D, Godbout C, et al. The utilization of recombinant prostanoid receptors to determine the affinities and selectivities of prostaglandins and related analogs. Biochim Biophys Acta 2000; 1483:285–93.
[171] Bastien L, Sawyer N, Grygorczyk R, Metters KM, Adam M. Cloning, functional expression, and characterization of the human prostaglandin E2 receptor EP2 subtype. J Biol Chem 1994;269:11873–7.
[172] Fujino H, Salvi S, Regan JW. Differential regulation of phosphorylation of the cAMP response element-binding protein after activation of EP2 and EP4 prostanoid receptors by prostaglandin E2. Mol Pharmacol 2005;68:251–9.
[173] Fujino H, West KA, Regan JW. Phosphorylation of glycogen synthase kinase-3 and stimulation of T-cell factor signaling following activation of EP2 and EP4 prostanoid receptors by prostaglandin E2. J Biol Chem 2002;277:2614–9.
[174] Bastien L, Sawyer N, Grygorczyk R, Metters K, Adam M. Cloning, functional expression, and characterization of the human prostaglandin E_2 receptor EP_2 subtype. J Biol Chem 1994;269:11873–7.
[175] Narko K, Saukkonen K, Ketola I, Butzow R, Heikinheimo M, Ristimaki A. Regulated expression of prostaglandin E(2) receptors EP2 and EP4 in human ovarian granulosa-luteal cells. J Clin Endocrinol Metab 2001;86:1765–8.
[176] Segi E, Sugimoto Y, Yamasaki A, Aze Y, Oida H, Nishimura T, et al. Patent ductus arteriosus and neonatal death in prostaglandin receptor EP4-deficient mice. Biochem Biophys Res Commun 1998;246:7–12.
[177] Lawrence RA, Jones RL. Investigation of the prostaglandin E (EP-) receptor subtype mediating relaxation of the rabbit jugular vein. Br J Pharmacol 1992;105:817–24.
[178] Schweda F, Klar J, Narumiya S, Nusing RM, Kurtz A. Stimulation of renin release by prostaglandin E2 is mediated by EP2 and EP4 receptors in mouse kidneys. Am J Physiol Renal Physiol 2004;287:F427–33.
[179] Bugge JF, Stokke ES, Vikse A, Kiil F. Stimulation of renin release by PGE2 and PGI2 infusion in the dog: enhancing effect of ureteral occlusion or administration of ethacrynic acid. Acta Physiol Scand 1990;138:193–201.
[180] Ito S, Carretero OA, Abe K, Beierwaltes WH, Yoshinaga K. Effect of prostanoids on renin release from rabbit afferent arterioles with and without macula densa. Kidney Int 1989; 35:1138–44.
[181] Nusing RM, Treude A, Weissenberger C, Jensen B, Bek M, Wagner C, et al. Dominant role of prostaglandin E2 EP4 receptor in furosemide-induced salt-losing tubulopathy: a model for hyperprostaglandin E syndrome/antenatal Bartter syndrome. J Am Soc Nephrol 2005;16:2354–62.
[182] Tan SY, Shapiro R, Franco R, Stockard H, Mulrow PJ. Indomethacin-induced prostaglandin inhibition with hyperkalemia. A reversible cause of hyporeninemic hypoaldosteronism. Ann Intern Med 1979;90:783–5.
[183] Kammerl MC, Nusing RM, Richthammer W, Kramer BK, Kurtz A. Inhibition of COX-2 counteracts the effects of diuretics in rats. Kidney Int 2001;60:1684–91.
[184] Reinalter SC, Jeck N, Brochhausen C, Watzer B, Nusing RM, Seyberth HW, et al. Role of cyclooxygenase-2 in hyperprostaglandin E syndrome/antenatal Bartter syndrome. Kidney Int 2002;62:253–60.
[185] Harding P, Sigmon DH, Alfie ME, Huang PL, Fishman MC, Beierwaltes WH, et al. Cyclooxygenase-2 mediates increased renal renin content induced by low-sodium diet. Hypertension 1997;29:297–302.
[186] Blackshear JL, Davidman M, Stillman MT. Identification of risk for renal insufficiency from nonsteroidal anti-inflammatory drugs. Arch Intern Med 1983;143:1130–4.
[187] Hockel G, Cowley A. Prostaglandin E2-induced hypertension in conscious dogs. Am J Physiol 1979;237:H449–54.
[188] Oliver JA, Pinto J, Sciacca RR, Cannon PJ. Increased renal secretion of norepinephrine and prostaglandin E2 during sodium depletion in the dog. J Clin Invest 1980;66:748–56.
[189] Hartner A, Cordasic N, Goppelt-Struebe M, Veelken R, Hilgers KF. Role of macula densa cyclooxygenase-2 in renovascular hypertension. Am J Physiol Renal Physiol 2002;:.
[190] Ahmad SR, Kortepeter C, Brinker A, Chen M, Beitz J. Renal failure associated with the use of celecoxib and rofecoxib. Drug Saf 2002;25:537–44.
[191] Perneger TV, Whelton PK, Klag MJ. Risk of kidney failure associated with the use of acetaminophen, aspirin, and nonsteroidal antiinflammatory drugs. N Engl J Med 1994;331: 1675–9.
[192] Yussim E, Schwartz E, Sidi Y, Ehrenfeld M. Acute renal failure precipitated by non-steroidal anti-inflammatory drugs (NSAIDs) in multiple myeloma. Am J Hematol 1998;58:142–4.
[193] Bek MJ, Wahle S, Muller B, Benzing T, Huber TB, Kretzler M, et al. Stra13, a prostaglandin E2-induced gene, regulates the cellular redox state of podocytes. Faseb J 2003;17:682–4.
[194] Martineau LC, McVeigh LI, Jasmin BJ, Kennedy CR. p38 MAP kinase mediates mechanically induced COX-2 and PG EP4 receptor expression in podocytes: implications for the actin cytoskeleton. Am J Physiol Renal Physiol 2004;286:F693–701.
[195] Stitt-Cavanagh EM, Faour WH, Takami K, Carter A, Vanderhyden B, Guan Y, et al. A maladaptive role for EP4 receptors in podocytes. J Am Soc Nephrol 2010;21:1678–90.
[196] Muro S, Tanaka I, Usui T, Kotani M, Koide S, Mukoyama M, et al. Expression of prostaglandin E receptor EP4 subtype in

rat adrenal zona glomerulosa: involvement in aldosterone release. Endocr J 2000;47:429–36.
[197] Galler M, Folkert VW, Schlondorff D. Reversible acute renal insufficiency and hyperkalemia following indomethacin therapy. JAMA 1981;246:154–5.
[198] Miller KP, Lazar EJ, Fotino S. Severe hyperkalemia during piroxicam therapy. Arch Intern Med 1984;144:2414–5.
[199] Inada M, Iwasaki K, Imai C, Hashimoto S. Hyperpotassemia and bradycardia in a bedridden elderly woman with selective hypoaldosteronism associated with low renin activity. Intern Med 2010;49:307–13.
[200] Baxter GS, Clayton JK, Coleman RA, Marshall K, Sangha R, Senior J. Characterization of the prostanoid receptors mediating constriction and relaxation of human isolated uterine artery. Br J Pharmacol 1995;116:1692–6.
[201] Kabashima K, Sakata D, Nagamachi M, Miyachi Y, Inaba K, Narumiya S. Prostaglandin E(2)-EP4 signaling initiates skin immune responses by promoting migration and maturation of Langerhans cells. Nat Med 2003;9:744–9.
[202] Miyaura C, Inada M, Suzawa T, Sugimoto Y, Ushikubi F, Ichikawa A, et al. Impaired bone resorption to prostaglandin E2 in prostaglandin E receptor EP4-knockout mice. J Biol Chem 2000;275:19819–23.
[203] Yoshida K, Oida H, Kobayashi T, Maruyama T, Tanaka M, Katayama T, et al. Stimulation of bone formation and prevention of bone loss by prostaglandin E EP4 receptor activation. Proc Natl Acad Sci USA 2002;99:4580–5.
[204] Watanabe K. Prostaglandin F synthase. Prostaglandins Other Lipid Mediat 2002;68-69:401–7.
[205] Lee SC, Levine L. Purification and regulatory properties of chicken heart prostaglandin E 9-ketoreductase. J Biol Chem 1975;250:4549–55.
[206] Roberts II LJ, Seibert K, Liston TE, Tantengco MV, Robertson RM. PGD2 is transformed by human coronary arteries to 9 alpha, 11 beta-PGF2, which contracts human coronary artery rings. Adv Prostaglandin Thromboxane Leukot Res 1987;17A:427–9.
[207] Sharif NA, Xu SX, Williams GW, Crider JY, Griffin BW, Davis TL. Pharmacology of [3H]prostaglandin E1/[3H]prostaglandin E2 and [3H]prostaglandin F2alpha binding to EP3 and FP prostaglandin receptor binding sites in bovine corpus luteum: characterization and correlation with functional data. J Pharmacol Exp Ther 1998;286:1094–102.
[208] Wallner EI, Wada J, Tramonti G, Lin S, Srivastava SK, Kanwar YS. Relevance of aldo-keto reductase family members to the pathobiology of diabetic nephropathy and renal development. Ren Fail 2001;23:311–20.
[209] Siragy HM, Senbonmatsu T, Ichiki T, Inagami T, Carey RM. Increased renal vasodilator prostanoids prevent hypertension in mice lacking the angiotensin subtype-2 receptor. J Clin Invest 1999;104:181–8.
[210] Siragy HM, Inagami T, Ichiki T, Carey RM. Sustained hypersensitivity to angiotensin II and its mechanism in mice lacking the subtype-2 (AT2) angiotensin receptor. Proc Natl Acad Sci USA 1999;96:6506–10.
[211] Siragy HM, Carey RM. The subtype 2 angiotensin receptor regulates renal prostaglandin F2 alpha formation in conscious rats. Am J Physiol 1997;273:R1103–7.
[212] Abramovitz M, Boie Y, Nguyen T, Rushmore TH, Bayne MA, Metters KM, et al. Cloning and expression of a cDNA for the human prostanoid FP receptor. J Biol Chem 1994;269:2632–6.
[213] Griffin BW, Williams GW, Crider JY, Sharif NA. FP prostaglandin receptors mediating inositol phosphates generation and calcium mobilization in Swiss 3T3 cells: a pharmacological study. J Pharmacol Exp Ther 1997;281:845–54.
[214] Kelly CR, Williams GW, Sharif NA. Real-time intracellular Ca^{2+} mobilization by travoprost acid, bimatoprost, unoprostone, and other analogs via endogenous mouse, rat, and cloned human FP prostaglandin receptors. J Pharmacol Exp Ther 2003;304:238–45.
[215] Woodward DF, Lawrence RA. Identification of a single (FP) receptor associated with prostanoid-induced Ca^{2+} signals in Swiss 3T3 cells. Biochem Pharmacol 1994;47:1567–74.
[216] Sugimoto Y, Yamasaki A, Segi E, Tsuboi K, Aze Y, Nishimura T, et al. Failure of parturition in mice lacking the prostaglandin F receptor. Science 1997;277:681–3.
[217] Chollet A, Tos EG, Cirillo R. Tocolytic effect of a selective FP receptor antagonist in rodent models reveals an innovative approach to the treatment of preterm labor. BMC Pregnancy Childbirth 2007;7(Suppl. 1):S16.
[218] Griffin BW, Klimko P, Crider JY, Sharif NA. AL-8810: a novel prostaglandin F2 alpha analog with selective antagonist effects at the prostaglandin F2 alpha (FP) receptor. J Pharmacol Exp Ther 1999;290:1278–84.
[219] Sharif NA, Kelly CR, Crider JY. Agonist activity of bimatoprost, travoprost, latanoprost, unoprostone isopropyl ester and other prostaglandin analogs at the cloned human ciliary body FP prostaglandin receptor. J Ocul Pharmacol Ther 2002;18:313–24.
[220] Saito O, Guan Y, Qi Z, Davis LS, Komhoff M, Sugimoto Y, et al. Expression of the prostaglandin F receptor (FP) gene along the mouse genitourinary tract. Am J Physiol Renal Physiol 2003;284:F1164–70.
[221] Yu Y, Lucitt MB, Stubbe J, Cheng Y, Friis UG, Hansen PB, et al. Prostaglandin F2alpha elevates blood pressure and promotes atherosclerosis. Proc Natl Acad Sci USA 2009;106:7985–90.
[222] Urade Y, Eguchi N. Lipocalin-type and hematopoietic prostaglandin D synthases as a novel example of functional convergence. Prostaglandins & Other Lipid Mediators 2002;68-69:375–82.
[223] Shimura C, Satoh T, Igawa K, Aritake K, Urade Y, Nakamura M, et al. Dendritic cells express hematopoietic prostaglandin D synthase and function as a source of prostaglandin D2 in the skin. Am J Pathol 2010;176:227–37.
[224] Vitzthum H, Abt I, Einhellig S, Kurtz A. Gene expression of prostanoid forming enzymes along the rat nephron. Kidney Int 2002;62:1570–81.
[225] Qu WM, Huang ZL, Xu XH, Aritake K, Eguchi N, Nambu F, et al. Lipocalin-type prostaglandin D synthase produces prostaglandin D2 involved in regulation of physiological sleep. Proc Natl Acad Sci USA 2006;103:17949–54.
[226] Eguchi N, Minami T, Shirafuji N, Kanaoka Y, Tanaka T, Nagata A, et al. Lack of tactile pain (allodynia) in lipocalin-type prostaglandin D synthase-deficient mice. Proc Natl Acad Sci USA 1999;96:726–30.
[227] Nakayama H, Echizen H, Gomi T, Shibuya Y, Nakamura Y, Nakano K, et al. Urinary lipocalin-type prostaglandin D synthase: a potential marker for early gentamicin-induced renal damage? Ther Drug Monit 2009;31:126–30.
[228] Uehara Y, Makino H, Seiki K, Urade Y. Urinary excretions of lipocalin-type prostaglandin D synthase predict renal injury in type-2 diabetes: a cross-sectional and prospective multicentre study. Nephrol Dial Transplant 2009;24:475–82.
[229] Ogawa M, Hirawa N, Tsuchida T, Eguchi N, Kawabata Y, Numabe A, et al. Urinary excretions of lipocalin-type prostaglandin D2 synthase predict the development of proteinuria and renal injury in OLETF rats. Nephrol Dial Transplant 2006;21:924–34.
[230] Tsuchida T, Eguchi N, Eguchi Y, Numabe A, Nakajima H, Oda H, et al. Lipocalin-type prostaglandin D synthase in urine in adriamycin-induced nephropathy of mice. Nephron Physiol 2004;96:p42–51.

[231] Ragolia L, Palaia T, Hall CE, Maesaka JK, Eguchi N, Urade Y. Accelerated glucose intolerance, nephropathy, and atherosclerosis in prostaglandin D2 synthase knock-out mice. J Biol Chem 2005;280:29946–55.
[232] Kanaoka Y, Ago H, Inagaki E, Nanayama T, Miyano M, Kikuno R, et al. Cloning and crystal structure of hematopoietic prostaglandin D synthase. Cell 1997;90:1085–95.
[233] Kanaoka Y, Urade Y. Hematopoietic prostaglandin D synthase. Prostaglandins Leukot Essent Fatty Acids 2003;69:163–7.
[234] Boie Y, Sawyer N, Slipetz DM, Metters KM, Abramovitz M. Molecular cloning and characterization of the human prostanoid DP receptor. J Biol Chem 1995;270:18910–6.
[235] Wright DH, Nantel F, Metters KM, Ford-Hutchinson AW. A novel biological role for prostaglandin D2 is suggested by distribution studies of the rat DP prostanoid receptor. Eur J Pharmacol 1999;377:101–15.
[236] Hirai H, Tanaka K, Yoshie O, Ogawa K, Kenmotsu K, Takamori Y, et al. Prostaglandin D2 selectively induces chemotaxis in T helper type 2 cells, eosinophils, and basophils via seven-transmembrane receptor CRTH2. J Exp Med 2001;193: 255–62.
[237] Toh H, Ichikawa A, Narumiya S. Molecular evolution of receptors for eicosanoids. FEBS Letters 1995;361:17–21.
[238] Kabashima K, Narumiya S. The DP receptor, allergic inflammation and asthma. Prostaglandins Leukot Essent Fatty Acids 2003;69:187–94.
[239] Koch KA, Wessale JL, Moreland R, Reinhart GA, Cox BF. Effects of BW245C, a prostaglandin dp receptor agonist, on systemic and regional haemodynamics in the anaesthetized rat. Clin Exp Pharmacol Physiol 2005;32:931–5.
[240] Hoeper MM, Schwarze M, Ehlerding S, Adler-Schuermeyer A, Spiekerkoetter E, Niedermeyer J, et al. Long-term treatment of primary pulmonary hypertension with aerosolized iloprost, a prostacyclin analogue. N Engl J Med 2000;342:1866–70.
[241] Yokoyama C, Yabuki T, Inoue H, Tone Y, Hara S, Hatae T, et al. Human gene encoding prostacyclin synthase (PTGIS): Genomic organization, chromosomal localization, and promoter activity. Genomics 1996;36:296–304.
[242] Tone Y, Inoue H, Hara S, Yokoyama C, Hatae T, Oida H, et al. The regional distribution and cellular localization of mRNA encoding rat prostacyclin synthase. Eur J Cell Biol 1997;72: 268–77.
[243] Yokoyama C, Yabuki T, Shimonishi M, Wada M, Hatae T, Ohkawara S, et al. Prostacyclin-deficient mice develop ischemic renal disorders, including nephrosclerosis and renal infarction. Circulation 2002;106:2397–403.
[244] Murata T, Ushikubi F, Matsuoka T, Hirata M, Yamasaki A, Sugimoto Y, et al. Altered pain perception and inflammatory response in mice lacking prostacyclin receptor. Nature 1997;388: 678–82.
[245] Hao CM, Redha R, Morrow J, Breyer MD. Peroxisome proliferator-activated receptor delta activation promotes cell survival following hypertonic stress. J Biol Chem 2002;277:21341–5.
[246] Lim H, Gupta RA, Ma WG, Paria BC, Moller DE, Morrow JD, et al. Cyclo-oxygenase-2-derived prostacyclin mediates embryo implantation in the mouse via PPARdelta. Genes Dev 1999; 13:1561–74.
[247] Namba T, Oida H, Sugimoto Y, Kakizuka A, Negishi M, Ichikawa A, et al. cDNA cloning of a mouse prostacyclin receptor: multiple signaling pathways and expression in thymic medulla. J Biol Chem 1994;269:9986–92.
[248] Oida H, Namba T, Sugimoto Y, Ushikubi F, Ohishi H, Ichikawa A, et al. In situ hybridization studies on prostacyclin receptor mRNA expression in various mouse organs. Br J Pharmacol 1995;116:2828–37.
[249] Fujino T, Nakagawa N, Yuhki K, Hara A, Yamada T, Takayama K, et al. Decreased susceptibility to renovascular hypertension in mice lacking the prostaglandin I2 receptor IP. J Clin Invest 2004;114:805–12.
[250] Egan KM, Lawson JA, Fries S, Koller B, Rader DJ, Smyth EM, et al. COX-2-derived prostacyclin confers atheroprotection on female mice. Science 2004;306:1954–7.
[251] Chevalier D, Lo-Guidice JM, Sergent E, Allorge D, Debuysere H, Ferrari N, et al. Identification of genetic variants in the human thromboxane synthase gene (CYP5A1). Mutat Res 2001; 432:61–7.
[252] Miyata A, Yokoyama C, Ihara H, Bandoh S, Takeda O, Takahashi E, et al. Characterization of the human gene (TBXAS1) encoding thromboxane synthase. Eur J Biochem 1994; 224:273–9.
[253] Zhang LQ, Chase MB, Shen RF. Molecular cloning and expression of murine thromboxane synthase. Biochem Biophys Res Commun 1993;194:741–8.
[254] Nusing R, Fehr PM, Gudat F, Kemeny E, Mihatsch MJ, Ullrich V. The localization of thromboxane synthase in normal and pathological human kidney tissue using a monoclonal antibody Tu 300. Virchows Arch 1994;424:69–74.
[255] Wilcox CS, Welch WJ. Thromboxane synthase and TP receptor mRNA in rat kidney and brain: effects of salt intake and ANG II. Am J Physiol Renal Physiol 2003;284:F525–31.
[256] Quest DW, Wilson TW. Effects of ridogrel, a thromboxane synthase inhibitor and receptor antagonist, on blood pressure in the spontaneously hypertensive rat. Jpn J Pharmacol 1998; 78:479–86.
[257] Vezza R, Mezzasoma AM, Venditti G, Gresele P. Prostaglandin endoperoxides and thromboxane A2 activate the same receptor isoforms in human platelets. Thromb Haemost 2002;87:114–21.
[258] Hirata M, Hayashi Y, Ushikubi F, Yokota Y, Kageyama R, Nakanishi S, et al. Cloning and expression of cDNA for a human thromboxane A2 receptor. Nature 1991;349:617–20.
[259] Abe T, Takeuchi K, Takahashi N, Tsutsumi E, Taniyama Y, Abe K. Rat kidney thromboxane receptor: molecular cloning, signal transduction, and intrarenal expression localization. J Clin Invest 1995;96:657–64.
[260] Francois H, Athirakul K, Mao L, Rockman H, Coffman TM. Role for thromboxane receptors in angiotensin-II-induced hypertension. Hypertension 2004;43:364–9.
[261] Boffa JJ, Just A, Coffman TM, Arendshorst WJ. Thromboxane receptor mediates renal vasoconstriction and contributes to acute renal failure in endotoxemic mice. J Am Soc Nephrol 2004;15:2358–65.
[262] Schnermann J, Traynor T, Pohl H, Thomas DW, Coffman TM, Briggs JP. Vasoconstrictor responses in thromboxane receptor knockout mice: Tubuloglomerular feedback and ureteral obstruction. Acta Physiol Scand 2000;168:201–7.
[263] Snoeijs MG, Hoogland PR, Boonen B, Coffman TM, Peutz-Kootstra CJ, Buurman WA, et al. Thromboxane receptor signalling in renal ischemia reperfusion injury. Free Radic Res 2011;45:699–706.
[264] Schuster VL. Prostaglandin transport. Prostaglandins Other Lipid Mediat 2002;68-69:633–47.
[265] Kanai N, Lu R, Satriano JA, Bao Y, Wolkoff AW, Schuster VL. Identification and characterization of a prostaglandin transporter. Science 1995;268:866–9.
[266] Chang HY, Locker J, Lu R, Schuster VL. Failure of postnatal ductus arteriosus closure in prostaglandin transporter-deficient mice. Circulation 2010;121:529–36.
[267] Bao Y, Pucci ML, Chan BS, Lu R, Ito S, Schuster VL. Prostaglandin transporter PGT is expressed in cell types that

synthesize and release prostanoids. Am J Physiol Renal Physiol 2002;282:F1103–10.
[268] Reid G, Wielinga P, Zelcer N, van der Heijden I, Kuil A, de Haas M, et al. The human multidrug resistance protein MRP4 functions as a prostaglandin efflux transporter and is inhibited by nonsteroidal antiinflammatory drugs. Proceedings of the National Academy of Sciences 2003;100:9244–9.
[269] Lin ZP, Zhu Y -L, Johnson DR, Rice KP, Nottoli T, Hains BC, et al. Disruption of cAMP and prostaglandin E2 transport by multidrug resistance protein 4 deficiency alters cAMP-mediated signaling and nociceptive response. Mol Pharmacol 2008; 73:243–51.
[270] Tomasoni S, Zappella S, Gotti E, Casiraghi F, Bonazzola S, Benigni A, et al. Upregulation of renal and systemic cyclooxygenase-2 in patients with active lupus nephritis. J Am Soc Nephrol 1998;9:1202–12.
[271] Schneider A, Harendza S, Zahner G, Jocks T, Wenzel U, Wolf G, et al. Cyclooxygenase metabolites mediate glomerular monocyte chemoattractant protein-1 formation and monocyte recruitment in experimental glomerulonephritis [see comments]. Kidney Int 1999;55:430–41.
[272] Zoja C, Benigni A, Verroust P, Ronco P, Bertani T, Remuzzi G. Indomethacin reduces proteinuria in passive Heymann nephritis in rats. Kidney Int 1987;31:1335–43.
[273] Takano T, Cybulsky AV, Cupples WA, Ajikobi DO, Papillon J, Aoudjit L. Inhibition of cyclooxygenases reduces complement-induced glomerular epithelial cell injury and proteinuria in passive Heymann nephritis. J Pharmacol Exp Ther 2003; 305:240–9.
[274] Kitahara M, Eitner F, Ostendorf T, Kunter U, Janssen U, Westenfeld R, et al. Selective cyclooxygenase-2 inhibition impairs glomerular capillary healing in experimental glomerulonephritis. J Am Soc Nephrol 2002;13:1261–70.
[275] Anderson GD, Hauser SD, McGarity KL, Bremer ME, Isakson PC, Gregory SA. Selective inhibition of cyclooxygenase (COX)-2 reverses inflammation and expression of COX-2 and interleukin 6 in rat adjuvant arthritis. J Clin Invest 1996;97:2672–9.
[276] Simon LS. Role and regulation of cyclooxygenase-2 during inflammation. Am J Med 1999;106:37S–42S.
[277] Mauer SM, Steffes MW, Ellis EN, Sutherland DE, Brown DM, Goetz FC. Structural–functional relationships in diabetic nephropathy. J Clin Invest 1984;74:1143–55.
[278] Najafian B, Alpers CE, Fogo AB. Pathology of human diabetic nephropathy. Contrib Nephrol 2011;170:36–47.
[279] Ciavarella A, Galuppi V, Forlani G, Vannini P. The prevalence of glomerular hyperfiltration in type 1 (insulin-dependent) diabetes mellitus. Diabete Metab 1988;14:73–4.
[280] Levine DZ, Iacovitti M, Robertson SJ, Mokhtar GA. Modulation of single-nephron GFR in the db/db mouse model of type 2 diabetes mellitus. Am J Physiol Regul Integr Comp Physiol 2006;290:R975–81.
[281] Qi Z, Fujita H, Jin J, Davis LS, Wang Y, Fogo AB, et al. Characterization of susceptibility of inbred mouse strains to diabetic nephropathy. Diabetes 2005;54:2628–37.
[282] Viberti GC, Benigni A, Bognetti E, Remuzzi G, Wiseman MJ. Glomerular hyperfiltration and urinary prostaglandins in type 1 diabetes mellitus. Diabet Med 1989;6:219–23.
[283] Craven PA, Caines MA, DeRubertis FR. Sequential alterations in glomerular prostaglandin and thromboxane synthesis in diabetic rats: relationship to the hyperfiltration of early diabetes. Metabolism 1987;36:95–103.
[284] Mathiesen ER, Hommel E, Olsen UB, Parving HH. Elevated urinary prostaglandin excretion and the effect of indomethacin on renal function in incipient diabetic nephropathy. Diabet Med 1988;5:145–9.
[285] Moel DI, Safirstein RL, McEvoy RC, Hsueh W. Effect of aspirin on experimental diabetic nephropathy. J Lab Clin Med 1987; 110:300–7.
[286] Cheng HF, Wang CJ, Moeckel GW, Zhang MZ, McKanna JA, Harris RC. Cyclooxygenase-2 inhibitor blocks expression of mediators of renal injury in a model of diabetes and hypertension. Kidney Int 2002;62:929–39.
[287] Khan KN, Stanfield KM, Harris RK, Baron DA. Expression of cyclooxygenase-2 in the macula densa of human kidney in hypertension, congestive heart failure, and diabetic nephropathy. Ren Fail 2001;23:321–30.
[288] Komers R, Lindsley JN, Oyama TT, Schutzer WE, Reed JF, Mader SL, et al. Immunohistochemical and functional correlations of renal cyclooxygenase-2 in experimental diabetes. J Clin Invest 2001;107:889–98.
[289] Xu S, Jiang B, Maitland KA, Bayat H, Gu J, Nadler JL, et al. The thromboxane receptor antagonist S18886 attenuates renal oxidant stress and proteinuria in diabetic apolipoprotein E-deficient mice. Diabetes 2006;55:110–9.
[290] Pelayo JC, Shanley PF. Glomerular and tubular adaptive responses to acute nephron loss in the rat. Effect of prostaglandin synthesis inhibition. J Clin Invest 1990;85:1761–9.
[291] Wang JL, Cheng HF, Shappell S, Harris RC. A selective cyclooxygenase-2 inhibitor decreases proteinuria and retards progressive renal injury in rats. Kidney Int 2000;57:2334–42.
[292] Cheng H, Zhang M, Moeckel GW, Zhao Y, Wang S, Qi Z, et al. Expression of mediators of renal injury in the remnant kidney of ROP mice is attenuated by cyclooxygenase-2 inhibition. Nephron Exp Nephrol 2005;101:e75–85.
[293] Funk CD, Chen X -S, Johnson EN, Zhao L. Lipoxygenase genes and their targeted disruption. Prostaglandins & Other Lipid Mediators 2002;68-69:303–12.
[294] Brash AR. Lipoxygenases: occurrence, functions, catalysis, and acquisition of substrate. J Biol Chem 1999;274:23679–82.
[295] Duroudier NP, Tulah AS, Sayers I. Leukotriene pathway genetics and pharmacogenetics in allergy. Allergy 2009;64: 823–39.
[296] Peters-Golden M, Henderson Jr. WR. Leukotrienes. N Engl J Med 2007;357:1841–54.
[297] Rinaldo-Matthis A, Haeggstrom JZ. Structures and mechanisms of enzymes in the leukotriene cascade. Biochimie 2010; 92:676–81.
[298] Jawien J, Gajda M, Rudling M, Mateuszuk L, Olszanecki R, Guzik TJ, et al. Inhibition of five lipoxygenase activating protein (FLAP) by MK-886 decreases atherosclerosis in apoE/LDLR-double knockout mice. Eur J Clin Invest 2006;36: 141–6.
[299] Samuelsson B, Funk CD. Enzymes involved in the biosynthesis of leukotriene B4. J Biol Chem 1989;264:19469–72.
[300] Shimizu T, Yokomizo T, Izumi T. Leukotriene-B4 receptor and signal transduction. Ernst Schering Res Found Workshop 2000;:125–41.
[301] Kolaczkowska E, Shahzidi S, Seljelid R, van Rooijen N, Plytycz B. Early vascular permeability in murine experimental peritonitis is co-mediated by resident peritoneal macrophages and mast cells: crucial involvement of macrophage-derived cysteinyl-leukotrienes. Inflammation 2002;26:61–71.
[302] Porreca E, Di Febbo C, Di Sciullo A, Angelucci D, Nasuti M, Vitullo P, et al. Cysteinyl leukotriene D4 induced vascular smooth muscle cell proliferation: a possible role in myointimal hyperplasia. Thromb Haemost 1996;76:99–104.
[303] Farrukh IS, Sciuto AM, Spannhake EW, Gurtner GH, Michael JR. Leukotriene D4 increases pulmonary vascular permeability and pressure by different mechanisms in the rabbit. Am Rev Respir Dis 1986;134:229–32.

[304 Fiedler VB, Mardin M, Abram TS. Leukotriene D4-induced vasoconstriction of coronary arteries in anaesthetized dogs. Eur Heart J 1984;5:253–60.
[305] Collin M, Rossi A, Cuzzocrea S, Patel NS, Di Paola R, Hadley J, et al. Reduction of the multiple organ injury and dysfunction caused by endotoxemia in 5-lipoxygenase knockout mice and by the 5-lipoxygenase inhibitor zileuton. J Leukoc Biol 2004; 76:961–70.
[306] Patel NS, Cuzzocrea S, Chatterjee PK, Di Paola R, Sautebin L, Britti D, et al. Reduction of renal ischemia-reperfusion injury in 5-lipoxygenase knockout mice and by the 5-lipoxygenase inhibitor zileuton. Mol Pharmacol 2004;66:220–7.
[307] Kitagawa K, Matsumoto M, Hori M. Cerebral ischemia in 5-lipoxygenase knockout mice. Brain Res 2004;1004:198–202.
[308] Di Gennaro A, Wågsäter D, Mäyränpää MI, Gabrielsen A, Swedenborg J, Hamsten A, et al. Increased expression of leukotriene C4 synthase and predominant formation of cysteinyl-leukotrienes in human abdominal aortic aneurysm. Proc Natl Acad Sci 2010;107:21093–7.
[309] Ardaillou R, Baud L, Sraer J. Leukotrienes and other lipoxygenase products of arachidonic acid synthesized in the kidney. Am J Med 1986;81:12–22.
[310] Badr KF. 15-Lipoxygenase products as leukotriene antagonists: Therapeutic potential in glomerulonephritis. Kidney Int Suppl 1992;38:S101–8.
[311] Kawasaki Y, Tanji M, Takano K, Fukuda Y, Isome M, Nozawa R, et al. The leukotriene B4 receptor antagonist ONO-4057 inhibits mesangioproliferative changes in anti-Thy-1 nephritis. Nephrology Dialysis Transplantation 2005;20:2697–703.
[312] Reinhold SW, Vitzthum H, Filbeck T, Wolf K, Lattas C, Riegger GA, et al. Gene expression of 5-, 12-, and 15-lipoxygenases and leukotriene receptors along the rat nephron. Am J Physiol Renal Physiol 2006;290:F864–72.
[313] Menegatti E, Roccatello D, Fadden K, Piccoli G, De Rosa G, Sena LM, et al. Gene expression of 5-lipoxygenase and LTA4 hydrolase in renal tissue of nephrotic syndrome patients. Clin Exp Immunol 1999;116:347–53.
[314] Badr KF. Five-lipoxygenase products in glomerular immune injury. J Am Soc Nephrol 1992;3:907–15.
[315] Katoh T, Lianos EA, Fukunaga M, Takahashi K, Badr KF. Leukotriene D4 is a mediator of proteinuria and glomerular hemodynamic abnormalities in passive Heymann nephritis. J Clin Invest 1993;91:1507–15.
[316] Natarajan R, Nadler JL. Lipid inflammatory mediators in diabetic vascular disease. Arterioscler Thromb Vasc Biol 2004; 24:1542–8.
[317] Dailey LA, Imming P. 12-Lipoxygenase: classification, possible therapeutic benefits from inhibition, and inhibitors. Curr Med Chem 1999;6:389–98.
[318] Zhao L, Moos MP, Grabner R, Pedrono F, Fan J, Kaiser B, et al. The 5-lipoxygenase pathway promotes pathogenesis of hyperlipidemia-dependent aortic aneurysm. Nat Med 2004; 10:966–73.
[319] Klein RF, Allard J, Avnur Z, Nikolcheva T, Rotstein D, Carlos AS, et al. Regulation of bone mass in mice by the lipoxygenase gene Alox15. Science 2004;303:229–32.
[320] Poeckel D, Funk CD. The 5-lipoxygenase/leukotriene pathway in preclinical models of cardiovascular disease. Cardiovasc Res 2010;86:243–53.
[321] Kang SW, Natarajan R, Shahed A, Nast CC, LaPage J, Mundel P, et al. Role of 12-lipoxygenase in the stimulation of p38 mitogen-activated protein kinase and collagen alpha5(IV) in experimental diabetic nephropathy and in glucose-stimulated podocytes. J Am Soc Nephrol 2003;14:3178–87.
[322] Kim YS, Xu ZG, Reddy MA, Li SL, Lanting L, Sharma K, et al. Novel interactions between TGF-{beta}1 actions and the 12/15-lipoxygenase pathway in mesangial cells. J Am Soc Nephrol 2005;16:352–62.
[323] Xu ZG, Li SL, Lanting L, Kim YS, Shanmugam N, Reddy MA, et al. Relationship between 12/15-lipoxygenase and COX-2 in mesangial cells: potential role in diabetic nephropathy. Kidney Int 2006;69:512–9.
[324] Gonzalez-Nunez D, Sole M, Natarajan R, Poch E. 12-Lipoxygenase metabolism in mouse distal convoluted tubule cells. Kidney Int 2005;67:178–86.
[325] Kang SW, Adler SG, Nast CC, LaPage J, Gu JL, Nadler JL, et al. 12-lipoxygenase is increased in glucose-stimulated mesangial cells and in experimental diabetic nephropathy. Kidney Int 2001;59:1354–62.
[326] Guo QY, Miao LN, Li B, Ma FZ, Liu N, Cai L, et al. Role of 12-lipoxygenase in decreasing P-cadherin and increasing angiotensin II type 1 receptor expression according to glomerular size in type 2 diabetic rats. Am J Physiol Endocrinol Metab 2011;300:E708–16.
[327] Xu ZG, Miao LN, Cui YC, Jia Y, Yuan H, Wu M. Angiotensin II type 1 receptor expression is increased via 12-lipoxygenase in high glucose-stimulated glomerular cells and type 2 diabetic glomeruli. Nephrol Dial Transplant 2009;24:1744–52.
[328] Capdevila JH, Harris RC, Falck JR. Microsomal cytochrome P450 and eicosanoid metabolism. Cell Mol Life Sci 2002; 59:780–9.
[329] McGiff JC. Cytochrome P-450 metabolism of arachidonic acid. Annu Rev Pharmacol Toxicol 1991;31:339–69.
[330] Camara NO, Martins JO, Landgraf RG, Jancar S. Emerging roles for eicosanoids in renal diseases. Curr Opin Nephrol Hypertens 2009;18:21–7.
[331] Spector AA. Arachidonic acid cytochrome P450 epoxygenase pathway. J Lipid Res 2009;50(Suppl.):S52–6.
[332] Kroetz DL, Zeldin DC. Cytochrome P450 pathways of arachidonic acid metabolism. Curr Opin Lipidol 2002;13:273–83.
[333] Scarborough PE, Ma J, Qu W, Zeldin DC. P450 subfamily CYP2J and their role in the bioactivation of arachidonic acid in extrahepatic tissues. Drug Metab Rev 1999;31:205–34.
[334] Lasker JM, Chen WB, Wolf I, Bloswick BP, Wilson PD, Powell PK. Formation of 20-hydroxyeicosatetraenoic acid, a vasoactive and natriuretic eicosanoid, in human kidney. Role of Cyp4F2 and Cyp4A11. J Biol Chem 2000;275:4118–26.
[335] Roman RJ. P-450 Metabolites of arachidonic acid in the control of cardiovascular function. Physiol Rev 2002;82:131–85.
[336] Imig J, Gebremedhin D, Zou A, Stec D, Harder D, Falck J, et al. Formation and actions of 20-hydroxyeicosatetraenoic acid in the renal microcirculation. Am J Physiol 1996;270:R217–27.
[337] Larsen BT, Gutterman DD, Hatoum OA. Emerging role of epoxyeicosatrienoic acids in coronary vascular function. Eur J Clin Invest 2006;36:293–300.
[338] Oltman CL, Weintraub NL, VanRollins M, Dellsperger KC. Epoxyeicosatrienoic acids and dihydroxyeicosatrienoic acids are potent vasodilators in the canine coronary microcirculation. Circ Res 1998;83:932–9.
[339] Wei Y, Lin DH, Kemp R, Yaddanapudi GS, Nasjletti A, Falck JR, et al. Arachidonic acid inhibits epithelial Na channel via cytochrome P450 (CYP) epoxygenase-dependent metabolic pathways. J Gen Physiol 2004;124:719–27.
[340] Wang S, Meng F, Xu J, Gu Y. Effects of lipids on ENaC activity in cultured mouse cortical collecting duct cells. J Membr Biol 2009;227:77–85.
[341] Sun P, Lin DH, Yue P, Jiang H, Gotlinger KH, Schwartzman ML, et al. High potassium intake enhances the inhibitory effect of 11,12-EET on ENaC. J Am Soc Nephrol 2010;21:1667–77.
[342] Athirakul K, Bradbury JA, Graves JP, DeGraff LM, Ma J, Zhao Y, et al. Increased blood pressure in mice lacking cytochrome P450 2J5. FASEB J 2008;22:4096–108.

[343] Holla VR, Adas F, Imig JD, Zhao X, Price Jr. E, Olsen N, et al. Alterations in the regulation of androgen-sensitive Cyp 4a monooxygenases cause hypertension. Proc Natl Acad Sci USA 2001;98:5211–6.

[344] Nakagawa K, Holla VR, Wei Y, Wang WH, Gatica A, Wei S, et al. Salt-sensitive hypertension is associated with dysfunctional Cyp4a10 gene and kidney epithelial sodium channel. J Clin Invest 2006;116:1696–702.

[345] Miyazono M, Zhu D, Nemenoff R, Jacobs ER, Carter EP. Increased epoxyeicosatrienoic acid formation in the rat kidney during liver cirrhosis. J Am Soc Nephrol 2003;14:1766–75.

[346] Hercule H, Oyekan A. Renal cytochrome p450 oxygenases and preglomerular vascular response to arachidonic acid and endothelin-1 following ischemia/reperfusion. J Pharmacol Exp Ther 2002;302:717–24.

[347] McCarthy ET, Sharma R, Sharma M. Protective effect of 20-hydroxyeicosatetraenoic acid (20-HETE) on glomerular protein permeability barrier. Kidney Int 2005;67:152–6.

[348] Yuhki K -I, Kojima F, Kashiwagi H, Kawabe J -I, Fujino T, Narumiya S, et al. Roles of prostanoids in the pathogenesis of cardiovascular diseases: novel insights from knockout mouse studies. Pharm Therap 2011;129:195–205.

This page intentionally left blank

CHAPTER

18

Extracellular Nucleotides and Renal Function

David G. Shirley[1], *Matthew A. Bailey*[2], *Scott S. P. Wildman*[3], *Frederick W. K. Tam*[4] *and Robert J. Unwin*[1]

[1]UCL Centre for Nephrology, University College London Medical School, UK
[2]British Heart Foundation Centre for Cardiovascular Science, University of Edinburgh, UK
[3]Medway School of Pharmacy, The Universities of Kent and Greenwich at Medway, UK
[4]Kidney and Transplant Institute, Imperial College School of Medicine, UK

Historically, the control of renal vascular and tubular function has been attributed solely to neural and endocrine regulation. However, in addition to these extrinsic factors, it is now recognized that several complex humoral control systems exist *within* the kidney that act in an autocrine and/or paracrine manner. One of these is the extracellular nucleotide/P2 receptor system.

Although physiological actions of extracellular adenine nucleotides were reported as long ago as 1929,[34] it was not until many years later (1972) that the importance of ATP as a transmitter for non-adrenergic, non-cholinergic neurones of the autonomic nervous system was proposed by Geoffrey Burnstock.[13] Since then it has become apparent that the function of extracellular nucleotides is not confined to neurones: rather, they are ubiquitous autocrine/paracrine agents regulating diverse physiological processes in almost every tissue in the body. Information on their roles in the kidneys has only really begun to emerge in the last decade.

P2 RECEPTORS

Extracellular nucleotides exert their effects by binding to and activating cell surface located receptors; P2 receptors. These are subdivided into P2X receptors, of which seven mammalian subunits have been cloned ($P2X_{1-7}$), and P2Y receptors, of which eight mammalian subtypes are currently recognized, $P2Y_{1,\ 2,\ 4,\ 6,}$ and $P2Y_{11-14}$.[14]

P2X Receptors

P2X receptor subunits are proteins with two transmembrane-spanning regions, the N- and C-termini being within the cell.[114] Three P2X subunits assemble to form a P2X receptor ion channel that, when activated, is permeable to small cations (Na^+, K^+, Ca^{2+}). Each of the seven P2X subunits can make homomeric ion channels, and can also form heteromeric assemblies involving more than one type of subunit. Until recently it had been thought that $P2X_7$ subunits could only make homomeric assemblies, but a $P2X_{4/7}$ heteromer has now been described.[51] As well as a non-selective ion channel, the $P2X_7$ receptor can form a larger membrane pore, and initiate cell death by necrosis or apoptosis.

The principal natural ligand for all P2X subunits is ATP. The $P2X_1$ subunit is the most sensitive (requiring sub-micromolar concentrations of ATP); $P2X_{2-6}$ subunits require micromolar concentrations, while the $P2X_7$ subunit is easily the least sensitive, requiring almost millimolar concentrations.

P2Y Receptors

P2Y receptors are G-protein-coupled receptors with seven transmembrane-spanning regions; the C-terminus is inside the cell and the N-terminus extracellular. In rodents, ATP is probably the principal natural ligand for $P2Y_{2,\ 4,}$ and $P2Y_{11}$ subtypes and, at sufficiently high dose and/or receptor density, can activate $P2Y_{1,\ 12,}$ and $P2Y_{13}$

Seldin and Giebisch's The Kidney, Fifth Edition.
DOI: http://dx.doi.org/10.1016/B978-0-12-381462-3.00018-5

© 2013 Elsevier Inc. All rights reserved.

subtypes. However, the natural ligand for $P2Y_{1,\ 12,}$ and $P2Y_{13}$ subtypes is ADP. Although $P2Y_6$ receptors can also be activated by ADP, UDP is much more potent. In rodents, UTP activates $P2Y_2$ and $P2Y_4$ subtypes with similar potency to ATP, an observation often used in physiological studies as an initial pointer to receptor identity. Human $P2Y_4$ receptors, however, are activated primarily by UTP (50-fold more potent than ATP[178]). This is a particularly striking example of species differences, serving to highlight the need for caution before extrapolating from findings in one species to another. The $P2Y_{14}$ receptor is exceptional in that its natural ligand is UDP-glucose; although originally believed to be unaffected by unglycosylated purine- or pyrimidine-based nucleotides, it is now known that UDP is also a full agonist at rat and human $P2Y_{14}$ receptors.[55]

P2Y receptors are coupled to either G_q or G_i signaling proteins. $P2Y_{1,\ 2,\ 4,\ 6,}$ and $P2Y_{11}$ subtypes are coupled to G_q/G_{11}, resulting in PLC-β activation and increased $[Ca^{2+}]_i$, while $P2Y_{12-14}$ are coupled to G_i/G_o, resulting in adenylyl cyclase inhibition and reduced cAMP levels. The $P2Y_{11}$ subtype is unusual, in that it can couple to both G_q and G_s, resulting in both PLC-β and adenylyl cyclase activation, causing increased cAMP levels.[172]

Heterodimeric Receptors and Dinucleotide Receptors

A further layer of complexity has been added to the picture with the finding that adenosine A1 receptors can be co-expressed with $P2Y_1$ or $P2Y_2$ receptors (and possibly other P2Y subtypes) as a discrete receptor type, at least in non-renal cells. The chimeric nature of such receptors is reflected in their mixed pharmacological and signaling properties.[200,201] The possible functional significance of these heterodimeric P1/P2Y receptors with regard to the kidneys is currently unknown.

Finally, a number of dinucleotides, in which the 5′-carbon positions of two nucleosides are linked by a polyphosphate chain, occur naturally in the body. These dinucleotides can be symmetrical (e.g., Ap_4A, where two adenosine moieties are linked by a chain of four phosphates) or asymmetrical (e.g., Up_4A, where a uridine moiety and an adenosine moiety are similarly linked). Dinucleotides can have both vascular and tubular effects within the kidneys (*vide infra*), but the receptors responsible are unknown; evidence for dinucleotide-specific receptors has been provided in other tissues, but several P2Y receptors ($P2Y_{1,\ 2,\ 4,}$ and $P2Y_6$) and P2X receptors ($P2X_{1-5}$) are known to be dinucleotide-sensitive.[81,143]

It is likely that both adenine-based and uracil-based nucleotides are released from most cells in the body (including renal cells); moreover, ecto-enzymes that metabolize nucleotides, either inactivating them or converting them to molecular forms that can stimulate different P2 receptor subtypes, are ubiquitous (*vide infra*). Figure 18.1 shows the molecular structures of some of the principal nucleotides involved, and Figure 18.2 provides a simplified overview of nucleotide release, degradation, and purinoceptor (i.e., P1 (adenosine) receptor and P2 receptor) activation.

Synthetic Agonists and Antagonists of P2 Receptors

Agonists

An ever-increasing range of synthetic nucleotide analogs and non-nucleotide agonists is being developed in an attempt to find agents that, unlike naturally occurring nucleotides, are not subject to degradation by ectonucleotidases, and can act as selective agonists for given receptor subtypes. Such exclusivity is rarely achieved, although substantial progress is now being made. Unfortunately, many of the initial observations on P2 receptor stimulation and renal function were made at a time when information on the selectivity of agonists was incomplete, and the agonists used were often more promiscuous than was appreciated, giving rise to misleading interpretations. Thus, although 2 meSADP, for example, has been used as an agonist for $P2Y_1$ receptors, it also activates $P2Y_{12}$ and $P2Y_{13}$ subtypes; the same applies to 2 meSATP which, additionally, can stimulate a number of P2X receptors, while ATPγS, originally used as a $P2Y_2$ and/or $P2Y_4$ agonist, is now known as a broad-spectrum agonist, being effective in a range of P2Y and P2X receptors. Another ATP analog, 2′3′-*O*-(4-benzoylbenzoyl)ATP (BzATP), has often been used as a "selective" $P2X_7$ agonist, given that it is more potent than ATP at this receptor subunit, but it is also effective at $P2X_{1,\ 3}$ and $P2Y_5$ subunits, so it is in reality only a non-selective P2X agonist. Furthermore, BzATP has been shown to act as an antagonist at $P2Y_4$ receptors.[185]

As our knowledge of truly selective P2 agonists expands, future investigations should provide more precise information about the purinoceptor subtype(s) involved in a given physiological response. That knowledge, however, is still limited. The *N*-methanocarba-ADP derivative MRS2365 is selective for $P2Y_1$ receptors; MRS2698 and INS365 (Up_4U or "diquafosol") are selective $P2Y_2$ agonists; and UDPβS, INS48823, and MRS2693 are selective $P2Y_6$ agonists.[14,72,178] At the time of writing, a selective agonist for $P2Y_4$ receptors has not been identified. Similarly, a truly selective agonist for any of the P2X subunits is still lacking.

Antagonists

As with agonists, nucleotide receptor-selective antagonists are something of a rarity. Probably the compound

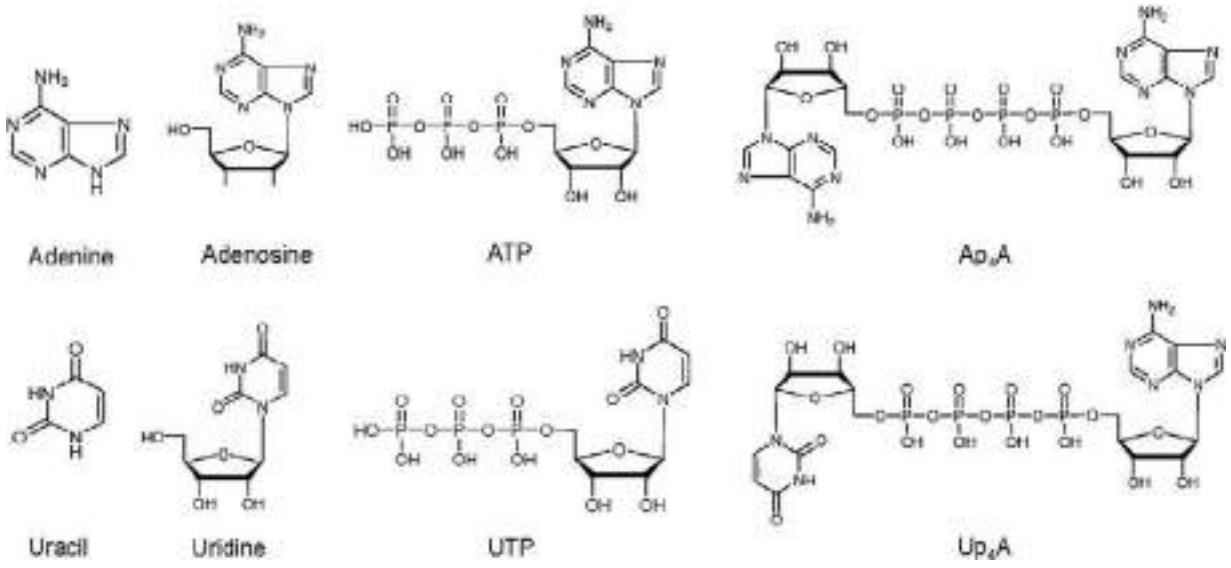

FIGURE 18.1 **Molecular structures of some of the principal nucleotides and their parent nucleosides and purine/pyrimidine bases.**

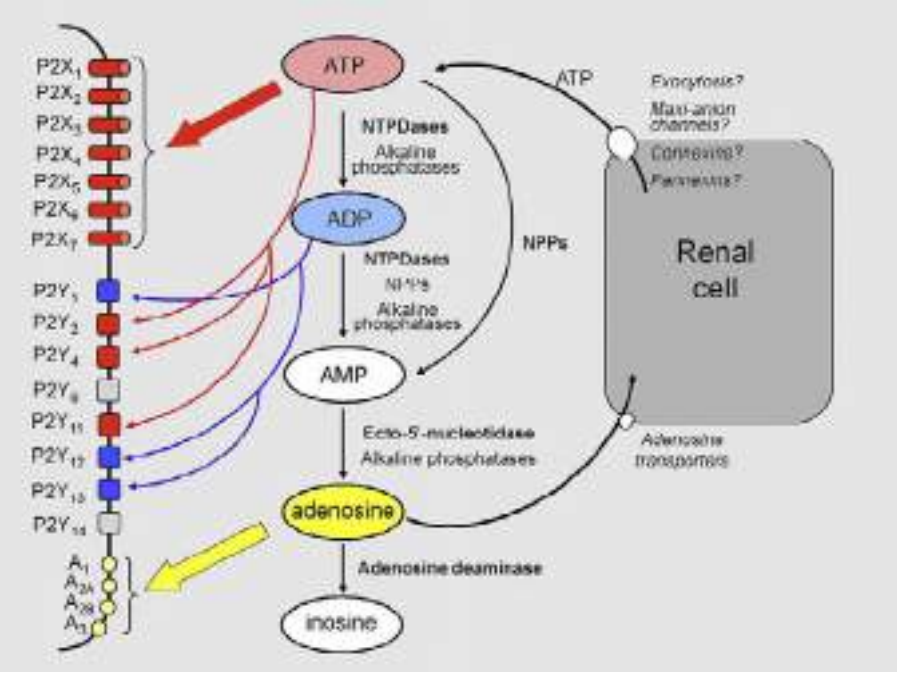

FIGURE 18.2 **The renal purinoceptor system and its modulation by the major renal ectonucleotidases.** The mechanism of ATP release from renal cells is still a matter of debate (see text for details). It is important to note that nucleotides derived from other bases are also likely to be secreted and are also hydrolyzed/synthesized by ectonucleotidases, but have been omitted for clarity. Uracil-based nucleotides are particularly significant: UTP is a potent agonist of $P2Y_2$ and $P2Y_4$ subtypes, and its derivative UDP is the major naturally occurring agonist of the $P2Y_6$ subtype.

most commonly used to inhibit P2 receptors is suramin, although it also affects a variety of other cellular processes. In sufficient concentration, suramin antagonizes practically every P2 receptor subtype, be it P2Y or P2X. The same comment applies to PPADS (pyridoxal-5-phosphate-6-azophenyl 2′,4′-disulphonic acid) and, to a lesser extent, reactive blue 2 (RB-2). However, a clutch of selective and potent antagonists is now available. Thus, the ADP derivatives MRS2179, MRS2279, and MRS2500 are selective $P2Y_1$ antagonists; AR-C126313 and AR-C118925 are selective $P2Y_2$ antagonists; MRS2578 is a selective $P2Y_6$ antagonist; INS49266, INS50589, and AZD6140 are selective $P2Y_{12}$ antagonists; and MRS2211 is a selective $P2Y_{13}$ antagonist.[14,72,178]

For P2X subunits, the list is shorter. Ip_5I is a selective $P2X_1$ antagonist,[14] and A-740003 and A-438079 are selective $P2X_7$ antagonists.[33] Trinitrophenyl-ATP (TNP-ATP) "selectively" antagonizes $P2X_{1-5}$ subunits without affecting P2Y receptors.

Assignment of Physiological Responses to Specific P2 Receptor Subtypes

The plasma membranes of any renal cell, be it vascular or tubular, can contain a variety of P2 receptor subtypes. Moreover, epithelial cells can have different (as well as the same) subtypes on their apical and basolateral membranes. This raises the question of how to attribute a given functional response to a particular subtype. A number of approaches can be used. First, it is useful to identify immunologically the subtypes present in the region of interest (although this, of course, depends on the availability of suitable antibodies) and, if possible, to localize the receptor to apical and/or basolateral membrane. In some cases, instead of the immunohistochemical approach, determination of mRNA has been used, although this obviously does not guarantee the presence of the receptor protein itself. Second, it is possible to try to mimic the effect of the naturally occurring nucleotide using "selective" agonists and antagonists. However, as indicated above, only a few of these are truly selective (although the situation is improving). Consequently, it is usually necessary to compare the individual responses to a variety of agonists (both natural and synthetic) to provide a pharmacological profile from which tentative conclusions can be drawn, but even then their effects will depend not only on agonist/antagonist concentration, but also on the number and distribution of receptor subtypes. Moreover, naturally occurring agonists are degraded by ectonucleotidases, making it difficult to control their absolute concentrations at the receptor site. A further limitation is the use of intracellular Ca^{2+} transients to assess responses to direct application of agonists, since these are not invariably associated with recognizable functional changes.

A completely different, and superficially more attractive, approach is to use "knockout" mice in which the gene encoding the receptor of interest has been deleted. However, this is not without its own potential problems. Life-long, global deletion of a receptor subtype that performs a vital function is likely to lead to compensatory changes in several organ systems. The P2 receptor profile within the kidney may then change in order to restore overall excretion rates, which could then lead to misleading conclusions about the role of the receptor. The *Cre-loxP* system adds a degree of refinement to the gene-targeting approach, permitting tissue- or cell-type-specific deletion. Nevertheless, compensatory changes in up- or downstream nephron segments cannot be excluded, and this approach is further complicated by incomplete (knockdown rather than knockout) and off-target deletion. Furthermore, genetically-engineered deletions have so far been restricted to mice, where $P2Y_2$ receptors seem to predominate in the renal tubule. There are important differences in the distributions of receptor subtypes between mice and rats – and presumably between mice and other species. Thus, for the foreseeable future it seems that we will need to continue to rely on a combination of approaches; as yet, there is no "silver bullet" when it comes to defining P2 receptor function.

Finally, to obviate the need for working with complex renal tubules, many investigators have made use of simpler systems: immortalized cell lines originally derived from renal-like tissue (e.g., Madin–Darby canine kidney (MDCK) cells). Unfortunately, these cell lines often express membrane proteins that differ from those found in native tissue. Consequently, in this chapter we will avoid deductions based solely on observations concerning P2 receptors in non-native renal tissue.

P2 RECEPTORS AND RENAL FUNCTION

The Renal Vasculature

Figure 18.3 summarizes current knowledge about the distribution of P2 receptors in renal vascular and tubular structures. P2 receptors are expressed widely in the renal vasculature, in the glomerulus, and in the extraglomerular mesangium. Immunohistochemical and Western analyses indicate that $P2X_1$ receptors are present in the vascular smooth muscle of the rat renal artery, arcuate and interlobular arteries, and the afferent arteriole, but not in the efferent arteriole.[19,171] Functional approaches have confirmed the expression of a $P2X_1$-like receptor in the afferent arteriole.[70] $P2X_2$ subunits have been immunolocalized in the smooth muscle of larger arteries and veins within the kidney,[66,171] and molecular evidence has recently been provided for $P2X_4$ subunits, at least in arcuate and interlobular arteries.[56] Of the P2Y receptors, $P2Y_1$ has an extensive distribution, being expressed in the endothelium of the large arteries, and both afferent and efferent arterioles.[171]

Most information concerning P2 receptor expression in the glomerulus comes from cell culture systems. On the basis of mRNA detection and/or agonist profiling, $P2Y_{1,2,4,}$ and $P2Y_6$ subtypes and $P2X_{2,3,4,5,}$ and $P2Y_7$ subunits have been identified in glomerular mesangial cells[53,65,132,151]; $P2Y_{1,2}$ and $P2Y_6$ subtypes in podocytes[41]; and $P2Y_1$ and $P2Y_2$ subtypes in glomerular endothelial cells.[12] Studies performed on RNA extracted from pools of intact glomeruli from rats found messages encoding $P2Y_{1,2,4}$ and $P2Y_6$

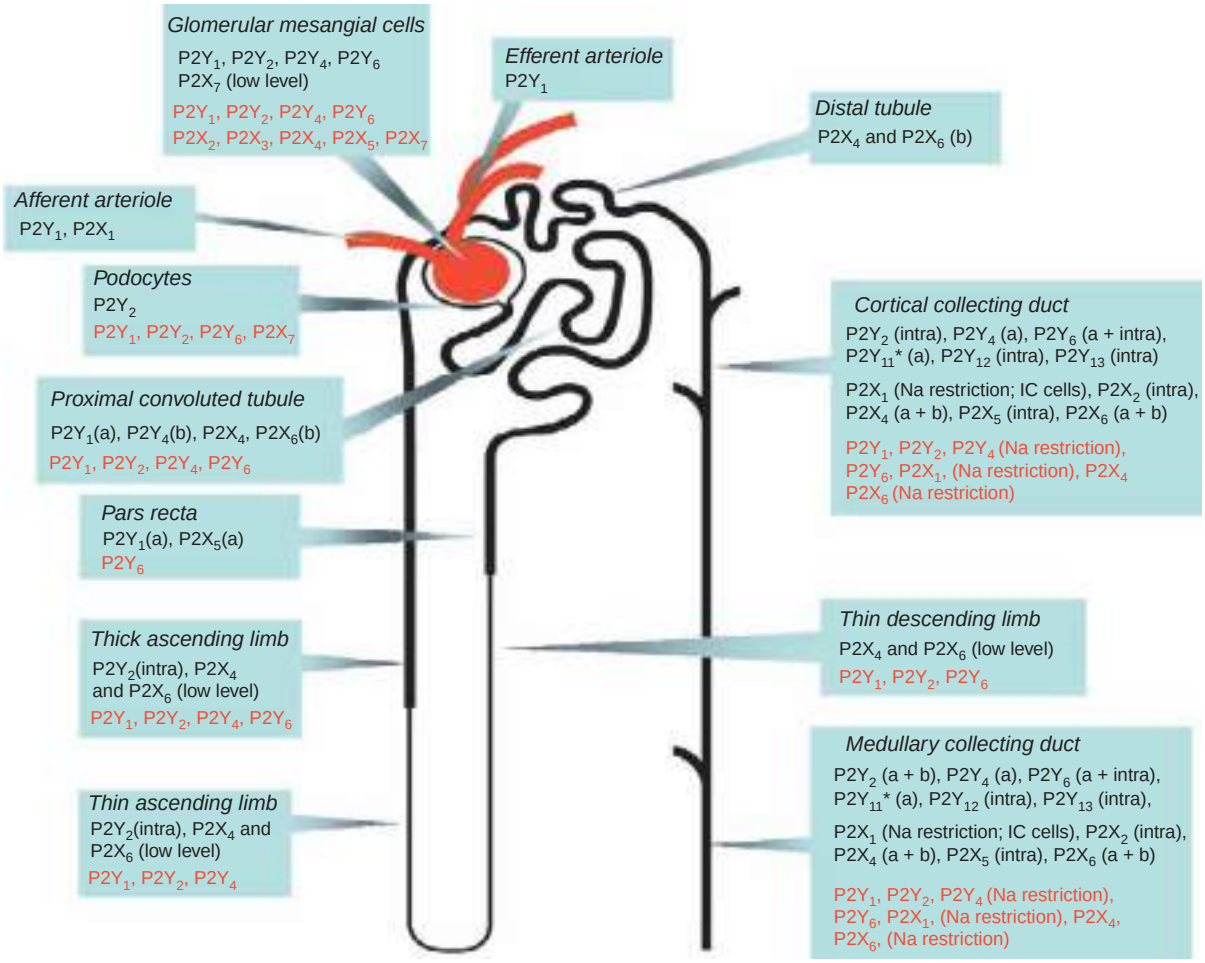
Glomerular mesangial cells
P2Y1, P2Y2, P2Y4, P2Y6
P2X7 (low level)
P2Y1, P2Y2, P2Y4, P2Y6
P2X2, P2X3, P2X4, P2X5, P2X7
Efferent arteriole
P2Y1
Distal tubule
P2X4 and P2X6 (b)
Afferent arteriole
P2Y1, P2X1
Podocytes
P2Y2
P2Y1, P2Y2, P2Y6, P2X7
Cortical collecting duct
P2Y2 (intra), P2Y4 (a), P2Y6 (a + intra),
P2Y11* (a), P2Y12 (intra), P2Y13 (intra)
P2X1 (Na restriction; IC cells), P2X2 (intra),
P2X4 (a + b), P2X5 (intra), P2X6 (a + b)
P2Y1, P2Y2, P2Y4 (Na restriction),
P2Y6, P2X1, (Na restriction), P2X4
P2X6 (Na restriction)
Proximal convoluted tubule
P2Y1(a), P2Y4(b), P2X4, P2X6(b)
P2Y1, P2Y2, P2Y4, P2Y6
Pars recta
P2Y1(a), P2X5(a)
P2Y6
Thin descending limb
P2X4 and P2X6 (low level)
P2Y1, P2Y2, P2Y6
Thick ascending limb
P2Y2(intra), P2X4
and P2X6 (low level)
P2Y1, P2Y2, P2Y4, P2Y6
Medullary collecting duct
P2Y2 (a + b), P2Y4 (a), P2Y6 (a + intra),
P2Y11* (a), P2Y12 (intra), P2Y13 (intra),
P2X1 (Na restriction; IC cells), P2X2 (intra),
P2X4 (a + b), P2X5 (intra), P2X6 (a + b)
P2Y1, P2Y2, P2Y4 (Na restriction),
P2Y6, P2X1, (Na restriction), P2X4,
P2X6, (Na restriction)
Thin ascending limb
P2Y2(intra), P2X4 and
P2X6 (low level)
P2Y1, P2Y2, P2Y4

FIGURE 18.3 **P2 receptors in the vasculature and tubules of the rat kidney.** Those receptors in the rat kidney for which firm evidence from immunohistochemical studies and/or Western blotting has been obtained are shown in black. Those receptors for which expression of mRNA has been documented are shown in red. Where possible, apical (a), basolateral (b) or intracellular (intra) location is indicated. *The antibody used to detect $P2Y_{11}$ was raised against an epitope of human, not rat, $P2Y_{11}$ receptors. Information is taken from ref. 4–7,19,41,53,83,132,151,171,187,203

subtypes[7]; the expression of other P2Y receptors was not assessed. Immunohistochemical analysis and measurements of agonist-induced phosphoinositide production confirmed the presence $P2Y_1$ and $P2Y_2$ subtypes in the rat glomerulus. On the basis of co-localization with cell-specific markers, $P2Y_1$ receptors were localized in mesangial cells and $P2Y_2$ receptors in podocytes[7,171]; expression of $P2Y_4$ and $P2Y_6$ receptor protein could not be confirmed, either functionally or immunologically. Of the P2X subtypes, only a low and variable expression of $P2X_7$ immunoreactivity was found in the rat glomerulus.[171]

Physiological Responses

Infusion of ATP into the renal artery has long been known to alter renal vascular resistance, although the nature and magnitude of the response are dependent upon species, basal vascular tone, and to some extent the experimental approach.[67] The larger renal arteries serve principally as conductance vessels,[202] and renal vascular resistance (and therefore renal blood flow) is regulated primarily through pressure-dependent vasoactivity of the preglomerular arterioles[153] and, to a lesser extent, the small interlobular arteries.[58] The responsiveness to ATP of the arcuate and interlobular arteries and the glomerular arterioles has been evaluated in rats using the isolated perfused kidney preparation.[70] The preglomerular arteries were relatively insensitive to ATP, with micromolar concentrations evoking transient vasoconstriction (Figure 18.4). In contrast, the afferent arteriole underwent sustained contraction at concentrations in the submicromolar range, whereas the efferent arteriole was unresponsive to extracellular ATP. Thus, in the isolated perfused rat kidney, intrarenal administration of ATP is normally vasoconstrictive. This vasoconstriction can be potentiated by inhibition of nitric oxide (NO) synthesis.[37] However, when baseline renal vascular resistance is

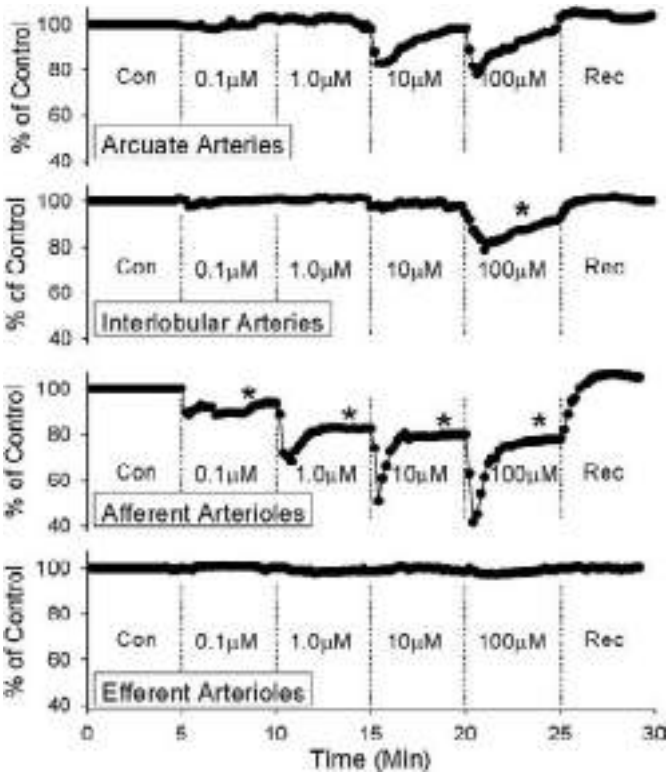

FIGURE 18.4 **ATP concentration–response relationships for pre- and post-glomerular vasculature.** The figure shows average segmental diameter responses evoked by ATP applied to the adventitial surface of arcuate arteries, interlobular arteries, afferent arterioles, and efferent arterioles of rat juxtamedullary vascular segments. After the control period (Con), increasing concentrations of ATP were applied at 5 min intervals; each protocol ended with a 5 min recovery period (Rec). Each data point is normalized as a percentage of the control diameter *(from ref. [67])*.

high, ATP induces *vasodilatation*, due to P2Y-mediated production of NO.[40] Thus, P2 receptor "tone" can influence renal vascular resistance, with P2Y/NO-mediated vasodilatation exerting a counterbalancing influence on $P2X_1$-mediated vasoconstriction. The dominant receptor pool, as well as the source and local concentration of extracellular nucleotide, will therefore influence the net physiological response to extracellular nucleotides. ATP released from renal nerve terminals, for example, will act directly on the vascular smooth muscle, promoting $P2X_1$-mediated vasoconstriction.[139,162] Conversely, release of ATP in the vicinity of the endothelial P2Y receptors would be expected to promote NO synthesis and vasodilatation.

Renal Autoregulation

The majority of vascular beds stabilize blood flow in the face of fluctuating blood pressure. This autoregulation of blood flow is an intrinsic property of the vasculature, and in the kidney it is highly efficient: over the physiological range, renal blood flow can be effectively independent of blood pressure.[26] Whole-kidney autoregulation is governed through the combined influence of at least two mechanisms, tubuloglomerular feedback (TGF) and the intrinsic myogenic response of the vascular smooth muscle; these regulatory systems have different, but overlapping, operational frequencies. Computational analysis of the dynamic frequencies of the two systems indicates a degree of interaction; constriction of the terminal afferent arteriole by TGF increases pressure in the upstream vasculature and the myogenic response is enhanced.[180]

Myogenic Responses to Altered Perfusion Pressure

Of the two major components, only the intrinsic myogenic response to altered perfusion pressure is both necessary and sufficient for full, whole kidney autoregulation.[26] The myogenic response operates along the preglomerular vascular tree, reacting to increased transmural pressure by channel-mediated calcium influx and reflex vasoconstriction of the vascular smooth muscle. The exact signaling mechanisms are not defined, but local release of ATP is implicated. In the afferent arteriole, pressure-mediated vasoconstriction is markedly blunted by PPADS or suramin, or by the saturation and subsequent desensitization of the P2 receptor system.[69] The central role of the P2 system is further underscored by experiments in $P2X_1$-deficient mice, in which pressure-induced reductions in afferent arteriole diameter are abolished[68] (Figure 18.5). Similarly, pharmacological[119] or pathological[50] maneuvers that impair $P2X_1$ receptor signaling significantly attenuate whole kidney autoregulation of blood flow both *in vivo* and *in vitro*. Furthermore, mice with a targeted deletion of the ectonucleotidase NTPDase1 (thereby prolonging the half-life of extracellular ATP – *vide infra*) exhibit enhanced pressure-induced vasocontriction in the mesenteric artery,[78] consistent with a key role for local nucleotide signaling in the general myogenic response.

Tubuloglomerular Feedback and the Juxtaglomerular Apparatus

Tubuloglomerular feedback (TGF) is a dynamic process whereby changes in the concentration of NaCl in the fluid emerging from the loop of Henle elicit inverse changes in the glomerular filtration rate of the nephron of origin. TGF is mediated by the juxtaglomerular apparatus (JGA), which includes a sensor, the macula densa, and an effector, the granulated cells of the afferent arteriole; other components of the JGA (e.g., mesangial cells) also play a role.

Bell and colleagues demonstrated the release of ATP across the basolateral membrane of the macula

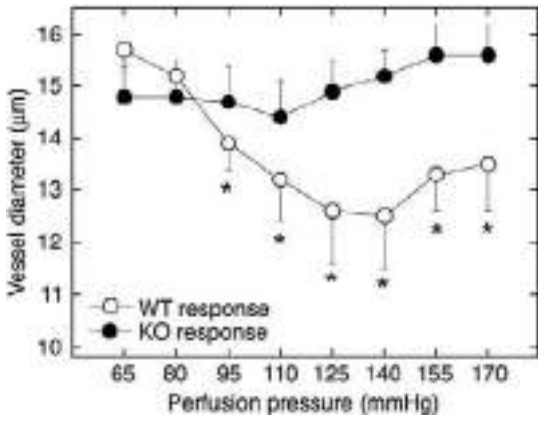

FIGURE 18.5 **Autoregulatory responses in P2X1 knockout (KO) mice versus wild-type (WT) mice.** The normal autoregulatory vasoconstrictor response to increases in perfusion pressure is absent in the KO mice. *(from ref. [68]).*

densa plaque in response to altered luminal NaCl concentration within the physiological range,[11,87] and the concentration of ATP in the cortical interstitium was shown to respond appropriately to inhibition or activation of TGF *in vivo*.[112] This compelling evidence suggests that ATP is the primary signaling molecule for TGF, the effects of which might well be modulated by other paracrine agents produced in the macula densa cell, such as nNOS- (NOS1-) derived NO and COX2-derived prostaglandin E_2.[10] Gene-targeting experiments, however, suggest that ATP may not be the ultimate signal through which TGF causes constriction of the afferent arteriole; hydrolysis of ATP to adenosine appears to be critical. *In vivo* TGF responses are attenuated in mice lacking either adenosine A_1 receptors[157] or ecto-5′-nucleotidase, the enzyme catalyzing the final stage of the degradation of ATP to adenosine.[15] This proposition is supported by a recent *in vivo* study in which the TGF response in mice (as assessed by changes in stop-flow pressure in the proximal tubule) was unaffected during intravenous infusion of PPADS or suramin.[136]

It would be rash, however, to conclude that the P2 receptor system has no role in TGF. Desensitization of this system inhibits TGF in rats,[113] and it is notable that *in vivo* manipulations of TGF affect the interstitial concentration of ATP, but not of adenosine.[67] Furthermore, an anatomical consideration argues strongly for involvement of the P2 receptor system in the TGF response: the ATP released from macula densa cells cannot directly activate P2 receptors in the afferent arteriole, being physically separated in most species by the extraglomerular mesangium. An intact mesangium is required for TGF responses,[129] and Peti-Peterdi has demonstrated that TGF activation causes a wave of increased cytosolic calcium to pass through the mesangium, to the granulated cells of the afferent arteriole and into the glomerular podocytes.[121] Propagation of this calcium wave was abolished by suramin, but not by adenosine receptor antagonism. The P2 receptor response was later shown to be dependent on gap junctional coupling, being inhibited by specific antagonists against connexins 37 and 40[159] (*vide infra* for discussion of connexins).

The basolateral membrane of macula densa cells expresses a $P2Y_2$-like receptor, the function of which is not yet known.[10] It is possible that this provides a negative feedback loop for TGF signaling or a mechanism through which ATP release can be coupled to production.

Glomerular and Medullary Microcirculation

Infusions of nucleotide analogs into the renal artery exert powerful effects on regional blood flow, which can be measured by laser-Doppler flow probes inserted into specific regions of the kidney. In the rabbit, ATP evokes a biphasic response, with vasoconstriction of the medullary blood flow being followed by hyperemia.[39] On the basis of relative agonist potency, the vasoconstriction was attributed to $P2X_1$ receptors; the secondary vasodilatation, which was independent of NO, was partially mediated by adenosine receptors. In the rat, the net effect of ATP is influenced by sodium status. In sodium-restricted rats, ATP increased medullary blood flow in a nitric oxide-dependent manner.[32] In rats fed a high-salt diet, ATP caused vasoconstriction in the outer medulla, without affecting inner medullary flow. The authors' speculated that the inner medullary vasodilatation reflected an effect of nucleotides on vasa recta pericytes. However, preliminary data from Peppiatt-Wildman's laboratory, obtained in slices of rat kidney, suggest that P2 receptor activation promotes vasoconstriction in this setting.[79]

Renin Release

The renin–angiotensin system is influenced by many factors, the final pathways of which converge at the level of altered $[Ca^{2+}]_i$ in the granular cell; renin secretion is inversely related to $[Ca^{2+}]_i$. The combined use of receptor-selective agonists and antagonists has demonstrated that A_1 receptors exert a tonic inhibitory effect on renin secretion at the level of the granular cell.[110] However, the adenosine receptor system is not vital for the control of renin secretion, since A_1 receptor knockout mice are able to raise their secretion appropriately in response to a low-salt diet,[140] a regimen that increases two-fold the sensitivity to luminal NaCl of ATP release by the macula densa.[87]

The role of the P2 receptor system in the regulation of renin release is not entirely clear, and is to some extent contradictory. Purinoceptor signaling is a prerequisite for synchronization of the intercellular calcium wave that controls renin secretion in the JGA,[198] and infusion of ATP into the isolated perfused rat kidney causes profound inhibition of renin secretion.[198] On the other hand, activation of an ADP-selective receptor, thought to be $P2Y_1$, was shown to stimulate renin secretion in rat renal cortical slices via a nitric oxide-dependent mechanism.[21] Resolution of this issue awaits further investigation.

Proximal Tubule

Immunohistochemical studies have identified apical expression of $P2Y_1$ and $P2X_5$ receptors in the S3 segment of the rat pars recta, and basolateral expression of $P2Y_4$ and $P2X_6$ receptors in the proximal convoluted tubule (PCT); low-level expression of $P2X_4$ protein was also seen in the PCT, although the membrane domain was not identified.[171] Western blot analysis has additionally shown the presence of $P2Y_1$ receptors in brush-border membrane vesicles from the S2 segment of rat PCT[6] (see Figure 18.3). Messenger RNA expression has been assessed for only four P2 receptor subtypes: $P2Y_{1,\ 2,\ 4}$ and $P2Y_6$ are all present in rat proximal tubule.[4,5] In terms of Ca^{2+} transients following application of P2 receptor agonists of varying selectivity, supportive evidence has been provided for apical $P2Y_1$-like receptors in an immortalized cell line with a proximal phenotype,[76] and for basolateral $P2Y_1$ receptors in native rat PCT[4,17]; Bailey and colleagues[5] also reported that basolateral UDP was effective in increasing $[Ca^{2+}]_i$, corroborating the presence of $P2Y_6$ receptors. Finally, ATP and UTP were equally effective in stimulating Ca^{2+} transients when applied to rat or rabbit basolateral membranes,[4,196] implying mediation by $P2Y_2$ or $P2Y_4$ receptors; the immunohistochemical evidence in rats favors $P2Y_4$ receptors.[171]

Using a stationary microperfusion technique in rat PCT *in vivo*, Bailey[2] showed that addition of adenosine nucleotides to the lumen inhibited bicarbonate reabsorption. ADP was more effective than ATP, implicating $P2Y_1$ receptors; this was supported by the observation that the $P2Y_1$ agonist 2 meSADP also had a potent inhibitory effect, which was blocked by the $P2Y_1$-selective antagonist MRS2179. (When the tubule was perfused with MRS2179 alone, a small increase in bicarbonate reabsorption was seen, suggesting a tonic inhibitory effect of endogenous nucleotides acting via $P2Y_1$ receptors.) The $P2Y_1$-mediated effect on bicarbonate reabsorption involved inhibition of the Na^+/H^+ exchanger NHE3, since it was not additive to that of EIPA. The effect was blocked by either U73122 or H89, indicating involvement of phospholipase C and protein kinase A. In apparent contrast to these findings from intraluminal perfusions, Diaz-Silvester et al.[31] found that addition of ATP to peritubular capillaries perfused *in vivo* caused an *increase* in transepithelial bicarbonate reabsorption in rat PCT. Conceivably, given the presence of ectonucleotidases in peritubular capillaries and the peritubular space (*vide infra*), degradation of ATP through to the nucleoside adenosine (which stimulates proximal tubular bicarbonate reabsorption[29]) could not be ruled out. However, increasing the viscosity of the peritubular perfusate also stimulated bicarbonate reabsorption, and this effect was blocked by peritubular suramin, suggesting P2 receptor mediation. (Shear stress was proposed as the activating factor.) Interestingly, the increase in bicarbonate reabsorption induced by ATP or by raised viscosity could be blocked by a nitric oxide synthase inhibitor.

In a preliminary study of membrane transporters in the tubules of $P2Y_2$ receptor knockout mice, Listhrop et al.[99] reported increased expression of NaPT2 protein in the proximal tubule (but no change in NHE3 abundance). In line with this, ATP has been shown to inhibit phosphate uptake (and mRNA for NaPT2) in primary cultures of rabbit PCTs.[94] Interestingly, in the same preparation, ATP *stimulates* sodium-glucose co-transport by increasing both SGLT1 and SGLT2 protein expression.[93]

A renal clearance study in rats, using lithium clearance as an index of end-proximal tubular fluid delivery,[165] reported remarkable effects of the naturally occurring diadenosine polyphosphate Ap_4A. When infused intravenously, Ap_4A increased lithium clearance almost two-fold, despite a fall in GFR, indicating a profound reduction in fractional proximal tubular reabsorption.[154] Although a fascinating observation, it is debatable whether intravenous infusion of relatively high-dose exogenous nucleotide provides physiologically useful information about normal autocrine/paracrine control by endogenous agents. It is also difficult to know which P2 receptor(s) is/are involved, since Ap_4A can stimulate a number of subtypes, including $P2Y_1$ and $P2Y_4$ receptors,[143,185] which are both expressed in the rat proximal tubule ($P2Y_1$ apically, $P2Y_4$ basolaterally); intravenous delivery of the agonist does not allow differentiation between these possibilities.

In addition to effects on proximal tubular transport, both adenine-based and uracil-based nucleotides can stimulate gluconeogenesis, an important metabolic function of this nephron segment.[16,109] Diadenosine polyphosphates also have this effect.[35] As these experiments were performed using tubule suspensions or isolated tubules, the agonists will presumably have gained access to both apical and basolateral membranes; moreover, ectonucleotidase-mediated

metabolism of the nucleotides is a possibility, hindering identification of the receptor subtype(s) responsible. However, ATP and UTP were equipotent in stimulating gluconeogenesis, implicating $P2Y_2$ or $P2Y_4$ receptors.[109] Although these authors plumped for $P2Y_2$ mediation, the fact that $P2Y_2$ receptors have not been found in rat proximal tubules, whereas $P2Y_4$ receptors have (*vide supra*), makes a basolateral $P2Y_4$-mediated effect more likely.

Loop of Henle

The pars recta (also called the thick descending limb of Henle), has been dealt with in the preceding section. In the rat thin descending limb there is some immunohistochemical evidence for $P2X_4$ and $P2X_6$ receptors (membrane domain not stated[171]), and indications, from measurements of $[Ca^{2+}]_i$ transients during superfusion of isolated segments with various agonists, of a basolateral pyrimidine receptor,[4] although no $P2Y_2$ or $P2Y_4$ protein has yet been identified. Messenger RNA is expressed for $P2Y_1$ and $P2Y_6$,[4,5] but again immunohistochemical evidence of receptor protein is lacking. In the rat thin ascending limb, similar evidence for a basolateral pyrimidine receptor[4] is in this case accompanied by immunohistochemical confirmation of (intracellular) $P2Y_2$ receptor protein; low-level $P2X_4$ and $P2X_6$ protein expression has also been reported.[171] Hardly surprisingly, given the paucity of information regarding normal transport processes in these nephron segments, the functional significance of P2 receptors in the thin limbs is unknown.

Consideration of P2 receptors in the thick ascending limb (TAL) of the loop of Henle must take account of species differences between rat and mouse. In the rat TAL, binding sites for ATPγS are present on the basolateral membrane[3]; this agonist stimulates several P2Y and most P2X subtypes. Immunohistochemistry has identified $P2Y_2$ (intracellularly), $P2X_4$, and $P2X_6$ (membrane domain not stated) receptor proteins.[171] In addition, mRNA is expressed for $P2Y_{1,2,4,}$ and $P2Y_6$ subtypes.[4,5,83] It has been reported that rat TAL segments are poorly responsive to basolateral application of nucleotides, at least in terms of Ca^{2+} transients,[4,5] which is in marked contrast to the situation in mice, where basolateral ATP and UTP were each found to evoke large Ca^{2+} transients, consistent with activation of $P2Y_2$ receptors.[3,120] A major role for $P2Y_2$ receptors in mice was supported by Jensen et al.[75] who showed, in mouse medullary TAL (mTAL) perfused *in vitro*, that luminal application of ATP or UTP caused almost identical increases in $Ca^{2+}{}_i$ and, importantly, that these increases were absent in $P2Y_2$ knockout mice. In the same study, however, significantly different results were obtained when the nucleotides were applied basolaterally: both ATP and UTP caused an initial peak in $[Ca^{2+}]_i$ followed by a sustained plateau, but whereas both phases were virtually abolished in mTAL from $P2Y_2$ knockout mice treated with UTP, the plateau phase in mTAL from $P2Y_2$ knockout mice treated with ATP persisted, suggesting the presence of an additional basolateral P2 receptor. Since the plateau phase was dependent on extracellular Ca^{2+}, the authors proposed a Ca^{2+}-permeable P2X receptor.[75]

Some information, albeit circumstantial, on the effects of $P2Y_2$ receptors on transport processes in the TAL has come from a comprehensive study of the renal phenotype of $P2Y_2$ knockout mice by Vallon's group. These animals were shown to exhibit increased expression of the apical $Na^+K^+2Cl^-$ co-transporter (NKCC-2) in mTAL, associated with an increased natriuretic response to furosemide.[130] The obvious implication is that nucleotide activation of $P2Y_2$ receptors inhibits NaCl transport in mouse TAL.

During the last decade, in a series of meticulously controlled experiments using cell suspensions or nephron segments perfused *in vitro*, Garvin's group has begun to piece together evidence for a functional role of ATP on TAL function in the rat. Using suspensions of rat mTAL, Silva et al.[146] showed that ATP increased intracellular NO production in a concentration-dependent manner, and that the response was significantly inhibited by suramin. Although the EC_{50} value for the NO response to ATP was high, at 37 μM, prevention of ATP hydrolysis by administration of the ectonucleotidase inhibitor ARL67156 reduced the EC_{50} to 0.8 μM. On the basis that the ATP analog βγmeATP caused an increase in NO production, it was argued that the response was mediated primarily by P2X receptors, although it was noted that UTP also had a weak effect. A recent study from the same group[148] has provided some insight into the signaling cascade involved in ATP-stimulated NO production. Confirmation that endothelial nitric oxide synthase (eNOS; or NOS3) is the enzyme responsible came from the finding that ATP was unable to stimulate NO production in TAL cells from NOS3 knockout mice, whereas a normal response was seen in wild-type mice given NOS1- or NOS2-selective inhibitors. The PI_3 kinase inhibitor LY294002 caused a major reduction in the response to ATP, and a similar reduction was seen in the presence of an Akt-selective inhibitor. This finding, together with the observation that ATP stimulated Akt1 (serine threonine kinase; also called protein kinase B) phosphorylation, whereas phosphorylation of Akt2 and Akt3 was either unchanged or reduced, led the authors to conclude that ATP increases NOS3-derived NO via activation of Akt1. A possible functional link between the recently observed effect of increased flow on nucleotide release in the TAL[75]; (*vide infra*) and the production of NO can be drawn from an earlier study by

Ortiz et al.,[118] in which increasing flow (in the physiological range) in isolated perfused TALs from rat caused markedly increased NO production (which was all but blocked by the NOS inhibitor L-NAME). Notably, increasing luminal flow caused a redistribution of NOS3 within the TAL cells, with translocation towards the apical membrane. It was already known that NO (and presumably therefore ATP) can reduce TAL transport by inhibiting NKCC-2 activity[117] and (to a lesser extent) Na^+/H^+ exchange,[45] but a recent study from this group explored the possibility that ATP might have a primary effect in reducing basolateral Na^+K^+-ATPase activity, and thereby Na^+ extrusion from the TAL cell.[149] Using rat mTAL suspensions, it was found that ATP reduced oxygen consumption in a dose-dependent manner and that this was blocked by suramin, but not by the adenosine receptor antagonist theophylline; it was also blocked by the NOS inhibitor L-NAME. The "2P2X-selective" agonist βγmeATP also reduced oxygen consumption concentration-dependently, while the "P2X-selective" antagonist NF023 blocked ATPs action. (However, as with nucleotide-stimulated NO production, it was found that UTP had a (weak) inhibitory effect on oxygen consumption, suggesting some P2Y involvement.) When NKCC-2 and Na^+/H^+ exchange were blocked with a combination of furosemide and dimethyl amiloride, oxygen consumption fell, and was no longer affected by ATP; while the Na^+ ionophore nystatin increased oxygen consumption to a similar extent in TALs treated with ATP or vehicle alone. These experiments provide powerful confirmatory evidence that ATP, by increasing NO production, can inhibit Na^+ transport in the rat TAL, not by inhibiting basolateral Na^+K^+-ATPase activity, but principally by reducing apical Na^+ entry, particularly via the $Na^+K^+2Cl^-$ co-transporter. Whilst this series of *in vitro* findings is strongly suggestive of a physiological role for nucleotides in autocrine/paracrine control of TAL function (a putative schema is shown in Figure 18.6), a full assessment awaits a comprehensive investigation of electrolyte transport in the loop of Henle *in vivo*.

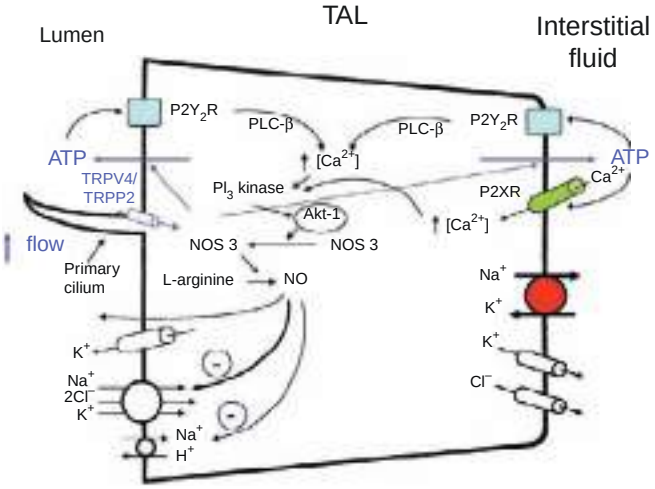

FIGURE 18.6 **Putative effects of flow-induced stimulation of ATP release in thick ascending limb of Henle (TAL).** According to this hypothesis, an increase in tubular flow is most likely detected by the primary cilium, and the consequent increase in Ca^{2+} influx stimulates ATP release. ATP, acting on apical and basolateral P2 receptors, stimulates (via intracellular 2nd messengers) PI_3 kinase which, in turn, phosphorylates Akt1. This kinase phosphorylates NOS3 (which itself may be translocated towards the apical membrane); thus activated, the enzyme stimulates the production of nitric oxide, which inhibits apical sodium entry into the cell via the $Na^+K^+2Cl^-$ co-transporter and the Na^+/H^+ exchanger, thereby inhibiting net Na^+ reabsorption. Information compiled from references [44,45,64,75,118,127,146,148,149]. $P2Y_2R$, $P2Y_2$ receptor; P2XR, P2X receptor; NO, nitric oxide; NOS3, nitric oxide synthase 3.

Distal Tubule

Little is known about P2 receptor distribution in this nephron segment (which, here, we arbitrarily define as distal convoluted tubule (DCT) plus connecting tubule (CNT); the final segment of the properly defined distal tubule – the initial collecting tubule – will be included under "Cortical Collecting Duct"). Immunohistochemical studies have identified $P2X_4$ and $P2X_6$ receptors on the basolateral membrane in rat distal tubule[171] (although it is not clear which region of the distal tubule was involved, as no markers of cell types were used in this study), and basolateral application of ATP to microdissected rat DCTs resulted in (weak) Ca^{2+} transients,[4] but no corresponding investigations have been made in other species or in CNT. Furthermore, no direct studies of distal tubular transport function have been made in native tissue, either *in vitro* or *in vivo*; the only information we have from whole-animal studies is that thiazide-sensitive sodium excretion is unaffected in $P2Y_2$ knockout mice, corresponding with a lack of change in Na^+-Cl^- co-transporter (NCC) abundance.[99,130] Consequently, our knowledge of the role of P2 receptors in these nephron segments is fragmentary and largely restricted to findings from studies of primary cultures of native cells or immortalized distal or "distal-like" cell lines.

Considerable evidence exists for the expression of a number of P2 receptor subtypes and for a range of P2-mediated actions in *Xenopus* A6 cells and Madin–Darby canine kidney (MDCK) cells, both widely used as "distal-like" cell lines. However, as indicated above, for reasons of physiological relevance it will not be considered here, as such cell lines often express membrane proteins different from those found in native tissue. Similar considerations may apply to immortalized cell lines derived from DCT: activation of apical receptors, characterized pharmacologically as $P2Y_2$ subtype, in immortalized rabbit DCT was shown to increase apical chloride

conductance[134]; while activation of receptors (membrane domain not stated) characterized pharmacologically as P2X, rather than P2Y, in immortalized mouse DCT was shown to inhibit magnesium reabsorption.[27] Finally, cultured cells from rabbit CNTs responded to extracellular ATP with an increase in $[Ca^{2+}]_i$ and inhibition of sodium and calcium absorption, although these inhibitory effects were not dependent on the Ca^{2+} transient.[88,173] Either apical or basolateral application of ATP was effective and, when ATP was added to both compartments, the inhibitory effects were additive. On the basis of pharmacological profiling, $P2Y_2$ receptors were implicated.[88]

It is difficult to build a coherent picture from these disparate findings. As with the loop of Henle, a comprehensive *in vivo* assessment of distal tubular function is required.

Collecting Duct

A large array of P2 receptor subtypes has been reported in rat collecting duct (CD) (Figure 18.3). Immunohistochemistry has indicated the expression of $P2Y_2$, $P2Y_4$, $P2Y_6$, $P2Y_{11}$, $P2Y_{12}$, and $P2Y_{13}$ subtypes, and $P2X_1$ (sodium-restricted rats only, intercalated cells only), $P2X_2$, $P2X_4$, $P2X_5$, and $P2X_6$ subunits[83,171,187] with, in some cases, differential expression in the different subsegments of the CD. With respect to membrane localization in principal cells, $P2Y_{4,6,}$ and $P2Y_{11}$ were reported to be exclusive to the apical membrane, whereas $P2Y_2$ and $P2X_4$ and $P2X_6$ were found in both apical and basolateral membranes; staining for $P2Y_{12}$ and $P2Y_{13}$ subtypes and $P2X_2$ and $P2X_5$ subunits was designated "intracellular".[187] In the mouse, immunohistochemistry has localized $P2X_1$ and $P2X_4$ subunits to the apical membrane of medullary CD cells.[97]

Expression of P2 receptor mRNA in the rat kidney broadly agrees with the immunohistochemical findings – at least in the one study in which both methodologies were used.[187] Messenger RNA has been identified for $P2Y_{1,2,4,}$ and $P2Y_6$ subtypes, and $P2X_4$ subunits in cortical (CCD) and outer medullary CD (OMCD),[4,5,187] and for $P2Y_{1,2,4}$ and $P2Y_6$ subtypes in inner medullary CD (IMCD).[83,203] Additionally, mRNA for $P2X_1$ and $P2X_6$ receptors has been reported in CCD and OMCD following dietary sodium restriction.[187] Messenger RNA levels for $P2Y_{11,12,13,}$ and $P2Y_{14}$ receptors have not yet been investigated. Studies using mice have so far focused on P2X receptors, and have identified mRNA for $P2X_{1,4,5,6,}$ and $P2X_7$ subunits in CCD and OMCD,[46,97] suggesting a species difference. As far as the human kidney is concerned, the only published information we have comes from a heroic study by Charbardès-Garonne and coworkers, in which the transcriptome from human kidneys was characterized using serial analysis of gene expression (SAGE). They found that, of tags for 258 genes conferring transport properties, the only P2X receptor detected in significant amounts in the CD was $P2X_4$.[18]

A complex picture is beginning to emerge concerning the role of P2 receptors in the CD. A combination of approaches has demonstrated that extracellular nucleotides, acting from both apical and basolateral sides, can have significant effects on water and electrolyte handling in this important nephron segment – the final site of regulation of urinary output.

Water

In the mid-1990s it was shown that activation of basolateral P2 receptors in rabbit CCD and rat IMCD, perfused *in vitro*, reversibly inhibited vasopressin-stimulated osmotic water permeability.[82,133] On the basis that UTP and ATP were equipotent, whereas other nucleotides were without effect, the inhibition found in the rat was attributed to basolateral $P2Y_2$ receptors[82]; this P2 receptor-mediated inhibition has been found to be PKC-dependent, and to result from decreased intracellular cAMP and increased PGE_2 levels.[181] The inhibitory action (at least in IMCD) appeared to be mediated only by basolateral receptors, since luminal application of ATP was without effect in this nephron segment.[36] Enhanced expression of $P2Y_2$ mRNA, and of the receptor protein itself, in the inner medulla of hydrated versus dehydrated rats, has provided additional evidence for a regulatory role for $P2Y_2$ receptors in modulating CD water reabsorption,[85] and this view is supported by the observation that chronic vasopressin V_2 receptor stimulation with dDAVP reduces inner medullary $P2Y_2$ mRNA and protein expression.[158] Gene deletion studies further substantiate a role for the $P2Y_2$ receptor in ATP-evoked inhibition of AVP-stimulated osmotic water permeability in the CD. Under basal conditions, $P2Y_2^{-/-}$ mice concentrated their urine to a greater degree, and their renal medullary aquaporin-2 (AQP2) abundance was significantly higher, compared with values in wild-type mice, despite almost identical plasma vasopressin levels,[130,205] and following chronic dDAVP treatment, inner medullary AQP2 expression was increased to a markedly greater extent in the $P2Y_2$ knockout animals.[205] In summary, the overall picture is that $P2Y_2$ receptor activation inhibits vasopressin-stimulated, AQP2-mediated water transport in the CD, and this results from decreased intracellular cAMP and increased intracellular PGE_2; the latter, in turn, can reduce cAMP levels and effect the retrieval of AQP2 from the apical membrane.[86]

A recent study from our laboratory, albeit in a cultured, immortalized mouse CCD cell line (mpkCCDc14), has provided additional evidence that P2 receptor activation may exert its inhibitory effect on water transport via altered AQP2 trafficking. Application of dDAVP to the basolateral membrane for four days resulted in marked AQP2

immunofluorescence in the apical membrane, but when ATP or ATPγS was then added to the medium, either apically or basolaterally, the AQP2 was internalized.[186] Treatment with dDAVP induced gene expression of $P2X_1$ in the apical domain, and led to translocation of $P2X_2$ and $P2Y_2$ to the apical and basolateral membranes, respectively. When these three subtypes were co-expressed with AQP2 in *Xenopus* oocytes, their activation reduced cell membrane AQP2 abundance and consequently reduced water permeability.[186] These findings suggest that: (1) in addition to basolateral $P2Y_2$ receptors, apically located P2 receptors can contribute to the downregulation of AQP2-stimulated water transport; (2) altered trafficking of AQP2 is involved; and (3) vasopressin itself can increase membrane abundance of P2 receptors (c.f. [158]). However, it must be stressed that the observations were confined to *in vitro* systems using a mouse CD-derived cell line and *Xenopus* oocytes. As such, they must be viewed with caution.

Potassium

Although early studies in MDCK cells reported that ATP activates K^+ channels,[42] evidence in native CD suggests that K^+ secretion by principal cells is *inhibited* by nucleotides. A patch-clamp investigation of split-open mouse CCDs (allowing access to the apical membrane) demonstrated that ATP reversibly inhibits the activity of the small-conductance K^+ (SK; also called ROMK) channels, which are believed to mediate most potassium secretion in the distal nephron.[104] On the basis of equipotency of ATP and UTP, and the absence of effect of αβmeATP and 2 meSATP, it was concluded that apical $P2Y_2$ receptors were responsible. That $P2Y_2$ knockout mice maintain a robust potassium excretion despite mild hypokalemia is consistent with this hypothesis.[130] It is worth noting that the inhibitory effect of ATP on SK channel activity observed by Lu and colleagues[104] could be blocked by the NOS inhibitor L-NAME, which implies that the NO-dependency of nucleotide-induced physiological actions may not be confined to the TAL (*vide supra*).

K^+ secretion in the distal nephron is generally enhanced when tubular flow rates are increased. This flow-induced increase in K^+ secretion is now thought to be mediated not by SK channels, but by large-conductance, maxi-K (big K; BK) channels.[191] Activation of BK channels is through increased $[Ca^{2+}]_i$,[100] and there is good evidence for a causal link between increased tubular flow rate, increased tubular nucleotide secretion, and increased $[Ca^{2+}]_i$ (*vide infra*). Although highly speculative at this stage, one implication of these various observations is that nucleotides may have conflicting effects on SK and BK channels.

Sodium

Studies into the effects of extracellular nucleotides on CD Na^+ transport have generally used sensitivity to amiloride as a basis for identifying ENaC-mediated transport; although occasionally sensitivity to benzamil – a more selective inhibitor of ENaC – has been employed. Koster and colleagues were the first to report that benzamil-sensitive transcellular Na^+ transport is inhibited by nucleotide activation of P2 receptors.[88] Using primary cultures of rabbit CD (and CNT) cells grown to confluence, they demonstrated that apically or basolaterally applied ATP inhibited benzamil-sensitive short circuit current (SCC; used as an index of Na^+ transport) across cell monolayers; the mechanism involved activation of PKC and/or PLC. The P2 receptor responsible for this inhibition was equally sensitive to ATP and UTP, but was insensitive to ADP. On this basis, the inhibition of ENaC was attributed to activation of $P2Y_2$ receptors. Subsequent studies using the mouse M1 cell line reported similar findings, except that the mechanism did not involve PKC.[25,164] Another CD cell model, the mouse mIMCD-K2, responded similarly to apical (but not basolateral) nucleotides, although in this case, on the basis of pharmacological profiling and mRNA expression, P2X receptors ($P2X_3$ and $P2X_4$) as well as P2Y receptors ($P2Y_1$ and $P2Y_2$) were thought to be responsible.[107] A more recent study, using the mouse IMCD-3 cell line, provided an exception to the "rule" of nucleotide-induced inhibition of CD transport: apical application of ATP induced an *increase* in SSC,[97] although sensitivity to amiloride or benzamil was not tested. Since this effect could be reproduced by the P2X agonist BzATP, it was inferred that the receptors responsible were $P2X_1$ and/or $P2X_4$, as located in native medullary collecting duct (*vide supra*), although UTP was able to increase SCC to some extent, implying a contribution from P2Y receptors.

Investigations of nucleotide effects on CD sodium transport are not limited to cell cultures: nucleotide-induced inhibition of Na^+ reabsorption in the CD has also been reported in native tissue. In mouse CCD perfused *in vitro*, ATP and UTP, applied either luminally or basolaterally, caused an increase in $[Ca^{2+}]_i$ (and subsequent activation of PKC), and inhibition of amiloride-sensitive SCC, an effect attributed to $P2Y_2$ receptor activation.[28,95] Subsequent single-channel patch-clamp experiments, using both rat and mouse CCD, showed that activation of apical P2 receptors with ATP decreased ENaC open probability (P_o), via PLC-dependent breakdown of PIP_2.[123] Although not tested in rats, it was found that in mice UTP was able to reduce P_o to the same extent as ATP. Further pharmacological profiling led to the conclusion that $P2Y_2$ receptors were responsible (at least in mice). The fact

that in $P2Y_2^{-/-}$ mice the effect of ATP on ENaC P_o was severely blunted provided strong support for this conclusion,[123] although a residual effect was still evident, suggesting partial involvement of other P2 receptors. A follow-up study from the same laboratory showed that increased dietary sodium causes a lowering of ENaC P_o in wild-type mice, but not in $P2Y_2$ knockout mice, implying a central role for $P2Y_2$ receptors in the CD response to changes in sodium intake.[124] More recently, the same group has extended this conclusion to implicate $P2Y_2$ receptors in the phenomenon of aldosterone escape – the restoration of normal sodium excretion rates in the face of chronically raised mineralocorticoid levels. Hitherto, aldosterone escape had been thought to rely on compensatory changes in more proximal segments of the nephron delivering an increased sodium load to the aldosterone-sensitive sites. However, Stockand and colleagues found that whereas wild-type mice on a high-sodium diet excreted appropriately high levels of sodium in the face of three days of deoxycorticosterone acetate treatment, owing partly to reduced ENaC activity, in $P2Y_2^{-/-}$ mice the reduction in ENaC activity was much less pronounced, and the natriuresis correspondingly compromised.[155]

At the time of writing, only one study of the effect of nucleotides on CD Na^+ reabsorption *in vivo* has been published.[144] Late distal tubules of rats were microperfused with artificial tubular fluid containing ^{22}Na, the urinary recovery of which was recorded. In animals fed a low-sodium diet (to upregulate ENaC activity), addition of ATPγS to the luminal perfusate was found to inhibit CD ^{22}Na reabsorption. Despite firm evidence from *in vitro* studies in mice for $P2Y_2$ mediation, "selective" $P2Y_2/P2Y_4$ agonists were ineffective *in vivo* in rats, and a P2X heteromer-mediated effect was suggested.[144] A recent patch-clamp investigation of split-open rat CCD (allowing access to the apical membrane) has provided evidence that both apical P2X and P2Y receptors can affect ENaC activity.[187] Activation of P2Y receptors, molecularly and pharmacologically characterized as $P2Y_2$ and/or $P2Y_4$ subtypes, inhibited ENaC activity by a PLC-dependent mechanism. Notably, activation of P2X receptors, characterized as $P2X_4$ and/or $P2X_{4/6}$ receptors, either inhibited or potentiated ENaC activity, depending on the luminal concentration of sodium. When luminal sodium was 145 mM (which is the concentration typically used in this type of *in vitro* experiment), $P2X_4$ and/or $P2X_{4/6}$ activation with 2 meSATP inhibited ENaC activity, whereas when luminal sodium concentration was 50 mM (which mimics the normal sodium concentration of fluid entering the CD *in vivo*), $P2X_4$ and/or $P2X_{4/6}$ activation with 2 meSATP potentiated ENaC activity (Figure 18.7). These findings led us to propose that $P2X_4$ and/or $P2X_{4/6}$ receptors might act as apically expressed sodium sensors for the local regulation of ENaC activity in the rat CD.[187] The situation is almost certainly more complex, since preliminary data from our laboratory, using the same electrophysiological techniques, have demonstrated that $P2X_4$ and $P2X_{4/6}$, and $P2Y_2$ and $P2Y_4$ receptor-mediated regulation of ENaC is also dependent on nucleotide concentration, duration of exposure to nucleotide, and tubular pH: higher nucleotide concentrations and prolonged exposure favor P2Y-mediated inhibition, while reducing tubular fluid acidity favors P2X-mediated increases in ENaC activity.[183] Staying with the $P2X_4$ theme, a causal link has been established between P2X activation, the apical insertion of ENaC, and enhancement of sodium transport, albeit in a "distal-like" cell line; activation of a basolateral $P2X_4$-like receptor in *Xenopus* A6 cells alters cell shape by a rearrangement of the cytoskeleton, which results in increased Na^+ transport[204] brought about by the unruffling of the apical membrane and insertion of ENaC.[49]

Gene deletion studies have so far concentrated on murine $P2Y_2$ knockout models, although studies using the $P2X_4^{-/-}$ mouse (which, like the $P2Y_2$ knockout, is hypertensive[197]) are afoot. Unsurprisingly (on the basis of the studies cited above), $P2Y_2$ gene deletion was found to result in facilitated Na^+ reabsorption in the kidney but, unexpectedly, this appeared to stem from increased expression of the $Na^+K^+2Cl^-$ co-transporter in the TAL (*vide supra*); expression of α-ENaC was *reduced*, while no overall change in amiloride-sensitive sodium transport was seen.[130] Subsequent studies using the $P2Y_2^{-/-}$ mouse have proposed that the $P2Y_2$ receptor tonically regulates ENaC activity by reducing ENaC P_o.[124] It has been suggested that in $P2Y_2$ knockout mice, the increase in ENaC P_o is compensated for in the longer-term by suppression of the renin–angiotensin–aldosterone system, resulting in downregulation of ENaC expression.[172]

In summary, a variety of approaches leaves little room for doubt that apical and basolateral nucleotides can alter ENaC-mediated Na^+ reabsorption in the CD, and more than likely play a role in blood pressure regulation. In simplistic terms, it appears that activation of $P2Y_2$ receptors inhibits ENaC activity, and activation of $P2X_4$ receptors stimulates ENaC activity. In reality, however, P2 receptor and ENaC interactions in the CD are complex, with an interplay between P2X and P2Y receptors dependent on a variety of factors yet to be unraveled.

Secretion of Nucleotides

As indicated earlier, it is thought that virtually all cells are able to release nucleotides,[127] renal vascular and epithelial cells included. Initial support for the

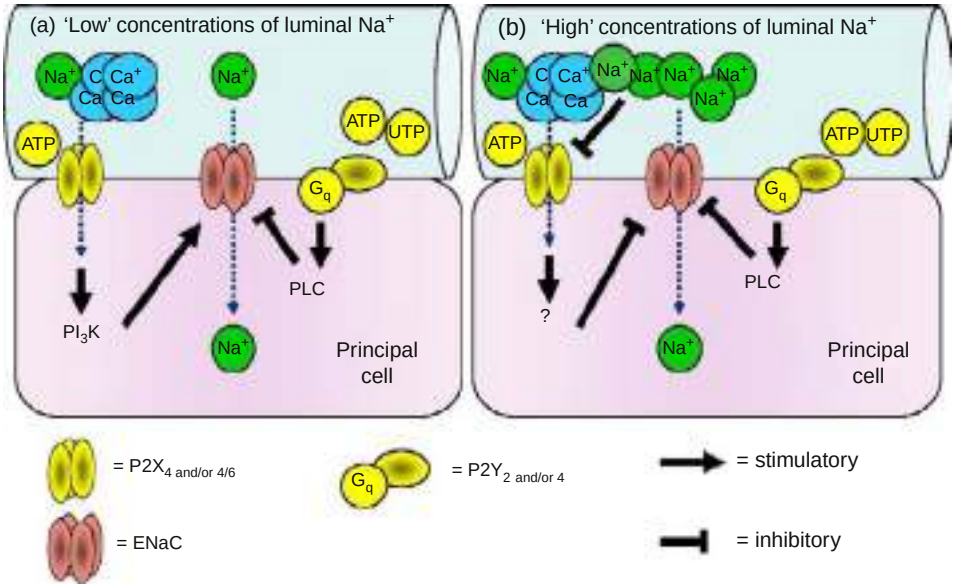

FIGURE 18.7 **Proposed regulation of ENaC activity by P2 receptors in principal cells of rat CD.** The hypothesis is that ENaC activity in the rat CD is differentially regulated by $P2X_4$ and/or $P2X_{4/6}$ receptors, depending on the concentration of luminal Na^+; i.e., that $P2X_4$ and/or $P2X_{4/6}$ receptors act as Na^+ sensors. Real time-PCR and immunohistochemistry suggest that levels of $P2Y_4$ and $P2X_4$ and/or $P2X_{4/6}$ are increased when ENaC is expressed. (a) When the concentration of luminal Na^+ is low (i.e., at 50 mM in our experiments), activation of apically expressed $P2X_4$ and/or $P2X_{4/6}$ receptors (which are highly permeable to Ca^{2+} and to a lesser extent to Na^+) increases ENaC activity through the activation of PI3K. In contrast, activation of apically expressed $P2Y_2$ and/or $P2Y_4$ receptors inhibits ENaC activity through the activation of PLC. N.B.The overall effect of P2 receptor activation (i.e., both P2X and P2Y, by using ATP) is a small degree of ENaC inhibition. (b) When the concentration of luminal Na^+ is high (i.e., at 145 mM in our experiments), activation of $P2X_4$ and/or $P2X_{4/6}$ receptors results in inhibition of ENaC activity by an unidentified mechanism, possibly involving an influx of Na^+. As before, activation of apically expressed $P2Y_2$ and/or $P2Y_4$ receptors inhibits ENaC activity through activation of PLC. The overall effect of P2 receptor activation (i.e., both P2X and P2Y, by using ATP) is a much larger degree of ENaC inhibition. *(from ref. [187]).*

latter came from studies using epithelial cultures and cell lines,[141,142,174] but clear evidence now exists that native renal tubules are also able to secrete ATP. (Cellular secretion of UTP and diadenosine polyphosphates also occurs,[74,199] but has not yet been firmly established in renal tubules.) The question of whether nucleotide release from renal tubular epithelia is constitutive (raising the concept of "purinergic tone"[127]) or is triggered by mechanical or agonist-induced stimuli, now appears to be resolved: both are likely.

Vekaria et al.[176] reported intraluminal ATP concentrations in rat PCTs *in vivo* of 200–300 nmol/l; these concentrations were markedly higher than those in the glomerular filtrate, suggesting secretion of ATP by PCT cells. Intraluminal concentrations in distal tubules were only ~30 nmol/l; the possibility that this ATP was merely flushed downstream, rather than secreted by distal tubular cells, could not be discounted. Using mouse medullary thick ascending limbs (mTALs) perfused *in vitro*, Leipziger's group demonstrated spontaneous oscillatory increases in $[Ca^{2+}]_i$ that appeared to require tubular nucleotide release.[47] An increase in intraluminal pressure from 10 to 80 cm H_2O also resulted in elevations in $[Ca^{2+}]_i$.[75] Convincing evidence was provided that this flow-induced Ca^{2+} transient was itself dependent on nucleotide release, being prevented by luminal or basolateral application of either apyrase (an ATP scavenger) or the P2 receptor blocker suramin. Moreover, both the oscillatory and flow-induced increases in $[Ca^{2+}]_i$ were greatly reduced in $P2Y_2$ receptor knockout mice. In an elegant follow-up study, the same group assessed agonist-induced, rather than flow-induced, nucleotide release in mouse mTAL, and made use of 132-1N1 astrocyte cells transfected with human $P2Y_2$ receptors, positioned at the outflow of perfused mTAL to act as biosensors for ATP[116]; these transfected cells respond dose-dependently to extracellular ATP by increasing their $[Ca^{2+}]_i$. Using this preparation, spontaneous nucleotide secretion was documented, while intraluminal vasopressin or dDAVP (10 nM) triggered $[Ca^{2+}]_i$ bursts. Since the 132-1N1 cells' response was mediated by $P2Y_2$ receptors, it was impossible to distinguish between ATP and UTP as the nucleotide in question, but calibration of the response to vasopressin revealed peak intraluminal nucleotide concentrations of 200–300 nmol/l, remarkably similar to *in vivo* ATP concentrations in the PCT.[176] In the same study, Odgaard et al.[116] found that vasopressin also triggered nucleotide secretion from mouse CCD perfused *in vitro*; intraluminal ATP/UTP

concentrations again reached values approaching 300 nmol/l. Unfortunately, no parallel studies in $P2Y_2$ knockout mice were reported.

It is open to debate whether the nucleotide concentrations measured intraluminally in the above studies reflect those in the vicinity of the P2 receptors in the cell membrane. Membrane-bound and soluble ectonucleotidases (*vide infra*) will rapidly metabolize secreted nucleotides, and it has been estimated that bulk-phase measurements could underestimate concentrations at the cell membrane by more than 20-fold, at least in astrocytes.[77]

Role of Primary Cilium in Flow-Induced Nucleotide Release

A discussion of nucleotide secretion in the tubule would be incomplete without reference to the possible role of the primary cilium. Most renal cells possess a primary cilium protruding from the centriole into the lumen; in the absence of fluid flow it is perpendicular to the cell membrane, but flow causes the cilium to bend, with a consequent increase in $[Ca^{2+}]_i$ in the relevant cell.[128] The question is whether this increase in $[Ca^{2+}]_i$ is triggered by nucleotide release. *In vitro* studies using a cell line (MDCK cells) provided support for nucleotide involvement, as ciliated cells released ATP (detected by biosensor cells downstream) in response to an increase in flow, whereas cells deciliated by means of chloral hydrate did not; apical apyrase or suramin also abolished the response.[127] It is thought that the link between the bending of the cilium and the release of ATP involves a member of the transient receptor potential vanilloid (TRPV) channels – TRPV4 – which is expressed along the TAL and all subsequent nephron segments.[166] Silva and Garvin[147] provided strong evidence that secretion of ATP by cell suspensions of mTAL in response to reduced tonicity depends on activation of TRPV4 channels: the response was reduced by ~75% after blockade of TRPV4 with ruthenium red, while treatment with siRNA against TRPV4 had a similar inhibitory effect. In MDCK cells, ruthenium red also inhibited flow-stimulated Ca^{2+} transients,[89] and it was noted that in these cells TRPV4 co-localizes in cilia with TRPP2 (polycystin 2), an ion channel that is required for cilia-mediated Ca^{2+} transients, but has no mechanosensitive properties. When these two channels were co-expressed in *Xenopus* oocytes, hypotonicity-induced cell swelling was found to cause a bigger increase in membrane currents than that seen when TRPV4 was expressed alone (no currents were sustained by TRPP2 alone).[89] The implication is that TRPV4 and TRPP2 form a sensory channel complex in the primary cilium, which mediates Ca^{2+} influx when the cilium is bent, thereby triggering the release of nucleotides into the surrounding extracellular space which, in turn, activate P2 receptors and cause a more general increase in $[Ca^{2+}]_i$.[127]

Further support for a role of the primary cilium came from a study of collecting duct principal cells derived from the Oak Ridge polycystic kidney (*orpk*) mouse model. These cells lack a well-formed apical cilium; however, they can be genetically rescued with the wild-type *orpk* gene. Constitutive ATP release under basal conditions was not different in mutant versus rescued monolayers of cells, but hypotonicity or increased flow rate induced markedly greater responses from the rescued cells than from those lacking primary cilia.[64]

The evidence thus far, then, favors a crucial role for the primary cilium, but the key question is whether it is equally important in native tissue. In this connection, Woda et al.[192] found comparable flow-induced increases in $[Ca^{2+}]_i$ in principal and intercalated cells of rabbit CCD, despite the fact that intercalated cells in rabbit CCDs do not have cilia.[101] However, the increases in $[Ca^{2+}]_i$ did not appear to depend on nucleotide secretion, since they were unaffected by suramin. It might be, therefore, that rabbits are a special case.

Mechanism of Nucleotide Release

The mechanism of secretion of nucleotides from renal tubular cells is not yet resolved. A large intracellular pool of ATP is available, but the exit route for the nucleotide is controversial, and it may well differ from segment to segment. In neurones and neuroendocrine cells, exocytosis of vesicles containing ATP is well-established, and circumstantial evidence has been provided for a similar mechanism in a proximal tubular cell line,[174] but confirmation is lacking. A variety of channels/transporters has been implicated in nucleotide release. A notable example is the ATP transport across the basolateral membrane of macula densa cells in response to increased NaCl delivery to this nephron site, which is mediated by maxi-anion channels (*vide supra*[10]). Speculation that CFTR channels can also mediate ATP release in the kidney[152] has not received firm support.[126]

In recent years, attention has focused on the possible role of connexin hemichannels in ATP release from renal cells. Connexins (Cxs) are a family of transmembrane proteins comprising approximately 20 members. Messenger RNA and immunohistochemistry studies indicate that several members of the connexin family are expressed in the renal vasculature and tubules.[52] When six connexins assemble, either as homomers or heteromers, they form a connexon. When

two connexons from neighboring cells dock, they form a gap junction; a channel with a central pore. Undocked connexons ("hemichannels") can also function independently as transmembrane channels. Although their functional role, if any, in the tubule remains to be clarified, it has been shown that dietary sodium intake can influence Cx30 and Cx37 expression in tubular cells,[108,156] and evidence is beginning to accumulate for involvement of connexin hemichannels in tubular ATP secretion, as has already been established in other cell types.[24] Evidence for such a role in the distal nephron has come from a recent study using Cx30 knockout mice.[150] Partially split-open CCDs were microperfused *in vitro* and PC12 cells (expressing $P2X_2$ receptors and used as ATP biosensors) were placed in direct contact with the apical membranes of principal cells and intercalated cells. In wild-type mice, increases in tubular flow or reductions in osmolality of the bathing solution evoked increases in $[Ca^{2+}]_i$ in the PC12 cells. Interestingly, these increases were much greater in PC12 cells placed in the vicinity of intercalated cells than in those placed in the vicinity of principal cells, which correlates with the observation that in the mouse distal nephron, immunohistochemical labeling for Cx30 is restricted to the apical membrane of intercalated cells.[108] Also notable was the calculated ATP concentration of 10–50 μmol/l, far in excess of concentrations measured in the bulk phase,[116] thus corroborating the view that bulk-phase measurements may be wide of the physiological mark. Responses were abolished by preincubation of the PC12 cells with suramin, and were almost absent in Cx30 knockout mice. These observations in themselves were striking enough, but the same study went on to assess their physiological significance by comparing pressure–natriuresis curves in wild-type and Cx30 knockout mice. While both groups responded to an imposed increase in renal perfusion pressure (to ~150 mmHg) by a natriuresis, the response in knockout mice was significantly blunted, despite almost identical GFRs in the two groups.[150]

There can be little doubt that these findings provide powerful evidence not only for a crucial role of Cx30 in ATP release in the CCD, but also for an important autocrine/paracrine function of nucleotides in the tubular response to elevations in blood pressure, at least under the conditions of the study. However, a cautionary note should be sounded concerning the physiological significance of the observations: the perfusion rates employed *in vitro* (2–20 nl/min) were far in excess of those found in mouse CCD *in vivo*, and it is clear that the authors used tubular flow rates in the rat, rather than in the mouse, as their reference point. Furthermore, connexin hemichannels appear to open only under non-physiological conditions, such as removal of extracellular divalent cations or major membrane depolarization.[127] In contrast, another group of proteins – the pannexins, which are structurally homologous to connexins and can also form hemichannels[8,135] – is permeable to ATP and can be activated by membrane depolarizations in the physiological range.[102] Further studies will be needed to determine their physiological or pathophysiological role in the kidney.

Ectonucleotidases

As indicated above, the nucleotides that are released from the renal vasculature and from apical and basolateral membranes of renal epithelial cells elicit a variety of autocrine/paracrine actions via P2 receptors. However, these nucleotides are rapidly degraded by surface-located and soluble enzymes (ectonucleotidases) to other nucleotides or nucleosides. Four families of ectonucleotidases, with differing but partly overlapping properties, exist: ectonucleoside triphosphate diphosphohydrolases (NTPDases); ectonucleotide pyrophosphatase phosphodiesterases (NPPs); ecto-5′-nucleotidase; and alkaline phosphatases. Members of all four families have been identified in the kidney,[145] where they will have a profound influence on the stimulation of purinoceptors, not only because the availability of nucleotide agonists is regulated by their hydrolysis, but also because the generation of other nucleotides (e.g., ADP) preferentially targets different P2 receptor subtypes, while the nucleoside derivative adenosine targets P1 (adenosine) receptors (Figure 18.2).

In addition to enzymes that break down nucleotides, two families of phosphorylating enzymes exist: nucleoside diphosphate kinases, which catalyze the transfer of the terminal phosphate of nucleoside 5′-triphosphates to nucleoside 5′-diphosphates (e.g., $ATP + GDP \rightleftharpoons ADP + GTP$), and adenylate kinases, which catalyze the production of ADP from ATP and AMP or *vice versa*, depending on the concentrations of the respective nucleotides ($ATP + AMP \rightleftharpoons 2ADP$). Although initially believed to be restricted to the cell cytosol, there is evidence that nucleoside diphosphate kinases are also present in the cell membrane[199]; mRNA and protein for these enzymes have been identified in rat kidney,[80] but their distribution is unknown. Adenylate kinases are also largely intracellular but, again, ecto-adenylate kinase activity has also been identified.[199] Adenylate kinase enzyme action has been documented along the nephron,[22] although the relative contributions of intracellular and extracellular activity could not be differentiated.

The principal catalytic activities of the ectonucleotidases and phosphorylating enzymes expressed in the kidney are summarized in Table 18.1. Since no

TABLE 18.1 Catalytic Activities of the Ectonucleotidases and Phosphorylating Enzymes Expressed in the Kidney

Enzyme	Hydrolysis Pathways
NTPDases	
NTPDase1	$ATP \rightarrow ADP + Pi \rightarrow AMP + 2P_i$
	$ADP \rightarrow AMP + P_i$
NTPDase2	$ATP \rightarrow ADP + P_i$
	$ADP \rightarrow AMP + P_i$
NTPDase3	$ATP \rightarrow ADP + P_i$
NTPDase8	$ADP \rightarrow AMP + P_i$
NPPs	
NPP1	$ATP \rightarrow AMP + PP_i$
NPP3	$ADP \rightarrow AMP + P_i$
	3′,5′-cAMP → AMP
	$Ap_nA \rightarrow AMP + Ap_{n-1}$
NPP2	$ATP \rightarrow AMP + PP_i$
	$ADP \rightarrow AMP + P_i$
	3′,5′-cAMP → AMP
	$Ap_nA \rightarrow AMP + Ap_{n-1}$
Ecto-5′-nucleotidase	$AMP \rightarrow adenosine + P_i$
Alkaline phosphatases	$ATP \rightarrow ADP + P_i$
	$ADP \rightarrow AMP + P_i$
	$AMP \rightarrow adenosine + P_i$
Nucleotide diphosphate kinases	$ADP + NTP \rightleftharpoons ATP + NDP$
Adenylate kinases	$ATP + AMP \rightleftharpoons 2ADP$

(Adapted from ref. [145].)
Major pathways are shown in black, others in gray. NB: In many cases, nucleotides derived from other bases (UTP, GTP, TTP, CTP, UDP, GDP, TDP, and CDP) can also act as substrates (NDP: nucleoside diphosphate; NTP: nucleoside triphosphate).

information is yet available on the possible functional relevance of the phosphorylating enzymes, in the account below we will restrict ourselves to ectonucleotidases. More detailed information can be found in recent reviews.[145,199]

Although the NTPDase family comprises eight members, only four of these (NTPDases 1, 2, 3, and 8) hydrolyze extracellular nucleotides. NTPDase1 hydrolyzes ATP and ADP with almost equal preference, whereas NTPDase2 has a much greater preference for ATP, therefore causing accumulation of ADP; NTPDases 3 and 8 are intermediate in their preference.[145] The possible functional consequence is that if NTPDase1 is present, P2 receptor stimulation will be abruptly terminated, whereas if NTPDase2 (and to some extent NTPDases 3 and 8) is expressed in the absence of NTPDase1 (or of NPPs), local production and accumulation of ADP would be expected to stimulate $P2Y_1$ (and $P2Y_{12}$ and $P2Y_{13}$) receptors.[172] In rats and mice, NTPDase1 is prominent throughout most of the renal vasculature (interlobular arteries, afferent arterioles, glomeruli, mesangial cells, peritubular capillaries) and is also present in the thin ascending limb of Henle and medullary CD.[84,175] NTPDase2 has been immunolocalized to Bowman's capsules and to most nephron segments beyond the proximal tubule[84,175]; the intrarenal expression of NTPDase3 has been investigated only in the rat where, like NTPDase2, it was found in TAL, distal tubule and CD.[175] Information on NTPDase8 is confined to porcine kidney and is incomplete.

The NPP family comprises seven members, but only NPPs 1–3 are able to hydrolyze nucleotides. NPPs can hydrolyze not only ATP and ADP to AMP, but also dinucleoside polyphosphates (again to AMP; see Table 18.1). Information on the intrarenal distribution of NPPs is limited. Staining for NPP1 protein has been identified in mouse proximal tubules and (more strongly) in basolateral membranes of distal tubules,[54] while prominent staining for NPP3 has been found in rat glomeruli and in the apical membrane of the pars recta, but not in more distal segments.[175]

Ecto-5′-nucleotidase catalyzes the final stage of nucleotide hydrolysis to nucleoside (e.g., AMP → adenosine + P_i). It has a high level of expression in the kidney; it is found in apical membranes of rat PCT and in intercalated cells throughout the distal nephron, as well as the peritubular space.[43,92,175]

An alkaline phosphatase has been identified in the apical membrane of PCT and pars recta of rat kidney.[9] Although alkaline phosphatases have broad substrate specificity, capable of breaking down ATP right through to adenosine, the K_m values for adenine nucleotides are in the low millimolar range, raising questions about the physiological significance of this enzyme, at least in relation to nucleotide degradation.

A summary of existing knowledge of the distribution of ectonucleotidases in the kidney is shown in Figure 18.8.

Given that our knowledge of ectonucleotidase location is incomplete, we can only make a limited number of speculations concerning their possible function in the kidney. The NTPDase1 located in the renal vasculature seems likely to fulfill an important function of that found elsewhere in the body: termination of the platelet aggregation response to extracellular ADP.[38] This enzyme may also terminate the vasoconstrictive action of locally produced ATP on $P2X_1$ receptors in afferent arterioles (*vide supra*) and, along with glomerular NPP3, may modulate the action of ATP on mesangial cells,[73] thereby influencing the ultrafiltration

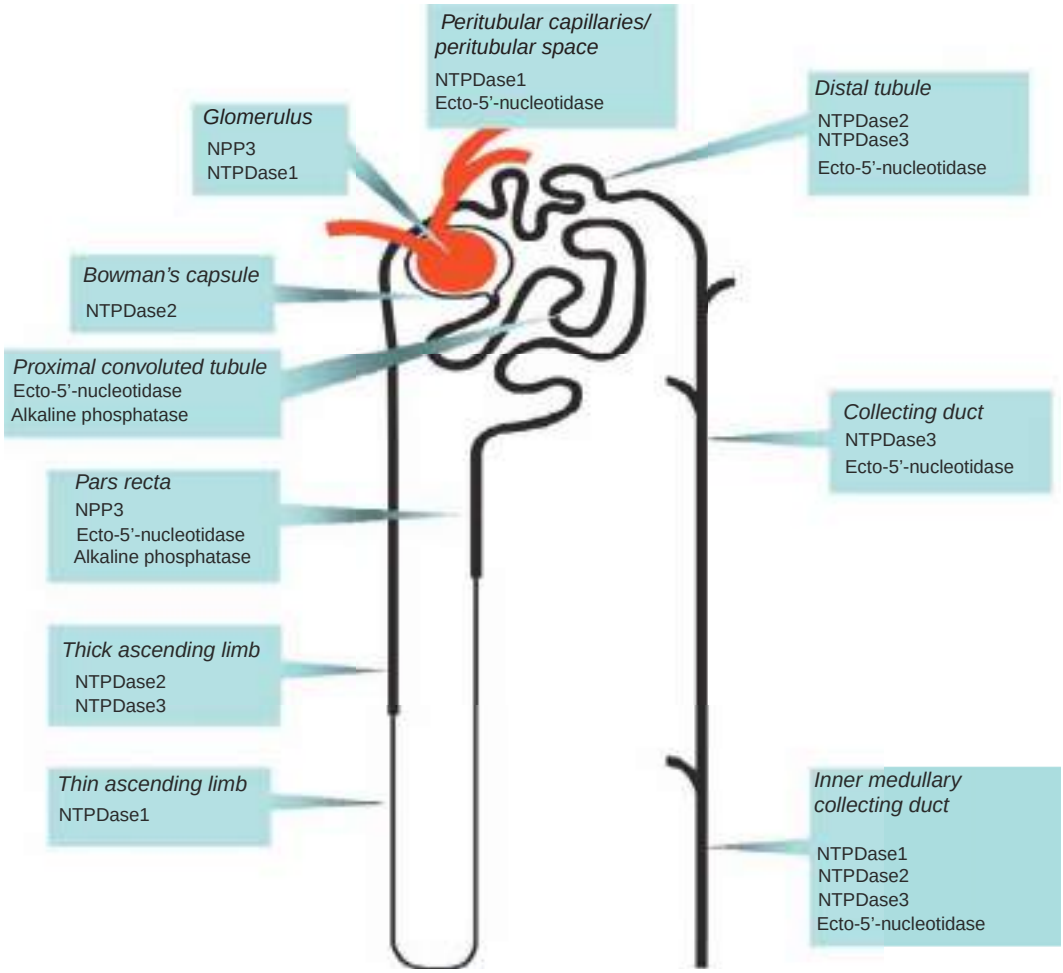

FIGURE 18.8 **Distribution of ectonucleotidases along the rat nephron.** Information compiled from [22,43,84,92,175]. N.B. No information is yet available concerning NPPs 1 and 2 in the rat. *(Adapted from ref. [145]).*

coefficient. The possible roles of ATP and adenosine in mediating TGF have already been discussed. In this context, NTPDase1, expressed in the peritubular space, and/or NPP1, present in basolateral membranes of mouse distal tubule, together with ecto-5′-nucleotidase, also expressed in the peritubular space, are available for the conversion of ATP to adenosine.

As yet, no enzymes that initiate the degradation of ATP have been identified in the PCT (although it should be noted that no suitable antibodies to rat NPP1 or NPP2 are available) and, as already indicated, it is unlikely that proximal tubular alkaline phosphatase could effect ATP degradation at the normal physiological concentrations of the nucleotide. However, it is worth noting that ATPase and ADPase activities have been described in porcine PCT apical membranes.[96] Any AMP produced in the proximal tubule will be converted rapidly to adenosine by the apical ecto-5′-nucleotidase present throughout this part of the nephron. The adenosine could then either activate adenosine A_1 receptors, increasing proximal tubular fluid reabsorption,[182] be converted to inosine or be transported into proximal tubular cells for reuse.[106] Finally, given the effects of extracellular nucleotides on solute and water transport in the distal nephron (*vide supra*), and the inhibitory effect of A_1 receptor activation on sodium reabsorption in the medullary collecting duct,[195] the NTPDases and ecto-5′-nucleotidase present throughout the distal nephron are likely to be of considerable functional significance.

In conclusion, although our knowledge of the intrarenal location of ectonucleotidases is still incomplete, it seems clear that their distribution varies along the nephron, and this provides scope for the rapid termination of the actions of locally produced ATP and/or initiation of ADP-mediated or adenosine-mediated effects.

Role of P2 Receptors in Renal Pathophysiology

The well-documented release of ATP from injured and dying cells at sites of injury and inflammation, and

from red cells and platelets during thrombus formation, suggests that the P2 receptor system could be involved in the pathophysiology of renal disease.[20] As well as producing changes in vascular tone and in fluid and electrolyte reabsorption or secretion (*vide supra*), stimulation of P2 receptors can influence renal cell growth[53,71,138] and – especially in the case of the $P2X_7$ receptor – can also result in cell death and promote inflammation.[59,137]

The published work supporting a pathophysiological role for P2 receptors in the kidney is still limited and remains somewhat speculative. Two disease models have been the main focus of interest: (1) renal cystic disease; and (2) glomerular injury and inflammation. The first stems from work on P2 receptors in secretory epithelia,[91] in particular the airway epithelium in cystic fibrosis,[115] and has been extrapolated to a potential role for these receptors in renal cyst growth in polycystic kidney disease.[142] The second concerns the broadly pro-proliferative effect of stimulating various P2Y receptor subtypes,[132] and the pro-apoptotic effect of activating the $P2X_7$ receptor, particularly when expressed by renal glomerular cells,[179] inflammatory macrophages,[167] and interstitial fibroblasts.[125]

Polycystic Kidney Disease

Mutations in polycystin 1, a membrane receptor, or polycystin 2, a putative Ca^{2+} channel (*vide supra*), give rise to polycystic kidney disease (PKD), a condition associated with uncontrolled proliferation of renal epithelial cells and disordered fluid transport, leading to tubular dilatation and formation and expansion of fluid-filled cysts, which eventually compress and destroy adjacent normal tissue.[189] Cyst-lining cells are thought to exhibit: (1) disordered regulation of proliferation and apoptosis; (2) abnormal secretion of fluid and electrolytes; and (3) disturbed polarity of membrane transport proteins and receptors, which is also believed to relate to a defect in mechanosensation (including detection of the flow of tubular fluid) due to mislocalization and dysfunction of the epithelial cell primary cilium.[193]

In culture, human PKD cells have been shown to release more ATP than normal proximal tubular cells, predominantly from their apical surface.[190] The cysts themselves accumulate and concentrate ATP (0.5–10 μM) and their ecto-ATPase activity appears to be diminished.[142] This extracellular ATP, acting on P2Y (and possibly P2X) receptors on cyst-lining cells, may not only promote cell growth and fluid secretion, but also, by activating the $P2X_7$ receptor, increase cell loss by apoptosis as part of the remodeling necessary for progressive cyst expansion (Figure 18.9); in this regard it is worth noting that inhibition of caspase-mediated apoptosis slows PKD progression.[161] However, much of the evidence in support of this appealing hypothesis is indirect and circumstantial. Schwiebert and

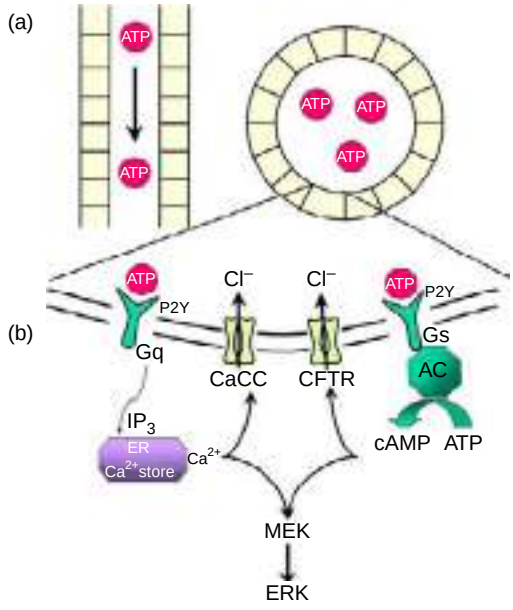

FIGURE 18.9 **Proposed role of P2 receptor signaling in cyst growth.** (a) Remodeling of the normal renal tubule (top left) into an enclosed cyst (top right) allows ATP to accumulate. Reduced nucleotidase activity, coupled with the large representation of P2 receptor subtypes likely to be present in these cyst lining epithelial cells, would allow an amplifying loop of autocrine signaling to occur that might promote osmotically driven fluid accumulation and cellular proliferation. (b) Exploded view of the apical cell membrane lining a hypothetical renal cyst. G-protein-coupled P2Y receptor activation triggers release of Ca^{2+} from the endoplasmic reticulum or production of cAMP via adenylyl cyclase (AC) and subsequent activation of calcium-sensitive chloride channels (CaCC) or CFTR, respectively. The facilitated transcellular transport of Cl^- creates a solute gradient that promotes the osmotic flow of water into the cyst lumen. The increase in $[Ca^{2+}]_i$ and cAMP can modulate the ERK pathway and consequently cellular proliferation. *(from ref. [167]).*

colleagues performed an *in vitro* analysis of P2 receptor signaling in cyst-derived epithelial cells. They confirmed ATP release and P2 receptor-mediated stimulation of SCC (Cl^- secretion), and they also documented mRNA expression for several P2Y and P2X receptor subtypes.[142] At the same time Hillman and co-workers demonstrated expression of the $P2X_7$ receptor (at mRNA and protein levels) in the cystic epithelium of the *cpk/cpk* mouse model of autosomal recessive PKD.[60] Using cells isolated from the *cpk/cpk* mouse, a three-dimensional (3D) suspension model of cyst development was used to study the effects of $P2X_7$ receptor activation on cyst development. The widely used P2X receptor agonist BzATP *reduced* cyst number, but not cyst size, in this model[61] (although BzATP is not selective for $P2X_7$ and can act as an antagonist at some P2Y receptors). In another 3D model of cyst formation using MDCK cells, cyst expansion was inhibited by BzATP; however, this appeared to depend on P2Y,

rather than P2X, stimulation.[168] In a rat model (Han-SPRD) of autosomal dominant PKD, although the $P2X_7$ subtype was detected in cyst-lining cells and its mRNA level increased, other P2X and P2Y receptors were also detected, with particular increases in $P2Y_{2,4}$, and $P2Y_6$ subtypes.[169] All this suggests a complex interplay of P2 receptor subtypes in PKD, with perhaps differing effects on cyst number and cyst size.

More mechanistically, expression of a C-terminal polycystin 1 construct, fused to a membrane expression cassette in a mouse CD cell line (M1), upregulated ATP-stimulated Cl^- secretion, which was associated with a rise in $[Ca^{2+}]_i$ due to an increase in Ca^{2+} entry.[63,184] However, more recent studies of cultured human PKD cells have described a loss of flow-mediated ATP release and the flow-dependent rise in $[Ca^{2+}]_i$, and this was attributed to reduced $P2X_7$ expression and function.[193,194] In this same model, expression of the ectonucleotidase NTPDase1 was also reduced, which would be expected to lead to an increase in local ATP levels. These human PKD cells have also been shown to have defective cilia, which are presumed to be the sensors for flow-activated cell signaling; in ciliated airway epithelia, cilial motion is increased by ATP and these cilia express a P2X receptor that is probably a heteromer of $P2X_{4/7}$,[105] P2X subtypes that are also found in PKD cells. However, although tantalizing, these findings provide more questions than answers, and the exact role of P2 receptors in PKD pathogenesis is still unclear.

The $P2X_7$ Receptor and Renal Inflammation

As already indicated, $P2X_7$ receptor expression is barely detectable in normal healthy kidney. However, its expression is increased in rodent models of glomerular injury, diabetes mellitus, and renin-dependent hypertension.[179] As well as the ability to form a non-selective cation channel or a larger membrane pore leading to cell death by necrosis or apoptosis, the $P2X_7$ receptor can mediate an inflammatory response by causing release of interleukin (IL)-1β (Figure 18.10).[30] Factors that determine whether $P2X_7$ receptor stimulation will cause cell necrosis or apoptosis, and/or inflammatory cytokine release, include the cell type, the concentration of ATP and duration of exposure to the nucleotide, as well as the level of $P2X_7$ receptor surface expression. In cultured human embryonic kidney cells expressing P2X7 receptors, membrane blebbing and microvesiculation are seen within seconds-to-minutes of receptor stimulation, which is associated with cell death by apoptosis.[188] More prolonged receptor stimulation leads to formation of a large membrane pore that permits leakage of vital intracellular components (including ATP) and loss of membrane potential, ultimately leading to cell death and necrosis[114]; somewhat paradoxically, lower concentrations of ATP (and perhaps tonic stimulation of P2X7) in at least some cell types seem to be able to enhance cell proliferation, rather than cause cell death.[1]

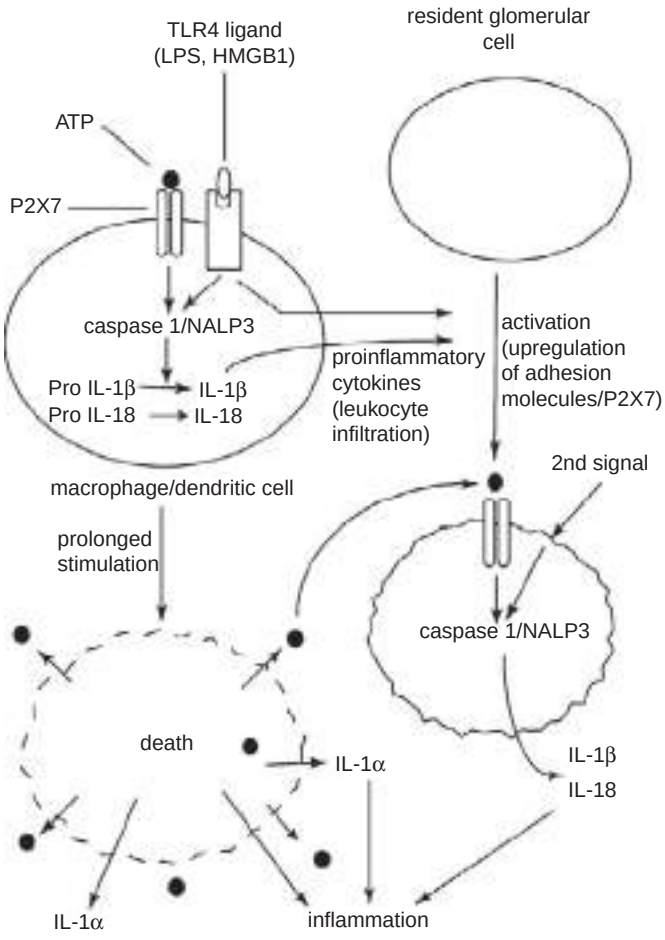

FIGURE 18.10 **Putative role of the P2X7 receptor in inflammatory glomerular disease.** Following initial injury to the kidney, ATP released from damaged cells, possibly together with endogenous Toll-like receptor 4 (TLR4) ligands such as High Mobility Group Box 1 (HMGB1) and lipopolysaccharide (LPS), stimulates the NALP3 inflammasome. Inflammasome activation leads to the maturation of caspase 1, which in turn promotes cleavage, maturation, and release of IL-1β and IL-18 from resident macrophages. Released cytokines promote leukocyte influx and stimulate upregulation of $P2X_7$ on intrinsic renal cells. Prolonged $P2X_7$ stimulation results in cell death with release of intracellular pro-inflammatory mediators such as ATP, IL-1α, and HMGB1, resulting in further rounds of $P2X_7$ stimulation. *(from ref. [167]).*

Activation of the $P2X_7$ receptor promotes release of mature IL-1β, IL-6, and IL-18 from activated macrophages, and both interferon-γ and tumor necrosis factor-α (TNF-α) can increase expression of $P2X_7$ receptors,[53,90,98,177] suggesting that this receptor can both regulate, and is regulated by, inflammatory cytokine processing and release. Moreover, we have observed a marked increase in glomerular expression of $P2X_7$ receptors in a rodent model of proliferative

glomerulonephritis, reaching a peak that coincides with the onset of proteinuria.[170] Macrophage infiltration and release of inflammatory cytokines are characteristic features of glomerular damage in many forms of glomerulonephritis.[160] $P2X_7$ receptor gene knockout or treatment with a $P2X_7$ receptor antagonist significantly reduced the severity of proliferative glomerulonephritis in mouse and rat models, respectively, as shown by reduced renal expression of CC chemokine ligand 2 (CCL2; monocyte chemoattractant-1 (MCP-1)), reductions in glomerular macrophage infiltration, glomerular capillary thrombosis and proteinuria, and a smaller rise in serum creatinine concentration.[163] In the rat diabetic model, both glomerular epithelial (podocytes) and mesangial cells express $P2X_7$ receptors[179]; damaged podocytes have been shown to release IL-13[111]; and both IL-13 and TNF-α are increased in diabetic glomeruli.[57] Thus, ATP, acting via the $P2X_7$ receptor, could interact with, and control, the inflammatory response, eventually leading to cell death, perhaps as a mechanism for deleting damaged cells without dispersal of their potentially toxic contents. Two auto-inflammatory rheumatic diseases, SAPHO and Schnitzler's syndrome, involve an enhanced interaction and dysregulation of the $P2X_7$ receptor with the inflammasome, leading to excessive IL-1β production and release,[23,122] which suggests a wider and more fundamental role for this receptor in tissue inflammation.

Fibrosis often follows inflammation, and it has always been a major goal to determine which factors during inflammation determine its resolution and repair, and which ones lead to chronicity and progressive fibrosis. The potential role of the $P2X_7$ receptor in renal fibrosis has been investigated in a mouse model of unilateral ureteric obstruction. Transient expression of $P2X_7$ receptors was detected in tubular epithelial cells following ureteric obstruction, and the severity of tubulo-interstitial macrophage infiltration, and expression of TGF-β and fibrosis, were reduced in $P2X_7$ receptor knockout mice.[48] In the kidney, interstitial fibroblasts are important in normal repair, and their $P2X_7$-mediated loss might contribute to post-injury fibrosis and scarring in this model.[125] A similar protective effect of $P2X_7$ gene deletion has been reported recently in a model of lung fibrosis.[131]

In another model of proliferative glomerulonephritis, the $P2Y_1$ receptor has been implicated.[62] Interestingly, the acute injury was similar in $P2Y_1$ knockout and wild-type mice (cf. $P2X_7$), but there was less glomerular capillary loss and fibrosis in the $P2Y_1$ knockouts at later time points (10 and 28 days). It would clearly be useful to explore the relationship and possible interaction between $P2Y_1$ and $P2X_7$ receptors in this and related models of acute glomerulonephritis, and whether there might be synergy in targeting therapeutically both receptors.

Finally, P2 receptor activation has also been implicated in the renal injury resulting from ischaemia-reperfusion (IR), a major cause of clinical acute renal failure. Such injury can result from a wide variety of insults, including transplantation, and a common unifying mechanism is therefore difficult to define. Nevertheless, the broad-spectrum P2 inhibitor suramin was found to attenuate the renal infiltration of leukocytes and tubular cell apopotosis that usually follows IR injury.[206] Furthermore, gene deletion of ecto-5′-nucleotidase also ameliorated IR-induced apoptotic and histological renal damage, while deletion of NTPDase1 aggravated it.[103]

CONCLUDING REMARKS

For extracellular nucleotides to be effective autocrine/paracrine agents, there are three fundamental requirements: release of nucleotides from cells; controlled degradation of the nucleotides once released; and the presence of specific nucleotide receptors that can initiate transduction of the signal to a functional response. In the fourth edition of this textbook it was established that these conditions were met, both in the vasculature and the tubule. Since then, significant advances have been made in all three areas, and the many and varied functions of nucleotides in the kidneys have received increased attention. Consequently, in some areas the situation is becoming clearer. For example, nucleotide-induced NO synthesis can account for an inhibitory effect on transport in the TALH; and, given NOs putative actions in the proximal tubule and CD, this might provide a unifying hypothesis to explain nucleotide-induced effects in these segments. On the other hand, several areas continue to defy understanding – for example, the mechanism(s) of release of nucleotides and the apparently differential effects of P2Y and P2X receptors on ENaC activity. As more and more sophisticated techniques are brought to bear, it is to be hoped that ongoing research will solve even the most intransigent problems. Furthermore, although much of the work on renal pathophysiology remains at a descriptive stage, altered P2 receptor signaling is strongly implicated, and the potential for novel therapeutic targets is high.

Acknowledgments

Work in the authors' laboratories was supported by the Wellcome Trust, the Medical Research Council, Kidney Research UK, the British Heart Foundation, the Biotechnology and Biological Sciences Research Council, the Diamond Fund (Imperial College Healthcare Charity) and St Peter's Trust for Kidney, Bladder & Prostate Research.

References

[1] Adinolfi E, Callegari MG, Cirillo M, Pinton P, Giorgi C, Cavagna D, et al. Expression of the $P2X_7$ receptor increases the Ca^{2+} content of the endoplasmic reticulum, activates NFATc1, and protects from apoptosis. J Biol Chem 2009;284:10120–8.

[2] Bailey MA. Inhibition of bicarbonate reabsorption in the rat proximal tubule by activation of luminal $P2Y_1$ receptors. Am J Physiol Renal Physiol 2004;287:F789–96.

[3] Bailey MA, Hillman KA, Unwin RJ. P2 receptors in the kidney. J Auton Nerv Syst 2000;81:264–70.

[4] Bailey MA, Imbert-Teboul M, Turner C, Marsy S, Srai K, Burnstock G, et al. Axial distribution and characterization of basolateral P2Y receptors along the rat renal tubule. Kidney Int 2000;58:1893–901.

[5] Bailey MA, Imbert-Teboul M, Turner C, Srai K, Burnstock G, Unwin RJ. Evidence for basolateral $P2Y_6$ receptors along the rat proximal tubule: functional and molecular characterization. J Am Soc Nephrol 2001;12:1640–7.

[6] Bailey MA, Shirley DG. Effects of extracellular nucleotides on renal tubular solute transport. Purinergic Signal 2009;5:473–80.

[7] Bailey MA, Turner CM, Hus-Citharel A, Marchetti J, Imbert-Teboul M, Milner P, et al. P2Y receptors present in the native and isolated rat glomerulus. Nephron Physiol 2004;96:p79–90.

[8] Barbe MT, Monyer H, Bruzzone R. Cell–cell communication beyond connexins: the pannexin channels. Physiology (Bethesda) 2006;21:103–14.

[9] Beliveau R, Brunette MG, Strevey J. Characterization of phosphate binding by alkaline phosphatase in rat kidney brush border membrane. Pflügers Arch 1983;398:227–32.

[10] Bell PD, Komlosi P, Zhang Z-R. ATP as a mediator of macula densa cell signaling. Purinergic Signal 2009;5:461–71.

[11] Bell PD, Lapointe JY, Sabirov R, Hayashi S, Peti-Peterdi J, Manabe K, et al. Macula densa cell signaling involves ATP release through a maxi anion channel. Proc Natl Acad Sci USA 2003;100:4322–7.

[12] Briner VA, Kern F. ATP stimulates Ca^{2+} mobilization by a nucleotide receptor in glomerular endothelial cells. Am J Physiol 1994;266:F210–7.

[13] Burnstock G. Purinergic nerves. Pharmacol Rev 1972;24:509–81.

[14] Burnstock G. Purine and pyrimidine receptors. Cell Mol Life Sci 2007;64:1471–83.

[15] Castrop H, Huang Y, Hashimoto S, Mizel D, Hansen P, Theilig F, et al. Impairment of tubuloglomerular feedback regulation of GFR in ecto-5′-nucleotidase/CD73-deficient mice. J Clin Invest 2004;114:634–42.

[16] Cha SH, Jung KY, Endou H. Effect of P2Y-purinoceptor stimulation on renal gluconeogenesis in rats. Biochem Biophys Res Commun 1995;211:454–61.

[17] Cha SH, Sekine T, Endou H. P2 purinoceptor localization along rat nephron and evidence suggesting existence of subtypes $P2Y_1$ and P_2Y_2. Am J Physiol 1998;274:F1006–14.

[18] Chabardès-Garonne D, Méjean A, Aude J-C, et al. A panoramic view of gene expression in the human kidney. Proc Natl Acad Sci USA 2003;100:13710–5.

[19] Chan CM, Unwin RJ, Bardini M, Oglesby IB, Ford AP, Townsend-Nicholson A, et al. Localization of $P2X_1$ purinoceptors by autoradiography and immunohistochemistry in rat kidneys. Am J Physiol 1998;274:F799–804.

[20] Chan CM, Unwin RJ, Burnstock G. Potential functional roles of extracellular ATP in kidney and urinary tract. Exp Nephrol 1998;6:200–7.

[21] Churchill PC, Ellis VR. Purinergic P2y receptors stimulate renin secretion by rat renal cortical slices. J Pharmacol Exp Ther 1993;266:160–3.

[22] Cole BR, Hays AE, Boylan JG, Burch HB, Lowry OH. Distribution of enzymes of adenylate and guanylate nucleotide metabolism in rat nephron. Am J Physiol 1982;243:F349–55.

[23] Colina M, Pizzirani C, Khodeir M, Falzoni S, Bruschi M, Trotta F, et al. Dysregulation of $P2X_7$ receptor-inflammasome axis in SAPHO syndrome: successful treatment with anakinra. Rheumatology (Oxford) 2010;49:1416–8.

[24] Cotrina ML, Lin JH, Alves-Rodrigues A, Liu S, Li J, Azmi-Ghadimi H, et al. Connexins regulate calcium signaling by controlling ATP release. Proc Natl Acad Sci USA 1998;95:15735–40.

[25] Cuffe JE, Bielfeld-Ackermann A, Thomas J, Leipziger J, Korbmacher C. ATP stimulates Cl^- secretion and reduces amiloride-sensitive Na^+ absorption in M-1 mouse cortical collecting duct cells. J Physiol 2000;524:77–90.

[26] Cupples WA, Braam B. Assessment of renal autoregulation. Am J Physiol Renal Physiol 2007;292:F1105–23.

[27] Dai L-J, Kang HS, Kerstan D, Ritchie G, Quamme GA. ATP inhibits Mg^{2+} uptake in MDCT cells via P2X purinoceptors. Am J Physiol Renal Physiol 2001;281:F833–40.

[28] Deetjen P, Thomas J, Lehrmann H, Kim SJ, Leipziger J. The luminal P2Y receptor in the isolated perfused mouse cortical collecting duct. J Am Soc Nephrol 2000;11:1798–806.

[29] Di Sole F. Adenosine and renal tubular function. Curr Opin Nephrol Hypertens 2008;17:399–407.

[30] Di Virgilio F. Liaisons dangereuses: $P2X_7$ and the inflammasome. Trends Pharmacol Sci 2007;28:465–72.

[31] Diaz-Sylvester P, Mac Laughlin M, Amorena C. Peritubular fluid viscosity modulates H^+ flux in proximal tubules through NO release. Am J Physiol Renal Physiol 2001;280:F239–43.

[32] Dobrowolski L, Walkowska A, Kompanowska-Jezierska E, Kuczeriszka M, Sadowski J. Effects of ATP on rat renal haemodynamics and excretion: role of sodium intake, nitric oxide and cytochrome P450. Acta Physiol (Oxford) 2007;189:77–85.

[33] Donnelly-Roberts DL, Jarvis MF. Discovery of $P2X_7$ receptor-selective antagonists offers new insights into $P2X_7$ receptor function and indicates a role in chronic pain states. Br J Pharmacol 2007;151:571–9.

[34] Drury AN, Szent-Gyorgyi A. The physiological activity of adenine compounds with special reference to their action upon the mammalian heart. J Physiol 1929;68:213–37.

[35] Edgecombe M, Craddock HS, Smith DC, McLennan AG, Fisher MJ. Diadenosine polyphosphate-stimulated gluconeogenesis in isolated rat proximal tubules. Biochem J 1997;323:451–6.

[36] Edwards RM. Basolateral, but not apical, ATP inhibits vasopressin action in rat inner medullary collecting duct. Eur J Pharmacol 2002;438:179–81.

[37] Eltze M, Ullrich B. Characterization of vascular P2 purinoceptors in the rat isolated perfused kidney. Eur J Pharmacol 1996;306:139–52.

[38] Enjyoji K, Sévigny J, Lin Y, et al. Targeted disruption of cd39/ATP diphosphohydrolase results in disordered hemostasis and thromboregulation. Nat Med 1999;5:1010–7.

[39] Eppel GA, Ventura S, Evans RG. Regional vascular responses to ATP and ATP analogues in the rabbit kidney *in vivo*: roles for adenosine receptors and prostanoids. Br J Pharmacol 2006;149:523–31.

[40] Fernández O, Wangensteen R, Osuna A, Vargas F. Renal vascular reactivity to P2-purinoceptor activation in spontaneously hypertensive rats. Pharmacology 2000;60:47–50.

[41] Fischer KG, Saueressig U, Jacobshagen C, Wichelmann A, Pavenstadt H. Extracellular nucleotides regulate cellular functions of podocytes in culture. Am J Physiol Renal Physiol 2001;281:F1075–81.

[42] Friedrich F, Weiss H, Paulmichl M, Woll E, Waldegger S, Lang F. Further analysis of ATP-mediated activation of K^+ channels in renal epithelioid Madin–Darby canine kidney (MDCK) cells. Pflügers Arch 1991;418:551–5.
[43] Gandhi R, Le Hir M, Kaissling B. Immunolocalization of ecto-5′-nucleotidase in the kidney by a monoclonal antibody. Histochemistry 1990;95:165–74.
[44] Garvin JL, Herrera M, Ortiz PA. Regulation of renal NaCl transport by nitric oxide, endothelin, and ATP: clinical implications. Annu Rev Physiol 2011;:73.
[45] Garvin JL, Hong NJ. Nitric oxide inhibits sodium/hydrogen exchange activity in the thick ascending limb. Am J Physiol Renal Physiol 1999;277:F377–82.
[46] George SN, Kennedy-Lydon T, Callaghan H, et al. Decreased $P2X_7$ receptor mRNA expression in the CCD of the $P2X_4^{-/-}$ mouse: a clue to the identity of the P2X luminal sodium sensor? J Am Soc Nephrol 2010; F-PO1611 (Abstract)
[47] Geyti CS, Odgaard E, Overgaard MT, Jensen ME, Leipziger J, Praetorious HA. Slow spontaneous $[Ca^{2+}]_i$ oscillations reflect nucleotide release from renal epithelia. Pflügers Arch 2008;455:1105–17.
[48] Goncalves RG, Gabrich L, Rosario Jr. A, Takiya CM, Ferreira ML, Chiarini LB, et al. The role of purinergic $P2X_7$ receptors in the inflammation and fibrosis of unilateral ureteral obstruction in mice. Kidney Int 2006;70:1599–606.
[49] Gorelik J, Zhang Y, Sanchez D, Shevchuk A, Frolenkov G, Lab M, et al. Aldosterone acts via an ATP autocrine/paracrine system: the Edelman ATP hypothesis revisited. Proc Natl Acad Sci USA 2005;102:15000–5.
[50] Guan Z, Fuller BS, Yamamoto T, Cook AK, Pollock JS, Inscho EW. Pentosan polysulfate treatment preserves renal autoregulation in Ang II-Infused hypertensive rats via normalization of $P2X_1$ receptor activation. Am J Physiol Renal Physiol 2011; in press.
[51] Guo C, Masin M, Qureshi OS, Murrell-Lagnado RD. Evidence for functional $P2X_4/P2X_7$ heteromeric receptors. Mol Pharmacol 2007;72:1447–56.
[52] Hanner F, Sorensen CM, Holstein-Rathlou N-H, Peti-Peterdi J. Connexins and the kidney. Am J Physiol Regul Integr Comp Physiol 2010;298:R1143–55.
[53] Harada H, Chan CM, Loesch A, Unwin R, Burnstock G. Induction of proliferation and apoptotic cell death via P2Y and P2X receptors, respectively, in rat glomerular mesangial cells. Kidney Int 2000;57:949–58.
[54] Harahap AR, Goding JW. Distribution of the murine plasma cell antigen PC-1 in non-lymphoid tissues. J Immunol 1988;141:2317–20.
[55] Harden TK, Sesma JI, Fricks IP, Lazarowski ER. Signaling and pharmacological properties of the $P2Y_{14}$ receptor. Acta Physiol (Oxford) 2010;199:149–60.
[56] Harhun MI, Povstyan OV, Gordienko DV. Purinoreceptor-mediated current in myocytes from renal resistance arteries. Br J Pharmacol 2010;160:987–97.
[57] Hasegawa G, Nakano K, Sawada M, Uno K, Shibayama Y, Ienaga K, et al. Possible role of tumor necrosis factor and interleukin-1 in the development of diabetic nephropathy. Kidney Int 1991;40:1007–12.
[58] Heyeraas KJ, Aukland K. Interlobular arterial resistance: influence of renal arterial pressure and angiotensin II. Kidney Int 1987;31:1291–8.
[59] Hillman KA, Burnstock G, Unwin RJ. The $P2X_7$ receptor in the kidney: a matter of life or death?. Nephron Exp Nephrol 2005;101:e24–30.
[60] Hillman KA, Johnson TM, Winyard PJ, Burnstock G, Unwin RJ, Woolf AS. $P2X_7$ receptors are expressed during mouse nephrogenesis and in collecting duct cysts of the cpk/cpk mouse. Exp Nephrol 2002;10:34–42.
[61] Hillman KA, Woolf AS, Johnson TM, Wade A, Unwin RJ, Winyard PJ. The $P2X_7$ ATP receptor modulates renal cyst development *in vitro*. Biochem Biophys Res Commun 2004;322:434–9.
[62] Hohenstein B, Renk S, Lang K, Daniel C, Freund M, Leon C, et al. $P2Y_1$ gene deficiency protects from renal disease progression and capillary rarefaction during passive crescentic glomerulonephritis. J Am Soc Nephrol 2007;18:494–505.
[63] Hooper KM, Unwin RJ, Sutters M. The isolated C-terminus of polycystin-1 promotes increased ATP-stimulated chloride secretion in a collecting duct cell line. Clin Sci (Lond) 2003;104:217–21.
[64] Hovater MB, Olteanu D, Hanson EL, et al. Loss of apical monocilia on collecting duct principal cells impairs ATP secretion across the apical cell surface and ATP-dependent and flow-induced calcium signals. Purinergic Signal 2008;4: 155–70.
[65] Huwiler A, Wartmann M, van den Bosch H, Pfeilschifter J. Extracellular nucleotides activate the p38-stress-activated protein kinase cascade in glomerular mesangial cells. Br J Pharmacol 2000;129:612–8.
[66] Inscho EW. Renal microvascular effects of P2 receptor stimulation. Clin Exp Pharmacol Physiol 2001;28:332–9.
[67] Inscho EW. ATP, P2 receptors and the renal microcirculation. Purinergic Signal 2009;5:447–60.
[68] Inscho EW, Cook AK, Imig JD, Vial C, Evans RJ. Physiological role for $P2X_1$ receptors in renal microvascular autoregulatory behavior. J Clin Invest 2003;112:1895–905.
[69] Inscho EW, Cook AK, Navar LG. Pressure-mediated vasoconstriction of juxtamedullary afferent arterioles involves P2-purinoceptor activation. Am J Physiol 1996;271:F1077–85.
[70] Inscho EW, Ohishi K, Navar LG. Effects of ATP on pre- and postglomerular juxtamedullary microvasculature. Am J Physiol Renal Physiol 1992;263:F886–93.
[71] Ishikawa S, Higashiyama M, Kusaka I, Saito T, Nagasaka S, Fukuda S, et al. Extracellular ATP promotes cellular growth of renal inner medullary collecting duct cells mediated via P2u receptors. Nephron 1997;76:208–14.
[72] Jacobson KA, Ivanov AA, de Castro S, Harden TK, Ko H. Development of selective agonists and antagonists of P2Y receptors. Purinergic Signal 2009;5:75–89.
[73] Jankowski M, Szczepanska-Konkel M, Kalinowski L, Angielski S. The role of P2Y-receptors in the regulation of glomerular volume. Med Sci Monit 2001;7:340–635.
[74] Jankowski V, Karadogan S, Vanholder R, et al. Paracrine stimulation of vascular smooth muscle proliferation by diadenosine polyphosphates released from proximal tubule epithelial cells. Kidney Int 2007;71:994–1000.
[75] Jensen ME, Odgaard E, Christensen MH, Praetorius HA, Leipziger J. Flow-induced $[Ca^{2+}]_i$ increase depends on nucleotide release and subsequent purinergic signaling in the intact nephron. J Am Soc Nephrol 2007;18:2062–70.
[76] Jin W, Hopfer U. Purinergic-mediated inhibition of Na^+-K^+-ATPase in proximal tubule cells: elevated cytosolic Ca^{2+} is not required. Am J Physiol 1997;272:C1169–77.
[77] Joseph SM, Buchakjian MR, Dubyak GR. Colocalization of ATP release sites and ecto-ATPase activity at the extracellular surface of human astrocytes. J Biol Chem 2003;278: 23331–42.
[78] Kauffenstein G, Drouin A, Thorin-Trescases N, Bachelard H, Robaye B, D'Orleans-Juste P, et al. Dase1 (CD39) controls nucleotide-dependent vasoconstriction in mouse. Cardiovasc Res 2010;85:204–13.

[79] Kennedy-Lydon T, Callaghan H, Sprott C, et al. P2 receptor-mediated changes in vasa recta diameter by *in situ* pericytes: evidence for tubular/vascular cross-talk?. J Am Soc Nephrol 2010; F-PO1742 (Abstract)

[80] Kimura N, Shimada N, Nomura K, Watanabe K. Isolation and characterization of a cDNA clone encoding rat nucleoside diphosphate kinase. J Biol Chem 1990;265:15744–9.

[81] King BF, Townsend-Nicholson A. Nucleotide and nucleoside receptors. Tocris Rev 2003;23:1–11.

[82] Kishore BK, Chou CL, Knepper MA. Extracellular nucleotide receptor inhibits AVP-stimulated water permeability in inner medullary collecting duct. Am J Physiol 1995;269:F863–9.

[83] Kishore BK, Ginns SM, Krane CM, Nielsen S, Knepper MA. Cellular localization of P_2Y_2 purinoceptor in rat renal inner medulla and lung. Am J Physiol Renal Physiol 2000;278: F43–51.

[84] Kishore BK, Isaac J, Fausther M, Tripp SR, Shi H, Gill PS, et al. Expression of NTPDase1 and NTPDase2 in murine kidney: Relevance to regulation of P2 receptor signaling. Am J Physiol Renal Physiol 2005;288:F1032–43.

[85] Kishore BK, Krane CM, Miller RL, Shi H, Zhang P, Hemmert A, et al. P_2Y_2 receptor mRNA and protein expression is altered in inner medullas of hydrated and dehydrated rats: relevance to AVP-independent regulation of IMCD function. Am J Physiol Renal Physiol 2005;288:F1164–72.

[86] Kishore BK, Nelson RD, Miller RL, et al. P_2Y_2 receptors and water transport in the kidney. Purinergic Signal 2009;5:491–9.

[87] Komlosi P, Peti-Peterdi J, Fuson AL, Fintha A, Rosivall L, Bell PD. Macula densa basolateral ATP release is regulated by luminal [NaCl] and dietary salt intake. Am J Physiol Renal Physiol 2004;286:F1054–8.

[88] Koster HPG, Hartog A, van Os CH, Bindels RJ. Inhibition of Na^+ and Ca^{2+} reabsorption by P2u purinoceptors requires PKC but not Ca^{2+} signaling. Am J Physiol 1996;270:F53–60.

[89] Köttgen M, Buchholz B, Garcia-Gonzalez MA, et al. TRPP2 and TRPV4 form a polymodal sensory channel complex. J Cell Biol 2008;182:437–47.

[90] Labasi JM, Petrushova N, Donovan C, McCurdy S, Lira P, Payette MM, et al. Absence of the $P2X_7$ receptor alters leukocyte function and attenuates an inflammatory response. J Immunol 2002;168:6436–45.

[91] Lazarowski ER, Boucher RC. UTP as an extracellular signaling molecule. News Physiol Sci 2001;16:1–5.

[92] Le Hir M, Kaissling B. Distribution of 5′-nucleotidase in the renal interstitium of the rat. Cell Tissue Res 1989;258:177–82.

[93] Lee YJ, Park SH, Han HJ. ATP stimulates Na^+-glucose co-transporter activity via cAMP and p38 MAPK in renal proximal tubule cells. Am J Physiol Cell Physiol 2005;289:C1268–1276.

[94] Lee YJ, Park SH, Jeung TO, Kim KW, Lee JH, Han HJ. Effect of adenosine triphosphate on phosphate uptake in renal proximal tubule cells: involvement of PKC and p38 MAP. J Cell Physiol 2005;205:68–76.

[95] Lehrmann H, Thomas J, Kim SJ, Jacobi C, Leipziger J. Luminal P_2Y_2 receptor-mediated inhibition of Na^+ absorption in isolated perfused mouse CCD. J Am Soc Nephrol 2002;13:10–8.

[96] Lemmens R, Kupers L, Sévigny J, Beaudoin AR, Grondin G, Kittel A, et al. Purification, characterization, and localization of an ATP diphosphohydrolase in porcine kidney. Am J Physiol Renal Physiol 2000;278:F978–88.

[97] Li L, Lynch IJ, Zheng W, Cash MN, Teng X, Wingo CS, et al. Apical P2XR contribute to $[Ca^{2+}]_i$ signaling and *I*sc in mouse renal MCD. Biochem Biophys Res Commun 2007;359:438–44.

[98] Lister MF, Sharkey J, Sawatzky DA, Hodgkiss JP, Davidson DJ, Rossi AG, et al. The role of the purinergic $P2X_7$ receptor in inflammation. J Inflamm 2007;4:5.

[99] Listhrop R, Nelson R, Ecelbarger CA, et al. Genetic deletion of P_2Y_2 receptor (P2Y2-R) alters the protein abundances of renal sodium transporters and channels. FASEB J 2007;21(937):4 (Abstract).

[100] Liu W, Morimoto T, Woda C, Kleyman TR, Satlin LM. Ca^{2+} dependence of flow-stimulated K secretion in the mammalian cortical collecting duct. Am J Physiol Renal Physiol 2007;293: F227–35.

[101] Liu W, Xu S, Woda C. Effect of flow and stretch on the $[Ca^{2+}]_i$ response of principal and intercalated cells in cortical collecting duct. Am J Physiol Renal Physiol 2003;285: F998–1012.

[102] Locovei S, Bao L, Dahl G. Pannexin 1 in erythrocytes: function without a gap. Proc Natl Acad Sci USA 2006;103:7655–9.

[103] Lu B, Rajakumar SV, Robson SC, Lee EK, Crikis S, d'Apice AJ, et al. The impact of purinergic signaling on renal ischemia-reperfusion injury. Transplantation 2008;86:1707–12.

[104] Lu M, MacGregor GG, Wang W, Giebisch G. Extracellular ATP inhibits the small-conductance K channel on the apical membrane of the cortical collecting duct from mouse kidney. J Gen Physiol 2000;116:299–310.

[105] Ma W, Korngreen A, Weil S, Cohen EB, Priel A, Kuzin L, et al. Pore properties and pharmacological features of the P2X receptor channel in airway ciliated cells. J Physiol 2006;571:503–17.

[106] Mangravite LM, Xiao G, Giacomini KM. Localization of human equilibrative nucleoside transporters, hENT1 and hENT2, in renal epithelial cells. Am J Physiol Renal Physiol 2003;284:F902–10.

[107] McCoy DE, Taylor AL, Kudlow BA, Karlson K, Slattery MJ, Schwiebert LM, et al. Nucleotides regulate NaCl transport in mIMCD-K2 cells via P2X and P2Y purinergic receptors. Am J Physiol 1999;277:F552–9.

[108] McCulloch F, Chambrey R, Eladari D, Peti-Peterdi J. Localization of connexin 30 in the luminal membrane of cells in the distal nephron. Am J Physiol Renal Physiol 2005;289: F1304–12.

[109] Mo J, Fisher MJ. Uridine nucleotide-induced stimulation of gluconeogenesis in isolated rat proximal tubules. Naunyn Schmiedebergs Arch Pharmacol 2002;366:151–7.

[110] Modlinger PS, Welch WJ. Adenosine A_1 receptor antagonists and the kidney. Curr Opin Nephrol Hypertens 2003;12:497–502.

[111] Niemir ZI, Stein H, Dworacki G, Mundel P, Koehl N, Koch B, et al. Podocytes are the major source of IL-1 alpha and IL-1 beta in human glomerulonephritides. Kidney Int 1997;52: 393–403.

[112] Nishiyama A, Majid DS, Walker III M, Miyatake A, Navar LG. Renal interstitial ATP responses to changes in arterial pressure during alterations in tubuloglomerular feedback activity. Hypertension 2001;37:753–9.

[113] Nishiyama A, Navar LG. ATP mediates tubuloglomerular feedback. Am J Physiol Regul Integr Comp Physiol 2002;283: R273–5 discussion R278-R279.

[114] North RA. Molecular physiology of P2X receptors. Physiol Rev 2002;82:1013–67.

[115] Novak I. ATP as a signaling molecule: the exocrine focus. News Physiol Sci 2003;18:12–7.

[116] Odgaard E, Praetorius HA, Leipziger J. AVP-stimulated nucleotide secretion in perfused mouse medullary thick ascending limb and cortical collecting duct. Am J Physiol Renal Physiol 2009;297:F341–9.

[117] Ortiz PA, Hong NJ, Garvin JL. NO decreases thick ascending limb chloride absorption by reducing $Na^+K^+2Cl^-$ co-transporter activity. Am J Physiol Renal Physiol 2001;281: F819–25.

[118] Ortiz PA, Hong NJ, Garvin JL. Luminal flow induces eNOS activation and translocation in the rat thick ascending limb. Am J Physiol Renal Physiol 2004;287:F274–80.
[119] Osmond DA, Inscho EW. $P2X_1$ receptor blockade inhibits whole kidney autoregulation of renal blood flow *in vivo*. Am J Physiol Renal Physiol 2010;298:F1360–8.
[120] Paulais M, Bandouin-Legros M, Teulon J. Extracellular ATP and UTP trigger calcium entry in mouse cortical thick ascending limb. Am J Physiol 1995;268:F496–502.
[121] Peti-Peterdi J. Calcium wave of tubuloglomerular feedback. Am J Physiol Renal Physiol 2006;291:F473–80.
[122] Pizzirani C, Falzoni S, Govoni M, et al. Dysfunctional inflammasome in Schnitzler's syndrome. Rheumatology (Oxford) 2009;48:1304–8.
[123] Pochynyuk O, Bugaj V, Rieg T, Insel PA, Mironova E, Vallon V, et al. Paracrine regulation of the epithelial Na^+ channel in the mammalian collecting duct by purinergic P_2Y_2 receptor tone. J Biol Chem 2008;283:36599–607.
[124] Pochynyuk O, Rieg T, Bugaj V, Schroth J, Fridman A, Boss GR, et al. Dietary Na^+ inhibits the open probability of the epithelial sodium channel in the kidney by enhancing apical P_2Y_2-receptor tone. FASEB J 2010;24:2056–65.
[125] Ponnusamy M, Ma L, Gong R, Pang M, Chin YE, Zhuang S. $P2X_7$ receptors mediate deleterious renal epithelial-fibroblast cross talk. Am J Physiol Renal Physiol 2011;300: F62–70.
[126] Praetorius HA, Leipziger J. ATP release from non-excitable cells. Purinergic Signal 2009;5:433–46.
[127] Praetorius HA, Leipziger J. Intrarenal purinergic signaling in the control of renal tubular transport. Annu Rev Physiol 2010;72:377–93.
[128] Praetorius HA, Spring KR. A physiological view of the primary cilium. Annu Rev Physiol 2005;67:515–29.
[129] Ren Y, Carretero OA, Garvin JL. Role of mesangial cells and gap junctions in tubuloglomerular feedback. Kidney Int 2002;62:525–31.
[130] Rieg T, Bundey RA, Chen Y, Deschenes G, Junger W, Insel PA, et al. Mice lacking $P2Y_2$ receptors have salt-resistant hypertension and facilitated renal Na^+ and water reabsorption. FASEB J 2007;21:3717–26.
[131] Riteau N, Gasse P, Fauconnier L, et al. Extracellular ATP is a danger signal activating $P2X_7$ receptor in lung inflammation and fibrosis. Am J Respir Crit Care Med 2010;182: 774–83.
[132] Rost S, Daniel C, Schulze-Lohoff E, Baumert HG, Lambrecht G, Hugo C. P2 receptor antagonist PPADS inhibits mesangial cell proliferation in experimental mesangial proliferative glomerulonephritis. Kidney Int 2002;62:1659–71.
[133] Rouse D, Leite M, Suki WN. ATP inhibits the hydrosmotic effect of AVP in rabbit CCT: evidence for a nucleotide P2u receptor. Am J Physiol 1994;267:F289–95.
[134] Rubera I, Tauc M, Bidet M, Verheecke-Mauze C, De Renzis G, Poujeol C, et al. Extracellular ATP increases $[Ca^{2+}]_i$ in distal tubule cells. II. Activation of a Ca^{2+}-dependent Cl^- conductance. Am J Physiol Renal Physiol 2000;279:F102–11.
[135] Scemes E, Spray DC, Meda P. Connexins, pannexins, innexins: novel roles of 'hemi-channels'. Pflügers Arch 2009;457:1207–26.
[136] Schnermann J. Maintained tubuloglomerular feedback responses during acute inhibition of P2 purinergic receptors in mice. Am J Physiol Renal Physiol 2011 in press.
[137] Schulze-Lohoff E, Hugo C, Rost S, Arnold S, Gruber A, Brune B, et al. Extracellular ATP causes apoptosis and necrosis of cultured mesangial cells via $P2Z/P2X_7$ receptors. Am J Physiol 1998;275:F962–71.
[138] Schulze-Lohoff E, Ogilvie A, Sterzel RB. Extracellular nucleotides as signaling molecules for renal mesangial cells. J Auton Pharmacol 1996;16:381–4.
[139] Schwartz DD, Malik KU. Renal periarterial nerve stimulation-induced vasoconstriction at low frequencies is primarily due to release of a purinergic transmitter in the rat. J Pharmacol Exp Ther 1989;250:764–71.
[140] Schweda F, Wagner C, Kramer BK, Schnermann J, Kurtz A. Preserved macula densa-dependent renin secretion in A_1 adenosine receptor knockout mice. Am J Physiol Renal Physiol 2003;284:F770–7.
[141] Schwiebert EM, Kishore BK. Extracellular nucleotide signaling along the renal epithelium. Am J Physiol Renal Physiol 2001;280:F945–63.
[142] Schwiebert EM, Wallace DP, Braunstein GM, King SR, Peti-Peterdi J, Hanaoka K, et al. Autocrine extracellular purinergic signaling in epithelial cells derived from polycystic kidneys. Am J Physiol Renal Physiol 2002;282:F763–75.
[143] Shaver SR, Rideout JL, Pendergast W, Douglass JG, Brown EG, Boyer JL, et al. Structure-activity relationships of dinucleotides: potent and selective agonists of P2Y receptors. Purinergic Signal 2005;1:183–91.
[144] Shirley DG, Bailey MA, Unwin RJ. *In vivo* stimulation of apical P2 receptors in collecting ducts: evidence for inhibition of sodium reabsorption. Am J Physiol Renal Physiol 2005;288: F1243–8.
[145] Shirley DG, Vekaria RM, Sévigny J. Ectonucleotidases in the kidney. Purinergic Signal 2009;5:501–11.
[146] Silva G, Beierwaltes WH, Garvin JL. Extracellular ATP stimulates NO production in rat thick ascending limb. Hypertension 2006;47:563–7.
[147] Silva GB, Garvin JL. TRPV4 mediates hypotonicity-induced ATP release by the thick ascending limb. Am J Physiol Renal Physiol 2008;295:F1090–5.
[148] Silva GB, Garvin JL. Akt1 mediates purinergic-dependent NOS3 activation in thick ascending limbs. Am J Physiol Renal Physiol 2009;297:F646–52.
[149] Silva GB, Garvin JL. Extracellular ATP inhibits transport in medullary thick ascending limbs: role of P2X receptors. Am J Physiol Renal Physiol 2009;297:F1168–73.
[150] Sipos A, Vargas SL, Toma I, Hanner F, Willecke K, Peti-Peterdi J. Connexin 30 deficiency impairs renal tubular ATP release and pressure natriuresis. J Am Soc Nephrol 2009;20:1724–32.
[151] Solini A, Iacobini C, Ricci C, Chiozzi P, Amadio L, Pricci F, et al. Purinergic modulation of mesangial extracellular matrix production: role in diabetic and other glomerular diseases. Kidney Int 2005;67:875–85.
[152] Souza-Menezes J, Morales MM. CFTR structure and function: is there a role in the kidney? Biophys Rev 2009;1:3–12.
[153] Steinhausen M, Blum M, Fleming JT, Holz FG, Parekh N, Wiegman DL. Visualization of renal autoregulation in the split hydronephrotic kidney of rats. Kidney Int 1989;35: 1151–60.
[154] Stiepanow-Trzeciak A, Jankowski M, Angielski S, Szczepanska-Konkel M. P^1,P^4-diadenosine tetraphosphate (Ap_4A) inhibits proximal tubular reabsorption of sodium in rats. Nephron Physiol 2007;106:p13–18.
[155] Stockand JD, Mironova E, Bugaj V, Rieg T, Insel PA, Vallon V, et al. Purinergic inhibition of ENaC produces aldosterone escape. J Am Soc Nephrol 2010;21:1903–11.
[156] Stoessel A, Himmerkus N, Bleich M, Bachmann S, Theilig F. Connexin 37 is localized in renal epithelia and responds to changes in dietary salt intake. Am J Physiol Renal Physiol 2010;298:F216–23.

[157] Sun D, Samuelson LC, Yang T, Huang Y, Paliege A, Saunders T, et al. Mediation of tubuloglomerular feedback by adenosine: evidence from mice lacking adenosine 1 receptors. Proc Natl Acad Sci USA 2001;98:9983–8.

[158] Sun R, Miller RL, Hemmert AC, Zhang P, Shi H, Nelson RD, et al. Chronic dDAVP infusion in rats decreases the expression of P_2Y_2 receptor in inner medulla and P_2Y_2 receptor-mediated PGE_2 release by IMC. Am J Physiol Renal Physiol 2005;289: F768–76.

[159] Takenaka T, Inoue T, Kanno Y, Okada H, Hill CE, Suzuki H. Connexins 37 and 40 transduce purinergic signals mediating renal autoregulation. Am J Physiol Regul Integr Comp Physiol 2008;294:R1–11.

[160] Tam FWK. Current pharmacotherapy for the treatment of crescentic glomerulonephritis. Expert Opin Investig Drugs 2006;15:1353–69.

[161] Tao Y, Kim J, Faubel S, Wu JC, Falk SA, Schrier RW, et al. Caspase inhibition reduces tubular apoptosis and proliferation and slows disease progression in polycystic kidney disease. Proc Natl Acad Sci USA 2005;102:6954–9.

[162] Tarasova O, Sjöblom-Widfeldt N, Nilsson H. Transmitter characteristics of cutaneous, renal and skeletal muscle small arteries in the rat. Acta Physiol Scand 2003;177:157–66.

[163] Taylor SR, Turner CM, Elliott JI, et al. $P2X_7$ deficiency attenuates renal injury in experimental glomerulonephritis. J Am Soc Nephrol 2009;20:1275–81.

[164] Thomas J, Deetjen P, Ko WH, Jacobi C, Leipziger J. P_2Y_2 receptor-mediated inhibition of amiloride-sensitive short circuit current in M-1 mouse cortical collecting duct cells. J Membr Biol 2001;183:115–24.

[165] Thomsen K, Shirley DG. The validity of lithium clearance as an index of sodium and water delivery from the proximal tubules. Nephron 1997;77:125–38.

[166] Tian W, Salanova M, Xu H, Lindsley JN, Oyama TT, Anderson S, et al. Renal expression of osmotically responsive cation channel TRPV4 is restricted to water-impermeant nephron segments. Am J Physiol Renal Physiol 2004;287:F17–24.

[167] Turner CM, Elliot JI, Tam FWK. P2 receptors in renal pathophysiology. Purinergic Signal 2009;5:513–20.

[168] Turner CM, King BF, Srai KS, Unwin RJ. Antagonism of endogenous putative P2Y receptors reduces the growth of MDCK-derived cysts cultured *in vitro*. Am J Physiol Renal Physiol 2007;292:F15–25.

[169] Turner CM, Ramesh B, Srai SK, Burnstock G, Unwin RJ. Altered ATP-sensitive P2 receptor subtype expression in the Han:SPRD cy/ + rat, a model of autosomal dominant polycystic kidney disease. Cells Tissues Organs 2004;178:168–79.

[170] Turner CM, Tam FWK, Lai PC, Tarzi RM, Burnstock G, Pusey CD, et al. Increased expression of the pro-apoptotic ATP-sensitive $P2X_7$ receptor in experimental and human glomerulonephritis. Nephrol Dial Transplant 2007;22:386–95.

[171] Turner CM, Vonend O, Chan C, Burnstock G, Unwin RJ. The pattern of distribution of selected ATP-sensitive P2 receptor subtypes in normal rat kidney: an immunohistological study. Cells Tissues Organs 2003;175:105–17.

[172] Vallon V. P2 receptors in the regulation of renal transport mechanisms. Am J Physiol Renal Physiol 2008;294:F10–27.

[173] van Baal J, Hoenderop JGJ, Groenendijk M, van Os CH, Bindels RJ, Willems PH, et al. Am J Physiol 1999;277: F899–906.

[174] Vekaria RM. Vesicular storage and release of ATP in a rat proximal tubule cell line. J Physiol 2004;560P:C17 (Abstract)

[175] Vekaria RM, Shirley DG, Sévigny J, Unwin RJ. Immunolocalization of ectonucleotidases along the rat nephron. Am J Physiol Renal Physiol 2006;290:F550–60.

[176] Vekaria RM, Unwin RJ, Shirley DG. Intraluminal ATP concentrations in rat renal tubules. J Am Soc Nephrol 2006;17:1841–7.

[177] Verhoef PA, Estacion M, Schilling W, Dubyak GR. $P2X_7$ receptor-dependent blebbing and the activation of Rho-effector kinases, caspases, and IL-1 beta release. J Immunol 2003;170:5728–38.

[178] von Kugelgen I. Pharmacological profiles of cloned mammalian P2Y-receptor subtypes. Pharmacol Ther 2006;110:415–32.

[179] Vonend O, Turner CM, Chan CM, Loesch A, Dell'Anna GC, Srai KS, et al. Glomerular expression of the ATP-sensitive P2X receptor in diabetic and hypertensive rat models. Kidney Int 2004;66:157–66.

[180] Walker III M, Harrison-Bernard LM, Cook AK, Navar LG. Dynamic interaction between myogenic and TGF mechanisms in afferent arteriolar blood flow autoregulation. Am J Physiol Renal Physiol 2000;279:F858–65.

[181] Welch BD, Carlson NG, Shi H, Myatt L, Kishore BK. $P2Y_2$ receptor-stimulated release of prostaglandin E_2 by rat inner medullary collecting duct preparations. Am J Physiol Renal Physiol 2003;285:F711–21.

[182] Wilcox CS, Welch WJ, Schreiner GF, Belardinelli L. Natriuretic and diuretic actions of a highly selective adenosine A_1 receptor antagonist. J Am Soc Nephrol 1999;10:714–20.

[183] Wildman SS, Brown SG. The complex nature of P2 receptor-mediated regulation of ENaC: dependence on Na concentration, nucleotide concentration and exposure time, and tubular pH. J Am Soc Nephrol 2010;: F-PO1610 (Abstract)

[184] Wildman SS, Hooper KM, Turner CM, Sham JS, Lakatta EG, King BF, et al. The isolated polycystin-1 cytoplasmic COOH terminus prolongs ATP-stimulated Cl^- conductance through increased Ca^{2+} entry. Am J Physiol Renal Physiol 2003;285: F1168–78.

[185] Wildman SS, Unwin RJ, King BF. Extended pharmacological profiles of rat $P2Y_2$ and rat $P2Y_4$ receptors and their sensitivity to extracellular H^+ and Zn^{2+} ions. Br J Pharmacol 2003;140:1177–86.

[186] Wildman SSP, Boone M, Peppiatt-Wildman CM, Contreras-Sanz A, King BF, Shirley DG, et al. Nucleotides downregulate aquaporin 2 via activation of apical P2 receptors. J Am Soc Nephrol 2009;20:1480–90.

[187] Wildman SSP, Marks J, Turner CM, Yew-Booth L, Peppiatt-Wildman CM, King BF, et al. Sodium-dependent regulation of renal amiloride-sensitive currents by apical P2 receptors. J Am Soc Nephrol 2008;19:731–42.

[188] Wilson HL, Wilson SA, Surprenant A, North RA. Epithelial membrane proteins induce membrane blebbing and interact with the $P2X_7$ receptor C terminus. J Biol Chem 2002;277: 34017–23.

[189] Wilson PD. Polycystic kidney disease. N Engl J Med 2004;350:151–64.

[190] Wilson PD, Hovater JS, Casey CC, Fortenberry JA, Schwiebert EM. ATP release mechanisms in primary cultures of epithelia derived from the cysts of polycystic kidneys. J Am Soc Nephrol 1999;10:218–29.

[191] Woda CB, Bragin A, Kleyman TR, Satlin LM. Flow-dependent K^+ secretion in the cortical collecting duct is mediated by a maxi-K channel. Am J Physiol Renal Physiol 2001;280: F786–93.

[192] Woda CB, Leite Jr M, Rohatgi R, Satlin LM. Effects of luminal flow and nucleotides on $[Ca^{2+}]_i$ in rabbit cortical collecting duct. Am J Physiol Renal Physiol 2002;283:F437–46.

[193] Xu C, Rossetti S, Jiang L, Harris PC, Brown-Glaberman U, Wandinger-Ness A, et al. Human ADPKD primary cyst

epithelial cells with a novel, single codon deletion in the PKD1 gene exhibit defective ciliary polycystin localization and loss of flow-induced Ca^{2+} signaling. Am J Physiol Renal Physiol 2007;292:F930–45.

[194] Xu C, Shmukler BE, Nishimura K, Kaczmarek E, Rossetti S, Harris PC, et al. Attenuated, flow-induced ATP release contributes to absence of flow-sensitive, purinergic Ca_i^{2+} signaling in human ADPKD cyst epithelial cells. Am J Physiol Renal Physiol 2009;296:F1464–76.

[195] Yagil C, Katni G, Yagil Y. The effects of adenosine on transepithelial resistance and sodium uptake in the inner medullary collecting duct. Pflügers Arch 1994;427:225–32.

[196] Yamada H, Seki G, Taniguchi S, Uwatoko S, Suzuki K, Kurokawa K. Mechanism of $[Ca^{2+}]_i$ increase by extracellular ATP in isolated rabbit renal proximal tubules. Am J Physiol 1996;270:C1096–104.

[197] Yamamoto K, Sokabe T, Matsumoto T, et al. Impaired flow-dependent control of vascular tone and remodeling in $P2X_4$-deficient mice. Nat Med 2006;12:133–7.

[198] Yao J, Suwa M, Li B, Kawamura K, Morioka T, Oite T. ATP-dependent mechanism for coordination of intercellular Ca^{2+} signaling and renin secretion in rat juxtaglomerular cells. Circ Res 2003;93:338–45.

[199] Yegutkin GG. Nucleotide- and nucleoside-converting ectoenzymes: important modulators of purinergic signaling cascade. Biochim Biophys Acta 2008;1783:673–94.

[200] Yoshioka K, Saitoh O, Nakata H. Heteromeric association creates a P2Y-like adenosine receptor. Proc Natl Acad Sci USA 2001;98:7617–22.

[201] Yoshioka K, Saitoh O, Nakata H. Agonist-promoted heteromeric oligomerization between adenosine A_1 and $P2Y_1$ receptors in living cells. FEBS Lett 2002;523:147–51.

[202] Zamir M, Phipps S. Morphometric analysis of the distributing vessels of the kidney. Can J Physiol Pharmacol 1987;65:2433–40.

[203] Zhang Y, Kohan DE, Nelson RD, Carlson NG, Kishore BK. Potential involvement of P_2Y_2 receptor in diuresis of postobstructive uropathy in rats. Am J Physiol Renal Physiol 2010;298:F634–42.

[204] Zhang Y, Sanchez D, Gorelik J, Klenerman D, Lab M, Edwards C, et al. Basolateral $P2X_4$-like receptors regulate the extracellular ATP-stimulated epithelial Na^+ channel activity in renal epithelia. Am J Physiol Renal Physiol 2007;292:F1734–40.

[205] Zhang Y, Sands JM, Kohan DE, Nelson RD, Martin CF, Carlson NG, et al. Potential role of purinergic signaling in urinary concentration in inner medulla: insights from P_2Y_2 receptor gene knockout mice. Am J Physiol Renal Physiol 2008;295:F1715–24.

[206] Zhuang S, Lu B, Daubert RA, Chavin KD, Wang L, Schnellmann RG. Suramin promotes recovery from renal ischemia/reperfusion injury in mice. Kidney Int 2009;75:304–11.

This page intentionally left blank

CHAPTER

19

Paracrine Regulation of Renal Function by Dopamine

Pedro A. Jose[1], *Robin A. Felder*[2] *and Gilbert M. Eisner*[3]

[1]Division of Nephrology, Department of Medicine, University of Maryland School of Medicine, USA
[2]University of Virginia Health Sciences Center, USA
[3]Georgetown University Medical Center, USA

HISTORICAL PERSPECTIVE

Classical transmitter ligands evolved about 1000 million years ago.[1] The role of dopamine as a neurotransmitter has evolved with time. In primordial and plant cells, dopamine is present, even though catecholamine signaling is not used. In invertebrate neural systems, dopamine is the pre-eminent catecholamine. In vertebrates, the catecholamine pathway terminates in norepinephrine and epinephrine.[2] Endogenous dopamine was mainly recognized as a precursor to norepinephrine and epinephrine[3] until the late 1950s, when Carlsson demonstrated that dopamine itself had a transmitter role.[4] This finding, for which he was awarded the Nobel Prize in Physiology or Medicine 2000, was revolutionary for the understanding of various central functions of the brain, including memory, learning, drug abuse, cognition, and attention; it has also enlightened us regarding the pathogenesis and treatment of various psychiatric and neurological disorders.

Since 1910, dopamine has been known to be a vasoconstrictor, but less potent than norepinephrine and epinephrine. However, in 1942 Holtz et al. reported that dopamine, via its oxidized form, decreases blood pressure in the guinea pig and rabbit.[5] In 1958, Hornykiewicz reported that the vasodepressor effect of dopamine is due to dopamine *per se*.[6] Goldberg et al. confirmed the depressor effect of low doses of dopamine in 1959, and demonstrated a direct negative effect of dopamine on vascular resistance in 1962.[7,8] The same group reported that dopamine increased renal blood flow, glomerular filtration rate, and sodium excretion in dogs and humans. In 1977, Lokhandwala and Buckley subsequently reported that presynaptic dopamine receptors may be responsible for the dopaminergic inhibition of renal neurogenic vasoconstriction.[10] In 1981, Morgunov and Baines demonstrated a positive relationship between renal sodium and dopamine excretion that was independent of renal nerves,[11] indicating that the kidney can synthesize dopamine. Dopamine had been shown to increase cAMP production in the canine renal artery in 1973,[12] and in renal particulate preparations containing tubules, glomeruli, and blood vessels in 1977.[13] In 1980 Nakajima and Kuruma reported that renal particulate preparations had two binding sites to a radio-labeled dopamine receptor antagonist, indicating two types of dopamine receptors.[14] In 1984, Felder et al. reported that renal tubules and glomeruli express D_1-like and D_2-like receptors, respectively.[15] That dopamine can directly inhibit sodium transport in the renal proximal tubule was demonstrated by Bello-Reuss et al. in 1982[16]; Aperia et al. in 1987[17] showed that this occurs, in part, by inhibition of Na^+,K^+-ATPase activity. Subsequently, renal endogenous dopamine was shown to be important in the regulation of renal sodium excretion[18–20] in normotensive rats, but not in spontaneously hypertensive rats (SHRs).[21] In mice, deletion of any of the dopamine receptor gene subtypes produces hypertension, the mechanism of which is specific to the particular dopamine receptor subtype deleted.[22–27]

Seldin and Giebisch's The Kidney, Fifth Edition.
DOI: http://dx.doi.org/10.1016/B978-0-12-381462-3.00019-7

© 2013 Elsevier Inc. All rights reserved.

OVERVIEW

Pharmacological doses of dopamine, such as those administered intravenously to increase blood pressure, achieve concentrations that stimulate other G-protein-coupled receptors (GPCRs) (e.g., α- and β-adrenergic receptors) in addition to dopamine receptors. In this dose range, the vasoconstrictor action of α-adrenergic receptors completely overcomes any vasodilatory effect of dopamine. Normal circulating concentrations of dopamine (picomolar range) are not sufficiently high to activate vascular dopamine receptors, but high nanomolar to low micromolar concentrations can be attained in dopamine-producing tissues.[10,28–32] The Ki of dopamine for its receptors may be as low as 5 nM[33] and as high as 2.5 μM.[34]

Dopamine is important in the regulation of water and electrolyte balance, and blood pressure,[29–31] partly by regulation of the secretion/release of hormones and humoral agents that affect water and electrolyte balance. Dopamine also modulates water and electrolyte intake via the "appetite" centers in the brain,[35] and regulates ion and water transport in the kidney[29–31] and gastrointestinal tract.[32] Physiological concentrations of locally produced dopamine, acting in an autocrine or paracrine manner, inhibit ion transporter/channel/pump activity directly by actions on enzyme or channel kinetics, and indirectly by regulating their protein expression and cellular distribution. The physiological effects of dopamine occur by occupation of its specific receptors, as well as via synergistic interaction with natriuretic agents/receptors such as atrial natriuretic peptide (ANP)/ANPA,[36] eicosanoids,[37,38] endothelin/ETBR,[39] nitric oxide,[40] prolactin,[41] urodilatin,[36] angiotensin III/AT_2R,[42] and negative interaction with antinatriuretic agents/receptors such as insulin,[43] renin,[44] angiotensin II/AT_1R,[45,46] and aldosterone.[37,47,48] In general, under normal conditions and especially when extracellular fluid volume is moderately expanded, dopamine impedes ion and water transport and facilitates their excretion. During normal or moderately increased NaCl intake, inhibition of D_1-like receptors decreases sodium chloride excretion by about 60%.[18–22,29–31,49] Dopamine, however, is not important in natriuresis with marked volume expansion with isotonic saline[20,49] or even moderate volume expansion with albumin[50] or hypotonic saline.[51] With volume deficit renal dopamine production decreases[52–54]; this may allow sodium retaining mechanisms to work more effectively. The decrease in renal dopamine production during volume depletion has been related to a decrease in angiotensin II-mediated renal tubular uptake of dopamine,[55] and an increase in renal MAO activity and dopamine turnover, without altering COMT activity.[52,55] Indeed, during volume deficit, exogenous dopamine may actually decrease sodium excretion, apparently caused by an increase in sodium reabsorption in the distal nephron.[56]

RENAL DOPAMINE PRODUCTION

Plasma dopamine is freely filtered through the glomerulus, but the concentration of free dopamine in the plasma is normally too low (below 1 nmol/L)[57] to account for any significant contribution to urinary dopamine, which is in the high nanomolar to low micromolar range.[23,32,58–63] Renal deconjugation of circulating conjugated dopamine probably does not occur and, therefore, cannot account for the free dopamine in the urine.[64] Intact afferent vagal pathways have been shown to mediate the increase in renal dopamine production during acute volume expansion with isotonic saline.[65] However, renal dopaminergic nerves[66] contribute less than 30% of renal dopamine production.[11,30,31] Moreover, renal denervation does not prevent the dopaminergic-mediated increase in sodium excretion associated with volume expansion with isotonic saline.[67]

The synthesis of dopamine differs between renal tubular and neural cells. Neural cells express tyrosine hydroxylase (TH), which converts tyrosine to L-3,4-dihydroxyphenylalanine (L-DOPA) that is subsequently decarboxylated to dopamine by aromatic acid decarboxylase (AADC). Non-neural tissues, such as the renal tubules (Figure 19.1), do not express TH,[68] and therefore cannot synthesize L-DOPA. Rather, L-DOPA is taken up intracellularly by renal tubule cells and converted to dopamine by AADC, which is expressed in many non-neuronal tissues, such as immune cells,[69] kidney,[68,70,71] liver,[72] adrenal,[72] spleen,[72] pancreas,[73] and thyroid,[74] among others. There is sexual dimorphism in the levels of AADC in mice; AADC protein expression and activity are higher in the kidneys of females than in males, while the converse is true in the intestines.[71]

Renal dopamine production is regulated by several factors, including the availability and renal tubular uptake of L-DOPA, activity of AADC, transport of dopamine from inside the proximal tubule cell into the tubular lumen and perivascular space, and metabolism of dopamine. However, sodium intake and intracellular sodium are probably the major stimuli in the renal tubular synthesis/release of dopamine in normal adults.[23,54,63,75]

Sources of L-DOPA

As previously mentioned, the major source of renal dopamine production is the renal tubular

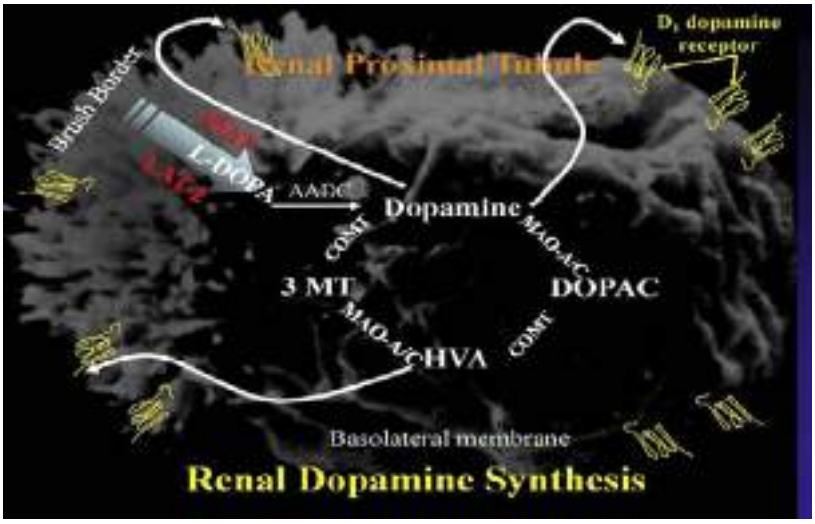

FIGURE 19.1 **Dopamine synthesis inside a renal proximal tubule cell (scanning electron microscopy).** The principal source of renal dopamine is from circulating L-dihydroxyphenylalanine (L-DOPA) which is found in the general circulation and is freely filtered by the glomerulus. Dopamine is produced in renal tubules following uptake by a sodium-independent and pH-sensitive L-type amino acid transporter (LAT2) and rBAT (related to Bo amino acid transporter and other transporters, including ASCT2, B0AT1, among others.), which is rate-limiting of the renal tubular dopamine synthesis. Renal proximal tubules convert L-DOPA to dopamine, via L-aromatic amino acid decarboxylase (AADC). In renal tubules, dopamine is produced from tyrosine and not converted to norepinephrine, because unlike neural tissue renal tubules do not express tyrosine hydroxylase or dopamine β-hydroxylase (COMT: catechol-*O*-methyl transferase; MAO: monoamine oxidase; 3MT: 3 methoxytyramine; HVA: homovanillic acid; DOPAC: 3,4 dihydroxymandelic acid).

decarboxylation of L-DOPA taken up by renal tubule cells from the glomerular filtrate and circulation.[76] Plasma L-DOPA, which is about 2 μM, reflects catecholamine turnover from sympathetically innervated tissues, such as skeletal muscle, heart, adrenal gland, and gut.[75,76] There are non-neuronal sources of plasma L-DOPA, because patients with pure autonomic failure have normal plasma levels of L-DOPA.[77] Indeed, L-DOPA is produced by non-neuronal cells that express TH in mesenteric organs (gastrointestinal tract, spleen, and pancreas[78]). Plasma L-DOPA sulfate levels increase after meals, possibly related to the amount of DOPA in the food.[79–83] Inhibition of the decarboxylation of L-DOPA during a protein meal doubles its plasma levels, indicating that normally a protein meal-induced increase in plasma L-DOPA is immediately decarboxylated.[82] Tyrosinase activation,[83] decreased degradation of L-DOPA, and renal demethylation of 3-O-methyl DOPA may be additional sources of urinary dopamine.[84–86]

Renal Tubular Uptake of L-DOPA

As already indicated, the rate-limiting step in the synthesis of dopamine by the kidney is the uptake of L-DOPA by renal tubule cells from the circulation and glomerular filtrate.[76,87] The conversion of L-DOPA to dopamine[66,88,89] occurs mainly in the proximal tubule, since AADC activity is highest in this nephron segment,[68,90] although AADC is also present in more distal nephron segments.[90–92] L-DOPA is taken up by the renal tubules via organic cation transporters[87,93] located at both apical and basolateral membranes.[94] These include sodium-dependent amino acid transporters, L-amino acid transporter-2 (LAT-2), and related to b0,+ amino acid transporter (rBAT), sodium-dependent L-amino acid transporters, ASCT2 and B0AT1, and as yet unidentified transporters.[95,96] rBAT is predominantly expressed at the apical membrane, while LAT-2 is expressed at both apical and basolateral membranes. In normotensive rats, LAT-2 and rBAT may account for more than 50% of the L-DOPA uptake in renal proximal tubules, while ASCT2 and B0AT1 may account for the rest.[95,96] In contrast in SHRs, 50% of L-DOPA uptake occurs via LAT-1, 25% via LAT-2, and 25% via ASCT2 and B0AT1.[95,97] Aging is associated with a decreased tubular uptake of L-DOPA resulting in a decrease in urinary dopamine production, the mechanism of which has not been determined.[98]

Aromatic Amino Acid Decarboxylase (AADC) Activity

Renal AADC activity is dependent on L-DOPA concentration and not on its Km. However, the increase in urinary dopamine in sodium-replete states may be caused, in part, by increased AADC activity.[89,99,100]

Patients with AADC deficiency have normal or increased levels of urinary dopamine that may be explained, in part, via tyramine hydroxylation by renal CYP2D6.[101] Hypertonic saline can increase the expression of AADC, that is mediated, in part, by TonEBP.

Dopamine Transporters

The accumulation of monoamines from the cytoplasm to storage organelles and their secretion are dependent on vesicular monoamine transporters 1 and 2 (VMAT-1, VMAT-2). VMAT-2 is expressed in neurons and certain neuroendocrine cells, while VMAT-1 is expressed in endocrine and rat renal proximal tubule cells.[60] VMAT-1 may participate in the dopaminergic regulation of renal ion transport, because renal tubular VMAT-1 mRNA and protein expression are increased by a high sodium diet.[60] However, dopamine synthesized in renal tubules is not stored, but is transported both to the basolateral membrane and into the tubular lumen, where it acts on its receptors locally.[31] Dopamine is secreted into the basolateral space via organic acid cationic transporters,[102] while dopamine probably diffuses into the lumen where it is concentrated, reaching high nanomolar to low micromolar concentrations (see above), as a result of water reabsorption and can stimulate its receptors in more distal nephron segments.[28–31]

Dopamine Metabolism

Dopamine that is synthesized in the renal tubule cells is probably not converted to norepinephrine or epinephrine. Dopamine β-hydroxylase (DBH) mRNA is not expressed in bovine or rat kidneys.[103] However, DBH is expressed in adrenergic nerves supplying the kidney, and inhibition of DBH increases renal dopamine concentration three-fold.[104] In tissues expressing phenylethanolamine-*N*-methyl transferase (PNMT) (e.g., adrenal medulla, heart, and some areas of the brain) norepinephrine is converted to epinephrine (Figure 19.1). PNMT is also not expressed in human renal proximal tubules, but is expressed in glomeruli, renal distal tubules, and endothelial cells.[105] Non-specific NMT, which is expressed in non-neuronal tissues including the kidney, enables the synthesis of epinephrine even after denervation.[106] More recent studies have also shown that TH and DBH are expressed in mesangial and renal proximal tubule cells in culture, in a pig renal tubular cell line (LLCPK) with proximal tubule and distal tubule characteristics,[107] in a canine distal tubular cell line, MDCK, and mouse inner medullary collecting duct cells.[91] Because TH is not expressed in renal proximal tubules,[68] the presence of TH in LLCPK could be indicative of its distal tubular characteristics.[107] Although dopamine may have access to non-specific NMT,[106] the increase in urinary dopamine with salt loading is not accompanied by an increase in urinary norepinephrine or epinephrine.[23,25,51,58]

In renal tubules, dopamine is degraded both by deamination via monoamine oxidase (MAO) to 3,4-dihydroxyphenylacetic acid (DOPAC), and by methylation via COMT to 3-methoxytyramine. Newly formed dopamine is metabolized predominantly by MAO-A rather than MAO-B, especially in the proximal tubule.[108] In contrast, dopamine is metabolized by COMT in more distal nephron segments.[109,110] A novel flavin adenine dinucleotide-dependent amine oxidase named renalase or MAO-C has been identified in the kidney, but its role in the intrarenal metabolism of renal dopamine is unknown.[111] Acute inhibition of COMT activity may be more important than MAO in the short-term,[112] while the converse is true for chronic inhibition.[110] The inhibition of dopamine degrading enzymes can increase its concentration. However, the increase in urinary dopamine with high salt intake is probably not related to any decrease in dopamine degradation.[62,99]

Dietary Influence Including Salt Intake

Feeding increases urinary dopamine that have been related to the amount of sodium in the diet. Most studies have shown that a low sodium intake is associated with low urinary dopamine, while the converse occurs with a high sodium diet.[31,50,53,58,62–65,92,113–117] This could be due to an increased spillover of L-DOPA into the arterial blood,[53,61] as ingestion of food/protein which contains sodium causes an increase in circulating L-DOPA.[80–84] However, plasma L-DOPA levels may not be increased by a high sodium diet.[32] Even if circulating L-DOPA is not increased by salt intake, the increase in urinary dopamine with salt loading is associated with an increase in urinary excretion of L-DOPA.[61] Therefore, the increase in urinary excretion of dopamine appears to be secondary to an increase in the uptake of L-DOPA by renal proximal tubules, presumably from the glomerular filtrate and circulation.[61,88,93–99,118–120] There may also be a mechanism by which L-DOPA is delivered to the kidney independent of circulating L-DOPA (e.g., via the adrenal gland).[121,122]

Chloride may be more important than sodium in the regulation of renal dopamine production, because an increase in the intake of chloride without sodium increases urinary dopamine, while sodium bicarbonate does not.[115] An increase in the intake of phosphate[112] or calcium[115,123] also increases renal dopamine production. Blockade of N-type, but not L-type, calcium channels can decrease urinary dopamine excretion.[124,125]

An important factor in the increase in urinary dopamine caused by sodium loading is the preferential egress of dopamine into the renal tubular lumen, rather than into the interstitium.[62,126] In LLC-PK1 cells dopamine egresses at the apical surface by a non-saturable process, while its egress at the basolateral surface is saturable, with the latter 5–7-fold higher than the former.[94] The egress of dopamine in LLC-PK1 is probably not related to VMAT-1, because the egress of dopamine is not inhibited by dopamine transporter inhibitors.[94] However, chronic sodium loading increases the expression of the VMAT-1 in the renal proximal tubule, which may contribute to the modification of the polarity of dopamine secretion during sodium loading.[60] Inhibition of sodium hydrogen exchanger (NHE) activity decreases efflux of dopamine into the peritubular space, which presumably favors luminal outflow. Thus, dopamine, by inhibiting proximal tubular luminal NHE activity,[127–133] may facilitate its own egress into the tubular lumen. The preferential luminal efflux and tubular fluid reabsorption result in high nanomolar to low micromolar concentrations[31,134] of dopamine in the tubular lumen, concentrations that approach the EC_{50} of dopamine and D_1-like receptor agonists to stimulate adenylyl cyclase and phospholipase C activity.[127,131,135–143] This mechanism, and the fact that dopamine can also be synthesized in more distal nephron segments, albeit to a lower extent relative to the proximal tubule, enables dopamine to stimulate its receptors in more distal nephron segments.

There may not always be a relationship among dietary sodium, urinary dopamine, and sodium excretion.[143–153] Mühlbauer and colleagues have claimed that food intake rather than sodium is responsible for the increase in urinary dopamine.[145–147] However, all the acute saline loading studies were performed in rats in which food, but not water, was withheld for 24 hours.[20,21,49,117] Differences in the amount[49,117] and duration[116,148–150] of the sodium load in the food, as well as differences in the strains of rats studied (see below) are possible explanations. In humans, increasing sodium intake from 20 to >200 mmol/day increases renal dopamine production that peaks by the second day, followed by a gradual decline to 50% of the peak value by the 5th day.[116] In rats, sodium chloride loading maximally increases dopamine excretion on the first few days, with the excretion decreasing close to control levels at 1 week, only to gradually increase again from 2 to 4 weeks.[148,149] Renal dopamine concentrations are not higher in non-salt loaded rats than in rats loaded with salt for 6 weeks.[150] There may also be an interaction between sodium and other substances in food, e.g., protein. Ingestion of food with very low sodium content (<0.02% sodium) is not associated with an increase in sodium excretion (unpublished data).

The renal production of dopamine is strain-dependent in rodents. Urine dopamine is lower in Sprague-Dawley than in Dahl salt-sensitive or -resistant rats[61] or in WKY and SHRs.[151] A strain of WKY rat increases urinary dopamine after 24 hours of salt loading at 4 weeks, but not at 12 weeks of age.[61] Uninephrectomy increases urinary dopamine in Wistar-Han from Harlan, but not from Charles-Rivers or WKY rats from Harlan.[97,152] The increase in urinary dopamine with chronic sodium chloride loading is less in the salt-sensitive C57BL/6 than the salt-resistant SJL mice from Jackson Laboratory.[153]

The renal production of dopamine is also age-dependent. Renal dopamine synthesis increases with development.[92] However, in contrast to the stimulatory effect of sodium intake on dopamine excretion in normal adult humans,[53,58,113,115,116] in pre-term infants sodium supplementation prevents, while sodium restriction increases, urinary dopamine[154]; the significance of this in terms of sodium balance remains to be determined. The stimulatory effect of increased dietary sodium on renal dopamine production and ability to excrete salt load are diminished with aging.[98,100,155–157] Urinary dopamine excretion is also decreased in patients with chronic renal failure, but due to loss of nephron number rather than an inability to synthesize dopamine.[158]

Gender may influence the urinary dopaminergic response to a sodium load. For example, sodium loading has been reported to increase urinary dopamine excretion in Chinese females, but not Chinese males.[159] Ethnic differences in the relationship between urine dopamine and sodium have been reported.[160–162] The blunted increase in urinary dopamine in response to acute volume expansion in blacks may be caused by reduced decarboxylation of L-DOPA.[125]

Patients with type 1 or type 2 diabetes have decreased basal urinary dopamine,[163,164] as well as a deficient response to high sodium chloride diet[165] or infusion.[166] Decreased dopamine production in human adults[164,167] and children[168] with type 2 diabetes[169] may affect the ability to excrete a sodium load. Rats with type 1 diabetes also have decreased renal dopamine production.[170]

Patients with salt-sensitive, low renin or non-modulating hypertension, and some with normal renin hypertension[161,171–174] have a blunted increase in urinary dopamine in response to salt loading, despite higher rates of L-DOPA excretion.[173] Protein intake[171] or high dietary sodium intake may not increase urinary dopamine in essential hypertensive patients or even normotensive subjects with a family history of hypertension.[159,165,172,175–177] However, salt-sensitive[173] and normal renin essential hypertensives[178] have normal basal urinary dopamine. Mild exercise has been reported to increase renal dopamine production in Stage 1 hypertensive subjects.[179] Borderline and young

hypertensives[180,181] have higher basal urinary dopamine than control subjects or stable hypertensive patients,[181,182] suggesting that the renal dopaminergic system may act as an early defense against hypertension that fails during its progression.[183]

There are also abnormalities in renal dopamine production in animal models of genetic hypertension. Renal dopamine production may be decreased in adult spontaneously hypertensive and Dahl salt-sensitive rats relative to their normotensive controls, the WKY and Dahl salt-resistant rat, respectively.[63,184] However, urinary free dopamine and renal tissue dopamine are actually increased in young SHRs in comparison with WKY rats,[184,185] but the difference disappears at age 16 weeks. In the young Dahl salt-sensitive rat, urinary dopamine is normal and increases with salt intake, as in Dahl salt-resistant rats,[63,186] although kidney levels of dopamine are lower in Dahl salt-sensitive than in salt-resistant rats on a high salt diet.[186] In adult Dahl salt-sensitive rats, the urinary excretion of dopamine is not increased or may even be decreased in response to acute volume expansion or salt loading.[185,187] Mice deficient of D_2 dopamine receptors have salt-sensitive hypertension and decreased renal dopamine production.[23,24]

Dopamine Receptor Subtypes

Dopamine receptors probably evolved from a common ancient ancestor over 750 million years ago, before the divergence of vertebrates and invertebrates.[188] Dopamine receptors belong to the α group of the rhodopsin-like family of GPCRs,[29–31,189–193] characterized by seven transmembrane domains. Based on their ability to stimulate or inhibit adenylyl cyclase, dopamine receptors have been classified into two families (Table 19.1): D_1-like receptors stimulate adenylyl cyclases, while D_2-like receptors inhibit adenylyl cyclases.[29–31,189–193] There are two D_1-like receptors in eutherian mammals, D_{1A} and D_{1B}, also known as D_1 and D_5 in humans; archosaurs have four D_1-like receptors, $D_{1A,}$ D_{1B}, D_{1C}, and D_{1D}; all other jawed vertebrates have three D1-like receptors, D_{1A}, D_{1B}, and D_{1C}.[194] The D_2-like receptors include D_2 (D_2R), D_3 (D_3R), and D_4 (D_4R).[29–31,189–193] The rank order affinity of dopamine to its receptors is: $D_3R \geq D_4R > D_5R \geq D_2R > D_1R$.[195]

Based on site-directed mutagenesis and protein modeling of some GPCRs, including D_2R, the binding of their respective agonist has been suggested to occur at the hydrophobic transmembrane domains, i.e., aspartate residues in transmembrane domains II and III, two serine residues in transmembrane V, and a phenylalanine residue in transmembrane VI.[190] Dopamine receptors have not been crystallized, but studies of the crystallized β2-adrenergic receptor suggest that agonist binding occurs at the extracellular ends of helices III, IV, V, and VII, with the cytosolic ends mediating G-protein activation.[196] Nuclear magnetic resonance spectroscopy has revealed three distinct conformations of the β_2AR: unliganded receptor or neutral antagonist, inverse agonist, and agonist.[197] The binding pocket of the A_{2A} adenosine receptor is slightly different, with the binding pocket closer to helices VI and VII, suggesting GPCR specificity.[198]

Dopamine Receptor Signaling

Receptor activation, at least for rhodopsin, occurs by a disruption of the Arg135/Glu134 ionic bond in transmembrane VI resulting in the formation of a new Arg135/Tyr223 interaction in transmembrane V261. This causes the GPCR to function as a guanine nucleotide exchange factor promoting the exchange of GDP with GTP on the Gα-subunit, resulting in the dissociation and release of the Gα-subunit from the Gβγ-subunit.[189,199] The dissociated G-protein-subunits then initiate the activation or inhibition of downstream effectors. Hydrolysis of GTP by the intrinsic GTPase activity of Gα promotes the reassociation of the G-protein-subunits. RGS (regulators of G-protein signaling) acting as a GTPase-activating protein (GAP), stimulate the hydrolysis of GTP and, therefore, the reassociation of the G-protein-subunits. RGS act as a GAP for GαS, Gαi and Gαq. While a primary function of RGS is to suppress G-protein signaling via GAP activity, RGS have non GAP actions such as direct antagonism of Gα and binding of Gβ/γ. Specific RGS have been reported to regulate dopamine receptors. For example, RGS7 with Gβ5 can regulate dopamine receptor signaling[200] and RGS9-2, but not RGS4, inhibits D_2R internalization,[201] while RGS19 inhibits D_2R signaling.[202] RGS4 may be involved in D_1R signaling.[203] In contrast, RGS2 may be regulated by both D_1R and D_2R.[204]

In some instances, agonist specific ligand binding does not cause dissociation of the protein subunits, but rather a conformational change.[205] Heterotrimeric G-proteins can also interact with proteins other than GPCRs to regulate physiological processes.[206] These include activators of G-protein signaling (AGS) which promote guanine nucleotide exchange independent of GPCRs and activate or inhibit adenylyl cyclase or phospholipase C. Dopamine receptors have been reported to decrease AGS1 expression.[207] In addition, GPCR signaling can be independent of G-protein-subunits.[208] For example, the inotropic effect of angiotensin II with occupation of $AT_{1a}R$ in cardiomyocytes occurs via a Gαq/PKC-independent, but GRK6/β-arrestin 2-dependent, mechanism.[209]

Both D_1-like receptors, D_1R and D_5R couple to $G\alpha_S$[29–31,189–193]and Gαq.[135,136,138–142] There are also

differences in G-protein linkage between D_1R and D_5R. For example, the D_1R, but not D_5R, also couples to Go[210] and $G\alpha_{Olf}$,[211] which is expressed in renal tubules and macula densa.[212] In contrast, D_5R, but not D_1R, couples to Gz and $G\alpha_{12/13}$.[211,213] $G\alpha_{12/13}$ proteins may have functions different from those ascribed to GPCR activation, including cell movement, actin cytoskeleton, and protein phosphatase 2A activity.[214] Because the recycling of D_1R is partly under the control of protein phosphatase 2A or a protein phosphatase 2-like enzyme,[215,216] this may be a mechanism for D_5R and D_1R cross-talk.

The linkage of G-protein-subunits to the specific D_1-like receptor may be tissue-specific. This apparently discordant linkage of D_1-like receptors to G-protein-subunits can be explained by recent observations that a specific ligand acting on the same receptor recruits specific signaling proteins that elicit a specific phenotype.[217] For example, most D_1-like receptor agonists stimulate both adenylyl cyclase and phospholipase C. However, there are exceptions; SKF83822 stimulates adenylyl cyclase but not phospholipase C,[218] whereas SKF83959 stimulates phospholipase C but actually inhibits adenylyl cyclase.[219]

Adenylyl Cyclase and Protein Kinase A (PKA)

As indicated above, D_1-like receptors are linked to stimulation of adenylyl cyclase which leads to the formation of cAMP. There are at least 10 isoforms of adenylyl cyclase (adenylyl cyclases I-IX and adenylyl cyclase short). In the neostriatum, the D_1R is linked to adenylyl cyclase V.[191] However, adenylyl cyclase V is not expressed in the rat renal proximal tubules[220] (but may be expressed in humans, unpublished observations). In kidney tubule cells, D_1R is linked to adenylyl cyclase VI, while D_5R is linked to adenylyl cyclase IV.[221] cAMP binds to the regulatory subunits of PKA resulting in the activation (disinhibition) of its catalytic subunits. There are two PKA isoforms, but D_1-like receptors, specifically D_1R, may utilize PKA II rather than PKA I.[222,223] There are several PKA substrates, among which are dopamine and cAMP-regulated 32 kDa phosphoprotein (DARPP-32) which inhibits protein phosphatase 1.[224] In contrast to the stimulatory effect of the D_1R/PKA pathway on DARPP-32, the D_1R/phospholipase C pathway inhibits DARPP-32.[225] The roles of PKA, DARPP-32, and protein-phosphatases in renal sodium transport are discussed below.

Phospholipase C

Phospholipase C catalyzes the formation of diacylglycerol and inositol phosphates. D_1-like receptors are linked to phospholipase C, via $G\alpha q$, independent of adenylyl cyclase, a phenomenon that was initially described in renal cortical tubules.[135,136,138–142] There are several isoforms of phospholipase C; the D_1R directly stimulates phospholipase $C\beta1$ in renal cortical[140] but not in medullary membranes, and indirectly stimulates phospholipase $C\gamma$ via PKA and PKC, in fibroblasts.[139]

In neuroblastoma cells, the D_1R is not linked to G_q[210] and in neurons, D_1R-mediated stimulation of phospholipase C may require the presence of D_2R[226] while D_5R, by itself, can increase phospholipase C-mediated calcium mobilization that is inhibited by D_2R.[227] However, in a pituitary adenoma rat cell line (GH4C1) transfected with the D_5R, the D_5R activation actually decreases inositol phosphate production.[228] The report that D_1-like receptor-stimulated phospholipase C persists in $D_1^{-/-}$ mice[229] has been taken to indicate that there is a D_1-like receptor other than D_1R that can stimulate phospholipase C. This is indeed the case, as the D_5R is also linked to phospholipase C activation in neural tissue (hippocampus, cortex, and striatum).[230]

Phospholipase D

Phospholipase D (PLD) hydrolyzes phospholipids, such as phosphatidylcholine, to form phosphatidic acid and the free polar head group of the phospholipid substrate. Phosphatidic acid can be cleaved by phosphatidic acid phosphohydrolase to produce diacylglycerol; both are important second messengers in the "late" response of cells to certain stimuli.[231] The two mammalian isoforms of PLD (PLD1 and PLD2) have ~50% identity, and are distributed widely in mammalian tissues and cells. They are believed to play an important role in the regulation of cell function and cell fate by a variety of extracellular signals.[231] D_5R inhibits PLD2 activity in renal proximal tubule cells,[232] while both D_1R and D_5R can inhibit phospholipase D activity in vascular smooth muscle cells.[233] These actions lead to inhibition of the production of reactive oxygen species (ROS).[232–234] The D_3R heterologously expressed in HEK293 cells has been reported to activate PLD, via Rho and independent of Gi/Go.[235] The relationship between PLD and endogenously expressed D_3R remains to be determined.

Protein Kinase C

Protein kinase C (PKC) isoforms are classified into three groups: (1) conventional PKCs (cPKC-α, -βI, -βII, and -γ); (2) novel PKCs (nPKC-δ, -ε, -θ, and -η/G); and (3) atypical PKCs (aPKC-$\lambda(\iota)$ and -ξ) and PKCμ, also called PKD which consists of PKD1, PKD2, and

PKD3.[236] In renal tubule cells, D_1-like receptors can stimulate PKCθ[237] and PKCξ,[237,238] and inhibit PKCδ.[237] The D_1R increases the phosphorylation of $PKC\theta^{S676}$ in human embryonic kidney (HEK293) cells.[239] D_1-like receptors can also translocate specific PKC isoforms. Thus, D_1-like receptors translocate conventional (α, β) and novel (ε) PKCs from renal tubule cytosol into membranes,[240,241] and the novel PKC-δ from membranes to cytosol.[240] Some studies have shown that the stimulation of PKC by dopamine may be secondary to PKA activation.[139,242]

While PKA and PKC mediate the actions of D_1R, both can also regulate D_1R signaling. PKC activation can produce differential D_1R and D_5R signaling. PKC can increase the membrane expression of D_1R in vascular smooth muscle cells.[243] In HEK293 cells, novel PKC isoforms stimulate D_1R signaling, but inhibit D_5R signaling.[244] However, in HEK293T cells, PKCα, β1, γ, δ, and ε constitutively phosphorylate and dampen D_1R signaling.[245] Ethanol enhances D_1R signaling by inhibiting PKCγ and PKCδ.[246] PKA and PKC have been reported to phosphorylate D_1R, modulating the rate of agonist-induced D_1R desensitization and intracellular trafficking.[243–248] RanBP9 and RanBP10 interact with both PKCδ/γ to increase the phosphorylation and desensitization of D_1R in neural and renal proximal tubule cells.[248] RanBP9 and RanBP10 may function as scaffolding proteins to regulate the spatial and temporal organization of D_1R and PKC. In renal proximal tubule cells, NHERF-1 is necessary for the D_1R-mediated stimulation of cAMP accumulation and PKC activity.[249]

D_2-Like Receptors

The D_2-like receptors couple to G-proteins $G\alpha_i$ and G_o, and inhibit adenylyl cyclases.[29–31,189–193]

There are two isoforms of D_2R; postsynaptic D_2R effects are mediated by the long isoform, $D_{2L}R$, while the presynaptic D_2R effects are mediated by the short isoform, $D_{2S}R$.[192,250] The $D_{2S}R$ is localized at the plasma membrane, while the $D_{2L}R$ is localized in the perinuclear region in several cell lines heterologously expressing $D_{2S}R$ and $D_{2L}R$.[251] However, in renal proximal tubule cells that express the $D_{2L}R$ rather than the $D_{2S}R$, the $D_{2L}R$ is expressed mainly at the plasma membrane.[252] The particular G-protein-subunit that interacts specifically with either D_2R isoform is not clear.[253] The D_2R can couple to the same extent to Gαi (Gαi2 and Gαi3) and Gz,[253] but Gαo may be the major G-protein that is activated by $D_{2S}R$ and $D_{2L}R$[254]; neither $D_{2S}R$ nor $D_{2L}R$ subtype is linked to Gq11 or $G\alpha_{12/13}$. A splice variant of Gαi2, $sG\alpha_{i2}$, is important in the intracellular localization of D_2R, and its dissociation from D_2R following D_2R agonist stimulation increases cell surface D_2R expression.[254]

The D_4R, like the D_2R, couples to Gαi ($G\alpha_{i2}$ and $G\alpha_{i3}$), Gαo, Gz, and Gαt2.[191,255] Different numbers of 16 amino acid repeats in the third cytoplasmic loop cause several human D_4R isoforms (e.g., D4-2, D4-4, and D4-7).[256] The role of these D_4R isoforms in cell function remains to be determined. However, the D_4R long (at least one 7 to 10 repeat) has been reported to be associated with higher diastolic and systolic blood pressure.[257]

The D_3R linkage to $G\alpha_i$ is not robust, in contrast to that observed for D_2R and D_4R.[258] In rat renal proximal tubule cells the D_3R stimulation of phospholipase C is via $G\alpha_{i3}$.[259] The signaling of D_3R, like the D_2R and D_4R, may be mediated by Gαo.[191] The utilization of G-proteins in D_2R and D_3R-mediated stimulation of extracellular signal-regulated kinase differs, D_2R utilizes $G\alpha_i$ while D_3R utilizes Gα/o and the βγ-subunit of G_i.[260] The D_3R also couples to Gz and, in the presence of pertussis toxin, the D_3R can also couple to Gαs.[253] The D_3R can also couple to Gq11.[259] The linkage of the D_3R to other effectors, such as inhibition of K^+ and Ca^{2+}, may be more sensitive than its weak linkage to G-proteins.[258] The D_3R is also insensitive to GTP, relative to the other dopamine receptor subtypes.[191] There could be seven distinct alternatively spliced D_3R variants.[261] The full-length D_3R and a shorter receptor isoform, the D_3S, bind to dopamine. The five other alternatively spliced D_3R variants do not bind dopamine, but one of them, D_3Rnf, regulates receptor dimerization.

Adenylyl Cyclase

Although D_2-like receptors inhibit adenylyl cyclase activity, in many cell lines heterologously expressing the D_3R, its linkage to $G\alpha_i$ is not robust.[258] However, the D_3R robustly inhibits adenylyl cyclase isoform V,[258] but because this adenylyl cyclase isoform is not expressed in the rat renal proximal tubule,[220] it is expressed in human renal proximal tubule cells (unpublished data). D_3R action in this rat nephron segment is not due to $G\alpha_i$ signaling. Because D_3R can couple to Gαs in the presence of pertussis toxin,[253] the D_3R could increase adenylyl cyclase activity in this nephron segment in the rat. This has not been directly tested, but D_1R and D_3R dimerization increases the ability of dopamine to stimulate adenylyl cyclase activity.[262] In contrast, the co-expression of D_2R with D_3R increases the ability of D_2-like agonists to inhibit adenylyl cyclase activity.[263] This becomes a conundrum in cells expressing these dopamine receptor subtypes, but at least in renal proximal tubules there is no evidence

of D_1R and D_2R or D_2R and D_3R heterodimerization (unpublished data). However, in the kidney and vascular smooth muscle D_1R and D_3R do interact, and this interaction probably predominates over the other possible D_1-like and D_2-like interactions.[264–266] While D_2R, by itself, stimulates Na^+K^+-ATPase activity,[267] simultaneous stimulation of D_1-like and other D_2-like receptors inhibits Na^+K^+-ATPase activity.[268] Furthermore, $D_{2L}R$ and $D_{4.4}R$ can potentiate PKC-stimulated adenylyl cyclase II activity through the release of β/γ-subunits,[269] and $D_{2L}R$ can sensitize adenylyl cyclase VI.[270] Although these adenylyl cyclase isoforms are expressed in renal proximal tubule cells, this interaction probably does not occur in renal proximal tubule cells because quinpirole, a D_2-like receptor agonist with preference for the D_3R and D_4R over the D_2R, does not stimulate adenylyl cyclase activity (unpublished studies). As stated above, there are species differences because adenylyl cyclase V is expressed in the human (unpublished data) but not in the rat renal proximal tubule.[220]

Phospholipase C

In neural cells, D_2R, via $G\beta/\gamma$, stimulates phospholipase C[191] and specifically phospholipase Cβ4 in the intermediate lobe of the pituitary gland[271]. D_1R and D_2R can interact to stimulate phospholipase C in neural cells,[226] but as stated above there is no evidence for D_2R and D_3R interaction in renal proximal tubule cells. D_2R and D_5R can also heterodimerize to stimulate phospholipase C in neural tissue and HEK-293 cells.[227] The $D_{2S}R$ can also stimulate phospholipase D,[272] but the latter enzyme is inhibited by D_5R.[232] These effects need not be counter-regulatory, because as previously mentioned the $D_{2S}R$ is presynaptic, while the D_5R inhibition of phospholipase D is postsynaptic in renal proximal tubule cells (in particular). In addition, presynaptic inhibition of adrenergic neurotransmitters by $D_{2S}R$ facilitates the inhibitory effects of dopamine on ion transport.

Dopamine Regulation of Ion Channels

D_1-like receptors inhibit voltage-gated K^+ channels and G-protein-regulated inward rectifying channels, but stimulate L-type Ca^{2+} channels.[191] D_1-like receptors inhibit G-protein-dependent inward rectifier K-like channels in medial prefrontal cortex via PKC.[273] In contrast, D_2-like receptors stimulate voltage-gated K^+ channels and G-protein-regulated inward rectifying channels, but inhibit L-type Ca^{2+} channels. Both D_1-like and D_2-like receptors inhibit N-, P-, and Q-type Ca^{2+} channels and transient sodium channels, but stimulate persistent P sodium channels.[191] We have reported that the D_3R-mediated vasorelaxation of rat mesenteric arteries is due to stimulation of small- and/or large-Ca^{2+}-activated K^+ channels.[264] In human coronary vascular smooth muscle cells, D_5R stimulates Ca^{2+}-activated big K^+ channel,[274] via cAMP-mediated stimulation of PKG.

Dopamine Regulation of Mitogen-Activated Protein (MAP) Kinase and other Kinases

D_1-like receptors may activate MAP kinases, including p38MAP kinase, and c-jun amino-terminal kinase.[191] In the brain, D_1-like receptors can also activate ERK,[275] but ERK1/2 is actually inhibited by D_5R but not by D_1R in human renal proximal tubule cells.[276] D_2-like receptors can also activate MAP kinase via $G\beta/\gamma$.[277] D_2-like receptor-mediated stimulation of Na^+ K^+-ATPase in the kidney is linked to the p44/42 MAP kinase pathway.[278] Aberrant D_1R activation of ERK1/2/MAP kinase has been reported in D_1R supersensitivity.[279] However, in the kidney, MAP kinase reduces D_1R affinity and G-protein coupling.[280]

Dopamine inhibits DNA synthesis of cultured human mesangial cells.[281] In rat vascular smooth muscle cells, D_1R or D_3R does not affect vascular smooth muscle cell proliferation, but inhibits the proliferative effect of insulin and norepinephrine.[282,283] D_2R, via inhibition of MAP kinase, inhibits angiotensin II-induced hypertrophy of cultured neonatal rat ventricular myocytes.[284] However, dopamine increases the phosphorylation of and activates p44/42 MAP kinases in rabbit renal proximal tubule cells in primary culture.[285] In human renal proximal tubule cells and Chinese hamster ovary cells, the D_3R promotes mitogenesis or cell proliferation through the activation of MAP kinases.[191,286,287] The variable effects of dopamine on MAP kinase in smooth muscle and epithelial cells may be related to tissue- or cell-specificity.

DARPP-32

As stated above, DARPP-32 was identified initially as a major target for dopamine-activated adenylyl cyclase in striatum.[224] Since the mid-1980s, DARPP-32 has been acknowledged as a crucial mediator of the biochemical, electrophysiological, transcriptional, and behavioral effects of dopamine.[288] The state of DARPP-32 phosphorylation has been shown to provide a mechanism for integrating information arriving at dopaminoceptive neurons, in multiple brain regions, via a variety of neurotransmitters, neuromodulators, neuropeptides, and steroid hormones. Activation of PKA or PKG stimulates DARPP-32

phosphorylation at Thr,[34] and thereby converts DARPP-32 into a potent inhibitor of protein phosphatase-1 (PP1). Protein phosphatase-2B (PP2B) is the most effective protein phosphatase in dephosphorylating DARPP-32 at Thr.[34] Thus, DARPP-32 acts as an amplifier of PKA and PKG-mediated signaling when it is phosphorylated on Thr,[34] which converts it into an inhibitor of PP1. The role of DARPP-32 in signaling has turned out to be very complex. Under basal conditions, DARPP-32 is phosphorylated at Thr[75] and inhibits PKA. Thus, DARPP-32 has the unique property of acting either as an inhibitor of PP1 or an inhibitor of PKA. However, under hyperdopaminergic conditions, the phosphorylated state of Thr[75] is reduced, allowing increased phosphorylation at Thr.[34] This positive feedback loop acts as a switch to potentiate dopaminergic signaling. Cdk5, a cyclin-dependent kinase family member, also phosphorylates DARPP-32 at Thr.[75] Furthermore, protein phosphatase 2A dephosphorylates DARPP-32 both at Thr[34] and Thr,[75] and the state of phosphorylation of DARPP-32 at Thr[34] depends on the phosphorylation state of two serine residues, Ser[102] and Ser.[137] DARPP-32 has been demonstrated with biochemical, immunohistochemical, and *in situ* hybridization techniques to have an anatomical distribution similar to that of dopaminoceptive cells possessing D_1Rs in the central nervous system.[289–291] DARPP-32 is also expressed in several peripheral tissues, including brown fat cells, parathyroid, retina, and renal tissue.[289,291–293] The ability of D_1R to stimulate protein phosphatase 2A[215,294] may serve as a negative feedback in the D_1R and DARPP-32 relationship, and prevent the inhibitory effect of DARPP-32 on PKA.

Regulation of Dopamine Receptor Function

Effect of Sodium on Dopamine Receptor Expression

While acute sodium loading generally increases renal dopamine production,[31,50,53,58,62–65,92,99,113,114,119] it may decrease brain[295] and renal D_1-like and D_2-like receptor density.[296,297] However, the decrease in renal D_1-like receptor expression occurs after 7–28 days of increased sodium intake during peak renal dopamine production.[148,149] In C57BL/6 mice, increasing NaCl diet to 6% for 5–7 days decreases renal D_1R expression, but increases renal D_3R expression without affecting the renal expression of D_2R, D_4R or D_5R (unpublished observations).

Dopamine Receptor Recycling

As with other GPCRs, dopamine receptor signal transduction is precisely regulated.[189–193,195,298,299] In the basal state, in human renal tubules, human D_1Rs exist as homooligomers in lipid raft microdomains.[300] Occupation of D_1Rs increases the amount of D_1R monomers associated with a transient increase in D_1R function, as a result of the recruitment of D_1R from an intracellular pool of D_1R to the lipid rafts of plasma membranes.[215,300–304] Following the transduction of the GPCR signals, there is a transient loss of receptor responsiveness (desensitization). This mechanism dampens short-term agonist effects following repeated agonist exposure. At least three families of regulatory molecules contribute to GPCR desensitization: second messenger-dependent protein kinase; G-protein-coupled receptor kinases (GRKs); and arrestins.[141,189–191,195,280,286,298,299,305–308] Homologous desensitization, in response to agonist stimulation, occurs via action of a member(s) of the GRK family. Heterologous desensitization, mediated by second messenger-dependent kinases, occurs when a decrease in receptor responsiveness is induced by a ligand other than its own specific ligand. The phosphorylation of GPCRs, including the D_1R, leads to the binding of a member(s) of the arrestin family, uncoupling of the receptor from its G-protein complex, and a decrease in its functional response. Desensitization of GPCRs involves phosphorylation, sequestration/internalization, and degradation of receptors. The D_1R (but not D_5R), expressed endogenously in renal proximal tubule cells,[288,299–307] is regulated to a lesser extent by GRK2 and to a greater extent by GRK4 in human kidneys,[299] but the converse may be true in rat kidneys.[305] Moreover, GRK4 may constitutively phosphorylate D_1R.[307] GRK3 regulates rat D_1R overexpressed in HEK293 cells.[308] It is not clear whether or not GRK5 regulates the rat D_1R.[308] GRK6 is not important in the regulation of D_1R in the kidney (unpublished), but it is important in the desensitization of the D_1R in intestinal crypt cells,[309] emphasizing the importance of cell type in D_1R regulation. The desensitization of D_5R, in contrast, does not involve GRKs, but rather sorting nexin 1.[310] Similarly, GRK is not involved in the first 20 minutes of D_1R desensitization in human renal proximal tubule cells,[299] but could be related to sorting nexins (unpublished data). It has also been suggested that GRK2 may negatively regulate D_2R signaling by a phosphorylation-independent mechanism.[311]

Heterologously expressed D_1Rs, after ligand stimulation, rapidly (but not completely) internalize (5–12 minutes) in cell lines (HEK-293 and Neuro2A neuroblastoma cells).[307] In HEK-293 cells heterologously expressing rat D_1R, 15 minutes of agonist stimulation does not completely desensitize D_1R.[307] Presumably, the internalized D_1R continues to function until it is completely desensitized.[312] Phosphorylation, desensitization, and internalization cannot be directly equated.[216,298,299] GPCR desensitization cannot be completely explained by phosphorylation; ubiquitination may also play a role.[46,313] AT_1R,[46] D_1R, and D_5R (unpublished data) are

ubiquitinated within the first 15 minutes following ligand stimulation; AT_1R and D_5R,[46] but not D_1R, are targeted for degradation following ligand occupation. Thus, desensitization may also occur at the plasma membrane.[216] Cell membrane invagination and endocytosis are important in D_1R trafficking; prevention of endocytosis with hypertonic sucrose abrogates ligand-induced D_1R desensitization in human renal proximal tubule cells.[314] The phosphorylated GPCR/β-arrestin complex undergoes endocytosis/internalization via clathrin-coated pits into a series of endosomal units, where it is dephosphorylated and recycled back to the plasma membrane or degraded. Dopamine receptors belong to Class A receptors that are rapidly recycled to the plasma membrane. In contrast, AT_1R receptors belong to Class B receptors that are slowly recycled to the plasma membrane, and some are actually degraded.[315] Protein phosphatases are involved in the resensitization of GPCRs in endosomes[316] and at the plasma membrane.[216] Protein phosphatases, including protein phosphatase 2A (PP2A),[215,294,317,318] a GPCR phosphatase,[216] and PP2B (calcineurin)[319] have been reported to resensitize D_1R, but PP2A is probably the major protein phosphatase involved in D_1R function and/or resensitization in renal tubule cells.[215,294,317]

The D_2R, like some GPCRs, is not desensitized by phosphorylation but rather by association with β-arrestin, but phosphorylation is required for its recycling.[256,311,320] The GRK regulating D_2R in renal tubule cells is not known, but D_2R in other cells is regulated by GRK2, GRK3, GRK5, and GRK6,[256,287,311,320] and constitutively desensitized by GRK2. GRK2 and GRK3 preferentially sequester $D_{2S}R$ over $D_{2L}R$, while β-arrestin 2 has the converse effect.[256] GRK2 or GRK3, but not GRK5 or GRK6, is involved in the desensitization of the calcium signal mediated by the interaction of D_1R/D_2R heterologously expressed in HEK293TSA cells.[321] The desensitization of D_3R is weakly regulated by GRK2 and GRK3,[322] but robustly by GRK4 (GRK4γ > GRK4α); GRK4 and D_3R colocalize and interact in human renal proximal tubule cells.[286] D_4R, like some GPCRs, e.g., AT_2R and β_1R, may not undergo internalization and is resistant to desensitization.[256,323] The GRK regulating D_4R is not clear, but does not seem to involve either GRK2 or GRK3. The GRK regulating D_5R is also not clear, but does not seem to involve GRK4.

Membrane Microdomains

Cholesterol rich domains in membranes are called lipid rafts and the rest are called non-lipid rafts.[324,325] Lipid rafts serve as signaling platforms for several signaling molecules such as G-protein-subunits, enzymes, and adaptor proteins. Lipid rafts can affect the function of GPCRs by inducing a conformational change and/or alteration of the physical properties of the membrane in which the GPCR is embedded. We have reported that angiotensin II does not affect the differential expression of AT_1R in lipid and non-lipid rafts in renal proximal tubule cells from normotensive rats, but increases the amount of glycosylated AT_1R in lipid rafts in renal proximal tubule cells from SHRs; this may lead to an increased ability of angiotensin II to stimulate the Cl^-/HCO_3^- exchanger.[326] D_1-like receptors also regulate NADPH oxidase activity and subunit expression in lipid microdomains of renal proximal tubule cells.[327] The D_2-like receptor antagonist, haloperidol, has been reported to disrupt lipid rafts.[328] Interestingly, high doses of simvastatin, a cholesterol depleting reagent, increase dopamine receptor expression in the rat prefrontal cortex.[329] In human renal tubule cells, heterologously or endogenously expressed D_1R exists as homo-oligomers; agonist stimulation increases the amount of D_1R monomers[300,330,331] consistent with other GPCRs.[332–334] D_1R oligomers exist in caveolae-like microdomains; decreasing caveolin expression or depleting cholesterol impairs D_1R-mediated generation of cAMP and oligomer formation.[300] Renal inhibition of caveolin-1 expression, an important component of lipid rafts, via caveolin-1 siRNA in the kidney impairs D_1-like receptor-mediated natriuresis in salt-loaded rats and produces hypertension.[335] Thus, the function of GPCRs, including dopamine receptors, can be regulated by cholesterol membrane microdomains.

Regulation of GPCR Membrane Expression

Plasma membrane expression of GPCRs requires proper folding that is aided by chaperones.[336] Homodimerization has been suggested to help in GPCR folding. Indeed, folding efficiency has been suggested to regulate the expression of D_4R.[337] A proper amount of calnexin, an endoplasmic reticulum chaperone, is important in the proper trafficking of both D_1R and D_2R to the plasma membrane.[338]

D_1R

Dopamine receptor interacting protein 78 (DRiP78) is an endoplasmic reticulum protein that regulates the transport of D_1R and other GPCRs, including AT_1R, and the assembly of G-protein β- and γ-subunits.[339] Increased expression of DRiP78 impairs the transport of D_1R from the endoplasmic reticulum to the plasma membrane.[340] In contrast, DRiP78 increases the plasma membrane expression of AT_1R,[341] another example of how certain proteins have contrasting effects on AT_1R, and dopamine receptor trafficking and expression.[45,46,342,343] Neurofilament-M specifically decreases the cell surface membrane expression of D_1R (not with D_2-like receptors and weakly with D_5R).[344] Calcyon is another D_1R interacting protein that may be important

in D_1R-calcium-mediated signaling in neural tissue.[345] Whether these proteins regulate D_1R endogenously expressed in renal tissue remains to be determined. However, RanBP9/10 which colocalizes with D_1R in renal and neural tissues, phosphorylates and impairs D_1R function.[248]

D_2R

Cbl-interacting protein of 85 kDa (CIN85) may be important in the trafficking of D_2R, at least in striatal tissue.[346] Absence of striatal CIN85 is associated with decreased endocytosis of D_2R and implicated in the hyperactivity of CIN85-deficient mice. A Ca^{2+}-binding protein, S100B, increases the ability of D_2R to inhibit adenylyl cyclase and stimulate ERK activity.[347] Two D_2R interacting proteins decrease the expression and/or function of D_2R, including neuronal calcium sensor 1[348] and protein kinase Cξ-interacting protein.[349] In neural cells, a spliced variant of the Gαi2 may also be important in the plasma membrane expression of the D_2R[350] and protein 4.1N for both D_2R and D_3R.[351]

D_3R

The D_3R has been reported to interact with proteins that affect plasma membrane localization. Filamin-A interacts with D_2R and D_3R, linking them to the cytoskeleton and increasing their plasma membrane localization.[322,352] In contrast, paralemmin specifically interacts with the D_3R decreasing its localization to the plasma membrane.[353] The role of these interacting proteins on D_3R function in renal proximal tubules or blood vessels remains to be determined.

D_4R

KLHL12, which can act as a ubiquitin ligase, interacts with the D_4R, but its ubiquitination does not result in its degradation.[354] Indeed, the D_4R is resistant to agonist-induced internalization and degradation.[323]

D_5R

The D_5R, but not the D_1R, requires N-glycosylation for membrane localization in transfected HEK-293 cells. However, it does not contribute to the radioligand-binding properties of D_5R.[355]

Renal Distribution of Dopamine Receptors

The expression of the dopamine receptors in the kidney (Table 19.1) of several mammals has been reported.

Tubular Distribution

The dopamine receptor subtypes are differentially expressed along the mammalian nephron.[213,252,356–365] However, their expression in the medulla is species-dependent. In the rat, the D_2R and D_4R are expressed in the inner medulla[357,365] (Table 19.1). The mouse kidney has no dopamine receptors in the inner medulla[360] (unpublished observations). High concentration of dopamine (100 μM) stimulates prostaglandin E2 production in the inner medulla and thin limb of Henle.[358] The dopamine receptor subtype expressed in the thin limb of Henle is not known, although dopamine (100 μM) stimulates prostaglandin E2 production in rat thin ascending limb cells[366.]

Immunohistochemical studies in human and rodent kidneys have shown expression of D_1R in the apical and basolateral membranes, as well as in the cytoplasm of proximal tubules (mouse:S3 > S1 = S2), distal convoluted tubules, medullary thick ascending limb (mTAL) of Henle, macula densa, and cortical collecting duct.[356,361,364,365] The presence of D_1R in the rat outer or inner medulla has not been shown consistently using immunohistochemistry[356,361,362,365] or *in situ* mRNA amplification,[367] and dopamine does not stimulate cAMP production via dopamine receptors,[368,369] in this nephron segment. Moreover, there is no D_1-like receptor radioligand-binding in the rat inner or outer medulla.[370,371] The human[372] and mouse kidney[360] (unpublished observations), do not express dopamine receptors in the inner medulla.

$D_{2L}R$ mRNA is expressed in the rat cortex, and outer and inner medulla.[252] Immunoreactive D_2R is present in rat[357] and human (unpublished observations) proximal tubule (mouse:S2 > S1/S3), distal convoluted tubule, and cortical and outer medullary collecting duct. The D_2R is expressed in the intercalated cells of the medullary collecting duct in the rat,[357] but not in the mouse (unpublished data). D_2R protein is also expressed in the OK cell, an opossum proximal tubule cell line that also exhibits distal tubular cell characteristics.[373]

D_3R mRNA is expressed in the rat cortex, and outer medulla and inner medulla.[252] Immunoreactive D_3R is expressed in rat apical and subapical areas, but not in the basolateral membrane of proximal tubules (S1 >> S2/S3) in three reports[357,373,375]; one study also showed immunoreactive D_3R in the distal convoluted tubule,[375] and two studies showed D_3R protein in the cortical collecting duct.[357,375] One[357] of three reports[374,375] found D_3R immunostaining in the inner medulla. Immunoreactive D_3R is present in mouse proximal tubule, thick ascending limb of Henle, and distal convoluted tubule, but not in the cortical collecting or outer and inner medullary collecting ducts (Table 19.1).

D_4R is present in the rat proximal tubule (S1 > S2 > S3), distal convoluted tubule, and especially in the cortical[357,376] and outer and inner medullary

collecting ducts, where it is more abundant at the luminal than at the basolateral areas.[365] In the mouse, D_4R is present in the proximal convoluted tubule (but not proximal straight tubule), thick ascending limb of Henle, and cortical and outer medullary collecting duct (unpublished observations). D_4R mRNA is expressed in the human kidney, but its expression along the nephron has not been reported.[377]

D_5R is expressed in the rat and mouse proximal tubule (S1 > S2/S3), thick ascending limb, and distal convoluted tubule and cortical and outer medullary collecting duct.[213,360,364] The expression of D_5R protein has not been reported in human kidney, but is expressed in human renal proximal tubule cells in culture,[46,276] and D_5R may be expressed preferentially over the D_1R in the thick ascending limb of Henle and the cortical collecting duct, while the D_1R is preferentially expressed in the proximal tubule[378](unpublished data).

VASCULAR RECEPTORS

D_1-Like Receptors

The D_5R may have chemo- and mechano sensory roles in primary cilia of mouse vascular endothelial cells.[379] D_1Rs, and to a greater extent D_5Rs, are expressed in the tunica media of rat mesenteric, pial, and renal arteries.[361,380,381] They are mainly located postjunctionally, which has been confirmed by insensitivity to chemical sympathectomy.[381] In the rat kidney, D_1R mRNA is also found in smooth muscle cells of large and small arteries, and afferent and efferent arterioles.[367] In humans D_1R protein is also present in vascular smooth muscle cells in the large intrarenal arteries, but not in renal veins.[372]

D_2-Like Receptors

The D_2-like receptors are expressed in the adventitia and adventitia–media border of arteries. D_2R and D_4R, but not D_3R, are expressed in rat mesenteric and pial arteries. Rat renal arterial branches express D_2R and D_3R.[380] Although renal arteries and arterioles in Wistar rats were not found to express D_4R,[380] a subsequent study in Sprague-Dawley rats showed expression of D_4R in large segmental, arcuate, interlobar, interlobular, and afferent and efferent arterioles.[376] Bilateral superior cervical ganglionectomy and renal denervation confirmed the prejunctional localization of the D_2-like receptors, and the location of D_2-like receptors in the renal artery suggest their prejunctional localization.[376,380] However, we have reported that D_3R stimulation relaxes mesenteric arterial rings, independent of the endothelium.[264] The failure of the endothelium to influence the vasorelaxant effect of D_3R stimulation is in agreement with the absence of D_2-like receptor expression in the intima.[380] One study could not find D_3R expression in renal vessels,[374] although another study found D_3R immunostaining in medial and adventitial layers of renal arteries[378] in agreement with the report of D_3R mRNA in renal microvessels.[252]

GLOMERULAR RECEPTORS

Radioligand binding and autoradiographic studies using D_1-like receptor ligands that recognize both D_1R and D_5R have failed to detect specific binding in rat and human glomeruli.[370,371,381,382] D_1R mRNA studied by *in situ* mRNA amplification is not detected in rat renal glomeruli[367] (Table 19.1). Immunoreactive D_1R[361,372] or D_5R[360,364] has not been demonstrated in rat or human glomeruli. In rat glomeruli isolated by sieving, two[383,384] of three[15] studies showed that dopamine, via an uncharacterized dopamine receptor, increased cAMP production. Dopamine increases cGMP, but not cAMP production in isolated dog glomeruli, also obtained by sieving.[385] However, because afferent and efferent arterioles express D_1R and D_5R (Table 19.1) it is possible that glomerular preparations that contain arterial vessels may confound the results. Nevertheless, rat glomerular mesangial cells[386] and mouse glomerular podocytes,[387] in culture, express D_1-like receptors, assessed by an increase in cAMP production in response to dopamine or D_1-like receptor agonist. Rat glomerular epithelial cells in culture do not increase cAMP production in response to dopamine.[386]

D_2-like receptors, $D_{2L}R$, D_3R, and D_4R, are present in rat glomeruli[252,357,375,381,388] (Table 19.1). Specifically, immunoreactive D_2R and D_3R have been reported in rat mesangial cells in one study[357] and in podocytes in another study.[375] However, there are three reports of the absence of D_4R receptors in rat glomeruli.[357,365,376] D_2-like receptor stimulation decreases cAMP production in rat glomeruli.[15] Dopamine attenuates the contractile response to angiotensin II in rat isolated glomeruli, but the receptor mediating this effect is not known.[389]

Receptors in Juxtaglomerular Apparatus

Rat[361,390] and mouse (unpublished observations) but not human[372] juxtaglomerular cells, *in situ*, and rat juxtaglomerular cells in culture[390] express D_1R (Table 19.1). Rat[361] and mouse (unpublished studies) but not human[372] macula densa cells express D_1R. Rat[364] but not mouse[360] juxtaglomerular or macula cells express

D_5R. Rat[361] but not mouse (unpublished studies) macula densa cells express D_1R. D_5R expression in human juxtaglomerular or macula cells has not been reported.

Rat, mouse, and human (unpublished studies) juxtaglomerular cells, *in situ*, do not express D_2R. Mouse juxtaglomerular cells, *in situ*, express D_3R (Table 19.1). In contrast, rat juxtaglomerular cells, *in situ*, also do not express D_3R[374,375] or D_4R,[365,376] but express D_3R and D_4R in culture.[391] Rat macula densa cells were found to express D_3R in one[375] of two reports.[374] Mouse macula densa cells express D_3R and D_4R (unpublished studies). D_2R is not expressed in human or mouse macula densa cells, but is expressed in rat macula densa (unpublished studies; Table 19.1); D_3R and D_4R expression has not been studied in human macula densa.

DOPAMINE AND RENAL HEMODYNAMICS

D_1-Like Receptors

Dopamine, administered in low doses intravenously or directly into the renal artery, increases renal blood flow and decreases renal vascular resistance.[9,392,393] The renal vasodilatory effect of dopamine is mimicked by D_1-like receptor agonists and blocked by the D_1-like receptor antagonists.[394–397] The contribution of D_1R and D_5R in this action remains to be determined. Dopamine and D_1-like receptor agonists dilate afferent and efferent arterioles to the same extent.[398,399] However, afferent arterioles are preferentially dilated in the hydronephrotic kidney.[400] Dopamine induces a greater vasodilatory effect in the renal artery than in the coronary artery,[401] mesenteric,[402] in agreement with the receptor density data.[403]

cAMP/PKA[12,404–406] is the primary signaling pathway of the renal vasodilatory effect of dopamine via D_1-like receptors. However, a dopamine-mediated stimulation of PKC is associated with increased expression of D_1-like receptors that enhances cAMP production in renal vascular smooth muscle cells.[243] However, as stated earlier in HEK293 cells, novel PKC isoforms stimulate D_1R[244] but inhibit D_5R signaling, while conventional PKCs and two of the novel PKCs (δ and ε) impair D_1R signaling.[245] In coronary arteries, the vasorelaxant effect of D_1-like receptors has also been attributed to PKA/PKG-dependent activation of K^+-ATP, calcium-, and voltage-activated K^+ channels.[274] Prostacyclins may also contribute to dopamine- and D_1-like receptor-mediated renal vasodilation.[407]

The effect of D_1-like receptors in the rat aorta and tail artery is complex. Dopamine has been reported to decrease both sodium influx and efflux by inhibition of NHE and Na^+/K^+-ATPase activity, respectively, in part via PKA, in rat aorta smooth muscle cells.[408] A predominant inhibitory effect on NHE activity would result in a decrease in intracellular sodium and a decrease in vessel tone, while a predominant inhibitory effect on Na^+/K^+-ATPase activity would result in an increase in intracellular sodium and an increase in vascular tone. The latter situation may explain the apparent vasoconstrictor action of a D_1-like receptor agonist in the rat tail artery.[409] In the rat tail artery, dopamine and SKF 38393, a D_1-like receptor agonist, inhibited Na^+/K^+-ATPase and increased vascular tone, an effect that was associated with activation of phospholipase C.[409] Since the effects were abolished by pertussis toxin, the D_1-like receptor in the rat tail artery is must be different from the D_1-like receptor in renal proximal tubules, because in this tissue phospholipase C is pertussis-toxin resistant and linked to Gq.[142,410] When phospholipase Cβ1 is not expressed, D_1-like agonists can be indirectly linked to phospholipase Cγ1 via PKA.[139] The effect of dopamine in resistance vessels may not be the same as that in conduit vessels (e.g., aorta) and in the rat tail artery, which may subserve a thermoregulatory function.

D_2-Like Receptors

Both the $D_{2S}R$ and $D_{2L}R$ may act as autoreceptors in certain nerves (GABA transmission), while the $D_{2S}R$ but not the $D_{2L}R$ regulates glutamate release.[411] However, the $D_{2S}R$ but not the $D_{2L}R$ is involved in presynaptic dopamine transmission, while postsynaptic dopamine transmission is via the $D_{2L}R$.[412] The D_3R[413] but not the D_4R[414] can also function as an autoreceptor (presumably located in prejunctional areas) and inhibit catecholamine release. Prejunctional D_2-like receptors in the kidney inhibit norepinephrine release.[415,416] This effect may explain the ability of bromocriptine (D_2R and D_3R agonist), but also with D_1-like antagonistic properties, to increase renal blood flow in the anesthetized rat,[417,418] and the renal vasodilatory effect of endogenous dopamine in humans on a low-sodium diet.[419]

The effect of postjunctional D_2-like receptors on the renal vasculature is inconsistent. When both α- and β-adrenergic receptors are blocked in the dog kidney, the renal vasodilatory effect of dopamine is antagonized by D_1-like but not by D_2-like receptor blockade.[395] However, in a similar preparation, bromocriptine has been reported to decrease renal blood flow.[420] In the conscious, chronically instrumented dog on a moderate sodium intake (40 mmol/day), low (picomolar) concentrations of quinpirole, a D_2-like receptor agonist with selectivity for the D_3R and D_4R over the D_2R, also produces vasoconstriction.[421] This result agrees with the report that D_3R stimulation constricts renal vessels in

volume-loaded rats.[422] In humans, D_2-like receptor blockade with L-sulpiride does not affect renal plasma flow but potentiates the renal vasoconstrictor effect of NO inhibition with L-NAME.[423] D_4R stimulation also enhances the contractile response of guinea pig vas deferens.[424]

In contrast to the above observations that D_2-like receptors induce vasoconstriction, in the preconstricted isolated perfused rat kidney bromocriptine (D_2R/D_3R agonist) induces vasodilation via postjunctional D_2-like receptors.[425] In the norepinephrine- or high-potassium-preconstricted rat mesenteric arterial rings, D_3R stimulation induces vasorelaxation.[264,426] The vasodilatory effect of D_3R is caused by activation of potassium channels (small- and/or large-conductance calcium-activated potassium channels).[264,426] Although the D_3R is present in the intima, the vasodilatory effects of the D_1R and D_3R agonists are endothelium independent; D_1R is not expressed in the intima.[264,426] In humans, the renal vasodilatory effect of D_2-like receptors is reduced during sodium loading and increased during sodium restriction.[419] This is in contrast to the lack of effect of sodium loading on the renal vasodilatory effect of D_1-like receptors.[427]

The D_3R can augment the vasodilatory effect of the D_1R by mechanisms independent of signal transduction. In embryonic thoracic aortic smooth muscle cells and coronary artery smooth muscle cells, stimulation of the D_1R increases D_1R and D_3R expression.[264,426] However, the additive vasorelaxant effects of D_1R and D_3R could not be explained by the increased expression of those two receptors, because the vasorelaxant effect occurs within minutes following agonist stimulation. Rather, the D_1R and D_3R may acutely and physically interact with each other; D_1R and D_3R co-immunoprecipitate within minutes after agonist stimulation, consistent with the timeframe of the additive vasodilation effect of D_1R and D_3R.[264]

The published studies show that D_1-like receptors cause renal vasodilation. Stimulation of pre-junctional D_2-like receptors should cause vasorelaxation, while stimulation of post-junctional D_2-like receptors can result in either vasodilation or vasoconstriction. With chronic sodium chloride loading, basal reactivity of renal vessels may be enhanced by an increase in levels of endogenous Na^+/K^+-ATPase inhibitor, e.g., ouabain, and an increase in intracellular sodium and calcium.[428] Ouabain, *per se*, can decrease renal D_1R expression and function.[429] Under these conditions, dopamine can further increase intracellular sodium by stimulating NHE1 activity via D_2-like receptors.[430] The increase in intracellular sodium increases sodium calcium exchanger activity. The increase in intracellular calcium increases vascular reactivity and, thus, dopamine, via D_2-like receptors which can then elicit vasoconstriction. When renal nerve activity is increased, as seen in renal nerve stimulation, low-sodium diet, hypovolemia or during anesthesia, the vasodilator effect of dopamine occurs via prejunctional D_2-like receptors,[415,416] presumably of the D_3R subtype.[264,426] In addition, when renal vascular resistance is increased, the D_2-like receptor effect at postjunctional sites would be that of vasodilation, since D_2-like receptors inhibit Ca^{2+} channels and stimulate K^+ channels, both of which can lead to vasorelaxation. Under these conditions, a synergistic effect between D_1- and D_2-like receptors may become evident.[264,394,398,426] The effect of dopamine on vascular tone may differ between conduit (e.g., aorta) and resistance (e.g., mesenteric and renal arterioles) vessels. The increase in vascular tone produced by D_1-like receptor agonists in conduit vessels may serve to increase perfusion in downstream vessels dilated by D_1-like receptors.

Glomerular Filtration

Although low concentrations (nM) of dopamine consistently increase renal blood flow, this is not the case for glomerular filtration rate.[427,431,432] Normally, low concentrations of dopamine dilate afferent and efferent arterioles to the same degree, and therefore transglomerular pressure remains unchanged.[368] However, dopamine can ameliorate the reduced glomerular filtration rate caused by amphotericin B,[433] radiocontrast material, and hypovolemic states.[434] This could be a direct effect on glomerular cells, since dopamine can attenuate the contractile effect of angiotensin II in isolated glomeruli.[389] This effect is probably exerted via D_2-like receptors, because D_1-like receptors are not expressed in glomerular mesangial cells, *in situ*.[15,360,361,364,367,370–372,381,382] It is only after culture that glomeruli express D_1-like receptors and their stimulation increases cAMP production.[383,384,386,387] In isolated dog glomeruli, dopamine increases cGMP formation[385] and in isolated rat glomeruli, dopamine decreases adenylyl activity,[15] in keeping with the presence of D_2-like receptors[252,357,376,381,388] (Table 19.1). *In vivo*, D_2-like receptors can decrease or increase glomerular filtration rate, depending upon the state of renal vascular D_2-like receptor activation. When the interaction of D_1- and D_2-like receptors results in a greater vasodilatory effect on afferent than efferent arterioles, glomerular filtration rate can increase.[435] D_2-like receptors are involved in the increase in glomerular filtration rate associated with amino acid infusion, an effect that is mediated by renal nerves.[436] The D_2-like receptor-mediated decrease in renal blood flow is associated with greater constriction of afferent than efferent arterioles, resulting in a greater decrease in glomerular

filtration rate than renal blood flow and, therefore, a fall in filtration fraction.[421,437]

Tubuloglomerular Feedback

Tubuloglomerular feedback describes a mechanism by which changes in distal tubular sodium chloride delivery induce changes in afferent glomerular arteriolar resistance mediated by the adenosine A_1 receptor.[438–441] Tubuloglomerular feedback is initiated by transport of sodium via sodium potassium 2 chloride transporters type A (NKCC2A) and type B (NKCC2B) at the macula densa.[441] Because dopamine stimulates NKCC2 activity,[442] it would be expected that dopamine should promote the tubuloglomerular feedback. However, dopamine inhibits tubuloglomerular feedback[443] by occupation of luminal D_1R but not D_2R on macula densa cells that may be more evident during sodium surfeit.[444] How can this be done when D_1R stimulates NKCC2?[442] There are several possible explanations. D_1-like receptors counteract the effect of adenosine A_1 receptors on the tubuloglomerular feedback.[134] The heterodimerization of the D_1R and adenosine A_1 receptor[445] and D_2-like and adenosine A_{2A} receptors[446] inhibit dopamine receptor function (see adenosine and dopamine receptor interaction). Adenosine A_{2A} receptors counteract the effect of adenosine A_1 receptors on tubuloglomerular feedback[447] and dopamine (probably via D_2-like receptors) counters the effects of adenosine A_{2A} receptors.[446] Superoxide anion activates 5′-nucleotidase, thereby increasing adenosine generation in the kidney. Dopamine also induces ecto-5′nucleotidase in glomeruli[448] and because ecto-5′-nucleotidase catalyzes the formation of adenosine, dopamine should enhance tubuloglomerular feedback.[438,440] However, the ability of dopamine receptors to inhibit ROS production[449] may also play a role, because ROS is also involved in tubuloglomerular feedback.[439] These counteracting effects of dopamine on adenosine formation, adenosine receptor action, NKCC2, and ROS may explain the variable effect of dopamine on tubuloglomerular feedback.

RENIN, ANGIOTENSINOGEN, AND ALDOSTERONE SECRETION

Dopamine can increase, decrease or have no effect on renin secretion, *in vivo*.[44] Dopamine can alter renin secretion directly or indirectly by effects on blood pressure and renal tubular ion transport. As indicated above, rat and mouse juxtaglomerular cells express the D_1R[361,367,390] (Table 19.1). The D_1R stimulates secretion of renin in rat primary cultured cells.[390,450] In pithed rats and anesthetized dogs, dopamine and D_1-like receptor agonists increase renin release.[451,452] However, in non-pithed rats, dopamine or a D_1-like receptor agonist inhibits renin secretion on a low or normal salt diet, by inhibiting cyclooxygenase 2 expression.[44] However, when cyclooxygenase 2 expression[44] is already inhibited, as is the case with salt-loading, D_1-like receptor stimulation increases renin secretion.[44] In humans on low or high sodium (300 mmol/day) intake D_1-like receptor stimulation does not affect renin secretion,[427] in agreement with the absence of D_1R in human juxtaglomerular cells.[372] D_1-like receptor stimulation also does not affect plasma renin activity in subjects with mild essential hypertension on an unmonitored sodium intake,[453] but increases it in hypertensive humans on a high (150 mmol Na)[454] or normal sodium intake.[455] The role of D_5R on renin secretion in the rat remains to be determined; D_5R is expressed in rat[364] but not in mouse[360] juxtaglomerular cells and deletion of *Drd5* does not affect plasma or renal renin levels.[360]

In salt replete humans, D_2-like receptor blockade with metoclopramide does not affect plasma renin activity[456] but another D_2-like receptor antagonist, domperidone, inhibits the fall in plasma renin activity induced by intravenous γ-L-glutamyl-L-dopa in humans on an unmonitored salt intake.[457] Disruption of the *Drd3* in mice leads to increased renin release and renin-dependent hypertension.[25] In contrast, deletion of *Drd4* does not affect plasma or renal renin levels.[26] D_2R also probably do not play a role in renin secretion, because they are not expressed in the juxtaglomerular cell in rat,[357] mouse or human kidney (unpublished observations). Whether or not the reported effects of dopamine and D_1-like and D_2-like receptors on renin secretion are exerted at the macula densa remains to be confirmed, but all the dopamine receptor subtypes have been found in macula densa cells, albeit with species variability (Table 19.1). These studies would suggest that in humans, the predominant effect of dopamine receptors on renin secretion is inhibitory, via D_2-like receptors. A stimulatory effect could occur in hypertensive humans (see above), similar to that suggested in Sprague-Dawley rats[44], which are salt-sensitive.

D_1R is expressed in the zona glomerulosa of rat adrenal glands[458] and increases aldosterone secretion in isolated and cultured rat adrenal glomerulosa cells.[459] In humans, dopamine does not affect aldosterone secretion in the salt-replete state[460] but dopamine[461] inhibits angiotensin II-induced aldosterone secretion. This would be in keeping with the attenuation of angiotensin II-induced aldosterone secretion by bromocriptine (D_2R/D_3R agonist) in human adrenal cortical and adenocarcinoma cells.[462] These observations are confounded by the report that stimulation of D_4R enhances[463] angiotensin II-stimulated aldosterone

TABLE 19.1 Renal Dopamine Receptor Subtype Expression (Normal Sodium Intake)

Dopamine Receptor Subtype	Species	Glomerulus		Proximal Tubule		TDL, ATL	TAL	DCT	Collecting Duct			Juxtaglomerular Apparatus		Arterial Vessel
		MC	Podocytes	PCT	PST				CCD	OMCD	IMCD	JGC	MD	
D_1R														
mRNA	mouse													
	rat	No[367]	No[367]	Yes[a,367]	No[367]	No[367]	Yes[367]	Yes[365,367]	No[367]	No[367]	Yes[367,390]	No[367]	Yes[367]	
	human													
Protein	mouse		Yes[387*]	Yes[b]		No[b]	Yes[b]	Yes[b]	Yes[b]	Yes[b]	No[b]	Yes[b]	Yes[b]	Yes[b]
	rat	Yes[356c] No[361, 364,365, 381,382]	No[356,361,364,365]	Yes[356,361,364]		No[361]	No[361] Yes[364]	Yes[361, 364]	Yes[356, 361,364d]	No[361] Yes[364d]	No[361] Yes[356]	Yes[a, 361]	Yes[361]	Yes[361]
	human	No[372, 381,382]	No[372,381,382]	Yes[372]			Yes[372]	Yes[372]	Yes[372]	Yes[372d]		No[372]	No[372]	Yes[372]
D_2R														
mRNA	mouse													
	rat	Yes[252]		Yes[252]						Yes[252]				Yes[252]
	human													
Protein	mouse	No[b]	No[b]	Yes[b]	Yes[b]	No[b]	Yes[b]	Yes[b]	Yes[b]	No[b]	No[b]	No[b]	No[b]	No[b]
	rat	Yes[357]	No[357]	Yes[357]		No[357]	Yes[b]	Yes[b]	Yes[357]		Yes[357,f]	No[b]	Yes[b]	
	human	No[b]	Yes[b]	Yes[b]	Yes[b]	No[b]	Yes[b]	Yes[b]	Yes[b]	Yes[b]	No[b]	No[b]	No[b]	Yes[b]
D_3R														
mRNA	mouse													
	rat	Yes[252,388]		Yes[252,388]					Yes[252,388]					Yes[252]
	human													
Protein	mouse	Yes[b]		Yes[b]	Yes[b]		Yes[b]	Yes[b]	No[b]	No[b]	No[b]	Yes[b]	Yes[b]	
	rat	Yes[357g,375] No[374]	Yes[375] No[374]	Yes[374,375]	No[374]	No[374]	No[374]	Yes[357,375] No[374]	Yes[357, 375] No[374]	No[374, 375]	Yes[357] No[374,375]	No[374, 375] Yes[391,i]	Yes[375] No[374]	Yes[375] No[374]
	human													

(*Continued*)

TABLE 19.1 (*Continued*)

Dopamine Receptor Subtype	Species	Glomerulus		Proximal Tubule		TDL, ATL	TAL	DCT	Collecting Duct			Juxtaglomerular Apparatus		Arterial Vessel
		MC	Podocytes	PCT	PST				CCD	OMCD	IMCD	JGC	MD	
D_4R														
mRNA	mouse													
	rat								Yes[365]					
	human													
Protein	mouse	Yes[b]		Yes[b]	No[b]	No[b]	Yes[b]	Yes[b]	Yes[b]	Yes[b]	No[b]		Yes[b]	Yes[b]
	rat	No[357,365,376]		Yes[357,376]			No[376]	Yes[376]	Yes[357,365,.376]	Yes[365,376]	Yes[357,365,376]	No[365, 376]	No[365, 376]	Yes[376h]
	human													
D_5R														
mRNA	mouse		Yes[387*]											
	rat			Yes[b]			Yes[b]	Yes[b]	Yes[b]					
	human													
Protein	mouse	No[360]	No[360]	Yes[360]	Yes[360]	No[360]	Yes[360]	Yes[360]	Yes[360]	Yes[360]	No[360]	No[360]	No[360]	Yes[360]
	rat	No[364]		Yes[213,364]			Yes[364]	Yes[364]	Yes[364d]	Yes[364d]		Yes[364]	Yes[b]	Yes[b]
	human													

[*] *did not distinguish D1R from D5R*
[a] *Yamaguchi I, Jose PA, Mouradian MM, et al. Expression of dopamine D1A receptor gene in proximal tubule of rat kidneys. Am J Physiol. 1993 Feb;264(2 Pt 2):F280–5.*
[b] *Unpublished data.*
[c] *Not universally expressed in the WKY rat, not expressed in the SHR.*[356]
[d] *Not indicated as to location in outer or inner medulla.*
[e] *Expressed in the WKY, not expressed in the SHR.*[357]
[f] *Expressed in intercalated cells.*
[g] *More in SHR than in WKY.*[357]
[h] *Disappeared with renal denervation.*
[i] *In culture.*

The renal expression of dopamine receptor subtypes is species dependent. In the rat, all the dopamine receptors except the D_5R are expressed in the outer and inner medulla[213,252,356-365]. The mouse kidney has no dopamine receptors in the inner medulla[360] (unpublished observations).

Abbreviations: Glom: glomerulus; MC: mesangial cell; PCT: proximal convoluted tubule; PST: proximal straight tubule; TDL: thin descending limb; ATL: ascending thin limb; TAL: thick ascending limb; DCT: distal convoluted tubule, CCD: cortical collecting duct, OMCD: outer medullary collecting duct; IMCD: inner medullary collecting duct; JGC: Juxtaglomerular cell; MD: Macula densa.

secretion in the same human adrenal cortical and adenocarcinoma cells. However, in hypertensive subjects, the D_2-like receptor agonist bromocriptine (D_2R/D_3R agonist) decreased renin and aldosterone secretion which was reversed by metoclopramide, a non-selective D_2-like receptor antagonist.[464] Metoclopramide did not affect aldosterone levels in saline-loaded normal and heart failure subjects.[465] Because saline loading normally decreases aldosterone levels, this study suggests that dopamine does not normally stimulate aldosterone secretion.[465] However, the inhibitory effect of D_2R on aldosterone secretion is consistent with the increase in urinary aldosterone in $D_2^{-/-}$ mice.[47] In contrast, urinary aldosterone is not different between $D_4^{-/-}$ and $D_4^{+/+}$ mice, $D_3^{-/-}$ and $D_3^{+/+}$ mice (unpublished studies) or $D_5^{-/-}$ and $D_5^{+/+}$ mice.[360] Thus, dopamine probably normally is inhibitory of aldosterone secretion, mainly via the D_2R.

Autocrine/Paracrine Regulation of Renal Function by Dopamine

The autocrine/paracrine regulation of renal tubular sodium transport, via D_1-like receptors, is mediated by tubular and not by hemodynamic mechanisms[18–21,371,466,467] (also see below). Systemically administered dopaminergic drugs may not mimic the autocrine/paracrine function of dopamine. The quantitative contribution of each dopamine receptor subtype on renal sodium transport remains to be determined. However, the D_1R is responsible for ≈80% of D_1-like receptor activity in renal proximal tubule cells[468]; D_5R may be more important in the distal nephron,[360] while the D_3R may regulate glomerular dynamics.[422] Each of the dopamine receptor subtypes, alone or via interaction with the other dopamine receptor subtypes or other GPCRs, regulates sodium transport in a unique fashion.[30] Indeed, disruption of any of the dopamine receptor genes results in hypertension, the pathogenesis of which is specific for each subtype.[22–27]

REGULATION OF ION AND WATER TRANSPORT

Ion Transport

Euvolemia and Moderate Volume Expansion

Dopamine and its receptors are important in the regulation of ion transport during euvolemia or moderate volume expansion, but have a minor role under marked volume expansion.[49,117] Inhibition of renal dopamine production by pharmacological inhibition of DOPA decarboxylase activity[469] or silencing of *Ddc* in mouse proximal tubule[470] impairs the ability to excrete a sodium load. In contrast, inhibition of the breakdown of renal tubular dopamine by inhibition of COMT but not MAO activity increases sodium excretion.[471] Deletion of *Comt* in mice, however, decreases the natriuretic response to an acute sodium load, apparently because in these mice, basal renal dopamine production is increased and is not futher increased by saline loading.[472] The increase in ion excretion caused by dopamine or D_1-like receptor agonists cannot be entirely ascribed to its ability to increase renal blood flow or glomerular filtration rate.[21,371,427,431,432,466,467,473] Reduction in renal blood flow to control values decreases but does not abolish the natriuretic effect of the D_1-like receptor agonist fenoldopam administered into the renal artery.[396] Rather, dopamine can directly inhibit renal tubular ion transport by inhibition of ion transporters, sodium channels, and sodium pump activity.[18–21,28–31] The short-term inhibition of ion transport by dopamine involves alteration in enzyme kinetics[89,474] and internalization of ion transporters/pump.[132,242,249,301,302,475–482] The long-term inhibition of sodium transport by dopamine may involve regulation of protein expression by decreasing gene transcription and translation, and increasing their degradation.[360]

The inhibitory effect of dopamine on ion transport is not simply a direct effect, but is modulated by its regulation of the release or secretion of other hormones/humoral substances. Hormones which directly inhibit ion transport interact with dopamine to increase (e.g., angiotensin III/AT_2R,[43] ANP/ANPA,[36,483–485] eicosanoids,[37,38,358,486] nitric oxide,[41,423,487,488] prolactin,[42,489] and urodilatin[36]) their inhibition of ion and water transport. In addition, dopamine negatively interacts with hormones that increase ion transport (e.g., angiotensin II,[45,46,490–494] insulin,[495,496] renin,[44] angiotensin II/AT_1R,[45,46] and aldosterone[37,47,48,461,463]) and water transport (e.g., vasopressin[51,365,497–499]). The natriuretic effect of D_1-like receptor stimulation persists even after renal denervation.[67]

The inhibitory effects of dopamine, via D_1-like receptors, on renal ion transport *in vivo* is well-established (*vide infra*). In contrast, the effect of D_2-like receptor agonists on ion transport *in vivo* has not been consistent; reports have found no effect,[395,418] a decrease[421,437,500] or an increase in sodium excretion.[24,419,501,502] The effect of blockade of D_2-like receptors may not become evident unless the nitric oxide mechanism is impaired.[423] The D_2R and D_2-like receptors have been reported to stimulate Na^+K^+-ATPase.[267,278,503,504] The D_2R/D_3R agonist, bromocriptine, transiently increases basolateral chloride transport in the isolated mTAL.[505] However, D_2-like receptor stimulation inhibits the stimulatory effect of angiotensin II on Na^+K^+-ATPase.[493]

Stimulation of D_3R also inhibits NHE3 activity.[506] The apparent discrepancies in these studies may be

related, in part, to the status of the extracellular fluid volume.[24,419] For example, a two-day administration of quinpirole, a D_2R/D_3R agonist, increased while a D_2R antagonist decreased sodium excretion in $D_2^{+/+}$ mice fed high but not normal sodium diet.[24] Because D_1-like receptor effect is increased with moderate sodium loading,[18–22,29–31,49,466,507] this would indicate the need of D_1-like receptors for D_2-like receptors to inhibit Na^+ transport.[268,473,508,509] A selective D_3R agonist, 7-OH-DPAT, increases sodium excretion in rats on a normal and high salt diet.[501] The natriuresis in rats with streptozotocin-induced diabetes is decreased by D_3R antagonist.[502] However, the natriuretic effect of another D_3R agonist, pramipexole, is blocked by a D_1-like receptor antagonist.[266] The natriuretic effect of dopamine has also been shown to depend on the activation of both D_1-like and D_2-like receptors.[508] Therefore, the inhibitory effect of D_2-like receptors on sodium transport may not be observed, unless the animals are salt-loaded, a state that enhances the natriuretic effect of D_1-like receptors.

In hypovolemic or euvolemic states where vasopressin levels are elevated, the ability of D_2-like receptor agonists, probably acting via the D_4R, to inhibit the effects of vasopressin[498,510] may obscure any stimulatory effect of D_2-like receptors, probably via the D_2R, on water and ion transport in more proximal parts of the nephron. However, preliminary studies suggest that D_4R stimulation inhibits NCC activity in mouse renal distal convoluted tubule cells.[511]

Dopamine inhibits ion and water transport in the proximal and distal nephron,[427,512–514] as estimated from lithium clearance studies. It must be noted that the renal tubular site of action of endogenous dopamine and its agonists on ion transport may not always match that given exogenously. Most of the renal dopamine is produced in the proximal tubule, and so its effects in the distal nephron could be limited while exogenously administered dopamine would reach all nephron segments equally.

Luminal Membrane

Proximal Tubule

As stated earlier, all the dopamine receptor subtypes are expressed in the proximal tubule. The stimulation of D_1-like receptors decreases the activity of several ion transporters, including the sodium hydrogen exchanger 3 (NHE3, SLC9A3),[22,127–133,515] sodium phosphate co-transporter (NaPi-IIa/SLC34A1 and NaPi-IIc/SLC34A3)[242,476,482,516–519] and Cl^-/HCO_3^- exchanger (SLC26A6)[520] at the luminal membrane. G-protein-dependent, cAMP/PKA-, PKC-, NHERF-1-, and phosphatase-dependent and -independent mechanisms are involved in the dopamine or D_1-like receptor inhibition of NHE3, $Na^+/Pi2$, Na^+/HCO_3, and Cl^-/HCO_3^- exchanger activity, including their translocation out of the brush border membranes into the cytosol.[127,130–133,249,476–482,515,518] The signaling pathways by which D_1-like receptors inhibit NHE3 activity may be species-specific, involving PKA only in rat and human renal proximal tubule cells (Figure 19.2), but involving both PKA and PKC in renal opossum kidney cells.[521] Specific PDZ domains of Pals-associated tight junction protein (PDZ 2, 4 or 5) or NHERF-1 (PDZ 2) may be important in organizing the signaling pathways by which dopamine inhibits sodium transporter/pump activity.[249,477–480,518,522] In contrast, NHERF3/4 regulates the internalization of NaPiIIa.[482]

The D_3R[506] and D_4R may also regulate NHE3 (Table 19.2) because its expression is increased in $D_3^{-/-}$ and $D_4^{-/-}$ mice on normal salt intake.[523] However, the inhibitory effect of the D_3R on NHE3 activity in renal proximal tubules is not linked to $G\alpha s$ because pretreatment of the cells with cholera toxin did not prevent the D_3R effect. Rather, the D_3R-mediated inhibition of NHE3 activity in renal proximal tubules is related to $G\alpha_{i3}$, stimulation of PKC, and modulation of intracellular calcium.[259] The effect of the D_3R, in the rat, is probably independent of changes in intracellular cAMP because renal proximal tubules do not express adenylyl cyclase V.[220] In mesenteric arteries, D_3R causes vasodilation that is mediated by inhibition of Ca^{2+} channels and modulation of K^+ channels,[264] in agreement with the suggestion that the linkage of the D_3R to other effectors, such as inhibition of K^+ and Ca^{2+} may be more sensitive than the weak linkage to G-proteins.[258]

Loop of Henle

The mTAL expresses the D_1R, D_3R (in the mouse but not in the rat), D_4R, and D_5R. D_1-like and D_2-like receptor agonists administered to the apical membrane of the rat mTAL do not affect chloride transport. However, their application to the basolateral membrane decreases chloride transport via D_1-like receptors[505] that is unrelated to PKA or PKC, but rather to PLA2-mediated formation of 20-HETE.[524] Incubation of mTAL suspensions with dopamine increases sodium potassium 2 chloride co-transporter (NKCC2, SLC12A1) activity.[442] Indeed, NKCC2 activity is stimulated by PKA and PKC, but inhibited by 20-HETE.[525] The PKA-mediated stimulation of Na^+/K^+-ATPase activity is observed only under oxygenated conditions, but is overridden by PLA2 inhibitory pathways under hypoxic conditions.[526] Therefore, overall ion transport is inhibited, probably because of inhibition of basolateral chloride[505] transport and Na^+/K^+-ATPase activity.[442,527] The D_1-like receptor-mediated stimulation of

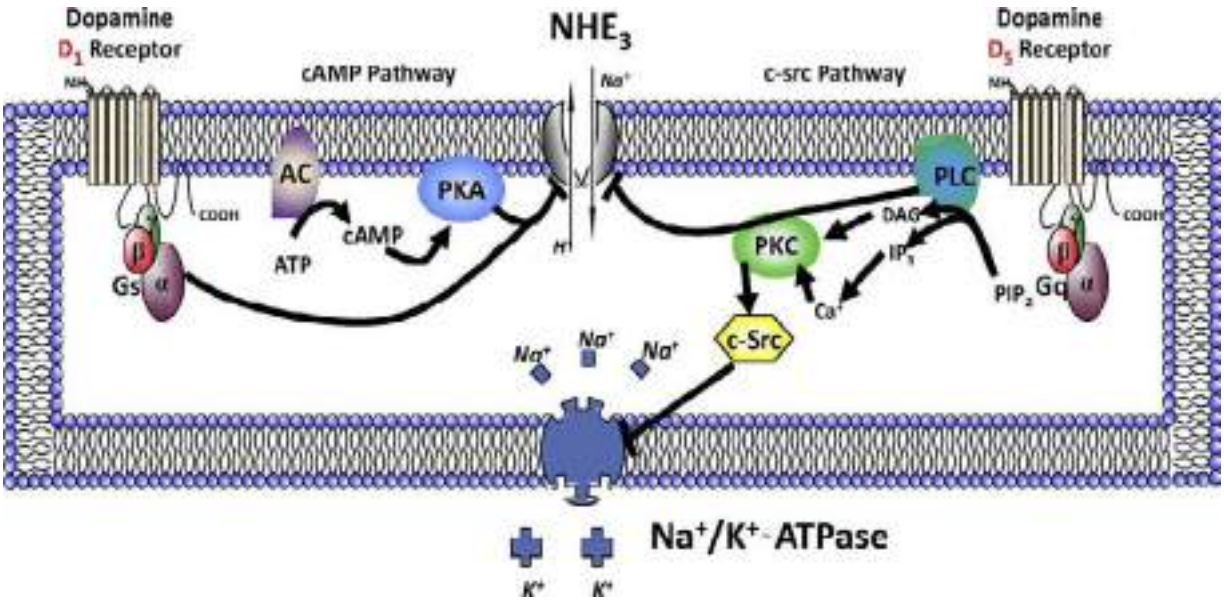

FIGURE 19.2 **Schematic model of the intracellular 2nd messenger pathways known for the dopamine-1 and dopamine-5 receptors (D_1R, D_5R) in the human renal proximal tubule cell.** The D_1R is coupled through Gas to stimulate adenylyl cyclase activity which converts ATP to cAMP. cAMP dependent protein kinase A (PKA) then inhibits the sodium hydrogen exchanger type 3 (NHE_3); GaS can also directly inhibit NHE_3. The D_5R interacts with Gaq to stimulate phospholipase C (PLC)[230] which converts phosphatidylinositol 4,5-bisphosphate (PIP_2) to diacylglycerol (DAG) and inositol 1,4,5-trisphosphate (IP_3) (The co-activation of D_1R and D_2R can also increase PLC activity.[226]) DAG and IP_3, through its release of intracellular calcium (Ca^{2+}), stimulate protein kinase C (PKC). Na^+/K^+-ATPase is then inhibited via a c-Src-mediated pathway. The inhibitory effect of D_1-like receptors on Na^+/K^+-ATPase also involves PKA in the distal convoluted tubule and cortical collecting duct, while eicosanoids are involved in all nephron segments, including the mTAL[241,522,530,539,540–544]; PKC may also be involved in the inhibition of Na^+/K^+-ATPase in the mTAL.[527] *(The authors acknowledge Robby Van Sciver for producing this diagram.)*

NKCC2 may be important in K^+ recycling in the mTAL.[442] Bromocriptine (D_2R/D_3R agonist) increases chloride transport, albeit transiently,[505] reminiscent of the ability of this agonist to increase Na^+/K^+-ATPase activity in renal proximal tubules.[267] However, the D_4R and D_5R may negatively regulate NKCC2 expression because its expression is increased in $D_4^{-/-}$ (unpublished) and $D_5^{-/-}$ mice.[360] NKCC2 expression is not altered in $D_2^{-/-}$ and $D_3^{-/-}$ mice and has not been reported in $D_1^{-/-}$ mice (Table 19.2).

Distal Convoluted Tubule

The distal convoluted tubule expresses all the dopamine receptor subtypes, but their effect on ion transport in this nephron segment has not been reported, except for D_4R which inhibits NCC.[511] However, the D_2R, D_3R, D_4R, and D_5R may regulate NCC because its expression is increased in $D_2^{-/-}$, $D_3^{-/-}$, $D_4^{-/-}$ and $D_5^{-/-}$ mice[360,528] (unpublished data). NCC expression has not been reported in $D_1^{-/-}$ mice (Table 19.2).

Cortical Collecting Duct

D_1-like receptor stimulation of the rabbit cortical collecting duct depolarizes the luminal membrane and increases cAMP production.[363,530] D_5R may regulate ENaC because α- and γ-subunit expressions are increased in $D_5^{-/-}$ mice[360]; sodium transporters in $D_1^{-/-}$ mice have not yet been quantified. Dopamine, via D_4R, at the basolateral membrane decreases sodium transport in the rabbit cortical collecting duct.[529] The D_4R may also inhibit the increase in sodium transport mediated by vasopressin, via a decrease in cAMP.[365,498] αENaC is increased in $D_4^{-/-}$ mice but only following a high salt diet (unpublished observations). ENaC expression is not altered in $D_2^{-/-}$ and $D_3^{-/-}$ mice. ENaC expression has not been reported in $D_1^{-/-}$ mice (Table 19.2).

Medullary Collecting Duct

The D_1R is expressed in the collecting duct or in the outer but probably not in the inner medulla, while the D_5R is also expressed in the outer but not in the inner medullary collecting duct in the mouse kidney.[360,528] Indeed, dopamine does not stimulate cAMP production in the rat inner medullary collecting duct.[369] D_2-like receptors are expressed in the medullary collecting duct; the D_2R is expressed in the intercalated cells,[357] while D_3R and D_4R are not differentially expressed between intercalated and principal cells.[357,528] A D_2-like

receptor has been shown to stimulate PGE2 production in rat inner medullary collecting duct cells.[358,359] The specific D_2-like receptor involved is not known, but only the D_4R is expressed in the inner medullary collecting duct; the expression of the D_2R has not been consistently shown (Table 19.2).[528] It is not clear if dopamine regulates ion transport in the medullary collecting duct. Indeed, the inhibitory effect of dopamine on vasopressin-induced water permeability and cAMP accumulation in the rat inner medullary collecting duct is mediated by the α_2 adrenergic receptor.[368]

Basolateral Membrane

D_1-like receptors inhibit the electrogenic Na^+/HCO_3^- co-transporter (NBCe1A, SLC4A4) expressed in the basolateral membrane of the proximal tubule[481] and Na^+/K^+-ATPase expressed at the basolateral membrane in all nephron segments studied (proximal tubule, thick ascending limb of Henle, cortical collecting duct).[17,38,89,268,293,301,304,318,319,477–480,495,522,526–543] Although stimulation of D_2-like receptors may increase Na^+/K^+-ATPase activity,[267,373,503] the inhibitory effect of dopamine on Na^+/K^+-ATPase activity may require simultaneous stimulation of D_1-like and D_2-like receptors,[268] and could result in a potentially greater inhibition of the sodium pump caused by D_1-like receptors. For example, in the rat proximal tubule (but not in the mTAL or cortical collecting duct) D_2-like receptors act in conjunction with D_1-like receptors to inhibit Na^+/K^+-ATPase activity and decrease sodium transport, similar to that proposed for NaPiII[545] and NHE3.[546] Under normal circumstances, dopamine receptors probably do not regulate the expression of the α-subunit of Na^+/K^+ATPase, because its expression is not altered in $D_2^{-/-}$, $D_3^{-/-}$, $D_4^{-/-}$, and $D_5^{-/-}$ mice on a normal salt intake[360,523,528] although this has not been studied in $D_1^{-/-}$ mice.

The inhibitory effect of D_1-like receptors on Na^+/K^+-ATPase is mediated by cAMP/PKA, certain PKC isoforms, and 20-HETE. The overall consequence of D_1-like receptor stimulation is internalization of $Na^+/$

TABLE 19.2 Characteristics of Mice With Knockout of Dopamine Receptor Subtype Gene (Normal Sodium Intake Unless Indicated)

Variable	$D_1^{-/-}$	$D_2^{-/-}$	$D_3^{-/-}$	$D_4^{-/-}$	$D_5^{-/-}$
Blood Pressure	High[22]	High[23,47]	High[25], Normal[560*]	High[26]	High[27,232,234]
Salt Sensitivity (chronic NaCl load)	Yes#	BP increased only with sodium load[24]	Yes#, No[560*]	Yes#	Yes[234,360]
Increased Na^+ transporter/exchanger, channel	ND	NHE3, NCC#	NHE3, NCC#	NHE3, NKCC2, NCC#	NKCC2, NCC, α & β ENaC subunits[360]
Na^+K^+ATPase, a subunit	ND	Low activity[23] and protein#	Normal#	High#	Normal[360]
GPCR (kidney)	ND	Normal AT_1R#, normal response to ARB, increased ETBR[23]	High AT_1R[342],	High AT_1R[26]	High AT_1R[a,46, 360]
Renin-Angiotensin	ND	ND	High[25]	Normal[26]	Normal[360]
Aldosterone	ND	High[47]	Normal#	Normal#	Normal[360]
Reactive Oxygen Species	ND	High[47]	Normal#	Normal#	High[a, 234]
Inflammation	ND	High#	Normal	Normal#	ND
Body Weight	Low [22,561]	Normal[23,24,47], Low[b]	Normal[25,560], Fat load increases body weight in males; increased body fat in males and females[c]	Normal[26]	Normal[360]

ND = not determined, # unpublished, *chronic administration of D_3R antagonist causes salt-dependent hypertension in rats.[501] Please read text for important details.

a. Asico L, Zhang X, Jiang J, et al. Lack of renal dopamine D5 receptors promotes hypertension. J Am Soc Nephrol. 20;22(1):82–89.

b. Kim KS, Yoon YR, Lee HJ, et al. Enhanced hypothalamic leptin signaling in mice lacking dopamine D2 receptors. J Biol Chem. 2010;285 (12):8905–8917.

c. McQuade JA, Benoit SC, Xu M, Woods SC, Seeley RJ. High-fat diet induced adiposity in mice with targeted disruption of the dopamine-3 receptor gene. 2004;151(1–2):313–319.

K^+-ATPase subunits.[301,477–480,533–536,540] The inhibitory effect of D_1-like receptors on Na^+/K^+-ATPase involves PKC in the proximal convoluted tubule (Figure 19.2) and PKA in the distal convoluted tubule and cortical collecting duct, while the eicosanoids are involved in all nephron segments, including the mTAL,[241,522,530,539,540,544] PKC may also be involved in the inhibition of Na^+/K^+-ATPase in the mTAL.[527] 20-HETE is important in the ability of dopamine to inhibit Na^+/K^+-ATPase activity in rat renal cortex, because it overrides the stimulatory effect of PKA.[38,544] In the renal medulla, but not in the renal cortex, PKA[544] and phosphatase inhibition also contribute to the inhibition of Na^+,K^+-ATPase activity that may be related to DARPP-32 inhibition of PP-1,[293,317,543] in the case of dopamine.

The effect of dopamine on Na^+/K^+-ATPase is tissue-specific. As stated above, dopamine inhibits Na^+/K^+-ATPase activity in renal cortical and medullary tubules.[17,38,89,268,293,301,304,318,319,477–480,495,522,526–543] However, the regulation of the phosphorylation of Na^+/K^+-ATPase at Ser-23 is different between the proximal convoluted tubule and thick ascending limb of Henle; PKC phosphorylates Na^+/K^+-ATPase at Ser-23 in the proximal tubule but not in the mTAL.[527] D_1-like receptors may actually stimulate Na^+/K^+-ATPase activity in human ciliary nonpigmented epithelial[547] and pulmonary alveolar cells.[548] $D_{2L}R$ also stimulates Na^+/K^+-ATPase in murine fibroblasts.[503] D_1R and D_2R, on the one hand, and Na^+/K^+-ATPase, on the other, can also negatively regulate each other in HEK293T cell by direct protein–protein interaction.[549] While the inhibition of Na^+/K^+-ATPase in the kidney by dopamine under conditions of sodium chloride excess is beneficial, inhibition of Na^+/K^+-ATPase activity in neuronal cells by high concentrations of dopamine can lead to cell death.[550] Inhibition of Na^+/K^+-ATPase activity in vascular smooth muscle cells would increase vascular resistance, as has been reported in the rat tail.[409] Low concentrations of dopamine, however, decrease systemic vascular resistance probably by mechanisms other than via regulation of sodium transporter or pump activity,[264,551,552] e.g., opening of potassium channels[274,553–555] (*vide supra*, "Dopamine and Renal Hemodynamics").

Water Transport

Dopamine may also regulate water transport.[497] Dopamine inhibits arginine vasopressin-mediated increase in water transport,[510] via the D_4R in the rat cortical collecting duct.[498] Dopamine has been reported also to inhibit vasopressin-stimulated increase in water permeability in inner medullary collecting duct cells.[368] Although it has been claimed to be exerted at a_2-adrenergic receptors, the effect could be[498] inhibited by clozapine, a D_4R antagonist. The dopamine-mediated reversal of vasopressin-mediated increase in water transport has been related to a decrease in expression, and increase in phosphorylation, of aquaporin 2 at the apical plasma membrane.[499] In addition, dopamine, via D_4R, increases the ubiquitin-mediated degradation of aquaporin 2 in lysosomes and decreases the aquaporin 2 transcription by decreasing vasopressin-induced increase in cAMP production.[497] D_1-like receptors probably do not play a role in the vasopressin-mediated transport, at least in the rat inner medullary collecting duct, because dopamine does not increase cAMP levels in this nephron segment.[369] Aquaporin 4-mediated increase in basolateral permeability is also impaired by dopamine, via a yet to be determined receptor subtype that is linked to PKC.[556] The D_2R can regulate aquaporin 4 in glial cells,[557] but is probably not the dopamine receptor involved in the medullary collecting duct because the D_2R is not expressed in principal cells of this nephron segment.[357] The diuresis associated with hypotonic saline loading has been related to the ability of D_1-like receptor antagonist to decrease vasopressin release.[51] However, dopamine is known to increase vasopressin secretion from the hypophysis.[558] This discrepancy could be taken to indicate that the dopamine-mediated release of vasopressin may be influenced by the state of volume expansion.

Hypovolemia

In contrast to the natriuretic effect of endogenous renal dopamine in euvolemic and in moderately volume-expanded states, in sodium-depleted states the D_1-like agonist, fenoldopam, does not affect sodium excretion,[427] while dopamine actually decreases sodium excretion.[56] A limited number of studies have assessed the dopamine receptor subtype that may increase renal sodium reabsorption in hypovolemic states. In conscious, chronically instrumented dogs on a sodium intake of 40 mmol/day, quinpirole (D_3R and D_4R agonist) decreased sodium excretion as a consequence of both a decrease in renal blood flow and an increase in tubular sodium reabsorption.[421] Dopamine has also been reported to stimulate NHE3 and Na^+/K^+-ATPase activity in rabbit renal proximal tubule cells[559] and NKCC2 in mTAL[442]; bromocriptine (D_2R/D_3R agonist) stimulates Na^+/K^+-ATPase activity in rat renal proximal tubule cells[267] and increases chloride transport in the mTAL.[505] Stimulation of the $D_{2S}R$ or $D_{2L}R$ heterologously expressed in murine LTK-cells increased Na^+/K^+-ATPase[503] and NHE1[430] activity. These may be the mechanisms by which dopamine increases sodium transport during hypovolemia.[56]

Dopamine Receptor Subtype Mutant Mice

The deletion of dopamine receptor subtype in mice has helped to determine the role of each dopamine receptor subtype in the regulation of renal function and blood pressure.[22–27,30,232,234,360,511,523,528,560] Each dopamine receptor subtype participates in the regulation of blood pressure by mechanisms specific for the subtype. As described above, some receptors influence epithelial transport. Others, as described below, regulate blood pressure by influencing the central and/or peripheral nervous system and regulating the secretion and receptors of several humoral agents (Table 19.2).

D_1R Mutant Mice

$D_1^{-/-}$ mice are growth retarded without obvious neurological defects, but exhibit a decrease in rearing behavior.[561] The low survival after weaning is caused by decreased feeding ability. $D_1^{-/-}$ mice and $D_1^{-/+}$ mice (C57BL/6 background) on a normal NaCl diet have higher systolic and diastolic blood pressures than D_1R wild-type ($D_1^{+/+}$) mice.[22] Homozygous $D_1^{-/-}$ mice do not increase renal tubular cAMP accumulation in response to dopamine stimulation, but the response to parathyroid hormone is intact. These data indicate D_1R specificity in the increased blood pressure in mice.[22] However, it is not clear why the other D_1-like receptor, D_5R, is unable to compensate for the lack of D_1R; D_5R expression is not altered in $D_1^{-/-}$ mice[193,229] and D_1R expression is not altered in $D_5^{-/-}$ mice.[27] The hypertension of $D_1^{-/-}$ mice is aggravated by an increase in salt intake (Table 19.2). The hypertension of $D_1^{-/-}$ mice is aggravated by an increase in salt intake (Table 19.2).

D_2R Mutant Mice

$D_2^{-/-}$ mice in C57BL/6J background have decreased motor activity but rotarod performance is not impaired.[192] D_1-like receptor binding may be decreased, while D_3R is transiently increased after birth in $D_2^{-/-}$ mice.[192] $D_2^{-/-}$ and $D_2^{-/+}$ mice (C57BL/6J) on a normal NaCl diet have higher systolic and diastolic blood pressures than D_2 wild-type ($D_2^{+/+}$) mice.[23] α-Adrenergic blockade decreases blood pressure to a greater extent in $D_2^{-/-}$ mice than in $D_2^{+/+}$ mice, but acute adrenalectomy decreases blood pressure to a similar level in $D_2^{-/-}$ and $D_2^{+/+}$ mice. ETB receptor expression is greater in $D_2^{-/-}$ mice than in $D_2^{+/+}$ mice, and ETB receptor blocker decreases blood pressure in $D_2^{-/-}$ mice but not $D_2^{+/+}$ mice. $D_2^{-/-}$ mice also have increased production of ROS; increasing antioxidant activity with hemin normalizes the increased blood pressure.[47] These data indicate that $D_2^{-/-}$ mice may have enhanced vascular reactivity caused by increased sympathetic and ETB receptor activities, and oxidative stress.[47] The $D_2^{-/-}$ mice also have increased production of aldosterone, and treatment with a mineralocorticoid receptor blocker normalizes blood pressure but not the increased oxidative stress in these mice,[47] indicating that the increased mineralocorticoid activity is distal to the increased oxidative stress. In an unspecified strain of $D_2^{-/-}$ mice, blood pressure is increased only when the mice are fed a high-salt diet; this is associated with a decrease in renal AADC activity and renal dopamine production. Sympathetic activity is not increased in these $D_2^{-/-}$ mice.[24] The differences between the two strains of $D_2^{-/-}$ mice could be related to differences in the genetic background,[153] similar to the differences in behavior of $D_2^{-/-}$ mice from different genetic backgrounds.[192,193]

D_3R Mutant Mice

The locomotor phenotype of $D_3^{-/-}$ mice does not resemble that of $D_2^{-/-}$ mice. $D_3^{-/-}$ mice may show a transient locomotor hyperactivity in a novel environment.[562] The D_3R may be involved in seeking behavior for natural reinforcers such as food in rodent models of obesity[563]; $D_3^{-/-}$ mice fed a high fat diet become obese.[564] $D_3^{-/-}$ and $D_3^{-/+}$ mice (C57BL/6J) on a normal NaCl diet have both higher systolic and diastolic blood pressure than their wild-type ($D_3^{+/+}$) littermates.[25] These $D_3^{-/-}$ and $D_3^{-/+}$ mice have increased renal renin production, but sustained decrease in blood pressure with AT_1R blockade is observed in the $D_3^{-/-}$ but not $D_3^{-/+}$ or $D_3^{+/+}$ mice.[25] An unspecified strain of $D_3^{-/-}$ mice has normal blood pressure regardless of salt intake.[560] Nevertheless, these two strains (C57BL/6 and an unspecified strain) of $D_3^{-/-}$ mice have decreased sodium excretion after an acute or chronic sodium chloride load. Differences in phenotypes can occur depending on the genetic background, and even the same mouse strain from different commercial sources. For example, the blood pressure of C57BL/6 from Jackson Laboratories is salt-sensitive while the blood pressure of C57BL/6 mice from Taconic is salt-resistant.[153] The salt-sensitive hypertensive phenotype of human G-protein-coupled receptor kinase type 4 (GRK4) 486V transgenic mice is dependent on the percentage of genetic background from salt-resistant SJL mice.[565]

D_4R Mutant Mice

D_4R deficient ($D_4^{-/-}$) mice have impaired photoreceptor response, reduced response to novelty, but attenuated locomotor response to amphetamine, but not to methylphenidate or cocaine.[192] Congenic $D_4^{-/-}$[26] but not $D_4^{-/+}$ (Table 19.2) mice have increased systolic and diastolic blood pressures. The blood pressure is increased further with increased sodium intake in

$D_4^{-/-}$ mice (Table 19.2) but the effect of sodium intake on blood pressure in $D_4^{-/+}$ has not been tested. $D_4^{-/-}$ mice do not have altered circulating or renal renin or aldosterone levels.[26] Renal and brain, but not cardiac, AT_1R expression is increased in $D_4^{-/-}$ mice. The hypotensive effect of a bolus intravenous injection of the angiotensin type 1 receptor blocker, losartan, persists longer in $D_4^{-/-}$ than in $D_4^{+/+}$ mice. Thus, the hypertension brought about by the absence of the D_4R is mediated, in part, by increased AT_1R expression , similar seen in $D_3^{-/-}$ and $D_5^{-/-}$ (*vide infra*).[26]

D_5R Mutant Mice

$D_5^{-/-}$ mice have no impairment in learning and memory.[27,192] $D_5^{-/-}$ mice have normal expression of the other dopamine receptors, including the D_1R, a feature found in the other dopamine receptor subtype knockout mice except for the $D_2^{-/-}$ mice.[192] $D_5^{-/-}$[27] and $D_5^{-/+}$ mice are hypertensive. As with the $D_4^{-/-}$ mice (Table 19.2), the blood pressure is increased further with increased sodium intake in $D_5^{-/-}$ mice.[360] Epinephrine/norepinephrine ratio and the hypotensive response to the acute administration of an α-adrenergic blocker are greater in $D_5^{-/-}$ mice than their $D_5^{+/+}$ littermates, indicating that increased sympathetic activity plays a role in the elevated blood pressure observed with deletion of the *Drd5* gene.[27] Central nervous system pathways involving glutaminergic, oxytocin, vasopressin, and adrenergic receptors are important in the pathogenesis of hypertension in $D_5^{-/-}$ mice.[27] Besides these central nervous system mechanisms, renal AT_1R[46,567] and increased production of ROS are also involved[232,234] in the hypertension of $D_5^{-/-}$ mice.

DOPAMINE RECEPTOR INTERACTIONS

Interaction among the Dopamine Receptors and with Other GPCRs in the Regulation of Renal Function and Blood Pressure

Dopamine Receptor Subtype Interaction

D_1-like and D_2-like receptors[266,473,508,509] interact to enhance the natriuretic effect of dopamine in sodium-replete states. In sodium-replete states, the synergistic interaction between D_1-like and D_2-like receptors to increase sodium excretion occurs by inhibiting NHE3[546] and Na^+/K^+-ATPase[38,268,362] activity, as stated above.

D_1R and D_3R

D_1R and D_3R synergistically interact to decrease sodium transport in renal proximal tubule cells[265,266,426] and to relax vascular smooth muscle cells.[264,283] D_1R and D_3R reciprocally regulate each other's function and trafficking in HEK293 cells heterologously expresses tagged D_1R and D_3R, but not D_5R.[262] This has to be reconciled to the fact that $G\alpha_S$, which by itself decreases NHE3 activity independently of PKA,[130] is linked to both D_1R[30,183–193,687] and D_3R.[253] Gαq/11, involved in the D_1-like receptor inhibition of Na^+/K^+-ATPase,[410] can also be linked to D_3R.[568] The natriuretic action of the D_3R agonist pramipexole is partially blocked by a D_1-like receptor antagonist.[266] The D_3R co-localizes with D_1R in renal proximal tubule cells of WKY rats and in these cells, stimulation of D_3R increases both the co-immunoprecipitation of D_1R with D_3R, and the protein expression of D_1R.[265] The individual inhibitory effect of either D_1-like receptors or the D_3R on transporters is not 100%, not always on the same transporter or in the same nephron segment, and thus, additive or even synergistic effects are possible with co-stimulation. In mouse brain, the ALG-2 interacting protein 1 may be important in the interaction between D_1R and D_3R.[569] Whether or not this protein is also important in D_1R and D_2R interaction in the kidney remains to be determined.

The D_3R promotes natriuresis, in the short-term, alone[388,501,502] and by interacting with the D_1R.[266] In the long-term, the D_3R increases the expression of D_1R.[426] The interaction between D_1R and D_3R receptors is absent or impaired in hypertension, and results in defective inhibition of sodium transport and relaxation of vascular smooth muscles and ultimately in the development or maintenance of high blood pressure.[264,265,283,426]

D_2R and D_3R

In HEK293 cells, activation of heterologous D_2R inhibits both adenylyl cyclases V and VI, while activation of D_3R inhibits only adenylyl cyclase V and does not affect the activity of adenylyl cyclase VI.[258] However, when D_2R and D_3R are co-expressed in a monkey kidney cell line, lower concentrations of a D_2-like receptor agonist are needed to induce inhibition of adenylyl cyclase VI than those needed in cells expressing only the D_2R.[263] This suggests that the D_2R/D_3R heterodimer may enable the G-protein coupling of the D_3R to adenylyl cyclase VI. The D_3R, however, cannot inhibit adenylyl cyclase V in the rat renal proximal tubule, because this isoform is not expressed in this rat nephron segment.[220]

D_1R, D_5R, and D_2R

D_1R and D_2R heterodimerize in expression systems[570] and neural tissues,[571] and the degree of receptor protein–protein interaction is significantly enhanced by concomitant addition of D_1R and D_2R receptor subtype-specific agonists.[570] The physical

interaction between D_1R and D_2R is increased by the chaperone, calnexin.[338] The co-activation of D_1R and D_2R increases phospholipase C products[571] and eicosanoids[572] which inhibit sodium transport. In the brain striatum, the D_1R and D_2R complex activates calcium−calmodulin-dependent protein kinase 2α.[573] The D_1R can inhibit the cellular sequestration of D_2R and could explain the synergy between these two dopamine receptor subtypes.[256] The D_2R also hetero-oligomerizes with D_5R, which causes a decrease in D_5R-mediated increase in intracellular calcium levels.[227] However, there is no evidence of a D_1R and D_2R or D_5R and D_2R heterodimerization in renal tubule cells. It remains to be determined whether or not D_1R and D_5R interact to regulate renal ion.

D_4R and Other Dopamine Receptor Subtypes

A direct interaction between D_4R and the other dopamine receptor subtypes has not been reported. However, the dopaminergic regulation of glutamate N-methyl-D-aspartate receptor activity in the amygdala may be due to a functional interaction between D_1R and D_4R.[574] Gene−gene interaction between D_2R and D_4R is associated with the development of conduct disorder and adult antisocial behavior in males.[575]

Dopamine Interaction with Other GPCRs

The dopamine receptor subtypes interact with several GPCRs, e.g., D_1R and μ opioid receptor,[576] and N-methyl-D-aspartic acid glutamate receptor.[577−579] Only those receptors that have been shown to be involved or have the potential to be involved in the regulation of renal function are included in this review.

Adenosine Receptors

Stimulation of renal adenosine receptors lowers glomerular filtration rate by constricting afferent arterioles, and exerts differential effects on NaCl transport along the nephron, depending upon the adenosine receptor subtype; the adenosine type 2 receptor decreases (adenosine A_{2b} promotes chloride secretion), while the adenosine A_1 receptor increases sodium transport. Adenosine antagonizes some effects of dopamine. The dopamine-mediated inhibition of tubuloglomerular feedback is antagonized by adenosine via the regulation of adenylyl cyclase activity in the macula densa.[134] In opossum kidney cells, low concentrations of an adenosine analog, via the adenosine A_1 receptor, stimulate NHE3 activity and attenuate dopamine-mediated inhibition of NHE3.[580] Adenosine A_1 receptor modulates D_1R; co-administration of adenosine A_1R receptor and D_1R agonists in HEK293 cells stably expressing both receptors potentiate the D_1R-mediated desensitization of D_1R.[581] Interestingly, adenosine A_1 receptor and D_1R have been shown to physically interact in the central nervous system, with the formation of a heteromeric complex that leads to the uncoupling of the D_1R from its Gs-like protein complex.[445,581] However, in COS-7 cells and fibroblasts heterologously expressing adenosine A_1 receptor, D_1R, and D_5R, activation of adenosine A_1 receptor blocks the desensitization of D_1R but not D_5R,[582] another instance of cell-specific effects or related gene overexpression. In contrast, in HEK293 cells heterologously expressing adenosine A_1 receptor, D_1R, activation of adenosine A_1 receptor desensitizes the D_1R.[581] These studies illustrate the importance of studying receptor function in cells where such GPCRs are endogenously expressed.

The adenosine A_2 receptor isoform, A_{2A} receptor, heterodimerizes with D_2R in striatal membranes and reduces the high affinity state of D_2Rs, especially the high-affinity agonists.[583] The heterodimerization of adenosine A_{2A} receptor and D_3R or D_4R also results in an impairment of D_3R and D_4R function.[584]

Adrenergic Receptors

β-Adrenergic receptor agonists interact with dopamine in the regulation of Na^+/K^+-ATPase activity in the rat kidney. Activation of β-receptors with isoproterenol increases D_1R translocation from the cytosol to the membranes and D_1R-mediated inhibition of Na^+/K^+-ATPase activity in renal proximal tubule cells.[585] However, as stated above, stimulation of β_2Rs reduces the uptake of L-DOPA and the production of dopamine.[586] Thus, endogenous renal β-adrenergic receptors may not always enhance the dopaminergic inhibition of sodium transport.

Dopamine receptors may counter-regulate the actions of α-adrenergic receptors on renal sodium transport (unpublished data) and vascular proliferation. Stimulation of α_1Rs increases proliferation of vascular smooth muscle cells. However, in the presence of D_1-like or D_3R agonists, the proliferative effect of norepinephrine, via α_1Rs, is inhibited, although D_1-like or D_3R agonists have no effect by themselves. Moreover, co-stimulation of D_1-like or D_3R has an additive inhibitory effect on norepinephrine-mediated vascular smooth muscle cell contraction and proliferation.[264] The failure of dopamine to induce natriuresis in sodium-depleted states may be a consequence of increased sympathomimetic activity.[56]

Angiotensin II and Angiotensin Receptors

AT_1R and Dopamine Receptors

There are several areas of interaction between the dopamine and the renin−angiotensin system (RAS).

The D_3R, D_4, and D_5R D_4R and D_5R or D_2R (Table 19.2), but not D_1R, decrease AT_1R expression in the kidney.[26,46,276] In contrast, the D_2R may negatively regulate the expression of AT_1R,[587] and angiotensin II may increase D_2R expression in neural cells.[588]

Angiotensin II inhibits the uptake of dopamine by rat renal tubule cells[589] and the intravenous infusion of angiotensin II in humans reduces urinary dopamine.[590] Angiotensin II, via AT_1R, causes renal vasoconstriction while at low concentrations of dopamine, D_1-like receptors cause vasodilation.[405,591] Activation of the RAS may cause the development of tolerance to the hypotensive action of D_1-like receptor agonists.[592] In the rat, dopamine attenuates the glomerular mesangial contractile response to angiotensin II independently of eicosanoids.[389] D_1-like receptor agonists block angiotensin II-induced afferent and efferent arteriolar constriction.[399,591] Blockade of AT_1R normalizes the impaired renal vasodilator effect of D_1-like receptor stimulation in the SHR.[492] The increased vasodilatory effect of a D_3R/D_4R agonist (quinpirole) after renal denervation may also depend on decreased activity of the RAS).[593]

Activation of the RAS has been suggested to cause attenuation of the natriuretic effect of the D_1-like receptor agonist, fenoldopam, in sodium-deplete states.[427] When angiotensin II generation is inhibited or AT_1Rs are blocked, the natriuretic effect of dopaminergic drugs is enhanced.[490,491,492] In humans, this effect is seen mainly in subjects on a low salt diet (Natarajan et al., unpublished studies). D_1- and D_2-like receptor agonists also antagonize the stimulatory effect of angiotensin II, acting on AT_1R, on renal proximal tubule sodium transport.[45,397,493,494,589] These counterbalancing effects of dopamine and angiotensin II on sodium transport occur by the regulation of sodium transporter/channel/pump activity in the short-term, and the regulation of receptor expression in the long-term.[477,534,528] The short-term counteracting actions may occur by differential cell membrane trafficking. Thus, angiotensin II, via the AT_1R, in renal proximal tubule cells, induces recruitment of Na^+/K^+-ATPase to the plasma membrane. At an intracellular concentration of sodium of 9 mM, angiotensin II increases Na^+/K^+-ATPase activity[534]; dopamine is without effect. Increasing intracellular sodium to 19 mM is associated with an increasing inhibition of Na^+/K^+-ATPase activity by dopamine and blunting of the stimulatory effect of angiotensin II. This is associated with the recruitment of D_1R to the plasma membrane and a reduction in plasma membrane AT_1R.[534]

The mechanism by which dopamine receptors interact with the angiotensin receptors is receptor subtype-specific. The D_1R[45,343] and the D_3R[342] inhibit angiotensin II effects via physical interaction (heterodimerization) with the AT_1R. In contrast, the D_5R and AT_1R can also heterodimerize but negatively regulate each other's expression. In renal proximal tubule cells, the D_5R (not the D_1R) decreases AT_1R expression and AT_1R-mediated extracellular signal-regulated kinase phosphorylation. The D_1-like receptor-induced decrease in AT_1R expression is reversed by tyrosine-kinase inhibition and proteasome inhibitor, demonstrating that the D_5R-mediated decrease in total cell AT_1R expression is a result of a c-Src- and proteasome-dependent process.[45,46,276,567] Dopamine has also been reported to decrease AT_1R mRNA expression in renal proximal tubules.[594] The D_4R also negatively regulates AT_1R expression, but the mechanism remains to be determined.[26]

AT_2R and Dopamine Receptors

In the rat striatum, AT_2R stimulation decreases dopamine synthesis.[595] However, stimulation of D_1-like receptors induces an AT_2R-dependent natriuresis.[596] Selective intrarenal activation of D_1-like receptors induces sustained natriuresis and diuresis in sodium-loaded Sprague-Dawley rats that is abolished by intrarenal AT_2R inhibition. D_1-like receptor-mediated natriuresis is accompanied by recruitment of both D_1Rs and AT_2Rs to the plasma membrane of renal proximal tubular cells. These observations suggest that D_1-like receptor-induced natriuresis and diuresis are modulated by functional AT_2Rs that are translocated from intracellular compartments to the plasma membrane of renal proximal tubule cells in response to D_1-like receptor activation, and that dopamine-induced natriuresis requires AT_2R activation.[596] Therefore, in the normotensive state, dopaminergic stimulation favors natriuresis not only via specific dopamine receptor subtype mechanisms, but also by enhancing AT_2R function[596]; D_1R increases AT_2R expression. In addition, dopamine impairs AT_1R function by decreasing AT_1R expression via D_3R,[342] D_4R,[27] and D_5R,[46,276,567] and a negative interaction of AT_1R with D_1R,[45,343] D_3R, and D_5R.[46,276,567]

Atrial Natriuretic Peptide (ANP)

The inhibition of dopamine synthesis or uptake impairs the ability of ANP to inhibit renal tubular Na^+K^+-ATPase activity.[597] The inhibitory effect of ANP on NHE3 activity becomes manifest in the presence of dopamine.[598] However, the ability of carbidopa to affect sodium excretion or the natriuretic effect of ANP in humans has not been consistent.[599–603] This could be related to the state of hydration.[599–603] The renal dopaminergic system is not responsible for the natriuresis caused by marked volume expansion,[49,117] and dopamine does not affect sodium excretion in subjects fed a low salt diet[427] and may actually decrease sodium excretion during hypovolemia.[56] The natriuretic effects of dopamine

and ANP are additive in humans.[604] Carbidopa or dopamine receptor blockade, especially by D_1-like receptor blocker, attenuates the natriuretic effect of ANP in rats[605–608] and the natriuretic effect of ANP is abolished in mice lacking *Ppp1r1b*, which is also involved in D_1R signaling.[224,225,288–293] The potentiation of the natriuretic effect of dopamine by ANP may be due to its ability to recruit D_1R to the plasma membrane.[609] The conflicting effects of carbidopa on the natriuretic effect of ANP may also be related to the fact that ANP can increase or decrease renal tubular dopamine synthesis.[597,610]

Cholecystokinin Receptors

There are two cholecystokinin receptors, namely, cholecystokinin type A receptor (CCKAR) and cholecystokinin type B receptor (CCKBR). Cholecystokinin modulates dopamine release in the nucleus accumbens through CCKAR. Cholecystokinin may also modulate D_2R expression in the nucleus accumbens; D_2R expression is higher in $CCKAR^{-/-}$ and lower in $CCKBR^{-/-}$ mice than in wild-type controls.[611] Also, activation of CCKBR reduces the affinity of the D_2R in the brain.[612,613] Cholecystokinin at low concentrations activates Na^+/K^+-ATPase activity via the CCKAR.[614] CCKBR is expressed in the kidney, and the postprandial increase in sodium excretion may be mediated by an increase in serum gastrin acting at CCKBR in the kidney to decrease Na^+/K^+-ATPase activity.[615]

Endothelin Receptors

There are two endothelin receptors, endothelin A receptor (ETAR) and endothelin B receptor (ETBR).[616] In the brain striatum, stimulation of the ETBR increases dopamine release, but dopamine does not increase endothelin-1 levels.[617] The ETB and dopamine receptors can interact to regulate renal function and blood pressure. Stimulation of the D_3R increases ETBR protein expression and D_3R/ETB receptor co-immunoprecipitation and co-localization in renal proximal tubules.[39,618] The interaction between D_3R and ETBR has physiological significance, because pretreatment with a D_3R agonist increases the ETBR-mediated inhibitory effect on Na^+/K^+-ATPase activity in renal proximal tubule cells from WKY rats.[39,618] Conversely, stimulation of ETBR increases D_3R expression and function in renal proximal tubule cells from WKY rats (unpublished data). The natriuretic effect of D_3R may be, in part, mediated by ETBR, because the natriuretic effect is attenuated in WKY rats when the renal ETBR is blocked.[39,618] In renal proximal tubule cells, the ability of D_3R to stimulate ETB expression is blocked by an L-type calcium channel blocker.[39]

The D_2R may also regulate ETB receptor expression. $D_2R^{-/-}$ mice have increased ETBR expression and an ETBR blocker normalized blood pressure in these mice, but did not affect blood pressure of D_2R wild-type littermates.[23] GPR37, a parkin-associated endothelin-like receptor, can associate with D_2R in HEK-293 cells.[619] In rat lactotrophs, D_2-like receptor stimulation antagonizes the ETAR-mediated activation of large-conductance K^+ channels.[620] The functional consequences of D_2R and ETBR interaction on renal ion transport remain to be determined.

Insulin and Insulin Receptors

Insulin and dopamine have opposite effects on Na^+/K^+-ATPase activity in renal proximal tubule cells, and may counter-regulate each other. Chronic exposure of renal proximal tubule cells to insulin causes a reduction in D_1R abundance and uncoupling from G-proteins, resulting in impairment of the inhibitory effect of dopamine on Na^+/K^+-ATPase.[621] This suggests a direct role of insulin in D_1R regulation.[495,622] Insulin causes renal D_1R desensitization via GRK2-mediated receptor phosphorylation (*vide infra*) involving PI3 kinase and PKC.[305] Hyperinsulinemic animals and patients with type 2 diabetes have a defective renal dopaminergic system.[623] In obese Zucker rats, a model of type 2 diabetes or in insulin-induced hypertension, renal D_1Rs are downregulated and dopamine fails to produce diuresis and natriuresis.[621] Treatment with an insulin sensitizer, rosiglitazone, decreases plasma insulin levels and restores D_1R function in obese Zucker rats.[622,624] Insulin has also been shown to increase the expression of the D_5R in renal proximal tubular cells from WKY rats, probably a compensatory response. In HEK293 cells heterologously expressing the D_5R, pretreatment with insulin increases the D_5R-mediated inhibition of Na^+/K^+-ATPase.[496] Both PKC and PI3 kinase are involved in the signaling pathway leading to increased D_5R expression.

Dopaminergic activity may influence insulin secretion, and *vice versa*. Insulin has been reported to increase renal proximal tubule uptake of L-DOPA, which should increase dopamine synthesis,[625] but this could be an attempt to compensate for the ability of insulin to decrease and uncouple D_1R.[621] The D_1-like receptor agonist fenoldopam improves peripheral insulin sensitivity and renal function in streptozotocin-induced type 2 diabetes in rats.[626] Normalizing blood sugar levels with insulin also normalizes renal D_1R expression and function in rats with sreptozotocin-induced diabetes.[627] D_2-like receptors in pancreatic β-cells inhibit[628] or stimulate glucose-stimulated insulin secretion, depending on dopamine concentration; an

inhibitory effect occurs at higher dopamine concentration (10^{-7}–10^{-4} M), while the effect is stimulatory at lower dopamine concentrations ($<10^{-8}$ M).[629] Bromocriptine (D_2R/D_3R agonist) decreases insulin levels and ameliorates several metabolic features in obese women.[630] The counter-regulatory actions of the insulin and dopamine receptors extend to their effects on vascular proliferation. Bromocriptine (D_2R/D_3R agonist) inhibits the insulin-like growth factor-mediated proliferation in rat vascular smooth muscle cells (A7r5) and human aortic smooth muscle cells.[631] Stimulation of D_1-like receptors or D_3R inhibits insulin receptor expression and insulin-mediated proliferative effects in vascular smooth muscle cells, showing an interaction between dopamine (D_1-like and D_3R) and insulin receptors.[40,632] A D_3R antagonist was found to be protective of renal injury in hypertensive type II diabetic SHR/Ncp rats.[633] In these rats, a D_3R antagonist ameliorated glomerulosclerosis and prevented mesangial cell proliferation. These apparent contradictory interactions between D_3R and insulin may be related to the biphasic effect of dopamine on insulin secretion.

Dopamine and Mineralocorticoid Receptor

Aldosterone increases catecholamine production in a pheochromocytoma cell line.[634] In the rabbit cortical collecting duct D_2-like, but not D_1-like, receptor stimulation at the basolateral surface depolarizes transepithelial voltage and decreases sodium transport.[529] It is possible that this effect is related to D_4-like negative interaction with the non-genomic effects of aldosterone.[48]

Dopamine and Prolactin

D_2R inhibits prolactin secretion by the pituitary gland.[189,193] However, prolactin is also expressed in the renal cortex and induces a natriuresis that requires an intact renal dopaminergic system. Prolactin recruits D_1Rs to the plasma membrane in renal proximal tubules which inhibits Na^+K^+-ATPase activity that involves activation of PKA, PKC, and PI-3 kinase.[42]

Dopamine and Prostaglandins

Earlier studies have suggested that the renal vasodilatory effect of dopamine is independent of prostaglandins because indomethacin, an inhibitor of prostaglandin synthase, did not affect the renal vasodilatory effect of dopamine or the D_1-like receptor agonist fenoldopam in the dog, rat[635] or humans.[636] The intrarenal arterial infusion of the D_1-like receptor agonist fenoldopam is also not associated with an increase in urinary prostaglandin E2 (PGE2) and $F_2\alpha$ in the dog.[396] Subsequent studies in normotensive humans revealed that the renal vasodilatory effect of dopamine was also not associated with an increase in urinary excretion of PGE2, but rather with 6-keto-PGF1α, a stable metabolite of prostacyclin. The effect of dopamine was blocked by metoclopramide or domperidone, D_2-like receptor antagonists, and two cyclooxygenase inhibitors.[407] These studies suggest that the dopamine and prostaglandin communication is via the D_2-like rather than D_1-like receptors. D_2-like but not D_1-like receptors may also regulate PGE2 synthesis in rat inner medullary collecting cells.[358] Dopamine stimulates medullary prostaglandin production, and may be involved in the attenuation of deoxycorticosterone acetate/high salt-induced increase in blood pressure.[37] Eicosanoids may act synergistically with D_1-like receptors to inhibit Na^+/K^+-ATPase activity in the proximal tubule, mTAL, and cortical collecting duct.[38,524,530,539,541] Moreover, the renal cortical expression of COX-2 is tonically suppressed by the renal D_1-like receptors secondary to inhibition of proximal tubular reabsorption.[44,637]

Regulation of Reactive Oxygen Species (ROS)

Dopamine regulates ROS production, stimulating production at high concentrations ($\geq 10\ \mu M$) but physiological concentrations of dopamine decrease ROS production via D_1-like receptors.[233,638,639] All the dopamine receptor subtypes are capable of decreasing ROS production. However, deletion of *Drd2* or *Drd5* but not *Drd3* or *Drd4* in mice is associated with increased ROS production. The D_1R inhibits NADPH oxidase activity via PKA and PKC cross-talk[239]; the D_5R inhibits NADPH oxidase directly and also indirectly, by inhibiting phospholipase D activity and independent of cAMP.[232,234] The D_5R may also positively regulate antioxidants such as heme oxygenase 1 (HO-1).[640] Plasma thiobarbituric acid-reactive substances (TBARS), an index of systemic oxidative stress, and PLD and NADPH oxidase subunit expression and activity are higher in $D_5R^{-/-}$ mice than in $D_5R^{+/+}$ mice[232,234] (Table 19.2). Chronic administration of apocynin, an NADPH inhibitor, normalizes blood pressure, plasma TBARs, and NADPH oxidase activity in the brain and kidney of $D_5R^{-/-}$ mice, suggesting that the D_5R keeps blood pressure in the normal range by preventing excessive ROS production.[234] The redox status of the $D_1R^{-/-}$ mice remains to be determined. ROS impair the function of renal D_1-like receptor. Rat renal proximal tubules treated with hydrogen peroxide, and those from streptozotocin-treated or old rats,

have increased oxidative stress and impaired D_1-like receptor function.[449,641–643] Oxidative stress causes the nuclear translocation of NFκB and subsequent activation of PKC and GRK2, which in turn increases D_1R phosphorylation, impairing its activity.[641,642]

The D_2R has also antioxidant activity. The neuroprotective effect of D_2R may be related to its ability to decrease ROS production by the mitochondria.[644] D_2R, similar to the D_1-like receptors, decreases oxidative stress by inhibition of NADPH oxidase and stimulation of HO-2,[47] $D_2^{-/-}$ mice are hypertensive and have increased urinary excretion of 8-isoprostane, a parameter of oxidative stress, as well as increased activity and expression of NADPH oxidase and decreased expression of the antioxidant enzyme HO-2 in the kidney. Apocynin (an NADPH inhibitor) or hemin (an inducer of HO) normalizes blood pressure in $D_2^{-/-}$ mice. Spironolactone normalizes the blood pressure in $D_2^{-/-}$ mice, but does not normalize the renal expression of NADPH oxidase, indicating that the increased ROS production is proximal to the increased aldosterone secretion in $D_2^{-/-}$ mice.[47]

The effect of D_3R receptors on ROS production is controversial. The D_3R has been reported to increase a dopamine autotrophic factor that has an antioxidant action, and thus the D_3R has antioxidant effect, albeit indirectly.[645] The selective D_3R agonist pramipexole inhibits lipid peroxidation,[646] increases the activity of antioxidant enzymes (glutathione peroxidase and catalase), and inhibits the production of ROS by the mitochondria, but this effect is not related to its dopamine agonist properties.[647] Moreover, the D_3R has been reported to stimulate PLD activity in HEK293 cells heterologously expressing the human D_3R.[235] The D_3R and D_4R may also have neuroprotective effects by inhibition of ROS production.[648,649]

Regulation of Inflammation

Lymphocytes can synthesize catecholamines, including dopamine.[650] All the dopamine receptor subtypes are expressed in normal human leukocytes, with the highest expression in B-lymphocytes and natural killer cells, followed by neutrophils and eosinophils, with least expression in T-lymphocytes and monocytes.[650–653] Dopamine, D_1- and D_2-like receptor subtype agonists can regulate the immune response and inhibit the inflammatory reaction,[654–657] the extent of their involvement is tissue-dependent. Dopamine inhibits the release of pro-inflammatory cytokines (e.g., interleukin-2 (IL-2), interferon (IFN)γ, IL-4,[657] but stimulates the production of the anti-inflammatory IL-10 in immune cells.[658] The D_1-like receptors and D_3R but not D_2R or D_4R can also stimulate TNFα secretion.[658] Indeed, the D_2R may actually decrease lipopolysaccharide-induced release of TNFα.[659] Dopamine or bromocriptine (D_2R/D_3R agonist), inhibits lymphocyte proliferation,[660] decreases the antigen-induced macrophage activation and the secretion of IL-2, IL-4 and IFNγ.[661]

Renal tubule cells produce pro-inflammatory cytokines and chemokines (e.g., IL-1, TNFα, IL-6, IL-8, IL-12, and macrophage chemoattractant protein (MCP)-1), as well as anti-inflammatory cytokines (e.g., IL-10).[662–664] Both pro-inflammatory and anti-inflammatory cytokines are secreted by tubular cells across their apical or basolateral membranes.[664] The pro-inflammatory cytokines contribute to the development and progression of glomerular and tubular injury.[662–664] Lipopolysaccharide causes dysfunction of renal D_1R and salt-sensitive hypertension,[665] but the D_2R may protect the kidney from the adverse effects of inflammation.[666] Silencing the D_2R in renal proximal tubule cells increases the expression of TNFα and MCP-1; expression of TNFα, MCP- 1, IL-6, and IL-10 are increased in the renal cortex of $D_2^{-/-}$ mice. These mice show renal injury and increased urinary albumin, suggesting that impaired D_2R function results in renal inflammation and injury.[666] The role of the other dopamine receptor subtypes in inflammation remains to be determined.

Dopamine and Essential Hypertension

About 50% of human essential hypertension is thought to be heritable, but the genetic causes of essential hypertension have been difficult to identify.[667] More than one gene is undoubtedly involved, because Mendelian dominant and recessive traits are not readily discernible in hypertensive subjects, except in those with monogenic forms of hypertension. Indeed, recent genome-wide association studies (GWAS) have been able to identify 2% of genetic factors believed to influence blood pressure.[668–674] However, the GWAS were not designed to identify predisposing genes engaged in a complex network of gene–gene and gene/environment interactions.[675] One example is salt sensitivity, a dietary sodium-induced increase in blood pressure that may or may not produce elevation in the hypertensive range. Several criteria have been suggested to link gene (s) to complex diseases such as hypertension and salt sensitivity, but the definitive evidence is swapping one phenotype for another (i.e., transgenic studies).[676] Many genes have been proposed to be causal of hypertension; however, their gene variants, including those identified in the GWAS, have not been shown to produce hypertension in mice. Many gene overexpression and deletion studies are performed in mice without

taking into account the salt sensitivity of the strain. C57BL/6 mice from Jackson Laboratories have an impaired ability to excrete a salt (NaCl) load with a resultant increase in blood pressure, while others are salt-resistant (e.g., SJL mice).[153]

GRK4 regulates renal D_1R[298] and D_3R.[286] Renal D_1-like receptor function is impaired in C57BL/6 Jackson mice, and is associated with increased expression of GRK4 upon salt loading.[153] Deletion of the *Grk4* gene in C57BL/6 mice prevents the development of salt-sensitive hypertension.[677] Renal cortical silencing of *Grk4* attenuates the increase in blood pressure with age in SHRs, but not in normotensive WKY rats.[306] Aging and obesity are associated with decreased D_1-like receptor dysfunction.[100,532,542] In obese rats, the D_1-like receptor dysfunction is acquired and has been related to increased GRK4 expression and membrane translocation of GRK2 due to insulin resistance.[624]

The GRK4 locus on human chromosome 4p16.3 is linked with hypertension.[678,679] Interestingly, adolescents with GRK4 65L, 142V, and A486 haplotype have a greater increase in blood pressure with age than those with the wild-type GRK4 haplotype.[680] GRK4 gene variants (65L, 142V, and 486V) are associated with essential hypertension in several ethnic groups: Caucasians, Chinese, Ghanaians, and Japanese.[681–686] In salt-sensitive hypertensive Japanese, the presence of three GRK4 variants impaired the natriuretic effect of a dopaminergic drug and predicted salt-sensitive hypertension correctly in 94% of cases.[683] In Ghanaians, the combination of angiotensin-converting enzyme insertion/deletion polymorphism and GRK4 65L has an estimated predictive accuracy for hypertension of 70%.[685,686] A meta-analysis revealed a significant association of GRK4 486V with hypertension with an odds ratio of 1.5 (95% CI: 1.2 to 1.9).[687] A re-analysis of a negative study in Han Chinese[688] found an association of GRK4 486V and other genes (GNB3A-350G) with essential hypertension.[682] One study, however, did not find an association of GRK4 486V with the top fifth percentile of diastolic blood pressure of subjects with white European ancestry; however, the authors did not test the association of GRK4 gene variants with hypertension.[689] Another study did not find an association between GRK4 142V and hypertension, but did find an association between variants of the promoter region of D_1R and hypertension.[690] The discordance of this report in European Caucasians[690] with other populations may be the influence of ethnicity in the phenotypic expression of a quantitative trait such as essential hypertension. Interestingly, low-renin hypertension is less frequent in Caucasians (15–20%)[708] than in other ethic groups (e.g., 40–60% in Japanese).[709] In the Japanese, the single best genetic model for low-renin hypertension included only GRK4 A142V, by itself, or GRK4 A142V and aldosterone synthase gene, CYP11B2, with an estimated predictive accuracy of 78%.[683] Ethnicity may also explain some of the discordances. GRK4 65L and GRK4 142V are less frequent, while GRK4 486V is more frequent in Asians than in African-Americans. GRK4 486V is also more frequent in Hispanic and non-Hispanic whites than in African-Americans.[710] The recent GWAS did not identify GRK4 as associated with hypertension.[669–673] This is probably because salt sensitivity was not taken into account and because previous studies have shown that it was critical to assess the role of GRK4 in conjunction with other single nucleotide polymorphisms and genes, e.g., ACE with GRK4 65L,[685,686] and *ADRB2* and *TH* with *GRK4 486V*.[682] While GRK4γ142V transgenic mice are hypertensive even on a normal salt diet,[298,691] GRK4γ486V transgenic mice develop hypertension only when stressed by a high salt diet.[692] Depending upon the genetic background of the mouse, overexpression of human GRK4γ wild-type converts a salt-sensitive phenotype to a salt-resistant phenotype, while overexpression of human GRK4γ486V converts a salt-resistant phenotype to a salt-sensitive phenotype.[692]

Polymorphisms in the non-coding region of the human D_1R gene are associated with decreased[690,693] and increased blood pressure.[694] However, D_1R and D_3R expression is not always decreased in hypertension.[29,30,141,298,343,426,695] Polymorphisms in the coding region of D_1R and D_3R genes[690,694,696] have also not been associated with essential hypertension. A D_2R variant may be associated with salt-sensitive human essential hypertension (unpublished studies). The D_4R long (at least one 7 to 10 repeat) has been reported to be associated with higher diastolic and systolic blood pressure.[697] There are inactivating mutations of D_5R,[698] but their association with hypertension has not been studied. D_1-like and D_2-like receptor functions are impaired in other rodent models of human essential hypertension, such as in the spontaneously hypertensive rat (SHR) and the Dahl salt-sensitive rat (DSS). As indicated earlier, deletion of any of the dopamine receptor genes causes hypertension,[22–27] and dopamine receptor dysfunction is found in several animal models of hypertension.[29,30]

Dopamine and Blood Pressure Regulation: Peripheral versus Central Nervous System

The effect of dopamine in the regulation of blood pressure differs in the kidney from that in the central nervous system. Overactivity of the dopaminergic system in the brain, e.g., the amygdala, is associated with

hypertension.[699] Hypertension induced in rats by decreasing blood flow to one kidney is also associated with increased levels of dopamine and dopamine metabolites in the brain striatum.[700] However, monkeys made hypertensive by constricting the aorta have decreased D_1-like receptor binding in the pre-frontal cortex,[701] and decreased post-synaptic dopaminergic and cholinergic functions in the ventrolateral striatum of SHR,[702] reinforcing the similarities and differences in the regulation of blood pressure between the dopaminergic system inside and outside the central nervous system.

Dopamine Pharmacogenetics and Hypertension

Current treatment of essential hypertension is empirical. It is not based on the molecular mechanisms of essential hypertension. Theoretically, drugs prescribed based on one's genetic make-up would be more effective, with fewer and lesser side-effects than empirical treatment. In African-American men with early hypertensive nephrosclerosis, GRK4 65L and 142V are associated with a poor response to β-adrenergic blockers, while GRK4 142V is associated with a good response to a β-adrenergic blocker.[703] In another study in two cohorts, GRK4 142V, but not GRK4 486V, was also associated with a blood pressure response to a β-adrenergic blocker.[704] There are at least two mechanisms by which β-adrenergic blockers may be beneficial in hypertensive subjects with GRK4 142V polymorphisms. The activity of GRK4, which decreases plasma membrane β-adrenergic receptor expression, can be blocked by β-adrenergic receptor antagonists.[705] As indicated above, normally the D_3R may be important in the negative regulation of renin secretion, at least in mice,[25] and because GRK4 142V can impair D_3R function, this may provide an explanation for the good response of subjects to β-adrenergic blockers. In an African hypertensive population, GRK4 142V is associated with a poor response to reduction in sodium intake,[706] in agreement with the report that human GRK4142V transgenic mice develop hypertension even on a normal salt intake.[298,691] In a Japanese population with essential hypertension ($n = 881$, unpublished data), carriers of the GRK4 142V allele had a larger drop in systolic blood pressure than non-carriers in response to angiotensin receptor blockade.[707] The addition of a diuretic to the non-responders ($n = 94$) decreased blood pressure which was associated with GRK4A486V,[707] in agreement with the reports that human GRK4γ 486V transgenic mice develop salt sensitivity that is dependent on genetic background.[692] Japanese with at least three GRK4 polymorphisms have salt-sensitive hypertension.[683]

CONCLUSION

Dopamine, one of the oldest hormones in phylogeny, serves not only as a precursor to norepinephrine and epinephrine, but also as a neurotransmitter. However, in non-neural cells, dopamine acts independently of the other catecholamines. Dopamine controls water and electrolyte balance and blood pressure by regulating the secretion/release of hormones and humoral agents that affect water and electrolyte balance, salt "appetite" centers in the brain, and ion and water transport in the kidney and gastrointestinal tract. Independent of innervation, the kidney and intestines synthesize dopamine from circulating or filtered L-DOPA (kidney only) that is not metabolized to norepinephrine or epinephrine. Sodium intake and intracellular sodium are probably the major determinants of the renal tubular synthesis/release of dopamine. In mammals, the actions of dopamine occur by occupation of two families of cell surface receptors, D_1-like receptors (D_1R and D_5R), and D_2-like receptors (D_2R, D_3R, and D_4R). The dopamine receptor subtypes interact among themselves, resulting in new signaling pathways. They also interact extensively with other GPCR, hormones, and humoral agents. D_1-like receptors are linked to vasodilation, while the effect of D_2-like receptors on the renal vasculature is probably dependent upon the state of renal nerve activity. The dopamine-induced increase in renal blood flow is not consistently associated with an increase in glomerular filtration rate. The autocrine/paracrine regulation of renal tubular sodium transport, mainly via D_1-like receptors, is mediated by tubular and not by hemodynamic mechanisms. The dopamine receptor subtypes are differentially expressed along the nephron and species-specific; all the five dopamine receptor subtypes are expressed in the proximal tubule, mTAL distal convoluted tubule, and cortical collecting duct, and only D_4R in the cortical TAL, D_1R, D_2R, D_4R, and D_5R in the outer medullary collecting duct, and only the D_2-like receptors, D_2R, D_3R, and D_4R in the inner medullary collecting duct. Dopamine inhibits ion transport in the proximal and distal nephron. D_1-like receptors inhibit NHE3, NaPi2 co-transporter, Cl^-/HCO_3^- exchanger, and ENaC at the apical membrane, and the electrogenic Na^+/HCO_3^- co-transporter and Na^+/K^+-ATPase at the basolateral membrane. Dopamine may also inhibit NCC but stimulates NKCC2, the latter effect for K^+ recycling. The inhibitory effects of dopamine and its receptors on ion transport are important under conditions of euvolemia and moderate volume expansion, but play a minor role under marked volume expansion. D_2-like receptors also participate in the inhibition of ion transport during conditions of

euvolemia and moderate volume expansion, but may increase ion transport in hypovolemic states. Dopamine also controls sodium transport and blood pressure by regulating the production of ROS and the inflammatory response. Aging, obesity, metabolic syndrome, and essential hypertension are associated with abnormalities in dopamine production, and receptor number, post-translational modification, and function.

Acknowledgment

This work was supported in part by grants from the National Institutes of Health, HL023081, DK039308, HL074940, HL068686, and HL092196.

References

[1] Walker RJ, Brooks HL, Holden-Dye L. Evolution and overview of classical transmitter molecules and their receptors. Parasitology 1996;113(Suppl.):S3–33.

[2] Stefano GB, Kream RM. Endogenous morphine synthetic pathway preceded and gave rise to catecholamine synthesis in evolution (Review). Int J Mol Med 2007;20(6):837–41.

[3] Shepherd DM, West GB. Hydroxytyramine and the adrenal medulla. J Physiol 1953;120(1-2):15–9.

[4] Carlsson A, Lindqvist M, Magnusson T, Waldeck B. On the presence of 3-hydroxy-tyramine in brain. Science 1958; 127(3296):471.

[5] Holtz P, Credner K, Koepp W. Die enzymatische entstehung von oxytyramin im organismus und die physiologische bedeutung der dopadecarboxylase. Naunyn Schmiedebergs Arch Exp Pathol Pharmakol 1942;200(2-5):356–88.

[6] Hornykiewicz O. The action of dopamine on the arterial blood pressure of the guinea-pig. Br J Pharmacol 1958;13(1):91–4.

[7] Goldberg LI, Sjoerdsma A. Effects of several monoamine oxidase inhibitors on the cardiovascular actions of naturally occurring amines in the dog. J Pharmacol Exp Ther 1959;127(3):212–8.

[8] Goldberg LI, Horwitz D, Sjoerdsma A. Attenuation of cardiovascular responses to exercise as a possible basis for effectiveness of monoamine oxidase inhibitors in angina pectoris. J Pharmacol Exp Ther 1962;137(1):39–46.

[9] McDonald Jr RH, Goldberg LI, McNay JL, Tuttle Jr EP. Effects of dopamine in man: augmentation of sodium excretion, glomerular filtration rate and renal plasma flow. J Clin Invest 1964;43(6):1116–24.

[10] Lokhandwala MF, Buckley JP. Presynaptic dopamine receptors as mediators of dopamine-induced inhibition of neurogenic vasoconstriction. Eur J Pharmacol 1977;45(3):305–9.

[11] Morgunov N, Baines AD. Renal nerves and catecholamine excretion. Am J Physiol 1981;240(1):F75–81.

[12] Murthy VV, Gilbert JC, Goldberg LI, Kuo JF. Dopamine-sensitive adenylate cyclase in canine renal artery. J Pharm Pharmacol 1976;28(7):567–71.

[13] Nakajima T, Naitoh F, Kuruma I. Dopamine-sensitive adenylate cyclase in the rat kidney particulate preparation. Eur J Pharmacol 1977;41(2):163–9.

[14] Nakajima T, Kuruma I. Characterization with 3H-haloperidol of the dopamine receptor in the rat kidney particulate preparation. Jpn J Pharmacol 1980;30(6):891–8.

[15] Felder RA, Blecher M, Eisner GM, Jose PA. Cortical tubular and glomerular dopamine receptors in the rat kidney. Am J Physiol 1984;246(5 Pt 2):F557–68.

[16] Bello-Reuss E, Higashi Y, Kaneda Y. Dopamine decreases fluid reabsorption in straight portions of rabbit proximal tubule. Am J Physiol 1982;242(6):F634–40.

[17] Aperia A, Bertorello A, Seri I. Dopamine causes inhibition of Na^+-K^+-ATPase activity in rat proximal convoluted tubule segments. Am J Physiol 1987;252(1 Pt 2):F39–45.

[18] Siragy HM, Felder RA, Howell NE, Chevalier RL, Peach MJ, Carey RM. Intrarenal dopamine acts at the dopamine-1 receptor to control renal function. J Hypertens Suppl 1988;6(4):S479–81.

[19] Felder RA, Robillard J, Eisner GM, Jose PA. Role of endogenous dopamine on renal sodium excretion. Semin Nephrol 1989; 9(1):91–3.

[20] Hegde SS, Jadhav AL, Lokhandwala MF. Role of kidney dopamine in the natriuretic response to volume expansion in rats. Hypertension 1989;13(6 Pt 2):828–34.

[21] Felder RA, Seikaly MG, Cody P, Eisner GM, Jose PA. Attenuated renal response to dopaminergic drugs in spontaneously hypertensive rats. Hypertension 1990;15(6 Pt 1):560–9.

[22] Albrecht FE, Drago J, Felder RA, Printz MP, Eisner GM, Robillard JE, et al. Role of the D_{1A} dopamine receptor in the pathogenesis of genetic hypertension. J Clin Invest 1996;97 (10):2283–8 Erratum in: J Clin Invest 1996;97(12):following 2925

[23] Li XX, Bek M, Asico LD, Yang Z, Grandy DK, Goldstein DS, et al. Adrenergic and endothelin B receptor-dependent hypertension in dopamine receptor type-2 knockout mice. Hypertension 2001;38 (3):303–8.

[24] Ueda A, Ozono R, Oshima T, Yano A, Kambe M, Teransihi Y, et al. Disruption of the type 2 dopamine receptor gene causes a sodium-dependent increase in blood pressure in mice. Am J Hypertens 2003;16(10):853–8.

[25] Asico LD, Ladines C, Fuchs S, Accili D, Carey RM, Semeraro C, et al. Disruption of the dopamine D3 receptor gene produces renin-dependent hypertension. J Clin Invest 1998;102(3):493–8.

[26] Bek MJ, Wang X, Asico LD, Jones JE, Zheng S, Li X, et al. Angiotensin-II type 1 receptor-mediated hypertension in D4 dopamine receptor-deficient mice. Hypertension 2006;47 (2):288–95 Erratum in: Hypertension. 2006;47(5):e[23]

[27] Hollon TR, Bek MJ, Lachowicz JE, et al. Mice lacking D5 dopamine receptors have increased sympathetic tone and are hypertensive. J Neurosci 2002;22(24):10801–10.

[28] Aperia AC. Intrarenal dopamine: a key signal in the interactive regulation of sodium metabolism. Annu Rev Physiol 2000;62:621–47.

[29] Banday AA, Lokhandwala MF. Dopamine receptors and hypertension. Curr Hypertens Rep 2008;10(4):268–75.

[30] Zeng C, Armando I, Luo Y, Eisner GM, Felder RA, Jose PA. Dysregulation of dopamine-dependent mechanisms as a determinant of hypertension: studies in dopamine receptor knockout mice. Am J Physiol Heart Circ Physiol 2008;294(2):H551–69.

[31] Wang ZQ, Siragy HM, Felder RA, Carey RM. Intrarenal dopamine production and distribution in the rat. Physiological control of sodium excretion. Hypertension 1997;29(1 Pt 2):228–34.

[32] Lucas-Teixeira VA, Hussain T, Serrão P, Soares-da-Silva P, Lokhandwala MF. Intestinal dopaminergic activity in obese and lean Zucker rats: response to high salt intake. Clin Exp Hypertens 2002;24(5):383–96.

[33] List SJ, Seeman P. [3H]dopamine labeling of D3 dopaminergic sites in human, rat, and calf brain. J Neurochem 1982;39(5):1363–73.

[34] Sunahara RK, Guan HC, O'Dowd BF, Seeman P, Laurier LG, Ng G, et al. Cloning of the gene for a human dopamine D5 receptor with higher affinity for dopamine than D1. Nature 1991;350(6319):614–9.

[35] Fulton S. Appetite and reward. Front Neuroendocrinol. 2010;31 (1):85–103.

[36] Citarella MR, Choi MR, Gironacci MM, Medici C, Correa AH, Fernández BE. Urodilatin and dopamine: a new interaction in the kidney. Regul Pept 2009;153(1-3):19–24.
[37] Yao B, Harris RC, Zhang MZ. Intrarenal dopamine attenuates deoxycorticosterone acetate/high salt-induced blood pressure elevation in part through activation of a medullary cyclooxygenase 2 pathway. Hypertension 2009;54(5):1077–83.
[38] Kirchheimer C, Mendez CF, Acquier A, Nowicki S. Role of 20-HETE in D1/D2 dopamine receptor synergism resulting in the inhibition of Na^+-K^+-ATPase activity in the proximal tubule. Am J Physiol Renal Physiol 2007;292(5):F1435–42.
[39] Yu C, Yang Z, Ren H, et al. D3 dopamine receptor regulation of ETB receptors in renal proximal tubule cells from WKY and SHRs. Am J Hypertens 2009;22(8):877–83.
[40] Venkatakrishnan U, Chen C, Lokhandwala MF. The role of intrarenal nitric oxide in the natriuretic response to dopamine-receptor activation. Clin Exp Hypertens 2000;22 (3):309–24.
[41] Crambert S, Sjöberg A, Eklöf AC, Ibarra F, Holtbäck U. Prolactin and dopamine 1-like receptor interaction in renal proximal tubular cells. Am J Physiol Renal Physiol 2010;299(1): F49–54.
[42] Padia SH, Kemp BA, Howell NL, Fournie-Zaluski MC, Roques BP, Carey RM. Conversion of renal angiotensin II to angiotensin III is critical for AT2 receptor-mediated natriuresis in rats. Hypertension 2008;51(2):460–5.
[43] Muhammad AB, Lokhandwala MF, Banday AA. Exercise reduces oxidative stress but does not alleviate hyperinsulinemia or renal dopamine D1 receptor dysfunction in obese rats. Am J Physiol Renal Physiol 2011;300(1):F98–104.
[44] Zhang MZ, Yao B, Fang X, Wang S, Smith JP, Harris RC. Intrarenal dopaminergic system regulates renin expression. Hypertension 2009;53(3):564–70.
[45] Khan F, Spicarová Z, Zelenin S, Holtbäck U, Scott L, Aperia A. Negative reciprocity between angiotensin II type 1 and dopamine D1 receptors in rat renal proximal tubule cells. Am J Physiol Renal Physiol 2008;295(4):F1110–6.
[46] Li H, Armando I, Yu P, et al. Dopamine 5 receptor mediates Ang II type 1 receptor degradation via a ubiquitin-proteasome pathway in mice and human cells. J Clin Invest 2008; 118(6):2180–9 Erratum in:* J Clin Invest. 2008 Aug;118(8):2986 Gildea, John J [added].
[47] Armando I, Wang X, Villar VA, Jones JE, Asico LD, Escano C, et al. Reactive oxygen species-dependent hypertension in dopamine D2 receptor-deficient mice. Hypertension 2007;49 (3):672–8.
[48] Schafer JA, Li L, Sun D. The collecting duct, dopamine and vasopressin-dependent hypertension. Acta Physiol Scand 2000;168(1):239–44.
[49] Hansell P, Fasching A. The effect of dopamine receptor blockade on natriuresis is dependent on the degree of hypervolemia. Kidney Int 1991;39(2):253–8.
[50] Faucheux B, Buu NT, Kuchel O. Effects of saline and albumin on plasma and urinary catecholamines in dogs. Am J Physiol 1977;232(2):F123–7.
[51] Angchanpen P, Marin-Grez M, Schnermann J. Effect of dopamine antagonists on the urine flow of rats infused with hypotonic saline. Br J Pharmacol 1988;93(1):151–5.
[52] De Luca Sarobe V, Nowicki S, Carranza A, Levin G, Barontini M, Arrizurieta E, et al. Low sodium intake induces an increase in renal monoamine oxidase activity in the rat. Involvement of an angiotensin II dependent mechanism. Acta Physiol Scand 2005;185(2):161–7.
[53] Goldstein DS, Stull R, Eisenhofer G, Gill Jr JR. Urinary excretion of dihydroxyphenylalanine and dopamine during alterations of dietary salt intake in humans. Clin Sci (Lond) 1989;76 (5):517–22.
[54] Carey RM, Van Loon GR, Baines AD, Ortt EM. Decreased plasma and urinary dopamine during dietary sodium depletion in man. J Clin Endocrinol Metab 1981;52(5):903–9.
[55] Choi MR, Lee BM, Medici C, Correa AH, Fernández BE. Effects of angiotensin II on renal dopamine metabolism: synthesis, release, catabolism and turnover. Nephron Physiol 2010;115 (1):1–7.
[56] Agnoli GC, Cacciari M, Garutti C, Ikonomu E, Lenzi P, Marchetti G. Effects of extracellular fluid volume changes on renal response to low-dose dopamine infusion in normal women. Clin Physiol 1987;7(6):465–79.
[57] Puyó AM, Levin GM, Armando I, Barontini MB. Free and conjugated plasma catecholamines in pheochromocytoma patients with and without sustained hypertension. Acta Endocrinol (Copenh) 1996;113(1):111–7.
[58] Alexander RW, Gill Jr JR, Yamabe H, Lovenberg W, Keiser HR. Effects of dietary sodium and of acute saline infusion on the interrelationship between dopamine excretion and adrenergic activity in man. J Clin Invest 1974;54(1):194–200.
[59] Chen N, Reith ME. Interaction between dopamine and its transporter: role of intracellular sodium ions and membrane potential. J Neurochem 2004;89(3):750–65.
[60] Maurel A, Spreux-Varoquaux O, Amenta F, Tayebati SK, Tomassoni D, Sequelas MH, et al. Vesicular monoamine transporter 1 mediates dopamine secretion in rat proximal tubular cells. Am J Physiol Renal Physiol 2007;292(5):F1592–8.
[61] Pinho MJ, Serrão MP, Soares-da-Silva P. High-salt intake and the renal expression of amino acid transporters in spontaneously hypertensive rats. Am J Physiol Renal Physiol 2007; 292(5):F1452–63.
[62] Baines AD. Effects of salt intake and renal denervation on catecholamine catabolism and excretion. Kidney Int 1982; 21(2):316–22.
[63] Grossman E, Hoffman A, Tamrat M, Armando I, Keiser HR, Goldstein DS. Endogenous dopa and dopamine responses to dietary salt loading in salt-sensitive rats. J Hypertens 1991; 9(3):259–63.
[64] Unger T, Buu NT, Kuchel O, Schürch W. Conjugated dopamine: peripheral origin, distribution, and response to acute stress in the dog. Can J Physiol Pharmacol 1980;58(1):22–7.
[65] Morgunov N, Baines AD. Vagal afferent activity and renal nerve release of dopamine. Can J Physiol Pharmacol 1985; 63(6):636–41.
[66] Dinerstein RJ, Vannice J, Henderson RC, Roth LJ, Goldberg LI, Hoffmann PC. Histofluorescence techniques provide evidence for dopamine-containing neuronal elements in canine kidney. Science 1979;205(4405):497–9.
[67] Jose PA, Felder RA, Holloway RR, Eisner GM. Dopamine receptors modulate sodium excretion in denervated kidney. Am J Physiol 1986;250(6 Pt 2):F1033–8.
[68] Bertorello A, Hökfelt T, Goldstein M, Aperia A. Proximal tubule Na^+-K^+-ATPase activity is inhibited during high-salt diet: evidence for DA-mediated effect. Am J Physiol 1988;254 (6 Pt 2):F795–801.
[69] Kokkinou I, Nikolouzou E, Hatzimanolis A, Fragoulis EG, Vassilacopoulou D. Expression of enzymatically active L-DOPA decarboxylase in human peripheral leukocytes. Blood Cells Mol Dis 2009;42(1):92–8.
[70] Soares Da Silva P, Pestana M, Fernandes MH. Involvement of tubular sodium in the formation of dopamine in the human renal cortex. J Am Soc Nephrol 1993;3(9):1591–9.
[71] López-Contreras AJ, Galindo JD, López-García C, Castells MT, Cremades A, Peñafiel R. Opposite sexual dimorphism of 3,4-

dihydroxyphenylalanine decarboxylase in the kidney and small intestine of mice. J Endocrinol 2008;196(3):615–24.
[72] Kubovcakova L, Krizanova O, Kvetnansky R. Identification of the aromatic L-amino acid decarboxylase gene expression in various mice tissues and its modulation by immobilization stress in stellate ganglia. Neuroscience 2004;126 (2):375–80.
[73] Borelli MI, Villar MJ, Orezzoli A, Gagliardino JJ. Presence of DOPA decarboxylase and its localisation in adult rat pancreatic islet cells. Diabetes Metab 1997;23(2):161–3.
[74] Maayan ML, Sellitto RV, Volpert EM. Dopamine and L-dopa: inhibition of thyrotropin-stimulated thyroidal thyroxine release. Endocrinology 1986;118(2):632–6.
[75] Grossman E, Hoffman A, Armando I, Abassi Z, Kopin IJ, Goldstein DS. Sympathoadrenal contribution to plasma dopa (3,4-dihydroxyphenylalanine) in rats. Clin Sci (Lond) 1992; 83(1):65–74.
[76] Goldstein DS, Udelsman R, Eisenhofer G, Stull R, Keiser HR, Kopin IJ. Neuronal source of plasma dihydroxyphenylalanine. J Clin Endocrinol Metab 1987;64(4):856–61.
[77] Goldstein DS, Polinsky RJ, Garty M, Robertson D, Brown RT, Biaggioni I, et al. Patterns of plasma levels of catechols in neurogenic orthostatic hypotension. Ann Neurol 1989;26 (4):558–63.
[78] Esplugues JV, Caramona MM, Moura D, Soares-da-Silva P. Effects of chemical sympathectomy on dopamine and noradrenaline content of the dog gastrointestinal tract. Auton Pharmacol 1985;5(3):189–95.
[79] Goldstein DS, Swoboda KJ, Miles JM, Coppack SW, Aneman A, Holmes C, et al. Sources and physiological significance of plasma dopamine sulfate. J Clin Endocrinol Metab 1999; 84(7):2523–31.
[80] Eldrup E, Moller SE, Andreasen J, Christensen NJ. Effects of ordinary meals on plasma concentrations of 3,4-dihydroxyphenylalanine, dopamine sulphate and 3,4-dihydroxyphenylacetic acid. Clin Sci (Lond) 1997;92(4):423–30.
[81] Eisenhofer G, Coughtrie MW, Goldstein DS. Dopamine sulphate: an enigma resolved. Clin Exp Pharmacol Physiol Suppl 1999;26:S41–53.
[82] Banwart B, Miller TD, Jones JD, Tyce GM. Plasma dopa and feeding. Proc Soc Exp Biol Med 1989;191(4):357–61.
[83] Williams M, Young JB, Rosa RM, Gunn S, Epstein FH, Landsberg L. Effect of protein ingestion on urinary dopamine excretion. Evidence for the functional importance of renal decarboxylation of circulating 3,4-dihydroxyphenylalanine in man. J Clin Invest 1986;78(6):1687–93.
[84] Rios M, Habecker B, Sasaoka T, Eisenhofer G, Tian H, Landis S, et al. Catecholamine synthesis is mediated by tyrosinase in the absence of tyrosine hydroxylase. J Neurosci 1999; 19(9):3519–26.
[85] Ibarra FR, Aguirre J, Nowicki S, Barontini M, Arrizurieta EE, Armando I. Demethylation of 3-O-methyldopa in the kidney: a possible source for dopamine in urine. Am J Physiol 1996;270(5 Pt 2):F862–8.
[86] Helkamaa T, Männistö PT, Rauhala P, Cheng ZJ, Finckenberg P, Huotari M, et al. Resistance to salt-induced hypertension in catechol-O-methyltransferase-gene-disrupted mice. J Hypertens 2003;21(12):2365–74.
[87] Soares-da-Silva P, Serrão MP. High- and low-affinity transport of L-leucine and L-DOPA by the hetero amino acid exchangers LAT1 and LAT2 in LLC-PK1 renal cells. Am J Physiol Renal Physiol 2004;287(2):F252–61.
[88] Baines AD, Chan W. Production of urine free dopamine from DOPA: a micropuncture study. Life Sci 1980;26 (4):253–9.
[89] Seri I, Kone BC, Gullans SR, Aperia A, Brenner BM, Ballermann BJ. Influence of Na^+ intake on dopamine-induced inhibition of renal cortical Na^+-K^+-ATPase. Am J Physiol 1990;258(1 Pt 2):F52–60.
[90] Hayashi M, Yamaji Y, Kitajima W, Saruta T. Aromatic L-amino acid decarboxylase activity along the rat nephron. Am J Physiol 1990;258(1 Pt 2):F28–33.
[91] Di Marco GS, Vio CP, Dos Santos OF, Schor N, Casarini DE. Catecholamine production along the nephron. Cell Physiol Biochem 2007;20(6):919–24.
[92] Meister B, Fried G, Holgert H, Aperia A, Hökfelt T. Ontogeny of aromatic L-amino acid decarboxylase-containing tubule cells in rat kidney. Kidney Int 1992;42(3):617–23.
[93] Gomes P, Serrão MP, Viera-Coelho MA, Soares-da-Silva P. Opossum kidney cells take up L-DOPA through an organic cation potential-dependent and proton-independent transporter. Cell Biol Int 1997;21(4):249–55.
[94] Soares-Da-Silva P, Serrão MP, Vieira-Coelho MA. Apical and basolateral uptake and intracellular fate of dopamine precursor L-dopa in LLC-PK1 cells. Am J Physiol 1998;274(2 Pt 2): F243–51.
[95] Pinho MJ, Serrão MP, Gomes P, Hopfer U, Jose PA, Soares-da-Silva P. Over-expression of renal LAT1 and LAT2 and enhanced L-DOPA uptake in SHR immortalized renal proximal tubular cells. Kidney Int 2004;66(1):216–26.
[96] Quiñones H, Collazo R, Moe OW. The dopamine precursor L-dihydroxyphenylalanine is transported by the amino acid transporters rBAT and LAT2 in renal cortex. Am J Physiol Renal Physiol 2004;287(1):F74–80.
[97] Pinho MJ, Serrão MP, José PA, Soares-da-Silva P. Organ specific underexpression renal of Na^+-dependent B^0AT1 in the SHR correlates positively with overexpression of NHE3 and salt intake. Mol Cell Biochem 2007;306(1-2):9–18.
[98] Armando I, Nowicki S, Aguirre J, Barontini M. A decreased tubular uptake of dopa results in defective renal dopamine production in aged rats. Am J Physiol 1995;268(6 Pt 2): F1087–92.
[99] Hayashi M, Yamaji Y, Kitajima W, Saruta T. Effects of high salt intake on dopamine production in rat kidney. Am J Physiol 1991;260(5):E675–9.
[100] Vieira-Coelho MA, Hussain T, Kansra V, Serrao MP, Guimaraes JT, Pestana M, et al. Aging, high salt intake, and renal dopaminergic activity in Fischer 344 rats. Hypertension 1999;34(4 Pt 1):666–72.
[101] Wassenberg T, Willemsen MA, Geurtz PB, Lammens M, Verrijp K, Wilmer M, et al. Urinary dopamine in aromatic L-amino acid decarboxylase deficiency: the unsolved paradox. Mol Genet Metab 2010;101(4):349–56.
[102] Wu X, Huang W, Ganapathy ME, Wang H, Kekuda R, Conway SJ, et al. Structure, function, and regional distribution of the organic cation transporter OCT3 in the kidney. Am J Physiol Renal Physiol 2000;279(3):F449–58.
[103] Hartman BK. Immunofluorescence of dopamine-β-hydroxylase. Application of improved methodology to the localization of the peripheral and central noradrenergic nervous system. J Histochem Cytochem 1973;21(4):312–32.
[104] Kinoshita S, Ohlstein EH, Felder RA. Dopamine-1 receptors in rat proximal convoluted tubule: regulation by intrarenal dopamine. Am J Physiol 1990;258(4 Pt 2):F1068–74.
[105] Kennedy B, Bigby TD, Ziegler MG. Nonadrenal epinephrine-forming enzymes in humans. Characteristics, distribution, regulation, and relationship to epinephrine levels. J Clin Invest 1995;95(6):2896–902.
[106] Ziegler MG, Kennedy B, Elayan H. Rat renal epinephrine synthesis. J Clin Invest 1989;84(4):1130–3.

[107] Jans DA, Hemmings BA. cAMP-dependent protein kinase activation affects vasopressin V2-receptor number and internalization in LLC-PK1 renal epithelial cells. FEBS Lett 1991;281 (1-2):267–71.
[108] Fernandes MH, Soares-da-Silva P. Role of monoamine oxidase and catechol-O-methyltransferase in the metabolism of renal dopamine. J Neural Transm Suppl 1994;41:101–5.
[109] Ibarra FR, Armando I, Nowicki S, Carranza A, De Luca Sarobe V, Azzurieta EE, et al. Dopamine is metabolised by different enzymes along the rat nephron. Pflugers Arch 2005;450(3):185–91.
[110] Wang Y, Berndt TJ, Gross JM, Peterson MA, So MJ, Knox FG. Effect of inhibition of MAO and COMT on intrarenal dopamine and serotonin and on renal function. Am J Physiol Regul Integr Comp Physiol 2001;280(1):R248–54.
[111] Xu J, Li G, Wang P, Velasquez H, Yao X, Li Y, et al. Renalase is a novel, soluble monoamine oxidase that regulates cardiac function and blood pressure. J Clin Invest 2005; 115(5):1275–80.
[112] Isaac J, Berndt TJ, Chinnow SL, Tyce GM, Dousa TP, Knox FG. Dopamine enhances the phosphaturic response to parathyroid hormone in phosphate-deprived rats. J Am Soc Nephrol 1992;2 (9):1423–9.
[113] Clark BA, Rosa RM, Epstein FH, Young JB, Landsberg L. Altered dopaminergic responses in hypertension. Hypertension 1992; 19(6 Pt 1):589–94.
[114] Akpaffiong MJ, Redfern PH, Woodward B. Factors affecting the release and excretion of dopamine in the rat. J Pharm Pharmacol 1980;32(12):839–43.
[115] Ball SG, Oats NS, Lee MR. Urinary dopamine in man and rat: effects of inorganic salts on dopamine excretion. Clin Sci Mol Med 1978;55(2):167–73.
[116] Oates NS, Ball SG, Perkins CM, Lee MR. Plasma and urine dopamine in man given sodium chloride in the diet. Clin Sci (Lond) 1979;56(3):261–4.
[117] Chen CJ, Lokhandwala MF. Role of endogenous dopamine in the natriuretic response to various degrees of iso-osmotic volume expansion in rats. Clin Exp Hypertens A. 1991;13(6-7):1117–26.
[118] Ball SG, Gunn IG, Douglas IH. Renal handling of dopa, dopamine, norepinephrine, and epinephrine in the dog. Am J Physiol 1982;242(1):F56–62.
[119] Boren DR, Henry DP, Selkurt EE, Weinberger MH. Renal modulation of urinary catecholamine excretion during volume expansion in the dog. Hypertension 1980;2(4):383–9.
[120] Chan YL. Cellular mechanisms of renal tubular transport of L-dopa and its derivatives in the rat: microperfusion studies. J Pharmacol Exp Ther 1976;199(1):17–24.
[121] Okubo M, Kaku K, Kaneko T, Yanaihara N. Effects of bombesin and gastrin releasing peptide on catecholamine secretion from rat adrenal gland, in vitro. Endocrinol Jpn 1985; 32(1):21–7.
[122] Abramczyk P, Ziecina R, Lisiecka A, Papierski K, Przybylski J. The adrenal renal vascular connection plays an essential role in the pathogenesis of renovascular hypertension in the rat. J Physiol Pharmacol 2000;51(1):35–40.
[123] Sutoo D, Akiyama K. Effect of dopamine receptor antagonists on the calcium-dependent central function that reduces blood pressure in spontaneously hypertensive rats. Neurosci Lett 1999;269(3):133–6.
[124] Takeda S, Ueshiba H, Hattori Y, Irie M. Cilnidipine, the N- and L-type calcium channel antagonist, reduced on 24-h urinary catecholamines and C-peptide in hypertensive non-insulin-dependent diabetes mellitus. Diabetes Res Clin Pract 1999;44(3):197–205.
[125] Damasceno A, Santos A, Pestana M, Serrao P, Caupers P, Soares-da-Silva P, et al. Acute hypotensive, natriuretic, and hormonal effects of nifedipine in salt-sensitive and salt-resistant black normotensive and hypertensive subjects. J Cardiovasc Pharmacol 1999;34(3):346–53.
[126] Wang ZQ, Siragy HM, Felder RA, Carey RM. Preferential release of renal dopamine into the tubule lumen: effect of chronic sodium loading. Clin Exp Hypertens 1997;19(1-2):107–16.
[127] Felder CC, Campbell T, Albrecht F, Jose PA. Dopamine inhibits Na^+-H^+ exchanger activity in renal BBMV by stimulation of adenylate cyclase. Am J Physiol 1990;259(2 Pt 2):F297–303.
[128] Gesek FA, Schoolwerth AC. Hormone responses of proximal Na^+-H^+ exchanger in spontaneously hypertensive rats. Am J Physiol 1991;261(3 Pt 2):F526–36.
[129] Jadhav AL, Liu Q. DA1 receptor mediated regulation of Na^+-H^+ antiport activity in rat renal cortical brush border membrane vesicles. Clin Exp Hypertens A. 1992;14(4):653–66.
[130] Felder CC, Albrecht FE, Campbell T, Eisner GM, Jose PA. Cyclic AMP- independent, G protein-linked inhibition of Na^+/H^+ exchange in renal brush border by D1 dopamine agonists. Am J Physiol 1993;264(6 Pt 2):F1032–7.
[131] Albrecht FE, Xu J, Moe OW, Hopfer U, Simonds WF, Orlowski J, et al. Regulation of NHE3 activity by G protein subunits in renal brush-border membranes. Am J Physiol Regul Integr Comp Physiol 2000;278(4):R1064–73.
[132] Bacic D, Kaissling B, McLeroy P, Zou L, Baum M, Moe OW. Dopamine acutely decreases apical membrane Na/H exchanger NHE3 protein in mouse renal proximal tubule. Kidney Int 2003;64(6):2133–41.
[133] Bobulescu IA, Quiñones H, Gisler SM, Di Sole F, Hu MC, Shi M, et al. Acute regulation of renal Na^+/H^+ exchanger NHE3 by dopamine: role of protein phosphatase 2A. Am J Physiol Renal Physiol 2010;298(5):F1205–13.
[134] Häberle DA, Königbauer B, Kawabata M, Ushiogi Y. Renal blood flow control by tubuloglomerular feedback (TGF) in normal and spontaneously hypertensive rats–a role for dopamine and adenosine. Klin Wochenschr 1991; 69(13):587–956.
[135] Felder CC, Blecher M, Jose PA. Dopamine-1-mediated stimulation of phospholipase C activity in rat renal cortical membranes. J Biol Chem 1989;264(15):8739–45.
[136] Gomes P, Soares-da-Silva P. Role of cAMP-PKA-PLC signaling cascade on dopamine-induced PKC-mediated inhibition of renal Na^+-K^+-ATPase activity. Am J Physiol Renal Physiol 2002;282(6):F1084–96.
[137] Felder RA, Kinoshita S, Ohbu K, Mouradian MM, Sibley DR, Monsma Jr FJ, et al. Organ specificity of the dopamine1 receptor/adenylyl cyclase coupling defect in spontaneously hypertensive rats. Am J Physiol 1993;264(4 Pt 2):R726–32.
[138] Vyas SJ, Eichberg J, Lokhandwala MF. Characterization of receptors involved in dopamine-induced activation of phospholipase-C in rat renal cortex. J Pharmacol Exp Ther 1992;260 (1):134–9.
[139] Yu PY, Eisner GM, Yamaguchi I, Mouradian MM, Felder RA, Jose PA. Dopamine D1A receptor regulation of phospholipase C isoform. J Biol Chem 1996;271(32):19503–8.
[140] Yu PY, Asico LD, Eisner GM, Jose PA. Differential regulation of renal phospholipase C isoforms by catecholamines. J Clin Invest 1995;95(1):304–8.
[141] Banday AA, Lokhandwala MF. Oxidative stress reduces renal dopamine D1 receptor-Gq/11α G protein-phospholipase C signaling involving G protein-coupled receptor kinase 2. Am J Physiol Renal Physiol 2007;293(1):F306–15.
[142] Felder CC, Jose PA, Axelrod J. The dopamine-1 agonist, SKF 82526, stimulates phospholipase C activity independent of adenylate cyclase. J Pharmacol Exp Ther 1989;248(1):171–5.

[143] Barendregt JN, Muizert Y, van Nispen tot Pannerden LL, Chang PC. Intrarenal production of dopamine and natriuresis following DOPA and saline infusions in healthy human volunteers. J Hum Hypertens 1995;9(3):187–94.
[144] Vieira-Coelho MA, Pestana M, Soares-da-Silva P. High sodium intake increases the urinary excretion of L-3,4-dihydroxyphenylalanine but fails to alter the urinary excretion of dopamine and amine metabolites in Wistar rats. Gen Pharmacol 1996; 27(8):1421–7.
[145] Luippold G, Benöhr P, Piesch C, Heyne N, Mühlbauer B. Urinary dopamine excretion in healthy volunteers: effect of sodium diet and acute water load. Pflugers Arch 2000;440 (1):28–33.
[146] Mühlbauer B, Osswald H. Feeding but not salt loading is the dominant factor controlling urinary dopamine excretion in conscious rats. Naunyn Schmiedebergs Arch Pharmacol 1992;346(4):469–71.
[147] Mühlbauer B, Osswald H. Feeding-induced increase in urinary dopamine excretion is independent of renal innervation and sodium intake. Am J Physiol 1994;266(4 Pt 2): F563–7.
[148] Jadhav AL, Lokhandwala MF. Dietary sodium-induced changes in renal noradrenergic and dopaminergic responses in rats. J Hum Hypertens 1990;4(2):163–4.
[149] Yoshimura M, Yamazaki H, Takashina R, Kambara S, Iyoda I, Sasaki S, et al. The significance of duration of salt loading on cardiovascular response and urinary excretion of catecholamine in rats. Endocrinol Jpn 1986;33(2):169–75.
[150] Petrovic T, Bell C. Catecholamines in kidneys of normotensive and genetically hypertensive rats. Effects of salt load. Hypertension 1986;8(2):122–7.
[151] Dantonello TM, Küster E, Mühlbauer B. Urinary dopamine and renal handling of L-DOPA in fasted spontaneously hypertensive rats. Kidney Blood Press Res 1998;21(6): 438–44.
[152] Sampaio-Maia B, Serrão P, Vieira-Coelho MA, Pestana M. Differences in the renal dopaminergic system activity between Wistar rats from two suppliers. Acta Physiol Scand 2003; 178(1):83–9.
[153] Escano CS, Armando I, Wang X, Asico LD, Pascua A, Yang Y, et al. Renal dopaminergic defect in C57BL/6J mice. Am J Physiol Regul Integr Comp Physiol 297(6):R1660-R1669.
[154] Sulyok E. Dopaminergic control of neonatal salt and water metabolism. Pediatr Nephrol 1988;2(1):163–5.
[155] Young JB, Troisi RJ, Weiss ST, Parker DR, Sparrow D, Landsberg L. Relationship of catecholamine excretion to body size, obesity, and nutrient intake in middle-aged and elderly men. Am J Clin Nutr 1992;56(5):827–34.
[156] Ferreira A, Bettencourt P, Pestana M, Correia F, Serrão P, Martins L, et al. Heart failure, aging, and renal synthesis of dopamine. Am J Kidney Dis 2001;38(3):502–9.
[157] Soares-Da-Silva P, Fernandes MH. A study on the renal synthesis of dopamine in aged rats. Acta Physiol Scand 1991;143 (3):287–93.
[158] Pestana M, Jardim H, Correia F, Vieira-Coelho MA, Soares-da-Silva P. Renal dopaminergic mechanisms in renal parenchymal diseases and hypertension. Nephrol Dial Transplant 2001;16(Suppl. 1):53–9.
[159] Chan TY, Critchley JA, Ho CS, Chan JC, Tomlinson B. Urinary dopamine and noradrenaline outputs during oral salt loading in healthy Chinese subjects with a family history of hypertension. J Auton Pharmacol 1996;16(1):1–6.
[160] Sowers JR, Zemel MB, Zemel P, Beck FW, Walsh MF, Zawada ET. Salt sensitivity in blacks. Salt intake and natriuretic substances. Hypertension 1988;12(5):485–90.
[161] Damasceno A, Santos A, Serrão P, Caupers P, Soares-da-Silva P, Polónia J. Deficiency of renal dopaminergic-dependent natriuretic response to acute sodium load in black salt-sensitive subjects in contrast to salt-resistant subjects. J Hypertens 1999; 17(12 Pt 2):1995–2001.
[162] Weder AB, Gleiberman L, Sachdeva A. Urinary dopamine excretion and renal responses to fenoldopam infusion in blacks and whites. J Clin Hypertens (Greenwich) 2009; 11(12):707–12.
[163] Gerdts E, Svarstad E, Myking OL, Lund-Johansen P, Omvik P. Salt sensitivity in hypertensive type-1 diabetes mellitus. Blood Press 1996;5(2):78–85.
[164] Segers O, Anckaert E, Gerlo E, Dupont AG, Somers G. Dopamine-sodium relationship in type 2 diabetic patients. Diabetes Res Clin Pract 1996;34(2):89–98.
[165] Rudberg S, Lemne C, Persson B, Krekula A, de Faire U, Aperia A. The dopaminuric response to high salt diet in insulin-dependent diabetes mellitus and in family history of hypertension. Pediatr Nephrol 1997;11(2):169–73.
[166] Stenvinkel P, Saggar-Malik AK, Wahrenberg H, Diczfalusy U, Bolinder J, Alvestrand A. Impaired intrarenal dopamine production following intravenous sodium chloride infusion in type 1 (insulin-dependent) diabetes mellitus. Diabetologia 1991;34(2):114–8.
[167] Shigetomi S, Yamada ZO, Ishii H, Sanada H, Watanabe H, Fukuchi S. Dopaminergic activity and endorenal dopamine synthesis in non-insulin dependent diabetes mellitus. Hypertens Res 1995;18(Suppl. 1):S125–30.
[168] Madácsy L, Sulyok E, Klujber L, Vámosi I, Barkai L, Baranyai Z. Decreased urinary excretion of dopamine and sodium in diabetic children with incipient nephropathy. Padiatr Padol 1991;26(6):253–6.
[169] Murabayashi S, Baba T, Tomiyama T, Takebe K. Urinary dopamine, noradrenaline and adrenaline in type 2 diabetic patients with and without nephropathy. Horm Metab Res 1989; 21(1):27–32.
[170] Carranza A, Karabatas L, Barontini M, Armando I. Decreased tubular uptake of L-3,4-dihydroxyphenylalanine in streptozotocin-induced diabetic rats. Horm Res 2001;55(6):282–7.
[171] Kuchel O, Buu NT, Unger T, Lis M, Genest J. Free and conjugated plasma and urinary dopamine in human hypertension. J Clin Endocrinol Metab 1979;48(3):425–9.
[172] Shikuma R, Yoshimura M, Kambara S, Yamazaki H, Takashina R, Takahashi H, et al. Dopaminergic modulation of salt sensitivity in patients with essential hypertension. Life Sci 1986;38(10):915–21.
[173] Gill Jr JR, Grossman E, Goldstein DS. High urinary dopa and low urinary dopamine-to-dopa ratio in salt-sensitive hypertension. Hypertension 1991;18(5):614–21.
[174] Gordon MS, Steunkel CA, Conlin PR, Hollenberg NK, Williams GH. The role of dopamine in nonmodulating hypertension. J Clin Endocrinol Metab 1989;69(2):426–32.
[175] Iimura O, Shimamoto K. Salt and hypertension: water-sodium handling in essential hypertension. Ann N Y Acad Sci 1993;676:105–21.
[176] Harvey JN, Casson IF, Clayden AD, Cope GF, Perkins CM, Lee MR. A paradoxical fall in urine dopamine output when patients with essential hypertension are given added dietary salt. Clin Sci (Lond) 1984;67(1):83–8.
[177] Saito I, Takeshita E, Saruta T, Nagano S, Sekihara T. Urinary dopamine excretion in normotensive subjects with or without family history of hypertension. J Hypertens 1986;4(1):57–60.
[178] Gill Jr JR, Gullner G, Lake CR, Lakatua DJ, Lan G. Plasma and urinary catecholamines in salt-sensitive idiopathic hypertension. Hypertension 1988;11(4):312–9.

[179] Sakai T, Ideishi M, Miura S, Maeda H, Tashiro E, Koga M, et al. Mild exercise activates renal dopamine system in mild hypertensives. J Hum Hypertens 1998;12(6):355–62.
[180] Saito I, Itsuji S, Takeshita E, Kawabe H, Nishino M, Wainai H, et al. Increased urinary dopamine excretion in young patients with essential hypertension. Clin Exp Hypertens 1994;16 (1):29–39.
[181] Castellano M, Beschi M, Agabiti-Rossi E, Muiesan ML, Romanelli G, Falo F, et al. Renal noradrenergic and dopaminergic activity in patients with borderline essential hypertension. J Cardiovasc Pharmacol 1986;8(Suppl. 5):S116–8.
[182] Kuchel O, Cuche JL, Buu NT, Genest J. An increase in urinary catecholamines of renal origin in patients with "borderline" hypertension. Am J Med Sci 1976;272(3):263–8.
[183] Kuchel O. Peripheral dopamine in essential hypertension. An early defense against hypertension failing during its progression? Am J Hypertens 1990;3(6 Pt 2):104S–7S.
[184] Sanada H, Watanabe H, Shigetomi S, Fukuchi S. Gene expression of aromatic L-amino acid decarboxylase mRNA in the kidney of normotensive and hypertensive rats. Hypertens Res 1995;18(Suppl. 1):S179–81.
[185] Kuchel O, Racz K, Debinski W, Falardeau P, Buu NT. Contrasting dopaminergic patterns in two forms of genetic hypertension. Clin Exp Hypertens A. 1987;9(5-6):987–1008.
[186] DeFeo ML, Jadhav AL, Lokhandwala MF. Dietary sodium intake and urinary dopamine and sodium excretion during the course of blood pressure development in Dahl salt-sensitive and salt-resistant rats. Clin Exp Hypertens A. 1987; 9(12):2049–60.
[187] Moller B, Hansell P. Sodium and dopamine excretion in prehypertensive Dahl rats during severe hypervolaemia. Acta Physiol Scand 1995;155(2):165–71.
[188] Cravchik A, Goldman D. Neurochemical individuality: Genetic diversity among human dopamine and serotonin receptors and transporters. Arch Gen Psychiatry 2000; 57(12):1105–14.
[189] Beaulieu JM, Gainetdinov RR. The physiology, signaling, and pharmacology of dopamine receptors. Pharmacol Rev. 2011; 63(1):182–217.
[190] Premont RT, Gainetdinov RR. Physiological roles of G protein-coupled receptor kinases and arrestins. Annu Rev Physiol 2007;69:511–34.
[191] Neve KA, Seamans JK, Trantham-Davidson H. Dopamine receptor signaling. J Recept Signal Transduct Res 2004; 24(3):165–205.
[192] Holmes A, Lachowicz JE, Sibley DR. Phenotypic analysis of dopamine receptor knockout mice; recent insights into the functional specificity of dopamine receptor subtypes. Neuropharmacology 2004;47(8):1117–34.
[193] Sibley DR. New insights into dopaminergic receptor function using antisense and genetically altered animals. Annu Rev Pharmacol Toxicol 1999;39:313–41.
[194] Kapsimali M, Dumond H, Le Crom S, Coudouel S, Vincent JD, Vernier P. [Evolution and development of dopaminergic neurotransmitter systems in vertebrates] [Article in French]. J Soc Biol 2000;194(2):87–93.
[195] Rondou P, Haegeman G, Van Craenenbroeck K. The dopamine D4 receptor: biochemical and signalling properties. Cell Mol Life Sci 2010;67(12):1971–86.
[196] Rosenbaum DM, Cherezov V, Hanson MA, Rasmussen SG, Thian FS, Kobilka TS, et al. GPCR engineering yields high-resolution structural insights into β_2-adrenergic receptor function. Science 2007;318(5854):1266–73.
[197] Bokoch MP, Zou Y, Rasmussen SG, Liu CW, et al. Ligand-specific regulation of the extracellular surface of a G-protein-coupled receptor. Nature 2010;463(7277):108–12.
[198] Jaakola VP, Griffith MT, Hanson MA, Cherezov V, Chien EY, Lane JR, et al. The 2.6 angstrom crystal structure of a human A2A adenosine receptor bound to an antagonist. Science 2008;322(5905):1211–7.
[199] Scheerer P, Park JH, Hildebrand PW, Kim YJ, Krauss N, Choe HW, et al. Crystal structure of opsin in its G protein interacting conformation. Nature 2008;455(7212):497–502.
[200] Anderson GR, Lujan R, Martemyanov KA. Changes in striatal signaling induce remodeling of RGS complexes containing Gbeta5 and R7BP subunits. Mol Cell Biol 2009;29(11):3033–44.
[201] Celver J, Sharma M, Kovoor A. RGS9-2 mediates specific inhibition of agonist-induced internalization of D2-dopamine receptors. J Neurochem 2010;114(3):739–49.
[202] Jeanneteau F, Guillin O, Diaz J, Griffon N, Sokoloff P. GIPC recruits GAIP (RGS19) to attenuate dopamine D2 receptor signaling. Mol Biol Cell 2004;15(11):4926–37.
[203] Stanwood GD, Parlaman JP, Levitt P. Genetic or pharmacological inactivation of the dopamine D1 receptor differentially alters the expression of regulator of G-protein signaling (Rgs) transcripts. Eur J Neurosci 2006;24(3):806–18.
[204] Taymans JM, Kia HK, Claes R, Cruz C, Leysen J, Langlois X. Dopamine receptor-mediated regulation of RGS2 and RGS4 mRNA differentially depends on ascending dopamine projections and time. Eur J Neurosci 2004;19(8):2249–6220.
[205] Zürn A, Zabel U, Vilardaga JP, Schindelin H, Lohse MJ, Hoffmann C. Fluorescence resonance energy transfer analysis of α_{2a}-adrenergic receptor activation reveals distinct agonist-specific conformational changes. Mol Pharmacol 2009; 75(3):534–41.
[206] Marty C, Ye RD. Heterotrimeric G protein signaling outside the realm of seven transmembrane domain receptors. Mol Pharmacol 2010;78(1):12–8.
[207] Schwendt M, McGinty JF. Amphetamine up-regulates activator of G-protein signaling 1 mRNA and protein levels in rat frontal cortex: The role of dopamine and glucocorticoid receptors. Neuroscience 2010;168(1):96–107.
[208] Rajagopal K, Lefkowitz RJ, Rockman HA. When 7 transmembrane receptors are not G protein-coupled receptors. J Clin Invest 2005;115(11):2971–4.
[209] Rajagopal K, Whalen EJ, Violin JD, Stilber JA, Rosenberg PB, Premont RT, et al. β-arrestin2-mediated inotropic effects of the angiotensin II type 1A receptor in isolated cardiac myocytes. Proc Natl Acad Sci USA 2006;103(44):16284–9.
[210] Kimura K, White BH, Sidhu A. Coupling of human D-1 dopamine receptors to different guanine nucleotide binding proteins: evidence that D-1 dopamine receptors can couple to both Gs and Go. J Biol Chem 1995;270(24):14672–8.
[211] Corvol JC, Studler JM, Schonn JS, Girault JA, Hervé D. $G\alpha_{olf}$ is necessary for coupling D1 and A2a receptors to adenylyl cyclase in the striatum. J Neurochem 2001;76(5):1585–8.
[212] Pluznick JL, Zou DJ, Zhang X, Yan Q, Rodriguez-Gil DJ, Eisner C, et al. Functional expression of the olfactory signaling system in the kidney. Proc Natl Acad Sci USA 2009; 106(6):2059–64.
[213] Zheng S, Yu P, Zeng C, Wang Z, Yang Z, Andrews PM, et al. $G_{\alpha 12}$- and $G\alpha_{13}$-protein subunit linkage of D_5 dopamine receptors in the nephron. Hypertension 2003;41(3):604–10.
[214] Yamaguchi Y, Katoh H, Mori K, Negishi MG. $G\alpha_{12}$ and $G\alpha_{13}$ interact with Ser/Thr protein phosphatase type 5 and stimulate its phosphatase activity. Curr Biol 2002;12(15):1353–8.

[215] Yu P, Asico LD, Luo Y, Andrews P, Eisner GM, Hopfer U, et al. D1 dopamine receptor hyperphosphorylation in renal proximal tubules in hypertension. Kidney Int 2006;70(6):1072–9.
[216] Gardner B, Liu ZF, Jiang D, Sibley DR. The role of phosphorylation/dephosphorylation in agonist-induced desensitization of D1 dopamine receptor function: evidence for a novel pathway for receptor dephosphorylation. Mol Pharmacol 2001; 59(2):310–21.
[217] Millar RP, Newton CL. The year in G protein-coupled receptor research. Mol Endocrinol 2010;24(1):261–74.
[218] O'Sullivan GJ, Roth BL, Kinsella A, Waddington JL. SK&F 83822 distinguishes adenylyl cyclase from phospholipase C-coupled dopamine D1-like receptors: behavioural topography. Eur J Pharmacol 2004;486(3):273–80.
[219] Jin LQ, Goswami S, Cai G, Zhen X, Friedman E. SKF83959 selectively regulates phosphatidylinositol-linked D1 dopamine receptors in rat brain. J Neurochem 2003;85(2):378–86.
[220] Bek MJ, Zheng S, Xu J, Yamaguchi I, Asico LD, Sun XG, et al. Differential expression of adenylyl cyclases in the rat nephron. Kidney Int 2001;60(3):890–9.
[221] Yu P, Zhang Y, Jose PA. Differential regulation of adenylyl cyclases in lipid rafts in human kidney cells. J Am Soc Nephrol 2010;21: 370A–370A.
[222] Dmitrieva RI, Lalli E, Doris PA. Regulation of adrenocortical cardiotonic steroid production by dopamine and PKA signaling. Front Biosci 2005;10:2489–95.
[223] Ventura AL, Sibley DR. Altered regulation of the D1 dopamine receptor in mutant Chinese hamster ovary cells deficient in cyclic AMP-dependent protein kinase activity. J Pharmacol Exp Ther 2000;293(2):426–34.
[224] Hemmings Jr HC, Greengard P, Tung HY, Cohen P. DARPP-32, a dopamine-regulated neuronal phosphoprotein, is a potent inhibitor of protein phosphatase-1. Nature 1984; 310(5977):503–5.
[225] Kuroiwa M, Bateup HS, Shuto T, Higashi H, Tanaka M, Nishi A. Regulation of DARPP-32 phosphorylation by three distinct dopamine D1-like receptor signaling pathways in the neostriatum. J Neurochem 2008;107(4):1014–26.
[226] Pollack A. Coactivation of D1 and D2 dopamine receptors: in marriage, a case of his, hers, and theirs. Sci STKE 2004; 2004(255):pe50.
[227] So CH, Verma V, Alijaniaram M, Cheng R, Rashid AJ, O'Dowd BF, et al. Calcium signaling by dopamine D5 receptor and D5-D2 receptor hetero-oligomers occurs by a mechanism distinct from that for dopamine D1-D2 receptor hetero-oligomers. Mol Pharmacol 2009;75(4):843–5.
[228] Sidhu A, Kimura K, Uh M, White BH, Patel S. Multiple coupling of human D5 dopamine receptors to guanine nucleotide binding proteins G_s and G_z. J Neurochem 1998;70(6):2459–67.
[229] Friedman E, Jin LQ, Cai GP, Hollon TR, Drago J, Sibley DR, et al. D_1-like dopaminergic activation of phosphoinositide hydrolysis is independent of D_{1A} dopamine receptors: evidence from D_{1A} knockout mice. Mol Pharmacol 1997;51(1):6–11.
[230] Sahu A, Tyeryar KR, Vongtau HO, Sibley DR, Undieh AS. D_5 dopamine receptors are required for dopaminergic activation of phospholipase C. Mol Pharmacol 2009;75 (3):447–53.
[231] Gomez-Cambronero J, Keire P. Phospholipase D: a novel major player in signal transduction. Cell Signal 1998;10(6):387–97.
[232] Yang Z, Asico LD, Yu P, Wang Z, Jones JE, Bai RK, et al. D5 dopamine receptor regulation of phospholipase D. Am J Physiol Heart Circ Physiol 2005;288(1):H55–61.
[233] Yasunari K, Kohno M, Kano H, Minami M, Yoshikawa J. Dopamine as a novel antioxidative agent for rat vascular smooth muscle cells through dopamine D1-like receptors. Circulation 2000;101(19):2302–8.
[234] Yang Z, Asico LD, Yu P, Wang Z, Jones JE, Escano CS, et al. D_5 dopamine receptor regulation of reactive oxygen species production, NADPH oxidase, and blood pressure. Am J Physiol Regul Integr Comp Physiol 2006;290(1): R96–104.
[235] Everett PB, Senogles SE. D3 dopamine receptor signals to activation of phospholipase D through a complex with Rho. J Neurochem 2010;112(4):963–71.
[236] Guo J, Gertsberg Z, Ozgen N, Sabri A, Steinberg SF. Protein kinase D isoforms are activated in an agonist-specific manner in cardiomyocytes. J Biol Chem 2011;286(8):6500–9.
[237] Yao LP, Li XX, Yu PY, Xu J, Asico LD, Jose PA. Dopamine D1 receptor and protein kinase C isoforms in spontaneously hypertensive rats. Hypertension 1998;32(6):1049–53.
[238] Efendiev R, Bertorello AM, Pedemonte CH. PKC-β and PKC-ζ mediate opposing effects on proximal tubule Na^+,K^+-ATPase activity. FEBS Lett 1999;456(1):45–8.
[239] Yu P, Han W, Villar VA, Li H, Arnaldo FB, Concepcion GP, et al. Dopamine D1 receptor-mediated inhibition of NADPH oxidase activity in human kidney cells occurs via protein kinase A-protein kinase C cross talk. Free Radic Biol Med 2011;50(7):832–40.
[240] Asghar M, Hussain T, Lokhandwala MF. Overexpression of PKCβ I and -δ contributes to higher PKC activity in the proximal tubules of old Fischer 344 rats. Am J Physiol Renal Physiol 2003;285(6):F1100–7.
[241] Nowicki S, Kruse MS, Brismar H, Aperia A. Dopamine-induced translocation of protein kinase C isoforms visualized in renal epithelial cells. Am J Physiol Cell Physiol 2000;279(6): C1812–8.
[242] Cunningham R, Biswas R, Brazie M, Steplock D, Shenolikar S, Weinman EJ. Signaling pathways utilized by PTH and dopamine to inhibit phosphate transport in mouse renal proximal tubule cells. Am J Physiol Renal Physiol 2009;296 (2):F355–61.
[243] Yasunari K, Kohno M, Murakawa K, Yokokawa K, Horio T, Takeda T. Interaction between a phorbol ester and dopamine DA1 receptors on vascular smooth muscle. Am J Physiol 1993;264(1 Pt 2):F24–30.
[244] Jackson A, Sedaghat K, Minerds K, James C, Tiberi M. Opposing effects of phorbol-12-myristate-13-acetate, an activator of protein kinase C, on the signaling of structurally related human dopamine D1 and D5 receptors. J Neurochem 2005;95 (5):1387–400.
[245] Rankin ML, Sibley DR. Constitutive phosphorylation by protein kinase C regulates D1 dopamine receptor signaling. J Neurochem 2010;115(6):1655–67.
[246] Rex EB, Rankin ML, Ariano MA, Sibley DR. Ethanol regulation of D1 dopamine deceptor signaling is mediated by protein kinase C in an isozyme-specific manner. Neuropsychopharmacology 2008; 33(12):2900–11.
[247] Mason JN, Kozell LB, Neve KA. Regulation of dopamine D_1 receptor trafficking by protein kinase A-dependent phosphorylation. Mol Pharmacol 2002;61(4):806–16.
[248] Rex EB, Rankin ML, Yang Y, Lu Q, Gerfen CR, Jose PA, et al. Identification of RanBP 9/10 as interacting partners for protein kinase C (PKC) γ/δ and the D1 dopamine receptor: regulation of PKC-mediated receptor phosphorylation. Mol Pharmacol 2010;78(1):69–80.
[249] Weinman EJ, Biswas R, Steplock D, Douglass TS, Cunningham R, Shenolikar S. Sodium-hydrogen exchanger regulatory factor 1 (NHERF-1) transduces signals that mediate dopamine inhibition of sodium-phosphate co-transport in mouse kidney. J Biol Chem 2010;285(18):13454–60.

[250] Centonze D, Usiello A, Gubellini P, Pisani A, Borrelli E, Bernardi G, et al. Dopamine D2 receptor-mediated inhibition of dopaminergic neurons in mice lacking D2L receptors. Neuropsychopharmacology 2002;27(5):723–6.

[251] Prou D, Gu WJ, Le Crom S, Vincent JD, Salamero J, Vernier P. Intracellular retention of the two isoforms of the D2 dopamine receptor promotes endoplasmic reticulum disruption. J Cell Sci 2001;114(Pt 19):3517–27.

[252] Gao DQ, Canessa LM, Mouradian MM, Jose PA. Expression of the D2 subfamily of dopamine receptor genes in kidney. Am J Physiol 1994;266(4 Pt 2):F646–50.

[253] Obadiah J, Avidor-Reiss T, Fishburn CS, Carmon S, Bayewitch M, Vogel Z, et al. Adenylyl cyclase interaction with the D2 dopamine receptor family; differential coupling to Gi, Gz, and Gs. Cell Mol Neurobiol 1999;19(5):653–64.

[254] Gazi L, Nickolls SA, Strange PG. Functional coupling of the human dopamine D_2 receptor with $G\alpha_{i1}$, $G\alpha_{i2}$, $G\alpha_{i3}$ and $G\alpha_o$ G proteins: evidence for agonist regulation of G protein selectivity. Br J Pharmacol 2003;138(5):775–86.

[255] Yamaguchi I, Harmon SK, Todd RD, O'Malley KL. The rat D4 dopamine receptor couples to cone transducin ($G\alpha t2$) to inhibit forskolin-stimulated cAMP accumulation. J Biol Chem 1997;272(26):16599–602.

[256] Cho DI, Beom S, Van Tol HH, Caron MG, Kim KM. Characterization of the desensitization properties of five dopamine receptor subtypes and alternatively spliced variants of dopamine D2 and D4 receptors. Biochem Biophys Res Commun 2006;350(3):634–40.

[257] Sen S, Nesse R, Sheng L, Stoltenberg SF, Gleiberman L, Burmeister M, et al. Association between a dopamine-4 receptor polymorphism and blood pressure. Am J Hypertens 2005;18(9 Pt 1):1206–10.

[258] Robinson SW, Caron MG. Selective inhibition of adenylyl cyclase type V by the dopamine D_3 receptor. Mol Pharmacol 1997;52(3):508–14.

[259] Pedrosa R, Gomes P, Hopfer U, Jose PA, Soares-da-Silva P. $Gi\alpha 3$ protein-coupled dopamine D_3 receptor-mediated inhibition of renal NHE3 activity in SHR proximal tubular cells is a PLC-PKC-mediated event. Am J Physiol Renal Physiol 2004;287(5):F1059–66.

[260] Beom S, Cheong D, Torres G, Caron MG, Kim KM. Comparative studies of molecular mechanisms of dopamine D_2 and D_3 receptors for the activation of extracellular signal-regulated kinase. J Biol Chem 2004; 279(27):28304–14.

[261] Richtand NM. Behavioral sensitization, alternative splicing, and D3 dopamine receptor-mediated inhibitory function. Neuropsychopharmacology 2006;31(11):2368–75.

[262] Fiorentini C, Busi C, Gorruso E, Gotti C, Spano P, Missale C. Reciprocal regulation of dopamine D_1 and D_3 receptor function and trafficking by heterodimerization. Mol Pharmacol 2008;74(1):59–69.

[263] Scarselli M, Novi F, Schallmach E, Lin R, Baragli A, Colzi A, et al. D_2/D_3 dopamine receptor heterodimers exhibit unique functional properties. J Biol Chem 2001;276(32):30308–14.

[264] Zeng C, Wang D, Yang Z, Wang Z, Asico LD, Wilcox CS, et al. Dopamine D_1 receptor augmentation of D_3 receptor action in rat aortic or mesenteric vascular smooth muscles. Hypertension 2004;43(3):673–9.

[265] Zeng C, Wang Z, Li H, Yu P, Zheng S, Wu L, et al. D_3 dopamine receptor directly interacts with D_1 dopamine receptor in immortalized renal proximal tubule cells. Hypertension 2006;47(3):573–9.

[266] Kaneko S, Albrecht F, Asico LD, Eisner GM, Robillard JE, Jose PA. Ontogeny of DA1 receptor-mediated natriuresis in the rat: In vivo and in vitro correlations. Am J Physiol 1992;263(3 Pt 2):R631–8.

[267] Hussain T, Abdul-Wahab R, Lokhandwala MF. Bromocriptine stimulates Na^+, K^+-ATPase in renal proximal tubules via the cAMP pathway. Eur J Pharmacol 1997;321(2):259–63.

[268] Bertorello A, Aperia A. Inhibition of proximal tubule Na^+-K^+-ATPase activity requires simultaneous activation of DA1 and DA2 receptors. Am J Physiol 1990;259(6 Pt 2):F924–8.

[269] Watts VJ, Neve KA. Activation of type II adenylate cyclase by D_2 and D_4 but not D_3 dopamine receptors. Mol Pharmacol 1997;52(2):181–6.

[270] Beazely MA, Watts VJ. Activation of a novel PKC isoform synergistically enhances D_{2L} dopamine receptor-mediated sensitization of adenylate cyclase type 6. Cell Signal 2005; 17(5):647–53.

[271] Hozumi Y, Watanabe M, Goto K. signaling cascade of diacylglycerol kinase β in the pituitary intermediate lobe: Dopamine D2 receptor/phospholipase $C\beta 4$/diacylglycerol kinase β/protein kinase $C\alpha$. J Histochem Cytochem 2010;58(2):119–29.

[272] Senogles SE. D2s dopamine receptor mediates phospholipase D and antiproliferation. Mol Cell Endocrinol 2003;209(1-2):61–9.

[273] Witkowski G, Szulczyk B, Rola R, Szulczyk P. D_1 dopaminergic control of G protein-dependent inward rectifier K^+ (GIRK)-like channel current in pyramidal neurons of the medial prefrontal cortex. Neuroscience 2008;155(1):53–63.

[274] Natarajan A, Han G, Chen SY, Yu P, White R, Jose P. The D_5 dopamine receptor mediates large-conductance, calcium- and voltage-activated potassium channel activation in human coronary artery smooth muscle cells. J Pharmacol Exp Ther 2010;332(2):640–9.

[275] Acquas E, Vinci S, Ibba F, Spiga S, De Luca MA, Di Chiara G. Role of dopamine D_1 receptors in caffeine-mediated ERK phosphorylation in the rat brain. Synapse 2010;64(5):341–9.

[276] Gildea JJ, Wang X, Jose PA, Felder RA. Differential D_1 and D_5 receptor regulation and degradation of the angiotensin type 1 receptor. Hypertension 2008;51(2):360–6.

[277] Choi EY, Jeong D, Park KW, Baik JH. G protein-mediated mitogen activated protein kinase activation by two dopamine D2 receptors. Biochem Biophys Res Commun 1999; 256(1):33–40.

[278] Narkar V, Hussain T, Lokhandwala M. Role of tyrosine kinase and p44/42 MAPK in D_2-like receptor-mediated stimulation of Na^+, K^+-ATPase in kidney. Am J Physiol Renal Physiol 2002;282(4):F697–702.

[279] Gerfen CR, Miyachi S, Paletzki R, Brown P. D1 dopamine receptor supersensitivity in the dopamine depleted striatum results from a switch in the regulation of ERK1/2/MAP kinase. J Neurosci 2002;22(12):5042–54.

[280] Banday AA, Fazili FR, Marwaha A, Lokhandwala MF. Mitogen-activated protein kinase upregulation reduces renal D1 receptor affinity and G-protein coupling in obese rats. Kidney Int 2007;71(5):397–406.

[281] Vlahović P, Stefanović V. Effect of dopamine on ecto-5′-nucleotidase expression in human glomerular mesangial cells. Arch Int Physiol Biochim Biophys 1994;102(3):171–3.

[282] Zeng C, Han Y, Huang H, Yu C, Ren H, Shi W, et al. D_1-like receptors inhibit insulin-induced vascular smooth muscle cell proliferation via down-regulation of insulin receptor expression. J Hypertens 2009;27(5):1033–41.

[283] Li Z, Yu C, Han Y, Ren H, Shi W, Fu C, et al. Inhibitory effect of D_1-like and D_3 dopamine receptors on norepinephrine-induced proliferation in vascular smooth muscle cells. Am J Physiol Heart Circ Physiol 2008;294(6):H2761–8.

[284] Li H, Shi S, Sun YH, Zhao YJ, Li QF, Li HZ, et al. Dopamine D2R receptor stimulation inhibits angiotensin II-induced

hypertrophy in cultured neonatal rat ventricular myocytes. Clin Exp Pharmacol Physiol 2009;36(3):312–8.

[285] Han JY, Heo JS, Lee YJ, Lee JH, Taub M, Han HJ. Dopamine stimulates $^{45}Ca^{2+}$ uptake through cAMP, PLC/PKC, and MAPKs in renal proximal tubule cells. J Cell Physiol 2007; 211(2):486–94.

[286] Villar VA, Jones JE, Armando I, Palmes-Saloma C, Yu P, Pascua AM, et al. G protein-coupled receptor kinase 4 (GRK4) regulates the phosphorylation and function of the dopamine D_3 receptor. J Biol Chem 2009;284(32):21425–34.

[287] Cho DI, Zheng M, Kim KM. Current perspectives on the selective regulation of dopamine D_2 and D_3 receptors. Arch Pharm Res 2010;33(10):1521–38.

[288] Svenningsson P, Nishi A, Fisone G, Girault JA, Nairn AC, Greengard P. DARPP-32: An integrator of neurotransmission. Annu Rev Pharmacol Toxicol. 2004;44:269–96.

[289] Meister B, Arvidsson U, Hemmings Jr HC, Greengard P, Hökfelt T. Dopamine- and adenosine-3′:5′-monophosphate (cAMP)-regulated phospho-protein of Mr 32,000 (DARPP-32) in the retina of cat, monkey and human. Neurosci Lett 1991;131(1):66–70.

[290] Ouimet CC, Miller PE, Hemmings Jr HC, Walaas SI, Greengard P. DARPP-32, a dopamine- and adenosine 3′:5′-monophosphate-regulated phosphoprotein enriched in dopamine-innervated brain regions. III. Immunocytochemical localization. J Neurosci 1984;4(1):111–24.

[291] Walaas SI, Greengard P. DARPP-32, a dopamine- and adenosine3′:5′-monophosphate-reglated phosphoprotein enriched in dopamine-innervated brain regions. I. Regional and cellular distribution in the brain. J Neurosci 1984; 4(1):84–98.

[292] Meister B, Askergren J, Tunevall G, Hemmings Jr HC, Greengard P. Identification of a dopamine- and 3′5′-cyclic adenosine monophosphate-regulated phosphoprotein of 32 kD (DARPP-32) in the parathyroid hormone-producing cells of the human parathyroid gland. J Endocrinol Invest 1991; 14(8):655–61.

[293] Meister B, Fryckstedt J, Schalling M, Cortes R, Hokfelt T, Aperia A, et al. Dopamine- and cAMP-regulated phosphoprotein (DARPP-32) and dopamine DA1 agonist-sensitive Na+, K+-ATPase in renal tubule cells. Proc Natl Acad Sci USA 1989;86(20):8068–72.

[294] Yu P, Asico LD, Eisner GM, Hopfer U, Felder RA, Jose PA. Renal protein phosphatase 2A activity and spontaneous hypertension in rats. Hypertension 2000;36(6):1053–8.

[295] Sharif NA, Nunes JL, Rosenkranz RP, Whiting RL, Eglen RM. Quantitative autoradiography demonstrates selective modulation of rat brain regional dopamine (D1 and D2) receptor subtypes after chronic manipulation of dietary salt. Neurochem Res 1995;20(2):121–8.

[296] Jadhav AL, Ricci A, Amenta F, Lokhandwala MF. Renal dopamine and changes in dopamine receptor ligand binding during high sodium intake. Clin. Exp. Hypertens. [A] 1991; 13(8):1371–81.

[297] Sharif NA, Nunes JL, Lake KD, McClelland DL, Corkins SF, Lakatos I, et al. Chronic manipulation of dietary salt modulates renal physiology and kidney dopamine receptor subtypes: functional and autoradiographic studies. Gen Pharmacol 1995;26(4):727–35.

[298] Felder RA, Sanada H, Xu J, Yu PY, Wang Z, Watanabe H, et al. G protein-coupled receptor kinase 4 gene variants in human essential hypertension. Proc Natl Acad Sci USA 2002;99 (6):3872–7.

[299] Watanabe H, Xu J, Bengra C, Jose PA, Felder RA. Desensitization of human renal D1 dopamine receptors by G protein-coupled receptor kinase 4. Kidney Int 2002; 62(3):790–8.

[300] Yu P, Yang Z, Jones JE, Wang Z, Owens SA, Mueller SC, et al. D1 dopamine receptor signaling involves caveolin-2 in HEK-293 cells. Kidney Int 2004;66(6):2167–8.

[301] Gildea JJ, Israel JA, Johnson AK, Zhang J, Jose PA, Felder RA. Caveolin-1 and dopamine-mediated internalization of NaKATPase in human renal proximal tubule cells. Hypertension 2009;54(5):1070–6.

[302] Adachi S, Scott L, Holtbäck U, Greengard P, Aperia A, Brismar H. Recruitment of renal dopamine 1 receptors requires an intact microtubulin network. Pflugers Arch 2003;445(5):534–9.

[303] Brismar H, Asghar M, Carey RM, Greengard P, Aperia A. Dopamine-induced recruitment of dopamine D1 receptors to the plasma membrane. Proc Natl Acad Sci USA 1998;95 (10):5573–8.

[304] Trivedi M, Narkar VA, Hussain T, Lokhandwala MF. Dopamine recruits D1A receptors to Na-K-ATPase-rich caveolar plasma membranes in rat renal proximal tubules. Am J Physiol Renal Physiol 2004;287(5):F921–31.

[305] Banday AA, Fazili FR, Lokhandwala MF. Insulin causes renal dopamine D1 receptor desensitization via GRK2-mediated receptor phosphorylation involving phosphatidylinositol 3-kinase and protein kinase C. Am J Physiol Renal Physiol 2007;293(3):F877–84.

[306] Sanada H, Yatabe J, Midorikawa S, Katoh H, Hashimoto S, Watanabe T, et al. Amelioration of genetic hypertension by suppression of renal G protein-coupled receptor kinase type 4 expression. Hypertension 2006;47(6):1131–9.

[307] Rankin ML, Marinec PS, Cabrera DM, Wang Z, Jose PA, Sibley DR. The D_1 dopamine receptor is constitutively phosphorylated by G protein-coupled receptor kinase 4. Mol Pharmacol 2006;69(3):759–69.

[308] Tiberi M, Nash SR, Bertrand L, Lefkowitz RJ, Caron MG. Differential regulation of dopamine D1A receptor responsiveness by various G protein-coupled receptor kinases. J Biol Chem 1996;271(7):3771–8.

[309] Fraga S, Jose PA, Soares-da-Silva P. Involvement of G protein-coupled receptor kinase 4 and 6 in rapid desensitization of dopamine D1 receptor in rat IEC-6 intestinal epithelial cells. Am J Physiol Regul Integr Comp Physiol 2004;287(4):R772–9.

[310] Heydorn A, Søndergaard BP, Hadrup N, Holst B, Haft CR, Schwartz TW. Distinct in vitro interaction pattern of dopamine receptor subtypes with adaptor proteins involved in post-endocytotic receptor targeting. FEBS Lett 2004;556(1-3):276–80.

[311] Namkung Y, Dipace C, Javitch JA, Sibley DR. G protein-coupled receptor kinase-2 constitutively regulates D2 dopamine receptor expression and signaling independently of receptor phosphorylation. J Biol Chem 2009;284(49):34103–15.

[312] Miaczynska M, Pelkmans L, Zerial M. Not just a sink: endosomes in control of signal transduction. Curr Opin Cell Biol 2004;16(4):400–6.

[313] Wojcikiewicz RJ. Regulated ubiquitination of proteins in GPCR-initiated signaling pathways. Trends Pharmacol Sci 2004;25(1):35–41.

[314] Zeng C, Watanabe H, Hopfer U, Felder RA, Jose PA. Desensitization of renal D1 dopamine receptor involves formation of endocytic vesicles. FASEB J 2005;19(5): A1137–A1137.

[315] Oakley RH, Laporte SA, Holt JA, Caron MG, Barak LS. Differential affinities of visual arrestin, βarrestin1, and βarrestin2 for G protein-coupled receptors delineate two major classes of receptors. J Biol Chem 2000;275(22):17201–10.

[316] Pitcher JA, Payne ES, Csortos C, DePaoli-Roach AA, Lefkowitz RJ. The G-protein-coupled receptor phosphatase: a protein

phosphatase type 2A with a distinct subcellular distribution and substrate specificity. Proc Natl Acad Sci USA 1995; 92(18):8343–7.

[317] Slobodyansky E, Aoki Y, Gaznabi AK, Aviles DH, Fildes RD, Jose PA. Dopamine and protein phosphatase activity in renal proximal tubules. Am J Physiol 1995;268(2 Pt 2):F279–84.

[318] Efendiev R, Yudowski GA, Zwiller J, Leibiger B, Katz AL, Berggren PO, et al. Relevance of dopamine signals anchoring dynamin-2 to the plasma membrane during Na^+,K^+-ATPase endocytosis. J Biol Chem 2002;277(46):44108–14.

[319] Aperia A, Fryckstedt J, Svensson L, Hemmings Jr HC, Nairn AC, Greengard P. Phosphorylated Mr 32,000 dopamine- and cAMP-regulated phosphoprotein inhibits Na + ,K + -ATPase activity in renal tubule cells. Proc Natl Acad Sci USA 1991; 88(7):2798–801.

[320] Iwata K, Ito K, Fukuzaki A, Inaki K, Haga T. Dynamin and rab5 regulate GRK2-dependent internalization of dopamine D2 receptors. Eur J Biochem 1999;263(2):596–602.

[321] So CH, Verma V, O'Dowd BF, George SR. Desensitization of the dopamine D_1 and D_2 receptor hetero-oligomer mediated calcium signal by agonist occupancy of either receptor. Mol Pharmacol 2007;72(2):450–62.

[322] Kim KM, Gainetdinov RR, Laporte SA, Caron MG, Barak LS. G protein-coupled receptor kinase regulates dopamine D_3 receptor signaling by modulating the stability of a receptor-filamin-β-arrestin complex. A case of autoreceptor regulation. J Biol Chem 2005;280(13):12774–80.

[323] Spooren A, Rondou P, Debowska K, Lintermans B, Vermeulen L, Samyn B, et al. Resistance of the dopamine D4 receptor to agonist-induced internalization and degradation. Cell Signal 2010;22(4):600–9.

[324] Lingwood D, Simons K. Lipid rafts as a membrane-organizing principle. Science 2010;327(5961):46–50.

[325] Insel PA, Head BP, Ostrom RS, Patel HH, Swaney JS, Tang CM, et al. Caveolae and lipid rafts: G protein-coupled receptor signaling microdomains in cardiac myocytes. Ann N Y Acad Sci 2005;1047:166–72.

[326] Pedrosa R, Villar VA, Pascua AM, Simao S, Hopfer U, Jose PA, et al. $H2O_2$ stimulation of the Cl^-/HCO_3^- exchanger by angiotensin II and angiotensin II type 1 receptor distribution in membrane microdomains. Hypertension 2008;51(5):1332–8.

[327] Li H, Han W, Villar VA, Keever LB, Lu Q, Hopfer U, et al. D_1-like receptors regulate NADPH oxidase activity and subunit expression in lipid raft microdomains of renal proximal tubule cells. Hypertension 2009;53(6):1054–61.

[328] Sánchez-Wandelmer J, Dávalos A, de la Peña G, Cano S, Giera M, Canfran-Duque A, et al. Haloperidol disrupts lipid rafts and impairs insulin signaling in SH-SY5Y cells. Neuroscience 2010;167(1):143–53.

[329] Wang Q, Ting WL, Yang H, Wong PT. High doses of simvastatin upregulate dopamine D_1 and D_2 receptor expression in the rat prefrontal cortex: possible involvement of endothelial nitric oxide synthase. Br J Pharmacol 2005;144(7):933–9.

[330] Han W, Li H, Villar VA, Pascua AM, Dajani MI, Wang X, et al. Lipid rafts keep NADPH oxidase in the inactive state in human renal proximal tubule cells. Hypertension 2008; 51(2):481–748.

[331] O'Dowd BF, Ji X, Alijaniaram M, Rajaram RD, Kong MM, Rashid A, et al. Dopamine receptor oligomerization visualized in living cells. J Biol Chem 2005;280(44):37225–35.

[332] Bulenger S, Marullo S, Bouvier M. Emerging role of homo- and heterodimerization in G-protein-coupled receptor biosynthesis and maturation. Trends Pharmacol Sci 2005;26 (3):131–7.

[333] Simpson LM, Taddese B, Wall ID, Reynolds CA. Bioinformatics and molecular modelling approaches to GPCR oligomerization. Curr Opin Pharmacol 2010;10(1):30–7.

[334] Milligan G. G protein-coupled receptor hetero-dimerization: contribution to pharmacology and function. Br J Pharmacol 2009;158(1):5–14.

[335] Gildea JJ, Kemp BA, Howell NL, Van Sciver RE, Carey RM, Felder RA. Inhibition of renal caveolin-1 reduces natriuresis and produces hypertension in sodium-loaded rats. Am J Physiol Renal Physiol 2011;300(4):F914–20.

[336] Achour L, Labbé-Jullié C, Scott MG, Marullo S. An escort for GPCRs: implications for regulation of receptor density at the cell surface. Trends Pharmacol Sci 2008;29(10):528–35 41

[337] Van Craenenbroeck K, Clark SD, Cox MJ, Oak JN, Liu F, Van Tol HH. Folding efficiency is rate-limiting in dopamine D_4 receptor biogenesis. J Biol Chem 2005;280(19):19350–7.

[338] Free RB, Hazelwood LA, Cabrera DM, Spadling HN, Namkung Y, Rankin ML, et al. D_1 and D_2 dopamine receptor expression is regulated by direct interaction with the chaperone protein calnexin. J Biol Chem 2007; 282(29):21285–300.

[339] Dupré DJ, Robitaille M, Richer M, Ethier N, Mamarbachi AM, Hébert TE. Dopamine receptor-interacting protein 78 acts as a molecular chaperone for Gγ subunits before assembly with Gβ. J Biol Chem 2007;282(18):13703–15.

[340] Bermak JC, Li M, Bullock C, Zhou QY. Regulation of transport of the dopamine D1 receptor by a new membrane-associated ER protein. Nat Cell Biol 2001;3(5):492–8.

[341] Leclerc PC, Auger-Messier M, Lanctot PM, Escher E, Leduc R, Guillemette G. A polyaromatic caveolin-binding-like motif in the cytoplasmic tail of the type 1 receptor for angiotensin II plays an important role in receptor trafficking and signaling. Endocrinology 2002;143(12):4702–10.

[342] Zeng C, Liu Y, Wang Z, He D, Huang L, Yu P, et al. Activation of D3 dopamine receptor decreases angiotensin II type 1 receptor expression in rat renal proximal tubule cells. Circ Res 2006;99(5):494–500.

[343] Zeng C, Wang Z, Hopfer U, et al. Rat strain effects of AT1 receptor activation on D1 dopamine receptors in immortalized renal proximal tubule cells. Hypertension 2005;46(4):799–805.

[344] Kim OJ, Ariano MA, Lazzarini RA, Levine MS, Sibley DR. Neurofilament-M interacts with the D_1 dopamine receptor to regulate cell surface expression and desensitization. J Neurosci 2002;22(14):5920–30.

[345] Bai J, He F, Novikova SI, Undie AS, Dracheva S, Haroutunian V, et al. Abnormalities in the dopamine system in schizophrenia may lie in altered levels of dopamine receptor-interacting proteins. Biol Psychiatry 2004;56(6):427–40.

[346] Shimokawa N, Haglund K, Hölter SM, et al. CIN85 regulates dopamine receptor endocytosis and governs behaviour in mice. EMBO J 2010;29(14):2421–32.

[347] Liu Y, Buck DC, Neve KA. Novel interaction of the dopamine D_2 receptor and the Ca^{2+} binding protein S100B: role in D_2 receptor function. Mol Pharmacol 2008;74(2):371–8.

[348] Negyessy L, Goldman-Rakic PS. Subcellular localization of the dopamine D_2 receptor and coexistence with the calcium-binding protein neuronal calcium sensor-1 in the primate prefrontal cortex. J Comp Neurol 2005;488(4):464–75.

[349] Kim OJ, Ariano MA, Namkung Y, Marinec P, Kim E, Han J, et al. D_2 dopamine receptor expression and trafficking is regulated through direct interactions with ZIP. J Neurochem 2008; 106(1):83–95.

[350] Tirotta E, Fontaine V, Picetti R. Signaling by dopamine regulates D2 receptors trafficking at the membrane. Cell Cycle 2008;7(14):2241–8.

[351] Binda AV, Kabbani N, Lin R, Levenson R. D_2 and D_3 dopamine receptor cell surface localization mediated by interaction with protein 4.1N. Mol Pharmacol 2002;62(3):507–13.

[352] Lin R, Karpa K, Kabbani N, Goldman-Rakic P, Levenson R. Dopamine D_2 and D_3 receptors are linked to the actin cytoskeleton via interaction with filamin A. Proc Natl Acad Sci USA 2001;98(9):5258–63.

[353] Basile M, Lin R, Kabbani N, Karpa K, Kilimann M, Simpson I, et al. Paralemmin interacts with D3 dopamine receptors: implications for membrane localization and cAMP signaling. Arch Biochem Biophys 2006;446(1):60–8.

[354] Rondou P, Skieterska K, Packeu A, Lintermans B, Vanhoenacker P, Vauquelin G, et al. KLHL12-mediated ubiquitination of the dopamine D4 receptor does not target the receptor for degradation. Cell Signal 2010;22(6):900–13.

[355] Karpa KD, Lidow MS, Pickering MT, Levenson R, Bergson C. N-linked glycosylation is required for plasma membrane localization of D_5, but not D_1, dopamine receptors in transfected mammalian cells. Mol Pharmacol 1999;56(5):1071–8.

[356] Sidhu A, Kumar U, Uh M, Patel S. Diminished expression of renal dopamine D1A receptors in the kidney inner medulla of the spontaneously hypertensive rat. J Hypertens 1998; 16(5):601–8.

[357] Shin Y, Kumar U, Patel Y, Patel SC, Sidhu A. Differential expression of D2-like dopamine receptors in the kidney of the spontaneously hypertensive rat. J Hypertens 2003;21 (1):199–207.

[358] Huo TL, Healy DP. Prostaglandin E2 production in rat IMCD cells. I. Stimulation by dopamine. Am J Physiol 1991;261(4 Pt 2):F647–f654.

[359] Huo T, Ye MQ, Healy DP. Characterization of a dopamine receptor (DA2K) in the kidney inner medulla. Proc Natl Acad Sci USA 1991;88(8):3170–4.

[360] Wang X, Luo Y, Escano CS, Yang Z, Asico LD, Li H, et al. Upregulation of renal sodium transporters in D5 dopamine receptor-deficient mice. Hypertension 2010;55(6):1431–7.

[361] O'Connell DP, Botkin SJ, Ramos SI, Sibley DR, Ariano MA, Felder RA, et al. Localization of dopamine D1A receptor protein in rat kidneys. Am J Physiol 1995;268(6 Pt 2): F1185–97.

[362] Takemoto F, Satoh T, Cohen HT, Katz AI. Localization of dopamine-1 receptors along the microdissected rat nephron. Pflugers Arch 1991;419(3-4):243–8.

[363] Ohbu K, Felder RA. DA1 dopamine receptors in renal cortical collecting duct. Am J Physiol 1991;261(5 Pt 2):F890–5.

[364] Amenta F, Barili P, Bronzetti E, Ricci A. Dopamine D1-like receptor subtypes in the rat kidney: a microanatomical study. Clin Exp Hypertens 1999;21(1-2):17–23.

[365] Sun D, Wilborn TW, Schafer JA. Dopamine D4 receptor isoform mRNA and protein are expressed in the rat cortical collecting duct. Am J Physiol 1998;275(5 Pt 2): F742–51.

[366] Grupp C, Begher M, Cohen D, Raghunath M, Franz HE, Müller GA. Isolation and characterization of the lower portion of the thin limb of Henle in primary culture. Am J Physiol 1998;274(4 Pt 2):F775–82.

[367] O'Connell DP, Aherne AM, Lane E, Felder RA, Carey RM. Detection of dopamine receptor D1A subtype-specific mRNA in rat kidney by in situ amplification. Am J Physiol 1998;274(1 Pt 2):F232–41.

[368] Edwards RM, Brooks DP. Dopamine inhibits vasopressin action in the rat inner medullary collecting duct via α_2-adrenoceptors. J Pharmacol Exp Ther 2001;298(3):1001–6.

[369] Maeda Y, Terada Y, Nonoguchi H, Knepper MA. Hormone and autacoid regulation of cAMP production in rat IMCD subsegments. Am J Physiol 1992;263(2 Pt 2):F319–27.

[370] Felder RA, Jose PA. Dopamine1 receptors in rat kidneys identified with 1251-Sch 23982. Am. J. Physiol. (Renal Fluid Electrolyte Physiol.) 1988;255(4):F970–6.

[371] Hedge SS, Ricci A, Amenta F, Lokhandwala MF. Evidence from functional and autoradiographic studies for the presence of tubular dopamine-1 receptors and their involvement in the renal effects of fenoldopam. J Pharmacol Exp Ther 1989; 251(3):1237–45.

[372] Ozono R, O'Connell DP, Wang ZQ, Moore AF, Sanada H, Felder RA, et al. Localization of the dopamine D1 receptor protein in the human heart and kidney. Hypertension 1997;30 (3 Pt 2):725–9.

[373] Narkar VA, Hussain T, Pedemonte C, Lokhandwala MF. Dopamine D2 receptor activation causes mitogenesis via p44/ 42 mitogen-activated protein kinase in opossum kidney cells. J Am Soc Nephrol 2001;12(9):1844–52.

[374] Nurnberger A, Rabiger M, Mack A, Diaz J, Sokoloff P, Muhlbauer B, et al. Subapical localization of the dopamine D3 receptor in proximal tubules of the rat kidney. J Histochem Cytochem 2004;52(12):1647–55.

[375] O'Connell DP, Vaughan CJ, Aherne AM, Botkin SJ, Wang ZQ, Felder RA, et al. Expression of the dopamine D3 receptor protein in the rat kidney. Hypertension 1998;32 (5):886–95.

[376] Ricci A, Marchal-Victorion S, Bronzetti E, Parini A, Amenta F, Tayebati SK. Dopamine D4 receptor expression in rat kidney: evidence for pre- and postjunctional localization. J Histochem Cytochem 2002;50(8):1091–6.

[377] Matsumoto M, Hidaka K, Tada S, Tasaki Y, Yamaguchi T. Full-length cDNA cloning and distribution of human dopamine D4 receptor. Brain Res Mol Brain Res 1995; 29(1):157–62.

[378] Amenta F. Light microscope autoradiography of peripheral dopamine receptor subtypes. Clin Exp Hypertens 1997;19(1-2):27–41.

[379] Abdul-Majeed S, Nauli SM. Dopamine receptor type 5 in the primary cilia has dual chemo- and mechano-sensory roles. Hypertension 2011;58(2):325–31.

[380] Amenta F, Barili P, Bronzetti E, Felici L, Mignini F, Ricci A. Localization of dopamine receptor subtypes in systemic arteries. Clin Exp Hypertens 2000;22(3):277–88.

[381] Amenta F. Density and distribution of dopamine receptors in the cardiovascular system and in the kidney. J Auton Pharmacol 1990;10(Suppl. 1):s11–8.

[382] Ricci A, Escaf S, Vega JA, Amenta F. Autoradiographic localization of dopamine D1 receptors in the human kidney. J Pharmacol Exp Ther 1993;264(1):431–7.

[383] Dousa TP, Shah SV, Abboud HE. Potential role of cyclic nucleotides in glomerular pathophysiology. Adv Cyclic Nucleotide Res 1980;12:285–99.

[384] Kotake C, Hoffmann PC, Goldberg LI, Cannon JG. Comparison of the effects of dopamine and beta-adrenergic agonists on adenylate cyclase of renal glomeruli and striatum. Mol Pharmacol 1981;20(2):429–34.

[385] Wargo AA, Slotkoff LM, Jose PA, Pelayo JC, Eisner GM. Cyclic nucleotide response to stimulation in isolated glomeruli from dog kidney. Nephron 1982;32(2):165–9.

[386] Shultz PJ, Sedor JR, Abboud HE. Dopaminergic stimulation of cAMP accumulation in cultured rat mesangial cells. Am J Physiol 1987;253(2 Pt 2):H358–64.

[387] Bek M, Fischer KG, Greiber S, Hupfer C, Mundel P, Pavenstädt H. Dopamine depolarizes podocytes via a D1-like receptor. Nephrol Dial Transplant 1999;14(3):581–7.
[388] Luippold G, Küster E, Joos TO, Mühlbauer B. Dopamine D3 receptor activation modulates renal function in anesthetized rats. Naunyn Schmiedebergs Arch Pharmacol 1998;358 (6):690–3.
[389] Barnett R, Singhal PC, Scharschmidt LA, Schlondorff D. Dopamine attenuates the contractile response to angiotensin II in isolated rat glomeruli and cultured mesangial cells. Circ Res 1986;59(5):529–33.
[390] Yamaguchi I, Yao L, Sanada H, et al. Characterization of dopamine D_{1A} receptors in rat juxtaglomerular cells. Hypertension 1997;29(4):962–8.
[391] Sanada H, Yao L, Jose PA, Carey RM, Felder RA. Dopamine D3 receptors in rat juxtaglomerular cells. Clin Exp Hypertens 1997;19(1-2):93–105.
[392] Olsen NV, Lund J, Jensen PF, Espersen K, Kanstrup IL, Plum I, et al. Dopamine, dobutamine, and dopexamine. A comparison of renal effects in unanesthetized human volunteers. Anesthesiology 1993;79(4):685–94.
[393] Smit AJ, Meijer S, Wesseling H, Donker AJ, Reitsma WD. Effect of metoclopramide on dopamine-induced changes in renal function in healthy controls and in patients with renal disease. Clin Sci (Lond) 1988;75(4):421–8.
[394] Hahn RA, Wardell Jr. JR. Renal vascular activity of SK&F 38393 and dopamine in anesthetized dogs. J Cardiovasc Pharmacol 1980;2(5):583–93.
[395] Frederickson ED, Bradley T, Goldberg LI. Blockade of renal effects of dopamine in the dog by the DA1 antagonist SCH 23390. Am J Physiol 1985;249(2 Pt 2):F236–40.
[396] Jose PA, Eisner GM, Robillard JE. Renal hemodynamics and natriuresis induced by the dopamine-1 agonist, SKF 82526. Am J Med Sci 1987;294(3):181–6.
[397] Yatsu T, Arai Y, Takizawa K, Kasai-Nakagawa C, Takanashi M, Uchida W, et al. Renal effect of YM435, a new dopamine D1 receptor agonist, in anesthetized dogs. Eur J Pharmacol 1997;322(1):45–53.
[398] Edwards RM. Comparison of the effects of fenoldopam, SK & F R-87516 and dopamine on renal arterioles in vitro. Eur J Pharmacol 1986;126(1-2):167–70.
[399] Takenaka T, Forster H, Epstein M. Characterization of the renal microvascular actions of a new dopaminergic (DA1) agonist, YM435. J Pharmacol Exp Ther 1993;264(3): 1154–9.
[400] Steinhausen M, Weis S, Fleming J, Dussel R, Parekh N. Responses of in vivo renal microvessels to dopamine. Kidney Int 1986;30(3):361–70.
[401] Lang WJ, Woodman OL. Comparison of the vasodilator action of dopamine and dopamine agonists in the renal and coronary beds of the dog. Br J Pharmacol 1982;77(1):23–82.
[402] van Kesteren RG, van Alphen MM, Charbon GA. Effects of dopamine on intestinal vessels in anesthetized dogs. Circ Shock 1988;25(1):41–51.
[403] Jin XH, Wang WZ, Zhao RR. Comparison of the characteristics and density of dopamine-1 receptors in membranes from different arteries using [^{3}H]SCH23390 binding. Methods Find Exp Clin Pharmacol 1995;17(7):455–61.
[404] Alkadhi KA, Sabouni MH, Ansari AF, Lokhandwala MF. Activation of DA1 receptors by dopamine or fenoldopam increases cyclic AMP levels in the renal artery but not in the superior cervical ganglion of the rat. J Pharmacol Exp Ther 1986;238(2):547–53.
[405] Chatziantoniou C, Ruan X, Arendshorst WJ. Defective G protein activation of the cAMP pathway in rat kidney during genetic hypertension. Proc Natl Acad Sci USA 1995; 92(7):2924–8.
[406] Tamaki T, Hura CE, Kunau Jr. RT. Dopamine stimulates cAMP production in canine afferent arterioles via DA1 receptors. Am J Physiol 1989;256(3 Pt 2):H626–9.
[407] Manoogian C, Nadler J, Ehrlich L, Horton R. The renal vasodilating effect of dopamine is mediated by calcium flux and prostacyclin release in man. J Clin Endocrinol Metab 1988;66 (4):678–83.
[408] Borin ML. Dual inhibitory effects of dopamine on Na^+ homeostasis in rat aorta smooth muscle cells. Am J Physiol 1997;272 (2 Pt 1):C428–38.
[409] Rashed SM, Songu-Mize E. Regulation of Na^+-pump activity by dopamine in rat tail arteries. Eur J Pharmacol 1995;284 (3):289–97.
[410] Hussain T, Lokhandwala MF. Renal dopamine DA1 receptor coupling with G_S and $G_{q/11}$ proteins in spontaneously hypertensive rats. Am J Physiol 1997;272(3 Pt 2):F339–f346.
[411] Centonze D, Gubellini P, Usiello A, Rossi S, Tscherter A, Bracci E, et al. Differential contribution of dopamine D2S and D2L receptors in the modulation of glutamate and GABA transmission in the striatum. Neuroscience 2004;129 (1):157–66.
[412] Lindgren N, Usiello A, Goiny M, Haycock J, Erbs E, Greengard P, et al. Distinct roles of dopamine D2L and D2S receptor isoforms in the regulation of protein phosphorylation at presynaptic and postsynaptic sites. Proc Natl Acad Sci USA 2003;100(7):4305–9.
[413] Chen PC, Lao CL, Chen JC. The D_3 dopamine receptor inhibits dopamine release in PC-12/hD3 cells by autoreceptor signaling via PP-2B, CK1, and Cdk-5. J Neurochem 2009; 110(4):1180–90.
[414] Tang L, Todd RD, O'Malley KL. Dopamine D2 and D3 receptors inhibit dopamine release. J Pharmacol Exp Ther 1994;270 (2):475–9.
[415] Lokhandwala MF, Steenberg ML. Selective activation by LY-141865 and apomorphine of presynaptic dopamine receptors in the rat kidney and influence of stimulation parameters in the action of dopamine. J Pharmacol Exp Ther 1984;228 (1):161–7.
[416] Rump LC, Schwertfeger E, Schuster MJ, Schaible U, Frankenschmidt A, Schollmeyer PJ. Dopamine DA2-receptor activation inhibits noradrenaline release in human kidney slices. Kidney Int 1993;43(1):197–204.
[417] Seri I, Eklöf AC, Aperia A. Role of dopamine2-receptors in mediating renal vascular response to low dose dopamine infusion in the rat. Acta Physiol Scand 1987;130(4):563–9.
[418] Stier Jr CT, Cowden EA, Allison ME. Effects of bromocriptine on single nephron and whole-kidney function in rats. J Pharmacol Exp Ther 1982;220(2):366–3670.
[419] Bughi S, Jost-Vu E, Antonipillai I, Nadler J, Horton R. Effect of dopamine2 blockade on renal function under varied sodium intake. J Clin Endocrinol Metab 1994;78(5):1079–84.
[420] Horn PT, Kohli JD. Absence of postsynaptic DA2 dopamine receptors in the dog renal vasculature. Eur J Pharmacol 1991;197(2-3):125–30.
[421] Siragy HM, Felder RA, Peach MJ, Carey RM. Intrarenal DA2 dopamine receptor stimulation in the conscious dog. Am J Physiol 1992;262(6 Pt 2):F932–8.
[422] Luippold G, Schneider S, Vallon V, Osswald H, Mühlbauer B. Postglomerular vasoconstriction induced by dopamine D_3 receptor activation in anesthetized rats. Am J Physiol Renal Physiol 2000;278(4):F570–5.
[423] Montanari A, Tateo E, Fasoli E, Donatini A, Cimolato B, Perinotto P, et al. Dopamine-2 receptor blockade potentiates

the renal effects of nitric oxide inhibition in humans. Hypertension 1998;31(1 Pt 2):277–82.
[424] Morishita H, Katsuragi T. Existence and pharmacological properties of dopamine D4 receptors in guinea pig vas deferens. Eur J Pharmacol 1999;374(2):255–61.
[425] Woodman OL, Rechtman MP, Lang WJ. A comparison of the responses to some dopamine-receptor agonists and antagonists in the isolated perfused rat kidney. Arch Int Pharmacodyn Ther 1980;248(2):203–11.
[426] Zeng C, Wang D, Asico LD, Welch WJ, Wilcox CS, Hopfer U, et al. Aberrant D1 and D3 dopamine receptor transregulation in hypertension. Hypertension 2004;43(3):654–60.
[427] Ragsdale NV, Lynd M, Chevalier RL, Felder RA, Peach MJ, Carey RM. Selective peripheral dopamine-1 receptor stimulation. Differential responses to sodium loading and depletion in humans. Hypertension 1990;15(6 Pt 2):914–21.
[428] Blaustein MP, Hamlyn JM. Signaling mechanisms that link salt retention to hypertension: endogenous ouabain, the Na^+ pump, the Na^+/Ca^{2+} exchanger and TRPC proteins. Biochim Biophys Acta 2010;1802(12):1219–29.
[429] Zhang Y, Yuan Z, Ge H, Ren Y. Effects of long-term ouabain treatment on blood pressure, sodium excretion, and renal dopamine D_1 receptor levels in rats. J Comp Physiol B 2010;180(1):117–24.
[430] Neve KA, Kozlowski MR, Rosser MP. Dopamine D2 receptor stimulation of Na^+/H^+ exchange assessed by quantification of extracellular acidification. J Biol Chem 1992;267(36):25748–53.
[431] O'Connell DP, Ragsdale NV, Boyd DG, Felder RA, Carey RM. Differential human renal tubular responses to dopamine type 1 receptor stimulation are determined by blood pressure status. Hypertension 1997;29(1 Pt 1):115–22.
[432] Pollock DM, Arendshorst WJ. Tubuloglomerular feedback and blood flow autoregulation during DA1-induced renal vasodilation. Am J Physiol 1990;258(3 Pt 2):F627–35.
[433] Reiner NE, Thompson WL. Dopamine and saralasin antagonism of renal vasoconstriction and oliguria caused by amphotericin B in dogs. J Infect Dis 1979;140(4):564–75.
[434] ter Wee PM, Donker AJ. Pharmacologic manipulation of glomerular function. Kidney Int 1994;45(2):417–24.
[435] Seri I, Aperia A. Contribution of dopamine 2 receptors to dopamine-induced increase in glomerular filtration rate. Am J Physiol 1988;254(2 Pt 2):F196–201.
[436] Mühlbauer B, Spöhr F, Schmidt R, Osswald H. Role of renal nerves and endogenous dopamine in amino acid-induced glomerular hyperfiltration. Am J Physiol 1997;273(1 Pt 2):F144–9.
[437] Siragy HM, Felder RA, Howell NL, Chevalier RL, Peach MJ, Carey RM. Evidence that dopamine-2 mechanisms control renal function. Am J Physiol 1990;259(5 Pt 2):F793–800.
[438] Vallon V. Tubuloglomerular feedback and the control of glomerular filtration rate. News Physiol Sci 2003;18:169–714.
[439] Wilcox CS. Redox regulation of the afferent arteriole and tubuloglomerular feedback. Acta Physiol Scand 2003; 179(3):217–23.
[440] Satriano J, Wead L, Cardus A, Deng A, Boss GR, Thomson SC, Blantz RC. Regulation of ecto-5'-nucleotidase by NaCl and nitric oxide: potential roles in tubuloglomerular feedback and adaptation. Am J Physiol Renal Physiol 2006;291(5):F1078–82.
[441] Castrop H, Schnermann J. Isoforms of renal Na-K-2Cl cotransporter NKCC2: Expression and functional significance. Am J Physiol Renal Physiol 2008;295(4):F859–66.
[442] Aoki Y, Albrecht FE, Bergman KR, Jose PA. Stimulation of Na^+-K^+-$2Cl^-$ co-transport in rat medullary thick ascending limb by dopamine. Am J Physiol 1996;271(6 Pt 2): R1561–1567.
[443] Schnermann J, Todd KM, Briggs JP. Effect of dopamine on the tubuloglomerular feedback mechanism. Am J Physiol 1990;258 (4 Pt 2):F790–8.
[444] Häberle DA, Königbauer B. Inhibition of tubuloglomerular feedback by the D1 agonist fenoldopam in chronically salt-loaded rats. J Physiol 1991;441:23–34.
[445] Fuxe K, Marcellino D, Borroto-Escuela DO, Guescini M, Fernandez-Duenas V, Tanganelli S, et al. Adenosine-dopamine interactions in the pathophysiology and treatment of CNS disorders. CNS Neurosci Ther 2010;16(3):e18–42.
[446] Trincavelli ML, Cuboni S, Catena Dell'osso M, Maggio R, Klotz KN, Novi F, et al. Receptor crosstalk: haloperidol treatment enhances A_{2A} adenosine receptor functioning in a transfected cell model. Purinergic Signal 2010;6(4):373–81.
[447] Carlström M, Wilcox CS, Welch WJ. Adenosine A2A receptor activation attenuates tubuloglomerular feedback responses by stimulation of endothelial nitric oxide synthase. Am J Physiol Renal Physiol 2011;300(2):F457–64.
[448] Vlahović P, Stefanović V. Effect of dopamine on ecto-5'-nucleotidase expression in human glomerular mesangial cells. Arch Int Physiol Biochim Biophys 1994;102(3):171–3.
[449] Zeng C, Villar VA, Yu P, Zhou L, Jose PA. Reactive oxygen species and dopamine receptor function in essential hypertension. Clin Exp Hypertens 2009;31(2):156–78.
[450] Kurtz A, Della Bruna R, Pratz J, Cavero I. Rat juxtaglomerular cells are endowed with DA-1 dopamine receptors mediating renin release. J Cardiovasc Pharmacol 1988;12(6): 658–63.
[451] Imbs JL, Schmidt M, Schwartz J. Effect of dopamine on renin secretion in the anesthetized dog. Eur J Pharmacol 1975; 33(1):151–7.
[452] Mizoguchi H, Dzau VJ, Siwek LG, Barger AC. Effect of intrarenal administration of dopamine on renin release in conscious dogs. Am J Physiol 1983;244(1):H39–45.
[453] Ventura HO, Messerli FH, Frohlich ED, Kobrin I, Oigman W, Dunn FG, et al. Immediate hemodynamic effects of a dopamine-receptor agonist (fenoldopam) in patients with essential hypertension. Circulation 1984;69(6):1142–5.
[454] Carey RM, Stote RM, Dubb JW, Townsend LH, Rose Jr CE, Kaiser DL. Selective peripheral dopamine-1 receptor stimulation with fenoldopam in human essential hypertension. J Clin Invest 1984;74(6):2198–207.
[455] Glück Z, Jossen L, Weidmann P, Gnädinger MP, Peheim E. Cardiovascular and renal profile of acute peripheral dopamine1-receptor agonism with fenoldopam. Hypertension 1987;10(1):43–54.
[456] Carey RM, Thorner MO, Ortt EM. Effects of metoclopramide and bromocriptine on the renin–angiotensin–aldosterone system in man. Dopaminergic control of aldosterone. J Clin Invest 1979;63(4):727–35.
[457] Worth DP, Harvey JN, Brown J, Worral A, Lee MR. Domperidone treatment in man inhibits the fall in plasma renin activity induced by intravenous γ-L-glutamyl-L-dopa. Br J Clin Pharmacol 1986;21(5):497–502.
[458] Aherne AM, Vaughan CJ, Carey RM, O'Connell DP. Localization of dopamine D1A receptor protein and messenger ribonucleic acid in rat adrenal cortex. Endocrinology 1997;138(3):1282–8.
[459] Gallo-Payet N, Chouinard L, Balestre MN, Guillon G. Mechanisms involved in the interaction of dopamine with angiotensin II on aldosterone secretion in isolated and cultured rat adrenal glomerulosa cells. Mol Cell Endocrinol 1991;81(1-3):11–23.
[460] Drake Jr CR, Ragsdale NV, Kaiser DL, Carey RM. Dopaminergic suppression of angiotensin II-induced

aldosterone secretion in man: differential responses during sodium loading and depletion. Metabolism 1984;33 (8):696–702.

[461] Drake Jr CR, Carey RM. Dopamine modulates sodium-dependent aldosterone responses to angiotensin II in humans. Hypertension 1984;6(2 Pt 2):I119–23.

[462] Chang HW, Chu TS, Huang HY, Chueh SC, Wu VC, Chen YM, et al. Down-regulation of D2 dopamine receptor and increased protein kinase Cμ phosphorylation in aldosterone-producing adenoma play roles in aldosterone overproduction. J Clin Endocrinol Metab 2007;92(5):1863–70.

[463] Chang HW, Wu VC, Huang CY, Huang HY, Chen YM, Chu TS, et al. dopamine receptor enhances angiotensin II-stimulated aldosterone secretion through PKC-ε and calcium signaling. Am J Physiol Endocrinol Metab 2008;294(3): E622–629.

[464] Luchsinger A, Grilli M, Forte P, Morales E, Velasco M. Metoclopramide blocks bromocriptine induced antihypertensive effect in hypertensive patients. Int J Clin Pharmacol Ther 1995;33(9):509–12.

[465] Alvelos M, Ferreira A, Bettencourt P, Pimenta J, Azevedo A, Serrao P, et al. Effect of saline load and metoclopramide on the renal dopaminergic system in patients with heart failure and healthy controls. J Cardiovasc Pharmacol 2005; 45(3):197–203.

[466] Siragy HM, Felder RA, Howell NL, Chevalier RL, Peach MJ, Carey RM. Evidence that intrarenal dopamine acts as a paracrine substance at the renal tubule. Am J Physiol 1989;257(3 Pt 2): F469–77.

[467] Pelayo JC, Fildes RD, Eisner GM, Jose PA. Effects of dopamine blockade on renal sodium excretion. Am J Physiol 1983;245(2): F247–53.

[468] Sanada H, Xu J, Watanabe H, Jose PA, Felder RA. Differential expression and regulation of dopamine-1 (D-1) and dopamine-5 (D-5) receptor function in human kidney. Am J Hypertens 2000;13: 156A-156A

[469] Ball SG, Lee MR. The effect of carbidopa administration on urinary sodium excretion in man.Is dopamine an intrarenal natriuretic hormone? Br J Clin Pharmacol 1977;4(2):115–9.

[470] Zhang MZ, Yao B, Wang S, Fan X, Wu G, Yang H, et al. Intrarenal dopamine deficiency leads to hypertension and decreased longevity in mice. J Clin Invest 2011;121 (7):2845–54.

[471] Odlind C, Fasching A, Liss P, Palm F, Hansell P. Changing dopaminergic activity through different pathways: consequences for renal sodium excretion, regional blood flow and oxygen tension in the rat. Acta Physiol Scand 2001;172 (3):219–26.

[472] Odlind C, Reenilä I, Männistö PT, Juvonen R, Uhlen S, Gogos JA, et al. Reduced natriuretic response to acute sodium loading in COMT gene deleted mice. BMC Physiol 2002;2:14.

[473] Ladines CA, Zeng C, Asico LD, et al. Impaired renal D1-like and D2-like dopamine receptor interaction in the spontaneously hypertensive rat. Am J Physiol Regul Integr Comp Physiol 2001;281(4):R1071–8.

[474] Gomes P, Soares-da-Silva P. Dopamine acutely decreases type 3 Na^+/H^+ exchanger activity in renal OK cells through the activation of protein kinases A and C signalling cascades. Eur J Pharmacol 2004;488(1-3):51–9.

[475] Amaral JS, Pinho MJ, Soares-da-Silva P. Regulation of amino acid transporters in the rat remnant kidney. Nephrol Dial Transplant 2009;24(7):2058–67.

[476] Bacic D, Capuano P, Baum M, Zhang J, Stange G, Biber J, et al. Activation of dopamine D_1-like receptors induces acute internalization of the renal Na^+/phosphate co-transporter NaPi-IIa in mouse kidney and OK cells. Am J Physiol Renal Physiol 2005;288(4):F740–7.

[477] Chen Z, Leibiger I, Katz AI, Bertorello AM. Pals-associated tight junction protein functionally links dopamine and angiotensin II to the regulation of sodium transport in renal epithelial cells. Br J Pharmacol 2009;158(2):486–93.

[478] Cinelli AR, Efendiev R, Pedemonte CH. Trafficking of Na-K-ATPase and dopamine receptor molecules induced by changes in intracellular sodium concentration of renal epithelial cells. Am J Physiol Renal Physiol 2008;295(4): F1117–25.

[479] Gomes P, Soares-da-Silva P. Dopamine-induced inhibition of Na^+-K^+-ATPase activity requires integrity of actin cytoskeleton in opossum kidney cells. Acta Physiol Scand 2002; 175(2):93–101.

[480] Khundmiri SJ, Weinman EJ, Steplock D, Cole J, Ahmad A, Baumann PD, et al. Parathyroid hormone regulation of Na^+, K^+ -ATPase requires the PDZ 1 domain of sodium hydrogen exchanger regulatory factor-1 in opossum kidney cells. J Am Soc Nephrol 2005;16(9):2598–607.

[481] Kunimi M, Seki G, Hara C, Taniguchi S, Uwatoko S, Goto A, et al. Dopamine inhibits renal Na^+:HCO_3^- co-transporter in rabbits and normotensive rats but not in spontaneously hypertensive rats. Kidney Int 2000;57(2):534–43.

[482] Lanaspa MA, Giral H, Breusegem SY, Halaihel N, Baile G, Catalan J, et al. Interaction of MAP17 with NHERF3/4 induces translocation of the renal Na/Pi IIa transporter to the trans-Golgi. Am J Physiol Renal Physiol 2007;292(1):F230–42.

[483] Correa AH, Choi MR, Gironacci M, Aprile F, Fernández BE. Atrial natriuretic factor decreases renal dopamine turnover and catabolism without modifying its release. Regul Pept 2008;146(1-3):238–42.

[484] Marin-Grez M, Angchanpen P, Gambaro G, Schnermann J, Schubert G, Briggs JP. Evidence for an involvement of dopamine receptors in the natriuretic response to atrial natriuretic peptide. Klin Wochenschr 1987;65(Suppl. 8):97–102.

[485] Hegde SS, Chen CJ, Lokhandwala MF. Involvement of endogenous dopamine and DA-1 receptors in the renal effects of atrial natriuretic factor in rats. Clin Exp Hypertens A 1991; 13(3):357–69.

[486] Bughi S, Horton R, Antonipillai I, Manoogian C, Ehrlich L, Nadler J. Comparison of dopamine and fenoldopam effects on renal blood flow and prostacyclin excretion in normal and essential hypertensive subjects. J Clin Endocrinol Metab 1989;69(6):1116–21.

[487] Costa MA, Elesgaray R, Loria A, Balaszczuk AM, Arranz C. Vascular and renal effects of dopamine during extracellular volume expansion: role of nitric oxide pathway. Life Sci 2006;78(14):1543–9.

[488] Venkatakrishnan U, Chen C, Lokhandwala MF. The role of intrarenal nitric oxide in the natriuretic response to dopamine-receptor activation. Clin Exp Hypertens 2000;22 (3):309–24.

[489] Ibarra F, Crambert S, Eklöf AC, Lundquist A, Hansell P, Holtbäck U. Prolactin, a natriuretic hormone, interacting with the renal dopamine system. Kidney Int 2005;68(4): 1700–7.

[490] Chen C, Lokhandwala MF. Potentiation by enalaprilat of fenoldopam-evoked natriuresis is due to blockade of intrarenal production of angiotensin-II in rats. Naunyn Schmiedebergs Arch Pharmacol 1995;352(2):194–200.

[491] Clark KL, Hilditch A, Robertson MJ, Drew GM. Effects of dopamine DA1-receptor blockade and angiotensin converting enzyme inhibition on the renal actions of fenoldopam in the anaesthetized dog. J Hypertens 1991;9(12):1143–50.

[492] de Vries PA, de Zeeuw D, de Jong PE, Navis G. The abnormal renal vasodilator response to D1-like receptor stimulation in conscious SHR can be normalized by AT1 blockade. J Cardiovasc Pharmacol 2004;44(5):571–6.
[493] Hussain T, Abdul-Wahab R, Kotak DK, Lokhandwala MF. Bromocriptine regulates angiotensin II response on sodium pump in proximal tubules. Hypertension 1998;32(6):1054–9.
[494] Sheikh-Hamad D, Wang YP, Jo OD, Yanagawa N. Dopamine antagonizes the actions of angiotensin II in renal brush-border membrane. Am J Physiol 1993;264(4 Pt 2):F737–43.
[495] Banday AA, Asghar M, Hussain T, Lokhandwala MF. Dopamine-mediated inhibition of renal Na,K-ATPase is reduced by insulin. Hypertension 2003;41(6):1353–8.
[496] Yang J, Cui Z, He D, Ren H, Han Y, Yu C, et al. Insulin increases D_5 dopamine receptor expression and function in renal proximal tubule cells fromWistar-Kyoto rats. Am J Hypertens 2009;22(7):770–6.
[497] Boone M, Kortenoeven ML, Robben JH, Tamma G, Deen PM. Counteracting vasopressin-mediated water reabsorption by ATP, dopamine, and phorbol esters: mechanisms of action. Am J Physiol Renal Physiol 2011;300(3):F761–71.
[498] Sun D, Schafer JA. Dopamine inhibits AVP-dependent Na^+ transport and water permeability in rat CCD via a D_4-like receptor. Am J Physiol 1996;271(2 Pt 2):F391–400.
[499] Nejsum LN, Zelenina M, Aperia A, Frøkiaer J, Nielsen S. Bidirectional regulation of AQP2 trafficking and recycling: Involvement of AQP2-S256 phosphorylation. Am J Physiol Renal Physiol 2005;288(5):F930–8.
[500] Bennett ED, Tighe D, Wegg W. Abolition, by dopamine blockade, of the natriuretic response produced by lower body positive pressure. Clin Sci (Lond) 1982;63(4):361–6.
[501] Luippold G, Zimmermann C, Mai M, Kloor D, Starck D, Gross G, et al. Dopamine D_3 receptors and salt-dependent hypertension. J Am Soc Nephrol 2001;12(11):2272–9.
[502] Luippold G, Beilharz M, Wehrmann M, Unger L, Gross G, Mühlbauer B. Effect of dopamine D3 receptor blockade on renal function and glomerular size in diabetic rats. Naunyn Schmiedebergs Arch Pharmacol 2005;371(5):420–7.
[503] Yamaguchi I, Walk SF, Jose PA, Felder RA. Dopamine D2L receptors stimulate Na^+/K^+-ATPase activity in murine LTK-cells. Mol Pharmacol 1996;49(2):373–8.
[504] Narkar VA, Hussain T, Lokhandwala MF. Activation of D_2-like receptors causes recruitment of tyrosine-phosphorylated NKA α1-subunits in kidney. Am J Physiol Renal Physiol 2002;283(6):F1290–5.
[505] Grider J, Kilpatrick E, Ott C, Jackson B. Effect of dopamine on NaCl transport in the medullary thick ascending limb of the rat. Eur J Pharmacol 1998;342(2-3):281–4.
[506] Pedrosa R, Gomes P, Hopfer U, Jose PA, Soares-da-Silva P. Giα3 protein-coupled dopamine D_3 receptor-mediated inhibition of renal NHE3 activity in SHR proximal tubular cells is a PLC-PKC-mediated event. Am J Physiol Renal Physiol 2004;287(5):F1059–1066.
[507] Chen CJ, Lokhandwala MF. An impairment of renal tubular DA-1 receptor function as the causative factor for diminished natriuresis to volume expansion in spontaneously hypertensive rats. Clin Exp Hypertens A. 1992;14(4):615–28.
[508] Eklöf AC. The natriuretic response to a dopamine DA1 agonist requires endogenous activation of dopamine DA2 receptors. Acta Physiol Scand 1997;160(4):311–4.
[509] Jose PA, Asico LD, Eisner GM, Pocchiari F, Semeraro C, Felder RA. Effects of costimulation of dopamine D_1- and D_2-like receptors on renal function. Am J Physiol 1998;275(4 Pt 2): R986–94.
[510] Muto S, Tabei K, Asano Y, Imai M. Dopaminergic inhibition of the action of vasopressin on the cortical collecting tubule. Eur J Pharmacol 1985;114(3):393–7.
[511] Upadhyay K, Jose P, Wang X. Inhibitory effect of dopamine 4 receptor on sodium chloride co-transporter in the renal distal convoluted tubule. Annual Meeting Pediatric Academic Societies 2011;: Abstract 3750.1
[512] Leyssac PP, Karlsen FM, Holstein-Rathlou NH, Skøtt O. On determinants of glomerular filtration rate after inhibition of proximal tubular reabsorption. Am J Physiol 1994;266(5 Pt 2): R1544–50.
[513] Nielsen CB, Pedersen EB. Abnormal distal tubular sodium reabsorption during dopamine infusion in patients with essential hypertension evaluated by the lithium clearance methods. Clin Nephrol 1997;47(5):304–9.
[514] Olsen NV, Olsen MH, Bonde J, Kanstrup IL, Plum I, Strandgaard S, et al. Dopamine natriuresis in salt-repleted, water-loaded humans: a dose–response study. Br J Clin Pharmacol 1997;43(5):509–20.
[515] Hu MC, Fan L, Crowder LA, Karim-Jimenez Z, Murer H, Moe OW. Dopamine acutely stimulates Na^+/H^+ exchanger (NHE3) endocytosis via clathrin-coated vesicles: dependence on protein kinase A-mediated NHE3 phosphorylation. J Biol Chem 2001;276(29):26906–15.
[516] Debska-Slizien A, Ho P, Drangova R, Baines AD. Endogenous renal dopamine production regulates phosphate excretion. Am J Physiol 1994;266(6 Pt 2):F858–67.
[517] Ba J, Brown D, Friedman PA. Calcium-sensing receptor regulation of PTH-inhibitable proximal tubule phosphate transport. Am J Physiol Renal Physiol 2003;285(6):F1233–43.
[518] Khundmiri SJ, Ahmad A, Bennett RE, Weinman EJ, Steplock D, Cole J, et al. Novel regulatory function for NHERF-1 in Npt2a transcription. Am J Physiol Renal Physiol 2008;294(4):F840–9.
[519] Weinman EJ, Biswas R, Steplock D, Wang P, Lau YS, Desir GV, et al. Increased renal dopamine and acute renal adaptation to a high-phosphate diet. Am J Physiol Renal Physiol 2011;300(5):F1123–9.
[520] Pedrosa R, Jose PA, Soares-da-Silva P. Defective D_1-like receptor-mediated inhibition of the Cl^-/HCO_3^- exchanger in immortalized SHR proximal tubular epithelial cells. Am J Physiol Renal Physiol 2004;286(6):F1120–6.
[521] Pedrosa R, Gomes P, Soares-da-Silva P. Distinct signalling cascades downstream to Gsα coupled dopamine D_1-like NHE3 inhibition in rat and opossum renal epithelial cells. Cell Physiol Biochem 2004;14(1-2):91–100.
[522] Salyer S, Lesousky N, Weinman EJ, Clark BJ, Lederer ED, Khundmiri SJ. Dopamine regulation of Na^+-K^+-ATPase requires the PDZ-2 domain of sodium hydrogen regulatory factor-1 (NHERF-1) in opossum kidney cells. Am J Physiol Cell Physiol 2011;300(3):C425–34.
[523] Wang X, Luo Y, Asico L, Jones JE, Escano CS, Jose PA. Increased renal sodium transporters are associated with hypertension in D4 dopamine receptor deficient mice. FASEB J 2007;21: A1366-A1366.
[524] Grider JS, Ott CE, Jackson BA. Dopamine D1 receptor-dependent inhibition of NaCl transport in the rat thick ascending limb: Mechanism of action. Eur J Pharmacol 2003;473(2-3):185–90.
[525] Amlal H, Legoff C, Vernimmen C, Paillard M, Bichara M. Na^+-K^+($NH4^+$)-$2Cl^-$ co-transport in medullary thick ascending limb: Control by PKA, PKC, and 20-HETE. Am J Physiol 1996;271(2 Pt 1):C455–63.
[526] Kiroytcheva M, Cheval L, Carranza ML, Martin PY, Favre H, Doucet A, et al. Effect of cAMP on the activity and the

phosphorylation of Na^+,K^+-ATPase in rat thick ascending limb of Henle. Kidney Int 1999;55(5):1819–31.

[527] Bertuccio CA, Cheng SX, Arrizurieta EE, Martín RS, Ibarra FR. Mechanisms of Na^+-K^+-ATPase phosphorylation by PKC in the medullary thick ascending limb of Henle in the rat. Pflugers Arch 2003;447(1):87–96.

[528] Wang X, Villar VM, Armando I, Eisner GM, Felder RA, Jose PA. Dopamine, kidney and hypertension: studies in dopamine receptor knockout mice. Pediatr Nephrol 2008;23 (12):2131–46.

[529] Saito O, Ando Y, Kusano E, Asano Y. Functional characterization of basolateral and luminal dopamine receptors in rabbit CCD. Am J Physiol Renal Physiol 2001;281(1):F114–22.

[530] Satoh T, Cohen HT, Katz AI. Different mechanisms of renal Na-K-ATPase regulation by protein kinases in proximal and distal nephron. Am J Physiol 1993;265(3 Pt 2):F399–405.

[531] Asghar M, Kansra V, Hussain T, Lokhandwala MF. Hyperphosphorylation of Na-pump contributes to defective renal dopamine response in old rats. J Am Soc Nephrol 2001;12(2):226–32.

[532] Banday AA, Hussain T, Lokhandwala MF. Renal dopamine D_1 receptor dysfunction is acquired and not inherited in obese Zucker rats. Am J Physiol Renal Physiol 2004;287(1):F109–16.

[533] Bertorello AM, Komarova Y, Smith K, Leibiger IB, Efendiev R, Pedemonte CH, et al. Analysis of Na^+,K^+-ATPase motion and incorporation into the plasma membrane in response to G protein-coupled receptor signals in living cells. Mol Biol Cell 2003;14(3):1149–57.

[534] Efendiev R, Budu CE, Cinelli AR, Bertorello AM, Pedemonte CH. Intracellular Na^+ regulates dopamine and angiotensin II receptors availability at the plasma membrane and their cellular responses in renal epithelia. J Biol Chem 2003;278(31): 28719–26.

[535] Efendiev R, Chen Z, Krmar RT, Uhles S, Katz AI, Pedemonte CH, et al. The 14-3-3 protein translates the Na^+,K^+-ATPase α1-subunit phosphorylation signal into binding and activation of phosphoinositide 3-kinase during endocytosis. J Biol Chem 2005;280(16):16272–7.

[536] Efendiev R, Cinelli AR, Leibiger IB, Bertorello AM, Pedemonte CH. FRET analysis reveals a critical conformational change within the Na,K-ATPase α1 subunit N-terminus during GPCR-dependent endocytosis. FEBS Lett 2006;580(21):5067–70.

[537] Eklöf AC, Holtbäck U, Sundelöf M, Chen S, Aperia A. Inhibition of COMT induces dopamine-dependent natriuresis and inhibition of proximal tubular Na^+,K^+-ATPase. Kidney Int 1997;52(3):742–7.

[538] Nishi A, Eklöf AC, Bertorello AM, Aperia A. Dopamine regulation of renal Na^+,K^+-ATPase activity is lacking in Dahl salt-sensitive rats. Hypertension 1993;21(6 Pt 1):767–71.

[539] Satoh T, Cohen HT, Katz AI. Intracellular signaling in the regulation of renal Na-K-ATPase. II. Role of eicosanoids. J Clin Invest 1993;91(2):409–15.

[540] Doné SC, Leibiger IB, Efendiev R, Katz AI, Leibiger B, Berggren PO, et al. Tyrosine 537 within the Na^+,K^+-ATPase alpha-subunit is essential for AP-2 binding and clathrin-dependent endocytosis. J Biol Chem 2002;277(19):17108–11.

[541] Ominato M, Satoh T, Katz AI. Regulation of Na-K-ATPase activity in the proximal tubule: role of the protein kinase C pathway and of eicosanoids. J Membr Biol 1996;152(3):235–43.

[542] Asghar M, George L, Lokhandwala MF. Exercise decreases oxidative stress and inflammation and restores renal dopamine D1 receptor function in old rats. Am J Physiol Renal Physiol 2007;293(3):F914–9.

[543] Li D, Aperia A, Celsi G, da Cruz e Silva EF, Greengard P, Meister B. Protein phosphatase-1 in the kidney: evidence for a role in the regulation of medullary Na^+-K^+-ATPase. Am J Physiol 1995;269(5 Pt 2):F673–80.

[544] Bełtowski J, Marciniak A, Wójcicka G, Górny D. The opposite effects of cyclic AMP-protein kinase a signal transduction pathway on renal cortical and medullary Na^+,K^+-ATPase activity. J Physiol Pharmacol 2002;53(2):211–31.

[545] Perrichot R, Garcia-Ocaña A, Couette S, Comoy E, Amiel C, Friedlander G. Locally formed dopamine modulates renal Na-Pi co-transport through DA1 and DA2 receptors. Biochem J. 1995;312(Pt 2):433–7.

[546] Wiederkehr MR, Di Sole F, Collazo R, Quinones H, Fan L, Murer H, et al. Characterization of acute inhibition of Na exchanger NHE-3 by dopamine in opossum kidney cells. Kidney Int 2001;59(1):197–209.

[547] Riese K, Beyer AT, Lui GM, Crook RB. Dopamine D1 stimulation of Na^+,K^+,Cl^- co-transport in human NPE cells: effects of multiple hormones. Invest Ophthalmol Vis Sci 1998;39 (8):1444–52.

[548] Bertorello AM, Sznajder JI. The dopamine paradox in lung and kidney epithelia: sharing the same target but operating different signaling networks. Am J Respir Cell Mol Biol 2005;33(5):432–7.

[549] Hazelwood LA, Free RB, Cabrera DM, Skinbjerg M, Sibley DR. Reciprocal modulation of function between the D_1 and D_2 dopamine receptors and the Na^+,K^+-ATPase. J Biol Chem 2008;283(52):36441–53.

[550] Bagh MB, Maiti AK, Jana S, Banerjee K, Roy A, Chakrabarti S. Quinone and oxyradical scavenging properties of N-acetylcysteine prevent dopamine mediated inhibition of Na^+, K^+-ATPase and mitochondrial electron transport chain activity in rat brain: implications in the neuroprotective therapy of Parkinson's disease. Free Radic Res 2008;42(6):574–81.

[551] Okamura T, Toda N. Comparison of the effect of dopamine in primate arteries and veins. Hypertens Res 1995;18(Suppl. 1): S35–7.

[552] Polakowski JS, Segreti JA, Cox BF, Hsieh GC, Kolasa T, Moreland RB, et al. Effects of selective dopamine receptor subtype agonists on cardiac contractility and regional haemodynamics in rats. Clin Exp Pharmacol Physiol 2004;31 (12):837–41.

[553] Han G, Kryman JP, McMillin PJ, White RE, Carrier GO. A novel transduction mechanism mediating dopamine-induced vascular relaxation: opening of BKCa channels by cyclic AMP-induced stimulation of the cyclic GMP-dependent protein kinase. J Cardiovasc Pharmacol 1999;34(5):619–27.

[554] Kawano H, Kawano T, Tanaka K, Eguchi S, Takahashi A, Nakaya A, et al. Effects of dopamine on ATP-sensitive potassium channels in porcine coronary artery smooth-muscle cells. J Cardiovasc Pharmacol 2008;51(2):196–201.

[555] White RE, Kryman JP, El-Mowafy AM, Han G, Carrier GO. cAMP-dependent vasodilators cross-activate the cGMP-dependent protein kinase to stimulate BK_{Ca} channel activity in coronary artery smooth muscle cells. Circ Res 2000;86(8):897–905.

[556] Zelenina M, Zelenin S, Bondar AA, Brismar H, Aperia A. Water permeability of aquaporin-4 is decreased by protein kinase C and dopamine. Am J Physiol Renal Physiol 2002; 283(2):F309–18.

[557] Pannicke T, Iandiev I, Uckermann O, Biedermann B, Kutzera F, Wiedemann P, et al. A potassium channel-linked mechanism of glial cell swelling in the postischemic retina. Mol Cell Neurosci 2004;26(4):493–502.

[558] Gálfi M, Baláspiri L, Tóth R, Pávó I, László F, Morschl E, et al. Inhibitory effect of galanin on dopamine-induced enhanced vasopressin secretion in rat neurohypophyseal tissue cultures. Regul Pept 2002;110(1):17–23.

[559] Laradi A, Sakhrani LM, Massry SG. Effect of dopamine on sodium uptake by renal proximal tubule cells of rabbit. Miner Electrolyte Metab 1986;12(5-6):303–7.

[560] Staudacher T, Pech B, Tappe M, Gross G, Mühlbauer B, Luippold G. Arterial blood pressure and renal sodium excretion in dopamine D_3 receptor knockout mice. Hypertens Res 2007;30(1):93–101.

[561] Drago J, Gerfen CR, Lachowicz JE, Steiner H, Hollon TR, Love PE, et al. Altered striatal function in a mutant mouse lacking D_{1A} dopamine receptors. Proc Natl Acad Sci USA 1994;91(26):12564–8.

[562] Accili D, Fishburn CS, Drago J, Steiner H, Lachowicz JE, Park BH, et al. A targeted mutation of the D_3 dopamine receptor gene is associated with hyperactivity in mice. Proc Natl Acad Sci USA 1996;93(5):1945–9.

[563] Thanos PK, Michaelides M, Ho CW, Wang GJ, Newman AH, Heidbreder CA, et al. The effects of two highly selective dopamine D_3 receptor antagonists (SB-277011A and NGB-2904) on food self-administration in a rodent model of obesity. Pharmacol Biochem Behav 2008;89(4):499–507.

[564] McQuade JA, Benoit SC, Xu M, Woods SC, Seeley RJ. High-fat diet induced adiposity in mice with targeted disruption of the dopamine-3 receptor gene. Behavioural Behav Brain Res 2004;151(1-2):313–9.

[565] Wang Z, Asico LD, Escano CS, Felder RA, Jose PA. Human G protein-coupled receptor kinase type 4 (hGRK4 γ) wild-type prevents salt sensitivity while its variant, hGRK4γ 486V, promotes salt sensitivity in transgenic mice: role of genetic background [Abstract]. Hypertension 2006;48:e27.

[566] Thanos PK, Bermeo C, Rubinstein M, Suchland KL, Wang GJ, Grandy DK, Volkow ND. Conditioned place preference and locomotor activity in response to methylphenidate, amphetamine and cocaine in mice lacking dopamine D4 receptors. J Psychopharmacol 2010;24(6):897–904.

[567] Zeng C, Yang Z, Wang Z, Jones J, Wang X, Altea J, et al. Interaction of angiotensin II type 1 and D_5 dopamine receptors in renal proximal tubule cells. Hypertension 2005;45(4):804–10.

[568] Newman-Tancredi A, Cussac D, Audinot V, Pasteau V, Gavaudan S, Millan MJ. G protein activation by human dopamine D_3 receptors in high-expressing Chinese hamster ovary cells: a guanosine-5′-O-(3-[^{35}S]thio)- triphosphate binding and antibody study. Mol Pharmacol 1999;55(3):564–74.

[569] Zhan L, Liu B, Jose-Lafuente M, Chibalina MV, Grierson A, Maclean A, et al. ALG-2 interacting protein AIP1: a novel link between D1 and D3 signalling. Eur J Neurosci 2008;27(7):1626–33.

[570] Dziedzicka-Wasylewska M, Faron-Górecka A, Andrecka J, Polit A, Kuśmider M, Wasylewski Z. Fluorescence studies reveal heterodimerization of dopamine D1 and D2 receptors in the plasma membrane. Biochemistry 2006;45(29):8751–9.

[571] Lee SP, So CH, Rashid AJ, Varghese G, Cheng R, Lanca AJ, et al. Dopamine D_1 and D_2 receptor co-activation generates a novel phospholipase C-mediated calcium signal. J Biol Chem 2004;279(34):35671–8.

[572] Kitaoka S, Furuyashiki T, Nishi A, Shuto T, Koyasu S, Matsuoka T, et al. Prostaglandin E_2 acts on EP1 receptor and amplifies both dopamine D_1 and D_2 receptor signaling in the striatum. J Neurosci 2007;27(47):12900–7.

[573] Ng J, Rashid AJ, So CH, O'Dowd BF, George SR. Activation of calcium/calmodulin-dependent protein kinase IIa in the striatum by the heteromeric D1-D2 dopamine receptor complex. Neuroscience 2010;165(2):535–41.

[574] Martina M, Bergeron R. D1 and D4 dopaminergic receptor interplay mediates coincident G protein-independent and dependent regulation of glutamate NMDA receptors in the lateral amygdala. J Neurochem 2008;106(6):2421–35.

[575] Beaver KM, Wright JP, DeLisi M, Walsh A, Vaughn MG, Boisvert D, et al. A gene × gene interaction between DRD2 and DRD4 is associated with conduct disorder and antisocial behavior in males. Behav Brain Funct 2007;3:30.

[576] Juhasz JR, Hasbi A, Rashid AJ, So CH, George SR, O'Dowd BF. Mu-opioid receptor heterooligomer formation with the dopamine D1 receptor as directly visualized in living cells. Eur J Pharmacol 2008;581(3):235–43.

[577] Guo Y, Wang HL, Xiang XH, Zhao Y. The role of glutamate and its receptors in mesocorticolimbic dopaminergic regions in opioid addiction. Neurosci Biobehav Rev 2009;33(6):864–73.

[578] Lee FJ, Xue S, Pei L, Vukusic B, Chery N, Wang Y, et al. Dual regulation of NMDA receptor functions by direct protein-protein interactions with the dopamine D1 receptor. Cell 2002;111(2):219–30.

[579] Scott L, Aperia A. Interaction between N-methyl-D-aspartic acid receptors and D1 dopamine receptors: an important mechanism for brain plasticity. Neuroscience 2009;158(1):62–6.

[580] Di Sole F, Cerull R, Petzke S, Casavola V, Burckhardt G, Helmle-Kolb C. Bimodal acute effects of A_1 adenosine receptor activation on Na^+/H^+ exchanger 3 in opossum kidney cells. J Am Soc Nephrol 2003;14(7):1720–30.

[581] Cao Y, Xie KQ, Zhu XZ. The enhancement of dopamine D_1 receptor desensitization by adenosine A_1 receptor activation. Eur J Pharmacol 2007;562(1-2):34–8.

[582] Le Crom S, Prou D, Vernier P. Autocrine activation of adenosine A_1 receptors blocks D_{1A} but not D_{1B} dopamine receptor desensitization. J Neurochem 2002;82(6):1549–52.

[583] Ferre S, von Euler G, Johansson B, Fredholm BB, Fuxe K. Stimulation of high-affinity adenosine A_2 receptors decreases the affinity of dopamine D_2 receptors in rat striatal membranes. Proc Natl Acad Sci USA 1991;88(16):7238–41.

[584] Torvinen M, Marcellino D, Canals M, Agnati LF, Lluis C, Franco R, et al. Adenosine A_{2A} receptor and dopamine D_3 receptor interactions: evidence of functional A_{2A}/D_3 heteromeric complexes. Mol Pharmacol 2005;67(2):400–7.

[585] Brismar H, Agren M, Holtback U. β-Adrenoceptor agonist sensitizes the dopamine-1 receptor in renal tubular cells. Acta Physiol Scand 2002;175(4):333–40.

[586] Carranza A, Nowicki S, Barontini M, Armando I. L-Dopa uptake and dopamine production in proximal tubular cells are regulated by β_2-adrenergic receptors. Am J Physiol Renal Physiol 2000;279(1):F77–83.

[587] Jenkins TA, Chai SY, Mendelsohn FA. Upregulation of angiotensin II AT1 receptors in the mouse nucleus accumbens by chronic haloperidol treatment. Brain Res 1997;748(1-2):137–42.

[588] Moore R, Krstew EV, Kirchhoff J, Davisson RL, Lawrence AJ. Central overexpression of angiotensin AT_{1A} receptors prevents dopamine D_2 receptor regulation of alcohol consumption in mice. Alcohol Clin Exp Res 2007;31(7):1128–37.

[589] Choi MR, Medici C, Gironacci MM, Correa AH, Fernández BE. Angiotensin II regulation of renal dopamine uptake and Na^+,K^+-ATPase activity. Nephron Physiol 2009;111(4):53–8.

[590] Eadington DW, Swainson CP, Frier BM, Johnston N, Samson RR, Lee MR. Urinary dopamine response to angiotensin II is not abnormal in type 1 (insulin-dependent diabetes mellitus. Nephrol Dial Transplant 1993;8(1):36–40.

[591] Chatziantoniou C, Ruan X, Arendshorst WJ. Interactions of cAMPmediated vasodilators with angiotensin II in rat kidney during hypertension. Am J Physiol 1993;265(6 Pt 2):F845–52.

[592] Lefèvre-Borg F, Lorrain J, Lechaire J, Thiry C, Hicks PE, Cavero I. Studies on the mechanisms of the development of

tolerance to the hypotensive effects of fenoldopam in rats. J Cardiovasc Pharmacol 1988;11(4):444–55.

[593] Luippold G, Max A, Albinus M, Osswald H, Mühlbauer B. Role of the renin-angiotensin system in the compensation of quinpirole-induced blood pressure decrease. Naunyn Schmiedebergs Arch Pharmacol 2003;367(5):427–33.

[594] Cheng HF, Becker BN, Harris RC. Dopamine decreases expression of type-1 angiotensin II receptors in renal proximal tubule. J Clin Invest 1996;97(12):2745–52.

[595] Mertens B, Vanderheyden P, Michotte Y, Sarre S. Direct angiotensin II type 2 receptor stimulation decreases dopamine synthesis in the rat striatum. Neuropharmacology 2010;58 (7):1038–44.

[596] Salomone LJ, Howell NL, McGrath HE, Kemp BA, Keller SR, Gildea JJ, et al. Intrarenal dopamine D_1-like receptor stimulation induces natriuresis via an angiotensin type-2 receptormechanism. Hypertension 2007;49(1):155–61.

[597] Correa AH, Choi MR, Gironacci M, Valera MS, Fernández BE. Signaling pathways involved in atrial natriuretic factor and dopamine regulation of renal Na^+, K^+ -ATPase activity. Regul Pept 2007;138(1):26–31.

[598] Winaver J, Burnett JC, Tyce GM, Dousa TP. ANP inhibits Na^+-H^+ antiport in proximal tubular brush border membrane: role of dopamine. Kidney Int 1990;38(6):1133–40.

[599] Castellano M, Beschi M, Agabiti-Rosei E, Rizzoni D, Rossini P, Poiesi C, et al. Renal and hemodynamic effects of atrial natriuretic peptide infusion are not mediated by peripheral dopaminergic mechanisms. Am J Hypertens 1991;4(4 Pt 1): 385–8.

[600] Stokes GS, Monaghan JC, Pillai DN. Effects of carbidopa and of intravenous saline infusion into normal and hypertensive subjects on urinary free and conjugated dopamine. J Hypertens 1997;15(7):761–8.

[601] Lucarini AR, Arrighi P, Favilla S, Simonini N, Salvetti A. The influence of dopamine-1 receptor blockade on the humoral and renal effects of low-dose atrial natriuretic factor in human hypertensives. J Hypertens Suppl 1989;7(6):S230–1.

[602] Kageyama S, Brown J, Causon R, O'Flynn M, Aber V. DOPA decarboxylase inhibition does not influence the diuretic and natriuretic response to exogenous alpha-atrial natriuretic peptide in man. Eur J Clin Pharmacol 1990;38(3):223–7.

[603] Lewis HM, Wilkins MR, Kendall MJ, Lee MR. Carbidopa does not affect the renal response to atrial natriuretic factor in man. Clin Sci (Lond) 1989;77(3):281–5.

[604] Hirata Y, Fukui K, Hayakawa H, et al. Renal effects of atrial natriuretic peptide during dopamine infusion. Am J Hypertens 1990;3(11):866–9.

[605] Webb RL, Della Puca R, Manniello J, Robson RD, Zimmerman MB, Ghai RD. Dopaminergic mediation of the diuretic and natriuretic effects of ANF in the rat. Life Sci 1986;38(25):2319–27.

[606] Hansell P, Fasching A, Sjoquist M, Anden NE, Ulfendahl HR. The dopamine receptor antagonist haloperidol blocks natriuretic but not hypotensive effects of the atrial natriuretic factor. Acta Physiol Scand 1987;130(3):401–7.

[607] Katoh T, Sophasan S, Kurokawa K. Permissive role of dopamine in renal action of ANP in volume-expanded rats. Am J Physiol 1989;257(2 Pt 2):F300–9.

[608] Ortola FV, Seri I, Downes S, Brenner BM, Ballermann BJ. Dopamine1-receptor blockade inhibits ANP-induced phosphaturia and calciuria in rats. Am J Physiol 1990;259(1 Pt 2): F138–46.

[609] Holtbäck U, Brismar H, DiBona GF, Fu M, Greengard P, Aperia A. Receptor recruitment: a mechanism for interactions between G protein-coupled receptors. Proc Natl Acad Sci USA 1999;96(13):7271–5.

[610] Soares-da-Silva P, Fernandes MH. Effect of α-human atrial natriuretic peptide on the synthesis of dopamine in the rat kidney. Br J Pharmacol 1992;105(4):869–74.

[611] Miyasaka K, Hosoya H, Takano S, Ohta M, Sekime A, Kanai S, et al. Differences in ethanol ingestion between cholecystokinin-A receptor deficient and -B receptor deficient mice. Alcohol Alcohol 2005;40(3):176–80.

[612] Li XM, Hedlund PB, Fuxe K. Cholecystokinin octapeptide in vitro and ex vivo strongly modulates striatal dopamine D2 receptors in rat forebrain sections. Eur J Neurosci 1995; 7(5):962–71.

[613] Dasgupta S, Li XM, Jansson A, Finnman UB, Matsui T, Rinken A, et al. Regulation of dopamine D_2 receptor affinity by cholecystokinin octapeptide in fibroblast cells cotransfected with human CCK_B and D_2L receptor cDNAs. Brain Res Mol Brain Res 1996;36(2):292–9.

[614] Roots K, Kairane C, Salum T, Koks S, Karelson E, Vasar E, et al. Very low levels of cholecystokinin octapeptide activate Na-pump in the cerebral cortex of CCK2 receptor-deficient mice. Int J Dev Neurosci 2006;24(6):395–400.

[615] Pisegna JR, Tarasova NI, Kopp JA, et al. Cholecystokinin type B receptors (CCKBRs) in the rat kidney mediate gastrin-stimulated urinary sodium excretion through inositol phosphate turnover (IP) and inhibition of Na^+/K^+ ATPase. Gastroenterology 2000;118(4): A301-A301

[616] Pollock JS, Pollock DM. Endothelin and NOS1/nitric oxide signaling and regulation of sodium homeostasis. Curr Opin Nephrol Hypertens 2008;17(1):70–5.

[617] Van Den Buuse M, Webber KM. Endothelin and dopamine release. Prog Neurobiol 2000;60(4):385–405.

[618] Zeng C, Asico LD, Yu C, Villar VA, Shi W, Luo Y, et al. Renal D_3 dopamine receptor stimulation induces natriuresis by endothelin B receptor interactions. Kidney Int 2008; 74(6):750–9.

[619] Dunham JH, Meyer RC, Garcia EL, Hall RA. GPR37 surface expression enhancement via N-terminal truncation or protein–protein interactions. Biochemistry 2009;48(43):10286–97.

[620] Kanyicska B, Freeman ME, Dryer SE. Endothelin activates large conductance K^+ channels in rat lactotrophs: Reversal by long-term exposure to dopamine agonist. Endocrinology 1997;138(8):3141–53.

[621] Hussain T, Beheray SA, Lokhandwala MF. Defective dopamine receptor function in proximal tubules of obese zucker rats. Hypertension 1999;34(5):1091–6.

[622] Umrani DN, Banday AA, Hussain T, Lokhandwala MF. Rosiglitazone treatment restores renal dopamine receptor function in obese Zucker rats. Hypertension 2002; 40(6):880–5.

[623] Tsuchida H, Imai G, Shima Y, Satoh T, Owada S. Mechanism of sodium load-induced hypertension in non-insulin dependent diabetes mellitus model rats: defective dopaminergic system to inhibit Na-K-ATPase activity in renal epithelial cells. Hypertens Res 2001;24(2):127–35.

[624] Trivedi M, Lokhandwala MF. Rosiglitazone restores renal D_{1A} receptor-G_s protein coupling by reducing receptor hyperphosphorylation in obese rats. Am J Physiol Renal Physiol 2005;289(2):F298–304.

[625] Carranza A, Musolino PL, Villar M, Nowicki S. Signaling cascade of insulin-induced stimulation of L-dopa uptake in renal proximal tubule cells. Am J Physiol Cell Physiol 2008;295(6): C1602–9.

[626] Umrani DN, Goyal RK. Fenoldopam treatment improves peripheral insulin sensitivity and renal function in STZ-induced type 2 diabetic rats. Clin Exp Hypertens 2003; 25(4):221–33.

[627] Moreira-Rodrigues M, Quelhas-Santos J, Serrão P, Fernandes-Cerqueira C, Sampaio-Maia B, Pestana M. Glycaemic control with insulin prevents the reduced renal dopamine D_1 receptor expression and function in streptozotocin-induced diabetes. Nephrol Dial Transplant 2010;25(9):2945–53.

[628] Rubı B, Ljubicic S, Pournourmohammadi S, Carrobio S, Armanet M, Bartley C, et al. Dopamine D_2-like receptors are expressed in pancreatic beta cells and mediate inhibition of insulin secretion. J Biol Chem 2005;280(44):36824–32.

[629] Shankar E, Santhosh KT, Paulose CS. Dopaminergic regulation of glucose-induced insulin secretion through dopamine D2 receptors in the pancreatic islets in vitro. IUBMB Life 2006; 58(3):157–63.

[630] Kok P, Roelfsema F, Frolich M, van Pelt J, Stokkel MP, Meinders AE, et al. Activation of dopamine D2 receptors simultaneously ameliorates various metabolic features of obese women. Am J Physiol Endocrinol Metab 2006;291(5): E1038–43.

[631] Zhang Y, Cincotta AH. Inhibitory effects of bromocriptine on vascular smooth muscle cell proliferation. Atherosclerosis 1997;133(1):37–44.

[632] Huang H, Han Y, Wang X, Chen C, Yu C, He D, et al. Inhibitory effect of the D_3 dopamine receptor on insulin receptor expression and function in vascular smooth muscle cells. Am J Hypertens 2011;24(6):654–60.

[633] Gross ML, Koch A, Mühlbauer B, Adamczak M, Ziebart H, Drescher K, et al. Renoprotective effect of a dopamine D3 receptor antagonist in experimental type II diabetes. Lab Invest 2006;86(3):262–74.

[634] Goto J, Otsuka F, Yamashita M, Suzuki J, Otani H, Takahashi H, et al. Enhancement of aldosterone-induced catecholamine production by bone morphogenetic protein-4 through activating Rho and SAPK/JNK pathway in adrenomedullar cells. Am J Physiol Endocrinol Metab 2009;296(4):E904–16.

[635] Robertson MJ, Horn NM, Chapman BJ. The depressor and renal vasodilator responses to dopamine in the rat do not depend on prostaglandin biosynthesis. J Pharm Pharmacol 1980;32(11):782–5.

[636] Glück Z, Jossen L, Weidmann P, Gnädinger MP, Peheim E. Cardiovascular and renal profile of acute peripheral dopamine1-receptor agonism with fenoldopam. Hypertension 1987;10(1):43–54.

[637] Zhang MZ, Yao B, McKanna JA, Harris RC. Cross talk between the intrarenal dopaminergic and cyclooxygenase-2 systems. Am J Physiol Renal Physiol 2005;288(4):F840–5.

[638] Grima G, Benz B, Parpura V, Cuénod M, Do KQ. Dopamine-induced oxidative stress in neurons with glutathione deficit: implication for schizophrenia. Schizophr Res 2003;62(3):213–24.

[639] Cosentino M, Rasini E, Colombo C, Marino F, Blandini F, Ferrari M, et al. Dopaminergic modulation of oxidative stress and apoptosis in human peripheral blood lymphocytes: evidence for a D1-like receptor-dependent protective effect. Free Radic Biol Med 2004;36(10):1233–40.

[640] Lu Q, Asico LD, Jones JE, et al. Impaired heme oxygenase activity, increased reactive oxygen species, and high blood pressure in D5 dopamine receptor deficient mice. J Am Soc Nephrol 2005;16: 163A-163A.

[641] Banday AA, Fazili FR, Lokhandwala MF. Oxidative stress causes renal dopamine D_1 receptor dysfunction and hypertension via mechanisms that involve nuclear factor-κB and protein kinase C. J Am Soc Nephrol 2007;18(5):1446–57.

[642] Asghar M, Banday AA, Fardoun RZ, Lokhandwala MF. Hydrogen peroxide causes uncoupling of dopamine D1-like receptors from G proteins via a mechanism involving protein kinase C and G-protein-coupled receptor kinase 2. Free Radic Biol Med 2006;40(1):13–20.

[643] Chugh G, Lokhandwala MF, Asghar M. Oxidative stress alters renal D1 and AT1 receptor functions and increases blood pressure in old rats. Am J Physiol Renal Physiol 2011;300(1): F133–8.

[644] Parvez S, Winkler-Stuck K, Hertel S, Schönfeld P, Siemen D. The dopamine-D2-receptor agonist ropinirole dose-dependently blocks the Ca^{2+}-triggered permeability transition of mitochondria. Biochim Biophys Acta 2010;1797(6-7):1245–50.

[645] Carvey PM, McGuire SO, Ling ZD. Neuroprotective effects of D3 dopamine receptor agonists. Parkinsonism Relat Disord 2001;7(3):213–23.

[646] Zou L, Xu J, Jankovic J, He Y, Appel SH, Le W. Pramipexole inhibits lipid peroxidation and reduces injury in the substantia nigra induced by the dopaminergic neurotoxin 1-methyl-4-phenyl-1,2,3,6-tetrahydropyridine in C57BL/6 mice. Neurosci Lett 2000;281(2-3):167–70.

[647] Le WD, Jankovic J, Xie W, Appel SH. Antioxidant property of pramipexole independent of dopamine receptor activation in neuroprotection. J Neural Transm 2000;107(10):1165–73.

[648] Gribkoff VK, Bozik ME. KNS-760704 [(6R)-4,5,6,7-tetrahydro-N6-propyl-2, 6-benzothiazole-diamine dihydrochloride monohydrate] for the treatment of amyotrophic lateral sclerosis. CNS Neurosci Ther 2008;14(3):215–26.

[649] Ishige K, Chen Q, Sagara Y, Schubert D. The activation of dopamine D4 receptors inhibits oxidative stress-induced nerve cell death. J Neurosci 2001;21(16):6069–76.

[650] Cosentino M, Fietta AM, Ferrari M, Rasini E, Bombelli R, Carcano E, et al. Human $CD4^+CD25^+$ regulatory T cells selectively express tyrosine hydroxylase and contain endogenous catecholamines subserving an autocrine/paracrine inhibitory functional loop. Blood 2007;109(2):632–42.

[651] Sarkar C, Basu B, Chakroborty D, Dasgupta PS, Basu S. The immunoregulatory role of dopamine: an update. Brain Behav Immun 2010;24(4):525–8.

[652] Ricci A, Bronzetti E, Mignini F, Tayebati SK, Zaccheo D, Amenta F. Dopamine D1-like receptor subtypes in human peripheral blood lymphocytes. J Neuroimmunol 1999;96 (2):234–40.

[653] McKenna F, McLaughlin PJ, Lewis BJ, Sibbring GC, Cummerson JA, Bowen-Jones D, et al. Dopamine receptor expression on human T- and B-lymphocytes, monocytes, neutrophils, eosinophils and NK cells: a flow cytometric study. J Neuroimmunol 2002;132(1-2):34–40.

[654] Nakano K, Yamaoka K, Hanami K, Saito K, Sasaguri Y, Yanagihara N, et al. Dopamine induces IL-6-dependent IL-17 production via D1-like receptor on CD4 naive T cells and D1-like receptor antagonist SCH-23390 inhibits cartilage destruction in a human rheumatoid arthritis/SCID mouse chimera model. J Immunol 2011;186(6):3745–52.

[655] Huang Y, Qiu AW, Peng YP, Liu Y, Huang HW, Qiu YH. Roles of dopamine receptor subtypes in mediating modulation of T lymphocyte function. Neuro Endocrinol Lett 2010;31 (6):782–91.

[656] Gomez F, Ruiz P, Briceño F, Rivera C, Lopez R. Macrophage Fcgamma receptors expression is altered by treatment with dopaminergic drugs. Clin Immunol 1999;90(3):375–87.

[657] Ghosh MC, Mondal AC, Basu S, Banerjee S, Majumder J, Bhattacharya D, et al. Dopamine inhibits cytokine release and expression of tyrosine kinases, Lck and Fyn in activated T cells. Int Immunopharmacol 2003;3(7):1019–26.

[658] Besser MJ, Ganor Y, Levite M. Dopamine by itself activates either D2, D3 or D1/D5 dopaminergic receptors in normal human T-cells and triggers the selective secretion

of either IL-10, TNFα or both. J Neuroimmunol 2005;169 (1-2):161–71.
[659] Haskó G, Szabó C, Merkel K, Bencsics A, Zingarelli B, Kvetan V, et al. Modulation of lipopolysaccharide-induced tumor necrosis factor-alpha and nitric oxide production by dopamine receptor agonists and antagonists in mice. Immunol Lett 1996;49(3):143–7.
[660] Morikawa K, Oseko F, Morikawa S. Immunosuppressive activity of bromocriptine on human T lymphocyte function in vitro. Clin Exp Immunol 1994;95(3):514–8.
[661] Ghosh MC, Mondal AC, Basu S, Banerjee S, Majumder J, Bhattacharya D, et al. Dopamine inhibits cytokine release and expression of tyrosine kinases, Lck and Fyn in activated T cells. Int Immunopharmacol 2003;3(7):1019–26.
[662] Godet C, Goujon JM, Petit I, Lecron JC, Hauet T, Mauco G, et al. Endotoxin tolerance enhances interleukin-10 renal expression and decreases ischemia-reperfusion renal injury in rats. Shock 2006;25(4):384–8.
[663] de Haij S, Woltman AM, Bakker AC, Daha MR, van Kooten C. Production of inflammatory mediators by renal epithelial cells is insensitive to glucocorticoids. Br J Pharmacol 2002;137 (2):197–204.
[664] Wang Y, Tay YC, Harris DC. Proximal tubule cells stimulated by lipopolysaccharide inhibit macrophage activation. Kidney Int 2004;66(2):655–62.
[665] Asghar M, Chugh G, Lokhandwala MF. Inflammation compromises renal dopamine D1 receptor function in rats. Am J Physiol Renal Physiol 2009;297(6):F1543–9.
[666] Zhang Y, Cuevas S, Asico LD, Escano C, Yang Y, Pascua AM, Wang LX, Jones JE, Grandy D, Eisner G, Jose PA, Armando I. Deficient dopamine D2 receptor function causes renal inflammation independently of high blood pressure. PLoS One 2012;7(6):e38745.
[667] Rafiq S, Anand S, Roberts R. Genome-wide association studies of hypertension: have they been fruitful? Cardiovasc Transl Res 2010;3(3):189–96.
[668] Harrap SB. Blood pressure genetics: time to focus. J Am Soc Hypertens 2009;3(4):231–7.
[669] Adeyemo A, Gerry N, Chen G, Herbert A, Doumatey A, Huang H, et al. A genome wide association study of hypertension and blood pressure in African-Americans. PLoS Genet 2009;5(7):e1000564.
[670] Cho YS, Go MJ, Kim YJ, Heo JY, Oh JH, Ban HJ, et al. A large-scale genome-wide association study of Asian populations uncovers genetic factors influencing eight quantitative traits. Nat Genet 2009;41(5):527–34.
[671] Johnson AD, Newton-Cheh C, Chasman DI, Ehret GB, Johnson T, Rose L, et al. Association of hypertension drug target genes with blood pressure and hypertension in 86 588 individuals. Hypertension 2011;57(5):903–10.
[672] Levy D, Ehret GB, Rice K. Genome-wide association study of blood pressure and hypertension. Nat Genet 2009;41(6):677–87.
[673] Newton-Cheh C, Johnson T, Gateva V, Tobin MD, Bochud M, Coin L, et al. Genome-wide association study identifies eight loci associated with blood pressure. Nat Genet 2009; 41(6):666–76.
[674] Wang Y, O'Connell JR, McArdle PF, Wade JB, Dorff SE, Shah SJ, et al. Whole-genome association study identifies STK39 as a hypertension susceptibility gene. Proc Natl Acad Sci USA 2009;106(1):226–321.
[675] Moore JH, Williams SM. New strategies for identifying gene-gene interactions in hypertension. Ann Med 2002;34(2):88–95.
[676] Glazier AM, Nadeau JH, Aitman TJ. Finding genes that underlie complex traits. Science 2002;298(5602):2345–9.
[677] Armando I, Jones JE, EscanoC, Asico L, Premont RT, Jose PA. Deletion of the GRK4 gene decreases blood pressure and reverses salt sensitivity. Proc Am Soc Hypertens 2008;:P-194.
[678] Allayee H, de Bruin TW, Michelle Dominguez K, Cheng LS, Ipp E, Cantor RM, et al. Genome scan for blood pressure in Dutch dyslipidemic families reveals linkage to a locus on chromosome 4p. Hypertension. 2001;38(4):773–8.
[679] Chen W, Li S, Srinivasan SR, Boerwinkle E, Berenson GS. Autosomal genome scan for loci linked to blood pressure levels and trends since childhood: the Bogalusa Heart Study. Hypertension 2005;45(5):954–9.
[680] Zhu H, Lu Y, Wang X, Treiber FA, Harshfield GA, Snieder H, et al. The G protein-coupled receptor kinase 4 gene affects blood pressure in young normotensive twins. Am J Hypertens 2006;19(1):61–6.
[681] Bengra C, Mifflin TE, Khripin Y, Manunta P, Williams SM, Jose PA, et al. Genotyping of essential hypertension single-nucleotide polymorphisms by a homogeneous PCR method with universal energy transfer primers. Clin Chem 2002;48 (12):2131–40.
[682] Gu D, Su S, Ge D, Chen S, Huang J, Li B, et al. Association study with 33 single-nucleotide polymorphisms in 11 candidate genes for hypertension in Chinese. Hypertension 2006;47 (6):1147–54.
[683] Sanada H, Yatabe J, Midorikawa S, Hashimoto S, Watanabe T, Moore JH, et al. Single-nucleotide polymorphisms for diagnosis of salt-sensitive hypertension. Clin Chem 2006; 52(3):352–60.
[684] Speirs HJ, Katyk K, Kumar NN, Benjafield AV, Wang WY, Morris BJ. Association of G-protein-coupled receptor kinase 4 haplotypes, but not HSD3B1 or PTP1B polymorphisms, with essential hypertension. J Hypertens 2004;22(5):931–6.
[685] Williams SM, Ritchie MD, Phillips III JA, Dawson E, Prince M, Dzhura E, et al. Multilocus analysis of hypertension: a hierarchical approach. Hum Hered 2004;57(1):28–38.
[686] Williams SM, Addy JH, Phillips 3rd JA, Dai M, Kpodonu J, Afful J, et al. Combinations of variations in multiple genes are associated with hypertension. Hypertension 2000;36(1):2–6.
[687] Zeng C, Villar VA, Eisner GM, Williams SM, Felder RA, Jose PA. G protein-coupled receptor kinase 4: Role in blood pressure regulation. Hypertension 2008;51(6):1449–55.
[688] Wang Y, Li B, Zhao W, Liu P, Zhao Q, Chen S, et al. Association study of G protein-coupled receptor kinase 4 gene variants with essential hypertension in northern Han Chinese. Ann Hum Genet 2006;70(Pt 6):778–83.
[689] Rana BK, Insel PA, Payne SH, Abel K, Beutler E, Ziegler MG, et al. Population-based sample reveals gene-gender interactions in blood pressure in White Americans. Hypertension 2007;49(1):96–106.
[690] Staessen JA, Kuznetsova T, Zhang H, Maillard M, Bochud M, Hasenkamp S, et al. Blood pressure and renal sodium handling in relation to genetic variation in the DRD1 promoter and GRK4. Hypertension 2008;51(6):1643–50.
[691] Wang Z, Armando I, Asico LD, Escano C, Wang X, Lu Q, et al. The elevated blood pressure of human GRK4γ A142V transgenic mice is not associated with increased ROS production. Am J Physiol Heart Circ Physiol 2007;292(5):H2083–92.
[692] Wang Z, Asico LD, Escano CS, Felder RA, Jose PA. Human G protein coupled receptor kinase type 4 (hGRK4 γ) wild-type prevents salt sensitivity while its variant, hGRK4γ 486V, promotes salt sensitivity in transgenic mice: role of genetic background [Abstract]. Hypertension 2006;48:e27.
[693] Doris PA. Promoting regulatory gene variation in sodium reabsorption. Hypertension 2008;52(4):623–4.

[694] Sato M, Soma M, Nakayama T, Kanmatsuse K. Dopamine D1 receptor gene polymorphism is associated with essential hypertension. Hypertension 2000;36(2):183–6.
[695] Sanada H, Jose PA, Hazen-Martin D, Yu PY, Xu J, Bruns DE, et al. Dopamine-1 receptor coupling defect in renal proximal tubule cells in hypertension. Hypertension 1999;33(4):1036–42.
[696] Soma M, Nakayama K, Rahmutula D, Uwabo J, Sato M, Kunimoto M, et al. Ser9Gly polymorphism in the dopamine D3 receptor gene is not associated with essential hypertension in the Japanese. Med Sci Monit 2002;8(1):CR1–4.
[697] Sen S, Nesse R, Sheng L, Stoltenberg SF, Gleiberman L, Burmeister M, et al. Association between a dopamine-4 receptor polymorphism and blood pressure. Am J Hypertens 2005;18(9 Pt 1):1206–10.
[698] Cravchik A, Gejman PV. Functional analysis of the human D5 dopamine receptor missense and nonsense variants: differences in dopamine binding affinities. Pharmacogenetics 1999; 9(2):199–206.
[699] De Brito Gariepy H, Carayon P, Ferrari B, Couture R. Contribution of the central dopaminergic system in the anti-hypertensive effect of kinin B1 receptor antagonists in two rat models of hypertension. Neuropeptides 2010; 44(2):191–8.
[700] Sawamura T, Nakada T. Role of dopamine in the striatum, renin–angiotensin system and renal sympathetic nerve on the development of two-kidney, one-clip Goldblatt hypertension. J Urol 1996;155(3):1108–11.
[701] Moore TL, Killiany RJ, Rosene DL, Prusty S, Hollander W, Moss MB. Hypertension-induced changes in monoamine receptors in the prefrontal cortex of rhesus monkeys. Neuroscience 2003;120(1):177–89.
[702] Fujita S, Adachi K, Lee J, Uchida T, Koshikawa N, Cools AR. Decreased postsynaptic dopaminergic and cholinergic functions in the ventrolateral striatum of spontaneously hypertensive rat. Eur J Pharmacol 2004;484(1):75–82.
[703] Bhatnagar V, O'Connor DT, Brophy VH, Schork NJ, Richard E, Salem RM, et al. G-protein-coupled receptor kinase 4 polymorphisms and blood pressure response to metoprolol among African Americans: sex-specificity and interactions. Am J Hypertens 2009;22(3):332–8.
[704] Vandell AG, Lobmeyer MT, Gawronski BE, Langaee TY, Gong Y, Gums JG, et al. G protein receptor kinase 4 polymorphisms: β-Blocker Pharmacogenetics and treatment-related outcomes in Hypertension. Hypertension 2012;60(4):957–64.
[705] Leineweber K, Rohe P, Beilfuss A, Wolf C, Sporkmann H, Bruck H, et al. G-protein-coupled receptor kinase activity in human heart failure: effects of β-adrenoceptor blockade. Cardiovasc Res 2005;66(3):512–9.
[706] Rayner B, Ramesar R, Steyn K, Levitt N, Lombard C, Charlton K. G-protein-coupled receptor kinase 4 polymorphisms predict blood pressure response to dietary modification in Black patients with mild-to-moderate hypertension. J Hum Hypertens 2011; 26(5):334–9.
[707] Sanada H, Yatabe J, Yatabe MS, et al. G Protein-coupled receptor type 4 gene variants and response to antihypertensive medication. Circulation 2009;120(18):S1087 (Abstract 5413)
[708] Grant FD, Romero JR, Jeunemaitre X, Hunt SC, Hopkins PN, Hollenberg NH, Williams GH. Low-renin hypertension, altered sodium homeostasis, and an α-adducin polymorphism. Hypertension 2002;39(2):191–6.
[709] Sugimoto K, Hozawa A, Katsuya T, Matsubara M, Ohkubo T, Tsuji I, et al. α-Adducin Gly460Trp polymorphism is associated with low renin hypertension in younger subjects in the Ohasama study. J Hypertens 2002;20(9):1779–84.
[710] Lohmueller KE, Wong LJ, Mauney MM, Jiang L, Felder RA, Jose PA, Williams SM. Patterns of genetic variation in the hypertension candidate gene GRK4: ethnic variation and haplotype structure. Ann Hum Genet 2006;70(Pt 1): 27–41.

This page intentionally left blank

SECTION 2

STRUCTURAL AND FUNCTIONAL ORGANIZATION OF THE KIDNEY

This page intentionally left blank

CHAPTER

20

Structural Organization of the Mammalian Kidney

Wilhelm Kriz[1] *and Brigitte Kaissling*[2]

[1]Department of Anatomy and Developmental Biology, Medical Faculty Mannheim, University of Heidelberg, Mannheim, Germany

[2]Institute for Anatomy, University of Zürich, Switzerland

KIDNEY TYPES AND RENAL PELVIS

The mammalian kidney is multiform. The basic architecture is best understood in the unipapillary kidney, which is common in all small species. A coronal section of this kidney shows the main structural parts (Figure 20.1a). The renal cortex, as a whole, is cup-shaped with inverted margins, and surrounds the renal medulla. The medulla can be roughly compared to a pyramid; its top portion, the papilla, projects into the renal pelvis. The pelvis is located within the renal sinus, which opens through the renal hilum to the medial surface of the kidney.

The cortical parenchyma is divided into the cortical labyrinth and the medullary rays. The uppermost part of the cortex, a continuous layer that covers the tops of the medullary rays, is called the cortex corticis. The medulla is divided into an outer medulla (subdivided into outer and inner stripes) and an inner medulla. The innermost part of the inner medulla generally forms the papilla.

The unipapillary kidney is the most simple kidney type; in comparative anatomy, such a kidney as a whole corresponds to a renculus. All other kidney types may be regarded as adaptations to larger body sizes. The crest kidney and the kidney with tubi maximi are magnifications of a one-reniculus unit. The multipapillary kidney (Figure 20.2) and the reniculus kidney multiply this unit.[1,2,3] The human kidney is a multipapillary kidney; however, it is particular because a variable number of papillae are generally fused, forming compound papillae.[4]

The renal pelvis (Figures 20.1a and b) or the renal calyces (Figure 20.2) are anchored to the renal parenchyma by connective and smooth-muscle tissues that follow the intrarenal arteries. The cavity of the pelvis and calyx surrounds the renal papilla (or its equivalent in other kidney types). In many species the pelvic cavity forms different kinds of pelvic extensions (Figure 20.1b).[5,6] Leaf-like extensions called "specialized fornices" accompany the large vessels for some distance along their entry into the renal parenchyma. Secondary pouches protrude toward the hilus, communicating with the primary pelvic cavity only above the free semilunar borders of the pelvic septa. These extensions increase the contact area between the pelvic cavity and the renal medulla, especially the outer medulla.[7]

RENAL VASCULATURE

Close to the renal hilum and afterwards within the renal sinus the renal artery undergoes several divisions, finally establishing the interlobar arteries which then enter the renal tissue at the border between the cortex and medulla (Figures 20.1a and 20.2). From there they follow an arc-like course and are therefore called arcuate arteries. They give rise to the cortical radial arteries, which ascend radially within the cortical labyrinth. The cortex is very densely penetrated by arteries; in contrast, no arteries enter the medulla. The renal veins (cortical radial (interlobular) veins, arcuate veins) accompany the corresponding arteries. In some species (cat, dog, man) the venous blood from the outer

Seldin and Giebisch's The Kidney, Fifth Edition.
DOI: http://dx.doi.org/10.1016/B978-0-12-381462-3.00020-3

© 2013 Elsevier Inc. All rights reserved.

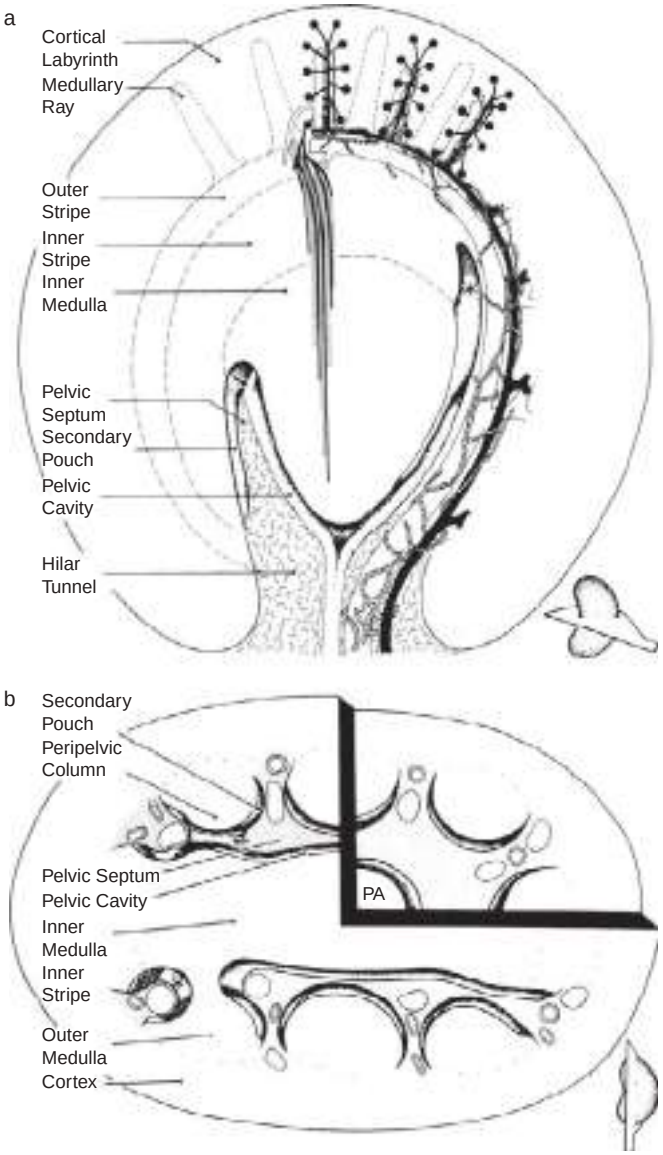

FIGURE 20.1 **Schematics of a coronal and two transverse (b) sections through the rabbit kidney.** The inset in the right lower corner indicates the section plane. The general architecture of the kidney and the renal pelvis is demonstrated. (a) Arterial vessels, including glomeruli and descending vasa recta, are shown in black, venous vessels are gray, and lymphatics are hatched. (b) The section plane of the main drawing runs through the middle part of the inner medulla; a deeper section through the papilla (PA) is shown in the upper right quarter. The cross-sectioned pelvic septa are stippled. The leaf-like extensions of the pelvic cavity are marked by a star, the free semilunar edges of the main pelvic septa by an arrow (in a and b). *(Adapted from Kaissling, B., and Kriz, W. (1979). Structured analysis of the rabbit kidney. Adv. Anat. Embryol. Cell Biol.* ***56****, 1–123, with permission.)*

cortex drains into veins on the renal surface (in man called "stellate veins") which are connected by additional cortical radial veins (interlobular veins) to arcuate veins. Such additional veins are not accompanied by arteries.[8]

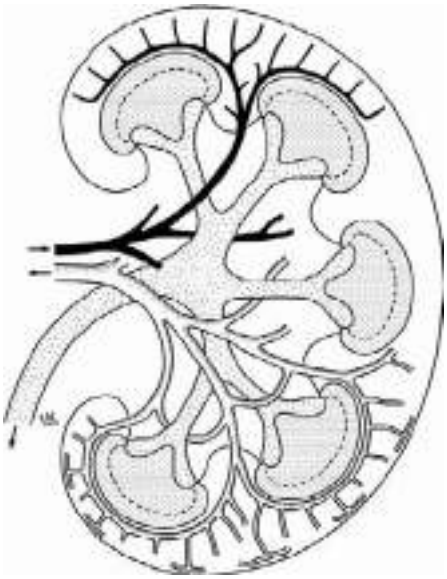

FIGURE 20.2 **Schematic illustration of a compound multipapillary kidney (coronal section) similar to the human kidney.** The renal cortex as a whole encloses several papillae; fused papillae typical for the human kidney are not shown. The central region, the renal sinus, contains the calyces and the pelvis (stippled), the pattern of branching arteries (black), and joining veins (white). The arcuate arteries, running at the cortico-medullary border, do not form true arches, but rather represent end-arteries. In contrast, the veins do form anastomoses at the level of the arcuate and interlobar veins. In the human kidney there are two types of cortical radial veins (interlobular veins); one group starting as stellate veins drains the most superficial cortex, the second group starts at deeper levels in the cortex; both drain into arcuate veins.

The microvasculature pattern of the kidney appears to be very similar among mamma*lian species; a basic pattern can be described (Figures 20.3 and 20.4a).[9–11] The afferent arterioles arise from the cortical radial arteries (a minor portion from the arcuate arteries) and supply the glomerular tufts of the renal corpuscles. The efferent arterioles drain the glomeruli. Several types of efferent arterioles have been described.[11,12] Basically, a distinction between superficial, midcortical, and juxtamedullary renal corpuscles is essential (Figures 20.3 and 20.5). The efferent arterioles of juxtamedullary glomeruli turn toward the medulla; they supply the medulla. Juxtamedullary glomeruli are best defined by this type of efferent arteriole. The superficial efferent arterioles extend to the kidney surface before dividing. Again, superficial glomeruli are best defined because of the typical pattern of their efferent arterioles. The efferent arterioles of midcortical nephrons (defined by exclusion) vary in length between those that branch abruptly near the glomerulus and others that extend to a medullary ray before splitting off into capillaries. All the efferent arterioles together (superficial, midcortical, and also small

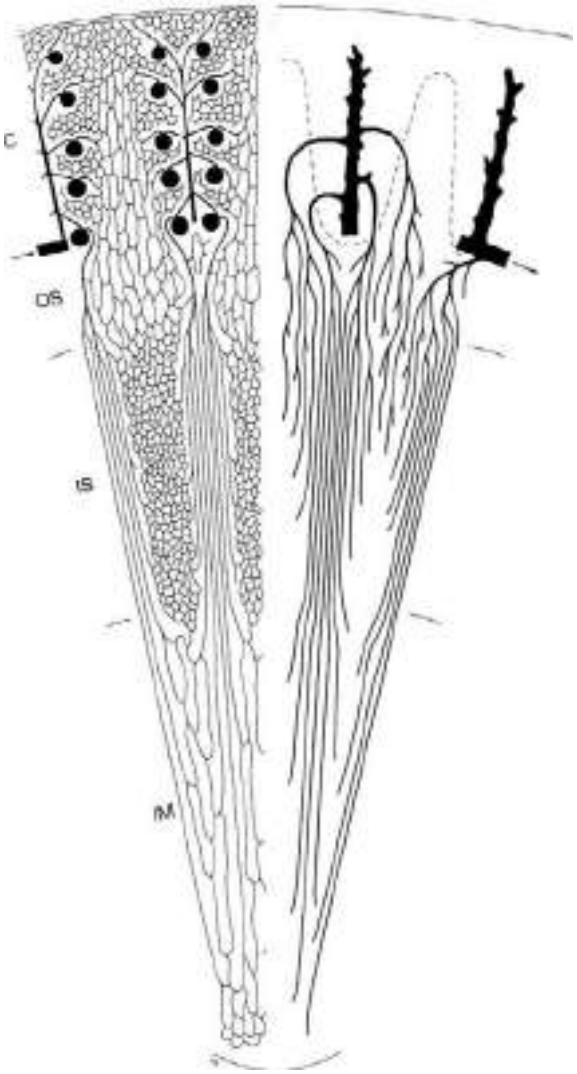

FIGURE 20.3 **Schematic of the microvasculature of the rat kidney** (C: cortex; OS: outer stripe; IS: inner stripe; IM: inner medulla). The left panel shows the arterial vessels and capillaries. An arcuate artery (arrow) gives rise to a cortical radial (interlobular) artery, from which afferent arterioles originate to supply the glomeruli. The efferent arterioles of the juxtamedullary glomeruli descend into the medulla and divide into the descending vasa recta, which, together with ascending vasa recta, form the vascular bundles of the renal medulla. At intervals, descending vasa recta leave the bundles to feed the adjacent capillaries. The right panel shows the venous vessels. The interlobular veins start in the superficial cortex. In the inner cortex they, together with the arcuate veins, receive the ascending vasa recta from the medulla. The vasa recta ascending from the inner medulla all traverse the inner stripe within the vascular bundles, whereas most of the vasa recta from the inner stripe ascend outside the bundles. Both of these types of ascending vasa recta traverse the outer stripe as wide, tortuous channels. *(Adapted from Kriz, W., and Lever, A. F. (1969). Renal countercurrent mechanisms: Structure and function. Am. Heart J.* ***78****(1), 101–118 and Rollhaeuser, H., and Kriz, W. (1964). The vascular system of the rat kidney. Z. Zellforsch. Mikrosk. Anat.* ***64****, 381–403, with permission.)*

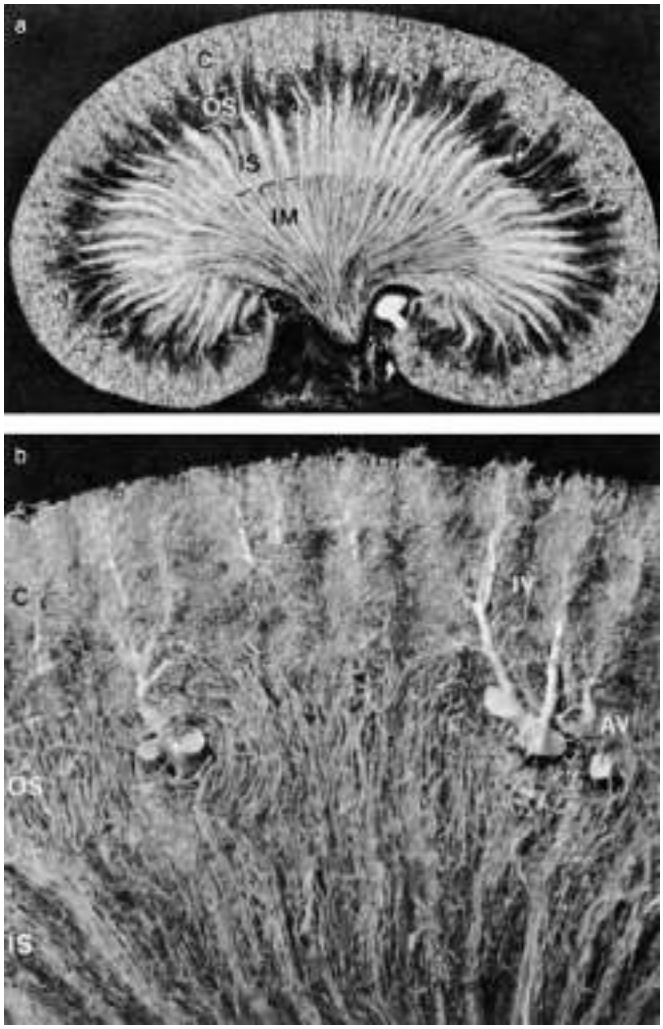

FIGURE 20.4 **Microvasculature.** (a) Rat kidney; silicon rubber (Microfil) filling of the arterial vessels. Cortex (C), outer stripe (OS), inner stripe (IS), and inner medulla (IM) are clearly distinguishable by their vessel patterns. The vascular bundles take shape along the OS and are best developed within the IS. Only a minor part of the descending vasa recta of each bundle enter the IM, where they gradually decrease in number toward the papilla. Note the scantiness of capillaries in the OS (×8). (b) Rabbit kidney; silicon rubber filling of the venous vessels. The interlobular veins (IV) accept the cortical capillaries and a major part of the ascending vasa recta. Note the density of ascending vasa recta within the OS. In the IS, ascending vasa recta are found within the bundles (mostly originating from the IM) and between the vascular bundles (draining the interbundle regions of the IS) (AV: arcuate vein; ×14). *(In cooperation with L. Bankir.)*

branches of the juxtamedullary efferent arterioles) supply the cortical peritubular capillaries. Direct aglomerular arterial supplies to the peritubular capillaries or to the medulla are sparse[13] and have frequently been shown to be the result of degeneration of the corresponding glomeruli.[14]

Within the capillary network of the cortex (Figures 20.3 and 20.4), a differentiation between two parts is necessary: namely, the dense, round-meshed

FIGURE 20.5 **Arterial vessels after filling with silicone rubber; rabbit kidney.** The broken lines show the renal surface and the corticomedullary border. Arcuate arteries (AA) give rise to cortical radial arteries which split into the afferent arterioles. The efferent arterioles of superficial glomeruli (arrow) ascend unbranched to the kidney surface before splitting into capillaries. The efferent arterioles of juxtamedullary nephrons (arrowheads) descend into the outer stripe and devide into the descending vasa recta (×80). *(From ref. [5].)*

capillary plexus of the cortical labyrinth (including the cortex corticis); and the less dense, long-meshed plexus of the medullary rays, both associated with the course of the tubules. Functionally these two plexuses are different with respect to their drainage. The blood from the medullary ray plexus has to pass the plexus of the cortical labyrinth to gain access to the interlobular veins. Therefore, the blood that has perfused the straight tubules within the medullary rays mixes with the blood that perfuses the convoluted tubules of the cortical labyrinth.

The medulla (Figures 20.3, 20.4, and 20.5) is exclusively supplied by the efferent arterioles of the juxtamedullary glomeruli.[5,8,10,11,15,16] These efferent arterioles descend through the outer stripe and divide into the descending vasa recta. In addition, the efferent arteriole and its first divisions give rise to small side branches that supply the sparse capillary plexus of the outer stripe of the outer medulla. This plexus is continuous with the cortical capillary plexus above and the capillary plexus of the inner stripe below. The descending vasa recta then penetrate the inner stripe of the outer medulla in cone-shaped vascular bundles. At intervals, descending vasa recta leave the bundles to join the capillary plexus at the adjacent medullary level, most leaving the bundle within the inner stripe. Only a small portion of the descending vasa recta penetrate the inner medulla, and even fewer reach the tip of the papilla.

The capillary plexuses of the renal medulla (Figures 20.3 and 20.4a) differ in the three regions. That of the outer stripe is sparse. In contrast, the capillary plexus of the inner stripe is very dense and characteristically round-meshed in appearance. In the inner medulla the capillary plexus is less dense and long-meshed.

The ascending vasa recta are the draining vessels of the renal medulla (Figures 20.3 and 20.4b). In the inner medulla they arise at every level and ascend as unbranched vessels to the border between the inner and outer medulla. At this point, they join the vascular bundles and traverse the inner stripe of the outer medulla within the vascular bundles. The ascending vasa recta, which drain the inner stripe, behave differently. Those of the lowermost part of the inner stripe (and therefore probably a minor portion) join the bundles as they pass through this region. Those from the middle and upper part (and thus probably the majority) do not join the bundles, but ascend directly within the interbundle regions to the outer stripe. There are, however, interspecies differences; in the sand rat (*Psammomys obesus*), all ascending vasa recta that drain the inner stripe ascend directly to the outer stripe without joining the bundles.[17]

Within the outer stripe, the vasa recta ascending within the bundles spread out and, together with the directly ascending vasa recta, traverse the outer stripe as individual tortuous channels with wide lumina (Figure 20.4b). They contact the tubules like true capillaries, and because the true capillaries which are derived from direct branches of efferent arterioles are few in the outer stripe (Figure 20.3a), they mainly affect the blood supply to the tubules in this region. At the corticomedullary border, the ascending venous vessels of the medulla empty into the arcuate veins or into the basal parts of interlobular veins. In some species, such as rat, guinea pig, and especially the sand rat (*Psammomys obesus*) some of the venous medullary vessels continue to ascend within the medullary rays of the cortex and finally empty into middle or even upper parts of interlobular veins.

Wall Structure of Intrarenal Vessels

The intrarenal arteries and the proximal portions of the afferent arterioles appear to be similar to arteries and arterioles of the same size elsewhere in the body. The terminal portions of the afferent arterioles are unique because of the occurrence of granular cells (renin producing cells) which replace ordinary smooth muscle cells in their wall.[18] It is generally agreed that granular cells are modified smooth muscle cells. Compared to proper smooth muscle cells, granular cells contain less myofilaments; thus, the contractile capacity of the very last portion of the afferent arteriole appears to be considerably decreased.[19] The endocrine function of granular cells will be considered later in the context of the juxtaglomerular apparatus. The glomerular capillaries will be described together with the glomerulus.

Efferent arterioles are already established inside the glomerular tuft. Thus, in contrast to afferent arterioles, efferent arterioles have an intraglomerular segment which passes through the glomerular stalk[20,21] (Figure 20.6a). After this, efferent arterioles have a segment which is narrowly associated with the extraglomerular mesangium (details will be given later in the context of the glomerulus). Thereafter, the efferent arterioles are established as arterioles with a proper media made up of smooth muscle cells.

Efferent arterioles from juxtamedullary glomeruli differ considerably from those of cortical (midcortical and superficial) glomeruli (compare Figures 20.6b and 20.6c). Juxtamedullary efferent arterioles are larger in diameter than cortical efferent arterioles; their size even exceeds that of their corresponding afferent arterioles. In the rabbit, the diameters of afferent arterioles throughout the cortex average approximately 20 μm; juxtamedullary efferent arterioles average 28 μm, and cortical efferent arterioles average only 12 μm.[22] Similar differences have been found in dog,[12] rat,[23] and human[24] kidneys.

Cortical efferent arterioles (Figure 20.6b) are only sparsely equipped with smooth muscle cells (generally not more than one layer). A striking feature of efferent arterioles (including those from juxtamedullary glomeruli) is the thick, irregular basement membrane. In contrast to the usual appearance of a basement membrane, basement membrane-like material fills the wide and irregular spaces between the endothelium and the muscle layer. The juxtamedullary efferent arterioles (Figure 20.6c) are surrounded by two to four layers of smooth muscle cells. Their endothelium is composed of a strikingly large number of longitudinally arranged cells; up to 30 individual cells may be found in cross-sections.[23,25]

In the descending vasa recta (Figure 20.6d) the smooth muscle cells are gradually replaced by

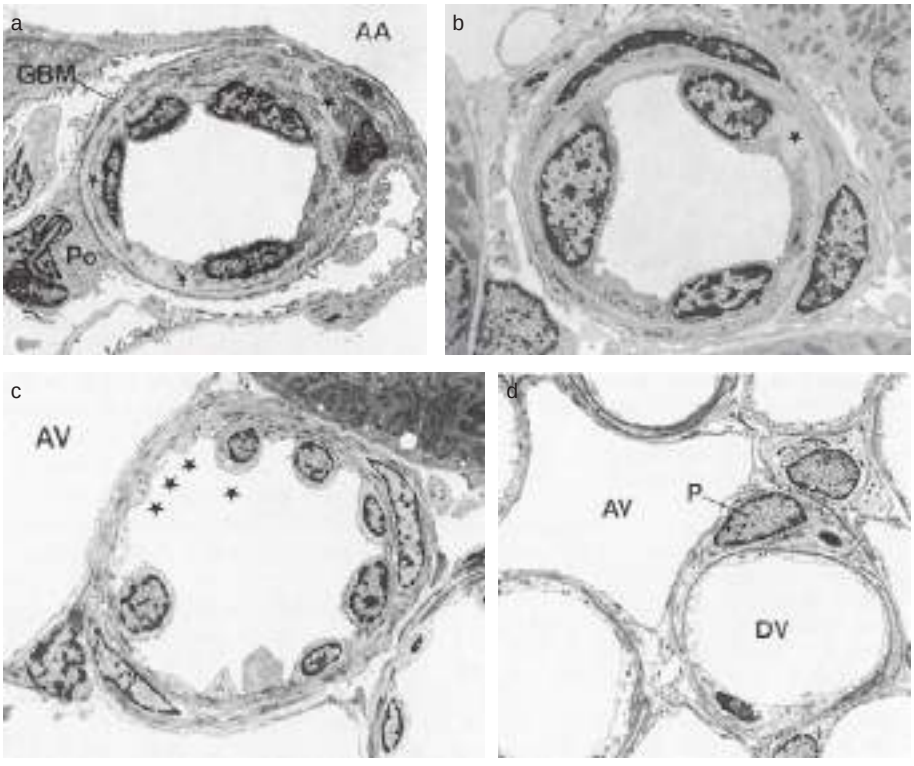

FIGURE 20.6 **Efferent arteriole.** (a) Intraglomerular segment of the efferent arteriole. Between the basement membrane (GBM) and the endothelium a mesangial layer is interposed. Note the intimate relationships of the afferent arteriole (AA) to the mesangium. PO: podocyte (Rat; TEM ×~4600). **(b)** Efferent arteriole of a superficial glomerulus. Note the irregular basement membrane-like material beneath the endothelium **(*)**. One to two layers of smooth muscle cells (SM) are encountered (Rabbit; TEM ×~3400). **(c)** Efferent arteriole of a juxtamedullary glomerulus. Note the many profiles of endothelial cells **(*)**; the tight junctions between them are shallow (Rat; TEM ×~2450). **(d)** Descending (DV) and ascending (AV) vasa recta of a vascular bundle are shown. The continuous endothelium of the descending vas rectum is surrounded by a pericyte (P). The endothelium of the ascending vas rectum is highly fenestrated **(**arrows**)** (Rabbit; TEM ×~2400).

pericytes, which form an incomplete layer around the vessel trunk. Pericytes should be regarded as contractile cells. The pattern of these cells, which encircle the endothelial tube-like hoops, and their dense assemblys of microfilaments strongly imply that they have a contractile function. In contrast to smooth muscle cells, they are not contacted by nerve terminals. The descending vasa recta finally lose their pericytes, and the concurrent appearance of endothelial fenestrations marks their gradual transformation into medullary capillaries.

The ultrastructure of the capillaries in the kidney is similar in both the cortex and the medulla (with the exception of glomerular capillaries; *vide infra*). The capillaries of the kidney are of the fenestrated type (Figure 20.7). The capillary wall consists of an extremely flat endothelium surrounded by a thin basement membrane. In non-nuclear regions the endothelial cells contain densely and regularly arranged fenestrations that (in contrast to the glomerular capillaries) are bridged by a thin diaphragm. An estimated 50% of the capillary circumference is composed of these fenestration-bearing areas.[23] The fenestrations themselves are of rather complex structure. In normal TEM sections the diaphragm appears as a very thin (5–6 nm) single-layered proteinaceous membrane provided with a central knob. Deep-etch freezing techniques have revealed a composition of radial fibrils converging to the central knob.[26] So far only one protein, PV1, a caveolar transmembrane protein, has been attributed to the diaphragm.[27] The diaphragm is considered to be permeable to water and small water-soluble substances.

FIGURE 20.7 **Freeze-fracture electron micrograph demonstrating the dense arrangement of fenestrations within the wall of a peritubular capillary (rabbit).** Pinocytotic vesicles (arrows) are found within areas of thicker cytoplasm, which connect the perikaryon and the more voluminous areas along the cell borders (not shown) (×7600). *(In cooperation with A. Schiller and R. Taugner.)*

The wall structure of the ascending vasa recta (Figure 20.6d) is similar to that of the capillaries. These draining vessels, with wide lumina, are bound for their entire length by an extremely flat endothelium with extensive fenestrations. The same structure is found in the large veins of the cortex and at the corticomedullary border (Figures 20.8 and 20.15). The interlobular and arcuate veins are not veins in the classic sense, but they have a wall structure fundamentally the same as that of the renal capillaries.[9,23] This wall consists solely of an extremely flattened, partly fenestrated endothelium that rests on a basement membrane.

NEPHRONS AND COLLECTING DUCT SYSTEM

The specific structural units of the kidney are the nephrons. In the rat, each kidney contains 30,000 to 35,000 nephrons[28]; each human kidney has an estimated 1 million,[29] but great interindividual differences exist.[30,31]

The nephron consists of a renal corpuscle connected to a complicated and twisted tube that finally drains into a collecting duct. Based on the location of the renal corpuscles within the cortex, three types of nephrons are distinguished: superficial; midcortical; and juxtamedullary nephrons. Exact definitions of these types, grounded on more than arbitrary decisions, can be based on the different patterns of the efferent arterioles (*vide supra*).

The tubular part of the nephron consists of a proximal and a distal portion connected by a loop of Henle. For details of subdivisions, see Figures 20.9 and 20.10.

According to the lengths of the loops of Henle, two types of nephrons are distinguished (Figure 20.9): those with long loops and those with short loops (including those with cortical loops). Short loops turn back in the outer medulla. In many species (rat, rabbit), the bends of the short loops are all located roughly at the same level of the inner stripe, namely, near the junction to the inner medulla. In other species (pig and human), short loops may form their bends at any level of the outer medulla, and even in the cortex (cortical loops).

The long loops turn back at successive levels of the inner medulla, many at its start; others reach intermediate levels, and only a few reach the tip of the papilla. Thus, the number of loops is successively reduced along the inner medulla toward the papilla. This decrease is paralleled by a decrease in collecting ducts

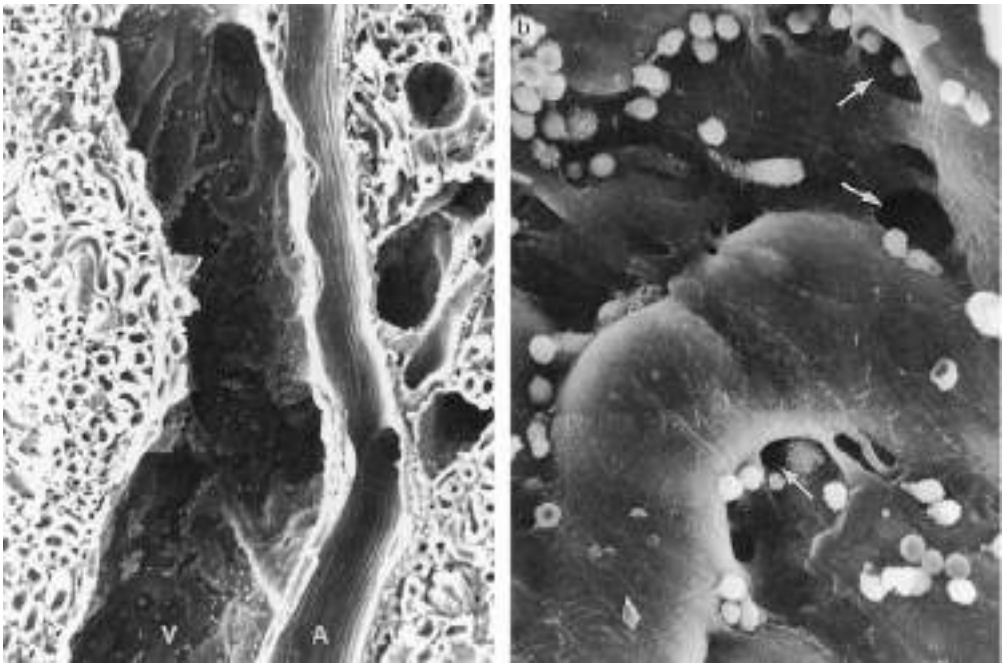

FIGURE 20.8 **Scanning electron micrographs of the inner surface of an arcuate artery and vein (Rat).** (a) The tubules underneath the venous wall are clearly discernible through the endothelium, which covers the tubules as a thin coat. (b) Higher magnification of the venous endothelium. The openings in the endothelial wall (arrows) mark the positions where venous vasa recta and capillaries empty into the vein. (a) ×~120; (b) ×~1900. *(From Frank, M., and Kriz, W. (1988). The luminal aspect of intrarenal arteries and veins in the rat as revealed by scanning electron microscopy. Anat. Embryol. (Berl) **177**(4), 371–376, with permission.)*

and vasa recta, leading to the characteristic form of the inner medulla, which in all species tapers from a broad basis to a papilla (or crest).

The division of nephrons according to the position of their corpuscles in the cortex does not coincide with the division based on the length of their loops. Among species, all three types of renal corpuscles may be attached to both short and long loops. However, within a given species (with short and long loops), the long loops always belong to the deeper renal corpuscles (i.e., juxtamedullary and deep midcortical) and the short loops to the more superficially situated corpuscles.

The number of short and long loops varies among species. Some species have only short loops (mountain beaver, muskrat), and consequently lack an inner medulla, which results in a poor ability to concentrate urine.[6] Only two species, cat and dog, are known to have just long loops. In comparison with other species, their urine concentrating ability is considered to be average. In the cat, however, many long loops penetrate into the inner medulla for a very short distance (less than 0.5 μm. Defining a loop by ultrastructural criteria (*vide infra*), a feline kidney does contain many loops resembling the short loops in other species. The formerly held presumption that rodent species with the most powerful ability to concentrate urine, like *Psammomys* or *Meriones*, have only long loops has been proved incorrect.[32] Most species have short and long loops whose ratio varies from species to species. A correlation between the ratio of short and long loops and urine concentrating ability is not obvious. Most rodent species that have a high urine concentrating ability (rat, mouse, golden hamster, *Psammomys*, *Meriones*) have more short loops than long loops.[32–34]

The collecting ducts are formed in the renal cortex by the joining of several nephrons (Figures 20.9 and 20.10). The location of the exact border between a nephron and a collecting duct is disputed. According to cytological criteria, a connecting tubule is interposed between a nephron and a cortical collecting duct. Whether this connecting tubule derives from the nephrogenic blastema, and therefore must be considered as a part of the nephron, or from the ureteral bud, and therefore is part of the collecting ducts, remains an open question.

Microanatomically, the connecting tubules of deep and superficial nephrons differ (Figure 20.9). The connecting tubules of deep nephrons generally join to form an arcade before draining into a collecting duct; superficial nephrons drain via an individual connecting tubule. The numerical ratio between nephrons draining through an arcade and those draining individually varies greatly among species. In rat, rabbit, and pig, the majority of nephrons drain via arcades; as Sperber[3] observed, some arcades probably exist in all mammalian kidneys. An arcade ascends within the cortical labyrinth before

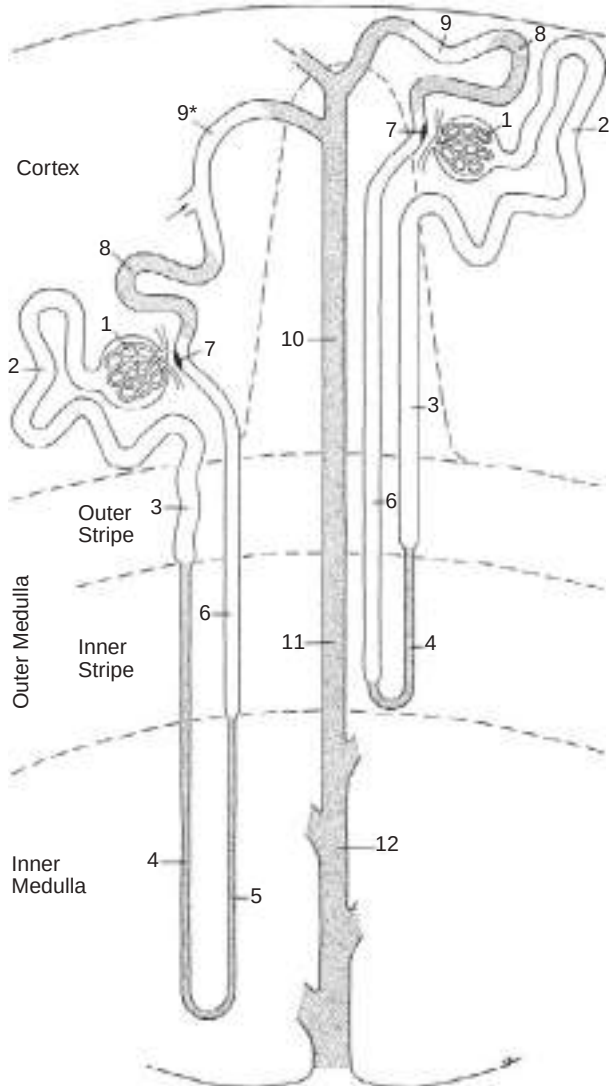

FIGURE 20.9 **Schematic of nephrons and collecting duct.** This scheme depicts a short-looped and a long-looped nephron, together with the collecting system. Not drawn to scale. Within the cortex a medullary ray is delineated by a dashed line. (*From Kriz, W., and Bankir, L. (1988). A standard nomenclature for structures of the kidney. The Renal Commission of the International Union of Physiological Sciences (IUPS). Kidney Int, 33, 1–7, with permission.*) 1: Renal corpuscle including Bowman's capsule and the glomerulus (glomerular tuft); 2: Proximal convoluted tubule; 3: Proximal straight tubule; 4: Descending thin limb; 5: Ascending thin limb; 6: Distal straight tubule (thick ascending limb); 7: Macula densa located within the final portion of the thick ascending limb; 8: Distal convoluted tubule; 9: Connecting tubule; 9*: Connecting tubule of the juxtamedullary nephron that forms an arcade; 10: Cortical collecting duct; 11: Outer medullary collecting duct; 12: Inner medullary collecting duct.

draining into a cortical collecting duct (Figure 20.9). Functionally, an arcade appears to serve as a device that prevents the addition of dilute distal urine to collecting ducts at the corticomedullary junction.[35]

The cortical collecting ducts descend within the medullary rays of the cortex and then, as unbranched tubes, traverse the outer medulla (outer medullary collecting ducts). On entering the inner medulla (inner medullary collecting ducts), they fuse successively. In the human kidney, an average of eight fusions has been found,[36] a number that may also be a good approximation for other species.[37] Because a cortical collecting duct in the human kidney accepts 11 nephrons on average, it can be calculated that a papillary duct (opening into the renal pelvis) drains a total of 2750 nephrons. In the rabbit kidney, which has only 6 nephron tributaries to a cortical collecting duct,[5] approximately 1000 nephrons are drained by a terminal collecting duct. It must be emphasized that an inner medullary collecting duct is not a single unbranched tube, but rather is a system of tubules that fuse successively.

INTERSTITIUM

Definition, Volume Fraction

The space between the basement membranes of the renal epithelia and the peritubular capillaries (Figure 20.11) is called the "*interstitial space*." Cells and extracellular matrix within this space constitute the "*interstitium*." The fractional volume of the interstitium in the cortex in healthy kidneys has been estimated between 4 to 9%,[38–41] in the outer stripe of the outer medulla and in the vascular bundle compartment ~3–5%. In the interbundle compartment of the inner stripe the fractional volume amounts to 10% in rat,[42,41] and in the inner zone the relative interstitial volume continuously increases from the base (10–15% fractional volume in rat, 20–25% in rabbit) to the tip of the papilla (~30% in rat; more than 40% in rabbit[42,43]). Reabsorption and secretion of fluid and solutes, as well as the transport for many regulatory substances from their site of production to their target site, implies a transit across the interstitial compartment.[44] In the cortex only about 26%[39] or 42%[40] of the total outer tubular surfaces are directly apposed to capillaries.

Cellular Constituents

The majority of cells in the interstitium of healthy kidneys are *interstitial fibroblasts* and *dendritic cells* (Figure 20.12). Other cell types (*macrophages* and *lymphocytes*) are scarce in healthy kidneys,[45] but they invade the interstitial spaces under inflammatory conditions.[46]

Interstitial Fibroblasts

Interstitial fibroblasts provide the scaffolding of the tissue, take part in the modeling of the extracellular matrix, and play a role in the production of regulatory

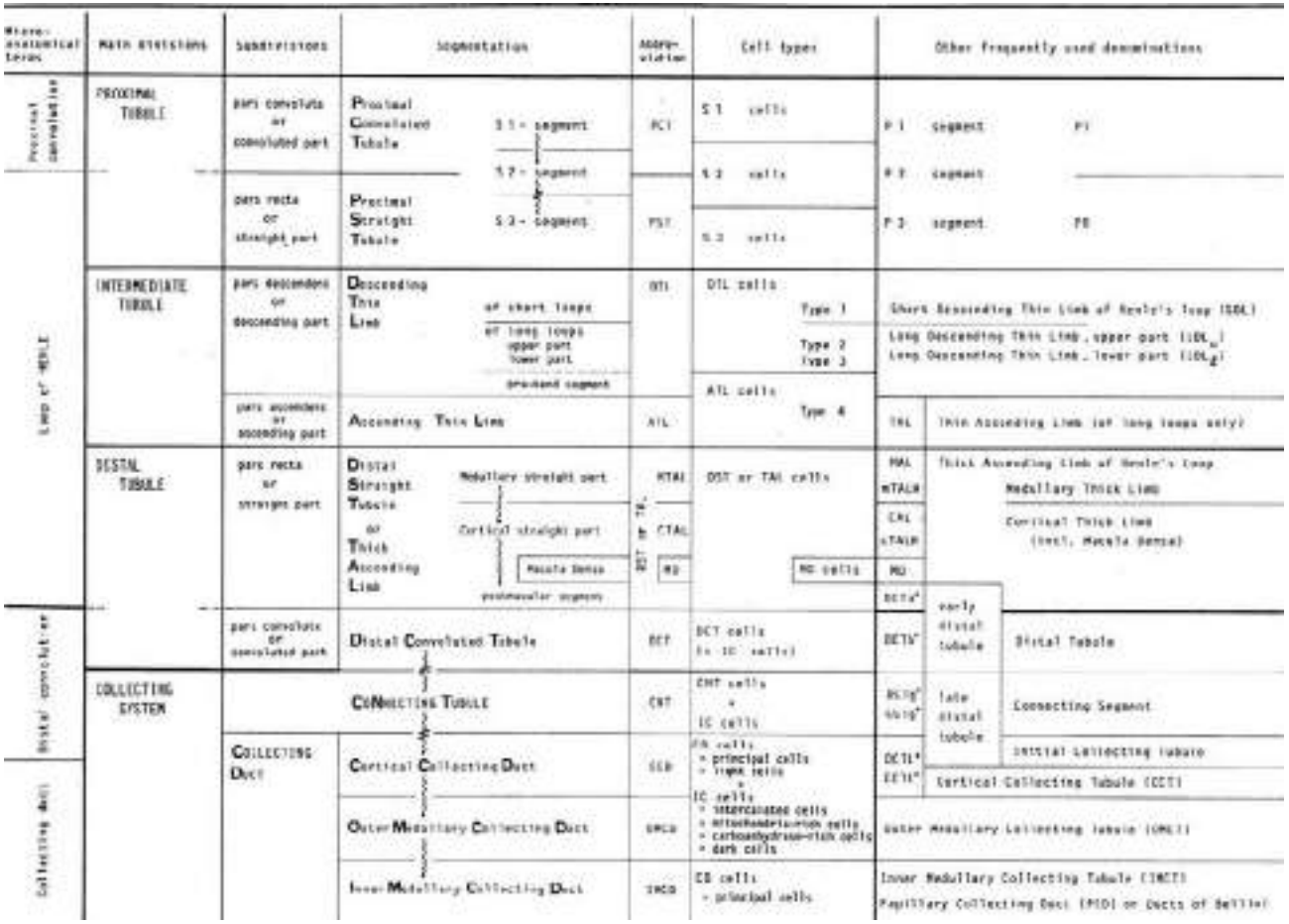

FIGURE 20.10 **Segmentation of the renal tubule.** This table summarizes the nomenclature of segments and cells of the renal tubule. A continuous serpentine arrow means that the transition between the two structures is gradual. An interrupted serpentine arrow means that the transition is gradual in some species, abrupt in others. *Abbreviations marked by a star were introduced by Morel and co-workers: Functional segmentation of the rabbit distal tubule by microdetermination of hormone-dependent adenylate cyclase activity. Kidney Int. 1976; **9**, 264–277* (DCTa: Distal convoluted tubule, initial portion; DCTb: Distal convoluted tubule, bright portion; DCTg: Distal convoluted tubule, granular portion; DCTl: Distal convoluted tubule, light portion; CCTg: Cortical collecting tubule, granular portion; CCTl: Cortical collecting tubule, light portion). *(From ref. [542].)*

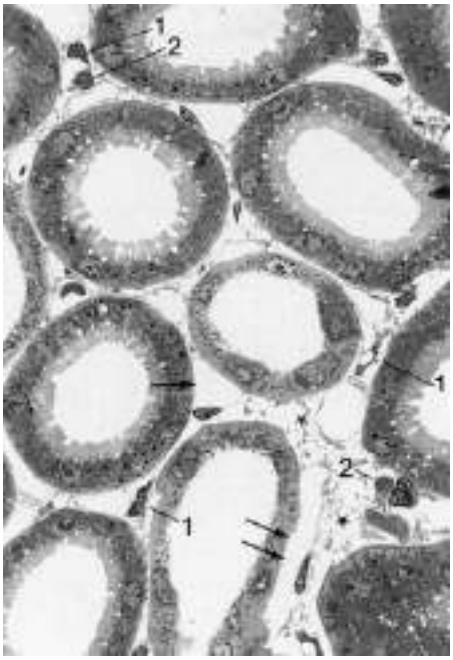

FIGURE 20.11 **Peritubular interstitium of the renal cortex with narrow (arrows) and wide (stars) portions.** Interstitial cells are resident fibroblasts (1) and temporarily sojourning dendritic/mononuclear cells (2) (rat kidney; TEM × ~720).

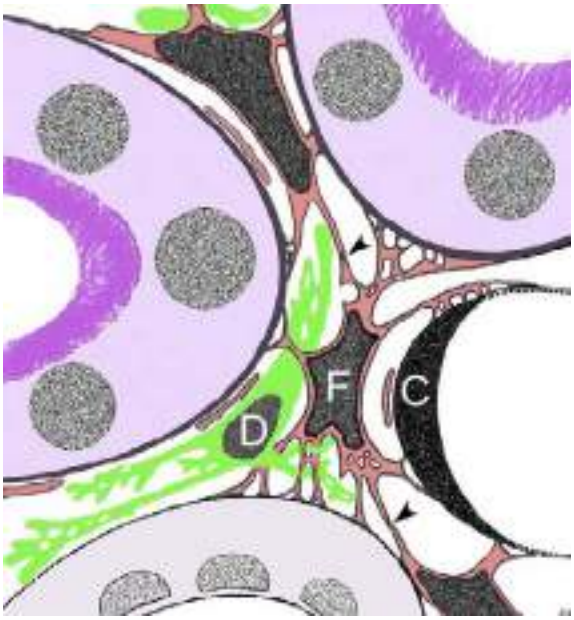

FIGURE 20.12 **Schematic representation of cortical interstitial fibroblast (F) and dendritic cell (D) in the cortical interstitial space of a healthy kidney.** The dark outline of fibroblasts indicates the f-actin layer under the plasma membrane (except for nuclei no cell organelles are shown); the fibroblasts are affixed to tubules and capillaries (C); the arrow heads indicate interconnection of fibroblasts by adhering junctions; the extensions of dendritic cells are narrowly intermingled with fibroblast cell processes.

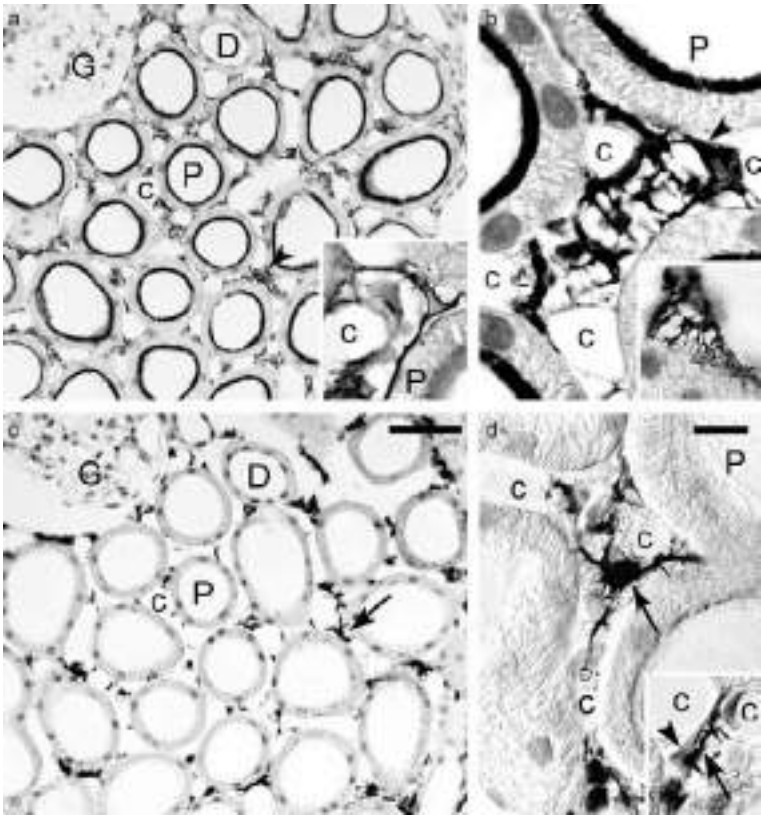

FIGURE 20.13 **Interstitial cells, labeled by immunogold staining for ecto-5′-nucleotidase (a,b) and MHC class II (c,d) on consecutive (a,c) cryostat sections.** P: Proximal tubule; D: Distal convoluted tubule; G: Glomerulus; C: Capillary; Arrowheads: Fibroblasts; Arrows: Dendritic cells. (a) 5′NT labeling highlights the abundance of interstitial fibroblasts (arrow) and the brush border of proximal tubules. Insert: Higher magnification of a fibroblast, labeled for 5′NT by enzyme-histochemistry, demonstrating the far extending processes within the interstitial space. (b) Fibroblasts (arrowheads) bridge the interstitial space between the basement membranes of tubules and capillaries. Insert: Detail of the attachment of a fibroblast process to a tubular basement membrane. (c) Dendritic cells (arrow) labeled for MHC class II, share the interstitial space with fibroblasts. (d) and insert: Differential interference contrast shows the narrow contact of dendritic cells and their extensions (arrow) to fibroblasts (arrowhead) (a,c × ~340; b,d × ~1200; Bars a,c ~50 μm; b,d ~10 μm).

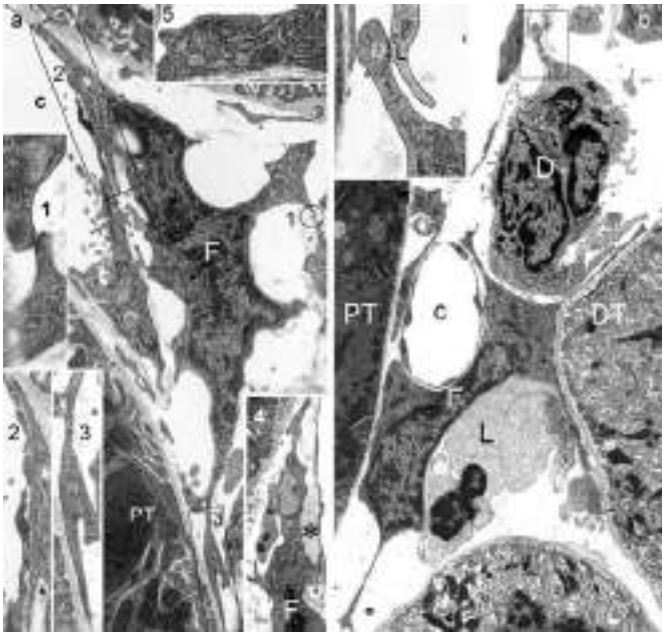

FIGURE 20.14 (a) Fibroblast with sharply outlined pericaryon in the cortical interstitium of a rat kidney; a filiform processes (1) is interconnected with another fibroblast by intermediate junctions (Insert 1); pedicle-like processes of the same fibroblast adhere to the basement membrane of a capillary (c) (2; Insert 2) and of a proximal tubule (PT) (3; Insert 3; Star: Extracellular matrix) with pedicle-like processes that reveal dense stress-fiber-like F-actin filaments; (Insert 4): collagen fibrils (asterisk) closely associated with a fibroblast extension (F) which encloses part of a dendritic cell (D); (Insert 5) the broad cytoplasmic extensions show abundant cisterns of rough endoplasmic reticulum (TEM ×~11,800; Inserts: 1 ×~50,000; 2,3 ×~23,000; 4 ×~11,800; 5 ×~23,000). (b) Fibroblast (F) in focal peritubular inflammation, caused by a lesion in a distal tubule; the fibroblast bridges the space between a healthy proximal tubule (PT), and a diseased distal tubule (DT), extends with thin processes closely along the basement membrane of the DT, partially encloses a profile of a peritubular capillary (C), and has close contact to migrating cells of the immune system (L: lymphocyte; D: dendritic cell; Insert: Higher magnification of the contact ("kiss") of the extension of the dendritic cell and a lymphocyte; TEM ×~6000; Insert ×~23,000).

substances. Interstitial fibroblasts bridge the interstitial space (Figures 20.12, 20.13 and 20.14). They are physically affixed to the basement membranes of tubules, renal corpuscles, and peritubular capillaries, they are interconnected by adhering junctions[44,45,47–49] (Figures 20.12 and 20.14), and narrowly contact all types of migrating cells within the interstitial space (Figures 20.12 and 20.13).

Cortical Interstitial Fibroblasts

In transmission electron microscopic (TEM) images (Figure 20.14), cortical interstitial fibroblasts display a heterochromatin-rich angular nucleus which is surrounded by a narrow organelle-free cytoplasmic rim. Filiform and leaf-like, perforated and filiform processes spread from the cell body, traverse the interstitial space and are affixed to the basement membranes of tubules, enveloping glomerular arterioles and cells of the immune system.[50] Characteristic for fibroblasts is the dense layer of f-actin filaments immediately under the plasmalemma (Figures 20.12 and 20.14). In the filiform processes and the pedicle- or spine-like attachments to the basement membranes, the f-actin is markedly dense[48] (Figures 20.12 and 20.14).

The anchorage of fibroblasts to tubular and capillary basement membranes and their interconnections suggests the possibility that each configurational change of tubules or capillaries (e.g., related with tubular/capillary growth, tubular/capillary dilatation or collapse) exerts mechanical forces on the f-actin frame of the fibroblasts and induces signaling pathways.[51,52] In concert with chemokines and other factors[53] the mechanical forces might be essential components in the cross-talk between fibroblasts and epi- or endothelia,

The production of *extracellular matrix* is another distinguishing characteristic of fibroblasts. The morphological correlate for matrix production is the prominent apparatus for protein synthesis, i.e., abundant large profiles of rough endoplasmic reticulum filled with flocculent, rather electron-dense material, as well as several sets of Golgi-fields. These organelles, including mitochondria, are predominantly located in the peripheral thicker parts of the leaf-like processes, close to the sites of release of matrix and collagen fibrils into the interstitial space (Figure 20.14).[47,48]

The *extracellular matrix* of the interstitium is composed of a network of fibers, proteoglycans, glycoproteins, and interstitial fluid.[44,54] Several types of fibers are found, among them typical interstitial collagen fibers (type 1, type 3, and type 6).[55] Microfibrils (collagen type 1) are found throughout the renal interstitium. Type 3 fibers correspond to the reticular fibers which form a network enveloping individual tubules. Proteoglycans are an important component of the interstitial matrix in the kidney.[56] As elsewhere in the body, various glycoproteins (fibronectin, laminin, and others) are found associated with tubular basement membranes, as well as with fibrillar structures. All these substances contribute to the scaffolding function of the interstitium. Furthermore, they are important substrates for migrating immune cells in the interstitial space.

Fibroblasts can accumulate *lipid droplets*. These are not common in cortical fibroblasts (in contrast to medullary fibroblasts, see below) of healthy kidneys; yet, they may also appear in cortical fibroblasts under specific functional conditions (e.g., anemia[38]). Lysosomal bodies are rarely observed under control conditions.

Cortical interstitial fibroblasts play important roles in the adaptive response to local and systemic hypoxia.

The cleavage of AMP by ecto-5′-nucleotidase (5′NT) on the plasmalemma of cortical fibroblasts generates *extracellular adenosine* (*ADO*) in the cortical interstitium.[57] ADO has been widely implicated in adaptive responses to local hypoxia[58] and in regulating local hemodynamics.[59] The particularly narrow sheathing of glomerular arterioles by 5′NT-positive fibroblasts[48,60] suggests a role of ADO in the regulation of glomerular blood flow and glomerular filtration rate. Indeed, purinergic receptors in afferent and efferent glomerular arterioles are implicated in the regulation of renal functions and hypertension.[61] Studies on 5′NT-deficient mice have confirmed that ADO mediates the vascular response elicited by changes in NaCl concentration at the macula densa.[62] Cortical fibroblasts also exhibit soluble guanylyl cyclase (sGC),[63] and a *b*-type cytochrome 558.[64]

Interstitial fibroblasts in the deep cortex are the source of renal erythropoietin.[65–67] The hypoxia-inducible factor (HIF Hif-2), which has also been located to 5′NT-positve fibroblasts,[68,69] mediates regulation of transcription of erythropoietin following changes in oxygen supply.[70] In conditions of anemia[38] and hypoxia, cortical interstitial fibroblasts from all cortical regions are rapidly recruited for EPO-synthesis.[71]

Extensive phenotypical modulations of cortical peritubular fibroblasts *in vivo* occur under the concerted action of inflammatory cytokines and growth factors.[72–74] Under these conditions, the interstitial fibroblasts proliferate and transform into *myofibroblasts*.[75] Morphologically myofibroblasts differ from interstitial fibroblasts of the healthy renal interstitium, having rounded, euchromatin-rich nuclei and large irregularly-shaped cellular extensions containing dramatically expanded cisterns of rER,[75] and by increased junctional coupling.[76] Differing from healthy interstitial fibroblasts, myofibroblasts express αSMA and vimentin, and 5′NT is internalized from the plasma membrane into the cytoplasm. Functionally, myofibroblasts have an increased capacity for quantitatively and qualitatively different matrix production,[72–74] and a reduced potential for erythropoietin gene expression.[70]

Medullary Interstitial Fibroblasts

The phenotype of fibroblasts in the medulla is basically the same as in the cortex, yet their three-dimensional configuration[50] changes in correlation with the change in tubular arrangement, from convolutions in the cortex to the strictly parallel course of tubules and vessels in the inner zone. The longitudinal axis of the pericaryon of inner medullary fibroblasts is oriented perpendicularly to the longitudinal axis of tubules and vessels (Figure 20.15), and in two-dimensional microscopic images they appear like "rungs of a ladder".[44]

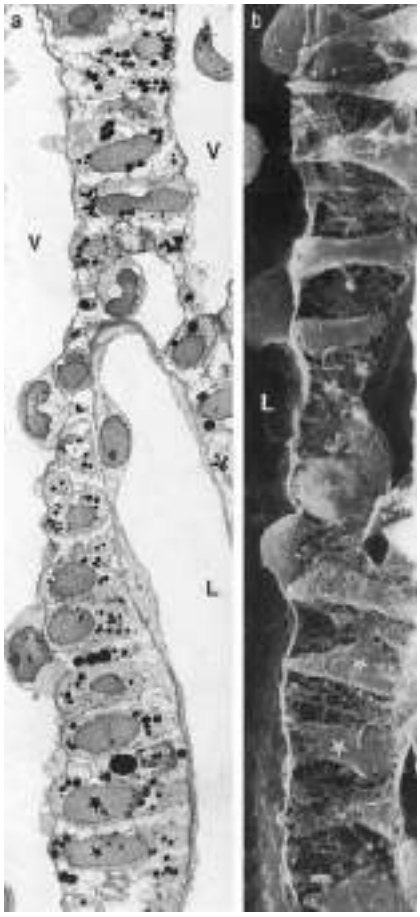

FIGURE 20.15 **Interstitial fibroblasts of the inner medulla, demonstrated in longitudinal sections.** The fibroblasts (asterisks) are arranged like the rungs of a ladder between parallel running tubules or vessels. The fibroblasts contain numerous lipid granules (black) of different sizes (visible in a). (L: loop limb; V: vessel; (a) *Psammomys*; TEM ×~1350; (b) Rat; SEM ×~3400). *(In cooperation with J. M. Barrett.)*

One noticeable change in the ultrastructure of medullary fibroblasts is the progressive increase in cytoskeletal elements towards the deep inner zone; actin filaments form a very prominent layer under the plasma membrane of the pericaryon (Figure 20.16) and the processes. The latter may be interconnected by a composite type of intercellular junction.[49] The increase in cytoskeletal elements in the cells in the inner zone most probably contributes to withstanding the increasing osmotic pressure towards the papillary tip. Furthermore, the occurrence of lipid granules increases progressively from the outer medulla towards the inner medulla where they may be so prominent that the cells were designated as "lipid-laden cells." However, inner medullary fibroblasts may also lack lipid droplets.[44] *In vitro* studies have revealed that the

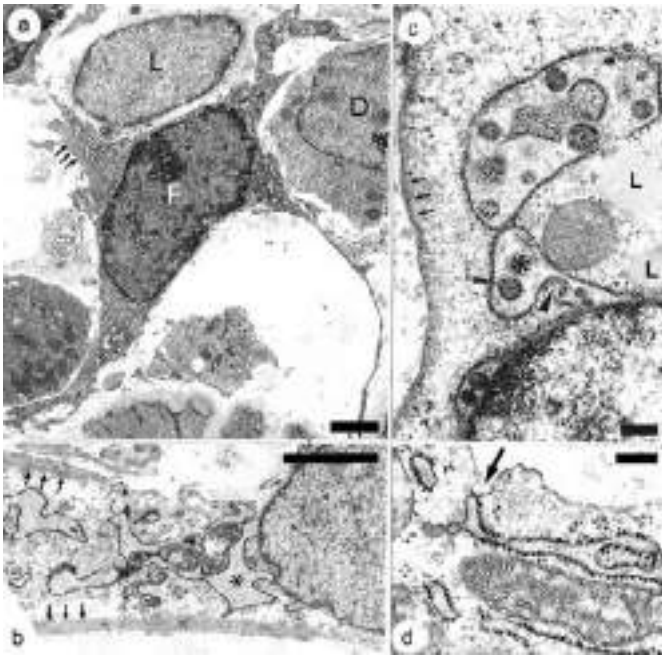

FIGURE 20.16 **Medullary fibroblasts, (a, b, d) human fibroblasts from a renal biopsy; (c) fibroblast from a perfusion-fixed rat kidney.** (a) Human fibroblast at the cortico-medullary border; stellate pericaryon and microfilament-rich cell processes (small arrows), extending between immune cells. (b) Part of a human fibroblast in the inner stripe of the outer medulla; the cisterns of the rough endoplasmic reticulum are widened and filled with flocculent material (Asterisk: Dilated perinuclear cistern; Small arrows: Accumulations of microfilaments along the plasma membrane). (c) Rat fibroblast from the inner medulla showing dilated perinuclear and endoplasmic reticulum cisterns (asterisk); infoldings of the ER into the cistern (arrow head) (L: Lipid droplets). (d) Fibroblast in the outer stripe of the outer medulla; a profile of rough endoplasmic reticulum in direct contact with the plasma membrane (arrow) (TEM (a): ×~4760; (b): ×~8500; (c) ×~37,400; (d) ×~33,150; Bars: (a,b): ~2 mm; (c,d): ~0.2 mm). *(From ref. [47].)*

occurrence and amount of lipid droplets in the inner medullary fibroblasts depends on the specific environment of the cells, conditioned by the presence of inner medullary collecting duct cells, and that inner medullary fibroblasts can transform to myofibroblasts with upregulation of alpha smooth muscle actin and desmin.[77] In medullary fibroblasts the cisterns of rough endoplasmic reticulum, including the perinuclear cistern, are often strikingly enlarged and they may narrowly enclose mitochondria (Figure 20.16). Occasionally the rER membranes are in direct contact with the plasma membrane (Figure 20.16). The functional interpretation of these particular features, only rarely observed in cortical fibroblasts, is still to be resolved.

The medullary fibroblasts do not display 5′NT or mRNA for EPO. A role of medullary interstitial cells has been proposed in the regulation of urinary osmolarity. *Glycosaminoglycans* are particularly abundant in the inner medullary interstitium,[78] and condensed hyaluronate-proteoglycan aggregates are associated with basement membranes, with collagen fibers, as well as with diffuse reticular structures.

The inner medulla has the greatest capacity for *renal prostaglandin* (PG) synthesis.[79,80] *Cyclooxygenase* (COX) isoforms, rate-limiting enzymes in PG biosynthesis, are expressed at substantially higher levels in the inner medulla than in the renal cortex.[81–84] COX-2 is found predominantly in inner medullary interstitial fibroblasts, and its expression increases under chronic salt loading.[84]

Dendritic Cells

Dendritic cells (DC) belong to the mononuclear phagocyte system and constitute the major antigen-presenting cell population in the healthy kidney.[85] Interstitial DCs continually probe the surrounding environment through dendrite extensions, and readily respond to insults to the parenchyma.[86–88] DCs have been recognized by their expression of MHC class II (Figures 20.12 and 20.13) and CD11c. In the healthy kidney DCs are present in their immature phenotype with comparatively low levels of MHC class II and of co-stimulatory proteins,[89] but with a high capacity for uptake of antigens.[86]

Similar to fibroblasts, DCs form an organ-spanning network,[88] located in very close contact with fibroblasts (Figures 20.12, 20.13 and 20.14).[45,47] DCs are constantly moving. Unlike fibroblasts, the pericaryon of DCs is large and confines the often rounded or elongated nucleus together with most cell organelles. The rER profiles of dendritic cells are narrow and less abundant than in fibroblasts. The intermediate filament protein vimentin is regularly present in the pericaryon of DCs, whereas it is absent in fibroblasts in the healthy renal cortex. Dendritic cells have, in comparison to macrophages and lymphocytes, more mitochondria, more rER, and a large Golgi apparatus. Lysosomes are less apparent than in macrophages. The so-called Birbeck granules, which are characteristic for dendritic cells, are a special formation of the endocytotic compartment serving as a loading compartment and/or reservoir of antigens before DC maturation.[90]

The ramified "veil-like" and perforated cellular extensions (Figure 20.12) lack the prominent stuffing with f-actin filaments, and are largely devoid of cell organelles, in marked contrast to fibroblasts. The long filiform processes of DCs have approximately the same diameter as the filiform fibroblast processes, but due to the lack of f-actin filaments are much less electron-dense (Figure 20.14). In contrast to fibroblasts, DCs

have no junctional connections among each other or with tubules or vessels. However, frequently the plasma membranes of dendritic cells and of fibroblasts or dendritic cells and lymphocytes form points of membrane adhesion, so-called "kisses" (Figure 20.14). Parts of dendritic cells are often nestled into the hollows of the pericaryon or the processes of fibroblasts. The narrow intermingling of both cell types (Figures 20.12, 20.13 and 20.14) suggests the possibility of extensive cross-talk between them.

Dendritic cells are abundant in the inner stripe in the outer medulla and, as in the cortex, are narrowly associated with fibroblasts. Accumulations of dendritic cells are particularly striking around collecting ducts and thick ascending limbs.

In the inner medulla the pericaryon of dendritic cells is often situated in the spaces between the "ladder rungs" formed by the fibroblasts, and their processes may extend over several "ladder rungs." In the lower two-thirds of the inner medulla bone marrow-derived cells are not detected in the healthy kidney.[45,47]

Macrophages and Lymphocytes

Macrophages and lymphocytes are rarely found in the healthy renal interstitium, but they massively invade the interstitial spaces under inflammatory conditions.[46] A large proportion of the invading mononuclear cells display the established "marker proteins" (CD 45, CD3, CD4, CD 8; ED1, ED2, CD44, etc.) and the protein S100A4.[35,91] Neutrophil granulocytes are found occasionally, basophil and eosinophil granulocytes and plasma cells are rare in the healthy cortical renal interstitium.

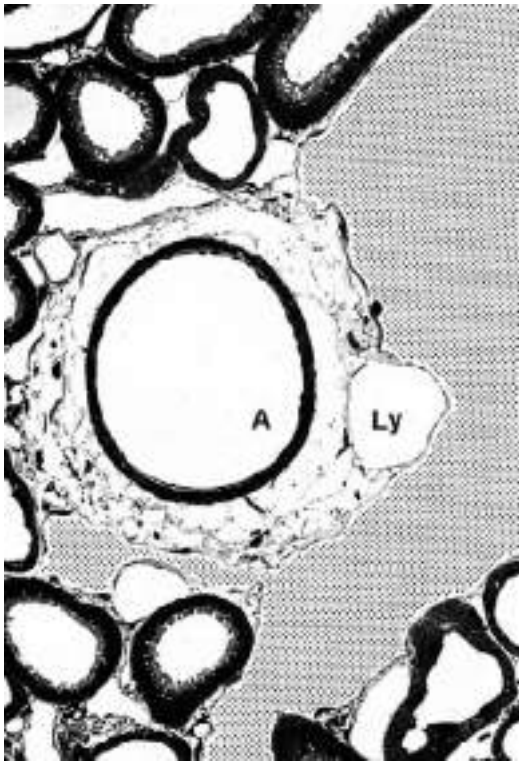

FIGURE 20.17 **Cross-section through the deep cortex (rat).** The cortical radial artery (A) is surrounded by a layer of loose connective tissue that contains the lymphatics (L_Y). The cortical radial vein is only partly shown; its lumen and those of direct tributaries have been highlighted by a dotted pattern. Note the intimate relationships of the artery, vein, and lymphatic, mediated by the periarterial loose connective tisue (TEM: $\times \sim 360$).

PERIARTERIAL CONNECTIVE TISSUE AND LYMPHATICS

The periarterial tissue is a sheath of loose connective tissue, surrounding the intrarenal arteries (arcuate arteries, cortical radial arteries). The considerable thickness of the periarterial sheath is apparent in quick-frozen specimens,[92] and in perfusion fixed tissue. It attenuates towards the end of the cortical radial arteries and terminates along the afferent arteriole at the vascular pole of the glomerulus (Figures 20.17, 20.18 and 20.19). The periarterial sheath is continuous with the peritubular interstitium and with the connective tissue underlying the epithelium of the renal pelvis and ureter at all sites. The renal veins are apposed to the periarterial sheath.[92]

The periarterial sheath constitutes wide meshes of the extremely attenuated processes of 5′NT-negative, but weakly alpha-smooth muscle actin- and vimentin-positive fibroblasts.[47] The meshes are filled with thick bundles of collageneous fibers and interstitial fluid and regularly confine some macrophages and dendritic cells.

The periarterial connective tissue sheath provides the path for renal nerves (see below) and for *renal lymphatics*.[92] Lymphatics start in the vicinity of the glomerular vascular pole[25] or at a more proximal level of the afferent arteriole, depending on the species, and travel along the branches of the renal arteries towards the renal hilum (Figures 20.17 and 20.18). Their recognition and distinction from blood capillaries at light microscopic levels is facilitated by their specific expression of podoplanin.[93] Also, 5′NT labels in rat and mice lymphatics, but not in blood vessels. Lymphatic endothelial cells secrete chemokines that attract dendritic cells. An increase in lymphatic microvessels has been observed, e.g., in tubulointerstitial fibrosis and progression to end-stage renal failure in remnant kidney.[93]

Regulatory substances that are released into the peritubular interstitium might access the systemic blood circulation via the lymphatics in the periarterial sheath. This suggestion has been made for renin,[92] and it may

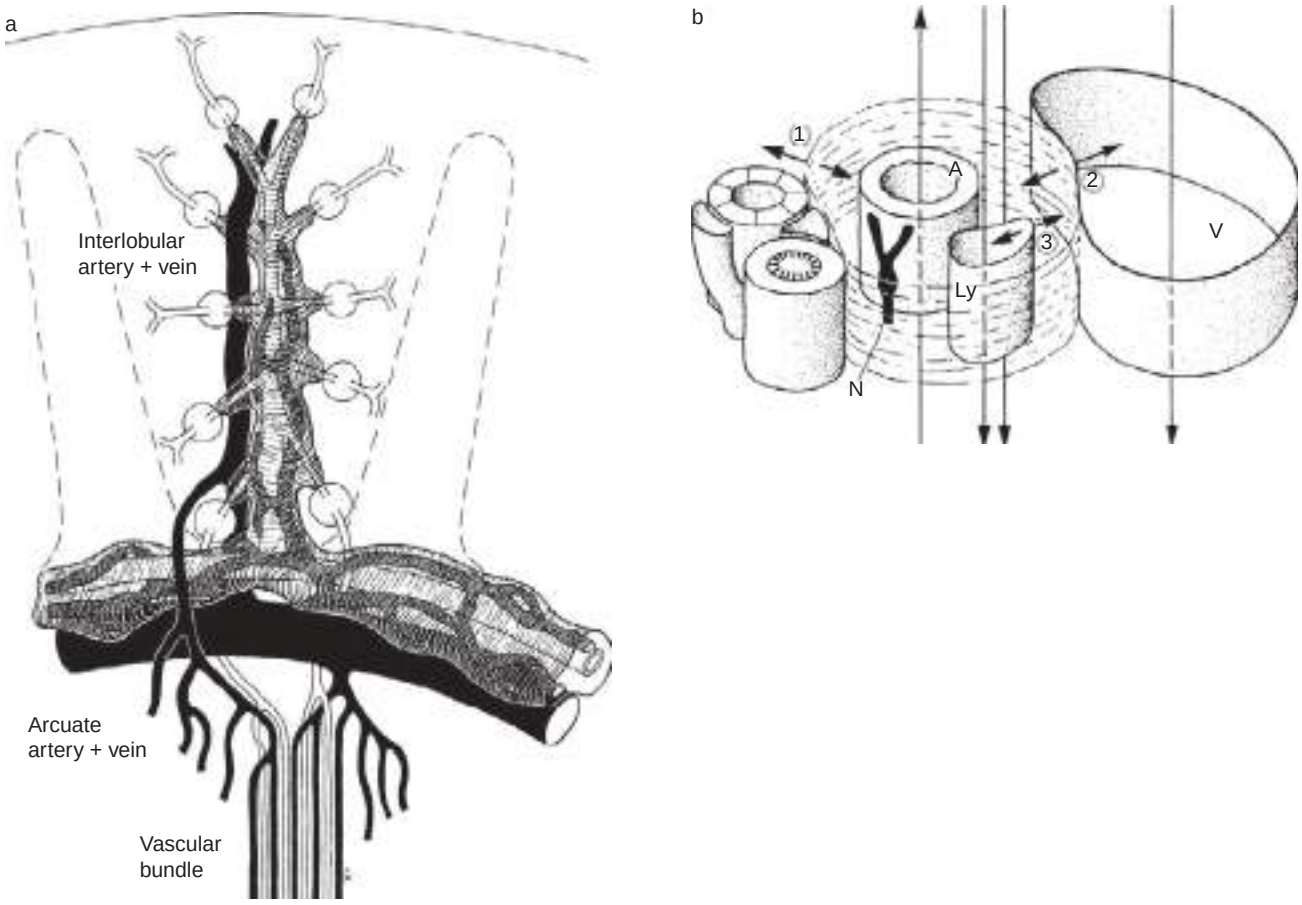

FIGURE 20.18 **Schematics to show (a) the distribution, and (b) the topographical relationships of the periarterial connective tissue sheath.** Not drawn to scale. (a) The periarterial sheath is schematically indicated as a wide "stocking" drawn over the intrarenal arteries and lymphatics. In reality this stocking has no limiting tissue that separates the interior from the surroundings. An arcuate artery transforms into a cortical radial artery, which gives rise to afferent arterioles. These segments are surrounded by the periarterial connective tissue sheath. The efferent arterioles, as well as the veins (drawn in black), are not included. The lymphatics (stippled) originate and travel within the periarterial sheath. Note there are no lymphatics coming up from the medulla. Within the cortex, medullary rays are indicated by a broken line. In (b) a transverse section through an cortical radial artery (A) shows the relationships of the periarterial sheath and the possibilities for functional exchanges (double-headed arrows) with surrounding structures: (1) with the peritubular interstitium; (2) with the accompanying vein (V); and (3) with lymphatics (Ly). The single-headed arrows indicate the flow of the respective fluid. Note the nerves (N) traveling through the periarterial tissue. In addition, two neighboring tubules, including an arcade and a proximal tubule, together with peritubular capillaries, are drawn. *(From ref. [92], with permission.)*

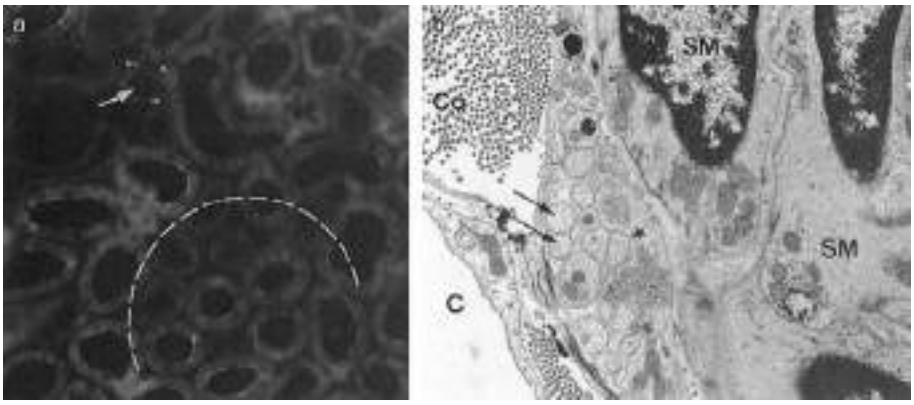

FIGURE 20.19 **The renal nerves accompany (a) the intrarenal arteries.** A cortical radial artery (arrow) is seen which is associated with three nerve bundles, identified by staining with a monoclonal antibody against protein gene product 9.5 (PGP 9.5) which is a universal marker for vertebrate neurons. Among the tubules no nerves are found. A medullary ray is delineated by a hatched line (Rat; LM $\times\sim$240). (*In cooperation with M. Siry, W. Kummer and S. Bachmann*). **(**b) A large terminal nerve accompanying an afferent arteriole. Several axons (arrows) and a varicosity (star) with synaptic vesicles are seen (SM: Smooth muscle cell; CO: Collagen; C: Capillary; Rabbit kidney: TEM $\times\sim$12,000).

apply to other protein hormones such as erythropoietin. The periarterial tissue sheaths have been interpreted as a mixing chamber for a variety of vasoactive substances, ultimately determining the contractile status of the renal resistance vessels. In addition to the lymphatics, the periarterial tissue itself constitutes a pathway for interstitial fluid drainage. Indeed, a tracer injected under the renal capsule can be followed within the periarterial tissue, as well as within the lymphatics.

While a fraction of cortical interstitial fluid gains access to the periarterial tissue, and eventually to lymphatics, there is no direct pathway for regulatory substances released in the cortical interstitium to reach medullary targets. It has been proposed that the intimate relationships between cortical radial arteries and veins permits countercurrent exchange of O_2, being responsible – at least in part – for the low partial pressure of O_2 in the superficial cortex.[94,95]

NERVES

The efferent nerves of the kidney are composed of sympathetic nerves and terminal axons, which accompany the intrarenal arteries, and the afferent and efferent arterioles (Figures 20.18 and 20.19).[96] The nerve fibers are monoaminergic. Norepinephrine[97–99] and dopamine have been identified.[100] In addition, several neuropeptides are co-localized with norepinephrine in renal nerves.[101] The presence of acetylcholinesterase in renal nerves cannot be taken to indicate cholinergic nerves, but rather that monoaminergic nerves obviously possess acetylcholinesterase activity.[97]

The nerve fibers run in the loose connective tissue around the arteries and arterioles. The descending vasa recta within the medulla are also innervated by adrenergic nerve terminals as far as they are enveloped by smooth muscle cells.[102,103] A dense assembly of nerves and terminal axons is found around the juxtaglomerular apparatus[99] which is described in more detail along with the JGA.

Tubules have direct relationships to terminal axons only when they are located around the arteries or arterioles.[96,99] Tubules adjacent to the juxtaglomerular apparatus (terminal portion of the cortical thick ascending limb) are more frequently touched by terminal axons than at other sites.[99] The density of nerve contacts to convoluted proximal tubules (located in the cortical labyrinth) is low[104]; nerve contacts to straight proximal tubules (located in the medullary rays and the outer stripe) have never been encountered. The overwhelming majority of tubular portions have no direct relationships to nerve terminals.

Consequently, morphologists are left with the question of how the neuronal influence on tubular function[105] is mediated. In addition to a systemic distribution of catecholamines, a more specific, but also indirect, mode seems possible for certain tubular segments.[5] Because nerve fibers do pass along the vascular pole of each glomerulus from afferent to efferent arterioles, the distribution of nerves in the renal cortex is dense. Catecholamines (and other transmitters) released from nerve terminals at the vascular poles and at the efferent arterioles may gain access to peritubular capillaries, and in this way may perfuse the convoluted tubules of the cortical labyrinth. Tubules arranged around the cortical radial arteries would be reached most easily by transmitters released from periarterially located nerve terminals. This may be of relevance with respect to arcades (connecting tubules), which have been shown to be sensitive to isoproterenol.[106] Exposure of the straight tubules within the medullary rays of the cortex to neural transmitters reaching them directly by diffusion from nerve terminal is improbable.

Tubules in the outer medulla may only be reached by neurotransmitters if they are either situated adjacent to vascular bundles (a minority of tubules) or secondarily, by a capillary distribution of the transmitters from nerve terminals accompanying the vascular bundles. The tubules of the inner medulla cannot be reached by neurotransmitters directly delivered from nerve terminals in the medulla.

Little is known about the afferent nerves of the kidney; they are commonly believed to be sparse, but the issue remains unresolved.[102,105,107–110]

TOPOGRAPHICAL RELATIONSHIPS

Cortex

The architectural pattern of the renal cortex is best understood when viewing a cross-section through the midcortex (Figures 20.20 and 20.21). Two portions within the cortical parenchyma, the labyrinth and the medullary rays, are distinguishable. Within the cortical labyrinth, the vascular axes, which consist of the cortical radial (interlobular) artery, vein, and a lymphatic, are regularly distributed. The renal corpuscles and the corresponding convoluted tubules (proximal and distal) are situated around each vascular axis. Barriers separating the population of renal corpuscles and convoluted tubules belonging to another vascular axis are not discernible. Thus, the cortical labyrinth is a continuous parenchymal layer that contains the vascular axes of the cortex and the medullary rays in a regular pattern. The straight tubules (proximal and distal), together with the collecting ducts, are located within the medullary rays. Because the number of straight tubules increases

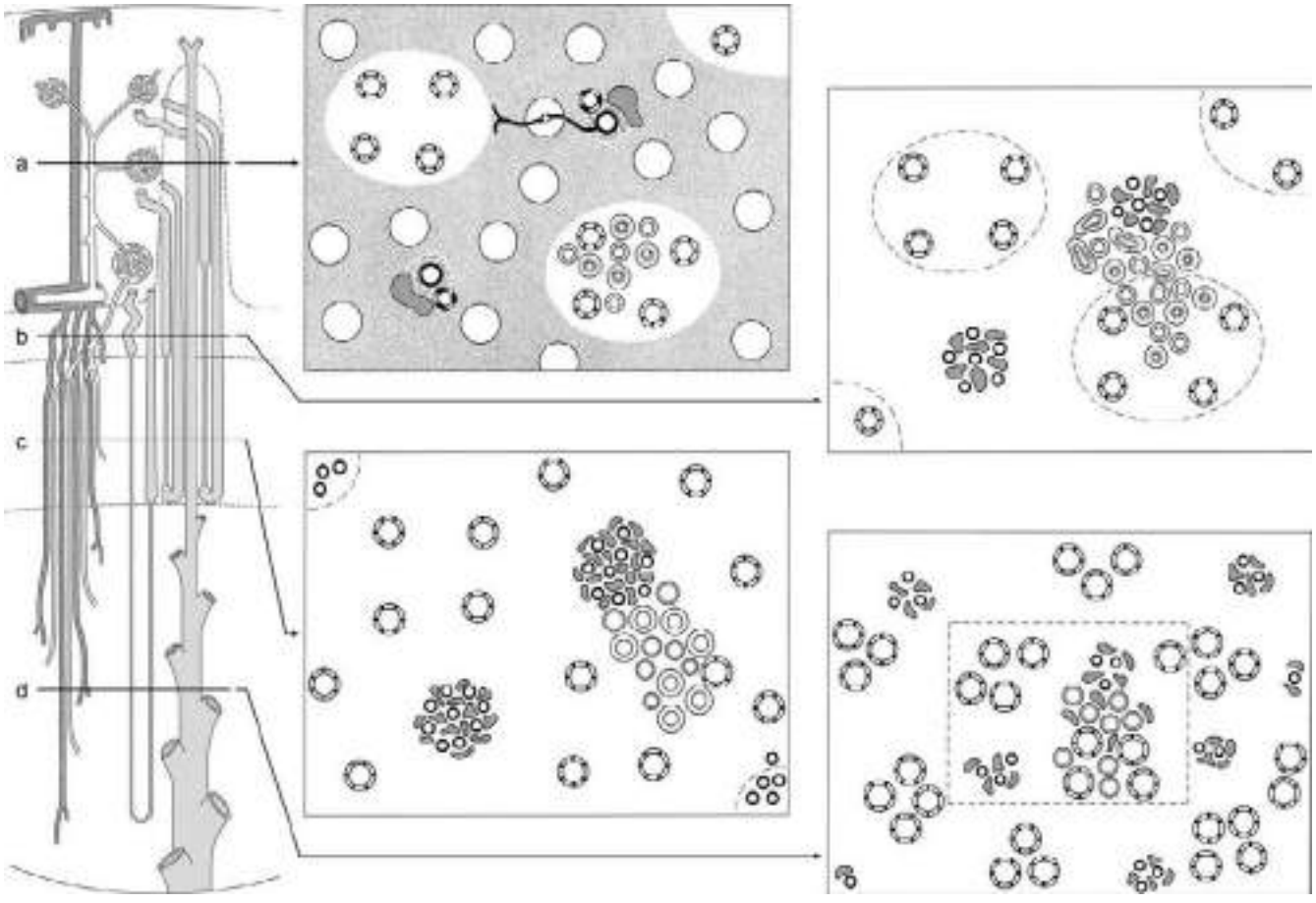

FIGURE 20.20 **Schematics of histotopography.** Histotopography of the kidney as revealed by four successive cross-sections through: (a) cortex; (b) outer stripe; (c) inner stripe; and (d) inner medulla. The simple type of the medulla (rabbit, man) is shown. (*From Koushanpour, E., and Kriz, W. (1986). In "Renal Physiology. Principles, Structure and Function." Springer-Verlag, New York, with permission.*) In the cortex the cortical labyrinth (shaded area) and the medullary rays (white**)** are shown. The labyrinth contains the cortical radial (interlobular) blood vessels, glomeruli, and the convoluted tubular portions (the latter are not shown). The arcades accompany the interlobular vessels. The medullary rays contain the collecting ducts and the straight proximal and distal tubules. Note the typical grouping of collecting ducts within a medullary ray. In the outer stripe, vascular bundles replace the interlobular vessel axis of the cortex. The continuations of the medullary rays are surrounded by hatched lines. Within these areas the collecting ducts and the loop limbs of superficial and midcortical nephrons are found. The loop limbs of juxtamedullary nephrons are situated around the vascular bundles. In the inner stripe, the vascular bundles are fully developed. Like in the outer stripe, the loop limbs of juxtamedullary nephrons are situated near the bundles, and those from superficial and midcortical nephrons together with the collecting ducts are located distant from the bundles. Note the heterogeneity of the thin limbs: Those of juxtamedullary nephrons lie near the bundles and are thicker in diameter, whereas those of the superficial nephrons lie distant from the bundles. Inner medulla. The area defined by the dashed rectangle corresponds to the entire area shown in section **(c)**. This reduction in size is because short loops and many vasa recta have turned back in the inner stripe. Note the grouping of collecting ducts reflecting their medullary ray arrangement in the cortex. Thin limbs (both descending and ascending) are associated with vasa recta or collecting ducts.

toward the corticomedullary border, the medullary rays increase in width toward the outer stripe.

A regular pattern of the convoluted tubules within the labyrinth is not apparent. Proximal and distal convoluted tubules (the latter constitute only a minor portion of profiles in comparison with proximal tubules) are equally embedded in the dense capillary plexus of this region. A strikingly constant position is occupied by the arcades (if they are present). They ascend within the cortical labyrinth and are grouped immediately around the vascular axes. The topographical relationships within the juxtaglomerular apparatus will be described later.

Within the medullary rays the straight tubules of superficial nephrons (proximal and distal) generally occupy a central position, and those of midcortical nephrons occupy a peripheral position. The collecting ducts are situated between the two groups, and therefore are situated neither in the center nor at the very border of a medullary ray. Efferent arterioles do not enter the medullary rays, but frequently break off into capillaries just at the border between the labyrinth and

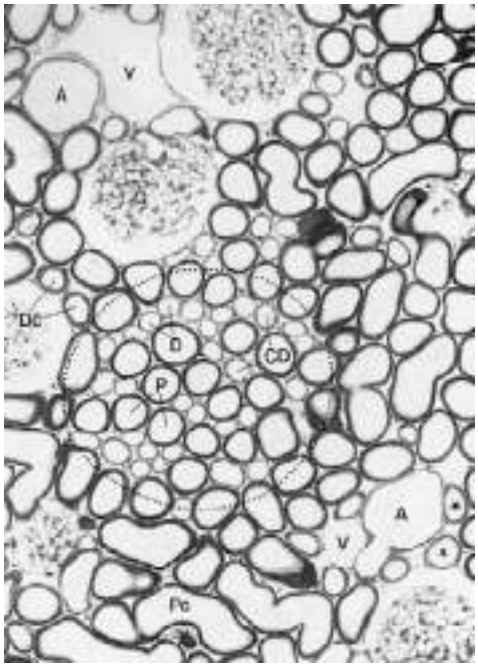

FIGURE 20.21 **Renal cortex of the rat; 1 μm cross-section.** The architectural pattern of the cortex is demonstrated. A medullary ray is delineated by a dashed line. It contains the straight proximal tubules (P), the straight distal tubules (thick ascending limb; asterisks), and the collecting ducts (C). The cortical radial vessels (A: Artery; V: Vein), glomeruli (G), and convoluted proximal (Pc) and distal (D) tubules establish the cortical labyrinth. Arcades (stars) ascend close to the cortical radial vessels (×∼200).

the medullary rays. As a result, the blood supply of the medullary ray tubules is as direct as that of the tubules within the cortical labyrinth. However, blood that perfuses the straight tubules of the medullary rays mixes afterwards with the blood that perfuses the convoluted tubules (*vide supra*).

Medulla

The three regions of the medulla contain different populations of nephron segments. The outer stripe contains straight parts of the proximal tubule (S_3 segments), straight parts of the distal tubule (thick ascending limbs), and collecting ducts. The inner stripe is composed of descending thin limbs, ascending thick limbs (distal straight tubules), and collecting ducts. The inner medulla contains thin descending and ascending limbs, and collecting ducts.

The architectural organization of the medulla can best be described by considering the vascular bundles as central axes and studying how the tubules are arranged around them.[33,112] A "simple" and a "complex" type of renal medulla are distinguished (Figure 20.22); the differences between both are mainly found in the inner stripe.

The vascular bundles develop in the outer stripe (Figures 20.20 and 20.23). At the very beginning of the bundles the straight proximal and distal tubules of juxtamedullary nephrons are grouped immediately around the bundles. In the continuation of the medullary rays, the tubules of superficial and midcortical nephrons, together with the collecting ducts, fill the spaces between the bundles and their adjacent juxtamedullary tubules. In the outer stripe straight proximal tubules and straight distal tubules (thick ascending limbs) should theoretically be present in equal numbers; however, a cross-section through the outer stripe shows that proximal tubular profiles are much more numerous than distal tubules. In the rat, proximal tubules occupy roughly 68% of the space in the outer stripe, in contrast to approximately 13% by the thick ascending limbs, and 5% by the collecting ducts.[41] The dominance of the proximal tubules is rooted in the fact that the straight proximal tubules of juxtamedullary nephrons are not straight (as their name indicates), but rather take a tortuous course when descending through the outer stripe; this holds true for the mouse kidney.[113] In addition, straight proximal tubules are much thicker in diameter than the straight distal tubules, and proximal tubules of juxtamedullary nephrons are even thicker than those of the midcortical and superficial nephrons.[5]

The tubules of the outer stripe are perfused by a specific "capillary" plexus. "True" capillaries, derived from direct branches of efferent arterioles, are few; the dominating "capillary" vessels in the outer stripe are the ascending vasa recta (Figures 20.3 and 20.4b). They traverse the outer stripe as wide tortuous channels closely contacting the tubules like proper capillaries. Because these vessels carry the entire venous blood from the medulla, the outer stripe tubules are mainly supplied by venous blood from deeper parts of the medulla.

The outer stripe varies considerably in thickness among species; in the rat[33] and mouse,[34] it is very well-developed and constitutes approximately one-third of the outer medulla. In contrast, in *Psammomys*,[32] cat,[37] dog,[114] and humans,[37] the outer stripe is very thin.

The inner stripe (Figures 20.20 and 20.24) of the outer medulla is the most constant part of the renal medulla, consisting of the regularly distributed vascular bundles (VB) leaving between them the interbundle region (IBR). Two types of vascular bundles can be distinguished, which form the basis for the discrimination of a "simple" and a "complex" type of medulla.

In most species[5,115] vascular bundles of the simple type are present, which exclusively contain descending and ascending vasa recta. The tubules are found in the IBR and are arranged around the bundles in a pattern similar to that found in the outer stripe. The loops of

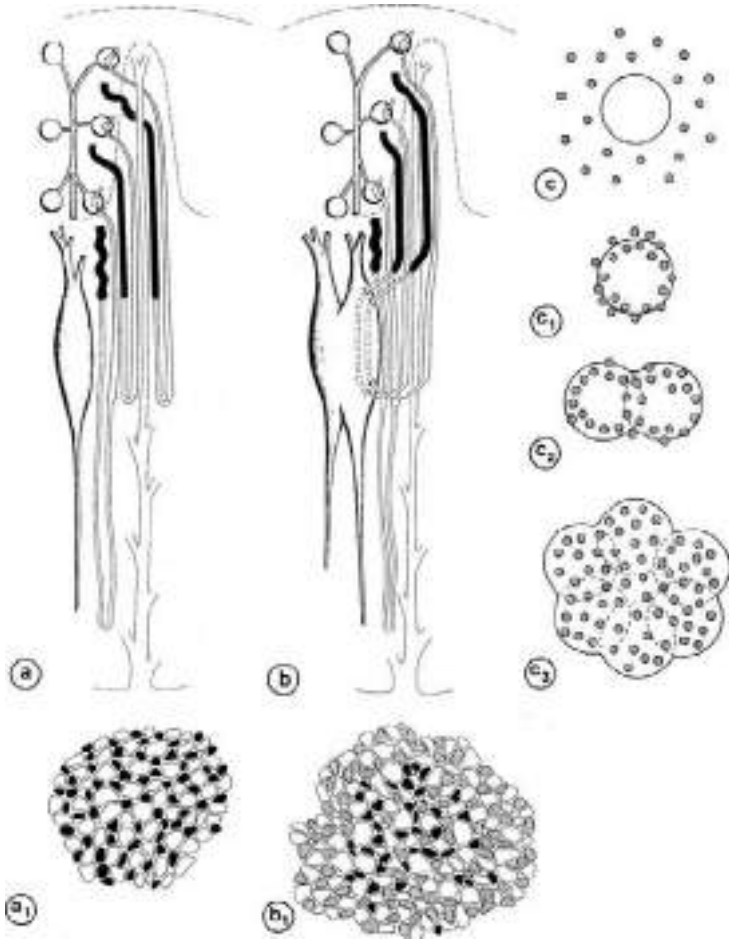

FIGURE 20.22 **Schematic to demonstrate the difference between the simple (a and a_1) and complex (b and b_1) types of medulla.** In the simple medulla (a), loops of Henle surround the vascular bundle according to the pattern established in the cortex. The long loops lie nearest to the bundle, the short loops of superficial nephrons farthest away. The collecting ducts are situated at a distance from the bundle. The bundle itself (a_1) contains only descending (black) and ascending (white) vasa recta. In the complex medulla (b), the descending thin limbs of short loops descend within the vascular bundles. The complex bundle (b_1) contains, in addition to descending (black) and ascending (white) vasa recta, the descending thin limbs of short loops (hatched). *(From ref. [133], with permission.)* (c−c_3): Schematics of cross-sections through vascular bundles to show different degrees of bundle fusing and loop integration in the complex type of renal medulla (c1−c_3) compared with the simple type (c) (Large circle: Vascular bundle; Small hatched circles: Descending thin limbs of short loops). In the simple type of medulla (c), the descending thin limbs of short loops are all located outside the bundle. Complex bundles (c_1−c_3) may be established in different degrees. In rat (c_1), descending thin limbs of short loops are arranged in the periphery of the bundles; bundles generally do not fuse. In mouse (c_2), bundles frequently fuse; descending thin limbs of short loops have penetrated deeper into the bundle. In *Psammomys* or *Meriones* (c_3), bundle fusing has produced giant bundles; descending thin limbs of short loops are distributed over the entire bundle area. *(From ref. [115], with permission.)*

Henle, originating from juxtamedullary nephrons (generally the longest long loops), lie nearest to the bundles, whereas the loops derived from superficial and midcortical nephrons (in most species, short loops) lie distant from the bundles. The collecting ducts are generally arranged in distant rings around the bundles, and are intermingled with loops derived from superficial and midcortical nephrons. Altogether, they are perfused by the dense capillary plexus of the IBR.

The complex type of vascular bundle (Figure 20.25) is present in several rodent species with a high urine concentrating ability, including rat,[33] mouse,[16,34] *Meriones*,[116] and *Psammomys*.[32] It differs from the simple type in that the descending thin limbs of short loops (only of short loops!) descend within the vascular bundle (Figure 20.26). Consequently, the bundles within the inner stripe change from the classic countercurrent arrangement of a rete mirabile, consisting of DVRs and AVRs, to a system in which one ascending tube (AVRs) is closely packed together with two descending tubes (DVRs and SDTLs). In addition, the vascular bundles in the complex type of medulla tend to fuse and to form larger bundles, up to giant bundles (*Psammomys*). These complex bundles are developed at the transition from the outer stripe to the inner stripe, and are maintained only throughout the inner stripe.

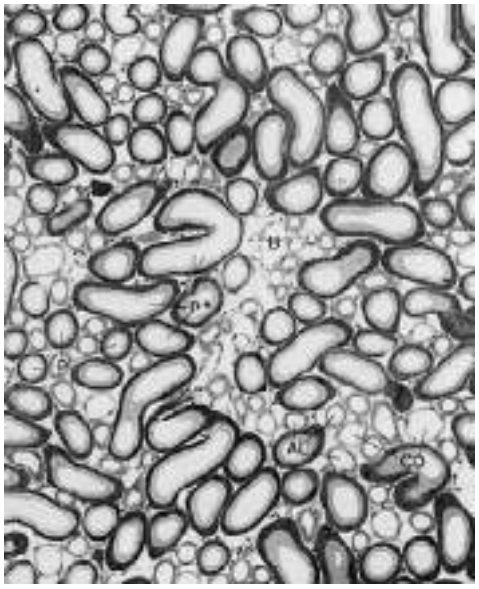

FIGURE 20.23 **Outer stripe of rat kidney; 1 μm cross-section.** The vascular bundle (VB) is surrounded by the straight proximal tubules of juxtamedullary nephrons (asterisk), which are larger in diameter than those of superficial and midcortical nephrons (P), which lie distant from the bundles (Asterisks: thick ascending limb; C: collecting duct). Interstitial spaces are sparsely developed (×∼220).

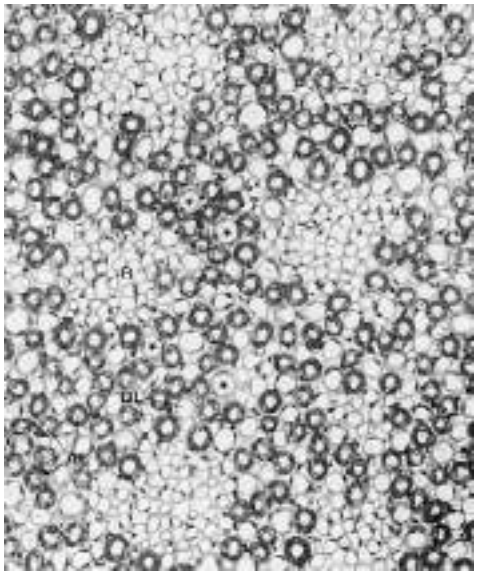

FIGURE 20.24 **Inner stripe of rabbit kidney (simple medulla); 1 μm cross-section.** The vascular bundles (VB) are regularly distributed. The collecting ducts (C) lie distant from the bundles. Descending thin limbs (asterisks) and thick ascending limbs (stars) are situated within the interbundle regions (×∼200).

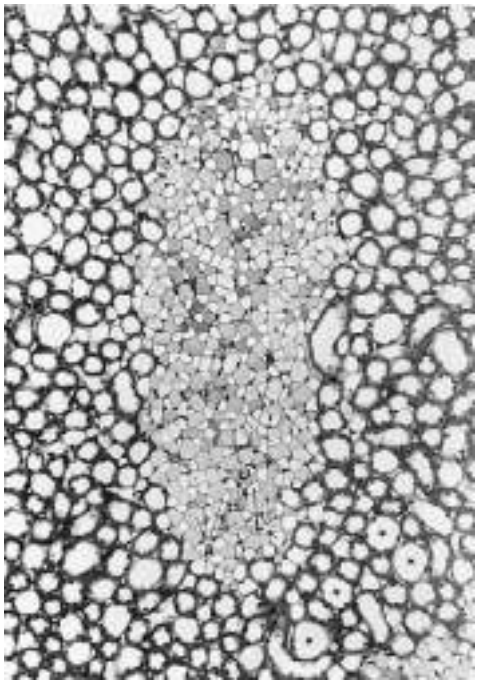

FIGURE 20.25 **Inner stripe of *Meriones shawii* kidney (complex medulla); paraffin cross-section.** The large vascular bundle originates by fusing of primary bundles. In addition to descending (D) and ascending (A) vasa recta, complex vascular bundles contain descending thin limbs of short loops (L). Collecting ducts (some are marked by asterisks) are situated distant from the bundles (×∼190).

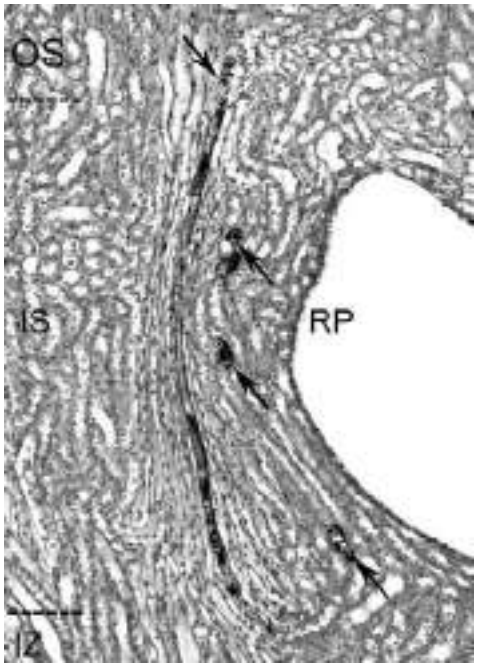

FIGURE 20.26 **Longitudinal section through a vascular bundle in the inner stripe of a gerbil kidney (complex medulla); paraffin section.** One superficial nephron has been injected with microfill; at the transition from the outer (OS) to the inner stripe (IS) the proximal tubule transforms to the intermediate tubule (thin descending limb; left arrow) which descends within the vascular bundle; the tubule leaves the bundle at the border between the inner stripe and the inner zone (IZ), and ascends as thick ascending limb (right arrows) within the interbundle region (RP: Extension of the renal pelvis; ×∼200).

At the border to the inner medulla, the SDTLs leave the bundles, and the fused bundles split into the original number of bundles. The characteristics of the complex type are developed to different degrees in the species so far investigated. A somewhat "gradual" transition from the rat, via the mouse, to *Meriones* and *Psammomys* is observed.

The tubular pattern around these complex bundles is different from that of the simple type. At the border between the outer stripe and inner stripe, the SDTLs leave their position distant from the bundles, then turn toward a bundle and descend within the bundle. Their TALs maintain a position distant from the bundles and near to a collecting duct throughout the outer medulla. As observed in the simple type, the tubules of the interbundle regions are embedded in the dense capillary plexus of the IBR. In contrast to what is observed in the simple type, it is worthwhile to stress the fact that in the complex type only the LDTLs, scattered among the TALs of short and long loops, traverse IBR. Specific variations of this pattern in mice[117] and *Psammomys*[17,32] are described elsewhere.

To understand the possible functional implications of the inner stripe architecture, as well as the differences between the simple type and the complex type, we have to consider precisely the composition of the vascular bundles. The vascular bundles of the simple type contain all descending and all ascending vasa recta servicing the inner medulla. Furthermore, they contain most of the descending vasa recta, which service the inner stripe, but only few of the ascending vasa recta, which drain the inner stripe. The numerical relationship between descending and ascending vasa recta is about 1 to 1 (at the level of the inner stripe). Thus, in the simple type of vascular bundle, the venous blood from the inner medulla contacts the arterial blood that supplies both the inner medulla and the inner stripe of the outer medulla in a countercurrent arrangement. Therefore, inner medullary venous blood may exchange not only with the arterial blood that is predetermined for the inner medulla, but also with blood predetermined for the inner stripe. Substances originating from the inner medulla could be trapped by countercurrent exchange to the inner medulla, but could also be shifted to the inner stripe capillary plexus, and thereby be offered to inner stripe tubules (see below).

In the complex type of medulla, the vascular bundles incorporate the descending thin limbs of short loops. In *Psammomys*, at the level of the inner stripe, the bundles consist of approximately 10% descending vasa recta, 45% ascending vasa recta, and 45% descending thin limbs,[32] with the descending thin limbs being completely surrounded by ascending vasa recta. The difference between the simple and the complex types of bundles is even more pronounced when it is realized that the bundles in *Psammomys* no longer contain any vasa recta servicing the inner stripe. All vasa recta present in the giant bundles of *Psammomys* either descend to the inner medulla or ascend from the inner medulla. The vasa recta servicing the inner stripe in *Psammomys* descend or ascend, respectively, independent of the bundles. Thus, the giant bundles of the inner stripe in *Psammomys* appear to form a countercurrent trap for the inner medullary blood that is located in the inner stripe. In other species with complex bundles (rat, mouse), vasa recta servicing the inner stripe are not as strictly excluded from the bundles as in *Psammomys*; even in these species the vascular bundles appear to be a countercurrent trap for mainly the inner medullary circulation.

The inner medulla develops very differently among species. Species with only short loops of Henle[6] do not have an inner medulla; their urine concentrating ability is poor. All species with high urine concentrating ability have a well-developed inner medulla.[3,118] It is characteristic for the inner medulla to taper from a broad basis to a papilla (or crest). The mass of the inner medulla is therefore unevenly distributed along the longitudinal axis. A study in the rat[2,119] has shown that the decrease in the mass of the inner medulla along the longitudinal axis follows an exponential function. The upper half of the inner medulla accounts for roughly 80% of the total inner medullary volume, and consequently only 20% are left for the papillary half.

With regard to the ratio between Henle's loops and collecting ducts along the inner medulla, considerable differences are found when comparing the base with the tip of the inner medulla, as well as notable interspecies differences.[42] In the rat, the ratio is about 2.5 (2.5 loops per one collecting duct) at the beginning of the inner medulla; this ratio rapidly decreases to about 1 toward the papilla. In the rabbit, the ratio increases from 3 at the beginning of the inner medulla to 9 within the papilla, then later decreases to 5 in the papillary tip. These data all await functional interpretation, thus indicating the limitation of our knowledge concerning structure–function correlations in the inner medulla.

An architectural pattern within the inner medulla is less apparent than in the outer medulla.[5,34,120] Constant histotopographical relationships between certain structures or spatial separations of others do not seem to be as important to the function of the inner medulla compared to the outer medulla. When entering the inner medulla, the vascular bundles already contain a drastically decreased number of vasa recta. Towards the papilla, this number continues to decrease; finally single descending vasa recta enter the tip of the papilla. Ascending vasa recta in the inner medulla generally ascend independent of the bundles, which they finally

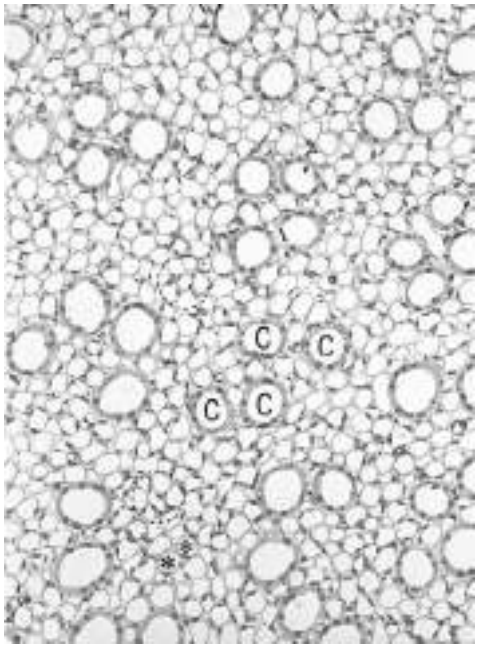

FIGURE 20.27 **Inner medulla of the rabbit kidney; 1 μm cross-section through the upper part.** The collecting ducts are still arranged in groups, reflecting the pattern in the medullary rays of the cortex. Vascular bundles (dashed circles) are poorly delineated. Thin loop limbs (asterisks) lie near collecting ducts (C), as well as near vasa recta of the vascular bundles (× ~240).

join at the border of the inner stripe. Thus, in the inner medulla, the vasa recta are never as closely packed to bundles as they are in the inner stripe.

As far as vascular bundles are discernible, the collecting ducts are generally distanced from them. At the very beginning of the inner medulla, collecting ducts are still arranged in groups that reflect their grouping within the medullary rays of the cortex (Figure 20.27). Joining of collecting ducts first occurs among the ducts of one group. Descending and ascending thin loop limbs, together with individually running vasa recta and capillaries, fill the spaces between the bundle centers and the collecting ducts. DTLs in general tend to be more distant from CDs, whereas ATLs tend to be positioned more closely to CDs[120,121]; a thin limb of Henle, regardless of whether descending or ascending, may be associated with both collecting ducts and/or vasa recta. Obviously, the interactions of the structures in the inner medulla are mediated through the wide interstitial spaces.

With regard to the functional connections of the inner medulla with the outer medulla, it is notable that all descending vasa recta servicing the inner medulla have already been established as individual vessels in the outer stripe and traverse the inner stripe within the bundles. All ascending vasa recta from the inner medulla traverse the inner stripe within the bundles without joining with ascending vasa recta from the inner stripe. The blood flow of the inner stripe and that of the inner medulla are apparently distinct from each other. In the outer stripe, however, venous vasa recta coming up from the inner medulla and those from the inner stripe finally take a similar route. Both traverse the outer stripe as wide capillary channels representing the major capillary supply of the outer stripe tubules.

GLOMERULUS (RENAL CORPUSCLE)

The renal corpuscle consists of a tuft of specialized capillaries that protrudes into Bowman's space (urinary space) surrounded by Bowman's capsule (BC). The tuft consists of specialized capillaries held together by the mesangium and covered – as a whole – by the glomerular basement membrane (GBM), followed by a layer of unique epithelial cells, the podocytes. Traditionally, this layer is called the visceral epithelium of BC, which – at the vascular pole of the glomerular tuft – reflects into the parietal epithelium of BC. Nowadays, the term Bowman's capsule is generally used only for this parietal cell layer which – together with its basement membrane (parietal, BM, PBM) – forms the outer wall of a glomerulus. At the urinary pole, BC transforms into the proximal tubule epithelium, Bowman's space opens into the tubular lumen (Figures 20.28 and 20.29).

The diameters of the – more or less – spherical renal corpuscles in different species range from approximately 100 μm (mouse) up to 300 μm (elephant), in humans they are approximately 200 μm, in rat 120 μm, and in rabbit 150 μm.[29,36,37] In many species (rodents) the diameter of juxtamedullary renal corpuscles may exceed that of midcortical and superficial nephrons by up to 50[22,29,34,37]; this does not hold true for the human kidney.[122]

Architecture of the Glomerulus

The reflection of the parietal epithelium of Bowman's capsule into the visceral epithelium creates an oval opening in the glomerulus, which is called the glomerular hilum. Actually, it is the reflection of the GBM into the PBM (i.e., the basement membrane of the parietal epithelium of Bowman's capsule) that borders the opening. Through it the glomerular arterioles, together with the glomerular mesangium, enter the inner space of the GBM, which forms a complex folded sack. Inside this sack the glomerular capillaries pursue a tortuous course around centrally located mesangial axes. Together, capillaries and mesangium totally fill the labyrinthine spaces inside the GBM. The outer

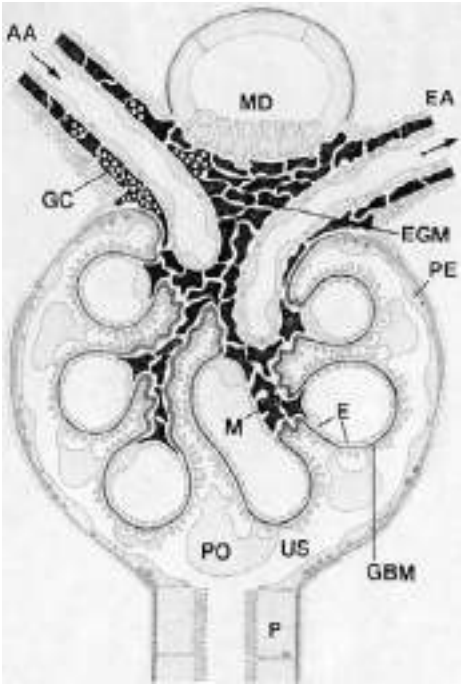

FIGURE 20.28 **Diagram of a longitudinal section through a glomerulus and its juxtaglomerular apparatus (JGA).** The capillary tuft consists of a network of specialized capillaries, which are outlined by a fenestrated endothelium. *(From Cunningham, R. et al. (2005). Am. J. Physiol. Renal Physiol. **289**(4), F933–938.)* Defective PTH regulation of sodium-dependent phosphate transport in NHERF1$^{-/-}$ renal proximal tubule cells and wild-type cells adapted to low-phosphate media. At the vascular pole, the afferent arteriole (AA) branches into capillaries immediately after its entrance; the efferent arteriole (EA) is established inside the tuft and passes through the glomerular stalk before leaving at the vascular pole. The capillary network, together with the mesangium, is enclosed in a common compartment bounded by the glomerular basement membrane (GBM). Note that there is no basement membrane at the interface between the capillary endothelium and the mesangium. The glomerular visceral epithelium consists of highly-branched podocytes (PO) which, in a typical interdigitating pattern, cover the outer aspect of the GBM. At the vascular pole, the visceral epithelium and the GBM are reflected into the parietal epithelium (PE) of Bowman's capsule, which passes over into the epithelium of the proximal tubule (PT) at the urinary pole. At the vascular pole, the glomerular mesangium is continuous with the extraglomerular mesangium (EGM) consisting of extraglomerular mesangial cells and an extraglomerular mesangial matrix. The extraglomerular mesangium, together with the granular cells (G) of the afferent arteriole and the macula densa (MD), establish the JGA. All cells which are suggested to be of smooth muscle origin are shown in black (F: foot processes; N: sympathetic nerve terminals; US: urinary space). *(Adapted from Kriz, W., and Sakai, T. et al. (1988). Morphological aspects of glomerular function.* In *"Nephrology," A. M. Davison, Vol. 1, Proceedings of the X International Congress of Nephrology," 3–23. Bailliere Tindall, London.)*

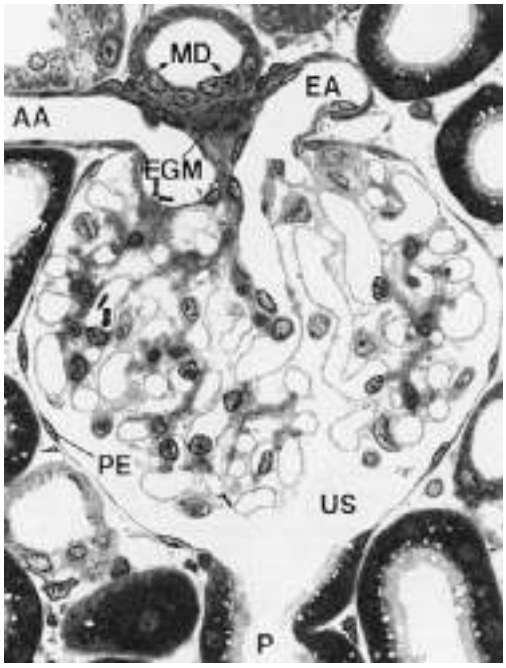

FIGURE 20.29 **Longitudinal section through a glomerulus (rat).** At the vascular pole the afferent arteriole (AA), the efferent arteriole (EA), the extraglomerular mesangium (EGM), and the macula densa (MD) are seen. At the urinary pole the beginning of the proximal tubule is seen (P) (PE: Parietal epithelial of Bowman's capsule; US: Urinary space; LM ×~490).

aspect of the GBM is covered by the visceral epithelium, i.e., by the podocytes. The glomerular tuft therefore consists of the glomerular capillaries and the mesangium inside the sack of the GBM (frequently called the "endocapillary compartment"), and the podocytes covering this sack from outside ("exocapillary compartment").

The glomerular capillaries are derived from the afferent arteriole which – strictly at the entrance level – divides into several (two to five) primary capillary branches.[20,123] Each of these branches gives rise to an anastomosing capillary network which runs toward the urinary pole and then turns back, running toward the vascular pole. Thereby, the glomerular tuft is subdivided into several (2–5) lobules, each of which contains an afferent and efferent capillary portion. The lobules are not strictly separated from each other; some anastomoses between lobules occur. The efferent portions of all lobules together establish the efferent domain of the capillary network out of which the efferent arteriole develops.

In contrast to the afferent arteriole, the efferent arteriole is already established inside the glomerular tuft; thus, the efferent arteriole has a significant intraglomerular segment which runs through the glomerular stalk (Figures 20.30, 20.31 and 20.32).[20] At this site, the efferent arteriole has close spatial relationships to the first branching of the afferent arteriole. After leaving the tuft, the efferent arteriole has a segment which is narrowly associated with the extraglomerular mesangium (see below). The intraglomerular segment is

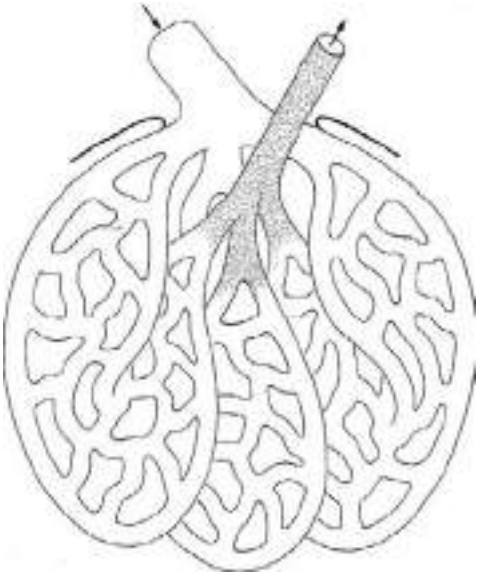

FIGURE 20.30 **Schematic to show the branching pattern of the glomerular tuft.** Immediately after its entrance into the tuft, the afferent arteriole splits into large superficially located capillaries which are the supplying vessels of glomerular lobules (three are shown). The capillaries run toward the urinary pole. After turning back they unite to establish the efferent arteriole still inside the glomerular tuft. Thus, in contrast to the afferent arteriole, the efferent arteriole has an intraglomerular segment (stippled). An afferent and an efferent capillary domain are distinguished. The efferent capillary domain occupies roughly a quarter sector of the tuft; it is partly covered by the afferent domain. *(From Winkler, D., and Elger, M. et al. (1991). Branching and confluence pattern of glomerular arterioles in the rat. Kidney Int. Suppl 32, S2–8, with permission.)*

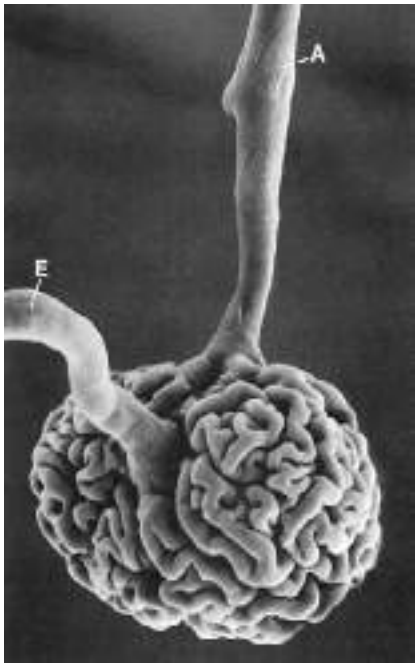

FIGURE 20.31 **Scanning electron micrograph of a vascular cast of a dog glomerulus with afferent (A) and efferent (E) arterioles.** Note the superficially located branching pattern of the afferent arteriole, out of which the afferent capillary domain is supplied. The efferent arteriole emerges from inside of the glomerular tuft.

made up by a continuous endothelium which is fully separated from the GBM by a "mesangial layer" consisting of mesangial cell processes and matrix. Thus, this initial segment of the EA is fully embedded into the mesangium. Along the course through the extraglomerular mesangium, the mesangial and/or extraglomerular mesangial cells in its wall are gradually replaced by smooth muscle cells.[20] Thereafter, the efferent vessel is established as a proper arteriole.

Glomerular capillaries are a specific type of blood vessel whose wall is made up of an endothelial tube only. A small strip of the outer circumference of this tube is in contact with the mesangium, the major part bulges toward the urinary space and is covered by the GBM, followed by the layer of podocyte foot processes. Taken together, these peripheral portions of the capillary wall represent the filtration area. The small juxtamesangial portion of the capillary wall is not underlain by a basement membrane, but directly abuts the mesangium.[124] The glomerular mesangium constitutes the axis of a glomerular lobule, to which the glomerular capillaries are attached by their juxtamesangial portion. Apart from this attachment site, the mesangium is bounded by the perimesangial part of the GBM. Like the peripheral GBM, it is covered at its outer aspect by podocyte processes. At the turning points of the GBM the opposing parts of the GBM are interconnected by podocyte processes that are strongly armed with actin filaments.

The Glomerular Basement Membrane (GBM)

The glomerular basement membrane represents the skeletal backbone of the glomerular tuft. Topographically, the GBM consists of a peripheral (pericapillary) and a perimesangial part. At the border between both parts, the GBM changes from a convex pericapillary into a concave perimesangial course; the turning points are called mesangial angles.[124]

During development, the GBM originates from the fusion of an endothelial and a podocytic basement membrane. In the adult, the collagen component of the GBM is solely derived from podocytes, whereas the laminin component originates from both podocytes and endothelial cells.[125] The GBM is a remarkably stable structure; the *in vivo* loss of protein radioactivity suggests a half-life of more than 100 days.[126] Nevertheless, a continuous turnover occurs,[127,128] but few details are known about where and how new

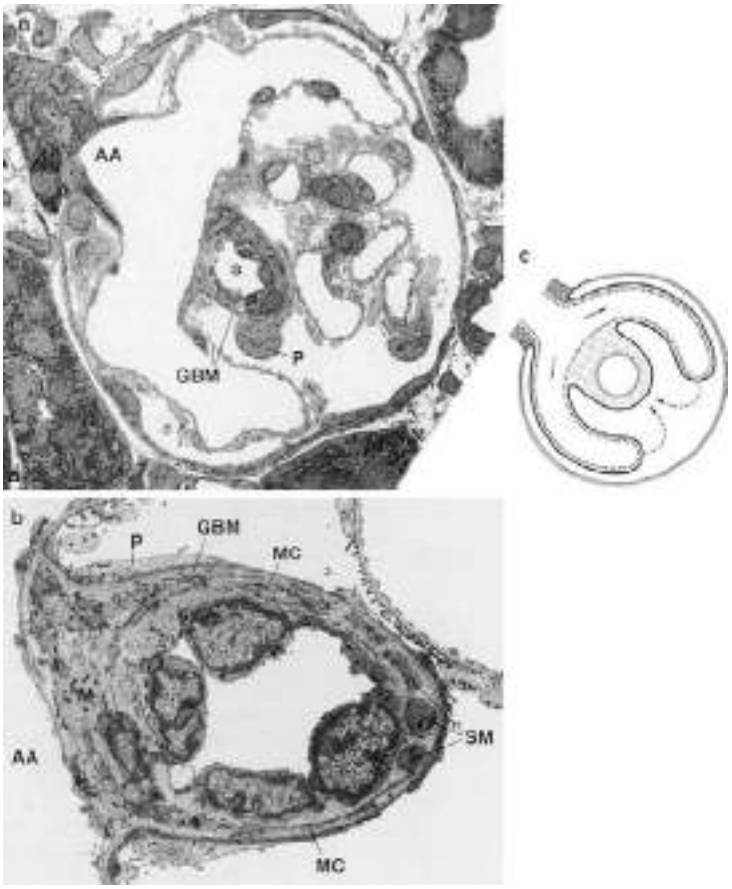

FIGURE 20.32 (a) Narrow association between the afferent arteriole (AA) and the intraglomerular segment of the efferent arteriole (*, EA) as seen in a section approximately 15 μm inside a glomerulus. The afferent arteriole (AA) splits into primary branches. The branching point of the AA has a narrow spatial relationship to the inraglomerular segment of the EA (asterisk), which is located in the center of the tuft. The intraglomerular segment of the EA is enclosed – together with the AA – in a common compartment bordered by the GBM. (b) Higher magnification of the intraglomerular segment in a subsequent section with several conspicuous features: the lumen is narrow; the continuous endothelium consists of four cell bodies that bulge into the lumen; the endothelium is surrounded by a mesangial envelope made up of mesangial cells (MC) and matrix; a few smooth muscle cell processes (*SM*) are interspersed. AA and EA are separated only by mesangial tissue (*M*); there is no basement membrane separating the AA and EA. *P*, cell body of a podocyte attached to the GBM surrounding the EA. (c) Schematic of a cross-section through the glomerular vascular pole, showing the spatial relationships of the AA and EA within the glomerular stalk corresponding to the situation in (a). Immediately after its entry into the glomerulus, the AA splits into wide capillary branches with open endothelial pores. The branching point of the AA has a narrow spatial association with the outflow segment of the EA. The outflow segment is enclosed, together with the AA, in a common compartment bordered by the GBM. The EA is completely surrounded by a layer of mesangial tissue (shown in gray), and is separated from the AA only by this layer; there is no basement membrane between AA and EA. Broken arrows represent blood flow from afferent branches through the capillary network to the outflow segment (TEMs: (a) ×~1500; (b) ×~4300). *(From ref. [20], with permission.)*

components are added, and others removed and degraded. Several extracellular matrix degrading enzymes have been found to be produced by podocytes and mesangial cells[129–131]; however, the relevance of these enzymes to the turnover of the GBM remains to be established.

The GBM varies in width among species. In humans the thickness ranges between 240 and 370 nm, in rat and other experimental animals it is between 110 and 190 nm. In electron micrographs of traditionally fixed tissue the GBM appears as a trilaminar structure made up of a lamina densa bounded by two less dense layers – the lamina rara interna and externa. Recent studies using freeze techniques reveal only one dense layer directly attached to the bases of the epithelium and endothelium.[132]

The major components of the mature GBM include type IV collagen, type II laminin (= laminin 521), heparan sulphate proteoglycans (agrin, perlecan), and the glycoproteins entactin/nidogen[133,134]; type V and VI collagen have also been demonstrated.[135]

The mature GBM is established during the development of a glomerulus from the S-shaped body to the capillary loop stage. During this transition, the collagen

IV α_1 and α_2 chains are replaced by α_3, α_4, and α_5 chains, and the laminin α_1 and β_1 chains are replaced by α_5 and β_2 chains, the γ_1 chain remains preserved, together forming laminin 521.[136,137] The components of the mature GBM are all synthesized by the podocytes. The functional importance of this specific composition of the GBM compared to basement membranes elsewhere in the body becomes evident when looking at their involvement in glomerular diseases: the various forms of Alport syndrome are caused by mutations in the genes encoding the α_3, α_4, and α_5 chains of collagen type IV; Goodpasture syndrome is mediated by antibodies against the α_3 collagen IV chain.[138]

Current models depict the basic structure of the basement membrane as a three-dimensional network of collagen type IV.[139] Monomers of type IV collagen consist of a triple helix of α_3, α_4, and α_5 chains measuring 400 nm in length which, at its carboxy-terminal end, has a large non-collagenous globular domain, called NC1. At the amino-terminus the helix possesses a triple helical rod 60 nm in length, the 7S domain. Interactions between the 7S domains of two triple helices or the NC1 domains of four triple helices allow collagen type IV monomers to form dimers and tetramers. In addition, triple helical strands interconnect by lateral associations via binding of NC1 domains to sites along the collagenous region.

Fibronectin, laminin, and entactin are the glycoproteins of the GBM[140]; the major one is laminin 521. Laminin forms a second network that is superimposed onto the collagenous network. Laminin is a noncollagenous glycoprotein consisting of three polypeptide chains, two of which are glycolylated and cross-linked by disulfide bridges.[137] Laminin, via entactin, binds to specific sites on the polymerized network of type IV collagen, as well as to integrin and dystroglycan surface receptors of the podocytes and endothelial cells (see later). This combined network of type IV collagen and laminin is considered to provide mechanical strength to the basement membrane, and to serve as a scaffold for alignment of other matrix components.

The proteoglycans of the GBM consist of core proteins and covalently bound glycosaminoclycans which are concentrated in the laminae rarae internae and externae. The electronegative charge of the GBM is mainly due to these polyanionic proteoglycans.[141] The major proteoglycans of the GBM are heparan sulfate proteoglycans; most prominent is agrin but perlecan is also present.[142,143] Proteoglycan molecules aggregate to form a meshwork that is kept highly hydrated by water molecules trapped in the interstices of the matrix. Within the GBM heparan sulfate proteoglycans may act as an anticlogging agent to prevent hydrogen bonding and adsorption of anionic plasma proteins and maintain an efficient flow of water through the membrane.

The Cells of the Glomerular Tuft

Within the glomerular tuft three cell types (Figure 20.33) are found which all contact the GBM: (1) mesangial cells; (2) endothelial cells; and (3) podocytes (visceral epithelial cells).

Mesangial cells, together with the mesangial matrix, establish the glomerular mesangium (Figure 20.34). Mesangial cells are quite irregular in shape, with many processes extending from the cell body towards the GBM.[144,145] In these processes (to a lesser extent also in cell bodies) dense assemblies of microfilaments are found which have been shown to contain actin, myosin, and α-actinin.[146]

The processes of mesangial cells run towards the GBM, to which they are attached either directly or mediated by the interposition of microfibrils (see below). The GBM represents the effector structure of mesangial contractility.[124,147] Mesangial–cell–GBM connections are

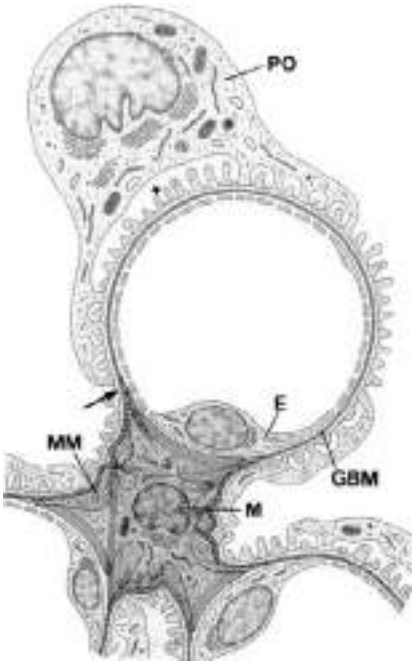

FIGURE 20.33 **Schematic to show the arrangement of the structures in the glomerular tuft.** Part of a glomerular lobule is shown with three glomerular capillaries (two are only partly shown) attached to a mesangial center. The glomerular capillary is made up of a fenestrated endothelium. The peripheral part of the endothelial tube is surrounded by the GBM which, at the mesangial angles (arrow), deviates from a pericapillary course and covers the mesangium. The interdigitated pattern of the podocyte (PO) foot processes form the external layer of the filtration barrier. Note the subcell body space (star). Podocyte foot processes are also found covering the paramesangial GBM. In the center a mesangial cell (M) is shown. Its many processes contain microfilament bundles and run towards the GBM, to which they are connected. The mesangial matrix (MM) contains an interwoven network of microfilaments. *(From Venkatachalam, M. A., and Kriz, W. (1992).* In *"Anatomy of the Kidney. Pathology of the Kidney," 1–92, Heptinstall, R. Little, Brown and Company, Boston, with permission.)*

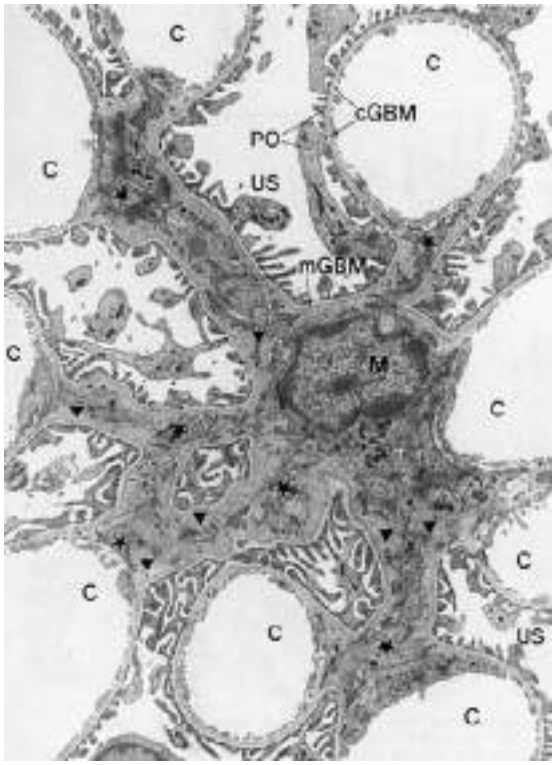

FIGURE 20.34 **Section through a glomerular lobule (rat).** The relationships of glomerular capillaries to the mesangium in the lobule center are seen. Glomerular capillaries (C) and the glomerular mesangium occupy a common compartment enclosed by the glomerular basement membrane (GBM). The mesangial cell body (M) gives rise to several processes (some are marked by stars) which extend toward the peripherally located capillaries. Note the abundant mesangial matrix **(**triangles**)**. The layer of podocytes (PO) covers the outer aspect of the GBM. Thus, neither the GBM, nor the podocyte layer encircle the capillaries completely; both together form a common surface cover around the entire lobule. Therefore, two subdomains of the GBM (as well as of the podocyte layer) can be delineated: the pericapillary (peripheral) GBM (cGBM; faced by podocytes and the endothelium); and the perimesangial GBM (mGBM) bordered by podocytes and the mesangium. The peripheral part of the capillary wall establishes the filtration barrier. Note the mesangial cell body (M) giving rise to many cell processes (some are marked by stars) which are embedded in the mesangial matrix (triangles**)** **(**US: Urinary space; TEM: $\times \sim 5500$).

especially prominent alongside the capillaries. At these sites mesangial cell processes (densely stuffed with microfilament bundles) extend underneath the capillary endothelium towards the mesangial angles of the GBM where they are anchored. Generally, these processes interconnect the GBM from two opposing mesangial angles (Figure 20.35b). Functionally, the microfilament bundles bridge the entire distance between both mesangial angles. In the axial mesangial region as well, numerous microfilament bundles extending through mesangial cell bodies and processes bridge opposing parts of the GBM. The connection of mesangial cell processes to the GBM is mediated by the integrin $\alpha 3\beta 1$ and the Lutheran glycoprotein, which both adhere to the laminin $\alpha 5$ chain.[148]

The mesangial matrix fills the highly irregular spaces between the mesangial cells and the perimesangial GBM (for review see [147,149]). A large number of common extracellular matrix proteins have been demonstrated within the mesangial matrix, including several types of collagen (III, IV, V, and VI), heparin sulfate proteoglycans (including the small proteoglycans biglycan and decorin),[150] fibronectin, laminin, and entactin, as well as fibrillin 1 and other specific elastic fiber proteins.[140,151–153] Among these components, fibronectin is the most abundant, and has been shown to be associated with microfibrils.[151,154]

The basic ultrastructural organization of the matrix is a network of microfibrils. In specimens prepared for TEM by routine methods a fine filamentous network is seen, which possibly corresponds to collagenous filaments. In specimens prepared by a technique that avoids osmium tetroxide and uses tannic acid for staining, the mesangial matrix is seen to contain abundant elastic microfibrils.[124,155] Microfibrils are unbranched, noncollagenous tubular structures that have an indefinite length and are about 15 nm in diameter. They form a dense three-dimensional network establishing a functionally continuous medium anchoring the mesangial cells to the GBM.[147,153] Distinct bundles of microfibrils may be regarded as "microtendons" that allow the transmission of contractile force of mesangial cells to specific sites of the GBM, predominantly to the mesangial angles.[124,155] α-8 integrin serves as a specific matrix receptor in the mesangium.[156]

Glomerular endothelial cells (Figures 20.33, 20.34 and 20.35) are large flat cells consisting of a cell body (which contains all the usual cell organelles) and densely perforated peripheral parts. These regions are extremely attenuated and characterized by round to oval pores varying in diameter between 50 and 100 nm. Unlike fenestrae (unfortunately, these pores are frequently also called "fenestrae"), the pores of glomerular endothelial cells lack a diaphragm, they are virtually open[26]; (Figures 20.36b and 20.37b). Fenestrae bridged by diaphragms in glomerular capillaries are only found along the intraglomerular segment of the efferent arteriole and its tributaries.[20] In rat, about 60% of the capillary surface is covered by the porous regions; the total area of pores occupies about 13% of the capillary surface.[157] Micropinocytotic vesicles are very rare in glomerular endothelial cells, corroborating the fact that the open pores make transcytotic processes unnecessary.

Glomerular endothelial cells contain the usual inventory of cytoplasmic organelles, generally located within the cell body cytoplasm. The endothelial skeleton comprises intermediate filaments and microtubules; individual pores are lined by clusters of microfilaments.[158]

The luminal membrane of endothelial cells is highly negatively charged, due to a cell coat that also fills the

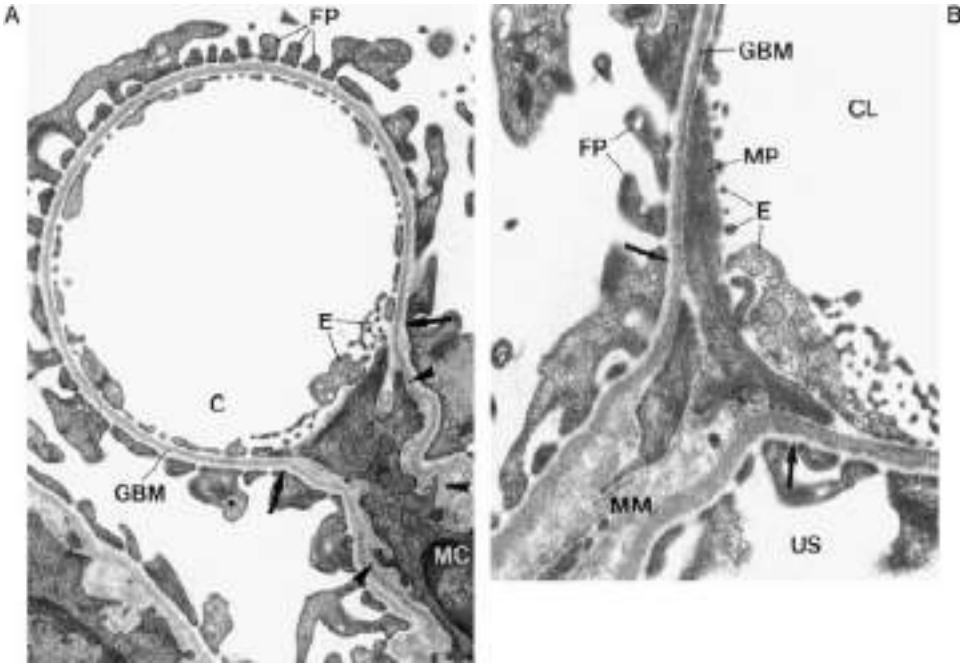

FIGURE 20.35 **(a) Overview of a glomerular capillary (mouse).** Within the mesangium, a mesangial cell (MC) is seen whose processes extend toward the peripherally located capillary (C). Microprojections (arrowheads) originating from the primary process extend toward the GBM. Note that the GBM (as well as the podocyte layer) deviates from its pericapillary course at the two mesangial angles (marked by arrows), continuing as a cover of the mesangium. Thus, the juxtamesangial part of the glomerular capillary lacks a basement membrane; at this site the endothelium is directly exposed to the mesangium. The capillary endothelium is thin and fenestrated. The podocyte layer consists of interdigitating foot processes (FP) which abut the GBM on its outside surface (TEM: ×~13,500). **(b) Capillary–mesangium interface (rat).** At this site a basement membrane is not developed. Beneath the endothelium, tongue-like mesangial cell processes (MP) are found which run toward both opposing mesangial angles. They contain microfilament bundles, which obviously interconnect the GBM of both mesangial angles (marked by arrows) (CL: capillary lumen; US: urinary space; MM: mesangial matrix; FP: foot processes; TEM: ×~23,000).

pores like "sieve plugs".[159] It consists of several polyanionic glycoproteins including a sialoprotein called podocalyxin, which is considered as the major surface polyanion of glomerular endothelial as well as epithelial cells.[160] Endothelial cells are active participants in the processes controlling coagulation, inflammation and immune processes. Glomerular endothelial cells synthesize and release endothelin-1, endothelium-derived relaxing factor (EDRF),[161] and PDGF B.[162] Glomerular endothelial cells have receptors for VEGF A and angiopoetin that are produced by podocytes.[163,164] The continuous stimulation of glomerular endothelial cells by podocyte-derived VEGF A has major relevance for the maintenance of glomerular capillaries and the formation of pores instead of fenestrae.[165]

Within the conspicuously narrow portion of the efferent arteriole (outflow segment) the endothelial cells are arranged in an eye-catching pattern: their cell bodies bulge into the lumen being longitudinally stretched, suggesting a specific shear stress receptor of glomerular capillaries.[20,166]

Mature podocytes are highly-differentiated cells. In the developing glomerulus at the S-shaped body stage, podocytes are a simple polygonal shape connected by apical tight junctions. At the transition to the capillary loop stage the mitotic activity of the cells is completed, the interdigitating foot process pattern with basally located slit membranes instead of apical tight junctions is established, and the final number of podocytes is determined. In rat this point is reached soon after birth, in man it is established during prenatal life. Differentiated podocytes are unavailable for regenerative cell replication[167]; thus in the adult, lost podocytes cannot be replaced by division of the remaining cells. The only way to replace the function of lost podocytes is the hypertrophy of the remaining podocytes.

Podocytes have a voluminous smooth surfaced cell body (Figures 20.36a and 20.37a), which floats within the urinary space; it appears to adapt in shape to the surrounding flow conditions created by the filtrate. The cells give rise to long primary processes (frequently branching another time) that extend towards the capillaries, finally splitting apart into terminal processes, called foot processes, which affix to the GBM (Figures 20.36 and 20.37a). The foot processes of neighbouring podocytes regularly interdigitate with each other, leaving meandering slits (filtration slits) between them, which are bridged by an extracellular structure,

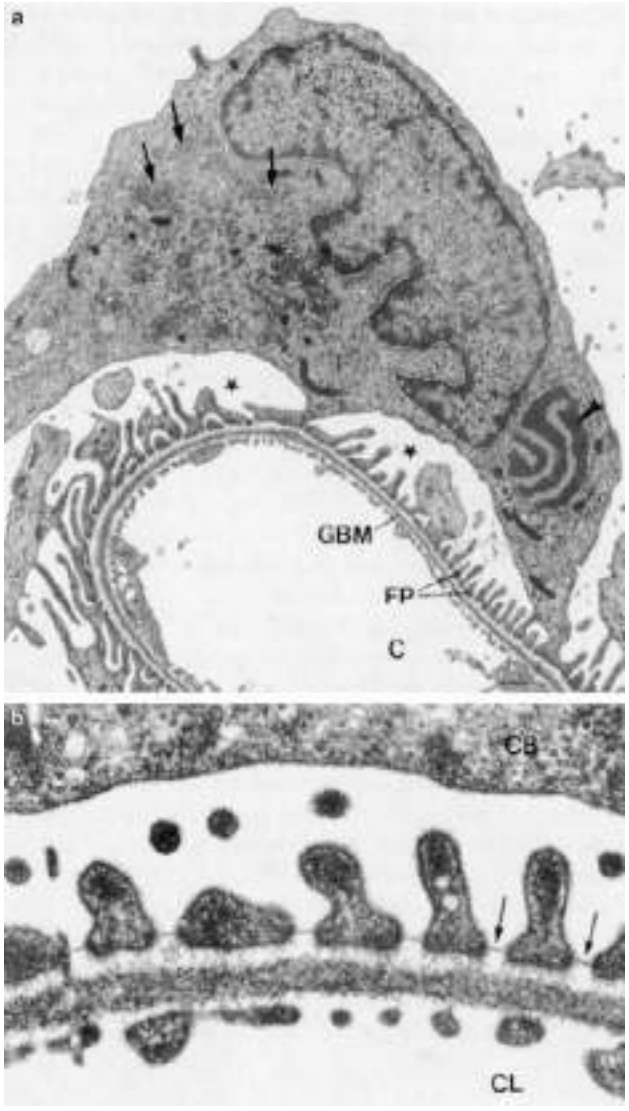

FIGURE 20.36 **(a) Podocyte (rat)**. The cell body contains a large nucleus with indentations. The cytoplasm contains a well-developed Golgi apparatus (arrows), and a conspicuous lamellated inclusion body (arrowhead). The cell processes run toward the GBM forming the interdigitating pattern of foot processes (FP) there. Note the subcellbody space (stars) (C: capillary; TEM: × ~7600). **(b) Filtration barrier (rat)**. The peripheral part of the glomerular capillary wall comprises three layers: the endothelium with large open pores; the basement membrane (GBM); and the layer of interdigitating podocyte foot processes. The GBM consists of a lamina densa, a lamina rara interna toward the endothelium, and a lamina rara externa toward the epithelium. Note the slit diaphrams bridging the floor of the filtrations slits (arrows) (CL: capillary lumen; CB: cell body of a podocyte; TEM: ×~57,000).

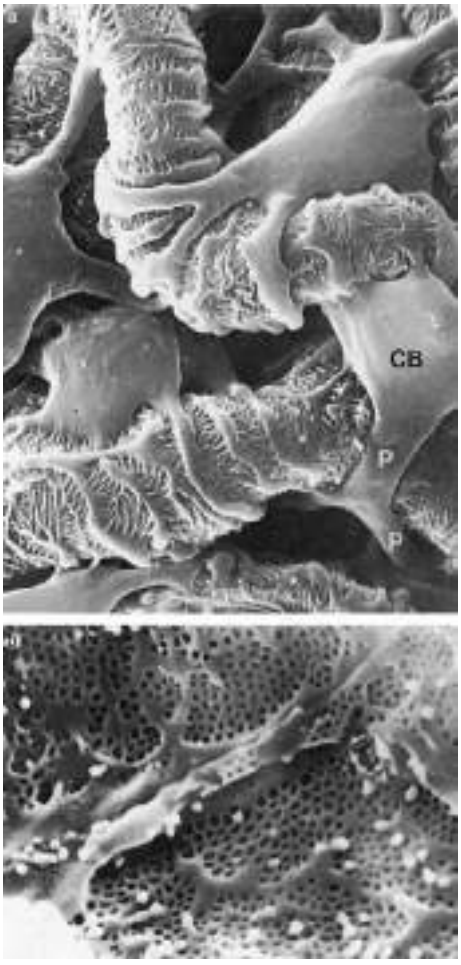

FIGURE 20.37 **(a) Outer surface of glomerular capillaries (rat).** Processes (P) of podocytes run from the cellbody (CB) toward the capillaries where they ultimately split into foot processes. By interdigitation, foot processes from neighbouring cells create the filtration slits (SEM: ×~3400). **(b) Inner surface of a glomerular capillary (rat).** The open fenestrations (not bridged by a diaphragm) are shown (SEM: ×~16,000).

the so-called slit diaphragm. Podocytes are polarized epithelial cells with a luminal and a basal cell membrane domain; the latter corresponds to the sole plates of the foot processes which are embedded into the GBM to a depth of 40 to 60 nm. The border between basal and luminal membrane is represented by the insertion of the slit diaphragm.[167]

The cell body contains a prominent nucleus, a well-developed Golgi system (Figure 20.36a), abundant rough and smooth endoplasmic reticulum, prominent lysosomes (including abundant multivesicular bodies), and many mitochondria. In contrast to the cell body, the cell processes contain only a few organelles (except from multivesicular bodies). The density of organelles in the cell body indicates a high level of anabolic, as well as catabolic, activity. In addition to the work necessary to sustain the structural integrity of these specialized cells, all components of the GBM are synthesized by podocytes.[133,143]

A well-developed cytoskeleton accounts for the complex shape of the cells. In the cell body and the primary processes, microtubules and intermediate filaments (vimentin, desmin) dominate, whereas

microfilaments are densely accumulated in the foot processes. In addition, in the cell body and the primary processes, microfilaments are seen as a thin layer underlying the cell membrane.[168,169]

The prominent bundles of microtubules in the large processes are associated with microtubule-associated proteins, including MAP3/MAP4 and tau.[170] Moreover, like in neuronal dendrites, the microtubules of the podocyte foot processes are non-uniformly arranged with peripheral plus- and minus-end microtubules associated with the specific protein CHO1/MKLP1.[171] In addition, the large processes contain the intermediate type filament protein vimentin.[168]

In the foot processes a complete microfilament-based contractile apparatus is present. The microfilaments form loop-shaped bundles, with their limbs running in the longitudinal axis of the foot processes. The bends of these loops are located centrally at the transition to the primary processes, and are probably connected to the microtubules by "tau" which is concentrated at those sites.[172] Tau is known from other places to mediate connections between microtubules and microfilaments.[173] The microfilament bundles contain actin, myosin II, α-actinin, and synaptopodin[168,174,175]; synaptopodin, a novel podocyte-specific actin-associated protein interacts with α-actinin inducing the formation of long unbranched parallel bundles of microfilaments.[176] Peripherally, the actin bundles anchor in the dense cytoplasm associated with the basal cell membrane of podocytes, i.e., the sole plates of foot processes.[167]

Anchoring of the sole plates to the GBM is achieved by specific transmembrane receptors; two systems are so far known (Figure 20.38). First, a specific integrin heterodimer, consisting of $\alpha_3\beta_1$ integrins, which bind within the GBM to collagen type IV, fibronectin, and laminin 521.[177–179] Second, a dystroglycan complex connects the intracellular molecule utrophin to laminin 521, agrin, and perlecan in the GBM.[180,181] Both integrins and dystroglycans are coupled via adapter molecules (paxillin, vinculin, α-actinin) to the podocyte cytoskeleton, allowing outside-in and inside-out signaling, as well as transmission of mechanical force in both directions. A major role in this issue is played by the integrin-linked kinase.[182]

A huge body of data has been accumulated in recent years concerning the inventory of receptors and signaling processes starting from podocytes. cGMP signaling

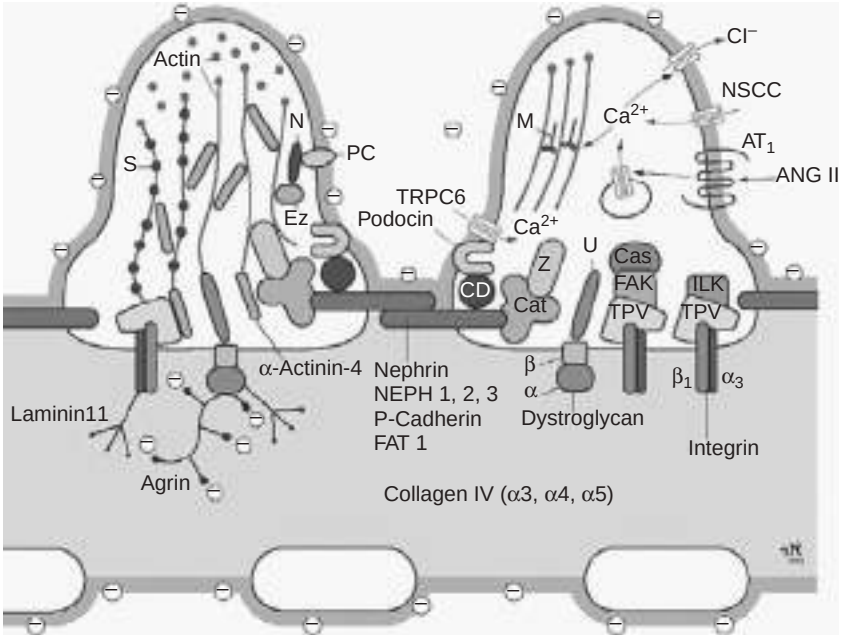

FIGURE 20.38 **Glomerular filtration barrier.** (*Modified from Endlich, K. H., Kriz, W., and Witzgall, R. (2001). Update in podocyte biology. Curr. Opin. Nephrol. Hypertens.* ***10****, 331–340.*) Two podocyte foot processes bridged by the slit membrane, the GBM, and the porous capillary endothelium are shown. The surfaces of podocytes and of the endothelium are covered by a negatively-charged glycocalyx containing the sialoprotein podocalyxin (PC). The GBM is mainly composed of collagen IV (α_3, α_4, and α_5), of laminin 11 (α_5, β_2, and γ_1 chains) and the heparan sulphate proteoglycan agrin. The slit membrane represents a porous proteinaceous membrane composed of (as far as is known) Nephrin, Neph1, 2, and 3, P-cadherin, and FAT1. The actin-based cytoskeleton of the foot processes connects to both the GBM and the slit membrane. With regard to the GBM, β_1/α_3 integrin dimers specifically interconnect the TVP complex (talin, paxillin, vinculin) to laminin 11; the β and α dystroglycans interconnect utrophin to agrin. The slit membrane proteins are joined to the cytoskeleton via various adaptor proteins, including Podocin, Zonula occludens protein 1 (ZO-1; Z), CD2-associated protein (CD), and catenins (Cat). TRPC6 associates with podocin (and nephrin; not shown) at the slit membrane. Among the many surface receptors only the angiotensin II (ANG II) type 1 receptor (AT1) is shown (Additional abbreviations: Cas: P130Cas; Ez: ezrin; FAK: focal adhesion kinase; ILK: integrin-linked kinase; M: myosin; N: NHERF2 (Na^+-H^+ exchanger regulatory factor); NSCC: Non-selelctive cation channel; S: Synaptopodin).

(stimulated by ANP, BNP, and CNP, as well as by NO), cAMP signaling (stimulated by prostaglandin E_2, dopamine, isoproterenol, PTH/PTHrP), and Ca^{2+} signaling (stimulated by a huge number of ligands including angiotensin II, acetylcholine, PGF_2, AVP, ATP, endothelin, histamine) have been identified. Among the cation channels, TRPC6, a nonselective Ca^{2+} channel, has recently received attention, since mutations in the respective gene lead to hereditary FSGS.[183,184] The major target of this signaling orchestra is the cytoskeleton, the concrete effects, however, are poorly-understood. Other receptors, such as for C3b,[185] TGFß,[186,187] FGF2,[188] and various other cytokines and chemokines have been shown to be involved in the development of podocyte diseases (for details see [189]). Megalin, a multi-ligand endocytotic receptor, is associated with coated bits[190–192]; it represents the major antigen of rat Heymann nephritis.[193]

The filtration slits are the site of convective fluid flow through the visceral epithelium. They have a width of 30 to 40 nm and are bridged by the slit membrane. The structure and molecular composition of this proteinaceous membrane is insufficiently understood. Chemically fixed and tannic acid treated tissue reveals a zipper-like structure with a row of "pores" approximately 4 × 14 nm on either side of a central bar.[194] According to its dimension and its components (as far as is known) the slit diaphragm may be considered as a specific adherens-like intercellular junction. Intensive research in recent years has uncovered several transmembrane proteins that participate in the formation of the slit membrane, including nephrin,[195] Neph1,[196] P-cadherin,[197] and FAT[198] (Figure 20.38). Other molecules, such as ZO1,[199] Podocin,[200] CD2AP,[201] and catenins mediate the connection to the actin cytoskeleton (see below). Nephrin is a member of the immunoglobin superfamily (IgCAM); its gene NPHS1 has been identified as the gene whose mutations cause congenital nephritic syndrome of the Finnish type.[195] In addition to its role as a structural component, nephrin acts as a signaling molecule that can activate MAP kinase cascades.[202] Neph1 is considered as a ligand for nephrin. Podocin belongs to the raft associated stomatin family, whose gene NPHS2 is mutated in a subgroup of patients with autosomol-recessive stereoid-resistent nephrotic syndrome.[200] These patients show disease onset in early childhood and rapid progression to end-stage renal failure. Podocin interacts with nephrin and CD2AP.[203] FAT is a novel member of the cadherin superfamily, with 34 tandem cadherin-like extracellular repeats and a molecular weight of 516 kDa.[204] Because FAT has a huge extracellular domain, it is speculated that it dominates the molecular structure of the slit membrane[198]; the FAT mutant mouse fails to develop a slit membrane.[205] P-cadherin[197] is thought to mediate the linkage to ß- and γ-catenin with its intracellular domain, a complex which then connects to the actin cytoskeleton via α-catenin and α-actinin. Taken together, many components of the slit membrane are known, but an integrative model of its substructure including all components is so far lacking.

The luminal membrane and the slit diaphragm are covered by a thick surface coat which is rich in sialoglycoproteins (including podocalyxin, podoendin, and others) that are responsible for the high negative surface charge of the podocytes.[206,207] Podocalyxin is anchored to the actin cytoskeleton beneath the cell membrane via the linker protein NHERF 2 (Na^+/H^+ exchanger regulatory factor 2) and ezrin.[208,209] The surface charge of podocytes contributes to the maintenance of the interdigitating pattern of the foot processes. In response to neutralization of the surface charge by cationic substances (e.g., protamine sulfate), the foot processes retract, resulting in what is called "foot process effacement".[210]

Filtration Barrier

The walls of glomerular capillaries represent a specific barrier which is very permeable to water, and yet able to prevent all but very minute losses of serum albumin and other major plasma proteins from the circulation. The glomerular capillary wall consists of three distinct layers (Figures 20.36b and 20.37). Starting at the capillary lumen, there is the porous endothelium, followed by the GBM, and the layer of interdigitating foot processes with the filtration slits in between.

The high hydraulic permeability of this barrier suggests that the filtrate pathway is entirely extracellular, passing through the endothelial fenestrae, across the GBM, and through the slit diaphragms of the filtration slits. According to a calculation by Drumond and Deen,[211] the hydraulic resistance of the endothelium is negligible. The GBM and the filtration slits each make up roughly one half of the total hydraulic resistance of the filtration barrier.

Charge, size, and shape determine the specific permeability of a macromolecule. It is now generally accepted that the charge barrier plays an important part in preventing polyanionic macromolecules such as albumin from passing through the glomerular filter. All components of the glomerular filter are heavily laden with negative charges.[212] Recent investigation[213,214] suggests that the negative residues of the endothelium play the major role in establishing a negative charge field which considerably decreases the entry of polyanionic macromolecules, i.e., albumin, into the filter.

With regard to the size selectivity, direct experimental findings,[211,215,216] as well as recent findings about the molecular composition of the slit membrane (see above) and the consequences of genetic mutations in these components, suggest that it is for the major part the slit membrane which is responsible for the size selectivity; it appears to be the main barrier for uncharged large molecules.

There is another major unresolved problem in glomerular physiology, namely the regulation of the ultrafiltration coefficient Kf. Kf is the product of the local hydraulic permeability and the filtration area. There has been a widespread belief that Kf is regulated through changes in the filtration area due to an action of the mesangium.[217] However, the structural arrangement of the mesangium,[124] as well as several morphometric studies,[218,219] do not support such an assumption. Dimensional changes in just the slit membrane area have also been regarded as a reasonable and, theoretically, very effective site to change Kf.[220] In pathological conditions, e.g., in membranous nephropathy,[221] the decrease in Kf correlates perfectly with the decrease in total slit length. With respect to acute regulatory mechanisms under physiological conditions, however, no convincing morphometric data have been published showing that changes in Kf are correlated with corresponding dimensional changes in the slit membrane. Thus, the question of where and how Kf is regulated remains an open problem.

Stability of the Glomerular Tuft

The glomerular tuft is constantly exposed to comparably high intraglomerular pressures within glomerular capillaries and mesangium. The high intraglomerular pressures challenge not only the glomerular capillaries themselves, but also the folding pattern of the glomerular tuft. Increased pressures lead to loss of the folding pattern, and to dilation of the glomerular capillaries. Therefore, we have to ask what are the specific structures and mechanisms that counteract the expansile forces in the glomerular tuft. To answer this question we have to distinguish between the structures and mechanisms maintaining: (1) the folding pattern of the glomerular tuft; and those maintaining (2) the width of glomerular capillaries (Figure 20.39).

The folding pattern of the glomerular tuft is primarily sustained by the mesangium.[124,147,222] Mesangial cells are connected to the GBM by their contractile processes (see above); by centripetal contractions they maintain the infoldings of the GBM, thereby allowing the capillaries to arrange in the peripheral expansion of the GBM. This supporting role of mesangial cells is best illustrated under circumstances with loss of mesangial cells, such as Thy-1 nephritis.[223] Under those circumstances the folding pattern of the GBM is progressively lost, finally resulting in mesangial aneurysms. Podocytes clearly contribute to the maintenance of the folding pattern by specific cell processes that interconnect opposing parts of the GBM from outside within the niches of the infoldings. This function is again clearly illustrated in Thy-1 nephritis under circumstances with loss of mesangial support: podocytes are capable of maintaining a high degree of the GBM folding pattern for 2–4 days, after which they fail and mesangial aneurysms become prominent.[223]

The width of glomerular capillaries, in the long run, is probably controlled by growth processes accounting for different-sized capillaries. The width of a given capillary, in an acute situation being exposed to changes in blood pressure, appears to be stabilized by the GBM which is a strong elastic structure[224] and, together with the mesangial cell bridges (see above), is capable of developing wall tension.[147,225] In addition, the tensile strength of the GBM is reinforced by podocytes. Podocytes are a kind of pericyte; their foot processes represent a unique type of pericyte process which, like elsewhere in the body, counteract the dilation of the vessel. Podocyte processes are firmly attached to the underlying GBM (see above); their cytoskeletal tonus counteracts the elastic extension of the GBM. Podocytes cannot be replaced by any other cell; failure in this function will lead to capillary dilation.

Parietal Epithelium of Bowman's Capsule

The parietal layer of Bowman's capsule consists of squamous epithelial cells resting on a basement

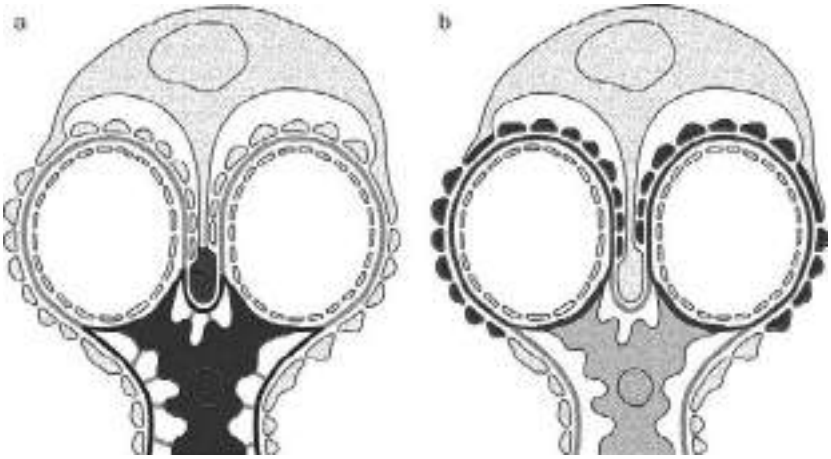

FIGURE 20.39 **Schematic to show the mechanisms that stabilize the glomerular tuft against expansion (relevant structures are highlighted in dark gray).** The folding pattern of the GBM is thus stained by mesangial cells from inside, and by specific podocyte processes located in the depth between two capillaries from outside. The width of capillaries against transmural pressure gradients is maintained by wall tension, which is generated by the rigidity of the GBM, by the mesangial cell processes that interconnect opposing turning points of the GBM, and by the tonus of podocyte foot processes.

membrane (Figure 20.29). The cells are of polygonal shape and contain prominent bundles of actin filaments running in all directions. Microfilament bundles are especially prominent in the parietal cells surrounding the vascular pole, where they are located within cytoplasmic ridges that run in a circular fashion around the glomerular entrance.[20]

The basement membrane of the parietal epithelium (PBM) is, at variance with the GBM, composed of several dense layers which are separated by translucent layers and contain bundles of fibrils.[226] Recent studies suggest a role of type XIV collagen in the organization of the multilayered PBM.[227] In contrast to the GBM, the predominant proteoglycan of the PBM is a chondroitin sulfate proteoglycan.[149] The transition from the GBM to the PBM borders the glomerular entrance. This transitional region is mechanically connected to the smooth muscle cells of the afferent and efferent arterioles as well as to extraglomerular mesangial cells.

At the urinary pole, the flat parietal cells transform into proximal tubule cells. In some cases the flat cells may continue for a certain distance as a so-called neck segment of the tubule (rabbit)[228] or the typical proximal tubule epithelium generally starts within the glomerular capsule. This is the case in the mouse,[824] most pronounced in males.

In rare cases, parietal epithelial cells may be replaced by podocytes ("parietal podocytes") which display a process pattern identical to that of podocyte proper of the tuft.[229] At such sites, the PBM is similar to the GBM and capillaries may attach from outside. As shown recently, parietal podocytes are regularly found when ß-catenin is deleted in renal epithelial cells during development at the S-shaped body stage.[230] Recent observations suggest that a niche of glomerular epithelial stem cells resides within the parietal epithelium at the transition to the proximal tubule.[231,232]

It is an intriguing hypothesis that proliferating stem cells from this locus may transform into podocytes and may reach the tuft via the transitions of the epithelia at the glomerular vascular pole. Migration of parietal cells via the vascular pole and subsequent transition into podocytes has been shown to occur in the new-born mouse.[233] However, evidence that such a process may be of any relevance in the adult has so far not been presented.[233]

STRUCTURAL ORGANIZATION OF RENAL ELECTROLYTE TRANSPORTING EPITHELIA

General Overview of Renal Epithelial Organization

The renal tubular epithelia function as selective barriers between the tubular fluid in the luminal compartment and the interstitial compartment that communicates with the blood compartment. The epithelium consists of a single layer of cells, resting on a basement membrane composed of extracellular matrix. The cells are interconnected by *junctional complexes* that encircle each individual cell like a belt. The *tight junction* (zonula occludens) separates the luminal compartment from the lateral intercellular space and is the boundary between the apical plasma membrane domain, facing the tubular fluid, and the basolateral membrane domain, which lines the intercellular compartments and is in contact with the basement membrane. The *intermediate junctions* (zonula adherens), and the patches of *desmosomes* (maculae adherentes) provide mechanical adherence. Gap junctions that provide intercellular communication exist exclusively in the proximal tubule.

This basic organization of the epithelium (Figure 20.40) implies two *transepithelial transport pathways* for solutes and macromolecules: (1) the paracellular pathway across the tight junctions and the lateral intercellular spaces (the passage of solutes through the paracellular pathway is driven by the transepithelial electrochemical and oncotic gradients); (2) the transcellular pathway across the luminal membrane domain, the cellular cytoplasm and the basolateral membrane domain, and *vice versa* (the passage of solutes via the transcellular pathway occurs mostly against electrochemical gradients and is energy-dependent).

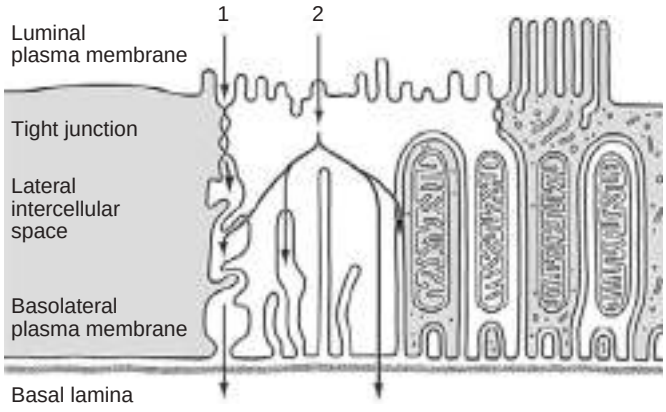

FIGURE 20.40 **Schematic drawing, demonstrating the essential structural features of renal transporting epithelia.** (1) Paracellular route through the tight junction and the lateral intercellular spaces; (2) Transcellular route, across the apical plasma membrane, which may be augmented by short microvilli, microfolds (not shown) or long microvilli of uniform length, called " brush border," across the cytoplasm, and across the basolateral plasma membrane; the latter may be augmented by infoldings of the basal plasma membrane or by basolateral processes of the cells, which narrowly interdigitate with each other. The lateral interdigitating processes contain large mitochondria.

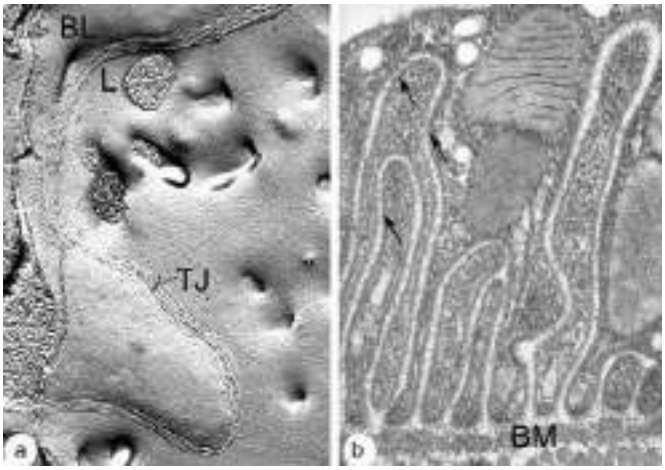

FIGURE 20.41 **Tight junction and intercellular space.** (a) Freeze-fracture electron micrograph of thick ascending limb cells. (b) The tight junction (TJ) consists of several densely arranged parallel strands (BL: basolateral membrane; L: luminal membrane; Rabbit: ×~45,000). (Cooperation with A.Schiller and R.Taugner).

Paracellular Pathway

As seen in freeze-fracture replicas, tight junctions are composed of globular particles, arranged in one or several roughly parallel strands or in a net-like pattern[234] (Figure 20.41a). The more-or-less densely packed particles in the strands presumably represent the transmembrane proteins that participate in the junction's formation.

The tight junctions function as barriers between the luminal compartment and the lateral intercellular spaces. At the same time they allow a selective, regulated paracellular flow of small inorganic cations,[235,236] and the passage of some large organic cations and of some uncharged molecules.[234,237] The selectivity of tight junctions for different solutes varies among the different tubular epithelia.[238,239] Claudins, a large family of integral membrane proteins, make up the bulk of tight junctional strands,[240–243] and play a key role in determining and regulating the paracellular permeability for small inorganic cations.[244] They act as size-, charge-, ion concentration- and pH-dependent channels or pores in the intercellular space,[245–247] and seem to be targets of the serine-threonine kinases WNK1 and WNK4.[248–251] The dynamic regulation of paracellular flux does not seem to involve structural changes of the tight junctional complexes. Mutations in claudin members[252,253] or defects in the WNK-signaling cascades may have major implications on volume homeostasis.[250,251,254–257] Occludin, another integral membrane protein, is interspersed with claudins in the tight junctional strands. The cytoplasmic domain of occludin is associated with ZO1, thereby providing a linkage for the membrane to its scaffolding actin cytoskeleton.[234,244] The interaction of occludins with the actin skeleton may be important in regulating the paracellular passage for larger molecules, and for "macropermeation" across the epithelium, as well as in the transduction of signals from apoptotic cells.[258] Further, ZO1 seems to be associated with the "fence" function of tight junctions,[258] i.e., the ability of the tight junction to prevent diffusion of lipids from the apical to the basolateral membrane domain. Via transcription factor zonula occludens 1 (ZO-1)-associated nucleic acid binding protein (ZONAB), it can also be involved in controlling cell proliferation.[259]

Cell adhesion proteins at the extracellular face of the basolateral surface of renal tubular cells maintain a basal level of cell–cell adhesion, in addition to strong cellular adhesion provided by the junctional complexes and/or desmosomes. The cell adhesion proteins in the intercellular spaces can be made visible by electron-microscopy with specific fixation procedures.[260] The "classical" cell adhesion proteins N- and E-cadherin,[261–264] as well as the "atypical" kidney-specific (ksp) cadherin 16[265,266] have been located by immunostainings on the basolateral membranes all along the tubular system. The classical cell adhesion molecules are linked to the scaffolding actin skeleton, as well as to β-catenin, at the cytoplasmic face of the basolateral cell membranes.[267] This connection provides a pathway for coupling extracellular signals (among others, binding of a hormone to its receptor, mechanical stresses) to intracellular signaling cascades that control various cellular responses, such as endocytosis, ubiquitination of proteins, transcription, proliferation or apotosis.[267]

Transcellular Pathway

The prerequisite for transcellular vectorial transport of solutes across epithelia is the asymmetric or polarized allocation of co-transporters, exchangers, channels, and enzymes, to the luminal and basolateral plasma membrane

LUMINAL MEMBRANE DOMAIN

The uptake of most solutes into the cell is coupled to passage of sodium via solute-specific co-transporters, via channels or via exchange against protons (H^+) in the luminal plasma membrane. The given assembly of transport proteins in the luminal membrane of the cells of a segment determines the segment-specific solute transport pattern. Enzymes (e.g., phosphatases, peptidases) in the luminal membrane hydrolyze poorly permeable organic compounds to readily permeable ones, and various receptor proteins (e.g., megalin, cubilin etc.[268]) mediate the uptake of their ligands into the cell.

Many of the apical transport proteins are linked to the actin-based cytoskeleton under the plasma

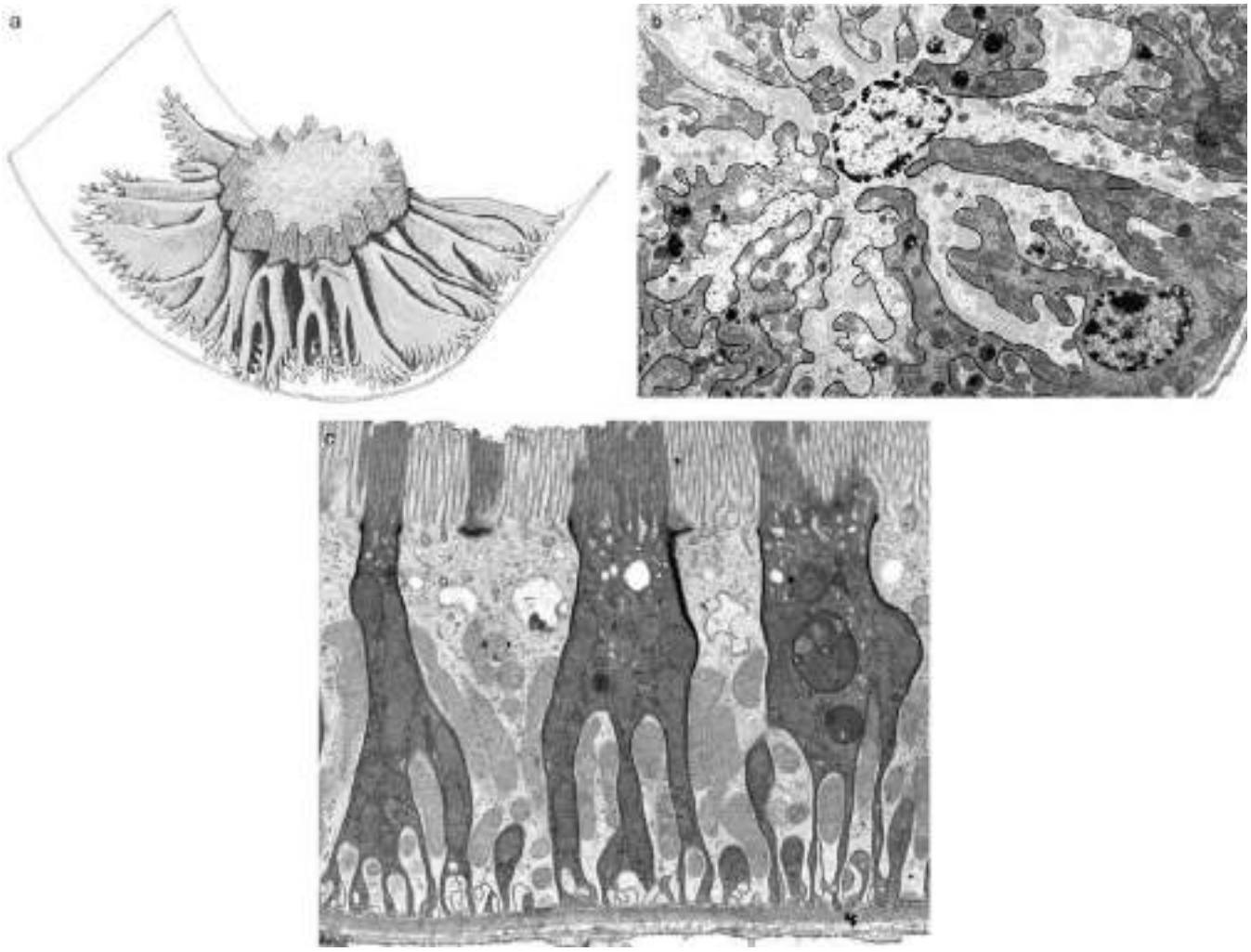

FIGURE 20.42 **Augmentation of apical and basolateral plasma membrane surfaces by microvilli and interdigitating lateral cell processes.** (a) Three-dimensional model of a rabbit proximal tubule cell. *(From Welling, L. W., and Welling, D. J. (1975). Surface areas of brush border and lateral cell walls in the rabbit proximal nephron. Kidney Int. 8(6), 343–348 ,with permission.)* The dark line indicates the position of the tight junctional belt between the apical and basolateral membrane domains; the apical membrane domain is amplified by microvilli, which form a brush border; the basolateral membrane domain is augmented by interdigitating lateral cell processes that split in an apico–basal direction to primary and secondary processes and basal plicae; the latter are anchored in the basement membrane. (b) and (c): Sections through S1 proximal tubule (*Psammomys obesus*); the dark contrast of the intercellular spaces (black lines), and the differential contrast of adjacent cells result from fixation with reduced osmium; (b) the section, cut approximately in parallel to the basement membrane through the center of the cell reveals the complex interdigitation of the lateral cell processes; (c) in the section in an apico–basal direction apical interdigitation by lateral processes is revealed by the different contrast in the brush border; the lateral interdigitating processes increasingly split up towards the cell base; the larger ones are filled out with mitochondria (TEM: $\times \sim 9000$).

membrane via adaptor proteins containing PDZ interactive domains,[269–273] namely NHERF1, 2, 3, and are thereby maintained in the specific cell membrane areas.[274]

The given assembly of transport proteins in the apical plasma membrane of a segment confers the *specificity* for transported solutes. The *rate* of solute permeation across the membrane critically depends on type (co-transporter, exchanger, channels) and *quantity of active transport systems* in the apical cell membrane domain. The latter is ultimately related to the available *surface area*. Thus, in many epithelia with high transport rates the apical membrane area is much larger than the area of a virtual plane at the level of the tight junctional belt.

Three modes of amplification of apical plasma membrane surface are distinguished (Figure 20.40): (1) densely arranged finger-like microvilli, all of similar dimensions, evenly distributed over the entire cell surface, forming the so-called "brush border" (Figures 20.42 and 20.44). The microvilli have an axial cytoskeleton of actin filaments, arranged in a 6 + 1

pattern, associated with villin and fimbrin in the microvillar core.[275] The actin filaments extend into the terminal web, located in the subapical cytoplasm immediately beneath the base of the microvilli. Brush border formation characterizes the proximal tubule: (2) short microvilli, found on all other tubular cells; their density and distribution on the cell surface varies considerably; (3) microfolds, found on cells in which regulation of the permeation rates for given solutes is associated with rapid transient modulation of the luminal cell surface area (subtypes of intercalated cells and occasionally also in collecting duct cells; see below).

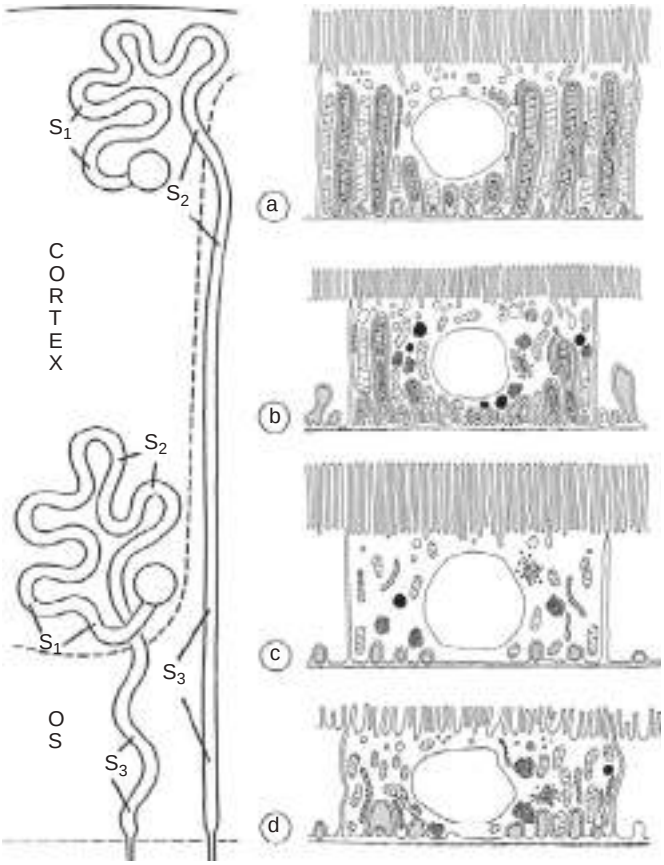

FIGURE 20.43 **Survey on location and ultrastructure of proximal tubule segments.** (a) S1 segments start at the urinary pole of the renal corpuscle in the cortex, and transform gradually to S2 segments within the labyrinth, S2 segments give way to S3 at different levels (depending on the nephron generation) within the medullary rays; S3 terminates at the border (dashed line) of the outer stripe (OS) and the inner stripe. (b) Salient features of S1, S2, and S3 proximal tubule cells; neighbouring cells are shaded in order to reveal the interdigitation by lateral cell processes; the vacuolar apparatus in the subapical cytoplasm, mitochondria, ER, Golgi apparatus, lysosomes (black spots), and peroxisomes (cross-hatched) are indicated; in rat S3 segments (c) the brush border micovilli are the highest, in rabbit (d) and most other species they are the shortest. *(Adapted from ref. [5], with permission).*

BASOLATERAL MEMBRANE DOMAIN

The entry of sodium-coupled solutes across the luminal membrane is driven by the enzymatic splitting of ATP by the Na-K-ATPase, the so-called sodium pump.[276] In renal epithelia ATP is mainly made available by mitochondria. The Na-K-ATPase is inserted in the basolateral membrane domain of all tubular cells, and is firmly linked to the actin cytoskeleton by interacting proteins, such as ankyrin, spectrin/fodrin, and NHERF.[277]

Segment-specific differences in Na-K-ATPase activity/protein[278,279] per unit tubular length rely on cell type-specific differences in the density of the enzyme molecules per area basolateral membrane, and on the available surface area of basolateral membrane per unit tubular length.[280,281] Basically two modes of increases of the basolateral membrane surface per unit tubular length are distinguished in renal epithelia:

1. *Lateral folding and interdigitation* (*basolateral interdigitations*): this mode increases the lateral membrane area[282] and implies an increase of the lateral intercellular space, the common compartment of para- and transcellular transport routes.[40] The width of the lateral intercellular spaces (about 20–50 nm) varies little with function.
   In interdigitated epithelia the tight junctions are composed of one or several parallel strands with more-or-less high particle density. The tall lateral plasma membrane folds, equipped with Na-K-ATPase, narrowly enclose large mitochondria. The folds split into complex basal ridges with densely packed actin filaments (but no Na-K-ATPase[283,284]), arranged in a circular manner,[285–287] which provide attachment to the underlying basememt membrane. This arrangement prevails in proximal (Figures 20.42, 20.43 and 20.44) and distal tubules (Figures 20.52, 20.53, 20.54, 20.56 and 20.57), and causes the characteristic basal striation of these segments in histological sections.
2. *Infoldings of the basal plasma membrane* into the cell body; the spaces between the infolded (Na-K-ATPase carrying) membranes open via so-called basal slits directly towards the underlying basement membrane, and have no continuity with the lateral intercellular spaces. Consequently, trans- and paracellular solute transport pathways are largely separated. The tight junctional belt consists of networks of anastomosing strands with high particle density. The width of the intercellular spaces can be narrow or dilated, depending on the functional conditions. The lateral membranes carry small finger-like villi or folds, and are often interconnected by small desmosomes, These might help to maintain mechanical cohesion under

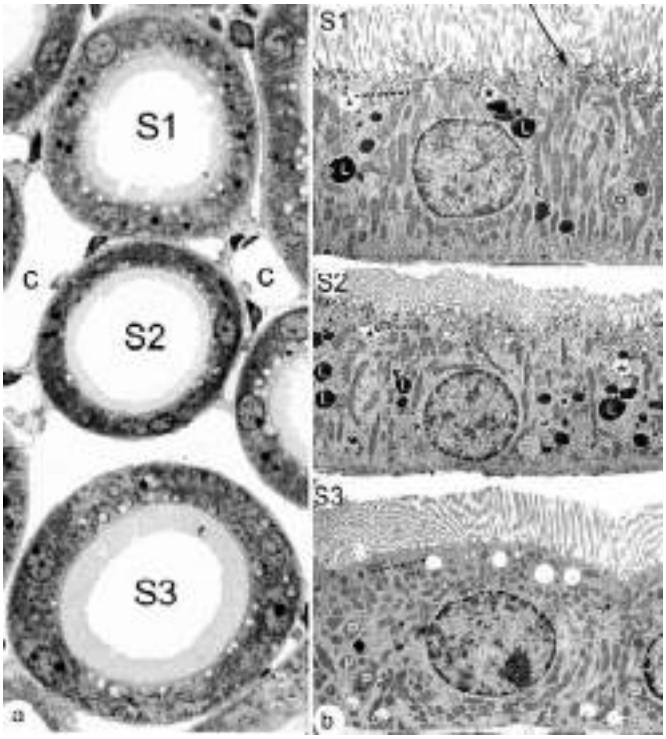

FIGURE 20.44 **Proximal tubule (rat).** (a) Profiles of S1, S2, and S3 segments of juxtamedullary proximal tubules; note the differences in brush border length, in cell height, cytoplasmic density, and outer diameter (c: Peritubular capillaries; Rat: 1 mm Epon section; ×~1000). (b) Ultrastructure of S1, S2, and S3 proximal tubule cells (Rat). The mitochondria in S1 and S2 are located in lateral cell processes, in S3 they are mainly scattered throughout the cytoplasm; the endocytotic apparatus in the subapical cytoplasm (roughly delimited by broken lines) is most prominent in S1 and early S2; endosomes (stars) and lysosomes (L) are located deeper in the cytoplasm; in S3 the vacuolar apparatus and lysosomes are virtually absent, whereas peroxisomes (P) are more frequent than in S1 and S2; interdigitation by lateral folds is almost lacking (TEM: ×~5400).

functionally-induced dilation of the intercellular space. This epithelial organization characterizes the collecting duct system. Increases in membrane area by lateral interdigitating folds and basal infoldings may well be found in the same cell (e.g., connecting tubule cells; Figures 20.56 and 20.58).

Correlation Between Structure and Transport

In defined nephron segments rather constant ratios have been found between Na-transport rates, Na-K-ATPase activity, basolateral plasma membrane surface area, and mitochondrial density.[276,279–281,288–294]

Acute changes in flow rates for a given solute across the luminal cell membrane may be sensed by local purinergic signaling and responded to by rapid adjustment in transport rates.[295,296] They depend on the availability of active transport systems in the cell, and can be effected by several mechanisms, e.g., by gating of transport channels (e.g., ENaC in collecting duct cells), that are present in the luminal plasma membrane,[277] by redistribution of the given protein between microdomains in the apical membrane (e.g., NHE3 in the brush border of proximal tubuli,[297,298] by cycling of luminal and vesicular membrane domains containing the respective transport proteins (e.g., AQP2 in collecting duct cells; H^+ATPase in intercalated cells) between the cell surface and intracellular vesicles[299] or by exocytotic insertion and endocytotic retraction of specific transport proteins into and from, respectively, the luminal membrane (e.g., ENaC[300]; NaPiIIa[301,302]).

Prolonged duration of increased transcellular flow rates stimulates, in addition to the acute responses, the transcription rates for the given transport proteins,[303] and finally results in cellular and epithelial hypertrophy, including cell proliferation.[304,305] Inversely, chronic decreases in Na-transport rates may result in epithelial hypotrophy, including a reduction of cell mass by apoptosis.[293,305–307] On this background it is tempting to interpret the internephron heterogeneity as a reflection of their different filtration and transport rates. In rats the juxtamedullary nephrons with the largest glomeruli and highest filtration rates[308] display the largest tubular diameter, the largest basolateral membrane area, Na-K-ATPase activity, and mitochondrial volume density.[41] The superficial nephrons have the smallest glomeruli, filtration rates, and tubular dimensions.

Primary Single Cilia

All renal cell types, except the intercalated cells, carry a central single primary cilium on their luminal surface. Primary cilia are regarded as mechanosensors that sense changes in luminal flow rate and circumferential stretch.[309–312] The extracellular mechanical stimulus caused by the urinary flow is transduced via the transmembrane proteins Polycystin 1 (PC-1) and Polycystin 2 (PC-2),[313] located in the membrane of the cilium.[314,315] Both together form a complex required for flow-mediated calcium entry in response to the deflection of the axoneme.[316] This subsequently results in release of calcium stores from the endoplasmic reticulum, possibly mediated by Polycystin 2.[309,311] On the one hand, this might induce local purinergic signaling and modulate renal tubular transport[317]; on the other hand, the primary cilia may be involved in the functional differentiation of polarized cells,[318] in the maintenance of normal tubular architecture,[309] in regulation of tissue morphogenesis,[319] and in gene transcription.[320] Cilia seem also to help to regulate and control mTOR and temper the response of this pathway to growth factors.[321] Loss-of-

function mutations in the genes for PC-1 or PC-2 cause ciliary abnormalities[322] and the autosomal dominant form of polycystic kidney disease (ADPKD).[315,323]

PROXIMAL TUBULE

The proximal tubule takes up the glomerular filtrate and recovers the major fraction of water, sodium, and solutes by reabsorption from the tubular lumen back to the blood compartment, and it clears the blood of various organic compounds by uptake from the blood compartment and secretion into the tubular lumen.[324,325] Furthermore, the epithelium removes almost completely filtered proteins from the tubular fluid by endocytosis.

The proximal tubule begins at the urinary pole of the renal corpuscle, and ends at the transition to the descending thin limb of Henle's loop which defines the border between the outer and the inner stripes. It has a convoluted part, situated in the cortical labyrinth, and a straight part (pars recta: the thick descending limb of Henle's loop), located in the cortical medullary rays and in the outer stripe (Figure 20.43). The volume fraction of proximal tubules is about 48% in the rat cortex and about 54% in the outer stripe.[41] From the collected tubular volume in the cortical labyrinth of an adult rat the convoluted proximal tubule takes a fraction of 80 to 85%.[38]

Morphology of Proximal Tubular Epithelium

The proximal tubule is lined by cells with complex, interdigitating folding of the basolateral plasma membrane and characteristic formation of a brush border at the apical pole. The largely amplified apical and basolateral plama membrane surfaces correspond to the high transcellular solute transport rates (see "Organization of Electrolyte Transporting Epithelia"). The lateral foldings narrowly ensheath large mitochondria. At the base the foldings are split into numerous basal ridges, which are densely filled with circular running f-actin filaments, and provide the anchoring of the cell to the underlying extracellular basement membrane. The tight junctions are shallow, mostly consisting of a single strand with low particle density,[275] in agreement with the low-resistance shunt pathway in parallel with a high-resistance pathway across the limiting cell membranes.[326,327] The proximal tubule cells are electrically coupled by gap junctions.

The subapical cytoplasm immediately under the base of the brush border microvilli is a membrane-rich region, called the "vacuolar apparatus".[268] It is the structural correlate of the early endocytotic apparatus (Figure 20.45a) and contains intermicrovillar more or less deep infoldings ("clefts") into the cytoplasm, small clathrin-coated vesicles, uncoated "dense apical tubules" (DAT) 70−90 nm in diameter, and large uncoated vesicles. The dimensions of the vacuolar apparatus are very variable, and depend on the rate of endocytosis (see below). The more or less abundant lysosomes, present in the center of the cells, are functionally related with the degradation of proteins. The nucleus is encircled in its equatorial plane by well-developed Golgi apparatus. Cisterns of rough ER are preferentially extended in parallel with the lateral cell membranes; ribosomes are abundant throughout the cytoplasm. Fenestrated cisterns of smooth ER are particularly abundant. In the terminal portions of the proximal tubule the cisterns of smooth ER contain xenobiotc-metabolizing enzymes[328] which contribute to detoxification processes. The cisterns of the smooth ER often extend along the lateral membranes and narrowly enwrap mitochondria and peroxisomes.[329] The latter are generally situated in the basal portions of the cells.[330] The amount of lysosomes, peroxisomes, and lipid droplets in proximal tubule cells strongly varies with the functional stage of the animal, food intake, and sex hormones.[331−333]

The proximal tubule is subdivided into three segments, S1, S2 and S3.[334,335] The subdivision is based on more-or-less gradually occurring quantitative changes along the proximal tubule. S1 cells line the initial half of the convoluted portion, and have the largest basolateral plasma membrane surface, Na-K-ATPase activity per unit membrane area, and mitochondrial density. They transform to S2 cells within the second half of the convoluted portion. All proximal tubule segments touching the renal capsule are S2 cella,[336] and S2 cells also form the beginning of the straight part in the medullary rays. In rats and rabbits the microvilli in S2 are markedly shorter than in S1 (in rat S1: ∼4.5 to 4.0 μm; S2: ∼4.0 to 1.5 μm). S2 cells usually have very prominent lysosomes. The basolateral surface area, Na-K-ATPase activity per unit membrane area, and mitochondrial density decrease from S1 to S3. S3 cells supersede S2 cells at various levels (depending on the nephron generation) in the medullary rays[34,113,268,336] and line the terminal portion of the proximal tubule. In rabbits, dog, and human the height of microvilli further decreases along S3.[5,114,334,335] In mice differences in the length of the brushborder microvilli among the three segments are little apparent,[113] whereas in rats the brush border microvilli of S3 are the longest from the three proximal tubule subsegments (Figure 20.44a). Lateral folding of the plasma membrane is lacking, and the S3 cells usually have a polygonal outline and a comparably small basolateral plasma membrane surface and

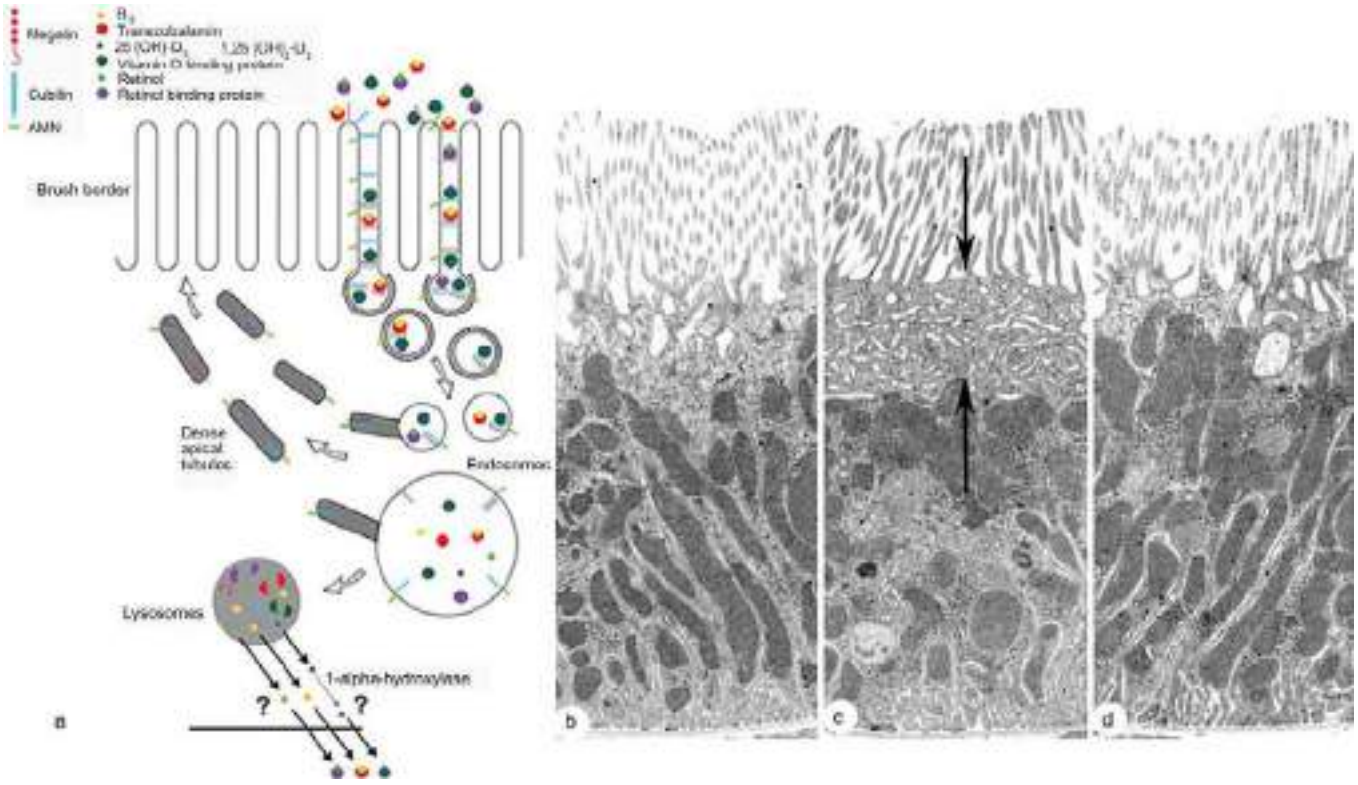

FIGURE 20.45 (a) Schematic representation of receptor-mediated endocytosis in the proximal tubule, exemplified for the megalin- and cubilin-mediated uptake of three vitamin carrier protein complexes: DBP-vitamin D3, TC-vitamin B12, and RBP-retinol in renal proximal tubule. Likewise, the cubilin chaperone protein amnionless, AMN, is indicated. Following receptor-mediated endocytosis via apical coated pits, the complexes accumulate in lysosomes for degradation of the proteins, while the receptors recycle to the apical plasma membrane via dense apical tubules. Megalin mediates the uptake of cubilin and its ligands. The mechanisms for the cellular release of the vitamins remain to be clarified. *(From ref. [346].)* (b)–(d) Transmission electron micrographs of S1 cells of the proximal tubule of rats; (b) control; (c) 15 min and (d) 60 min after a single PTH-injection; PTH induces rapid downregulation of the sodium phosphate co-transporter NaPi-IIa in the brush border membrane by endocytotic mechanisms, associated with a transient expansion of the vacuolar apparatus (between arrows) in the subapical vesicular compartment (TEM ~10,000). *(Modified from ref. [356].)*

Na-K-ATPase activity. Yet, the volume density of mitochondria in S3 of rat and mice is rather high. The mitochondria are scattered throughout the cytoplasm. Structural correlates for endocytosis and lysosomes are almost absent in S3, whereas amount and size of peroxisomes increases from S2 towards S3.

Functional Aspects

Structural Correlate for Receptor-Mediated Endocytosis

Receptor-mediated endocytosis (Figure 20.45a) is the most efficient mechanism for cellular uptake of filtered proteins[268,337,338] and plays an important role in the acute downregulation of transport rates by selective retraction of transport proteins from the microvillous membrane rapid (e.g., NaPiIIa, Figures 20.45b,c,d; see below). By multiphoton microscopy the passage of proteins across the different endocytotic compartments has been directly observed *in vivo*.[339,340]

The first requirement for cellular uptake of a protein by endocytosis is binding of a ligand to a receptor protein on the surface of the tubular cell. The multireceptors megalin, cubilin, and amnionless[341,342] have all been located in the proximal tubule, mainly on the base of the microvillous plasma membrane, in the intermicrovillar membrane invaginations ("clefts"), and in subapical clathrin-coated pits. Megalin belongs to the LDL-receptor family, and is bound with its cytoplasmic tail to cytoplasmic adaptor proteins.[343,344] It forms a tandem with the peripheral protein cubilin which is associated with the membrane by amnionless.[345,346] Megalin is responsible for the internalization of its own ligands and of cubilin with its ligands.[338] The receptor–ligand complexes are gathered in the clathrin-coated membrane pits, and are directed by clathrin-coated vesicles to larger, uncoated early and late

endosomes, located slightly deeper in the cytoplasm. In the endosomes the receptors are cleaved from the ligands and travel back to the luminal membrane via uncoated "dense apical tubules" (DAT).[347–350] The DAT form an elaborate, moving dynamic network of anastomosing tubules,[348,351] which are transiently connected to the larger endosomes, and which display at their other end small clathrin-coated domains.[352–354] From the endosomes the ligands are sorted either for degradation to lysosomes or for ubiquitination via the proteasome pathway.

The trafficking of internalized material from the vacuolar apparatus to lysosomes critically depends on the microtubular system.[355] Microtubules normally form a loose network across the proximal tubule cells, and become highly oriented in the apico–basal direction during vesicular transport of endocytosed cargo to lysosomes.[356] The dimensions of the vacuolar apparatus and the abundance of megalin in proximal tubule cells are correlated with the rate of endocytosis. If endocytosis does not take place, either due to paucity of ligands in the tubular fluid (e.g., normally in S3) or due to lack or low levels of the endocytosis receptor,[338,357,358] the vacuolar apparatus is barely developed.

The processing of material in the vesicular compartments of the endocytotic pathway relies on acidification. NHE3, the proton-ATPase, and the chloride channel ClC-5 (for a review see [359]), are all highly expressed and co-localized in the intermicrovillous clefts and in the vesicular membranes of the early endocytotic pathway.[360–362] Dysfunction of one or several of these acidifying proteins may cause primary defects in endocytosis. Knockout of the ClC-5 channel, for instance, impairs the clearance of PTH from the tubular fluid, bringing about hyperphosphaturia and hypercalciuria.[361,362] This mechanism can explain the high incidence of kidney stones in Dent's disease, with functionally impaired ClC-5 channels.[363–367]

The role of basolateral endocytosis is interesting, since the basolateral cell membrane is the site of different hormone receptors,[368] e.g., the insulin receptor. After binding to the receptors peptide hormones seem to be, at least in part, taken up by the cells and are transported to the lysosomes.[369]

Sodium Proton Exchange

Apical Na^+-H^+ exchange in the proximal tubule and the reabsorption of the bulk of filtered sodium is mediated by the sodium/hydrogen exchanger NHE3 in the microvillous plasma membrane[361,370–372] and in the plasma membrane of the intermicrovillous invaginations.[297] The sodium/hydrogen exchanger is enriched in the intermicrovillar microdomain,[370] where it interacts with the scavenger receptor megalin (see above, [298]). Changes in Na/H exchange activity correlate with changes in cell surface expression of NHE-3, mediated by sgk2.[373] Rapid and reversible redistribution of NHE3 between the two microdomains in the microvillous plasma membrane domain and the intervillous plasma membrane invaginations ("clefts") may also alter the surface expression of NHE3 and activity of Na/H exchange.[298,374–377]

Reabsorption of Water and Solutes

The plasma membrane of the microvilli is covered by a glycocalyx containing hydrolases (phosphatases, peptidases, nucleotidases) which cleave their substrates in the tubular fluid (ecto-enzymes). The microvillous membrane holds a large variety of transport proteins for uptake of water and solutes from the tubular fluid. The density of a given transport protein in the microvillous membrane can be dissimilar along the segments of the proximal tubule and among nephron generations. Many of the transport proteins are anchored by adaptor proteins, such as PDZ-proteins and NHERF1/2, to the underlying apical scaffold.[372,373,378,379]

Transcellular water reabsorption in the proximal tubule is mediated by the constitutive water channel, aquaporin 1 (AQP1) located in the microvillous- and basolateral plasma membrane domains.[380–384] Orthogonal arrays of intramembrane particles in the basolateral membranes of S3 of mice[385] are associated with another water channel, AQP4, AQP7, which is probably involved in the reabsorption of glycerol (see review in [386]) and is expressed in the brush border, especially of S3 in rats and mice, as shown by immunocytochemistry.[387,388]

Sodium-coupled solute uptake from the lumen into the cells is mediated by co-transport proteins located in the plasma membrane of the microvilli. The proximal tubule usually recovers all filtered glucose. The sodium–glucose co-transporter SGLT2 is found primarily in S1, and is responsible for 90% of glucose reabsorption. SLGT*1* is located in S3, and is responsible for only 10% of reabsorption (reviewed by Hediger and Rhoads[389,390]). SGLT*1* is more highly expressed in females than in males.[391] The exit of glucose across the basolateral plasma membrane occurs by the glucose transporters GLUT2 (low affinity in S1) and GLUT1(high affinity in S3).[392]

Inorganic phosphate (Pi) transport is mediated by at least three different brush border Na^+/P(i) co-transporter proteins, the electrogenic transporter NaPi IIa, Pit-2, and the electroneutral transporter NaPi Iic.[393,394] Their expressions and activities appear to be tightly regulated.

Low dietary intake of Pi increases mRNA and brush border expression of NaPi IIa.[395] High dietary Pi intake, parathyroid hormone (PTH) and activation of dopamine receptors[358] rapidly downregulate NaPiIIa-mRNA[395] and NaPiIIa in the brush border,[396–398] and induce phosphaturia. Downregulation of NaPiIIa in

the brush border involves receptor-mediated endocytosis (see above) and subsequent lysosomal degradation.[355,356,358,399,400]

The passage of NaPi-IIa across the successive endocytotic compartments namely, the megalin-containing clefts, the clathrin-coated-vesicle compartment,[401] through the early and late endosomal compartment, and finally its disposal in lysosomes, where NaPi-IIa is degraded, has been tracked by immunofluorescence.[301] The shifting of the protein through the early endocytotic compartments goes along with a dramatic, rapidly transient expansion and remodeling of the vacuolar apparatus in the subapical compartment[356] (Figure 20.45). PTH also reduces Pit-2 expression and activity, whereas NaPi-IIc is inhibited and internalized with a delay of several hours after PTH application.[394]

Recently Klotho has been recognized as a phosphatonin, and an important regulator of phosphate homeostasis. In partnership with the FGF-R, Klotho functions as an obligate co-receptor for FGF23.[402] Secreted soluble Klotho inhibits Pi transport by altering the trafficking of the proximal tubule Na-coupled phosphate transporter.[402]

Neutral amino acids, which represent about 80% of circulating amino acids, are transported by the low affinity Na^+-co-transporter B(0)AT1, located in the early proximal tubule. The high affinity transporter B(0)AT3 is located in the late proximal tubule, at least in mice. In addition, there are several other apical and basolateral amino acid transporters (for a recent review see [403]). Similarly the short-chain peptide, di-, and tripeptide carriers PEPT1, high capacity, low affinity, and PEPT2 low capacity, high affinity are located in mainly S1 and S3, respectively.[404,405]

Secretion of organic amphiphilic electrolytes from the blood into the tubular fluid is a pathway for clearance and detoxification of xenobiotics and drugs, including diuretics.[325,406–410] The uptake into the proximal tubule epithelium proceeds via multispecific organic anion transporters (OAT) and organic cation transporters (OCT) in the basolateral membrane domain. The majority of members of the OAT- and OCT-family have been immunolocalized to the basolateral cell membrane of S3 proximal tubule,[411–413] yet OAT 1 has been detected mainly in S2,[414] a few also in S1. The expression of the OATs and OCTs is strongly regulated by sex hormones.[415–420]

The export into the tubular lumen of both conjugated and unconjugated lipophilic anionic substrates involves various OATs and primarily active transporters with ATP-binding casette motifs, belonging to the MRP-family,[421] and located in the brush border membrane of S1, S2, and S3 proximal tubule segments.[421,422]

The role of basolateral endocytosis is interesting, since the basolateral cell membrane is the site of different hormone receptors,[368] e.g., the insulin receptor. After binding to the receptors peptide hormones seem to be, at least in part, taken up by the cells and are transported to the lysosomes.[369]

THIN LIMBS OF HENLE'S LOOP (INTERMEDIATE TUBULE)

The intermediate tubule comprises the thin tubular portions, interposed between the proximal and the distal tubules (Figure 20.46). Ultrastructurally, the intermediate tubule has four structurally different segments: (1) the descending thin limbs of short loops (SDTL); (2) the upper part; (3) the lower part of descending thin limbs of long loops (LDTLup and LDTL lp); and (4) the ascending thin limbs (ATL). This pattern has been observed in various species, including rat,[423,424] mouse,[34,425] golden hamster,[426] rabbit,[5,427] *Perognathus*,[428] *Octodon degus*,[429] *Meriones shawii*,[116] and *Psammomys obesus*.[430–432] An additional subsegment of thin limbs has been identified in Chinchilla.[433] The thin limbs in human have so far not been studied in comparable completeness.[434–436]

Surprisingly, by lightmicroscopy these simple-looking epithelia are strikingly different from each other with respect to ultrastructure and function, not only the ascending from the descending limbs but, most remarkably, the descending limbs of short from those of long loops. Furthermore, within the descending segments (SDTL, LDTLup, LDTLlp) the proximal portion, although structurally no different from the distal portion, displays considerable functional differences. In the IM a high percentage of thin limbs was found that consisted of a patchwork of descending and ascending type epithelia.[437,438] Beyond all these heterogeneities, there are prominent differences among species. This complex situation appears to account for the persistent discussion about the integrated function of thin limbs in the urine concentrating process.

The type I epithelium (Figure 20.47), which is characteristic for descending thin limbs of short loops (SDTL), has a simple and uniform organization. It is composed of flat, non-interdigitating cells reposing on a thin basement membrane. The luminal cell membrane bears only a few short microvilli that are mainly found along the cell borders. The tight junction consists of several anastomosing junctional strands; desmosomes are frequently encountered. The SDTLs in the rat have, among all other thin limb segments, a particularly prominent cytoskeleton with a high content of cytokeratins and desmoplakins.[439] Cell organelles, such as mitochondria, profiles of rough and smooth

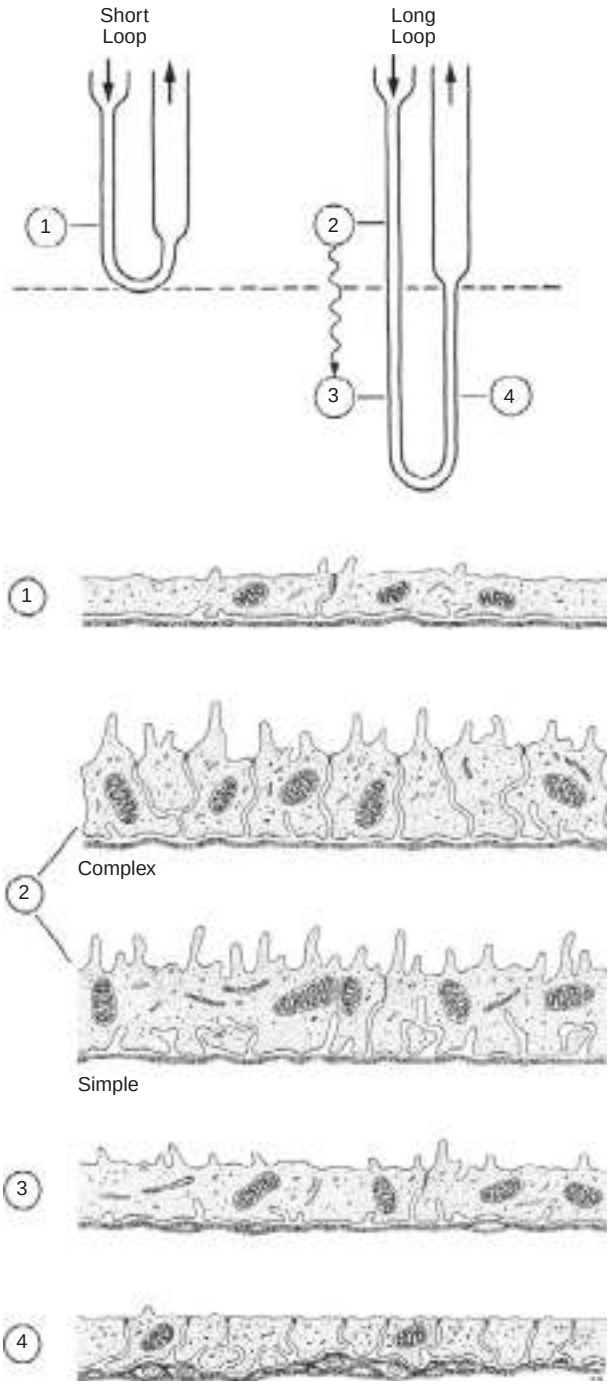

FIGURE 20.46 **Survey of thin limb ultrastructure.** Four thin limb segments are discernible: (1) Descending thin limb of short loops. (2) Descending thin limbs of long loops, upper part. This segment is differently developed among species: a complex type (upper panel) found e.g., in rat, mouse, and *Psammomys* is distinguished from a simple type (lower panel) found e.g., in rabbit and guinea pig. (3) Descending thin limb of long loops, lower part. The transition between upper and lower parts is gradual. (4) Ascending thin limb. *(Adapted from Kriz, W., and Schiller, A. et al. (1980). In "Comparative and Functional Aspects of Thin Loop Limb Ultrastructure. Functional Ultrastructure of the Kidney," 239–250, Maunsbach, A. B. Academic Press, London, and Kaissling, B., and Kriz, W. (1992). In "Morphology of the Loop of Henle, Distal Tubule and Collecting Duct. Handbook of Physiology: Section on Renal Physiology," 109–167, Windhager, E. E. Oxford University Press, New York, with permission).*

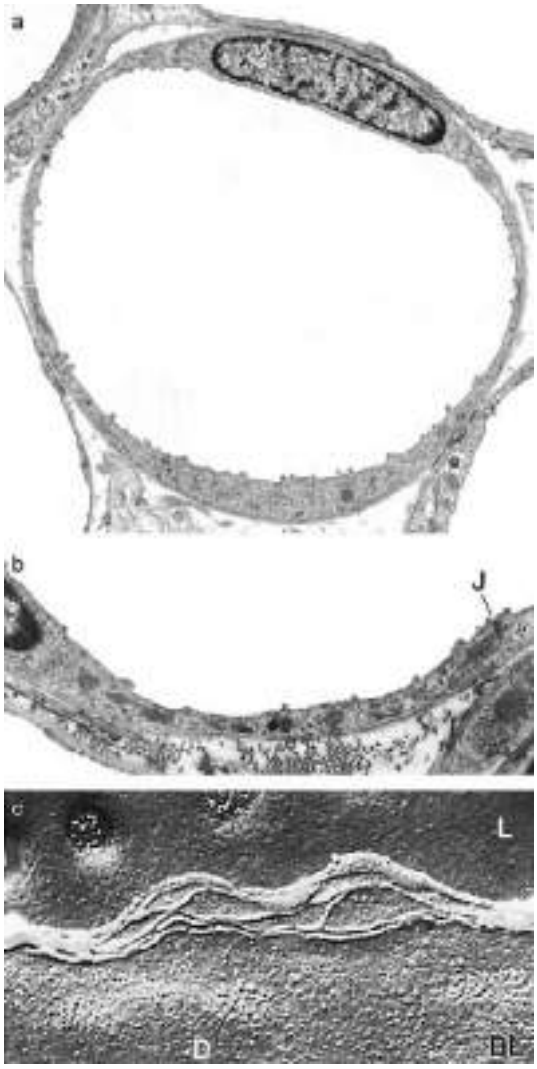

FIGURE 20.47 **Thin descending limbs of short loops. (**a) Cross-sectional profile (rat; TEM: ×~4100). (b) The simplicity of the epithelium is demonstrated (J: Junctional complex; Rat: TEM: × ~11,000). (c) Freeze-fracture electron micrograph. The tight junction consists of several anastomosing strands (L: luminal membrane; BL: basolateral membrane; D: desmosome; Rabbit: ×~71,000).

endoplasmic reticulum, etc., are exceedingly sparse in type I epithelium.

Apart from an initial stretch of maximally 400 μm in about 10% of SDTLs in mouse, these nephron segments do not show any labeling for aquaporin 1 (AQP1), thus they are rather impermeable to water.[440] The lower parts of SDTLs contain the urea transporter UT-A2 in its cell membranes.[382,441,442] In species with complex vascular bundles (e.g., rat, mouse), the short descending limbs lie within the vascular bundles[115]; in these surroundings, the thin limbs are in an ideal position to recycle urea from the ascending vasa recta into the short loop nephrons (see below).

This simple type I epithelium is also found in many descending loop profiles in the inner stripe of feline and canine kidneys which, by microanatomical definition, possess only "long" loops. Consequently, it may be assumed that these simple profiles belong to those long loops that descend into the inner medulla for only very short distances, frequently less than 500 μm.[443] The epithelial characteristics of these loops may be more important than their short descent into the inner zone for determining their functional role. From this point of view, "short loops" are also present in the cat kidney. The short descending thin limbs of cortical loops – studied in the minipig[444] and guinea pig (unpublished results from our laboratory) – are also established by the simple type 1 epithelium.

The descending thin limbs of long loops are generally much larger in diameter, and have a thicker epithelium than those of short loops. Moreover, the LDTLs are heterogeneous; obviously, those of the "longest" long loops begin in the inner stripe as a much thicker tubule than those of "shorter" long loops. The character of the epithelium gradually changes as the limbs descend toward and into the inner medulla. The subdivision of these thin limbs into an upper part (type 2 epithelium) (Figure 20.48a) and a lower part (type 3 epithelium) (Figure 20.48b) is an approximation, and reflects the gradual change to a more and more structurally simplified epithelium. Moreover, this process of epithelial simplification appears to be individually related to the length of each loop. It occurs earlier and more quickly in "short" long loops and is delayed in the longest of the long loops.[34,260,424,432,445] This explains the heterogeneity among descending thin limb profiles in a given cross-section through the medulla: profiles lined with the lower-part epithelium (type 3) may already be found at the end of the inner stripe. Even deep in the inner medulla, profiles with the upper part epithelium (type 2; in reduced elaboration) are still present.

Furthermore, considerable interspecies differences, concerning in particular the upper parts of LDTLs, complicate understanding of the long descending thin limbs. Two patterns may be distinguished[260]; in one group of species (mouse, rat, golden hamster, *Perognathus*, *Psammomys*, *O. degus*, cat), the epithelium (type 2) of the LDTLup is characterized by an extremely high degree of cellular interdigitation. In a single cross-section, more than 100 cell processes may be encountered (Figures 20.48a and 20.49a,b). The tight junctions are extremely shallow, usually consisting of one junctional strand. Thus, the most characteristic features of this epithelium are the prominent paracellular pathways. The junctions are "leaky," and the amount of junctional area available per unit area of epithelial surface is increased several-fold by the tortuosity of the junction due to cellular interdigitation. The lateral cellular spaces form an elaborate "labyrinth," bordered by correspondingly amplified basolateral membranes. Additional structural characteristics of the epithelium are numerous apical microvilli, considerable numbers of mitochondria, and a strikingly high density of uniform intramembranous particles in the luminal and basolateral membrane. In addition, cytochemical and immunohistochemical studies have revealed that the LDTLup exhibits a sodium–potassium ATPase in both membranes,[446,447] suggesting active salt secretion. In addition, salt transport may occur through the tight

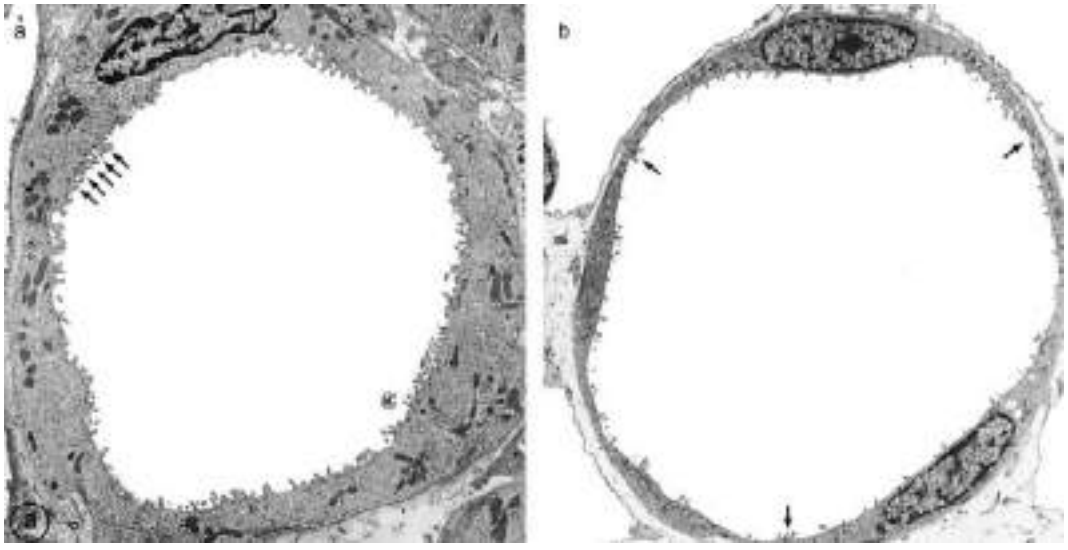

FIGURE 20.48 **Descending thin limbs of long loops, upper part.** (a) Complex type; note the many tight junctions (arrows) (*Psammomys*: TEM: ×~3000). (b) Simple type; only three junctions are encountered (arrows) (rabbit: TEM: ×~3000).

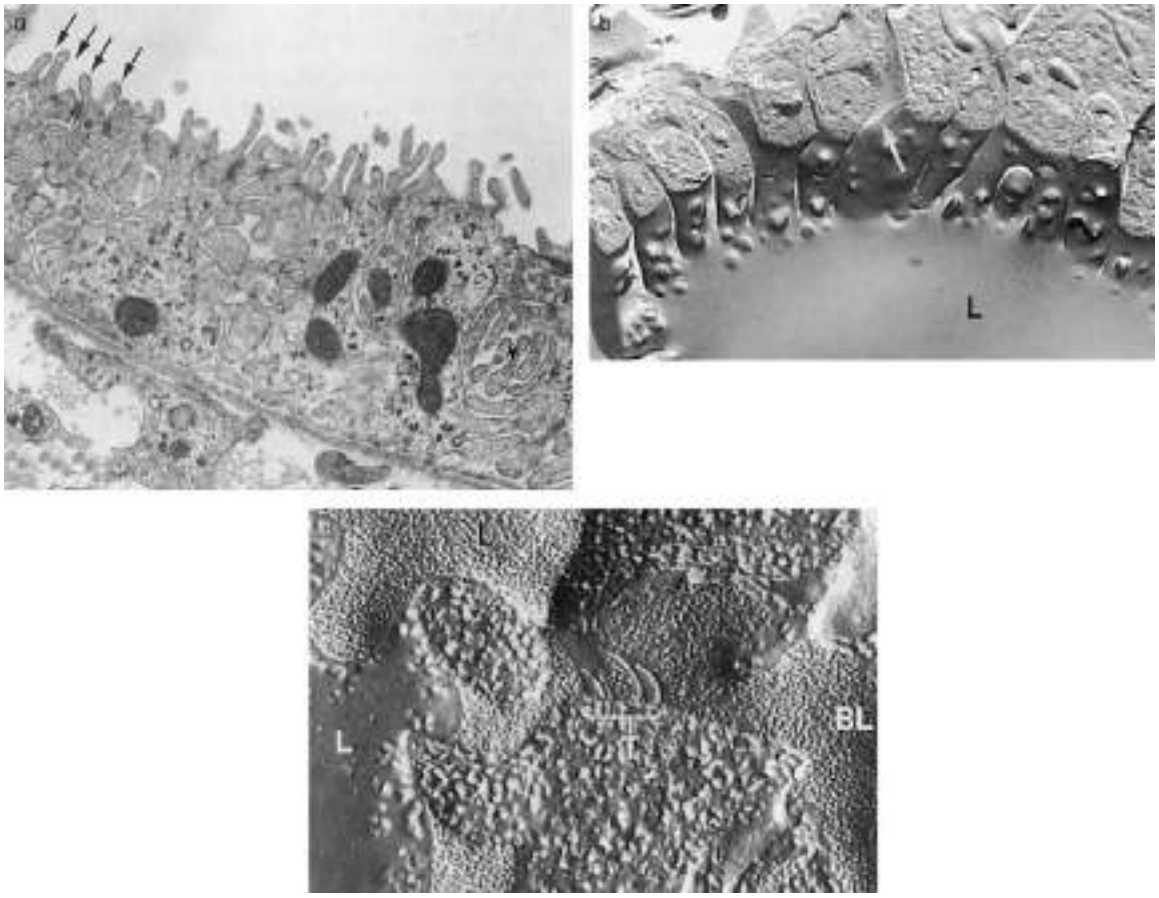

FIGURE 20.49 **Descending thin limbs of long loops, upper part.** (a) The complex epithelium is characterized by numerous tight junctions (arrows) indicating the extensive intercellular digitation. The interdigitation of the basolateral membrane forms a "labyrinth" of extracellular spaces within the cell body (*) (rat: TEM: ×∼11,000). (b) Freeze-fracture electron micrograph exhibiting the luminal aspect of the complex epithelium demonstrating the extensive cellular interdigitation. The tight junction consists of one strand only (arrow) (L: lumen of the tubule; Rat: TEM: ×∼13,000). *(From Kriz, W., and Schiller, A. et al. (1980). In "Comparative and Functional Aspects of Thin Loop Limb Ultrastructure. Functional Ultrastructure of the Kidney," 239–250, Maunsbach, A. B. Academic Press, London, with permission.)* (c) Freeze-fracture electron micrograph of the simple type epithelium. The tight junction (T) consists of several junctional strands. Note the dense pattern of intramembrane particles on the P face of luminal (L) and basolateral (BL) membranes (an equally dense particle pattern is also found in the complex type) (L: Tubular lumen; Rabbit: × ∼66,000). *(From Schiller, A., and Taugner, R. et al. (1980). The thin limbs of Henle's loop in the rabbit. A freeze fracture study. Cell Tissue Res.* ***207****(2), 249–265, with permission.)*

junctions, which contain claudin 2.[261,448] LDTLups are highly permeable to water due to the abundancy of the constitutive water channel aquaporin 1 (AQD1) in both membranes,[449] probably correlating with the high density of intramembrane particles. Carbonic anhydrase activity was found in both short and long descending thin limbs.[450]

In a second group of species that includes rabbit,[427,451] minipig[444] and guinea pig (unpublished data from our laboratory), the upper parts of LDTLs are more simply organized. The prominent paracellular pathway typical of the first group is lacking. The epithelial cells in this group do not interdigitate, and are joined by much deeper tight junctions consisting of several anastomosing junctional strands (Figures 20.48b and 20.49c). In other respects, however, the epithelia are similar in the two groups. Numerous luminal microvilli, many mitochondria, and the dense assembly of intramembrane particles in luminal and basolateral membranes are present in type 2 epithelium also in this group. The high density of intramembrane particles may be partially due to the high density of aquaporin 1 (AQP1) channels in both membranes; corresponding to the decrease of particle density along its descending course the density of AQP1 channels decreases.[452–454]

The epithelium of the lower part of LDTL (type 3 epithelium) is comparably simple (Figure 20.50); interspecies differences are no longer prominent. The epithelium consists of relatively flat, noninterdigitating

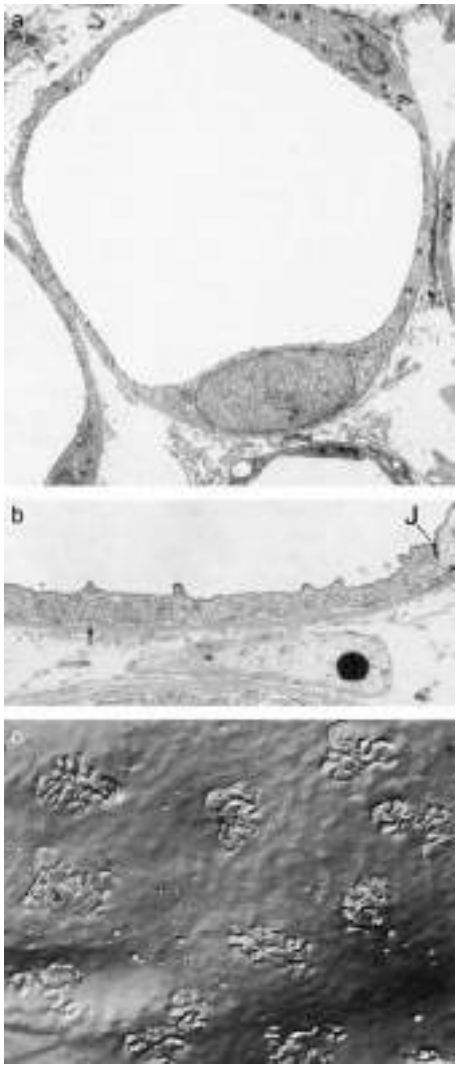

FIGURE 20.50 **Descending thin limbs of long loops, lower part.** (a) Cross-sectional profile (rat: TEM: ×~3800). (b) The epithelium is simply organized; basal infoldings (arrow) are regularly encountered (J: Junctional complex; Rabbit: TEM: ×~10,200). (c) Freeze-fracture electron micrograph demonstrating the regular pattern of basal infoldings within the basal cell membrane (*) (*Psammomys*: ×~12,800). *(In cooperation with A. Schiller and R. Taugner.)*

cells bearing some sparse microvilli; in the rat it is covered by an unusually thick surface coat.[424] The tight junctions are of an intermediate apicobasal depth, composed of several junctional strand (in rabbit: 138 ±37 nm and 3.5 ±0.7 strands; in *Psammomys*, 51 ± 28 nm).[260] The basolateral membrane regularly forms basal infoldings, similar to those found in the simple type of LDTLup.[260] The fluid spaces between the infoldings are not continuous with the lateral intercellular spaces, and thus they are not part of a paracellular pathway route. The pattern and density of intramembrane particles in the luminal and basolateral membranes are inconspicuous; the dense packing, typical for the upper parts, has disappeared. This appears to correlate with the decrease in density of AQP1 channels that, in the terminal portions of this segment, may completely disappear. Thus, the water permeability probably decreases toward the loop bend[452,453]; the terminal segment may accordingly be thought to have a very low water permeability. Regarding the permeability to urea and the distribution of the urea transporter UT-A, conflicting data are published, especially when comparing data from different species.[438,442,452,455–457] In the mouse in antidiuretic conditions, the UTA2 urea transporter is upregulated in LDTLep.[458] Also, claudin 8 has been found in this segment.[240]

With respect to the descending thin limbs of the human kidney, the published data do not allow a final conclusion. In an older TEM investigation[459] a thin limb profile is shown with a heavily interdigitated epithelium corresponding to the thin limb epithelium described above as the complex type in other species. However, in the text the descending thin limbs in the human kidney are described as being outlined by a simply structured epithelium. In 1967, when this paper was published, it was not yet known that there were four different thin limb epithelia.

The axial, the internephron, as well as the interspecies differences in descending thin limb epithelia, is surprisingly prominent compared to all other nephron segments. Differences among thin limb segments were also found with respect to the cholesterol content of their cell membranes.[460] Binding studies with various lectins have revealed distinct labeling patterns in the descending, as well as the ascending, thin limbs in rat and rabbit.[461–463]

The ascending thin limb is present only in long loop nephrons, and is uniformly organized among mammals (Figure 20.51). Generally, the transition from the type 3 epithelium of the descending limb to the type 4 epithelium of the ascending limb occurs a short, but fairly constant, distance before the bend ("pre-bend segment[34,120,121,431]). Therefore, functionally, the entire bend should be regarded as part of the ascending thin limb. The type 4 epithelium is characterized by very flat but heavily interdigitating cells joined by shallow tight junctions, consisting of only one prominent junctional strand. This leaky organization of the paracellular pathways corresponds with functional studies,[464,465] which all demonstrate that the ascending thin limbs are highly permeable for ions.

The change from the type 3 epithelium to the type 4 epithelium coincides with the disappearance of the urea transporter UT-A 2, and the abrupt beginning of the expression of the chloride channel ClC-K1[437,452,466]; aquaporins are completely lacking. Thus, the ascending thin limb is water- and urea-impermeable, but highly

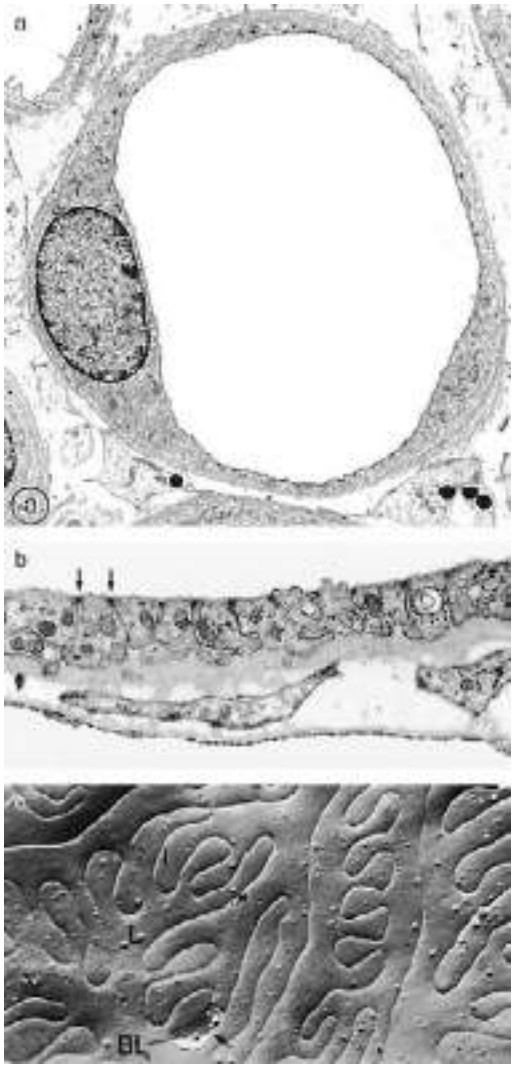

FIGURE 20.51 **Ascending thin limbs.** (a) Cross-sectional profile; note the many junctions (arrows) (*Psammomys*: TEM: ×~3500). (b) Epithelium exhibiting extensive intercellular interdigitation; numerous tight junctions are encountered (arrows) (C: Capillary; Golden hamster: TEM: ×~13,500). (c) Freeze-fracture electron micrograph. Luminal aspect of the tubule demonstrating the mode of cellular interdigitation and the shallow tight junction (arrow) (L: luminal membrane; BL: basolateral membrane; *Psammomys*: ×~4800). *(From Kriz, W., and Schiller, A. et al. (1981). Freeze-fracture studies on the thin limbs of Henle's loop in Psammomys obesus. Am. J. Anat.* ***162****(1), 23–33, with permission.)*

permeable for Cl^- and also Na^+. The relevance of the expression of claudin 4[261] is poorly-understood. Surprisingly, in mouse, rat, and rabbit a high fraction of "mixed" thin limbs was found consisting of alternating stretches of descending and ascending type epithelia.

In most species the transition from the ascending thin limb to the thick ascending limb (distal straight tubule) is abrupt over the length of one cell. The level of this transition defines the border between the inner medulla and the inner stripe of the outer medulla. In the canine[467] and human kidney,[459] a gradual transition between the thin and thick ascending parts of the limb has been observed.

THICK ASCENDING LIMB OF HENLE'S LOOP

The **T**hick **A**scending **L**imb (TAL = distal straight tubule – DST) absorbs NaCl in excess of water.[468] The subtraction of salt from the tubular fluid contributes to rendering the surrounding interstitium hypertonic, a crucial prerequisite for the urinary concentration process. The tubular fluid delivered by the segment into the cortex becomes progressively diluted. In addition, the TAL plays a prominent role in acid–base homeostasis, and recovers important fractions of filtered Mg^{2+} and Ca^{2+} via the paracellular transport route.

The beginning and end of the TAL epithelium are sharply demarcated from the preceding thin limb epithelium, and the successive DCT epithelium. The TAL of nephrons with long loops begins at the border between inner and outer medulla, and that of nephrons with short loops at various levels within the inner stripe of the outer medulla (in cortical loops even in the medullary rays in the cortex). It ascends through the outer medulla and the cortical medullary rays, enters the cortical labyrinth for a short distance, and contacts with the "macula densa," the vascular pole of its parent glomerulus (Figure 20.52). After a short "post-macula" segment the TAL transforms to the **d**istal **c**onvoluted **t**ubule (DCT). The length of the post-macula segment varies not only among species (< 500 μm in rabbits), but also among nephrons within the same kidney.[5,37,260] An association of its length with nephron types has not been established.

Long-looped nephrons have a thinner epithelium than nephrons with short loops.[5,308,469] The thickness of the epithelium decreases gradually, although considerably in the flow direction along the segment (Figures 20.52 and 20.53).[308]

The organization of the TAL-epithelium is exemplary for electrolyte transporting epithelia (see above: "Organization of Electrolyte Transporting Epithelia") (Figure 20.52). The cells display prominent lateral membrane foldings (Figure 20.22a)[5,470] which narrowly interdigitate with adjacent cells and enclose plate-like large mitochondria, and occasionally a few cisterns of rough endoplasmic reticulum (rER)[470] (Figure 20.53). Except in the deep inner stripe the lateral folding extends over the entire cell height. Hence, the luminal outline and tight junctional belt are much longer in upstream portions than in the deep inner stripe,[471] evident by the very frequent hits of the tortuous tight junctional belt in sections of cortical TAL

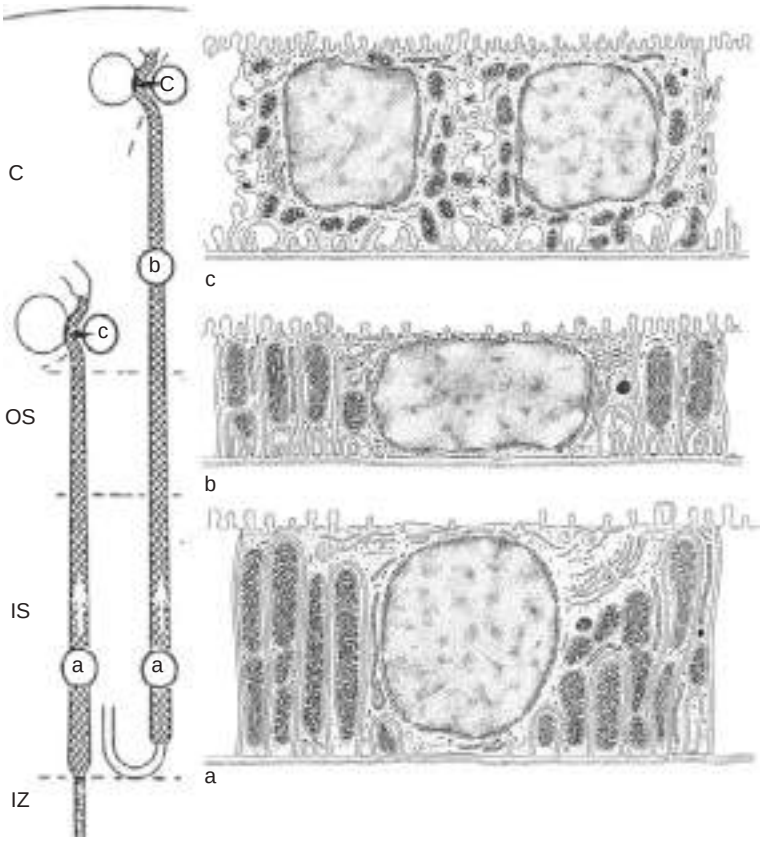

FIGURE 20.52 **Survey on location and ultrastructure of the thick ascending limb of Henle's loop.** (TAL: distal straight tubule, including macula densa; C: cortex; IS: inner stripe; OS: outer stripe; IZ: inner zone.) The direction of the urinary flow is indicated by white arrows, interdigitated cells with large mitochondria, enclosed in the lateral processes; (a) medullary part; (b) cortical part; (c) macula densa; note the difference in the organization of the lateral intercellular spaces between macula densa cells and other TAL cells. *(Adapted from Kaissling, B., and Kriz, W. (1979). Structural analysis of the rabbit kidney. Adv. Anat. Embryol. Cell Biol.* ***56****, 1–123, and Kaissling, B., and Kriz, W. (1992). In "Morphology of the Loop of Henle, Distal Tubule and Collecting Duct. Handbook of Physiology: Section on Renal Physiology," 109–167, Windhager, E. E. Oxford University Press, New York, with permission).*

epithelium (Figure 20.53b). The tight junction is organized by a few strands, arranged in parallel, and with a high particle density (Figure 20.41a).

The large nucleus usually (except in the deep inner stripe) spans the entire cell height. The cytoplasm in the nuclear region displays small, round mitochondrial profiles, a particularly extensive Golgi apparatus,[308] polyribosomes, and some short cisterns of rER. The varying amounts of narrow tubular profiles and smooth vesicles in the subapical cytoplasm might be related with trafficking of apical transport proteins (see below). The apical membrane of the cells carries short stubby microvilli,[114,472] which usually border the tight junctional belt[471] and are less abundant in the center of the cell and in the vicinity of the single cilium. Scanning electron microscopy revealed that "rough" cells with numerous microvilli may be present side-by-side with rather smooth cells with only a few microvilli.[469] The latter cells display strong immunoreactivity for EGF, which seems to play a role in the regulation of growth and differentiation of cells in the loop of Henle.[473]

Role of the TAL in NaCl Reabsorption

The major fraction of salt reabsorption by the TAL (including the macula densa cells) proceeds via the $Na^+,K^+,2Cl^-$ (NKCC2) symporter[468] in the luminal membrane[474–476] which is specifically inhibited by loop diuretics, such as bumetanide and furosemide.[477] The apical entry of Na^+,K^+ and $2Cl^-$ is driven by the Na-K-ATPase in the basolateral plasma membrane. The density of Na-K-ATPase in the TAL exceeds by far that of more proximal tubular sites.[278,279]

The inwardly rectifying renal outer medullary K channel, ROMK, which recycles the K^+ ions entering the cell via NKCC2 over the apical membrane, is particularly abundant in the apical plasma membrane of TAL cells.[365,478–483] The basolateral extrusion of Cl^- occurs passively through ClC-K and ClC-Kb channels.[479,484]

Role in Bicarbonate Reabsorption

In addition to its role in salt reabsorption, the TAL has also an important function in maintaining acid–base homeostasis. It reabsorbs about 15–20% of the filtered bicarbonate[485–488] via the sodium/hydrogen exchangers NHE3 and NHE2 in the luminal plasma membrane of the TAL cells[370,489–491] and the NEM-sensitive vacuolar H^+-ATPase.[492] The apical Na/H exchange is tightly coupled with the basolateral Cl^-/HCO_3^- exchange that proceeds by the Cl^-/HCO_3^-

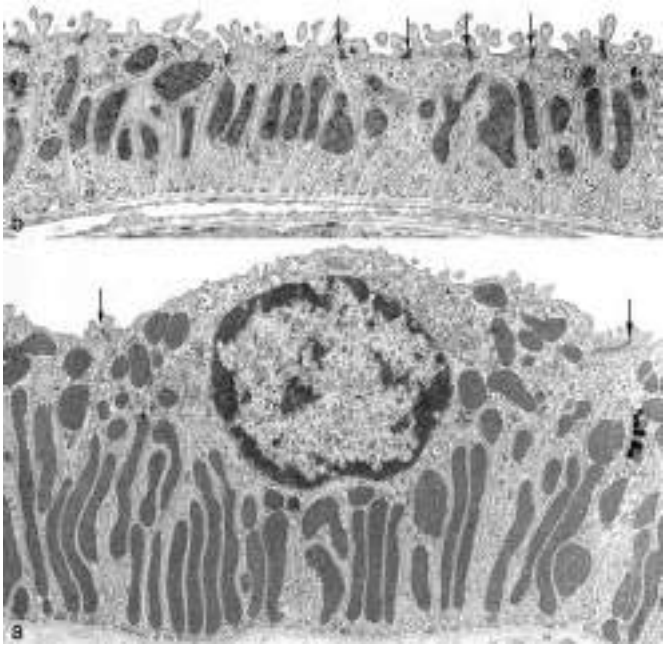

FIGURE 20.53 **Thick ascending limb cells.** (a) Deep level of the inner stripe; the lateral interdigitated foldings contain large mitochondria and do not reach up to the lumen; (b) Cortical part; in the much lower cells the lateral interdigitated foldings reach up to the lumen, causing a folded course of the tight junctions (arrows) (rat: TEM: × ~14,500). *(Adapted from and Kaissling, B., and Kriz, W. (1992). In "Morphology of the Loop of Henle, Distal Tubule and Collecting Duct. Handbook of Physiology: Section on Renal Physiology," 109–167, Windhager, E. E. Oxford University Press, New York, with permission).*

exchanger AE2.[493,494] The abundance of the NHE3 protein in the apical plasma membrane of the TAL has been shown to increase with functional adaptation to reduced renal mass,[487] under metabolic acidosis,[495] and with high levels of glucocorticoids.[496]

Role in Mg^{2+} and Ca^{2+} Recovery

Although virtually impermeable to water, the junctions in the TAL display a selective permeability for Mg^{2+} and Ca^{2+}. 40–70% of the filtered Mg^{2+} is recovered by the TAL in a passive paracellular manner facilitated by tight junction proteins claudin-16 and claudin-19 protein.[252,497]The much greater length of the tight junctional belt in the CTAL than in the MTAL might explain the higher paracellular movement of Mg^{2+} and Ca^{2+} in the CTAL than in the MTAL.[497,498] Impaired function of paracellin 1 (claudin 16) leads to urinary losses, specifically of magnesium and calcium.[499–506]

Regulation of salt transport rates in the TAL involves peptide hormones, among them vasopressin and glucagons, which bind to receptors on the basolateral plasma membranes. Via the cAMP messenger system they increase the abundance of the NKCC2 co-transporter and the K-channel in the luminal membrane.[106,117,474,468,507–512]

The acute response to decreases or increases of cAMP seem to involve endocytotic and exocytotic, respectively, membrane translocation.[513] The various amounts of NKCC2-displaying vesicular and tubular structures in the apical cytoplasm of TAL cells[270,510,514] might well be part of the membrane pool, available for translocation. Similar to the proximal tubule, endocytosis requires NHE3-mediated acidification, and needs the chloride channel CLC5. NHE3 and ClC5 are both located in the apical cytoplasm of TAL cells.[480,515] The basolateral extrusion of Cl occurs passively through ClC-K and ClC-Kb channels.[479] The trafficking of ClC-K to the basolateral membrane depends on the protein barttin.[479]

Cyclooxygenase 2 (COX2) has been located in the TAL cells, including the macula densa cells, and contributes through local production of prostaglandins[479,516–518] to the handling of ions by the TAL.

All maneuvers that chronically affect the salt transport rates by the TAL finally result in structural hyper- or hypotrophy of the TAL epithelium. The plasticity of the TAL epithelium in response to variations in plasma levels of vasopressin (ADH) or cAMP had been revealed by studies on Brattleboro rats, which genetically lack ADH and suffer from diabetes insipidus (DI).[519] In these rats the medullary and cortical portion of the TAL are equally thin.[520] In healthy rats with chronic low plasma levels of ADH due to chronic high water intake the structural appearance of the TAL resembles that seen in DI-rats.[521] Several weeks of substitution of ADH in DI rats or of endogeneously increased ADH-levels, associated with chronic water restriction, restore the normal axial heterogeneity.[522,523]

The transport rates by the TAL epithelium are correlated with the DNA synthesis rate of TAL cells. Specific inhibition of NaCl reabsorption in the TAL of rats by furosemide transiently reduces the incidence of TAL cells showing DNA synthesis (assessed by nuclear detection of the proliferating cell nuclear antigen, PCNA, and incorporation of the thymidine analog bromodesoxyuridine) from about 1%, the basal rate in the rat TAL epithelium, to zero.[305]

With the given background it is likely that the structural heterogeneity regarding cell height, mitochondrial density, and basolateral plasma membrane surface along the TAL represents the physiologically lower tubular salt load, and ensuing lower transport rates in the cortical than in the medullary portions.[468] In rabbits the overall reduction of the cell height, membrane area and mitochondrial volume (per unit tubular

length) along the TAL is much more pronounced than in rats and mice.

Disruption of genes coding for NKCC2 (SLC12A1) or for one or several proteins and/or channels associated with the NaCl-transport via NKCC2 (e.g., chloride channels ClCKA, ClCkB or the Barttin subunit, CLC5, NHE3), involved in regulation of its surface expression, or of the respective signaling cascades causes more or less severe renal salt-wasting, characteristic of "Bartter" syndrome. Symptoms of the Bartter syndrome are, e.g., lowered blood pressure, hypokalemic metabolic alkalosis, and hypercalciuria, with variable risk of kidney stones.[479,483–484,524–527]

The Tamm-Horsfall glycoprotein (THP), the most abundant urinary protein in mammals, is synthesized exclusively by the renal TAL epithelium. It is located in high density on the apical plasma membrane, in low density also on the basolateral plasma membrane.[528,529] Uromodulin has been linked to water–electrolyte balance and to kidney innate immunity.[530] THP is thought to be relevant in the pathogenesis of cast nephropathy and urolithiasis. By its property to compete efficiently with urothelial cell receptors, such as uroplakins, in adhering to type I fimbriated *Escherichia coli*, it may play a role in defense against urinary tract infection.[531] Mutations in the gene encoding uromodulin lead to rare autosomal dominant diseases, collectively referred to as uromodulin-associated kidney diseases.[532] Recently, it has been shown that THP-deficient ($THP^{-/-}$) mice showed moderately impaired urinary concentrating abilityuromodulin plays a permissive role in TAL reabsorptive fu/uromodulin plays a permissive role in TAL reabsorptive function.[533]

SEGMENTS DOWNSTREAM OF THE TAL: DISTAL CONVOLUTED TUBULE, CONNECTING TUBULE, AND COLLECTING DUCT

Electrolyte transports by the tubular epithelia distal of the loop of Henle provide the fine tuning of urinary electrolyte- and water-excretion. Located downstream of the macula densa, their transepithelial solute transport rates are no more directly submitted to tubuloglomerular feedback control but, rather, they are regulated by systemic hormones and a multitude of local factors.[296,317]

The structural subdivision of these portions in the cortex into the distal convoluted tubule (DCT), the connecting tubule (CNT), and the cortical collecting duct (CCD) goes back to light microscopic observations made in sections and microdissected tubules from kidneys of rabbits, human, mouse, sheep, cat, pig, beef, and dolphin by Karl Peter early in the 20th century.[37] More than half-a-century later, microdissection studies of nephrons from rabbits and mice by the group of Morel[534] revealed that the distribution of sensitivities for several peptide hormones was bound to the morphological segmentation. Detailed electron microscopic investigations of the distal tubular portions in rabbits,[5] rats,[291,535,536] *Psammomys obesus*,[35] and mice[537,538] further confirmed and extended the earlier findings. The few studies on the human nephron[459,539–541] agree with the data obtained from experimental animals.

In contrast to the preceding tubular portions, the epithelial lining of each of the segments following the TAL display at least two distinct cell types: one cell type is segment-specific and called accordingly DCT cell, CNT cell, and CD cell; the other one, the intercalated cell (IC cell), is interspersed in differing amounts among the specific cells of each segment.[542] The transition from one segment to the next may be sharp and unequivocally definable, e.g., as in rabbits[5,268] or they may develop gradually, involving more-or-less long transitional portions with a mixture of cells from the successive segments or with cells showing features intermediate between the segment-specific cell types of the given segments.[535] The presence of a rather long transitional portion between the definite DCT and CNT in rats,[543,544] in mice,[537,538] and in humans[539] claimed a subdivision of the DCT in these species into the "early" DCT and the "transitional portion"[538,545] or the DCT 1 and the DCT 2,[537] respectively. Taken the morphological data of the various species (except rabbits!) together it is obvious that the segmentation of the cortical tubular portion distal of Henle's loop is a matter of definition.[544] The nowadays conventionally-used segment definitions for the DCT, the CNT and the CCD (Figure 20.55) take into account the structural data and the distribution of the major apical salt and water transport proteins (Figure 20.55). The uptake by the cell type-specific transport proteins in the luminal plasma membrane into the cell and the movement across and out of the cell is facilitated by a bunch of "auxiliary" cytoplasmic and/or basolateral membrane proteins (e.g., Na-K-ATPase, Ca-binding proteins, K-channels, hormone receptors, etc.). These "auxiliary" proteins are not restricted to the given cell type and thus, are not segment-specific. The inventory of gene expressions (*in situ* hybridization of mouse kidney sections with annotations) in given segments can be looked up in the "Euregene Expression Database." "The Kidney Atlas" (http://www.euregene.org/portal/pages/index.html).

The segmentation of the CD into cortical (CCD), outer medullary (OMCD), and inner medullary CD (IMCD) is based mainly on the location in the given zones. The structural differences between the CCD and

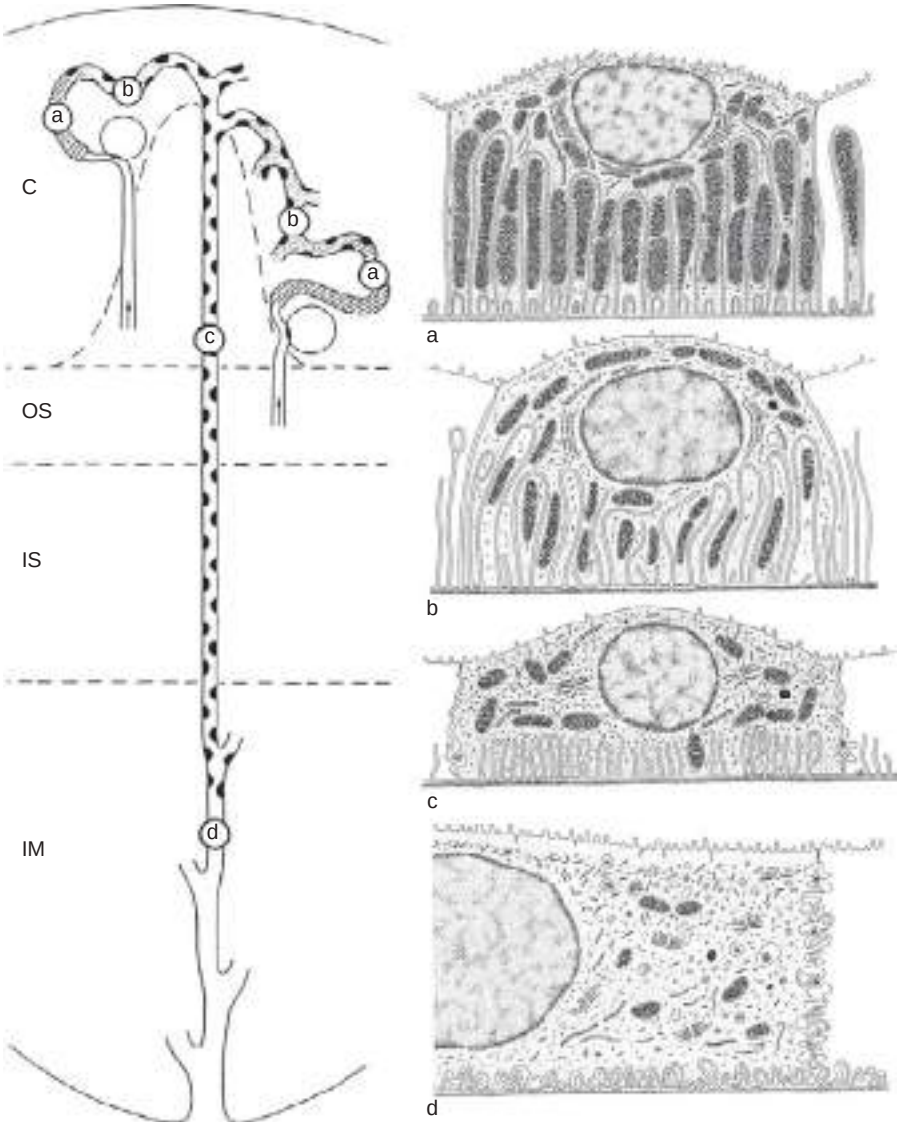

FIGURE 20.54 **Survey on organization of the cortical distal segments and collecting ducts (left panel) and on ultrastructure of the segment-specific cells (right panel).** (C: cortex; OS: outer stripe; IS: inner stripe of the outer medulla; IM: inner medulla; Dashed line: delimits the medullary ray; (a): distal convoluted tubule (DCT) and DCT-cell; (b): connecting tubule (CNT) and CNT-cell; (c): CCD and CCD cell; (d): inner medulla (IM) and IMCD cell; Black semicircles indicate the occurrence of intercalated (IC) cells.) Each DCT opens into one CNT. In superficial nephrons the CNT opens directly into a CCD; connecting tubules of deeper nephrons join to form an arcades which ascend in the cortical labyrinth, before they open into a CCD. The collecting ducts descend in the medullary rays and through the outer and inner stripes of the outer medulla; the lower two-thirds of the collecting duct are lined by IMCD cells exclusively; the IMCD open as papillary ducts on the renal papilla. *(Adapted from and Kaissling, B., and Kriz, W. (1992). In "Morphology of the Loop of Henle, Distal Tubule and Collecting Duct. Handbook of Physiology: Section on Renal Physiology," 109–167, Windhager, E. E. Oxford University Press, New York, with permission).*

OMCD cells are quantitative rather than qualitative. Usually, the IMCD does not display any more IC cells in its two lower thirds and the lining cells (IMCD cells) are regarded as a separate cell type[546] (Figure 20.54).

Distal Convoluted Tubule (DCT)

The DCT reabsorbs 5–10% of the filtered Na-load[547] and determines the final urinary Mg^{2+} concentration through active transcellular transport.[548] In addition, the transitional portion (DCT2) participates (together with the subsequent CNT; see below) in regulation of calcium excretion by transcellular calcium reabsorption.[538,549] The DCT epithelium is water-impermeable, similar as the preceding TAL.

The abrupt increase in epithelial height (Figure 20.56)[550,544] marks the beginning of the DCT. This prominent feature in the tubular epithelium has been observed in all mammalian species investigated so far, and it coincides exactly with the replacement in the luminal membrane of the NKCC2, characterizing the TAL cells, by the thiazide-inhibitable sodium chloride co-transporter, NCC, characterizing the DCT cells.[547] The NCC characterizes all DCT cells (DCT1 and DCT2). The breaking off of NCC expression defines the end of the DCT.[537] It is sharp in rabbits,[551] but it drops off over a more or less long distance in mice and rat.[538]

The DCT epithelium is organized by laterally interdigitating cells (Figures 20.57 and 20.58a) similar to the TAL, yet the lateral folding excludes the apical cell portion in DCT cells. The amount of Na-K-ATPase,[279] the

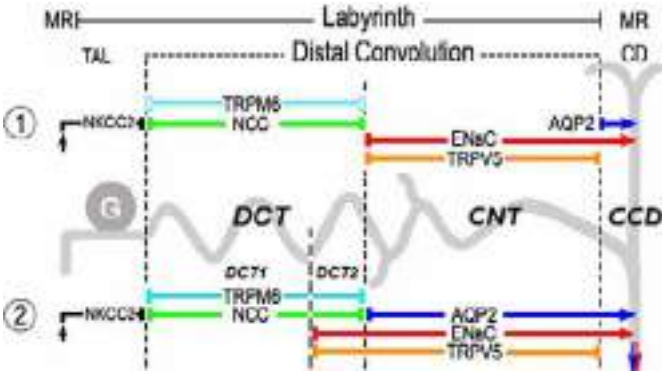

FIGURE 20.55 **Schematic distribution of the major apical transport proteins (NKCC2, NCC, TRPM6, TRPV5, ENaC, and AQP2) along the cortical distal segments.** (1) In rabbit; and (2) in rat, mouse, and human (MR: medullary ray; TAL: thick ascending limb; G: renal corpuscle; DCT: distal convoluted tubule; CNT: connecting tubule; CCD: cortical collecting duct). Sharp beginning and stop of a transporter along the cortical nephron is indicated by vertical bars, the continuation along the CD by arrows.

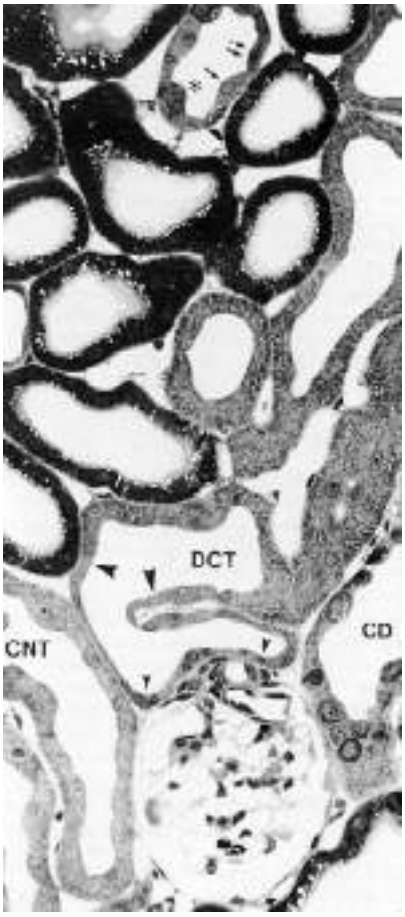

FIGURE 20.56 **Distal tubular segments beyond the macula densa.** Small arrowheads delimit the macula densa, large arrowheads point to the transition from the epithelium of the thick ascending limb to the distal convoluted tubule (DCT) (CNT: connecting tubule; CD: cortical collecting duct). The tubule profile in the upper portion of the micrograph has a mixed cell population, composed of CNT cells (arrow), CD cells (double arrow), and IC cells (asterisk) and represents the transition from a CNT to a cortical CD (rat: TEM: ×~500).

surface area of basolateral membranes and the volume density of mitochondria[280] are the highest of all tubular cells[41] (Figure 20.26). The large lamella-like mitochondria are narrowly enveloped by the lateral interdigitating plasma membrane foldings, all other cell organelles are situated in the apical cytoplasm: the nucleus; the distinct Golgi apparatus; numerous small mitochondrial profiles; short cisterns of rough endoplasmic reticulum; and abundant smooth small, invaginated vesicles closely beneath the apical plasma membrane.[260,552] Lysosomes are less frequently observed in DCT cells. The microtubular system in DCT cells is much more prominent than in proximal tubule cells. The tight junctional belt has a similar organization as in the TAL, but is shorter since the apical portions of the DCT cells have a polygonal outline.The intercellular space has a regular width of about 50 nm and is bridged by an intercellular skeleton.[553] The apical plasma membrane carries numerous stubby microvilli. Single cilia are present on the center of all DCT cells.

In the transitional portion (DCT-2) the lateral folding is progressively superseded by infoldings of the basal plasmalemma which may extend into the apical cell pole. The infolded membranes carry a few caveolae on their cytoplasmic face.[260] This structural observation is confirmed by the finding of caveolin in late DCT cells.[554,555] Size and volume density of mitochondria slightly decrease along the DCT2.

In rats, mice, and humans the appearance of basal plasmalemma infoldings of the DCT cells coincides with the most upstream appearance of intercalated cells. In rabbits, a species that lacks a transitional segment (DCT2), infoldings of the basal plasmalemma and the most upstream appearance of IC cells mark the beginning of the CNT.

Functional Data

Sodium chloride reabsorption by the DCT proceeds via the electro-neutral Na^+-Cl^- co-transporter (NCC) in the apical plasma membrane of DCT cells. NCC is specifically inhibitable by thiazide diuretics,[547,556] which are frequently used in the treatment of hypertension.[547] The driving force for influx of NaCl via NCC is generated by the Na-K-ATPase activity in the basolateral membrane of DCT cells. The basolateral chloride channel, subunit b (ClC-Kb),[479,556,557] extrudes Cl^- ions at the basolateral side of DCT cells. Potassium handling, associated with NCC-mediated transport,

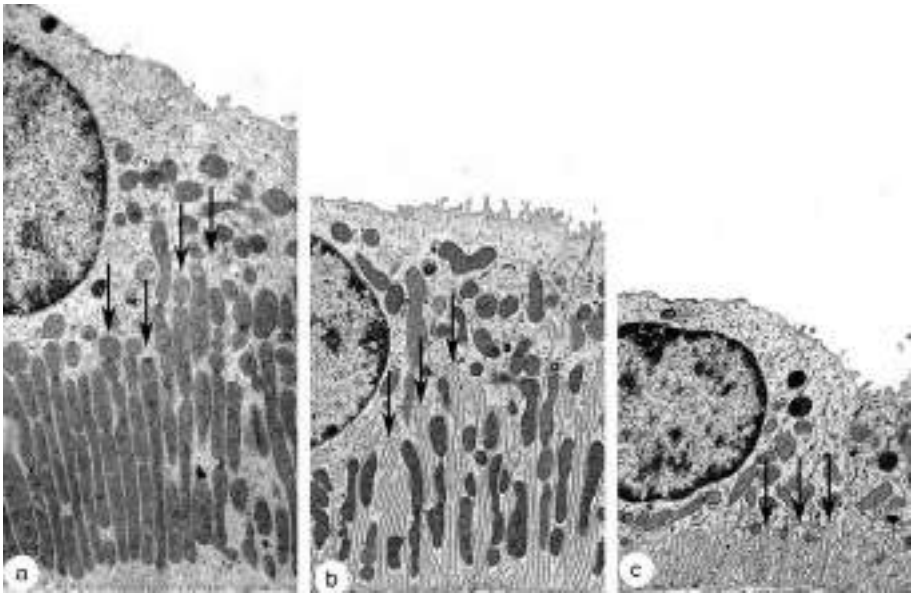

FIGURE 20.57 Organization of distal and collecting duct cells in the renal cortex; (a) and (b) *Psammomys obesus*; (c) rat; fixation by reduced osmium. (a) DCT cell, interdigitating, lateral cell processes (arrows) narrowly enclose large mitochondria; (b) CNT cell, displaying a few interdigitating lateral cell processes and abundant infoldings of the basal plasma membrane (arrows), extending up into the apical cell half; most mitochondria are aligned between the infolded membranes; (c) non-interdigitating CCD cell; all infoldings of the basal plasma membrane are restricted to the basal cell portion; the location of mitochondria above the basal rim of infolded membranes is characteristic for CD cells (TEM: ×~10 000).

involves ROMK, detectable by immunomethods in the cytoplasm of DCT1,[481,558] and in the apical membrane of DCT2 cells, and BK channels.[558,559]

The NaCl transport rates by the DCT epithelium are linked with NCC surface expression. It is regulated (among others) by the luminal NaCl-load,[560] dietary salt,[561] by angiotensin II,[562–564] and by sex hormones.[565] Although mineralocorticoid receptors have been detected in the DCT,[547] aldosterone has no effect on NCC-mediated transport since beta hydroxysteroid-dehydrogenase, which confers mineralocorticoid specificity to the receptor, is lacking in DCT1.[562]

Changes in NCC surface expression are effected by trafficking of the co-transporter from the subapical vesicular compartment into[564] and removal by endocytosis[566] from, respectively, the apical plasmalemma, and by altering the NCC degradation rate through the lysosomal pathway.[567,568]

Kinases, such as the serum- and glucocorticoid-inducible kinase, SGK1, with-no-lysine kinases WNK1 and WNK4, both themselves controlled by NaCl intake, play an important role in this regulation.[559,561,569–571] WNKs promote NCC-targeting to the lysosome for degradation.[572] WNK signaling is implicated in the coordination of transcellular and paracellular flux to achieve NaCl and K^+ homeostasis.[250]

Recent data obtained in genetically vasopressin-deficient Brattleboro rats suggest that vasopressin and the vasopressin-V2 receptor-NCC signaling cascade might play a role in the short-term regulation of NCC in the apical plasmalemma of DCT cells.[573,574]Vasopressin-dependent increases in cAMP had not been recorded in the DCT of rats and other species.[534,575]

Chronic increases in the NaCl-transport rates in the DCT, induced in rabbits by high dietary Na-intake combined with low K-intake[280,281] or in rats by rises in NaCl-delivery due to impaired NaCl-reabsorption in the preceding TAL, provoke extensive structural compensatory hypertrophy in the DCT,[290,292,304,576,577] including substantial increases in the DNA synthesis rate in DCT cells.[305,578] These changes occur in the presence, but also in the absence, of increased plasma levels of mineralocorticoids,[578] and are mediated most probably by angiotensin II.[562]

In line with these earlier structural observations are recent studies in a ROMK-deficient mice model for Bartter's syndrome with loss of TAL function. The ROMK-deficient mice reveal hypertrophy of the DCT epithelium, with compensatory upregulation of NaCl reabsorption via the thiazide-sensitive NCC co-transporter.[579,580]

The renal abundance and the NCC-labeling in DCT were found to be profoundly and selectively decreased in aldosterone-escape rats, suggesting that the thiazide-sensitive NaCl co-transporter may be the chief molecular target for regulatory processes responsible for mineralocorticoid escape via a post-transcriptional mechanism.[581]

The DCT determines the final urinary Mg^{2+} concentration through active transcellular transport.[504,548,582,583] The transient receptor potential channel melastatin subtype 6 (TRPM6),[548,584] co-localizes with NCC, at least in the early DCT (DCT1), and is regarded as a likely candidate for influx of Mg^{2+} across the luminal membrane. This influx apparently requires the presence of the gamma subunit of the renal Na-K-APTase in the basolateral membrane of the

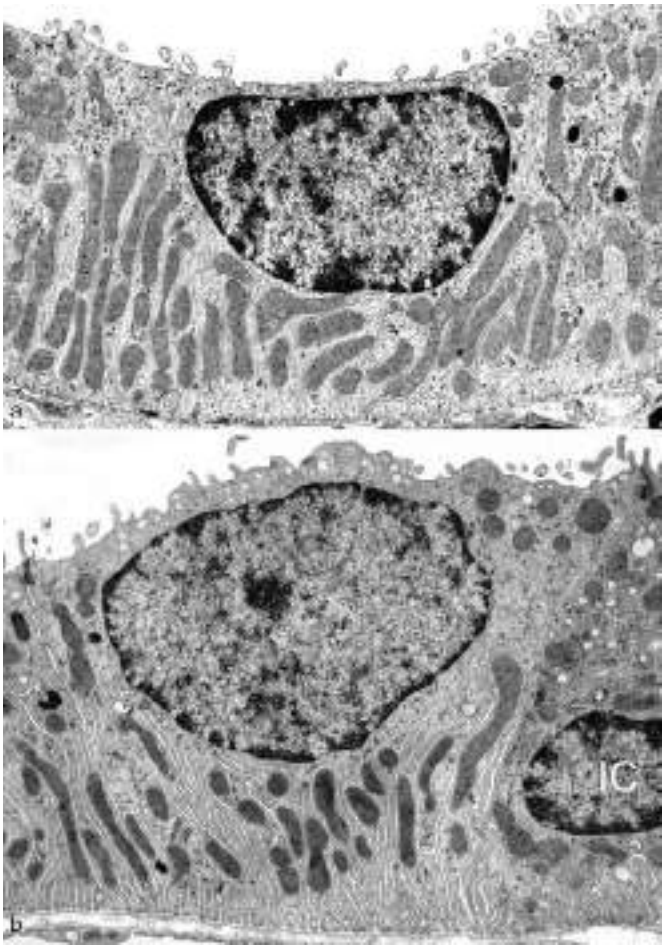

FIGURE 20.58 **Ultrastructure of distal convoluted tubule cells (rat kidney).** (a) Cell in the early and (b) late portion of the DCT; in (a) characteristic apical position of the nucleus and location of the mitochondria in basolateral interdigitating cell processes; the volume density of mitochondria is high; in (b) the amount of basal plasma membrane infoldings is higher than in (a), the amount of mitochondria is lower; the most upstream appearance of intercalated cells (IC) is in the late DCT (TEM: ×~5400).

DCT cells.[276,585] Transcription factor HNF1B (hepatocyte nuclear factor 1 homeobox B) is proposed to regulate the expression of the g-subunit of the Na^+/K^+-ATPase.[586] In addition to the Na-K-ATPase, the DCT cells weakly display the plasma membrane $Ca^{2+}(Mg^{2+})$-ATPase (PMCA)[307,587] and the sodium–calcium exchanger (NCX).[544]

The epidermal growth factor (EGF) expressed by the DCT epithelium[473,588,589] seems to be involved in TRPM6-mediated regulation of active Mg^{2+} reabsorption. Transcellular magnesium reabsorption via TRPM6 seems to critically depend on low levels of free intracellular magnesium, putatively kept low by the cytoplasmic calcium-binding protein parvalbumin (PV). PV has a several-fold higher binding capacity for magnesium than the calcium-binding protein calbindinD28k, and is prominent in the early part of the DCT of mice.[537,538] PV seems also to play a role in the endogeneous NCC expression in DCT cells by modulating intracellular Ca^{2+} signaling in response to ATP.[590]

The key players for paracellular Mg^{2+}-transport, Claudin 16 (paracellin1) and Claudin 19, are both detected in the DCT tight junction,[497] and may enable paracellular Mg^{2+}-movement across the DCT epithelium in addition to the transcellular Mg^{2+}-transport. The tight junction protein Claudin 7 has been found to be highly expressed in the distal convoluted tubules (and collecting ducts) of the mature kidney, suggesting that it may play a role in paracellular NaCl and K handling.[240,591,592]

DCT 2

This transitional segment expresses, in addition to NCC, the amiloride-sensitive epithelial sodium channel, ENaC. The onset of ENaC in the apical plasma membrane coincides with the most upstream appearance of intercalated cells (see below), apical immunoexpression of ROMK. The eyecatching beginning of prominent cytoplasmic immunostaining for Vitamin D-dependent calbindin-D28k, and the marked increase in immunostaining for PMCA and NCX in the basolateral plasma membrane go along with the onset in the luminal membrane of the epithelial calcium channel, TRPV5,[538] the gatekeeper for renal epithelial Ca^{2+} transport.[593] ENaC and TRPV5 are coexpressed in the CNT and will be discussed there.

Rabbits have no DCT2; in this species the transition from the DCT to the CNT is sharp and marked by an abrupt change in cell structure,[280] coinciding with the abrupt onset of ENaC[538] in the apical membrane, as well as the onset of the TRPV5[594] (Figure 20.55), and also the appearance of IC cells.

Dysfunctions of NaCl Reabsorption in the DCT

Inhibition of NCC in rats treated for three to four days with thiazide diuretics induces massive rates of apoptotic cell death of DCT cells in the early part of the DCT, while the late part of the segment with the additional sodium entry pathway ENaC remains intact.[307] If the transport activity of the early DCT cells is inhibited for only a few days, the epithelium rapidly and fully recovers within a few days after removal of the drug.

In loss-of-function mutations of the NCC gene in mice,[595] permanent, dramatic atrophy of the early DCT portion is seen.[545] These data highlight the eminent importance of the transport activity in maintaining and modeling the tubular epithelium. Loss-of-function mutations in the NCC-gene in humans cause "Gitelman's syndrome." This syndrome is characterized by mild

renal sodium-wasting, hypocalciuria, hypomagnesaemia, hypokaliemic alkalosis, and reduced blood pressure in humans.[596–599]

Mutations in the NCC-regulating WNK1 and WNK4 increase NCC activity, and cause Gordon's Syndrome (Pseudohypoaldosteronism type II - PAH II). The symptoms of this disease comprise arterial hypertension, hyperkaliaemia, hypercalciuria and hypermagnesaemia, and mirror Gitelman's disease.[251,567,600] Loss-of-function mutations of one or several of the genes involved in Mg^{2+} reabsorption are associated with hypomagnesemia,[601] characteristic for Gordon's syndrome.[602]

Connecting Tubule (CNT)

In all species the epithelium of the CNT is lined by two distinct cell types (Figure 20.59): the segment-specific CNT cells; and the intercalated cells (IC cells) (see below). The segment-specific CNT cells display the calcium channel TRPV5 and the amiloride-sensitive epithelial sodium channel (ENaC) in their apical plasma membrane. In rats, mice, and humans they display, in addition, the vasopressin-regulated water channel, aquaporin-2 (AQP2) (Figure 20.55). In these species the emergence of AQP2 in the apical plasmalemma in the epithelial lining defines the beginning of the CNT, since TRPV5 and ENaC already appear in the transitional region (DCT2) (see Figure 20.55). Contrastingly, in rabbits vasopressin-regulated water channels are lacking in the CNT. In rabbits the beginning of the CNT is defined by a distinct change in epithelial structure, expression of TRPV5 and ENaC, and the first incidence of intercalated cells[544] (Figure 20.55). Evidently, the CNT shares cytological and functional features ascribed to both the nephron (derived from the metanephrogenic blastema) and the collecting duct (derived from the ureteric bud). The assignment of the CNT to either the nephron or the collecting ducts is disputed.[36,37,603,604]

CNT Cell Organization

The organization of CNT cells (Figures 20.54b, 20.57b, and 20.59b) is similar to that of DCT2 cells, i.e., intermediate between the DCT cells with basolateral membrane surface augmentation by interdigitating lateral folds and the non-interdigitating epithelia (CD cells) with basal plasma membrane infoldings.

The apical and the basal outlines of CNT cells approach a polygonal shape, and the cells are smoothly apposed to each other. The basolateral plasma membrane area is increased predominantly by folding of the basal plasma membrane into the cell. The infolded plasma membranes may extend into the most apical cell portion, and are endowed with abundant caveolae on their cytoplasmic face[260,554] (Figure 20.59). The extracellular spaces between the basal plasma membrane foldings and the lateral intercellular spaces have no direct continuity and are usually narrow.[260] The apical plasma membrane with short slender microvilli is delimited from the lateral plasma membrane by rather deep tight junctions, composed of several anastomosing strands.[427] The nucleus, the Golgi apparatus, polyribosomes, very short profiles of rER, and elongated and small round mitochondrial profiles are located in the cytoplasm between or above the infolded membranes. Smooth vesicles are particularly abundant in the apical half of CNT cells. In contrast to DCT cells, small lysosomes are frequent in CNT cells.

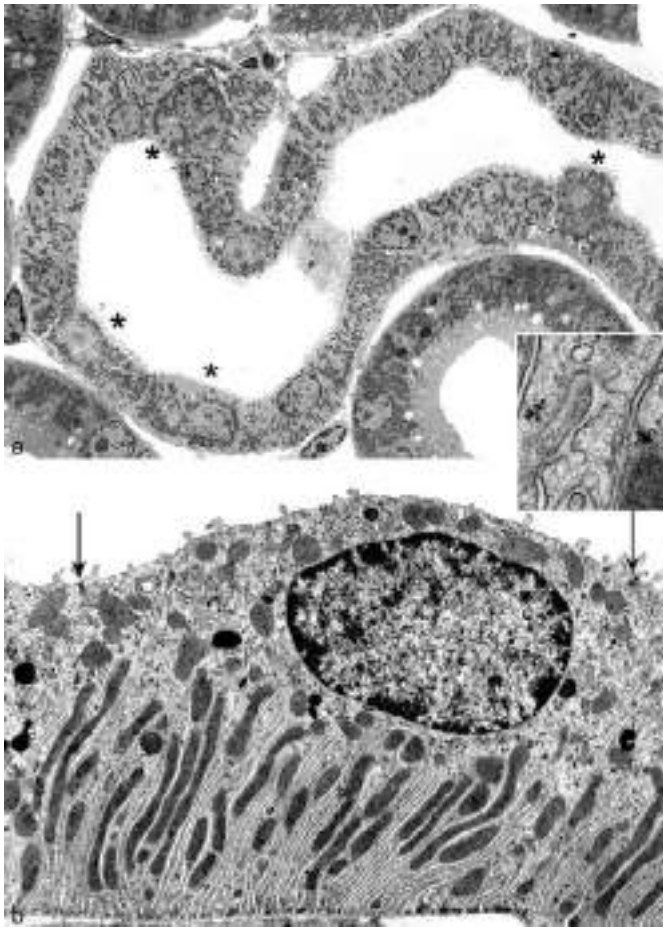

FIGURE 20.59 **Connecting tubule (rat kidney).** (a) The epithelium is composed of CNT cells and IC cells, (asterisks). (b) Characteristic CNT cell with abundant infoldings of the basal cell membrane; the arrows point to the tight junction. Insert: The infolded plasma membranes reveal numerous caveolae (TEM (a): ×~1400; (b): ×~6100).

From the beginning to the end of the segment, the height of the CNT cells, the extent of basal plasma membrane, and their volume density of mitochondria decrease. The steepness of the axial changes is more pronounced in rabbits[280] and mice than in rats, and varies with the functional conditions.[605,606]

Functional Aspects

Calcium Reabsorption

Microperfusion[607] and micropuncture studies had located active Ca^{2+} reabsorption to the distal convolution, including the DCT and CNT (for review see [608]) a long time before the specific Ca^{2+}-channel in the distal segments, TRPV5, was known.. The localization of TRPV5[609] in the apical plasmalemma of the late distal tubule (DCT2 cells and CNT cells[538]) (Figure 20.55) unequivocally identified these segments as sites for active transcellular Ca^{2+} reabsorption in the kidney. The paracellular pathway in these segments is impermeable for Ca^{2+}.

The cytoplasmic calcium-binding protein, calbindin D28k, the sodium calcium exchanger, NCX, and the plasma membrane calcium-Mg ATPase, PMCA, located in the basolateral plasma membrane, are auxiliary proteins necessary for TRPV5-mediated transcellular calcium movement. All three reveal very heavy immunostaining in DCT2 and CNT cells.[537,538] Upon its entry into the cell via TRPV5, calbindinD28k buffers Ca^{2+} and the basolateral Ca^{2+} transporters NCX and PMCA extrude Ca^{2+} into the interstitial compartment.[593] Interestingly, in tubular flow direction immunostaining for TRPV5 progressively shifts from the apical plasma membrane into the cytoplasm,[538] associated with parallel decreases of immuno-traceability for cytoplasmic calbindinD28k, for basolateral PMCA and for NCX. These changes most probably indicate respective changes of transcellular calcium transport rates.

Regulation of transcellular Ca^{2+} transport rates involves changes in the apical channel abundance and direct TRPV5 channel activation.[610] Via binding to its receptor (PTH/PTHrP) in the basolateral plasma membrane of CNT cells,[611–613] parathyroid hormone (PTH) increases the protein expression of TRPV5[593,614] and via a cAMP-PKA signaling pathway PTH increases the channel opening probability.[615] Transcription of the Ca^{2+} channel is regulated by the active form of vitamin D_3, 1,25-dihydroxyvitamin D_3 ($1,25(OH)_2D_3$).[594,616] The male and female sex hormones, estrogens and androgens, also play a role in renal Ca^{2+} handling.[617]

Urinary klotho stimulates TRPV5 channel activity at the apical membrane, whereas intracellular klotho enhances basolateral Na-K-ATPase surface expression that activates NCX-mediated Ca^{2+} efflux.[593] Urinary tissue kallikrein (TK) activates a bradykinin receptor (BK2) in the apical membrane of segment-specific CNT cells,[618] and thereby stimulates TRPV5-mediated Ca^{2+} influx.[615,619–621] The sites of TK synthesis in the kidney are approximately congruent with the sites of calcium reabsorption, i.e, the late DCT and CNT.[618] These findings suggest that TK may be a physiologic regulator of renal tubular calcium transport.[622,623] Kallikrein synthesis in the CNT and its subsequent release into the urine are stimulated by aldosterone,[624] dietary Na^+ restriction,[618] and in particular by dietary K^+ loading.[625,626] TK knockout mice display a somewhat delayed kaliuretic response to potassium loading.[623,627]

Sodium Reabsorption

The amiloride-sensitive sodium channel, ENaC, is the key player in the final sodium recovery by the kidney.[628,629] ENaC is a heteromultimeric channel composed of three homologous subunits (α, β, γ).[630] Full activity of ENaC requires the co-expression of all three subunits in the luminal membrane.

The activity of amiloride-sensitive transport is under the tight control of aldosterone.[631] Therefore, all segments with ENaC-mediated sodium reabsorption – DCT2, CNT, and CD – are collectively designated as "aldosterone-sensitive distal nephron" (ASDN[632]). While the mineralocorticoid receptor (MR) is expressed in all distal segments,[633] only the renal ENaC-expressing portions display the enzyme 11-β-hydroxysteroid dehydrogenase type 2 (11βHSD2),[605,606,634–639] which confers mineralocorticoid specificity to the MR. The rate-limiting factor for transepithelial Na^+ transport in the ASDN is the activity and abundance of ENaC in the luminal membrane of the ENaC-expressing cells.

Under control conditions[605,606] all three EnaC subunits are well detectable by immunostainings in the apical plasma membrane of the DCT2- and CNT-cells.[605,606] Along the course of the CNT and CD-segments all three subunits become undetectable in the apical plasmalemma, but heavily accumulate in the cytoplasm.[605,606,639] The decline in available channels in the luminal membrane is paralleled by reduction of basal infoldings and of mitochondria, most evident along the CNT epithelium and by a respective progressive decline of Na^+ transport activity along the axis of the ASDN (CNT > CCD).[604,640] The physiological relevance of ENaC-mediated Na^+ transport in the CNT is highlighted by the observation that the collecting duct-specific deletion of the alpha ENaC gene in mice[604] is fully compensated by the residual activity of ENaC in the upstream located CNT (and in the DCT2).[604]

In fact, recent data on the three-dimensional reconstruction of the mouse nephron show that five to seven nephrons are connected via a CNT to a single CCD.[34] Thus, the collected luminal surface for ENaC-mediated sodium reabsorption in the late DCTs and the CNT,[37,641] is several-fold greater than that available in the CCD itself.

All factors involved in regulation of sodium transport rates in the ASDN (hormones, proteases, intra-, and extracellular ion concentrations, tubular flow rate, as well as kinases and interacting proteins (for review see [562,642–644]), ultimately target the ENaC channel activity or abundance in the apical plasma membrane. Changes in ENaC abundance in the luminal plasma membrane involve channel synthesis, exocytotic delivery of subunits to the cell surface, and endocytotic retrieval of channels from the luminal membrane and their degradation.[300,562,628,644,645]

Endogeneous increases in plasma aldosterone levels rapidly induce (within hours) activation and redistribution of ENaC subunits from intracellular compartments to the apical plasma membrane[605,631,639,646] and a decrease of internalization of ENaC through the synthesis of SGK1.[647–649] Prolonged changes in EnaC-mediated sodium transport promote respective changes in cell height, abundance of basolateral plasma membrane infoldings, and the density of mitochondria,[280,290,292,293] which all together reflect the changes in Na^+ transport rates.

ENaC channel activity and abundance in the apical plasma membrane of the ASDN is also target of other hormones. The co-expression of ENaC with vasopressin receptors (V1 and V2) and vasopressin-sensitive water channels AQP2 in rat-, mice-, and human-segment-specific CNT (not in rabbit CNT cells) suggests the mutual interaction of sodium and water transport.[650,651] Indeed, vasopressin facilitates the translocation of ENaC to the apical membrane[652] and on removal of a V2R agonist ENaC is endocytosed from the membrane surface and reorganized into recycling vesicles, with a mechanism similar to that described for AQP2 regulation.[653] The delivery of somewhat water-depleted tubular fluid from the CNTs to the cortical collecting duct might enhance the urinary concentration process in the CD. Interestingly, in rabbits, in which the CNT lacks vasopressin-sensitive water channels, the arcades open at a much higher cortical level into the cortical collecting duct than in rats, mice or humans.[37]

Insulin and insulin-like growth factor,[610] angiotensin II[654–656] kinases, interacting proteins, intra-, and extracellular ion concentrations, osmolarity (for review see [645]), locally released nucleotides, and tubular flow rate (for review see [657]) have also been shown to modulate ENaC-mediated Na-transport activity.

Potassium Transport

In all ENaC-displaying cells renal outer medulla potassium channel ROMK is strongly expressed in the luminal membrane, where it co-localizes with PDZ proteins (NHERF2).[272] ENaC-mediated sodium reabsorption is coupled in a fixed ratio with K secretion via the ROMK. K^+ enters the cell by the activity of the Na-K-ATPase in the basolateral membrane, and exits into the tubular fluid via ROMK. The ratio of sodium-reabsorption and K-secretion by the segment-specific (CNT; CD cells)[658] can be modulated by intercalated cells which are bound to ENaC-displaying epithelia. The proton secretion by IC cells via a H-K-ATPase can apparently be coupled with K reabsorption.[659] Therefore, the ASDN is also the tubular site for net renal potassium (K^+) excretion.[482,660] The main factors regulating K^+ secretion are dietary K^+ intake and aldosterone (for review see [562]).

Mutations in the genes coding for ENaC subunits,[628,629] and for proteins involved in ENaC-associated K-secretion (ROMK),[661] as well as the correct targeting into or removal from the membrane (e.g., SGK1, Nedd4-2; for review see [645]) are associated with severe disturbances of blood pressure regulation.[662]

Transition From CNT tO CCD

In rodents and humans no marked structural change indicates the transition from the CNT to the CCD. Morphologically, the CCD can be defined by its location in the medullary ray. In difference, in rabbits the clear-cut onset of vasopressin-regulated water permeability marks the beginning of the CCD. It is associated with the appearance of dilated intercellular spaces in the epithelium[5,280] and the change of segment-specific cells, i.e., from CNT- to CD-cells.

By immunostaining, the beginning of the CCD is defined in rodents and rabbits by the break-off of TRPV5 (Figure 20.55) and related proteins (NCX, calbindin D28k[538,544]). In humans, NCX and calbindin D28k have also been detected in the CCD.[539]

Collecting Ducts

The CCD, the OMCD, and the upper part of the IMCD are composed of segment-specific cells (CD cells) and intercalated cells (IC cells; see subsequent sections) (Figure 20.54). The CD cells (Figures 20.54, 20.57, 20.60 and 20.61) have simple polygonal basal and apical outlines. Their most characteristic feature is the narrowly arranged basal plasmalemma infoldings of uniform height (Figures 20.54, 20.57, and 20.60) at the base of the cells, easily recognizable in light- and electron-microscopy as a basal light rim. All major cell organelles – the nucleus, small

mitochondria, numerous small Golgi-fields, abundant profiles of smooth ER, and a few of rough ER, lysosomes, multivesicular bodies, and occasional glycogen accumulations – are located in the zone above the infolded membranes. The subapical zone often reveals small round or elongated vesicles, oriented either perpendicularly or at an oblique angle to the luminal membrane (Figure 20.61c). These vesicles contain aggregates of AQP2, and are called aggrephores. Many of the aggrephores carry spherical clathrin-coated heads. The tight junctional belt is deep and consists of anastomosing strands with high particle density.[663] The apical plasma membrane generally bears only a few short slender microvilli or microfolds. The prominent central single cilia on the collecting duct-specific cells (Figure 20.62a) have been proposed as the key structural element in the Ca^{2+} response to fluid shear stress.[312,664] Short microvilli or folds of the lateral plasma membrane project into the intercellular space, and are connected by small desmosomes with those of adjacent cells (Figure 20.62b). In marked contrast to the water-impermeable epithelia of the TAL and the DCT, the width of the intercellular spaces between CD cells as well as the space between the infolded basal plasma membranes may be largely dilated or narrow, correlating with bulk water flow across the epithelium (see below).

The cytoskeleton is particularly prominent in CD cells. Actin filaments and microtubules form a dense meshwork along the apical and lateral plasma membrane. The cytoskeleton is essential for the shuttling of AQP2 to and from the plasmalemma (see below). Furthermore, the prominent cytoskeleton may be one mean, among others, to withstand the varying osmotic pressure in the collecting duct.

The CD cell undergoes gradual, although considerable, changes from the deep cortex (CCD) downstream to the upper third of the inner zone (IMCD) (Figure 20.61). The extent of basal plasma membrane foldings and the volume density of mitochondria decrease from the cortex towards the inner zone, whereas the volume density of lysosomes and the density of cytoskeletal proteins increase. The degree of changes along the CD differs among species.[5,260,540]

The CD cells in the lower two-thirds of the inner medulla are distinguished as inner medullary collecting duct cells (IMCD cells).[552] In rabbit[5] and guinea pig, IMCD cells increase in height toward the papilla up to 20-fold. A substantial, albeit less dramatic, increase occurs in rhesus monkey[665] and in human kidney.[540] In other species (e.g., rat, mouse, *Psammomys*, and dog[260]) the epithelium near the tip of the papilla is cuboidal or low columnar. The luminal membrane of IMCD cells is covered by numerous stubby microvilli, and generally lacks the central cilium.[546] The lateral intercellular spaces are conspicuous by their dense assembly of microvilli and microfolds, projecting from the lateral cell membranes. In the beginning of the inner medullary collecting duct (IMCD) the tight junctions are complex and consist of several anastomosing strands.[260] Toward the papillary tip in rat and rabbit, there is a considerable decrease in the number of strands, and in the apico–basal depth of the junction.[260]

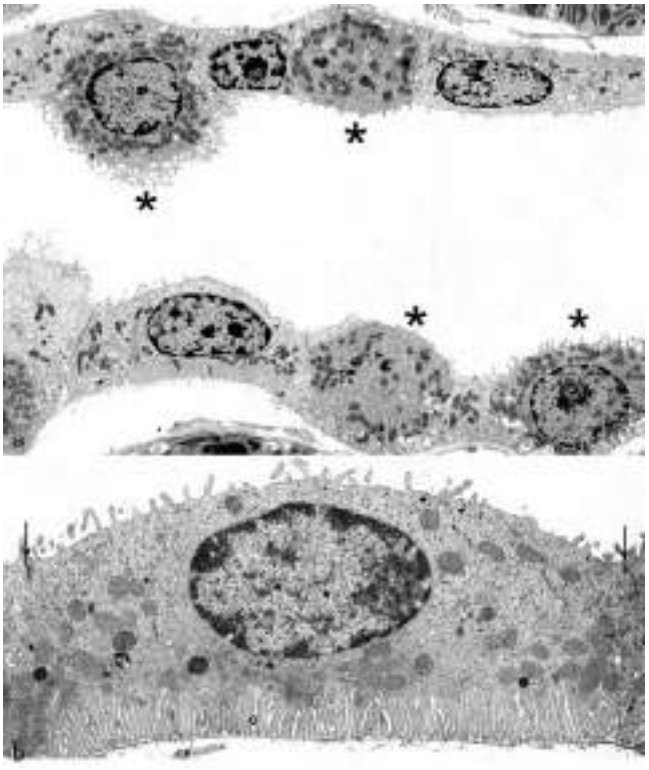

FIGURE 20.60 **Cortical collecting duct (rat kidney).** (a) The epithelium is composed of CD cells and IC cells. (b) CCD cell – infoldings of the basal plasma membrane are restricted to the basal cell portion; all mitochondria and cell organelles are located above the infolded membranes (Arrows: Tight junctions; TEM (a): ×~2700; (b): ×~8500). *(Adapted from and Kaissling, B., and Kriz, W. (1992). In "Morphology of the Loop of Henle, Distal Tubule and Collecting Duct. Handbook of Physiology: Section on Renal Physiology," 109–167, Windhager, E. E. Oxford University Press, New York, with permission).*

Sodium Reabsorption in the Collecting Duct

Together with the vasopressin-regulated water-channel AQP2, the CD cells consistently express the amiloride-sensitive Na-channel ENaC (see CNT)[666] (Figure 20.55) and ROMK. The coexistence of the differentially regulated pathways for water- and Na-reabsorption in the same cell suggest the possibility for mutual interactions.[650,666,667]

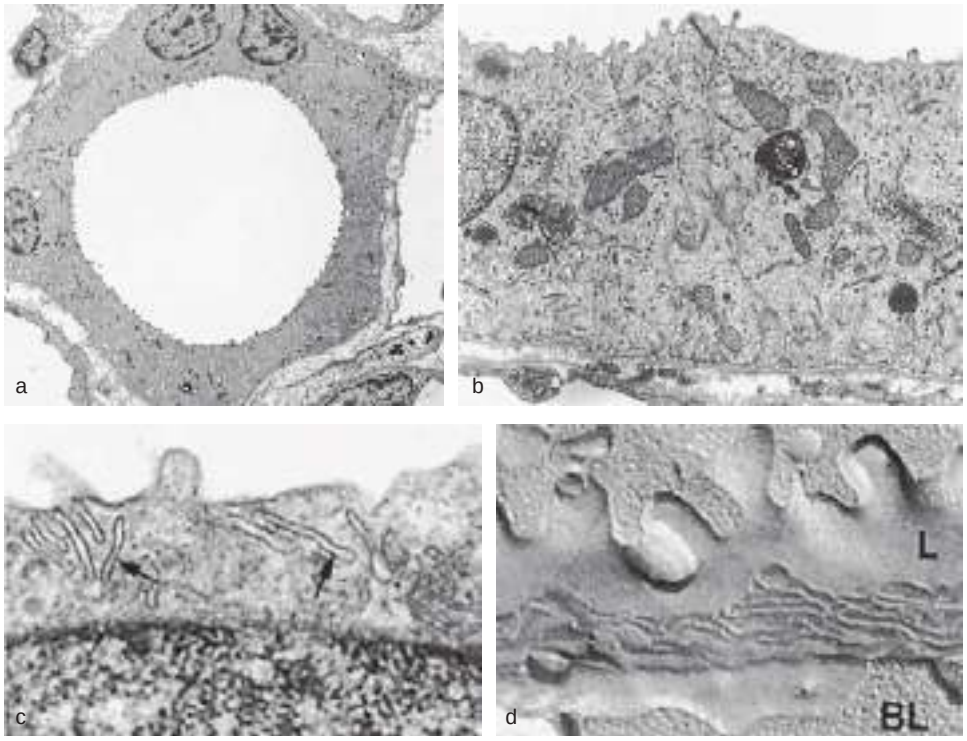

FIGURE 20.61 **Inner medullary collecting duct.** (a) Tubular profile showing the homogenous epithelium (rat: TEM: ×~3400). (b) Epithelium of the middle portion of an IMCD. Within the epithelium three zones are seen: a basal zone with basal infoldings, a middle zone containing Golgi fields, mitochondria and lysosomal elements, and a thin apical zone with tubular and vesicular profiles. Note the deep tight junction (rat: TEM: ×~17,000). (c) Apical zone of a CD cell with many elongated tubular profiles (arrows) which are believed to represent agrophores (rat: TEM: ×~38,000). (d) Freeze-fracture electron micrograph to show the multistranded tight junction of the collecting duct epithelium (L: luminal membrane; BL: basolateral membrane; Rabbit: ×~34,000).

Recently, a second pathway for electroneutral NaCl absorption has been revealed in the collecting duct epithelium, This pathway is located in the intercalated cells (see below) and is insensitive to amiloride but inhibited by thiazides, and couples 2 anion exchangers, pendrin and Na-driven chloride/bicarbonate exchanger (NDCBE)[668,669] (see "Intercalated Cells").

Paracrine and autocrine regulation by the purinergic system[296,657,670,671] mediates flow-and metabolic rate-dependent changes of Na^+ and water transport in the collecting duct.

Vasopressin-Regulated Water and Urea Reabsorption in the Collecting Duct

Collecting ducts are the canonical targets for vasopressin-sensitive water and urea reabsorption.[672] They display receptors for vasopressin (V_1 and V_2) in the basolateral plasma membrane of the segment-specific cells, the CD cells,[519] and vasopressin-sensitive water channels AQP2. Water permeability of the luminal membrane is achieved by exocytotic insertion of the vasopressin-regulated water-channel AQP2 from subapical vesicles (aggrephores) into the apical cell membrane. The exocytosis is triggered by binding of vasopressin (ADH) to the V2-receptor at the basolateral membrane of CD cells and the subsequent signal transduction cascade. The aggregates of AQP2 in the aggrephores are colocalized with dynein and dynactin.[673] Many of the aggrephores carry spherical clathrin-coated heads. With low levels of vasopressin, the AQP2-containing membrane portions recycle back into the subapical cytoplasm.[299,674–676] The movement of aggrephores critically depends on microtubules and actin filaments in the apical cytoplasm.

High levels of vasopressin-independent AQP2 surface expression have been observed under long-term[677] and acute[678] exposure of rats and mice to statins. Applied chronically, statins decrease membrane cholesterol[679] and clathrin-mediated endocytosis of AQP2. Acutely, the statins seem to decrease endocytosis of AQP2 and vesicle trafficking by modulating Rho-GTPase,[678] which is involved in regulation of the cytoskeleton, endocytosis, and vesicle trafficking.[680,681] The water channels AQP3 and AQP4 are both located in the basolateral membrane of CD cells.[682] AQP3 is permeable to glycerol, urea, and water; AQP4 is associated with orthogonal arrays of intramembrane particles, as

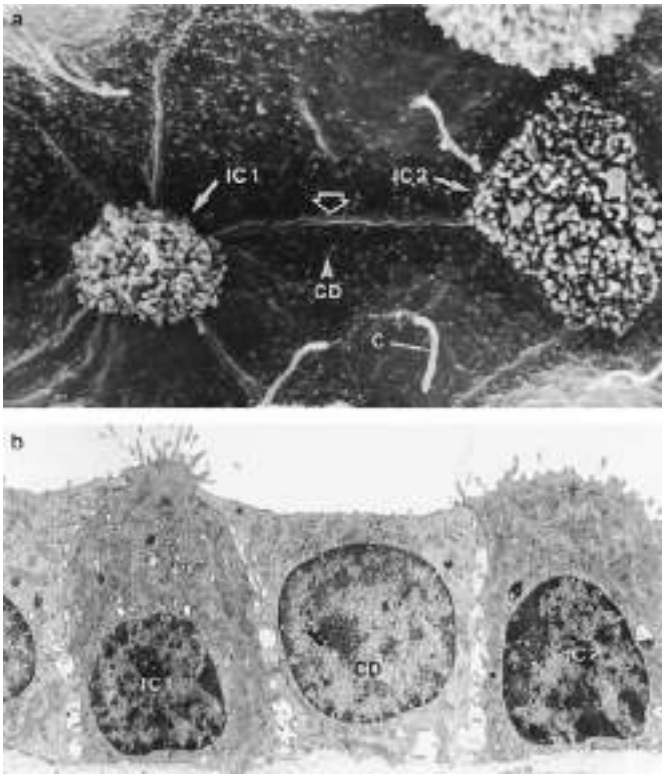

FIGURE 20.62 **Intercalated cells from the rabbit.** (a) Scanning electron micrograph of a cortical collecting duct with collecting duct-specific CD cells (CD) and intercalated cells (IC). The CD cells carry single cilia (C) and short microvilli (arrowhead). The straight ridges (open arrow) represent the cell borders between CD cells. From the IC cells one (IC 1) has a narrow, constricted apical cell pole, the other one (IC 2) a large apical cell pole, both adorned with numerous long microvilli (TEM: ×~13,000). (b) Section across corresponding cells. Note the position and accumulation of flat vesicles (asterisk) in the apical cell pole of the IC cells (TEM: ×~7500).

revealed by freeze-fracture studies in the outer medullary collecting duct.[683,684]

The IMCD cells co-express, in addition to vasopressin-regulated AQP2, the vasopressin-regulated urea transporters UT-A1/3 and possibly UT-A4 (for review see [148]). The abundance of UT-A1/3 in the apical membrane is rate-limiting for transepithelial, vasopressin-dependent urea reabsorption.[571,685] The basolateral membranes of the IMCD cells display the water channel AQP3. The abundance of UT-A1/3 in the apical membrane is rate-limiting for transepithelial, vasopressin-dependent urea reabsorption.[571,685] In the basolateral membranes of the IMCD cells the water channels AQP3,[682] permeability to glycerol, urea and water,[686] and AQP4[683,687] with an apparently low urea permeability have been demonstrated.

The genes coding for proteins, which are involved in cellular accumulation of organic osmolytes, such as the vasopressin-regulated urea transporter UT-A and heat shock protein 70,[688] are target genes of the tonicity-response enhancer binding protein (TonEBP), a transcriptional activator of the REL-family. During kidney development, expression of TonEBP precedes that of the urea transporter. It is first detected in the renal medulla of mice at the fetal age of 16 days and increases up to postnatal day 21, when the medulla is fully developed and the urinary concentrating ability is achieved.[689]

Intercalated Cells (IC Cells)

Intercalated cells (IC cells) are interspersed as single cells among the epithelium of the ASDN (i.e., among ENaC-displaying epithelia, the late DCT (DCT2), the CNT (Figure 20.59a), and the CD (Figure 20.60a). IC cells play a decisive role in the final regulation by the collecting system of acid−base excretion, in potassium reabsorption and secretion, in ammonia excretion and, as discovered recently, intercalated cells participate together with the segment-specific cells in electroneutral sodium reabsorption.

Consistent Structural Features of Intercalated Cells

Intercalated cells reveal conspicuous structural heterogeneity (Figure 20.61). IC cells usually do not form a continous epithelial layer, but at least their luminal poles are entirely surrounded by the segment-specific cells. The luminal outline of IC cells is in most cases rather circular (Figure 20.62a),[291,540,690−692] IC cells generally reveal a specific surface pattern of microprojections (Figure 20.62a) and lack, at least in the cortex, the central cilium which is apparent on other cells (Figure 20.62b). Among the most consistent distinguishing intracellular features is the distribution pattern of mitochondria: the often rounded mitochondrial profiles lack the systematic association to basolateral cell membranes[35,693,694] evident in other tubular cells. The generally small, more or less round vesicles often reveal an invagination bordered by a thin smooth membrane ("invaginated vesicles"[5]); they participate in endocytosis[695−697]; the elongated slender profiles − "tubules" − probably represent sections through flat saccules or collapsed large spherical vesicles ("flat vesicles").[5] Occasionally they are found to be continuous with the luminal membrane, and are often in close juxtaposition with mitochondria.[5] Transitional forms between the two vesicle types can be seen; the presence of specific particles in one or several membrane domains (luminal, basolateral, and/or tubulo-vesicular) have been observed. In TEM preparations the membranes reveal a coat of densely arranged, approximately rectangular large particles, so-called "studs," on their cytoplasmic face. The "studs" are 10 nm spherical

structures (Figure 20.65a,c,d), which represent the H^+-ATPase.[698,699] In freeze-fracture preparations dense arrays of intramembrane particles, so-called "rod-shaped" particles appear on the P-face of the membranes (Figure 20.65b).[543,700] The presence of "studs" and of "rod-shaped" particles on the cytoplasmic membrane faces often coincides. Clathrin-coated pits on either the luminal or the basal cell membrane and clathrin heads on the "studded" vesicles are regularly found. The nucleus generally reveals more heterochromatin condensations and looks darker than that of the adjacent CNT or CD cells.

Proteins Related to Intercalated Cell Functions

All intercalated cells display high levels of cabonic anhydrase II in the cytoplasm.[450,472,701–704] All IC cells express the electrogenic V-type proton-ATPase, the proton pump[698] in at least one of their membrane domains, and all express an anion exchanger, either anion exchanger 1 (AE1, gene Slc4A1; band 3[705]) or Pendrin (Slc 26A4[706]) in one membrane domain. Pendrin is an aldosterone-sensitive Na^+-independent Cl^-/HCO_3^- exchanger that mediates Cl^- absorption and HCO_3^- secretion in the cortical collecting duct (CCD).[669] Furthermore, studies on isolated CCDs suggested that the parallel action of the Na^+-driven Cl^-/HCO_3^- exchanger (NDCBE/SLC4A8) and the Na^+-independent Cl^-/HCO_3^- exchanger (pendrin/SLC26A4) account for the electroneutral thiazide-sensitive sodium transport in the CCD (where the thiazide sensitive electroneutral NaCl co-transporter NCC is not expressed), a finding that challenges the current concept of a functional separation between principal cells for the regulation of sodium and potassium balance, and intercalated cells for acid–base regulation.[668]

All IC cells express the Rhesus glycoproteins, Rh B Glycoprotein (Rhbg[707]) and Rh C Glycoprotein (Rhcg[708]). These proteins are recently recognized ammonia transporters in the distal tubule and collecting duct. Rhcg is present in both the apical and basolateral plasma membrane, is expressed in parallel with renal ammonia excretion, and mediates a critical role in renal ammonia excretion and collecting duct ammonia transport. Rhbg is expressed specifically in the basolateral plasma membrane.[709]

Subtypes of Intercalated Cells

By morphological criteria and distribution patterns of specific transport proteins (Table 20.1) three different manifestation of IC cells have been described, type A cells, type B cells,[694] and type nonA-nonB cells.[710]

TYPE A IC CELLS

Morphologically, the type A IC cells usually have a broad protruding apical cell pole, which is adorned with numerous slender microfolds and/or finger-like microvilli giving rise to a very complex surface pattern[5,691,694](Figures 20.63a and 20.64a). The cytoplasmic membrane face of the microprojections and of the esicles in the apical cell pole are "studded"[594] (Figure 20.65a). "Rod-shaped" particles (Figure 20.64b) have also been demonstrated.[700] The mitochondria are particularly numerous, and are accumulated in the apical cell pole above the large round nucleus (Figure 20.64a). They are often found very closely adjacent to the luminal cell membrane. They possess narrower cristae, and their matrix appears more electron-dense than in other cell types. The Golgi apparatus and other cell organelles are only slightly apparent among the numerous mitochondria. Polyribosomes may be exceedingly frequent. Some profiles of RER are

TABLE 20.1 Proteins with Defined Functional Relevance (see text) in Renal Intercalated Cell (IC) Subtypes

Intercalated Cells Protein	Type A	Type B	Type nonA-nonB	References
Carbonic anhydrase II	yes; a	yes; c	yes; c	450,812–819
H^+-ATPase	**yes; a**	**yes; b**	yes; **diff**	698,699,714–719
AE1 (Slc4A1; Band 3)	**yes; a**	absent	absent	705,709,721,740,820
Pendrin(Slc 26A4)	absent	**yes; a**	**yes; a**	740,820
RhBG	yes; b	absent	yes; b	494,709,730
RhCG	yes; a	absent	yes; a	709,730,732,821,822
H + -K-ATPase (gastric and non-gastric)	yes; a	?	?	823–830
5′NT	yes; a	yes; a (b)	?	57,753

Localization in: a: apical membrane domain; b: basolateral membrane domain; (b): occasionally; diff: diffuse vesicular; c: cytoplasmic; ?: not determined.
bold: marker combination for IC subtype diagnosis.

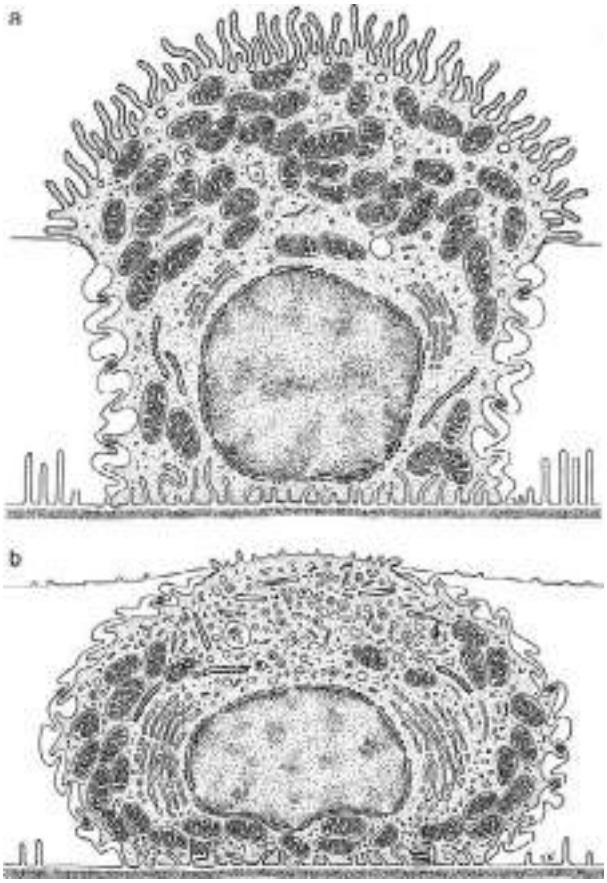

FIGURE 20.63 **Survey of ultrastructure of intercalated cells.** (a) A-type IC cell; (b) B-type IC cell. . *(Adapted from and Kaissling, B., and Kriz, W. (1992).* In *"Morphology of the Loop of Henle, Distal Tubule and Collecting Duct. Handbook of Physiology: Section on Renal Physiology," 109–167, Windhager, E. E. Oxford University Press, New York, with permission)*

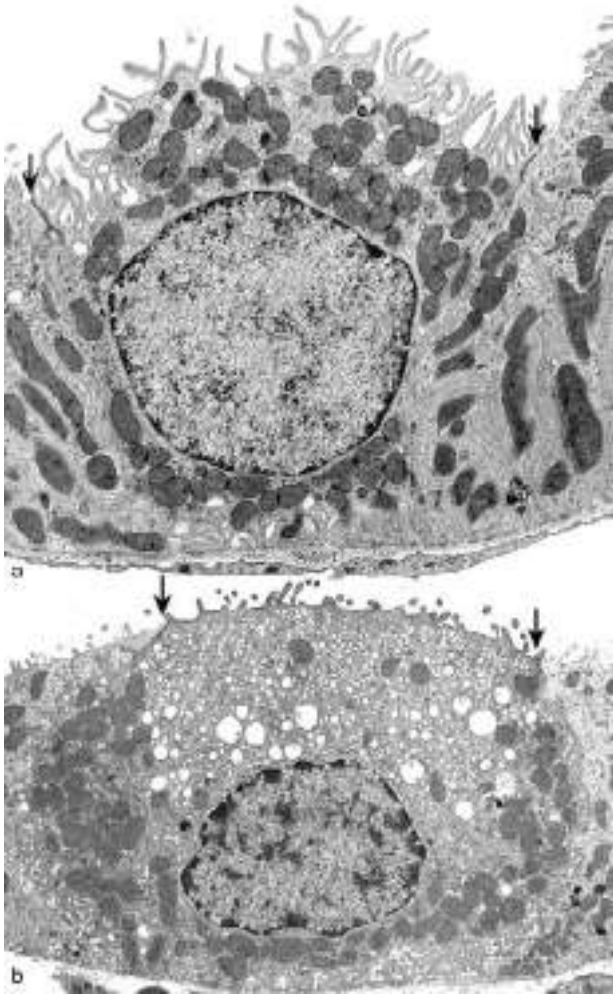

FIGURE 20.64 **Intercalated cells (rat).** (a) Type A cell with many luminal microfolds and abundant mitochondria in the apical cell pole. (b) Type B cell with a rather narrow apical cell pole, a narrow rim of dense cytoplasm with no vesicles under the apical plasma membrane, abundant smooth-surfaced vesicles in the apical cytoplasm, and a huge Golgi complex (G), with abundant mitochondria along the basolateral plasma membrane (Arrows: Tight junction; TEM: ×~7000).

generally found in basal cell portions. Basal infoldings can be extensive in the rat,[694,711] yet in the rabbit they are virtually absent.[712]

Some structural variation within type A cells exist among and even within individuals. They concern essentially the extent of studded membrane projections on the luminal cell surface, and the abundance of studded tubulo-vesicular profiles in the apical cell pole. The membrane surface area of the microfolds seems to be inversely related that of the tubular-vesicular profiles; both vary with functional conditions. For instance, under acute metabolic and respiratory acidosis[711] and/or potassium depletion the vesicular pool decreases and the apical membrane increases. Mitochondria with rather short profiles and narrowly arranged cristae are amassed in the apical cell pole, in particularly close vicinity to the apical cell membrane. Many microtubules and clathrin-coated vesicles are apparent between the tubulo-vesicular profiles and the mitochondria. The nucleus is shifted to the basal cell portion (Figures 20.63a and 20.64a) (for review see [492,698,713]).

IC cells in the outer medulla and the initial part of the inner medullary CD (rats) appear slightly different from the cortical type A cells. In rats, the apical cell pole is often narrower than the basal cell pole.[268] The mitochondrial profiles are fewer and smaller than in cortical type A, the Golgi apparatus and the SER are less apparent than in cortical type A cells, the basal infoldings are less extensive compared to cortical type A cells and the nucleus has a characteristic elongated flattened profile. Among the "studded" vesicles in the apical cell pole very large round profiles and

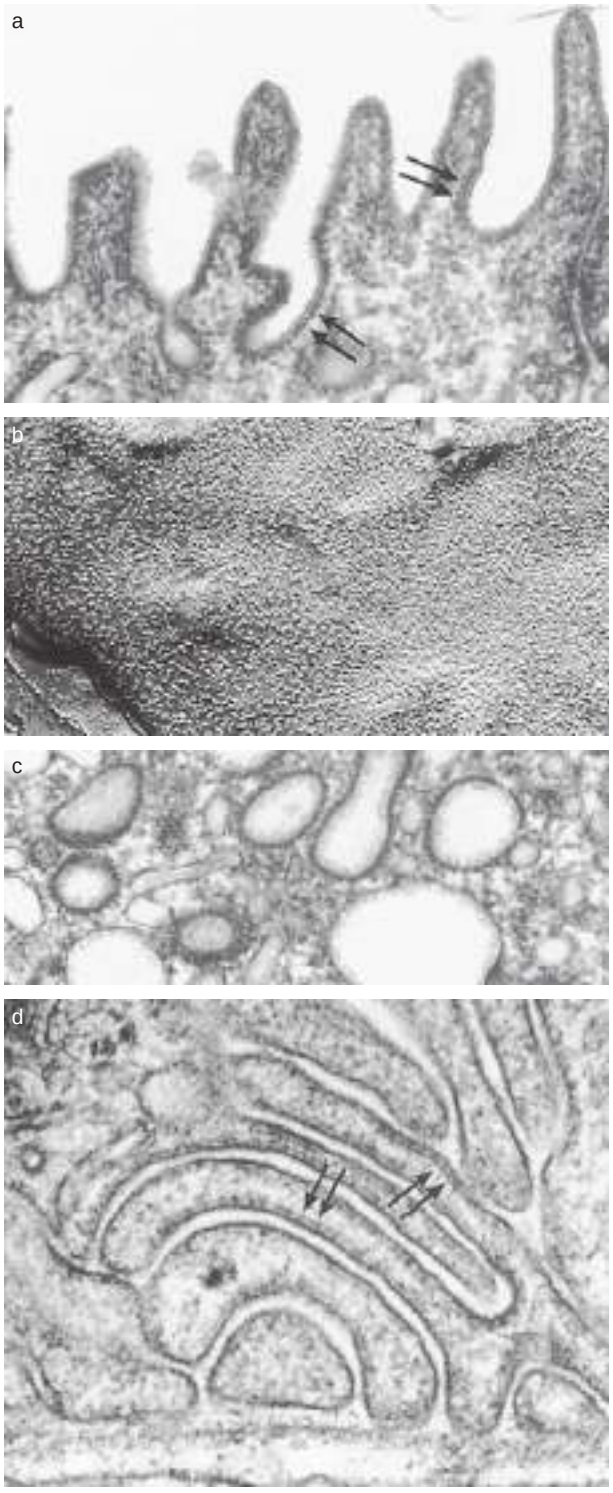

FIGURE 20.65 **Intercalated cells (rat).** (a) Luminal membrane; its cytoplasmic face is coated with studs (arrows) (TEM: ×~61,000). (b) Freeze-fracture electron micrograph showing the rod-shaped intramembrane particles (stars) of a luminal membrane (TEM: ×~32,000). (c) Apical cytoplasm of a type A cell. The specific vesicles are coated with studs (TEM: ×~64,000). (d) Membrane of basal infoldings of type B cell; its cytoplasmic face is covered with studs (arrows) (TEM: ×~61,000).

particularly long flat vesicles often predominate over other cell organelles.

Type A IC cells are considered as the proton-secreting cells. Their apical membrane domain possesses various subunits of H^+-ATPase, among them the B1- and d-subunits which possess a high selectivity for intercalated cells.[698,699,715–719] The proton-ATPase functions in series with a bicarbonate/Cl (HCO_3^- /Cl^-) exchanger located in the basolateral membrane domain (for review see [492]). In type A IC cells the HCO_3^- /Cl^- exchanger is the anion exchanger AE1 (SLC4A1, band 3), a splice variant product of the erythrocyte band 3 gene.[705,720] The presence of AE1 in the basolateral membrane is decisive for diagnosis of type A IC cells.[705,721]

In addition to the V-type proton-ATPase type A IC cells – at least in the outer stripe – also display a P-type (gastric-type) K-H-ATPase, shown so far in rat and rabbit.[578,659,722–726] This K-reabsorbing ATPase seems to be associated with clusters of rod-shaped particles, revealed by freeze-fracture studies on the P-face of cell membranes in rabbit IC cells.[700] Thus, the type A IC cells could be involved in recovering potassium, secreted via ROMK, in association with EnaC-mediated Na-reabsorption by the segment-specific cells. Type A cells also express the chloride channel ClC 5.[727] The secretory isoform of the Na-K-Cl-co-transporter, NKCC 1, has been detected in the basolateral membrane of type A cells in the outer stripe.[728]

The type A IC cells express apically and basolaterally non-erythroid Rh-associated glycoproteins Rhcg and basolaterally Rhbg,[492,494,709,729–731] which mediate transport of ammonia/ammonium (NH_4^+/NH_3)[494,732] when expressed in *Xenopus laevis* oocytes.[733]

In chronic metabolic acidosis and prolonged high proton secretion the type A IC cells hypertrophy (for review see [492]), and IC cells in the OMCD and IMCD show increased RhCG expression.[734] However, genetic ablation of the RhBG gene is not a critical determinant of NH_4^+ excretion by the kidney under acidic or under control conditions.[729] Under chronic acidosis the type A IC cells proliferate, as evidenced by upregulation of cell cycle proteins, by incorporation of the thymidine analog bromo-deoxyuridine (BrdU) and mitotic figures.[735]

TYPE B IC CELLS

Morphologically, Type B IC cells reveal a relatively small, occasionally slightly polygonal luminal outline and protrude only slightly into the lumen (Figures 20.60a, 20.63b, and 20.64b[711]). The cells seem to be partly covered by the adjacent CD cells, and their sectional profiles often appear almost elliptical (Figures 20.63b and 20.64b). The luminal membrane, with only a few short microprojections, lacks "studs".[736] In contrast, "studs" may be apparent on

fragments or even along the entire lateral and often extensive formation of infoldings of the basal plasma membrane (Figure 20.65d). The small short mitochondria are accumulated in the basal cell portion and along the lateral cell faces (Figures 20.63b and 20.64b), but they are never found immediately beneath the luminal membrane. The cytoplasm above the plane of the tight junctional belt may be completely devoid of any cell organelles. The nucleus often reveals some basal indentations,[711] and is often situated eccentrically. The center of the cell is occupied by a conspicously developed Golgi apparatus, a few short profiles of RER, polyribosomes, and microtubules, as well as lysosomes of varying dimensions, and autophagosomes containing frequently recognizable remnants of mitochondria or membranes. A striking feature of these cells is the high abundance of narrow-meshed profiles of smooth ER, often with clathrin-coated heads.[329] The SER is intermingled with a great amount of small, generally "unstudded" invaginated vesicles, which are preferentially found in the apical cell portion, but may be accumulated also in the direct vicinity of the basal cell membrane. "Studded" vesicles are sparse or lacking.

The type B cells also display different manifestations. Between cells which are densely stuffed with SER and display very few mitochondria and very few "studded" membrane domains, and cells which contain large amounts of mitochondria, of "studded" vesicles, and which may be even densely covered with short microvilli, all intermediates can be found. Another configuration of possibly type B cells is found in the cortex of rabbits. These cells appear "constricted" at the level of the tight junctional belt where a prominent web of microfilaments is evident. Some elongated profiles of "studded" vesicles are found within and beneath this web. The narrow, apical cell pole is adorned with a tuft of long microvilli.[260]

Type B IC cells mediate secretion of HCO_3^- through apical Cl^-/ HCO_3^- exchange, which functions in series with H^+-ATPase-mediated H^+ efflux across the basolateral plasma membrane.[737] They are characterized by apical pendrin (Slc4A1)[738–740] and basolateral H^+-ATPase. Type B cells reveal less carbonic anhydric activity than type A cells,[702] and they express the chloride channel ClC 3[727] in the apical cell pole.

Metabolic alkalosis is compensated in the kidney by reducing bicarbonate reabsorption and increased bicarbonate secretion by type B IC cells. Type B IC cells adapt under chronic metabolic alkalosis with cellular hypertrophy.[741] DNA synthesis and mitoses of type B cells have been recorded under this situation.[742] Adaptive downregulation of pendrin in metabolic acidosis indicates the important role of this exchanger in acid–base regulation in the CCD.[741] The type B intercalated cell does not express either Rhbg or Rhcg detectable by immunohistochemistry.

NON A-NON B CELLS

A third type of IC cells without evident polarity with respect to proton-APTase, and so far with undefined function, are called "non A-non B" cells.[738] These cells are often much larger and protrude much more into the lumen than type A or B.[709] In contrast to type A and B IC cells, neither the luminal nor the basolatreal plasma membranes reveal "studs," at best "studs" are found on membranes of vesicular profiles in the cytoplasm. In mice this latter population of intercalated cells is more frequent than in rats.[743] It decreases in either pronounced chronic metabolic acidosis or pronounced chronic metabolic alkalosis.[492,711,744]

On their apical plasma membrane they display, similar to type B IC cells, the anion exchanger pendrin (Slc4A1) and diffusely distributed H^+-ATPase, occasionally also in the apical membrane. They express apical, but not basolateral, Rhcg and basolateral Rhbg.[709]

The observations on non A-non B cells, the striking structural diversity[713,745] and the apparent plasticity of IC cells raised the question whether one, two or more distinct cell types are subsumed in the IC cell population or whether the different appearances are manifestations of different functional stages of the same cell type. Based on studies in collecting ducts *in vitro* from adult rabbits and IC cells cultured *in vitro*,[746–749] (IC cells with the morphology of type B were identified by apical binding to peanut lectin),[750] it was speculated that the IC cells might reverse their polarity in response to specific functional environmental conditions. Type A would present the terminal differentiation of IC cells. This hypothesis received support from studies *in vitro* showing that the matrix protein hensin could reverse the functional phenotype of cultured intercalated cells (for review see [492]), and induce the type A IC cells. The non A-non B cells might represent intermediate stages. The diminution of this latter population under chronic acidotic or alkalotic conditions would agree with this hypothesis.

Another view was that the non A-non B cells could be precursors for either A or B cells or only of B cells (for review see [492]). This hypothesis would also be supported by the finding of a diminution of non A-non-B cells under chronic acidosis or alkalosis. The observations on mitosis in fully-differentiated type A,[735,751] as well as in type B IC cells[742] do not agree with the hypothesis on reversal of polarity, nor with the hypothesis claiming a common precursor cell of type A and B.

Most IC cells also display on at least one membrane domain (more often on the luminal and vesicular than on the basolateral) the AMP-degrading phosphatidyl-inositol-anchored ecto-enzyme 5′nucleotidase

(5′NT)[57,60,740,752,753] and the protein Connexin 30, that might function as plasma membrane ATP channel.[754] It has been shown that increased flow in the distal nephron induces K secretion through the large-conductance, calcium-activated K channel (BK), which is primarily expressed in intercalated cells (IC). High distal flows and shear stress induce BK-dependent K efflux and ATP release from IC cells.[295] These mechanisms might play a role in the purinergic autocrine and/or paracrine regulation of salt and water reabsorption.[317]

The intergral membrane proteins syntaxin 3[755] and synaptotagmin VIII demonstrated in the basolateral membrane of IC cells,[756] are possibly involved in the targeting of acid−base transporters and may participate in the basolateral membrane remodeling of IC cells in response to systemic acid−base perturbations.

Interestingly, it had been reported that IC cells lack significant levels of Na-K-ATPase in the basolateral membranes.[283] However, more recently, weak to moderate Na-K-ATPase was revealed in cortical and outer medullary IC cells, whereas IC cells in the upper part of the inner medullary collecting duct showed a staining intensity that was similar or even stronger to that in adjacent IMCD cells.[757]

Distribution of IC Cells

The ratio of intercalated cells to other tubular cell types varies among and within species, and along the distal segments (DCT, CNT, upper and lower half of cortical collecting duct, outer and inner stripe collecting duct). Possibly, it may be altered by some functional conditions.[744] Discrepancies in reported data for a given species may be rooted in poor definition of the investigated kidney region, and also in the criteria used for the recognition of cells. The relative number of intercalated cells (all forms) in the various segments is roughly ∼25−30% in the CNT, ∼40% in the CCD and OMCD, and ∼10% in the initial IMCD.[699,718,743,758] IC cells are absent in deeper levels of the inner medulla in most species.

In the rat, taking the morphological, cyto-, and immunochemical data together, it can be deduced that among the IC cells in the CNT the type A cells prevail. Type B cells are in the minority among the IC cells in the CNT in rat, but not in mouse. Type B IC cells constitute the majority of IC cells in the CCD, of which a varying proportion may present proton-ATPase in the basolateral cell membrane. Based on the different distribution of the proton-ATPase in non-type A intercalated cells, it has been suggested type B IC cells with only basolateral proton-ATPase staining and non-A/non-B IC cells with bipolar or luminal proton-ATPase staining should be distinguished.[743] However, both subpopulations carry pendrin staining, and may represent different states of activity.

In the CCD type A cells are in the minority, and often appear in their apparently functionally less active form, with less microprojections, but more intracellular "studded" vesicles than type A cells in the CNT.[759] Accordingly, they display a slightly weaker luminal, but often a diffuse cytoplasmic, staining for the proton-ATPase. Apparently only one type of IC cells exists in the OMCD of rats, mice, and humans. It resembles the type A cells in the cortex.

Disruption of IC Cell Characteristic Genes

Inheritable forms of distal renal tubular acidosis (dRTA) most often affect the physiology of type A IC cells.[760] Disruption of one of the IC cell characteristic genes leads to profound structural alterations of IC cell types. In mice with functional deletion of carbonic anhydrase II, the frequency of IC cells is drastically reduced.[701]

The genetic disruption of pendrin (Slc26a4) leads to marked reduction of type B cell size, with reduced H^+/OH^- transporter expressions.[506,738] In mice with disruption of the Foxi1 gene, upstream of several anion transporters, proton pumps, and anion exchange proteins expressed by intercalated cells, and of the collecting ducts cells, the normal collecting duct epithelium with its two major cell populations − collecting ducts cells (principal) and intercalated cells − has been replaced by a single cell type positive for both principal and intercalated cell markers.[761]

ARCHITECTURAL−FUNCTIONAL RELATIONSHIPS

So far we have always emphasized the relationships between structure and function. However, we have neglected the important relationships between architecture and function − i.e., arrangements through which the close relationships between certain nephron and vascular portions permit the carrying out and coordination of complex regulatory functions. The two most obvious examples in this respect are the juxtaglomerular apparatus (JGA), regulating glomerular perfusion and renin secretion, and the renal medulla permitting the production of urine, varying in dilution and concentration.

Juxtaglomerular Apparatus

The juxtaglomerular apparatus (JGA) is a composite assembly of specialized structures at the vascular pole of the glomerulus (Figures 20.28 and 20.29). The thick ascending limb of Henle's loop (TAL) returns to its parent glomerulus and extends through the angle

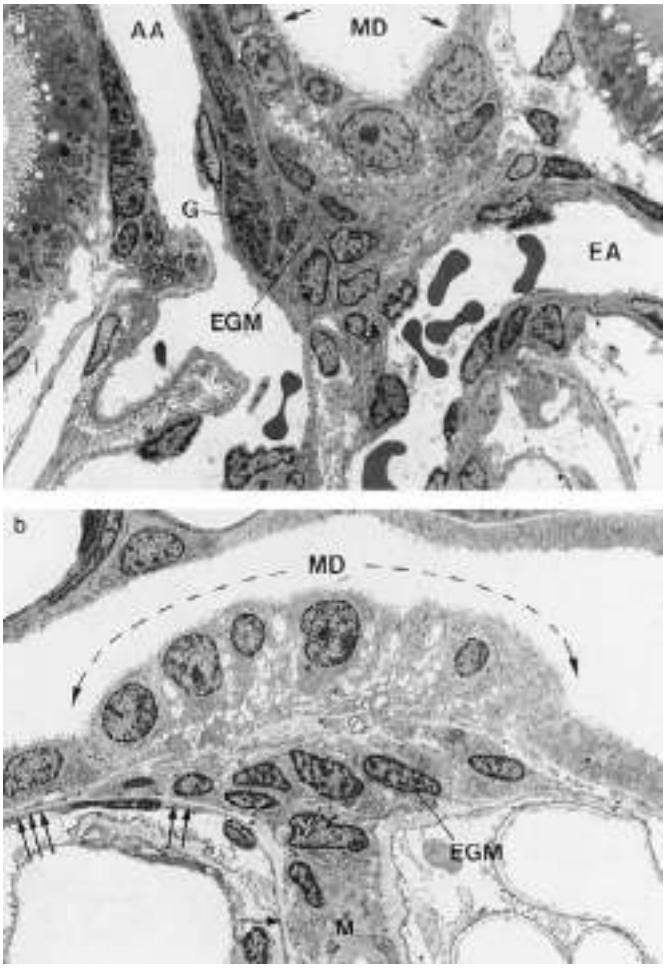

FIGURE 20.66 **Juxtaglomerular apparatus.** (a) Meridional section through a glomerulus which runs through both glomerular arterioles (rat). The macula densa (MD) is attached to the extraglomerular mesangium (EGM), which fills the angle between the afferent (AA) and efferent (EA) arteriole. Within the wall of the afferent arteriole granular cells (G) are seen. Note the intraglomerular segment of the efferent arteriole (TEM: ×~1850). (b) Meridional section through a glomerulus running in between both arterioles (rabbit). The macula densa (MD) is a prominent cell plaque within the thick ascending limb. It covers the extraglomerular mesangium (EGM). Within the glomerular stalk the EGM continues into the mesangium (M). The EGM interconnects opposing parts of the GBM (one arrow) to the basement membrane of Bowman's capsule (BCBM) (two arrows), as well as the first parts of the BCBM (three arrows). Note the dilated intercellular spaces between macula densa cells (TEM: ×~8100).

between afferent and efferent arterioles, where it is firmly attached to the extraglomerular mesangium (Figure 20.66a). At the attachment point, the TAL changes its character: a plaque of specialized cells, known as the macula densa (MD), represents the contact site of the tubule. Around this attachment, other specialized structures are developed which, together with the macula densa, comprise the JGA. These are: the terminal portion of the afferent arteriole housing the renin producing granular cells; the initial portion of the efferent arteriole; and the extraglomerular mesangium (EGM). The latter is in continuity with the intraglomerular mesangium, and has intimate relationships with the parietal epithelium of Bowman's capsule.[20] The JGA, more precisely the granular cells and the smooth muscle cells of afferent and efferent arterioles, are richly innervated by sympathetic nerves.

Macula Densa

Shortly before its end, the TAL passes between the afferent and efferent arterioles of its original glomerulus. At this site the basal face of the tubule is affixed to the extracellular matrix, enveloping the cells of the extraglomerular mesangium (EGM), tying together both arterioles. The TAL cells in contact with the EGM are transformed into the "macula densa" (MD). The MD is a cell plaque comprising some 20 to 30 specialized epithelial cells (in juxtamedullary nephrons more than in superficial nephrons). The MD completely and consistently overlaps the EGM, and may extend over variable portions of the afferent and efferent arterioles.[429,762] The specific histo-topographical relationship of the epithelial tubular cells and the other components of the JGA at the glomerular vascular pole are established already during nephron formation. The prospective MD cells are affixed to the mesenchymal cells accompanying the capillary loops that invade the distal cleft of the S-shaped body of the nephron-anlage to form the glomerular tuft.[763] This occurs before the epithelial cells of the prospective loop of Henle have elongated into a tubule.

The cells of the MD (Figure 20.66) differ from the surrounding cells of the thick ascending limb in several aspects. The most eye-catching feature of the MD are the closely packed nuclei, usually located in the apical cell pole.[5,764] This feature, well recognizable even in light microscopic preparations at low magnification, conferred the name "macula densa" to the cell plaque.

Most importantly, and in marked contrast to the cells of the thick ascending limb, MD cells do not interdigitate with each other by large lateral folding; rather, the lateral cell membranes of MD cells run in a fairly straight fashion from the tight junction toward the base of the epithelium.[5,764] They possess slender microplicae or microvilli that protrude into the lateral intercellular spaces, and contact (frequently by desmosomes) corresponding protrusions from opposite cells. At the very base the cells ramify into slender processes. They are fixed to the basement membrane of the MD cells which is fused with the basement membrane-like material

surrounding the extraglomerular mesangial cells. The tight junctions are morphologically similar as in the TAL, but they may be slightly deeper (e.g., in rabbit). Like all other TAL cells, MD cells do not display gap junctions.

The cytoplasm of MD cells is relatively sparse and displays the usual organelles comprising some small mitochondria. The Golgi apparatus is large, smooth endoplasmic reticulum and free ribosomes are abundant, but rough endoplasmic reticulum is infrequent.

The luminal cell membrane is densely studded by short stubby microvilli and displays, like the other tubular cells, single cilia. In some species (e.g., rabbit[5]) the MD cells are distinctly taller than the surrounding TAL cells, so that the entire plaque of the MD protrudes into the tubule lumen.

The inventory of transport proteins in MD cells is essentially the same as in the other TAL cells, i.e., they display the bumetanide-sensitive NKCC2 co-transporter,[537,765,766] ROMK,[767,768] and NHE3[769] in the apical plasma membrane, and express cyclooxygenase-1.[516] They specifically express cyclooxygenase-2[516] and nitric oxide synthetase 1.[770,771] In contrast to the TAL, MD cells lack the Tamm-Horsfall protein.[528]

Recent findings[772] detected by RT-PCR and by immunohistochemistry demonstrated olfactory-related adenylate cyclase 3 (AC3) and the olfactory G-protein limited to the distal convoluted tubule and especially the MD.[772] These findings suggest a role of the olfactory machinery in the regulation of renin secretion and glomerular filtration rate.[772]

In contrast to all other TAL cells, the lateral intercellular spaces in the MD epithelium have been found to be dilated under most physiological conditions, usually regarded as "normal" conditions.[754,764,773–776] In agreement with the suggestion that water flow through the MD-epithelium is secondary to active sodium reabsorption, compounds that block sodium transport by MD cells (e.g., furosemide), as well as high osmolalities of impermeable solutes in the tubular fluid (e.g., mannitol), are associated with narrow intercellular spaces.[764,773] These observations suggested that the MD epithelium might be a water-permeable cell plaque within the water-impermeable TAL epithelium,[764] but so far direct evidence for this suggestion is missing. The lack of immunoreactivity for TRPV4, a nonselective cation channel of the transient receptor potential (TRP) family, gated by hypotonicity, had been interpreted as indirect support for this assumption.[777]

The granular cells (often termed juxtaglomerular cells) (Figure 20.67)[778] are assembled in clusters (up to 15 cells, but generally not more than 4 or 5) within the wall of the terminal portion of the afferent arteriole, replacing ordinary smooth muscle cells. Occasionally, they are also found within the wall of the efferent arteriole, again occupying the space where one would otherwise expect to find an ordinary smooth muscle cell. In rare cases, extraglomerular mesangial cells may also be replaced by granular cells. The name "granular" cell points to the specific cytoplasmic granules which may densely fill the cell body cytoplasm. They are electron-dense, membrane-bound, and irregular in size and

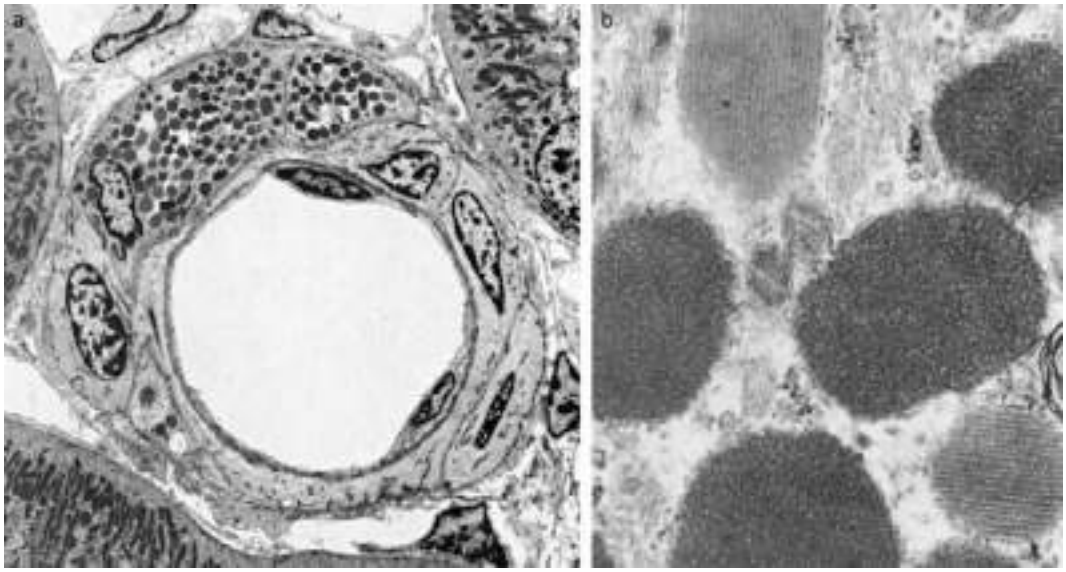

FIGURE 20.67 (a) Juxtaglomerular portion of an afferent arteriole. Smooth muscle cells are replaced by two granular cells (rabbit: TEM: ×~2700). (b) Granular cell. Renin granules are membrane-bound. Granules with a crystalline substructure are considered as "protogranules" which will develop into mature amorphous granules (rat: TEM: ×~48,000).

shape. Small granules with crystalline substructure represent protogranules, which are developed within the prominent Golgi apparatus and are then transformed into the major amorphous granules. Immunocytochemical studies with two antibodies against the renin prosegment and against mature renin have shown that only protogranules are prosegment-positive, whereas a signal of mature renin was found in mature as well as protogranules. These findings show that the cleavage of the prosegment, i.e., the maturation of renin, takes place in the juvenile granules; mature renin is then stored in the electron-dense granules. However, it is suggested that a major fraction of pro-renin never matures to renin, but is constitutively secreted as pro-renin – together with an unknown fraction of renin. Mature renin is segregated into storage granules for regulated release. The release mode of renin is not fully-understood. In addition to classic exocytosis, other mechanisms may also be involved.[18] It is important to know that renin release occurs into the surrounding interstitium, not into the lumen of the afferent arteriole, as has been frequently suggested.

Granular cells are modified smooth muscle cells. Within the peripheral parts of the cytoplasm, especially within the many cell processes, granular cells contain myofibrils. In situations that require enhanced renin synthesis (e.g., volume depletion or stenosis of the renal artery) additional smooth muscle cells located upstream in the wall of the afferent arteriole transform into granular cells.[19]

Granular cells have processes of manifold shapes.[99] Because of them, granular cells have extensive membrane contacts to all surrounding cells, e.g., other granular cells, smooth muscle cells, and extraglomerular mesangial cells. At these contacts, gap junctions are frequently encountered.[19] Like ordinary smooth muscle cells, granular cells also have membrane contacts to endothelial cells, in the manner that foot-like processes of endothelial cells penetrate the basement membrane and come into contact with granular cells; gap junctions are found at these contact sites.[99]

Peripolar cells have first been described in sheep, where they are regularly found[779]; in most other species, including man, they are rare.[780] Peripolar cells are parietal cells of Bowman's capsule which are located around the glomerular hilum (i.e., at the vascular pole, therefore: peripolar), and which contain numerous cytoplasmic membrane-bound granules filled homogeneously with electron-dense fibrillogranular material.[779] Subsequent studies have shown that these granules contain a neuron-specific enolase-like protein[781] and transthyretin[782]; their function is unknown. The number of cells and the number of granules per cell vary greatly among species and, furthermore, are dependent on age.[780] In the rat kidney, granulated peripolar cells have only rarely been found.[780]

Extraglomerular mesangial cells (EGM-cells, Goormaghtigh cells, lacis cells) together with the surrounding matrix establish the extraglomerular mesangium (polar cushion). The EGM represents a solid cell complex that is not penetrated by blood vessels or lymphatic capillaries. Nerves pass on both sides of it from the afferent to the efferent arteriole, but do not enter the cell complex.[99]

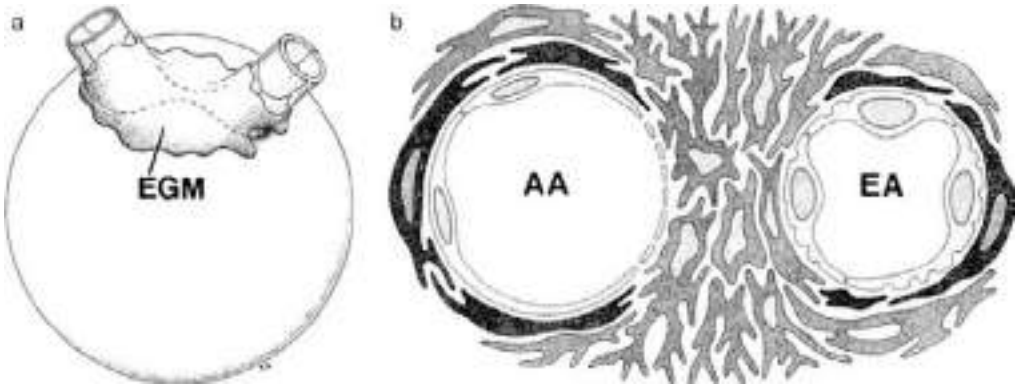

FIGURE 20.68 (a) Schematic of the extraglomerular mesangium (*EGM*). The glomerulus is shown as a globe. Its outer aspect is represented by the parietal basement membrane of Bowman's capsule (*PBM*). The EGM lies between the two arterioles above the opening of Bowman's capsule (broken line). It is attached to the PBM and has extensive contacts with the two arterioles. The macula densa and the smooth muscle layers of the arterioles are not shown. (b) Schematic cross-section through the vascular pole just above Bowman's capsule. Afferent and efferent arterioles (*AA*, *EA*) are cut transversely. Extraglomerular mesangial cells (*EGM*) are shown in moderate gray, smooth muscle cells in dark gray, and endothelial cells in light gray. Note differences in the walls of AA and EA; the AA already displays endothelial fenestration on the side facing the EGM. Conversely, the EA has a continuous endothelium with many cell bodies. In both AA and EA the smooth muscle layer (*SM*) is not complete; towards the center of the EGM the SM cells are replaced by EGM cells. *(Elger, M., and Sakai, T. et al. (1998). The vascular pole of the renal glomerulus of rat. Adv. Anat. Embryol. Cell Biol.**139**, 1–98, with permission).*

The EGM is located within the triangular space bordered by the two glomerular arterioles and the macula densa (Figures 20.66 and 20.68).[778] Reconstruction studies have shown that EGM-cells are flat and elongated, separating into two bunches of long cell processes at their poles.[783] They are arranged in several layers parallel to the base of the macula densa. The cells nearest to the glomerular stalk, thus filling the deepest portion of the triangle, lose this parallel grouping, but extend into the stalk of the glomerular tuft mixing with mesangial cells proper. The cells are separated by a conspicuous matrix which appears to be different from the intraglomerular mesangial matrix by the fact that microfibrils are rarely found in the EGM[20]; details are largely unknown.

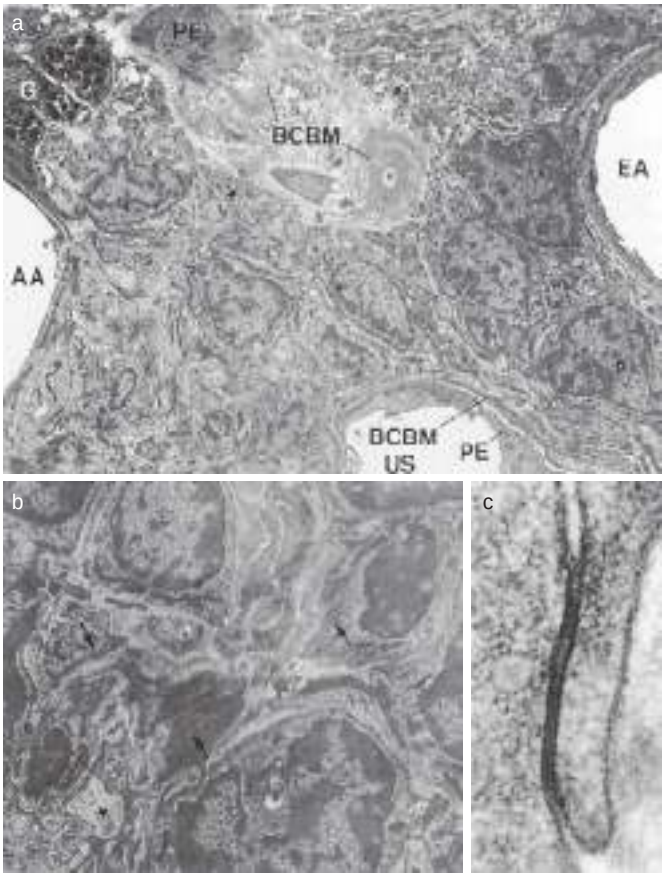

FIGURE 20.69 **Flat section through the extraglomerular mesangium (rat).** (a) The section crosses the afferent (AA) and the efferent (EA) arteriole; it grazes the top of Bowman's capsule, showing the basement membrane of Bowman's capsule (BCBM), and the parietal epithelium (PE), as well as the urinary space (US). The extraglomerular mesangium forms a complicated texture by which the structures of the vascular pole are interconnected. Note that toward their insertion in the BCBM the extraglomerular mesangial cells fall apart into many processes (stars) (G: Granular cells; TEM: ×~2650). (b) Higher magnification of extraglomerular mesangial cells. Note the microfilament bundles within the periphery of cell bodies, as well as within cell processes (arrows). Note the irregular extracellular spaces filled with a matrix of varying appearance (star) (TEM: ×~6000). (c) Gap junction between two mesangial cells (rat: TEM: ×~147,000).

EGM cells are characterized by the scantness of their cytoplasm and their extensive ramifications (Figure 20.69).[778,784] A Golgi apparatus and some profiles of granulated endoplasmic reticulum are regularly encountered. Although direct evidence is lacking, EGM-cells can be expected to be contractile for several reasons. First, they contain a good amount of microfilaments, mainly in their processes and peripherally within cell bodies. Second, intimate structural similarities are found among arteriolar smooth muscle cells, granular cells, and intra- and EGM cells, suggesting that they have the same origin. Third, they are extensively coupled by gap junctions. Gap junctions not only bridge different cells, but also regularly bridge individual processes of the same cell.[785] Moreover, gap junction contacts consistently occur to all other cells of the JGA (except the macula densa!), i.e., to granular cells, to ordinary smooth muscle cells of both arterioles, and to the mesangial cells proper.[19]

From a biomechanical point of view, the contractile apparatus of EGM cells is conspicuous. Microfilament bundles are contained within the periphery of cell bodies and within the cell processes, which are connected to the walls of both glomerular arterioles and to the basement membrane of the parietal layer of Bowman's capsule (PBM) surrounding the glomerular hilum (Figures 20.68 and 20.69). As a whole, the EGM can be considered as a spider-like contractile clamp sitting above the glomerular entrance interconnecting all structures at this site.[20] The EGM probably represents some sort of closure device of the glomerular entrance, maintaining the structural integrity of the entrance against the distending forces exerted on it by the high intraglomerular pressure. Moreover, from the viewpoint that the glomerular mesangium represents a high pressure compartment (mesangial interstitial pressures are expected to range in the same magnitude as glomerular capillary pressures[147]), the EGM would seem to be the structure which mediates a gradual pressure drop toward the cortical interstitium and toward the base of the macula densa.[20]

The function of the EGM cells is obscure. Because of their central position within the JGA, their constant relationships to the macula densa and their gap junction coupling to all smooth muscle-derived cells of the JGA, the EGM cells have repeatedly been considered as the necessary functional link between the macula densa and any possible effector cell within the regulatory mechanisms of the JGA.[20,99] Thus, they are widely considered as an integrating system of signals derived

from the reabsorptive function of the MD and the function of the EGM as a pressure sentinel mirroring the blood pressure in the afferent–efferent arteriolar system, but details are unknown.

The intimate and systematic juxtaposition of tubular and vascular cells within the JGA has given rise to early speculations about a feedback system between tubular and glomerular function.[786] It has now become clear that the JGA serves two different functions: it regulates the flow resistance of afferent arterioles in the so-called tubuloglomerular feedback mechanism; and it participates in the control of renin synthesis and release from granular cells in the afferent arteriole.[787] Researchers originally assumed that the two responses might be related to each other, in that renin released from the granular cells not only has systematic relevance, but locally triggers the formation of angiotensin II, and thus is responsible for afferent vasoconstriction as well; however, it now appears that the final activation of smooth muscle and granular effector cells occurs through largely independent pathways. Renin release from granular cells is the major source of systemic angiotensin II, and thus plays an essential role in controlling extracellular volume and blood pressure, whereas the vasoconstriction of the afferent arteriole locally serves to modulate the filtration of this nephron.

For both mechanisms, it is well-established that a change in NaCl concentration in the tubular fluid at the MD initiates the appropriate signal. Thus, the MD, situated at the very end of the TAL, controls the work of the TAL; the short postmacula segment of the TAL may be interpreted to guarantee that the composition of the tubular fluid at the MD might not be influenced by the function of the subsequent DCT. Expressed in general terms, the MD translates changes in the tubular fluid Na-Cl concentration into a graded release of mediators that reach their target by diffusion, thus acting in a paracrine fashion. Note that the extraglomerular mesangium that mediates the contact between the MD and the effector cells is not vascularized, so that the build-up of any paracrine agent would not be perturbed by blood flow.

With respect to renin release, the most likely paracrine mediators of this process are prostaglandin E 2 and nitric oxide.[18,788–790] With respect to the vasoconstrictor response purinergic mediators, either ATP or adenosine, as first suggested by Oswald and colleagues[791] appear to play the major role.[62,787,792] For an up to-date discussion of the function of the JGA see the reviews by Schnermann and Levine,[787,793] Persson and colleagues,[794] and Komlosi and colleagues.[795,796]

THE RENAL MEDULLA

During phylogeny the renal medulla has developed in response to the necessity to conserve water by excreting concentrated urine.[29] Loops of Henle, collecting ducts, and a specific blood supply through vascular bundles have developed into a complex structural system that accounts for this function. However, the details are insufficiently understood.

The overall mechanism (Figure 20.70) is clear: reabsorption of NaCl from the MTALs in the outer medulla represents the driving force to produce an interstitial cortico-medullary osmotic gradient that provokes osmotic water withdrawal from the collecting duct when the latter descend toward the papillary tip. The reabsorbed water is brought back into the systemic circulation by venous vasa.[2,797]

The unresolved problem is the generation of a cortico-papillary solute gradient, notably in the inner medulla. In discussions concerning the formation of a medullary solute gradient "countercurrent multiplication" has occupied a center-stage as the decisive mechanism. This mechanism has been experimentally established in artificial tubes,[798] and has been imposed on the renal medulla, conceding immense deviations from the original conditions. From a structural point of view, the preconditions for countercurrent multiplication in the renal medulla would appear to be quite incompletely developed: at no site are the limbs of Henle's loop juxtaposed to each other. Even when allowing a mediating interstitial space between both loop limbs, the DTLs do not case behave homogenously in an adequate way, but they change their function gradually on their descent, and even change their transport characteristics to the ascending limb type a considerable distance before the bend; most relevant in the present context is that the terminal third of the SDTLs in the mouse kidney is equipped with TAL epithelium.[16,34] Without going into more details, everyone who has been engaged in this problem knows that the principle of countercurrent multiplication has been extensively bent to make it fit with the structural organization of the renal medulla – in our view, with little benefit in facilitating the understanding of the function of the renal medulla. If at all, this principle can only be applied to describe the mechanism in the outer medulla. In the inner medulla, a process that could be regarded as a "single concentrating effect" is not apparent. Several "passive models"[452,799–802] attempting to explain the concentrating mechanism in the inner medulla have greatly refined our understanding of the problem, but have never reached the level of a convincing theory.

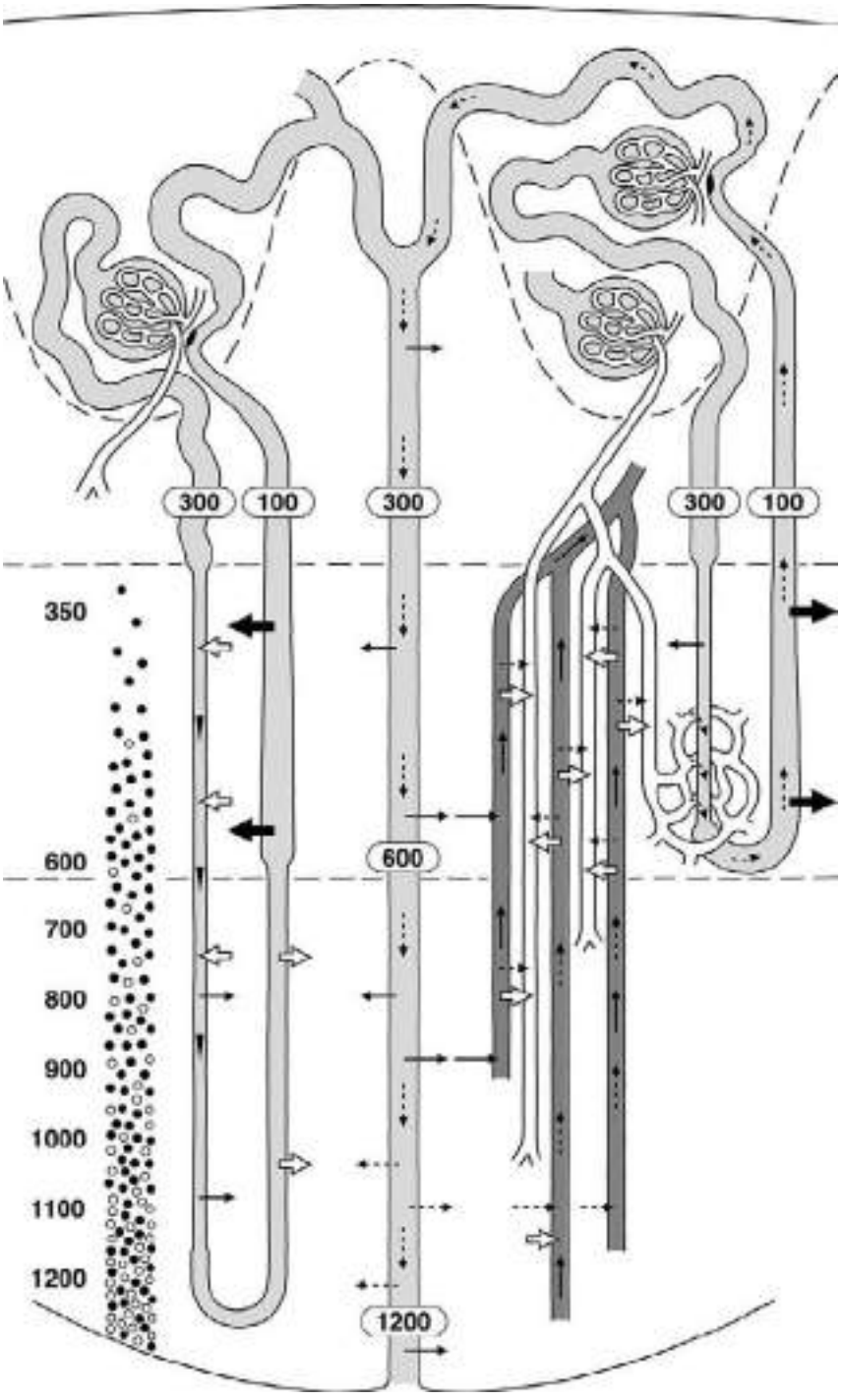

FIGURE 20.70 **Schematic to show the functional interactions in the medulla as they are derived from the histotopography of the structures, the distribution of channels and transporters and direct measurements of transport characteristics in the various tubular and vessel segments.** A long looped nephron, a short looped nephron, and a collecting duct are shown in light gray. Descending vasa recta (DVRs) derived from the efferent arteriole of a juxtamedullary glomerulus are shown in white (including the capillaries), ascending vasa recta (AVRs) in dark gray: both together establish a vascular bundle. The osmolar concentration in the medulla rises from the cortico-medullary border to the papillary tip from 300 to 12,000 mosmol/l, mainly established by the increase in the concentration of salt (indicated by dark dots) and urea (indicated by open circles). The driving force of the concentrating mechanism is the dumping of salt into the medullary interstitium from TALs (thick black arrows), leaving behind a diluted fluid (indicated by an osmolar concentration of 100 mosmol/l at the re-entry into the cortex). Osmotic water withdrawal from CCDs (slim arrows) into the cortical circulation again elevates the tubular urine to 300 mosmol/l upon re-entry into the medulla. Continuous water reabsorption along the MCDs (slim arrows) will produce a final urine concentration of about 12,000 mosmol/l (in humans). The source for the inner medullary solute gradient is shown to consist of: (1) dragging of salt from the IS into the IM by LDTLs (arrow heads); and (2) re-entry of urea from the CDs into the terminal portion of the IM (hatched arrows). The gain in osmotic energy by urea re-entry originates from urea recycling, which starts with a shift of urea from the AVRs into the SDTLs in the IS (follow the hatched arrows), and concentration of this urea by water reabsorption in the CCDs, OMCDs, and starting portions of IMCDs (see text for further explanation). The removal of the water from the medulla regained from the CDs (thus the final step in urine concentration) is effected by AVRs (follow the slim arrows). These vessels are the core structures in the complex countercurrent exchange system of the medulla equilibrating at any level with the local concentrations of salt and urea. Open thick arrows show passive movements of salt (see text).

In this situation it might be worth an attempt, opposite to the usual, to start with the available functional data – including the recent data on the distribution of transporters – confronting them with the structure, i.e., the architecture of the renal medulla, as well as the cellular organization of the individual components, in order to arrive at a novel view of "function–structure–correlation."

Let us first regard the three regions of the medulla with such an approach. The most constant region is the IS; there is no renal medulla known without an IS. In contrast, an OS is frequently quite incompletely developed, and an IM may be fully absent.

The Inner Stripe of the Outer Medulla

The IS (Figures 20.20 and 20.24) is made up of two portions: the vascular bundles (VBs) and the interbundle region (IBR). The IBR contains the tubules (DTLs, TALs, CDs) supplied by a dense capillary plexus which is drained upwards by the gradual transition of capillaries into AVRs that directly ascend into the OS. Since all the salt reabsorbed by MTALs accumulates in this area, the interstitium of the IBR is rich in salt.[803]

The VBs, structurally, are part of the IS but, functionally, they belong to the IM. They represent a quite perfectly developed countercurrent exchange system primarily handling the blood descending to and ascending from the IM by respective DVRs and AVRs. However, since the DVRs also supplying the capillary plexus of the IBR of the IS are contained within the VBs (not the respective AVRs), the VBs provide the possibility of shifting solutes coming up from the IM into the IBR of the IS. Since the dominating solute of the IM is urea, the VBs are rich in urea. The handling of urea as a main function of the VBs becomes most obvious in the complex bundles (see below).

The Inner Medulla

The IM (Figures 20.20 and 20.27) including the papilla, at the transverse level, is homogenously organized; a separation into VBs and an IBR is no longer possible. Even if there may be a certain prevalence that the ATLs are more frequently gathered around CDs than DTLs,[34,804] it appears quite doubtful that this is of any functional relevance. The AVRs (including the capillaries) are homogenously distributed among all other components and, most importantly, a wide homogenous interstitial space permits the interaction of every descending tube with every ascending tube. The IM provides strict countercurrent arrangements of all involved structures, but without giving prevalence to any specific lateral interaction. Thus, the IM as a whole may be considered as a countercurrent system that allows countercurrent exchange – mediated by the interstitium – between all descending (DVRs, DTLs, CDs) and all ascending tubes (AVRs, ATLs), according to the transport characteristics of the individual tubes.

A most important feature of the IM is its particular shape reflecting its longitudinal organization. The inner medulla tapers from a broad basis to a tiny papilla[2] (see also above). This shape perfectly reflects what happens with the structures within the inner medulla: loops of Henle, vasa recta, and collecting ducts (by fusing together) all decrease rapidly in number from the base to the tip of the papilla.[119,805] For the rat, it has been calculated that, of an estimated 10,000 long loops entering the inner medulla at its base, only about 1500 reach the papillary half of the inner medulla, and only a few of these the papillary tip.[2] The majority of long loops, the "short" long loops, turn back shortly after entering the inner medulla, a smaller but still substantial number of long loops reach the middle part of the inner medulla, and only a small population of "long" long loops really reach the papilla.

The Outer Stripe of the Outer Medulla

The OS (Figures 20.20 and 20.23) is a transitional region which separates the medulla from the cortex, mediating the transition between an hyperosmotic and an isoosmotic environment. The OS does not seem to make any particular contribution to the creation of the cortico-medullary solute gradient, but it greatly helps to maintain it. The OS contains the nascent (or dissolving) VBs (performing the same function as in the IS but quantitatively of minor importance) and the AVRs which are directly coming up form the IBR of the IS (Figure 20.71). Together with the AVRs spreading out from the dissolving VBs, the AVRs as a whole traverse the OS as individual vessels intimately associated with the tubules of this region; actually they represent the major "capillary" supply of the OS (see above). In addition, among all regions of the kidney, the OS exhibits the smallest fraction of interstitial space, thus the vessels are most closely juxtaposed to the tubules (note: lymphatics are absent from the entire medulla[25]). Since the PSTs of juxtamedullary nephrons, in contrast to their name, take a tortuous course when descending through the OS, the majority of tubular profiles in the OS consists of PSTs (S3 segments). This arrangement – AVRs closely associated with descending PTs (and, to some extent, also CDs) represent an ultimate countercurrent trap to prevent the loss of osmotic energy into the systemic circulation (Figure 20.71 right panel). Since reabsorption from PTs is isoosmotic, the hypertonic environment created by AVRs will allow water withdrawal not only from CDs (starting the concentrating process), but also from the PTs, increasing their osmolarity already at the level of the OS – with a clear prevalence of the PTs of juxtamedullary nephrons (tortuous course!) that give rise to the "long long loops." The TALs of the OS are already of the cortical type (equipped with a comparably flat epithelium; see above) capable of maintaining and even increasing a large salt gradient, but incapable of transporting large quantities.[308]

So far, we have a summary of the essential architectural features of the three medullary regions; let us now talk about the functional connections between them. This needs, first, to talk about the overall mechanism

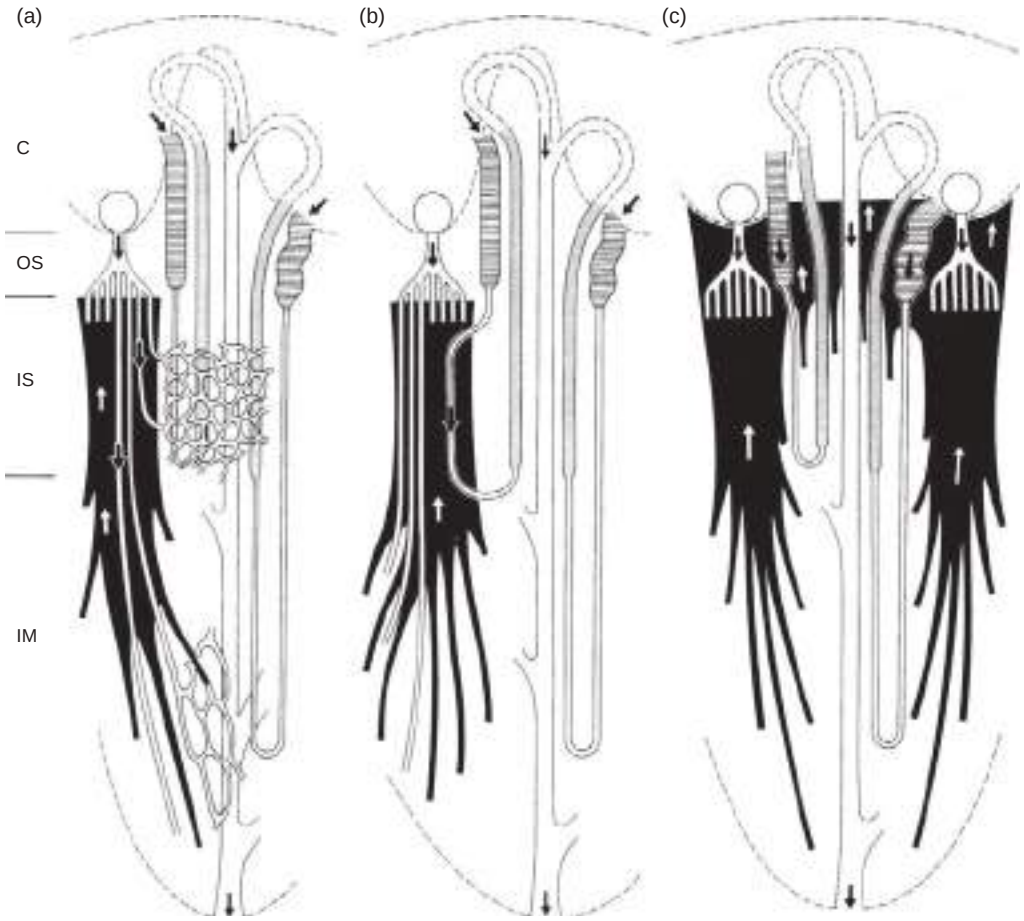

FIGURE 20.71 **Schematics to demonstrate the possible recycling routes within the medulla.** A short loop and a long loop of Henle and a collecting duct are shown. The straight proximal tubules are hatched; the thin limbs, collecting ducts, and capillaries are white; the thick ascending limbs are gray. Ascending vasa recta are drawn black en bloc (C: cortex; OS: outer stripe; IS: inner stripe; IM: inner medulla). (a) Simple type of medulla: recycling route from the ascending vasa recta in the inner stripe, via descending vasa recta, to inner stripe tubules. (b) Complex type of medulla: recycling route from ascending vasa recta in the inner stripe to descending thin limbs of short loops. (c) Recycling route from the ascending vasa recta in the outer stripe to descending tubules (proximal tubules and collecting ducts); valid for both the simple type and the complex type of medulla. *(Adapted from Kaissling, B., and Kriz, W. (1979). Structural analysis of the rabbit kidney. Adv. Anat. Embryol. Cell Biol.* ***56****, 1–123, and Kriz, W., and Barrett, J. M. et al. (1976). The renal vasculature. In "Anatomical–Functional Aspects. Kidney and Urinary Tract Physiology II, 1–21, Thruau, K. Tokyo University Park Press, Baltimore, London.)*

underlying urine concentration in some more detail, and afterwards to talk about the individual mechanisms.

The Basic Mechanism in Some Detail

The renal medulla contains the phylogenetically ancient "diluting segments" of the nephron, i.e., the TALs which separate salt from water (Figure 20.70). The salt is dumped into the medullary interstitium, the water is carried up into the cortex and – in the case that ADH is available – is recovered by the systemic circulation through osmotic withdrawl from the CCDs. Thus, the tubular urine that re-enters the renal medulla in the collecting duct is isoosmotic with respect to plasma concentration, and considerably reduced in quantity compared to the amount that originally entered the renal medulla in descending limbs after filtration. Thus, the salt that is available to drive the concentrating mechanism has emerged from a much larger quantity of isoosmotic fluid than the quantity of isoosmotic fluid that is subject to concentration. Moreover, along with the increasing concentration of the CD urine, less and less water has to be reclaimed to achieve the same increment in concentration; the work that is necessary to account for a progressively increasing urine concentration decreases steeply toward the tip of the papilla.

In the IM, in addition to salt, urea is a major solute accounting for the solute gradient toward the tip of the papilla. Since in the IM neither any up-hill transport of salt nor of urea is known, the crucial problem consists of explaining the increasing concentration of salt (flat increase) and of urea (steep increase) in the IM toward

the papillary tip. If both depend on the work of the TALs in the OM, how can part of the osmotic energy be carried down from the OM into the IM and piled up there to a steep solute gradient toward the tip of the papilla?

In our view, three major mechanisms have become apparent that are responsible for the distribution of salt and urea into a cortico-papillary gradient in the IM (Figure 20.70). They all depend on salt reabsorption by TALs in the OM; they all fit with the morphology, even more: specific structural elaborations in highly concentrating species support their relevance. These are: (1) salt dragging by flow to deeper medullary levels; (2) countercurrent exchange of solutes and water to maintain the cortico-papillary gradient; and (3) urea recycling by short loops of Henle as a major mechanism to create the solute gradient toward the papilla.

Dragging of Solutes by Flow to Deeper Medullary Levels

In all descending tubes of the renal medulla (DVRs, DTLs, CDs) solutes are dragged by flow to deeper medullary levels. This appears to be relevant for salt in the DTLs and for urea in the CDs (see urea recycling).

Continuous uptake and dragging of salt by SDTLs down to their bends at the end of the IS has been considered as an essential mechanism in the original countercurrent multiplication concept. In the light of current knowledge such a mechanism in short DTLs may not be of crucial importance. In contrast to previous reports, SDTLs (apart from some of them; see above) do not express aquaporin, and thus must be considered as fairly water-impermeable. Also, the Na^+ and Cl^- permeability was found to be low.[806] Thus, the increasing concentration towards the bend of SDTLs seems to be predominantly accounted for by urea entry into the lower part (see below: urea recycling). However, in any case the salt left from filtration at the end of the proximal tubule that enters the SDTLs in the OS will be dragged down by flow until the loop bends and will return in the TALs to be reabsorbed there. In case that, despite low salt permeability, a small part of the reabsorbed salt may – via the interstitium – re-enter the descending limb, thus being trapped within the SDTLs, this salt transfer from the TALs to the SDTLs represents the only esssential step that would be left from the countercurrent multiplication principle.

In contrast, continuous uptake of salt by LDTLs in the OM and dragging it by flow down into the IM appears to be the essential mechanism for salt accumulation in the IM; no other source of salt (apart from a small quantity reabsorbed by IMCDs) for the IM is obvious. Available models of the inner medullary concentrating process do not put so much emphasis on this mechanism, but the structural data strongly do suggest it. Layton and colleagues[452] were the first to include this idea into a model. The structural arguments are the following:

1. The upper portions of the LDTLs, most obvious in the IS, have an epithelial organization that suggests ion transport through extensively developed (Figure 20.48a) claudin 2 (cation pore) and claudin 10 (anion and cation pore) containing tight junctions.[261,807] Since the salt concentration is certainly higher outside the LDTLs (see below), salt can readily be expected to diffuse into the lumen. This process may become reinforced by active salt-secretion into the lumen, based on the abundant occurrence of Na^+-K^+-ATPase in the upper portions of LDTLs.[446,447] Moreover, the LDTLups are the only thin limb segments with abundant expression of aquaporin 1 channels (see below). No question, the salt concentrations within LDTLs at the transition from the OM to the IM may be expected to be quite high. Measured data are not available, but it seems reasonable to suggest considerably higher salt concentrations inside than outside.
2. The LDTLs on their descent through the inner stripe always pass through the sodium richest area, i.e., distant from the vascular bundles among the TALs of short loops[803] (Figure 20.22). In the mouse kidney, two specific modifications in this system appear to reinforce the ability of LDTLs for salt uptake. First, the LDTLs take a tortuous course when descending through the IS (increasing their length by 27%[34]) and, second, at the end of the IS before entering the IM, they traverse the so-called "innermost stripe," which has a thickness of about half of the IS proper and in which the SDTLs are already equipped with the TAL epithelium.[16,34] Thus, the density of TALs dumping salt into the interstitium at this level is dramatically higher (5 versus 3 per unit area) than at any other level of the OM. Consequently, the interstitial salt concentration should be very high. The LDTLs traverse this region and may readily be expected to take up some of the accumulated salt.
3. After challenging urine concentration in rats by water deprivation (or treatment with ADH) the TALs hypertrophy, with the most prominent increase in epithelial salt transport capacity of the initial portions in the deep IS.[520,808] Thus again, a prominent "surplus" in salt accumulation occurs just at the border to the inner medulla.
4. As described above, the LDTLs are quite heterogeneous with respect to their actual length,

and with respect to the epithelial differentiation of their upper parts.[435,803] Most important, the actual length of an LDTL strictly correlates with the degree of epithelial elaboration of its upper part in the IS. The small fraction of longest long loops extending down into the papilla clearly have the most prominent upper parts in the IS: they are thicker, with larger lumina and with more elaborate epithelia composed of heavily interdigitating cells; also their abundance in Na-K-ATPase is spectacular.[446] Comparing these longest long loops with those extending down into the IM for only short or intermediate distances, there is a continuous spectrum also with respect to the epithelial elaboration in the IS. Thus, the idea is plausible that salt is taken up by the upper portions of LDTLs, and subsequently carried down through the salt impermeable lower portions to the bend region. Beginning abruptly with a prebend segment, the loop becomes ion-permeable, allowing the salt to be dumped into the interstitium. In the mouse, the prebend segments are quite prominent comprising a length up to 700 μm.[34] Thus, the entire loop bend appears to represent a loop segment that delivers salt into the interstitium.

Since the lower portions of LDTLS are also water-permeable (to what extent is not clear[452,453]), water withdrawal may further increase the salt concentration in these segments. The problem consists of the driving force for such a process. A possibility offered from a structural view is that the heterogeneous longitudinal distribution of loops within the inner medulla (as describe above) might account for a cascade-like transport of salt toward the papilla. The large fraction of "short" long loops carries salt into the first third of the IM. Together with some urea (emerging from reabsorption by papillary CDs and subsequent recycling; see later) the total interstitial osmolality will be elevated above DTL fluid osmolality at the respective level allowing reclaimation of water from DTLs, elevating the total osmolality and salt concentration in all the DTLs underway to deeper medullary levels. A major fraction of those will reach an intermediate level of the IM before bending, dumping a major fraction of its salt at this level into the interstitium. Again, together with some urea a driving force will be established accounting for some water withdrawal from the small fraction of "long" long loops that will carry their salt into the papillary tip. No question, this is quite a hypothetical idea, but from a structural point of view would be worth modeling. Ideas in this direction have been published previously,[435] and also mathematical models for some features of such a mechanism have been presented.[452]

Countercurrent Exchange of Solutes and Water

Countercurrent exchange in a U-type countercurrent exchanger may have two functions: (1) trapping of solutes within the system by transfer of solutes from the ascending to the descending limb; and (2) preventing water from entering the system by short circuiting from the descending to the ascending limb. Both mechanisms *per se* do not build up any solute gradient; they are only capable of maintaining a gradient (with little loss). However, incorporated into the complex countercurrent arrangement of the renal medulla they decisively participate in the creation of the cortico-papillary gradient. In agreement with others,[797] in our view, the relevance of countercurrent exchange has always been underestimated compared to countercurrent multiplication in the urine concentrating mechanism. Actually, from a structural point of view, the renal medulla should best be considered as an extremely complex countercurrent exchange system that is fuelled by two mechanisms at two sites: by salt reabsorption through TALs in the OS; and by urea addition through terminal CDs in the IM. These solutes are distributed by countercurrent exchange into a cortico-medullary gradient that − due to continuous fueling − allows water withdrawal from CDs and the transport of this water into the systemic circulation in the cortex.

As already discussed above, a more-or-less direct countercurrent exchange between juxtaposed countercurrent tubes may only occur within the VBs of the IS. In contrast, in the IBR of the IS, and within the entire IM, the countercurrent tubes are consistently separated from each other by comparably wide interstitial spaces, thus any exchange at a transverse level is mediated by the interstitium. No doubt, this decreases the effectiveness of the exchanges, but allows countercurrent exchanges between more than two structures. Any solute dumped into the inner medullary interstitium, i.e., predominantly salt from LDTLs (at their bends) and urea from CDs (at their terminal portion) or left in ATL and AVRs at their beginning in the IM, will be subject to countercurrent trapping (or used to drive countercurrent short-circuiting of water; see below), between AVRs and ATLs on the one site and DVRs and DTLs on the other.

In addition to solute trapping, countercurrent exchange of water preventing the flow of water to deeper levels by short circuiting seems of major relevance. The recent elucidation of the distribution of aquaporins in medullary structures has shed considerable light on the handling of water in the urine concentrating process. Among the thin limbs only the LDTLups have regularly been found to be equipped with aquaporin 1 channels; in rat, also, the LDTLlps have been reported to express AQP1[453]; DVRs are abundantly equipped

with AQP1 channels[453]; the water permeability of CDs is ADH-dependent (see above). The only ascending structures that are water-permeable are the AVRs (based on the hydrophilic fenestrae providing a direct route of water flow through the endothelium). Thus, any water withdrawn from any descending structure finally enters an AVR, by which it is brought back to the cortex. This cardinal function of AVRs has recently been analyzed in detail by Pallone and colleagues.[797]

The ability of AVRs to take up water appears to be based on an elevated oncotic pressure (resulting from short circuiting of water between DVRs and AVRs within the VBs), and on the reasonable assumption that the blood in capillaries at any level of the medulla is in osmotic equilibrium with the interstitial fluid (due to the hydrophilic fenestrae in capillary and AVR endothelia). Thus, when capillary blood at any level of the medulla starts to assemble in AVRs and to ascend, it will – after any small ascent – become hyperosmotic compared to the surrounding interstitium. Due to the abundant hydrophilic fenestrae of the AVR endothelium osmotic equilibrium will most easily be achieved by water uptake.

The water to be taken up originates mainly from the CDs, but water may also originate from DTLs. In LTDLs, the upper parts have abundant aquaporins (type 1) in both membranes surprisingly contained in an epithelium that exhibits the features of an ion-permeable epithelium, i.e., an extremely lengthened leaky tight junction due to extensive cellular interdigitation. Thus, this epithelium, in addition to being water-permeable, obviously allows the transport of large amounts of ions. From what we have argued above, that salt dragging by flow in LDTLs appears to be the only mechanism to bring down the salt into the IM, large volumes of salt-enriched urine would be the best precondition for this goal. It appears to us that the actual transport capabilities of the upper portions of LDTLs have not been completely elucidated. Along the lower portions of LDTLs in the IM, the water permeability progressively decreases and fully ceases at the transition to the prebend segment.[437,438] This offers the possibility (described already above) that water withdrawal from the LDTLs by an osmotic driving force established at each medullary level by salt and urea might lead to a "cascade-like" transport of salt toward the tip of the papilla.

Urea Recycling

Solute recycling is a different mechanism compared to solute trapping by countercurrent exchange; this difference is rarely appreciated. Urea appears to be the only solute, recycling of which plays an essential role in the urine concentrating process. Recycling of urea defines a process that starts with a molecule of urea in the inner medullary interstitium and brings this molecule back into the IM via the normal tubular route, finally re-entering the inner medullary interstitium via exit from the terminal IMCD (Figure 20.70). As described above, the terminal portion of the IMCDs contains the urea transporters UTA_1 and UTA_3 which allow the facilitated diffusion of urea from the CD into the surrounding interstitium.[809] A precondition for this reuptake of urea is that the concentration of urea in the tubular urine of IMCDs has reached a higher level than in the medullary interstitium at the same level. This is achieved by water removal through urea-impermeable tubular segments, i.e., CNTs and CCDs in the cortex, OMCDs and upper IMCDs in the medulla. The reabsorption of urea through IMCDs compromises the reclaiming of water through IMCDs, decreasing urine concentration instead of increasing it. Thus, urea does both: on the one hand, reabsorption of urea increases the inner medullary solute gradient, thereby decreasing urine osmolality; on the other hand, the increased solute gradient increases the driving force for water reabsorption, thereby increasing urine osmolality. This sounds like a story from Baron Münchhausen, who was able to help himself getting out of a swamp by pulling on his own hairs.

However, the two opposing functions of urea have a solid base: a given molecule of urea may become active a second (or a third) time, this is what urea recycling means. After entering the inner medullary interstitium from an IMCD, a given molecule of urea will travel towards the cortex within an AVR, thereby balancing (together with other molecules and other solutes) a certain amount of water that enters the AVR along its ascent, and that finally has to be delivered into the systemic circulation at the cortico-medullary border. However, this specific molecule of urea participates in water balancing on its way from a hyperosmotic to an isoosmotic environment only up to an intermediate level, i.e., up to the IS. Here it re-enters the nephron; its relevance in balancing water that continuously enters the AVR and needs to be transported further up into the cortex is taken over by salt which, due to the active Na^+ reabsorption by TALs, is available in abundance at this level. Thus, the urea molecule has spent only part of its osmotic energy for the transport of water before it re-enters the nephron, precisely the SDTL, and becomes again subject of a concentrating process in subsequent urea-impermeable, but water-permeable, tubular segments. This urea molecule started the intratubular concentrating process at a higher energy level than a urea molecule that entered the tubule by filtration. In our view, this difference in osmotic energy between a recycling

and a freshly filtered urea molecule, entering the nephron in the IS versus in the cortex, and becoming subject to a concentrating process by water removal along the DCT, CNT, CCD, OMCD, and upper IMCD represents a real gain in osmotic energy that is finally available for water reabsorption in the inner medulla. Entry of urea to the LTDLs somewhere in the IM (i.e., recycling of urea via long loops) would not have a similar effect, simply because at this site there is no surplus salt available to replace urea in its role of water balancing.

At the present stage of knowledge, urea recycling via short loops appears as an essential process in urine concentration, and represents the most obvious evidence for the numerical dominance of short loops of Henle in every highly concentrating species. Note that also species which by definition are commonly reported to have 100% long loops (e.g., *Psammomys obesus*) in reality have a majority of short loops.

Moreover, as described above, the SDTLs in such highly concentrating rodent species are directly incorporated into the vascular bundles, and thus provide a more direct route for urea recycling than the simple bundles (Figures 20.22, 20.25, 20.26, and 20.71).[16,32,115,435] Within the VBs of such species, AVRs coming up from the IM are arranged in a countercurrent fashion not only with DVRs but, most prominently, also with the SDTLs. Thus urea, by countercurrent exchange, may directly enter the SDTLs through the urea transporter UT-A2[441,809] (the hydrophilic fenestrae of the endothelium of the AVRs may readily be expected to be highly permeable for urea). In a renal medulla with "simple" vascular bundles (as they are found in most species) countercurrent exchange of urea first occurs from AVRs to DVRs (which contain the urea transporter UT-B1[810,811]), which afterwards will deliver their blood to the capillary plexus of the IBR in the IS, which perfuses the SDTLs on their descending way. Thus, even if probably much less effective, urea from the inner medulla has access to the SDTLs[435,803,809] and may start its recycling route to the terminal CD in the papilla.[435,809,811]

The locus of urea redelivery, i.e., in the papilla, thus at the "ultimate bend" of the complex countercurrent exchange system in the papilla, is optimal, since by countercurrent exchange in vasa recta and thin limbs, urea is largely trapped and distributed in a longitudinal gradient within the inner medulla. The fraction of urea that escapes this process in the inner medulla is subject to recycling via short loops (starting in the IS) back into the inner medulla, and is thus available another time within the papillary interstitium ready to withdraw and/or to balance water reabsorption from the collecting duct.

CONCLUSION

The urine concentrating mechanism certainly does not belong to the most urgent of problems in medicine, but it represents a highly challenging biological enigma. We are aware that several aspects of our view are hypothetical, but they are based on particular structural features (the ultrastructural organization and particular histotopographical relationships of LDTLs, the incorporation of SDTLs into the VBs in highly concentrating rodent species) for which no better functional relevance is available. Whether the proposed mechanisms are sufficient to build up an effective solute gradient in the IM (in rodents up to several osmoles) or whether there are additional sources complementing the solute gradients (continuous production of osmotic active substances) is presently unknown.

References

[1] Hodson J. The lobar structure of the kidney. Br J Urol 1972;44:246.
[2] Jamison R, Kriz W. Urinary concentrating mechanism. Structure and function. New York: Oxford University Press; 1982.
[3] Sperber J. Studies of the mammalian kidney. Zool Bidrag 1944;22:249–431.
[4] Inke G. The protolobar structure of the human kidney. New York: Alan R. Liss, Inc; 1988.
[5] Kaissling B, Kriz W. Structural analysis of the rabbit kidney. Adv Anat Embryol Cell Biol 1979;56:1–123.
[6] Schmidt-Nielsen B, Pfeiffer E. Urea and urinary concentrating ability in the mountain beaver, *Aplodontia rufa*. Am J Physiol 1970;218:1370–5.
[7] Lacy E. The mammalian renal pelvis: physiological implications from morphometric analyses. Anat Embryol 1980; 160:131–44.
[8] Fourman J, Moffat D. The blood vessels of the kidney. Oxford: Blackwell Scientific; 1971.
[9] Lemley K, Kriz W. Structure and function of the renal vasculature. In: Tisher C, Brenner B, editors. Renal pathology. Philadelphia: Lippincott,J.B.; 1989. p. 926–64.
[10] Moffat D, Fourman J. The vascular pattern of the rat kidney. J Anat 1963;97:543–53.
[11] Rollhäuser H, Kriz W, Heinke W. Das Gefässsystem der Rattenniere. Z Zellforsch Mikrosk Anat 1964;64:381–403.
[12] Beeuwkes R. Efferent vascular patterns and early vascular-tubular relations in the dog kidney. Am J Physiol 1971;221:1361–74.
[13] Casellas D, Mimran A. Shunting in renal microvasculature of the rat: a scanning electron microscopic study of corosion casts. Anat Rec 1981;201:237–48.
[14] Moffat D. The Mammalian Kidney. London: Cambridge University; 1975.
[15] Beeuwkes R, Bonventre J. Tubular organization and vascular–tubular relations in the dog kidney. Am J Physiol 1975;229:695–713.
[16] Kriz W, Koepsell H. The structural organization of the mouse kidney. Z Anat Entwicklungsgesch 1974;144:137–63.
[17] Bankir L, Kaissling B, de Rouffignac C, Kriz W. The vascular organization of the kidney of *Psammomys obesus*. Anat Embryol 1979;155:149–60.

[18] Kurtz A. Renin release: sites, mechanisms, and control. Annu Rev Physiol 2011;73:377–99.
[19] Taugner R, Hackenthal E. In: Springer-Verlag, editor. The juxtaglomerular apparatus. Berlin,Heidelberg: Springer-Verlag; 1989.
[20] Elger M, Sakai T, Kriz W. The vascular pole of the renal glomerulus of rat. Adv Anat Embryol Cell Biol 1998;139:1–98.
[21] Schnabel E, Kriz W, Steinhausen M. Outflow segment of the efferent arteriole of the rat glomerulus investigated by *in vivo* and electron microscopy. Ren Physiol 1987;10:318–26.
[22] Bankir L, Farman N. Hétérogénéité des glomérules chez le lapin. Arch Anat Microsc Morphol Exp 1973;62:281–91.
[23] Dieterich H. Die Struktur der Blutgefäbe in der Rattenniere. In: Bargmann W, Doerr W, editors. Normale und pathologische anatomie. Bd.35. Stuttgart: Thieme; 1978. p. 1–127.
[24] Edwards J. Efferent arterioles of glomeruli in the juxtamedullary zone of the human kidney. Anat Rec 1956;125:521–9.
[25] Kriz W, Dieterich H. The supplying and draining vessels of the renal medulla in mammals. Proceedings of the 4th international congress of nephrology. Basel: Karger; 1970138–144
[26] Bearer E, Orci L. Endothelial fenestral diaphragms: a quick-freeze, deep-etch study. J Cell Biol 1985;100:418–28.
[27] Stan R, Kubitza M, Palade G. PV-1 is a component of the fenestral and stomatal diaphragms in fenestrated endothelia. Proc Natl Acad Sci USA 1999;96:13203–7.
[28] Baines A, de Rouffignac C. Functional heterogeneity of nephrons. II. Filtration rates, intraluminal flow velocities and fractional water reasorption. Pflugers Arch 1969;308:260–76.
[29] Smith H. The kidney: structure and function in health and disease. New York: Oxford University Press; 1951.
[30] Amann K, Plank C, Dotsch J. Low nephron number – a new cardiovascular risk factor in children? Pediatr Nephrol 2004; 19:1319–23.
[31] Bertram J, Douglas-Denton R, Diouf B, Hughson M, Hoy W. Human nephron number: implications for health and disease. Pediatr Nephrol 2011;26:1529–33.
[32] Kaissling B, de Rouffignac C, Barrett J, Kriz W. The structural organization of the kidney of the desert rodent *Psammomys obesus*. Anat Embryol 1975;148:121–43.
[33] Kriz W. Der architektonische und funktionelle Aufbau der Rattenniere. Z Zellforsch Mikrosk Anat 1967;82:495–535.
[34] Zhai X, Thomsen J, Birn H, Kristoffersen I, Andreasen A, Christensen E. Three-dimensional reconstruction of the mouse nephron. J Am Soc Nephrol 2006;17:77–88.
[35] Kaissling B. Ultrastructural organization of the transition from the distal nephron to the collecting duct in the desert rodent *Psammomys obesus*. Cell Tissue Res 1980;212:475–95.
[36] Oliver J. Nephrons and kidneys. New York/Evanston/London: Harper & Row, Hoeber Medical; 1968.
[37] Peter K. Untersuchungen über bau und entwicklung der niere. Jena: Gustav Fischer; 1909.
[38] Kaissling B, Spiess S, Rinne B, Le Hir M. Effects of anemia on the morphology of the renal cortex of rats. Am J Physiol 1993;264:F608–17.
[39] Kriz W, Napiwotzky P. Structural and functional aspects of the renal interstitium. In: Berlyne G, editor. Contr Nephrol. Basel: Karger; 1979. p. 104–8.
[40] Pedersen J, Persson A, Maunsbach A. Ultrastructure and quantitative characterization of the cortical interstitium in the rat kidney. In: Maunsbach A, Olsen T, Christensen E, editors. Functional ultrastructure of the kidney. London: Academic Press; 1980. p. 443–57.
[41] Pfaller W. Structure function correlation in rat kidney. Quantitative correlation of structure and function in the normal and injured rat kidney. Adv Anat Embryol Cell Biol 1982; 70:1–106.
[42] Knepper M, Danielson R, Saidel G, Post R. Quantitative analysis of renal medullary anatomy in rats and rabbits. Kidney Int 1977;12:313–23.
[43] Wolgast M, Larson M, Nygren K. Functional characteristics of the renal interstitium. Am J Physiol 1981;241:F105–11.
[44] Lemley K, Kriz W. Anatomy of the renal interstitium. Kidney Int 1991;39:370–81.
[45] Kaissling B, Le Hir M. Characterization and distribution of interstitial cell types in the renal cortex of rat. Kidney Int 1994;45:709–20.
[46] Eddy A, McCulloch L, Adams J, Liu E. Interstitial nephritis induced by protein-overload proteinuria. Am J Pathol 1989; 135:718–9.
[47] Kaissling B, Hegyi I, Loffing J, Le Hir M. Morphology of interstitial cells in the healthy kidney. Anat Embryol 1996;193:303–18.
[48] Kaissling B, Le Hir M. The renal cortical interstitium: morphological and functional aspects. Histochem Cell Biol 2008;130:247–62.
[49] Schiller A, Taugner R. Junctions between interstitial cells of the renal medulla: a freeze-fracture study. Cell Tissue Res 1979; 203:231–40.
[50] Takahashi-Iwanaga H. The three-dimensional spaces of the kidney. Cell Tissue Res 1991;264:269–81.
[51] Fletcher D, Mullins R. Cell mechanics and the cytoskeleton. Nature 2010;463:485–92.
[52] Fujigaki Y, Muranaka Y, Sun D, Goto T, Zhou H, Sakakima M, et al. Transient myofibroblast differentiation of interstitial fibroblastic cells relevant to tubular dilatation in uranyl acetate-induced acute renal failure in rats. Virchows Arch 2005;446:164–76.
[53] van Kooten C, Daha M. Cytokine cross-talk between tubular epithelial cells and interstitial immunocompetent cells. Curr Opin Nephrol Hypertens 2001;10:55–9.
[54] Postlethwaite A, Kang A. Fibroblasts and matrix proteins. In: Gallin J, Goldstein I, Snyderman R, editors. Inflammation: basic principles and clinical correlates. New York: Raven Press; 1992. p. 747–73.
[55] Karkavelas G, Kefalides N. Comparative ultrastructural localization of collagen types III, IV, VI and laminin in rat uterus and kidney. J Ultrastruct Mol Struct Res 1988;100:137–55.
[56] Pitcock J, Lyons H, Brown P, Rightsel W, Muirhead E. Glycosaminoglycans of the rat renomedullary interstitium: ultrastructural and biochemical observations. Exp Mol Pathol 1988;49:373–87.
[57] Le Hir M, Kaissling B. Distribution and regulation of renal ecto-5′-nucleotidase: implications for physiological functions of adenosine. Am J Physiol 1993;264:F377–87.
[58] Eltzschig H, Ibla J, Furuta G, Leonard M, Jacobson K, Enjyoji K, et al. Coordinated adenine nucleotide phosphohydrolysis and nucleoside signaling in posthypoxic endothelium: role of ectonucleotidases and adenosine A2B receptors. J Exp Med 2003; 198:783–96.
[59] Vallon V. Tubuloglomerular feedback and the control of glomerular filtration rate. News Physiol Sci 2003;18:169–74.
[60] Gandhi R, Le Hir M, Kaissling B. Immunolocalization of ecto-5′nucleotidase in the kidney by a monoclonal antibody. Histochemie 1990;95:165–74.
[61] Franco M, Bautista R, Tapia E, Soto V, Santamaria J, Osorio H, et al. Contribution of renal purinergic receptors to renal vasoconstriction in angiotensin II-induced hypertensive rats. Am J Physiol Renal Physiol 2011;300:F1301–9.
[62] Castrop H, Huang Y, Hashimoto S, Mizel D, Hansen P, Theilig F, et al. Impairment of tubuloglomerular feedback regulation

of GFR in ecto-5′-nucleotidase/CD73-deficient mice. J Clin Invest 2004;114:634–42.
[63] Theilig F, Bostanjoglo M, Pavenstadt H, Grupp C, Holland G, Slosarek I, et al. Cellular distribution and function of soluble guanylyl cyclase in rat kidney and liver. J Am Soc Nephrol 2001;12:2209–20.
[64] Bachmann S, Ramasubbu K. Immunohistochemical colocalization of the alpha-subunit of neutrophil NADPH oxidase and ecto-5′-nucleotidase in kidney and liver. Kidney Int 1997;51:479–82.
[65] Bachmann S, Le Hir M, Eckardt K. Co-localization of erythropoietin mRNA and ecto-5′-nucleotidase immunoreactivity in peritubular cells of rat renal cortex indicates that fibroblasts produce erythropoietin. J Histochem Cytochem 1993;41: 335–41.
[66] Fisher J, Koury S, Ducey T, Mendel S. Erythropoietin production by interstitial cells of hypoxic monkey kidneys. Br J Haematol 1996;95:27–32.
[67] Maxwell P, Osmond M, Pugh C, Heryet A, Nicholls L, Tan C, et al. Identification of the renal erythropoietin-producing cells using transgenic mice. Kidney Int 1993;44:1149–62.
[68] Rosenberger C, Griethe W, Gruber G, Wiesener M, Frei U, Bachmann S, et al. Cellular responses to hypoxia after renal segmental infarction. Kidney Int 2003;64:874–86.
[69] Rosenberger C, Rosen S, Heyman S. Current understanding of HIF in renal disease. Kidney Blood Press Res 2005;28: 325–40.
[70] Maxwell P. HIF-1: an oxygen response system with special relevance to the kidney. J Am Soc Nephrol 2003;14: 2712–22.
[71] Eckardt K, Koury S, Tan C, Schuster S, Kaissling B, Ratcliffe P, et al. Distribution of erythropoietin producing cells in rat kidneys during hypoxic hypoxia. Kidney Int 1993;43: 815–23.
[72] Alpers C, Hudkins K, Floege J, Johnson R. Human renal cortical interstitial cells with some features of smooth muscle cells participate in tubulointerstitial and crescentic glomerular injury. J Am Soc Nephrol 1994;5:201–10.
[73] Desmouliere A, Gabbiani G. Myofibroblast differentiation during fibrosis. Exp Nephrol 1995;3:134–9.
[74] Diamond J, van Goor H, Ding G, Engelmyer E. Myofibroblasts in experimental hydronephrosis. Am J Pathol 1995;146:121–9.
[75] Picard N, Baum O, Vogetseder A, Kaissling B, Le Hir M. Origin of renal myofibroblasts in the model of unilateral ureter obstruction in the rat. Histochem Cell Biol 2008;130: 141–55.
[76] Sappino A, Schurch W, Gabbiani G. Different repertoire of fibroblastic cells: expression of cytoskeletal proteins as markers of phenotypic modulations. Lab Invest 1990;63: 144–61.
[77] Grupp C, Lottermoser J, Cohen D, Begher M, Franz H, Mueller G. Transformation of rat inner medullary fibroblasts to myofiblasts *in vitro*. Kidney Int 1997;52:1279–90.
[78] Lüllmann-Rauch R. Lysosomal storage of sulfated glycosaminoglycans in renal interstitial cells of rats treated with tilorone. Cell Tissue Res 1987;250:641–8.
[79] Muirhead E. Discovery of the renomedullary system of blood pressure control and its hormones. Hypertension 1990; 15:114–6.
[80] Vernace M, Mento P, Maita M, Girardi E, Chang M, Nord E, et al. Osmolar regulation of endothelin signaling in rat medullary interstitial cells. J Clin Invest 1995;96:183–91.
[81] Breyer M, Harris R. Cyclooxygenase 2 and the kidney. Curr Opin Nephrol Hypertens 2001;10:89–98.
[82] Jensen B, Kurtz A. Differential regulation of renal cyclooxygenase mRNA by dietary salt intake. Kidney Int 2004;52: 1242–9.
[83] Yang T, Singh I, Pham H, Sun D, Smart A, Schnermann J, et al. Regulation of cyclooxygenase expression in the kidney by dietary salt intake. Am J Physiol 1998;274:F481–9.
[84] Ye W, Zhang H, Hillas E, Kohan D, Miller R, Nelson R, et al. Expression and function of COX isoforms in renal medulla: evidence for regulation of salt sensitivity and blood pressure. Am J Physiol Renal Physiol 2006;290:F542–9.
[85] Austyn J, Hankins D, Larsen C, Morris P, Rao A, Roake J. Isolation and characterization of dendritic cells from mouse heart and kidney. J Histochem Cytochem 1994;41:335–41.
[86] Dong X, Swaminathan S, Bachman L, Croatt A, Nath K, Griffin M. Antigen presentation by dendritic cells in renal lymph nodes is linked to systemic and local injury to the kidney. Kidney Int 2005;68:1096–108.
[87] John R, Nelson P. Dendritic cells in the kidney. J Am Soc Nephrol 2011;18:2628–35.
[88] Soos T, Sims T, Barisoni L, Link K, Littman D, Dustin M, et al. CX3CR1 + interstitial dendritic cells form a contiguous network throughout the entire kidney. Kidney Int 2006; 70:591–6.
[89] Kruger T, Benke D. Identification and functional characterization of dendritic cells in the healthy murine kidney and in experimental glomerulonephritis. J Am Soc Nephrol 2004;15:613–21.
[90] McDermott R, Ziylan U, Spehner D, Bausinger H, Lipsker D, Mommaas M, et al. Birbeck granules are subdomains of endosomal recycling compartment in human epidermal Langerhans cells, which form where Langerin accumulates. Mol Biol Cell 2002;13:317–35.
[91] Le Hir M, Hegyi I, Loffing-Cueni D, Loffing J, Kaissling B. Characterization of renal interstitial fibroblast-specific protein 1/S100A4-positive cells in healthy and inflamed rodent kidneys. Histochem Cell Biol 2005;123:335–46.
[92] Kriz W. A periarterial pathway for intrarenal distribution of renin. Kidney Int 1987;31:S-51–6.
[93] Matusi K, Nagy-Bojarsky K, Laakkonen P, Krieger S, Mechtler K, Uchida S, et al. Lymphatic microvessels in the rat remnant kidney model of renal fibrosis: aminopeptidase p and podoplanin are discriminatory markers for endothelial cells of blood and lymphatic vessels 4432. J Am Soc Nephrol 2003;14:1981–9.
[94] Gardiner B, Smith D, O'Connor P, Evans R. A mathematical model of diffusional shunting of oxygen from arteries to veins in the kidney. Am J Physiol Renal Physiol 2011;300: F1339–52.
[95] Schurek H, Jost U, Baumgärtl H, Bertram H, Heckmann U. Evidence for a preglomerular oxygen diffusion shunt in rat renal cortex. Am J Physiol 1990;259:F910–5.
[96] Barajas L, Wang P. Myelinated nerves of the rat kidney. A light and electron microscopic study. J Ultrastruct Res 1978; 65:148–62.
[97] Barajas L, Wang P. Demonstration of acetylcholinesterase in the adrenergic nerves of the renal glomerular arterioles. J Ultrastruct Res 1975;53:244–53.
[98] Dolezel S, Edvinsson L, Owman C, Owman T. Fluorescence histochemistry and autoradiography of adrenergic nerves in the renal juxtaglomerular complex of mammals and man, with special regard to the efferent arteriole. Cell Tissue Res 1976;169:211–20.
[99] Gorgas K. Structure and innervation of the juxtaglomerular apparatus of the rat. Adv Anat Embryol Cell Biol 1978;54:5–84.

[100] Dinerstein R, Vannice J, Henderson R, Roth L, Goldberg L, Hoffmann P. Histofluorescence techniques provide evidence for dopamine-containing neuronal elements in canine kidney. Science 1979;205:497–9.
[101] Unwin R, Ganz M, Sterzel R. Brain-gut peptides, renal function and cell growth. Kidney Int 1990;37:1031–47.
[102] Dieterich H. Electron microscopic studies of the innervation of the rat kidney. Z Anat Entwicklungsgesch 1974;145:169–86.
[103] Fourman J. The adrenergic innervation of the efferent arterioles and the vasa recta in the mammalian kidney. Experientia 1970;26:293–4.
[104] Barajas L, Powers K. Innervation of the renal proximal convoluted tubule of the rat. Am J Anat 1989;186:378–88.
[105] DiBona G, Kopp U. Neural control of renal function. Physiol Rev 1997;77:75–197.
[106] Morel F, Chabardes D, Imbert-Teboul M. Heterogeneity of hormonal control in the distal nephron. In: Barcelo R, editor. Proceedings of the VII international congress of nephrology. Basel: Karger; 1978. p. 209–16.
[107] Ciriello J, de Oliveira C. Renal afferents and hypertension. Curr Hypertens Rep 2002;4:136–42.
[108] DiBona G. Differentiation of vasoactive renal sympathetic nerve fibers. Acta Physiol Scand 2000;168:195–200.
[109] Eppel G, Luff S, Denton K, Evans R, Neuropeptide Y. (Y1) receptors and {alpha}1-adrenoceptors in the neural control of regional renal perfusion. Am J Physiol Regul Integr Comp Physiol 2006;290(2):R331–40.
[110] Ferguson M, Bell C. Ultrastructural localization and characterization of sensory nerves in the rat kidney. J Comp Neurol 1988;274:9–16.
[112] von Mollendorff W. Der Exkretionsapparat. Berlin: Springer-Verlag; 1930.
[113] Zhai X, Birn H, Jensen K, Thomsen J, Andreasen A, Christensen E. Digital three-dimensional reconstruction und ultrastructure of the mouse proximal tubule. J Am Soc Nephrol 2003;14:611–9.
[114] Bulger R, Cronin R, Dobyan D. Survey of the morphology of the dog kidney. Anat Rec 1979;194:41–66.
[115] Kriz W. Structural organization of the renal medulla: comparative and functional aspects. Am J Physiol 1981;241:R3–16.
[116] Kriz W, Dieterich H, Hoffmann S. Aufbau der Gefässbündel im Nierenmark von Wüstenmäusen. Naturwissenschaften 1968;55:40.
[117] Morel F, Imbert-Teboul M, Chabardes D. Receptors to vasopressin and other hormones in the mammalian kidney. Kidney Int 1987;31:512–20.
[118] Schmidt-Nielsen B, O'Dell R. Structure and concentrating mechanism in the mammalian kidney. Am J Physiol 1961; 200:1119–24.
[119] Han J, Thompson K, Chou C, Knepper M. Experimental tests of three-dimensional model of urinary concentrating mechanism. J Am Soc Nephrol 1992;2:1677–88.
[120] Kriz W, Schnermann J, Koepsell H. The position of short and long loops of Henle in the rat kidney. Z Anat Entwicklungsgesch 1972;138:301–19.
[121] Pannabecker T, Dantzler W. Three-dimensional lateral and vertical relationships of inner medullary loops of Henle and collecting ducts. Am J Physiol Renal Physiol 2004;287:F767–74.
[122] Samuel T, Hoy W, Douglas-Denton R, Hughson M, Bertram J. Determinants of glomerular volume in different cortical zones of the human kidney. J Am Soc Nephrol 2005;16:3102–9.
[123] Murakami T, Miyoshi M, Fujita T. Glomerular vessels of the rat kidney with special reference to double efferent arterioles. A scanning electron microscope study of corrosion casts. Arch Histol Jpn 1971;3:179–98.
[124] Sakai T, Kriz W. The structural relationship between mesangial cells and basement membrane of the renal glomerulus. Anat Embryol 1987;176:373–86.
[125] Abrahamson D, Hudson B, Stroganova L, Borza D, St John P. Cellular origins of type IV collagen networks in developing glomeruli. J Am Soc Nephrol 2009;20:1471–9.
[126] Price R, Spiro R. Studies on the metabolism of the renal glomerular basement membrane. Turnover measurements in the rat with the use of radiolabeled amino acids. J Biol Chem 1977;252:8597–602.
[127] Abrahamson D. Origin of the glomerular basement membrane visualized after *in vivo* labeling of laminin in newborn rat kidneys. J Cell Biol 1985;100:1988–2000.
[128] Reddi A. Metabolism of glomerular basement membrane in normal, hypophysectomized, and growth-hormone-treated diabetic rats. Exp Mol Pathol 1985;43:196–208.
[129] Davies M, Thomas G, Shrewing L, Mason R. Mesangial cell proteoglycans: synthesis and metabolism. J Am Soc Nephrol 1992;2(10 Suppl):S88–94.
[130] Martin J, Eynstone L, Davies M, Steadman R. Induction of metalloproteinases by glomerular mesangial cells stimulated by proteins of the extracellular matrix. J Am Soc Nephrol 2001;12:88–96.
[131] Martin J, Steadman R, Knowlden J, Williams J, Davies M. Differential regulation of matrix melalloproteinases and their inhibitors in human glomerular epithelial cells *in vitro*. J Am Soc Nephrol 1998;9:1629–37.
[132] Inoue S. Ultrastructural architecture of basement membranes. Contrib Nephrol 1994;107:21–8.
[133] Abrahamson D. Structure and development of the glomerular capillary wall and basement membrane. Am J Physiol 1987; 253:F783–94.
[134] Yurchenco P. Assembly of laminin and type IV collagen into basement membrane networks. In: Yurchenco P, Birk D, Mecham R, editors. Extracellular matrix assembly and structure. San Diego: Academic Press; 1994. p. 351–88.
[135] Martinez-Hernandez A, Gay S, Miller E. Ultrastructural localization of type V collagen in rat kidney. J Cell Biol 1982;92:343.
[136] Miner J. Building the glomerulus: a matricentric view. J Am Soc Nephrol 2005;16:857–61.
[137] Miner J, Yurchenco P. Laminin functions in tissue morphogenesis. Annu Rev Cell Dev Biol 2004;20:255–84.
[138] Hudson B, Reeders S, Tryggvason K. Type IV collagen: structure, gene organization and role in human diseases. J Biol Chem 1993;268:26033–6.
[139] Timpl R, Brown J. Supramolecular assembly of basement membranes. BioEssays 1996;18(2):123–32.
[140] Martinez-Hernandez A, Chung A. The ultrastructural localization of two basement membrane components entactin and laminin – in rat tissue. J Histochem Cytochem 1984;32:289.
[141] Stow J, Sawada H, Farquhar M. Basement membrane heparan sulfate proteoglycans are concentrated in the laminae rarae and in the podocytes of the rat renal glomerulus. Proc Natl Acad Sci USA 1985;82:3296.
[142] Groffen A, Buskens C, van Kuppevelt T, Veerkamp J, Monnens L, van den Heuvel L. Primary structure and high expression of human agrin in basement membranes of adult lung and kidney. Eur J Biochem 1998;254:123–8.
[143] Miner J. Renal basement membrane components. Kidney Int 1999;56:2016–24.
[144] Farquhar M, Palade G. Functional evidence for the existence of a third cell type in the renal glomerulus. Phagocytosis of filtration residues by a distinctive "third" cell. J Cell Biol 1962;13:55–87.

[145] Zimmermann K. Ueber den Bau des Glomerulus der Saeugerniere. Z Mikrosk Anat Forsch 1933;32:176–278.
[146] Elger M, Drenckhahn D, Nobiling R, Mundel P, Kriz W. Cultured rat mesangial cells contain smooth muscle a-actin not found *in vivo*. Am J Pathol 1993;142:497–509.
[147] Kriz W, Elger M, Mundel P, Lemley K. Structure-stabilizing forces in the glomerular tuft. J Am Soc Nephrol 1995;5:1731–9.
[148] Kikkawa Y, Virtanen I, Miner J. Mesangial cells organize the glomerular capillaries by adhering to the G domain of laminin a5 in the glomerular basement membrane. J Cell Biol 2003; 161:187–96.
[149] Couchman J, Beavan L, McCarthy K. Glomerular matrix: synthesis, turnover and role in mesangial expansion. Kidney Int 1994;45:328–35.
[150] Schaefer L, Gröne H, Raslik I, Robenek H, Ugorcakova J, Budny S, et al. Small proteoglycans of normal adult human kidney: distinct expression patterns of decorin, biglycan, fibromodulin, and lumican. Kidney Int 2000;58:1557–68.
[151] Courtoy P, Timpl R, Farquhar M. Comparative distribution of laminin, type IV collagen, and fibronectin in the rat glomerulus. J Histochem Cytochem 1982;30:874.
[152] Madri J, Roll F, Furthmayr H, Foidart J. Ultrastructural localization of fibronectin and laminin in the basement membranes of the murine kidney. J Cell Biol 1980;86:G82–7.
[153] Sterzel R, Hartner A, Schlotzer-Schrehard U, Voit S, Hausknecht B, Doliana R, et al. Elastic fiber proteins in the glomerular mesangium *in vivo* and in cell culture. Kidney Int 2000;58:1588–602.
[154] Schwartz E, Goldfischer S, Coltoff-Schiller B, Blumenfeld O. Extracellular matrix microfibrils are composed of core proteins coated with fibronectin. J Histochem Cytochem 1985;33: 268–74.
[155] Mundel P, Elger M, Sakai T, Kriz W. Microfibrils are a major component of the mesangial matrix in the glomerulus of the rat kidney. Cell Tissue Res 1988;254:183–7.
[156] Bieritz B, Spessotto P, Colombatti A, Jahn A, Prols F, Hartner A. Role of alpha8 integrin in mesangial cell adhesion, migration, and proliferation. Kidney Int 2003;64:119–27.
[157] Bulger R, Eknoyan G, Purcell D, Dobyan D. Endothelial characteristics of glomerular capillaries in normal, mercuric chloride-induced, and gentamicin-induced acute renal failure in the rat. J Clin Invest 1983;72:128–41.
[158] Vasmant D, Maurice M, Feldmann G. Cytoskeleton ultrastructure of podocytes and glomerular endothelial cells in man and in the rat. Anat Rec 1984;210:17–24.
[159] Rostgaard J, Qvortrup K. Sieve plugs in fenestrae of glomerular capillaries – site of the filtration barrier? Cells Tissues Organs 2002;170:132–8.
[160] Horvat R, Hovorka A, Dekan G, Poczewski H, Kerjaschki D. Endothelial cell membranes contain podocalyxin: the major sialoprotein of visceral glomerular epithelial cells. J Cell Biol 1986;102:484–91.
[161] Savage C. The biology of the glomerulus: endothelial cells. Kidney Int 1994;45:314–9.
[162] Betsholtz C, Lindblom P, Bjarnegard M, Enge M, Gerhardt H, Lindahl P. Role of platelet-derived growth factor in mesangium development and vasculopathies: lessons from platelet-derived growth factor and platelet-derived growth factor receptor mutations in mice. Curr Opin Nephrol Hypertens 2005;13:45–52.
[163] Eremina V, Quaggin S. The role of VEGF-A in glomerular development and function. Curr Opin Nephrol Hypertens 2004; 13:9–15.
[164] Satchell S, Anderson K, Mathieson P. Angiopoietin 1 and vascular endothelial growth factor modulate human glomerular cell barrier properties. Am Soc Nephrol 2004;15: 566–74.
[165] Ballermann B. Glomerular endothelial cell differentation. Kidney Int 2005;67:1668–71.
[166] Fretschner M, Endlich K, Fester C, Parekh N, Steinhausen M. A narrow segment of the efferent arteriole controls efferent resistance in the hydronephrotic rat kidney. Kidney Int 1990; 37:1227–39.
[167] Mundel P, Kriz W. Structure and function of podocytes: an update. Anat Embryol 1995;192:385–97.
[168] Drenckhahn D, Franke R. Ultrastructural organization of contractile and cytoskeletal proteins in glomerular podocytes of chicken, rat, and man. Lab Invest 1988;59:673–82.
[169] Ichimura K, Kurihara H, Sakai T. Actin filament organization of foot-processes in rat podocytes. J Histochem Cytochem 2003;51:1589–600.
[170] Huber G, Matus A. Microtubule-associated protein 3 (MAP3) expression in non-neuronal tissues. J Cell Sci 1990;95: 237–46.
[171] Kobayashi N, Reiser J, Kuriyama R, Kriz W, Mundel P. Nonuniform microtubular polarity established by CHO1/MKLP1 motor protein is necessary for process formation of podocytes. J Cell Biol 1998;143:1961–70.
[172] Sanden W, Elger M, Mundel P, Kriz W. The architecture of podocyte cytoskeleton suggests a role in glomerular filtration dynamics. Ann Anat 1995;177:44–5.
[173] Cross D, Vial C, Maccioni R. A tau-like protein interacts with stress fibers and microtubules in human and rodent cultured cell lines. J Cell Sci 1993;105:51–60.
[174] Lloyd C, Minto A, Dorf M, Proudfoot A, Wells T, Salant D, et al. RANTES and monocyte chemoattractant protein-1 (MCP-1) play an important role in the inflammatory phase of crescentic nephritis, but only MCP-1 is involved in crescent formation and interstitial fibrosis. J Exp Med 1997;185:1371–80.
[175] Volk K, Sigmund R, Snyder P, McDonald F, Welsh M, Stokes J. rENaC is the predominant Na^+ channel in the apical membrane of the rat renal inner medullary collecting duct. J Clin Invest 1995;96:2748–57.
[176] Asanuma K, Kim K, Oh J, Giardino L, Chabanis S, Faul C, et al. Synaptopodin regulates the actin-bundling activity of alpha-actinin in an isoform-specific manner. J Clin Invest 2005;1:1.
[177] Adler S. Characterization of glomerular epithelial cell matrix receptors. Am J Pathol 1992;141:571–8.
[178] Cybulsky A, Carbonetto S, Huang Q, McTavish A, Cyr M. Adhesion of rat glomerular epithelial cells to extracellular matrices: role of b1 integrins. Kidney Int 1992;42:1099–106.
[179] Kreidberg J, Symons J. Integrins in kidney development, function, and disease. Am J Physiol Renal Physiol 2000;279(2): F233–42.
[180] Raats C, van den Born J, Bakker M, Oppers-Walgreen B, Pisa B, Dijkman H, et al. Expression of agrin, dystroglycan, and utrophin in normal renal tissue and in experimental glomerulopathies. Am J Pathol 2000;156(5):1749–65.
[181] Regele H, Fillipovic E, Langer B, Poczewki H, Kraxberger I, Bittner R, et al. Glomerular expression of dystroglycans is reduced in minimal change nephrosis but not in focal segmental glomerulosclerosis. J Am Soc Nephrol 2000;11(3): 403–12.
[182] Blattner S, Kretzler M. Integrin-linked kinase in renal disease: connecting cell–matrix interaction to the cytoskeleton. Curr Opin Nephrol Hypertens 2005;14:404–10.
[183] Reiser J, Polu K, Moller C, Kenlan P, Altintas M, Wei C, et al. TRPC6 is a glomerular slit diaphragm-associated channel required for normal renal function. Nat Genet 2005;37: 739–44.
[184] Winn M, Conlon P, Lynn K, Farrington M, Creazzo T, Hawkins A, et al. A mutation in the TRPC6 cation channel causes familial focal segmental glomerulosclerosis. Science 2005;308:1801–4.

[185] Kazatchkine M, Fearon D, Appay M, Mandet C, Bariety J. Immunohistochemical study of the human glomerular C3b receptor in normal kidney and in seventy-five cases of renal diseases. J Clin Invest 1982;69:900–12.
[186] Schiffer M, Schiffer L, Gupta A, Shaw A, Roberts I, Mundel P, et al. Inhibitory smads and TGF-ß signaling in glomerular cells. J Am Soc Nephrol 2002;13:2657–66.
[187] Wogensen L, Nielsen C, Hjorth P. Under control of the Ren-1c promoter, locally produced transforming growth factor-beta1 induced accumulation of glomerular extracellular matrix in transgenic mice. Diabetes 1999;48:182–92.
[188] Kriz W, Haehnel B, Rosener S, Elger M. Long-term treatment of rats with FGF-2 results in focal segmental glomerulosclerosis. Kidney Int 1995;48:1435–50.
[189] Pavenstadt H, Kriz W, Kretzler M. Cell biology of the glomerular podocyte. Physiol Rev 2003;83:253–307.
[190] Kerjaschki D, Exner M, Ullrich R, Susani M, Curtiss L, Witztum J, et al. Pathogenic antibodies inhibit the binding of apolipoproteins to megalin/gp330 in passive Heymann nephritis. J Clin Invest 1997;100:2303–9.
[191] Kerjaschki D, Farquhar M. Immunocytochemical localization of the Heymann antigen (gp 330) in glomerular epithelial cells of normal Lewis rats. J Exp Med 1983;157:667–86.
[192] Orlando R, Rader K, Authier F, Yamazaki H, Posner B, Farquhar M. Megalin is an endocytic receptor for insulin. J Am Soc Nephrol 1998;9:1759–66.
[193] Saito A, Pietromonaco S, Loo A, Farquhar M. Complete cloning and sequencing of rat gp330/"megalin," a distinctive member of the low density lipoprotein receptor gene family. Proc Natl Acad Sci USA 1994;91:9725–9.
[194] Rodewald R, Karnovsky M. Porous substructure of the glomerular slit diaphragm in the rat and mouse. J Cell Biol 1974;60:423–33.
[195] Ruotsalainen V, Ljungberg P, Wartiovaara J, Lenkkeri U, Kestila M, Jalanko H, et al. Nephrin is specifically located at the slit diaphragm of glomerular podocytes. Proc Natl Acad Sci USA 1999;96(14):7962–7.
[196] Donoviel D, Freed D, Vogel H, Potter D, Hawkins E, Barrish J, et al. Proteinuria and perinatal lethality in mice lacking NEPH1, a novel protein with homology to nephrin. Mol Cell Biol 2001;21:4829–36.
[197] Reiser J, Kriz W, Kretzler M, Mundel P. The glomerular slit diaphragm is a modified adherens junction. J Am Soc Nephrol 2000;11:1–8.
[198] Inoue T, Yaoita E, Kurihara H, Shimizu F, Sakai T, Kobayashi T, et al. Fat is a component of glomerular slit diaphragms. Kidney Int 2001;59:1003–12.
[199] Schnabel E, Anderson J, Farquhar M. The tight junction protein ZO-1 is concentrated along slit diaphragms of the glomerular epithelium. J Cell Biol 1990;111:1255–63.
[200] Boute N, Gribouval O, Roselli S, Benessy F, Lee H, Fuchshuber A, et al. NPHS2, encoding the glomerular protein podocin, is mutated in autosomal recessive steroid-resistant nephrotic syndrome. Nat Genet 2000;24:349–54.
[201] Li C, Ruotsalainen V, Tryggvason K, Shaw A, Miner J. CD2AP is expressed with nephrin in developing podocytes and is found widely in mature kidney and elsewhere. Am J Physiol Renal Physiol 2000;279(4):F785–92.
[202] Huber T, Kottgen M, Schilling B, Walz G, Benzing T. Interaction with podocin facilitates nephrin signaling. J Biol Chem 2001; 276:41543–6.
[203] Schwarz K, Simons M, Reiser J, Saleem M, Faul C, Kriz W, et al. Podocin, a raft-associated component of the glomerular slit diaphragm, interacts with CD2AP and nephrin. J Clin Invest 2001;108:1621–9.
[204] Dunne J, Hanby A, Poulsom R, Jones T, Sheer D, Chin W, et al. Molecular cloning and tissue expression of FAT, the human homologue of the *Drosophila* fat gene that is located on chromosome 4q34-q35 and encodes a putative adhesion molecule. Genomics 1995;30:207–23.
[205] Ciani L, Patel A, Allen N, ffrench-Constant C. Mice lacking the giant protocadherin mFAT1 exhibit renal slit junction abnormalities and a partially penetrant cyclopia and anophthalmia phenotype. Mol Cell Biol 2003;23:3575–82.
[206] Huang T, Langlois J. Podoendin. A new cell surface protein of the podocyte and endothelium. J Exp Med 1985;162: 245–67.
[207] Sawada H, Stukenbrok H, Kerjaschki D, Farquhar M. Epithelial polyanion (podocalyxin) is found on the sides but not the soles of the foot processes of the glomerular epithelium. Am J Pathol 1986;125:309–18.
[208] Hugo C, Nangaku M, Shankland S, Pichler R, Gordon K, Amieva M, et al. The plasma membrane-actin linking protein, ezrin, is a glomerular epithelial cell marker in glomerulogenesis, in the adult kidney and in glomerular injury. Kidney Int 1998;54:1934–44.
[209] Takeda T, McQuistan T, Orlando R, Farquhar M. Loss of glomerular foot processes is associated with uncoupling of podocalyxin from the actin cytoskeleton. J Clin Invest 2001; 108:289–301.
[210] Seiler M, Rennke H, Venkatachalam M, Cotran R. Pathogenesis of polycation-induced alteration (fusion) of glomerular epithelium. Lab Invest 1977;36:48–61.
[211] Drumond M, Deen W. Structural determinants of glomerular hydraulic permeability. Am J Physiol 1994;266:F1–12.
[212] Kanwar Y, Venkatachalam M. Renal Physiology. In: Windhager E, editor. Handbook of physiology. New York: Oup; 1992. p. 3–40.
[213] Bolton G, Deen W, Daniels B. Assessment of the charge selectivity of glomerular basement membrane using Ficoll sulfate. Am J Physiol 1998;274:F889–96.
[214] Daniels B. Increased albumin permeability *in vitro* following alterations of glomerular charge is mediated by the cells of the filtration barrier. J Lab Clin Med 1994;124(2):224–30.
[215] Drumond M, Deen W. Hindered transport of macromolecules through a single row of cylinders: application to glomerular filtration. J Biomech Eng 1995;117:414–22.
[216] Edwards A, Daniels B, Deen W. Hindered transport of macromolecules in isolated glomeruli. II. Convection and pressure effects in basement membrane. Biophys J 1997;72: 214–22.
[217] Dworkin L, Brenner B. Biophysical basis of glomerular filtration. In: Seldin D, Giebisch G, editors. The kidney: physiology and pathophysiology. New York: Raven Press; 1992. p. 979–1016.
[218] Anderson W, Alcorn D, Gilchrist A, Whiting J, Ryan G. Glomerular actions of ANG II during reduction of renal artery pressure: a morphometric analysis. Am J Physiol 1989;256: F1021–6.
[219] Denton K, Fennessy P, Alcorn D, Anderson W. Morphometric analysis of the actions of angiotensin II on renal arterioles and glomeruli. Am J Physiol 1992;262:F367–72.
[220] Andrews P. Morphological alterations of the glomerular (visceral) epithelium in response to pathological and experimental situations. J Electron Microsc Tech 1988;9:115–44.
[221] Drumond M, Kristal B, Myers B, Deen W. Structural basis for reduced glomerular filtration capacity in nephrotic humans. J Clin Invest 1994;94:1187–95.
[222] Kriz W, Elger M, Lemley K, Sakai T. Structure of the glomerular mesangium: a biomechanical interpretation. Kidney Int 1990;38:S2–9.

[223] Kriz W, Haehnel B, Hosser H, Ostendorf T, Kränzlin B, Gretz N, et al. Pathways to recovery and loss of nephrons in anti-Thy-1 nephritis. J Am Soc Nephrol 2003;14:1904–26.
[224] Welling L, Zupka M, Welling D. Mechanical properties of basement membrane. News Physiol Sci 1995;10(1):30–5.
[225] Kriz W, Mundel P, Elger M. The contractile apparatus of podocytes is arranged to counteract GBM expansion. Contrib Nephrol 1994;107:1–9.
[226] Mbassa G, Elger M, Kriz W. The ultrastructural organization of the basement membrane of Bowman's capsule in the rat renal corpuscle. Cell Tissue Res 1988;253:151–63.
[227] Lethias C, Aubert-Foucher E, Dublet B, Eichenberger D, Font B, Goldschmidt D, et al. Structure, molecular assembly and tissue distribution of facit collagen molecules. Contrib Nephrol 1994; 107:57–63.
[228] Schonheyder H, Maunsbach A. Ultrastructure of a specialized neck region in the rabbit nephron. Kidney Int 1975;7:145–53.
[229] Gibson I, Downie I, Downie T, Han S, More I, Lindop G. The parietal podocyte: a study of the vascular pole of the human glomerulus. Kidney Int 1992;41:211–4.
[230] Grouls S, Iglesias D, Wentzensen N, Moeller M, Bouchard M, Kemler R, et al. ß-catenin/wnt-signaling is required for lineage specification of parietal epithelial cells of the glomerulus. J Am Soc Nephrol 2011;: in press:nn.
[231] Ronconi E, Sagrinati C, Angelotti M, Lazzeri E, Mazzinghi B, Ballerini L, et al. Regeneration of glomerular podocytes by human renal progenitors. J Am Soc Nephrol 2009;20:322–32.
[232] Sagrinati C, Netti G, Mazzinghi B, Lazzeri E, Liotta F, Frosali F, et al. Isolation and characterization of multipotent progenitor cells from the Bowman's capsule of adult human kidneys. J Am Soc Nephrol 2006;17:2443–56.
[233] Appel D, Kershaw D, Smeets B, Yuan G, Fuss A, Freye B, et al. Recruitment of podocytes from glomerular parietal epithelial cells. J Am Soc Nephrol 2008;20:333–43.
[234] Schneeberger E, Lynch R. Sodium transport deficiency and sodium balance in gene-targeted mice. Am J Physiol Cell Physiol 2004;286:C1213–28.
[235] Mitic L, Anderson J. Molecular architecture of tight junctions. Annu Rev Physiol 1998;60:121–42.
[236] Tsukita S, Furuse M. Multifunctional strands in tight junctions 4437. Nat Rev Mol Cell Biol 2001;2:285–93.
[237] Matlin K. Clues to occludin. Focus on "Knockdown of occludin expression leads to diverse phenotypic alterations in epithelial cells.". Am J Physiol Cell Physiol 2011;288:C1191–2.
[238] Denker B, Sabath E. The biology of epithelial cell tight junctions in the kidney. J Am Soc Nephrol 2011;22:622–5.
[239] Madara J. Regulation of the movement of solutes across tight junctions. Annu Rev Physiol 1998;60:143–59.
[240] Li W, Huey C, Yu A. Expression of claudin-7 and -8 along the mouse nephron. Am J Physiol Renal Physiol 2004;286:F1063–71.
[241] Peter Y, Goodenough D. Claudins. Curr Opin Cell Biol 2004;14:R293–4.
[242] Yu A. Claudins and epithelial paracellular transport: the end of the beginning 4441. Curr Opin Nephrol Hypertens 2003;12:503–9.
[243] Yu A, Enck A. Claudin-8 expression in Madin–Darby canine kidney cells augments the paracellular barrier to cation permeation. J Biol Chem 2003;278:17350–9.
[244] Tsukita S, Furuse M. Claudin-based barrier in simple and stratified cellular sheets. Curr Opin Cell Biol 2002;14:531–6.
[245] Colegio O, Van Itallie C. Claudins create charge-selective channels in the paracellular pathway between epithelial cells. Am J Physiol Cell Physiol 2002;283:C142–7.
[246] Colegio O, Van Itallie C. Claudin extracellular domains determine paracellular charge selectivity and resistance but not tight junction fibril architecture. Am J Physiol Cell Physiol 2003;284:C1346–54.
[247] Tang V, Goodenough D. Paracellular ion channel at the tight junction. Biophys J 2003;84:1660–73.
[248] Clarke H, Marano C. Modification of tight junction function by protein kinase C isoforms. Adv Drug Delivery Rev 2000;41:283–301.
[249] Hopkins A, Li D. Modulation of tight junction function by G protein-coupled events. Adv Drug Delivery Rev 2000; 41:329–40.
[250] Kahle K, Gimenez I. WNK4 regulates apical and basolateral Cl^- flux in extrarenal epithelia. Proc Natl Acad Sci USA 2004;101:2064–9.
[251] Yang C, Angell J. WNK kinases regulate thiazide-sensitive Na-Cl co-transport. J Clin Invest 2003;111:1039–45.
[252] Simon D, Lu Y. Paracellin-1 a renal tight junction protein required for paracellular Mg^{2+} resorption. Science 1999; 285:103–6.
[253] Wilcox E, Burton Q. Mutations in the gene encoding tight junction claudin-14 cause autosomal recessive deafness. Cell 2001;104:165–72.
[254] Choate K, K. Kahle. WNK1 a kinase mutated in inherited hypertension with hyperkalemia, localizes to diverse Cl^--transporting epithelia. Proc Natl Acad Sci USA 2003;100:663–8.
[255] Kahle K, Wilson F. WNK4 regulates the balance between renal NaCl reabsorption and K^+ secretion. Nat Genet 2003;35:372–6.
[256] Wilson F, Disse-Nicodeme S. Human hypertension caused by mutations in WNK kinases. Science 2001;293:1107–12.
[257] Wilson F, Kahle K. Molecular pathogenesis of inherited hypertension with hyperkalemia: the Na-Cl co-transporter is inhibited by wild-type but not mutant WNK4. Proc Natl Acad Sci USA 2003;100:680–4.
[258] Yu A, McCarthy K. Knockdown of occludin expression leads to diverse phenotypic alterations in epithelial cells. Am J Physiol Cell Physiol 2005;288:C1231–41.
[259] Lima WR, Parreira K, Devuyst O, Caplanusi A, N'kuli F, Marien B, et al. ZONAB promotes proliferation and represses differentiation of proximal tubule epithelial cells. J Am Soc Nephrol 2010;21:478–88.
[260] Kaissling B, Kriz W. Morphology of the loop of Henle, distal tubule and collecting duct. In: Windhager E, editor. Handbook of physiology: section on renal physiology. New York, N.Y.: Oxford University Press; 1992. p. 109–67.
[261] Kiuchi-Saishin Y, Gotoh S, Furuse M, Takasuga A, Tano Y, Tsukita S. Differential expression patterns of claudins, tight junction membrane proteins, in mouse nephron segments. J Am Soc Nephrol 2002;13:875–86.
[262] Piepenhagen P, Nelson W. Differential expression of cell–cell and cell–substratum adhesion proteins along the kidney nephron 4461. Am J Physiol 1995;269:C1433–49.
[263] Piepenhagen P, Peters L, Lux S, Nelson W. Differential expression of Na(+)-K(+)-ATPase, ankyrin, fodrin, and E-cadherin along the kidney nephron. Am J Physiol 1995;269: C1417–32.
[264] Prozialeck W, Lamar P, Appelt D. Differential expression of E-cadherin, N-cadherin and beta-cadherin in proximal and distal segments of the rat nephron. BMC Physiol 2004;4:10.
[265] Rybak J, Ettorre A, Kaissling B, Giavazzi R, Neri D, Elia G. *In vivo* protein biotinylation for identification of organ-specific antigens accessible from the vasculature. Nat Methods 2005; 2:291–8.
[266] Thomson R, Aronson P. Immunolocalization of Ksp-cadherin in the adult and developing rabbit kidney. Am J Physiol Renal Physiol 1999;277:F146–56.

[267] Nelson W, Nusse R. Convergence of Wnt, beta-catenin, and cadherin pathways. Science 2004;303:1483–7.
[268] Christensen E, Wagner C, Kaissling B. The uriniferous tubule: structural and functional organization. In: American Physiological Society, editor. Compr physiol. Wiley Blackwell; 2012. p. 1–57.
[269] Donowitz M, Cha B, Zachos N, Brett C, Sharma A, Tse C, et al. Family and NHE3 regulation 4469. J Physiol 2005;567:3–11.
[270] Ecelbarger C, Kim G, Wade J, Knepper M. Regulation of the abundance of renal sodium transporters and channels by vasopressin 4467. Exp Neurol 2001;171:227–34.
[271] Wade J, Stanton B, Brown D. Structural correlates of transport in distal tubule and collecting duct segments. In: Windhager E, editor. Handbook of physiology: renal. New York: Oxford Univerity Press; 1992. p. 1–10.
[272] Wade J, Welling P, Donowitz M, Shenolikar S, Weinman E. Differential renal distribution of NHERF isoforms and their colocalization with NHE3, ezrin, and ROMK. Am J Physiol Cell Physiol 2001;280:C192–8.
[273] Weinman E, Cunningham R, Wade J, Shenolikar S. The role of NHERF-1 in the regulation of renal proximal tubule sodium-hydrogen exchanger 3 and sodium-dependent phosphate co-transporter 2a 4470. J Physiol 2005;567:27–32.
[274] Cha B, Kenworthy A, Murtazina R, Donowitz M. The lateral mobility of NHE3 on the apical membrane of renal epithelial OK cells is limited by the PDZ domain proteins NHERF1/2, but is dependent on an intact actin cytoskeleton as determined by FRA. J Cell Sci 2004;117:3353–65.
[275] Rodman J, Mooseker M, Farquhar M. Cytoskeletal proteins of the rat kidney proximal tubule brush border. Eur J Cell Biol 1986;42:313.
[276] Geering K. FXYD proteins: new regulators of Na-K-ATPase. J Physiol Renal Physiol 2006;290:F241–50.
[277] Brown D. Targeting of membrane transporters in renal epithelia: when cell biology meets physiology. Am J Physiol Renal Physiol 2000;278:F192–201.
[278] Doucet A, Katz A, Morel F. Determination of Na-K-ATPase activity in single segments of the mammalian nephron 4474. Am J Physiol 1979;237:F105–13.
[279] Katz A, Doucet A, Morel F. Na-K-ATPase activity along the rabbit, rat and mouse nephron. Am J Physiol 1979;237: F114–20.
[280] Kaissling B, Le Hir M. Distal tubular segments in the rabbit kidney after adaptation to altered Na- and K-intake. I. Structural changes. Cell Tissue Res 1982;224:469–92.
[281] Le Hir M, Kaissling B, Dubach U. Distal tubular segments of the rabbit kidney after adaption to altered Na- and K-intake. II. Changes in Na-K-ATPase activity. Cell Tissue Res 1982; 224:493–504.
[282] Welling D, Urani J, Welling L, Wagner E. Fractal analysis and imaging of the proximal nephron cell. Am J Physiol 1996;270: C953–63.
[283] Kashgarian M, Biemesderfer D, Caplan M, Forbush B. Monocloal antibody to Na,K-ATPase: immunocytochemical localization along nephron segments. Kidney Int 1985; 28:899–913.
[284] Koob R, Zimmermann M, Schoner W, Drenckhahn D. Colocalization and coprecipitation of ankyrin and Na^+,K^+-ATPase in kidney epithelial cells. Eur J Cell Biol 1988; 45:230–7.
[285] Rostgaard J, Kristensen B, Nielsen L. Electron microscopy of filaments in the basal part of rat kidney tubule cells, and their *in situ* interaction with heavy meromyosin. Z Zellforsch Mikrosk Anat 1972;132:497–521.
[286] Rostgaard J, Thuneberg L. Electron microscopic evidence suggesting a contractile system in the base of tubular cells of rat kidney. J Ultrastruct Res 1969;29:570–7.
[287] Trenchev P, Dorling J, Webb J, Holborrow E. Localization of smooth muscle-like contractile proteins in kidney by immunoelectron microscopy. J Anat 1976;121:85–95.
[288] Guder W, Wagner S, Wirthensohn G. Metabolic fuels along the nephron: pathways and intracellular mechanisms of interaction. Kidney Int 1986;29:41–5.
[289] Kaissling B. Structural aspects of adaptive changes in renal electrolyte excretion. Am J Physiol 1982;243:F211–26.
[290] Kaissling B, Stanton B. Adaptation of distal tubule and collecting duct to increased sodium delivery. I. Ultrastructure. Am J Physiol 1988;255:F1256–68.
[291] Madsen K, Verlander J, Tisher C. Relationship between structure and function in distal tubule and collecting duct. J Electron Microsc Tech 1988;9:187–208.
[292] Stanton B, Kaissling B. Adaptation of distal tubule and and collecting duct to increased Na delivery. II. Na^+ and K^+ transport. Am J Physiol 1988;255:F1269–75.
[293] Stanton B, Kaissling B. Regulation of renal ion transport and cell growth by sodium. Am J Physiol 1989;257:F1–10.
[294] Wade J, O'Neil R, Pryor J, Boulpaep E. Modulation of cell membrane area in renal collecting tubules by corticosteroid hormones. J Cell Biol 1979;81:439–45.
[295] Holtzclaw J, Cornelius R, Hatcher L, Sansom S. Coupled ATP and potassium efflux from intercalated cells. Am J Physiol Renal Physiol 2011;300:F1319–26.
[296] Praetorius H, Leipziger J. Intrarenal purinergic signaling in the control of renal tubular transport. Annu Rev Physiol 2010; 72:377–93.
[297] Biemesderfer D, DeGray D. Active (9.6 s) and inactive (21 s) oligomers of NHE3 in microdomains of the renal brush border 4478. J Biol Chem 2001;276:10161–7.
[298] McDonough A, Biemesderfer D. Does membrane trafficking play a role in regulating the sodium/hydrogen exchanger isoform 3 in the proximal tubule? Curr Opin Nephrol Hypertens 2003;12:533–41.
[299] Brown D. The ins and outs of aquaporin-2 trafficking. Am J Physiol Renal Physiol 2003;284:F893–901.
[300] Butterworth M. Regulation of the epithelial sodium channel (ENaC) by membrane trafficking. Biochim Biopyhs Acta 2010;1802:1166–77.
[301] Bacic D, Le Hir M, Biber J, Kaissling B, Murer H, Wagner C. The renal Na^+/phosphate co-transporter NaPi-IIa is internalized via the receptor-mediated endocytic route in response to parathyroid hormone. Kidney Int 2006;69:495–503.
[302] Thomas C, Itani O. New insights into epithelial sodium channel function in the kidney: site of action, regulation by ubiquitin ligases, serum- and glucocorticoid-inducible kinase and proteolysis 4482. Curr Opin Nephrol Hypertens 2004; 13:541–8.
[303] Ecelbarger C, Knepper M. Increased abundance of distal sodium transporters in rat kidney during vasopressin escape. J Am Soc Nephrol 2001;12:207–17.
[304] Kaissling B, Bachmann S, Kriz W. Structural adaptation of the distal convoluted tubule to prolonged furosemide treatment. Am J Physiol Renal Fluid Electrolyte Physiol 1985;248:F374–81.
[305] Loffing J, Le Hir M, Kaissling B. Modulation of salt transport rate affects DNA sythesis *in vivo* in rat renal tubules. Kidney Int 1995;47:1615–23.
[306] Kaissling B, Loffing J. Cell growth and cell death in renal distal tubules, associated with diuretic treatment. Nephrol Dial Transplant 1998;13:1341–3.
[307] Loffing J, Loffing-Cueni D, Hegyi I, Kaplan M, Hebert S, Le Hir M, et al. Thiazide treatment of rats provokes apoptosis in distal tubule cells. Kidney Int 1996;50:1180–90.
[308] Bankir L, Bouby N, Trinh-Trang-Tan M, Kaissling B. The thick ascending limb of Henle's loop. Anatomical and functional

characteristics and role in the urine concentration mechanism. In: Crosnier J, Funck-Brentano J, Bach J, Grünfeld J, editors. Actualités nephrologiques de l'Hopital Necker. Paris: Flammarion Medicine-Sciences; 1987.

[309] Calvert J. New insights into ciliary function: kidney cysts and photoreceptors 4484. Proc Natl Acad Sci USA 2003;100: 5583–5.

[310] Liu W, Xu S, Woda C, Kim P, Weinbaum S, Satlin L. Effect of flow and stretch on the $[Ca^{2+}]$i response of principal and intercalated cells in cortical collecting duct. Am J Physiol Renal Physiol 2003;285:F998–1012.

[311] Luo Y, Vassilev P, Li X, Kawanabe Y, Zhou J. Native polycystin 2 functions as a plasma membrane Ca^{2+}-permeable cation channel in renal epithelia. Mol Biol Cell 2003;23:2600–7.

[312] Weinbaum S, Duan Y, Satlin L, Wang T, Weinstein A. Mechanotransduction in the renal tubule 4491. Am J Physiol Renal Physiol 2010;299:F1220–36.

[313] Yoder B, Hou X, Guay-Woodford L. The polycystic kidney disease proteins, polycystin-1, polycystin-2, polaris, and cystin, are co-localized in renal cilia. J Am Soc Nephrol 2002;13: 2508–16.

[314] Li Q, Montalbetti N, Shen P, Dai X, Cheeseman C, Karpinski E, et al. Alpha-actinin associates with polycystin-2 and regulates its channel activity. Hum Mol Genet 2005;14:1587–603.

[315] Zhang Q, Taulman P, Yoder B. Cystic kidney diseases: all roads lead to the cilium 4489. Physiology 2004;19:225–30.

[316] Davenport J, Yoder B. An incredible decade for the primary cilium: a look at a once-forgotten organelle 4486. Am J Physiol Renal Physiol 2005;289:F1159–69.

[317] Leipziger J. Luminal nucleotides are tonic inhibitors of renal tubular transport. Curr Opin Nephrol Hypertens 2011; 20:518–22.

[318] Hou X, Mrug M, Yoder B, Lefkowitz E, Kremmidiotis G, D'Eustachio P, et al. Cystin, a novel cilia-associated protein, is disrupted in the cpk mouse model of polycystic kidney disease. J Clin Invest 2002;109:533–40.

[319] Nauli S, Alenghat F, Luo Y, Williams E, Vassilev P, Li X, et al. Polycystins 1 and 2 mediate mechanosensation in the primary cilium of kidney cells 4494. Nat Genet 2003;33:129–37.

[320] Zhou J. Polycystins and primary cilia: primers for cell cycle progression. Annu Rev Physiol 2009;71:83–113.

[321] Bell P, Fitzgibbon W, Sas K, Stenbit A, Amria M, Houston A, et al. Loss of primary cilia upregulates renal hypertrophic signaling and promotes cystogenesis 4496. J Am Soc Nephrol 2011; 22:839–48.

[322] Igarashi P, Somlo S. Genetics and pathogenesis of polycystic kidney disease. J Am Soc Nephrol 2002;13:2384–98.

[323] Nishio S, Hatano M, Nagata M, Horie S, Koike T, Tokuhisa T, et al. Pkd1 regulates immortalized proliferation of renal tubular epithelial cells through p53 induction and JNK activation. J Clin Invest 2005;115:910–8.

[324] Orlando R, Takeda T, Zak B, Schmieder S, Benoit V, McQuistan T, et al. The glomerular epithelial cell anti-adhesion podocalyxin associates with the actin cytoskeleton through interactions with ezrin. J Am Soc Nephrol 2001;12:1589–98.

[325] Wright S, Dantzler W. Molecular and cellular physiology of renal organic cation and anion transport. Physiol Rev 2004;84:987–1049.

[326] Grandchamp A, Boulpaep E. Pressure control of sodium reabsorption and intercellular backflux across proximal kidney tubule. J Clin Invest 1974;54:69.

[327] Lutz M, Cardinal J, Burg B. Electrical resistance of renal proximal tubule perfused *in vitro*. Am J Physiol 1973;225:729.

[328] Lock E, Reed C. Xenobiotic metabolizing enzymes of the kidney. Toxicol Pathol 1998;26:18–25.

[329] Bergeron M, Gaffiero P, Thiery G. Segmental variations in the organization of the endoplasmic reticulum of the rat nephron. A stereomicroscopic study. Cell Tissue Res 1987;247: 215–25.

[330] Zaar K. Structure and function of peroxisomes in the mammalian kidney. Eur J Cell Biol 1992;59:233–54.

[331] Daigeler R. Sex-dependent changes in the rat kidney after hypophysectomy. Cell Tissue Res 1981;216:423–43.

[332] Schiebler T, Danner K. The effect of sex hormones on the proximal tubules in the rat kidney. Cell Tissue Res 1978; 192:527–49.

[333] Zabel M, Schiebler T. Histochemical, autoradiographic and electron microscopic investigations of the renal proximal tubule of male and female rats after castration. Histochemie 1980;69:255–76.

[334] Maunsbach A. The influence of different fixatives and fixation methods on the ultrastructure of rat kidney proximal tubule cells: I. Comparison of different perfusion fixation methods and of glutaraldehyde, formaldehyde and osmium tetroxide fixatives. J Ultrastruct Res 1966;15:242–82.

[335] Maunsbach A. The influence of different fixatives and fixation methods on the ultrastructure of rat kidney proximal tubule cells: II. Effects of varying osmolality, ionic strength, buffer system and fixative concentration of glutaraldehyde solutions. J Ultrastruct Res 1966;15:283.

[336] Dorup J, Maunsbach A. Three-dimensional organization and segmental ultrastructure of rat proximal tubules. Exp Nephrol 1997;5:305–17.

[337] Birn H, Willnow T, Nielsen R, Norden A, Bönsch C, Moestrup S, et al. Megalin is essential for renal proximal tubule reabsorption and accumulation of transcobalamin-B(12). Am J Physiol Renal Physiol 2002;282:F408–16.

[338] Christensen E, Gburek J. Protein reabsorption in renal proximal tubule – function and dysfunction in kidney pathophysiology. Pediatr Nephrol 2004;19:714–21.

[339] Hall A, Crawford C, Unwin R, Duchen M, Peppipiatt-Wildman C. Multiphoton imaging of the functioning kidney. J Am Soc Nephrol 2011;22:1297–304.

[340] Molitoris B, Sandoval R. Intravital multiphoton mircroscopy of dynamic renal processes. Am J Physiol Renal Physiol 2005;288: F1084–9.

[341] He Q, Madsen M. Amnionless function is required for cubilin brush-border expression and intrinsic factor-cobalamin (vitamin B12) absorption *in vivo*. Blood 2005;106:1447–53.

[342] Moestrup S, Nielsen L. The role of the kidney in lipid metabolism. Curr Opin Lipidol 2005;16:301–6.

[343] Nagai J, Christensen E. Mutually dependent localization of megalin and Dab2 in the renal proximal tubule. Am J Physiol Renal Physiol 2005;289:F569–76.

[344] Takeda T, Yamazaki H, Farquhar M. Identification of an apical sorting determinant in the cytoplasmic tail of megalin. Am J Physiol Cell Physiol 2003;284:C1105–13.

[345] Verroust P, Birn H, Nielsen R, Kozyraki R, Christensen E. The tandem endocytic receptors megalin and cubilin are important proteins in renal pathology. Kidney Int 2002;62:745–56.

[346] Verroust P, Christensen E. Megalin and cubilin – the story of two multipurpose receptors unfolds. Nephrol Dial Transplant 2002;17:1867–71.

[347] Christensen E, Nielsen S, Moestrup S, Borre C, Maunsbach A, de Heer E, et al. Segmental distribution of the endocytosis receptor gp330 in renal proximal tubules. Eur J Cell Biol 1995;66:349–64.

[348] Hatae T, Ichimura T, Ishida T, Sakurai T. Apical tubular network in the rat kidney proximal tubule cells studied by thick-section and scanning electron microscopy. Cell Tissue Res 1997;288:317–25.

[349] Maunsbach A. Observations on the segmentation of the proximal tubule in the rat kidney. J Ultrastruct Res 1966; 16:239–58.
[350] Maunsbach A. Functional ultrastructure of the proximal tubule. In: Windhager E, editor. Handbook of physiology: section on renal physiology. New York, N.Y.: Oxford University Press; 1992. p. 41–108.
[351] Cui S, Mata L, Maunsbach A, Christensen E. Ultrastructure of the vacuolar apparatus in the renal proximal tubule microinfused *in vivo* with the cytological stain light green. Exp Nephrol 1998;6:359–67.
[352] Cui S, Christensen E. Three-dimensional organization of the vacuolar apparatus involved in endocytosis and membrane recycling of rat kidney proximal tubule cells. An electronmicroscopic study of serial sections. Exp Nephrol 1993;1: 175–84.
[353] Cui S, Verroust P, Moestrup S, Christensen E. Megalin/gp 330 mediates uptake of albumin in renal proximal tubule. Am J Physiol 1996;271:F900–7.
[354] Farquhar M, Saito A, Kerjaschki D, Orlando R. The Heymann nephritis antigenic complex: megalin (gp330) and RAP. J Am Soc Nephrol 1995;6:35–47.
[355] Lotscher M, Kaissling B, Biber J, Murer H, Levi M. Role of microtubules in the rapid regulation of renal phosphate transport in response to acute alterations in dietary phosphate content. J Clin Invest 1997;99:1302–12.
[356] Lotscher M, Scarpetta Y, Levi M, Halaihel N, Wang H, Zajicek H, et al. Rapid downregulation of rat renal Na/P(i) co-transporter in response to parathyroid hormone involves microtubule rearrangement. J Clin Invest 1999;104:483–94.
[357] Bachmann S, Schlichting U, Geist B, Mutig K, Petsch T, Bacic D, et al. Kidney-specific inactivation of the megalin gene impairs trafficking of renal inorganic sodium phosphate co-transporter (NaPi-IIa). J Am Soc Nephrol 2004; 15:892–900.
[358] Bacic D, Capuano P, Gisler S, Pribanic S, Christensen E, Biber J, et al. Impaired PTH-induced endocytotic down-regulation of the renal type IIa Na^+/Pi-co-transporter in RAP-deficient mice with reduced megalin expression. Pflugers Arch 2003; 446:475–84.
[359] Marshansky V, Ausiello D, Brown D. Physiological importance of endosomal acidification: potential role in proximal tubulopathies. Curr Opin Nephrol Hypertens 2002;11: 527–37.
[360] Gekle M, Völker K, Mildenberger S, Freudinger R, Shull G, Wiemann M. NHE3 $Na^+/H+$ exchanger supports proximal tubular protein reabsorption *in vivo*. Am J Physiol Renal Physiol 2004;287:F469–73.
[361] Honegger K, Capuano P, Winter C, Bacic D, Stange G, Wagner C, et al. Regulation of sodium-proton exchanger isoform 3 (NHE3) by PKA and exchange protein directly activated by cAMP (EPAC). Proc Natl Acad Sci USA 2006;103:803–8.
[362] Wang Y, Cai H, Cebotaru L, Hryciw D, Weinman E, Donowitz M, et al. ClC-5: role in endocytosis in the proximal tubule. Am J Physiol Renal Physiol 2005;289:F850–62.
[363] Devuyst O. Chloride channels and endocytosis: new insights from Dent's disease and CLC-5 knockout mice. Bull Mem Acad R Med Belg 2004;159:212–7.
[364] Jentsch T. Chloride transport in the kidney: lessons from human disease and knockout mice. J Am Soc Nephrol 2005;16:1549–61.
[365] Jentsch T, Hübner C, Fuhrmann J. Ion channels: function unravelled by dysfunction. Nat Cell Biol 2004;6:1039–47.
[366] Marshanky V, Ausiello D, Brown D. Physiological importance of endosomal acidification: potential role in proximal tubulopathies. Curr Opin Nephrol Hypertens 2002;11:527–37.
[367] Novarino G, Weinert S, Rickheit G, Jentsch T. Endosomal chloride-proton exchange rather than chloride conductance is crucial for renal endocytosis. Science 2010;328:1398–401.
[368] Rabkin R, Mahoney C. Hormones and the kidney. In: Schrier R, Gottschalk C, editors. Diseases of the kidney. Boston: Little Brown; 1988. p. 309.
[369] Nielsen S, Nielsen J, Christensen E. Luminal and basolateral uptake of insulin in isolated, perfused proximal tubules. Am J Physiol Renal Fluid Electrolyte Physiol 1987;253: F857–67.
[370] Amemiya M, Loffing J, Lötscher M, Kaissling B, Alpern R, Moe O. Expression of NHE-3 in the apical membrane of rat renal proximal tubule and thick ascending limb. Kidney Int 1995;48:1206–15.
[371] Aronson P. Ion exchangers mediating NaCl transport in the renal proximal tubule. Cell Biochem Biophys 2002; 36:147–53.
[372] Bobulescu I, Moe O. Luminal Na(+)/H (+) exchange in the proximal tubule. Pflugers Arch 2009;458:5–21.
[373] Pao A, Bhargava A, Di Sole F, Quigley R, Saho X, Wang J, et al. Expression and role of serum and glucocorticoid-regulated kinase 2 in the regulation of Na^+/H^+ exchanger 3 in the mammalian kidney. Am J Physiol Renal Physiol 2010;299: F1496–506.
[374] Besse-Eschmann V, Klisic J, Nief V, Le Hir M, Kaissling B, Ambühl P. Regulation of the proximal tubular sodium/proton exchanger NHE3 in rats with puromycin aminonucleoside (PAN)-induced nephrotic syndrome. J Am Soc Nephrol 2002;13:2199–206.
[375] Kobayashi K, Monkawa T, Hayashi M, Saruta T. Expression of the Na^+/H^+ exchanger regulatory protein family in genetically hypertensive rats. J Hypertens 2004;22:1723–30.
[376] McDonough A, Leong P, Yang L. Mechanisms of pressure natriuresis: how blood pressure regulates renal sodium transport. Ann NY Acad Sci 2003;986:669–77.
[377] Yang L, Maunsbach A, Leong P, McDonough A. Differential traffic of proximal tubule Na^+ transporters during hypertension or PTH: NHE3 to base of microvilli vs. NaPi2 to endosomes. Am J Physiol Renal Physiol 2004;287:F896–906.
[378] Biber J, Gisler S, Hernando N, Wagner C, Murer H. PDZ interactions and proximal tubular phosphate reabsorption. Am J Physiol Renal Physiol 2004;287:F871–5.
[379] Gisler S, Pribanic S, Bacic D, Forrer P, Gantenbein A, Sabourin L, et al. PDZK1: I. A major scaffolder in brush borders of proximal tubular cells. Kidney Int 2003;64:1733–45.
[380] Maunsbach A, Marples D, Chin E, Ning G, Bondy C, Agre P, et al. Aquaporin-1 water channel expression in human kidney. J Am Soc Nephrol 1997;8:1–14.
[381] Nielsen S. Renal aquaporins: an overview. BJU Int 2002;90:1–6.
[382] Nielsen S, Frokiaer J. Aquaporins in the kidney: from molecules to medicine. Physiol Rev 2002;82:205–44.
[383] Sabolic I, Valenti G, Verbavatz J, van Hoek A, Verkman A. Localization of the CHIP28 water channel in rat kidney. Am J Physiol 1992;263:C1225–33.
[384] Schnermann J, Chou C, Ma T, Traynor T, Knepper M, Verkman A. Defective proximal tubular fluid reabsorption in transgenic aquaporin-1 null mice. Proc Natl Acad Sci USA 1998;95:9660–4.
[385] van Hoek A, Ma T, Yang B, Verkman A, Brown D. Aquaporin-4 is expressed in basolateral membranes of proximal tubule S3 segments in mouse kidney. Am J Physiol Renal Physiol 2000;278:F310–6.
[386] Sohara E, Uchida S, Sasaki S. Function of aquaporin-7 in the kidney and the male reproductive system. Handb Exp Pharmacol 2009;190:219–31.

[387] Ishibashi K, Imai M, Sasaki S. Cellular localization of aquaporin 7 in the rat kidney. Exp Nephrol 2000;8:252–7.
[388] Nesjum L, Elkjaer M, Hager H, Frokiaer J, Kwon T, Nielsen S. Localization of aquaporin-7 in rat and mouse kidney using RT-PCR, immunoblotting, and immunocytochemistry. Biochem Biophys Res Commun 2000;277:164–70.
[389] Bakris G, Fonseca V, Sharma K, Wright E. Renal sodium-glucose transport: role in diabetes mellitus and potential clinical implications. Kidney Int 2009;75:1272–7.
[390] Hediger M, Rhoads D. Molecular physiology of sodium-glucose co-transporters. Physiol Rev 1994;74:993–1026.
[391] Sabolic I, Skarica M, Gorboulev V, Ljubojevic M, Balen D, Herak-Kramberger C, et al. Rat renal glucose transporter SGLT1 exhibits zonal distribution and androgen-dependent gender differences. Am J Physiol Renal Physiol 2006;290:F913–26.
[392] Rahmoune H, Thompson P, Ward J, Smith C, Hong G, Brown J. Glucose transporters in human renal proximal tubular cells isolated from the urine of patients with non-insulin-dependent diabetes. Diabetes 2005;54:3427–34.
[393] Forster I, Hernando N, Biber J, Murer H. Proximal tubular handling of phosphate: a molecular perspective. Kidney Int 2006;70:1548–59.
[394] Villa-Bellosta R, Ravera S, Sorribas V, Stange G, Levi M, Murer H, et al. The Na^+-Pi co-transporter PiT-2 (SLC20A2) is expressed in the apical membrane of rat renal proximal tubules and regulated by dietary Pi. Am J Physiol Renal Physiol 2009;296:F691–9.
[395] Ritthaler T, Traebert M, Lötscher M, Biber J, Murer H, Kaissling B. Effects of phosphate intake on distribution of type ll Na/P-co-transporter mRNA in rat kidney. Kidney Int 1998;:.
[396] Levi M, Lötscher M, Sorribas V, Custer M, Arar M, Kaissling B, et al. Cellular mechanisms of acute and chronic adaptation of rat renal Pi-transporter to alterations in dietary Pi. Am J Physiol 1994;267:F900–8.
[397] Lötscher M, Kaissling B, Biber J, Murer H, Levi M. Role of microtubules in the rapid regulation of renal phosphate transport in response to acute alterations in dietary phosphate content. J Clin Invest 1997;99:1302–12.
[398] Murer H, Forster I, Hernando N, Biber J. Proximal tubular handling of phosphate: Na/Pi-co-transporters and their regulation. In: Alpern R, Hebert S, editors. Seldin and Giebisch's the kidney. New York: Academic Press; 2008. p. 1979–88.
[399] Kempson S, Lötscher M, Kaissling B, Biber J, Murer H, Levi M. Parathyroid hormone action on phosphate transporter mRNA and protein in rat renal proximal tubules. Am J Physiol 1995;268:F784–91.
[400] Keusch I, Traebert M, Lotscher M, Kaissling B, Murer H, Biber J. Parathyroid hormone and dietary phosphate provoke a lysosomal routing of the proximal tubular Na/Pi cotransporter type II. Kidney Int 1998;54:1224–32.
[401] Traebert M, Roth J, Biber J, Murer H, Kaissling B. Internalization of proximal tubular type II Na-P(i) co-transporter by PTH: Immunogold electron microscopy. Am J Physiol Renal Physiol 2000;278:F148–54.
[402] Huang C, Moe O. Klotho: a novel regulator of calcium and phosphorus homeostasis. Pflugers Arch 2011;462:185–93.
[403] Verrey F, Singer D, Ramadan T, Vuille-dit-Bille R, Mariotta L, Camargo S. Kidney amino acid transport. Pflugers Arch 2009;458:53–60.
[404] Daniel H, Rubio-Aliaga I. An update on renal peptide transporters. Am J Physiol Renal Physiol 2003;284:F885–92.
[405] Shen H, Smith D, Yang T, Huang Y, Schnermann J. Brosius F3. Localization of PEPT1 and PEPT2 proton-coupled oligopeptide transporter mRNA and protein in rat kidney. Am J Physiol 1999;276:F658–65.
[406] Koepsell H. Polyspecific organic cation transporters: their functions and interactions with drugs. Trends Pharmacol Sci 2004;25:375–81.
[407] Lee W, Kim R. Transporters and renal drug elimination. Annu Rev Pharmacol Toxicol 2004;44:137–66.
[408] Rafey M, Lipkowitz M, Leal-Pinto E, Abramson R. Uric acid transport. Curr Opin Nephrol Hypertens 2003;12:511–6.
[409] Wright S. Role of organic cation transporters in the renal handling of therapeutic agents and xenobiotics. Toxicol Appl Pharmacol 2005;204:309–19.
[410] You G. Structure, function, and regulation of renal organic anion transporters. Med Res Rev 2011;22:602–16.
[411] Karbach U, Kricke J, Meyer-Wentrup F, Gorboulev V, Volk C, Loffing-Cueni D, et al. Localization of organic cation transporters OCT1 and OCT2 in rat kidney. Am J Physiol Renal Physiol 2000;279:F679–87.
[412] Urakami Y, Okuda M, Masuda S, Akazawa M, Saito H, Inui K. Distinct characteristics of organic cation transporters, OCT1 and OCT2, in the basolateral membrane of renal tubules. Pharm Res 2001;18:1528–34.
[413] Urakami Y, Okuda M, Masuda S, Saito H, Inui K. Functional characteristics and membrane localization of rat multispecific organic cation transporters, OCT1 and OCT2, mediating tubular secretion of cationic drugs. J Pharmacol Exp Ther 1998;287:800–5.
[414] Tojo A, Sekine T, Nakajima N, Hosoyamada M, Kanai Y, Kimura K, et al. Immunohistochemical localization of multispecific renal organic anion transporter 1 in rat kidney. J Am Soc Nephrol 1999;10:464–71.
[415] Burckhardt B, Burckhardt G. Transport of organic anions across the basolateral membrane of proximal tubule cells. Rev Physiol Biochem Pharmacol 2003;146:95–158.
[416] Kato Y, Kuge K, Kusuhara H, Meier P, Sugiyama Y. Gender difference in the urinary excretion of organic anions in rats. J Pharmacol Exp Ther 2002;302:483–9.
[417] Kato Y, Sai Y, Yoshida K, Watanabe C, Hirata T, Tsuji A. PDZK1 directly regulates the function of organic cation/carnitine transporter OCTN2. Mol Pharmacol 2005;67:734–43.
[418] Ljubojevic M, Herak-Kramberger C, Hagos S, Bahn A, Endou H, Burckhardt G, et al. Rat renal cortical OAT1 and OAT3 exhibit gender differences determined by both androgen stimulation and estrogen inhibition. Am J Physiol Renal Physiol 2004;287:F124–38.
[419] Urakami Y, Nakamura N, Takahashi K, Okuda M, Saito H, Hashimoto Y, et al. Gender differences in expression of organic cation transporter OCT2 in rat kidney. FEBS Lett 1999;461:339–42.
[420] Urakami Y, Okuda M, Saito H, Inui K. Hormonal regulation of organic cation transporter OCT2 expression in rat kidney. FEBS Lett 2000;473:173–6.
[421] Sekine T, Miyazaki H, Endou H. Molecular physiology of renal organic anion transporters. Am J Physiol Renal Physiol 2006;290:F251–61.
[422] Schaub T, Kartenbeck J, König J, Vogel O, Witzgall R, Kriz W, et al. Expression of the conjugate export pump encoded by the mrp2 gene in the apical membrane of kidney proximal tubules. J Am Soc Nephrol 1997;8:1213–21.
[423] Kriz W, Schnermann J, Dieterich H. Differences in the morphology of descending limbs of short and long loops of Henle in the rat kidney. In: Wirz H, Spinelli F, editors. Recent advances in renal physiology. Basel: Karger; 1972. p. 140–4.
[424] Schwartz M, Venkatachalam M. Structural differences in thin limbs of Henle: physiological implications. Kidney Int 1974;6:193–208.

[425] Dieterich H, Barrett J, Kriz W, Bülhoff J. The ultrastructure of the thin loop limbs of the mouse kidney. Anat Embryol 1975;147:1–18.
[426] Bachmann S, Kriz W. Histotopography an ultrastructure of the thin limbs of the loop of Henle in the hamster. Cell Tissue Res 1982;225:111–27.
[427] Schiller A, Forssmann W, Taugner R. The tight junctions of the renal tubules in the cortex and outer medulla. A quantitative study of the kidney of six species. Cell Tissue Res 1980; 212:395–413.
[428] Nagle R, Altschuler E, Dobyan D, Dong S, Bulger R. The ultrastructure of the thin limbs of Henle in kidneys of the desert heteromyid (*Perognathus penicillatus*). Am J Anat 1981; 161:33–47.
[429] Barajas L. The ultrastructure of the juxtaglomerular apparatus as disclosed by three-dimensional reconstruction from serial sections: the anatomical relationship between the tubular and vascular components. J Ultrastruct Res 1970;33: 116–47.
[430] Barrett J, Kriz W, Kaissling B, de Rouffignac C. The ultrastructure of the nephrons of the desert rodent (*Psammomys obesus*) kidney. I. Thin limbs of Henle of short looped nephrons. Am J Anat 1978;151:487–98.
[431] Barrett J, Kriz W, Kaissling B, de Rouffignac C. The ultrastructure of the nephrons of the desert rodent (*Psammomys obesus*) kidney. II. Thin limbs of Henle of long-looped nephrons. Am J Anat 1978;151:499–514.
[432] Kriz W, Schiller A, Taugner R. Freeze-fracture studies on the thin limbs of Henle's loop in *Psammomys obesus*. Am J Anat 1981;162:23–34.
[433] Chou C, Nielsen S, Knepper M. Structural–functional correlation in chinchilla long loop of Henle thin limbs: a novel papillary subsegment. Am J Physiol 1993;265:F863–74.
[434] Dobyan D, Jamison R. Structure and function of the renal papilla. Semin Nephrol 1984;4:5.
[435] Kriz W. Structural organization of the renal medullary counterflow system. Fed Proc 1983;42:2379–85.
[436] Kriz W, Kaissling B. Structural organization of the mammalian kidney. In: Seldin D, Giebisch G, editors. The kidney. Philadelphia: Lippincott Williams and Wilkens; 2000. p. 587–654.
[437] Pannabecker T, Abbott D, Dantzler W. Three-dimensional functional reconstruction of inner medullary thin limbs of Henle's loop. Am J Physiol Renal Physiol 2004;286: F38–45.
[438] Pannabecker T, Dahmann A, Brokl O, Dantzler W. Mixed descending- and ascending-type thin limbs of Henle's loop in mammalian renal inner medulla. Am J Physiol Renal Physiol 2000;278:F202–8.
[439] Bachmann S, Kriz W, Kuhn C, Franke W. Differentiation of cell types of the mammalian kidney by immunofluorescence microscopy using antibodies to intermediate filament proteins and desmoplakins. Histochemistry 1983;77:365–94.
[440] Zhai X, Fenton R, Andreasen A, Thomsen J, Christensen E. Aquaporin-1 is not expressed in descending thin limbs of short-loop nephrons. J Am Soc Nephrol 2007;18:2937–44.
[441] Bankir L, Trinh-Trang-Tan M. Renal urea transporters. Direct and indirect regulation by vasopressin. Exp Physiol 2000;85:243S–52S.
[442] Kim Y, Kim D, Han K, Jung J, Sands J, Knepper M, et al. Expression of urea transporters in the developing rat kidney. Am J Physiol Renal Physiol 2002;282:F530–40.
[443] Küttler T. Verlauf und histotopographische beziehungen oberflächlich gelegener nephrone der katzenniere. Heidelberg: Dissertation; 1980.
[444] Dobyan D, Bulger R. Morphology of the minipig kidney. J Electron Microsc Tech 1988;9:213–34.
[445] Schwartz M, Karnovsky M, Venkatachalam M. Ultrastructural differences between rat inner medullary descending and ascending vasa recta. Lab Invest 1976;35:161–70.
[446] Ernst S, Schreiber J. Ultrastructural localization of Na^+, K^+-ATPase in rat and rabbit kidney medulla. J Cell Biol 1981;91:803–13.
[447] Majack R, Paull W, Barrett J. The ultrastructural localization of membrane ATPase in rat thin limbs of the loop of Henle. Histochemie 1979;63:23–33.
[448] Van Itallie C, Anderson J. Claudins and epithelial paracellular transport. Annu Rev Physiol 2006;68:403–29.
[449] Nielsen S, Digiovanni S, Christensen E, Knepper M, Harris H. Cellular and subcellular immunolocalization of vasopressin-regulated water channel in rat kidney. Proc Natl Acad Sci USA 1993;90:11663–7.
[450] Dobyan D, Magill L, Friedman P, Herbert S, Bulger R. Carbonic anhydrase histochemistry in rabbit and mouse kidneys. Anat Rec 1982;204:185–97.
[451] Schiller A, Taugner R, Kriz W. The thin limbs of Henle's loop in the rabbit: a freeze-fracture study. Cell Tissue Res 1980; 207:249–65.
[452] Layton A, Pannabecker T, Dantzler W, Layton H. Two modes for concentrating urine in rat inner medulla. Am J Physiol Renal Physiol 2004;287:F816–39.
[453] Nielsen S, Pallone T, Smith B, Christensen E, Agre P, Maunsbach A. Aquaporin-1 water channels in short and long loop descending thin limbs and in descending vasa recta in rat kidney. Am J Physiol Renal Physiol 1995; 268:1023–37.
[454] Verbavatz J, Brown D, Sabolic I, Valenti G, Ausiello D, van Hoek A, et al. Tetrameric assembly of CHIP28 water channels in liposomes and cell membranes: a freeze-fracture study. J Cell Biol 1993;123:605–18.
[455] Hediger M, Knepper M. Introduction: recent insights into the urinary concentrating mechanism: from cDNA cloning to dodelin renal function. Am J Physiol 1998;275:F317.
[456] Shayakul C, Knepper M, Smith C, Digiovanni S, Hediger M. Segmental localization of urea transporter mRNAa in rat kidney. Am J Physiol 1997;272:F654–60.
[457] Trinh-Trang-Tan M, Bankir L. Integrated function of urea transporters in the mammalian kidney. Exp Nephrol 1998; 6:471–9.
[458] Wade J, Lee A, Liu C, Ecelbarger C, Mitchell C, Bradford A, et al. UT-A2: A 55-kDa urea transporter in thin descending limb whose abundance is regulated by vasopressin. Am J Physiol Renal Physiol 2000;278:F52–62.
[459] Bulger R, Tisher C, Myers C, Trump B. Human renal ultrastructure. II. The thin limb of Henle's loop and the interstitium in healthy individuals. Lab Invest 1967;16:124–41.
[460] Orci L, Brown D. Distribution of filipin-sterol complexes in plasma membranes of the kidney. II. The thin limbs of Henle's loop. Lab Invest 1983;48:80–9.
[461] Le Hir M, Dubach U. The cellular specificity of lectin binding in the kidney. I. A light microscopical study in the rat. Histochemie 1982;74:521–30.
[462] Le Hir M, Dubach U. The cellular specificity of lectin binding in the kidney. II. A light microscopical study in the rabbit. Histochemie 1982;74:531–40.
[463] Roth J, Taatjes D. Glycocalix heterogeneity of rat kidney urinary tubule: demonstration with lectin-gold technique specific for sialic acid. Eur J Cell Biol 1985;39:449–57.
[464] Imai M. Function of the thin ascending limb of Henle of rats and hamsters perfused *in vitro*. Am J Physiol 1977;232:F201–9.

[465] Jamison R. Micropuncture study of segments of thin loops of Henle in the rat. Am J Physiol 1968;215:236–42.
[466] Uchida S, Sasaki S, Nitta K, Uchida K, Horita S, Nihei H, et al. Localization and functional characterization of rat kidney-specific chloride channel, CIC-K1. J Clin Invest 1995;95: 104–13.
[467] Bulger R. The shape of rat kidney tubular cells. Am J Anat 1965;116:237–56.
[468] Hebert S, Culpepper R, Andreoli T. NaCl transport in mouse medullary thick ascending limbs. I. Functional nephron heterogeneity and ADH-stimulated NaCl co-transport. Am J Physiol 1981;241:F412–31.
[469] Allen F, Tisher C. Morphology of the ascending thick limb of Henle. Kidney Int 1976;9:8–22.
[470] Welling L, Welling D, Hill J. Shape of cells and intercellular channals in rabbit thick ascending limb of Henle. Kidney Int 1978;13:144–51.
[471] Kone B, Madsen K, Tisher C. Ultrastructure of the thick ascending limb of Henle in the rat kidney. Am J Anat 1984;171:217–26.
[472] Bulger R, Dobyan D. Recent structure–function relationships in normal and injured mammalian kidneys. Anat Rec 1983; 205:1–11.
[473] Jung J, Song J, Li C, Yang C, Kang T, Won M, et al. Expression of epidermal growth factor in the developing rat kidney. Am J Physiol Renal Physiol 2005;288:F227–35.
[474] Ecelbarger C, Terris J, Hoyer J, Nielsen S, Wade J, Knepper M. Localization and regulation of the rat renal Na^+-K^+-$2Cl^-$ co-transporter,BSC-1. Am J Physiol 1996;271:F619–28.
[475] Nielsen S, Maunsbach A, Ecelbarger C, Knepper M. Ultrastructural localization of Na-K-2Cl co-transporter in thick ascending limb and macula densa of rat kidney. Am J Physiol Renal Physiol 1998;275:F885–93.
[476] Obermüller N, Kunchaparty S, Ellison D, Bachmann S. Expression of the Na-K-2Cl co-transporter by macula densa and thick ascending limb cells of rat and rabbit nephron. J Clin Invest 1996;98:635–40.
[477] Greger R, Schlatter E, Lang F. Evidence for electroneutral sodium chloride co-transport in the cortical thick ascending limb of Henle's loop of rabbit kidney. Pflugers Arch 1983;396:308–14.
[478] Giebisch G. Renal potassium channels: function, regulation, and structure. Kidney Int 2001;60:436–45.
[479] Hebert S. Bartter syndrome. Curr Opin Nephrol Hypertens 2003;12:527–32.
[480] Lin D, Sterling H, Wang W. The protein tyrosine kinase-dependent pathway mediates the effect of K intake on renal K secretion. Physiology 2005;20:140–6.
[481] Wade J, Fang L, Coleman R, Liu J, Grimm P, Wang T, et al. Differential regulation of ROMK (Kir1.1) in distal nephron segments by dietary potassium. Am J Physiol Renal Physiol 2011;300:F1385–93.
[482] Wang W. Renal potassium channels: recent developments. Curr Opin Nephrol Hypertens 2004;13:549–55.
[483] Wang W. Regulation of ROMK (Kir1.1) channels: new mechanisms and aspects. Am J Physiol Renal Physiol 2006;290: F14–9.
[484] Krämer B, Bergler T, Stoelcker B, Waldegger S. Mechanisms of disease: the kidney-specific chloride channels CICKA and CICKB, the Barttin subunit and their clinical relevance. Nat Clin Pract Nephrol 2008;4:38–46.
[485] Burckhardt G, Di Sole F, Helmle-Kolb C. The Na^+/H^+ exchanger gene family. J Nephrol 2002;(Suppl. 5):S3–21.
[486] Burckhardt G, Wolff N, Bahn A. Molecular characterization of the renal organic anion transporter 1. Cell Biochem Biophys 2002;36:169–74.
[487] Capasso G, Rizzo M, Pica A, Di Maio F, Moe O, Alpern R, et al. Bicarbonate reabsorption and NHE-3 expression: abundance and activity are increased in Henle's loop of remnant rats. Kidney Int 2002;62:2126–35.
[488] Capasso G, Unwin R. Bicarbonate transport along the loop of Henle: molecular mechanisms and regulation. J Nephrol 2002; (Suppl. 5):S88–96.
[489] Biemesderfer D, Rutherford P, Nagy T, Pizzonnia J, Abu-Alfa A, Aronson P. Monoclonal antibodies for high-resolution localization of NHE-3 in adult and neonatal rat kidney. Am J Physiol 1997;273:F289–99.
[490] Sun A, Liu Y, Dworkin L, Tse C, Donowitz M, Yip K. Na^+/H^+ exchanger isoform 2 (NHE2) is expressed in the apical membrane of the medullary thick ascending limb. J Membr Biol 1997;160:85–90.
[491] Wright F, Giebisch G. Regulation of potassium excretion. In: Seldin D, Giebisch G, editors. The kidney: physiology and pathophysiology. New York: Raven Press; 1985. p. 1223–49.
[492] Wagner C, Finberg K, Breton S, Marshanky V, Brown D, Geibel J. Renal vacuolar H^+-ATPase. Physiol Rev 2004; 84:1263–314.
[493] Pushkin A, Kurtz I. SLC4 base (HCO_3^- , CO_3^{2-}) transporters: classification, function, structure, genetic diseases, and knockout models. Am J Physiol Renal Physiol 2006;290: F580–99.
[494] Quentin F, Eladari D, Cheval L, Lopez C, Goossens D, Colin Y, et al. RhBG and RhCG, the putative ammonia transporters, are expressed in the same cells in the distal nephron. J Am Soc Nephrol 2003;14:545–54.
[495] Ambühl P, Amemiya M, Danzkay M, Lötscher M, Kaissling B, Moe O, et al. Chronic metabolic acidosis inicreases NHE-3 protein abundance in rat kidney. Am J Physiol 1996;271:F917–25.
[496] Loffing J, Lötscher M, Kaissling B, Biber J, Murer H, Seikaly M, et al. Renal Na/H exchanger NHE-3 and Na-PO_4 co-transporter NaPi-2 protein expression in glucocorticoid excess and deficient states. J Am Soc Nephrol 1998;9:1560–7.
[497] Konrad M, Schlingmann K, Gudermann T. Insights into the molecular nature of magnesium homeostasis. Am J Physiol Renal Physiol 2004;286:F599–605.
[498] Konrad M, Weber S. Recent advances in molecular genetics of hereditary magnesium-losing disorders. J Am Soc Nephrol 2003;14:249–60.
[499] Ellison D. Divalent cation transport by the distal nephron: insights from Bartter's and Gitelman's syndromes. Am J Physiol Renal Physiol 2000;279:F616–25.
[500] Gunzel D, Yu A. Function and regulation of claudins in the thick ascending limb of Henle. Pflugers Arch 2009;458:77–88.
[501] Hou J, Renigunta A, Gomes A, Hou M, Paul D, Waldegger S, et al. Claudin-16 and claudin-19 interaction is required for their assembly into tight junctions and for renal reabsorption of magnesium. Proc Natl Acad Sci USA 2009;106:15350–5.
[502] Knohl S, Scheinman S. Inherited hypercalciuric syndromes: dent's disease (CLC-5) and familial hypomagnesemia with hypercalciuria (paracellin-1). Semin Nephrol 2004;24: 55–60.
[503] Konrad M, Schaller A, Seelow D, Pandey A, Waldegger S, Lesslauer A, et al. Mutations in the tight-junction gene claudin 19 (CLDN19) are associated with renal magnesium wasting, renal failure, and severe ocular involvement. Am J Hum Genet 2006;79:949–57.
[504] Quamme G, de Rouffignac C. Epithelial magnesium transport and regulation by the kidney. Front Biosci 2000;5:D694–711.
[505] Unwin R, Capasso G, Shirley D. An overview of divalent cation and citrate handling by the kidney. Nephron Physiol 2004;98:15–20.

[506] Wagner C. Metabolic acidosis: new insights from mouse models. Curr Opin Nephrol Hypertens 2007;16:471–6.
[507] Chabardes D, Gagnan-Brunette M, Imbert-Teboul M, Gontcharevskaia O, Montegut M, Clique A, et al. Adenylate cyclase responsiveness to hormones in various portions of the human nephron. J Clin Invest 1980;65:439–48.
[508] de Rouffignac C, Di Stefano A, Wittner M, Roinel N, Elalouf J. Consequences of differential effects of ADH and other peptide hormones on thick ascending limb of mammalian kidney. Am J Physiol 1991;260:R1023–35.
[509] Hebert S, Andreoli T. Control of Nal transport in the thick ascending limb. Am J Physiol 1984;246:F745–56.
[510] Knepper M, Kim G, Fernandez-Llama P, Ecelbarger C. Regulation of thick ascending limb transport by vasopressin. J Am Soc Nephrol 1999;10:628–34.
[511] Molony D, Reeves W, Hebert S, Andreoli T. ADH increases apical Na^+, K^+, $2Cl^-$ entry in mouse medullary thick ascending limbs of Henle. Am J Physiol 1987;252:F177–87.
[512] Wittner M, Di Stefano A, Mandon B, Roinel N, de Rouffignac C. Stimulation of NaCl reabsorption by antidiuretic hormone in the cortical thick ascending limb of Henle's loop of the mouse. Pflugers Arch 1991;419:212–4.
[513] Meade P, Hoover R, Plata C, Vázquez N, bobadilla N, Gamba G, et al. cAMP-dependent activation of the renal-specific Na^+-K^+-$2Cl^-$ co-transporter is mediated by regulation of co-transporter trafficking. Am J Physiol Renal Physiol 2003;284: F1145–54.
[514] Kim G, Ecelbarger C, Mitchell C, Packer R, Wade J, Knepper M. Vasopressin increases Na-K-2Cl co-transporter expression in thick ascending limb of Henle's loop. Am J Physiol 1999;276: F96–103.
[515] Pham P, Devuyst O, Phamt P, Matsumoto N, Shih R, Jo O, et al. Hypertonicity increases CLC-5 expression in mouse medullary thick ascending limb cells. Am J Physiol Renal Physiol 2004;287:F747–52.
[516] Harris R, McKanna J, Akai Y, Jacobson H, Dubois R, Breyer M. Cyclooxygenase-2 is associated with the macula densa of rat kidney and increases with salt restriction. J Clin Invest 1994;94:2504–10.
[517] Jeck N, Schlingmann K, Reinalter S, Kömhoff M, Peters M, Waldegger S, et al. Salt handling in the distal nephron: lessons learned from inherited human disorders. Am J Physiol Regul Integr Comp Physiol 2005;288:R782–95.
[518] Vio C, Cespedes C, Gallardo P, Masferrer J. Renal identification of cyclooxygenase-2 in a subset of thick ascending limb cells. Hypertension 1997;30:687–92.
[519] Valtin H. Physiological effects of vasopressin on the kidney. In: Gash D, Boer G, editors. Vasopressin. New York: Plenum; 1987. p. 369–87.
[520] Trinh-Trang-Tan M, Bouby N, Kriz W, Bankir L. Functional adaptation of the thick ascending limb and internephron heterogeneity to urine concentration. Kidney Int 1987;31:549–55.
[521] Bankir L, Fischer C, Fischer S, Jukkala K, Specht H, Kriz W. Adaptation of the rat kidney to altered water intake and urine concentration. Pflugers Arch 1988;412:42–53.
[522] Bouby N, Bankir L. Effect of high protein intake on sodium, potassium-dependent adenosine triphosphatase activity in the thick ascending limb of Henle's loop in the rat. Clin Sci 1988;74:319–29.
[523] Bouby N, Trinh-Trang-Tan M, Coutaud C, Bankir L. Vasopressin is involved in renal effects of high-protein diet: study in homozygous Brattleboro rats. Am J Physiol 1991;260: F96–100.
[524] Lu M, Wang T, Yan Q, Wang W, Giebisch G, Hebert S. ROMK is required for expression of the 70-pS K channel in the thick ascending limb. Am J Physiol Renal Physiol 2004;286:F490–5.
[525] Nomura N, Tajima M, Sugawara N, Morimoto T, Kondo Y, Ohno M, et al. Generation and analyses of R8L barttin knockin mouse. Am J Physiol Renal Physiol 2011;301:F297–307.
[526] Schnermann J. Sodium transport deficiency and sodium balance in gene-targeted mice. Acta Physiol Scand 2001; 173:59–66.
[527] Teulon J, Eladari D. A new mouse model for Bartter's syndrome. Am J Physiol Renal Physiol 2011;301:F295–6.
[528] Bachmann S, Koeppen-Hagemann I, Kriz W. Ultrastructural localization of Tamm-Horsfall glycoprotein (THP) in rat kidney as revealed by protein A-gold immunocytochemistry. Histochemistry 1985;83:531–8.
[529] Bachmann S, Metzger R, Bunnemann B. Tamm-Horsfall protein-mRNA synthesis is localized to the thick ascending limb of Henle's loop in rat kidney. Histochemistry 1990;94:517–23.
[530] Rampoldi L, Scolari F, Amoroso A, Ghiggeri G, Devuyst O. The rediscovery of uromodulin (Tamm-Horsfall protein): from tubulointerstitial nephropathy to chronic kidney disease. Kidney Int 2011;80:338–47.
[531] Serafini-Cessi F, Malagolini N, Cavallone D. Tamm-Horsfall glycoprotein: biology and clinical relevance. Am J Kidney Dis 2003;42:658–76.
[532] Bernascone J, Janas S, Ikehata M, Trudu M, Corbelli A, Schaeffer C, et al. A transgenic mouse model for uromodulin-associated kidney diseases shows specific tubulo-interstitial damage, urinary concentrating defect and renal failure. Hum Mol Genet 2010;19:2898–3010.
[533] Mutig K, Kahl T, Godes M, Persson P, Bates J, Raffi H, et al. Activation of the bumetanide-sensitive Na^+,K^+,$2Cl^-$ co-transporter (NKCC2) is facilitated by Tamm-Horsfall protein in a chloride-sensitive manner. J Biol Chem 2011;286:30200–10.
[534] Morel F, Chabardes D, Imbert-Teboul M. Functional segmentation of the rabbit distal tubule by microdetermination of hormone-dependent adenylate cyclase activity. Kidney Int 1976; 9:264–77.
[535] Crayen M, Thoenes W. Architecture and cell structures in the distal nephron of the rat kidney. Cytobiol 1978;17:197–211.
[536] Schmitt R, Ellison D, Farman N, Rossier B, Reilly R, Reeves W, et al. Developmental expression of sodium entry pathways in rat nephron. Am J Physiol 1999;276:F367–81.
[537] Campean V, Kricke J, Ellison D, Luft F, Bachmann S. Localization of thiazide-sensitive Na(+)-Cl(−) co-transport and associated gene products in mouse DCT. Am J Physiol Renal Physiol 2001;281:F1028–35.
[538] Loffing J, Loffing-Cueni D, Valderrabano V, Klausli L, Hebert S, Rossier B, et al. Distribution of transcellular calcium and sodium transport pathways along mouse distal nephron. Am J Physiol Renal Physiol 2001;281:F1019–20.
[539] Biner H, Arpin-Bott M, Loffing J, Wang X, Kneper M, Hebert S, et al. Human cortical distal nephron: distribution of electrolyte and water transport pathways. J Am Soc Nephrol 2002; 13:836–47.
[540] Myers C, Bulger R, Tisher C, Trump B. Human renal ultrastructure. IV. Collecting duct of healthy individuals. Lab Invest 1966;15:1921–50.
[541] Tisher C, Bulger R, Trump B. Human renal ultrastructure. III. The distal tubule in healthy individuals. Lab Invest 1968; 18:655–68.
[542] Kriz W, Bankir L. A standard nomenclature for structure of the kidney. The Renal Commission of the International Union of Physiological Sciences (IUPS). Kidney Int 1988;33:1–7.

[543] Dorup J. Ultrastructure of distal nephron cells in rat renal cortex. J Ultrastruct Res 1985;92:101–18.
[544] Loffing J, Kaissling B. Sodium and calcium transport pathways along the mammalian distal nephron from rabbit to human. Am J Physiol Renal Physiol 2003;284:F628–43.
[545] Loffing J, Vallon V, Loffing-Cueni D, Aregger F, Richter K, Pietri L, et al. Altered renal distal tubule structure and renal $Na(^{+})$ and $Ca(^{2+})$ handling in a mouse model for Gitelman's syndrome. J Am Soc Nephrol 2004;15:2276–88.
[546] Clapp W, Madsen K, Verlander J, Tisher C. Intercalated cells of the rat inner medullary collecting duct. Kidney Int 1987;31:1080–7.
[547] Reilly R, Ellison D. Mammalian distal tubule: physiology, pathophysiology, and molecular anatomy. Physiol Rev 2000;80:277–313.
[548] Voets T, Nilius B, Hoefs S, van der Kemp A, Droogmans G, Bindels R, et al. TRPM6 forms the Mg^{2+} influx channel involved in interstitial and renal Mg^{2+} absorption. J Biol Chem 2004;279:19–25.
[549] Nijenhuis T, Hoenderop J, Loffing J, van der Kemp A, van Os C, Bindels R. Thiazide-induced hypocalciuria is accompanied by a decreased expression of Ca^{2+} transport proteins in kidney. Kidney Int 2003;64:555–64.
[550] Kaissling B, Peter S, Kriz W. The transition of the thick ascending limb of Henle's loop into the distal convoluted tubule in the nephron of the rat kidney. Cell Tissue Res 1977;182:111–8.
[551] Loffing J, Loffing-Cueni D, Macher A, Hebert S, Olson B, Knepper M, et al. Localization of epithelial sodium channel and aquaporin-2 in rabbit cortex. Am J Physiol Renal Physiol 2000;272:530.
[552] Madsen K, Clapp W, Verlander J. Structure and function of the inner medullary-collecting duct. Kidney Int 1988;34:441–54.
[553] Stoessel A, Himmerkus N, Bleich M, Bachmann S, Theilig F. Connexin 37 is localized in renal epithelia and responds to changes in dietary salt intake. Am J Physiol Renal Physiol 2010;298:F216–23.
[554] Breton S, Lisanti M, Tyszkowski R, McLaughlin M, Brown D. Basolateral distribution of caveolin-1 in the kidney: absence from H^{+}-ATPase-coated endocytic vesicles in intercalated cells. J Histochem Cytochem 1998;46:205–14.
[555] Voldstedlund M, Thuneberg L, Tranum-Jensen J, Vinten J, Christensen E. Caveolae, caveolin and cav-p60 in smooth muscle and renin-producing cells in the rat kidney. Acta Physiol Scand 2003;179:179–88.
[556] Gamba G. The thiazide-sensitive Na^{+}-Cl-co-transporter: molecular biology, functional properties, and regulation by WNKs. Am J Physiol Renal Physiol 2009;297:F838–48.
[557] Estevez R, Boettger T, Stein V, Birkenhager R, Otto E, Hildebrandt F, et al. Barttin is a Cl^{-} channel beta-subunit crucial for renal Cl-reabsorption and inner ear K^{+} secretion. Nature 2001;414:558–61.
[558] Rieg T, Vallon V, Sausbier M, Kaissling B, Ruth P, Osswald H. The role of the BK channel in potassium homeostasis and flow-induced renal potassium excretion. Kidney Int 2007; 72:566–73.
[559] Rodan A, Cheng C, Huang C. Recent advances in distal tubular potassium handling. Am J Physiol Renal Physiol 2011;300: F821–7.
[560] Yang L, Sandberg M, Can A, Pihakaski-Maunsbach K, McDonough A. Effects of dietary salt on renal Na^{+} transporter subcellular distribution, abundance, and phosphorylation status. Am J Physiol Renal Physiol 2008;295: F1003–16.
[561] Vallon V, Schroth J, Lang F, Kuhl D, Uchida S. Expression and phosphorylation of the Na^{+}-Cl^{-} co-transporter NCC *in vivo* is regulated by dietary salt, potassium, and SGK1. Am J Physiol Renal Physiol 2009;297:F704–12.
[562] Arroyo P, Ronzaud C, Lagnaz D, Staub O, Gamba G. Aldosterone paradox: differential regulation of ion transport in distal nephron. Physiology 2011;26:115–23.
[563] Lee D, Riquier A, Yang L, Leong P, Maunsbach A, McDonough A. Acute hypertension provokes acute trafficking of distal tubule Na-Cl-co-transporter (NCC) to subapical cytoplasmic vesicles. Am J Physiol Renal Physiol 2009;296: F810–8.
[564] Sandberg M, Riquier A, Pihakaski-Maunsbach K, McDonough A, Maunsbach A. ANG II provokes acute trafficking of distal tubule Na^{+}-$Cl(^{-})$ co-transporter to apical membrane. Am J Physiol Renal Physiol 2007;293:F662–9.
[565] Verlander J, Tran T, Zhang L, Kaplan M, Hebert S. Estradiol enhances thiazide-sensitive NaCl co-transporter density in the apical plasma membrane of the distal convoluted tubule in ovariectomized rats. J Clin Invest 1998;101:1661–9.
[566] Ko B, Kamsteeg E, Cooke L, Moddes L, Deen P, Hoover R. RasGRP1 stimulation enhances ubiquitation and endocytosis. Am J Physiol Renal Physiol 2010;299:F300–9.
[567] Golbang A, Cope G, Hamad A, Murthy M, Liu C, Cuthbert A, et al. Regulation of the expression of the Na/Cl co-transporter by WNK4 and WNK1: evidence that accelerated dynamin-dependent endocytosis is not involved. Am J Physiol Renal Physiol 2006;291:F1369–76.
[568] Subramanya A, Ellison D. Sorting out lysosomal trafficking of the thiazide-sensitive Na-Cl co-transporter. J Am Soc Nephrol 2010;21:7–9.
[569] Gamba G. Role of WNK kinases in regulating tubular salt and potassium transport and in the development of hypertension. Am J Physiol Renal Physiol 2005;288:F245–52.
[570] Hadouchel J, Soukaseum C, Büsst C, Zhou X, Baudrie V, Zürrer T, et al. Decreased ENaC expression compensates the increased NCC activity following inactivation of the kidney specific isoform of WNK1 and prevents hypertension. Proc Natl Acad Sci USA 2010;107:18109–14.
[571] Yang B, Bankir L. Urea and urine concentrating ability: new insights from studies in mice. Am J Physiol Renal Physiol 2005;288:F881–96.
[572] Zhou B, Zhuang J, Gu D, Wang H, Cebotaru L, Guggino W, et al. WNK4 enhances the degradation of NCC through a sortilin-mediated lysosomal pathway. J Am Soc Nephrol 2010;21:82–92.
[573] Mutig K, Saritas T, Uchida S, Kahl T, Borowski T, Paliege A, et al. Short-term stimulation of the thiazide-sensitive Na^{+}-Cl^{-} co-transporter by vasopressin involves phosphorylation and membrane translocation. Am J Physiol Renal Physiol 2010;298: F502–9.
[574] Pedersen N, Hofmeister M, Rosenbaek L, Nielsen J, Fenton R. Vasopressin induces phosphorylation of the thiazide-sensitive chloride co-transporter in the distal convoluted tubule. Kidney Int 2010;78:160–9.
[575] Imbert-Teboul M, Chabardes D, Morel F. Vasopressin and catecholamine sites of action along rabbit, mouse and rat nephron. In: Bahlman J, Brod J, editors. Contributions to nephrology: disturbance of water and electrolyte metabolism. Basel: Karger; 1980. p. 41–7.
[576] Ellison D, Velazquez H, Wright F. Thiazide-sensitive sodium chloride co-transport in early distal tubule. Am J Physiol 1987; 253:F546–54.
[577] Koechlin N, Elalouf J, Kaissling B, Roinel N, de Rouffignac C. A structural study of the rat proximal and distal nephron:

effect of peptide and thyroid hormones. Am J Physiol 1989;256:F814–22.
[578] Stanton B. Renal potassium transport: morphological and functional adaptations. Am J Physiol 1989;257:R989–97.
[579] Cantone A, Yang X, Yan Q, Giebisch G, Hebert S, Wang T. Mouse model of type II Bartter's syndrome. I. Upregulation of thiazide-sensitive Na-Cl co-transporter activity. Am J Physiol Renal Physiol 2008;294:F1366–72.
[580] Wagner C, Loffing-Cueni D, Yan Q, Schulz N, Fakitsas P, Carrel M, et al. Mouse model of type II Bartter's syndrome. II. Altered expression of renal soldium- and water-transporting proteins. Am J Physiol Renal Physiol 2008;294:F1373–80.
[581] Wang X, Masilamani S, Nielsen S, Kwon T, Brooks H, Nielsen S, et al. The renal thiazide-sensitive Na-Cl co-transporter as mediator of the aldosterone-escape phenomenon. J Clin Invest 2001;108:215–22.
[582] Glaudermans B, Knoers N, Hoenderop J, Bindels R. New molecular players facilitating $Mg^{(2+)}$ reabsorption in the distal convoluted tubule. Kidney Int 2010;77:17–22.
[583] Satoh J, Romero M. Mg^{2+} transport in the kidney. Biometals 2002;15:285–95.
[584] Schlingmann K, Gudermann T. A critical role of TRPM channel-kinase for human magnesium transport. J Physiol 2005;566:301–8.
[585] Meij I, Koenderink J, de Jong J, De Pont J, Monnens L, van den Heuvel L, et al. Dominant isolated renal magnesium loss is caused by misrouting of the Na^+,K^+-ATPase gamma-subunit. Ann NY Acad Sci 2003;986:437–43.
[586] Adalat S, Woolf A, Johnstone K, Wirsing A, Harries L, Long D, et al. HNF1B mutations associate with hypomagnesemia and renal magnesium wasting. J Am Soc Nephrol 2009;20: 1123–31.
[587] Borke J, Caride A, Verma A, Penniston J, Kumari R. Plasma membrane calcium pump and 28-KDa calcium binding protein in cells of rat kidney distal tubules. Am J Physiol 1989;257: F842–9.
[588] Salido E, Fisher D, Barajas L. Immunoelectron microscopy of epidermal growth factor in mouse kidney. J Ultrastruct Mol Struct Res 1986;96:105–13.
[589] Salido E, Lakshmanan J, Fisher D, Shapiro L, Barajas L. Expression of epidermal growth factor in the rat kidney. An immunocytochemical and *in situ* hybridization study. Histochemie 1991;96:65–72.
[590] Belge H, Gailly P, Schwaller B, Loffing J, Debaix H, Riveira-Munoz E, et al. Renal expression of parvalbumin is critical for NaCl handling and response to diuretics. Proc Natl Acad Sci USA 2007;104:14849–54.
[591] Tatum R, Zhang Y, Salleng K, Lu Z, Lin J, Lu Q, et al. Renal salt wasting and chronic dehydration in claudin-7-deficient mice. Am J Physiol Renal Physiol 2010;298:F24–34.
[592] Turksen K. Wasted salts and wasted bodies: new insight into the role of claudin-7 in the kidney. Am J Physiol Renal Physiol 2010;298:F22–3.
[593] Boros S, Bindels R, Hoenderop J. Active $Ca^{(2+)}$ reabsorption in the connecting tubule. Pflugers Arch 2009;458:99–109.
[594] van Abel M, Hoenderop J, van der Kemp A, Friedlaender M, van Leeuwen J, Bindels R. Coordinated control of renal $Ca^{(2+)}$ transport proteins by parathyroid hormone. Kidney Int 2005;68:1708–21.
[595] Schultheis P, Lorenz J, Meneton P, Nieman M, Riddle T, Flagella M, et al. Phenotype resembling Gitelman's syndrome in mice lacking the apical Na^+-Cl^- co-transporter of the distal convoluted tubule. J Biol Chem 1998;273: 29150–5.
[596] Cruz D, Shaer A, Bia M, Lifton R, Simon D. Gitelman's syndrome revisited: an evaluation of symptoms and health-related quality of life. Kidney Int 2001;59:710–7.
[597] De Jong J, Van der Vliet W, van den Heuvel L, Willems P, Knoers N, Bindels R. Functional expression of mutations in the human NaCl co-transporter: evidence for impaired routing mechanisms in Gitelman's syndrome. J Am Soc Nephrol 2002;13:1442–8.
[598] Melander O, Orho-Melander M, Bengtsson K, Lindblad U, Rastam L, Groop L, et al. Genetic variants of thiazide-sensitive NaCl-co-transporter in Gitelman's syndrome and primary hypertension. Hypertension 2000;36:389–94.
[599] Reissinger A, Ludwig M, Utsch B, Prömse A, Baulmann J, Weisser B, et al. Novel NCCT gene mutations as a cause of Gitelman's syndrome and a systematic review of mutant and polymorphic NCCT alleles. Kidney Blood Press Res 2002; 25:354–62.
[600] Kahle K, Macgregor G, Wilson F, van Hoek A, Brown D, Ardito T, et al. Paracellular Cl^- permeability is regulated by WNK4 kinase: insight into normal physiology and hypertension. Proc Natl Acad Sci USA 2004;101:14877–82.
[601] San-Cristobal P, Dimke H, Hoenderop J, Bindels R. Novel molecular pathways in renal Mg^{2+} transport: a guided tour along the nephron. Curr Opin Nephrol Hypertens 2010; 19:456–62.
[602] Lang F, Capasso G, Schwab M, Waldegger S. Renal tubular transport and the genetic basis of hypertensive disease. Clin Exp Nephrol 2005;9:91–9.
[603] Osathanondh V, Potter E. Development of human kidney as shown by microdissection. III. Formation and interrelationship of collecting tubules and nephrons. Arch Pathol 1963; 76:290–302.
[604] Rubera I, Loffing J, Palmer L, Frindt G, Fowler-Jaeger N, Sauter D, et al. Collecting duct-specific gene inactivation of alphaENacC in the mouse kidney does not impair sodium and potassium balance. J Clin Invest 2003;112:554–65.
[605] Loffing J, Pietri L, Aregger F, Bloch-Faure M, Ziegler U, Meneton P, et al. Differential subcellular localization of ENaC subunits in mouse kidney in response to high- and low-Na diets. Am J Physiol Renal Physiol 2000;279:F252–8.
[606] Loffing J, Zecevic M, Feraille S, Kaissling B, Asher C, Rossier B, et al. Aldosterone induces rapid apical translocation of ENaC in early portion of renal collecting system: possible role of SGK. Am J Physiol Renal Physiol 2001;280:F675–82.
[607] Costanzo L, Windhager E. Calcium and sodium transport by the distal convoluted tubule of the rat. Am J Physiol 1978;235: F492–506.
[608] Friedman P. Mechanism of renal calcium transport. Exp Nephrol 2000;8:343–50.
[609] Hoenderop J, van der Kemp A, Hartog A, van de Graaf S, van Os C, Willems P, et al. Molecular identification of the apical Ca^{2+} channel in 1, 25-dihydroxyvitamin D3-responsive epithelia. J Biol Chem 1999;274:8375–8.
[610] Markadieu N, Bindels R, Hoenderop J. The renal connecting tubule: resolved and unresolved issues in Ca^{2+} transport. Int J Biochem Cell Biol 2011;43:1–4.
[611] Riccardi D, Hall A, Chattopadhyay N, Yu J, Brown E, Hebert S. Localization of the extracellular Ca^{2+}/polyvalent cation-sensing protein in rat kidney. Am J Physiol 1998;274: F611–22.
[612] Riccardi D, Lee W, Lee K, Segre G, Brown E, Hebert S. Localization of the extracellular Ca^{2+}-sensing receptor and PPTH/PTHrP receptor in rat kidney. Am J Physiol 1996;271:F951–6.
[613] Yang T, Hassan S, Huang Y, Smart A, Briggs J, Schnermann J. Expression of PTHrP, PTH/PTHrP receptor, and Ca^{2+}-sensing

receptor mRNAs along the rat nephron. Am J Physiol 1997; 272:F751–8.
[614] Riccardi D, Brown E. Physiology and pathophysiology of the calcium-sensing receptor in the kidney. Am J Physiol Renal Physiol 2010;298:F485–99.
[615] de Groot T, Bindels R, Hoenderop J. TRPV5: an ingeniously controlled calcium channel. Kidney Int 2008;74:1241–6.
[616] Hoenderop J, Nilius B, Bindels R. ECaC: the gatekeeper of transepithelial Ca^{2+} transport. Biochim Biopyhs Acta 2002; 1600:6–11.
[617] Hsu Y, Dimke H, Schoeber J, Hsu S, Lin S, Chu P, et al. Testosterone increases urinary calcium excretion and inhibits expression of renal calcium transport proteins. Kidney Int 2010;77:601–8.
[618] Omata K, Carretero O, Itoh S, Scicli A. Active and inactive kallikrein in rabbit connecting tubules and urine during low and normal sodium intake. Kidney Int 1983;24:714–8.
[619] Cha S, Huang C. WNK4 kinase stimulates caveola-mediated endocytosis of TRPV5 amplifying the dynamic range of regulation of the channel by protein kinase C. J Biol Chem 2010;285:6604–11.
[620] Gkika D, Topala C, Chang Q, Picard N, Thebault S, Houillier P, et al. Tissue kallikrein stimulates $Ca^{(2+)}$ reabsorption via PKC-dependent plasma membrane accumulation of TRPV5. EMBO J 2006;25:4707–16.
[621] Topala C, Bindels R, Hoenderop J. Regulation of the epithelial calcium channel TRPV5 by extracellular factors. Curr Opin Nephrol Hypertens 2007;16:319–24.
[622] Ardiles L, Loyola F, Ehrenfeld P, Burgos M, Flores C, Valderrama G, et al. Modulation of renal kallikrein by a high potassium diet in rats with intense proteinuria. Kidney Int 2006;69:53–9.
[623] Picard N, Van A, Campone C, Seiler M, Bloch-Faure M, Hoenderop J, et al. Tissue kallikrein-deficient mice display a defect in renal tubular calcium absorption. J Am Soc Nephrol 2005;16:3602–10.
[624] Marchetti J, Imbert-Teboul M, Alhenc-Gelas F, Allegrini J, Menard J, Morel F. Kallikrein along the rabbit microdissected nephron: a micromethod for its measurement. Effect of adrenalectomy and DOCA treatment. Pflugers Arch 1984; 401:27–33.
[625] Guder W, Hallbach J, Fink E, Kaissling B, Wirthensohn G. Kallikrein (kininogenese) in the mouse nephron: effect of dietary potassium. Biol Chem Hoppe Seyler 1987;368:637–45.
[626] Vio C, Figueroa C. Evidence for a stimulatory effect of high potassium diet on renal kallikrein. Kidney Int 1987;31: 1327–34.
[627] El Moghrabi S, Houillier P, Picard N, Sohet F, Wootla B, Bloch-Faure M, et al. Tissue kallikrein permits early renal adaptation of potassium load. Proc Natl Acad Sci USA 2010;107:13526–31.
[628] Rossier B, Pradervand S, Schild L, Hummler E. Epithelial sodium channel and the control of sodium balance: interaction between genetic and enviromental factors. Annu Rev Physiol 2002;64:877–97.
[629] Warnock D, Rossier B. Renal sodium handling: the role of the epithelial sodium channel. J Am Soc Nephrol 2005;322:302–7.
[630] Duc C, Farman N, Canessa C, Bonvalet J, Rossier B. Cell-specific expression of epithelial sodium channel a,b,and G subunits in aldosterone-responsive epithelia from the rat: localization by *in situ* hybridization and immunocytochemistry. J Cell Biol 1994;127:1907–21.
[631] Masilamani S, Kim G, Mitchell C, Wade J, Knepper M. Aldosterone-mediated regulation of ENaC alpha, beta and gama subunit proteins in the rat kidney. J Clin Invest 1999;104: R19–23.
[632] Verrey F, Loffing J, Zecevic M, Heitzmann D, Staub O. SGK1: aldosterone-induced relay of Na^+ transport regulation in distal kidney nephron cells. Cell Physiol Biochem 2003; 13:21–8.
[633] Ellison D. The thiazide-sensitive Na-CL co-transporter and human disease: reemergence of an old player. J Am Soc Nephrol 2003;14:538–40.
[634] Ackermann D, Gresko N, Carrel M, Loffing-Cueni D, Habermehl D, Gomez-Sanchez C, et al. *In vivo* nuclear translocation of mineralocorticoid and glucocorticoid receptors in rat kidney: differential effect of corticosteroids along the distaltubule. Am J Physiol Renal Physiol 2011;299: F1473–85.
[635] Bostanjoglo M, Reeves W, Reilly R, Velazquez H, Robertson N, Litwack G, et al. Molecular segmentation of the rat distal tubule: Co-expression of the thiazide-sensitive Na-Cl co-transporter with 11b-hydroxysteroid dehydrogenase. J Am Soc Nephrol 1998;9:1347–58.
[636] Brown R, Diaz R, Robson A, Kotelevtsev Y, Mullins J, Kaufman M, et al. The ontogeny of 11b-hydroxysteroid dehydrogenase type 2 and mineralocorticoid receptor gene expression reveal intricate control of glucocorticoid action in development. Endocrinology 1996;137:794–7.
[637] Farman N, Rafestin-Oblin M. Multiple aspects of mineralocorticoid selectivity. Am J Physiol Renal Physiol 2001;280: F181–92.
[638] Kyossev Z, Walker P, Reeves W. Immunolocalization of NAD-dependent 11b-hydroxysteroid dehydrogenase in human kidney and colon. Kidney Int 1996;49:271–81.
[639] Loffing J, Summa V, Zecevic M, Verrey F. Mediators of aldosterone action in the renal tubule. Curr Opin Nephrol Hypertens 2001;10:667–75.
[640] Frindt G, Palmer L. Surface expression of sodium channels and transporters in rat kidney: effects of dietary sodium. Am J Physiol Renal Physiol 2009;297:F1249–55.
[641] Coleman R, Wu D, Liu J, Wade J. Expression of aquaporin in the renal connecting tubule. Am J Physiol Renal Physiol 2000;279:F874–83.
[642] Kleyman T, Myerburg M, Hughey R. Regulation of ENaC by protease: an increasingly complex story. Kidney Int 2006; 70:1391–2.
[643] Planes C, Caughey G. Regulation of the epithelial Na^+ channel by peptidase. Curr Top Dev Biol 2007;78:23–46.
[644] Rossier B, Stutts M. Activation of the epithelial sodium channel (ENaC) by serine protease. Annu Rev Physiol 2009; 71:361–79.
[645] Loffing J, Korbmacher C. Regulated sodium transport in the renal connecting tubule (CNT) via the epithelial sodium channel (ENaC). Pflugers Arch 2009;458:111–35.
[646] Dijkink L, Hartog A, Deen P, van Os C, Bindels R. Time-dependent regulation by aldosterone of the amiloride-sensitive Na^+ channel in rabbit kidney. Pflugers Arch 1999;438:354–60.
[647] Debonneville C, Flores S, Kamynina E, Plant P, Tauxe C, Thomas M, et al. Phosphorylation of Nedd4-2 by Sgk1 regulates epithelial $Na^{(+)}$ channel cell surface expression. EMBO J 2001;20:7052–9.
[648] Flores S, Loffing-Cueni D, Kamynina E, Daidié D, Gerbex C, Chabanel S, et al. Aldosterone-induced serum and glucocorticoid-induced kinase 1 expression is accompanied by Nedd4-2 phosphorylation and increased Na^+ transport in cortical collecting duct cells. J Am Soc Nephrol 2005;16:2279–87.
[649] Snyder P, Olson D, Thomas B. Serum and glococorticoid-regulated kinase modulates Nedd4-2-mediated inhibition of the epithelial Na channel. J Biol Chem 2002;277:5–8.

[650] Bankir L, Bichet D, Bouby N. Vasopressin V2 receptors. ENaC, and sodium reabsorption: a risk factor for hypertension? Am J Physiol Renal Physiol 2010;299:F917–28.

[651] Bugaj V, Pochynyuk O, Stockand J. Activation of the epithelial Na^+ chanel in the collecting duct by vasopressin contributes to water reabsorption. Am J Physiol Renal Physiol 2009;297: F1411–8.

[652] Boulkroun S, Ruffieux-Daidiè D, Vitagliano J, Poirot O, Charles R, Lagnaz D, et al. Vasopressin-inducible ubiquitin-specific protease 10 increases ENaC cell surface expression by deubiquitylating and stabilizing sorting nexin 3. Am J Physiol Renal Physiol 2008;295:F889–900.

[653] Butterworth M, Edinger R, Johnson J, Frizzell R. Acute ENaC stimulation by cAMP in a kidney cell line is mediated by exocytic insertion from a recycling channel pool. J Gen Physiol 2005;125:81–101.

[654] Cruz D, Simon D, Nelson-Williams C, Farhi A, Finberg K, Burleson L, et al. Mutations in the Na-Cl co-transporter reduce blood pressure in humans. Hypertension 2001;37:1458–64.

[655] Harrison-Bernard L, Navar L, Ho H, Vinson G, El-Dahr S. Immunohistochemical localization of ANG II AT1 receptor in adult rat kidney using a monoclonal antibody. Am J Physiol 1997;273:F170–7.

[656] Mujais S, Kauffman S, Katz A. Aingiotensin II binding sites in individual segments of the rat nephron. J Clin Invest 1986; 77:315–8.

[657] Vallon V, Rieg T. Regulation of renal NaCl and water transport by the ATP/UTP/P2Y2 receptor system. Am J Physiol Renal Physiol 2011;301:F463–75.

[658] Wang T, Giebisch G. Effects of angiotensin II on electrolyte transport in the early and late distal tubule in rat kidney. Am J Physiol 1996;271:F143–9.

[659] Wingo C, Smolka A. Function and structure of H-K-ATPase immunoreactivity in cortical and outer medullary collecting duct. Am J Physiol Renal Physiol 1995;269:F1–16.

[660] Kovacikova J, Winter D, Loffing-Cueni D, Loffing J, Finberg K, Lifton R, et al. The connecting tubule is the main site of the furosemide-induced urinary acidification by the vacuolar H^+-ATPase. Kidney Int 2006;70:1706–16.

[661] Simon D, Karet F, Rodriguez-Soriano J, Hamdan J, DiPietro A, Trachtman H, et al. Genetic heterogeneity of Bartter's syndrome revealed by mutations in the K^+ channel, ROMK. Nat Genet 1996;14:152–6.

[662] Palmer B, Alpern R. Liddle's syndrome. Am J Med 1998; 104:301–9.

[663] Schiller A, Taugner R. Heterogeneity of tight junctions along the collecting duct in the renal medulla. A freeze-fracture study in rat and rabbit. Cell Tissue Res 1982;223:603–14.

[664] Liu W, Morimoto T, Woda C, Kleyman T, Satlin L. Ca^{2+} dependence of flow-stimulated K secretion in the mammalian cortical collecting duct. Am J Physiol Renal Physiol 2007;293:F227–35.

[665] Andrews P. Scanning electron microscopy of human and rhesus monkey kidneys. Lab Invest 1975;32:610–8.

[666] Nielsen J, Kwon T, Praetorius J, Frokiaer J, Knepper M, Nielsen S. Aldosterone increases urine production and decreases apical AQP2 expression in rats with diabetes insipitus. Am J Physiol Renal Physiol 2006;290:F438–49.

[667] Nicco C, Wittner M, DiStefano A, Jounier S, Bankir L, Bouby N. Chronic exposure to vasopressin upregulates ENaC and sodium transport in the rat renal collecting duct and lung. Hypertension 2001;38:1143–9.

[668] Leviel F, Hübner C, Houillier P, Morla L, El Moghrabi S, Brideau G, et al. The Na^+-dependent chloride-bicarbonate exchanger SLC4A8 mediates an electroneural Na^+ reabsorption process in the renal cortical collecting duct of mice. J Clin Invest 2010;120:1627–35.

[669] Pech V, Pham T, Hong S, Weinstein A, Spencer K, Duke B, et al. Pendrin modulates ENaC function by changing luminal HCO_3. J Am Soc Nephrol 2010;21:1928–41.

[670] Kishore B, Nelson R, Miller R, Carlson N, Kohan D. P2Y2 receptors and water transport in the kidney. Purinergic Signal 2009;5:491–9.

[671] Shirley D, Vekaria R, Sévigny J. Ectonucleotidases in the kidney. Purinergic Signal 2009;5:501–11.

[672] Moeller H, Olesen E, Fenton R. Regulation of the water channel aquaporin-2 by posttranslational modifications. Am J Physiol Renal Physiol 2011;300:F1062–73.

[673] Marples D, Schroer T, Ahrens N, Taylor A, Knepper M, Nielsen S. Dynein and dynactin colocalize with AQP2 water channels in intracellular vesicles from kidney collecting duct. Am J Physiol 1998;274:F384–94.

[674] Nielsen S, Chou C, Marples D, Christensen E, Kishore B, Knepper M. Vasopressin increases water permeability of kidney collecting duct by inducing translocation of aquaporin-CD water channels to plasma membrane. Proc Natl Acad Sci USA 1995;92:1013–7.

[675] Sabolic I, Brown D. Water channels in renal and nonrenal tissues. News Physiol Sci 1995;10:12–7.

[676] Verkman A, Shi L, Frigeri A, Hasegawa H, Farinas J, Mitra A, et al. Structure and function of kidney water channels. Kidney Int 1995;48:1081–96.

[677] Lu H, Sun T, Bouley R, Blackburn K, McLaughlin M, Brown D. Inhibition of endocytosis causes phosphorylation (S256)-independent plasma membrane accumulation of AQP2. Am J Physiol Renal Physiol 2004;286:F233–43.

[678] Li W, Zhang Y, Bouley R, Chen Y, Matsuzaki T, Nunes P, et al. Simvastatin enhances aquaporin-2 surface expression and urinary concentration in vasopressin-deficient Brattleboro rats through modulation of Rho GTPase. Am J Physiol Renal Physiol 2011;301:F309–18.

[679] Procino G, Barbieri C, Carmosino M, Rizzo F, Valenti G, Svelto M. Lovastatin-induced cholesterol depletion affects both apical sorting and endocytosis of aquaporin-2 in renal cells. Am J Physiol Renal Physiol 2010;298:F266–78.

[680] Ridley A. Rho GTPase and actin dynamics in membrane protrusions and vesicle trafficking. Trends Cell Biol 2011; 16:522–9.

[681] Rikitake Y, Liao J. Rho GTPase, statins, and nitric oxide. Circ Res 2005;97:1232–5.

[682] Knepper M, Wade J, Terris J, Ecelbarger C, Marples D, Mandon B, et al. Renal aquaporins. Kidney Int 1996;49:1712–7.

[683] Terris J, Ecelbarger C, Marples D, Knepper M, Nielsen S. Distribution of aquaporin-4 water channel expression within rat kidney. Am J Physiol 1995;269:F775–85.

[684] Verkman A. Lessons on renal physiology from transgenic mice lacking aquaporin wter channels. J Am Soc Nephrol 1999; 10:1126–35.

[685] Nielsen S, Knepper M. Vasopressin activates collecting duct urea transporters and water channels by distinct physical processes. Am J Physiol 1993;265:F204–13.

[686] Ishibashi K, Sasaki S, Fushimi K, Yamamoto T, Kuwahara M, Marumo F. Immunolocalization and effect of dehydration on AQP3, a basolateral water channel of kidney collecting ducts. Am J Physiol 1997;272:F235–41.

[687] Frigeri A, Gropper M, Truck C, Verkman A. Immunolocalization of the mercurial-insensitive water channel and glycerol intrinsic protein in epithelial cell plasma membranes. Proc Natl Acad Sci USA 1995;92:4328–31.

[688] Han K, Woo S, Kim W, Park S, Cha J, Kim J, et al. Maturation of TonEBP expression in developing rat kidney. Am J Physiol Renal Physiol 2004;287:F878–85.
[689] Kultz D. Hypertonicity and TonEBP promote development of the renal concentrating system. Am J Physiol Renal Physiol 2004;287:F876–7.
[690] Dorup J. Structural adaptation of intercalated cells in rat renal cortex to acute metabolic acidosis and lakalosis. J Ultrastruct Res 1985;92:119–31.
[691] LeFurgey A, Tisher C. Morphology of rabbit collecting duct. Am J Anat 1979;155:111–24.
[692] Tisher C, Madsen K. Anatomy of the kidney. In: Brenner B, editor. The kidney. Philadelphia: Saunders; 1996. p. 3–71.
[693] Kaissling B. Cellular heterogeneity of the distal nephron and its relation to function. Klin Wochenschr 1985;63:868–76.
[694] Madsen K, Tisher C. Structural–functional relationships along the distal nephron. Am J Physiol 1986;250:F1–15.
[695] Brown D, Weyer P, Orci L. Nonclathrin-coated vesicles are involved in endocytosis in kidney collecting duct intercalated cells. Anat Rec 1987;218:237–42.
[696] Gluck S, Cannon C, Al-Awqati Q. Exocytosis regulates urinary acidification in turtle bladder by rapid insertion of H^+ pumps into the luminal membrane. Proc Natl Acad Sci USA 1982; 79:4327–31.
[697] Schwartz G, Barasch J, Al-Awqati Q. Plasticity of functional epithelial polarity. Nature 1985;318:368–71.
[698] Brown D, Gluck S, Hartwig J. Structure of the novel membrane-coating material in proton-secreting epithelial cells and identification as an H^+-ATPase. J Cell Biol 1987;105: 1637–48.
[699] Brown D, Hirsch S, Gluck S. Localization of a proton-pumping ATPase in rat kidney. J Clin Invest 1988;82:2114–26.
[700] Stetson D, Wade J, Giebisch G. Morphologic alterations in the rat medullary collecting duct following potassium depletion. Kidney Int 1980;17:45–56.
[701] Breton S, Alper S, Gluck S, Sly W, Barker J, Brown D. Depletion of intercalated cells from collecting ducts of carbonic anhydrase ll-deficient (CAR null) mice. Am J Physiol 1995;269:F761–74.
[702] Kim J, Tisher C, Linser P, Madsen K. Ultrastructural localization of carbonic anhydrase ll in subpopulations of intercalated cells of the rat kidney. J Am Soc Nephrol 1990;1:245–56.
[703] Ridderstrale Y, Wistrand P, Tashian R. Membrane-associated carbonic anhydrase activity in the kidney of CA ll-deficient mice. J Histochem Cytochem 1992;40:1665–73.
[704] Schwartz G, Winkler C, Zavilowitz B, Bargiello T. Carbonic anhydrase ll mRNA is induced in rabbit kidney cortex during chronic metabolic acidosis. Am J Physiol 1993;265: F764–72.
[705] Drenckhahn D, Schluter K, Allen D, Bennett V. Colocalization of band 3 with ankyrin and spectrin at the basal membrane of intercalated cells in the rat kidney. Science 1985;230:1287–9.
[706] Verlander J, Kim Y, Shin W, Pham T. Dietary $Cl^{(-)}$ restriction upregulates pendrin expression within the apical plasma membrane of type B intercalated cells. Am J Physiol Renal Physiol 2006;291:F833–9.
[707] Bishop J, Verlander J, Lee H, Nelson R, Weiner A, Handlogten M, et al. Role of the Rhesus glycoprotein, RhB glycoprotein, in renal ammonia excretion. Am J Physiol Renal Physiol 2010;299: F1065–77.
[708] Lee H, Verlander J, Bishop J, Nelson R, Handlogten M, Weiner I. Effect of intercalated cell-specific Rh C glycoprotein deletion on basal and metabolic acidosis-stimulated renal ammonia excretion. Am J Physiol Renal Physiol 2010; 299:F369–79.
[709] Weiner I, Verlander J. Role of NH3 and NH4 transporters in renal acid–base transport. Am J Physiol Renal Physiol 2011; 300:F11–23.
[710] Kim J, Kim Y, Cha J, Tisher C, Madsen K. Intercalated cells subtypes in connecting tubule and cortical collecting duct of rat and mouse. J Am Soc Nephrol 1999;10:1–12.
[711] Verlander J, Madsen K, Tisher C. Effect of acute respiratory acidosis on two populations of intercalated cells in rat cortical collecting duct. Am J Physiol Renal Fluid Electrolyte Physiol 1987;253:F1142–56.
[712] Kaissling B, Koeppen B, Wade J. Effect of mineralocorticoids on the structure of intercalated cells. Acta Anat 1981;111:72.
[713] Bastani B. Immunocytochemical localization of the vacuolar H^+-ATPase pump in the kidney. Histopathology 1997; 12:769–79.
[714] Brown D, Hirsch S, Gluck S, An H. ATPase in opposite plasma membrane domains in kidney epithelial cell subpopulations. Nature 1988;331:622–4.
[715] Nelson R, Guo X, Masood K, Kalkbrenner M, Gluck S. Selectively amplified expression of an isoform of the vacuolar H(+)-ATPase 56-kilodaltons subunit in renal intercalated cells. Proc Natl Acad Sci USA 1992;89:3541–5.
[716] Oka T, Murata Y, Namba M, Yoshimizu T, Toyumura T, Yamamoto A, et al. A4, a unique kidney-specific isoform of mouse vacuolar H^+-ATPase subunit a. J Biol Chem 2001;276:40050–4.
[717] Smith A, Jouret F, Bord S, Brothwick K, Al-Lamki R, Wagner C, et al. Vacuolar H^+-ATPase d2 subunit: molecular characterization, developmental regulation, and localization to specialized proton pumps in kidney and bone. J Am Soc Nephrol 2005;16:1245–56.
[718] Stehberger P, Schulz N, Finberg K, Karet F, Giebisch G, Lifton R, et al. Localization and regulation of the ATP6V0A4 (a4) vacuolar H^+-ATPase subunit defective in an inherited form of distal renal tubular acidosis. J Am Soc Nephrol 2003;14: 3027–38.
[719] Sun-Wada G, Murata Y, Namba M, Yamamoto A, Wada Y, Futai M. Mouse proton pump ATPase C subunit isoforms (C2-a and C2-b9) specifically expressed in kidney and lung. J Biol Chem 2003;278:44843–51.
[720] Alper S. The band 3-related anion exchanger (AE) gene family. Annu Rev Physiol 1991;53:549–64.
[721] Alper S, Natale J, Gluck S, Lodish H, Brown D. Subtypes of intercalated cells in rat kidney collecting duct defined by antibodies against erythroid band 3 and renal vascular H^+-ATPase. Proc Natl Acad Sci USA 1989;80:5429–33.
[722] Emmons C, Kurtz I. H^+/base transport pathways in the cortical collecting duct. Exp Nephrol 1993;1:325–33.
[723] Greenlee M, Lynch I, Gumz M, Cain B, Wingo C. Mineralocorticoids stimulate the activity and expression of renal H^+,K^+-ATPases. J Am Soc Nephrol 2011;22:49–58.
[724] Gunz M, Lynch I, Greenlee M, Cain B, Wingo C. The renal H -K -ATPases: physiology, regulation, and structure. Am J Physiol Renal Physiol 2010;298:F12–21.
[725] Silver R, Frindt G, Mennitt P, Satlin L. Characterization and regulation of H-K-ATPase in intercalated cells of rabbit cortical collecting duct. J Exp Zool 1997;279:443–55.
[726] Wingo C, Cain B. The renal H-K-ATPase: physiological significance and role in potassium homeostasis. Annu Rev Physiol 1993;55:323.
[727] Obermüller N, Gretz N, Kriz W, Reilly R, Witzgall R. The swelling-activated chloride channel CIC-2, the chloride channel CIC-3, and CIC-5, a chloride channel mutated in kidney stone disease, are expressed in distinct subpopulations of renal epithelial cells. J Clin Invest 1998;101:635–42.

[728] Ginns S, Knepper M, Ecelbarger C, Terris J, Coleman R, He X, et al. Immunolocalization of the secretory isoform of Na-K-Cl co-transporter in rat renal intercalated cells. J Am Soc Nephrol 1996;7:2533–42.
[729] Chambrey R, Goossens D, Bourgeois S, Picard N, Bloch-Faure M, Leviel F, et al. Genetic ablation of Rhbg in the mouse does not impair renal ammonium excretion. Am J Physiol Renal Physiol 2005;289:F1281–90.
[730] Verlander J, Miller R, Frank A, Royaux I, Kim Y, Weiner I. Localization of the ammonium transporter proteins RhBG and RhCG in mouse kidney. Am J Physiol 2003;284:F323–37.
[731] Weiner I, Miller R, Verlander J. Localization of the ammonium transporters, Rh B glycoprotein and Rc C glycoprotein, in the mouse liver. Gastroenterology 2011;5:1432–40.
[732] Eladari D, Cheval L, Quentin F, Bertrand O, Mouro I, Cherif-Zahar B, et al. Expression of RhCG, a new putative NH(3)/NH(4)(+) transporter, along the rat nephron. J Am Soc Nephrol 2002;13:1999–2008.
[733] Mak D, Dang B, Weiner I, Foskett J, Westhoff C. Characterization of ammonia transport by the kidney Rh glycoproteins RhBG and RhCG. Am J Physiol Renal Physiol 2006;290:F297–305.
[734] Seshadri R, Klein J, Kozlowski S, Sands J, Kim Y, Han K, et al. Renal expression of the ammonia transporters, Rhbg and Rhcg, in response to chronic metabolic acidosis. Am J Physiol Renal Physiol 2006;290:397–408.
[735] Welsh-Bacic D, Nowik M, Kaissling B, Wagner C. Proliferation of acid-secretory 1 cells in the kidney during adaptive remodelling of the collecting duct. PLOS one 2011;6(10):e25240.
[736] Munkacsi I. Distribution of the intrarenal moonoaminergic nerves in the kidney of the desert rat (*Dipodomys merriami*) and the white rat (*Rattus norvegicus*). Acta Anat 1969;73: 56–68.
[737] Milton A, Weiner I. Regulation of B-type intercalated cell apical anion exchange activity by CO2/HCO3. Am J Physiol 1998;275:F1086–94.
[738] Kim Y, Verlander J, Matthews S, Kurtz I, Shin W, Weiner I, et al. Intercalated cell H^+/OH^- transporter expression is reduced in Slc26a4 null mice. Am J Physiol Renal Physiol 2005;289: F262–72.
[739] Quentin F, Eladari D, Frische S, Cambillau M, Nielsen S, Alper S, et al. Regulation of the Cl^-/HCO_3^- exchanger AE2 in rat thick ascending limb of Henle's loop in response to changes in acid–base and sodium balance. J Am Soc Nephrol 2004;15:2988–97.
[740] Royaux I, Wall S, Karniski L, Everett L, Suzuki K, Knepper M, et al. Pendrin, encoded by the Pendred syndrome gene, resides in the apical region of renal intercalated cells and mediates bicarbonate secretion. Proc Natl Acad Sci USA 2001; 98:4221–6.
[741] Petrovic S, Wang Z, Ma L, Soleimani M. Regulation of the apical Cl^-/IICO-3 exchanger pendrin in rat cortical collecting duct in metabolic acidosis. Am J Physiol Renal Physiol 2003; 284:F103–12.
[742] Wehrli P, Loffing-Cueni D, Kaissling B, Loffing J. Replication of segment-specific and intercalated cells in the mouse renal collecting system. Histochem Cell Biol 2007;127: 389–98.
[743] Teng-Umnuay P, Verlander J, Yuan W, Tisher C, Madsen K. Identification of distinct subpopulations of intercalated cells in the mouse collecting duct. J Am Soc Nephrol 1996;7: 260–74.
[744] Wagner C, Devuyst O, Bourgeois S, Mohebbi N. Regulated acid–base transport in the collecting duct. Pflugers Arch 2009;458:137–56.
[745] Bastani B, Haragsim L. Immunocytochemistry of renal H-ATPase. Miner Electrolyte Metab 1996;22:382–95.
[746] Matsumoto T, Fejes-Toth G, Schwartz G. Postnatal differentiation of rabbit collecting duct intercalated cells. Pediatr Res 1996;39:1–12.
[747] Matsumoto T, Feyes-Toth G, Schwartz G. Developmental expression of acid–base-related proteins in the rabbit kidney. Pediatr Nephrol 1993;7:792–7.
[748] Schwaderer A, Vijayakumar S, Al-Awqati Q, Schwartz G. Glectin-3 expression is induced in renal beta-intercalated cells during metabolic acidosis. Am J Physiol Renal Physiol 2006;290:F148–58.
[749] Schwartz G, Satlin L. Fluorescent characterization of intercalated cells in the rabbit renal cortical collecting duct. Semin Nephrol 1989;9:79–82.
[750] Le Hir M, Kaissling B, Koeppen B, Wade J. Binding of peanut lectin to specific epithelial cell types in the kidney. Am J Physiol 1982;242:C117–20.
[751] van Huyen D, Cheval L, Bloch-Faure M, Belair M, Heudes D, Bruneval P, et al. GDF15 triggers homeostatic proliferation of acid-secreting collecting duct cells. J Am Soc Nephrol 2008; 19:1965–74.
[752] Brown D, Waneck G. Glycosyl-phosphatidylnositol-anchored membrane proteins. J Am Soc Nephrol 1992;3:895–906.
[753] Dawson T, Gandhi R, Le Hir M, Kaissling B. Ecto-5′-nucleotidase: localization in rat kidney by light microscopic histochemical methods. J Histochem Cytochem 1989;37:39–47.
[754] McCulloch F, Chambrey R, Eladari D, Peti-Peterdi J. Localization of connexin 30 in the luminal membrane of cells in the distal nephron. Am J Physiol Renal Physiol 2005;289: F1304–12.
[755] Mandon B, Nielsen S, Kishore B, Knepper M. Expression of syntaxins in rat kidney. Am J Physiol 1997;273:F718–30.
[756] Kishore B, Wade J, Schorr K, Inoue T, Mandon B, Knepper M. Expression of synaptotagmin Vlll in rat kidney. Am J Physiol 1998;275:F131–42.
[757] Sabolic I, Herak-Kramberger C, Breton S, Brown D. Na/KATPase in intercalated cells along the rat nephron revealed by antigen. J Am Soc Nephrol 1999;10:913–22.
[758] Kim J, Kim Y, Cha J, Tisher C, Madsen K. Intercalated cell subtypes in connecting tubule and cortical collecting duct of rat and mouse. J Am Soc Nephrol 1999;10:1–12.
[759] Schon D, Backman K, Hayslett J. Role of the medullary collecting duct in potassium excretion in potassium-adapted animals. Kidney Int 1981;20:655–62.
[760] Nicoletta J, Schwartz G. Distal renal tubular acidosis. Curr Opin Pediatr 2004;16:194–8.
[761] Blomqvist S, Vidarsson H, Fitzgerald S, Johansson B, Ollerstam A, Brown R, et al. Distal renal tubular acidosis in mice that lack the forkhead transcription factor Foxi1. J Clin Invest 2004;113:1560–70.
[762] Christensen J, Bjaerke H, Meyer D, Bohle A. The normal juxtaglomerular apparatus in the human kidney. A morphological study. Acta Anat 1979;103:374–83.
[763] Kriz W. Ontogenetic development of the filtration barrier. Nephron Exp Nephrol 2007;106:e44–50.
[764] Kaissling B, Kriz W. Variability of intercellular spaces between macula densa cells: a transmission electron microscopic study in rabbits and rats. Kidney Int 1982;22:9–17.
[765] Bachmann S, Velazquez H, Obermüller N, Reilly R, Moser D, Ellison D. Expression of the thiazide-sensitive Na-Cl co-transporter in rat and human kidney. Am J Physiol 1995;96: 2510–4.
[766] Haas M, Forbush BI. The Na-K-Cl contransporters. J Bioenerg Biomembr 1998;30:161–72.

[767] Boim M, Ho K, Shuck M, Bienkowski M, Block J, Slighton J, et al. ROMK inwardly rectifying ATP-sensitive K^+ channel. II. Cloning and distribution of alternative forms. Am J Physiol 1995;268:F1132–40.
[768] Mennitt P, Wade J, Ecelbarger C, Palmer L, Frindt G. Localization of ROMK channels in the rat kidney. J Am Soc Nephrol 1997;8:1823–30.
[769] Kim G, Ecelbarger C, Knepper M, Packer R. Regulation of thick ascendig limb ion transporter abundance in response to altered acid/base intake. J Am Soc Nephrol 1999;10:935–42.
[770] Mundel P, Bachmann S, Bader M, Fischer A, Kummer W, Mayer B, et al. Expression of nitric oxide synthase in kidney macula densa cells. Kidney Int 1992;42:1017–9.
[771] Wilcox C, Welch W. Macula densa nitric oxide synthase: expression, regulation, and function. Kidney Int 1998;67:7–53.
[772] Pluznick J, Zou D, Zhang X, Yan Q, Rodriguez-Gil D, Eisner C, et al. Functional expression of the olfactory signaling system in the kidney. Proc Natl Acad Sci USA 2009;106: 2059–64.
[773] Alcorn D, Anderson W, Ryan G. Morphological changes in the renal macula densa during natriuresis and diuresis. Ren Physiol 1986;9:335–47.
[774] Bell P, Komlosi P, Zhang Z. ATP as a mediator of macula densa cell signaling. Purinergic Sigal 2009;5:461–71.
[775] Kirk K, Bell P, Barfuss D, Ribadeneira M. Direct visualization of the isolated and perfused macula densa. Am J Physiol 1985;248:F890–4.
[776] Rosivall L, Mirzahosseini S, Toma I, Sipos A, Peti-Peterdi J. Fluid flow in the juxtaglomerular interstitium visualized *in vivo*. Am J Physiol Renal Physiol 2006;291:F1241–7.
[777] Tian W, Salanova M, Xuk H, Lindsley J, Oyama T, Anderson S, et al. Renal expression of osmotically responsive cation channel TRPV4 is restricted to water-impermeant nephron segments. Am J Physiol Renal Physiol 2004; 287:F17–24.
[778] Barajas L. The JGA: anatomical considerations in feedback control of glomerular filtration rate. Fed Proc 1981; 40:78–86.
[779] Ryan G, Coghlan J, Scoggins B. The granulated peripolar epithelial cell: a potential secretory component of the renal juxtaglomerular complex. Nature 1979;277:655–6.
[780] Gall J, Alcorn D, Butkus A, Coghlan J, Ryan G. Distribution of glomerular peripolar cells in different mammalian species. Cell Tissue Res 1986;244:203–8.
[781] Trahair J, Ryan G. Co-localization of neuron-specific enolase-like and kallikrein-like immunoreactivity in ductal and tubular epithelium of sheep salivary gland and kidney. J Histochem Cytochem 1989;37:309–14.
[782] Hollywell C, Jaworowski A, Thumwood C, Alcorn D, Ryan G. Immunohistochemical localization of transthyretin in glomerular peripolar cells of newborn sheep. Cell Tissue Res 1992;267:193–7.
[783] Spanidis A, Wunsch H, Kaissling B, Kriz W. Three-dimensional shape of a Goormaghtigh cell and its contact with a granular cell in the rabbit kidney. Anat Embryol 1982; 165:239–52.
[784] Satlin G, Schwartz J. Cellular remodeling of HCO_3-secreting cells in rabbit renal collecting duct in response to an acidic environment. J Cell Biol 1989;109:1279–88.
[785] Spanidis A, Wunsch H. Rekonstruktion einer goormaghtigh'schen und einer epitheloiden zelle der kaninchenniere. Heidelberg: Dissertation University of Heidelberg; 1979.
[786] Goormaghtigh N. Facts in favour of an endocrine function of the renal arterioles. J Pathol Bacteriol 1945;57:392.
[787] Schnermann J, Levine D. Paracrine factors in tubuloglomerular feedback: adenosine, ATP, and nitric oxide. Annu Rev Physiol 2003;65:501–29.
[788] Peti-Peterdi J, Komlosi P, Fuson A, Guan Y, Schneider A, Qi Z, et al. Luminal NaCl delivery regulates basolateral PGE_2 release from macla densa cells. J Clin Invest 2003;112:76–82.
[789] Schweda F, Kurtz A. Cellular mechanism of renin release. Acta Physiol Scand 2004;181:383–90.
[790] Wilcox C, Welch W, Murad F, Gross S, Taylor G, Levi R, et al. Nitric oxide synthase in macula densa regulates glomerular capillary pressure. Proc Natl Acad Sci USA 1992; 89:11993–7.
[791] Osswald H, Nabakowski G, Hermes H. Adenosine as a possible mediator of metabolic control of glomerular filtration rate. Int J Biochem 1980;12:263–7.
[792] Thomson S, Bao D, Deng A, Vallon V. Adenosine formed by 5′-nucleotidase mediates tubuloglomerular feedback. J Clin Invest 2000;106:289–98.
[793] Schnermann J, Briggs J. Tubuloglomerular feedback: mechanistic insights from gene-manipulated mice. Kidney Int 2008;74:418–26.
[794] Persson A, Ollerstam A, Liu R, Brown R. Mechanism for macula densa cell release of renin. Acta Physiol Scand 2004;181: 471–4.
[795] Komlosi P, Fintha A, Bell P. Current mechanisms of macula densa cell signaling. Acta Physiol Scand 2004;181:463–9.
[796] Vallon V, Mühlbauer B, Osswald H. Adenosine and kidney function. Physiol Rev 2006;86:901–40.
[797] Pallone T, Turner M, Edwards A, Jamison R. Countercurrent exchange in the renal medulla. Am J Physiol Regul Integr Comp Physiol 2003;284:R1153–75.
[798] Wirz H. Countercurrent principle. Protoplasma 1967;63:322–7.
[799] Kokko J, Rector Jr F. Countercurrent multiplication system without active transport in inner medulla. Kidney Int 1972;2:214–23.
[800] Stephenson J. Concentration of urine in a central core model of the renal counterflow system. Kidney Int 1972;2:85–94.
[801] Thomas S. Cycles and separations in a model of the renal medulla. Am J Physiol 1998;275:F671–90.
[802] Wexler A, Kalaba R, Marsh D. Three-dimensional anatomy and renal concentrating mechanism. I. Modeling results. Am J Physiol 1991;260:F368–83.
[803] Lemley K, Kriz W. Cycles and separations: the histotopography of the urinary concentrating process. Kidney Int 1987; 31:538–48.
[804] Koepsell H, Kriz W, Schnermann J. Pattern of luminal diameter changes along the descending and ascending thin limbs of the loop of Henle in the inner medullary zone of the rat kidney. Z Anat Entwicklungsgesch 1972;138: 321–8.
[805] Becker B. Quantitative beschreibung der innenzone der rattenniere. Muenster: Inaugural Dissertation; 1978.
[806] Imai M, Hayashi M, Araki M. Functional heterogeneity of the descending limbs of Henle's loop. I. Internephron heterogeneity in the hamster kidney. Pflugers Arch 1984;402:385–92.
[807] Van Itallie C, Anderson J. The molecular physiology of tight junction pores. Physiology 2004;19:331–8.
[808] Bankir L, Kriz W. Adaptation of the kidney to protein intake and to urine concentrating activity: similar consequences in health and CFR. Kidney Int 1995;47:7–24.
[809] Bankir L, Trinh-Trang-Tan M. Urea and the kidney. In: Brenner B, editor. The kidney. Philadelphia: Saunders; 2000. p. 637–79.
[810] Bankir L, Chen K, Yang B. Lack of UT-B in vasa recta and red blood cells prevents urea-induced improvement of urinary concentrating ability. Am J Physiol Renal Physiol 2004;286:F144–51.

[811] Trinh-Trang-Tan M, Lasbennes F, Gane P, Roudier N, Ripoche P, Cartron J, et al. UT-B1 proteins in rat: tissue distribution and regulation by antidiuretic hormone in kidney. Am J Physiol Renal Physiol 2002;283:F912–22.

[812] Brown D, Kumpulainen J, Roth J, Orci L. Immunohistochemical localization of carbonic anhydrase in postnatal and adult rat kidney. Am J Physiol 1983;245:F110–8.

[813] Brown D, Kumpulainen T. Immunocytochemical localization of carbonic anhydrase on ultrathin frozen sections with protein A-gold. Histochemistry 1985;83:153–8.

[814] Brown D, Roth J, Kumpulainen T, Orci L. Ultrastructural immunocytochemical localization of carbonic anhydrase. Presence in intercalated cells of the rat collecting tubule. Histochemistry 1982;75:209–13.

[815] Dobyan D, Bulger R. Renal carbonic anhydrase. Am J Physiol 1982;243:F311–24.

[816] Holthofer H, Schulte B, Pasternack G, Siegel G, Spicer S. Immunocytochemical characterization of carbonic anhydrase-rich cells in the rat kidney collecting duct. Lab Invest 1987; 57:150–6.

[817] Holthofer H, Schulte B, Pasternack G, Siegel G, Spicer S. Three distinct cell populations in rat kidney collecting duct. Am J Physiol 1987;253:C323–8.

[818] Lönnerholm G, Ridderstrale Y. Intracellular distribution of carbonic anhydrase in the rat kidney. Kidney Int 1980;17:162–74.

[819] Lönnerholm G, Wistrand P. Carbonic anhydrase in the human kidney: a histochemical and immunocytochemical study. Kidney Int 1984;25:86–898.

[820] Kim Y, Kwon T, Frische S, Kim J, Tisher C, Madsen K, et al. Immunocytochemical localization of pendrin in intercalated cell subtypes in rat and mouse kidney. Am J Physiol Renal Physiol 2002;283:F744–54.

[821] Brown A, Hallouane D, Mawby W, Karet F, Saleem M, Howie A, et al. RhCG is the mahor putative ammonia transporter expressed in the human kidney, and RhBG is not expressed at detectable levels. Am J Physiol Renal Physiol 2009;296: F1279–90.

[822] Kim H, Verlander J, Bishop J, Cain B, Han K, Igarashi P, et al. Basolateral expression of the ammonia transporter family member Rh C glycoprotein in the mouse kidney. Am J Physiol Renal Physiol 2009;296:F543–55.

[823] Ahn K, Park K, Kim K, Kone B. Chronic hypokalemia enhances expression of the H(+)-K(+)-ATPase alpha 2-subunit gene in renal medulla. Am J Physiol 1996;271:F314–21.

[824] Codina J, Delmas-Mata J, DuBose TJ. Expression of HKalpha2 protein is increased selectively in renal medulla by chronic hypokalemia. Am J Physiol 1998;275:F433–40.

[825] DuBose TJ, Codina J, Burges A, Pressley T. Regulation of H (+)-K(+)-ATPase expression in kidney. Am J Physiol 1995;269: F500–7.

[826] Jaisser F, Escoubet B, Coutry N, Eugene E, Bonvalet J, Farman N. Differential regulation of putative $K(^{+})$-ATPase by low K^{+} diet and corticocosteroids in rat distal colon and kidney. Am J Physiol 1996;270:C679–87.

[827] Kraut J, Helander K, Helander H, Iroezi N, Marcus E, Sachs G. Detection and localization of H^{+}-K^{+}-ATPase isoforms in human kidney. Am J Physiol Renal Physiol 2001;281:F763–8.

[828] Ryan G, Karnovsky M. Distribution of endogenous albumin in the rat glomerulus. Role of hemodynamic factors in glomerular barrier function. Kidney Int 1976;9:36–45.

[829] Sangan P, Rajendran V, Mann A, Kashgarian M, Binder H. Regulation of colonic H-K-ATPase in large intestine and kidney by dietary Na depletion and dietary K depletion. Am J Physiol 1987;272:C685–96.

[830] Verlander J, Moudy R, Campbell W, Cain B, Wingo C. Immunohistochemical localization of H-K-ATPase alpha(2c)-subunit in rabbit kidney. Am J Physiol Renal Physiol 2001;281: F357–65.

This page intentionally left blank

CHAPTER

21

Biophysical Basis of Glomerular Filtration

Scott C. Thomson and Roland C. Blantz

University of California and VA San Diego Healthcare System, San Diego, CA, USA

INTRODUCTION

Marcello Malpighi (1628–1694) discovered the renal corpuscle and proposed that each glomerular body embraces the ampullar extremity of a tubule to form a "glandular follicle".[81] Thereafter, progress toward understanding the structure and function of the nephron stalled for two centuries, until William Bowman finally established the proper anatomic relationship between the glomerular arterioles, capillary tuft, and uriniferous tubule in 1842.[1,16] In that same year, Carl Ludwig, in his *Habilitations* thesis, addressed the driving force that separates the watery and crystalloid constituents of the plasma from its "proteid" constituents. He dismissed both the "nonexistent" vital force and chemical theories for converting blood to urine, and deduced from geometric considerations that local hydraulic forces drive filtration of blood plasma through porous glomerular capillary walls[78] (Figure 21.1). Ludwig's theory was not universally accepted at the time and other influential figures, such as Heidenhain, continued to advocate the secretory formation of urine.[54] Ludwig also had the foresight to envision that the hyperproteinemia resulting from glomerular filtration causes concentration of the urine by endosmosis into the peritubular capillaries.[79] Several decades later, vant Hoff and others began to describe osmosis in terms of pressure using thermodynamic principles,[143] which inspired Ernest Henry Starling to contemplate a role for the osmotic pressure of the plasma colloids in glomerular filtration. Starling wondered whether the minimum blood pressure below which formation of urine ceases might equal the osmotic pressure of the plasma colloids that oppose filtration. In 1897, he tested this hypothesis using a colloid osmometer of his own design[131] with which he estimated the osmotic pressure of the blood plasma protein to be 25–30 mmHg or about 0.4 mmHg-gram^{-1}/liter^{-1}. Then he observed that raising the ureteral pressure to within 30–45 mmHg of the arterial blood pressure would stop the flow of urine in a dog undergoing diuresis. Thus, the hydraulic pressure across the glomerular epithelium must exceed the plasma colloid osmotic pressure by some small amount in order for urine to form. On this basis, Ludwig's filtration hypothesis was deemed credible. Further evidence for glomerular filtration was published in 1924 by Wearn and Richards, who directly visualized the passage of indigo carmine into Bowman's space from the blood in the course of performing the first-ever micropuncture experiments. Wearn and Richards interpreted their own findings as "indirect evidence that the process in the glomerulus is physical".[148]

Glomerular filtration eventually received theoretical consideration as a case of coupled transport, subject to the basic rules of non-equilibrium thermodynamics, which were articulated by Onsager in 1931[95] and adapted to describe the permeability of biological membranes by several investigators in the 1950s. Prior to the 1950s, the conventional description of transport through membranes simply combined Fick's diffusion equation for solute flux with Darcy's equation for water flux, such that the function of a membrane which is to "prescribe the road along which the system strives toward equilibrium",[132] was defined by two permeability coefficients, one for diffusion of solute and one for bulk flow of water. By the 1950s it had become clear that these "conventional" permeability equations for solute and volume flow could not fully describe the physical behavior of membranes, so attempts were made to supplement them. The most cited contribution in this area came from Kedem and Katchalsky,[69] who pointed out that the prior approach was incomplete due to the fact that it included only two coefficients, whereas Onsager's theory calls for exactly three coefficients to characterize permeability for a solute–solvent system. Qualitatively, the

Seldin and Giebisch's The Kidney, Fifth Edition.
DOI: http://dx.doi.org/10.1016/B978-0-12-381462-3.00021-5

© 2013 Elsevier Inc. All rights reserved.

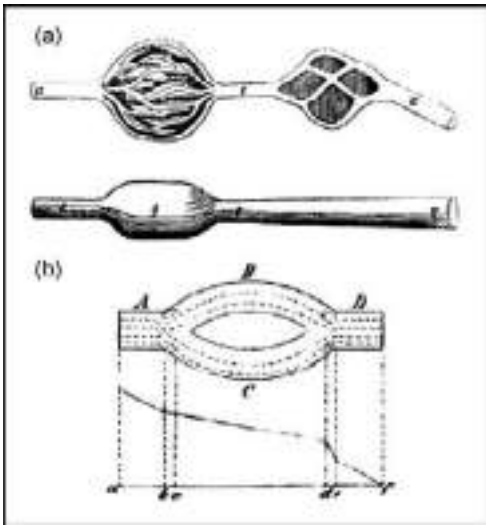

FIGURE 21.1 **Ludwig's representation of renal microvasculature (a) and (b) pressure profiles along the glomerular capillary** *(from ref. [56]).*

hydrodynamic resistance to free diffusion is due to friction between solute and solvent alone, and is determined by a single diffusion coefficient. But passage through a membrane involves two additional factors, namely, the friction between solute and membrane, and the friction between solvent and membrane. Hence, three processes are at play, and three coefficients are required to account for them all. Kedem and Katchalsky then proceeded with a formal argument, starting from the rate of entropy production and invoking Onsager's theory for a solute–solvent system which is paraphrased as follows:

For present purposes, we are interested in the transmembrane flux of a two-component system consisting of a water (w) and a non-electrolyte solute (s). Each of these components is driven by a conjugate force equivalent to its difference in free energy across the membrane. The conjugate forces for water and non-electrolyte solute are:

$$\Delta\mu_w = V_w\Delta P + RT\Delta\ln\gamma_w X_w \tag{21.1a}$$

$$\Delta\mu_s = V_s\Delta P + RT\Delta\ln\gamma_s X_s \tag{21.1b}$$

where V is a partial molar volume, ΔP is the pressure difference, X is the mole fraction, and γ is an activity function, empirically derived as a function of X. Since water flux affects X_s and solute flux affects X_w, the two conjugate forces and fluxes are coupled. For a small deviation from equilibrium this coupling can be taken into account by the following linear flux equations:

$$J_w = L_{11}\Delta\mu_w + L_{12}\Delta\mu_s \tag{21.2a}$$

$$J_s = L_{21}\Delta\mu_w + L_{22}\Delta\mu_s \tag{21.2b}$$

where Lxy are the so-called phenomenological constants. Onsager's theory says that $L_{21} = L_{12}$. Therefore, if the three coefficients, L_{11}, L_{22}, and $L_{21} = L_{12}$ are known, along with baseline values of J_w and J_s, then one can predict the changes in J_w and J_s that will arise from any alteration in $\Delta\mu_w$ or $\Delta\mu_s$. However, the physical meanings of the phenomenological constants are difficult to appreciate, and a more familiar form of the Onsager equations was provided in 1958 by Kedem and Katchalsky to describe transport across biological membranes[69]:

$$J_v = L_P\cdot(\Delta P - \sigma_s\Delta\Pi) \tag{21.3a}$$

$$J_s = P_s\cdot\Delta C_s + J_V(1-\sigma_s)\cdot\overline{C_s} \tag{21.3b}$$

When applied to movement across a capillary wall, J_v and J_s denote respectively the flux of volume (substituting volume for water is allowable for dilute solutions) and solute; ΔP, $\Delta\Pi$, and ΔC are differences in hydrostatic pressure, osmotic pressure, and concentration integrated across the membrane; σ_s is the reflection coefficient of the membrane for s; L_p is the hydraulic permeability per unit area of membrane; and P_s is the diffusive permeability of the membrane to s; $\overline{C_s}$ is the mean concentration of s within the membrane. Π is a function of C. σ_s assumes a value between zero and one. Three of these parameters, L_p, P_s, and σ_s, are characteristics of the membrane, in keeping with the Onsager theory which requires exactly three coefficients to describe the coupled transport of the two entities, v and s. Equation (21.3a) is often referred to as the "Starling equation." Equation (21.3b) expresses J_s as the sum of diffusive and convective components. Equations (21.3a) and (21.3b) are coupled. J_s explicitly depends on J_v. J_v depends on J_s because J_s affects $\Delta\Pi$.

There are limitations to irreversible thermodynamics and to the simplified equations, beginning with the assumption of a linear relationship between fluxes and forces. For example, one can imagine how increasing ΔP might cause a capillary wall to stretch, thereby changing the geometry of its pores and altering L_p. Also, $\overline{C_s}$ can take a variety of forms, depending on whether σ is taken to be active throughout the membrane or to be a membrane entrance phenomenon, and this will affect how J_s is parsed into its diffusive and convective components.[67] Finally, protein accumulates near the capillary wall during filtration, which could raise the local colloid osmotic pressure at the wall and cause L_p to be underestimated when calculated based on Π for the bulk plasma. Nonetheless, these equations remain the basis for all current understanding of the physical factors that determine transport of water and solutes between the glomerular capillary plasma and the urinary space.

Depending on the context, different simplifying assumptions are made that streamline the description of capillary flux in the glomerulus. For example, when considering J_v (i.e., glomerular filtration), the solutes

are divided into two groups, large and small. Large solutes are the colloids, and it is assumed that P_s for these is zero and σ_s is unity. All other solutes are assumed to be small, and it is assumed that σ_s (and ΔC) for these is zero. Solutes with intermediate permeability are ignored. Therefore, $\Delta\Pi$ can be substituted by the colloid osmotic pressure of the glomerular plasma, and a full description of J_v is provided by Eq. (21.3a). This obviates the need to consider coupled transport. Although the contribution of filtered macromolecules to the transcapillary oncotic pressure may be negligible, there are times when it is critical to understand the sieving properties of the glomerulus for large molecules. In such cases, simplifying assumptions are made regarding the geometry of the filtration barrier and the shape of the solute molecules, so that the process can be conveniently described using hydrodynamic theory.

THE MAGNITUDE OF RENAL BLOOD FLOW AND GLOMERULAR FILTRATION

In humans, the kidneys constitute 0.5% of the body weight, but receive 20% of the cardiac output. The low resistance to renal blood flow is owing to the large number of parallel conductances, with each human kidney containing about 1 million glomeruli.[124] Approximately 8000 liters per day of blood plasma transits the extrarenal organs, of which about 20 liters is filtered into interstitial spaces and returned to the blood as lymph.[71] In contrast, the kidneys form 180 liters per day of glomerular filtrate from 900 liters of blood plasma. The high rate of filtration by the kidney relative to other organs is due to a greater ultrafiltration coefficient, not to greater Starling force.[44,99,149] The surface area available for filtration in the human kidney is in the order of 1.2 m^2 overall or 0.6 mm^2 per glomerulus. A meaningful number is difficult to assign to the capillary surface area in other major organs where the number of capillaries perfused at any given moment is highly variable. The hydraulic permeability L_p of fenestrated glomerular capillaries has been estimated from 2.5–4.0 $\mu l/min/mmHg/cm^2$ in rats and humans,[33,114,115] which is 50-fold higher than L_p for non-fenestrated skeletal muscle.[123]

GLOMERULAR HEMODYNAMICS BY INFERENCE

Having first identified inulin and PAH as a markers of GFR renal plasma flow (RPF),[121,126] Homer Smith and colleagues used clearance of these markers to make logical judgments about the regulation of GFR. Smith observed a reciprocal relationship between RPF and filtration fraction in human subjects injected with pyrogens,[23] and recognized that this is contrary to what should occur if the changes in RPF were mediated by a preglomerular resistance. He used equations to argue that the renal resistance changed in these experiments due to dilation and constriction of the efferent arteriole. His formulation required a strong inverse effect of efferent resistance on filtration fraction, which could be achieved by assuming that the net ultrafiltration pressure vanishes at some point along the capillary, as hydrostatic pressure declines and plasma oncotic pressure increases. Based on knowledge that this occurs in the mesenteric circulation, Smith was willing to assume that this also happens in the kidney, and coined the term "filtration pressure equilibrium" in reference to the phenomenon[125] (see Figure 21.2). Smith later recanted his notion of filtration pressure equilibrium in the glomerular capillary, arguing on teleologic grounds that the hydrostatic null point should occur in the proximal portion of the efferent arteriole in order to promote maximal GFR and maximal reabsorption in the peritubular capillary.[124] His revised thinking was likely influenced by the contemplations of Gomez.[47]

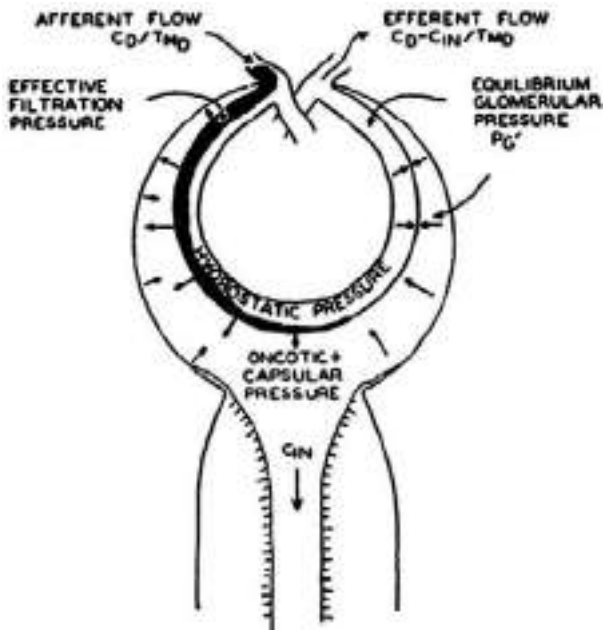

FIGURE 21.2 **Filtration equilibrium illustrated in the glomerulus** *(from ref. [29]).*

GLOMERULAR HEMODYNAMICS AND MICROPUNCTURE

A full and direct assessment of the filtration forces and hydraulic permeability in a mammalian glomerulus was first published by Brenner et al. in 1971.[19] Three

developments made this possible. First, a mutant rat strain (Munich Wistar) was discovered with glomeruli on the kidney surface making them accessible for glomerular micropuncture. Second, a servo-null device was invented that enabled accurate and rapid pressure measurements in capillaries and tubules.[41] Third, a microadaptation of the Lowry method[77] was developed for measuring the protein concentration in a few nanoliters of plasma which could be obtained by micropuncture from a postglomerular arteriole.[17]

Given values for the pressure in the glomerular capillary P_{GC} and Bowman's space P_{BS}, pre- and postglomerular plasma protein concentrations c_0 and c_1, single nephron ^{3}H-inulin clearance *SNGFR*, and a simple mathematical model for computing changes in the ultrafiltration pressure P_{UF} along the glomerular capillary, it is possible to obtain values for the glomerular plasma flow Q_0 and ultrafiltration coefficient *LpA*. *LpA* is the product of the hydraulic permeability *Lp* (see Eq. (21.3a)) and the filtration surface area *A*.

The mathematical model for computing the physical determinants of *SNGFR* from micropuncture data was developed by Deen, Robertson, and Brenner in 1972.[31] This model treats the glomerular capillary as a circular cylinder of unit length and surface area, uniform permeability to water and small solutes, and zero permeability to protein (see Figure 21.3). As in Eq. (21.3a), the filtration flux at any point along the capillary is equal to the product of the Starling force, $\Delta P - \Delta\Pi$, and the hydraulic permeability, *Lp*. *SNGFR* is obtained by integrating the flux along the capillary length:

$$\begin{aligned} SNGFR &= \int_0^1 Jv \cdot dx \\ &= LpA \int_0^1 (\Delta P - \Delta\Pi) dx \\ &= LpA \langle P_{UF} \rangle \end{aligned} \tag{21.4}$$

where $\Delta P = P_{GC} - P_{BS}$, $\Delta\Pi + \Pi_{GC} - \Pi_{BS}$ and $\langle P_{UF} \rangle$ is the mean ultrafiltration pressure. The term *LpA* represents the product of the hydraulic permeability *Lp* and filtration surface area *A*. For the non-dimensionalized capillary, *A* equals unity. For the real capillary, micropuncture data do not distinguish between changes in *Lp* and changes in *A*.

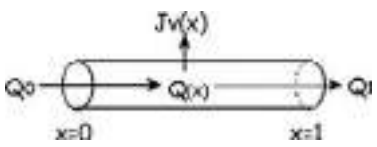

FIGURE 21.3 **Glomerular capillary represented by a homogerous circular circular cylinder with unit length and surface area (Q: Plasma flow; Jv: Filtration water flux; X: Axial position along the capillary).**

To perform the integration in Eq. (21. 4) it is necessary to know how the integrand varies along the capillary. In theory, both ΔP and $\Delta\Pi$ should change along the capillary, since P_{GC} must decline due to axial flow resistance and Π_{GC} must rise as water moves from the plasma into Bowman's space. It has always been assumed that the decline in P_{GC} along the capillary is small relative to the increase in Π_{GC}. This assumption was eventually justified by a three-dimensional reconstruction of the rat glomerulus submitted to computational analysis.[104] It is our custom to ignore the small axial pressure drop and represent ΔP as a constant, since including a 1−2 mmHg axial pressure drop in the model has a minimal effect on $\langle P_{UF} \rangle$. However, to better illustrate certain principles in this chapter, we have incorporated a 1 mmHg decline in P_{GC} from the beginning to the end of the glomerular capillary.

For the purposes of determining $\Delta\Pi$ it is assumed that all solutes in the system are either completely impermeant plasma proteins that exert their full osmotic potential ($\sigma = 1$, $Ps = 0$) and reside solely in the plasma or small molecules that are freely filtered ($\sigma = 0$) and contribute nothing to $\Delta\Pi$. Thus, $\Delta\Pi$ is reduced to the plasma oncotic pressure, Π_{GC}. The oncotic pressure in a plasma sample is determined from the protein concentration *c*, according to an empiric relationship developed by Landis and Pappenheimer:

$$\Pi = \alpha_1 c + \alpha_2 c^2 \tag{21.5}$$

The values of α_1 and α_2 in Eq. (21.5) vary according to the ratio of albumin to globulin in the plasma. When Π is expressed in mmHg and *c* in grams per 100 ml, for rat plasma, α_1 and α_2 are 1.73 and 0.28, respectively.[71] According to Eq. (21.5), Π_{GC} will increase from 18 to 35 mmHg along the length of a glomerular capillary if the systemic plasma contains 6 g/dl of protein and the nephron filtration fraction is 0.29. Such values are typical of the rat.

LpA is computed from *SNGFR* and $\langle P_{UF} \rangle$, according to Eq. (21.4). To obtain $\langle P_{UF} \rangle$ it is necessary to know the profile for Π_{GC} along the capillary. This profile is computed from the following mass balance considerations for protein and water. First are three conservation of mass equations:

$$Q_0 = SNGFR\left(\frac{c_1}{c_1 - c_0}\right) \tag{21.6a}$$

$$cQ = c_0 Q_0 \tag{21.6b}$$

$$J_v = -\frac{dQ}{dx} \tag{21.6c}$$

where Q_0 is the nephron plasma flow and c_0 and c_1 are the pre- and post-capillary plasma protein

concentrations. Differentiating Eq. (21.6b) and substituting Eqs. (21.6c), (21.5), and (21.3a):

$$\frac{dc}{dx} = \frac{c^2}{c_0 Q_0} J_v \tag{21.7a}$$

$$= \frac{Lp \cdot c^2}{c_0 Q_0} (\Delta P - (\alpha_1 c + \alpha_2 c^2)) \tag{21.7b}$$

A standard root-finding algorithm is used to obtain a value for *LpA* by numerical integration of Eq. (21.7) along the entire capillary to obtain an estimate for the plasma protein concentration at the end of the capillary (c_1*) and adjust the value of *LpA* until c_1* is arbitrarily close to the measured value of c_1.

$$c_1^* = c_0 + \frac{LPA}{c_0 Q_0} \int_0^1 c^2 (\Delta P - (\alpha_1 c + \alpha_2 c^2)) \cdot dx \tag{21.8}$$

In a typical experiment, *SNGFR*, ΔP, and c_1 are measured in several nephrons. Most often, these parameters are not obtained from the same nephrons. The mean values for an experiment are inserted into the model to calculate the determinants of SNGFR for an idealized nephron.

From the foregoing description, we see that *SNGFR* is fully determined by ΔP, Q_0, c_0, and *LpA*. Typical values for these parameters are shown in Table 21.1 for Munich Wistar rats from two different breeding colonies under different volume states. Conceptually, *SNGFR* can be made to increase by raising ΔP, Q_0 or *LpA* or by reducing c_0. But the magnitude of the dependence on each of the four determinants depends on the values of the other three. Some of these interactions are shown in Figures 21.4–21.7 and discussed below.

Ultrafiltration Coefficient, *LpA*, and Filtration Pressure Equilibrium

If the ratio of *LpA* to Q_0 is great enough, then Π_{GC} will rise to become arbitrarily near to ΔP at some point along the glomerular capillary, resulting in filtration pressure equilibrium. The remaining capillary surface downstream from the equilibration point will not contribute to the flux. It is possible to infer the presence of filtration equilibrium from micropuncture data, but it is not possible to know at what point along the length of the capillary equilibrium occurs. Therefore, it is not possible to compute actual values for $\langle P_{UF} \rangle$ or *LpA* for nephrons in filtration equilibrium. When Eqs. (21.4)–(21.8) are applied to data from a nephron in filtration pressure equilibrium, the values generated for *LpA* and $\langle P_{UF} \rangle$ are respective

TABLE 21.1 Representative Micropuncture Data in Munich Wistar Rats from the Blantz Lab in San Diego and Brenner Lab in Boston.

Laboratory	State of Hydration	SNGFR (nl/min)	ΔP (mmHg)	Π_0 (mmHg)	Q_0 (nl/min)	*LpA* (nl/s/mmHg)	Filtration Pressure Equilibrium	Reference
Blantz	Hydropenia	30	30.5	18.3	86	0.08*	Yes	9
	Euvolemia	31	37.2	19.7	121	0.06	No	137
	Acute 2.5% plasma volume expansion	45	42.2	18.2	177	0.05	No	137
Brenner	Hydropenia	21	35.3	19.4	65	0.08*	Yes	19
	Euvolemia	32	33.4	19.4	114	0.08*	Yes	59
	Acute 5% plasma volume expansion	50	41.2	22.9	201	0.08	No	33

Minimum estimate due to filtration pressure equilibrium. LpA values that show differently from the original papers were originally calculated based on a linear estimate of the oncotic pressure profile and are recalculated here using the non-linear model.

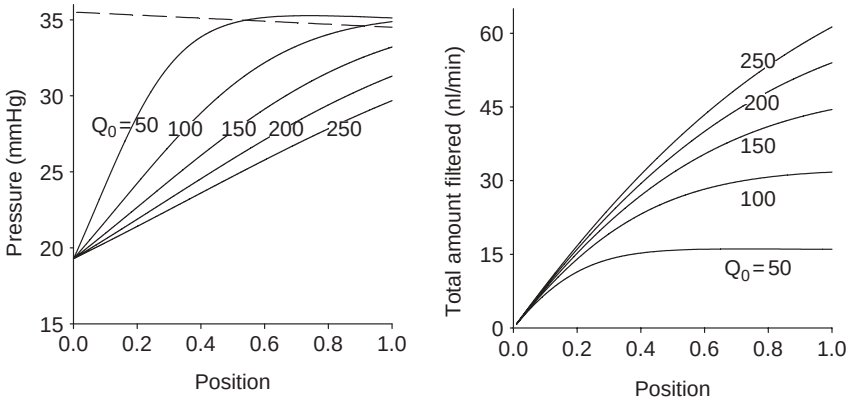

FIGURE 21.4 **Pressure (left) and total flux (right) along the length of the glomerular capillary.** In left panel solid curves represent plasma oncotic pressure which rises due to removal of water, while dashed line represents ΔP, which declines by 1 mmHg along the capillary due to flow resistance. *SNGFR* is the total amount filtered at position 1. Other inputs include systemic plasma protein concentration 5.8 mg/dl, and LpA 0.08 nl/s/mmHg. Filtration ceases where oncotic pressure rises to equal ΔP, which occurs when incoming plasma flow, Q_0, is low.

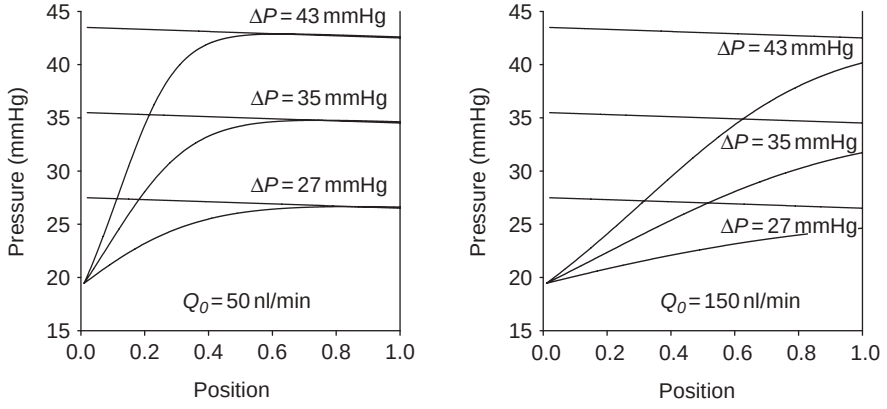

FIGURE 21.5 **ΔP (lines) and Π_{GC} (curves) along the length of a glomerular capillary for three different values of ΔP.** Left panel: $Q_0 = 50$ nl/min. Right panel: $Q_0 = 150$ nl/min. Other inputs include systemic plasma protein concentration 5.8 g/dl, and LpA = 0.06 nl/s/mmHg. ΔP has little effect on whether or not filtration pressure equilibrium is achieved. In contrast, increasing Q_0 from 50 to 150 nl/min eliminates filtration equilibrium regardless of ΔP.

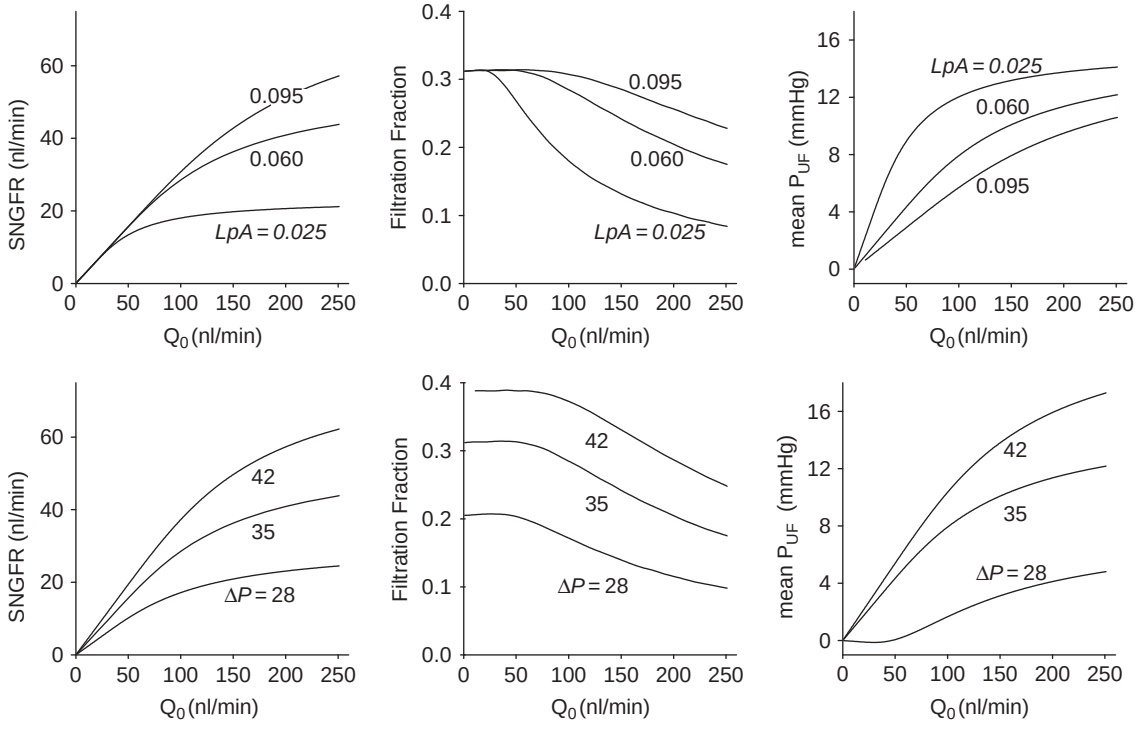

FIGURE 21.6 ***SNGFR*, filtration fraction or mean ultra-filtration pressure (P_{UF}) as a function of nephron plasma flow, Q_0.** Curves in top panels were generated for three different values of LpA. Curves in the bottom panel were generated for three values of ΔP. Unless otherwise stated, LpA = 0.06 nl/s/mmHg; ΔP = 35 mmHg; Systemic plasma oncotic pressure = 19.5 mmHg. Values over this range occur in the rat under varying levels of volume expansion.

minimum and maximum estimates for actual *LpA* and $\langle P_{UF} \rangle$. If a change in *LpA* occurs while a nephron remains in filtration pressure equilibrium, the equilibrium point will shift along the capillary, but *SNGFR* will not be affected. In order for *SNGFR* to be affected by a change in *LpA*, the nephron must not be in filtration equilibrium.

A debate over whether filtration pressure equilibrium occurs dates back to Homer Smith, who used conjecture and teleology to argue both sides of the issue at different points in his career (*vide supra*). Brenner and colleagues found filtration equilibrium in each of 12 consecutive published series, suggesting that filtration equilibrium is universal for hydropenic or euvolemic Munich Wistar rats. However, contrary data were generated by other micropuncture laboratories. At one point, this led to consternation.[92] The issue was resolved after experiments done with rats exchanged between different laboratories led to the conclusion that filtration equilibrium prevails in some rat strains or breeding colonies but not in others, and that the difference is attributable to differences in *LpA*.[4] This finding detracts somewhat from teleologic arguments for or against filtration pressure equilibrium.

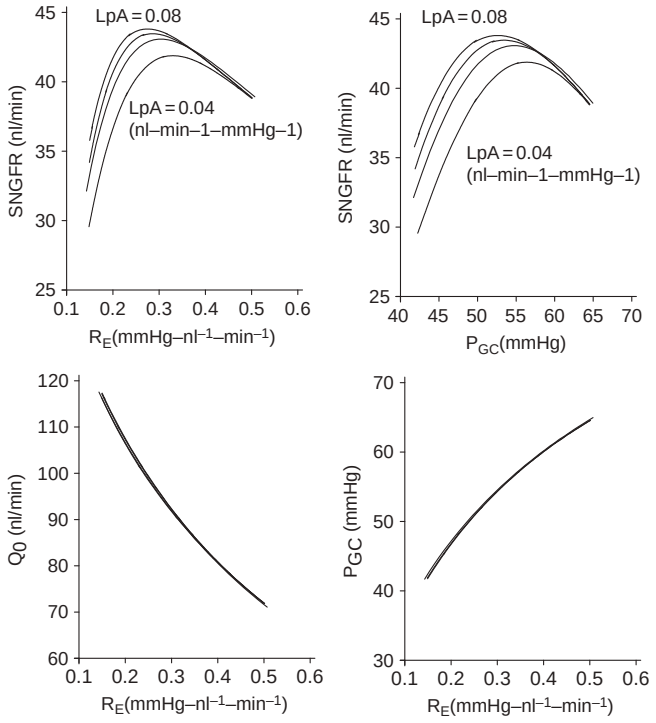

FIGURE 21.7 **Effects of efferent arteriolar resistance (R_E) on *SNGFR*, nephron plasma flow (Q_0), and glomerular capillary pressure (P_{GC}).** In top right panel, P_{GC} is made an independent variable by manipulating R_E. Effects on Q_0 and P_{GC} are nonlinear, because the filtration fraction rises along with R_E such that a lesser fraction of the blood flow transits the efferent arteriole. The Q_0 and P_{GC} curves (bottom) are insensitive to LpA. The apex of the *SNGFR* curve occurs within the physiological range of P_{GC} (48–52 mmHg). Medical treatments for glomerular capillary hypertension that reduce R_E until P_{GC} is normal will not reduce *SNGFR*. However, for P_{GC} <48 mmHg, reducing R_E will cause *SNGFR* to decline.

Nephron Plasma Flow, Q_0

Q_0 does not appear in the Starling equation for water flux (Eq. (21.3a)) or in the flux integral that defines *SNGFR* (Eq. (21.4)). Nonetheless, Q_0 is an important determinant of *SNGFR*. In fact, increased renal plasma flow underlies many of the physiologic increases in GFR that occur in the normal course of life, such as during pregnancy[6] or after protein feeding.[57,103,120] *SNGFR* is the simple product of *LpA* and $\langle P_{UF} \rangle$ (Eq. (21.4)). $\langle P_{UF} \rangle$ becomes greater if the average plasma oncotic pressure along the capillary is less. Removing a given amount of water from the plasma will cause a lesser increase in the plasma oncotic pressure if that water is subtracted from a larger initial plasma volume. Hence, increasing Q_0 will cause oncotic pressure to rise more slowly along the capillary. Therefore, increasing Q_0 causes $\langle P_{UF} \rangle$ to increase. The precise effect of Q_0 on the rate of rise in plasma protein concentration along the nephron is described mathematically in Eq. (21.7). *SNGFR* will be most sensitive to changes in Q_0 under conditions of filtration pressure equilibrium where the filtration fraction remains constant as Q_0 increases. In filtration disequilibrium, c_1, *ergo* filtration fraction, will decline with increasing Q_0 to reduce the impact of Q_0 on *SNGFR*. Homer Smith recognized that renal plasma flow should affect GFR by this mechanism, and that his experiments (*vide supra*) failed to confirm a plasma flow dependence of *GFR* only because the particular tools that he employed to manipulate the renal blood flow were confounded by offsetting effects on P_{GC}.[125]

Systemic Plasma Protein Concentration, c_0

In the idealized glomerulus, an isolated change in c_0 will cause opposite changes in $\langle P_{UF} \rangle$ and, therefore, *SNGFR*. However, it is difficult to demonstrate this experimentally because it is nearly impossible to manipulate oncotic pressure of the arterial plasma without affecting the neurohumoral milieu of the entire body, thereby altering other determinants of *SNGFR*. In fact, the circumstances associated with low oncotic pressure in real life (e.g., generalized capillary leak, sepsis, malnutrition or nephrosis) are generally associated with a low GFR. When c_0 is manipulated by whatever means, changes in other determinants occur to offset the impact on *SNGFR*. These changes are discussed below under "Interactions Among the Determinants of SNGFR."

Hydrostatic Pressure, P_{GC}, and ΔP

Whereas *SNGFR* is insensitive to *LpA* when Q_0 is low and insensitive to Q_0 when *LpA* is low, *SNGFR* will always be sensitive to an isolated change in ΔP unless ΔP is so low as to be exceeded by the incoming plasma oncotic pressure, in which case *SNGFR* will be zero. This is true because the proportional increase in $\langle P_{UF} \rangle$ brought about by any increment in $\Delta P - \Pi_0$ is relatively insensitive to the other determinants of SNGFR. This is illustrated in Figure 21.5 and in the lower half of Figure 21.6.

The interposition of the efferent arteriole between the glomerulus and peritubular capillary provides a simple mechanism for regulating ΔP independently of Q_0. Furthermore, this arrangement provides an opportunity to elicit reciprocal changes in P_{GC} and pressure in the downstream peritubular capillary P_{PTC}. Tying an increase in P_{GC} to a decrease in P_{PTC} has teleologic appeal, as this will facilitate homeostasis of the effective circulating blood volume while stabilizing GFR. If the efferent arteriole reacts to sustain P_{GC} and reduce P_{PTC} during a decline in renal perfusion pressure or effective circulating blood volume, then GFR will be relatively spared from declining while filtration

fraction will increase, thus affecting both the hydraulic and oncotic components of the Starling force that drives reabsorption by the peritubular capillary.

Regulating the efferent arteriole in this way is largely the purview of the renin–angiotensin system, which figures prominently among the myriad neurohumoral mechanisms contained in models of blood pressure and salt homeostasis. Angiotensin II is antinatriuretic and constricts arterioles throughout the body but, on balance, its effect on the glomerulus is always to elevate ΔP.[52,55,119,142] Thus, in spite of being a renal vasoconstrictor, angiotensin II protects GFR from total decline when the arterial blood pressure is low or when the preglomerular resistance is high.

While unduly low P_{GC} must impair glomerular filtration, P_{GC} and *SNGFR* are poorly correlated under normal circumstances, as are P_{GC} and arterial blood pressure. This implies that the kidney generally protects P_{GC} against the influence of arterial blood pressure and employs determinants other than ΔP to effect physiologically those changes in *SNGFR* that normally occur throughout life. Furthermore, it has recently been demonstrated that the preglomerular myogenic elements, long associated with static renal blood flow autoregulation, efficiently buffer the glomerular capillary against systolic pressure pulses delivered at the heart-rate frequency.[76] Teleologic reasoning behind sheltering the glomerular capillary from high pressure is that high P_{GC} augments wall stress in the glomerular capillary, which elicits a trophic response. If unchecked, this response will ultimately sclerose and destroy the glomerulus. Therefore, high P_{GC} is always pathologic, and treating glomerular capillary hypertension has been a cornerstone of nephrology practice for more than two decades. Some examples of glomerular capillary hypertension include angiotensin II-mediated hypertension,[46] experimental glomerulonephritis,[10,45] and residual nephrons after subtotal nephrectomy.[3] It has been asserted, and commonly accepted, that glomerular capillary hypertension also underlies glomerular hyperfiltration in early diabetes mellitus.[58,151] However, there are more than 10 published micropuncture studies in which diabetic hyperfiltration occurred in the absence of glomerular capillary hypertension or in which glomerular capillary hypertension was treated with no mitigating effect on diabetic hyperfiltration.[27,62,79,83,84,89,90,106,118,122,141,152] This does not detract from the salutary effect of therapy to reduce P_{GC}, which applies to all glomerular diseases.[5,73,82,136]

Interactions Among the Determinants of *SNGFR*

According to the standard model of Deen and Brenner, *SNGFR* is completely determined by a set of four parameters, which include P, Q_0, LpA, and c_0 (or Π_0). To state that *SNGFR* can be calculated from these four determinants is a mathematical truism which requires no consideration of how the four determinants might correlate in actual physiology. In fact, the individual components of the glomerular microvasculature that influence determinants of *SNGFR* generally affect more than one of them at a time. For example, an isolated increase in resistance of the preglomerular arteriole will directly reduce both ΔP and Q_0 and will reliably reduce *SNGFR*. In contrast, an isolated increase in resistance of the efferent arteriole will directly augment ΔP and reduce Q_0. Since these two effects exert opposing influences on *SNGFR*, increasing efferent arteriolar resistance might cause *SNGFR* to increase, decrease or remain the same, depending on other circumstances. For example if P_{GC} is low enough to be at or below Π_{GC}, then raising the efferent resistance can only cause *SNGFR* to increase whereas, if efferent resistance increases toward infinity, Q_0 must tend toward zero while P_{GC} cannot exceed the arterial blood pressure and, therefore, *SNGFR* must decline. The point where the impact of increasing the efferent resistance switches from positive to negative is within the domain of values that occur *in vivo*. Much of the acute renal failure encountered in contemporary medical practice occurs when drugs that reduce the ratio of efferent: afferent resistance are taken by patients who operate to the left of that point (see Figure 21.7).

There are other correlations between determinants of *SNGFR* that are more difficult to explain. For example, since *LpA* is computed as the ratio of *SNGFR* to $\langle P_{UF} \rangle$, random uncorrelated errors in ΔP and SNGFR will cause an inverse correlation to appear between ΔP and *LpA*. Also, an isolated reduction in *LpA*, if sufficient to reduce *SNGFR*, will remove a shunt pathway for fluid to bypass the efferent arteriole, thereby increasing ΔP. Furthermore, the physical orientation of the glomerular mesangium relative to the intraglomerular portion of the efferent arteriole allows activation of the same contractile elements to simultaneously reduce *LpA* and constrict the efferent arteriole.[40] This appears to explain why angiotensin II, the prototype effector of glomerular hemodynamics, simultaneously increases ΔP and reduces *LpA*,[12] and why lyzing mesangial cells with an antibody negates the effects of angiotensin II on both ΔP and *LpA*.[11]

Another interesting interaction among two determinants of *SNGFR* involves ΔP and the systemic plasma oncotic pressure Π_0. As mentioned above, experiments targeted at confirming the role of Π_0 as a determinant of *SNGFR* are encumbered by the difficulty in manipulating the plasma protein concentration independent of the neurohumoral environment. To get around this, Brenner[7] and Blantz[9,13,140] drew

upon a wide variety of infusion and exchange protocols to alter the systemic plasma protein concentration in multiple ways that were likely to yield contrary effects on the effective circulating volume and hematocrit. These differences were roughly intended to cancel each other out and reveal the underlying impact of Π_0 on *SNGFR*, ΔP, Q_0, and *LpA*. Both groups of investigators confirmed that the four determinants of *SNGFR* are not independent of one another. In particular, they discovered that, regardless of the experimental means for invoking a change in Π_0, a change in Π_0 causes a parallel change in ΔP, and reciprocal change in *LpA*. In contrast, neither *SNGFR* nor Q_0 are predictably tied to Π_0. Most remarkably, ΔP is so strongly dependent on Π_0 that the afferent effective filtration pressure, $\Delta P - \Pi_0$, is independent of Π_0. A biophysical or anatomic explanation for this interaction between Π_0 and ΔP has not been forthcoming. It seems, instead, that a physiological mechanism is involved in autoregulating the afferent effective filtration pressure (see Table 21.2).

Brenner and Blantz also both observed an inverse correlation between Π_0 and *LpA*. It is possible that this is an artifact of concentration polarization which causes plasma proteins to accumulate near the capillary wall. Concentration polarization will lead to an overestimate of P_{UF}, because the calculation of P_{UF} will be based on a lower value of Π than is present at the plasma interface with the capillary wall. Using an overestimate of $\langle P_{UF} \rangle$ in Eq. (21.4) will lead to an underestimate for *LpA*. If concentration polarization occurs in the glomerular capillary, the effect will be greatest when c_0 is least. Hence, the appearance could arise of an inverse dependence of *LpA* on c_0, even though c_0 has no actual effect on the capillary wall. However, there is likely to be enough scrubbing by red blood cells to prevent concentration polarization. Furthermore, concentration polarization cannot explain the correlation between Π_0 and ΔP. Finally, we have already discussed a mechanism for the inverse relationship between ΔP and *LpA*.

TABLE 21.2 Multivariate Regression Applied to Combined Micropuncture Data from Brenner[7] and Blantz[126] to Test for Interactions between ΔP and the other Determinants of SNGFR*

Dependent Variable	Independent Terms in Multivariate Regression		
P (mmHg)	Π_0 (mmHg)	*LpA* (nl/sec/mmHg)	Q_0 (nl/min)
Regression coefficient	0.84 ± 0.09	-72 ± 10	~ 0
P-Value associated with regression coefficient	2×10^{-10}	1×10^{-10}	0.750

*The original regression model included the protocol for manipulating the systemic plasma protein and the lab where the work was performed, neither of which influenced the result.

Therefore, the inverse correlation of between *LpA* and Π_0 might arise because *LpA* is affected, as an innocent bystander, by a mechanism that is postulated to autoregulate afferent P_{UF}.

THE FILTRATION BARRIER AND FILTRATION OF MACROMOLECULES

A striking feature of glomerular filtration is the ability of the capillary wall to discriminate among molecules of varying size. Solutes up to the size of inulin pass freely from the plasma to Bowman's space, while passage becomes progressively difficult for substances that are larger such that all but the smallest plasma proteins are screened almost entirely. Hence, when describing the determinants of SNGFR, the concentration of macromolecules in the filtrate is low enough that these contribute negligibly to the Starling forces. However, the filtration of small amounts of macromolecules is important for other reasons. For example, the plasma transiting a normal pair of human kidneys in one day contains 50,000 grams of protein, while the appearance of one gram per day of protein in the urine is sufficient to establish the presence of glomerular disease. Discerning how this small amount of protein winds up in Bowman's space is key to explaining how the filtration barrier operates normally, and to understanding the physical aspects of glomerular disease.

The filtration of a macromolecule is most often quantified in terms of its sieving coefficient, Θ, which is the ratio of solute concentration in the filtrate relative to filtrand. The earliest direct test for protein in mammalian glomerular filtrate was performed by Walker in 1941, who reported that micropuncture fluid obtained from Bowman's space in rat, guinea pig or opossum contained "either no protein or, at most, very small amounts." The assay in use at the time would have detected an overall sieving coefficient for protein of 0.4%, which made it insensitive by later standards.[146] Several subsequent micropuncture studies during the 1970s yielded widely varying amounts of albumin in proximal tubular fluid, even within an experiment. This variability was reasonably ascribed to contamination of samples by extratubular proteins, since only 1% contamination of a tubular fluid sample with plasma from the peritubular capillary would markedly alter the apparent result.[93] Performing micropuncture with a system of concentric pipettes to reduce contamination, Tojo succeeded in confirming a strong inverse relationship between TF/P inulin and albumin concentration in fluid collected from rat proximal tubules due to removal of filtered albumin along the proximal tubule. By linear extrapolation to TF/P inulin of unity,

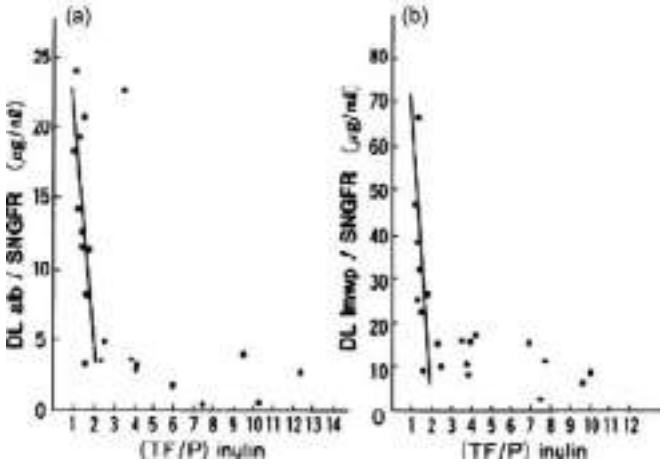

FIGURE 21.8 **Albumin (a) and low molecular weight protein (LMWP) delivery (b) along the nephron.** Linear regression over the domain of TF/Pinulin from 1 to 2 was used to calculate the protein concentration in Bowman's space *(from ref. [80])*.

which represents Bowman's space, the sieving coefficient for albumin was estimated at 0.062%. Meanwhile, the sieving coefficient of low molecular weight proteins was almost 99%, confirming the size-selective nature of protein sieving[138] (see Figure 21.8). However, micropuncture remains an unwieldy technique for studying glomerular sieving of macromolecules, and most of what is known about glomerular sieving has been learned by other means (*vide infra*).

Pore Theory

The glomerular capillary wall clearly screens solutes according to size, and it is usually taught that the glomerulus also screens macromolecules according to charge. The physical basis of molecular sieving is often modeled using pore theory. In pore theory, the coupled flux equations (Eq. (21.3a,b)) are modified to fit an idealized model of the glomerular capillary wall. The usual model consists of a solid barrier perforated by cylindrical pores. In some models, the pores form a homogenous population, while other models employ a mixture of pores of different sizes. This paradigm for describing the flow of material through porous membranes was applied to diffusion and filtration of solutes by capillaries, and an early review of the subject was published by Pappenheimer in 1953.[98] Mathematical descriptions were developed for pores shaped like circular cylinders or rectangular slits. At about the same time, theories were developed by others to explain the migration of large solutes through fibrous gels.[91] Given what is now known about the physical structure of the glomerular capillary wall, pores, slits, and fibrous gels are all relevant to glomerular sieving. Hence, descriptions based solely on cylindrical pores have become more obviously phenomenological. Nonetheless, pore theory remains the most popular paradigm for describing nuances of glomerular sieving in humans.[13,29,72,86]

Pore theory builds on the Kedem–Katchalsky flux equations (Eq. (21.3a,b)) by associating the three membrane parameters, Lp, P_s, and σ_s with an idealized physical structure. This structure incorporates the membrane geometry, the Stokes–Einstein radius of the solute molecules, temperature, viscosity, and the Boltzman constant. The solutes are represented by rigid spheres that interact with the solvent medium and with the pores, but not with each other. This makes the problem mathematically tractable. The filtration properties of a membrane with circular pores turn out to depend on two things: (1) the ratio of pore diameter to membrane thickness; and (2) the overall fraction of the membrane area covered by pores.

An explanation begins with Fick's first law of diffusion for a solute s:

$$J_s^{diffusion} = -D_s \frac{dC_s}{dx} \tag{21.9}$$

where:

$$D_s = \frac{RT}{fN} \tag{21.10}$$

is the diffusion coefficient, N is Avogadro's number, and f is the frictional force that opposes diffusion of s.

According to Stokes' law, a sphere of radius a falling at unit velocity in a medium of viscosity:

$$J_s^{diffusion} = D_0 \frac{A_p}{\delta} \Delta C_s$$

η faces a frictional force given by:

$$f = 6\pi\eta a \tag{21.11}$$

Einstein[39] combined Fick's law of diffusion and Stokes law to derive the diffusion coefficient for a spherical molecule in free solution, D_0, in terms of its molecular radius a:

$$D_0 = \frac{RT}{6\pi\eta a N} \tag{21.12}$$

Since actual molecules are not spherical, the Stokes–Einstein radius, a, of a molecule is a virtual quantity represented by a sphere of equivalent radius. Using the Stokes–Einstein radius of a marker solute to estimate the size of pores in a membrane will overestimate the actual pore radius if the marker solute is flexible and can squeeze through a smaller pore than a rigid sphere with the same Stokes-Einstein radius.

For the diffusion of small molecules through a membrane that contains large pores, Fick's first law is rewritten:

$$J_s^{diffusion} = D_0 \frac{A_p}{\delta} \Delta C_s \tag{21.13}$$

where A_p is the fraction of the membrane surface covered by pores and δ is the membrane thickness. Therefore, the diffusion through a membrane of a small solute with known D_0 is a convenient method to determine the ratio of pore area to thickness for the membrane.

However, when the molecular radius of the solute molecule is on the same scale as the pore size, diffusion through the membrane is less than predictable from Eq. (21.13). In other words, mobility of the solute is restricted. There are two factors that contribute to restricted mobility. First, there is steric hindrance to the solute entering or residing within the pore. Second, solute molecules within the pore experience greater friction than predicted by Stokes' law for solute molecules in free solution. While it makes sense to us to represent the steric hindrance by a reduced effective pore area and the increased friction as a reduced effective diffusion coefficient, most of the literature combines both effects into an expression for the effective pore area. This is described below.

Diffusion through a Porous Membrane: Steric Hindrance and Altered Friction

Restricted passage of solutes of increasing molecular radius is a basic property of membrane structures made of impermeable matrix with pores or fibrous gels. The basis for molecular sieving in all cases is the exclusion of large solute molecules from a portion of the membrane that is otherwise available to be occupied by water and other small molecules. The formulae for describing steric hindrance are different for pores than for gels. Here we will describe the phenomenon for cylindrical pores.

The center of a spherical molecule cannot approach any closer than its own radius to the edge of any pore. Hence, the fraction of a cylindrical pore, area Vp and radius r, that is available to be occupied by a solute with molecular radius a, is:

$$\frac{V}{V_p} = \frac{\pi(r-a)^2}{\pi r^2} = \left(1-\frac{a}{r}\right)^2 \tag{21.14}$$

Introducing solvent flow makes the steric hindrance more complex. This was first addressed by Ferry who added a term to account for laminar flow within the pore[43]:

$$\frac{V}{Vp} = \left(1-\frac{a}{r}\right)^2 \cdot \left(2-\left(1-\frac{a}{r}\right)^2\right) \tag{21.15}$$

The frictional drag on a solute molecule moving through a pore is also different from that described by Stokes' law for a solute in an unbounded free solution. The drag according to Stokes' law for the unbounded condition and the drag encountered in a pore are given by Eq. (21.16a,b) for a solute moving with velocity u in a fluid with velocity v. k_1 and k_2 are component drag coefficients that weight the contributions of the particle and fluid velocities. k_1 and k_2 are functions of a/r.

Theoretical treatments have provided approximate solutions for k_1 and k_2 for particles in cylindrical tubes.[51] Determining values for k_1 and k_2 is computationally intense. For this reason, k_1 and k_2 were originally provided for only a few values of a/r and a polynomial equation was fit to these points to allow interpolation. This approximation expression was inaccurate for $a/r > 0.6$, but this was the only method available until better computers were built in the 1970s.[97]

$$f_{unbounded} = 6\pi\eta a(u-v) \tag{21.16a}$$

$$f_{pore} = 6\pi\eta a(u\cdot k_1 - v\cdot k_2) \tag{21.16b}$$

Accounting for steric hindrance and dividing Eq. (21.16b) by Eq. (21.16a) to correct for the departure from Stokes' law, the diffusive flux is rewritten from Eq. (13) to become:

$$\begin{aligned} J_s^{diffusion} &= D_0 \frac{A_p}{\delta}\left(\left(1-\frac{a}{r}\right)^2\left(2-\left(1-\frac{a}{r}\right)^2\right)\right) \\ &\quad \cdot \left(\frac{u-v}{uk_1 - vk_2}\right)\Delta C_s \\ &= D_0 \frac{A_{eff}}{\delta}\Delta C_s \end{aligned} \tag{21.17}$$

where A_{eff} represents the "effective" pore area and depends on a/r as well as the solute and bulk flow velocities. The combined effects of steric hindrance and friction on A_{eff} are illustrated in Figure 21.9 using published values for k_1 and k_2.[97] The approximation equation used by Landis and Pappenheimer in 1963 is also shown[71] where:

$$\frac{f_{unbounded}}{f_{pore}} = 1 - 2.104\cdot\left(\frac{a}{r}\right) + 2.09\left(\frac{a}{r}\right)^3 - 0.95\left(\frac{a}{r}\right)^5 + \cdots \tag{21.18}$$

From Figure 21.9 it is clear that restricted diffusion will cause a membrane to discriminate between two solute molecules of different radii, even when the radii of both are considerably less than the radius of the pore. Also, note that Eq. (21.17) reduces to Eq. (21.13) in the absence of bulk flow and as a/r approaches zero.

Pore Theory and Hydrodynamic Flow

It is allowable to describe bulk flow within a cylindrical pore using Poiseulle's law as long as the pore

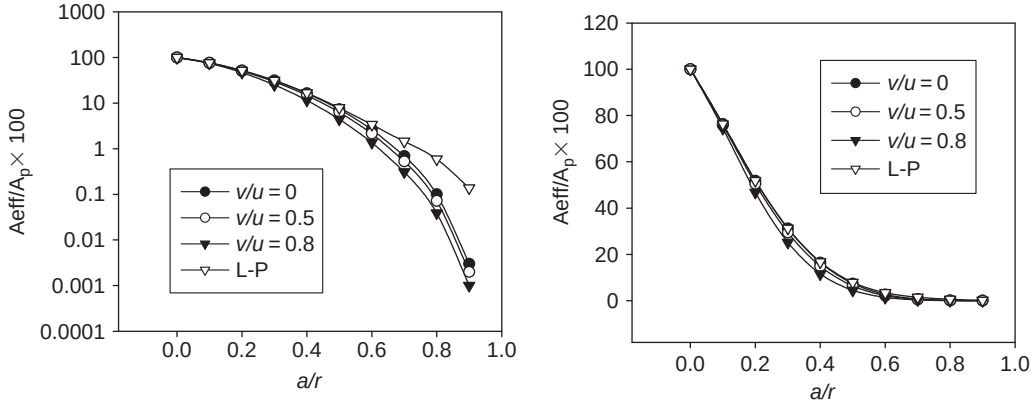

FIGURE 21.9 **Ratio of effective pore area A_{eff} to physical pore area A_P that applies to diffusion of solute with radius a through circular pore with radius r.** The model accounts for steric hindrance and for friction; u and v are respective solute and bulk flow velocities. Friction is calculated based on published coefficients.[97] L–P refers to result generated by older method of Landis and Pappenheimer, which works well for a/r <0.6. Results shown in semi-log (left) and linear (right) formats.

radius is several-fold the radius of a water molecule. Accordingly:

$$q = \frac{-\pi r^4}{8\eta}\frac{dP}{dy} \tag{21.19}$$

where q represents bulk flow within a single pore and dP/dy is the axial pressure gradient along the pore. For flow per unit area across a membrane, pressure is replaced by the Starling forces[113,117] such that:

$$Jv = \frac{n\pi r^4}{8\eta\delta}(\Delta P - \Delta\Pi) = \frac{A_w r^2}{8\eta\delta}(\Delta P - \Delta\Pi) \tag{21.20}$$

where n is the number of pores per unit area and A_w is the restricted pore area available to water. Comparing Eq. (20) to Eq. (3a), the hydraulic permeability L_p for an isoporous membrane is given in terms of the pore radius r and the ratio of total pore area to membrane thickness A_w/δ.

$$L_p = \frac{A_w r^2}{8\eta\delta} \tag{21.21}$$

Combining Bulk Flow and Restricted Diffusion

The solute flux equation (Eq. (21.3b)) includes terms for diffusion and advection. Advective transport and restricted diffusion occur simultaneously in the glomerulus, and each contributes to the presence of large molecules in the filtrate. Furthermore, convection and diffusion are coupled, and this coupling must be unraveled for a full understanding of glomerular sieving. We shall present two approaches to this that are both based on pore theory and rely on the sieving coefficient, Θ, to draw inferences regarding the filtration barrier. The first approach is the early work of Pappenheimer, and the second approach is that of Chang and Deen who based their method on the prior work of Patlak. It is the latter approach to interpreting sieving data that is used by most authors who publish in the physiology or clinical literature nowadays.

There are some intuitive features of glomerular sieving, and some that are not so intuitive. First, it is intuitive that Θ cannot be a negative number, nor can it exceed unity. If Θ exceeds unity, a model other than pore theory is required to explain the flux. It is also intuitive that Θ will approach unity for small solutes, and that Θ will equal zero for any solute that is larger than the largest pore. A feature that is not so intuitive is how intermediate Θ can arise from an isoporous membrane, although we have shown intermediate A_{eff} for an isoporous membrane in Figure 21.9. Intermediate Θ also owes to the effect of filtration rate on molecular sieving, which appears as the second term in Eq. (21.3b). If the passage of a solute is restricted relative to the passage of water, then the filtrate will become diluted during filtration. This will give rise to a concentration gradient for diffusion. Thus, the overall sieving coefficient is determined by competition between the filtration rate, which tends to dilute the filtrate, and the restricted diffusion, which fights to reduce the concentration difference that arises from molecular sieving.

It is intuitive that, if A_{eff} is non-zero and J_v is low enough, then solute will eventually equilibrate between the plasma and Bowman's space ($\Theta = 1$). It is also intuitive that, at high rates of J_v, Θ will approach the ratio of restricted pore area for solute relative to water. Pappenheimer provided a quantitative expression for Θ that satisfies these two conditions.[71] This derivation begins with a bulk-flow sieving step to create an initial filtrate to plasma concentration ratio:

$$\frac{C_{fitrate}}{C_{plasma}} = (1 - \sigma_s) = \frac{A_s}{A_w} \tag{21.22}$$

where C is the concentration of the solute in question, A_w and A_s are the effective pore areas for water and solute, and σ_s is the sieving coefficient from Eq. (21.3). Next, diffusion is superimposed according to Fick's law. Assuming that the concentration gradient is constant within the membrane:

$$J_s^{diffusion} = D_0 \frac{A_s}{\delta}(C_{plasma} - C_{filtrate}) \tag{21.23}$$

where D_0 is the free solute diffusion coefficient and δ is the membrane thickness. Summing the effects of bulk-flow sieving and diffusion:

$$C_{filtrate} = \left(\frac{A_s}{A_w}\right) C_{plasma} + \frac{J_s^{diffusion}}{J_v} \tag{21.24}$$

Inserting Eq. (21.23) into Eq. (21.24) and rearranging yields:

$$\Theta = \frac{C_{filtrate}}{C_{plasma}} = \frac{\left(1 + \frac{D_0 A w}{J_v \delta}\right)}{\left(\frac{A_w}{A_s} + \frac{D_0 A w}{J_v \delta}\right)} \tag{21.25}$$

The assumption of a constant solute gradient within the membrane is a shortcoming of Pappenheimer's approach. This shortcoming was later overcome, based on the work of Patlak[100] who developed a more rigorous approach for quantifying filtration–diffusion interactions in isoporous membranes. Variations on the Patlak approach form the basis for the pore models that are applied to animal and clinical investigations of glomerular sieving nowadays.[2] A modified Patlak equation for solute flux begins again with the Kedem–Katchalsky solute flux equation (Eq. (21.3b)). Diffusion-advection coupling in Eq. (21.3b) is contained in the parameter $\overline{C_s}$, which is the average value of C_s within the membrane. However, $\overline{C_s}$ can't be measured or derived without prior knowledge of the coupled flux that we are trying to determine. Therefore, the challenge is to come up with a form of Eq. (21.3b) that doesn't contain $\overline{C_s}$. The first step toward accomplishing this is to divide the capillary wall of thickness δ into a series of infinitesimally thin laminae. The Kedem–Katchalsky equation for a thin lamina is:

$$J_s = -D_s \frac{dC_s}{dy} + J_v(1 - \sigma_s)C_s \tag{21.26}$$

where y is the position along the length of the pore, which runs perpendicular to the membrane surface. Next, separating variables and integrating across the membrane yields:

$$\int_{plasma}^{filtrate} \frac{dy}{-D_s} = \int_{plasma}^{filtrate} \frac{dC_s}{J_s - J_v(1 - \sigma_s)C_s} \tag{21.27a}$$

$$\frac{\delta}{-D_s} = \frac{1}{-P_s} = \frac{1}{-J_v(1 - \sigma_s)} [\ln(J_s - J_v(1 - \sigma_s)C_s)]_{plasma}^{filtrate} \tag{21.27b}$$

$$\exp\left(\frac{J_v(1 - \sigma_s)}{P_s}\right) = \left[\frac{J_s - J_v(1 - \sigma_s)C_{filtrate}}{J_s - J_v(1 - \sigma_s)C_{plasma}}\right] \tag{21.27c}$$

Making the substitutions:

$$P_e = \frac{J_v(1 - \sigma_s)}{P_s} \quad \text{and} \quad C_{filtrate} = \frac{J_s}{J_v} \tag{21.28}$$

and rearranging Eq. (21.24c) to solve for J_s yields:

$$J_s = \frac{C_{plasma} J_v(1 - \sigma_s)}{1 - \sigma_s \exp(-P_e)} \tag{21.29}$$

Equation (21.29) expresses the solute flux as a function of plasma solute concentration, filtration rate, and the membrane characteristics σ_s and P_s, without referring to C_s anywhere inside the membrane. P_e is the Peclet number, which represents the ratio of advective to diffusive solute flux.

The remaining steps involve relating P_s and σ_s to the idealized membrane geometry using the equations for the hydrodynamics of cylindrical pores developed above.

$$P_s = \frac{D_0 A_s}{\delta A_p} \quad \text{and} \quad \sigma_s = 1 - \frac{A_s}{A_w} \tag{21.30}$$

PORE THEORY AND EXPERIMENTS IN THE GLOMERULUS

To characterize the filtration properties of a particular membrane by applying pore theory as described above, one begins with tracer solute(s) of known concentration (s) and Stokes–Einstein radii and a membrane of unknown microscopic dimensions. The water flux and sieving coefficient of the tracer solute(s) are measured along with the filtrand tracer concentration(s) and transmembrane pressure. A best fit of these data is made to the theoretical model, in order to determine the size and density of idealized pore(s). A better fit can always be achieved by allowing subpopulations of pores with various sizes. This is often justifiable on grounds of common sense. For example, in glomerular disease there is increased permeability to macromolecules, but not to water. This is easily explained by the appearance of a small population of large pores (sometimes called "shunts") that allow for the passage of macromolecules that are excluded from the main population of small pores. A scant population of shunt pores could account for most of the macromolecular sieving, but contribute negligibly to the ultrafiltration coefficient, LpA, because the pore area available to water is much larger.

To convert solute flux to overall sieving for the glomerulus, flux must be integrated over the entire capillary surface. Using C_{plasma} to represent the plasma concentration of s and x as the position along the capillary:

$$\Theta_s = \frac{1}{C_{plasma}(0)} \cdot \frac{\int_0^1 J_s dx}{\int_0^x J_v dx} \tag{21.31}$$

But the forces driving J_v and J_s change along the length of the capillary, since C_{plasma} rises as filtration occurs and J_v declines as oncotic pressure in the capillary pressure rises. For the idealized cylindrical capillary of unit length:

$$C_{plasma}(x) = \frac{C_{plasma}(0)Q_0 - \int_0^x J_s(z)dz}{Q_0 - \int_0^x J_v(z)dz} \quad (21.32a)$$

$$J_v(x) = Lp(\Delta P - \Pi(x)) \quad (21.32b)$$

where Q_0 is the incident plasma flow, and the oncotic pressure Π is given by Eq. (21.5).

To solve for the total sieving of solute by a glomerular capillary, Eq. (21.32) is iterated to provide the inputs for Eq. (21.29), which is then integrated along the capillary according to Eq. (21.31). Although the actual glomerular capillary bed is a complex and heterogeneous network of branching blood vessels, the sieving coefficients predicted for the idealized homogeneous circular cylinder differ negligibly from those predicted from a reconstruction that incorporates the complex anatomy.[105]

SIEVING CURVES

In order to compute the size-selective properties of the glomerular barrier it is necessary to know the sieving coefficient Θ for multiple tracer solutes with different radii. Therefore, tracer solutes are required whose concentration in Bowman's space can be measured or inferred. Direct sampling from Bowman's space is inconvenient or impossible in most circumstances, so it is usually necessary to infer sieving coefficient(s) from urinary clearance(s). The sieving coefficient of a tracer solute is equal to its urinary clearance divided by the GFR, as long as the test solute is not secreted, reabsorbed or metabolized by the tubule. Polysaccharides fulfill this criterion of being impervious to processing by the tubule. Also, it is possible to generate mixtures of polysaccharides with a range of Stokes–Einstein radii. These mixtures can be used to plot Θ as a function of Stokes–Einstein radius with many data points in a single experiment. These sieving curves can be used to determine pore size and relative abundance of different pores in heteroporous models.

The most commonly used tracer polysaccharide is dextran, an inert polymer of glucopyranose. There are over 50 published human and animal studies in which the size selective characteristics of the glomerular barrier have been analyzed from dextran sieving curves. As a rule, dextran sieving data are consistent with a two pore model[109] of the glomerular capillary wall where the vast majority are small pores with radius of 4.8–6.0 nm and the remainder are shunt pores with radius exceeding 10 nm (reviewed in [144]). However, this use of dextran is seriously encumbered because the equations of pore theory were developed for rigid spheres, whereas dextran exists as a flexible random coil.[48] Due to its flexibility, a dextran molecule is far less hindered at crossing the filtration barrier than a rigid spherical molecule of equivalent Stokes–Einstein radius.[108] Based on pore sizes computed from dextran sieving data, Θ for albumin (Stokes–Einstein radius 3.6 nm) should exceed the experimental value by roughly 500-fold. The realization that this discrepancy in Θ between albumin and 3.6 nm neutral dextran owes mainly to the flexibility of the dextran molecule has reduced the need explain the low sieving coefficient for albumin based on something other than size. Hence, there is a lesser emphasis placed on the charge selectivity of the glomerular capillary wall these days than there was during the 1970s. Clearly, one must be cautious when using dextran sieving data to predict the sieving of non-dextrans. Nonetheless, dextran sieving is reproducible and precise, and predicts the structural changes that befall diseased glomeruli, even though they give a biased estimate of pore size.

Ficoll is an inert spherical sucrose polymer with internal cross-linking that confers some rigidity.[14] Ficoll has been tested against dextran in rats and found to have a sieving coefficient substantially less than size-matched dextran for Stokes–Einstein radii greater than 3 nm.[15,94] Lower sieving coefficients for Ficoll relative to size-matched dextran have also been confirmed in healthy and nephrotic humans.[1,13] However, Ficoll is less convenient to use than dextran in humans, because potential toxicity limits the amount that can be given. Also, Ficoll molecules are more compressible than globular proteins, such that pore sizes estimated from Ficoll sieving data will overestimate the sieving coefficients of like-sized globular proteins, albeit to a lesser degree than dextran.[144]

The glomerular sieving of polysaccharides is useful to the extent that it helps explain the permselectivity for endogenous proteins. Ultimately, however, the predictions based on polysaccharide sieving must be verified for proteins. As already discussed, the direct approach of measuring protein sieving by micropuncture is difficult. There are other strategies that have been employed to estimate sieving coefficients for proteins without requiring micropuncture. We will mention two of these. One alternative to micropuncture is to reduce the tubular processing of proteins by cooling the isolated perfused rat kidney to 8°C (cold IPK) to stop the tubule from degrading or transporting filtered proteins, then assuming that the filtered protein equals the protein excretion. Adding furosemide and nitroprusside to the cold IPK eliminates water reabsorption almost completely, and reportedly yields stable values for albumin fractional clearance. However, GFR is low in the

cold IPK and perfusate flow is high, which means that the determinants of glomerular filtration are quite different than *in vivo*. This should pose a problem for the cold IPK, since fractional solute clearance must depend on the determinants of glomerular filtration rate given that convection and diffusion both contribute to solute transport.[22] Nonetheless, cooling seems to have minimal effect on the urine to plasma ratio for Ficoll, and the cold IPK has been used to address a variety of issues related to glomerular protein sieving.[53,64–66,74,75,128]

More recently, Tenstad et al. have made direct estimates of glomerular sieving coefficents for proteins based on tracer radioactivity retained in the kidney six minutes after administering radiolabeled proteins to rats. The rationale behind this approach is that there exists a several-minute window of opportunity when a tracer protein will remain in the kidney after being filtered and taken up by the proximal tubule, and before being degraded or reabsorbed back into the body. An estimate of this time window was first made using cystatin C, which is a freely filtered protein that is completely degraded by the tubule. As such, the rate at which cystatin C enters the urinary space is equal to its plasma concentration × GFR. Administering a bolus of labeled cystatin C along with a GFR marker, then stopping the experiment at various time points and counting tracer activity in the kidney, revealed that cystatin C remains in the kidney for at least six minutes after undergoing filtration.[135] In tracer uptake experiments using neutral horseradish peroxidase, myoglobin, and charge-neutralized albumin, the sieving coefficients for each of these proteins was significantly less than for Ficoll or dextran of equal hydrodynamic radius.[80] The principle pore radius computed by pore theory is 3.75, 4.6, and 5.5 nm for protein, Ficoll, and dextran, respectively[144] (see Figure 21.10).

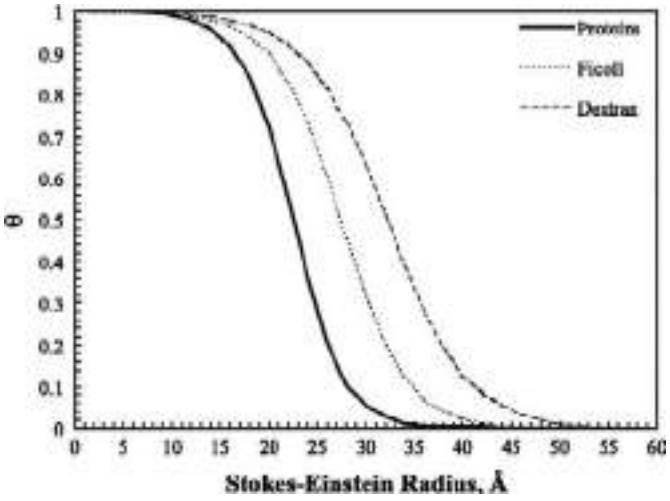

FIGURE 21.10 **Sieving curves for dextran, Ficoll, and neutral proteins constructed from the literature** *(taken from ref. [98]).*

COMBINING FIBER MATRIX THEORY WITH THE PORE MODEL

Using a wider range of dextran radii than previously employed by others, Katz generated dextran sieving curves that were not uniformly convex upward, but flattened out slightly above 4 nm.[68] This nuance could be explained by a two-pore model in which the pores were filled with a fiber matrix, but it could not be explained by any open-pore model of equal complexity. Citing the location of albumin molecules found in glomerular sections[112] and confocal tracking of dextran in isolated glomeruli,[25] it was hypothesized that the albumin barrier does not reside in the GBM anyway, and that the endothelial fenestrae, filled with fibrous glycocalyx, justify the mathematical model. The pore-matrix model has features corresponding to the pore theory model described above. For example, there is steric hindrance due to the presence of the gel fibers. There is also reduced solute mobility due to the gel fibers. The specific formulae for these were developed from the theoretical groundwork for gel permeation by solutes provided by Ogston,[91] and combined with pore theory by Katz.[68]

Intravital Microscopy and Albumin Sieving

Glomerular permeability to albumin has also been examined using intravital dual-photon microscopy. The first measurements of glomerular albumin sieving by the dual-photon method were reported in 2007 by Russo et al. who administered fluorophore-labeled albumin to rats, compared fluorescence intensity in Bowman's space to plasma, and concluded that the albumin sieving coefficient is approximately 0.03, which is 50-fold higher than previously reported by any other method dating from the 1940s.[113] Subsequent application of the dual-photon technique by Tanner, who used the same facility but a different brand of microscope, failed to reproduce the finding, instead corroborating the traditional view of an albumin sieving coefficient less than 0.004, which was his lower limit of detection.[133] Peti-Peterdi also examined the filtration barrier using dual-photon microscopy and came to the same conclusion as Tanner, namely that the Russo finding was in error.[101] Peti-Peterdi has also argued that fluorescence imaging is poorly suited to measuring glomerular sieving coefficients, because light absorption and scattering by RBCs suppresses the apparent fluorescence of plasma proteins, which will lead to an overestimate of Θ.[102] So, after initial excitement over the Russo finding, the prevailing opinion among

investigators in this field remains that the glomerular sieving coefficient of albumin is approximately 0.0006.

Charge Selectivity of the Filtration Barrier

Since the 1970s it has been generally accepted that the glomerular capillary wall is less permeable to proteins that are negatively charged. In addition to the low Θ for albumin compared to neutral dextran for equivalent Stokes–Einstein radius, the impression of charge selectivity was supported by experiments that compared sieving of anionic, neutral, and cationic dextrans.[18,21] It has since been learned that anionic dextran sulfate can be taken up by glomerular cells, desulfated, then secreted to appear in the urine as neutral dextran.[134,145] In addition, sieving of dextran sulfate is reduced through binding to plasma proteins.[49] These effects could create the appearance of charge selectivity of the filtration barrier where none exists. Furthermore, other experiments using Ficoll or hydroxyethyl starch failed to show a charge-selective barrier to either of these alternative polysaccharide molecules.[50,116]

Although the notion of charge selectivity for polysaccharides has lost some of its currency, the bulk of evidence still favors the notion that charge selectivity applies to the filtration of globular proteins. Rennke showed a lesser sieving coefficient for anionic horseradish peroxidase (HRP) than neutral HRP in rats,[107] allowing that part of the effect may have been due to degradation of anionic HRP during filtration.[96] Lindström showed charge selectivity for the somewhat larger protein, lactate dehydrogenase.[75] Making use of the tissue tracer uptake technique described above, Lund calculated sieving coefficients and reflection coefficients for several proteins, including charge-neutralized and native anionic human serum albumin. Θ for anionic albumin was remarkably similar to the micropuncture result of Tojo (*vide supra*) while Θ for neutral albumin was 10-fold higher[80] (Table 21.3).

TABLE 21.3 Charge Permselectivity of the Glomerulus in Rats Confirmed by the Tracer Uptake Method Using Neutralized or Native Anionic Human Serum Albumin

	Stokes–Einstein Radius (Å)	Isoelectric pH	Θ	σ
neutral albumin	35.0	7.4	0.0055	0.996
anionic albumin	35.5	4.9	0.0006	0.9997

Adapted from data in Lund et al. (2003). Am. J. Physiol.[80]
Θ: glomerular sieving coefficient; σ: Staverman reflection coefficient. Since these experiments were performed *in vivo*, they reflect the normal contributions of diffusion and convection to albumin flux.

Theory of Charge Selective Sieving

Deen presented a theory for glomerular filtration of charged solutes based on a homogeneous distribution of fixed negative charges within the glomerular capillary wall[32] as idealized in Figure 21.11. The mathematical description of this model begins with an equation for flux through an imaginary thin surface within a membrane. This is the same as Eq. (21.26), except that the full electrochemical potential is included in the diffusion force to yield:

$$Js = -D_s\left(\frac{dC_s}{dx} + z_s C_s \frac{d\psi}{dx}\right) + J_v(1-\sigma_s)C_s \qquad (21.33)$$

where $D_s = D_0 \cdot A_{eff}$, z_s is the valence of s and ψ is a dimensionless electrical potential.

Next, it is assumed that there is electrochemical equilibrium at both membrane-solution interfaces. This allows the step change in C_s at each interface to be calculated from the Nernst equation and the steric hindrance:

$$\begin{aligned} C_s'(0) &= C_{plasma}(1-\sigma_s)\exp(z_s(\psi_{plasma} - \psi'(0))) \\ C_s'(\delta) &= C_{filtrate}(1-\sigma_s)\exp(z_s(\psi_{B.S.} - \psi'(\delta))) \end{aligned} \qquad (21.34)$$

where (′) refers to values within the membrane just inside its interface with the plasma or Bowman's space, and *B.S.* refers to Bowman's space. Within the membrane, $d\psi/dx$ is small so that the same integration can be done as was done to Eq. (21.27). Integrating from 0 to δ within the membrane and substituting and rearranging yields the following charged-solute flux equation which is analogous to Eq. (21.29):

$$J_s = \frac{C_{plasma}J_v(1-\sigma)\exp(z_s(\psi_{plasma} - \psi'(0)))}{1-\exp(-P_e)(1-(1-\sigma)\exp(z_s(\psi_{B.S.} - \psi'(\delta))))} \qquad (21.35)$$

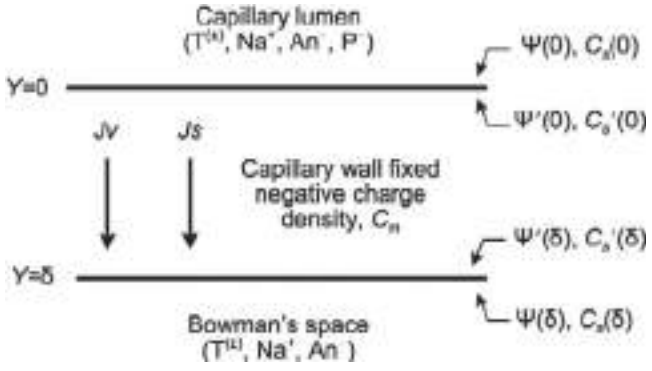

FIGURE 21.11 **Idealized capillary wall with fixed negative charge density C_m, which causes Donnan potentials ($\Psi - \Psi'$) to form at interfaces of the membrane with the capillary lumen and Bowman's space.** These Donnan potentials retard the flux of anionic tracer T^- and accelerate the flux of cationic tracer T^+ according to formulae developed in the text (A_n: mobile anions; P^-: anionic proteins) *(adapted from ref. [125]).*

The two electrical potential differences in Eq. (21.35) are next to be determined. These cannot be measured, but are given by the Donnan potentials for Na^+:

$$\psi - \psi' = \ln\left(\frac{C'_{Na^+}}{C_{Na^+}}\right) \tag{21.36}$$

Since there must be zero net charge in each compartment:

$$C_{Na} = C_{An} \text{ and } C'_{Na} = C'_{An} + C_m \tag{21.37}$$

where *An* refers to mobile anions and *Cm* is the density of negative charges in the membrane. At Donnan equilibrium:

$$\frac{C'_{An}}{C_{An}} = \frac{C_{Na}}{C'_{Na}} \tag{21.38}$$

Combining Eqs. (21.37) and (21.38) yields a quadratic equation for C'_{Na} with the positive root:

$$C'_{Na^+} = \frac{C_m + \sqrt{C_m^2 + 4C_{Na^+}C_{An^-}}}{2} \tag{21.39}$$

Inserting Eq. (21.39) into the numerator of Eq. (21.36) gives the Donnan potentials. Inserting these into Eq. (21.35) gives an expression for solute flux that incorporates the effect of C_m. If C_m or z_s is zero, this reduces to Eq. (21.29), as it should. Θ_s for the glomerulus is obtained by integrating J_s along the capillary surface as per Eq. (21.31).

Deen's model predicts that a single parameter, C_m, can account for charge selective sieving. This is shown in Figure 21.12, where the theory was applied to anionic dextran sulfate based on other model inputs from the normal rat in which neutral dextran was used to determine a pore radius.

This theory of charge-selective filtration has been criticized, because isolated GBM was found to have too low a density of anionic charge to satisfy model predictions for what is required of the GBM to operate as barrier to albumin.[24] However, the inflated 5 nm pore radius calculated from neutral dextran sieving may account for the discrepancy. It should also be noted that this model explains charge-related sieving entirely on the basis of Donnan potentials at the two membrane interfaces. It makes no allowance for any effect that the fixed membrane charges might have on the steric hindrance or friction within the pore. Such effects are likely, and would further reduce the amount of fixed negative membrane charge required to account for any degree of charge selectivity. To date, there is no theory for quantifying this, although it has been argued that the phenomenon of "charge screening" can be used to show reduced partitioning of anionic proteins in the glomerular capillary wall (*vide infra*). Furthermore, the relevant Donnan potential may arise at the plasma interface with the negatively charged endothelial glycocalyx rather than the basement membrane, in which case the charge density of the GBM is not the appropriate straw man for arguments against charge-based sieving (*vide infra*).

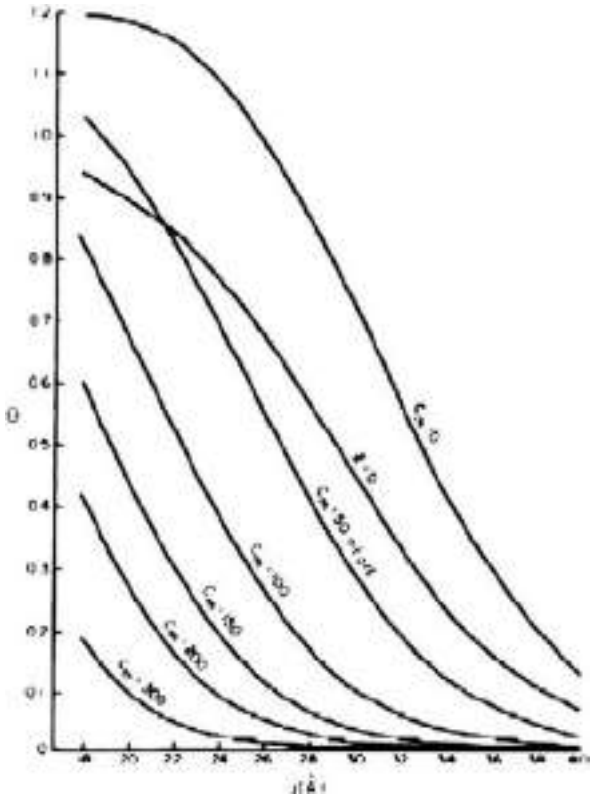

FIGURE 21.12 **Sieving coefficent (Θ) for dextran sulfate as function of Stokes–Einstein radius, a.** Cm-membrane fixed negative charge density in mEq/liter. Valence, z, of dextran = 0.245 × a. z = 0 is curve for neutral dextran *(from ref. [126]).*

Endothelial Glycocalyx as the Barrier to Macromolecules

It has been a challenge to determine which individual layer of the glomerular filtration barrier contributes most to macromolecular sieving. Various investigators at various times and with various methods have argued for the GBM,[20,42,60] filtration slit diaphragm,[139] and endothelium.[112] Overall, the glomerular endothelium has received less attention than GBM and slit diaphragm with respect to permselectivity. Nonetheless, it is arguably unwise to ignore the possibility of a proximal barrier, since the filter should clog if albumin is allowed to permeate downstream and wedge against the slit diaphragm.[127]

The glomerular endothelium is perforated with fenestrae 20 times the diameter of albumin. So if the

endothelium serves as a selective barrier to filtration of macromolecules this property owes to the glycocalyx that fills these fenestrae. Information about the molecular dimensions and electrical properties of the endothelial glycocalyx has accrued slowly, and lack of such information has forestalled a definitive analysis. Nonetheless, both experimental data and logical arguments have emerged for the glycocalyx as an important size and charge-selective barrier. The endothelial glycocalyx forms a hydrated gel within the fenestrae, and contains fixed negative charges on its gel fibers. The effective permeability of a solute in a gel relative to free solution (D_{eff}) can be expressed as the product of its diffusion coefficient in the gel relative to free solution (D_{gel}/D_0) and the fraction of the gel volume available to be occupied by the protein (e.g., its partition coefficient, Φ).

$$D_{eff} = \frac{D_{gel}}{D_0}\Phi \tag{21.40}$$

Considering charge selectivity, it is conceivable that electrostatic interactions with a negatively charged gel might impede the transit of like-charged molecules by reducing D_{gel} or Φ.

One way to study the role of electrostatic interactions between proteins and gels is to inhibit these interactions by increasing the ionic strength of the solvent, which is the standard method for separating proteins by size and charge on agarose gels in the laboratory. Ions in the solvent have the effect of screening the charged solute protein from the coulomb forces that would otherwise be exerted on it by the fixed charges on the gel fibers.

The following brief digression into the physical theory of colloids (also known as Debye–Hückel theory) explains how this phenomenon works. Adding a point charge at a fixed position in any medium generates an electric field that attracts mobile ions of opposite charge. An electric field formed by those charges will offset the field associated with the fixed charge so that at some distance from the fixed charge, one can no longer "sense" its presence. If a fixed charge is added, mobile charges will reposition in response, and it can be shown from the density of repositioned charges that the influence of the fixed charge decays exponentially with distance. The reciprocal of the decay constant is known as the Debye length. The Debye length can be deduced by rearranging the equation for electrochemical potential into a Boltzman distribution for the concentration of redistributed charges, using a linear approximation for the Boltzmann distribution to obtain charge concentration as a function of voltage, then inserting the result into the Poisson equation from classical electrical theory, which expresses the second derivative of voltage as a function of charge density. This yields:

$$C(r) = \frac{l}{d}\exp\left(\frac{-r}{d}\right) \text{where } d = \sqrt{\frac{k_B T\varepsilon}{q^2 C_0}} \tag{21.41}$$

$C(r)$ is the probability density of relocated charges at distance r from the fixed charge, d is the Debye length, k_B is Boltzmann's constant, ε is the permittivity, q is the elementary charge, and C_0 is the baseline concentration of mobile charges, e.g., the ionic strength of the buffer. Accordingly, increasing the salinity of the buffer will shorten the Debye length and the influence of the fixed charge wanes almost completely beyond two or three Debye lengths. For a material with a typical dielectric constant and 0.15 molar mobile charges, the Debye length is about 0.2 nm, which is similar to the difference between the main pore radius estimated from sieving of neutral proteins (3.75 nm, *vide supra*) and the molecular radius of albumin (3.6 nm).

Johnson et al. made use of charge screening to examine the role of electrostatic interactions on diffusion and partitioning of bovine serum albumin in 6% sulfated agarose gels by varying the ionic strength of the buffer from 0.01 to 1.0 molar. Increasing the ionic strength to shorten the Debye length and reduce the distance over which repulsive coulomb forces from gel anions can be "felt" had minimal effect on the diffusion coefficient for albumin, but caused a major increase in its partitioning coefficient, Φ. Therefore, the anionic gel poses a selective barrier to sieving of anionic proteins not because it restricts the diffusive mobility of albumin within the gel, but because electrostatic forces reduce the amount of space available within the gel to be occupied by albumin.[63]

The notion of altering buffer strength to manipulate the Debye length has also been applied to study the filtration of charged proteins in the cold isolated perfused kidney.[129] Perfusion with physiologic concentration of buffer salts (152 mM) yielded respective sieving coefficients of 0.11 and 0.045 for neutral and anionic horseradish peroxidase (HRP). Reducing the total salts in the buffer from 152 to 34 mM did not affect the sieving of neutral HRP, but reduced the sieving coefficient for anionic HRP by about half. Thus, there appears to be selective screening-out of anionic HRP by the glomerulus that increases along with the distance over which coulomb forces between the barrier and albumin are able to act. A note of caution is warranted when ascribing the effect of buffer salinity to charge screening within the membrane, since increasing the buffer salinity will also reduce the Donnan potential at the membrane–solution interface, according to Eqs. (21.35)–(21.39).

Glomerular sieving properties have also been examined in the cold isolated perfused kidney of mice

treated with glycosaminoglycan-degrading enzymes intended to disrupt the endothelial glycocalyx. This treatment was estimated to reduce the fiber charge density by 10% and increased the sieving coefficient for albumin by five-fold, but only increased sieving of Ficoll by 1.5-fold, thus demonstrating that hyaluronic acid, chondroitin sulfate, and heparan sulfate are important for glomerular charge selectivity.[61] If the endothelial glycocalyx contributes to the screening of albumin, this removes some of the burden of showing how the GBM can do this when it appears that the GBM contains too few fixed charges. Screening by the glycocalyx at the interface with the well-stirred plasma also reduces the burden on the epithelial slit diaphragm which might otherwise clog.

Recent inroads to understanding the filtration properties of the endothelial glycocalyx have also been made with mathematics. Using computed autocorrelation functions of electron micrographs, Squire et al. found quasi-periodic 20 nm spacing of 10 nm fibers in the endothelial glycocalyx of frog mesentery, and suggested that the glycocalyx in fenestrated glomerular capillaries could be similarly organized.[131] Inspired by Squire et al., Zhang developed a formula for reflection coefficients in a periodic array of parallel fibers. The Zhang model predicts a reflection coefficient for albumin of approximately 0.6, but it does not account for electrical charge, and requires that flow occurs parallel to the fiber axis.[150] Bhalla and Deen also developed a model based on Squire's version of glycocalyx geometry in which they applied Debye–Hückel theory to incorporate the effects of charge on osmotic reflection coefficients of macromolecules in a membrane of parallel fibers bearing like surface charge with flow parallel to the fiber axis.[8] This involved computing the electrostatic free energy for a charged sphere interacting with a hexagonal array of charged fibers. The sphere was assigned a size and surface charge resembling albumin (-0.2 coulomb-m^{-2}). Charge densities were ascribed to the fiber array up to the predicted charge density on chondroitin sulfate. At zero fiber charge, the reflection coefficient matched the prediction of the Zhang model. The reflection coefficient was steeply dependent on fiber charge, rising almost to unity within the tested range. So the current idealized models suggest that the endothelium is a major barrier to albumin, whereas the GBM is probably not.

Serial Membrane Models

The glomerular filtration barrier is built of multiple layers arranged in series. The sieving coefficient for the whole assembly differs from what is predicted by deriving individual sieving coefficients for each layer based on its own physical properties, then multiplying these coefficients together. Conversely, the physical characteristics of a given layer cannot be inferred from its sieving coefficient as measured *in situ*. This is because the sieving coefficient of a given layer is determined by its own physical characteristics, and by the physical characteristics of all downstream layers. In other words, for a filtration barrier consisting of two layers arranged in series with upstream and downstream layers denoted by respective subscripts 1 and 2 and overall sieving coefficient $\Theta = \Theta_1\Theta_2$, it can be shown that Θ_1 depends on Θ_2. There are several consequences of this. The most striking is that placing a less selective layer upstream of a more selective layer actually causes the upstream sieving coefficient to exceed unity, and causes the overall barrier function to deteriorate. This counterintuitive result can be deduced from the solute flux equation, as follows.

We wish to describe the sieving of a solute that exists in low concentration in the plasma. Solute concentration at the boundary interface between the two layers is C_B. By conservation of mass, J_s and J_v are constant throughout the barrier and solute concentration in the terminal filtrate is J_s/J_v. $\Theta_2 = C_{filtrate}/C_B$ rearranges to $C_B = J_s/(J_v\Theta_2)$. Starting with the solute flux equation for the downstream layer, separating variables, integrating, defining the Peclet number, and rearranging to solve for Θ_2 gives:

$$\exp(-Pe_2) = \frac{Js - Jv(1-\sigma_2)C_B}{Js - Jv(1-\sigma_2)C_{filtrate}}$$

$$\Theta_2 \equiv \frac{C_{filtrate}}{C_B} = \frac{1-\sigma_2}{1-\exp(-Pe_2) + (1-\sigma_2)\exp(-Pe_2)} \tag{21.42}$$

Next, we take the same approach to the upstream layer and substitute $J_s/(J_v\Theta_2)$ for C_B to yield

$$\exp(-Pe_1) = \frac{Js - Jv(1-\sigma_1)C_{plasma}}{Js - Jv(1-\sigma_1)\left(\frac{Js}{Jv\cdot\Theta_2}\right)}$$

$$\Theta_1 \equiv \frac{C_B}{Cplasma} = \frac{1-\sigma_1}{\Theta_2(1-\exp(-Pe_1)) + (1-\sigma_1)\exp(-Pe_1)} \tag{21.43}$$

Note that the expression for Θ_2 (Eq. (21.42)) contains no reference to upstream events, whereas Θ_1 is affected by Θ_2 (Eq. (21.43)) such that reducing the sieving coefficient of the downstream membrane increases the sieving coefficient of the upstream membrane without altering any of its physical properties Extending this approach to the ith component of a membrane with n series components gives:

$$\Theta_i = \frac{1-\sigma_i}{\Theta_{i+1}\Theta_{i+2}\ldots\Theta_n(1-\exp(-Pe_i)) + (1-\sigma_i)\exp(-Pe_i))} \tag{21.44}$$

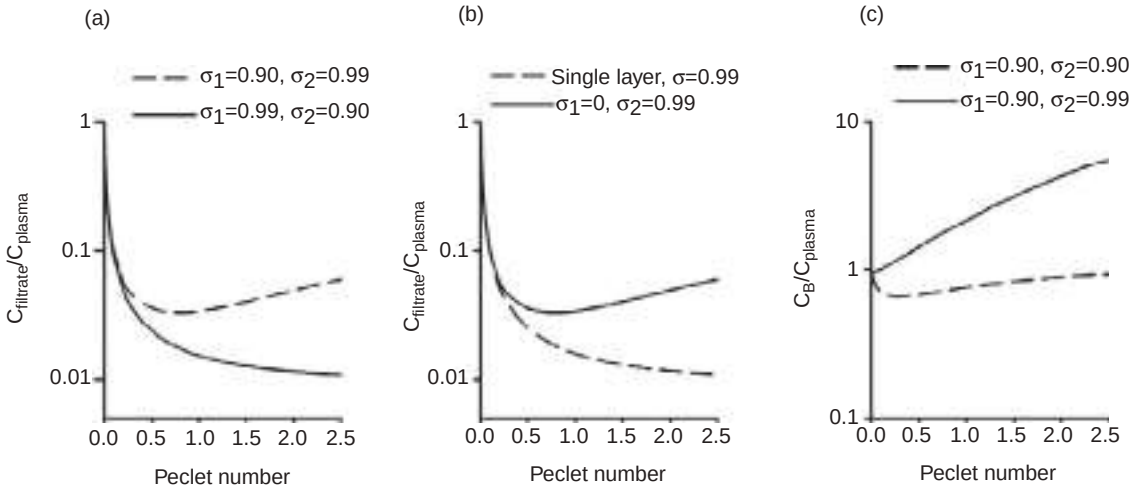

FIGURE 21.13 **Sieving coefficients for a filtration barrier consisting of two layers shown over a range of Peclet numbers.** The upstream and downstream layers are designated *1* and *2*, respectively. Each layer has its own inherent reflection coefficient, σ. C_{plasma}, $C_{filtrate}$, and C_B are the respective solute concentrations in plasma, filtrate, and at the boundary between the two layers. When the Peclet number is zero, there is no bulk flow and the system comes to diffusion equilibrium with equal solute concentrations everywhere (all sieving coefficients = unity). (a) One layer has $\sigma = 0.99$ and the other has $\sigma = 0.90$. The overall efficiency as a filtration barrier is markedly diminished when the less restrictive layer is placed upstream of the more restrictive layer. (b) Placing a permeable layer ($\sigma = 0$) upstream of a restrictive layer yields a barrier that is less efficient than the restrictive layer alone. (c) The sieving coefficient of the upstream layer (C_B/C_{plasma}) is strongly influenced by the reflection coefficient of the downstream layer. Remarkably, when the downstream layer is only 10% more restrictive than the upstream layer, the upstream sieving coefficient can exceed unity by several-fold. In other words, there is concentration polarization in the upstream layer. This acts like a force for diffusion through the downstream layer, and explains the separation of the two curves in panel (a).

Some implications of the double layer filtration barrier are shown graphically in Figure 21.13. Note that all components of Θ approach unity as the Peclet number approaches zero. This corresponds to zero *SNGFR*, where the solute comes to diffusion equilibrium across the membrane. For a single layer membrane at high Peclet number (corresponding to high *SNGFR*) diffusion becomes irrelevant, and Θ approaches $1 - \sigma$. Placing a more selective layer downstream of a less selective layer actually causes the upstream sieving coefficient, Θ_1, to exceed unity, and the overall barrier function deteriorates. Adding an upstream layer of equivalent selectivity to the downstream layer is equivalent to doubling the thickness of a homogeneous membrane. As expected, this halves the diffusion permeability, as manifest by $\Theta_1 \approx 0.5$ at low Peclet number. Peclet numbers haven't been measured for cell layers of the glomerular filtration barrier, but Deen has presented a logical argument against small Pe for albumin in the endothelial or epithelial layers.[28]

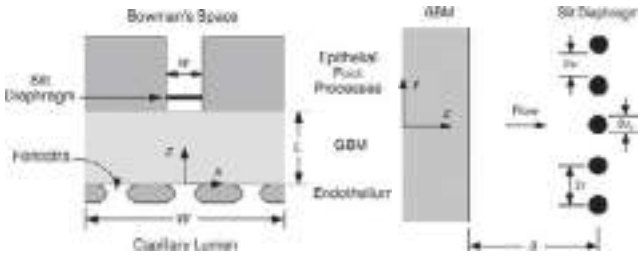

FIGURE 21.14 Left: Idealized structural unit of glomerular capillary wall corresponding to one filtration slit. Right: Idealized structure of slit diaphragm in relation to GBM. Dimensions in nm: W 360, L 200, w 39, rf 30, rc 2, 2u 20 ± 15, Δ 500, fractional area of fenestrae 0.2, fractional area of filtration slits 0.11 *(from ref. [145]).*

Structure-Based Models of the Glomerular Capillary

Since the 1990s there has been progress toward relating the filtration properties of the glomerulus to its actual physical structure. This is mainly the work of Deen and colleagues, who apply modern numerical methods in fluid mechanics to a specific structural model that is based on morphometry.[30,35] The defined structural elements of the model include the endothelial cells and fenestrae, the GBM represented as homogeneous porous material, and the epithelial cell foot processes with filtration slits bridged by slit diaphragms. These elements form a filtering subunit that is repeated many times to comprise the glomerular capillary. Each filtration subunit consists of one filtration slit, several fenestrae, and the GBM in between (see Figure 21.14). Water movement is assumed to be paracellular. In some instances

consideration is given to the endothelial glycocalyx, although untestable assumptions are required for this, since the permeability characteristics of the glycocalyx are not known.

The hydraulic conductances of the endothelium, GBM and filtration slits are treated as separate conductances arranged in series such that the overall conductance is given by a reciprocal of summed resistance:

$$\frac{P_{UF}}{Jv} = \frac{1}{k} = \frac{1}{k_{endo}} + \frac{1}{k_{GBM}} + \frac{1}{k_{epi}} \tag{21.45}$$

where P_{UF} is the ultrafiltration pressure and k is the hydraulic permeability.

By analogy to the first term in Eq. (21.3a), the hydraulic permeability for a single endothelial fenestra is equal to:

$$k_{endo} = \frac{\varepsilon_F \overline{v}_Z}{(P_G - \overline{P}_0)} \tag{21.46}$$

where z is the direction perpendicular to the membrane, v_Z is the average z-component of the flow velocity within the fenestra, P_0 is the average pressure at the outflow, P_G is the capillary pressure, and ε_F is the fraction of the endothelial surface covered by fenestrae. P_0 and v_Z are determined from pressure and velocity fields calculated by finite element analysis applied to a simplified Navier–Stokes'equation, which relates fluid flow to pressure and external forces acting on a fluid.

Hydraulic permeability of the basement membrane is estimated from Darcy's law, which describes the flow of water through porous media when the structural details of the media are unknown:

$$v = -\nabla P \frac{k_D}{\mu} \tag{21.47}$$

where v is the velocity vector, μ is the viscosity and k_D is the so-called Darcy permeability of the medium. The Darcy permeability is related to Lp in Eq. (21.3a), and must be determined empirically. Values for k_D/μ are available from measurements made on isolated glomerular basement membrane.[26,37,110] It is a complicated problem to solve for the pressures and flows within the GBM due to streaming and bulging of the velocity and pressure fields that arise, because fluid must enter only through fenestrae and leave only through epithelial slits that cover only part of the basement membrane. These pressure and flow fields are determined numerically after setting the appropriate conditions for zero flow in the z-direction at boundary areas covered by cells, and setting the divergence of flow equal to zero to satisfy conservation of mass for a noncompressible fluid. Calculating k_{GBM} in this way is somewhat artificial, inasmuch as the apparent conductance of the GBM will increase along with the fraction of its surface that is covered by fenestrae and filtration slits. Therefore, as the number of fenestrae and filtration slits declines, the apparent hydraulic resistance of the GBM will increase even though there has been no actual change to the GBM.

Hydraulic permeability of the epithelial layer is calculated, again by applying the simplified Navier–Stokes' equation, this time to an ultrastructural model of the filtration slit as a rectangular channel bridged by fibers.[34] This particular geometry for the slit diaphragm is based on microscopy of Rodewald and Karnovsky, who suggested that the filtration slit consists of a central fiber connected by bridging fibers to the cell membranes on either side (see Figure 21.15).[111] Solving the model reveals that the slit diaphragm is the main site of resistance to flow through the filtration slit, and that there is little resistance to flow along the remainder of the filtration slit, which is a channel whose walls are formed by two adjacent foot processes. One caveat to these predictions has arisen from molecular sieving data, which suggest that the true pore dimensions provided by the Rodewald–Karnovsky model are too small, and are better explained if the slit diaphragm is represented by a single row of parallel cylindrical fibers rather than two rows of pores separated by a central fiber.[38] However, a more detailed image of the slit diaphragm has now been obtained by electron tomography which validates the basic zipper-like configuration with pores on each side that approximate the dimension of

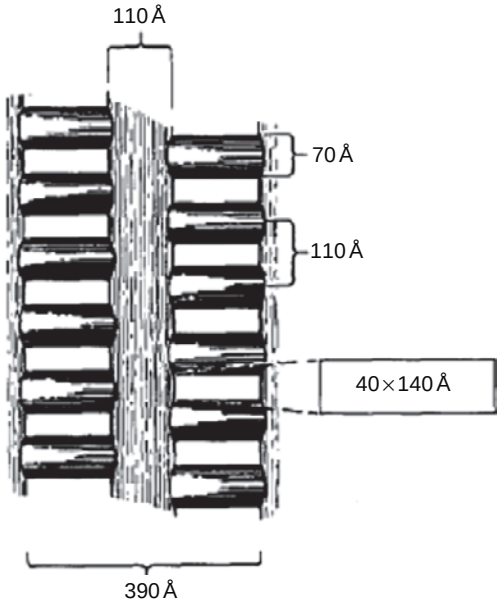

FIGURE 21.15 **Schematic drawing of the epithelial slit diaphragm.** Typical cross-sectional dimensions of pores between cross-bridges are 40 × 140 D *(from ref. [144])*.

TABLE 21.4 Microstructural Parameters and Ultrafiltration Coefficient in the Rat used by Drumond et al.*

Width of filtration unit	360 nm
Thickness of GBM	200 nm
Width of filtration slit	39 nm
Fractional area of fenestrae	0.2
Number of fenestrae per unit	3
Fractional area of slits	0.11
Darcy permeability of GBM	2.7 nm^2
k_{endo}	2.0×10^{-7} m-s^{-1}-Pa^{-1}
k_{GBM}	8.3×10^{-9} m-s^{-1}-Pa^{-1}
k_{epi}	8.6×10^{-9} m-s^{-1}-Pa^{-1}
k	4.1×10^{-9} m-s^{-1}-Pa^{-1}
k estimated from micropuncture and morphometry	3×10^{-9}–5×10^{-9} m-s^{-1}-Pa^{-1}

Drumond et al. (1994). Am. J. Physiol. Renal Fluid Electrolyte Physiol. 266, F1–F12.[35] See also Figure 21.14.

albumin. As depicted by electron tomography, these pores appear more irregular and tortuous than previously imagined.[147]

The morphometric parameters and hydraulic permeabilities calculated from the ultrastructural model of Deen et al. are shown in Table 21.4, which also shows that the hydraulic permeability predicted by the model is consistent with values obtained by micropuncture in normal rats. Some other predictions of the model cannot be tested by micropuncture. For example, a main prediction of the model is that the GBM and epithelial layers contribute equally and, together, account for most of the resistance to glomerular filtration. The endothelial fenestrae pose little resistance to bulk flow, except that reducing their fractional area reduces the apparent permeability of the GBM. Furthermore, as already mentioned, most resistance of the filtration slit is due to the slit diaphragm, rather than to drag along the length of the slit.

An important test of the model is that it predicts changes in the ultrafiltration coefficient that occur when the glomerular structure is altered. The model has successfully forecast changes in ultrafiltration coefficient brought about by manipulating dietary protein and/or renal mass to alter glomerular morphology in rats with adriamycin nephrosis.[85]

Computation based on morphometry has also been employed to estimate glomerular ultrafiltration coefficient from renal biopsies in patients with reduced GFR due to membranous or minimal change nephropthies[36] and pre-eclampsia.[70] In each of these conditions, GFR was reduced in spite of normal PAH clearance. In order for GFR to decline while nephron plasma flow remains constant, there must be a decrease in either glomerular ultrafiltration pressure or ultrafiltration coefficient. While it is not possible to measure ultrafiltration pressure in humans, the determinants of *SNGFR* have been extensively evaluated in a wide range of animal models of glomerular disease. With the single exception of cyclosporine toxicity,[137] low pressure in the glomerular capillary does not provide the basis for low *SNGFR* in any of these models. Therefore, it is reasonable to assume that ultrafiltration pressure is not reduced in humans with idiopathic nephrotic syndrome or pre-eclampsia, and that the low filtration fraction in these patients is likely to be the consequence of a decline in ultrafiltration coefficient. Once this premise is accepted, there are several potential explanations for an apparent decline in ultrafiltration coefficient in a glomerulus. First, this could be due to a loss of capillary surface area. Second, it could result from mismatched blood flow among capillary loops within the glomerulus, such that those loops with low flow manifest filtration equilibrium early in their course, which eliminates their latter portions from contributing to the working area. A third mechanism for reducing ultrafiltration coefficient could be to alter the chemical composition of the GBM or slit diaphragm to make them less permeable to water. Finally, ultrafiltration coefficient could decline due to changes in geometry of the individual filtration unit. The latter of these possibilities is amenable to testing by applying computational fluid dynamics to morphometry. Based on this approach, changes in geometry of the filtration unit predict that the ultrafiltration coefficient will be different between normal subjects and those with minimal change disease, membranous nephropthy, and pre-eclampsia. Although each disease has its own morphology, reduced frequency of filtration slits, increased basement membrane thickness, loss of fenestral area or loss of capillary surface area predicted changes in the ultrafiltration coefficient consistent with what would be necessary to explain the associated declines in GFR, given the reasonable assumption that glomerular capillary pressure was not profoundly reduced, and a less certain assumption that the Darcy permeability for the GBM is unaffected. One interesting prediction of the model is that, while the GBM is thickened in membranous nephropathy, this has little importance to the GFR because an even greater augmentation of the average distance traveled from fenestra to slit diaphragm results from the lower filtration slit density, which requires much of the filtrate to stream obliquely through the GBM rather than crossing it directly.

In 2005 it was recognized that the visceral epithelial cell body attaches to the GBM in such a way as to create a semi-confined space downstream of the filtration

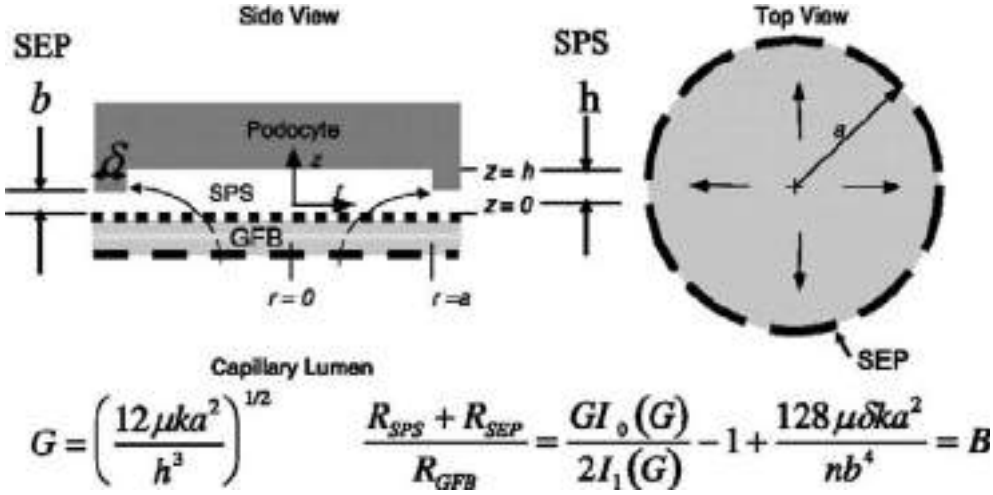

FIGURE 21.16 **Flow across the glomerular filtration barrier and through the subpodocyte space (SPS).** Resistance depends on height of subpodocyte space (h), the path length (a), and the area draining into SPS (πa^2) *(reprinted from ref. [88]).*

slit and upstream of the rest of Bowman's space[87] (see Figure 21.16). It was further estimated that 60% of the filtration surface is covered by this subpodocyte space, and that the space between attachments constitute pores through which filtrate must pass en route to Bowman's space. When analyzed in greater detail and subject to mathematical modeling, it was estimated that the resistance encountered by filtrate in exiting the subepithelial space is likely to exceed that of the traditional 3-layer filtration barrier, and that pressure in this space could, therefore, be three-fold greater than in Bowman's space.[88] This poses a problem for prior structure-based models, which accurately predict the hydraulic permeability without this contribution to the barrier.

SUMMARY

Details about the physics of glomerular filtration have become known over the past century. Different approaches to describing glomerular filtration employ different admixtures of phenomenology and structural detail. The spectrum of useful models extends from the glomerular capillary as an idealized circular cylinder with homogenous permeability to water and small solutes and zero permeability to macromolecules, to a tube perforated by discreet cylindrical pores with differential permeability to solutes based on size and electrical charge, to fiber matrix models based on the physical theory of colloids, to representations that incorporate actual physical dimensions to determine the contributions of endothelial, basement membrane, and epithelial layers to the filtration barrier.

Acknowledgment

This work was performed with grant support from NIH, RO1 DK28602 and RO1 DK56248 and the Department of Veterans Affairs Research Service.

References

[1] Andersen S, Blouch K, Bialek J, Deckert M, Parving HH, Myers BD. Glomerular permselectivity in early stages of overt diabetic nephropathy. Kidney Int 2000;58:2129–37.
[2] Anderson JL, Quinn JA. Restricted transport in small pores. A model for steric exclusion and hindered particle motion. Biophys J 1974;14:130–50.
[3] Anderson S, Meyer TW, Rennke HG, Brenner BM. Control of glomerular hypertension limits glomerular injury in rats with reduced renal mass. J Clin Invest 1985;76(2):612–9.
[4] Arendshorst WJ, Gottschalk CW. Glomerular ultrafiltration dynamics: historical perspective. Am J Physiol 1985;248(2 Pt 2): F163–74.
[5] Bakris GL, Weir MR. Angiotensin-converting enzyme inhibitor-associated elevations in serum creatinine: is this a cause for concern? Arch Intern Med 2000;160(5):685–93.
[6] Baylis C. The mechanism of the increase in glomerular filtration rate in the twelve-day pregnant rat. J Physiol 1980;305:405–14.
[7] Baylis C, Ichikawa I, Willis WT, Wilson CB, Brenner BM. Dynamics of glomerular ultrafiltration. IX. Effects of plasma protein concentration. Am J Physiol 1977;232(1):F58–71.
[8] Bhalla G, Deen WM. Effects of charge on osmotic reflection coefficients of macromolecules in fibrous membranes. Biophys J 2009;97(6):1595–605.
[9] Blantz RC. Effect of mannitol on glomerular ultrafiltration in the hydropenic rat. J Clin Invest 1974;54(5):1135–43.
[10] Blantz RC, Gabbai F, Gushwa LC, Wilson CB. The influence of concomitant experimental hypertension and glomerulonephritis. Kidney Int 1987;32(5):652–63.
[11] Blantz RC, Gabbai FB, Tucker BJ, Yamamoto T, Wilson CB. Role of mesangial cell in glomerular response to volume and angiotensin II. Am J Physiol 1993;264(1 Pt 2):F158–65.

[12] Blantz RC, Konnen KS, Tucker BJ. Angiotensin II effects upon the glomerular microcirculation and ultrafiltration coefficient of the rat. J Clin Invest 1976;57(2):419–34.
[13] Blantz RC, Rector Jr FC, Seldin DW. Effect of hyperoncotic albumin expansion upon glomerular ultrafiltration in the rat. Kidney Int 1974;6(4):209–21.
[14] Blouch K, Deen WM, Fauvel JP, Bialek J, Derby G, Myers BD. Molecular configuration and glomerular size selectivity in healthy and nephrotic humans. Am J Physiol 1997;273:F430–7.
[15] Bohrer MP, Deen WM, Robertson CR, Troy JL, Brenner BM. Influence of molecular configuration on the passage of macromolecules across the glomerular capillary wall. J Gen Physiol 1979;74(5):583–93.
[16] Bowman W. On the Structure and Use of the Malpighian Bodies of the Kidney, with Observations on the Circulation. London: Printed by R. and J. E. Taylor, 1842. Offprint from *Philosophical Transactions of the Royal Society, Part I for 1842*.
[17] Brenner BM, Falchuk KH, Keimowitz RI, Berliner RW. The relationship between peritubular capillary protein concentration and fluid reabsorption by the renal proximal tubule. J Clin Invest 1969;48(8):1519–31.
[18] Brenner BM, Hostetter TH, Humes HD. Glomerular permselectivity: barrier function based on discrimination of molecular size and charge. Am J Physiol Renal Fluid Electrolyte Physiol 1978;234:F455–60.
[19] Brenner BM, Troy JL, Daugharty TM. The dynamics of glomerular ultrafiltration in the rat. J Clin Invest 1971;50(8):1776–80.
[20] Caulfield JP, Farquhar MG. The permeability of glomerular capillaries to graded dextrans. Identification of the basement membrane as the primary filtration barrier. J Cell Biol 1974; 63(3):883–903.
[21] Chang RL, Deen WM, Robertson CR, Brenner BM. Permselectivity of the glomerular capillary wall. III. Restricted transport of polyanions. Kidney Int 1975;8:212–8.
[22] Chang RL, Robertson CR, Deen WM, Brenner BM. Permselectivity of the glomerular capillary wall to macromolecules. I. Theoretical considerations. Biophys J 1975;15(9):861–86.
[23] Chasis H, Ranges HA, Goldring W, Smith HW. The control of renal blood flow and glomerular filtration in normal man. J Clin Invest 1938;17:683–97.
[24] Comper WD, Lee AS, Tay M, Adal Y. Anionic charge concentration of rat kidney glomeruli and glomerular basement membrane. Biochem J. 1993;289:647–52.
[25] Daniels BS, Deen WM, Mayer G, Meyer T, Hostetter TH. Glomerular permeability barrier in the rat. Functional assessment by *in vitro* methods. J Clin Invest 1993;92(2):929–36.
[26] Daniels BS, Hauser EH, Deen WM, Hostetter TH. Glomerular basement membrane: *in vitro* studies of water and protein permeability. Am J Physiol Renal Fluid Electrolyte Physiol 1992;262:F919–26.
[27] De Nicola L, Blantz RC, Gabbai FB. Renal functional reserve in the early stage of experimental diabetes. Diabetes 1992;41 (3):267–73.
[28] Deen WM. Cellular contributions to glomerular size selectivity. Kidney Int 2006;69(8):1295–7.
[29] Deen WM, Bridges CR, Brenner BM, Myers BD. Heteroporous model of glomerular size selectivity: application to normal and nephrotic humans. Am J Physiol 1985;249:F374 –F389.
[30] Deen WM, Lazzara MJ, Myers BD. Structurual determinants of glomerular permeability. Am J Physiol Renal Physiol 2001;281: F579–96.
[31] Deen WM, Robertson CR, Brenner BM. A model of glomerular ultrafiltration in the rat. Am J Physiol 1971;223:1178–83.
[32] Deen WM, Satvat B, Jamieson JM. Theoretical model for glomerular filtration of charged solutes. Am J Physiol 1980;238(2):F126–39.
[33] Deen WM, Troy JL, Robertson CR, Brenner BM. Dynamics of glomerular ultrafiltration in the rat. IV. Determination of the ultrafiltration coefficient. J Clin Invest 1973;52(6):1500–8.
[34] Drumond MC, Deen WM. Stokes flow through a row of cylinders between parallel walls: model for the glomerular slit diaphragm. J Biomech Eng 1994;116(2):184–9.
[35] Drumond MC, Deen WH. Structural determinants of glomerular hydraulic permeability. Am J Physiol Renal Fluid Electrolyte Physiol 1994;266:F1–12.
[36] Drumond MC, Kristal B, Myers BD, Deen WM. Structural basis for reduced glomerular filtration capacity in nephrotic humans. J Clin Invest 1994;94(3):1187–95.
[37] Edwards A, Daniels BS, Deen WM. Hindered transport of macromolecules in isolated glomeruli II. Convection and pressure effects in basememt membrane. Biophys J 1997;72: 214–22.
[38] Edwards A, Daniels BS, Deen WM. Ultrastructural model for size selectivity in glomerular filtration. Am J Physiol 1999;276(6 Pt 2):F892–902.
[39] Einstein A. Uber die von der molekularkinetistchen Theorie der Waerme geforderte Bewegung von in ruhenden Fluessigkeiten suspendierten Teilchen. Ann Physik 1905;17:549–60.
[40] Elger M, Sakai T, Kriz W. The vascular pole of the renal glomerulus of rat. Adv Anat Embryol Cell Biol 1998;139:1–98.
[41] Falchuk HK, Berliner RW. Hydrostatic pressures in peritubular capillaries and tubules in the rat kidney. Am J Physiol 1971;220:1422–6.
[42] Farquhar MG, Palade GE. Glomerular permeability. II. Ferritin transfer across the glomerular capillary wall in nephrotic rats. J Exp Med 1961;114:699–716.
[43] Ferry JD. Ultrafilter membranes and ultrafiltration. Chem Rev 1936;18:373.
[44] Fronek K, Zweifach BW. Microvascular pressure distribution in skeletal muscle and the effect of vasodilation. Am J Physiol 1975;228(3):791–6.
[45] Gabbai FB, Gushwa LC, Wilson CB, Blantz RC. An evaluation of the development of experimental membranous nephropathy. Kidney Int 1987;31(6):1267–78.
[46] Gabbai FB, Gushwa LC, Peterson OW, Wilson CB, Blantz RC. Analysis of renal function in the two-kidney Goldblatt model. Am J Physiol 1987;252(1 Pt 2):F131–7.
[47] Gomez DM. Evaluation of renal resistances, with special reference to changes in essential hypertension. J Clin Invest 1951;30:1143–55.
[48] Granath KA. Solution properties of branched dextrans. J Colloid Sci 1958;13:308–28.
[49] Guasch A, Deen WM, Myers BD. Charge selectivity of the glomerular filtration barrier in healthy and nephrotic humans. J Clin Invest 1993;92:2274–82.
[50] Guimarães MA, Nikolovski J, Pratt LM, Greive K, Comper WD. Anomalous fractional clearance of negatively charged Ficoll relative to uncharged Ficoll. Am J Physiol Renal Physiol 2003;285:F1118–24.
[51] Haberman WL, Sayre RM. David Taylor Model Basin. Report No. 1143 Motion of rigid and fluid spheres in stationary and moving liquids inside cylindrical tubes. Washington DC: U.S. Navy; 1958
[52] Hall JE, Guyton AC, Smith Jr MJ, Coleman TG. Blood pressure and renal function during chronic changes in sodium intake: role of angiotensin. Am J Physiol 1980;239(3):F271–80.
[53] Haraldsson BS, Johnsson EK, Rippe B. Glomerular permselectivity is dependent on adequate serum concentrations of orosomucoid. Kidney Int 1992;41(2):310–6.
[54] Heidenhain RP. Absonderungsvorgaenge. Sechster Abschnitt. Die Harnabsonderung (Viertes Capitel. Die Absonderung der

festen Harnbestandteile). In: Leipzig HL, editor. Handbuch d Physiol Fuenfter Teil. Germany: Vogel; 1883. p. 341–3.
[55] Heller J, Horacek V. Angiotensin II: preferential efferent constriction? Ren Physiol 1986;9(6):357–65.
[56] Hierholzer K, Ullrich KJ. History of renal physiology in Germany during the 19th century. Am J Nephrol 1999; 19(2):243–56.
[57] Hostetter TH. Human renal response to a meat meal. Am J Physiol 1986;250(4 Pt 2):F613–8.
[58] Hostetter TH, Troy JL, Brenner BM. Glomerular hemodynamics in experimental diabetes mellitus. Kidney Int 1981;19(3):410–5.
[59] Ichikawa I, Brenner BM. Local intrarenal vasoconstrictor–vasodilator interactions in mild partial ureteral obstruction. Am J Physiol 1979;236(2):F131–40.
[60] Jarad G, Cunningham J, Shaw AS, Miner JH. Proteinuria precedes podocyte abnormalities inLamb2$^{-/-}$ mice, implicating the glomerular basement membrane as an albumin barrier. J Clin Invest 2006;116(8):2272–9.
[61] Jeansson M, Haraldsson B. Glomerular size and charge selectivity in the mouse after exposure to glucosaminoglycan-degrading enzymes. J Am Soc Nephrol 2003;14(7):1756–65.
[62] Jensen PK, Christiansen JS, Steven K, Parving HH. Renal function in streptozotocin-diabetic rats. Diabetologia 1981; 21(4):409–14.
[63] Johnson EM, Berk DA, Jain RK, Deen WM. Diffusion and partitioning of proteins in charged agarose gels. Biophys J 1995; 68(4):1561–8.
[64] Johnsson E, Haraldsson B. An isolated perfused rat kidney preparation designed for assessment of glomerular permeability characteristics. Acta Physiol Scand 1992;144(1): 65–73.
[65] Johnsson E, Rippe B, Haraldsson B. Analysis of the pressure-flow characteristics of isolated perfused rat kidneys with inhibited tubular reabsorption. Acta Physiol Scand 1994; 150(2):189–99.
[66] Johnsson E, Rippe B, Haraldsson B. Reduced permselectivity in isolated perfused rat kidneys following small elevations of glomerular capillary pressure. Acta Physiol Scand 1994; 150(2):201–9.
[67] Katz MA, Bressler EH. Osmosis. In: Staub N, Taylor A, editors. Edema: Basic science and clinical manifestations. NY: Raven Press; 1984. p. 39–60.
[68] Katz MA, Schaeffer Jr RC, Gratrix M, Mucha D, Carbajal J. The glomerular barrier fits a two-pore-and-fiber-matrix model: derivation and physiologic test. Microvasc Res 1999;57(3): 227–43.
[69] Kedem O, Katchalsky A. Thermodynamic analysis of the permeability of biological membranes to non-electrolytes. Biochim Biophys Acta 1958;27:229–46.
[70] Lafayette RA, Druzin M, Sibley R, Derby G, Malik T, Huie P, et al. Nature of glomerular dysfunction in pre-eclampsia. Kidney Int 1998;54(4):1240–9.
[71] Landis EM, Pappenheimer JR. Exchange of substances through the capillary walls. In: Hamilton WF, Dow P, editors. *Handbook of Physiology*. *Circulation*. Washington DC: Am Physiol Soc; 1963. p. p961–1034. Section 2. Vol II. Chapter 29
[72] Lemley KV, Blouch K, Abdullah I, Boothroyd DB, Bennett PH, Myers BD, et al. Glomerular permselectivity at the onset of nephropathy in type 2 diabetes mellitus. J Am Soc Nephrol 2000;11:2095–105.
[73] Lewis EJ, Hunsicker LG, Bain RP, Rohde RD, for the Collaborative Study Group. The effect of angiotensin-converting-enzyme inhibition on diabetic nephropathy. N Engl J Med 1993;329:1456–62.
[74] Lindströöm KE, Blom A, Johnsson E, Haraldsson B, Fries E. High glomerular permeability of bikunin despite similarity in charge and hydrodynamic size to serum albumin. Kidney Int 1997;51(4):1053–8.
[75] Lindströöm KE, Johnsson E, Haraldsson B. Glomerular charge selectivity for proteins larger than serum albumin as revealed by lactate dehydrogenase isoforms. Acta Physiol Scand 1998;162 (4):481–8.
[76] Loutzenhiser R, Bidani A, Chilton L. Renal myogenic response: kinetic attributes and physiological role. Circ Res 2002;90 (12):1316–24.
[77] Lowry OH, Rosebrough NJ, Farr AL, Randall RJ. Protein measurement with the Folin phenol reagent. J Biol Chem 1951;193:265–75.
[78] Ludwig CFW. Beitraege zur lehre vom mechanismus der harnsekretion. Marburg: N.G. Elwert; 1843.
[79] Ludwig C. De viribus physicis secretionem urinae adjuvantibus Thesis, Marburg. 1842. Reprinted with a translation into English in Kidney Int 1994;(Suppl 46):1–23.
[80] Lund U, Rippe A, Venturoli D, Tenstad O, Grubb A, Rippe B. Glomerular filtration rate dependence of sieving of albumin and some neutral proteins in rat kidneys. Am J Physiol Renal Physiol 2003;284:F1226–34.
[81] Malpighi M. De viscerum structura exercitatio anatomica Bononias Iacoi Montiz, 1666. For English translation see: JM Hayman Jr. Maipighi's "Concerning the structure of the kidney." Ann Med Hist 1925;7:242–63.
[82] Maschio G, Alberti D, Janin G, Locatelli F, Mann JF, Motolese M, et al. Effect of the angiotensin-converting-enzyme inhibitor benazepril on the progression of chronic renal insufficiency: The Angiotensin-Converting-Enzyme Inhibition in Progressive Renal Disease trial. N Engl J Med 1996;334: 939–45.
[83] Michels LD, Davidman M, Keane WF. Determinants of glomerular filtration and plasma flow in experimental diabetic rats. J *Lab Clin Med* 1981;8(6):869–85.
[84] Michels LD, O'Donnell MP, Keane WF. Glomerular hemodynamic and structural correlations in long-term experimental diabetic rats. J Lab Clin Med 1984;103(6):840–7.
[85] Miller PL, Scholey JW, Rennke HG, Meyer TW. Glomerular hypertrophy aggravates epithelial cell injury in nephrotic rats. J Clin Invest 1990;85(4):1119–26.
[86] Myers BD, Nelson RG, Williams GW, Bennett PH, Hardy SA, Berg RL, et al. Glomerular function in Pima Indians with noninsulin-dependent diabetes mellitus of recent onset. J Clin Invest 1991;88(2):524–30.
[87] Neal CR, Crook H, Bell E, Harper SJ, Bates DO. Three-dimensional reconstruction of glomeruli by elecron microscopy reveals a distinct restrictive urinary subpodocyte space. J Am Soc Nephrol 2005;16:1223–35.
[88] Neal CR, Muston PR, Njegovan D, Verrill R, Harper SJ, Deen WM, et al. Glomerular filtration into the subpodicyte space is highly restricted under physiological perfusion conditions. Am J Physiol 2007;293(6):F1787–98.
[89] O'Donnell MP, Kasiske BL, Daniels FX, Keane WF. Effects of nephron loss on glomerular hemodynamics and morphology in diabetic rats. Diabetes 1986;35(9):1011–5.
[90] O'Donnell MP, Kasiske BL, Keane WF. Glomerular hemodynamic and structural alterations in experimental diabetes mellitus. FASEB J 1988;8:2339–47.
[91] Ogston AG. The spaces in a uniform random suspension of fibres. Trans Faraday Soc 1958;54:1754–7.
[92] Oken DE, Choi SC. Filtration pressure equilibrium: a statistical analysis. Am J Physiol 1981;241(2):F196–200.
[93] Oken DE, Flamenbaum W. Micropuncture studies of proximal tubule albumin concentrations in normal and nephrotic rats. J Clin Invest 1971;50(7):1498–505.

[94] Oliver JD, Anderson S, Troy JL, Brenner BM, Deen WH. Determination of glomerular size-selectivity in the normal rat with Ficoll. J Am Soc Nephrol 1992;3:214–8.
[95] Onsager L. Reciprocal relations in irreversible processes. I. I *Phys Rev* 1931;37:405–91.
[96] Osicka TM, Comper WD. Glomerular charge selectivity for anionic and neutral horseradish peroxidase. Kidney Int 1995;47:1630–7.
[97] Paine PL, Scherr P. Drag coefficients for the movement of rigid spheres through liquid-filled cylindrical pores. Biophysical Journal 1975;15:1087–91.
[98] Pappenheimer JR. Passage of molecules through capillary walls. Physiol Rev 1953;33:387–423.
[99] Parazynski SE, Tucker BJ, Aratow M, Crenshaw A, Hargens AR. Direct measurement of capillary blood pressure in the human lip. J Appl Physiol 1993;74(2):946–50.
[100] Patlak CS, Goldstein DA, Hoffman JF. The flow of solute and solvent across a two-membrane system. J. Theoretical Biology 1963;5:426–42.
[101] Peti-Peterdi J. Independent two-photon measurements of albumin GSC give low values. Am J Physiol Renal Physiol 2009;296(6):F1255–7.
[102] Peti-Peterdi J, Sipos A. A high-powered view of the filtration barrier. J Am Soc Nephrol 2010;21(11):1835–41.
[103] Pullman TN, Alving AS, Dern RJ, Landowne M. The influence of dietary protein intake on specific renal functions in normal man. J Lab Clin Med 1954;44:320–32.
[104] Remuzzi A, Brenner BM, Pata V, Tebaldi G, Mariano R, Belloro A, et al. Three-dimensional reconstructed glomerular capillary network: Blood flow distribution and local filtration. Am J Physiol 1992;263(3 Pt 2):F562–72.
[105] Remuzzi A, Ene-Iordache B. Capillary network structure does not affect theoretical analysis of glomerular size selectivity. Am J Physiol 1995;268(5 Pt 2):F972–9.
[106] Remuzzi A, Fassi A, Sangalli F, Malanchini B, Mohamed EI, Bertani T, et al. Prevention of renal injury in diabetic MWF rats by angiotensin II antagonism. Exp Nephrol 1998;6(1): 28–38.
[107] Rennke HG, Patel Y, Venkatachalam MA. Glomerular filtration of proteins: clearance of anionic, neutral, and cationic horseradish peroxidase in the rat. Kidney Int 1978;13:278–88.
[108] Rennke HG, Venkatachalam MA. Glomerular permeability of macromolecules. Effect of molecular configuration on the fractional clearance of uncharged dextran and neutral horseradish peroxidase in the rat. J Clin Invest 1979;63(4):713–7.
[109] Rippe B, Haraldsson B. Transport of macromolecules across microvascular walls: the two-pore theory. Physiol Rev 1994;74:163–219.
[110] Robinson GB, Walton HA. Glomerular basement membrane as a compressible ultrafilter. Microvasc Res 1989;38:36–48.
[111] Rodewald R, Karnovsky MJ. Porous substructure of the glomerular slit diaphragm in the rat and mouse. J Cell Biol 1974;60(2):423–33.
[112] Russo PA, Bendayan M. Distribution of endogenous albumin in the glomerular wall of proteinuric patients. Am J Pathol 1990;137(6):1481–90.
[113] Russo LM, Sandoval RM, McKee M, Osicka TM, Collins AB, Brown D, et al. The normal kidney filters nephrotic levels of albumin retrieved by proximal tubule cells: retrieval is disrupted in nephrotic states. Kidney Int 2007;71(6):504–13.
[114] Savin VJ. Ultrafiltration in single isolated human glomeruli. Kidney Int 1983;24(6):748–53.
[115] Savin VJ, Terreros DA. Filtration in single isolated mammalian glomeruli. Kidney Int 1981;20(2):188–97.
[116] Schaeffer Jr RC, Gratrix ML, Mucha DR, Carbajal JM. The rat glomerular filtration barrier does not show negative charge selectivity. Microcirculation 2002;9:329–42.
[117] Schlogl R. Zurtheorie der anomalen Osmose. Z *Physik Chem* 1955;3:73–102.
[118] Scholey JW, Meyer TW. Control of glomerular hypertension by insulin administration in diabetic rats. J Clin Invest 1989; 83(4):1384–9.
[119] Schor N, Ichikawa I, Brenner BM. Glomerular adaptations to chronic dietary salt restriction or excess. Am J Physiol 1980; 238(5):F428–36.
[120] Shannon JA, Jolliffe N, Smith HW. The excretion of urine in the dog IV. The effect of maintenance diet, feeding, etc., upon the quantity of the glomerular filtrate. Am J Physiol 1932;101:625–38.
[121] Shannon JA, Smith HW. The excretion of inulin, xylose and urea by normal and phlorinized man. J Clin Invest 1935;112:405–13.
[122] Slomowitz LA, Peterson OW, Thomson SC. Converting enzyme inhibition and the glomerular hemodynamic response to glycine in diabetic rats. J Am Soc Nephrol 1999;10(7): 1447–54.
[123] Smaje L, Zweifach BW, Intaglietta M. Micropressures and capillary filtration coefficients in single vessels of the cremaster muscle of the rat. Microvasc Res 1970;2(1):96–110.
[124] Smith HW. The kidney: Structure and function in health and disease. New York: Oxford Univ. Press; 1951.
[125] Smith HW, Chasis H, Goldring W, Ranges HA. Glomerular dynamics in the normal human kidney. J Clin Invest 1940;19:751–64.
[126] Smith HW, Finkelstein N, Aliminosa L, Crawford B, Graber M. The renal clearance of substituted hippuric acid derivatives and other aromatic acids in dog and man. J Clin Invest 1945;24:388–404.
[127] Smithies O. Why the kidney glomerulus does not clog: a gel permeation/diffusion hypothesis of renal function. Proc Natl Acad Sci USA 2003;100(7):4108–13.
[128] Sorensson J, Ohlson M, Lindströöm K, Haraldsson B. Glomerular charge selectivity for horseradish peroxidase and albumin at low and normal ionic strengths. Acta Physiol Scand 1998;163(1):83–91.
[129] Sorensson J, Ohlson M, Lindströöm K, Haraldsson B. Glomerular charge selectivity for horseradish peroxidase and albumin at low and normal ionic strengths. Acta Physiol Scand 1998;163(1):83–91.
[130] Squire JM, Chew M, Nneji G, Neal C, Barry J, Michel C. Quasi-periodic substructure in the microvessel endothelial glycocalyx: a possible explanation for molecular filtering? J Struct Biol 2001;136(3):239–55.
[131] Starling EH. The glomerular functions of the kidney. J Physiol London 1899;24:317–30.
[132] Staverman AJ. Non-equilibrium thermodynamics of membrane processes. Trans Faraday Soc 1952;48:176–85.
[133] Tanner GA. Glomerular sieving coefficient of serum albumin in the rat: a two-photon microscopy study. Am J Physiol Renal Physiol 2009;296(6):F1258–65.
[134] Tay M, Comper WD, Singh AK. Charge selectivity in kidney ultrafiltration is associated with glomerular uptake of transport probes. Am J Physiol Renal Fluid Electrolyte Physiol 1991;260: F549–54.
[135] Tenstad O, Roald AB, Grubb A, Aukland K. Renal handling of radiolabelled human cystatin C in the rat. Scand J Clin Lab Invest 1996;56:409–14.
[136] The Sixth Report of the Joint National Committee on Prevention, Detection, Evaluation and Treatment of High Blood Pressure. Arch Intern Med. 1997;157:2413-2446

[137] Thomson SC, Tucker BJ, Gabbai FB, Blantz RC. Functional effects on glomerular hemodynamics of short-term chronic cyclosporine in male rats. J Clin Invest 1989;83:960–9.

[138] Tojo A, Endou H. Intrarenal handling of proteins in rats using fractional micropuncture technique. Am J Physiol 1992;263(4 Pt 2):F601–6.

[139] Tryggvason K, Wartiovaara J. Molecular basis of glomerular permselectivity. Curr Opin Nephrol Hypertens 2001;10:543–9.

[140] Tucker BJ, Blantz RC. Effects of glomerular filtration dynamics on the glomerular permeability coefficient. Am J Physiol 1981;240(3):F245–54.

[141] Tucker BJ, Anderson CM, Thies RS, Collins RC, Blantz RC. Glomerular hemodynamic alterations during acute hyperinsulinemia in normal and diabetic rats. Kidney Int 1992;42(5): 1160–8.

[142] Tucker BJ, Mundy CA, Blantz RC. Adrenergic and angiotensin II influences on renal vascular tone in chronic sodium depletion. Am J Physiol 1987;252(5 Pt 2):F811–7.

[143] van't Hoff J. Chemical equilibria in gaseous systems or strongly diluted solutions), 1885. From *Nobel Lectures*, *Chemistry 1901-1921* L'Équilibre chimique dans les Systè mes gazeux ou dissous à l'État dilué. Amsterdam: Elsevier Publishing Company; 1966

[144] Venturoli D, Rippe B. Ficoll and dextran vs. globular proteins as probes for testing glomerular permselectivity: effects of molecular size, shape, charge, and deformability. Am J Physiol Renal Physiol 2005;288(4):F605–13.

[145] Vyas SV, Comper WD. Dextran sulfate binding to isolated rat glomeruli and glomerular basement membrane. Biochim Biophys Acta 1994;1201:367–72.

[146] Walker AM, Bott PA, Oliver J, MacDowell M. The collection and analysis of fluid from single nephrons of the mammalian kidney. Am J Physiol 1941;134:580–5.

[147] Wartiovaara J, Ofverstedt LG, Khoshnoodi J, Zhang J, Makela E, Sandin S, et al. Nephrin strands contribute to a porous slit diaphragm scaffold as revealed by electron tomography. J Clin Invest 2004;114(10):1475–83.

[148] Wearn JT, Richards AN. From: Observations on the composition of glomerular urine, with particular reference to the problem of reabsorption in the renal tubules. Am J Physiol 1924;71:209 –227.

[149] Wiederhielm CA, Weston BV. Microvascular, lymphatic, and tissue pressures in the unanesthetized mammal. Am J Physiol 1973;225(4):992–6.

[150] Zhang X, Curry FR, Weinbaum S. Mechanism of osmotic flow in a periodic fiber array. Am J Physiol Heart Circ Physiol 2006;290(2):H844–52.

[151] Zatz R, Dunn BR, Meyer TW, Anderson S, Rennke HG, Brenner BM. Prevention of diabetic glomerulopathy by pharmacological amelioration of glomerular capillary hypertension. J Clin Invest 1986;77(6):1925–30.

[152] Zatz R, Meyer TW, Rennke HG, Brenner BM. Predominance of hemodynamic rather than metabolic factors in the pathogenesis of diabetic glomerulopathy. Proc Natl Acad Sci USA 1985;82(17):5963–7.

This page intentionally left blank

CHAPTER

22

Glomerular Cell Biology

Yoshiro Maezawa[1], *Davide Cina*[1,2] *and Susan E. Quaggin*[1,2,3]

[1]Samuel Lunenfeld Research Institute, Mount Sinai Hospital

[2]Institute of Medical Science

[3]Division of Nephrology, St. Michael's Hospital University of Toronto, Toronto, Ontario, Canada

CELL BIOLOGY OF THE GLOMERULUS

Structure and Function of the Glomerulus (Renal Corpuscle)

The glomerulus or renal corpuscle is comprised of the glomerular tuft surrounded by Bowman's capsule and space. The tuft is a specialized microvascular bed which contains three cell types including the fenestrated or sinusoidal glomerular endothelial cells, the visceral epithelial cells known as podocytes, and mesangial cells. The glomerular filtration barrier is made up of the endothelial cells and podocytes together with an intervening glomerular basement membrane, and is the site of formation of the primary urinary filtrate. In the average adult human with normal renal function, 180 L of primary urinary filtrate is formed each day. The filtration barrier must permit free passage of water and small solutes into the urine, while retaining larger macromolecules in the blood. The demands of such "high flux" filtration require that the cell types of the glomerulus exhibit many specialized features, which will be discussed in this chapter.

In all mammals, the renal corpuscle appears as a spherical structure, although its diameter varies to some degree with the size of the organism. In humans, glomeruli are approximately 200 μm in diameter, in elephants 300 μm, in rats 120 μm, and in rabbits 150 μm.[209,215,271] A normal human kidney contains approximately one million individual glomeruli.

The central component of the renal corpuscle is composed of a plexus of sinusoidal or fenestrated capillaries that extend into Bowman's space where the primary urinary filtrate accumulates. The capillary loops are held together by the mesangial cells, and they are covered by a continuous layer of podocytes (Figure 22.1). At the vascular pole, the podocyte layer is continuous with the parietal epithelium of Bowman's capsule. Cells with intermediate phenotypes (between podocyte and parietal epithelium) can be observed at the transition zone. At the urinary pole of the renal corpuscle, the parietal epithelium is continuous with the epithelium of the proximal tubule (Figure 22.2c).

At the site of transition between parietal and visceral epithelium, the afferent and efferent arterioles enter and exit the glomerulus respectively, this is known as the glomerular hilum. After entering, the afferent arteriole branches to form a complex plexus of fenestrated capillaries with loops at the urinary pole.[64,197] The mesangium is required for proper structure and formation of this plexus, and in its absence only a single ballooned capillary loop forms.[64] The capillary loops come into direct contact with the mesangium at discrete points in a small region known as the juxtamesangial portion. However, the majority of the loops are found within Bowman's space and are covered entirely by the glomerular basement membrane and podocyte foot processes.[246] This is the surface area across which filtration occurs. The branches of the afferent arteriole give rise to individual vascular lobules within the glomerular tuft; each of these lobules contains its own afferent and efferent capillary with some connections between lobules. After looping at the urinary pole, the efferent capillaries join to form the larger efferent arteriole, which exits the tuft at the glomerular hilum. Along the length of the efferent arteriole, the

Seldin and Giebisch's The Kidney, Fifth Edition.
DOI: http://dx.doi.org/10.1016/B978-0-12-381462-3.00022-7

© 2013 Elsevier Inc. All rights reserved.

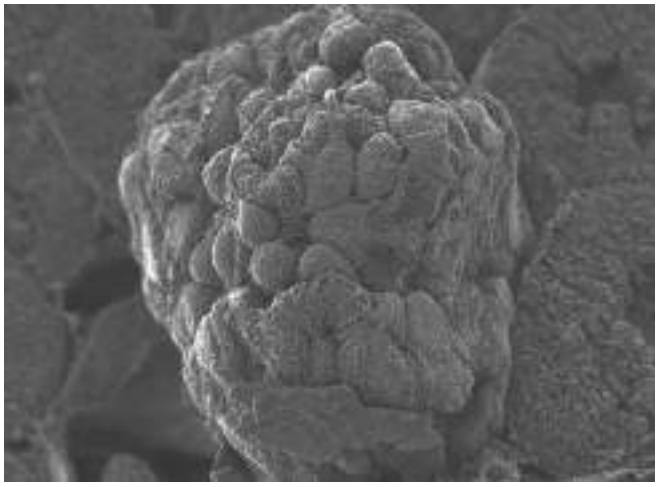

FIGURE 22.1 **Scanning electron micrograph of a normal mouse glomerulus.** Glomeruli are spherical bundles of capillary loops, covered by structurally unique podocytes and their foot processes (SEM × 1900). *(Courtesy of Dr. Marie Jeansson, Mount Sinai Hospital, Toronto, ON.)*

extraglomerular mesangium is gradually replaced by typical smooth muscle cells[64] (Figures 22.3 and 22.4).

GLOMERULAR ENDOTHELIAL CELLS

General Description

Glomerular endothelial cells are large, highly flattened cells that form the innermost layer of the glomerular capillary. Peripherally these cells are extremely thin, and the cell body contains the nucleus and all the cell organelles. The peripheral portions of the endothelial cells contain numerous fenestrae, which are 50−100 nm pores that penetrate the cytoplasm[158,241] (Figure 22.5). The luminal side of endothelial cells is covered by a thick layer consisting of glycoproteins that form "sieve plugs" in the fenestrae and the glycocalyx.[241]

Formation of Glomerular Capillaries

Several transplantation studies have demonstrated that the glomerular capillaries are formed largely by vasculogenesis: endothelial cells are derived from angioblasts believed to be intrinsic to the metanephric mesenchyme.[120,234,235] At E12.5, in mice before the formation of immature vasculature, kinase insert domain receptor (Kdr, also known as vascular endothelial growth factor receptor 2 (Vegfr-2) or Flk-1) positive angioblasts are present in the metanephric mesenchyme.[235] In the S-shaped stage of the developing nephron, immature podocytes start expressing vascular endothelial growth factor-A (Vegfa), thereby attracting Kdr-expressing endothelial cells to migrate to the vascular cleft.[65,68,225] Transforming growth factor-β1 (Tgfb1) induces apoptosis of the endothelial cells and opens the capillary lumens.[73]

Fenestrae and Diaphragms

Ultrastructural analysis demonstrates that diaphragms are often observed in fenestrae of glomerular endothelial cells in rodent embryos. Diaphragmed fenestrae are formed in the S-shaped stage, and then the diaphragms disappear from the capillary loop stage onwards.[121] The main component of the fenestration diaphragm is type II transmembrane glycoprotein plasmalemmal vesicle-associated protein-1 (Pv-1), but its precise function is still unknown.[249] Fenestrae in adult glomerular endothelial cells do not have diaphragms[121] (Figure 22.5); however, fenestrae bridged by diaphragms can be found along the intraglomerular segment of the efferent arteriole and its derivatives.[64] Diaphragms can also be observed in a drug-induced nephritis model, suggesting that diaphragms are required in the development and remodeling of fenestrations, thereby compensating for the immaturity of the barrier function in these settings.[121]

Glycocalyx/Sieve Plugs

The luminal membrane of endothelial cells is covered by a highly negatively-charged layer called the endothelial surface layer (ESL). The relatively dense, membrane-associated part of this layer is called the glycocalyx, and the larger, less compact component is known as the endothelial cell coat (Figure 22.6). The main components of the ESL are glycoproteins, glycoaminoglycans (GAGs), and membrane-associated and secreted proteoglycans.[104] Ultrastructural examinations with sophisticated specialized fixation techniques have revealed that this layer also fills the fenestrae with slit diaphragm-like "sieve plugs".[241] The thickness of the glycocalyx is estimated to be 50−100 nm, and that of the loose endothelial cell coat is considered to be 200−400 nm.[115,129,165,242] The relative importance of the ESL and sieve plug in the glomerular filtration barrier is still controversial.

Functional Maintenance of Glomerular Endothelial Cells: Insights from Studies of Angiogenic Factors

A number of factors are involved in the maintenance of glomerular endothelial structure and function, and coordinate an elaborate cross-talk between endothelial

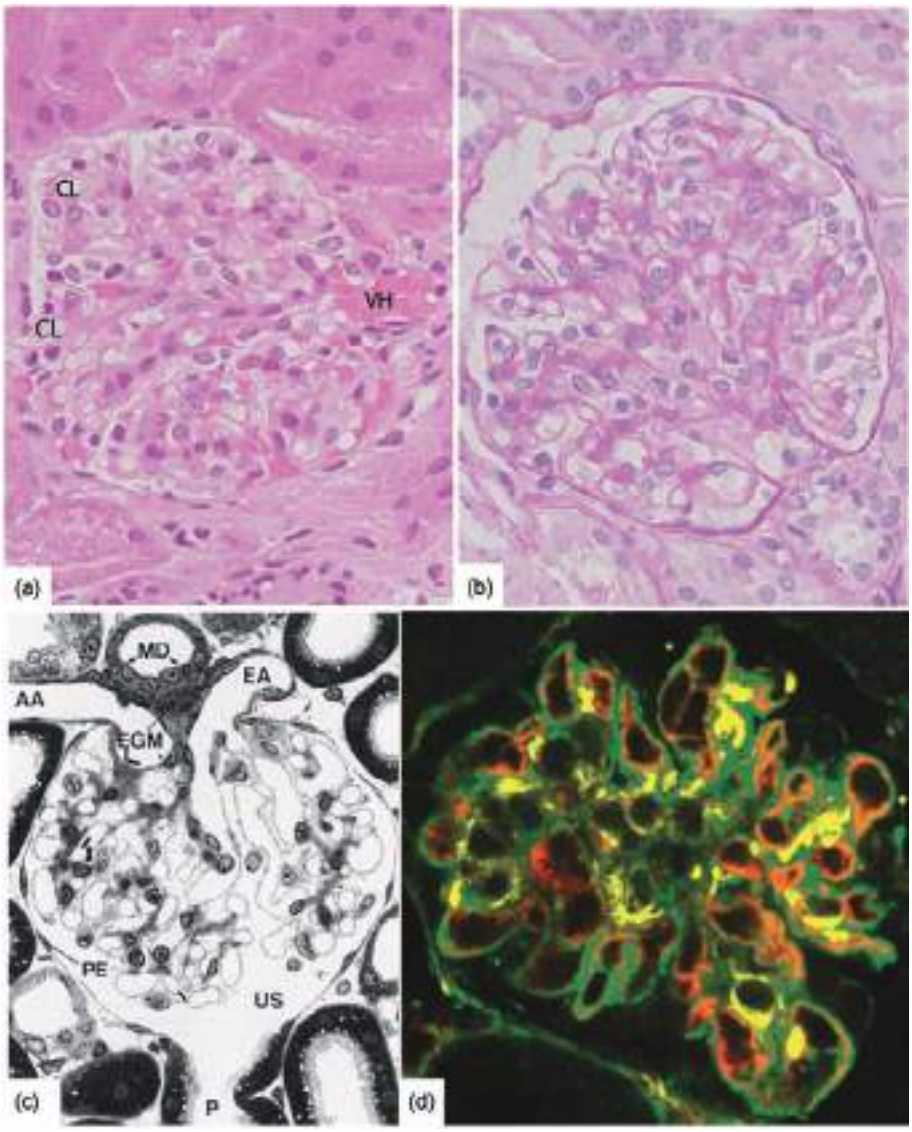

FIGURE 22.2 (a): Histology of normal human glomerulus. Hematoxylin-eosin (HE) staining showing patent capillary loops (CL) and vascular hilum (VH) (LM × 600). (b): Histology of normal human glomerulus. Periodic acid Schiff (PAS) staining (LM × 600). (c): Rat glomerulus sectioned through the vascular pole and the urinary pole. The afferent arteriole (AA), the efferent arteriole (EA), the extraglomerular mesangium (EGM), and the macula densa (MD) can be observed in this section. The orifice of proximal tubule (P) can be seen at the urinary pole (PE: parietal epithelial cells of Bowman's capsule; US: urinary space; LM × 490). (d): Immunostaining shows the three cell types found within the glomerular tuft (mouse glomerulus is shown) (Green: Zo-1 = podocytes; red: CD31 = endothelial cells; yellow: desmin = mesangial cells). The capillary loops are outlined by podocytes. Mesangial cells are located within the capillary tuft and connect capillary loops with each other (× 400). *(a and b: Courtesy of Dr. Paul S. Thorner, The Hospital for Sick Children, Toronto, ON.)*

cells and other cell types of the glomerulus (Figure 22.7).

Pdgfb/Pdgfrb

Platelet-derived growth factor B (Pdgfb) is secreted from endothelial cells and binds its receptor (Pdgfrb) on mesangial cells.[161,165,272] Pdgfb or Pdgfrb knockout mice have a defect in mesangial migration and a single, dilated glomerular capillary loop[14,161,272] (Figure 22.8). Endothelial specific deletion of Pdgfb results in the same phenotype as that seen in mice with a systemic knockout.[14,166] Also, this paracrine system requires retention of the ligands in the pericellular space, because mutants with deletion of the Pdgfb retention motif demonstrate delayed mesangial migration and, later on, proteinuria and glomerulosclerosis.[69,166]

Vegfa

Vegfa facilitates the formation of fenestrae in cultured glomerular endothelial cells.[67,69] Podocytes produce large amounts of Vegfa that can bind to Kdr on endothelial cells.[67,68] Cell-selective deletion of Vegfa from podocytes demonstrates that Vegfa signaling is required for formation and maintenance of the glomerular vasculature, its fenestrated phenotype and the filtration barrier. Mice treated with soluble fms-related tyrosine kinase-1 (sFlt-1, discussed below), a decoy receptor of Vegfa, show striking attenuation of endothelial fenestration, highlighting the necessity for Vegfa in the maintenance of fenestration[132] (Figure 22.5). In mutant mice that carry a podocyte-specific gene deletion of *Vegfa*, a few endothelial cells migrate into the developing glomeruli but they fail

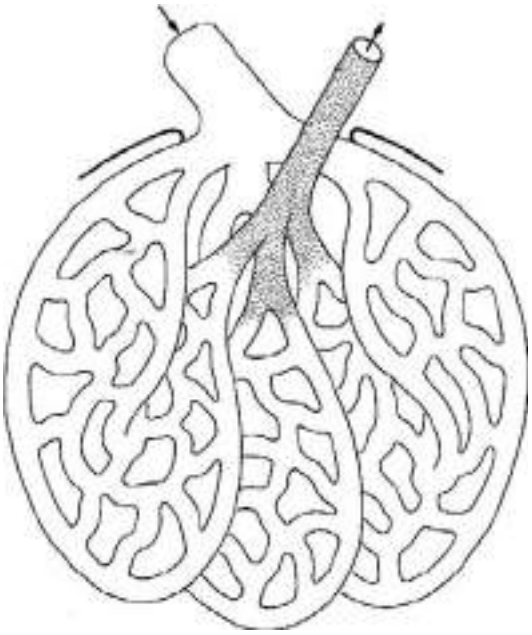

FIGURE 22.3 **Schematic diagram shows the branching pattern of glomerular capillaries.** As soon as the afferent arteriole enters the glomerulus, it divides into two to five branches to form the glomerular capillaries. The capillaries run toward the urinary pole, continuing to branch, and then loop back to the vascular pole to unify and form the efferent arteriole within the glomerular tuft. The efferent arteriole possesses a significant intraglomerular portion (*stippled*), whereas the afferent arteriole does not. *(From Winkler, D., Elger, M., et al. (1991). Branching and confluence pattern of glomerular arterioles in the rat. Kidney Int. Suppl.* ***32****: S2–8, with permission.)*

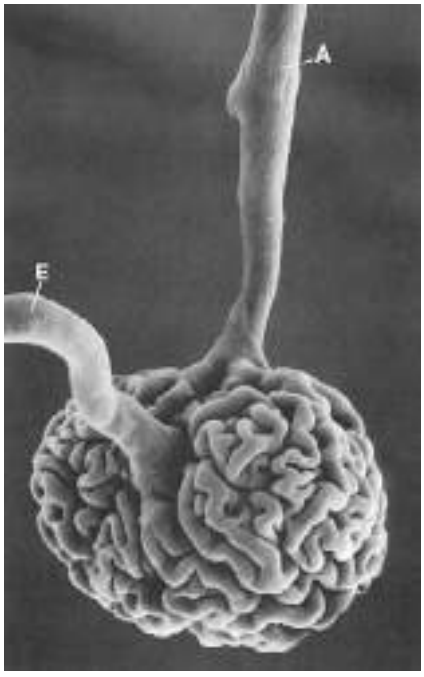

FIGURE 22.4 **Scanning electron micrograph of a glomerular vascular cast.** Afferent (A) and efferent (E) arterioles can be seen.

to develop fenestrations and rapidly disappear, causing renal failure and neonatal death.[67,68] The deletion of one allele of the *Vegfa* gene from podocytes leads to a glomerular defect known as endotheliosis, characterized by endothelial swelling and loss of fenestrations – a universal feature found in thrombotic microangiopathies. Overexpression of the major angiogenic Vegfa 164 isoform in podocytes results in collapse of the glomerular tuft.[67,98] Additionally, patients receiving anti-VEGF therapy may develop proteinuria due to thrombotic microangiopathy (TMA) of the glomerulus with prominent endotheliosis[66,98] (Figure 22.9). Indeed, deletion of *Vegfa* in mature podocytes of adult mice leads to TMA.[66,162] Taken together, these results indicate an indispensable role for Vegfa in the development, maintenance, and function of the glomerular vasculature and filtration barrier. They also highlight the importance of Vegfa paracrine signaling from the podocyte to Kdr on glomerular endothelial cells.

sFlt-1 is an alternatively spliced soluble form of VEGF receptor 1 (VEGFR-1)/Flt-1, and binds to VEGF as a decoy, thereby acting as a potent inhibitor of VEGF activity. Treatment of mice with adenoviral-induced sFlt-1 leads to a massive reduction of endothelial fenestrae[133] (Figure 22.5b). sFlt-1 blood levels are elevated in patients with pre-eclampsia[162,179] and administration of sFlt-1 to pregnant rats causes hypertension and proteinuria with histological glomerular endotheliosis. The endothelium is the most common glomerular region affected in pre-eclampsia,[157,179] suggesting a functional role for sFlt-1 in the function of the glomerular endothelium. A recent study also implicated sFlt-1 in the pathogenesis of PR3-ANCA-associated vasculitis affecting the glomeruli.[157,167]

Tgfb1

Infusion of a neutralizing antibody against transforming growth factor β1 (Tgfb1) to neonatal rats causes a delay in glomerular capillary formation, including the development of fenestrations.[167,173] In the choroid plexus, neutralization of both Tgfb1 and Vegfa leads to decreased cerebral perfusion, vascular thorombi, and a defect of fenestration, which does not occur when either of these treatments are administered individually.[173,279] Thus, Tgfb1 also plays a crucial role in the development and maintenance of glomerular endothelial cells, and may work in concert with Vegfa. Additionally, blood levels of soluble endoglin, an antagonist of Tgfb1 are elevated in patients with pre-eclampsia, and correlate with disease severity. Administration of soluble endoglin in combination with sFlt-1 to pregnant rats results in severe pre-

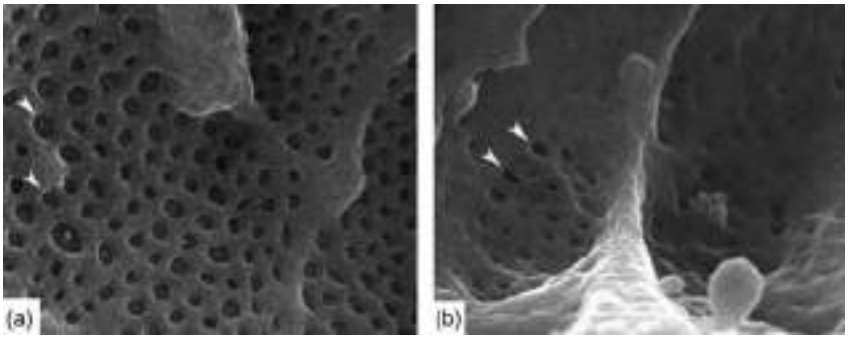

FIGURE 22.5 (a): Scanning electron micrograph shows the inner surface of a healthy glomerular capillary and its beautifully fenestrated endothelium. (B): Endothelial fenestrae are largely reduced after 14 days treatment of mice with soluble Flt-1 (SEM × 18,000). *(From Kamba, T., and McDonald, D. M. (2007). Mechanisms of adverse effects of anti-VEGF therapy for cancer. British Journal of Cancer* ***96****: 1788–1795, with permission.)*

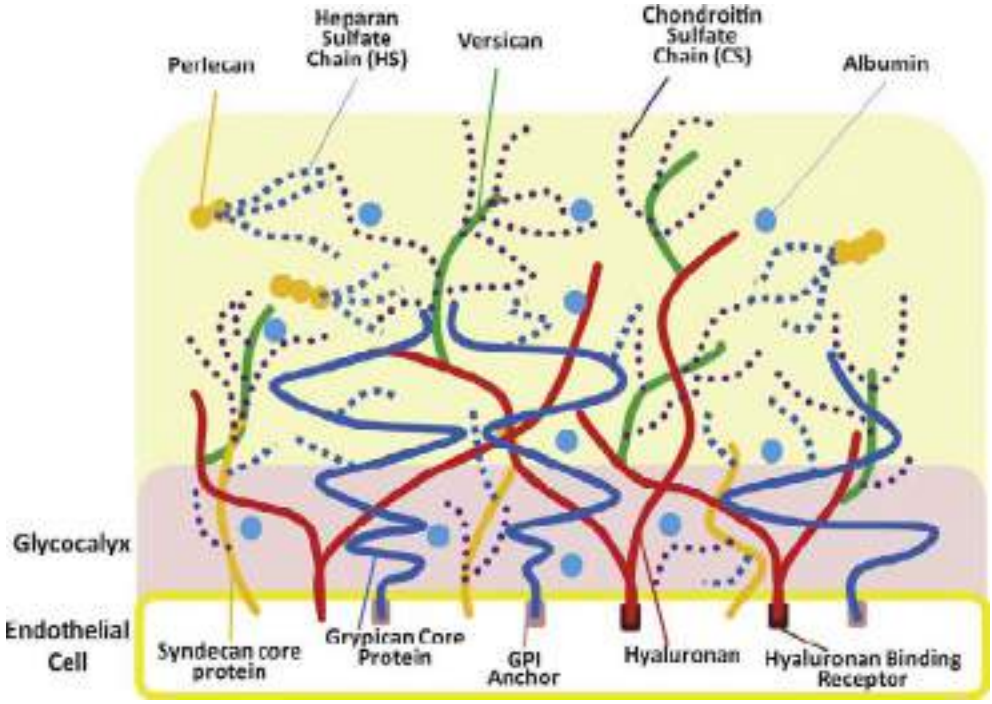

FIGURE 22.6 **Schematic diagram showing the endothelial surface layer (ESL).** The relatively dense part of the layer close to the endothelial cells form the glycocalyx, which consists of membrane-bound proteoglycans (PG), including syndecan and glypican. Syndecan carries both chondroitin sulfate (CS) and heparan sulfate (HS) side chains, and glypican carries HS side chains. The ESL is comprised of secreted proteoglycans such as perlecan (mainly HS) and versican (mainly CS), as well as secreted glycosaminoglycans (GAG) including hyaluronan. It also traps some plasma proteins such as albumin. *(Modified from Haraldsson, B., Nystrom, J., and Deen, W. M. (2008). Properties of the glomerular barrier and mechanisms of proteinuria. Physiol. Rev.* ***88****: 451–487, with permission.)*

eclampsia, including HELLP syndrome (hemolysis, elevated liver enzymes, and low platelets).[292]

Angiopoietins

Another family of angiogenic factors required for the development and homeostasis of glomerular endothelial cells is the Angiopoetin–Tek signaling system. Angiopoietin 1 (Angpt1) and Angiopoietin 2 (Angpt2) are ligands for Tek tyrosine kinase (Tek/Tie-2). Angpt1 binds to the Tek receptor expressed on endothelial cells, and causes its phosphorylation. This signal leads to enhanced survival of endothelial cells, stabilization of the endothelial cell-to-cell connection, and reduced permeability.[174,253,279] Angpt2 is considered to be a competitive antagonist of Angpt1 by binding Tek but not activating any intracellular signaling.[174,253,320] There is some data, however, that suggests that Angpt2 can activate Tek signaling under certain conditions.[319,320] Angpt1, Angpt2 and Tek are all expressed in developing kidneys.[319] Angpt1 is expressed widely in the condensing mesenchyme in the developing kidney and its derivatives,[250,319] and in mature podocytes.[250,318] Angpt2 shows a more restricted expression pattern, localizing to endothelial cells, pericytes, smooth muscle cells of cortical and large blood vessels, and immature mesangial cells.[318,319] Tek is expressed

both in mature and immature glomerular endothelial cells.[279,319] Angpt1 conventional knockout mice die at embryonic day 12.5, thus precluding any analysis of its role in the glomerular vasculature.[146,279] In mouse metanephric organ culture, recombinant Angpt1 enhances the growth of interstitial capillaries.[146,247] A recent report demonstrated that Angpt1 treatment of isolated rat glomeruli reduced vascular permeability and increased the depth of the glycocalyx layer.[159,247] Cell type-specific/inducible knockout approaches, however, have revealed a crucial role for Angpt1 in glomeruli. Deletion of Angpt1 at E10.5 leads to a single, dilated glomerular capillary loop without mesangial migration in a portion (~10%) of glomeruli that is reminiscent of the Pdgfb/Pdgfrb mouse mutant phenotype (Figure 22.10a,b). Although deletion of Angpt1 after E13.5 doesn't cause any immediate vascular phenotype, streptozotocin-induced diabetic mice with global or glomerular-specific Angpt1 deletion develop increased urinary albumin excretion, severe mesangial expansion, glomerular sclerosis, and early mortality (Figure 22.10c,d). Another report also demonstrated that treatment of diabetic mice with Angpt1 recombinant protein is protective for renal function.[127,159] Angpt1 is therefore dispensable in quiescent, mature glomeruli, but is essential in development and in the vascular response to injury.[80,127,217]

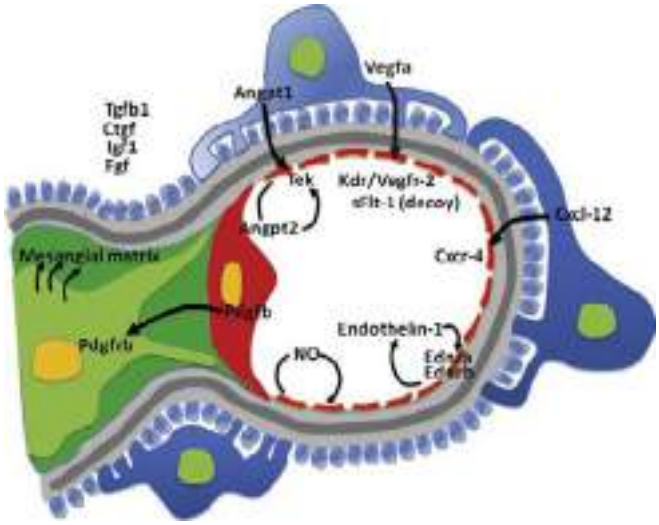

FIGURE 22.7 **Soluble factors involved in the maintenance of endothelial cells and the glomerular capillary structure.** Schematic diagram shows the location of secretion of soluble factors, and where the associated receptors are expressed. Vegfa from podocytes is required for the recruitment, survival, and maintenance of the endothelial cells, and binds to its receptor Kdr. sFlt-1 works as a decoy, but its precise function is still unknown. Angpt-1 is expressed in podocytes and binds to the endothelial Tie-2/Tek receptor in a paracrine fashion, whereas its antagonist, Angpt-2 is secreted from endothelial cells and binds to the Tie-2/Tek receptor in an autocrine fashion. Cxcl12 is secreted from podocytes and interstitial cells, and acts on Cxcr4 in endothelial cells to regulate vascular development and function. Pdgfb secreted by endothelial cells signals to the Pdgfrb receptor expressed by mesangial cells, and is a critical factor for their migration and maintenance. Endothelial cells also express some vasoactive factors including NO and endothelins. Expression of growth factors such as Tgfb, Ctgf, Igf, and Fgf are increased in disease conditions such as diabetic nephropathy, but their precise functions under normal conditions are still unclear.

Angpt2 knockout mice are briefly viable in the postnatal period, and exhibit increased pericyte coverage of peritubular capillaries. The mice die soon after birth however, precluding analysis of the role of Angpt2 in more mature capillary beds.[52,80,217] Angpt2 overexpression in podocytes causes proteinuria and podocyte apoptosis in formed glomeruli.[52,308]

Angiopoietin ligands seem to function in concert with Vegfa. In Vegfa-rich conditions, Vegfa and Angpt2 work together to promote sprouting.[84,299,308] The precise degree of cross-talk between these pathways is still under investigation.

Ephrin-Eph Family

Ephrin-Eph molecules are another family of tyrosine kinase signaling factors that are widely expressed in the developing kidney. In other organs, they are involved in the specification of arteries and veins, as well as in neural development.[84,282,299] In the developing kidney, the Ephrin B2 ligand is expressed in podocyte precursors, but later it is expressed by endothelial

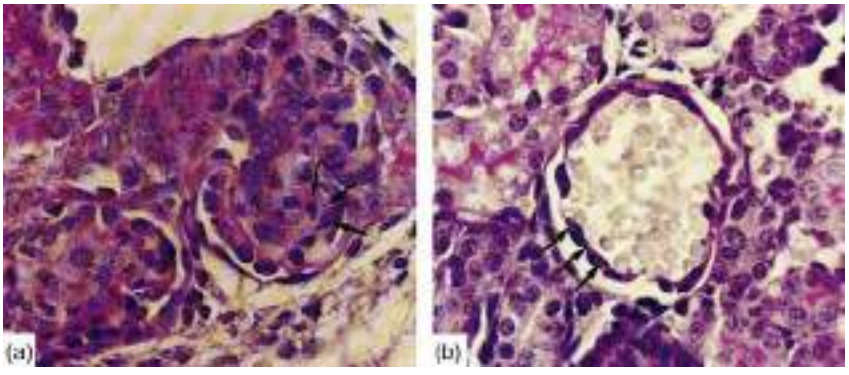

FIGURE 22.8 **PAS stain of glomeruli from E17.5 mouse embryos.** (a): Normal mouse glomerulus. Arrows show normal fold of the basement membrane. (b): Pdgfb$^{-/-}$ glomerulus shows a single open aneurysm-like capillary loop without any mesangium (failure of mesangial migration). There is no fold of basement membrane (arrows).*(From Betsholtz, C. (1995). Role of platelet-derived growth factor in mouse development. Int. J. Dev. Biol. **39**: 817–825 with permission.)*

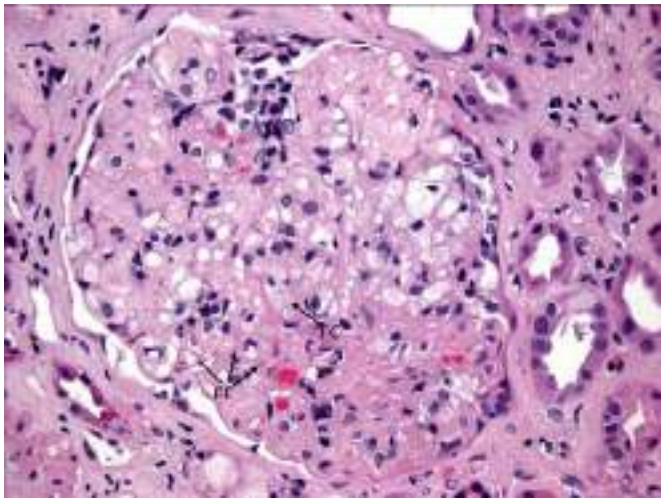

FIGURE 22.9 A glomerulus showing thrombotic microangiopathy from a patient who received anti-VEGF therapy, showing fragmentation of erythrocytes (FE: arrows) and foamy change (FC: arrow) of endothelium.*(Courtesy of Dr. Laura Barisoni, New York University School of Medicine, New York, NY.)*

and mesangial cells.[282,307] In adults, the EphB4 receptor is mainly expressed in podocytes.[5,307] Overexpression of the EphB4 receptor causes defects of glomerular arteriolar formation.[5,307] Deletion of Ephrin B2 from Pdgfrb-expressing pericytes and the mesangial cell population results in abnormal glomerular tuft formation.[7,76] Pharmacologic inhibition of EphB4 leads to delayed recovery and extended injury of endothelial cells and podocytes in a rat mesangial injury model.[280,307] Therefore, it seems this family is involved in glomerular tuft formation and maintenance, but the precise mechanism is still unclear.

CXCR4/CXCR7/CXCL12 Axis

Chemokine CXC motif receptor type 4 (CXCR4), CXCR7, and Chemokine CXC motif ligand 12 (CXCL12) are also critical factors in the development and maintenance of glomerular vasculature. Cxcr4 and Cxcr7 are seven-transmembrane G-protein coupled receptors, and Sdf-1/Cxcl12 is their cognate chemokine ligand.[7,281] A deficiency of Cxcr4 or Cxcl12 leads to a

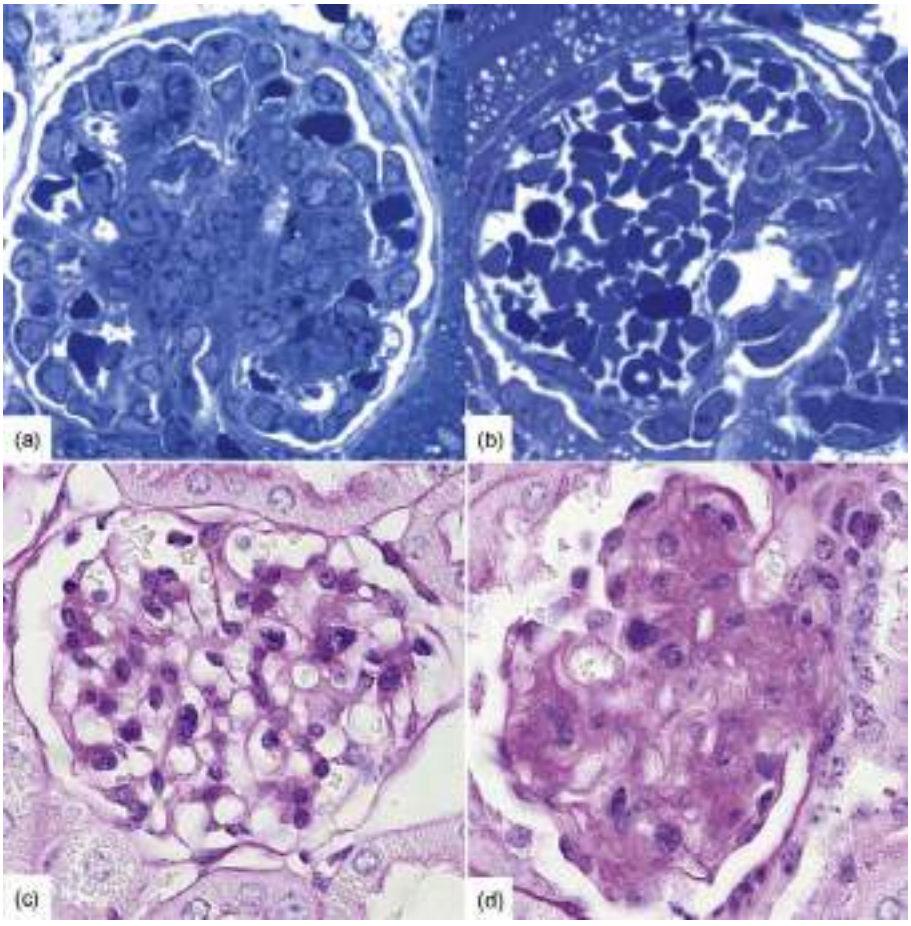

FIGURE 22.10 **Conditional deletion of Angpt1 results in glomerular developmental defects and enhanced diabetic glomerular injury.** (a): A normal glomerulus at embryonic day 17.5 (E17.5). (b): Early conditional deletion of Angpt1 gene at embryonic day 10.5 (midgestation) results in some abnormal glomeruli with single open capillary loops similar to that of Pdgfb-null mouse at E17.5. (c) and (d): Late deletion of Angpt1 at E16.5 doesn't lead to any immediate phenotype. However, after 20 weeks of streptozotocin-induced diabetes, the diabetic mutant mice that carry Angpt1 deletion show an increase in mesangial matrix expansion and sclerosis (d) compared with that of diabetic controls (c) (LM × 1000). *(Courtesy of Dr. Marie Jeansson, Mount Sinai Hospital, Toronto, ON.)*

failure of vasculogenesis and embryonic lethality.[55,280] During renal development, Cxcr4$^{-/-}$ or Cxcl12$^{-/-}$ knockout mice show a ballooning of the glomerular capillary loops which is reminiscent of Pdgfb/Pdgfrb knockout mice.[51,251,281] On the other hand, activation of the CXCR4/CXCR7/CXCL12 axis appears to underlie some glomerular diseases, such as rapidly progressive glomerulonephritis (RPGN),[55,216] diabetic nephropathy,[51,251,281] and hemolytic uremic syndrome (HUS).[116,212,216] It appears that Cxcl12 is secreted from podocytes or interstitial cells, and acts on Cxcr4 expressed by the endothelial cells to regulate vascular development and function.[212,281]

Glomerular Endothelial Cells as a Source of Vasoregulators

Glomerular endothelial cells produce both nitric oxide, a vasodilator, and endothelin-1, a vasoconstrictor. Nitric oxide is produced by NO synthases. Both endothelial and inducible NO synthases are expressed by glomerular endothelial cells *in vitro* and *in vivo*.[116,212,288,310] eNOS expression and activation is at least partially influenced by Vegfa.[212,288] In many rodent disease models and human patients with kidney diseases, overproduction of NO and its derivatives has been observed.[116,288,310] It is considered that excessive NO production generated by inducible NO synthase (iNOS) results in glomerular injury, whereas NO generated from endothelial NO synthase (eNOS) is protective by preserving endothelial survival and function.[200,288,324] In diabetic patients, eNOS expression is increased in renal endothelial cells, whereas iNOS expression is preferentially upregulated in inflammatory cells. The degree of eNOS expression is related to the severity of the glomerular lesion and proteinuria.[116,286] Diabetic eNOS knockout mice develop more severe glomerular lesions and greater albuminuria.[114,200,324] In addition, excretion of NO-related products is often reduced in diabetic patients with nephropathy.[286,305]

Endothelin-1 is a potent vasoconstrictor which binds to one of two receptors: endothelin receptor type A (Ednra); and endothelin receptor type B (Ednrb). Binding of endothelin-1 to Ednra results in vasconstriction, while binding to Ednrb causes vasodilation.[114,315] In glomerular endothelial cells, Ednrb is dominant, whereas Ednra is expressed by mesangial cells.[71,305]

Glomerular endothelial cells are also involved in the renin–angiotensin–aldosterone system (RAAS). They express angiotensin-converting enzyme (ACE) and produce angiotensin II.[63,315] The relative contribution of the glomerular endothelium compared to the systemic endothelium with regard to angiotensin II production, however, is still unknown. Furthermore, the potential role of angiotensin receptors in endothelial cells is also unknown.

Summary

Glomerular endothelial cells form the first permselective barrier in the glomerulus. The relationship between their elaborate, fenestrated cell shape and function is maintained by a network of various angiogenic factors. Glomerular endothelial cells also contribute to the charge-selective barrier through the negatively-charged glycocalyx.

MESANGIAL CELLS

Description

Mesangial cells are irregularly shaped cells which extend processes from their cell body towards the glomerular basement membrane (GBM). The "mesangium" refers to the mesangial cells together with the mesangial matrix they produce[71,141] (Figures 22.11 and 22.12). Mesangial cells provide structural support to the glomerular tuft, produce and maintain mesangial matrix, communicate with other glomerular cells by secreting soluble factors, and may contribute to the glomerular capillary flow via their contractile properties.

Mesangial Cells Provide Structural Support to the Glomerular Tuft

The mesangium forms the central core of the glomerular tuft. The processes which they extend towards the GBM are densely populated by bundles of actin, myosin, and β-actinin microfilaments.[63,152] These processes attach directly or by interposition of microfibrils to the GBM. They also extend underneath glomerular endothelial cells toward the mesangial angles of the GBM, anchoring two opposing mesangial angles together through their microfilament bundles (Figure 22.12b). These microfilament bundles cross the mesangial cells to tether opposing parts of the GBM through α3β1 integrin and the basal cell adhesion molecule (BCAM) glycoprotein, which bind laminin α5 in the GBM.[141] These structures are believed to supply protection from hydraulic pressure by providing inward-directed tension.[152]

Mesangial Cells Produce and Maintain Mesangial Matrix

The *mesangial matrix* fills the remaining spaces between the mesangial cells and the perimesangial glomerular basement membrane (GBM, for review

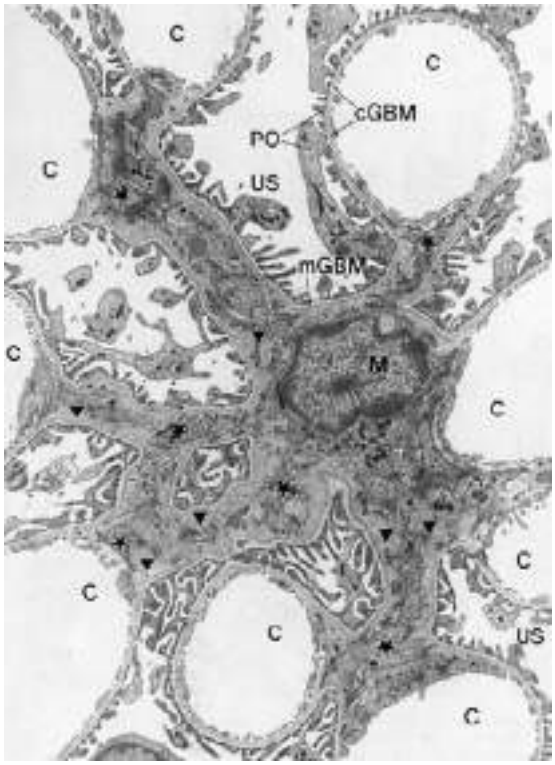

FIGURE 22.11 **Transmission electron micrograph showing all components of the glomerular tuft.** The glomerular tuft is marked by the GBM, which includes the pericapillary GBM (cGBM; between podocytes and the endothelium) and the perimesangial GBM (mGBM; between podocytes and mesangium). Glomerular capillaries (C) are covered by podocytes at the periphery, and connected to the mesangium, proximally. The mesangial cell body (M) possesses several processes (some are marked by *stars*) which extend toward the peripherally located capillaries. In the mesangial area, abundant mesangial matrix (*triangles*) can be seen (US: urinary space; TEM × 5500).

see [152]). This matrix is composed of a diverse array of common matrix proteins including collagens type III, IV, V, and VI; heparan sulfate proteoglycans including biglycan and decorin[252]; and the elastic fiber proteins fibronectin, laminin, entactin, and fibrillin-1, among others.[42,87,172,177,276] Fibronectin is the most abundant of these, and is associated with microfibrils which network to form the basic ultrastructure of the matrix.[42,260] These microfibrils are unbranched and non-collagenous with a diameter of 15 nm, and form a dense three-dimensional network that contributes to the anchoring of mesangial cells to the GBM.[152] It is thought that these microfibrils allow for the transmission of mesangial cell contractile forces to the GBM.

Mesangial phenotypic changes are a hallmark of certain glomerular diseases such as diabetic nephropathy. This condition is characterized by glomerular sclerosis due to an accumulation of mesangial matrix and thickening of the GBM. The sclerotic lesion contains an abundance of type IV collagen normally present in the glomerulus, but also contains types I and III collagen which are usually absent but are produced by injured mesangial cells.[175]

Signaling Molecules Involved in Mesangial Cell Biology

Integrins

In addition to $\alpha3\beta1$ integrin observed in connections between the GBM and mesangial processes, $\alpha1\beta1$, $\alpha2\beta1$, and fibronectin receptors $\alpha5\beta1$ and $\alpha8\beta1$ integrins are expressed in the mesangial cells,[13,142] and are able to activate integrin-linked cell signaling. In the

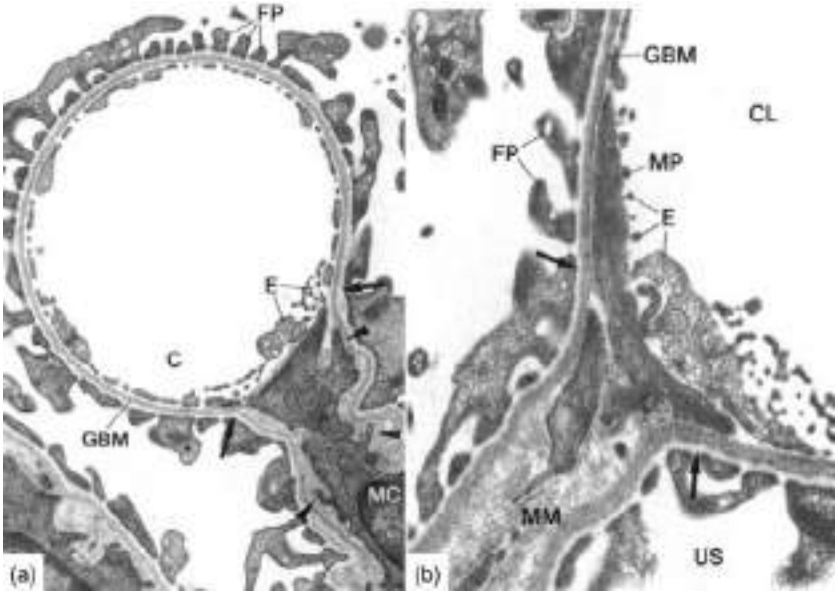

FIGURE 22.12 (a): Transmission electron micrograph showing a mouse glomerular capillary. A mesangial cell (MC) extends its processes to a capillary loop (C). Microprojections (*arrowheads*) from the primary process run toward the glomerular basement membrane (GBM). As shown by arrows, the endothelial cells are directly connected to the mesangium. Podocyte foot processes (FP) and fenestrated endothelium (E) are shown (TEM × 13,500). (b): High magnification of the juxtamesangial part of the capillary loop showing direct contact of mesangium to endothelium. Endothelial cells are attached to the mesangial cell processes (MP) that connect opposing mesangial angles. (arrows) (CL: capillary lumen; US: urinary space; MM: mesangial matrix; FP: foot processes; TEM × 23,000).

absence of α1 integrin, cultured mesangial cells show decreased proliferation, increased matrix production, and altered intracellular signaling. Mice lacking α1 integrin exhibit more severe Adriamycin and diabetes-induced glomerular injury,[34,323] highlighting the importance of matrix-related signaling. On the other hand, removal of α2 integrin in mice leads to amelioration of glomerular damage in an Adriamycin and partial renal ablation model.[18] α8 integrin seems to promote adhesion, but inhibits migration and proliferation of mesangial cells *in vitro*.[13]

Pdgfrb

Pdgfb is secreted from endothelial cells and binds to Pdgfrb expressed in mesangial cells, where it exerts a crucial role in mesangial migration and glomerular tuft formation. Without mesangial cell migration, the looping of glomerular capillaries does not occur. This interaction is discussed further in the endothelial section.

Ephrin B2

As mentioned in the section on the glomerular endothelium, deletion of Ephrin B2 from mesangial cells and pericytes leads to abnormal glomerular tuft formation and reduced numbers of capillary loops.[76] It's receptor, EphB4 is expressed in podocytes, suggesting an interaction between the mesangium and podocytes.

Other Secretary Molecules and Receptors

Mesangial cells produce, and are also influenced by, many growth factors including Tgfb1,[257] connective tissue growth factor (Ctgf),[44,297] insulin like growth factor (Igf),[220,221] fibroblast growth factor (Fgf),[75,221] and hepatocyte growth factor (Hgf).[46,48] Among these factors, Hgf antagonizes the pro-fibrotic actions of Tgfb1, whereas the other factors are upregulated by mesangial cells in disease conditions including diabetes or Thy1.1 nephritis, and facilitate glomerular matrix accumulation.[75,297] Vasoactive factors such as angiotensin II and endothelins promote mesangial proliferation, and this effect may be mediated by transactivation of the Egf receptor.[54,118] However, because of the lack of effective tools for deleting genes specifically from mesangial cells, the precise functions of these factors in normal physiology remain to be determined.

Contractile Ability of Mesangial Cells

Because of the microfibrils and the contractile ability of cultured mesangial cells, it has been assumed that the mesangial cells regulate glomerular filtration by controlling the capillary surface area, but concrete *in vivo* evidence is lacking.[85]

THE GLOMERULAR BASEMENT MEMBRANE

Description

The glomerular basement membrane (GBM) is a specialized extracellular matrix that sits between the podocytes and vascular side of the filtration barrier. During glomerulogenesis, components of the GBM are synthesized by both the glomerular endothelial cells and podocytes, forming a bilayered structure that later fuses.[189] Compared to basement membranes in other tissues the GBM is unusually thick, measuring 240–370 nm in adults.[189,210,274] Ultrastructural analysis of the mature GBM shows a trilaminar structure made up of a lamina densa surrounded by the lamina rara interna and externa, which appear less dense.

Similar to other basement membranes, the GBM is primarily made up of laminin, collagen type IV, nidogen, and heparan sulfate proteoglycans. However, the GBM contains different members of some of these families compared to other basement membranes, including laminin-521, collagen a3a4a5(IV), and agrin.[2] Laminin and collagen type IV appear to be particularly important for function of the GBM, as mutations in these factors are associated with glomerular filtration defects and renal disease.[189] Components of the GBM are continuously "turned over",[1] but it is not yet clear how new components are added and old ones removed.

Given the location of the GBM between the relatively "open pores" of the endothelium and the podocyte foot processes and filtration slits bridged by the slit diaphragms, a major role for the GBM is to restrict the passage of plasma proteins into Bowman's space. From the time of classic electron micrographic studies of the GBM in the 1950s attempting to define the specific characteristics of the GBM that impart its permselective properties, to the current molecular era, it is still hotly debated which component represents the major barrier. Current models suggest that all three layers of the filtration barrier are likely important (including the glycocalyx of the endothelial layer), but relative contributions remain unknown. However, it is clear that mutations in genes encoding specific GBM proteins are sufficient to cause proteinuria and renal failure, underscoring the importance of this layer to the barrier.[189]

Laminin

Laminins are secreted as heterotrimers, which are stabilized by disulfide interchain bonding. Each laminin heterotrimer is composed of α, β, and γ chains that combine with each other in nonrandom combinations to form at least 15 different heterotrimers. The laminins

are named by their composition; for example: α5β2γ1 is named laminin-521 or LM-521.[40,192] The heterotrimer structure appears as a "cross" with one longer and three shorter arms. At the COOH end of all α chains is a laminin globular chain (LG) that extends beyond the long arm. This LG domain interacts with cell surface receptors such as integrins and dystroglycans that are expressed by the podocytes.

Interactions between the laminin heterotrimers themselves are mediated by subdomains found in the shorter arms of the "cross." Laminin also binds to the network of type IV collagen via nidogen, and to agrin, a heparan sulfate proteoglycan of the GBM.[189] The combined network of type IV collagen (see below) and laminin provides mechanical properties to the basement membrane, serving as a scaffold for the placement of other matrix components.

During glomerular formation, laminin trimer compostion changes from LM-111 to LM-511, and finally to LM-521.[150,187,192] In the adult, laminins continue to be produced by both endothelial cells and podocytes, as the protein can be identified in the endoplasmic reticula of both cell types.[273]

A series of reports confirm an important role for laminins in GBM function. A mutation of laminin β2 results in Pierson syndrome in humans that is characterized by ocular and neurological symptoms, and congenital nephrotic syndrome.[204] This observation was confirmed using knockout mice of laminin β2 that develop proteinuria even before the onset of visible ultrastructural changes to the podocytes.[125] Recently, the phenotype of the laminin β2 knockout mouse was rescued by overexpression of laminin β1, suggesting redundancy between laminin β1 and β2.[117] Also, deletion of laminin α5 in mice prevents the transition from LM-111 to the mature LM-521 that leads to breakdown of the GBM and failure of glomerular vascularization.[185] A mouse carrying a hypomorphic mutation of laminin α5 also shows glomerular proteinuria, hematuria, and cystic kidneys, suggesting the gene dosage of the laminin α5 chain is crucial for the maintenance of the GBM.[119]

Type IV Collagen

Collagen IV is another major component of the GBM. Similar to other collagens, collagen IV is a trimeric extracelluluar matrix component made up of α chains that are rich in Gly-X-Y amino acid repeats.[119,154] The type IV collagen family includes six genetically distinct α chains that trimerize with each other in specific combinations to make three types of trimers with each other: $(\alpha1)_2\alpha2$; $\alpha3\alpha4\alpha5$; and $(\alpha5)_2\alpha6$. Each of these trimers is referred to as a protomer. Protomers are secreted into the extracellular matrix, where they self-polymerize and are subsequently cross-linked by specific enzymes.[188]

Similar to laminin, the composition of type IV collagen trimers undergoes a developmental switch in the GBM. Early in glomerulogenesis (S-shaped stage), the GBM is composed of α2/α1 chains, which are replaced at the capillary loop stage by α3α4α5.[3] Although a basement membrane can form in the absence of type IV collagen its structure is compromised, resulting in variable defects in the filtration barrier depending on the specific genetic mutation.[188] In the adult kidney, the type IV collagen α3α4α5 network is produced only by podocytes.[3]

Mutations in any of the α3, α4 or α5 genes are associated with glomerular disease in patients, emphasizing the key role that type IV collagen plays in glomerular barrier function. The defects can be minimal, as observed in patients with thin basement membrane disease (also known as benign familial hematuria). This disease is inherited in an autosomal dominant fashion, and patients present with isolated microscopic hematuria. As suggested by its name, the GBMs show thinning. Thirty to forty per cent of the patients exhibit mutations in COL4A3 or COL4A4. Although originally assumed to be benign, FSGS has been reported in Cypriot families with this disease.[295]

The same mutations in COL4A3 and COL4A4 inherited in a homozygous fashion as an autosomal recessive disease result in a more severe disease known as Alport's syndrome, a hereditary basement membrane disease associated with progressive glomerulopathy that leads to renal failure, and is associated with deafness and ocular abnormalities. The commonest form of Alport syndrome is X-linked, caused by mutations in the α5 chain (Figure 22.13). Goodpasture syndrome, an autoimmune disease characterized by glomerulonephritis and lung hemorrhage, is mediated by antibodies against the type IV collagen α3 chain.[119]

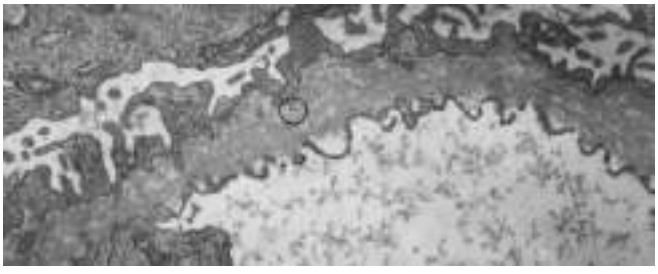

FIGURE 22.13 **Transmission electron micrograph of the GBM in a patient with Alport syndrome.** Thickening, splitting and lamination of the GBM can be seen (TEM × 14,900). *(From Rumpelt, H. J. (1987). Alport's syndrome: Specificity and pathogenesis of glomerular basement membrane alterations. Pediatr. Nephrol. **1**: 422–427, with permission.)*

Intriguingly, recent studies have shown that a mutation of the type IV collagen α1 chain causes hereditary angiopathy with nephropathy, aneurysms, and muscle cramps (HANAC syndrome); the renal manifestations are characterized by hematuria and large bilateral cysts.[107] A rodent model of this mutation leads to defects of the GBM,[89] suggesting a functional role for the α1 chain in the GBM, despite the prominence of a3a4a5 trimers in mature type IV collagen.

Nidogen

Nidogen-1 and -2 (previously known as entactin-1 and entactin-2) are virtually ubiquitous basement membrane glycoproteins. Nidogen-1 binds both laminin and type IV collagen,[77] suggesting that it is involved in forming the GBM. However, it was demonstrated that a single knockout of either nidogen-1 or nidogen-2 in mice results in no GBM phenotype.[199,262] Although deletion of both nidogen genes results in perinatal lethality, suggesting some overlapping roles of the two genes,[11] the glomerular basement membrane still forms apparently normally. The exact role and requirement of nidogen in the GBM is not yet known.

Proteoglycans

Heparan sulfate proteoglycans of the GBM are concentrated in the laminae rarae internae and externae, and provide an electronegative charge to the GBM.[136,277] The major proteoglycans of the GBM are heparan sulfate proteoglycans; most prominent is agrin, but perlecan is also present.[92,205] Although classical studies suggested that the negative charge of the GBM was essential to retard passage of neutral and negatively-charged macromolecules across the barrier, this model has been challenged due to results obtained from genetically modified mice. Podocyte-specific knockout mice for agrin and/or perlecan, either in isolation or together, does not result in proteinuria or overt filtration defects.[88,108] Current thoughts on the glomerular charge barrier are discussed later in the chapter.

PODOCYTES

Podocyte Morphology

Mature podocytes are highly-differentiated, polarized epithelial cells that sit on the glomerular basement membrane in Bowman's space. They function as vascular support cells, wrapping around the underlying glomerular capillaries, providing growth factors necessary for endothelial health and survival. Podocytes are characterized by a highly arborized and unique cytoskeleton. They have a large cell body (Figure 22.14a) that gives rise to a complex network of processes including primary, major processes, which then continue to branch as they extend around the glomerular capillary loops until they form terminal foot processes. The foot processes are the only point of contact between the podocyte and the GBM (Figure 22.15a). The foot processes of neighbouring podocytes interdigitate (Figure 22.14b), and are connected to one another through a specialized intercellular junction known as the slit diaphragm (SD). The SD bridges the porous filtration slits; these structures have been recently visualized at high magnification[79,236] (Figures 22.14b, and 22.15b). In disease, these structures can be dysregulated, causing a disorganization of foot processes and breakdown of the GFB (Figure 22.15c,d).

While the podocyte is terminally differentiated and largely post-mitotic, the podocyte cell body contains a number of organelles that are crucial to maintain its high metabolic activity and secretory function, including a large nucleus, abundant lysosomes, and many mitochondria.[196] In addition to producing factors necessary for maintaining their own specialized architectural cytoskeleton and protecting adjacent endothelial cells, podocytes must synthesize many of the components of the GBM in the mature glomerulus (reviewed in [189]).

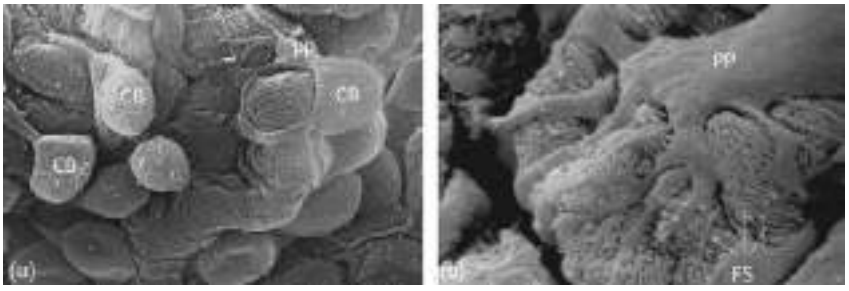

FIGURE 22.14 **Scanning electron micrograph shows podocytes wrapping around glomerular capillary loops.** (a): Mouse podocytes have a large, smooth-surfaced cell body (CB) which branches into primary processes (PP), which continue to branch as they wrap around the capillary loop forming the actin-based foot processes (SEM × 5600). (b): Scanning electron micrograph of rat podocytes. The filtration slits are created between the interdigitating foot processes, the terminal ends of the branching processes (FS) (SEM × 5670). (Courtesy of Dr. Monika Wnuk, Mount Sinai Hospital, Toronto, ON.)

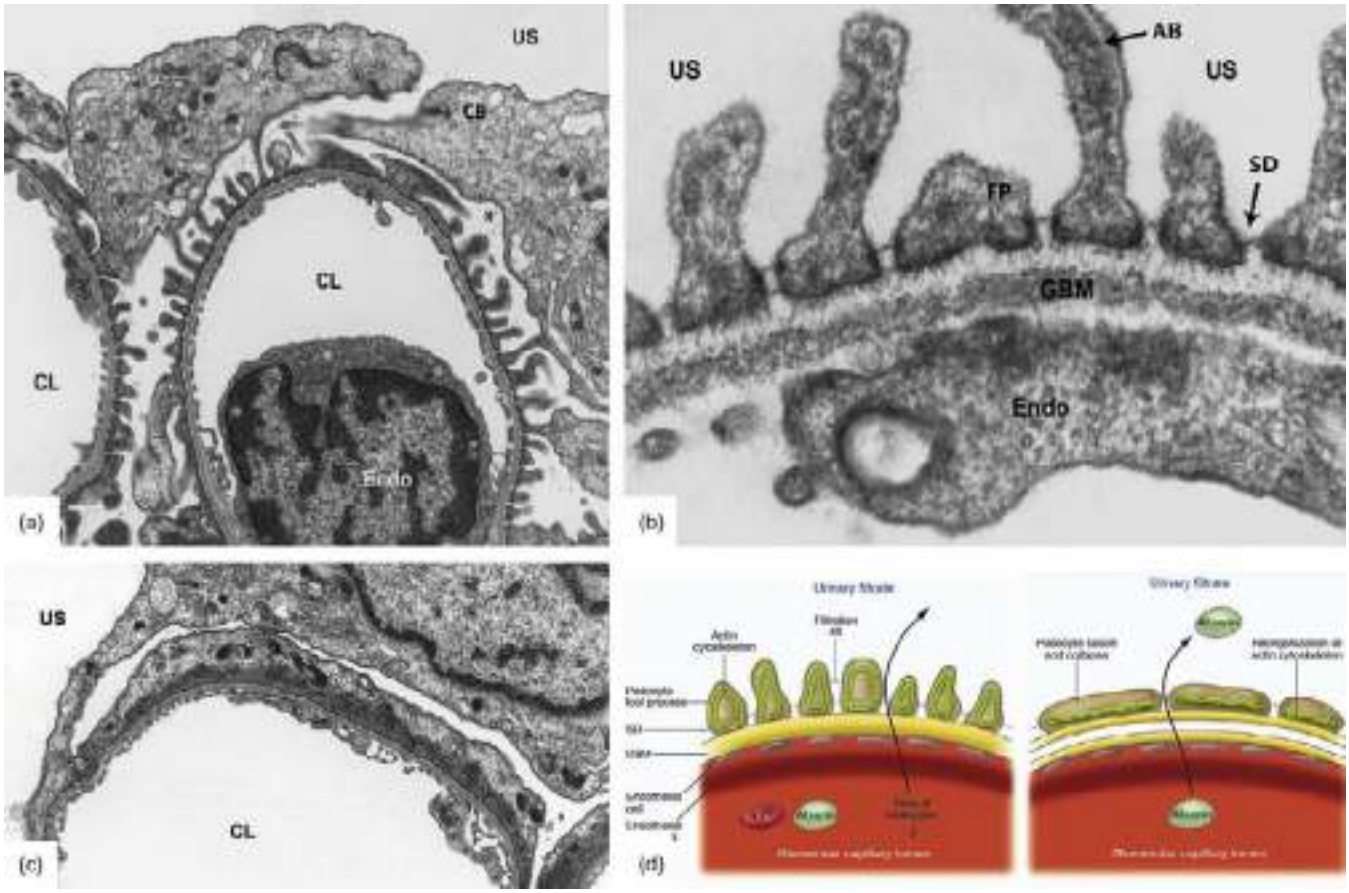

FIGURE 22.15 **Transmission electron micrograph of a normal and abnormal human podocytes.** (a): Coronal section of a podocyte intimately associated and lining a glomerular capillary loop (CL) cell body (CB) can be seen. Note the space (*) between the cell body and the basement membrane as the foot processes are the only point of contact between the podocyte and the GBM. (b): High power transmission EM shows podocyte foot processes (FP) attached to the glomerular basement membrane (GBM). Foot processes contain actin bundles (AB), and adjacent foot processes are attached by their slit diaphragms (SDs). (c): Transmission electron micrograph of podocyte foot process effacement in human focal segmental glomerulosclerosis (FSGS). (d): Scheme of podocyte foot process flattening. Left panel shows normal podocyte foot processes, actin cytoskeleton supports its elaborated shape. Once the actin cytoskeleton is disorganized, podocytes are no longer able to keep the foot process assembly, which results in fusion and flattening of foot processes (right panel). *((a)–(c): Courtesy of Dr. Dontscho Kerjaschki, Medical University Vienna, Vienna, Austria; (b): From Ronco, P. (2007). Proteinuria: Is it all in the foot? J. Clin. Invest.* ***117****: 2079–2082, with permission.)*

The structure of the cell body and the primary major processes is determined by microtubules and intermediate filaments (vimentin, desmin, and nestin), while the shape (width and length) of the foot processes is largely determined by actin microfilament bundles. The actin bundles form continuous loops that run longitudinally in the foot processes and end at the sole plates, connecting adjacent foot processes associated with a single, primary, major process (Figure 22.15b). The loops of actin bundles are tethered to the microtubules and intermediate filaments of the major processes.[196] This connection is thought to be mediated by Tau, which is known to form connections between microtubules and microfilaments and is concentrated at these areas.[145] In the foot processes, a complex system links the slit diaphragm proteins, GBM receptors on the basolateral side, and the actin cytoskeleton to regulate the functional morphology of podocytes; this will be discussed at greater length later.

Podocyte Development, Transcription Factors, and Notch

Podocyte precursors first appear in the "S-shaped body" phase of glomerular development as a columnar epithelium attached along their lateral membrane by a cadherin junction containing P-cadherin.[36] This nascent glomerulus is also populated by a thin epithelial layer called the Bowman's capsule, and a capillary loop that begins to enter the glomerular cleft. As glomerular development progresses, the primitive podocytes

extend themselves around the capillary loop by an unknown mechanism and differentiate into mature podocytes. A number of transcription factors have been identified that are expressed in the immature and mature podocytes, including Wt-1, Pod1 (Tcf21), Lmx1b, Kreisler (Maf1), and Foxc2.

Wt-1

The transcription factor Wt-1 is first expressed in the metanephric mesenchyme, which contains progenitors of the tubular and glomerular epithelium. As renal development continues, its expression becomes restricted to the renal vesicle, comma, and the S-shaped body. Later on, its expression is observed in immature and mature podocytes, which persists throughout life.

Wt-1 is a transcription factor with four zinc fingers that can bind both DNA and RNA.[24,25,61] There are four major splice variants of Wt-1 mRNA, which may be responsible for its variety of functions in development and normal physiology.[99] Embryonic loss of Wt-1 in mice leads to complete renal and gonadal agenesis,[149] defects in the epicardium, lack of sub-epicardial mesenchymal cells, and adrenal agenesis,[194] suggesting its important role in multiple organs.

Several mouse models underscore the importance of Wt-1 function during nephrogenesis and in podocytes. Postnatal deletion of the Wt-1 gene results in glomerulosclerosis with loss of podocyte foot processes and molecular markers of differentiation such as nephrin, atrophy of the exocrine pancreas and spleen, severe reduction in bone and fat mass, and failure of erythropoiesis.[30] In Wt-1 knockout mice, restitution of Wt-1 expression using a human derived Wt-1-YAC transgene leads to a rescue of cardiac defects, but incomplete glomerular development.[194] Furthermore, Wt-1 haploinsufficient mice develop adult onset mesangiosclerosis and glomerulonephritis.[96,184]

In humans, Wt-1 mutations are associated with two glomerulopathies: Denys–Drash syndrome (DDS) and Frasier syndrome (FS), which can both present early in life and cause abnormal glomerular development. DDS is caused by heterozygous mutations of the *Wt-1* gene that predominantly affect the zinc finger regions in exons 8 (zinc finger II) and 9 (zinc finger III), and directly interfere with the DNA-binding capacity of Wt-1.[214] The characteristic clinical picture of DDS is a triad of congenital nephrotic syndrome, XY pseudohermaphroditism, and Wilm's tumor.[53,59] The characteristic renal lesion in these patients is diffuse mesangiosclerosis due to increased matrix deposition on the vascular side of the glomerular basement membrane. Expression of the DDS mutation in mice, either in podocytes or systemically, leads to various glomerular lesions similar to those of humans. Wt-1 is expressed in podocytes, which are found on the opposite side of the glomerular basement membrane (GBM) to the mesangium. The glomerular lesion in DDS therefore highlights the importance of interactions that occur between podocytes on one side of the GBM and endothelial cells or mesangial cells on the other side of the GBM. Frasier syndrome (FS) is characterized by focal segmental glomerular sclerosis, male-to-female sex reversal, but no tumors. It results from a dominant mutation that causes an inability to include an alternatively spliced lysine-threonine-serine (KTS) sequence after the third zinc finger[102] of *Wt-1*. Interestingly, mice engineered to exclusively express the variant that is +KTS or −KTS display normal induction of the metanephric mesenchyme by the ureteric bud, but have malformed glomeruli. These findings suggest different roles for the alternatively spliced variants of Wt-1 in glomerular development and maintenance.

While the contribution of Wt-1 to renal development and maintenance is undeniable, its precise role is still being elucidated. Human and animal models seem to indicate it plays a role in regulating the expression of a number of developmental genes. During early renal development the regulatory gene Pax-2 is expressed in the induced metanephric mesenchyme and ureteric bud, but is absent in the mature renal epithelium. In podocytes, the expression of Wt-1 coincides with a downregulation of Pax-2, suggesting a role for Wt-1 in transcriptional repression of this gene.[244] Indeed, in patients with DDS, downregulation of Wt-1 was associated with increased Pax-2 expression[311]; however, it is unclear if this increased Pax-2 expression is pathogenic. Recent advances in high-throughput technology for assessing transcription factor activity have elucidated a number of other Wt-1 regulated genes that are known to play a role in renal development, including Six2, Bmp7, Sall1, and HeyL.[107]

Wt-1 also plays a role in maintaining podocyte homeostasis beyond development. The essential podocyte slit diaphragm protein nephrin has been identified as a transcriptional target of Wt-1, and is downregulated in the glomeruli of mice lacking the Wt-1(−KTS) splice variant.[95,298] Furthermore, Wt-1 modulates the podocyte glycocalyx through transcriptional regulation of Podocalyxin[213] and 6-O-endosulfatases Sulf1 and Sulf2,[259] which play a role in maintaining the charge of the glomerular filtration barrier, podocyte foot process separation, and bioavailability of essential growth factors such as vascular endothelial growth factor-α (Vegfa) and fibroblast growth factor (Fgf)-2. In addition to post-translational regulation of Vegfa bioavailability, Wt-1 can also directly regulate expression of Vegfa, which is essential to the maintainenance of the glomerular vasculature.[103,107] Given this wide range of regulatory functions, it is still unclear what is responsible for the pathology observed in DDS and FS patients, but it

is likely a convergence of a number of these signaling networks.

Lmx1b

Lmx1b encodes a Lim-domain protein that is mutated in Nail–Patella syndrome.[31,60] In mice lacking Lmx1b, podocytes retain their immature cuboidal phenotype, fail to form foot processes or endothelial fenestrations, and have a split glomerular basement membrane.[237] These findings are associated with a concomitant downregulation of Vegfa, Synaptopodin, Nphs2, type III collagen α4 (Col3a4), and type IV collagen α4 (Col4a4). Lmx1b-binding elements in the Nphs2 and Col4a4 promoter regions suggest that this occurs through direct transcriptional regulation.[191,237]

Tcf21

Tcf21 (also known as Pod1/Capsulin/Epicardin) encodes a basic helix-loop-helix transcription factor that is highly-expressed in the developing kidney, lung, intestine, and pancreas at sites of mesenchymal–epithelial interaction.[224] In the developing mouse kidney, it is expressed in the condensing mesenchyme, and knockdown of Tcf21 expression in renal explants causes decreased mesenchymal condensation and ureteric bud branching.[224] Subsequently, *Tcf21* expression is restricted to the primitive podocytes of the S-shaped bodies, and genetic deletion of Tcf21 in mice leads to failure of podocyte terminal differentiation[223] (Figure 22.16). $Tcf21^{-/-}$ knockout mice have a marked reduction in glomerular number, and the remaining glomeruli are developmentally arrested between S-shaped body and capillary loop stages.

Kreisler

Kreisler (Mafb) encodes a basic domain leucine zipper transcription factor that is expressed in podocytes at the capillary loop stage of glomerular development.[245] Mice with a homozygous enu mutation of Kreisler show a similar but milder phenotype to those with a Tcf21 deletion. They are born with glomeruli arrested at the capillary loop stage, and podocytes that adhere to the GBM but fail to form foot processes.[245] Kreisler mutants, however, express Tcf21, suggesting that Tcf21 is either upstream of Kreisler in podocyte development or acts by a different mechanism.

Foxc2

Foxc2 is a winged helix transcription factor that was identified during a screen of enriched genes in mRNA isolated from glomeruli at different stages of development.[284] Foxc2 is first expressed in putative podocytes during the comma shaped body stage of glomerular development, and as such is the earliest known podocyte marker. Glomeruli from $Foxc2^{-/-}$ mice display aberrant podocyte foot process formation, mesangial cell clustering at the base of the glomerular tuft, and swollen endothelial cells lacking fenestrae,[284] similar to $Tcf21^{-/-}$ mutant mice. In these mice, the endothelial and mesangial defects are thought to be secondary to the podocyte defects. Gene array of $Foxc2^{-/-}$ glomeruli identified over 700 differentially regulated genes. Notably, however, there was a strong downregulation of Nphs2, Col4α3, and Col4α4, which are fundamental to slit diaphragm assembly and GBM formation.

Notch

The Notch family includes four well-conserved genes that encode transmembrane receptors involved in cell fate specification and development from invertebrates to mammals. Notch is fundamental in the segmentation of the metanephric mesenchyme into 20 functionally-distinct cell types segregated into different compartments along the nephron.

During normal development, Notch2 is expressed in condensing structures of the metanephric mesenchyme, such as the metanephric vesicles, comma-shaped bodies, and S-shaped bodies, but is eventually restricted to differentiating podocytes in more mature glomeruli.[181] Jag1 is the Notch2 ligand thought to be important for glomerular differentiation. During development, it is expressed in renal vesicles, comma-shaped bodies, and S-shaped bodies.[32] In more mature glomeruli it then localizes to the inner region of the glomerular tuft to endothelial and/or mesangial cells.[181] Mice homozygous for a hypomorphic mutation

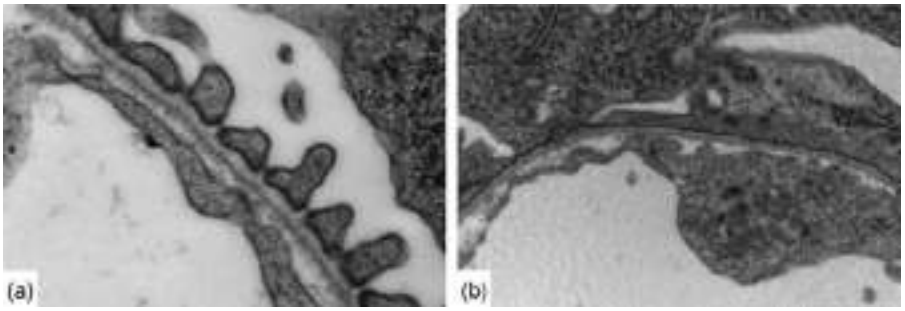

FIGURE 22.16 **Transmission electron micrograph of podocyte foot processes at E18.5.** Normal mouse podocytes show organized foot processes assembly (a), whereas Tcf21 null mouse podocytes demonstrate defects of foot process development (b).

in the *Notch2* gene exhibit hypoplastic kidneys, and an arrest of glomerular development prior to the capillary loop stage.[181] A conditional inactivation of Notch2 from nephron progenitor cells results in a more severe "distal tubule only" phenotype, with a complete failure of glomerulogenesis and proximal tubule formation.[35]

In humans, mutations in Jag1 or Notch2 cause Alagille syndrome, an autosomal dominant disorder characterized by the presence of cholestatic liver disease, cardiac disease, ocular abnormalities, skeletal abnormalities, and characteristic facial features.[164,182,206] A large proportion of Alagille patients also develop renal disease characterized by glomerular lesions, cystic kidneys, and ultimately renal failure.[182] Taken together these studies suggest an important role for Notch signaling in establishing the proximal–distal orientation of the nephron, and segmentation of the proximal structures.

Recent evidence also reports a crucial role for the Notch pathway in the maintenance of mature podocytes. In patients with a variety of proteinuric nephropathies, including diabetic nephropathy and FSGS, activation of the Notch pathway was observed in podocytes.[198,202] Furthermore, upregulation of Notch expression in podocytes of transgenic mice results in severe proteinuria and glomerulosclerosis with dedifferentiation of podocytes.[300]

Podocyte Slit Diaphragm Assembly

The attachments between foot processes are comprised of the "slit diaphragm" (SD). SD assembly is an important part of glomerular development, as it is integral to the correct interdigitation of podocyte foot processes. The SD, which is visible by high power electron microscopy, is a structure that connects adjacent foot processes. It consists of a complex of transmembrane proteins and cytoskeletal adaptor proteins that link adjacent foot processes to the complex actin cytoskeleton of the podocyte and make up a component of the protein barrier (reviewed in [101,115,129,242,289]). While the relative importance of the endothelial layer versus the glomerular basement membrane versus the podocyte SD in maintaining the perm-selectivity of the glomerular filtration barrier is debatable, studies in humans and mice have shown that SD components are essential to this function.

In 1974 Rodewald and Karnovsky described the slit diaphragm as rod-like units connected in the center to a linear bar forming a zipper-like pattern with pores.[76,236] They hypothesized that because of the size of these pores (40 Å × 140 Å), the slit-diaphragm was the principal filtration barrier to plasma proteins in the kidney.

Nephrin

While this first description of the SD shed light on the filtration function of podocytes, the molecular composition of the SD remained poorly-defined. However, the discovery that a mutation in the *NPHS1* gene causes Congenital Nephrotic syndrome of the Finnish variety[143,160] suggested that dysregulation of SD structure can cause glomerular disease. This disease is characterized by massive proteinuria *in utero*, lack of a slit diaphragm, and abnormal foot process formation. The *NPHS1* gene encodes a 180 kDa transmembrane protein of the immunoglobulin superfamily called nephrin that is expressed in the glomerular podocyte, and localizes specifically to the SD.[117,243] These findings defined the importance of nephrin to the formation and maintenance of a normal SD, and led to the postulation of a "zipper-like model" of nephrin assembly in the SD. Accordingly, it is considered that the SD is the principle structure of the glomerular filtaration barrier and nephrin is its main component. Subsequent work, however, has also elucidated an important role for nephrin as a mediator of actin cytoskeletal organization by binding Src homology domain SH2/SH3 containing Nck adaptor proteins.[131] The cytoplasmic tail of nephrin contains three tyrosine-aspartic acid-x-valine (YDxV) residues which, when phosphrylated by Src family kinases, recruit the SH2 Nck adaptor proteins and induce local actin polymerization[15] (Figure 22.17). Following the identification of nephrin, intensive research has led to the discovery of several other transmembrane proteins that participate in the formation of the slit diaphragm (Figure 22.18).

Podocin

NPHS2 is a gene that is mutated in some forms of steroid-resistant nephrotic syndrome[19] that cause early onset proteinuria, and focal and segmental glomerulosclerosis. This gene encodes a protein called podocin, which associates in podocyte lipid rafts with nephrin and another SD component, CD2AP, via its C-terminal domain.[163,261,268] Nephrin is thought to contribute directly to the formation of the SD, while podocin and CD2AP are thought to mediate its connection to the podocyte actin cytoskeleton. Mouse models in which any of these three components are disrupted lead to a congenital nephrotic syndrome.[222,239,269]

Neph Proteins

The C-terminal domain of podocin also interacts with another group of three immunoglobulin superfamily transmembrane proteins called Neph1, 2, and 3 that bear significant homology to nephrin. This family is defined by their well-conserved cytoplasmic tail with a centrally located tyrosine residue required for

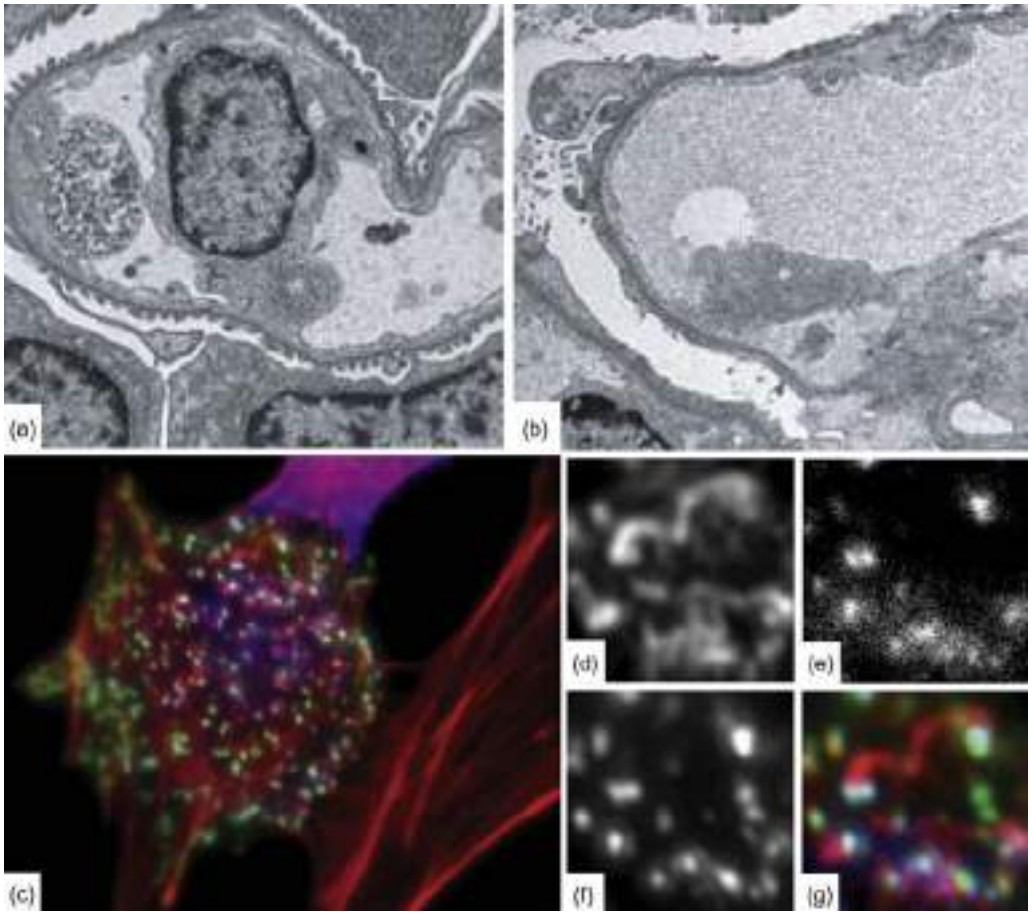

FIGURE 22.17 Transmission electron micrograph of distinct mouse podocyte foot-processes present at 4 days of birth (a), but absent in Nck knockout mice (b). (c)–(g): Cellular immunostaining showing co-localization of Nck2, nephrin at the actin tail. Nck-nephrin interaction is required for nephrin-dependent actin reorganization (Green: nephrin; purple: Nck2; red: palloidin = actin). (d), (e), and (f) show actin, nck2, and nephrin staining, respectively. *((a) and (b): From Jones, N., et al. (2006). Nck adaptor proteins link nephrin to the actin cytoskeleton of kidney podocytes. Nature **440**: 818–823, with permission; (c)–(g): Courtesy of Drs. Tony Pawson and Nina Jones.)*

interacting with podocin.[265] The extracellular domain of Neph1 interacts with nephrin in the SD, and is essential for the regulation of glomerular perm-selectivity.[168] In addition to podocin, the C-terminal (intracellular) domain binds the tight junction protein-1 (Tjp-1/ZO-1), which in turn tethers it to the podocyte actin cytoskeleton.[168] Like nephrin, Neph1 plays a role in intracellular signaling, and is tyrosine phosphorylated at the SD, particularly in certain disease models.[105] Mutations in Neph1 result in proteinuria and perinatal lethality in mice, but the phenotype is less dramatic than that observed in nephrin knockout mice, suggesting that nephrin may be more crucial to maintain the SD.[57] This Nephrin-centric view of the slit diaphragm was called into question by a recent study showing that chickens and developing chicks lack nephrin, but express all three Neph proteins.[296] Ultrastructurally, however, chickens are still able to assemble a SD in the glomerular filtration barrier. These SDs lacking nephrin still express P-cadherin and the large protocadherin Fat-1, suggesting that heterophilic interactions between Neph proteins and these other cadherins may be sufficient to allow SD assembly.[190]

Cadherin and Catenins

In addition to these atypical junctions, the slit diaphragm contains adherens junction proteins P-cadherin, and α, β, γ catenins.[230] P-cadherin is a transmembrane protein, and the extracellular domain is thought to contribute to slit diaphragm formation, while its cytoplasmic tail connects to β or γ catenin. Linkage of this complex to the actin cytoskeleton is believed to occur through an interaction between α catenin and Tjp-1/ZO-1 or α-actinin-4, both of which can directly bind actin.

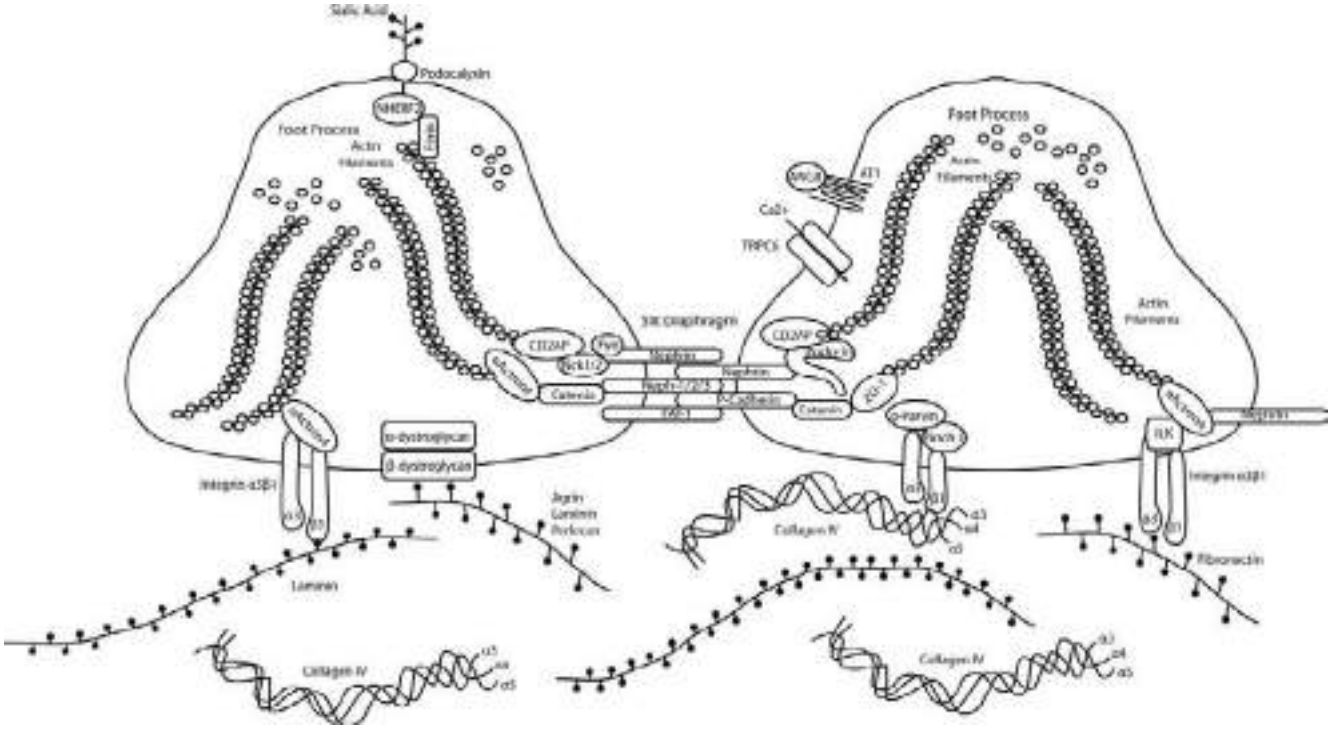

FIGURE 22.18 **Schematic diagram of the podocyte foot process and slit diaphragm with associated molecules.**

The occludens protein Tjp-1/ZO-1 is expressed specifically at the points of insertion of the slit diaphragms in mature glomeruli.[256] Tjp-1/ZO-1 appears early on in podocyte development when the apical junctional complexes between podocytes are composed of typical tight and adherens junctions, and persists as these junctional complexes migrate to the basolateral side and ultimately form the SDs. These findings suggest that tight junction proteins play a role in podocyte SD development and function, independent of their ability to form tight junctions.

α-Actinin-4

In humans, mutations in α-actinin-4 result in an autosomal dominant familial FSGS.[111,137] *In vitro* the mutant form of α-actinin-4 binds F-actin more strongly than wild-type. This is thought to reduce the podocytes' ability to respond dynamically to the hydrostatic pressure required for normal glomerular filtration, and ultimately leads to podocyte injury.[303] In addition, α-actinin-4 is thought to mediate the interaction between the actin cytoskeleton and integrins to regulate podocyte adhesion to the glomerular basement membrane.[50]

FAT1

FAT1 is another member of the cadherin superfamily expressed in the podocyte at the SD, and has 34 tandem cadherin-like extracellular repeats. With its large extracellular domain, FAT1 is a major molecular component of the SD, and is required for normal foot process formation as FAT1 knockout mice lack SDs.[37,123] Because of its localization to the cell−cell contact sites and tips of cellular processes, FAT1 may be involved in the initial steps of cell−cell interaction between podocytes.[313]

Rho GTPases

Given the actin rich nature of the podocyte cytoskeleton, it is not surprising that Rho GTPases − master regulators of cytoskeletal dynamics − are important in podocyte biology. At the leading edge, Rac1 and Cdc42 promote lamellipodia and fillipodia formation, thus enhancing cell motility. In contrast, RhoA promotes a contractile phenotype by inducing formation of actin-myosin stress fibers.[70,227] In this sense, it is believed that a balance between the opposing activities of RhoA and Cdc42/Rac1 regulates podocyte cytoskeletal dynamics. Both overexpression and inhibition of these small Rho GTPases in podocytes causes glomerular injury in mouse models. Podocyte-specific deletion of Cdc42 leads to a congenital nephropathy in transgenic mice by impairing actin polymerization at sites of nephrin clustering[263] (Figure 22.19), while RhoA deletion does not result in proteinuria. By contrast, overexpression of RhoA in podocytes results in an FSGS phenotype in mice.[325]

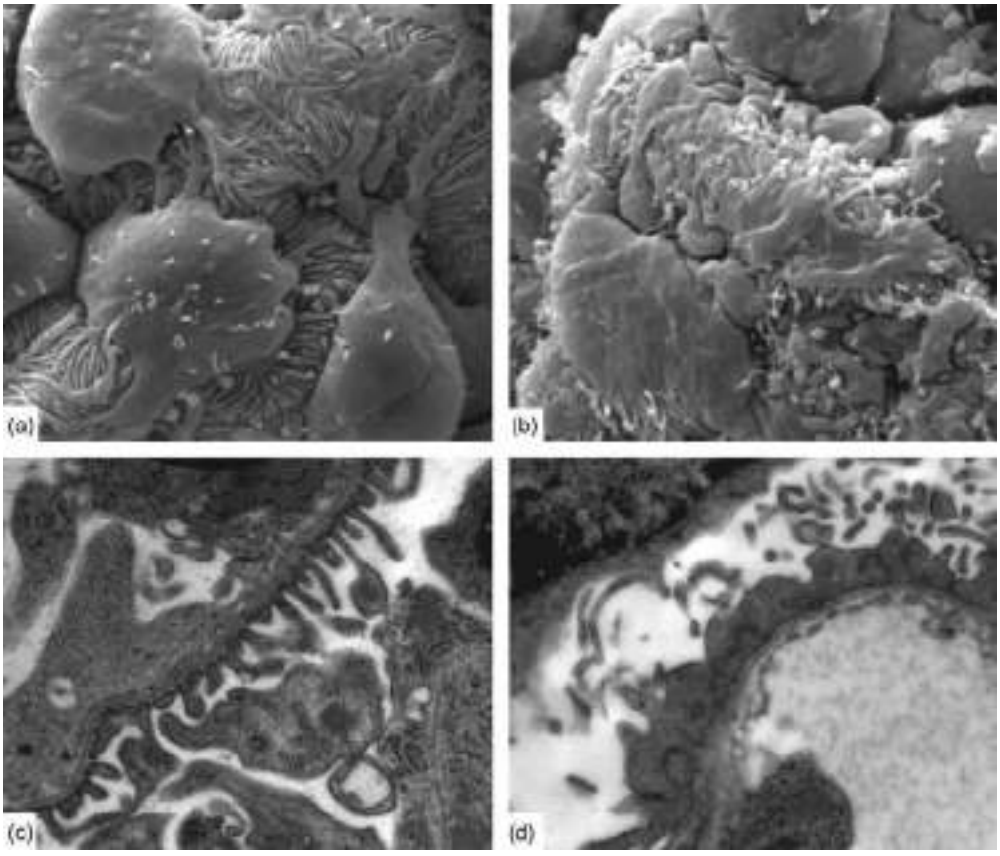

FIGURE 22.19 **Scanning ((a) and (b)) and transmission ((c) and (d)) electron micrograph of murine podocytes.** (a) and (c): Normal appearance of podocytes. (b) and (d): Podocytes lacking Cdc42 show extensive effacement of foot process at postnatal day 5 ((a), (b) × 11, 000; (c), (d) × 27,000). *(From Scott, R. P., et al. (2012) Podocyte-specific loss of Cdc42 leads to congenital nephropathy. J. Am. Soc. Nephrol. **23**(7): 1149–1154 with permission.)*

Recently, dysregulation of Rho-GTPase signaling has also been linked to human glomerular disease. *ARHGAP24* is a RhoA-activated Rac1 GTPase-activating protein (Rac1-GAP); a mutation that impairs Rac1-GAP activity results in FSGS in humans.[4] Two recent reports also showed that mutations in the Inverted Formin 2 (*IFN2*) gene result in autosomal dominant FSGS.[20,82] INF2 interacts with other diaphanous related formins such as Cdc42; disease causing mutations in *INF2* result in decreased CDC42 targeting to the plasma membrane, and impaired actin polymerization and depolymerization in podocytes.[20]

Podocyte–GBM Interaction

The podocyte actin cytoskeleton is not only required for formation of podocyte foot processes and the slit diaphragm, but is also involved in a dynamic and bidirectional cross-talk with the glomerular basement membrane (GBM). In addition to production of GBM components, podocytes also express transmembrane molecules on their basolateral surface which interact with the GBM to regulate intracellular signaling. These include α3β1 integrin, αvβ3 integrin, and α- and β-dystroglycans.

α3β1 Integrin

α3β1 integrin is a heterodimeric cell adhesion receptor with specificity for collagen types I and VI, laminins, fibronectin, and nidogen.[147] α3β1 integrin is highly-expressed on the basolateral surface of mature and developing podocytes, and plays an important role in the development and maintenance of podocyte foot processes.[147,228] Mice with a targeted mutation of the α3 integrin gene lack podocyte foot processes, and have a reduced number of capillary loops.[148] Furthermore, the podocyte-derived basement membrane fails to fuse with the endothelium-derived basement membrane and becomes fragmented and disorganized. A recent paper reported three paediatric patients who have mutations in *ITGA3*, which encodes α3 integrin; they presented with congenital nephrotic syndrome and severe basement membrane abnormalities.[109] Taken together, these findings indicate that

α3β1 integrin is not only a receptor for GBM components, but is also required for its development and maintenance. Similarly, podocyte specific ablation of the β1 integrin gene in mice results in massive proteinuria, abnormal capillary morphogenesis, podocyte foot process effacement, and podocyte apoptosis.[134,219]

αvβ3 Integrin

While α3β1 integrin is the primary integrin expressed in podocytes, more recent work has identified a role for αvβ3 integrin in podocyte homeostasis. αvβ3 integrin is a vitronectin receptor that localizes to podocyte foot processes, and is predominantly associated with non-lipid raft fractions of the cell membrane. Genetic deletion of β3 integrin does not result in an overt renal phenotype, but these mice are protected from LPS-induced proteinuria,[302] suggesting that αvβ3 integrin activation may play a role in the pathogenesis of proteinuria in the setting of glomerular injury. Further work by Wei et al. showed that activation of β3 integrin by soluble urokinase receptor (suPAR) may occur in primary focal segmental glomerular sclerosis; the authors suggest that suPAR may be the circulating factor responsible for recurrence of FSGS after transplant.[301] While these data suggest that αvβ3 integrin activation may injure the podocyte, other work shows that αv integrins act as receptors for osteopontin, which is a protective factor in stretch-induced podocyte injury.[258]

Dystroglycan

Integrins are not the only adhesion proteins to be expressed in podocyte foot processes. The dystrophin−glycoprotein complex (DGC) is a group of proteins that includes α- and β-dystroglycan, utrophin, and dystrophin, and plays a central role in stabilizing skeletal muscle cell membranes by tethering the cytoskeleton to the basement membrane components laminin, perlecan, and agrin. α- and β-dystroglycan have also been localized to podocyte foot processes, and their expression is diminished in several mouse models of glomerular disease and human minimal change disease.[226,229] However, recent studies have shown that genetic deletion of dystroglycan from podocytes in mice does not result in a glomerular phenotype or increased susceptibility to injury, suggesting that integrins may be the primary functional extracellular matrix receptors in the podocyte.[126]

Integrin-Linked Kinase

Given the central, non-redundant role of α3β1 integrin in the development and maintenance of the glomerular filtration barrier, it is of interest to identify its interacting proteins in podocytes. Integrin-linked kinase (ILK) is a serine/threonine kinase with kinase-dependent and -independent functions that interact with the cytoplasmic domains of β1 and β3 integrins.[309] Detailed molecular studies have elucidated a role for ILK in podocyte morphology and health. ILK forms a complex with Pinch1 and α-Parvin to regulate matrix adhesion, foot process formation, and inhibit podocyte apoptosis.[312] ILK also forms a ternary complex with α-actinin-4 and α3β1 integrin, providing a link between the GBM, the actin cytoskeleton, and nephrin in the SD.[47] ILK was first identified as a potential mediator of glomerular disease by two groups showing that it is upregulated in glomeruli of patients with diabetic nephropathy,[97] congenital nephrotic syndrome of the Finnish type, and two proteinuric mouse models.[151] Indeed, activation of ILK *in vivo* using a rodent model of puromycin-associated nephropathy, and *in vitro* by overexpression of a kinase-active ILK transgene, caused activation of β-catenin, podocyte detachment and apoptosis, and transcriptional repression of the SD components P-cadherin and Cd2ap.[285] However, while ILK activation may contribute to podocyte injury in disease, it also plays a fundamentally important role in normal podocyte physiology. Mice with a podocyte-specific deletion of the ILK gene appear normal at birth, but develop focal segmental glomerular sclerosis with GBM thickening, and podocyte foot process effacement characterized by an aberrant distribution of α-actinin-4 and nephrin.[47,62,134] The deletion of ILK causes an upregulation of focal adhesion kinase (FAK),[134] a non-receptor tyrosine kinase which is involved in focal adhesion turnover, cell spreading, and motility. This result is supported by recent work showing that FAK is activated in LPS and anti-GBM models of podocyte injury, and genetic deletion of FAK protects mice from proteinuria.[171]

Tetraspanin CD151

CD151 is a tetraspanin family protein with affinity for α3β1 integrin[314] that is expressed abundantly in the glomerulus.[275] While CD151 is not absolutely required for α3β1 integrin binding to the extracellular matrix, it stabilizes the active conformation of α3β1 integrin and strengthens this interaction.[203] A nonsense mutation in CD151 causes hereditary nephropathy in patients characterized by a splitting and thickening of the GBM, along with pretibial epidermis bullosa, sensorineural deafness, and thalassemia.[138] A podocyte specific knockout mouse model recapitulates this renal phenotype. Mechanistically, CD151 causes a redistribution of α3β1 integrin at the interface between the podocyte and GBM, increasing its binding affinity for laminin-511/521. These findings suggest that CD151 may strengthen the adhesion of podocytes to the GBM, protecting them from higher glomerular pressures.

Negative Charge on the Surface of Podocytes

Although heparan sulfate proteoglycans are key components of the GBM and endothelial cell layer (as discussed above), they are also expressed by podocytes. The two major families of heparan sulfates expressed by the podocyte are Podocalyxin and Syndecans (primarily Syndecan I and Syndecan IV). Podocalyxin and Syndecans are transmembrane proteins involved in regulation of the podocyte actin cytoskeleton through regulation of signaling pathways (see below). While heparan sulfates provide a negative charge to the surface of the podocyte, sialyation of glycoproteins (including podocalyxin) and gangliosides also imparts a negative charge. Both are important components of glomerular barrier function.[33]

Podocalyxin

Podocalyxin is a CD34-related sialomucin protein that is highly-expressed by podocytes and also by mesothelia, vascular endothelial cells, hematopoietic stem cells, and platelets. Mice with a conventional knockout of the podocalyxin gene die within the first 24 hours of life from renal failure. Importantly, podocyte foot processes do not form, and intercellular junctions between adjacent foot processes are abnormal and appear immature. These data provide functional evidence that podocalyxin is a key molecule in podocyte development.[58] Cell biologic experiments have shown that podocalyxin interacts with the Na^+/H^+ exchanger regulatory factor 2 (NHERF2) and phosphorylated ezrin in a complex, connecting it to the actin cytoskeleton of the podocyte foot process. Disruption of this interaction results in nephrotic syndrome.[178,255,283] Podocalyxin appears to regulate foot process architecture through activation of the small Rho-GTPase, RhoA, mediated by its interaction with the NHERF/Ezrin complex.[255]

Sialyation Defects and the Podocyte

Podocytes express a number of sialyated proteins including podocalyxin (as described above), other proteoglycans, and gangliosides. Loss of sialyation of podocalyxin has been identified in various nephrotic syndrome experimental models, such as in rodents injected with sialidase, puromycin aminonucleoside or protaimine sulfate, which neutralizes negative charges.[140,153,264] All of these compounds cause an abrupt onset of proteinuria, together with foot process effacement. Simultaneous infusion of sialic acid prevents the proteinuria and podocyte foot process fusion observed with puromycin injection, presumably due to resialylation of critical glomerular proteins.[195] More recently, loss of sialyation of podocalyxin was observed in a transgenic rat model of minimal change disease due to overexpression of Anptl4.[39]

Although many studies have focused on sialylation defects of podocalyxin, the podocyte expresses other sialylated glycoproteins and gangliosides. Mutations in sialylating enzymes have also been associated with glomerular defects and proteinuria. For example, a point mutation in a gene encoding one of the key enzymes needed for sialic acid biosynthesis (uridine diphospho-N-acetylglucosamine (UDP-GlcNAc) 2-epimerase/N-acetyl-mannosamine (ManNAc) kinase (GNE/MNK)) results in severe perinatal glomerular disease in mice, characterized by splitting of the glomerular basement membrane, hematuria, and proteinuria.[81] The phenotype was partially rescued by dietary supplementation with ManNAc. Intriguingly, ManNAc supplementation also appeared to rescue the Anptl4-induced sialyation defect in rats, suggesting it might represent a new therapy for certain forms of glomerular disease.

Podocytes and Metabolism

Although the majority of podocyte studies to date have focused on its unique cytoskeletal architecture and its role as a structural component of the filtration barrier, recent studies have highlighted the importance of metabolic regulatory pathways in podocyte function.

mTOR

The mechanistic target of rapamycin (mTOR) is an evolutionarily-conserved serine-threonine kinase that interacts with regulatory associated protein of mTOR (Rptor) or Rptor-independent companion of MTOR (Rictor) to form mTORC1 and mTORC2 complexes, respectively. mTORC1 is a key regulator of cellular metabolism, including protein translation, ribosomal biogenesis, cell growth and proliferation, and suppression of autophagy in response to amino acids, growth factors, and elevated cellular ATP levels.[326] mTORC2 is regulated primarily by growth factors to promote actin cytoskeletal rearrangement, cell survival, and cell cycle progression.[124] Rapamycin is an mTOR inhibitor that is used clinically and is thought to specifically inhibit mTORC1 function.[94] In certain cell types including the podocyte, however, chronic inhibition of mTORC1 by rapamycin also results in downregulation of mTORC2 functions.[248,294,321] The importance of mTOR in podocyte biology was first suggested by the clinical observation that rapamycin causes proteinuria.[23,266]

Deletion of *mTOR* itself or R*ptor* in podocytes of mice results in proteinuria.[38,90] Conversely, ectopic mTORC1 activation in mouse podocytes, accomplished by deletion of its suppressor *Tsc1*, results in kidney

disease with many of the features of diabetic nephropathy (DN), including podocyte hypertrophy and loss and proteinuria, and is attributed to endoplasmic reticulum stress.[122] Although mTORC1 appears to be crucial for podocyte function, loss of Rictor from podocytes of mice does not result in a phentoype.[90]

Given its central role in cellular metabolism, mTOR is likely to play multiple roles in podocyte biology. Regulation of autophagy is one pathway regulated by mTOR that appears to be crucial for podocyte function. Autophagy is a lysosomal-dependent cellular survival response to starvation or lack of growth factors in which cells degrade cellular constituents from proteins to entire organelles, such as mitochondria, in order to provide a supply of nutrients under conditions of stress. A basal level of autophagy is, however, necessary to remove damaged organelles, excessive lipids, and long-lived or misfolded proteins. The basal level of autophagy appears to be increased in podocytes,[106,201] and it has been suggested that autophagy may be required to protect this long-living cell from injury. In keeping with this model, deletion of Atg5, a key component of the autophagic pathway, results in late onset of glomerular disease in mice at 20 to 24 months of age due to the accumulation of damaged organelles and ubiquitinated protein complexes.[106] In contrast, deletion of mTOR from podocytes results in disruption of autophagic flux, with subsequent accumulation of autophagolysomes in the podocyte[38] (Figure 22.20). Clinically, dysregulation of autophagy is observed in patients with lysosomal storage diseases such as Fabry's disease, Aspartilglucoseaminuria or Scheie's disease, where the inability to acidify lysosomes causes a failure of lysosomal reformation[317]; these patients are prone to developing proteinuria,[74] providing additional support that the autophagic pathway is clinically relevant.

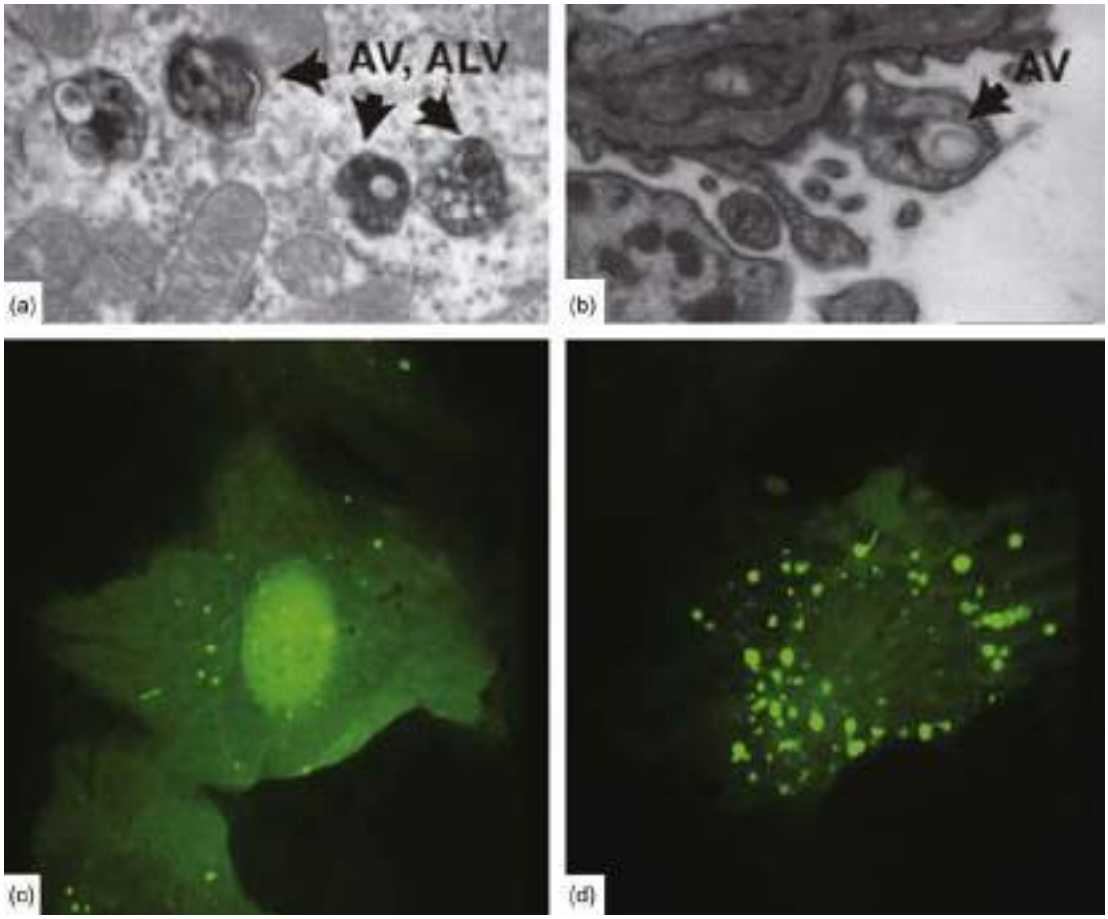

FIGURE 22.20 (a) and (b): Transmission electron micrographs of podocytes from 3 week old podocyte-specific mTor knockout mice showing an accumulation of autophagosomal vesicles (AV) and autophagolysosomal vesicles (ALV). *(From Cina, D. et al. (2012). Inhibition of MTOR disrupts autophagic flux in podocytes. J. Am. Soc. Nephrol.* ***23****: 412–420, with permission.)* (c): LC3 positive autophagosomes are visualized by green fluorescent protein in cultured human podocyte. (d): Treatment of the podocytes with rapamycin induces massive activation of autophagy.

Insulin Signaling

mTORC1 hyperactivation is associated with a phosphorylation of IRS1/2 and decreased insulin sensitivity, suggesting that podocytes might be a direct cellular target for insulin.[155] A recent study confirmed this hypothesis; genetic deletion of the insulin receptor from podocytes recapitulates many of the features of diabetic nephropathy (DN).[304] *In vitro*, insulin binds the insulin receptor on podocytes and acts through the mitogen-activated protein kinase and phosphor-inositol-3-kinase pathways to induce cytoskeletal rearrangement.[43,304] Taken together, these findings suggest that strategies aimed at increasing insulin sensitivity in podocytes may be a therapeutic option in DN.

Calcium Signaling

TRPC6

The identification of mutations in the Transient Receptor Potential Cation Channel 6 (TRPC6) in patients with autosomal dominant familial FSGS[231,306] emphasizes the key role that calcium signaling plays in glomerular function. Atlhough a variety of different mutations were identified, a number of them result in enhanced calcium signaling within the podocyte. These human genetic findings helped explain results why other factors (such as complement 5b-9,[45] protamine sulfate,[264] bradykinin,[8] and angiotensin (ANG) II[112]), which are associated with increased cytosolic Ca^{2+} concentrations in cultured podocytes, also cause injury. Furthermore, ANG II was shown to signal to the non-selective cation channels TRPC5 and TRPC6 through the AT1 receptor,[287] suggesting that these channels may play a role in podocyte injury beyond the familial FSGS described by Winn et al.[306]

Calcineurin and Synaptopodin

Calcineurin-mediated, NFAT-independent[72] and -dependent[254] signaling pathways in podocytes have also been associated with activating mutations of TRPC6. The link between Ca^{2+}, calcineurin, and synaptopodin provided a clue that TRPC channels may be involved in regulating the actin cytoskeleton, as synaptopodin is known to regulate small Rho GTPases – master regulators of actin cytoskeletal dynamics. The opposing action of RhoGTPases – RhoA which promotes F-actin stabilization, and Cdc42 or Rac1 that promote F-actin turnover – are thought to maintain the podocyte FP dynamic.[91] Podocyte-specific overexpression of TRPC6 led to a Ca^{2+}-mediated increase in RhoA activity,[130] while genetic deletion of TRPC6 led to increased Rac1 activity and podocyte motility.[287] This cumulative body of work outlines an important role for intracellular Ca^{2+} in regulating the actin cytoskeleton of podocytes, and more work in the area will yield interesting insights into the intersection of metabolism, Ca^{2+} signaling, and cytoskeleton in podocytes.

GLOMERULAR PARIETAL EPITHELIUM

Description

The parietal layer of Bowman's capsule consists of a heterogenous population of squamous and cuboidal epithelial cells resting on a basement membrane.[100] The heterogeneity of this population is rendered more complex by the identification of a peripolar cell population, which by morphology[86] and molecular markers[12] resemble visceral podocytes, and extend up to 100 μm along Bowman's capsule. The glomerular parietal epithelial cells (PECs) are rich in actin microfilament bundles which are particularly prominent in the cells surrounding the vascular pole.[64] In this cell population, the actin bundles are located in cytoplasmic grooves that run circularly around the vascular stalk.[64]

As the visceral and parietal layers of the glomerulus are continuous, so are the basement membranes. The transition region occurs around the vascular stalk, and is connected to the smooth muscle cells of the afferent and efferent arterioles and the extraglomerular mesangial cells. Despite this continuity, however, the parietal basement membrane layer is considerably different. Ultrastructurally, the parietal basement membrane is multilayered, with translucent laminae on the extracellular matrix.[180] Further immunohistochemical studies have identified type I, III, IV, and V collagens, heparin sulfate proteoglycans, laminin, enactin, fibronectin, and nidogen.[180] Of these, however, only type IV and V collagen[238] and heparin sulfated proteoglycans[277] have been confirmed by electron microscopy. Compared to the tubular and glomerular basement membrane, the parietal basement membrane is particularly enriched in collagen type IV as opposed to laminin.[238]

Podocyte Progenitors

It has been long assumed that because of podocytes' limited replicative ability, podocyte loss is a largely irreversible event, ultimately leading to end-stage kidney disease. However, under physiologic conditions and in the event of reversible glomerular disease in humans and animals, podocytes are reportedly shed into the urine at a rate that is not compatible with recovery.[78,176,293,316] This would suggest that there is another mechanism allowing for the replenishment of podocytes. Indeed, seminal experiments involving

irreversible triple labeling of parietal epithelial cells in the Bowman's capsule of mice show the existence of a population of cells near the glomerular vascular stalk that can migrate into the glomerulus and differentiate into podocytes.[6]

Parietal Epithelial Cell-Fate Specification and Wnt Signaling

Given the presence of podocyte progenitors in the parietal epithelium and the podocyte-like cells that seem to populate the transition zone between visceral and parietal epithelium, it is important to understand the developmental cues that push their common progenitors in the S-shaped body stage of glomerular development towards either phenotype. To elucidate this, a conditional deletion of *β-catenin* from the renal epithelium and developing collecting ducts showed that in the absence of β-catenin/Wnt signaling, well-differentiated podocytes replace the parietal epithelium of Bowman's capsule.[93] These "parietal podocytes" were not a result of podocytes migrating from the glomerular tuft, but rather were derived from parietal precursors in the S-shaped body phase by direct lineage switch.

PECs in Glomerular Injury

Glomerulosclerosis

While PECs can promote recovery from physiologic podocyte loss or milder forms of injury, they can also contribute to sclerotic lesions in certain mouse models of glomerulosclerosis.[270] Lineage tracing of podocytes in a mouse model of podocyte depletion showed that PECs, but not podocytes, avidly proliferated and migrated into the visceral side, developing a lesion that is similar to idiopathic FSGS.[10]

Crescent Formation

A role for PECs has also been demonstrated in crescentic formation in inflammatory models of murine glomerular injury. Unlike in the sclerotic lesions, anti-GBM glomerular nephritis induced the proliferation of both podocytes and PECs.[193] In this model, podocytes undergo a profound phenotypic change, losing all their typical markers, and form a bridge between the tuft and Bowman's capsule.[156,193] This bridging event then induces the proliferation of PECs, and both cell types can be found in the cellular crescents that are the hallmark of severe inflammatory glomerular injury.[270]

Glomerular Permeability

In the setting of inflammatory injury, the tight junctions between PECs are also disturbed and become permeable to texas-red labeled dextran and ovalbumin.[207] These findings suggest that, along with their basement membrane, PECs also form a second barrier to protein, and the perturbation of this cell layer may be responsible for the periglomerular inflammation typical of anti-GBM glomerulonephritis.

THE GLOMERULAR FILTRATION BARRIER

As discussed above, the glomerular filtration barrier has multiple components that contribute to its size and charge perm-selectivity.[104] It begins at the glomerular capillary loop with its fenestrated endothelium, endothelial surface layer, and glycocalyx, then progresses to the glomerular basement membrane, and finally to the podocyte foot processes with their filtration slits bridged by the slit diaphragms.

Size Barrier

Many classical experiments using dextrans,[29] ficolls,[16] and proteins[170] have incontrovertibly established the existence of a size barrier to permeability. Some reports support the idea that the GBM is the principle filtration barrier. Infusion of dextrans with different molecular weights in rats shows that the particles can reach the subendothelial part of the GBM, but cannot go further.[26] Knockout mice for laminin β2, a major component of the GBM, develop massive proteinuria, even before the onset of visible ultrastructural changes to the podocytes.[125] Mutations in this gene cause Pierson syndrome in patients, an autosomal recessive condition characterized by nephrotic syndrome and ocular abnormalities.[322] Mutations in the gene encoding type IV collagen α5 chain (*COL4A5*) cause X-linked Alport syndrome, characterized by hereditary nephrotic syndrome, hearing loss, and lens defects. Furthermore, homozygous mutations in *COL4A3* or *COL4A4* also affect the collagen network of the GBM structure, and result in an autosomal recessive form of Alport syndrome.[139]

On the other hand, the sieve-like structure of the slit diaphragm[290] also seems to be of paramount importance to the size-selective glomerular filtration barrier. Evidence from human mutations and genetic mouse models which affect slit diaphragm components (discussed above), leads to massive proteinuria, providing evidence that the slit membrane plays a major role in size selectivity. Therefore, current literature supports a role for both the GBM and the podocyte slit diaphragm in size perm-selectivity.

TABLE 22.1 Genetic Mutations that Result in Glomerular Disease (Humans)

Gene	Protein	Disease	Inheritance	Clinical Features	Reference
NPHS1	Nephrin	Congenital nephrotic syndrome of the Finnish type	AR	Massive proteinuria *in utero* and treatment resistant nephrotic syndrome	143
NPHS2	Podocin	Steroid-resistant nephrotic syndrome	AR	Variable onset nephropathy that is steroid resistant	19
CD2AP	CD2AP	Sporadic FSGS	n/a	FSGS	144
ACTN4	α-Actinin-4	FSGS	AD	Progressive proteinuria starting in adolescence with adult onset FSGS (variable penetrance)	137
COQ2	Coenzyme Q10 biosynthesis mono-oxigenase 2	Steroid-resistant nephrotic syndrome	AR	Steroid resistant nephrotic syndrome,epileptic encephalopathy	56
COQ6	Coenzyme Q10 biosynthesis mono-oxigenase 6	Steroid-resistant nephrotic syndrome	AR	Nephrotic syndrome with sensorineural deafness	110
PLCE1	PLCε1	Inherited nephrotic syndrome	AR	Nephrosis and diffuse mesangial sclerosis leading to renal failure	113
LAMB2	Laminin β2	Pierson's syndrome	AR	Congenital nephrosis, mesangial sclerosis, and microcoria	322
ITGA3	Integrin α3	Congenital nephrotic syndrome	AR	Congenital nephrotic syndrome, interstitial lung disease, and skin fragility	109
TRPC6	TRPC6	FSGS	AD	High grade proteinuria with adult onset, and progression to renal failure	306
MYH9	MYH9	Epstein syndrome Fechtner's syndrome	AD	Proteinuria, microhematuria, thrombocytopenia, and sensorineural deafness	9
LMX1B	LMX1B	Nail–Patella syndrome	AD	Nephrotic syndrome with nail and skeletal abnormalities in children	60
WT1	WT1	Denis–Drash syndrome (DDS) Frasier syndrome (FS)	AD	Pseudohermaphroditism, diffuse mesangial sclerosis and renal failure with varying onset depending on the mutation	214
SYNPO	Synaptopodin	Sporadic FSGS	n/a	FSGS risk in Chinese patients	49
MYOE1	Myosin 1E	Childhood FSGS	n/a	Childhood onset FSGS	183
APOL1	Apolipoprotein L-1	Sporadic FSGS	n/a	Risk of FSGS in African-American patients	83
GPC5	Glypican 5	Acquired nephrotic syndrome	n/a	Increased risk of nephrotic syndrome	208
INF2	Formin	Charcot–Marie Tooth	AD	Adolescent onset proteinuria with progression to FSGS and renal failure	20,82
PTPRO/ GLEPP1	Protein-tyrosine phosphatase receptor type O [PTPRO or GLEPP1]	FSGS	AR	Childhood nephrotic syndrome with FSGS and progression to renal failure	211
COL4A1	Collagen IV α1	Alport's syndrome	X-linked	Nephrotic syndrome with hematuria and sensorineural hearing loss (α1,3,4,5)	41,169,186,218,233
COL4A3	Collagen IV α3		AR		
COL4A4	Collagen IV α4		AR		
COL4A5	Collagen IV α5			Intracerebral hemorrhage and strokes (α1)	
ARHGAP24	Arhgap24	FSGS	AD	Early onset FSGS	4

AR: autosomal recessive; AD: autosomal dominant.

Charge Barrier

The presence of a charge barrier was demonstrated by sequential classical analyses that show retardation of anionic macromolecules from passing through the glomerular filtration barrier as compared to neutral molecules with a similar size.[21,22,28]

GBM as a Charge Barrier

Electron microscopy with perfusion of cationic lysozyme demonstrated the presence of anionic sites in all three layers of the GBM.[27] Studies using ferritins with different isometric points showed that cationic ferritin could distribute widely into the GBM, whereas filtration of its neutral counterpart was restricted at the level of the endothelium and subendothelial layer of the GBM.[232] Treatment of rats with heparinase reduced the restriction of neutral ferritin and allowed the ferritin particles[135] and bovine albumin[240] into the GBM. These results were considered to be conclusive evidence that the negative charges of heparan sulfate proteoglycans in the GBM play a major role in maintaining the charge barrier. Recently, however, podocyte-specific genetic deletion of agrin, both agrin and the heparan sulfated side chains of perlecan, and a systemic deletion of COLXVIII[88,108,291] were reported. Although they are the main components of heparan sulfate proteoglycans in the GBM, none of the mutant mice developed significant proteinuria, as discussed above in the section on GBM. Moreover, a study using isolated GBM showed the sieving coefficients of negatively-charged ficoll sulfate were not different from those of neutral ficoll at physiological ionic strength.[17] Given these recent results, it is unlikely that the GBM is the main charge selective barrier in the glomerulus.

Endothelial Surface Layer as a Charge Barrier

Several experiments have been performed to reduce the endothelial charge barrier by enzymatic digestion of glycosaminoglycans (GAGs). GAGs are major contributors to the GBM negative charge, but they are also expressed on the endothelial surface layer. Perfusion of mice with heparanase, chondroitinase, and hyaluronidase reduces the charge density and thickness of the endothelial surface layer and increases the fractional clearance of albumin.[128,129] In these studies the authors assume that it is most unlikely that the enzymes affect the GBM or podocytes, because they are large molecules and are therefore restricted largely to the vascular lumen. Indeed, the ultrastructure of the endothelium, GBM, and podocytes were not affected by this enzymatic digestion. Since the GBM is no longer considered as the principal charge barrier, these data support the notion of an endothelial charge barrier.

References

[1] Abrahamson DR. Origin of the glomerular basement membrane visualized after *in vivo* labeling of laminin in newborn rat kidneys. J Cell Biol 1985;100(6):1988–2000.

[2] Abrahamson DR. Structure and development of the glomerular capillary wall and basement membrane. Am J Physiol 1987;253 (5 Pt 2):F783–94.

[3] Abrahamson DR, Hudson BG, Stroganova L, Borza D-B St, John PL. Cellular origins of type IV collagen networks in developing glomeruli. J Am Soc Nephrol 2009;20(7):1471–9.

[4] Akilesh S, Suleiman H, Yu H, Stander MC, Lavin P, Gbadegesin R, et al. Arhgap24 inactivates Rac1 in mouse podocytes, and a mutant form is associated with familial focal segmental glomerulosclerosis. J Clin Invest 2011;121(10):4127–37.

[5] Andres A-C, Munarini N, Djonov V, Bruneau S, Zuercher G, Loercher S, et al. EphB4 receptor tyrosine kinase transgenic mice develop glomerulopathies reminiscent of aglomerular vascular shunts. Mech Dev 2003;120(4):511–6.

[6] Appel D, Kershaw DB, Smeets B, Yuan G, Fuss A, Frye B, et al. Recruitment of podocytes from glomerular parietal epithelial cells. J Am Soc Nephrol 2009;20(2):333–43.

[7] Ara T, Tokoyoda K, Okamoto R, Koni PA, Nagasawa T. The role of CXCL12 in the organ-specific process of artery formation. Blood 2005;105(8):3155–61.

[8] Ardaillou N, Blaise V, Costenbader K, Vassitch Y, Ardaillou R. Characterization of a B2-bradykinin receptor in human glomerular podocytes. Am J Physiol 1996;271(3 Pt 2):F754–61.

[9] Arrondel C, Vodovar N, Knebelmann B, Grünfeld J-P, Gubler M-C, Antignac C, et al. Expression of the nonmuscle myosin heavy chain IIA in the human kidney and screening for MYH9 mutations in Epstein and Fechtner syndromes. J Am Soc Nephrol 2002;13(1):65–74.

[10] Asano T, Niimura F, Pastan I, Fogo AB, Ichikawa I, Matsusaka T. Permanent genetic tagging of podocytes: fate of injured podocytes in a mouse model of glomerular sclerosis. J Am Soc Nephrol 2005;16(8):2257–62.

[11] Bader BL, Smyth N, Nedbal S, Miosge N, Baranowsky A, Mokkapati S, et al. Compound genetic ablation of nidogen 1 and 2 causes basement membrane defects and perinatal lethality in mice. Mol Cell Biol 2005;25(15):6846–56.

[12] Bariety J, Mandet C, Hill GS, Bruneval P. Parietal podocytes in normal human glomeruli. J Am Soc Nephrol 2006;17 (10):2770–80.

[13] Bieritz B, Spessotto P, Colombatti A, Jahn A, Prols F, Hartner A. Role of alpha8 integrin in mesangial cell adhesion, migration, and proliferation. Kidney Int 2003;64(1):119–27.

[14] Bjarnegård M, Enge M, Norlin J, Gustafsdottir S, Fredriksson S, Abramsson A, et al. Endothelium-specific ablation of PDGFB leads to pericyte loss and glomerular, cardiac and placental abnormalities. Development 2004;131(8):1847–57.

[15] Blasutig IM, New LA, Thanabalasuriar A, Dayarathna TK, Goudreault M, Quaggin SE, et al. Phosphorylated YDXV motifs and Nck SH2/SH3 adaptors act cooperatively to induce actin reorganization. Mol Cell Biol 2008;28(6):2035–46.

[16] Blouch K, Deen WM, Fauvel JP, Bialek J, Derby G, Myers BD. Molecular configuration and glomerular size selectivity in healthy and nephrotic humans. Am J Physiol 1997;273(3 Pt 2): F430–7.

[17] Bolton GR, Deen WM, Daniels BS. Assessment of the charge selectivity of glomerular basement membrane using Ficoll sulfate. Am J Physiol 1998;274(5 Pt 2):F889–96.

[18] Borza CM, Su Y, Chen X, Yu L, Mont S, Chetyrkin S, et al. Inhibition of integrin $\alpha 2\beta 1$ ameliorates glomerular injury. J Am Soc Nephrol 2012;23(6):1027–38.

[19] Boute N, Gribouval O, Roselli S, Benessy F, Lee H, Fuchshuber A, et al. NPHS2, encoding the glomerular protein podocin, is mutated in autosomal recessive steroid-resistant nephrotic syndrome. Nat Genet 2000;24(4):349–54.

[20] Boyer O, Nevo F, Plaisier E, Funalot B, Gribouval O, Benoit G, et al. INF2 mutations in Charcot-Marie-Tooth disease with glomerulopathy. N Engl J Med 2011;365(25):2377–88.

[21] Brenner BM, Baylis C, Deen WM. Transport of molecules across renal glomerular capillaries. Physiol Rev 1976;56(3):502–34.

[22] Brenner BM, Bohrer MP, Baylis C, Deen WM. Determinants of glomerular permselectivity: insights derived from observations *in vivo*. Kidney Int 1977;12(4):229–37.

[23] Budde K, Becker T, Arns W, Sommerer C, Reinke P, Eisenberger U, et al. Everolimus-based, calcineurin-inhibitor-free regimen in recipients of *de novo* kidney transplants: an open-label, randomised, controlled trial. Lancet 2011;377 (9768):837–47.

[24] Call KM, Glaser T, Ito CY, Buckler AJ, Pelletier J, Haber DA, et al. Isolation and characterization of a zinc finger polypeptide gene at the human chromosome 11 Wilms' tumor locus. Cell 1990;60(3):509–20.

[25] Caricasole A, Duarte A, Larsson SH, Hastie ND, Little M, Holmes G, et al. RNA binding by the Wilms tumor suppressor zinc finger proteins. Proc Natl Acad Sci USA 1996;93 (15):7562–6.

[26] Caulfield JP, Farquhar MG. The permeability of glomerular capillaries to graded dextrans. Identification of the basement membrane as the primary filtration barrier. J Cell Biol 1974;63 (3):883–903.

[27] Caulfield JP, Farquhar MG. Distribution of annionic sites in glomerular basement membranes: their possible role in filtration and attachment. Proc Natl Acad Sci USA 1976;73(5): 1646–50.

[28] Chang RL, Deen WM, Robertson CR, Brenner BM. Permselectivity of the glomerular capillary wall: III. Restricted transport of polyanions. Kidney Int 1975;8(4):212–8.

[29] Chang RL, Ueki IF, Troy JL, Deen WM, Robertson CR, Brenner BM. Permselectivity of the glomerular capillary wall to macromolecules. II. Experimental studies in rats using neutral dextran. Biophys J 1975;15(9):887–906.

[30] Chau Y-Y, Brownstein D, Mjoseng H, Lee W-C, Buza-Vidas N, Nerlov C, et al. Acute multiple organ failure in adult mice deleted for the developmental regulator Wt1. PLoS Genet 2011;7 (12):e1002404.

[31] Chen H, Lun Y, Ovchinnikov D, Kokubo H, Oberg KC, Pepicelli CV, et al. Limb and kidney defects in Lmx1b mutant mice suggest an involvement of LMX1B in human Nail Patella syndrome. Nat Genet 1998;19(1):51–5.

[32] Chen L, Al-Awqati Q. Segmental expression of Notch and Hairy genes in nephrogenesis. Am J Physiol Renal Physiol 2005;288(5):F939–52.

[33] Chen S, Wassenhove-McCarthy DJ, Yamaguchi Y, Holzman LB, van Kuppevelt TH, Jenniskens GJ, et al. Loss of heparan sulfate glycosaminoglycan assembly in podocytes does not lead to proteinuria. Kidney Int 2008;74(3):289–99.

[34] Chen X, Moeckel G, Morrow JD, Cosgrove D, Harris RC, Fogo AB, et al. Lack of integrin alpha1beta1 leads to severe glomerulosclerosis after glomerular injury. Am J Pathol 2004;165 (2):617–30.

[35] Cheng H-T, Kim M, Valerius MT, Surendran K, Schuster-Gossler K, Gossler A, et al. Notch2, but not Notch1, is required for proximal fate acquisition in the mammalian nephron. Development 2007;134(4):801–11.

[36] Cho EA, Patterson LT, Brookhiser WT, Mah S, Kintner C, Dressler GR. Differential expression and function of cadherin-6 during renal epithelium development. Development 1998;125 (5):803–12.

[37] Ciani L, Patel A, Allen ND, ffrench-Constant C. Mice lacking the giant protocadherin mFAT1 exhibit renal slit junction abnormalities and a partially penetrant cyclopia and anophthalmia phenotype. Mol Cell Biol 2003;23(10):3575–82.

[38] Cinà DP, Onay T, Paltoo A, Li C, Maezawa Y, De Arteaga J, et al. Inhibition of MTOR disrupts autophagic flux in podocytes. J Am Soc Nephrol 2011;23(3):412–20.

[39] Clement LC, Avila-Casado C, Macé C, Soria E, Bakker WW, Kersten S, et al. Podocyte-secreted angiopoietin-like-4 mediates proteinuria in glucocorticoid-sensitive nephrotic syndrome. Nat Med 2011;17(1):117–22.

[40] Colognato H, Yurchenco PD. Form and function: the laminin family of heterotrimers. Dev Dyn 2000;218(2):213–34.

[41] Cosgrove D, Meehan DT, Grunkemeyer JA, Kornak JM, Sayers R, Hunter WJ, et al. Collagen COL4A3 knockout: a mouse model for autosomal Alport syndrome. Genes Dev 1996;10 (23):2981–92.

[42] Courtoy PJ, Timpl R, Farquhar MG. Comparative distribution of laminin, type IV collagen, and fibronectin in the rat glomerulus. J Histochem Cytochem 1982;30(9):874–86.

[43] Coward RJM, Welsh GI, Yang J, Tasman C, Lennon R, Koziell A, et al. The human glomerular podocyte is a novel target for insulin action. Diabetes 2005;54(11):3095–102.

[44] Crean JKG, Finlay D, Murphy M, Moss C, Godson C, Martin F, et al. The role of p42/44 MAPK and protein kinase B in connective tissue growth factor induced extracellular matrix protein production, cell migration, and actin cytoskeletal rearrangement in human mesangial cells. J Biol Chem 2002;277 (46):44187–94.

[45] Cybulsky AV, Bonventre JV, Quigg RJ, Lieberthal W, Salant DJ. Cytosolic calcium and protein kinase C reduce complement-mediated glomerular epithelial injury. Kidney Int 1990;38 (5):803–11.

[46] Dai C, Liu Y. Hepatocyte growth factor antagonizes the profibrotic action of TGF-beta1 in mesangial cells by stabilizing Smad transcriptional corepressor TGIF. J Am Soc Nephrol 2004;15(6):1402–12.

[47] Dai C, Stolz DB, Bastacky SI, St-Arnaud R, Wu C, Dedhar S, et al. Essential role of integrin-linked kinase in podocyte biology: Bridging the integrin and slit diaphragm signaling. J Am Soc Nephrol 2006;17(8):2164–75.

[48] Dai C, Yang J, Bastacky S, Xia J, Li Y, Liu Y. Intravenous administration of hepatocyte growth factor gene ameliorates diabetic nephropathy in mice. J Am Soc Nephrol 2004;15(10):2637–47.

[49] Dai S, Wang Z, Pan X, Wang W, Chen X, Ren H, et al. Functional analysis of promoter mutations in the ACTN4 and SYNPO genes in focal segmental glomerulosclerosis. Nephrol Dial Transplant 2010;25(3):824–35.

[50] Dandapani SV, Sugimoto H, Matthews BD, Kolb RJ, Sinha S, Gerszten RE, et al. Alpha-actinin-4 is required for normal podocyte adhesion. J Biol Chem 2007;282(1):467–77.

[51] Darisipudi MN, Kulkarni OP, Sayyed SG, Ryu M, Migliorini A, Sagrinati C, et al. Dual blockade of the homeostatic chemokine CXCL12 and the proinflammatory chemokine CCL2 has additive protective effects on diabetic kidney disease. Am J Pathol 2011;179(1):116–24.

[52] Davis B, Dei Cas A, Long DA, White KE, Hayward A, Ku C-H, et al. Podocyte-specific expression of angiopoietin-2 causes proteinuria and apoptosis of glomerular endothelia. J Am Soc Nephrol 2007;18(8):2320–9.

[53] Denys P, Malvaux P, Van Den Berghe H, Tanghe W, Proesmans W. Association of an anatomo-pathological syndrome of male pseudohermaphroditism, Wilms' tumor, parenchymatous

nephropathy and XX/XY mosaicism. Arch Fr Pediatr 1967;24 (7):729–39.
[54] Ding G, Zhang A, Huang S, Pan X, Zhen G, Chen R, et al. ANG II induces c-Jun NH2-terminal kinase activation and proliferation of human mesangial cells via redox-sensitive transactivation of the EGFR. Am J Physiol Renal Physiol 2007;293(6): F1889–97.
[55] Ding M, Cui S, Li C, Jothy S, Haase V, Steer BM, et al. Loss of the tumor suppressor Vhlh leads to upregulation of Cxcr4 and rapidly progressive glomerulonephritis in mice. Nat Med 2006;12(9):1081–7.
[56] Diomedi-Camassei F, Di Giandomenico S, Santorelli FM, Caridi G, Piemonte F, Montini G, et al. COQ2 nephropathy: A newly described inherited mitochondriopathy with primary renal involvement. J Am Soc Nephrol 2007;18(10): 2773–80.
[57] Donoviel DB, Freed DD, Vogel H, Potter DG, Hawkins E, Barrish JP, et al. Proteinuria and perinatal lethality in mice lacking NEPH1, a novel protein with homology to nephrin. Mol Cell Biol 2001;21(14):4829–36.
[58] Doyonnas R, Kershaw DB, Duhme C, Merkens H, Chelliah S, Graf T, et al. Anuria, omphalocele, and perinatal lethality in mice lacking the CD34-related protein podocalyxin. J Exp Med 2001;194(1):13–27.
[59] Drash A, Sherman F, Hartmann WH, Blizzard RM. A syndrome of pseudohermaphroditism, Wilms' tumor, hypertension, and degenerative renal disease. J Pediatr 1970;76(4):585–93.
[60] Dreyer SD, Zhou G, Baldini A, Winterpacht A, Zabel B, Cole W, et al. Mutations in LMX1B cause abnormal skeletal patterning and renal dysplasia in nail patella syndrome. Nat Genet 1998;19 (1):47–50.
[61] Drummond IA, Rupprecht HD, Rohwer-Nutter P, Lopez-Guisa JM, Madden SL, Rauscher FJ, et al. DNA recognition by splicing variants of the Wilms' tumor suppressor, WT1. Mol Cell Biol 1994;14(6):3800–9.
[62] El-Aouni C, Herbach N, Blattner SM, Henger A, Rastaldi MP, Jarad G, et al. Podocyte-specific deletion of integrin-linked kinase results in severe glomerular basement membrane alterations and progressive glomerulosclerosis. J Am Soc Nephrol 2006;17(5):1334–44.
[63] Elger M, Drenckhahn D, Nobiling R, Mundel P, Kriz W. Cultured rat mesangial cells contain smooth muscle alpha-actin not found *in vivo*. Am J Pathol 1993;142(2):497–509.
[64] Elger M, Sakai T, Kriz W. The vascular pole of the renal glomerulus of rat. Adv Anat Embryol Cell Biol 1998;139:1–98.
[65] Eremina V, Cui S, Gerber H, Ferrara N, Haigh J, Nagy A, et al. Vascular endothelial growth factor a signaling in the podocyte-endothelial compartment is required for mesangial cell migration and survival. J Am Soc Nephrol 2006;17 (3):724–35.
[66] Eremina V, Jefferson JA, Kowalewska J, Hochster H, Haas M, Weisstuch J, et al. VEGF inhibition and renal thrombotic microangiopathy. N Engl J Med 2008;358(11):1129–36.
[67] Eremina V, Quaggin SE. The role of VEGF-A in glomerular development and function. Curr Opin Nephrol Hypertens 2004;13(1):9–15.
[68] Eremina V, Sood M, Haigh J, Nagy A, Lajoie G, Ferrara N, et al. Glomerular-specific alterations of VEGF-A expression lead to distinct congenital and acquired renal diseases. J Clin Invest 2003;111(5):707–16.
[69] Esser S, Wolburg K, Wolburg H, Breier G, Kurzchalia T, Risau W. Vascular endothelial growth factor induces endothelial fenestrations *in vitro*. J Cell Biol 1998;140(4):947–59.
[70] Etienne-Manneville S, Hall A. Rho GTPases in cell biology. Nature 2002;420(6916):629–35.
[71] Farquhar MG, Palade GE. Functional evidence for the existence of a third cell type in the renal glomerulus: phagocytosis of filtration residues by a distinctive "third" cell. J Cell Biol 1962;13 (1):55–87.
[72] Faul C, Donnelly M, Merscher-Gomez S, Chang YH, Franz S, Delfgaauw J, et al. The actin cytoskeleton of kidney podocytes is a direct target of the antiproteinuric effect of cyclosporine A. Nat Med 2008;14(9):931–8.
[73] Fierlbeck W, Liu A, Coyle R, Ballermann BJ. Endothelial cell apoptosis during glomerular capillary lumen formation *in vivo*. J Am Soc Nephrol 2003;14(5):1349–54.
[74] Fischer EG, Moore MJ, Lager DJ. Fabry disease: a morphologic study of 11 cases. Mod Pathol 2006;19(10):1295–301.
[75] Floege J, Burg M, Hugo C, Gordon KL, Van Goor H, Reidy M, et al. Endogenous fibroblast growth factor-2 mediates cytotoxicity in experimental mesangioproliferative glomerulonephritis. J Am Soc Nephrol 1998;9(5):792–801.
[76] Foo SS, Turner CJ, Adams S, Compagni A, Aubyn D, Kogata N, et al. Ephrin-B2 controls cell motility and adhesion during blood-vessel-wall assembly. Cell 2006;124(1):161–73.
[77] Fox JW, Mayer U, Nischt R, Aumailley M, Reinhardt D, Wiedemann H, et al. Recombinant nidogen consists of three globular domains and mediates binding of laminin to collagen type IV. EMBO J 1991;10(11):3137–46.
[78] Fries JW, Sandstrom DJ, Meyer TW, Rennke HG. Glomerular hypertrophy and epithelial cell injury modulate progressive glomerulosclerosis in the rat. Lab Invest 1989;60(2):205–18.
[79] Gagliardini E, Conti S, Benigni A, Remuzzi G, Remuzzi A. Imaging of the porous ultrastructure of the glomerular epithelial filtration slit. J Am Soc Nephrol 2010;21(12):2081–9.
[80] Gale NW, Thurston G, Hackett SF, Renard R, Wang Q, McClain J, et al. Angiopoietin-2 is required for postnatal angiogenesis and lymphatic patterning, and only the latter role is rescued by Angiopoietin-1. Dev Cell 2002;3(3):411–23.
[81] Galeano B, Klootwijk R, Manoli I, Sun M, Ciccone C, Darvish D, et al. Mutation in the key enzyme of sialic acid biosynthesis causes severe glomerular proteinuria and is rescued by N-acetylmannosamine. J Clin Invest 2007;117(6):1585–94.
[82] Gbadegesin RA, Lavin PJ, Hall G, Bartkowiak B, Homstad A, Jiang R, et al. Inverted formin 2 mutations with variable expression in patients with sporadic and hereditary focal and segmental glomerulosclerosis. Kidney Int 2012;81(1):94–9.
[83] Genovese G, Friedman DJ, Ross MD, Lecordier L, Uzureau P, Freedman BI, et al. Association of trypanolytic ApoL1 variants with kidney disease in African Americans. Science 2010;329 (5993):841–5.
[84] Gerety SS, Anderson DJ. Cardiovascular ephrinB2 function is essential for embryonic angiogenesis. Development 2002;129 (6):1397–410.
[85] Ghayur MN, Krepinsky JC, Janssen LJ. Contractility of the renal glomerulus and mesangial cells: lingering doubts and strategies for the future. Med Hypotheses Res 2008;4(1):1–9.
[86] Gibson IW, Downie I, Downie TT, Han SW, More IA, Lindop GB. The parietal podocyte: a study of the vascular pole of the human glomerulus. Kidney Int 1992;41(1):211–4.
[87] Gibson MA, Kumaratilake JS, Cleary EG. The protein components of the 12-nanometer microfibrils of elastic and nonelastic tissues. J Biol Chem 1989;264(8):4590–8.
[88] Goldberg S, Harvey SJ, Cunningham J, Tryggvason K, Miner JH. Glomerular filtration is normal in the absence of both agrin and perlecan-heparan sulfate from the glomerular basement membrane. Nephrol Dial Transplant 2009;24(7):2044–51.
[89] Gould DB, Phalan FC, van Mil SE, Sundberg JP, Vahedi K, Massin P, et al. Role of COL4A1 in small-vessel disease and hemorrhagic stroke. N Engl J Med 2006;354(14):1489–96.

[90] Gödel M, Hartleben B, Herbach N, Liu S, Zschiedrich S, Lu S, et al. Role of mTOR in podocyte function and diabetic nephropathy in humans and mice. J Clin Invest 2011;121(6):2197–209.
[91] Greka A, Mundel P. Cell biology and pathology of podocytes. Annu Rev Physiol 2012;74:299–323.
[92] Groffen AJ, Ruegg MA, Dijkman H, van de Velden TJ, Buskens CA, van den Born J, et al. Agrin is a major heparan sulfate proteoglycan in the human glomerular basement membrane. J Histochem Cytochem 1998;46(1):19–27.
[93] Grouls S, Iglesias DM, Wentzensen N, Moeller MJ, Bouchard M, Kemler R, et al. Lineage specification of parietal epithelial cells requires β-catenin/Wnt signaling. J Am Soc Nephrol 2012;23(1):63–72.
[94] Guertin DA, Sabatini DM. The pharmacology of mTOR inhibition. Sci Signal 2009;2(67):pe24.
[95] Guo G, Morrison DJ, Licht JD, Quaggin SE. WT1 activates a glomerular-specific enhancer identified from the human nephrin gene. J Am Soc Nephrol 2004;15(11):2851–6.
[96] Guo J-K, Menke AL, Gubler M-C, Clarke AR, Harrison D, Hammes A, et al. WT1 is a key regulator of podocyte function: reduced expression levels cause crescentic glomerulonephritis and mesangial sclerosis. Hum Mol Genet 2002;11(6): 651–9.
[97] Guo L, Sanders PW, Woods A, Wu C. The distribution and regulation of integrin-linked kinase in normal and diabetic kidneys. Am J Pathol 2001;159(5):1735–42.
[98] Gurevich F, Perazella MA. Renal effects of anti-angiogenesis therapy: update for the internist. Am J Med 2009;122(4):322–8.
[99] Haber DA, Sohn RL, Buckler AJ, Pelletier J, Call KM, Housman DE. Alternative splicing and genomic structure of the Wilms tumor gene WT1. Proc Natl Acad Sci USA 1991;88 (21):9618–22.
[100] Haensly WE, Lee JC. Metaplasia of the parietal layer of Bowman's capsule: a histopathological survey of the human kidney. Histol Histopathol 1986;1(4):363–7.
[101] Hamano Y, Grunkemeyer JA, Sudhakar A, Zeisberg M, Cosgrove D, Morello R, et al. Determinants of vascular permeability in the kidney glomerulus. J Biol Chem 2002;277(34): 31154–62.
[102] Hammes A, Guo JK, Lutsch G, Leheste JR, Landrock D, Ziegler U, et al. Two splice variants of the Wilms' tumor 1 gene have distinct functions during sex determination and nephron formation. Cell 2001;106(3):319–29.
[103] Hanson J, Gorman J, Reese J, Fraizer G. Regulation of vascular endothelial growth factor, VEGF, gene promoter by the tumor suppressor, WT1. Front Biosci 2007;12:2279–90.
[104] Haraldsson B, Nyström J, Deen WM. Properties of the glomerular barrier and mechanisms of proteinuria. Physiol Rev 2008;88(2):451–87.
[105] Harita Y, Kurihara H, Kosako H, Tezuka T, Sekine T, Igarashi T, et al. Neph1, a component of the kidney slit diaphragm, is tyrosine-phosphorylated by the Src family tyrosine kinase and modulates intracellular signaling by binding to Grb2. J Biol Chem 2008;283(14):9177–86.
[106] Hartleben B, Gödel M, Meyer-Schwesinger C, Liu S, Ulrich T, Köbler S, et al. Autophagy influences glomerular disease susceptibility and maintains podocyte homeostasis in aging mice. J Clin Invest 2010;120(4):1084–96.
[107] Hartwig S, Ho J, Pandey P, Macisaac K, Taglienti M, Xiang M, et al. Genomic characterization of Wilms' tumor suppressor 1 targets in nephron progenitor cells during kidney development. Development 2010;137(7):1189–203.
[108] Harvey SJ, Jarad G, Cunningham J, Rops AL, van der Vlag J, Berden JH, et al. Disruption of glomerular basement membrane charge through podocyte-specific mutation of agrin does not alter glomerular permselectivity. Am J Pathol 2007;171 (1):139–52.
[109] Has C, Spartà G, Kiritsi D, Weibel L, Moeller A, Vega-Warner V, et al. Integrin α3 mutations with kidney, lung, and skin disease. N Engl J Med 2012;366(16):1508–14.
[110] Heeringa SF, Chernin G, Chaki M, Zhou W, Sloan AJ, Ji Z, et al. COQ6 mutations in human patients produce nephrotic syndrome with sensorineural deafness. J Clin Invest 2011;121 (5):2013–24.
[111] Henderson JM, Alexander MP, Pollak MR. Patients with ACTN4 mutations demonstrate distinctive features of glomerular injury. J Am Soc Nephrol 2009;20(5):961–8.
[112] Henger A, Huber T, Fischer KG, Nitschke R, Mundel P, Schollmeyer P, et al. Angiotensin II increases the cytosolic calcium activity in rat podocytes in culture. Kidney Int 1997;52 (3):687–93.
[113] Hinkes B, Wiggins RC, Gbadegesin R, Vlangos CN, Seelow D, Nürnberg G, et al. Positional cloning uncovers mutations in PLCE1 responsible for a nephrotic syndrome variant that may be reversible. Nat Genet 2006;38(12):1397–405.
[114] Hirata Y, Emori T, Eguchi S, Kanno K, Imai T, Ohta K, et al. Endothelin receptor subtype B mediates synthesis of nitric oxide by cultured bovine endothelial cells. J Clin Invest 1993;91(4):1367–73.
[115] Hjalmarsson C, Johansson BR, Haraldsson B. Electron microscopic evaluation of the endothelial surface layer of glomerular capillaries. Microvasc Res 2004;67(1):9–17.
[116] Hohenstein B, Hugo CPM, Hausknecht B, Boehmer KP, Riess RH, Schmieder RE. Analysis of NO-synthase expression and clinical risk factors in human diabetic nephropathy. Nephrol Dial Transplant 2008;23(4):1346–54.
[117] Holthöfer H, Ahola H, Solin ML, Wang S, Palmen T, Luimula P, et al. Nephrin localizes at the podocyte filtration slit area and is characteristically spliced in the human kidney. Am J Pathol 1999;155(5):1681–7.
[118] Hua H, Munk S, Whiteside CI. Endothelin-1 activates mesangial cell ERK1/2 via EGF-receptor transactivation and caveolin-1 interaction. Am J Physiol Renal Physiol 2003;284(2): F303–12.
[119] Hudson BG, Tryggvason K, Sundaramoorthy M, Neilson EG. Alport's syndrome, Goodpasture's syndrome, and type IV collagen. N Engl J Med 2003;348(25):2543–56.
[120] Hyink DP, Tucker DC St, John PL, Leardkamolkarn V, Accavitti MA, Abrass CK, et al. Endogenous origin of glomerular endothelial and mesangial cells in grafts of embryonic kidneys. Am J Physiol 1996;270(5 Pt 2):F886–99.
[121] Ichimura K, Stan RV, Kurihara H, Sakai T. Glomerular endothelial cells form diaphragms during development and pathologic conditions. J Am Soc Nephrol 2008;19(8):1463–71.
[122] Inoki K, Mori H, Wang J, Suzuki T, Hong S, Yoshida S, et al. mTORC1 activation in podocytes is a critical step in the development of diabetic nephropathy in mice. J Clin Invest 2011;121 (6):2181–96.
[123] Inoue T, Yaoita E, Kurihara H, Shimizu F, Sakai T, Kobayashi T, et al. FAT is a component of glomerular slit diaphragms. Kidney Int 2001;59(3):1003–12.
[124] Jacinto E, Loewith R, Schmidt A, Lin S, Rüegg MA, Hall A, et al. Mammalian TOR complex 2 controls the actin cytoskeleton and is rapamycin insensitive. Nat Cell Biol 2004;6(11):1122–8.
[125] Jarad G, Cunningham J, Shaw AS, Miner JH. Proteinuria precedes podocyte abnormalities inLamb2$^{-/-}$ mice, implicating the glomerular basement membrane as an albumin barrier. J Clin Invest 2006;116(8):2272–9.
[126] Jarad G, Pippin JW, Shankland SJ, Kreidberg JA, Miner JH. Dystroglycan does not contribute significantly to kidney

development or function, in health or after injury. Am J Physiol Renal Physiol 2011;300(3):F811–20.
[127] Jeansson M, Gawlik A, Anderson G, Li C, Kerjaschki D, Henkelman M, et al. Angiopoietin-1 is essential in mouse vasculature during development and in response to injury. J Clin Invest 2011;121(6):2278–89.
[128] Jeansson M, Haraldsson B. Glomerular size and charge selectivity in the mouse after exposure to glucosaminoglycan-degrading enzymes. J Am Soc Nephrol 2003;14(7):1756–65.
[129] Jeansson M, Haraldsson B. Morphological and functional evidence for an important role of the endothelial cell glycocalyx in the glomerular barrier. Am J Physiol Renal Physiol 2006;290 (1):F111–6.
[130] Jiang L, Ding J, Tsai H, Li L, Feng Q, Miao J, et al. Over-expressing transient receptor potential cation channel 6 in podocytes induces cytoskeleton rearrangement through increases of intracellular Ca^{2+} and RhoA activation. Exp Biol Med (Maywood) 2011;236(2):184–93.
[131] Jones N, Blasutig IM, Eremina V, Ruston JM, Bladt F, Li H, et al. Nck adaptor proteins link nephrin to the actin cytoskeleton of kidney podocytes. Nature 2006;440(7085):818–23.
[132] Kamba T, McDonald DM. Mechanisms of adverse effects of anti-VEGF therapy for cancer. Br J Cancer 2007;96(12):1788–95.
[133] Kamba T, Tam BYY, Hashizume H, Haskell A, Sennino B, Mancuso MR, et al. VEGF-dependent plasticity of fenestrated capillaries in the normal adult microvasculature. Am J Physiol Heart Circ Physiol 2006;290(2):H560–76.
[134] Kanasaki K, Kanda Y, Palmsten K, Tanjore H, Lee SB, Lebleu VS, et al. Integrin beta1-mediated matrix assembly and signaling are critical for the normal development and function of the kidney glomerulus. Dev Biol 2008;313(2):584–93.
[135] Kanwar YS, Linker A, Farquhar MG. Increased permeability of the glomerular basement membrane to ferritin after removal of glycosaminoglycans (heparan sulfate) by enzyme digestion. J Cell Biol 1980;86(2):688–93.
[136] Kanwar YS, Danesh FR, Chugh SS. Contribution of proteoglycans towards the integrated functions of renal glomerular capillaries: a historical perspective. Am J Pathol 2007;171 (1):9–13.
[137] Kaplan JM, Kim SH, North KN, Rennke H, Correia LA, Tong HQ, et al. Mutations in ACTN4, encoding alpha-actinin-4, cause familial focal segmental glomerulosclerosis. Nat Genet 2000;24(3):251–6.
[138] Karamatic Crew V, Burton N, Kagan A, Green CA, Levene C, Flinter F, et al. CD151, the first member of the tetraspanin (TM4) superfamily detected on erythrocytes, is essential for the correct assembly of human basement membranes in kidney and skin. Blood 2004;104(8):2217–23.
[139] Kashtan CE. Alport syndromes: phenotypic heterogeneity of progressive hereditary nephritis. Pediatr Nephrol 2000;14 (6):502–12.
[140] Kerjaschki D. Polycation-induced dislocation of slit diaphragms and formation of cell junctions in rat kidney glomeruli: the effects of low temperature, divalent cations, colchicine, and cytochalasin B. Lab Invest 1978;39(5):430–40.
[141] Kerjaschki D, Farquhar MG. Immunocytochemical localization of the Heymann nephritis antigen (GP330) in glomerular epithelial cells of normal Lewis rats. J Exp Med 1983;157 (2):667–86.
[142] Kerjaschki D, Ojha PP, Susani M, Horvat R, Binder S, Hovorka A, et al. A beta 1-integrin receptor for fibronectin in human kidney glomeruli. Am J Pathol 1989;134(2):481–9.
[143] Kestilä M, Lenkkeri U, Männikkö M, Lamerdin J, McCready P, Putaala H, et al. Positionally cloned gene for a novel glomerular protein – nephrin – is mutated in congenital nephrotic syndrome. Mol Cell 1998;1(4):575–82.
[144] Kim JM, Wu H, Green G, Winkler CA, Kopp JB, Miner JH, et al. CD2-associated protein haploinsufficiency is linked to glomerular disease susceptibility. Science 2003;300(5623): 1298–300.
[145] Kobayashi N, Mundel P. A role of microtubules during the formation of cell processes in neuronal and non-neuronal cells. Cell Tissue Res 1998;291(2):163–74.
[146] Kolatsi-Joannou M, Li XZ, Suda T, Yuan HT, Woolf AS. Expression and potential role of angiopoietins and Tie-2 in early development of the mouse metanephros. Dev Dyn 2001;222(1):120–6.
[147] Kreidberg JA. Functions of alpha3beta1 integrin. Curr Opin Cell Biol 2000;12(5):548–53.
[148] Kreidberg JA, Donovan MJ, Goldstein SL, Rennke H, Shepherd K, Jones RC, et al. Alpha 3 beta 1 integrin has a crucial role in kidney and lung organogenesis. Development 1996;122 (11):3537–47.
[149] Kreidberg JA, Sariola H, Loring JM, Maeda M, Pelletier J, Housman D, et al. WT-1 is required for early kidney development. Cell 1993;74(4):679–91.
[150] Kreidberg JA, Symons JM. Integrins in kidney development, function, and disease. Am J Physiol Renal Physiol 2000;279(2): F233–42.
[151] Kretzler M, Teixeira VP, Unschuld PG, Cohen CD, Wanke R, Edenhofer I, et al. Integrin-linked kinase as a candidate downstream effector in proteinuria. FASEB J 2001;15(10):1843–5.
[152] Kriz W, Elger M, Mundel P, Lemley KV. Structure-stabilizing forces in the glomerular tuft. J Am Soc Nephrol 1995;5 (10):1731–9.
[153] Kurihara H, Anderson JM, Kerjaschki D, Farquhar MG. The altered glomerular filtration slits seen in puromycin aminonucleoside nephrosis and protamine sulfate-treated rats contain the tight junction protein ZO-1. Am J Pathol 1992;141 (4):805–16.
[154] Kühn K. Basement membrane (type IV) collagen. Matrix Biol 1995;14(6):439–45.
[155] Laplante M, Sabatini DM. mTOR signaling in growth control and disease. Cell 2012;149(2):274–93.
[156] Le Hir M, Keller C, Eschmann V, Hähnel B, Hosser H, Kriz W. Podocyte bridges between the tuft and Bowman's capsule: an early event in experimental crescentic glomerulonephritis. J Am Soc Nephrol 2001;12(10):2060–71.
[157] Le Roux S, Pepper RJ, Dufay A, Néel M, Meffray E, Lamandé N, et al. Elevated soluble Flt1 inhibits endothelial repair in PR3-ANCA-associated vasculitis. J Am Soc Nephrol 2012;23 (1):155–64.
[158] Lea PJ, Silverman M, Hegele R, Hollenberg MJ. Tridimensional ultrastructure of glomerular capillary endothelium revealed by high-resolution scanning electron microscopy. Microvasc Res 1989;38(3):296–308.
[159] Lee S, Kim W, Kim DH, Moon S-O, Jung YJ, Lee AS, et al. Protective effect of COMP-angiopoietin-1 on cyclosporine-induced renal injury in mice. Nephrol Dial Transplant 2008;23 (9):2784–94.
[160] Lenkkeri U, Männikkö M, McCready P, Lamerdin J, Gribouval O, Niaudet PM, et al. Structure of the gene for congenital nephrotic syndrome of the Finnish type (NPHS1) and characterization of mutations. Am J Hum Genet 1999;64(1):51–61.
[161] Levéen P, Pekny M, Gebre-Medhin S, Swolin B, Larsson E, Betsholtz C. Mice deficient for PDGF B show renal, cardiovascular, and hematological abnormalities. Genes Dev 1994;8 (16):1875–87.

[162] Levine RJ, Maynard SE, Qian C, Lim K-H, England LJ, Yu KF, et al. Circulating angiogenic factors and the risk of preeclampsia. N Engl J Med 2004;350(7):672–83.
[163] Li C, Ruotsalainen V, Tryggvason K, Shaw AS, Miner JH. CD2AP is expressed with nephrin in developing podocytes and is found widely in mature kidney and elsewhere. Am J Physiol Renal Physiol 2000;279(4):F785–92.
[164] Li L, Krantz ID, Deng Y, Genin A, Banta AB, Collins CC, et al. Alagille syndrome is caused by mutations in human Jagged1, which encodes a ligand for Notch1. Nat Genet 1997;16 (3):243–51.
[165] Lindahl P, Hellström M, Kalén M, Karlsson L, Pekny M, Pekna M, et al. Paracrine PDGF-B/PDGF-Rbeta signaling controls mesangial cell development in kidney glomeruli. Development 1998;125(17):3313–22.
[166] Lindblom P, Gerhardt H, Liebner S, Abramsson A, Enge M, Hellstrom M, et al. Endothelial PDGF-B retention is required for proper investment of pericytes in the microvessel wall. Genes Dev 2003;17(15):1835–40.
[167] Liu A, Dardik A, Ballermann BJ. Neutralizing TGF-beta1 antibody infusion in neonatal rat delays *in vivo* glomerular capillary formation 1. Kidney Int 1999;56(4):1334–48.
[168] Liu G, Kaw B, Kurfis J, Rahmanuddin S, Kanwar YS, Chugh SS. Neph1 and nephrin interaction in the slit diaphragm is an important determinant of glomerular permeability. J Clin Invest 2003;112(2):209–21.
[169] Lu W, Phillips CL, Killen PD, Hlaing T, Harrison WR, Elder FF, et al. Insertional mutation of the collagen genes Col4a3 and Col4a4 in a mouse model of Alport syndrome. Genomics 1999;61(2):113–24.
[170] Lund U, Rippe A, Venturoli D, Tenstad O, Grubb A, Rippe B. Glomerular filtration rate dependence of sieving of albumin and some neutral proteins in rat kidneys. Am J Physiol Renal Physiol 2003;284(6):F1226–34.
[171] Ma H, Togawa A, Soda K, Zhang J, Lee S, Ma M, et al. Inhibition of podocyte FAK protects against proteinuria and foot process effacement. J Am Soc Nephrol 2010;21(7):1145–56.
[172] Madri JA, Roll FJ, Furthmayr H, Foidart JM. Ultrastructural localization of fibronectin and laminin in the basement membranes of the murine kidney. J Cell Biol 1980;86(2):682–7.
[173] Maharaj ASR, Walshe TE, Saint-Geniez M, Venkatesha S, Maldonado AE, Himes NC, et al. VEGF and TGF-beta are required for the maintenance of the choroid plexus and ependyma. J Exp Med 2008;205(2):491–501.
[174] Maisonpierre PC, Suri C, Jones PF, Bartunkova S, Wiegand SJ, Radziejewski C, et al. Angiopoietin-2, a natural antagonist for Tie2 that disrupts in vivo angiogenesis. Science 1997;277 (5322):55–60.
[175] Makino H, Kashihara N, Sugiyama H, Kanao K, Sekikawa T, Shikata K, et al. Phenotypic changes of the mesangium in diabetic nephropathy. J Diabetes Complicat 1995;9(4):282–4.
[176] Marshall CB, Shankland SJ. Cell cycle and glomerular disease: a minireview. Nephron Exp Nephrol 2006;102(2):e39–48.
[177] Martinez-Hernandez A, Chung AE. The ultrastructural localization of two basement membrane components: entactin and laminin in rat tissues. J Histochem Cytochem 1984;32 (3):289–98.
[178] Matsui T, Maeda M, Doi Y, Yonemura S, Amano M, Kaibuchi K, et al. Rho-kinase phosphorylates COOH-terminal threonines of ezrin/radixin/moesin (ERM) proteins and regulates their head-to-tail association. J Cell Biol 1998;140(3):647–57.
[179] Maynard SE, Min J-Y, Merchan J, Lim K-H, Li J, Mondal S, et al. Excess placental soluble fms-like tyrosine kinase 1 (sFlt1) may contribute to endothelial dysfunction, hypertension, and proteinuria in preeclampsia. J Clin Invest 2003;111(5):649–58.
[180] Mbassa G, Elger M, Kriz W. The ultrastructural organization of the basement membrane of Bowman's capsule in the rat renal corpuscle. Cell Tissue Res 1988;253(1):151–63.
[181] McCright B, Gao X, Shen L, Lozier J, Lan Y, Maguire M, et al. Defects in development of the kidney, heart and eye vasculature in mice homozygous for a hypomorphic Notch2 mutation. Development 2001;128(4):491–502.
[182] McDaniell R, Warthen DM, Sanchez-Lara PA, Pai A, Krantz ID, Piccoli DA, et al. NOTCH2 mutations cause Alagille syndrome, a heterogeneous disorder of the notch signaling pathway. Am J Hum Genet 2006;79(1):169–73.
[183] Mele C, Iatropoulos P, Donadelli R, Calabria A, Maranta R, Cassis P, et al. MYO1E mutations and childhood familial focal segmental glomerulosclerosis. N Engl J Med 2011;365 (4):295–306.
[184] Menke AL, IJpenberg A, Fleming S, Ross A, Medine CN, Patek CE, et al. The wt1-heterozygous mouse; a model to study the development of glomerular sclerosis. J Pathol 2003;200 (5):667–74.
[185] Miner JH, Li C. Defective glomerulogenesis in the absence of laminin alpha5 demonstrates a developmental role for the kidney glomerular basement membrane. Dev Biol 2000;217 (2):278–89.
[186] Miner JH, Sanes JR. Molecular and functional defects in kidneys of mice lacking collagen alpha 3(IV): implications for Alport syndrome. J Cell Biol 1996;135(5):1403–13.
[187] Miner JH. Building the glomerulus: a matricentric view. J Am Soc Nephrol 2005;16(4):857–61.
[188] Miner JH. Organogenesis of the kidney glomerulus: focus on the glomerular basement membrane. Organogenesis 2011;7 (2):75–82.
[189] Miner JH. The glomerular basement membrane. Exp Cell Res 2012;318(9):973–8.
[190] Miner JH. Life without nephrin: it's for the birds. J Am Soc Nephrol 2012;23(3):369–71.
[191] Miner JH, Morello R, Andrews KL, Li C, Antignac C, Shaw AS, et al. Transcriptional induction of slit diaphragm genes by Lmx1b is required in podocyte differentiation. J Clin Invest 2002;109(8):1065–72.
[192] Miner JH, Yurchenco PD. Laminin functions in tissue morphogenesis. Annu Rev Cell Dev Biol 2004;20:255–84.
[193] Moeller MJ, Soofi A, Hartmann I, Le Hir M, Wiggins R, Kriz W, et al. Podocytes populate cellular crescents in a murine model of inflammatory glomerulonephritis. J Am Soc Nephrol 2004;15(1):61–7.
[194] Moore AW, McInnes L, Kreidberg J, Hastie ND, Schedl A. YAC complementation shows a requirement for Wt1 in the development of epicardium, adrenal gland and throughout nephrogenesis. Development 1999;126(9):1845–57.
[195] Muchitsch E, Pichler L, Schwarz HP, Ulrich W. Effects of human alpha-1-acid glycoprotein on aminonucleoside-induced minimal change nephrosis in rats. Nephron 1999;81(2):194–9.
[196] Mundel P, Kriz W. Structure and function of podocytes: an update. Anat Embryol 1995;192(5):385–97.
[197] Murakami T, Miyoshi M, Fujita T. Glomerular vessels of the rat kidney with special reference to double efferent arterioles. A scanning electron microscope study of corrosion casts. Arch Histol Jpn 1971;33(3):179–98.
[198] Murea M, Park J-K, Sharma S, Kato H, Gruenwald A, Niranjan T, et al. Expression of Notch pathway proteins correlates with albuminuria, glomerulosclerosis, and renal function. Kidney Int 2010;78(5):514–22.

[199] Murshed M, Smyth N, Miosge N, Karolat J, Krieg T, Paulsson M, et al. The absence of nidogen 1 does not affect murine basement membrane formation. Mol Cell Biol 2000;20 (18):7007–12.

[200] Nakagawa T, Sato W, Glushakova O, Heinig M, Clarke T, Campbell-Thompson M, et al. Diabetic endothelial nitric oxide synthase knockout mice develop advanced diabetic nephropathy. J Am Soc Nephrol 2007;18(2):539–50.

[201] Narita M, Young ARJ, Arakawa S, Samarajiwa SA, Nakashima T, Yoshida S, et al. Spatial coupling of mTOR and autophagy augments secretory phenotypes. Science 2011;332(6032):966–70.

[202] Niranjan T, Bielesz B, Gruenwald A, Ponda MP, Kopp JB, Thomas DB, et al. The Notch pathway in podocytes plays a role in the development of glomerular disease. Nat Med 2008;14(3):290–8.

[203] Nishiuchi R, Sanzen N, Nada S, Sumida Y, Wada Y, Okada M, et al. Potentiation of the ligand-binding activity of integrin alpha3beta1 via association with tetraspanin CD151. Proc Natl Acad Sci USA 2005;102(6):1939–44.

[204] Noakes PG, Miner JH, Gautam M, Cunningham JM, Sanes JR, Merlie JP. The renal glomerulus of mice lacking s-laminin/ laminin beta 2: nephrosis despite molecular compensation by laminin beta 1. Nat Genet 1995;10(4):400–6.

[205] Noonan DM, Fulle A, Valente P, Cai S, Horigan E, Sasaki M, et al. The complete sequence of perlecan, a basement membrane heparan sulfate proteoglycan, reveals extensive similarity with laminin A chain, low density lipoprotein-receptor, and the neural cell adhesion molecule. J Biol Chem 1991;266 (34):22939–47.

[206] Oda T, Elkahloun AG, Pike BL, Okajima K, Krantz ID, Genin A, et al. Mutations in the human Jagged1 gene are responsible for Alagille syndrome. Nat Genet 1997;16(3):235–42.

[207] Ohse T, Chang AM, Pippin JW, Jarad G, Hudkins KL, Alpers CE, et al. A new function for parietal epithelial cells: A second glomerular barrier. Am J Physiol Renal Physiol 2009;297(6): F1566–74.

[208] Okamoto K, Tokunaga K, Doi K, Fujita T, Suzuki H, Katoh T, et al. Common variation in GPC5 is associated with acquired nephrotic syndrome. Nat Genet 2011;43(5):459–63.

[209] Oliver J, MacDowell M. Nephrons and kidneys: a quantitative study of developmental and evolutionary mammalian renal architectonics. New York: Hoeber Medical Division, Harper & Row; 1968.

[210] Osterby R. Morphometric studies of the peripheral glomerular basement membrane in early juvenile diabetes. I. Development of initial basement membrane thickening. Diabetologia 1972;8 (2):84–92.

[211] Ozaltin F, Ibsirlioglu T, Taskiran EZ, Baydar DE, Kaymaz F, Buyukcelik M, et al. Disruption of PTPRO causes childhood-onset nephrotic syndrome. Am J Hum Genet 2011;89(1): 139–47.

[212] Pala L, Cresci B, Manuelli C, Maggi E, Yamaguchi YF, Cappugi P, et al. Vascular endothelial growth factor receptor-2 and low affinity VEGF binding sites on human glomerular endothelial cells: biological effects and advanced glycosilation end products modulation. Microvasc Res 2005;70(3):179–88.

[213] Palmer RE, Kotsianti A, Cadman B, Boyd T, Gerald W, Haber DA. WT1 regulates the expression of the major glomerular podocyte membrane protein Podocalyxin. Curr Biol 2001;11 (22):1805–9.

[214] Pelletier J, Bruening W, Kashtan CE, Mauer SM, Manivel JC, Striegel JE, et al. Germline mutations in the Wilms' tumor suppressor gene are associated with abnormal urogenital development in Denys–Drash syndrome. Cell 1991;67(2):437–47.

[215] Peter K. Untersuchungen über bau und entwickelung der niere. Jena: Gustav Fischer; 1909.

[216] Petruzziello-Pellegrini TN, Yuen DA, Page AV, Patel S, Soltyk AM, Matouk CC, et al. The CXCR4/CXCR7/SDF-1 pathway contributes to the pathogenesis of Shiga toxin-associated hemolytic uremic syndrome in humans and mice. J Clin Invest 2012;122(2):759–76.

[217] Pitera JE, Woolf AS, Gale NW, Yancopoulos GD, Yuan HT. Dysmorphogenesis of kidney cortical peritubular capillaries in angiopoietin-2-deficient mice. Am J Pathol 2004;165 (6):1895–906.

[218] Plaisier E, Gribouval O, Alamowitch S, Mougenot B, Prost C, Verpont MC, et al. COL4A1 mutations and hereditary angiopathy, nephropathy, aneurysms, and muscle cramps. N Engl J Med 2007;357(26):2687–95.

[219] Pozzi A, Jarad G, Moeckel GW, Coffa S, Zhang X, Gewin L, et al. Beta1 integrin expression by podocytes is required to maintain glomerular structural integrity. Dev Biol 2008;316(2):288–301.

[220] Pricci F, Pugliese G, Romano G, Romeo G, Locuratolo N, Pugliese F, et al. Insulin-like growth factors I and II stimulate extracellular matrix production in human glomerular mesangial cells. Comparison with transforming growth factor-beta. Endocrinology 1996;137(3):879–85.

[221] Pugliese G, Pricci F, Locuratolo N, Romeo G, Romano G, Giannini S, et al. Increased activity of the insulin-like growth factor system in mesangial cells cultured in high glucose conditions. Relation to glucose-enhanced extracellular matrix production. Diabetologia 1996;39(7):775–84.

[222] Putaala H, Soininen R, Kilpeläinen P, Wartiovaara J, Tryggvason K. The murine nephrin gene is specifically expressed in kidney, brain and pancreas: inactivation of the gene leads to massive proteinuria and neonatal death. Hum Mol Genet 2001;10(1):1–8.

[223] Quaggin SE, Schwartz L, Cui S, Igarashi P, Deimling J, Post M, et al. The basic-helix-loop-helix protein pod1 is critically important for kidney and lung organogenesis. Development 1999;126(24):5771–83.

[224] Quaggin SE, Vanden Heuvel GB, Igarashi P. Pod-1, a mesoderm-specific basic-helix-loop-helix protein expressed in mesenchymal and glomerular epithelial cells in the developing kidney. Mech Dev 1998;71(1–2):37–48.

[225] Quaggin SE, Kreidberg JA. Development of the renal glomerulus: good neighbors and good fences. Development 2008;135 (4):609–20.

[226] Raats CJ, van den Born J, Bakker MA, Oppers-Walgreen B, Pisa BJ, Dijkman HB, et al. Expression of agrin, dystroglycan, and utrophin in normal renal tissue and in experimental glomerulopathies. Am J Pathol 2000;156(5):1749–65.

[227] Raftopoulou M, Hall A. Cell migration: rho GTPases lead the way. Dev Biol 2004;265(1):23–32.

[228] Rahilly MA, Fleming S. Differential expression of integrin alpha chains by renal epithelial cells. J Pathol 1992;167 (3):327–34.

[229] Regele HM, Fillipovic E, Langer B, Poczewki H, Kraxberger I, Bittner RE, et al. Glomerular expression of dystroglycans is reduced in minimal change nephrosis but not in focal segmental glomerulosclerosis. J Am Soc Nephrol 2000;11 (3):403–12.

[230] Reiser J, Kriz W, Kretzler M, Mundel P. The glomerular slit diaphragm is a modified adherens junction. J Am Soc Nephrol 2000;11(1):1–8.

[231] Reiser J, Polu KR, Möller CC, Kenlan P, Altintas MM, Wei C. TRPC6 is a glomerular slit diaphragm-associated channel required for normal renal function. Nat Genet 2005;37 (7):739–44.

[232] Rennke HG, Venkatachalam MA. Glomerular permeability: *in vivo* tracer studies with polyanionic and polycationic ferritins. Kidney Int 1977;11(1):44–53.
[233] Rheault MN, Kren SM, Thielen BK, Mesa HA, Crosson JT, Thomas W, et al. Mouse model of X-linked Alport syndrome. J Am Soc Nephrol 2004;15(6):1466–74.
[234] Robert B St, John PL, Abrahamson DR. Direct visualization of renal vascular morphogenesis in Flk1 heterozygous mutant mice. Am J Physiol 1998;275(1 Pt 2):F164–72.
[235] Robert B St, John PL, Hyink DP, Abrahamson DR. Evidence that embryonic kidney cells expressing flk-1 are intrinsic, vasculogenic angioblasts. Am J Physiol 1996;271(3 Pt 2): F744–53.
[236] Rodewald R, Karnovsky MJ. Porous substructure of the glomerular slit diaphragm in the rat and mouse. J Cell Biol 1974;60(2):423–33.
[237] Rohr C, Prestel J, Heidet L, Hosser H, Kriz W, Johnson RL, et al. The LIM-homeodomain transcription factor Lmx1b plays a crucial role in podocytes. J Clin Invest 2002;109(8):1073–82.
[238] Roll FJ, Madri JA, Albert J, Furthmayr H. Codistribution of collagen types IV and AB2 in basement membranes and mesangium of the kidney. An immunoferritin study of ultrathin frozen sections. J Cell Biol 1980;85(3):597–616.
[239] Roselli S, Heidet L, Sich M, Henger A, Kretzler M, Gubler M-C, et al. Early glomerular filtration defect and severe renal disease in podocin-deficient mice. Mol Cell Biol 2004;24 (2):550–60.
[240] Rosenzweig LJ, Kanwar YS. Removal of sulfated (heparan sulfate) or nonsulfated (hyaluronic acid) glycosaminoglycans results in increased permeability of the glomerular basement membrane to 125I-bovine serum albumin. Lab Invest 1982;47 (2):177–84.
[241] Rostgaard J, Qvortrup K. Electron microscopic demonstrations of filamentous molecular sieve plugs in capillary fenestrae. Microvasc Res 1997;53(1):1–13.
[242] Rostgaard J, Qvortrup K. Sieve plugs in fenestrae of glomerular capillaries – site of the filtration barrier? Cells Tissues Organs (Print) 2002;170(2–3):132–8.
[243] Ruotsalainen V, Ljungberg P, Wartiovaara J, Lenkkeri U, Kestilä M, Jalanko H, et al. Nephrin is specifically located at the slit diaphragm of glomerular podocytes. Proc Natl Acad Sci USA 1999;96(14):7962–7.
[244] Ryan G, Steele-Perkins V, Morris JF, Rauscher FJ, Dressler GR. Repression of Pax-2 by WT1 during normal kidney development. Development 1995;121(3):867–75.
[245] Sadl V, Jin F, Yu J, Cui S, Holmyard D, Quaggin S, et al. The mouse Kreisler (Krml1/MafB) segmentation gene is required for differentiation of glomerular visceral epithelial cells. Dev Biol 2002;249(1):16–29.
[246] Sakai T, Kriz W. The structural relationship between mesangial cells and basement membrane of the renal glomerulus. Anat Embryol 1987;176(3):373–86.
[247] Salmon AHJ, Neal CR, Sage LM, Glass CA, Harper SJ, Bates DO. Angiopoietin-1 alters microvascular permeability coefficients *in vivo* via modification of endothelial glycocalyx. Cardiovasc Res 2009;83(1):24–33.
[248] Sarbassov DD, Ali SM, Sengupta S, Sheen J-H, Hsu PP, Bagley AF, et al. Prolonged rapamycin treatment inhibits mTORC2 assembly and Akt/PKB. Mol Cell 2006;22(2): 159–68.
[249] Satchell SC, Braet F. Glomerular endothelial cell fenestrations: an integral component of the glomerular filtration barrier. Am J Physiol Renal Physiol 2009;296(5):F947–56.
[250] Satchell SC, Harper SJ, Tooke JE, Kerjaschki D, Saleem MA, Mathieson PW. Human podocytes express angiopoietin 1, a potential regulator of glomerular vascular endothelial growth factor. J Am Soc Nephrol 2002;13(2):544–50.
[251] Sayyed SG, Hägele H, Kulkarni OP, Endlich K, Segerer S, Eulberg D, et al. Podocytes produce homeostatic chemokine stromal cell-derived factor-1/CXCL12, which contributes to glomerulosclerosis, podocyte loss and albuminuria in a mouse model of type 2 diabetes. Diabetologia 2009;52 (11):2445–54.
[252] Schaefer L, Grone HJ, Raslik I, Robenek H, Ugorcakova J, Budny S, et al. Small proteoglycans of normal adult human kidney: distinct expression patterns of decorin, biglycan, fibromodulin, and lumican. Kidney Int 2000;58(4):1557–68.
[253] Scharpfenecker M, Fiedler U, Reiss Y, Augustin HG. The Tie-2 ligand angiopoietin-2 destabilizes quiescent endothelium through an internal autocrine loop mechanism. J Cell Sci 2005;118(Pt 4):771–80.
[254] Schlondorff J, Del Camino D, Carrasquillo R, Lacey V, Pollak MR. TRPC6 mutations associated with focal segmental glomerulosclerosis cause constitutive activation of NFAT-dependent transcription. Am J Physiol, Cell Physiol 2009;296(3): C558–69.
[255] Schmieder S, Nagai M, Orlando RA, Takeda T, Farquhar MG. Podocalyxin activates RhoA and induces actin reorganization through NHERF1 and Ezrin in MDCK cells. J Am Soc Nephrol 2004;15(9):2289–98.
[256] Schnabel E, Anderson JM, Farquhar MG. The tight junction protein ZO-1 is concentrated along slit diaphragms of the glomerular epithelium. J Cell Biol 1990;111(3):1255–63.
[257] Schnaper HW, Hayashida T, Hubchak SC, Poncelet A-C. TGF-beta signal transduction and mesangial cell fibrogenesis. Am J Physiol Renal Physiol 2003;284(2):F243–52.
[258] Schordan S, Schordan E, Endlich K, Endlich N. AlphaV-integrins mediate the mechanoprotective action of osteopontin in podocytes. Am J Physiol Renal Physiol 2011;300(1):F119–32.
[259] Schumacher VA, Schlötzer-Schrehardt U, Karumanchi SA, Shi X, Zaia J, Jeruschke S. WT1-dependent sulfatase expression maintains the normal glomerular filtration barrier. J Am Soc Nephrol 2011;22(7):1286–96.
[260] Schwartz E, Goldfischer S, Coltoff-Schiller B, Blumenfeld OO. Extracellular matrix microfibrils are composed of core proteins coated with fibronectin. J Histochem Cytochem 1985;33 (4):268–74.
[261] Schwarz K, Simons M, Reiser J, Saleem MA, Faul C, Kriz W, et al. Podocin, a raft-associated component of the glomerular slit diaphragm, interacts with CD2AP and nephrin. J Clin Invest 2001;108(11):1621–9.
[262] Schymeinsky J, Nedbal S, Miosge N, Pöschl E, Rao C, Beier DR, et al. Gene structure and functional analysis of the mouse nidogen-2 gene: nidogen-2 is not essential for basement membrane formation in mice. Mol Cell Biol 2002;22(19):6820–30.
[263] Scott RP, Hawley SP, Ruston J, Du J, Brakebusch C, Jones N, et al. Podocyte-specific loss of Cdc42 leads to congenital nephropathy. J Am Soc Nephrol 2012;: [epub ahead of print]
[264] Seiler MW, Rennke HG, Venkatachalam MA, Cotran RS. Pathogenesis of polycation-induced alterations ("fusion") of glomerular epithelium. Lab Invest 1977;36(1):48–61.
[265] Sellin L, Huber TB, Gerke P, Quack I, Pavenstädt H, Walz G. NEPH1 defines a novel family of podocin interacting proteins. FASEB J 2003;17(1):115–7.
[266] Serra AL, Poster D, Kistler AD, Krauer F, Raina S, Young J, et al. Sirolimus and kidney growth in autosomal dominant polycystic kidney disease. N Engl J Med 2010;363(9):820–9.
[267] Shannon MB, Patton BL, Harvey SJ, Miner JH. A hypomorphic mutation in the mouse laminin alpha5 gene causes polycystic kidney disease. J Am Soc Nephrol 2006;17(7):1913–22.

[268] Shih NY, Li J, Cotran R, Mundel P, Miner JH, Shaw AS. CD2AP localizes to the slit diaphragm and binds to nephrin via a novel C-terminal domain. Am J Pathol 2001;159 (6):2303–8.
[269] Shih NY, Li J, Karpitskii V, Nguyen A, Dustin ML, Kanagawa O, et al. Congenital nephrotic syndrome in mice lacking CD2-associated protein. Science 1999;286(5438):312–5.
[270] Smeets B, Kuppe C, Sicking E-M, Fuss A, Jirak P, van Kuppevelt TH, et al. Parietal epithelial cells participate in the formation of sclerotic lesions in focal segmental glomerulosclerosis. J Am Soc Nephrol 2011;22(7):1262–74.
[271] Smith HW. The kidney. USA: Oxford University Press; 1951.
[272] Soriano P. Abnormal kidney development and hematological disorders in PDGF beta-receptor mutant mice. Genes Dev 1994;8(16):1888–96.
[273] St John PL, Abrahamson DR. Glomerular endothelial cells and podocytes jointly synthesize laminin-1 and -11 chains. Kidney Int 2001;60(3):1037–46.
[274] Steffes MW, Barbosa J, Basgen JM, Sutherland DE, Najarian JS, Mauer SM. Quantitative glomerular morphology of the normal human kidney. Lab Invest 1983;49(1):82–6.
[275] Sterk LMT, Geuijen CAW, van den Berg JG, Claessen N, Weening JJ, Sonnenberg A. Association of the tetraspanin CD151 with the laminin-binding integrins alpha3beta1, alpha6-beta1, alpha6beta4 and alpha7beta1 in cells in culture and *in vivo*. J Cell Sci 2002;115(Pt 6):1161–73.
[276] Sterzel RB, Hartner A, Schlotzer-Schrehardt U, Voit S, Hausknecht B, Doliana R, et al. Elastic fiber proteins in the glomerular mesangium *in vivo* and in cell culture. Kidney Int 2000;58(4):1588–602.
[277] Stow JL, Sawada H, Farquhar MG. Basement membrane heparan sulfate proteoglycans are concentrated in the laminae rarae and in podocytes of the rat renal glomerulus. Proc Natl Acad Sci USA 1985;82(10):3296–300.
[278] Suh JH, Jarad G, VanDeVoorde RG, Miner JH. Forced expression of laminin beta1 in podocytes prevents nephrotic syndrome in mice lacking laminin beta2, a model for Pierson syndrome. Proc Natl Acad Sci USA 2011;108(37):15348–53.
[279] Suri C, Jones PF, Patan S, Bartunkova S, Maisonpierre PC, Davis S, et al. Requisite role of angiopoietin-1, a ligand for the TIE2 receptor, during embryonic angiogenesis. Cell 1996;87 (7):1171–80.
[280] Tachibana K, Hirota S, Iizasa H, Yoshida H, Kawabata K, Kataoka Y, et al. The chemokine receptor CXCR4 is essential for vascularization of the gastrointestinal tract. Nature 1998;393(6685):591–4.
[281] Takabatake Y, Sugiyama T, Kohara H, Matsusaka T, Kurihara H, Koni PA, et al. The CXCL12 (SDF-1)/CXCR4 axis is essential for the development of renal vasculature. J Am Soc Nephrol 2009;20(8):1714–23.
[282] Takahashi T, Takahashi K, Gerety S, Wang H, Anderson DJ, Daniel TO. Temporally compartmentalized expression of ephrin-B2 during renal glomerular development. J Am Soc Nephrol 2001;12(12):2673–82.
[283] Takeda T, McQuistan T, Orlando RA, Farquhar MG. Loss of glomerular foot processes is associated with uncoupling of podocalyxin from the actin cytoskeleton. J Clin Invest 2001;108 (2):289–301.
[284] Takemoto M, He L, Norlin J, Patrakka J, Xiao Z, Petrova T, et al. Large-scale identification of genes implicated in kidney glomerulus development and function. EMBO J 2006;25(5): 1160–74.
[285] Teixeira V de PC, Blattner SM, Li M, Anders H-J, Cohen CD, Edenhofer I, et al. Functional consequences of integrin-linked kinase activation in podocyte damage. Kidney Int 2005;67(2):514–23.
[286] Tessari P, Cecchet D, Cosma A, Vettore M, Coracina A, Millioni R, et al. Nitric oxide synthesis is reduced in subjects with type 2 diabetes and nephropathy. Diabetes 2010;59(9): 2152–9.
[287] Tian D, Jacobo SMP, Billing D, Rozkalne A, Gage SD, Anagnostou T, et al. Antagonistic regulation of actin dynamics and cell motility by TRPC5 and TRPC6 channels. Sci Signal 2010;3(145):ra77.
[288] Trachtman H. Nitric oxide and glomerulonephritis. Semin Nephrol 2004;24(4):324–32.
[289] Tryggvason K, Wartiovaara J. Molecular basis of glomerular permselectivity. Curr Opin Nephrol Hypertens 2001;10 (4):543–9.
[290] Tryggvason K, Patrakka J, Wartiovaara J. Hereditary proteinuria syndromes and mechanisms of proteinuria. N Engl J Med 2006;354(13):1387–401.
[291] Utriainen A, Sormunen R, Kettunen M, Carvalhaes LS, Sajanti E, Eklund L, et al. Structurally altered basement membranes and hydrocephalus in a type XVIII collagen deficient mouse line. Hum Mol Genet 2004;13(18):2089–99.
[292] Venkatesha S, Toporsian M, Lam C, Hanai J-I, Mammoto T, Kim YM, et al. Soluble endoglin contributes to the pathogenesis of preeclampsia. Nat Med 2006;12(6):642–9.
[293] Vogelmann SU, Nelson WJ, Myers BD, Lemley KV. Urinary excretion of viable podocytes in health and renal disease. Am J Physiol Renal Physiol 2003;285(1):F40–8.
[294] Vollenbröker B, George B, Wolfgart M, Saleem MA, Pavenstädt H, Weide T. mTOR regulates expression of slit diaphragm proteins and cytoskeleton structure in podocytes. Am J Physiol Renal Physiol 2009;296(2):F418–26.
[295] Voskarides K, Damianou L, Neocleous V, Zouvani I, Christodoulidou S, Hadjiconstantinou V, et al. COL4A3/COL4A4 mutations producing focal segmental glomerulosclerosis and renal failure in thin basement membrane nephropathy. J Am Soc Nephrol 2007;18(11):3004–16.
[296] Völker LA, Petry M, Abdelsabour-Khalaf M, Schweizer H, Yusuf F, Busch T, et al. Comparative analysis of Neph gene expression in mouse and chicken development. Histochem Cell Biol 2012;137(3):355–66.
[297] Wada J, Makino H, Kanwar YS. Gene expression and identification of gene therapy targets in diabetic nephropathy. Kidney Int 2002;61(1 Suppl):S73–8.
[298] Wagner N, Wagner K-D, Xing Y, Scholz H, Schedl A. The major podocyte protein nephrin is transcriptionally activated by the Wilms' tumor suppressor WT1. J Am Soc Nephrol 2004;15(12):3044–51.
[299] Wang HU, Anderson DJ. Eph family transmembrane ligands can mediate repulsive guidance of trunk neural crest migration and motor axon outgrowth. Neuron 1997;18(3): 383–96.
[300] Waters AM, Wu MYJ, Onay T, Scutaru J, Liu J, Lobe CG, et al. Ectopic notch activation in developing podocytes causes glomerulosclerosis. J Am Soc Nephrol 2008;19(6):1139–57.
[301] Wei C, Hindi El S, Li J, Fornoni A, Goes N, Sageshima J, et al. Circulating urokinase receptor as a cause of focal segmental glomerulosclerosis. Nat Med 2011;17(8):952–60.
[302] Wei C, Möller CC, Altintas MM, Li J, Schwarz K, Zacchigna S, et al. Modification of kidney barrier function by the urokinase receptor. Nat Med 2008;14(1):55–63.
[303] Weins A, Schlondorff JS, Nakamura F, Denker BM, Hartwig JH, Stossel TP, et al. Disease-associated mutant alpha-actinin-4 reveals a mechanism for regulating its F-actin-binding affinity. Proc Natl Acad Sci USA 2007;104(41):16080–5.
[304] Welsh GI, Hale LJ, Eremina V, Jeansson M, Maezawa Y, Lennon R, et al. Insulin signaling to the glomerular podocyte is

critical for normal kidney function. Cell Metab 2010;12 (4):329–40.
[305] Wendel M, Knels L, Kummer W, Koch T. Distribution of endothelin receptor subtypes ETA and ETB in the rat kidney. J Histochem Cytochem 2006;54(11):1193–203.
[306] Winn MP, Conlon PJ, Lynn KL, Farrington MK, Creazzo T, Hawkins AF, et al. A mutation in the TRPC6 cation channel causes familial focal segmental glomerulosclerosis. Science 2005;308(5729):1801–4.
[307] Wnuk M, Hlushchuk R, Janot M, Tuffin G, Martiny-Baron G, Holzer P, et al. Podocyte EphB4 signaling helps recovery from glomerular injury. Kidney Int 2012;81(12):1212–25.
[308] Woolf AS. Angiopoietins: Vascular growth factors looking for roles in glomeruli. Curr Opin Nephrol Hypertens 2010;19 (1):20–5.
[309] Wu C, Dedhar S. Integrin-linked kinase (ILK) and its interactors: A new paradigm for the coupling of extracellular matrix to actin cytoskeleton and signaling complexes. J Cell Biol 2001;155(4):505–10.
[310] Yamagishi S-I, Matsui T. Nitric oxide, a janus-faced therapeutic target for diabetic microangiopathy: friend or foe? Pharmacol Res 2011;64(3):187–94.
[311] Yang Y, Jeanpierre C, Dressler GR, Lacoste M, Niaudet P, Gubler MC. WT1 and PAX-2 podocyte expression in Denys–Drash syndrome and isolated diffuse mesangial sclerosis. Am J Pathol 1999;154(1):181–92.
[312] Yang Y, Guo L, Blattner SM, Mundel P, Kretzler M, Wu C. Formation and phosphorylation of the PINCH-1-integrin linked kinase-alpha-parvin complex are important for regulation of renal glomerular podocyte adhesion, architecture, and survival. J Am Soc Nephrol 2005;16(7):1966–76.
[313] Yaoita E, Kurihara H, Yoshida Y, Inoue T, Matsuki A, Sakai T, et al. Role of Fat1 in cell–cell contact formation of podocytes in puromycin aminonucleoside nephrosis and neonatal kidney. Kidney Int 2005;68(2):542–51.
[314] Yauch RL, Kazarov AR, Desai B, Lee RT, Hemler ME. Direct extracellular contact between integrin alpha(3)beta(1) and TM4SF protein CD151. J Biol Chem 2000;275(13):9230–8.
[315] Ye M, Wysocki J, William J, Soler MJ, Cokic I, Batlle D. Glomerular localization and expression of Angiotensin-converting enzyme 2 and Angiotensin-converting enzyme: Implications for albuminuria in diabetes. J Am Soc Nephrol 2006;17(11):3067–75.
[316] Yu D, Petermann A, Kunter U, Rong S, Shankland SJ, Floege J. Urinary podocyte loss is a more specific marker of ongoing glomerular damage than proteinuria. J Am Soc Nephrol 2005;16(6):1733–41.
[317] Yu L, McPhee CK, Zheng L, Mardones GA, Rong Y, Peng J, et al. Termination of autophagy and reformation of lysosomes regulated by mTOR. Nature 2010;465(7300):942–6.
[318] Yuan HT, Suri C, Landon DN, Yancopoulos GD, Woolf AS. Angiopoietin-2 is a site-specific factor in differentiation of mouse renal vasculature. J Am Soc Nephrol 2000;11 (6):1055–66.
[319] Yuan HT, Suri C, Yancopoulos GD, Woolf AS. Expression of angiopoietin-1, angiopoietin-2, and the Tie-2 receptor tyrosine kinase during mouse kidney maturation. J Am Soc Nephrol 1999;10(8):1722–36.
[320] Yuan HT, Khankin EV, Karumanchi SA, Parikh SM. Angiopoietin 2 is a partial agonist/antagonist of Tie2 signaling in the endothelium. Mol Cell Biol 2009;29(8):2011–22.
[321] Zeng Z, Sarbassov DD, Samudio IJ, Yee KWL, Munsell MF, Ellen Jackson C, et al. Rapamycin derivatives reduce mTORC2 signaling and inhibit AKT activation in AML. Blood 2007;109 (8):3509–12.
[322] Zenker M, Aigner T, Wendler O, Tralau T, Müntefering H, Fenski R, et al. Human laminin beta2 deficiency causes congenital nephrosis with mesangial sclerosis and distinct eye abnormalities. Hum Mol Genet 2004;13(21):2625–32.
[323] Zent R, Yan X, Su Y, Hudson BG, Borza D-B, Moeckel GW. Glomerular injury is exacerbated in diabetic integrin alpha1-null mice. Kidney Int 2006;70(3):460–70.
[324] Zhao HJ, Wang S, Cheng H, Zhang M-Z, Takahashi T, Fogo AB, et al. Endothelial nitric oxide synthase deficiency produces accelerated nephropathy in diabetic mice. J Am Soc Nephrol 2006;17(10):2664–9.
[325] Zhu L, Jiang R, Aoudjit L, Jones N, Takano T. Activation of RhoA in podocytes induces focal segmental glomerulosclerosis. J Am Soc Nephrol 2011;22(9):1621–30.
[326] Zoncu R, Efeyan A, Sabatini DM. mTOR: from growth signal integration to cancer, diabetes and ageing. Nat Rev Mol Cell Biol 2011;12(1):21–35.

This page intentionally left blank

CHAPTER

23

Function of the Juxtaglomerular Apparatus: Control of Glomerular Hemodynamics and Renin Secretion

Jürgen B. Schnermann[1] *and Hayo Castrop*[2]

[1]National Institute of Diabetes, and Digestive and Kidney Diseases, National Institutes of Health, Bethesda, MD, USA
[2]Institute of Physiology, University of Regensburg, Germany

CELLULAR ELEMENTS OF THE JUXTAGLOMERULAR APPARATUS (JGA)

More than a century ago, Golgi observed that "the ascending limb of the loop of Henle returns with invariable constancy to its capsule of origin".[1] At this point of contact at the glomerular hilum, the afferent and efferent arterioles together with the adherent distal tubule form a wedge-shaped compartment which contains the three defining cell types of the juxtaglomerular apparatus (JGA) (Figure 23.1). The *macula densa* (MD) cells in the wall of the tubule abut on a cushion of closely packed interstitial cells called *Goormaghtigh* or lacis cells. These cells are indistinguishable in their fine structure from mesangial cells[2] and are also referred to as extraglomerular mesangial (EGM) cells. The third specialized cell type of the JGA is the *juxtaglomerular granular* (JG) cell, a modified smooth muscle cell in the media of the arteriolar wall.

The anatomical relationships in the vicinity of the JGA have been extensively studied, since they may reveal pathways for functional connections. The most extensive and regular contact of the MD cells is with the underlying extraglomerular mesangium.[3] Regions of adherence between the afferent arteriole and the thick ascending limb outside the MD, and between afferent arterioles and the distal and connecting tubule, have also been observed.[4–7] Less extensive and consistent contacts exist between the MD and efferent arterioles, although the efferent arteriole can be adjacent to the distal tubule and to the thick ascending limb, either immediately before or immediately after the MD.[2,8]

Macula Densa Cells

Morphology

The MD cells form an elliptical plaque of epithelial cells located at the distal end of the thick ascending limb, approximately 100 to 200 μm upstream from the transition to the distal convoluted tubule.[2,9] An MD plaque has been reported to consist of 14 cells in rat and about 25 cells in rabbit.[10,11] Cellular plasticity is suggested by the finding that this number increased by about 30% following chronic angiotensin II receptor blockade, probably by transdifferentiation of adjacent TAL cells.[11] MD cells are morphologically characterized by a high nucleus-to-cytoplasm ratio, absence of basal infoldings, and numerous mitochondria that are typically not in contact with the basal membrane.[2,12] The basement membrane is thinner than that found in other areas of the tubule, and shows discontinuities in scanning electron micrographs.[13] The difference in basement membrane appearance is paralleled by a macromolecular composition that differs from that of adjacent TAL cells.[14]

NaCl and Water Movement

Although morphologically distinct, MD cells and neighboring thick ascending limb (TAL) cells share similar NaCl transport mechanisms (Figure 23.2). As in TAL cells, NaCl uptake is mostly through the apical Na,K,2Cl co-transporter (NKCC2/BSC1). Conventional electrophysiology and patch-clamp evidence has established its presence functionally.[15–17] Presence of the NKCC2 co-transporter has also been shown at mRNA

Seldin and Giebisch's The Kidney, Fifth Edition.
DOI: http://dx.doi.org/10.1016/B978-0-12-381462-3.00023-9

© 2013 Elsevier Inc. All rights reserved.

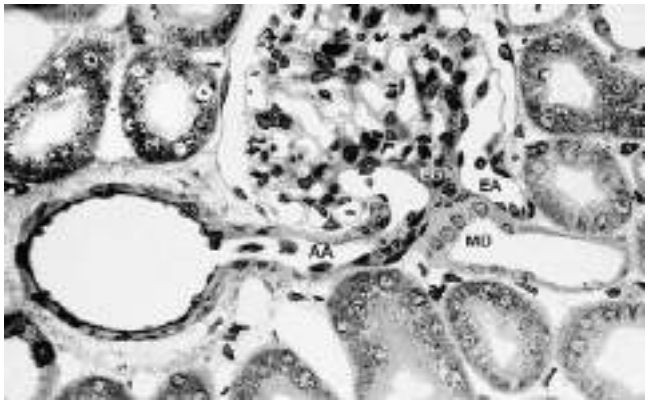

FIGURE 23.1 **Low power electron micrograph of the juxtaglomerular apparatus and surrounding cortical tissue** (mag. ×320) (AA: afferent arteriole; EA: efferent arteriole; MD: macula densa; EGM: extraglomerular mesangium). *(Courtesy of Brigitte Kaissling and Wilhelm Kriz.)*

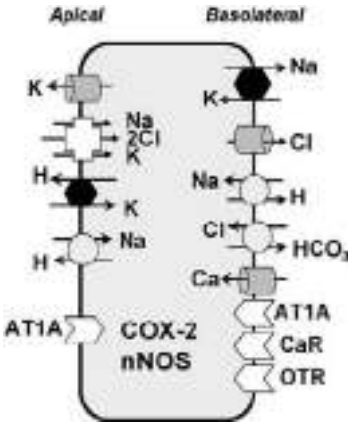

FIGURE 23.2 **Representation of transport proteins and receptors in apical and basolateral membranes of macula densa cells.** Experimental evidence comes from work in both rats and rabbits.

and protein expression levels.[18–20] Of the three full length isoforms of the co-transporter, both the A and the B types are expressed in the MD.[20–23] In contrast to TAL cells, in which NKCC2 phosphorylation is strongly enhanced by vasopressin, MD cells have a constitutively high presence of phospho-NKCC2 even in the complete absence of vasopressin.[24] From the rates of MD cell acidification by luminal ammonium it has been concluded that apical NKCC2-mediated flux rates are not markedly different from those in TAL cells.[25] Apical membranes of MD cells are rich in low conductance K channels of the ROMK type that are required for K recycling.[16,17,26–28] Na/H exchange through NHE2 provides a second pathway for a smaller fraction of Na uptake by MD cells.[29–32] In the rabbit, the apical membrane may also be a site of active Na extrusion, since the luminal presence of ouabain has been found to elevate intracellular Na concentration in both MD and TAL cells; in addition, luminal ouabain prevented the recovery of intracellular Na from the elevated levels resulting from increased luminal NaCl.[33] Apical Na efflux in MD cells may be mediated by a luminal H,K-ATPase, as colonic H,K-ATPase has been shown previously to mediate active Na efflux.[34] Its presence in MD cells is supported by immunocytochemical and functional evidence.[33,35]

Na,K-ATPase abundance and activity in the basolateral membrane of MD cells in rabbit kidneys appears to be low compared to neighboring TAL cells, a finding that is probably mainly due to the absence of basolateral membrane infoldings.[33,36,37] In the rat, basolateral membranes of MD cells identified by nNOS counterstaining clearly express α1 Na,K-ATPase, together with β1- and γ-subunits.[38–43] Cl exit across the basolateral membrane occurs through abundant Cl channels.[17,44] Immunocytochemical evidence indicates the presence of the AE2 anion exchanger in basolateral membranes of MD cells in both the rat and the mouse, and Cl/HCO_3 exchange activity has been observed in isolated rabbit JGA preparations.[45,46] Together with the apical Na/H exchanger, basolateral AE2 may play a role in the absorption of HCO_3 or it may act as a pHi-controlling housekeeping gene.

The effect of changes in luminal fluid composition on the volume of macula densa cells has remained a controversial issue. At constant luminal osmolarity of around 300 mOsm, changes in luminal NaCl concentration caused parallel changes in the volume of MD cells.[47–49] Changes in volume were to some extent transient, indicating some ability of MD cells for volume regulation.[49] Both increases and decreases in MD cell volume have been observed with concomitant increments in Na (25 to 135 mM) and osmolarity (210 to 300 mOsm).[10,47] When NaCl concentration was kept constant, MD cells behaved like osmometers, swelling with a reduction and shrinking with an increase in osmolarity.[49] Transcellular osmotic water permeability of MD cells, assessed from the initial cell volume change in response to an osmotic step change, was estimated to be similar to that of cortical collecting tubules in the absence of ADH.[50,51] The main restriction to water movement resides in the apical membrane.[50] Transmembrane channels for water movement have not been identified; apical membranes of MD cells lack aquaporin 1,[52] and the presence of other aquaporins has not been established. Vasopressin receptors of both the V1a and V2 varieties have been found in MD cells, but there is no evidence that MD water permeability is regulated.[24,53]

Other Cellular Characteristics

Nitric oxide synthase type I (NOS I or nNOS), a constitutive and Ca-dependent NOS isoform, is highly and

selectively expressed in MD cells, and has become a useful marker of this cell type.[54,55] Alternative splicing leads to the generation of several nNOS variants with NO synthase activity.[56] The presence of three of these variants, nNOSα, β, and γ in MD cells and their regulation by salt intake has recently been demonstrated.[57] Catalysis of the conversion of L-arginine to NO and L-citrulline by NOS requires the participation of a number of co-factors. One of these co-factors is NADPH, and it is possible that the relatively high activity of glucose-6-phosphate dehydrogenase (G6PDH) in MD cells is related to the NADPH requirement of NOS.[58] A functional connection between nNOS and G6PDH is suggested by the parallel upregulation of the expression of both enzymes during NaCl restriction.[58–60] Alternatively, the high pentose shunt activity suggested by the abundance of G6PDH may serve to provide ribose-5-phosphate for nucleic acid synthesis. Avid uptake of labeled uridine has been shown to occur in MD cells, a process inhibited by actinomycin D, and therefore indicative of incorporation of the pyrimidine precursor into the RNA pool.[61]

Cyclooxygenase-2 (COX-2), typically induced by LPS and cytokines in the inflammatory process, is constitutively expressed both in the renal medulla and to a lesser extent in the cortex.[62,63] Cortical expression of COX-2 in the mature rat and rabbit kidney is restricted to a subgroup of MD and perimacular cells of the TAL.[62,64–66] MD expression of COX-2 has also been observed in humans older than 60 years, and in patients with Bartter syndrome.[67,68] Condensation of COX-2 expression is the remnant of a more intense expression in early postnatal kidneys, where the enzyme can be found in a more contiguous pattern in TAL cells proximal and distal of the MD. At this early stage, COX-2 appears to be specifically excluded from MD cells.[69] Conversion of PGH_2 into the bioactive PGE_2 is catalyzed by prostaglandin E2 synthases, of which both a microsomal and cytosolic isoform have been described.[70] Immunocytochemical evidence has demonstrated the presence of a membrane-associated PGE_2 synthase in MD cells of both rats and rabbits.[71,72] Co-localization of COX-2 with phospholipase A2 has been described in the MD at the level of single cells.[66] Table 23.1 lists a number of other differences in the expression pattern of MD compared to surrounding TAL cells where the function has remained unclear.

TABLE 23.1 List of Proteins with an Expression Pattern that Differs between Macula Densa and Surrounding Tubular Cells

Macula Densa	Comments	Reference
Tamm-Horsfall protein	Neg, ideal negative selection marker	596
Epidermal growth factor	Neg, present in TAL and DCT	597
Hepcidin	Neg, present in TAL, apical	598
PKD2	Neg, present in TAL, mostly basolateral	599
TRPV4	Neg, present in TAL and DCT	600
Oxytocin receptors	Pos, not in TAL, mostly basolateral	601
Angiotensin II receptors	Pos, apical and basolateral	602
Benzodiazepine receptors	Pos, peripheral type receptors	603
Ca-sensing receptor	Pos, basolateral	604
PTHrP	Pos, microvessels, PCT and DCT	605
Stanniocalcin	Pos, also in TAL, DCT, and CD	606
Integrin-β6	Pos, fibronectin receptor	607
P2Y receptors	Pos, basolateral	608
WNK4	Pos also in TAL and DCT	609
P38 MAP Kinase	Pos more than other tubular segments	610
SGLT1	Pos also in cTAL	611
IQGAP1	Pos apical, also in DCT, less inTAL	612

Extraglomerular Mesangial (EGM) Cells

Morphology

The EGM cells (Goormaghtigh or lacis cells are synonyms) are the cells of the JGA which have the most intimate and regular contact with the MD.[3] MD cells and EGM cells are separated by an interstitial cleft of variable width that does not appear to be bridged by gap junctional connections. In three-dimensional reconstructions EGM cells are elongated cells with long cytoplasmic processes, which in general run parallel to the base of the MD cells.[73] Commensurate with extensive gap junctional coupling of EGM cells with each other as well as with mesangial cells and granular cells,[74,75] connexins 40, 37, and perhaps 43 or 45 are expressed to various degrees in extra- and intraglomerular mesangium.[76,77] The presence of myofilaments in EM cells suggests that EGM cells, like mesangial cells, have contractile potential.[78]

The extraglomerular mesangial cell field is free of capillaries, lymph terminals or nerve fibers. The absence of blood capillaries may cause a retardation of fluid entry and fluid removal from this compartment. In fact, the interstitial volume density of the EGM cell field increased from 17% during volume depletion to 29% during volume expansion, while no changes were

noted in the peritubular interstitium.[79] Nevertheless, recent studies of the flow dynamics across the JGA interstitium using lucifer yellow as a fluorescent marker indicate rapid exchange between afferent arterioles and tubular lumen, presumably mediated by bulk fluid flow.[80]

Biochemical and Functional Aspects

Localization studies using histochemical, autoradiographic or immunological methods usually do not distinguish between intra- and extraglomerular mesangial expression patterns. Nevertheless, in some cases it seems justified to assume parallel expression in both cell types. For example, autoradiographic localization of angiotensin II and atrial natriuretic factor binding suggests the presence of receptors on both intra- and extraglomerular mesangial cells.[81,82] Relative predominance of AT1 receptor mRNA in EGM cells has been observed by *in situ* hybridization.[83] While EGM cells normally do not synthesize renin, they can be recruited to form renin with long-standing stimulation such as chronic diuretic abuse.[7,84]

Differential expression patterns in intra- and extraglomerular mesangium are relatively discrete. EGM cells do not stain with antibodies against Thy-1, while the glomerular mesangium does.[85] Conversely, decay accelerating factor (DAF), a glycoprotein that limits complement activation on cell surfaces, is restricted to the EGM cells, at least in the human kidney.[86] HSP 25 expression has also been reported in extraglomerular, but not intraglomerular, mesangium.[87] Of unknown significance is the observation that two Na,K-ATPase-associated proteins, the FXYD protein phospholemman (FXYD1) and the β2-subunit, are expressed in the extraglomerular mesangium, while being excluded from both MD cells and intraglomerular mesangial cells.[43] Conventional mesangial cell cultures have been used as a model to study JGA-specific issues such as NO and PGE_2 production, but whether or not this approach permits inferences about the JGA signaling mechanisms *in vivo* has remained unclear.[88–90]

Granular Cells

Morphology

The granular cells in the arteriolar walls are the main renin-producing cells of the kidney. With a rough endoplasmic reticulum, a well-developed Golgi apparatus, and numerous cytoplasmic granules, they have the fine structure of protein-secreting cells.[2,78] The renin-containing granules are membrane-bound. Some granules, believed to be the more newly formed, have a crystalline lattice appearance and may mainly contain pro-renin; others, with an amorphous electron-dense content, are believed to represent the mature form.[7,91] Myofibrils and smooth muscle myosin are sparse, and may be even absent in granular cells at the vascular pole.[92] In the mature rat kidney under control conditions, granular cells are clustered at the vascular pole over a length of about 30 μm or about 20% of the afferent arteriole, but single ring-like renin-positive regions in more proximal locations are sometimes seen.[93] In the developing kidney, as well as during stimulation of renin synthesis, for example with converting enzyme blockade, renin-positive cells can be found all along the afferent arteriole and also in larger vessels.[94,95]

Coexistence of renin and angiotensin II in granules of rat and human epithelioid cells has been shown by light and electron microscopy.[96,97] Granular angiotensin II appears to increase in parallel to renin following adrenalectomy and renal artery stenosis.[97,98] Granular angiotensin II may reflect uptake through either nonspecific endocytosis, receptor internalization or intracellular *de novo* generation.[99,100] Not unexpectedly, granular cells contain AT1 receptor mRNA, with rats expressing both AT1A and AT1B receptor mRNA and mice expressing only AT1A receptor mRNA.[101,102] Granular cells express the mRNA for both D1-like and D2-like dopamine receptors mediating stimulation and inhibition of renin secretion.[103,104] The gap junctional connexins 40 and 37 have been shown to co-localize with renin, indicating functional connections among granular cells.[105–107] Other proteins found in JG cells include cyclic guanylate kinase II,[108] the ubiquitous basolateral form of the Na,2Cl,K co-transporter NKCC1/BSC2,[109] and GLUT4.[110]

Functional Aspects

Renin release has been found to be episodic or quantal, an observation most consistent with granule exocytosis.[111] Nevertheless, EM images rarely document the classic omega configuration with an open pore to the cell exterior,[7] and no evidence in support of the presence of vesicle or target membrane SNARE proteins in JG cells has been published. On the other hand, isoproterenol and cAMP caused an increase in membrane capacitance in isolated JG cells, an observation usually interpreted to be the result of an exocytotic membrane fusion event.[112] An attempt to observe exocytosis has been made in dissected glomerulus/vessel preparations using optical labeling of renin granules with quinacrine and LysoTracker-Red, fluorophores that are taken up into acidic organelles. When stimulated by isoproterenol or a low arteriolar pressure, labeled granules disappeared at a rate of about 5–10 granules per minute.[113] In renin-releasing As4.1 cells, the extinction of individual granules was followed by the appearance of an extracellular quinacrine cloud, presumably representing the released granule contents.[113]

Studies of the membrane characteristics of JG cells in the hydronephrotic mouse kidney by the whole cell patch-clamp technique have identified an inward rectifying K current whose inhibition was shown to be partly responsible for the depolarizing effect of angiotensin II.[114] In addition, JG cells expressed Ca-activated Cl channels in high density.[114] In contrast, inwardly rectifying K channels were not detected in isolated JG cells from rat kidneys.[115] Instead, Ca-dependent and voltage-gated large conductance K channels (BK_{Ca}) were identified that largely determined the resting potential of −32 mV.[115] Presence of BK_{Ca} channels was verified at the mRNA level by RT-PCR, and at the protein level by immunocytochemistry. The increased outward current caused by cAMP was also due to activation of BK_{Ca} channels, suggesting that they were of the cAMP-stimulated ZERO splice variant.[115] There is also evidence for the presence of K-ATP channels in JG cells, but their functional role is not clear.[116] While earlier studies failed to obtain functional evidence for the presence of voltage-dependent Ca channels,[117] the presence of L-type Ca channels and their activation by strong depolarizations has been established in isolated JG cells.[118] JG cells express NKCC1, the ubiquitous isoform of the Na,K,2Cl co-transporter, and its inhibition by furosemide stimulates renin exocytosis, as evidenced by increased membrane capacitance.[119]

MACULA DENSA CONTROL OF VASCULAR TONE

The Tubuloglomerular Feedback Loop

Effect of Distal Tubule Flow Perturbations on SNGFR

The tubuloglomerular feedback (TGF) response is defined as the change of *SNGFR* resulting from a change in tubular fluid flow exiting the proximal convoluted tubule, a practical experimental variable to predictably alter tubular fluid composition in the MD segment of the tubule.[120] The average reduction of *SNGFR* in superficial nephrons of rats caused by a saturating flow increase in 15 independent studies was 13 ±1 nl/min or 40 ±3%.[52] In addition to the rat, TGF responses were found in all mammalian species tested thus far (dog, hamster, mouse, humans), as well as in two non-mammalian species (*Amphiuma means* and *Necturus maculosus*).[52] Fitting *SNGFR* measurements at eight different loop perfusion rates to a four parameter logistic equation (Figures 23.3 and 23.4) revealed that TGF responses occur over a defined flow range and show nonlinear saturation kinetics.[121] $V_{½}$, the flow resulting in the half-maximum response, was 17.5 nl/min, a value close to the ambient end-proximal flow

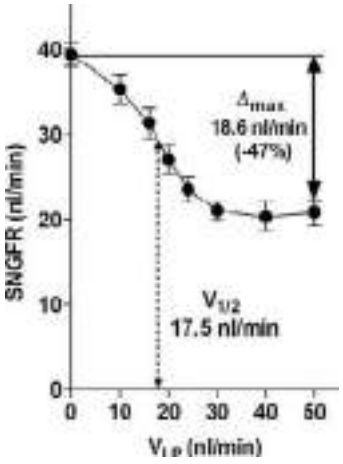

FIGURE 23.3 **Relationship between *SNGFR* and loop of Henle perfusion rate (V_{LP}).** The diagram shows mean values from 9 tubules in which *SNGFR* was determined at 8 different flow rates[121] (Δ_{max}: maximum reduction of *SNGFR*; $V_{½}$: perfusion rate causing half-maximal reduction of *SNGFR*).

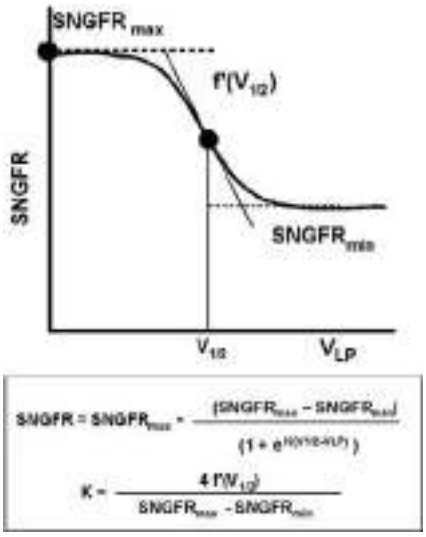

FIGURE 23.4 **Four parameter equation (logistic equation) used to describe the sigmoidal relationship between *SNGFR* and lat proximal flow rate (V_{LP}).** Parameters are $SNGFR_{max}$, $SNGFR_{min}$, $V_{½}$, the flow rate at which the response is half-maximum, and f′ $V_{½}$, the slope at the midpoint.[594]

rate in the rat (Figure 23.3). The precise location of the TGF operating point has been determined by adding or withdrawing small volumes of fluid from the proximal tubule and determining the resulting changes in proximal flow rate.[122] In these studies, small increases and decreases in loop flow rate were equally and maximally effective in altering *SNGFR*, an observation that directly demonstrates the position of the operating point at the midpoint of the feedback function curve.[122,123] Consistent with the conclusion of tonic suppression of GFR by TGF are observations showing

that *SNGFR* based on fluid collections in the proximal tubule where the TGF signal is eliminated is usually higher than *SNGFR* based on distal collections where the TGF signal is intact (Figure 23.5[52]). Systematically higher values of *SNGFR* of superficial nephrons determined in proximal compared to distal tubule segments have also been demonstrated in the dog and mouse.[124,125] TGF responses were also observed in juxtamedullary nephrons of both rats and hamsters, where increased flow past the MD by perfusion of thin ascending limbs produced a reduction in *SNGFR* by about 25 nl/min or approximately 50%.[126,127]

The vasoconstriction elicited by TGF at the level of the JGA may be partially offset by a tubular vasodilator effect that appears to be mediated by a tubulovascular contact area at the level of the connecting tubule.[128] This dilator mechanism, called cTGF, is activated by high Na concentrations and inhibited by amiloride or benzamil, suggesting that it is initiated by activation of ENaC-dependent Na transport.[128] Activation of cTGF seems to require relatively high flow rates, and may therefore play an important role only under special circumstances.[129] Nevertheless, the implications of these observations are potentially far-reaching for the interpretation of previous microperfusion studies, and for the understanding of the physiology of TGF regulation of GFR.

TGF Oscillations

In both rats and mice the operation of the TGF system in the closed-loop mode can result in stable oscillations of filtration pressure and filtration rate with a periodicity of 2–3 cycles/min (30–50 mHz).[125,134,135] Synchronous pressure oscillations were seen in efferent arteriolar blood flow, with blood flow leading tubular pressure by about a 1 second lag. This phase shift suggests that oscillations in blood flow were the cause of changes in tubular pressure.[130] Oscillations were principally of single nephron origin, since oscillations in random nephrons were not in phase.[131] However, synchronized pressures were observed in adjacent nephrons whose afferent arterioles originate from the same interlobular artery.[132,133] The simultaneous assessment of the oscillatory pattern of many nephrons on the surface of the kidney using the novel approach of laser speckle contrast imaging has shown that synchronized TGF oscillations can sometimes be observed among nephrons that are not located in the immediate vicinity of each other.[134] Pressure oscillations were abolished by loop diuretics, and they were absent in mice that lack TGF responses, suggesting that they were generated by the TGF system.[125,135] This contention was further supported by the finding that distal flow rate and Cl concentrations oscillate with the same frequency, but with a fixed phase shift.[136] Mathematical modeling of the TGF system indicates that oscillations are the result of a relatively high feedback gain, in combination with delays in the transmission of the signal across the JGA and along the nephron.[137,138]

In addition to the slow TGF-dependent oscillations, laser-Doppler velocimetry identified oscillations in star vessel blood flow with a frequency of about 100–200 mHz, probably reflecting myogenic vessel activity.[130] Since TGF and myogenic mechanisms are targeted to identical arteriolar smooth muscle cells, they are expected to interact and become synchronized. As an expression of the interaction, the power of the myogenic oscillations increased during inhibition of TGF, and decreased during TGF saturation.[130,139] In contrast to the synchronized oscillations of normal animals, irregular fluctuations of proximal tubular pressure have been observed in spontaneously hypertensive as well as Goldblatt hypertensive rats, but not in salt-sensitive Dahl rats with hypertension.[140–142] Mathematical modeling has shown that desynchronizations like those seen in the hypertensive models can result from parameter variations of the TGF system or from increases in interaction strength, particularly when nephrons are electrotonically coupled.[143,144] Oxygen tension on the renal surface has also been found to oscillate at the 30 mHz TGF frequency,

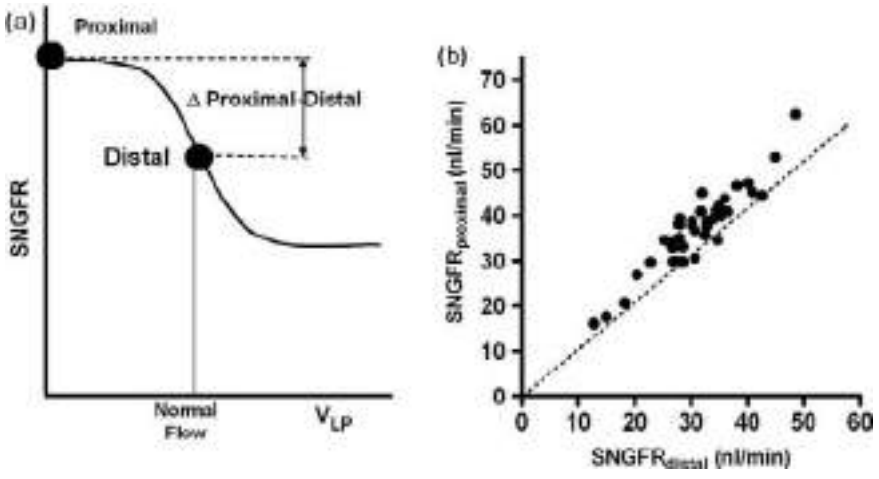

FIGURE 23.5 (a) Difference between *SNGFR* measured in the distal and in the proximal tubule (Δ proximal–distal); its magnitude is an index of the *SNGFR*-reducing effect of ambient flow rates past the macula densa. (b) Relationship between measurements of *SNGFR* in proximal and distal segments of the same nephron. Each point is the mean of an experimental series taken from the literature (for references see [52]). Proximal *SNGFR* exceeded distal *SNGFR* by an average of 6.0 ± 0.54 nl/min, suggesting TGF-dependent suppression of the GFR of superficial nephrons by about 16%

and it has been speculated that a switch of TAL cell energy production from aerobic to anaerobic metabolism may cause the instability in MD NaCl concentration that activates TGF oscillations.[145]

The Tubular Signal and the Sensing Mechanism

Effect of Loop of Henle Flow on MD NaCl Concentration

Although flow rate changes are frequently used to activate TGF, their mechanical consequences *per se* do not appear to be sufficient cause for vasomotor responses *in vivo*. Flow rate changes do not elicit TGF responses as long as they are not accompanied by changes in NaCl, and conversely, full TGF responses can be induced by low flows, as long as NaCl is supplied at sufficiently high concentrations.[120,146–148] Furthermore, widely varying TGF responses can be observed at identical flow rates.[148,149] However, in a recent study using the isolated perfused JGA preparation, changes in flow even in the absence of NaCl were observed to elicit vasoconstriction and increases of cytosolic calcium in vascular cells at the glomerular pole, an effect attributed to the consequences of mechanical deflection of the central cilium of MD cells.[150,151] The reasons for this major discrepancy between the *in vivo* and *in vitro* effects of flow are not known.

Nevertheless, extensive experimental evidence *in vivo* favors the notion that the MD cells respond to changes in luminal NaCl concentration, and that the flow dependency of TGF responses reflects flow dependence of luminal [NaCl] in the MD region of the nephron.[152] *In situ* microperfusion of loops of Henle has revealed a biphasic relationship between flow rate and distal [NaCl] measured 300–600 μm downstream from the MD, the earliest accessible site along the distal convoluted tubule.[120,153,154] The increase of distal solute concentrations at subnormal flow rates is the result of modifications of tubular fluid between the MD region and the distal tubule. NaCl influx along the early post-MD epithelium causes [NaCl] to increase over the levels existing at the MD, and the effect of this addition of NaCl is particularly evident at low flow rates.[153,155]

Effect of MD NaCl Concentration on SNGFR

The precise relationship between MD NaCl concentration and *SNGFR* was established by perfusing loops of Henle from their distal ends in a retrograde direction.[148] In this approach, the distance between perfusion and sensing sites is greatly shortened, the changes in perfusate composition by tubular transport activities are minimized, and the effects of perfusate composition on *SNGFR* can be studied at constant flow rate and pressure. At a flow rate of 20 nl/min, *SNGFR* varied inversely with changes in perfusate NaCl concentration between 15 and 60 mM (or 30 and 120 mOsm), values which extend over the hypotonic range normally occurring at the end of the thick ascending limb.[146,148,156] Increments in NaCl concentration above 60 mM did not further suppress filtration rate. Maximum changes of *SNGFR* caused by saturating flow rates during orthograde perfusion and by saturating NaCl concentrations during retrograde perfusion were identical. Fitting the equation of a hyperbolic tangent to these results (Figure 23.6) indicates that the half-maximum decrease in *SNGFR* is caused by a NaCl concentration of 33.5 mM, and that the maximum slope is about 0.5 nl/min mM.

Studies designed to discriminate between ionic or osmotic effects of the perfusion fluid indicate that total solute concentration at the MD does not seem to measurably participate in TGF-mediated reductions of *SNGFR*. Orthograde perfusion with isotonic mannitol solutions in the rat is usually not associated with sustained reductions in *SNGFR*, even though distal tubular fluid osmolality is greatly increased.[120,147,157] TGF responses correlating with alterations in osmolality have been observed during orthograde perfusion with various perfusion solutions, but the variations in distal osmolality were outside the critical osmolality range of 30 to 120 mOsm observed in retrograde perfusion studies.[158] In retrograde perfusion experiments in which fluid osmolality and NaCl concentration were varied independently, TGF responses were exclusively determined by NaCl concentration, and not by osmolality in a range between 130 and 400 mOsm.[149] Finally, the pattern of *SNGFR* responses during retrograde perfusion with isotonic solutions in which either Na or Cl was replaced, but in which osmolality was kept constant, indicates dependence on the ionic composition and independence of osmolality.[148,156]

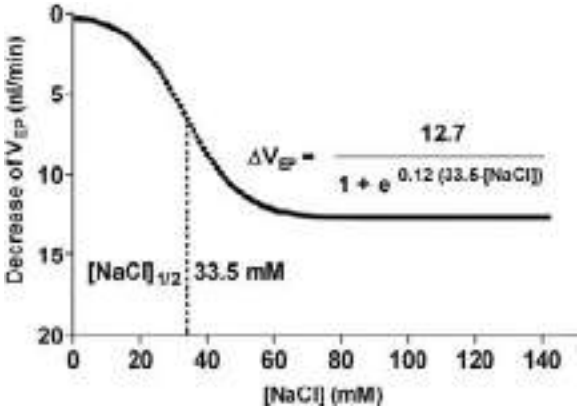

FIGURE 23.6 **Logistic equation describing the relationship between NaCl at the macula densa and early proximal flow rate (V_{EP}), a close correlate of *SNGFR*.** Changes in NaCl concentration at the macula densa were produced by retrograde microperfusion.[148] $[NaCl]_{1/2}$, NaCl concentration causing half-maximum reduction of V_{EP}.

TGF Response and NaCl Transport

EFFECTS OF LOOP DIURETICS

The observation that inhibition of NaCl transport along the loop of Henle is associated with blockade of the TGF mechanism has been of fundamental importance in understanding the initiation of the TGF signaling pathway.[159] TGF inhibition has been rather uniformly observed in the presence of loop diuretics such as furosemide, bumetanide, piretanide, ethacrynic acid, triflocin or l-ozolinone.[52] Concentrations causing half-maximal inhibition of transport and feedback appear to be similar, about 5×10^{-5} M for furosemide and about 10^{-6} M for bumetanide[160] (own unpublished data). Furosemide also blocked TGF responses during retrograde perfusion, suggesting that metabolic consequences of TAL inhibition are not transmitted by convective transport to the MD cells.[161,162] Since distal Na and Cl concentrations are greatly elevated during loop NaCl transport inhibition, TGF responses do not appear to be caused by luminal NaCl concentration changes *per se*, but by changes in cellular NaCl uptake mediated by the furosemide-inhibitable Na,K,2Cl co-transporter NKCC2. The concentration dependence of feedback responses is probably the result of concentration dependence of NaCl uptake. Studies in mice with selective deletions of the A or B isoform of NKCC2 indicate that NKCC2B mediates TGF in the low NaCl concentration range, while NKCC2A is required for responsiveness to higher NaCl concentrations.[22,163] Thus, the presence of two isoforms of NKCC2 in the macula densa extends the NaCl range over which TGF operates (Figure 23.7). The concept that TGF responses are generated by the successive activation of NKCC2B and NKCC2A is supported by expression studies in *Xenopus* oocytes that have shown a higher Cl affinity of NKCC2B than NKCC2A, 9 mM versus 45 mM.[21] Other aspects, such as the dependence of the inhibitory potency of furosemide on Cl concentration, have also been found to hold true for the TGF response.[162,164] Diuretic agents with primary actions outside the loop of Henle such as acetazolamide, chlorothiazide, and amiloride do not possess TGF-inhibitory properties.[159,165]

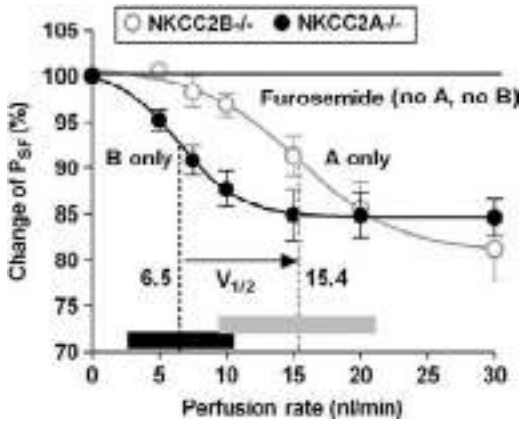

FIGURE 23.7 Relationship between loop of Henle perfusion rate and the relative reduction of P_{SF} (± SEM) in mice lacking NKCC2B (circles: (A) only) or NKCC2A (dots: (B) only). Dashed lines indicate the positions of $V_{1/2}$, the flow rates causing half-maximum reduction of P_{SF}; bars indicate the flow ranges over which 90% of the total responses occur. *(Data from .[22,163])*

EFFECT OF K CHANNEL BLOCKADE

Retrograde application of the K channel blocker U37883A caused an almost complete inhibition of TGF responses.[166] This effect is mediated by inhibition of ROMK type K channels, since TGF responses were largely absent in mice with targeted ROMK deletion,[167] a finding that has been confirmed in mice in which selective breeding of surviving animals has generated ROMK-deficient mice with less compromised kidney function and well-maintained blood pressure.[168,169] The observation that inhibition of NKCC2 and ROMK has similar effects on TGF responses argues against a specific "sensor" function of these transport proteins, and for a critical role of some consequence of MD NaCl transport. Since ambient distal K concentrations near the MD are close to the K affinity of the co-transporter, it is possible that variations in luminal K may in part regulate TGF response magnitude.[166] Nevertheless, the increase in distal K concentration accompanying acute hyperkalemia was associated with attenuation, not enhancement, of TGF responses.[170]

ION SUBSTITUTION STUDIES

That NaCl uptake by NKCC2 is the initial step in the feedback transmission pathway is further supported by parallels in the ionic requirements for both TGF- and NKCC2-mediated NaCl transport across TALH. During retrograde perfusion of the MD segment (Figure 23.8a), TGF responses were not seen during perfusion with isotonic or hypotonic solutions of Na salts such as $NaHCO_3$, $NaNO_3$, NaI, NaSCN, Na acetate, Na gluconate or Na isethionate.[148,156] In contrast, isotonic solutions of Cl salts (Figure 23.8b) accompanied by small monovalent cations such as K, Rb, Cs or NH_4 elicited full TGF responses, as did the bromide salts of Na and K[148]. It is to be noted that some of these small cations have been found to be substrates for either the Na or the K site on the NKCC2 co-transporter.[164,171]

The requirement for sizable Cl or Br concentrations, and the apparent lack of dependence on Na concentration, are consistent with an involvement of Na,K,2Cl co-transport, since the apparent overall affinity of NKCC2 for Cl in both TAL and MD cells is much lower than that for Na or K.[172,173] Thus, the relatively low Cl affinity would predictably create an apparent Cl dependency of transport, while the small amounts of Na or K entering

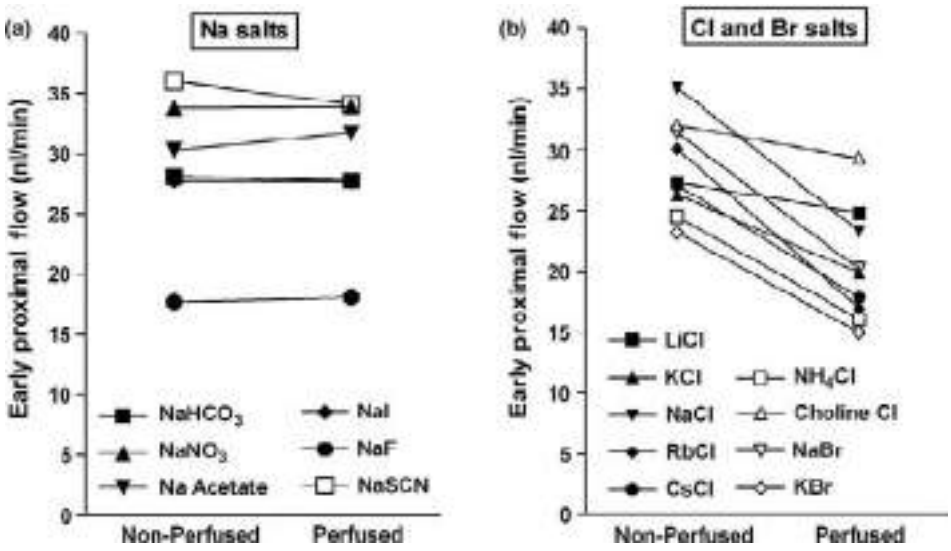

FIGURE 23.8 (a) Effect of Na salts with various anionic substitutions on the response of V_{EP} to retrograde perfusion of the macula densa segment. (b) Effect of Cl and Br salts with various cationic substitutions on the response of V_{EP} to retrograde perfusion of the macula densa segment. *(Data from ref. [148]).*

initially Na- or K-free solutions are sufficient to sustain near normal NKCC2 activity. When Na was replaced with large cations such as choline or TMA, TGF responses of normal magnitude were not seen, even though Cl was present in sufficiently high concentrations.[148,156] Considering the cationic selectivity of the paracellular shunt, replacing luminal Na for choline will result in a sizable lumen positive Na diffusion potential[172] that is predicted to reduce NaCl absorption by increasing Cl backflux. This explanation is consistent with the observation that NaCl transport rates of isolated TAL were found unaltered when studied under symmetric conditions with high choline Cl on both sides of the epithelium.[172] In this case, Na backdiffusion and voltage-dependent inhibition of NaCl absorption is not to be expected as long as low concentrations of Na and K are present.

ACTIVE NaCl TRANSPORT

Transport inhibition caused by metabolic inhibitors such as cyanide, antimycin A or uncouplers of oxidative phosphorylation has also been found to reduce TGF responsiveness.[159,174] TGF responses are not affected by peritubular application of ouabain, and this is probably related to the fact that the α1 Na,K-ATPase in rodents is rather insensitive to cardiac glycoside inhibition.[175] In fact, when α1 Na,K-ATPase was genetically engineered to become ouabain-sensitive, intravenous or luminal administration of the glycoside caused marked reductions of TGF responses.[176] The effect of luminal ouabain may not be related to H,K-ATPase inhibition, since TGF responses were unaltered in H,K-ATPase-deficient mice.[176] The striking effect of loop transport blockade suggests that NaCl uptake through the furosemide sensitive Na,K,2Cl co-transporter, and Na extrusion through an energy-dependent pathway are critical steps in generating feedback responses.

The Vascular Effector Mechanism

The vascular response to a change in perfusion of single loops of Henle occurs without alterations in systemic arterial pressure, renal sympathetic tone or in the resistance of larger renal vessels such as the cortical radial arteries (interlobular arteries). Therefore, the alteration in the hemodynamic determinants of filtration must be caused by a change in the contractile state of glomerular vascular elements. To determine the effect of TGF on glomerular arteriolar resistance, both the pressure fall and the rate of arteriolar blood flow have to be assessed while the perfusion in the loop of Henle of the same nephron is altered.

Pressure Gradients

GLOMERULAR CAPILLARY PRESSURE (P_{GC})

Direct measurements in superficial glomeruli of Munich-Wistar rats have shown that saturating flow increments cause a significant fall in P_{GC}, with fractional decreases ranging between 15 and 22%.[123,177–180] The slope of the P_{GC} change in the most sensitive flow range was 1.3 mmHg min/nl.[123] P_{GC} measured directly in an *in vitro* preparation of juxtamedullary nephrons also fell during TGF activation.[181] P_{GC} in nephrons without superficial glomeruli can be estimated from measurements of stop flow pressure (P_{SF}).[182] In response to a saturating increase in loop flow, mean P_{SF} of 23 studies fell by 22%, from 39.0 ± 0.8 to 30.3 ± 0.8 mmHg.[52] A reduction in P_{SF} was also observed in the dog when loop flow was increased from zero to normal and supranormal values.[183,184] In the mouse, TGF responses of P_{SF} are similar in magnitude as those seen in rats, but the sensitivity range is shifted to lower flows.[185] Since multiple determinations of P_{SF} can be made in the same nephron with small

perfusion flow increments, the nonlinear relationship between loop of Henle flow and P_{SF} was apparent long before a similar feedback function for *SNGFR* was defined.[186] In 15 experimental series, the maximum P_{SF} decrease averaged 7.9 ± 0.6 mmHg, with a mean $V_{1/2}$ of 20.1 ± 1.1 nl/min. The maximum sensitivity varied substantially between different studies, but in general was between 1 and 2 mmHg min/nl.[52] Two laboratories have reported that the TGF-induced change in P_{SF} was identical to the TGF-induced change in P_{GC}.[178,179]

The main uncertainty in the determination of feedback-induced changes in the glomerular arteriolar pressure drop results from the evidence that, at least in the rat, a portion of the preglomerular resistance resides in the cortical radial arteries rather than in the afferent arterioles.[187,188] As a consequence, afferent arteriolar resistance, calculated from the artery-to-glomerulus pressure difference, overestimates true afferent resistance, while the relative change caused by the TGF mechanism is underestimated. If preglomerular resistance is equally apportioned between interlobular artery and afferent arteriole, the TGF-induced resistance change along the afferent arteriole would be about 15% greater.

Glomerular Plasma Flow

Estimation of glomerular plasma flow (GPF) by micropuncture requires measurements of *SNGFR* and single nephron filtration fraction (SNFF), with SNFF being derived from the increase in protein concentration or hematocrit in collected samples of early postglomerular blood. Increasing loop perfusion rate reduced plasma flow entering the glomerulus by about 20%, a change accompanied by a fall in SNFF.[189,190] Laser-Doppler shift analysis showed that saturation of the TGF mechanism caused about a 40% reduction in efferent arteriolar blood flow, while TGF inhibition with furosemide increased blood flow by about 25%.[130] Supportive evidence for TGF-induced reductions in GPF came from the observation that glomerular blood flow, estimated from the change in the arrival of fluorescent particles in a single glomerular capillary,[191] fell by about 25–30% when loop flow was increased (M. Steinhausen and J. Schnermann, unpublished). A 30% reduction in afferent arteriolar blood flow was also seen in *Amphiuma* and *Necturus* kidneys when distal flow rate was increased.[192,193]

Effector Site

PREGLOMERULAR RESISTANCE

The micropuncture studies agree that increasing loop of Henle flow produces a 30–40% increase in preglomerular resistance.[189,190] TGF-induced reductions in afferent arteriolar diameter have been directly observed in the blood-perfused juxtamedullary nephron preparation, and in an isolated perfused tubule/vessel preparation.[181,194,195] TGF-induced resistance changes estimated from such diameter observations are consistently much larger than those measured with the micropuncture approach. As suggested above, the location of a sizable resistance along large intrarenal arteries would lead to an underestimation of the TGF-induced resistance change. It is also possible that in the small preglomerular arterioles resistance estimates may deviate from Poiseuille's law. Finally, cTGF, the vasodilator effect at the level of the connecting tubule, may blunt TGF *in vivo*, but would be absent in the perfused tubule.[128,196]

The ultimate cause for TGF-induced vasoconstriction is a rise in intracellular calcium that, at least to a large extent, is mediated by activation of voltage-dependent calcium channels. Depolarization of afferent arteriolar smooth muscle cells during TGF activation has recently been demonstrated using voltage-sensitive dyes.[197] A role for the resulting activation of L-type Ca channels in TGF is supported by the TGF inhibitory effects of intravenous or peritubular application of Ca channel blockers.[198–200] A decrease in protein kinase A activation may be an additional component of TGF-mediated vasoconstriction of the afferent arteriole, since Db-cAMP in the presence of 50 μM IBMX or the luminal application of forskolin, a stimulator of adenyl cyclase, significantly reduced the TGF response magnitude.[201,202]

Observation of the TGF response indicates that the afferent arteriole immediately adjacent to the glomerulum is the main direct target of the TGF mediator.[181] The glomerular entrance segment of the vessel is the part of the afferent arteriole in which agents affecting TGF response magnitude, such as adenosine and angiotensin II, exert their largest constrictor action.[203,204] TGF-induced local constriction may elicit a vascular conducted response that spreads to proximal portions of the arteriole by electrotonic coupling or myogenic excitation.[205,206] Spreading of contractile responses during local application of KCl has been observed in juxtamedullary nephrons, indicating electrotonic coupling of afferent arteriolar smooth muscle cells.[207] Upstream propagation of TGF-induced vasoconstriction is also responsible for the functional coupling of nephrons that are supplied by a common interlobular artery.[132,208,209] It is probable that conducted vasoconstriction relies on the presence of various connexins in endothelial and smooth muscle cells.[76,210] In view of the functional connection between afferent arteriolar smooth muscle cells, one may conclude that the total vasoconstrictor response to a NaCl step-change is composed of a local MD-generated effect and an upstream myogenic constrictor component.

POSTGLOMERULAR RESISTANCE

Evidence for a concomitant constriction of efferent arterioles during TGF activation has been obtained by micropuncture studies showing a reduction of GFR with unaltered glomerular capillary pressure, therefore suggesting proportional increases in the tone of afferent and efferent vessels.[179,190,211] Furthermore, an increase of flow within the low-to-ambient flow range is associated with a greater change of *SNGFR* than of P_{SF}, suggesting that either there was balanced afferent and efferent vasoconstriction, with the *SNGFR* fall being a consequence of the reduced plasma flow or that total resistance did not change and the *SNGFR* change was a consequence of a reduced K_f.[123,212] Direct observations of juxtamedullary efferent arterioles during TGF activation did not reveal any vasoactivity.[181] In contrast to these observations, luminal NaCl has been observed to dilate efferent vessels in the double-perfused nephron preparation of the rabbit, an effect that was prevented by antagonists of A2 adenosine receptors.[213] There is some experimental evidence in support of the possibility that a reduction in the filtration coefficient may contribute to TGF-induced reduction of GFR.[190]

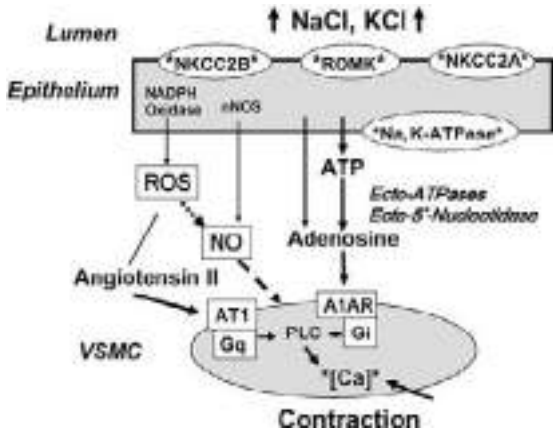

FIGURE 23.9 **Schematic summary of our current understanding of the pathway by which an increase in luminal NaCl at the macula densa causes activation of vascular smooth muscle cells (VSMC) in the afferent arteriole.** Some consequence of NaCl uptake is linked to the release of ATP, subsequent generation of adenosine, interaction with adenosine 1 receptors (A1AR), Gi-dependent activation of PLC, and increases in Ca by release from stores and opening of Ca channels. Angiotensin II is an important co-factor that augments the impact of A1AR activation. NO is a response-attenuating factor whose levels are to some extent modulated by reactive oxygen species (ROS).

Purinergic Mediation of the Vascular Response

As discussed in the previous sections, an increase in loop of Henle flow rate produces increases in NaCl concentration and NaCl transport at the MD, and this functional alteration elicits a vasoconstrictor response of the glomerular microvasculature, as well as a reduction in the rate of renin secretion. Propagation of the signal across the JGA interstitium and subsequent changes in vasomotor tone occurs through the transport-dependent generation and action of purinergic mediators (Figure 23.9).

ADENOSINE

Adenosine was originally proposed as a mediator of the TGF response, since it provided a conceptual link between the energy expended for NaCl transport and the generation of a vasoactive ATP metabolite.[214,215] Stimulation of Na transport in the proximal tubule is in fact associated with a decrease in cellular ATP, and increased NaCl secretion in the shark rectal gland causes a decrease in ATP, as well as an increase in adenosine release.[216,217]

The vasomotor action of adenosine in most organs and vascular beds consists of vasorelaxation that reflects the wide distribution of the two types of A2 adenosine receptors, A2aAR and A2bAR. Although the kidney is usually considered an exception to this rule,[218] several studies have shown that the steady-state response to an intravenous administration of adenosine is a clear reduction of renal vascular resistance, whereas the initial constrictor response is only short-lasting.[219] In contrast, persistent vasoconstriction of afferent arterioles by adenosine and A1 adenosine (A_1) analogs was observed in the hydronephrotic kidney and in isolated perfused afferent arterioles when adenosine receptors were activated from the interstitial aspect of the vessel.[203,220–222] The constrictor effect was absent in arterioles from A1 adenosine receptor (A1AR)-deficient mice.[203,223] Thus, adenosine causes a lasting vasoconstriction only when the nucleoside is generated in a restricted interstitial region so that A1AR can be accessed without general activation of the more dominant A2 receptors. Expression data, as well as functional observations, indicate that the terminal afferent arteriole is a vessel with high representation of A1AR.[222,224] A1AR-mediated vasoconstriction of afferent arterioles is initiated by Gi-dependent activation of phospholipase C, release of Ca from intracellular stores, and subsequent Ca entry through L-type Ca channels.[203,225,226] The A1AR-mediated vasoconstrictor effect of adenosine in afferent arterioles was stable for extended periods of time, indicating absence of rapid receptor desensitization.[203,225] Tubular administration of A1AR agonists augments the vasoconstrictor response to increased loop flow rates.[161,227] This effect does not appear to be mediated through apical A1AR, but rather to reflect a direct interaction with A1AR on afferent arterioles, and it thereby demonstrates the vasoconstrictor potency of A1AR activation and its effect on glomerular capillary pressure *in vivo*.[228]

Two laboratories have independently generated mouse strains with targeted deletion of A1AR, and both groups observed a complete absence of TGF responses in $A1AR^{-/-}$ animals using micropuncture measurements of stop flow pressure or single nephron GFR (Figure 23.10).[229,230] Furthermore, specific A1AR antagonists such as 8-cyclopentyl-1,3-dipropylxanthine (DPCPX) or PSB-36 inhibit TGF responses when added to either the tubular lumen or the peritubular blood.[228,231] A similar effect has been seen earlier with non-specific blockers such as theophylline or 3-isobutyl-1-methylxanthine, IBMX.[161,201,214,232] Addition of the nonxanthine A_1 receptor antagonist FK838 to the perfusate or bath also eliminated TGF responses in an isolated tubule preparation.[233] There is evidence that adenosine generated during TGF activation may also interact with A2 adenosine receptors, but the site of action is unclear. Enhanced TGF responses have been observed during A2AR blockade, suggesting that activation of A2AR tonically diminishes A1AR-mediated vasoconstriction of afferent arterioles, perhaps through the release of nitric oxide.[231,234] On the other hand, adenosine is able to vasodilate preconstricted efferent arterioles through A2AR, and A2AR inhibition has been found to block TGF-mediated vasodilatation of efferent arterioles in the isolated perfused JGA preparation.[213,235] The latter findings are difficult to reconcile with the absence of *in vivo* evidence for a reduction of efferent arteriolar resistance during TGF activation.

ATP

The preponderance of current evidence indicates that extracellular ATP serves as the major source for the generation of adenosine in the JG interstitium. Strong support for this notion is furnished by the demonstration that basolateral membranes of MD cells appear to have an ATP release pathway that is modulated by changes in luminal NaCl. Release of ATP by MD cells is suggested by the observation that PC12 or mesangial cells placed near the basolateral MD cell membrane responded to changes in luminal NaCl over the 20−60 mM range with an increase in cytosolic calcium.[236,237] This Ca response of the biosensor cells reflects P2 receptor activation, since it was inhibited by suramin.[236,237] Patch-clamp studies in cell-attached and excised patches of the basolateral membrane of MD cells showed the presence of an anion channel of 380 pS whose activity was dependent on the presence of extracellular NaCl, and that was active in the presence of ATP as the only anion.[236,237] Channel activity was blocked by gadolinium, but not by the Cl channel inhibitors DPC or NPPB.[236] The molecular nature of this large conductance anion channel has not been identified, but it may be identical to a functionally described maxi-anion channel that is widely expressed throughout the body.[238] Release of ATP across connexin hemichannels would be another possibility, but the evidence for the presence of connexins in the basolateral membrane of MD cells is weak.[76,239]

It is likely that ATP released into the JGA interstitium serves as substrate for membrane-bound ecto-ATPases and nucleotidases, ultimately resulting in the formation of the vascular mediator adenosine. In fact, TGF responses have been found to be greatly reduced in mice with deletion of NTPDase1/CD39, the major renal ecto-ATPase that dephosphorylates both ATP and ADP to AMP.[240] Furthermore, evidence has been obtained suggesting that adenosine formation by

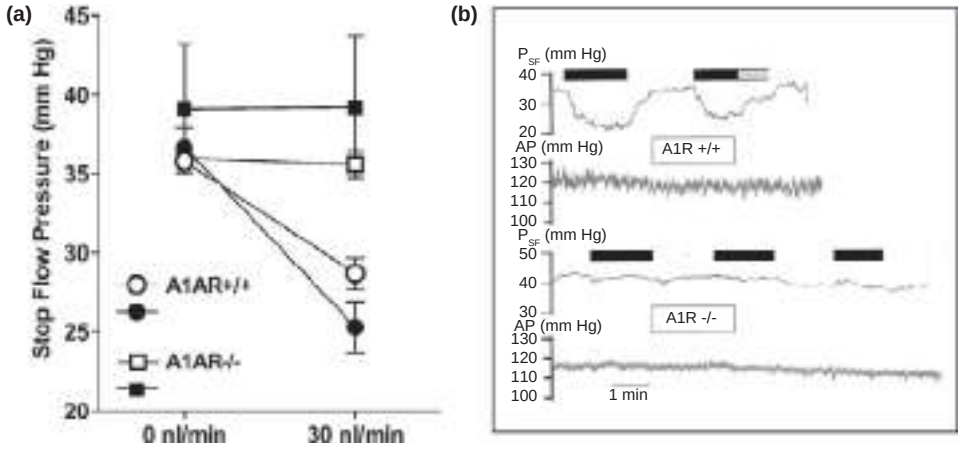

FIGURE 23.10 (a) Mean responses of stop flow pressure to an increase in loop of Henle perfusion rate from 0 to 30 nl/min in wild-type ($A1AR^{+/+}$) and in adenosine 1 receptor-deficient mice ($A1AR^{-/-}$). Gene targeting and phenotypic studies were performed by two independent groups of investigators (Closed symbols: data from [229]; Open symbols: data from [230]). (b) Recordings of stop-flow pressure (P_{SF}) and arterial blood pressure (AP) in a wild-type mouse ($A1R^{+/+}$) and in an adenosine 1 receptor-deficient mouse ($A1R^{-/-}$). During periods indicated by black bars, loop of Henle perfusion rate was increased to activate the TGF mechanism. Note absence of perfusion-related changes of P_{SF} in the nephron of the A1 receptor-deficient animal.

e-5′NT/CD73 may be critical in the generation of adenosine during the TGF response. Blocking adenosine formation with the e-5′NT-inhibitor α,β-methylene adenosine 5′-diphosphate (MADP) significantly reduced the compensatory TGF efficiency and the slope of the TGF relationship.[241] When the level of TGF activation was fixed by saturating concentrations of CHA, TGF efficiency was further reduced, and retrograde administration of MADP in combination with CHA caused vasoconstriction and abolition of TGF response.[241] Consistent with these data are observations in mice with targeted deletion of e-5′NT/CD73 in which TGF responses were found to be markedly compromised.[242,243] Finally, in the double-perfused JGA preparation, bath addition of the ecto-ATPase apyrase enhanced, and MADP abolished, TGF responses, suggesting that extracellular generation of adenosine from ATP is critical for JGA signaling.[244] Exogenous e-5′NT was also found to improve the defective TGF component of renal autoregulation in Thy-1 nephritic rats.[245] Dephosphorylation of ATP and AMP is likely to occur through enzymes anchored to the surface of mesangial cells.[246,247] Whether adenosine levels in the JG interstitium are regulated by adenosine release across equilibrative nucleoside transporters (ENT) is unclear, since evidence based on the effect of ENT inhibitors such as dipyridamole or dilazep on TGF responses is inconclusive.[214,248,249]

As an alternative to a role of ATP as precursor for adenosine, it has been proposed that ATP may directly elicit TGF responses, most likely through activation of P2 receptors on extraglomerular mesangial cells and gap junctional transmission of the resulting increase of cytosolic Ca to the afferent arteriole.[150,236,250,251] ATP may also directly activate arteriolar P2 receptors, with P2X1 receptors being the most likely receptor subtype since its presence in afferent arterioles has been well-documented.[252] In fact, ATP causes rapid and reversible constriction of afferent arterioles, an effect that may be more pronounced in juxtamedullary than superficial nephrons.[222,250] A similar effect is seen with the P2X receptor-specific ligand α,ß-methylene ATP, suggesting mediation of vasoconstriction by P2X purinoceptors.[250] Nevertheless, unequivocal evidence in support of a P2 receptor-mediated action of ATP in TGF *in vivo* is not available. TGF responses in superficial nephrons of P2X1 knockout mice were not statistically distinguishable from wild-type animals.[169] Likewise, TGF responses were not significantly affected by the infusion of the broad-spectrum inhibitors of P2 receptors PPADS or suramin, although these agents clearly diminished the blood pressure response to the P2 agonist α,ß-methylene ATP.[253] Results from the double-perfused JGA preparation are controversial. In an earlier study on rabbit tissue, suramin had been without effect on the response of afferent arteriolar diameter to an increase of luminal NaCl.[244] Since acceleration of ATP breakdown enhanced, and inhibition of 5′-ecto nucleotidase and of A1 adenosine receptors blocked, the arteriolar diameter response, these results were consistent with the ATP dephosphorylation/adenosine paradigm.[233,244] However, in similar preparations from rabbit or mouse, suramin was recently found to abolish afferent arteriolar Ca and constrictor responses, while the A1AR antagonist DPCPX was without effect.[150,151] The reasons for this divergence are presently unclear, but it is to be noted that a novel approach was used in at least part of the latter study, in that only the macula densa cells of the perfused nephron were maintained, while all thick ascending limb cells were removed by microdissection.[151] While it is conceivable that the presence of thick ascending limb cells is required for the "conventional" TGF response that is flow-independent, NaCl-dependent, and affects vascular tone through A1AR activation, the possibility of technical reasons for the obvious discrepancies cannot be excluded.

LINK BETWEEN NaCl TRANSPORT AND TGF

Exactly how an increase of NaCl transport by MD cells is coupled to the release of ATP or the subsequent activation of the purinergic signaling pathway is one of the major open questions in TGF physiology. Cell swelling is a very common cause for eliciting ATP release, and this mechanism may be the critical factor for linking NaCl transport to ATP egress in MD cells. Nevertheless, as discussed above, the relationship between the compositional changes associated with elevated loop flow rates and MD cell volume is not entirely clear. ATP release could also be related to any of the changes caused by stimulation of NaCl transport acrosss apical or basal membranes of MD cells. NKCC2 activation is followed by increases in cytosolic Na and Cl concentrations, increases in cytosolic pH, and membrane depolarization.[16,30,33,173,254] MD depolarization by about 30 mV following an increase of luminal [NaCl] to 150 mM occurs over the 20−60 mM range, and it therefore parallels the TGF response curve.[255] Depolarization may be directly involved in TGF responses, since the cation ionophore nystatin elicited afferent arteriolar vasoconstriction in the presence of low luminal NaCl and furosemide.[256] TGF responses were also seen when MD cells were depolarized by luminal application of the K ionophore valinomycin, together with 50 mM KCl. The valinomycin-induced vascular response was not affected by the Cl channel inhibitor NPPB (5-nitro-2-(3-phenylpropylamino) benzoic acid), whereas the normal NaCl-induced response was fully blocked by NPPB.[256] Thus, it appears that TGF responses depend upon MD cell depolarization

independent of the specific mechanism underlying the PD change, but evidence is needed to establish that the depolarization by valinomycin or nystatin is restricted to MD cells, and does not affect arteriolar smooth muscle cells.

MD cell depolarization may be linked to TGF responsiveness through its effect on MD cytosolic calcium $[Ca]_i$. Transport-induced changes in MD $[Ca]_i$ have been suggested to play a specific role in coupling the luminal electrolyte signal to the vascular response.[257] The Ca ionophore A 23187 in the presence of luminal Ca enhanced TGF responsiveness, whereas blocking Ca release from intracellular stores with 8-(N,N-diethyl-amino)-octyl-3,4,5-trimethoxybenzoate (TMB 8) and chelation of Ca with BAPTA-AM diminished it.[257–259] Ca entry may occur through a voltage-activated and nifedipine-sensitive Ca channel in the basolateral membrane,[260] but increased flux across a 20 pS non-selective cation channel with finite Ca permeability reduced Ca extrusion by Na/Ca exchange, and utilization of a conductive Ca entry pathway across the apical cell membrane is an alternative possibility.[259,261,262] Despite the evidence supporting an important role of $[Ca]_i$ it is far from certain that the $[Ca]_i$ changes occurring in response to fluctuations of luminal NaCl between 20 and 60 mM *in vivo* are large and consistent enough to establish a systematic and causal association between MD $[Ca]_i$ and the TGF response. In fact, the relationship between luminal NaCl and MD cytosolic calcium has been described as positive,[260] negative[49] or entirely absent,[150] perhaps indicating that the changes of $[Ca]^i$ in MD cells may be too small to be safely distinguishable from experimental noise in this technically demanding experimental approach.

A novel role for MD cell depolarization may be activation of NADPH oxidase and generation of superoxide that may directly or by scavenging NO enhance TGF.[263] An increase in NaCl delivery to the MD in the isolated perfused JGA preparation caused about a three-fold increase in superoxide production that was largely inhibited by tempol or apocynin.[264,265] Activation of NADPH oxidase appears to be the direct result of depolarization, since depolarization with valinomycin increased superoxide production and the hyperpolarization following furosemide-induced inhibition of NaCl uptake reduced it.[265] The enhanced activity of the NOX2 isoform of NADPHase oxidase following membrane depolarization may be associated with translocation of the small GTP-binding protein Rac to the plasma membrane.[266–268]

Integrated Function of the TGF Mechanism

The JGA control system is constructed as a negative, homeostatic feedback loop. The physiological purpose of this regulatory loop has been the subject of a substantial body of investigation using both experimental approaches and mathematical modeling. One potential effect of the operation of the TGF feedback loop is to reduce fluctuations of NaCl concentration at the MD, thus reducing the variability in the delivery of NaCl into the relatively low-capacity transport system of the distal nephron. Another role hypothesized for the TGF loop is in the autoregulatory adjustments in vascular resistance that promote constancy of GFR when arterial pressure changes.

The two hypothesized roles, regulation of distal salt delivery and control of GFR, are functionally interrelated; the feedback loop may contribute to stabilization of NaCl excretion, rendering it relatively independent of fast and irregular fluctuations in perturbing forces that are not the expression of an adaptation to a change in body Na balance. Such variations are represented, for example, by the marked fluctuations in blood pressure that have been observed to occur throughout the day and with changing body activities.[269] In the absence of tight control of vascular resistance, glomerular capillary pressure, and hence GFR, would be expected to fluctuate in parallel with blood pressure, causing changes in Na excretion unrelated to the NaCl status of the organism. Since, however, changes in GFR will in general be followed by parallel changes in distal NaCl concentration, the TGF system can dampen the amplitude of the predicted GFR changes. Similar rapid hemodynamic adjustments will occur with other acute perturbations of MD NaCl concentration resulting from variations in cardiac output, renal blood flow or proximal tubular transport. As discussed below, the TGF mechanism changes its response characteristics when perturbations of MD NaCl concentration are sustained for extended periods of time.[270] The homeostatic efficiency of TGF in the regulation of distal salt delivery and *SNGFR* is greatest in the vicinity of the operating point where fractional compensations of small input perturbations may be between 0.6 and 0.75, corresponding to an open loop gain of around 3.[122,271]

Participation of TGF in autoregulation

Acute changes in mean arterial pressure induce adjustments in renal vascular resistance which stabilize renal blood flow and glomerular filtration rate over a wide range of pressures. Pressure-induced resistance changes in the kidney have been proposed to be TGF-mediated.[272,273] A role of TGF in steady-state autoregulation was first supported by the observation in both dogs and rats that interruption of the TGF loop in single nephrons causes *SNGFR* and P_{SF} to vary directly with arterial pressure.[124,184,274–279] Pressure dependency of *SNGFR* was noted regardless of whether the TGF loop was physically disrupted by injecting an oil

block, blocked acutely by adding furosemide to the perfusate[274] or inhibited by chronic treatment with DOCA and a high salt diet.[274] In contrast, arterial pressure had little effect on GFR when the TGF loop was intact.[124,274–278] In the *in vitro* perfused juxtamedullary nephron preparation, interference with the TGF mechanism by furosemide or physical interruption of the feedback loop markedly diminished autoregulatory diameter alterations of afferent arterioles,[195,280,281] and constancy of afferent arteriolar blood flow was no longer maintained.[281]

There is equally solid evidence for the existence of TGF-independent autoregulatory resistance changes. Glomerular arterioles in kidney tissue transplanted to the cheek pouch of the hamster showed marked autoregulation of vessel diameters.[282] In the hydronephrotic kidney model which does not possess an operating TGF system, a decrease in arterial pressure increased vessel diameters along the entire preglomerular vasculature, except for the portion of the afferent arteriole near the glomerulus.[283] Isolated afferent arterioles and interlobular arteries of the rabbit maintained their diameter when luminal pressure increased,[284,285] while perfused afferent arterioles from the mouse showed an 11% diameter reduction with a doubling of perfusion pressure from 40–80 mmHg accompanied by a linear increase in wall tension.[286] The nature of the TGF-independent regulator is unclear, but an intrinsic myogenic mechanism responding to wall tension or mechanical stress is the most likely possibility.

Existence of at least two regulators is further supported by studies in which the dynamic response of renal blood flow to random fluctuations of blood pressure has been analyzed. Frequency domain analysis of renal blood flow using linear techniques revealed the presence of a regulator with a frequency response compatible with the TGF mechanism, about 0.01 Hz, and a faster mechanism with a frequency characteristic consistent with myogenic vasomotion, about 0.1 Hz.[287–289] Since the TGF system is nonlinear, it is important that a similar conclusion has been reached from the more recent application of nonlinear system analysis.[290–292] The existence of two regulators with similar frequencies has also been established in spontaneously hypertensive and Dahl rats.[293–295] There is evidence for the operation of two regulating mechanisms in conscious dogs and mice.[296,297] Interference with the slow component was observed in a number of experimental models of TGF interruption, including A1AR-deficient mice, ureteral obstruction, converting enzyme inhibition, and the perfused hydronephrotic kidney.[294,298–300] Temporal resolution of the adjustment of renal vascular resistance to step-changes in renal arterial pressure is consistent with the sequential operation of several mechanisms with different response times.[301–303] Various approaches and analyses have concluded that the quantitative contribution of TGF to autoregulation may be between 30 and 60%.[181,274,275,278,281,302] In addition to the TGF and myogenic components, evidence for the presence of a third mechanism with a slow response time has been obtained that may be of particular importance at low perfusion pressures.[302,303] Furthermore, an afferent arteriolar constrictor mechanism has been identified that responds to the systolic pressure peaks rather than to mean arterial pressure, and therefore must possess a response time in the frequency of the heart rate.[304,305] This mechanism is thought to protect the glomerular vasculature against the high pressures exerted during systole.

Interaction between the two autoregulatory mechanisms may lead to amplification of vascular responses. Models of autoregulation suggest that a TGF-dependent vasoconstriction can induce a myogenic response in upstream vascular regions and amplify the resistance increase.[206,306,307] In fact, mathematical modeling suggests that a myogenic contribution from proximal vascular segments is necessary for distal mechanisms such as TGF to contribute to resistance regulation.[308] Spatial separation between the two regulatory mechanisms along the afferent arteriole has been noted, with TGF being most effective in the region of the afferent arteriole close to the glomerulus, and the myogenic component being more pronounced in more proximal portions of the afferent arteriole.[195] Interactions between the myogenic response and TGF have been demonstrated at both the single nephron and the whole kidney level,[290,309] and they have been the subject of extensive mathematical modeling.[292,310,311] One of the conclusions is that elimination of a variable TGF signal enhances myogenic responsiveness.[301,309,310,312] Recent evidence indicates that the restraining effect of TGF on the myogenic mechanism is mediated by nitric oxide.[313,314] Functional coupling of small ensembles of nephrons by ascending myogenic or conducted vascular responses adds to the complexity of regulation of preglomerular vascular tone.[132,209] Enhanced nephron-to-nephron coupling has been suggested to be responsible for the more efficient dynamic autoregulation in spontaneously hypertensive rats.[133,207,293]

Role of TGF in Response to Transport Alterations

HYPERTONIC NaCl

Administration of hypertonic NaCl causes vasodilatation in most vascular beds, but in the kidney it results in an anomalous vasoconstriction.[315] This response may be a whole kidney equivalent of the response of *SNGFR* to increased loop flow rate. Both TGF- and NaCl-induced vasoconstriction are enhanced by salt

depletion[316,317] and inhibited by furosemide, theophylline or DOCA-salt treatment.[159,232,318–320] Furthermore, hypertonic non-chloride containing solutions usually do not produce vasoconstriction.[317] A micropuncture study in the rat revealed that an infusion of hypertonic NaCl reduced proximal tubular fluid absorption and increased loop flow rate, and that *SNGFR* fell as a result of these changes.[321]

PROTEIN FEEDING

The vasodilatation caused by acute and chronic protein feeding may include a TGF-dependent component. In conscious dogs, furosemide and ethacrynic acid blocked the acute rise in GFR following a meat meal, suggesting that the postprandial vasodilatation may be TGF-dependent.[322] It has been proposed that the rise in filtered amino acids causes an increase in proximal Na and fluid absorption, and a decrease in MD Na delivery.[322]

Chronic consumption of a high-protein diet induced a rightward resetting in the feedback curve of normal and Goldblatt hypertensive rats, so that higher flows were necessary to suppress GFR than in control or low-protein fed animals.[323,324] In normotensive animals the response amplitude and the slope of the feedback function were unaltered.[324] These effects appear to be due to alterations in transport along the loop of Henle, since NaCl concentrations in distal tubular fluid during loop perfusion were 30% lower in rats on a high-protein diet than in rats on a low-protein diet.[325] Consistent with this notion is the observation that TGF responses were the same in the two groups of rats when loops of Henle were perfused in a retrograde fashion, indicating that functional changes in the loop of Henle rather than at the level of the JGA were responsible for the protein-induced changes in TGF characteristics. The increased rate of NaCl transport along the loop of Henle caused by high-protein feeding may result from structural adaptations.[326]

INHIBITION OF PROXIMAL TRANSPORT

Diuretics that inhibit predominantly proximal tubular fluid absorption may cause a TGF-dependent decrease in GFR as a result of increased distal NaCl delivery. In support of this hypothesis, several studies using carbonic anhydrase inhibitors, as well as chlorothiazide, suggest that these agents cause *SNGFR* to fall more with the TGF loop intact than with the TGF loop interrupted.[165,211,327] In view of the Cl dependency of TGF, however, the acute TGF activation by carbonic anhydrase inhibition is unexpected since these drugs, while causing an increase of early distal [Na], do not elevate distal Cl concentrations.[165,327] There is no evidence to show that HCO_3 can substitute for Cl in initiating TGF responses. In fact, recent studies have shown that the effect of benzolamide to reduce GFR and RBF was maintained in $A1AR^{-/-}$ mice which are unable to generate a TGF response.[328] Thus, the mechanism of the renal vasoconstriction caused by CA inhibitors is not entirely clear, but a rise in tubular pressure may be an important contributor.[329,330] In addition, studies in rats and mice indicate that major increases in urine flow, including those caused by furosemide, may lead to increases in total renal vascular resistance even when participation of TGF is *a priori* unlikely.[331,332]

SNGFR of mice with targeted deletion of AQP1 was found to be significantly reduced compared to wild-type when it was determined in distal nephron segments with the TGF pathway intact.[333] The fall in GFR was dependent upon distal fluid delivery, since it was not observed when *SNGFR* was measured in the proximal tubule with the TGF loop interrupted.[333] Mice deficient in both AQP1 and A1AR which combine a proximal transport defect with absent TGF responsiveness, have been found to have a normal distal *SNGFR*, supporting the notion that the fall of GFR in $AQP1^{-/-}$ mice is TGF-mediated.[334]

Very similar results were obtained in mice with a knockout mutation in the apical Na/H exchanger NHE3, another model of established proximal tubular NaCl and fluid malabsorption.[335] Considering that distal flow rates were not different between wild-type and AQP1 or NHE3 knockout mice, it seems unlikely that TGF activation is due to an increased NaCl concentration at the MD. Resetting of the TGF function curve (discussed below) subsequent to extracellular volume depletion seems to be more likely as causation for enhanced TGF engagement.

Adaptation of TGF Response Characteristics

EXTRACELLULAR FLUID VOLUME

Adaptations in the TGF function occur whenever MD NaCl concentrations deviate from normal for an extended period of time. Typically, such deviations result from alterations in body Na content, with volume expansion associated with persistently increased, and volume depletion associated with decreased, MD NaCl concentrations. Formally, two types of adaptation in the TGF relationship can be distinguished. TGF *resetting* refers to a shift in the range over which the system is operating, either a shift to the right, to higher flows or concentrations or a shift to the left, to lower flows or concentrations. A change in TGF response *sensitivity* refers to an altered response, either altered slope and/or maximum response magnitude. By and large, volume depletion is associated with a left shift and an increase in response magnitude, and volume expansion with the opposite, but the actual adaptation observed has varied with the protocol used.

A number of studies have established that acute expansion of the extracellular space by infusion of isotonic saline or plasma reduces the TGF response magnitude and slope, and increases $V_{½}$ in both superficial and juxtamedullary nephrons.[127,336–341] Impaired TGF responses have been observed during chronic volume expansion caused by the administration of DOCA together with isotonic saline as drinking fluid.[274,320,342] The combination of a right shift and a reduced response magnitude is not invariant. Short-term volume expansion by a bolus injection of dilute rat plasma shifted the responsive range to higher flows, although this protocol produced an increase rather than a decrease in the maximum response magnitude[343]; *SNGFR* at zero loop flow rose 60%, whereas kidney GFR and free flow *SNGFR* rose only moderately with the position of the operating point and a large proximal–distal *SNGFR* difference indicating that the suppressing effect of the TGF mechanism was greater than normal. Thus, in these studies, the TGF mechanism appeared to counteract TGF-independent vasodilator influences on the renal vasculature. These data are consistent with closed-loop studies in which acute volume expansion with plasma did not reduce the maximum homeostatic efficiency, but shifted it away from ambient flows to lower flows, enhancing its dilatory and reducing its constrictor potency.[122]

The effects of an acute decrease of ECV have been studied in rats after acute hypotensive hemorrhage,[344,345] and in dehydrated rats.[346] In general, these interventions are accompanied by an increase in TGF response magnitude. Hypotensive hemorrhage induced a shift of the feedback curve to the left.[344,345,347] Since proximal absorption increased at the same time, the operating point tended to move toward the shoulder of the reset feedback function.[344] Thus, in this circumstance, the resetting results in reduced dilatory and enhanced constrictor capacity.

Studies have been performed to determine the time course of TGF adaptation. When single nephrons were perfused for extended periods of time, resetting developed over the initial 30–40 minutes of hyperperfusion, whereas changes in response magnitude were slower, requiring 40–60 minutes.[270] Similarly, acute volume depletion by furosemide restored TGF responses in chronically volume-expanded rats within 60–120 minutes.[342]

Other Conditions Associated with TGF Adaptation

URETERAL AND NEPHRON OBSTRUCTION

In the first few hours following complete unilateral ureteral obstruction (UUO), TGF reactivity appears to be completely abolished.[348–350] Elimination of the restraining effect of TGF is reflected by increased renal and glomerular plasma flows and elevated glomerular capillary pressures.[351] After persistence of ureteral obstruction for 24 hours, TGF activity is restored and possibly slightly enhanced, as indicated by a reduced $V_{½}$.[350,352] Augmentation of TGF responses in hydronephrotic kidneys appears to be caused by increased superoxide formation and NO deficiency, since nNOS blockade was without effect and tempol administration normalized TGF responsiveness in hydronephrotic animals.[353,354] The dominant effect of prolonged ureteral obstruction is a marked reduction of glomerular capillary pressure and glomerular plasma flow, changes which result in a dramatic reduction of GFR.[349,355] The apparent absence of a luminal signal suggests that vasoconstriction is not equivalent to the standard TGF response discussed so far. On the other hand, obstruction of a single nephron for 4 hours also causes marked vasoconstriction, indicating that persistent interruption of distal delivery produces a local constrictor signal of unknown nature.[356–358]

Following release of short-lasting ureteral obstruction TGF reactivity is increased,[349] and it is maintained in its somewhat activated state after release of an obstruction of 24 hours duration.[350,352] It is possible that the activated TGF mechanism is in part responsible for the continued vasoconstriction following release of both ureteral and single nephron obstruction.[352] However, additional mechanisms appear to contribute to the reduction in filtration after release of obstruction, since *SNGFR* at zero flow increased only slightly above distal values.[352] Furthermore, nephron and kidney filtration rates were also markedly suppressed after release of bilateral ureteral obstruction, even though in this experimental condition TGF responses were blunted rather than enhanced.[350,352]

During partial unilateral ureteral obstruction for 3–6 weeks, TGF reactivity appears to be in the normal range.[359,360] During volume expansion, on the other hand, TGF reactivity increased in the hydronephrotic kidney whereas it was strongly inhibited in the nonobstructed contralateral kidney.[359] The enhanced TGF reactivity seen in hydronephrotic kidneys during volume expansion could be prevented by thromboxane synthase inhibition.[360] A similar paradoxical enhancement of TGF reactivity by volume expansion was less pronounced during chronic bilateral ureteral obstruction.[361]

LOSS OF RENAL MASS

In the first hours following unilateral nephrectomy, TGF responses in the residual kidney may be enhanced and ambient distal flows may exert a GFR-depressing effect as judged from an increase in the proximal–distal *SNGFR* difference, without a change in the proximal value.[362] However, at later time points

uninephrectomy or 5/6 ablation has been shown to shift the TGF function to the right, with[363] or without increasing the maximum response.[364,365] A similar response to nephrectomy was noted in transplanted kidneys.[364] On the other hand, a striking variability in *SNGFR* responses to loop of Henle perfusion was noted in rats with subtotal nephrectomy, in which the average TGF response was zero. Unexpectedly, AT1 blockade restored TGF responses for reasons that are not clear.[366] To the extent that the most striking change is a TGF-independent increase in GFR (Y-intercept of the TGF function or proximal *SNGFR*) these results are reminiscent of the findings during growth-related increases in renal weight, and suggest an adaptation of the TGF function curve to a primary increase in GFR.[121,367]

HYPERGLYCEMIA

Moderate hyperglycemia produced by either acute glucose infusion[368] or streptozotocin-induced diabetes mellitus[369] reduced the amplitude of the TGF response and shifted $V_{1/2}$ to higher flow rates.[368] Type 2 diabetic rats of the OLETF strain have significantly diminished TGF responses accompanied by reduced autoregulatory efficiency even in the pre-diabetic stage.[370] Reduced TGF responses have also been observed in the Akita mouse model of type 1 diabetes mellitus, as well as in hydrated db/db mice, a model of type 2 diabetes.[371,372] This reduced capacity to compensate for experimentally-induced perturbations was also demonstrable under closed-loop conditions.[373] The reduction in the TGF response magnitude may in part be caused by a reduction in NaCl concentration, and the presence of glucose in tubular perfusion fluid.[368,374,375]

It has been suggested that the hyperfiltration of early diabetes is caused by TGF, as a result of excessive salt reabsorption in nephron segments upstream from the MD and the resulting reduction in MD NaCl concentration.[376,377] This hypothesis is supported by the demonstration that tubular transport proximal to the macula densa is in fact enhanced in diabetic animals.[378,375] Structural adaptations participate in tubular hyper-reabsorption; inhibition of the enzyme ornithine decarboxylase blocked the renal hypertrophy in a rat model of diabetes mellitus,[379] and attenuated both the enhanced proximal reabsorption and the increase in GFR.[378] On the other hand, it has been argued that TGF may actually prevent excessive hyperfiltration in diabetes.[380] A protective action of TGF is supported by the finding that diabetic mice of the Akita strain display an exaggerated hyperfiltration when TGF is rendered inoperative by A1AR deletion.[371] Hyperfiltration in alloxan-diabetic mice deficient in A1AR also suggests that TGF is not the primary cause of hyperfiltration in this diabetic model.[381]

Both in streptozotocin-treated rats and in diabetic humans, a paradoxical relationship between salt intake and GFR or renal plasma flow has been observed, with high salt intake producing a decrease instead of the expected rise of GFR,[375,382] an effect which was absent when kidney growth was suppressed by inhibition of ornithine decarboxylase.[383] These observations are consistent with the notion that the TGF adaptation during changes in extracellular fluid volume may be defective in diabetic animals. Whereas TGF desensitization normally prevents a non-homeostatic reduction of GFR during volume expansion, absent or incomplete resetting of TGF in diabetes appears to permit persistent GFR deviations. Altered resetting in diabetic animals could be a consequence of abnormal RAS activation or dysregulation of NO generation, factors thought to be involved in TGF adaptation.[372,384,385] Nevertheless, the paradoxical low salt-induced increase and high salt-induced decrease of GFR has not been found in all studies of diabetic patients and animals.[386–388] Differences in the dietary background, aside from NaCl content, may be an important modifying factor.[389]

RENAL SYMPATHETIC NERVE ACTIVITY

Whereas some experiments did not detect an effect of acute denervation or renal nerve stimulation on the TGF function curve in normotensive animals,[390,391] other studies have reported that denervation causes a time-dependent resetting of TGF to higher values of $V_{1/2}$ without changes in the maximum response.[392] Changes in TGF function persisted for at least one week, and were associated with increased GFR and Na excretion.[393]

Mechanisms of TGF Adaptation

RENIN–ANGIOTENSIN SYSTEM

The local activity of the renin–angiotensin system appears to be the most consistent determinant of TGF sensitivity. Converting enzyme inhibitors or angiotensin-receptor blockers in relatively high doses cause a reduction of the TGF response magnitude by about 50–60%.[394–398] An essentially complete inhibition of TGF responsiveness was seen in mice with a null mutation in the AT1A receptor, the major renal receptor for angiotensin I[185]. Similarly, TGF responses were essentially absent in ACE knockout mice, an effect that was in part reversible with infusion of subpressor doses of angiotensin II.[399] Studies in mice with deletion of tissue ACE or with selective expression of ACE in either blood vessels or proximal tubules suggest that the angiotensin II that is required for full TGF responsiveness is derived both from the action of membrane-associated ACE in endothelial cells, and from systemic

ACE,[400] while exclusive expression of ACE in proximal tubules is unable to sustain normal TGF responses.[401] This conclusion is consistent with earlier observations that angiotensin infusion partly restored feedback responsiveness during captopril-induced TGF inhibition.[402,403] Intravenous or peritubular infusion of angiotensin II enhanced TGF responses in untreated control rats, a property not shared by other vasoconstrictors such as vasopressin and norepinephrine.[404,212] Conversely, the arteriolar constrictor response to angiotensin II was greater during simultaneous TGF activation in both the isolated afferent arteriole/MD double-perfusion approach, and in the blood-perfused juxtamedullary nephron preparation.[405,406] Since local adenosine levels are thought to increase during TGF activation, this augmentation is possibly due to the effect of adenosine in preventing angiotensin II desensitization.[407] In accordance with the role of TGF in autoregulation, angiotensin II has been noted to enhance the TGF component of dynamic autoregulation.[408–410] The suppression of TGF responsiveness caused by acute volume expansion could be fully overcome by the infusion of angiotensin II at doses that restored normal plasma angiotensin II levels.[341] Taken together, these results indicate that an AT1A receptor-mediated effect of angiotensin II is a required constituent of the TGF pathway. The requirement for angiotensin II may result from the well-described synergistic interaction between the vascular effects of angiotensin II and of the TGF mediator adenosine.[223,226,411–413] The mechanism of this interaction has been suggested to result from an intracellular action of adenosine that enhances the calcium sensitivity of myosin light chain phosphorylation or prevents desensitization of angiotensin II receptors.[407,414] Contributing factors may be upregulation of MD NaCl transport by angiotensin II or enhanced production of feedback-enhancing superoxide radicals.[266,415]

The TGF-modifying effect of angiotensin II gains special importance in view of the fact that changes in NaCl in the tubular fluid in the MD region not only affect vascular tone, but also regulate renin secretion (see below). This dual effect of MD NaCl has the potential to automatically adjust TGF sensitivity to the NaCl status of the organism. When the combined external forces determining GFR and proximal and loop of Henle absorption cause deflections in MD NaCl concentration which exceed the range over which TGF operates effectively, persistent changes in MD NaCl occur which will cause an inverse change in renin secretion. The change in angiotensin II concentration resulting from the altered rate of renin secretion, in turn, is predicted to alter TGF sensitivity. For example, an increase in MD NaCl resulting from extracellular volume expansion will decrease renin secretion, and the decrease of angiotensin II concentration expected to gradually develop is then predicted to uncouple GFR from MD control.

EICOSANOIDS

The presence of both isoforms of cyclooxygenase (COX) in the juxtaglomerular region raises the possibility of a participation of prostaglandins in JGA cell-to-cell signaling. COX-1 is expressed in mesangial cells and in endothelial cells of afferent arterioles,[416] whereas COX-2 activity has been demonstrated in epithelial cells of thick ascending limb and MD.[417] Maximum TGF responses have been found to be inhibited by the intravenous or luminal application of high concentrations of non-specific COX inhibitors, as well as specific inhibitors of both COX-2 and COX-1.[418–422] The conclusion that the net effect of PGs on TGF is enhanced vasoconstriction is supported by the finding that arachidonic acid elicits a constrictor rather than a dilator response when administered by retrograde luminal infusion.[423] Thromboxane (TP) is a vasoconstrictor prostaglandin that has been implicated in TGF on the basis of the finding that the intravenous administration of inhibitors of TP receptors or of TP synthesis reduced the magnitude of the TGF-induced vasoconstrictor response.[360,398,422] TP receptor blockade also interfered with the TGF reducing effects of COX-2 and COX-1 inhibitors, indicating that these effects were TP-dependent.[418] Conversely, activation of TP receptors by U-46,619 or by the isoprostane 8-isoprostaglandin F2α enhanced TGF responses,[424] and COX-1 generated prostaglandins, presumably TP, may contribute to the TGF-enhancing effects of angiotensin II.[425] Low levels of glomerular thromboxane synthase may limit thromboxane formation under basal and low-salt conditions[426,427]; in fact, attenuation of TGF responses by systemic or luminal application of blockers of TP receptors or of TP synthesis has not been found in all laboratories,[360,398,422,423] and normal TGF responses have been observed in TP receptor knockout mice.[428] Administration of a high-salt diet, on the other hand, caused a 20-fold increase of thromboxane synthase expression, as well as a stimulation of TP receptor levels.[426,429] These observations provide an explanation for the finding that the TGF response in the presence of the TP mimetic U-46,619 is augmented in high-salt fed animals.[426] TP receptor activation may also contribute to the exaggerated TGF responses observed in young spontaneously hypertensive rats (SHR).[430] In contrast to these conclusions, studies in the blood-perfused juxtamedullary nephron preparation indicate that TGF activation is accompanied by nNOS-dependent enhancement of COX-2 activity and subsequent generation of vasodilatory PG metabolites which counteract TGF-mediated vasoconstriction.[431]

There is some evidence that 20-hydroxyeicosatetraenoic acid (20-HETE), an arachidonic acid metabolite endogenously generated in afferent arterioles by the 4A family of cytochrome P450 enzymes, may be involved in the TGF response.[432] Two inhibitors of cytochrome P450 enzymes, 17-octadecynoic acid (ODYA) and clotrimazole, caused a marked attenuation of the TGF response when added to the luminal perfusate for an extended period of time, and this inhibition could be overcome by the administration of exogenous 20-HETE.[433] The presence of the mRNAs for cytochrome P450 4A2, 4A3, and 4A8 has recently been demonstrated by RT-PCR in glomeruli and most segments of the tubule, while preglomerular arterioles appear to express only the 4A2 isoform.[434] Immunocytochemistry with a polyclonal non-specific P450 4A antibody showed cortical presence of P450 4A protein in proximal tubules, thick ascending limbs, glomeruli, and preglomerular arterioles.[434] Exactly how locally formed 20-HETE affects the TGF pathway is unclear. In addition to its vasoconstrictor properties, 20-HETE has been shown to inhibit TAL NaCl transport by blocking Na,K,2Cl co-transport, Na,K-ATPase, and by closing K channels.[435] This combination of effects should result in a powerful inhibition of NaCl transport in thick ascending limb and presumably MD cells, so that increments in 20-HETE production would be expected to attenuate, not enhance, TGF responses. It is conceivable, therefore, that ODYA and clotrimazole inhibit the TGF response in a non-specific way by causing a reduction in baseline afferent arteriolar tone.[436] It is also possible that 20-HETE acts as an intracellular second messenger for the TGF-mediating agent.[432,437]

NITRIC OXIDE

Luminal application of non-specific and nNOS-selective inhibitors of NO synthases has been shown to enhance MD-mediated vasoconstrictor responses both *in vivo* and *in vitro*.[55,438–441] These findings demonstrate tonic attenuation of TGF responsiveness by NO generated by nNOS in MD cells, an effect that is cGMP-dependent.[442] TGF responses of stop flow pressure *in situ* and afferent arteriolar diameter reductions *in vitro* in response to elevated MD [NaCl] were similar in nNOS-deficient and wild-type mice,[443,444] but the specific mutation in these mice does not exclude the possibility of maintained expression of β and γ splice variants of nNOS.[57] Nevertheless, the proximal–distal *SNGFR* difference was significantly higher in the $nNOS^{-/-}$ animals, and luminal administration of a non-specific NOS inhibitor (NLA 10^{-3} M) caused an augmentation of TGF responses only in wild-type, but not in nNOS knockout, mice.[444] Luminal and systemic administration of NOS inhibitors reversed the attenuation of TGF responses caused by an acute saline infusion, suggesting that NO contributes to the TGF resetting caused by volume expansion.[445]

NO may affect TGF by altering the function of MD cells. In the isolated double-perfused JGA preparation, inhibition of soluble guanylate cyclase or cGMP-dependent protein kinase mimicked the TGF-potentiating effect of a nNOS inhibitor when administered from the tubular side, whereas there was no effect when inhibitors were added to the vascular perfusate.[446] The cGMP-dependent mechanism may be inhibition of NaCl uptake, since inhibition of Cl fluxes by NO is mediated by soluble guanylate cyclase in TAL cells.[447] Formation of NO may occur in MD cells, but a contribution of NO produced by eNOS in TAL cells appears to also affect MD cell function.[448]

The relationship between luminal NaCl concentration and NO formation in MD cells has been addressed by using the NO-binding agents DAF-AM DA and DAF-AM. Two independent studies agree that an increase in luminal NaCl causes an increase in fluorescence in MD cells, as well as in their surroundings, and that this increase was prevented by an inhibitor of nNOS.[48,449,450] Since the concentration steps causing increased NO formation were between 35 and 135 mM in one study and between 60 and 150 mM in the other, it has been concluded that supraphysiological NaCl changes are necessary to stimulate NOS.[449] That the stimulation of nNOS activity by high luminal NaCl is Ca-dependent is unlikely, since NaCl does not consistently elevate $[Ca]_i$, and since an activation of NOS was seen in Ca-free medium.[48] Another explanation for the increased formation of NO is based on the fact that the pH optimum of NOS is in the slightly alkaline range.[451] Since an increase in luminal NaCl caused cell alkanization, it is conceivable that pH-dependent disinhibition of nNOS is responsible for the enhanced NO generation.[30] This notion is supported by the observation that dimethyl amiloride increased TGF responses, and that an nNOS-specific inhibitor in the presence of the NHE blocker did not further enhance the TGF reaction.[450,452] Furthermore, amiloride as well as 7-nitroindazole blunted the increase in NO formation caused by elevated luminal NaCl.[450] Stimulation of NO formation by high-luminal NaCl is consistent with the earlier observations that the effect of NOS blockade on TGF-dependent vasoconstriction is greater at high than at low flows.[453] Increases in luminal flow rate also stimulate NO formation by TAL cells, but in contrast to MD cells stimulation is strictly shear stress-dependent, and independent of NaCl transport.[454,455] NaCl independence is difficult to reconcile with direct NO measurements performed with carbon fiber electrodes in the distal tubule which have shown an increase in the amount of NO and in NO concentration during perfusion of loops of

Henle with furosemide, suggesting that transport inhibition along the entire loop of Henle stimulates emission and downstream convection of NO.[456] These results seem consistent with observations in an MD cell line showing increased NO generation during exposure to low chloride or furosemide.[457]

In the absence of hemoglobin, the biological half-life of NO in relation to the diffusion distance across the JGA would seem long enough to permit a direct interaction of NO released by MD cells with smooth muscle cells of the afferent arterioles. Nevertheless, NO inactivation may be an important modulator of the effect of NO on TGF. Reactive oxygen species have been identified as a factor that can markedly reduce bioactive NO levels. MD cells express NADPH oxidase isoforms NOX2 and NOX4, together with the required constituents of the active enzyme complex p47phox, p67phox, p22phox, and Rac.[268,458] A high-luminal NaCl appears to activate NADPH oxidase, and this activation is pH-dependent since blocking Na/H exchange with dimethyl amiloride or acidification of the luminal perfusate diminished superoxide production.[459] Production of the NO scavenger may limit the impact of NO that is stimulated in MD cells at the same time by the same mechanism. The membrane-permeant superoxide dismutase mimetic tempol can diminish TGF responses *in vivo* and in the perfused JGA preparation, but this effect is usually not very pronounced under control conditions.[263,354,460,461] Since tempol had no effect in the presence of a NOS inhibitor, it appears that any effect is due to an increase in NO bioavailability.[263,460] In spontaneously hypertensive rats (SHR) the expression of NADPH oxidase subunits is elevated, and the TGF-inhibiting effect of tempol is enhanced compared to normotensive controls, suggesting increased oxidative stress in SHR and reduced bioavailability of NO.[458,461] This observation is in accordance with the earlier finding that inhibition of nNOS did not enhance TGF responses in SHR.[462] Angiotensin II may be in part responsible for the activation of NADPH oxidase in SHR, since candesartan restored normal TGF responses to NOS inhibition.[463] A high salt intake may be another situation in which the generation of superoxide is increased as indicated by increased expression of NADPH oxidase subunits, and increased excretion of isoprostanes.[464] However, the TGF-enhancing effect of NOS inhibition was augmented rather than reduced in rats on a high-salt diet.[465,466] NO availability may also be regulated by ADMA (asymmetric dimethylarginine), an endogenous NOS inhibitor that also inhibits cellular uptake of the NOS substrate arginine. In fact, ADMA in the luminal perfusate enhanced TGF responses, and this effect appears to be the result of both inhibition of arginine uptake and of NOS activity.[467,468] Finally, NO may reduce TGF responses by inhibition of ecto-5′-nucleotidase, an intervention that would be predicted to reduce extracellular adenosine levels.[469,470]

OTHER VASOACTIVE FACTORS

A reduction in TGF reactivity has been observed subsequent to the systemic administration of renal vasodilators such as atrial natriuretic factor,[471,472] histamine,[436] dopamine,[473] high concentrations of PGI_2,[474] bradykinin,[348] uroguanylin,[475] and a number of vasodilating drugs.[199,200,436,476] Inhibition of heme oxygenase with stannous mesoporphyrin enhanced TGF-induced vasoconstriction in the isolated tubule/vessel preparation, and the administration of the CO-releasing agent CORM-3 (tricarbonylchloro[glycinato]rutheniumII) inhibited it, suggesting that carbon monoxide reduces TGF.[477] Since the presence of heme oxygenases in the MD has not been established, it is likely that carbon monoxide affects TGF by its vasodilatory properties.[478,479] Furthermore, TGF reactivity is decreased by an acute reduction of arterial blood pressure,[309] probably as a consequence of non-TGF-mediated autoregulatory vasodilatation. It seems unlikely that all these agents specifically interact with the TGF mechanism at the JGA level to cause a reduction of renal vascular resistance. Rather, the adjustment of TGF responsiveness may be the non-specific consequence of vasodilatation, reflecting a dependency of vascular resistance changes on the initial wall thickness−radius ratio.[480] Since the predominant effector of the TGF response is the afferent arteriole, a resistance change at this site would appear to be most likely to modulate TGF sensitivity.

INTERSTITIAL PRESSURE

TGF reactivity has been shown to increase during peritubular capillary perfusion with a hyperoncotic solution, whereas perfusion with protein-free solutions reduced TGF responses.[481] Changes in response were seen after a time delay of about 20 minutes.[481] Based on these observations, the concept was developed that net interstitial pressure (the difference between interstitial hydrostatic pressure and interstitial oncotic pressure) may be an important determinant of TGF reactivity in general. It was subsequently shown that TGF reactivity correlated inversely with net interstitial pressure during acute NaCl infusion,[336,337,339,482] during short-lasting ureteral obstruction,[349] and after contralateral nephrectomy.[363,483] In all these conditions, $V_{1/2}$ increased and the TGF response amplitude decreased. Conversely, net interstitial pressure was found to be reduced by 24 hours of dehydration,[346,482] and before and after release of 24 hour unilateral ureteral occlusion.[350] TGF reactivity was increased in these experimental situations. Exactly how net interstitial pressure affects TGF reactivity is unclear.

RESETTING BY LUMINAL FACTORS

There are a number of circumstances in which unidentified factors in tubular fluid have been shown to modify responses. During chronic dietary salt-loading, TGF control was inhibited when native tubular fluid was used as perfusate, whereas responses were only slightly blunted during perfusion with an artificial fluid.[484] A luminal factor has also been reported to modify TGF during the infusion of atrial natriuretic peptide,[485] but this factor appears to enhance TGF responses compared to the blunting observed with artificial solutions. Loop of Henle perfusion with electrolyte-free plasma dialysates from patients with acute renal failure and liver dysfunction produced exaggerated TGF responses which could not be blocked by furosemide,[486] suggesting that the plasma in certain disease states contains a factor which can elicit NaCl-independent vasoconstriction when present in the tubular lumen.

MACULA DENSA CONTROL OF RENIN SECRETION

Following Goormaghtigh's early speculation,[487] Vander suggested that renin release might be influenced by tubular fluid composition at the macula densa.[488] During a variety of experimental conditions, plasma renin activity and sodium excretion appeared to be inversely correlated, whereas there was no correlation between renin and mean arterial pressure or renal blood flow.[489,490] The overall conclusion from these studies was that an increased delivery of NaCl to the MD cells inhibits renin secretion. These early observations have now been corroborated by additional evidence from whole animal studies and from isolated *in vitro* systems which have established the concept that a high NaCl concentration at the macula densa inhibits renin secretion.[488,491]

Evidence for Macula Densa Control of Renin Secretion

Studies in Intact Animals

Vander's proposal that renin secretion depends upon MD NaCl concentration was studied more directly by comparing renin secretion from normal or nonfiltering kidneys. In dogs in which basal levels of renin were elevated by thoracic caval constriction, intrarenal infusion of NaCl or KCl inhibited renin secretion, but such a response was not seen in similarly treated animals in which the infused kidney had been rendered nonfiltering by ureteral occlusion.[492] In conscious mice, acute infusion of isotonic saline, a maneuver that has been shown to result in increased distal tubular NaCl concentrations, leads to a suppression of renin secretion.[493,494]

Attempts have been made to evaluate the effect of changes in MD NaCl concentration at the single nephron level *in vivo*. In these studies in rats, renin concentration in proximal tubular fluid and in postglomerular blood collected by micropuncture was found to vary inversely with changes in distal NaCl.[495]

Studies in the Isolated Perfused TAL/Glomerulus Preparation

With the isolated perfused tubule technique it has been possible to study MD-dependent renin secretion in the absence of baroreceptor and regulated adrenergic inputs, and during precise control of tubular fluid composition.[491] Another important aspect of the isolated JGA preparation is that it limits the possible sites of tubulovascular information transfer to MD cells and possibly a small number of surrounding TAL cells as the only cells present in the area of contact. In this preparation (Figure 23.11) there is unequivocal

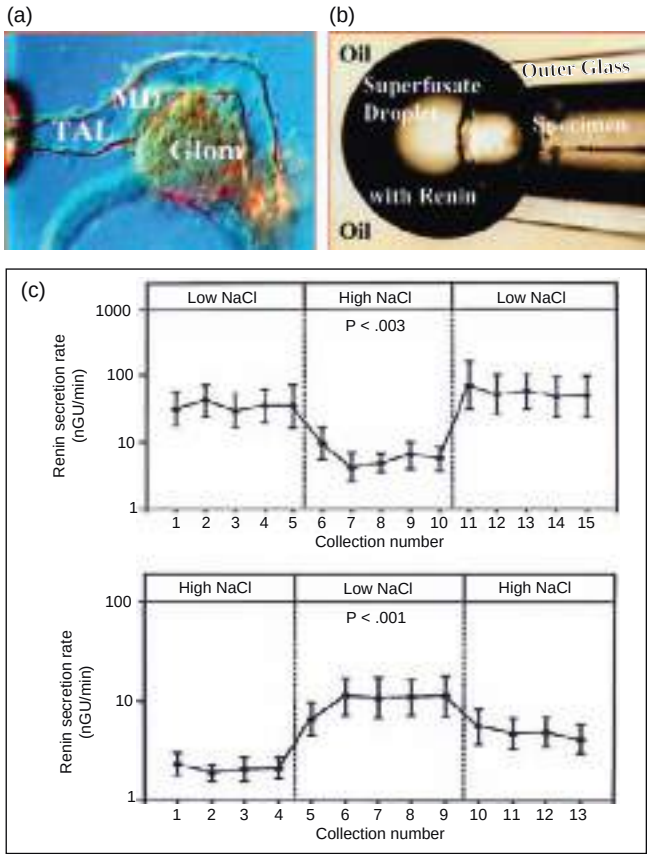

FIGURE 23.11 (a) Isolated perfused thick ascending limb (TAL) with attached glomerulus (glom); macula densa (MD) cells can be seen to protrude into the luminal space. (b) The perfused specimen is superfused through an outer glass pipette; emerging superfusate containing the secreted renin is collected under oil in defined time intervals.[595] (c) Macula densa-mediated changes in renin secretion showing the time course of changes in renin release to an increase (top) and decrease (bottom) in perfusate NaCl concentration.[497,498]

evidence that increasing NaCl concentration in the tubular perfusate suppresses renin secretion and reducing NaCl concentration stimulates it.[496–499] MD-dependent renin secretion is characterized by a rapid onset and offset following step-changes in NaCl concentration, and by reversibility of the induced changes.[497,499] Renin responses were independent of whether the tubule was perfused in an orthograde fashion from the TALH or in a retrograde fashion from the distal convoluted tubule.[497] Similar to the TGF response, MD-dependent renin secretion was not altered when NaCl concentration was reduced from isotonicity to about 80 mM, but the full renin response was seen when NaCl concentrations were varied between 7 and 61 mM of Cl and between 26 and 80 mM of Na, i.e., within the range that is physiologically relevant.[500] In the most sensitive concentration range between 7 and 47 mM of Cl, renin secretion increased by about 2 nGU/min per mM, whereas it fell by 0.4 nGU/min per mM when NaCl concentration was raised from 47 to 87 mM.[500] The NaCl concentration causing a half-maximum renin response is between 25 and 30 mM, values close to the estimated ambient NaCl concentration and close to the NaCl concentration causing a half-maximum TGF response. Although both decreases and increases of NaCl concentration are predicted to affect renin secretion, MD-dependent renin secretion is asymmetric around the operating point, with most of the responses occurring in the subnormal concentration range. Quantitative extrapolation from this *in vitro* system to the *in vivo* response must be made with caution, mainly because renin secretory responses *in vitro* are assessed in the absence of stabilizing feedback loops that may dampen MD-dependent changes in renin secretion *in vivo*.

Sensing Mechanism for Macula Densa-Mediated Renin Secretion

Renin Secretory Response and NaCl Transport

Early studies in intact animals suggested that, in certain conditions, renin secretion correlates more closely with distal tubular NaCl load than NaCl concentration, for example, during the infusion of hypertonic mannitol.[490,501,502] However, a reinvestigation of early distal NaCl concentration during mannitol diuresis showed a clear concentration decrease, in agreement with the stimulation of renin release typically seen in this condition.[503] In the isolated JGA preparation, an 80% reduction in luminal NaCl load by decreasing perfusate flow at constant NaCl concentration caused only a small, approximately two-fold increase in the rate of renin secretion. In contrast, when NaCl load was reduced to a similar degree by decreasing perfusate NaCl concentration, renin secretion increased nearly eight-fold, indicating that NaCl concentration is a more important determinant of renin release than NaCl delivery.[497]

Based on the stimulatory effect of loop diuretics in intact animals, it was concluded that MD NaCl transport plays a critical role as an early step in NaCl-dependent control of renin secretion.[488,490,504–507] Recent studies in mice deficient in the NKCC2A isoform of the co-transporter have shown that the inhibitory effect of an acute volume load on renin release is absent, supporting the notion that intact salt transport is required for salt-sensing by MD cells.[163] Direct evidence for an MD-mediated effect of transport inhibition on renin secretion was obtained in non-perfused afferent arterioles in which furosemide stimulated renin release only when the MD segment was included in the dissected specimen, but not in its absence.[508] In the isolated perfused JGA preparation, luminal application of bumetanide at 10^{-6} M increased renin secretion during perfusion with high NaCl solutions.[498] Furthermore, the presence of furosemide at 5×10^{-5} M essentially abolished the dependence of renin secretion on luminal NaCl concentration.[500]

Although NKCC2 mediates the bulk of MD Na reabsorption, apical expression of the Na^+/H^+ exchanger 2 (NHE2) may contribute to Na^+ transport, as well as to the regulation of intracellular pH.[30,32] In NHE2-deficient mice, renal renin content and plasma renin concentration were elevated compared to wild-type controls, and the stimulation of the renin system by a salt-depleted diet was blunted.[509] Increased baseline renin secretion in $NHE2^{-/-}$ mice was paralleled by enhanced MD COX-2 and mPGES expression. Recent studies have shown that plasma renin concentration is significantly elevated in NKCC1-deficient compared to wild-type mice.[510] Studies in isolated JG cells indicate that NKCC1 exerts a direct inhibitory effect on basal renin release.[119] This effect appears to be independent of the NKCC2-dependent inhibitory pathway through the macula densa, since the stimulatory effect of furosemide on renin release was essentially normal in $NKCC1^{-/-}$ mice.

Ion Specificity of Renin Secretion

MD control of renin secretion shows an apparent Cl dependency that is reminiscent of that described for TGF responses. Whereas the acute or chronic administration of various Cl or Br salts without Na inhibited renin secretion, Na salts without Cl as the accompanying anion had no effect.[493,511] Furthermore, changes in renin secretion under these conditions correlated with loop of Henle Cl absorption.[512] Conversely, an acute selective depletion of Cl by peritoneal dialysis increased plasma renin activity,[513] and substitution of

Cl by nitrate or thiocyanate in the perfusate of isolated kidneys stimulated renin secretion.[514] In the isolated perfused JGA, ion selectivity has been examined by measuring the inhibitory effect of adding various Na and Cl salts to a low NaCl perfusate. The inhibitory response was unchanged when most luminal Na was replaced by choline or rubidium.[498] On the other hand, substituting Cl by isethionate or acetate virtually eliminated the response to increased Na concentration.[498] Cl dependency is supported by studies in conscious mice showing that suppression of renin secretion following acute intravenous salt-loading is observed with infusion of NaCl, but not $NaHCO_3$.[515] These results support the hypothesis that the initiating signal for MD control of renin secretion is a change in the rate of NaCl uptake predominantly via a luminal Na,K,2Cl cotransporter whose physiological activity is determined by a change in luminal Cl concentration.

Organic Compounds and Renin Secretion

In addition to their function as sensors of TAL Cl concentration, MD cells are equipped with receptors for organic compounds, like the citric acid intermediate succinate. The succinate receptor GPR91 (succinate receptor 1, SUCNR1) has been shown to be localized in the apical membrane of cells of the cortical TAL, including the MD.[516] Increases in tubular succinate concentration result in the induction of the same intracellular signaling pathways that are activated by a low NaCl concentration. Incubation of cultured MD cells with succinate induced phosphorylation of p38 and Erk1/2 MAP kinases, and subsequent stimulation of COX-2 activity and expression in MD cells and enhanced PGE_2 release.[517] During streptozotocin-induced diabetes mellitus, renocortical COX-2 and renin content were upregulated in wild-type mice, and this stimulation of the renin system was markedly reduced in GPR91-deficient mice.[517] GPR91 expression in the vicinity of the JG cells, however, is not restricted to MD cells. GPR91 is also present in endothelial cells of the afferent arteriole, and may mediate renin release by stimulating endothelial prostanoid and NO formation.[518,519]

Furthermore, components of the olfactory system are present in MD cells.[520] MD cells rather specifically express the olfactory adenylate cyclase isoform 3 (AC3), as well as the olfactory trimeric G-protein G_{olf}. The olfactory receptor Olfr90 was detected in a MD cell line, and was also present in the native kidney.[520] Plasma renin concentration in AC3-deficient mice was reduced by about 50% compared to wild-types, despite increased MD COX-2 expression and augmented nNOS activity. The reason for these alterations of the MD–JG axis is unclear, and the ligands that may activate olfactory receptors on MD cells *in vivo* remain to be determined.

The Stimulus–Response Coupling Mechanism

Nitric Oxide

The presence of NOS I in MD cells raises the possibility that NO may act as an epithelium-derived factor that participates in MD control of renin secretion. This notion is supported by observations showing that the expression of MD nNOS changes in parallel with renin expression in a number of circumstances. MD cells of rats on a low-salt diet have increased levels of nNOS mRNA and protein expression.[59,60,521–523] Furthermore, the administration of furosemide also causes a marked increase in MD nNOS expression,[59,521] as does renal artery constriction.[59,521] The mechanism responsible for the upregulation of nNOS expression in these states is unclear, but a reduced NaCl transport at the MD is a common feature. Since the expression and secretion of renin is known to be elevated in these conditions, it is possible that NO generation is an upstream signal in the control of the RAS. The suggestion that a chronically reduced NaCl transport may stimulate MD nNOS expression is not immediately reconcilable with the evidence discussed earlier that acute increases in NaCl concentration appear to increase nNOS activity and NO formation. The expression of nNOS in MD cells is stabilized by negative feedback influences exerted by angiotensin II and PGE_2, since nNOS expression was markedly upregulated in mice with AT1 receptor or angiotensinogen deficiencies, as well as in COX-$2^{-/-}$ mice.[524–526]

Understanding the role of NO in renin secretion is complicated by the fact that NO can elicit both stimulatory and inhibitory effects. The inhibitory effect appears to result from activation of cGMP-dependent protein kinases (cGK), while the stimulatory effects are related to changes in intracellular cAMP levels. Two isoforms of cGK have been identified, cGK I and cGK II, and both isoforms have been found in granular cells.[108] A direct activator of cGK, 8-para-chlorophenylthio-cGMP, has been shown to inhibit isoproterenol- or forskolin-stimulated renin secretion in isolated perfused rat kidneys and microdissected afferent arterioles, and this stimulation could be reversed by an inhibitor of cGK.[527] A role for cGKII is suggested by the finding that 8-bromo-cGMP reduced basal and forskolin stimulated renin secretion in JG cells isolated from wild-type and cGK $I^{-/-}$ mice, but that it had no effect in cultures from cGK $II^{-/-}$ mice.[528]

The mechanism of the stimulatory effect of NO on renin secretion is related to an activation of the cAMP/protein kinase A pathway, and this activation results from an inhibition of PDEIII, a cAMP degrading phosphodiesterase that is inhibited by cGMP.[529] An early report showing that the PDEIII inhibitor milrinone increased basal and isoproterenol stimulated renin

release in conscious rabbits has now been corroborated by substantial additional evidence.[530] In the isolated perfused rat kidney, Na nitroprusside increased renin secretion, and this increase was attenuated by the protein kinase A inhibitor Rp-8-CPT-cAMPS. Since membrane-permeable cGMP analogs also reduced the stimulatory effect of SNP, stimulation of renin secretion by NO was clearly related to the A kinase, not G kinase pathway.[531] Inhibition of PDE IV, a phosphodiesterase with predominant effects on cGMP degradation, also increased renin secretion,[532] and this effect was blunted by nNOS inhibition suggesting that nNOS contributed to cGMP formation.

NO IN MD-DEPENDENT RENIN RELEASE

In view of the dual effects of NO on renin secretion and the ambiguity about the directional changes of juxtaglomerular NO with changes in loop of Henle flow rates, it is not surprising that the precise role of NO in MD control of renin release has remained equivocal. In the isolated perfused JGA preparation during perfusion with a low NaCl concentration, the luminal addition of l-arginine stimulated renin secretion and this stimulation was abolished by NOS blockade, suggesting that in this setting NO is renin-stimulatory.[533] Consistent with this conclusion is the observation that the NaCl dependency of renin secretion was essentially abolished in the presence of an NOS blocker in the tubular lumen, a change that was due entirely to prevention of the rise of renin secretion caused by a low luminal NaCl.[533] The conclusion that a low NaCl concentration at the MD stimulates renin secretion in an NO-dependent fashion is also supported by findings showing that the increased renin secretion caused by a reduction in arterial or perfusion pressure in kidneys of conscious dogs and in isolated rat kidneys was markedly and consistently blunted by NOS inhibition.[534,535] In other studies, the administration of a loop diuretic has been used to simulate a reduction in MD NaCl concentration. In dissected rat renal microvessels, NOS inhibition abolished the increase in renin release caused by furosemide pretreatment.[536] Similarly, the stimulation of renin secretion by furosemide *in vivo* was inhibited by the administration of NOS inhibitors.[504,537,538] Plasma renin activity in nNOS knockout mice and basal renin secretion in isolated perfused kidneys from $nNOS^{-/-}$ or $eNOS^{-/-}$ mice were found to be consistently lower than in wild-type animals, suggesting that tonic release of NO enhances renin release in mice.[505,526] The relative increases of renin secretion by furosemide were essentially normal in $nNOS^{-/-}$ or $eNOS^{-/-}$ mice, but were markedly reduced by general NOS inhibition.[505] Furthermore, the administration of the NO donor SNAP in kidneys in which endogenous NO production was blocked by L-NAME completely restored the stimulatory effect of loop diuretics. According to this recent evidence, it would appear that exposition of JG cells to NO regardless of its exact cellular source is necessary for the MD pathway to operate normally. The nature of this permissive effect of NO may be to inhibit PDEIII, and thereby to sensitize the renin secretory mechanism to the renin mediator that we assume to act through activation of the cAMP/PKA pathway (Figure 23.12).

Prostaglandins

Starting with the early observations by Larsson et al. that arachidonic acid increases and indomethacin reduces plasma renin activity,[539] various metabolites of arachidonic acid, most notably prostaglandins, have been established as potent regulators of renin secretion in a variety of experimental conditions.[506] Stimulation of renin secretion is most consistently seen with administration of prostaglandins of the E and I series.[540] The effect of prostaglandins on renin secretion are mediated by G_s-protein-coupled receptors, IP receptors in the case of PGI2, and EP2/EP4 receptors in the case of PGE_2.[541] Selective deletion of floxed $G_{s\alpha}$ in JG cells by cre recombinase driven by the endogenous renin promoter was associated with marked reductions of plasma renin concentration.[542]

RELATIONSHIP BETWEEN MD COX-2 AND RENIN

Cyclooxygenases catalyze the hydroxylation and oxygenation of arachidonic acid that lead to the generation of endoperoxides (or PGH2). Subsequent processing by a number of enzymes converts PGH2 into the biologically active spectrum of prostaglandins. The potential of prostaglandins to regulate renin secretion became highly relevant for the MD-dependent pathway by the demonstration that one of the cyclooxygenases, the inducible isoform COX-2, was constitutively expressed in MD

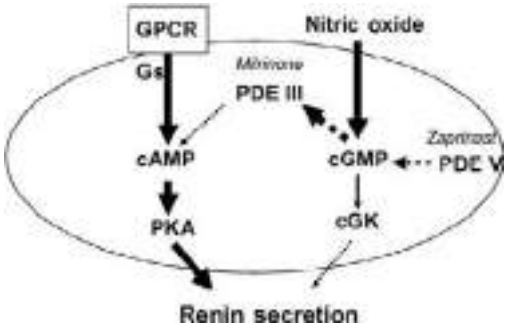

FIGURE 23.12 **Schematic representation of the pathways by which nitric oxide can inhibit or stimulate renin secretion.** Inhibition of PDEIII by cGMP and subsequent reduced degradation of cAMP appears to be the dominant pathway under many conditions. Milrinone, an inhibitor of PDEIII, consistently stimulates renin secretion.

cells.[62] The abundance of COX-2 in the MD and adjacent TAL cells is highly regulated, and the pattern of COX-2 regulation parallels that of nNOS in the macula densa and of renin in JG cells. Parallel increases in COX-2 and renin have been observed in rats treated chronically with furosemide, and in patients with Bartter syndrome, suggesting that COX-2 expression, like nNOS, may be in some way linked to NaCl uptake by MD cells.[543–547] An increase of MD COX-2 expression and of JG cell renin is induced by administration of a low NaCl diet or by renal artery stenosis.[62,63,548–550] Stimulation of COX-2 expression has also been found following partial renal ablation and in active lupus nephritis.[551,552] A low NaCl diet also caused a two- to three-fold increase in the expression of PGE_2 synthase in MD cells.[71] Conversely, mice with genetic COX-2 deficiency have a marked reduction of renin expression and of plasma renin concentration.[553,554] On the other hand, angiotensin II appears to play the role of a negative feedback regulator of COX-2 synthesis: a strong and consistent stimulation of COX-2 expression is induced by ACE inhibition or AT1 receptor blockade, and COX-2 expression is increased in AT1 receptor knockout mice,[543,555,556] as well as in other states of low angiotensin action.[542]

REGULATION OF PGE_2 PRODUCTION

The application of a biosensor technique has provided a missing piece of evidence linking MD NaCl delivery to local PGE_2 release.[557] In this approach, HEK293 cells were stably transfected with the mouse PGE_2 receptor EP1, a receptor subtype that is coupled to the IP3 pathway, and whose activation therefore causes an increase in cytosolic Ca. In perfused TAL/MD preparations dissected from kidneys of salt-restricted rabbits, a transfected and fura-2 loaded sensor cell was positioned at the basolateral aspect of MD cells, and changes in $[Ca]_i$ were used as an index of PGE_2 release. In this preparation, removal of luminal NaCl caused a significant increase in sensor cell $[Ca]_i$, while no effect was seen when NaCl was reduced to zero in the presence of luminal furosemide (Figure 23.13b). This effect appeared to be cell-specific, since the positioning of the sensor cell close to a TAL cell had no effect on $[Ca]_i$. Of major importance is the observation that most of the change in $[Ca]_i$ occurred in a NaCl concentration range of between 20 and 40 mM, exactly the concentration range in which NaCl concentration affects renin secretion in a similar preparation (Figure 23.13a).

Studies in the isolated rabbit JGA have shown that acute, non-specific COX inhibition with flufenamic acid or flurbiprofen virtually completely abolished the increase in renin secretion caused by a decrease in MD NaCl concentration.[496] Since the concentration change from minimal to maximal was done in a single step, it is not clear whether the effect of these agents was symmetrical around the midpoint or whether it mainly affected the stimulation in the subnormal concentration range. Direct evidence for a role of COX-2 has been obtained in an extension of these studies in which the specific COX-2 inhibitor NS-398 was also found to prevent the stimulation of renin secretion by low NaCl, while the putative COX-1 blocker valerylsalicylate did not have this effect (Figure 23.13c).[558] The significance of these findings is substantial since as pointed out earlier, the isolated perfused rabbit JGA preparation is the only currently available technique capable of assessing MD-dependent renin release unencumbered by simultaneous sympathetic and baroreceptor input.

The mechanisms by which a reduction in luminal NaCl may cause stimulation of PGE_2 release and COX-2 expression have been studied in cell lines derived from the MD and from TAL cells.[559,560] In both lines of cells a reduction in medium NaCl caused a prompt and dose-dependent increase in PGE_2 release that was essentially completely inhibited by NS-398, and was therefore largely mediated by COX-2. The onset of this response preceded any increase in COX-2 expression, suggesting that it was the result of an increase in COX-2 activity and/or of an activation of PLA2 followed by increased availability of arachidonic acid. Presence of PLA2 in macula densa cells and regulation of PLA2 in parallel to that of COX-2 has recently been demonstrated.[66] In both TAL and MD cells in culture, a reduction in medium NaCl also augmented the expression of the mRNA and protein expression of COX-2.[559,560] Ion substitution studies indicate that the extracellular signal for COX-2 stimulation appears to be a reduction in Cl rather than in Na concentration, a finding that is remarkably concordant with the Cl-dependency of renin secretion shown earlier in an entirely different preparation. The intracellular signaling events leading to the stimulation of COX-2 activity and expression are initiated by rapid phosphorylation of p38 and Erk1/2 kinases (Figure 23.14).[560] Participation of MAP kinases in COX-2 expression is supported by the inhibitory effects of SB 203580 and PD 98059, inhibitors of p38- and Erk1/2-mediated signaling events.[559,560] The role of the MAP kinase pathway in Cl-dependent COX-2 expression that appears to reflect both a transcriptional activation and an increased stability of the mRNA[561] is similar to the involvement of MAP kinases in mediating the effects of cytokines, growth factors, and hypertonicity on COX-2 expression in other cell types.[562–564]

Chronic interference with COX-2 signaling is associated with a reduction of renin expression that has secondary consequences for acute renin secretory responses. Thus, COX-2-deficient mice have been shown to have a markedly reduced renin mRNA expression and plasma renin, and this effect was greater on 129J or C57Bl/6 than on mixed genetic

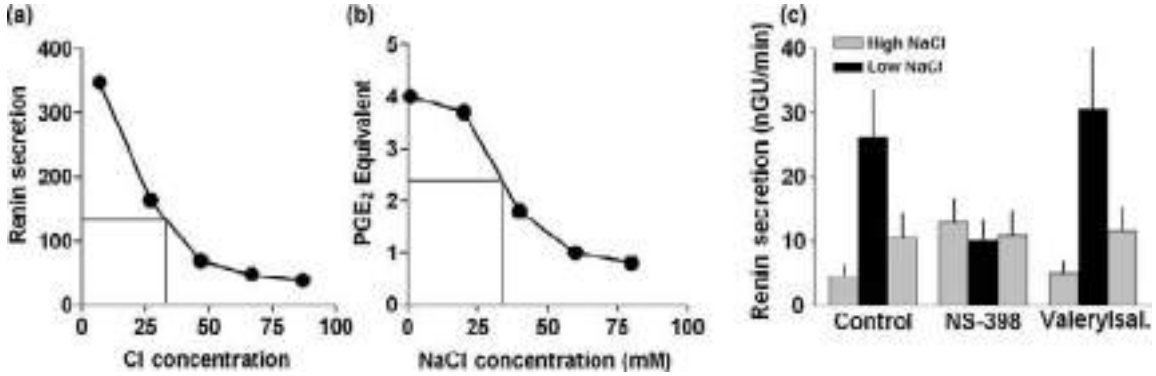

FIGURE 23.13 (a) Relationship between perfusate Cl concentration and renin release in the isolated perfused JGA preparation; data from [500]. (b) Relationship between perfusate NaCl concentration and PGE_2 release by macula densa cells.[557] The PGE2 equivalent corresponds to the EP1-mediated increase in cytosolic Ca in HEK cells transfected with EP1 receptor cDNA, and placed at the basolateral aspect of macula densa cells.[557] (c) Renin secretion in the perfused thick ascending limb/glomerulus preparation of the rabbit in response to perfusion with solutions containing high and low NaCl concentrations during control conditions, during inhibition of COX-2 with NS-398, and during inhibition of COX-1 with valerylsalicylate.[558]

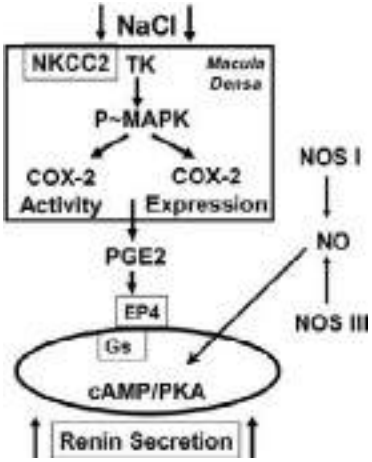

FIGURE 23.14 **Schematic summary of the pathway by which a decrease in luminal NaCl concentration causes stimulation of renin secretion.** Activation of several MAP kinases causes activation of COX-2, as well as transcriptional upregulation of COX-2 synthesis, augmented release of PGE2, and stimulation of the cAMP/PKA pathway through EP4 receptors. Nitric oxide, derived from both NOS I and NOC III, supports renin secretion by stabilizing cAMP.

background.[553,554,565] Chronic administration of COX-2 blockers, on the other hand, did not consistently reduce renin expression.[566–568] Acute stimulation of renin release by furosemide, hydralazine or isoproterenol was markedly reduced in COX-2-deficient compared to wild-type mice, suggesting that the acute release response was dependent upon basal renin expression levels.[553] Thus, when low renin release in COX-2-deficient mice was overcome by chronic prestimulation of their renin system, *acute* renin secretory responses to various stimuli were reconstituted to levels observed in wild-type animals. Furthermore, stimulation of renin release by angiotensin converting enzyme or AT1 blockers was also markedly reduced in animals with genetic or pharmacologic COX-2-deficiency.[553,555,565] Overall these studies reveal that the level of renin expression is an important and non-specific determinant of the acute secretory response, independent of whether the stimulus acts through the MD, baroreceptor, sympathetic or any other pathway. The strong relationship between basal levels of renin release or its surrogate, plasma renin, and the acute release response suggests the existence of an acutely releasable renin pool in JG cells whose magnitude depends on renin synthesis.[553,569]

In addition to the MD, the renal vasculature including the afferent arteriole appears to be a significant source of prostanoids in the vicinity of the JGA in some species. In humans, expression levels of COX-2 in the MD are low and are exceeded by vascular COX-2 expression, in particular in close vicinity to the JG cells.[570] In patients with renal artery stenosis this vascular expression of COX-2 was enhanced, and therefore prostaglandins from non-MD sources may contribute to enhanced renin secretion in this condition. In addition, stimulation of the renin system *in vivo* after loop diuretics may not be exclusively mediated by the MD pathway, but may be at least partly related to enhanced vascular prostanoid formation.[571] Furthermore, the reduced stimulatory capacity of loop diuretics on renin secretion in the presence of COX inhibitors appears to be to some extent related to blockade of vascular prostanoid formation.[572,573]

Adenosine

In general, exogenous adenosine inhibits renin release in intact rats or dogs,[574–576] an effect that is produced by activation of A1AR.[575] Nevertheless, it is unclear to what extent adenosine participates in the renin inhibition caused by high luminal NaCl concentrations. In the

isolated perfused JGA, the selective A1AR blocker 8-cyclopentyl-1,3-dipropylxanthine (CPX) blunted the fall in renin secretion caused by an elevation in luminal NaCl, but did not abolish it.[499] Adenosine itself was found to be only a weak inhibitor of MD-stimulated renin secretion when added to the bathing fluid.[577] This may reflect effective degradation of exogenous adenosine, since the addition of the adenosine deaminase inhibitor pentostatin (deoxycoformycin) augmented the renin-inhibitory effect of adenosine somewhat.[577] Additional studies may have clarified the role of adenosine in MD-dependent renin release. In isolated perfused kidneys, it was found that the stimulation of renin release by bumetanide was not measurably different between wild-type and A1AR-deficient mice.[578] This observation argues against a role of A1AR and adenosine in the stimulation of renin secretion during inhibition of NaCl transport below ambient levels. On the other hand, renin secretion fell when NaCl at the MD was acutely increased by a bolus injection of NaCl, and this effect was not seen in A1AR-deficient mice, suggesting that the renin-inhibitory effect of increased NaCl concentrations is mediated by adenosine, whereas the renin-stimulatory effect is not (Figure 23.15).

The cellular mechanisms of inhibition of renin release by adenosine are not clear, but it is likely that an increase in $[Ca]_i$ may play a role. Considerable progress has been made in understanding the paradoxical inhibition of renin release by elevated $[Ca]_i$. In primary cultures of JG cells it has been observed that an increase of $[Ca]_i$ by thapsigargin, angiotensin II or endothelin was associated with a marked decrease in isoproterenol- or forskolin-stimulated cellular cAMP and a decrease of renin release.[579] Conversely, a decrease of $[Ca]_i$ by the Ca chelator BAPTA-AM caused an increase in cellular cAMP, accompanied by an increase in renin release.[580] The inverse relation between $[Ca]_i$ and cAMP was suggested to reflect regulation of adenylyl cyclase (AC) by $[Ca]_i$. In fact, the Ca-inhibitable AC5 and AC6 isoforms were shown to be expressed in JG cells,[579,580] and siRNAs directed against AC5 and AC6 were able to prevent cAMP stimulation by forskolin or isoproterenol ,as well as renin secretion in As4.1 cells (Figure 23.16).[579]

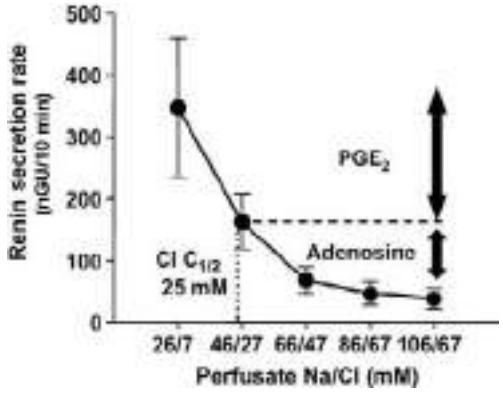

FIGURE 23.15 **Control of macula densa-dependent renin secretion by PGE2 and adenosine, with PGE2 being responsible for the larger stimulatory effect during reduced luminal NaCl, and adenosine causing a smaller inhibitory effect during increases in macula densa NaCl.**

Ionic and Osmotic Effects

Changes in external juxtaglomerular osmolarity may mediate the renin secretory response to a change of luminal NaCl. In a number of different preparations hypoosmolarity stimulates and hyperosmolarity inhibits renin secretion, and such changes would seem to be directionally plausible in mediating MD-dependent renin release.[581–584] Hypotonicity-stimulated renin secretion appears to be initiated by AQP1-mediated water flux leading to COX-2-dependent PGE_2 production and cAMP formation.[585] However, a recent study in isolated perfused rat or mouse kidneys established a direct rather than an inverse relationship between renin release and external osmolarity,[569] a finding that confirms an earlier *in vivo* observation.[586] Osmotic stimulation of renin release was not prevented by L-NAME, indomethacin or bumetanide, and was therefore

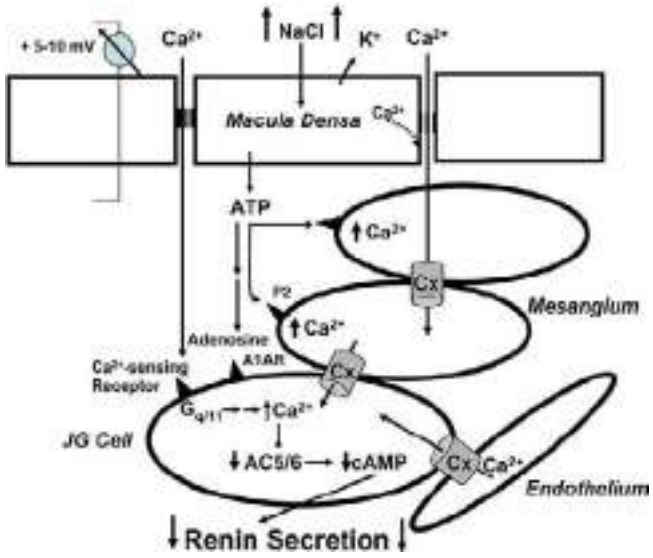

FIGURE 23.16 **Schematic summary of the pathways by which an increase in TAL/macula densa NaCl reabsorption mediates Ca-dependent suppression of renin secretion.** TAL/macula densa transepithelial NaCl transport and concomitant K recycling generate a lumen-positive potential which drives paracellular Ca absorption. Ca-sensing receptors on JG cells translate changes in interstitial Ca into a modulation of Ca_i. Cell coupling by calcium-permeable connexins (Cx), activation of Ca_i-mobilizing P2 receptors by ATP, and A1AR activation in JG cells are additional pathways for raising JG cell calcium. Ca-inhibited adenylyl cyclases (AC5 and AC6) link the increase of Ca_i to a reduction of cAMP formation in JG cells.

suggested to reflect a direct effect on JG cells.[569] In addition to changes in interstitial osmolarity, direct ionic effect may influence renin secretion. Thus, JG cells express the calcium receptor CaR which renders renin-producing cells capable of translating changes in extracellular calcium into changes in intracellular calcium.[587] In fact, the calcimimetic R-568 partially blunted the stimulation of renin secretion in response to isoproterenol, furosemide, and enalapril, while having little effect on basal renin release.[588] It remains to be determined under which conditions changes in interstitial Ca concentrations may occur *in vivo*. In theory, increased TAL/MD NaCl reabsorption would be expected to augment the tubular lumen-positive potential, and would enhance the driving force for paracellular Ca uptake; this would result in an increased interstitial Ca concentration. In line with this concept, interstitial renal cortical Ca concentration as determined by *in situ* microdialysis techniques in Wistar rats was shown to rise by 25% during chronic oral salt loading.[589] A role of Ca in the MD-JG signal transmission is further supported by the finding that an increased tubular flow rate triggers a Ca wave that originates around the MD, spreads throughout the JGA, and eventually increases Ca_i of the JG cells. Both cell–cell coupling in the JGA via connexins and ATP-dependent mechanisms appear to participate in the propagation of this Ca wave.[150,590] Gap junction uncoupling by α-glycyrrhetinic acid and ATP degradation by apyrase markedly diminished changes in Ca_i in the most distal portion of the afferent arteriole.[150] Connexin 45 expression was detected in vascular smooth muscle cells of the afferent and efferent arteriole, the mesangium, and JG cells. In cultured vascular smooth muscle cells from mice with local deletion of connexin 45 the speed of a cell-to-cell Ca wave was reduced by 60% compared to wild-type controls.[590] Furthermore, mice with deletion of connexin 45 in the JGA showed increased PRC accompanied by elevated blood pressure suggesting an inadequate inhibitory input on renin secretion.[590] However, connexin 45 probably is not the only connexin involved in a Ca-dependent signal transmission from MD cells to renin granular cells. In particular, connexin 40 was shown to mediate Ca transmission from endothelial to JG cells,[591] a finding consistent with major derangements in JG cell renin secretion and topology in connexin 40-deficient mice.[592,593]

Acknowledgment

Research from the laboratory of the authors was supported by intramural funds of the National Institute of Diabetes, and Digestive and Kidney Diseases, National Institutes of Health, and by funding from the Deutsche Forschungsgemeinschaft.

References

[1] Golgi C. Annotazioni intorno all'istologia dei reni dell'uomo e di altri mammiferi e sull'istogenesi dei canalicoli oriniferi. Atti della Reale Accademia dei Lincei 1889;5:334–42.
[2] Kaissling B, Kriz W. Structural analysis of the rabbit kidney. Adv Anat Embryol Cell Biol 1979;56:1–123.
[3] Christensen JA, Meyer DS, Bohle A. The structure of the human juxtaglomerular apparatus. A morphometric, lightmicroscopic study on serial sections. Virchows Arch A Pathol Anat Histol 1975;367:83–92.
[4] Christensen JA, Bohle A. The juxtaglomerular apparatus in the normal rat kidney. Virchows Arch A Pathol Anat Histol 1978;379:143–50.
[5] Dorup J, Morsing P, Rasch R. Tubule–tubule and tubule–arteriole contacts in rat kidney distal nephrons. A morphologic study based on computer-assisted three-dimensional reconstructions. Lab Invest 1992;67:761–9.
[6] Komlosi P, Banizs B, Fintha A, Steele S, Zhang ZR, Bell PD. Oscillating cortical thick ascending limb cells at the juxtaglomerular apparatus. J Am Soc Nephrol 2008;19:1940–6.
[7] Taugner R, Hackenthal E. The juxtaglomerular apparatus. Berlin Heidelberg: Springer-Verlag; 1989.
[8] Barajas L. Anatomy of the juxtaglomerular apparatus. Am J Physiol 1979;237:F333–343.
[9] Kaissling B, Peter S, Kriz W. The transition of the thick ascending limb of Henle's loop into the distal convoluted tubule in the nephron of the rat kidney. Cell Tissue Res 1977;182:111–8.
[10] Peti-Peterdi J, Morishima S, Bell PD, Okada Y. Two-photon excitation fluorescence imaging of the living juxtaglomerular apparatus. Am J Physiol Renal Physiol 2002;283:F197–201.
[11] Razga Z, Nyengaard JR. The effect of angiotensin II on the number of macula densa cells through the AT1 receptor. Nephron Physiol 2009;112:37–43.
[12] Zimmermann KW. Ueber den Bau des Glomerulus der Saeugerniere. Z Mikr Anat Forsch 1933;32:176–278.
[13] Bonsib SM. The macula densa tubular basement membrane: a unique plaque of basement membrane specialization. J Ultrastruct Mol Struct Res 1986;97:103–8.
[14] Ojeda JL, Piedra S. Lectin-binding sites and silver affinity of the macula densa basement membranes in the rabbit kidney. J Anat 1994;185:529–35.
[15] Lapointe JY, Bell PD, Cardinal J. Direct evidence for apical Na^+:$2Cl^-$:K^+ co-transport in macula densa cells. Am J Physiol Renal Physiol 1990;258:F1466–1469.
[16] Schlatter E, Salomonsson M, Persson AE, Greger R. Macula densa cells sense luminal NaCl concentration via furosemide sensitive $Na^+2Cl^-K^+$ co-transport. Pflugers Arch 1989;414:286–90.
[17] Schlatter E. Effect of various diuretics on membrane voltage of macula densa cells. Whole-cell patch-clamp experiments. Pflugers Arch 1993;423:74–7.
[18] Nielsen S, Maunsbach AB, Ecelbarger CA, Knepper MA. Ultrastructural localization of Na-K-2Cl co-transporter in thick ascending limb and macula densa of rat kidney. Am J Physiol Renal Physiol 1998;275:F885–893.
[19] Obermuller N, Kunchaparty S, Ellison DH, Bachmann S. Expression of the Na-K-2Cl co-transporter by macula densa and thick ascending limb cells of rat and rabbit nephron. J Clin Invest 1996;98:635–40.
[20] Yang T, Huang YG, Singh I, Schnermann J, Briggs JP. Localization of bumetanide- and thiazide-sensitive Na-K-Cl co-transporters along the rat nephron. Am J Physiol 1996;271: F931–939.
[21] Gimenez I, Isenring P, Forbush B. Spatially distributed alternative splice variants of the renal Na-K-Cl co-transporter exhibit

dramatically different affinities for the transported ions. J Biol Chem 2002;277:8767–70.
[22] Oppermann M, Mizel D, Huang G, et al. Macula densa control of renin secretion and preglomerular resistance in mice with selective deletion of the B isoform of the Na,K,2Cl co-transporter. J Am Soc Nephrol 2006;17:2143–52.
[23] Payne JA, Forbush B. Alternatively spliced isoforms of the putative renal Na-K-Cl co-transporter are differently distributed within the rabbit kidney. Proc Nat Acad Sci USA 1994; 91:4544–8.
[24] Mutig K, Paliege A, Kahl T, Jons T, Muller-Esterl W, Bachmann S. Vasopressin V2 receptor expression along rat, mouse, and human renal epithelia with focus on TAL. Am J Physiol Renal Physiol 2007;293:F1166–1177.
[25] Laamarti MA, Lapointe JY. Determination of NH_4^+/NH_3 fluxes across apical membrane of macula densa cells: A quantitative analysis. Am J Physiol Renal Physiol 1997;273:F817–824.
[26] Hurst AM, Lapointe JY, Laamarti A, Bell PD. Basic properties and potential regulators of the apical K^+ channel in macula densa cells. J Gen Physiol 1994;103:1055–70.
[27] Nusing RM, Pantalone F, Grone HJ, Seyberth HW, Wegmann M. Expression of the potassium channel ROMK in adult and fetal human kidney. Histochem Cell Biol 2005;123:553–9.
[28] Xu JZ, Hall AE, Peterson LN, Bienkowski MJ, Eessalu TE, Hebert SC. Localization of the ROMK protein on apical membranes of rat kidney nephron segments. Am J Physiol Renal Physiol 1997;273:F739–48.
[29] Amemiya M, Loffing J, Lotscher M, Kaissling B, Alpern RJ, Moe OW. Expression of NHE-3 in the apical membrane of rat renal proximal tubule and thick ascending limb. Kidney Int 1995;48:1206–15.
[30] Fowler BC, Chang YS, Laamarti A, Higdon M, Lapointe JY, Bell PD. Evidence for apical sodium proton exchange in macula densa cells. Kidney Int 1995;47:746–51.
[31] Kwon TH, Nielsen J, Kim YH, Knepper MA, Frokiaer J, Nielsen S. Regulation of sodium transporters in the thick ascending limb of rat kidney: response to angiotensin II. Am J Physiol Renal Physiol 2003;285:F152–165.
[32] Peti-Peterdi J, Chambrey R, Bebok Z, Biemesderfer St D, John PL, Abrahamson DR, et al. Macula densa $Na(^+)/H(^+)$ exchange activities mediated by apical NHE2 and basolateral NHE4 isoforms. Am J Physiol Renal Physiol 2000;278:F452–463.
[33] Peti-Peterdi J, Bebok Z, Lapointe JY, Bell PD. Novel regulation of cell $[Na(^+)]$ in macula densa cells: apical $Na(^+)$ recycling by H-K-ATPase. Am J Physiol Renal Physiol 2002;282:F324–329.
[34] Rajendran VM, Sangan P, Geibel J, Binder HJ, Ouabain-sensitive H. K-ATPase functions as Na,K-ATPase in apical membranes of rat distal colon. J Biol Chem 2000;275:13035–40.
[35] Verlander JW, Moudy RM, Campbell WG, Cain BD, Wingo CS. Immunohistochemical localization of H-K-ATPase alpha(2c)-subunit in rabbit kidney. Am J Physiol Renal Physiol 2001;281: F357–365.
[36] Kashgarian M, Biemesderfer D, Caplan M, Forbush III B. Monoclonal antibody to Na,K-ATPase: immunocytochemical localization along nephron segments. Kidney Int 1985; 28:899–913.
[37] Schnermann J, Marver D. ATPase activity in macula densa cells of the rabbit kidney. Pflugers Arch 1986;407:82–6.
[38] Arystarkhova E, Wetzel RK, Sweadner KJ. Distribution and oligomeric association of splice forms of $Na(^+)$-$K(^+)$-ATPase regulatory gamma-subunit in rat kidney. Am J Physiol Renal Physiol 2002;282:F393–407.
[39] Farman N, Fay M, Cluzeaud F. Cell-specific expression of three members of the FXYD family along the renal tubule. Ann NY Acad Sci 2003;986:428–36.
[40] Pu HX, Cluzeaud F, Goldshleger R, Karlish SJ, Farman N, Blostein R. Functional role and immunocytochemical localization of the gamma a and gamma b forms of the Na,K-ATPase gamma subunit. J Biol Chem 2001;276:20370–8.
[41] Sweadner KJ, Arystarkhova E, Donnet C, Wetzel RK. FXYD proteins as regulators of the Na,K-ATPase in the kidney. Ann NY Acad Sci 2003;986:382–7.
[42] Wetzel RK, Sweadner KJ. Immunocytochemical localization of Na-K-ATPase alpha- and gamma-subunits in rat kidney. Am J Physiol Renal Physiol 2001;281:F531–545.
[43] Wetzel RK, Sweadner KJ. Phospholemman expression in extraglomerular mesangium and afferent arteriole of the juxtaglomerular apparatus. Am J Physiol Renal Physiol 2003;285: F121–129.
[44] Lapointe JY, Bell PD, Hurst AM, Cardinal J. Basolateral ionic permeabilities of macula densa cells. Am J Physiol Renal Physiol 1991;260:F856–860.
[45] Alper SL, Stuart-Tilley AK, Biemesderfer D, Shmukler BE, Brown D. Immunolocalization of AE2 anion exchanger in rat kidney. Am J Physiol Renal Physiol 1997;273:F601–614.
[46] Komlosi P, Frische S, Fuson AL, Fintha A, Zsmbery A, Peti-Peterdi J, et al. Characterization of basolateral chloride/bicarbonate exchange in macula densa cells. Am J Physiol Renal Physiol 2005;288:F380–386.
[47] Komlosi P, Fintha A, Bell PD. Unraveling the relationship between macula densa cell volume and luminal solute concentration/osmolality. Kidney Int 2006;70:865–71.
[48] Liu R, Pittner J, Persson AE. Changes of cell volume and nitric oxide concentration in macula densa cells caused by changes in luminal NaCl concentration. J Am Soc Nephrol 2002;13:2688–96.
[49] Liu R, Persson AE. Simultaneous changes of cell volume and cytosolic calcium concentration in macula densa cells caused by alterations of luminal NaCl concentration. J Physiol 2005;205:895–901.
[50] Gonzalez E, Salomonsson M, Muller-Suur C, Persson AE. Measurements of macula densa cell volume changes in isolated and perfused rabbit cortical thick ascending limb. II. Apical and basolateral cell osmotic water permeabilities. Acta Physiol Scand 1988;133:159–66.
[51] Gonzalez E, Salomonsson M, Muller-Suur C, Persson AE. Measurements of macula densa cell volume changes in isolated and perfused rabbit cortical thick ascending limb. I. Isosmotic and anisosmotic cell volume changes. Acta Physiol Scand 1988;133:149–57.
[52] Schnermann J, Briggs JP. Function of the juxtaglomerular apparatus: control of glomerular hemodynamics and renin secretion. In: Seldin DW, Giebisch G, editors. The kidney physiology and pathophysiology, vol. 1. Philadelphia: Lippincott Williams &Wilkins; 2000. p. 945–80.
[53] Aoyagi T, Izumi Y, Hiroyama M, Matsuzaki T, Yasuoka Y, Sanbe A, et al. Vasopressin regulates the renin–angiotensin–aldosterone system via V1a receptors in macula densa cells. Am J Physiol Renal Physiol 2008;295:F100–107.
[54] Mundel P, Bachmann S, Bader M, Fischer A, Kummer W, Mayer B, et al. Expression of nitric oxide synthase in kidney macula densa cells. Kidney Int 1992;42:1017–9.
[55] Wilcox CS, Welch WJ, Murad F, Gross SS, Taylor G, Levi R, et al. Nitric oxide synthase in macula densa regulates glomerular capillary pressure. Proc Natl Acad Sci USA 1992;89:11993–7.
[56] Brenman JE, Chao DS, Gee SH, McGee AW, Craven SE, Santillano DR, et al. Interaction of nitric oxide synthase with the postsynaptic density protein PSD-95 and alpha1-syntrophin mediated by PDZ domains. Cell 1996;84:757–67.

[57] Lu D, Fu Y, Lopez-Ruiz A, Juncos R, Liu H, Manning Jr RD, et al., Salt-sensitive splice variant of nNOS expressed in the macula densa cells. Am J Physiol Renal Physiol 298: F1465–71.
[58] Norgaard T. Quantitation of glucose-6-phosphate dehydrogenase activity in cortical fractions of the nephron in sodium-depleted and sodium-loaded rabbits. Histochemistry 1980;69:49–59.
[59] Schricker K, Potzl B, Hamann M, Kurtz A. Coordinate changes of renin and brain-type nitric-oxide-synthase (b-NOS) mRNA levels in rat kidneys. Pflugers Arch 1996;432:394–400.
[60] Singh I, Grams M, Wang WH, Yang T, Killen P, Smart A, et al. Coordinate regulation of renal expression of nitric oxide synthase, renin, and angiotensinogen mRNA by dietary salt. Am J Physiol Renal Physiol 1996;270:F1027–1037.
[61] Vandewalle A, Farman N, Cluzeaud F, Bonvalet JP. Heterogeneity of uridine incorporation along the rabbit nephron. I. Autoradiographic study. Am J Physiol 1984;246:F417–426.
[62] Harris RC, McKanna JA, Akai Y, Jacobson HR, Dubois RN, Breyer MD. Cyclooxygenase-2 is associated with the macula densa of rat kidney and increases with salt restriction. J. Clin. Invest 1994;94:2504–10.
[63] Yang T, Singh I, Pham H, Sun D, Smart A, Schnermann JB, et al. Regulation of cyclooxygenase expression in the kidney by dietary salt intake. Am J Physiol Renal Physiol 1998;274: F481–9.
[64] Guan Y, Chang M, Cho W, Zhang Y, Redha R, Davis L, et al. Cloning, expression, and regulation of rabbit cyclooxygenase-2 in renal medullary interstitial cells. Am J Physiol Renal Physiol 1997;273:F18–26.
[65] Hartner A, Goppelt-Struebe M, Hilgers KF. Coordinate expression of cyclooxygenase-2 and renin in the rat kidney in renovascular hypertension. Hypertension 1998;31:201–5.
[66] Mangat H, Peterson LN, Burns KD. Hypercalcemia stimulates expression of intrarenal phospholipase A_2 and prostaglandin H synthase-2 in rats. J Clin Invest 1997;100:1941–50.
[67] Komhoff M, Seyberth HW, Nusing RM, Breyer MD. Cyclooxygenase-2 expression is associated with the macula densa in kidneys from patients with Bartter like syndrome. J Am Soc Nephrol 1999;10:437A (abstract)
[68] Nantel F, Meadows E, Denis D, Connolly B, Metters KM, Giaid A. Immunolocalization of cyclooxygenase-2 in the macula densa of human elderly. FEBS Lett 1999;457:475–7.
[69] Zhang MZ, Wang JL, Cheng HF, Harris RC, McKanna JA. Cyclooxygenase-2 in rat nephron development. Am J Physiol Renal Physiol 1997;273:F994–1002.
[70] Murakami M, Nakatani Y, Tanioka T, Kudo I. Prostaglandin E synthase. Prostaglandins Other Lipid Mediat 2002;68-69:383–99.
[71] Campean V, Theilig F, Paliege A, Breyer M, Bachmann S. Key enzymes for renal prostaglandin synthesis: site-specific expression in rodent kidney (rat, mouse). Am J Physiol Renal Physiol 2003;285:F19–32.
[72] Fuson AL, Komlosi P, Unlap TM, Bell PD, Peti-Peterdi J. Immunolocalization of a microsomal prostaglandin E synthase in rabbit kidney. Am J Physiol Renal Physiol 2003;285:F558–564.
[73] Spanidis A, Wunsch H, Kaissling B, Kriz W. Three-dimensional shape of a Goormaghtigh cell and its contact with a granular cell in the rabbit kidney. Anat Embryol (Berl) 1982;165:239–52.
[74] Pricam C, Humbert F, Perrelet A, Orci L. Gap junctions in mesangial and lacis cells. J Cell Biol 1974;63:349–54.
[75] Taugner R, Schiller A, Kaissling B, Kriz W. Gap junctional coupling between the JGA and the glomerular tuft. Cell Tissue Res 1978;186:279–85.
[76] Hanner F, Sorensen CM, Holstein-Rathlou NH, Peti-Peterdi J. Connexins and the kidney. Am J Physiol Regul Integr Comp Physiol 2010;298:R1143–1155.
[77] Kurtz L, Madsen K, Kurt B, Jensen BL, Walter S, Banas B, et al. High-level connexin expression in the human juxtaglomerular apparatus. Nephron Physiol 2010;116:p1–8.
[78] Latta H, Maunsbach AB. The juxtaglomerular apparatus as studied electron microscopically. J Ultrastruct Res 1962;6:547–61.
[79] Schnabel E, Kriz W. Morphometric studies of the extraglomerular mesangial cell field in volume expanded and volume depleted rats. Anat Embryol (Berl) 1984;170:217–22.
[80] Rosivall L, Mirzahosseini S, Toma I, Sipos A, Peti-Peterdi J. Fluid flow in the juxtaglomerular interstitium visualized *in vivo*. Am J Physiol Renal Physiol 2006;291:F1241–1247.
[81] Bacay AC, Mantyh CR, Cohen AH, Mantyh PW, Fine LG. Glomerular atrial natriuretic factor receptors in primary glomerulopathies: studies on human renal biopsies. Am J Kidney Dis 1989;14:386–95.
[82] Osborne MJ, Droz B, Meyer P, Morel F, Angiotensin II. Renal localization in glomerular mesangial cells by autoradiography. Kidney Int 1975;8:245–54.
[83] Kakinuma Y, Fogo A, Inagami T, Ichikawa I. Intrarenal localization of angiotensin II type 1 receptor mRNA in the rat. Kidney Int 1993;43:1229–35.
[84] Christensen JA, Bohle A, Mikeler E, Taugner R. Renin-positive granulated Goormaghtigh cells. Immunohistochemical and electron-microscopic studies on biopsies from patients with pseudo-Bartter syndrome. Cell Tissue Res 1989;255:149–53.
[85] Paul LC, Rennke HG, Milford EL, Carpenter CB. Thy-1.1 in glomeruli of rat kidneys. Kidney Int 1984;25:771–7.
[86] Cosio FG, Sedmak DD, Mahan JD, Nahman Jr. NS. Localization of decay accelerating factor in normal and diseased kidneys. Kidney Int 1989;36:100–7.
[87] Muller E, Neuhofer W, Ohno A, Rucker S, Thurau K, Beck FX. Heat shock proteins HSP25, HSP60, HSP72, HSP73 in isoosmotic cortex and hyperosmotic medulla of rat kidney. Pflugers Arch 1996;431:608–17.
[88] Kremer SG, Breuer WV, Skorecki KL. Vasoconstrictor hormones depolarize renal glomerular mesangial cells by activating chloride channels. J Cell Physiol 1989;138:97–105.
[89] Okuda T, Yamashita N, Kurokawa K. Angiotensin II and vasopressin stimulate calcium-activated chloride conductance in rat mesangial cells. J Clin Invest 1986;78:1443–8.
[90] Tsukahara H, Krivenko Y, Moore LC, Goligorsky MS. Decrease in ambient [Cl^-] stimulates nitric oxide release from cultured rat mesangial cells. Am J Physiol Renal Physiol 1994;267: F190–195.
[91] Barajas L. The development and ultrastructure of the juxtaglomerular cell granule. J Ultrastruct Res 1966;15:400–13.
[92] Taugner R, Rosivall L, Buhrle CP, Groschel-Stewart U. Myosin content and vasoconstrictive ability of the proximal and distal (renin-positive) segments of the preglomerular arteriole. Cell Tissue Res 1987;248:579–88.
[93] Casellas D, Dupont M, Kaskel FJ, Inagami T, Moore LC. Direct visualization of renin–cell distribution in preglomerular vascular trees dissected from rat kidney. Am J Physiol Renal Physiol 1993;265:F151–156.
[94] Gomez RA, Chevalier RL, Everett AD, Elwood JP, Peach MJ, Lynch KR, et al. Recruitment of renin gene-expressing cells in adult rat kidneys. Am J Physiol 1990;259:F660–665.
[95] Sauter A, Machura K, Neubauer B, Kurtz A, Wagner C. Development of renin expression in the mouse kidney. Kidney Int 2008;73:43–51.
[96] Celio MR, Inagami T. Angiotensin II immunoreactivity coexists with renin in the juxtaglomerular granular cells of the kidney. Proc Natl Acad Sci USA 1981;78:3897–900.
[97] Taugner R, Mannek E, Nobiling R, Buhrle CP, Hackenthal E, Ganten D, et al. Coexistence of renin and angiotensin II in

epitheloid cell secretory granules of rat kidney. Histochemistry 1984;81:39–45.
[98] Cantin M, Gutkowska J, Lacasse J, Ballack M, Ledoux S, Inagami T, et al. Ultrastructural immunocytochemical localization of renin and angiotensin II in the juxtaglomerular cells of the ischemic kidney in experimental renal hypertension. Am J Pathol 1984;115:212–24.
[99] Mercure C, Ramla D, Garcia R, Thibault G, Deschepper CF, Reudelhuber TL. Evidence for intracellular generation of angiotensin II in rat juxtaglomerular cells. FEBS Lett 1998;422:395–9.
[100] Naruse K, Inagami T, Celio MR, Workman RJ, Takii Y. Immunohistochemical evidence that angiotensins I and II are formed by intracellular mechanism in juxtaglomerular cells. Hypertension 1982;4:70–4.
[101] Burson JM, Aguilera G, Gross KW, Sigmund CD. Differential expression of angiotensin receptor 1A and 1B in mouse. Am J Physiol 1994;267:E260–267.
[102] Gasc JM, Shanmugam S, Sibony M, Corvol P. Tissue-specific expression of type 1 angiotensin II receptor subtypes. An *in situ* hybridization study. Hypertension 1994;24:531–7.
[103] Sanada H, Yao L, Jose PA, Carey RM, Felder RA. Dopamine D3 receptors in rat juxtaglomerular cells. Clin Exp Hypertens 1997;19:93–105.
[104] Yamaguchi I, Yao L, Sanada H, Ozono R, Mouradian MM, Jose PA, et al. Dopamine D1A receptors and renin release in rat juxtaglomerular cells. Hypertension 1997;29:962–8.
[105] Haefliger JA, Demotz S, Braissant O, Suter E, Waeber B, Nicod P, et al. Connexins 40 and 43 are differentially regulated within the kidneys of rats with renovascular hypertension. Kidney Int 2001;60:190–201.
[106] Kurtz L, Janssen-Bienhold U, Kurtz A, Wagner C. Connexin expression in renin-producing cells. J Am Soc Nephrol 2009;20:506–12.
[107] Wagner C, de Wit C, Kurtz L, Grunberger C, Kurtz A, Schweda F. Connexin40 is essential for the pressure control of renin synthesis and secretion. Circ Res 2007;100:556–63.
[108] Gambaryan S, Hausler C, Markert T, Pohler D, Jarchau T, Walter U, et al. Expression of type II cGMP-dependent protein kinase in rat kidney is regulated by dehydration and correlated with renin gene expression. J Clin Invest 1996;98:662–70.
[109] Kaplan MR, Plotkin MD, Brown D, Hebert SC, Delpire E. Expression of the mouse Na-K-2Cl co-transporter, mBSC2, in the terminal inner medullary collecting duct, the glomerular and extraglomerular mesangium, and the glomerular afferent arteriole. J Clin Invest 1996;98:723–30.
[110] Anderson TJ, Martin S, Berka JL, James DE, Slot JW, Stow JL. Distinct localization of renin and GLUT-4 in juxtaglomerular cells of mouse kidney. Am J Physiol 1998;274:F26–33.
[111] Skott O. Episodic release of renin from single isolated superfused rat afferent arterioles. Pflugers Arch 1986;407:41–5.
[112] Friis UG, Jensen BL, Hansen PB, Andreasen D, Skott O. Exocytosis and endocytosis in juxtaglomerular cells. Acta Physiol Scand 2000;168:95–9.
[113] Peti-Peterdi J, Fintha A, Fuson AL, Tousson A, Chow RH. Real-time imaging of renin release *in vitro*. Am J Physiol Renal Physiol 2004;287:F329–335.
[114] Kurtz A, Penner R. Angiotensin II induces oscillations of intracellular calcium and blocks anomalous inward rectifying potassium current in mouse renal juxtaglomerular cells. Proc Natl Acad Sci USA 1989;86:3423–7.
[115] Friis UG, Jorgensen F, Andreasen D, Jensen BL, Skott O. Molecular and functional identification of cyclic AMP-sensitive BKCa potassium channels (ZERO variant) and L-type voltage-dependent calcium channels in single rat juxtaglomerular cells. Circ Res 2003;93:213–20.
[116] Russ U, Rauch U, Quast U. Pharmacological evidence for a KATP channel in renin-secreting cells from rat kidney. J Physiol 1999;517(Pt 3):781–90.
[117] Kurtz A, Skott O, Chegini S, Penner R. Lack of direct evidence for a functional role of voltage-operated calcium channels in juxtaglomerular cells. Pflugers Arch 1990;416:281–7.
[118] Friis UG, Jorgensen F, Andreasen D, Jensen BL, Skott O. Membrane potential and cation channels in rat juxtaglomerular cells. Acta Physiol Scand 2004;181:391–6.
[119] Castrop H, Lorenz JN, Hansen PB, Friis U, Mizel D, Oppermann M, et al. Contribution of the basolateral isoform of the Na-K-2Cl$^-$ co-transporter (NKCC1/BSC2) to renin secretion. Am J Physiol Renal Physiol 2005;289:F1185–1192.
[120] Schnermann J, Wright FS, Davis JM, Stackelberg WV, Grill G. Regulation of superficial nephron filtration rate by tubuloglomerular feedback. Pflugers Arch 1970;318:147–75.
[121] Briggs JP, Schubert G, Schnermann J. Quantitative characterization of the tubuloglomerular feedback response: effect of growth. Am J Physiol Renal Physiol 1984;247:F808–15.
[122] Thomson SC, Blantz RC. Homeostatic efficiency of tubuloglomerular feedback in hydropenia, euvolemia, and acute volume expansion. Am J Physiol Renal Physiol 1993;264: F930–936.
[123] Thomson S, Vallon V, Blantz RC. Asymmetry of tubuloglomerular feedback effector mechanism with respect to ambient tubular flow. Am J Physiol Renal Physiol 1996;271:F1123–30.
[124] Navar LG, Burke TJ, Robinson RR, Clapp JR. Distal tubular feedback in the autoregulation of single nephron glomerular filtration rate. J Clin Invest 1974;53:516–25.
[125] Vallon V, Richter K, Huang DY, Rieg T, Schnermann J. Functional consequences at the single-nephron level of the lack of adenosine A1 receptors and tubuloglomerular feedback in mice. Pflugers Arch 2004;448:214–21.
[126] Muller-Suur R, Ulfendahl HR, Persson AE. Evidence for tubuloglomerular feedback in juxtamedullary nephrons of young rats. Am J Physiol Renal Physiol 1983;244:F425–431.
[127] Muller-Suur R, Persson AE. Influence of water-diuresis or saline volume expansion on deep nephron tubuloglomerular feedback. Acta Physiol Scand 1986;126:139–46.
[128] Ren Y, Garvin JL, Liu R, Carretero OA. Crosstalk between the connecting tubule and the afferent arteriole regulates renal microcirculation. Kidney Int 2007;71:1116–21.
[129] Wang H, Garvin JL, D'Ambrosio MA, Ren Y, Carretero OA. Connecting tubule glomerular feedback (CTGF) antagonizes tubuloglomerular feedback (TGF) *in vivo*. Am J Physiol Renal Physiol 2010;299:F1374–8.
[130] Yip KP, Holstein-Rathlou NH, Marsh DJ. Mechanisms of temporal variation in single-nephron blood flow in rats. Am J Physiol Renal Physiol 1993;264:F427–434.
[131] Leyssac PP, Baumbach L. An oscillating intratubular pressure response to alterations in Henle loop flow in the rat kidney. Acta Physiol Scand 1983;117:415–9.
[132] Holstein-Rathlou NH. Synchronization of proximal intratubular pressure oscillations: evidence for interaction between nephrons. Pflugers Arch 1987;408:438–43.
[133] Yip KP, Holstein-Rathlou NH, Marsh DJ. Dynamics of TGF-initiated nephron–nephron interactions in normotensive rats and SHR. Am J Physiol Renal Physiol 1992;262:F980–988.
[134] Holstein-Rathlou NH, Sosnovtseva OV, Pavlov AN, Cupples WA, Sorensen CM, Marsh DJ. Nephron blood flow dynamics measured by laser speckle contrast imaging. Am J Physiol Renal Physiol 2011;300:F319–29.
[135] Leyssac PP, Holstein-Rathlou NH. Effects of various transport inhibitors on oscillating TGF pressure responses in the rat. Pflugers Arch 1986;407:285–91.

[136] Holstein-Rathlou NH, Marsh DJ. Oscillations of tubular pressure, flow, and distal chloride concentration in rats. Am J Physiol Renal Physiol 1989;256:F1007–1014.
[137] Holstein-Rathlou NH, Marsh DJ. A dynamic model of the tubuloglomerular feedback mechanism. Am J Physiol Renal Physiol 1990;258:F1448–1459.
[138] Layton HE, Pitman EB, Moore LC. Bifurcation analysis of TGF-mediated oscillations in SNGFR. Am J Physiol Renal Physiol 1991;261:F904–919.
[139] Marsh DJ, Sosnovtseva OV, Pavlov AN, Yip KP, Holstein-Rathlou NH. Frequency encoding in renal blood flow regulation. Am J Physiol Regul Integr Comp Physiol 2005;288: R1160–1167.
[140] Holstein-Rathlou NH, Leyssac PP. TGF-mediated oscillations in the proximal intratubular pressure: differences between spontaneously hypertensive rats and Wistar-Kyoto rats. Acta Physiol Scand 1986;126:333–9.
[141] Karlsen FM, Leyssac PP, Holstein-Rathlou NH. Tubuloglomerular feedback in Dahl rats. Am J Physiol Renal Physiol 1998;274: R1561–1569.
[142] Yip KP, Holstein-Rathlou NH, Marsh DJ. Chaos in blood flow control in genetic and renovascular hypertensive rats. Am J Physiol Renal Physiol 1991;261:F400–408.
[143] Laugesen JL, Sosnovtseva OV, Mosekilde E, Holstein-Rathlou NH, Marsh DJ. Coupling-induced complexity in nephron models of renal blood flow regulation. Am J Physiol Regul Integr Comp Physiol 298:R997–1006.
[144] Layton AT, Moore LC, Layton HE. Multistability in tubuloglomerular feedback and spectral complexity in spontaneously hypertensive rats. Am J Physiol Renal Physiol 2006;291: F79–97.
[145] Schurek HJ, Johns O. Is tubuloglomerular feedback a tool to prevent nephron oxygen deficiency? Kidney Int 1997;51:386–92.
[146] Bell PD, Navar LG. Relationship between tubulo-glomerular feedback responses and perfusate hypotonicity. Kidney Int 1982;22:234–9.
[147] Briggs J, Schubert G, Schnermann J. Further evidence for an inverse relationship between macula densa NaCl concentration and filtration rate. Pflugers Arch 1982;392:372–8.
[148] Schnermann J, Ploth DW, Hermle M. Activation of tubuloglomerular feedback by chloride transport. Pfluegers Arch 1976;362:229–40.
[149] Briggs JP, Schnermann J, Wright FS. Failure of tubule fluid osmolarity to affect feedback regulation of glomerular filtration. Am J Physiol Renal Physiol 1980;239:F427–432.
[150] Peti-Peterdi J. Calcium wave of tubuloglomerular feedback. Am J Physiol Renal Physiol 2006;291:F473–480.
[151] Sipos A, Vargas SL, Peti-Peterdi J. Direct demonstration of tubular fluid flow sensing by macula densa cells. Am J Physiol Renal Physiol 2010;299:F1087–93.
[152] Thurau K, Schnermann J. The Na concentration at the macula densa cells as a factor regulating glomerular filtration rate (micropuncture studies). 1965 [classical article]. J Am Soc Nephrol 1998;9:925–34.
[153] Gutsche HU, Muller-Suur R, Hegel U, Hierholzer K. Electrical conductivity of tubular fluid of the rat nephron. Micropuncture study of the diluting segment *in situ*. Pflugers Arch 1980;383:113–21.
[154] Morgan T, Berliner RW. A study by continuous microperfusion of water and electrolyte movements in the loop of Henle and distal tubule of the rat. Nephron 1969;6:388–405.
[155] Schnermann J, Briggs J, Schubert G. *In situ* studies of the distal convoluted tubule in the rat. I. Evidence for NaCl secretion. Am J Physiol 1982;243:F160–166.
[156] Seney FD, Wright FS. Signal for tubuloglomerular feedback control of GFR: separate changes of sodium and chloride at constant osmolality. Kidney Int 1986;29:388.
[157] Wright FS, Mandin H, Persson AE. Studies of the sensing mechanism in the tubuloglomerular feedback pathway. Kidney Int Suppl 1982;12:S90–96.
[158] Bell PD, McLean CB, Navar LG. Dissociation of tubuloglomerular feedback responses from distal tubular chloride concentration in the rat. Am J Physiol Renal Physiol 1981;240:F111–119.
[159] Wright FS, Schnermann J. Interference with feedback control of glomerular filtration rate by furosemide, triflocin, and cyanide. J Clin Invest 1974;53:1695–708.
[160] Mason J, Takabatake T, Olbricht C, Thurau K. The early phase of experimental acute renal failure. III. Tubologlomerular feedback. Pflugers Arch 1978;373:69–76.
[161] Franco M, Bell PD, Navar LG. Effect of adenosine A1 analogue on tubuloglomerular feedback mechanism. Am J Physiol Renal Physiol 1989;257:F231–236.
[162] Schnermann J, Briggs JP. Concentration-dependent sodium chloride transport as the signal in feedback control of glomerular filtration rate. Kidney Int 1982;22(Suppl. 12):S82–9.
[163] Oppermann M, Mizel D, Kim SM, Chen L, Faulhaber-Walter R, Huang Y, et al. Renal function in mice with targeted disruption of the A isoform of the Na-K-2Cl co-transporter. J Am Soc Nephrol 2007;18:440–8.
[164] Kinne R, Koenig B, Hannafin J, Kinne-Saffran E, Scott DM, Zierold K. The use of membrane vesicles to study the NaCl/KCl co-transporter involved in active transepithelial chloride transport. Pflugers Arch 1985;405(Suppl. 1):S101–105.
[165] Okusa MD, Persson AE, Wright FS. Chlorothiazide effect on feedback-mediated control of glomerular filtration rate. Am J Physiol Renal Physiol 1989;257:F137–144.
[166] Vallon V, Osswald H, Blantz RC, Thomson S. Potential role of luminal potassium in tubuloglomerular feedback. J Am Soc Nephrol 1997;8:1831–7.
[167] Lorenz JN, Baird NR, Judd LM, Noonan WT, Andringa A, Doetschman T, et al. Impaired renal NaCl absorption in mice lacking the ROMK potassium channel, a model for type II Bartter's syndrome. J Biol Chem 2002;277:37871–80.
[168] Lu M, Wang T, Yan Q, Yang X, Dong K, Knepper MA, et al. Absence of small conductance K^+ channel (SK) activity in apical membranes of thick ascending limb and cortical collecting duct in ROMK (Bartter's) knockout mice. J Biol Chem 2002;277:37881–7.
[169] Schnermann J, Briggs JP. Tubuloglomerular feedback: mechanistic insights from gene-manipulated mice. Kidney Int 2008;74:418–26.
[170] Braam B, Boer P, Koomans HA. Tubuloglomerular feedback and tubular reabsorption during acute potassium loading in rats. Am J Physiol Renal Physiol 1994;267:F223–230.
[171] Kinne R, Kinne-Saffran E, Schutz H, Scholermann B. Ammonium transport of medullary thick ascending limb of rabbit kidney: involvement of the Na^+,K^+,Cl-co-transporter. J Membr Biol 1986;94:279–84.
[172] Greger R. Ion transport mechanism in thick ascending limb of Henle's loop of mammalian nephron. Physiol Rev 1985;65:760–97.
[173] Lapointe JY, Laamarti A, Hurst AM, Fowler BC, Bell PD. Activation of Na:2Cl:K co-transport by luminal chloride in macula densa cells. Kidney Int 1995;47:752–7.
[174] Briggs JP, Schnermann J. The effect of metabolic inhibitors on feedback response of nephron filtration rate. Pflugers Arch 1981;389(*Suppl*):R40.
[175] Price EM, Lingrel JB. Structure–function relationships in the Na,K-ATPase alpha subunit: Site-directed mutagenesis of

glutamine-111 to arginine and asparagine-122 to aspartic acid generates a ouabain-resistant enzyme. Biochemistry 1988;27:8400–8.

[176] Lorenz JN, Dostanic-Larson I, Shull GE, Lingrel JB. Ouabain inhibits tubuloglomerular feedback in mutant mice with ouabain-sensitive alpha1 Na,K-ATPase. J Am Soc Nephrol 2006;17:2457–63.

[177] Bell PD, Reddington M, Ploth D, Navar LG. Tubuloglomerular feedback-mediated decreases in glomerular pressure in Munich-Wistar rats. Am J Physiol Renal Physiol 1984;247:F877–880.

[178] Briggs JP. Effect of loop of Henle flow rate on glomerular capillary pressure. Ren Physiol 1984;7:311–20.

[179] Persson AE, Gushwa LC, Blantz RC. Feedback pressure-flow responses in normal and angiotensin-prostaglandin-blocked rats. Am J Physiol Renal Physiol 1984;247:F925–931.

[180] Peterson OW, Gushwa LC, Wilson CB, Blantz RC. Tubuloglomerular feedback activity after glomerular immune injury. Am J Physiol Renal Physiol 1989;257:F67–71.

[181] Casellas D, Moore LC. Autoregulation and tubuloglomerular feedback in juxtamedullary glomerular arterioles. Am J Physiol Renal Physiol 1990;258:F660–669.

[182] Gertz KH, Mangos JA, Braun G, Pagel HD. Pressure in the glomerular capillaries of the rat kidney and its relation to arterial blood pressure. Pflugers Arch Gesamte Physiol Menschen Tiere 1966;288:369–74.

[183] Bell PD, Thomas C, Williams RH, Navar LG. Filtration rate and stop-flow pressure feedback responses to nephron perfusion in the dog. Am J Physiol 1978;234:F154–165.

[184] Navar LG, Chomdej B, Bell PD. Absence of estimated glomerular pressure autoregulation during interrupted distal delivery. Am J Physiol 1975;229:1596–603.

[185] Schnermann J, Traynor T, Yang T, Huang YG, Oliverio MI, Coffman T, et al. Absence of tubuloglomerular feedback responses in AT1A receptor-deficient mice. Am J Physiol Renal Physiol 1997;273:F315–320.

[186] Schnermann J, Persson AE, Agerup B. Tubuloglomerular feedback. Nonlinear relation between glomerular hydrostatic pressure and loop of Henle perfusion rate. J Clin Invest 1973;52:862–9.

[187] Boknam L, Ericson AC, Aberg B, Ulfendahl HR. Flow resistance of the interlobular artery in the rat kidney. Acta Physiol Scand 1981;111:159–63.

[188] Heyeraas Tonder KJ, Aukland K. Interlobular arterial pressure in the rat kidney. Renal Physiol 1979/80;2:214–21.

[189] Briggs JP, Wright FS. Feedback control of glomerular filtration rate: site of the effector mechanism. Am J Physiol 1979;236:F40–47.

[190] Ichikawa I. Direct analysis of the effector mechanism of the tubuloglomerular feedback system. Am J Physiol Renal Physiol 1982;243:F447–455.

[191] Steinhausen M, Zimmerhackl B, Thederan H, Dussel R, Parekh N, Esslinger HU, et al. Intraglomerular microcirculation: measurements of single glomerular loop flow in rats. Kidney Int 1981;20:230–9.

[192] Persson BE, Sakai T, Marsh DJ. Juxtaglomerular interstitial hypertonicity in *Amphiuma*: tubular origin-TGF signal. Am J Physiol 1988;254:F445–449.

[193] Persson BE, Sakai T, Ekblom M, Marsh DJ. Effect of bumetanide on tubuloglomerular feedback in *Necturus maculosus*. Acta Physiol Scand 1989;137:93–9.

[194] Ito S, Carretero OA. An *in vitro* approach to the study of macula densa-mediated glomerular hemodynamics. Kidney Int 1990;38:1206–10.

[195] Moore LC, Casellas D. Tubuloglomerular feedback dependence of autoregulation in rat juxtamedullary afferent arterioles. Kidney Int 1990;37:1402–8.

[196] Morsing P, Velazquez H, Ellison D, Wright FS. Resetting of tubuloglomerular feedback by interrupting early distal flow. Acta Physiol Scand 1993;148:63–8.

[197] Marsh DJ, Toma I, Sosnovtseva OV, Peti-Peterdi J, Holstein-Rathlou NH. Electrotonic vascular signal conduction and nephron synchronization. Am J Physiol Renal Physiol 2009;296:F751–761.

[198] Haberle DA, Kawata T, Davis JM. The site of action of nitrendipine in the rat kidney. J Cardiovasc Pharmacol 1987;9(Suppl. 1):S17–23.

[199] Mitchell KD, Navar LG. Tubuloglomerular feedback responses during peritubular infusions of calcium channel blockers. Am J Physiol Renal Physiol 1990;258:F537–544.

[200] Muller-Suur R, Gutsche HU, Schurek HJ. Acute and reversible inhibition of tubuloglomerular feedback mediated afferent vasoconstriction by the calcium-antagonist verapamil. Curr Probl Clin Biochem 1976;6:291–8.

[201] Bell PD. Cyclic AMP-calcium interaction in the transmission of tubuloglomerular feedback signals. Kidney Int 1985;28:728–32.

[202] Schnermann J. Juxtaglomerular cell complex in the regulation of renal salt excretion. Am J Physiol Renal Physiol 1998;274: R263–279.

[203] Hansen PB, Castrop H, Briggs J, Schnermann J. Adenosine induces vasoconstriction through GI-dependent activation of phospholipase C in isolated perfused afferent arterioles of mice. J Am Soc Nephrol 2003;14:2457–65.

[204] Weihprecht H, Lorenz JN, Briggs JP, Schnermann J. Vasoconstrictor effect of angiotensin and vasopressin in isolated rabbit afferent arterioles. Am J Physiol Renal Physiol 1991;261:F273–282.

[205] Gustafsson F, Holstein-Rathlou N. Conducted vasomotor responses in arterioles: characteristics, mechanisms and physiological significance. Acta Physiol Scand 1999;167:11–21.

[206] Moore LC, Rich A, Casellas D. Ascending myogenic autoregulation: interactions between tubuloglomerular feedback and myogenic mechanisms. Bull Math Biol 1994;56:391–410.

[207] Wagner AJ, Holstein-Rathlou NH, Marsh DJ. Internephron coupling by conducted vasomotor responses in normotensive and spontaneously hypertensive rats. Am J Physiol 1997;272: F372–379.

[208] Chen YM, Yip KP, Marsh DJ, Holstein-Rathlou NH. Magnitude of TGF-initiated nephron–nephron interactions is increased in SHR. Am J Physiol Renal Physiol 1995;269:F198–204.

[209] Kallskog O, Marsh DJ. TGF-initiated vascular interactions between adjacent nephrons in the rat kidney. Am J Physiol Renal Physiol 1990;259:F60–64.

[210] Wagner C. Function of connexins in the renal circulation. Kidney Int 2008;73:547–55.

[211] Tucker BJ, Steiner RW, Gushwa LC, Blantz RC. Studies on the tubulo-glomerular feedback system in the rat. The mechanism of reduction in filtration rate with benzolamide. J Clin Invest 1978;62:993–1004.

[212] Schnermann J, Briggs JP. Single nephron comparison of the effect of loop of Henle flow on filtration rate and pressure in control and angiotensin II-infused rats. Miner Electrolyte Metab 1989;15:103–7.

[213] Ren Y, Garvin JL, Carretero OA. Efferent arteriole tubuloglomerular feedback in the renal nephron. Kidney Int 2001;59:222–9.

[214] Osswald H, Nabakowski G, Hermes H. Adenosine as a possible mediator of metabolic control of glomerular filtration rate. Int J Biochem 1980;12:263–7.

[215] Spielman WS, Thompson CI. A proposed role for adenosine in the regulation of renal hemodynamics and renin release. Am J Physiol 1982;242:F423–435.

[216] Beck JS, Breton S, Mairbaurl H, Laprade R, Giebisch G. Relationship between sodium transport and intracellular ATP in isolated perfused rabbit proximal convoluted tubule. Am J Physiol 1991;261:F634–639.
[217] Kelley GG, Aassar OS, Forrest Jr. JN. Endogenous adenosine is an autacoid feedback inhibitor of chloride transport in the shark rectal gland. J Clin Invest 1991;88:1933–9.
[218] Vallon V, Muhlbauer B, Osswald H. Adenosine and kidney function. Physiol Rev 2006;86:901–40.
[219] Hansen PB, Hashimoto S, Oppermann M, Huang Y, Briggs JP, Schnermann J. Vasoconstrictor and vasodilator effects of adenosine in the mouse kidney due to preferential activation of A1 or A2 adenosine receptors. J Pharmacol Exp Ther 2005;315:1150–7.
[220] Holz FG, Steinhausen M. Renovascular effects of adenosine receptor agonists. Renal Physiol 1987;10:272–82.
[221] Nishiyama A, Inscho EW, Navar LG. Interactions of adenosine A_1 and A_{2a} receptors on renal microvascular reactivity. Am J Physiol Renal Physiol 2001;280:F406–14.
[222] Weihprecht H, Lorenz JN, Briggs JP, Schnermann J. Vasomotor effects of purinergic agonists in isolated rabbit afferent arterioles. Am J Physiol Renal Physiol 1992;263:F1026–1033.
[223] Lai EY, Patzak A, Steege A, Mrowka R, Brown R, Spielmann N, et al. Contribution of adenosine receptors in the control of arteriolar tone and adenosine–angiotensin II interaction. Kidney Int 2006;70:690–8.
[224] Weaver DR, Reppert SM. Adenosine receptor gene expression in rat kidney. Am J Physiol Renal Physiol 1992;263:F991–995.
[225] Hansen PB, Schnermann J. Vasoconstrictor and vasodilator effects of adenosine in the kidney. Am J Physiol Renal Physiol 2003;285:F590–599.
[226] Lai EY, Patzak A, Persson AE, Carlstrom M. Angiotensin II enhances the afferent arteriolar response to adenosine through increases in cytosolic calcium. Acta Physiol (Oxf) 2009;196:435–45.
[227] Schnermann J. Effect of adenosine analogues on tubuloglomerular feedback responses. Am J Physiol Renal Physiol 1988;255: F33–42.
[228] Schnermann J, Weihprecht H, Briggs JP. Inhibition of tubuloglomerular feedback during adenosine1 receptor blockade. Am J Physiol Renal Physiol 1990;258:F553–561.
[229] Brown R, Ollerstam A, Johansson B, Skøtt O, Gebre-Medhin S, Fredholm B, et al. Abolished tubuloglomerular feedback and increased plasma renin in adenosine A1 receptor-deficient mice. Am J Physiol Regul Integr Comp Physiol 2001;281: R1362–1367.
[230] Sun D, Samuelson LC, Yang T, Huang Y, Paliege A, Saunders T, et al. Mediation of tubuloglomerular feedback by adenosine: evidence from mice lacking adenosine 1 receptors. Proc Natl Acad Sci USA 2001;98:9983–8.
[231] Carlstrom M, Wilcox CS, Welch WJ. Adenosine A(2) receptors modulate tubuloglomerular feedback. Am J Physiol Renal Physiol 2010;299:F412–417.
[232] Schnermann J, Osswald H, Hermle M. Inhibitory effect of methylxanthines on feedback control of glomerular filtration rate in the rat. Pflugers Arch 1977;369:39–48.
[233] Ren Y, Arima S, Carretero OA, Ito S. Possible role of adenosine in macula densa control of glomerular hemodynamics. Kidney Int 2002;61:169–76.
[234] Carlstrom M, Wilcox CS, Welch WJ. Adenosine A2A receptor activation attenuates tubuloglomerular feedback responses by stimulation of endothelial nitric oxide synthase. Am J Physiol Renal Physiol 2011;300:F457–64.
[235] Al-Mashhadi RH, Skott O, Vanhoutte PM, Hansen PB. Activation of A(2) adenosine receptors dilates cortical efferent arterioles in mouse. Kidney Int 2009;75:793–9.
[236] Bell PD, Lapointe JY, Sabirov R, Hayashi S, Peti-Peterdi J, Manabe K, et al. Macula densa cell signaling involves ATP release through a maxi anion channel. Proc Natl Acad Sci USA 2003;100:4322–7.
[237] Komlosi P, Peti-Peterdi J, Fuson AL, Fintha A, Rosivall L, Bell PD. Macula densa basolateral ATP release is regulated by luminal [NaCl] and dietary salt intake. Am J Physiol Renal Physiol 2004;286:F1054–1058.
[238] Sabirov RZ, Okada Y. The maxi-anion channel: a classical channel playing novel roles through an unidentified molecular entity. J Physiol Sci 2009;59:3–21.
[239] Stoessel A, Himmerkus N, Bleich M, Bachmann S, Theilig F. Connexin 37 is localized in renal epithelia and responds to changes in dietary salt intake. Am J Physiol Renal Physiol 2010;298:F216–223.
[240] Oppermann M, Friedman DJ, Faulhaber-Walter R, Mizel D, Castrop H, Enmjyoji K, et al. Tubuloglomerular feedback and renin secretion in NTPDase1/CD39-deficient mice. Am J Physiol Renal Physiol 2008;294:F965–970.
[241] Thomson S, Bao D, Deng A, Vallon V. Adenosine formed by 5′-nucleotidase mediates tubuloglomerular feedback. J Clin Invest 2000;106:289–98.
[242] Castrop H, Huang Y, Hashimoto S, Mizel D, Hansen P, Theilig F, et al. Impairment of tubuloglomerular feedback regulation of GFR in ecto-5′-nucleotidase/CD73-deficient mice. J Clin Invest 2004;114:634–42.
[243] Huang DY, Vallon V, Zimmermann H, Koszalka P, Schrader J, Osswald H. Ecto-5′-nucleotidase (cd73)-dependent and -independent generation of adenosine participates in the mediation of tubuloglomerular feedback *in vivo*. Am J Physiol Renal Physiol 2006;291:F282–288.
[244] Ren Y, Garvin JL, Liu R, Carretero OA. Role of macula densa adenosine triphosphate (ATP) in tubuloglomerular feedback. Kidney Int 2004;66:1479–85.
[245] Takenaka T, Okada H, Kanno Y, Inoue T, Ryuzaki M, Nakamoto H, et al. Exogenous 5′-nucleotidase improves glomerular autoregulation in Thy-1 nephritic rats. Am J Physiol Renal Physiol 2006;290:F844–853.
[246] Le Hir M, Kaissling B. Distribution and regulation of renal ecto-5′-nucleotidase: implications for physiological functions of adenosine. Am J Physiol 1993;264:F377–387.
[247] Stefanovic V, Savic V, Vlahovic P, Ardaillou N, Ardaillou R. Ecto-5′-nucleotidase of cultured rat mesangial cells. Ren Physiol Biochem 1988;11:89–102.
[248] Kawabata M, Haneda M, Wang T, Imai M, Takabatake T. Effects of a nucleoside transporter inhibitor, dilazep, on renal microcirculation in rats. Hypertens Res 2002;25:615–21.
[249] Vallon V, Osswald H. Dipyridamole prevents diabetes-induced alterations of kidney function in rats. Naunyn Schmiedebergs Arch Pharmacol 1994;349:217–22.
[250] Inscho EW. P2 receptors in regulation of renal microvascular function. Am J Physiol Renal Physiol 2001;280:F927–944.
[251] Navar LG, Inscho EW, Majid SA, Imig JD, Harrison-Bernard LM, Mitchell KD. Paracrine regulation of the renal microcirculation. Physiol Rev 1996;76:425–536.
[252] Chan CM, Unwin RJ, Bardini M, Oglesby IB, Ford AP, Townsend-Nicholson A, et al. Localization of P2X1 purinoceptors by autoradiography and immunohistochemistry in rat kidneys. Am J Physiol 1998;274:F799–804.
[253] Schnermann J. Maintained tubuloglomerular feedback responses during acute inhibition of P2 purinergic receptors in mice. Am J Physiol Renal Physiol 2011;300:F339–44.
[254] Salomonsson M, Gonzalez E, Westerlund P, Persson AE. Chloride concentration in macula densa and cortical thick ascending limb cells. Kidney Int Suppl 1991;32:S51–54.

[255] Bell PD, Lapointe JY, Cardinal J. Direct measurement of basolateral membrane potentials from cells of the macula densa. Am J Physiol Renal Physiol 1989;257:F463–468.
[256] Ren Y, Yu H, Wang H, Carretero OA, Garvin JL. Nystatin and valinomycin induce tubuloglomerular feedback. Am J Physiol Renal Physiol 2001;281:F1102–1108.
[257] Bell PD, Navar LG. Cytoplasmic calcium in the mediation of macula densa tubulo-glomerular feedback responses. Science 1982;215:670–3.
[258] Bell PD, Reddington M. Intracellular calcium in the transmission of tubuloglomerular feedback signals. Am J Physiol Renal Physiol 1983;245:F295–302.
[259] Ren Y, Liu R, Carretero OA, Garvin JL. Increased intracellular Ca^{++} in the macula densa regulates tubuloglomerular feedback. Kidney Int 2003;64:1348–55.
[260] Peti-Peterdi J, Bell PD. Cytosolic [Ca^{2+}] signaling pathway in macula densa cells. Am J Physiol Renal Physiol 1999;277: F472–476.
[261] Lapointe JY, Bell PD, Sabirov RZ, Okada Y. Calcium-activated nonselective cationic channel in macula densa cells. Am J Physiol Renal Physiol 2003;285:F275–280.
[262] Naruse M, Inoue T, Nakayama M, Sato T, Kurokawa K. Effect of luminal Cl^- and Ca^{2+} on tubuloglomerular feedback mechanism. Jpn J Physiol 1994;44:S269–272.
[263] Liu R, Ren Y, Garvin JL, Carretero OA. Superoxide enhances tubuloglomerular feedback by constricting the afferent arteriole. Kidney Int 2004;66:268–74.
[264] Hong NJ, Garvin JL. Flow increases superoxide production by NADPH oxidase via activation of Na-K-2Cl co-transport and mechanical stress in thick ascending limbs. Am J Physiol Renal Physiol 2007;292:F993–998.
[265] Liu R, Garvin JL, Ren Y, Pagano PJ, Carretero OA. Depolarization of the macula densa induces superoxide production via NAD(P)H oxidase. Am J Physiol Renal Physiol 2007;292:F1867–1872.
[266] Fu Y, Zhang R, Lu D, Liu H, Chandrashekar K, Juncos LA, Liu R. NOX2 is the primary source of angiotensin II-induced superoxide in the macula densa. Am J Physiol Regul Integr Comp Physiol 2010;298:R707–712.
[267] Liu R, Juncos LA. GTPase-Rac enhances depolarization-induced superoxide production by the macula densa during tubuloglomerular feedback. Am J Physiol Regul Integr Comp Physiol 2010;298:R453–458.
[268] Zhang R, Harding P, Garvin JL, Juncos R, Peterson E, Juncos LA, et al. Isoforms and functions of NAD(P)H oxidase at the macula densa. Hypertension 2009;53:556–63.
[269] Marsh DJ, Osborn JL, Cowley Jr. AW. 1/f fluctuations in arterial pressure and regulation of renal blood flow in dogs. Am J Physiol 1990;258:F1394–1400.
[270] Thomson SC, Blantz RC, Vallon V. Increased tubular flow induces resetting of tubuloglomerular feedback in euvolemic rats. Am J Physiol Renal Physiol 1996;270:F461–468.
[271] Holstein-Rathlou NH. A closed-loop analysis of the tubuloglomerular feedback mechanism. Am J Physiol Renal Physiol 1991;261:F880–889.
[272] Guyton AC, Langston JB, Navar G. Theory for renal autoregulation by feedback at the juxtaglomerular apparatus. Circ Res. 1964;15(Suppl):187–97.
[273] Thurau K. Renal hemodynamics. Am J Med 1964;36:850–60.
[274] Moore LC, Schnermann J, Yarimizu S. Feedback mediation of SNGFR autoregulation in hydropenic and DOCA- and salt-loaded rats. Am J Physiol Renal Physiol 1979;237:F63–74.
[275] Moore LC. Tubuloglomerular feedback and SNGFR autoregulation in the rat. Am J Physiol Renal Physiol 1984;247: F267–276.
[276] Ploth DW, Schnermann J, Dahlheim H, Hermle M, Schmidmeier E. Autoregulation and tubuloglomerular feedback in normotensive and hypertensive rats. Kidney Int 1977;12:253–67.
[277] Ploth DW, Dahlheim H, Schmidmeier E, Hermle M, Schnermann J. Tubuloglomerular feedback and autoregulation of glomerular filtration rate in Wistar-Kyoto spontaneously hypertensive rats. Pflugers Arch 1978;375:261–7.
[278] Schnermann J, Briggs JP, Weber PC. Tubuloglomerular feedback, prostaglandins, and angiotensin in the autoregulation of glomerular filtration rate. Kidney Int 1984;25:53–64.
[279] Sjoquist M, Goransson A, Kallskog O, Ulfendahl HR. The influence of tubulo-glomerular feedback on the autoregulation of filtration rate in superficial and deep glomeruli. Acta Physiol Scand 1984;122:235–42.
[280] Sanchez-Ferrer CF, Roman RJ, Harder DR. Pressure-dependent contraction of rat juxtamedullary afferent arterioles. Circ Res 1989;64:790–8.
[281] Takenaka T, Harrison-Bernard LM, Inscho EW, Carmines PK, Navar LG. Autoregulation of afferent arteriolar blood flow in juxtamedullary nephrons. Am J Physiol Renal Physiol 1994;267:F879–887.
[282] Gilmore JP, Cornish KG, Rogers SD, Joyner WL. Direct evidence for myogenic autoregulation of the renal microcirculation in the hamster. Circ Res 1980;47:226–30.
[283] Steinhausen M, Blum M, Fleming JT, Holz FG, Parekh N, Wiegman DL. Visualization of renal autoregulation in the split hydronephrotic kidney of rats. Kidney Int 1989;35:1151–60.
[284] Edwards RM. Segmental effects of norepinephrine and angiotensin II on isolated renal microvessels. Am J Physiol 1983;244: F526–534.
[285] Harder DR, Gilbert R, Lombard JH. Vascular muscle cell depolarization and activation in renal arteries on elevation of transmural pressure. Am J Physiol 1987;253:F778–781.
[286] Lai EY, Onozato ML, Solis G, Aslam S, Welch WJ, Wilcox CS. Myogenic responses of mouse isolated perfused renal afferent arterioles: effects of salt intake and reduced renal mass. *Hypertension* 2010;55:983–9.
[287] Daniels FH, Arendshorst WJ. Tubuloglomerular feedback kinetics in spontaneously hypertensive and Wistar-Kyoto rats. Am J Physiol Renal Physiol 1990;259:F529–534.
[288] Holstein-Rathlou NH, Wagner AJ, Marsh DJ. Tubuloglomerular feedback dynamics and renal blood flow autoregulation in rats. Am J Physiol Renal Physiol 1991;260: F53–68.
[289] Young DK, Marsh DJ. Pulse wave propagation in rat renal tubules: implications for GFR autoregulation. Am J Physiol 1981;240:F446–458.
[290] Chon KH, Chen YM, Marmarelis VZ, Marsh DJ, Holstein-Rathlou NH. Detection of interactions between myogenic and TGF mechanisms using nonlinear analysis [published erratum appears in Am J Physiol Renal Physiol 1994 Dec;267(6 Pt 3): section F following table of contents] Am J Physiol Renal Physiol 1994;267:F160–173.
[291] Chon KH, Chen YM, Holstein-Rathlou NH, Marmarelis VZ. Nonlinear system analysis of renal autoregulation in normotensive and hypertensive rats. IEEE Trans Biomed Eng 1998;45:342–53.
[292] Holstein-Rathlou NH, Marsh DJ. Renal blood flow regulation and arterial pressure fluctuations: a case study in nonlinear dynamics. Physiol Rev 1994;74:637–81.
[293] Chen YM, Holstein-Rathlou NH. Differences in dynamic autoregulation of renal blood flow between SHR and WKY rats. Am J Physiol Renal Physiol 1993;264:F166–174.

[294] Daniels FH, Arendshorst WJ, Roberds RG. Tubuloglomerular feedback and autoregulation in spontaneously hypertensive rats. Am J Physiol Renal Physiol 1990;258:F1479–1489.
[295] Karlsen FM, Andersen CB, Leyssac PP, Holstein-Rathlou NH. Dynamic autoregulation and renal injury in Dahl rats. Hypertension 1997;30:975–83.
[296] Iliescu R, Cazan R, McLemore Jr. GR, Venegas-Pont M, Ryan MJ. Renal blood flow and dynamic autoregulation in conscious mice. Am J Physiol Renal Physiol 2008;295: F734–740.
[297] Wittmann U, Nafz B, Ehmke H, Kirchheim HR, Persson PB. Frequency domain of renal autoregulation in the conscious dog. Am J Physiol 1995;269:F317–322.
[298] Cupples WA, Loutzenhiser RD. Dynamic autoregulation in the *in vitro* perfused hydronephrotic rat kidney. Am J Physiol Renal Physiol 1998;275:F126–130.
[299] He J, Marsh DJ. Effect of captopril on fluctuations of blood pressure and renal blood flow in rats. Am J Physiol Renal Physiol 1993;264:F37–44.
[300] Just A, Arendshorst WJ. A novel mechanism of renal blood flow autoregulation and the autoregulatory role of A1 adenosine receptors in mice. Am J Physiol Renal Physiol 2007;293: F1489–1500.
[301] Just A, Ehmke H, Toktomambetova L, Kirchheim HR. Dynamic characteristics and underlying mechanisms of renal blood flow autoregulation in the conscious dog. Am J Physiol Renal Physiol 2001;280:F1062–1071.
[302] Just A, Arendshorst WJ. Dynamics and contribution of mechanisms mediating renal blood flow autoregulation. Am J Physiol Regul Integr Comp Physiol 2003;285:R619–631.
[303] Wronski T, Seeliger E, Persson PB, Forner C, Fichtner C, Scheller J, et al. The step response: a method to characterize mechanisms of renal blood flow autoregulation. Am J Physiol Renal Physiol 2003;285:F758–764.
[304] Loutzenhiser R, Bidani A, Chilton L. Renal myogenic response: kinetic attributes and physiological role. Circ Res 2002;90:1316–24.
[305] Loutzenhiser R, Bidani AK, Wang X. Systolic pressure and the myogenic response of the renal afferent arteriole. Acta Physiol Scand 2004;181:407–13.
[306] Davis JM, Haberle DA, Kawata T. The control of glomerular filtration rate and renal blood flow in chronically volume-expanded rats. J Physiol (Lond) 1988;402:473–95.
[307] Haberle DA. Hemodynamic interactions between intrinsic blood flow control mechanisms in the rat kidney. Ren Physiol Biochem 1988;11:289–315.
[308] Feldberg R, Colding-Jorgensen M, Holstein-Rathlou NH. Analysis of interaction between TGF and the myogenic response in renal blood flow autoregulation. Am J Physiol Renal Physiol 1995;269:F581–593.
[309] Schnermann J, Briggs JP. Interaction between loop of Henle flow and arterial pressure as determinants of glomerular pressure. Am J Physiol Renal Physiol 1989;256:F421–9.
[310] Chon KH, Raghavan R, Chen YM, Marsh DJ, Yip KP. Interactions of TGF-dependent and myogenic oscillations in tubular pressure. Am J Physiol Renal Physiol 2005;288: F298–307.
[311] Marsh DJ, Sosnovtseva OV, Chon KH, Holstein-Rathlou NH. Nonlinear interactions in renal blood flow regulation. Am J Physiol Regul Integr Comp Physiol 2005;288: R1143–1159.
[312] Walker III M, Harrison-Bernard LM, Cook AK, Navar LG. Dynamic interaction between myogenic and TGF mechanisms in afferent arteriolar blood flow autoregulation. Am J Physiol Renal Physiol 2000;279:F858–865.
[313] Just A, Arendshorst WJ. Nitric oxide blunts myogenic autoregulation in rat renal but not skeletal muscle circulation via tubuloglomerular feedback. J Physiol 2005;569:959–74.
[314] Shi Y, Wang X, Chon KH, Cupples WA. Tubuloglomerular feedback-dependent modulation of renal myogenic autoregulation by nitric oxide. Am J Physiol Regul Integr Comp Physiol 2006;290:R982–991.
[315] Nashat FS, Tappin JW, Wilcox CS. The renal blood flow and the glomerular filtration rate of anaesthetized dogs during acute changes in plasma sodium concentration. J Physiol 1976;256:731–45.
[316] Dev B, Drescher C, Schnermann J. Resetting of tubulo-glomerular feedback sensitivity by dietary salt intake. Pflugers Arch 1974;346:263–77.
[317] Wilcox CS. Regulation of renal blood flow by plasma chloride. J Clin Invest 1983;71:726–35.
[318] Gerber JG, Branch RA, Nies AS, Hollifield JW, Gerkens JF. Influence of hypertonic saline on canine renal blood flow and renin release. Am J Physiol 1979;237:F441–446.
[319] Gerkens JF, Heidemann HT, Jackson EK, Branch RA. Aminophylline inhibits renal vasoconstriction produced by intrarenal hypertonic saline. J Pharmacol Exp Ther 1983;225:611–5.
[320] Schnermann J, Hermle M, Schmidmeier E, Dahlheim H. Impaired potency for feedback regulation of glomerular filtration rate in DOCA escaped rats. Pflugers Arch 1975;358:325–38.
[321] Schnermann J, Briggs J, Wright FS. Feedback-mediated reduction of glomerular filtration rate during infusion of hypertonic saline. Kidney Int 1981;20:462–8.
[322] Woods LL, DeYoung DR, Smith BE. Regulation of renal hemodynamics after protein feeding: effects of loop diuretics. Am J Physiol Renal Physiol 1991;261:F815–823.
[323] Schnermann J, Gokel M, Weber PC, Schubert G, Briggs JP. Tubuloglomerular feedback and glomerular morphology in Goldblatt hypertensive rats on varying protein diets. Kidney Int 1986;29:520–9.
[324] Seney Jr. FD, Wright FS. Dietary protein suppresses feedback control of glomerular filtration in rats. J Clin Invest 1985;75:558–68.
[325] Seney Jr. FD, Persson EG, Wright FS. Modification of tubuloglomerular feedback signal by dietary protein. Am J Physiol Renal Physiol 1987;252:F83–90.
[326] Bouby N, Trinh-Trang-Tan MM, Kriz W, Bankir L. Possible role of the thick ascending limb and of the urine concentrating mechanism in the protein-induced increase in GFR and kidney mass. Kidney Int Suppl 1987;22:S57–61.
[327] Persson AEG, Wright FS. Evidence for feedback mediated reduction of glomerular filtration rate during infusion of acetazolamide. Acta Physiol Scand 1982;114:1–7.
[328] Hashimoto S, Huang YG, Castrop H, Hansen PB, Mizel D, Briggs J, et al. Effect of carbonic anhydrase inhibition on GFR and renal hemodynamics in adenosine-1 receptor-deficient mice. Pflugers Arch 2004;448:621–8.
[329] Leyssac PP, Karlsen FM, Skott O. Dynamics of intrarenal pressures and glomerular filtration rate after acetazolamide. Am J Physiol Renal Physiol 1991;261:F169–178.
[330] Leyssac PP, Karlsen FM, Holstein-Rathlou NH, Skott O. On determinants of glomerular filtration rate after inhibition of proximal tubular reabsorption. Am J Physiol Renal Physiol 1994;266:R1544–1550.
[331] Janssen BJ, Eerdmans PH, Smits JF. Mechanisms of renal vasoconstriction following furosemide in conscious rats. Naunyn Schmiedebergs Arch Pharmacol 1994;349:528–37.
[332] Oppermann M, Hansen PB, Castrop H, Schnermann J. Vasodilatation of afferent arterioles and paradoxical increase

of renal vascular resistance by furosemide in mice. Am J Physiol Renal Physiol 2007;293:F279–287.
[333] Schnermann J, Chou C-L, Ma T, Traynor T, Knepper MA, Verkman AS. Defective proximal tubular fluid reabsorption in transgenic aquaporin-1 null mice. Proc Natl Acad Sci 1998;95:9660–4.
[334] Hashimoto S, Huang Y, Mizel D, Briggs J, Schnermann J. Compensation of proximal tubule malabsorption in AQP1-deficient mice without TGF-mediated reduction of GFR. Acta Physiol Scand 2004;181:455–62.
[335] Lorenz JN, Schultheis PJ, Traynor T, Shull GE, Schnermann J. Micropuncture analysis of single-nephron function in NHE3-deficient mice. Am J Physiol Renal Physiol 1999;277:F447–53.
[336] Boberg U, Persson AE. Tubuloglomerular feedback during elevated renal venous pressure. Am J Physiol Renal Physiol 1985;249:F524–531.
[337] Boberg U, Persson AE. Increased tubuloglomerular feedback activity in Milan hypertensive rats. Am J Physiol Renal Physiol 1986;250:F967–974.
[338] Persson AE, Schnermann J, Wright FS. Modification of feedback influence on glomerular filtration rate by acute isotonic extracellular volume expansion. Pflugers Arch 1979;381:99–105.
[339] Persson AE, Bianchi G, Boberg U. Tubuloglomerular feedback in hypertensive rats of the Milan strain. Acta Physiol Scand 1985;123:139–46.
[340] Ploth DW, Rudulph J, Thomas C, Navar LG. Renal and tubuloglomerular feedback responses to plasma expansion in the rat. Am J Physiol Renal Physiol 1978;235:F156–162.
[341] Schnermann J, Briggs JP. Restoration of tubuloglomerular feedback in volume-expanded rats by angiotensin II. Am J Physiol Renal Physiol 1990;259:F565–572.
[342] Moore LC, Yarimizu S, Schubert G, Weber PC, Schnermann J. Dynamics of tubuloglomerular feedback adaptation to acute and chronic changes in body fluid volume. Pflugers Arch 1980;387:39–45.
[343] Davis JM, Takabatake T, Kawata T, Haberle DA. Resetting of tubuloglomerular feedback in acute volume expansion in rats. Pflugers Arch 1988;411:322–7.
[344] Moore LC, Mason J. Perturbation analysis of tubuloglomerular feedback in hydropenic and hemorrhaged rats. Am J Physiol Renal Physiol 1983;245:F554–563.
[345] Moore LC, Mason J. Tubuloglomerular feedback control of distal fluid delivery: effect of extracellular volume. Am J Physiol Renal Physiol 1986;250:F1024–1032.
[346] Selen G, Muller-Suur R, Persson AE. Activation of the tubuloglomerular feedback mechanism in dehydrated rats. Acta Physiol Scand 1983;117:83–9.
[347] Kaufman JS, Hamburger RJ, Flamenbaum W. Tubuloglomerular feedback response after hypotensive hemorrhage. Ren Physiol 1982;5:173–81.
[348] Morsing P, Persson AE. Kinin and tubuloglomerular feedback in normal and hydronephrotic rats. Am J Physiol Renal Physiol 1991;260:F868–873.
[349] Persson AE, Wahlberg J, Safirstein R, Wright FS. The effect of 2 hours of complete unilateral ureteral obstruction on tubuloglomerular feedback control. Acta Physiol Scand 1984;122:35–43.
[350] Wahlberg J, Stenberg A, Wilson DR, Persson AE. Tubuloglomerular feedback and interstitial pressure in obstructive nephropathy. Kidney Int 1984;26:294–301.
[351] Dal Canton A, Stanziale R, Corradi A, Andreucci VE, Migone L. Effects of acute ureteral obstruction on glomerular hemodynamics in rat kidney. Kidney Int 1977;12:403–11.
[352] Tanner GA. Tubuloglomerular feedback after nephron or ureteral obstruction. Am J Physiol Renal Physiol 1985;248: F688–697.
[353] Carlstrom M, Brown RD, Edlund J, Sällström J, Larsson E, Teerlink T, et al. Role of nitric oxide deficiency in the development of hypertension in hydronephrotic animals. Am J Physiol Renal Physiol 2008;294:F362–370.
[354] Carlstrom M, Brown RD, Sallstrom J, Larsson E, Zilmer M, Zabihi S, et al. SOD1 deficiency causes salt sensitivity and aggravates hypertension in hydronephrosis. Am J Physiol Regul Integr Comp Physiol 2009;297:R82–92.
[355] Dal Canton A, Corradi A, Stanziale R, Maruccio G, Migone L. Effects of 24-hour ureteral obstruction on glomerular hemodynamics in rat kidney. Kidney Int 1979;15:457–62.
[356] Arendshorst WJ, Finn WF, Gottschalk CW. Nephron stop-flow pressure response to obstruction for 24 hours in the rat kidney. J Clin Invest 1974;53:1497–500.
[357] Tanner GA. Effects of kidney tubule obstruction on glomerular function in rats. Am J Physiol 1979;237:F379–385.
[358] Tanner GA. Nephron obstruction and tubuloglomerular feedback. Kidney Int Suppl 1982;12:S213–218.
[359] Morsing P, Stenberg A, Muller-Suur C, Persson AE. Tubuloglomerular feedback in animals with unilateral, partial ureteral occlusion. Kidney Int 1987;32:212–8.
[360] Morsing P, Stenberg A, Persson AE. Effect of thromboxane inhibition on tubuloglomerular feedback in hydronephrotic kidneys. Kidney Int 1989;36:447–52.
[361] Morsing P, Stenberg A, Wahlin N, Persson AE. Tubuloglomerular feedback in rats with chronic partial bilateral ureteral obstruction. Ren Physiol Biochem 1995;18:27–34.
[362] Blantz RC, Peterson OW, Thomson SC. Tubuloglomerular feedback responses to acute contralateral nephrectomy. Am J Physiol Renal Physiol 1991;260:F749–756.
[363] Muller-Suur R, Norlen BJ, Persson AE. Resetting of tubuloglomerular feedback in rat kidneys after unilateral nephrectomy. Kidney Int 1980;18:48–57.
[364] Norlen BJ, Muller-Suur R, Persson AE. Tubulo-glomerular feedback response and excretory characteristics of the transplanted rat kidney. Scand J Urol Nephrol 1978;12:27–33.
[365] Salmond R, Seney FJ. Reset tubuloglomerular feedback permits and sustains glomerular hyperfunction after extensive renal ablation. Am J Physiol Renal Physiol 1991;260:F395–401.
[366] Singh P, Deng A, Blantz RC, Thomson SC. Unexpected effect of angiotensin AT1 receptor blockade on tubuloglomerular feedback in early subtotal nephrectomy. Am J Physiol Renal Physiol 2009;296:F1158–1165.
[367] Pollock CA, Bostrom TE, Dyne M, Gyory AZ, Field MJ. Tubular sodium handling and tubuloglomerular feedback in compensatory renal hypertrophy. Pflugers Arch 1992;420:159–66.
[368] Blantz RC, Peterson OW, Gushwa L, Tucker BJ. Effect of modest hyperglycemia on tubuloglomerular feedback activity. Kidney Int Suppl 1982;12:S206–212.
[369] Jensen PK, Kristensen KS, Rasch R, Persson AEG. Decreased sensitivity of the tubuloglomerular feedback mechanism in experimental diabetic rats. In: Persson AEG, Boberg U, editors. The Juxtaglomerular Apparatus. Amsterdam: Elsevier; 1988. p. 333–8.
[370] Hashimoto S, Yamada K, Kawata T, Mochizuki T, Schnermann J, Koike T. Abnormal autoregulation and tubuloglomerular feedback in prediabetic and diabetic OLETF rats. Am J Physiol Renal Physiol 2009;296:F598–604.
[371] Faulhaber-Walter R, Chen L, Oppermann M, Kim SMK, Huang Y, Hiramatsu MJ, et al. Lack of A1 adenosine receptors augments diabetic hyperfiltration and glomerular injury. J Am Soc Nephrol 2008;19:722–30.
[372] Levine DZ, Iacovitti M, Robertson SJ, Mokhtar GA. Modulation of single-nephron GFR in the db/db mouse model

of type 2 diabetes mellitus. Am J Physiol Regul Integr Comp Physiol 2006;290:R975–981.
[373] Vallon V, Blantz RC, Thomson S. Homeostatic efficiency of tubuloglomerular feedback is reduced in established diabetes mellitus in rats. Am J Physiol Renal Physiol 1995;269:F876–883.
[374] Blantz RC, Konnen KS. Relation of distal tubular delivery and reabsorptive rate to nephron filtration. Am J Physiol Renal Physiol 1977;233:F315–324.
[375] Vallon V, Huang DY, Deng A, Richter K, Blantz RC, Thomson S. Salt-sensitivity of proximal reabsorption alters macula densa salt and explains the paradoxical effect of dietary salt on glomerular filtration rate in diabetes mellitus. J Am Soc Nephrol 2002;13:1865–71.
[376] Thomson SC, Vallon V, Blantz RC. Kidney function in early diabetes: the tubular hypothesis of glomerular filtration. Am J Physiol Renal Physiol 2004;286:F8–15.
[377] Vallon V, Blantz RC, Thomson S. Glomerular hyperfiltration and the salt paradox in early [corrected] type 1 diabetes mellitus: a tubulo-centric view. J Am Soc Nephrol 2003;14:530–7.
[378] Thomson SC, Deng A, Bao D, Satriano J, Blantz RC, Vallon V. Ornithine decarboxylase, kidney size, and the tubular hypothesis of glomerular hyperfiltration in experimental diabetes. J Clin Invest 2001;107:217–24.
[379] Pedersen SB, Flyvbjerg A, Richelsen B. Inhibition of renal ornithine decarboxylase activity prevents kidney hypertrophy in experimental diabetes. Am J Physiol 1993;264:C453–456.
[380] Pollock CA, Lawrence JR, Field MJ. Tubular sodium handling and tubuloglomerular feedback in experimental diabetes mellitus. Am J Physiol Renal Physiol 1991;260:F946–952.
[381] Sallstrom J, Carlsson PO, Fredholm BB, Larsson E, Persson AE, Palm F. Diabetes-induced hyperfiltration in adenosine A(1)-receptor deficient mice lacking the tubuloglomerular feedback mechanism. Acta Physiol (Oxf) 2007;190:253–9.
[382] Vallon V, Kirschenmann D, Wead LM, Lortie MJ, Satriano J, Blantz RC, et al. Effect of chronic salt loading on kidney function in early and established diabetes mellitus in rats. J Lab Clin Med 1997;130:76–82.
[383] Miracle CM, Rieg T, Mansoury H, Vallon V, Thomson SC. Ornithine decarboxylase inhibitor eliminates hyperresponsiveness of the early diabetic proximal tubule to dietary salt. Am J Physiol Renal Physiol 2008;295:F995–1002.
[384] Bell TD, DiBona GF, Biemiller R, Brands MW. Continuously measured renal blood flow does not increase in diabetes if nitric oxide synthesis is blocked. Am J Physiol Renal Physiol 2008;295:F1449–1456.
[385] Thomson SC, Deng A, Komine N, Hammes JS, Blantz RC, Gabbai FB. Early diabetes as a model for testing the regulation of juxtaglomerular NOS I. Am J Physiol Renal Physiol 2004;287:F732–738.
[386] Allen TJ, Waldron MJ, Casley D, Jerums G, Cooper ME. Salt restriction reduces hyperfiltration, renal enlargement, and albuminuria in experimental diabetes. Diabetes 1997;46:19–24.
[387] Bank N, Lahorra G, Aynedjian HS, Wilkes BM. Sodium restriction corrects hyperfiltration of diabetes. Am J Physiol 1988;254: F668–676.
[388] Campese VM, Wurgaft A, Safa M, Bianchi S. Dietary salt intake, blood pressure and the kidney in hypertensive patients with non-insulin dependent diabetes mellitus. J Nephrol 1998;11:289–95.
[389] O'Neill H, Kwon TH, Ring T, et al. Restriction of dietary NaCl decreases urinary output in diabetic rats: absence of the salt paradox in uncontrolled type 1 diabetes mellitus. J Am Soc Nephrol 2008;19:849A (abstract).
[390] Hermansson K, Kallskog O, Wolgast M. Effect of renal nerve stimulation on the activity of the tubuloglomerular feedback mechanism. Acta Physiol Scand 1984;120:381–5.
[391] Takabatake T, Ushiogi Y, Ohta K, Hattori N. Attenuation of enhanced tubuloglomerular feedback activity in SHR by renal denervation. Am J Physiol Renal Physiol 1990;258:F980–985.
[392] Thorup C, Kurkus J, Morsing P, Persson AE. Acute renal denervation causes time-dependent resetting of the tubuloglomerular feedback mechanism. Acta Physiol Scand 1995;153:43–9.
[393] Thorup C, Kurkus J, Ollerstam A, Persson AE. Effects of acute and chronic unilateral renal denervation on the tubuloglomerular feedback mechanism. Acta Physiol Scand 1996;156:139–45.
[394] Ploth DW, Rudulph J, LaGrange R, Navar LG. Tubuloglomerular feedback and single nephron function after converting enzyme inhibition in the rat. J Clin Invest 1979;64:1325–35.
[395] Ploth DW, Roy RN. Renal and tubuloglomerular feedback effects of [Sar1,Ala8]angiotensin II in the rat. Am J Physiol Renal Physiol 1982;242:F149–157.
[396] Schnermann J, Briggs JP, Schubert G, Marin-Grez M. Opposing effects of captopril and aprotinin on tubuloglomerular feedback responses. Am J Physiol Renal Physiol 1984;247: F912–918.
[397] Stowe N, Schnermann J, Hermle M. Feedback regulation of nephron filtration rate during pharmacologic interference with the renin–angiotensin and adrenergic systems in rats. Kidney Int 1979;15:473–86.
[398] Welch WJ, Wilcox CS. Feedback responses during sequential inhibition of angiotensin and thromboxane. Am J Physiol Renal Physiol 1990;258:F457–466.
[399] Traynor T, Yang T, Huang YG, Krege JH, Briggs JP, Smithies O, et al. Tubuloglomerular feedback in ACE-deficient mice. Am J Physiol Renal Physiol 1999;276:F751–757.
[400] Hashimoto S, Adams JW, Bernstein KE, Schnermann J. Micropuncture determination of nephron function in mice without tissue angiotensin converting enzyme. Am J Physiol Renal Physiol 2005;288:F445–52.
[401] Kessler SP, Hashimoto S, Senanayake PS, Gaughan C, Sen GC, Schnermann J. Nephron function in transgenic mice with selective vascular or tubular expression of Angiotensin-converting enzyme. J Am Soc Nephrol 2005;16:3535–42.
[402] Huang WC, Bell PD, Harvey D, Mitchell KD, Navar LG. Angiotensin influences on tubuloglomerular feedback mechanism in hypertensive rats. Kidney Int 1988;34:631–7.
[403] Ploth DW, Roy RN. Renin–angiotensin influences on tubuloglomerular feedback activity in the rat. Kidney Int Suppl 1982;12:S114–121.
[404] Mitchell KD, Navar LG. Enhanced tubuloglomerular feedback during peritubular infusions of angiotensins I and II. Am J Physiol Renal Physiol 1988;255:F383–390.
[405] Ikenaga H, Fallet RW, Carmines PK. Contribution of tubuloglomerular feedback to renal arteriolar angiotensin II responsiveness. Kidney Int 1996;49:34–9.
[406] Ren YL, Carretero OA, Ito S. Influence of NaCl concentration at the macula densa on angiotensin II-induced constriction of the afferent arteriole. Hypertension 1996;27:649–52.
[407] Lai EY, Martinka P, Fahling M, Mrowka R, Steege A, Gericke A, et al. Adenosine restores angiotensin II-induced contractions by receptor-independent enhancement of calcium sensitivity in renal arterioles. Circ Res 2006;99:1117–24.
[408] DiBona GF, Sawin LL. Effect of endogenous angiotensin II on the frequency response of the renal vasculature. Am J Physiol Renal Physiol 2004;287:F1171–1178.
[409] Guan Z, Willgoss DA, Matthias A, Manley SW, Crozier S, Gobe G, et al. Facilitation of renal autoregulation by angiotensin II is mediated through modulation of nitric oxide. Acta Physiol Scand 2003;179:189–201.

[410] Just A, Ehmke H, Wittmann U, Kirchheim HR. Role of angiotensin II in dynamic renal blood flow autoregulation of the conscious dog. J Physiol 2002;538:167–77.
[411] Schnermann J, Levine DZ. Paracrine factors in tubuloglomerular feedback: adenosine, ATP, and nitric oxide. Annu Rev Physiol 2003;65:501–29.
[412] Traynor T, Yang T, Huang YG, Arend L, Oliverio MI, Coffman T, et al. Inhibition of adenosine-1 receptor-mediated preglomerular vasoconstriction in AT1A receptor-deficient mice. Am J Physiol Renal Physiol 1998;275:F922–927.
[413] Weihprecht H, Lorenz JN, Briggs JP, Schnermann J. Synergistic effects of angiotensin and adenosine in the renal microvasculature. Am J Physiol Renal Physiol 1994;266:F227–239.
[414] Patzak A, Lai EY, Fahling M, Sendeski M, Martinka P, Persson PB, et al. Adenosine enhances long term the contractile response to angiotensin II in afferent arterioles. Am J Physiol Regul Integr Comp Physiol 2007;293:R2232–2242.
[415] Kovacs G, Peti-Peterdi J, Rosivall L, Bell PD. Angiotensin II directly stimulates macula densa Na-2Cl-K co-transport via apical AT(1) receptors. Am J Physiol Renal Physiol 2002;282: F301–306.
[416] Smith WL, Bell TG. Immunohistochemical localization of the prostaglandin-forming cyclooxygenase in renal cortex. Am J Physiol Renal Physiol 1978;235:F451–7.
[417] Harris RC, Breyer MD. Physiological regulation of cyclooxygenase-2 in the kidney. Am J Physiol Renal Physiol 2001;281: F1–11.
[418] Araujo M, Welch WJ. Cyclooxygenase 2 inhibition suppresses tubuloglomerular feedback: Roles of thromboxane receptors and nitric oxide. Am J Physiol Renal Physiol 2009;296:F790–794.
[419] Morsing P, Persson AE. Effect of prostaglandin synthesis inhibition on the tubuloglomerular feedback control in the rat kidney. Ren Physiol Biochem 1992;15:66–72.
[420] Schnermann J, Schubert G, Hermle M, Herbst R, Stowe NT, Yarimizu S, et al. The effect of inhibition of prostaglandin synthesis on tubuloglomerular feedback in the rat kidney. Pflugers Arch 1979;379:269–79.
[421] Schnermann J, Weber PC. Reversal of indomethacin-induced inhibition of tubuloglomerular feedback by prostaglandin infusion. Prostaglandins 1982;24:351–61.
[422] Welch WJ, Wilcox CS. Modulating role for thromboxane in the tubuloglomerular feedback response in the rat. J Clin Invest 1988;81:1843–9.
[423] Franco M, Bell PD, Navar LG. Evaluation of prostaglandins as mediators of tubuloglomerular feedback. Am J Physiol Renal Physiol 1988;254:F642–649.
[424] Welch WJ. Effects of isoprostane on tubuloglomerular feedback: roles of TP receptors, NOS, and salt intake. Am J Physiol Renal Physiol 2005;288:F757–762.
[425] Araujo M, Welch WJ. Tubuloglomerular feedback is decreased in COX-1 knockout mice after chronic angiotensin II infusion. Am J Physiol Renal Physiol 2010;298:F1059–1063.
[426] Welch WJ, Peng B, Takeuchi K, Abe K, Wilcox CS. Salt loading enhances rat renal TxA2/PGH2 receptor expression and TGF response to U-46,619. Am J Physiol Renal Physiol 1997;273: F976–983.
[427] Yanagisawa H, Jin Z, Kurihara N, Klahr S, Morrissey J, Wada O. Increases in glomerular eicosanoid production in rats with bilateral ureteral obstruction are mediated by enhanced enzyme activities of both the cyclooxygenase and 5-lipoxygenase pathways. Proc Soc Exp Biol Med 1993;203:291–6.
[428] Schnermann J, Traynor T, Pohl H, Thomas DW, Coffman TM, Briggs JP. Vasoconstrictor responses in thromboxane receptor knockout mice: tubuloglomerular feedback and ureteral obstruction. Acta Physiol Scand 2000;168:201–7.
[429] Wilcox CS, Welch WJ. Thromboxane synthase and TP receptor mRNA in rat kidney and brain: effects of salt intake and ANG II. Am J Physiol Renal Physiol 2003;284:F525–531.
[430] Brannstrom K, Arendshorst WJ. Thromboxane A_2 contributes to the enhanced tubuloglomerular feedback activity in young SHR. Am J Physiol Renal Physiol 1999;276:F758–66.
[431] Ichihara A, Imig JD, Inscho EW, Navar LG. Cyclooxygenase-2 participates in tubular flow-dependent afferent arteriolar tone: interaction with neuronal NOS. Am J Physiol Renal Physiol 1998;275:F605–612.
[432] Zhao X, Imig JD. Kidney CYP450 enzymes: biological actions beyond drug metabolism. Curr Drug Metab 2003;4:73–84.
[433] Zou AP, Imig JD, Ortiz de Montellano PR, Sui Z, Falck JR, Roman RJ. Effect of P-450 omega-hydroxylase metabolites of arachidonic acid on tubuloglomerular feedback. Am J Physiol Renal Physiol 1994;266:F934–941.
[434] Ito O, Alonso-Galicia M, Hopp KA, Roman RJ. Localization of cytochrome P-450 4A isoforms along the rat nephron. Am J Physiol 1998;274:F395–404.
[435] Sarkis A, Roman RJ. Role of cytochrome P450 metabolites of arachidonic acid in hypertension. Curr Drug Metab 2004;5:245–56.
[436] Schnermann J. Vascular tone as a determinant of tubuloglomerular feedback responsiveness. In: Persson AEG, Boberg U, editors. The juxtaglomerular apparatus. Amsterdam: Elsevier; 1988. p. 167–76.
[437] Harder DR, Lange AR, Gebremedhin D, Birks EK, Roman RJ. Cytochrome P450 metabolites of arachidonic acid as intracellular signaling molecules in vascular tissue. J Vasc Res 1997;34:237–43.
[438] Braam B, Koomans HA. Reabsorption of nitro-L-arginine infused into the late proximal tubule participates in modulation of TGF responsiveness. Kidney Int 1995;47:1252–7.
[439] Ito S, Ren YL. Evidence for the role of nitric oxide in macula densa control of glomerular hemodynamics. J Clin Invest 1993;92:1093–8.
[440] Thorup C, Persson AE. Macula densa derived nitric oxide in regulation of glomerular capillary pressure. Kidney Int 1996;49:430–6.
[441] Vallon V, Thomson S. Inhibition of local nitric oxide synthase increases homeostatic efficiency of tubuloglomerular feedback. Am J Physiol Renal Physiol 1995;269:F892–9.
[442] Thomson SC, Deng A. Cyclic GMP mediates influence of macula densa nitric oxide over tubuloglomerular feedback. Kidney Blood Press Res 2003;26:10–8.
[443] Ren YL, Garvin JL, Ito S, Carretero OA. Role of neuronal nitric oxide synthase in the macula densa. Kidney Int 2001;60:1676–83.
[444] Vallon V, Traynor T, Barajas L, Huang YG, Briggs JP, Schnermann J. Feedback control of glomerular vascular tone in neuronal nitric oxide synthase knockout mice. J Am Soc Nephrol 2001;12:1599–606.
[445] Brown R, Ollerstam A, Persson AE. Neuronal nitric oxide synthase inhibition sensitizes the tubuloglomerular feedback mechanism after volume expansion. Kidney Int 2004; 65:1349–56.
[446] Ren YL, Garvin JL, Carretero OA. Role of macula densa nitric oxide and cGMP in the regulation of tubuloglomerular feedback. Kidney Int 2000;58:2053–60.
[447] Ortiz PA, Garvin JL. NO Inhibits NaCl absorption by rat thick ascending limb through activation of cGMP-stimulated phosphodiesterase. Hypertension 2001;37:467–71.
[448] Wang H, Carretero OA, Garvin JL. Nitric oxide produced by THAL nitric oxide synthase inhibits TGF. Hypertension 2002;39:662–6.

[449] Kovacs G, Komlosi P, Fuson A, Peti-Peterdi J, Rosivall L, Bell PD. Neuronal nitric oxide synthase: its role and regulation in macula densa cells. J Am Soc Nephrol 2003;14:2475–83.
[450] Liu R, Carretero OA, Ren Y, Garvin JL. Increased intracellular pH at the macula densa activates nNOS during tubuloglomerular feedback. Kidney Int 2005;67:1837–43.
[451] Yaqoob M, Edelstein CL, Wieder ED, Alkhunaizi AM, Gengaro PA, Nemenoff RA, et al. Nitric oxide kinetics during hypoxia in proximal tubules: effects of acidosis and glycine. Kidney Int 1996;49:1314–9.
[452] Wang H, Carretero OA, Garvin JL. Inhibition of apical Na^+/H^+ exchangers on the macula densa cells augments tubuloglomerular feedback. Hypertension 2003;41:688–91.
[453] Welch WJ, Wilcox CS. Tubuloglomerular feedback and macula densa-derived NO. In: Goligorsky MS, Gross SS, editors. Nitric oxide and the kidney. New York: Chapman & Hall; 1997. p. 216–32.
[454] Cabral PD, Hong NJ, Garvin JL. Shear stress increases nitric oxide production in thick ascending limbs. Am J Physiol Renal Physiol 2010;299:F1185–1192.
[455] Ortiz PA, Hong NJ, Garvin JL. Luminal flow induces eNOS activation and translocation in the rat thick ascending limb. Am J Physiol Renal Physiol 2004;287:F274–280.
[456] Levine DZ, Burns KD, Jaffey J, Iacovitti M. Short-term modulation of distal tubule fluid nitric oxide *in vivo* by loop NaCl reabsorption. Kidney Int 2004;65:184–9.
[457] Kawada H, Yasuoka Y, Fukuda H, Kawahara K. Low [NaCl]-induced neuronal nitric oxide synthase (nNOS) expression and NO generation are regulated by intracellular pH in a mouse macula densa cell line (NE-MD). J Physiol Sci 2009;59:165–73.
[458] Chabrashvili T, Tojo A, Onozato ML, Kitiyakara C, Quinn MT, Fujita T, et al. Expression and cellular localization of classic NADPH oxidase subunits in the spontaneously hypertensive rat kidney. Hypertension 2002;39:269–74.
[459] Liu R, Carretero OA, Ren Y, Wang H, Garvin JL. Intracellular pH regulates superoxide production by the macula densa. Am J Physiol Renal Physiol 2008;295:F851–856.
[460] Ren Y, Carretero OA, Garvin JL. Mechanism by which superoxide potentiates tubuloglomerular feedback. Hypertension 2002;39:624–8.
[461] Welch WJ, Tojo A, Wilcox CS. Roles of NO and oxygen radicals in tubuloglomerular feedback in SHR. Am J Physiol Renal Physiol 2000;278:F769–776.
[462] Welch WJ, Tojo A, Lee JU, Kang DG, Schnackenberg CG, Wilcox CS. Nitric oxide synthase in the JGA of the SHR: expression and role in tubuloglomerular feedback. Am J Physiol Renal Physiol 1999;277:F130–138.
[463] Welch WJ, Wilcox CS. AT1 receptor antagonist combats oxidative stress and restores nitric oxide signaling in the SHR. Kidney Int 2001;59:1257–63.
[464] Kitiyakara C, Chabrashvili T, Chen Y, Blau J, Karber A, Aslam S, et al. Salt intake, oxidative stress, and renal expression of NADPH oxidase and superoxide dismutase. J Am Soc Nephrol 2003;14:2775–82.
[465] Welch WJ, Wilcox CS. Role of nitric oxide in tubuloglomerular feedback: effects of dietary salt. Clin Exp Pharmacol Physiol 1997;24:582–6.
[466] Wilcox CS, Deng X, Welch WJ. NO generation and action during changes in salt intake: roles of nNOS and macula densa. Am J Physiol 1998;274:R1588–1593.
[467] Tojo A, Welch WJ, Bremer V, Kimoto M, Kimura K, Omata M, et al. Colocalization of demethylating enzymes and NOS and functional effects of methylarginines in rat kidney. Kidney Int 1997;52:1593–601.
[468] Welch WJ, Wilcox CS. Macula densa arginine delivery and uptake in the rat regulates glomerular capillary pressure. Effects of salt intake. J Clin Invest 1997;100:2235–42.
[469] Satriano J, Wead L, Cardus A, Deng A, Boss GR, Thomson SC, et al. Regulation of ecto-5′-nucleotidase by NaCl and nitric oxide: potential roles in tubuloglomerular feedback and adaptation. Am J Physiol Renal Physiol 2006;291:F1078–1082.
[470] Siegfried G, Amiel C, Friedlander G. Inhibition of ecto-5′-nucleotidase by nitric oxide donors. Implications in renal epithelial cells. J Biol Chem 1996;271:4659–64.
[471] Briggs JP, Steipe B, Schubert G, Schnermann J. Micropuncture studies of the renal effects of atrial natriuretic substance. Pflugers Arch 1982;395:271–6.
[472] Huang CL, Cogan MG. Atrial natriuretic factor inhibits maximal tubuloglomerular feedback response. Am J Physiol Renal Physiol 1987;252:F825–828.
[473] Schnermann J, Todd KM, Briggs JP. Effect of dopamine on the tubuloglomerular feedback mechanism. Am J Physiol Renal Physiol 1990;258:F790–798.
[474] Boberg U, Hahne B, Persson AE. The effect of intraarterial infusion of prostacyclin on the tubuloglomerular feedback control in the rat. Acta Physiol Scand 1984;121:65–72.
[475] Wang T, Kawabata M, Haneda M, Takabatake T. Effects of uroguanylin, an intestinal natriuretic peptide, on tubuloglomerular feedback. Hypertens Res 2003;26:577–82.
[476] Wang T, Takabatake T. Effects of vasopeptidase inhibition on renal function and tubuloglomerular feedback in spontaneously hypertensive rats. Hypertens Res 2005;28:611–8.
[477] Ren Y, D'Ambrosio MA, Wang H, Liu R, Garvin JL, Carretero OA. Heme oxygenase metabolites inhibit tubuloglomerular feedback (TGF). Am J Physiol Renal Physiol 2008;295:F1207–1212.
[478] Kozma F, Johnson RA, Zhang F, Yu C, Tong X, Nasjletti A. Contribution of endogenous carbon monoxide to regulation of diameter in resistance vessels. Am J Physiol 1999;276: R1087–1094.
[479] Thorup C, Jones CL, Gross SS, Moore LC, Goligorsky MS. Carbon monoxide induces vasodilation and nitric oxide release but suppresses endothelial NOS. Am J Physiol 1999;277: F882–889.
[480] Folkow B. Physiological aspects of primary hypertension. Physiol Rev 1982;62:347–504.
[481] Persson AE, Muller-Suur R, Selen G. Capillary oncotic pressure as a modifier for tubuloglomerular feedback. Am J Physiol Renal Physiol 1979;236:F97–102.
[482] Selen G, Persson AE. Hydrostatic and oncotic pressures in the interstitium of dehydrated and volume expanded rats. Acta Physiol Scand 1983;117:75–81.
[483] Hahne B, Persson AEG. Prevention of interstitial pressure change at unilateral nephrectomy by prostaglandin synthesis inhibition. Kidney Int 1984;25:42–6.
[484] Haberle DA, Davis JM. Resetting of tubuloglomerular feedback: evidence for a humoral factor in tubular fluid. Am J Physiol Renal Physiol 1984;246:F495–500.
[485] Pollock DM, Arendshorst WJ. Native tubular fluid attenuates ANF-induced inhibition of tubuloglomerular feedback. Am J Physiol Renal Physiol 1990;258:F189–198.
[486] Wunderlich PF, Brunner FP, Davis JM, Haberle DA, Tholen H, Thiel G. Feedback activation in rat nephrons by sera from patients with acute renal failure. Kidney Int 1980;17:497–506.
[487] Goormaghtigh N. Une glande endocrine dans la paroi des arterioles renales. Bruxelles Med 1939;19:1541–9.
[488] Vander AJ. Control of renin release. Physiol Rev 1967; 47:359–82.
[489] Vander AJ, Miller R. Control of renin secretion in the anesthetized dog. Am J Physiol 1964;207:537–46.

[490] Vander AJ. Renin secretion during mannitol diuresis and ureteral occlusion. Proc Soc Exp Biol Med 1968;128:518–20.
[491] Skott O, Briggs JP. Direct demonstration of macula densa-mediated renin secretion. Science 1987;237:1618–20.
[492] Shade RE, Davis JO, Johnson JA, Witty RT. Effects of renal arterial infusion of sodium and potassium on renin secretion in the dog. Circ Res 1972;31:719–27.
[493] Kirchner KA, Kotchen TA, Galla JH, Luke RG. Importance of chloride for acute inhibition of renin by sodium chloride. Am J Physiol 1978;235:F444–450.
[494] Kotchen TA, Galla JH, Luke RG. Contribution of chloride to the inhibition of plasma renin by sodium chloride in the rat. Kidney Int 1978;13:201–7.
[495] Leyssac PP. Changes in single nephron renin release are mediated by tubular fluid flow rate. Kidney Int 1986;30:332–9.
[496] Greenberg SG, Lorenz JN, He XR, Schnermann JB, Briggs JP. Effect of prostaglandin synthesis inhibition on macula densa-stimulated renin secretion. Am J Physiol Renal Physiol 1993;265:F578–583.
[497] Lorenz JN, Weihprecht H, Schnermann J, Skott O, Briggs JP. Characterization of the macula densa stimulus for renin secretion. Am J Physiol Renal Physiol 1990;259:F186–193.
[498] Lorenz JN, Weihprecht H, Schnermann J, Skott O, Briggs JP. Renin release from isolated juxtaglomerular apparatus depends on macula densa chloride transport. Am J Physiol Renal Physiol 1991;260:F486–493.
[499] Weihprecht H, Lorenz JN, Schnermann J, Skott O, Briggs JP. Effect of adenosine1-receptor blockade on renin release from rabbit isolated perfused juxtaglomerular apparatus. J Clin Invest 1990;85:1622–8.
[500] He XR, Greenberg SG, Briggs JP, Schnermann J. Effects of furosemide and verapamil on the NaCl dependency of macula densa-mediated renin secretion. Hypertension 1995;26: 137–42.
[501] Churchill PC, Churchill MC, McDonald FD. Effects of saline and mannitol on renin and distal tubule Na in rats. Circ Res 1979;45:786–92.
[502] DiBona GF. Effect of mannitol diuresis and ureteral occlusion on distal tubular reabsorption. Am J Physiol 1971;221: 511–4.
[503] Leyssac PP, Holstein-Rathlou NH, Skott O. Renal blood flow, early distal sodium, and plasma renin concentrations during osmotic diuresis. Am J Physiol Regul Integr Comp Physiol 2000;279:R1268–1276.
[504] Beierwaltes WH. Selective neuronal nitric oxide synthase inhibition blocks furosemide- stimulated renin secretion *in vivo*. Am J Physiol Renal Physiol 1995;269:F134–139.
[505] Castrop H, Schweda F, Mizel D, Huang Y, Briggs J, Kurtz A, et al. Permissive role of nitric oxide in macula densa control of renin secretion. Am J Physiol Renal Physiol 2004;286(5): F848–857 .
[506] Keeton TK, Campbell WB. The pharmacologic alteration of renin release. Pharmacol Rev 1980;32:81–227.
[507] Vander AJ, Carlson J. Mechanism of the effects of furosemide on renin secretion in anesthetized dogs. Circ Res 1969; 25:145–52.
[508] Itoh S, Carretero OA. Role of the macula densa in renin release. Hypertension 1985;7:I49–54.
[509] Hanner F, Chambrey R, Bourgeois S, Meer E, Mucsi I, Rosivall L, et al. Increased renal renin content in mice lacking the Na^+/H^+ exchanger NHE2. Am J Physiol Renal Physiol 2008;294: F937–944.
[510] Castrop HW, Hansen PB, Huang YG, et al. Direct effects of furosemide on renin secretion and preglomerular resistance. J Am Soc Nephrol 2004;15:199A (abstract)
[511] Kotchen TA, Luke RG, Ott CE, Galla JH, Whitescarver S. Effect of chloride on renin and blood pressure responses to sodium chloride. Ann Intern Med 1983;98:817–22.
[512] Welch WJ, Ott CE, Lorenz JN, Kotchen TA. Effects of chlorpropamide on loop of Henle function and plasma renin. Kidney Int 1986;30:712–6.
[513] Abboud HE, Luke RG, Galla JH, Kotchen TA. Stimulation of renin by acute selective chloride depletion in the rat. Circ Res 1979;44:815–21.
[514] Rostand SG, Work J, Luke RG. Effect of reduced chloride reabsorption on renin release in the isolated rat kidney. Pflugers Arch 1985;405:46–51.
[515] Kim SM, Mizel D, Huang YG, Briggs JP, Schnermann J. Adenosine as a mediator of macula densa-dependent inhibition of renin secretion. Am J Physiol Renal Physiol 2006;290: F1016–1023.
[516] Robben JH, Fenton RA, Vargas SL, Schweer H, Peti-Peterdi J, Deen PM, et al. Localization of the succinate receptor in the distal nephron and its signaling in polarized MDCK cells. Kidney Int 2009;76:1258–67.
[517] Vargas SL, Toma I, Kang JJ, Meer EJ, Peti-Peterdi J. Activation of the succinate receptor GPR91 in macula densa cells causes renin release. J Am Soc Nephrol 2009;20:1002–11.
[518] Baumbach L, Leyssac PP, Skinner SL. Studies on renin release from isolated superfused glomeruli: effects of temperature, urea, ouabain and ethacrynic acid. J Physiol 1976;258: 243–56.
[519] Toma I, Kang JJ, Sipos A, Vargas S, Bansal E, Hanner F, et al. Succinate receptor GPR91 provides a direct link between high glucose levels and renin release in murine and rabbit kidney. J Clin Invest 2008;118:2526–34.
[520] Pluznick JL, Zou DJ, Zhang X, Yan Q, Rodriguez-Gil DJ, Eisner C, et al. Functional expression of the olfactory signaling system in the kidney. Proc Natl Acad Sci USA 2009;106: 2059–64.
[521] Bosse HM, Bohm R, Resch S, Bachmann S. Parallel regulation of constitutive NO synthase and renin at JGA of rat kidney under various stimuli. Am J Physiol Renal Physiol 1995;269: F793–805.
[522] Murakami K, Tsuchiya K, Naruse M, Naruse K, Demura H, Arai J, et al. Nitric oxide synthase I immunoreactivity in the macula densa of the kidney is angiotensin II dependent. Kidney Int Suppl 1997;63:S208–210.
[523] Tojo A, Madsen KM, Wilcox CS. Expression of immunoreactive nitric oxide synthase isoforms in rat kidney. Effects of dietary salt and losartan. Jpn Heart J 1995;36:389–98.
[524] Kihara M, Umemura S, Kadota T, Yabana M, Tamura K, Nyuui N, et al. The neuronal isoform of constitutive nitric oxide synthase is up-regulated in the macula densa of angiotensinogen gene-knockout mice. Lab Invest 1997;76:285–94.
[525] Kihara M, Umemura S, Sugaya T, Toya Y, Yabana M, Kobayashi S, et al. Expression of neuronal type nitric oxide synthase and renin in the juxtaglomerular apparatus of angiotensin type-1a receptor gene-knockout mice. Kidney Int 1998;53:1585–93.
[526] Paliege A, Mizel D, Medina C, Pasumarthy A, Huang YG, Bachmann S, et al. Inhibition of nNOS expression in the macula densa by COX-2-derived prostaglandin E(2). Am J Physiol Renal Physiol 2004;287:F152–159.
[527] Gambaryan S, Wagner C, Smolenski A, Walter U, Poller W, Haase W, et al. Endogenous or overexpressed cGMP-dependent protein kinases inhibit cAMP-dependent renin release from rat isolated perfused kidney, microdissected glomeruli, and isolated juxtaglomerular cells. Proc Natl Acad Sci USA 1998;95:9003–8.

[528] Wagner C, Pfeifer A, Ruth P, Hofmann F, Kurtz A. Role of cGMP-kinase II in the control of renin secretion and renin expression. J Clin Invest 1998;102:1576–82.
[529] Harrison SA, Reifsnyder DH, Gallis B, Cadd GG, Beavo JA. Isolation and characterization of bovine cardiac muscle cGMP-inhibited phosphodiesterase: a receptor for new cardiotonic drugs. Mol Pharmacol 1986;29:506–14.
[530] Chiu T, Reid IA. Role of cyclic GMP-inhibitable phosphodiesterase and nitric oxide in the beta adrenoceptor control of renin secretion. J Pharmacol Exp Ther 1996;278:793–9.
[531] Kurtz A, Gotz KH, Hamann M, Kieninger M, Wagner C. Stimulation of renin secretion by NO donors is related to the cAMP pathway. Am J Physiol Renal Physiol 1998;274:F709–717.
[532] Sayago CM, Beierwaltes WH. Nitric oxide synthase and cGMP-mediated stimulation of renin secretion. Am J Physiol Regul Integr Comp Physiol 2001;281:R1146–1151.
[533] He XR, Greenberg SG, Briggs JP, Schnermann JB. Effect of nitric oxide on renin secretion. II. Studies in the perfused juxtaglomerular apparatus. Am J Physiol Renal Physiol 1995;268: F953–959.
[534] Persson PB, Baumann JE, Ehmke H, Hackenthal E, Kirchheim HR, Nafz B, et al. Endothelium-derived NO stimulates pressure-dependent renin release in conscious dogs. Am J Physiol 1993;264:F943–947.
[535] Scholz H, Kurtz A. Involvement of endothelium-derived relaxing factor in the pressure control of renin secretion from isolated perfused kidney. J Clin Invest 1993;91:1088–94.
[536] Chatziantoniou C, Pauti MD, Pinet F, Promeneur D, Dussaule JC, Ardaillou R. Regulation of renin release is impaired after nitric oxide inhibition. Kidney Int 1996;49:626–33.
[537] Reid IA, Chou L. Effect of blockade of nitric oxide synthesis on the renin secretory response to frusemide in conscious rabbits. Clin Sci (Colch) 1995;88:657–63.
[538] Schricker K, Hamann M, Kurtz A. Nitric oxide and prostaglandins are involved in the macula densa control of the renin system. Am J Physiol Renal Physiol 1995;269:F825–830.
[539] Larsson C, Weber P, Anggard E. Arachidonic acid increases and indomethacin decreases plasma renin activity in the rabbit. Eur J Pharmacol 1974;28:391–4.
[540] Jensen BL, Schmid C, Kurtz A. Prostaglandins stimulate renin secretion and renin mRNA in mouse renal juxtaglomerular cells. Am J Physiol Renal Physiol 1996;271:F659–69.
[541] Jensen BL, Mann B, Skott O, Kurtz A. Differential regulation of renal prostaglandin receptor mRNAs by dietary salt intake in the rat. Kidney Int 1999;56:528–37.
[542] Chen L, Kim SM, Oppermann M, Faulhaber-Walter R, Huang Y, Mizel D, et al. Regulation of renin in mice with Cre recombinase-mediated deletion of G protein Gsalpha in juxtaglomerular cells. Am J Physiol Renal Physiol 2007;292:F27–37.
[543] Castrop H, Schweda F, Schumacher K, Wolf K, Kurtz A. Role of renocortical cyclooxygenase-2 for renal vascular resistance and macula densa control of renin secretion. J Am Soc Nephrol 2001;12:867–74.
[544] Kammerl MC, Nusing RM, Richthammer W, Kramer BK, Kurtz A. Inhibition of COX-2 counteracts the effects of diuretics in rats. Kidney Int 2001;60:1684–91.
[545] Komhoff M, Jeck ND, Seyberth HW, Grone HJ, Nusing RM, Breyer MD. Cyclooxygenase-2 expression is associated with the renal macula densa of patients with Bartter-like syndrome. Kidney Int 2000;58:2420–4.
[546] Mann B, Hartner A, Jensen BL, Kammerl M, Kramer BK, Kurtz A. Furosemide stimulates macula densa cyclooxygenase-2 expression in rats. Kidney Int 2001;59:62–8.
[547] Reinalter SC, Jeck N, Brochhausen C, Watzer B, Nüsing RM, Seyberth HW, et al. Role of cyclooxygenase-2 in hyperprostaglandin E syndrome/antenatal Bartter syndrome. Kidney Int 2002;62:253–60.
[548] Hartner A, Cordasic N, Goppelt-Struebe M, Veelken R, Hilgers KF. Role of macula densa cyclooxygenase-2 in renovascular hypertension. Am J Physiol Renal Physiol 2003;284: F498–502.
[549] Jensen BL, Kurtz A. Differential regulation of renal cyclooxygenase mRNA by dietary salt intake. Kidney Int 1997;52:1242–9.
[550] Wang JL, Cheng HF, Harris RC. Cyclooxygenase-2 inhibition decreases renin content and lowers blood pressure in a model of renovascular hypertension. Hypertension 1999;34:96–101.
[551] Tomasoni S, Noris M, Zappella S, Gotti E, Casiraghi F, Bonazzola S, et al. Upregulation of renal and systemic cyclooxygenase-2 in patients with active lupus nephritis. J Am Soc Nephrol 1998;9:1202–12.
[552] Wang JL, Cheng HF, Zhang MZ, McKanna JA, Harris RC. Selective increase of cyclooxygenase-2 expression in a model of renal ablation. Am J Physiol Renal Physiol 1998;275:F613–622.
[553] Kim SM, Chen L, Mizel D, Huang YG, Briggs JP, Schnermann J. Low plasma renin and reduced renin secretory responses to acute stimuli in conscious COX-2-deficient mice. Am J Physiol Renal Physiol 2007;292:F415–22.
[554] Yang T, Endo Y, Huang YG, Smart A, Briggs JP, Schnermann J. Renin expression in COX-2-knockout mice on normal or low-salt diets. Am J Physiol Renal Physiol 2000;279:F819–825.
[555] Cheng HF, Wang JL, Zhang MZ, Miyazaki Y, Ichikawa I, McKanna JA, et al. Angiotensin II attenuates renal cortical cyclooxygenase-2 expression. J Clin Invest 1999;103:953–61.
[556] Wolf K, Castrop H, Hartner A, Goppelt-Strube M, Hilgers KF, Kurtz A. Inhibition of the renin-angiotensin system upregulates cyclooxygenase-2 expression in the macula densa. Hypertension 1999;34:503–7.
[557] Peti-Peterdi J, Komlosi P, Fuson AL, Guan Y, Schneider A, Qi Z, et al. Luminal NaCl delivery regulates basolateral PGE2 release from macula densa cells. J Clin Invest 2003;112:76–82.
[558] Traynor TR, Smart A, Briggs JP, Schnermann J. Inhibition of macula densa-stimulated renin secretion by pharmacological blockade of cyclooxygenase-2. Am J Physiol Renal Physiol 1999;277:F706–10.
[559] Cheng HF, Wang JL, Zhang MZ, McKanna JA, Harris RC. Role of p38 in the regulation of renal cortical cyclooxygenase-2 expression by extracellular chloride. J Clin Invest 2000;106:681–8.
[560] Yang T, Park JM, Arend L, Huang Y, Topaloglu R, Pasumarthy A, et al. Low chloride stimulation of prostaglandin E2 release and cyclooxygenase-2 expression in a mouse macula densa cell line. J Biol Chem 2000;275:37922–9.
[561] Cheng HF, Harris RC. Cyclooxygenase-2 expression in cultured cortical thick ascending limb of Henle increases in response to decreased extracellular ionic content by both transcriptional and post-transcriptional mechanisms. Role of p38-mediated pathways. J Biol Chem 2002;277:45638–43.
[562] Guan Z, Buckman SY, Miller BW, Springer LD, Morrison AR. Interleukin-1beta-induced cyclooxygenase-2 expression requires activation of both c-Jun NH2-terminal kinase and p38 MAPK signal pathways in rat renal mesangial cells. J Biol Chem 1998;273:28670–6.
[563] Xie W, Herschman HR. Transcriptional regulation of prostaglandin synthase 2 gene expression by platelet-derived growth factor and serum. J Biol Chem 1996;271:31742–8.
[564] Yang T, Huang Y, Heasley LE, Berl T, Schnermann JB, Briggs JP. MAPK mediation of hypertonicity-stimulated cyclooxygenase-2 expression in renal medullary collecting duct cells. J Biol Chem 2000;275:23281–6.

[565] Cheng HF, Wang JL, Zhang MZ, Wang SW, McKanna JA, Harris RC. Genetic deletion of COX-2 prevents increased renin expression in response to ACE inhibition. Am J Physiol Renal Physiol 2001;280:F449–456.

[566] Fujino T, Nakagawa N, Yuhki K, Hara A, Yamada T, Takayama K, et al. Decreased susceptibility to renovascular hypertension in mice lacking the prostaglandin I2 receptor IP. J Clin Invest 2004;114:805–12.

[567] Hocherl K, Kammerl MC, Schumacher K, Endemann D, Grobecker HF, Kurtz A. Role of prostanoids in regulation of the renin–angiotensin–aldosterone system by salt intake. Am J Physiol Renal Physiol 2002;283:F294–301.

[568] Kammerl MC, Nusing RM, Seyberth HW, Riegger GA, Kurtz A, Kramer BK. Inhibition of cyclooxygenase-2 attenuates urinary prostanoid excretion without affecting renal renin expression. Pflugers Arch 2001;442:842–7.

[569] Kurtz A, Schweda F. Osmolarity-induced renin secretion from kidneys: evidence for readily releasable renin pools. Am J Physiol Renal Physiol 2006;290:F797–805.

[570] Therland KL, Stubbe J, Thiesson HC, Ottosen PD, Walter S, Sørensen GL, et al. Cycloxygenase-2 is expressed in vasculature of normal and ischemic adult human kidney and is colocalized with vascular prostaglandin E2 EP4 receptors. J Am Soc Nephrol 2004;15:1189–98.

[571] Liguori A, Casini A, Di Loreto M, Andreini I, Napoli C. Loop diuretics enhance the secretion of prostacyclin *in vitro*, in healthy persons, and in patients with chronic heart failure. Eur J Clin Pharmacol 1999;55:117–24.

[572] Hocherl K, Kees F, Kramer BK, Kurtz A. Cyclosporine A attenuates the natriuretic action of loop diuretics by inhibition of renal COX-2 expression. Kidney Int 2004;65:2071–80.

[573] Stichtenoth DO, Marhauer V, Tsikas D, Gutzki FM, Frolich JC. Effects of specific COX-2-inhibition on renin release and renal and systemic prostanoid synthesis in healthy volunteers. Kidney Int 2005;68:2197–207.

[574] Arend LJ, Haramati A, Thompson CI, Spielman WS. Adenosine-induced decrease in renin release: dissociation from hemodynamic effects. Am J Physiol Renal Physiol 1984;247:F447–452.

[575] Churchill PC, Churchill MC. A1 and A2 adenosine receptor activation inhibits and stimulates renin secretion of rat renal cortical slices. J Pharmacol Exp Ther 1985;232:589–94.

[576] Tagawa H, Vander AJ. Effects of adenosine compounds on renal function and renin secretion in dogs. Circ Res 1970;26:327–38.

[577] Lorenz JN, Weihprecht H, He XR, Skott O, Briggs JP, Schnermann J. Effects of adenosine and angiotensin on macula densa-stimulated renin secretion. Am J Physiol Renal Physiol 1993;265:F187–194.

[578] Schweda F, Wagner C, Kramer BK, Schnermann J, Kurtz A. Preserved macula densa-dependent renin secretion in A1 adenosine receptor knockout mice. Am J Physiol Renal Physiol 2003;284:F770–777.

[579] Grunberger C, Obermayer B, Klar J, Kurtz A, Schweda F. The calcium paradoxon of renin release: Calcium suppresses renin exocytosis by inhibition of calcium-dependent adenylate cyclases AC5 and AC6. Circ Res 2006;99:1197–206.

[580] Ortiz-Capisano MC, Ortiz PA, Harding P, Garvin JL, Beierwaltes WH. Decreased intracellular calcium stimulates renin release via calcium-inhibitable adenylyl cyclase. Hypertension 2007;49:162–9.

[581] Frederiksen O, Leyssac PP, Skinner SL. Sensitive osmometer function of juxtaglomerular cells *in vitro*. J Physiol 1975;252:669–79.

[582] Jensen BL, Skott O. Osmotically sensitive renin release from permeabilized juxtaglomerular cells. Am J Physiol 1993;265: F87–95.

[583] Schricker K, Kurtz A. Role of membrane-permeable ions in renin secretion by renal juxtaglomerular cells. Am J Physiol 1995;269:F64–69.

[584] Skott O. Do osmotic forces play a role in renin secretion? Am J Physiol 1988;255:F1–10.

[585] Friis UG, Madsen K, Svenningsen P, Hansen PB, Gulaveerasingam A, Jorgensen F, et al. Hypotonicity-induced Renin exocytosis from juxtaglomerular cells requires aquaporin-1 and cyclooxygenase-2. J Am Soc Nephrol 2009;20:2154–61.

[586] Young DB, Rostorfer HH. Renin release responses to acute alterations in renal arterial osmolarity. Am J Physiol 1973;225:1009–14.

[587] Ortiz-Capisano MC, Ortiz PA, Garvin JL, Harding P, Beierwaltes WH. Expression and function of the calcium-sensing receptor in juxtaglomerular cells. Hypertension 2007;50:737–43.

[588] Maillard MP, Tedjani A, Perregaux C, Burnier M. Calcium-sensing receptors modulate renin release *in vivo* and *in vitro* in the rat. J Hypertens 2009;27:1980–7.

[589] Palmer CE, Rudd MA, Bukoski RD. Renal interstitial Ca^{2+} during sodium loading of normotensive and Dahl-salt hypertensive rats. Am J Hypertens 2003;16:771–6.

[590] Hanner F, von Maltzahn J, Maxeiner S, Toma I, Sipos A, Kruger O, et al. Connexin45 is expressed in the juxtaglomerular apparatus and is involved in the regulation of renin secretion and blood pressure. Am J Physiol Regul Integr Comp Physiol 2008;295:R371–380.

[591] Toma I, Bansal E, Meer EJ, Kang JJ, Vargas SL, Peti-Peterdi J. Connexin 40 and ATP-dependent intercellular calcium wave in renal glomerular endothelial cells. Am J Physiol Regul Integr Comp Physiol 2008;294:R1769–1776.

[592] Krattinger N, Capponi A, Mazzolai L, Aubert JF, Caille D, Nicod P, et al. Connexin40 regulates renin production and blood pressure. Kidney Int 2007;72:814–22.

[593] Kurtz L, Schweda F, de Wit C, Kriz W, Witzgall R, Warth R, et al. Lack of connexin 40 causes displacement of renin-producing cells from afferent arterioles to the extraglomerular mesangium. J Am Soc Nephrol 2007;18:1103–11.

[594] Briggs J. A simple steady-state model for feedback control of glomerular filtration rate. Kidney International 1982;22(Suppl. 12):S143–50.

[595] Skott O, Briggs JP. A method for superfusion of the isolated perfused tubule. Kidney Int 1988;33:1009–12.

[596] Hoyer JR, Sisson SP, Vernier RL. Tamm-Horsfall glycoprotein: Ultrastructural immunoperoxidase localization in rat kidney. Lab Invest 1979;41:168–73.

[597] Salido EC, Yen PH, Shapiro LJ, Fisher DA, Barajas L. *In situ* hybridization of prepro-epidermal growth factor mRNA in the mouse kidney. Am J Physiol 1989;256:F632–638.

[598] Kulaksiz H, Theilig F, Bachmann S, Gehrke SG, Rost D, Janetzko A, et al. The iron-regulatory peptide hormone hepcidin: expression and cellular localization in the mammalian kidney. J Endocrinol 2005;184:361–70.

[599] Obermuller N, Gallagher AR, Cai Y, Gassler N, Gretz N, Somlo S, et al. The rat pkd2 protein assumes distinct subcellular distributions in different organs. Am J Physiol 1999;277: F914–925.

[600] Tian W, Salanova M, Xu H, Lindsley JN, Oyama TT, Anderson S, et al. Renal expression of osmotically responsive cation channel TRPV4 is restricted to water-impermeant nephron segments. Am J Physiol Renal Physiol 2004;287:F17–24.

[601] Stoeckel ME, Freund-Mercier MJ. Autoradiographic demonstration of oxytocin-binding sites in the macula densa [published erratum appears in Am J Physiol Renal Physiol 1990 Jan;258(1 Pt 2):preceding F1] Am J Physiol Renal Physiol. 1989;257:F310–314.

[602] Harrison-Bernard LM, Navar LG, Ho MM, Vinson GP, el-Dahr SS. Immunohistochemical localization of ANG II AT1 receptor in adult rat kidney using a monoclonal antibody. Am J Physiol 1997;273:F170–177.

[603] Beaumont K, Healy DP, Fanestil DD. Autoradiographic localization of benzodiazepine receptors in the rat kidney. Am J Physiol 1984;247:F718–724.

[604] Riccardi D, Hall AE, Chattopadhyay N, Xu JZ, Brown EM, Hebert SC. Localization of the extracellular Ca^{2+}/polyvalent cation-sensing protein in rat kidney. Am J Physiol 1998;274: F611–622.

[605] Massfelder T, Stewart AF, Endlich K, Soifer N, Judes C, Helwig JJ. Parathyroid hormone-related protein detection and interaction with NO and cyclic AMP in the renovascular system. Kidney Int 1996;50:1591–603.

[606] Haddad M, Roder S, Olsen HS, Wagner GF. Immunocytochemical localization of stanniocalcin cells in the rat kidney. Endocrinology 1996;137:2113–7.

[607] Breuss JM, Gillett N, Lu L, Sheppard D, Pytela R. Restricted distribution of integrin beta 6 mRNA in primate epithelial tissues. J Histochem Cytochem 1993;41:1521–7.

[608] Liu R, Bell PD, Peti-Peterdi J, Kovacs G, Johansson A, Persson AE. Purinergic receptor signaling at the basolateral membrane of macula densa cells. J Am Soc Nephrol 2002;13:1145–51.

[609] O'Reilly M, Marshall E, Macgillivray T, Mittel M, Xue W, Kenyon CJ, et al. Dietary electrolyte-driven responses in the renal WNK kinase pathway *in vivo*. J Am Soc Nephrol 2006;17:2402–13.

[610] Komers R, Lindsley JN, Oyama TT, Cohen DM, Anderson S. Renal p38 MAP kinase activity in experimental diabetes. Lab Invest 2007;87:548–58.

[611] Balen D, Ljubojevic M, Breljak D, Brzica H, Zlender V, Koepsell H, et al. Revised immunolocalization of the Na^+-D-glucose co-transporter SGLT1 in rat organs with an improved antibody. Am J Physiol Cell Physiol 2008;295: C475–489.

[612] Lai LW, Yong KC, Lien YH. Site-specific expression of IQGAP1, a key mediator of cytoskeleton, in mouse renal tubules. J Histochem Cytochem 2008;56:659–66.

This page intentionally left blank

CHAPTER

24

Renal Cortical and Medullary Microcirculations: Structure and Function

Thomas L. Pallone and Chunhua Cao

Division of Nephrology, Department of Medicine, University of Maryland at Baltimore, Baltimore, MD, USA

ANATOMY OF THE RENAL CIRCULATION

Cortical Microcirculation

The basic vascular pattern of the kidney is preserved across mammalian species[1,3–9] (Figure 24.1). The renal artery branches into interlobar arteries that ascend within the renal pelvis to enter the parenchyma. In multipapillate organisms, the interlobar arteries travel toward the cortex along the columns of Bertin. These vessels change direction and follow an arc-like course near the corticomedullary border to become arcuate arteries. The arcuate artery gives rise to the interlobular arteries that ascend, in radial fashion, toward the cortical surface. Afferent arterioles arise from interlobular arteries at angles that vary with their cortical depth. Afferents that supply deep glomeruli near the corticomedullary junction (juxtamedullary glomeruli) leave the interlobular artery at a recurrent angle. In contrast, superficial afferent arterioles that supply glomeruli near the surface of the kidney line up with the interlobular artery at its termination.

In some species (rat, cat, dog, and *Meriones*) a pair of intra-arterial "cushions" exist as parallel ridges that project from the origin of the juxtamedullary afferent arteriole into the lumen of the parent intralobular artery (Figure 24.2a).[10,11] The cushions are 18–30 μm in length, composed of a ground substance in which smooth muscle cells are embedded and covered by a layer of continuous endothelium (Figure 24.2b).[12] The cushions are ideally placed to regulate blood flow distribution within the cortex. Given that blood flow to the renal medulla arises largely from the efferent flow of juxtamedullary glomeruli, it is also plausible that the cushions play a role in the regulation of blood flow to the medulla. The cushions have been hypothesized to separate plasma and red blood cells, and alter medullary hematocrit by "skimming" plasma from a red cell-free layer near the vessel wall.[10,13]

The structure of afferent and efferent arterioles varies with cortical location. Afferent arterioles are composed of one to three layers of smooth muscle cells. Muscle and elastic tissue diminish near the glomerulus and the media is replaced by granular cells of the juxtaglomerular apparatus. The diameters of efferent arterioles vary from as small as 12 μm in the superficial cortex to 28 μm for juxtamedullary glomeruli. Efferent arterioles in the superficial cortex branch to form a dense peritubular capillary plexus. Ten different branching patterns have been described.[14] In contrast to the efferent arterioles of superficial glomeruli, those of juxtamedullary glomeruli most frequently cross the corticomedullary junction to enter the outer stripe of the outer medulla, where they give rise to descending vasa recta (DVR). DVR are transitional vessels along which smooth muscle is replaced by contractile pericytes.[8,15] A small fraction of blood flow to the renal medulla may bypass juxtamedullary glomeruli in "shunt" vessels (dashed line, Figure 24.1). Casellas and Mimran have described variations of those shunts as: (1) branches of afferent arterioles; (2) continuous vessels from which afferent arterioles arise as side branches; (3) short vascular connections between

Seldin and Giebisch's The Kidney, Fifth Edition.
DOI: http://dx.doi.org/10.1016/B978-0-12-381462-3.00024-0

© 2013 Elsevier Inc. All rights reserved.

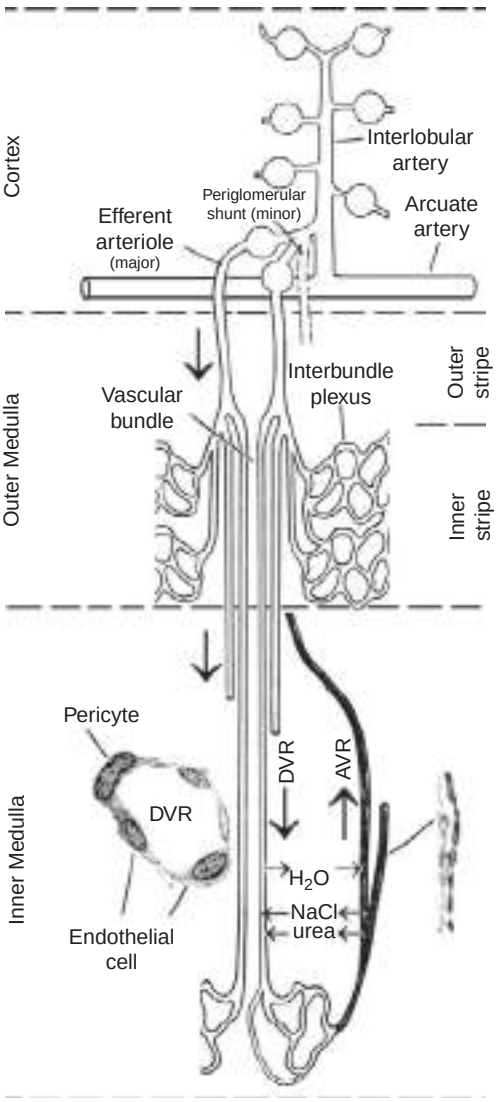

FIGURE 24.1 Microcirculation of the renal cortex and medulla. Within the renal cortex, interlobular arteries, derived from the arcuate artery, ascend toward the cortical surface. Superficial and midcortical glomeruli arise at obtuse and right angles, while juxtamedullary glomeruli arise at an acute, recurrent angle from the interlobular artery. The majority of blood flow to the medulla arises from juxtamedullary efferent arterioles. A minor fraction might also be derived from periglomerular shunt pathways (dashed lines). In the outer stripe of the outer medulla, juxtamedullary efferent arterioles give rise to DVR that combine with AVR, and sometimes thin descending limbs of Henle, to form vascular bundles. Vascular bundles are the prominent feature of the inner stripe of the outer medulla. DVR on the periphery of vascular bundles perfuse the interbundle capillary plexus that supplies nephrons (thick ascending limb, collecting duct, long looped thin descending limbs, not shown). DVR in the center of the bundles continue across the inner–outer medullary junction to perfuse the inner medulla. In some species, thin descending limbs of short looped nephrons migrate toward or become associated with vascular bundles. In the inner medulla, vascular bundles disappear and vasa recta become dispersed with thin loops of Henle and collecting ducts. Blood from the interbundle capillary plexus is returned without rejoining vascular bundles. DVR have a continuous endothelium (inset) and are surrounded by contractile pericytes. Like cortical peritubular capillaries, the AVR endothelium is highly fenestrated. As blood flows toward the papillary tip, NaCl and urea diffuse into DVR and out of AVR. Transmural gradients of NaCl and urea drive water efflux across the DVR wall via aquaporin-1 water channels. The increasing size of the circled "P" is to represent the rise in DVR plasma protein concentration with medullary depth. *(Reproduced with permission from ref. [31].)*

afferent and efferent arterioles; and (4) pelvic arterioles derived from afferent arterioles near the renal hilus (Figure 24.3).[16] Several reviews of arteriolar patterns in the renal cortex have been written.[4,11,17]

The bulk of glomerular filtrate is reabsorbed by the proximal convoluted tubule. That reabsorbate is conducted through the cortical interstitium and taken up by peritubular capillaries. The peritubular interstitium of the cortex has been divided into "narrow" and "wide" portions comprising 0.6 and 3.4% of tissue volume.[18,19] The narrow interstitium is flanked by a highly fenestrated capillary wall on one side and the basolateral membrane of the PCT on the other (Figure 24.4).[9,20] Since only 26% of the tubular surface faces the narrow interstitium it follows that substantial quantities of fluid must flow from the wide to the narrow portion, implying that hydrostatic pressure gradients exist within the cortical interstitium.[18,21]

Medullary Microcirculation

Blood flow to the renal medulla is supplied by DVR. Descending vasa recta (DVR) arise largely from efferent arterioles of juxtamedullary glomeruli and supply all blood flow to the renal medulla (Figure 24.1). The afferent arterioles that supply juxtamedullary glomeruli arise from interlobular arterioles (cortical penetrating arterioles) at recurrent angles. Muscular intra-arterial cushions exist at the origins of afferent arterioles (Figure 24.2), particularly near the corticomedullary junction, and have been proposed to participate in reduction of medullary hematocrit by "plasma skimming" (see below).[10,11] Juxtamedullary efferent arterioles are larger, longer, and have a more robust smooth muscle layer than those derived from superficial or midcortical glomeruli (Figure 24.5).[15,17] They often divide into branches that either remain in the cortex to supply cortical peritubular

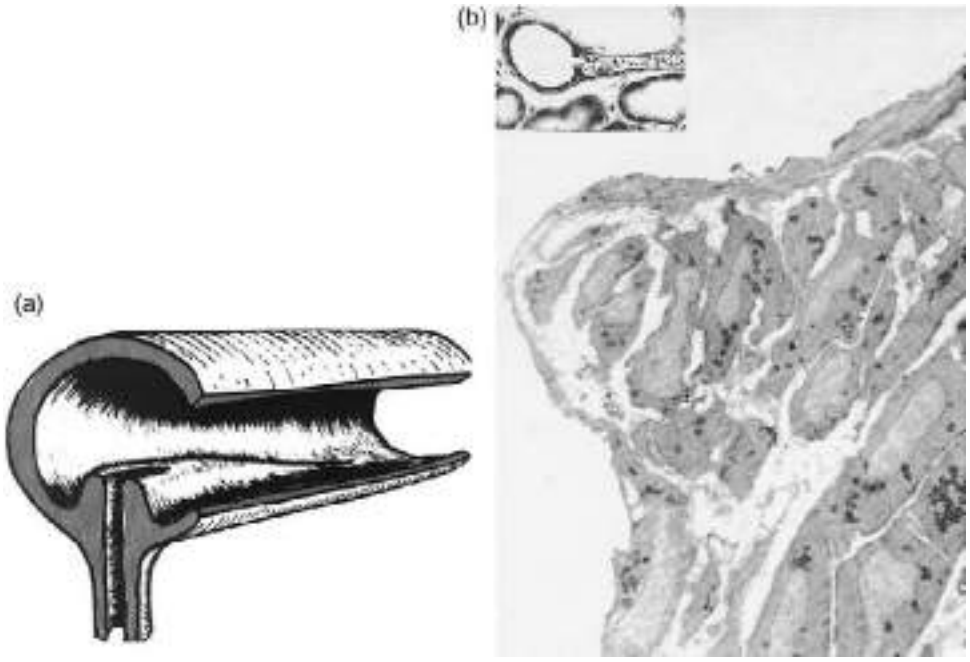

FIGURE 24.2 **The intra-arterial cushion.** (a) In some species intra-arterial cushions are present where juxtamedullary afferent arterioles arise from interlobular arterioles. (b) A longitudinal section through an afferent arteriole shows an intra-arterial cushion at its origin from the interlobular artery (inset: ×160). The cushion protrudes into the lumen of the parent vessel. Smooth muscle cells of the cushion are embedded in a copious matrix (×4000). Intra-arterial cushions might affect the relative volume fraction of RBCs versus plasma (hematocrit) that is directed from intralobular arterioles to juxtamedullary glomeruli and renal medulla. It is also conceivable that they regulate the relative distribution of blood flow between the superficial and juxtamedullary cortex (see text). *(Reproduced with permission from ref. [11,12]).*

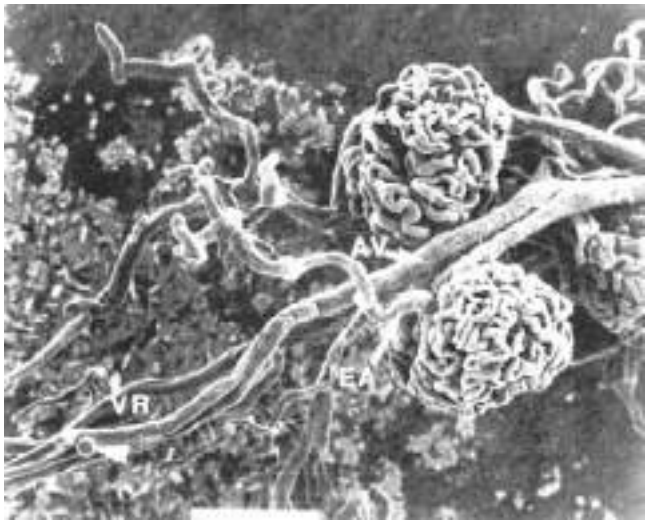

FIGURE 24.3 **Corrosion cast showing a periglomerular shunt vessel at the corticomedullary junction.** The afferent arteriole (AA) of a juxtamedullary glomerulus gives rise to a side branch (AV) which forms descending vasa recta (VR). The efferent arteriole (EA) of the juxtamedullary glomerulus is visible (Arrowhead: 16 μm sphere; Bar: 100 μm). It is probable that some blood flow that reaches the renal medulla bypasses juxtamedullary glomeruli by shunts such as the one illustrated, but the overall fraction of medullary blood flow derived from shunts is probably small (i.e., <10%). *(Reproduced with permission from ref. [16]).*

capillaries or, alternatively, descend into the medulla to form DVR.[14,22,23] DVR are about one half of the diameter of parent juxtamedullary efferent arterioles, in the range of 12 to 18 μm; some may be as large as 20 μm. DVR branch from their parent efferent arteriole in the outer stripe of the outer medulla and then coalesce within vascular bundles in the inner stripe of the outer medulla[4,5,8,24,25] (Figure 24.1). Larger diameter DVR lie in the center of vascular bundles and penetrate to the deepest regions of the inner medulla.[15,17,26] DVR are transitional vessels, wherein smooth muscle is replaced by contractile pericytes.[27] Pericytes become increasingly scarce with medullary depth, but are retained well into the inner medulla[28] (Figure 24.6). DVR have a continuous endothelium with tight junctions. In contrast, ascending vasa recta (AVR) that arise from DVR are highly fenestrated[25,29,30](Figure 24.7). DVR peel off from the periphery of the vascular bundles as they pass through the inner stripe to supply the interbundle capillary plexus (Figure 24.8a,b,c). AVR within vascular bundles are only those that originate from the inner medulla.[24] Blood flow from the outer medullary interbundle capillary plexus returns to the cortex without rejoining vascular bundles. Thus, countercurrent exchange in the vascular bundles of the inner stripe of the outer medulla involves all DVR, but only those AVR that return from the inner medulla.

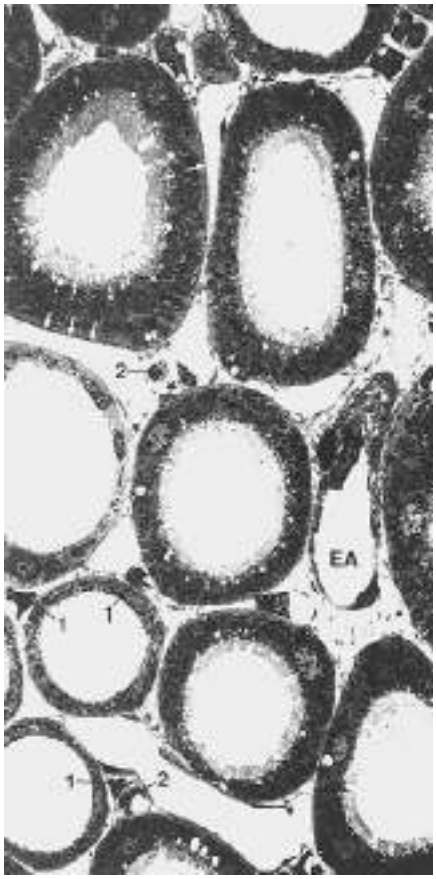

FIGURE 24.4 **Peritubular interstitium of the renal cortex.** The narrow portion of the cortical interstitium (arrows) lies immediately adjacent to the basement membrane of the proximal tubule. The wide portion (stars) lies between peritubular capillaries and cortical nephrons. Interstitial cells are fibroblast-like[780] or rounded[746] (EA: efferent arteriole (× 1000). *(Reproduced with permission from ref. [20]).*

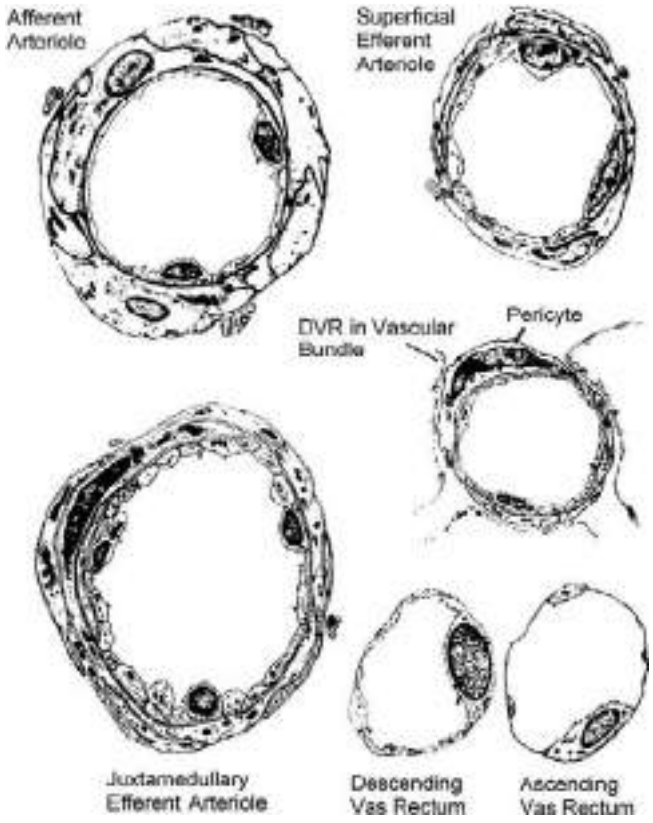

FIGURE 24.5 **Structure and transition of cortical and medullary vessels.** The proximal afferent arteriole is composed of at least two layers of smooth muscle cells. The muscularity and size of cortical efferent arterioles differ with location. Note the difference between the superficial and juxtamedullary efferent arterioles. The juxtamedullary efferent arteriole is larger, has a thicker, multilayered media, and its endothelium is composed of more numerous endothelial cells. In the illustration, a descending vas rectum (DVR) in a vascular bundle is adjacent to three fenestrated ascending vasa recta (AVR). The DVR wall is surrounded by a contractile pericyte. At the bottom right, DVR and AVR from the inner medulla are shown. Inner medullary DVR have a continuous endothelium through most of their length as pericytes become scarcer with medullary depth. Terminal DVR and the entire AVR wall is fenestrated. *(Reproduced with permission from ref. [15]).*

The most striking characteristic of the outer medullary circulation is its separation into vascular bundles and the dense capillary plexus that supplies the interbundle region of the inner stripe[4,5,15,17,24–26,31] (Figures 24.1, and 24.8). Species variation exists with respect to the association of nephrons with vascular bundles. The "simple" vascular bundle of the rabbit, guinea pig, dog, cat, monkey, and man is comprised only of DVR and AVR, excluding nephrons.[4,17,26] The "complex" vascular bundle of some rodents incorporates the descending thin limbs of short looped nephrons (nephrons that return from the inner–outer medullary junction). The degree to which thin descending limbs of Henle are incorporated into vascular bundles varies with species, and is highly developed in the mouse[4,17,26,32] (Figure 24.9). *Psammomys obesus* is a desert-dwelling rodent in which vascular bundles combine in the outer stripe of the outer medulla to form "giant" vascular bundles (Figure 24.8a).[5] By anatomical inference, the parallel arrangement of DVR within vascular bundles of all species contributes to the regulation of regional blood flow distribution in the kidney. Constriction of DVR on the vascular bundle periphery should favor perfusion of the inner medulla. Conversely, constriction of DVR in the bundle center should preferentially favor flow to the capillary plexus of the interbundle region. Experimental evidence that supports such differential regulation of perfusion of the outer and inner medulla is sparse, because few studies have simultaneously measured outer and inner medullary blood flow.[33]

The vascular bundles that are characteristic of the inner stripe of the outer medulla disappear below the inner–outer medullary junction. Throughout the medulla, AVR are larger and more numerous than DVR. As a consequence, during passage of blood from the

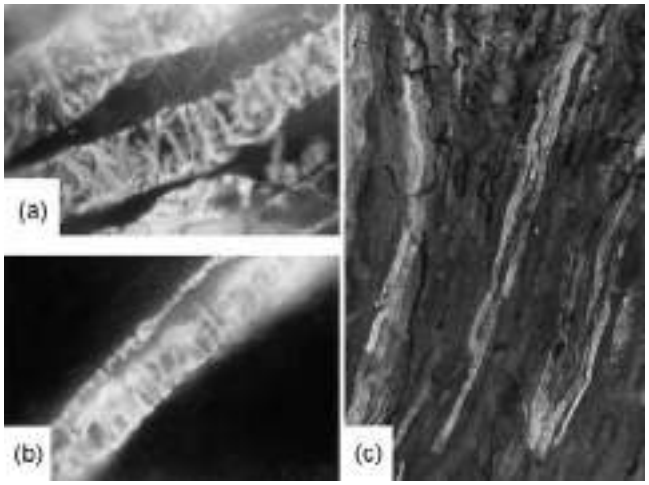

FIGURE 24.6 **Distribution of descending vasa recta pericytes.** (a) (b) Immunofluorescent staining of DVR pericytes using anti α-smooth muscle actin as primary antibody. The pericytes are present on DVR from outer medullary vascular bundles (Panel a), and those from the inner medulla (Panel b) (×1000). (c) Low power image of immunofluorescent staining of DVR pericytes using anti α-smooth muscle actin antibody. Some vessels show pericytes throughout their length to the papillary tip. Black vessels are filled with Indian ink (×100). *(Reproduced with permission from ref. [28]).*

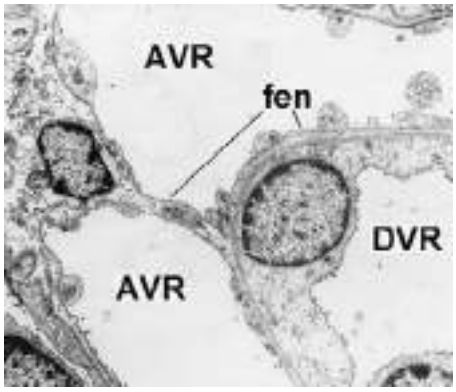

FIGURE 24.7 **Electron micrograph of DVR and AVR.** Electron micrograph of DVR and AVR in rat vascular bundles. DVR have a continuous endothelium and AVR are fenestrated. Note the minimal interstitium that exists between vessels in this region (×12,400). *(Reproduced with permission from ref. [111]).*

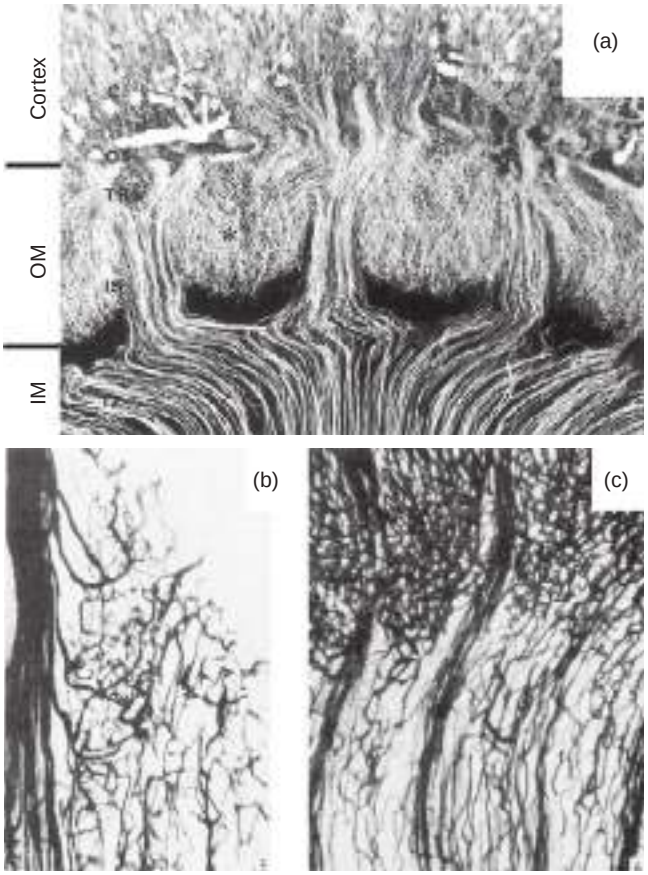

FIGURE 24.8 **Arterial injection of *Psammomys obesus*.** (a) Photograph of the microvasculature of the desert rodent *Psammomys obesus* obtained by injecting the arteries of the kidney with Microfil and digesting the tissue. The distinct arteriolar patterns of the cortex, outer, and inner medulla are apparent. In *Psammomys*, the separation of the outer medulla into vascular bundles and the dense capillary plexus of the interbundle region (*) is striking, because vasa recta coalesce into giant vascular bundles (OM: outer medulla; IM: inner medulla). Designations on the original figure are: c: cortex; TR: transitional region (outer stripe of the outer medulla); IS: inner stripe of the outer medulla; IZ: inner zone (inner medulla).*(Reproduced with permission from ref. [5]).* (b),(c) Indian ink injection study of vascular bundles in the outer medulla of the rat. In contrast to *Psammomys*, individual vascular bundles do not coalesce into giant bundles. The bundles are more evenly dispersed throughout the inner stripe of the outer medulla. This pattern is typical of many mammalian species including the rat, mouse and human. *(Reproduced with permission from ref. [790]).*

juxtamedullary efferent arteriole to DVR and then AVR, single vessel flow rate falls as overall microvessel cross-sectional area increases.[17,31,34–36] The latter increases transit time, presumably to favor greater equilibration of solute concentrations between AVR blood and interstitium. Outer medullary vascular bundles have little interstitial space. In contrast, the fraction of medullary cross-section attributable to interstitium rises substantially toward the deepest regions of the inner medulla, particularly near the papillary tip.[17,20,37] In some species, renal medullary interstitial cells (RMIC) of the inner medulla appear to be tethered between thin limbs of Henle and vasa recta[20,25,36] (Figure 24.10). It is likely that the horizontal arrangement of RMIC helps to preserve corticomedullary solute gradients by limiting axial diffusion along the medulla.[20,38] RMIC have receptors for vasoactive peptides such as angiotensin II, bradykinin, and endothelin. In addition, they release vasoactive agents such as PGE_2 and medullipin. RMIC are contractile and respond to various paracrine factors.[39–42]

Three-dimensional computer reconstructions of images derived from immunostained serial sections have yielded insight into relationships between tubules,

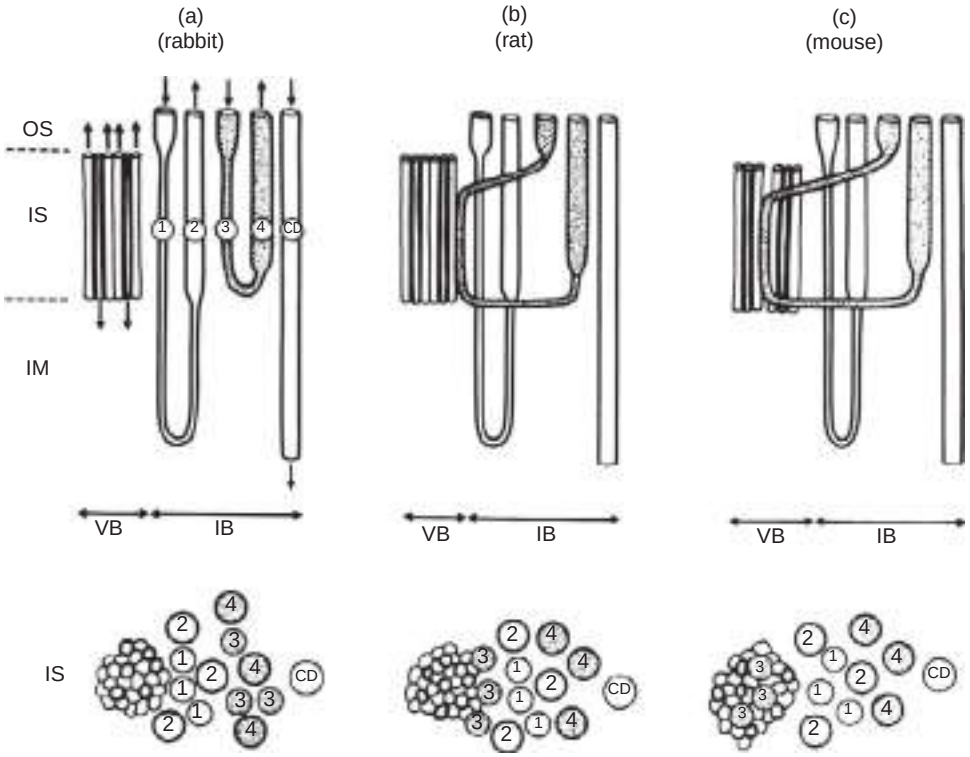

FIGURE 24.9 **Tubular-vascular relationships in the outer medulla.** Organization of the inner stripe of the outer medulla. Top and bottom panels show longitudinal and cross-sectional views, respectively. The extent to which the thin descending limbs (tDLH) of short looped nephrons associate with vascular bundles varies between species. In the rabbit (a) no association exists, whereas in the rat (b) and mouse (c), the tDLH migrates to the periphery or becomes incorporated within vascular bundles, respectively (Abbreviations: VB: vascular bundle; IB: interbundle region; 1 and 2: thin descending and thick ascending limbs of long looped nephrons; 3 and 4: thin descending and thick ascending limbs of short looped nephrons.) *(Reproduced with permission from ref. [4]).*

collecting ducts, and the vasculature in rats and mice.[25,32,43–46] Specifically, collecting ducts (CD), descending thin limbs of Henle (DLH), ascending thin limbs of Henle (ALH), descending vasa recta (DVR), and ascending vasa recta (AVR) are identified by their respective expression of aquaporin 2 (AQP2), aquaporin 1 (AQP1), chloride channel (ClCK1), urea transporter type B (UTB), and the fenestral protein, PV-1. Thin DLH frequently lack AQP1 expression, and are identified as thin limbs lacking ClCK1 but expressing α,β-crystallin, an antigen that is present along the entire loop of Henle.[47,48] Thin DLH include an entirely AQP1-null group that turns early in the inner medulla, and longer limbs that are AQP1-positive for the first ~40% of their length; the latter turn to form thin ALH within deeper regions of the inner medulla. More than 50% of the AQP1-positive DLH also express ClC-K1. AQP1-positive segments have semilunar cell bodies that regularly jut into the lumen.[49] Murine tubulovascular relationships in the outer medulla may exhibit an important characteristic, in that some thick ascending limbs of long looped nephrons may lie within vascular bundles. In that species, short looped thin DLH are known to be incorporated into the more peripheral parts of vascular bundles.[4,20,26,32]

Pannabecker and colleagues have described clustering of collecting ducts that eventually coalesce to form single large collecting ducts in the deep medulla (Figure 24.11). The tubules and vessels that surround the collecting duct clusters occupy structured patterns.[43,46–48] DVR and DLH occupy regions outside the clusters, while AVR and ALH are diffusely distributed both within the central regions of the CD clusters and throughout the surrounding inner medulla. Within clusters, four AVR abut individual CDs.[25] AVR closely approach the CD wall and appear to be tethered to it. That arrangement may be critical to vascular reabsorption in the medulla, allowing interstitial pressure to exceed AVR luminal pressure without inducing collapse.[38,50,51] The implications of those tubulovascular relationships have been examined in mathematical simulations.[52–55] The organization of the outer medulla into vascular bundles and the peribundle region enhances the delivery of high osmolality fluid to the inner medulla by long looped DLH and CD. Reduction of the number of DVR that reach the inner–outer medullary junction is predicted to favor enhancement of urinary concentration, as is a high AVR solute permeability. The striking observation of thick ascending limbs of Henle within vascular bundles

FIGURE 24.10 **Renal medullary interstitial cells (RMIC).** RMIC from the rat kidney appear to be tethered between thin limbs and vasa recta in the inner medulla. Interstitial spaces lie between the cells, and the cells are stacked like rungs of a ladder. RMIC are contractile and secrete vasoactive paracrine agents (see text). The stacked arrangement or RMICs in some species has been suggested to help retard axial diffusion that would otherwise tend to dissipate corticomedullary gradients of NaCl and urea (V: venous or ascending vasa recta; Arrows point to lipid droplets within RMIC). *(Reproduced with permission from ref. [20]).*

of the mouse[32] may have important implications for urinary concentration, because sodium chloride reabsorption from those structures might raise vicinal osmolality to favor water uptake from AQP1-expressing DVR, thereby concentrating their contents en route to the inner medulla.

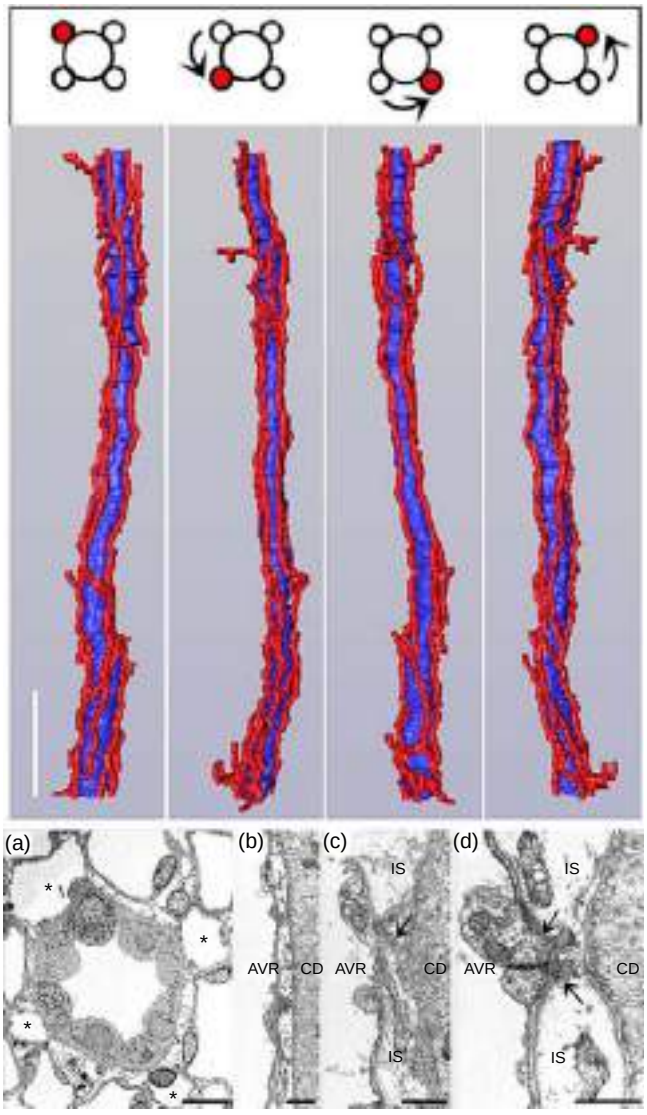

FIGURE 24.11 **Relationship between vasa recta and collecting duct clusters.** Upper panel: A single collecting duct (blue) with adjacent AVR (red) is shown in four 90° rotated views (Bar = 100 microns). Lower panel: (a–c) Electron micrographs of sections through a collecting duct (CD) and adjacent AVR, demonstrating the close apposition and interstitial space (IS). (d) Close approximation of AVR and CD where the two appear to be tethered with microvilli (arrows). *(Reproduced with permission from ref. [25]).*

TRANSPORT FUNCTIONS AND PROPERTIES

The Renal Cortex and Capillary Uptake of Tubular Reabsorbate

Cortical peritubular capillaries are fenestrated, have a large surface area and high hydraulic conductivity. It is generally accepted that fluid is driven into the cortical interstitium from the PCT due to the generation of a locally hypertonic fluid within the lateral intercellular space between PCT epithelial cells. The local hypertonicity results from the secretion of small hydrophilic solutes by proximal tubular cells. Dilution of the interstitium in the vicinity of the capillary wall with protein-free fluid both lowers interstitial oncotic pressure and raises interstitial hydraulic pressure. These effects generate Starling forces that favor capillary reabsorption.

A substantial body of evidence has demonstrated that modulation of cortical peritubular capillary oncotic pressure alters PCT reabsorption. Intra-aortic injection or peritubular perfusion of colloid free or hyperoncotic fluid leads to decreases or increases proximal reabsorption, respectively.[56–58] While it seems inviting to surmise that protein oncotic pressure acts directly to enhance fluid movement out of the PCT, several lines of evidence

suggest otherwise. Oncotic pressure changes fail to modulate reabsorption when active transport by PCT epithelia is inhibited,[59] PCT reabsorption rates correlate with GFR (glomerulotubular balance) but not with interstitial Starling forces,[60] hydropenia blunts the capacity of hyperoncotic albumin to enhance PCT reabsorption,[61] and elevation of luminal pressure in the PCT fails to enhance reabsorption.[62] The osmotic water permeability of the proximal convoluted tubule ($P_f = 0.1 - 0.4$ cm/s) is probably too low for small oncotic pressure changes to substantially affect transmembrane water flux.[63,64] It has been suggested that peritubular oncotic pressure might modulate PCT volume reabsorption by affecting solute reabsorption rate[65,66] or by enhancing paracellular backleak into the PCT lumen.[67] More recently, attention has turned to mechanosensation of luminal shear forces as a transducer of glomerulotubular balance.[68–70]

Whatever mechanisms converge to influence PCT reabsorption it is immense, and its removal from the interstitium is the task of the cortical microcirculation. Since lymphatics remove less than 1% of the reabsorbate,[71] the route for return to the systemic circulation must be via peritubular capillaries. As reviewed by Aukland et al., the high oncotic pressure of postglomerular plasma cannot be invoked as the primary driving force for capillary uptake in all cases. Older rats in which renal lymphatic (and therefore presumably interstitial) protein concentration is equal to that of plasma continue to reabsorb tubular fluid.[18,71] Furthermore, PCT reabsorption occurs even in kidneys perfused with colloid free solutions.[72] Particularly in the latter case, it is apparent that interstitial pressure must exceed intracapillary luminal pressure to provide the driving force for transcapillary volume flux. It also follows that the peritubular capillaries must be tethered to the interstitium in a way that prevents an inwardly directed transmural pressure from collapsing the lumen.

The Renal Medulla and Countercurrent Exchange

Like the capillary bed of other organs, the renal medullary microcirculation supplies oxygen and nutrients to the surrounding tissue. Additionally, however, corticomedullary gradients of NaCl and urea must be preserved to enable urinary concentration. This task is accommodated by countercurrent exchange between DVR and AVR.[17,31,73,74] Countercurrent exchange is an adaptation found throughout nature. The maintenance of high gas tensions in swim bladders of deep sea fish, and the minimization of heat loss from the extremities of aquatic and arctic animals relies upon this strategy.[31,75]

The microcirculation of the renal medulla traps NaCl and urea deposited to the interstitium by the loops of Henle and collecting ducts. Countercurrent exchange provides the means by which blood flow through the medulla is concentrated and then diluted to preserve corticomedullary solute gradients established by countercurrent multiplication. The hypothesis that vasa recta are a purely "U-tube" diffusive countercurrent exchanger implies the following function. NaCl and urea diffuse from interstitium into DVR plasma en route from the corticomedullary junction toward the papillary tip. The solutes diffuse out from AVR plasma to be returned to the interstitium as blood returns to the cortex. That theory predicts that countercurrent exchanger efficiency will be enhanced if permeability to solute is high.

In fact, vasa recta probably do not function as a purely diffusive countercurrent exchanger. Several features point to greater complexity. Tubulovascular relationships in the outer and inner medulla differ markedly (Figures 24.1, 24.9, 24.11), and the endothelium of DVR and AVR are continuous and fenestrated, respectively (Figure 24.7). The discoveries of aquaporin-1 (AQP1) water channels and the facilitated urea carrier, UTB, in DVR endothelia (see below) shows that transcellular as well as paracellular pathways involving water and urea are involved in equilibration of DVR plasma with the interstitium. Efflux of water across the DVR wall to the medullary interstitium occurs across AQP1 water channels, and AQP1 excludes NaCl and urea implying that both water removal and diffusive influx of solute contribute to transmural equilibration.[31,76–78] Expression of AQP1 within the vasculature has been found to vary with axial location, greater in those DVR that turn in the outer portion of the inner medulla.[45,46]

Transport of Small Solutes and Water by Vasa Recta and Red Blood Cells

Transport of Water across the DVR Wall: Small Solutes, Osmotic Pressure, and Starling Forces

Mass balance dictates that water, NaCl, and urea must be removed from the medullary interstitium at a rate that equals deposition by the loops of Henle and collecting tubules.[17,79] Papillary micropuncture studies in the hydropenic rat[80] and hamster[81,82] have shown that DVR and AVR plasma osmolality rises in parallel with tubular fluid from the loops of Henle and collecting ducts. DVR plasma protein also becomes concentrated along the direction of flow, implying that water is lost from DVR lumen to the interstitium (Table 24.1, Figure 24.1).[83,84] Uptake of fluid into AVR exceeds that lost from DVR, accounting for mass balance in the medulla.[15,85–88] Volume efflux from the DVR occurs despite an intracapillary oncotic pressure that exceeds hydraulic pressure, so that "Starling forces" cannot fully explain transmural volume efflux. According to Starling, volume flux (J_v) across a

TABLE 24.1 Vasa Recta Plasma Protein Concentration, Hydraulic and Oncotic Pressures Measured in Rats and Hamsters

Location	VR/P	Cp (g/dl)	Oncotic Pressure (mmHg)	Hydraulic Pressure (mmHg)	Osmolality (mOsm)	Condition (Reference)
DVR-base	1.76	7.1	26.0	9.2		Hydropenia
DVR-tip	–	–	–	–		83
AVR-base	1.38	5.6	18.1	7.8		
DVR-base	1.43	7.1	26.0	6.6	688	Hydropenia
DVR-tip	1.66	6.4	21.8	7.4	759	84
AVR-base	–	–	–	–		
DVR-base	1.0 to 1.8[a]					Hydropenia
DVR-tip	2.1 to 2.9					87
DVR-base	1.42	5.1	16.0	–		Hydropenia
DVR-tip	–	–	–	–		88
AVR-base	1.11	4.0	11.2	–		
DVR-base				15.7		Hydropenia
DVR-tip				11.4		429
AVR-base				10.2		
DVR-base	1.08	5.2	16.7	9.5	573	Hydropenia
DVR-tip	1.42	6.8	18.2	9.1	1011	86
AVR-base	–	–	–	–	–	
DVR-base	1.10	5.4	17.6	12.2	356	Furosemide
DVR-tip	1.12	5.5	18.2	11.2	377	86
AVR-base	–	–	–	–	–	
DVR-base	1.19	5.7	18.6	11.7	380	Furosemide
DVR-tip	–	–	–	11.2	386	187
AVR-base	1.17	5.6	18.4	9.6	–	
AVR-mid		5.2	16.7	8.0		Hydropenia
AVR-mid		5.2	16.7	16.0		Furosemide
						143
DVR-mid				9.1 to 15.5[b]		Plasma/ANP[c]
AVR-mid				7.8 to 14.3		Plasma/ANP
DVR-mid				8.4 to 10.8		Plasma/Furosemide
AVR-mid				7.8 to 10.0		Plasma/Furosemide
						792

[a] *Ratio measured from ^{131}I-albumin activity.*
[b] *Values refer to changes before and after administration of either ANP or furosemide.*
[b] *Measured after replacement of surgical fluid losses with plasma.*
Abbreviations: VR/P: vasa recta to plasma ratio; Cp: plasma protein concentration; DVR: descending vasa recta; AVR: ascending vasa recta; base, mid, tip, micropuncture site along exposed papilla (inner 1/3 of the inner medulla, blood flows from base to tip in DVR and tip to base in AVR); ANP: atrial natriuretic peptide.

capillary wall is a function of capillary (P_c) and interstitial hydraulic pressure (P_i), and luminal (π_c) and interstitial (π_i) oncotic pressure.[89]

$$J_V = L_P[(P_c - P_i) - (\pi_c - \pi_i)] \quad (24.1)$$

where L_p is the hydraulic conductivity. In order to explain volume efflux from the DVR in a manner compatible with Eq. (24.1), a negative interstitial hydraulic pressure or very high interstitial oncotic pressure has to be postulated. In either of those cases, however, interstitial driving forces would prevent volume uptake by AVR violating mass balance. Neither possibility can be the explanation.[17,84,90]

Due to the lag in equilibration of DVR plasma with the interstitium, NaCl and urea concentrations in the interstitium exceed those in DVR so that a transendothelial osmotic gradient favors water efflux across the DVR wall. That driving force could account for water efflux only if there is a transendothelial pathway across which small solutes are effective to drive water movement.[84] Volume flux across a membrane can be simulated by Eq. (24.2) that accounts for osmotic reflection coefficients (σ) to individual solutes. In the current context, small solutes (σ_{ss}) and proteins (σ_{pr}) are of importance, leading to[91]:

$$J_V = L_P[\Delta P - \sigma_{pr}\Delta\pi_{pr} - \sigma_{ss}\Delta\pi_{ss}] \quad (24.2)$$

where ΔP is transmembrane hydraulic pressure, and $\Delta\pi_{pr}$ and $\Delta\pi_{SS}$ are the transmembrane osmotic pressure due to protein and small solutes, respectively.[84] The hypothesis that small solutes act to promote volume movement across the DVR is equivalent to postulating that $\sigma_{ss} > 0$. Support for this was readily obtained. Volume efflux from DVR was prevented by elimination of corticomedullary (and therefore transendothelial) NaCl and urea gradients by furosemide,[86] and *in vivo* microperfusion of DVR with buffers made hypertonic or hypotonic to the papillary interstitium generated volume uptake or efflux, respectively ($\sigma_{NaCl} > 0$).[92]

DVR Hydraulic Conductivity and Osmotic Water Permeability

The predominant pathway that conducts water efflux across the DVR is the AQP1 water channel. AQP1 but not other aquaporins are expressed by DVR endothelia.[36,45,93,94] *Diffusional* water permeability (P_D) of isolated, microperfused DVR, measured by efflux of ^3H_2O, was reduced by the AQP1 blocking mercurial agent p-chloromercuribenzene sulfonate (pCMBS). Dramatic confirmation was provided by the demonstration that *osmotic* water permeability (P_f) of microperfused DVR, measured by driving water flux with transmural gradients of NaCl, was driven from ~1100 μm/s to nearly zero by pCMBS (Figure 24.12a). In contrast, when albumin rather than NaCl was used to drive water flux, P_f was much higher, ~16,700 μm/s and insensitive to pCMBS, implying that a different pathway conducts transmural volume flux driven by oncotic pressure.[77,78] The results support the notion that NaCl and urea drive water flux across the DVR wall exclusively through AQP1 (contribution to total transmural water conductivity is P_f ~1100 μm/s), while hydraulic pressure and oncotic pressure drive most water flux through a high conductivity parallel pathway (paracellular or other). Mathematically, the AQP1 and parallel pathways are best stimulated as[85,95]:

$$J_{V,P} = L_{P,P}[\Delta P - \sigma_{pr}\Delta\pi_{pr}] \text{ and, } J_{V,C} = L_{P,C}[\Delta P - \textstyle\sum_i \Delta\pi_i] \quad (24.3a, b)$$

where the additional subscript "P" (probably pericellular) refers to the high conductivity pathway for which $\sigma_{NaCl} = \sigma_{urea} = 0$,[96] and the subscript "C" refers to the transcellular AQP1 pathway for which $\sigma_{NaCl} = \sigma_{urea} = 1$. Hydraulic conductivity (Lp) and osmotic water permeability (P_f) are related according to $Lp = (P_f \times V_w)/(RT)$, where V_W is the partial molar volume of water. Existing measurements of DVR osmotic water permeability are summarized in Table 24.2. A rigorous discussion of the measurement of, and relationships between, these transport parameters has been provided.[78,96]

The AQP1 knockout mouse provided additional confirmation of the role of AQP1 in DVR water transport. P_f of DVR in AQP1 knockout mice, driven by NaCl, was indeed very low (Figure 24.12b). An intriguing finding was that urea and larger solutes (raffinose, MW 594, glucose, MW[97]) drive significant water flux despite AQP1 deletion, a finding that implies the existence of a non-AQP1 route across which those solutes are osmotically active. A potential candidate for the non-AQP1, pCMBS insensitive pathway is the UTB urea transporter (see below) which is expressed by the DVR endothelium and can function as a water channel.[98–102]

Insights from Modeling: AQP1 and the Enhancement of Exchanger Efficiency

Mathematical models of urinary concentration have played an important role in the evolution of our understanding. Simulation of both nephrons and the microcirculation is difficult, so that investigators prefer to account for one while neglecting the other. Vasa recta models typically assume specified corticomedullary solute concentrations, and simulate transport properties of the vessel wall. Wang and Michel revised this approach by specifying the rate of deposition of NaCl, urea, and water to the medullary interstitium as though they are generated within the interstitium. In agreement with electron probe measurements, they predicted an exponential increase in corticomedullary solute

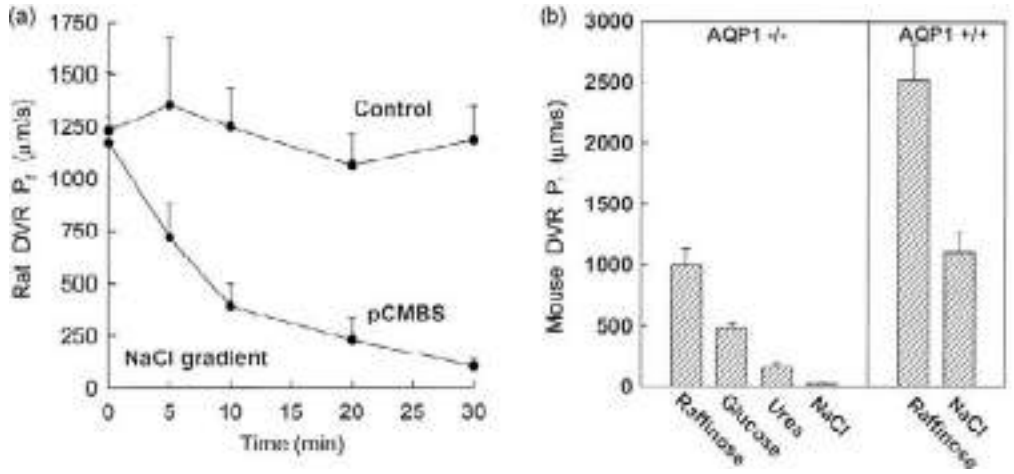

FIGURE 24.12 **Osmotic water permeability (P_f) of outer medullary DVR.** (a) Pf was measured in glutaraldehyde-fixed rat DVR by measuring the rate of transmural water flux generated by a bath > lumen NaCl gradient. Sequential measurements in controls were stable. In contrast, exposure to p-chloromercuribenzene sulfonate (pCMBS, 2 mM), an agent that covalently binds to cysteine residues on aquaporin-1, reduced Pf to nearly zero. In these experiments, glutaraldehyde fixation was necessary to prevent deterioration of the vessel caused by pCMBS and other harsh conditions of the experiment. (b) Pf was measured in AQP1-null($^{-/-}$) or replete($^{+/+}$) murine DVR by transmural gradients of NaCl, urea, glucose or raffinose. When NaCl was the solute used to drive water flux, deletion of AQP1 reduced Pf from ~1100 μm/s to nearly zero. Water flux driven by raffinose (MW 564) was markedly reduced by AQP1deletion (compare AQP1$^{-/-}$ to $^{+/+}$), but remained unexpectedly high. Similarly, glucose (MW 180) and urea (MW 60) gradients drove measurable water flux across AQP1($^{-/-}$) DVR. *(Reproduced with permission from ref. [76,77]).*

TABLE 24.2 Hydraulic Conductivity, Osmotic Water Permeability and Solute Reflection Coefficients of Vasa Recta

Parameter	Driving Force	OMDVR	IMDVR	IMAVR	Reference
$L_p \times 10^{-613}$ ($cm \bullet s^{-780} \bullet mmHg^{-780}$)	Albumin Gradient		1.4[a]		187
$L_p \times 10^{-613}$ ($cm \bullet s^{-780} \bullet mmHg^{-780}$)	Albumin Gradient	1.6			96
$L_p \times 10^{-613}$ ($cm \bullet s^{-780} \bullet mmHg^{-780}$)	NaCl Gradient	0.12[b]			76,77
$L_p \times 10^{-613}$ ($cm \bullet s^{-780} \bullet mmHg^{-780}$)	Hydraulic Pressure			12.5	50,92
Parameter	**Method**	**OMDVR**	**IMDVR**	**IMAVR**	**Reference**
$\sigma_{albumin}$	Sieving	0.89[c]			96
$\sigma_{albumin}$	Sieving			0.78	128
$\sigma_{albumin}$	Osmotic			0.70	50
σ_{Na}	Osmotic		<0.05[d]	0.00[d]	92,129
σ_{Na}	Osmotic	~0.03[d]			78
σ_{Na}	Sieving	~1.0[e]			78
$\sigma_{Raffinose}$	Sieving	~1.0[e]			78

[a] *Assumes a reflection coefficient to albumin of 1.0.*
[b] *Evidence shows that transmural NaCl gradients drive water flux exclusively through water channels, whereas albumin drives water flux predominantly through water channels along with a small component via other pathway(s), see text and references .[77,78,96]*
[c] *Not significantly different from 1.0.*
[d] *Measurement of σ_{Na} for the vessel wall as a whole.*
[e] *σ_{Na}, $\sigma_{Raffinose}$ for the putative aquaporin-1 water channel pathway through which NaCl gradients drive water flux, see text and references [77,78].*

concentration in the medulla.[103–105] A weakness of models that neglect simulation of loops of Henle and collecting ducts is that solute generation rates in the interstitium are assigned as inputs and interstitial solute concentrations calculated as predictions. Variations of blood flow and transport properties cannot affect the interstitial appearance of NaCl, urea, and water from nephrons as would occur *in vivo*. Convincing evidence has been provided that structure and properties of nephrons can abruptly vary with medullary depth.[28,40,49,106,107]

Many key parameters needed to simulate microvascular exchange in the renal medulla (solute permeabilities, reflection coefficients, hydraulic conductivities) have been measured. That data has been combined with more complete simulations of transcellular pathways for urea and water transport to perform additional simulations. The models predict that AQP1 might play an important role to raise medullary interstitial osmolality by driving water efflux from DVR to the medullary interstitium across AQP1 water channels (see above); that water movement effectively shunts DVR plasma volume to the AVR reducing blood flow to the deep medulla; and that favors high diffusive exchanger efficiency in the deep inner medulla where urea is added to the interstitium from the collecting duct. Stated another way, it reduces the lag in equilibration that leads to solute "washout" from the deep medulla.[76,108,109] The net effect is to enhance interstitial osmolality (Figure 24.13). Interest in this intriguing prediction is heightened by the observation that transmural water flux can be driven across the wall of AQP1-null mice by solutes other than NaCl (Figure 24.12b). If the non-AQP1 pathway is important *in vivo*, it might also enhance shunting of water from DVR to AVR.[31,76,108]

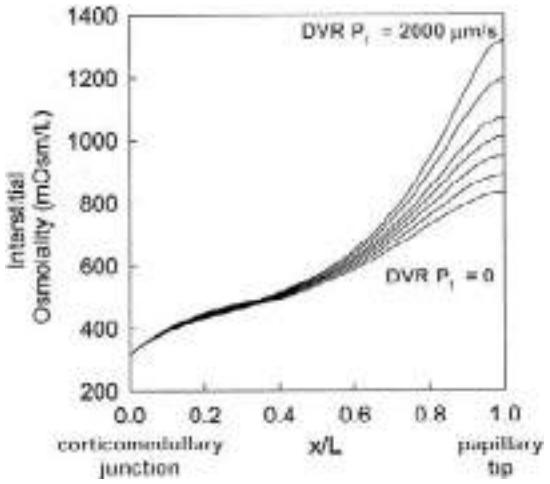

FIGURE 24.13 **Effect of AQP1 deletion on predictions of renal medullary interstitial osmolality.** A mathematical simulation of the renal medulla was solved to predict interstitial osmolality. Interstitial osmolality is shown as a function of corticomedullary axis (x/L = 0 is the corticomedullary junction; x/L = 1 is the papillary tip). Various curves denote predictions for different values of Pf (DVR osmotic water permeability). Pf was varied between 0 (equivalent to AQP1 deletion) and 2000 μm/s. AQP1 expression in DVR is predicted to enhance concentrating ability by conducting water flux from DVR to interstitium where after it is taken up by AVR. The net result is a secondary reduction of blood flow in the deepest regions of the inner medulla (papillary tip). *(Reproduced with permission from ref. [76]).*

Transport of Small Hydrophilic Solutes across the DVR Wall

It is likely that the majority of NaCl and urea equilibration across the DVR wall occurs by diffusive influx. AQP1 contributes to the process of equilibration through molecular sieving. Evidence supports the notion that small hydrophilic solutes (NaCl, urea) diffuse through the same "shared" pathway that conducts the component of water flux driven by Starling forces, because DVR permeability to tracers (^{22}Na, ^{36}Cl, ^{3}Hraffinose, ^{14}Cinulin) correlate with each other and hydraulic conductivity.[31,96,110,111] Urea transport across the DVR wall is more complicated, because it diffuses both via paracellular and transcellular routes. A summary of available solute diffusive permeability measurements is provided in Table 24.3.

Facilitated Transport of Urea across DVR and RBCs

Transmural flux of urea across the DVR wall is complicated, because DVR endothelia express a facilitated urea carrier.[112,113] Sodium and urea have similar free water diffusivity, and are therefore expected to have the same transvessel permeability if they diffuse, sterically unrestricted, through a large pore. In contrast to this, some outer medullary DVR have low or moderate P_{Na} but high P_U (Figure 24.14). DVR permeability to ^{14}C urea can be partially inhibited by phloretin, pCMBS, and structural analogs of urea, verifying the presence of an endothelial carrier.[111,112] Histochemical evidence and *in situ* hybridization studies have shown that the DVR urea carrier is the same as that in the RBC (urea transporter type B, UTB), and is distinct from the urea carrier in the thin limbs of Henle (UTA2) and collecting duct (UTA1, UTA3, UTA4).[100,114–118]

Rat UTB carries the Kidd blood group antigen, has 62% identity to UTA2, and is expressed in RBCs, DVR endothelium, papillary surface, and pelvic epithelium of the kidney.[100,119] The presence of UTB in the DVR endothelium and RBCs facilitates medullary urea recycling. Urea tends to exit the renal medulla in AVR plasma and RBCs. To prevent associated dissipation of corticomedullary urea gradients, urea recycles from AVR into DVR plasma and RBCs via UTB, and into thin limbs of Henle via UTA2 (Figure 24.15). Those processes are highly evolved in the outer medullary inner stripe where DVR and AVR are closely

TABLE 24.3 Diffusional Permeability of Vasa Recta to Hydrophilic Solutes

Permeability $\times 10^{-590}$ cm/s	Species	OMDVR[a]	IMDVR[b]	IMAVR[b]	Reference
P_{Na}	Hamster		28	51	35
P_{Na}	Rat	76	75	115	111
P_{Na}	Rat		67	116	92,129
P_{Na}	Mouse	207– 314			76
P_{Urea}	Rat		47		130
P_{Urea}	Rat	360	76	121	111
P_{Urea}	Rat	343 → 191[c]			112
P_{Urea}	Mouse	661[d]			76
P_D	Rat	476[e]			93,110
$P_{raffinose}$	Rat	40			110,96
$P_{raffinose}$	Mouse	80, 111[d]			76
Permeability Ratio	**Species**	**OMDVR[a]**	**IMDVR[b]**	**IMAVR[b]**	**Reference**
P_{Urea}/P_{Na}	Rat	4.7	1.1	0.98	76,110,111
	Mouse[d]	3.2			
P_{Cl}/P_{Na}	Rat	1.3			
$P_{raffinose}/P_{Na}$	Rat	0.35			
	Mouse	0.35, 0.39[d]			
P_{Inulin}/P_{Na}	Rat	0.22			
	Mouse	0.31[d]			

[a]*Values obtained with* in vitro *microperfusion are highly dependent upon perfusion rate, see text and references* [77,110,96].
[b]*Values obtained with* in vivo *microperfusion in the exposed papilla, probably underestimated due to boundary layer effects, see text.*
[c]*Values are before and after inhibition with 50 mM thiourea.*
[d]*Value from DVR of AQP1 null mice.*[76]
[e]*Diffusional water permeability measured with* ^3H_2O *efflux.*
Abbreviations: OMDVR: outer medullary descending vasa recta; IMDVR: inner medullary descending vasa recta; IMAVR: inner medullary ascending vasa recta.

positioned in vascular bundles. Many water-conserving species also incorporate UTA2 expressing thin limbs of Henle within or on the periphery of vascular bundles[5,6,15,24,26] (Figure 24.9). Interesting insights into function have been obtained from the study of UTB-null mice. UTB deficiency results in reduced urinary concentrating ability, reduced urea clearance, and an increased plasma urea concentration.[100,114,118] In contrast to wild-type mice, infusion of urea into UTB-null animals fails to enhance urinary concentrating ability.[114] Acute regulation of UTB by vasopressin or other factors has not been demonstrated. In contrast to upregulation of UTA transporters,[119] chronic vasopressin treatment may reduce UTB expression.[99,120] UTB expression in the renal medulla increases during osmotic diuresis induced by urea, but not NaCl or glucose infusion.[121] In contrast, UTB expression is depressed by ureteral obstruction, lithium treatment, potassium deficiency, and cyclosporine toxicity.[122–125]

UTB expression in RBCs should limit AQP1-mediated water transport and the associated osmotic shrinking and swelling that would otherwise accompany RBC transit through the medulla. Macey and Yousef proposed that this might prevent osmotic lysis.[126] Against this hypothesis is the finding that humans devoid of Kidd antigen have mildly depressed urinary concentrating ability, but no hemolytic anemia. It seems most likely that RBC expression of UTB serves to increase the overall mass of urea that is efficiently recycled from the AVR and DVR lumens in the renal inner medulla.[98,100,102]

Transport of Solutes and Water across the AVR Wall

Transport of solutes and water in AVR has not been as thoroughly evaluated as that in DVR, because AVR cannot be isolated for *in vitro* microperfusion. Measurements of AVR transport properties have been performed by *in vivo* micropuncture and microperfusion of vessels on the surface of the exposed papilla (inner

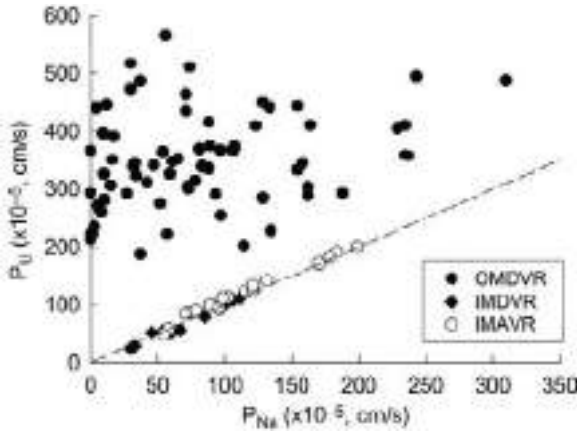

FIGURE 24.14 **Vasa recta solute permeabilities.** [^{14}C]urea permeability (P_U, ordinate) versus ^{22}Na permeability (P_{Na}: abscissa) is shown for outer medullary DVR (OMDVR) isolated from Sprague-Dawley rats and perfused *in vitro*. Results are also shown for inner medullary DVR and AVR (IMDVR, IMAVR) perfused on the surface of the exposed papilla of Munich-Wistar rats *in vivo*. The dashed line is identity. P_U and P_{Na} are highly correlated and nearly equal in inner medullary vasa recta. In contrast, P_U of outer medullary DVR is always very high and is not correlated with P_{Na}. The dissociation of P_{Na} and P_U in OMDVR results (at least in part) from the expression of the UTB facilitated urea carrier. In separate experiments (not shown), P_U of OMDVR was inhibited by exposure to urea analogs or phloretin. *(Data reproduced with permission from ref. [111]).*

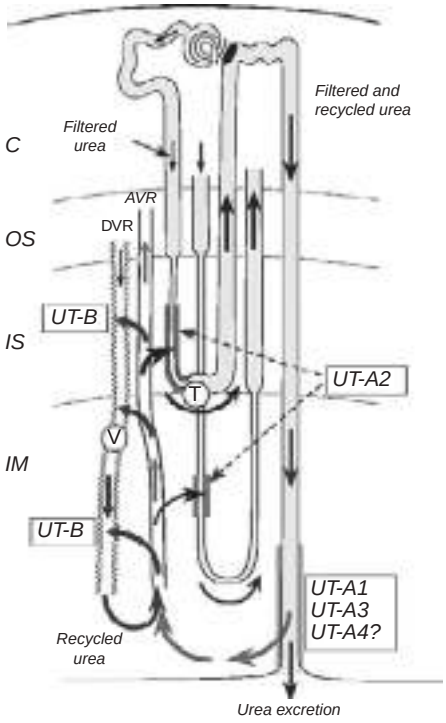

FIGURE 24.15 **UTB and urea recycling in the medulla.** Schematic of vascular and tubular urea recycling in the kidney. Short and long loops of Henle and vasa recta are shown. The UTA2 urea transporter is expressed in the thin descending limbs of Henle. The UTB urea transporter is expressed in DVR endothelium and red blood cells (not shown). Thin descending limbs of short looped nephrons become associated with vascular bundles (see Figure 24.9) so that urea recycling from thin limbs to DVR via UTA2 and UTB is accommodated. UTB is not expressed by the AVR endothelium, but AVR are fenestrated and urea permeability is high. Thus, urea in AVR plasma and RBCs can readily recycle back to DVR in vascular bundles using UTB in the RBC membrane and DVR endothelium. The UTA1, A3, and A4 collecting duct conduct urea transporters conduct urea from the lumen to the inner medullary interstitium (C: cortex; OS: outer stripe of outer medulla; IS: inner stripe of outer medulla; IM: inner medulla). *(Reproduced with permission from ref. [100]).*

third of the inner medulla) of rats. Some reliable measurements of AVR hydraulic conductivity (Lp) have been obtained. Consistent with the highly fenestrated endothelium, Lp is high, about 12.5×10^{-6} ^{13} cm/(s•mmHg) (P_f = 13.4 cm/s).[50,127] The reflection coefficient of the AVR wall to albumin has been measured by molecular sieving[128] and by osmosis.[50] Mean values of 0.78 and 0.70 were obtained, respectively. A summary of AVR hydraulic conductivity and reflection coefficient measurements is provided in Table 24.2.

When blood ascends toward the cortex in AVR it encounters decreasing NaCl and urea concentrations, so that luminal osmolality exceeds that of the adjacent interstitium. Perfusing AVR *in vivo* with buffers made hypertonic or hypotonic to the papillary interstitium with NaCl generated no measurable water flux, suggesting that, for the AVR wall, $\sigma_{SS} = 0$ (Eq. (24.2)).[129] Transmural AVR NaCl and urea gradients *in vivo* are likely to be smaller than those in DVR, because AVR blood flow rates are lower. AVR are larger in diameter and more numerous than DVR.[34,35,88] Consequently, high permeability, high surface area, and an increased transit time of blood all favor a high degree of equilibration between AVR plasma and interstitium.[90,95]

Vasa recta diffusional solute permeabilities, measured in the rat[129,130] and hamster,[35] are higher than those in DVR (Table 24.3). Even so, AVR permeabilities have probably been underestimated, because all measurements relied upon ^{22}Na and ^{14}Curea efflux during microperfusion *in vivo*. That method probably underestimates permeability, because accumulation of tracers near the abluminal surface during microperfusion violates the assumption that abluminal tracer concentrations are zero.[92,129]

Transport of Macromolecules in the Cortex and Medulla

It is generally accepted that lymphatics are sparse in the outer medulla, and absent from the inner medulla.[79,131] It has long been recognized that proteins permeate the walls of capillaries[89,132,133] to be drained

by lymphatics and returned to the systemic circulation. Given the absence of lymphatics in the inner medulla, the mechanisms that regulate interstitial oncotic pressure and protein trafficking through the interstitium have been enigmatic. Early studies led to the conclusion that a large extravascular pool of albumin is present within the medulla.[134–136] Leakage of fluorescent albumin[137,138] and Evans blue dye-labeled albumin[139,140] into the medullary interstitium were observed. Ultrastructural studies with horseradish peroxidase (molecular radius 50 Å), catalase (elliptical molecule, 240,000 Da, major axis 240 Å), and ferritin (spherical molecule, 500,000 D, 110 Å) demonstrated that these markers can cross the fenestrations of cortical peritubular cortical capillaries[141] and medullary AVR.[142]

Measurements of albumin transport rates across the DVR and AVR walls have been technically limited. Using molecular sieving of Texas red-labeled albumin, Turner estimated the reflection coefficient of the DVR wall to albumin to be 0.89 (not significantly different from unity).[96] In separate studies with different methods, the reflection coefficient of the AVR wall to albumin was estimated to be 0.7 and 0.78.[50,128] No reliable measurements of the diffusional permeability of either the DVR or AVR wall to albumin exist. Attempts have been made to determine Starling forces within the medullary interstitium through direct measurement of interstitial protein concentration. Using a differential centrifugation technique, MacPhee and Michel obtained a mean value of 0.9 g/dl.[50] By an alternative approach, interstitial protein concentrations of 4 to 6 g/dl were predicted and interstitial hydraulic pressures in the range of 5 to 10 mmHg were found.[143]

Whatever the concentration of albumin in the medullary interstitium, the fundamental question remains, in the absence of lymphatics, how is medullary interstitial protein deposited and cleared by the microcirculation? Protein transport into the AVR lumen by convective influx is the most likely answer.[50,74,143] Michel pointed out that molecular sieving at the AVR wall would indicate convective movement of protein into the AVR lumen, were it not for continuous deposition of protein-free fluid by medullary nephrons.[74] The plausibility of convective protein uptake is also supported by the finding that papillary AVR withstand an inwardly-directed hydraulic pressure without collapsing.[51] Pinter and colleagues have suggested that the combined effects of negative charge exclusion resulting from compartmentation of hyaluron and albumin, Donnan equilibrium, and hydrostatic pressure variation from ureteral contractions provide key driving forces for fluid movements and urinary concentration.[144,145]

INTRARENAL HEMATOCRIT

When the volumes of distribution of plasma and red blood cells within the kidney were examined by injecting labeled albumin and red blood cells (RBCs), intrarenal hematocrit was found to be less than systemic hematocrit. Given the observation of Fahraeus that red cells migrate to the center of small vessels, Pappenheimer and Kinter proposed that cell free blood is "skimmed" from the periphery of the interlobular arteries to enter the afferent arterioles of deep glomeruli,[13,146] an effect which might be facilitated by intraarterial cushions[10–12] (Figure 24.2). This possibility was tested by Lilienfield et al. who found that RBC transit time was shorter than plasma transit time, and that tissue hematocrit varies with medullary axis.[147] Rasmussen performed a technically superior examination using ^{131}I-IgM, a larger and therefore more reliable plasma marker. Simultaneous injection with ^{51}Cr-RBCs, led to the estimates of tissue hematocrit shown in Figure 24.16.[148] Using videomicroscopic techniques, Zimmerhackl estimated the "dynamic" or "tube" hematocrit of the papillary DVR and AVR to be 26 and 25%, respectively.[149] Direct measurements with micropuncture gave similar results. A low microvessel hematocrit in the renal medulla has been consistently found.

In addition to plasma skimming,[10,13] other mechanisms could reduce medullary hematocrit. Fahraeus demonstrated that the hematocrit of a microvessel is reduced by migration of RBCs to the centerline where the velocity of flow is highest.[146] Based on this alone,

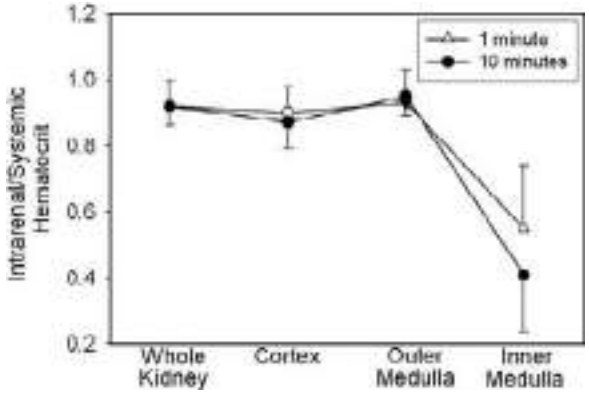

FIGURE 24.16 **Distribution of hematocrit in the kidney.** ^{51}Cr-RBC's and ^{131}I-IgM (plasma volume marker) were simultaneously infused into the kidney. An equilibration period of either 1 or 10 minutes followed before ligation of the renal artery and vein. The distribution of RBCs and plasma were inferred by measuring activity of the isotopes in tissue and dividing their ratio by the systemic ratio. Results show that the hematocrit of inner medullary blood is lower than that whole kidney, cortex or outer medulla. *(Data redrawn with permission from ref. [148]).*

vasa recta (10–20 μm diameter) are expected to have hematocrits reduced by 40 to 50% of that in a large vessel.[150] Pries et al. have shown that a "network" Fahraeus effect can further reduce microvessel hematocrit by as much as 20%. When a vessel bifurcates, the higher flow branch receives blood of higher hematocrit. Conservation of RBC and plasma dictates that the increase of hematocrit in one branch must be less than the reduction in the other branch, tending to reduce average capillary hematocrit.[151] Shrinkage of RBCs in the hypertonic medulla must also tend to lower medullary microvessel hematocrit.[17]

METHODS FOR MEASUREMENT OF REGIONAL BLOOD FLOW TO THE CORTEX AND MEDULLA

The relative contribution of various renal microvessels to renal vascular resistance can be inferred from the luminal hydrostatic pressure profile. As shown in Figure 24.17, the largest pressure drop, and therefore the dominant resistance, is the afferent arteriole. Glomerular capillaries, due to their large combined cross-sectional area, are thought to offer little resistance to flow. Efferent arterioles and DVR contribute significantly to renal vascular resistance, but less than that attributed to afferent arterioles. Vasoactivity of the afferent arteriole is governed by myogenic autoregulation and tubuloglomerular feedback via the macula densa, important topics that are covered by other chapters of this text. The afferent and efferent arterioles may also be influenced by other nephron to vascular crosstalk mechanisms.[152,153] Measurement of regional blood flows in the kidney that result from the actions and distributions of resistance arterioles has been the frequently pursued. Early approaches to the measurement of regional blood flow within the kidney relied upon tracers, gave widely varying estimates of tissue blood flow, and have fallen into disfavor. Results from those methods are summarized in Table 24.4 from which one can conclude that inner medullary tissue blood flow rate is much lower than that of the cortex.[34,148,154–173] The associated details have been reviewed in prior versions of this text and other sources.[1,17,174] Videomicroscopic measurement of RBC velocity is a more reliable means for calculating single vessel blood flow rates, but it is limited to surface microvessels in the cortex or exposed papilla.[149,175] Use of a pencil lens camera for measurement of glomerular and cortical peritubular RBC velocities has been described by Goligorsky and colleagues.[176] It has been used to examine effects of pharmaceutical calcium channel blockers on glomerular arteriolar tone *in situ*.[177] Laser-Doppler flowmetry is the dominant method for examining regional blood flow, due to the ease of applying optical fibers to the kidney surface or inserting them into otherwise inaccessible regions within the parenchyma[167]; laser speckle[178,179] and ultrasound imaging of microbubbles[180,181] may offer future improvements.

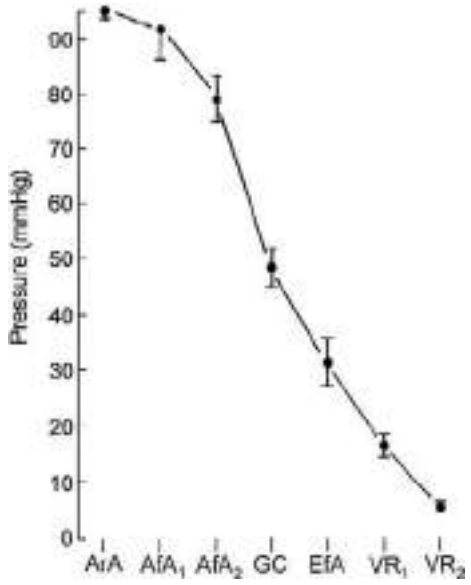

FIGURE 24.17 **Microvessel pressure distribution within the kidney.** The values on the ordinate were obtained by micropuncture and servo-nulling pressure measurements using the juxtamedullary nephron preparation. Pressure falls successively from the arcuate artery to vasa recta (ArA: arcuate artery; AfA_1 and AfA_2: early and late afferent arteriole; GC: glomerular capillaries; EfA: efferent arterioles; VR_1: descending vasa recta; VR_2: ascending vasa recta). *(Reproduced with permission from ref. [202]).*

Videomicroscopy

Measurement of microvessel diameter and RBC velocity (V_{RBC}) can be combined to calculate single vessel blood flow rates.[35] Gussis and colleagues measured V_{RBC} in vasa recta on the surface of the exposed renal papilla, following which Holliger and co-workers coupled V_{RBC} with diameter measurement to calculate single vessel blood flow rates.[34,182] In later refinements, contrast between red cells, plasma, and the capillary wall was enhanced by injection of fluorescein isothiocyanate-labeled gamma globulin, and V_{RBC} was determined from the video images captured with a silicon intensified target camera. Additionally, the Fahraeus effect[146] was accounted for by calibrating RBC streaming effects in quartz capillaries.[175] Application of videomicroscopy to measurement of renal blood flow is limited by regional accessibility. Observation of the medulla for videomicroscopy is limited to the papilla (distal third of the inner medulla) because only that

TABLE 24.4 Regional Tissue Plasma Inflow Rates Measured in the Kidney

Method	Species	Inflow Rate, ml • min • g^{-780} Cortex	Outer Medulla	Inner Medulla	Reference
Dye Transit	Dog		1.3	0.2–0.7	171
	Dog	5.35	3.22	0.38	165
^{32}P Transit	Dog		1.8	0.5–0.7	172
^{85}Kr Washout	Dog	4.72	1.32	0.17	170
H_2 Washout	Dog	2.6–5.0			154
^{86}Rb Uptake	Dog	4.4–7.4	1.2–2.3	1.1	169
	Dog	4.84	2.81	0.8	155
	Rat	4.76	1.35	0.66	163
	Rat		0.60–0.88[a]	0.2–0.3[a]	159
	Rat	5.2	1.5–2.2	0.69	164
	Rat	4.7–7.3	2.4	2.4	173
Albumin Accumulation	Dog			0.25	166
	Dog			0.22	160
	Dog			0.23	157
	Rat			0.38–0.42	161,162
	Rat			0.32	168
	Rat			0.27	156
	Rat			0.36	158
	Rat			0.38–0.64	148
	Rat			0.06–0.08[b]	148
	Rat			0.18[c,d]	167
	Rat			0.31[c,e]	167
RBC velocity	Rat			1.3–5.9[c,f]	34

[a] *Probably underestimated.*
[b] *RBC inflow rate.*
[c] *Total blood (RBC and plasma) inflow rate.*
[d] *Young rats.*
[e] *Old rats.*
[f] *Probably overestimated.*
Abbreviations: RBC: red blood cell.

part of the medulla can be exposed for visualization by excising the ureter of young rodents.

Laser-Doppler

The laser-Doppler method for measuring tissue blood flow rates relies upon the frequency shift of light emitted from a laser due to scattering by flowing RBCs.[183] Among other advantages, sequential measurements in the same region are possible, and signals can be obtained on the renal surface or from optical fibers implanted into the parenchyma. The counterflow arrangement of vasa recta within the medulla would appear to violate the requirement that the laser-Doppler receive random backscattered light. Despite this concern, agreement between laser-Doppler and videomicroscopy[184] or ^{51}Cr-RBC accumulation[167] has been demonstrated. The laser-Doppler device provides a voltage proportional to tissue perfusion in the immediate vicinity of the fiber-optic probe. Calibration to convert the signal to absolute units that quantitatively describe local perfusion is generally not possible. This limits absolute comparisons of measurements between regions of the kidney of the same or different animals.

METHODS FOR DIRECT MEASUREMENTS OF MICROVESSEL REACTIVITY

Other important methods for investigation of the regulation of regional blood flow examine the effects of vasoactive agents on pressurized microvessels. Important information on the sites of action, the concentrations at which specific hormones modulate reactivity, and receptor subtypes responsible for mediating vasoactivity can be obtained. Extrapolation of results to arrive at conclusions concerning the effects of hormones and autocoids on regional blood flow within the kidney is fraught with uncertainty. This topic has been frequently reviewed.[1,2,15,185–188]

In Vitro Microperfusion

The *in vitro* microperfusion method commonly used for study of transport processes in renal tubules has also been applied to microvessels[189,190](Figure 24.18). The first applications of this method were in canine glomeruli.[191] Subsequent adaptations in rabbits permitted examination of vasomotor tone in afferent and efferent arterioles.[192–196] Using this approach, it has been possible to measure effects of vasoactive agents on afferent arterioles (Figure 24.19a) and vasa recta[111,197,198] (Figure 24.19b,c). As with all methods, limitations exist. Hormones that cause vasoconstriction often activate compensatory mechanisms that inhibit their actions. Endothelium-dependent vasodilators such as nitric oxide, prostacyclin, and hyperpolarizing factors[199] might be blunted, substrate-limited[200] or simply diluted into the bathing buffer. The actions of nitric oxide (NO) might be enhanced *in vitro* due to the absence of hemoglobin, a NO scavenger[201] or reduced by endothelial damage during vessel isolation.

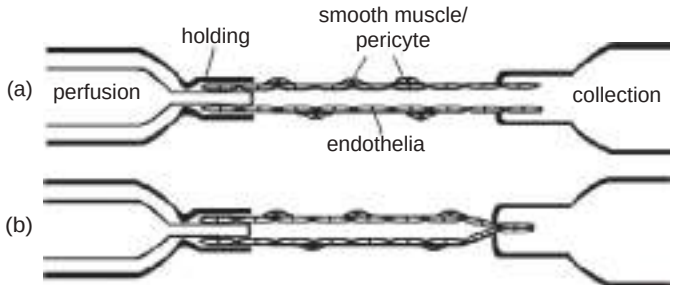

FIGURE 24.18 ***In vitro* microperfusion.** (a) An isolated microvessel is cannulated on concentric pipettes by drawing the vessel into an outer holding pipette and cannulating its orifice with a perfusion pipette. By pressurizing the perfusion pipette, fluid is forced to flow through the vessel lumen into a collection pipette. (b) The collection end can be crimped to create a "stop-flow" condition in which the lumen is pressurized to that of the holding pipette in the absence of flow. *(Reproduced with permission from ref. [393]).*

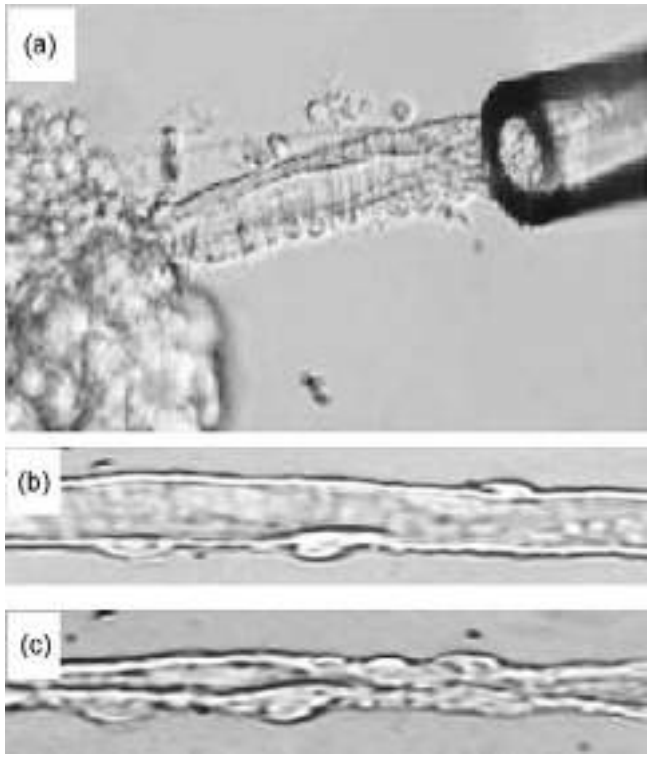

FIGURE 24.19 ***In vitro* microperfusion.** (a) An afferent arteriole is cannulated with concentric pipettes and perfused toward the glomerulus. *(Reproduced with permission from ref. [197]).* (b), (c) Perfusion of an isolated DVR. Images obtained before (b) and after (c) exposure to angiotensin II. Compare the thick smooth muscle layer of the afferent arteriole to the sporadically distributed pericyte cell bodies of DVR.

Juxtamedullary Nephron Preparation

The ingenious blood-perfused juxtamedullary nephron preparation was devised by Casellas and Navar (Figure 24.20, top panel). The surgically isolated kidney, perfused with artificial buffers or blood, is hemisected. Dissection of perihilar fat and reflection of the papilla exposes the juxtamedullary circulation to enable observation of RBC flow and microvessel diameters. Advantages of the method are many, including relative preservation of tubulovascular relationships, continuous oxygenation of the tissue under study, the ability to measure pressures by servo-nulling, and the ability to control hormone concentrations in the perfusate and superfusate.[202]

The Split Hydronephrotic Kidney

Steinhausen et al. developed a method for reducing the kidney to a transparent layer of tissue within which transilluminated microvessels are readily visualized. After transient ischemia to the kidney, ureteral ligation is performed, inducing hydronephrosis. Weeks later,

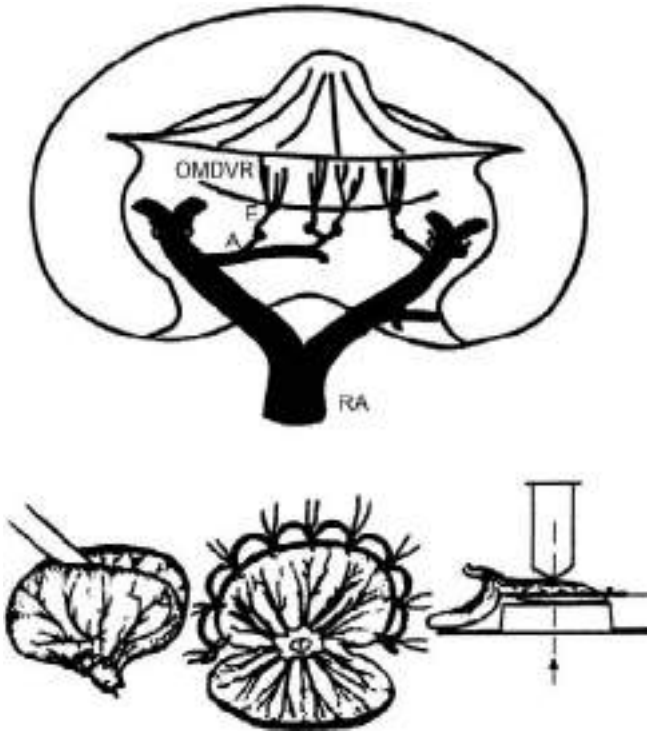

FIGURE 24.20 **Juxtamedullary nephron and split hydronephrotic kidney preparations.** Top panel: The juxtamedullary nephron preparation is created by perfusing the kidney, sectioning it longitudinally and reflecting the papilla to expose the underlying microvasculature (RA: renal artery; A and E: afferent and efferent arterioles; OMDVR: outer medullary descending vasa recta). Bottom panel: The split hydronephrotic kidney preparation is created by ligating the ureter for 3 to 10 weeks prior to isolation of the kidney. Ureteral ligation eventually reduces the kidney to a thin sheet of tissue in which tubules have atrophied but the vasculature remains. The kidney is exposed, split along the greater curvature, and sutured onto a chamber for observation and experimentation. *(Reproduced with permission from ref. [2]).*

the hydronephrotic kidney, reduced to a thin layer, can be split along its curvature and suspended on a microscope stage for study[203,204] (Figure 24.20, bottom panel). The actions of vasoactive agents can be studied by infusing them into the rat or by applying them directly onto the preparation. Changes in blood flow rate can be measured by videomicroscopy, and the reactivity of microvessels quantitated as changes in luminal diameter. The possibility of phenotypic drift in the altered tissue has to be considered.

VASOACTIVITY OF THE RENAL MICROCIRCULATION: ION CHANNEL ARCHITECTURE

Voltage-Gated Ca^{2+} Channels

Contraction of microvessels is generally tied to elevation of cytoplasmic calcium ($[Ca^{2+}]_{CYT}$) of smooth muscle cells (SMC). The increase of $[Ca^{2+}]_{CYT}$ is often mediated by influx through voltage-gated channels that are activated by membrane depolarization. This is observed experimentally, exposing SMC to high extracellular KCl induces depolarization by raising the K^+ equilibrium potential (Keq), activating voltage-gated Ca^{2+} entry and inducing vasoconstriction. Studies have shown that KCl depolarization constricts afferent arterioles more than efferent arterioles.[205–207] A role for high voltage-gated, L-type channels to mediate afferent SMC contraction is supported by the observation that both $[Ca^{2+}]_{CYT}$ elevation and vasoconstriction are blocked by diltiazem.[208,209] In the split hydronephrotic kidney preparation, angiotensi II constricts both afferent and efferent arterioles, but depolarizes only the former.[210] Application of agonists such as angiotensin II, endothelin, and ATP to preglomerular smooth muscle preparations consistently elicits $[Ca^{2+}]_{CYT}$ and current responses that are sensitive to L-type antagonists.[211–215] Taken together, sensitivity of the preglomerular microcirculation to L-type calcium channel blockade has been a very consistent finding.[216–221] Reduction of afferent vasoconstriction due to impairment of L-channel function could conceivably lead to transmission of elevated pressures to the glomerulus, resulting in injury. Such a mechanism has been invoked in rodent models of diabetes and hypertension.[222–224]

Voltage-gated Ca^{2+} channels (CaV) exist as a variety of subtypes and splice variants thereof. The nomenclature has evolved. Modern CaV classification follows the identity of the pore forming α-subunit (Table 24.5). Isoforms of classic high voltage-activated (HVA), L-channels are CaV 1.1– 1.3, and those of low voltage-activated (LVA) T-type channels are CaV 3.1–3.3. Other HVA types, originally identified in neurons, are the P/Q, R, and N which are CaV 2.1–2.3. Recently, RT-PCR and immunochemistry have been used to examine the distribution of voltage-gated Ca^{2+} channel α-subunits in the kidney. In addition to the anticipated expression of L-type (CaV 1.x) in the afferent circulation, T-type as well as unexpected P/Q-type Ca^{2+} channels were found.[206,225–229] Consistent with the earlier literature (see above), superficial efferent arterioles were not found to express L-type channels.[206]

Functional confirmation of CaV expression in the afferent and efferent circulation has been obtained in various studies. The CaV 1.x, L-type blocker diltiazem, partially reversed angiotensin II vasoconstriction and $[Ca^{2+}]_{CYT}$ elevation in DVR pericytes.[230,231] Similarly, the L-type blocker calciseptine and nonselective T-type blockers nilvadipine, mibefradil, pimozide, and Ni^{2+} reversed KCl and angiotensin II-induced constriction of afferent and efferent arterioles.[206,227,228,232,233] Elegant patch-clamp recordings by Gordienko et al. demonstrated signature currents consistent with both

TABLE 24.5 Expression of Voltage Activated Ca^{2+} Cannels (CaV) in the Renal Microcirculation[225,206,226,227,228,355,320,236]

		CaV	α-subunit	Renal SMC[a]	Locations Found
HVA	L	1.1	1S	−	Preglomerular SMC
	L	1.2	1C	+	Afferent arteriole
	L	1.3	1D	−	Mesangial cells
	L	1.4	1F	−	JM efferent arteriole
					DVR
HVA	P/Q	2.1	1A	+	Afferent arteriole
	N	2.2	1B	−	Mesangial cells
	R	2.3	1E	−	DVR
LVA	T	3.1	1G	+	Afferent arteriole
	T	3.2	1H	+	Efferent arteriole
	T	3.3	1I	−	DVR

[a]*Detection by immunochemistry, polymerase chain reaction.*
Abbreviations: SMC: smooth muscle cell; HVA: high voltage activated by depolarization to > -40 mV; LVA: low voltage activated by depolarization to > -55 mV.

high (L-type) and low (T-type) voltage-gated Ca^{2+} entry into isolated preglomerular smooth muscle.[234] Glomerular mesangial cells have a smooth muscle phenotype and express L-type dihydropyridine-sensitive voltage-gated Ca^{2+} channels.[235]

It is now clear that CaV are not just confined to the preglomerular circulation; juxtamedullary efferent arterioles and DVR express them. Despite positive immunostaining for T-type and P/Q-type channels in DVR pericytes,[206,225] a rigorous search for signature currents found only L-type activity.[236] Feng and colleagues examined the roles of arteriolar CaV with the juxtamedullary nephron preparation. Pimozide and mibefradil (T-type blockers) reduced basal tone of both afferent and efferent arterioles. In contrast, successful blockade with diltiazem (L-type blocker) occurred only in afferent arteriole, except when generation of NO was prevented by NO synthase inhibition. In their hands, T-type channel blockade with pimozide reversed both afferent and efferent contraction by angiotensin II.[232,237,238] Elegant studies in the renal cortex, performed *in vivo* using a pencil lens camera, have also documented that efferent arterioles are dilated by nonselective CCB, such as efonidipine and mibefradil.[239] Taken together, a role for CaV, particularly T-type channels, to participate in myogenic tone and agonist-induced contraction of juxtamedullary efferent arterioles is well-supported, and the ability of combined T- and L-type blockade to provide renoprotection through efferent dilation has thus become the subject of clinical investigation.[240–242]

Nonselective Cation Channels, Store Operated Channels, TRP Channels

Early study of store operated Ca^{2+} entry (SOC) in mast cells pointed to a highly Ca^{2+} selective pathway of immeasurably low single channel conductance that was referred to as a "calcium release activated current" (CRAC or I_{CRAC}).[243] That pathway is been attributed to the ER anchored stromal interacting molecule (STIM1) as the putative sensor and Orai, possibly interacting with TRPC1 as the selective pore.[244–247] Other pathways may participate in cellular Ca^{2+} entry in response to receptor activation and intracellular Ca^{2+} store depletion.[248] The routes involved are not always highly selective for Ca^{2+}, but instead also conduct other cations including Na^+. Their promiscuous transport of cations led to the designation "nonselective cation channels" (NSCC). Both receptor operated and store operated Ca^{2+} entry into cells can occur via NSCC, and channels of the transient receptor potential (TRP) families are now recognized as the major participants.[249] Fellner and Arendshorst showed that store operated Ca^{2+} entry into renal SMCs occurs and may be increased in the spontaneously hypertensive rat,[223,250] and that using SKF-96365 as an NSCC blocker, it has been shown that angiotensin II induced Ca^{2+} responses[215] and vasoconstriction[251] of the efferent arteriole involves NSCC. Assigning subtype-specific functional roles to the ubiquitously expressed TRP channel family members has proven generally difficult.[249] Takenaka and colleagues demonstrated that TRPC1 is expressed in glomerular arterioles and might conduct store or receptor operated Ca^{2+} entry.[249,251] The presence and activation of SOC has been most thoroughly examined in glomerular mesangial cells. Sansom and colleagues identified a small, 2.1 pS cation channel that is activated by thapsigargin-induced store depletion.[249,252] In whole cell patch-clamp experiments, identical currents were elicited by either thapsigargin or epidermal growth factor activation.[253,254] Activation of the pathway requires signaling through PKCα.[255,256] TRPC1 and TRPC4 are expressed in the murine mesangium, where antisense-induced suppression of TRPC4 was accompanied by inhibition of store operated currents.[257] TRPC4 has also been identified in DVR pericytes and endothelium, where it is in physical association with isoform 2 of the Na^+/H^+ exchange regulatory factor (NHERF-2), a scaffolding protein that facilitates protein−protein interactions.[258] The function of the NHERF-TRPC4 association is unknown.

Chloride Channels

For CaV to mediate Ca^{2+} entry into smooth muscle, they must depolarize the cell membrane to potentials greater than the CaV activation threshold. The equilibrium potential for K^+ ion is about -90 mV and SMC

membrane potential is held at negative values because overall conductance of the cell membrane is dominated by permeability to K^+. In many SMCs, depolarization that presages CaV-mediated Ca^{2+} entry is achieved by increasing the conductance to Cl^- ion, the equilibrium potential of which is generally −35 to −20 mV. This is accomplished through activation of Ca^{2+}-dependent Cl^- channels (CaCC).[259,260] The identity of CaCC had been confusing and enigmatic, but has recently been traced to TMEM16A and the family of proteins dubbed "anoctamins".[261,262] It seems likely that anoctamins are SMC CaCC, but confirmatory evidence in the renal vasculature is currently lacking. In the kidney, activation of CaCC channels has been described to participate in angiotnsin II-, endothelin-, and adenosine-induced constriction of afferent but not efferent arterioles.[263–267] Presumably, based on the juxtamedullary efferent expression of CaV,[206] CaCC plays a similar role in that location, but this has not been demonstrated. DVR pericyte depolarization and constriction is dependent upon CaCC activation.[268–270] In pericytes, cyclic CaCC stimulation participates in angiotensin II-induced oscillations of membrane potential,[271,272] and CaCC activity can be regulated by kinase blockade.[273] It has also been shown that high concentrations of angiotensin II also depolarize DVR pericytes by inhibiting K^+ channels.[274] The extent to which Cl^- channel activity regulates overall renal vascular resistance is uncertain.[229,248,275]

Potassium Channels

Most smooth muscle cells (SMC) express an array of K^+ channels. These include inward rectifier (K_{IR}), calcium-dependent (K_{Ca}), voltage-dependent (K_V), and ATP-dependent (K_{ATP}) varieties.[276] SMC of renal vessels are no exception, and many studies have been dedicated to the determination of their distribution and function (Table 24.6).

K_{Ca} channels are activated by depolarization and elevation of $[Ca^{2+}]_{CYT}$. They can be further subdivided into larger conductance (maxiK_{Ca} or BK_{Ca}) channels sensitive to charybdotoxin and iberotoxin, and medium and low conductance channels blocked by apamin. K_{Ca} channels are ubiquitous in smooth muscle. When stimulated by Ca^{2+} entry, they may provide a "breaking" function that opposes depolarization and deactivates CaV.

K_V channels, also refered to as delayed rectifiers, activate with depolarization, are insensitive to $[Ca^{2+}]_{CYT}$, and are specifically blocked by 4-aminopyridine. K_V can contribute to resting potential, and their voltage-dependent activation probably limits membrane depolarization.

K_{IR} are named for their avid permeation of K^+ at membrane potentials that lie below Keq. Above Keq, where the physiological function of K_{IR} occurs, K_{IR} conduct K^+ efflux from cells in a complex manner. Conductance, at membrane potentials greater than Keq, declines as the difference between membrane potential and Keq increases. The latter property imparts a very important characteristic. Small elevations of extracellular K^+ (e.g., 5–20 mM) raise Keq to a level that enhances K_{IR} conductance, but still lies below the resting membrane potential. The result is hyperpolarization of the membrane that favors inhibition of Ca^{2+} entry and vasodilation.[277] That mechanism may enable extracellular K^+ ion to function as an endothelium-dependent hyperpolarizing factor (EDHF). The increase in extracellular K^+ needed for the EDHF process to occur is thought to arise from endothelial K^+ secretion. Vasodilators, such as bradykinin and acetylcholine, increase $[Ca^{2+}]_{CYT}$ and stimulate endothelial K_{Ca} channels so that they secrete K^+ ion into the extracellular space of adjacent SMCs.[97,278–280] Stated another way, K^+ may be an EDHF, the function of which depends upon endothelial K^+ secretion and SMC K_{IR} expression. Extracellular K^+ can also activate electrogenic Na^+K^+-ATPase activity in SMC which, by exchanging $3Na^+$ for $2K^+$, favors hyperpolarization. Participation of Na^+ pumps versus K_{IR} in SMC hyperpolarization must be experimentally distinguished, generally by examining the component that is sensitive to ouabain.

SMC K_{ATP} channels are generally comprised of four K_{IR} 6.1 α-subunits combined with four type 2B sulfonurea

TABLE 24.6 Potassium Channel Expression in the Renal Microcirculation

Site	K_{Ca}	Kv	K_{IR}	K_{ATP}	Reference
Main renal artery	+	+	N.D.	N.D.	281,284,285
Preglomerular SMCs	+	+	+	+	283,291,292,299,301,302,307
Interlobular artery	+	+	N.D.	N.D.	234,282,296,300
Arcuate artery	+	+	+	N.D.	234,282,286,289,290
Interlobular arteriole	+	+	N.D.	N.D.	287,288,293,294
Afferent arteriole	+	+	+	+	298,303–306,308–310–316
Mesangial cells	+	+	N.D.	+	320–328,330–334,793
Efferent arteriole	+	N.D.	+	+	311,317
DVR	+	N.D.	+	+	231,274,318,319,467

Table entries are + for existence of functional evidence based on electrophysiology, vasoactivity and use of specific channel blockers. Abbreviations: K_{Ca}: small, medium or large/maxi calcium dependent potassium channel; Kv: voltage-gated (delayed rectifier) potassium channel; K_{IR}: inward rectifier potassium channel; K_{ATP}: ATP-dependent potassium channel; N.D.: no data; DVR: descending vasa recta.

receptors (SUR2B). Despite the participation of K_{IR} 6.1, K_{ATP} channels lack the strongly inward rectifying characteristics of other K_{IR} isoforms. K_{ATP} channels are widely expressed in SMC and, with high specificity, are inhibited by antagonists such as glybenclamide that bind to the SUR-subunits. K_{ATP} channels are named for their inhibition by intracellular ATP. In addition to ATP, nucleotide diphosphates (NDPs) regulate most K_{ATP} channels. It was historically thought that reduction of cellular ATP related to metabolic stress activates K_{ATP} channels favoring hyperpolarization, microvessel dilation, and enhancement of perfusion. It is now recognized that this is an oversimplification, because K_{ATP} channels can contribute to resting potential and are sensitive to a variety of regulatory influences.[277]

SMC of the main renal artery, interlobular, and arcuate arteries have been shown to express both BK_{Ca} and K_V channels that exhibit slow inactivation after depolarization.[234,281–286] Preglomerular renal microvessels of varying caliber obtained by hand dissection or by filling them with iron oxide particles and isolating them from collagenase-digested tissue with a magnet have provided preparations for study. SK_{Ca}, BK_{Ca}, and K_V channels have been observed in afferent SMCs.[287–289] The P450 cyclooxygenase constrictor, 20-hydroxyeicosatetraenoic acid (20-HETE), inhibits preglomerular K_{Ca} channel activity,[290–292] probably through activation of MAP kinase.[293] Preglomerular K_{Ca} channels can be activated by NO,[294] 11,12-epoxyeicosatrienoic acid (11, 12-EET),[295] and CO generated by hemoxygenase.[296] The cytochrome P450 synthesis of epoxyeicosatrienoic acids (EETs) has been shown to activate BK_{Ca}, and may participate in the function of EETs as an EDHF.[297–299] NO-mediated inhibition of 20-HETE synthesis may be the primary mechanism (versus cyclic GMP generation) that favors BK_{Ca} activation in preglomerular SMC.[291,300] Preglomerular expression of K_{ATP} component subunits has been variably observed.[301,302]

Afferent arterioles are the dominant resistance of the renal microcirculation, and play vital roles in autoregulation through myogenic constriction and tubuloglomerular feedback. The K^+ channel architecture of afferent arterioles has been intensely studied, and evidence for expression of K_{Ca}, K_{IR}, K_V, and K_{ATP} channels has been obtained. Afferent dilation by acetylcholine during inhibition of NO and prostaglandin synthesis has been traced to the participation of K_{IR} and K_{Ca} channels, because it is blocked by the combined K_{Ca} inhibitors, charybdotoxin and apamin.[298,303] As described above, the EDHF response may be related to local elevations of K^+ outside the SMC membrane. Direct participation of K_{IR} has been demonstrated by Chilton and Loutzenhiser, who found that small elevations of K^+ dilate afferent arterioles. The dilation is sensitive to low concentrations of Ba^{2+} ($<100\ \mu M$) that selectively blocks K_{IR} channels.[304–306] Juxtaglomerular cells express the strong inward rectifier, K_{IR} 2.1, where it plays a role in setting membrane potential.[307] Vasodilation of afferent arterioles by the K^+ channel activator, NS-1619, supports a role for K_{Ca} channels in that structure.[307,308] Myogenic constriction appears to be modulated through PKC that acts, at least in part, by inhibiting 4-aminopyridine sensitive K_V channels.[309] A role for K_{ATP} channel activity to affect afferent arterioles has been repeatedly verified. K_{ATP} channels activated by hypoxia, pinacidil, calcitonin gene related peptide (CGRP) or adenosine modulate constriction[310–313] and levakromlin hyperpolarizes renin-secreting cells of the afferent arteriole.[314] K_{ATP} expression in afferent arterioles is supported by the observation of [^{3}H]P-1075 binding to membranes.[315] Multiple classes of K^+ channels contribute to resting tone of afferent arterioles, and enhancement of K_{IR} and K_{ATP} activity may contribute to vasodilation and glomerular hypertension in diabetes.[316]

The role of K^+ channels in the activity of the efferent circulation has not been as thoroughly explored as that of afferent smooth muscle. The K_{ATP} opener, pinacidil, dilates the efferent arteriole.[311] Pinacidil both dilates DVR and hyperpolarizes DVR smooth muscle/pericytes.[231] High concentrations of angiotensin II inhibit DVR K^+ channel activity.[274] A modulatory role for K_{IR} and K_{Ca} channels to affect $[Ca^{2+}]_{CYT}$ signaling by angiotensin II in efferent arteriolar smooth muscle has been described.[317] Roles for strong K_{IR} isoforms to modulate contraction and membrane potential of glomerular arterioles and vasa recta pericytes have been verified.[304,318,319]

Mesangial cells are smooth muscle pericytes that contract to modulate filtration by glomerular capillaries.[320] The ability to study mesangial cells in culture has permitted study of their channel architecture. Molecular evidence exists for expression of K_V, K_{ATP}, and K_{Ca} channels in rat primary and immortalized murine mesangial cells.[321,322] Both medium and large conductance K_{Ca} channels are present.[289,323–328] The BK_{Ca} channel in mesangial cells is activated by arachidonic acid[329] and Ca^{2+}-calmodulin-dependent protein kinase.[330] Atrial natriuretic peptide[331] or nitric oxide, acting through cGMP-dependent protein kinase, also activatesK_{Ca} channels through phosphorylation of the β1-subunit.[332] Mesangial BK_{Ca} activation is favored by protein phosphatase 2A inhibition,[333] and enhancement of activity and expression by insulin-induced MAPK activation.[334]

Connexins

In addition to permitting exchange of ions with the extracellular space, specialized channel proteins, the

connexins, electrically couple smooth muscle and endothelia in the vascular wall. Of more than 20 connexins, Cx37, Cx40, Cx43, and Cx45 have been found in the vasculature where they form endothelial and myoendothelial gap junctions. Connexins are four transmembrane spanning proteins with two extracellular loops that combine as homomeric or heteromeric hexamers. Docking of the extracellular loops combines two hexameric hemichannels from adjacent cells into the transcellular "connexon" conduit that mediates cell−cell communication. Mimetic peptides have been designed that interfere with binding of the extracellular loops.[335] Connexons are true channels that generally have high conductivity (15−300 pS), high open probability, and can occupy multiple subconductance states. They are regulated by pH, Ca^{2+}, signaling molecules, and phosphorylation events. Their pores are sufficiently large to pass signaling molecules, anions, and cations. Communication between cells is often documented by cell-to-cell spreading of fluorescent molecules (e.g., Lucifer yellow 457 Da).[336−338] The physiological roles of vascular gap junctions are under study. A role for endothelial to smooth muscle transfer of vasodilators has been postulated.[97,278] This has received support from the observation that Cx40 deficient mice are hypertensive, have abnormal vasomotion, and deficient spreading of vasodilation.[336,339,340] Endothelial deficiency of Cx43 also leads to abnormal spreading of vasodilation,[341,342] and targeting of Cx43 and Cx37 with the extracellular peptide mimetic, Gap27, inhibits myogenic responses.[343]

The renal microcirculation expresses gap junctions Cx37, Cx40, Cx43, and Cx45.[29,344−352] NO- and COX-independent (EDHF-mediated) dilation of the main renal artery with carbachol was shown to be sensitive to Gap27.[353] Similarly, arachidonic acid- and bradykinin-mediated, NO- and COX-independent dilation of arcuate and interlobar arterioles was inhibited by the gap junction blocker, 18-α glycyrrhetinic acid.[354] Salmonsson and colleagues have documented Ca^{2+} spreading along interlobular arterioles that is likely to be mediated by gap junctions.[355] Cx40 is highly expressed in endothelial cells of renal vessels and glomeruli,[347,356] and may play an important role in tubuloglomerular feedback and autoregulation.[348] Endothelial cells of preglomerular arteries and arterioles also express Cx37 and Cx43. Cx37 is found in arcuate and interlobular arteries, and afferent arterioles.[352] Cx40 bridging endothelial cells are most abundantly localized in large intrarenal arteries, including interlobular artery and the proximal portion of the afferent arteriole, but then markedly decreases as the arteriole approaches a glomerulus.[347] Deficiency of Cx40 leads to ectopic renin production.[357−359] Afferent arterioles have considerably more connexin expression than efferent arterioles where Cx43 is largely present in the endothelium. Cx37 and Cx40 are expressed in juxtaglomerular cells and extraglomerular mesangial cells.[352] Cx43 is localized to extraglomerular mesangium and is found in isolated glomeruli.[360,361,362] Intraglomerular mesangial cells have primarily Cx40.[352,363] In the renal medullary microcirculation, DVR pericytes express Cx37 while the endothelia express Cx40 and Cx43 (Figure 24.21). DVR endothelia, but not pericytes, are highly connected as an electrical syncytium. DVR conduct Ca^{2+} responses to mechanical stimulation that can be inhibited by gap junction blockade.[364]

REGULATION OF BLOOD FLOW AND MICROVESSEL CONTRACTION

The most effective locations at which regional perfusion of cortex and medulla can be controlled are readily inferred from renal microanatomy (Figure 24.1). For example, constriction of intralobular arterioles should favor redistribution of blood flow toward the medulla via the juxtamedullary glomeruli. Similarly, closure of juxtamedullary intra-arterial cushions (Figure 24.2) or constriction of juxtamedullary afferent or efferent arterioles should favor perfusion of the superficial cortex. DVR are the final resistance vessels involved in the

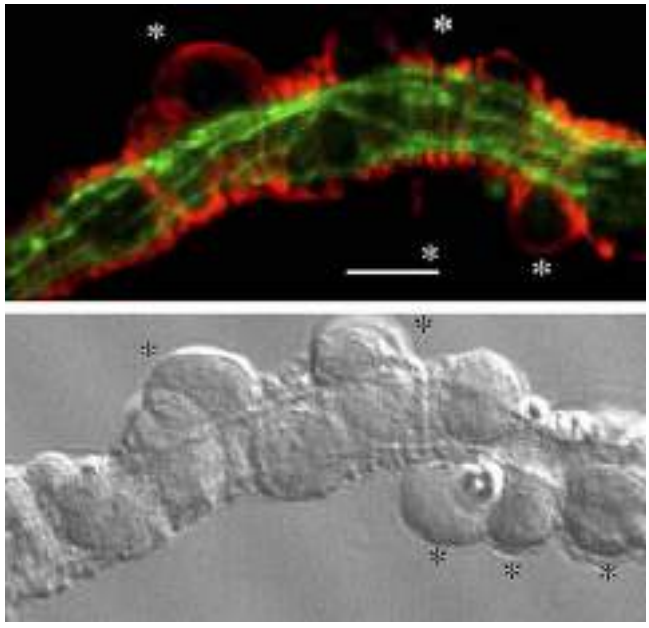

FIGURE 24.21 **Connexin staining in DVR.** Immunostaining with antibody directed against α-smooth muscle actin (SMA red, pericyte marker) or Cx40 (green) along with corresponding white light micrograph. Cx40 is linear and confined to the endothelium with very little SMA colocalization. Abluminal pericyte cell bodies (*) protrude from the outer rim of the vessel (Bar = 10 microns). *(Reproduced with permission from ref. [364]).*

control of medullary perfusion. The fraction of the total resistance to blood flow into the renal medulla accounted for by DVR, versus juxtamedullary afferent and efferent arterioles, is uncertain. The parallel arrangement of DVR within vascular bundles does, however, imply a probable role for them to modulate regional perfusion to the outer versus inner medulla. For example, contraction of DVR that are destined to perfuse the inner medulla should favor redirection of blood flow toward the outer medullary interbundle capillary plexus. Factors that control regional perfusion within the kidney are the subject of intense investigation.

Autoregulation and Pressure Natriuresis

Blood flow to the kidney remains relatively constant despite physiological variation of renal perfusion pressure (RPP), a phenomenon called autoregulation. Two major mechanisms account for renal autoregulation. The first is "myogenic," whereby stretch of the afferent arteriole leads to reflex vasoconstriction.[365] The second component, that reacts more slowly than the myogenic reflex, is tubuloglomerular feedback (TGF). TGF occurs when an increase in renal perfusion pressure, transiently transmitted to glomerular capillaries, results in a rise in glomerular filtration rate. After a delay traversing the nephron, the increased tubular fluid delivery is sensed at the macula densa, where a signaling cascade leads to release of ATP and adenosine formation via 5′-ecto-nucleotidase. The adenosine so formed constricts the afferent arteriole, thereby reducing filtration pressure and returning glomerular filtration rate to its set point.[366–371]

The phenomenon of "pressure natriuresis" may be tied to variation of medullary autoregulation. Pressure natriuresis refers to the observation that elevation of renal perfusion pressure (RPP) causes natriuresis even in isolated, denervated kidneys.[372,373] Increased RPP leads to increased sodium delivery to papillary thin descending limbs of Henle, implying that a mechanism exists to inhibit reabsorption by the proximal tubule of deep nephrons.[374,375] Internalization of proximal Na^+/H^+ exchanger from the apical membrane might participate. Pressure natriuresis has been traced to alteration of renal interstitial hydrostatic pressure (RIHP). An increase in RIHP occurs when RPP is elevated,[376] and both the increase in RIHP and natriuresis can be blunted through renal decapsulation.[377] Garcia-Estan and Roman have suggested that residual effects after decapsulation might be traced to the inability of decapsulation to modulate interstitial pressure in the renal medulla.[378] A role for RIHP in the phenomenon of pressure natriuresis is supported by experiments in which it has been altered without changing RPP. Infusion of 2.5% albumin into the renal interstitium increases RIHP and causes natriuresis through inhibition of sodium reabsorption by superficial and deep nephrons.[379,380]

It is accepted that renal cortical blood flow is autoregulated over a physiological range of renal perfusion pressure. In contrast, the extent to which medullary blood flow is autoregulated is controversial. It has been proposed that lack of medullary autoregulation is essential to pressure natriuresis, and the control of salt and water excretion.[76,184,381–385] The renal medulla is largely perfused by postglomerular blood. Flow through a small population of shunt vessels that bypass glomeruli has been invoked to explain the escape of the medulla from tubuloglomerular feedback-mediated autoregulation (Figures 24.1 and 24.3).[16,381] Nearly 50 years of investigation have failed to completely support or refute the hypothesis that blood flow to the renal medulla lacks autoregulation. Work with microvascular transit time indicators favored lack of autoregulation,[171] but several early studies favored its presence.[183,386,387] Studies performed in the rat suggest that the efficiency of medullary autoregulation is a function of volume status. Measurement of blood flow to the cortex and medulla using videomicroscopy or laser-Doppler probes placed on the renal surface[388] or within the parenchyma[389] showed that medullary blood flow of volume-expanded rats does not autoregulate, but instead increases with perfusion pressure (Figure 24.22). Both an increase in single vessel blood flow rate and recruitment of flow through

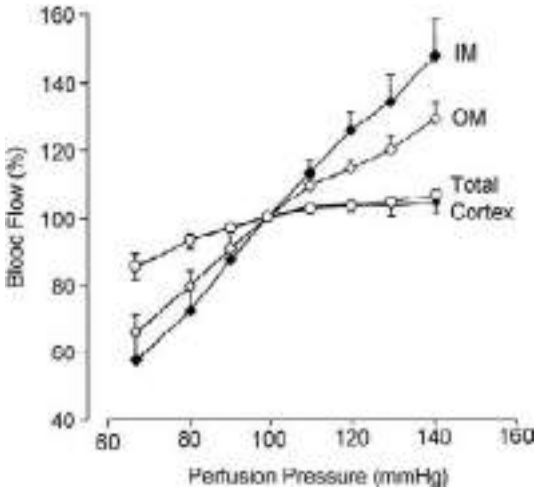

FIGURE 24.22 **Autoregulation in different regions of the kidney.** An electromagnetic flow device on the renal artery was used to measure total renal blood flow. Laser-Doppler flow probes were inserted into the renal parenchyma at various depths to measure regional blood flow in the outer and inner medulla. Total renal blood flow and cortical tissue blood flow shows intact autoregulation (stability of blood flow over a range of perfusion pressure). In contrast, in these volume-expanded rats (see text) the small fraction of blood flow that reaches the outer or inner medulla is not autoregulated. *(Reproduced with permission from ref. [389]).*

previously unperfused vasa recta may contribute to the process.[388] In contrast to volume-expanded animals, hydropenic rats autoregulate medullary blood flow and minimal pressure natriuresis[381,382,384,390](Figure 24.23). Studies of regional blood flow in sodium-replete dogs by Majid, and in rabbits by Eppel et al. support intact medullary autoregulation.[391,392] Zhang and colleagues recently demonstrated that pressurizing the DVR lumen leads to endothelial $[Ca^{2+}]_{CYT}$ elevation and generation of NO.[393] If transmission of pressure to the medulla is a key event in pressure natriuresis, release of NO could conceivably inhibit salt reabsorption by adjacent nephrons generating pressure natriuresis. Such a paracrine role for NO to signal between the vasculature and nephrons is frequently postulated.[382,394–397]

Blood flow to the renal medulla is dependent on generation of NO.[382,384] This is particularly true in the spontaneously hypertensive rat (SHR).[398] Roald and colleagues observed poor autoregulation of juxtamedullary blood flow in the SHR. They proposed that the tendency toward early tissue damage in the juxtaglomerular cortex is due to poor autoregulation.[399] The superoxide dismutase mimetic, tempol, enhances tissue NO levels by eliminating its reaction with superoxide.[400] Feng and colleagues found that tempol reduced blood pressure and enhanced medullary blood flow in the SHR.[401]

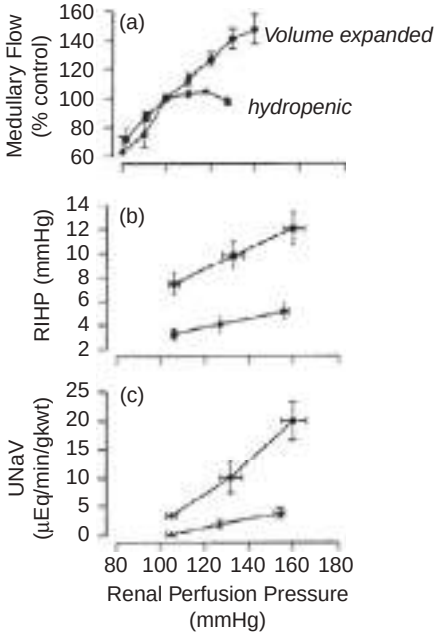

FIGURE 24.23 **Pressure natriuresis.** Panel a: Medullary blood flow is autoregulated in hydropenic but not volume-expanded rats. Panel b: Renal interstitial hydrostatic pressure (RIHP) is higher and increases to a greater degree with renal perfusion pressure in volume-expanded animals. Panel c: When renal perfusion pressure is increased, urinary sodium excretion (UNaV) increases much more markedly in volume-expanded than in hydropenic animals. *(Reproduced with permission from ref. [381]).*

Vasopressin and Excretion of Water

Changes in medullary blood flow might have a diuretic effect by reducing the efficiency of countercurrent exchange, leading to "solute washout" and loss of corticomedullary axial gradients of NaCl and urea.[17] The role of vasopressin to modulate medullary blood flow during antidiuresis has been the focus of much investigation.[2,381,390,402] Early studies, based on indicator transit times, showed that vasopressin reduces medullary blood flow.[171] Homozygous Brattleboro rats that lack vasopressin secretion have elevated papillary plasma flow.[156] The effect of vasopressin and specific V_1 (vasoconstrictor) and V_2 (antidiuretic) receptor subtype inhibitors on vasa recta blood flow was studied with videomicroscopy. Vasopressin reduces vasa recta blood flow in a manner that was partially blocked with either vasopressin V1 or V2 receptor subtype inhibitors.[403–405]

Studies with laser-Doppler and implantable probes confirmed that intrarenal infusion of a selective V_1 receptor agonist reduces inner medullary blood flow more than outer medullary blood flow.[406] Similarly, elevation of circulating vasopressin, stimulated by depriving conscious rats of water, led to selective reduction of only inner medullary blood flow, sparing perfusion of the cortex and outer medulla. Infusion of a V_1-antagonist into the medullary parenchyma blocked the decline in inner medullary perfusion and interfered with urinary concentration.[33] When vasopressin was infused into decerebrate rats to maintain plasma levels within a physiological range of 2.9 to 11.2 pg/ml (about 1 to 10 pM), inner medullary blood flow fell to an extent that correlated with urinary osmolality[33] (Figure 24.24). Those studies support the V_1-mediated vascular effect of vasopressin as a modulator of inner medullary blood flow favoring antidiuresis. The renal cortex might be spared from V_1

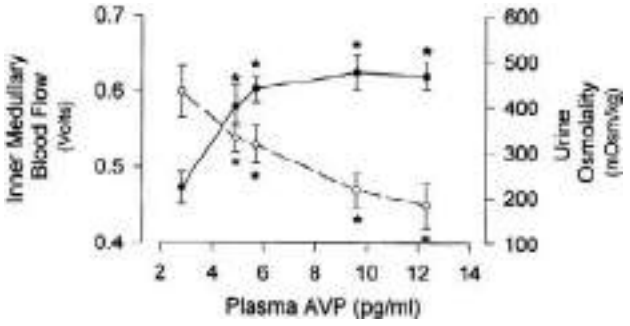

FIGURE 24.24 **Effect of arginine vasopressin (AVP) on inner medullary blood flow and urine osmolality.** To control plasma vasopressin concentrations, decerebrate rats were infused with AVP. Increasing AVP concentration within the physiological range caused a reduction of inner medullary blood flow and an improvement in urinary concentration. *(Reproduced with permission from ref. [33]).*

receptor-mediated vasoconstriction by reflex generation of vasodilator epoxyeicosatrienoic acids.[407]

Vasopressin reduces inner medullary perfusion by acting at various sites. It constricts juxtamedullary afferent (1 pM−1 nM) and efferent (1 nM) arterioles in isolated, perfused rat kidneys.[408] Afferent AVP constriction is dependent upon voltage-gated Ca^{2+} entry, whereas efferent constriction may be related to Ca^{2+} mobilization from stores.[409] Vasopressin also constricts rabbit afferent arterioles,[410] efferent arterioles (0.1 pM−100 nM), and rat outer medullary DVR (100 pM−1 microM) *in vitro*.[411,412] Correia and colleagues showed that vasopressin V_1-agonist reduced medullary blood flow in rabbits, but did not constrict either juxtamedullary afferent or efferent arterioles. They concluded that DVR might be the primary site at which vasopressin acts to regulate inner medullary blood flow.[413]

In addition to the constrictor effects of vasopressin, mediated by the V1 receptor, it has been demonstrated that vasodilation of some vessels can be mediated through vascular V2 receptors, leading to elevation of nitric oxide.[414−417] Selective V2 agonists have been shown to dilate preconstricted afferent arterioles[418] and outer medullary DVR[412] *in vitro*. In contrast, however, efforts to date have failed to show V2 receptor mRNA in dissected renal microvessels by RT-PCR.[419] Chronic infusion of the V2 agonist dDAVP was shown to elevate renal medullary nitric oxide and increase medullary blood flow,[420] an effect that may be related to release of NO by collecting duct.[421,422] Blockade of NO production during vasopressin elevation leads to hypertension. That finding suggests that V2-mediated NO production in the medulla serves as a buffer to protect the outer medulla from ischemia, as well as to prevent salt retention and hypertension.[423,424] The probable source of V2-mediated NO production is the inner medullary collecting duct.[421]

Angiotensins

Studies that employ isolated microvessel perfusion,[193,194,198,396,410,421,425,426] the juxtamedullary nephron preparation[205,263,427] or the split hydronephrotic kidney,[204,210] have all shown that angiotensin II constricts afferent arterioles, efferent arterioles, and DVR. Cultured mesangial cells also contract in response to angiotensin II.[320] Angiotensin II tonically constricts the juxtamedullary microcirculation *in vivo*[160,428−430] in a manner that is modulated by vasodilators and renal nerves.[431−435] Several vasodilators modulate angiotensin II-induced vasoconstriction. Blockade of NOS induces basal constriction of afferent arterioles and DVR, and intensifies constriction by angiotensin II stimulation.[193,194,436−438] Paracrine agents such as prostaglandin E_2 (PGE_2) and adenosine counteract angiotensin II constriction of glomerular arterioles and DVR.[198,439−441] Blockade of prostaglandin production may have a greater effect in augmenting constriction of juxtamedullary than superficial glomerular arterioles.[439]

Angiotensin II exerts its effects through type 1 ($AT1_A$ and $AT1_B$) and type 2 (AT2) receptors. AT1 stimulation activates phospholipase C (PLC) to generate inositol trisphosphate (IP_3) and elevate $[Ca^{2+}]_{CYT}$.[211,215] $AT1_A$ receptor-null mice have blunted afferent and absent efferent arteriolar responses to angiotensin II .[442] Study of the distribution of receptors on juxtamedullary efferent arterioles revealed expression of $AT1_A$, $AT1_B$, and AT2 on muscular efferents destined to perfuse the medulla. In contrast, the $AT1_B$ subtype was absent in efferent arterioles that give rise to juxtamedullary capillary plexus in the cortex.[443] AT2 receptor activation has been reported to favor vasodilation via generation of nitric oxide.[444,445] In the afferent arteriole, however, AT2 stimulation favors synthesis of vasodilatory CYP450 epoxygenase products (EETs)[436,437,446] rather than NO. The evidence favors compensatory NO generation due to AT1 stimulation.[447,448] AT2 activation also vasodilates efferent arterioles[449] and DVR, where it both inhibits reactive oxygen species formation and facilitates endothelium-dependent $[Ca^{2+}]_{CYT}$ signaling in response to vasodilators.[395,450,451] The vasodilatory response to AT2 receptors may be impaired in forms of hypertension.[452,453] Both AT1 and AT2 receptors are widely expressed in vascular and tubular elements of the kidney.[454]

The role of angiotensin II AT1 and AT2 receptors to modulate regional perfusion in the kidney has been investigated. Angiotensin II constricts DVR that supply the medulla,[198,395] but angiotensin II infusion largely reduces blood flow to the renal cortex, sparing the medulla.[432,434,435] Moreover, there are reports that angiotensin II enhances medullary perfusion in rats and rabbits.[431,455,456] The resistance of the renal medulla to angiotensin II-induced vasoconstriction has been traced to reflex generation of compensatory vasodilators, particularly NO.[394,395,455,457−459] Recent studies favor the role of endothelial nitric oxide synthase (eNOS, NOS3) to maintain basal perfusion and stimulation of neuronal nitric oxide synthase (nNOS, NOS1) to blunt vasoconstriction by angiotensin II .[460] Pressure natriuresis has been tied to renal medullary perfusion (see above). Possibly related to this, AT2 receptor-null mice are hypertensive and lack the pressure natriuretic response.[461]

Angiotensin II constricts renal microvessels over a broad range of concentrations, with efferent arterioles and DVR showing the greatest sensitivity (EC_{50} ~0.5 nM). Although circulating plasma angiotensin II concentrations are in the range of 100 pM, renal interstitial and intratubular concentrations approach 1 to 10 nM, implying that there is an intrarenal mechanism

for generation and sequestration (Figure 24.25). Interstitial concentrations are greatest in the renal medulla, where angiotensin II receptor density is high.[462–466] At very high concentrations of 1 to 10 nM, angiotensin II acting via the AT1 receptor blunts DVR endothelial $[Ca^{2+}]_{CYT}$ responses to bradykinin and acetylcholine, an effect that is partially counteracted by concomitant AT2 receptor activation.[395,450] At high concentrations, angiotensin II inhibits K^+ channel activity of DVR pericytes[274,467,468] while stimulating Ca^{2+}-dependent Cl^- channel-mediated depolarization[268,270,273] to favor voltage-gated Ca^{2+} entry.[231,236] In DVR pericytes, angiotensin II often induces oscillations of $[Ca^{2+}]_{CYT}$ and Cl^- ion conductance.[271,272] Taken together, the results favor the interpretation that high levels of angiotensin II prevent vasodilatory compensation within vasa recta by blocking NO generation and K^+ channel activation, while stimulating NO generation by adjacent nephrons. Hypothetically, DVR on the vascular bundle periphery dilate in response to NO from adjacent epithelia to preferentially maintain outer medullary perfusion.[394,459,469–471]

Angiotensin II is derived from angiotensin I through the actions of angiotensin-converting enzyme (ACE).

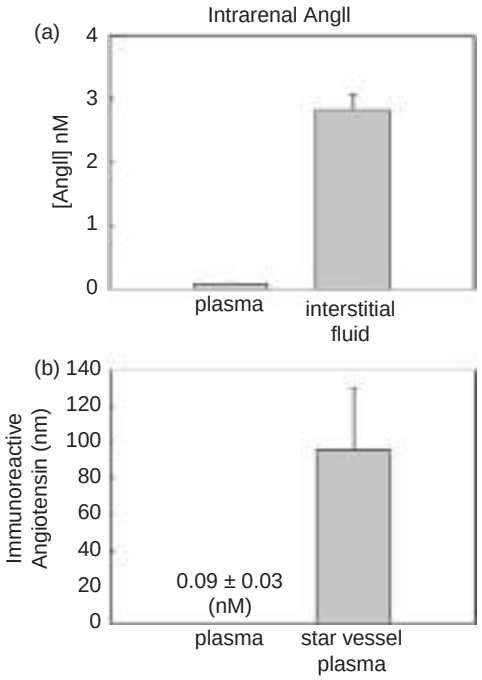

FIGURE 24.25 **Intrarenal angiotensin II concentrations.** (a) Graph shows a comparison of angiotensin II concentration in plasma and renal interstitial fluid obtained by microdialysis. Cortical interstitial angiotensin II concentrations are markedly higher than plasma values. (b) Comparison of immunoreactive angiotensins in systemic plasma and star vessel plasma (efferent arteriolar, precapillary blood) by micropuncture of the rat kidney. Angiotensin II concentration is estimated to be ~10–25% of the immunoreactive angiotensins in various compartments. *(Results redrawn from published data [465,466]).*

Angiotensin II has a short half-life, and is itself degraded by angiotensinases to form several fragments, including angiotensin [1–7] and angiotensin [3–8]. Angiotensin-converting enzyme type 2 (ACE2) is a metalloprotease that hydrolyzes angiotensin I and angiotensin II to form the heptapeptide, angiotensin [1–7]. ACE2 is not blocked by conventional converting enzyme inhibitors. ACE2 reduces formation of angiotensin II by degrading angiotensin I to other fragments.[444,464,472] Angiotensin [1–7] is a dilator of the renal and other capillary beds,[473] and accumulates during ACE inhibition, potentially contributing to antihypertensive actions of those pharmaceuticals.[474] In the kidney, angiotensin [1–7] specifically binds to the Mas receptor. Mas-null mice lack binding, aortic relaxation, and antidiuretic response to angiotensin [1–7].[475] Renoprotective roles for angiotensin [1–7] are emerging.[476–478]

Aldosterone

Aldosterone increases transcription of molecular machinery dedicated to salt reabsorption in the distal nephron. It has been shown to increase mRNA for renin in juxtaglomerular cells in a manner that is blocked by the mineralocorticoid receptor antagonist, spironoloactone.[479] Recently, it has also been shown that aldosterone acts as a paracrine agent in the vasculature to have acute "nongenomic" effects on vasoactivity.[480] This was uncovered by Schmidt and colleagues, who showed that aldosterone increased human forearm blood flow. With NOS inhibition, aldosterone enhanced blood flow reduction mediated by phenyephrine. The data were interpreted to show that aldosterone causes vasoconstriction via smooth muscle activation and compensatory vasodilation via release of NO.[481] Similarly, Arima et al. showed that aldosterone caused concentration-dependent constriction of both afferent and efferent arterioles, an effect that was insensitive to spironoloactone. The constriction was prevented by PLC inhibition, involved voltage-gated Ca^{2+} entry mediated principally by L-type and T-type channels in the afferent and efferent arterioles, respectively, and is partially offset by NO generation.[482–485]

Adrenomedullin

Adrenomedullin and adrenomedullin-2/intermedin are peptide hormones with homology to calcitonin gene related peptide (CGRP). It circulates in picomolar concentrations and is widely synthesized by tissues including vascular smooth muscle and endothelium. It has potent vasodilatory and hypotensive effects, at least partially mediated by NO.[486–488] Deletion of the gene for adrenomedullin is lethal *in utero*.

Heterozygotes live to adulthood but are hypertensive, have defective synthesis of NO, and are vulnerable to renal ischemia.[489,490] Renal synthesis of adrenomedullin is enhanced by hypoxia.[491] Intrarenal infusion induces vasodilation that is attenuated by NO synthase inhibition[492–494] and was found to increase canine cortical and medullary blood flow.[493] Adrenomedullin has been shown to dilate both afferent and efferent arterioles of the hydronephrotic kidney preparation.[495] Chronic infusion of adrenomedullin was found to limit hypertensive injury in deoxycorticosterone (DOCA) salt hypertensive rats[496,497] and limits injury during ureteral obstruction.[498] It may partially act by limiting generation of reactive oxygen species.[499]

Intermedin, also known as adrenomedullin-2, shares many of the properties of adrenomedullin. Its receptor profile overlaps that of CGRP and adrenomedullin, and its adult expression is largely in the hypothalamus, pituitary, and kidney.[500,501] Intra-arterial infusion enhances renal blood flow and induces diuresis.[502] Like adrenomedullin, intermedin has been found to ameliorate renal tissue damage in pathological models,[503] and its expression is reduced in forms of renal injury.[504]

Nitric Oxide

Endothelia and transporting epthelia secrete paracrine modulators of vascular tone, including nitric oxide (NO), prostacyclin (prostaglandin I_2, PGI_2), and endothelium-derived hyperpolarizing factors (EDHF). Nitric oxide regulates vessel tone, regional distribution of blood flow, autoregulation, pressure natriuresis, tubuloglomerular feedback, and salt reabsorption. Its effects on the microcirulation of the kidney are protean and have been frequently reviewed.[382–385,457,505–517] Nitric oxide synthase (NOS) isoforms are expressed by nephrons and vessels throughout the kidney,[384,385,510,513] but expression is greatest in the inner medullary collecting duct and vasa recta.[518] It has also been shown that NO generation by collecting duct is regulated by uptake of L-arginine via the CAT1 cationic amino acid transporter.[519–522] Infusion of competing cationic amino acids reduced medullary NO, reduced medullary blood flow, and induced hypertension.[519] Asymmetric dimethyl arginine (ADMA) is an endogenous NOS inhibitor that is metabolized by dimethylaminohydrolase (DDAH).[523–525] ADMA equilibrates with the cytoplasm via cationic amino acid transporters (CATs), competes with their ability to transport L-arginine, and inhibits NOS.[524] The DDAH2 isoform predominates to remove ADMA in the vasculature. The role of ADMA and DDAH in endothelial function and dysfunction is the subject of much current investigation.[526,527]

Infusion of the NO synthase inhibitor Nw-nitro-L-arginine methyl ester (L-NAME) into the renal artery of rats and dogs increases renal vascular resistance and blunts pressure natriuresis.[528,529] NOS inhibition constricts the preglomerular microcirculation of the juxtamedullary nephron preparation, an effect that is enhanced when RBCs, that consume NO, are included in the perfusate.[530,531] The ability of NO to modulate afferent arteriolar tone results both from its synthesis by the endothelium[193–195,532] and signaling in the macula densa.[196] Similar to cortical microvessels, NOS inhibition constricts isolated DVR, largely by preventing the consumption of superoxide by NO.[425,438]

NOS inhibition interferes with pressure natriuresis.[531,533] Infusion of an NO synthase inhibitor into rats was found to restore medullary autoregulation and blunt the pressure natriuretic response.[383] Similarly, infusion of L-arginine both altered medullary autoregulation and normalized pressure natriuresis in the spontaneously hypertensive rat (SHR).[534] Exogenous L-arginine increases NO production in cultured cells and the isolated perfused kidney.[535] Moreover, it can abrogate hypertension and renal damage in hypertension induced by chronic angiotensin II infusion.[536,537]

Chronic, global NOS inhibition causes a selective reduction of renal medullary blood flow.[538,539] Nitric oxide (NO) production in the renal medulla exceeds that in the cortex.[385,540–543] L-arginine supplementation enhances NO levels in the renal medullary interstitium,[543] and abrogates hypertension in the Dahl rat and SHR.[534,544,545] In contrast to global NOS inhibition, reduction of nNOS activity induces hypertension without affecting medullary perfusion, suggesting that the saliuretic effects of NO generated by those isoforms is of predominant importance.[546–549] Thus, NO generated by eNOS may primarily affect basal vascular resistance, while NO derived from other NOS isoforms, particularly nNOS, affects renal epithelial Na^+ reabsorption and adaptation to a high-salt diet.[550–552]

NO is released in response to administration of the vasoconstrictor agents norepinephrine, angiotensin II, and vasopressin.[420,424,458,459,553,554] Evidence also favors an important role for NO to abrogate tissue hypoxia that would otherwise arise from the action of vasoconstrictors. Low dose, subpressor infusion of L-NAME into the renal interstitium does not affect MBF or pO_2, but enables otherwise ineffective doses of angiotensin II,[459] norepinephrine[553,554] or vasopressin[424,555] to reduce those parameters. Reduced expression of NOS isoforms and NO generation in the Dahl rat may contribute to its sensitivity to angiotensin II and hypertension.[458] In the absence of NOS blockade, constrictors enhance medullary NO levels, implying that a reflex increase in medullary NO probably serves to protect the hypoxic medulla from ischemia. NO generation has

also been found to protect the medulla from the blood flow redistribution induced by endotoxemic hypotension[556,557] and radiocontrast agents.[558]

Given that NO has both vasodilatory and saliuretic effects and is widely synthesized by nephrons and endothelium, attention has been drawn to possible tubulovascular interactions. NO generated by the medullary thick ascending limb has been proposed to influence DVR tone to mitigate medullary hypoperfusion and hypoxia.[269,382,394,395,450,559,560] NO generation by DVR is highly perfusion-dependent,[393] and NOS inhibition constricts *in vitro* perfused DVR, implying a substantial tonic role for intrinsic endothelial NO generation to modify DVR function.[425] The bioavailability and actions of NO are predicted to be under the influence of opposing generation of reactive oxygen species.[471,561] Mathematical simulations of NO and superoxide trafficking in the medulla favor a role for DVR endothelial NO generation to influence tissue NO levels,[469,470] leading to the consideration that DVR might influence salt reabsorption by adjacent nephrons. The latter might mechanistically link medullary perfusion and pressure natriuresis.[393] Stated another way, hemoglobin in outer medullary vascular bundles degrades NO so that NO from transporting epithelia and DVR endothelium must generate gradients directed toward the vascular bundle centers. Accordingly, elevation of NO outside vascular bundles in the vicinity of nephrons is likely to arise from both epithelial and endothelial NO generation.

Reactive Oxygen Species

Oxygen free radicals are generated by one and two electron reductions of O_2 that generate superoxide (O_2^-) and hydrogen peroxide (H_2O_2). In turn, reactions of those species yield hypochlorous acid and hydroxyl radical (OH). Reaction of NO with O_2^- forms peroxynitrite ($ONOO^-$), reducing the availability of NO to act as a vasodilator. Oxygen-derived radicals are collectively referred to as "reactive oxygen species" (ROS). ROS can be generated through many pathways. Autooxidation of cysteine can generate O_2^- and H_2O_2. Oxygen utilizing enzymes such as cyclooxygenase, lipoxygenase, epoxygenase, and xanthine oxidase can generate ROS. When oxidative stress reduces the ratio of the NOS co-factor tetrahydrobiopterin (BH_4) relative to dihydrobiopterin (BH_2), NOS produces O_2^- rather than NO. It is generally accepted that the dominant source of ROS for bacterocidal activity in leukocytes and signaling in other cells is NADPH oxidase. NADPH oxidase consists of cytosolic components ($p47^{phox}$, $p67^{phox}$), a G-protein (Rac1 or Rac2), and membrane-associated cytochrome b_{558} comprised of $p22^{phox}$ and $gp91^{phox}$. In nonphagocytic cells, the $gp91^{phox}$-subunit may be substituted by another isoform, such as RENOX/NOX4.[400] Antioxidant systems exist within all cells. Superoxide dismutase (SOD) catalyzes the conversion of O_2^- to H_2O_2 which is then converted to water by catalase. Extracellular, cytoplasmic (Cu/ZnSOD), and mitochondrial (MnSOD) forms of SOD participate in the control of oxidative stress. Endogenous free radical scavengers also serve to limit the potential for oxidative damage to cellular macromolecules.[562]

Tissue NO levels are modulated through reaction with ROS. Generation of oxygen free radicals is known to affect agonist-induced constriction of renal microvessels in cortex and medulla,[563–565] and play a prominent role in hypertension.[516,566] The cell permeant superoxide dismutase (SOD) mimetic, tempol, prevents afferent arteriolar constriction by the TxA_2/prostaglandin H_2 (TP) receptor agonist U-46,619.[567] Similarly, tempol increased detection of NO in bradykinin stimulated DVR and vasodilated DVR preconstricted with angiotensin II.[560] Zhang et al. found that ROS are generated upon stimulation of DVR with angiotensin II and protein kinase C agonists, and angiotensin II-stimulated ROS generation was enhanced when AT2 receptors were blocked with PD123,319.[451] The role of ROS in the mediation of vasoconstriction probably varies with the vasoactive stimulus.[568] Studies of ROS generation by the medullary thick ascending limb show that reactions with superoxide from the mTAL might limit NO delivery and vasodilation of vascular bundle DVR.[394,569,570]

Intrarenal generation of ROS plays a role in vasoactivity and generation of hypertension.[506,515,566,571,572] Blood pressure elevation in the SHR is associated with enhanced urinary excretion of the ROS marker, 8-iso prostaglandin F2α. Both hypertension and 8-Iso PGF2α excretion are blunted by the superoxide dismutase (SOD) mimetic, tempol. Infusion of L-NAME eliminates the antihypertensive effect of tempol, implying that reduction of NO availability through reaction with O_2^- partially underlies the genesis of SHR hypertension.[573,574] Slow pressor hypertension due to chronic infusion of angiotensin II is also associated with an increase in cortical ROS generation,[575] but the medulla may be spared in that model.[576] Intrarenal oxygen tension and the efficiency of renal oxygen utilization are low in rodent models of hypertension, suggesting a shunt of oxygen toward formation of ROS.[577–579]

Enhancement of renal medullary ROS generation occurs in hypertensive models and intramedullary infusion of the SOD inhibitor, diethylthiocarbamate, reduces medullary blood flow and raises arterial blood pressure.[580–582] Conversely, infusion of the SOD mimetic, tempol, increases medullary blood flow and

sodium excretion, an effect that is enhanced when H_2O_2 is eliminated with catalase.[580,581,583] A role for renal medullary generation of ROS was reinforced by Meng et al. who showed that hypertension of Dahl salt-sensitive rats is accompanied by reduced expression of Cu/Zn SOD and Mn SOD in the medulla.[584] In contrast to those findings, slow pressor hypertension generated by chronic angiotensin II infusion failed to increase ROS generation by isolated DVR.[576] Instead, angiotensin II hypertension was accompanied by increased DVR generation of NO, a finding that agrees with earlier reports by Zou and Cowley.[382,459] It is possible that ROS production by medullary nephrons contributes to angiotensin II, slow pressor hypertension. NO is an endogenous diuretic, and its consumption by ROS could favor hypertension.[550,551] Enhanced generation of ROS may also play a role in enhancing arteriolar constriction in diabetes.[316,585–589]

Carbon Monoxide and Hemoxygenase

Hemoxygenases-1 and -2 (HO-1, HO-2) are microsomal enzymes that degrade heme to form carbon monoxide (CO) and biliverdin. CO, like NO, induces vasodilation via cGMP generation, while biliverdin is converted to bilirubin by biliverdin reductase. Bilirubin is a highly effective free radical scavenger and inhibits ROS generation via NADPH oxidase and protein kinase C.[590] Constitutive expression of HO isoforms in the kidney predominate in the medulla[591] under transcriptional control of oxygen and superoxide anion. Hypoxia inducible factor α1,[592,593] urea concentration, and medullary hypertonicity[594] all influence HO expression. HO inhibition with zinc deuteroporphyrin 2,4-bis glycol via the renal interstitium reduces medullary blood flow and cGMP content.[591] Treatment with cobalt protoporphyrin upregulates HO-1, reduces intrarenal levels of 20-HETE, and ameliorates SHR hypertension.[595] Exacerbation and protection of the kidney from ischemic injury can be accomplished by inhibiting or upregulating HO-1.[596] Acute HO inhibition blunts pressure natriuresis, and chronic inhibition raises blood pressure.[597–599] HO pre-induction blocks slow-pressor angiotensin II-induced hypertension.[600,601] Inducing HO also minimizes radiocontrast injury.[602,603] The protean and beneficial effects of HO upregulation have attracted considerable attention, pointing to a potential target for therapeutic intervention.[590,604]

Adenosine and P1 Purinoceptors

Adenosine acts via A1, $A2_A$, $A2_B$, and A3 receptors (P_1 purinoceptors). In the kidney, A1 and A2 receptors predominate, $A2_A$ are primarily vascular, and A3 may be absent.[605,606] Through its action, adenosine modulates vasoactivity and epithelial transport.[605,607–610] Acting via the P2X1 receptor, adenosine may be a primary mediator of renal autoregulation.[611] The microvascular effects of adenosine vary with intrarenal location.[612] Adenosine A1 receptor activation transiently reduces cortical and medullary blood flow, and constricts afferent arterioles.[613–615] When afferent A1 receptors are blocked, however, A2 mediated vasodilation can be elicited.[616] The effects of adenosine in the efferent arteriole may be primarily vasodilatory.[153,617,618] Afferent constriction by adenosine is of particular importance, because evidence supports it as a key mediator of tubuloglomerular feedback (TGF).[619–624] ATP release from macula densa cells via maxi-anion channels followed by ecto-5′-nucleotidase-mediated hydrolysis are the likely steps in its formation.[366–368,370,625] A role for adenosine to act on both afferent and efferent arterioles has been proposed as integral to the TGF response.[153,626] Adenosine constriction of the afferent arteriole is complex, because proximal portions away from the glomerulus may be regulated by both A2-mediated dilatory and A1-mediated contractile interactions. In contrast, the afferent arteriole near the glomerlar hilus may lack A2 receptors, so that it constricts as adenosine concentration is increased.[264,607]

Adenosine A2 receptor stimulation leads to preferential vasodilation, saliuresis, and enhanced perfusion of the medulla[612,613,627](Figure 24.26). Both A1 and A2 receptors are expressed by DVR,[628] and their respective stimulation induces constriction or dilation.[396] Interstitial adenosine concentrations are near the affinity for the A2 receptor, so that changes should modulate vasodilatory and saliuretic effects.[629] In preglomerular vessels, A1-induced constriction is mediated by pertussis toxin sensitive G_i-protein and phospholipase C activation.[630] A2-mediated dilation has been traced to activation of K_{ATP} channels,[313] probably activated through 11,12-epoxyeicosatrienoic acid.[631]

Evidence for and against synergism between angiotensin II and adenosine exists.[197,625] Several studies have favored the interdependence of adenosine A1 receptor- and angiotensin II AT1 receptor-mediated constriction,[632–636] while others have not.[614,637,638] The availability of adenosine A1 and angiotensin II $AT1_A$ receptor-deficient mice have permitted re-examination of the issue. Infusion of angiotensin II led to less reduction of renal blood flow and less constriction of afferent arterioles in A1 knockout mice.[197] Similarly, favoring synergism, intranephron infusion of an adenosine A1 agonist induced greater reduction of stop-flow pressure (reflecting afferent constriction) in wild-type than in angiotensin II $AT1_A$ receptor-deficient mice.[639]

A consequence of countercurrent exchange is that renal medullary oxygen tensions (pO_2) are low[640]

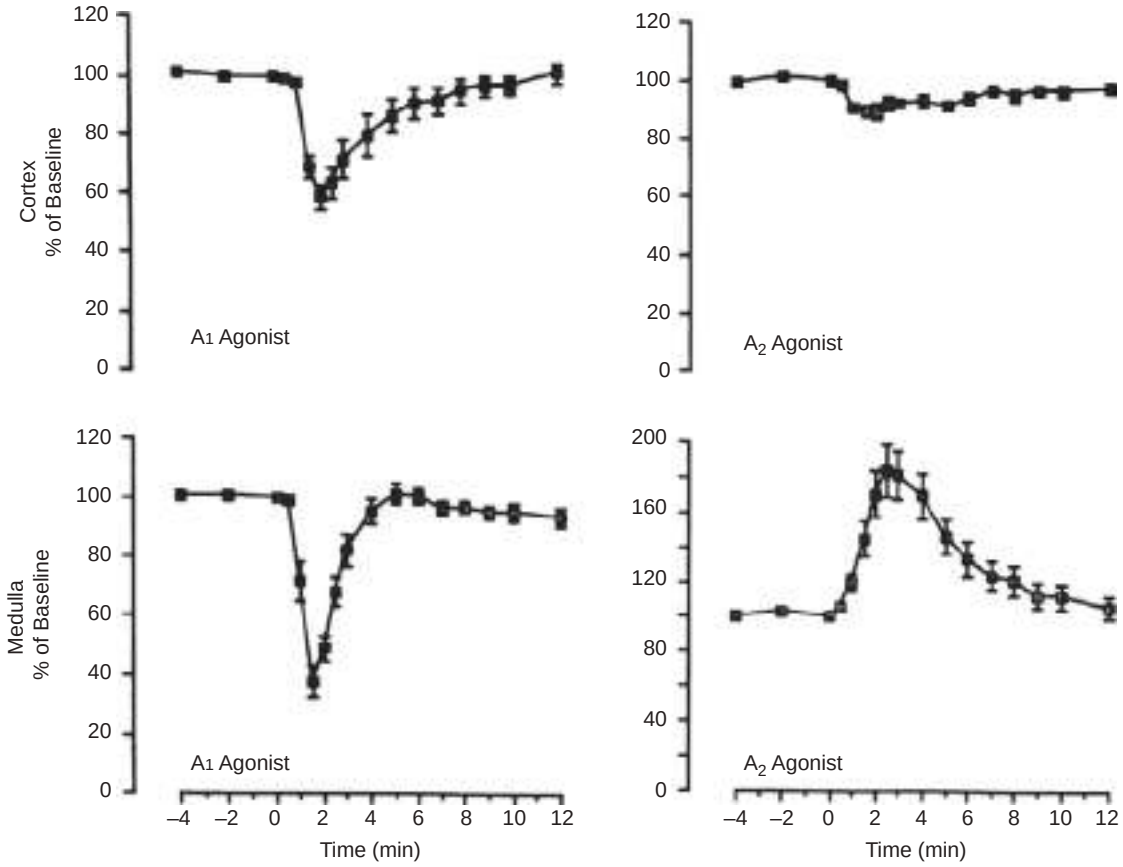

FIGURE 24.26 **Effect of intrarenal infusion of adenosine receptor A1 or A2 subtype agonists.** Top and bottom panels show the effect of adenosine agonist infusions on intrarenal blood flow. Cortical and medullary measurements were obtained using laser-Doppler flowmetry with optical fibers placed on the kidney surface or inserted into the renal parenchyma, respectively. Left and right panels show the respective effects of either A1 or A2 receptor stimulation with subtype specific agonists. At time = 0, the A1 agonist N^6-cyclopentyladenosine (left panels) or the A2 agonist CGS-21680C (right panels) were transiently infused (1 minute) into the renal parenchyma. The A1 agonist transiently reduced both cortical and medullary blood flow, while the A2 agonist caused a preferential increase in blood flow to the medulla. *(Reproduced with permission from ref. [613,465]).*

(Figure 24.27). During hypoxia, the medullary thick ascending limb of Henle (mTAL) synthesizes adenosine.[641] That finding, coupled with the close proximity of the mTAL to outer medullary vascular bundles, led to the hypothesis that adenosine, like NO and prostaglandins (see above), acts as a paracrine vasodilator to preserve medullary perfusion, raising medullary pO_2.[642] Inhibition of mTAL transport by adenosine A2 receptor activation, like the effects of furosemide, probably raises medullary pO_2 by reducing O_2 consumption.[642,643] Rats fed a high-salt diet increase tissue adenosine levels and downregulate A1 receptor expression, the activation of which encourages sodium reabsorption.[644]

Extracellular ATP and Renal P_2 Purinoceptors

In addition to the actions of adenosine mediated by P1 purinoceptors (A1, A2 adenosine receptors), micromolar concentrations of ATP modulate vasoactivity through P2 purinoceptors.[611,625,638,645–647] P2 receptors are subdivided into P2X and P2Y families, encoded by separate genes, that yield either ligand-gated nonselective cation channels or seven transmembrane spanning G-protein coupled receptors, respectively. Unlike adenosine receptors, P2 receptors seem confined to the preglomerular microcirculation.[648–650] P2 antagonists such as suramin are somewhat nonselective, however α,β-methylene-ATP and β,γ-methylene-ATP are relatively selective agonists for P2X receptors. UTP largely stimulates P2Y.[638,648,651,652] The experimental effects of ATP on the vasculature are variable, depending upon luminal versus abluminal application, the preparation, and species.[651] Both constrictor and dilator effects can be observed. Intrarenal infusion of α,β-methylene-ATP leads to constriction, but ATP (mixed P2X, P2Y agonist) and UTP (selective P2Y agonist) yield NO dependent dilation at low concentrations or constriction at high

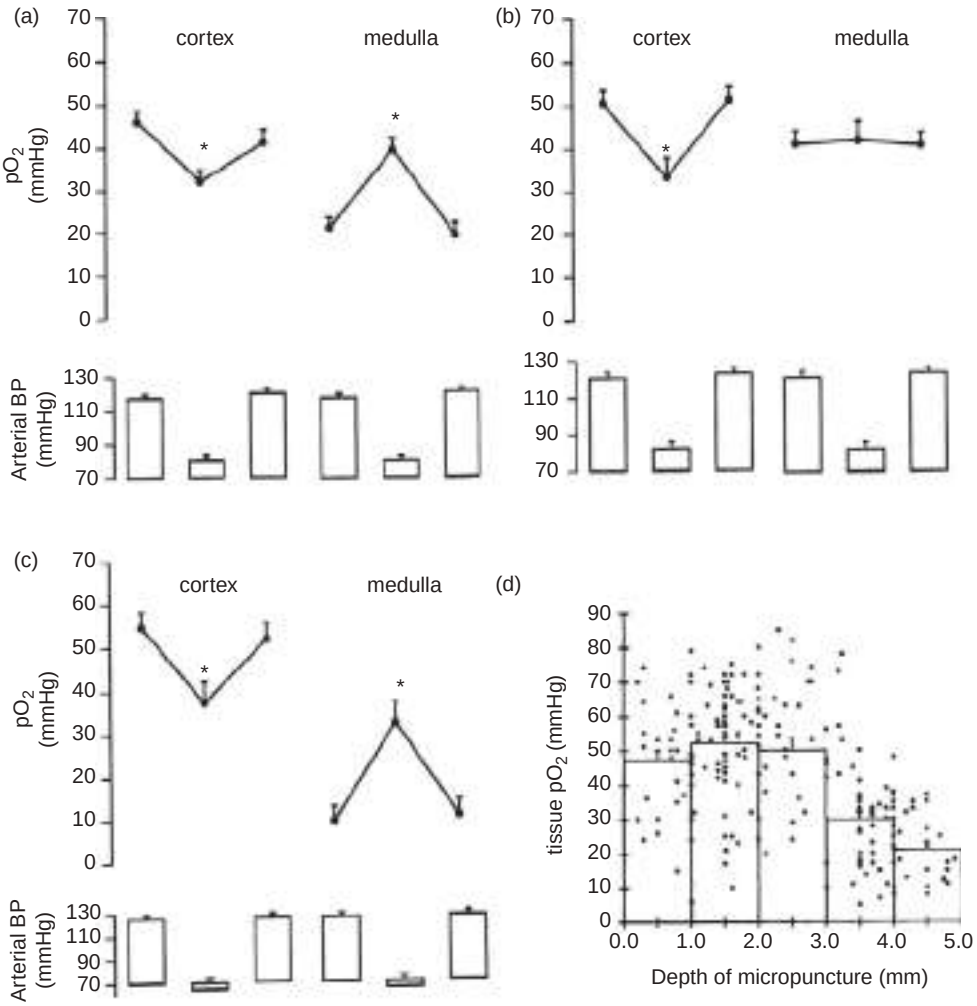

FIGURE 24.27 **Hemodynamic effects on intrarenal oxygenation.** Intrarenal oxygen tension (pO_2) was measured in the cortex and medulla with a microelectrode. Cortical pO_2 falls and medullary pO_2 increases during an episode of hypotension induced by hemorrhage, aortic ligation or nitroprusside infusion (Panel a). Inhibition of transport in the thick ascending limb of Henle with a loop diuretic (Panel b) increases basal pO_2 in the medulla (compare to Panel a), and eliminates the effect of hypotension to raise medullary pO_2. Inhibition of vasodilatory prostaglandins and nitric oxide or blockade of adenosine receptors reduces basal pO_2 in the medulla and accentuates the increase in pO_2 caused by hypotension (Panel c). Intrarenal tissue pO_2 decreases with medullary depth (Panel d). *(Reproduced with permission from ref. [643,791]).*

concentrations.[653] Exposure of preconstricted afferent arterioles of rabbit and human kidneys to ATP leads to dilation via NO generation.[647,651,654] In the juxtamedullary nephron preparation of the rat, activation of P2X leads to afferent but not efferent constriction that is dependent upon generation of 20-HETE and Ca^{2+} influx involving L-type Ca^{2+} channel blockade.[655–658] Stimulation of P2Y receptors yields sustained constriction that is independent of 20-HETE, and dependent upon Ca^{2+} release from cellular stores.[213,659,660]

Of great importance, myogenic autoregulatory constriction of afferent arterioles has been traced to activation of P2 receptors (Figure 24.28). In the juxtamedullary nephron preparation, prior desensitization or nonspecific blockade of P2 receptors attenuated pressure-induced afferent constriction.[661] Similarly, infusion of excess ATP into the dog kidney during NO sythase blockade eliminated autoregulatory constriction.[662,663] Finally, P2X1 receptor-deficient mice were shown to retain tubuloglomerular feedback responses, but to lack autoregulatory adjustments to changes in perfusion pressure.[611,645,664] Pharmacological blockade of P2X1 receptors eliminates renal whole-organ autoregulation in the rat.[611]

Arachidonic Acid Metabolites

Once liberated from the membrane by phospholipases, arachidonic acid undergoes metabolism to a very large array of metabolites that function as paracrine, autocrine, and intracellular signaling molecules (Figure 24.29). These metabolites have profound effects

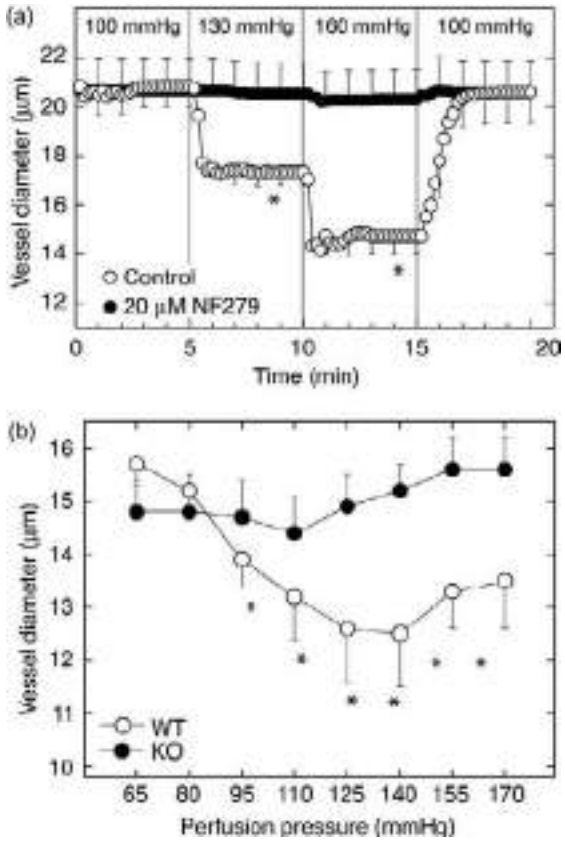

FIGURE 24.28 **Autoregulation and purinoceptors.** (a) Panel shows the effect of a P2X receptor blocker (NF279) on autoregulatory afferent arteriolar constriction resulting from step-changes in perfusion pressure from 100 to 120 and 160 mmHg. P2X blockade eliminates the afferent myogenic response associated with autoregulation. (b) Summary of the changes in murine afferent arteriolar diameter elicited by graded change of perfusion pressure. Autoregulatory vasoconstriction occurs in wild-type (WT) but not $P2X_1$ receptor-null mice. Data obtained using the juxtamedullary nephron preparation. *(Reproduced with permission from ref. [664]).*

on vascular tone, as well as on solute and water excretion. Three generalized pathways are recognized, cyclo-oxygenases (COX) that generate prostaglandins (PG) and thromboxanes (TBX), lipoxygenases that generate leukotrienes (LT) and hydroxyeicosatetraenoic acids (HETE), and cytochrome P450 pathways that synthesize HETEs and epoxyeicosatrienoic acids (EET).

Prostaglandins

Prostaglandins (PGs) are generated from arachidonic acid by cyclooxygenase (COX) (Figure 24.29a) and exert wide effects on solute reabsorption, tubuloglomerular feedback, and intrarenal hemodynamics. When injected into the renal artery, PGE_2 and PGI_2 enhance renal blood flow.[665] Early efforts showed that stimulation of PG synthesis redistributes blood flow toward the juxtamedullary cortex.[666,667] A consistent finding has been that renal medullary perfusion is protected from vasoconstrictors by NO (see above) and PGs.[668,669] Nonselective COX blockade decreased vasa recta blood flow,[670] and augmented the ability of angiotensin II infusion to decrease single vessel blood flow in the exposed papilla.[428] Laser-Doppler studies indicate that COX blockade reduces medullary blood flow with relative sparing of cortical perfusion.[671–674] Radiocontrast agents can lower cortical and medullary oxygen content, predisposing to hypoxic insult. Indomethacin potentiates medullary hypoxia and the parenchymal damage induced by either radiocontrast agents or ureteral excision.[675–677]

COX-1 and COX-2 isoforms contribute to renal PG synthesis. Of the two, COX-1 is expressed to a greater extent, while COX-2 is more highly regulated.[678–682] In a manner that predicts the effects of its inhibition, COX-2 expression is pronounced in macula densa.[678] Release of renin by juxtaglomerular cells and release of PGE_2 by the macula densa is COX-2-dependent.[683–685] In the macula densa, COX-2 is co-expressed with NOS1. Simultaneous inhibition of COX-2 and NOS in the dog markedly enhances sensitivity to vasoconstriction. Norepinephrine infusion, which otherwise has minor effects, induces a remarkable rise in renal vascular resistance and sharp reduction of GFR.[686] COX-2 blockade blunts adaptation of tubuloglomerular feedback[687] and augments afferent constriction associated with benzolamide inhibition of proximal transport.[688] Renomedullary interstitial cells express receptors for vasoconstrictors, release paracrine substances such as PGE_2 and medullipin, and express both COX-1 and COX-2.[41,678] Zhang et al. showed that COX-2 expression is stimulated by medullary tonicity.[689] Genetic deficiency of COX-2 or its inhibition leads to reduction of medullary perfusion, salt-sensitive hypertension, and enhanced response to infusion of angiotensin II.[690–694]

In isolated vessels, Edwards first showed that prostaglandins dilate *in vitro* perfused rabbit afferent (PGE_2 and PGI_2) and efferent (PGI_2) arterioles.[695] In contrast, Inscho et al. found that PGE_2 enhanced angiotensin II and norepinephrine constriction of the afferent arteriole, while PGI_2 counteracted their effects.[696] In rabbit afferent arterioles, indomethacin enhanced vasoconstriction when perfusate passed through the glomerulus, but not during retrograde perfusion, implying that glomerular PGs influence efferent vasoactivity.[697] Abluminal PGE_2 blunts angiotensin II-induced constriction of DVR.[198,397] Few studies of the effects of selective COX-2 inhibition in isolated vessel preparations are available. Wang et al. determined that augmented constriction of afferent arterioles during slow pressor angiotensin II hypertension is partially mediated by a COX-2 product from the endothelium.[698] PGE_2 is very abundant in the kidney, and its local actions are governed by the receptor subtype activated.

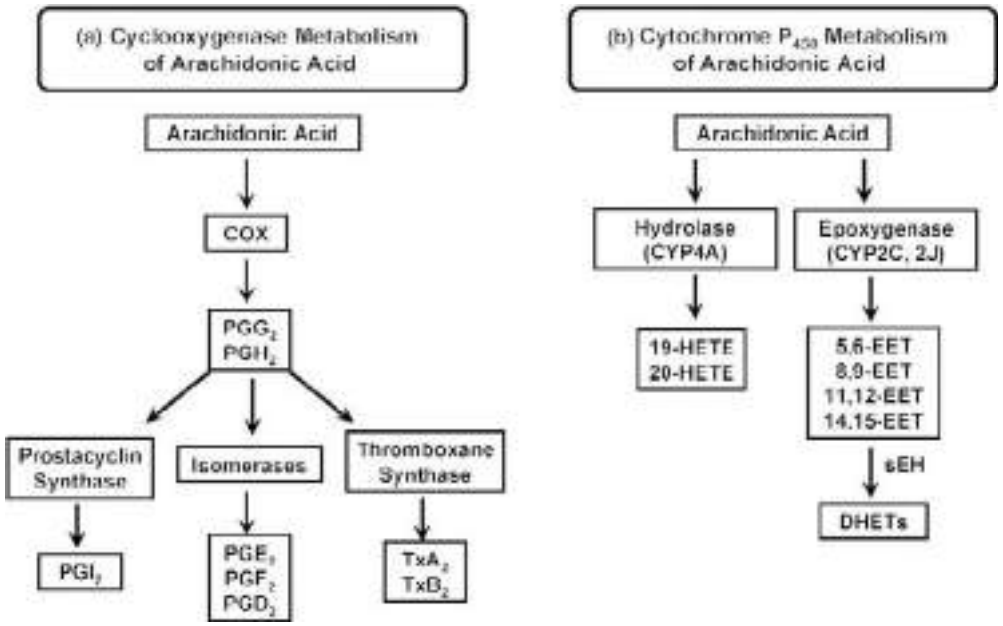

FIGURE 24.29 **Arachidonic acid metabolites.** (a) Abbreviated schematic showing signaling molecules generated from arachadonic acid by cyclo-oxygenase (COX). Prostaglandins (PG) and thromboxanes (Tx) are vasoactive end products. (b) Abbreviated schematic showing signaling molecules generated cytochrome P450 metabolism of arachidonic acid (COX). Hydrolases generate the potent constrictor 20-hydroxyeicosatetraenoic acid (20-HETE), and epoxygenases generate the epoxyeicosatrienoic acids (EETs) that most often function as vasodilators. The lipoxygenase pathway of arachidonic acid metabolism is not shown.

For example, stimulation of the EP3 receptor inhibits cAMP formation, favoring vasoconstriction, while stimulation of EP2 and EP4 receptors increases cAMP, favoring vasodilation.[297] The ability of PGE_2 to act as a vasoconstrictor has also been observed,[696] and EP3 receptor deficiency leads to reduction of renal vascular resistance.[297,699]

COX products can be metabolized by thromboxane synthase to stimulate the thromboxane/PGH_2 receptor and induce vasoconstriction. In the afferent arteriole and DVR, angiotensin II-induced constriction is reduced by TP receptor blockade, inhibition of COX with indomethacin or inhibition of thromboxane synthesis.[440,700–702] Thromboxane-mediated constriction may be exaggerated during angiotensin II slow pressor hypertension, due to enhanced sythesis of reactive oxygen species.[698,703]

Cytochrome P450 Metabolites of Arachadonic Acid

Vasoactive products of arachidonic acid are generated by cytochrome P450 (CYP) isoforms (Figure 24.29B) in the form of epoxyeicosatrienoic acids (EETs), the hydroxyeicosatetraenoic acids (HETEs) and their products, dihydroxyeicosatetraneoic acids (DHETs).[704] More than 400 CYP isoforms are recognized in various species. Those that have >40% homology are classified by an Arabic numeral and those with >55% homology by a capital letter. CYP monooxygenases metabolize arachadonic acid to 19- and 20-HETE (ω/ω-1 hyroxylase) and to 5,6-, 8,9-, 11,12-, and 14,15-EETs (epoxygenases). For the purposes of focusing on the microvasculature of the kidney, it is important to recognize that CYP2C and CYC2J isoforms are largely responsible for synthesis of EETs, and CYP4A isoforms for synthesis of the HETEs. This topic has been frequently reviewed.[280,291,704–714]

The 20 ω-hydroxylation product, 20-HETE, is a potent vasoconstrictor the synthesis of which is rate-limited by O_2.[715,716] 20-HETE depolarizes and increases $[Ca^{2+}]_{CYT}$ in smooth muscle[290] and mediates constriction by angiotensin II,[436,717] endothelin-1,[708,718] and ATP via P2X stimulation.[658] 20-HETE plays an important role in blood flow autoregulation of the cerebral and renal microcirculations.[704,719] 20-HETE inhibits K_{Ca} channel activity[292–294,299,713,716] through the actions of tyrosine and MAP kinases.[293] It is generally recognized that NO inhibits vascular smooth muscle contraction through cGMP formation. Roman and colleagues have shown that the majority of NO effects in the kidney involve inhibition of CYP4A and reduction of 20-HETE synthesis.[300,720] 20 ω-Hydroxylation products play a role in blood pressure regulation, and blockade of 20-HETE synthesis interferes with pressure natriuresis.[721] Chronic inhibition of 20-HETE synthesis induces salt-sensitive hypertension in the rat,[722,723] and exacerbates ischemia reperfusion injury.[711] Similarly, disruption of murine CYP4A14 leads to hypertension, and a variant of the CYP4A11 homolog in humans has been associated with essential hypertension.[724–726]

The EET epoxygenase metabolite arachidonic acid has several important roles in the renal microcirculation. In addition, EETs have been broadly identified as endothelium-dependent hyperpolarizing factors (EDHF).[97,278] The EETs are largely vasodilatory, but some of their metabolites can induce COX-dependent vasoconstriction.[297,727,728] Stimulation of preglomerular arteriolar $A2_A$ adenosine receptors leads to enhanced synthesis of EETs and vasodilation.[631] Similarly, angiotensin II dilation via AT2 receptor stimulation has been traced to these epoxygenase products.[436,446] Afferent vasodilation by 11,12-EET is partially mediated by PKA.[729] In contrast to inhibition by 20-HETE, 11,12-EET and 5,6-EET are associated with K_{Ca} channel activation.[292,295,713,730–732]

The ability to activate large conductance K_{Ca} channels may be tied to the role of 11,12-EET as an EDHF. Putative EDHFs are agents that elevate endothelial $[Ca^{2+}]_{CYT}$, hyperpolarize endothelium and smooth muscle and vasodilate, independent of NO and COX. Work in this area has failed to identify a single EDHF, but much evidence points to a role for EET formation and K_{Ca} channel activation in the endothelium. Adjacent smooth muscle hyperpolarization may be tied to diffusion of secondary signaling molecules or electrogenic spread of current from the endothelium via myoendothelial gap junctions.[279,280] It might also be tied to release of K^+ ion into the myoendothelial intercellular space via EET-stimulated endothelial K_{Ca} channels, resulting in hyperpolarization via activation of smooth muscle K_{IR} or Na^+,K^+-ATPase.[97,278] In the kidney, evidence points to a role for afferent arteriolar EET formation in the EDHF related actions of bradykinin[733] and acetylcholine.[298] Evidence for K_{IR} expression in afferent smooth muscle has been provided.[304,305] Reduction of vasodilatory EET formation may accompany hypertension. Imig et al. showed that enhanced afferent constriction during slow pressor angiotensin II hypertension is reversed by an 11,12-EET analog, and that reduction of EET degradation through soluble epoxide hydrolase inhibition reverses angiotensin II hypertension.[734,735] Lack of ability to upregulate CYP2C and CYP2J isoforms of P450 might underlie the abnormality.[736] Similarly, it has been found that enhancement of EET through inhibition of soluble epoxide hydrolase reverses hypertension, and protects the kidney from damage.[694,706,707,737,738]

Endothelins

Endothelins are 21 amino acid vasoactive peptides synthesized by a variety of cell types in the kidney. Three ETs have been identified (ET1, ET2, ET3). These agents are autocrine/paracrine hormones derived from ~200 amino acid preproendothelins that undergo successive proteolytic cleavage to form large (Big ET) intermediates that are processed by endothelin-converting enzymes. ETs stimulate ETA and ETB receptors on smooth muscle to induce potent vasoconstriction. Endothelia express ETB receptors, stimulation of which leads to synthesis of NO. In addition to their vascular actions, ETs have an important role to inhibit sodium reabsorption through inhibition of transport by NO and downregulation of the epithelial Na^+ of the collecting duct.[739–742] Renal ET receptors have been identified on collecting ducts, vascular bundles, and RMIC.[743–745]

The highest concentrations of ET1 occur in the renal medulla where it is synthesized by collecting duct and other cells.[746,747] ET1 is a potent vasoconstrictor and reduces overall renal blood flow via combined ETA and ETB stimulation. Isolated ETB receptor stimulation, however, can have net vasodilatory effects.[748] In the renal cortex, ET1 constricts afferent and efferent arterioles, arcuate and interlobular arteries.[2,749–754] Afferent constriction by ET1 partially depends upon voltage-gated Ca^{2+} entry, is modulated by endothelial generation of NO,[195,755] and is mediated by 20-HETE and COX products.[708,718] Preglomerular smooth muscle cells show biphasic $[Ca^{2+}]_{CYT}$ responses to ETA agonists, but small or absent responses to ETB agonists.[756–758] Isolated DVR from the outer medulla are intensely constricted by low concentrations of endothelins.[27,269,397]

The actions of ETB stimulation in the medulla favor natriuresis and vasodilation, at least partially by activating NO generation through NOS1.[743,759,760] Bolus injection of ET1 (a mixed ETA and ETB receptor agonist) selectively reduced cortical blood flow while transiently increasing medullary blood flow. Medullary vasodilation and saliuresis is abrogated by blocking ETB receptors or synthesis of NO.[423,752,753,761,762] The effects on medullary blood flow may vary with dietary salt intake.[763] ETB receptor deficient "spotted lethal" rats have been identified that have been rescued from lethal abnormalities by selective ETB gene replacement into ganglionic cells of the intestine. Those rats have salt-sensitive hypertension.[764,765] Injection of Big ET1 into ETB receptor-deficient rats or wild-type rats in which ETB receptor has been blocked fails to elicit saliuresis.[753,766] Chronic angiotensin II infusion, combined with salt-loading, increases cortical and medullary immunoreactive ET.[767,768] Reduction of endothelin-induced saliuresis may play a role in human and rodent models of hypertension.[740,767,769–771] ETs might play a significant roles in other pathological states.[743,747,772]

Natriuretic Peptides

The diuretic effect of injection of extracts of atrial tissue extracts into rats led to the discovery of atrial

(ANP), brain (BNP), and C natriuretic peptides (CNP). Each is derived by proteolytic cleavage of different gene products. They act through stimulation of guanylyl cyclase A (GC-A) (ANP, BNP ligands), GC-B type (CNP ligand), and GC-C receptors. GC-C may play a role in peptide clearance and inhibition. Deletion of ANP or its receptor leads to hypertension, while overexpression results in hypotension.[773] In the kidney, expression and alternate processing of ANP prohormone yields urodilatin.[774,775] Studies showed that that ANP infusions increased renal blood flow, glomerular filtration rate, papillary plasma flow, and sodium excretion. Diuresis and natriuresis, however, begin before the increase in medullary blood flow, so that medullary dilation is not required for the natriuretic effect.[776–779] Examination of the vasoactive effects of natriuretic peptides generally uncovered dilation of preglomerular vasculature.[780–783] Edwards and Weidley found no effect of ANP on *in vitro* perfused rabbit afferent or efferent arterioles.[784] In the efferent arteriole, either a lack of effect[783,784] or constriction[785] was reported, while urodilatin mediated vasodilation.[786] Vasodilatory effects of ANP may be mediated through cGMP formation, activation of smooth muscle K_{Ca} channels, hyperpolarization and inhibition of Ca^{2+} signaling.[320,332] Natriuresis from an oral salt load is more brisk than that from an intravenous route, a finding that may be related to intestinal release of guanylin and uroguanylin, peptide hormones that activate ANP receptors. Like ANP, these agents inhibit tubuloglomerular feedback, but their specific effects on renal arterioles have not been reported.[787,788] Trials of ANP as a renoprotective agent have yielded inconclusive results.[789]

Acknowledgments

Efforts have been supported by NIH R37 DK42495, R01 DK67621, and P01 HL078870.

References

[1] Navar LG, Arendshorst WJ, Pallone TL, Inscho EW, Imig JD, Bell PD. The Renal Microcirculation. In: Tuma RF, Duran WN, Ley K, editors. Handbook of physiology: microcirculation. San Diego: Elsevier; 2008. p. 550–683.
[2] Navar LG, Inscho EW, Majid SA, Imig JD, Harrison-Bernard LM, Mitchell KD. Paracrine regulation of the renal microcirculation. Physiol Rev 1996;76:425–536.
[3] Bankir L, Bouby N, Trinh-Trang-Tan MM. Heterogeneity of nephron anatomy. Kidney Int Suppl 1987;20:S25–39.
[4] Bankir L, de Rouffignac C. Urinary concentrating ability: insights from comparative anatomy. Am J Physiol 1985;249: R643–66.
[5] Bankir L, Kaissling B, de Rouffignac C, Kriz W. The vascular organization of the kidney of *Psammomys obesus*. Anat Embryol (Berl) 1979;155:149–60.
[6] Kaissling B, de Rouffignac C, Barrett JM, Kriz W. The structural organization of the kidney of the desert rodent *Psammomys obesus*. Anat Embryol (Berl) 1975;148:121–43.
[7] Kaissling B, Kriz W. Structural analysis of the rabbit kidney. Adv Anat Embryol Cell Biol 1979;56:1–123.
[8] Kriz W. Structural organization of the renal medulla: comparative and functional aspects. Am J Physiol-Regul, Integr Comp Physiol 1981;241:R3–16.
[9] Kriz W, Napiwotzky P. Structural and functional aspects of the renal interstitium. Contrib Nephrol 1979;16:104–8.
[10] Fourman J, Moffat DB. The effect of intra-arterial cushions on plasma skimming in small arteries. J Physiol 1961;158:374–80.
[11] Fourman J, Moffat DB. The blood vessels of the kidney. Blackwell Scientific, Oxford, UK. 1971.
[12] Moffat DB, Creasey M. The fine structure of the intra-arterial cushions at the origins of the juxtamedullary afferent arterioles in the rat kidney. J Anat 1971;110:409–19.
[13] Pappenheimer JR, Kinter WB. Hematocrit ratio of blood within mammalian kidney and its significance for renal hemodynamics. Am J Physiol 1956;185:377–90.
[14] Beeuwkes III R. The vascular organization of the kidney. Ann Rev Physiol 1980;42:531–42.
[15] Jamison RL, Kriz W. Urinary concentrating mechanism: structure and function. New York-Oxford, Oxford University Press, 1982.
[16] Casellas D, Mimran A. Shunting in renal microvasculature of the rat: a scanning electron microscopic study of corrosion casts. Anat Rec 1981;201:237–48.
[17] Pallone TL, Robertson CR, Jamison RL. Renal medullary microcirculation. Physiol Rev 1990;70:885–920.
[18] Aukland K, Bogusky RT, Renkin EM. Renal cortical interstitium and fluid absorption by peritubular capillaries. Am J Physiol 1994;266:F175–84.
[19] Pedersen JC, Persson AEG, Maunsbach AB. Ultrastructure and quantitative characterization of the cortical interstitium in the rat kidney. Functional ultrastructure of the kidney. London: Academic Press; 1980443–457
[20] Lemley KV, Kriz W. Anatomy of the renal interstitium. Kidney Int 1991;39:370–81.
[21] Wolgast M, Larson M, Nygren K. Functional characteristics of the renal interstitium. Am J Physiol 1981;241:F105–11.
[22] Beeuwkes III R, Bonventre JV. Tubular organization and vascular–tubular relations in the dog kidney. Am J Physiol 1975;229:695–713.
[23] Evan AP, Dail Jr WG. Efferent arterioles in the cortex of the rat kidney. Anat Rec 1977;187:135–45.
[24] Lemley KV, Kriz W. Cycles and separations: the histotopography of the urinary concentrating process. Kidney Int 1987;31:538–48.
[25] Pannabecker TL, Dantzler WH. Three-dimensional architecture of inner medullary vasa recta. Am J Physiol Renal Physiol 2006;290:F1355–66.
[26] Kriz W. Structural organization of the renal medulla: comparative and functional aspects. Am J Physiol 1981;241:R3–16.
[27] Pallone TL, Silldorff EP. Pericyte regulation of renal medullary blood flow. Exp Nephrol 2001;9:165–70.
[28] Park F, Mattson DL, Roberts LA, Cowley Jr AW. Evidence for the presence of smooth muscle alpha-actin within pericytes of the renal medulla. Am J Physiol 1997;273:R1742–8.
[29] Mink D, Schiller A, Kriz W, Taugner R. Interendothelial junctions in kidney vessels. Cell Tissue Res 1984;236:567–76.
[30] Schwartz MM, Karnovsky MJ, Vehkatachalam MA. Ultrastructural differences between rat inner medullary descending and ascending vasa recta. Lab Invest 1976;35:161–70.
[31] Pallone TL, Turner MR, Edwards A, Jamison RL. Countercurrent exchange in the renal medulla. Am J Physiol Regul Integr Comp Physiol 2003;284:R1153–75.

[32] Zhai XY, Thomsen JS, Birn H, Kristoffersen IB, Andreasen A, Christensen EI. Three-dimensional reconstruction of the mouse nephron. J Am Soc Nephrol 2006;17:77–88.
[33] Franchini KG, Cowley Jr AW. Renal cortical and medullary blood flow responses during water restriction: role of vasopressin. Am J Physiol 1996;270:R1257–64.
[34] Holliger C, Lemley KV, Schmitt SL, Thomas FC, Robertson CR, Jamison RL. Direct determination of vasa recta blood flow in the rat renal papilla. Circ Res 1983;53:401–13.
[35] Marsh DJ, Segel LA. Analysis of countercurrent diffusion exchange in blood vessels of the renal medulla. Am J Physiol 1971;221:817–28.
[36] Pannabecker TL, Dantzler WH. Three-dimensional architecture of collecting ducts, loops of Henle, and blood vessels in the renal papilla. Am J Physiol Renal Physiol 2007;293:F696–704.
[37] Knepper MA, Danielson RA, Saidel GM, Post RS. Quantitative analysis of renal medullary anatomy in rats and rabbits. Kidney Int 1977;12:313–23.
[38] Takahashi-Iwanaga H. The three-dimensional cytoarchitecture of the interstitial tissue in the rat kidney. Cell Tissue Res 1991;264:269–81.
[39] Hughes AK, Barry WH, Kohan DE. Identification of a contractile function for renal medullary interstitial cells. J Clin Invest 1995;96:411–6.
[40] Thomas CJ, Woods RL, Evans RG, Alcorn D, Christy IJ, Anderson WP. Evidence for a renomedullary vasodepressor hormone. Clin Exp Pharmacol Physiol 1996;23:777–85.
[41] Zhuo JL. Renomedullary interstitial cells: a target for endocrine and paracrine actions of vasoactive peptides in the renal medulla. Clin Exp Pharmacol Physiol 2000;27:465–73.
[42] Zusman RM, Keiser HR. Prostaglandin biosynthesis by rabbit renomedullary interstitial cells in tissue culture. Stimulation by angiotensin II, bradykinin, and arginine vasopressin. J Clin Invest 1977;60:215–23.
[43] Kim J, Pannabecker TL. Two-compartment model of inner medullary vasculature supports dual modes of vasopressin-regulated inner medullary blood flow. Am J Physiol Renal Physiol 2010;299:F273–9.
[44] Pannabecker TL. Loop of Henle interaction with interstitial nodal spaces in the renal inner medulla. Am J Physiol Renal Physiol 2008;295:F1744–51.
[45] Pannabecker TL, Henderson CS, Dantzler WH. Quantitative analysis of functional reconstructions reveals lateral and axial zonation in the renal inner medulla. Am J Physiol Renal Physiol 2008;294:F1306–14.
[46] Yuan J, Pannabecker TL. Architecture of inner medullary descending and ascending vasa recta: pathways for countercurrent exchange. Am J Physiol Renal Physiol 2010; 299:F265–72.
[47] Pannabecker TL, Abbott DE, Dantzler WH. Three-dimensional functional reconstruction of inner medullary thin limbs of Henle's loop. Am J Physiol Renal Physiol 2004;286:F38–45.
[48] Pannabecker TL, Dantzler WH. Three-dimensional lateral and vertical relationships of inner medullary loops of Henle and collecting ducts. Am J Physiol Renal Physiol 2004;287:F767–74.
[49] Pannabecker TL, Dahlmann A, Brokl OH, Dantzler WH. Mixed descending- and ascending-type thin limbs of Henle's loop in mammalian renal inner medulla. Am J Physiol Renal Physiol 2000;278:F202–8.
[50] MacPhee PJ, Michel CC. Fluid uptake from the renal medulla into the ascending vasa recta in anaesthetized rats. J Physiol 1995;487(Pt 1):169–83.
[51] MacPhee PJ, Michel CC. Subatmospheric closing pressures in individual microvessels of rats and frogs. J Physiol 1995; 484(Pt 1):183–7.
[52] Layton AT, Layton HE. A region-based mathematical model of the urine concentrating mechanism in the rat outer medulla. I. Formulation and base-case results. Am J Physiol Renal Physiol 2005;289:F1346–66.
[53] Layton AT, Layton HE. A region-based mathematical model of the urine concentrating mechanism in the rat outer medulla. II. Parameter sensitivity and tubular inhomogeneity. Am J Physiol Renal Physiol 2005;289:F1367–81.
[54] Layton AT, Pannabecker TL, Dantzler WH, Layton HE. Two modes for concentrating urine in rat inner medulla. Am J Physiol Renal Physiol 2004;287:F816–39.
[55] Layton AT, Pannabecker TL, Dantzler WH, Layton HE. Functional implications of the three-dimensional architecture of the rat renal inner medulla. Am J Physiol Renal Physiol 2010;298:F973–87.
[56] Brenner BM, Falchuk KH, Keimowitz RI, Berliner RW. The relationship between peritubular capillary protein concentration and fluid reabsorption by the renal proximal tubule. J Clin Invest 1969;48:1519–31.
[57] Brenner BM, Troy JL. Postglomerular vascular protein concentration: evidence for a causal role in governing fluid reabsorption and glomerulotublar balance by the renal proximal tubule. J Clin Invest 1971;50:336–49.
[58] Spitzer A, Windhager EE. Effect of peritubular oncotic pressure changes on proximal tubular fluid reabsorption. Am J Physiol 1970;218:1188–93.
[59] Sapirstein LA. Regional blood flow by fractional distribution of indicators. Am J Physiol 1958;193:161–8.
[60] Tucker BJ, Blantz RC. Determinants of proximal tubular reabsorption as mechanisms of glomerulotubular balance. Am J Physiol 1978;235:F142–50.
[61] Ott CE, Haas JA, Cuche JL, Knox FG. Effect of increased peritubule protein concentration on proximal tubule reabsorption in the presence and absence of extracellular volume expansion. J Clin Invest 1975;55:612–20.
[62] Grantham JJ, Qualizza PB, Welling LW. Influence of serum proteins on net fluid reabsorption of isolated proximal tubules. Kidney Int 1972;2:66–75.
[63] Andreoli TE, Schafer JA, Troutman SL. Perfusion rate-dependence of transepithelial osmosis in isolated proximal convoluted tubules: estimation of the hydraulic conductance. Kidney Int 1978;14:263–9.
[64] Green R, Giebisch G. Luminal hypotonicity: a driving force for fluid absorption from the proximal tubule. Am J Physiol 1984;246:F167–74.
[65] Baum M, Berry CA. Peritubular protein modulates neutral active NaCl absorption in rabbit proximal convoluted tubule. Am J Physiol 1985;248:F790–5.
[66] Green R, Giebisch G, Unwin R, Weinstein AM. Coupled water transport by rat proximal tubule. Am J Physiol 1991;261:F1046–54.
[67] Imai M, Kokko JP. Effect of peritubular protein concentration on reabsorption of sodium and water in isolated perfused proxmal tubules. J Clin Invest 1972;51:314–25.
[68] Du Z, Yan Q, Duan Y, Weinbaum S, Weinstein AM, Wang T. Axial flow modulates proximal tubule NHE3 and H-ATPase activities by changing microvillus bending moments. Am J Physiol Renal Physiol 2006;290:F289–96.
[69] Wang T. Flow-activated transport events along the nephron. Curr Opin Nephrol Hypertens 2006;15:530–6.
[70] Weinstein AM, Weinbaum S, Duan Y, Du Z, Yan Q, Wang T. Flow-dependent transport in a mathematical model of rat proximal tubule. Am J Physiol Renal Physiol 2007;292:F1164–81.
[71] Pinter GG, Gartner K. Peritubular capillary, interstitium, and lymph of the renal cortex. Rev Physiol Biochem Pharmacol 1984;99:184–202.

[72] Schurek HJ, Alt JM. Effect of albumin on the function of perfused rat kidney. Am J Physiol 1981;240:F569–76.
[73] Kuhn W, Ryffel R. Herstellung konzentrierter Losungen aus verdunnten durch blosse Membranwirkung. (Ein Modellversuch zur Function der Niere). Hoppe-Seylers Z Physiol Chem 1942;276:145–78.
[74] Michel CC. Renal medullary microcirculation: architecture and exchange. Microcirculation 1995;2:125–39.
[75] Scholander PF. The wonderful net. Scient Am 1957;196:96–107.
[76] Pallone TL, Edwards A, Ma T, Silldorff EP, Verkman AS. Requirement of aquaporin-1 for NaCl-driven water transport across descending vasa recta. J Clin Invest 2000;105:215–22.
[77] Pallone TL, Kishore BK, Nielsen S, Agre P, Knepper MA. Evidence that aquaporin-1 mediates NaCl-induced water flux across descending vasa recta. Am J Physiol 1997;272:F587–96.
[78] Pallone TL, Turner MR. Molecular sieving of small solutes by outer medullary descending vasa recta. Am J Physiol 1997;272: F579–86.
[79] Kriz W, Dieterich HJ. [The lymphatic system of the kidney in some mammals. Light and electron microscopic investigations]. Z Anat Entwicklungsgesch 1970;131:111–47.
[80] Johnston PA, Battilana CA, Lacy FB, Jamison RL. Evidence for a concentration gradient favoring outward movement of sodium from the thin loop of Henle. J Clin Invest 1977;59:234–40.
[81] Gottschalk CW, Mylle M. Micropuncture study of the mammalian urinary concentrating mechanism: evidence for the countercurrent hypothesis. Am J Physiol 1959;196:927–36.
[82] Marsh DJ, Azen SP. Mechanism of NaCl reabsorption by hamster thin ascending limbs of Henle's loop. Am J Physiol 1975;228:71–9.
[83] Sanjana VM, Johnston PA, Deen WM, Robertson CR, Brenner BM, Jamison RL. Hydraulic and oncotic pressure measurements in inner medulla of mammalian kidney. Am J Physiol 1975;228:1921–6.
[84] Sanjana VM, Johnston PA, Robertson CR, Jamison RL. An examination of transcapillary water flux in renal inner medulla. Am J Physiol 1976;231:313–8.
[85] Edwards A, Pallone TL. A multiunit model of solute and water removal by inner medullary vasa recta. Am J Physiol 1998;274: H1202–10.
[86] Pallone TL, Yagil Y, Jamison RL. Effect of small-solute gradients on transcapillary fluid movement in renal inner medulla. Am J Physiol 1989;257:F547–53.
[87] Thurau K, Sugiura T, Lilienfield LS. Micropuncture of renal vasa recta in hydropenic hamsters. Circ Res 1960;8:383.
[88] Zimmerhackl B, Robertson CR, Jamison RL. Fluid uptake in the renal papilla by vasa recta estimated by two methods simultaneously. Am J Physiol 1985;248:F347–53.
[89] Landis EM, Pappenheimer JR. Exchange of substances through the capillary wall. Handbook of physiology. Circulation. Washington: Am. Physiol. Soc; 1963962–1034.
[90] Pallone TL, Morgenthaler TI, Deen WM. Analysis of microvascular water and solute exchanges in the renal medulla. Am J Physiol 1984;247:F303–15.
[91] Kedem O, Katchalsky A. Thermodynamic analysis of the permeability of biological membranes to non-electrolytes. Biochim Biophys Acta 1958;27:229–46.
[92] Pallone TL. Effect of sodium chloride gradients on water flux in rat descending vasa recta. J Clin Invest 1991;87:12–9.
[93] Nielsen S, Pallone T, Smith BL, Christensen EI, Agre P, Maunsbach AB. Aquaporin-1 water channels in short and long loop descending thin limbs and in descending vasa recta in rat kidney. Am J Physiol 1995;268:F1023–37.
[94] Nielsen S, Smith BL, Christensen EI, Agre P. Distribution of the aquaporin CHIP in secretory and resorptive epithelia and capillary endothelia. Proc Natl Acad Sci U S A 1993;90:7275–9.
[95] Edwards A, Pallone TL. Facilitated transport in vasa recta: theoretical effects on solute exchange in the medullary microcirculation. Am J Physiol 1997;272:F505–14.
[96] Turner MR, Pallone TL. Hydraulic and diffusional permeabilities of isolated outer medullary descending vasa recta from the rat. Am J Physiol 1997;272:H392–400.
[97] Fleming I. Cytochrome P450 epoxygenases as EDHF synthase (s). Pharmacol Res 2004;49:525–33.
[98] Layton AT. Role of UTB urea transporters in the urine concentrating mechanism of the rat kidney. Bull Math Biol 2007;69:887–929.
[99] Promeneur D, Bankir L, Hu MC, Trinh-Trang-Tan MM. Renal tubular and vascular urea transporters: influence of antidiuretic hormone on messenger RNA expression in Brattleboro rats. J Am Soc Nephrol 1998;9:1359–66.
[100] Yang B, Bankir L. Urea and urine concentrating ability: new insights from studies in mice. Am J Physiol Renal Physiol 2005;288:F881–96.
[101] Yang B, Verkman AS. Urea transporter UT3 functions as an efficient water channel. Direct evidence for a common water/urea pathway. J Biol Chem 1998;273:9369–72.
[102] Zhang W, Edwards A. Theoretical effects of UTB urea transporters in the renal medullary microcirculation. Am J Physiol Renal Physiol 2003;285:F731–47.
[103] Koepsell H, Nicholson WA, Kriz W, Hohling HJ. Measurements of exponential gradients of sodium and chlorine in the rat kidney medulla using the electron microprobe. Pflugers Arch 1974;350:167–84.
[104] Wang W, Michel CC. Effects of anastomoses on solute transcapillary exchange in countercurrent systems. Microcirculation 1997;4:381–90.
[105] Wang W, Parker KH, Michel CC. Theoretical studies of steady-state transcapillary exchange in countercurrent systems. Microcirculation 1996;3:301–11.
[106] Chou CL, Knepper MA. *In vitro* perfusion of chinchilla thin limb segments: segmentation and osmotic water permeability. Am J Physiol 1992;263:F417–26.
[107] Chou CL, Nielsen S, Knepper MA. Structural–functional correlation in chinchilla long loop of Henle thin limbs: a novel papillary subsegment. Am J Physiol 1993;265:F863–74.
[108] Edwards A, Delong MJ, Pallone TL. Interstitial water and solute recovery by inner medullary vasa recta. Am J Physiol Renal Physiol 2000;278:F257–69.
[109] Thomas SR. Cycles and separations in a model of the renal medulla. Am J Physiol 1998;275:F671–90.
[110] Pallone TL, Nielsen S, Silldorff EP, Yang S. Diffusive transport of solute in the rat medullary microcirculation. Am J Physiol 1995;269:F55–63.
[111] Pallone TL, Work J, Myers RL, Jamison RL. Transport of sodium and urea in outer medullary descending vasa recta. J Clin Invest 1994;93:212–22.
[112] Pallone TL. Characterization of the urea transporter in outer medullary descending vasa recta. Am J Physiol 1994;267: R260–7.
[113] Promeneur D, Rousselet G, Bankir L, Bailly P, Cartron JP, Ripoche P, et al. Evidence for distinct vascular and tubular urea transporters in the rat kidney. J Am Soc Nephrol 1996;7:852–60.
[114] Bankir L, Chen K, Yang B. Lack of UT-B in vasa recta and red blood cells prevents urea-induced improvement of urinary concentrating ability. Am J Physiol Renal Physiol 2004;286:F144–51.
[115] Shayakul C, Knepper MA, Smith CP, DiGiovanni SR, Hediger MA. Segmental localization of urea transporter mRNAs in rat kidney. Am J Physiol 1997;272:F654–60.

[116] Shayakul C, Steel A, Hediger MA. Molecular cloning and characterization of the vasopressin-regulated urea transporter of rat kidney collecting ducts. J Clin Invest 1996;98:2580–7.
[117] Xu Y, Olives B, Bailly P, Fischer E, Ripoche P, Ronco P, et al. Endothelial cells of the kidney vasa recta express the urea transporter HUT11. Kidney Int 1997;51:138–46.
[118] Yang B, Bankir L, Gillespie A, Epstein CJ, Verkman AS. Urea-selective concentrating defect in transgenic mice lacking urea transporter UT-B. J Biol Chem 2002;277:10633–7.
[119] Sands JM. Renal urea transporters. Curr Opin Nephrol Hypertens 2004;13:525–32.
[120] Trinh-Trang-Tan MM, Lasbennes F, Gane P, Roudier N, Ripoche P, Cartron JP, et al. UT-B1 proteins in rat: tissue distribution and regulation by antidiuretic hormone in kidney. Am J Physiol Renal Physiol 2002;283:F912–22.
[121] Kim D, Klein JD, Racine S, Murrell BP, Sands JM. Urea may regulate urea transporter protein abundance during osmotic diuresis. Am J Physiol Renal Physiol 2005;288:F188–97.
[122] Jung JY, Madsen KM, Han KH, Yang CW, Knepper MA, Sands JM, et al. Expression of urea transporters in potassium-depleted mouse kidney. Am J Physiol Renal Physiol 2003;285: F1210–24.
[123] Klein JD, Gunn RB, Roberts BR, Sands JM. Down-regulation of urea transporters in the renal inner medulla of lithium-fed rats. Kidney Int 2002;61:995–1002.
[124] Li C, Klein JD, Wang W, Knepper MA, Nielsen S, Sands JM, et al. Altered expression of urea transporters in response to ureteral obstruction. Am J Physiol Renal Physiol 2004;286:F1154–62.
[125] Lim SW, Li C, Sun BK, Han KH, Kim WY, Oh YW, et al. Long-term treatment with cyclosporine decreases aquaporins and urea transporters in the rat kidney. Am J Physiol Renal Physiol 2004;287:F139–51.
[126] Macey RI, Yousef LW. Osmotic stability of red cells in renal circulation requires rapid urea transport. Am J Physiol 1988;254:C669–74.
[127] Pallone TL. Resistance of ascending vasa recta to transport of water. Am J Physiol 1991;260:F303–10.
[128] Pallone TL. Molecular sieving of albumin by the ascending vasa recta wall. J Clin Invest 1992;90:30–4.
[129] Pallone TL. Transport of sodium chloride and water in rat ascending vasa recta. Am J Physiol 1991;261:F519–25.
[130] Morgan T, Berliner RW. Permeability of the loop of Henle, vasa recta, and collecting duct to water, urea, and sodium. Am J Physiol 1968;215:108–15.
[131] Bell RD, Keyl MJ, Shrader FR, Jones EW, Henry LP. Renal lymphatics: the internal distribution. Nephron 1968;5:454–63.
[132] LeBrie SJ. Renal peritubular capillary permeability to macromolecules. Am J Physiol 1967;213:1225–32.
[133] Renkin EM. Capillary transport of macromolecules: pores and other endothelial pathways. J Appl Physiol 1985;58:315–25.
[134] Lassen NA, Longley JB, Lilienfield LS. Concentration of albumin in renal papilla. Science 1958;128:720–1.
[135] Lilienfield LS, Maganzini HC, Bauer MH. Blood flow in the renal medulla. Circ Res 1961;9:614–7.
[136] Slotkoff LM, Lilienfield LS. Extravascular renal albumin. Am J Physiol 1967;212:400–6.
[137] Carone FA, Everett BA, Blondeel NJ, Stolarczyk J. Renal localization of albumin and its function in the concentrating mechanism. Am J Physiol 1967;212:387–93.
[138] Pomerantz RM, Slotkoff LM, Lilienfield LS. Histochemical and microanatomical differences between renal cortical and medullary interstitium. In: Kass EH, editor. Progress in pyelonephritis. Philadelphia: F.A. Davis Co.; 1965. p. 434–525.
[139] Moffat DB. Extravascular protein in the renal medulla. Q J Exp Physiol Cogn Med Sci 1969;54:60–7.
[140] Wilde WS, Vorburger C. Albumin multiplier in kidney vasa recta analyzed by microspectrophotometry of T-1824. Am J Physiol 1967;213:1233–43.
[141] Venkatachalam MA, Karnovsky MJ. Extravascular protein in the kidney. An ultrastructural study of its relation to renal peritubular capillary permeability using protein tracers. Lab Invest 1972;27:435–44.
[142] Shimamura T, Morrison AB. Vascular permeability of the renal medullary vessels in the mouse and rat. Am J Pathol 1973;71:155–63.
[143] Pallone TL. Extravascular protein in the renal medulla: analysis by two methods. Am J Physiol 1994;266:R1429–36.
[144] Pinter GG, Shohet JL. Two fluid compartments in the renal inner medulla: a view through the keyhole of the concentrating process. Philos Transact A Math Phys Eng Sci 2006;364:1551–61.
[145] Pinter GG, Shohet JL. An inner medullary concentrating process actuated by renal pelvic/calyceal muscle contractions: assessment and hypothesis. Nephron Physiol 2009;113:1–6.
[146] Fahraeus R. The suspension stability of blood. Physiol Rev 1929;9:241–74.
[147] Lilienfield LS, Rose JC, Lassen NA. Diverse distribution of red cells and albumin in the dog kidney. Circ Res 1958;6:810–5.
[148] Rasmussen SN. Red cell and plasma volume flows to the inner medulla of the rat kidney: determinations by means of a step function input indicator technique. Pflugers Arch 1978;373:153–9.
[149] Zimmerhackl B, Dussel R, Steinhausen M. Erythrocyte flow and dynamic hematocrit in the renal papilla of the rat. Am J Physiol 1985;249:F898–902.
[150] Gaehtgens P. Flow of blood through narrow capillaries: Rheological mechanisms determining capillary hematocrit and apparent viscosity. Biorheology 1980;17:183–9.
[151] Pries AR, Ley K, Gaehtgens P. Generalization of the Fahraeus principle for microvessel networks. Am J Physiol 1986;251: H1324–32.
[152] Ren Y, Garvin JL, Liu R, Carretero OA. Crosstalk between the connecting tubule and the afferent arteriole regulates renal microcirculation. Kidney Int 2007;71:1116–21.
[153] Ren Y, Garvin JL, Liu R, Carretero OA. Possible mechanism of efferent arteriole (Ef-Art) tubuloglomerular feedback. Kidney Int 2007;71:861–6.
[154] Aukland K, Bower BF, Berliner RW. Measurement of local blood flow with hydrogen gas. Circ Res 1964;14:164–87.
[155] Balint P, Bartha J, Fekete A. Intrarenal distribution of blood flow in the dog. Acta Physiol Acad Sci Hung 1969;36:1–11.
[156] Bayle F, Eloy L, Trinh-Trang-Tan MM, Grunfeld JP, Bankir L. Papillary plasma flow in rats. I. Relation to urine osmolality in normal and Brattleboro rats with hereditary diabetes insipidus. Pflugers Arch 1982;394:211–6.
[157] Chou SY, Spitalewitz S, Faubert PF, Park IY, Porush JG. Inner medullary hemodynamics in chronic salt-depleted dogs. Am J Physiol 1984;246:F146–54.
[158] Chuang EL, Reineck HJ, Osgood RW, Kunau Jr RT, Stein JH. Studies on the mechanism of reduced urinary osmolality after exposure of renal papilla. J Clin Invest 1978;61:633–9.
[159] Coelho JB. Heterogeneity of intracortical peritubular plasma flow in the rat kidney. Am J Physiol 1977;233:F333–41.
[160] Faubert PF, Chou SY, Porush JG. Regulation of papillary plasma flow by angiotensin II. Kidney Int 1987;32:472–8.
[161] Ganguli M, Tobian L, Azar S, O'Donnell M. Evidence that prostaglandin synthesis inhibitors increase the concentration of sodium and chloride in rat renal medulla. Circ Res 1977;40: I135–9.
[162] Ganguli M, Tobian L, Dahl L. Low renal papillary plasma flow in both Dahl and Kyoto rats with spontaneous hypertension. Circ Res 1976;39:337–41.

[163] Harsing L, Pelley K. [The determination of renal medullary blood flow based on Rb-86 deposit and distribution]. Pflugers Arch Gesamte Physiol Menschen Tiere 1965;285:302–12.
[164] Karlberg L, Kallskog O, Ojteg G, Wolgast M. Renal medullary blood flow studied with the 86-Rb extraction method. Methodological considerations. Acta Physiol Scand 1982;115:11–8.
[165] Kramer K, Thurau K, Deetjen P. [Hemodynamics of kidney medullary substance. Part I. Capillary passage time, blood volume, circulation, tissue hematocrit and oxygen consumption of kidney medullary substance *in situ*.]. Pflugers Arch Gesamte Physiol Menschen Tiere 1960;270:251–69.
[166] Lilienfield LS, Maganzini HC, Bauer MH. Renal medullary blood flow. Fed Proc 1960;19:363–5.
[167] Roman RJ, Smits C. Laser-Doppler determination of papillary blood flow in young and adult rats. Am J Physiol 1986;251: F115–24.
[168] Solez K, Kramer EC, Fox JA, Heptinstall RH. Medullary plasma flow and intravascular leukocyte accumulation in acute renal failure. Kidney Int 1974;6:24–37.
[169] Steiner SH, King RD. Nutrient renal blood flow and its distribution in the unanesthetized dog. J Surg Res 1970;10:133–46.
[170] Thorburn GD, Kopald HH, Herd JA, Hollenberg M, O'Morchoe CC, Barger AC. Intrarenal distribution of nutrient blood flow determined with krypton 85 in the unanesthetized dog. Circ Res 1963;13:290–307.
[171] Thurau K. Renal hemodynamics. Am J Med 1964;36:698–719.
[172] Wolgast M. Studies on the regional renal blood flow with p32-labelled red cells and small beta-sensitive semiconductor detectors. Acta Physiol Scand Suppl 1968;313:1–109.
[173] Yarger WE, Boyd MA, Schrader NW. Evaluation of methods of measuring glomerular and nutrient blood flow in rat kidneys. Am J Physiol 1978;235:H592–600.
[174] Pallone TL. The extraglomerular circulation of the kidney. In: Seldin DW, Giebisch G, editors. The kidney: physiology and pathophysiology. Philadelphia, PA: Lippincott Williams and Wilkins; 2000. p. 791–822.
[175] Zimmerhackl B, Tinsman J, Jamison RL, Robertson CR. Use of digital cross-correlation for on-line determination of single-vessel blood flow in the mammalian kidney. Microvasc Res 1985;30:63–74.
[176] Yamamoto T, Tada T, Brodsky SV, Tanaka H, Noiri E, Kajiya F, et al. Intravital videomicroscopy of peritubular capillaries in renal ischemia. Am J Physiol Renal Physiol 2002;282:F1150–5.
[177] Hayashi K, Wakino S, Sugano N, Ozawa Y, Homma K, Saruta T. Ca^{2+} channel subtypes and pharmacology in the kidney. Circ Res 2007;100:342–53.
[178] Draijer M, Hondebrink E, van LT, Steenbergen W. Review of laser speckle contrast techniques for visualizing tissue perfusion. Lasers Med Sci 2009;24:639–51.
[179] Humeau A, Steenbergen W, Nilsson H, Stromberg T. Laser-Doppler perfusion monitoring and imaging: novel approaches. Med Biol Eng Comput 2007;45:421–35.
[180] Correas JM, Claudon M, Tranquart F, Helenon AO. The kidney: imaging with microbubble contrast agents. Ultrasound Q 2006;22:53–66.
[181] Sullivan JC, Wang B, Boesen EI, D'Angelo G, Pollock JS, Pollock DM. Novel use of ultrasound to examine regional blood flow in the mouse kidney. Am J Physiol Renal Physiol 2009;297:F228–35.
[182] Gussis GL, Jamison RL, Robertson CR. Determination of erythrocyte velocities in the mammalian inner renal medulla by a video velocity-tracking system. Microvasc Res 1979;18:370–83.
[183] Stern MD, Bowen PD, Parma R, Osgood RW, Bowman RL, Stein JH. Measurement of renal cortical and medullary blood flow by laser-Doppler spectroscopy in the rat. Am J Physiol 1979;236:F80–7.
[184] Fenoy FJ, Roman RJ. Effect of volume expansion on papillary blood flow and sodium excretion. Am J Physiol 1991;260: F813–22.
[185] Aukland K. Methods for measuring renal blood flow: total flow and regional distribution. Annu Rev Physiol 1980;42:543–55.
[186] Carmines PK, Fleming JT. Control of the renal microvasculature by vasoactive peptides. FASEB J 1990;4:3300–9.
[187] Pallone TL, Work J, Jamison RL. Resistance of descending vasa recta to the transport of water. Am J Physiol 1990;259:F688–97.
[188] Roman RJ, Carmines PK, Loutzenhiser R, Conger JD. Direct studies on the control of the renal microcirculation. J Am Soc Nephrol 1991;2:136–49.
[189] Burg M, Grantham J, Abramow M, Orloff J. Preparation and study of fragments of single rabbit nephrons. Am J Physiol 1966;210:1293–8.
[190] Pallone TL. Microdissected perfused vessels. Methods Mol Med 2003;86:443–56.
[191] Osgood RW, Patton M, Hanley MJ, Venkatachalam M, Reineck HJ, Stein JH. *In vitro* perfusion of the isolated dog glomerulus. Am J Physiol 1983;244:F349–54.
[192] Edwards RM. Segmental effects of norepinephrine and angiotensin II on isolated renal microvessels. Am J Physiol 1983;244: F526–34.
[193] Ito S, Arima S, Ren YL, Juncos LA, Carretero OA. Endothelium-derived relaxing factor/nitric oxide modulates angiotensin II action in the isolated microperfused rabbit afferent but not efferent arteriole. J Clin Invest 1993;91:2012–9.
[194] Ito S, Johnson CS, Carretero OA. Modulation of angiotensin II-induced vasoconstriction by endothelium-derived relaxing factor in the isolated microperfused rabbit afferent arteriole. J Clin Invest 1991;87:1656–63.
[195] Ito S, Juncos LA, Nushiro N, Johnson CS, Carretero OA. Endothelium-derived relaxing factor modulates endothelin action in afferent arterioles. Hypertension 1991;17:1052–6.
[196] Ito S, Ren Y. Evidence for the role of nitric oxide in macula densa control of glomerular hemodynamics. J Clin Invest 1993;92:1093–8.
[197] Hansen PB, Hashimoto S, Briggs J, Schnermann J. Attenuated renovascular constrictor responses to angiotensin II in adenosine 1 receptor knockout mice. Am J Physiol Regul Integr Comp Physiol 2003;285:R44–9.
[198] Pallone TL. Vasoconstriction of outer medullary vasa recta by angiotensin II is modulated by prostaglandin E2. Am J Physiol 1994;266:F850–7.
[199] Newby AC, Henderson AH. Stimulus-secretion coupling in vascular endothelial cells. Annu Rev Physiol 1990;52:661–74.
[200] Buckley BJ, Mirza Z, Whorton AR. Regulation of $Ca^{(2+)}$-dependent nitric oxide synthase in bovine aortic endothelial cells. Am J Physiol 1995;269:C757–65.
[201] Martin W, Villani GM, Jothianandan D, Furchgott RF. Selective blockade of endothelium-dependent and glyceryl trinitrate-induced relaxation by hemoglobin and by methylene blue in the rabbit aorta. J Pharmacol Exp Ther 1985;232:708–16.
[202] Casellas D, Navar LG. *In vitro* perfusion of juxtamedullary nephrons in rats. Am J Physiol 1984;246:F349–58.
[203] Steinhausen M, Ballantyne D, Fretschner M, Parekh N. Sex differences in autoregulation of juxtamedullary glomerular blood flow in hydronephrotic rats. Am J Physiol 1990;258:F863–9.
[204] Steinhausen M, Kucherer H, Parekh N, Weis S, Wiegman DL, Wilhelm KR. Angiotensin II control of the renal microcirculation: effect of blockade by saralasin. Kidney Int 1986;30:56–61.

[205] Carmines PK, Morrison TK, Navar LG. Angiotensin II effects on microvascular diameters of *in vitro* blood-perfused juxtamedullary nephrons. Am J Physiol 1986;251:F610–8.
[206] Hansen PB, Jensen BL, Andreasen D, Skott O. Differential expression of T- and L-type voltage-dependent calcium channels in renal resistance vessels. Circ Res 2001;89:630–8.
[207] Loutzenhiser R, Hayashi K, Epstein M. Divergent effects of KCl-induced depolarization on afferent and efferent arterioles. Am J Physiol 1989;257:F561–4.
[208] Conger JD, Falk SA. KCl and angiotensin responses in isolated rat renal arterioles: effects of diltiazem and low-calcium medium. Am J Physiol 1993;264:F134–40.
[209] Inscho EW, Mason MJ, Schroeder AC, Deichmann PC, Stiegler KD, Imig JD. Agonist-induced calcium regulation in freshly isolated renal microvascular smooth muscle cells. J Am Soc Nephrol 1997;8:569–79.
[210] Loutzenhiser R, Chilton L, Trottier G. Membrane potential measurements in renal afferent and efferent arterioles: actions of angiotensin II. Am J Physiol 1997;273:F307–14.
[211] Arendshorst WJ, Brannstrom K, Ruan X. Actions of angiotensin II on the renal microvasculature. J Am Soc Nephrol 1999;10 (Suppl. 11):S149–61.
[212] Helou CM, Marchetti J. Morphological heterogeneity of renal glomerular arterioles and distinct $[Ca^{2+}]i$ responses to ANG II. Am J Physiol 1997;273:F84–96.
[213] Inscho EW, Schroeder AC, Deichmann PC, Imig JD. ATP-mediated Ca^{2+} signaling in preglomerular smooth muscle cells. Am J Physiol 1999;276:F450–6.
[214] Iversen BM, Arendshorst WJ. ANG II and vasopressin stimulate calcium entry in dispersed smooth muscle cells of preglomerular arterioles. Am J Physiol 1998;274:F498–508.
[215] Loutzenhiser K, Loutzenhiser R. Angiotensin II-induced $Ca^{(2+)}$ influx in renal afferent and efferent arterioles: differing roles of voltage-gated and store-operated $Ca^{(2+)}$ entry. Circ Res 2000;87:551–7.
[216] Carmines PK, Navar LG. Disparate effects of Ca channel blockade on afferent and efferent arteriolar responses to ANG II. Am J Physiol 1989;256:F1015–20.
[217] Fleming JT, Parekh N, Steinhausen M. Calcium antagonists preferentially dilate preglomerular vessels of hydronephrotic kidney. Am J Physiol 1987;253:F1157–63.
[218] Loutzenhiser R, Epstein M, Horton C. Inhibition by diltiazem of pressure-induced afferent vasoconstriction in the isolated perfused rat kidney. Am J Cardiol 1987;59:72A–5A.
[219] Loutzenhiser RD, Epstein M, Fischetti F, Horton C. Effects of amlodipine on renal hemodynamics. Am J Cardiol 1989;64:122I–7I.
[220] Navar LG, Inscho EW, Imig JD, Mitchell KD. Heterogeneous activation mechanisms in the renal microvasculature. Kidney Int Suppl 1998;67:S17–21.
[221] Takenaka T, Ohno Y, Hayashi K, Saruta T, Suzuki H. Governance of arteriolar oscillation by ryanodine receptors. Am J Physiol Regul Integr Comp Physiol 2003;285:R125–31.
[222] Carmines PK, Ohishi K, Ikenaga H. Functional impairment of renal afferent arteriolar voltage-gated calcium channels in rats with diabetes mellitus. J Clin Invest 1996;98:2564–71.
[223] Fellner SK, Arendshorst WJ. Store-operated Ca^{2+} entry is exaggerated in fresh preglomerular vascular smooth muscle cells of SHR. Kidney Int 2002;61:2132–41.
[224] Iversen BM, Arendshorst WJ. Exaggerated Ca^{2+} signaling in preglomerular arteriolar smooth muscle cells of genetically hypertensive rats. Am J Physiol 1999;276:F260–70.
[225] Hansen PB, Jensen BL, Andreasen D, Friis UG, Skott O. Vascular smooth muscle cells express the alpha(1A) subunit of a P-/Q-type voltage-dependent $Ca^{(2+)}$ channel, and it is functionally important in renal afferent arterioles. Circ Res 2000;87:896–902.
[226] Jensen BL, Friis UG, Hansen PB, Andreasen D, Uhrenholt T, Schjerning J, et al. Voltage-dependent calcium channels in the renal microcirculation. Nephrol Dial Transplant 2004;19:1368–73.
[227] Ozawa Y, Hayashi K, Nagahama T, Fujiwara K, Saruta T. Effect of T-type selective calcium antagonist on renal microcirculation: studies in the isolated perfused hydronephrotic kidney. Hypertension 2001;38:343–7.
[228] Ozawa Y, Hayashi K, Nagahama T, Fujiwara K, Wakino S, Saruta T. Renal afferent and efferent arteriolar dilation by nilvadipine: studies in the isolated perfused hydronephrotic kidney. J Cardiovasc Pharmacol 1999;33:243–7.
[229] Salomonsson M, Sorensen CM, Arendshorst WJ, Steendahl J, Holstein-Rathlou NH. Calcium handling in afferent arterioles. Acta Physiol Scand 2004;181:421–9.
[230] Rhinehart K, Zhang Z, Pallone TL. $Ca^{(2+)}$ signaling and membrane potential in descending vasa recta pericytes and endothelia. Am J Physiol Renal Physiol 2002;283:F852–60.
[231] Zhang Z, Rhinehart K, Pallone TL. Membrane potential controls calcium entry into descending vasa recta pericytes. Am J Physiol Regul Integr Comp Physiol 2002;283:R949–57.
[232] Feng MG, Navar LG. Angiotensin II-mediated constriction of afferent and efferent arterioles involves T-type Ca channel activation. Am J Nephrol 2004;24:641–8.
[233] Hayashi K, Ozawa Y, Wakino S, Kanda T, Homma K, Takamatsu I, et al. Cellular mechanism for mibefradil-induced vasodilation of renal microcirculation: studies in the isolated perfused hydronephrotic kidney. J Cardiovasc Pharmacol 2003;42:697–702.
[234] Gordienko DV, Clausen C, Goligorsky MS. Ionic currents and endothelin signaling in smooth muscle cells from rat renal resistance arteries. Am J Physiol 1994;266:F325–41.
[235] Hall DA, Carmines PK, Sansom SC. Dihydropyridine-sensitive $Ca^{(2+)}$ channels in human glomerular mesangial cells. Am J Physiol Renal Physiol 2000;278:F97–103.
[236] Zhang Z, Lin H, Cao C, Khurana S, Pallone TL. Voltage gated divalent currents in descending vasa recta pericytes. Am J Physiol Renal Physiol 2010.
[237] Feng MG, Li M, Navar LG. T-type calcium channels in the regulation of afferent and efferent arterioles in rats. Am J Physiol Renal Physiol 2004;286:F331–7.
[238] Feng MG, Navar LG. Nitric oxide synthase inhibition activates L- and T-type Ca^{2+} channels in afferent and efferent arterioles. Am J Physiol Renal Physiol 2006;290:F873–9.
[239] Honda M, Hayashi K, Matsuda H, Kubota E, Tokuyama H, Okubo K, et al. Divergent renal vasodilator action of L- and T-type calcium antagonists *in vivo*. J Hypertens 2001;19:2031–7.
[240] Hart P, Bakris GL. Calcium antagonists: do they equally protect against kidney injury? Kidney Int 2008;73:795–6.
[241] Saruta T, Kanno Y, Hayashi K, Konishi K. Antihypertensive agents and renal protection: calcium channel blockers. Kidney Int Suppl 1996;55:S52–6.
[242] Sasaki H, Saiki A, Endo K, Ban N, Yamaguchi T, Kawana H, et al. Protective effects of efonidipine, a T- and L-type calcium channel blocker, on renal function and arterial stiffness in type 2 diabetic patients with hypertension and nephropathy. J Atheroscler Thromb 2009;16:568–75.
[243] Parekh AB. Store-operated Ca^{2+} entry: dynamic interplay between endoplasmic reticulum, mitochondria and plasma membrane. J Physiol 2003;547:333–48.
[244] Cioffi DL, Barry C, Stevens T. Store-operated calcium entry channels in pulmonary endothelium: the emerging story of TRPCS and Orai1. Adv Exp Med Biol 2010;661:137–54.

[245] Putney Jr JW. Capacitative calcium entry: sensing the calcium stores. J Cell Biol 2005;169:381–2.
[246] Putney JW. Capacitative calcium entry: from concept to molecules. Immunol Rev 2009;231:10–22.
[247] Vaca L. SOCIC: the store-operated calcium influx complex. Cell Calcium 2010;47:199–209.
[248] Fellner SK, Arendshorst WJ. Angiotensin II-stimulated Ca^{2+} entry mechanisms in afferent arterioles: role of transient receptor potential canonical channels and reverse Na^+/Ca^{2+} exchange. Am J Physiol Renal Physiol 2008;294:F212–9.
[249] Clapham DE. TRP channels as cellular sensors. Nature 2003;426:517–24.
[250] Fellner SK, Arendshorst WJ. Capacitative calcium entry in smooth muscle cells from preglomerular vessels. Am J Physiol 1999;277:F533–42.
[251] Takenaka T, Suzuki H, Okada H, Inoue T, Kanno Y, Ozawa Y, et al. Transient receptor potential channels in rat renal microcirculation: actions of angiotensin II. Kidney Int 2002;62:558–65.
[252] Ma R, Smith S, Child A, Carmines PK, Sansom SC. Store-operated $Ca^{(2+)}$ channels in human glomerular mesangial cells. Am J Physiol Renal Physiol 2000;278:F954–61.
[253] Li WP, Tsiokas L, Sansom SC, Ma R. Epidermal growth factor activates store-operated Ca^{2+} channels through an inositol 1,4,5-trisphosphate-independent pathway in human glomerular mesangial cells. J Biol Chem 2004;279:4570–7.
[254] Ma R, Sansom SC. Epidermal growth factor activates store-operated calcium channels in human glomerular mesangial cells. J Am Soc Nephrol 2001;12:47–53.
[255] Ma R, Kudlacek PE, Sansom SC. Protein kinase C-alpha participates in activation of store-operated Ca^{2+} channels in human glomerular mesangial cells. Am J Physiol Cell Physiol 2002;283:C1390–8.
[256] Ma R, Pluznick J, Kudlacek P, Sansom SC. Protein kinase C activates store-operated $Ca^{(2+)}$ channels in human glomerular mesangial cells. J Biol Chem 2001;276:25759–65.
[257] Wang X, Pluznick JL, Wei P, Padanilam BJ, Sansom SC. TRPC4 forms store-operated Ca^{2+} channels in mouse mesangial cells. Am J Physiol Cell Physiol 2004;287:C357–64.
[258] Lee-Kwon W, Wade JB, Zhang Z, Pallone TL, Weinman EJ. Expression of TRPC4 channel protein that interacts with NHERF-2 in rat descending vasa recta. Am J Physiol Cell Physiol 2005;288:C942–9.
[259] Kitamura K, Yamazaki J. Chloride channels and their functional roles in smooth muscle tone in the vasculature. Jpn J Pharmacol 2001;85:351–7.
[260] Large WA, Wang Q. Characteristics and physiological role of the $Ca^{(2+)}$-activated Cl^- conductance in smooth muscle. Am J Physiol 1996;271:C435–54.
[261] Duran C, Thompson CH, Xiao Q, Hartzell HC. Chloride channels: often enigmatic, rarely predictable. Annu Rev Physiol 2010;72:95–121.
[262] Hartzell HC, Yu K, Xiao Q, Chien LT, Qu Z. Anoctamin/TMEM16 family members are Ca^{2+}-activated Cl^- channels. J Physiol 2009;587:2127–39.
[263] Carmines PK. Segment-specific effect of chloride channel blockade on rat renal arteriolar contractile responses to angiotensin II. Am J Hypertens 1995;8:90–4.
[264] Hansen PB, Friis UG, Uhrenholt TR, Briggs J, Schnermann J. Intracellular signalling pathways in the vasoconstrictor response of mouse afferent arterioles to adenosine. Acta Physiol (Oxf) 2007;191:89–97.
[265] Hansen PB, Jensen BL, Skott O. Chloride regulates afferent arteriolar contraction in response to depolarization. Hypertension 1998;32:1066–70.
[266] Jensen BL, Ellekvist P, Skott O. Chloride is essential for contraction of afferent arterioles after agonists and potassium. Am J Physiol 1997;272:F389–96.
[267] Takenaka T, Kanno Y, Kitamura Y, Hayashi K, Suzuki H, Saruta T. Role of chloride channels in afferent arteriolar constriction. Kidney Int 1996;50:864–72.
[268] Pallone TL, Huang JM. Control of descending vasa recta pericyte membrane potential by angiotensin II. Am J Physiol Renal Physiol 2002;282:F1064–74.
[269] Pallone TL, Zhang Z, Rhinehart K. Physiology of the renal medullary microcirculation. Am J Physiol Renal Physiol 2003;284:F253–66.
[270] Zhang Z, Huang JM, Turner MR, Rhinehart KL, Pallone TL. Role of chloride in constriction of descending vasa recta by angiotensin II. Am J Physiol Regul Integr Comp Physiol 2001;280:R1878–86.
[271] Edwards A, Pallone TL. Mechanisms underlying angiotensin II-induced calcium oscillations. Am J Physiol Renal Physiol 2008;295:F568–84.
[272] Zhang Q, Cao C, Zhang Z, Wier WG, Edwards A, Pallone TL. Membrane current oscillations in descending vasa recta pericytes. Am J Physiol Renal Physiol 2008;294:F656–66.
[273] Lin H, Pallone TL, Cao C. Murine vasa recta pericyte chloride conductance is controlled by calcium, depolarization andkinase activity. Am J Physiol Regul Integr Comp Physiol 2010 .
[274] Pallone TL, Cao C, Zhang Z. Inhibition of K^+ conductance in descending vasa recta pericytes by ANG II. Am J Physiol Renal Physiol 2004;287:F1213–22.
[275] Steendahl J, Holstein-Rathlou NH, Sorensen CM, Salomonsson M. Effects of chloride channel blockers on rat renal vascular responses to angiotensin II and norepinephrine. Am J Physiol Renal Physiol 2004;286:F323–30.
[276] Nelson MT, Quayle JM. Physiological roles and properties of potassium channels in arterial smooth muscle. Am J Physiol 1995;268:C799–822.
[277] Quayle JM, Nelson MT, Standen NB. ATP-sensitive and inwardly rectifying potassium channels in smooth muscle. Physiol Rev 1997;77:1165–232.
[278] Busse R, Edwards G, Feletou M, Fleming I, Vanhoutte PM, Weston AH. EDHF: bringing the concepts together. Trends Pharmacol Sci 2002;23:374–80.
[279] Popp R, Brandes RP, Ott G, Busse R, Fleming I. Dynamic modulation of interendothelial gap junctional communication by 11,12-epoxyeicosatrienoic acid. Circ Res 2002;90:800–6.
[280] Quilley J, Fulton D, McGiff JC. Hyperpolarizing factors. Biochem Pharmacol 1997;54:1059–70.
[281] Betts LC, Kozlowski RZ. Electrophysiological effects of endothelin-1 and their relationship to contraction in rat renal arterial smooth muscle. Br J Pharmacol 2000;130:787–96.
[282] Fergus DJ, Martens JR, England SK. Kv channel subunits that contribute to voltage-gated K^+ current in renal vascular smooth muscle. Pflugers Arch 2003;445:697–704.
[283] Gebremedhin D, Kaldunski M, Jacobs ER, Harder DR, Roman RJ. Coexistence of two types of $Ca^{(2+)}$-activated K^+ channels in rat renal arterioles. Am J Physiol 1996;270:F69–81.
[284] Gelband CH, Hume JR. Ionic currents in single smooth muscle cells of the canine renal artery. Circ Res 1992;71:745–58.
[285] Gelband CH, Ishikawa T, Post JM, Keef KD, Hume JR. Intracellular divalent cations block smooth muscle K^+ channels. Circ Res 1993;73:24–34.
[286] Prior HM, Yates MS, Beech DJ. Functions of large conductance Ca^{2+}-activated (BKCa), delayed rectifier (KV) and background K^+ channels in the control of membrane potential in rabbit renal arcuate artery. J Physiol 1998;511(Pt 1):159–69.

[287] Martens JR, Gelband CH. Alterations in rat interlobar artery membrane potential and K^+ channels in genetic and nongenetic hypertension. Circ Res 1996;79:295–301.
[288] Martens JR, Gelband CH. Ion channels in vascular smooth muscle: alterations in essential hypertension. Proc Soc Exp Biol Med 1998;218:192–203.
[289] Prior HM, Yates MS, Beech DJ. Role of K^+ channels in A2A adenosine receptor-mediated dilation of the pressurized renal arcuate artery. Br J Pharmacol 1999;126:494–500.
[290] Ma YH, Gebremedhin D, Schwartzman ML, Falck JR, Clark JE, Masters BS, et al. 20-Hydroxyeicosatetraenoic acid is an endogenous vasoconstrictor of canine renal arcuate arteries. Circ Res 1993;72:126–36.
[291] Maier KG, Roman RJ. Cytochrome P450 metabolites of arachidonic acid in the control of renal function. Curr Opin Nephrol Hypertens 2001;10:81–7.
[292] Zou AP, Fleming JT, Falck JR, Jacobs ER, Gebremedhin D, Harder DR, et al. 20-HETE is an endogenous inhibitor of the large-conductance $Ca^{(2+)}$-activated K^+ channel in renal arterioles. Am J Physiol 1996;270:R228–37.
[293] Sun CW, Falck JR, Harder DR, Roman RJ. Role of tyrosine kinase and PKC in the vasoconstrictor response to 20-HETE in renal arterioles. Hypertension 1999;33:414–8.
[294] Sun CW, Alonso-Galicia M, Taheri MR, Falck JR, Harder DR, Roman RJ. Nitric oxide-20-hydroxyeicosatetraenoic acid interaction in the regulation of K^+ channel activity and vascular tone in renal arterioles. Circ Res 1998;83:1069–79.
[295] Imig JD, Dimitropoulou C, Reddy DS, White RE, Falck JR. Afferent arteriolar dilation to 11,12-EET analogs involves PP2A activity and Ca^{2+}-activated K^+ channels. Microcirculation 2008;15:137–50.
[296] Kaide JI, Zhang F, Wei Y, Jiang H, Yu C, Wang WH, et al. Carbon monoxide of vascular origin attenuates the sensitivity of renal arterial vessels to vasoconstrictors. J Clin Invest 2001;107:1163–71.
[297] Imig JD. Eicosanoid regulation of the renal vasculature. Am J Physiol Renal Physiol 2000;279:F965–81.
[298] Wang D, Borrego-Conde LJ, Falck JR, Sharma KK, Wilcox CS, Umans JG. Contributions of nitric oxide, EDHF, and EETs to endothelium-dependent relaxation in renal afferent arterioles. Kidney Int 2003;63:2187–93.
[299] Zou AP, Fleming JT, Falck JR, Jacobs ER, Gebremedhin D, Harder DR, et al. Stereospecific effects of epoxyeicosatrienoic acids on renal vascular tone and $K^{(+)}$-channel activity. Am J Physiol 1996;270:F822–32.
[300] Alonso-Galicia M, Sun CW, Falck JR, Harder DR, Roman RJ. Contribution of 20-HETE to the vasodilator actions of nitric oxide in renal arteries. Am J Physiol 1998;275:F370–8.
[301] Li L, Wu J, Jiang C. Differential expression of Kir6.1 and SUR2B mRNAs in the vasculature of various tissues in rats. J Membr Biol 2003;196:61–9.
[302] Sun X, Cao K, Yang G, Huang Y, Hanna ST, Wang R. Selective expression of Kir6.1 protein in different vascular and non-vascular tissues. Biochem Pharmacol 2004;67:147–56.
[303] Wang X, Trottier G, Loutzenhiser R. Determinants of renal afferent arteriolar actions of bradykinin: evidence that multiple pathways mediate responses attributed to EDHF. Am J Physiol Renal Physiol 2003;285:F540–9.
[304] Chilton L, Loutzenhiser K, Morales E, Breaks J, Kargacin GJ, Loutzenhiser R. Inward rectifier $K^{(+)}$ currents and Kir2.1 expression in renal afferent and efferent arterioles. J Am Soc Nephrol 2008;19:69–76.
[305] Chilton L, Loutzenhiser R. Functional evidence for an inward rectifier potassium current in rat renal afferent arterioles. Circ Res 2001;88:152–8.
[306] Eckman DM, Nelson MT. Potassium ions as vasodilators: role of inward rectifier potassium channels. Circ Res 2001;88:132–3.
[307] Leichtle A, Rauch U, Albinus M, Benohr P, Kalbacher H, Mack AF, et al. Electrophysiological and molecular characterization of the inward rectifier in juxtaglomerular cells from rat kidney. J Physiol 2004;560:365–76.
[308] Fallet RW, Bast JP, Fujiwara K, Ishii N, Sansom SC, Carmines PK. Influence of $Ca^{(2+)}$-activated $K^{(+)}$ channels on rat renal arteriolar responses to depolarizing agonists. Am J Physiol Renal Physiol 2001;280:F583–91.
[309] Kirton CA, Loutzenhiser R. Alterations in basal protein kinase C activity modulate renal afferent arteriolar myogenic reactivity. Am J Physiol 1998;275:H467–75.
[310] Loutzenhiser RD, Parker MJ. Hypoxia inhibits myogenic reactivity of renal afferent arterioles by activating ATP-sensitive K^+ channels. Circ Res 1994;74:861–9.
[311] Reslerova M, Loutzenhiser R. Divergent mechanisms of ATP-sensitive K^+ channel-induced vasodilation in renal afferent and efferent arterioles. Evidence of L-type Ca^{2+} channel-dependent and -independent actions of pinacidil. Circ Res 1995;77:1114–20.
[312] Reslerova M, Loutzenhiser R. Renal microvascular actions of calcitonin gene-related peptide. Am J Physiol 1998;274: F1078–85.
[313] Tang L, Parker M, Fei Q, Loutzenhiser R. Afferent arteriolar adenosine A2a receptors are coupled to KATP in *in vitro* perfused hydronephrotic rat kidney. Am J Physiol 1999;277: F926–33.
[314] Russ U, Rauch U, Quast U. Pharmacological evidence for a KATP channel in renin-secreting cells from rat kidney. J Physiol 1999;517(Pt 3):781–90.
[315] Metzger F, Quast U. Binding of [^{3}H]-P1075, an opener of ATP-sensitive K^+ channels, to rat glomerular preparations. Naunyn Schmiedebergs Arch Pharmacol 1996;354:452–9.
[316] Troncoso Brindeiro CM, Fallet RW, Lane PH, Carmines PK. Potassium channel contributions to afferent arteriolar tone in normal and diabetic rat kidney. Am J Physiol Renal Physiol 2008;295:F171–8.
[317] Marchetti J, Praddaude F, Rajerison R, Ader JL, Alhenc-Gelas F. Bradykinin attenuates the $[Ca^{(2+)}](_i)$ response to angiotensin II of renal juxtamedullary efferent arterioles via an EDHF. Br J Pharmacol 2001;132:749–59.
[318] Cao C, Goo JH, Lee-Kwon W, Pallone TL. Vasa recta pericytes express a strong inward rectifier K^+ conductance. Am J Physiol Regul Integr Comp Physiol 2006;290:R1601–7.
[319] Cao C, Lee-Kwon W, Payne K, Edwards A, Pallone TL. Descending vasa recta endothelia express inward rectifier potassium channels. Am J Physiol Renal Physiol 2007;293: F1248–55.
[320] Stockand JD, Sansom SC. Glomerular mesangial cells: electrophysiology and regulation of contraction. Physiol Rev 1998;78:723–44.
[321] Barber RD, Woolf AS, Henderson RM. Potassium conductances and proliferation in conditionally immortalized renal glomerular mesangial cells from the H-2Kb-tsA58 transgenic mouse. Biochim Biophys Acta 1997;1355:191–203.
[322] Szamosfalvi B, Cortes P, Alviani R, Asano K, Riser BL, Zasuwa G, et al. Putative subunits of the rat mesangial KATP: a type 2B sulfonylurea receptor and an inwardly rectifying K^+ channel. Kidney Int 2002;61:1739–49.
[323] Grimm PR, Sansom SC. BK channels in the kidney. Curr Opin Nephrol Hypertens 2007;16:430–6.
[324] Matsunaga H, Yamashita N, Miyajima Y, Okuda T, Chang H, Ogata E, et al. Ion channel activities of cultured rat mesangial cells. Am J Physiol 1991;261:F808–14.

[325] Sansom SC, Stockand JD. Physiological role of large, Ca^{2+}-activated K^+ channels in human glomerular mesangial cells. Clin Exp Pharmacol Physiol 1996;23:76–82.
[326] Stockand JD, Sansom SC. Large $Ca(^{2+})$-activated K^+ channels responsive to angiotensin II in cultured human mesangial cells. Am J Physiol 1994;267:C1080–6.
[327] Stockand JD, Sansom SC. Activation by methylene blue of large $Ca(^{2+})$-activated K^+ channels. Biochim Biophys Acta 1996;1285:123–6.
[328] Stockand JD, Sansom SC. Role of large $Ca(^{2+})$-activated K^+ channels in regulation of mesangial contraction by nitroprusside and ANP. Am J Physiol 1996;270:C1773–9.
[329] Stockand JD, Silverman M, Hall D, Derr T, Kubacak B, Sansom SC. Arachidonic acid potentiates the feedback response of mesangial BKCa channels to angiotensin II. Am J Physiol 1998;274:F658–64.
[330] Sansom SC, Ma R, Carmines PK, Hall DA. Regulation of $Ca(^{2+})$-activated $K(^{+})$ channels by multifunctional $Ca(^{2+})$/calmodulin-dependent protein kinase. Am J Physiol Renal Physiol 2000;279:F283–8.
[331] Cermak R, Kleta R, Forssmann WG, Schlatter E. Natriuretic peptides increase a K^+ conductance in rat mesangial cells. Pflugers Arch 1996;431:571–7.
[332] Kudlacek PE, Pluznick JL, Ma R, Padanilam B, Sansom SC. Role of hbeta1 in activation of human mesangial BK channels by cGMP kinase. Am J Physiol Renal Physiol 2003;285:F289–94.
[333] Sansom SC, Stockand JD, Hall D, Williams B. Regulation of large calcium-activated potassium channels by protein phosphatase 2A. J Biol Chem 1997;272:9902–6.
[334] Foutz RM, Grimm PR, Sansom SC. Insulin increases the activity of mesangial BK channels through MAPK signaling. Am J Physiol Renal Physiol 2008;294:F1465–72.
[335] Dhein S. Peptides acting at gap junctions. Peptides 2002;23:1701–9.
[336] De Wit C. Connexins pave the way for vascular communication. News Physiol Sci 2004;19:148–53.
[337] Evans WH, Martin PE. Gap junctions: structure and function (Review). Mol Membr Biol 2002;19:121–36.
[338] Figueroa XF, Isakson BE, Duling BR. Connexins: gaps in our knowledge of vascular function. Physiology (Bethesda) 2004;19:277–84.
[339] De Wit C, Roos F, Bolz SS, Kirchhoff S, Kruger O, Willecke K, et al. Impaired conduction of vasodilation along arterioles in connexin40-deficient mice. Circ Res 2000;86:649–55.
[340] De Wit C, Roos F, Bolz SS, Pohl U. Lack of vascular connexin 40 is associated with hypertension and irregular arteriolar vasomotion. Physiol Genomics 2003;13:169–77.
[341] Figueroa XF, Paul DL, Simon AM, Goodenough DA, Day KH, Damon DN, et al. Central role of connexin40 in the propagation of electrically activated vasodilation in mouse cremasteric arterioles *in vivo*. Circ Res 2003;92:793–800.
[342] Liao Y, Day KH, Damon DN, Duling BR. Endothelial cell-specific knockout of connexin 43 causes hypotension and bradycardia in mice. Proc Natl Acad Sci USA 2001;98:9989–94.
[343] Earley S, Resta TC, Walker BR. Disruption of smooth muscle gap junctions attenuates myogenic vasoconstriction of mesenteric resistance arteries. Am J Physiol Heart Circ Physiol 2004;287:H2677–86.
[344] Arensbak B, Mikkelsen HB, Gustafsson F, Christensen T, Holstein-Rathlou NH. Expression of connexin 37, 40, and 43 mRNA and protein in renal preglomerular arterioles. Histochem Cell Biol 2001;115:479–87.
[345] Braunstein TH, Sorensen CM, Holstein-Rathlou NH. Connexin abundance in resistance vessels from the renal microcirculation in normo- and hypertensive rats. APMIS 2009;117:268–76.
[346] Gustafsson F, Mikkelsen HB, Arensbak B, Thuneberg L, Neve S, Jensen LJ, et al. Expression of connexin 37, 40 and 43 in rat mesenteric arterioles and resistance arteries. Histochem Cell Biol 2003;119:139–48.
[347] Hwan SK, Beyer EC. Heterogeneous localization of connexin40 in the renal vasculature. Microvasc Res 2000;59:140–8.
[348] Just A, Kurtz L, de WC, Wagner C, Kurtz A, Arendshorst WJ. Connexin 40 mediates the tubuloglomerular feedback contribution to renal blood flow autoregulation. J Am Soc Nephrol 2009;20:1577–85.
[349] Silverstein DM, Thornhill BA, Leung JC, Vehaskari VM, Craver RD, Trachtman HA, et al. Expression of connexins in the normal and obstructed developing kidney. Pediatr Nephrol 2003;18:216–24.
[350] Takenaka T, Inoue T, Kanno Y, Okada H, Hill CE, Suzuki H. Connexins 37 and 40 transduce purinergic signals mediating renal autoregulation. Am J Physiol Regul Integr Comp Physiol 2008;294:R1–11.
[351] Takenaka T, Inoue T, Kanno Y, Okada H, Meaney KR, Hill CE, et al. Expression and role of connexins in the rat renal vasculature. Kidney Int 2008;73:415–22.
[352] Zhang J, Hill CE. Differential connexin expression in preglomerular and postglomerular vasculature: accentuation during diabetes. Kidney Int 2005;68:1171–85.
[353] Karagiannis J, Rand M, Li CG. Role of gap junctions in endothelium-derived hyperpolarizing factor-mediated vasodilatation in rat renal artery. Acta Pharmacol Sin 2004;25:1031–7.
[354] Udosen IT, Jiang H, Hercule HC, Oyekan AO. Nitric oxide–epoxygenase interactions and arachidonate-induced dilation of rat renal microvessels. Am J Physiol Heart Circ Physiol 2003;285:H2054–63.
[355] Salomonsson M, Gustafsson F, Andreasen D, Jensen BL, Holstein-Rathlou NH. Local electric stimulation causes conducted calcium response in rat interlobular arteries. Am J Physiol Renal Physiol 2002;283:F473–80.
[356] Haefliger JA, Krattinger N, Martin D, Pedrazzini T, Capponi A, Doring B, et al. Connexin43-dependent mechanism modulates renin secretion and hypertension. J Clin Inves 2006;116:405–13.
[357] Kurtz L, Gerl M, Kriz W, Wagner C, Kurtz A. Replacement of connexin 40 by connexin 45 causes ectopic localization of renin-producing cells in the kidney but maintains *in vivo* control of renin gene expression. Am J Physiol Renal Physiol 2009;297:F403–9.
[358] Kurtz L, Madsen K, Kurt B, Jensen BL, Walter S, Banas B, et al. High-level connexin expression in the human juxtaglomerular apparatus. Nephron Physiol 2010;116:1–8.
[359] Kurtz L, Schweda F, De Wit C, Kriz W, Witzgall R, Warth R, et al. Lack of connexin 40 causes displacement of renin-producing cells from afferent arterioles to the extraglomerular mesangium. J Am Soc Nephrol 2007;18:1103–11.
[360] Barajas L, Liu L, Tucker M. Localization of connexin43 in rat kidney. Kidney Int 1994;46:621–6.
[361] Guo R, Liu L, Barajas L. RT-PCR study of the distribution of connexin 43 mRNA in the glomerulus and renal tubular segments. Am J Physiol 1998;275:R439–47.
[362] Hillis GS, Duthie LA, Mlynski R, McKay NG, Mistry S, MacLeod AM, et al. The expression of connexin 43 in human kidney and cultured renal cells. Nephron 1997;75:458–63.
[363] Haefliger J-A, Demotz S, Braissant O, Suter E, Waeber B, Nicod P, et al. Connexins 40 and 43 are differentially regulated within the kdineys of rats with renovascular hypertension. Kidney Int 2001;60:190–201.
[364] Zhang Q, Cao C, Mangano M, Zhang Z, Silldorff EP, Lee-Kwon W, et al. Descending vasa recta endothelium is an

electrical syncytium. Am J Physiol Regul Integr Comp Physiol 2006;291:R1688–99.
[365] Loutzenhiser R, Bidani AK, Wang X. Systolic pressure and the myogenic response of the renal afferent arteriole. Acta Physiol Scand 2004;181:407–13.
[366] Bell PD, Lapointe JY, Peti-Peterdi J. Macula densa cell signaling. Annu Rev Physiol 2003;65:481–500.
[367] Bell PD, Lapointe JY, Sabirov R, Hayashi S, Peti-Peterdi J, Manabe K, et al. Macula densa cell signaling involves ATP release through a maxi anion channel. Proc Natl Acad Sci USA 2003;100:4322–7.
[368] Castrop H, Huang Y, Hashimoto S, Mizel D, Hansen P, Theilig F, et al. Impairment of tubuloglomerular feedback regulation of GFR in ecto-5′-nucleotidase/CD73-deficient mice. J Clin Invest 2004;114:634–42.
[369] Komlosi P, Fintha A, Bell PD. Current mechanisms of macula densa cell signalling. Acta Physiol Scand 2004;181:463–9.
[370] Ren Y, Garvin JL, Liu R, Carretero OA. Role of macula densa adenosine triphosphate (ATP) in tubuloglomerular feedback. Kidney Int 2004;66:1479–85.
[371] Schnermann J, Homer W. Smith Award lecture. The juxtaglomerular apparatus: from anatomical peculiarity to physiological relevance. J Am Soc Nephrol 2003;14:1681–94.
[372] Granger JP, Alexander BT, Llinas M. Mechanisms of pressure natriuresis. Curr Hypertens Rep 2002;4:152–9.
[373] Kaloyanides GJ, DiBona GF, Raskin P. Pressure natriuresis in the isolated kidney. Am J Physiol 1971;220:1660–6.
[374] Haas JA, Granger JP, Knox FG. Effect of renal perfusion pressure on sodium reabsorption from proximal tubules of superficial and deep nephrons. Am J Physiol 1986;250: F425–9.
[375] Roman RJ. Pressure-diuresis in volume-expanded rats. Tubular reabsorption in superficial and deep nephrons. Hypertension 1988;12:177–83.
[376] Khraibi AA, Haas JA, Knox FG. Effect of renal perfusion pressure on renal interstitial hydrostatic pressure in rats. Am J Physiol 1989;256:F165–70.
[377] Khraibi AA, Knox FG. Effect of renal decapsulation on renal interstitial hydrostatic pressure and natriuresis. Am J Physiol 1989;257:R44–8.
[378] Garcia-Estan J, Roman RJ. Role of renal interstitial hydrostatic pressure in the pressure diuresis response. Am J Physiol 1989;256:F63–70.
[379] Granger JP, Haas JA, Pawlowska D, Knox FG. Effect of direct increases in renal interstitial hydrostatic pressure on sodium excretion. Am J Physiol 1988;254:F527–32.
[380] Haas JA, Granger JP, Knox FG. Effect of intrarenal volume expansion on proximal sodium reabsorption. Am J Physiol 1988;255:F1178–82.
[381] Cowley Jr AW. Role of the renal medulla in volume and arterial pressure regulation. Am J Physiol 1997;273:R1–15.
[382] Cowley Jr AW, Mori T, Mattson D, Zou AP. Role of renal NO production in the regulation of medullary blood flow. Am J Physiol Regul Integr Comp Physiol 2003;284:R1355–69.
[383] Fenoy FJ, Ferrer P, Carbonell L, Garcia-Salom M. Role of nitric oxide on papillary blood flow and pressure natriuresis. Hypertension 1995;25:408–14.
[384] Mattson DL. Importance of the renal medullary circulation in the control of sodium excretion and blood pressure. Am J Physiol Regul Integr Comp Physiol 2003;284:R13–27.
[385] Mattson DL, Wu F. Control of arterial blood pressure and renal sodium excretion by nitric oxide synthase in the renal medulla. Acta Physiol Scand 2000;168:149–54.
[386] Cohen HJ, Marsh DJ, Kayser B. Autoregulation in vasa recta of the rat kidney. Am J Physiol 1983;245:F32–40.
[387] Galskov A, Nissen OI. Autoregulation of directly measured blood flows in the superficial and deep venous drainage areas of the cat kidney. Circ Res 1972;30:97–103.
[388] Roman RJ, Cowley Jr AW, Garcia-Estan J, Lombard JH. Pressure-diuresis in volume-expanded rats. Cortical and medullary hemodynamics. Hypertension 1988;12:168–76.
[389] Mattson DL, Lu S, Roman RJ, Cowley Jr AW. Relationship between renal perfusion pressure and blood flow in different regions of the kidney. Am J Physiol 1993;264:R578–83.
[390] Cowley Jr AW. Control of the renal medullary circulation by vasopressin V1 and V2 receptors in the rat. Exp Physiol 2000;85: Spec No:223S-231S
[391] Eppel GA, Bergstrom G, Anderson WP, Evans RG. Autoregulation of renal medullary blood flow in rabbits. Am J Physiol Regul Integr Comp Physiol 2003;284:R233–44.
[392] Majid DS, Godfrey M, Omoro SA. Pressure natriuresis and autoregulation of inner medullary blood flow in canine kidney. Hypertension 1997;29:210–5.
[393] Zhang Z, Pallone TL. Response of descending vasa recta to luminal pressure. Am J Physiol Renal Physiol 2004;287:F535–42.
[394] Dickhout JG, Mori T, Cowley Jr AW. Tubulovascular nitric oxide crosstalk: buffering of angiotensin II-induced medullary vasoconstriction. Circ Res 2002;91:487–93.
[395] Pallone TL, Silldorff EP, Zhang Z. Inhibition of calcium signaling in descending vasa recta endothelia by ANG II. Am J Physiol Heart Circ Physiol 2000;278:H1248–55.
[396] Silldorff EP, Kreisberg MS, Pallone TL. Adenosine modulates vasomotor tone in outer medullary descending vasa recta of the rat. J Clin Invest 1996;98:18–23.
[397] Silldorff EP, Yang S, Pallone TL. Prostaglandin E2 abrogates endothelin-induced vasoconstriction in renal outer medullary descending vasa recta of the rat. J Clin Invest 1995;95:2734–40.
[398] Racasan S, Joles JA, Boer P, Koomans HA, Braam B. NO dependency of RBF and autoregulation in the spontaneously hypertensive rat. Am J Physiol Renal Physiol 2003;285: F105–12.
[399] Roald AB, Ofstad J, Iversen BM. Attenuated buffering of renal perfusion pressure variation in juxtamedullary cortex in SHR. Am J Physiol Renal Physiol 2002;282:F506–11.
[400] Taniyama Y, Griendling KK. Reactive oxygen species in the vasculature: molecular and cellular mechanisms. Hypertension 2003;42:1075–81.
[401] Feng MG, Dukacz SA, Kline RL. Selective effect of tempol on renal medullary hemodynamics in spontaneously hypertensive rats. Am J Physiol Regul Integr Comp Physiol 2001;281: R1420–5.
[402] Bankir L. Antidiuretic action of vasopressin: quantitative aspects and interaction between V1a and V2 receptor-mediated effects. Cardiovasc Res 2001;51:372–90.
[403] Gussis GL, Robertson CR, Jamison RL. Erythrocyte velocity in vasa recta: effect of antidiuretic hormone and saline loading. Am J Physiol 1979;237:F326–32.
[404] Kiberd B, Robertson CR, Larson T, Jamison RL. Effect of V2-receptor-mediated changes on inner medullary blood flow induced by AVP. Am J Physiol 1987;253:F576–81.
[405] Zimmerhackl B, Robertson CR, Jamison RL. Effect of arginine vasopressin on renal medullary blood flow. A videomicroscopic study in the rat. J Clin Invest 1985;76:770–8.
[406] Nakanishi K, Mattson DL, Gross V, Roman RJ, Cowley Jr AW. Control of renal medullary blood flow by vasopressin V1 and V2 receptors. Am J Physiol 1995;269:R193–200.
[407] Rajapakse NW, Roman RJ, Falck JR, Oliver JJ, Evans RG. Modulation of V1-receptor-mediated renal vasoconstriction by epoxyeicosatrienoic acids. Am J Physiol Regul Integr Comp Physiol 2004;287:R181–7.

[408] Harrison-Bernard LM, Carmines PK. Juxtamedullary microvascular responses to arginine vasopressin in rat kidney. Am J Physiol 1994;267:F249–56.
[409] Fallet RW, Ikenaga H, Bast JP, Carmines PK. Relative contributions of Ca^{2+} mobilization and influx in renal arteriolar contractile responses to arginine vasopressin. AJP - Renal Physiology 2005;288:F545–51.
[410] Weihprecht H, Lorenz JN, Briggs JP, Schnermann J. Vasoconstrictor effect of angiotensin and vasopressin in isolated rabbit afferent arterioles. Am J Physiol 1991;261:F273–82.
[411] Edwards RM, Trizna W, Kinter LB. Renal microvascular effects of vasopressin and vasopressin antagonists. Am J Physiol 1989;256:F274–8.
[412] Turner MR, Pallone TL. Vasopressin constricts outer medullary descending vasa recta isolated from rat kidneys. Am J Physiol 1997;272:F147–51.
[413] Correia AG, Denton KM, Evans RG. Effects of activation of vasopressin-V1-receptors on regional kidney blood flow and glomerular arteriole diameters. J Hypertens 2001;19:649–57.
[414] Aki Y, Tamaki T, Kiyomoto H, He H, Yoshida H, Iwao H, et al. Nitric oxide may participate in V2 vasopressin-receptor-mediated renal vasodilation. J Cardiovasc Pharmacol 1994;23: 331–6.
[415] Liard JF. L-NAME antagonizes vasopressin V2-induced vasodilatation in dogs. Am J Physiol 1994;266:H99–106.
[416] Naitoh M, Suzuki H, Murakami M, Matsumoto A, Ichihara A, Nakamoto H, et al. Arginine vasopressin produces renal vasodilation via V2 receptors in conscious dogs. Am J Physiol 1993;265:R934–42.
[417] Rudichenko VM, Beierwaltes WH. Arginine vasopressin-induced renal vasodilation mediated by nitric oxide. J Vasc Res 1995;32:100–5.
[418] Tamaki T, Kiyomoto K, He H, Tomohiro A, Nishiyama A, Aki Y, et al. Vasodilation induced by vasopressin V2 receptor stimulation in afferent arterioles. Kidney Int 1996;49:722–9.
[419] Park F, Mattson DL, Skelton MM, Cowley Jr AW. Localization of the vasopressin V1a and V2 receptors within the renal cortical and medullary circulation. Am J Physiol 1997;273:R243–51.
[420] Park F, Zou AP, Cowley Jr AW. Arginine vasopressin-mediated stimulation of nitric oxide within the rat renal medulla. Hypertension 1998;32:896–901.
[421] Mori T, Dickhout JG, Cowley Jr AW. Vasopressin increases intracellular NO concentration via $Ca^{(2+)}$ signaling in inner medullary collecting duct. Hypertension 2002;39:465–9.
[422] O'Connor PM, Cowley Jr AW. Vasopressin-induced nitric oxide production in rat inner medullary collecting duct is dependent on V2 receptor activation of the phosphoinositide pathway. Am J Physiol Renal Physiol 2007;293:F526–32.
[423] Evans RG, Madden AC, Denton KM. Diversity of responses of renal cortical and medullary blood flow to vasoconstrictors in conscious rabbits. Acta Physiol Scand 2000;169:297–308.
[424] Szentivanyi Jr M, Park F, Maeda CY, Cowley Jr AW. Nitric oxide in the renal medulla protects from vasopressin-induced hypertension. Hypertension 2000;35:740–5.
[425] Cao C, Edwards A, Sendeski M, Lee-Kwon W, Cui L, Cai CY, et al. Intrinsic nitric oxide and superoxide production regulates descending vasa recta contraction. Am J Physiol Renal Physiol 2010.
[426] Yuan BH, Robinette JB, Conger JD. Effect of angiotensin II and norepinephrine on isolated rat afferent and efferent arterioles. Am J Physiol 1990;258:F741–50.
[427] Harrison-Bernard LM, Carmines PK. Impact of cyclo-oxygenase blockade on juxtamedullary microvascular responses to angiotensin II in rat kidney. Clin Exp Pharmacol Physiol 1995;22:732–8.
[428] Cupples WA, Sakai T, Marsh DJ. Angiotensin II and prostaglandins in control of vasa recta blood flow. Am J Physiol 1988;254:F417–24.
[429] Goransson A, Sjoquist M, Ulfendahl HR. Superficial and juxtamedullary nephron function during converting enzyme inhibition. Am J Physiol 1986;251:F25–33.
[430] Roman RJ, Kaldunski ML, Scicli AG, Carretero OA. Influence of kinins and angiotensin II on the regulation of papillary blood flow. Am J Physiol 1988;255:F690–8.
[431] Evans RG, Head GA, Eppel GA, Burke SL, Rajapakse NW. Angiotensin II and neurohumoral control of the renal medullary circulation. Clin Exp Pharmacol Physiol 2010; 37:e58–69.
[432] Mori T, Cowley Jr AW, Ito S. Molecular mechanisms and therapeutic strategies of chronic renal injury: physiological role of angiotensin II-induced oxidative stress in renal medulla. J Pharmacol Sci 2006;100:2–8.
[433] Navar LG, Prieto-Carrasquero MC, Kobori H. Molecular aspects of the renal renin–angiotensin system. In: Re R, DiPette DJ, Schiffrin EL, Sowers JR, editors. *Molecular mechanisms in hypertension*. Taylor & Francis group. 2006. p. 3–14.
[434] Patzak A, Persson AE. Angiotensin II–nitric oxide interaction in the kidney. Curr Opin Nephrol Hypertens 2007;16:46–51.
[435] Sadowski J, Badzynska B. Specific features and roles of renal circulation: angiotensin II revisited. J Physiol Pharmacol 2006;57(Suppl. 11):169–78.
[436] Kohagura K, Arima S, Endo Y, Chiba Y, Ito O, Abe M, et al. Involvement of cytochrome P450 metabolites in the vascular action of angiotensin II on the afferent arterioles. Hypertens Res 2001;24:551–7.
[437] Kohagura K, Endo Y, Ito O, Arima S, Omata K, Ito S. Endogenous nitric oxide and epoxyeicosatrienoic acids modulate angiotensin II-induced constriction in the rabbit afferent arteriole. Acta Physiol Scand 2000;168:107–12.
[438] Yang S, Silldorff EP, Pallone TL. Effect of norepinephrine and acetylcholine on outer medullary descending vasa recta. Am J Physiol 1995;269:H710–6.
[439] Matsuda H, Hayashi K, Arakawa K, Kubota E, Honda M, Tokuyama H, et al. Distinct modulation of superficial and juxtamedullary arterioles by prostaglandin *in vivo*. Hypertens Res 2002;25:901–10.
[440] Silldorff EP, Pallone TL. Adenosine signaling in outer medullary descending vasa recta. Am J Physiol Regul Integr Comp Physiol 2001;280:R854–61.
[441] Tang L, Loutzenhiser K, Loutzenhiser R. Biphasic actions of prostaglandin E(2) on the renal afferent arteriole: role of EP(3) and EP(4) receptors. Circ Res 2000;86:663–70.
[442] Harrison-Bernard LM, Cook AK, Oliverio MI, Coffman TM. Renal segmental microvascular responses to ANG II in AT1A receptor null mice. Am J Physiol Renal Physiol 2003;284: F538–45.
[443] Helou CM, Imbert-Teboul M, Doucet A, Rajerison R, Chollet C, Alhenc-Gelas F, et al. Angiotensin receptor subtypes in thin and muscular juxtamedullary efferent arterioles of rat kidney. Am J Physiol Renal Physiol 2003;285:F507–14.
[444] Carey RM. Update on the role of the AT2 receptor. Curr Opin Nephrol Hypertens 2005;14:67–71.
[445] Carey RM, Jin X, Wang Z, Siragy HM. Nitric oxide: a physiological mediator of the type 2 (AT2) angiotensin receptor. Acta Physiol Scand 2000;168:65–71.
[446] Arima S, Endo Y, Yaoita H, Omata K, Ogawa S, Tsunoda K, et al. Possible role of P-450 metabolite of arachidonic acid in vasodilator mechanism of angiotensin II type 2 receptor in the isolated microperfused rabbit afferent arteriole. J Clin Invest 1997;100:2816–23.

[447] Patzak A, Kleinmann F, Lai EY, Kupsch E, Skelweit A, Mrowka R. Nitric oxide counteracts angiotensin II induced contraction in efferent arterioles in mice. Acta Physiol Scand 2004;181:439–44.
[448] Patzak A, Lai EY, Mrowka R, Steege A, Persson PB, Persson AE. AT1 receptors mediate angiotensin II-induced release of nitric oxide in afferent arterioles. Kidney Int 2004;66:1949–58.
[449] Endo Y, Arima S, Yaoita H, Omata K, Tsunoda K, Takeuchi K, et al. Function of angiotensin II type 2 receptor in the postglomerular efferent arteriole. Kidney Int Suppl 1997;63:S205–7.
[450] Rhinehart K, Handelsman CA, Silldorff EP, Pallone TL. ANG II AT2 receptor modulates AT1 receptor-mediated descending vasa recta endothelial Ca^{2+} signaling. Am J Physiol Heart Circ Physiol 2003;284:H779–89.
[451] Zhang Z, Rhinehart K, Kwon W, Weinman E, Pallone TL. ANG II signaling in vasa recta pericytes by PKC and reactive oxygen species. Am J Physiol Heart Circ Physiol 2004;287:H773–81.
[452] Endo Y, Arima S, Yaoita H, Tsunoda K, Omata K, Ito S. Vasodilation mediated by angiotensin II type 2 receptor is impaired in afferent arterioles of young spontaneously hypertensive rats. J Vasc Res 1998;35:421–7.
[453] Goto M, Mukoyama M, Sugawara A, Suganami T, Kasahara M, Yahata K, et al. Expression and role of angiotensin II type 2 receptor in the kidney and mesangial cells of spontaneously hypertensive rats. Hypertens Res 2002;25:125–33.
[454] Miyata N, Park F, Li XF, Cowley Jr AW. Distribution of angiotensin AT1 and AT2 receptor subtypes in the rat kidney. Am J Physiol 1999;277:F437–46.
[455] Badzynska B, Grzelec-Mojzesowicz M, Dobrowolski L, Sadowski J. Differential effect of angiotensin II on blood circulation in the renal medulla and cortex of anaesthetised rats. J Physiol 2002;538:159–66.
[456] Duke LM, Eppel GA, Widdop RE, Evans RG. Disparate roles of AT2 receptors in the renal cortical and medullary circulations of anesthetized rabbits. Hypertension 2003;42:200–5.
[457] Navar LG, Ichihara A, Chin SY, Imig JD. Nitric oxide-angiotensin II interactions in angiotensin II-dependent hypertension. Acta Physiol Scand 2000;168:139–47.
[458] Szentivanyi Jr M, Zou AP, Mattson DL, Soares P, Moreno C, Roman RJ, et al. Renal medullary nitric oxide deficit of Dahl S rats enhances hypertensive actions of angiotensin II. Am J Physiol Regul Integr Comp Physiol 2002;283:R266–72.
[459] Zou AP, Wu F, Cowley Jr AW. Protective effect of angiotensin II-induced increase in nitric oxide in the renal medullary circulation. Hypertension 1998;31:271–6.
[460] Mattson DL, Meister CJ. Renal cortical and medullary blood flow responses to L-NAME and ANG II in wild-type, nNOS null mutant, and eNOS null mutant mice. Am J Physiol Regul Integr Comp Physiol 2005;289:R991–7.
[461] Gross V, Schunck WH, Honeck H, Milia AF, Kargel E, Walther T, et al. Inhibition of pressure natriuresis in mice lacking the AT2 receptor. Kidney Int 2000;57:191–202.
[462] Navar LG. The intrarenal renin–angiotensin system in hypertension. Kidney Int 2004;65:1522–32.
[463] Navar LG, Nishiyama A. Why are angiotensin concentrations so high in the kidney? Curr Opin Nephrol Hypertens 2004;13:107–15.
[464] Nishiyama A, Seth DM, Navar LG. Renal interstitial fluid angiotensin I and angiotensin II concentrations during local angiotensin-converting enzyme inhibition. J Am Soc Nephrol 2002;13:2207–12.
[465] Nishiyama A, Seth DM, Navar LG. Angiotensin II type 1 receptor-mediated augmentation of renal interstitial fluid angiotensin II in angiotensin II-induced hypertension. J Hypertens 2003;21:1897–903.
[466] Seikaly MG, Arant Jr BS, Seney Jr FD. Endogenous angiotensin concentrations in specific intrarenal fluid compartments of the rat. J Clin Invest 1990;86:1352–7.
[467] Cao C, Lee-Kwon W, Silldorff EP, Pallone TL. KATP channel conductance of descending vasa recta pericytes. Am J Physiol Renal Physiol 2005;289:F1235–45.
[468] Pallone TL, Turner MR. Ion channel architecture of the renal microcirculation. Current Hypertension Reviews 2006;2:69–81.
[469] Edwards A, Layton AT. Nitric oxide and superoxide transport in a cross-section of the rat outer medulla. I. Effects of low medullary oxygen tension. Am J Physiol Renal Physiol 2010.
[470] Edwards A, Layton AT. Nitric oxide and superoxide transport in a cross-section of the rat outer medulla. II. Reciprocal interactions and tubulo-vascular cross-talk. Am J Physiol Renal Physiol 2010.
[471] Zhang W, Edwards A. A model of nitric oxide tubulovascular cross talk in a renal outer medullary cross section. Am J Physiol Renal Physiol 2007;292:F711–22.
[472] Ferrario CM, Chappell MC. Novel angiotensin peptides. Cell Mol Life Sci 2004;61:2720–7.
[473] Sampaio WO, Nascimento AA, Santos RA. Systemic and regional hemodynamic effects of angiotensin-(1–7) in rats. Am J Physiol Heart Circ Physiol 2003;284:H1985–94.
[474] Stegbauer J, Oberhauser V, Vonend O, Rump LC. Angiotensin-(1–7) modulates vascular resistance and sympathetic neurotransmission in kidneys of spontaneously hypertensive rats. Cardiovasc Res 2004;61:352–9.
[475] Santos RA, Simoes e Silva AC, Maric C, Silva DM, Machado RP, de BI, et al. Angiotensin-(1–7) is an endogenous ligand for the G protein-coupled receptor Mas. Proc Natl Acad Sci USA 2003;100:8258–63.
[476] Batlle D, Soler MJ, Wysocki J. New aspects of the renin–angiotensin system: angiotensin-converting enzyme 2 – a potential target for treatment of hypertension and diabetic nephropathy. Curr Opin Nephrol Hypertens 2008;17:250–7.
[477] Chappell MC. Emerging evidence for a functional angiotensin-converting enzyme 2-angiotensin-(1–7)-MAS receptor axis: more than regulation of blood pressure? Hypertension 2007;50:596–9.
[478] Dilauro M, Burns KD. Angiotensin-(1–7) and its effects in the kidney. Scientific World Journal 2009;9:522–35.
[479] Klar J, Vitzthum H, Kurtz A. Aldosterone enhances renin gene expression in juxtaglomerular cells. Am J Physiol Renal Physiol 2004;286:F349–55.
[480] Uhrenholt TR, Jensen BL, Skott O. Rapid nongenomic effect of aldosterone on vasoconstriction. Hypertension 2004;43:e30.
[481] Schmidt BM, Oehmer S, Delles C, Bratke R, Schneider MP, Klingbeil A, et al. Rapid nongenomic effects of aldosterone on human forearm vasculature. Hypertension 2003;42:156–60.
[482] Arima S. Aldosterone and the kidney: rapid regulation of renal microcirculation. Steroids 2006;71:281–5.
[483] Arima S. Rapid non-genomic vasoconstrictor actions of aldosterone in the renal microcirculation. J Steroid Biochem Mol Biol 2006;102:170–4.
[484] Arima S, Kohagura K, Xu HL, Sugawara A, Abe T, Satoh F, et al. Nongenomic vascular action of aldosterone in the glomerular microcirculation. J Am Soc Nephrol 2003;14:2255–63.
[485] Arima S, Kohagura K, Xu HL, Sugawara A, Uruno A, Satoh F, et al. Endothelium-derived nitric oxide modulates vascular action of aldosterone in renal arteriole. Hypertension 2004;43:352–7.
[486] Brain SD, Grant AD. Vascular actions of calcitonin gene-related peptide and adrenomedullin. Physiol Rev 2004;84:903–34.
[487] Bunton DC, Petrie MC, Hillier C, Johnston F, McMurray JJ. The clinical relevance of adrenomedullin: a promising profile? Pharmacol Ther 2004;103:179–201.

[488] Hinson JP, Kapas S, Smith DM. Adrenomedullin, a multifunctional regulatory peptide. Endocr Rev 2000;21:138–67.
[489] Nishimatsu H, Hirata Y, Shindo T, Kurihara H, Kakoki M, Nagata D, et al. Role of endogenous adrenomedullin in the regulation of vascular tone and ischemic renal injury: studies on transgenic/knockout mice of adrenomedullin gene. Circ Res 2002;90:657–63.
[490] Shindo T, Kurihara Y, Nishimatsu H, Moriyama N, Kakoki M, Wang Y, et al. Vascular abnormalities and elevated blood pressure in mice lacking adrenomedullin gene. Circulation 2001;104:1964–71.
[491] Nagata D, Hirata Y, Suzuki E, Kakoki M, Hayakawa H, Goto A, et al. Hypoxia-induced adrenomedullin production in the kidney. Kidney Int 1999;55:1259–67.
[492] Gardiner SM, Kemp PA, March JE, Bennett T. Regional haemodynamic effects of human and rat adrenomedullin in conscious rats. Br J Pharmacol 1995;114:584–91.
[493] Majid DS, Kadowitz PJ, Coy DH, Navar LG. Renal responses to intra-arterial administration of adrenomedullin in dogs. Am J Physiol 1996;270:F200–5.
[494] Minami K, Segawa K, Uezono Y, Shiga Y, Shiraishi M, Ogata J, et al. Adrenomedullin inhibits the pressor effects and decrease in renal blood flow induced by norepinephrine or angiotensin II in anesthetized rats. Jpn J Pharmacol 2001;86:159–64.
[495] Hirata Y, Hayakawa H, Suzuki Y, Suzuki E, Ikenouchi H, Kohmoto O, et al. Mechanisms of adrenomedullin-induced vasodilation in the rat kidney. Hypertension 1995;25:790–5.
[496] Mori Y, Nishikimi T, Kobayashi N, Ono H, Kangawa K, Matsuoka H. Long-term adrenomedullin infusion improves survival in malignant hypertensive rats. Hypertension 2002;40:107–13.
[497] Nishikimi T, Mori Y, Kobayashi N, Tadokoro K, Wang X, Akimoto K, et al. Renoprotective effect of chronic adrenomedullin infusion in Dahl salt-sensitive rats. Hypertension 2002;39:1077–82.
[498] Ito K, Yoshii H, Asano T, Seta K, Mizuguchi Y, Yamanaka M, et al. Adrenomedullin increases renal nitric oxide production and ameliorates renal injury in mice with unilateral ureteral obstruction. J Urol 2010;183:1630–5.
[499] Oba S, Hino M, Fujita T. Adrenomedullin protects against oxidative stress-induced podocyte injury as an endogenous antioxidant. Nephrol Dial Transplant 2008;23:510–7.
[500] Bell D, McDermott BJ. Intermedin (adrenomedullin-2): a novel counter-regulatory peptide in the cardiovascular and renal systems. Br J Pharmacol 2008;153(Suppl. 1):S247–62.
[501] Fujisawa Y, Nagai Y, Miyatake A, Miura K, Shokoji T, Nishiyama A, et al. Roles of adrenomedullin 2 in regulating the cardiovascular and sympathetic nervous systems in conscious rats. Am J Physiol-Heart Circ Physiol 2006;290:H1120–7.
[502] Fujisawa Y, Nagai Y, Miyatake A, Takei Y, Miura K, Shoukouji T, et al. Renal effects of a new member of adrenomedullin family, adrenomedullin2, in rats. Eur J Pharmacol 2004;497:75–80.
[503] Hagiwara M, Bledsoe G, Yang ZR, Smith Jr RS, Chao L, Chao J. Intermedin ameliorates vascular and renal injury by inhibition of oxidative stress. Am J Physiol Renal Physiol 2008;295:F1735–43.
[504] Hirose T, Totsune K, Mori N, Mori T, Morimoto R, Metoki H, et al. Expression of adrenomedullin 2/intermedin, a possible reno-protective peptide, is decreased in the kidneys of rats with hypertension or renal failure. Am J Physiol Renal Physiol 2010;299:F128–34.
[505] Baylis C. Nitric oxide deficiency in chronic kidney disease. Am J Physiol Renal Physiol 2008;294:F1–9.
[506] Cowley Jr AW. Renal medullary oxidative stress, pressure-natriuresis, and hypertension. Hypertension 2008;52:777–86.
[507] Goligorsky MS, Brodsky SV, Noiri E. NO bioavailability, endothelial dysfunction, and acute renal failure: new insights into pathophysiology. Semin Nephrol 2004;24:316–23.
[508] Goligorsky MS, Li H, Brodsky S, Chen J. Relationships between caveolae and eNOS: everything in proximity and the proximity of everything. Am J Physiol Renal Physiol 2002;283: F1–10.
[509] Kone BC. Nitric oxide synthesis in the kidney: isoforms, biosynthesis, and functions in health. Semin Nephrol 2004;24:299–315.
[510] Kone BC, Baylis C. Biosynthesis and homeostatic roles of nitric oxide in the normal kidney. Am J Physiol 1997;272:F561–78.
[511] Kone BC, Kuncewicz T, Zhang W, Yu ZY. Protein interactions with nitric oxide synthases: controlling the right time, the right place, and the right amount of nitric oxide. Am J Physiol Renal Physiol 2003;285:F178–90.
[512] Majid DS, Navar LG. Nitric oxide in the control of renal hemodynamics and excretory function. Am J Hypertens 2001;14:74S–82S.
[513] Mattson DL, Lu S, Cowley Jr AW. Role of nitric oxide in the control of the renal medullary circulation. Clin Exp Pharmacol Physiol 1997;24:587–90.
[514] Pallone TL, Mattson DL. Role of nitric oxide in regulation of the renal medulla in normal and hypertensive kidneys. Curr Opin Nephrol Hypertens 2002;11:93–8.
[515] Wilcox CS. Effects of tempol and redox-cycling nitroxides in models of oxidative stress. Pharmacol Ther 2010;126:119–45.
[516] Wilcox CS, Pearlman A. Chemistry and antihypertensive effects of tempol and other nitroxides. Pharmacol Rev 2008;60:418–69.
[517] Zou AP, Cowley Jr AW. Reactive oxygen species and molecular regulation of renal oxygenation. Acta Physiol Scand 2003;179:233–41.
[518] Mattson DL, Wu F. Nitric oxide synthase activity and isoforms in rat renal vasculature. Hypertension 2000;35:337–41.
[519] Kakoki M, Kim HS, Arendshorst WJ, Mattson DL. L-Arginine uptake affects nitric oxide production and blood flow in the renal medulla. Am J Physiol Regul Integr Comp Physiol 2004;287:R1478–85.
[520] Kakoki M, Wang W, Mattson DL. Cationic amino acid transport in the renal medulla and blood pressure regulation. Hypertension 2002;39:287–92.
[521] Wu F, Cholewa B, Mattson DL. Characterization of L-arginine transporters in rat renal inner medullary collecting duct. Am J Physiol Regul Integr Comp Physiol 2000;278:R1506–12.
[522] Zewde T, Wu F, Mattson DL. Influence of dietary NaCl on L-arginine transport in the renal medulla. Am J Physiol Regul Integr Comp Physiol 2004;286:R89–93.
[523] Palm F, Onozato ML, Luo Z, Wilcox CS. Dimethylarginine dimethylaminohydrolase (DDAH): expression, regulation, and function in the cardiovascular and renal systems. Am J Physiol Heart Circ Physiol 2007;293:H3227–45.
[524] Teerlink T, Luo Z, Palm F, Wilcox CS. Cellular ADMA: regulation and action. Pharmacol Res 2009;60:448–60.
[525] Tojo A, Welch WJ, Bremer V, Kimoto M, Kimura K, Omata M, et al. Colocalization of demethylating enzymes and NOS and functional effects of methylarginines in rat kidney. Kidney Int 1997;52:1593–601.
[526] Wang D, Gill PS, Chabrashvili T, Onozato ML, Raggio J, Mendonca M, et al. Isoform-specific regulation by N^G,N^G-dimethylarginine dimethylaminohydrolase of rat serum asymmetric dimethylarginine and vascular endothelium-derived relaxing factor/NO. Circ Res 2007;101:627–35.
[527] Wang D, Strandgaard S, Iversen J, Wilcox CS. Asymmetric dimethylarginine, oxidative stress, and vascular nitric oxide

synthase in essential hypertension. Am J Physiol Regul Integr Comp Physiol 2009;296:R195–200.
[528] Beierwaltes WH, Sigmon DH, Carretero OA. Endothelium modulates renal blood flow but not autoregulation. Am J Physiol 1992;262:F943–9.
[529] Majid DS, Williams A, Navar LG. Inhibition of nitric oxide synthesis attenuates pressure-induced natriuretic responses in anesthetized dogs. Am J Physiol 1993;264:F79–87.
[530] Imig JD, Gebremedhin D, Harder DR, Roman RJ. Modulation of vascular tone in renal microcirculation by erythrocytes: role of EDRF. Am J Physiol 1993;264:H190–5.
[531] Imig JD, Roman RJ. Nitric oxide modulates vascular tone in preglomerular arterioles. Hypertension 1992;19:770–4.
[532] Juncos LA, Ito S, Carretero OA, Garvin JL. Removal of endothelium-dependent relaxation by antibody and complement in afferent arterioles. Hypertension 1994;23:I54–9.
[533] Hoffend J, Cavarape A, Endlich K, Steinhausen M. Influence of endothelium-derived relaxing factor on renal microvessels and pressure-dependent vasodilation. Am J Physiol 1993;265: F285–92.
[534] Larson TS, Lockhart JC. Restoration of vasa recta hemodynamics and pressure natriuresis in SHR by L-arginine. Am J Physiol 1995;268:F907–12.
[535] Kakoki M, Kim HS, Edgell CJ, Maeda N, Smithies O, Mattson DL. Amino acids as modulators of endothelium-derived nitric oxide. Am J Physiol Renal Physiol 2006;291:F297–304.
[536] Rajapakse NW, De MC, Das S, Mattson DL. Exogenous L-arginine ameliorates angiotensin II-induced hypertension and renal damage in rats. Hypertension 2008;52:1084–90.
[537] Rajapakse NW, Mattson DL. Role of L-arginine in nitric oxide production in health and hypertension. Clin Exp Pharmacol Physiol 2009;36:249–55.
[538] Mattson DL, Lu S, Nakanishi K, Papanek PE, Cowley Jr AW. Effect of chronic renal medullary nitric oxide inhibition on blood pressure. Am J Physiol 1994;266:H1918–26.
[539] Nakanishi K, Mattson DL, Cowley Jr AW. Role of renal medullary blood flow in the development of L-NAME hypertension in rats. Am J Physiol 1995;268:R317–23.
[540] Biondi ML, Dousa T, Vanhoutte P, Romero JC. Evidence for the existence of endothelium-derived relaxing factor in the renal medulla. Am J Hypertens 1990;3:876–8.
[541] McKee M, Scavone C, Nathanson JA. Nitric oxide, cGMP, and hormone regulation of active sodium transport. Proc Natl Acad Sci USA 1994;91:12056–60.
[542] Moridani BA, Kline RL. Effect of endogenous L-arginine on the measurement of nitric oxide synthase activity in the rat kidney. Can J Physiol Pharmacol 1996;74:1210–4.
[543] Zou AP, Cowley Jr AW. Nitric oxide in renal cortex and medulla. An *in vivo* microdialysis study. Hypertension 1997;29:194–8.
[544] Miyata N, Cowley Jr AW. Renal intramedullary infusion of L-arginine prevents reduction of medullary blood flow and hypertension in Dahl salt-sensitive rats. Hypertension 1999;33:446–50.
[545] Miyata N, Zou AP, Mattson DL, Cowley Jr AW. Renal medullary interstitial infusion of L-arginine prevents hypertension in Dahl salt-sensitive rats. Am J Physiol 1998;275:R1667–73.
[546] Kakoki M, Zou AP, Mattson DL. The influence of nitric oxide synthase 1 on blood flow and interstitial nitric oxide in the kidney. Am J Physiol Regul Integr Comp Physiol 2001;281:R91–7.
[547] Mattson DL, Bellehumeur TG. Neural nitric oxide synthase in the renal medulla and blood pressure regulation. Hypertension 1996;28:297–303.
[548] Mattson DL, Maeda CY, Bachman TD, Cowley Jr AW. Inducible nitric oxide synthase and blood pressure. Hypertension 1998;31:15–20.
[549] Mattson DL, Meister CJ. Sodium sensitivity of arterial blood pressure in L-NAME hypertensive but not eNOS knockout mice. Am J Hypertens 2006;19:327–9.
[550] Garvin JL, Ortiz PA. The role of reactive oxygen species in the regulation of tubular function. Acta Physiol Scand 2003;179:225–32.
[551] Ortiz PA, Garvin JL. Role of nitric oxide in the regulation of nephron transport. Am J Physiol Renal Physiol 2002;282: F777–84.
[552] Ortiz PA, Garvin JL. Superoxide stimulates NaCl absorption by the thick ascending limb. Am J Physiol Renal Physiol 2002;283:F957–62.
[553] Szentivanyi Jr M, Zou AP, Maeda CY, Mattson DL, Cowley Jr AW. Increase in renal medullary nitric oxide synthase activity protects from norepinephrine-induced hypertension. Hypertension 2000;35:418–23.
[554] Zou AP, Cowley Jr AW. Alpha^2-adrenergic receptor-mediated increase in NO production buffers renal medullary vasoconstriction. Am J Physiol Regul Integr Comp Physiol 2000;279: R769–77.
[555] Yuan B, Cowley Jr AW. Evidence that reduced renal medullary nitric oxide synthase activity of Dahl S rats enables small elevations of arginine vasopressin to produce sustained hypertension. Hypertension 2001;37:524–8.
[556] Heyman SN, Rosen S, Darmon D, Goldfarb M, Bitz H, Shina A, et al. Endotoxin-induced renal failure. II. A role for tubular hypoxic damage. Exp Nephrol 2000;8:275–82.
[557] James PE, Bacic G, Grinberg OY, Goda F, Dunn JF, Jackson SK, et al. Endotoxin-induced changes in intrarenal PO_2, measured by *in vivo* electron paramagnetic resonance oximetry and magnetic resonance imaging. Free Radic Biol Med 1996;21:25–34.
[558] Sendeski M, Patzak A, Pallone TL, Cao C, Persson AE, Persson PB. Iodixanol, constriction of medullary descending vasa recta, and risk for contrast medium-induced nephropathy. Radiology 2009;251:697–704.
[559] Mori T, Cowley Jr AW. Angiotensin II-NAD(P)H oxidase-stimulated superoxide modifies tubulovascular nitric oxide cross-talk in renal outer medulla. Hypertension 2003;42:588–93.
[560] Rhinehart KL, Pallone TL. Nitric oxide generation by isolated descending vasa recta. Am J Physiol Heart Circ Physiol 2001;281:H316–24.
[561] Zhang W, Pibulsonggram T, Edwards A. Determinants of basal nitric oxide concentration in the renal medullary microcirculation. Am J Physiol Renal Physiol 2004;287:F1189–203.
[562] Droge W. Free radicals in the physiological control of cell function. Physiol Rev 2002;82:47–95.
[563] Araujo M, Welch WJ. Oxidative stress and nitric oxide in kidney function. Curr Opin Nephrol Hypertens 2006;15:72–7.
[564] Schnackenberg CG. Physiological and pathophysiological roles of oxygen radicals in the renal microvasculature. Am J Physiol Regul Integr Comp Physiol 2002;282:R335–42.
[565] Welch WJ. Angiotensin II-dependent superoxide: effects on hypertension and vascular dysfunction. Hypertension 2008;52:51–6.
[566] Wilcox CS. Oxidative stress and nitric oxide deficiency in the kidney: a critical link to hypertension? Am J Physiol Regul Integr Comp Physiol 2005;289:R913–35.
[567] Schnackenberg CG, Welch WJ, Wilcox CS. TP receptor-mediated vasoconstriction in microperfused afferent arterioles: roles of $O_2^{(-)}$ and NO. Am J Physiol Renal Physiol 2000;279:F302–8.
[568] Ozawa Y, Hayashi K, Wakino S, Kanda T, Homma K, Takamatsu I, et al. Free radical activity depends on underlying vasoconstrictors in renal microcirculation. Clin Exp Hypertens 2004;26:219–29.

[569] Abe M, O'Connor P, Kaldunski M, Liang M, Roman RJ, Cowley Jr AW. Effect of sodium delivery on superoxide and nitric oxide in the medullary thick ascending limb. Am J Physiol Renal Physiol 2006;291:F350–7.
[570] Mori T, O'Connor PM, Abe M, Cowley Jr AW. Enhanced superoxide production in renal outer medulla of Dahl salt-sensitive rats reduces nitric oxide tubular-vascular cross-talk. Hypertension 2007;49:1336–41.
[571] Palm F, Onozato M, Welch WJ, Wilcox CS. Blood pressure, blood flow, and oxygenation in the clipped kidney of chronic 2-kidney, 1-clip rats: effects of tempol and angiotensin blockade. Hypertension 2010;55:298–304.
[572] Sedeek M, Hebert RL, Kennedy CR, Burns KD, Touyz RM. Molecular mechanisms of hypertension: role of Nox family NADPH oxidases. Curr Opin Nephrol Hypertens 2009;18:122–7.
[573] Schnackenberg CG, Welch WJ, Wilcox CS. Normalization of blood pressure and renal vascular resistance in SHR with a membrane-permeable superoxide dismutase mimetic: role of nitric oxide. Hypertension 1998;32:59–64.
[574] Schnackenberg CG, Wilcox CS. Two-week administration of tempol attenuates both hypertension and renal excretion of 8-Iso prostaglandin f2alpha. Hypertension 1999;33:424–8.
[575] Chabrashvili T, Kitiyakara C, Blau J, Karber A, Aslam S, Welch WJ, et al. Effects of ANG II type 1 and 2 receptors on oxidative stress, renal NADPH oxidase, and SOD expression. Am J Physiol Regul Integr Comp Physiol 2003;285:R117–24.
[576] Zhang Z, Rhinehart K, Solis G, Pittner J, Lee-Kwon W, Welch WJ, et al. Chronic ANG II infusion increases NO generation by rat descending vasa recta. Am J Physiol Heart Circ Physiol 2005;288:H29–36.
[577] Welch WJ. Intrarenal oxygen and hypertension. Clin Exp Pharmacol Physiol 2006;33:1002–5.
[578] Welch WJ, Baumgartl H, Lubbers D, Wilcox CS. Renal oxygenation defects in the spontaneously hypertensive rat: role of AT1 receptors. Kidney Int 2003;63:202–8.
[579] Welch WJ, Blau J, Xie H, Chabrashvili T, Wilcox CS. Angiotensin-induced defects in renal oxygenation: role of oxidative stress. Am J Physiol Heart Circ Physiol 2005;288:H22–8.
[580] Chen YF, Cowley Jr AW, Zou AP. Increased $H(_2)O(_2)$ counteracts the vasodilator and natriuretic effects of superoxide dismutation by tempol in renal medulla. Am J Physiol Regul Integr Comp Physiol 2003;285:R827–33.
[581] Makino A, Skelton MM, Zou AP, Cowley Jr AW. Increased renal medullary H_2O_2 leads to hypertension. Hypertension 2003;42:25–30.
[582] Makino A, Skelton MM, Zou AP, Roman RJ, Cowley Jr AW. Increased renal medullary oxidative stress produces hypertension. Hypertension 2002;39:667–72.
[583] Zou AP, Li N, Cowley Jr AW. Production and actions of superoxide in the renal medulla. Hypertension 2001;37:547–53.
[584] Meng S, Roberts LJ, Cason GW, Curry TS, Manning Jr RD. Superoxide dismutase and oxidative stress in Dahl salt-sensitive and -resistant rats. Am J Physiol Regul Integr Comp Physiol 2002;283:R732–8.
[585] Carmines PK. The renal vascular response to diabetes. Curr Opin Nephrol Hypertens 2010;19:85–90.
[586] Ishii N, Patel KP, Lane PH, Taylor T, Bian K, Murad F, et al. Carmines PK. Nitric oxide synthesis and oxidative stress in the renal cortex of rats with diabetes mellitus. J Am Soc Nephrol 2001;12:1630–9.
[587] Kanwar YS, Wada J, Sun L, Xie P, Wallner EI, Chen S, et al. Diabetic nephropathy: mechanisms of renal disease progression. Exp Biol Med (Maywood) 2008;233:4–11.
[588] Pollock JS, Carmines PK. Diabetic nephropathy: nitric oxide and renal medullary hypoxia. Am J Physiol Renal Physiol 2008;294:F28–9.
[589] Schoonmaker GC, Fallet RW, Carmines PK. Superoxide anion curbs nitric oxide modulation of afferent arteriolar ANG II responsiveness in diabetes mellitus. Am J Physiol Renal Physiol 2000;278:F302–9.
[590] Abraham NG, Kappas A. Heme oxygenase and the cardiovascular–renal system. Free Radic Biol Med 2005;39:1–25.
[591] Zou AP, Billington H, Su N, Cowley Jr AW. Expression and actions of heme oxygenase in the renal medulla of rats. Hypertension 2000;35:342–7.
[592] Yang ZZ, Zhang AY, Yi FX, Li PL, Zou AP. Redox regulation of HIF-1alpha levels and HO-1 expression in renal medullary interstitial cells. Am J Physiol Renal Physiol 2003;284: F1207–15.
[593] Yang ZZ, Zou AP. Transcriptional regulation of heme oxygenases by HIF-1alpha in renal medullary interstitial cells. Am J Physiol Renal Physiol 2001;281:F900–8.
[594] Tian W, Bonkovsky HL, Shibahara S, Cohen DM. Urea and hypertonicity increase expression of heme oxygenase-1 in murine renal medullary cells. Am J Physiol Renal Physiol 2001;281:F983–91.
[595] Abraham NG, Botros FT, Rezzani R, Rodella L, Bianchi R, Goodman AI. Differential effect of cobalt protoporphyrin on distributions of heme oxygenase in renal structure and on blood pressure in SHR. Cell Mol Biol (Noisy-le-grand) 2002;48:895–902.
[596] Akagi R, Takahashi T, Sassa S. Cytoprotective effects of heme oxygenase in acute renal failure. Contrib Nephrol 2005;148:70–85.
[597] Li N, Chen L, Yi F, Xia M, Li PL. Salt-sensitive hypertension induced by decoy of transcription factor hypoxia-inducible factor-1alpha in the renal medulla. Circ Res 2008;102:1101–8.
[598] Li N, Yi F, dos Santos EA, Donley DK, Li PL. Role of renal medullary heme oxygenase in the regulation of pressure natriuresis and arterial blood pressure. Hypertension 2007;49:148–54.
[599] Li N, Yi F, Sundy CM, Chen L, Hilliker ML, Donley DK, et al. Expression and actions of HIF prolyl-4-hydroxylase in the rat kidney. Am J Physiol Renal Physiol 2007;292:F207–16.
[600] Vera T, Kelsen S, Stec DE. Kidney-specific induction of heme oxygenase-1 prevents angiotensin II hypertension. Hypertension 2008;52:660–5.
[601] Vera T, Kelsen S, Yanes LL, Reckelhoff JF, Stec DE. HO-1 induction lowers blood pressure and superoxide production in the renal medulla of angiotensin II hypertensive mice. Am J Physiol Regul Integr Comp Physiol 2007;292:R1472–8.
[602] Curtis LM, Agarwal A. Hope for contrast-induced acute kidney injury. Kidney Int 2007;72:907–9.
[603] Goodman AI, Olszanecki R, Yang LM, Quan S, Li M, Omura S, et al. Heme oxygenase-1 protects against radiocontrast-induced acute kidney injury by regulating anti-apoptotic proteins. Kidney Int 2007;72:945–53.
[604] Jarmi T, Agarwal A. Heme oxygenase and renal disease. Curr Hypertens Rep 2009;11:56–62.
[605] Jackson EK, Zhu C, Tofovic SP. Expression of adenosine receptors in the preglomerular microcirculation. Am J Physiol Renal Physiol 2002;283:F41–51.
[606] Vitzthum H, Weiss B, Bachleitner W, Kramer BK, Kurtz A. Gene expression of adenosine receptors along the nephron. Kidney Int 2004;65:1180–90.
[607] Hansen PB, Schnermann J. Vasoconstrictor and vasodilator effects of adenosine in the kidney. Am J Physiol Renal Physiol 2003;285:F590–9.

[608] Jackson EK, Dubey RK. Role of the extracellular cAMP-adenosine pathway in renal physiology. Am J Physiol Renal Physiol 2001;281:F597–612.
[609] Vallon V, Muhlbauer B, Osswald H. Adenosine and kidney function. Physiol Rev 2006;86:901–40.
[610] Vallon V., Osswald H. Adenosine receptors and the kidney. Handb Exp Pharmacol 2009;(193):443–70.
[611] Osmond DA, Inscho EW. P2X(1) receptor blockade inhibits whole kidney autoregulation of renal blood flow *in vivo*. Am J Physiol Renal Physiol 2010;298:F1360–8.
[612] McCoy DE, Bhattacharya S, Olson BA, Levier DG, Arend LJ, Spielman WS. The renal adenosine system: structure, function, and regulation. Semin Nephrol 1993;13:31–40.
[613] Agmon Y, Dinour D, Brezis M. Disparate effects of adenosine A1- and A2-receptor agonists on intrarenal blood flow. Am J Physiol 1993;265:F802–6.
[614] Carmines PK, Inscho EW. Renal arteriolar angiotensin responses during varied adenosine receptor activation. Hypertension 1994;23:I114–9.
[615] Weihprecht H, Lorenz JN, Briggs JP, Schnermann J. Vasomotor effects of purinergic agonists in isolated rabbit afferent arterioles. Am J Physiol 1992;263:F1026–33.
[616] Nishiyama A, Inscho EW, Navar LG. Interactions of adenosine A1 and A2a receptors on renal microvascular reactivity. Am J Physiol Renal Physiol 2001;280:F406–14.
[617] Al-Mashhadi RH, Skott O, Vanhoutte PM, Hansen PB. Activation of A^2 adenosine receptors dilates cortical efferent arterioles in mouse. Kidney Int 2009;75:793–9.
[618] Blantz RC, Vallon V. Tubuloglomerular feedback responses of the downstream efferent resistance: unmasking a role for adenosine? Kidney Int 2007;71:837–9.
[619] Brown R, Ollerstam A, Johansson B, Skott O, Gebre-Medhin S, Fredholm B, et al. Abolished tubuloglomerular feedback and increased plasma renin in adenosine A1 receptor-deficient mice. Am J Physiol Regul Integr Comp Physiol 2001;281:R1362–7.
[620] Castrop H. Mediators of tubuloglomerular feedback regulation of glomerular filtration: ATP and adenosine. Acta Physiol (Oxf) 2007;189:3–14.
[621] Oppermann M, Mizel D, Kim SM, Chen L, Faulhaber-Walter R, Huang Y, et al. Renal function in mice with targeted disruption of the A isoform of the Na-K-2Cl co-transporter. J Am Soc Nephrol 2007;18:440–8.
[622] Oppermann M, Qin Y, Lai EY, Eisner C, Li L, Huang Y, et al. Enhanced tubuloglomerular feedback in mice with vascular overexpression of A1 adenosine receptors. Am J Physiol Renal Physiol 2009;297:F1256–64.
[623] Schnermann J. Adenosine mediates tubuloglomerular feedback. Am J Physiol Regul Integr Comp Physiol 2002;283: R276–7.
[624] Thomson S, Bao D, Deng A, Vallon V. Adenosine formed by 5′-nucleotidase mediates tubuloglomerular feedback. J Clin Invest 2000;106:289–98.
[625] Inscho EW, Cook AK, Imig JD, Vial C, Evans RJ. Renal autoregulation in P2X1 knockout mice. Acta Physiol Scand 2004;181:445–53.
[626] Blantz RC, Deng A. Coordination of kidney filtration and tubular reabsorption: considerations on the regulation of metabolic demand for tubular reabsorption. Acta Physiol Hung 2007;94:83–94.
[627] Miyamoto M, Yagil Y, Larson T, Robertson C, Jamison RL. Effects of intrarenal adenosine on renal function and medullary blood flow in the rat. Am J Physiol 1988;255:F1230–4.
[628] Kreisberg MS, Silldorff EP, Pallone TL. Localization of adenosine-receptor subtype mRNA in rat outer medullary descending vasa recta by RT-PCR. Am J Physiol 1997;272:H1231–8.
[629] Baranowski RL, Westenfelder C. Estimation of renal interstitial adenosine and purine metabolites by microdialysis. Am J Physiol 1994;267:F174–82.
[630] Hansen PB, Castrop H, Briggs J, Schnermann J. Adenosine induces vasoconstriction through Gi-dependent activation of phospholipase C in isolated perfused afferent arterioles of mice. J Am Soc Nephrol 2003;14:2457–65.
[631] Cheng MK, Doumad AB, Jiang H, Falck JR, McGiff JC, Carroll MA. Epoxyeicosatrienoic acids mediate adenosine-induced vasodilation in rat preglomerular microvessels (PGMV) via A2A receptors. Br J Pharmacol 2004;141:441–8.
[632] Dietrich MS, Endlich K, Parekh N, Steinhausen M. Interaction between adenosine and angiotensin II in renal microcirculation. Microvasc Res 1991;41:275–88.
[633] Hall JE, Granger JP. Adenosine alters glomerular filtration control by angiotensin II. Am J Physiol 1986;250:F917–23.
[634] Osswald H, Schmitz HJ, Heidenreich O. Adenosine response of the rat kidney after saline loading, sodium restriction and hemorrhagia. Pflugers Arch 1975;357:323–33.
[635] Spielman WS, Osswald H. Blockade of postocclusive renal vasoconstriction by an angiotensin II antagonists: evidence for an angiotensin–adenosine interaction. Am J Physiol 1979;237: F463–7.
[636] Weihprecht H, Lorenz JN, Briggs JP, Schnermann J. Synergistic effects of angiotensin and adenosine in the renal microvasculature. Am J Physiol 1994;266:F227–39.
[637] Barrett RJ, Droppleman DA. Interactions of adenosine A1 receptor-mediated renal vasoconstriction with endogenous nitric oxide and ANG II. Am J Physiol 1993;265:F651–9.
[638] Inscho EW. Modulation of renal microvascular function by adenosine. Am J Physiol Regul Integr Comp Physiol 2003;285: R23–5.
[639] Traynor T, Yang T, Huang YG, Arend L, Oliverio MI, Coffman T, et al. Inhibition of adenosine-1 receptor-mediated preglomerular vasoconstriction in AT1A receptor-deficient mice. Am J Physiol 1998;275:F922–7.
[640] Dinour D, Brezis M. Effects of adenosine on intrarenal oxygenation. Am J Physiol 1991;261:F787–91.
[641] Beach RE, Watts III BA, Good DW, Benedict CR, DuBose Jr TD. Effects of graded oxygen tension on adenosine release by renal medullary and thick ascending limb suspensions. Kidney Int 1991;39:836–42.
[642] Beach RE, Good DW. Effects of adenosine on ion transport in rat medullary thick ascending limb. Am J Physiol 1992;263: F482–7.
[643] Brezis M, Agmon Y, Epstein FH. Determinants of intrarenal oxygenation. I. Effects of diuretics. Am J Physiol 1994;267: F1059–62.
[644] Zou AP, Wu F, Li PL, Cowley Jr AW. Effect of chronic salt loading on adenosine metabolism and receptor expression in renal cortex and medulla in rats. Hypertension 1999; 33:511–6.
[645] Guan Z, Osmond DA, Inscho EW. P2X receptors as regulators of the renal microvasculature. Trends Pharmacol Sci 2007;28: 646–52.
[646] Guan Z, Osmond DA, Inscho EW. Purinoceptors in the kidney. Exp Biol Med (Maywood) 2007;232:715–26.
[647] Inscho EW. Renal microvascular effects of P2 receptor stimulation. Clin Exp Pharmacol Physiol 2001;28:332–9.
[648] Bailey MA, Hillman KA, Unwin RJ. P2 receptors in the kidney. J Auton Nerv Syst 2000;81:264–70.
[649] Chan CM, Unwin RJ, Bardini M, Oglesby IB, Ford AP, Townsend-Nicholson A, et al. Localization of P2X1 purinoceptors by autoradiography and immunohistochemistry in rat kidneys. Am J Physiol 1998;274:F799–804.

[650] Lewis CJ, Evans RJ. P2X receptor immunoreactivity in different arteries from the femoral, pulmonary, cerebral, coronary and renal circulations. J Vasc Res 2001;38:332–40.
[651] Inscho EW. P2 receptors in regulation of renal microvascular function. Am J Physiol Renal Physiol 2001;280:F927–44.
[652] Ralevic V, Burnstock G. Receptors for purines and pyrimidines. Pharmacol Rev 1998;50:413–92.
[653] Churchill PC, Ellis VR. Pharmacological characterization of the renovascular P2 purinergic receptors. J Pharmacol Exp Ther 1993;265:334–8.
[654] Rump LC, Oberhauser V, von KI. Purinoceptors mediate renal vasodilation by nitric oxide dependent and independent mechanisms. Kidney Int 1998;54:473–81.
[655] Inscho EW, Ohishi K, Cook AK, Belott TP, Navar LG. Calcium activation mechanisms in the renal microvascular response to extracellular ATP. Am J Physiol 1995;268:F876–84.
[656] Inscho EW, Ohishi K, Navar LG. Effects of ATP on pre- and postglomerular juxtamedullary microvasculature. Am J Physiol 1992;263:F886–93.
[657] Zhao X, Falck JR, Gopal VR, Inscho EW, Imig JD. P2X receptor-stimulated calcium responses in preglomerular vascular smooth muscle cells involves 20-hydroxyeicosatetraenoic acid. J Pharmacol Exp Ther 2004;311:1211–7.
[658] Zhao X, Inscho EW, Bondlela M, Falck JR, Imig JD. The CYP450 hydroxylase pathway contributes to P2X receptor-mediated afferent arteriolar vasoconstriction. Am J Physiol Heart Circ Physiol 2001;281:H2089–96.
[659] Inscho EW, LeBlanc EA, Pham BT, White SM, Imig JD. Purinoceptor-mediated calcium signaling in preglomerular smooth muscle cells. Hypertension 1999;33:195–200.
[660] White SM, Imig JD, Kim TT, Hauschild BC, Inscho EW. Calcium signaling pathways utilized by P2X receptors in freshly isolated preglomerular MVSMC. Am J Physiol Renal Physiol 2001;280:F1054–61.
[661] Inscho EW, Cook AK, Navar LG. Pressure-mediated vasoconstriction of juxtamedullary afferent arterioles involves P2-purinoceptor activation. Am J Physiol 1996;271:F1077–85.
[662] Majid DS, Inscho EW, Navar LG. P2 purinoceptor saturation by adenosine triphosphate impairs renal autoregulation in dogs. J Am Soc Nephrol 1999;10:492–8.
[663] Majid DS, Navar LG. Suppression of blood flow autoregulation plateau during nitric oxide blockade in canine kidney. Am J Physiol 1992;262:F40–6.
[664] Inscho EW, Cook AK, Imig JD, Vial C, Evans RJ. Physiological role for P2X1 receptors in renal microvascular autoregulatory behavior. J Clin Invest 2003;112:1895–905.
[665] Chatziantoniou C, Arendshorst WJ. Prostaglandin interactions with angiotensin, norepinephrine, and thromboxane in rat renal vasculature. Am J Physiol 1992;262:F68–76.
[666] Itskovitz HD, Stemper J, Pacholczyk D, McGiff JC. Renal prostaglandins: determinants of intrarenal distribution of blood flow in the dog. Clin Sci Mol Med Suppl 1973;45(Suppl. 1):321s–4s.
[667] Larsson C, Anggard E. Increased juxtamedullary blood flow on stimulation of intrarenal prostaglandin biosynthesis. Eur J Pharmacol 1974;25:326–34.
[668] Gomez SI, Strick DM, Romero JC. Role of nitric oxide and prostaglandin in the maintenance of cortical and renal medullary blood flow. Braz J Med Biol Res 2008;41:170–5.
[669] Sadowski J, Badzynska B. Intrarenal vasodilator systems: NO, prostaglandins and bradykinin. An integrative approach. J Physiol Pharmacol 2008;59(Suppl. 9):105–19.
[670] Lemley KV, Schmitt SL, Holliger C, Dunn MJ, Robertson CR, Jamison RL. Prostaglandin synthesis inhibitors and vasa recta erythrocyte velocities in the rat. Am J Physiol 1984;247:F562–7.
[671] Badzynska B, Grzelec-Mojzesowicz M, Sadowski J. Prostaglandins but not nitric oxide protect renal medullary perfusion in anaesthetised rats receiving angiotensin II. J Physiol 2003;548:875–80.
[672] Oliver JJ, Eppel GA, Rajapakse NW, Evans RG. Lipoxygenase and cyclo-oxygenase products in the control of regional kidney blood flow in rabbits. Clin Exp Pharmacol Physiol 2003;30:812–9.
[673] Parekh N, Zou AP. Role of prostaglandins in renal medullary circulation: response to different vasoconstrictors. Am J Physiol 1996;271:F653–8.
[674] Roman RJ, Lianos E. Influence of prostaglandins on papillary blood flow and pressure-natriuretic response. Hypertension 1990;15:29–35.
[675] Agmon Y, Peleg H, Greenfeld Z, Rosen S, Brezis M. Nitric oxide and prostanoids protect the renal outer medulla from radiocontrast toxicity in the rat. J Clin Invest 1994;94:1069–75.
[676] Heyman SN, Brezis M, Epstein FH, Spokes K, Silva P, Rosen S. Early renal medullary hypoxic injury from radiocontrast and indomethacin. Kidney Int 1991;40:632–42.
[677] Heyman SN, Fuchs S, Jaffe R, Shina A, Ellezian L, Brezis M, et al. Renal microcirculation and tissue damage during acute ureteral obstruction in the rat: effect of saline infusion, indomethacin and radiocontrast. Kidney Int 1997;51:653–63.
[678] Campean V, Theilig F, Paliege A, Breyer M, Bachmann S. Key enzymes for renal prostaglandin synthesis: site-specific expression in rodent kidney (rat, mouse). Am J Physiol Renal Physiol 2003;285:F19–32.
[679] Cheng HF, Harris RC. Cyclooxygenases, the kidney, and hypertension. Hypertension 2004;43:525–30.
[680] Harris RC, Breyer MD. Physiological regulation of cyclooxygenase-2 in the kidney. Am J Physiol Renal Physiol 2001;281: F1–11.
[681] Harris RC, Zhang MZ, Cheng HF. Cyclooxygenase-2 and the renal renin–angiotensin system. Acta Physiol Scand 2004;181:543–7.
[682] Yang T. Regulation of cyclooxygenase-2 in renal medulla. Acta Physiol Scand 2003;177:417–21.
[683] Fujino T, Nakagawa N, Yuhki K, Hara A, Yamada T, Takayama K, et al. Decreased susceptibility to renovascular hypertension in mice lacking the prostaglandin I2 receptor IP. J Clin Invest 2004;114:805–12.
[684] Paliege A, Mizel D, Medina C, Pasumarthy A, Huang YG, Bachmann S, et al. Inhibition of nNOS expression in the macula densa by COX-2-derived prostaglandin E(2). Am J Physiol Renal Physiol 2004;287:F152–9.
[685] Peti-Peterdi J, Komlosi P, Fuson AL, Guan Y, Schneider A, Qi Z, et al. Luminal NaCl delivery regulates basolateral PGE2 release from macula densa cells. J Clin Invest 2003;112:76–82.
[686] Lopez R, Llinas MT, Roig F, Salazar FJ. Role of nitric oxide and cyclooxygenase-2 in regulating the renal hemodynamic response to norepinephrine. Am J Physiol Regul Integr Comp Physiol 2003;284:R488–93.
[687] Deng A, Wead LM, Blantz RC. Temporal adaptation of tubuloglomerular feedback: effects of COX-2. Kidney Int 2004;66:2348–53.
[688] Ichihara A, Imig JD, Inscho EW, Navar LG. Cyclooxygenase-2 participates in tubular flow-dependent afferent arteriolar tone: interaction with neuronal NOS. Am J Physiol 1998;275: F605–12.
[689] Zhang MZ, Sanchez LP, McKanna JA, Harris RC. Regulation of cyclooxygenase expression by vasopressin in rat renal medulla. Endocrinology 2004;145:1402–9.
[690] Birck R, Krzossok S, Knoll T, Braun C, Der Woude FJ, Rohmeiss P. Preferential COX-2 inhibitor, meloxicam,

compromises renal perfusion in euvolemic and hypovolemic rats. Exp Nephrol 2000;8:173–80.
[691] Green T, Rodriguez J, Navar LG. Augmented cyclooxygenase-2 effects on renal function during varying states of angiotensin II activity. Am J Physiol Renal Physiol 2010;299(5):F954–962.
[692] Qi Z, Hao CM, Langenbach RI, Breyer RM, Redha R, Morrow JD, et al. Opposite effects of cyclooxygenase-1 and -2 activity on the pressor response to angiotensin II. J Clin Invest 2002;110:61–9.
[693] Zewde T, Mattson DL. Inhibition of cyclooxygenase-2 in the rat renal medulla leads to sodium-sensitive hypertension. Hypertension 2004;44:424–8.
[694] Zhao X, Yamamoto T, Newman JW, Kim IH, Watanabe T, Hammock BD, et al. Soluble epoxide hydrolase inhibition protects the kidney from hypertension-induced damage. J Am Soc Nephrol 2004;15:1244–53.
[695] Edwards RM. Effects of prostaglandins on vasoconstrictor action in isolated renal arterioles. Am J Physiol 1985;248:F779–84.
[696] Inscho EW, Carmines PK, Navar LG. Prostaglandin influences on afferent arteriolar responses to vasoconstrictor agonists. Am J Physiol 1990;259:F157–63.
[697] Arima S, Ren Y, Juncos LA, Carretero OA, Ito S. Glomerular prostaglandins modulate vascular reactivity of the downstream efferent arterioles. Kidney Int 1994;45:650–8.
[698] Wang D, Chabrashvili T, Wilcox CS. Enhanced contractility of renal afferent arterioles from angiotensin-infused rabbits: roles of oxidative stress, thromboxane prostanoid receptors, and endothelium. Circ Res 2004;94:1436–42.
[699] Audoly LP, Ruan X, Wagner VA, Goulet JL, Tilley SL, Koller BH, et al. Role of EP(2) and EP(3) PGE(2) receptors in control of murine renal hemodynamics. Am J Physiol Heart Circ Physiol 2001;280:H327–33.
[700] Hayashi K, Loutzenhiser R, Epstein M. Direct evidence that thromboxane mimetic U44069 preferentially constricts the afferent arteriole. J Am Soc Nephrol 1997;8:25–31.
[701] Silldorff EP, Hilbun LR, Pallone TL. Angiotensin II constriction of rat vasa recta is partially thromboxane dependent. Hypertension 2002;40:541–6.
[702] Wilcox CS, Welch WJ, Snellen H. Thromboxane mediates renal hemodynamic response to infused angiotensin II. Kidney Int 1991;40:1090–7.
[703] Kawada N, Dennehy K, Solis G, Modlinger P, Hamel R, Kawada JT, et al. TP receptors regulate renal hemodynamics during angiotensin II slow pressor response. Am J Physiol Renal Physiol 2004;287:F753–9.
[704] Harder DR, Campbell WB, Roman RJ. Role of cytochrome P-450 enzymes and metabolites of arachidonic acid in the control of vascular tone. J Vasc Res 1995;32:79–92.
[705] Fleming I. Cytochrome p450 and vascular homeostasis. Circ Res 2001;89:753–62.
[706] Imig JD. Eicosanoids and renal vascular function in diseases. Clin Sci (Lond) 2006;111:21–34.
[707] Imig JD. Targeting epoxides for organ damage in hypertension. J Cardiovasc Pharmacol 2010;56(4):329–35.
[708] Imig JD, Pham BT, LeBlanc EA, Reddy KM, Falck JR, Inscho EW. Cytochrome P450 and cyclooxygenase metabolites contribute to the endothelin-1 afferent arteriolar vasoconstrictor and calcium responses. Hypertension 2000;35:307–12.
[709] McGiff JC, Quilley J. 20-HETE and the kidney: resolution of old problems and new beginnings. Am J Physiol 1999;277: R607–23.
[710] Ortiz PA, Garvin JL. Intrarenal transport and vasoactive substances in hypertension. Hypertension 2001;38:621–4.
[711] Regner KR, Zuk A, Van Why SK, Shames BD, Ryan RP, Falck JR, et al. Protective effect of 20-HETE analogues in experimental renal ischemia reperfusion injury. Kidney Int 2009;75:511–7.
[712] Roman RJ. P-450 metabolites of arachidonic acid in the control of cardiovascular function. Physiol Rev 2002;82:131–85.
[713] Roman RJ, Maier KG, Sun CW, Harder DR, Alonso-Galicia M. Renal and cardiovascular actions of 20-hydroxyeicosatetraenoic acid and epoxyeicosatrienoic acids. Clin Exp Pharmacol Physiol 2000;27:855–65.
[714] Sarkis A, Lopez B, Roman RJ. Role of 20-hydroxyeicosatetraenoic acid and epoxyeicosatrienoic acids in hypertension. Curr Opin Nephrol Hypertens 2004;13:205–14.
[715] Harder DR, Narayanan J, Birks EK, Liard JF, Imig JD, Lombard JH, et al. Identification of a putative microvascular oxygen sensor. Circ Res 1996;79:54–61.
[716] Imig JD, Zou AP, Stec DE, Harder DR, Falck JR, Roman RJ. Formation and actions of 20-hydroxyeicosatetraenoic acid in rat renal arterioles. Am J Physiol 1996;270:R217–27.
[717] Alonso-Galicia M, Maier KG, Greene AS, Cowley Jr AW, Roman RJ. Role of 20-hydroxyeicosatetraenoic acid in the renal and vasoconstrictor actions of angiotensin II. Am J Physiol Regul Integr Comp Physiol 2002;283:R60–8.
[718] Hercule HC, Oyekan AO. Cytochrome P450 omega/omega-1 hydroxylase-derived eicosanoids contribute to endothelin(A) and endothelin(B) receptor-mediated vasoconstriction to endothelin-1 in the rat preglomerular arteriole. J Pharmacol Exp Ther 2000;292:1153–60.
[719] Zou AP, Imig JD, Kaldunski M, Ortiz de Montellano PR, Sui Z, Roman RJ. Inhibition of renal vascular 20-HETE production impairs autoregulation of renal blood flow. Am J Physiol 1994;266:F275–82.
[720] Alonso-Galicia M, Drummond HA, Reddy KK, Falck JR, Roman RJ. Inhibition of 20-HETE production contributes to the vascular responses to nitric oxide. Hypertension 1997;29:320–5.
[721] Williams JM, Sarkis A, Lopez B, Ryan RP, Flasch AK, Roman RJ. Elevations in renal interstitial hydrostatic pressure and 20-hydroxyeicosatetraenoic acid contribute to pressure natriuresis. Hypertension 2007;49:687–94.
[722] Hoagland KM, Flasch AK, Roman RJ. Inhibitors of 20-HETE formation promote salt-sensitive hypertension in rats. Hypertension 2003;42:669–73.
[723] Stec DE, Mattson DL, Roman RJ. Inhibition of renal outer medullary 20-HETE production produces hypertension in Lewis rats. Hypertension 1997;29:315–9.
[724] Capdevila JH, Falck JR. The CYP P450 arachidonic acid monooxygenases: from cell signaling to blood pressure regulation. Biochem Biophys Res Commun 2001;285:571–6.
[725] Capdevila JH, Nakagawa K, Holla V. The CYP P450 arachidonate monooxygenases: enzymatic relays for the control of kidney function and blood pressure. Adv Exp Med Biol 2003;525:39–46.
[726] Gainer JV, Bellamine A, Dawson EP, Womble KE, Grant SW, Wang Y, et al. Functional variant of CYP4A11 20-hydroxyeicosatetraenoic acid synthase is associated with essential hypertension. Circulation 2005;111:63–9.
[727] Imig JD, Navar LG, Roman RJ, Reddy KK, Falck JR. Actions of epoxygenase metabolites on the preglomerular vasculature. J Am Soc Nephrol 1996;7:2364–70.
[728] Spiecker M, Liao JK. Vascular protective effects of cytochrome p450 epoxygenase-derived eicosanoids. Arch Biochem Biophys 2005;433:413–20.
[729] Imig JD, Inscho EW, Deichmann PC, Reddy KM, Falck JR. Afferent arteriolar vasodilation to the sulfonimide analog of 11,12-epoxyeicosatrienoic acid involves protein kinase A. Hypertension 1999;33:408–13.
[730] Fukao M, Mason HS, Kenyon JL, Horowitz B, Keef KD. Regulation of BK(Ca) channels expressed in human embryonic

kidney 293 cells by epoxyeicosatrienoic acid. Mol Pharmacol 2001;59:16–23.
[731] Pomposiello SI, Quilley J, Carroll MA, Falck JR, McGiff JC. 5,6-Epoxyeicosatrienoic acid mediates the enhanced renal vasodilation to arachidonic acid in the SHR. Hypertension 2003;42:548–54.
[732] Regner KR, Zuk A, Van Why SK, Shames BD, Ryan RP, Falck JR, et al. Protective effect of 20-HETE analogues in experimental renal ischemia reperfusion injury. Kidney Int 2009;75:511–7.
[733] Imig JD, Falck JR, Wei S, Capdevila JH. Epoxygenase metabolites contribute to nitric oxide-independent afferent arteriolar vasodilation in response to bradykinin. J Vasc Res 2001;38:247–55.
[734] Imig JD, Zhao X, Capdevila JH, Morisseau C, Hammock BD. Soluble epoxide hydrolase inhibition lowers arterial blood pressure in angiotensin II hypertension. Hypertension 2002;39:690–4.
[735] Imig JD, Zhao X, Falck JR, Wei S, Capdevila JH. Enhanced renal microvascular reactivity to angiotensin II in hypertension is ameliorated by the sulfonimide analog of 11,12-epoxyeicosatrienoic acid. J Hypertens 2001;19:983–92.
[736] Zhao X, Pollock DM, Inscho EW, Zeldin DC, Imig JD. Decreased renal cytochrome P450 2C enzymes and impaired vasodilation are associated with angiotensin salt-sensitive hypertension. Hypertension 2003;41:709–14.
[737] Yu Z, Huse LM, Adler P, Graham L, Ma J, Zeldin DC, et al. Increased CYP2J expression and epoxyeicosatrienoic acid formation in spontaneously hypertensive rat kidney. Mol Pharmacol 2000;57:1011–20.
[738] Yu Z, Xu F, Huse LM, Morisseau C, Draper AJ, Newman JW, et al. Soluble epoxide hydrolase regulates hydrolysis of vasoactive epoxyeicosatrienoic acids. Circ Res 2000;87:992–8.
[739] Kotelevtsev Y, Webb DJ. Endothelin as a natriuretic hormone: the case for a paracrine action mediated by nitric oxide. Cardiovasc Res 2001;51:481–8.
[740] Krum H, Viskoper RJ, Lacourciere Y, Budde M, Charlon V. The effect of an endothelin-receptor antagonist, bosentan, on blood pressure in patients with essential hypertension. Bosentan Hypertension Investigators. N Engl J Med 1998;338:784–90.
[741] Naicker S, Bhoola KD. Endothelins: vasoactive modulators of renal function in health and disease. Pharmacol Ther 2001;90:61–88.
[742] Plato CF, Garvin JL. Nitric oxide, endothelin and nephron transport: potential interactions. Clin Exp Pharmacol Physiol 1999;26:262–8.
[743] Kohan DE. The renal medullary endothelin system in control of sodium and water excretion and systemic blood pressure. Curr Opin Nephrol Hypertens 2006;15:34–40.
[744] Terada Y, Tomita K, Nonoguchi H, Marumo F. Different localization of two types of endothelin receptor mRNA in microdissected rat nephron segments using reverse transcription and polymerase chain reaction assay. J Clin Invest 1992;90:107–12.
[745] Zhuo J, Dean R, Maric C, Aldred PG, Harris P, Alcorn D, et al. Localization and interactions of vasoactive peptide receptors in renomedullary interstitial cells of the kidney. Kidney Int Suppl 1998;67:S22–8.
[746] Abassi ZA, Ellahham S, Winaver J, Hoffman A. The intrarenal endothelin system and hypertension. News Physiol Sci 2001;16:152–6.
[747] Kohan DE. Endothelins in the normal and diseased kidney. Am J Kidney Dis 1997;29:2–26.
[748] Just A, Olson AJ, Arendshorst WJ. Dual constrictor and dilator actions of ET(B) receptors in the rat renal microcirculation: interactions with ET(A) receptors. Am J Physiol Renal Physiol 2004;286:F660–8.
[749] Bloom IT, Bentley FR, Wilson MA, Garrison RN. *In vivo* effects of endothelin on the renal microcirculation. J Surg Res 1993;54:274–80.
[750] Cavarape A, Bartoli E. Effects of BQ-123 on systemic and renal hemodynamic responses to endothelin-1 in the rat split hydronephrotic kidney. J Hypertens 1998;16:1449–58.
[751] Endlich K, Hoffend J, Steinhausen M. Localization of endothelin ETA and ETB receptor-mediated constriction in the renal microcirculation of rats. J Physiol 1996;497(Pt 1):211–8.
[752] Kitamura K, Tanaka T, Kato J, Eto T, Tanaka K. Regional distribution of immunoreactive endothelin in porcine tissue: abundance in inner medulla of kidney. Biochem Biophys Res Commun 1989;161:348–52.
[753] Konishi F, Okada Y, Takaoka M, Gariepy CE, Yanagisawa M, Matsumura Y. Role of endothelin ET(B) receptors in the renal hemodynamic and excretory responses to big endothelin-1. Eur J Pharmacol 2002;451:177–84.
[754] Loutzenhiser R, Epstein M, Hayashi K, Horton C. Direct visualization of effects of endothelin on the renal microvasculature. Am J Physiol 1990;258:F61–8.
[755] Edwards RM, Trizna W, Ohlstein EH. Renal microvascular effects of endothelin. Am J Physiol 1990;259:F217–21.
[756] Fellner SK, Arendshorst WJ. Endothelin A and B receptors of preglomerular vascular smooth muscle cells. Kidney Int 2004;65:1810–7.
[757] Pollock DM, Jenkins JM, Cook AK, Imig JD, Inscho EW. L-type calcium channels in the renal microcirculatory response to endothelin. Am J Physiol Renal Physiol 2004.
[758] Schroeder AC, Imig JD, LeBlanc EA, Pham BT, Pollock DM, Inscho EW. Endothelin-mediated calcium signaling in preglomerular smooth muscle cells. Hypertension 2000;35:280–6.
[759] Nakano D, Pollock DM. Contribution of endothelin A receptors in endothelin 1-dependent natriuresis in female rats. Hypertension 2009;53:324–30.
[760] Nakano D, Pollock JS, Pollock DM. Renal medullary ETB receptors produce diuresis and natriuresis via NOS1. Am J Physiol Renal Physiol 2008;294:F1205–11.
[761] Gurbanov K, Rubinstein I, Hoffman A, Abassi Z, Better OS, Winaver J. Differential regulation of renal regional blood flow by endothelin-1. Am J Physiol 1996;271:F1166–72.
[762] Hoffman A, Abassi ZA, Brodsky S, Ramadan R, Winaver J. Mechanisms of big endothelin-1-induced diuresis and natriuresis: role of ET(B) receptors. Hypertension 2000;35:732–9.
[763] Vassileva I, Mountain C, Pollock DM. Functional role of ETB receptors in the renal medulla. Hypertension 2003;41:1359–63.
[764] Gariepy CE, Ohuchi T, Williams SC, Richardson JA, Yanagisawa M. Salt-sensitive hypertension in endothelin-B receptor-deficient rats. J Clin Invest 2000;105:925–33.
[765] Gariepy CE, Williams SC, Richardson JA, Hammer RE, Yanagisawa M. Transgenic expression of the endothelin-B receptor prevents congenital intestinal aganglionosis in a rat model of Hirschsprung disease. J Clin Invest 1998;102:1092–101.
[766] Pollock DM. Contrasting pharmacological ETB receptor blockade with genetic ETB deficiency in renal responses to big ET-1. Physiol Genomics 2001;6:39–43.
[767] Pollock DM. Renal endothelin in hypertension. Curr Opin Nephrol Hypertens 2000;9:157–64.
[768] Sasser JM, Pollock JS, Pollock DM. Renal endothelin in chronic angiotensin II hypertension. Am J Physiol Regul Integr Comp Physiol 2002;283:R243–8.
[769] Dhaun N, Goddard J, Kohan DE, Pollock DM, Schiffrin EL, Webb DJ. Role of endothelin-1 in clinical hypertension: 20 years on. Hypertension 2008;52:452–9.

[770] Dhaun N, Goddard J, Webb DJ. The endothelin system and its antagonism in chronic kidney disease. J Am Soc Nephrol 2006;17:943–55.
[771] Molero MM, Giulumian AD, Reddy VB, Ludwig LM, Pollock JS, Pollock DM, et al. Decreased endothelin binding and $[Ca^{2+}]_i$ signaling in microvessels of DOCA-salt hypertensive rats. J Hypertens 2002;20:1799–805.
[772] Kohan DE. Biology of endothelin receptors in the collecting duct. Kidney Int 2009.
[773] Kuhn M. Molecular physiology of natriuretic peptide signalling. Basic Res Cardiol 2004;99:76–82.
[774] Levin ER, Gardner DG, Samson WK. Natriuretic peptides. N Engl J Med 1998;339:321–8.
[775] Vesely DL. Atrial natriuretic peptides in pathophysiological diseases. Cardiovasc Res 2001;51:647–58.
[776] Janssen WM, Beekhuis H, de Bruin R, de Jong PE, de Zeeuw D. Noninvasive measurement of intrarenal blood flow distribution: kinetic model of renal 123I-hippuran handling. Am J Physiol 1995;269:F571–80.
[777] Kiberd BA, Larson TS, Robertson CR, Jamison RL. Effect of atrial natriuretic peptide on vasa recta blood flow in the rat. Am J Physiol 1987;252:F1112–7.
[778] Takezawa K, Cowley Jr AW, Skelton M, Roman RJ. Atriopeptin III alters renal medullary hemodynamics and the pressure-diuresis response in rats. Am J Physiol 1987;252: F992–1002.
[779] Tsuchiya K, Sanaka T, Nitta K, Ando A, Sugino N. Effects of atrial natriuretic peptide on regional renal blood flow measured by a thermal diffusion technique. Jpn J Exp Med 1989;59:27–35.
[780] Aalkjaer C, Mulvany MJ, Nyborg NC. Atrial natriuretic factor causes specific relaxation of rat renal arcuate arteries. Br J Pharmacol 1985;86:447–53.
[781] Hayashi K, Epstein M, Loutzenhiser R. Determinants of renal actions of atrial natriuretic peptide. Lack of effect of atrial natriuretic peptide on pressure-induced vasoconstriction. Circ Res 1990;67:1–10.
[782] Marin-Grez M, Fleming JT, Steinhausen M. Atrial natriuretic peptide causes pre-glomerular vasodilatation and post-glomerular vasoconstriction in rat kidney. Nature 1986;324:473–6.
[783] Veldkamp PJ, Carmines PK, Inscho EW, Navar LG. Direct evaluation of the microvascular actions of ANP in juxtamedullary nephrons. Am J Physiol 1988;254:F440–4.
[784] Edwards RM, Weidley EF. Lack of effect of atriopeptin II on rabbit glomerular arterioles *in vitro*. Am J Physiol 1987;252: F317–21.
[785] Endlich K, Steinhausen M. Natriuretic peptide receptors mediate different responses in rat renal microvessels. Kidney Int 1997;52:202–7.
[786] Endlich K, Forssmann WG, Steinhausen M. Effects of urodilatin in the rat kidney: comparison with ANF and interaction with vasoactive substances. Kidney Int 1995;47:1558–68.
[787] Lorenz JN, Nieman M, Sabo J, Sanford LP, Hawkins JA, Elitsur N, et al. Uroguanylin knockout mice have increased blood pressure and impaired natriuretic response to enteral NaCl load. J Clin Invest 2003;112:1244–54.
[788] Wang T, Kawabata M, Haneda M, Takabatake T. Effects of uroguanylin, an intestinal natriuretic peptide, on tubuloglomerular feedback. Hypertens Res 2003;26:577–82.
[789] Ejaz AA, Heinig ME, Kazory A, Bihorac A, Hobson CE, Beaver TM. The rise and fall of natriuretic peptides in acute kidney injury: a misunderstood relationship? Rev Cardiovasc Med 2007;8(Suppl 5):S32–7.
[790] Moffat DB, Fourman J. The vascular pattern of the rat kidney. J Anat 1963;97:543–53.
[791] Brezis M, Heyman SN, Dinour D, Epstein FH, Rosen S. Role of nitric oxide in renal medullary oxygenation. Studies in isolated and intact rat kidneys. J Clin Invest 1991;88:390–5.
[792] Mendez RE, Dunn BR, Troy JL, Brenner BM. Atrial natriuretic peptide and furosemide effects on hydraulic pressure in the renal papilla. Kidney Int 1988;34:36–42.
[793] Ma R, Pluznick JL, Sansom SC. Ion channels in mesangial cells: function, malfunction, or fiction. Physiology (Bethesda) 2005;20:102–11.

This page intentionally left blank

CHAPTER

25

Molecular and Cellular Mechanisms of Kidney Development

Kevin T. Bush[1], *Hiroyuki Sakurai*[2] *and Sanjay K. Nigam*[1,3,4,5]

[1]Departments of Pediatrics, University of California San Diego, La Jolla, CA, USA
[2]Kyorin University School of Medicine, Mitaka, Tokyo, Japan
[3]Cellular and Molecular Medicine, University of California San Diego, La Jolla, CA, USA
[4]Medicine (Division of Nephrology and Hypertension), University of California San Diego, La Jolla, CA, USA
[5]Bioengineering, University of California San Diego, La Jolla, CA, USA

OVERVIEW

In the course of its development, the mammalian kidney goes through three distinct forms: the pronephros; the mesonephros; and the metanephros, ultimately leading to the formation of the mature kidney (Figure 25.1). At day 22 of gestation in humans or at day 8 in mice, an epithelial streak called the pronephric duct arises in the cervical region of the developing embryo from intermediate mesodermal cells induced to undergo the transition to epithelial cells in response to signals arising from the somite and surface ectoderm.[1–3] The pronephric duct then extends caudally to form the nephric duct or Wolffian duct. The most primitive kidney, the pronephros, is formed as the pronephric duct induces surrounding mesenchyme to form the pronephric tubules. Glomerulus-like structures (glomera) are also seen, but are not physically connected to the tubules forming a non-integrated nephron.[4] The pronephros is functional only in fish and amphibians; it is thought to be rudimentary and non-functional in higher vertebrates.

Next, a more complex "protokidney," the mesonephros, arises just caudal to the pronephros at day 24 in humans or day 9.5 in mice. As with the pronephros, mesonephric development starts with induction of the surrounding mesenchyme by the Wolffian duct. Unlike the pronephros, however, the mesonephros glomeruli are linked to the Wolffian duct via mesonephric tubules. In humans, about 30 nephrons are observed in the mesonephros; their function is unclear. The mesonephric duct and some tubules persist, and are ultimately integrated into the male genital system forming, in part, the vas deferens and tubules of the epididymis.[5] In females, the mesonephros degenerates and disappears.

The permanent kidney of amniotes, the metanephros, starts to form at day 28 in humans or day 11 in mice. Unlike the pronephros and mesonephros, which are induced by the Wolffian duct, metanephric tubules are induced by an epithelial structure derived from the Wolffian duct: the ureteric bud. The ureteric bud is induced to evaginate from the Wolffian duct in response to signals arising from the metanephric mesenchyme, a loose aggregation of intermediate mesodermal cells.[6,7] The emergence of this epithelial progenitor tissue of the metanephric kidney is a key initiating event, and depends upon differentiation of the metanephric mesenchyme from the intermediate mesodermal cells.[8,9] As the ureteric bud invades the surrounding mesenchyme, it induces the mesenchymal cells to form epithelial metanephric tubules that eventually differentiate into the proximal through distal portions of the nephron. The ureteric bud, reciprocally induced by the metanephric mesenchyme, undergoes branching morphogenesis, eventually giving rise to the collecting system. Morphologically, nephron formation is completed by birth in humans, although only after birth does the nephron become fully functional.[7]

Seldin and Giebisch's The Kidney, Fifth Edition.
DOI: http://dx.doi.org/10.1016/B978-0-12-381462-3.00025-2

© 2013 Elsevier Inc. All rights reserved.

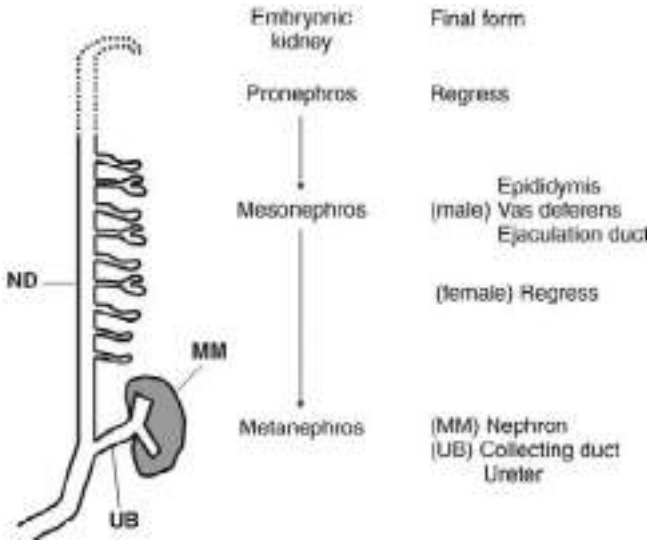

FIGURE 25.1 **Schematic illustration of mammalian kidney development.** The pronephros appears at a relatively higher position in the embryo. Then the mesonephros forms caudally around the nephric duct (ND) or Wolffian duct. In the male, the mesonephric tubules become a part of the genital system. The permanent kidney, the metanephros, forms caudally to the mesonephros. The ureteric bud (UB) derives from the Wolffian duct, ultimately becoming the collecting system. The metanephric mesenchyme, induced by the ureteric bud, forms nephron tubules and glomeruli.

DEVELOPMENT OF THE METANEPHROS

Here, the development of the metanephros is described in more detail (Figure 25.2), since it becomes the final kidney in mammals. As discussed in the previous section, the ureteric bud, the inducer of metanephric development, is formed from the Wolffian duct. This structure invades the metanephric mesenchyme, whereupon mesenchymal cells condense at the tip of the ureteric bud. The condensed mesenchymal cells then differentiate into epithelial cells: the so-called mesenchymal-to-epithelial transformation (MET). The newly formed epithelial cells gradually develop into distinct structures called "comma-shaped bodies," which subsequently become "S-shaped bodies." The S-shaped bodies, which begin to exhibit tubular morphology, continue to elongate; the end closest to the ureteric bud connects to it, while the opposite end forms podocytes and Bowman's capsule. The middle part ultimately differentiates into the proximal through distal tubules of the nephron. At the same time, the tips of the ureteric bud, induced by the metanephric mesenchyme, continue to branch to ultimately form the collecting ducts, renal pelvis, calyces, and papillae.

The process of collecting system development has been studied in detail by microdissection of the human kidney.[10,11] Initial ureteric bud branching is dichotomous and symmetric; the ureteric bud takes on a T-shape in this early stage of metanephrogenesis. Subsequently, the ureteric bud elongates and bifurcates at the tips, and eventually branches again dichotomously. At later branching events, the angle between branches lessens and branching may not be completely symmetrical, so that somehow the ureteric tree structure "fits" into the final shape of the kidney.[8] The initial branches become dilated to form the renal pelvis, while terminal branches become collecting

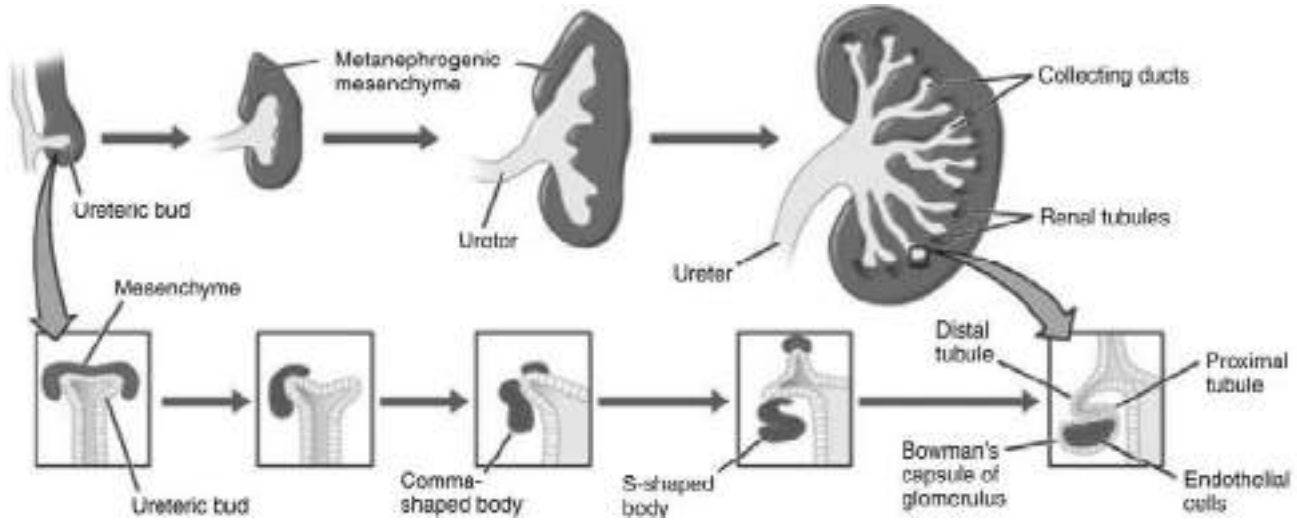

FIGURE 25.2 **Schematic illustration of metanephros development.** Top panels show a macroscopic view of kidney collecting system development through ureteric bud branching morphogenesis. Bottom panels show nephron development from metanephric mesenchyme. *adapted from ref. [82]).*

ducts. As the ureteric bud undergoes branching morphogenesis, its tips continue to induce more nephrons from the metanephric mesenchyme.

Vascular development occurs along with nephron development. Dissection of the developing kidney reveals that large vessels branch off from the dorsal aorta invading into the kidneys.[12] As will be discussed later, the extent to which the microvasculature of the kidney is derived from cells of the metanephric mesenchyme versus cells from outside the kidney is still unclear (reviewed in [13]). The origin of the mesangial cells, which closely associate with the endothelial cells in the glomerulus, also remains uncertain.

Thus, the reciprocal mutual induction and feedback between the ureteric bud and the metanephric mesenchyme represent key events in metanephric epithelial tissue development leading to a functional kidney. These reciprocal interactions induce branching morphogenesis of the ureteric bud, together with epithelialization and tubulogenesis of the metanephric mesenchyme (Figure 25.3). To better understand the mechanisms underlying induction, it is necessary to identify and analyze the key molecules that mediate signals between the metanephric mesenchyme and the ureteric bud.

EXPERIMENTAL APPROACHES TO KIDNEY DEVELOPMENT

Over the years, a variety of experimental approaches have been used for evaluation of the mechanistic details of the induction process between the ureteric bud and metanephric mesenchyme. For example, the developing kidney has been found to be amenable to extensive *in vitro* analysis. In addition to this "whole embryonic kidney organ culture," it has been demonstrated that progenitor tissues (i.e., Wolffian duct, ureteric bud, and metanephric mesenchyme) can be isolated and cultured individually. Advances in genetic manipulation have allowed the analysis of kidney development *in vivo* in genetically-engineered mice. As *in vitro* culture techniques and *in vivo* genetic manipulation become increasingly sophisticated, it is becoming clear that these approaches should be viewed as complementary.

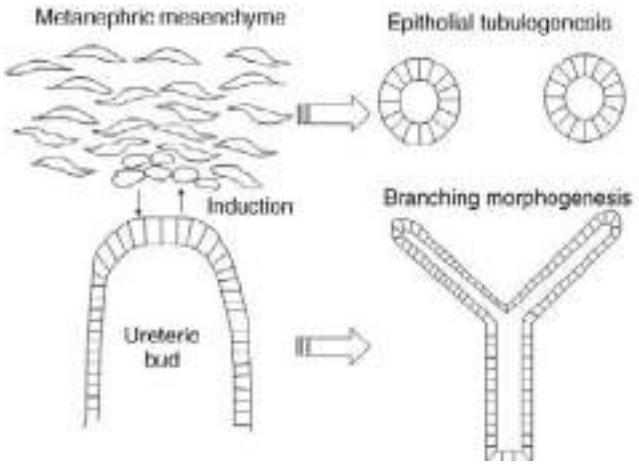

FIGURE 25.3 **Schematic illustrations of mutual induction.** The metanephric mesenchyme cells become epithelial nephron tubules (induced by the ureteric bud), while the ureteric bud undergoes branching morphogenesis to form the collecting system (induced by the metanephric mesenchyme).

Organ Culture

Whole Embryonic Kidney Organ Culture

The transfilter culture system, used by Grobstein and co-workers in the 1950s,[14–16] has been the mainstay of *in vitro* organ culture work in the developing kidney. In this system, microdissected kidneys, from as early as the beginning of metanephrogenesis (gestational day 11.5 in mice or day 13.5 in rats), are cultured on top of filters for several days. In the presence of appropriately defined serum-free medium, kidney rudiments grow and differentiate.[17] It is possible to observe branching morphogenesis of the ureteric bud, induction of the metanephric mesenchyme, and formation of nephrons by microscopy as the cultured embryonic kidneys develop (Figure 25.4a). Only vascular development does not occur to an appreciable extent. Thus, not only does the whole embryonic kidney culture resemble *in vivo* developmental processes, but it also appears to retain the inherent spatiotemporal complexity.

In this whole embryonic kidney culture, it is possible to manipulate humoral factors that play a role in nephrogenesis. The effects of growth factors or their inhibitors on kidney development can be evaluated *in vitro* by analysis of total kidney size, ureteric bud branching events, and metanephric mesenchyme tubulogenesis. For example, ureteric bud branching can be assayed by staining with a fluorescently-labeled lectin from *Dolichos biflorus*, which has been shown to bind specifically to the cells derived from the ureteric bud[18] (Figure 25.4b). However, the organ culture method is not without its limitations. For example, when antibodies and antisense oligonucleotides are used to perturb *in vitro* nephrogenesis, care must be taken to ensure that the agent is delivered to the sites of interest, since antisense oligonucleotides do not seem to penetrate the ureteric bud as well as the metanephric mesenchyme.[19] In addition, oligonucleotide toxicity may, in some instances, nonspecifically inhibit kidney growth.[19] However, recent development of RNAi technology to perturb specific gene function may prove useful in this setting.[20,21]

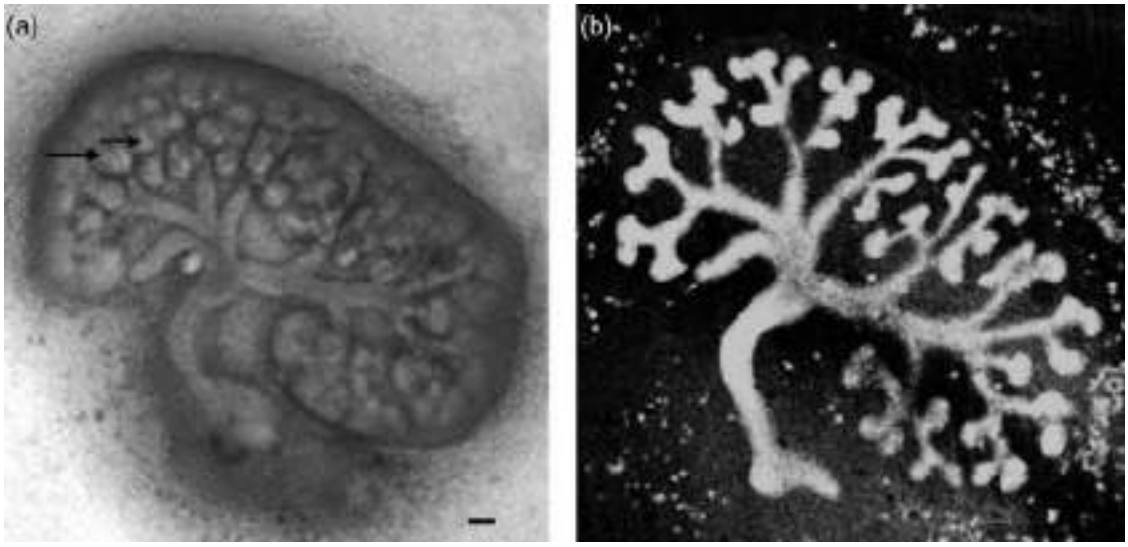

FIGURE 25.4 **(a) Embryonic rat kidney isolated at embryonic day 13 and cultured for 3 days on Transwell filter. Ureteric bud branches and epithelial nephron formation (arrows) are visible. (b) Cultured kidney stained with fluorescent-labeled lectin from Dolichos biflorus to visualize ureteric bud-derived structures** (Bars: 100 μm). See color plate section at the end of the book.

Isolated Wolffian Duct Culture

It is possible to culture the entire mesonephros −metanephros area on top of transfilters. Addition of humoral factors can induce outgrowth of ureteric bud-like structures from the Wolffian duct.[22−26] For example, the addition of glial cell-derived neurotrophic factor (GDNF) induces numerous budding events at multiple foci along the length of the cultured Wolffian duct (Figure 25.5). The epithelial Wolffian ducts can also be dissected away from most of the non-epithelial mesoderm and cultured in the presence of soluble growth factors to induce the outgrowth of ureteric bud-like structures.[23−25,27−30] However, in this culture system GDNF alone is insufficient to induce the outgrowth of ureteric bud-like structures, and supplementation with other growth factors is required[23,24] (Figure 25.6). The Wolffian duct can also be cultured as a "naked" epithelial tube cleared of all surrounding mesodermal cells, although these isolated ducts must be cultured within a three-dimensional extracellular matrix.[25] The ureteric bud-like structures can be excised from the Wolffian duct and induced to branch in culture (Figure 25.7), indicating that the *in vitro* ureteric bud possesses the ability to branch and grow in a manner similar to that seen with the *in vivo* ureteric bud (see below). These *ex vivo* culture systems have proven useful in the elucidation of the mechanism of ureteric bud budding, and have allowed for the identification of multiple modulators/regulators (e.g., growth factors, signal transduction pathways, etc.) of this process.[23−25,27−30]

Isolated Ureteric Bud Culture

Since the 1950s, *in vitro* culture of the two individual components of metanephros, the ureteric bud and the metanephric mesenchyme, has been attempted. Of the two progenitor tissues, *in vitro* growth of the isolated ureteric bud proved to be more difficult, and it was argued that cell−cell contact between the ureteric bud

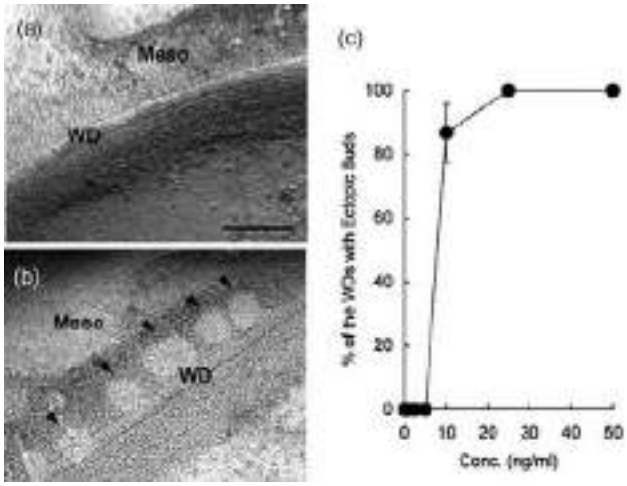

FIGURE 25.5 (a), (b) Photomicrographs of whole mesonephros (Meso) with attached Wolffian duct (WD) cultured for 4 days in the absence (a) or presence (b) of GDNF. (c) Graph depicting quantitative analysis of ureteric bud emergence (Scale bar: 200 μm; Arrowheads: ectopic ureteric buds). *(from ref. [24]).*

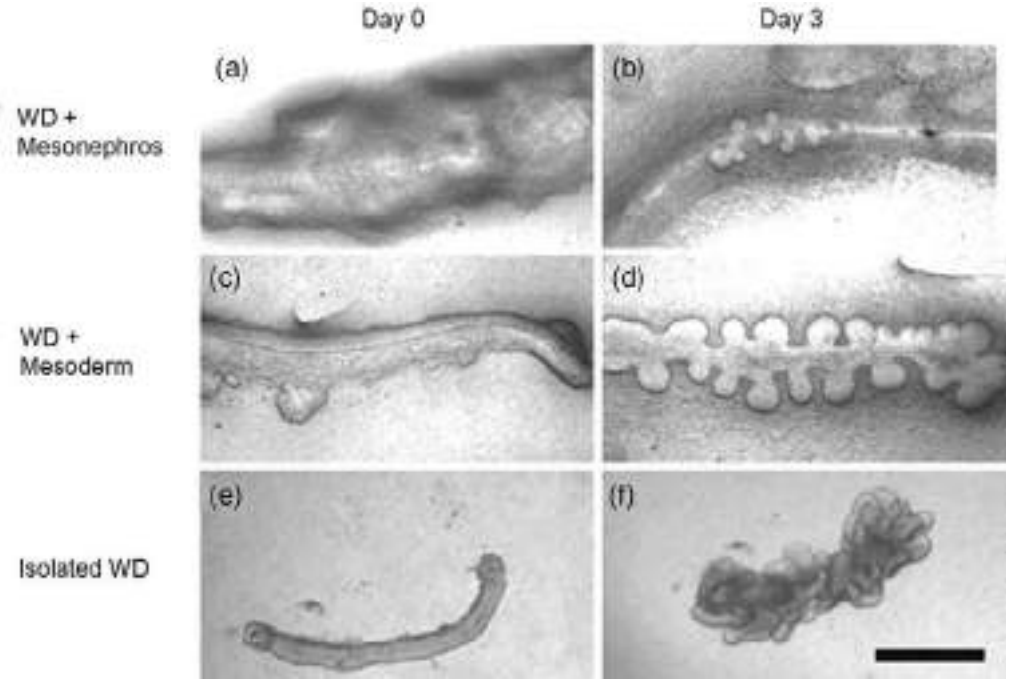

FIGURE 25.6 (a–f) Photomicrographs of isolated mesonephric tissues at Day 0 (a, c, e) or after 3 days of culture in the presence of GDNF (b, d, f). (a), (b) Entire mesonephros with attached Wolffian duct (WD). (c), (d) Wolffian duct (WD) dissected free from most of surrounding mesonephros. (e), (f) Wolffian duct (isolated WD) isolated free of surrounding mesonephros and mesodermal cells which must be cultured within an extracellular matrix gel (Scale bar: 500 μm). *(from ref. [25]).*

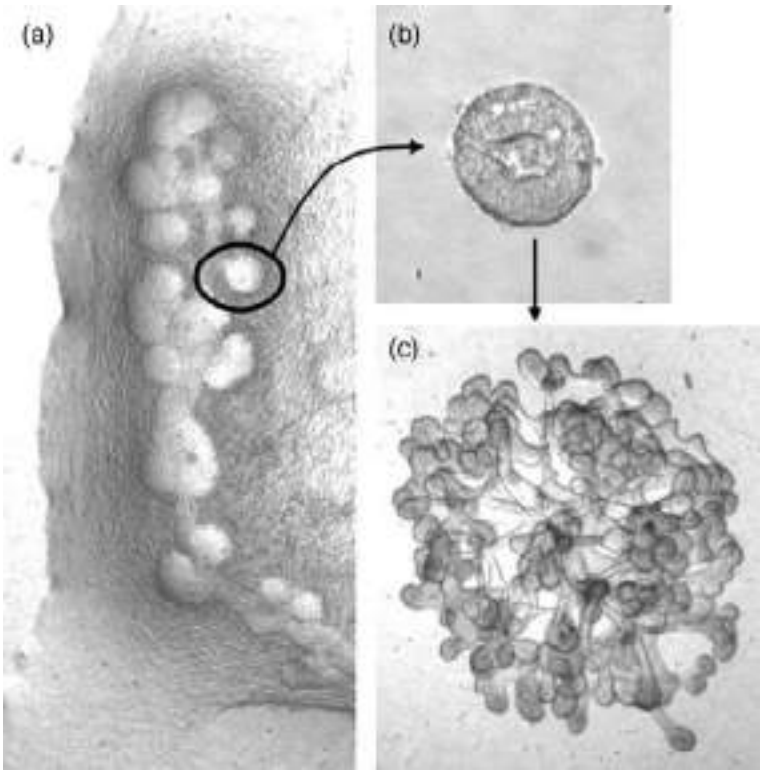

FIGURE 25.7 (a) Wolffian duct dissected free from most of mesonephros cultured for 4 days in the presence of GDNF. (b) High magnification view of a single ureteric bud-like structure isolated from cultured Wolffian duct in (a). (c) Single ureteric bud-like structure in (b) cultured within a three-dimensional extracellular matrix gel in the presence of branch-inducing growth factors. *(from ref. [25]).*

and metanephric mesenchyme was an important component in the process of ureteric bud branching. However, the isolated ureteric bud has since been shown to grow and branch extensively in the presence of appropriate extracellular matrix and soluble factors in the absence of direct contact with the metanephric mesenchyme[31] (Figure 25.8). The epithelial cells of the ureteric bud in this culture system appear to retain similar morphological characteristics to those of the ureteric bud in the whole embryonic kidney culture.[32] This system has allowed for the isolation and identification of numerous molecules, including soluble factors that modulate ureteric bud branching morphogenesis.[31–47]

Isolated Metanephric Mesenchyme Culture: Recombination with Heterologous Inductive Tissues

Another setting in which organ culture has been used focuses on metanephric mesenchyme induction and transformation to an epithelial phenotype. In this system, the isolated mesenchyme is cultured on one side of a filter while, on the other side of the filter, heterologous inducing tissues are placed. Various stages of metanephric mesenchyme induction (i.e., condensation, epithelialization, and tubulogenesis) can be observed, depending on the inductive capacity of the tissue. Using this method, it has been shown that embryonic spinal cord, salivary gland, and other tissues can induce the metanephric mesenchyme.[48,49] As is the case for isolated ureteric bud branching described previously, a key question here is the relative contribution of humoral factor(s) or cell–cell contact in this process. Electron microscopic examination revealed that the inducing tissue can contact the metanephric mesenchyme via cellular processes extending through the filter.[50] In fact, filters with pore sizes greater than 0.1 μm are unable to block cell-to-cell contact completely,[7] indicating the importance of cell–cell contact. However, complete mesenchymal induction has been demonstrated in the presence of soluble factors without cell–cell contact with inductive tissue.[51,52]

Isolated Metanephric Mesenchyme Culture: Recombination with Isolated Ureteric Bud

It has been shown that when co-cultured with freshly isolated metanephric mesenchyme, the isolated ureteric bud in culture (as described previously) is capable of inducing nephron tubules from the metanephric mesenchyme.[31] At the same time, the pattern of ureteric bud growth is altered by the presence of the metanephric mesenchyme; it is only through contact with metanephric mesenchyme that the ureteric bud undergoes vectorial branching with elongation and tapering of newly induced branches, similar to those seen in cultured whole embryonic kidneys[44] (Figure 25.9). Although this

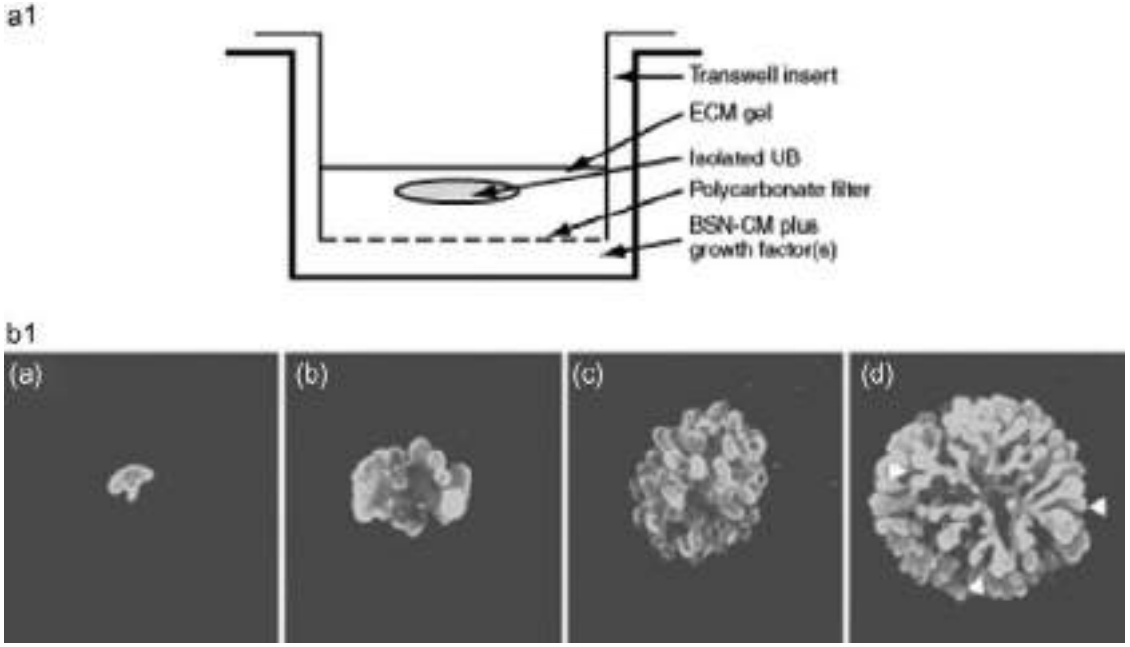

FIGURE 25.8 (a1) Illustration of isolated ureteric bud culture system. (b1) Cultured ureteric buds stained with fluorescein-conjugated lectin from Dolichos biflorus at (a) 0 days; (b) 3 days; (c) 6 days; and (d) 12 days. Arrows indicate branch points. *(adapted from ref. [31]).*

patterning effect on the ureteric bud appears to be modulated, in part, by soluble factors, cell contact with the metanephric mesenchyme and/or short-acting factors produced by the interaction of these two progenitor tissues plays a key role in determining the arborization pattern.[44] Another potential application of this "recombination" system is to pinpoint the defective tissue in knockout mice with a kidney phenotype. Through recombination of wild-type and gene knockout tissues (e.g., wild-type ureteric bud with knockout metanephric mesenchyme), it may be possible to determine the source of the kidney defect. For example, kidneys lacking heparan sulfate 2-O sulfotransferase ($Hs2st^{-/-}$) display renal agenesis, presumably due to defects in the inductive responsiveness of the ureteric bud to undergo branching morphogenesis.[53] However, examination of cultures of recombined wild-type and $Hs2st^{-/-}$ ureteric buds and metanephric mesenchyme (Figure 25.10) provided evidence that the key defect in the knockout kidney is the inability of the metanephric mesenchyme to undergo induction.[46]

The aforementioned tissue culture systems allow one to observe certain key phenomenon in metanephric kidney development *in vitro/ex vivo*. The analysis of genetically-engineered kidneys (and/or their component tissues) in these *in vitro* systems, in combination with an advanced method of gene perturbation (e.g., RNAi), will undoubtedly provide a more mechanistic picture of kidney development.

Genetically-Engineered Mice

Genetically-engineered mice allow one to manipulate the process of kidney development *in vivo*. Introducing null mutations of the gene of interest into mouse embryonic stem cells can be used to generate gene knockout mice.[54–56] Generally speaking, knockout mice grow from conception without normal expression of the gene product. If the mice develop beyond the stage of kidney development, the effect of the gene disruption on nephrogenesis can be observed *in vivo* by direct examination of the tissue histology. In such cases, the abnormal kidney phenotype can be directly or indirectly ascribed to disruption of the gene. In fact, many important molecules involved in kidney development have been identified by gene knockout technology.[57,58] In particular, the contribution of many transcription factors, molecules acting in the nucleus to regulate gene expression in the cell, have been demonstrated by this technique. However, knockout technology has its limitations. For example, although gene knockout mice can demonstrate the indispensability of a particular gene, how the gene product acts in the complex process of kidney development often remains unclear, owing to the spatiotemporal complexity of the

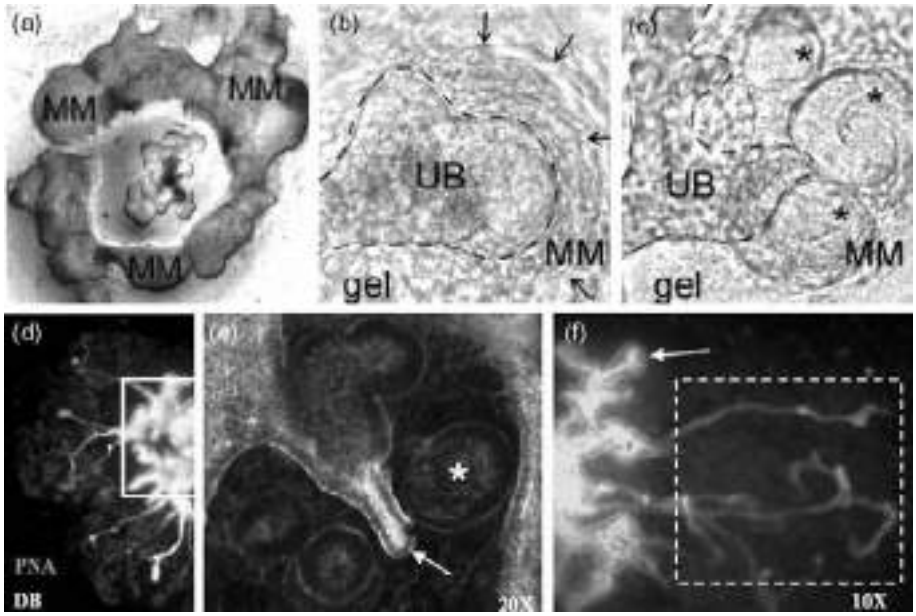

FIGURE 25.9 (a–c) Photomicrogrpahs of uninduced metanephric mesenchyme (MM) placed around the cultured UB (a); and co-cultured for 7 days (b–c). (d–f) UB and MM recombinations after 8 days of co-culture visualized with UB-specific lectin (*Dolichos biflorus*) and antibody against E-cadherin. Structures derived from mesenchymal-to-epithelial transformation, including cap-condensate (b: arrows) and coronas (indicated by asterisks) are observed. (f) Boxed area indicates elongation of UB branches and vectorial growth toward the MM; arrow indicates an area of the UB that has not undergone recombination with the MM and maintains its original architecture. *(adapted from ref. [44]).*

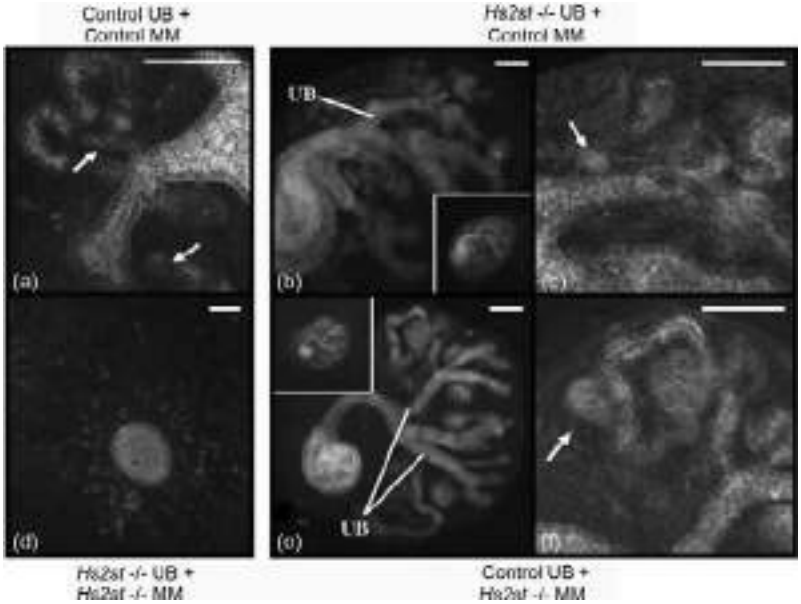

FIGURE 25.10 (a–f) Confocal photomicrographs of mix-and-match recombination cultures between heparan sulfate 2-O-sulfotransferase (Hs2st) knockout and control tissues. E-cadherin staining reveals epithelial structures derived from either ureteric bud (UB) or metanpehric mesenchyme (arrows). Mutual induction can be seen in co-cultures of control tissues recombined with control (a) or Hs2st$^{-/-}$ tissues (b), (c), (e), (f). Recombination of UB and MM from Hs2st$^{-/-}$ kidneys results in no mutual induction (d) (Scale bars: 100 μm). *(from ref. [46]).*

developing organ. Thus, if one observes defective ureteric bud branching in knockout mice, the deleted/disrupted gene product could be affecting the ureteric bud directly or it could be affecting the metanephric mesenchyme, resulting in incompetent induction of the ureteric bud. To resolve this problem, some have used organ culture type approaches ("recombination").[46,59] Another limitation of gene knockouts is that the mice may not have an apparent phenotype due to redundancy. In other words, the expression of other molecules with features or functions that overlap with the targeted gene could compensate for the defect from the gene knockout.

Perhaps the major drawback of conventional knockouts for studying genes involved in development of the kidney is the possibility that the targeted gene is critical for early embryonic survival, rendering the analysis of kidney development impossible as the embryo dies before organogenesis. In recent years, this issue (as well as some of the others listed above) has been overcome by the use of tissue-specific knockout technologies which provides the means for gene disruption in a time- and organ-specific manner.[60] This gene targeting system utilizes site-specific recombinases to excise out genes or portions of genes from the genomic DNA, resulting in the inactivation of the gene of interest.[61] Cre-loxP is the most commonly employed site-specific recombinase for these "conditional" deletions, although other site-specifc recombinases are available, including Flp-FRT and Dre-Rox. In the case of the Cre-loxP system (although the general principles are shared), conditional deletion of a gene of interest is performed by crossing two transgenic mouse lines: (1) "floxed" mice that carry the gene of interest with flanking loxP sites which can be cleaved by the enzyme; and (2) Cre-recombinase transgenic mice under the control of a tissue-specific promoter.[62] For example, deletion of β1 integrin from the epithelial cells destined to become the ureteric bud using Cre recombinase under the control of the HoxB7 promoter disrupts ureteric bud branching morphogenesis, and variably retards kidney growth, leading in a few instances to renal agenesis.[45,63] While such approaches have proven useful, the main drawback of these conditional deletions in the study of the kidney is the availability of cell-specific promoters.[61] The use of tet-operon and tamoxifen to induce recombinase activity and the modulation of gene activity have also proven to be useful.[61] In these systems, animals are exposed to tetracycline or tamoxifen which activates the site-specific recombinase under its control, resulting in the modulation of gene activity. These systems have the advantage of being under the control of the investigator; however, they are not without problems, including the toxicity of the inducing agent.[61] Nevertheless, these spatiotemporal conditional deletions have rapidly established themselves as an invaluable tool for investigating the development of the kidney.

Cell Culture

Cell culture models have the advantage of simplicity. Since they use homogenous cell populations grown under controlled conditions, it is possible to perform biochemical analysis in great detail. Moreover, gene introduction by plasmid transfection and gene knockdown by RNAi is simpler in comparison to the organ culture system. Here, the most relevant system for branching morphogenesis of the ureteric bud, the three-dimensional cell culture system, is discussed.

When certain kidney-derived epithelial cells are suspended in an extracellular matrix gel (type I collagen or a collagen–Matrigel mixture) in the presence of morphogenetic humoral factors, they form tubules and undergo branching morphogenesis *in vitro*. The tubules in the three-dimensional culture have lumens and retain apical–basolateral polarity.[64] The effect of humoral factors in epithelial tube and/or branch formation can be studied here. In addition to the humoral factors, the effect of extracellular matrix composition on morphogenesis and the cellular details of morphogenesis can be examined in this system. MDCK cells and murine inner medullary collecting duct (mIMCD3) cells have been used in the past,[65–68] but these have the limitation of being derived from mature renal epithelial cells. To address this issue, an *in vitro* cell culture system using ureteric bud (UB) cells directly derived from embryonic day (E) 11.5 mouse ureteric bud has also been established.[69] Although there is some difference in the responsiveness of the different cell lines to growth factors, all three cell lines respond to soluble factors produced by the metanephric mesenchyme by forming branching tubules.

A detailed mechanism of hepatocyte growth factor (HGF)-induced MDCK cell tubulogenesis model has been described.[70] There appear to be two steps involved in this process of invasion: epithelial–mesenchymal transition; and the re-establishment of epithelial intercellular junctions. However, it has also been shown that ureteric buds in *in vitro* culture undergo branching morphogenesis through budding, a process in which epithelial cells never lose their junctions.[32] It remains to be seen where and when these two morphogenetic processes, branching through invasion ("invadopodia") and branching through budding, are utilized *in vivo*.[71]

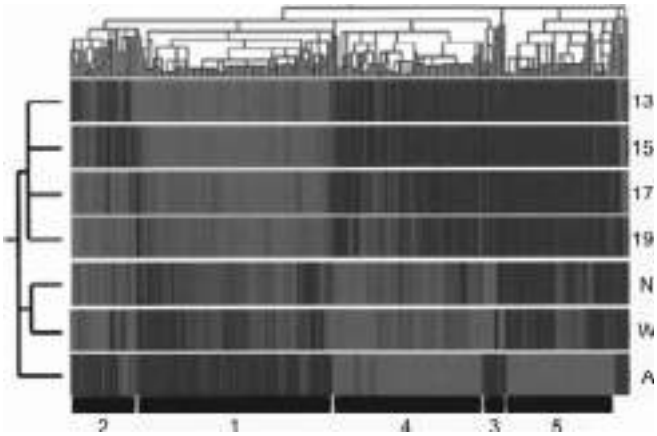

FIGURE 25.11 **Hierarchical clustering of 873 genes identified as changing significantly at some point in kidney development (out of 8740 genes examined).** Numbers at the bottom indicate group numbers derived from k-means clustering. Group 1 genes are upregulated (red) in the early embryonic period and decrease thereafter. Group 2 genes rise to a mid-late embryonic peak. Group 3 genes peak in the neonatal period. Group 4 genes rise somewhat linearly throughout development. Group 5 genes display a distinct peak in the adult versus all earlier times (13, 15, 17, 19: embryonic days; N: newborn; W: 1 week old; A: adult). *(from ref. [72]).*

MOLECULAR APPROACHES TO KIDNEY DEVELOPMENT

The development of high-density DNA microarray technology and global gene profiling has made it possible to analyze patterns of gene expression throughout embryonic and postnatal development and into adulthood in the whole developing rodent kidney.[72,73] It has also been possible to analyze gene expression changes in *in vitro* culture systems such as the isolated UB and MM.[39,42,74] For example, initial microarray analysis of a global time series of gene expression in the developing rat kidney revealed five discrete patterns or groups of gene expression[72] (Figure 25.11). mRNA encoding transcription factors and growth factors were found to be upregulated early in organogenesis (group 1). Among the genes whose expression level peaked in the middle of kidney organogenesis (group 2), many extracellular matrix related genes were found.[72] Further representing the global time series gene expression data as self-organizing maps (SOMs) made it possible to define roughly six stages of gene expression during pre- and postnatal kidney development in the rat.[73] Computational analysis suggested points of stability and transition based solely on gene expression and correlations where classically described anatomical changes were not intuitively obvious[73] (Figure 25.12). The most profound changes appear to occur at birth, when there is a sudden burst in the expression of many genes involved in redox metabolism and transport, including multispecific drug transporters such as Oat1 and Oct1.[75]

There has also been a massive effort to create an atlas of gene expression in the developing kidney, the genitourinary developmental molecular anatomy project or GUDMAP.[76–80] This multi-group international project is still continuing and has not only provided an atlas of localization information (e.g., ureteric bud, comma-shaped bodies, S-shaped bodies, renal vesicle), but has also yielded specific gene signatures for developing structures like branching ureteric bud tips. Although the function of many of these genes remains unknown, at a minimum they represent useful markers.

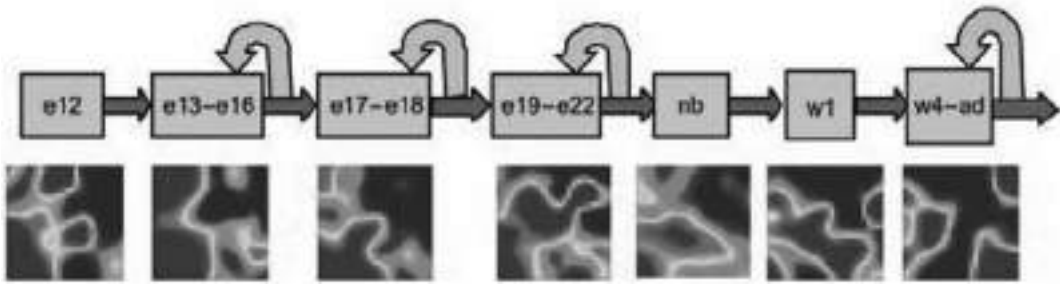

FIGURE 25.12 **Representative SOMs from each stage (Stage 1: e12; stage 2: e13 to e16; stage 3: e17 to e18; stage 4: e19 to e22; stage 5: nb (P0 to P1); stage 6: w1; stage 7: w4 to ad).** Curved arrows represent putative negative feedback loops that potentially stabilize the previous stage. *(from ref. [73]).*

One of the key tasks in the future will be to place this localization information in the context of global gene expression time series data, to obtain a more accurate picture of the dynamics of kidney organogenesis and suggest new points of regulation. Growth factor-selective heparan sulfation interactions have been proposed as important regulators of the switching between stages.[46,47] Moreover, based on current knockout and *in vitro* data, it has been suggested that key "hubs" in the network of genes regulating kidney development include the process of GDNF-dependent budding early on, and late tubulogenesis involving cilia-associated genes such as those implicated in various types of cystic kidney disease.[81,82] It is becoming increasingly clear that an abundance of knockouts reported to have "renal phenotypes" cluster around these processes. *In vivo* branching morphogenesis, especially in the middle phases, appears largely protected from disruption in many knockouts of gene products known to be involved in *in vitro* branching. When branching phenotypes are reported, it is usually in the form of a small reduction in nephron number. One interpretation, supported by a wealth of *in vitro* data, is that there are many growth factor−heparan sulfate-dependent pathways regulating branching, and deletion of any single one is likely to be compensated by another. Double knockouts, for example of the EGF receptor and the HGF receptor (c-met), are beginning to provide support for this view.[83]

In addition to these high-throughput gene profiling approaches, epigenetic transcriptional controls are becoming rapidly appreciated. These dynamic cell-inheritable processes alter transcriptional activity without affecting DNA sequence, and include covalent modifications of DNA and histones, DNA packaging, chromatin folding, and regulatory noncoding microRNAs (miRNAs).[84,85] For example, conditional deletion of Dicer, the RNase involved in the production of miRNAs (which control gene expression at the post-transcriptional level), from cells of the nephron lineage lead to elevated apoptosis and premature termination of nephrogenesis.[86] In addition, deletion of Dicer from ureteric bud epithelium disrupts branching morphogenesis, and leads to the development of renal cysts.[86] Together with other studies on Dicer and miRNAs, the data clearly indicate a role for Dicer and Dicer-dependent miRNA activity in the development of the kidney, as well as in the development and progression of kidney disease.[84,86–93]

Ultimately, high-throughput gene profiling, together with a thorough epigenetic analysis, may provide mechanistic insight into the very complex system of gene expression regulating kidney development. This may enable the development of a systems perspective on nephrogenesis. Attempts at creation of "coarse grained" models of kidney development have clearly begun.[40,82,94,95] In the following section, a number of molecules which have been shown to be involved in kidney development are discussed. Over the past two decades, a large number of developing kidney phenotypes has been reported in gene knockout studies. Together with *in vitro* studies, they provide a great deal of functional information. We will highlight some of the results below. Several recent reviews describe them in much more detail.[96–98] Moreover, we do not discuss in great detail the impressive amount of work that has been done in relation to the formation of the glomerular filtration barrier (reviewed in [99]), polycystic kidney disease (reviewed in [100]) or late nephron differentiation and acquisition of mature transport function (reviewed in [96–98,101]). We focus largely on the WD, UB, and early MM-derived structures.

TRANSCRIPTION FACTORS IN METANEPHROGENESIS

Transcription factors bind to DNA and regulate the expression of other genes that are involved in, among other things, morphogenesis and differentiation. As a result of many gene disruption studies,

several important transcription factors in kidney development have been demonstrated. With careful molecular marker analysis, it will soon be possible to draw a whole network of these molecules in this process.

Transcription Factors Regulating Glial Cell Line-Derived Neurotrophic Growth Factor

As will be described later, a key molecule in the process of the initial stage of metanephros development (i.e., ureteric bud formation and outgrowth from the Wolffian duct) is glial cell line-derived neurotrophic growth factor (GDNF). Many transcription factors regulating expression of this growth factor affect ureteric bud development, and thus kidney development.

Hox Genes

Hox genes, mammalian homologs of *Drosophilia* homeotic genes, have been shown to be critically important for early nephrogenesis. While null mutants for *Hoxa11* or *Hoxd11* mice do not have a kidney phenotype, double knockouts of *Hoxa11* and *Hoxd11* show kidney agenesis or hypogenesis.[102] Moreover, complete elimination of *Hox11* paralogs (*Hoxa11*, *Hoxc11*, and *Hoxd11*) result in a lack of ureteric bud outgrowth from the Wolffian duct.[103] In this mutant, expression of another transcription factor, *Six2* as well as *Gdnf* is lacking, suggesting that *Hox11* paralogs regulate *Gdnf* expression.

Pax Genes

Additional members of the homeotic gene family, the *Pax* genes, have been implicated in nephrogenesis. Compared with *Hox* genes, *Pax* genes appear to be restricted to certain tissues or organs. *Pax2* and *Pax8* have been shown to be expressed in the kidney. These *Pax* genes can be considered as early nephric lineage specification genes, as they are first expressed in the pronephric duct, and their simultaneous disruption causes failure in the formation of the epithelial pronephric duct from the intermediate mesoderm.[1] After the pronephric duct, *Pax2* expression is sequentially found in its extension, the Wolffian duct, the ureteric bud, as well as the condensed metanephric mesenchyme and the newly formed nephron tubules. As the kidney tubules mature, *Pax2* expression decreases.[104,105] The expression pattern suggests a role for *Pax2* in mesenchymal–epithelial transformation. Homozygous null mutant mice lacking *Pax2* show only a partially developed Wolffian duct, leading to kidney agenesis.[106] It has also been shown that the mutant Wolffian duct does not respond to GDNF to form the ureteric bud. Furthermore, the mutant metanephric mesenchyme not only lacks *Gdnf* expression, it is not competent to form nephron tubules in response to wild-type spinal cord.[22] Heterozygous *Pax2* mutant mice have hypoplastic kidneys.[106] In fact, there are Pax2-binding sites in the promoter region of *Gdnf*, and Pax2 can promote *Gdnf* expression *in vitro*.[22] Pax2 has also been shown to promote the assembly of an H3K4 methyltransferase complex, which is involved in epigenetic transcriptional regulation.[85]

Pax8 has a similar tissue expression pattern to *Pax2*; however, *Pax8* expression peaks later than *Pax2*.[107] Although kidney development is apparently normal in *Pax8* knockout mice,[108] double knockouts of *Pax2* and *Pax8* show a complete absence of a urogenital system, due to failure in the formation of the pronephric duct from the intermediate mesoderm,[1] suggesting some overlap in the roles of these two *Pax* genes in pronephric duct induction. Analysis of kidney development in mice heterozygous for *Pax2* and for *Pax8*, which form kidneys (albeit hypodysplastic with fewer ureteric bud tips and a reduced nephron number), indicates a dramatic reduction in the expression levels of *Lim1*.[109] Although normal levels of *Ret* and *Gdnf* were seen, *Wnt11* (an important downstream target of Gdnf signaling, see below) was reduced. Thus, it has been postulated that *Pax2* and *Pax8* play a key cooperative role in nephron differentiation and branching of the ureteric bud.[109]

Eya1, Six1, and Six2 Genes

These genes have been implicated in *Drosophila* eye development together with *Pax6*,[110] and are expressed in the metanephric mesenchyme in the kidney. Homozygous null mutants for *Eya1* show kidney agenesis with loss of *Gdnf* and *Six* expression,[111] suggesting that EYA1 acts upstream of SIX, and together they regulate *Gdnf* expression. In fact, EYA1 is shown to act as a co-activator[111] of the genes regulated by SIX.[112] In *Six1* knockouts, which show various kidney phenotypes ranging from hypogenesis to agenesis, *Gdnf* expression is reduced, but *Eya1* expression is preserved.[112,113] Interestingly, metanephric mesenchyme derived from *Six1* knockout mice is not competent in nephron tubule formation when it is cultured with spinal cord, a potent inducer of nephron tubulogenesis, suggesting that these factors not only control *Gdnf* expression, but also have a role in maintaining certain characteristics of metanephric mesenchyme.[113] As described previously, another member of the *Six* family, *Six2* appears to regulate *Gdnf* expression downstream of *Hox11* paralogs.[103] Although *Six1* and *Six2* show overlapping areas of expression, the fact that *Six2* expression is reduced in *Six1* knockouts[112,113] suggests a close relationship between these two molecules. *Six2* expression *in vivo* has been found to be directly

activated by a novel protein complex composed of the Hox11 paralogous proteins, Pax2 and Eya1, which clearly demonstrates that *Six2* and *Gdnf* are downstream targets of the Hox11 paralogs.[114] Moreover, *Six2* defines nephron progenitor populations in the metanephric mesenchyme and it cell-autonomously maintains progenitor populations.[6]

Sall1

Sall1 is a transcription-related protein expressed in the metanephric mesenchyme of the developing kidney.[115] It is also expressed in extrarenal tissues such as the limb buds and central nervous systems. Knockout of this gene results in failure of the ureteric bud to undergo branching after invading the metanephric mesenchyme.[116] Although *Gdnf* expression just before ureteric bud formation is reported to be normal, its expression in the metanephric mesenchyme subsequently decreases.[115] It is unclear whether this reduction of *Gdnf* expression is due to a direct effect of the *Sall1* mutation or if it is secondary to a loss of a ureteric bud-derived signal. Interestingly, exogenous Gdnf was unable to rescue branching in cultures of *Sall1* knockout kidneys despite expression of *Ret*, suggesting that the ureteric buds are unable to respond to Gdnf.[116] *In situ* hybridization demonstrates the expression of the stalk-specific marker, *Wnt9b*, as well as the β-catenin target gene *Axin2*, in the ureteric bud tips of *Sall1* knockout kidneys.[116] Since reduction of β-catenin levels in *Sall1* mutants rescued ureteric bud branching and overexpression of *Wnt9b*-inhibited branching in normal ureteric buds, the data indicate that *Sall1*-dependent signals regulate the initiation of ureteric bud branching by modulating the expression of ureteric bud tip-specific genes.[116] In addition, among metanephric mesenchyme cells, only those cells which express high levels of *Sall1* are capable of nephron formation, suggesting the possibility that activation of this gene is key for nephron-forming capacity in the metanephric mesenchyme.[117] Given the fact that *Six2* maintains nephron progenitor cells, *Sall1* may act together with *Six2* to ensure multipotency of nephron progenitors.

Foxc1

Although some of the aforementioned genes affect a number of other genes, they all normally stimulate *Gdnf* expression. However, it is also important to restrict the area of *Gdnf* expression, to avoid multiple kidneys arising from a single Wolffian duct. In this regard, a member of the forkhead transcription factor superfamily, *Foxc1*, appears to restrict *Gdnf* expression to the intermediate mesoderm around the Wolffian duct (i.e., metanephric mesenchyme). *Foxc1* homozygous null mutants display ectopic ureteric bud outgrowth resulting in duplex kidneys.[118] In this mutant, the restrictive expression pattern of *Gdnf* as well as *Eya1* is perturbed, and is abnormally extended along the Wolffian duct.

Transcription Factors Regulating Ureteric Bud Formation (or Early Kidney Development)

Lim1

Lim1 is a homeotic gene expressed in both the central nervous system and kidneys. By whole-mount *in situ* hybridization, its transcript is detected from the pronephric stage to the metanephros.[119] In the metanephros, its expression is detected in the renal vesicles, S-shaped bodies, and ureteric bud branches.[119] Knockout of *Lim1* leads to kidney agenesis, suggesting its distinct role in early nephrogenesis.[120] Since *Pax2* expression in the mesonephros is detected in *Lim1* knockouts,[121] and the ectopic expression of *Pax2* was found to induce *Lim1* in the intermediate mesoderm,[1] it is likely that *Lim1* acts downstream of *Pax2* in pronephros development. However, the exact role of *Lim1* in metanephrogenesis remains to be determined.

Wt1

One of the Wilms tumor suppressor genes, *Wt1*, a zinc-finger transcription factor, is required for kidney development. *Wt1* generally acts as a transcriptional repressor, and has been shown to repress *Igf2*,[122] *Igf1* receptor,[123] *Pax2*,[124] *Myc*,[125] and *Bcl2*[125] expression. Most of these genes are related to cell proliferation, supporting the notion that loss of *Wt1*-mediated repression could lead to disregulated proliferation (i.e., cancer). It seems paradoxical that the *Wt1* knockout suffers from kidney agenesis, not tumors.[126] In the homozygous deletion mutant of *Wt1*, the ureteric bud fails to form, despite relatively normal development of the mesonephros and in the presence of *Gdnf* expression,[127] suggesting that factor(s) other than GDNF might be required for ureteric bud initiation. In normal embryonic kidneys, *Wt1* is expressed in uninduced mesenchyme, renal vesicles, and glomerular podocytes.[128] *Wt1* mutant mesenchyme is not responsive to the inductive signal from wild-type spinal cord, while the mutant Wolffian duct can induce wild-type metanephric mesenchyme, suggesting that the primary defect is in the mesenchyme.[127] Interestingly, the mechanism(s) of WT1 remain to be fully elucidated. Genome-wide expression profiling analysis in cells expressing inducible WT1 identified some direct WT1-target genes, including EGF receptor ligands, chemokines, and transcription factors.[129]

Limb Deformity Gene/*Fmn1*

Kidney agenesis is observed in mice homozygous for the *limb deformity* (*ld*) gene, *Fmn1*, mutation. The initial outgrowth of the ureteric bud is not observed in mutant mice. The metanephric mesenchyme from *Fmn1* mutant mice is induced by embryonic spinal cord, suggesting that the defect is in the ureteric bud.[130] The *Fmn* gene encodes formin, a gene product, which is present in both the ureteric bud and the metanephric mesenchyme.[131,132] Although knockouts of certain formin isoforms display limb deformity and kidney defects, specific elimination of isoform 4 results in a pure kidney phenotype.[133]

Myc Genes

The *Myc* family members were first recognized as proto-oncogenes that function as transcription factors. While *Myc* is expressed in the uninduced metanephric mesenchyme and newly formed epithelium, *Nmyc1* is transiently expressed in the area of mesenchymal–epithelial transformation.[134] Another *Myc* family member, *Lmyc1*, is expressed in ureteric bud-derived structures, and its expression increases as these structures mature.[134] Both *Myc* and *Nmyc1* gene knockouts are lethal at E9.5–10.5 and E10.5–12.5, respectively.[135–137] *Myc* mutants apparently have no specific kidney phenotype. In *Nmyc1* mutants, mesonephric development is affected. In both cases, mice die before metanephric development, which therefore cannot be assessed. The distinct pattern of expression of the various *Myc* genes makes them useful as markers: mesenchymal stromal cells are negative for *Myc*; *Nmyc1* is a marker for induced mesenchyme or early mesenchymal epithelialization; *Lmyc1* is a marker for the collecting duct.

Transcription Factors Regulating Ureteric Bud Survival/Branching

Emx2

Disruption of a homeotic gene, *Emx2* results in urogenital defects in mice.[59] In mutant mice, the initial formation of the Wolffian duct and ureteric bud is normal, as is the initial induction of the metanephric mesenchyme. Normal *Pax2* expression is observed in these structures. However, the ureteric bud starts to degenerate around E12.5. At the same time, the expression of *Pax2* and *Ret*, a receptor tyrosine kinase normally expressed at the tip of growing ureteric bud, is greatly reduced. Recombinant organ culture between wild-type and mutant ureteric bud and metanephric mesenchyme indicates a defect in the ureteric bud. *Emx2* expression is observed at a later stage of epithelialization than *Pax2* in normal mice. The expression pattern suggests that *Emx2* regulates maturation and/or survival of epithelial cells, rather than formation of epithelial cells.

Timeless

By differential gene expression screening in the epithelial cell three-dimensional culture system for branching tubulogenesis, the mammalian ortholog of *Timeless* gene was identified as a candidate for regulation of epithelial branching morphogenesis. Its expression is detected in the active region of ureteric bud branching in the developing kidney. Selective inhibition of this gene in various *in vitro* culture models resulted in inhibition of ureteric bud branching.[33] Deletion of this gene is embryonic lethal prior to the onset of kidney development.[138] The kidney (or ureteric bud)-specific knockout data are needed to provide a definitive role of this molecule in kidney development.

ETS Transcription Factor Genes

Etv4 and *Etv5*, two members of the Pea3 family of E-twenty six (ETS) domain transcription factors, which are believed to function as transcriptional activator proteins,[139] were identified in an analysis of gene expression in ureteric buds cultured in the absence or presence of Gdnf.[140,141] *Etv4* and *Etv5* were found to have overlapping expression in ureteric bud tips which was positively enhanced by Gdnf.[140,141] Gene dosage reductions and/or deletions of these transcription factors indicated a role in the formation of the ureteric bud tip domain.[140,141]

Sox Genes

Sox genes are developmental regulators containing a DNA-binding domain with high homology with the HMG box of the sex-determining gene *Sry*. Mice with double deletions of *Sox9* and *Sox8* have kidney defects, including renal agenesis.[142] *In situ* hybridization demonstrates reduced expression of a number of downstream targets of Gdnf-Ret signaling, including *Etv4*, *Etv5*, *Met*, and *Spry1* in the ureteric bud tips. Together, the data indicate that *Sox8* and *Sox9* have key roles in Gdnf-Ret signaling regulating/modulating ureteric bud branching morphogenesis.[142]

Transcription Factors Regulating Stroma Development

Foxd1

Study of one of the forkhead box transcription factor superfamily members, *Foxd1* (*Bf2*), shed light on the

role of the third cellular component of the developing kidney, the stroma. In developing kidneys, *Foxd1* is expressed by the cortical stromal mesenchyme. Homozygous null mutants for *Foxd1* die soon after birth due to renal failure. Mutant kidneys are small, fused, and located in the pelvis.[143] Both ureteric bud branching morphogenesis and kidney tubulogenesis in the metanephric mesenchyme-derived segments are perturbed. Further analysis of this knockout mouse reveals that the mutant kidney capsule abnormally contains cells expressing bone morphogenetic protein (BMP) 4 or PECAM (endothelial marker). Abnormal signals from these cells are likely to cause disruption of normal ureteric bud branching and nephrogenesis.[144] One of the target genes for this transcription factor is placental growth factor, a family member of vascular endothelial growth factor.[145]

Pod1

The *Pod1* gene, a transcription factor expressed in mesenchymal cells surrounding the ureteric bud and visceral glomerular podocytes in the developing kidney,[146] also plays a role in regulating ureteric bud branching and nephron formation. Null mutants for this gene exhibit a phenotype similar to that seen in *Foxd1* knockouts; initial ureteric budding and mesenchymal condensation occurs, but the process appears to slow down beyond this point.[147] By chimeric mouse analysis, *Pod1* expression was shown to be critical for the medullary stroma.[148]

Pbx1

Pbx1 gene encodes a homeodomain containing transcription factor expressed in metanephric mesenchyme, and both cortical and medullary stroma in the developing kidney. The kidney phenotype of *Pbx1* knockouts is similar to that of *Pod1*/*Foxd1* knockouts.[149] It appears that expression of these genes is not dependent upon the others, and all three genes are required for the functioning stroma to be capable of supporting ureteric bud branching and nephron differentiation. Identifying the molecular nature of this "stromal effect" will provide considerable insight into kidney development.

Retinoic Acid Receptor Genes

One possible mechanism for control of ureteric bud branching morphogenesis by the stromal cells is through the vitamin A/retinoic acid pathway. Vitamin A deficiency has been known to result in small kidneys.[150] Dietary vitamin A is converted to its active form, retinoic acid, and its signal is mediated through the retinoic acid receptor, which acts as a transcription factor. Retinoic acid synthesizing enzyme localizes to the cortical stromal cells,[151] and double knockout of retinoic acid receptor *Rara* and *Rarb2* results in *Ret* downregulation and impaired ureteric branching.[152]

Transcription Factors Regulating Functional Maturation of Nephron Tubules

Hnf1

Hepatocyte nuclear factor (*Hnf*)*-1* is a homeotic gene mainly expressed in liver and kidney. *Hnf1* knockout mice have an enlarged liver and Fanconi syndrome, resulting in urinary wasting of sugars, amino acids, and electrolytes that normally are reabsorbed in the renal proximal tubules,[153] suggesting an important role for *Hnf1* in regulating the expression of proximal tubule transporters.

Brn1

Maturation of Henle's loop and distal tubule is controlled by *Brn1*, a POU transcription factor. *Brn1* is expressed only in part of the mesenchymal condensate, then the prospective Henle's loop and distal tubule in the maturing kidney. There is no expression in the glomerulus, proximal tubule or collecting duct. Knockout of this transcription factor results in an elongation and maturation defect of the Henle's loop, macula densa, and distal tubule.[154]

URETERIC BUD OUTGROWTH FROM THE WOLFFIAN DUCT

Outgrowth of the ureteric bud from the Wolffian duct in response to signals arising from the metanephric mesenchyme is the initiating event in the development of the mammalian kidney.[7] The major growth factor involved in this process is Glial-derived neurotrophic factor (Gdnf) (see below).There are several levels of regulation surrounding the GDNF pathway.

Restriction of GDNF Expressed Region by *Slit-Robo*

The secreted protein *Slit2* and its receptor *Robo2*, previously reported as a chemo-repellant factor for axon guidance,[155] also functions to restrict *Gdnf* expression. Null mutations of either *Slit2* or *Robo2* result in supernumerary ureteric buds, caused by an abnormally extended *Gdnf* expression area.[156]

Regulators for GDNF Signaling Pathway

Sprouty

Sprouty (Spry) is an intercellular protein that acts as a negative feedback regulator for FGF and other receptor tyrosine kinase-mediated signaling.[157] Knockouts of *Spry1* display multiple ureters and multiplex kidneys.[158] It appears that mutant Wolffian ducts are abnormally more sensitive to GDNF, as reduction of *Gdnf* expression rescues the phenotype.[158] Double knockouts of *Spry* and *Gdnf* ($Spry^{-/-}$; $Gdnf^{-/-}$) rescue normal ureteric bud outgrowth and kidney development.[159] When *Fgf10* was also deleted from these mice ureteric bud outgrowth failed to occur, suggesting that *Fgf10* is likely to function as the receptor tyrosine kinase responsible for ureteric bud outgrowth in the absence of *Spry* and *Gdnf*.[159]

Activin and FGF

One of the puzzles in early nephrogenesis has been that a substantial fraction of Ret knockouts develop very rudimentary kidneys, suggesting the existence of a "bypass" pathway for ureteric bud formation. A GDNF-independent pathway for *in vitro* budding has been described that appears to involve a FGF,[22] but it is possible that inhibition of activin signaling also enables a "bypass" of the GDNF-ret pathway.[23,24] The FGF-dependent bypass pathway has been recently supported by *in vivo* evidence.[159]

NPY and *BMP* through PKA

Utilizing *ex vivo* cultured Wolffian ducts, microarray analysis of ducts maintained in the absence or presence of Gdnf identified neuropeptide Y (*Npy*) as a novel modulator of ureteric bud outgrowth.[28] Npy also rescues budding in Bmp4-treated Wolffian ducts, suggesting that this neuropeptide is reciprocally regulated by Gdnf and Bmps.[28] Comparison of budded and non-budded portions of Gdnf-induced cultured Wolffian ducts also reveals an almost 15-fold increase in protein kinase A (PKA) activity in non-budded Wolffian ducts.[30] Microarray analysis reveals a marked decrease in the expression of *Ret* following activation of the PKA pathway in cultured Wolffian duct. *Bmp2* expression is also increased in unbudded Wolffian ducts, and exogenous Bmp2 inhibits *ex vivo* budding from the Wolffian duct with a three-fold increase in PKA activity.[30] Taken together, the data suggest a role for PKA in regulating the site of ureteric bud outgrowth, potentially via a Bmp-dependent downregulation of *Ret*/*Gfrα1* co-receptor expression.[30]

GDF11

Another member of this family, growth/differentiation factor (*Gdf*)11 is expressed in the Wolffian duct and the metanephric mesenchyme. Knockouts of this gene result in kidney hypoplasia to agenesis, thought to be caused by downregulation of *Gdnf* in the mesenchyme.[160,161] In these mice, molecules known to regulate *Gdnf* expression such as *Eya1*, *Six2*, *Pax2*, and *Wt1* are expressed in the metanephric mesenchyme region, and the metanephric mesenchyme from this mutant undergoes nephron tubule formation when it is cultured with embryonic spinal cord. Molecular markers for the Wolffian duct such as *Ret*, *Pax2*, *Emx2*, and *Lim1* were expressed in the right place, and mutant Wolffian duct responds to exogenous GDNF.[160] Thus, GDF11 is likely to be indispensable for *Gdnf* expression.

Outside the kidney, this mutant mouse shows deranged anterior/posterior patterning, with alteration of *Hox* gene expression pattern.[161] Given the fact that *Hox11* paralogs control *Gdnf* expression,[103] downregulation of *Gdnf* in *Gdf11* mutants may be mediated through *Hox11* expression. GDF11 acts through the activin receptor (ACVR) IIA and IIB,[162] and knockouts of *Acvr2b* result in a similar though milder phenotype than that of *Gdf11* knockouts.[163]

Unidentified Signal(s) from Metanephric Mesenchyme

Another pathway involved in the regulation of ureteric bud outgrowth is revealed by single deletions of *Fgfr2* (but not *Fgfr1*, which appeared to be normal) from the metanephric mesenchyme, which leads to the outgrowth of duplicated ureteric buds from the Wolffian duct.[164] Although it is not clear which factors are secreted from metanephric mesenchyme, this result suggests that certain FGF signaling plays a role in the metanephric mesenchyme to suppress ectopic ureteric bud formation.

URETERIC BUD BRANCHING MORPHOGENESIS

As discussed previously, ureteric bud branching morphogenesis is induced by signals from the metanephric mesenchyme. Soluble growth factors, direct cell-to-cell contact, and cell−matrix contact play key roles in the process. The molecules likely to be involved in ureteric bud branching morphogenesis are summarized in Table 25.1.

TABLE 25.1 Molecules Likely to be Involved in Ureteric Bud Outgrowth and Branching Morphogenesis

Process	Soluble Factors	Transcription Factors	ECM/ Protease/ Integrin
Initiation	GDNF	*Pax2*	
	WNT2b	*Lim1*	
	Slit/Robo	*Six1, 2*	
	Activin (inhibitory)	*Eya1*	
	BMP2/4 (inhibitory)	*Wt1*	
	Sprouty (intracellular molecule)	*Hox11 paralogs*	
		Formin	
		Foxc1	
		Sox9	
		Sall1	
Branching morphogenesis	GDNF	*Sall1*	Proteoglycans
	Pleiotrophin	*Timeless*	MMP9
	Wnt11	*Sox9*	Integrin $\alpha_3\beta_1$
	Gremlin	*Etv4*	Integrin $\beta1$
	TGFβ superfamily	*Etv5*	
	HGF		
	IGF		
	FGFs		
	FGFR2		
Maintenance/ maturation of collecting system	EGFR ligands	*Emx2*	
	Wnt9b, Wnt7b	*Foxd1*	
		Pbx1	
		Pod1	

ECM: extracellular matrix; EGFR: epidermal growth factor receptor; GDNF: glial cell line-derived neurotrophic growth factor; HGF: hepatocyte growth factor; IGF: insulin-like growth factor; TGF: transforming growth factor.

Growth Factors

The embryonic kidney or isolated metanephric mesenchyme can induce branching morphogenesis of MDCK, mIMCD3 or UB cells grown in type I collagen gels in the absence of apparent cell contact.[65,69,165] Moreover, isolated ureteric buds from E13 rats have been shown to undergo branching morphogenesis in the presence of soluble factors.[31] This suggests that the metanephric mesenchyme elaborates soluble growth factors capable of inducing branching morphogenesis in the ureteric bud. A number of key growth factors have been identified.

Glial Cell Line-Derived Neurotrophic Factor

The importance of GDNF and its receptors GFRa1 and RET in kidney development is strongly supported by gene knockout data. Kidney agenesis or severe kidney hypogenesis is found in *Gdnf*,[166–168] *Gfra1*[169] or *Ret* knockout mice.[170,171] GDNF is expressed in the prospective metanephric mesenchyme area, while GFRa1 and RET are expressed in the Wolffian duct at the time of ureteric bud induction. As discussed previously, a wide variety of genetic manipulations affecting the transcription of the GDNF/GFRα1/Ret axis lead to disruption of kidney development. Moreover, *in vitro* application of GDNF-soaked beads to the whole genitourinary tract culture induces ectopic budding of the Wolffian duct.[172] GDNF is also important in subsequent branching morphogenesis of the ureteric bud, as inhibition of this factor perturbs further branching of the isolated ureteric bud *in vitro*.[31] Gene dosage of *Gdnf* is important, as heterozygous null mutants of this gene have smaller kidneys.[173] However, unlike ureteric budding from the Wolffian duct, where GDNF appears necessary and sufficient, GDNF is necessary but not sufficient to support ureteric bud branching morphogenesis, at least in the isolated ureteric bud culture system.[31]

Fibroblast Growth Factors and Receptors

Many fibroblast growth factors (FGFs) and their receptors are expressed in the developing kidney.[174] Initial demonstration of the importance of this signaling pathway came from an analysis of transgenic mice that overexpress a soluble chimera of FGFR 2IIIb and human IgG Fc. In these animals, where FGF signaling is broadly inhibited, kidney agenesis or severe hypogenesis ensues.[175] In addition, minor kidney defects are reported in *Fgf7*,[176] *Fgf10*,[177] and *Fgfr2IIIb*[178] knockout mice. In the isolated ureteric bud culture system, FGF2 and FGF7 induce a less branched globular ureteric bud growth, while FGF1 and FGF10 support branching growth,[36] suggesting that FGFs may play a role in ureteric bud morphogenesis. Consistent with this, a ureteric bud-specific knockout of *Fgfr2*, (but not *Fgfr1*) was found to result in abnormal ureteric bud growth, as well as abnormally thickened cortical stroma.[164] Three-dimensional reconstructive imaging reveals decreases in ureteric bud tip number and increases in the length of the ureteric bud segments.[179,180]

Pleiotrophin

This heparin-binding growth factor has been implicated in neurite outgrowth[181] and mesenchymal–epithelial interaction during organogenesis.[182] In the context of kidney development, pleiotrophin (isolated from the conditioned medium made by metanephric mesenchyme-derived cells) was found to induce ureteric bud branching morphogenesis in the presence of GDNF in the *in vitro* culture system.[37] It is present in the developing kidney at the basement membrane of the ureteric bud. Although pleiotrophin may act as a mitogen for the ureteric bud after its budding through GDNF action, knockout of this gene does not appear to have a major affect in kidney development.[183]

Wnts and Related Molecules (Frizzled-Related Proteins)

A member of the WNT family of secreted glycoprotein, WNT2b is expressed in the stroma, and its presence promotes ureteric bud branching *in vitro*.[184] Null mutants of the gene encoding another member of WNT family, *Wnt11*, result in decreased ureteric bud branching with reduced *Gdnf* expression in the mesenchyme.[185] *Ret* knockout mice also show reduced expression of *Wnt11*.[185] In the trunk or stalk region of the ureteric bud, *Wnt9b* is expressed, and genetic deletion of this molecule results in cystic kidneys, presumably due to the disruption of the planar cell polarity (non-canonical beta catenin-independent) pathway of Wnt signaling.[186] Later in collecting duct development, collecting duct-specific inactivation of *Wnt7b* displays a similar phenotype.[187]

Secreted frizzled-related proteins (sFRPs) are secreted proteins that function as WNT modulators. sFRP1 is expressed in the stroma and periureter area; sFRP2 is expressed in early mesenchymal condensates and also in the periureter area in the developing kidney.[188,189] Exogenous administration of sFRP1 to embryonic kidney organ culture leads to decreased ureteric bud branching and nephron induction. While exogenous sFRP2 alone does not have a major effect, its administration to the organ culture treated with sFRP1 partially reverses the inhibitory effect of sFRP1.[189]

Transforming Growth Factor β Superfamily

Most of the soluble factors discussed thus far facilitate ureteric bud branching and growth. However, unopposed proliferation and branching is not desirable for normal kidney development. Potential candidates for these "negative regulators" include members of the transforming growth factor (TGF) β superfamily. Generally, TGFβ inhibits epithelial cell growth. In organ culture, exogenous TGFβ1 or another member of the TGFβ superfamily, activin, inhibits ureteric bud development and/or disrupts the branching pattern,[190] suggesting their role not only in regulating proliferation, but also in correct patterning. In this regard, it is interesting that TGFβ selectively inhibits HGF-induced mIMCD3 branching events with little effect on tubule formation[67]; HGF plus TGFβ induces long, straight tubules, whereas HGF alone induces branching tubules. Furthermore, detailed image analysis reveals alteration in the ureteric bud branching pattern in embryonic kidneys treated with TGFβ superfamily members.[40] In isolated ureteric bud culture, administration of TGFβ superfamily members causes growth inhibition, as well as morphological changes similar (although not so striking) to that observed in mIMCD cell culture.[40]

Heterozygous mutation of another family member, bone morphogenetic protein (*Bmp*) 4 reveals loss of ureteric bud elongation, together with ectopic budding from the Wolffian duct.[191] Its expression is detected at the intermediate mesoderm surrounding the Wolffian duct and metanephric mesenchyme surrounding the stalk of the ureteric bud.[191,192] Taken together, these data suggest that TGFβ superfamily members inhibit branching events, but have somewhat less effect on ureteric bud elongation (and may even facilitate it in the presence of stimulatory growth factors), and play a role in regulating the pattern of ureteric bud branching.

Gremlin

Gremlin is a secreted BMP antagonist[193] expressed initially in the Wolffian duct, followed by induced mesenchyme in metanephros development.[194] Knockout of this gene results in kidney agenesis. The ureteric bud forms but fails to invade the metanephric mesenchyme.[194] Subsequently, the metanephric mesenchyme undergoes apoptosis. Although the kidney phenotype of *Gremlin1* knockouts resembles that of *Sall1* knockouts, *Sall1* expression is unchanged in *Gremlin1* knockouts.[194] However, inactivation of one copy of the *Bmp4* gene or the complete absence of *Bmp7* in gremlin knockout animals rescues ureteric bud invasion and branching.[191,192] Thus, it possible that gremlin antagonization of BMP activity at ureteric bud tips acts to restrict and guide ureteric bud outgrowth and branching, although the mechanism remains unclear.[195,196] Furthermore, treatment of embryonic kidneys from *Six1* knockout animals with gremlin restores ureteric bud branching morphogenesis, while heterozygous inactivation of *Bmp4* ($Bmp4^{+/-}$) also rescues ureteric bud branching morphogenesis and kidney development in Six1 knockout animals.[197] Taken together, the

data indicate that interplay between Bmps, gremlin, and Six1 likely plays a key role in the regulation/modulation of ureteric bud growth and branching.[197]

Hepatocyte Growth Factor

Embryonic kidneys express HGF and its receptor Met.[165] Neutralizing anti-HGF antibodies inhibit the growth of the embryonic kidney and disrupt ureteric bud branching morphogenesis in serum-free organ culture.[165] These results support the notion that HGF is an important morphogen for the ureteric bud that is secreted from metanephric mesenchyme. However, kidney development appears to be unaffected up to embryonic day 14 in *Hgf* or *Met* knockout mice, which die around this time from liver failure.[198,199] Although HGF may act at later stages of ureteric bud branching morphogenesis, it is probably not critically important in the initial stages.

Epidermal Growth Factor Receptor Ligands

Epidermal growth factor (EGF), transforming growth factor α (TGFα), heparin-binding epidermal growth factor-like growth factor (HBEGF), amphiregulin, and betacellulin all bind and activate the EGF receptor.[200] TGFα is present in the embryonic kidney, and disruption of TGFα signaling by neutralizing antibodies results in a small, less well-developed kidney in organ culture.[201] As mentioned above, when mIMCD3 cells grown in collagen gels are co-cultured with embryonic kidney, the cells undergo branching morphogenesis. Unlike MDCK cells, which only undergo branching morphogenesis in the presence of HGF,[165,202] mIMCD3 cells respond to EGF receptor ligands as well.[65,68] Similar results are obtained with the UB cell three-dimensional culture system.[69] Moreover, *Met* (HGF receptor) knockout kidney epithelial cells grown in three-dimensional extracellular matrix (ECM) gels undergo *in vitro* tubulogenesis in response to EGF or TGFα.[203] A conditional deletion of *Met* from the ueteric bud results in kidneys with a reduced number of nephrons and increased epidermal growth factor (EGF) receptor expression.[83] Mice which lack both normal *Egfr* and *Met* signaling have decreased ureteric bud branching and small kidneys with a reduced number of glomeruli, suggesting that *Met* and *Egfr* can act cooperatively to regulate ureteric bud branching.[83] Although *Tgfα* knockout mice do not have a kidney phenotype,[204,205] knockout of the *EGF* receptor in mice with a certain genetic background leads to dilated collecting ducts and renal dysfunction.[206] These results suggest an important role for EGF receptor ligands in later collecting duct development.

Insulin-Like Growth Factors

In serum-free organ culture, the embryonic kidney produces insulin-like growth factors (IGFs) 1 and 2.[207] When neutralizing antibodies against IGFs are added to the culture, kidney growth is suppressed.[207] The ureteric bud expresses IGF1 receptor.[208] Addition of antisense oligonucleotides against IGF1 receptor to the embryonic kidney in organ culture leads to a small kidney with disrupted ureteric bud branching morphogenesis.[208] However, knockout mice for either *Igf1* or *Igf2* do not display a kidney phenotype.[209,210] Molecular redundancy may be part of the explanation; however, as with HGF, the apparent discrepancies between the *in vitro* and *in vivo* data need to be addressed experimentally.

Extracellular Matrix

Soluble growth factors are not the only molecules involved in ureteric bud branching morphogenesis. Cells of the ureteric bud are surrounded by ECM proteins, and to form branching tubules the cells must digest the ECM. Cells have receptors for ECM proteins, such as integrins, as well as other specific receptors. Integrins can transmit signals to cytosolic and intranuclear proteins in a fashion similar to growth factor receptors. The cell modifies its behavior in response to the combined signals from growth factors and ECM proteins.[211]

The importance of the specific composition of the ECM in kidney epithelial cell branching morphogenesis has been shown using the three-dimensional cell culture model. When MDCK cells are cultured in type I collagen gels in the presence of HGF, the cells undergo branching morphogenesis. When MDCK cells are suspended in growth factor-reduced Matrigel, a basement membrane protein mixture secreted by EHS sarcoma cells, HGF-induced tubulogenesis is inhibited.[212] By mixing individual Matrigel component proteins into type I collagen gels, it was found that collagen I, laminin, fibronectin, and entactin facilitate MDCK cell tubulogenesis, whereas collagen IV, vitronectin, and heparan sulfate proteoglycan inhibit it.[212] However, a mixture of type I collagen and Matrigel, not pure type I collagen, is the optimum ECM for UB cell (a cell line derived from embryonic kidney tissue) tubulogenesis. Interestingly, when these cells are cultured in growth factor-reduced Matrigel alone, UB cells develop into cystic structures (Figure 25.13).[69] Together with the fact that isolated ureteric buds can be cultured in an ECM containing Matrigel but not in pure type 1 collagen gels,[31] this indicates that ECM composition modulates tubulogenesis and branching morphogenesis.

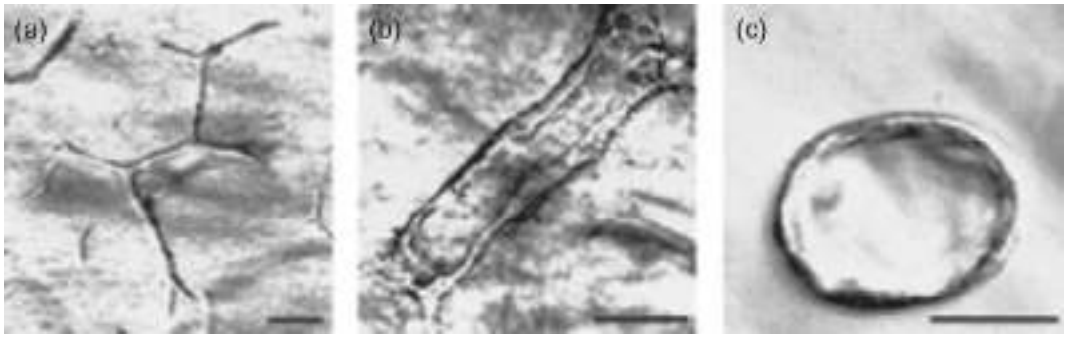

FIGURE 25.13 **Photomicrograph of ureteric bud (UB) cells cultured in three-dimensional extracellular matrix (ECM) gels.** In the presence of conditioned medium from metanephric mesenchyme cells, UB cells form branching cordlike structures in 3 to 5 days (a). In 10 to 15 days tubules with clear lumens can be observed (b). UB cells form multicellular cysts when cultured in pure Matrigel (c) instead of collagen I/Matrigel mixture (A and B) (Bars: 50 μm). *(from ref. [69]).*

Laminin

Laminins are the major component of the mature basement membrane. The role of laminin in epithelial branching morphogenesis has been shown in lung organ culture *in vitro.* Antilaminin antibodies perturb branching morphogenesis of embryonic lung in culture.[213] In the kidney, studies have shown a role for laminin in epithelial cell formation from the induced metanephric mesenchyme. It is known that antibodies against nidogen, a basement membrane protein secreted by mesenchymal cells, perturb epithelial morphogenesis in lung and kidney.[214] Nidogen binds to the γ1 chain of laminin. Thus, it is conceivable that the mesenchyme regulates epithelial branching morphogenesis through nidogen–laminin interaction. Moreover, knockouts of one of the laminin receptors, α3β1 integrin, result in decreased ureteric bud branching morphogenesis.[215] In *in vitro* whole organ culture and isolated ureteric bud culture, branching is inhibited in the presence of blocking antibodies against integrins α3, α6, β1 or β4. Interestingly, a common ligand for α3β1 and α6β4, laminin-5, is present in the developing ureteric bud, and its inhibition results in decreased branching in both whole embryonic kidney culture and isolated ureteric bud culture.[38]

Proteoglycans

Proteoglycans are protein molecules containing many bound glycosaminoglycan (GAG) chains.[216] The common GAG chains include chondroitin sulfate, dermatan sulfate, heparan sulfate, heparin, and keratan sulfate. Proteoglycans are mostly found at the cell surface or in the extracellular matrix. In embryonic kidneys, sulfated proteoglycans are concentrated around the tip of the ureteric bud, and perturbation of their synthesis by β-D-xyloside results in the inhibition of ureteric bud branching morphogenesis.[217,218] This perturbation also abolishes the expression of *Wnt11* at the tip of the ureteric bud.[219] As described previously, loss of *Wnt11* expression at the tip of the ureteric bud can lead to loss of *Gdnf* expression in the metanephric mesenchyme. However, the linking mechanism between inhibition of sulfated proteoglycan and the loss of *Wnt11* expression is unclear. Along the same lines, genetic inactivation of an enzyme, heparan sulfate 2-O-sulfotransferase, involved in heparan sulfate proteoglycan synthesis results in kidney agenesis.[53] In this case, the ureteric bud forms from the Wolffian duct, but subsequent invasion of the metanephric mesenchyme is perturbed. As for the mesenchyme, initial specification of the metanephric mesenchyme appears intact, but subsequent mesenchymal condensation is affected. Consistent with the *in vitro* result described above, heparan sulfate biosynthesis perturbation results in loss of *Wnt11* expression and reduced *Gdnf* expression. Given the fact that many growth factors that regulate branching morphogenesis of the ureteric bud are heparin (a heavily sulfated form of GAG chain)-binding, it is likely that global inhibition of GAG chain synthesis or its sulfation could compromise actions of these heparin-binding growth factors.

In contrast, inhibition of specific heparan sulfate proteoglycans results in less clear effects. One exception is *glypican* (*Gpc*) 3, a gene encoding a heparan sulfate proteoglycan linked to the cell surface via a glycosyl-phosphatidylinositol anchor. *Gpc3* knockout mice display enhanced ureteric branching and dysplastic kidneys.[220] *Gpc3* is expressed in the ureteric bud cells and modulates BMP and FGF action on the ureteric bud.[220] A potent angiogenesis inhibitor, endostatin, a breakdown product of extracellular proteoglycan, collagen XVIII, inhibits ureteric bud branching

morphogenesis.[35] Interestingly, this action is likely to be mediated through its binding to glypicans.[35]

Although it is not a proteoglycan in the strict sense, because it lacks a protein core, hyaluronic acid (HA) also plays a role in branching morphogenesis. Synthetic enzymes for this GAG are expressed in the developing kidney, and the addition of HA to three-dimensional culture of UB cells promotes tubulogenesis and survival of cells. Blocking antibodies against its receptor CD44 abolishes this effect.[221] In addition, supplementation of cultures of isolated ureteric bud or whole kidneys with hyaluronidase inhibited branching morphogenesis.[222] Specific sizes and concentrations of HA were also found to act independently in regulating UB branching, and in tubular maturation.[222]

While the protein core of proteoglycans, particularly the heparan sufate proteoglycans, play important roles in many developmental and physiologic processes, most of the function of these proteoglycans are mediated by the variably sulfated heparan sulfate GAG chain. For example, mice deficient in heparan sufate 2-O sulfotransferase, a heparan sulfate biosynthetic enzyme, display renal agenesis.[53] As described above, this is likely due to a defect in the induction of the metanephric mesenchyme.[46] On the other hand, ureteric bud branching morphogenesis appears to be more dependent upon 6-O sulfated heparan sulfate.[47]

Fibrillin1

Fibrillin1 is made in the metanephric mesenchyme and binds to integrin $\alpha 3\beta 1$, which is expressed in the ureteric bud. Antisense oligonucleotides directed against this extracellular matrix molecule induce dysmorphogenesis of cultured metanephros,[223] suggesting a role for this protein in kidney development.

Extracellular Proteinases and their Inhibitors

The idea that ECM-degrading proteases are involved in branching morphogenesis is supported by work from *in vitro* three-dimensional culture and organ culture. Two classes of proteases appear to be involved: metalloproteases (MMPs) and serine proteases. In HGF-induced MDCK cell tubulogenesis, inhibitors of collagenase (MMP1) perturb the morphogenetic events when the cells are suspended in type I collagen gels.[224] The broadly active MMP inhibitor, 1,10-phenanthroline, inhibits TGFα- or HGF-induced mIMCD3 cell tubulogenesis in collagen gels.[68] Furthermore, tubulogenic growth factors, such as HGF or EGF receptor ligands, upregulate the expression of MMPs and urokinase in the epithelial cells as they undergo tubulogenesis.[68,71] Interestingly, in the case of long, non-branching mIMCD3 cell tubules induced by HGF plus TGFβ, the balance between proteases (MMP1 and urokinase) and their inhibitors (TIMP1 and PAI1) expressed by mIMCD3 cells changes in parallel with tubular morphology.[67] In embryonic ureteric bud-derived UB cells, expression of MMPs and TIMPs changes in response to surrounding ECM and soluble factors.[34] These results suggest that tubulogenic growth factors act, at least in part, through changing the expression patterns of extracellular proteases and their inhibitors in *in vitro* tubulogenesis. It has also been shown that "tubulogenic ECM" and highly tubulogenic conditioned medium secreted by metanephric mesenchyme-derived cells contain MMP activity, and that the expression level of regulators for these MMPs in UB cells alters as branching morphogenesis progresses,[34] suggesting local control of proteolytic activity is important in the morphogenetic process. In the embryonic kidney in organ culture, antibodies against MMP9, but not MMP2, inhibit the branching morphogenesis of the ureteric bud.[225] Although *Mmp9* knockout mice do not show a kidney phenotype in some genetic backgrounds,[226] in the C57BL/6 background deletion of Mmp9 results in a $\sim$30% reduction in nephron number.[227] This is most likely through its anti-apoptotic effect in the mesenchyme, and its ability to stimulate ureteric bud branching morphogenesis.[227] Both of these enzymes act as a gelatinase, which is required to digest ECMs in basement membranes. In another study, however, antisense oligonucleotides against mesenchymal MMP2 or epithelial cell surface-expressed membrane type (MT)1-MMP inhibit metanephrogenesis in organ culture.[228]

In summary, ureteric bud branching outgrowth and morphogenesis is modulated in large part by a combination of positive and negative soluble growth factors secreted by the metanephric mesenchyme that act synergistically. In many cases, these pathways are more parallel than interdependent. These growth factors subsequently regulate downstream effector molecules such as ECM or ECM-degrading proteinases (Figure 25.14).

TUBULOGENESIS AFTER INDUCTION OF THE METANEPHRIC MESENCHYME

Early mesenchymally-derived nephrons, which will go on to form Bowman's capsule, as well as the proximal and distal tubules, are induced in the metanephric mesenchyme by the ureteric bud. In the process, mesenchymal cells transform into epithelial cells. The induced epithelial cells differentiate into kidney tubules. This transformation can be induced by a number of inducer tissues other than the ureteric bud, including embryonic spinal cord, embryonic salivary

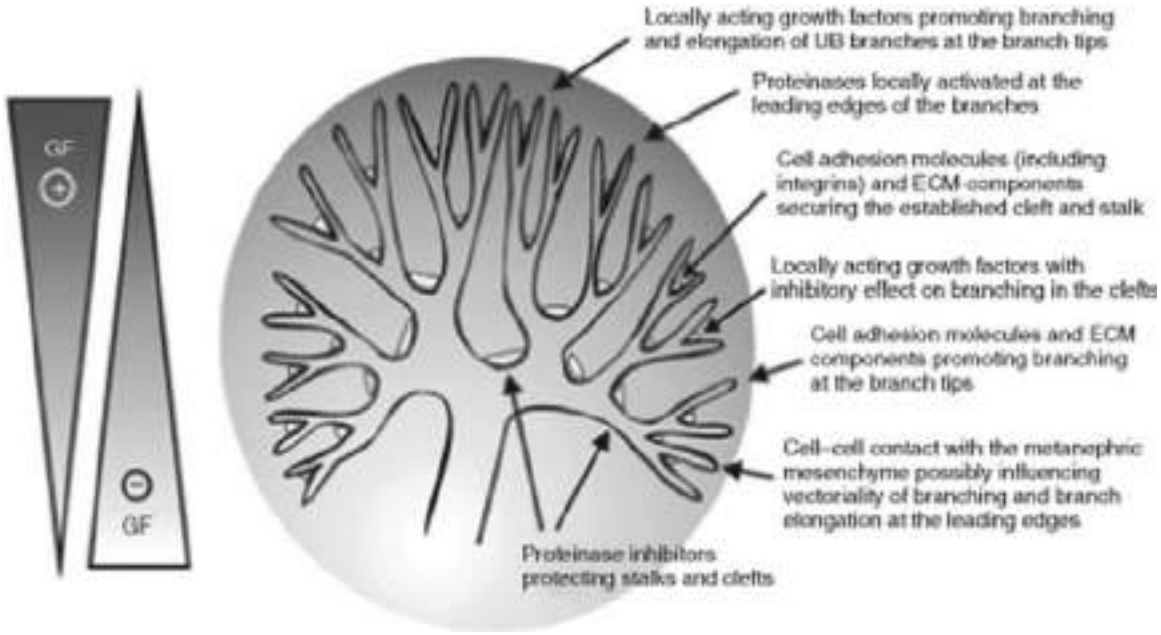
Locally acting growth factors promoting branching and elongation of UB branches at the branch tips
Proteinases locally activated at the leading edges of the branches
Cell adhesion molecules (including integrins) and ECM components securing the established cleft and stalk
Locally acting growth factors with inhibitory effect on branching in the clefts
Cell adhesion molecules and ECM components promoting branching at the branch tips
Cell–cell contact with the metanephric mesenchyme possibly influencing vectoriality of branching and branch elongation at the leading edges
Proteinase inhibitors protecting stalks and clefts
GF
GF

FIGURE 25.14 **Model for ureteric bud branching morphogenesis.** After induction of the ureteric bud (UB), in which GDNF appears to play a critical role, branching may be guided by gradients of promoting (GF +) and inhibiting growth factors (GF −). Distal effector molecules probably include facilitating and inhibiting extracellular matrix (ECM) components, together with signal transducing−cell adhesion molecules such as integrins, CD44, membrane-bound proteinase activators such as MT1-MMP, and active proteinases (e.g., MMP9), as well as proteinase inhibitors such as TIMP3, which binds to the ECM and could protect the matrix around the stalks from degradation. *(Reprinted with permission from the* Annual Review of Physiology, *Volume 62 © 2000 by Annual Reviews www.annualreviews.org.)*

mesenchyme, and embryonic bone.[48,49,229] Many embryonic epithelial, neural or mesenchymal tissues can thus induce the metanephric mesenchyme, although various tissues have different potency. For example, brain can only induce metanephric mesenchyme to the condensation stage, while spinal cord can induce tubule formation.[230] Thus, it is conceivable that there are several steps in the induction process: (1) rescue of metanephric mesenchyme and/or later tubular structures from apoptosis; (2) mesenchymal cell condensation; (3) epithelial polarization and junction formation; and (4) tubule formation. The molecules likely involved in the process are summarized in Table 25.2.

Prevention of Apoptosis

During kidney tubule development, apoptosis is observed among cells surrounding newly formed epithelial tubules.[231] In fact, significant levels of apoptosis appear to be occurring in many parts of the kidney during development.[232] When the metanephric mesenchyme is cultured with inducer tissues or EGF, apoptosis becomes less prominent.[231,232] These results suggest that an important early signal from the inducer tissue prevents metanephric mesenchyme cell apoptosis. In *in vitro* culture of metanephric mesenchyme, conditioned medium from UB cells also exhibits an anti-apoptotic effect.[233] One of the anti-apoptotic molecules in UB-conditioned medium is FGF2.[234] Consistent with these findings, RUB cell (derived from rat ureteric bud)-conditioned medium requires supplementation of FGF2 and TGFα to induce kidney tubule formation in the absence of inductive tissues.[235]

In addition, analysis of bone morphogenetic protein (*Bmp*)*7*-deficient mice suggests that BMP7 may act as an anti-apoptotic factor.[236,237] BMP7 belongs to the TGFβ superfamily and is expressed in the Wolffian duct, ureteric bud, and nephron structures after induction.[236] *Bmp7* knockout mice exhibit defects in eye and kidney development. Although there is a difference in the early kidney phenotype between knockout mice created by different groups, ureteric bud formation and initial induction appears unaffected; at least a few comma- and S-shaped bodies are observed at E12.5.[236,237] However, soon after this, both the ureteric bud and the metanephric mesenchyme start to degenerate, ultimately resulting in nonfunctioning disorganized kidneys. This raises the possibility that BMP7 maintains induced tubules, inhibiting them from apoptosis rather than directly inducing the metanephric mesenchyme.[236] On the other hand, *in vitro* application of BMP7 has been reported to induce E11.5 mouse metanephric mesenchyme to form epithelial glomeruli

TABLE 25.2 Molecules Likely to be Involved in Metanephric Mesenchyme Induction

Process	Transcription Factors	Soluble Factors	ECM/Other Molecules
Define	*Wt1*		
nephrogenic	*Pax2*		
mesenchyme	*Six1 Six2 Sall1 high*		
	Myc (uninduced MM)		
Rescue from apoptosis		FGF2, FGF8	
		EGFR ligands	
		BMP7	
Condensation/ epithelialization	*Pax2*	Wnt9b	Laminin
	Pax8	LIF	(γ1chain)/laminin receptor
	Nmyc	TGFβ2	(α6β1 integrin, nonmuscle dystroglycan)
	Foxd1	Lipocalin	
	Pod1	Wnt4	
	Pbx1		α8β1 integrin
Tubule formation	*Hnf1* (proximal tubule)		Laminin (γ1chain)/laminin
	Brn1 (Henle, distal)		receptor

ECM: extracellular matrix; LIF: leukemia-inhibiting factor; TGF: transforming growth factor.

without inductive tissues.[238] Whether BMP7 directly induces the metanephric mesenchyme remains to be determined.

Molecules Involved in Metanephric Mesenchyme Induction and Nephron Tubule Formation

As discussed in the transcription factor section, certain transcription factors such as *Pax2*, *Wt1*, *Six1*, *Six2* or *Sall1* are necessary to retain competency of the metanephric mesenchyme to respond to the signals from the ureteric bud. Early experiments using transfilter coculture of the metanephric mesenchyme with various inductive tissues defined several expected characteristics of "inductive molecules".[7] Experiments using different pore-size filters and multiple filters to separate the metanephric mesenchyme and inducer suggest that inductive molecules do not simply diffuse, rather, they seem to require close association of cells. In other words, direct cell-to-cell contact and/or soluble molecules associated with the cell surface are likely to be required for induction. In fact, direct interaction between the inductive tissue and the metanephric mesenchyme cells have been observed through the filter pores by electron microscopy.[239]

However, *in vitro* work indicates that combinations of soluble factors are sufficient to induce tubulogenesis of the metanephric mesenchyme. Leukemia inhibitory factor (LIF), FGF2, and TGFβ[51] or this combination plus TGFβ2[52] can induce nephron tubules in metanephric mesenchyme cultured in the absence of inductive tissues. A member of the lipocalin superfamily, 24p3, has also been shown to induce epithelialization of metanephric mesenchyme in the presence of FGFs,[240] and to deliver iron to the cell (iron is required for mesenchymal induction by this molecule[240]).

Cell surface glycoproteins of the Wnt family are candidate molecules for coordinating morphogenesis at the interface of metanephric mesenchyme and inductive tissues, as WNT1-expressing fibroblasts induce the metanephric mesenchyme to form glomeruli.[241] Although the *Wnt1* gene is not expressed in embryonic kidneys,[242] this result raises the possibility of an important role for other Wnt family members in nephrogenesis. Another Wnt family member, *Wnt4*, is expressed in the embryonic kidneys; it first appears in condensed metanephric mesenchyme, and its expression continues in comma- and S-shaped bodies, finally becoming restricted to the area where newly formed epithelial tubules are connected to collecting ducts.[243] WNT9b, secreted from the ureteric bud, triggers mesenchymal epithelial transformation, as metanephric mesenchyme induction is not observed in *Wnt9b*$^{-/-}$ mice.[244] Six2, a transcription factor important for nephron progenitor maintenance, counteracts WNT9b signaling.[6] Downstream of WNT9b, WNT4 plays an important role in metanephric mesenchyme induction as an autocrine factor for metanephric mesenchymal cells.[244] The metanephric mesenchyme of mutant mice lacking the *Wnt4* gene is able to condense around the branching ureteric bud, but fails to form peritubular aggregates.[243] There is no apparent kidney tubule development in these knockout animals. The expression of markers for early mesenchymal induction, *Pax2* and *Nmyc*, does not seem to be affected in *Wnt4* mutant mice, suggesting that *Wnt4* acts at a later stage than *Pax2* or *Nmyc*. However, *Pax8* expression by metanephric mesenchyme-derived structures cannot be detected in the mutant mice.

Another autocrine factor for metanephric mesenchyme induction is FGF8. Site specific, conditional deletion of Fgf8, either in the metanephric mesenchyme[245] or in all mesodermal tissues,[179,246] results in hypoplastic,

dysmorphic kidneys displaying disruptions in nephron formation. Conditional deletion of both *Fgfr1* and *Fgfr2* from the metanephric mesenchyme results in renal dysgenesis, due to defects in the formation of the metanephric mesenchyme and early ureteric bud.[247]

The cell-surface-signaling molecule Notch has also been implicated in tubulogenesis. Binding of Notch by its ligands (Jagged1 (Jag1), Jag2, Delta-like (Dll) 1, Dll3 or Dll4)) results in the shedding of its extracellular domain, cleavage of its transmembrane domain by γ-secretase, and translocation of its intracellular domain to the nucleus where it promotes transcription of target genes (reviewed in [248–250]). *Notch 1*, *2*, and *3* have been shown to be expressed in the developing kidney.[58,251–255] *Notch2* mutation leads to hypoplastic kidneys with glomerular defects,[256] while conditional deletion of *Notch2*, but not *Notch1*, causes the loss of glomeruli and proximal tubules.[248] However, proteolytic cleavage of Notch1 by γ-secretase is required for Notch activation, and this inhibition in kidney organ culture results in decreased S-shaped bodies despite having normal condensation.[257] Knockout and partial rescue of *Presenilin1* and *2* that are required for γ-secretase activity lead to a similar phenotype.[258] In addition, augmenting Notch1 signaling by inactivating Mint (an inhibitor of Notch-mediated transcription[250,259–262]) has the ability to partially rescue nephron development in Notch2 knockout kidneys.[250] Taken together, the data suggest that Notch1 and Notch2 likely act in concert to regulate proximal tubule and glomerular development.[250]

Extracellular matrix proteins are important for maintaining epithelial tubular structures. Much work has been done on the basement membrane glycoprotein laminin and the integrins that bind laminin. Laminin1 is composed of three chains: α1; β1; and γ1. Of these, β1- and γ1-expression increases early (day 1) when the metanephric mesenchyme is induced, while the α1 chain is expressed after epithelial cell polarization begins.[263,264] The laminin α1 chain is exclusively expressed by the epithelial cells,[263] and perturbation of this chain by antibodies inhibits kidney tubulogenesis *in vitro*.[265] The kidney epithelial cell has at least two laminin receptors: $\alpha_6\beta_1$ integrin and nonmuscle dystroglycan. Perturbation of these receptors inhibits kidney tubulogenesis *in vitro*.[38,266] Moreover, in *in vitro* culture of embryonic lung, it has been demonstrated that heterotypic cell-to-cell contact between epithelial cells and mesenchymal cells is required to synthesize the laminin α_1 chain.[267] If this result is applicable to embryonic kidney, further differentiation after cell-to-cell contact may be a function of expression of the laminin α_1 chain.

In addition to laminin-binding integrins, knockouts of integrin α8 have been shown to produce severe defects in kidney development.[268] The ureteric bud initiation and initial mesenchymal induction appear unaffected; the metanephric mesenchyme cells condense around the ureteric bud and start to express *Pax2* and p75 NGFR. However, further steps toward epithelialization and tubule formation are not observed. In normal mice, α8β1 integrin is transiently expressed in the condensing mesenchymal cells. Both spatiotemporal localization and knockout phenotype suggest that $\alpha_8\beta_1$ integrin plays an important role after the initial induction step of mesenchymal–epithelial transformation.

Evidence is beginning to accumulate on the functional maturation of the kidney tubules. Kidney tubules further differentiate into several segments. In each segment the tubular cells express different sets of transporters. For example, Northern blot analysis shows that the organic anion transporter Oat1 begins to be expressed at around E16 kidney.[269] It is likely that expression of many transporters, characteristic of mature tubules, is tightly regulated. In this regard, elucidation of the roles of transcription factors *Hnf1* (proximal tubules) and *Brn1* (Henle's loop and distal tubule) is important, and other unknown factors may be involved in this process.

VASCULAR AND GLOMERULAR DEVELOPMENT

The origin of glomerular endothelial cells and mesangial cells, and how the vascular system is integrated in the developing kidney, has been an area of controversy for years (reviewed in[13]). Vascular development occurs by: (1) angiogenesis, in which new vessels arise from existing vasculature; and/or (2) vasculogenesis, in which *de novo* endothelial cells are formed. As mentioned previously, *in vitro* kidney organ culture gives rise to epithelial glomerular structures, not mesangial cells nor endothelial cells, suggesting that either the culture conditions are not suitable for endothelial cell growth or there are no angioblasts in the metanephric mesenchyme. To study kidney vascular development, interspecies grafting techniques have been used in which E11 murine embryonic kidneys are transplanted into chick chorioallantoic-membranes (CAM).[270] When E11 mouse kidneys, which have no apparent vascular development, are grown in chick CAM, the kidneys form glomeruli containing blood vessels from the chick, as determined by staining with species-specific antibodies against basement membranes.[271,272] However, when E11 mouse kidneys are grafted into the rat anterior eye chamber, newly formed glomerular endothelial cells appear to be derived from the graft.[273] Moreover, the same group has demonstrated that vascular endothelial cell growth factor (Vegf) receptor FLK1-positive cells are

found in the E12 mouse kidney, and these cells are likely to be angioblasts, which differentiate into blood vessels in the glomeruli.[274] Thus, depending on the culture and grafting conditions, glomerular capillaries can be derived by an angiogenic process (i.e., outside of the metanephric mesenchyme or a vasculogenic process; inside of the metanephric mesenchyme). Which of these processes is more important *in vivo* remains uncertain, and it is of course possible that both are important.

The origin of mesangial cells also remains uncertain, although it has been recently proposed that they are derived from cap mesenchymal cells.[6,275] In the aforementioned different kidney graft systems, mesangial cells appear to behave similarly to glomerular endothelial cells: in CAM grafts, the mesangial cells are derived from the hosts[276,277]; while in the anterior eye chamber grafts, they are derived from the grafts.[273] Platelet-derived growth factor (*Pdgf*)-B receptor knockout mice do not have mesangial cells, and exhibited dilated capillary loops resulting in defective glomeruli.[278,279]

Recently, genetic fate tracing of *Six2*-positive nephron progenitor cells revealed that neither vasucular endothelial cells nor mesangial cells are derived from nephron progenitors.[280] This does not mean that blood vessel and mesangial cells are extrarenal in origin, because metanephric mesenchyme contains non-nephron progenitor cells. Nevertheless, it should be noted that endothelial and mesangial cells and nephron epithelial cells are derived from distinct sources.

In addition, deletion of *Crim1*, a transmembrane protein expressed in mesangial cells and podocytes, was found to induce abnormal glomerular development, characterized by simplified glomerular capillary networks with dilated capillaries.[281–283] Together with the observed mislocalization of Vegf-A, as well as increased activation of Flk1, *Crim1* appears to regulate the spatial distribution of Vegf-A during glomerular development.[282] Knockout of Semaphorin3a (*Sema3a*) also disrupts kidney vascular patterning.[101,284,285] Decreased apoptosis of endothelial cells is observed in kidneys from *Sema3a* knockout animals, while whole organ culture also indicates that Sema3a is a chemorepellant and inhibits endothelial cell migration.[101,284,285] Together with the fact that Vegf-A promotes endothelial cell survival and acts as a chemoattractant for endothelial cells,[286,287] the data suggest that endothelial cell number and vascular patterning is regulated by a balance of Vegf-A and Sema3a signaling.[284,285]

TERMINATION OF KIDNEY DEVELOPMENT

Despite the wealth of literature describing the molecules and mechanisms regulating the various morphogenetic processes involved in the development of the metanephric kidney, how the overall process is brought to an end has received little attention. In humans, kidney organogenesis is complete before birth; however, in other mammals, including rats and mice, kidney development continues into the postnatal period. Examination of this postnatal period in mice reveals the loss of nephrogenic mesenchyme by day three after birth.[288] This was not due to an increase in apoptosis, but rather appeared to result from the synchronous conversion of the remaining nephrogenic mesenchyme into new nephrons.[288] Since, during this time, the ureteric bud tips retain the capacity to induce nephrogenesis *in vitro*, this indicates that this loss of nephrogeneic mesenchyme demarcates the beginning of the end of kidney development.[288] This time period also correlates with the observed sudden burst in the expression of many genes involved in redox metabolism and transport, including multispecific drug transporters such as Oat1 and Oct1.[75] Together, the data suggest that parturition and the end of kidney development is characterized by rapid changes in: (1) the remaining metanephric mesenchyme, leading to the formation of new nephrons (which completes metanephrogenesis and sets the final nephron number); and (2) the differentiation state of existing nephrons.[75,288]

Acknowledgments

The authors thank Dr. Wei Wu for providing valuable comments on this manuscript. S. K. Nigam is funded by the National Institutes of Health.

References

[1] Bouchard M, Souabni A, Mandler M, Neubuser A, Busslinger M. Nephric lineage specification by Pax2 and Pax8. Genes Dev 2002;16(22):2958–70.
[2] Mauch TJ, Yang G, Wright M, Smith D, Schoenwolf GC. Signals from trunk paraxial mesoderm induce pronephros formation in chick intermediate mesoderm. Dev Biol 2000;220(1):62–75.
[3] Obara-Ishihara T, Kuhlman J, Niswander L, Herzlinger D. The surface ectoderm is essential for nephric duct formation in intermediate mesoderm. Development 1999;126(6):1103–8.
[4] Vize PD, Seufert DW, Carroll TJ, Wallingford JB. Model systems for the study of kidney development: use of the pronephros in the analysis of organ induction and patterning. Dev Biol 1997;188(2):189–204.
[5] Smith C, Mackay S. Morphological development and fate of the mouse mesonephros. J Anat 1991;174:171–84.
[6] Kobayashi A, Valerius MT, Mugford JW, Carroll TJ, Self M, Oliver G, et al. Six2 defines and regulates a multipotent self-renewing nephron progenitor population throughout mammalian kidney development. Cell Stem Cell 2008;3(2):169–81.
[7] Saxen L, Organogenesis of the Kidney. In: Barlow P, Green P, White C, editors. Cambridge, U.K.: Cambridge University Press; 1987; 184.

[8] Costantini F. GDNF/Ret signaling and renal branching morphogenesis: from mesenchymal signals to epithelial cell behaviors. Organogenesis 2010;6(4):252–62.
[9] Sajithlal G, Zou D, Silvius D, Xu PX. Eya 1 acts as a critical regulator for specifying the metanephric mesenchyme. Dev Biol 2005;284(2):323–36.
[10] Osathanondh V, Potter EL. Development of human kidney as shown by microdissection. III. Formation and interrelationship of collecting tubules and nephrons. Arch Pathol 1963; 76:290–302.
[11] Osathanondh V, Potter EL. Development of human kidney as shown by microdissection. II. Renal pelvis, calyces, and papillae. Arch Pathol 1963;76:277–89.
[12] Osathanondh V, Potter EL. Development of human kidney as shown by microdissection. V. Development of vascular pattern of glomerulus. Arch Pathol 1966;82(5):403–11.
[13] Sequeira Lopez ML, Gomez RA. Development of the renal arterioles. J Am Soc Nephrol 2011;22(12):2156–65.
[14] Grobstein C. Morphogenetic interaction between embryonic mouse tissues separated by a membrane filter. Nature 1953;172 (4384):869–70.
[15] Grobstein C. Inductive epitheliomesenchymal interaction in cultured organ rudiments of the mouse. Science 1953;118(3054): 52–5.
[16] Grobstein C. Inductive tissue interaction in development. Adv Cancer Res 1956;4:187–236.
[17] Ekblom P, Thesleff I, Miettinen A, Saxen L. Organogenesis in a defined medium supplemented with transferrin. Cell Differ 1981;10(5):281–8.
[18] Laitinen L, Virtanen I, Saxen L. Changes in the glycosylation pattern during embryonic development of mouse kidney as revealed with lectin conjugates. J Histochem Cytochem 1987;35 (1):55–65.
[19] Durbeej M, Soderstrom S, Ebendal T, Birchmeier C, Ekblom P. Differential expression of neurotrophin receptors during renal development. Development 1993;119(4):977–89.
[20] Davies JA, Ladomery M, Hohenstein P, Michael L, Shafe A, Spraggon L, et al. Development of an siRNA-based method for repressing specific genes in renal organ culture and its use to show that the Wt1 tumour suppressor is required for nephron differentiation. Hum Mol Genet 2004;13(2):235–46.
[21] Sakai T, Larsen M, Yamada KM. Fibronectin requirement in branching morphogenesis. Nature 2003;423(6942):876–81.
[22] Brophy PD, Ostrom L, Lang KM, Dressler GR. Regulation of ureteric bud outgrowth by Pax2-dependent activation of the glial derived neurotrophic factor gene. Development 2001;128 (23):4747–56.
[23] Maeshima A, Sakurai H, Choi Y, Kitamura S, Vaughn DA, Tee JB, et al. Glial cell-derived neurotrophic factor independent ureteric bud outgrowth from the Wolffian duct. J Am Soc Nephrol 2007;18(12):3147–55.
[24] Maeshima A, Vaughn DA, Choi Y, Nigam SK. Activin A is an endogenous inhibitor of ureteric bud outgrowth from the Wolffian duct. Dev Biol 2006;295(2):473–85.
[25] Rosines E, Sampogna RV, Johkura K, Vaughn DA, Choi Y, Sakurai H, et al. Staged *in vitro* reconstitution and implantation of engineered rat kidney tissue. Proc Natl Acad Sci USA 2007;104(52):20938–43.
[26] Tang MJ, Cai Y, Tsai SJ, Wang YK, Dressler GR. Ureteric bud outgrowth in response to RET activation is mediated by phosphatidylinositol 3-kinase. Dev Biol 2002;243(1):128–36.
[27] Bush KT, Vaughn DA, Li X, Rosenfeld MG, Rose DW, Mendoza SA, et al. Development and differentiation of the ureteric bud into the ureter in the absence of a kidney collecting system. Dev Biol 2006;298(2):571–84.
[28] Choi Y, Tee JB, Gallegos TF, Shah MM, Oishi H, Sakurai H, et al. Neuropeptide Y functions as a facilitator of GDNF-induced budding of the Wolffian duct. Development 2009;136(24): 4213–24.
[29] Rosines E, Johkura K, Zhang X, Schmidt HJ, Decambre M, Bush KT, et al. Constructing kidney-like tissues from cells based on programs for organ development: toward a method of *in vitro* tissue engineering of the kidney. Tissue Eng Part A 2010;6 (18):2441–55.
[30] Tee JB, Choi Y, Shah MM, Dnyanmote A, Sweeney DE, Gallegos TF, et al. Protein kinase A regulates GDNF/RET-dependent but not GDNF/Ret-independent ureteric bud outgrowth from the Wolffian duct. Dev Biol 2010;347(2):337–47.
[31] Qiao J, Sakurai H, Nigam SK. Branching morphogenesis independent of mesenchymal-epithelial contact in the developing kidney. Proc Natl Acad Sci USA 1999;96(13):7330–5.
[32] Meyer TN, Schwesinger C, Bush KT, Stuart RO, Rose DW, Shah MM, et al. Spatiotemporal regulation of morphogenetic molecules during *in vitro* branching of the isolated ureteric bud: toward a model of branching through budding in the developing kidney. Dev Biol 2004;275(1):44–67.
[33] Li Z, Stuart RO, Qiao J, Pavlova A, Bush KT, Pohl M, et al. A role for Timeless in epithelial morphogenesis during kidney development. Proc Natl Acad Sci USA 2000;97(18):10038–43.
[34] Pohl M, Sakurai H, Bush KT, Nigam SK. Matrix metalloproteinases and their inhibitors regulate *in vitro* ureteric bud branching morphogenesis. Am J Physiol Renal Physiol 2000;279(5): F891–900.
[35] Karihaloo A, Karumanchi SA, Barasch J, Jha V, Nickel CH, Yang J, et al. Endostatin regulates branching morphogenesis of renal epithelial cells and ureteric bud. Proc Natl Acad Sci USA 2001;98(22):12509–14.
[36] Qiao J, Bush KT, Steer DL, Stuart RO, Sakurai H, Wachsman W, et al. Multiple fibroblast growth factors support growth of the ureteric bud but have different effects on branching morphogenesis. Mech Dev 2001;109(2):123–35.
[37] Sakurai H, Bush KT, Nigam SK. Identification of pleiotrophin as a mesenchymal factor involved in ureteric bud branching morphogenesis. Development 2001;128(17):3283–93.
[38] Zent R, Bush KT, Pohl ML, Quaranta V, Koshikawa N, Wang Z, et al. Involvement of laminin binding integrins and laminin-5 in branching morphogenesis of the ureteric bud during kidney development. Dev Biol 2001;238(2):289–302.
[39] Stuart RO, Bush KT, Nigam SK. Changes in gene expression patterns in the ureteric bud and metanephric mesenchyme in models of kidney development. Kidney Int 2003;64(6): 1997–2008.
[40] Bush KT, Sakurai H, Steer DL, Leonard MO, Sampogna RV, Meyer TN, et al. TGF-beta superfamily members modulate growth, branching, shaping, and patterning of the ureteric bud. Dev Biol 2004;266(2):285–98.
[41] Steer DL, Shah MM, Bush KT, Stuart RO, Sampogna RV, Meyer TN, et al. Regulation of ureteric bud branching morphogenesis by sulfated proteoglycans in the developing kidney. Dev Biol 2004;272(2):310–27.
[42] Sakurai H, Bush KT, Nigam SK. Heregulin induces glial cell line-derived neurotrophic growth factor-independent, nonbranching growth and differentiation of ureteric bud epithelia. J Biol Chem 2005;280(51):42181–7.
[43] Meyer TN, Schwesinger C, Sampogna RV, Vaughn DA, Stuart RO, Steer DL, et al. Rho kinase acts at separate steps in ureteric bud and metanephric mesenchyme morphogenesis during kidney development. Differentiation 2006;74(9-10):638–47.
[44] Shah MM, Tee JB, Meyer T, Meyer-Schwesinger C, Choi Y, Sweeney DE, et al. The instructive role of metanephric

mesenchyme in ureteric bud patterning, sculpting, and maturation and its potential ability to buffer ureteric bud branching defects. Am J Physiol Renal Physiol 2009;297(5):F1330–41.
[45] Wu W, Kitamura S, Truong DM, Rieg T, Vallon V, Sakurai H, et al. Beta1-integrin is required for kidney collecting duct morphogenesis and maintenance of renal function. Am J Physiol Renal Physiol 2009;297(1):F210–7.
[46] Shah MM, Sakurai H, Sweeney DE, Gallegos TF, Bush KT, Esko JD, et al. Hs2st mediated kidney mesenchyme induction regulates early ureteric bud branching. Dev Biol 2010;339(2):354–65.
[47] Shah MM, Sakurai H, Gallegos TF, Sweeney DE, Bush KT, Esko JD, et al. Growth factor-dependent branching of the ureteric bud is modulated by selective 6-O sulfation of heparan sulfate. Dev Biol 2011;356(1):19–27.
[48] Grobstein C. Trans-filter induction of tubules in mouse metanephrogenic mesenchyme. Exp Cell Res 1956;10(2):424–40.
[49] Saxen L, Lehtonen E. Embryonic kidney in organ culture. Differentiation 1987;36(1):2–11.
[50] Lehtonen E, Wartiovaara J, Nordling S, Saxen L. Demonstration of cytoplasmic processes in Millipore filters permitting kidney tubule induction. J Embryol Exp Morphol 1975; 33(1):187–203.
[51] Barasch J, Yang J, Ware CB, Taga T, Yoshida K, Erdjument-Bromage H, et al. Mesenchymal to epithelial conversion in rat metanephros is induced by LIF. Cell 1999;99(4):377–86.
[52] Plisov SY, Yoshino K, Dove LF, Higinbotham KG, Rubin JS, Perantoni AO. TGF beta 2, LIF and FGF2 cooperate to induce nephrogenesis. Development 2001;128(7):1045–57.
[53] Bullock SL, Fletcher JM, Beddington RS, Wilson VA. Renal agenesis in mice homozygous for a gene trap mutation in the gene encoding heparan sulfate 2-sulfotransferase. Genes Dev 1998;12(12):1894–906.
[54] Capecchi MR. Altering the genome by homologous recombination. Science 1989;244(4910):1288–92.
[55] Capecchi MR. Targeted gene replacement. Sci Am 1994;270 (3):52–9.
[56] Galli-Taliadoros LA, Sedgwick JD, Wood SA, Korner H. Gene knock-out technology: a methodological overview for the interested novice. J Immunol Methods 1995;181(1):1–15.
[57] Lechner MS, Dressler GR. The molecular basis of embryonic kidney development. Mech Dev 1997;62(2):105–20.
[58] Yu J, McMahon AP, Valerius MT. Recent genetic studies of mouse kidney development. Curr Opin Genet Dev 2004;14 (5):550–7.
[59] Miyamoto N, Yoshida M, Kuratani S, Matsuo I, Aizawa S. Defects of urogenital development in mice lacking Emx2. Development 1997;124(9):1653–64.
[60] Ly JP, Onay T, Quaggin SE. Mouse models to study kidney development, function and disease. Curr Opin Nephrol Hypertens 2011;20(4):382–90.
[61] Birling MC, Gofflot F, Warot X. Site-specific recombinases for manipulation of the mouse genome. Methods Mol Biol 2009;561:245–63.
[62] Gawlik A, Quaggin SE. Deciphering the renal code: advances in conditional gene targeting. Physiology (Bethesda) 2004;19: 245–52.
[63] Zhang X, Mernaugh G, Yang DH, Gewin L, Srichai MB, Harris RC, et al. beta1 integrin is necessary for ureteric bud branching morphogenesis and maintenance of collecting duct structural integrity. Development 2009;136(19):3357–66.
[64] Santos OF, Moura LA, Rosen EM, Nigam SK. Modulation of HGF-induced tubulogenesis and branching by multiple phosphorylation mechanisms. Dev Biol 1993;159(2):535–48.
[65] Barros EJ, Santos OF, Matsumoto K, Nakamura T, Nigam SK. Differential tubulogenic and branching morphogenetic activities of growth factors: implications for epithelial tissue development. Proc Natl Acad Sci USA 1995;92(10):4412–6.
[66] Cantley LG, Barros EJ, Gandhi M, Rauchman M, Nigam SK. Regulation of mitogenesis, motogenesis, and tubulogenesis by hepatocyte growth factor in renal collecting duct cells. Am J Physiol 1994;267(2 Pt 2):F271–80.
[67] Sakurai H, Nigam SK. Transforming growth factor-beta selectively inhibits branching morphogenesis but not tubulogenesis. Am J Physiol 1997;272(1 Pt 2):F139–46.
[68] Sakurai H, Tsukamoto T, Kjelsberg CA, Cantley LG, Nigam SK. EGF receptor ligands are a large fraction of *in vitro* branching morphogens secreted by embryonic kidney. Am J Physiol 1997; 273(3 Pt 2):F463–72.
[69] Sakurai H, Barros EJ, Tsukamoto T, Barasch J, Nigam SK. An *in vitro* tubulogenesis system using cell lines derived from the embryonic kidney shows dependence on multiple soluble growth factors. Proc Natl Acad Sci USA 1997;94(12):6279–84.
[70] Zegers MM, O'Brien LE, Yu W, Datta A, Mostov KE. Epithelial polarity and tubulogenesis *in vitro*. Trends Cell Biol 2003;13 (4):169–76.
[71] Stuart RO, Barros EJ, Ribeiro E, Nigam SK. Epithelial tubulogenesis through branching morphogenesis: relevance to collecting system development. J Am Soc Nephrol 1995;6(4):1151–9.
[72] Stuart RO, Bush KT, Nigam SK. Changes in global gene expression patterns during development and maturation of the rat kidney. Proc Natl Acad Sci USA 2001;98(10):5649–54.
[73] Tsigelny IF, Kouznetsova VL, Sweeney DE, Wu W, Bush KT, Nigam SK. Analysis of metagene portraits reveals distinct transitions during kidney organogenesis. Sci Signal 2008;1 (49):ra16.
[74] Schmidt-Ott KM, Masckauchan TN, Chen X, Hirsh BJ, Sarkar A, Yang J, et al. Beta-catenin/TCF/Lef controls a differentiation-associated transcriptional program in renal epithelial progenitors. Development 2007;134(17):3177–90.
[75] Sweeney DE, Vallon V, Rieg T, Wu W, Gallegos TF, Nigam SK. Functional maturation of drug transporters in the developing, neonatal, and postnatal kidney. Mol Pharmacol 2011;80 (1):147–54.
[76] Brunskill EW, Aronow BJ, Georgas K, Rumballe B, Valerius MT, Aronow J, et al. Atlas of gene expression in the developing kidney at microanatomic resolution. Dev Cell 2008;15(5): 781–91.
[77] Georgas KM, Chiu HS, Lesieur E, Rumballe BA, Little MH. Expression of metanephric nephron-patterning genes in differentiating mesonephric tubules. Dev Dyn 2011;240(6):1600–12.
[78] Harding SD, Armit C, Armstrong J, Brennan J, Cheng Y, Haggarty B, et al. The GUDMAP database–an online resource for genitourinary research. Development 2011;138(13):2845–53.
[79] Little MH, Brennan J, Georgas K, Davies JA, Davidson DR, Baldock RA, et al. A high-resolution anatomical ontology of the developing murine genitourinary tract. Gene Expr Patterns 2007;7(6):680–99.
[80] McMahon AP, Aronow BJ, Davidson DR, Davies JA, Gaido KW, Grimmond S, et al. GUDMAP: the genitourinary developmental molecular anatomy project. J Am Soc Nephrol 2008;19(4): 667–71.
[81] Nigam SK, Shah MM. How does the ureteric bud branch? J Am Soc Nephrol 2009;20(7):1465–9.
[82] Sampogna RV, Nigam SK. Implications of gene networks for understanding resilience and vulnerability in the kidney branching program. Physiology (Bethesda) 2004;19:339–47.
[83] Ishibe S, Karihaloo A, Ma H, Zhang J, Marlier A, Mitobe M, et al. Met and the epidermal growth factor receptor act cooperatively to regulate final nephron number and maintain collecting duct morphology. Development 2009;136(2):337–45.

[84] Pastorelli LM, Wells S, Fray M, Smith A, Hough T, Harfe BD, et al. Genetic analyses reveal a requirement for Dicer1 in the mouse urogenital tract. Mamm Genome 2009;20(3): 140–51.
[85] Patel SR, Kim D, Levitan I, Dressler GR. The BRCT-domain containing protein PTIP links PAX2 to a histone H3, lysine 4 methyltransferase complex. Dev Cell 2007;13(4): 580–92.
[86] Nagalakshmi VK, Ren Q, Pugh MM, Valerius MT, McMahon AP, Yu J. Dicer regulates the development of nephrogenic and ureteric compartments in the mammalian kidney. Kidney Int 2011;79(3):317–30.
[87] Harvey SJ, Jarad G, Cunningham J, Goldberg S, Schermer B, Harfe BD, et al. Podocyte-specific deletion of dicer alters cytoskeletal dynamics and causes glomerular disease. J Am Soc Nephrol 2008;19(11):2150–8.
[88] Ho J, Ng KH, Rosen S, Dostal A, Gregory RI, Kreidberg JA. Podocyte-specific loss of functional microRNAs leads to rapid glomerular and tubular injury. J Am Soc Nephrol 2008;19(11): 2069–75.
[89] Ho JJ, Marsden PA. Dicer cuts the kidney. J Am Soc Nephrol 2008;19(11):2043–6.
[90] Saal S, Harvey SJ. MicroRNAs and the kidney: coming of age. Curr Opin Nephrol Hypertens 2009;18(4):317–23.
[91] Shi S, Yu L, Chiu C, Sun Y, Chen J, Khitrov G, et al. Podocyte-selective deletion of dicer induces proteinuria and glomerulosclerosis. J Am Soc Nephrol 2008;19(11):2159–69.
[92] Tang KF, Song GB, Shi YS, Yuan L, Li YH. Dicer knockdown induces fibronectin-1 expression in HEK293T cells via induction of Egr1. Biochim Biophys Acta 2010;1800(3):380–4.
[93] Wei Q, Bhatt K, He HZ, Mi QS, Haase VH, Dong Z. Targeted deletion of Dicer from proximal tubules protects against renal ischemia-reperfusion injury. J Am Soc Nephrol 2010;21(5): 756–61.
[94] Monte JC, Sakurai H, Bush KT, Nigam SK. The developmental nephrome: systems biology in the developing kidney. Curr Opin Nephrol Hypertens 2007;16(1):3–9.
[95] Nigam SK. From the ureteric bud to the penome. Kidney Int 2003;64(6):2320–2.
[96] Costantini F, Kopan R. Patterning a complex organ: branching morphogenesis and nephron segmentation in kidney development. Dev Cell 2010;18(5):698–712.
[97] Dressler GR. Patterning and early cell lineage decisions in the developing kidney: the role of Pax genes. Pediatr Nephrol 2011;26(9):1387–94.
[98] Little M, Georgas K, Pennisi D, Wilkinson L. Kidney development: two tales of tubulogenesis. Curr Top Dev Biol 2010; 90:193–229.
[99] Miner JH. Organogenesis of the kidney glomerulus: focus on the glomerular basement membrane. Organogenesis 2011;7 (2):75–82.
[100] Chapin HC, Caplan MJ. The cell biology of polycystic kidney disease. J Cell Biol 2010;191(4):701–10.
[101] Reidy KJ, Rosenblum ND. Cell and molecular biology of kidney development. Semin Nephrol 2009;29(4):321–37.
[102] Davis AP, Witte DP, Hsieh-Li HM, Potter SS, Capecchi MR. Absence of radius and ulna in mice lacking hoxa-11 and hoxd-11. Nature 1995;375(6534):791–5.
[103] Wellik DM, Hawkes PJ, Capecchi MR. Hox11 paralogous genes are essential for metanephric kidney induction. Genes Dev 2002;16(11):1423–32.
[104] Dressler GR, Deutsch U, Chowdhury K, Nornes HO, Gruss P. Pax2, a new murine paired-box-containing gene and its expression in the developing excretory system. Development 1990; 109(4):787–95.
[105] Dressler GR, Douglass EC. Pax-2 is a DNA-binding protein expressed in embryonic kidney and Wilms tumor. Proc Natl Acad Sci USA 1992;89(4):1179–83.
[106] Torres M, Gomez-Pardo E, Dressler GR, Gruss P. Pax-2 controls multiple steps of urogenital development. Development 1995;121(12):4057–65.
[107] Plachov D, Chowdhury K, Walther C, Simon D, Guenet JL, Gruss P. Pax8, a murine paired box gene expressed in the developing excretory system and thyroid gland. Development 1990;110(2):643–51.
[108] Mansouri A, Chowdhury K, Gruss P. Follicular cells of the thyroid gland require Pax8 gene function. Nat Genet 1998;19 (1):87–90.
[109] Narlis M, Grote D, Gaitan Y, Boualia SK, Bouchard M. Pax2 and pax8 regulate branching morphogenesis and nephron differentiation in the developing kidney. J Am Soc Nephrol 2007;18(4):1121–9.
[110] Wawersik S, Purcell P, Maas RL. Pax6 and the genetic control of early eye development. Results Probl Cell Differ 2000; 31:15–36.
[111] Xu PX, Adams J, Peters H, Brown MC, Heaney S, Maas R. Eya1-deficient mice lack ears and kidneys and show abnormal apoptosis of organ primordia. Nat Genet 1999;23(1):113–7.
[112] Li X, Oghi KA, Zhang J, Krones A, Bush KT, Glass CK, et al. Eya protein phosphatase activity regulates Six1-Dach-Eya transcriptional effects in mammalian organogenesis. Nature 2003;426(6964):247–54.
[113] Xu PX, Zheng W, Huang L, Maire P, Laclef C, Silvius D. Six1 is required for the early organogenesis of mammalian kidney. Development 2003;130(14):3085–94.
[114] Gong KQ, Yallowitz AR, Sun H, Dressler GR, Wellik DM. A Hox-Eya-Pax complex regulates early kidney developmental gene expression. Mol Cell Biol 2007;27(21):7661–8.
[115] Nishinakamura R, Matsumoto Y, Nakao K, Nakamura K, Sato A, Copeland NG, et al. Murine homolog of SALL1 is essential for ureteric bud invasion in kidney development. Development 2001;128(16):3105–15.
[116] Kiefer SM, Robbins L, Stumpff KM, Lin C, Ma L, Rauchman M. Sall1-dependent signals affect Wnt signaling and ureter tip fate to initiate kidney development. Development 2010;137 (18):3099–106.
[117] Nishinakamura R, Osafune K. Essential roles of Sall family genes in kidney development. J Physiol Sci 2006;56(2):131–6.
[118] Kume T, Deng K, Hogan BL. Murine forkhead/winged helix genes Foxc1 (Mf1) and Foxc2 (Mfh1) are required for the early organogenesis of the kidney and urinary tract. Development 2000;127(7):1387–95.
[119] Fujii T, Pichel JG, Taira M, Toyama R, Dawid IB, Westphal H. Expression patterns of the murine LIM class homeobox gene lim1 in the developing brain and excretory system. Dev Dyn 1994;199(1):73–83.
[120] Shawlot W, Behringer RR. Requirement for Lim1 in head-organizer function. Nature 1995;374(6521):425–30.
[121] Tsang TE, Shawlot W, Kinder SJ, Kobayashi A, Kwan KM, Schughart K, et al. Lim1 activity is required for intermediate mesoderm differentiation in the mouse embryo. Dev Biol 2000;223(1):77–90.
[122] Drummond IA, Madden SL, Rohwer-Nutter P, Bell GI, Sukhatme VP, Rauscher III FJ. Repression of the insulin-like growth factor II gene by the Wilms tumor suppressor WT1. Science 1992;257(5070):674–8.
[123] Werner H, Re GG, Drummond IA, Sukhatme VP, Rauscher III FJ, Sens DA, et al. Increased expression of the insulin-like growth factor I receptor gene, IGF1R, in Wilms tumor is correlated with modulation of IGF1R promoter activity by the WT1

Wilms tumor gene product. Proc Natl Acad Sci USA 1993;90 (12):5828–32.
[124] Ryan G, Steele-Perkins V, Morris JF, Rauscher III FJ, Dressler GR. Repression of Pax-2 by WT1 during normal kidney development. Development 1995;121(3):867–75.
[125] Hewitt SM, Hamada S, McDonnell TJ, Rauscher III FJ, Saunders GF. Regulation of the proto-oncogenes bcl-2 and c-myc by the Wilms' tumor suppressor gene WT1. Cancer Res 1995;55(22):5386–9.
[126] Kreidberg JA, Sariola H, Loring JM, Maeda M, Pelletier J, Housman D, et al. WT-1 is required for early kidney development. Cell 1993;74(4):679–91.
[127] Donovan MJ, Natoli TA, Sainio K, Amstutz A, Jaenisch R, Sariola H, et al. Initial differentiation of the metanephric mesenchyme is independent of WT1 and the ureteric bud. Dev Genet 1999;24(3-4):252–62.
[128] Mundlos S, Pelletier J, Darveau A, Bachmann M, Winterpacht A, Zabel B. Nuclear localization of the protein encoded by the Wilms' tumor gene WT1 in embryonic and adult tissues. Development 1993;119(4):1329–41.
[129] Kim HS, Kim MS, Hancock AL, Harper JC, Park JY, Poy G, et al. Identification of novel Wilms' tumor suppressor gene target genes implicated in kidney development. J Biol Chem 2007;282 (22):16278–87.
[130] Maas R, Elfering S, Glaser T, Jepeal L. Deficient outgrowth of the ureteric bud underlies the renal agenesis phenotype in mice manifesting the limb deformity (ld) mutation. Dev Dyn 1994;199(3):214–28.
[131] Chan DC, Wynshaw-Boris A, Leder P. Formin isoforms are differentially expressed in the mouse embryo and are required for normal expression of fgf-4 and shh in the limb bud. Development 1995;121(10):3151–62.
[132] Mass RL, Zeller R, Woychik RP, Vogt TF, Leder P. Disruption of formin-encoding transcripts in two mutant limb deformity alleles. Nature 1990;346(6287):853–5.
[133] Wynshaw-Boris A, Ryan G, Deng CX, Chan DC, Jackson-Grusby L, Larson D, et al. The role of a single formin isoform in the limb and renal phenotypes of limb deformity. Mol Med 1997;3(6):372–84.
[134] Mugrauer G, Ekblom P. Contrasting expression patterns of three members of the myc family of protooncogenes in the developing and adult mouse kidney. J Cell Biol 1991;112(1):13–25.
[135] Charron J, Malynn BA, Fisher P, Stewart V, Jeannotte L, Goff SP, et al. Embryonic lethality in mice homozygous for a targeted disruption of the N-myc gene. Genes Dev 1992;6 (12A):2248–57.
[136] Davis AC, Wims M, Spotts GD, Hann SR, Bradley A. A null c-myc mutation causes lethality before 10.5 days of gestation in homozygotes and reduced fertility in heterozygous female mice. Genes Dev 1993;7(4):671–82.
[137] Stanton BR, Perkins AS, Tessarollo L, Sassoon DA, Parada LF. Loss of N-myc function results in embryonic lethality and failure of the epithelial component of the embryo to develop. Genes Dev 1992;6(12A):2235–47.
[138] Gotter AL, Manganaro T, Weaver DR, Kolakowski Jr. LF, Possidente B, Sriram S, et al. A time-less function for mouse timeless. Nat Neurosci 2000;3(8):755–6.
[139] Guo B, Panagiotaki N, Warwood S, Sharrocks AD. Dynamic modification of the ETS transcription factor PEA3 by sumoylation and p300-mediated acetylation. Nucleic Acids Res 2011;39 (15):6403–13.
[140] Kuure S, Chi X, Lu B, Costantini F. The transcription factors Etv4 and Etv5 mediate formation of the ureteric bud tip domain during kidney development. Development 2010;137 (12):1975–9.
[141] Lu BC, Cebrian C, Chi X, Kuure S, Kuo R, Bates CM, et al. Etv4 and Etv5 are required downstream of GDNF and Ret for kidney branching morphogenesis. Nat Genet 2009;41(12): 1295–302.
[142] Reginensi A, Clarkson M, Neirijnck Y, Lu B, Ohyama T, Groves AK, et al. SOX9 controls epithelial branching by activating RET effector genes during kidney development. Hum Mol Genet 2011;20(6):1143–53.
[143] Hatini V, Huh SO, Herzlinger D, Soares VC, Lai E. Essential role of stromal mesenchyme in kidney morphogenesis revealed by targeted disruption of Winged Helix transcription factor BF-2. Genes Dev 1996;10(12):1467–78.
[144] Levinson RS, Batourina E, Choi C, Vorontchikhina M, Kitajewski J, Mendelsohn CL. Foxd1-dependent signals control cellularity in the renal capsule, a structure required for normal renal development. Development 2005;132(3):529–39.
[145] Zhang H, Palmer R, Gao X, Kreidberg J, Gerald W, Hsiao L, et al. Transcriptional activation of placental growth factor by the forkhead/winged helix transcription factor FoxD1. Curr Biol 2003;13(18):1625–9.
[146] Quaggin SE, Vanden Heuvel GB, Igarashi P. Pod-1, a mesoderm-specific basic-helix-loop-helix protein expressed in mesenchymal and glomerular epithelial cells in the developing kidney. Mech Dev 1998;71(1-2):37–48.
[147] Quaggin SE, Schwartz L, Cui S, Igarashi P, Deimling J, Post M, et al. The basic-helix-loop-helix protein pod1 is critically important for kidney and lung organogenesis. Development 1999;126(24):5771–83.
[148] Cui S, Schwartz L, Quaggin SE. Pod1 is required in stromal cells for glomerulogenesis. Dev Dyn 2003;226(3):512–22.
[149] Schnabel CA, Godin RE, Cleary ML. Pbx1 regulates nephrogenesis and ureteric branching in the developing kidney. Dev Biol 2003;254(2):262–76.
[150] Wilson JG, Roth CB, Warkany J. An analysis of the syndrome of malformations induced by maternal vitamin A deficiency. Effects of restoration of vitamin A at various times during gestation. Am J Anat 1953;92(2):189–217.
[151] Batourina E, Gim S, Bello N, Shy M, Clagett-Dame M, Srinivas S, et al. Vitamin A controls epithelial/mesenchymal interactions through Ret expression. Nat Genet 2001;27(1):74–8.
[152] Mendelsohn C, Batourina E, Fung S, Gilbert T, Dodd J. Stromal cells mediate retinoid-dependent functions essential for renal development. Development 1999;126(6):1139–48.
[153] Pontoglio M, Barra J, Hadchouel M, Doyen A, Kress C, Bach JP, et al. Hepatocyte nuclear factor 1 inactivation results in hepatic dysfunction, phenylketonuria, and renal Fanconi syndrome. Cell 1996;84(4):575–85.
[154] Nakai S, Sugitani Y, Sato H, Ito S, Miura Y, Ogawa M, et al. Crucial roles of Brn1 in distal tubule formation and function in mouse kidney. Development 2003;130(19):4751–9.
[155] Wong K, Park HT, Wu JY, Rao Y. Slit proteins: molecular guidance cues for cells ranging from neurons to leukocytes. Curr Opin Genet Dev 2002;12(5):583–91.
[156] Grieshammer U, Le M, Plump AS, Wang F, Tessier-Lavigne M, Martin GR. SLIT2-mediated ROBO2 signaling restricts kidney induction to a single site. Dev Cell 2004;6(5):709–17.
[157] Kramer S, Okabe M, Hacohen N, Krasnow MA, Hiromi Y. Sprouty: a common antagonist of FGF and EGF signaling pathways in *Drosophila*. Development 1999;126(11):2515–25.
[158] Basson MA, Akbulut S, Watson-Johnson J, Simon R, Carroll TJ, Shakya R, et al. Sprouty1 is a critical regulator of GDNF/RET-mediated kidney induction. Dev Cell 2005;8(2):229–39.
[159] Michos O, Cebrian C, Hyink D, Grieshammer U, Williams L, D'Agati V, et al. Kidney development in the absence of Gdnf and Spry1 requires Fgf10. PLoS Genet 2010;6(1):e1000809.

[160] Esquela AF, Lee SJ. Regulation of metanephric kidney development by growth/differentiation factor 11. Dev Biol 2003;257 (2):356–70.
[161] McPherron AC, Lawler AM, Lee SJ. Regulation of anterior/posterior patterning of the axial skeleton by growth/differentiation factor 11. Nat Genet 1999;22(3):260–4.
[162] Oh SP, Yeo CY, Lee Y, Schrewe H, Whitman M, Li E. Activin type IIA and IIB receptors mediate Gdf11 signaling in axial vertebral patterning. Genes Dev 2002;16(21):2749–54.
[163] Oh SP, Li E. The signaling pathway mediated by the type IIB activin receptor controls axial patterning and lateral asymmetry in the mouse. Genes Dev 1997;11(14):1812–26.
[164] Zhao H, Kegg H, Grady S, Truong HT, Robinson ML, Baum M, et al. Role of fibroblast growth factor receptors 1 and 2 in the ureteric bud. Dev Biol 2004;276(2):403–15.
[165] Santos OF, Barros EJ, Yang XM, Matsumoto K, Nakamura T, Park M, et al. Involvement of hepatocyte growth factor in kidney development. Dev Biol 1994;163(2):525–9.
[166] Moore MW, Klein RD, Farinas I, Sauer H, Armanini M, Phillips H, et al. Renal and neuronal abnormalities in mice lacking GDN. Nature 1996;382(6586):76–9.
[167] Pichel JG, Shen L, Sheng HZ, Granholm AC, Drago J, Grinberg A, et al. Defects in enteric innervation and kidney development in mice lacking GDN. Nature 1996;382(6586):73–6.
[168] Sanchez MP, Silos-Santiago I, Frisen J, He B, Lira SA, Barbacid M. Renal agenesis and the absence of enteric neurons in mice lacking GDN. Nature 1996;382(6586):70–3.
[169] Enomoto H, Araki T, Jackman A, Heuckeroth RO, Snider WD, Johnson Jr. EM, et al. GFR alpha1-deficient mice have deficits in the enteric nervous system and kidneys. Neuron 1998;21 (2):317–24.
[170] Durbec P, Marcos-Gutierrez CV, Kilkenny C, Grigoriou M, Wartiowaara K, Suvanto P, et al. GDNF signalling through the Ret receptor tyrosine kinase. Nature 1996;381(6585):789–93.
[171] Schuchardt A, D'Agati V, Pachnis V, Costantini F. Renal agenesis and hypodysplasia in ret-k-mutant mice result from defects in ureteric bud development. Development 1996;122 (6):1919–29.
[172] Sainio K, Suvanto P, Davies J, Wartiovaara J, Wartiovaara K, Saarma M, et al. Glial-cell-line-derived neurotrophic factor is required for bud initiation from ureteric epithelium. Development 1997;124(20):4077–87.
[173] Cullen-McEwen LA, Drago J, Bertram JF. Nephron endowment in glial cell line-derived neurotrophic factor (GDNF) heterozygous mice. Kidney Int 2001;60(1):31–6.
[174] Cancilla B, Davies A, Cauchi JA, Risbridger GP, Bertram JF. Fibroblast growth factor receptors and their ligands in the adult rat kidney. Kidney Int 2001;60(1):147–55.
[175] Celli G, LaRochelle WJ, Mackem S, Sharp R, Merlino G. Soluble dominant-negative receptor uncovers essential roles for fibroblast growth factors in multi-organ induction and patterning. Embo J 1998;17(6):1642–55.
[176] Qiao J, Uzzo R, Obara-Ishihara T, Degenstein L, Fuchs E, Herzlinger D. FGF-7 modulates ureteric bud growth and nephron number in the developing kidney. Development 1999;126 (3):547–54.
[177] Ohuchi H, Hori Y, Yamasaki M, Harada H, Sekine K, Kato S, et al. FGF10 acts as a major ligand for FGF receptor 2 IIIb in mouse multi-organ development. Biochem Biophys Res Commun 2000;277(3):643–9.
[178] Revest JM, Spencer-Dene B, Kerr K, De Moerlooze L, Rosewell I, Dickson C. Fibroblast growth factor receptor 2-IIIb acts upstream of Shh and Fgf4 and is required for limb bud maintenance but not for the induction of Fgf8, Fgf10, Msx1, or Bmp4. Dev Biol 2001;231(1):47–62.
[179] Bates CM. Role of fibroblast growth factor receptor signaling in kidney development. Am J Physiol Renal Physiol 2011;301 (2):F245–51.
[180] Sims-Lucas S, Argyropoulos C, Kish K, McHugh K, Bertram JF, Quigley R, et al. Three-dimensional imaging reveals ureteric and mesenchymal defects in Fgfr2-mutant kidneys. J Am Soc Nephrol 2009;20(12):2525–33.
[181] Li YS, Milner PG, Chauhan AK, Watson MA, Hoffman RM, Kodner CM, et al. Cloning and expression of a developmentally regulated protein that induces mitogenic and neurite outgrowth activity. Science 1990;250(4988):1690–4.
[182] Mitsiadis TA, Salmivirta M, Muramatsu T, Muramatsu H, Rauvala H, Lehtonen E, et al. Expression of the heparin-binding cytokines, midkine (MK) and HB-GAM (pleiotrophin) is associated with epithelial-mesenchymal interactions during fetal development and organogenesis. Development 1995;121 (1):37–51.
[183] Amet LE, Lauri SE, Hienola A, Croll SD, Lu Y, Levorse JM, et al. Enhanced hippocampal long-term potentiation in mice lacking heparin-binding growth-associated molecule. Mol Cell Neurosci 2001;17(6):1014–24.
[184] Lin Y, Liu A, Zhang S, Ruusunen T, Kreidberg JA, Peltoketo H, et al. Induction of ureter branching as a response to Wnt-2b signaling during early kidney organogenesis. Dev Dyn 2001;222(1):26–39.
[185] Majumdar A, Vainio S, Kispert A, McMahon J, McMahon AP. Wnt11 and Ret/Gdnf pathways cooperate in regulating ureteric branching during metanephric kidney development. Development 2003;130(14):3175–85.
[186] Karner CM, Chirumamilla R, Aoki S, Igarashi P, Wallingford JB, Carroll TJ. Wnt9b signaling regulates planar cell polarity and kidney tubule morphogenesis. Nat Genet 2009;41 (7):793–9.
[187] Yu J, Carroll TJ, Rajagopal J, Kobayashi A, Ren Q, McMahon APA. Wnt7b-dependent pathway regulates the orientation of epithelial cell division and establishes the cortico-medullary axis of the mammalian kidney. Development 2009;136(1): 161–71.
[188] Lescher B, Haenig B, Kispert A. sFRP-2 is a target of the Wnt-4 signaling pathway in the developing metanephric kidney. Dev Dyn 1998;213(4):440–51.
[189] Yoshino K, Rubin JS, Higinbotham KG, Uren A, Anest V, Plisov SY, et al. Secreted Frizzled-related proteins can regulate metanephric development. Mech Dev 2001;102(1-2):45–55.
[190] Ritvos O, Tuuri T, Eramaa M, Sainio K, Hilden K, Saxen L, et al. Activin disrupts epithelial branching morphogenesis in developing glandular organs of the mouse. Mech Dev 1995;50 (2-3):229–45.
[191] Miyazaki Y, Oshima K, Fogo A, Hogan BL, Ichikawa I. Bone morphogenetic protein 4 regulates the budding site and elongation of the mouse ureter. J Clin Invest 2000;105(7): 863–73.
[192] Raatikainen-Ahokas A, Hytonen M, Tenhunen A, Sainio K, Sariola H. BMP-4 affects the differentiation of metanephric mesenchyme and reveals an early anterior–posterior axis of the embryonic kidney. Dev Dyn 2000;217(2):146–58.
[193] Hsu DR, Economides AN, Wang X, Eimon PM, Harland RM. The *Xenopus* dorsalizing factor Gremlin identifies a novel family of secreted proteins that antagonize BMP activities. Mol Cell 1998;1(5):673–83.
[194] Michos O, Panman L, Vintersten K, Beier K, Zeller R, Zuniga A. Gremlin-mediated BMP antagonism induces the epithelial–mesenchymal feedback signaling controlling metanephric kidney and limb organogenesis. Development 2004;131 (14):3401–10.

[195] Goncalves A, Zeller R. Genetic analysis reveals an unexpected role of BMP7 in initiation of ureteric bud outgrowth in mouse embryos. PLoS One 2011;6(4):e19370.
[196] Michos O, Goncalves A, Lopez-Rios J, Tiecke E, Naillat F, Beier K, et al. Reduction of BMP4 activity by gremlin 1 enables ureteric bud outgrowth and GDNF/WNT11 feedback signalling during kidney branching morphogenesis. Development 2007;134(13):2397–405.
[197] Nie X, Xu J, El-Hashash A, Xu PX. Six1 regulates Grem1 expression in the metanephric mesenchyme to initiate branching morphogenesis. Dev Biol 2011;352(1):141–51.
[198] Bladt F, Riethmacher D, Isenmann S, Aguzzi A, Birchmeier C. Essential role for the c-met receptor in the migration of myogenic precursor cells into the limb bud. Nature 1995;376 (6543):768–71.
[199] Schmidt C, Bladt F, Goedecke S, Brinkmann V, Zschiesche W, Sharpe M, et al. Scatter factor/hepatocyte growth factor is essential for liver development. Nature 1995;373(6516): 699–702.
[200] Massague J, Pandiella A. Membrane-anchored growth factors. Annu Rev Biochem 1993;62:515–41.
[201] Rogers SA, Ryan G, Hammerman MR. Metanephric transforming growth factor-alpha is required for renal organogenesis *in vitro*. Am J Physiol 1992;262(4 Pt 2):F533–9.
[202] Montesano R, Matsumoto K, Nakamura T, Orci L. Identification of a fibroblast-derived epithelial morphogen as hepatocyte growth factor. Cell 1991;67(5):901–8.
[203] Kjelsberg C, Sakurai H, Spokes K, Birchmeier C, Drummond I, Nigam S, et al. $Met^{-/-}$ kidneys express epithelial cells that chemotax and form tubules in response to EGF receptor ligands. Am J Physiol 1997;272(2 Pt 2):F222–8.
[204] Luetteke NC, Qiu TH, Peiffer RL, Oliver P, Smithies O, Lee DC. TGF alpha deficiency results in hair follicle and eye abnormalities in targeted and waved-1 mice. Cell 1993;73(2): 263–78.
[205] Mann GB, Fowler KJ, Gabriel A, Nice EC, Williams RL, Dunn AR. Mice with a null mutation of the TGF alpha gene have abnormal skin architecture, wavy hair, and curly whiskers and often develop corneal inflammation. Cell 1993;73(2):249–61.
[206] Threadgill DW, Dlugosz AA, Hansen LA, Tennenbaum T, Lichti U, Yee D, et al. Targeted disruption of mouse EGF receptor: effect of genetic background on mutant phenotype. Science 1995;269(5221):230–4.
[207] Rogers SA, Ryan G, Hammerman MR. Insulin-like growth factors I and II are produced in the metanephros and are required for growth and development *in vitro*. J Cell Biol 1991;113 (6):1447–53.
[208] Wada J, Liu ZZ, Alvares K, Kumar A, Wallner E, Makino H, et al. Cloning of cDNA for the alpha subunit of mouse insulin-like growth factor I receptor and the role of the receptor in metanephric development. Proc Natl Acad Sci USA 1993;90 (21):10360–4.
[209] Baker J, Liu JP, Robertson EJ, Efstratiadis A. Role of insulin-like growth factors in embryonic and postnatal growth. Cell 1993;75(1):73–82.
[210] Powell-Braxton L, Hollingshead P, Warburton C, Dowd M, Pitts-Meek S, Dalton D, et al. IGF-I is required for normal embryonic growth in mice. Genes Dev 1993;7(12B):2609–17.
[211] Kanwar YS, Wada J, Lin S, Danesh FR, Chugh SS, Yang Q, et al. Update of extracellular matrix, its receptors, and cell adhesion molecules in mammalian nephrogenesis. Am J Physiol Renal Physiol 2004;286(2):F202–15.
[212] Santos OF, Nigam SK. HGF-induced tubulogenesis and branching of epithelial cells is modulated by extracellular matrix and TGF-beta. Dev Biol 1993;160(2):293–302.
[213] Schuger L, O'Shea S, Rheinheimer J, Varani J. Laminin in lung development: effects of anti-laminin antibody in murine lung morphogenesis. Dev Biol 1990;137(1):26–32.
[214] Ekblom P, Ekblom M, Fecker L, Klein G, Zhang HY, Kadoya Y, et al. Role of mesenchymal nidogen for epithelial morphogenesis *in vitro*. Development 1994;120(7):2003–14.
[215] Kreidberg JA, Donovan MJ, Goldstein SL, Rennke H, Shepherd K, Jones RC, et al. Alpha 3 beta 1 integrin has a crucial role in kidney and lung organogenesis. Development 1996;122(11): 3537–47.
[216] Kjellen L, Lindahl U. Proteoglycans: structures and interactions. Annu Rev Biochem 1991;60:443–75.
[217] Klein DJ, Brown DM, Moran A, Oegema Jr. TR, Platt JL. Chondroitin sulfate proteoglycan synthesis and reutilization of beta-D-xyloside-initiated chondroitin/dermatan sulfate glycosaminoglycans in fetal kidney branching morphogenesis. Dev Biol 1989;133(2):515–28.
[218] Lelongt B, Makino H, Dalecki TM, Kanwar YS. Role of proteoglycans in renal development. Dev Biol 1988;128(2):256–76.
[219] Kispert A, Vainio S, Shen L, Rowitch DH, McMahon AP. Proteoglycans are required for maintenance of Wnt-11 expression in the ureter tips. Development 1996;122(11):3627–37.
[220] Grisaru S, Cano-Gauci D, Tee J, Filmus J, Rosenblum ND. Glypican-3 modulates BMP- and FGF-mediated effects during renal branching morphogenesis. Dev Biol 2001;231(1): 31–46.
[221] Pohl M, Sakurai H, Stuart RO, Nigam SK. Role of hyaluronan and CD44 in *in vitro* branching morphogenesis of ureteric bud cells. Dev Biol 2000;224(2):312–25.
[222] Rosines E, Schmidt HJ, Nigam SK. The effect of hyaluronic acid size and concentration on branching morphogenesis and tubule differentiation in developing kidney culture systems: potential applications to engineering of renal tissues. Biomaterials 2007;28(32):4806–17.
[223] Kanwar YS, Ota K, Yang Q, Kumar A, Wada J, Kashihara N, et al. Isolation of rat fibrillin-1 cDNA and its relevance in metanephric development. Am J Physiol 1998;275(5 Pt 2):F710–23.
[224] Montesano R, Soriano JV, Pepper MS, Orci L. Induction of epithelial branching tubulogenesis *in vitro*. J Cell Physiol 1997;173 (2):152–61.
[225] Lelongt B, Trugnan G, Murphy G, Ronco PM. Matrix metalloproteinases MMP2 and MMP9 are produced in early stages of kidney morphogenesis but only MMP9 is required for renal organogenesis *in vitro*. J Cell Biol 1997;136(6):1363–73.
[226] Andrews KL, Betsuyaku T, Rogers S, Shipley JM, Senior RM, Miner JH, et al. (MMP-9) is not essential in the normal kidney and does not influence progression of renal disease in a mouse model of Alport syndrome. Am J Pathol 2000;157(1): 303–11.
[227] Arnould C, Lelievre-Pegorier M, Ronco P, Lelongt B. MMP9 limits apoptosis and stimulates branching morphogenesis during kidney development. J Am Soc Nephrol 2009;20(10): 2171–80.
[228] Kanwar YS, Ota K, Yang Q, Wada J, Kashihara N, Tian Y, et al. Role of membrane-type matrix metalloproteinase 1 (MT-1-MMP), MMP-2, and its inhibitor in nephrogenesis. Am J Physiol 1999;277(6 Pt 2):F934–47.
[229] Unsworth B, Grobstein C. Induction of kidney tubules in mouse metanephrogenic mesenchyme by various embryonic mesenchymal tissues. Dev Biol 1970;21(4):547–56.
[230] Lombard MN, Grobstein C. Activity in various embryonic and postembryonic sources for induction of kidney tubules. Dev Biol 1969;19(1):41–51.
[231] Koseki C, Herzlinger D, al-Awqati Q. Apoptosis in metanephric development. J Cell Biol 1992;119(5):1327–33.

[232] Coles HS, Burne JF, Raff MC. Large-scale normal cell death in the developing rat kidney and its reduction by epidermal growth factor. Development 1993;118(3):777–84.
[233] Barasch J, Pressler L, Connor J, Malik A. A ureteric bud cell line induces nephrogenesis in two steps by two distinct signals. Am J Physiol 1996;271(1 Pt 2):F50–61.
[234] Barasch J, Qiao J, McWilliams G, Chen D, Oliver JA, Herzlinger D. Ureteric bud cells secrete multiple factors, including bFGF, which rescue renal progenitors from apoptosis. Am J Physiol 1997;273(5 Pt 2):F757–67.
[235] Karavanova ID, Dove LF, Resau JH, Perantoni AO. Conditioned medium from a rat ureteric bud cell line in combination with bFGF induces complete differentiation of isolated metanephric mesenchyme. Development 1996;122 (12):4159–67.
[236] Dudley AT, Lyons KM, Robertson EJ. A requirement for bone morphogenetic protein-7 during development of the mammalian kidney and eye. Genes Dev 1995;9(22):2795–807.
[237] Luo G, Hofmann C, Bronckers AL, Sohocki M, Bradley A, Karsenty G. BMP-7 is an inducer of nephrogenesis, and is also required for eye development and skeletal patterning. Genes Dev 1995;9(22):2808–20.
[238] Vukicevic S, Kopp JB, Luyten FP, Sampath TK. Induction of nephrogenic mesenchyme by osteogenic protein 1 (bone morphogenetic protein 7). Proc Natl Acad Sci USA 1996;93 (17):9021–6.
[239] Lehtonen E. Epithelio–mesenchymal interface during mouse kidney tubule induction *in vivo*. J Embryol Exp Morphol 1975;34(3):695–705.
[240] Yang J, Blum A, Novak T, Levinson R, Lai E, Barasch J. An epithelial precursor is regulated by the ureteric bud and by the renal stroma. Dev Biol 2002;246(2):296–310.
[241] Herzlinger D, Qiao J, Cohen D, Ramakrishna N, Brown AM. Induction of kidney epithelial morphogenesis by cells expressing Wnt-1. Dev Biol 1994;166(2):815–8.
[242] Wilkinson DG, Bailes JA, McMahon AP. Expression of the proto-oncogene int-1 is restricted to specific neural cells in the developing mouse embryo. Cell 1987;50(1):79–88.
[243] Stark K, Vainio S, Vassileva G, McMahon AP. Epithelial transformation of metanephric mesenchyme in the developing kidney regulated by Wnt-4. Nature 1994;372(6507):679–83.
[244] Carroll TJ, Park JS, Hayashi S, Majumdar A, McMahon AP. Wnt9b plays a central role in the regulation of mesenchymal to epithelial transitions underlying organogenesis of the mammalian urogenital system. Dev Cell 2005;9(2):283–92.
[245] Grieshammer U, Cebrian C, Ilagan R, Meyers E, Herzlinger D, Martin GR. FGF8 is required for cell survival at distinct stages of nephrogenesis and for regulation of gene expression in nascent nephrons. Development 2005;132(17):3847–57.
[246] Perantoni AO, Timofeeva O, Naillat F, Richman C, Pajni-Underwood S, Wilson C, et al. Inactivation of FGF8 in early mesoderm reveals an essential role in kidney development. Development 2005;132(17):3859–71.
[247] Poladia DP, Kish K, Kutay B, Hains D, Kegg H, Zhao H, et al. Role of fibroblast growth factor receptors 1 and 2 in the metanephric mesenchyme. Dev Biol 2006;291(2):325–39.
[248] Cheng HT, Kim M, Valerius MT, Surendran K, Schuster-Gossler K, Gossler A, et al. Notch2 but not Notch1, is required for proximal fate acquisition in the mammalian nephron. Development 2007;134(4):801–11.
[249] Kopan R, Cheng HT, Surendran K. Molecular insights into segmentation along the proximal–distal axis of the nephron. J Am Soc Nephrol 2007;18(7):2014–20.
[250] Surendran K, Boyle S, Barak H, Kim M, Stomberski C, McCright B, et al. The contribution of Notch1 to nephron segmentation in the developing kidney is revealed in a sensitized Notch2 background and can be augmented by reducing Mint dosage. Dev Biol 2010;337(2):386–95.
[251] Mitsiadis TA, Lardelli M, Lendahl U, Thesleff I. Expression of Notch 1, 2 and 3 is regulated by epithelial–mesenchymal interactions and retinoic acid in the developing mouse tooth and associated with determination of ameloblast cell fate. J Cell Biol 1995;130(2):407–18.
[252] Mitsiadis TA, Gayet O, Zhang N, Carroll P. Expression of Deltex1 during mouse embryogenesis: comparison with Notch1, 2 and 3 expression. Mech Dev 2001;109(2):399–403.
[253] McCright B. Notch signaling in kidney development. Curr Opin Nephrol Hypertens 2003;12(1):5–10.
[254] Chen L, Al-Awqati Q. Segmental expression of Notch and Hairy genes in nephrogenesis. Am J Physiol Renal Physiol 2005;288(5):F939–52.
[255] Cheng HT, Kopan R. The role of Notch signaling in specification of podocyte and proximal tubules within the developing mouse kidney. Kidney Int 2005;68(5):1951–2.
[256] McCright B, Gao X, Shen L, Lozier J, Lan Y, Maguire M, et al. Defects in development of the kidney, heart and eye vasculature in mice homozygous for a hypomorphic Notch2 mutation. Development 2001;128(4):491–502.
[257] Cheng HT, Miner JH, Lin M, Tansey MG, Roth K, Kopan R. Gamma-secretase activity is dispensable for mesenchyme-to-epithelium transition but required for podocyte and proximal tubule formation in developing mouse kidney. Development 2003;130(20):5031–42.
[258] Wang P, Pereira FA, Beasley D, Zheng H. Presenilins are required for the formation of comma- and S-shaped bodies during nephrogenesis. Development 2003;130(20):5019–29.
[259] Oswald F, Kostezka U, Astrahantseff K, Bourteele S, Dillinger K, Zechner U, et al. SHARP is a novel component of the Notch/RBP-Jkappa signalling pathway. Embo J 2002;21 (20):5417–26.
[260] Oswald F, Winkler M, Cao Y, Astrahantseff K, Bourteele S, Knochel W, et al. RBP-Jkappa/SHARP recruits CtIP/CtBP corepressors to silence Notch target genes. Mol Cell Biol 2005;25 (23):10379–90.
[261] Tsuji M, Shinkura R, Kuroda K, Yabe D, Honjo T. Msx2-interacting nuclear target protein (Mint) deficiency reveals negative regulation of early thymocyte differentiation by Notch/RBP-J signaling. Proc Natl Acad Sci USA 2007;104(5):1610–5.
[262] Yabe D, Fukuda H, Aoki M, Yamada S, Takebayashi S, Shinkura R, et al. Generation of a conditional knockout allele for mammalian Spen protein Mint/SHARP. Genesis 2007;45 (5):300–6.
[263] Ekblom M, Klein G, Mugrauer G, Fecker L, Deutzmann R, Timpl R, et al. Transient and locally restricted expression of laminin A chain mRNA by developing epithelial cells during kidney organogenesis. Cell 1990;60(2):337–46.
[264] Klein G, Ekblom M, Fecker L, Timpl R, Ekblom P. Differential expression of laminin A and B chains during development of embryonic mouse organs. Development 1990;110(3):823–37.
[265] Klein G, Langegger M, Timpl R, Ekblom P. Role of laminin A chain in the development of epithelial cell polarity. Cell 1988;55(2):331–41.
[266] Falk M, Salmivirta K, Durbeej M, Larsson E, Ekblom M, Vestweber D, et al. Integrin alpha 6B beta 1 is involved in kidney tubulogenesis *in vitro*. J Cell Sci 1996;109(Pt 12):2801–10.
[267] Schuger L, Skubitz AP, Zhang J, Sorokin L, He L. Laminin alpha1 chain synthesis in the mouse developing lung: requirement for epithelial–mesenchymal contact and possible role in bronchial smooth muscle development. J Cell Biol 1997;139 (2):553–62.

[268] Muller U, Bossy B, Venstrom K, Reichardt LF. Integrin alpha 8 beta 1 promotes attachment, cell spreading, and neurite outgrowth on fibronectin. Mol Biol Cell 1995;6(4):433–48.
[269] Lopez-Nieto CE, You G, Bush KT, Barros EJ, Beier DR, Nigam SK. Molecular cloning and characterization of NKT, a gene product related to the organic cation transporter family that is almost exclusively expressed in the kidney. J Biol Chem 1997;272(10):6471–8.
[270] Preminger GM, Koch WE, Fried FA, Mandell J. Utilization of the chick chorioallantoic membrane for *in vitro* growth of the embryonic murine kidney. Am J Anat 1980;159(1):17–24.
[271] Ekblom P, Sariola H, Karkinen-Jaaskelainen M, Saxen L. The origin of the glomerular endothelium. Cell Differ 1982;11 (1):35–9.
[272] Sariola H, Ekblom P, Lehtonen E, Saxen L. Differentiation and vascularization of the metanephric kidney grafted on the chorioallantoic membrane. Dev Biol 1983;96(2):427–35.
[273] Hyink DP, Abrahamson DR. Origin of the glomerular vasculature in the developing kidney. Semin Nephrol 1995;15(4):300–14.
[274] Robert St B, John PL, Hyink DP, Abrahamson DR. Evidence that embryonic kidney cells expressing flk-1 are intrinsic, vasculogenic angioblasts. Am J Physiol 1996;271(3 Pt 2):F744–53.
[275] Faa G, Gerosa C, Fanni D, Monga G, Zaffanello M, Van Eyken P, et al. Morphogenesis and molecular mechanisms involved in human kidney development. J Cell Physiol 2012;227 (3):1257–68.
[276] Sariola H, Kuusela P, Ekblom P. Cellular origin of fibronectin in interspecies hybrid kidneys. J Cell Biol 1984;99(6):2099–107.
[277] Sariola H, Timpl R, von der Mark K, Mayne R, Fitch JM, Linsenmayer TF, et al. Dual origin of glomerular basement membrane. Dev Biol 1984;101(1):86–96.
[278] Leveen P, Pekny M, Gebre-Medhin S, Swolin B, Larsson E, Betsholtz C. Mice deficient for PDGF B show renal, cardiovascular, and hematological abnormalities. Genes Dev 1994;8 (16):1875–87.
[279] Soriano P. Abnormal kidney development and hematological disorders in PDGF beta-receptor mutant mice. Genes Dev 1994;8(16):1888–96.
[280] Humphreys BD, Valerius MT, Kobayashi A, Mugford JW, Soeung S, Duffield JS, et al. Intrinsic epithelial cells repair the kidney after injury. Cell Stem Cell 2008;2(3):284–91.
[281] Wilkinson L, Gilbert T, Sipos A, Toma I, Pennisi DJ, Peti-Peterdi J, et al. Loss of renal microvascular integrity in postnatal Crim1 hypomorphic transgenic mice. Kidney Int 2009;76 (11):1161–71.
[282] Wilkinson L, Gilbert T, Kinna G, Ruta LA, Pennisi D, Kett M, et al. Crim1KST264/KST264 mice implicate Crim1 in the regulation of vascular endothelial growth factor-A activity during glomerular vascular development. J Am Soc Nephrol 2007;18 (6):1697–708.
[283] Pennisi DJ, Wilkinson L, Kolle G, Sohaskey ML, Gillinder K, Piper MJ, et al. Crim1KST264/KST264 mice display a disruption of the Crim1 gene resulting in perinatal lethality with defects in multiple organ systems. Dev Dyn 2007;236(2): 502–11.
[284] Reidy K, Tufro A. Semaphorins in kidney development and disease: modulators of ureteric bud branching, vascular morphogenesis, and podocyte-endothelial crosstalk. Pediatr Nephrol 2011;26(9):1407–12.
[285] Reidy KJ, Villegas G, Teichman J, Veron D, Shen W, Jimenez J, et al. Semaphorin3a regulates endothelial cell number and podocyte differentiation during glomerular development. Development 2009;136(23):3979–89.
[286] Tufro A, Norwood VF, Carey RM, Gomez RA. Vascular endothelial growth factor induces nephrogenesis and vasculogenesis. J Am Soc Nephrol 1999;10(10):2125–34.
[287] Tufro A. VEGF spatially directs angiogenesis during metanephric development *in vitro*. Dev Biol 2000;227(2):558–66.
[288] Hartman HA, Lai HL, Patterson LT. Cessation of renal morphogenesis in mice. Dev Biol 2007;310(2):379–87.

CHAPTER

26

Molecular and Cellular Mechanisms of Glomerular Capillary Development

Jeffrey H. Miner[1] *and Dale R. Abrahamson*[2]

[1]Department of Medicine, Renal Division, Washington University School of Medicine, St. Louis, MO, USA
[2]Department of Anatomy and Cell Biology, University of Kansas Medical Center, Kansas City, KS, USA

Among all of the capillaries in the body, the glomerulus is arguably the most unusual and important, if not the most aesthetically interesting. In this chapter, we review the morphogenesis of this unique capillary, discuss the origins of its cells and extracellular matrices, and describe some of the primary regulatory events that occur during glomerular development.

GLOMERULAR MORPHOGENESIS

Formation of the permanent, metanephric kidney begins at embryonic day 11 in mice, day 12 in rats, and during the 4th-5th week of gestation in humans. As the ureteric bud projects from the mesonephric duct and enters the metanephric anlage, mesenchymal cells condense around the bud's advancing tip. Soon thereafter, the condensed mesenchyme converts to an epithelial phenotype and proceeds through a developmental sequence of nephric structures, which are termed vesicle, comma-, and S-shaped, developing capillary loop, and maturing glomerulus stages.[1,2] Bud tip stimulation of mesenchymal cell induction and aggregation, conversion to epithelium, and glomerular and tubule differentiation occur repeatedly until the full complement of nephrons has developed. Nephrogenesis concludes ~1 week after birth in rodents,[2] and during the 34th gestational week in humans.[3]

Vesicle Stage

At the inception of the vesicle stage of nephron development, the aggregated mesenchymal cells near the ureteric bud tips convert to a cluster of epithelial cells (vesicle), and begin assembling a basement membrane matrix containing collagen type IV, laminin, and basement membrane proteoglycans around the basal surface of the vesicle.[4–6] As development progresses through the comma- and then S-shaped stages, a groove (vascular cleft) forms in the lower aspect of the vesicle, into which endothelial precursor cells (angioblasts) migrate (Figure 26.1). Two epithelial layers can be distinguished beneath the vascular cleft: visceral epithelial cells (which ultimately differentiate into podocytes); and parietal epithelial cells (which will become the thin epithelium lining Bowman's capsule of the mature nephron). Epithelial cells above the vascular cleft ultimately develop into proximal, Henle's loop, and distal tubule epithelium. During the S-shaped phase of nephron development, the distal segment fuses with the same ureteric bud branch tip that initially induced the nephric structure, so that the lumen of the forming nephron is now continuous with that of the developing collecting system. Continued growth and branching of the ureteric bud leads to the induction of new mesenchymal aggregates, and glomerulo- and tubulogenesis continues until the full complement of nephrons is achieved.[2]

Vascular Clefts of Comma- and S-Shaped Stage

With the progressive invasion and differentiation of endothelial cells, the developing capillary endothelium assembles a subendothelial basement membrane matrix.

Seldin and Giebisch's The Kidney, Fifth Edition.
DOI: http://dx.doi.org/10.1016/B978-0-12-381462-3.00026-4

© 2013 Elsevier Inc. All rights reserved.

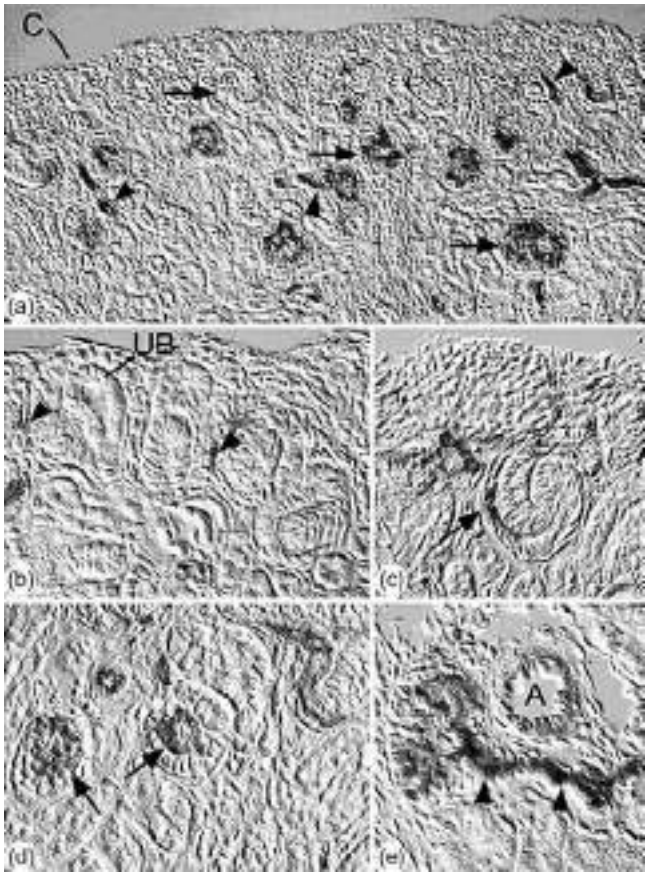

FIGURE 26.1 **Sections of developing kidney from a heterozygous Flk1/LacZ transgenic mouse.** Blue reaction product reflects cellular sites of Flk1 (VEGFR2) gene transcription. (a) Kidney cortex contains a range of glomeruli at different stages of development (arrows) that are lined by endothelial cells expressing Flk1. Vascular endothelium throughout the cortex also express Flk1 (arrowheads) (C: capsule). (b) Higher magnification view of outer cortex. Note blue cells scattered in mesenchyme (arrowheads) (UB: branch of ureteric bud). (c) Nephric figure at S-shaped stage. Endothelial cells expressing Flk1 can be seen migrating into the vascular cleft (arrow), which is the initial site of glomerular formation. (d) Two capillary loop stage glomeruli can be seen (arrows). (e) Maturing stage glomerulus with attached arteriole (arrowheads) (A: small artery). *(Reprinted from ref. [26], with permission).*

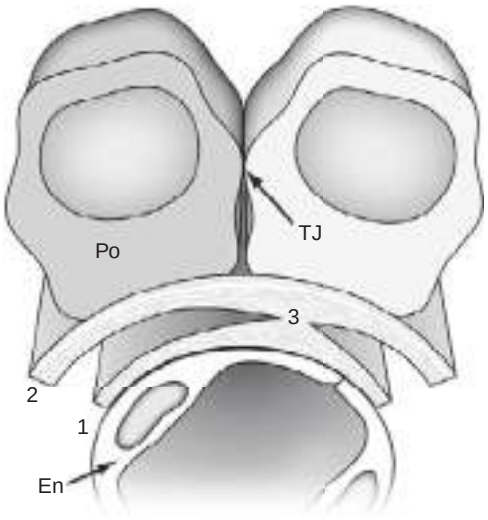

FIGURE 26.2 **Diagram showing spatial relationships during development of glomerular capillary wall.** During initial glomerular development, endothelial cells (En) migrate into vascular clefts of comma- and S-shaped nephrons. Dual sheets of subendothelial (1) and subepithelial (2) basement membranes separate the endothelium from the developing podocyte (Po) cell layers. Areas of basement membrane fusion can be seen (3). The immature GBM contains laminin α1,β1,γ1, laminin α4,β1,γ1 and collagen α1,α2(IV) at this time point. Apical tight junctional complexes (TJ) exist between immature podocytes.

Similarly, the developing podocyte cell layer assembles a subepithelial basement membrane, so that two distinct basal laminae can be seen between the endothelial and epithelial cells (Figure 26.2). As nephrons develop further, these two basement membranes layers merge to form the glomerular basement membrane (GBM), with endothelial cells lining its inner surface, and podocytes adherent to its outer surface.[7]

Capillary Loop

As glomerular capillary loops begin to form, the endothelial cells gradually flatten and become extensively fenestrated (Figures 26.3 and 26.4). Initially, the fenestrations are spanned by diaphragms, but these structures soon disappear. The epithelial podocytes, which originally were columnar with apical junctional complexes, also begin to flatten and begin sending out basolateral cytoplasmic projections that interdigitate with similar projections from neighboring cells (Figure 26.3). As glomeruli mature, these projections go on to develop into the podocyte pedicels or foot processes (Figures 26.3 and 26.4). The apical junctional complexes migrate basolaterally between these cellular projections and, although the mechanism is not fully-understood (see below), convert into the slit diaphragm complex between foot processes[8] (Figure 26.4). Metabolic labeling studies, histochemical and immunohistochemical techniques, and inter-species transplantation experiments[6,9–12] have all shown that both the endothelium and epithelium are actively synthesizing glomerular basement membrane (GBM) proteins at this time.[4]

Maturing Glomeruli

Here, capillary loop diameters expand, and endothelial and podocyte cell layers differentiate further until the

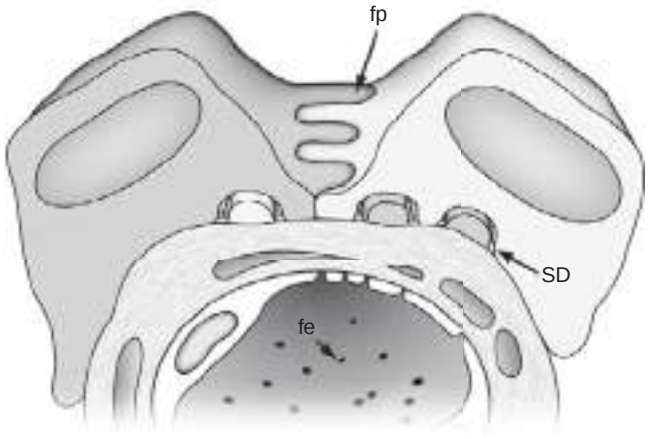

FIGURE 26.3 **During intermediate, capillary loop and maturing stages of glomerular development, fenestrae form in the endothelial cells.** Foot process (fp) extension occurs between podocytes and epithelial slit diaphragms (SD) first appear. Remodeling and splicing of newly synthesized GBM into existing, fused, GBM takes place, and new isoforms of GBM laminin and type IV collagen are seen.

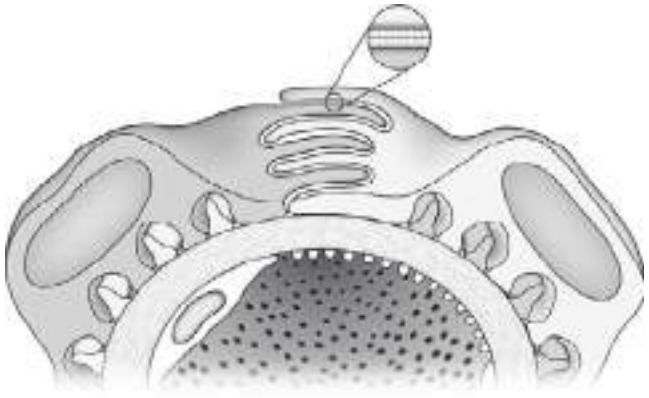

FIGURE 26.4 **As glomeruli approach full maturation, the endothelium becomes extensively fenestrated, and the mature GBM laminin and collagen type IV isoforms are now in place.** In the podocyte layer, foot process extension and interdigitation finalizes, and epithelial slit diaphragms completely span the filtration slits. Inset shows structure of SD viewed *en face*.

fully mature glomerular morphology is achieved. Unfused basement membranes are rarely seen in maturing glomeruli. On the other hand, complex, irregular projections of basement membrane are commonly found beneath podocytes at this stage, particularly in areas where foot processes are broad and their formation into relatively narrow pedicels is still incomplete. *In vivo* labeling studies have shown that these subepithelial basement membrane segments are somehow spliced or inserted into the existing fused GBM, possibly to provide the additional GBM material necessary for the inflating capillaries.[13,14] Shortly after the initial, vascular cleft stage, and continuing into maturing glomeruli, modification and remodeling of the GBM occurs, with the appearance of new basement membrane protein isoforms and the disappearance of earlier species. As discussed later, however, we do not understand how these events are regulated at either the gene or protein level. Additionally, once the glomerulus is fully mature (Figure 26.4), matrix synthesis and cell morphogenesis virtually halt (except for some poorly-understood activities responsible for GBM "maintenance" or "turnover"), and how these processes are downregulated is also not known.

ORIGIN OF THE GLOMERULAR ENDOTHELIUM

Extrarenal Origins

Although compelling evidence has accumulated showing that nephron epithelial cells, including the visceral and parietal epithelium of Bowman's capsule, all derive originally from the metanephric mesenchyme, the origin of vascular endothelial cells during kidney organogenesis has been more difficult to understand.[15] Studies conducted nearly 30 years ago convincingly showed that cells of extrarenal origin grew into the metanephros and established the microvasculature, including the glomerular capillary tufts. These studies involved the grafting of embryonic, avascular mouse or quail kidney rudiments onto avian chorioallantoic membranes. After culturing *in ovo*, the kidney grafts contained glomerular endothelial and mesangial cells stemming from host chorioallantoic tissues, therefore signifying the ingress of vessel progenitors from sites outside the kidney.[12,16]

Intrarenal Origins

Contrary to the results discussed above, several lines of evidence from a number of more recent experiments have shown that the metanephros contains its own pool of endothelial progenitors (angioblasts) capable of vascularizing nephrons *in vivo*.[17] The first clues about the existence of these intrinsic metanephric angioblasts came from transplantation studies between mice and rats. For example, when E12 mouse kidneys are grafted into anterior eye chambers of rats, the vascular and glomerular basement membranes that develop within the grafts after transplantation are almost entirely of mouse (graft) origin.[18] Similarly, when E12 kidneys are transplanted under kidney capsules of adult ROSA26 mice (which bear a

ubiquitously expressed LacZ reporter gene useful as a cell lineage marker), all of the microvascular and glomerular endothelial *cells* within grafts are derived from the engrafted kidney, not from the host.[19] Furthermore, when kidneys from E12 ROSA26 mice are grafted into the nephrogenic renal cortices of newborn wild-type hosts, endothelial cells stemming from the grafts can be seen integrating into host vasculature.[19] In additional experiments, when embryonic kidneys from Flk1 (VEGF receptor-2)−LacZ heterozygous mice are grown under routine organ culture conditions, Flk1-LacZ-positive microvessels do not develop *in vitro*, despite the extensive formation of metanephric tubules and avascular glomerular epithelial tufts.[20] When these same cultured kidneys are then transplanted into anterior eye chambers of wild-type host mice, the grafts develop microvessels and vascularized glomeruli lined by Flk1-LacZ-expressing cells, indicating again that the endothelium originates from the engrafted kidney itself, and not from the host.[20] Several other research groups have reached similar conclusions independently. For example, when avascular metanephroi from E11 Tie1/LacZ transgenic mice are transplanted into newborn wild−type hosts, widespread expression of Tie1/LacZ is found within glomeruli developing within grafts.[21] Others have immunolocalized putative angioblasts in the metanephric mesenchyme of prevascular embryonic rat kidney.[22]

Although current evidence shows that the embryonic kidney contains a pool of angioblasts capable of establishing the glomerular endothelium, whether these progenitors originate initially from outside the metanephric blastema or instead stem directly from metanephric mesenchyme is not yet clear. Nevertheless, immunolabeling experiments in developing rat kidney shows that endothelial, as well as mesangial, cell precursors share common markers during glomerulogenesis (RECA-1 and Thy1.1, respectively), suggesting that they may indeed derive from metanephric mesenchyme.[23] Other immunolocalization and transplantation experiments have shown that juxtaglomerular cells in developing kidney also originate from metanephric mesenchyme, although they appear to stem from a different lineage than endothelial and mesangial cells.[24]

ENDOTHELIAL CELL RECRUITMENT AND DIFFERENTIATION

Mechanisms controlling vascular development are highly complex and involve several different transcription factors, cell-cell and cell-matrix interactions, and many membrane receptor−ligand signaling cascades. Although our knowledge of these systems in a variety of vascular beds has improved dramatically during the past several years, many key questions regarding temporal and spatial controls still persist. With respect to the formation of glomerular capillaries, the process can be considered to progress through four interrelated events: (1) angioblast survival, proliferation and differentiation into endothelium; (2) glomerular endothelial cell recruitment; (3) initial assembly of the glomerular capillary tuft and associated mesangium; and (4) glomerular capillary stabilization and maturation.[25,26]

VEGF Signaling

Among all of the mechanisms involved with development of the systemic vasculature, signals evoked by binding of VEGF to its cellular receptors, VEGFR-1 and VEGFR-2, are singularly critical. Mice with homozygous *Vegfa* gene deletions die by E9.5 with severe vascular deficits. Remarkably, *Vegfa* heterozygote mutants also succumb by E12 with vascular phenotypes, indicating that a single *Vegfa* allele is insufficient to direct normal vascular development.[27,28] Homozygous (but not heterozygous) *Vegfr1* and *Vegfr2* mutants die at midgestation, due to failure of endothelial differentiation[29] and vessel integrity,[30] respectively.

Developing podocytes are key sources of VEGF,[31] and its secretion and binding to angioblasts bearing VEGF receptors may initiate their recruitment into the vascular cleft of comma- and S-shaped nephrons,[32] which is the initial site of glomerulogenesis. Because *Vegfa* and *Vegfr2* knockout mice die with vascular phenotypes before glomerulogenesis commences, the precise role of this ligand-receptor pair in mediating glomerular endothelial development has been difficult to analyze fully. Nevertheless, and underscoring the importance of the VEGF signaling system, injection of VEGF-blocking antibodies into developing mouse kidney cortex inhibits glomerular capillary formation *in vivo*.[33] With the advent of cell selective and/or inducible gene deletion technologies, additional evidence for the importance of podocyte-derived VEGF has been obtained. For example, homozygous deletion of *Vegfa* selectively in podocytes (obtained in bi-transgenic mice carrying nephrin-cre recombinase and floxed *Vegfa* alleles) results in animals which die perinatally with non-vascularized glomeruli.[34] Heterozygous deletion of *Vegfa* causes no evident phenotype initially. By 2.5 weeks of age, however, mice become proteinuric, and glomeruli contain swollen endothelial cells and hyaline deposits similar to those seen in patients with preeclampsia. By contrast, overexpression of the $VEGF_{164}$ isoform specifically in podocytes leads to collapsing glomerulopathy and death at ~5 days of age.[35] When *Vegfa* is selectively deleted in podocytes of adult mice (using a Tet-On conditional expression model), mice become severely proteinuric and hypertensive, and glomeruli resemble those of humans with thrombotic

microangiopathy (mesangiolysis, endothelial swelling, red cell fragmentation, and fibrin deposition).[196] Clearly, the cellular controls for maintaining VEGF protein expression within an optimal range are critically important for the appropriate establishment and maintenance of the glomerular capillary.

Regulation of Endothelial Development

Hypoxia-Inducible Transcription Factors (HIFs)

Transcription of VEGF and VEGFR genes is activated by hypoxia-inducible transcription factors (HIFs), which consist of heterodimers of HIF α- and β-subunits.[36] Under normal oxygen concentrations, the HIF α-subunit undergoes prolyl hydroxylation, binding to von Hippel Lindau protein (VHL), polyubiquitination, and proteasomal degradation. In hypoxia, the prolyl hydroxylase enzyme is inhibited, and HIF α chain degradation is avoided. Hypoxia-stabilized HIF α/β heterodimers bind to hypoxia-responsive elements (HREs) located in promoter/enhancer regions of inducible genes,[37] many of which are proteins expressed in response to hypoxic stress. For example, erythropoietin, transferrin, VEGF, VEGFR1, and VEGFR2 are among the more than 70 distinct genes known to be transcriptionally activated by HIFs.[36]

There are at least three distinct HIF α- and two β-subunits known at present, making a variety of different HIF isoforms possible. Because HIF stabilization is enhanced in cells experiencing subnormal oxygen tensions, such as those in rapidly growing tissues, robust VEGF and VEGFR synthesis commonly occurs during organogenesis. Increased VEGF/VEGFR signaling stimulates mitosis in endothelial progenitor cells, phosphorylation of the antiapoptotic kinases Akt/PKB[38] and focal adhesion kinase (FAK),[39] and upregulation of the survival factors Bcl2 and A1.[38] In time, these events can lead to the creation of new blood vessels, which can then provide appropriate levels of oxygen specifically to the formerly hypoxic tissue sites.

Renal HIF Expression

The expression patterns for several of the different HIF α- and β-subunits have been documented in developing human, rat, and mouse kidney using *in situ* hybridization and immunohistochemistry. In general, both HIF-1 and HIF-2α are found in glomeruli, with specific immunolocalization of HIF-2α protein to immature podocytes (which are rich sources of VEGF).[40,41] HIF-2α is also expressed by developing vascular endothelial cells in the kidney (most of which express VEGFR-2), whereas HIF-1α is found in cortical and medullary collecting duct epithelium. HIF-1α and HIF-2α protein are undetectable in fully mature glomeruli. Mice with a global deletion of *Hif2α* show no defects in glomerular development or function, and no deficits in VEGF or Flk1 expression.[197] Interestingly, HIF-1β is apparently ubiquitously expressed by all cells in the kidney, but HIF-2β distribution is greatly restricted during development and, in mice, becomes confined to nuclei in cells of the thick ascending limb of Henle's loop.[42]

The selective expression of certain HIF isoforms in different tissue compartments of developing kidney may reflect the coordinated regulation of different sets of HIF target genes.[43] Importantly, individuals with mutations in VHL, a key protein in mediating HIF α chain degradation, and thereby reducing expression of HIF target genes, are prone to developing hemangioblastomas and clear cell-renal cell carcinomas.[44–46] Some studies have shown that HIF-1α and HIF-2α had differential and sometimes antagonistic effects on the growth of clear cell-renal cell carcinomas, with HIF-1α retarding and HIF-2α promoting tumor growth.[47] These findings provide further evidence for differential effects of different HIF isoforms, and call for more studies examining the expression of HIF and HIF gene targets in the developing kidney. Surprisingly, when *Vhl* is selectively deleted in podocytes, glomerular vascularization patterns are not affected, and kidneys develop normally.[198] On the other hand, mice become proteinuric by 4 weeks of age, and there is ectopic deposition of collagen $(\alpha1)_2\alpha2$(IV) in peripheral loop GBMs, and upregulation of an ancient oxygen-binding protein, neuroglobin, specifically in podocytes.[198]

Once glomeruli are vascularized and fully mature, podocytes still continue VEGF synthesis. Likewise, expression of Flk1 is also maintained by glomerular endothelial cells of mature kidneys. VEGF-Flk1 signaling in glomeruli therefore probably exerts functions extending well beyond those needed for mobilization of angioblasts and initial formation of the capillary tuft. For example, in co-cultures of epithelial cells with endothelium, epithelial-derived VEGF has been shown to induce fenestrae formation in the endothelium.[48] When *Vegfr2* is inducibly deleted in adult mice, podocytes appear normal, but there is loss of viable glomerular endothelial cells.[199] Perhaps the continued expression of VEGF by podocytes and Flk1 by glomerular endothelial cells *in vivo* is necessary for maintenance of the highly-differentiated state seen in the endothelium.

Other Growth Factor/Receptors

Beyond VEGF and VEGFR, several other growth factor-receptor signaling systems important for vessel

development systemically are also crucial for glomerular capillary formation, including the Tie/angiopoietin and PDGFR/PDGF families.[25,26] Developing glomerular endothelial cells express Tie-2, and and one of its ligands, angiopoietin-1, is important for vascular organization and remodeling. Another Tie-2 ligand, angiopoietin-2, may mediate vascular integrity and permeability. The coordinated expression of these two angiopoietins may therefore regulate the maturation and stabilization phases of glomerular development (reviewed in [49]). Additionally, Tie-2 and at least some members of the angiopoietins contain defined HREs in their promoters, making their transcriptional regulation by hypoxia/HIFs seem likely.[36] Similarly, an HRE is found in the PDGFB gene promoter, although this may not necessarily be responsive to hypoxia.[50] During early glomerular development, PDGFB protein is expressed by podocytes. This may be important for the glomerular recruitment of immature mesangial cells, which express the PDGFB receptor, PDGFRβ.[51] In later developmental stages, both PDGF and PDGFRβ expression becomes confined to the mesangium, which may provide autocrine signals required for mesangial cell proliferation and/or maturation[51] (see below).

Like other developing vessels, at least some neuronal axon guidance receptors and ligands are also found in developing glomeruli.[52–54] For example, neuropilin-1 (Np1), which is a co-receptor with VEGFR2 for $VEGF_{164}$ (but lacks a cytoplasmic signaling domain), immunolocalizes to glomerular endothelial cells. Semaphorins-3A and -3F, which are ligands for Np1, have been found on podocytes, suggesting that semaphorin-Np1 signaling between podocytes and endothelium may help pattern glomerular morphogenesis.[55] One study, however, has also reported that Np1 is expressed by podocytes *in vivo*.[56] Recent experiments also showed that podocyte-derived VEGF may act as an autocrine survival factor for cultured podocytes *in vitro*.[57] Additionally, these same studies found an upregulation of VEGFR2 in cultured podocytes, suggesting that VEGF/VEGFR2 signaling is important not only for glomerular capillary formation and maintenance, but also for podocyte differentiation.[57]

Other receptor-ligand signaling systems probably crucial for glomerular capillary formation include members of the Eph/ephrin receptor/counter-receptor families.[20,25] Specifically, the receptor tyrosine kinase EphB1 and its ligand, ephrin-B1, which itself is also a transmembrane protein receptor, are both expressed in similar distribution patterns in developing kidney microvasculature.[58] Although the precise roles for Eph/ephrin signaling in the glomerulus are still uncertain, knockout mice display lethal vascular phenotypes, including defects in vessel patterning, sprouting, and remodeling (reviewed in [25]). Reciprocal gradients of Eph and ephrin protein concentrations have been identified in the developing brain, where they appear to direct accurate neuronal patterning in the visual system. Perhaps analogous events take place in the developing glomerulus, where spatial signals conveyed between endothelial cells help target them to correct microanatomical domains.[25]

DEVELOPMENT OF THE MESANGIUM

Fundamentals regarding the development of the intercapillary mesangium, as well as the origin and recruitment of mesangial cell progenitors, are still largely unresolved issues in glomerular biology. Nevertheless, we have known for some time that PDGFB and its receptor, PDGFRβ, are both expressed by mesangial cells of mature glomeruli.[51] Additionally, studies in developing kidney have shown that immature podocytes produce PDGFB which may help recruit mesangial cell progenitors expressing PDGFRβ into glomeruli. Later, podocyte expression of PDGF declines, and the synthesis of both PDGF and PDGFRβ becomes confined to the mesangial cells, perhaps to promote their proliferation or maturation.[51] Gene deletion studies in mice have conclusively shown an absolute requirement for PDGFB/PDGFRβ signaling. Null mutants for either genes die perinatally, with massive hemorrhaging systemically.[59,60] Importantly, glomeruli in these mutants entirely lack mesangial cells and consist of one or only a few large, swollen capillary loops.[59,60]

Interestingly, once the glomerulus has fully matured, there appears to be a small population of extraglomerular mesangial cells capable of completely repopulating the glomerulus if the intraglomerular mesangium becomes severely injured. These mesangial reserve cells reside in the juxtaglomerular apparatus, and are distinct from renin-secreting cells, macrophages, vascular smooth muscle cells, and endothelial cells.[61] In an anti-Thy-1 model of proliferative glomerulonephritis in rats, these extraglomerular mesangial reserve cells migrate into the glomerulus and entirely restore the depleted intraglomerular mesangium.[61] Alternatively, some studies suggest that bone marrow hematopoitic stem cells can be a source of mesangial cells.[62] Perhaps additional studies based on these fascinating observations can shed more light on the origin and development of mesangial cells during glomerulogenesis. Similarly, much more work needs to be done on the assembly and maintenance of the mesangial matrix. Although this matrix undergoes morphologic and compositional changes throughout glomerulogenesis, it has not yet been the topic of thorough study. Whether the mesangial matrix is produced exclusively by mesangial cells

or whether glomerular endothelial cells and podocytes also contribute components, are also not understood. On the other hand, and as discussed later, considerable progress has been made in understanding the assembly of the GBM (see below).

FACTORS REGULATING PODOCYTE DIFFERENTIATION

Determination of podocyte identity and regulation of podocyte differentiation are fundamental aspects of glomerulogenesis about which much remains to be learned. Although the podocyte transcription factors described below have been shown to be crucial for proper differentiation, exactly how these regulators interact to orchestrate the complex acquisition of the podocyte phenotype remains a mystery. Studies aimed at defining the entire glomerular transcriptome[63,64] have been very useful for defining what genes may play important roles in podocyte determination, differentiation, and function; however, we have only just begun to gain an understanding of how the podocyte achieves its unique and important properties through interacting pathways.[65]

WT1

The protein that likely has one of the earliest roles in podocyte differentiation is Wilms tumor 1 (WT1), a zinc-finger protein that is involved in both transcription and RNA processing.[66] WT1 is expressed at the initial stages of nephrogenesis, when it has been shown to regulate such developmentally important genes as *Bmp7*, *Six2*, and *Sall1*.[67] But once glomerulogenesis begins, there is a dramatic increase in the level of WT1 in podocyte precursors, and podocytes continue to express WT1 throughout life (reviewed in [68]). One potentially important function of WT1 is to downregulate expression of Pax2 in the immature podocytes of S-shape stage nephrons,[69] as artificial overexpression of Pax2 widely, including in podocytes, causes severe nephrotic syndrome.[70] In addition, WT1 has been shown to regulate a number of genes, including NPHS1,[71,72] the gene encoding nephrin (discussed below). This provides a clear mechanism whereby alteration in WT1 function directly affects glomerular function.

Several lines of investigation reveal important roles for WT1 in promoting proper podocyte differentiation (reviewed in [66,68,73]). Most notable is that heterozygous mutations that affect the zinc-finger structure of WT1 cause Denys–Drash syndrome in humans. This rare disease is characterized by proteinuria, nephrotic syndrome, diffuse mesangial sclerosis, and ESRD. Expression of mutant WT1 forms associated with Denys–Drash syndrome in transgenic mice, either globally or specifically in podocytes, causes various glomerular and podocyte defects that are consistent with the human pathology.[66,74] Moreover, heterozygous mutations in WT1 that affect the normal pattern of WT1 RNA alternative splicing to generate the so-called +KTS and −KTS isoforms of WT1, cause Frasier syndrome.[75] The renal component of this disease includes proteinuria that begins in early childhood and progresses to FSGS, but the course to ESRD is slower than observed in Denys–Drash syndrome. Mice engineered to express only the +KTS or the −KTS isoforms develop severe podocyte and glomerular defects, further emphasizing the important role that WT1 and these specific splice variants play in glomerular development and function.[76]

Lmx1b

Lmx1b, a LIM-homeodomain protein, is another transcription factor expressed in podocytes that is affected in human disease. Heterozygous mutations in LMX1B cause Nail–Patella syndrome,[77] an autosomal dominant disease with skeletal abnormalities, nail hypoplasia, and variably penetrant nephropathy associated with accumulation of fibrillar material in the GBM that appears to be collagen type III.[78] Although $Lmx1b^{+/-}$ mice do not exhibit a phenotype, $Lmx1b^{-/-}$ mice die shortly after birth with abnormalities in dorsal limb structures, including absence of nails and patellae, abnormal glomeruli, attenuated podocyte maturation with lack of normal slit diaphragms, and tubular protein casts.[79] Analysis of gene expression in $Lmx1b^{-/-}$ podocytes has revealed decreases in collagen α3 and α4(IV), podocin, and CD2AP,[80–82] which are all known to be important for proper glomerular filtration. The reduced expression in $Lmx1b^{-/-}$ mice suggests a basis for the partially penetrant nephropathy in $LMX1B^{+/-}$ humans, but gene expression studies in affected individuals do not support this hypothesis.[78] Thus, exactly how LMX1B haploinsufficiency causes nephropathy in humans remains a mystery. If there really is no reduction in the expression of relevant podocyte genes, then perhaps there is a lack of repression, either direct or indirect, of genes injurious to glomerular function, as previously proposed.[83]

Pod1/Tcf21

Pod1, a basic helix-loop-helix transcription factor also known as epicardin, capsulin, and Tcf21, is highly expressed early during kidney development in

condensing metanephric mesenchyme and in stromal cells. In the developing nephron, Pod1 is expressed in podocyte precursors at the S-shaped stage, and persists in adult podocytes.[73,84] The kidney phenotype in Pod1$^{-/-}$ mice, which die at birth due to heart and lung defects, is complex, but it is clear that there are fewer glomeruli associated with defects in ureteric bud branching. In addition, there is a striking arrest of glomerular development at the capillary loop stage, and podocytes fail to mature properly, elaborating only rudimentary foot processes.[85] Gene expression profiling studies of Pod1$^{-/-}$ glomeruli revealed 3986 genes expressed differently than in wild-type glomeruli, demonstrating that Pod1 has profound effects on gene expression.[86]

Kreisler/Mafb

Kreisler/Mafb is a basic domain leucine zipper transcription factor expressed in podocytes from the capillary loop stage onwards.[87] Mice that are homozygous for a point mutation affecting the kreisler DNA-binding domain die within 24 hours of birth. The podocytes of these mice fail to extend foot processes or establish slit diaphragms, and there is a significant reduction in expression of nephrin, podocin, and CD2AP.[88] Interestingly, whereas Pod1 is expressed in kreisler$^{-/-}$ podocytes, kreisler is not expressed in Pod1$^{-/-}$ podocytes. This suggests the existence of a transcriptional hierarchy in which Pod1 may activate expression of kreisler.[87]

Foxc2

Foxc2 is a member of the forkhead/winged-helix family of transcription factors. During nephrogenesis, Foxc2 is first expressed in a subset of cells in the comma-shaped body and then is expressed in developing podocytes at the S-shaped and capillary loop stages, and more weakly at maturity.[89] Foxc2$^{-/-}$ mice exhibit small kidneys and reduced numbers of glomeruli with ballooned capillaries, suggesting a defect in adhesion of mesangial cells (which are present) to the glomerular basement membrane (GBM). Ultrastructural analyses revealed that podocytes fail to extend processes or assemble slit diaphragms, and endothelial cells fail to become fenestrated, suggesting an arrest of differentiation of these two cell types. Gene expression profiling studies of Foxc2$^{-/-}$ glomeruli showed reductions in a number of known podocyte genes, such as kreisler/Mafb, Nphs2 (podocin), and Podxl1 (podocalyxin), although others, such as Nphs1, Wt1, and Cd2ap, were not affected.[89] Interestingly, in the *Xenopus* pronephros, the combined knockdown of WT1 and Foxc2 resulted in the loss of all podocyte marker gene expression.[65]

Notch2

Notch2 is expressed in developing podocytes from as early as the comma-shaped stage.[90] Although the total absence of Notch2 in mice results in embryonic lethality at E11.5 before glomerulogenesis begins, homozygosity for a hypomorphic Notch2 allele allows survival until 24 hours after birth. These latter Notch2$^{-/-}$ mice exhibit small kidneys with cortical vascular lesions. Some glomeruli arrested before the capillary loop stage and were not vascularized, whereas others became vascularized but had ballooned capillaries due to an absence of mesangial cells. In addition, genetic interaction studies demonstrated that Jagged1, a Notch ligand, is required for proper Notch2 signaling during glomerulogenesis.[90] Additional studies using a conditional Notch2 allele showed that Notch2 (but not Notch1) is required for acquisition of podocyte and proximal tubule cell fates.[91,92]

FORMATION OF THE SLIT DIAPHRAGM COMPLEX

In mature glomeruli, the slit diaphragm (SD) represents the only known connection between adjacent podocytes and podocyte foot processes. The SD spans the space between the interdigitated foot processes (Figure 26.4), and has been proposed to play a crucial role in glomerular filtration by serving as the major barrier to albumin,[93] although some data do not support this view.[94,95] The SD has also been shown to mediate important signaling events that are responsible for maintaining podocyte survival and differentiation,[96,97] suggesting that it plays dual roles in ensuring proper glomerular function. But interestingly, mutant mice without slit diaphragms due to lack of nephrin have dramatic leakage of albumin into the urine, but they do not have major alterations in podocyte survival or gene expression.[98]

Slit Diaphragm Components

Nephrin and the Neph Family

The explosion of research into SD composition and function began with the identification of the nephrin gene (*NPHS1*), as mutated in congenital nephrotic syndrome of the Finnish type,[99] and the nephrin protein as an integral component of the SD[100,101] (Figure 26.5). Nephrin is an immunoglobulin superfamily member containing eight extracellular Ig-like domains, a

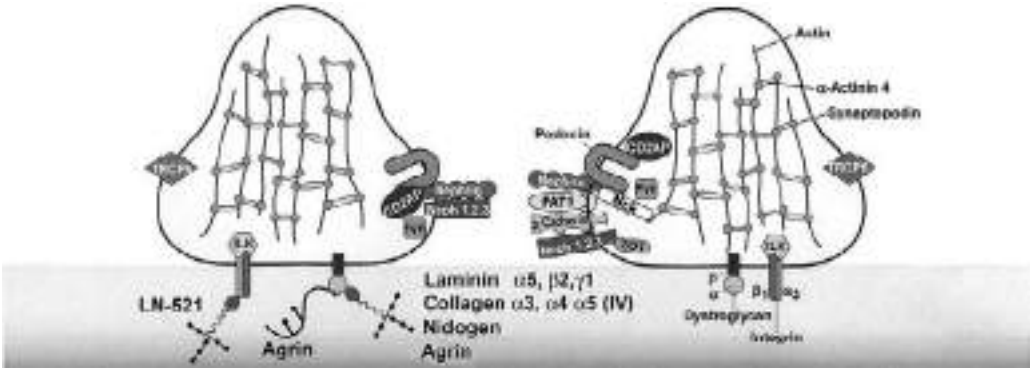

FIGURE 26.5 **Diagram showing clustering of the slit diaphragm complex proteins at the basolateral surfaces of podocyte foot processes, which are attached to the underlying GBM (shown in blue).** Molecules are not drawn to scale, but many known extracellular and intracellular protein:protein interactions are represented. Exactly how the several protein ectodomains interact to form the characteristic SD ultrastructure is not yet fully defined. See text for details. See color section at the end of the book.

fibronectin type III domain, a single-pass transmembrane domain, and a cytoplasmic tail of ~155 amino acids, including several tyrosines that have been predicted to be important for its function, perhaps by interacting with actin-binding Nck adapter proteins.[102–106] Humans and mice lacking nephrin never establish SDs, demonstrating the importance of nephrin for SD formation. A group of three related Ig superfamily molecules that interact with nephrin, Neph1-3, are also found at the SD, as well as in other tissues, and it is clear that at least Neph1 is required for maintenance of the filtration barrier.[107] Interestingly, nephrin interacts directly with the Neph proteins[108–110] (Figure 26.5), and disturbing their association *in vivo* causes proteinuria.[111]

Further evidence for the importance of nephrin-Neph interactions come from the model organisms *Drosophila* (fruitflies) and *C. elegans* (nematodes), which have conserved homologs of nephrin and Neph proteins. In both these invertebrates, a nephrin homolog on one cell interacts with a Neph homolog on another cell to promote a developmental event.[112–114] Amazingly, all three mouse Neph proteins can partially compensate for the nematode Neph-like protein SYG-1.[115] Together with data from mouse, these results suggest that nephrin-Neph interactions are conserved across phyla.

ZO-1 and Podocin

Before the identification of nephrin, zonula occludens-1 (ZO-1), an epithelial tight junction protein, was shown to be localized to the cytoplasmic face of the SD.[116] ZO-1 has recently been shown to interact with Neph1–3, which may serve to anchor it to the SD. In turn, podocin, whose encoding gene (*NPHS2*) is mutated in familial steroid resistant nephrotic syndrome, appears important for anchoring nephrin and the Neph family to the SD (Figure 26.5). Podocin is a hairpin-shaped integral membrane protein that interacts with the cytoplasmic tails of nephrin and Neph family members,[117] and is required to target nephrin to lipid raft microdomains, which have been proposed to be crucial for SD organization and function.[118]

Cadherins

Consistent with the notion that the SD is a modified adherens junction,[119] two cadherins, P-cadherin and the FAT1 protocadherin, have been localized to the SD. P-cadherin was found to associate with ZO-1 and the catenins at the SD, but the functional importance of P-cadherin at the SD has yet to be demonstrated, and humans with mutations in the P-cadherin gene (*CDH3*) are not reported to have kidney disease. FAT1, an extremely large member of the cadherin family, is involved in regulating actin cytoskeleton dynamics and cell polarization.[120] Mice lacking FAT1 die within two days of birth, and their podocytes lack SDs and significant foot process formation. This underscores the importance of FAT1 in the establishment or maintenance of SDs. A model of the SD that can accommodate the very large extracellular domain of FAT1 has not yet been presented, but FAT1 may somehow contribute to the central density of the SD that is apparent in ultrastructural analyses.[93,121]

CD2AP

CD2-associated protein (CD2AP) is a modular cytoplasmic docking protein that interacts with multiple slit diaphragm components, including nephrin and podocin, as well as with the actin cytoskeleton[122,123] (Figure 26.5). Mice lacking CD2AP exhibit congenital nephrotic syndrome with progressive loss of SDs and foot processes, and they die at 6–7 weeks of age.[124] In addition, CD2AP haploinsufficiency has been associated with renal disease in both mice and humans,[125,126] and a

patient homozygous for a premature stop codon mutation (R612X) lacking the final 28 amino acids of 639 total exhibited proteinuria, FSGS, and kidney failure by 3 years of age.[127] CD2AP is thought to be an adaptor that forms a bridge between the SD and the cytoskeleton,[128] but it also appears to play a role in the trafficking of endocytic vesicles.[122,126] Although CD2AP is very widely expressed, it seems to be required only in the podocyte[129]; this could be due to compensation by a paralog of CD2AP, CIN85, although CIN85 activity in podocytes appears to be detrimental.[130]

Nck

That mice lacking CD2AP are able to form normal foot processes and SDs initially suggests the existence of other adaptor proteins in podocytes that might play an earlier role in organizing SDs and linking them to the cytoskeleton. Indeed, the Nck adaptor proteins (Nck1 and Nck2), which contain three Src homology 3 (SH3) domains and one SH2 domain, bind to phosphotyrosine-containing motifs in the cytoplasmic tail of nephrin via their SH2 domains. In addition, clustering of nephrin-Nck complexes reorganized the actin cytoskeleton in transfected cells.[102,105] Importantly, genetically-engineered mice lacking Nck1 and Nck2 in podocytes failed to elaborate foot processes or assemble SDs,[102] and inducible deletion of Nck1 and Nck2 in adult podocytes rapidly leads to proteinuria and glomerulosclerosis.[131] These exciting findings establish a potentially pivotal role for the Nck adaptor proteins in organizing and maintaining SDs, and suggest one mechanism whereby the Fin minor mutation in NPHS1, which results in a nephrin protein lacking most of its cytoplasmic tail and all of the intracellular tyrosines,[99] causes congenital nephrotic syndrome.

TRPC6

TRPC6 is a member of the transient receptor potential family of cation channel proteins, and is associated with the SD. Mutations in TRPC6 have been shown to cause autosomal dominant FSGS in several different families, and this was associated with increased calcium current amplitude in some cases.[132,133] Calcium flux mediated by TRPC6 could have an important role in regulating podocyte and SD homeostasis, perhaps by regulating actin dynamics and motility[134] and calcium-sensitive transcription factors such as those in the NFAT family.[135]

Slit Diaphragm Assembly Mechanisms

As mentioned earlier, the slit diaphragm bears some relationship to adherens junctions, and ZO-1 immunolocalizes to the cytoplasmic domains on the lateral surfaces of podocytes adjacent to the extracellular diaphragm spanning the slit pore. The synthetic patterns of all of the SD components during glomerular development have not yet been studied in detail. However, nephrin and podocin first appear during the late S-shaped and early capillary loop stages of nephron development, which is when foot process interdigitation first occurs, simultaneous with the first ultrastructural appearance of SDs.[100,136] Also occurring at this stage of development is the apical-to-basal translocation of protein complexes involved in cell polarity, an event crucial for proper slit diaphragm and foot process formation.[137,138] The precise sequence of SD assembly, including how the linkages between the ectodomains of SD proteins are made, as well as connections with the internal cytoskeleton and associated elements, are not known. Similarly, the extent to which the SD may be dynamic and undergo modification with age is poorly-understood. Nevertheless, an increasing number of studies have shown that the SD does not merely represent a static component of the glomerular filtration barrier, but it also functions to influence podocyte behavior.[97]

Signaling at the Slit Diaphragm

The first evidence that the SD complex may have a signaling role came from studies of nephrin activity in cultured cells. Transfection of cells with nephrin increased activator protein-1 (AP1)-mediated transcriptional activation, and this effect on intracellular signaling was augmented by cotransfection with podocin, to which nephrin binds.[139] These authors later showed that podocin recruits nephrin to lipid rafts,[118] which are cholesterol-enriched plasma membrane microdomains associated with high concentrations of signaling proteins and high levels of signaling activity. Furthermore, as alluded to above, nephrin contains multiple tyrosines in its cytoplasmic tail. Some of these can be phosphorylated by the Src-family tyrosine kinase, Fyn,[106] and clustering of nephrin by Fyn increases phosphorylation.[103] Phosphorylation of nephrin both augments its interaction with podocin[104] and allows Nck adaptor proteins to bind its tail and influence the organization of the adjacent actin cytoskeleton.[102,105] Consistent with this, $Fyn^{-/-}$ mice have variably coarsened or effaced foot processes.[106] In addition, trans-heterozgyous $Fyn^{+/-}$; $Cd2ap^{+/-}$ mice exhibit marked proteinuria and FSGS, and CD2AP can be immunoprecipitated with Fyn from glomerular lysates. These findings demonstrate that Fyn-mediated signaling likely depends upon interactions with CD2AP.[125]

Nephrin-mediated signaling has also been shown to involve stimulation of phosphoinositide 3-OH kinase (PI3K). Nephrin and CD2AP interact with the p85

regulatory subunit of PI3K, recruit PI3K to the plasma membrane and, in conjunction with podocin, stimulate PI3K activation of AKT signaling in podocytes.[140] This is proposed to regulate the behavior of podocytes and protect them from detachment–induced apoptosis (anoikis), which suggests that proper signaling at the SD is important for maintaining podocyte health.

Neph family proteins, like nephrin, have cytoplasmic tails containing tyrosines that can be phosphorylated. Also like nephrin, Neph1 can induce AP-1-mediated transcriptional activation.[117] ZO-1, which binds to the cytoplasmic tail of Neph proteins, enhances tyrosine phosphorylation of Neph1 and augments AP-1 activation.[141] As ZO-1 can also interact with the actin cytoskeleton, one can envisage how the podocin-CD2AP-nephrin-Neph-ZO-1 complex can activate signaling in podocytes and provide stability to the SD via linkage to actin (Figure 26.5). Interfering with any of these interactions likely leads to abnormal podocyte behavior and proteinuria; in this regard, the actin cytoskeleton in podocyte foot processes also has specialized components. These include α-actinin-4, which is mutated in autosomal dominant FSGS,[142] and synaptopodin, which regulates α-actinin's actin bundling activity[143] and binds to CD2AP.[125] That trans-heterozygous Synpo$^{+/-}$; Cd2ap$^{+/-}$ mice develop proteinuria and FSGS-like lesions[125] underscores the importance of the SD-actin cytoskeleton linkage in maintaining podocyte health, structure, and function. Further support comes from a study showing that the action of cyclosporine A in reducing proteinuria has to do with a protective effect on synaptopodin and on the podocyte's actin cytoskeleton.[144]

DEVELOPMENTAL-ORGANIZATIONAL ROLE OF THE GLOMERULAR BASEMENT MEMBRANE

An important extracellular matrix component of developing and mature glomeruli is the glomerular basement membrane (GBM). Basement membranes are the thin sheets of specialized extracellular matrix that underlie all epithelial cells, including the vascular endothelium. The GBM is somewhat unique in that it is an unusually thick basement membrane that forms by fusion of two independent basement membranes, one secreted by podocytes and one by endothelial cells. Thus, both cell types contribute components to the GBM. Like all basement membranes, the GBM contains laminin, type IV collagen, nidogen/entactin, and sulfated proteoglycans.[145] These are all relatively large glycoproteins of which there are multiple isoforms, but only specific ones are found in the GBM.[146] These isoforms are thought to impart properties to the GBM that are important for maintaining glomerular structure and function.

Laminin

Most laminins are cruciform heterotrimers consisting of evolutionarily related α, β, and γ chains.[147] There are five α, four β, and three γ chains that associate nonrandomly and become disulfide bonded to each other to form at least 15 different heterotrimers, most of which are ~800 kDa.[148] Assembly of trimers occurs intracellularly within the endoplasmic reticulum, and then trimers are secreted into the extracellular space where they interact with cellular receptors, such as integrins and dystroglycan, and polymerize with each other to form laminin networks.[149] This network provides the foundation of the basement membrane; as shown in knockout mice, basement membranes do not form without laminin.[148]

Only a subset of the known laminin heterotrimers are expressed in glomeruli, and only a single heterotrimer, laminin α5β2γ1 (designated LM-521),[147] is found in the mature GBM[146] (Figure 26.4). The mesangial matrix, on the other hand, which is structurally and compositionally similar but distinct from basement membranes, contains an assortment of laminins, including LM-111, LM-211, LM-411, and LM-511.[146] Whether these mesangial laminins have any specific functions in glomerular biology is not yet clear, but they could certainly influence the behavior of mesangial cells and interact with laminins or other components of the GBM to strengthen the adhesion of the mesangium to GBM segments at the bases of the glomerular capillary loops. In contrast, as discussed below, the laminin content of the GBM is well-known to be extremely important for both glomerular development and function.

Developmental Transitions in GBM Laminin Composition

During glomerulogenesis there are well-characterized developmental transitions in the deposition of laminin isoforms in the GBM and its precursor.[150] From the comma-shape through the S-shape stage, LM-111 and LM-411 are present, but they are eliminated from the GBM during the transition to the capillary loop stage (Figures 26.2 and 26.3). At the S-shape stage, LM-511 is first deposited in the nascent GBM by the presumptive podocytes and the invading endothelial cells. At the capillary loop stage, both LM-511 and LM-521 are present in the maturing GBM, but LM-511 is gradually eliminated as the glomerulus begins functioning as a filter. LM-521 is from then on the major GBM laminin.[150] While little is known about

the transcriptional control of these isoform transitions during glomerular development, it is clear that the *in vivo* setting is important, as metanephroi grown *ex vivo* do not deposit LM-521. This deficiency is rescued upon reimplantation and subsequent glomerular vascularization *in vivo*, suggesting that glomerular endothelial cells are required for proper laminin isoform substitution.[151]

LAMININ A CHAIN TRANSITIONS

Experiments primarily in knockout mice have revealed the importance of some of these developmental transitions for successful glomerulogenesis and proper glomerular function. A targeted mutation in Lama5, the gene encoding laminin α5, results in breakdown of the GBM at the stage when LM-511 should begin to replace LM-111 (late S-shape stage).[152] In the absence of LM-511, LM-111 is still eliminated from the nascent GBM, and without a full-size laminin trimer, GBM architecture cannot be maintained. The loss of the GBM at this critical stage of glomerulogenesis has severe consequences, as podocytes lose their cup-shaped arrangement and instead contract into a ball of cells, leaving no place for the endothelial and mesangial cells to form capillaries. Thus, glomerular vascularization completely fails.[152] Additional studies aimed at defining the function of the laminin α5 COOH-terminal globular (α5LG) domain in glomerulogenesis showed that this domain is not important for maintenance of GBM integrity, but rather serves as a ligand for mesangial cells to adhere to the GBM at the bases of the glomerular capillary loops so that they can maintain and perhaps modulate capillary loop structure and diameter, as previously proposed.[153] When this ligand is missing, the capillaries balloon in a fashion similar to that observed in the absence of mesangial cells (discussed above), yet here mesangial cells are clearly present but apparently unable to adhere to the GBM under the stress of capillary blood flow.[154] These studies show that the GBM and the laminin that it contains serve important organizational roles, both during and after glomerulogenesis.

LAMININ β CHAIN TRANSITIONS

In contrast to the requirement for laminin α5 for successful glomerulogenesis, laminin β2 is dispensable. This is best demonstrated by the structurally normal glomeruli that form in Lamb2$^{-/-}$ mice, which correlates with maintenance of GBM integrity during glomerulogenesis.[155] The GBM is able to remain intact without LM-521, the only isoform normally found in mature GBM, because of the persistence or continued expression of laminin β1, resulting in a GBM containing LM-511 instead of LM-521. However, despite normal glomerulogenesis, Lamb2$^{-/-}$ mice exhibit congenital nephrotic syndrome and are proteinuric.[155] Similarly, humans with mutations in LAMB2 exhibit congenital nephrotic syndrome and diffuse mesangial sclerosis that is sometimes associated with distinct ocular and other abnormalities, a disease entity called Pierson syndrome.[156–158] Together these results show that laminin β2 in the GBM (as part of LM-521) is uniquely qualified to ensure that the glomerular barrier to protein is intact. This could be due to either direct effects on GBM porosity or indirect effects on behavior of the attached endothelium and overlying podocytes, as well as assembly and function of the slit diaphragm complex.

Post-fixation immunoelectron microscopy of wild-type mouse kidney has shown that the laminin α1, α5, β1, and β2 chains all originate in both glomerular endothelial cells and podocytes during glomerular development.[151] Similarly, in transgenic mice that overexpress human *LAMA5*, endothelial cells and podocytes were both positive for human laminin α5 protein.[200]

Collagen Type IV

There are six genetically distinct collagen IV chains, called α chains, that assemble in a defined fashion to form three different triple helical protomers.[159,160] These are designated $(\alpha1)_2\alpha2$, $\alpha3\alpha4\alpha5$, and $(\alpha5)_2\alpha6$. Like all collagen chains, collagen IV chains contain long stretches of Gly-X-Y amino acid triplet repeats that favor formation of a triple helix. However, unlike most other collagens, type IV contains interspersed interruptions of the triplet repeats that provide flexibility both to the protomers and to the collagen IV network. This is in turn thought to impart needed flexibility to basement membranes.[161]

Collagen IV protomers interact with each other via both covalent and non-covalent interactions to form a chicken wire-like network, and a substantial amount of cross-linking stabilizes the network. Surprisingly, knockout mice demonstrate that collagen IV is not absolutely required for basement membrane formation, but it is crucial for basement membrane maintenance and stability.[162]

Most basement membranes in the body contain the $\alpha(1)_2\alpha2$ protomer, and this is also true of the early nephrogenic epithelial structures (Figure 26.2). As is the case for the laminins, $\alpha1\alpha2\alpha1$ collagen(IV) originates in both endothelial cells and podocytes.[163] However, at the capillary loop stage, the α3, α4, and α5 chains become detectable in the GBM[150] (Figure 26.3), and have been shown to be made exclusively by podocytes.[163] At maturity, the $\alpha3\alpha4\alpha5$ protomer represents the major collagen IV component of the

GBM (Figure 26.4), although apparently small amounts of presumably residual $(\alpha1)_2\alpha2$ can also be detected, more so in human than in mouse GBM. On the other hand, the α1 and α2(IV) chains are abundant in the mesangial matrix, whereas the α3, α4, and α5 chains are absent.[146] Interestingly, the basement membrane of Bowman's capsule contains $(\alpha1)_2\alpha2$ and $(\alpha5)_2\alpha6$ protomers.[164]

As implied by the existence of only three different collagen IV protomers *in vivo*, the α3 and α4(IV) chains exist exclusively in combination with α5(IV) to make the α3α4α5 protomer.[159,160] Thus, if any one of the three genes encoding these chains is altered by genetic mutation, this protomer is affected. Mutations that prevent proper assembly of this protomer cause Alport syndrome or hereditary glomerulonephritis, in humans, dogs, and mice,[159,160] as discussed in detail in Chapter 90. In the absence of the α3α4α5 protomer, there are no defects in glomerulogenesis, primarily due to compensation by the collagen IV network containing the $(\alpha1)_2\alpha2$ protomer. However, as affected individuals age, the abnormal GBM develops characteristic lesions, including thickening and splitting, that eventually lead to renal failure in most cases.[165] Heterozygous mutations in human and mouse Col4a1 have also been shown to cause disease that includes defects in kidney function.[166–169]

Nidogen–Entactin

Nidogens are dumbbell-shaped molecules.[145] There are two isoforms of nidogen, nidogen-1 and -2, and both have been reported to be present in the GBM.[170] Nidogen-1 was previously considered to be an obligatory link between the laminin and collagen IV networks, because it binds well to each of them.[145] However, mutant mice lacking both nidogens-1 and -2 survive to birth with most basement membranes intact, demonstrating that nidogen is not required for the integrity of all basement membranes.[171] Although the double knockouts died on the day of birth, urine removed from their bladders showed only a marginal increase in low molecular weight proteins,[171] suggesting that the glomerular barrier to albumin was intact and therefore not dependent on the presence of nidogen in the GBM.

Nidogen-1 binds to laminin trimers via a high-affinity interaction with a specific domain of the laminin γ1 chain.[172] To determine the biological importance of this interaction, 56 amino acids encompassing this domain of γ1 were deleted in mice such that nidogen-1 could no longer bind laminin.[173] Interestingly, the result was a phenotype that is in many ways more severe than the total absence of both nidogen-1 and -2. For example, homozygotes died immediately after birth rather than surviving for many hours. Renal agenesis was very common, and glomerular capillary aneurisms and hydronephrosis occurred in those few kidneys that did form.[173] Together, the results of these two studies[171,173] suggest that the alteration to laminin γ1 affects more than just its ability to bind nidogens, but the phenotype of this Lamc1 mutant also underscores the importance of laminin for proper glomerulogenesis.

Sulfated Proteoglycans

Proteoglycans consist of a core protein with covalently attached glycosaminoglycan side chains (GAGs). Those proteoglycans present in basement membranes are usually modified further on their GAGs by addition of heparan sulfate and/or chondroitin sulfate. The anionic character of these sulfate-containing adducts provides much of the basement membrane's net negative charge. A large number of experiments performed in animals suggest that the glomerular filtration barrier possesses charge selectivity, and the sulfated proteoglycans that are present in the GBM are attractive candidates to provide the basis for at least part of this selectivity against the passage of negatively charged molecules into the urine. However, recent studies suggest that anionic charges within the GBM may not be involved in establishment of the glomerular filtration barrier under normal circumstances.[174,175]

Perlecan

There are four major sulfated proteoglycans with relevance to the glomerulus, and the best-studied biochemically is perlecan. Perlecan consists of a 400 kDa core protein with three heparan sulfate chains linked to residues near the NH2-terminus. It is widely found in basement membranes, and is abundant in the mesangial matrix, but perlecan is only weakly detected in the GBM.[176] Cleavage of the COOH-terminus of perlecan produces a fragment with antiangiogenic activity called endorepellin.[177]

Knockout mice lacking perlecan die during embryogenesis or in the neonatal period with multiple developmental defects. Most basement membranes form normally, but mechanical stress causes disruptions in meningeal and cardiomyocyte basement membranes. Perlecan is also normally found in cartilage extracellular matrix, and this matrix is severely disrupted in perlecan mutants.[178,179] No defects in kidneys were noted in these mice.

To investigate further the function of perlecan as a heparan sulfate proteoglycan, a deletion was made that affects only the small part of the protein to which the GAGs are normally attached. Mice carrying this

mutation are viable, but they have defects in the lens capsule.[180] Neither functional nor structural defects were noted in kidney glomeruli under normal circumstances, but these mice exhibit elevated levels of urinary protein after bovine serum albumin overload.[181] Because little perlecan is detectable in the GBM, it is somewhat surprising that removal of its GAGs can have an effect on the filtration barrier.

Agrin

Agrin is a widely expressed modular proteoglycan that consists of a core protein of ~220 kDa with two glycosaminoglycan side chains that carry heparan sulfate and/or chondroitin sulfate. These increase the molecular weight of agrin to greater than 400 kDa. Agrin exhibits robust binding to the coiled-coil domain of the laminin γ1 chain *in vitro*,[182] and this might indicate that agrin is involved in organization of basement membrane architecture.

Agrin has been intensively studied by the neuroscience community because a specific splice form of agrin is deposited by motor neurons on developing skeletal muscle fibers, where it serves as a signal that is in part responsible for maintaining the aggregation of acetylcholine receptors to ensure the proper assembly of the neuromuscular junction.[183,184] In kidney, agrin is highly concentrated in the GBM,[185] significantly more so than perlecan, but there is as yet no evidence that it serves any signaling functions. Agrin has, however, been proposed to be responsible for the anionic charge that is present in the GBM, and that is presumed to be involved in establishing the charge-selective aspect of the glomerular barrier to protein.

Several different mutations have been made in the mouse agrin gene. Whereas all but the most subtle of these have dramatic effects on the differentiation of the neuromuscular junction, no defects in the kidney have been found. Because agrin mutant mice die at birth due to an inability to breathe, agrin-null kidneys beyond the neonatal period have not been studied. Nevertheless, no defects in glomerulogenesis were noted in agrin-deficient kidneys at perinatal stages.[175] In addition, a conditional knockout of agrin in podocytes using the Cre/loxP system was successful at removing both agrin and fixed anionic sites from the GBM, yet there were no detectable defects in glomerular filtration.[175] These results show that agrin likely plays no role either in glomerulogenesis or in establishment of the glomerular barrier to protein. Further, these findings suggest that glomerular charge selectivity may be contributed by podocyte and endothelial cell surface molecules, rather than by GBM proteoglycans.

Other Proteoglycans

Although perlecan and agrin are the best-studied GBM proteoglycans, two others have been shown to be present. Collagen XVIII, the COOH-terminus of which is cleaved to form the antiangiogenic molecule endostatin,[177] is unique in that it is a basement membrane collagen with heparan sulfate glycosaminoglycan side chains.[186] It is present in the GBM, but its function there, if any, is unknown. Mutant mice lacking collagen XVIII have no reported glomerular defects, but do exhibit abnormal blood vessel formation in the eye and retinal defects.[187] Consistent with this, Knobloch syndrome in humans is caused by mutations in COL18A1.[188]

A basement membrane chondroitin sulfate proteoglycan that exhibits transient deposition in postnatal rat GBM has been described.[189] Although nothing is known about the function of this protein, of potential interest is the fact that increased levels of this proteoglycan were detected in the GBM of diabetic rats, compared to the normal situation where it is not detected in mature GBM.[190]

RECEPTORS AND RECEPTOR-ASSOCIATED PROTEINS MEDIATING GLOMERULAR CELL INTERACTIONS WITH THE GBM

In order for glomerular cells to interact appropriately with the GBM, they must express the required matrix receptors and the associated cytoplasmic proteins that mediate responses to the engagement of ligand. While there is a plethora of these molecules, only a limited set have been studied in the context of glomerulogenesis and glomerular function.

The best characterized matrix receptors are the integrins. Integrins are a large family of transmembrane αβ heterodimers that bind to extracellular matrix proteins, mediate adhesion, and transduce signals that govern cell proliferation, survival, and migration. The most studied integrin in the glomerulus is α3β1. This is primarily a laminin-binding integrin, although it has also been shown to bind collagen IV. Biochemical studies suggest that α3β1 preferentially binds laminins containing the α3 and α5 chains. This would include the LM-511 and LM-521 heterotrimers that, as discussed above, are so important for glomerular development and function.

The first indication that integrin α3β1 is important for glomerulogenesis came from studies of Itga3 mutant mice, which lack integrin α3.[191] These mice die in the neonatal period due to defects in both kidney and lung. Glomerulogenesis occurs in a mostly normal

fashion, but ultrastructural analysis reveals that formation of podocyte foot processes is defective, and the GBM appears highly disorganized.[191] These data are consistent with the fact that podocytes express integrin α3β1 at a high level, and suggest that α3β1 is involved in organizing GBM architecture, perhaps by modulating polymerization of secreted laminins, and in regulating foot process extension. Integrin α3β1 also serves as a mesangial cell receptor for the COOH-terminal LG domain of laminin α5 in the GBM. Their interaction at the base of the glomerular capillary loops allows mesangial cells to maintain loop structure. If this interaction is impaired, either by alteration of the composition of the LG domain or by deletion of integrin α3, then capillary ballooning occurs.[154,191] Ballooning is more severe in the former case, indicating that there is likely a receptor on mesangial cells besides integrin α3β1 that mediates binding to the GBM. One possibility is integrin α8β1, as older Itga8$^{-/-}$ mice exhibit widening of the glomerular capillaries, although the effect is mild.[192]

Integrin α3β1 is one of many integrins that use the integrin-linked kinase (ILK) as an intermediate in signal transduction. ILK binds to integrins and to various actin-binding proteins, and therefore serves to bridge the actin cytoskeleton with the cell's major linkage to the extracellular matrix. Whereas mice lacking ILK die as very early peri-implantation embryos, mice with a podocyte-specific deletion of ILK survive for a few months, but they eventually succumb to an end-stage renal disease that begins with thickening and broadening of the GBM, followed by focal segmental glomerulosclerosis.[193] Mutation of CD151, a tetraspanin family protein expressed by podocytes that interacts with and modulates integrin function, can also cause GBM defects and glomerular disease.[194,195] These data further underscore the importance of the podocyte in organizing GBM architecture.

CONCLUDING REMARKS

Although much progress has been made in understanding certain aspects of glomerular development, many important questions remain. First and foremost, the fundamental morphogenic events that initiate, propel, and conclude glomerulogenesis are still poorly-defined. In this chapter, we discussed a series of different transcription factors, intracellular and transmembrane proteins, growth factors, and various signaling mechanisms associated with glomerular endothelial cell and podocyte biology. With only a few exceptions, however, most of these individual proteins and processes are expressed by many other cells and tissues throughout the body, and therefore are not likely to be solely or directly responsible for development of the glomerulus. On the other hand, there are a few features of the glomerulus that are both compositionally and structurally distinct, and these include the GBM and epithelial slit diaphragm. Similarly, the intercapillary mesangial cell and its matrix are also unusual structures not found in other vascular beds. We believe that more research aimed at investigating the regulation of the synthesis, assembly, and maintenance of the GBM, SD, and mesangium specifically may yield detailed new insights into how the glomerulus develops and is maintained normally. Perhaps new therapies that retrace parts of the normal developmental pathway could then be designed and used successfully to repair injured glomeruli.

Acknowledgments

We thank Erin Cambron and the late Eileen Roach for help with the illustrations. Our supporting funds came from the National Institutes of Health.

References

[1] Abrahamson DR. Glomerulogenesis in the developing kidney. Sem Nephrol 1991;11:375–89.
[2] Saxen L. Organogenesis of the kidney. Cambridge, UK: Cambridge University Press; 1987.
[3] Woolf AS. The life of the human kidney before birth: its secrets unfold. Pediatr Res 2001;49:8–10.
[4] Abrahamson DR. Structure and development of the glomerular capillary wall and basement membrane. Am J Physiol 1987;253: F783–794.
[5] Ekblom P. Formation of basement membranes in the embryonic kidney: an immunohistological study. J Cell Biol 1981;91:1–10.
[6] Lelongt B, Makino H, Kanwar YS. Maturation of the developing renal glomerulus with respect to basement membrane proteoglycans. Kidney Int 1987;32:498–506.
[7] Abrahamson DR, Wang R. Development of the glomerular capillary and its basement membrane. In: Vize PD, Woolf AS, Bard JBL, editors. The Kidney. From normal development to congenital disease. London: Academic Press; 2003. p. 221–49.
[8] Reeves W, Caulfield JP, Farquhar MG. Differentiation of epithelial foot processes and filtration slits: sequential appearance of occluding junctions, epithelial polyanion, and slit membranes in developing glomeruli. Lab Invest 1978;39:90–100.
[9] Abrahamson DR. Origin of the glomerular basement membrane visualized after *in vivo* labeling of laminin in newborn rat kidneys. J Cell Biol 1985;100:1988–2000.
[10] Kanwar YS, Jakubowski ML, Rosenzweig LJ, Gibbons JT. *De novo* cellular synthesis of sulfated proteoglycans of the developing renal glomerulus *in vivo*. Proc Natl Acad Sci USA 1984;81:7108–11.
[11] Reeves WH, Kanwar YS, Farquhar MG. Assembly of the glomerular filtration surface. differentiation of anionic sites in glomerular capillaries of newborn rat kidney. J Cell Biol 1980;85:735–53.
[12] Sariola H, Peault B, LeDouarin N, Buck C, Dieterlen-Lievre F, Saxen L. Extracellular matrix and capillary ingrowth in interspecies chimeric kidneys. Cell Diff 1984;15:43–51.

[13] Abrahamson DR, Perry EW. Evidence for splicing new basement membrane into old during glomerular development in newborn rat kidneys. J Cell Biol 1986;103:2489–98.
[14] Desjardins M, Bendayan M. Ontogenesis of glomerular basement membrane: structural and functional properties. J Cell Biol 1991;113:689–700.
[15] Hyink DP, Abrahamson DR. Origin of the glomerular vasculature in the developing kidney. Semin Nephrol 1995;15:300–14.
[16] Sariola H, Ekblom P, Lehtonen E, Saxen L. Differentiation and vascularization of the metanephric kidney grafted on the chorioallantoic membrane. Dev Biol 1983;96:427–35.
[17] Abrahamson DR. Development of kidney glomerular endothelial cells and their role in basement membrane assembly. Organogenesis 2009;5:275–87.
[18] Hyink DP, Tucker DC, St John PL, Leardkamolkarn V, Accavitti MA, Abrass CK, et al. Endogenous origin of glomerular endothelial and mesangial cells in grafts of embryonic kidneys. Am J Physiol 1996;270:F886–899.
[19] Robert St. B, John PL, Hyink DP, Abrahamson DR. Evidence that embryonic kidney cells expressing flk-1 are intrinsic, vasculogenic angioblasts. Am J Physiol 1996;271:F744–753.
[20] Robert B, St John PL, Abrahamson DR. Direct visualization of renal vascular morphogenesis in Flk1 heterozygous mutant mice. Am J Physiol 1998;275:F164–172.
[21] Loughna S, Hardman P, Landels E, Jussila L, Alitalo K, Woolf AS. A molecular and genetic analysis of renalglomerular capillary development. Angiogenesis 1997;1:84–101.
[22] Tufro A, Norwood VF, Carey RM, Gomez RA. Vascular endothelial growth factor induces nephrogenesis and vasculogenesis. J Amer Soc Nephrol 1999;10:2125–34.
[23] Ricono JM, Xu YC, Arar M, Jin DC, Barnes JL, Abboud HE. Morphological insights into the origin of glomerular endothelial and mesangial cells and their precursors. J Histochem Cytochem 2003;51:141–50.
[24] Sequeira Lopez ML, Pentz ES, Robert B, Abrahamson DR, Gomez RA. Embryonic origin and lineage of juxtaglomerular cells. Am J Physiol Renal Physiol 2001;281:F345–356.
[25] Daniel TO, Abrahamson D. Endothelial signal integration in vascular assembly. Annu Rev Physiol 2000;62:649–71.
[26] Robert B, Abrahamson DR. Control of glomerular capillary development by growth factor/receptor kinases. Pediatr Nephrol 2001;16:294–301.
[27] Carmeliet P, Ferreira V, Breier G, Pollefeyt S, Kieckens L, Gertsenstein M, et al. Abnormal blood vessel development and lethality in embryos lacking a single VEGF allele. Nature 1996;380:435–9.
[28] Ferrara N, Carver-Moore K, Chen H, Dowd M, Lu L, O'Shea KS, et al. Heterozygous embryonic lethality induced by targeted inactivation of the VEGF gene. Nature 1996;380:439–42.
[29] Shalaby F, Rossant J, Yamaguchi TP, Gertsenstein M, Wu XF, Breitman ML, et al. Failure of blood-island formation and vasculogenesis in Flk-1-deficient mice. Nature 1995;376:62–6.
[30] Fong GH, Rossant J, Gertsenstein M, Breitman ML. Role of the Flt-1 receptor tyrosine kinase in regulating the assembly of vascular endothelium. Nature 1995;376:66–70.
[31] Simon M, Grone HJ, Johren O, Kullmer J, Plate KH, Risau W, et al. Expression of vascular endothelial growth factor and its receptors in human renal ontogenesis and in adult kidney. Am J Physiol 1995;268:F240–250.
[32] Tufro A. VEGF spatially directs angiogenesis during metanephric development *in vitro*. Dev Biol 2000;227:558–66.
[33] Kitamoto Y, Tokunaga H, Tomita K. Vascular endothelial growth factor is an essential molecule for mouse kidney development: Glomerulogenesis and nephrogenesis. J Clin Invest 1997;99:2351–7.
[34] Eremina V, Cui S, Gerber H, Ferrara N, Haigh J, Nagy A, et al. Vascular endothelial growth factor-A signaling in the podocyte-endothelial compartment is required for mesangial cell migration and survival. J Am Soc Nephrol 2006;17:724–35.
[35] Eremina V, Sood M, Haigh J, Nagy A, Lajoie G, Ferrara N, et al. Glomerular-specific alterations of VEGF-A expression lead to distinct congenital and acquired renal diseases. J Clin Invest 2003;111:707–16.
[36] Wenger RH, Stiehl DP, Camenisch G. Integration of oxygen signaling at the consensus HRE. Sci STKE 2005;306:re12.
[37] Maxwell PH, Ratcliffe PJ. Oxygen sensors and angiogenesis. Semin Cell Dev Biol 2002;13:29–37.
[38] Gerber HP, Dixit V, Ferrara N. Vascular endothelial growth factor induces expression of the antiapoptotic proteins Bcl-2 and A1 in vascular endothelial cells. J Biol Chem 1998;273:13313–6.
[39] Abedi H, Zachary I. Vascular endothelial growth factor stimulates tyrosine phosphorylation and recruitment to new focal adhesions of focal adhesion kinase and paxillin in endothelial cells. J Biol Chem 1997;272:15442–51.
[40] Bernhardt WM, Schmitt R, Rosenberger C, Munchenhagen PM, Grone HJ, Frei U, et al. Expression of hypoxia-inducible transcription factors in developing human and rat kidneys. Kidney Int 2006;69:114–22.
[41] Freeburg PB, Robert St B, John PL, Abrahamson DR. Podocyte expression of hypoxia-inducible factor (HIF)-1 and HIF-2 during glomerular development. J Am Soc Nephrol 2003;14:927–38.
[42] Freeburg PB, Abrahamson DR. Divergent expression patterns for hypoxia-inducible factor-1beta and aryl hydrocarbon receptor nuclear transporter-2 in developing kidney. J Am Soc Nephrol 2004;15:2569–78.
[43] Freeburg PB, Abrahamson DR. Hypoxia-inducible factors and kidney vascular development. J Amer Soc Nephrol 2003;14:2723–30.
[44] Haase VH. Hypoxia-inducible factors in the kidney. Am J Physiol Renal Physiol 2006;291:F271–281.
[45] Haase VH. The VHL/HIF oxygen-sensing pathway and its relevance to kidney disease. Kidney Int 2006;69:1302–7.
[46] Kaelin Jr WG. The von Hippel-Lindau tumor suppressor gene and kidney cancer. Clin Cancer Res 2004;10:6290S–5S.
[47] Raval RR, Lau KW, Tran MG, Sowter HM, Mandriota SJ, Li JL, et al. Contrasting properties of hypoxia-inducible factor 1 (HIF-1) and HIF-2 in von Hippel-Lindau-associated renal cell carcinoma. Mol Cell Biol 2005;25:5675–86.
[48] Esser S, Wolburg K, Wolburg H, Breier G, Kurzchalia T, Risau W. Vascular endothelial growth factor induces endothelial fenestrations *in vitro*. J Cell Biol 1998;140:947–59.
[49] Woolf AS, Yuan HT. Angiopoietin growth factors and Tie receptor tyrosine kinases in renal vascular development. Pediatr Nephrol 2001;16:177–84.
[50] Ulleras E, Wilcock A, Miller SJ, Franklin GC. The sequential activation and repression of the human PDGF-B gene during chronic hypoxia reveals antagonistic roles for the depletion of oxygen and glucose. Growth Factors 2001;19:233–45.
[51] Alpers CE, Seifert RA, Hudkins KL, Johnson RJ, Bowen-Pope DF. Developmental patterns of PDGF B-chain, PDGF-receptor, and alpha-actin expression in human glomerulogenesis. Kidney Int 1992;42:390–9.
[52] Eichmann A, Makinen T, Alitalo K. Neural guidance molecules regulate vascular remodeling and vessel navigation. Genes Dev 2005;19:1013–21.
[53] Klagsbrun M, Eichmann A. A role for axon guidance receptors and ligands in blood vessel development and tumor angiogenesis. Cytokine Growth Factor Rev 2005;16:535–48.
[54] Robert B, Zhao X, Abrahamson DR. Coexpression of neuropilin-1, Flk1, and VEGF(164) in developing and mature mouse kidney glomeruli. Am J Physiol Renal Physiol 2000;279:F275–282.

[55] Villegas G, Tufro A. Ontogeny of semaphorins 3A and 3F and their receptors neuropilins 1 and 2 in the kidney. Mech Dev 2002;119(Suppl. 1):S149–153.
[56] Harper SJ, Xing CY, Whittle C, Parry R, Gillatt D, Peat D, et al. Expression of neuropilin-1 by human glomerular epithelial cells *in vitro* and *in vivo*. Clin Sci 2001;101:439–46.
[57] Guan F, Villegas G, Teichman J, Mundel P, Tufro A. Autocrine VEGF-A system in podocytes regulates podocin and its interaction with CD2AP. Am J Physiol Renal Physiol 2006;291:F422–428.
[58] Daniel TO, Stein E, Cerretti DP, St John PL, Robert B, Abrahamson DR. ELK and LERK-2 in developing kidney and microvascular endothelial assembly. Kidney Int Supp 1996;57: S73–81.
[59] Leveen P, Pekny M, Gebre-Medhin S, Swolin B, Larsson E, Betsholtz C. Mice deficient for PDGF B show renal, cardiovascular, and hematological abnormalities. Genes Dev 1994;8:1875–87.
[60] Soriano P. Abnormal kidney development and hematological disorders in PDGF beta- receptor mutant mice. Genes Dev 1994;8:1888–96.
[61] Hugo C, Shankland SJ, Bowen-Pope DF, Couser WG, Johnson RJ. Extraglomerular origin of the mesangial cell after injury. A new role of the juxtaglomerular apparatus. J Clin Invest 1997;100:786–94.
[62] Masuya M, Drake CJ, Fleming PA, Reilly CM, Zeng H, Hill WD, et al. Hematopoietic origin of glomerular mesangial cells. Blood 2003;101:2215–8.
[63] Lindenmeyer MT, Eichinger F, Sen K, Anders HJ, Edenhofer I, Mattinzoli D, et al. Systematic analysis of a novel human renal glomerulus-enriched gene expression dataset. PLoS ONE 2010;5:e11545.
[64] Takemoto M, He L, Norlin J, Patrakka J, Xiao Z, Petrova T, et al. Large-scale identification of genes implicated in kidney glomerulus development and function. EMBO J 2006;25:1160–74.
[65] White JT, Zhang B, Cerqueira DM, Tran U, Wessely O. Notch signaling, wt1 and foxc2 are key regulators of the podocyte gene regulatory network in *Xenopus*. Development 2010;137: 1863–73.
[66] Hastie ND. Life, sex, and WT1 isoforms–three amino acids can make all the difference. Cell 2001;106:391–4.
[67] Hartwig S, Ho J, Pandey P, Macisaac K, Taglienti M, Xiang M, et al. Genomic characterization of Wilms' tumor suppressor 1 targets in nephron progenitor cells during kidney development. Development 2010;137:1189–203.
[68] Kreidberg JA. Podocyte differentiation and glomerulogenesis. J Am Soc Nephrol 2003;14:806–14.
[69] Ryan G, Steele-Perkins V, Morris JF, Rauscher 3rd FJ, Dressler GR. Repression of Pax-2 by WT1 during normal kidney development. Development 1995;121:867–75.
[70] Dressler GR, Wilkinson JE, Rothenpieler UW, Patterson LT, Williams-Simons L, Westphal H. Deregulation of Pax-2 expression in transgenic mice generates severe kidney abnormalities. Nature 1993;362:65–7.
[71] Guo G, Morrison DJ, Licht JD, Quaggin SE. WT1 activates a glomerular-specific enhancer identified from the human nephrin gene. J Am Soc Nephrol 2004;15:2851–6.
[72] Wagner N, Wagner KD, Xing Y, Scholz H, Schedl A. The major podocyte protein nephrin is transcriptionally activated by the Wilms' tumor suppressor WT1. J Am Soc Nephrol 2004;15: 3044–51.
[73] Quaggin SE. Transcriptional regulation of podocyte specification and differentiation. Microsc Res Tech 2002;57:208–11.
[74] Natoli TA, Liu J, Eremina V, Hodgens K, Li C, Hamano Y, et al. A mutant form of the Wilms' tumor suppressor gene WT1 observed in Denys-Drash syndrome interferes with glomerular capillary development. J Am Soc Nephrol 2002;13:2058–67.
[75] Salomon R, Gubler MC, Niaudet P. Genetics of the nephrotic syndrome. Curr Opin Pediatr 2000;12:129–34.
[76] Hammes A, Guo JK, Lutsch G, Leheste JR, Landrock D, Ziegler U, et al. Two splice variants of the Wilms' tumor 1 gene have distinct functions during sex determination and nephron formation. Cell 2001;106:319–29.
[77] Dreyer SD, Zhou G, Baldini A, Winterpacht A, Zabel B, Cole W, et al. Mutations in LMX1B cause abnormal skeletal patterning and renal dysplasia in nail patella syndrome. Nat Genet 1998;19:47–50.
[78] Heidet L, Bongers EM, Sich M, Zhang SY, Loirat C, Meyrier A, et al. *In vivo* expression of putative LMX1B targets in nail-patella syndrome kidneys. Am J Pathol 2003;163:145–55.
[79] Chen H, Lun Y, Ovchinnikov D, Kokubo H, Oberg KC, Pepicelli CV, et al. Limb and kidney defects in Lmx1b mutant mice suggest an involvement of LMX1B in human nail patella syndrome. Nat Genet 1998;19:51–5.
[80] Miner JH, Morello R, Andrews KL, Li C, Antignac C, Shaw AS, et al. Transcriptional induction of slit diaphragm genes by Lmx1b is required in podocyte differentiation. J Clin Invest 2002;109:1065–72.
[81] Morello R, Zhou G, Dreyer SD, Harvey SJ, Ninomiya Y, Thorner PS, et al. Regulation of glomerular basement membrane collagen expression by LMX1B contributes to renal disease in nail patella syndrome. Nat Genet 2001;27:205–8.
[82] Rohr C, Prestel J, Heidet L, Hosser H, Kriz W, Johnson RL, et al. The LIM-homeodomain transcription factor Lmx1b plays a crucial role in podocytes. J Clin Invest 2002;109:1073–82.
[83] Mutter WP, Peng H, Goldring MB, Knebelmann B, Karumanchi A. Role of LMX1B in proteinuria. J Am Soc Nephrol 2005;16:670A.
[84] Quaggin SE, Vanden Heuvel GB, Igarashi P. Pod-1, a mesoderm-specific basic-helix-loop-helix protein expressed in mesenchymal and glomerular epithelial cells in the developing kidney. Mech Dev 1998;71:37–48.
[85] Quaggin SE, Schwartz L, Cui S, Igarashi P, Deimling J, Post M, et al. The basic-helix-loop-helix protein pod1 is critically important for kidney and lung organogenesis. Development 1999;126: 5771–83.
[86] Cui S, Li C, Ema M, Weinstein J, Quaggin SE. Rapid isolation of glomeruli coupled with gene expression profiling identifies downstream targets in Pod1 knockout mice. J Am Soc Nephrol 2005;16:3247–55.
[87] Sadl V, Jin F, Yu J, Cui S, Holmyard D, Quaggin S, et al. The mouse Kreisler (Krml1/MafB) segmentation gene is required for differentiation of glomerular visceral epithelial cells. Dev Biol 2002;249:16–29.
[88] Moriguchi T, Hamada M, Morito N, Terunuma T, Hasegawa K, Zhang C, et al. MafB is essential for renal development and F4/80 expression in macrophages. Mol Cell Biol 2006;26:5715–27.
[89] Takemoto M, Asker N, Gerhardt H, Lundqvist A, Johansson BR, Saito Y, et al. A new method for large scale isolation of kidney glomeruli from mice. Am J Pathol 2002;161:799–805.
[90] McCright B, Gao X, Shen L, Lozier J, Lan Y, Maguire M, et al. Defects in development of the kidney, heart and eye vasculature in mice homozygous for a hypomorphic Notch2 mutation. Development 2001;128:491–502.
[91] Cheng HT, Kim M, Valerius MT, Surendran K, Schuster-Gossler K, Gossler A, et al. Notch2, but not Notch1, is required for proximal fate acquisition in the mammalian nephron. Development 2007;134:801–11.
[92] Cheng HT, Miner JH, Lin M, Tansey MG, Roth K, Kopan R. Gamma-secretase activity is dispensable for mesenchyme-to-epithelium transition but required for podocyte and proximal tubule formation in developing mouse kidney. Development 2003;130:5031–42.

[93] Wartiovaara J, Ofverstedt LG, Khoshnoodi J, Zhang J, Makela E, Sandin S, et al. Nephrin strands contribute to a porous slit diaphragm scaffold as revealed by electron tomography. J Clin Invest 2004;114:1475–83.
[94] Gagliardini E, Conti S, Benigni A, Remuzzi G, Remuzzi A. Imaging of the porous ultrastructure of the glomerular epithelial filtration slit. J Amer Soc Nephrol 2010;21:2081–9.
[95] Jarad G, Cunningham J, Shaw AS, Miner JH. Proteinuria precedes podocyte abnormalities in Lamb2$^{-/-}$ mice, implicating the glomerular basement membrane as an albumin barrier. J Clin Invest 2006;116:2272–9.
[96] Aaltonen P, Holthofer H. The nephrin-based slit diaphragm: new insight into the signalling platform identifies targets for therapy. Nephrol Dial Transplant 2007;22:3408–10.
[97] Huber TB, Benzing T. The slit diaphragm: a signaling platform to regulate podocyte function. Curr Opin Nephrol Hypertens 2005;14:211–6.
[98] Done SC, Takemoto M, He L, Sun Y, Hultenby K, Betsholtz C, et al. Nephrin is involved in podocyte maturation but not survival during glomerular development. Kidney Int 2008;73:697–704.
[99] Kestila M, Lenkkeri U, Mannikko M, Lamerdin J, McCready P, Putaala H, et al. Positionally cloned gene for a novel glomerular protein– nephrin– is mutated in congenital nephrotic syndrome. Mol Cell 1998;1:575–82.
[100] Holzman LB, John PL, Kovari IA, Verma R, Holthofer H, Abrahamson DR. Nephrin localizes to the slit pore of the glomerular epithelial cell. Kidney Int 1999;56:1481–91.
[101] Ruotsalainen V, Ljungberg P, Wartiovaara J, Lenkkeri U, Kestila M, Jalanko H, et al. Nephrin is specifically located at the slit diaphragm of glomerular podocytes. Proc Natl Acad Sci USA 1999;96:7962–7.
[102] Jones N, Blasutig IM, Eremina V, Ruston JM, Bladt F, Li H, et al. Nck adaptor proteins link nephrin to the actin cytoskeleton of kidney podocytes. Nature 2006.
[103] Lahdenpera J, Kilpelainen P, Liu XL, Pikkarainen T, Repenon P, Ruotsalainen V, et al. Clustering-induced tyrosine phosphorylation of nephrin by Src family kinases. Kidney Int 2003;64:404–13.
[104] Li H, Lemay S, Aoudjit L, Kawachi H, Takano T. SRC-family kinase Fyn phosphorylates the cytoplasmic domain of nephrin and modulates its interaction with podocin. J Am Soc Nephrol 2004;15:3006–15.
[105] Verma R, Kovari I, Soofi A, Nihalani D, Patrie K, Holzman LB. Nephrin ectodomain engagement results in Src kinase activation, nephrin phosphorylation, Nck recruitment, and actin polymerization. J Clin Invest 2006;116:1346–59.
[106] Verma R, Wharram B, Kovari I, Kunkel R, Nihalani D, Wary KK, et al. Fyn binds to and phosphorylates the kidney slit diaphragm component Nephrin. J Biol Chem 2003;278:20716–23.
[107] Donoviel DB, Freed DD, Vogel H, Potter DG, Hawkins E, Barrish JP, et al. Proteinuria and perinatal lethality in mice lacking neph1, a novel protein with homology to nephrin. Mol Cell Biol 2001;21:4829–36.
[108] Barletta GM, Kovari IA, Verma RK, Kerjaschki D, Holzman LB. Nephrin and Neph1 co-localize at the podocyte foot process intercellular junction and form cis hetero-oligomers. J Biol Chem 2003;278:19266–71.
[109] Gerke P, Huber TB, Sellin L, Benzing T, Walz G. Homodimerization and heterodimerization of the glomerular podocyte proteins nephrin and NEPH1. J Am Soc Nephrol 2003;14:918–26.
[110] Gerke P, Sellin L, Kretz O, Petraschka D, Zentgraf H, Benzing T, et al. NEPH2 is located at the glomerular slit diaphragm, interacts with nephrin and is cleaved from podocytes by metalloproteinases. J Am Soc Nephrol 2005;16:1693–702.
[111] Liu G, Kaw B, Kurfis J, Rahmanuddin S, Kanwar YS, Chugh SS. Neph1 and nephrin interaction in the slit diaphragm is an important determinant of glomerular permeability. J Clin Invest 2003;112:209–21.
[112] Shelton C, Kocherlakota KS, Zhuang S, Abmayr SM. The immunoglobulin superfamily member Hbs functions redundantly with Sns in interactions between founder and fusion-competent myoblasts. Development 2009;136:1159–68.
[113] Shen K, Fetter RD, Bargmann CI. Synaptic specificity is generated by the synaptic guidepost protein SYG-2 and its receptor, SYG-1. Cell 2004;116:869–81.
[114] Zhuang S, Shao H, Guo F, Trimble R, Pearce E, Abmayr SM. Sns and Kirre, the *Drosophila* orthologs of Nephrin and Neph1, direct adhesion, fusion and formation of a slit diaphragm-like structure in insect nephrocytes. Development 2009;136:2335–44.
[115] Neumann-Haefelin E, Kramer-Zucker A, Slanchev K, Hartleben B, Noutsou F, Martin K, et al. A model organism approach: defining the role of Neph proteins as regulators of neuron and kidney morphogenesis. Hum Mol Genet 2010;19:2347–59.
[116] Schnabel E, Anderson JM, Farquhar MG. The tight junction protein ZO-1 is concentrated along slit diaphragms of the glomerular epithelium. J Cell Biol 1990;111:1255–63.
[117] Sellin L, Huber TB, Gerke P, Quack I, Pavenstadt H, Walz G. NEPH1 defines a novel family of podocin interacting proteins. FASEB J 2003;17:115–7.
[118] Huber TB, Simons M, Hartleben B, Sernetz L, Schmidts M, Gundlach E, et al. Molecular basis of the functional podocin-nephrin complex: mutations in the NPHS2 gene disrupt nephrin targeting to lipid raft microdomains. Hum Mol Genet 2003;12:3397–405.
[119] Reiser J, Kriz W, Kretzler M, Mundel P. The glomerular slit diaphragm is a modified adherens junction. J Am Soc Nephrol 2000;11:1–8.
[120] Moeller MJ, Soofi A, Braun GS, Li X, Watzl C, Kriz W, et al. Protocadherin FAT1 binds Ena/VASP proteins and is necessary for actin dynamics and cell polarization. EMBO J 2004;23:3769–79.
[121] Rodewald R, Karnovsky MJ. Porous substructure of the glomerular slit diaphragm in the rat and mouse. J Cell Biol 1974;60:423–33.
[122] Welsch T, Endlich N, Gokce G, Doroshenko E, Simpson JC, Kriz W, et al. Association of CD2AP with dynamic actin on vesicles in podocytes. Am J Physiol Renal Physiol 2005;289: F1134–1143.
[123] Yuan H, Takeuchi E, Salant DJ. Podocyte slit-diaphragm protein nephrin is linked to the actin cytoskeleton. Am J Physiol Renal Physiol 2002;282:F585–591.
[124] Shih N-Y, Li J, Karpitskii V, Nguyen A, Dustin ML, Kanagawa O, et al. Congenital nephrotic syndrome in mice lacking CD2-associated protein. Science 1999;286:312–5.
[125] Huber TB, Kwoh C, Wu H, et al. A bigenic mouse model of focal segmental glomerulosclerosis involving pairwise interaction of CD2AP, Fyn and synaptopodin. J Clin Invest 2006;116:1337–45.
[126] Kim JM, Wu H, Green G, Winkler CA, Kopp JB, Miner JH, et al. CD2-associated protein haploinsufficiency is linked to glomerular disease susceptibility. Science 2003;300:1298–300.
[127] Lowik MM, Groenen PJ, Pronk I, Lilien MR, Goldschmeding R, Dijkman HB, et al. Focal segmental glomerulosclerosis in a patient homozygous for a CD2AP mutation. Kidney Int 2007;72:1198–203.
[128] Shih N-Y, Li J, Cotran R, Mundel P, Miner JH, Shaw AS. CD2AP localizes to the slit diaphragm and binds to nephrin via a novel C-terminal domain. Am J Pathol 2001;159:2303–8.

[129] Grunkemeyer JA, Kwoh C, Huber TB, Shaw AS. CD2-associated protein (CD2AP) expression in podocytes rescues lethality of CD2AP deficiency. J Biol Chem 2005;280:29677–81.
[130] Tossidou I, Teng B, Drobot L, Meyer-Schwesinger C, Worthmann K, Haller H, et al. CIN85/RukL is a novel binding partner of nephrin and podocin and mediates slit diaphragm turnover in podocytes. J Biol Chem 2010;285:25285–95.
[131] Jones N, New LA, Fortino MA, Eremina V, Ruston J, Blasutig IM, et al. Nck proteins maintain the adult glomerular filtration barrier. J Amer Soc Nephrol 2009;20:1533–43.
[132] Reiser J, Polu KR, Moller CC, Kenlan P, Altintas MM, Wei C, et al. TRPC6 is a glomerular slit diaphragm-associated channel required for normal renal function. Nat Genet 2005;37:739–44.
[133] Winn MP, Conlon PJ, Lynn KL, Farrington MK, Creazzo T, Hawkins AF, et al. A mutation in the TRPC6 cation channel causes familial focal segmental glomerulosclerosis. Science 2005;308:1801–4.
[134] Tian D, Jacobo SM, Billing D, Rozkalne A, Gage SD, Anagnostou T, et al. Antagonistic regulation of actin dynamics and cell motility by TRPC5 and TRPC6 channels. Sci Signal 2010;3:ra77.
[135] Wang Y, Jarad G, Tripathi P, Pan M, Cunningham J, Martin DR, et al. Activation of NFAT signaling in podocytes causes glomerulosclerosis. J Amer Soc Nephrol 2010;21:1657–66.
[136] Moeller MJ, Sanden SK, Soofi A, Wiggins RC, Holzman LB. Podocyte-specific expression of cre recombinase in transgenic mice. Genesis 2003;35:39–42.
[137] Hartleben B, Schweizer H, Lubben P, Bartram MP, Moller CC, Herr R, et al. Neph-Nephrin proteins bind the Par3-Par6-atypical protein kinase C (aPKC) complex to regulate podocyte cell polarity. J Biol Chem 2008;283:23033–8.
[138] Huber TB, Hartleben B, Winkelmann K, Schneider L, Becker JU, Leitges M, et al. Loss of podocyte aPKClambda/iota causes polarity defects and nephrotic syndrome. J Amer Soc Nephrol 2009;20:798–806.
[139] Huber TB, Kottgen M, Schilling B, Walz G, Benzing T. Interaction with podocin facilitates nephrin signaling. J Biol Chem 2001;276:41543–6.
[140] Huber TB, Hartleben B, Kim J, Schmidts M, Schermer B, Keil A, et al. Nephrin and CD2AP associate with phosphoinositide 3-OH kinase and stimulate AKT-dependent signaling. Mol Cell Biol 2003;23:4917–28.
[141] Huber TB, Schmidts M, Gerke P, Schermer B, Zahn A, Hartleben B, et al. The carboxy terminus of Neph family members binds to the PDZ domain protein Zonula occludens-1. J Biol Chem 2003;278:13417–21.
[142] Kaplan JM, Kim SH, North KN, Rennke H, Correia LA, Tong HQ, et al. Mutations in ACTN4, encoding alpha-actinin-4, cause familial focal segmental glomerulosclerosis. Nat Genet 2000;24:251–6.
[143] Asanuma K, Kim K, Oh J, Giardino L, Chabanis S, Faul C, et al. Synaptopodin regulates the actin-bundling activity of alpha-actinin in an isoform-specific manner. J Clin Invest 2005;115:1188–98.
[144] Faul C, Donnelly M, Merscher-Gomez S, Chang YH, Franz S, Delfgaauw J, et al. The actin cytoskeleton of kidney podocytes is a direct target of the antiproteinuric effect of cyclosporine A. Nat Med 2008;14:931–8.
[145] Timpl R. Structure and biological activity of basement membrane proteins. Eur J Biochem 1989;180:487–502.
[146] Miner JH. Renal basement membrane components. Kidney Int 1999;56:2016–24.
[147] Aumailley M, Bruckner-Tuderman L, Carter WG, et al. A simplified laminin nomenclature. Matrix Biol 2005;24:326–32.
[148] Miner JH, Yurchenco PD. Laminin functions in tissue morphogenesis. Annu Rev Cell Dev Biol 2004;20:255–84.
[149] Colognato H, Yurchenco PD. Form and function: the laminin family of heterotrimers. Dev Dyn 2000;218:213–34.
[150] Miner JH. Developmental biology of glomerular basement membrane components. Curr Opin Nephrol Hypertens 1998;7:13–9.
[151] St. John PL, Wang R, Yin Y, Miner JH, Robert B, Abrahamson DR. Glomerular laminin isoform transitions: errors in metanephric culture are corrected by grafting. Am J Physiol Renal Physiol 2001;280:F695–705.
[152] Miner JH, Li C. Defective glomerulogenesis in the absence of laminin α5 demonstrates a developmental role for the kidney glomerular basement membrane. Dev Biol 2000;217:278–89.
[153] Kriz W, Elger M, Mundel P, Lemley KV. Structure-stabilizing forces in the glomerular tuft. J Am Soc Nephrol 1995;5:1731–9.
[154] Kikkawa Y, Virtanen I, Miner JH. Mesangial cells organize the glomerular capillaries by adhering to the G domain of laminin alpha5 in the glomerular basement membrane. J Cell Biol 2003;161:187–96.
[155] Noakes PG, Miner JH, Gautam M, Cunningham JM, Sanes JR, Merlie JP. The renal glomerulus of mice lacking s-laminin/laminin beta2: nephrosis despite molecular compensation by laminin beta1. Nat Genet 1995;10:400–6.
[156] Zenker M, Aigner T, Wendler O, Tralau T, Müntefering H, Fenski R, et al. Human laminin beta2 deficiency causes congenital nephrosis with mesangial sclerosis and distinct eye abnormalities. Hum Mol Genet 2004;13:2625–32.
[157] Zenker M, Pierson M, Jonveaux P, Reis A. Demonstration of two novel LAMB2 mutations in the original Pierson syndrome family reported 42 years ago. Am J Med Genet A 2005;138:73–4.
[158] Zenker M, Tralau T, Lennert T, Pitz S, Mark K, Madlon H, et al. Congenital nephrosis, mesangial sclerosis, and distinct eye abnormalities with microcoria: an autosomal recessive syndrome. Am J Med Genet A 2004;130:138–45.
[159] Hudson BG. The molecular basis of Goodpasture and Alport syndromes: beacons for the discovery of the collagen IV family. J Am Soc Nephrol 2004;15:2514–27.
[160] Hudson BG, Tryggvason K, Sundaramoorthy M, Neilson EG. Alport's syndrome, Goodpasture's syndrome, and type IV collagen. N Engl J Med 2003;348:2543–56.
[161] Hudson BG, Reeders ST, Tryggvason K. Type IV collagen: structure, gene organization, and role in human diseases. J Biol Chem 1993;268:26033–6.
[162] Poschl E, Schlotzer-Schrehardt U, Brachvogel B, Saito K, Ninomiya Y, Mayer U. Collagen IV is essential for basement membrane stability but dispensable for initiation of its assembly during early development. Development 2004;131:1619–28.
[163] Abrahamson DR, Hudson BG, Stroganova L, Borza DB, St John PL. Cellular origins of type IV collagen networks in developing glomeruli. J Am Soc Nephrol 2009;20:1471–9.
[164] Ninomiya Y, Kagawa M, Iyama K, Naito I, Kishiro Y, Seyer JM, et al. Differential expression of two basement membrane collagen genes, COL4A6 and COL4A5, demonstrated by immunofluorescence staining using peptide-specific monoclonal antibodies. J Cell Biol 1995;130:1219–29.
[165] Kashtan CE. Alport syndrome. Kidney Int 1997;51(Suppl. 58): S-69–71.
[166] Gould DB, Phalan FC, Breedveld GJ, van Mil SE, Smith RS, Schimenti JC, et al. Mutations in Col4a1 cause perinatal cerebral hemorrhage and porencephaly. Science 2005;308:1167–71.
[167] Gould DB, Phalan FC, van Mil SE, Sundberg JP, Vahedi K, Massin P, et al. Role of COL4A1 in small-vessel disease and hemorrhagic stroke. N Engl J Med 2006;354:1489–96.

[168] Plaisier E, Chen Z, Gekeler F, Benhassine S, Dahan K, Marro B, et al. Novel COL4A1 mutations associated with HANAC syndrome: a role for the triple helical CB3[IV] domain. Am J Med Genet A 2010;152A:2550–5.

[169] Plaisier E, Gribouval O, Alamowitch S, Mougenot B, Prost C, Verpont MC, et al. COL4A1 mutations and hereditary angiopathy, nephropathy, aneurysms, and muscle cramps. N Engl J Med 2007;357:2687–95.

[170] Miosge N, Kother F, Heinemann S, Kohfeldt E, Herken R, Timpl R. Ultrastructural colocalization of nidogen-1 and nidogen-2 with laminin-1 in murine kidney basement membranes. Histochem Cell Biol 2000;113:115–24.

[171] Bader BL, Smyth N, Nedbal S, Miosge N, Baranowsky A, Mokkapati S, et al. Compound genetic ablation of nidogen 1 and 2 causes basement membrane defects and perinatal lethality in mice. Mol Cell Biol 2005;25:6846–56.

[172] Mayer U, Nischt R, Poschl E, Mann K, Fukuda K, Gerl M, et al. A single EGF-like motif of laminin is responsible for high affinity nidogen binding. EMBO J 1993;12:1879–85.

[173] Willem M, Miosge N, Halfter W, Smyth N, Jannetti I, Burghart E, et al. Specific ablation of the nidogen-binding site in the laminin gamma1 chain interferes with kidney and lung development. Development 2002;129:2711–22.

[174] Goldberg S, Harvey SJ, Cunningham J, Tryggvason K, Miner JH. Glomerular filtration is normal in the absence of both agrin and perlecan-heparan sulfate from the glomerular basement membrane. Nephrol Dial Transplant 2009;24:2044–51.

[175] Harvey SJ, Jarad G, Cunningham J, Rops AL, van der Vlag J, Berden JH, et al. Disruption of glomerular basement membrane charge through podocyte-specific mutation of agrin does not alter glomerular permselectivity. Am J Pathol 2007;171:139–52.

[176] Groffen AJA, Hop FWH, Tryggvason K, Dijkman H, Assmann KJ, Veerkamp JH, et al. Evidence for the existence of multiple heparan sulfate proteoglycans in the human glomerular basement membrane and mesangial matrix. Eur J Biochem 1997;247:175–82.

[177] Bix G, Iozzo RV. Matrix revolutions: "Tails" of basement-membrane components with angiostatic functions. Trends Cell Biol 2005;15:52–60.

[178] Arikawa-Hirasawa E, Watanabe H, Takami H, Hassell JR, Yamada Y. Perlecan is essential for cartilage and cephalic development. Nat Genet 1999;23:354–8.

[179] Costell M, Gustafsson E, Aszodi A, Morgelin M, Bloch W, Hunziker E, et al. Perlecan maintains the integrity of cartilage and some basement membranes. J Cell Biol 1999;147:1109–22.

[180] Rossi M, Morita H, Sormunen R, Airenne S, Kreivi M, Wang L, et al. Heparan sulfate chains of perlecan are indispensable in the lens capsule but not in the kidney. EMBO J 2003;22:236–45.

[181] Morita H, Yoshimura A, Inui K, Ideura T, Watanabe H, Wang L, et al. Heparan sulfate of perlecan is involved in glomerular filtration. J Am Soc Nephrol 2005;16:1703–10.

[182] Kammerer RA, Schulthess T, Landwehr R, Schumacher B, Lustig A, Yurchenco PD, et al. Interaction of agrin with laminin requires a coiled-coil conformation of the agrin-binding site within the laminin gamma1 chain. EMBO J 1999;18:6762–70.

[183] Gautam M, Noakes PG, Moscoso L, Rupp F, Scheller RH, Merlie JP, et al. Defective neuromuscular synaptogenesis in agrin-deficient mutant mice. Cell 1996;85:525–35.

[184] Misgeld T, Kummer TT, Lichtman JW, Sanes JR. Agrin promotes synaptic differentiation by counteracting an inhibitory effect of neurotransmitter. Proc Natl Acad Sci USA 2005;102:11088–93.

[185] Groffen AJ, Ruegg MA, Dijkman H, van de Velden TJ, Buskens CA, van den Born J, et al. Agrin is a major heparan sulfate proteoglycan in the human glomerular basement membrane. J Histochem Cytochem 1998;46:19–27.

[186] Halfter W, Dong S, Schurer B, Cole GJ. Collagen XVIII is a basement membrane heparan sulfate proteoglycan. J Biol Chem 1998;273:25404–12.

[187] Fukai N, Eklund L, Marneros AG, Oh SP, Keene DR, Tamarkin L, et al. Lack of collagen XVIII/endostatin results in eye abnormalities. EMBO J 2002;21:1535–44.

[188] Suzuki OT, Sertie AL, Der Kaloustian VM, Kok F, Carpenter M, Murray J, et al. Molecular analysis of collagen XVIII reveals novel mutations, presence of a third isoform, and possible genetic heterogeneity in Knobloch syndrome. Am J Hum Genet 2002;71:1320–9.

[189] McCarthy KJ, Bynum St. K, John PL, Abrahamson DR, Couchman JR. Basement membrane proteoglycans in glomerular morphogenesis: chondroitin sulfate proteoglycan is temporally and spatially restricted during development. J Histochem Cytochem 1993;41:401–14.

[190] McCarthy KJ, Abrahamson DR, Bynum St KR, John PL, Couchman JR. Basement membrane-specific chondroitin sulfate proteoglycan is abnormally associated with the glomerular capillary basement membrane of diabetic rats. J Histochem Cytochem 1994;42:473–84.

[191] Kreidberg JA, Donovan MJ, Goldstein SL, Rennke H, Shepherd K, Jones RC, et al. Alpha3 beta1 integrin has a crucial role in kidney and lung organogenesis. Development 1996;122:3537–47.

[192] Haas CS, Amann K, Schittny J, Blaser B, Muller U, Hartner A. Glomerular and renal vascular structural changes in alpha8 integrin-deficient mice. J Am Soc Nephrol 2003;14:2288–96.

[193] El-Aouni C, Herbach N, Blattner SM, Henger A, Rastadi MP, Jarad G, et al. Podocyte specific deletion of integrin-linked kinase results in severe glomerular basement membrane alterations and progressive glomerulosclerosis. J Am Soc Nephrol 2006;17:1334–44.

[194] Baleato RM, Guthrie PL, Gubler MC, Ashman LK, Roselli S. Deletion of CD151 results in a strain-dependent glomerular disease due to severe alterations of the glomerular basement membrane. Am J Pathol 2008;173:927–37.

[195] Sachs N, Kreft M, van den Bergh WMA, Beynon AJ, Peters TA, et al. Kidney failure in mice lacking the tetraspanin CD151. J Cell Biol 2006;175:33–9.

[196] Eremina V, Jefferson JA, Kowalewska J, Hochster H, Haas M, Weisstuch J, et al. VEGF inhibition and renal thrombotic microangiopathy. N England J Med 2008;358:1129–36.

[197] Steenhard BM, Freeburg PB, Isom K, Stroganova L, Borza DB, Hudson BG, et al. Kidney development and gene expression in the HIF2α knockout mouse. Dev Dyn 2007;236:1115–25.

[198] Steenhard BM, Isom K, Stroganova L, St John PL, Zelenchuk A, Freeburg PB, et al. Deletion of von Hippel-Lindau in gomerular podocytes results in glomerular basement membrane thickening, extopic subepithelial deposition of collagen α1, α2, α1(IV), expression of neuroglobin, and proteinuria. Am J Pathol 2010;177:84–96.

[199] Sison K, Eremina V, Baelde H, Min W, Hirashima M, Fantus IG, et al. Glomerular structure and function require paracrine, not autocrine, VEGFVEGFR-2 signaling. J Am Soc Nephrol 2010;21:1691–701.

[200] Steenhard BM, Zelenchuk A, Stroganova L, Isom K, St John PL, Andrews GK, et al. TRansgenic expression of human LAMA5 suppresses murine LAma5 mRNA and laminin α5 protein deposition. PLoS ONE 2011;6(9):e23926.

CHAPTER

27

Postnatal Renal Development

Michel Baum[1,2], *Jyothsna Gattineni*[1] *and Lisa M. Satlin*[3]

[1]Departments of Pediatrics and University of Texas Southwestern Medical Center, Dallas, TX, USA
[2]Internal Medicine, University of Texas Southwestern Medical Center, Dallas, TX, USA
[3]Departments of Pediatrics and Medicine, Mount Sinai School of Medicine, New York, NY, USA

RENAL BLOOD FLOW AND GLOMERULAR FILTRATION RATE

Renal Blood Flow

The renal blood flow in the adult human is 660 ml/min which is 20–25% of the cardiac output. In contrast, the fetal kidney receives only 2% of the cardiac output from mid-gestation to term.[178] The developmental increase in renal blood flow is due in part to an increase in cardiac output, but predominantly to a decrease in renal vascular resistance.[92,117,220] When corrected for a body surface area of 1.73 m^2, the human neonate has a renal blood flow of only 15–20% of that measured in adults.[51,177] Renal blood flow doubles in the first month of life, and is comparable to adults by one to two years of age when corrected for body surface area.[177] The maturational changes in renal vascular resistance are due to anatomical changes in the renal vasculature, as well as changes in the balance between vasoconstrictors, such as catecholamines and angiotensin II, and vasodilators, such as nitric oxide.[169] The kidney develops in a centrifugal fashion. Juxtamedullary nephrons are formed before those in the superficial cortex. The renal blood flow distribution, measured by both xenon washout and injection of microspheres, shows a paucity of blood flow to the outer cortex compared to the deep cortex in neonates.[18,117,155] During postnatal maturation there is a redistribution of blood flow, with enhanced perfusion of the outer cortex due to a decrease in renal vascular resistance.[18,117,155]

Autoregulation

Renal blood flow (RBF) and glomerular filtration rate (GFR) remain stable over a wide range of perfusion pressures.[251] As perfusion pressure falls there is vasodilatation of the afferent arteriole and vasoconstriction of the efferent arteriole which maintains RBF and GFR. As blood pressure increases during development, the range in pressure where autoregulation of renal blood flow and GFR occurs shifts accordingly.[118] While neonates can autoregulate GFR in response to changes in blood pressure, this protective mechanism is far less developed than the autoregulatory capability of adults due, at least in part, to an attenuated release and efferent arteriolar response to angiotensin II.[251]

Glomerular Filtration Rate

Initiation of glomerular filtration, as evidenced by the flow of urine, begins between nine and twelve weeks gestation in the human.[85] The glomerular filtration rate (GFR) is lower in neonates than adults, even when corrected for body surface area.[15,177] In premature human infants creatinine clearance increases as a function of postconceptual age (the sum of gestational age and postnatal age).[15] GFR is constant at ~0.5 ml/min in infants with a postconceptional age of 28–34 weeks, despite the increase in renal size.[14] GFR increases to 1.0 ml/min at 34–37 weeks and to 2 ml/min at a postconceptional age of 40 weeks.[14] In absolute terms, the GFR increases 25-fold from birth to adulthood. Corrected for a surface area of 1.73 m^2, the GFR in the human term neonate is 30 ml/min/1.73 m^2 in the first week of life.[15,67] GFR continues to increase during the first ~1–2 years of life to reach adult levels when factored for body surface area[177](Figure 27.1).

At birth, juxtamedullary glomeruli have a larger volume and greater single nephron GFR than superficial

Seldin and Giebisch's The Kidney, Fifth Edition.
DOI: http://dx.doi.org/10.1016/B978-0-12-381462-3.00027-6

© 2013 Elsevier Inc. All rights reserved.

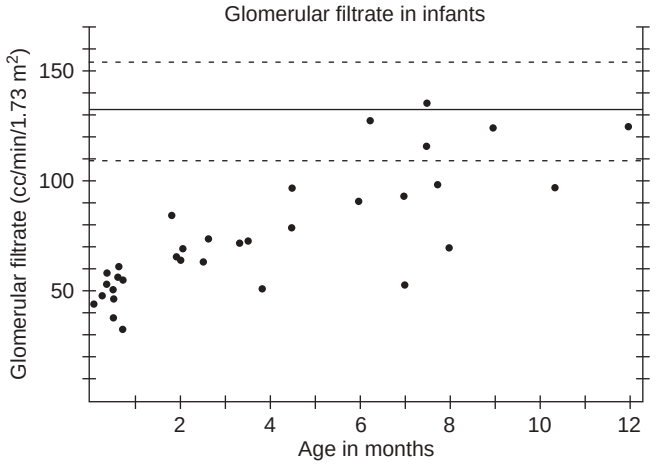

FIGURE 27.1 **Glomerular filtration rate (GFR) in infants in the first year of life (values are corrected for a surface area of 1.73 m^2).** The horizontal line is the mean adult value, and the broken line represents one standard deviation. *(from ref. [177] with permission.)*

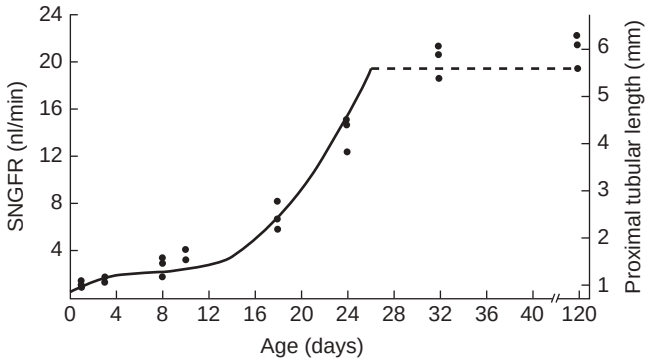

FIGURE 27.2 **Single nephron GFR (SNGFR) in guinea pigs with age.** Each point represents two to six determinations of SNGFR in an animal *(from ref. [219])*.

nephrons.[219] In the guinea pig there is a 7-fold increase in GFR in the first month of life.[219] The increase in total kidney GFR during the first week of life, a time when superficial nephron GFR is relatively constant, is predominantly due to an increase in juxtamedullary nephron GFR.[219] After two weeks of age, however, the rise in total kidney GFR is predominantly due to an increase in GFR in superficial nephrons[219](Figure 27.2).

The increase in single nephron GFR with postnatal maturation is due to a number of factors. Single nephron GFR is the product of the net ultrafiltration pressure and the glomerular ultrafiltration coefficient, K_f. The effective ultrafiltration pressure is the difference between the hydrostatic and oncotic pressures across the glomerular capillary bed. Studies comparing newborn rats and guinea pigs to adults have shown a maturational increase in effective ultrafiltration pressure.[3,220] However, these changes contribute at most 10% to the 20-fold increase in single nephron GFR.[113,220,232] The maturational increase in GFR is predominantly the result of the increase in K_f, which is the product of the hydraulic permeability of the glomerular capillary and the glomerular capillary surface area.[88,115,129,232] Studies using neutral dextrans have found that the permeability characteristics change only slightly with maturation.[88] The increase in K_f, and thus single nephron GFR, is predominately due to the 7.5-fold increase in glomerular capillary surface area during renal maturation.[115,129]

SODIUM CHLORIDE TRANSPORT

The transition from fetal to neonatal life is characterized by a dramatic decrease in urinary sodium excretion, despite an increase in GFR. The early fetus excretes ~20% of the filtered sodium, while the late gestation fetus excretes only ~0.2%.[173,211] Term neonates are able to maintain a positive sodium balance over a wide range of sodium intake which is essential for growth.[9,218] Compared to adults, neonates have a limited capacity to excrete an acute sodium load, and will develop volume expansion and hypernatremia with a sodium load.[9,65] This phenomenon is exemplified in a study where adult and neonatal dogs were given an isotonic saline infusion equal in volume to 10% of the animal's weight.[87] The results of the cumulative excretion of sodium with time are shown in Figure 27.3. Adult dogs had a brisk natriuresis and diuresis, excreting 50% of the sodium within two hours of the infusion. Dogs less than one week of age excreted less than 10% of the sodium infused by two hours. The limited ability to excrete a sodium load in neonates was not explained by a low GFR, since there was a comparable change with volume expansion in neonates and adults. Premature neonates have high urinary sodium losses and fractional excretion of sodium compared to term neonates.[2,7,9,75] The following section discusses the maturation of tubular transport, which maintains the positive sodium balance in growing neonates.

Glomerulotubular Balance

Glomerulotubular balance remains fairly constant under a number of conditions which alter the GFR in the adult. During postnatal development, the maturational increase in the GFR is paralleled by a concomitant increase in the rate of tubule solute absorption.[109,219] If this did not occur, there would be loss of essential solutes which would jeopardize the life of the neonate as GFR increases during development.[109,219]

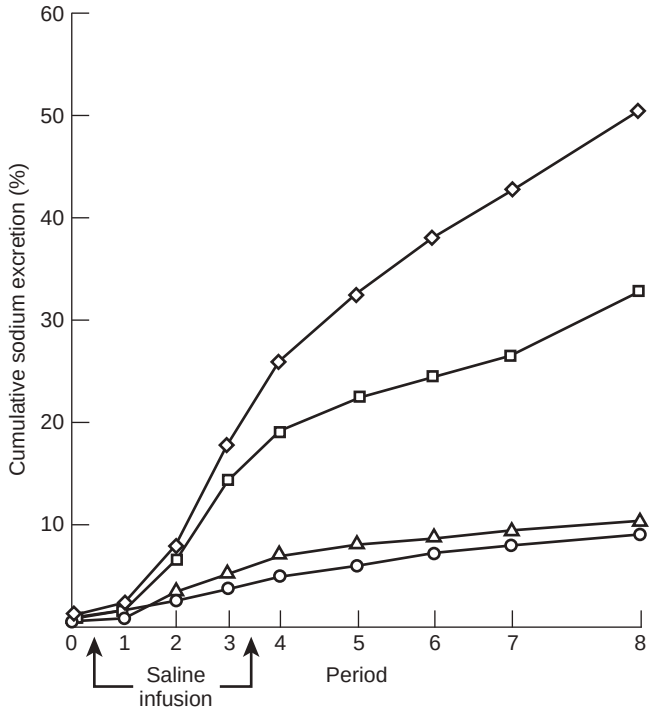

FIGURE 27.3 **Cumulative sodium excretion in dogs of various ages after infusion of isotonic saline equal to 10% of body weight over 30 minutes.** Period 8 is approximately 120 minutes after initiation of saline infusion. *(from ref. [87]).*

In the fetus, however, the GFR and delivery of solutes and water to the tubules can surpass the reabsorptive capacity of the tubules. In a clearance study examining the fractional reabsorption of volume and sodium after salt-loading in fetal, young, and adult guinea pigs, the fractional reabsorption of volume and sodium were lower in the fetus and in one-day-old animals. By 2–5 days of age, the fractional reabsorption of sodium and water were at the adult level.[149] The glomerular–tubular imbalance is not only present in the fetus, but can also be manifest in the premature neonate. This is exemplified by the fact that glucosuria is frequently present in premature human neonates born before 30 weeks of gestation.[14,235] In human neonates born before 34 weeks gestation, 93% of the filtered glucose is reabsorbed,[14] which is comparable to the fractional reabsorption in the guinea pig fetus.[149] By 34 weeks of gestation, the human neonate can reabsorb over 99% of the filtered glucose load.[14]

Maturation of Proximal Tubule Volume Reabsorption

The developing kidney exhibits a centrifugal pattern of nephron maturation, with juxtamedullary nephrons being formed before superficial nephrons.[76] The glomerular and tubular morphology of juxtamedullary nephrons are more mature than those in the superficial cortex.[76] In many species, including the mouse, rat, and rabbit, nephrogenesis continues after birth in the superficial cortex. Nephrogenesis also continues postnatally in humans born prior to 34 weeks gestation.

The reabsorptive capacity of the neonatal superficial and juxtamedullary proximal tubule is less than that of adults. The rate of volume absorption in superficial proximal convoluted tubules increases two-fold between a 22–24-day-old weanling and a 40–45-day-old adult rat.[11] In rabbit superficial proximal tubules the rate of volume absorption increased four-fold between one week and one month of age,[130] while the rate of volume absorption in rabbit juxtamedullary proximal convoluted tubules did not change appreciably during that time.[190] However, there is a two-fold increase in volume absorption in juxtamedullary nephrons between 4 and 6 weeks of age in the rabbit.[190] Proximal tubule transport for each solute is the sum of transport mediated by passive diffusion, solvent drag, and active transport, which are discussed below.

Na^+/K^+-ATPase Activity

The basolateral Na^+/K^+-ATPase provides the driving force for all sodium-dependent transport along the nephron by generating and maintaining a low intracellular sodium concentration. Inhibition of Na^+/K^+-ATPase with ouabain reduces the rate of volume absorption to zero in neonatal and adult isolated rabbit proximal convoluted tubules.[190] Thus, maturation of Na^+/K^+-ATPase activity plays a key role in the maturation of solute transport along the nephron.

The Na^+/K^+-ATPase is made up of an α-subunit and a regulatory ß-subunit. There are four α isoforms and three ß isoforms.[41] The α-subunit is the catalytic subunit, and has an ATP-binding site as well as the binding site for cardiac glycosides. The adult kidney predominantly expresses the α1 and ß1 isoforms. There is a postnatal increase in renal Na^+/K^+-ATPase activity.[12,13,188,191] In dissected rabbit tubules, the neonatal Na^+/K^+-ATPase activity is lower than the adult in each nephron segment examined[188] (Figure 27.4). The V_{max} Na^+/K^+-ATPase activity increases five-fold during renal maturation, with no change in the K_m for sodium, potassium or ATP.

The increase in Na^+/K^+-ATPase activity in the rabbit juxtamedullary proximal convoluted tubule lags behind the maturational increase in bicarbonate and volume absorption by one week,[188] consistent with the maturational increase in apical membrane transport being the driving force for the increase in basolateral

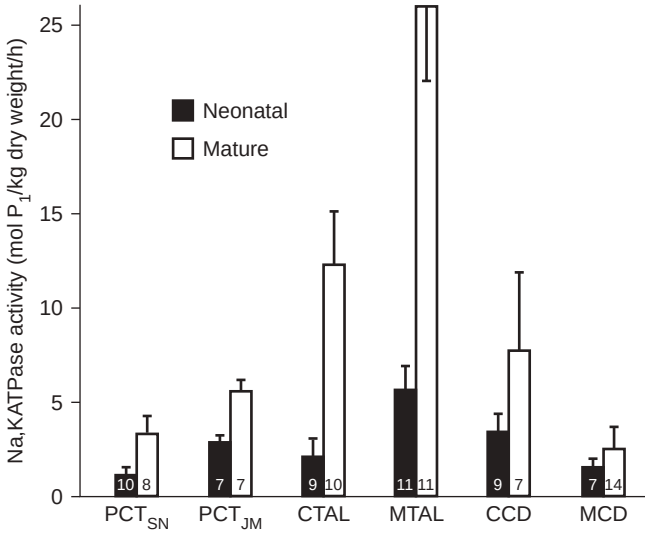

FIGURE 27.4 **Na^+/K^+-ATPase activity in neonatal and adult rabbit nephron segments** (PCT_{SN}: superficial proximal convoluted tubule; PCT_{JM}: juxtamedullaryproximal convoluted tubule; CTAL and MTAL: cortical and medullary thick ascending limbs; CCD and MCD: cortical and medullary collecting ducts) *(from ref. [188]).*

Na^+/K^+-ATPase. Several studies have supported this hypothesis. In rat proximal tubule cells in culture, stimulation of the Na^+/H^+ exchanger increases intracellular sodium and leads to an increase in Na^+/K^+-ATPase activity.[101] An increase in intracellular sodium not only increases pump activity, but also increases α and ß Na^+/K^+-ATPase subunit mRNA and protein abundance.[61] Chronic increases in Na^+/H^+ exchanger activity in rats induced by metabolic acidosis result in an increase in Na^+/K^+-ATPase activity in growing but not adult rats, an effect not seen when the rats were administered amiloride, an inhibitor of the Na^+/H^+ exchanger.[81] Thus, the maturational increase in Na^+/H^+ exchanger activity may be responsible for the increase in Na^+/K^+-ATPase activity.

Maturation of Proximal Tubule NaCl Transport

In the early proximal tubule there is preferential reabsorption of bicarbonate over chloride ions. This leaves the proximal tubule luminal fluid with a higher chloride concentration and a lower bicarbonate concentration than the peritubular fluid. Chloride transport is the sum of active transcellular reabsorption and chloride diffusion across the paracellular pathway down its concentration gradient. In the adult rabbit proximal convoluted tubule, two-thirds of NaCl transport is active and transcellular and one-third is passive and paracellular.[23] In the adult rat proximal convoluted tubule one-third of NaCl transport is active, and two-thirds is mediated by passive diffusion.[4]

Active chloride transport by the proximal convoluted tubule is mediated by the parallel operation of the Na^+/H^+ and Cl^-/base exchangers.[17,204,208] Cl^-/OH^-, Cl^-/oxalate, and Cl^-/formate exchange have all been found to mediate chloride uptake into the proximal tubule[17]; however, the relative importance of these transporters remains controversial. In the rabbit superficial convoluted tubule there is evidence for both Cl^-/OH^- and Cl^-/formate exchangers.[208] However, in juxtamedullary proximal convoluted tubules only Cl^-/OH^- exchange is present.[208] In the guinea pig there is a large increase in Na^+/H^+ exchanger activity and Cl^-/formate exchange in brush border membrane vesicles during the transition from fetus to newborn.[93] In isolated perfused rabbit proximal straight tubules the rate of active NaCl transport was two-fold greater in adult proximal straight tubules compared to neonatal tubules.[203] Both Cl^-/OH^- and Na^+/H^+ exchange activities were five-fold less in neonatal tubules compared to that in adult tubules.[203]

The relative contribution of passive chloride transport to total NaCl transport may be species-specific. In the adult rat the late proximal tubular chloride concentration is significantly higher than that in the glomerular ultrafiltrate.[133] However, in the neonatal rat, the proximal tubule luminal chloride concentration remains the same as that in the glomerular ultrafiltrate. The constant luminal chloride concentration could be due to equal rates of chloride and bicarbonate reabsorption by the immature segment or to a higher chloride permeability in the neonate mediating higher rates of passive chloride transport than in adults.[133] Direct measurements of chloride permeability and the relative contributions of passive chloride transport have not been examined *in vivo*. Thus, the reason for the lack of the chloride gradient in neonatal rat proximal tubules is unknown.

Developmental Changes in the Paracellular Transport

Direct measurements of rabbit proximal convoluted tubule chloride and bicarbonate permeabilities demonstrate that neonatal segments have a lower permeability to both solutes than in the adult.[162,165,206] In addition, the resistance of the proximal tubule is higher in the neonatal rabbit proximal tubule than the adult, providing further evidence that there are developmental changes in the paracellular pathway.[165] Finally, studies have demonstrated that solvent drag does not contribute significantly to volume absorption in the neonatal tubule, as the reflection coefficients for both

NaCl and $NaHCO_3$ were not different from one.[164] Passive chloride transport has been characterized in the rabbit using *in vitro* microperfusion.[165,203,206] In both neonates and adults chloride permeability is extremely low, indicating that passive chloride transport does not contribute significantly to chloride absorption in this nephron segment.[206] The permeability of chloride in neonatal juxtamedullary proximal convoluted tubules is more than 10-fold lower than that of the adult segment.[206] In adult rabbit proximal straight tubules there is a substantive rate of passive chloride transport[165,203]; however, the neonatal rabbit proximal straight tubule is impermeable to chloride. Thus, there is no passive NaCl transport in the neonatal proximal straight tubule.[165,203]

The maturational changes in passive paracellular transport indicate there must be a developmental change in the composition of tight junction proteins. The tight junction creates a barrier and mediates the paracellular properties of the paracellular pathway.[236] Occludin, a protein with a ubiquitous distribution, and claudins, a family of tight junction proteins that number over 20, have four membrane spanning domains forming two extracellular loops that adjoin with their partner on the neighboring cell.[236] The permeability properties, including the ion permeability and resistance of epithelia, are determined predominantly by the isoforms of the claudins in the tight junction. Using semiquantitative real-time PCR of individually dissected tubules, there was no difference in the mRNA expression of claudins 1, 2, 10a, 12, and occludin in neonates compared to adult proximal tubules. However, claudins 6 and 9 were present in neonatal proximal tubules, but were absent in the adult segment.[1] Expression of claudins 6 and 9 in Madin–Darby canine kidney II (MDCK II) cells, which have a low resistance and do not express these claudin isoforms, resulted in an increase in the paracellular resistance and increased sodium-to-chloride and bicarbonate-to-chloride permeability ratios.[179] In addition, expression of claudin 6 and claudin 9 in MDCK II cells resulted in a decrease in the transepithelial chloride permeability.[179] Thus, the expression of claudin 6 and 9 in neonatal proximal tubule is likely the cause for the higher resistance and the lower chloride permeability than in the adult tubule.

Distal Tubule NaCl Transport

The thick ascending limb and distal convoluted tubule reabsorb NaCl, and are impermeable to water. The osmolality of the luminal fluid collected by micropuncture of rat early distal tubules is 40% lower in adults compared to neonates,[253] and the fraction of filtered sodium remaining in the early distal tubule is higher in neonatal than adult rats,[10] consistent with a maturational increase in the rate of sodium transport in the thick ascending limb. *In vivo* micropuncture of 13- to 39-day-old rats showed an increase in loop NaCl reabsorption during postnatal maturation,[133] and *in vitro* microperfusion of the rabbit cortical thick ascending limb demonstrated that the rate of sodium transport in the adult segment is five-fold greater than that of the neonate.[107] Both rat and rabbit cortical and medullary thick ascending limb Na^+/K^+-ATPase activity increase approximately four-fold during postnatal maturation, consistent with a large developmental increase in sodium reabsorption by both segments.[167,188] A direct comparison of NaCl transport in neonatal and adult medullary thick ascending limb has not been performed; however, there is a maturational increase in Na^+/K^+-ATPase activity in this segment.[69,167,188]

Compared to adults, neonates have a limited capacity to excrete a sodium load which is not due solely to a lower GFR.[9,65,87] None of the nephron segments discussed thus far is responsible for this phenomenon, as this requires a segment where the relative transport rates are higher in neonates than in adults. The adult distal convoluted tubule reabsorbs only 5% of the filtered sodium, but sodium transport rates are higher in neonates.[10] In an *in vivo* micropuncture study, distal tubule transport was assayed during hydropenia and during volume expansion in 24- and 40-day-old rats. While 24-day-old hydropenic rats had a higher fraction of filtered sodium remaining in the early distal tubule than 40-day-old animals, this difference had disappeared by the late distal tubule puncture site. With volume expansion there was a comparable fraction of filtered sodium remaining in the early distal tubule in the two age groups, but there was enhanced late distal tubule sodium reabsorption in the younger rats.[10] Thus this segment is, at least in part, responsible for the blunted natriuresis with salt-loading in neonates.

The cortical collecting duct is the nephron segment responsible for the final modulation of sodium transport under the control of aldosterone. In the isolated perfused cortical collecting tubule, there is a three- to five-fold increase in sodium transport between one-week-old and adult rabbits.[180,237] Most of the maturational increase occurs between the first and second weeks of life. Sodium entry in the neonatal and adult cortical collecting tubule is via an apical sodium channel termed ENaC. ENaC is the rate-limiting step in collecting tubule sodium transport, and neonatal cortical collecting ducts have fewer apical conducting sodium channels than adult segments[112,184](Figure 27.5). ENaC is composed of α-, ß-, and γ- subunits, and the mRNA and protein abundance of each increases during postnatal life.[112,238,241,254] The driving force for conductive sodium entry across the apical conductance is the

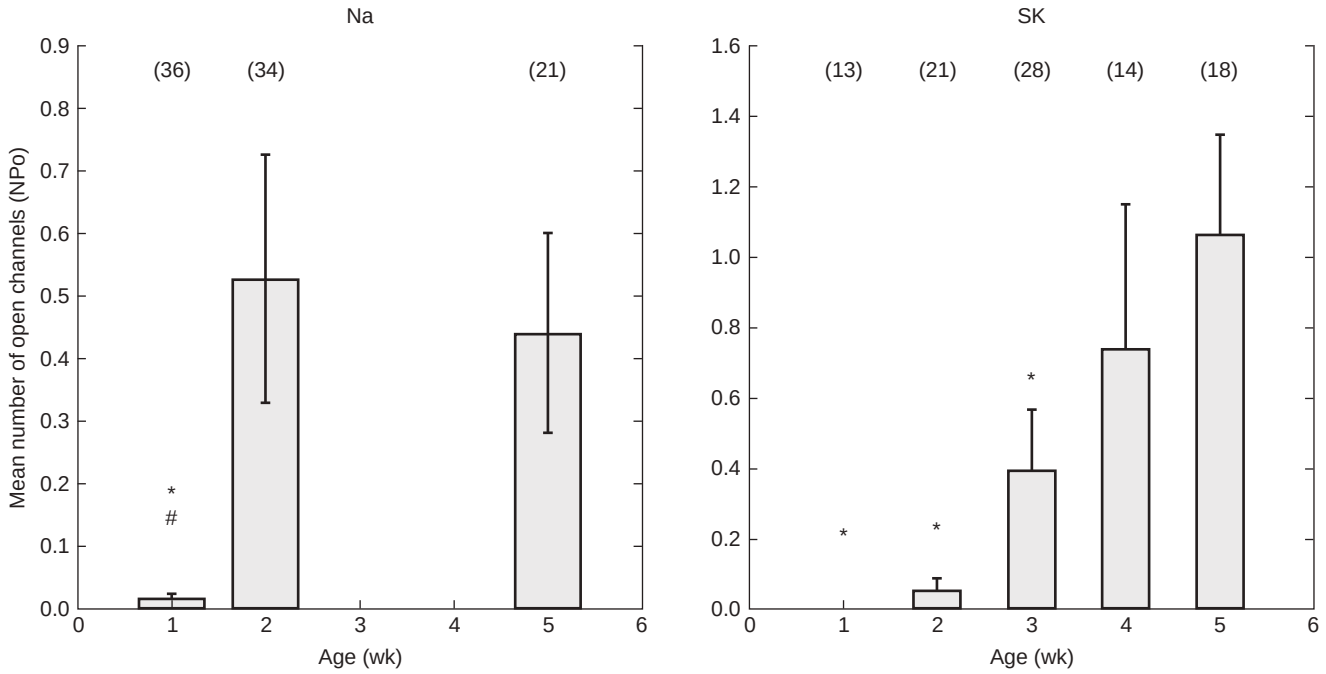

FIGURE 27.5 **Postnatal changes in number of conducting Na (ENaC) and secretory potassium (SK) channels per cell-attached patch of apical membrane of rabbit principal cells.** The number of functional Na channels increased ~30-fold between the first and second weeks of life, whereas the number of SK channels increased gradually after the second postnatal week *(from ref. [184] with permission).*

basolateral Na^+/K^+-ATPase, which increases in activity two-fold during maturation in this segment.[188] Interestingly, the fetal collecting duct expresses the Na^+/K^+-ATPase on the apical membrane; the significance of this is unknown.[50,108]

REGULATION OF SODIUM TRANSPORT

Renin–Angiotensin–Aldosterone

Plasma renin activity is higher in the neonate than the adult, and increases appropriately to a reduction in extracellular fluid volume in the fetus, premature infant, and neonate.[71,86,141,225] Plasma aldosterone levels are also significantly higher in preterm and term neonates than in adults.[8,34,141,210,225] Cord blood from term infants born to mothers who ingested a normal salt diet had significantly lower plasma aldosterone levels than those whose mothers ingested a low-salt diet or who were taking diuretics.[34] These data imply that the human fetus can also respond to volume contraction with an increase in serum aldosterone. The plasma aldosterone level has also been shown to vary inversely with sodium intake in preterm infants with respiratory distress syndrome.[210] Although the newborn can increase aldosterone secretion, the effect of aldosterone to increase distal tubule sodium reabsorption and potassium secretion is blunted compared to adults.[8,141,225] For example, in adult rats, adrenalectomy produces a 40-fold increase in urinary Na/K ratio, but in neonatal rats adrenalectomy has no effect on urinary electrolyte excretion.[222] Administration of exogenous aldosterone to adult adrenalectomized rats decreases the urinary Na/K ratio profoundly, but administration of aldosterone has no effect on urinary electrolytes in adrenalectomized neonatal rats.[222] Isolated perfused cortical collecting tubules from adult rabbits treated with mineralocorticoid had a significant increase in sodium absorption compared to control rabbits, but neonatal cortical collecting tubules were unaffected by prior mineralocorticoid treatment.[237] This resistance to aldosterone in neonatal rats is not due to a paucity of mineralocorticoid receptors, but is a postreceptor phenomenon.[222] However, in the mouse the blunted effect of aldosterone may also be due to fewer mineralocorticoid receptors compared to adults.[141]

Angiotensin II augments proximal and distal tubule sodium reabsorption by binding to both basolateral and luminal receptors. While neonatal rats have a blunted diuresis and natriuresis in response to volume expansion,

this was not the case in neonates which received Losartan, an AT_I receptor blocker, consistent with angiotensin II playing an important role in the regulation of sodium absorption in the neonate.[56]

Renal Nerves and Catecholamines

Renal nerve stimulation produces an increase in renal vascular resistance and reduction in renal blood flow in the fetus and newborn, although the effect is less in immature animals compared to adults.[174] Renal denervation of the fetal and neonatal lamb does not significantly alter renal blood flow, GFR or renal sodium handling, indicating that basal renal function is not significantly affected by renal nerves.[172,214,215] However, in the transition from fetal to neonatal life, renal nerves play a role in the decrease in sodium excretion that occurs during this period.[216] Sheep with denervated kidneys had a greater urine volume and sodium excretion in the first 24 hours after birth, as well as lower plasma atrial natriuretic peptide and renin levels.[216] There is no difference in urinary sodium or volume excretion after the first day of life, indicating that other unknown variables play an important role in mediating the profound decrease in urinary sodium and volume excretion after birth.[216]

Dopamine is a natriuretic hormone whose plasma levels are increased with volume expansion. Dopamine increases renal blood flow and GFR, and inhibits sodium transport in the proximal tubule, thick ascending limb, and collecting duct.[6] The concentration of dopamine is higher in fetal rat plasma and amniotic fluid than in the maternal blood.[39] Administration of exogenous dopamine to human premature neonates with respiratory distress syndrome increases GFR, and produces a natriuresis and diuresis.[234] However, comparative studies demonstrate that the effect of dopamine on the Na^+/H^+ exchanger and Na^+/K^+-ATPase is less in neonatal than adult tubules.[6,82,119,136]

RENAL ACIDIFICATION

The serum bicarbonate concentration in human infants in the first year of life averages 22 mEq/l, a value significantly less than that of adults.[74] Premature human neonates can have serum bicarbonate levels as low as 14.5 mEq/l.[193] The lower serum bicarbonate concentration in neonates and infants is due to a lower threshold for bicarbonate by the immature kidney.[74] This section will discuss the salient differences between the neonatal and adult kidney with regard to renal acidification.

Proximal Tubules

The adult proximal tubule reabsorbs 80% of the filtered bicarbonate. The lower bicarbonate threshold in neonates is, in large part, due to a lower bicarbonate reabsorptive capacity of the neonatal proximal tubule. In rabbit juxtamedullary proximal convoluted tubules perfused *in vitro*, the rate of bicarbonate reabsorption in proximal tubules from one-week-old rabbits is one-third that of the adult proximal tubule.[190] The rate of bicarbonate absorption does not change significantly until the time of weaning at four weeks of age. At six weeks of age, the rate of bicarbonate absorption is comparable to the adult. The maturational pattern of glucose and total volume reabsorption is quite similar to that for bicarbonate absorption.[190] The rate of bicarbonate absorption has not been directly measured in superficial nephrons. However, micropuncture studies in rats and *in vitro* microperfusion studies in rabbits have demonstrated a similar maturational increase in the rate of volume absorption in these segments.[11,130,133] Since a substantial fraction of volume absorption reflects bicarbonate absorption, a similar maturational pattern for bicarbonate is likely.

There are several potential explanations for the lower rate of bicarbonate transport in neonatal proximal tubules. In the adult proximal tubule there is a preferential reabsorption of bicarbonate over chloride ions. This leaves the luminal fluid with a higher chloride concentration and a lower bicarbonate concentration than that in the peritubular capillaries. This bicarbonate concentration difference could potentially allow bicarbonate to diffuse from the peritubular capillaries back to the luminal fluid. The amount of bicarbonate passive backflux is dependent upon the permeability of the paracellular pathway of the neonatal proximal tubule to bicarbonate.[123,162,165,203,205,206] However, bicarbonate permeability in juxtamedullary rabbit proximal convoluted tubules is less in neonatal juxtamedullary proximal tubules perfused *in vitro* than that of the adult segment.[162] Thus, the lower rate of bicarbonate transport in neonatal juxtamedullary proximal tubules is not explained by enhanced back diffusion, but is entirely due to a lower rate of active transcellular bicarbonate transport.

In the adult proximal tubule, two-thirds of apical proton secretion is mediated by the Na^+/H^+ exchanger and one-third is via an H^+-ATPase.[21,160] The driving force for the Na^+/H^+ exchanger is the low intracellular sodium concentration generated by the Na^+/K^+-ATPase. In the adult proximal tubule bicarbonate, exit is via the $Na(HCO_3)_3$ co-transporter. A lower rate of bicarbonate reabsorption by the neonatal proximal tubule could be due to a lower activity of any of these transport processes.

Studies using a variety of different techniques have demonstrated a maturational increase in proximal tubule apical membrane Na^+/H^+ exchanger activity.[20,21,31,202] In isolated perfused rabbit juxtamedullary proximal convoluted tubules the rate of Na^+/H^+ exchanger activity is approximately one-third that of the adult rate, and adult values are reached at six weeks of age.[20] These results compare well to the maturational changes in bicarbonate absorption measured in isolated perfused rabbit convoluted tubules.[190] While this study solely examined juxtamedullary proximal tubules, similar findings have been demonstrated in brush border membrane vesicles from the renal cortex.[31] Na^+/H^+ exchanger activity in late rabbit fetal kidney cortex is 25% that of the adult cortex. This difference is entirely due to a lower V_{max}, and not to a difference in the K_M for sodium.[31]

The H^+-ATPase, present on the apical membrane of the adult proximal tubules, does not contribute significantly to bicarbonate absorption in the neonatal proximal tubule. To study the relative contribution of the Na^+/H^+ exchanger and the H^+-ATPase to proximal tubule acidification, the rates of these two transporters were assayed by measuring proton secretory rates in adult and neonatal proximal convoluted tubules in response to an intracellular acid load.[21] As has previously been demonstrated, the rate of neonatal Na^+/H^+ exchanger activity is less than that in the adult. In the adult rabbit proximal tubule two-thirds of the pH recovery from an acid load is due to the Na^+/H^+ exchanger, and one-third is due to the the H^+-ATPase. In the neonate, 95% of pH recovery is due to the Na^+/H^+ exchanger, and only 5% is due to a sodium-independent mechanism. Thus, both the Na^+/H^+ exchanger and the H^+-ATPase undergo a significant increase in activity during maturation, and presumably limit bicarbonate absorption by the neonatal proximal tubule.

Three isoforms of the Na^+/H^+ exchanger, NHE1, NHE3, and NHE8 have been localized to the proximal tubule.[39,40,91,255] NHE1 has a ubiquitous distribution in tissues, and is found on the basolateral membrane of the proximal tubule.[40] NHE1 protein abundance does not vary significantly with postnatal maturation.[24] NHE3 is the apical membrane Na^+/H^+ exchanger mediating most luminal proton secretion by the adult proximal tubule.[39,249] There is a substantive postnatal maturational increase in NHE3 mRNA and protein abundance.[24] Interestingly, neonates have Na^+/H^+ exchanger activity at a time when NHE3 protein abundance is barely detectable.[202] The disparity between the presence of Na^+/H^+ exchanger activity and the paucity of NHE3 in the proximal tubule of neonates is due to the presence of NHE8.[33] NHE8 is predominantly an intracellular sodium–hydrogen exchanger that is also abundantly expressed on the apical membrane in neonates. Brush border membrane NHE8 decreases in abundance during postnatal maturation[33] (Figure 27.6). The factors responsible for this isoform switch will be discussed below.

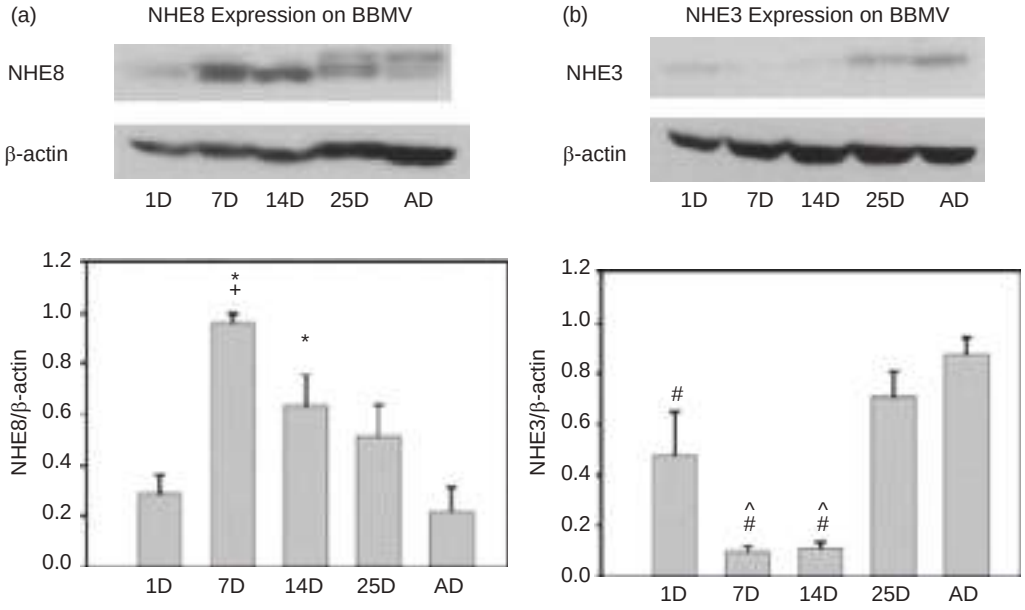

FIGURE 27.6 **Developmental change in brush border membra 33 ne NHE8 (a) and NHE3 (b) compared to β-actin.** NHE8 increased during postnatal development with a reciprocal increase in NHE3. *$P < 0.05$ vs. 1D and AD; +$P < 0.05$ vs. 26D; #$P < 0.05$ vs. 26D and AD; ^$P < 0.05$ vs. 1D. *(from ref. [33] with permission).*

The basolateral membrane $Na(HCO_3)_3$ co-transporter facilitates bicarbonate exit from the proximal tubule. $Na(HCO_3)_3$ symporter activity in neonates is only slightly less than that of adults.[20] This transporter not only plays a role in bicarbonate exit, but is also the predominate mechanism for the defense against changes in intracellular pH by the proximal tubule.[20]

Distal Tubule Acidification

The adult cortical collecting duct can absorb or secrete bicarbonate depending on the acid–base status of the animal.[146] Proton and bicarbonate secretion are mediated by α- and β-intercalated cells, respectively, which are far fewer in number than principal cells, the predominant cell in the cortical collecting duct. The number of α- and β-intercalated cells per millimeter of tubular length increases several-fold during maturation of the rabbit cortical collecting duct.[77,183] β-intercalated cells start to appear in the mouse cortical collecting tubule in the first week of life.[217] While β-intercalated cells are present in the outer medullary collecting duct of the neonate, they disappear by apoptosis and are no longer present in this segment by 2–3 weeks of age.[48,217]

Net bicarbonate transport in the cortical collecting tubule is dependent on the relative rates of bicarbonate absorption and secretion. In isolated perfused cortical collecting tubules from neonatal rabbits there is no net bicarbonate transport, whereas adult cortical collecting ducts secrete bicarbonate.[147] Bicarbonate secretion by the β-intercalated cell is via an apical chloride-bicarbonate exchanger that functions at a reduced rate in the neonatal segment.[183] Removal of bath chloride inhibits basolateral membrane chloride-base exchange on α-intercalated cells and inhibits luminal proton secretion. Removal of bath chloride had no effect on the rate of bicarbonate transport in cortical collecting tubules from neonatal rabbits, but increased net bicarbonate secretion in adult segments, indicating that there is a maturational increase in the cortical collecting tubule to secrete bicarbonate.[147] The bicarbonate absorptive capacity of the α-intercalated cell in the cortical collecting duct also increases during postnatal maturation.[183,186] The outer medullary collecting duct is an important segment for urinary acidification. Unlike the cortical collecting tubule, the number of intercalated cells per millimeter of tubular length does not change significantly with postnatal development.[77,186] The rate of bicarbonate absorption is only slightly less in the neonatal outer medullary collecting ducts compared to the adult rabbit segment.[147] Thus, there is a significant difference in the relative maturity of the cortical and medullary segments in neonates.

Titratable Acid and Ammonia Excretion

In addition to reclaiming the filtered load of bicarbonate, the kidney must excrete an amount of acid equivalent to the acid generated from metabolism. The growing animal must also excrete protons liberated during the formation of bone.[125,126] This is in part compensated for by the gastrointestinal absorption of alkali in the neonate,[125,126,240] but as in the adult, the neonatal kidney plays a major role in acid excretion. Thus, the kidney of the growing neonate must excrete 50–100% more acid per kg than the adult.

To excrete the quantity of acid generated from metabolism of proteins and growing bones, there must be urinary buffers to accept the secreted protons. If there were no titratable acids and ammonia in our urine, the secretion of a few protons would decrease the urine pH to levels that would inhibit further proton secretion. Net acid excretion, the sum of ammonium and titratable acid excretion per kg body weight, is significantly less in neonates than adults.[144] However, by seven days of age cows milk formula-fed infants have comparable rates of ammonium and titratable acid excretion as that of adults when normalized per kg of body weight.[142,144] Breast milk-fed infants, however, have significantly less phosphate intake and lower rates of titratable acid excretion than infants fed cows milk formula.[66,80,102,144] Thus, the rate of renal maturation of net acid excretion is quite brisk. However, unlike adults, human neonates function at near maximal capacity of net acid excretion to eliminate metabolically generated acid,[142] and have a limited ability to respond to an exogenous acid-load by increasing titratable acid and ammonia excretion.[142] In comparison to adults, neonates given an acid-load have a smaller increase in both titratable acid and ammonium excretion, making them more prone to develop acidosis when so challenged.[60,102] By one month of age the rate of net acid excretion in response to an acid-load is comparable to that of adults.[74,90,152,158,228] However, young infants respond to an acid-load with higher rates of titratable acid excretion to compensate for the lower rates of ammonium excretion.[74,152] *In vitro* studies have shown that the rate of renal ammonia production in kidney slices is lower in neonates compared to adults.[105] The low rate of ammonia production is in part due to lower glutamine synthetase activity limiting glutamine availability, but predominantly due to lower glutaminase activity.[89,239] As in adults, glutaminase activity increases substantively in response to an acid-load.[36] Premature neonates have significantly lower rates of titratable acid and ammonia excretion than term infants.[124,226,229] Preterm infants are thus less tolerant of a high protein formula than term infants, because sulfur containing amino acids generate an

acid-load which cannot be eliminated due to the low rates of net acid excretion.[63,228] Administration of NH_4Cl to premature infants resulted in an increase in net acid excretion, but premature infants had lower rates of ammonium and titratable acid excretion, and a higher urine pH, than term neonates.[90,124,226,227,229] As with term infants, there is a rapid maturation of the ability of premature infants to excrete an exogenous acid-load.[124,226,229]

Carbonic Anhydrase Activity

Carbonic anhydrase facilitates the reversible hydration of CO_2 to H_2CO_3.[161,192] Carbonic anhydrase is localized to all acidifying nephron segments, where it plays an important role in acidification. For example, carbonic anhydrase inhibition results in a 90% decrease in the rate of proximal tubule bicarbonate reabsorption.[139] There are 15 carbonic acid isoforms, with both species- and nephron segment-specificity.[161]

Carbonic anhydrase II is located in the cytosol of all acidifying renal tubules, and comprises 95% of carbonic anhydrase activity in the kidney.[120] Carbonic anhydrase IV comprises approximately 5% of total renal carbonic anhydrase activity, and is located on the apical and basolateral membrane of the proximal tubule and on the apical membrane of acid-secreting cells in the distal nephron.[192,194,195,245] Carbonic anhydrase XII is present on the basolateral membrane of acidifying segments.[156] In rodents, carbonic anhydrase XIV is also expressed on the apical membrane of the proximal tubule and thick ascending limb.[161] Carbonic anhydrase II protein abundance, normalized per millimeter of tubular length, increases approximately 10-fold in rat proximal convoluted tubules, cortical collecting tubules, and outer medullary collecting tubules between one and twelve weeks of age.[120] In the rabbit, carbonic anhydrase II increases only two-fold during postnatal maturation compared to carbonic anhydrase IV, which undergoes a ten-fold increase in mRNA and protein abundance with cortical maturation.[195,245] Thus, the developmental increase in carbonic anhydrase may be a factor in the postnatal increase in renal acidification.

INDUCTION OF NEPHRON MATURATION

As noted above, there are a number of quantitative and qualitative changes that occur in all nephron segments during postnatal development. Most of the studies examining the factors responsible for the postnatal changes during development come from studies of the proximal tubule, which will be the focus here. There are a number of potential factors which may be responsible for the postnatal maturational changes in proximal tubule transport. The maturational increase in GFR may induce the maturation of transporters on the apical membrane by increasing solute delivery. As previously discussed, an increase in apical membrane sodium transport could increase intracellular sodium and play a potential role in the maturational increase in Na^+/K^+-ATPase activity.[61,101,131] There are also significant postnatal maturational changes in several hormones which affect proximal tubular transport, including thyroid hormone and glucocorticoids, which increase 3-fold and 20-fold, respectively, in the postnatal period.[104]

Glucocorticoids increase renal cortical Na^+/H^+ exchanger activity. This effect can, in part, be mediated by an increase in GFR which will increase sodium delivery to the proximal tubule. However, glucocorticoids and thyroid hormone have a direct epithelial action on the proximal tubule to increase the rate of bicarbonate absorption and Na^+/H^+ exchanger activity.[22,25] This effect of glucocorticoids and thyroid hormone on NHE3 is due to an increase in NHE3 transcription.[22,52] However, glucocorticoids also increase apical membrane NHE3 by increasing the rate of exocytosis.[42] Administration of glucocorticoids to pregnant rabbits two days prior to the delivery increases the V_{max} of the Na^+/H^+ exchanger in neonates to levels the same as those seen in adults.[31] The K_m for sodium is comparable in neonates and adults. Similarly, proximal convoluted tubules from neonatal rabbits whose mothers received dexamethasone before delivery had infants with an almost two-fold increase in the rate of bicarbonate absorption to levels comparable to that measured in adult animals.[27] In addition, the rate of Na^+/H^+ exchanger and $Na(HCO_3)_3$ activity in proximal tubules increased two-fold in dexamethasone treated neonates.[27] The effect of dexamethasone is specific for the NHE3 isoform, the isoform present on the apical membrane of the proximal tubule and responsible for the majority of Na^+/H^+ exchanger activity in adults.[24] Prevention of the maturational increase of either glucocorticoids or thyroid hormone prevents the maturational increase in Na^+/H^+ exchanger activity and NHE3 protein abundance.[26,95] While glucocorticoids are the most important factor causing the maturational increase in NHE3, adrenalectomy in the neonatal period does not totally prevent an increase in both Na^+/H^+ exchanger activity and NHE3 protein and mRNA abundance, suggesting that thyroid hormone can compensate, to some extent, in the absence of glucocorticoids.[95] This was definitively demonstrated in studies using hypothyroid-glucocorticoid-deficient rats, where the maturational

increase in both hormones was prevented, and where Na^+/H^+ exchanger activity, NHE3 protein, and mRNA abundance remained at neonatal levels into adulthood.[94] As noted, there is an isoform switch from NHE8 to NHE3 during postnatal development.[33] The maturational decrease in NHE8 on the apical membrane of the proximal tubule is due the postnatal increase in thyroid hormone.[84] Administration of thyroid hormone to neonates resulted in a premature decrease in NHE8 and increase in NHE3 on brush border membranes, while prevention of developmental increase in thyroid hormone prevented the decrease in brush border membrane NHE8 abundance.[84] The regulation of NHE8 by thyroid hormone is due to a direct epithelial effect to decrease NHE8 surface expression, likely by post-transcriptional regulation.[84]

As will be discussed, there is a maturational decrease in the rate of phosphate transport during postnatal maturation.[57,66,106] This is observed at a time when there is an increase in serum glucocorticoid levels.[104] Administration of glucocorticoids to neonatal rats produced a significant inhibition in the rate of sodium-dependent phosphate uptake. This is due to a reduction in the V_{max} with no change in the K_M for phosphate.[16] This glucocorticoid-induced decrease in phosphate uptake was not accompanied by a change in NaPi-2a mRNA abundance; however, there was a three-fold decrease in NaP_i transporter protein abundance.[16] Thus, glucocorticoids play a role in the maturational decrease in phosphate transport.

Thyroid hormone appears to play an important role in postnatal development of mitochondrial enzymes in the rat proximal convoluted tubule. The normal maturational increase in the proximal tubule mitochondrial enzymes 3-keto acid-CoA transferase, an enzyme involved in ketone body oxidation, and citrate synthase and carnitine acetyltransferase were impaired in hypothyroid rats.[243] The enzyme activities were restored with thyroid replacement. Acetoacetyl-CoA thiolase, however, is not decreased in 21-day-old hypothyroid rats.[243] Finally, thyroid hormone plays a role in the maturational changes that occur in the permeability properties of the paracellular pathway.[28,205] As noted above, the adult rabbit proximal straight tubule has a high chloride permeability which results in high rates of passive chloride transport.[205] The neonatal rabbit proximal straight tubule is impermeable to chloride.[165] Neonatal proximal straight tubules have higher P_{Na}/P_{Cl} (sodium to chloride permeability ratio) and P_{HCO3}/P_{Cl} ratios than adult segments. Many, but not all, of the maturational changes in paracellular permeability properties of the proximal tubule can be accelerated by administration of thyroid hormone to neonates[205] or prevented if the neonates are made hypothyroid.[205]

PHOSPHATE TRANSPORT

Phosphate is essential for growth, and unlike adults growing animals are in positive phosphate balance. Human neonates and infants have a higher serum phosphate concentration than that of adults. While the high serum phosphate in neonates could be due to the lower GFR compared to adults, this is not the case. Studies have demonstrated that increasing the GFR by arginine infusion in young rats does not increase phosphate excretion, and lowering the GFR in adult rats by constricting the abdominal aorta does not increase the rate of phosphate absorption to that seen in the neonate.[99] The tubular reabsorptive capacity for phosphate is higher in neonates and infants than in adults.[57,66,106,171] Approximately 90–95% of the filtered phosphate is reabsorbed in human neonates during the first week of life, and growing children continue to maintain a higher maximal tubular reabsorption of phosphate than adults.[57,106]

A number of variables, such as intrinsic properties of phosphate transport in the proximal tubule, dietary phosphate content, parathyroid hormone, and growth factors can modulate phosphate transport, and could potentially explain the higher rate of phosphate transport by the neonatal kidney. The role of these factors has been extensively studied and will be reviewed in this section. A higher intrinsic rate of renal phosphate transport has been demonstrated in the isolated perfused guinea pig kidney where other *in vivo* factors were eliminated.[116] The maximal tubular reabsorption of phosphate per volume of glomerular filtrate in 3–7-day-old neonatal guinea pig kidneys is 40% greater than that measured in adult animals.[107] A higher intrinsic rate of proximal tubular phosphate reabsorption was also directly demonstrated in micropuncture studies, where 5–14 day neonatal guinea pigs reabsorbed a higher fraction of filtered phosphate than adults.[122] The maximal rate of phosphate uptake in brush border membrane vesicles (V_{max}) is five-fold higher in neonates than in adults, in the absence of a maturational change in the K_M for phosphate in growing animals.[154]

In addition to the difference in the rate of sodium-dependent phosphate co-transport with maturation, other intrinsic proximal tubular factors may play a role in the higher rates of phosphate transport in growing animals. The intracellular phosphate concentration (P_i) measured in isolated perfused kidneys using NMR was 40% lower in growing animals than in adults.[19] This provides a greater driving force for phosphate transport in growing animals. The lower intracellular phosphate concentration in the presence of a higher rate of apical phosphate transport implies that the rate

of basolateral phosphate exit is also higher in growing animals, although this has not been directly examined.

Membrane fluidity also has been shown to affect phosphate transport.[134,135,151] The brush border membrane content of cholesterol, sphingomyelin, and phosphatidylinositol increases with age.[135] This change in lipid composition decreases membrane fluidity,[135,151] which directly decreases the rate of phosphate transport.[134,151] Thus, the lipid composition and high membrane fluidity of the neonate and growing animal provides an environment which increases the V_{max} of the NaPi co-transporter. Glucocorticoids, which increase during the time of weaning, decrease membrane fluidity, and likely play a role in the postnatal decrease in phosphate transport.[16]

There are two sodium-dependent phosphate co-transporters, designated as NaPi-2a and NaPi-2c, present on the apical membrane of the proximal tubule that are primarily responsible for phosphate reabsorption.[140,197] In mice, NaPi-2a has been identified as the most important phosphate transporter in the kidney, responsible for ~70% of phosphate reabsorption.[32] NaPi-2a mRNA is first detected in early proximal convolutions in the post S-shaped body segment of the developing nephron.[189] However, NaPi-2a protein is not detected until the proximal tubules have a distinct brush border membrane.[231] Brush border membrane NaPi-2a expression is two-fold higher in 4-week-old juvenile rats than in adult rats, consistent with the higher rate of phosphate transport in growing animals.[246] A growth-specific NaPi co-transporter was postulated to be responsible for the increased phosphate transport in the weaning animals,[213] which was later identified as NaPi-2c.[197] NaPi-2c mRNA and protein expression is highest in the brush border of the convoluted proximal tubules of weanling rodents,[197] whereas it plays a negligible role in renal phosphate absorption in adults.[150,199,200] In contrast to rodents, NaPi-2c plays an important role in phosphate transport in humans. Mutations in NaPi-2c result in an autosomal recessive disorder termed hereditary hypophosphatemic rickets with hypercalciuria that is characterized by hypophosphatemia, due to renal phosphate-wasting, rickets, hypervitaminosis D, hypercalcemia, and hypercalciuria.[37,114]

Dietary phosphate content regulates renal phosphate transport in adult and in growing animals.[54,121,153,246] Thyroparathyroidectomized growing rats had a greater increase in their maximal tubular capacity for phosphate reabsorption in response to a low-phosphate diet and a blunted decrease in phosphate reabsorption on a high-phosphate diet compared to adult thyroparathyroidectomized rats.[54,153] In addition, the adaptive increase in maximal tubular capacity of phosphate reabsorption in response to phosphate deprivation took longer to occur in adult animals than in growing animals.[54] A low phosphate diet increases the rate of sodium-dependent phosphate uptake by brush border membrane vesicles in growing rats.[55] In addition, ingestion of a low-phosphate diet increases the abundance of Na-Pi transporters on the apical membrane of the proximal tubule, whereas a high-phosphate diet produces the opposite effect.[246] The dietary changes in phosphorus affect both brush border membrane NaPi-2a and NaPi-2c expression.[197,198]

The plasma concentration of PTH is lower in human neonates than in adults.[64] Fetal and neonatal rats can respond to changes in serum calcium with appropriate changes in PTH levels,[230] although there is a blunted response to PTH secretion.[242] Infusion of PTH in one-day-old human neonates produces no increase in urinary phosphate excretion.[57,137] By three days of age, infusion of parathyroid hormone results in an increase in phosphate excretion and increase in urinary cAMP.[57,137,145] However, the phosphaturic response to PTH is markedly lower in neonates than adults.[137] Furthermore, in micropuncture studies, the proximal tubule response to infusion of pharmacologic doses of PTH is attenuated in young rats compared to adults.[246] Despite the fact that PTH did not significantly increase phosphate excretion in young animals, the urinary cAMP corrected for GFR in response to PTH infusion was similar in all ages.[242] Thus, there is clearly a disassociation between the PTH-induced increase in cAMP production in neonates and the effect on phosphate excretion. The blunted response to PTH in the neonate compared to the adult is due to lower levels of phospholipase A2 activity in response to PTH and cAMP.[207]

Growth hormone administration can result in an increase in serum phosphate.[103] Brush border membrane vesicle phosphate transport is increased in dogs that received growth hormone compared to controls.[97] The effect of growth hormone on phosphate transport is mediated by IGF-1.[163] While growth hormone is not a significant regulator of phosphate transport in the adult, this may not be the case in the growing animal. Administration of growth hormone-releasing factor antagonist, which suppresses growth hormone secretion, has no effect on the maximal rate of phosphate absorption in adult rats, but significantly reduces phosphate absorption in growing rats.[100]

In addition to PTH, there are a number of hormones, known as phosphatonins, that regulate phosphate transport, including fibroblast growth factor-23 (FGF23),[29,209] secreted frizzled-related protein 4 (sFRP-4),[38] matrix extracellular phosphoglycoprotein,[49] fibroblast growth factor 7 (FGF7),[53] and dentin matrix protein-1(DMP1).[78] These hormones are dysregulated in a number of diseases with aberrant phosphate regulation, incuding X-linked hypophosphatemia and

tumor-induced osteomalacia.[83] The role of these phosphatonins in the developmental changes in phosphate transport remains to be elucidated.

POTASSIUM TRANSPORT

Potassium is transported actively across the placenta from mother to fetus,[201] ensuring that the fetal plasma potassium concentration is maintained at levels exceeding 5 mEq/L, even in the face of maternal potassium deficiency.[62,201] Both premature and term neonates have very low rates of renal potassium excretion, which maintains a positive potassium balance necessary for growth.[68,225] The low rate of renal potassium excretion is also responsible, at least in part, for the higher serum potassium concentration in neonates than in adults.[225] Renal potassium clearance in infants less than one year of age is less than that of older children, even if corrected for GFR.[181,225] Neonates can respond to potassium-loading with net tubular secretion, but this response is less than that of adults.[138,233]

The proximal tubule of neonatal and adult rats reabsorbs approximately 50% of the filtered potassium.[133] There is a maturational increase in potassium reabsorption by the loop of Henle.[70,133] The loop of Henle of adult rats has been shown to reabsorb 79% of the delivered load, while only 56% was reabsorbed by 13–15-day-old neonates.[133] The limited capability of the thick ascending limb of the neonate to reabsorb potassium will increase distal delivery of potassium. Thus, neither the proximal tubule nor the loop of Henle is responsible for the limited capability of the neonate to excrete potassium.

The distal convoluted and connecting tubules and cortical collecting duct ultimately regulate potassium excretion in adults and neonates. Clearance studies in dogs have demonstrated that the amiloride-sensitive (i.e., EnaC-dependent) component of potassium secretion is substantially less in neonates than adults, providing indirect evidence for a limited distal nephron potassium secretory capacity.[138] The developmental maturation of potassium transport in the distal nephron has been directly examined in the rabbit cortical collecting duct by *in vitro* microperfusion.[180] Baseline potassium secretory rates are not different than zero during the first three weeks of life, and did not reach mature rates until six weeks of age.[180]

The limited capacity of the distal nephron for net potassium secretion could be due to either an unfavorable electrochemical gradient across the apical membrane and/or a limited apical potassium permeability. The rate of net sodium absorption in the cortical collecting duct of the two-week-old animal is approximately 60% of that measured in the adult,[81] reflecting the rapid appearance of conducting ENaC channels in the apical membrane of this segment between the first and second weeks of life.[184] Thus, the electrochemical gradient is not considered to be limiting for potassium secretion at this age. While low rates of luminal flow and distal sodium delivery can limit potassium secretion in adults, these are unlikely to be significant variables in neonates, which have high rates of distal nephron flow and sodium delivery.[10,133]

In support of the notion that a paucity of plasma membrane potassium channels limits potassium secretion early in life is the observation that the intracellular potassium concentration in the distal nephron at birth is comparable to that measured in the adult,[182] despite Na^+/K^+-ATPase activity that is only 50% of that measured in adult.[59,188] Direct analysis of the apical potassium conductance of CCDs isolated from maturing rabbits showed that the mean number of open channels per patch (NPo) increased progressively after birth[185] (Figure 27.5).

Two populations of apical potassium channels have been identified by patch-clamp analysis in the collecting duct. The secretory K (SK) channel, encoded by ROMK and restricted to principal cells, is a small conductance channel with a high open probability. The SK/ROMK channel is considered to mediate baseline potassium secretion.[185] High conductance BK channels, present in both principal and intercalated cells, are activated by increases in intracellular calcium concentration and stretch, but are rarely open at physiological membrane potentials. BK channels mediate flow-induced potassium secretion, which does not appear until the fifth week of postnatal life.[247,248] The temporal delay between the postnatal increases in SK/ROMK and BK channel activity accounts for the sequential appearance of basal- and then flow-induced net potassium secretion at 3 and 5 weeks, respectively, of postnatal life in the rabbit. Specifically, SK/ROMK channel activity increases progressively after the second week of postnatal life,[185] whereas functional BK channel activity does not appear until 5 weeks of age in the cortical collecting duct.[248] Both developmental processes closely parallel increases in channel-specific mRNA levels and immunodetectable protein at the apical membrane of the CCD.[35,248,254]

The H^+/K^+-ATPase is a third potassium transporter, present in the apical membrane of intercalated cells in the distal nephron. The H^+/K^+-ATPase has little functional role except under conditions of potassium deficiency and metabolic acidosis, when it mediates potassium absorption and proton secretion. The activity of this transporter is comparable in neonates and adult collecting tubules.[58]

URINARY CONCENTRATING AND DILUTING ABILITY

Deprived of water for sufficient time, an adult human can concentrate urine to 1200 mOsm/Kg water, while the term and premature neonatal kidney can achieve urine osmolalities of only 400−600 mOsm/Kg water.[79,98,157,159] By six months of age, the human infant can increase the urine osmolality to 600 mOsm/Kg water[159] and by 1 to 1.5 years the human infant can concentrate the urine to levels comparable to that of an adult.[159,244] The neonate also has a limited capacity to excrete free water compared to that of adults.[132,143] However, both term and premature infants can excrete dilute urine with an osmolality approaching 50 mOsm/Kg water.[176] Thus, the primary limiting factor in the ability of the neonate to excrete free water is the low GFR that limits the distal delivery of fluid.

The ability to maximally concentrate urine requires vasopressin secretion from the neurohypophysis, a hypertonic renal medulla and a renal collecting duct that responds to vasopressin by increasing water permeability. In the developing human, there are a number of factors in the concentrating mechanism that limit the ability to maximally concentrate urine. The neonate and late gestation fetus respond to changes in plasma osmolality and volume with appropriate changes in plasma vasopressin.[96,168] These changes in plasma vasopressin are of comparable magnitude to that measured under similar conditions in the adult.[168] Perinatal stress also results in the secretion of vasopressin.[96,170] However, infusion of vasopressin in the late gestation fetal sheep resulted in a smaller increase in urinary osmolality than that measured in adult animals.[175] Thus, while the fetus and neonate can secrete vasopressin at concentrations comparable to the adult, there is a hyporesponsiveness to the renal effect of vasopressin to increase urinary osmolality.

The osmotic gradient in the renal medulla is composed of urea and sodium chloride. The urea concentration in the neonatal renal medulla is limited in part by the low dietary protein intake and the high volume of fluid ingested.[72,73] Augmentation of protein or addition of urea to the diet of neonates increases their maximal concentrating ability, albeit not to the levels measured in adults.[72,73] Urea must get into the interstitium, which is facilitated by the urea transporter (UTA) located in the inner medulla. The abundance of UTA-1, which is also regulated by vasopressin, increases during postnatal maturation.[128] The capacity of the thick ascending limb to reabsorb sodium chloride, necessary to generate a hypertonic medulla, is less in the neonate compared to that of an adult.[10,107,110,167,188,253] The developmental changes that occur in transport with age in the thick ascending limb are paralleled by an increase in the concentration of sodium and urea in the medulla and papilla.[168,221] In addition, the sorbitol concentration in the inner medulla, a major intracellular osmolyte formed by aldose reductase, is significantly less than that in the adult.[196] Fluid restriction increases aldose reductase activity in the adult medulla, but not in the neonate.[196]

The urinary concentrating ability of neonatal rats can be induced prematurely by the administration of glucocorticoids,[168,224] likely due to the premature induction of the NKCC2 in the medullary thick limb.[224,252] Adrenalectomy in rats on day 16 of life prevents the maturational increase in papillary sodium and urea concentration, but not the growth of the papilla, consistent with a role of glucocorticoids in the maturation of the tubular transport processes responsible for development of maximally concentrated urine.[168] However, adrenalectomy at 10 days of life in rats results in a poorly-developed papilla and an increase in medullary cyclooxygenase-2 protein abundance and PGE_2 levels. Administration of glucocorticoids alone to adrenalectomized neonatal rats increased, but did not normalize, urine osmolality,[223] which required both glucocorticoid and mineralocorticoid replacement.[223] The requirement for mineralocorticoids may be due to their effect of decreasing medullary cyclooxygenase-2 levels, since prostaglandins cause a natriuresis and diuresis.[223]

The osmotic water permeability of the adult and neonatal inner medullary collecting duct are very low in the absence of vasopressin.[212] Vasopressin causes an increase in cAMP that increases protein kinase A activity. Protein kinase A phosphorylates aquaporin 2, resulting in trafficking of the protein to the apical membrane and an increase in apical membrane water permeability.[43] In both the outer and inner medullary collecting collecting duct, vasopressin results in an increase in osmotic permeability, yet the response is far less than that measured in the adult segment.[111,212]

The limited response to vasopressin by the neonatal collecting tubule is due to several factors. There are fewer vasopressin-binding sites in the medullary and cortical collecting duct in the neonatal rat compared to the adult,[5,43] but is not likely to be a significant factor limiting renal concentrating ability.[30,166] Aquaporin-2 is less abundant in the renal medulla of neonatal rats than in adult animals.[45,250,252] Both aquaporin-2 mRNA and protein abundance increase with neonatal betamethasone administration,[252] providing further evidence that glucocorticoids are important in the maturation of the urinary concentrating mechanism. In the neonatal rat kidney aquaporin-2 expression and trafficking increase appropriately in response to both water deprivation and vasopressin administration.[45] The

basolateral water channels, aquaporin-3 and -4 do not change significantly with postnatal development.[30,127,250]

The basal cAMP level is comparable in immature and adult cortical collecting ducts. However, there is a diminished stimulation of cAMP production in response to vasopressin in neonates compared to that of adults.[46] Forskolin, which directly activates adenylate cyclase, does not stimulate cAMP levels in the cortical collecting duct to the same extent as the adult tubule,[46] due to elevated phosphodiesterase activity which degrades cAMP in neonatal tubules compared to adult tubules.[166] In the presence of inhibitor of phosphodiesterase IV, the neonatal collecting duct water permeability was comparable to the adult in response to vasopressin.[166] Thus, developmental change in phosphodiesterase plays an important role in the development of the concentrating ability by degrading the generated cAMP. The limited vasopressin-mediated increase in cAMP levels in the neonatal collecting tubule due to increased degradation is the predominant factor impairing the action of vasopressin to increase water permeability.[46]

Prostaglandins could also play a role in the limited response of the neonatal collecting duct to vasopressin, since prostaglandins impair cAMP production.[46] While one study showed decreased PGE_2 production in neonatal cortical collecting tubules,[187] others have demonstrated both higher rates of production and greater abundance of G_i-coupled EP_3 (prostaglandin) receptors.[44,148] cAMP production in response to forskolin and vasopressin in neonatal and adult tubules are comparable when incubated with indomethacin to inhibit prostaglandin production.[44] However, when neonatal collecting ducts were perfused *in vitro*, there was no difference in water permeability in the response to vasopressin in presence or absence of indomethacin.[47] Thus, the role of prostaglandins in the limited response to vasopressin in the neonatal collecting duct remains unclear.

References

[1] Abuazza G, Becker A, Williams SS, Chakravarty S, Truong HT, Lin F, Baum M. Claudins 6, 9, and 13 are developmentally expressed renal tight junction proteins. Am J Physiol Renal Physiol 2006;291(6):F1132–41.

[2] Al-Dahhan J, Haycock GB, Chantler C, Stimmler L. Sodium homeostasis in term and preterm neonates. Arch Dis Child 1983;58:335–42.

[3] Allison ME, Lipham EM, Gottschalk CW. Hydrostatic pressure in the rat kidney. Am J Physiol 1972;223(4):975–83.

[4] Alpern RJ, Howlin KJ, Preisig PA. Active and passive components of chloride transport in the rat proximal convoluted tubule. J Clin Invest 1985;76(4):1360–6.

[5] Ammar A, Roseau S, Butlen D. Postnatal ontogenesis of vasopressin receptors in the rat collecting duct. Mol Cell Endocrinol 1992;86(3):193–203.

[6] Aperia A. Intrarenal dopamine: a key signal in the interactive regulation of sodium metabolism. Annu Rev Physiol 2000;62:621–47.

[7] Aperia A, Broberger O, Elinder G, Herin P, Zetterstrom R. Postnatal development of renal function in pre-term and full-term infants. Acta Paediatr Scand 1981;70(2):183–7.

[8] Aperia A, Broberger O, Herin P, Zetterstrom R. Sodium excretion in relation to sodium intake and aldosterone excretion in newborn preterm and fullterm infants. Acta Paediatr Scand 1979;68:813–7.

[9] Aperia A, Broberger O, Thodenius K, Zetterstrom R. Renal response to an oral sodium load in newborn full-term infants. Acta Paediatr Scand 1972;61:670–6.

[10] Aperia A, Elinder G. Distal tubular sodium reabsorption in the developing rat kidney. Am J Physiol 1981;240(6):F487–91.

[11] Aperia A, Larrson L. Corrrelation between fluid reabsorption and proimal tubule ultrastructure during development of the rat kidney. Acta Physiol Scand 1979;105:11–22.

[12] Aperia A, Larrson L. Induced development of proximal tublar Na,K-ATPase, basolateral cell membranes and fluid reabsorption. Acta Physiol Scand 1984;121:133–41.

[13] Aperia A, Larrson L, Zetterstrom R. Hormonal induction of Na-K-ATPase in developing proximal tubular cells. Am J Physiol 1981;241:F356–60.

[14] Arant Jr BS. Developmental patterns of renal functional maturation compared in the human neonate. J Pediatr 1978;92:705–12.

[15] Arant Jr BS, Edelmann Jr CM, Nash MA. The renal reabsorption of glucose in the developing canine kidney: a study of glomerulotubular balance. Pediatr Res 1974;8:638–46.

[16] Arar M, Levi M, Baum M. Maturational effects of glucocorticoids on neonatal brush-border membrane phosphate transport. Pediatr Res 1994;35:474–8.

[17] Aronson PS. Role of ion exchangers in mediating NaCl transport in the proximal tubule. Kidney Int 1996;49(6):1665–70.

[18] Aschinberg LC, Goldsmith DI, Olbing H, Spitzer A, Edelmann Jr CM, Blaufox MD. Neonatal changes in renal blood flow distribution in puppies. Am J Physiol 1975;228(5):1453–61.

[19] Barac-Nieto M, Dowd TL, Gupta RK, Spitzer A. Changes in NMR-visible kidney cell phosphate with age and diet: relationship to phosphate transport. Am J Physiol 1991;261(1 Pt 2):F153–62.

[20] Baum M. Neonatal rabbit juxtamedullary proximal convoluted tubule acidification. J Clin Invest 1990;85:499–506.

[21] Baum M. Developmental changes in rabbit juxtamedullary proximal convoluted tubule acidification. Pediatr Res 1992;31(4 Pt 1):411–4.

[22] Baum M, Amemiya M, Dwarakanath V, Alpern RJ, Moe OW. Glucocorticoids regulate NHE-3 transcription in OKP cells. Am J Physiol 1996;270(1 Pt 2):F164–9.

[23] Baum M, Berry CA. Evidence for neutral transcellular NaCl transport and neutral basolateral chloride exit in the rabbit convoluted tubule. J Clin Invest 1984;74:205–11.

[24] Baum M, Biemesderfer D, Gentry D, Aronson PS. Ontogeny of rabbit renal cortical NHE3 and NHE1: effect of glucocorticoids. Am J Physiol 1995;268(5 Pt 2):F815–20.

[25] Baum M, Cano A, Alpern RJ. Glucocorticoids stimulate Na^+/H^+ antiporter in OKP cells. Am J Physiol 1993;264(6 Pt 2):F1027–31.

[26] Baum M, Dwarakanath V, Alpern RJ, Moe OW. Effects of thyroid hormone on the neonatal renal cortical Na^+/H^+ antiporter. Kidney Int 1998;53(5):1254–8.

[27] Baum M, Quigley R. Prenatal glucocorticoids stimulate neonatal juxtamedullary proximal convoluted tubule acidification. Am J Physiol 1991;261(5 Pt 2):F746–52.

[28] Baum M, Quigley R. Thyroid hormone modulates rabbit proximal straight tubule paracellular permeability. Am J Physiol-Renal Physiol 2004;286(3):F477–82.
[29] Baum M, Schiavi S, Dwarakanath V, Quigley R. Effect of fibroblast growth factor-23 on phosphate transport in proximal tubules. Kidney Int 2005;68(3):1148–53.
[30] Baum MA, Ruddy MK, Hosselet CA, Harris HW. The perinatal expression of aquaporin-2 and aquaporin-3 in developing kidney. Pediatr Res 1998;43(6):783–90.
[31] Beck JC, Lipkowitz MS, Abramson RG. Ontogeny of Na/H antiporter activity in rabbit renal brush border membrane vesicles. J Clin Invest 1991;87(6):2067–76.
[32] Beck L, Karaplis AC, Amizuka N, Hewson AS, Ozawa H, et al. Targeted inactivation of Npt2 in mice leads to severe renal phosphate wasting, hypercalciuria, and skeletal abnormalities. Proc Natl Acad Sci USA 1998;95(9):5372–7.
[33] Becker AM, Zhang J, Goyal S, Dwarakanath V, Aronson PS, Moe OW, et al. Ontogeny of NHE8 in the rat proximal tubule. Am J Physiol Renal Physiol 2007;293:F255–61.
[34] Beitins IZ, Bayard F, Levitsky L, Ances IG, Kowarski A, Migeon CJ. Plasma aldosterone concentration at delivery and during the newborn period. J Clin Invest 1972;51(2):386–94.
[35] Benchimol C, Zavilowitz B, Satlin LM. Developmental expression of ROMK mRNA in rabbit cortical collecting duct. Pediatr Res 2000;47(1):46–52.
[36] Benyajati S, Goldstein L. Renal glutaminase adaptation and ammonia excretion in infant rats. Am J Physiol 1975;228 (3):693–8.
[37] Bergwitz C, Roslin NM, Tieder M, Loredo-Osti JC, Bastepe M, Abu-Zahra H, et al. SLC34A3 mutations in patients with hereditary hypophosphatemic rickets with hypercalciuria predict a key role for the sodium-phosphate co-transporter NaPi-IIc in maintaining phosphate homeostasis. Am J Hum Genet 2006;78 (2):179–92.
[38] Berndt T, Craig TA, Bowe AE, Vassiliadis J, Reczek D, Finnegan R, et al. Secreted frizzled-related protein 4 is a potent tumor-derived phosphaturic agent. J Clin Invest 2003;112(5):785–94.
[39] Biemesderfer D, Pizzonia J, Abu-Alfa A, Exner M, Reilly R, Igarashi P, et al. NHE3: a Na^+/H^+ exchanger isoform of renal brush border. Am J Physiol 1993;265(5 Pt 2):F736–42.
[40] Biemesderfer D, Reilly RF, Exner M, Igarashi P, Aronson PS. Immunocytochemical characterization of $Na(^+)$-H^+ exchanger isoform NHE-1 in rabbit kidney. Am J Physiol 1992;263(5 Pt 2): F833–40.
[41] Blanco G, Mercer RW. Isozymes of the Na-K-ATPase: heterogeneity in structure, diversity in function. Am J Physiol 1998;275(5 Pt 2):F633–50.
[42] Bobulescu IA, Dwarakanath V, Zou L, Zhang J, Baum M, Moe OW. Glucocorticoids acutely increase cell surface Na^+/H^+ exchanger-3 (NHE3) by activation of NHE3 exocytosis. Am J Physiol Renal Physiol 2005;289(4):F685–91.
[43] Bonilla-Felix M. Development of water transport in the collecting duct. Am J Physiol Renal Physiol 2004;287(6):F1093–101.
[44] Bonilla-Felix M, Jiang W. Expression and localization of prostaglandin EP3 receptor mRNA in the immature rabbit kidney. Am J Physiol 1996;271(1 Pt 2):F30–6.
[45] Bonilla-Felix M, Jiang W. Aquaporin-2 in the immature rat: expression, regulation, and trafficking. J Am Soc Nephrol 1997;8 (10):1502–9.
[46] Bonilla-Felix M, John-Phillip C. Prostaglandins mediate the defect in AVP-stimulated cAMP generation in immature collecting duct. Am J Physiol 1994;267(1 Pt 2):F44–8.
[47] Bonilla-Felix M, Vehaskari VM, Hamm LL. Water transport in the immature rabbit collecting duct. Pediatr Nephrol 1999;13 (2):103–7.
[48] Bonnici B, Wagner CA. Postnatal expression of transport proteins involved in acid–base transport in mouse kidney. Pflugers Arch 2004;448(1):16–28.
[49] Bresler D, Bruder J, Mohnike K, Fraser WD, Rowe PS. Serum MEPE-ASARM-peptides are elevated in X-linked rickets (HYP): implications for phosphaturia and rickets. J Endocrinol 2004;183 (3):R1–9.
[50] Burrow CR, Devuyst O, Li X, Gatti L, Wilson PD. Expression of the beta2-subunit and apical localization of Na^+-K^+-ATPase in metanephric kidney. Am J Physiol 1999;277(3 Pt 2):F391–403.
[51] Calcagno PL, Rubin MI. Renal extraction of para-aminohippurate in infants and children. J Clin Invest 1963;42:1632–9.
[52] Cano A, Baum M, Moe OW. Thyroid hormone stimulates the renal Na/H exchanger NHE3 by transcriptional activation. Am J Physiol 1999;276(1 Pt 1):C102–8.
[53] Carpenter TO, Ellis BK, Insogna KL, Philbrick WM, Sterpka J, Shimkets R. Fibroblast growth factor 7: an inhibitor of phosphate transport derived from oncogenic osteomalacia-causing tumors. J Clin Endo Med 2005;90(2):1012–20.
[54] Caverzasio J, Bonjour JP, Fleisch H. Tubular handling of Pi in young growing and adult rats. Am J Physiol 1982;242(6): F705–10.
[55] Caverzasio J, Murer H, Fleisch H, Bonjour JP. Phosphate transport in brush border membrane vesicles isolated from renal cortex of young growing and adult rats. Comparison with whole kidney data. Pflugers Arch 1982;394(3):217–21.
[56] Chevalier RL, Thornhill BA, Belmonte DC, Baertschi AJ. Endogenous angiotensin II inhibits natriuresis after acute volume expansion in the neonatal rat. Am J Physiol 1996;270(2 Pt 2):R393–7.
[57] Connelly JP, Crawford JD, Watson J. Studies of neonatal hyperphosphatemia. Pediatrics 1962;30:425–32.
[58] Constantinescu A, Silver RB, Satlin LM. H-K-ATPase activity in PNA-binding intercalated cells of newborn rabbit cortical collecting duct. Am J Physiol 1997;272(2 Pt 2):F167–77.
[59] Constantinescu AR, Lane JC, Mak J, Zavilowitz B, Satlin LM. $Na(^+)$-$K(^+)$-ATPase-mediated basolateral rubidium uptake in the maturing rabbit cortical collecting duct. Am J Physiol Renal Physiol 2000;279(6):F1161–8.
[60] Cort JP, McCrane RA. The renal response of puppies to an acidosis. J Physiol (London) 1954;124:358–69.
[61] Cramb G, Cutler CP, Lamb JF, McDevitt T, Ogden PH, Owler D, et al. The effects of monensin on the abundance of mRNA (alpha) and of sodium pumps in human cultured cells. Q J Exp Physiol 1989;74(1):53–63.
[62] Dancis J, Springer D. Fetal homeostasis in maternal malnutrition: potassium and sodium deficiency in rats. Pediatr Res 1970;4(4):345–51.
[63] Darrow DC, DaSilva MM, Stevenson SS. Production of acidosis in premature infants by protein milk. J Pediatr 1945;27:43–58.
[64] David L, Anast CS. Calcium metabolism in newborn infants. The interrelationship of parathyroid function and calcium, magnesium, and phosphorus metabolism in normal, "sick," and hypocalcemic newborns. J Clin Invest 1974;54(2):287–96.
[65] Dean RF, McCance RA. The renal response of infants and adults to the administration of hypertonic solutions of sodium chloride and urea. J Physiol (London) 1949;109:81–7.
[66] Dean RF, McCance RA. Phosphate clearance in infants and adults. J Physiol (London) 1948;107:182–6.
[67] Dean RFA, McCance RA. Inulin, diodone, creatinine and urea clearance in newborn infants. J Physiol (London) 1947;106:431–9.

[68] Delgado MM, Rohatgi R, Khan S, Holzman IR, Satlin LM. Sodium and potassium clearances by the maturing kidney: clinical–molecular correlates. Pediatr Nephrol 2003;18 (8):759–67.
[69] Djouadi F, Wijkhuisen A, Bastin J. Coordinate development of oxidative enzymes and Na-K-ATPase in thick ascending limb: role of corticosteroids. Am J Physiol 1992;263(2 Pt 2):F237–42.
[70] Dlouha H. A micropuncture study of the development of renal function in the young rat. Biol Neonate 1976;29(1–2):117–28.
[71] Drukker A, Goldsmith DI, Spitzer A, Edelmann Jr. CM, Blaufox MD. The renin angiotensin system in newborn dogs: developmental patterns and response to acute saline loading. Pediatr Res 1980;14(4 Pt 1):304–7.
[72] Edelmann Jr CM, Barnett HL, Stark H. Effect of urea on concentration of urinary nonurea solute in premature infants. J Appl Physiol 1966;21(3):1021–5.
[73] Edelmann Jr CM, Barnett HL, Troupkou V. Renal concentrating mechanisms in newborn infants. Effect of dietary protein and water content, role of urea, and responsiveness to antidiuretic hormone. J Anat 1960;1062–9.
[74] Edelmann CMJ, Soriano JR, Boichis H, Gruskin AB, Acosta M. Renal bicarbonate reabsorption and hydrogen ion excretion in normal infants. J Clin Invest 1967;46:1309–17.
[75] Engelke SC, Shah GL, Vasan J, Raye JR. Sodium blance in very low-birth-weight infants. J Pediatr 1978;93:837–41.
[76] Evan AP, Gattone II, Schwartz GJ. Development of solute transport in rabbit proximal tubule. II. Morphologic segmentation. Am J Physiol 1983;245:F391–407 Renal Fluid Electrolyte Physiol 14
[77] Evan AP, Satlin LM, Gattone VH, Connors B, Schwartz GJ. Postnatal maturation of rabbit renal collecting duct. II. Morphological observations. Am J Physiol 1991;261(1 Pt 2): F91–107.
[78] Feng JQ, Ward LM, Liu SG, Lu YB, Xie YX, Yuan BZ, et al. Loss of DMP1 causes rickets and osteomalacia and identifies a role for osteocytes in mineral metabolism. Nat Genet 2006;38 (11):1310–5.
[79] Fisher DA, Pyle Jr HR, Porter JC, Beard AG, Panos TC. Control of water balance in the newborn. Am J Dis Child 1963;106:137–46.
[80] Fomon SJ, Harris DM, Jensen RL. Acidification of the urine by infants fed human milk and whole cow's milk. Pediatrics 1959;23:113–20.
[81] Fukuda Y, Aperia A. Differentiation of Na^+-K^+ pump in rat proximal tubule is modulated by Na^+-H^+ exchanger. Am J Physiol 1988;255(3 Pt 2):F552–7.
[82] Fukuda Y, Bertorello A, Aperia A. Ontogeny of the regulation of Na^+,$K(^+)$-ATPase activity in the renal proximal tubule cell. Pediatr Res 1991;30(2):131–4.
[83] Gattineni J, Baum M. Regulation of phosphate transport by fibroblast growth factor 23 (FGF23): implications for disorders of phosphate metabolism. Pediatr Nephrol 2010;25(4):591–601.
[84] Gattineni J, Sas D, Dagan A, Dwarakanath V, Baum M. Effect of thyroid hormone on the postnatal renal expression of NHE8. Am J Physiol Renal Physiol 2008;294(1):F198–204.
[85] Gersh I. The correlation of structure and function in the developing mesonephros and metanephros. Contrib Embryol 1937;153:35–58.
[86] Godard C, Geering JM, Geering K, Vallotton MB. Plasma renin activity related to sodium balance, renal function and urinary vasopressin in the newborn infant. Pediatr Res 1979;13 (6):742–5.
[87] Goldsmith DI, Drukker A, Blaufox MD, Edelmann Jr CM, Spitzer A. Hemodynamic and excretory response of the neonatal canine kidney to acute volume expansion. Am J Physiol 1979;237(5):F392–7.
[88] Goldsmith DI, Jodorkovsky RA, Sherwinter J, Kleeman SR, Spitzer A. Glomerular capillary permeability in developing canines. Am J Physiol 1986;251(3 Pt 2):F528–31.
[89] Goldstein L. Ammonia metabolism in kidneys of suckling rats. Am J Physiol 1971;220(1):213–7.
[90] Gordon HH, McNamara H, Benjamin HR. The response of young infants to ingestion of ammonium chloride. Pediatrics 1948;2:290–302.
[91] Goyal S, Vanden Heuvel G, Aronson PS. Renal expression of novel Na^+/H^+ exchanger isoform NHE8. Am J Physiol Renal Physiol 2003;284(3):F467–73.
[92] Gruskin AB, Edelmann Jr CM, Yuan S. Maturational changes in renal blood flow in piglets. Pediatr Res 1970;4 (1):7–13.
[93] Guillery EN, Huss DJ. Developmental regulation of chloride/formate exchange in guinea pig proximal tubules. Am J Physiol 1995;269(5 Pt 2):F686–95.
[94] Gupta N, Dwarakanath V, Baum M. Maturation of the Na/H antiporter (NHE3) in the proximal tubule of the hypothroid adrenalectomized rat. Am J Physiol Renal Physiol 2004;287: F521–7.
[95] Gupta N, Tarif SR, Seikaly M, Baum M. Role of glucocorticoids in the maturation of the rat renal Na^+/H^+ antiporter (NHE3). Kidney Int 2001;60(1):173–81.
[96] Hadeed AJ, Leake RD, Weitzman RE, Fisher DA. Possible mechanisms of high blood levels of vasopressin during the neonatal period. J Pediatr 1979;94:805–8.
[97] Hammerman MR, Karl IE, Hruska KA. Regulation of canine renal vesicle Pi transport by growth hormone and parathyroid hormone. Biochim Biophys Acta 1980;603(2):322–35.
[98] Hansen JOL, SmithC. A. Effects of withholding fluid in the immediate post-natal period. Pediatrics 1953;12:99–113.
[99] Haramati A, Mulroney SE. Enhanced tubular capacity for phosphate reabsorption in immature rats: role of glomerular–filtration rate (Gfr). Fed Proc 1987;46(4):1288.
[100] Haramati A, Mulroney SE, Lumpkin MD. Regulation of renal phosphate reabsorption during development: implications from a new model of growth hormone deficiency. Pediatr Nephrol 1990;4(4):387–91.
[101] Harris RC, Seifter JL, Lechene C. Coupling of Na-H exchange and Na-K pump activity in cultured rat proximal tubule cells. Am J Physiol 1986;251(5 Pt 1):C815–24.
[102] Hatemi N, McCance RA. Response to acidifying drugs. Acta Paediatr Scand 1961;50:603–16.
[103] Henneman PH, Forbes AP, Moldawer M, Dempsey EF, Carroll EL. Effects of human growth hormone in man. J Clin Invest 1960;39:1223–38.
[104] Henning SJ. Plasma concentrations of total and free corticosterone during development in the rat. Am J Physiol 1978;235(5): E451–6.
[105] Hines HE, McCance RA. Ammonia formation from glutamine by kidney slices from adult and newborn animals. J Physiol (London) 1954;124:8–16.
[106] Hohenauer L, Rosenberg TF, Oh W. Calcium and phosphorus homeostasis on the first day of life. Biol Neonate 1970;15 (12):49–56.
[107] Horster M. Loop of Henle functional differentiation: *in vitro* perfusion of the isolated thick ascending segment. Pflugers Arch 1978;378(1):15–24.
[108] Horster M, Huber S, Tschop J, Dittrich G, Braun G. Epithelial nephrogenesis. Pflugers Arch 1997;434(6):647–60.
[109] Horster M, Valtin H. Postnatal development of renal function: micropuncture and clearance studies in the dog. J Clin Invest 1971;50(4):779–95.

[110] Horster MF, Gilg A, Lory P. Determinants of axial osmotic gradients in the differentiating countercurrent system. Am J Physiol 1984;246(2 Pt 2):F124–32.
[111] Horster MF, Zink H. Functional differentiation of the medullary collecting tubule: influence of vasopressin. Kidney Int 1982;22(4):360–5.
[112] Huber SM, Braun GS, Horster MF. Expression of the epithelial sodium channel (ENaC) during ontogenic differentiation of the renal cortical collecting duct epithelium. Pflugers Arch 1999;437(3):491–7.
[113] Ichikawa I, Maddox DA, Brenner BM. Maturational development of glomerular ultrafiltration in the rat. Am J Physiol 1979;236(5):F465–71.
[114] Ichikawa S, Sorenson AH, Imel EA, Friedman NE, Gertner JM, Econs MJ. Intronic deletions in the SLC34A3 gene cause hereditary hypophosphatemic rickets with hypercalciuria. J Clin Endocrinol Metab 2006;91(10):4022–7.
[115] John E, Goldsmith DI, Spitzer A. Quantitative changes in the canine glomerular vasculature during development: physiologic implications. Kidney Int 1981;20(2):223–9.
[116] Johnson V, Spitzer A. Renal reabsorption of phosphate during development: whole-kidney events. Am J Physiol 1986;251(2 Pt 2):F251–6.
[117] Jose PA, Slotkoff LM, Lilienfield LS, Calcagno PL, Eisner GM. Sensitivity of neonatal renal vasculature to epinephrine. Am J Physiol 1974;226(4):796–9.
[118] Jose PA, Slotkoff LM, Montgomery S, Calcagno PL, Eisner G. Autoregulation of renal blood flow in the puppy. Am J Physiol 1975;229(4):983–8.
[119] Kaneko S, Albrecht F, Asico LD, Eisner GM, Robillard JE, Jose PA. Ontogeny of DA1 receptor-mediated natriuresis in the rat: *in vivo* and *in vitro* correlations. Am J Physiol 1992;263(3 Pt 2): R631–8.
[120] Karashima S, Hattori S, Ushijima T, Furuse A, Nakazato H, Matsuda I. Developmental changes in carbonic anhydrase II in the rat kidney. Pediatr Nephrol 1998;12(4):263–8.
[121] Karlen J. Renal response to low and high phosphate intake in weanling, adolescent and adult rats. Acta Physiol Scand 1989;135(3):317–22.
[122] Kaskel FJ, Kumar AM, Feld LG, Spitzer A. Renal reabsorption of phosphate during development: tubular events. Pediatr Nephrol 1988;2(1):129–34.
[123] Kaskel FJ, Kumar AM, Lockhart EA, Evan A, Spitzer A. Factors affecting proximal tubular reabsorption during development. Am J Physiol 1987;252:F188–97 Renal Fluid Electrolyte Physiol. 21
[124] Kerpel-Fronius E, Heim T, Sulyok E. The development of the renal acidifying processes and their relation to acidosis in low-birth-weight infants. Biol Neonate 1979;15:156–68.
[125] Kildeberg P, Engel K, Winters RW. Balance of net acid in growing infants. Endogenous and transintestinal aspects. Acta Paediatr Scand 1969;58(4):321–9.
[126] Kildeberg P, Winters R. Infant feeding and blood acid–base status. Pediatrics 1972;49(6):801–2.
[127] Kim YH, Earm JH, Ma T, Verkman AS, Knepper MA, Madsen KM, et al. Aquaporin-4 expression in adult and developing mouse and rat kidney. J Am Soc Nephrol 2001;12 (9):1795–804.
[128] Kim YH, Kim DU, Han KH, Jung JY, Sands JM, Knepper MA, et al. Expression of urea transporters in the developing rat kidney. Am J Physiol Renal Physiol 2002;282(3): F530–40.
[129] Knutson DW, Chieu F, Bennett CM, Glassock RJ. Estimation of relative glomerular capillary surface area in normal and hypertrophic rat kidneys. Kidney Int 1978;14(5):437–43.
[130] Larsson L, Horster M. Ultrastructure and net fluid transport in isolated perfused developing proximal tubules. J Ultrastruct Res 1976;54:276–85.
[131] Larsson SH, Rane S, Fukuda Y, Aperia A, Lechene C. Changes in Na influx precede post-natal increase in Na, K-ATPase activity in rat renal proximal tubular cells. Acta Physiol Scand 1990;138(1):99–100.
[132] Leake RD, Zakauddin S, Trygstad CW, Fu P, Oh W. The effects of large volume intravenous fluid infusion on neonatal renal function. J Pediatr 1976;89(6):968–72.
[133] Lelievre-Pegorier M, Merlet-Benichou D, Roinel N, DeRouffignac C. Developmental pattern of water and electrolyte transport in rat superficial nephrons. Am J Physiol 1983;245:F15–21.
[134] Levi M, Baird BM, Wilson PV. Cholesterol modulates rat renal brush border membrane phosphate transport. J Clin Invest 1990;85:231–7.
[135] Levi M, Jameson DM, van der Meer BW. Role of BBM lipid composition and fluidity in impaired renal pi transport in aged rat. Am J Physiol 1989;256(1 Pt 2):F85–94.
[136] Li XX, Albrecht FE, Robillard JE, Eisner GM, Jose PA. Gbeta regulation of Na/H exchanger-3 activity in rat renal proximal tubules during development. Am J Physiol Regul Integr Comp Physiol 2000;278(4):R931–6.
[137] Linarelli LG. Nephron urinary cyclic AMP and developmental renal responsiveness to parathyroid hormone. Pediatrics 1972;50:14–23.
[138] Lorenz JM, Kleinman LI, Disney TA. Renal response of newborn dog to potassium loading. Am J Physiol 1986;251(3 Pt 2): F513–9.
[139] Lucci MS, Pucacco LR, DuBose Jr. TD, Kokko JP, Carter NW. Direct evaluation of acidification by rat proximal tubule: role of carbonic anhydrase. Am J Physiol 1980;238(5):F372–9.
[140] Magagnin S, Werner A, Markovich D, Sorribas V, Stange G, Biber J, et al. Expression cloning of human and rat renal cortex Na/Pi co-transport. Proc Natl Acad Sci USA 1993;90 (13):5979–83.
[141] Martinerie L, Pussard E, Foix-L'Helias L, Petit F, Cosson C, Boileau P, et al. Physiological partial aldosterone resistance in human newborns. Pediatr Res 2009;66(3):323–8.
[142] McCance RA, Hatemi N. Control of acid–base stability in the newly born. Lancet 1961;1:293–7.
[143] McCance RA, Naylor NJ, Widdowson EM. The response of infants to a large dose of water. Arch Dis Child 1954;29 (144):104–9.
[144] McCance RA, Widdowson EM. Renal aspects of acid–base control in the newly born. Acta Paediatr Scand 1960;49:409–14.
[145] McCrory WW, Forman CW, McNamara H, Barnett HL. Renal excretion of inorganic phosphate in newborn infants. J Clin Invest 1952;31(4):357–66.
[146] McKinney TD, Burg MB. Bicarbonate transport by rabbit cortical collecting tubules. Effect of acid and alkali loads *in vivo* on transport *in vitro*. J Clin Invest 1977;60(3):766–8.
[147] Mehrgut FM, Satlin LM, Schwartz GJ. Maturation of HCO_3^- transport in rabbit collecting duct. Am J Physiol 1990;259(5 Pt 2):F801–8.
[148] Melendez E, Reyes JL, Escalante BA, Melendez MA. Development of the receptors to prostaglandin E2 in the rat kidney and neonatal renal functions. Dev Pharmacol Ther 1989;14(2):125–34.
[149] Merlet-Benichou C, Pegorier M, Muffat-Joly M, Augeron D. Functional and morphologic patterns of renal maturation in the developing guinea pig. Am J Physiol 1981;36:H1467–75.
[150] Miyamoto K, Ito M, Tatsumi S, Kuwahata M, Segawa H. New aspect of renal phosphate reabsorption: the type IIc sodium-

dependent phosphate transporter. Am J Nephrol 2007;27 (5):503–15.
[151] Molitoris BA, Simon FR. Renal cortical brush-border and basolateral membranes: cholesterol and phospholipid composition and relative turnover. J Membr Biol 1985;83(3):207–15.
[152] Monnens L, Schretlen E, van Munster P. The renal excretion of hydrogen ions in infants and children. Nephron 1973;12:29–43.
[153] Mulroney SE, Haramati A. Renal adaptation to changes in dietary phosphate during development. Am J Physiol 1990;258(6 Pt 2):F1650–6.
[154] Neiberger RE, Barac-Nieto M, Spitzer A. Renal reabsorption of phosphate during development: transport kinetics in BBMV. Am J Physiol 1989;257(2 Pt 2):F268–74.
[155] Olbing H, Blaufox MD, Aschinberg LC, Silkalns GI, Bernstein J, Spitzer A, et al. Postnatal changes in renal glomerular blood flow distribution in puppies. J Clin Invest 1973;52 (11):2885–95.
[156] Parkkila S, Parkkila AK, Saarnio J, Kivela J, Karttunen TJ, Kaunisto K, et al. Expression of the membrane-associated carbonic anhydrase isozyme XII in the human kidney and renal tumors. J Histochem Cytochem 2000;48(12):1601–8.
[157] Pellegrini L, Burke DF, von Delft F, Mulloy B, Blundell TL. Crystal structure of fibroblast growth factor receptor ectodomain bound to ligand and heparin. Nature 2000;407 (6807):1029–34.
[158] Peonides A, Levin B, Young WF. The renal excretion of hydrogen ions in infants and children. Arch Dis Child 1965;40:33–9.
[159] Polacek E, Vocel J, Neugebaurova L, Sebkova M, Vechetova E. The osmotic concentrating ability in healthy infants and children. Arch Dis Child 1965;40:291–5.
[160] Preisig PA, Ives HE, Cragoe Jr. EJ, Alpern RJ, Rector Jr. FC. Role of the Na^+/H^+ antiporter in rat proximal tubule bicarbonate absorption. J Clin Invest 1987;80(4):970–8.
[161] Purkerson JM, Schwartz GJ. The role of carbonic anhydrases in renal physiology. Kidney Int 2007;71(2):103–15.
[162] Quigley R, Baum M. Developmental changes in rabbit juxtamedullary proximal convoluted tubule bicarbonate permeability. Pediatr Res 1990;28(6):663–6.
[163] Quigley R, Baum M. Effects of growth hormone and insulin-like growth factor I on rabbit proximal convoluted tubule transport. J Clin Invest 1991;88(2):368–74.
[164] Quigley R, Baum M. Developmental changes in rabbit juxtamedullary proximal convoluted tubule water permeability. Am J Physiol 1996;271(4 Pt 2):F871–6.
[165] Quigley R, Baum M. Developmental changes in rabbit proximal straight tubule paracellular permeability. Am J Physiol Renal Physiol 2002;283(3):F525–31.
[166] Quigley R, Chakravarty S, Baum M. Antidiuretic hormone resistance in the neonatal cortical collecting tubule is mediated in part by elevated phosphodiesterase activity. Am J Physiol Renal Physiol 2004;286(2):F317–22.
[167] Rane S, Aperia A. Ontogeny of Na-K-ATPase activity in thick ascending limb and of concentrating capacity. Am J Physiol 1985;249(5 Pt 2):F723–8.
[168] Rane S, Aperia A, Eneroth P, Lundin S. Development of urinary concentrating capacity in weaning rats. Pediatr Res 1985;19(5):472–5.
[169] Ratliff B, Rodebaugh J, Sekulic M, Dong KW, Solhaug M. Nitric oxide synthase and renin–angiotensin gene expression and NOS function in the postnatal renal resistance vasculature. Pediatr Nephrol 2009;24(2):355–65.
[170] Rees L, Forsling ML, Brook CG. Vasopressin concentrations in the neonatal period. Clin Endocrinol (Oxf) 1980;12(4): 357–62.
[171] Richmond JB, Kravitz H, Segar W, Kravitz H. Renal clearance of endogenous phosphate in infants and children. Proc Soc Exp Biol Med 1951;77:83–7.
[172] Robillard JE, Nakamura KT, DiBona GF. Effects of renal denervation on renal responses to hypoxemia in fetal lambs. Am J Physiol 1986;250(2 Pt 2):F294–301.
[173] Robillard JE, Sessions C, Kennedey RL, Hamel-Robillard L, Smith Jr FG. Interrelationship between glomerular filtration rate and renal transport of sodium and chloride during fetal life. Am J Obstet Gynecol 1977;128(7):727–34.
[174] Robillard JE, Smith FG, Nakamura KT, Sato T, Segar J, Jose PA. Neural control of renal hemodynamics and function during development. Pediatr Nephrol 1990;4(4):436–41.
[175] Robillard JE, Weitzman RE. Developmental aspects of the fetal renal response to exogenous arginine vasopressin. Am J Physiol 1980;238(5):F407–14.
[176] Rodriguez-Soriano J, Vallo A, Oliveros R, Castillo G. Renal handling of sodium in premature and full-term neonates: a study using clearance methods during water diuresis. Pediatr Res 1983;17(12):1013–6.
[177] Rubin MI, Bruck E, Rapoport M. Maturation of renal function in childhood: clearance studies. J Clin Invest 1949;28: 1144–62.
[178] Rudolph AM, Heymann MA. Circulatory changes during growth in the fetal lamb. Circ Res 1970;26(3):289–99.
[179] Sas D, Hu MC, Moe OW, Baum M. Effect of claudins 6 and 9 on paracellular permeability in MDCK II cells. Am J Physiol-Regul Integr and Comp Physiol 2008;295(5):R1713–9.
[180] Satlin LM. Postnatal maturation of potassium transport in rabbit cortical collecting duct. Am J Physiol 1994;266(1 Pt 2): F57–65.
[181] Satlin LM. Regulation of potassium transport in the maturing kidney. Semin Nephrol 1999;19(2):155–65.
[182] Satlin LM, Evan AP, Gattone III VH, Schwartz GJ. Postnatal maturation of the rabbit cortical collecting duct. Pediatr Nephrol 1988;2(1):135–45.
[183] Satlin LM, Matsumoto T, Schwartz GJ. Postnatal maturation of rabbit renal collecting duct. III. Peanut lectin-binding intercalated cells. Am J Physiol 1992;262(2 Pt 2):F199–208.
[184] Satlin LM, Palmer LG. Apical Na^+ conductance in maturing rabbit principal cell. Am J Physiol 1996;270(3 Pt 2):F391–7.
[185] Satlin LM, Palmer LG. Apical K^+ conductance in maturing rabbit principal cell. Am J Physiol 1997;272(3 Pt 2):F397–404.
[186] Satlin LM, Schwartz GJ. Postnatal maturation of rabbit renal collecting duct: Intercalated cell function. Am J Physiol 1987;253(4 Pt 2):F622–35.
[187] Schlondorff D, Satriano JA, Schwartz GJ. Synthesis of prostaglandin E2 in different segments of isolated collecting tubules from adult and neonatal rabbits. Am J Physiol 1985;248(1 Pt 2): F134–44.
[188] Schmidt U, Horster M. Na-K-activated ATPase: activity maturation in rabbit nephron segments dissected *in vitro*. Am J Physiol 1977;233(1):F55–60.
[189] Schmitt R, Ellison DH, Farman N, Rossier BC, Reilly RF, Reeves WB, et al. Developmental expression of sodium entry pathways in rat nephron. Am J Physiol 1999;276(3 Pt 2): F367–81.
[190] Schwartz GH, Evan AP. Development of solute transport in rabbit proximal tubule. I. HCO3 and glucose absorption. Am J Physiol 1983;245:F382–90 Renal Fluid Electrolyte Physiol. 14
[191] Schwartz GH, Evan AP. Development of solute transport in rabbit proximal tubule. III. Na-K-ATPase activity. Am J Physiol 1984;246:F845–52 Renal Fluid Electrolyte Physiol. 15
[192] Schwartz GJ. Physiology and molecular biology of renal carbonic anhydrase. J Nephrol 2002;15(Suppl 5):S61–74.

[193] Schwartz GJ, Haycock GB, Edelmann Jr. CM, Spitzer A. Late metabolic acidosis: a reassessment of the definition. J Pediatr 1979;95(1):102–7.
[194] Schwartz GJ, Kittelberger AM, Barnhart DA, Vijayakumar S. Carbonic anhydrase IV is expressed in $H^{(+)}$-secreting cells of rabbit kidney. Am J Physiol Renal Physiol 2000;278(6): F894–904.
[195] Schwartz GJ, Olson J, Kittelberger AM, Matsumoto T, Waheed A, Sly WS. Postnatal development of carbonic anhydrase IV expression in rabbit kidney. Am J Physiol 1999;276(4 Pt 2): F510–20.
[196] Schwartz GJ, Zavilowitz BJ, Radice AD, Garcia-Perez A, Sands JM. Maturation of aldose reductase expression in the neonatal rat inner medulla. J Clin Invest 1992;90(4):1275–83.
[197] Segawa H, Kaneko I, Takahashi A, Kuwahata M, Ito M, Ohkido I, et al. Growth-related renal type II Na/Pi co-transporter. J Biol Chem 2002;277(22):19665–72.
[198] Segawa H, Kawakami E, Kaneko I, Kuwahata M, Ito M, Kusano K, et al. Effect of hydrolysis-resistant FGF23-R179Q on dietary phosphate regulation of the renal type-II Na/Pi transporter. Pflugers Arch 2003;446(5):585–92.
[199] Segawa H, Onitsuka A, Furutani J, Kaneko I, Aranami F, Matsumoto N, et al. Npt2a and Npt2c in mice play distinct and synergistic roles in inorganic phosphate metabolism and skeletal development. Am J Physiol Renal Physiol 2009;297(3): F671–8.
[200] Segawa H, Onitsuka A, Kuwahata M, Hanabusa E, Furutani J, Kaneko I, et al. Type IIc sodium-dependent phosphate transporter regulates calcium metabolism. J Am Soc Nephrol 2009;20(1):104–13.
[201] Serrano CV, Talbert LM, Welt LG. Potassium deficiency in the pregnant dog. J Clin Invest 1964;43:27–31.
[202] Shah M, Gupta N, Dwarakanath V, Moe OW, Baum M. Ontogeny of Na^+/H^+ antiporter activity in rat proximal convoluted tubules. Pediatr Res 2000;48(2):206–10.
[203] Shah M, Quigley R, Baum M. Maturation of rabbit proximal straight tubule chloride/base exchange. Am J Physiol 1998;274 (5 Pt 2):F883–8.
[204] Shah M, Quigley R, Baum M. Neonatal rabbit proximal tubule basolateral membrane Na^+/H^+ antiporter and Cl^-/base exchange. Am J Physiol 1999;276(6 Pt 2):R1792–7.
[205] Shah M, Quigley R, Baum M. Maturation of proximal straight tubule NaCl transport: role of thyroid hormone. Am J Physiol Renal Physiol 2000;278(4):F596–602.
[206] Sheu JN, Baum M, Bajaj G, Quigley R. Maturation of rabbit proximal convoluted tubule chloride permeability. Pediatr Res 1996;39(2):308–12.
[207] Sheu JN, Baum M, Harkins EW, Quigley R. Maturational changes in rabbit renal cortical phospholipase A2 activity. Kidney Int 1997;52(1):71–8.
[208] Sheu JN, Quigley R, Baum M. Heterogeneity of chloride/base exchange in rabbit superficial and juxtamedullary proximal convoluted tubules. Am J Physiol 1995;268(5 Pt 2):F847–53.
[209] Shimada T, Kakitani M, Hasegawa H, Yamazaki Y, Ohguma A, Takeuchi Y, et al. Targeted ablation of FGF-23 causes hyperphosphatemia, increased 1,25-dihydroxyvitamin D level and severe growth retardation. J Bone Miner Res 2002;17:S168.
[210] Siegel SR, Fisher DA, Oh W. Serum aldosterone concentrations related to sodium balance in the newborn infant. Pediatrics 1974;53(3):410–3.
[211] Siegel SR, Oh W. Renal function as a marker of human fetal maturation. Acta Paediatr Scand 1976;65:481–5.
[212] Siga E, Horster MF. Regulation of osmotic water permeability during differentiation of inner medullary collecting duct. Am J Physiol 1991;260(5 Pt 2):F710–6.
[213] Silverstein DM, Barac-Nieto M, Murer H, Spitzer A. A putative growth-related renal $Na^{(+)}$-Pi co-transporter. Am J Physiol 1997;273(3 Pt 2):R928–33.
[214] Smith FG, Sato T, McWeeny OJ, Klinkefus JM, Robillard JE. Role of renal sympathetic nerves in response of the ovine fetus to volume expansion. Am J Physiol 1990;259(5 Pt 2):R1050–5.
[215] Smith FG, Sato T, McWeeny OJ, Torres L, Robillard JE. Role of renal nerves in response to volume expansion in conscious newborn lambs. Am J Physiol 1989;257(6 Pt 2):R1519–25.
[216] Smith FG, Smith BA, Guillery EN, Robillard JE. Role of renal sympathetic nerves in lambs during the transition from fetal to newborn life. J Clin Invest 1991;88(6):1988–94.
[217] Song HK, Kim WY, Lee HW, Park EY, Han KH, Nielsen S, et al. Origin and fate of pendrin-positive intercalated cells in developing mouse kidney. J Am Soc Nephrol 2007;18 (10):2672–82.
[218] Spitzer A. The role of the kidney in sodium homeostasis during maturation. Kidney Int 1982;21(4):539–45.
[219] Spitzer A, Brandis M. Functional and morphologic maturation of the superficial nephrons. Relationship to total kidney function. J Clin Invest 1974;53(1):279–87.
[220] Spitzer A, Edelmann Jr CM. Maturational changes in pressure gradients for glomerular filtration. Am J Physiol 1971;221 (5):1431–5.
[221] Stanier MW. Development of intra-renal solute gradients in foetal and post-natal life. Pflugers Arch 1972;336(3):263–70.
[222] Stephenson G, Hammet M, Hadaway G, Funder JW. Ontogeny of renal mineralocorticoid receptors and urinary electrolyte responses in the rat. Am J Physiol 1984;247(4 Pt 2):F665–71.
[223] Stubbe J, Madsen K, Nielsen FT, Bonde RK, Skott O, Jensen BL. Postnatal adrenalectomy impairs urinary concentrating ability by increased COX-2 and leads to renal medullary injury. Am J Physiol Renal Physiol 2007;293(3):F780–9.
[224] Stubbe J, Madsen K, Nielsen FT, Skott O, Jensen BL. Glucocorticoid impairs growth of kidney outer medulla and accelerates loop of Henle differentiation and urinary concentrating capacity in rat kidney development. Am J Physiol Renal Physiol 2006;291(4):F812–22.
[225] Sulyok E, Nemeth M, Tenyi I, Csaba IF, Varga F, Gyory E, et al. Relationship between maturity, electrolyte balance and the function of the renin–angiotensin–aldosterone system in newborn infants. Biol Neonate 1979;35(1–2):60–5.
[226] Sulyok EHT. Assessment of maximal urinary acidification in prematuare infants. Biol Neonate 1971;19:200–10.
[227] Sulyok EHT. The influence of matauarity on renal control of acidosis in newborn infants. Biol Neonate 1972;21:418–35.
[228] Svenningsen NW. Renal acid–base titration studies in infants with and without metabolic acidosis in the postneonatal period. Pediatr Res 1973;8:659–72.
[229] Svenningsen NW, Lindquist B. Postnatal development of renal hydrogen ion excretion capacity in relation to age and protein intake. Acta Paediatr Scand 1974;63:721–31.
[230] Thomas ML, Anast CS, Forte LR. Regulation of calcium homeostasis in the fetal and neonatal rat. Am J Physiol 1981;240(4):E367–72.
[231] Traebert M, Lotscher M, Aschwanden R, Ritthaler T, Biber J, Murer H, et al. Distribution of the sodium/phosphate transporter during postnatal ontogeny of the rat kidney. J Am Soc Nephrol 1999;10(7):1407–15.
[232] Tucker BJ, Blantz RC. Factors determining superficial nephron filtration in the mature, growing rat. Am J Physiol 1977;232(2): F97–104.
[233] Tudvad F, McNamara H, Barnett HL. Renal response of premature infants to administration of bicarbonate and potassium. Pediatrics 1954;13(1):4–16.

[234] Tulassay T, Rascher W, Hajdu J, Lang RE, Toth M, Seri I. Influence of dopamine on atrial natriuretic peptide level in premature infants. Acta Paediatr Scand 1987;76(1):42–6.
[235] Tuvad F, Vesterdal J. The maximal tubular transfer of glucose and para-aminohippurate in premature infants. Acta Paediatr Scand 1953;42:337–45.
[236] Van Itallie CM, Anderson JM. Claudins and epithelial paracellular transport. Annu Rev Physiol 2006;68:403–29.
[237] Vehaskari VM. Ontogeny of cortical collecting duct sodium transport. Am J Physiol 1994;267(1 Pt 2):F49–54.
[238] Vehaskari VM, Hempe JM, Manning J, Aviles DH, Carmichael MC. Developmental regulation of ENaC subunit mRNA levels in rat kidney. Am J Physiol 1998;274(6 Pt 1):C1661–6.
[239] Wacker GR, Zarkowsky HS, Bruch HB. Changes in kidney enzymes of rats after birth. Am J Physiol 1961;200:367–9.
[240] Wamberg S, Kildeberg P, Engel K. Balance of net base in the rat. II. Reference values in relation to growth rate. Biol Neonate 1976;28:171–90.
[241] Watanabe S, Matsushita K, McCray Jr. PB, Stokes JB. Developmental expression of the epithelial Na^+ channel in kidney and uroepithelia. Am J Physiol 1999;276(2 Pt 2):F304–14.
[242] Webster SK, Haramati A. Developmental changes in the phosphaturic response to parathyroid hormone in the rat. Am J Physiol 1985;249(2 Pt 2):F251–5.
[243] Wijkhuisen A, Djouadi F, Vilar J, Merlet-Benichou C, Bastin J. Thyroid hormones regulate development of energy metabolism enzymes in rat proximal convoluted tubule. Am J Physiol 1995;268(4 Pt 2):F634–42.
[244] Winberg J. Determination of renal concentrating capacity in infants and children without renal disease. Acta Paediatrica Scandinavia 1959;48:318–28.
[245] Winkler CA, Kittelberger AM, Watkins RH, Maniscalco WM, Schwartz GJ. Maturation of carbonic anhydrase IV expression in rabbit kidney. Am J Physiol Renal Physiol 2001;280(5): F895–903.
[246] Woda C, Mulroney SE, Halaihel N, Sun L, Wilson PV, Levi M, et al. Renal tubular sites of increased phosphate transport and NaPi-2 expression in the juvenile rat. Am J Physiol Regul Integr Comp Physiol 2001;280(5):R1524–33.
[247] Woda CB, Bragin A, Kleyman TR, Satlin LM. Flow-dependent K^+ secretion in the cortical collecting duct is mediated by a maxi-K channel. Am J Physiol Renal Physiol 2001;280(5): F786–93.
[248] Woda CB, Miyawaki N, Ramalakshmi S, Ramkumar M, Rojas R, Zavilowitz B, et al. Ontogeny of flow-stimulated potassium secretion in rabbit cortical collecting duct: Functional and molecular aspects. Am J Physiol Renal Physiol 2003;285(4): F629–39.
[249] Wu MS, Biemesderfer D, Giebisch G, Aronson PS. Role of NHE3 in mediating renal brush border Na^+-H^+ exchange. Adaptation to metabolic acidosis. J Biol Chem 1996;271 (51):32749–52.
[250] Yamamoto T, Sasaki S, Fushimi K, Ishibashi K, Yaoita E, Kawasaki K, et al. Expression of AQP family in rat kidneys during development and maturation. Am J Physiol 1997;272(2 Pt 2):F198–204.
[251] Yared A, Yoshioka T. Autoregulation of glomerular filtration in the young. Semin Nephrol 1989;9(1):94–7.
[252] Yasui M, Marples D, Belusa R, Eklof AC, Celsi G, Nielsen S, et al. Development of urinary concentrating capacity: role of aquaporin-2. Am J Physiol 1996;271(2 Pt 2):F461–8.
[253] Zink H, Horster M. Maturation of diluting capacity in loop of Henle of rat superficial nephrons. Am J Physiol 1977;233(6): F519–24.
[254] Zolotnitskaya A, Satlin LM. Developmental expression of ROMK in rat kidney. Am J Physiol 1999;276(6 Pt 2):F825–36.
[255] Zweifach A, Desir GV, Aronson PS, Giebisch G. Inhibition of Ca-activated K^+ channels from renal microvillus membrane vesicles by amiloride analogs. J Membr Biol 1992;128 (2):115–22.

This page intentionally left blank

CHAPTER

28

Renal Hyperplasia and Hypertrophy

Paul T. Brinkkoetter[1], *Sian V. Griffin*[2] *and Stuart J. Shankland*[3]

[1]University Hospital Cologne, Cologne, Germany
[2]University Hospital Wales, Health Park, Cardiff, Wales
[3]University of Washington, Seattle, Washington, USA

INTRODUCTION

The tight regulation of cell growth and division within an organ is essential for the development and maintenance of correct structure and function. Perturbations of renal growth occurring either developmentally or following injury to mature renal cells contribute to the abnormalities observed in a wide range of diseases. The changes in growth are increasingly recognized as an influence on the progression of the initial disease process, and the ultimate clinical outcome. Abnormal cell growth is classified according to the presence of an increase in cell number or cell size. Hyperplasia refers to abnormal growth resulting in an increased absolute number of cells, whereas hypertrophy refers to an increase in individual cell size. Both processes may be present in a given cell population and contribute to the increase in overall kidney size.

Of particular interest to clinical nephrologists and renal pathologists is the fact that the kidney has several different resident cell types. Within the glomerulus, the growth responses of the mesangial cell, podocyte, parietal epithelial cell, and endothelial cell differ. The tubulointerstitial cells and vascular smooth muscle cells also vary in their growth responses following injury. Thus, characterizing the mechanisms that regulate each cell's growth response enables the potential development of specific therapies that will modify the response to injury. We recognize that renal cell hyperplasia and hypertrophy are regulated by numerous pathways, involving growth factors, signaling pathways, and transcription factors. However, the focus of this review is to update the reader on recent advances in the regulation of these growth processes at the level of the cell cycle. We will first describe cell cycle regulation by specific cell cycle proteins, and then discuss hyperplasia and hypertrophy for individual glomerular and tubular cell types.

Although highly metabolically active, under normal conditions the cells of the mature kidney are relatively quiescent with respect to cell cycle entry. Following injury to either the glomerulus or the tubules, cell cycle progression with proliferation is often an essential part of the reparative process. However, if unchecked, proliferation can lead to compromise of renal function. Similarly, renal hypertrophy may occur as a compensatory physiological response, but unregulated hypertrophy is maladaptive, and is one of the hallmarks of diabetic nephropathy.

Cell proliferation is ultimately regulated at the level of the cell cycle, which occurs within the nucleus. Within the kidney, the control of the cell cycle is particularly intriguing, given the contrasting responses of the various resident cell types to injury. For example, the mesangial cell is capable of marked proliferation, often accompanied by the deposition of extracellular matrix. In contrast, the podocyte has been considered a relatively inert cell, although this view has recently been challenged, and the reparative proliferation of glomerular endothelial cells following injury has also been described. Renal tubular cells readily undergo both proliferative and hypertrophic responses following injury. The last decade has seen a rapid expansion in our understanding of the molecular mechanisms underlying the cell cycle, and therapeutic options for its manipulation are becoming available. There is currently increasing awareness of the need to reduce the progression of renal diseases. Knowledge of the cell cycle and an understanding of how this can be

Seldin and Giebisch's The Kidney, Fifth Edition.
DOI: http://dx.doi.org/10.1016/B978-0-12-381462-3.00028-8

© 2013 Elsevier Inc. All rights reserved.

influenced may be crucial to the prevention, control, and amelioration of a wide range of renal diseases.

MEASUREMENT OF CELL GROWTH

Hyperplasia

During a hyperplastic response, the number of proliferating cells is increased. A number of methods are available for measuring this increase, both *in vivo* and in cell culture. The majority of these have as their basis the detection of increased DNA synthesis. This may be done by determining the presence of proteins known to be associated with DNA synthesis, such as proliferating cell nuclear antigen (PCNA) or Ki-67, or by exogenously labeling cells with a compound known to be incorporated into newly synthesized DNA, such as ^{3}H thymidine or bromodeoxyuridine (BrdU). In cell culture, a convenient and high-throughput method for determining cell number is the MTT assay, in which the yellow tetrazolium salt is reduced in metabolically active cells to form insoluble formazan crystals, which are solubilized by the addition of detergent. The color intensity may then be quantified spectrophotometrically, allowing quantification of changes in proliferation. A caveat for this method is that a decrease in cell viability will mimic a decrease in proliferation, and concomitant apoptosis should be excluded. Analysis by fluorescent activated cell sorting (FACS) is a valuable tool for the assessment of hyperplasia, because it also allows quantification of the number of cells in each phase of the cell cycle.

Hypertrophy

Cellular hypertrophy may be defined as an increase in cell size due to an increase in protein and RNA content without DNA replication,[1,2] and this forms the basis for the majority of methods for detection of hypertrophy. Upon entry into G1, cells undergo a physiologic increase in protein synthesis prior to the DNA synthesis of S-phase. Thus, one mechanism underlying hypertrophy is cell cycle arrest at the G1/S checkpoint, so that while protein synthesis and hence content, increase, there is no subsequent increase in DNA. Hypertrophy may also occur independently of the cell cycle, due to an inhibition of protein synthesis, and this mechanism is considered to contribute to tubular cell hypertrophy.[3,4] Measurement of leucine or proline incorporation and comparison to ^{3}H thymidine incorporation allow determination of cell protein/DNA content, and hence assessment of hypertrophy. FACS analysis is also useful and enables direct measurement of cell size. Defining the growth response to a given stimulus as either hyperplastic or hypertrophic is important, as each will result from different alterations in cell signaling pathways, with implications for possible interventions.

CELL CYCLE AND CELL CYCLE REGULATORY PROTEINS

Cell Cycle

The cell cycle is divided into distinct phases, each representing a different function, and each being regulated by specific proteins[5] (Figure 28.1). Quiescent cells are termed as in G0, and upon mitogenic stimuli enter the cell cycle at early G1. Cells pass through the restriction point in late G1, beyond which they are typically unresponsive to extracellular cues, and are committed to complete the cell cycle despite the withdrawal of mitogenic stimuli. DNA synthesis occurs in S-phase. Cells then progress through G2, in preparation for mitosis (M-phase). Ultimately, cell division follows during cytokinesis. Our current understanding suggests there are at least two checkpoints to ensure fidelity of DNA duplication, at G1/S and G2/M, where cell cycle progression may be arrested. The length of the cell cycle is cell-type-specific, but this variability is largely due to differences in the duration of G1. For mammalian cells, the typical duration of G1 is approximately 12 hours, S- and G2-phases 6 hours, and mitosis 30 minutes.

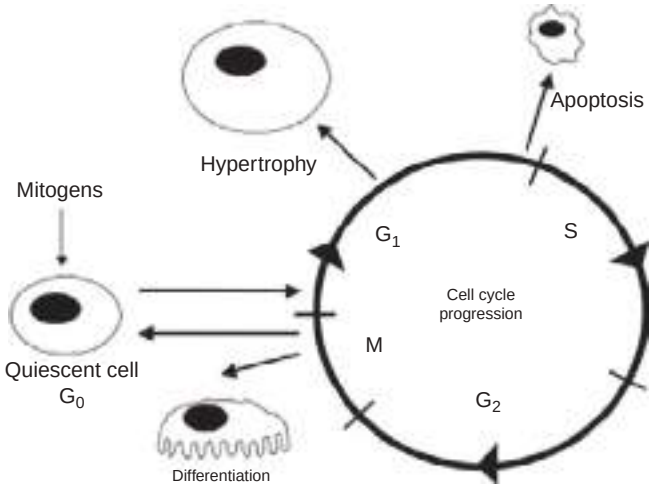

FIGURE 28.1 **The cell cycle and possible consequences of cell cycle exit.** Mitogens stimulate quiescent cells to engage the cell cycle at G1-phase. Hyperplasia then requires a coordinated and sequential series of events, including DNA synthesis at S-phase, followed by a resting G2-phase and mitosis in M-phase. This is followed by cell division. Cells that then exit the cell cycle and are quiescent again are in many cases differentiated. Of note is that if cells arrest at the G1/S-phase, they can develop a hypertrophic phenotype. Cell cycle exit with apoptosis may also occur.

Cyclins and Cyclin-Dependent Kinases: Positive Regulators of the Cell Cycle

Overview

The progress of a somatic cell through the cell cycle is dependent on the sequential and coordinated activation of the cyclin-dependent kinases (Cdks) by their specific partners, called cyclins (Figure 28.2). Cdks belong to the family of proline-directed serine/threonine kinases with a specific (K/R) (S*/T*) PX (K/H/R)-phosphorylation motif. Once active, Cdks phosphorylate downstream targets, ultimately to induce DNA synthesis.[6] While the levels of the Cdk catalytic subunits remain constant throughout the cell cycle, they are only functional following the binding of their specific cyclin partners. In contrast, cyclins are unstable proteins that are sequentially expressed and subsequently degraded by ubiquitination throughout the cell cycle,[7] which activate their partner Cdks by inducing conformational changes. Originally described for their fluctuation during the cell cycle,[8] members of the cyclin family are now defined by the presence of a conserved 100 amino acid cyclin box, which binds their complementary Cdk. In addition, the binding of inhibitors and accessory proteins, subcellular localization, and both inhibitory and activating phosphorylations influence the functional activity of the Cdk–cyclin complex.[9]

Jumpstarting the Cycle

The cell cycle is initiated by the mitogen-driven induction of cyclin D.[10–12] Depending on the cell type, three forms of cyclin D have been described (D1, D2, and D3), which interact allosterically with Cdk4 and Cdk6. Receptor-activated Ras signaling pathways lead to accumulation of cyclin D by three mechanisms: gene transcription; assembly; and stabilization of the cyclin D–Cdk complex.[13] The Ras-Raf-1-mitogen-activated, protein kinase kinase (MEK), extracellular signal-related protein kinase (ERK) pathway both induces cyclin D transcription and promotes assembly of cyclin D–Cdk.[14,15] The rate of degradation of cyclin D is controlled by a separate Ras signaling pathway involving phosphatidylinositol 3-kinase (PI3K) and protein kinase B (PKB/Akt), which inhibits the phosphorylation of cyclin D on threonine-286 (Thr-286) by glycogen synthase kinase 3β (GSKβ).[16] Thr-286 phosphorylated cyclin D would otherwise be exported to the cytoplasm for ubiquitination and degradation.[17] This requirement for mitogen signaling prevents the cell from autonomous cycling. Although ectopic expression of cyclin D is insufficient to drive cell cycle progression, constitutive activation of the cyclin D pathway can reduce the reliance of the cell on mitogenic stimulation, and lower the threshold for oncogenic transformation.[18] The cyclin D–Cdk4/6 complex enters the cell nucleus and is phosphorylated by Cdk-activating kinase (CAK).[19]

Once DNA replication begins, active cyclin D-dependent kinase activity is not required until mitosis is complete, and the cell re-enters the next G1 phase.[20] In continuously dividing cells, cyclin D1 is exported to the cytoplasm during S-phase, and its turnover is accelerated.[16,21] However, cyclin D1 synthesis stimulated by Ras is stabilized in G2 as described above, allowing reaccumulation before cells divide.[22] Hence, in the presence of continuous mitogen stimulation, the second and subsequent cell cycles are shorter than the first. Withdrawal of mitogens results in a rapid decline in cyclin D kinase activity, and cell cycle exit.

Active cyclin D-dependent kinases phosphorylate the retinoblastoma protein (pRb), which in quiescent cells has a growth-inhibitory effect.[23,24] In its hypophosphorylated state, pRb suppresses the transcription of several genes whose proteins are required for DNA synthesis, including the E2F transcription factors. Upon phosphorylation of pRb, the E2Fs are released from inhibition, leading to the transcription of cyclins E and A, and many genes whose products are required for DNA replication.[25] Furthermore, cyclin D–Cdk4 complexes also phosphorylate Smad3, negatively regulating the functions of transcriptional proteins responsible for mediating the growth inhibitory effects of transforming growth factor β (TGFβ).[26] Cyclin D-dependent kinases therefore affect the activity of at least two pathways that

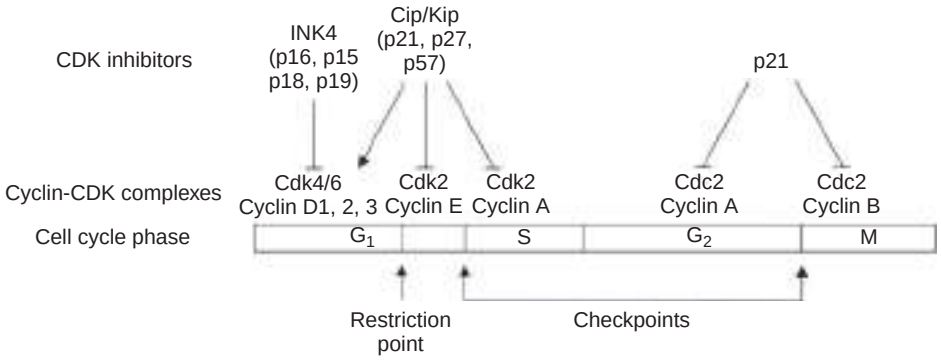

FIGURE 28.2 **Cell cycle progression: timing of activation of cyclins and Cdks, and site of action of Cdk inhibitors.** Each Cdk is activated by a partner cyclin in each phase of the cell cycle, and the resulting cyclin–Cdk complex can be inhibited by specific Cdk inhibitors.

independently inhibit the expression of cell cycle promoting genes.

The activity of cyclin E–Cdk2 is maximal at the G1- to S-phase transition,[27,28] when its function to further phosphorylate pRb releases the cell from mitogen dependency.[29,30] In addition to preferentially phosphorylating pRb on different sites to the cyclin D-dependent kinases, which may modify the interaction with E2Fs,[31] cyclin E–Cdk2 phosphorylates a second set of substrates involved in cell replication, thus affecting histone gene expression, and centrosome duplication.[32] The timing of expression and wider range of substrates suggest a role for cyclin E–Cdk2 in coordinating G1 regulation and the core cell cycle machinery.

The abrupt decline in cyclin E–Cdk2 activity in early S-phase results from cyclin E degradation. Phosphorylation by GSK-3β and Cdk2 itself target cyclin E for ubiquitination by the SCF^{Fbw7} E3 ligase, leading to proteasomal destruction.[33–35]

Low levels of cyclin A–Cdk2 activity are first detected in late G1-phase, increase as cells begin to replicate their DNA, and decline as cyclin A is degraded in early mitosis. The substrate specificity of cyclin A–Cdk2 is different from that of cyclin E–Cdk2. In S-phase, cyclin A–Cdk2 is thought to phosphorylate substrates that control the start of DNA replication from preassembled replication initiation complexes,[36–38] and control the integration of the end of S-phase with the activation of the mitotic Cdks.[39] The apparently central role of Cdk2 in coordinating cell cycle progression through S-phase and entry into mitosis has been challenged by the surprising observation that Cdk2 null mice are viable.[40,41] The possibility that other Cdks compensate for the loss of Cdk2 is currently a focus of intense research.

The entry to mitosis is controlled by cyclin B–Cdc2.[42,43] Cell cycle-regulated transcription of cyclin B begins at the end of S-phase. Phosphorylation on Thr161 by CAK parallels cyclin B binding to Cdc2.[44] During G2, cyclin B–Cdc2 complexes are maintained in an inactive state by phosphorylation on two inhibitory sites, Thr14 and tyrosine 15 (Tyr15) (Figure 28.3). Phosphorylation on Tyr15 is mediated by the nuclear Wee1 kinases,[166] and that on Thr14 by the membrane-bound Myt1.[45] In late G2 phase, both Thr14 and Tyr15 are dephosphorylated by Cdc25, thus activating cyclin B–Cdc2, and initiating mitosis.[46] Inappropriate triggering of mitosis is also prevented by the translocation of cyclin B to the cytoplasm by the nuclear export factor CRM1 (exportin 1) during S- and G2-phases.[47] Phosphorylation of cyclin B is thought to promote nuclear import at the G2/M transition.[48] Cyclin B–Cdc2 phosphorylates numerous downstream targets responsible for the structural reorganization of the cell to enable mitosis.

Although what is described above represents the basic paradigm of the control of cell cycle progression in mammalian cells, recent studies of knockout mice have demonstrated that much fetal development can occur normally despite the absence of cyclins and Cdks formerly considered to be vital.[49] Clearly, individual cyclins and Cdks are able to act more promiscuously than previously appreciated to enable compensation for the lack of a specific cell cycle protein.

Stopping the Cell Cycle: Cdk Inhibitors Act as Negative Regulators

In essence, Cdk inhibitors bind and inhibit target cyclin–Cdk complexes. Two classes of Cdk inhibitors have been described, the *INK4 proteins* and the *Cip/Kip family*.[50,51] Within each family, individual proteins are named according to their molecular weight. INK4 proteins were originally named for their ability to *in*hibit Cd*k4*. This family comprises four proteins, namely $p16^{INK4a}$, $p15^{INK4b}$, $p18^{INK4c}$, and $p19^{INK4d}$. Structurally these proteins are made up of multiple ankyrin repeats, and bind only to the catalytic subunits Cdk4 and Cdk6, thus inhibiting G1 progression. An alternate reading frame of the genetic locus encoding $p16^{INK4a}$ also encodes a second structurally and functionally unrelated protein named $p19^{ARF}$ in the mouse ($p14^{ARF}$ in the human).[52] Whereas $p16^{INK4a}$ acts to stabilize Rb by inhibition of Cdk4/6, $p19^{ARF}$ stabilizes p53 by binding its negative regulator, Mdm2.[53] Data from knockout mice suggest that $p19^{ARF}$, rather than $p16^{INK4a}$, is responsible for the tumor suppressor function of this locus.[54]

The second class of Cdk inhibitors is the Cip/Kip family, which includes $p21^{Cip1}$, $p27^{Kip1}$, and $p57^{Kip2}$,

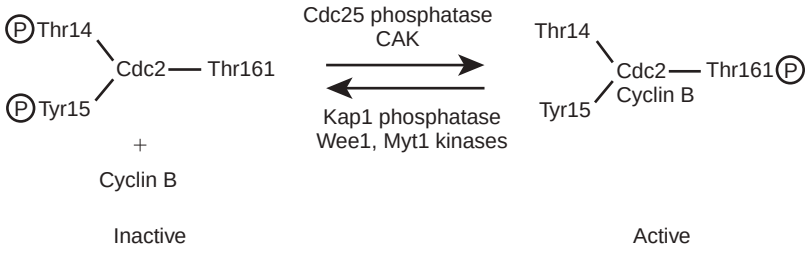

FIGURE 28.3 **Regulation of the phosphorylation status of Cdc2.** Wee1 and Myt1 kinases phosphorylate Cdc2 on Thr14 and Tyr15, inhibiting activity. Phosphorylation by CAK on Thr161 results in a 200-fold increase in kinase activity. Cdk2 is similarly phosphorylated on Thr160.

which share a conserved N-terminal Cdk-binding domain.[50] They are capable of binding a wider range of targets, and can variably affect the activities of cyclin D-, E-, A-, and B-dependent kinases.[43,51,55,56] Although potent inhibitors of cyclin E- and A-dependent CDK2, and to a lesser extent Cdc2, the Cip/Kip proteins have recently also been characterized, paradoxically, as positive regulators of the cyclin D-dependent kinases.[57]

The first member of the family to be identified was $p21^{Cip1}$,[58–60] and it is usually present at a low level in quiescent cells. As the cell enters the replicative cycle, $p21^{Cip1}$ levels rise, displace INK4 proteins from binding to Cdk 4/6, and promote the assembly of cyclin D-Cdk complexes.[61,62] This stabilizes the active complex and additionally provides a nuclear localization signal (NLS). The transcription of $p21^{Cip1}$ is increased by both p53-dependent[27] and -independent[63] pathways, such as those mediated by TGFβ.[64] The inhibitory role of $p21^{Cip1}$ becomes dominant later in the cell cycle, and levels are also increased in senescent cells.[65]

In contrast to $p21^{Cip1}$, the level of $p27^{Kip1}$ is usually high in quiescent cells, where its primary role is as an inhibitor of cell division.[66,67] Whereas $p21^{Cip1}$ is a principal mediator of the p53-dependent G1 arrest that occurs following DNA damage,[37] $p27^{Kip1}$ appears to be primarily responsible for mediating extracellular antiproliferative signals.[66,67] The levels and activity of $p27^{Kip1}$ are post-transcriptionally regulated by changes in the rates of translation, ubiquitination, and phosphorylation.[68,69] As cyclin D levels rise in response to mitogens, both $p21^{Cip1}$ and $p27^{Kip1}$ are sequestered by cyclin D–Cdk complexes, and therefore are unable to inhibit Cdk2.[51] Cyclin E–Cdk2 phosphorylates $p27^{Kip1}$ on Thr 187,[70,71] proving a recognition motif for an E3 ligase that targets $p27^{Kip1}$ for ubiquitination and proteasomal degradation.[72,73]

The most recently identified member of the family, $p57^{Kip2}$, was cloned in 1995.[74,75] While tissue expression of $p21^{Cip1}$ and $p27^{Kip1}$ is widespread, that of $p57^{Kip2}$ is restricted to placenta, muscle, heart, brain, lung, and kidney. In addition to the Cdk inhibitory domain and putative C terminal NLS, $p57^{Kip2}$ also has a proline-rich domain containing a consensus ERK phosphorylation site, and an acidic domain, the functions of which are not known.[74,75] A role for $p57^{Kip2}$ in the cell cycle exit that accompanies terminal differentiation has been suggested.

Despite their structural similarities, knockout studies have demonstrated divergent roles for the three Cip/Kip Cdk inhibitors. While $p21^{Cip1}$ and $p27^{Kip1}$ are not essential for normal embryogenesis,[50,76,77] lack of $p57^{Kip2}$ results in profound developmental abnormalities.[78–80] Most $p57^{Kip2}$ null mice die shortly after birth and have severe cleft palates, abdominal wall and gastrointestinal tract defects, and abnormal skeletal ossification. Unlike adult $p21^{Cip1-/-}$ mice,[81,82] $p27^{Kip1-/-}$ mice are larger than wild-type animals, and have hyperplasia of organs that usually express high levels of $p27^{Kip1}$, such as the thymus, spleen, adrenal and pituitary glands, testes, and ovaries.[50,76] In contrast, only 10% of $p57^{Kip2-/-}$ mice survive the weaning period and are much smaller than wild-type.[78] The kidneys of $p57^{Kip2-/-}$ mice have medullary dysplasia, although glomerular development appears normal.

HYPERPLASIA: AN INCREASE IN CELL NUMBER DUE TO PROLIFERATION

Glomerular Hyperplasia

Mesangial Cell Proliferation

Mesangial cell proliferation characterizes many forms of both experimental and human glomerular disease, including IgA nephropathy, lupus nephritis, diabetic nephropathy, and other forms of membranoproliferative glomerulonephritis (Figure 28.4). It is frequently associated with, and likely underlies, matrix expansion and subsequent glomerulosclerosis, the significance of which has been shown in a range of experimental models.[83–89] This simple observation provides the impetus for understanding what switches mesangial proliferation on and what switches it off. Several growth factors and cytokines are mitogens for mesangial cells, including platelet-derived growth factor (PDGF),[90,91] basic fibroblast growth factor (bFGF),[92] interleukin 6,[93,94] and the product of growth arrest-specific gene 6 (Gas6).[95] Intervention to reduce mesangial proliferation also reduces matrix

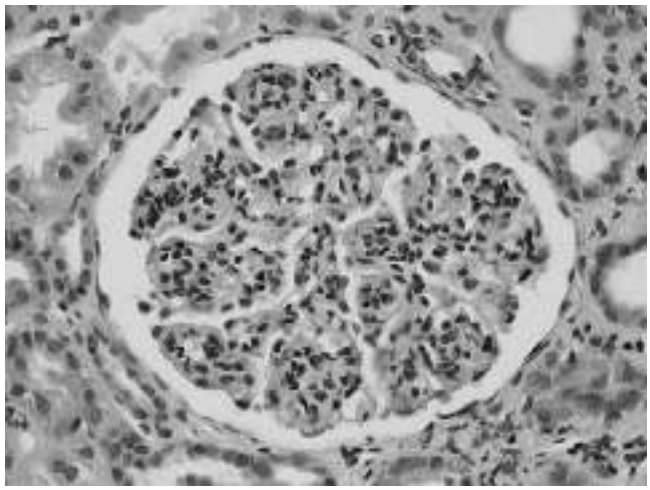

FIGURE 28.4 **Global mesangial cell proliferation occurring in the context of membranoproliferative glomerulonephritis (haematoxylin and eosin ×400).** *(Histology courtesy of Dr Meryl Griffiths, Addenbrooke's Hospital, Cambridge.)*

expansion, confirming the tight link between these two processes. This has been achieved in experimental models using complement depletion,[96,97] heparin infusion,[91] blocking the action PDGF[92,98] and bFGF,[83] and inhibiting their specific intracellular signaling pathways with phosphodiesterase inhibitors.[86] Warfarin has been used with mixed results in the treatment of glomerular diseases since the 1970s, and was originally hypothesized to reduce fibrin deposition. However, low-dose warfarin may also be effective, suggesting a mechanism of action not directly related to anticoagulation. Gas6 is a vitamin K-dependent growth factor for mesangial cells, and its inhibition by warfarin is likely to underlie the reported benefits of this treatment in human disease.[95] Careful research since the mid-1990s has delineated the role of individual cell cycle proteins in mesangial cell proliferation, and also its resolution by apoptosis (Figure 28.5).

ROLE OF CDK2 IN MESANGIAL CELL PROLIFERATION

Cdk2 protein and kinase activity increase in cultured mesangial cells in response to mitogenic growth factors.[99,100] The Thy1 model of experimental mesangial proliferative glomerulonephritis, induced in rats by an antibody directed against the mesangial Thy1 antigen, has provided an opportunity to study the regulation and consequences of mesangial cell proliferation *in vivo*.[101,102] The initial complement-dependent mesangiolysis is followed by a phase of marked mesangial proliferation, paralleled by an increase in extracellular matrix accumulation and a decline in renal function. This model is useful as not only may the fluctuations of cell cycle proteins during proliferation be defined, but also the effect of their manipulation. Mesangial cell proliferation is associated with an increase in cyclin D1 and A, and their partners Cdk4 and Cdk2.[103] Cdk2 expression is absent in the normal rat glomerulus. Proliferation is associated with increased Cdk2 activity, measured by the histone H1 kinase assay on protein extracted from isolated glomeruli. Bokemeyer et al. identified activation of the map kinase ERK as an upstream regulator of Cdk2 activity in the Thy1 model.[104] Inhibition of ERK was associated with decreased cell proliferation by 67%.[105] Cdk2 protein levels are also increased in the remnant kidney model, a nonimmune glomerular disease associated with mesangial proliferation.[106] Taken together, these studies show that in contrast to most nonrenal cells,[103] Cdk2 protein is at low levels in quiescent mesangial cells, and its levels and activity increase following injury.

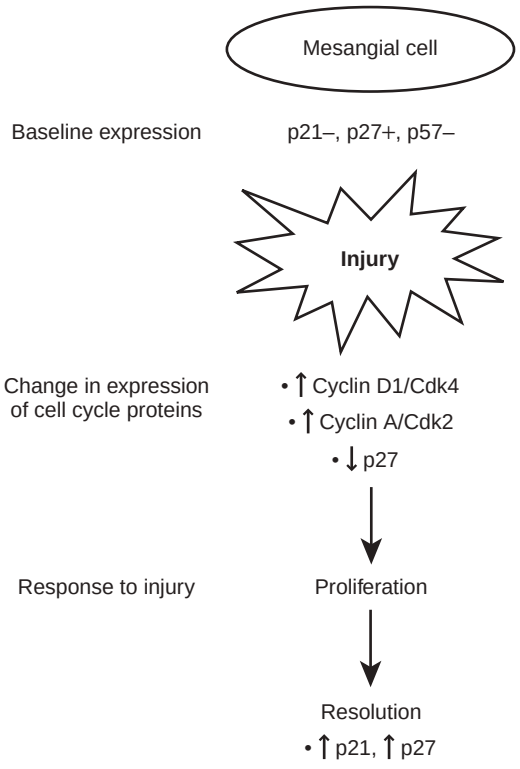

FIGURE 28.5 **Changes in cell cycle protein activity following injury to glomerular mesangial cells.** At baseline, quiescent mesangial cells express $p27^{Kip1}$, but not $p21^{Cip1}$ or $p57^{Kip2}$. Following injury, there is an increase in the positive cell cycle regulators cyclin D1/Cdk4 and cyclin A/Cdk2, with a decline in $p27^{Kip1}$, resulting in promotion of cell cycle progression and proliferation. During the resolution phase, there is an increase in the Cdk-inhibitors $p21^{Cip1}$ and $p27^{Kip1}$, with cessation of proliferation.

Cdk Inhibitors and Mesangial Cell Proliferation

The Cdk inhibitor $p27^{Kip1}$ is constitutively expressed in quiescent mesangial cells both *in vitro*[107] and *in vivo*,[103] whereas $p21^{Cip1}$ and $p57^{Kip2}$ are essentially absent.[103,108] In cultured mesangial cells, proliferation induced by mitogenic growth factors reduces $p27^{Kip1}$ levels.[107] Mesangial cells derived from $p27^{Kip1-/-}$ mice have augmented proliferation in response to mitogens,[109] and lowering $p27^{Kip1}$ levels with antisense oligonucleotides has a similar effect in rat mesangial cells.[107]

Complement-induced injury in the Thy1 model is associated with a marked decrease in $p27^{Kip1}$ levels.[103] However, there is *de novo* synthesis of $p21^{Cip1}$ in the resolution phase of the disease, coincident with a decrease in proliferation. To further explore the role of $p27^{Kip1}$ in inflammatory disease, we induced experimental glomerulonephritis in $p27^{Kip1-/-}$ mice.[110] Our results showed a marked increase in the onset and magnitude of glomerular cell proliferation and cellularity in nephritic $p27^{Kip1-/-}$ mice compared to control nephritic $p27^{Kip1+/+}$ mice. Moreover, this was associated with increased extracellular matrix proteins and a decline in renal function. To demonstrate that this

result was not specific to glomerular cells or immune-mediated injury, we also obstructed a ureter by ligation to induce nonimmune injury to tubuloepithelial cells.[110] Our results showed that tubuloepithelial proliferation was increased in obstructed $p27^{Kip1-/-}$ mice compared to obstructed $p27^{Kip1+/+}$ mice. Taken together, these studies were the first to show that in inflammatory diseases, renal cell proliferation is regulated by the CKI $p27^{Kip1}$, supporting a role for $p27^{Kip1}$ in controlling the threshold at which proliferation occurs.

Little is known about the role of the Cdk inhibtiors $p21^{Cip1}$ and $p57^{Kip2}$. In an immune-mediated model of MC disease, the absence $p21^{Cip1}$ was associated with increased focal segmental tuft necrosis, mesangiolysis, and mesangial hypercellularity.[111]

Role of Cell Cycle Proteins in Resolution of Mesangial Hyperplasia: Apoptosis

Although a characteristic response to mesangial cell injury is proliferation, apoptosis is often simultaneously increased.[85] Studies have shown that apoptosis is a vital mechanism required to normalize cell number in the reparative phase of injury.[112] However, the cellular pathways linking these opposing responses remain unclear. Many cells undergoing apoptosis have entered the cell cycle, but rather than completing their replication, they are destined to leave by programmed cell death. This suggests a role for the cell cycle proteins in directing these alternative outcomes.

Evidence to support this hypothesis was the observation that the resolution phase of Thy1 mesangial proliferation in the rat is characterized by mesangial cell apoptosis, a process that peaks when the levels of $p27^{Kip1}$ are at their lowest.[103] Considering glomerulonephritis or unilateral ureteric obstruction in $p27^{Kip1-/-}$ mice as described above, in addition to the increase in either glomerular or tubuloepithelial cell proliferation following injury, there was a marked increase in apoptosis in the $p27^{Kip1-/-}$ mice compared to wild-type disease controls.[110] Moreover, apoptosis was also increased in $p27^{Kip1-/-}$ mesangial cells in culture following growth factor deprivation or cycloheximide, and reconstituting $p27^{Kip1}$ levels by transfection-rescued cells from apoptosis.[109] In wild-type rat mesangial cells, apoptosis was increased following treatment with anti-$p27^{Kip1}$ antisense oligonucleotides.[109] These results showed for the first time that $p27^{Kip1}$ has a role beyond the regulation of proliferation, in that it also protects cells from apoptosis. This dual role of regulating the proliferative threshold and governing apoptosis makes $p27^{Kip1}$ a potent regulator of overall mesangial cell numbers. In contrast, $p21^{Cip1}$ showed no effect on MC apoptosis.[111]

HOW DOES $P27^{KIP1}$ PROTECT CELLS FROM APOPTOSIS?

A clue to a possible mechanism was the increase in Cdk2 activity in $p27^{Kip1-/-}$ mesangial cells when deprived of growth factors.[109] The increase was due specifically to cyclin A–Cdk2, and not cyclin E–Cdk2. Moreover, inhibition of cyclin A–Cdk2 activity by roscovitine or a dominant negative mutant reduced apoptosis in mesangial cells and fibroblasts. In apoptotic $p27^{Kip1-/-}$ mesangial cells, Cdk2 was bound to cyclin A, without a preceding increase in cyclin E–Cdk2 activity. We suggest that, in the absence of $p27^{Kip1}$, uncoupling of Cdk2 activity from the scheduled sequence of cell cycle protein expression may lead to an inappropriate and premature initiation of G_1/S-phase transition, causing the cell to respond by undergoing apoptosis, rather than inappropriately progressing through an unscheduled cell cycle.

HOW MIGHT Cdk2 CONTROL GROWTH AND APOPTOTIC FATE OF CELLS?

Apoptosis typically begins in the cytoplasm, whereas DNA synthesis and mitosis are nuclear events. Accordingly, we tested the hypothesis that the subcellular localization of Cdk2 determines if cells undergo apoptosis or proliferation.[113] As expected, Cdk2 protein was cytoplasmic in quiescent, and nuclear in proliferating, mesangial cells. However, in proliferating cells injured by an apoptotic stimulus, Cdk2 localized to the cytoplasm, was no longer nuclear, and importantly, remained active. Our results also showed that cyclin A, and not cyclin E, co-localized to the cytoplasm with Cdk2 in apoptotic cells, to form an active cytoplasmic cyclin A–Cdk2 complex. The translocation of Cdk2 is not p53-dependent, and inhibiting the nuclear localization signal has no effect. That inhibiting Cdk2 decreased apoptosis provides further support for a critical role for cytoplasmic Cdk2 in triggering programmed cell death. Thus, the subcellular localization of active Cdk2 determines the fate of a cell: when nuclear, cells proliferate; when cytoplasmic, cells die by apoptosis. The mechanism by which nuclear Cdk2 is translocated to the cytoplasm remains to be elucidated. These studies provide the novel paradigm that specific cell cycle regulatory proteins have a role in glomerular disease beyond the regulation of proliferation.

Therapeutic Inhibition of Mesangial Proliferation at Cell Cycle Level

In vitro and animal studies have recently revealed the potential of several novel therapies to modulate glomerular cell proliferation: the purine analog roscovitine, which inhibits Cdk2 activity; retinoids, derived from vitamin A; and lipoxins, endogenously produced

eicosanoids. Roscovitine and retinoids have also been used to beneficial effect in the treatment of podocyte diseases, discussed in the next sections.

ROSCOVITINE

The significance of increased Cdk2 activity in mesangial proliferation was demonstrated by Pippin et al.,[114] using roscovitine to inhibit Cdk2 in rats with Thy1 mesangioproliferative gomerulonephritis. Given immediately after disease induction, roscovitine significantly reduced mesangial cell proliferation. Moreover, administering roscovitine to rats once mesangial proliferation was already established also reduced proliferation. This inhibition of Cdk2 activity was accompanied by a marked reduction in the accumulation of glomerular extracellular matrix proteins (collagen IV, laminin, and fibronectin), and an improvement in renal function compared to controls. These results suggest that inhibiting Cdk2 may be a potential therapeutic target in glomerular diseases characterized by proliferation.

RETINOIDS

Retinoic acid (RA) has an established role in kidney development.[115,116] RA binds to specific nuclear receptors, and the RA receptor complex then binds to DNA−RA response elements to cause the transcription of target genes.[117] RA is used therapeutically in acute promyelocytic leukemia to slow proliferation and promote differentiation. RA-induced cell cycle arrest in nonrenal cells has been reported to involve reduction in c-Myc, cyclin D1, and cyclin E levels, with upregulation of $p21^{Cip1}$ and $p27^{Kip1}$.[118–120] The treatment of rats with experimental Thy1 glomerulonephritis with RA reduced mesangial cell proliferation, glomerular lesions, and albuminuria.[121] In addition to a direct antiproliferative action, RA has also been reported to modulate both the renin−angiotensin system[122] and TGFβ signaling,[123] in addition to anti-inflammatory and immune modulatory effects.[116] The efficacy of RA in the treatment of glomerulonephritis is likely due to its pleiotropic effects on these numerous pathways.

LIPOXINS

Lipoxins are endogenously produced eicosanoids with potent anti-inflammatory actions,[124] and are generated during the resolution phase of an acute inflammatory insult.[125] Lipoxin A_4 biosynthesis has been demonstrated in glomerulonephritis,[126] and its effects include modulation of leukocyte trafficking and phagocytic clearance of apoptotic cells.[124,125] *In vitro*, lipoxin A4 inhibits PDGF-induced activation of Akt/PKB in human mesangial cells, and modulates PDGF-induced decrements of $p21^{Cip1}$ and $p27^{Kip1}$.[127] PDGF-induced increases in Cdk2−cyclin E complex formation are also inhibited by lipoxin A_4. Prolonged exposure of mesangial cells to PDGF is associated with autocrine TGFβ production, and this is ameliorated by lipoxin A_4.

In vivo, lipoxins are rapidly metabolized. To enable study of these compounds in disease models, stable synthetic analogs have been developed that are modified at C-15, C-16, and/or C20.[128] These compounds retain the biological activity and receptor-binding affinity of the native lipoxin. The effect of a lipoxin A_4 analog, 15-epi-16-(FPho)-LXA-Me, has been studied in the immediate phase of experimental anti-GBM nephritis in mice, and found to inhibit neutrophil infiltration and glomerular nitrotyrosine staining.[129] Although animal studies with lipoxins are at an earlier stage than those with roscovitine or retinoids, their potential to augment the resolution phase of glomerulonephritis suggests that they may in the future have an important therapeutic role.

The Podocyte and Cell Cycle: Why Is Lack of Podocyte Proliferation Important?

The podocyte, or visceral glomerular epithelial cell, is a highly specialized, terminally differentiated cell overlying the outer aspect of the glomerular basement membrane. In contrast to the mesangial cell, numerous studies of both animal models and human disease have shown that aside from a few specific conditions, podocytes do not typically proliferate *in vivo* (Figure 28.6). Indeed, following injury, podocyte numbers may become depleted, because following cell loss by detachment or apoptosis, the lack of proliferation prevents normalization of podocyte number. Although initially the remaining podocytes may undergo a degree of compensatory hypertrophy, the decrease in podocyte number will eventually result in areas of "denuded" basement membrane, which is thought to predispose to the formation of synechiae between the GBM and Bowman's capsule, leading to the development of secondary focal glomerulosclerosis and subsequent decline in renal function.[130–134] Podocytes provide a size- and charge-dependent barrier to protein leakage into the urine, and are therefore a critical component of the glomerular filtration apparatus. Several studies in diverse renal diseases have shown a close correlation between the onset and progression of proteinuria and reduced podocyte number.[135–141] These events provide a compelling rationale to define the mechanisms underlying the lack of podocyte proliferation.

MATURE PODOCYTE HAS EXITED CELL CYCLE AND IS POSTMITOTIC

During glomerulogenesis, immature podocytes are capable of proliferation.[108,142] However, during the critical S-shaped body stage of glomerular development,

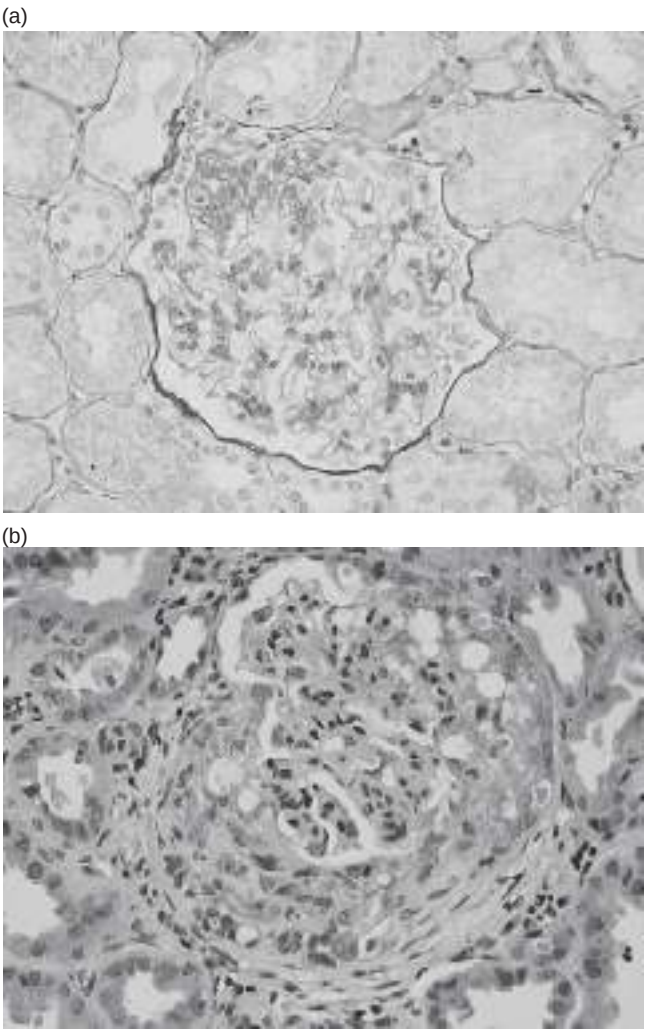

FIGURE 28.6 **The podocyte response to injury in human glomerulonephritis – to proliferate or not to proliferate?** (a) No proliferation, with development of segmental sclerosis, as occurs in idiopathic focal and segmental. (b) Proliferation, with the glomerulosclerosis (Periodic Acid Schiff, development of a cellular crescent in a patient with vasculitis (haematoxylin and eosin ×400). *(Histology courtesy of Dr Meryl Griffiths, Addenbrooke's Hospital, Cambridge.)*

podocytes exit the cell cycle in order to become terminally differentiated and quiescent, which are necessary requirements for normal function. Thus, in podocytes, proliferation and differentiation are closely linked, akin to neurons and cardiac myocytes. In both mouse and human glomerulogenesis, immunostaining for $p27^{Kip1}$ and $p57^{Kip2}$ is absent in proliferating podocytes during the S-shaped body stage.[108,142] On cessation of proliferation, there is strong expression of both Cdk inhibitors, so that $p27^{Kip1}$ and $p57^{Kip2}$ are constitutively expressed in mature podocytes. The Cdk inhibitors $p21^{Cip1}$, $p27^{Kip1}$, and $p57^{Kip2}$ alone are not required for normal glomerular development because, as described previously, the glomeruli from null mice are histologically normal. However, functional redundancy of $p27^{Kip1}$ and $p57^{Kip2}$, at least within the podocyte, has been suggested by studies of E13.5 embryonic metanephroi from double $p27^{Kip1}/p57^{Kip2-/-}$ mice. Glomeruli from these mice have been reported to be significantly larger than those from wild-type or single mutants, due to an increase in podocyte number. Differentiation of podocytes was judged to be normal by electron microscopy and immunostaining for WT-1, suggesting a synergistic role for $p27^{Kip1}$ and $p57^{Kip2}$ in determining the final complement of podocytes.

RESISTANCE OF PODOCYTES TO PROLIFERATION: ROLE OF CELL CYCLE REGULATORY PROTEINS

Studies have shown that the frequently observed lack of podocyte proliferation may be due to abnormalities in DNA synthesis or mitosis and cytokinesis (Figure 28.7).

The passive Heymann nephritis (PHN) model, induced by the administration of an antibody reactive against the Fx1A antigen on the rat podocyte, has many similarities to human membranous nephropathy.[143,144] In common with the Thy1 model of mesangial proliferative glomerulonephritis, PHN is complement (C5b-9)-dependent. However, in contrast to the observed mesangial cell proliferation in response

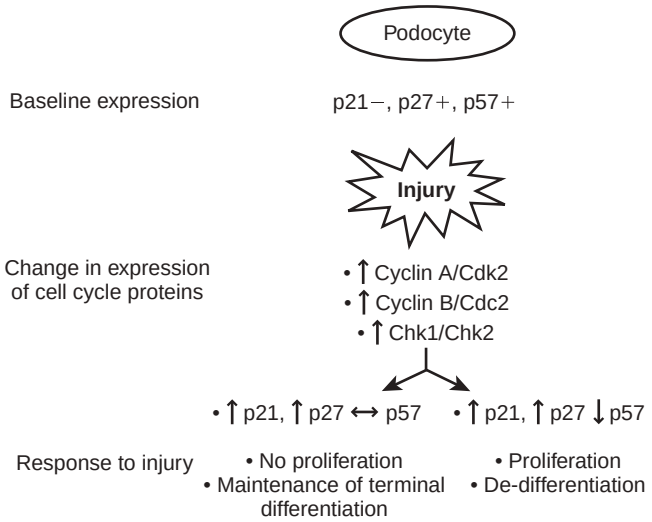

FIGURE 28.7 **Changes in cell cycle protein activity following injury to glomerular podocytes: the critical role of Cdk inhibitors in determining podocyte fate.** In contrast to mesangial cells, at baseline quiescent podocytes express both $p27^{Kip1}$ and $p57^{Kip2}$. Following injury, there is an increase in the positive cell cycle regulators cyclin A/Cdk2 and cyclin B/Cdc2; however, this is accompanied by an increase in checkpoint kinases 1 and 2. The subsequent podocyte response depends on changes in the Cdk inhibitors. If $p21^{Cip1}$ and $p27^{Kip1}$ increase, cell cycle entry remains inhibited, there is no proliferation, and terminal differentiation is maintained. However, if there is a decline in the levels of $p21^{Cip1}$, $p27^{Kip1}$, and $p57^{Kip2}$, then the cell cycle is engaged and proliferation and de-differentiation occur.

to complement-mediated injury, there is no increase in podocyte number. Mitotic figures and an increase in ploidy are seen in the acute phase of disease, but over time the number of podocytes decreases. The comparison of patterns of expression of cell cycle proteins between the PHN and Thy-1 disease models has provided an opportunity to elucidate the role of cell cycle proteins in experimental podocyte disease.

Following C5b-9-induced injury in PHN rats, protein levels for cyclin A and Cdk2 rise,[145] indicating engagement of the cell cycle. However, only a limited increase in DNA synthesis occurs, suggesting the presence of an inhibitor to cell cycle progression. Indeed, the levels of the Cdk inhibitors $p21^{Cip1}$ and $p27^{Kip1}$ increase specifically in podocytes following the induction of PHN.[145] The increase in $p21^{Cip1}$ is attenuated by administering the mitogen bFGF to PHN rats, and this augments the increase in podocyte DNA synthesis and ploidy. Furthermore, upregulation of M-phase cell cycle proteins Cdc2 and cyclin B is also observed in PHN podocytes, suggesting that a disturbance in cytokinesis is ultimately responsible for the development of polynucleated cells and lack of podocyte proliferation in this experimental glomerular disease.[146]

Cell culture studies have further explored the inability of podocytes to proliferate following C5b-9-induced injury, and support the hypothesis of a defect in completing mitosis. When cultured podocytes are exposed to sublytic C5b-9 attack, the cells engage the cell cycle. However, there is a delay or inhibition in entering mitosis, suggesting a block in the G_2/M transition, and involvement of mechanisms that regulate this checkpoint. This response is typical of that following DNA damage, to which podocytes appear to be particularly susceptible. The occurrence of DNA damage following exposure to sublytic C5b-9 has subsequently been confirmed,[147] together with increased checkpoint kinase-1 and -2 protein levels, thus arresting cells at G_2/M. The mechanism by which DNA damage occurs in podocytes is not currently well-understood, but is thought to involve the generation of reactive oxygen radicals.

A key role for $p21^{Cip1}$ in limiting the proliferative response of podocytes has been demonstrated in studies using $p21^{Cip1}$ knockout mice.[148,149] The administration of an antiglomerular antibody to induce experimental podocyte injury caused podocyte dedifferentiation and proliferation in $p21^{Cip1-/-}$ mice compared to control mice receiving the same antibody. Glomerular extracellular matrix accumulation was also increased in $p21^{Cip1-/-}$ mice, and was associated with a significant decrease in renal function. Additional *in vitro* data could link the pro-apoptotic effect of TGF-beta1 in podocytes to $p21^{Cip1}$.[150] Podocyte apoptosis induced by TGF-beta1 required sufficient $p21^{Cip1}$ levels.

Intravenous application of the podocyte toxin Adriamycin resembles the histological findings of focal segemental glomerulosclerosis (FSGS) in mice. Diseased $p21^{Cip1-/-}$ mice presented with increased podocyte apotosis and decreased podocyte number, leading to aggravated glomerular disease including worse albuminuria, glomerulosclerosis, and increased BUN compared to control animals.[151]

The resistance of podocytes to proliferation in the majority of animal models has been confirmed in human diseases, and similar underlying mechanisms have been observed. Normal quiescent podocytes express $p27^{Kip1}$ and $p57^{Kip2}$, and immunostaining for these proteins is maintained in conditions without proliferation, namely minimal change diseases and membranous glomerulopathy.[152] In contrast, expression of both these proteins is uniformly decreased in diseases characterized by podocyte proliferation, that is, cellular FSGS, collapsing glomerulopathy, and HIV-associated nephropathy. This is accompanied by the *de novo* expression of $p21^{Cip1}$. The mechanisms by which the podocyte eludes the usual constraints on proliferation are discussed below.

RESISTANCE OF PODOCYTES TO PROLIFERATION: ROLE OF MECHANICAL STRETCH

An additional factor reported to influence the proliferative capacity of the podocyte is the presence of mechanical stress.[153] Independent of the site of initial injury, a common pathway to progressive glomerulosclerosis is an increase in intraglomerular pressure, also known as glomerular hypertension.[130,132,154] Lowering intraglomerular pressure reduces progression in a number of glomerular diseases, including diabetic nephropathy.[155] Glomerular hypertension is associated with glomerular hypertrophy (see below), and the resultant mechanical stretch causes injury to all three glomerular cell types. Whereas applying mechanical stretch to cultured mesangial cells increases proliferation,[156] the opposite response is seen in cultured podocytes.[157,171] Stretching mouse podocytes in culture decreased the levels of cyclins D1, A, B1, and Cdc2, in association with an increase in the Cdk inhibitors. Stretch caused an early increase in $p21^{Cip1}$, followed by an increase in $p27^{Kip1}$ at 24 hours and $p57^{Kip2}$ at 72 hours. In contrast to the growth arrest seen in wild-type cells exposed to stretch, $p21^{Cip1-/-}$ podocytes exposed to stretch continued to proliferate, suggesting a role for $p21^{Cip1}$ in the inability of the podocyte to progress through the cell cycle in response to stretch. These studies show that in addition to being injurious to mesangial cells, mechanical stretch affects podocytes and reduces their proliferative potential by altering specific cell cycle proteins.

PODOCYTE PROLIFERATION

Although the majority of both experimental animal models of podocyte injury and human podocyte diseases are not associated with proliferation, this has been reported to occur in a limited number of settings. The true ability of the mature podocyte to proliferate remains controversial, principally because glomerular cells believed to be proliferating podocytes frequently lack defining cell-type-specific markers.[158] However, the use of transgenic animals has been invaluable in resolving the debate. A well-studied animal model of podocyte proliferation is crescentic glomerulonephritis in the mouse, which has been examined in detail by several groups. In this model, predictable proliferation of glomerular cells occurs, and early in the course of the disease this is not associated with rupture of Bowman's capsule, nor with the presence of infiltrating cells.[159] It is therefore a useful model for studying the contribution of intrinsic glomerular cells to crescent formation. Moeller et al. generated a mouse with constitutive expression of β galactosidase specifically in podocytes *in vivo*.[160] Experimental crescentic nephritis was induced by injecting rabbit IgG ip, followed six days later by an intravenous injection of rabbit anti-mouse GBM antibody. The crescents contained numerous β-galactosidase-expressing cells, confirming their podocyte origin. Furthermore, expression of the nuclear proliferation marker Ki-67 by these cells demonstrated the capability of these podocyte-derived cells to undergo proliferation. Matsusaka et al. generated a transgenic mouse with podocyte-specific expression of human CD25.[161] Injury was then induced using an immunotoxin, resulting in a proliferative glomerular lesion. However, immunohistochemistry indicated that the proliferating cells were of parietal epithelial origin, not podocytes. The disparity between these two results likely results from the different initiating injuries used, but illustrates the ongoing debate which was further fueled by recent data.[162] Smeets et al. could show, by lineage tracing of either podocytes or parietal epithelial cells (PECs), that the majority of cells within extracapillary proliferative leasions were PECs, and only a minority were of podocyte origin. This held true in the nephrotoxic nephritis model of inflammatory crescentic glomerulonephritis, and in the Thy-1.1 transgenic mouse model of collapsing glomerulopathy. As described above, once podocytes proliferate they lose several of their defining characteristic proteins, such as WT-1, making identification difficult. However, there is broad agreement that the proliferating resident glomerular cells making up crescents are of epithelial origin, although the relative contributions of parietal cells and podocytes remains disputed.

In human disease, podocyte proliferation is considered to occur in collapsing glomerulopathy, cellular focal segmental glomerulosclerosis, and HIV-associated nephropathy.[163,164] In these diseases, there is increased expression of cyclin A and the proliferation marker Ki-67, with a marked reduction in $p27^{Kip1}$ and $p57^{Kip2}$.[152,164] In contrast, all other diseases of podocytes in humans, including membranous nephropathy, minimal change disease, and focal segmental glomerulosclerosis, are not associated with a decrease in Cdk inhibitor levels, and typical markers of proliferation are absent. Interestingly, the rate of progression to end-stage renal failure is increased in glomerular diseases characterized by podocyte proliferation.[165,166] The pathogenesis of HIV-associated nephropathy has been further detailed using transgenic mice expressing HIV-1 genes.[167–169] The Tg26 mouse model develops murine HIVAN secondary o renal expression of HIV-1 mRNAs from the HIV-1 NL4-3 gag-pol proviral transgene.[169] This model has enabled characterization of the cellular effects of HIV-1 using both the intact animal and conditionally immortalized podocytes in culture. HIV-1 induces loss of contact inhibition in podocytes,[170] and expression of cyclin D1 and phosphorylation of pRb.[171] The cells become dedifferentiated, with loss of specific podocyte-expressed proteins.[167,172] Interestingly, there have been reports of reversibility of HIV nephropathy in both mice (discussed below) and human disease[173] following treatment with highly active antiretroviral therapy, suggesting that once the virus is cleared the podocyte is capable of exiting the cell cycle and redifferentiating to its mature phenotype.

ATYPICAL EFFECTS OF CELL CYCLE PROTEINS ON PODOCYTES

The traditional view of cell cycle proteins focuses on the regulation of cellular proliferation. The view on cell cycle proteins has since been broadened by the discovery of atypical cyclin proteins and dependent kinases. These include cyclin C-Cdk8, cyclin H-cdk7, cyclin K-Cdk9, cyclin T-Cdk9 or cyclin I-Cdk5.[174] We could show that cyclin I null mice are normal consistent with the notion that cyclin I is not required for cell differentation. Cyclin I is predominantly expressed in terminally differentiated cells, including neurons and podocytes. Lack of cyclin I rendered podocytes more susceptible to apoptosis.[175] A potential mechanism included a decreased expression and protein stability of p21.

The Cdk partner of cyclin I remained elusive since its discovery. We could identify Cdk5 as the Cdk partner of cyclin I.[176] Cdk5 itself is essential for normal development, as Cdk5 null mice die from developmental deficits, but little is known about its

function in the kidney. Cdk5 is mainly activated by the non-cyclin proteins p35 and p39. The latter is not expressed in podocytes, but p35−Cdk5 has been shown to be present in podocytes.[177] In 2004, Griffin et al. demonstrated an essential role for p35−Cdk5 in podocyte differentation, proliferation, and maintenance. Cdk5 levels decline in experimental disease associated with podocyte dedifferentation and proliferation, including anti-glomerular antibody disease and HIV-associated nephropathy. More recent *in vivo* and *in vitro* data support the model that Cdk5 is central to podocyte survival, and is dually regulated by cyclin I and p35. Downstream targets of Cdk5 were the pro-survival proteins Bcl-2 and Bcl-XL.[174,176,178]

Therapeutic Inhibition of Podocyte Proliferation at Cell Cycle Level

As with glomerular diseases principally affecting the mesangial cell, both roscovitine and retinoids have shown promise as therapeutic agents in modulating the podocyte response to injury. In addition, recent data suggest a direct effect of glucocorticoids on podocytes at the cell cycle level.

ROSCOVITINE

We hypothesized that inhibition of podocyte proliferation with the Cdk2 inhibitor roscovitine in a mouse model of crescentic glomerulonephritis would improve renal outcome,[179] similar to that observed following inhibition of mesangial cell proliferation in Thy 1 nephritis described previously.[114] Inhibition of Cdk2 activity was confirmed by a histone kinase assay, and podocyte DNA synthesis measured by incorporation of BrdU. Compared to control nephritic animals receiving the vehicle, in mice treated with roscovitine there was a significant decrease in BrdU at day 5 of nephritis. This was accompanied by less accumulation of laminin at day 14, and significantly improved renal function, suggesting a similar intervention may be beneficial in human diseases. Roscovitine has also been demonstrated to be beneficial in the treatment of Tg26 mice at doses that did not decrease HIV-1 transgene expression, suggesting an effect mediated by inhibition of cell cycle progression.[180]

RETINOIDS

Retinoids are particularly attractive agents for the treatment of podocyte disease, as it has been demonstrated that following podocyte injury, both decrease podocyte proliferation and maintain the expression of markers of differentiation.[181,182] The promoter region of the human nephrin gene (NPHS1) contains three putative retinoic acid-response elements, and shows enhancer activity in response to all-trans-retinoic acid (ATRA) in a dose-dependent manner. We have recently demonstrated that ATRA *in vitro* significantly retards podocyte proliferation, as measured by the MTT assay, while inducing process formation and increasing the expression of both nephrin and podocin.[182] Similarly, in mice with antiglomerular antibody nephritis, treatment with ATRA both reduces podocyte proliferation and prevents the decreases in nephrin, podocin, and synaptopodin in experimental animals. This was accompanied by a reduction in proteinuria. The dual roles of retinoids to both inhibit proliferation while promoting differentiation underscore their potential value as therapeutic agents for human podocyte diseases.

GLUCOCORTICOIDS

Glucocorticods are the clinical backbone to treat patients with glomerular diseases. Their mode of action is poorly-understood, particularly in patients with steroid-sensitive nephritic syndrome which lacks any signs of inflammation in the glomerulus. *In vitro* data in human podocytes revealed direct effects of dexamethasone on human podocytes.[183] Incubation with steroids led to decreased expression of p21 and suppression of inflammatory chemokines (IL-6/IL-8), but did not induce apoptosis.

Parietal Epithelial Cell Proliferation

As outlined above, there is an ongoing debate on the cellular origin of extracapillary proliferative lesions in glomerular disease. The parietal epithelial cell (PEC) has long been neglected, but recently moved into the center of glomerular research.[184] PECs share a common lineage with podocytes until the S-shaped stage of glomerulogenesis. Between the S-shaped body and capillary loop stages, each cell begins to express distinct genes, used as "cell-specific markers." For example, Wilm's tumor suppressor protein 1 (WT-1) expression is no longer detected in PECs, whereas podocytes maintain WT-1 and gain vimentin expression. In mice, PECs express CD10 in the capillary loop stage of development.[158] Potential mechanisms underlying PEC proliferation result from studies of cell cycle proteins. In contrast to podocytes, expression of the Cdk inhibitors $p21^{Cip1}$ and $p57^{Kip2}$ were not detected in healthy PECs, whereas $p27^{Kip1}$ was expressed at low levels. In experimental and human forms of FSGS, PECs showed increased DNA-synthesis. The increased expression of Ki-67 and cyclin A were accompanied by decreased $p27^{Kip1}$ expression in the absence of $p21^{Cip1}$ and $p57^{Kip2}$.[185] Suzuki et al. recently showed in a mouse model of FSGS, that PEC proliferation was in part regulated by $p21^{Cip1}$.[186]

Glomerular Endothelial Cell Proliferation

The endothelial cells of mature glomeruli are quiescent, but retain the capacity to proliferate and form new capillaries following injury.[187] The degree of proliferation appears to be dependent on the local balance of proangiogenic factors, such as vascular endothelial growth factor (VEGF), and antiangiogenic factors, such as thrombospondin-1. An inadequate proliferative response may lead to loss of the glomerular microvasculature, and contribute to glomerulosclerosis and progressive renal impairment. The beneficial effects of VEGF administration have been demonstrated in animal models of acute glomerulonephritis,[188–190] suggesting that amelioration of human diseases may be achieved by augmenting the reparative potential of the glomerular endothelial cells. However, the underlying role of individual cyclins, Cdk, and Cdk inhibitors in these cells remains unknown.

Tubular Cell Hyperplasia

Renal tubular hyperplasia is most frequently encountered during the reparative phase following an acute injury, such as ischemia or toxin exposure.[191] Tubular injury results in cell loss by either necrosis or apoptosis, and therefore there is a requirement for the remaining cells to spread and migrate to cover the exposed basement membrane. These cells then dedifferentiate and proliferate to restore cell number, and finally differentiate again to restore the functional integrity of the nephron. Interestingly, the tubular repair recapitulates organogenesis in patterns of gene expression, including vimentin, neural cell adhesion molecule, growth factors such as IGF-1, fibroblast growth factor, and hepatocyte growth factor; and matrix molecules such as osteopontin.[191] This dedifferentiated phenotype is likely to be important for the spreading and proliferative properties of the viable tubular epithelial cells as they cover the denuded basement membrane to replace lost cells. However, the factors controlling the reversion to a less-differentiated phenotype, and the subsequent re-establishment of the mature phenotype, remain poorly-understood.

As might be expected, the proliferation observed following a transient ischemic injury is associated with an increase in the mRNA and protein expression of cyclins D1, D3, and B, mRNA expression of cyclin A, and protein expression of Cdks 2 and 4.[192] Both cyclin-D and -E kinase activities are increased.[192] Thus, the proliferative response is due to increased expression of both the regulatory and catalytic subunits of the G1 kinases, and an increase in their activity.

The Cdk inhibitors appear to have a critical role in limiting the proliferative response. Following acute renal injury induced by ischemia, ureteral obstruction or cisplatin, $p21^{Cip1}$ protein expression is increased in the thick ascending limb of the loop of Henle, and in the distal convoluted tubule.[193] Induction of the same injury in $p21^{Cip1-/-}$ mice was associated with increased proliferation, as assessed by BrdU incorporation and PCNA staining.[194] The $p21^{Cip-/-}$ mice had a more rapid onset of acute renal failure, developed more severe morphological damage, and had a higher mortality, emphasizing the requirement for proliferation following injury to be at a controlled and appropriate level.

HYPERTROPHY

Hypertrophy has been described in most segments of the nephron, but proximal tubular hypertrophy is observed most frequently. Hypertrophy of the proximal tubule has been described in compensatory renal growth, chronic metabolic acidosis and chronic hypokalemia, diabetes mellitus, and during protein-loading.[195] In compensatory renal growth, there is also hypertrophy of the glomerulus and collecting tubules; in diabetes, hypertrophy of glomerular cells is well-described, and with prolonged protein-loading hypertrophy of the initial segments of the thick ascending limb occurs.

As mentioned previously, cellular hypertrophy may result from either cell cycle-dependent or -independent mechanisms. Within the glomerulus, an increase in cell size is predominantly due to cell cycle re-entry without progression, whereas in the tubules there appears to be a more significant contribution from the inhibition of protein synthesis.

Glomerular Hypertrophy

Glomerular cell hypertrophy occurs during many forms of chronic renal disease, and may herald the development of glomerulosclerosis.[130,196,197] Glomerular diseases associated with glomerular hypertrophy include diabetic nephropathy,[198] minimal change nephropathy,[199] focal segmental glomerulosclerosis,[200,201] and a reduction in renal mass.[202] However, there are clear differences in the prognosis of glomerular hypertrophy, depending on the underlying disease. Following uninephrectomy, the hypertrophy is compensatory, and is not typically associated with the development of glomerulosclerosis. In contrast, the hypertrophy of diabetic nephropathy antecedes and probably underlies the development of glomerulosclerosis.[169] Diabetic nephropathy is the leading cause of end-stage renal disease in Western countries, and is

discussed further below. Pathological glomerular hypertrophy leads to progressive glomerulosclerosis and scarring by a number of different mechanisms.[196] The increased metabolic rate of cells undergoing hypertrophy results in enhanced mitochondrial oxygen consumption, which may lead to tissue injury due to the generation of reactive oxygen radicals and the subsequent peroxidation of proteins and lipids. The hypertrophy is often initiated by growth factors that also stimulate the cells to increase production of extracellular matrix components, such as type IV collagen.

Diabetic Nephropathy

Diabetes mellitus is now the most frequent cause of end-stage renal failure in Western countries, and the pathogenesis of diabetic nephropathy is discussed in detail elsewhere in this book. The focus of this chapter is on the disordered cell growth seen in association with diabetic renal involvement. The hallmarks of human diabetic nephropathy are similar in both type I and type II diabetes, and consist of mesangial cell hypertrophy and podocyte loss, with accumulation of extracellular matrix in the mesangium and tubulointerstitium, resulting in glomerulosclerosis and tubulointerstitial fibrosis.[203–205] Research has concentrated principally on the ability of hyperglycemia and TGF-β to induce mesangial cell hypertrophy, and more recently the roles of RAGE[206] and hyperinsulinemia[207] have also been studied.

DIABETES AND MESANGIAL CELLS

HYPERGLYCEMIA *In vitro* culture of mesangial cells in high glucose media causes cell cycle entry and a biphasic growth response.[208] Following initial proliferation, the cells arrest in G1-phase, and there is progressive hypertrophy. Both kidney and glomerular hypertrophy induced by hyperglycemia are associated with an early and sustained increase in expression of cyclin D1 and activation of Cdk4.[209] An arrested cell cycle suggests a role for the Cdk inhibitors in mediating hypertrophy, and indeed high glucose increases the levels of both $p21^{Cip1}$ [210] and $p27^{Kip1}$ [211] in cultured mesangial cells. This is mediated by a number of factors, including glucose itself, TGF-β, which then acts in an autocrine fashion,[212,213] and CTGF.[214] High glucose directly stimulates the transcription of $p21^{Cip1}$,[215] and activates MAP kinases, which prolong the half-life of $p27^{Kip1}$ by phosphorylation on serine residues.[216] Lowering $p21^{Cip1}$ [217] or $p27^{Kip1}$ [211] levels with antisense oligonucleotides reduces the hypertrophic effects of high glucose. Moreover, hypertrophy is not induced by high glucose in $p21^{Cip1-/-}$ (unpublished observations) and $p27^{Kip1-/-}$[218] mesangial cells *in vitro*. Indeed, high glucose increases proliferation in $p27^{Kip1-/-}$ mesangial cells, whereas it arrests cell cycle progression in $p27^{Kip1+/+}$ mesangial cells.[218] Reconstituting $p27^{Kip1}$ levels in $p27^{Kip1-/-}$ mesangial cells by transfection restores the hypertrophic phenotype.[218] These studies show a compelling role for the Cdk inhibitors $p21^{Cip1}$ and $p27^{Kip1}$ in mediating the hypertrophy induced by high glucose.

These *in vitro* findings have been confirmed in experimental models of both type I and type II diabetic nephropathy. Considering type I diabetes, the glomerular protein levels of $p21^{Cip1}$ are increased in the streptozotocin (STZ)-induced model in the mouse,[210] and both $p21^{Cip1}$ and $p27^{Kip1}$ levels are increased in the glomeruli of diabetic BBdp rats.[64] A similar increase was noted in glomeruli of *db/db* mice[215] and the Zucker diabetic fatty rat,[219] models of type II diabetic nephropathy. Diabetic $p21^{Cip1-/-}$ mice are protected from glomerular hypertrophy.[220] Diabetic $p27^{Kip1-/-}$ mice have only mild mesangial expansion and no glomerular or renal hypertrophy compared to control diabetic $p27^{Kip1+/+}$ mice, despite upregulation of glomerular TGF-β.[221] These results support a critical role for the Cdk inhibitors $p21^{Cip1}$ and $p27^{Kip1}$ in mediating the glomerular hypertrophy seen not only in association with diabetes, but also as described in the following, a reduction in nephron number.

TRANSFORMING GROWTH FACTOR β The cytokine TGF-β has been shown in numerous settings to be a key mediator of progressive fibrosis in renal disease.[222–224] TGF-β also decreases proliferation in mesangial cells, an effect that appears to be independent of $p21^{Cip1}$ and $p27^{Kip1}$, and induces cell hypertrophy.[225–227] To determine the role of Cdk inhibitors in mediating the hypertrophic effects of TGF-β, mesangial cells derived from single and double null mice were studied.[226] Compared to wild-type mice, hypertrophy was significantly reduced in double $p21^{Cip1}/p27^{Kip1-/-}$ mesangial cells. A less marked reduction in hypertrophy was seen in the single $p21^{Cip1-/-}$ and $p27^{Kip1-/-}$ cells. These results show that although $p21^{Cip1}$ and $p27^{Kip1}$ each contribute to the hypertrophic action of TGF-β, the presence of both is required for maximal effect.

The expression of Cdk inhibitors has also been explored in response to CTGF, considered to be a principle mediator of the downstream effects of TGF-β. Abdel Wahab et al.[214] demonstrated that CTGF is a hypertrophic factor for human mesangial cells, and that this hypertrophy is associated with the induction of $p15^{INK4b}$, $p21^{Cip1}$, and $p27^{Kip1}$, with the maintenance of pRb in a hypophosphorylated state.

Diabetes and Podocytes

Morphometric analyses have demonstrated that the podocyte undergoes hypertrophy early in the course of

both animal models of diabetic nephropathy[219,228–230] and in human disease.[140,231] This hypertrophy may be in direct response to the metabolic changes associated with diabetes or compensatory, consequent to the loss of podocytes that is known to occur.[232,233]

At the level of the cell cycle, mRNA and protein expression of $p27^{Kip1}$ is increased in both cultured podocytes exposed to high glucose, and in glomeruli isolated from streptozotocin-induced diabetic rats.[230] The $p27^{Kip1}$ gene appears to be haplo-insufficient, as diabetic $p27^{Kip1+/-}$ mice exhibited an intermediate degree of functional and structural renal injury.[234] High glucose also significantly increased angiotensin II levels both in cell lysates and media compared with normal glucose, and exogenous angiotensin II increased $p27^{Kip1}$ mRNA and protein expression. Exposure of cultured cells and treatment of diabetic rats with an angiotensin II receptor antagonist (ARB) inhibited the increase in $p27^{Kip1}$. Glomerular hypertrophy was also significantly prevented by ARB treatment. It appears likely that similar cell cycle mechanisms drive both mesangial cell and podocyte hypertrophy in diabetic nephropathy, suggesting that podocytes in this setting are also capable of engaging the cell cycle.

Compensatory Glomerular Hypertrophy

A reduction in nephron number results in compensatory hypertrophy in the remaining viable nephron.[235] Uninephrectomy does not alter the protein expression of cyclins D1 or D2, nor of Cdk2 or Cdk4, when total renal lysates are studied at day 7.[236] However, there may be a differential effect in specific renal compartments,[187] and an increase in tubular cyclin E–Cdk2 activity was demonstrated during compensatory hypertrophy following uninephrectomy. Prior to hypertrophy, severe renal ablation produced by 5/6 nephrectomy resulted in an early proliferative glomerular response, associated with an increase in cyclin E expression and phosphorylation of pRb.[106]

A role for the Cdk inhibitors is now emerging in the pathogenesis of glomerular hypertrophy. Following partial renal ablation, $p21^{Cip1-/-}$ mice develop glomerular hyperplasia rather than hypertrophy and increased intraglomerular pressure, with protection from the development of progressive renal failure.[237] Increased intraglomerular pressure is a final pathway toward glomerulosclerosis in systemic hypertension, diabetes, and focal segmental glomerulosclerosis (FSGS). This glomerular hypertension causes stress-tension, or stretch, on resident glomerular cells, with differing consequences for the different cell types. Exposure of mesangial cells to cyclical mechanical stretch results in cell cycle entry and proliferation.[238] In contrast, mechanical stretch reduces cell cycle progression and induces podocyte hypertrophy *in vitro*.[157] This is unchanged in $p27^{Kip1-/-}$ cells, but hypertrophy was not induced in $p21^{Cip1}$ and double $p21^{Cip1}/p27^{Kip1-/-}$ podocytes, indicating a requirement for $p21^{Cip1}$. Stretch-induced hypertrophy required cell cycle entry, and was prevented by specifically blocking Erk1/2 or Akt. However, it is not clear whether podocyte hypertrophy represents a beneficial adaptive response to raised intraglomerular pressure or whether this change in podocyte phenotype is accompanied by a disturbance in function that is detrimental to the glomerulus.

TUBULAR HYPERTROPHY

The compensatory growth capacity of the kidney was known to the ancient Greeks: Aristotle (384–322 BC) described that animals born with a single kidney have a larger organ compared to those born with two. More contemporary studies have documented that the increase in renal size following nephron reduction by disease or surgical resection is due primarily to proximal tubular epithelial hypertrophy.[183,239] The initial hypertrophic response is considered adaptive;[77,235,240] however, with time persistent hypertrophy is associated with the infiltration of macrophages, T-cells, and fibroblasts into the tubulointerstitial space.[87,196] This hypertrophy is no longer beneficial to organ function, and the cellular infiltrate results in tubular atrophy and tubulointerstitial fibrosis, the final convergent pathway of many renal diseases of diverse etiologies.

Cell Cycle-Dependent Tubular Cell Hypertrophy

TRANSFORMING GROWTH FACTOR β

As in the glomerulus, TGF-β is an important mediator of tubular cell hypertrophy. The hypertrophy induced by both angiotensin II and high glucose[241] is also dependent on TGF-β. TGF-β converts a mitogen-induced proliferative response to cellular hypertrophy, and this has been studied in detail in cultures of proximal tubule cells by examining the effects of epidermal growth factor (EGF) plus TGF-β. TGF-β alone has an antiproliferative effect on tubular cell growth, but does not induce hypertrophy.[242] EGF-induced hyperplasia is associated with cell cycle entry, hyperphosphorylation of pRb, and an increase in thymidine incorporation, but no change in cell size or protein/DNA ratio.[242] In the presence of additional TGF-β, cell cycle entry is not impaired and cyclin-E protein levels increase, but there is no increase in DNA synthesis and pRb remains hypophosphorylated, with arrest of the cells in mid- to late-G1. Inactivation of pRb by expression of either SV40 large-T antigen (inactivates both pRb and p53) or

HPV E7 (inactivates pRb alone) prevents TGF-β from converting EGF-induced hyperplasia to hypertrophy. In contrast, inactivation of p53 alone with HPV E6 has no effect on the induction of hypertrophy, confirming the importance of pRb in the cell cycle arrest of tubular cells resulting from TGF-β.

The maintenance of pRb in its hypophosphorylated state suggests TGF-β modifies the activity of G1 kinases. Consistent with the observation that cell cycle entry is not impaired in the presence of TGF-β, TGF-β has no effect on EGF-induced increase in Cdk4/6−cyclin D kinase activity.[243,244] However, there is no increase in cyclin E kinase activity, with a decreased number of Cdk2−cyclin E complexes and retention of p57, but not p27 or p21, in those complexes that do form.

In summary, the proposed paradigm for the development of hypertrophy in response to TGF-β in renal tubular cells is as follows. After a proliferative stimulus, there is cell cycle entry and activation of cyclin D kinase. This is associated with an increase in protein synthesis, and hence cell size. As the cell reaches mid- to late-G1, if cyclin E kinase is sufficiently activated, pRb is further phosphorylated and becomes inactivated, allowing the cell to progress to S-phase and hyperplasia to occur. However, in the presence of TGF-β, cyclin E kinase is not sufficiently activated, pRb remains hypophosphorylated, the cell is arrested, and hypertrophy results.

ANGIOTENSIN II

Angiotensin II has an established role in stimulating hypertrophy of proximal tubular cells, mediated by the high-affinity AT_1 receptor.[245] Both angiotensin II and EGF induce the expression of early immediate genes in tubule cells, suggesting that angiotensin II-mediated hypertrophy is also dependent on cell cycle entry.[246] Indeed, angiotensin II-treated cells are arrested in G1, and do not progress to S-phase,[245,247] reminiscent of cells exposed to TGF-β. It has subsequently been shown that angiotensin II stimulates the transcription and protein synthesis of TGF-β in proximal tubule cells.[248] Exposure of cells to a neutralizing antibody to TGF-β abrogated the ability of angiotensin II to induce hypertrophy, demonstrating its dependency on the induction and autocrine activity of TGF-β.[248] In contrast to proximal tubules cells exposed to EGF and TGF-β, angiotensin II increases protein (but not mRNA) levels for $p27^{Kip1}$.[249] To characterize the functional role of $p27^{Kip1}$ in angiotensin II-mediated hypertrophy, proximal tubule cells were cultured from $p27^{Kip1}$ null mice,[250] which responded to angiotensin II with cell cycle progression but no hypertrophy. Cdk4/6−cyclin D kinase activity was stimulated in both wild-type and null cells, but Cdk2−cyclin E kinase activity only increased in the null cells, indicating that $p27^{Kip1}$ inhibits this complex, and is required for angiotensin II-mediated hypertrophy of proximal tubular cells.

The mechanism by which angiotensin II increases $p27^{Kip1}$ expression has been studied in detail.[251] Angiotensin II upregulates p22phox, a subunit of membrane-bound NADPH oxidase, and hence increases the concentration of intracellular reactive oxygen species. This results in phosphorylation and activation of the mitogen-activated protein kinases Erk 1,2, that in turn leads to serine phosphorylation of $p27^{Kip1}$.[216,252] Serine phosphorylated $p27^{Kip1}$ has increased stability and decreased degradation by the ubiquitin pathway.[216] Atrial natriuretic peptide attenuates angiotensin II-mediated $p27^{Kip1}$ expression and proximal tubule cell hypertrophy, by a mechanism that appears to involve activation of the phosphatase MKP-1, which dephosphorylates Erk1,2.[253] The importance of this pathway has also been shown *in vivo*.[254] Infusion of angiotensin II into normal rats for 7 days increased the formation of reactive oxygen species in tubular cells and augmented $p27^{Kip1}$ expression. Immunostaining for PCNA decreased, indicating G1 cell cycle arrest, although hypertrophy was not observed.

As occurs with mesangial cells, a role for CTGF has been described in mediating tubular cell hypertrophy in response to angiotensin II. Systemic infusion of angiotensin II into normal rats induced overexpression of CTGF in glomeruli, tubules, and renal arteries, with associated tubular injury and increase in fibronectin expression.[255] A similar effect was demonstrated in cultured tubular cells, with angiotensin II acting through the AT_1 receptor. The importance of CTGF in angiotensin II-mediated hypertrophy was explored in detail by another group using HK2 cells.[256] Angiotensin II induced CTGF expression, G1 cell cycle arrest, and cell hypertrophy, which were reversed by treatment with an anti-CTGF antibody. In addition to the well-described roles in apoptosis and fibrosis, further detrimental renal effects of angiotensin II are likely to be secondary to its recently described effects of cell cycle arrest and hypertrophy.

A summary of the changes in cell cycle proteins occurring in glomerular and tubular hyperplasia, and in cell cycle-dependent hypertrophy, is shown in Table 28.1. Data from knockout mice are shown in Table 28.2.

Cell Cycle-Independent Tubular Cell Hypertrophy

In addition to increased new protein synthesis, a decrease in the rate of protein breakdown may contribute to cell hypertrophy.[3] Within the kidney, this is best characterized for tubular cells. Although diabetes and acidosis are catabolic states, both are associated with decreases in renal proteolysis, which makes a significant contribution to the associated growth of the kidney.[257−259]

TABLE 28.1 Summary of Cell Cycle Proteins in Hyperplasia and Hypertrophy of Renal Cells

		Cyclin CDK			CDK Inhibitor			
	Experiment	**Increased**	**Decreased**	**No Change**	**Increased**	**Decreased**	**No Change**	**Reference**
MESANGIAL CELL								
Proliferation	*In vitro* exposure to mitogens (PDGF, bFGF)	D1, E, A			p21	p27	p57	176,193,99
	Animal models		Cdk4,2					
	Thy1	D1, E Cdk4, 2			p15, p21	p27		200
	Remnant kidney	E, Cdk2		Cdk4				199
Suppression of proliferation hypertrophy	*In vitro* exposure to antimitogens (TGFβ, SPARC, heparin)		D1, E, A Cdk4, 2		p15, p21, p27			193,203,246
	In vitro exposure Glucose			Cdk2	p21, p27			112,245
	TGFβ				p16, p21, p27			201,248
	CTGF				p15, p21, p27			1
	Animal models							
	Type I diabetes (STZ mouse, BBdp rat)			E, A	p21, p27			112,248
	Type II diabetes (*db*/*db* mouse, Zucker rat)			Cdk2	p27			88,243
Apoptosis	Cytoplasmic location of Cdk2							85
PODOCYTE								
Immune injury	*In vitro* exposure to C5b9				p21			43
	Animals models							
	PHN	A, Cdk2			p21	p57		176,98
	Antiglomerular antibody	A, Cdk2			p21, p27	p57		203
Proliferation	*In vitro* exposure to HIV-1	D_1						151
	Human disease							
	Collapsing GN	A				p27, p57		10,202
Response to stretch	*In vitro*		D, A, B		D, A p21, p27, p57			171
TUBULAR EPITHELIAL CELL								
Proliferation	Animal models							
	Uninephroctomy	E, Cdk2						122
	Ischemic injury	D1, D3, A, B Cdk2, 4						137,164
	UUO, cisplatin				p21			164
Hypertrophy	In vitro exposure EGF + TGFβ	D, Cdk4	E					62,120

TABLE 28.2 Data from Knockout Mice

	Experiment	Outcome	Reference
$p21^{-/-}$	Mesangial cells exposed to high glucose *in vitro*	Resistant to hypertrophy	—[a]
	Animal models STZ diabetes Antiglomerular antibody Remnant kidney Acute tubular injury (ischemia, UUO, cisplatin)	Reduced glomerular hypertrophy	3
		Increased podocyte proliferation	100
		Glomerular hyperplasia, not hypertrophy	135
		Increased proliferation, worse renal function, increased mortality	136
$p27^{-/-}$	Mesangial cells exposed to high glucose *in vitro*	Resistant to hypertrophy	244
	Mesangial cells deprived of growth factors	Increased apoptosis	84
	Animal models STZ diabetes Antiglomerular antibody	Reduced glomerular hypertrophy	5
		Increased mesangial cell proliferation and apoptosis	158
	UUO	Increased tubular apoptosis	158
$p57^{-/-}$	Unmanipulated animal	Normal glomerulogenesis in embryonic mice	217,257,263

[a]*Unpublished.*
UUO: Unilateral ureteral obstruction.

An estimated 60% of total intracellular proteolysis in renal tubular cells occurs by the ubiquitin–proteasome pathway;[260] however, this does not appear to be a major factor in the regulation of proteolysis during the hypertrophic response of renal tubular cells. Two lines of evidence support an alteration in lysosomal function as underlying the reduced proteolysis observed in certain cases of tubular hypertrophy, and a possible mechanism by which this occurs has recently begun to be clarified.[261] First, in addition to stimulating cell cycle entry, EGF increases protein half-life by approximately 30% in cultured primary proximal tubular cells, primarily by affecting lysosomal proteolysis.[260] Second, exposure of tubular cells to ammonia leads to alkalinization of acidic intracellular compartments, including lysosomes, thus modifying their function, and stimulates hypertrophy that is independent of cell cycle entry.[262]

Several studies have demonstrated proximal tubule cell hypertrophy in response to ammonia *in vitro*,[262–264] and renal ammonia synthesis is increased in several apparently diverse clinical conditions associated with hypertrophy.[195,265] In chronic metabolic acidosis and chronic hypokalemia, mitochondrial ammoniagenesis is directly stimulated. In contrast, the increase in ammonia in diabetes mellitus, following uninephrectomy and during protein-loading, is thought to be stimulated by an increase in single-nephron glomerular filtration rate (SNGFR). Cell culture studies involving either reducing the media pH[182] or lowering potassium concentration[266] do not induce hypertrophy, indicating that it is not changes in the extracellular milieu *per se* that initiate the hypertrophic growth response. The results from direct application of ammonium chloride suggest that the accumulation of this molecule, in response to acidosis or hypokalemia, drives the development of hypertrophy. This hypothesis is supported by studies of hypertrophy in the setting of chronic hypokalemia in the rat.[267] In this model, renal ammonia production is significantly increased. Administration of bicarbonate both decreases the rate of ammonia synthesis and the hypertrophy. Renal generation of ammonia has recently been studied in patients with metabolic acidosis and normal renal function.[263] Compared to individuals with normal acid– base balance, kidney protein degradation was significantly lower and urinary ammonia excretion significantly higher. As with cell and animal studies, it was suggested that in human metabolic acidosis the increased ammonia synthesis drives the decrease in protein degradation, and is potentially responsible for kidney hypertrophy.

What is the mechanism by which altered lysosomal function affects protein degradation? Chaperone-mediated autophagy allows lysosomal import of proteins containing a specific consensus sequence, KFERQ, by the binding of heat-shock cognate protein 73 (Hsc73) to lysosomal membrane protein 2a (LAMP2a). In cultured

NRK-52E cells (a rat kidney epithelial cell line) exposed to EGF or ammonia (but not TGF-β alone), there was an increase in the half-life of KFERQ-containing proteins[261] associated with a decrease in total cellular and lysosomal LAMP2a. Furthermore, declines in LAMP2a and Hsc73 have also been demonstrated in lysosomes isolated from the hypertrophied cortex of acutely diabetic rats, and was accompanied by an increase in KFERQ-containing proteins.[268] Other lysosomal pathways may also be affected during renal hypertrophy.[3] EGF-induced suppression of proteolysis in NRK-52E cells was prevented by inhibitors of Ras and PI-3 kinase, but not by inhibitors of MAP kinase or Src.[269] PI-3 kinase and Akt activities are increased in the renal cortex of diabetic *db/db* mice and correlate with hypertrophy.[270] Products of the PI-3 kinase pathway control membrane and protein trafficking, and the suppression of chaperone-mediated autophagy may be part of a generalized abnormality in trafficking to and from lysosomes.

CONCLUSIONS

The last two decades have seen an explosion in our understanding of the underlying mechanisms governing renal hyperplasia and hypertrophy which has literally burgeoned since 1991. The goal for the next 15 years will be to identify specific modifiable targets to alter or even reverse these pathological processes. Numerous agents have been demonstrated to be beneficial in ameliorating the course of animal models of disease, and the hope is that certain of these will transfer to be of use in human disease. Indeed, Cdk2 inhibitors are now in human trials for treatment of proliferative glomerulonephritis. With the discovery of drugs that target either the network of mitogens responsible for stimulating abnormal cell growth or specific cell cycle-regulatory proteins, potential therapies may be on the horizon for patients with renal diseases in which hyperplasia or hypertrophy is a dominant feature. Much has been learned, but in addition to characterizing the role of conventional cyclins, Cdks, and Cdk inhibitors, the challenge remains to identify novel cell cycle proteins, determine their role in renal disease, and the consequences of their manipulation.

References

[1] Fine L. The biology of renal hypertrophy. Kidney Int 1986;29 (3):619–34.

[2] Fine LG, Norman J. Cellular events in renal hypertrophy. Annu Rev Physiol 1989;51:19–32.

[3] Franch HA. Pathways of proteolysis affecting renal cell growth. Curr Opin Nephrol Hypertens 2002;11(4):445–50.

[4] Preisig P. A cell cycle-dependent mechanism of renal tubule epithelial cell hypertrophy. Kidney Int 1999;56(4):1193–8.

[5] Nurse P. A long twentieth century of the cell cycle and beyond. Cell 2000;100(1):71–8.

[6] Harper JW, Adams PD. Cyclin-dependent kinases. Chem Rev 2001;101(8):2511–26.

[7] Koepp DM, Harper JW, Elledge SJ. How the cyclin became a cyclin: regulated proteolysis in the cell cycle. Cell 1999;97(4):431–4.

[8] Evans T, Rosenthal ET, Youngblom J, Distel D, Hunt T. Cyclin: a protein specified by maternal mRNA in sea urchin eggs that is destroyed at each cleavage division. Cell 1983;33(2):389–96.

[9] Pines J. Cyclins and cyclin-dependent kinases: a biochemical view. Biochem J 1995;308(Pt 3):697–711.

[10] Aktas H, Cai H, Cooper GM. Ras links growth factor signaling to the cell cycle machinery via regulation of cyclin D1 and the Cdk inhibitor p27KIP1. Mol Cell Biol 1997;17(7):3850–7.

[11] Filmus J, Robles AI, Shi W, Wong MJ, Colombo LL, Conti CJ. Induction of cyclin D1 overexpression by activated ras. Oncogene 1994;9(12):3627–33.

[12] Winston JT, Coats SR, Wang YZ, Pledger WJ. Regulation of the cell cycle machinery by oncogenic ras. Oncogene 1996;12(1):127–34.

[13] Gille H, Downward J. Multiple ras effector pathways contribute to G(1) cell cycle progression. J Biol Chem 1999;274 (31):22033–40.

[14] Cheng M, Sexl V, Sherr CJ, Roussel MF. Assembly of cyclin D-dependent kinase and titration of p27Kip1 regulated by mitogen-activated protein kinase kinase (MEK1). Proc Natl Acad Sci USA 1998;95(3):1091–6.

[15] Peeper DS, Upton TM, Ladha MH, Neuman E, Zalvide J, Bernards R, et al. Ras signalling linked to the cell-cycle machinery by the retinoblastoma protein. Nature 1997;386 (6621):177–81.

[16] Diehl JA, Cheng M, Roussel MF, Sherr CJ. Glycogen synthase kinase-3beta regulates cyclin D1 proteolysis and subcellular localization. Genes Dev 1998;12(22):3499–511.

[17] Diehl JA, Zindy F, Sherr CJ. Inhibition of cyclin D1 phosphorylation on threonine-286 prevents its rapid degradation via the ubiquitin-proteasome pathway. Genes Dev 1997;11(8):957–72.

[18] Sherr CJ. Mammalian G1 cyclins. Cell 1993;73(6):1059–65.

[19] Kaldis P, Sutton A, Solomon MJ. The Cdk-activating kinase (CAK) from budding yeast. Cell 1996;86(4):553–64.

[20] Matsushime H, Roussel MF, Ashmun RA, Sherr CJ. Colony-stimulating factor 1 regulates novel cyclins during the G1 phase of the cell cycle. Cell 1991;65(4):701–13.

[21] Baldin V, Lukas J, Marcote MJ, Pagano M, Draetta G. Cyclin D1 is a nuclear protein required for cell cycle progression in G1. Genes Dev 1993;7(5):812–21.

[22] Guo Y, Stacey DW, Hitomi M. Post-transcriptional regulation of cyclin D1 expression during G2 phase. Oncogene 2002;21 (49):7545–56.

[23] Matsushime H, Quelle DE, Shurtleff SA, Shibuya M, Sherr CJ, Kato JY. D-type cyclin-dependent kinase activity in mammalian cells. Mol Cell Biol 1994;14(3):2066–76.

[24] Weinberg RA. The retinoblastoma protein and cell cycle control. Cell 1995;81(3):323–30.

[25] Trimarchi JM, Lees JA. Sibling rivalry in the E2F family. Nat Rev Mol Cell Biol 2002;3(1):11–20.

[26] Matsuura I, Denissova NG, Wang G, He D, Long J, Liu F. Cyclin-dependent kinases regulate the antiproliferative function of Smads. Nature 2004;430(6996):226–31.

[27] Dulic V, Lees E, Reed SI. Association of human cyclin E with a periodic G1-S phase protein kinase. Science 1992;257 (5078):1958–61.

[28] Koff A, Giordano A, Desai D, Yamashita K, Harper JW, Elledge S, et al. Formation and activation of a cyclin E-cdk2 complex during the G1 phase of the human cell cycle. Science 1992;257(5077):1689–94.
[29] Kitagawa M, Higashi H, Jung HK, Suzuki-Takahashi I, Ikeda M, Tamai K, et al. The consensus motif for phosphorylation by cyclin D1-Cdk4 is different from that for phosphorylation by cyclin A/E-Cdk2. EMBO J 1996;15(24):7060–9.
[30] Lundberg AS, Weinberg RA. Functional inactivation of the retinoblastoma protein requires sequential modification by at least two distinct cyclin-cdk complexes. Mol Cell Biol 1998;18 (2):753–61.
[31] Harbour JW, Dean DC. The Rb/E2F pathway: expanding roles and emerging paradigms. Genes Dev 2000;14 (19):2393–409.
[32] Yu Q, Sicinski P. Mammalian cell cycles without cyclin E-CDK2. Cell Cycle 2004;3(3):292–5.
[33] Clurman BE, Sheaff RJ, Thress K, Groudine M, Roberts JM. Turnover of cyclin E by the ubiquitin-proteasome pathway is regulated by cdk2 binding and cyclin phosphorylation. Genes Dev 1996;10(16):1979–90.
[34] Welcker M, Singer J, Loeb KR, Grim J, Bloecher A, Gurien-West M, et al. Multisite phosphorylation by Cdk2 and GSK3 controls cyclin E degradation. Mol Cell 2003;12(2):381–92.
[35] Won KA, Reed SI. Activation of cyclin E/CDK2 is coupled to site-specific autophosphorylation and ubiquitin-dependent degradation of cyclin E. EMBO J 1996;15(16):4182–93.
[36] Coverley D, Laman H, Laskey RA. Distinct roles for cyclins E and A during DNA replication complex assembly and activation. Nat Cell Biol 2002;4(7):523–8.
[37] Hua XH, Newport J. Identification of a preinitiation step in DNA replication that is independent of origin recognition complex and cdc6, but dependent on cdk2. J Cell Biol 1998;140 (2):271–81.
[38] Krude T, Jackman M, Pines J, Laskey RA. Cyclin/Cdk-dependent initiation of DNA replication in a human cell-free system. Cell 1997;88(1):109–19.
[39] Mitra J, Enders GH. Cyclin A/Cdk2 complexes regulate activation of Cdk1 and Cdc25 phosphatases in human cells. Oncogene 2004;23(19):3361–7.
[40] Berthet C, Aleem E, Coppola V, Tessarollo L, Kaldis P. Cdk2 knockout mice are viable. Curr Biol 2003;13(20):1775–85.
[41] Ortega S, Prieto I, Odajima J, Martin A, Dubus P, Sotillo R, et al. Cyclin-dependent kinase 2 is essential for meiosis but not for mitotic cell division in mice. Nat Genet 2003;35(1):25–31.
[42] Atherton-Fessler S, Parker LL, Geahlen RL, Piwnica-Worms H. Mechanisms of p34cdc2 regulation. Mol Cell Biol 1993;13 (3):1675–85.
[43] Smits VA, Medema RH. Checking out the G(2)/M transition. Biochim Biophys Acta 2001;1519(1–2):1–12.
[44] Krek W, Nigg EA. Differential phosphorylation of vertebrate p34cdc2 kinase at the G1/S and G2/M transitions of the cell cycle: identification of major phosphorylation sites. EMBO J 1991;10(2):305–16.
[45] Li J, Meyer AN, Donoghue DJ. Requirement for phosphorylation of cyclin B1 for *Xenopus* oocyte maturation. Mol Biol Cell 1995;6(9):1111–24.
[46] Nilsson I, Hoffmann I. Cell cycle regulation by the Cdc25 phosphatase family. Prog Cell Cycle Res 2000;4:107–14.
[47] Yang J, Bardes ES, Moore JD, Brennan J, Powers MA, Kornbluth S. Control of cyclin B1 localization through regulated binding of the nuclear export factor CRM1. Genes Dev 1998;12 (14):2131–43.
[48] Hagting A, Jackman M, Simpson K, Pines J. Translocation of cyclin B1 to the nucleus at prophase requires a phosphorylation-dependent nuclear import signal. Curr Biol 1999;9(13):680–9.
[49] Sherr CJ, Roberts JM. Living with or without cyclins and cyclin-dependent kinases. Genes Dev 2004;18(22):2699–711.
[50] Nakayama K, Ishida N, Shirane M, Inomata A, Inoue T, Shishido N, et al. Mice lacking p27(Kip1) display increased body size, multiple organ hyperplasia, retinal dysplasia, and pituitary tumors. Cell 1996;85(5):707–20.
[51] Sherr CJ, Roberts JM. CDK inhibitors: positive and negative regulators of G1-phase progression. Genes Dev 1999;13 (12):1501–12.
[52] Quelle DE, Zindy F, Ashmun RA, Sherr CJ. Alternative reading frames of the INK4a tumor suppressor gene encode two unrelated proteins capable of inducing cell cycle arrest. Cell 1995;83 (6):993–1000.
[53] Sherr CJ. The INK4a/ARF network in tumour suppression. Nat Rev Mol Cell Biol 2001;2(10):731–7.
[54] Sherr CJ. Parsing Ink4a/Arf: "pure" p16-null mice. Cell 2001;106(5):531–4.
[55] Bunz F, Dutriaux A, Lengauer C, Waldman T, Zhou S, Brown JP, et al. Requirement for p53 and p21 to sustain G2 arrest after DNA damage. Science 1998;282(5393):1497–501.
[56] Smits VA, Klompmaker R, Vallenius T, Rijksen G, Makela TP, Medema RH. p21 inhibits Thr161 phosphorylation of Cdc2 to enforce the G2 DNA damage checkpoint. J Biol Chem 2000;275 (39):30638–43.
[57] Cheng M, Olivier P, Diehl JA, Fero M, Roussel MF, Roberts JM, et al. The p21(Cip1) and p27(Kip1) CDK "inhibitors" are essential activators of cyclin D-dependent kinases in murine fibroblasts. EMBO J 1999;18(6):1571–83.
[58] el-Deiry WS, Tokino T, Velculescu VE, Levy DB, Parsons R, Trent JM, et al. WAF1, a potential mediator of p53 tumor suppression. Cell 1993;75(4):817–25.
[59] Harper JW, Adami GR, Wei N, Keyomarsi K, Elledge SJ. The p21 Cdk-interacting protein Cip1 is a potent inhibitor of G1 cyclin-dependent kinases. Cell 1993;75(4):805–16.
[60] Xiong Y, Hannon GJ, Zhang H, Casso D, Kobayashi R, Beach D. p21 is a universal inhibitor of cyclin kinases. Nature 1993;366 (6456):701–4.
[61] LaBaer J, Garrett MD, Stevenson LF, Slingerland JM, Sandhu C, Chou HS, et al. New functional activities for the p21 family of CDK inhibitors. Genes Dev 1997;11(7):847–62.
[62] Parry D, Mahony D, Wills K, Lees E. Cyclin D-CDK subunit arrangement is dependent on the availability of competing INK4 and p21 class inhibitors. Mol Cell Biol 1999;19 (3):1775–83.
[63] Parker SB, Eichele G, Zhang P, Rawls A, Sands AT, Bradley A, et al. p53-independent expression of p21Cip1 in muscle and other terminally differentiating cells. Science 1995;267 (5200):1024–7.
[64] Wolf G, Wenzel U, Ziyadeh FN, Stahl RA. Angiotensin converting-enzyme inhibitor treatment reduces glomerular p16INK4 and p27Kip1 expression in diabetic BBdp rats. Diabetologia 1999;42(12):1425–32.
[65] Noda A, Ning Y, Venable SF, Pereira-Smith OM, Smith JR. Cloning of senescent cell-derived inhibitors of DNA synthesis using an expression screen. Exp Cell Res 1994;211 (1):90–8.
[66] Polyak K, Lee MH, Erdjument-Bromage H, Koff A, Roberts JM, Tempst P, et al. Cloning of p27Kip1, a cyclin-dependent kinase inhibitor and a potential mediator of extracellular antimitogenic signals. Cell 1994;78(1):59–66.
[67] Toyoshima H, Hunter T. p27, a novel inhibitor of G1 cyclin-Cdk protein kinase activity, is related to p21. Cell 1994;78 (1):67–74.

[68] Hengst L, Reed SI. Translational control of p27Kip1 accumulation during the cell cycle. Science 1996;271(5257):1861–4.
[69] Pagano M, Tam SW, Theodoras AM, Beer-Romero P, Del Sal G, Chau V, et al. Role of the ubiquitin-proteasome pathway in regulating abundance of the cyclin-dependent kinase inhibitor p27. Science 1995;269(5224):682–5.
[70] Sheaff RJ, Groudine M, Gordon M, Roberts JM, Clurman BE. Cyclin E-CDK2 is a regulator of p27Kip1. Genes Dev 1997;11 (11):1464–78.
[71] Vlach J, Hennecke S, Amati B. Phosphorylation-dependent degradation of the cyclin-dependent kinase inhibitor p27. EMBO J 1997;16(17):5334–44.
[72] Bloom J, Pagano M. Deregulated degradation of the cdk inhibitor p27 and malignant transformation. Semin Cancer Biol 2003;13(1):41–7.
[73] Elledge SJ, Harper JW. The role of protein stability in the cell cycle and cancer. Biochim Biophys Acta 1998;1377(2):M61–70.
[74] Lee MH, Reynisdottir I, Massague J. Cloning of p57KIP2, a cyclin-dependent kinase inhibitor with unique domain structure and tissue distribution. Genes Dev 1995;9(6):639–49.
[75] Matsuoka S, Edwards MC, Bai C, Parker S, Zhang P, Baldini A, et al. p57KIP2, a structurally distinct member of the p21CIP1 Cdk inhibitor family, is a candidate tumor suppressor gene. Genes Dev 1995;9(6):650–62.
[76] Fero ML, Rivkin M, Tasch M, Porter P, Carow CE, Firpo E, et al. A syndrome of multiorgan hyperplasia with features of gigantism, tumorigenesis, and female sterility in p27(Kip1)-deficient mice. Cell 1996;85(5):733–44.
[77] Wolf G, Neilson EG. Molecular mechanisms of tubulointerstitial hypertrophy and hyperplasia. Kidney Int 1991;39 (3):401–20.
[78] Takahashi K, Nakayama K. Mice lacking a CDK inhibitor, p57Kip2, exhibit skeletal abnormalities and growth retardation. J Biochem 2000;127(1):73–83.
[79] Yan Y, Frisen J, Lee MH, Massague J, Barbacid M. Ablation of the CDK inhibitor p57Kip2 results in increased apoptosis and delayed differentiation during mouse development. Genes Dev 1997;11(8):973–83.
[80] Zhang P, Liegeois NJ, Wong C, Finegold M, Hou H, Thompson JC, et al. Altered cell differentiation and proliferation in mice lacking p57KIP2 indicates a role in Beckwith-Wiedemann syndrome. Nature 1997;387(6629):151–8.
[81] Deng C, Zhang P, Harper JW, Elledge SJ, Leder P. Mice lacking p21CIP1/WAF1 undergo normal development, but are defective in G1 checkpoint control. Cell 1995;82(4):675–84.
[82] Wolf G, Ziyadeh FN. Molecular mechanisms of diabetic renal hypertrophy. Kidney Int 1999;56(2):393–405.
[83] Couser WG, Johnson RJ. Mechanisms of progressive renal disease in glomerulonephritis. Am J Kidney Dis 1994;23(2):193–8.
[84] Fogo A, Ichikawa I. Evidence for the central role of glomerular growth promoters in the development of sclerosis. Semin Nephrol 1989;9(4):329–42.
[85] Baker AJ, Mooney A, Hughes J, Lombardi D, Johnson RJ, Savill J. Mesangial cell apoptosis: the major mechanism for resolution of glomerular hypercellularity in experimental mesangial proliferative nephritis. J Clin Invest 1994;94(5):2105–16.
[86] Tsuboi Y, Shankland SJ, Grande JP, Walker HJ, Johnson RJ, Dousa TP. Suppression of mesangial proliferative glomerulonephritis development in rats by inhibitors of cAMP phosphodiesterase isozymes types III and IV. J Clin Invest 1996;98 (2):262–70.
[87] Klahr S, Schreiner G, Ichikawa I. The progression of renal disease. N Engl J Med 1988;318(25):1657–66.
[88] Pesce CM, Striker LJ, Peten E, Elliot SJ, Striker GE. Glomerulosclerosis at both early and late stages is associated with increased cell turnover in mice transgenic for growth hormone. Lab Invest 1991;65(5):601–5.
[89] Striker LJ, Doi T, Elliot S, Striker GE. The contribution of glomerular mesangial cells to progressive glomerulosclerosis. Semin Nephrol 1989;9(4):318–28.
[90] Hudkins KL, Gilbertson DG, Carling M, Taneda S, Hughes SD, Holdren MS, et al. Exogenous PDGF-D is a potent mesangial cell mitogen and causes a severe mesangial proliferative glomerulopathy. J Am Soc Nephrol 2004;15(2):286–98.
[91] Floege J, Eng E, Young BA, Couser WG, Johnson RJ. Heparin suppresses mesangial cell proliferation and matrix expansion in experimental mesangioproliferative glomerulonephritis. Kidney Int 1993;43(2):369–80.
[92] Floege J, Eng E, Lindner V, Alpers CE, Young BA, Reidy JM, et al. Rat glomerular mesangial cells synthesize basic fibroblast growth factor. Release, upregulated synthesis, and mitogenicity in mesangial proliferative glomerulonephritis. J Clin Invest 1992;90(6):2362–9.
[93] Ruef C, Budde K, Lacy J, Northemann W, Baumann M, Sterzel RB, et al. Interleukin 6 is an autocrine growth factor for mesangial cells. Kidney Int 1990;38(2):249–57.
[94] Ryffel B, Car BD, Gunn H, Roman D, Hiestand P, Mihatsch MJ. Interleukin-6 exacerbates glomerulonephritis in (NZB × NZW)F1 mice. Am J Pathol 1994;144(5):927–37.
[95] Yanagita M. The role of the vitamin K-dependent growth factor Gas6 in glomerular pathophysiology. Curr Opin Nephrol Hypertens 2004;13(4):465–70.
[96] Brandt J, Pippin J, Schulze M, Hansch GM, Alpers CE, Johnson RJ, et al. Role of the complement membrane attack complex (C5b-9) in mediating experimental mesangioproliferative glomerulonephritis. Kidney Int 1996;49(2):335–43.
[97] Floege J, Johnson RJ, Gordon K, Iida H, Pritzl P, Yoshimura A, et al. Increased synthesis of extracellular matrix in mesangial proliferative nephritis. Kidney Int 1991;40(3):477–88.
[98] Gesualdo L, Di Paolo S, Ranieri E, Schena FP. Trapidil inhibits human mesangial cell proliferation: effect on PDGF beta-receptor binding and expression. Kidney Int 1994;46 (4):1002–9.
[99] Caspary T, Cleary MA, Perlman EJ, Zhang P, Elledge SJ, Tilghman SM. Oppositely imprinted genes p57(Kip2) and igf2 interact in a mouse model for Beckwith-Wiedemann syndrome. Genes Dev 1999;13(23):3115–24.
[100] Schoecklmann HO, Rupprecht HD, Zauner I, Sterzel RB. TGF-beta1-induced cell cycle arrest in renal mesangial cells involves inhibition of cyclin E-cdk 2 activation and retinoblastoma protein phosphorylation. Kidney Int 1997;51(4):1228–36.
[101] Yamamoto T, Wilson CB. Complement dependence of antibody-induced mesangial cell injury in the rat. J Immunol 1987;138(11):3758–65.
[102] Yamamoto T, Wilson CB. Quantitative and qualitative studies of antibody-induced mesangial cell damage in the rat. Kidney Int 1987;32(4):514–25.
[103] Shankland SJ, Hugo C, Coats SR, Nangaku M, Pichler RH, Gordon KL, et al. Changes in cell-cycle protein expression during experimental mesangial proliferative glomerulonephritis. Kidney Int 1996;50(4):1230–9.
[104] Bokemeyer D, Panek D, Kitahara M, et al. The map kinase ERK regulates renal activity of cyclin-dependent kinase 2 in experimental glomerulonephritis. Nephrol Dial Transplant 2007;22(12):3431–41.
[105] Bokemeyer D, Panek D, Kramer HJ, Lindemann M, Kitahara M, Boor P, et al. *In vivo* identification of the mitogen-activated protein kinase cascade as a central pathogenic pathway in experimental mesangioproliferative glomerulonephritis. J Am Soc Nephrol 2002;13(6):1473–80.

[106] Shankland SJ, Hamel P, Scholey JW. Cyclin and cyclin-dependent kinase expression in the remnant glomerulus. J Am Soc Nephrol 1997;8(3):368–75.
[107] Shankland SJ, Pippin J, Flanagan M, Coats SR, Nangaku M, Gordon KL, et al. Mesangial cell proliferation mediated by PDGF and bFGF is determined by levels of the cyclin kinase inhibitor p27Kip1. Kidney Int 1997;51(4):1088–99.
[108] Hiromura K, Haseley LA, Zhang P, Monkawa T, Durvasula A, Petermann AT, et al. Podocyte expression of the CDK-inhibitor p57 during development and disease. Kidney Int 2001;60 (6):2235–46.
[109] Hiromura K, Pippin JW, Fero ML, Roberts JM, Shankland SJ. Modulation of apoptosis by the cyclin-dependent kinase inhibitor p27(Kip1). J Clin Invest 1999;103(5):597–604.
[110] Ophascharoensuk V, Fero ML, Hughes J, Roberts JM, Shankland SJ. The cyclin-dependent kinase inhibitor p27Kip1 safeguards against inflammatory injury. Nat Med 1998;4 (5):575–80.
[111] Monkawa T, Pippin J, Yo Y, Kopp JB, Alpers CE, Shankland SJ. The cyclin-dependent kinase inhibitor p21 limits murine mesangial proliferative glomerulonephritis. Nephron Exp Nephrol 2006;102(1):e8–18.
[112] Savill J. Regulation of glomerular cell number by apoptosis. Kidney Int 1999;56(4):1216–22.
[113] Hiromura K, Pippin JW, Blonski MJ, Roberts JM, Shankland SJ. The subcellular localization of cyclin dependent kinase 2 determines the fate of mesangial cells: role in apoptosis and proliferation. Oncogene 2002;21(11):1750–8.
[114] Pippin JW, Qu Q, Meijer L, Shankland SJ. Direct *in vivo* inhibition of the nuclear cell cycle cascade in experimental mesangial proliferative glomerulonephritis with Roscovitine, a novel cyclin-dependent kinase antagonist. J Clin Invest 1997;100 (10):2512–20.
[115] Gilbert T, Merlet-Benichou C. Retinoids and nephron mass control. Pediatr Nephrol 2000;14(12):1137–44.
[116] Xu Q, Lucio-Cazana J, Kitamura M, Ruan X, Fine LG, Norman JT. Retinoids in nephrology: promises and pitfalls. Kidney Int. 2004;66(6):2119–31.
[117] Marill J, Idres N, Capron CC, Nguyen E, Chabot GG. Retinoic acid metabolism and mechanism of action: a review. Curr Drug Metab 2003;4(1):1–10.
[118] Dimberg A, Bahram F, Karlberg I, Larsson LG, Nilsson K, Oberg F. Retinoic acid-induced cell cycle arrest of human myeloid cell lines is associated with sequential down-regulation of c-Myc and cyclin E and posttranscriptional up-regulation of p27(Kip1). Blood 2002;99(6):2199–206.
[119] Hsu SL, Hsu JW, Liu MC, Chen LY, Chang CD. Retinoic acid-mediated G1 arrest is associated with induction of p27(Kip1) and inhibition of cyclin-dependent kinase 3 in human lung squamous carcinoma CH27 cells. Exp Cell Res 2000;258 (2):322–31.
[120] Seewaldt VL, Dietze EC, Johnson BS, Collins SJ, Parker MB. Retinoic acid-mediated G1-S-phase arrest of normal human mammary epithelial cells is independent of the level of p53 protein expression. Cell Growth Differ 1999;10(1):49–59.
[121] Dechow C, Morath C, Peters J, Lehrke I, Waldherr R, Haxsen V, et al. Effects of all-trans retinoic acid on renin–angiotensin system in rats with experimental nephritis. Am J Physiol Renal Physiol 2001;281(5):F909–19.
[122] Wagner J, Dechow C, Morath C, Lehrke I, Amann K, Waldherr R, et al. Retinoic acid reduces glomerular injury in a rat model of glomerular damage. J Am Soc Nephrol 2000; 11(8):1479–87.
[123] Morath C, Dechow C, Lehrke I, Haxsen V, Waldherr R, Floege J, et al. Effects of retinoids on the TGF-beta system and extracellular matrix in experimental glomerulonephritis. J Am Soc Nephrol 2001;12(11):2300–9.
[124] McMahon B, Mitchell S, Brady HR, Godson C. Lipoxins: revelations on resolution. Trends Pharmacol Sci. 2001;22(8):391–5.
[125] Levy BD, Clish CB, Schmidt B, Gronert K, Serhan CN. Lipid mediator class switching during acute inflammation: signals in resolution. Nat Immunol 2001;2(7):612–9.
[126] Papayianni A, Serhan CN, Phillips ML, Rennke HG, Brady HR. Transcellular biosynthesis of lipoxin A4 during adhesion of platelets and neutrophils in experimental immune complex glomerulonephritis. Kidney Int 1995;47(5):1295–302.
[127] Mitchell D, Rodgers K, Hanly J, McMahon B, Brady HR, Martin F, et al. Lipoxins inhibit Akt/PKB activation and cell cycle progression in human mesangial cells. Am J Pathol 2004;164(3):937–46.
[128] Clish CB, Gronert K, Serhan CN. Local and systemic delivery of an aspirin-triggered lipoxin stable analog inhibits neutrophil trafficking. Ann NY Acad Sci 2000;905:274–8.
[129] Ohse T, Ota T, Kieran N, Godson C, Yamada K, Tanaka T, et al. Modulation of interferon-induced genes by lipoxin analogue in anti-glomerular basement membrane nephritis. J Am Soc Nephrol 2004;15(4):919–27.
[130] Fries JW, Sandstrom DJ, Meyer TW, Rennke HG. Glomerular hypertrophy and epithelial cell injury modulate progressive glomerulosclerosis in the rat. Lab Invest 1989;60(2):205–18.
[131] Kriz W. Podocyte is the major culprit accounting for the progression of chronic renal disease. Microsc Res Tech 2002;57 (4):189–95.
[132] Kriz W, Gretz N, Lemley KV. Progression of glomerular diseases: is the podocyte the culprit? Kidney Int 1998;54 (3):687–97.
[133] Kriz W, Lemley KV. The role of the podocyte in glomerulosclerosis. Curr Opin Nephrol Hypertens 1999;8(4):489–97.
[134] Rennke HG. How does glomerular epithelial cell injury contribute to progressive glomerular damage? Kidney Int Suppl 1994;45:S58–63.
[135] Dalla Vestra M, Masiero A, Roiter AM, Saller A, Crepaldi G, Fioretto P. Is podocyte injury relevant in diabetic nephropathy? Studies in patients with type 2 diabetes. Diabetes 2003;52 (4):1031–5.
[136] Hishiki T, Shirato I, Takahashi Y, Funabiki K, Horikoshi S, Tomino Y. Podocyte injury predicts prognosis in patients with IgA nephropathy using a small amount of renal biopsy tissue. Kidney Blood Press Res 2001;24(2):99–104.
[137] Lemley KV, Lafayette RA, Safai M, Derby G, Blouch K, Squarer A, et al. Podocytopenia and disease severity in IgA nephropathy. Kidney Int 2002;61(4):1475–85.
[138] Meyer TW, Bennett PH, Nelson RG. Podocyte number predicts long-term urinary albumin excretion in Pima Indians with Type II diabetes and microalbuminuria. Diabetologia 1999;42 (11):1341–4.
[139] Nakamura T, Ushiyama C, Hara M, Osada S, Ugai K, Shimada N, et al. Comparative effects of plasmapheresis and intravenous cyclophosphamide on urinary podocyte excretion in patients with proliferative Lupus nephritis. Clin Nephrol 2002;57(2):108–13.
[140] White KE, Bilous RW. Structural alterations to the podocyte are related to proteinuria in type 2 diabetic patients. Nephrol Dial Transplant 2004;19(6):1437–40.
[141] White KE, Bilous RW, Marshall SM, El Nahas M, Remuzzi G, Piras G, et al. Podocyte number in normotensive type 1 diabetic patients with albuminuria. Diabetes 2002;51(10):3083–9.
[142] Nagata M, Nakayama K, Terada Y, Hoshi S, Watanabe T. Cell cycle regulation and differentiation in the human podocyte lineage. Am J Pathol 1998;153(5):1511–20.

[143] Cybulsky AV, Rennke HG, Feintzeig ID, Salant DJ. Complement-induced glomerular epithelial cell injury. Role of the membrane attack complex in rat membranous nephropathy. J Clin Invest 1986;77(4):1096–107.

[144] Salant DJ, Darby C, Couser WG. Experimental membranous glomerulonephritis in rats. Quantitative studies of glomerular immune deposit formation in isolated glomeruli and whole animals. J Clin Invest 1980;66(1):71–81.

[145] Shankland SJ, Floege J, Thomas SE, Nangaku M, Hugo C, Pippin J, et al. Cyclin kinase inhibitors are increased during experimental membranous nephropathy: potential role in limiting glomerular epithelial cell proliferation *in vivo*. Kidney Int 1997;52(2):404–13.

[146] Petermann AT, Pippin J, Hiromura K, Monkawa T, Durvasula R, Couser WG, et al. Mitotic cell cycle proteins increase in podocytes despite lack of proliferation. Kidney Int 2003;63 (1):113–22.

[147] Pippin JW, Durvasula R, Petermann A, Hiromura K, Couser WG, Shankland SJ. DNA damage is a novel response to sublytic complement C5b-9-induced injury in podocytes. J Clin Invest 2003;111(6):877–85.

[148] Kim YG, Alpers CE, Brugarolas J, Johnson RJ, Couser WG, Shankland SJ. The cyclin kinase inhibitor p21CIP1/WAF1 limits glomerular epithelial cell proliferation in experimental glomerulonephritis. Kidney Int 1999;55(6):2349–61.

[149] Shankland SJ, Wolf G. Cell cycle regulatory proteins in renal disease: role in hypertrophy, proliferation, and apoptosis. Am J Physiol Renal Physiol 2000;278(4):F515–29.

[150] Wada T, Pippin JW, Terada Y, Shankland SJ. The cyclin-dependent kinase inhibitor p21 is required for TGF-beta1-induced podocyte apoptosis. Kidney Int 2005;68(4):1618–29.

[151] Marshall CB, Krofft RD, Pippin JW, Shankland SJ. The CDK-inhibitor p21 is pro-survival in adriamycin(R)-induced podocyte injury, *in vitro* and *in vivo*. Am J Physiol Renal Physiol 2010.

[152] Shankland SJ, Eitner F, Hudkins KL, Goodpaster T, D'Agati V, Alpers CE. Differential expression of cyclin-dependent kinase inhibitors in human glomerular disease: role in podocyte proliferation and maturation. Kidney Int 2000;58(2):674–83.

[153] Petermann AT, Hiromura K, Blonski M, Pippin J, Monkawa T, Durvasula R, et al. Mechanical stress reduces podocyte proliferation *in vitro*. Kidney Int 2002;61(1):40–50.

[154] Brenner BM. Nephron adaptation to renal injury or ablation. Am J Physiol 1985;249(3 Pt 2):F324–37.

[155] Weir MR. Diabetes and hypertension: blood pressure control and consequences. Am J Hypertens 1999;12(12 Pt 1–2): 170S–8S.

[156] Harris RC, Haralson MA, Badr KF. Continuous stretch-relaxation in culture alters rat mesangial cell morphology, growth characteristics, and metabolic activity. Lab Invest 1992;66 (5):548–54.

[157] Petermann AT, Pippin J, Durvasula R, Pichler R, Hiromura K, Monkawa T, et al. Mechanical stretch induces podocyte hypertrophy *in vitro*. Kidney Int 2005;67(1):157–66.

[158] Nagata M, Tomari S, Kanemoto K, Usui J, Lemley KV. Podocytes, parietal cells, and glomerular pathology: the role of cell cycle proteins. Pediatr Nephrol 2003;18(1):3–8.

[159] Ophascharoensuk V, Pippin JW, Gordon KL, Shankland SJ, Couser WG, Johnson RJ. Role of intrinsic renal cells versus infiltrating cells in glomerular crescent formation. Kidney Int 1998;54(2):416–25.

[160] Moeller MJ, Soofi A, Hartmann I, Le Hir M, Wiggins R, Kriz W, et al. Podocytes populate cellular crescents in a murine model of inflammatory glomerulonephritis. J Am Soc Nephrol 2004;15(1):61–7.

[161] Matsusaka T, Xin J, Niwa S, Kobayashi K, Akatsuka A, Hashizume H, et al. Genetic engineering of glomerular sclerosis in the mouse via control of onset and severity of podocyte-specific injury. J Am Soc Nephrol 2005;16(4):1013–23.

[162] Smeets B, Uhlig S, Fuss A, Mooren F, Wetzels JF, Floege J, et al. Tracing the origin of glomerular extracapillary lesions from parietal epithelial cells. J Am Soc Nephrol 2009;20 (12):2604–15.

[163] Barisoni L, Kriz W, Mundel P, D'Agati V. The dysregulated podocyte phenotype: a novel concept in the pathogenesis of collapsing idiopathic focal segmental glomerulosclerosis and HIV-associated nephropathy. J Am Soc Nephrol 1999;10 (1):51–61.

[164] Barisoni L, Mokrzycki M, Sablay L, Nagata M, Yamase H, Mundel P. Podocyte cell cycle regulation and proliferation in collapsing glomerulopathies. Kidney Int 2000;58(1):137–43.

[165] Detwiler RK, Falk RJ, Hogan SL, Jennette JC. Collapsing glomerulopathy: a clinically and pathologically distinct variant of focal segmental glomerulosclerosis. Kidney Int 1994;45 (5):1416–24.

[166] Schwartz MM, Evans J, Bain R, Korbet SM. Focal segmental glomerulosclerosis: prognostic implications of the cellular lesion. J Am Soc Nephrol 1999;10(9):1900–7.

[167] Barisoni L, Bruggeman LA, Mundel P, D'Agati VD, Klotman PE. HIV-1 induces renal epithelial dedifferentiation in a transgenic model of HIV-associated nephropathy. Kidney Int 2000;58(1):173–81.

[168] Bruggeman LA, Dikman S, Meng C, Quaggin SE, Coffman TM, Klotman PE. Nephropathy in human immunodeficiency virus-1 transgenic mice is due to renal transgene expression. J Clin Invest 1997;100(1):84–92.

[169] Dickie P, Felser J, Eckhaus M, Bryant J, Silver J, Marinos N, et al. HIV-associated nephropathy in transgenic mice expressing HIV-1 genes. Virology 1991;185(1):109–19.

[170] Schwartz EJ, Cara A, Snoeck H, Ross MD, Sunamoto M, Reiser J, et al. Human immunodeficiency virus-1 induces loss of contact inhibition in podocytes. J Am Soc Nephrol 2001;12(8): 1677–84.

[171] Nelson PJ, Sunamoto M, Husain M, Gelman IH. HIV-1 expression induces cyclin D1 expression and pRb phosphorylation in infected podocytes: cell-cycle mechanisms contributing to the proliferative phenotype in HIV-associated nephropathy. BMC Microbiol 2002;2:26.

[172] Conaldi PG, Bottelli A, Baj A, Serra C, Fiore L, Federico G, et al. Human immunodeficiency virus-1 that induces hyperproliferation and dysregulation of renal glomerular epithelial cells. Am J Pathol 2002;161(1):53–61.

[173] Scheurer D. Rapid reversal of renal failure after initiation of HAART: a case report. AIDS Read 2004;14(8):443–7.

[174] Brinkkoetter PT, Pippin JW, Shankland SJ. Cyclin I-Cdk5 governs survival in post-mitotic cells. Cell Cycle 2010;9 (9):1729–31.

[175] Griffin SV, Olivier JP, Pippin JW, Roberts JM, Shankland SJ. Cyclin I protects podocytes from apoptosis. J Biol Chem 2006;281(38):28048–57.

[176] Brinkkoetter PT, Olivier P, Wu JS, Henderson S, Krofft RD, Pippin JW, et al. Cyclin I activates Cdk5 and regulates expression of Bcl-2 and Bcl-XL in postmitotic mouse cells. J Clin Invest 2009.

[177] Griffin SV, Hiromura K, Pippin J, Petermann AT, Blonski MJ, Krofft R, et al. Cyclin-dependent kinase 5 is a regulator of podocyte differentiation, proliferation, and morphology. Am J Pathol 2004;165(4):1175–85.

[178] Brinkkoetter PT, Wu JS, Ohse T, Krofft RD, Schermer B, Benzing T, et al. p35, the non-cyclin activator of Cdk5, protects

podocytes against apoptosis *in vitro* and *in vivo*. Kidney Int 2010;77(8):690–9.
[179] Griffin SV, Krofft RD, Pippin JW, Shankland SJ. Limitation of podocyte proliferation improves renal function in experimental crescentic glomerulonephritis. Kidney Int 2005;67(3):977–86.
[180] Gherardi D, D'Agati V, Chu TH, Barnett A, Gianella-Borradori A, Gelman IH, et al. Reversal of collapsing glomerulopathy in mice with the cyclin-dependent kinase inhibitor CYC202. J Am Soc Nephrol 2004;15(5):1212–22.
[181] Suzuki A, Ito T, Imai E, Yamato M, Iwatani H, Kawachi H, et al. Retinoids regulate the repairing process of the podocytes in puromycin aminonucleoside-induced nephrotic rats. J Am Soc Nephrol 2003;14(4):981–91.
[182] Tovbin D, Franch HA, Alpern RJ, Preisig PA. Media acidification inhibits TGF beta-mediated growth suppression in cultured rabbit proximal tubule cells. Proc Assoc Am Physicians 1997;109(6):572–9.
[183] Xing CY, Saleem MA, Coward RJ, Ni L, Witherden IR, Mathieson PW. Direct effects of dexamethasone on human podocytes. Kidney Int 2006;70(6):1038–45.
[184] Ohse T, Pippin JW, Chang AM, Krofft RD, Miner JH, Vaughan MR, et al. The enigmatic parietal epithelial cell is finally getting noticed: a review. Kidney Int 2009;76 (12):1225–38.
[185] Nitta K, Horita S, Honda K, Uchida K, Watanabe T, Nihei H, et al. Glomerular expression of cell-cycle-regulatory proteins in human crescentic glomerulonephritis. Virchows Arch 1999;435 (4):422–7.
[186] Suzuki T, Matsusaka T, Nakayama M, Asano T, Watanabe T, Ichikawa I, et al. Genetic podocyte lineage reveals progressive podocytopenia with parietal cell hyperplasia in a murine model of cellular/collapsing focal segmental glomerulosclerosis. Am J Pathol 2009;174(5):1675–82.
[187] Kang DH, Kanellis J, Hugo C, Truong L, Anderson S, Kerjaschki D, et al. Role of the microvascular endothelium in progressive renal disease. J Am Soc Nephrol 2002;13 (3):806–16.
[188] Kang DH, Hughes J, Mazzali M, Schreiner GF, Johnson RJ. Impaired angiogenesis in the remnant kidney model: II. Vascular endothelial growth factor administration reduces renal fibrosis and stabilizes renal function. J Am Soc Nephrol 2001;12(7):1448–57.
[189] Kim YG, Suga SI, Kang DH, et al. Vascular endothelial growth factor accelerates renal recovery in experimental thrombotic microangiopathy. Kidney Int 2000;58(6):2390–9.
[190] Masuda Y, Shimizu A, Mori T, Ishiwata T, Kitamura H, Ohashi R, et al. Vascular endothelial growth factor enhances glomerular capillary repair and accelerates resolution of experimentally induced glomerulonephritis. Am J Pathol 2001;159 (2):599–608.
[191] Bonventre JV. Dedifferentiation and proliferation of surviving epithelial cells in acute renal failure. J Am Soc Nephrol 2003;14 (Suppl. 1):S55–61.
[192] Park SK, Kang MJ, Kim W, Koh GY. Renal tubule regeneration after ischemic injury is coupled to the up-regulation and activation of cyclins and cyclin dependent kinases. Kidney Int 1997;52(3):706–14.
[193] Megyesi J, Udvarhelyi N, Safirstein RL, Price PM. The p53-independent activation of transcription of p21 WAF1/CIP1/SDI1 after acute renal failure. Am J Physiol 1996;271(6 Pt 2): F1211–6.
[194] Megyesi J, Safirstein RL, Price PM. Induction of p21WAF1/CIP1/SDI1 in kidney tubule cells affects the course of cisplatin-induced acute renal failure. J Clin Invest 1998;101 (4):777–82.
[195] Kurtz I. Role of ammonia in the induction of renal hypertrophy. Am J Kidney Dis 1991;17(6):650–3.
[196] Hostetter TH. Progression of renal disease and renal hypertrophy. Annu Rev Physiol 1995;57:263–78.
[197] Zatz R, Fujihara CK. Glomerular hypertrophy and progressive glomerulopathy. Is there a definite pathogenetic correlation? Kidney Int Suppl. 1994;45:S27–29; discussion S30-21.
[198] Ziyadeh FN, Sharma K. Role of transforming growth factor-beta in diabetic glomerulosclerosis and renal hypertrophy. Kidney Int Suppl 1995;51:S34–6.
[199] Toth T, Takebayashi S. Glomerular hypertrophy in relapsing minimal change nephropathy. Nephron 1996;74(1):64–71.
[200] Fogo A, Hawkins EP, Berry PL, Glick AD, Chiang ML, MacDonell Jr RC, et al. Glomerular hypertrophy in minimal change disease predicts subsequent progression to focal glomerular sclerosis. Kidney Int 1990;38(1):115–23.
[201] Muda AO, Feriozzi S, Cinotti GA, Faraggiana T. Glomerular hypertrophy and chronic renal failure in focal segmental glomerulosclerosis. Am J Kidney Dis 1994;23(2):237–41.
[202] Tenschert S, Elger M, Lemley KV. Glomerular hypertrophy after subtotal nephrectomy: relationship to early glomerular injury. Virchows Arch 1995;426(5):509–17.
[203] McGowan T, McCue P, Sharma K. Diabetic nephropathy. Clin Lab Med 2001;21(1):111–46.
[204] Pagtalunan ME, Miller PL, Jumping-Eagle S, Nelson RG, Myers BD, Rennke HG, et al. Podocyte loss and progressive glomerular injury in type II diabetes. J Clin Invest 1997;99(2):342–8.
[205] Ritz E, Keller C, Bergis K, Strojek K. Pathogenesis and course of renal disease in IDDM/NIDDM: differences and similarities. Am J Hypertens 1997;10(9 Pt 2):202S–7S.
[206] Brizzi MF, Dentelli P, Rosso A, et al. RAGE- and TGF-beta receptor-mediated signals converge on STAT5 and p21waf to control cell-cycle progression of mesangial cells: a possible role in the development and progression of diabetic nephropathy. FASEB J 2004;18(11):1249–51.
[207] Cusumano AM, Bodkin NL, Hansen BC, Iotti R, Owens J, Klotmant PE, et al. Glomerular hypertrophy is associated with hyperinsulinemia and precedes overt diabetes in aging rhesus monkeys. Am J Kidney Dis 2002;40(5):1075–85.
[208] Young BA, Johnson RJ, Alpers CE, Eng E, Gordon K, Floege J, et al. Cellular events in the evolution of experimental diabetic nephropathy. Kidney Int 1995;47(3):935–44.
[209] Feliers D, Frank MA, Riley DJ. Activation of cyclin D1-Cdk4 and Cdk4-directed phosphorylation of RB protein in diabetic mesangial hypertrophy. Diabetes 2002;51(11):3290–9.
[210] Kuan CJ, al-Douahji M, Shankland SJ. The cyclin kinase inhibitor p21WAF1, CIP1 is increased in experimental diabetic nephropathy: potential role in glomerular hypertrophy. J Am Soc Nephrol 1998;9(6):986–93.
[211] Wolf G, Schroeder R, Ziyadeh FN, Thaiss F, Zahner G, Stahl RA. High glucose stimulates expression of p27Kip1 in cultured mouse mesangial cells: relationship to hypertrophy. Am J Physiol 1997;273(3 Pt 2):F348–56.
[212] Wolf G, Sharma K, Chen Y, Ericksen M, Ziyadeh FN. High glucose-induced proliferation in mesangial cells is reversed by autocrine TGF-beta. Kidney Int 1992;42(3):647–56.
[213] Ziyadeh FN, Sharma K, Ericksen M, Wolf G. Stimulation of collagen gene expression and protein synthesis in murine mesangial cells by high glucose is mediated by autocrine activation of transforming growth factor-beta. J Clin Invest 1994;93 (2):536–42.
[214] Abdel-Wahab N, Weston BS, Roberts T, Mason RM. Connective tissue growth factor and regulation of the mesangial cell cycle: role in cellular hypertrophy. J Am Soc Nephrol 2002;13(10):2437–45.

[215] Wolf G, Schroeder R, Thaiss F, Ziyadeh FN, Helmchen U, Stahl RA. Glomerular expression of p27Kip1 in diabetic db/db mouse: role of hyperglycemia. Kidney Int 1998;53(4):869–79.
[216] Wolf G, Reinking R, Zahner G, Stahl RA, Shankland SJ. Erk 1,2 phosphorylates p27(Kip1): functional evidence for a role in high glucose-induced hypertrophy of mesangial cells. Diabetologia 2003;46(8):1090–9.
[217] Fan YP, Weiss RH. Exogenous attenuation of p21(Waf1/Cip1) decreases mesangial cell hypertrophy as a result of hyperglycemia and IGF-1. J Am Soc Nephrol 2004;15(3):575–84.
[218] Wolf G, Schroeder R, Zahner G, Stahl RA, Shankland SJ. High glucose-induced hypertrophy of mesangial cells requires p27 (Kip1), an inhibitor of cyclin-dependent kinases. Am J Pathol 2001;158(3):1091–100.
[219] Hoshi S, Shu Y, Yoshida F, Inagaki T, Sonoda J, Watanabe T, et al. Podocyte injury promotes progressive nephropathy in zucker diabetic fatty rats. Lab Invest 2002;82(1):25–35.
[220] Al-Douahji M, Brugarolas J, Brown PA, Stehman-Breen CO, Alpers CE, Shankland SJ. The cyclin kinase inhibitor p21WAF1/CIP1 is required for glomerular hypertrophy in experimental diabetic nephropathy. Kidney Int 1999;56 (5):1691–9.
[221] Awazu M, Omori S, Ishikura K, Hida M, Fujita H. The lack of cyclin kinase inhibitor p27(Kip1) ameliorates progression of diabetic nephropathy. J Am Soc Nephrol 2003;14(3):699–708.
[222] Kopp JB, Factor VM, Mozes M, Nagy P, Sanderson N, Böttinger EP, et al. Transgenic mice with increased plasma levels of TGF-beta 1 develop progressive renal disease. Lab Invest 1996;74(6):991–1003.
[223] Roberts AB, McCune BK, Sporn MB. TGF-beta: regulation of extracellular matrix. Kidney Int 1992;41(3):557–9.
[224] Shankland SJ, Johnson RJ. TGF-beta in glomerular disease. Miner Electrolyte Metab 1998;24(2–3):168–73.
[225] MacKay K, Striker LJ, Stauffer JW, Doi T, Agodoa LY, Striker GE. Transforming growth factor-beta. Murine glomerular receptors and responses of isolated glomerular cells. J Clin Invest 1989;83(4):1160–7.
[226] Monkawa T, Hiromura K, Wolf G, Shankland SJ. The hypertrophic effect of transforming growth factor-beta is reduced in the absence of cyclin-dependent kinase-inhibitors p21 and p27. J Am Soc Nephrol 2002;13(5):1172–8.
[227] Wolf G. Molecular mechanisms of renal hypertrophy: role of p27Kip1. Kidney Int 1999;56(4):1262–5.
[228] Gross ML, El-Shakmak A, Szabo A, Koch A, Kuhlmann A, Munter K, et al. ACE-inhibitors but not endothelin receptor blockers prevent podocyte loss in early diabetic nephropathy. Diabetologia 2003;46(6):856–68.
[229] Gross ML, Ritz E, Schoof A, Adamczak M, Koch A, Tulp O, et al. Comparison of renal morphology in the Streptozotocin and the SHR/N-cp models of diabetes. Lab Invest 2004;84 (4):452–64.
[230] Xu ZG, Yoo TH, Ryu DR, Cheon Park H, Ha SK, Han DS, et al. Angiotensin II receptor blocker inhibits p27Kip1 expression in glucose-stimulated podocytes and in diabetic glomeruli. Kidney Int 2005;67(3):944–52.
[231] White KE, Bilous RW. Estimation of podocyte number: a comparison of methods. Kidney Int 2004;66(2):663–7.
[232] Bhathena DB. Glomerular basement membrane length to podocyte ratio in human nephronopenia: implications for focal segmental glomerulosclerosis. Am J Kidney Dis 2003;41 (6):1179–88.
[233] Petermann AT, Pippin J, Krofft R, Blonski M, Griffin S, Durvasula R, et al. Viable podocytes detach in experimental diabetic nephropathy: potential mechanism underlying glomerulosclerosis. Nephron Exp Nephrol 2004;98(4):e114–23.
[234] Wolf G, Schanze A, Stahl RA, Shankland SJ, Amann K. p27 (Kip1) Knockout mice are protected from diabetic nephropathy: evidence for p27(Kip1) haplotype insufficiency. Kidney Int 2005;68(4):1583–9.
[235] Wolf G. Changing concepts of compensatory renal growth: from humoral pathology to molecular biology. Am J Nephrol 1992;12(5):369–73.
[236] Park SK, Kang SK, Lee DY, Kang MJ, Kim SH, Koh GY. Temporal expressions of cyclins and cyclin dependent kinases during renal development and compensatory growth. Kidney Int 1997;51(3):762–9.
[237] Megyesi J, Price PM, Tamayo E, Safirstein RL. The lack of a functional p21(WAF1/CIP1) gene ameliorates progression to chronic renal failure. Proc Natl Acad Sci USA 1999;96 (19):10830–5.
[238] Ingram AJ, Ly H, Thai K, Kang M, Scholey JW. Activation of mesangial cell signaling cascades in response to mechanical strain. Kidney Int 1999;55(2):476–85.
[239] Rabkin R, Fervenza FC. Renal hypertrophy and kidney disease in diabetes. Diabetes Metab Rev 1996;12(3):217–41.
[240] Wolf G. Cellular mechanisms of tubule hypertrophy and hyperplasia in renal injury. Miner Electrolyte Metab 1995;21 (4–5):303–16.
[241] Chen S, Hoffman BB, Lee JS, Kasama Y, Jim B, Kopp JB, et al. Cultured tubule cells from TGF-beta1 null mice exhibit impaired hypertrophy and fibronectin expression in high glucose. Kidney Int 2004;65(4):1191–204.
[242] Franch HA, Shay JW, Alpern RJ, Preisig PA. Involvement of pRB family in TGF beta-dependent epithelial cell hypertrophy. J Cell Biol 1995;129(1):245–54.
[243] Liu B, Preisig P. TGF-beta1-mediated hypertrophy involves inhibiting pRB phosphorylation by blocking activation of cyclin E kinase. Am J Physiol 1999;277(2 Pt 2):F186–94.
[244] Preisig P. What makes cells grow larger and how do they do it? Renal hypertrophy revisited. Exp Nephrol 1999;7(4):273–83.
[245] Wolf G, Neilson EG. Angiotensin II induces cellular hypertrophy in cultured murine proximal tubular cells. Am J Physiol 1990;259(5 Pt 2):F768–77.
[246] Wolf G, Kuncio GS, Sun MJ, Neilson EG. Expression of homeobox genes in a proximal tubular cell line derived from adult mice. Kidney Int 1991;39(5):1027–33.
[247] Burns KD, Harris RC. Signaling and growth responses of LLC-PK1/Cl4 cells transfected with the rabbit AT1 ANG II receptor. Am J Physiol 1995;268(4 Pt 1):C925–35.
[248] Wolf G, Mueller E, Stahl RA, Ziyadeh FN. Angiotensin II-induced hypertrophy of cultured murine proximal tubular cells is mediated by endogenous transforming growth factor-beta. J Clin Invest 1993;92(3):1366–72.
[249] Wolf G, Stahl RA. Angiotensin II-stimulated hypertrophy of LLC-PK1 cells depends on the induction of the cyclin-dependent kinase inhibitor p27Kip1. Kidney Int 1996;50(6): 2112–9.
[250] Wolf G, Jablonski K, Schroeder R, Reinking R, Shankland SJ, Stahl RA. Angiotensin II-induced hypertrophy of proximal tubular cells requires p27Kip1. Kidney Int 2003;64(1): 71–81.
[251] Hannken T, Schroeder R, Stahl RA, Wolf G. Angiotensin II-mediated expression of p27Kip1 and induction of cellular hypertrophy in renal tubular cells depend on the generation of oxygen radicals. Kidney Int 1998;54(6):1923–33.
[252] Hannken T, Schroeder R, Zahner G, Stahl RA, Wolf G. Reactive oxygen species stimulate p44/42 mitogen-activated protein kinase and induce p27(Kip1): role in angiotensin II-mediated hypertrophy of proximal tubular cells. J Am Soc Nephrol 2000;11(8):1387–97.

[253] Hannken T, Schroeder R, Stahl RA, Wolf G. Atrial natriuretic peptide attenuates ANG II-induced hypertrophy of renal tubular cells. Am J Physiol Renal Physiol 2001;281(1): F81–90.

[254] Wolf G, Wenzel U, Hannken T, Stahl RA. Angiotensin II induces p27(Kip1) expression in renal tubules *in vivo*: role of reactive oxygen species. J Mol Med 2001;79(7):382–9.

[255] Ruperez M, Ruiz-Ortega M, Esteban V, Lorenzo O, Mezzano S, Plaza JJ, et al. Angiotensin II increases connective tissue growth factor in the kidney. Am J Pathol 2003;163(5): 1937–47.

[256] Liu BC, Sun J, Chen Q, Ma KL, Ruan XZ, Phillips AO. Role of connective tissue growth factor in mediating hypertrophy of human proximal tubular cells induced by angiotensin II. Am J Nephrol 2003;23(6):429–37.

[257] Olbricht CJ, Geissinger B. Renal hypertrophy in streptozotocin diabetic rats: role of proteolytic lysosomal enzymes. Kidney Int 1992;41(4):966–72.

[258] Shechter P, Boner G, Rabkin R. Tubular cell protein degradation in early diabetic renal hypertrophy. J Am Soc Nephrol 1994;4(8):1582–7.

[259] Shechter P, Shi JD, Rabkin R. Renal tubular cell protein breakdown in uninephrectomized and ammonium chloride-loaded rats. J Am Soc Nephrol 1994;5(5):1201–7.

[260] Franch HA, Curtis PV, Mitch WE. Mechanisms of renal tubular cell hypertrophy: mitogen-induced suppression of proteolysis. Am J Physiol 1997;273(3 Pt 1):C843–51.

[261] Franch HA, Sooparb S, Du J, Brown NS. A mechanism regulating proteolysis of specific proteins during renal tubular cell growth. J Biol Chem 2001;276(22):19126–31.

[262] Franch HA, Preisig PA. NH_4Cl-induced hypertrophy is mediated by weak base effects and is independent of cell cycle processes. Am J Physiol 1996;270(3 Pt 1):C932–8.

[263] Garibotto G, Sofia A, Robaudo C, Saffioti S, Sala MR, Verzola D, et al. Kidney protein dynamics and ammoniagenesis in humans with chronic metabolic acidosis. J Am Soc Nephrol 2004;15(6):1606–15.

[264] Ling H, Vamvakas S, Gekle M, Schaefer L, Teschner M, Schaefer RM, et al. Role of lysosomal cathepsin activities in cell hypertrophy induced by NH_4Cl in cultured renal proximal tubule cells. J Am Soc Nephrol 1996;7(1):73–80.

[265] Nath KA, Hostetter MK, Hostetter TH. Increased ammoniagenesis as a determinant of progressive renal injury. Am J Kidney Dis 1991;17(6):654–7.

[266] Walsh-Reitz MM, Toback FG. Kidney epithelial cell growth is stimulated by lowering extracellular potassium concentration. Am J Physiol 1983;244(5):C429–32.

[267] Tolins JP, Hostetter MK, Hostetter TH. Hypokalemic nephropathy in the rat. Role of ammonia in chronic tubular injury. J Clin Invest 1987;79(5):1447–58.

[268] Sooparb S, Price SR, Shaoguang J, Franch HA. Suppression of chaperone-mediated autophagy in the renal cortex during acute diabetes mellitus. Kidney Int 2004;65(6):2135–44.

[269] Franch HA, Wang X, Sooparb S, Brown NS, Du J. Phosphatidylinositol 3-kinase activity is required for epidermal growth factor to suppress proteolysis. J Am Soc Nephrol 2002;13(4):903–9.

[270] Feliers D, Duraisamy S, Faulkner JL, Duch J, Lee AV, Abboud HE, et al. Activation of renal signaling pathways in *db*/*db* mice with type 2 diabetes. Kidney Int 2001;60(2):495–504.

CHAPTER

29

Stem Cells and Generation of New Cells in the Adult Kidney

Juan A. Oliver[1] *and Qais Al-Awqati*[2]

[1]Department of Medicine, Columbia University, New York, NY, USA

[2]Departments of Medicine and Physiology, Columbia University, New York, NY, USA

EMBRYONIC ORIGIN OF RENAL CELLS

The idea that the kidney is an organ needs to be tempered by the realization that it is the nephron that is the organ. Each nephron, as far as we know, is independent from other nephrons, and the kidney is to a first approximation a collection of these mini-organs put together in a complex three-dimensional assembly. The nephrons of all mammals are remarkably similar in size, function, and origin (as far as we know), and the differences among species are largely if not entirely due to the number of these units in the assembly, with mice having 10,000 and whales having 250 million in each kidney. But while the epithelial character of the nephron garners most of the attention, one needs to be reminded that the kidney has a very extensive vascular network with multiple distinct morphological and functional domains, as well as an abundant interstitial cell population that unfortunately is still poorly understood (see Kaissiling and Le Hir[1] for a review). While the taxonomy of the renal epithelial cells is nearly complete, that of the cells of the vascular and interstitial compartments awaits detailed characterization. Hence, analysis of renal regeneration after injury, as well as search for putative renal stem cells in the adult kidney, has essentially been restricted to the epithelial compartment. However, as epithelial cells are likely instructed by mesenchymal signals and epithelia-mesenchymal cross-talk is critical for renal epithelial differentiation and function,[2] there is a need for deeper understanding of the cell types that comprise the renal vascular and interstitial compartments, and their roles in kidney homeostasis and repair from injury. For example, in many organs including the kidney, mesenchymal cells with characteristics of precursor/stem cells have been found to reside near or in the vascular wall,[3–5] but the exact origin and normal function of these cells is unknown.

The different cellular compartments of the adult kidney have been traditionally recognized by their morphological characteristics or by their embryonic origin, since it was long ago recognized that the adult (metanephric) kidney derives from two distinct elements of the intermediate mesoderm: the metanephric mesenchyme and the ureteric bud. Within the kidney, the ureteric bud gives rise to the collecting duct cells, while some metanephric mesenchyme cells give rise to the rest of the nephron.[6] However, over the last few decades, the discovery of several genes that are expressed in the restricted group of cells of the renal anlage has allowed a different taxonomic approach that has greatly illuminated our understanding of the distinct cell populations in the adult kidney. Moreover, it has allowed development of research tools with which it is possible to probe in the adult kidney the function of specific cells, of specific genes in specific cells, and importantly for the present discussion, to identify the daughter cells of different cell types by *in vivo* genetic cell lineage methods. Thus, we briefly review the embryonic origin of the distinct cells in the adult kidney, emphasizing those aspects that might clarify the origin of new cells in the adult organ.

Epithelial Cells

All epithelial cells of the adult kidney are believed to derive from the intermediate mesoderm, from which both the ureteric bud (a branch of the Wolffian duct) and the metanephric mesenchyme originate. Renal

Seldin and Giebisch's The Kidney, Fifth Edition.
DOI: http://dx.doi.org/10.1016/B978-0-12-381462-3.00029-X

© 2013 Elsevier Inc. All rights reserved.

morphogenesis starts when the ureteric bud invades the metanephric mesenchyme and starts branching. The cells in the tip of each ureteric bud branch give rise to the collecting duct cells and the metanephric mesenchyme cells in contact with each ureteric bud tip give rise, after a series of morphogenic steps, to the cells of the remaining nephron segments spanning from the connecting tubule to the glomerulus. The ureteric bud, like the Wolffian duct, expresses the homeobox gene *HoxB7*,[7] and transgenic mice expressing *HoxB7*-GFP or *HoxB7*-Cre recombinase have been used to label most, if not all, of the cells in the ureteric bud branches of the embryonic collecting duct,[8] and their progeny in the adult kidney.

The metanephric mesenchymal cells undergo simultaneous differentiation (to generate a nephron for each ureteric bud tip) and growth, so that the appropriate number of nephrons will be generated for the branches of the ureteric bud. It was recently found that the metanephric mesenchymal cells that are in contact with the tips of the ureteric bud, referred to as the cap mesenchyme, are the progenitor cells of all nephron epithelia (except the collecting duct). These cells were found to express the transcription factors *Cited1*[9] and *Six2*,[10] thereby allowing generation of transgenic mice that label all nephron epithelial cells except those of the collecting ducts. More relevant to the present discussion is that these mice can be used to permanently identify the progeny of adult nephron epithelial cells,[9,10] thus providing an invaluable tool for analysis of epithelial cell regeneration after kidney injury and/or disease,[11] as discussed below.

Mesenchymal/Stromal Cells

Like renal epithelial cells, the vast majority of the stroma cells in the adult kidney derive from the intermediate mesoderm[12] that in the kidney gives rise to a cell population that expresses the forkhead transcription factor *Foxd1*.[2,13,14] These cells generate many renal interstitial cells, as well as mesangial cells, vascular smooth muscle, pericytes, and renal capsule, and likely mesenchymal stem cells.[5] *Foxd1*-expressing cells are absolutely required for normal kidney development,[2,13,14] and their adult progeny is of extreme interest because it likely contains pluripotent MSC[5] and pericytes,[4] although a clear-cut distinction between these two cell types is not yet possible. In addition, identification of *Foxd1* as marker of these cells has made it possible to develop transgenic mice that can be used to label the stroma cell progeny in the adult kidney.[15]

Another population of renal stromal cells derives from the paraxial mesoderm,[16] but the precise contribution of these cells to the interstitial and mesenchymal cell populations of the adult kidney remains to be defined. Finally, an area of the intermediate mesoderm located ventro–lateral to the dorsal aorta generates renal interstitial cells that express the stem cell factor receptor (*c-kit*).[17] During embryogenesis, these cells appear to be involved in the maintenance of the metanephric mesenchyme-derived cells, but identification of their progeny in the adult kidney remains to be established.

Endothelial Cells

The renal circulation is both anatomically and functionally complex, and likely contains many types of endothelial cells. Their exact origin is still poorly-understood. It is clear that once kidney development starts, the renal anlage contains angioblats[18,19] that give rise to endothelial cells. It is currently unknown whether these endothelial precursors migrate into the developing kidney or differentiated from cells that reside in the metanephric mesenchyme. The latter appears more likely, as we found that many cells in the renal anlage express tyrosine kinases that are characteristic of adult endothelial cells.[20] Interestingly, in addition to being endothelial precursors, angioblasts in the renal anlage appear to provide signals important for development and differentiation of the metanephric mesenchyme.[21] It is currently unknown if there exists interaction in the adult kidney between endothelial cells and either interstitial or epithelial cells that might be involved in maintaining kidney homeostasis or repair from injury. Recent work by Lin et al.[22] suggests that endothelial-to-pericyte cross-talk is involved in the generation of kidney myofibroblats, as detailed below.

NEW CELLS IN THE ADULT KIDNEY

Normal Conditions

As assayed by a variety of methods, the normal adult kidney has a low rate of cellular proliferation.[23–26] Using antibodies to Ki67, a nuclear protein expressed in cycling cells during G0 and G1, between 0.4–1% of all cells were cycling in the adult rat kidney.[24,25] Interestingly, age has a profound effect in the abundance of proliferating cells found in the kidney. Vogesterder et al.[25] found that while only ~0.4% of all renal cells were positive for Ki67 in the kidneys of 16- to 20-week-old rats, in animals that were only 4 weeks old the number of cycling cells was ~5%. This suggests that in the kidney there is an age-dependent progressive decline in the number of cycling cells, and that workers examining renal cell proliferation should take into account the age of the animal as an important variable.

Proliferating cells in the renal cortex of 4-week-old rats were found preferentially located to the S3 segment of the proximal tubule, when compared to the S1 and S2 segments.[25] This interesting result might have important implications in designing strategies to identify renal stem cells, a subject to which we will return below. In contrast, in 1-year-old rats, we found that most of the kidney parenchyma had a homogeneous fraction of ~1% of Ki67 positive cells Figure 29.1. There were two exceptions to this, however, the body of the papilla where there were extremely low numbers of cycling cells (<0.1% of the cells were positive for Ki67), and the upper part of the papilla (at the papilla–medullary junction), where we found the highest frequency of cycling cells (~2.5%),[24] indicating that it is an area of privileged cellular proliferation in the adult rat. Detailed morphological observations indicate that terminally differentiated tubular epithelia cells can generate new cells,[27,28] but these observations don't exclude the possibility that there are epithelial stem cells.

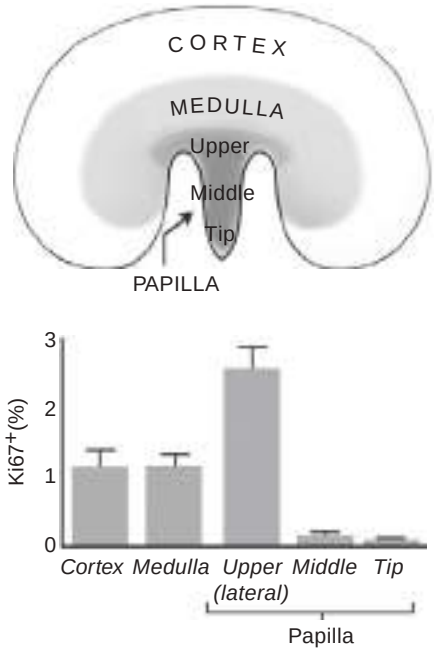

FIGURE 29.1 **Cellular proliferation in adult kidney.** Top: Kidney regions were examined for cellular proliferation. Bottom: Fraction of Ki67-positive cells in different kidney regions. Cortex and medulla had a similar number of Ki67-positive cells, but the lateral side of the papilla had significantly more Ki67-positive cells than the cortex and medulla, as well as the other regions of the papilla. The middle and tip of the papilla had significantly fewer Ki67 positive cells than other regions of the kidney. *(From ref. [27].)*

Organ Repair from Injury

In contrast to normal conditions, the kidney displays a remarkable proliferation capacity shortly after transient injury. For example, injury induced by 30–45 minutes of complete renal artery occlusion in rodents causes functional failure, and widespread cellular apoptosis and necrosis that are followed by diffuse cellular proliferation and functional recovery. What is the origin of these new cells? While the kidney has multiple cell types, studies on the generation of new cells after injury have fundamentally focused on the epithelial cells, likely because of their better-understood functional importance and easier identification. It is now established that the new epithelial cells after kidney injury develop from within the parenchyma, rather than being derived from extrarenal sources such as the bone marrow,[29,30] and thus three possibilities appear likely: (1) any surviving terminally differentiated epithelial cell can generate identical cells; (2) there exist kidney epithelial stem cells capable of generating any epithelial cell type, similar to what was found in the interfollicular epidermis;[31,32] and (3) pluripotent renal stem cells generate epithelial as well as other cell types, as in the case of the stem cells in the bulge of the skin.[33–36]

Morphological observations[35,37] and functional studies with nucleotide analogs[27,38] have provided strong evidence that terminally-differentiated epithelial cells generate new epithelial cells after injury. More recent elegant genetic cell fate-mapping studies have confirmed this suspicion; Humpreys et al.[11] used reporter mice in which the renal epithelial cell compartment was labeled by a Cre recombinase driven by the promoter of *Six2*, a gene that is specifically expressed in embryonic epithelial precursors (see above), and examined their response to acute kidney injury. They found that injury induced massive cellular proliferation, and that all new epithelial cells expressed the reporter gene (Figure 29.2). Since RT-PCR of adult kidney tissue could neither detect *Six2* nor *Cre*, it is apparent that the labeled cells originated from epithelial cells labeled previously during kidney development, thus excluding the interstitial/stroma cell compartment as the origin of new epithelial cells. Needless to say, this experiment does not address whether there exists a group of restricted epithelial cells that are responsible for all the new epithelia generated after injury; these cells could function as adult renal epithelial stem cells. In a recent study, Humphreys et al.[39] examined this possibility by labeling cycling cells after transient kidney injury with two different thymidine analogs administered sequentially. Since the number of epithelial cells that were positive for both nucleotides was very low, these workers concluded that surviving epithelial cells repopulate the nephron epithelium in a stochastic manner,

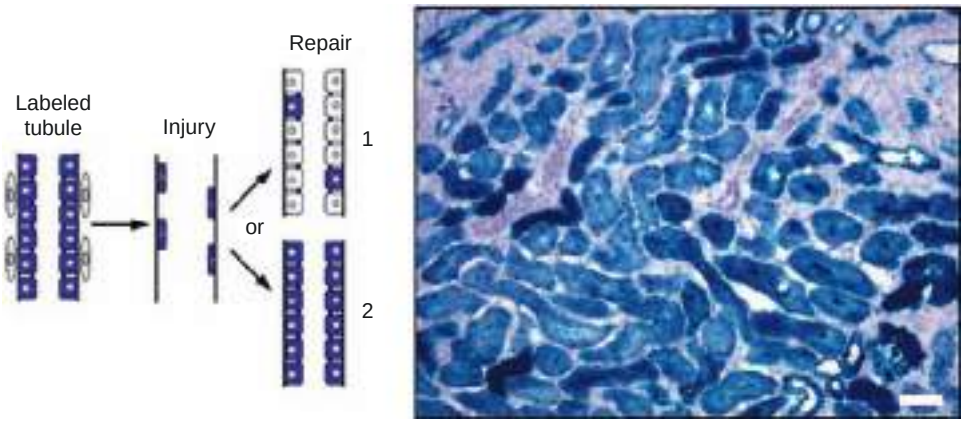

FIGURE 29.2 **Surviving epithelial cells after injury generate new epithelial cells.** (Left) New cells after acute kidney injury in mice with genetically labeled epithelial tubules will not carry the label if they derive from cells outside the epithelial cell compartment (#1), but will carry the label if they derive from terminally differentiated epithelial cells (#2). (Right) Fifteen days after transient ischemic injury and repair, there was no dilution on the number of labeled cells (dark) despite marked cellular proliferation, indicating that they derived from epithelial cells. *(From ref. [14].)*

suggesting that the nephron epithelia has no stem cells.[39] However, while control experiments clearly showed appropriate specificity of both antibodies, detection of closely related thymidine analogs during conditions that, unlike in the control experiments, probably result in incorporation of very different amounts of the two analogs in a given cell are fraught with potential problems. More importantly, their conclusion is based on the implicit assumption that a putative population of epithelial stem cells would be a small fraction of the total number of cells. Under these conditions, to repopulate the damaged epithelia the stem cell progeny would need to divide rapidly, and would thus incorporate both nucleotide analogs. However, as detailed below, stem cells in *Drosophila* Malpighian tubules are a very large fraction of the total cells, and there is no reason why this may not also be the case in mammalian kidneys. Similarly, in organs other than the kidney such as the adult airway epithelia, stem cells account for about one-third of the total number of cells.[40,41]

Identification of the site where cellular proliferation first starts after transient injury could potentially facilitate identification of precursor/stem cells. Unfortunately, for most insults that cause acute kidney injury with functional failure, cellular proliferation has most often been examined one or a few days afterwards, at which time cell proliferation, while very prominent in the S3 segment of the proximal tubule, is also widespread in other parts of the kidney parenchyma, particularly the medulla.[38,42–44]

Following acute kidney injury by renal artery occlusion we could not detect proliferating cells until ~24 hours later when we examined kidney sections of ~5 μm thickness, as is done routinely. However, with 100 μm vibrotome sections, one hour after injury we found that the upper part of the papilla had more proliferative cells than other parts of the kidney[24] (see Figure 29.3), suggesting that this is the site of initial cellular proliferation after kidney injury, which we previously found to be the site of enhanced cell cycling under normal conditions (see above). Interestingly, Vinsonneau et al.[45] reported that the first cells that they found cycling after ischemia reperfusion injury to the kidney were uro-epithelial cells in the upper part of the urinary (intrarenal) space and neighboring interstitial cells; detailed analysis with Ki67 and BrdU incorporation showed that these cells were proliferating ~16 hours after ischemic injury and ~4 hours before proliferation could be detected elsewhere in the kidney. The site identified by Vinsonneau et al.[45] is where the base of the papilla attaches to the medulla, it is in close proximity to the cortex, and appears to be the same proliferating site we identified in the upper papilla. Needless to say, identification of these "early" proliferating cells and of their progeny would be of extreme interest.

An additional observation merits mention. In the few studies that identified the cells that first started proliferating after injury, either after transient ischemic injury[44] or aminoglycoside toxicity,[46,47] it is remarkable that in all instances they were interstitial cells, perhaps suggesting that some interstitial cell plays a critical role in initiating epithelial regeneration. Indeed, the likelihood of renal functional recovery after injury was found to correlate with increases in the number of interstitial cells, many of which were likely myofibroblasts.[43,48,49] Although these results raise the possibility that myofibroblasts might be involved in epithelial regeneration, other interstitial cells such as macrophages are known

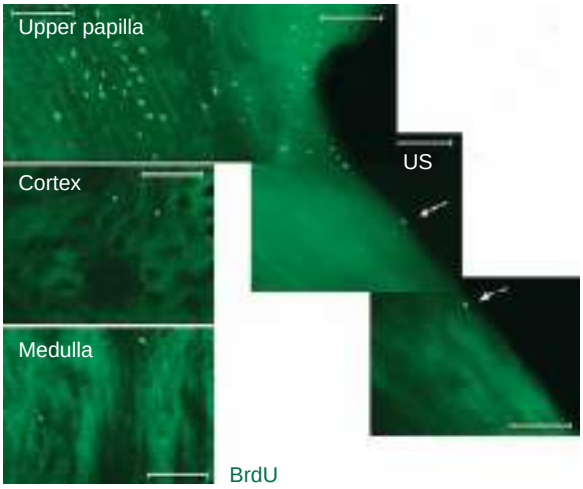

FIGURE 29.3 **Cellular proliferation was first detected in the upper papilla following kidney injury.** There was a selective increase of cells in S-phase in the upper papilla during the first hour after transient ischemic injury. Note abundant BrdU-labeled cells in the upper papilla, whereas the cortex and medulla revealed very rare BrdU-labeled cells (US: urinary space). Photomicrographs were done in 100 μm tissue sections obtained with a vibratome.*(From ref. [27].)*

to be involved in kidney repair,[50] and a detailed characterization of the interstitial cell compartment following transient kidney injury is lacking.

Effect of Age

For many organs, including the kidney,[51] the capacity to recover from injury decreases with age, an observation familiar to most practicing nephrologists. In most organs, it remains to be determined whether this is due to a decrease in the number of organ-specific stem cells or to the inability of the stem cells to be activated, but recent work suggest that the latter is more likely (reviewed by Liu and Rando[52]). For example, it was recently found that aging muscle had a normal number of satellite cells, but the cells failed to activate in response to exercise.[53] Interestingly, progenitor/stem cells in advanced age can display a "young" response by exposure to a young systemic environment,[54] indicating that the changes responsible for the functional decrease of precursor/stem cells are potentially reversible.

While the effect of age on the renal proliferative capacity after injury has not been studied in detail, it appears that cell proliferation after acute kidney injury decreases with age,[55] in agreement with the poor prognosis of recovery from acute kidney injury in elderly patients.[51] Mechanisms that could account for these observations include telomere shortening[56] and increased expression by renal epithelial cells of zinc-α^2-glycoprotein (Zag), an adipokine associated with cachexia.[58] To examine whether the poor regenerative capacity of the aging kidney is due to a decrease in the numbers or in the functionality of putative renal stem/progenitor cells awaits definitive identification of these cells.

In sum, both during normal conditions and particularly after transient kidney injury, the S3 segment of the proximal tubule is a site of intense cell proliferation, suggesting the presence of progenitor cells in this part of the nephron. In addition, the upper part of the papilla and close to the urinary space is also a site of robust cell cycling, both under normal conditions[24] and after transient kidney injury.[24,45]

IDENTIFICATION OF POTENTIAL PRECURSOR/STEM CELLS IN THE ADULT KIDNEY

Studies from several laboratories have presented evidence characterizing renal precursor cells in the adult kidney, but none of these cells meet strict criteria for traditional adult, organ-specific stem cells; i.e., asymmetric cell division and multipotency. Nonetheless, since our ultimate aim is to understand the origin of new cells in the adult kidney so that the responsible mechanisms might be manipulated, these studies are worth reviewing. In addition, the results of these studies are likely to be useful for future work to identify adult renal stem cells. Several strategies have been used to identify and characterize adult kidney precursor/stem cells, and the robustness of the obtained results varies widely. In our view, the methodological approach used for cell identification and/or isolation of the cells best separates these studies.

Cellular Markers

Several workers have isolated cells from the adult kidney using a candidate gene approach. For example, Busolatti et al.[59] used the transmembrane glycoprotein Cd133, which is expressed in hematopoietic stem cells, endothelial progenitor cells, neuronal, glial, and glioblastoma stem cells, as well as some other cell types (see Mizrak et al.[60] for a review), to select cells from the adult human kidney. The isolated cells showed strong clonogenic capacity, and when subcutaneously transplanted to SCID mice formed tubules which expressed some renal epithelial markers. Finally, when the cells were injected intravenously into mice with glycerol-mediated acute kidney injury, they integrated into tubules. However, the functional significance of the integration was not explored.

Using a somewhat similar approach, Dekel et al.[61] used Sca-1, a protein identified in several progenitor cells, to isolate a cell population from mouse kidneys. However, because Sca-1 is also expressed in renal epithelia, these workers used a collagenase digestion approach that appeared to yield interstitial cells. The *in vitro* differentiation of these cells suggested that they were mesenchymal-like stem cells, since they differentiated into myogenic, osteogenic, adipogenic, and neural lineages. When injected into kidneys with acute kidney injury, they also incorporated into tubules.

In Vitro Growth Behavior

Several laboratories have isolated cells from adult kidneys based on their characteristics when cultured *in vitro*. For example, cells were selected because of their high clonogenic potential, ability to outlast all other cultured cells or their ability to change their phenotype. For example, Gupta et al.,[62] cultured cells from collagenase digested rat kidneys, and after ~5 weeks in culture they obtained a cell population with substantial proliferative potential (which in fact was the characteristic that lead to isolation of the cells) and expressing transcription factors such as *Pax-2* and *Oct4* that are either involved in renal development or in determining cell fate. When the cells were injected into the subcapsular space of normal kidneys, some of them incorporated into tubules.

Kitamura et al.[63] used a slightly different strategy by isolating single nephrons from adult rat kidneys and culturing them *in vitro*. Cells growing out from these nephrons were harvested and individually cultured; and the clone with the fastest proliferation capacity was characterized. These clonal cells expressed several proteins important in kidney development and proteins characteristic of mature nephrons. When the cells were injected in the subcapsular region of a kidney with acute kidney injury, the cells engrafted into renal tubules.

More recently, Lee et al.[64] used a mouse with a targeted mutation in which GFP is expressed under the control of *Myh9*, a gene expressed in interstitial cells (among others). After isolation of the GFP^+ cells from the kidney and subsequent culture for eight weeks, they isolated a cell line that expressed renal embryonic or stem cell markers such as *Oct-4*, *Pax-2*, *Wnt-4*, and *WT-1*. Immunolocation of the endogenous $Oct\text{-}4^+$ and GFP^+ cells in the kidney found them in the interstitial space of the medulla and papilla. Finally, when the cells were injected directly into kidneys after acute kidney injury, they incorporated into tubules and partially decreased the functional consequences of the injury.

In Vivo Growth Behavior

The hypothesis that adult, organ-specific stem cells divide infrequently has been a powerful tool in locating and identifying several stem/precursor cells. According to this hypothesis, due to their low cycling behavior, stem cells retain S-phase labels (traditionally ^{3}H-Thymidine or a thymidine analog such as BrdU) when given as a short pulse followed by a long time of chase. Recent work has, however, demonstrated that there is more complexity than originally thought[65–67] (see Fuchs[68] for an informed discussion), as not all stem cells are low cycling and "label retention" experiments identify a heterogeneous group of cells. Nonetheless, populations of "label-retaining cells" from several organs are enriched for stem cells,[66,69–72] and identification of a "label-retaining" group of cells is of great interest. To detect low cycling cells, an S-phase label is only administered during a short period of intense growth (e.g., embryonic life or shortly after birth), so that all cells are cycling and incorporate the label; during the subsequent period of chase the label is diluted and lost by the progeny of dividing cells and selectively retained by low- or non-cycling cells. Cells cycling infrequently were thus named "label-retaining cells" (LRC). Several investigators have used this approach in the kidney.

Maeshima et al.[38] administered BrdU for one week to adult rats that were then "chased" for two weeks, and found that there were many BrdU-retaining cells the kidney parenchyma, particularly in the proximal tubules. Following transient ischemic injury, most of the tubular cells that were proliferating (expressing proliferating nuclear antigen; PCNA) were also BrdU-labeled cells. These results led Maeshima et al.[38] to conclude that a "label-retaining" cell population was the precursor of new cells during kidney repair from injury. However, the long pulse and short period of chase complicate the interpretation of these results. In addition, the increased number of BrdU-labeled cells after injury was likely due to detection of the cells loaded with BrdU during the "pulse" plus their immediate progeny after injury. Nonetheless, because a relatively small population of cells were labeled during the one-week "pulse" and many of these cells were also PCNA positive after injury, this experiment suggests that both during normal conditions and during repair from injury a group of renal epithelial cells cycles at a much higher frequency that most other epithelial cells. This raises the possibility that these cells could be adult, renal epithelial precursors.

We exploited the low cycling frequency of adult stem cells by giving BrdU to newborn rats or mice during a short pulse, and "chased" the animals to

adulthood.[73] In addition, to circumvent the use of BrdU, we[24] also followed the suggestion of Tumbar et al.[74] and used transgenic mice that expressed a fusion protein of histone 2B and GFP (referred as H2B-GFP mice) under the control of a tetracycline-responsive element. Pregnant females given doxycycline give birth to pups where all cells are GFP^+ cells, but when these pups are chased to adulthood, only low-cycling cells remain GFP^+. As shown in the Figure 29.4, after 2–3 months of chase, label-retaining cells were only found in the kidney papilla. When isolated, the cells showed pluripotency and, like other stem cells, formed spheres.[24,73]

Under normal conditions, most of these papillary label-retaining cells (LRC) in the adult kidney are, unsurprisingly, in growth arrest, but we found in the upper papilla a small population of them that were cycling[24] (see Figure 29.5), indicating that they generate new cells and explaining that the number of papillary LRC slowly decreased with age. In marked contrast to the normally low-cycling frequency of the papillary LRC, many of these cells proliferated shortly after acute kidney injury, likely generating many daughter cells, since after a few weeks the S-phase label disappeared from the papilla (see Figure 29.6). Hence, the cells we identified in the kidney papilla showed two cycling characteristics: first, during normal homeostasis, the cells are low-cycling (and thus they are LRC) except for a small population of them that are cycling in the upper papilla; second, and in marked contrast to normal conditions, may of the papillary LRC start cycling shortly after injury. These results strongly suggest that the population of LRC of the kidney papilla is involved in kidney repair, and that within the LRC cells are renal stem/precursor cells.

Because the renal capsule contains a population of nestin-expressing cells,[75] and this intermediate filament protein has been found in a variety of precursor cells,[76] Park and co-workers[77] searched for low-cycling cells in this part of the kidney. They administered a short pulse of BrdU to 4-week-old mice, and followed the pulse by a chase period of two months. They found that the kidney capsule had a sparse population of BrdU-retaining cells which further characterization showed them to be $CD29^{+,}$ $Sca\text{-}1^+$, $vimentin^+$, and $nestin^+$, but that did not express hematopoietic or endothelial markers. These cells showed marked proliferative and clonogenic capacities, and could differentiate towards adipogenic, chondrogenic, and osteogenic lineages, suggesting that they were MSC or MSC-like. The function of these cells *in vivo* remains unknown, and it would be of great interests to determine whether kidney injury induces their proliferation.

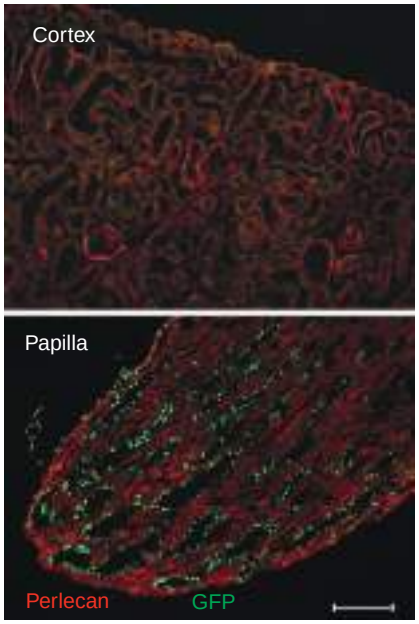

FIGURE 29.4 **Papillary LRCs in mice expressing histone 2B-GFP.** The kidney of an 11-week-old mouse pulsed with doxycycline during embryonic life showed low cycling cells (i.e., GFP- retaining) in the papilla but not the cortex or medulla. *(From ref. [27].)*

Cellular Function

Since first used to enrich for hematopoietic stem cells,[78–80] the *Side Population* discrimination assay has been used to identify stem cells and progenitor cells in a variety of organs and tumors.[81] The assay can be useful when stem cell-specific markers are not available, and it is based on the differential ability of cells to efflux a lipophilic fluorescent dye via the ATP-binding cassette transporter protein ABCG2. Many stem/precursor cells rapidly efflux the Hoechst 33342 dye, a process that can be blocked with ABC transporter inhibitors. By flow cytometry, such cells are recognized as being "Hoechst low" (versus "Hoechst high") and as they are a very small fraction of the total cells, they were termed side population (SP) cells. Because the assay is dependent on normal cellular metabolic function in freshly isolated cells, it is extremely challenging (for a detailed discussion see Golebiewska et al.[81]), and uncertainty exists about the significance of some of the results. Nonetheless several workers have isolated SP cells from the adult kidney.[82–85] The frequency of these cells has been reported to vary from ~5%[84] to ~0.1%.[83,85] In one study, exogenous administration of the isolated cells to mice with cisplatin-induced acute kidney injury improved the kidney's functional response.[84] These provocative results need further analysis, particularly because the SP of the kidney

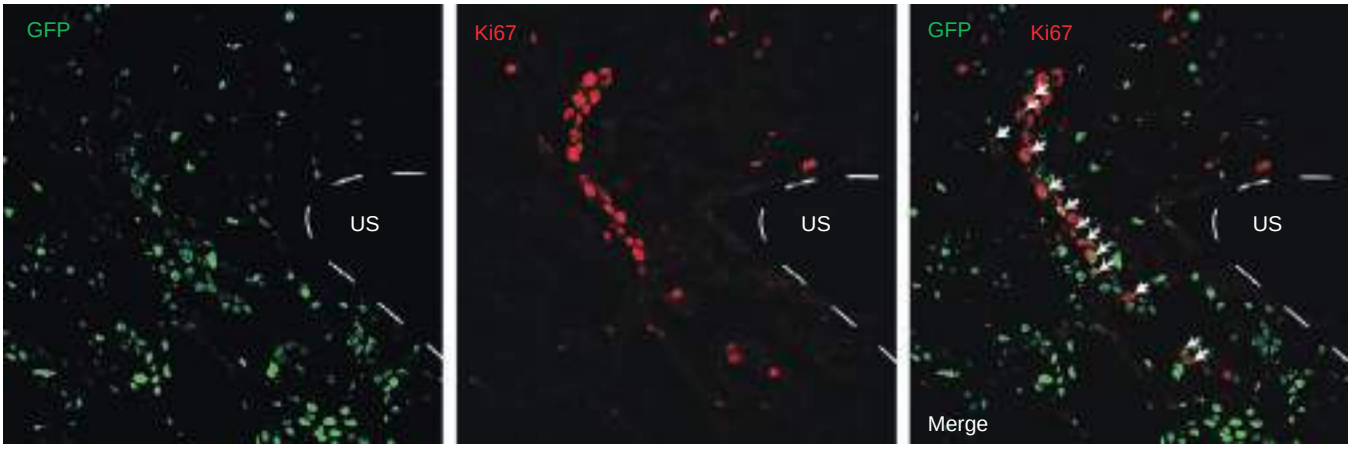

FIGURE 29.5 **LRC in the upper papilla from chains of proliferating cells.** LRCs (GFP^+: top) and proliferating cells (Ki67-positive: middle) in the upper papilla. The merged image shows that several cells are positive for both Ki67 and GFP (arrows). Broken white line depicts papillary edge (US: urinary space). *(From ref. [27].)*

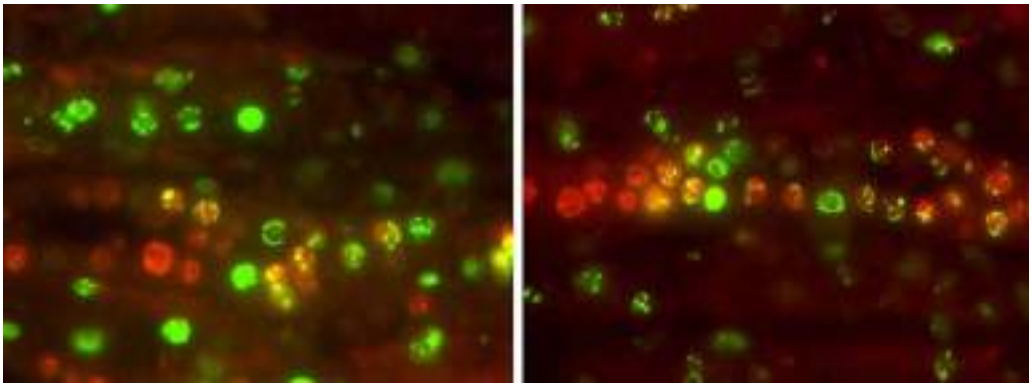

FIGURE 29.6 **Proliferation of papillary LRC after transient ischemic injury.** Cellular proliferation of papillary LRC after transient renal ischemia. Thirty-six hours after ischemic injury, many LRC of the papilla (FITC fluorescin) were cycling and labeled by a Ki67 antibody (rhodamine) (Scale bars: 50 μm). *(From ref. [76].)*

appears to show considerable heterogeneity.[83] However, the kidney is a transporting organ with a large number of ABC-type transporters expressed in several of its segments including ABCG2, the putative transporter of the Hoechst33342 dye. Hence, the presence of cells that pump the dye out may not be the best marker for progenitor cells.

Another cellular function that has been exploited to isolate putative renal stem/precursor cells is the *aldehyde dehydrogenase activity* (ALDH). This enzyme oxidizes intracellular aldehydes (for a review see Sophos and Vasiliou[86]), and it is believed to have a role in cellular differentiation by its ability to oxidize retinol to retinoic acid.[87] Hematopoietic, neural, and some cancer stem/precuror cells were found to have high ALDH enzymatic activity.[88] Similarly, Lindgren et al.[89] recently isolated from the human kidneys cells with progenitor characteristics. Using an ALDH enzymatic assay in suspensions of renal cortical cells deprived of glomeruli, they separated the cells into $ALDH^{low}$ and $ALDH^{high}$ populations. Interestingly, transcription analysis of the populations showed that one of the most upregulated genes in the $ALDH^{high}$ cells was Cd133, a membrane protein found in some progenitor/stem cells and used to isolate other renal progenitors (see above and the section on podocyte precursors next). *In vitro*, the cells showed some stem/precursor cell characteristics, but of particular interest is their finding by immunohistochemistry that there is a population of Cd133-positive cells scattered through the proximal tubule, clearly showing that there is some heterogeneity in the proximal tubular cells. Analyses of kidney biopsies of patients with acute tubular necrosis showed that in areas of regeneration tubular cells positive for Cd133 in their luminal membrane were frequently found to be also positive for vimentin in their

basolateral membrane. Since tubular epithelial cells expressing vimentin have been observed during the recovery phase of acute kidney injury,[90,91] it is possible that these Cd133- and vimentin-expressing cells might be specialized epithelial precursors.

Podocyte Precursors

It had long been assumed that in adult kidneys podocytes, the specialized epithelial cells that surround the glomerular capillary loops, have extremely low or no cycling activity. Yet, these cells are clearly renewed because they can be captured in the urine of normal subjects.[92] Interest in the origin of podocytes and their life cycle has been spurred by observations that their numbers can decrease during diseases caused by several mutations that disrupt their proteins, leading to glomerular sclerosis (reviewed by D'Agati[93]). In addition, it was recently found that a variable fraction of the cells in the glomerular "crescents" (layers of abnormal cells attached to the Bowman's capsule) often present in glomerulonephritis were found to express nestin.[94] Since normal podocytes express nestin, these results raised the possibility that cells in crescents might derive from podocytes or that podocytes and cells in crescents share a common lineage. Regardless, these interesting observations suggested that both podocyte loss and/or their uncontrolled proliferation might be involved in renal diseases.

Analyzing human kidney sections, Sagrinati et al.[95] found that a subpopulation of the parietal epithelial cells of Bowman's capsule expressed Cd24 and Cd133, two cell surface proteins found in a variety of adult stem cells. Isolation of these cells from glomerular cultures showed them to possess high cloning efficiency and some differentiation potential. In addition, when the cells were intravenously administered to mice with acute kidney injury, there was improvement in the morphological and functional renal response.[95,96] The observation that some epithelial cells in the parietal side of the Bowman's capsule had progenitor characteristics led to the hypothesis that these cells could be podocyte precursors.[97,98] With this in mind, Ronconi et al.[98] analyzed human kidneys sections, and confirmed that a group of cells in the parietal epithelia of the Bowman's capsule expressed Cd133 and Cd24 and that, in contrast, fully differentiated podocytes only expressed proteins used to identify them such as nestin, complement receptor-1, and podocalyxin. Interestingly, they also identified a third cell population that expressed Cd133, Cd24, and podocyte markers, suggesting that it could be a podocyte precursor. Isolation of these three different cell populations by FACS using Cd133, Cd24, and podocalyxin and their culture *in vitro* showed that a cell clone derived from a cell only positive for Cd133 and Cd24 contained cells that expressed both tubular epithelial markers and podocyte markers. In contrast, clones of cells derived from cells positive for Cd133, Cd24 plus podocalyxin only expressed podocyte markers. When these two different types of cells were intravenously administered to mice that had received the podocyte toxin adriamycin, they found that cells only positive for Cd133 and Cd24, but not cells positive for Cd133, Cd24, and podocalyxin, were capable of reducing urinary protein excretion and morphologic damage. Finally, labeling the cells with vital dyes showed that the former, but not the latter, localized to glomeruli. These results were interpreted as indicating that in adult kidney, podocytes derive from a precursor cell population that resides in the parietal epithelium of Bowman's capsule. One might conclude that the study shows heterogeneity in the parietal epithelial cells of Bowman's capsule, and that *in vitro* these cell types express different genes. The mechanism responsible for the functional recovery after cell injection and its significance is harder to define, since the large majority of epithelial cells administered intravenously are likely to lodge into the lung vascular bed.

The hypothesis that parietal epithelial cells might migrate into the glomerular capillaries and differentiate into podocytes was also examined by Appel et al.[97] in a detailed and elegant study. These authors reported that in adult rats, cells that had morphological characteristics of both glomerular parietal epithelial cells and podocytes could be detected by electron microscopy in the glomerular vascular stacks. That these cells could be transitional cells between parietal epithelial cells and podocytes was examined in 10-day-old mice with a variety of approaches. By immune-detection they found that some cells had markers of both parietal epithelial cells and podocytes. Administration of BrdU to young rats for two weeks showed that, while a substantial number of parietal epithelial cells were labeled with BrdU, only $\sim$0.5% of podocytes were labeled. However, as the animals aged, the number of $BrdU^+$ parietal epithelial cells decreased, while that of $BrdU^+$ podocytes increased, suggesting that the latter derived from the former. In a final genetic fate-mapping experiment, these workers generated triple-transgenic mice in which labeling of the parietal epithelial cells and their progeny could be temporarily controlled by doxycycline administration. In 5-day-old and 10-day-old mice they found that the number of podocytes that derived from parietal epithelial cells increased as the animals aged. This elegant study provides strong evidence that podocytes derive from parietal epithelial cells, at least in the young. This is a very exciting result, because even if this process only occurs at very young

ages, understanding of its controlling mechanisms might allow its modulation. An additional conclusion appears also important; it is clear that as our understanding of the homeostasis of the renal cell populations advances, the distinction between embryonic and adult lives is becoming less clear-cut than previously believed (i.e., "development" appears to be a life-long process), a subject to which we return below.

Because a variety of glomerulonephritis types are associated with hyperplasia of Bowman's capsule (a histological finding long ago termed "crescents"), the possibility that unregulated proliferation of a precursor cell could be responsible for their generation was examined. In a study of human kidney biopsies, the hypercellular lesions of crescentic glomerulonephritis were analyzed with antibodies and RT-PCR after laser capture of the lesions.[99] The authors found that these lesions contained three kinds of cells: $Cd133^+$, $Cd24^+$, $podocalyxin^-$ and $nestin^-$ (presumed podocyte precursors), $Cd133^+$, $Cd24^+$, $podocalyxin^+$ and $nestin^+$ (named intermediate cells), and finally, $Cd133^-$, $Cd24^-$ but $podocalyxin^+$ and $nestin^+$ (same profile as that of differentiated podocytes). When the lesions were examined for the presence of proliferating cells with a Ki67 antibody, most of the cells that were cycling were only positive for $Cd133^+$, $Cd24^+$. Further, *in vitro*, $Cd133^+$, $Cd24^+$, $podocalyxin^-$ and $nestin^-$ cells responded robustly to TGFβ induction of extracellular proteins. These results were taken as evidence that generation of glomerular crescents is likely due to proliferation of "podocyte progenitors." In a related experimental study, Smeets et al.[100] induced crescentic glomerulonephritis in triple-transgenic mice in which parietal epithelial cells and their progeny could be labeled by the administration of doxycycline. In these mice, "crescents" could be detected to be positive by enzymatic X-gal staining, strongly suggesting that these cells derived from epithelial cells of the Bowman's capsule. In contrast, podocyte genetic labeling experiments did not show that the cells in the crescents derived from podocytes. These interesting results strongly suggest that some cells in the parietal epithelium of the Bowman's capsule, and not the podocytes, proliferate in response to injury.

However, in a fascinating study, Ding et al.[101] found that deletion of the product of the von Hippel-Lindau gene (*Vhlh*, encoding VHL) specifically in podocytes caused glomerulonephritis with crescent formation. Loss of VHL stabilizes the hypoxia-inducible factor (HIF) α-subunit and activates hypoxia-response genes. Of great interest is their finding that the cells in the crescents were derived from podocytes; this was elegantly shown by laser-capture of the crescents and PCR demonstrating the rearrangement of the genomic DNA induced in the podocytes (a tour de force control experiment which unfortunately is rarely done). In addition, because the gene expression profile revealed induction of *Cxcr4* expression in glomeruli, Ding and co-workers overexpressed this receptor in podocytes; this resulted in podocyte proliferation and glomerulonephritis. This extremely interesting study therefore indicates that under some conditions, podocytes can proliferate, likely by the effect of Cxcl12 (SDF-1) the ligand of Cxcr4, and that their proliferation can lead to "crescent" formation.

Renal Mesenchymal Stem Cells and/or Pericytes

Mesenchymal stem cells (MSC) from the bone marrow were originally characterized by their ability to adhere to culture surfaces and when cultured with appropriate differentiation media, by their differentiation potential into adipocytes, osteoblasts, chondrocytes, and, sometimes, myoblasts. In other organs including the kidneys, MSC identification and characterization remains to be formalized, since they might be a heterogeneous population that expresses a variety of cell surface markers.[5] Nonetheless, there is widespread interest in MSC because, in addition to their differentiation potential, they appear to be present in most if not all organs[4,5] including the kidney,[5,102] and their precise function remains to be defined. They preferentially locate in the perivascular space[4,5] of even large blood vessels such as the aorta and vena cava,[5] and have pericycte-like characteristics.[3] In the kidney, mesangial cells also have MSC-like characteristics,[5] and might be the glomerular cells that express $Cd146^+$ and $Cd133^-$ found by Bruno et al.[103] in glomeruli. Because of their perivascular location and mesenchymal origin, pericytes are difficult to distinguish from MSCs, and how these two cells differ and relate is still poorly-understood. Although true renal pericytes can only be unambiguously identified by their anatomical location surrounding capillary endothelial cells, these cells have been implicated in myofibrobalst generation during renal fibrogenesis,[15] and are discussed in detail below. In organs other than the kidney, pericytes have been found to have MSC-like characteristics,[104] and in the most detailed study to date, perivascular cells from skeletal muscle, bone marrow, and adipose tissue were found to express several pericyte markers, as well as MSC markers and MSC differentiation potential,[4] suggesting that MSC and pericytes might be the same cells in different locations. It has been shown that during tooth growth and in response to injury, pericytes can give rise to MSC, although in the same organ MSC have an additional, pericyte-independent origin,[105] so that lineage analysis between MSC and pericytes is likely to be complex. In the kidney, mesangial cells,

vascular smooth muscle, pericytes, and likely, MSC derive from the *Foxd1* embryonic cellular compartment described above but as stated, the exact relationship among these different cells remains to be defined.

It is currently unknown whether renal pericytes/MSCs generate daughter cells important for normal kidney homeostasis or for repair from injury. However, recent studies showing that pericytes characterized as $Cd73^+$, platelet-derived growth factor $receptor^+$ and smooth muscle actin negative, give rise to myofibroblasts during renal fibrosis[15] have generated a great deal of interest, a finding that we discuss below. However, morphological observations indicating the transient presence of myofibroblasts after transient kidney injury[43,106] suggest that these cells, long studied from a pathogenic perspective, might also be involved in organ repair, a possibility that we believe deserves attention. Regardless, since like other organs, the kidney contains perivascular cells that are pericytes, MSC or their immediate progenitors,[15] their full characterization and role in normal renal homeostasis and if any, in organ repair from injury, would be of great interest.

POTENTIAL SITES HARBORING RENAL STEM CELLS

Given the kidney's anatomical complexity, identification of stem cells within it might be facilitated by focusing on sites that might harbor them. Several strategies are possible to locate candidate sites, but we believe that current evidence already suggests the presence of sites likely to contain stem cells.

Highly Proliferative Regions

Because many adult stem cells are low-cycling (see [37] and [107] for recent reviews), to generate needed new cells they frequently give rise to an immediate progeny that experience several "transit amplifying" (TA) divisions prior to their differentiation. In this way, many new cells can be regenerated from infrequent stem cell cycling. Hence, adult stem cells can be located close to sites of increased cell cycling. Indeed a seminal discovery in this field showed that there was postnatal neurogenesis in the granular zone of the dentate gyrus in the hippocampus,[57] and led to the discovery that the subgranular zone harbored neural stem cells (reviewed in Zhao et al.[108]). Hence, proliferative regions during normal homeostasis or after kidney injury are good candidates to harbor renal stem cells.

After nephrogenesis is completed in young rats and during normal homeostasis, it was found that the S3 segment of the proximal tubule displayed high cycling activity[25,28]: over a two-week period in 4-week-old rats, 90% of the cells of the S3 segment had cycled, a remarkable rate of proliferation. While this may reflect morphogenetic requirements of a growing kidney, the high proliferative capacity of these cells raises the possibility that they could be "transit amplifying" daughter cells of a proximal tubule stem cell. Other findings support that the S3 segment of the proximal tubule might contain stem cells. Shortly after several types of kidney injury, high proliferation activity was particularly prominent in cells from the S3 segment.[25,42,43] Moreover, Gupta et al.[62] found cells in the cortico–medullary junction which expressed Oct-4 and had progenitor characteristics, and Kitamura et al.[63] isolated a highly proliferative cell type from the S3 segment of rat kidneys that, at least *in vitro*, also expressed precursor cell markers. Whether these putative stem cells relate to the recently described podocyte precursor (see above) or renal proximal tubule progenitors[95] remains to be determined.

The S3 segment of the proximal tubule is of additional interest as a potential site to harbor renal stem cells, because indirect determinations of oxygen tension have shown that this part of the nephron surprisingly exists in a hypoxic environment quite different from other parts of the kidney cortex.[109] A low oxygen tension is characteristic of sites where stem cells in other organs reside, a subject that we discuss below.

To determine whether the adult kidney contained regions of increased cell proliferation, we used kidneys of one-year-old rats, because we reasoned that fully grown older animals would not have proliferating cells needed for organ growth. We found cycling cells by staining for Ki67, a marker of cellular proliferation.[24] As shown in Figure 29.1, Ki67-positive cells were rare in the cortex and medulla, and were solitary and of a similar frequency (~1 % of the total cells). In contrast, the papilla showed marked heterogeneity in its abundance of Ki67-positive cells; they were extremely rare in its tip and middle part (~0.1 %), but were readily apparent in the upper part of the peripheral papilla, adjacent to the urinary space (US) where the kidney parenchyma forms a narrow angle which provides an easily identifiable landmark and the papilla meets the medulla; it is also very close to the kidney cortex. In this region, and unlike other areas of the kidney, Ki67-positive cells frequently formed chain-like structures and accounted for ~2.5 % of the total cells, a significant difference from other parts of the kidney. When cellular proliferation was assayed 24 hours after labeling cells in S-phase by administration of a single dose of BrdU, proliferating cells were very rarely detected in the cortex and medulla but again, the lateral part of the upper papilla consistently contained cycling cells; i.e.,

BrdU-labeled (not shown). We also obtained similar results in kidney of six-month-old rats.

Interestingly, after acute kidney injury, the lateral part of the upper papilla is also the site in which we first detected the increased cell cycling that follows injury; rats were subjected to 45 minutes of unilateral kidney ischemia, following which were given a single dose of BrdU and sacrificed one hour later. Thus, only cells that were in S-phase during this hour could be labeled, and using 5 μm kidney sections, we saw only equally rare labeled cells in normal kidneys or in the kidneys subjected to ischemia. However, examination of 100 μm vibratome sections showed abundant cells in S-phase in the upper papilla (Figure 29.3), next to the urinary space (US) only in the kidneys subjected to ischemia. In the aggregate, these results indicate that the lateral upper part of the kidney papilla contains more proliferating cells than other parts of the kidney under normal conditions, and that it contains the first cells that start cycling in response to transient injury. As reviewed above, Vinsonneau et al.[45] found that the first intrarenal area that contains Ki67 positive cells after ischemia reperfusion injury was the uro-epithelium and adjacent interstitial space in the upper part of the urinary space at the papilla–medullary junction.

In sum, because of their proliferative behavior, both under homeostatic conditions and during repair from several types of kidney injury, the S3 segment of the proximal tubule and the lateral part of the upper papilla are domains of the kidney where stem cells appear likely to reside.

Stem Cell "Niches"

Adult stem cells receive critical signaling from their immediate microenvironment, a domain that is distinct from the rest of the organ (see Morrison and Spradling[110] for a review). In these locations (referred to as "niches"), stem cells interact with other cells and the extracellular matrix, a process that is best understood in the *Drosophila* germline stem cells (see Fuller and Spradling for a review[111]). The stem cell "niche" provides positional information that regulates both proliferation activity and cell fate identity, and in fact it can even redirect cell fate similar to what often happens during embryogenesis.[112] While characterization of mammalian stem cell niches is still very limited, some common motifs are emerging that might be useful to identify the location of renal stem cells. Among those, a hypoxic environment is a prominent characteristic. Several organ-specific stem cells such as hematopoietic stem cells[113–115] and neural stem cells[116] reside in hypoxic regions, and a large body of *in vitro* work has shown the critical role of oxygen on stem cell regulation (see Mohyeldin et al.[117] for a review). Moreover, in both hematopoietic stem cells and neural stem cells, it was recently found that regulation of the oxygen-sensitive gene *HIF-1α* is critical for the cells' maintenance and fate decisions.[114–116,118]

The kidney parenchyma possesses steep oxygen gradients,[119] and variations in renal oxygenation are undoubtedly sensed as they regulate erythropoietin synthesis. While direct determinations of oxygen tension in the kidney papilla have not been reported, it is likely that papillary pO_2 ranges are ~4–10 mmHg.[119] The presence of low-cycling cells in this very hypoxic environment[24,39,73,120] and that many of these cells express nestin,[24] an intermediate filament protein identified in a variety of progenitor/stem cells,[76] suggests that the papilla harbors renal stem cells. Interestingly, using a nestin-GFP-expressing mouse,[75] nestin$^+$ cells were detected in large clusters within the papilla, along the *vasa rectae* and, at least *in vitro*, these papillary nesting-expressing cells were found to migrate upwards in the papilla towards the cortex, an observation compatible with our *in vivo* experiments with vital dyes in which we found upward migration of papillary cells, some of which were "label-retaining cells".[24]

Several other findings also suggest that the kidney papilla is a niche for renal stem/precursor cells. Dekel and co-workers[61] isolated a population of purportedly renal stem cells from the renal interstitium that expressed the stem cell antigen-1 (Sca-1) and were enriched for β1-integrin; when the cells were located *in vivo*, they were found to be particularly abundant in the renal papilla. Using a different approach, Lee et al.[64] identified a renal interstitial cell that expressed several potential renal progenitor cell markers, such as *Oct-4*, *Pax-2*, *Wnt-4*, and *WT-1*. *In vivo*, Oct-4$^+$ cells were located in the medulla as well as in the papilla, leading these authors to suggest that the interstitium in these regions of the kidney is a "niche" for renal stem cells. Finally, and with a very different approach, Curtis et al.[121] examined whether cells from different regions of the kidneys were equally capable of contributing to cell regeneration after acute kidney injury. These workers isolated from mice constitutively expressing β-galactosidase in certain cells from the kidney cortex, medulla or papilla, and implanted them under the capsule of kidneys subjected to ischemia-reperfusion injury. Seven days later, implanted cells deriving from the three different regions of the kidney could be detected in the tubules of the renal medulla, but cells obtained from the papilla exhibited the most robust engraftment. These results suggest that cells deriving from all regions of the kidney might contribute to the reparative response of the organ after injury, and that some cells in the papilla are particularly capable of contributing to repair and might be stem cells.

RENAL STEM CELLS IN NON-MAMMALS

Renal Progenitors in Fish

Unlike mammals, fish appear to be capable of generating new nephrons during adult life, and their kidneys possess a clearly identifiable "nephrogenic zone".[122] This zone decreases in volume as the animal ages, likely because the nephron number increases with age.[123] In addition and of great interest, the nephrogenic zone can be stimulated in adult fish. For example, in the little skate the cellular proliferation and morphological complexity of the zone increased after partial nephrectomy,[122] a process that resembled embryonic nephrogenesis in mammals. While this morphological response strongly suggests *de novo* generation of nephrons, confirmation that new and functional nephrons developed remains to be established. Following acute kidney injury due to gentamicin, zebrafish can regenerate their nephrons, a process that starts shortly after injury with expression of *wt1b* (the zebrafish homolog of *Wilm's Tumor 1*) in individually dispersed cells of the mesonephric interstitium.[123]

These studies suggest that the fish could be a useful model to explore mechanisms of kidney repair where one can derive information that might facilitate identification of mammalian adult renal stem cells. Indeed, in a recent elegant study, Diep et al.[124] used zebrafish to search for potential nephron precursor cells. They reasoned that if adult kidney contains nephron progenitors these cells could be transplanted. They induced acute kidney injury by gentamicin administration, and performed a series of transplant experiments using cells from transgenic fish expressing reporters such as EGFP or Cherry with *cdh17*, thereby locating the fluorescent reporters in the distal nephron. When they injected unpurified whole kidney marrow cells (5×10^2 cells), mostly comprised of non-tubular interstitial cells, they found that the donor cells generated new nephrons in the host in 100% of the cases (Figure 29.7). Nephron number increased with time after injection and at later times, donor-derived nephrons were found at sites distal from the injection site, indicating that the cells migrated. Importantly, they found that these donor-generated nephrons connected to the host renal tubules and to the host's circulation, as shown by the fact that they could filter fluorescent dextran. Because in cell transplantation experiments it is frequently impossible to be certain that fusion of donor and recipient cells did not occur, to exclude this possibility Diep et al.[124] injected Cherry labeled cells into EGFP recipients and found that all engrafted nephrons were Cherry$^+$ and EGFP negative, indicating that cell-to-cell fusion did not take place. To identify the cells responsible for the genesis of new nephrons, the authors examined the zebrafish homologs of transcription factors know to be expressed in the mammalian renal vesicles (the precursors of the nephron). They found that kidneys from adult zebrafish transgenics expressing *lhx1:EFGP* (the homolog of Lh1/Lim 1[125,126]) contained ~100 aggregates of ~30 EGFP$^+$ cells per kidney. Examination of the evolution of these aggregates showed that they emerged from the assembly of ~3-4*lhx1:EFGP*$^+$ cells that expanded to form a renal vesicle (expressing *wt1b*, the homolog of mammalian *WT1*), which in turn elongated into a nephron. Interestingly, laser ablation of a single aggregate of *lhx1:EFGP*$^+$ cells prevented nephron formation without affecting neighboring nephrons, indicating that *lhx1:EFGP*$^+$ cells are required for nephrogenesis. However, transplantation of single *lhx1:EGFP*$^+$ cells to conditioned hosts failed to engraft, but transplantation of aggregates of *lhx1:EFGP*$^+$ cells generated nephrons. Thus, *lhx1:EFGP*$^+$ aggregates contain nephron progenitors and several cells are needed to generate a nephron. Whether the cell aggregates are clonal or contain several nephron progenitors with more restrictive differentiation potential is unclear. Nonetheless, demonstration in adult zebrafish of nephron progenitors capable of kidney regeneration and identification of their "genetic signature" is likely to facilitate design of new studies searching for renal stem cells in adult mammalian kidney.

Renal Progenitors in Invertebrates

The nephron is the basic structure of the vertebrate kidney, but many insects have tubular excretory systems with "nephron-like" features, suggesting that at least some components of the vertebrate kidneys derive from invertebrate ancestors. In addition, to regulate the composition of hemolymph, *Drosophila* has filtration cells that possess fly orthologs of the major components of the slit diaphragm, indicating that these cells are podocyte-like.[127] The similarity of the fly's excretory system to that of the nephron in vertebrates suggests that analysis of renal stem cells in *Drosophila* might be of considerable interest. Indeed, Singh et al.[128] used lineage tracing, molecular marking analysis, and BrdU incorporation to follow the fate of the different cells in the Malpigian tubules of adult flies. These tubules contain four types of cells, and Singh et al.[128] found that one type of cell was multipotent and could generate all the cell types of the Malpigian tubules of adult flies, indicating that they are renal stem cells. Singh et al. additionally found that autocrine JAK-STAT signaling in the renal stem cells regulated their renewal, and absence of signaling promoted their differentiation with loss of the stem cell

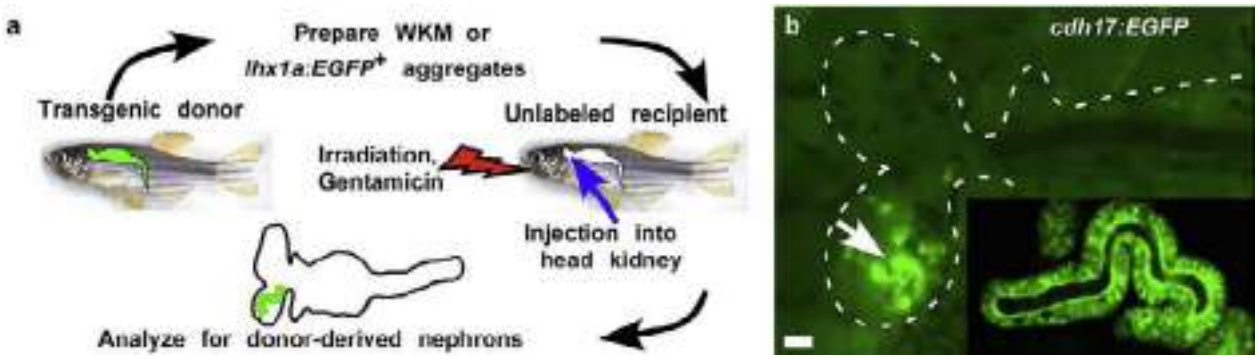

FIGURE 29.7 **The kidney of the adult zebrafish contains progenitor cells that generate new nephrons.** (a) Transplantation assay. Whole kidney marrow cells mostly comprising interstitial cells were isolated from genetically labeled donors. (b) Injection of the cells into recipients with damaged nephrons due to genatmicin injection resulted in donor-derived nephrons. *(From ref. [127].)*

population. Of great interest was their additional finding that these stem cells are present in the lower tubules and ureters, very much resembling the initial location of the nephron precursors recently identified in zebrafish,[124] and raising the possibility that the sharp distinction currently being made in mammalian adult kidneys between collecting ducts and the rest of the nephron might require re-evaluation. Also remarkable is that these stem cells are a large fraction of the total number of cells of the Malpighian tubules, rather than the anticipated small minority, another characteristic worth noting for workers on the renal stem field.

NEW CELLS IN DISEASED KIDNEYS

Renal Fibroblast and Myofibroblasts

In addition to dendritic cells, the normal adult kidney contains a network of interstitial fibroblasts and other cells that remain poorly-characterized, as they are technically difficult to detect and there is no general agreement on markers that identify them.[1] However, during many kidney diseases the renal interstitial compartment changes dramatically, with a marked increase in the number of renal fibroblasts and the invasion of the interstitium by a new type of cell called a myofibroblast. Myofibroblasts have fibroblast-like characteristics, but also express α smooth muscle actin (αSMA), and are believed to have great migratory capacity. It is currently thought that the marked proliferation of fibroblasts and myofibroblasts plus the expansion of their secreted extracellular matrix, i.e., renal fibrogenesis, is itself pathogenic as it disrupts the normal renal architecture and is the final common pathway of many kidney diseases. Indeed, expansion of the fibroblast and myofibroblast populations and the extracellular matrix are tightly correlated with the slow and inexorable progressive loss-of-function that characterizes many kidney diseases. There is thus great interest in the mechanisms responsible for appearance of these cells during diseases.

Several possibilities have attracted attention. First, the cells might derive from resident renal interstitial "fibroblasts." In this view, the disease process induces fibroblast proliferation and in some of them, a change in their phenotype that results in expression of αSMA. Detailed morphological studies suggest that at least in some forms of renal fibrosis, such as that due to unilateral ureteral obstruction (UUO), this is likely the case.[129] More recent genetic cell fate tracing studies by Humphreys et al.[15] have suggested that myofibroblasts after unilateral ureteral obstruction (UUO) or after acute ischemic kidney injury derive from interstitial cells that are likely pericytes, since they were positive for Cd73 and platelet-derived growth factor receptor β (PGDFR β). Interestingly, pericyte differentiation and proliferation appears to be dependent on endothelial cell action, since blockade of their VEGF receptor 2 attenuates the fibrogenic process.[22] However, while Cd73 and PGDFR β appear to be present in most pericytes, there is no definitive marker profile for these cells, as they can only be unambiguously identified by their location around capillary endothelium. Moreover, new studies have shown that most, if not all, organs possess a population of perivascular mesenchymal stem cells,[4,5] and the distinction between these cells and pericytes is poorly-understood (see Corselli et al.[130] for a review). Hence, whether myofibroblasts solely derive from resident interstitial fibroblasts, pericytes, mesenchymal stem cells or from a combination of these cells remains to be clarified, and must await a detailed characterization of these three interstitial cell types.

Another possibility is that myofibroblasts could derive from bone marrow mesenchymal stem cells

(MSC); i.e., cells characterized by their ability to differentiate into adipocytes, osteoblasts, chondrocytes, and, sometimes, myoblasts. While Iwano et al.[131] found a small number of bone marrow-derived fibroblasts in the renal interstitium, little additional evidence has been obtained to support that bone marrow precursor cells could be the origin of the myofibroblasts.

Another possible origin of the renal fibroblasts and myofibroblasts found in kidney diseases is that they derive from renal epithelial cells by epithelial-mesenchymal transition (EMT), a process in which epithelial cells lose the ability to maintain close contacts with their neighbors as well as apico–basal polarity, and instead develop a mesenchymal phenotype that includes migratory capacity. The process of EMT is of course widely used during embryogenesis and in some disease processes, particularly cancer (for a recent review see Thiery et al.[132]). It is of great interest that in nonrenal cells, it has been found that EMT might generate cells with the properties of stem cells,[133] but this possibility appears not to have been examined in the kidney.

There is little doubt, at least *in vitro*, that epithelial cells from both embryonic[134] and adult kidneys[15,135] can undergo EMT. However, there is currently a debate whether this process might generate fibroblasts and myofibroblasts *in vivo* (see Kapus and Quaggin[136] and Kriz et al.[137] for informed discussions). Morphological and cell marker studies during renal fibrosis have provided some evidence supporting EMT *in vivo*, both in experimental models[90,138–142] and in human diseases,[90,91,143,144] but other studies have failed to support this.[129,145] The most robust method currently to determine whether myofibroblasts might derive from renal epithelial cells is based on studies using genetic cell fate analysis. In these studies epithelial cells are genetically labeled so that their progeny (e.g., fibroblasts or myofibroblasts) can be easily identified. Using the UUO model of renal fibrogenesis, Iwano et al.[131] found that a substantial number of renal fibroblasts derived from renal epithelial cells. However, three subsequent studies with UUO plus other models of renal fibrogenesis and using different epithelial genes to drive Cre recombinase and label epithelial cells in reporter mice found no evidence that renal fibroblasts and myofibroblasts derived from epithelial cells.[15,146,147] There is currently no clear explanation for these conflicting results, and it is apparent that additional studies are needed.

Finally, another potential origin of renal fibroblasts and myofibroblasts are endothelial cells. Genetic cell fate experiments have shown that Cre recombinase driven by Tie2 (a tyrosine kinase receptor believed to be endothelial-specific in the adult) identified a reporter gene in renal fibroblasts in UUO and streptozotocin-induced renal fibrogenesis.[148,149] This unexpected result is of particular interest, because adult endothelial cells have been shown to have the capacity to transform into mesenchymal stem-like cells by activation of activin-like kinase-2,[153] and two ligands well-known to be involved in renal fibrogenesis, TGFβ and BMP4, phosphorylated activin-like kinase-2 and induced a mesenchymal phenotype in cultured endothelial cells.[150]

This brief survey shows that the precise origin of the renal fibroblasts and myofibroblasts during renal diseases remains undefined, and given the medical importance of this issue additional studies are needed. Needless to say, it is also likely that these cells might have more than one origin. While studies based on morphology and/or cell identification by cell-specific markers offer at best indirect evidence, genetic-based cell lineage tracing experiments have their own potential pitfalls (see the review by Matthaei[151]). In particular, two potential problems might complicate their interpretation. The first is that it is assumed that the reporter gene is expressed in all cells and for the duration of the animal's life, as well as during the disease process. Definitive proof of this is lacking and, for example, in the adult kidney, the robustness of the reporter expression in the *Rosa26* locus (frequently used to introduce the reporter gene) was found to be less than anticipated ([152] and our unpublished results). In addition, cell fate-mapping studies can give markedly different results depending on the genetic construct of the reporter.[153] The second, and potentially more confounding, problem in the interpretation of genetic cell-fate analyses is that the gene used to activate the reporter gene is chosen because of its restricted expression to a specific cell type during embryogenesis, and lack of expression during adult life and after injury, when the analysis is done. However, the possibility that the gene is activated later in life or by the disease process in a small number of cells might be very difficult to detect.

KIDNEY REPAIR BY EXOGENOUS STEM/PRECURSOR CELLS

While analysis of the kidney's ability to repair from injury has naturally focused on the intrinsic renal cell population, reports that cells derived from the bone marrow could generate new renal cells and perhaps contribute to organ repair generated a great deal of interest.[154–157] However, subsequent studies have firmly established that most if not all the new cells generated after kidney injury derived from other renal cells.[29,30] Nonetheless, and stimulated from work in other organs, the possibility that exogenous cells might

either facilitate kidney repair or diminish the consequences of injury has been examined in multiple studies. Indeed, clinical trials with bone marrow-derived MSC are already underway or in planned stages in a variety of diseases, particularly for myocardial infarction, but also including the kidney (http://www3.niddk.nih.gov/fund/other/akiworkshop/). In experimental animals, the potential therapeutic effect of several cell types in acute kidney injury has been examined under a variety of protocols.

Mesenchymal Stem Cells (MSC)

When HSC and bone marrow-derived MSC were administered to mice it was found that the latter, but not the former, protected the animals from the functional consequences of acute kidney injury due to cisplatin.[156] Multiple studies have confirmed that extrarenal MSC can either diminish the functional consequences of acute kidney injury or accelerate recovery of kidney function after injury. In addition to MSC derived from the bone marrow,[23,158–161] MSC from human cord blood[162] or even the kidney[163] have been shown to be effective. In these studies, acute kidney injury was induced by several methods and the cells were administered through a variety of routes: intravenously, intra-arterially and by direct intrarenal injection.

What are the potential mechanisms by which exogenous MSC might protect the kidney from injury or facilitate its repair? Although initial observations suggested incorporation of the cells into the renal parenchyma,[156] more recent studies have shown that their mechanism of action is likely to be that the cells provide endocrine/paracrine factors, perhaps growth factors[23,161,164] or chemokines such as IL10.[161] In this view, the mechanism of action of the MSC would be similar to that of directly delivering growth factors in transient kidney injury (reviewed by Hammerman and Miller[165]). Unfortunately, very little information is available on the identity of these beneficial factors, and whether MSC are more or less effective than isolated growth factors alone.

Another possible mechanism is that the transplanted MSC might modulate the host immune response by effects on macrophages,[166,167] dendritic cells,[168,169] T-cells[168] or B-cells.[170] Given the complexity of the kidney's response to the insults used to induce functional acute renal failure, it is apparent that there might be multiple mechanisms whereby exogenous cells could protect this organ from injury or facilitate its repair. An additional problem complicating analysis of these studies is that because MSC are identified *a posteriori* (based on a variety of characteristics such as high proliferation capacity and ability to differentiate into several mesenchymal lineages) there are no strict identification criteria for the administered cells, making comparison across studies extremely difficult.

Regardless, given the clinical severity and epidemiological importance of acute kidney failure, the finding that MSC can improve its evolution is of extreme interest, and studies that illuminate their mechanisms of action are urgently needed. Work in other organs has begun to provide answers. In an elegant study in myocardial repair from ischemic myocardial infarction, Lee et al.[171] found that human MSC (hMSC) administered intravenously acutely embolized into the lungs where they upregulated multiple genes, including the anti-inflamatory protein TSG-6 (the product of tumor necrosis factor-stimulated gene 6). Similar to the observations in kidney injury, the injected hMSC reduced the myocardial inflammatory response to ischemia, decreased infarct size, and improved myocardial function. Administration of recombinant TSG-6 had similar effects as hMSC, but hMSC that were transduced with TSG-6 siRNA did not. This interesting study provides a detailed mechanistic explanation of why hMSC facilitate myocardial repair without engraftment into the organ, and opens new therapeutic avenues for research.

Other Bone Marrow-Derived Cells

Earlier experiments with bone marrow-derived stem cells (other than MSC) suggested that they could ameliorate the functional consequences of transient acute kidney injury.[154] While the possibility that these cells exerted this effect by generating significant numbers of renal epithelia cells has been ruled out,[29,30] their mechanism of action remains unexplained and little explored. Lie et al.[172] used human $Cd34^+$ hematopoietic stem/progenitor cells isolated from peripheral blood after granulocyte colony stimulating factor mobilization, and injected them into mice. They found that, whereas the cells did not localize to normal kidneys, they did so in injured kidneys. Moreover, administration of the cells increased cellular proliferation in the injured kidneys, accelerated kidney functional recovery, and increased animal survival. The exact mechanism(s) whereby these cells exerted these effects remain to be determined, and many possibilities exist. For example, in the heart where bone marrow-derived cells also had significant regenerative effects, their action appears to be mediated by resident cardiac stem cells. In a model of myocardial infarction by coronary ligation, Loffredo et al.[173] administered a population of purified $c\text{-}kit^+$ bone marrow-derived cells and found that they stimulated endogenous cardiomyocite progenitors. These progenitors are capable of differentiating into several cell types, including cardiac muscle cells, and their stimulation resulted in improved

cardiac repair and enhanced function. In contrast, MSC were unable to stimulate endogenous myocardial progenitors.

Kidney Cells

A variety of studies have examined whether administration of cells derived from the kidney might facilitate this organ's repair from injury. All the cells used in these studies possess some "precursor/stem" characteristics, but were poorly-characterized and even their exact *in vivo* location is somewhat uncertain. Administration of cells derived from the S3 segment of the proximal tubule had no effect on the functional response to acute kidney injury due to ischemia-reperfusion.[62,63] However, when the kidney was injured by cisplatin, subcapsular transplantation of the cells facilitated kidney functional recovery.[174]

Several studies have used cells from the kidney that were captured by their expression of Cd24 and Cd133, either from embryonic kidney[175] or adult kidneys.[95,96] In these studies, intravenous administration of the cells facilitated kidney functional recovery from rhabdomyolysis induced by glycerol administration. Lee et al.[64] used a renal interstitial cell population expressing *Oct4*, *Pax2*, *Wnt 4*, and *WT1* (discussed above), and found that intrarenal injection of the cells markedly blunted the functional consequences of kidney injury from transient ischemia.

What is to be concluded form these experiments with exogenous cells? That the administration of MSC might improve the kidney's functional response to injury appears well-established; however, that of other bone marrow cells or renal-derived cells appears to be less robust. Significant problems in many of these studies include: (1) poor characterization of the cell population used; (2) less than ideal monitoring of the kidney functional response, notoriously difficult to do in mice; and (3) lack of analysis of where the majority of the injected cells locate. Most cells injected into the renal artery are retained by glomeruli[176] and the vast majority of intravenously injected cells remain in the lungs.[171] The recent discovery that under specific culture conditions, MSC reduce their size such that when they are injected intravenously they can cross the pulmonary circulation[166] is a finding that may allow the systemic delivery of MSC to the kidney. It is of course possible that injected cells that locate at sites other than the kidney might be responsible for the observed beneficial effects on renal function. Regardless of the location and potential mechanism of action of the injected cells, these initial results suggesting that exogenous cell therapy might be beneficial in acute kidney injury need confirmation and further analysis.

CONCLUDING REMARKS

Whether the adult mammalian kidney contains stem cells that self-renew and are pluripotent is currently unknown. However, given its multiple cell types and by analogy with other organs, it is very likely that renal stem cells might indeed be present. In contrast to the mammalian kidney, it is established that the Malpighian tubule of *Drosophila* contains true stem cells, and that the zebrafish kidney can be regenerated from a small number of specialized epithelial precursor cells, strongly suggesting that it also contains stem cells. Most work searching for a renal stem cell has focused on the epithelial cellular compartment, likely because of its understood important functional role and the relative ease with which it can be identified. However, the adult kidney also contains an abundant population of interstitial cells that are just now beginning to be understood; the discovery that the transcription factor *Foxd1* (*Bcl2*) is expressed during embryonic development in many of these cells has provided an important new research tool that should illuminate their role.

While *bona fide* adult stem cells in the mammalian kidney remain to be identified, several observations suggest that some stem/precursor cells exist in several locations. Perhaps the best evidence that a specialized precursor exists is in the glomerular podocytes, although it also appears likely that, at least under pathological conditions, podocytes themselves can generate other cell types. Perhaps podocytes are not solely terminally-differentiated cells, but can give rise to other cell progeny. A surprisingly variable cell identity was recently discovered in some of the progeny of hair follicle stem cells; these daughter cells were found to return to the stem cell niche and serve as future stem cells.[177]

Confirming classical morphological observations, new genetic cell lineage tracing experiments have provided strong evidence that after acute kidney injury epithelial cells give rise to new epithelia cells, but it remains unclear whether there exist distinct epithelial stem/precursor cells. In fact, multiple observations are compatible with the presence of specialized epithelial progenitors/stem cells in the S3 segment of the proximal tubule. Is it possible that some of the conflicting results could be explained by the presence of two types of stem/precursor cells: one that normally divides to provide new cells during homeostatic conditions and a low-cycling stem cell that is activated during organ repair, as appears to be the case in other organs (see Fuchs[68] and Li and Clevers[107] for reviews)?

Finally, several lines of evidence strongly suggest that the kidney papilla is a "niche" for renal stem cells. This very hypoxic part of the kidney contains many

low-cycling cells (identified as "label-retaining cells") that slowly disappear as the animal ages, and that after acute kidney injury quickly start cycling and markedly decrease in number after repair. While *in vitro* characterization of these cells has shown them to have many properties of stem/precursor cells, no array of specific cell markers can yet identify them, so that their identity and the identity of their progeny remains to be defined. It is our hope that genetic cell lineage analysis will allow us to answer these questions.

References

[1] Kaissling B, Le Hir M. The renal cortical interstitium: morphological and functional aspects. Hematol Cell Biol 2008;130:247–62.

[2] Hatini V, Huh SO, Herzlinger D, Soares VC, Lai E. Essential role of stromal mesenchyme in kidney morphogenesis revealed by targeted disruption of Winged Helix transcription factor BF-2. Genes Dev 1996;10:1467–78.

[3] Covas DT, Panepucci RA, Fontes AM, Silva Jr WA, Orellana MD, Freitas MC, et al. Multipotent mesenchymal stromal cells obtained from diverse human tissues share functional properties and gene-expression profile with CD146+ perivascular cells and fibroblasts. Exp Hematol 2008;36:642–54.

[4] Crisan M, Yap S, Casteilla L, Chen CW, Corselli M, Park TS, et al. A perivascular origin for mesenchymal stem cells in multiple human organs. Cell Stem Cell 2008;3:301–13.

[5] da Silva Meirelles L, Chagastelles PC, Nardi NB. Mesenchymal stem cells reside in virtually all post-natal organs and tissues. J Cell Sci 2006;119:2204–13.

[6] Herzlinger D, Koseki C, Mikawa T, al-Awqati Q. Metanephric mesenchyme contains multipotent stem cells whose fate is restricted after induction. Development 1992;114:565–72.

[7] Kress C, Vogels R, De Graaff W, Bonnerot C, Meijlink F, Nicolas JF, et al. Hox-2.3 upstream sequences mediate lacZ expression in intermediate mesoderm derivatives of transgenic mice. Development 1990;109:775–86.

[8] Srinivas S, Goldberg MR, Watanabe T, D'Agati V, al-Awqati Q, Costantini F. Expression of green fluorescent protein in the ureteric bud of transgenic mice: a new tool for the analysis of ureteric bud morphogenesis. Dev Genet 1999;24:241–51.

[9] Boyle S, Misfeldt A, Chandler KJ, Deal KK, Southard-Smith EM, Mortlock DP, et al. Fate mapping using Cited1-CreERT2 mice demonstrates that the cap mesenchyme contains self-renewing progenitor cells and gives rise exclusively to nephronic epithelia. Dev Biol 2008;313:234–45.

[10] Kobayashi A, Valerius MT, Mugford JW, Carroll TJ, Self M, Oliver G, et al. Six2 defines and regulates a multipotent self-renewing nephron progenitor population throughout mammalian kidney development. Cell Stem Cell 2008;3:169–81.

[11] Humphreys BD, Valerius MT, Kobayashi A, Mugford JW, Soeung S, Duffield JS, et al. Intrinsic epithelial cells repair the kidney after injury. Cell Stem Cell 2008;2:284–91.

[12] Mugford JW, Sipila P, McMahon JA, McMahon AP. Osr1 expression demarcates a multi-potent population of intermediate mesoderm that undergoes progressive restriction to an Osr1-dependent nephron progenitor compartment within the mammalian kidney. Dev Biol 2008;324:88–98.

[13] Levinson RS, Batourina E, Choi C, Vorontchikhina M, Kitajewski J, Mendelsohn CL. Foxd1-dependent signals control cellularity in the renal capsule, a structure required for normal renal development. Development 2005;132:529–39.

[14] Mendelsohn C, Batourina E, Fung S, Gilbert T, Dodd J. Stromal cells mediate retinoid-dependent functions essential for renal development. Development 1999;126:1139–48.

[15] Humphreys BD, Lin SL, Kobayashi A, Hudson TE, Nowlin BT, Bonventre JV, et al. Fate tracing reveals the pericyte and not epithelial origin of myofibroblasts in kidney fibrosis. Am J Pathol 2010;176:85–97.

[16] Guillaume R, Bressan M, Herzlinger D. Paraxial mesoderm contributes stromal cells to the developing kidney. Dev Biol 2009;329:169–75.

[17] Schmidt-Ott KM, Chen X, Paragas N, Levinson RS, Mendelsohn CL, Barasch J. c-kit delineates a distinct domain of progenitors in the developing kidney. Dev Biol 2006;299:238–49.

[18] Robert B St, John PL, Abrahamson DR. Direct visualization of renal vascular morphogenesis in Flk1 heterozygous mutant mice. Am J Physiol 1998;275:F164–72.

[19] Robert B St, John PL, Hyink DP, Abrahamson DR. Evidence that embryonic kidney cells expressing flk-1 are intrinsic, vasculogenic angioblasts. Am J Physiol 1996;271:F744–53.

[20] Oliver JA, Barasch J, Yang J, Herzlinger D, Al-Awqati Q. Metanephric mesenchyme contains embryonic renal stem cells. Am J Physiol Renal Physiol 2002;283:F799–809.

[21] Gao X, Chen X, Taglienti M, Rumballe B, Little MH, Kreidberg JA. Angioblast-mesenchyme induction of early kidney development is mediated by Wt1 and Vegfa. Development 2005;132:5437–49.

[22] Lin SL, Chang FC, Schrimpf C, Chen YT, Wu CF, Wu VC, et al. Targeting endothelium-pericyte cross talk by inhibiting VEGF receptor signaling attenuates kidney microvascular rarefaction and fibrosis. Am J Pathol 2011;178:911–23.

[23] Bi B, Schmitt R, Israilova M, Nishio H, Cantley LG. Stromal cells protect against acute tubular injury via an endocrine effect. J Am Soc Nephrol 2007;18:2486–96.

[24] Oliver JA, Klinakis A, Cheema FH, Friedlander J, Sampogna RV, Martens TP, et al. Proliferation and migration of label-retaining cells of the kidney papilla. J Am Soc Nephrol 2009;20:2315–27.

[25] Vogetseder A, Picard N, Gaspert A, Walch M, Kaissling B, Le Hir M. Proliferation capacity of the renal proximal tubule involves the bulk of differentiated epithelial cells. Am J Physiol Cell Physiol 2008;294:C22–28.

[26] Witzgall R, Brown D, Schwarz C, Bonventre JV. Localization of proliferating cell nuclear antigen, vimentin, c-Fos, and clusterin in the postischemic kidney. Evidence for a heterogenous genetic response among nephron segments, and a large pool of mitotically active and dedifferentiated cells. J Clin Invest 1994;93:2175–88.

[27] Vogetseder A, Karadeniz A, Kaissling B, Le Hir M. Tubular cell proliferation in the healthy rat kidney. Histochem Cell Biol 2005;124:97–104.

[28] Vogetseder A, Palan T, Bacic D, Kaissling B, Le Hir M. Proximal tubular epithelial cells are generated by division of differentiated cells in the healthy kidney. Am J Physiol Cell Physiol 2007;292:C807–13.

[29] Duffield JS, Park KM, Hsiao LL, Kelley VR, Scadden DT, Ichimura T, et al. Restoration of tubular epithelial cells during repair of the postischemic kidney occurs independently of bone marrow-derived stem cells. J Clin Invest 2005;115:1743–55.

[30] Lin F, Moran A, Igarashi P. Intrarenal cells, not bone marrow-derived cells, are the major source for regeneration in postischemic kidney. J Clin Invest 2005;115:1756–64.

[31] Ghazizadeh S, Taichman LB. Multiple classes of stem cells in cutaneous epithelium: a lineage analysis of adult mouse skin. Embo J 2001;20:1215–22.

[32] Ro S, Rannala B. A stop-EGFP transgenic mouse to detect clonal cell lineages generated by mutation. EMBO Rep 2004;5:914–20.

[33] Blanpain C, Lowry WE, Geoghegan A, Polak L, Fuchs E. Self-renewal, multipotency, and the existence of two cell populations within an epithelial stem cell niche. Cell 2004;118:635–48.
[34] Morris RJ, Liu Y, Marles L, Yang Z, Trempus C, Li S, et al. Capturing and profiling adult hair follicle stem cells. Nat Biotechnol 2004;22:411–7.
[35] Oliver J, Mac DM, Tracy A. The pathogenesis of acute renal failure associated with traumatic and toxic injury; renal ischemia, nephrotoxic damage and the ischemic episode. J Clin Invest 1951;30:1307–439.
[36] Oshima H, Rochat A, Kedzia C, Kobayashi K, Barrandon Y. Morphogenesis and renewal of hair follicles from adult multipotent stem cells. Cell 2001;104:233–45.
[37] Haagsma BH, Pound AW. Mercuric chloride-induced tubulonecrosis in the rat kidney: the recovery phase. Br J Exp Pathol 1980;61:229–41.
[38] Maeshima A, Yamashita S, Nojima Y. Identification of renal progenitor-like tubular cells that participate in the regeneration processes of the kidney. J Am Soc Nephrol 2003;14:3138–46.
[39] Humphreys BD, Czerniak S, Dirocco DP, Hasnain W, Cheema R, Bonventre JV. Repair of injured proximal tubule does not involve specialized progenitors. Proc Natl Acad Sci USA 2011;108:9226–31.
[40] Rock JR, Gao X, Xue Y, Randell SH, Kong YY, Hogan BL. Notch-dependent differentiation of adult airway basal stem cells. Cell Stem Cell 2011;8:639–48.
[41] Rock JR, Onaitis MW, Rawlins EL, Lu Y, Clark CP, Xue Y, et al. Basal cells as stem cells of the mouse trachea and human airway epithelium. Proc Natl Acad Sci U S A 2009;106:12771–5.
[42] Fujigaki Y, Goto T, Sakakima M, Fukasawa H, Miyaji T, Yamamoto T, et al. Kinetics and characterization of initially regenerating proximal tubules in S3 segment in response to various degrees of acute tubular injury. Nephrol Dial Transplant 2006;21:41–50.
[43] Sun DF, Fujigaki Y, Fujimoto T, Yonemura K, Hishida A. Possible involvement of myofibroblasts in cellular recovery of uranyl acetate-induced acute renal failure in rats. Am J Pathol 2000;157:1321–35.
[44] Vansthertem D, Caron N, Decleves AE, Cludts S, Gossiaux A, Nonclercq D, et al. Label-retaining cells and tubular regeneration in postischaemic kidney. Nephrol Dial Transplant 2008;23:3786–97.
[45] Vinsonneau C, Girshovich A, M'Rad MB, Perez J, Mesnard L, Vandermersch S, et al. Intrarenal urothelium proliferation: an unexpected early event following ischemic injury. Am J Physiol Renal Physiol 2010;299:F479–86.
[46] Nonclercq D, Wrona S, Toubeau G, Zanen J, Heuson-Stiennon JA, Schaudies RP, et al. Tubular injury and regeneration in the rat kidney following acute exposure to gentamicin: a time-course study. Ren Fail 1992;14:507–21.
[47] Nouwen EJ, Verstrepen WA, Buyssens N, Zhu MQ, De Broe ME. Hyperplasia, hypertrophy, and phenotypic alterations in the distal nephron after acute proximal tubular injury in the rat. Lab Invest 1994;70:479–93.
[48] Kwon O, Hong SM, Sutton TA, Temm CJ. Preservation of peritubular capillary endothelial integrity and increasing pericytes may be critical to recovery from postischemic acute kidney injury. Am J Physiol Renal Physiol 2008;295:F351–9.
[49] Sun DF, Fujigaki Y, Fujimoto T, Goto T, Yonemura K, Hishida A. Mycophenolate mofetil inhibits regenerative repair in uranyl acetate-induced acute renal failure by reduced interstitial cellular response. Am J Pathol 2002;161:217–27.
[50] Lin SL, Li B, Rao S, Yeo EJ, Hudson TE, Nowlin BT, et al. Macrophage Wnt7b is critical for kidney repair and regeneration. Proc Natl Acad Sci U S A 2010;107:4194–9.
[51] Schmitt R, Coca S, Kanbay M, Tinetti ME, Cantley LG, Parikh CR. Recovery of kidney function after acute kidney injury in the elderly: a systematic review and meta-analysis. Am J Kidney Dis 2008;52:262–71.
[52] Liu L, Rando TA. Manifestations and mechanisms of stem cell aging. J Cell Biol 2011;193:257–66.
[53] Carlson ME, Suetta C, Conboy MJ, Aagaard P, Mackey A, Kjaer M, et al. Molecular aging and rejuvenation of human muscle stem cells. EMBO Mol Med 2009;1:381–91.
[54] Conboy IM, Conboy MJ, Wagers AJ, Girma ER, Weissman IL, Rando TA. Rejuvenation of aged progenitor cells by exposure to a young systemic environment. Nature 2005;433:760–4.
[55] Schmitt R, Cantley LG. The impact of aging on kidney repair. Am J Physiol Ren Physiol 2008;294:F1265–1272.
[56] Westhoff JH, Schildhorn C, Jacobi C, Homme M, Hartner A, Braun H, et al. Telomere shortening reduces regenerative capacity after acute kidney injury. J Am Soc Nephrol 2010;21:327–36.
[57] Altman J, Das GD. Postnatal neurogenesis in the guinea-pig. Nature 1967;214:1098–101.
[58] Schmitt R, Marlier A, Cantley LG. Zag expression during aging suppresses proliferation after kidney injury. J Am Soc Nephrol 2008;19:2375–83.
[59] Bussolati B, Bruno S, Grange C, Buttiglieri S, Deregibus MC, Cantino D, et al. Isolation of renal progenitor cells from adult human kidney. Am J Pathol 2005;166:545–55.
[60] Mizrak D, Brittan M, Alison MR. CD133: molecule of the moment. J Pathol 2008;214:3–9.
[61] Dekel B, Zangi L, Shezen E, Reich-Zeliger S, Eventov-Friedman S, Katchman H, et al. Isolation and characterization of nontubular sca-1 + lin − multipotent stem/progenitor cells from adult mouse kidney. J Am Soc Nephrol 2006;17:3300–14.
[62] Gupta S, Verfaillie C, Chmielewski D, Kren S, Eidman K, Connaire J, et al. Isolation and characterization of kidney-derived stem cells. J Am Soc Nephrol 2006;17:3028–40.
[63] Kitamura S, Yamasaki Y, Kinomura M, Sugaya T, Sugiyama H, Maeshima Y, et al. Establishment and characterization of renal progenitor like cells from S3 segment of nephron in rat adult kidney. Faseb J 2005;19:1789–97.
[64] Lee PT, Lin HH, Jiang ST, Lu PJ, Chou KJ, Fang HC, et al. Mouse kidney progenitor cells accelerate renal regeneration and prolong survival after ischemic injury. Stem Cells 2010;28:573–84.
[65] Barker N, van Es JH, Kuipers J, Kujala P, van den Born M, Cozijnsen M, et al. Identification of stem cells in small intestine and colon by marker gene Lgr5. Nature 2007;449:1003–7.
[66] Foudi A, Hochedlinger K, Van Buren D, Schindler JW, Jaenisch R, Carey V, et al. Analysis of histone 2B-GFP retention reveals slowly cycling hematopoietic stem cells. Nat Biotechnol 2009;27:84–90.
[67] Kiel MJ, He S, Ashkenazi R, Gentry SN, Teta M, Kushner JA, et al. Haematopoietic stem cells do not asymmetrically segregate chromosomes or retain BrdU. Nature 2007;449:238–42.
[68] Fuchs E. The tortoise and the hair: slow-cycling cells in the stem cell race. Cell 2009;137:811–9.
[69] Cotsarelis G, Cheng SZ, Dong G, Sun TT, Lavker RM. Existence of slow-cycling limbal epithelial basal cells that can be preferentially stimulated to proliferate: implications on epithelial stem cells. Cell 1989;57:201–9.
[70] Marshman E, Booth C, Potten CS. The intestinal epithelial stem cell. Bioessays 2002;24:91–8.
[71] Wilson A, Laurenti E, Oser G, van der Wath RC, Blanco-Bose W, Jaworski M, et al. Hematopoietic stem cells reversibly switch from dormancy to self-renewal during homeostasis and repair. Cell 2008;135:1118–29.

[72] Zhang YV, Cheong J, Ciapurin N, McDermitt DJ, Tumbar T. Distinct self-renewal and differentiation phases in the niche of infrequently dividing hair follicle stem cells. Cell Stem Cell 2009;5:267–78.
[73] Oliver JA, Maarouf O, Cheema FH, Martens TP, Al-Awqati Q. The renal papilla is a niche for adult kidney stem cells. J Clin Invest 2004;114:795–804.
[74] Tumbar T, Guasch G, Greco V, Blanpain C, Lowry WE, Rendl M, et al. Defining the epithelial stem cell niche in skin. Science 2004;303:359–63.
[75] Patschan D, Michurina T, Shi HK, Dolff S, Brodsky SV, Vasilieva T, et al. Normal distribution and medullary-to-cortical shift of Nestin-expressing cells in acute renal ischemia. Kidney Int 2007;71:744–54.
[76] Wiese C, Rolletschek A, Kania G, Blyszczuk P, Tarasov KV, Tarasova Y, et al. Nestin expression: a property of multi-lineage progenitor cells? Cell Mol Life Sci 2004;61:2510–22.
[77] Park HC, Yasuda K, Kuo MC, Ni J, Ratliff BB, Chander PN, et al. Renal capsule as a stem cell niche. Am J Physiol Renal Physiol 2010;298:F1254–62.
[78] Goodell MA, Brose K, Paradis G, Conner AS, Mulligan RC. Isolation and functional properties of murine hematopoietic stem cells that are replicating *in vivo*. J Exp Med 1996;183:1797–806.
[79] Matsuzaki Y, Kinjo K, Mulligan RC, Okano H. Unexpectedly efficient homing capacity of purified murine hematopoietic stem cells. Immunity 2004;20:87–93.
[80] Zhou S, Schuetz JD, Bunting KD, Colapietro AM, Sampath J, Morris JJ, et al. The ABC transporter Bcrp1/ABCG2 is expressed in a wide variety of stem cells and is a molecular determinant of the side-population phenotype. Nat Med 2001;7:1028–34.
[81] Golebiewska A, Brons NH, Bjerkvig R, Niclou SP. Critical appraisal of the side population assay in stem cell and cancer stem cell research. Cell Stem Cell 2011;8:136–47.
[82] Asakura A, Rudnicki MA. Side population cells from diverse adult tissues are capable of *in vitro* hematopoietic differentiation. Exp Hematol 2002;30:1339–45.
[83] Challen GA, Bertoncello I, Deane JA, Ricardo SD, Little MH. Kidney side population reveals multilineage potential and renal functional capacity but also cellular heterogeneity. J Am Soc Nephrol 2006;17:1896–912.
[84] Hishikawa K, Marumo T, Miura S, Nakanishi A, Matsuzaki Y, Shibata K, et al. Musculin/MyoR is expressed in kidney side population cells and can regulate their function. J Cell Biol 2005;169:921–8.
[85] Iwatani H, Ito T, Imai E, Matsuzaki Y, Suzuki A, Yamato M, et al. Hematopoietic and nonhematopoietic potentials of Hoechst (low)/side population cells isolated from adult rat kidney. Kidney Int 2004;65:1604–14.
[86] Sophos NA, Vasiliou V. Aldehyde dehydrogenase gene superfamily: the 2002 update. Chem Biol Interact 2003;143–144:5–22.
[87] Chute JP, Muramoto GG, Whitesides J, Colvin M, Safi R, Chao NJ, et al. Inhibition of aldehyde dehydrogenase and retinoid signaling induces the expansion of human hematopoietic stem cells. Proc Nat Acad Sci USA 2006;103:11707–12.
[88] Ginestier C, Hur MH, Charafe-Jauffret E, Monville F, Dutcher J, Brown M, et al. ALDH1 is a marker of normal and malignant human mammary stem cells and a predictor of poor clinical outcome. Cell Stem Cell 2007;1:555–67.
[89] Lindgren D, Bostrom AK, Nilsson K, Hansson J, Sjolund J, Moller C, et al. Isolation and characterization of progenitor-like cells from human renal proximal tubules. Am J Pathol 2011;178:828–37.
[90] Grone HJ, Weber K, Grone E, Helmchen U, Osborn M. Coexpression of keratin and vimentin in damaged and regenerating tubular epithelia of the kidney. Am J Pathol 1987;129:1–8.
[91] Moll R, Hage C, Thoenes W. Expression of intermediate filament proteins in fetal and adult human kidney: modulations of intermediate filament patterns during development and in damaged tissue. Lab Invest 1991;65:74–86.
[92] Vogelmann SU, Nelson WJ, Myers BD, Lemley KV. Urinary excretion of viable podocytes in health and renal disease. Am J Physiol Renal Physiol 2003;285:F40–8.
[93] D'Agati VD. Podocyte injury in focal segmental glomerulosclerosis: lessons from animal models (a play in five acts). Kidney Int 2008;73:399–406.
[94] Thorner PS, Ho M, Eremina V, Sado Y, Quaggin S. Podocytes contribute to the formation of glomerular crescents. J Am Soc Nephrol: J Am Soc Nephrol 2008;19:495–502.
[95] Sagrinati C, Netti GS, Mazzinghi B, Lazzeri E, Liotta F, Frosali F, et al. Isolation and characterization of multipotent progenitor cells from the Bowman's capsule of adult human kidneys. J Am Soc Nephrol: J Am Soc Nephrol 2006;17:2443–56.
[96] Mazzinghi B, Ronconi E, Lazzeri E, Sagrinati C, Ballerini L, Angelotti ML, et al. Essential but differential role for CXCR4 and CXCR7 in the therapeutic homing of human renal progenitor cells. J Exp Med 2008;205:479–90.
[97] Appel D, Kershaw DB, Smeets B, Yuan G, Fuss A, Frye B, et al. Recruitment of podocytes from glomerular parietal epithelial cells. J Am Soc Nephrol 2009;20:333–43.
[98] Ronconi E, Sagrinati C, Angelotti ML, Lazzeri E, Mazzinghi B, Ballerini L, et al. Regeneration of glomerular podocytes by human renal progenitors. J Am Soc Nephrol 2009;20:322–32.
[99] Smeets B, Angelotti ML, Rizzo P, Dijkman H, Lazzeri E, Mooren F, et al. Renal progenitor cells contribute to hyperplastic lesions of podocytopathies and crescentic glomerulonephritis. J Am Soc Nephrol 2009;20:2593–603.
[100] Smeets B, Uhlig S, Fuss A, Mooren F, Wetzels JF, Floege J, et al. Tracing the origin of glomerular extracapillary lesions from parietal epithelial cells. J Am Soc Nephrol 2009;20:2604–15.
[101] Ding M, Cui S, Li C, Jothy S, Haase V, Steer BM, et al. Loss of the tumor suppressor Vhlh leads to upregulation of Cxcr4 and rapidly progressive glomerulonephritis in mice. Nat Med 2006;12:1081–7.
[102] Plotkin MD, Goligorsky MS. Mesenchymal cells from adult kidney support angiogenesis and differentiate into multiple interstitial cell types including erythropoietin-producing fibroblasts. Am J Physiol Renal Physiol 2006;291:F902–12.
[103] Bruno S, Bussolati B, Grange C, Collino F, di Cantogno LV, Herrera MB, et al. Isolation and characterization of resident mesenchymal stem cells in human glomeruli. Stem Cells Dev 2009;18:867–80.
[104] Farrington-Rock C, Crofts NJ, Doherty MJ, Ashton BA, Griffin-Jones C, Canfield AE. Chondrogenic and adipogenic potential of microvascular pericytes. Circulation 2004;110:2226–32.
[105] Feng J, Mantesso A, De Bari C, Nishiyama A, Sharpe PT. Dual origin of mesenchymal stem cells contributing to organ growth and repair. Proc Natl Acad Sci U S A 2011;108:6503–8.
[106] Fujigaki Y, Muranaka Y, Sun D, Goto T, Zhou H, Sakakima M, et al. Transient myofibroblast differentiation of interstitial fibroblastic cells relevant to tubular dilatation in uranyl acetate-induced acute renal failure in rats. Virchows Arch 2005;446:164–76.
[107] Li L, Clevers H. Coexistence of quiescent and active adult stem cells in mammals. Science 2010;327:542–5.
[108] Zhao C, Deng W, Gage FH. Mechanisms and functional implications of adult neurogenesis. Cell 2008;132:645–60.

[109] Rosenberger C, Rosen S, Paliege A, Heyman SN. Pimonidazole adduct immunohistochemistry in the rat kidney: detection of tissue hypoxia. Methods Mol Biol 2009;466:161–74.
[110] Morrison SJ, Spradling AC. Stem cells and niches: mechanisms that promote stem cell maintenance throughout life. Cell 2008;132:598–611.
[111] Fuller MT, Spradling AC. Male and female *drosophila* germline stem cells: two versions of immortality. Science 2007;316:402–4.
[112] Bonfanti P, Claudinot S, Amici AW, Farley A, Blackburn CC, Barrandon Y. Microenvironmental reprogramming of thymic epithelial cells to skin multipotent stem cells. Nature 2010;466:978–82.
[113] Parmar K, Mauch P, Vergilio JA, Sackstein R, Down JD. Distribution of hematopoietic stem cells in the bone marrow according to regional hypoxia. Proc Natl Acad Sci U S A 2007;104:5431–6.
[114] Simsek T, Kocabas F, Zheng J, Deberardinis RJ, Mahmoud AI, Olson EN, et al. The distinct metabolic profile of hematopoietic stem cells reflects their location in a hypoxic niche. Cell Stem Cell 2010;7:380–90.
[115] Takubo K, Goda N, Yamada W, Iriuchishima H, Ikeda E, Kubota Y, et al. Regulation of the HIF-1alpha level is essential for hematopoietic stem cells. Cell Stem Cell 2010;7:391–402.
[116] Mazumdar J, O'Brien WT, Johnson RS, LaManna JC, Chavez JC, Klein PS, et al. O_2 regulates stem cells through Wnt/beta-catenin signalling. Nat Cell Biol 2010;12:1007–13.
[117] Mohyeldin A, Garzon-Muvdi T, Quinones-Hinojosa A. Oxygen in stem cell biology: a critical component of the stem cell niche. Cell Stem Cell 2010;7:150–61.
[118] Kranc KR, Schepers H, Rodrigues NP, Bamforth S, Villadsen E, Ferry H, et al. Cited2 is an essential regulator of adult hematopoietic stem cells. Cell Stem Cell 2009;5:659–65.
[119] Zhang W, Edwards A. Oxygen transport across vasa recta in the renal medulla. Am J Physiol Heart Circ Physiol 2002;283: H1042–55.
[120] Adams DC, Oxburgh L. The long-term label retaining population of the renal papilla arises through divergent regional growth of the kidney. Am J Physiol Renal Physiol 2009;297: F809–15.
[121] Curtis LM, Chen S, Chen B, Agarwal A, Klug CA, Sanders PW. Contribution of intrarenal cells to cellular repair after acute kidney injury: subcapsular implantation technique. Am J Physiol Renal Physiol 2008;295:F310–4.
[122] Elger M, Hentschel H, Litteral J, Wellner M, Kirsch T, Luft FC, et al. Nephrogenesis is induced by partial nephrectomy in the elasmobranch *Leucoraja erinacea*. J Am Soc Nephrol 2003;14:1506–18.
[123] Zhou W, Boucher RC, Bollig F, Englert C, Hildebrandt F. Characterization of mesonephric development and regeneration using transgenic zebrafish. Am J Physiol Renal Physiol 2010;299:F1040–7.
[124] Diep CQ, Ma D, Deo RC, Holm TM, Naylor RW, Arora N, et al. Identification of adult nephron progenitors capable of kidney regeneration in zebrafish. Nature 2011;470:95–100.
[125] Georgas K, Rumballe B, Valerius MT, Chiu HS, Thiagarajan RD, Lesieur E, et al. Analysis of early nephron patterning reveals a role for distal RV proliferation in fusion to the ureteric tip via a cap mesenchyme-derived connecting segment. Dev Biol 2009;332:273–86.
[126] Kobayashi A, Kwan KM, Carroll TJ, McMahon AP, Mendelsohn CL, Behringer RR. Distinct and sequential tissue-specific activities of the LIM-class homeobox gene Lim1 for tubular morphogenesis during kidney development. Development 2005;132:2809–23.
[127] Weavers H, Prieto-Sanchez S, Grawe F, Garcia-Lopez A, Artero R, Wilsch-Brauninger M, et al. The insect nephrocyte is a podocyte-like cell with a filtration slit diaphragm. Nature 2009;457:322–6.
[128] Singh SR, Liu W, Hou SX. The adult *Drosophila* malpighian tubules are maintained by multipotent stem cells. Cell Stem Cell 2007;1:191–203.
[129] Picard N, Baum O, Vogetseder A, Kaissling B, Le Hir M. Origin of renal myofibroblasts in the model of unilateral ureter obstruction in the rat. Histochem Cell Biol 2008;130:141–55.
[130] Corselli M, Chen CW, Crisan M, Lazzari L, Peault B. Perivascular ancestors of adult multipotent stem cells. Arterioscler Thromb Vasc Biol 2010;30:1104–9.
[131] Iwano M, Plieth D, Danoff TM, Xue C, Okada H, Neilson EG. Evidence that fibroblasts derive from epithelium during tissue fibrosis. J Clin Invest 2002;110:341–50.
[132] Thiery JP, Acloque H, Huang RY, Nieto MA. Epithelial-mesenchymal transitions in development and disease. Cell 2009;139:871–90.
[133] Mani SA, Guo W, Liao MJ, Eaton EN, Ayyanan A, Zhou AY, et al. The epithelial–mesenchymal transition generates cells with properties of stem cells. Cell 2008;133:704–15.
[134] Oliver JA, Barasch J, Yang J, Herzlinger D, Al-Awqati Q. Metanephric mesenchyme contains embryonic renal stem cells. Am J Physiol Renal Physiol 2002;283:F799–809.
[135] Okada H, Danoff TM, Kalluri R, Neilson EG. Early role of Fsp1 in epithelial-mesenchymal transformation. Am J Physiol 1997;273:F563–74.
[136] Quaggin SE, Kapus A. Scar wars: mapping the fate of epithelial–mesenchymal–myofibroblast transition. Kidney Int 2011;80:41–50.
[137] Kriz W, Kaissling B, Le Hir M. Epithelial–mesenchymal transition (EMT) in kidney fibrosis: fact or fantasy? J Clin Invest 2011;121:468–74.
[138] Burns WC, Twigg SM, Forbes JM, Pete J, Tikellis C, Thallas-Bonke V, et al. Connective tissue growth factor plays an important role in advanced glycation end product-induced tubular epithelial-to-mesenchymal transition: implications for diabetic renal disease. J Am Soc Nephrol 2006;17:2484–94.
[139] Cheng S, Lovett DH. Gelatinase A (MMP-2) is necessary and sufficient for renal tubular cell epithelial–mesenchymal transformation. Am J Pathol 2003;162:1937–49.
[140] Li Y, Yang J, Dai C, Wu C, Liu Y. Role for integrin-linked kinase in mediating tubular epithelial to mesenchymal transition and renal interstitial fibrogenesis. J Clin Invest 2003;112:503–16.
[141] Strutz F, Okada H, Lo CW, Danoff T, Carone RL, Tomaszewski JE, et al. Identification and characterization of a fibroblast marker: FSP1. J Cell Biol 1995;130:393–405.
[142] Zhang G, Kernan KA, Collins SJ, Cai X, Lopez-Guisa JM, Degen JL, et al. Plasmin(ogen) promotes renal interstitial fibrosis by promoting epithelial-to-mesenchymal transition: role of plasmin-activated signals. J Am Soc Nephrol 2007;18:846–59.
[143] Nishitani Y, Iwano M, Yamaguchi Y, Harada K, Nakatani K, Akai Y, et al. Fibroblast-specific protein 1 is a specific prognostic marker for renal survival in patients with IgAN. Kidney Int 2005;68:1078–85.
[144] Rossini M, Cheunsuchon B, Donnert E, Ma LJ, Thomas JW, Neilson EG, et al. Immunolocalization of fibroblast growth factor-1 (FGF-1), its receptor (FGFR-1), and fibroblast-specific protein-1 (FSP-1) in inflammatory renal disease. Kidney Int 2005;68:2621–8.
[145] Faulkner JL, Szcykalski LM, Springer F, Barnes JL. Origin of interstitial fibroblasts in an accelerated model of angiotensin II-induced renal fibrosis. Am J Pathol 2005;167:1193–205.

[146] Koesters R, Kaissling B, Lehir M, Picard N, Theilig F, Gebhardt R, et al. Tubular overexpression of transforming growth factor-beta1 induces autophagy and fibrosis but not mesenchymal transition of renal epithelial cells. Am J Pathol 2010;177:632–43.
[147] Li L, Zepeda-Orozco D, Black R, Lin F. Autophagy is a component of epithelial cell fate in obstructive uropathy. Am J Pathol 2010;176:1767–78.
[148] Li J, Qu X, Bertram JF. Endothelial–myofibroblast transition contributes to the early development of diabetic renal interstitial fibrosis in streptozotocin-induced diabetic mice. Am J Pathol 2009;175:1380–8.
[149] Zeisberg EM, Potenta SE, Sugimoto H, Zeisberg M, Kalluri R. Fibroblasts in kidney fibrosis emerge via endothelial-to-mesenchymal transition. J Am Soc Nephrol 2008;19:2282–7.
[150] Medici D, Shore EM, Lounev VY, Kaplan FS, Kalluri R, Olsen BR. Conversion of vascular endothelial cells into multipotent stem-like cells. Nat Med 2010;16:1400–6.
[151] Matthaei KI. Genetically manipulated mice: a powerful tool with unsuspected caveats. J Physiol 2007;582:481–8.
[152] Duffield JS, Humphreys BD. Origin of new cells in the adult kidney: results from genetic labeling techniques. Kidney Int 2011;79:494–501.
[153] Madisen L, Zwingman TA, Sunkin SM, Oh SW, Zariwala HA, Gu H, et al. A robust and high-throughput Cre reporting and characterization system for the whole mouse brain. Nat Neurosci 2010;13:133–40.
[154] Kale S, Karihaloo A, Clark PR, Kashgarian M, Krause DS, Cantley LG. Bone marrow stem cells contribute to repair of the ischemically injured renal tubule. J Clin Invest 2003;112:42–9.
[155] Lin F, Cordes K, Li L, Hood L, Couser WG, Shankland SJ, et al. Hematopoietic stem cells contribute to the regeneration of renal tubules after renal ischemia-reperfusion injury in mice.. J Am Soc Nephrol 2003;14:1188–99.
[156] Morigi M, Imberti B, Zoja C, Corna D, Tomasoni S, Abbate M, et al. Mesenchymal stem cells are renotropic, helping to repair the kidney and improve function in acute renal failure. J Am Soc Nephrol 2004;15:1794–804.
[157] Poulsom R, Forbes SJ, Hodivala-Dilke K, Ryan E, Wyles S, Navaratnarasah S, et al. Bone marrow contributes to renal parenchymal turnover and regeneration. J Pathol 2001;195:229–35.
[158] Hauser PV, De Fazio R, Bruno S, Sdei S, Grange C, Bussolati B, et al. Stem cells derived from human amniotic fluid contribute to acute kidney injury recovery. Am J Pathol 2010;177:2011–21.
[159] Herrera MB, Bussolati B, Bruno S, Morando L, Mauriello-Romanazzi G, Sanavio F, et al. Exogenous mesenchymal stem cells localize to the kidney by means of CD44 following acute tubular injury. Kidney Int 2007;72:430–41.
[160] Lange C, Togel F, Ittrich H, Clayton F, Nolte-Ernsting C, Zander AR, et al. Administered mesenchymal stem cells enhance recovery from ischemia/reperfusion-induced acute renal failure in rats. Kidney Int 2005;68:1613–7.
[161] Togel F, Hu Z, Weiss K, Isaac J, Lange C, Westenfelder C. Administered mesenchymal stem cells protect against ischemic acute renal failure through differentiation-independent mechanisms. Am J Physiol Renal Physiol 2005;289:F31–42.
[162] Morigi M, Rota C, Montemurro T, Montelatici E, Lo Cicero V, Imberti B, et al. Life-sparing effect of human cord blood-mesenchymal stem cells in experimental acute kidney injury. Stem Cells 2010;28:513–22.
[163] Chen J, Park HC, Addabbo F, Ni J, Pelger E, Li H, et al. Kidney-derived mesenchymal stem cells contribute to vasculogenesis, angiogenesis and endothelial repair. Kidney Int 2008;74:879–89.
[164] Togel F, Weiss K, Yang Y, Hu Z, Zhang P, Westenfelder C. Vasculotropic, paracrine actions of infused mesenchymal stem cells are important to the recovery from acute kidney injury. Am J Physiol Renal Physiol 2007;292:F1626–35.
[165] Hammerman MR, Miller SB. Therapeutic use of growth factors in renal failure. J Am Soc Nephrol 1994;5:1–11.
[166] Bartosh TJ, Ylostalo JH, Mohammadipoor A, Bazhanov N, Coble K, Claypool K, et al. Aggregation of human mesenchymal stromal cells (MSCs) into 3D spheroids enhances their antiinflammatory properties. Proc Natl Acad Sci U S A 2010;107:13724–9.
[167] Nemeth K, Leelahavanichkul A, Yuen PS, Mayer B, Parmelee A, Doi K, et al. Bone marrow stromal cells attenuate sepsis via prostaglandin E(2)-dependent reprogramming of host macrophages to increase their interleukin-10 production. Nat Med 2009;15:42–9.
[168] Huang Y, Johnston P, Zhang B, Zakari A, Chowdhry T, Smith RR, et al. Kidney-derived stromal cells modulate dendritic and T cell responses. J Am Soc Nephrol 2009;20:831–41.
[169] Zhang B, Liu R, Shi D, Liu X, Chen Y, Dou X, et al. Mesenchymal stem cells induce mature dendritic cells into a novel Jagged-2-dependent regulatory dendritic cell population. Blood 2009;113:46–57.
[170] Corcione A, Benvenuto F, Ferretti E, Giunti D, Cappiello V, Cazzanti F, et al. Human mesenchymal stem cells modulate B-cell functions. Blood 2006;107:367–72.
[171] Lee RH, Pulin AA, Seo MJ, Kota DJ, Ylostalo J, Larson BL, et al. Intravenous hMSCs improve myocardial infarction in mice because cells embolized in lung are activated to secrete the anti-inflammatory protein TSG-6. Cell Stem Cell 2009;5:54–63.
[172] Li B, Cohen A, Hudson TE, Motlagh D, Amrani DL, Duffield JS. Mobilized human hematopoietic stem/progenitor cells promote kidney repair after ischemia/reperfusion injury. Circulation 2010;121:2211–20.
[173] Loffredo FS, Steinhauser ML, Gannon J, Lee RT. Bone marrow-derived cell therapy stimulates endogenous cardiomyocyte progenitors and promotes cardiac repair. Cell Stem Cell 2011;8:389–98.
[174] Kinomura M, Kitamura S, Tanabe K, Ichinose K, Hirokoshi K, Takazawa Y, et al. Amelioration of cisplatin-induced acute renal injury by renal progenitor-like cells derived from the adult rat kidney. Cell Transplant 2008;17:143–58.
[175] Lazzeri E, Crescioli C, Ronconi E, Mazzinghi B, Sagrinati C, Netti GS, et al. Regenerative potential of embryonic renal multipotent progenitors in acute renal failure. J Am Soc Nephrol 2007;18:3128–38.
[176] Kunter U, Rong S, Boor P, Eitner F, Muller-Newen G, Djuric Z, et al. Mesenchymal stem cells prevent progressive experimental renal failure but maldifferentiate into glomerular adipocytes. J Am Soc Nephrol 2007;18:1754–64.
[177] Hsu YC, Pasolli HA, Fuchs E. Dynamics between stem cells, niche, and progeny in the hair follicle. Cell 2011;144:92–105.

SECTION 3

FLUID AND ELECTROLYTE REGULATION AND DYSREGULATION

This page intentionally left blank

CHAPTER

30

Epithelial Na^+ Channels

Shaohu Sheng[1], *Kenneth R. Hallows*[1,2] *and Thomas R. Kleyman*[1,2]

[1]Renal-Electrolyte Division, Department of Medicine, University of Pittsburgh, Pittsburgh, PA, USA

[2]Department of Cell Biology and Physiology, University of Pittsburgh, Pittsburgh, PA, USA

INTRODUCTION

From the late distal convoluted tubule, connecting tubule, and throughout the collecting duct, Na^+ exits the urinary space by passive diffusion through an apical membrane epithelial Na^+ channel, referred to as ENaC. Na^+ exits cells across basolateral membranes via the Na^+,K^+-ATPase. Koefoed-Johnson and Ussing initially proposed this model of electrogenic transepithelial Na^+ transport, with diffusion of Na^+ across an apical membrane conductance pathway, in 1958.[1] Studies using both noise analysis and single channel recordings demonstrated the presence of apical membrane Na^+ selective ion channels.[2–4] Subsequent to the cloning of ENaC, knockout studies have confirmed the role of ENaC in the reabsorption of filtered Na^+ in the distal nephron, as well as its role in facilitating renal K^+ secretion.[5–7]

Electrophysiologic Characteristics

The basic electrophysiologic characteristics of epithelial Na^+ channels have been defined using both macroscopic and single channel studies, and are presented in Figure 30.1. ENaCs are Na^+- and Li^+-permeable channels that exhibit negligible K^+ conductance, with a single channel conductance of 4 to 5 pS at room temperature with Na^+ as the charge carrier.[3,8,9] These channels exhibit a slight increase in open probability under hyperpolarizing membrane potentials.[10,11] ENaCs characteristically exhibit long open and closed times, in the order of seconds to tens of seconds, although a population of ENaCs has been described that has brief open times and long closed times that likely represent channels that have not been processed by proteases.[11–13] Channels are blocked by submicromolar concentrations of amiloride, a pyrazinoylguanidine derivative.[14,15] Amiloride is a weak base and has a pK_a of 8.8 in water. It is the charged, or protonated, form of amiloride that blocks ENaC.[15] Other organic weak bases, including triamterene, trimethoprim, and pentamidine also inhibit ENaC.[16–19]

Biochemical and Molecular Characteristics of ENaC

Amiloride was first demonstrated to inhibit electrogenic transepithelial Na^+ transport in 1968.[14] With an IC_{50} of ~100 nM, amiloride and several related compounds proved to be highly selective Na^+ channel inhibitors.[15] Prior to the cloning of ENaC subunits, several different approaches were used to isolate a Na^+ channel complex.[20–22] The relationship of this channel complex to ENaC is still unclear, although antibodies raised against a subunit of the cloned Na^+ channel have been observed to recognize a polypeptide within the purified channel complex.[23]

The molecular characteristics of this channel were elucidated in studies from Canessa and co-workers and Lingueglia and co-workers in 1993 and 1994.[9,24–26] An expression cloning technique led to the identification of a cDNA, termed α ENaC, whose cRNA induced expression of amiloride-sensitive Na^+ currents when injected into *Xenopus* oocytes.[24,25] However, Na^+ currents were lower than expected. Two subsequent cDNA clones were isolated based on their ability to complement α ENaC cRNA in the expression of amiloride-sensitive Na^+ currents in *Xenopus* oocytes, and were termed β and γ ENaC.[9] *Xenopus* oocytes coinjected with the three cRNA species expressed amiloride-sensitive Na^+ channels with characteristics nearly identical to that of Na^+ channels expressed in renal

Seldin and Giebisch's The Kidney, Fifth Edition.
DOI: http://dx.doi.org/10.1016/B978-0-12-381462-3.00030-6

© 2013 Elsevier Inc. All rights reserved.

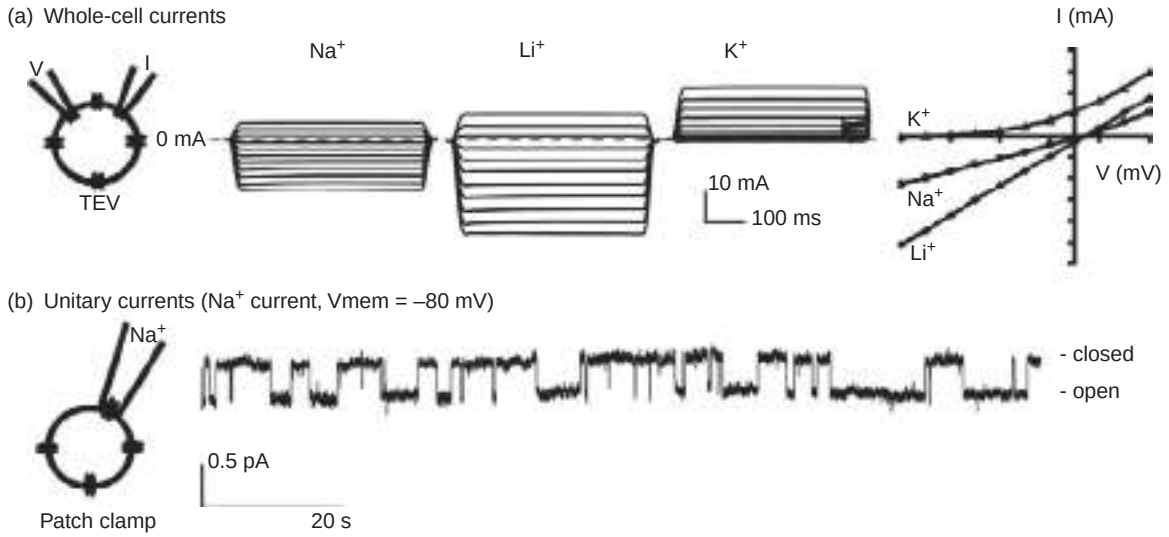

FIGURE 30.1 **Biophysical properties of epithelial Na^+ channels.** (a) Whole-cell currents were recorded in *Xenopus* oocytes expressing αβγ ENaC that were bathed with NaCl, LiCl or KCl solutions. Current-voltage curves are shown on the right. (b) Single channel recording was performed with cell-attached patch and NaCl in the pipette *(Recordings in part (a) are reprinted with permission from ref. [170]).*

cortical collecting tubules and in cultured cell lines derived from the distal nephron. Na^+ currents were not observed when either the β- or γ-subunits were expressed alone.

The three ENaC subunits are likely derived from a common ancestral gene, given their limited (~30 to 40%) sequence identity. ENaC subunits have been cloned from a variety of species, including rat, human, mouse, rabbit, guinea pig, chicken, cattle, sheep, salamander, clawed African frog (*Xenopus laevis*), and bullfrog.[9,24–34] The human α-subunit gene *Scnn1a* spans 17 kb on human chromosome 12p13. The β- and γ-subunit genes *Scnn1b* and *Scnn1g* are closely linked on human chromosome 16p12-p13.[35,36] The genes encoding the three ENaC subunits have a conserved exon–intron architecture, with 13 exons.[37,38] Splice variants have been described that alter the cytoplasmic N-termini or alter the extracellular domains.[39–41] Variants that result in a termination codon in the region coding the extracellular domain of the α-subunit have also been reported.[41–43] Some of these variants are associated with a reduction or loss of channel activity when expressed in heterologous systems, and with an autosomal recessive loss of function phenotype (pseudohypoaldosteronism) in humans.[42]

ENaC/Degenerin Gene Family

Canessa and co-workers noted that ENaC subunits were related to genes identified in *Caenorhabditis elegans* that participate in mechanosensation specific mutations of which result in degeneration of selected neurons.[44–46] ENaCs belong to the ENaC/Degenerin gene family (Figure 30.2). There are two additional ENaC subunits, referred to as δ and ε, that appear to be functionally related to the α-subunit. δ ENaC is a proton-activated channel expressed in primates, although its physiologic role is still unclear.[47,48] The ε-subunit was identified in *Xenopus*, and has an altered Na^+ self-inhibition response suggesting altered gating properties.[49] Members of this family also include genes identified in *C. elegans* that are involved in mechanosensation (*mecs* and *degs*) or control of defecation rhythm (*flrs*);

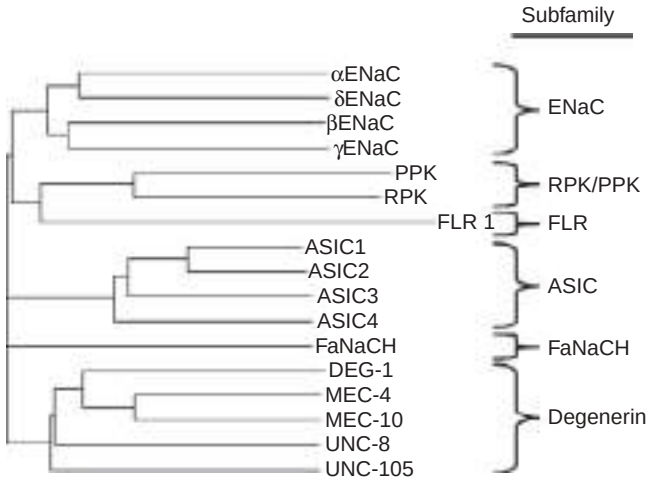

FIGURE 30.2 **Phylogenetic tree of the ENaC/DEG superfamily.** Family members are grouped into six subfamilies: ENaCs: RPK (ripped pocket)/PPK (pickpocket), expressed in *Drosophila*; FLR: expressed in *C. elegans*; ASICs or acid-sensing ion channels; FaNaCh: a peptide-gated channel expressed in marine snails; and degenerins: expressed in *C. elegans*.

H^+-gated channels (referred to as acid-sensing ion channels (or ASICs)) that are expressed in mammalian central and peripheral nervous systems and have a role in nociception, mechanosensation, fear-related behavior, and seizure termination;[50–55] a family of 16 genes expressed in *Drosophila*, referred to as pickpocket, that may have roles in airway fluid clearance, mechanosensation, salt sensation, and detection of pheromones;[56–61] and peptide-gated channels expressed in marine snails.[62–64]

Structure and Function of ENaC

Each ENaC subunit has only two predicted membrane spanning domains, similar to the topology of members of the Kir family of K^+ channels, and members of the P2X family of purinergic receptors that are ligand-gated ion channels[65,66] (Figure 30.3). Three independent groups published topologic analyses of ENaC subunits.[67,68] Each subunit has intracellular amino and carboxyl termini and two α helical membrane spanning domains connected by a large extracellular domain. The cytoplasmic domains have kinase phosphorylation sites, as well as protein–protein and protein–lipid interaction motifs that affect channel gating or trafficking.

Jasti and colleagues resolved the crystal structure of ASIC1, a member of the ENaC/Degenerin family.[69,70] Although initially lacking the N- and C-terminal cytoplasmic regions, this structure provided important insights into the structural organization of ASIC and related family members, including ENaC. ASIC1 is a trimer, suggesting that ENaC has a subunit stoichiometry of α1β1γ1, in contrast to the higher ordered stoichiometry that had been proposed based on biophysical and biochemical studies.[71–74] The extracellular region is a highly ordered structure that resembles an outstretched hand containing a ball, and has clearly defined domains termed wrist, finger, thumb, palm, knuckle, and β-ball[69] (see Figure 30.3). Jasti et al. suggested that ASIC1 proton-dependent gating occurs in conjunction with conformational changes within the thumb and finger domains, which are transmitted to the transmembrane domains.[69] The three ENaC subunits contribute residues that line the channel's pore. The resolved ASIC1 structure suggests that the channel's gate resides in the outer part of the pore,[70,75] in the vicinity of the "degenerin" site where the introduction of bulky residues in: (1) ENaC subunits; (2) mec4 or mec10 (a component of the mechanosensitive channel in *C. elegans*); and (3) ASIC subunits result in a dramatic increase in channel open probability.[46,76–79]

ASIC1 is the only member of the ENaC/Degenerin gene family whose structure has been resolved.[69] This structure provides a starting point to generate models of ENaC subunits. Kashlan and co-workers have built models of the extracellular region of the α-subunit of ENaC based, in part, on homology to ASIC1.[80–82] The extracellular regions of ENaC subunits and ASIC1 are reasonably homologous, except in the finger domain. For example, the α-subunit of ENaC has 73 additional residues when compared to ASIC (see [81,82]). The α-subunit is proteolytically processed at specific sites within its finger domain, releasing an inhibitory tract.[83–85] To determine the molecular architecture of the α-subunit finger domain, sites within α ENaC that interact with an 8 residue inhibitory peptide derived from the portion of the

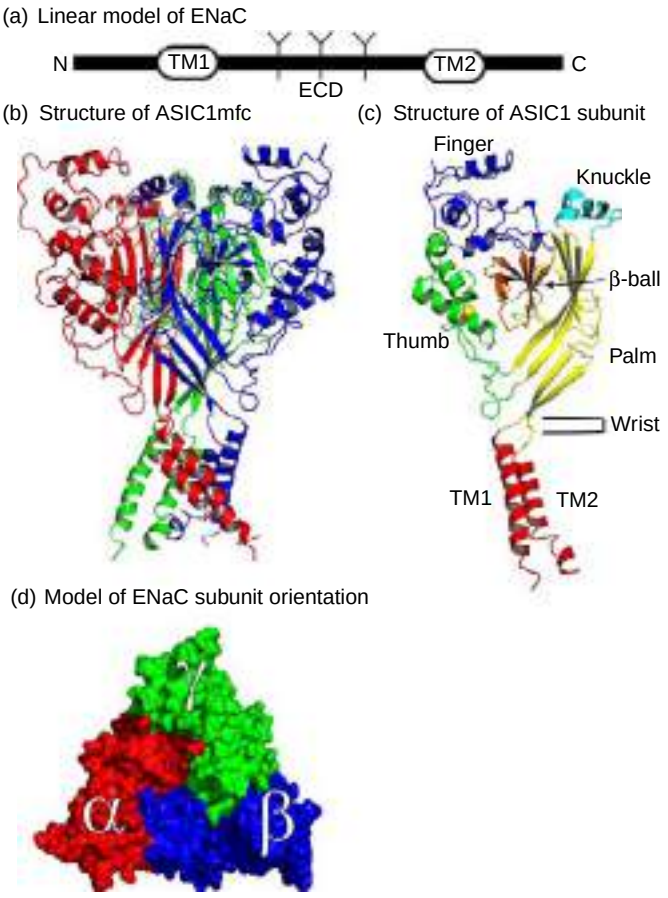

FIGURE 30.3 **Structural features of ENaC subunits.** (a) Linear model of an ENaC subunit (TM1, TM2: the first and second transmembrane domains; ECD: extracellular domain connecting TM1 and TM2; N: amino terminus; C: carboxyl terminus). Several glycosylation sites are shown as branched lines. (b) Structure of the minimally functional chicken ASIC1.[70] Three identical ASIC1 subunits are shown as ribbons with colors of red, green, and blue for the three subunits. (c) Defined subdomains within the large extracellular domain. (d) Proposed subunit orientation of ENaC, viewed from above.[187,191] Surface rendering of the relative locations of the α- (red), β- (blue), and γ- (green) subunits are shown. The structural models in this figure were generated from coordinates of ASIC1.[70]

α-subunit that is removed by furin cleavage were determined.[86] The working hypothesis was that the inhibitory tract within a non-cleaved α-subunit and the 8 residue inhibitory peptide share common binding sites. Distance constraints were introduced to construct a model of the α-subunit.[81,82] The model places the inhibitory tract at an interface of the finger and thumb domains. Kashlan and co-workers suggested that the inhibitory tract blocks channel activity by stabilizing the movement of the finger domain relative to the thumb domain.[81,82]

Stockand and co-workers have also generated a model of an ENaC trimer, based on the structure of ASIC1.[87] To generate the model areas that lacked sequence similarity within the finger regions of ENaC subunits were removed. Although this limits the utility of the model, the model provides important insights regarding sites of intersubunit interactions.

ENaC Biogenesis

Na^+ channel subunits likely undergo assembly in the endoplasmic reticulum (ER), where core, high mannose Asn- (or N)-linked glycans are added at specific sites.[88–97] Each subunit is modified by N-linked glycosylation at multiple sites. For example, rat α-, β-, and γ-subunits have six, twelve, and five consensus sites (Asn-X-Ser/Thr) for N-linked oligosaccharide addition, respectively. Exit of assembled channels from the ER appears to be inefficient.[96,98] A motif that facilitates the exit of ENaC from the ER was found in the proximal cytoplasmic carboxyl terminus of the α-subunit.[98]

Channel subunits that do not exit the ER are likely degraded via proteasome-mediated ER associated degradation (ERAD).[99–102] Integral membrane proteins such as ENaC are co-translationally inserted into the ER. The proper folding and assembly of polypeptides synthesized in the ER involves interactions with a variety of chaperone proteins.[103–105] Specific chaperones that participate in ENaC folding and assembly or targeting misfolded subunits for degradation are starting to be defined. These include members of the luminal Hsp40s, the small heat shock protein alpha A-crystallin, and calreticulin.[100–102,106,107] Cytoplasmic Hsp70s also have roles in channel trafficking, although at present it is unclear whether their roles are related to facilitating ER exit or post-ER trafficking events.[106]

The half-life of newly synthesized subunits, determined by metabolic labeling/pulse-chase experiments, is approximately an hour,[89,91–93,96,99,108] consistent with the notion that the majority of ENaC subunits synthesized within the ER are targeted for degradation via ERAD. A longer-lived pool of channels is apparent in pulse-chase studies, which likely reflects properly assembled channels that have exited the ER.[99] Several groups have determined the half-life of channels that have reached the surface. The rate of degradation of channels that have reached the surface may be in the order of many hours to days,[92,109–111] although some investigators have reported a shorter half-life for channels that have reached the cell surface of A6 cells and MDCK cells expressing exogenous ENaCs.[91,93] These differences in the half-life of channels that have reached the cell surface could result from differences in cell type, and whether ENaCs are expressed endogenously or exogenously.

ENaC Processing in the Biosynthetic Pathway

As assembled ENaCs exit the ER, it has been thought that channels follow the route used by other proteins in the secretory pathway. This involves trafficking through the Golgi where most N-glycans are processed, and the trans-Golgi network where channels are sorted into endosomes that are delivered to the apical membrane. N-glycan processing is often monitored by the enzyme endoglycosidase H, an enzyme that removes high mannose N-linked glycans prior to processing events that occur in the medial Golgi complex.

N-glycans on all three subunits of assembled channels are modified to complex-type Endo H-resistant forms.[93,97] Surprisingly, subunits with endoglycosidase H sensitive N-glycans have also been described.[97] Hughey and co-workers reported that two distinct pools of ENaC subunits were expressed at the plasma membrane: subunits with processed N-glycans and cleaved α- and γ-subunits; and full-length subunits that have non-processed N-glycans.[97] Processing of subunits within a channel complex appears to be an all-or-nothing event.[112] These findings suggest that a population of channel complexes exiting the ER transits through Golgi and post-Golgi compartments where subunits are processed (Figure 30.4). These processed channels likely represent the pool of active, functional channels. A distinct population of channels exiting the ER appears to bypass Golgi and post-Golgi processing events. This distinct pool of non-processed channels is likely a functionally inactive pool, as proteolysis of ENaC subunits appears to have a dramatic effect on increasing channel open probability.[13,83,113–115] Proteolytic cleavage of these inactive channels provides a potential mechanism to increase rates of Na^+ transport in the distal nephron. The role of proteolysis of ENaC subunits in regulating channel gating is discussed in detail later in this chapter.

Intracellular Trafficking of ENaC

Functional channels are delivered to the apical plasma membrane via the traditional secretory

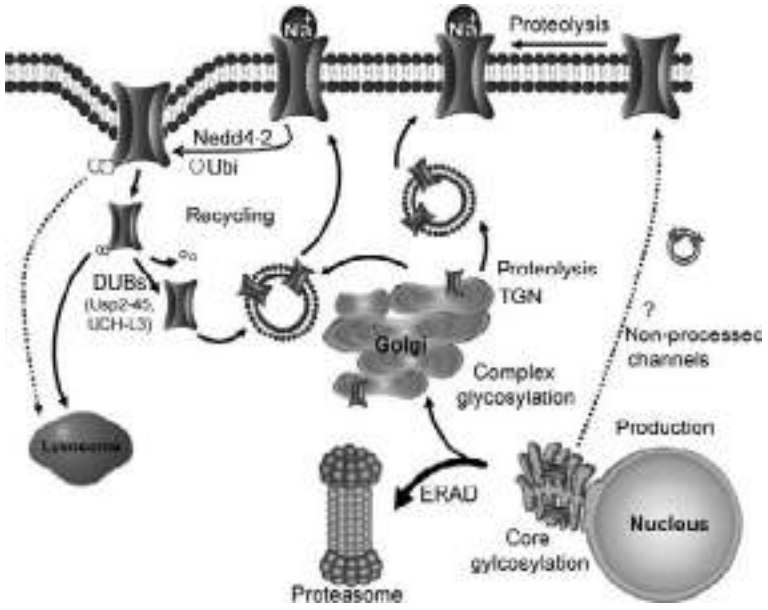

FIGURE 30.4 **Model of ENaC biogenesis and intracellular trafficking.** ENaC subunits are assembled and undergo addition of high mannose asparagine (N)-linked glycans within the endoplasmic reticulum (ER). The majority of newly synthesized subunits are targeted for ER associated degradation (ERAD) that occurs within proteasomes. Assembled ENaCs that exit the ER transit to the apical plasma membrane via distinct routes. ENaCs traffic through the Golgi, where most N-glycans are processed, and through the trans-Golgi network (TGN), where channels are processed by the protease furin prior to delivery to the apical membrane. Alternatively, ENaCs exiting the ER may be delivered directly to the apical plasma membrane, bypassing processing steps that occur in the Golgi and TGN. These non-processed channels are functionally inactive, but are potentially activated by proteases present at the plasma membrane or within the urinary space. ENaCs at the plasma membrane are targeted for internalization following Nedd4-2-dependent ubiquitination (Ubi). Internalized channels are degraded within lysosomes or proteasomes. Alternatively, internalized channels are likely deubiquitinated by specific deubiquitinating enzymes (DUBs), and recycled to the plasma membrane in a regulated manner.

pathway[112] (Figure 30.4). The exocytic insertion of channels into the apical plasma membrane occurs as a regulated process that is increased in response to a variety of hormones, including vasopressin, aldosterone, and insulin. Vesicle and target SNAREs (soluble N-ethylmaleimide sensitive factor attachment protein receptors) participate in this process, and overexpression of specific SNARE proteins disrupts the intracellular trafficking of ENaC subunits.[116–119] Channels at the plasma membrane appear to reside within specific compartments. Several groups have reported that a population of channels resides within lipid-rich microdomains, referred to as lipid rafts,[120,121] although other groups have not confirmed this finding.[91] While lipid rafts have been reported to facilitate the co-localization of membrane proteins and signaling molecules, the functional consequences of ENaCs within lipid rafts are still unclear. ENaCs interact with cytoskeletal elements, including actin and α-spectrin, which may have a role in localizing the channel to the plasma membrane and in modulating ENaC activity.[122–125]

The residency time of channels at the plasma membrane has been examined by several groups, with reported half-lives in the order of minutes to hours.[91,93,110,111,126,127] Mutations within a carboxyl-terminal PY motif within the β- and γ-subunits are associated with increases in the half-life of the channel at the plasma membrane via mechanisms that are discussed later in this chapter.[126,128] Internalization of channels from the plasma membrane has been proposed to occur via a dynamin-dependent process.[126] Dynamin is required for clathrin-dependent endocytosis, as well as for caveolae-dependent endocytosis.[129–131] Ubiquitin conjugation of defined lysine residues within ENaC subunits at the plasma membrane targets the channels for endocytosis,[132] presumably via a clathrin-dependent mechanism (Figure 30.4).[133] Once internalized, some channels are targeted for degradation via proteasomes or possibly lysosomes.[93,108,132] A significant fraction of the pool of endocytosed channels may undergo recycling to the plasma membrane in a regulated manner[111] (Figure 30.4). Specific deubiquitination enzymes have a role in removing ubiquitin from internalized channels, facilitating the recycling of channels to the plasma membrane.[134–136]

Localization within the Kidney and Other Organs

The aldosterone-sensitive distal nephron is the final site of Na^+ reabsorption within the nephron. ENaCs

are expressed in principal cells in the late distal convoluted tubule, connecting tubule, and through the collecting duct, and are the major pathway for Na^+ entry across the apical plasma membrane. In the more proximal segments of the aldosterone-sensitive distal nephron, Na^+ reabsorption via ENaC is coupled to K^+ secretion mediated by apical membrane K^+ channels, including Kir1.1 (or ROMK) and the large conductance Ca^{2+}-activated K^+ channel (maxi-K).[137–139] ENaC-dependent reabsorption of Na^+ in the distal nephron has a major role in the control of extracellular fluid volume, blood pressure, and renal K^+ secretion.

The cellular localization of individual ENaC subunits may differ within the nephron. When maintained on normal laboratory diet, β- and γ-subunits were localized within an intracellular compartment in principal cells within the cortical and outer medullary segments of the rat aldosterone-sensitive distal nephron.[140] One group reported that the α-subunit was localized primarily to apical part of principal cells,[140] whereas other groups have observed either modest cytoplasmic localization or have failed to detect the α-subunit.[141,142] Within the inner medullary collecting duct, all three ENaC subunits were localized primarily within an intracellular compartment.[140] When placed on a low-Na^+ diet or following administration of aldosterone, all three subunits were expressed at the apical membrane of principal cells.[141,143]

Mice lacking expression of the β- or γ-subunits or that have reduced expression of the α-subunit exhibit renal Na^+-wasting.[5–7,144] Mice that lack expression of the α-subunit are unable to clear airway fluids at birth, leading to death in the early postnatal period.[145] Recent work suggests that the density of ENaC expression may be greatest in the connecting tubule, an early segment within the aldosterone-sensitive distal nephron that connects the distal convoluted tubule to the collecting tubule.[146] Mice that lack expression of α ENaC beyond the connecting tubule are able to maintain Na^+ and K^+ balance, even in the setting of dietary Na^+ restriction or K^+-loading.[147]

In addition to its expression in the nephron, ENaCs are expressed within numerous other organs. They are expressed throughout the airways, as well as in both type I and type II alveolar cells.[148–152] ENaC has a key role in the reabsorption of airway fluids.[145,153] Maintaining an appropriate volume of airway surface liquids has an important role in facilitating mucociliary clearance.[153,154] ENaCs are also expressed in the distal colon, sweat ducts, salivary ducts, inner ear, lingular epithelium, keratinocytes, lymphocytes, and vascular smooth muscle. ENaC expression has also been reported in endothelia and in various sites within the eye, including epithelia within the retina, lens, and pigmented ciliary body and iris.[9,155–162] The functional roles of ENaCs within many of these tissues are unclear.

ENaC STRUCTURE AND FUNCTION

Specific structural features within channel subunits have key roles in defining the biophysical properties of ENaC. All three ENaC subunits contribute to the formation of the conduction pore, as pore properties are altered by mutations within each of the three subunits.[163] The published structures of ASIC1 reveal a homomeric trimer[69,70] (Figure 30.3). The structures of the extracellular domain (ECD) and transmembrane domain (TM) are well-defined, while the cytoplasmic amino- and carboxyl-terminal domains are not resolved in the crystal structures. The cASIC1 structures confirm a longstanding notion that the channel pore is formed largely by the second transmembrane domain (TM2s) that determines the basic biophysical properties of ENaC. Both the extracellular and cytoplasmic domains have roles in modulating channel-gating and trafficking. The functional roles of individual domains within ENaC subunits, and potential mechanisms of ion permeation, ion selectivity, channel-gating, and amiloride block are reviewed below with insights from the ASIC1 structures.

Functional Domains within ENaC Subunits

Amino-Terminus

The cytoplasmic amino-termini have regions that affect channel-gating, trafficking, and regulation by intracellular factors. Chalfant and co-workers identified a Lys-Gly-Asp-Lys tract within the rat α-subunit corresponding to residues 47–50, that may function as an endocytic signal that regulates the number of channels in the plasma membrane.[164] A domain that affects channel-gating has been characterized within the distal portion of the amino-terminus of the α-subunit, which includes a highly-conserved His-Gly tract.[165,166] A mutation in the corresponding Gly in the β-subunit was described in a patient with pseudohypoaldosteronism. Reduced channel activity attributed to a decreased open probability was observed with a mutation of the conserved Gly in each subunit, suggesting that the His-Gly tract within the amino termini of all three subunits influences channel-gating.[42,165,166] A recent study showed that mutations of this Gly in the α and γ ENaC subunits induced a strong inward rectification in the whole cell currents, reflecting voltage-dependent gating.[167] Mutations at other sites have also

been found to reduce channel activity and induce voltage-dependent gating.[168–171]

Phosphatidylinositol 4,5-bisphosphate (PIP2) activates ENaCs,[172,173] an effect that reflects an increase in channel open probability as a result of direct interactions between PIP2 and ENaC. Several groups have proposed that the amino-termini of the β- and γ-subunits of ENaC harbor putative PIP2-binding domains containing basic amino acid residues.[172,174,175] In addition, Helms and co-workers suggest that PIP3 mediates aldosterone-induced ENaC activity and trafficking, and interacts with γ ENaC.[176] The ENaC amino-termini also contain Cys residues that may interact with intracellular metals (Cd^{2+} and Zn^{2+}) and thiol-reactive chemicals, leading to a reduction in channel open probability.[177] Palmitoylation of amino-terminal Cys-43 and carboxyl-terminal Cys-557 of mouse β ENaC enhances channel open probability (see below).[98]

First Transmembrane Domain (TM1)

The ASIC1 structures were apparently resolved in a desensitized state. In these structures, the channel pore is primarily lined by TM2 helices from three identical subunits, with the three TM1 helices packed tangentially behind the TM2 helices and contacting the lipid bilayer. The TM1 helix from an individual subunit also makes extensive interactions with the TM2 helix of the same subunit, as well as specific contacts with helices from an adjacent subunit.[70] The closed-pore conformation of ENaC may be similar to that of ASIC1. A Trp scanning of the TM1 of α ENaC showed that mutations within the amino-terminal portion of αTM1 alter channel activity, selectivity, and gating,[178] consistent with the extensive intrasubunit interaction between TM1 and TM2 helices revealed in the ASIC1 structures.[69,70] A recent Cys scanning of ASIC1 TM domains is also consistent with the relative locations of TM1 and TM2 helices in the resolved structures.[75]

Extracellular Domain (ECD)

Each ENaC subunit has a large, ~450 residue extracellular region with 16 conserved Cys residues clustered within two Cys-rich domains.[179] Other members of the ENaC/DEG family also possess extracellular Cys-rich domains.[180] The size and the apparently conserved structural organization of the extracellular domain suggest that this region has important functional roles. Recent studies have examined the role of the ECD in modulating channel-gating in response to proteases, sheer stress, external Na^+, metals, H^+, and Cl^-.[49,80,97,179,181–193] These functional studies and insights from the ASIC1 structure suggest that the ECD of ENaC functions as a sensor or receptor for a variety of extracellular signals. The extracellular domains also facilitate the assembly of the heteroligomeric channel complex within the endoplasmic reticulum, and influence intracellular trafficking.[179,193,194]

Several proteases, including prostasin and related channel-activating proteases, furin, trypsin, chymotrypsin, and elastase have been shown to activate ENaC.[83,113,114,195–199] Activation of ENaC by proteases is a result of proteolytic cleavage of ENaC subunits within their extracellular domains at defined sites, releasing intrinsic inhibitory tracts.[81,84,85,200] Mechanisms by which proteases activate ENaCs are discussed below.

ENaCs are inhibited by extracellular Na^+, which presumably binds to sites within the ECD. This response, referred to as self-inhibition, reflects a reduction in channel open probability.[2,115,182,185,201,202] The structural basis of Na^+ self-inhibition has begun to emerge from mutagenesis studies.[80,182,185,186,188,190–193] At present, the sites of Na^+-binding, as well as the subsequent allosteric changes that lead to a reduction in channel open probability, have not been defined. In addition to Na^+, other external cations such as Ni^{2+}, Zn^{2+}, Cu^{2+}, Cd^{2+}, and Hg^{2+} affect ENaC activity, presumably by binding to sites within the ECDs and altering channel open probability.[181,184,187,203–206] The effects of these metals on ENaC are both metal- and species-specific.

Extracellular anions also interact at sites within the extracellular domains of ENaC subunits and alter ENaC gating. Collier and Snyder found that external Cl^- regulates ENaC activity in part through enhancing Na^+ self-inhibition. Their findings provide a mechanism by which changes in extracellular Cl^- modulates epithelial Na^+ absorption.[190] They identified two Cl^- inhibitory sites in ENaC, one formed by residues in the thumb domain of the α-subunit and the palm domain of the β-subunit, and the other formed by residues at the interface of the thumb domain of the β-subunit and the palm domain of the γ-subunit. Based on the effects of mutagenesis on Cl^- inhibition, the additive nature of mutations, and on differences in the mechanisms of Cl^- inhibition, the authors propose a model in which ENaC subunits assemble in an αγβ-orientation when viewed from above[191] (Figure 30.3). This subunit arrangement is also suggested by Chen et al., based on the identification of a putative Cu^{2+}-binding site at the α- and β-subunit interface within the ECD of human ENaC.[187] However, the model is based on the assumption that the functional ENaC complex is a heterotrimer. The possibility that multiple arrangements co-exist needs to be tested.

Within the ENaC extracellular domains are 16 Cys residues, which are largely conserved among other members of the ENaC/degenerin family. Firsov and colleagues proposed that specific Cys residues (the first and sixth Cys in all three subunits, as well as the

eleventh and twelfth Cys in the α- and β-subunits) have an essential role in the efficient transport of assembled channels to the plasma membrane.[179] A mutation of the first cysteine residue in the human α-subunit (aC133Y) is associated with PHA-1.[207] Sheng et al. proposed that there are several intrasubunit disulfide bonds, based on analyses of additivity of double Cys mutations and responses to sulfhydryl reagent of single and double mutants.[183] These predicted disulfide bonds (Cys1-Cys6, Cys4-Cys5, Cys7-Cys16, Cys11-Cys12, Cys10-Cys13, and Cys8-Cys15 (conserved Cys numbered sequentially)) were present in the resolved ASIC1 structure.[69] ASIC subunits have 14 conserved Cys residues within the ECD that form seven intrasubunit disulfide bonds, one in β-ball, one in palm, and five in thumb domain.[69] The locations of the disulfide bonds are consistent with their roles in stabilizing the conformations of these domains.

Second Transmembrane Domain (TM2)

The TM2 region is thought to be the segment that lines the conduction pore and contains important functional sites, including the degenerin (DEG) site, amiloride-binding site, and selectivity filter site[169,208,209] (Figure 30.5). The structure of the ENaC pore is expected to be similar to that of ASIC1, given the high degree of sequence homology and similar biophysical properties. For example, three ENaC TM2s likely line the channel pore, while TM1s contact the lipid bilayer. As the resolved ASIC1 structures likely represent non-conducting states, they provide limited information regarding the roles of TM2 residues in ion permeation and selectivity. Two distinct TM domain structures of ASIC1 have been described,[69,70] adding an additional layer of complexity in interpreting structure and function relationships of the TM2 domains from the resolved ASIC1 structures. Here we discuss mutagenesis results, mainly in reference to the most recent ASIC1 structure.[70]

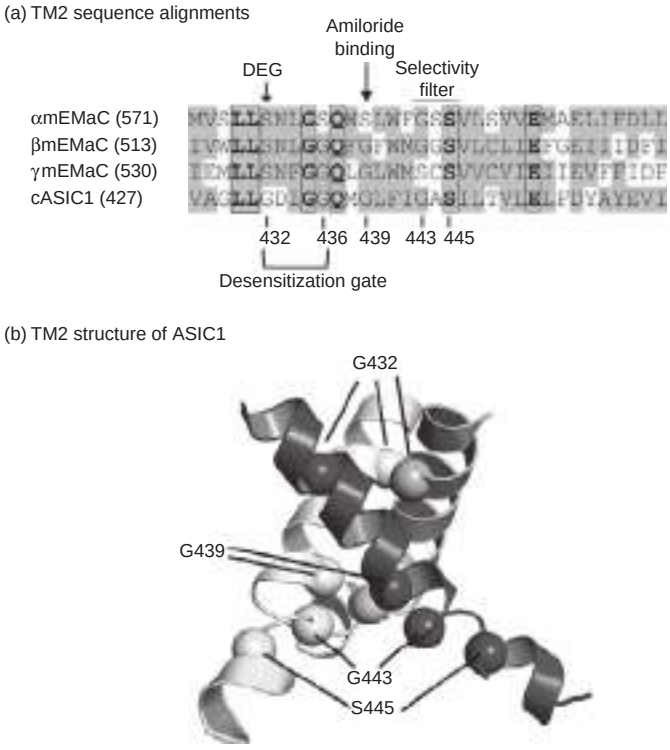

FIGURE 30.5 ENaC/ASIC pore structures. (a) Sequence alignments of the second transmembrane domains (TM2) of mouse α-, β- and γ-subunits and chicken ASIC1. Identical residues are shown as boxed and bold letters and the similar residues are shaded. Key functional sites are labeled. Selected ASIC1 residues are identified below by residue numbers. Location of the proposed desensitization gate of ASIC1[70] is indicated by a square bracket. (b) Model of the TM2 bundles of ASIC1.[70] The three TM2 helices are shown. Spheres represent α-carbons of ASIC1 residues identified in panel (a).

AMILORIDE BINDING

Schild and co-workers identified a ring of residues at homologous positions within each of the three subunits (αS583, βG525, and γG537 in rat ENaC) as a putative amiloride-binding site[163] (Figure 30.5). The substitution of βG525 or γG537 weakened amiloride IC_{50} by about three orders of magnitude. In contrast, the substitution of αS583 with amino acids bearing side chains with different functional groups (e.g., Gly, Leu, Asn, Gln) had only a slight effect on amiloride block, suggesting that the side chain of αS583 does not participate in amiloride binding.[171] However, amino acids with aromatic side chains introduced at αS583 led to a large reduction in amiloride affinity, suggesting that large side chains at position α583 protrude into the pore, and limit access of amiloride to this site.[171] The effects of Cys substitutions at the amiloride-binding ring on the inhibitory constant largely reflected an increase in the microscopic k_{off} rate, consistent with an effect on the bound complex.[210] An adjacent three residue Gly/Ser-X-Ser tract that forms the primary selectivity filter may also have an important role in amiloride binding. Mutations introduced in the first position of this tract in the α- or β-subunit were associated with a large reduction in amiloride affinity,[211–213] suggesting that amiloride also interacts with this site.

The introduction of Cys residues at the amiloride-binding ring rendered channels sensitive to block by external Zn^{2+}-, Cd^{2+}-, and sulfhydryl-reactive methanthiosulfonate (MTS) derivatives.[72,76,163,209,212] Moreover, mutations of these residues reduced single channel conductance.[163,171] This site was also shown to be located within the membrane electrical field.[76,163,171] These observations suggest that this ring of residues

line the conducting pore, as was observed in the homologous residue in the resolved ASIC1 structure.[70]

SELECTIVITY FILTER

A three residue tract (Gly/Ser-X-Ser) starting four residues distal to the amiloride-binding site has a key role in conferring cation selectivity (Figure 30.5). Systematic examination of the ENaC TM2 domains by several groups found that mutations of either the first and/or third residue within the Gly/Ser-X-Ser tract of the α-, β-, and γ-subunits resulted in significant K^+ permeation.[169,208,209,211,212,214] Certain substitutions of the third residue within this tract in the α-subunit allow for permeation of divalent cations.[208]

It is unclear whether backbone carbonyl oxygens or side chains within this three residue Gly/Ser-X-Ser tract face the lumen.[213–215] Kellenberger et al. initially proposed that carbonyl oxygen atoms from third position Ser residues provide a Na^+-binding site, based on a positive correlation between increases in K^+ permeability and the volumes of several substituted residues at αSer589.[214] Alternatively, Sheng et al. proposed that the side chains of the selectivity filter residues faced the pore lumen, based on the sensitivity of channels with an introduced Cys at the first or third residue in the selectivity filter to externally applied Cd^{2+}.[213] This proposed side chain orientation is also consistent with the need for a hydroxyl group at position α589 to prevent K^+ permeation.[169] The dispute regarding the orientation of residue side chains within the selectivity filter will likely remain until a high-resolution structure of ENaC or ASIC in an open state is available.

The distal (C-terminal) portions of the TM2 domains have three well-conserved negatively charged residues that likely line one face of an α helix. The introduction of mutations at specific sites containing acidic residues has been reported to reduce channel activity without altering surface expression[216] and result in K^+ permeation, suggesting that some of these residues may also have a direct or indirect role in conferring cation selectivity.[170]

CHANNEL GATE

A five residue motif (G^{432}DIGG^{436}) in the outer part of the ASIC1 TM2 domain has been proposed to function as the desensitization gate[70] (Figure 30.5). Gly432 is conserved among ASICs and is homologous to Ala442 in MEC4, the degenerin site where substitutions with a bulky residue result in degeneration of specific neurons in *Caenorhabditis elegans*.[217,218] The three ENaC subunits bear a Ser at this site. Mutations at the degeneration site in MECs, ASICs, and ENaCs have the common phenotype of an increase in channel open probability,[76,78,79,219] suggesting similar gating machinery. ENaCs with a Cys substitution at the degenerin site are activated by externally applied sulfhydryl reagents.[76,79,219] Modification of Cys residues at the degenerin site is dependent on channels being in an open state, suggesting that either: (1) there is an extracellular gate controlling access to the degenerin site or (2) that this site undergoes a conformational change in association with channel-gating that alters the accessibility of the cysteine side chain to chemical reagents.[79] The desensitization gate of ASIC1 is formed by a helical bundle crossing, which favors the second possibility.[70]

In addition to the degenerin site, external sulfhydryl reagents activate channels with Cys substitutions at nearby sites with a periodicity suggestive of an α-helical structure,[76] suggesting that an extended helical region functions as a gating domain.[76] Consistent with the hypothesis, the sulfhydryl reactive agent MTSET transitions channels with an introduced Cys distal to the α-subunit degenerin site to a high open probability state. Furthermore, these modified channels lose their response to external Na^+ and to laminar shear stress.[182,220] Carattino and co-workers reported that mutations at multiple sites within the TM2 of the α-subunit altered the magnitude and time course of ENaC activation by laminar shear stress, suggesting that this region has a role in the channel's response to external mechanical forces.[221] While ENaCs do not undergo desensitization, these results suggest that the primary gate within ENaCs is located in the same region as the ASIC1 desensitization gate.

Previous studies also suggest that there are additional sites within the TM1 and TM2 domains that affect rates of ion permeation or channel-gating. Several amiloride-binding site mutants (see above) exhibited an altered single channel conductance, although cation selectivity was preserved.[72,163,171] Moreover, channels with a cysteine residue at the γ-subunit amiloride-binding site (γG537) had a high open probability, failed to respond to shear stress stimulus, and lacked a Na^+ self-inhibition response.[222] These results suggest that the αS583-βG525-γG537 ring participates, either directly or indirectly, in ion permeation and channel-gating, in addition to its role in amiloride-binding. The carboxyl-terminal portion of TM2 may also have a role in the regulation of gating.[223,224]

STRUCTURE OF THE PORE

Analogous to the ASIC1 pore structure, the ENaC pore is likely lined primarily by the TM2 helices. The TM1 helices may insulate the TM2 helices from the lipid bilayer. However, uncertainties regarding the ENaC pore structure remain, due in part to the distinct pore structures of the two ASIC1 structures that

apparently were resolved from channels in the desensitized state.[69,70] It is not clear which structure represents the native pore conformation and the extent to which structural distortion was generated by crystal lattice contacts. It remains possible that these two structures represent two native conformations that are captured at different stages of desensitization. The TM domains in the original structure[69] are asymmetric with the TM2 helices of two of the subunits showing a $\sim 30-33^\circ$ kink at Gly 435, with the third subunit being nearly straight. The kinks bring the TM2 helices close together, allowing Leu 440 side chains to occlude the pore and separate the outer and inner vestibules. In contrast, the second structure has a symmetric pore design with all TM helices tilted at $\sim 50^\circ$ relative to the membrane normal, with the TM2 helices crossing at the proposed desensitization gate ($G^{432}DIGG^{436}$) that separates the extracellular and intracellular vestibules.[70] The defined degenerin site is located at the top of the gate. Assuming that the ENaC pore has a similar structure, the amiloride-binding and selectivity filter sites would be located within the intracellular vestibule. Mutagenesis studies of the ENaC pore are consistent with an asymmetric open state pore structure.[76,163,169,171,208,210–213,219]

Cytoplasmic Carboxyl-Terminus

The region immediately following TM2 contains clusters of basic residues that effect channel-gating through interactions with acidic phospholipids, such as PIP3, as well as cation selectivity.[175,225–228] A major function of the carboxyl-termini appears to be related to the internalization of the channel complex, through a well-characterized Pro-Tyr (PY) motif (PPPXYXXL) that interacts with the ubiquitin ligase Nedd4-2.[128,132,229,230] ENaC subunit ubiquitination serves as a signal for channel internalization from the plasma membrane.[132] It is unclear whether the YXXL sequence within this motif serves as an independent signal for channel internalization. Other sites within the carboxyl termini may influence rates of channel endocytosis. For example, an A663T polymorphism in the α-subunit of the human ENaC affects rates of channel internalization from the plasma membrane.[231,232] ER exit of ENaC is regulated by a signal within the α-subunit carboxyl cytoplasmic tail.[99]

The carboxyl-termini have sites that are targeted by specific protein kinases that modulate ENaC activity via phosphorylation. These kinases include an extracellular regulated kinase (ERK), casein kinase 2 (CK2), a serum and glucocorticoid regulated kinase (SGK1), and a G-protein-coupled receptor kinase (Grk2).[233–237] ERK1/2-dependent phosphorylation of the carboxyl-termini of the β- and γ-subunits enhances ENaC's interactions with Nedd4.[233] Both forskolin and phorbol 12-myristate 13-acetate (PMA) have been reported to enhance phosphorylation of the β- and γ-subunits, although the target residues that are phosphorylated have not been identified.[238] A region in the proximal part of the carboxyl-terminus of the α-subunit has a role in conferring sensitivity to a staurosporine-sensitive kinase that has not been identified.[239] The carboxyl termini also bind α spectrin and possibly actin, linking the channel to the cytoskeleton.[122,124] Grk2 activates ENaC by phosphorylating the carboxyl terminus of the β-subunit, and prevents Nedd4-2-dependent inhibition of ENaC.[236] Cysteine residues in the amino and carboxyl termini of ENaC subunits may participate in the inhibition of ENaC that is observed with intracellular thiol reactive reagents.[177] Selected cytoplasmic cysteine residues in the β- and γ-subunits are targets of modified palmitoylation.[98] β-Subunit palmitoylation modulates channel-gating, possibly by facilitating interactions between cytoplasmic domains and the plasma membrane.[98]

Cation Permeation and Selectivity

While a detailed understanding of the molecular mechanisms underlying permeation and selectivity awaits a high-resolution structure of ENaC in the open state, there is a growing body of information regarding ion permeation and selectivity.[81,240,241] Organic or inorganic cations larger than Na^+ are unable to pass through the channel, in contrast to voltage-gated Na^+ channels, suggesting that permeant cations must dehydrate to cross the narrowest part of the channel pore (i.e., the selectivity filter).[242,243] Within the Gly/Ser-X-Ser tract that comprises ENaCs selectivity filter,[169,211,214] backbone carbonyl oxygens or hydroxyl oxygens present on the side chains of Ser residues may coordinate permeating Na^+ or Li^+ ions.[213,214]

The selectivity sequence of ENaC ($Li^+ > Na^+ >>> K^+$, organic cations) suggests that the relative permeability of an ion is inversely related to its ionic size, a relationship consistent with a mechanism in which ENaC discriminates cations through molecular sieving.[208,214] Alternatively, cation selectivity could be achieved by placing a negatively (or partially negatively) charged site with strong field strength that preferentially binds small cations within the channel pore.[242,243] In this regard, the selectivity sequence for ENaC corresponds to sequence XI of Eisenman. This sequence was determined based on the presence of strong electrostatic interactions between ions and the selectivity site that override differences in dehydration energies for ions.[244] Interestingly, the selectivity filter of a voltage-gated Na^+ channel has a high-field-strength anionic coordination site.[245]

Selectivity filters appear to be flexible, not static, structures.[246–250] A dynamic selectivity filter of ENaC

has been suggested,[76] and appears to be likely in the light of the resolved ASIC1 structures. Both ASIC1 structures likely represent a desensitized state, and the selectivity filter residues are not in close proximity.[81] We speculate that these residues are brought sufficiently close in the open state to interact with permeating cations. A recent study of ASIC1 is consistent with this notion.[75]

Mechanisms of ENaC-Gating

ENaC-gating is characterized by unusually long open and closed times (up to seconds or even tens of seconds) compared to other channels such as voltage-gated channels (Figure 30.1). This gating pattern seems appropriate for this channel, given its major physiological role of mediating bulk Na^+ transport across the apical membrane of epithelial cells, for which slow transitions between open and closed states may be beneficial for transport efficiency. Transitions between open and closed states appear to occur spontaneously. Another feature of ENaC-gating is the high variability in open probability observed in patch-clamp recordings.[11,251,252] Subunit composition and regulatory factors that affect gating may account for this variability.[252,253] As discussed in detail below, proteolytic cleavage of ENaC subunits converts channels that have a low open probability to channels that exhibit either an intermediate or high open probability.[13,83,97,113] Mechanical forces, external metals, and temperature have also been shown to affect channel-gating.[181,182,184,202,220,221] Studies on Na^+ self-inhibition and effects of metals on ENaC-gating have raised the question of whether ENaCs should be considered a ligand-gated channel, similar to FaNaCh and ASIC.[81,184,254]

A detailed understanding of ENaC-gating mechanisms is lacking, despite the identification of several sites within ENaC where the introduction of mutations affects ENaC-gating kinetics. These sites are present within the amino-terminal domain,[165,166] the extracellular domain,[13,83,113,181,182,184,255] TM2,[76,79,219,221,224] and the intracellular carboxyl-terminal domain.[226,227,256] However, it is unclear whether these different regions control channel-gating in an independent or coordinated manner, nor is it known whether there is a single gate or multiple gates. The location of the ENaC gate is another open question, although the region corresponding to the desensitization gate of ASIC1 is an attractive candidate.

Several recent studies have suggested that the pore helix of cation channels may be a central gating structure.[221,257–260] Yeh and co-workers suggested that the regulation of TRPV5 (a member of the transient receptor potential channel subfamily)-gating by extracellular and intracellular protons is mediated by a rotational movement of the pore helix, and the subsequent closing of a gate within the selectivity filter gate.[260] As the amino-terminal helical portion of the TM2 helices of ENaC participates in channel-gating,[76,79,219] it is possible that rotation of the TM2 helix that is initiated by conformational changes at other sites of the channels alters ENaC-gating kinetics, as suggested for ASIC1.[261] Li and co-workers proposed a gating motion for ASIC1 involving a straightening of the tilt of TM2 without significant rotation.[75]

Permeation and gating of ion channels were proposed to be two independent processes 60 years ago.[262] While previous studies have supported this concept, recent studies suggest that connections exist between permeation and gating.[263,264] For example, channel gating is often modulated by permeant or blocking ions.[265,266] Mutations within selectivity filters are associated with changes in gating kinetics in K^+ channels, voltage-gated Na^+ channels, and ENaC.[168,211,221] Lu and co-workers provided evidence suggesting conformational changes of the selectivity filter contribute directly to the spontaneous gating of an inward rectifier K^+ channel (Kir2.1).[267] Significant differences in the selectivity filter structure of KcsA K^+ channel were observed when the crystals were soaked in low-K^+ and high-K^+ solutions,[268] suggesting that the selectivity filter of this channel is flexible. Molecular simulations using the high resolution structures of bacterial K^+ channels support this idea of a flexible selectivity filter.[269,270] Conformational changes in the selectivity filter have been proposed to occur in the ligand-initiated gating of cyclic nucleotide-gated ion channels.[271] A similar notion has been proposed for inward rectifier K^+ channels.[272,273] We anticipate that future studies will examine whether ENaC's selectivity filter also serves as a gate.

ENaC REGULATION

ENaC is subject to a wide variety of regulatory influences that alter channel activity over long or short time periods in order to respond to the physiologic needs of the organism. In the kidney, these regulatory influences determine the final Na^+ concentration of urine, which may vary from virtually Na^+ free to >100 mM. Abnormalities in these regulatory mechanisms in the cortical collecting duct have been convincingly linked to excess Na^+ reabsorption and hypertension, when disordered regulation leads to gain-of-function; and salt-wasting, hypotension and hyperkalemia when abnormal regulation leads to loss-of-function.[207] Altered or abnormal regulation of ENaC in the lung

has been linked to abnormal alveolar fluid clearance in disease states such as cystic fibrosis, high altitude pulmonary edema, and acute lung injury.[153,154,274–276] In many cases, studies of abnormal ENaC function in disease states have complemented basic observations concerning channel function made in experimental settings, and led to remarkable insights concerning molecular mechanisms of regulation of channel activity.

Channel activity is subject to regulation through alteration of one of its intrinsic kinetic properties, either its number, open probability or single channel conductance. Since significant changes in single channel conductance are not found under physiologic conditions, channel regulation may be considered primarily as a matter of alterations in channel number and/or open probability. Thinking about channel regulation from this perspective would seem to simplify the subject, and certainly provides a framework within which regulation may be considered. However, the subject remains enormously complex given the number of regulatory influences that may modify either channel number or open probability.

There has been a significant paradigm shift, in that we now recognize that "near silent" channels are present in the membrane, in addition to constitutively active channels.[11–13] These "near silent" channels are capable of activation and may be viewed as the extreme case of open probability regulation, where channels move from very low to a measurable open probability, giving the appearance of increased numbers of channels.[13] The levels of "near silent" channel expression in the distal nephron under various physiological and pathological conditions are currently unclear. Channel regulation serves to either enhance or diminish Na^+ reabsorption from luminal fluids of the distal nephron, lung or colon, in accord with the needs of the organism. Given the wide variations in rates of Na^+ reabsorption and luminal Na^+ gradients that this involves, other intrinsic regulatory influences are required to maintain constant cell volume and ion gradients. To respond to these needs under normal physiologic conditions, channel activity is regulated by a number of hormones, including steroids, vasopressin, and insulin; by a variety of accessory proteins; by kinases, proteases, methyltransferases, and other signaling mediators; by other channels such as CFTR; and by ion concentrations and pH.

Cellular Regulation

Ubiquitination and Deubiquitination

Liddle syndrome is a hereditary form of salt-sensitive hypertension associated with increased ENaC activity.[207,277,278] The most common defects in ENaC primary structure leading to this disorder involve the proline-rich regions in carboxyl-termini of the β- or γ-subunit.[277,279–281] Rotin and colleagues used this region of the β-subunit as bait in a yeast two-hybrid screen to identify proteins that interact with ENaC and might regulate ENaC expression. They isolated the protein Nedd4 (Neuronal precursor cells Expressed Developmentally Downregulated) using this technique. In a series of elegant studies they examined the role of this protein in the regulation of ENaC expression.[132,282,283] Nedd4 is an E3 ubiquitin ligase composed of a C2 domain, three or four WW domains that are protein interaction modules, and a ubiquitin ligase Hect domain. The WW domains of Nedd4 bind ENaC, with the strongest interaction being between the carboxyl-terminus of the β-subunit and the third WW domain.[284] The Hect domain is an E3 ligase that receives ubiquitin from an E2 protein and transfers ubiquitin to lysines on target proteins. The C2 region is a Ca^{2+}- and phospholipid-binding domain. It is not present on all Nedd4 isoforms and, based on oocyte studies, does not appear to be essential for inhibition of ENaC expression.[230,285,286] This domain does, however, serve to localize Nedd4 to plasma membrane in response to an increase in cytosolic [Ca^{2+}],[287] and mediates association with annexin XIIIb, which may be involved in apical membrane targeting in epithelia.[288]

Nedd4-2, the isoform most active in binding ENaC, is detected in tissues that express ENaC. The Nedd4-2 WW domains interact *in vitro* with the proline-rich region of carboxyl terminus of the β- and γ- (and possibly α-) subunits of ENaC.[289–291] Considerable evidence indicates that the interaction between Nedd4-2 and ENaC results in ubiquitination of the channel (Figure 30.6). ENaC has been shown to be ubiquitinated in endogenously expressing A6 cells, and when overexpressed along with Nedd4-2 in HEK-293 cells.[108,132] Co-expression studies with Nedd4-2 and ENaC in oocytes demonstrated that Nedd4-2 decreases ENaC surface expression, and that this is dependent both on the E3 ligase domain of Nedd4-2 and on the presence of Lys residues on the amino-termini of the target subunits.[132] Taken together, these studies strongly support the model that surface expression of ENaC is regulated by ubiquitination, which serves as a signal for retrieval from the plasma membrane. It is likely that ENaC is ubiquitinated at other cellular sites, including the endoplasmic reticulum. Unassembled subunits are likely degraded by the proteasome by a process involving polyubiquitination, while fully assembled trimeric channels are degraded by either the proteasome or lysosomal–endosomal pathway following ubiquitination at the cell surface.[93,95,108,132] At present, it is unclear whether monoubiquitination of

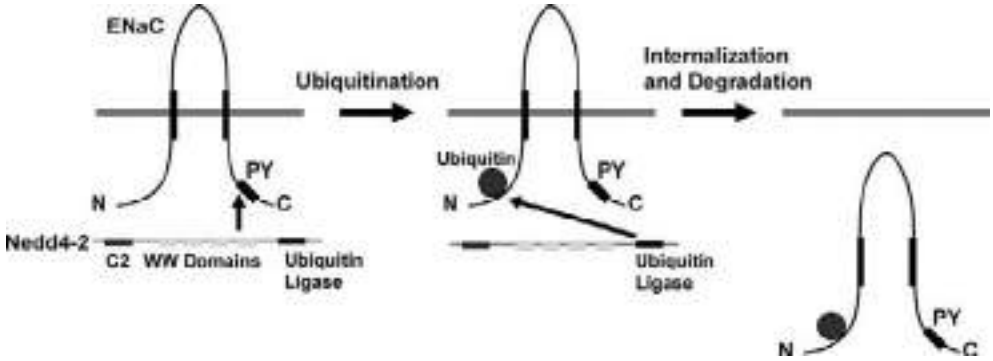

FIGURE 30.6 **Nedd4-2-dependent regulation of ENaC surface expression.** Nedd4-2 binding to ENaC subunits is facilitated through interactions between WW domains on Nedd4-2 and the PY motifs on the β- and γ-subunits. Nedd4-2-dependent ubiquitination of ENaC subunits targets the channel for internalization and degradation. *(adapted from ref. [295]).*

ENaC occurs at the cell surface. However, there is considerable evidence suggesting that ubiquitination is a signal for channel internalization from the plasma membrane,[292] and that channel internalization is a dynamin-dependent,[126] clathrin-dependent,[133] as well as caveolin-dependent process.[293]

The interaction between Nedd4-2 and ENaC is itself subject to regulation by specific hormones and kinases.[233,236,294–300] The regulation of ENaC by Nedd4-2 represents a final common pathway of several regulatory influences affecting ENaC surface expression, providing further evidence for the importance of this interaction in ENaC regulation (see below).

Recent work has elucidated an important role for deubiquitinating enzymes (DUBs) in the regulation of ENaC expression and trafficking in cells.[134,135] Specifically, the DUB Usp2-45 was found to be upregulated by aldosterone in mouse polarized collecting duct ($mpkCCD_{c14}$) cells, which causes deubiquitination of ENaC, and an increase in ENaC surface expression and activity.[134] The subcellular site(s) of action of Usp2-45 on ENaC and its precise physiological role are currently unclear. Butterworth and colleagues identified another DUB, UCH-L3, in the early endosomal compartment of these cells, which also deubiquitinates ENaC, and enhances the recycling of ENaC to the apical membrane.[135] UCH-L3 may play an important role in reversing Nedd4-2-mediated ubiquitination of ENaC upon retrieval from the plasma membrane, thereby rescuing ENaC from degradation and promoting apical recycling of the channel (Figure 30.4). Finally, Usp10 was recently identified as a vasopressin-stimulated DUB, leading to enhanced ENaC abundance and activity at the plasma membrane.[301] In summary, DUBs may respond to hormonal inputs and appear to antagonize Nedd4-2-dependent ubiquitination and inhibition of ENaC, promoting ENaC stabilization and function at the plasma membrane.[302]

Kinases

Protein phosphatase inhibitors, such as okadaic acid, activate ENaC,[303] while nonspecific kinase inhibitors, such as staurosporine, inhibit basal channel activity,[239,304] suggesting that kinases play an important role in regulating the channel. In many cases, the regulation of ENaC by a protein kinase is indirect, with kinase activation occurring within a pathway of hormonal regulation or cellular stress. Examples of this are: (1) SGK1 activation by steroid hormones induces SGK1-dependent phosphorylation of Nedd4-2 (the subsequent binding of 14-3-3 proteins to phosphorylated Nedd4-2 prevents the interaction of Nedd4-2 with ENaC subunits, and reduces ubiquitin-based retrieval of channels from the plasma membrane[305–309]) (Figure 30.7); (2) insulin-dependent activation of phosphatidyl-inositol 3 kinase and 3-phosphoinositide-dependent kinase 1 results in the phosphorylation and activation of SGK1 and ENaC;[307,310] (3) activation of protein kinase A by adenylate cyclase and cAMP in response to vasopressin or beta-adrenergic agonists leads to phosphorylation of Nedd4-2 at sites that overlap the SGK1 phosphorylation sites, and a reduction in ENaC endocytosis,[297] as well as exocytotic insertion of Na^+ channels into the plasma membrane;[111,311,312] (4) activated IKKβ, the kinase-regulating NF-κB, interacts with the cytoplasmic carboxyl terminus of β ENaC[313] and phosphorylates Nedd4-2 at a residue that is also targeted by SGK1 and PKA, reducing channel endocytosis[300] (IKKβ provides a mechanism of integrating inflammatory cascades and ENaC activation); (5) endothelin-dependent activation of Src kinase results in a decrease in channel open probability without directly phosphorylating channel subunits[314]; (6) selected protein kinase C isoforms also reduce channel open probability in a Ca^{2+}-dependent manner, protein kinase C also decreases expression of the β- and γ-subunits, which is dependent on activated

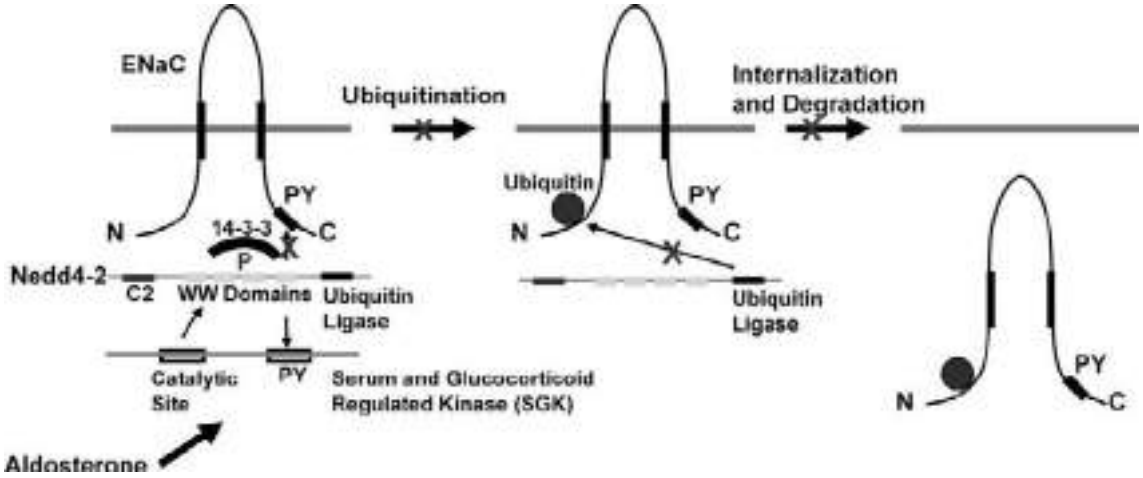

FIGURE 30.7 **Aldosterone modulates the interaction between Nedd4-2 and ENaC.** Sgk1 is targeted to Nedd4-2 through interactions between a PY motif on Sgk1 and WW domains on Nedd4-2. Sgk1-dependent phosphorylation of Nedd4-2 results in the recruitment of a 14-3-3 protein that prevents Nedd4-2 binding to ENaC. *(adapted from ref. [295]).*

ERK kinase[315–317]; (7) AMP-activated protein kinase (AMPK) is a ubiquitous metabolic sensor that phosphorylates Nedd4-2, enhances Nedd4-2 binding to β ENaC, and inhibits ENaC activity and surface expression.[77,299,318]

ENaC is also a substrate for kinases that are involved in its regulation. Studies of ENaC expressed in MDCK cells have demonstrated increased phosphorylation of the β- and γ-subunits in response to stimulation by aldosterone and insulin.[238] Phosphopeptide mapping indicated that the phosphorylated sites were carboxyl terminal Ser and Thr residues.[238] Shi and colleagues described phosphorylation of Ser631 in the β-subunit and Thr599 in the γ-subunit by the pleiotropic but essential kinase CK2.[234] Kunzelmann and colleagues found that a specific CK2 inhibitor blocked ENaC activity, and expression of a trimeric channel lacking both CK2 sites inhibited ENaC conductance and rendered ENaC insensitive to CK2.[237] They concluded that phosphorylation by CK2 is essential for ENaC activation and partly regulates ENaC surface expression. Garty and colleagues also described phosphorylation of βThr613 and γThr623 by the extracellular regulated kinase (ERK).[233] ERK-dependent phosphorylation of ENaC facilitates interactions between the channel and Nedd4-2, thereby inhibiting ENaC activity. SGK1 increases channel open probability by directly phosphorylating the carboxyl-terminus of the α-subunit at Ser-621.[235] Finally, insulin has been described to increase phosphorylation of a fully mature 65 kDa form of α ENaC in cultured epithelial cells, which correlated with an increase in channel activity.[319] The kinase-mediating of this effect was not directly identified, but the protein kinase C inhibitor chelerythrine blocked the insulin stimulation of transport and subunit phosphorylation.

It has also been reported that the G-protein-coupled receptor kinase, Grk2, phosphorylates Ser-633 in the carboxyl-terminus of the β-subunit.[236] Phosphorylation at this site renders the channel insensitive to regulation by Nedd4-2, resulting in increased surface expression and channel activity. This finding is intriguing, as: (1) it is the first report of a G-protein receptor kinase directly regulating an ion channel; and (2) increased Grk2 activity has been associated with hypertension.[320] Grk2 may also phosphorylate Nedd4-2, although the relevant site(s) and functional significance of this phosphorylation are unclear.[321] A recent study suggests that Grk2 may also stimulate ENaC via a kinase-independent mechanism that requires its interaction with α-subunits of the Gq/11 family.[322]

Another family of kinases linked to human hypertension is the WNK (with no lysine) family of serine-threonine kinases.[323] These kinases are prominently expressed in the distal convoluted tubule, connecting segment, and cortical collecting duct of the kidney (i.e., the aldosterone-sensitive distal nephron), where they coordinate with angiotensin II and aldosterone signaling pathways.[324] WNK mutations lead to hypertension and hyperkalemia typical of pseudohypoaldosteronism type II (PHA II).[325] WNK4 inhibits the renal Na,Cl cotransporter (NCC) and ROMK, and mutations associated with hypertension relieve the inhibition of NCC, but enhance inhibition of ROMK.[323] These observations suggested that under normal physiologic conditions, WNK4 regulates the balance between renal Na^+ reabsorption and K^+ excretion, but mutations would lead to exaggerated Na^+ reabsorption and hypertension

with hyperkalemia, due to impaired K^+ excretion. In addition to NCC and ROMK, one group found that WNK4 also inhibits ENaC *in vitro*, and this inhibition by WNK4 is relieved by SGK1 phosphorylation near the WNK4 C-terminus.[326] In contrast, another group suggested that WNK4 activates ENaC.[327] Another member of this family, WNK1, has also been implicated in activating ENaC.[327] Interestingly, intronic deletions that could lead to hypertension and hyperkalemia result in overexpression of WNK1.[328] Aldosterone has also been shown to stimulate expression of a kidney-specific isoform of WNK1, and overexpression of this kinase stimulates Na^+ reabsorption in cultured collecting duct cells, and in overexpression systems.[329] WNK1 expression activates SGK1 in a PI-3 kinase-dependent manner, indicating that the kinase activates ENaC by increasing its expression at the apical membrane of collecting duct cells, contributing to the human hypertension seen in association with PHA II.[327,330]

As suggested above, the E3 ubiquitin ligase Nedd4-2 has emerged as a central convergence point for the regulation of ENaC and other transport proteins in cells. A growing number of kinases have been shown to phosphorylate Nedd4-2, modulate Nedd4-2 function, and thereby regulate ENaC.[331] These include the aldosterone-induced kinase SGK1,[306] vasopressin-stimulated PKA,[297] the metabolic sensor AMPK,[299] the NF-κB inflammatory mediator IKKβ,[300] Grk2,[321] and the insulin-stimulated kinase Akt1.[332] In general, these kinases modulate the apparent binding affinity of Nedd4-2 for ENaC and/or 14-3-3 scaffolding proteins. Of note, additional putative Nedd4-2 phosphorylation sites have been recently identified by mass spectrometry that may be targets of the c-Jun N-terminal kinase (JNK1), and possibly other kinases.[333] Unlike the above paradigm, where kinases regulate protein−protein interactions involving Nedd4-2, these novel target phosphorylation sites appear to play an important role in regulating Nedd4-2 catalytic function.[333]

Proteases

Proteolysis of ENaC subunits has an important role in regulating ENaC activity. The first hint that proteases modulated ENaC activity was that serine protease inhibitors reduced transepithelial Na^+ transport across toad urinary bladder.[334] Subsequent studies identified a channel-activating protease, or CAP,[195] and demonstrated that extracellular trypsin activated ENaC by increasing channel open probability.[114] Following these initial observations, other proteases have been identified that activate ENaC when either co-expressed with the channel in heterologous expression systems or when added to a solution bathing cells expressing ENaCs. These channel activating proteases include prostasin (also referred to as CAP1), TMPRSS4 (transmembrane protease serine 4 or CAP2), and matriptase (or CAP3), elastase, chymotrypsin, kallikrein, and plasmin.[113,114,195,199,335–339]

Proteolytic processing of ENaC subunits occurs within the biosynthetic pathway. This is likely mediated by furin, a member of the proprotein convertase family of serine proteases that is expressed primarily in the trans-Golgi network.[83,340] There are two furin cleavage sites within the extracellular domain of the α-subunit, and a single site within the extracellular domain of the γ-subunit.[83,85] Furin-dependent cleavage of the α-subunit excises a 26 residue inhibitory fragment. Simply deleting this 26 residue tract from the α-subunit in the absence of subunit cleavage was sufficient to activate the channel.[84] Furthermore, a synthetic peptide corresponding to the released fragment is a reversible channel inhibitor.[84] An 8 residue tract, embedded within the 26 residue fragment, is responsible for the inhibitory properties of this fragment.[86]

While the α-subunit is cleaved by furin twice, releasing an inhibitory fragment, the γ-subunit is cleaved only once by furin. As was observed with α-subunit processing by furin, cleavage at two sites spanning an inhibitory tract within the γ-subunit increases channel activity. While furin cleaves the γ-subunit at a site preceding an embedded inhibitory tract,[200] multiple proteases have been shown to cleave the γ-subunit at sites distal to the inhibitory tract. Among the proteases that cleave the γ-subunit distal to the inhibitory tract are prostasin, TMPRSS4 (CAP2), elastase, and plasmin.[199,200,338,339,341] Deleting the γ-subunit inhibitory tract dramatically increases channel activity, even in the absence of γ-subunit cleavage.[200,342] An 11 residue tract is responsible for the inhibitory properties of the released fragment.[342] With regard to channel activation, release of the γ-subunit inhibitory tract has a more profound effect than release of the α-subunit inhibitory tract.[343]

At the single channel level, ENaCs exhibit a highly variable open probability. While ENaCs often exhibit open and closed times in the order of seconds to tens of seconds, a distinct population of ENaCs have very brief open times and long closed times.[11–13] Caldwell and co-workers have shown that this latter population of channels responds to external trypsin, with a dramatic increase in channel open probability.[13] These inactive channels likely represent a population of channels whose subunits have not been processed by proteases. Channels with α-subunit furin site mutations that have retained α- and γ-subunit inhibitory tracts have a very low open probability that reflects a dramatically enhanced reduction in ENaC activity in response to external Na^+ (referred to as Na^+ self-inhibition). When these channels are examined in the

presence of a low external [Na^+], their activity dramatically increases.[115]

Both processed (i.e., cleaved) and unprocessed subunits are expressed at the cell surface.[93,112] These nonprocessed channels provide a pool of ENaCs that could be activated by proteases in a regulated manner. In this regard, rats placed on a low-Na^+ diet or receiving exogenous aldosterone have increased levels of whole kidney expression of the processed form of the γ-subunit.[142,344–347]

The sites of protease cleavage in the α- and γ-subunits are located with the finger domain. A model of the α-subunit generated by Kashlan and co-workers suggests that the α-subunit inhibitory tract binds to sites at an interface of the finger and thumb domains. They proposed that the inhibitory tract reduces channel activity by stabilizing the movement of the finger domain relative to the thumb domain.[81,82]

Syntaxins

The factors regulating ENaC delivery to the apical membrane in epithelial cells have not been fully-defined. The SNARE proteins (soluble N-ethylmaleimide sensitive factor attachment protein receptors) have been linked to directed exocytosis and intracellular trafficking in a number of tissues.[348] A typical interaction involves binding of vesicle-associated v-SNARES to target membrane-associated t-SNARES. These interactions may be regulated by accessory proteins such as Munc 18.[349] The t-SNARE syntaxin 1A has been demonstrated to interact directly with ENaC in co-immunoprecipitation experiments, and overexpression of this protein inhibited ENaC expression in oocytes.[116,350] This effect was blocked by co-expression of Munc 18. These findings implicate the SNARE proteins in the process of exocytosis of ENaC, but are somewhat counterintuitive in that overexpression of the trafficking partners results in downregulation of the channel. The results suggest that the balance of t- and v-SNAREs may regulate this process, and that overexpression alters this interaction in a negative fashion.

The direct interaction of syntaxin 1A and ENaC suggests that there are cargo-specific interactions between SNARE proteins and apical membrane resident proteins such as ENaC. In a series of studies, Condliffe and colleagues identified domain-specific interactions between the carboxyl-termini of ENaC subunits and the H3 domain of syntaxin 1A. Interestingly, there was an effect of the H3 domain to decrease ENaC open probability, suggesting that SNARE proteins may regulate both channel exocytosis and gating.[118,119] A more recent study suggests that syntaxin 1A regulates ENaC function by multiple mechanisms that include PKA, phospholipase C, PI-3 kinase, and MAP kinase signaling systems.[351] Distinct inhibitory and stimulatory domains of syntaxin 1A interact with ENaC subunits, and the overall effect of syntaxin 1A on ENaC function depends on distinct physiological conditions.

Cystic Fibrosis Transmembrane Conductance Regulator (CFTR)

Patients with cystic fibrosis (CF) have increased amiloride-sensitive transport in airway epithelia.[352] Indeed, increased ENaC activity in airway epithelia has been proposed as one mechanism for the drying of airway fluids, which promotes progression of airway disease. Lung specific overexpression of β ENaC or knockout of Nedd4-2 in mice results in a phenotype similar to CF airway disease in humans.[153,353] CF is caused by function impairing mutations in the cystic fibrosis transmembrane conductance regulator (CFTR), an ATP-gated Cl^- channel.[354] On the basis of studies comparing ENaC activity in the presence and absence of CFTR expressed in MDCK cells, Stutts and colleagues proposed that CFTR functions as a cAMP-dependent regulator of ENaC, and the absence of this function in CF airways explained the increased ENaC activity in CF patients.[355,356] Ling and co-workers demonstrated that inhibiting CFTR expression in a renal distal nephron cell line (A6) led to an increase in ENaC open probability.[357] Studies in *Xenopus* oocytes or other overexpression systems have demonstrated that CFTR inhibits ENaC activity,[355,358,359] although this has been disputed.[360,361] However, several recent studies have questioned the role of CFTR in modulating ENaC activity.[362,363] There is also evidence that ENaC enhances the activity of CFTR, due to an increase in the number of channels expressed at the plasma membrane, as well as an increase in CFTR open probability.[364]

It is unclear if the interaction between CFTR and ENaC is indirect or results from a direct physical interaction. Changes in the intracellular [Cl^-], as well as electrochemical coupling, have been proposed as potential mechanisms by which CFTR regulates ENaC.[360,365] One group has proposed that there are interactions between the regulatory domain of CFTR and ENaC,[366] although the manner in which this interaction results in ENaC regulation is not clear. Moreover, ENaC–CFTR interactions appear to vary depending on the tissue of expression. For example, in sweat ducts, CFTR enhances ENaC activity.[367] Although both CFTR and ENaC are expressed in collecting duct principal cells, no significant abnormalities of renal Na^+ handling have been described in CF patients. In airway epithelial cells, CFTR and ENaC co-immunoprecipitate, and interestingly expression of the most common CF-causing ΔF508 CFTR mutation was recently found to increase the proportion of cleaved to uncleaved α ENaC that was bound to CFTR.[368] These

findings suggest that wild-type CFTR may normally impede the proteolytic stimulation of ENaC in airway cells, although mechanistic details of how this may occur are unclear. Elastase is one of perhaps several proteases that are present in inflamed CF airways and could contribute to an increase in the extent of γ ENaC subunit proteolysis.[113,199,337] Another recent study suggested that CFTR regulates the whole cell and surface expression of ENaC in airway epithelial cells, and that absence of this regulation may foster ENaC hyperactivity in CF airway epithelia.[369] In summary, with current data it is difficult to explain the regulatory interactions between CFTR and ENaC solely on the basis of physical interactions or alterations in electrochemical driving forces or the intracellular Cl^- concentration. The regulatory interactions may reflect changes in ENaC open probability (cleavage status) and surface expression, and vary among differing tissues, suggesting that other proteins or factors not yet recognized may be critical for functional CFTR−ENaC interactions.[370]

Methyltransferases

Methylation reactions have long been implicated in the activation of ENaC by aldosterone.[371,372] Aldosterone stimulates carboxylmethylation of proteins and phospholipids, and inhibition of these reactions blunts the ENaC response to steroid stimulation.[373] A few potential targets of methyltransferases have been identified: k-ras, β ENaC, and more recently, histones involved in the aldosterone-dependent control of transcription. Aldosterone induces k-ras in a *Xenopus* distal nephron cell line (A6) cells, and this small G-protein is methylated by isoprenylcysteine carboxylmethyltransferase (PCMTase). PCMTase is not induced by aldosterone, but is regulated by the enzyme S-adenosyl-homocysteine hydrolase that is stimulated by aldosterone and results in increased activity of PCMTase.[374] The enzyme (PCMTase) itself does not appear to stimulate ENaC, so it is unlikely to directly methylate the channel. Induction and processing of k-ras appears to be important for regulation of ENaC in A6 cells, but it is not clear that this occurs in mammalian tissues.[375] Direct methylation of β ENaC has been demonstrated using a partially purified membrane preparation as a source of enzyme, but the enzyme itself has not been identified. Methylation of ENaC in planar lipid bilayers has been shown to lead to an increase in open probability of the channel.[376] Edinger and co-workers identified a methyltransferase that activates ENaC when co-expressed with the channel in oocytes.[377] Methylation does not appear to play a role in basal channel activity.

Several recent studies have explored the role of Dot1a, which has histone H3K79 methyltransferase activity and is widely expressed in the kidney,[378] in the transcriptional control of α ENaC in response to aldosterone.[379] Aldosterone releases repression of α ENaC by reducing expression of Dot1a and its partner AF9,[380] and by impairing Dot1a−AF9 interaction via SGK1-mediated AF9 phosphorylation.[381] This network also appears to regulate transcription of several other aldosterone target genes, including SGK1.[382]

Calcium

Increases in intracellular calcium have been shown to inhibit ENaC activity by several groups.[252,383–385] This appears to happen as a biphasic process with a very quick early response and a slower downregulation after 5 minutes.[385] This is likely an indirect effect on the channel, as the activity of channels from cortical collecting ducts in excised patches exposed to increased cytosolic [Ca^{2+}] was not altered.[383] Activation of protein kinase C has been suggested to mediate the Ca^{2+}-dependent inhibition of ENaC, since this is known to decrease channel activity.[315] A second intriguing possibility, related to the delayed effect of Ca^{2+} on ENaC activity, is Ca^{2+}-dependent recruitment of Nedd4-2 isoforms that possess the Ca^{2+}-binding C2 domain to the plasma membrane,[285,286] with a subsequent increase in channel retrieval from the apical membrane.

pH and Oxidative Stress

Acidic intracellular pH, below 7.2, has been shown to decrease amiloride-sensitive Na^+ transport in isolated epithelial tissues, suggesting that intracellular pH may act as an intrinsic regulator of ENaC activity.[383,386,387] In conditions of ischemia or hypoxia where intracellular pH might fall, activation of AMPK might act to decrease channel activity, as noted above.[77] Hypoxia is known to decrease activity of ENaC through a decrease in channel expression in cultured type II alveolar cells, but the mechanism of this response is unknown. The effect of pH on channel activity appears to be direct. In excised, inside-out patches from apical membranes of rat cortical collecting tubule, a fall in pH from 7.4 to 6.4 resulted in a progressive and dramatic fall in open probability of the channel. The mechanism of this regulation is unknown. However, ENaC activity is clearly downregulated under cellular conditions where ATP is limiting.[388] It has been proposed that ENaC may be sensitive to changes in intracellular redox potential through oxidation of intracellular cysteine residues.[177] It has also been shown that transcription and expression of α ENaC subunit variants are suppressed by oxidative stress in lung epithelial cells.[389] Conversely, oxidative stress induced by hydrogen peroxide exposure appears to stimulate ENaC activity through a PI 3-kinase-dependent pathway in cultured kidney collecting duct cells.[390] Such oxidative stress-induced stimulation of

ENaC has been proposed to contribute to the pathogenesis of salt-sensitive hypertension. Similarly, superoxide formation and release by NADPH oxidase (NOX2) downstream of epidermal growth factor and Rac1 has been reported to stimulate ENaC open probability in the lung.[391]

Nitric Oxide

Several studies have shown that nitric oxide (NO) inhibits ENaC activity in both alveolar type II (AT II) cells and in cultured renal epithelial cells.[392–394] This effect may be important in inflammatory conditions such as acute respiratory distress syndrome, where NO levels may be elevated due to increased expression of inducible nitric oxide synthase (iNOS).[393] NO appears to inhibit the open probability of the channel in a cGMP-dependent manner.[392] Interestingly, aldosterone has also been shown to inhibit NO production from ATII cells, and this appears to be related to an effect of SGK1.[395] These results suggest a second, novel mechanism by which SGK1 could enhance ENaC activity through downregulation of iNOS activity, and a decrease in NO inhibition of ENaC open probability. In addition, the superoxide generation that occurs with oxidative stress appears to antagonize the NO-mediated inhibition of ENaC in lung slice patch-clamp experiments.[396]

Lipids

A number of membrane lipids and lipid intermediates have been shown to modify ENaC activity, often in complex ways. Inhibition of phospholipase A2 (PLA2) by aristolochic acid reduced arachidonic acid (AA) levels and increased ENaC activity in both *Xenopus* oocytes and A6 cells in culture.[127,397] Direct application of AA to rat cortical collecting ducts markedly reduced ENaC activity in a dose-dependent manner. While this effect was not reproduced by application of a non-metabolized analog of AA, 5,8,11,14-eicosatetraynoic acid (ETYA), it was reproduced by the CYP-epoxygenase metabolite 11,12-epoxyeicosatrienoic acid (EET).[398] A recent study found that, along with 11,12-EET, 8,9-EET, and 14,15-EET are additional eicosanoids that inhibit ENaC activity downstream of CYP2C8.[399] These results suggest that arachidonic acid effects are mediated by CYP epoxygenase metabolites. In contrast, in A6 cells current stimulation by PLA2 inhibition was blocked by ETYA, suggesting a direct effect of arachidonic acid on the channel, rather than the effect of a metabolite. The effect of ETYA on ENaC was to reduce open probability.[397] In oocytes, however, both arachidonic acid and ETYA inhibited ENaC, and this was due to an alteration in the number of surface channels. Analysis of ENaC surface expression showed a downregulation of channels consistent with a trafficking effect mediated by both increased endocytosis and decreased exocytosis.[127] Taken together, these experimental observations indicate that PLA2 activity leads to increased arachidonic acid levels that inhibit ENaC activity, but the precise molecular mechanisms remain in dispute.

Cellular phosphoinositides also affect ENaC function. Phosphatidylinositol-4,5-bisphosphate (PIP2) is a signaling molecule related to a number of intracellular processes, including endocytosis[400] and exocytosis.[401] It has also been implicated in the activation of several ion channels.[401] Patch-clamp studies have shown that anionic phospholipids, including PIP2 and PI-3,4,5-P3, can directly alter channel activity presumably by binding to cationic sequences within β and γ ENaC.[172,173] A distinct PIP3-binding site has been identified in the initial part of the carboxyl-terminus of the γ-subunit.[227] PIP2 also directly interacts with ENaC at a site distinct from the PIP3 binding site, and may be permissive for channel gating.[228] Interestingly, increases in cellular PIP2 levels have also been shown to increase surface expression of ENaC, presumably by stimulating exocytosis.[402] Kunzelmann and colleagues demonstrated that purinergic inhibition of ENaC by extracellular ATP in tracheal epithelia resulted in depletion of PIP2 from cells, and appeared to require a PIP2-binding region of the amino-terminus of the β-subunit.[174]

There are three isoforms of phosphoinositide-5-kinase, which produces PI-4,5-P2 from PI4P. These kinases have differing effects on cellular processes such as endocytosis.[400,403] PIP2 may thus induce varying effects on ENaC function, depending on the isoform of PI5K that is activated or the spatial localization of kinases and phosphatases that regulate PIP2 activity within the cellular microenvironment.[404] In summary, phosphoinositides functioning either as signaling agents or directly binding to ENaC affect channel activity.

Intracellular cytoplasmic Cys residues in β- and γ-subunits are modified by palmitoylation. Two Cys residues (Cys43 and Cys557) in the mouse β-subunit were shown to be modified by palmitoylation. Mutation of these Cys to Ala to prevent palmitoylation at these sites was associated with a reduction in channel open probability.[98] Secondary structural predictions suggest that Cys557 is within an amphipathic α helix near the second transmembrane domain, while Cys43 is in proximity to the first transmembrane α helix. Mueller and co-workers suggested that β-subunit palmitoylation modulates channel-gating by enhancing interactions between cytoplasmic domains and the plasma membrane.[98]

Intracellular Na^+

Since ENaC is present in epithelia that generate a steep lumen-to-bath Na^+ gradient, it is potentially

exposed to significant variations in both internal and external [Na^+]. ENaC is modulated by both intracellular and extracellular [Na^+]. Low levels of extracellular [Na^+] increase ENaC activity while elevated levels decrease activity, a process known as Na^+ self-inhibition.[405] Cytoplasmic [Na^+] is usually maintained quite low through the action of the Na^+,K^+-ATPase on the basolateral surface of epithelial cells. Since the pump is normally functioning well below its maximum capacity, Na^+ entry into cells is the rate-limiting step for Na^+ reabsorption. Under conditions of rapid increases in ENaC activity, regulation may also be achieved through increases in the intracellular [Na^+], a process referred to as feedback inhibition. This phenomenon has been observed in epithelial cells and *Xenopus* oocytes.[385,406] Feedback inhibition in response to an increase in the intracellular [Na^+] is a slow process that occurs over a period of minutes, in contrast to Na^+ self-inhibition, which occurs over seconds.[252] Studies in rat cortical collecting ducts suggested that PKC activation plays an important role in ENaC feedback inhibition.[407] Studies in oocytes indicated that this feedback inhibition was not readily seen in cells expressing ENaC with Liddle mutations that inhibit Nedd4-2-binding and ubiquitin-dependent internalization.[408] This finding focused attention on Nedd4-2 as the potential mediator of Na^+ feedback inhibition. In a series of studies in mouse mandibular duct cells, it was demonstrated that Na^+ feedback inhibition was dependent on Nedd4-2, and required binding of the second and third WW domains to carboxyl termini of β and γ ENaC.[409,410] More recent studies have suggested that the A-kinase anchoring protein 15 (AKAP-15) may bind to PKC and act in concert with PKC to regulate Na^+ feedback inhibition[411] or that intracellular [Na^+] may directly modulate the proteolytic activation of ENaC.[412] In summary, a few potential signaling pathways/mechanisms have been implicated in ENaC feedback inhibition by intracellular [Na^+], although the relative contributions for each and how they may integrate with one another in different cell types are still unclear.

Extracellular Na^+

Increases in extracellular [Na^+] inhibit ENaC activity, a process referred to as Na^+ self-inhibition. This phenomenon was originally observed in studies of native epithelial tissues in the setting of a rapid increase in extracellular Na^+ concentration.[413] This process reflects a decrease in channel open probability, and is not dependent on Na^+ influx.[2,182,201,202] Chraibi and Horisberger demonstrated that Na^+ self-inhibition is an intrinsic property of EnaC, and can be abolished by treatment with extracellular proteases.[202] Na^+ self-inhibition is a temperature-dependent phenomenon and has a large activation energy, suggesting that a conformational change occurs in association with the inhibition of channel activity by extracellular Na^+ that is presumably initiated by Na^+-binding to an extracellular site.[202,414] Numerous sites within the extracellular domains of the α- and γ-subunits have been identified where mutations alter Na^+ self-inhibition.[80,182,185,186,188,191,192] A number of important questions remain to be addressed regarding the Na^+ self-inhibition response, including: (1) where are the external Na^+-binding site(s); (2) what are the conformational changes that occur in response to Na^+-binding that result in a reduction in channel open probability; and (3) how do external proteases, presumably by cleaving ENaC subunits, diminish the Na^+ self-inhibition response?

Peroxisome Proliferators-Activated Receptors (PPARs)

The peroxisome proliferators-activated receptors (PPAR) have been implicated in the regulation of a wide variety of cellular processes. PPARγ is the pharmacological target of thiazolidinediones (TZDs) that have been used in the management of hyperglycemia associated with type II diabetes mellitus.[415] PPARγ is localized along the collecting duct in kidney,[416] and it is known that a side-effect of PPAR stimulation by TZDs is fluid retention.[417] It has been shown that TZD-induced weight gain was prevented in mice by amiloride or by deletion of the gene encoding PPARγ from collecting duct.[417] These studies suggested that TZDs increase ENaC activity in collecting duct cells, and increased mRNA for γ ENaC. These interesting results implicate PPARs in the regulation of transcription of at least one ENaC subunit that apparently leads to increased ENaC activity. More recent studies have suggested that the PPARγ-induced Na^+ reabsorption via ENaC in the kidney may be mediated through increased SGK1 expression.[418,419] In contrast, work from other groups suggest that PPARγ agonists do not activate ENaC[420] in cultured principal cells or decrease ENaC expression in the kidney.[421]

ATP

Luminal ATP signals through P2Y2 receptors and inhibits ENaC activity through activation of phospholipase C, activation of protein kinase C, and reducing cellular levels of PIP2 and channel open probability.[228,422,423] Recent studies suggest that this signaling pathway may have an important role in aldosterone escape, and the enhanced rates of Na^+ excretion in animals on a high-Na^+ diet.[424–426] Cellular release of ATP may be occurring through connexin 30 hemi-channels.[426]

Hormonal Regulation

Aldosterone

The major hormones regulating ENaC activity in a broad variety of tissues are corticosteroids. ENaC regulation by steroids is the subject of a separate chapter in this volume, and will not be discussed in detail here. Although non-genomic actions of aldosterone have been described in vascular and non-absorptive tissues,[427] the bulk of the available evidence supports the notion that steroid regulation of ENaC in Na^+-absorptive epithelia is mediated by processes dependent on transcription and translation. This transcriptional activity is driven by translocation of the steroid receptor to the nucleus following binding to its cognate ligand, and binding to specific domains within the genome. Interestingly, ENaC regulation varies somewhat by tissue. Steroid regulation of ENaC activity is largely due to an increase in the number of active channels in the apical membrane, although there is evidence for effects on open probability as well.[12,428,429] The increase in the number of active channels is not apparently a simple one-step procedure. An early increase in channels appears to be a trafficking event, with altered insertion or retrieval of already synthesized subunits.[142,143] A large part, but not all, of this effect is regulated by the aldosterone-induced proteins SGK1 and GILZ1 altering Nedd4-2-ENaC interactions and leading to increased membrane expression of the channel[305–307,430–433] (Figure 30.7). Synthesis and delivery of new channel subunits can be detected somewhat later in the course of steroid action in responsive tissues and, interestingly, also varies somewhat by tissue. In kidney, the predominant induced subunit is α, while in colon, the β- and γ-subunits are primarily induced.[434] This is true both at the mRNA and protein level. This phenomenon has been referred to as non-coordinate regulation, and suggests a degree of complexity of ENaC trafficking that is still not fully-understood.[92,435]

Vasopressin

Vasopressin has been shown to stimulate ENaC activity in the kidney and a number of epithelial cell lines derived from kidney.[252,312,436] The response is relatively rapid, with a time course of minutes, and does not appear to depend on transcription or translation of new proteins, at least in its initial phase.[252] Vasopressin binds to V_2 receptors on the basolateral surface of responsive epithelia, and activates adenylate cyclase. In almost all tissues studied, the action of vasopressin on Na^+ transport is fully reproduced by exogenous cAMP, and is felt to be secondary to activation of protein kinase A (PKA).[252,437,438] PKA has not been shown to phosphorylate any subunit of the channel, so its actions are felt to be indirect.[437] There has been no consistent demonstration of an effect of PKA on ENaC open probability, so it is likely that the primary effect of PKA on ENaC is to increase the number of channels at the plasma membrane. Indeed, there are now numerous demonstrations that PKA stimulation leads to an increase in surface expression of ENaC by biochemical, immunohistochemical, and electrophysiologic techniques.[111,312,439–441] By analogy to its well-described effects on insertion of aquaporins in kidney cortex and medulla, it seems reasonable to expect that the primary event in PKA stimulation of ENaC is the exocytosis of channels into the apical membrane from some pre-existing cytoplasmic pool. Strong evidence supports this likelihood. Studies by patch-clamp indicate a rapid increase in the number of surface channels in response to cAMP stimulation.[442] Stimulation of adenylate cyclase by forskolin or by addition of cAMP analogs leads to an increase in biochemical and immunohistochemically measured apical channel number,[312,439] and this increase is temporally associated with an increase in apical membrane capacitance typical of exocytic events.[111,441] Butterworth and colleagues have recently proposed that cAMP stimulation leads to exocytic insertion of channels from a subapical recycling pool of channels that is distinct from constitutive turnover of the channel, analogous to vasopressin regulation of water channels[111] (Figure 30.4).

It is also likely that vasopressin, acting through cAMP and Nedd4-2, alters channel retrieval. Snyder and colleagues reported that Nedd4-2 is a substrate for PKA phosphorylation, and they related cAMP regulation of ENaC to inhibition of Nedd4-ENaC interactions.[297] Indeed, PKA appears to phosphorylate Nedd4-2 at sites that overlap the SGK1 target phosphorylation sites, suggesting a similar mechanism of action in promoting the sequestration of Nedd4-2 through binding to 14-3-3 proteins.[308,309] There is an obvious interplay between the hormonal regulation of ENaC by aldosterone and vasopressin, and it is possible that it occurs at the point of kinase regulation. However, the fact that aldosterone and vasopressin are synergistic, and that ENaCs with Liddle's mutations which should be unresponsive to Nedd4-2 inhibition are still responsive to vasopressin stimulation,[436] suggests that, at a minimum, some distinct pathways are involved in the regulation of ENaC by these two hormones. It is also interesting to note that a long-term (days) effect of vasopressin to stimulate transcription of ENaC subunits would clearly complement and be synergistic with aldosterone effects in situations of significant Na^+ avidity.[443]

Insulin

Insulin stimulates ENaC activity in renal epithelia.[252,444] The exact mechanism(s) of this effect are a

subject of considerable controversy. This would seem odd, as it is clear that insulin stimulates phosphoinositide 3-kinase (PI3K), which in turn regulates the activity of 3-phosphoinositide-dependent kinase 1. The latter kinase phosphorylates SGK1 and converts it to an active form.[445] This represents an obvious convergence point for the effects of aldosterone and insulin, which have been shown to be synergistic, on the stimulation of ENaC activity.[445–447] Indeed, noise analysis indicates that the primary effect of insulin is to increase the number of active apical membrane channels, with little effect on open probability.[446] All of these observations are consistent with insulin increasing ENaC activity via decreasing Nedd4-2-dependent retrieval.

It is possible, however, that the action of insulin is more complex. Stimulation of ENaC activity by insulin is quite rapid (minutes), and has been associated with exocytosis and delivery of preformed channels to the apical membrane in a PI3K-dependent manner.[310] Additionally it has been proposed that insulin may directly activate channels by phosphorylation that is dependent on protein kinase C[319] or by interaction with active metabolites of PI3K, phosphoinositol 3,4 phosphate, and phosphoinositol 3,4,5 phosphate, both of which activate ENaC in excised patches.[448] As with aldosterone and vasopressin, although a great deal has been learned about the regulation and trafficking of ENaC, the final control mechanisms by which hormones regulate the channel are complex and only partially-understood.

Angiotensin II

Angiotensin II activates ENaC by signaling through angiotensin II type 1 receptors.[449–451] The signaling mechanism appears to involve activation of a Ca^{2+}-independent protein kinase C isoform and activation of NADPH oxidase, leading to an increase in channels at the plasma membrane, as well as an increase in channel open probability.[450,451]

Endothelin

Endothelin-1 signaling through ETB receptors results in a decrease in ENaC open probability. The intracellular signaling pathways subsequent to ETB receptor activation involve Src kinase and MAP kinase 1/2 signaling pathways.[314,452,453]

Regulation by Mechanical Forces

Members of the ENaC/DEG family expressed in *C. elegans* are mechanosensitive ion channels. Early studies directed at examining the mechanosensitivity of ENaC produced conflicting results that have led to lively debates.[454] Different responses of ENaC expressed in *Xenopus* oocytes to cell swelling or shrinking have been reported.[455,456] Application of a negative hydrostatic pressure to rat CCD cells by patch pipettes led to a variable increase in the open probability of Na^+ channels.[11]

The distal nephron is subject to varying flow rates and volumes, dependent in part on extracellular volume status and the use of pharmacologic agents, such as loop and thiazide diuretics. Changes in flow rates within the distal nephron affect ENaC activity. Micropuncture and microperfusion studies of distal nephron segments have demonstrated that increases in flow rates within the physiologic range led to increases in the rates of net transepithelial Na^+ flux.[457–459] Increases in tubular flow rates expose channels to a variety of mechanical forces, including hydrostatic pressure and shear stress. Carattino and co-workers demonstrated that ENaCs expressed in oocytes are activated when exposed to laminar shear stress at levels that are likely to be present at the surface of principal cells within collecting ducts exposed to flow rates within a physiologic range.[220,221] The increase in ENaC activity is due to an increase in channel open probability.[204,220,221,460] While mutations introduced at sites within the channel pore alter the channel's response to shear stress, evidence suggest that the large extracellular regions function as flow sensors.[188,221,461,462] ENaC subunits are also expressed in vascular smooth muscle, where they are also exposed to mechanical forces. ENaC subunits, possibly in conjunction with ASIC subunits, form mechanosensitive channels that function as arterial baroreceptors and participate in the myogenic response in vascular beds.[160,463–470]

ENaC AND HUMAN DISORDERS

Liddle syndrome is a rare, autosomal dominant disorder characterized by extracellular fluid volume expansion, hypertension, and hypokalemia. Mutations have been described in patients with this disorder in genes encoding the β- or γ-subunits of ENaC that result in either a truncation or frameshift within the intracellular carboxyl termini or amino acid substitutions within the PY motifs.[277,279–281] These mutations disrupt the binding of Nedd4-2 to ENaC, prevent Nedd4-2-dependent ubiquitination of ENaC subunits, and significantly retard rates of channel internalization from the plasma membrane and degradation.[126,128,282,471,472] Liddle's mutations are also associated with an increase in channel open probability that may reflect an increase in the proteolytic processing of subunits, in association with an increased residency time at the plasma membrane.[473]

It is likely that rare mutations that result in a Liddle syndrome phenotype that are not associated with the

PY motif will be identified. These mutations would result in either an increase in channel open probability or an increase in surface expression. For example, a γ-subunit N530K mutation has been described in a patient with diabetic nephropathy.[474] This mutation is within a region where mutations or chemical modification of substituted cysteine residues lead to an increase in channel open probability.[76,79,219] Common human epithelial Na^+ channel polymorphisms segregate with blood pressure, including βT594M and αA663T,[475,476] and are associated with altered channel activity.[231,477,478] A homozygous missense mutation in the gene encoding SCNN1A (α-subunit) resulting in a Ser243Pro mutation was noted in an infant with severe renal Na^+-wasting.[479] This mutation was associated with enhanced Na^+ self-inhibition, as well as enhanced Na^+ feedback inhibition (an inhibition of channel activity due to an increase in intracellular [Na^+]). Another report described an individual with atypical cystic fibrosis who was heterozygous for the ΔF508 CFTR mutation.[192] This individual also had a mutation in the α-subunit (αW493R) that resulted in a profound loss in Na^+ self-inhibition. While it is unclear whether the αW493R mutation contributed to the pulmonary symptoms, individuals who are heterozygous for the ΔF508 mutation in the cystic fibrosis transmembrane conductance regulator (CFTR) generally lack overt pulmonary symptoms. Specific disorders of mineralocorticoid and glucocorticoid metabolism are also associated with increases in ENaC activity and hypertension.

A decrease in airway fluid volume has been observed in patients with cystic fibrosis. As discussed above, it has been suggested the CFTR, a cAMP-regulated Cl^- channel, inhibits ENaC activity in airway epithelia. In the absence of functional CFTR, the activity of ENaC in airways appears to be increased,[352,355,357] although conflicting observations have been reported.[362,363]

Renal Na^+ retention occurs in nephrotic syndrome, even in the absence of activation of known volume regulatory hormones. Recent studies suggest that plasminogen is filtered by damaged glomeruli, and is converted to plasmin by urokinase that lines kidney tubules.[338,339,480] Plasmin cleaves the γ-subunit and activates ENaC, raising the possibility that aberrant activation of ENaC by plasmin may have an important role in the activation of renal Na^+ retaining mechanisms in nephrotic syndrome.[338,339,480]

ENaC loss-of-function mutations have been described in the autosomal recessive variant of type I pseudohypoaldosteronism. This disorder is characterized by volume depletion, hypotension, and hyperkalemia. Many of the mutations described to date are due to a frameshift or premature stop codon.[42] A missense mutation within the β-subunit G37S led to the identification of an N-terminal domain that affects channel-gating.[165,166]

References

[1] Koefoed-Johnson V, Ussing HH. The nature of frog skin potential. Acta Physiol Scand 1958;42:298–308.

[2] Van Driessche W, Lindemann B. Concentration dependence of currents through single sodium-selective pores in frog skin. Nature 1979;282(5738):519–20.

[3] Palmer LG, Frindt G. Epithelial sodium channels: characterization by using the patch-clamp technique. Fed Proc 1986;45 (12):2708–12.

[4] Hamilton KL, Eaton DC. Single-channel recordings from amiloride-sensitive epithelial sodium channel. Am J Physiol 1985;249(3 Pt 1):C200–7.

[5] Hummler E, Barker P, Talbot C, Wang Q, Verdumo C, Grubb B, et al. A mouse model for the renal salt-wasting syndrome pseudohypoaldosteronism. Proc Natl Acad Sci USA 1997;94 (21):11710–5.

[6] McDonald FJ, Yang B, Hrstka RF, Drummond HA, Tarr DE, McCray Jr PB, et al. Disruption of the beta subunit of the epithelial Na^+ channel in mice: Hyperkalemia and neonatal death associated with a pseudohypoaldosteronism phenotype. Proc Natl Acad Sci USA 1999;96(4):1727–31.

[7] Pradervand S, Barker PM, Wang Q, Ernst SA, Beermann F, Grubb BR, et al. Salt restriction induces pseudohypoaldosteronism type 1 in mice expressing low levels of the beta-subunit of the amiloride-sensitive epithelial sodium channel. Proc Natl Acad Sci USA 1999;96(4):1732–7.

[8] Hamilton KL, Eaton DC. Single-channel recordings from two types of amiloride-sensitive epithelial Na^+ channels. Membr Biochem 1986;6(2):149–71.

[9] Canessa CM, Schild L, Buell G, Thorens B, Gautschi I, Horisberger JD, et al. Amiloride-sensitive epithelial Na^+ channel is made of three homologous subunits. Nature 1994;367 (6462):463–7.

[10] Palmer LG, Frindt G. Conductance and gating of epithelial Na channels from rat cortical collecting tubule. Effects of luminal Na and Li. J Gen Physiol 1988;92(1):121–38.

[11] Palmer LG, Frindt G. Gating of Na channels in the rat cortical collecting tubule: effects of voltage and membrane stretch. J Gen Physiol 1996;107(1):35–45.

[12] Kemendy AE, Kleyman TR, Eaton DC. Aldosterone alters the open probability of amiloride-blockable sodium channels in A6 epithelia. Am J Physiol 1992;263(4 Pt 1):C825–37.

[13] Caldwell RA, Boucher RC, Stutts MJ. Serine protease activation of near-silent epithelial Na^+ channels. Am J Physiol Cell Physiol 2004;286(1):C190–4.

[14] Bentley PJ. Amiloride: a potent inhibitor of sodium transport across the toad bladder. J Physiol 1968;195(2):317–30.

[15] Kleyman TR, Cragoe Jr EJ. Cation transport probes: the amiloride series. Methods Enzymol 1990;191:739–55.

[16] Salako LA, Smith AJ. Effects of the diuretics, triamterene and mersalyl on active sodium transport mechanisms in isolated frog skin. Br J Pharmacol 1971;41(3):552–7.

[17] Choi MJ, Fernandez PC, Patnaik A, Coupaye-Gerard B, D'Andrea D, Szerlip H, et al. Brief report: trimethoprim-induced hyperkalemia in a patient with AIDS. N Engl J Med 1993;328(10):703–6.

[18] Schlanger LE, Kleyman TR, Ling BN. $K(^+)$-sparing diuretic actions of trimethoprim: inhibition of Na^+ channels in A6 distal nephron cells. Kidney Int 1994;45(4):1070–6.

[19] Kleyman TR, Roberts C, Ling BN. A mechanism for pentamidine-induced hyperkalemia: inhibition of distal nephron sodium transport. Ann Intern Med 1995;122(2):103–6.
[20] Benos DJ, Saccomani G, Brenner BM, Sariban-Sohraby S. Purification and characterization of the amiloride-sensitive sodium channel from A6 cultured cells and bovine renal papilla. Proc Natl Acad Sci USA 1986;83(22):8525–9.
[21] Benos DJ, Saccomani G, Sariban-Sohraby S. The epithelial sodium channel. Subunit number and location of the amiloride binding site. J Biol Chem 1987;262(22):10613–8.
[22] Kleyman TR, Kraehenbuhl JP, Ernst SA. Characterization and cellular localization of the epithelial Na^+ channel. Studies using an anti-Na^+ channel antibody raised by an antiidiotypic route. J Biol Chem 1991;266(6):3907–15.
[23] Ismailov II, Berdiev BK, Bradford AL, Awayda MS, Fuller CM, Benos DJ. Associated proteins and renal epithelial Na^+ channel function. J Membr Biol 1996;149(2):123–32.
[24] Canessa CM, Horisberger JD, Rossier BC. Epithelial sodium channel related to proteins involved in neurodegeneration. Nature 1993;361(6411):467–70.
[25] Lingueglia E, Voilley N, Waldmann R, Lazdunski M, Barbry P. Expression cloning of an epithelial amiloride-sensitive Na^+ channel. A new channel type with homologies to *Caenorhabditis elegans* degenerins. FEBS Lett 1993;318(1):95–9.
[26] Lingueglia E, Renard S, Waldmann R, Voilley N, Champigny G, Plass H, et al. Different homologous subunits of the amiloride-sensitive Na^+ channel are differently regulated by aldosterone. J Biol Chem 1994;269(19):13736–9.
[27] Ahn YJ, Brooker DR, Kosari F, Harte BJ, Li J, Mackler SA, et al. Cloning and functional expression of the mouse epithelial sodium channel. Am J Physiol 1999;277(1 Pt 2):F121–9.
[28] McDonald FJ, Price MP, Snyder PM, Welsh MJ. Cloning and expression of the beta- and gamma-subunits of the human epithelial sodium channel. Am J Physiol 1995;268(5 Pt 1): C1157–63.
[29] McDonald FJ, Snyder PM, McCray Jr PB, Welsh MJ. Cloning, expression, and tissue distribution of a human amiloride-sensitive Na^+ channel. Am J Physiol 1994;266(6 Pt 1):L728–34.
[30] Fuller CM, Awayda MS, Arrate MP, Bradford AL, Morris RG, Canessa CM, et al. Cloning of a bovine renal epithelial Na^+ channel subunit. Am J Physiol 1995;269(3 Pt 1):C641–54.
[31] Puoti A, May A, Canessa CM, Horisberger JD, Schild L, Rossier BC. The highly selective low-conductance epithelial Na channel of *Xenopus laevis* A6 kidney cells. Am J Physiol 1995;269(1 Pt 1): C188–97.
[32] Jensik P, Holbird D, Cox T. Cloned bullfrog skin sodium (fENaC) and xENaC subunits hybridize to form functional sodium channels. J Comp Physiol [B] 2002;172(7):569–76.
[33] Goldstein O, Asher C, Garty H. Cloning and induction by low NaCl intake of avian intestine Na^+ channel subunits. Am J Physiol 1997;272(1 Pt 1):C270–7.
[34] Schnizler M, Mastroberardino L, Reifarth F, Weber WM, Verrey F, Clauss W. cAMP sensitivity conferred to the epithelial Na^+ channel by alpha-subunit cloned from guinea-pig colon. Pflugers Arch 2000;439(5):579–87.
[35] Voilley N, Bassilana F, Mignon C, Merscher S, Mattei MG, Carle GF, et al. Cloning, chromosomal localization, and physical linkage of the beta and gamma subunits (SCNN1B and SCNN1G) of the human epithelial amiloride-sensitive sodium channel. Genomics 1995;28(3):560–5.
[36] Brooker DR, Kozak CA, Kleyman TR. Epithelial sodium channel genes Scnn1b and Scnn1g are closely linked on distal mouse chromosome 7. Genomics 1995;29(3):784–6.
[37] Ludwig M, Bolkenius U, Wickert L, Marynen P, Bidlingmaier F. Structural organisation of the gene encoding the alpha-subunit of the human amiloride-sensitive epithelial sodium channel. Hum Genet 1998;102(5):576–81.
[38] Thomas CP, Auerbach SD, Zhang C, Stokes JB. The structure of the rat amiloride-sensitive epithelial sodium channel gamma subunit gene and functional analysis of its promoter. Gene 1999;228(1–2):111–22.
[39] Thomas CP, Auerbach S, Stokes JB, Volk KA. 5′ heterogeneity in epithelial sodium channel alpha-subunit mRNA leads to distinct NH2-terminal variant proteins. Am J Physiol 1998;274(5 Pt 1):C1312–23.
[40] Chraibi A, Verdumo C, Merillat AM, Rossier BC, Horisberger JD, Hummler E. Functional analyses of a N-terminal splice variant of the alpha subunit of the epithelial sodium channel. Cell Physiol Biochem 2001;11(3):115–22.
[41] Tucker JK, Tamba K, Lee YJ, Shen LL, Warnock DG, Oh Y. Cloning and functional studies of splice variants of the alpha-subunit of the amiloride-sensitive Na^+ channel. Am J Physiol 1998;274(4 Pt 1):C1081–9.
[42] Chang SS, Grunder S, Hanukoglu A, Rosler A, Mathew PM, Hanukoglu I, et al. Mutations in subunits of the epithelial sodium channel cause salt wasting with hyperkalaemic acidosis, pseudohypoaldosteronism type 1. Nat Genet 1996;12(3): 248–53.
[43] Bonny O, Chraibi A, Loffing J, Jaeger NF, Grunder S, Horisberger JD, et al. Functional expression of a pseudohypoaldosteronism type I mutated epithelial Na^+ channel lacking the pore-forming region of its alpha subunit. J Clin Invest 1999;104 (7):967–74.
[44] Huang M, Chalfie M. Gene interactions affecting mechanosensory transduction in *Caenorhabditis elegans*. Nature 1994;367 (6462):467–70.
[45] Corey DP, Garcia-Anoveros J. Mechanosensation and the DEG/ENaC ion channels. Science 1996;273(5273):323–4.
[46] Goodman MB, Ernstrom GG, Chelur DS, O'Hagan R, Yao CA, Chalfie M. MEC-2 regulates *C. elegans* DEG/ENaC channels needed for mechanosensation. Nature 2002;415(6875): 1039–42.
[47] Waldmann R, Champigny G, Bassilana F, Voilley N, Lazdunski M. Molecular cloning and functional expression of a novel amiloride-sensitive Na^+ channel. J Biol Chem 1995;270 (46):27411–4.
[48] Yamamura H, Ugawa S, Ueda T, Nagao M, Shimada S. Protons activate the delta-subunit of the epithelial Na^+ channel in humans. J Biol Chem 2004;279(13):12529–34.
[49] Babini E, Geisler HS, Siba M, Grunder S. A new subunit of the epithelial Na^+ channel identifies regions involved in Na^+ self-inhibition. J Biol Chem 2003;278(31):28418–26.
[50] Waldmann R, Champigny G, Bassilana F, Heurteaux C, Lazdunski M. A proton-gated cation channel involved in acid-sensing. Nature 1997;386(6621):173–7.
[51] Price MP, Snyder PM, Welsh MJ. Cloning and expression of a novel human brain Na^+ channel. J Biol Chem 1996;271(14): 7879–82.
[52] Wemmie JA, Askwith CC, Lamani E, Cassell MD, Freeman Jr JH, Welsh MJ. Acid-sensing ion channel 1 is localized in brain regions with high synaptic density and contributes to fear conditioning. J Neurosci 2003;23(13):5496–502.
[53] Wemmie JA, Coryell MW, Askwith CC, Lamani E, Leonard AS, Sigmund CD, et al. Overexpression of acid-sensing ion channel 1a in transgenic mice increases acquired fear-related behavior. Proc Natl Acad Sci USA 2004;101(10):3621–6.
[54] Ziemann AE, Allen JE, Dahdaleh NS, Drebot II, Coryell MW, Wunsch AM, et al. The amygdala is a chemosensor that detects carbon dioxide and acidosis to elicit fear behavior. Cell 2009;139 (5):1012–21.

[55] Ziemann AE, Schnizler MK, Albert GW, Severson MA, Howard III MA, Welsh MJ, et al. Seizure termination by acidosis depends on ASIC1a. Nat Neurosci 2008;11(7):816–22.
[56] Adams CM, Anderson MG, Motto DG, Price MP, Johnson WA, Welsh MJ. Ripped pocket and pickpocket, novel *Drosophila* DEG/ENaC subunits expressed in early development and in mechanosensory neurons. J Cell Biol 1998;140(1):143–52.
[57] Darboux I, Lingueglia E, Pauron D, Barbry P, Lazdunski M. A new member of the amiloride-sensitive sodium channel family in *Drosophila melanogaster* peripheral nervous system. Biochem Biophys Res Commun 1998;246(1):210–6.
[58] Take-Uchi M, Kawakami M, Ishihara T, Amano T, Kondo K, Katsura I. An ion channel of the degenerin/epithelial sodium channel superfamily controls the defecation rhythm in *Caenorhabditis elegans*. Proc Natl Acad Sci USA 1998;95(20):11775–80.
[59] Liu L, Johnson WA, Welsh MJ. *Drosophila* DEG/ENaC pickpocket genes are expressed in the tracheal system, where they may be involved in liquid clearance. Proc Natl Acad Sci USA 2003;100(4):2128–33.
[60] Liu L, Leonard AS, Motto DG, Feller MA, Price MP, Johnson WA, et al. Contribution of *Drosophila* DEG/ENaC genes to salt taste. Neuron 2003;39(1):133–46.
[61] Lin H, Mann KJ, Starostina E, Kinser RD, Pikielny CWA. *Drosophila* DEG/ENaC channel subunit is required for male response to female pheromones. Proc Natl Acad Sci USA 2005;102(36):12831–6.
[62] Lingueglia E, Champigny G, Lazdunski M, Barbry P. Cloning of the amiloride-sensitive FMRFamide peptide-gated sodium channel. Nature 1995;378(6558):730–3.
[63] Cottrell GA. The first peptide-gated ion channel. J Exp Biol 1997;200(Pt 18):2377–86.
[64] Jeziorski MC, Green KA, Sommerville J, Cottrell GA. Cloning and expression of a FMRFamide-gated $Na(^+)$ channel from *Helisoma trivolvis* and comparison with the native neuronal channel. J Physiol 2000;526(Pt 1):13–25.
[65] Ho K, Nichols CG, Lederer WJ, Lytton J, Vassilev PM, Kanazirska MV, et al. Cloning and expression of an inwardly rectifying ATP-regulated potassium channel. Nature 1993;362(6415):31–8.
[66] Valera S, Hussy N, Evans RJ, Adami N, North RA, Surprenant A, et al. A new class of ligand-gated ion channel defined by P2x receptor for extracellular ATP. Nature 1994;371(6497):516–9.
[67] Renard S, Lingueglia E, Voilley N, Lazdunski M, Barbry P. Biochemical analysis of the membrane topology of the amiloride-sensitive Na^+ channel. J Biol Chem 1994;269(17):12981–6.
[68] Canessa CM, Merillat AM, Rossier BC. Membrane topology of the epithelial sodium channel in intact cells. Am J Physiol 1994;267(6 Pt 1):C1682–90.
[69] Jasti J, Furukawa H, Gonzales EB, Gouaux E. Structure of acid-sensing ion channel 1 at 1.9 A resolution and low pH. Nature 2007;449(7160):316–23.
[70] Gonzales EB, Kawate T, Gouaux E. Pore architecture and ion sites in acid-sensing ion channels and P2X receptors. Nature 2009;460(7255):599–604.
[71] Firsov D, Gautschi I, Merillat AM, Rossier BC, Schild L. The heterotetrameric architecture of the epithelial sodium channel (ENaC). Embo J 1998;17(2):344–52.
[72] Kosari F, Sheng S, Li J, Mak DO, Foskett JK, Kleyman TR. Subunit stoichiometry of the epithelial sodium channel. J Biol Chem 1998;273(22):13469–74.
[73] Snyder PM, Cheng C, Prince LS, Rogers JC, Welsh MJ. Electrophysiological and biochemical evidence that DEG/ENaC cation channels are composed of nine subunits. J Biol Chem 1998;273(2):681–4.
[74] Anantharam A, Palmer LG. Determination of epithelial Na^+ channel subunit stoichiometry from single-channel conductances. J Gen Physiol 2007;130(1):55–70.
[75] Li T, Yang Y, Canessa CM. Outlines of the pore in open and closed conformations describe the gating mechanism of ASIC1. Nat Commun 2011;2:399.
[76] Sheng S, Li J, McNulty KA, Kieber-Emmons T, Kleyman TR. Epithelial sodium channel pore region. Structure and role in gating. J Biol Chem 2001;276(2):1326–34.
[77] Carattino MD, Edinger RS, Grieser HJ, Wise R, Neumann D, Schlattner U, et al. Hallows KR. Epithelial sodium channel inhibition by AMP-activated protein kinase in oocytes and polarized renal epithelial cells. J Biol Chem 2005;280(18):17608–16.
[78] Adams CM, Snyder PM, Price MP, Welsh MJ. Protons activate brain Na^+ channel 1 by inducing a conformational change that exposes a residue associated with neurodegeneration. J Biol Chem 1998;273(46):30204–7.
[79] Snyder PM, Bucher DB, Olson DR. Gating induces a conformational change in the outer vestibule of ENaC. J Gen Physiol 2000;116(6):781–90.
[80] Kashlan OB, Boyd CR, Argyropoulos C, Okumura S, Hughey RP, Grabe M, et al. Allosteric inhibition of the epithelial Na^+ channel through peptide binding at peripheral finger and thumb domains. J Biol Chem 2010;285(45):35216–23.
[81] Kashlan OB, Kleyman TR. ENaC structure and function in the wake of a resolved structure of a family member. Am J Physiol Renal Physiol 2011;301(4):F684–96.
[82] Kashlan OB, Adelman JL, Okumura S, Blobner BM, Zuzek Z, Hughey RP, et al. Constraint-based, homology model of the extracellular domain of the epithelial Na^+ channel alpha subunit reveals a mechanism of channel activation by proteases. J Biol Chem 2011;286(1):649–60.
[83] Hughey RP, Bruns JB, Kinlough CL, Harkleroad KL, Tong Q, Carattino MD, et al. Epithelial sodium channels are activated by furin-dependent proteolysis. J Biol Chem 2004;279(18):18111–4.
[84] Carattino MD, Sheng S, Bruns JB, Pilewski JM, Hughey RP, Kleyman TR. The epithelial Na^+ channel is inhibited by a peptide derived from proteolytic processing of its alpha subunit. J Biol Chem 2006;281(27):18901–7.
[85] Kleyman TR, Carattino MD, Hughey RP. ENaC at the cutting edge: regulation of epithelial sodium channels by proteases. J Biol Chem 2009;284(31):20447–51.
[86] Carattino MD, Passero CJ, Steren CA, Maarouf AB, Pilewski JM, Myerburg MM, et al. Defining an inhibitory domain in the alpha-subunit of the epithelial sodium channel. Am J Physiol Renal Physiol 2008;294(1):F47–52.
[87] Stockand JD, Staruschenko A, Pochynyuk O, Booth RE, Silverthorn DU. Insight toward epithelial Na^+ channel mechanism revealed by the acid-sensing ion channel 1 structure. IUBMB Life 2008;60(9):620–8.
[88] Adams CM, Snyder PM, Welsh MJ. Interactions between subunits of the human epithelial sodium channel. J Biol Chem 1997;272(43):27295–300.
[89] May A, Puoti A, Gaeggeler HP, Horisberger JD, Rossier BC. Early effect of aldosterone on the rate of synthesis of the epithelial sodium channel alpha subunit in A6 renal cells. J Am Soc Nephrol 1997;8(12):1813–22.
[90] Prince LS, Welsh MJ. Cell surface expression and biosynthesis of epithelial Na^+ channels. Biochem J 1998;336(Pt 3):705–10.
[91] Hanwell D, Ishikawa T, Saleki R, Rotin D. Trafficking and cell surface stability of the epithelial Na^+ channel expressed in epithelial Madin–Darby canine kidney cells. J Biol Chem 2002;277(12):9772–9.

[92] Weisz OA, Wang JM, Edinger RS, Johnson JP. Non-coordinate regulation of endogenous epithelial sodium channel (ENaC) subunit expression at the apical membrane of A6 cells in response to various transporting conditions. J Biol Chem 2000;275(51):39886–93.

[93] De La Rosa DA, Li H, Canessa CM. Effects of aldosterone on biosynthesis, traffic, and functional expression of epithelial sodium channels in A6 cells. J Gen Physiol 2002;119(5): 427–42.

[94] Cheng C, Prince LS, Snyder PM, Welsh MJ. Assembly of the epithelial Na^+ channel evaluated using sucrose gradient sedimentation analysis. J Biol Chem 1998;273(35):22693–700.

[95] Rotin D, Kanelis V, Schild L. Trafficking and cell surface stability of ENaC. Am J Physiol Renal Physiol 2001;281(3):F391–9.

[96] Valentijn JA, Fyfe GK, Canessa CM. Biosynthesis and processing of epithelial sodium channels in *Xenopus* oocytes. J Biol Chem 1998;273(46):30344–51.

[97] Hughey RP, Mueller GM, Bruns JB, Kinlough CL, Poland PA, Harkleroad KL, et al. Maturation of the epithelial Na^+ channel involves proteolytic processing of the alpha- and gamma-subunits. J Biol Chem 2003;278(39):37073–82.

[98] Mueller GM, Maarouf AB, Kinlough CL, Sheng N, Kashlan OB, Okumura S, et al. Cys palmitoylation of the beta subunit modulates gating of the epithelial sodium channel. J Biol Chem 2010;285(40):30453–62.

[99] Mueller GM, Kashlan OB, Bruns JB, Maarouf AB, Aridor M, Kleyman TR, et al. Epithelial sodium channel exit from the endoplasmic reticulum is regulated by a signal within the carboxyl cytoplasmic domain of the alpha subunit. J Biol Chem 2007;282(46):33475–83.

[100] Kashlan OB, Mueller GM, Qamar MZ, Poland PA, Ahner A, Rubenstein RC, et al. Small heat shock protein alphaA-crystallin regulates epithelial sodium channel expression. J Biol Chem 2007;282(38):28149–56.

[101] Buck TM, Kolb AR, Boyd CR, Kleyman TR, Brodsky JL. The endoplasmic reticulum-associated degradation of the epithelial sodium channel requires a unique complement of molecular chaperones. Mol Biol Cell 2010;21(6):1047–58.

[102] Kolb AR, Buck TM, Brodsky JL. *Saccharomyces cerivisiae* as a model system for kidney disease: what can yeast tell us about renal function? Am J Physiol Renal Physiol 2011;301(1):F1–11.

[103] Kopito RR. ER quality control: the cytoplasmic connection. Cell 1997;88(4):427–30.

[104] Ellgaard L, Molinari M, Helenius A. Setting the standards: quality control in the secretory pathway. Science 1999;286 (5446):1882–8.

[105] Fewell SW, Travers KJ, Weissman JS, Brodsky JL. The action of molecular chaperones in the early secretory pathway. Annu Rev Genet 2001;35:149–91.

[106] Goldfarb SB, Kashlan OB, Watkins JN, Suaud L, Yan W, Kleyman TR, et al. Differential effects of Hsc70 and Hsp70 on the intracellular trafficking and functional expression of epithelial sodium channels. Proc Natl Acad Sci USA 2006;103 (15):5817–22.

[107] Sugahara T, Koga T, Ueno-Shuto K, Shuto T, Watanabe E, Maekawa A, et al. Calreticulin positively regulates the expression and function of epithelial sodium channel. Exp Cell Res 2009;315(19):3294–300.

[108] Malik B, Schlanger L, Al-Khalili O, Bao HF, Yue G, Price SR, et al. ENaC degradation in A6 cells by the ubiquitin-proteosome proteolytic pathway. J Biol Chem 2001;276(16):12903–10.

[109] Kleyman TR, Zuckerman JB, Middleton P, McNulty KA, Hu B, Su X, et al. Cell surface expression and turnover of the alpha-subunit of the epithelial sodium channel. Am J Physiol Renal Physiol 2001;281(2):F213–21.

[110] Mohan S, Bruns JR, Weixel KM, Edinger RS, Bruns JB, Kleyman TR, et al. Differential current decay profiles of epithelial sodium channel subunit combinations in polarized renal epithelial cells. J Biol Chem 2004;279(31):32071–8.

[111] Butterworth MB, Edinger RS, Johnson JP, Frizzell RA. Acute ENaC stimulation by cAMP in a kidney cell line is mediated by exocytic insertion from a recycling channel pool. J Gen Physiol 2005;125(1):81–101.

[112] Hughey RP, Bruns JB, Kinlough CL, Kleyman TR. Distinct pools of epithelial sodium channels are expressed at the plasma membrane. J Biol Chem 2004;279(47):48491–4.

[113] Caldwell RA, Boucher RC, Stutts MJ. Neutrophil elastase activates near-silent epithelial Na^+-channels and increases airway epithelial Na^+-transport. Am J Physiol Lung Cell Mol Physiol 2005;288(5):L813–9.

[114] Chraibi A, Vallet V, Firsov D, Hess SK, Horisberger JD. Protease modulation of the activity of the epithelial sodium channel expressed in *Xenopus* oocytes. J Gen Physiol 1998;111 (1):127–38.

[115] Sheng S, Carattino MD, Bruns JB, Hughey RP, Kleyman TR. Furin cleavage activates the epithelial Na^+ channel by relieving Na^+ self-inhibition. Am J Physiol Renal Physiol 2006;290(6): F1488–96.

[116] Saxena S, Quick MW, Tousson A, Oh Y, Warnock DG. Interaction of syntaxins with the amiloride-sensitive epithelial sodium channel. J Biol Chem 1999;274(30):20812–7.

[117] Berdiev BK, Jovov B, Tucker WC, Naren AP, Fuller CM, Chapman ER, et al. ENaC subunit-subunit interactions and inhibition by syntaxin 1A. Am J Physiol Renal Physiol 2004;286 (6):F1100–6.

[118] Condliffe SB, Zhang H, Frizzell RA. Syntaxin 1A regulates ENaC channel activity. J Biol Chem 2004;279(11):10085–92.

[119] Condliffe SB, Carattino MD, Frizzell RA, Zhang H. Syntaxin 1A regulates ENaC via domain-specific interactions. J Biol Chem 2003;278(15):12796–804.

[120] Hill WG, An B, Johnson JP. Endogenously expressed epithelial sodium channel is present in lipid rafts in A6 cells. J Biol Chem 2002;277(37):33541–4.

[121] Shlyonsky VG, Mies F, Sariban-Sohraby S. Epithelial sodium channel activity in detergent-resistant membrane microdomains. Am J Physiol Renal Physiol 2003;284(1):F182–8.

[122] Rotin D, Bar-Sagi D, O'Brodovich H, Merilainen J, Lehto VP, Canessa CM, et al. An SH3 binding region in the epithelial Na^+ channel (alpha rENaC) mediates its localization at the apical membrane. Embo J 1994;13(19):4440–50.

[123] Zuckerman JB, Chen X, Jacobs JD, Hu B, Kleyman TR, Smith PR. Association of the epithelial sodium channel with Apx and alpha-spectrin in A6 renal epithelial cells. J Biol Chem 1999;274 (33):23286–95.

[124] Copeland SJ, Berdiev BK, Ji HL, Lockhart J, Parker S, Fuller CM, et al. Regions in the carboxy terminus of alpha-bENaC involved in gating and functional effects of actin. Am J Physiol Cell Physiol 2001;281(1):C231–40.

[125] Berdiev BK, Latorre R, Benos DJ, Ismailov II. Actin modifies Ca^{2+} block of epithelial Na^+ channels in planar lipid bilayers. Biophys J 2001;80(5):2176–86.

[126] Shimkets RA, Lifton RP, Canessa CM. The activity of the epithelial sodium channel is regulated by clathrin-mediated endocytosis. J Biol Chem 1997;272(41):25537–41.

[127] Carattino MD, Hill WG, Kleyman TR. Arachidonic acid regulates surface expression of epithelial sodium channels. J Biol Chem 2003;278(38):36202–13.

[128] Schild L, Lu Y, Gautschi I, Schneeberger E, Lifton RP, Rossier BC. Identification of a PY motif in the epithelial Na channel subunits as a target sequence for mutations causing channel

activation found in Liddle syndrome. Embo J 1996;15 (10):2381–7.
[129] Takei K, McPherson PS, Schmid SL, De Camilli P. Tubular membrane invaginations coated by dynamin rings are induced by GTP-gamma S in nerve terminals. Nature 1995;374 (6518):186–90.
[130] Henley JR, Krueger EW, Oswald BJ, McNiven MA. Dynamin-mediated internalization of caveolae. J Cell Biol 1998;141 (1):85–99.
[131] Oh P, McIntosh DP, Schnitzer JE. Dynamin at the neck of caveolae mediates their budding to form transport vesicles by GTP-driven fission from the plasma membrane of endothelium. J Cell Biol 1998;141(1):101–14.
[132] Staub O, Gautschi I, Ishikawa T, Breitschopf K, Ciechanover A, Schild L, et al. Regulation of stability and function of the epithelial Na^+ channel (ENaC) by ubiquitination. Embo J 1997;16 (21):6325–36.
[133] Wang H, Traub LM, Weixel KM, Hawryluk MJ, Shah N, Edinger RS, et al. Clathrin-mediated endocytosis of the epithelial sodium channel. Role of epsin J Biol Chem 2006;281 (20):14129–35.
[134] Fakitsas P, Adam G, Daidie D, van Bemmelen MX, Fouladkou F, Patrignani A, et al. Early aldosterone-induced gene product regulates the epithelial sodium channel by deubiquitylation. J Am Soc Nephrol 2007;18(4):1084–92.
[135] Butterworth MB, Edinger RS, Ovaa H, Burg D, Johnson JP, Frizzell RA. The deubiquitinating enzyme UCH-L3 regulates the apical membrane recycling of the epithelial sodium channel. J Biol Chem 2007;282(52):37885–93.
[136] Oberfeld B, Ruffieux-Daidie D, Vitagliano JJ, Pos KM, Verrey F, Staub O. Ubiquitin-specific protease 2-45 (Usp2-45) binds to epithelial Na^+ channel (ENaC)-ubiquitylating enzyme Nedd4-2. Am J Physiol Renal Physiol 2011;301(1):F189–96.
[137] Xu JZ, Hall AE, Peterson LN, Bienkowski MJ, Eessalu TE, Hebert SC. Localization of the ROMK protein on apical membranes of rat kidney nephron segments. Am J Physiol 1997;273 (5 Pt 2):F739–48.
[138] Woda CB, Miyawaki N, Ramalakshmi S, Ramkumar M, Rojas R, Zavilowitz B, et al. Ontogeny of flow-stimulated potassium secretion in rabbit cortical collecting duct: functional and molecular aspects. Am J Physiol Renal Physiol 2003;285(4): F629–39.
[139] Woda CB, Bragin A, Kleyman TR, Satlin LM. Flow-dependent K^+ secretion in the cortical collecting duct is mediated by a maxi-K channel. Am J Physiol Renal Physiol 2001;280(5): F786–93.
[140] Hager H, Kwon TH, Vinnikova AK, Masilamani S, Brooks HL, Frokiaer J, et al. Immunocytochemical and immunoelectron microscopic localization of alpha-, beta-, and gamma-ENaC in rat kidney. Am J Physiol Renal Physiol 2001;280(6):F1093–106.
[141] Loffing J, Pietri L, Aregger F, Bloch-Faure M, Ziegler U, Meneton P, et al. Differential subcellular localization of ENaC subunits in mouse kidney in response to high- and low-Na diets. Am J Physiol Renal Physiol 2000;279(2):F252–8.
[142] Masilamani S, Kim GH, Mitchell C, Wade JB, Knepper MA. Aldosterone-mediated regulation of ENaC alpha, beta, and gamma subunit proteins in rat kidney. J Clin Invest 1999;104 (7):R19–23.
[143] Loffing J, Zecevic M, Feraille E, Kaissling B, Asher C, Rossier BC, et al. Aldosterone induces rapid apical translocation of ENaC in early portion of renal collecting system: possible role of SGK. Am J Physiol Renal Physiol 2001;280(4): F675–82.
[144] Barker PM, Nguyen MS, Gatzy JT, Grubb B, Norman H, Hummler E, et al. Role of gammaENaC subunit in lung liquid clearance and electrolyte balance in newborn mice. Insights into perinatal adaptation and pseudohypoaldosteronism. J Clin Invest 1998;102(8):1634–40.
[145] Hummler E, Barker P, Gatzy J, Beermann F, Verdumo C, Schmidt A, et al. Early death due to defective neonatal lung liquid clearance in alpha-ENaC-deficient mice. Nat Genet 1996;12(3):325–8.
[146] Frindt G, Palmer LG. Na channels in the rat connecting tubule. Am J Physiol Renal Physiol 2004;286(4):F669–74.
[147] Rubera I, Loffing J, Palmer LG, Frindt G, Fowler-Jaeger N, Sauter D, et al. Collecting duct-specific gene inactivation of alphaENaC in the mouse kidney does not impair sodium and potassium balance. J Clin Invest 2003;112(4):554–65.
[148] Burch LH, Talbot CR, Knowles MR, Canessa CM, Rossier BC, Boucher RC. Relative expression of the human epithelial Na^+ channel subunits in normal and cystic fibrosis airways. Am J Physiol 1995;269(2 Pt 1):C511–8.
[149] Talbot CL, Bosworth DG, Briley EL, Fenstermacher DA, Boucher RC, Gabriel SE, et al. Quantitation and localization of ENaC subunit expression in fetal, newborn, and adult mouse lung. Am J Respir Cell Mol Biol 1999;20(3):398–406.
[150] Matsushita K, McCray Jr PB, Sigmund RD, Welsh MJ, Stokes JB. Localization of epithelial sodium channel subunit mRNAs in adult rat lung by *in situ* hybridization. Am J Physiol 1996;271(2 Pt 1):L332–9.
[151] Jain L, Chen XJ, Malik B, Al-Khalili O, Eaton DC. Antisense oligonucleotides against the alpha-subunit of ENaC decrease lung epithelial cation-channel activity. Am J Physiol 1999;276(6 Pt 1):L1046–51.
[152] Borok Z, Liebler JM, Lubman RL, Foster MJ, Zhou B, Li X, et al. Na transport proteins are expressed by rat alveolar epithelial type I cells. Am J Physiol Lung Cell Mol Physiol 2002;282 (4):L599–608.
[153] Mall M, Grubb BR, Harkema JR, O'Neal WK, Boucher RC. Increased airway epithelial Na^+ absorption produces cystic fibrosis-like lung disease in mice. Nat Med 2004;10 (5):487–93.
[154] Boucher RC. Regulation of airway surface liquid volume by human airway epithelia. Pflugers Arch 2003;445 (4):495–8.
[155] Duc C, Farman N, Canessa CM, Bonvalet JP, Rossier BC. Cell-specific expression of epithelial sodium channel alpha, beta, and gamma subunits in aldosterone-responsive epithelia from the rat: localization by *in situ* hybridization and immunocytochemistry. J Cell Biol 1994;127(6 Pt 2):1907–21.
[156] Kretz O, Barbry P, Bock R, Lindemann B. Differential expression of RNA and protein of the three pore-forming subunits of the amiloride-sensitive epithelial sodium channel in taste buds of the rat. J Histochem Cytochem 1999;47(1): 51–64.
[157] Brouard M, Casado M, Djelidi S, Barrandon Y, Farman N. Epithelial sodium channel in human epidermal keratinocytes: expression of its subunits and relation to sodium transport and differentiation. J Cell Sci 1999;112(Pt 19):3343–52.
[158] Grunder S, Muller A, Ruppersberg JP. Developmental and cellular expression pattern of epithelial sodium channel alpha, beta and gamma subunits in the inner ear of the rat. Eur J Neurosci 2001;13(4):641–8.
[159] Couloigner V, Fay M, Djelidi S, Farman N, Escoubet B, Runembert I, et al. Location and function of the epithelial Na channel in the cochlea. Am J Physiol Renal Physiol 2001;280(2): F214–22.
[160] Drummond HA, Gebremedhin D, Harder DR. Degenerin/epithelial Na^+ channel proteins: components of a vascular mechanosensor. Hypertension 2004;44(5):643–8.

[161] Mirshahi M, Nicolas C, Mirshahi S, Golestaneh N, d'Hermies F, Agarwal MK. Immunochemical analysis of the sodium channel in rodent and human eye. Exp Eye Res 1999;69(1):21–32.
[162] Bubien JK, Watson B, Khan MA, Langloh AL, Fuller CM, Berdiev B, et al. Expression and regulation of normal and polymorphic epithelial sodium channel by human lymphocytes. J Biol Chem 2001;276(11):8557–66.
[163] Schild L, Schneeberger E, Gautschi I, Firsov D. Identification of amino acid residues in the alpha, beta, and gamma subunits of the epithelial sodium channel (ENaC) involved in amiloride block and ion permeation. J Gen Physiol 1997;109(1):15–26.
[164] Chalfant ML, Denton JS, Langloh AL, Karlson KH, Loffing J, Benos DJ, et al. The $NH(_2)$ terminus of the epithelial sodium channel contains an endocytic motif. J Biol Chem 1999;274 (46):32889–96.
[165] Grunder S, Firsov D, Chang SS, Jaeger NF, Gautschi I, Schild L, et al. A mutation causing pseudohypoaldosteronism type 1 identifies a conserved glycine that is involved in the gating of the epithelial sodium channel. Embo J 1997;16(5):899–907.
[166] Grunder S, Jaeger NF, Gautschi I, Schild L, Rossier BC. Identification of a highly conserved sequence at the N-terminus of the epithelial Na^+ channel alpha subunit involved in gating. Pflugers Arch 1999;438(5):709–15.
[167] Kucher V, Boiko N, Pochynyuk O, Stockand JD. Voltage-dependent gating underlies loss of ENaC function in Pseudohypoaldosteronism type 1. Biophys J 2011;100 (8):1930–9.
[168] Waldmann R, Champigny G, Lazdunski M. Functional degenerin-containing chimeras identify residues essential for amiloride-sensitive Na^+ channel function. J Biol Chem 1995;270 (20):11735–7.
[169] Sheng S, Li J, McNulty KA, Avery D, Kleyman TR. Characterization of the selectivity filter of the epithelial sodium channel. J Biol Chem 2000;275(12):8572–81.
[170] Sheng S, McNulty KA, Harvey JM, Kleyman TR. Second transmembrane domains of ENaC subunits contribute to ion permeation and selectivity. J Biol Chem 2001;276(47):44091–8.
[171] Kashlan OB, Sheng S, Kleyman TR. On the interaction between amiloride and its putative alpha-subunit epithelial Na^+ channel binding site. J Biol Chem 2005;280(28):26206–15.
[172] Yue G, Malik B, Yue G, Eaton DC. Phosphatidylinositol 4,5-bisphosphate (PIP2) stimulates epithelial sodium channel activity in A6 cells. J Biol Chem 2002;277(14):11965–9.
[173] Ma HP, Saxena S, Warnock DG. Anionic phospholipids regulate native and expressed epithelial sodium channel (ENaC). J Biol Chem 2002;277(10):7641–4.
[174] Kunzelmann K, Bachhuber T, Regeer R, Markovich D, Sun J, Schreiber R. Purinergic inhibition of the epithelial Na^+ transport via hydrolysis of PIP2. Faseb J 2005;19(1):142–3.
[175] Pochynyuk O, Tong Q, Medina J, Vandewalle A, Staruschenko A, Bugaj V, et al. Molecular determinants of PI(4,5)P2 and PI (3,4,5)P3 regulation of the epithelial Na^+ channel. J Gen Physiol 2007;130(4):399–413.
[176] Helms MN, Liu L, Liang YY, Al-Khalili O, Vandewalle A, Saxena S, et al. Phosphatidylinositol 3,4,5-trisphosphate mediates aldosterone stimulation of epithelial sodium channel (ENaC) and interacts with gamma-ENaC. J Biol Chem 2005;280 (49):40885–91.
[177] Kellenberger S, Gautschi I, Pfister Y, Schild L. Intracellular thiol-mediated modulation of epithelial sodium channel activity. J Biol Chem 2005;280(9):7739–47.
[178] Kashlan OB, Maarouf AB, Kussius C, Denshaw RM, Blumenthal KM, Kleyman TR. Distinct structural elements in the first membrane-spanning segment of the epithelial sodium channel. J Biol Chem 2006;281(41):30455–62.
[179] Firsov D, Robert-Nicoud M, Gruender S, Schild L, Rossier BC. Mutational analysis of cysteine-rich domains of the epithelium sodium channel (ENaC). Identification of cysteines essential for channel expression at the cell surface. J Biol Chem 1999;274 (5):2743–9.
[180] Mano I, Driscoll M. DEG/ENaC channels: a touchy superfamily that watches its salt. Bioessays 1999;21(7):568–78.
[181] Sheng S, Perry CJ, Kleyman TR. External nickel inhibits epithelial sodium channel by binding to histidine residues within the extracellular domains of alpha and gamma subunits and reducing channel open probability. J Biol Chem 2002;277 (51):50098–111.
[182] Sheng S, Bruns JB, Kleyman TR. Extracellular histidine residues crucial for Na^+ self-inhibition of epithelial Na^+ channels. J Biol Chem 2004;279(11):9743–9.
[183] Sheng S, Maarouf AB, Bruns JB, Hughey RP, Kleyman TR. Functional role of extracellular loop cysteine residues of the epithelial Na^+ channel in Na^+ self-inhibition. J Biol Chem 2007;282(28):20180–90.
[184] Sheng S, Perry CJ, Kleyman TR. Extracellular Zn^{2+} activates epithelial Na^+ channels by eliminating Na^+ self-inhibition. J Biol Chem 2004;279(30):31687–96.
[185] Maarouf AB, Sheng N, Chen J, Winarski KL, Okumura S, Carattino MD, et al. Novel determinants of epithelial sodium channel gating within extracellular thumb domains. J Biol Chem 2009;284(12):7756–65.
[186] Winarski KL, Sheng N, Chen J, Kleyman TR, Sheng S. Extracellular allosteric regulatory subdomain within the gamma subunit of the epithelial Na^+ channel. J Biol Chem 2010;285(34):26088–96.
[187] Chen J, Myerburg MM, Passero CJ, Winarski KL, Sheng S. External Cu^{2+} inhibits human epithelial Na^+ channels by binding at a subunit interface of extracellular domains. J Biol Chem 2011;286(31):27436–46.
[188] Shi S, Ghosh DD, Okumura S, Carattino MD, Kashlan OB, Sheng S, et al. Base of the thumb domain modulates epithelial sodium channel gating. J Biol Chem 2011;286(17):14753–61.
[189] Collier DM, Snyder PM. Extracellular protons regulate human ENaC by modulating Na^+ self-inhibition. J Biol Chem 2009;284 (2):792–8.
[190] Collier DM, Snyder PM. Extracellular chloride regulates the epithelial sodium channel. J Biol Chem 2009;284(43):29320–5.
[191] Collier DM, Snyder PM. Identification of epithelial Na^+ channel (ENaC) intersubunit Cl^- inhibitory residues suggests a trimeric alpha gamma beta channel architecture. J Biol Chem 2011;286(8):6027–32.
[192] Rauh R, Diakov A, Tzschoppe A, Korbmacher J, Azad AK, Cuppens H, et al. A mutation of the epithelial sodium channel associated with atypical cystic fibrosis increases channel open probability and reduces Na^+ self inhibition. J Physiol 2010;588 (Pt 8):1211–25.
[193] Edelheit O, Hanukoglu I, Dascal N, Hanukoglu A. Identification of the roles of conserved charged residues in the extracellular domain of an epithelial sodium channel (ENaC) subunit by alanine mutagenesis. Am J Physiol Renal Physiol 2011;300(4):F887–97.
[194] Bruns JB, Hu B, Ahn YJ, Sheng S, Hughey RP, Kleyman TR. Multiple epithelial Na^+ channel domains participate in subunit assembly. Am J Physiol Renal Physiol 2003;285(4):F600–9.
[195] Vallet V, Chraibi A, Gaeggeler HP, Horisberger JD, Rossier BC. An epithelial serine protease activates the amiloride-sensitive sodium channel. Nature 1997;389(6651):607–10.
[196] Vuagniaux G, Vallet V, Jaeger NF, Pfister C, Bens M, Farman N, et al. Activation of the amiloride-sensitive epithelial sodium channel by the serine protease mCAP1 expressed in a mouse

cortical collecting duct cell line. J Am Soc Nephrol 2000;11 (5):828–34.
[197] Adachi M, Kitamura K, Miyoshi T, Narikiyo T, Iwashita K, Shiraishi N, et al. Activation of epithelial sodium channels by prostasin in *Xenopus* oocytes. J Am Soc Nephrol 2001;12 (6):1114–21.
[198] Guipponi M, Vuagniaux G, Wattenhofer M, Shibuya K, Vazquez M, Dougherty L, et al. The transmembrane serine protease (TMPRSS3) mutated in deafness DFNB8/10 activates the epithelial sodium channel (ENaC) *in vitro*. Hum Mol Genet 2002;11(23):2829–36.
[199] Adebamiro A, Cheng Y, Rao US, Danahay H, Bridges RJ. A segment of gamma ENaC mediates elastase activation of Na^+ transport. J Gen Physiol 2007;130(6):611–29.
[200] Bruns JB, Carattino MD, Sheng S, Maarouf AB, Weisz OA, Pilewski JM, et al. Epithelial Na^+ channels are fully activated by furin- and prostasin-dependent release of an inhibitory peptide from the gamma-subunit. J Biol Chem 2007;282 (9):6153–60.
[201] Garty H, Benos DJ. Characteristics and regulatory mechanisms of the amiloride-blockable Na^+ channel. Physiol Rev 1988;68 (2):309–73.
[202] Chraibi A, Horisberger JD. Na self inhibition of human epithelial Na channel: temperature dependence and effect of extracellular proteases. J Gen Physiol 2002;120(2):133–45.
[203] Segal A, Cucu D, Van Driessche W, Weber WM. Rat ENaC expressed in *Xenopus laevis* oocytes is activated by cAMP and blocked by $Ni(^{2+})$. FEBS Lett 2002;515(1–3):177–83.
[204] Althaus M, Bogdan R, Clauss WG, Fronius M. Mechano-sensitivity of epithelial sodium channels (ENaCs): laminar shear stress increases ion channel open probability. FASEB J 2007;21 (10):2389–99.
[205] Chen J, Winarski KL, Sheng S. Mutations in extracellular domains reverse Zn^{2+}. Activation of human epithelial Na^+ channels. Biophys J 2010;98(3, Suppl. 1):532a.
[206] Yu L, Eaton DC, Helms MN. Effect of divalent heavy metals on epithelial Na^+ channels in A6 cells. Am J Physiol Renal Physiol 2007;293(1):F236–44.
[207] Rossier BC, Pradervand S, Schild L, Hummler E. Epithelial sodium channel and the control of sodium balance: interaction between genetic and environmental factors. Annu Rev Physiol 2002;64:877–97.
[208] Kellenberger S, Gautschi I, Schild L. A single point mutation in the pore region of the epithelial Na^+ channel changes ion selectivity by modifying molecular sieving. Proc Natl Acad Sci USA 1999;96(7):4170–5.
[209] Snyder PM, Olson DR, Bucher DB. A pore segment in DEG/ENaC $Na(^+)$ channels. J Biol Chem 1999;274(40): 28484–90.
[210] Kellenberger S, Gautschi I, Schild L. Mutations in the epithelial Na^+ channel ENaC outer pore disrupt amiloride block by increasing its dissociation rate. Mol Pharmacol 2003;64 (4):848–56.
[211] Kellenberger S, Hoffmann-Pochon N, Gautschi I, Schneeberger E, Schild L. On the molecular basis of ion permeation in the epithelial Na^+ channel. J Gen Physiol 1999;114(1):13–30.
[212] Li J, Sheng S, Perry CJ, Kleyman TR. Asymmetric organization of the pore region of the epithelial sodium channel. J Biol Chem 2003;278(16):13867–74.
[213] Sheng S, Perry CJ, Kashlan OB, Kleyman TR. Side chain orientation of residues lining the selectivity filter of epithelial Na^+ channels. J Biol Chem 2005;280(9):8513–22.
[214] Kellenberger S, Auberson M, Gautschi I, Schneeberger E, Schild L. Permeability properties of ENaC selectivity filter mutants. J Gen Physiol 2001;118(6):679–92.
[215] Takeda AN, Gautschi I, van Bemmelen MX, Schild L. Cadmium trapping in an epithelial sodium channel pore mutant. J Biol Chem 2007;282(44):31928–36.
[216] Langloh AL, Berdiev B, Ji HL, Keyser K, Stanton BA, Benos DJ. Charged residues in the M2 region of alpha-hENaC play a role in channel conductance. Am J Physiol Cell Physiol 2000;278(2): C277–91.
[217] Driscoll M, Chalfie M. The mec-4 gene is a member of a family of *Caenorhabditis elegans* genes that can mutate to induce neuronal degeneration. Nature 1991;349(6310):588–93.
[218] Hong K, Driscoll M. A transmembrane domain of the putative channel subunit MEC-4 influences mechanotransduction and neurodegeneration in *C. elegans*. Nature 1994;367 (6462):470–3.
[219] Kellenberger S, Gautschi I, Schild L. An external site controls closing of the epithelial Na^+ channel ENaC. J Physiol 2002;543 (Pt 2):413–24.
[220] Carattino MD, Sheng S, Kleyman TR. Epithelial Na^+ channels are activated by laminar shear stress. J Biol Chem 2004;279 (6):4120–6.
[221] Carattino MD, Sheng S, Kleyman TR. Mutations in the pore region modify epithelial sodium channel gating by shear stress. J Biol Chem 2005;280(6):4393–401.
[222] Carattino MD, Sheng S, Kleyman TR. Mutations in the pore region modify epithelial sodium channel gating by shear stress. J Biol Chem 2005;280(6):4393–401.
[223] Zhang P, Fyfe GK, Grichtchenko II, Canessa CM. Inhibition of alphabeta epithelial sodium channels by external protons indicates that the second hydrophobic domain contains structural elements for closing the pore. Biophys J 1999;77(6):3043–51.
[224] Fyfe GK, Zhang P, Canessa CM. The second hydrophobic domain contributes to the kinetic properties of epithelial sodium channels. J Biol Chem 1999;274(51):36415–21.
[225] Ji HL, Parker S, Langloh AL, Fuller CM, Benos DJ. Point mutations in the post-M2 region of human alpha-ENaC regulate cation selectivity. Am J Physiol Cell Physiol 2001;281(1):C64–74.
[226] Booth RE, Tong Q, Medina J, Snyder PM, Patel P, Stockand JD. A region directly following the second transmembrane domain in gamma ENaC is required for normal channel gating. J Biol Chem 2003;278(42):41367–79.
[227] Pochynyuk O, Staruschenko A, Tong Q, Medina J, Stockand JD. Identification of a functional phosphatidylinositol 3,4,5-trisphosphate binding site in the epithelial Na^+ channel. J Biol Chem 2005;280(45):37565–71.
[228] Pochynyuk O, Bugaj V, Stockand JD. Physiologic regulation of the epithelial sodium channel by phosphatidylinositides. Curr Opin Nephrol Hypertens 2008;17(5):533–40.
[229] Snyder PM, Price MP, McDonald FJ, Adams CM, Volk KA, Zeiher BG, et al. Mechanism by which Liddle's syndrome mutations increase activity of a human epithelial Na^+ channel. Cell 1995;83(6):969–78.
[230] Kamynina E, Debonneville C, Bens M, Vandewalle A, Staub O. A novel mouse Nedd4 protein suppresses the activity of the epithelial Na^+ channel. Faseb J 2001;15(1):204–14.
[231] Samaha FF, Rubenstein RC, Yan W, Ramkumar M, Levy DI, Ahn YJ, et al. Functional polymorphism in the carboxyl terminus of the alpha-subunit of the human epithelial sodium channel. J Biol Chem 2004;279(23):23900–7.
[232] Yan W, Suaud L, Kleyman TR, Rubenstein RC. Differential modulation of a polymorphism in the carboxyl terminus of the alpha subunit of the human epithelial sodium channel by protein kinase C {delta}. Am J Physiol Renal Physiol 2005;290(2): F279–88.
[233] Shi H, Asher C, Chigaev A, Yung Y, Reuveny E, Seger R, et al. Interactions of beta and gamma ENaC with Nedd4 can be

facilitated by an ERK-mediated phosphorylation. J Biol Chem 2002;277(16):13539–47.
[234] Shi H, Asher C, Yung Y, Kligman L, Reuveny E, Seger R, et al. Casein kinase 2 specifically binds to and phosphorylates the carboxy termini of ENaC subunits. Eur J Biochem 2002;269 (18):4551–8.
[235] Diakov A, Korbmacher C. A novel pathway of epithelial sodium channel activation involves a serum- and glucocorticoid-inducible kinase consensus motif in the C terminus of the channel's alpha-subunit. J Biol Chem 2004;279(37):38134–42.
[236] Dinudom A, Fotia AB, Lefkowitz RJ, Young JA, Kumar S, Cook DI. The kinase Grk2 regulates Nedd4/Nedd4-2-dependent control of epithelial Na^+ channels. Proc Natl Acad Sci USA 2004;101(32):11886–90.
[237] Bachhuber T, Almaca J, Aldehni F, Mehta A, Amaral MD, Schreiber R, et al. Regulation of the epithelial Na^+ channel by the protein kinase CK2. J Biol Chem 2008;283(19):13225–32.
[238] Shimkets RA, Lifton R, Canessa CM. *In vivo* phosphorylation of the epithelial sodium channel. Proc Natl Acad Sci USA 1998;95(6):3301–5.
[239] Volk KA, Snyder PM, Stokes JB. Regulation of epithelial sodium channel activity through a region of the carboxyl terminus of the alpha-subunit. Evidence for intracellular kinase-mediated reactions. J Biol Chem 2001;276(47):43887–93.
[240] Palmer LG. Epithelial Na channels: the nature of the conducting pore. Ren Physiol Biochem 1990;13(1–2):51–8.
[241] Kellenberger S, Schild L. Epithelial sodium channel/degenerin family of ion channels: a variety of functions for a shared structure. Physiol Rev 2002;82(3):735–67.
[242] Benos DJ, Mandel LJ, Simon SA. Cationic selectivity and competition at the sodium entry site in frog skin. J Gen Physiol 1980;76(2):233–47.
[243] Palmer LG. Ion selectivity of the apical membrane Na channel in the toad urinary bladder. J Membr Biol 1982;67(2):91–8.
[244] Eisenman G. Cation selective glass electrodes and their mode of operation. Biophys J 1962;2((2)Pt 2):259–323.
[245] Payandeh J, Scheuer T, Zheng N, Catterall WA. The crystal structure of a voltage-gated sodium channel. Nature 2011;475 (7356):353–8.
[246] Khakh BS, Lester HA. Dynamic selectivity filters in ion channels. Neuron 1999;23(4):653–8.
[247] Roux B. Ion conduction and selectivity in $K(^+)$ channels. Annu Rev Biophys Biomol Struct 2005;34:153–71.
[248] Berneche S, Roux B. A gate in the selectivity filter of potassium channels. Structure (Camb) 2005;13(4):591–600.
[249] Cuello LG, Jogini V, Cortes DM, Pan AC, Gagnon DG, Dalmas O, et al. Structural basis for the coupling between activation and inactivation gates in $K(^+)$ channels. Nature 2010;466 (7303):272–5.
[250] Cuello LG, Jogini V, Cortes DM, Perozo E. Structural mechanism of C-type inactivation in $K(^+)$ channels. Nature 2010;466 (7303):203–8.
[251] Chalfant ML, Peterson-Yantorno K, O'Brien TG, Civan MM. Regulation of epithelial Na^+ channels from M-1 cortical collecting duct cells. Am J Physiol 1996;271(4 Pt 2):F861–70.
[252] Garty H, Palmer LG. Epithelial sodium channels: function, structure, and regulation. Physiol Rev 1997;77(2):359–96.
[253] Fyfe GK, Canessa CM. Subunit composition determines the single channel kinetics of the epithelial sodium channel. J Gen Physiol 1998;112(4):423–32.
[254] Horisberger JD, Chraibi A. Epithelial sodium channel: a ligand-gated channel? Nephron Physiol 2004;96(2):p37–41.
[255] Kelly O, Lin C, Ramkumar M, Saxena NC, Kleyman TR, Eaton DC. Characterization of an amiloride binding region in the alpha-subunit of ENaC. Am J Physiol Renal Physiol 2003;285 (6):F1279–90.
[256] Ji HL, Fuller CM, Benos DJ. Intrinsic gating mechanisms of epithelial sodium channels. Am J Physiol Cell Physiol 2002;283(2): C646–50.
[257] Liu J, Siegelbaum SA. Change of pore helix conformational state upon opening of cyclic nucleotide-gated channels. Neuron 2000;28(3):899–909.
[258] Alagem N, Yesylevskyy S, Reuveny E. The pore helix is involved in stabilizing the open state of inwardly rectifying K^+ channels. Biophys J 2003;85(1):300–12.
[259] Seebohm G, Westenskow P, Lang F, Sanguinetti MC. Mutation of colocalized residues of the pore helix and transmembrane segments S5 and S6 disrupt deactivation and modify inactivation of KCNQ1 K^+ channels. J Physiol 2005; 563(Pt 2):359–68.
[260] Yeh BI, Kim YK, Jabbar W, Huang CL. Conformational changes of pore helix coupled to gating of TRPV5 by protons. Embo J 2005;24(18):3224–34.
[261] Tolino LA, Okumura S, Kashlan OB, Carattino MD. Insights into the mechanism of pore opening of acid-sensing ion channel 1a. J Biol Chem 2011;286(18):16297–307.
[262] Hodgkin AL, Huxley AF. A quantitative description of membrane current and its application to conduction and excitability in nerve. Journal of Physiology 1952;117:500–44.
[263] Zheng J, Sigworth FJ. Selectivity changes during activation of mutant Shaker potassium channels. J Gen Physiol 1997;110 (2):101–17.
[264] Zhang ZR, McDonough SI, McCarty NA. Interaction between permeation and gating in a putative pore domain mutant in the cystic fibrosis transmembrane conductance regulator. Biophys J 2000;79(1):298–313.
[265] Swenson Jr. RP, Armstrong CM. $K.^+$ channels close more slowly in the presence of external K^+ and Rb^+. Nature 1981;291(5814):427–9.
[266] Demo SD, Yellen G. Ion effects on gating of the $Ca(^{2+})$-activated K^+ channel correlate with occupancy of the pore. Biophys J 1992;61(3):639–48.
[267] Lu T, Ting AY, Mainland J, Jan LY, Schultz PG, Yang J. Probing ion permeation and gating in a K^+ channel with backbone mutations in the selectivity filter. Nat Neurosci 2001;4 (3):239–46.
[268] Zhou Y, Morais-Cabral JH, Kaufman A, MacKinnon R. Chemistry of ion coordination and hydration revealed by a K^+ channel-Fab complex at 2.0 Å resolution. Nature 2001;414 (6859):43–8.
[269] Domene C, Grottesi A, Sansom MS. Filter flexibility and distortion in a bacterial inward rectifier K^+ channel: simulation studies of KirBac1.1. Biophys J 2004;87(1):256–67.
[270] Domene C, Sansom MS. Potassium channel, ions, and water: simulation studies based on the high resolution X-ray structure of KcsA. Biophys J 2003;85(5):2787–800.
[271] Matulef K, Zagotta WN. Cyclic nucleotide-gated ion channels. Annu Rev Cell Dev Biol 2003;19:23–44.
[272] Xiao J, Zhen XG, Yang J. Localization of PIP2 activation gate in inward rectifier K^+ channels. Nat Neurosci 2003;6(8):811–8.
[273] Proks P, Antcliff JF, Ashcroft FM. The ligand-sensitive gate of a potassium channel lies close to the selectivity filter. EMBO Rep 2003;4(1):70–5.
[274] Matalon S, Lazrak A, Jain L, Eaton DC. Invited review: Biophysical properties of sodium channels in lung alveolar epithelial cells. J Appl Physiol 2002;93(5):1852–9.
[275] Donaldson SH, Boucher RC. Sodium channels and cystic fibrosis. Chest 2007;132(5):1631–6.

[276] Eaton DC, Helms MN, Koval M, Bao HF, Jain L. The contribution of epithelial sodium channels to alveolar function in health and disease. Annu Rev Physiol 2009;71:403–23.
[277] Shimkets RA, Warnock DG, Bositis CM, Nelson-Williams C, Hansson JH, Schambelan M, et al. Liddle's syndrome: heritable human hypertension caused by mutations in the beta subunit of the epithelial sodium channel. Cell 1994;79 (3):407–14.
[278] Warnock DG. Liddle syndrome: genetics and mechanisms of Na^+ channel defects. Am J Med Sci 2001;322(6):302–7.
[279] Tamura H, Schild L, Enomoto N, Matsui N, Marumo F, Rossier BC. Liddle disease caused by a missense mutation of beta subunit of the epithelial sodium channel gene. J Clin Invest 1996;97(7):1780–4.
[280] Hansson JH, Schild L, Lu Y, Wilson TA, Gautschi I, Shimkets R, et al. A *de novo* missense mutation of the beta subunit of the epithelial sodium channel causes hypertension and Liddle syndrome, identifying a proline-rich segment critical for regulation of channel activity. Proc Natl Acad Sci USA 1995;92 (25):11495–9.
[281] Hansson JH, Nelson-Williams C, Suzuki H, Schild L, Shimkets R, Lu Y, et al. Hypertension caused by a truncated epithelial sodium channel gamma subunit: Genetic heterogeneity of Liddle syndrome. Nat Genet 1995;11(1):76–82.
[282] Staub O, Dho S, Henry P, Correa J, Ishikawa T, McGlade J, et al. WW domains of Nedd4 bind to the proline-rich PY motifs in the epithelial Na^+ channel deleted in Liddle's syndrome. Embo J 1996;15(10):2371–80.
[283] Staub O, Abriel H, Plant P, Ishikawa T, Kanelis V, Saleki R, et al. Regulation of the epithelial Na^+ channel by Nedd4 and ubiquitination. Kidney Int 2000;57(3):809–15.
[284] Snyder PM, Olson DR, McDonald FJ, Bucher DB. Multiple WW domains, but not the C2 domain, are required for inhibition of the epithelial Na^+ channel by human Nedd4. J Biol Chem 2001;276(30):28321–6.
[285] Itani OA, Campbell JR, Herrero J, Snyder PM, Thomas CP. Alternate promoters and variable splicing lead to hNedd4-2 isoforms with a C2 domain and varying number of WW domains. Am J Physiol Renal Physiol 2003;285(5):F916–29.
[286] Itani OA, Stokes JB, Thomas CP. Nedd4-2 isoforms differentially associate with ENaC and regulate its activity. Am J Physiol Renal Physiol 2005;289(2):F334–46.
[287] Plant PJ, Yeger H, Staub O, Howard P, Rotin D. The C2 domain of the ubiquitin protein ligase Nedd4 mediates Ca^{2+}-dependent plasma membrane localization. J Biol Chem 1997;272(51):32329–36.
[288] Plant PJ, Lafont F, Lecat S, Verkade P, Simons K, Rotin D. Apical membrane targeting of Nedd4 is mediated by an association of its C2 domain with annexin XIIIb. J Cell Biol 2000;149 (7):1473–84.
[289] Fotia AB, Dinudom A, Shearwin KE, Koch JP, Korbmacher C, Cook DI, et al. The role of individual Nedd4-2 (KIAA0439) WW domains in binding and regulating epithelial sodium channels. Faseb J 2003;17(1):70–2.
[290] Lott JS, Coddington-Lawson SJ, Teesdale-Spittle PH, McDonald FJ. A single WW domain is the predominant mediator of the interaction between the human ubiquitin-protein ligase Nedd4 and the human epithelial sodium channel. Biochem J 2002;361(Pt 3):481–8.
[291] Kamynina E, Staub O. Concerted action of ENaC, Nedd4-2, and Sgk1 in transepithelial $Na(^+)$ transport. Am J Physiol Renal Physiol 2002;283(3):F377–87.
[292] Lu C, Pribanic S, Debonneville A, Jiang C, Rotin D. The PY motif of ENaC, mutated in Liddle syndrome, regulates channel internalization, sorting and mobilization from subapical pool. Traffic 2007;8(9):1246–64.
[293] Lee IH, Campbell CR, Song SH, Day ML, Kumar S, Cook DI, et al. The activity of the epithelial sodium channels is regulated by caveolin-1 via a Nedd4-2-dependent mechanism. J Biol Chem 2009;284(19):12663–9.
[294] McCormick JA, Bhalla V, Pao AC, Pearce D. SGK1: a rapid aldosterone-induced regulator of renal sodium reabsorption. Physiology (Bethesda) 2005;20:134–9.
[295] Snyder PM. The epithelial Na^+ channel: cell surface insertion and retrieval in Na^+ homeostasis and hypertension. Endocr Rev 2002;23(2):258–75.
[296] Snyder PM. Regulation of epithelial Na^+ channel trafficking. Endocrinology 2005;146(12):5079–85.
[297] Snyder PM, Olson DR, Kabra R, Zhou R, Steines JC. cAMP and serum and glucocorticoid-inducible kinase (SGK) regulate the epithelial $Na(^+)$ channel through convergent phosphorylation of Nedd4-2. J Biol Chem 2004;279(44):45753–8.
[298] Bhalla V, Daidie D, Li H, Pao AC, LaGrange LP, Wang J, et al. Serum- and glucocorticoid-regulated kinase 1 regulates ubiquitin ligase neural precursor cell-expressed, developmentally downregulated protein 4-2 by inducing interaction with 14-3-3. Mol Endocrinol 2005;19(12):3073–84.
[299] Bhalla V, Oyster NM, Fitch AC, Wijngaarden MA, Neumann D, Schlattner U, et al. AMP-activated kinase inhibits the epithelial Na^+ channel through functional regulation of the ubiquitin ligase Nedd4-2. J Biol Chem 2006;281(36):26159–69.
[300] Edinger RS, Lebowitz J, Li H, Alzamora R, Wang H, Johnson JP, et al. Functional regulation of the epithelial Na^+ channel by IkappaB kinase-beta occurs via phosphorylation of the ubiquitin ligase Nedd4-2. J Biol Chem 2009;284(1):150–7.
[301] Boulkroun S, Ruffieux-Daidie D, Vitagliano JJ, Poirot O, Charles RP, Lagnaz D, et al. Vasopressin-inducible ubiquitin-specific protease 10 increases ENaC cell surface expression by deubiquitylating and stabilizing sorting nexin 3. Am J Physiol Renal Physiol 2008;295(4):F889–900.
[302] Rotin D, Staub O. Role of the ubiquitin system in regulating ion transport. Pflugers Arch 2011;461(1):1–21.
[303] Becchetti A, Malik B, Yue G, Duchatelle P, Al-Khalili O, Kleyman TR, et al. Phosphatase inhibitors increase the open probability of ENaC in A6 cells. Am J Physiol Renal Physiol 2002;283(5):F1030–45.
[304] Volk KA, Husted RF, Snyder PM, Stokes JB. Kinase regulation of hENaC mediated through a region in the COOH-terminal portion of the alpha-subunit. Am J Physiol Cell Physiol 2000;278(5):C1047–54.
[305] Snyder PM, Olson DR, Thomas BC. Serum and glucocorticoid-regulated kinase modulates Nedd4-2-mediated inhibition of the epithelial Na^+ channel. J Biol Chem 2002;277(1):5–8.
[306] Debonneville C, Flores SY, Kamynina E, Plant PJ, Tauxe C, Thomas MA, et al. Phosphorylation of Nedd4-2 by Sgk1 regulates epithelial $Na(^+)$ channel cell surface expression. Embo J 2001;20(24):7052–9.
[307] Flores SY, Loffing-Cueni D, Kamynina E, Daidie D, Gerbex C, Chabanel S, et al. Aldosterone-induced serum and glucocorticoid-induced kinase 1 expression is accompanied by Nedd4-2 phosphorylation and increased Na + transport in cortical collecting duct cells. J Am Soc Nephrol 2005;16(8):2279–87.
[308] Bhalla V, Daidie D, Li H, Pao AC, Lagrange LP, Wang J, et al. SGK1 regulates ubiquitin ligase Nedd4-2 by inducing interaction with 14-3-3. Mol Endocrinol 2005;19(12):3073–84.
[309] Ichimura T, Yamamura H, Sasamoto K, Tominaga Y, Taoka M, Kakiuchi K, et al. 14-3-3 proteins modulate the expression of epithelial Na^+ channels by phosphorylation-dependent

interaction with Nedd4-2 ubiquitin ligase. J Biol Chem 2005;280(13):13187–94.
[310] Blazer-Yost BL, Esterman MA, Vlahos CJ. Insulin-stimulated trafficking of ENaC in renal cells requires PI 3-kinase activity. Am J Physiol Cell Physiol 2003;284(6):C1645–53.
[311] Snyder PM. Liddle's syndrome mutations disrupt cAMP-mediated translocation of the epithelial Na(+) channel to the cell surface. J Clin Invest 2000;105(1):45–53.
[312] Morris RG, Schafer JA. cAMP increases density of ENaC subunits in the apical membrane of MDCK cells in direct proportion to amiloride-sensitive Na(+) transport. J Gen Physiol 2002;120(1):71–85.
[313] Lebowitz J, Edinger RS, An B, Perry CJ, Onate S, Kleyman TR, et al. Ikappab kinase-beta (ikkbeta) modulation of epithelial sodium channel activity. J Biol Chem 2004;279(40):41985–90.
[314] Gilmore ES, Stutts MJ, Milgram SL. SRC family kinases mediate epithelial Na^+ channel inhibition by endothelin. J Biol Chem 2001;276(45):42610–7.
[315] Ling BN, Eaton DC. Effects of luminal Na^+ on single Na^+ channels in A6 cells, a regulatory role for protein kinase C. Am J Physiol 1989;256(6 Pt 2):F1094–103.
[316] Yue G, Edinger RS, Bao HF, Johnson JP, Eaton DC. The effect of rapamycin on single ENaC channel activity and phosphorylation in A6 cells. Am J Physiol Cell Physiol 2000;279(1):C81–8.
[317] Booth RE, Stockand JD. Targeted degradation of ENaC in response to PKC activation of the ERK1/2 cascade. Am J Physiol Renal Physiol 2003;284(5):F938–47.
[318] Woollhead AM, Scott JW, Hardie DG, Baines DL. Phenformin and 5-aminoimidazole-4-carboxamide-1-beta-D-ribofuranoside (AICAR) activation of AMP-activated protein kinase inhibits transepithelial Na^+ transport across H441 lung cells. J Physiol 2005;566(Pt 3):781–92.
[319] Zhang YH, Alvarez de la Rosa D, Canessa CM, Hayslett JP. Insulin-induced phosphorylation of ENaC correlates with increased sodium channel function in A6 cells. Am J Physiol Cell Physiol 2005;288(1):C141–7.
[320] Feldman RD. Deactivation of vasodilator responses by GRK2 overexpression: a mechanism or the mechanism for hypertension? Mol Pharmacol 2002;61(4):707–9.
[321] Sanchez-Perez A, Kumar S, Cook DI. GRK2 interacts with and phosphorylates Nedd4 and Nedd4-2. Biochem Biophys Res Commun 2007;359(3):611–5.
[322] Lee IH, Song SH, Campbell CR, Kumar S, Cook DI, Dinudom A. Regulation of the epithelial Na^+ channel by the RH domain of G protein-coupled receptor kinase, GRK2, and Galphaq/11. J Biol Chem 2011;286(22):19259–69.
[323] Kahle KT, Wilson FH, Leng Q, Lalioti MD, O'Connell AD, Dong K, et al. WNK4 regulates the balance between renal NaCl reabsorption and K^+ secretion. Nat Genet 2003;35(4):372–6.
[324] Furgeson SB, Linas S. Mechanisms of type I and type II pseudohypoaldosteronism. J Am Soc Nephrol 2010;21(11):1842–5.
[325] Wilson FH, Disse-Nicodeme S, Choate KA, Ishikawa K, Nelson-Williams C, Desitter I, et al. Human hypertension caused by mutations in WNK kinases. Science 2001;293(5532):1107–12.
[326] Ring AM, Leng Q, Rinehart J, Wilson FH, Kahle KT, Hebert SC, et al. An SGK1 site in WNK4 regulates Na^+ channel and K^+ channel activity and has implications for aldosterone signaling and K^+ homeostasis. Proc Natl Acad Sci USA 2007;104(10):4025–9.
[327] Heise CJ, Xu BE, Deaton SL, Cha SK, Cheng CJ, Earnest S, et al. Serum and glucocorticoid-induced kinase (SGK) 1 and the epithelial sodium channel are regulated by multiple with no lysine (WNK) family members. J Biol Chem 2010;285(33):25161–7.
[328] Xu BE, Stippec S, Chu PY, Lazrak A, Li XJ, Lee BH, et al. WNK1 activates SGK1 to regulate the epithelial sodium channel. Proc Natl Acad Sci USA 2005;102(29):10315–20.
[329] Naray-Fejes-Toth A, Snyder PM, Fejes-Toth G. The kidney-specific WNK1 isoform is induced by aldosterone and stimulates epithelial sodium channel-mediated Na^+ transport. Proc Natl Acad Sci USA 2004;101(50):17434–9.
[330] Xu BE, Stippec S, Lazrak A, Huang CL, Cobb MH. WNK1 activates SGK1 by a PI-3 kinase-dependent and non-catalytic mechanism. J Biol Chem 2005;280(40):34218–23.
[331] Snyder PM. Downregulating destruction: Phosphorylation regulates the E3 ubiquitin ligase Nedd4-2. Sci Signal 2009;2(79):pe41.
[332] Lee IH, Dinudom A, Sanchez-Perez A, Kumar S, Cook DI. Akt mediates the effect of insulin on epithelial sodium channels by inhibiting Nedd4-2. J Biol Chem 2007;282(41):29866–73.
[333] Hallows KR, Bhalla V, Oyster NM, Wijngaarden MA, Lee JK, Li H, et al. Phosphopeptide screen uncovers novel phosphorylation sites of Nedd4-2 that potentiate its inhibition of the epithelial Na^+ channel. J Biol Chem 2010;285(28):21671–8.
[334] Orce GG, Castillo GA, Margolius HS. Inhibition of short-circuit current in toad urinary bladder by inhibitors of glandular kallikrein. Am J Physiol 1980;239(5):F459–65.
[335] Vuagniaux G, Vallet V, Jaeger NF, Hummler E, Rossier BC. Synergistic activation of ENaC by three membrane-bound channel-activating serine proteases (mCAP1, mCAP2, and mCAP3) and serum- and glucocorticoid-regulated kinase (Sgk1) in *Xenopus* oocytes. J Gen Physiol 2002;120(2):191–201.
[336] Picard N, Eladari D, El Moghrabi S, Planes C, Bourgeois S, Houillier P, et al. Defective ENaC processing and function in tissue kallikrein-deficient mice. J Biol Chem 2008;283(8):4602–11.
[337] Harris M, Firsov D, Vuagniaux G, Stutts MJ, Rossier BC. A novel neutrophil elastase inhibitor prevents elastase activation and surface cleavage of the epithelial sodium channel expressed in *Xenopus laevis* oocytes. J Biol Chem 2007;282(1):58–64.
[338] Svenningsen P, Bistrup C, Friis UG, Bertog M, Haerteis S, Krueger B, et al. Plasmin in nephrotic urine activates the epithelial sodium channel. J Am Soc Nephrol 2009;20(2):299–310.
[339] Passero CJ, Mueller GM, Rondon-Berrios H, Tofovic SP, Hughey RP, Kleyman TR. Plasmin activates epithelial Na^+ channels by cleaving the gamma subunit. J Biol Chem 2008;283(52):36586–91.
[340] Thomas G. Furin at the cutting edge: from protein traffic to embryogenesis and disease. Nat Rev Mol Cell Biol 2002;3(10):753–66.
[341] Passero CJ, Mueller GM, Myerburg MM, Carattino MD, Hughey RP, Kleyman TR. TMPRSS4-dependent activation of the epithelial sodium channel requires cleavage of the gamma subunit distal to the furin cleavage site. Am J Physiol Renal Physiol 2011;302(1):F1–8.
[342] Passero CJ, Carattino MD, Kashlan OB, Myerburg MM, Hughey RP, Kleyman TR. Defining an inhibitory domain in the gamma subunit of the epithelial sodium channel. Am J Physiol Renal Physiol 2010;299(4):F854–61.
[343] Carattino MD, Hughey RP, Kleyman TR. Proteolytic processing of the epithelial sodium channel gamma subunit has a dominant role in channel activation. J Biol Chem 2008;283(37):25290–5.
[344] Nielsen J, Kwon TH, Masilamani S, Beutler K, Hager H, Nielsen S, et al. Sodium transporter abundance profiling in

kidney: effect of spironolactone. Am J Physiol Renal Physiol 2002;283(5):F923–33.
[345] Frindt G, Masilamani S, Knepper MA, Palmer LG. Activation of epithelial Na channels during short-term Na deprivation. Am J Physiol Renal Physiol 2001;280(1):F112–8.
[346] Frindt G, Ergonul Z, Palmer LG. Surface expression of epithelial Na channel protein in rat kidney. J Gen Physiol 2008;131 (6):617–27.
[347] Frindt G, Palmer LG. Surface expression of sodium channels and transporters in rat kidney: effects of dietary sodium. Am J Physiol Renal Physiol 2009;297(5):F1249–55.
[348] Gerst JE. SNAREs and SNARE regulators in membrane fusion and exocytosis. Cell Mol Life Sci 1999;55(5):707–34.
[349] Sollner TH. Regulated exocytosis and SNARE function (Review). Mol Membr Biol 2003;20(3):209–20.
[350] Qi J, Peters KW, Liu C, Wang JM, Edinger RS, Johnson JP, et al. Regulation of the amiloride-sensitive epithelial sodium channel by syntaxin 1A. J Biol Chem 1999;274(43):30345–8.
[351] Saxena SK, Singh M, Kaur S, George C. Distinct domain-dependent effect of syntaxin1A on amiloride-sensitive sodium channel (ENaC) currents in HT-29 colonic epithelial cells. Int J Biol Sci 2007;3(1):47–56.
[352] Mall M, Bleich M, Greger R, Schreiber R, Kunzelmann K. The amiloride-inhibitable Na^+ conductance is reduced by the cystic fibrosis transmembrane conductance regulator in normal but not in cystic fibrosis airways. J Clin Invest 1998;102(1):15–21.
[353] Kimura T, Kawabe H, Jiang C, Zhang W, Xiang YY, Lu C, et al. Deletion of the ubiquitin ligase Nedd4L in lung epithelia causes cystic fibrosis-like disease. Proc Natl Acad Sci USA 2011;108(8):3216–21.
[354] Dalemans W, Barbry P, Champigny G, Jallat S, Dott K, Dreyer D, et al. Altered chloride ion channel kinetics associated with the delta F508 cystic fibrosis mutation. Nature 1991;354(6354):526–8.
[355] Stutts MJ, Canessa CM, Olsen JC, Hamrick M, Cohn JA, Rossier BC, et al. CFTR as a cAMP-dependent regulator of sodium channels. Science 1995;269(5225):847–50.
[356] Stutts MJ, Rossier BC, Boucher RC. Cystic fibrosis transmembrane conductance regulator inverts protein kinase A-mediated regulation of epithelial sodium channel single channel kinetics. J Biol Chem 1997;272(22):14037–40.
[357] Ling BN, Zuckerman JB, Lin C, Harte BJ, McNulty KA, Smith PR, et al. Expression of the cystic fibrosis phenotype in a renal amphibian epithelial cell line. J Biol Chem 1997;272(1): 594–600.
[358] Chabot H, Vives MF, Dagenais A, Grygorczyk C, Berthiaume Y, Grygorczyk R. Downregulation of epithelial sodium channel (ENaC) by CFTR co-expressed in *Xenopus* oocytes is independent of Cl^- conductance. J Membr Biol 1999;169(3):175–88.
[359] Konstas AA, Koch JP, Korbmacher C. cAMP-dependent activation of CFTR inhibits the epithelial sodium channel (ENaC) without affecting its surface expression. Pflugers Arch 2003; 445(4):513–21.
[360] Horisberger JD. ENaC-CFTR interactions: the role of electrical coupling of ion fluxes explored in an epithelial cell model. Pflugers Arch 2003;445(4):522–8.
[361] Nagel G, Barbry P, Chabot H, Brochiero E, Hartung K, Grygorczyk R. CFTR fails to inhibit the epithelial sodium channel ENaC, when expressed in *Xenopus laevis* oocytes. J Physiol 2005;564(Pt 3):671–82.
[362] Itani OA, Chen JH, Karp PH, Ernst S, Keshavjee S, Parekh K, et al. Human cystic fibrosis airway epithelia have reduced Cl^- conductance but not increased Na^+ conductance. Proc Nat Acad Sci USA 2011;108(25):10260–5.
[363] Chen JH, Stoltz DA, Karp PH, Ernst SE, Pezzulo AA, Moninger TO, et al. Loss of anion transport without increased sodium absorption characterizes newborn porcine cystic fibrosis airway epithelia. Cell 2010;143(6):911–23.
[364] Jiang Q, Li J, Dubroff R, Ahn YJ, Foskett JK, Engelhardt J, et al. Epithelial sodium channels regulate cystic fibrosis transmembrane conductance regulator chloride channels in *Xenopus* oocytes. J Biol Chem 2000;275(18):13266–74.
[365] Bachhuber T, Konig J, Voelcker T, Murle B, Schreiber R, Kunzelmann K. Cl^- interference with the epithelial Na^+ channel ENaC. J Biol Chem 2005;280(36):31587–94.
[366] Schreiber R, Hopf A, Mall M, Greger R, Kunzelmann K. The first-nucleotide binding domain of the cystic-fibrosis transmembrane conductance regulator is important for inhibition of the epithelial Na^+ channel. Proc Natl Acad Sci USA 1999;96 (9):5310–5.
[367] Reddy MM, Quinton PM. Functional interaction of CFTR and ENaC in sweat glands. Pflugers Arch 2003;445(4):499–503.
[368] Gentzsch M, Dang H, Dang Y, Garcia-Caballero A, Suchindran H, Boucher RC, et al. The cystic fibrosis transmembrane conductance regulator impedes proteolytic stimulation of the epithelial Na^+ channel. J Biol Chem 2010;285(42):32227–32.
[369] Rubenstein RC, Lockwood SR, Lide E, Bauer R, Suaud L, Grumbach Y. Regulation of endogenous ENaC functional expression by CFTR and DeltaF508-CFTR in airway epithelial cells. Am J Physiol Lung Cell Mol Physiol 2011;300(1): L88–101.
[370] Huang P, Gilmore E, Kultgen P, Barnes P, Milgram S, Stutts MJ. Local regulation of cystic fibrosis transmembrane regulator and epithelial sodium channel in airway epithelium. Proc Am Thorac Soc 2004;1(1):33–7.
[371] Sariban-Sohraby S, Burg M, Wiesmann WP, Chiang PK, Johnson JP. Methylation increases sodium transport into A6 apical membrane vesicles: possible mode of aldosterone action. Science 1984;225(4663):745–6.
[372] Stockand JD, Edinger RS, Eaton DC, Johnson JP. Toward understanding the role of methylation in aldosterone-sensitive $Na(^+)$ transport. News Physiol Sci 2000;15:161–5.
[373] Wiesmann WP, Johnson JP, Miura GA, Chaing PK. Aldosterone-stimulated transmethylations are linked to sodium transport. Am J Physiol 1985;248(1 Pt 2):F43–7.
[374] Stockand JD, Edinger RS, Al-Baldawi N, Sariban-Sohraby S, Al-Khalili O, Eaton DC, et al. Isoprenylcysteine-O-carboxyl methyltransferase regulates aldosterone-sensitive $Na(^+)$ reabsorption. J Biol Chem 1999;274(38):26912–6.
[375] Stockand JD, Spier BJ, Worrell RT, Yue G, Al-Baldawi N, Eaton DC. Regulation of $Na(^+)$ reabsorption by the aldosterone-induced small G protein K-Ras2A. J Biol Chem 1999;274(50): 35449–54.
[376] Rokaw MD, Wang JM, Edinger RS, Weisz OA, Hui D, Middleton P, et al. Carboxylmethylation of the beta subunit of xENaC regulates channel activity. J Biol Chem 1998;273 (44):28746–51.
[377] Edinger RS, Yospin J, Perry C, Kleyman TR, Johnson JP. Regulation of epithelial Na^+ channels (ENaC) by methylation: a novel methyltransferase stimulates ENaC activity. J Biol Chem 2006;281(14):9110–7.
[378] Zhang W, Hayashizaki Y, Kone BC. Structure and regulation of the mDot1 gene, a mouse histone H3 methyltransferase. Biochem J 2004;377(Pt 3):641–51.
[379] Zhang W, Xia X, Jalal DI, Kuncewicz T, Xu W, Lesage GD, et al. Aldosterone-sensitive repression of ENaCalpha transcription by a histone H3 lysine-79 methyltransferase. Am J Physiol Cell Physiol 2006;290(3):C936–46.

[380] Zhang W, Xia X, Reisenauer MR, Hemenway CS, Kone BC. Dot1a-AF9 complex mediates histone H3 Lys-79 hypermethylation and repression of ENaCalpha in an aldosterone-sensitive manner. J Biol Chem 2006;281(26):18059–68.

[381] Zhang W, Xia X, Reisenauer MR, Rieg T, Lang F, Kuhl D, et al. Aldosterone-induced Sgk1 relieves Dot1a-Af9-mediated transcriptional repression of epithelial Na^+ channel alpha. J Clin Invest 2007;117(3):773–83.

[382] Reisenauer MR, Wang SW, Xia Y, Zhang W. Dot1a contains three nuclear localization signals and regulates the epithelial Na^+ channel (ENaC) at multiple levels. Am J Physiol Renal Physiol 2010;299(1):F63–76.

[383] Palmer LG, Frindt G. Effects of cell Ca and pH on Na channels from rat cortical collecting tubule. Am J Physiol 1987;253(2 Pt 2):F333–9.

[384] Garty H, Asher C, Yeger O. Direct inhibition of epithelial Na^+ channels by a pH-dependent interaction with calcium, and by other divalent ions. J Membr Biol 1987;95(2):151–62.

[385] Ishikawa T, Marunaka Y, Rotin D. Electrophysiological characterization of the rat epithelial Na^+ channel (rENaC) expressed in MDCK cells. Effects of Na^+ and Ca^{2+}. J Gen Physiol 1998;111(6):825–46.

[386] Harvey BJ, Thomas SR, Ehrenfeld J. Intracellular pH controls cell membrane Na^+ and K^+ conductances and transport in frog skin epithelium. J Gen Physiol 1988;92(6):767–91.

[387] Chalfant ML, Denton JS, Berdiev BK, Ismailov II, Benos DJ, Stanton BA. Intracellular H^+ regulates the alpha-subunit of ENaC, the epithelial Na^+ channel. Am J Physiol 1999;276(2 Pt 1):C477–86.

[388] Ishikawa T, Jiang C, Stutts MJ, Marunaka Y, Rotin D. Regulation of the epithelial Na^+ channel by cytosolic ATP. J Biol Chem 2003;278(40):38276–86.

[389] Xu H, Chu S. ENaC alpha-subunit variants are expressed in lung epithelial cells and are suppressed by oxidative stress. Am J Physiol Lung Cell Mol Physiol 2007;293(6):L1454–62.

[390] Ma HP. Hydrogen peroxide stimulates the epithelial sodium channel through a phosphatidylinositide 3-kinase-dependent pathway. J Biol Chem 2011;286(37):32444–53.

[391] Takemura Y, Goodson P, Bao HF, Jain L, Helms MN. Rac1-mediated NADPH oxidase release of O_2^- regulates epithelial sodium channel activity in the alveolar epithelium. Am J Physiol Lung Cell Mol Physiol 2010;298(4):L509–20.

[392] Jain L, Chen XJ, Brown LA, Eaton DC. Nitric oxide inhibits lung sodium transport through a cGMP-mediated inhibition of epithelial cation channels. Am J Physiol 1998;274(4 Pt 1):L475–84.

[393] Ding JW, Dickie J, O'Brodovich H, Shintani Y, Rafii B, Hackam D, et al. Inhibition of amiloride-sensitive sodium-channel activity in distal lung epithelial cells by nitric oxide. Am J Physiol 1998;274(3 Pt 1):L378–87.

[394] Hardiman KM, McNicholas-Bevensee CM, Fortenberry J, Myles CT, Malik B, Eaton DC, et al. Regulation of amiloride-sensitive $Na(^+)$ transport by basal nitric oxide. Am J Respir Cell Mol Biol 2004;30(5):720–8.

[395] Helms MN, Yu L, Malik B, Kleinhenz DJ, Hart CM, Eaton DC. Role of SGK1 in nitric oxide inhibition of ENaC in Na^+-transporting epithelia. Am J Physiol Cell Physiol 2005;289(3):C717–26.

[396] Helms MN, Jain L, Self JL, Eaton DC. Redox regulation of epithelial sodium channels examined in alveolar type 1 and 2 cells patch-clamped in lung slice tissue. J Biol Chem 2008;283(33):22875–83.

[397] Worrell RT, Bao HF, Denson DD, Eaton DC. Contrasting effects of cPLA2 on epithelial Na^+ transport. Am J Physiol Cell Physiol 2001;281(1):C147–56.

[398] Wei Y, Lin DH, Kemp R, Yaddanapudi GS, Nasjletti A, Falck JR, et al. Arachidonic acid inhibits epithelial Na channel via cytochrome P450 (CYP) epoxygenase-dependent metabolic pathways. J Gen Physiol 2004;124(6):719–27.

[399] Pavlov TS, Ilatovskaya DV, Levchenko V, Mattson DL, Roman RJ, Staruschenko A. Effects of cytochrome P-450 metabolites of arachidonic acid on the epithelial sodium channel (ENaC). Am J Physiol Renal Physiol 2011;301(3):F672–81.

[400] Padron D, Wang YJ, Yamamoto M, Yin H, Roth MG. Phosphatidylinositol phosphate 5-kinase Ibeta recruits AP-2 to the plasma membrane and regulates rates of constitutive endocytosis. J Cell Biol 2003;162(4):693–701.

[401] Hilgemann DW, Feng S, Nasuhoglu C. The complex and intriguing lives of PIP2 with ion channels and transporters. Sci STKE 2001;2001(111):RE19.

[402] Staruschenko A, Nichols A, Medina JL, Camacho P, Zheleznova NN, Stockand JD. Rho small GTPases activate the epithelial $Na(^+)$ channel. J Biol Chem 2004;279(48):49989–94.

[403] Weixel KM, Edinger RS, Kester L, Guerriero CJ, Wang H, Fang L, et al. Phosphatidylinositol 4-phosphate 5-kinase reduces cell surface expression of the epithelial sodium channel (ENaC) in cultured collecting duct cells. J Biol Chem 2007;282(50):36534–42.

[404] Butterworth MB, Edinger RS, Frizzell RA, Johnson JP. Regulation of the epithelial sodium channel by membrane trafficking. Am J Physiol Renal Physiol 2009;296(1):F10–24.

[405] Van Driessche W, Zeiske W. Ionic channels in epithelial cell membranes. Physiol Rev 1985;65(4):833–903.

[406] Awayda MS. Regulation of the epithelial $Na(^+)$ channel by intracellular $Na(^+)$. Am J Physiol 1999;277(2 Pt 1):C216–24.

[407] Frindt G, Palmer LG, Windhager EE. Feedback regulation of Na channels in rat CCT. IV. Mediation by activation of protein kinase C. Am J Physiol 1996;270(2 Pt 2):F371–6.

[408] Kellenberger S, Gautschi I, Rossier BC, Schild L. Mutations causing Liddle syndrome reduce sodium-dependent downregulation of the epithelial sodium channel in the *Xenopus* oocyte expression system. J Clin Invest 1998;101(12):2741–50.

[409] Harvey KF, Dinudom A, Cook DI, Kumar S. The Nedd4-like protein KIAA0439 is a potential regulator of the epithelial sodium channel. J Biol Chem 2001;276(11):8597–601.

[410] Harvey KF, Dinudom A, Komwatana P, Jolliffe CN, Day ML, Parasivam G, et al. All three WW domains of murine Nedd4 are involved in the regulation of epithelial sodium channels by intracellular Na. J Biol Chem 1999;274(18):12525–30.

[411] Bengrine A, Li J, Awayda MS. The A-kinase anchoring protein 15 regulates feedback inhibition of the epithelial Na^+ channel. FASEB J 2007;21(4):1189–201.

[412] Knight KK, Wentzlaff DM, Snyder PM. Intracellular sodium regulates proteolytic activation of the epithelial sodium channel. J Biol Chem 2008;283(41):27477–82.

[413] Fuchs W, Larsen EH, Lindemann B. Current–voltage curve of sodium channels and concentration dependence of sodium permeability in frog skin. J Physiol 1977;267(1):137–66.

[414] Chraibi A, Horisberger JD. Dual effect of temperature on the human epithelial Na^+ channel. Pflugers Arch 2003;447(3):316–20.

[415] Yki-Jarvinen H. Thiazolidinediones. N Engl J Med 2004;351(11):1106–18.

[416] Guan Y, Zhang Y, Davis L, Breyer MD. Expression of peroxisome proliferator-activated receptors in urinary tract of rabbits and humans. Am J Physiol 1997;273(6 Pt 2):F1013–22.

[417] Guan Y, Hao C, Cha DR, Rao R, Lu W, Kohan DE, et al. Thiazolidinediones expand body fluid volume through PPARgamma stimulation of ENaC-mediated renal salt absorption. Nat Med 2005;11(8):861–6.

[418] Artunc F, Sandulache D, Nasir O, Boini KM, Friedrich B, Beier N, et al. Lack of the serum and glucocorticoid-inducible kinase SGK1 attenuates the volume retention after treatment with the PPARgamma agonist pioglitazone. Pflugers Arch 2008;456 (2):425–36.

[419] Renauld S, Tremblay K, Ait-Benichou S, Simoneau-Roy M, Garneau H, Staub O, et al. Stimulation of ENaC activity by rosiglitazone is PPARgamma-dependent and correlates with SGK1 expression increase. J Membr Biol 2010;236(3):259–70.

[420] Nofziger C, Chen L, Shane MA, Smith CD, Brown KK, Blazer-Yost BL. PPARgamma agonists do not directly enhance basal or insulin-stimulated $Na(^+)$ transport via the epithelial $Na(^+)$ channel. Pflugers Arch 2005;451(3):445–53.

[421] Borsting E, Cheng VP, Glass CK, Vallon V, Cunard R. Peroxisome proliferator-activated receptor gamma agonists repress epithelial sodium channel expression in the kidney. Am J Physiol Renal Physiol 2012;302(5):F540–51.

[422] Pochynyuk O, Bugaj V, Vandewalle A, Stockand JD. Purinergic control of apical plasma membrane PI(4,5)P2 levels sets ENaC activity in principal cells. Am J Physiol Renal Physiol 2008;294(1):F38–46.

[423] Ma HP, Chou CF, Wei SP, Eaton DC. Regulation of the epithelial sodium channel by phosphatidylinositides: experiments, implications, and speculations. Pflugers Arch 2007;455(1): 169–80.

[424] Pochynyuk O, Rieg T, Bugaj V, Schroth J, Fridman A, Boss GR, et al. Dietary Na^+ inhibits the open probability of the epithelial sodium channel in the kidney by enhancing apical P2Y2-receptor tone. FASEB J 2010;24(6):2056–65.

[425] Stockand JD, Mironova E, Bugaj V, Rieg T, Insel PA, Vallon V, et al. Purinergic inhibition of ENaC produces aldosterone escape. J Am Soc Nephrol 2010;21(11):1903–11.

[426] Mironova E, Peti-Peterdi J, Bugaj V, Stockand JD. Diminished paracrine regulation of the epithelial Na^+ channel by purinergic signaling in mice lacking connexin 30. J Biol Chem 2011;286 (2):1054–60.

[427] Zhou ZH, Bubien JK. Nongenomic regulation of ENaC by aldosterone. Am J Physiol Cell Physiol 2001;281(4):C1118–30.

[428] Stockand JD, Zeltwanger S, Bao HF, Becchetti A, Worrell RT, Eaton DC. S-adenosyl-L-homocysteine hydrolase is necessary for aldosterone-induced activity of epithelial $Na(^+)$ channels. Am J Physiol Cell Physiol 2001;281(3):C773–85.

[429] Thomas SV, Kathpalia PP, Rajagopal M, Charlton C, Zhang J, Eaton DC, et al. Epithelial sodium channel regulation by cell surface-associated serum- and glucocorticoid-regulated kinase 1. J Biol Chem 2011;286(37):32074–85.

[430] Soundararajan R, Melters D, Shih IC, Wang J, Pearce D. Epithelial sodium channel regulated by differential composition of a signaling complex. Proc Natl Acad Sci USA 2009;106 (19):7804–9.

[431] Soundararajan R, Wang J, Melters D, Pearce D. Glucocorticoid-induced Leucine zipper 1 stimulates the epithelial sodium channel by regulating serum- and glucocorticoid-induced kinase 1 stability and subcellular localization. J Biol Chem 2010;285(51):39905–13.

[432] Soundararajan R, Zhang TT, Wang J, Vandewalle A, Pearce D. A novel role for glucocorticoid-induced leucine zipper protein in epithelial sodium channel-mediated sodium transport. J Biol Chem 2005;280(48):39970–81.

[433] Soundararajan R, Pearce D, Hughey RP, Kleyman TR. Role of epithelial sodium channels and their regulators in hypertension. J Biol Chem 2010;285(40):30363–9.

[434] Asher C, Wald H, Rossier BC, Garty H. Aldosterone-induced increase in the abundance of Na^+ channel subunits. Am J Physiol 1996;271(2 Pt 1):C605–11.

[435] Weisz OA, Johnson JP. Noncoordinate regulation of ENaC: Paradigm lost? Am J Physiol Renal Physiol 2003;285(5): F833–42.

[436] Auberson M, Hoffmann-Pochon N, Vandewalle A, Kellenberger S, Schild L. Epithelial Na^+ channel mutants causing Liddle's syndrome retain ability to respond to aldosterone and vasopressin. Am J Physiol Renal Physiol 2003;285(3): F459–71.

[437] Benos DJ, Awayda MS, Ismailov II, Johnson JP. Structure and function of amiloride-sensitive Na^+ channels. J Membr Biol 1995;143(1):1–18.

[438] Ecelbarger CA, Kim GH, Wade JB, Knepper MA. Regulation of the abundance of renal sodium transporters and channels by vasopressin. Exp Neurol 2001;171(2):227–34.

[439] Kleyman TR, Ernst SA, Coupaye-Gerard B. Arginine vasopressin and forskolin regulate apical cell surface expression of epithelial Na^+ channels in A6 cells. Am J Physiol 1994;266(3 Pt 2): F506–11.

[440] Erlij D, De Smet P, Mesotten D, Van Driessche W. Forskolin increases apical sodium conductance in cultured toad kidney cells (A6) by stimulating membrane insertion. Pflugers Arch 1999;438(2):195–204.

[441] Butterworth MB, Helman SI, Els WJ. cAMP-sensitive endocytic trafficking in A6 epithelia. Am J Physiol Cell Physiol 2001;280 (4):C752–62.

[442] Marunaka Y, Eaton DC. Effects of vasopressin and cAMP on single amiloride-blockable Na channels. Am J Physiol 1991;260 (5 Pt 1):C1071–84.

[443] Ecelbarger CA, Kim GH, Terris J, Masilamani S, Mitchell C, Reyes I, et al. Vasopressin-mediated regulation of epithelial sodium channel abundance in rat kidney. Am J Physiol Renal Physiol 2000;279(1):F46–53.

[444] Wiesmann WP, Sinha S, Klahr S. Insulin stimulates active sodium transport in toad bladder by two mechanisms. Nature 1976;260(5551):546–7.

[445] Pearce D. The role of SGK1 in hormone-regulated sodium transport. Trends Endocrinol Metab 2001;12(8):341–7.

[446] Blazer-Yost BL, Liu X, Helman SI. Hormonal regulation of ENaCs: Insulin and aldosterone. Am J Physiol 1998;274(5 Pt 1): C1373–9.

[447] Faletti CJ, Perrotti N, Taylor SI, Blazer-Yost BL. sgk: an essential convergence point for peptide and steroid hormone regulation of ENaC-mediated Na^+ transport. Am J Physiol Cell Physiol 2002;282(3):C494–500.

[448] Tong Q, Gamper N, Medina JL, Shapiro MS, Stockand JD. Direct activation of the epithelial $Na(^+)$ channel by phosphatidylinositol 3,4,5-trisphosphate and phosphatidylinositol 3,4-bisphosphate produced by phosphoinositide 3-OH kinase. J Biol Chem 2004;279(21):22654–63.

[449] Peti-Peterdi J, Warnock DG, Bell PD. Angiotensin II directly stimulates ENaC activity in the cortical collecting duct via AT (1) receptors. J Am Soc Nephrol 2002;13(5):1131–5.

[450] Sun P, Yue P, Wang WH. Angiotensin II stimulates epithelial sodium channels (ENaC) in the cortical collecting duct of the rat kidney. Am J Physiol Renal Physiol 2012;302(6): F679–87.

[451] Mamenko M, Zaika O, Ilatovskaya DV, Staruschenko A, Pochynyuk O. Angiotensin II increases activity of the epithelial Na^+ channel (ENaC) in distal nephron additively to aldosterone. J Biol Chem 2012;287(1):660–71.

[452] Bugaj V, Pochynyuk O, Mironova E, Vandewalle A, Medina JL, Stockand JD. Regulation of the epithelial Na^+ channel by endothelin-1 in rat collecting duct. Am J Physiol Renal Physiol 2008;295(4):F1063–70.

[453] Bugaj V, Mironova E, Kohan DE, Stockand JD. Collecting duct-specific endothelin B receptor knockout increases ENaC activity. Am J Physiol Cell Physiol 2012;302(1):C188–94.
[454] Rossier BC. Mechanosensitivity of the epithelial sodium channel (ENaC): Controversy or pseudocontroversy? J Gen Physiol 1998;112(2):95–6.
[455] Awayda MS, Subramanyam M. Regulation of the epithelial Na^+ channel by membrane tension. J Gen Physiol 1998;112 (2):97–111.
[456] Ji HL, Fuller CM, Benos DJ. Osmotic pressure regulates alpha beta gamma-rENaC expressed in *Xenopus* oocytes. Am J Physiol 1998;275(5 Pt 1):C1182–90.
[457] Engbretson BG, Stoner LC. Flow-dependent potassium secretion by rabbit cortical collecting tubule *in vitro*. Am J Physiol 1987;253(5 Pt 2):F896–903.
[458] Malnic G, Berliner RW, Giebisch G. Flow dependence of K^+ secretion in cortical distal tubules of the rat. Am J Physiol 1989;256(5 Pt 2):F932–41.
[459] Satlin LM, Sheng S, Woda CB, Kleyman TR. Epithelial $Na(^+)$ channels are regulated by flow. Am J Physiol Renal Physiol 2001;280(6):F1010–8.
[460] Morimoto T, Liu W, Woda C, Carattino MD, Wei Y, Hughey RP, et al. Mechanism underlying flow stimulation of sodium absorption in the mammalian collecting duct. Am J Physiol Renal Physiol 2006;291(3):F663–9.
[461] Carattino MD, Liu W, Hill WG, Satlin LM, Kleyman TR. Lack of a role of membrane-protein interactions in flow-dependent activation of ENaC. Am J Physiol Renal Physiol 2007;293(1): F316–24.
[462] Abi-Antoun T, Shi S, Tolino LA, Kleyman TR, Carattino MD. Second transmembrane domain modulates epithelial sodium channel gating in response to shear stress. Am J Physiol Renal Physiol 2011;300(5):F1089–95.
[463] Drummond HA, Price MP, Welsh MJ, Abboud FM. A molecular component of the arterial baroreceptor mechanotransducer. Neuron 1998;21(6):1435–41.
[464] Drummond HA, Welsh MJ, Abboud FM. ENaC subunits are molecular components of the arterial baroreceptor complex. Ann NY Acad Sci 2001;940:42–7.
[465] Drummond HA, Grifoni SC, Jernigan NL. A new trick for an old dogma: ENaC proteins as mechanotransducers in vascular smooth muscle. Physiology (Bethesda) 2008;23:23–31.
[466] Jernigan NL, Drummond HA. Vascular ENaC proteins are required for renal myogenic constriction. Am J Physiol Renal Physiol 2005;289(4):F891–901.
[467] Jernigan NL, Drummond HA. Myogenic vasoconstriction in mouse renal interlobar arteries: role of endogenous beta and gammaENaC. Am J Physiol Renal Physiol 2006;291(6): F1184–91.
[468] Jernigan NL, LaMarca B, Speed J, Galmiche L, Granger JP, Drummond HA. Dietary salt enhances benzamil-sensitive component of myogenic constriction in mesenteric arteries. Am J Physiol Heart Circ Physiol 2008;294(1):H409–20.
[469] Guan Z, Pollock JS, Cook AK, Hobbs JL, Inscho EW. Effect of epithelial sodium channel blockade on the myogenic response of rat juxtamedullary afferent arterioles. Hypertension 2009;54 (5):1062–9.
[470] Grifoni SC, Chiposi R, McKey SE, Ryan MJ, Drummond HA. Altered whole kidney blood flow autoregulation in a mouse model of reduced beta-ENaC. Am J Physiol Renal Physiol 2010;298(2):F285–92.
[471] Kamynina E, Tauxe C, Staub O. Distinct characteristics of two human Nedd4 proteins with respect to epithelial $Na(^+)$ channel regulation. Am J Physiol Renal Physiol 2001;281(3): F469–77.
[472] Goulet CC, Volk KA, Adams CM, Prince LS, Stokes JB, Snyder PM. Inhibition of the epithelial Na^+ channel by interaction of Nedd4 with a PY motif deleted in Liddle's syndrome. J Biol Chem 1998;273(45):30012–7.
[473] Knight KK, Olson DR, Zhou R, Snyder PM. Liddle's syndrome mutations increase Na^+ transport through dual effects on epithelial Na^+ channel surface expression and proteolytic cleavage. Proc Natl Acad Sci USA 2006;103(8):2805–8.
[474] Melander O, Orho M, Fagerudd J, Bengtsson K, Groop PH, Mattiasson I, et al. Mutations and variants of the epithelial sodium channel gene in Liddle's syndrome and primary hypertension. Hypertension 1998;31(5):1118–24.
[475] Baker EH, Dong YB, Sagnella GA, Rothwell M, Onipinla AK, Markandu ND, et al. Association of hypertension with T594M mutation in beta subunit of epithelial sodium channels in black people resident in London. Lancet 1998;351 (9113):1388–92.
[476] Ambrosius WT, Bloem LJ, Zhou L, Rebhun JF, Snyder PM, Wagner MA, et al. Genetic variants in the epithelial sodium channel in relation to aldosterone and potassium excretion and risk for hypertension. Hypertension 1999;34(4 Pt 1): 631–7.
[477] Baker EH, Duggal A, Dong Y, Ireson NJ, Wood M, Markandu ND, et al. Amiloride, a specific drug for hypertension in black people with T594M variant? Hypertension 2002;40(1):13–7.
[478] Cui Y, Su YR, Rutkowski M, Reif M, Menon AG, Pun RY. Loss of protein kinase C inhibition in the beta-T594M variant of the amiloride-sensitive Na^+ channel. Proc Natl Acad Sci USA 1997;94(18):9962–6.
[479] Dirlewanger M, Huser D, Zennaro MC, Girardin E, Schild L, Schwitzgebel VM. A homozygous missense mutation in SCNN1A is responsible for a transient neonatal form of pseudohypoaldosteronism type 1. Am J Physiol Endoc M 2011;301 (3):E467–73.
[480] Passero CJ, Hughey RP, Kleyman TR. New role for plasmin in sodium homeostasis. Curr Opin Nephrol Hypertens 2010;19 (1):13–9.

This page intentionally left blank

CHAPTER

31

Anion Channels

Owen M. Woodward and William B. Guggino

Department of Physiology, The Johns Hopkins University School of Medicine, Baltimore, MD, USA

INTRODUCTION

The mammalian kidney evolved to allow for the efficient secretion of metabolic waste without excess loss of water in terrestrial environments, for the maintenance of the ionic balance in the extracellular milieu, for the regulation of blood pressure, and for the recapture of essential solutes like proteins and sugars. These functions all deferentially depended on the conductance/transport of Cl^- and other anions across individual cell membranes. A classic example is NaCl reabsorption in the distal nephron, where Na^+, Cl^-, and K^+ enter the cell across the apical membrane via the NKCC2 co-transporter, driven by the Na^+ gradient established by the Na^+/K^+-ATPase, and the Cl^- gradient maintained by basolateral ClC-Kb Cl^- channels. Mutations in these basolateral Cl^- channels result in the severe salt-wasting characteristic of Type III Bartter's syndrome. As more of the major Cl^- channel family molecular identities are resolved, our understanding of the role of Cl^- channels in kidney disease will increase proportionally, and hopefully shed light on some of the long-standing mysteries of kidney function.

Although anions and negatively charged organic solutes were appreciated as necessary to balance the charges accumulated by the cations, Na^+, K^+, and Ca^{2+}, they were believed to be passive players. Cl^-, by far the most abundant physiological anion, was believed to be balanced across the membrane, a belief supported by early studies of skeletal muscle, where the resting Cl^- permeability was found to be very high,[27] and thus Cl^- was mostly known for its contribution to the "leak" current.[131] Even as later studies demonstrated that Cl^- was being actively transported in squid axons or secreted as HCl in the stomach,[27] less interest was given to anion conductances. Initial patch-clamp studies of Cl^- channels discovered that Cl^- channels are not really even Cl^- channels; their general promiscuity toward all anions makes them more accurately described as anion channels. The tide first began to change as neuroscientists found, and later cloned, the GABA- and glycine-gated Cl^- channels that worked to inhibit synaptic transmission, proving that Cl^- was not in equilibrium at rest and could be harnessed by cells to do work. But it was the cloning of two major classes of Cl^- channels, the CLCs and CFTR, which lead to an explosion of interest in Cl^- channels, and exponentially increased our understanding of their ubiquity, importance in human disease, and function in the mammalian kidney.

Anion channels are usually grouped into five major classes, based on how they are activated or regulated. There are the voltage-dependent Cl^- channels (the CLCs); ligand-gated Cl^- channels (the GABA and glycine receptor channels); cAMP-activated channels (CFTR); Ca^{2+}-activated Cl^- channels (the TMEM16 channels); and the volume-regulated anion channels (the VRAC channels). This chapter will examine the expression and function of these major classes of Cl^- channels in the kidney, but will also discuss at length Cl^- channels that are expressed ubiquitously or for which expression and functional information does not yet exist. The chapter dives right in to survey the major anion channel families and their relevance in the kidney, focusing on the CLC, CFTR, TMEM16, VRAC, and SLC26A7/9 Cl^- channels. However, the chapter will also look at a number of less well-understood anion channel genes that have currently unclear physiological relevance. Lastly, we will delve deeply into Cl^- channelopathies that affect the kidney both directly and indirectly, seeking insight into how Cl^- channels contribute to normal kidney physiology.

Seldin and Giebisch's The Kidney, Fifth Edition.
DOI: http://dx.doi.org/10.1016/B978-0-12-381462-3.00031-8

© 2013 Elsevier Inc. All rights reserved.

What's "New"?

Recent work on Cl^- channels has paid disproportionate dividends for Cl^- channel researchers, including advances in our understanding of Cl^- channel structure, molecular identity, and discovery of new Cl^- channels in familiar but surprising places. The most important advance in Cl^- channel knowledge came in 2008, when three independent groups using three novel approaches all identified the TMEM16A gene as the molecular identity of the classic Ca^{2+}-activated Cl^- channel (CaCC). The TMEM16 family of genes has 10 human homologs that are expressed widely, including in the kidney. As more and more work is done describing their function, biophysical characteristics, and expression patterns, the more certain it becomes that TMEM16a is the classic CaCC. Second, crystal structures solved for bacterial orthologs of the voltage-dependent CLC Cl^- channel family revealed via homology that a number of the human CLCs (ClC-3, 4, 5, 6, and 7) are not in fact channels, but H^+/Cl^- exchangers, a finding with ramifications in the kidney. And third, two members of a well-known anion transporter family, SLC26A7 and A9, appear to behave almost exclusively as anion channels, with no appreciable transport of bicarbonate. Which, taken in conjunction with the recent reclassification of a number of the CLC channels as exchangers, suggests a fine line between anion transporter and anion channel. Each of the recent advances mentioned above will be discussed in depth in the following chapter.

MAJOR CLASSES OF IDENTIFIED ANION CHANNELS

Similar to the study of other ion channels, extensive research into the biophysical and physiological characteristics and functions of Cl^- channels preceded the identification of their molecular identity or their corresponding human genes. One reason that the molecular identification of Cl^- channels lagged far behind that of cation channels is that there were no highly specific inhibitors that could be used for cloning Cl^- channels in a manner similar to that done for many cation channels. However, with a considerable amount of effort, more and more of the Cl^- channels recognized for their biophysical characteristics now have mammalian gene candidates, identifications of which have quickly expanded our knowledge of the roles of Cl^- channels in cellular functions and in human disease. The molecular identification has also shown just how difficult identification of all the Cl^- channels is. There is no homology between any of the identified gene families containing Cl^- channels, and very little commonality in structure.[27] Their demonstrated convergence of function, so different from the common homology of many of the families of cation channels, presents no easy bioinformatic road map to the discovery of Cl^- channel identities. Instead, a narrowly focused approach has been used on each of the functional classes of Cl^- channels to identify the known Cl^- channel families (Figure 31.1), a growing list that now includes the CLC voltage-dependent channels, CFTR, TMEM16/Anoctamins Ca^{2+}-activated Cl^- channels,

Anion Channel	Regulation	Channel Properties	Kidney Localization	Physiological Role	Human Disease
CFTR	Activated by cAMP-dependent phosphorylation	Linear I/V; $Cl^->I^-$	Proximal and distal tubule, collecting duct	Cl^-secretion from epithelium	Cystic fibrosis; Polycystic kidney disease
ClC-2	Activated by hyperpolarization and cell swelling	Inward rectifying I/V; $Cl^->I^-$	Proximal tubule	Unknown	Unknown
ClC-Ka and Kb	Weak voltage activation and requires barttin subunit	Moderate outward rectifying I/V;$Cl^->I^-$	ClC-Ka: tAL;ClC-Ka: TAL, distal tubule, collecting duct	Basolateral Cl^- secretion	Bartter's syndrome type III and IV
TMEM16 (A)	Activated by cytosolic Ca^{2+}	Outward rectifying I/V; $I^->Cl^-$	Unknown	Ca^+ dependent Cl^- secretion from epithelium	Unknown
SLC26A7	Constitutively active and pH sensitive	Linear I/V; $Cl^->I^-$	Collecting duct	pH sensor or Cl^- shunt in acid secreting cells	Unknown
VRAC/Maxi-anion	Activated by cell swelling	Outward rectifying, depolarization induced inactivation; $I^->Cl^-$	Ubiquitous; maxi-anion; macula densa cells	Regulatory volume decrease; salt-sensing and ATP secretion	Unknown

FIGURE 31.1 **Anion Channels of the human kidney.**

SLC26A7/9, GABA and glycine receptor channels, VDAC, and a myriad of less well-studied groups including the bestrophins, intracellular CLICs, CLCA, and tweety (hTTYH3). The long search for molecular identities of the Cl^- channels has lead to many ambiguous discoveries, dead ends, and great success stories. Below we review the Cl^- channels with known molecular identities, and known physiological and kidney specific functions, but we will also discuss those genes that code for proteins that can conduct Cl^-, but do not yet have known physiological functions.

CLC Cl^- Channels

Our discussion about the specific families of Cl^- channels begins with CLC Cl^- channels (Figure 31.2). Unlike CFTR, which was not immediately recognized as a Cl^- channel and appeared to be a very divergent type of ABC transporter,[27] the canonical ClC-0 shared close homology with proteins from a large gene family with members expressed across all phyla, including nine members expressed in humans. Two decades of subsequent work have revealed much about the CLC family, their biophysical properties, and their importance in human disease, yet many of the mammalian orthologs still only have vaguely defined physiological functions. However, the relevance of the CLCs in the human kidney is clear. Eight of nine human CLC orthologs are expressed in the kidney, and their dysfunction leads directly to Dent's disease and Type III Bartter's syndrome.[25]

For years the mammalian CLCs were divided into two classes, based on cellular localization with ClC-1, 2, and ClC-Ka, b channels being expressed in the plasma membranes, and the remaining ClC-3, 4, 5, 6, and 7 all being expressed on intracellular membranes. Recent evidence has substantially shifted this paradigm of understanding, with the plasma membrane CLCs now simply classified as the voltage-dependent Cl^- channel CLCs with the rest now classified as Cl^-/H^+ exchangers. It turns out that the vast majority of all CLC family members across all phyla are Cl^-/H^+ exchangers and not Cl^- channels. For the mammalian CLC proteins this has meant a revision of functions and physiological roles for the previously designated intracellular CLCs. Intrinsically, the difference between a CLC Cl^- channel and a CLC Cl^-/H^+ exchanger is little more than a few strategically placed glutamate residues; extrinsically, their thermodynamic properties are completely different.[79] These newly classified exchangers will be covered briefly below, but this section will mostly focus on the remaining CLC Cl^- channels and their functions in the kidney.

The early work investigating CLC Cl^- channels found they have very distinct biophysical properties, which immediately set them apart from the known cation channels and would later set them apart from all other known Cl^- channels. ClC-0 can be described as voltage-dependent, pH-dependent, and dependent on the Cl^- gradient across the pore, as can most of the CLC Cl^- channels.[19] The "kidney" Cl^- channels, ClC-Ka and ClC-Kb, are additionally dependent on a smaller beta-subunit, barttin (BSND); a dependence with ramifications for NaCl reuptake in the thick ascending loop and Bartter's syndrome. The halide selectivity sequence for ClC-0 is $Cl^- > Br^- > I^-$, and in most physiological circumstances it forms functional homodimers, although heterodimers from ClC-0, 1, and 2 can be formed heterologously.[19,54] ClC-0 single channel currents appeared at first glance to be two separate channels, albeit with identical conductances; however, even though the two conductances or protopores appeared to open and close independently, sporadically they both closed simultaneously and remained closed for prolonged periods before opening again.[19,70a,78] The coexpression of ClC-0 and ClC-2 heterodimers resulted in the same strange phenomenon, but this time the two protopore conductances were different. The difference in protopore conductances correlated with the varying protopore size between ClC-0, 1, and 2, being 10 pS, 1.5 pS, and 3 pS respectively.[27] This prompted the conclusion that ClC Cl^- channels function as dimers, with two separate protopores, each independently gated by a separate "fast" gate, but both gated simultaneously by a "slow" gate.[55]

This hypothesis was proven correct after the crystallization of the prokaryotic CLC proteins from *E. coli* and *Salmonella typhimurium*.[28] These prokaryotic CLCs formed dimers, with each subunit forming its own protopore. Each subunit consists of 18 membrane "embedded" domains, where many of the helices do not project completely through the bilayer.[28] Interestingly, each subunit has structurally similar halves that "twist" in an antiparallel structure that forms an hourglass shaped protopore toward the center.[28] Further work on the *E. coli* CLC, EcClC-1, crystal revealed that there are three Cl^--binding sites within the hourglass shaped pore, and in the outermost site the Cl^- appears to compete with the carboxyl group of a negatively-charged glutamate.[29] When this glutamate is replaced with a non-charged amino acid in the ClC-0 channel, the voltage-dependent gating properties are altered.[29] This suggests that the central "gating" glutamate is key in the voltage- and Cl^--dependence of CLC gating,[55] and represents the fast gate regulating each protopore. The possible protonation of the gating glutamate, thereby allowing Cl^- to enter the pore, may also help explain the pH-dependence observed for many CLCs.[27]

The reconstitution of EcClC-1 in lipid bilayers revealed that it is not a Cl^- channel, but a Cl^-/H^+

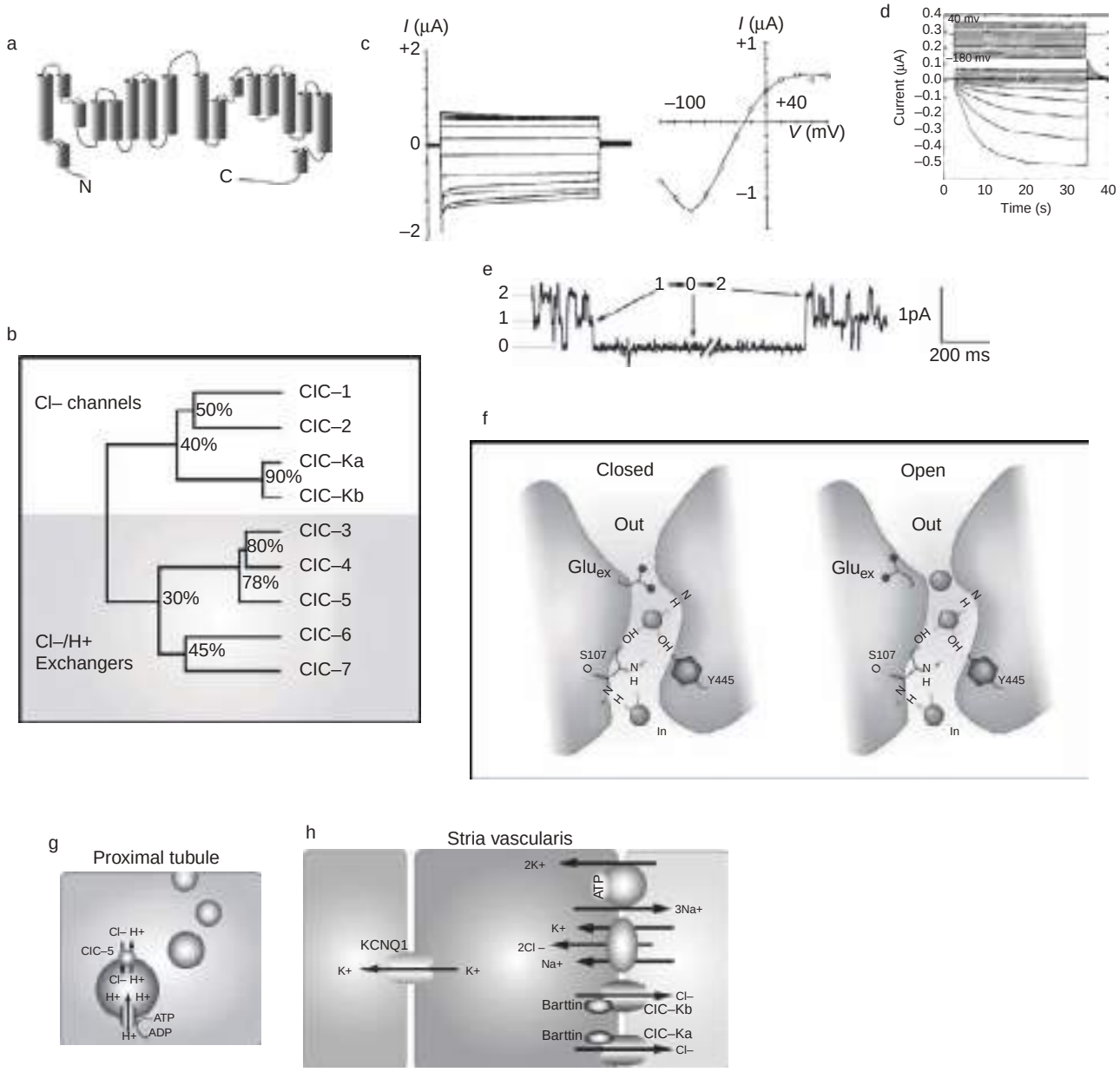

FIGURE 31.2 **CLC Gene family.** (a) Topography of representative CLC protein. (b) Dendrogram of mammalian CLC proteins. (c) Whole cell currents and I/V relationship of ClC-1 expressed in *Xenopus* oocytes. (d) Whole cell currents from ClC-2 expressing *Xenopus* oocytes. (e) Single channel ClC-0 openings with two clear substates or protopores. (f) Drawing of the closed and opened states of ClC channels and exchangers. In the closed state the "gating" glutamate side chain is bound to the uppermost Cl^- binding site, to open the channel the side chain must be moved or bind an H^+. (g) ClC-5 acts to balance the positive charge build-up resulting from the acidification of endosomes. (h) In the inner ear the two ClC proteins Ka and Kb secret Cl^- across the basolateral membrane, allowing high concentrations of K^+ to be conducted across the apical membrane into the stria media facilitating the function of the hair cells. ((c), (d), (e), (f): *Reprinted by permission from Macmillan Publishers Ltd. (c) Steinmeyer, K., Ortland, C., Jentsch, T. J. (1991). Primary structure and functional expression of a developmentally regulated skeletal muscle chloride channel. Nature* ***354****, 301–304.*[118] *(d) Thiemann, A., Grunder, S., Pusch, M., Jentsch, T. J. (1992). A chloride channel widely expressed in epithelial and non-epithelial cells. Nature* ***356****, 57–60.* [125] *(e) Lisal, J., and Maduke, M. (2008). The ClC-0 chloride channel is a broken Cl^-/H^+ antiporter. Nat. Struct. Mol. Bio.* ***15****, 805–810.*[71a] *(f) Miller, C. (2006). ClC chloride channels viewed through a transporter lens. Nature* ***440****, 484–489.*[79] *)*

exchanger, where two Cl^- ions are substituted for one H^+.[55] Further mutational studies discovered the H^+ exchange depended on both the gating glutamate, and a second glutamate near the cytosolic surface, but not in the protopore.[79] These characteristics suggest that both protons and Cl^- are gated by the "gating" glutamate, after which they travel separate permeation paths to the cytoplasm. This theory is supported by

experiments where this second glutamate was mutated in the EcClC-1, making the protein exclusively a Cl^- channel, not an exchanger.[1] The human CLCs ClC-3, 4, 5, 6, and 7 all have this second glutamate marking them as exchangers, and mutating both glutamates in ClC-4 and 5 converted them into Cl^- channels,[96,109] demonstrating just how fine the line is between Cl^- channel and exchanger.

The pharmacology of CLC Cl^- channels, like many of the other anion channels, has been plagued by the lack of specific high affinity inhibitors. Although the mammalian CLCs are highly conserved, they do differ somewhat in their susceptibility to the classic Cl^- channel inhibitors. ClC-0, ClC-1, and ClC-2 all differ in their affinity for 9-anthracene carboxylic acid (9-AC), with ClC-1 effectively blocked by 100 μM, whereas ClC-0 and ClC-2 require mM levels.[118,125] The CLCs are also affectively inhibited by the clofibric acid derivatives 2-(-p-chlorophenoxy) propionic acid (CPP) and 2-(-p-chlorophenoxy) acetic acid (CPA).[19,131] Stilibenes can also be weakly inhibitory and can block ClC-2, as can DPC and NPPB at 0.5 to >1 mM concentrations.[131] ClC-2 is also inhibited by divalent cations like zinc and cadmium with IC_{50} in the μM range[131] as the other CLC Cl^- channels can be. Because of their human disease relevance the kidney CLCs, Ka and Kb have been scrutinized more than the others. Specifically, inhibitors could regulate dieresis and possibly blood pressure, and therapeutic activators could aid patients with Bartter's Syndrome.[70] The close shared homology of the ClC-Ks obviously suggested similar sensitivities to inhibitors, but both CPP and DIDS are more affective at blocking CLC-Ka than Kb.[28,131] Niflumic acid (NFA), another classic Cl^- channel inhibitor, was actually shown to activate the CLC-Ks at low concentrations (50−100 μM),[70] but inhibit them at higher concentrations,[131] a finding that prompted Liantonio et al.[70] to manipulate the CPP structure to recapitulate characteristics of the NFA molecule, in order to create a better inhibitor. They found that their rationally designed benzofuran carboxyl acid derivatives could inhibit both ClC-Ka and Kb with low μM IC_{50}s.[70] Their work, and the insight provided by the EcClC-1 crystal structure, make finding potential therapeutic activators and inhibitors of the CLC-Ks a real likelihood, therapies that could impact millions of patients.

Physiological Function of Mammalian CLC Cl^- Channels

With the recent identification of the intracellular CLCs as exchangers, only four human CLCs remain for further in-depth discussion: ClC-1, ClC-2, and the CLC-Ks. ClC-1 (the human gene is *CLCN1*), is the only CLC that is not expressed in the kidney.[25] It is a plasma membrane localized Cl^- channel found almost exclusively in skeletal muscle. There it represents about 80% of the resting conductance of the muscle.[55] When the muscle depolarizes along the T-tubule, and Ca^{2+} is released from the sarcoplasmic reticulum, ClC-1 is further activated. The ClC-1 activation repolarizes the muscle cell and brings it back to its negative resting potential. Cl^- and not K^+, as in most other excitable cells, is used for repolarization because it is thought that in the microdomains of T-tubules extracellular K^+ would quickly build up, causing unsolicited depolarizations.[55] The physiological importance of ClC-1 became clear after causal ClC-1 mutations were found first in myotonic mice and later in humans.[55] The human form of the disease, myotonia or "muscle stiffness" is characterized by muscles that suffer prolonged contractions, exactly the phenotype expected if repolarization cannot occur after the initial depolarizing stimulus. Humans can have either the recessive form of the disease (Becker type) with complete ClC-1 functionality loss or the dominant form (Thomsen's) with the retention of some ClC-1 function and less severe debilitation.[55,131]

ClC-2

ClC-2 is broadly expressed in many different tissues, but is prominent in epithelium (including kidney), neurons, glia, and heart muscle.[125] Unlike ClC-1, ClC-2 is inwardly rectifying and hyperpolarization activated.[108,131] It can also be activated by cell swelling, but is clearly not the ubiquitous VRAC current, which differs in selectivity, voltage-dependence, rectification, and single channel conductance.[55] Unfortunately, little is yet known about its function. Even the development of $Clnc2^{-/-}$ knockout mice has provided only minimal hints at its broad functions. $Clcn2^{-/-}$ mice did display some disease phenotypes; however, knockout mice displayed degeneration of photo receptors and seminiferous tubules in testicles.[131] There is also some evidence that ClC-2 is involved in Cl^- secretion in lung epithelium, and that it could provide an alternative source of Cl^- secretion in patients with aberrant CFTR function.[112] To that end, the FDA approved lubiprostone, the only CLC-targeted drug yet approved, for treatment in cystic fibrosis (CF).[23,131] More recent work suggests that ClC-2 may be localized more on the basolateral membrane and not apical, at least in gut epithelium,[55] and that lubiprostome may also activate CFTR or other apical Cl^- channels, not necessarily just ClC-2.[6,131] Unfortunately, $Clcn2^{-/-}$ mice have no kidney phenotype, even though ClC-2 is believed to be expressed in the proximal tubule.[128] It is possible that, like in the gut, they may be expressed on the basolateral membrane and involved in the reabsorption of Cl^- along the nephron, but to what extent is unclear.

CLC Exchangers

Before progressing to the in-depth analysis of the remaining kidney CLC Cl^- channels, it is necessary to briefly touch on the CLC intracellular exchangers, in particular ClC-5 because of its relevance in kidney function. Like most other CLCs, ClC-5 is a Cl^-/H^+ exchanger that exchanges two Cl^- for every H^+. ClC-5 is localized to the proximal tubule and to the α-intercalated cells of the cortical collecting duct.[25] ClC-5 is specifically localized to the endosomes in these cell types, alongside the v-type H^+-ATPase.[25,43,98] The human ClC-5 gene *CLCN5* was identified independently, first through positional cloning in families with Dent's disease,[25] and confirmed through homology cloning.[55] Dent's disease is an X-linked renal tubular disorder characterized by low molecular weight proteinuria (LMWP), hypercalciuria, nephrocalcinosis, kidney stones, and renal failure.[25] More than 40 mutations have been identified in human *CLCN5* that cause Dent's disease, with a wide range of severity.[55] Recapitulating some of the disease-causing mutations in ClC-5 expressed in heterologous systems showed they almost universally resulted in reduction or loss of Cl^- conductance (ClC-5 when overexpressed reaches the plasma membrane).[25] This, along with its known localization to subapical endosomes alongside H^+-ATPases, prompted the hypothesis that ClC-5 was functioning to provide Cl^- influx to offset the positive charge build-up from the acidification of the endosomes.[25,98] A Cl^- shunt would prevent a slowdown of H^+ pumping into the endosomes from positive charge build-up. Importantly, the then presumed channel characteristics of ClC-5 didn't match this function well, ClC-5 is outwardly rectifying, and most importantly is inhibited by acidic pH.[25] The creation of a $Clcn5^{-/-}$ knockout mouse allowed the testing of the role ClC-5 plays in endosomal acidification. The two models[97,135] both reproduced the LWMP and defective apical endocytosis, seemingly supporting the hypothesis that ClC-5 aids in acidification.[25,55,128] In addition, *in vitro* disruption of ClC-5 function caused reduced acidification of the endosomes.[87] But with the discovery that ClC-5 is not in fact a Cl^- channel, but a Cl^-/H^+ exchanger it became far less clear how it could provide the shunt current for acidification, and how it could be influencing the endocytosis of low molecular weight proteins. Recent work by Noarino et al.[87] addressed this question directly by comparing mouse models with either $Clcn5^{-/-}$ knockout or the knockin of a mutated Clcn5 (Clcn5unc) that removed the "gating" glutamate, uncoupling the Cl^-/H^+ exchange and thereby creating a ClC-5 Cl^- channel, not exchanger. They found, as reported previously, endosomes from the Clcn5 knockout showed reduced acidification and defective endocytosis; however, the Clcn5unc knockin mice showed normal acidification, but still had defective endocytosis.[87] These data strongly suggest that ClC-5 plays a role in acidification by acting as a charge shunt; however, as a Cl^-/H^+ exchanger it plays a further yet to be explained role in endocytosis unrelated to its role as a shunt. Novarino et al.[87] suggest the intra-endosome absolute Cl^- concentration may be key in regulating endocytosis, not just the negative charge.

CLC-Ks

There are two mammalian CLC-K channels, named because of their localization to kidney tissues, although they are now also known to be expressed in the inner ear. Mammals possess two CLC-Ks, ClC-K1 and K2, and the human orthologs are termed ClC-Ka and -Kb, respectively. The CLC-Ks are highly conserved with the rodent homologs, ClC-K1 and K2, sharing 80% homology and the human pair being over 90% homologous.[61] After the homology cloning of rodent ClC-K1 and -K2, they were heterologously expressed in *Xenopus* oocytes, but only ClC-K1 expression resulted in Cl^- currents.[127] These ClC-K1 currents displayed a linear I/V relationship, with little voltage-dependence.[133] Like the rodent ClC-K2 that failed to produce currents, the heterologous expression of the human ClC-Ka and -Kb failed to yield any Cl^- currents,[61] prompting the supposition that a β-subunit may be necessary for function. The discovery of the subunit came tangentially from the successful positional cloning of a gene mutated in human type IV Bartter's syndrome, BSND, which codes for the protein barttin.[14] Barttin has two transmembrane domains, and both N- and C-termini located in the cytoplasm.[32] The expression of barttin along with either of the human CLC-Ks resulted in robust Cl^- currents with ion selectivity similar to that of other CLC Cl^- channels, inhibited by low extracellular pH, and stimulated by extracellular Ca^{2+}[62]. The main function of barttin appears to be to increase dramatically the amount of CLC-Ks that make it to the plasma membrane, although it also appears to subtly alter gating.[134] Interestingly, the voltage-dependence described for other CLCs is absent in the CLC-Ks,[128] a phenomenon that appears connected to the "gating" glutamate described in the EcClC-1 exchanger; the two ClC-K channels in humans lack the gating glutamate and instead have a valine at the same position. However, if the valine is mutated to a glutamate, strong voltage dependence is recapitulated.[133]

Although human CLC-Ks share close homology and do have overlapping kidney expression patterns, there does appear to be some divergence in localization that is supported by a divergence in function as well. ClC-

K1 (and presumably ClC-Ka) is expressed in the cortex, inner, and outer medulla, specifically localized in the thin ascending limb (tAL) of the loop of Henle; ClC-K2 is expressed in the cortex, inner, and outer medulla, specifically localizing to the thick ascending limb (TAL), distal convoluted tubule, and the α-intercalated cells of the collecting duct. Barttin expression is co-localized with the two CLC-Ks.[25,55,61,130] All three proteins, ClC-Ka, b, and barttin, are also expressed together in the stria vascularis of the inner ear.[61]

Function of the CLC-Ks

The discussion on function will concentrate on three areas, the tAL, the TAL, and the inner ear. These are not the only areas of the nephron where the CLC-Ks have significant function, but they are the areas most directly attributed to their roles in human disease. An additional discussion of Bartter's syndrome and CLC-Kb will come at the end of the chapter.

Currently there are no described human diseases with an isolated defect in the ClC-Ka gene, *CLCNKA*.[61] Although there has been one report of an association between salt-sensitive hypertension and single nucleotide polymorphisms in humans *CLCNKA*,[7] it is not clear how the SNPs or resulting haplotypes would alter ClC-Ka function. This lack of recognized human diseases from mutant ClC-Ka may be due to functional redundancies or poor sampling, because evidence has accumulated suggesting that ClC-Ka plays an important role in the urine concentrating mechanism of the loop of Henle. As mentioned above, ClC-K1 (Ka) is localized to the tAL, the area of the nephron with the highest Cl^- permeability,[25] and early studies comparing the characteristics of heterologously expressed ClC-K1/barttin currents versus those described from *in vitro* perfusion studies found striking similarities.[128] Subsequent work demonstrated that ClC-K1 was expressed in both the basolateral and apical membranes of tAL epithelium,[25] and interestingly, dehydration appears to increase the tAL expression of ClC-K1 in rats.[61] This loose connection between volume sensing and ClC-K1 expression in the tAL may be through the skg1 protein kinase. The SKG1 gene and protein expression increases when the cell volume diminishes and, in turn, can upregulate ClC-K1/barttin currents.[31] Barttin has a PY site on its C-terminus which facilitates the binding of WW domain-containing ubiquitin ligases like Nedd4-2; sgk1 can phosphorylate Nedd4-2, preventing the ubquitination of barttin and increasing the half-life of ClC-K1/barttin at the plasma membrane.[31] Upregulation of Cl^- vectorial transport in the tAL in times of dehydration would work to increase the concentrating mechanism of the inner medulla, and allow for increased water reabsorption via Aquaporin-2 in the collecting duct principle cells. However, it wasn't until the creation of the $Clcnk1^{-/-}$ knockout mouse that the physiological significance of ClC-K1 was clearly demonstrated.

$Clcnk1^{-/-}$ mice display no physical phenotypes, no renal organ phenotype or changes in plasma creatinine, Na^+, K^+ or HCO_3^-. However, they do display a four- to five-fold increase in the volume of excreted urine and other symptoms similar to the human condition nephrogenic diabetes insipidus (NDI).[77,128] The concentrating of urine depends on the reuptake of water in the collecting duct, a process which in turn depends on the osmolarity gradient across the inner medulla.[25] The high interstitial osmolarity of the inner medulla depends on the reabsorption of $NaCl^-$ and the recycling of urea in the tAL. The dysfunction of any part of the complicated concentrating mechanism will lead to diabetes insipidus, qualified as "nephrogenic" if the application of vasopressin (AVP) has no effect on the water lost in urine.[25] The $Clcnk1^{-/-}$ mice demonstrated an increase in urinary AVP secretion, no tAL Cl^- transport, and reduction in papillary osmolarity due to decreased accumulation of NaCl and urea in the inner medulla.[77] These results clearly and unambiguously demonstrated that ClC-K1 (Ka) is solely responsible for the vectorial Cl^- transport of the tAL, and that it constitutes an important part of the urine concentrating mechanism.

The function of ClC-K2 (Kb) became clear after the mapping of human mutations in the *CLCNKB* in patients with Bartter's syndrome, a condition that includes renal salt-wasting.[61] This discovery, coupled with the localization of ClC-Kb to the TAL, prompted a model of NaCl reapportion in the TAL, where the ClC-K2 (Kb) is responsible for the basolateral Cl^- conductance out of the cell. More specifically, in TAL cells, the apical membrane contains the NKCC2 co-transporter (SLC12A1) and ROMK K^+ channels; Na^+, Cl^-, and K^+ all enter the cell via the NKCC2, K^+ exits again apically via the ROMK channel, Na^+ is pumped into the interstitium via the Na^+/K^+-ATPase, and the Cl^- moves down its gradient through basolateral ClC-Kb channels into the interstitium.[61] This model is well-supported by the human genetics underlying Bartter's syndrome, and will be discussed further at the end of the chapter. In contrast, gain-of-function mutations have also been identified in the human *CLCNKB*, most notably the T481S polymorphism prevalent in both African and Caucasian populations, with minor allele frequencies of 0.22 and 0.12 respectively.[53] The T481S mutation in ClC-Kb increases currents 20-fold, possibly by alterations to the channels open probability,[53] and was thought therefore to lead to increased salt reabsorption and thus hypertension; however, studies have mostly shown that there is no association between the T481S mutation and hypertension.[55]

More recently, ClC-Ka, ClC-Kb, and barttin have all been shown to be expressed outside the kidney, in the stria vascularis of the inner ear. This was discovered only after a connection between deafness in some patients suffering from Bartter's syndrome was made to a mutation in the barttin protein. Barttin and the CLC-Ks are expressed on the basolateral membrane of the stria vascularis epithelium, where they function to reduce the Cl^- concentration in the stria vascularis. The fluid of the stria media has a very high concentration of K^+, and an unusually low concentration of Na^+. The excess K^+ is necessary to depolarize the hair cells via mechanosensory apical K^+ channels. The high K^+ is established by the movement of K^+ out of the stria vascularis epithelium via apical KCNQ1/KCNE1 K^+ channels. The K^+ enters the stria vascularis cells via basolateral Na^+/K^+-ATPases and the NKCC1 transporter, which imports two Cl^- for every K^+. Excess Na^+ is pumped out via the Na^+/K^+-ATPase and the Cl^- is extruded through basolateral CLC-K channels.[55,61] Human mutations in either one or the other CLC-K does not result in deafness, only in the dysfunction of their common barttin subunit or in very rare cases an individual has a mutation in both CLC-K genes.[55] This suggests redundancy in function that may also occur in the kidney and help explain why human disease does not result from *CLCNKA* mutations. Intriguingly, individuals carrying at least one copy of the T481S ClC-Kb gain-of-function mutation mentioned above display a lower hearing threshold than wild-type individuals.[35]

CFTR

Cystic fibrosis (CF) is the most common autosomal recessive genetic disease in Caucasians, and is debilitating and fatal; thus, long before the cloning of the Cystic Fibrosis Transmembrane Conductance Regulator (CFTR) gene, CF had been the focus of extensive physiological study. It was apparent that lung epithelium from patients with CF was lacking cAMP-activated Cl^- conductance, as well as dramatically increased apical Na^+ conductance.[25] These seemingly irreconcilable phenotypes resulted in the naming of the "CF" gene as a regulator of conductances, not as a Cl^- channel.[103] In fact, even after the successful cloning of the CFTR gene in 1989,[57,103,104] it wasn't until the creation of a $CFTR^{-/-}$ knockout mouse in 1993 that CFTR was definitively described as a Cl^- channel.[38] The $CFTR^{-/-}$ knockout demonstrated that there are actually two Cl^- conductances that are dysfunctional in CF patients and in the $CFTR^{-/-}$ mouse, and that the CFTR biophysical characteristics did not match the large outwardly rectifying currents (ORCC) that were for years believed to be the dominant Cl^- conductance.[38] Instead, CFTR regulated these ORCC currents.[25] Later work demonstrated that CFTR could regulate other channels like the epithelial sodium channel ENaC and the ATP sensitive K^+ channel ROMK2.[113]

CFTR (Figure 31.3) is now known to be a member of the ABC (ATP-binding cassette) superfamily of transporters; a vast gene family found in all phyla, responsible for transporting everything from metabolic products, lipids, and sterols, to drugs[3] and uric acid.[140] CFTR is a member of the C branch of the ABC family (ABCC7), characterized by having two large multihelix transmembrane domains (TMD) and two intracellular nucleotide-binding domains (NBD).[3] CFTR, uniquely among the ABC proteins, also possesses an extra, highly-charged cytoplasmic domain, termed the regulatory or "R" domain.[103] Perhaps not coincidentally, CFTR is also the only ABC transporter, among 48 expressed in humans,[3] shown to conduct Cl^-. Both the N- and C-terminus of the protein are cytosolic, and the C-terminus contains the amino acid sequence DTRL, a sequence that is known to interact with the "PDZ" domains often found on scaffolding and linker proteins upon which regulatory protein complexes can be built.[41,82] CFTR is therefore a single channel among a large family of anion transporters, much like the CLC and SLC26A gene families, further demonstrating the relative uniqueness of proteins that are Cl^- channels and how many appear to be derivatives of exchangers or transporters.

CFTR can most aptly be characterized as activated by cAMP-dependent phosphorylation, although the activation of the channel is actually a complicated and slow process. First, the R domain needs to be phosphorylated by the catalytic subunit of protein kinase A (PKA) (activated directly by cAMP-binding)[38]; second, ATP needs to be bound (and hydrolyzed) within the conserved walker A- and B-binding sites of the NBD domains.[39] Once activated, the Cl^- currents show little or no voltage-dependence, display a linear I/V relation, show no Ca^{2+}-dependence, and have an anion selectivity sequence of $Br^- > Cl^- > I^- > F^-$.[3,131] Single channel properties are reflective of the whole cell current characteristics: linear I/V relationship under symmetrical Cl^- concentrations; 10–11 pS single channel conductance; activation by catalytic subunit of PKA; and channel-gating coupled to ATP hydrolysis.[145]

In a reccurring theme that may be the single common characteristic among the various identified Cl^- channels, for many years there was no identified high affinity or specific CFTR inhibitors. Common Cl^- channel inhibitors like glibenclamide, DPC, NPPB, and niflumic acid provided low affinity pore blocking, but DIDS and other stilbene derivatives have little effect. In the CF lung there would be little use for CFTR

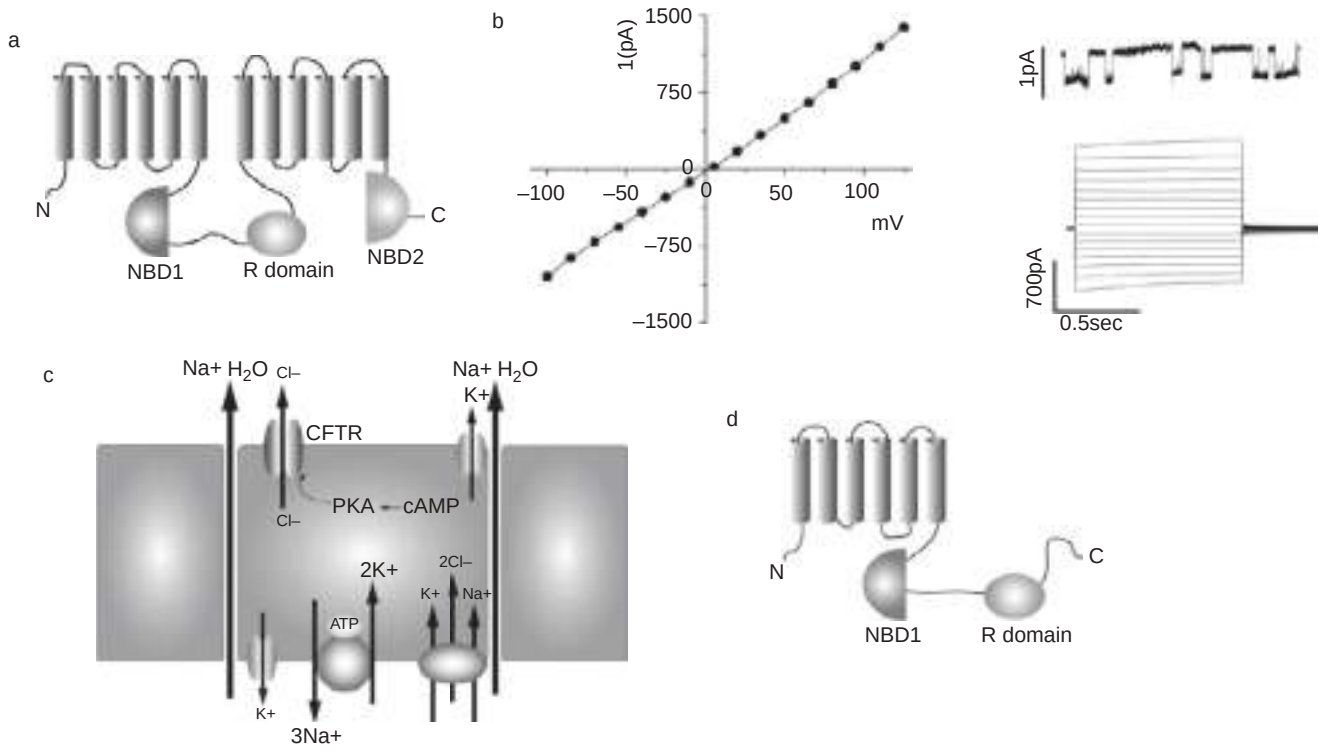

FIGURE 31.3 **Cystic fibrosis transmembrane conductance regulator (CFTR).** (a) Topography of CFTR. (b) I/V relationship, single channel recordings, and whole cell current records of CFTR heterologously expressed in CHO cells (Woodward and Guggino, unpublished data). (c) CFTR mediated Cl^- conductance drives fluid secretion in secretory airway epithelium cells. (d) Topography of kidney localized CFTR splice variant TNR-CFTR.

inhibitors therapeutically; however, CFTR expression has also been linked to fluid secretion in the kidney (see discussion of polycystic kidney disease below) and in the human gut. Specifically, toxin from *Cholera* increases cAMP levels and induces secretory diarrhea, a loss of fluids and salts that can be lethal.[74,131] The severity and pervasiveness of cholera has led to a substantial commitment of time and money to finding specific inhibitors of the cAMP-dependent Cl^- secretion of the gut epithelium. High-throughput screens of small drug-like molecules, using a fluorescent halide-based assay has yielded two classes of specific CFTR inhibitors.[74,131] The first class includes members of the 2-thioxo-4-thiazolidinone chemical class, in particular a compound named CFTRinh-172 with an IC_{50} of 300 nM.[74] CFTRinh-172 inhibits by blocking the intracellular pore in a voltage-independent fashion and prolongs the channels closed time, is non-toxic at high concentrations, is excreted with little metabolism,[131] and has been shown to effectively reduce *Cholera*-induced fluid loss by 90% in mouse models.[74] The second class of inhibitors includes the glycine hydrazides, and specifically GlyH-101.[83] It appears to block the CFTR pore from the extracellular side, is voltage- and Cl^- concentration-dependent, and in a closed loop model of cholera, GlyH-101 reduced fluid secretion by 80%.[83,131] Both classes and their lead compounds, CFTRinh-172 and GlyH-101, appear to represent therapeutic avenues for cholera and polycystic kidney disease; however, the assays used to find them also present the possibility of finding CFTR activators. The past decade has seen the discovery of a number of correctors and potentiators, small molecules targeted to bind directly to the CFTR molecule and aid in folding or in changing the gating characteristics. A number of these compounds have begun clinical trials for treating CF patients, and represent a valid avenue for chronic CF therapy.

Before progressing to a discussion of CFTRs specific role in the kidney, it is appropriate to introduce CFTR function first in the context of the human lung. CFTR was originally cloned as the gene responsible for cystic fibrosis, a disease characterized by chronic lung infection, deteriorating lung function, pancreatic exocrine insufficiency, male infertility, meconium ileus, and gastrointestinal complications.[131] In each phenotype the dysfunction stems from the reduction in fluid secretion at each relevant epithelium. CFTR is normally apically localized, and when activated Cl^- leaves the cells and enters the lumen or airway this drives paracellular Na^+, leading to water movement into the lumen.[68] In the lung, the loss of the CFTR Cl^- conductance lowers

the airway surface liquid volume (ASL), reduces the activity of the epithelial cilia, and reduces or abolishes the mucus clearance, leading to chronic infection.[124]

Currently, over 1500 CFTR mutations have been found in CF patients, representing a spectrum of disease severity directly proportional to the level of residual CFTR function. Null mutations result in no protein being produced, whereas other mutations can result in minor changes to channel-gating or cell surface expression. By far the most common CFTR mutation is the deletion of phenylalanine residue at position 508 (Δ508), carried by 90% of CF patients,[131] a mutation that causes misprocessing and trafficking, and results in no CFTR being expressed at the cell surface. Human CFTR mutations have been classified based on their severity into five classes. Class I mutants produce no CFTR, Class II includes the folding and processing mutants like Δ508, and Class III mutants produce CFTR that is trafficked to the membrane but have dysfunctional Cl^- conductance; all three classes result in severe lung disease and pancreatic insufficiency. Class IV mutants display less pronounced conductance abnormalities and often have no lung phenotypes, and Class V mutants are often asymptomatic and diagnosed only after they are found to be infertile or present with idiopathic pancreatitis.[20,21]

CFTR in the Kidney

CFTR expression is abundant in the human kidney. Early studies looking at CFTR mRNA or using RT-PCR found evidence for CFTR expression generally in the cortex and outer medulla. More specifically, CFTR was found all along the nephron, including proximal and distal tubules, thin and thick ascending limbs, and the collecting duct.[80,81] Immunostaining of CFTR protein showed CFTR expression again in the proximal and distal tubules, the tAL, and the cortical and inner medullary collecting ducts.[81] Functional studies using patch-clamp have identified CFTR-like currents in the proximal and distal tubules and the collecting ducts.[81] CFTR is also known to be expressed in the embryonic kidney, with upregulation in the ureteric bud during the later stages of branching morphogenesis.[25] Intriguingly, a large proportion of the overall CFTR expression in the kidney consists of a CFTR splice variant termed TNR-CFTR.[80] The TNR-CFTR mRNA is missing the final 145 bp including exons 13 and 14, creating an early stop codon. The splicing may be regulated by snRNAs U11 and U12, which co-localize to the same areas of the kidney as the TNR-CFTR isoform.[117] This truncation corresponds to a loss of the second TMD and NBD, as well as 7% of the R domain in the final protein. The TNR-CFTR is therefore a "half" transporter, similar to many other members of the ABC family, and like those other ABC transporters, the remaining half molecule is enough to give the protein function. When expressed in *Xenopus* oocytes the TNR-CFTR is a functional Cl^- channel, is still activated my cAMP and PKA, and possesses many of the same biophysical traits as the wild-type CFTR.[80] Its processing, however, seems less efficient,[80] and little makes it to the plasma membrane, but instead it localizes to intracellular vesicles.[81] More generally, TNR-CFTR is found mostly in the renal medulla, and has an interesting developmental expression pattern. In mice, the expression of TNR-CFTR increases throughout embryonic kidney development, reaching its highest level at birth.[81] The functional significance of TNR-CFTR remains a complete mystery.

CFTR as a Kidney Cl^- Channel

Although the expression levels of CFTR in kidney are comparable to those of the lung, there is no clear CF kidney phenotype, with the exception of increased risk of hyperoxaluria or insufficient citrate-induced kidney stones; a fact that many have taken as evidence that CFTR is not very important in salt handling in the kidney, and yet CFTR is known to play important roles in renal diseases like ADPKD. Many have attributed the lack of phenotypes to a redundancy in Cl^- channels present in the kidney. Mouse $CFTR^{-/-}$ knockout models often show little or no lung CF phenotype, a discrepancy explained by the upregulation of Ca^{2+}-activated Cl^- channels (TMEM16s; [62]) to compensate for the loss of CFTR Cl^- conductances. Likewise in the kidney, other types of Cl^- channels could be compensating for the missing functional CFTR in CF patients. However, CFTRs functional role in the kidney could be more regulatory, thus CF renal phenotypes more subtle. Recent work looking at CFTR in the apical membrane of mouse cortical collecting duct principal cells demonstrates the difficulty in establishing CFTRs function as a Cl^- channel and not as a regulator of other channels. Lu et al.[72] definitively demonstrated CFTR Cl^- channel activity on the apical membrane of mouse principal cells, and plausibly suggest that it could represent a short-circuit current meant to regulate Na^+ absorption and K^+ secretion. However, they concede that it is just as likely that phosphorylation of CFTR could act as a modulatory switch on ROMK activity, and thus exert an influence on K^+ secretion.[72] To complicate matters further, the prevailing model of ion movement in principal cells has Cl^- being reabsorbed mainly through a paracellular pathway, suggesting that for CFTR to have an effect it would need to represent a very large conductance, much larger than that measured by Lu et al. in mouse principal cells.[72] In fact, there is ample evidence that in the kidney and elsewhere CFTRs main function may be to regulate other ion channels.

CFTR as a Regulator of ENaC

From before its initial molecular identification, CFTR has been shown to regulate an ORCC Cl^- conductance and a Na^+ conductance.[113] In the airway of CF patients (but not in the sweat ducts), increased Na^+ absorption via the epithelial sodium channel, ENaC, is observed due to loss of the normal CFTR-mediated inhibition; however, the mechanism of regulation remains unclear. Currently, there are multiple hypotheses to explain how CFTR regulates ENaC. One possibility is that intracellular Cl^- regulates ENaC activity. This is supported by data showing that CFTR Cl^- conductance is necessary for ENaC regulation, and in some but not all cell types replacing CFTR Cl^- current with CLC-mediated Cl^- currents can also inhibit ENaC currents.[12] These data are conflicted by the lack of identified Cl^--binding sites on ENaCs intracellular domains, and by studies showing that alternative Cl^- channels like CaCCs cannot inhibit ENaC.[12]

A second theory proposes CFTR exerts its regulatory effects through intermediary proteins as part of a large protein complex. CFTR contains a PDZ-binding domain that enables it to interact with linking proteins like ezrin-binding phosphoprotein 50 (EB50) and NHERF1. NHERF1, through its PZD2 region, can bind YAP65 which recognizes the PY motif on the C-terminus of ENaC, creating a complex with both CFTR and ENaC. C-Yes, a c-Src kinase, is a known inhibitor of ENaC and can bind to YAP65. Thus, CFTR, in aiding the assembly of the protein complex, inhibits the activity of ENaC and the dissolution of the complex, e.g., from CFTR dysfunction or mutation, liberates ENaC from C-Yes inhibition.[42] However, this possibility has not been demonstrated in heterologous expression systems.[12]

A third possibility involves CFTR interacting directly with ENaC to cause inhibition. Patch-clamp studies of ENaC subunits and CFTR in proteoliposomes, presumably free of contaminating complex proteins, showed that CFTR directly affects the gating of ENaC single channels. FRET studies have demonstrated an association of less than 10 nM of the two proteins *in vitro*, and co-immunoprecipitation experiments show the two physically interact.[12] However, with the exception of the single channel results, the evidence does not strictly rule out the possibility of CFTR and ENaC interacting indirectly as part of a protein complex.

The relationship between CFTR and ENaC in the kidney appears as conflicting as that found for the airways and seat ducts. Some work has shown that CFTR inhibits ENaC in the kidney, similar to the relationship found in airways. Experiments in M-1 cortical collecting duct cells showed that activation of PKA reduced the amiloride-sensitive apical Na^+ current.[66] However, other studies have found CCD cells from mice carrying a mutation in ENaC, known to cause Liddles's syndrome (deletion of the PY motif in the c-terminus as the β-subunit ENaC), display increased Na^+ absorption as compared to wild-type when treated with dD-arginine vasopressin. A similar increase is seen in the CFTR-mediated apical current, implying vasopressin causes increases in both conductances,[130] an idea consistent with the cAMP-induced increases in both CFTR and ENaC seen in sweat ducts.[101] Simply put, the evidence for CFTR regulating ENaC in the kidney is sparse, and it remains unknown whether or not it acts as an inhibitor, activator or neither. It may require a final determination of how CFTR regulates ENaC in airway tissue before a renewed focus can be brought on CFTR and ENaC in the kidney.

CFTR as a Regulator of ROMK

The inward rectifier potassium channel ROMK (Kir1.1) and its isoforms are expressed highly in the distal nephron, where it plays a major role in ATP sensitive K^+ secretion.[72] Some of their defining traits are lack of sensitivity to the common K^+ channel blocker tetraethylammonium (TEA), and inhibition by ATP and sulfonylureas like glibenclamide.[113] But when the ROMK2 isoform was expressed in the *Xenopus* oocytes, it was no longer sensitive to glibenclamide. Other ATP-sensitive K^+ channels require ABC transporter subunits, SUR1 and SUR2 (ABCC8 and ABCC9), for glibenclamide sensitivity, but neither SUR1 nor SUR2 is known to be expressed in the kidney. However, CFTR is expressed in the same distal nephron cells as ROMK channels, and when CFTR and ROMK2 are co-expressed in *Xenopus* oocytes, the glibenclamide sensitivity is restored.[113] Subsequent work has demonstrated that CFTR is also necessary for ROMK's sensitivity to Mg-ATP in CCD mouse cells. Lu et al.[72] hypothesize that water diuresis and the resulting low cAMP-PKA would promote the CFTR−ROMK interaction, and so cytoplasmic ATP would inhibit excessive K^+ secretion. However, during antidiuresis when PKA levels are high, the phosphorylation of CFTR will free ROMK from ATP sensitivity and promote K^+ secretion.[72] The specifics of the ROMK−CFTR interaction are unknown, but it is probably similar to the better-understood Kir6.x/SUR complex of pancreatic β-cells. Kir6.x-subunits form tetramers, with each subunit associated with a SURx subunit to create an eight unit complex.[2] Although the CFTR regulation of ROMK appears functionally very important, there is no reported K^+ secretion phenotype in the distal nephron in CF patients.

CFTR as a Regulator of SLC26As

CFTR is also a demonstrated regulator of transporters from the SLC family of anion transporters. Earlier research showed that CFTR could interact with and activate SLC26A3 and A6, conferring cAMP sensitivity on these two transporters.[116] In the pancreatic ducts, HCO_3 secretion is a critical component of the function of the secretory epithelium, a function disrupted in patients with severe CF. Wang et al.[136] showed specifically that the SLC26A6 HCO_3^-/Cl^- exchanger was critical for HCO_3^- secretion, and that its function was regulated by co-localized CFTR expression in the luminal membrane. Further work demonstrated that a conserved region of the SLC26A transporters, the STAS domain, interacted directly with the R domain of CFTR.[59] The binding of the STAS and R domains activates SLC26A6, but also dramatically increase the Cl^- conductance of CFTR by increasing the channels open probability six-fold.[59] Interestingly, SLC26A6 is expressed throughout the kidney, but appears most prominently in the apical–luminal membrane of the proximal tubule where it is responsible for Cl^-, HCO_3^-, oxalate, and formate exchange.[59] CFTR expression is also reported in the proximal tubule, and although there is no current evidence of their interaction in the kidney it seems plausible.

CFTR more recently has also been demonstrated to be a regulator of one of the two true Cl^- channel members of the SLC26A family, SLC26A9. Both SLC26A9 and CFTR co-localize to the apical membrane of human bronchial epithelial (HBE) cells, where cAMP leads to the co-activation of SLC26A9 and CFTR Cl^- channels.[13] The nature of the CFTR–SLC26A9 interaction is similar to the other CFTR–SLC interactions, the conserved STAS domain of SLC26A9 binds directly to the R domain of CFTR.[17] However, there are conflicting reports as to the exact regulatory nature of the CFTR–SLC26A9 relationship. Bertrand et al.[13] report that endogenous SLC26 currents in HBE cells are activated by functional CFTR; whereas Chang et al.[17] report heterologous co-expression of an NBD + R domain CFTR construct with SLC26A9 in *Xenopus* oocytes results in the inhibition of SLC26A9 currents. What is clear is that the conserved STAS domain of the SLC26A channels and transporters strongly interacts with CFTR, an interaction that may extend to many of the SLC26A members. SLC26A9 is expressed mainly in the lung, but the other described SLC26A pure Cl^- channel, SLC26A7, is expressed throughout the kidney, and in particular cells of the cortical collecting ducts, an area also high in CFTR expression. The role of a possible interaction between SLC26A7 and CFTR in the cortical collecting duct is an important area for future investigation.

CFTR and Endocytosis

A new area of CFTR research has begun investigating CFTRs role in acidification of endosomes of the proximal tubule. Generally, CF patients have shown increased renal clearance of some drugs including aminoglycosides, and more specifically a cohort of patients with at least one copy of the Δ508 CFTR mutation showed significantly higher levels of albuminuria and LMW proteinuria.[56] $CFTR^{-/-}$ knockout mice have significantly increased excretion of LMW Clara Cell protein (CC16), and decreased uptake of radio-labeled ^{124}I-β2microglobulin and aminoglycosides, similar to human CF patients. Significantly, the $CFTR^{-/-}$ mice also demonstrated decreased cubilin expression in the S3 segment of the proximal tubule, a finding correlating with the observed increase of cubilin excretion.[56] Cubilin is a lipoprotein receptor and, along with megalin, is critical for the uptake of LMW proteins. In the $CFTR^{-/-}$ mouse, however, megalin is not affected, thus it appears CFTR is specifically reducing cubilin expression. Cubilin recycling to the apical membrane via endosomes is critical to maintain apical cubilin expression and for LWM protein uptake. The sorting and recycling of endosomes is pH-dependent.[56] CFTR has been localized to the apical region in proximal tubule cells and specifically it co-distributes with ClC-5 and Rab5a in endosomes,[56] where it is proposed to aid in providing a negative current shunt for the interior of the endosomes. CFTR would offset the build-up of positively-charged H^+ during acidification, a role similar to that proposed for the Cl^-/H^+ exchanger ClC-5.[56] The evidence of CFTRs involvement in receptor-mediated endocytosis from CF patient studies and $CFTR^{-/-}$ mice is compelling, but the mechanism remains unconfirmed, although it seems likely CFTR, along with ClC-5 and possibly other Cl^- channels, all contribute to the pH regulation of the proximal tubule endosomes.

Ca^{2+}-Activated Cl^- Channels (CaCC): TMEM16/Anoctamin

For 30 years Ca^{2+}-activated Cl^- channels (CaCC) with similar biophysical characteristics have been studied in a wide range of tissue and cell types, including secretory epithelia, egg cells, cardiac, smooth, and skeletal muscles, neurons, olfactory and photoreceptors, hepatocytes, and beta cells.[45,47] The classic CaCC characteristics are best described by the endogenous CaCCs of *Xenopus* oocytes or the CaCCs of acinar cells in the salivary gland (Figure 31.4). These classic CaCC channels are activated by small amounts of cytosolic Ca^{2+} (0.2–5 μM)[45] either from extracellular influx or store release. Activation appears to occur through direct binding of Ca^{2+} to the channel. When cytosolic Ca^{2+} is

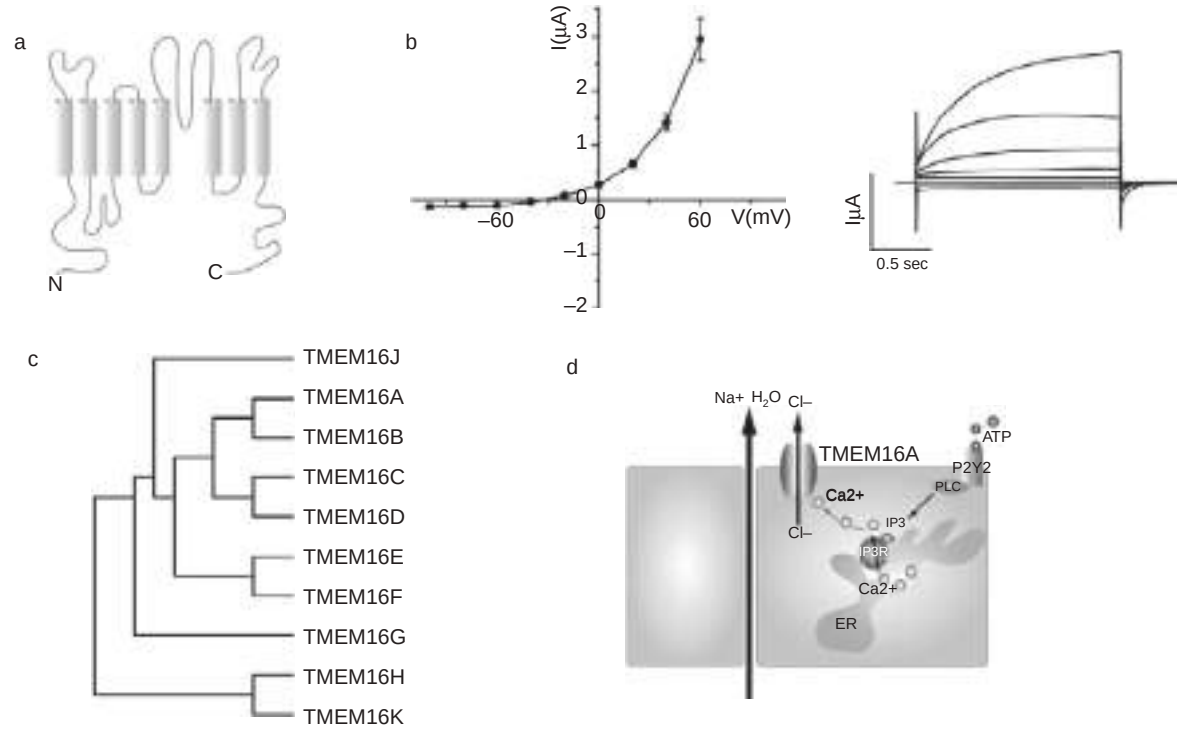

FIGURE 31.4 **Ca^{2+} activated Cl^- channels (CaCC), the TMEM16s.** (a) Topography of TMEM16A. (b) I/V relationship and whole cell classical endogenous CaCC currents of *Xenopus* oocytes mediated by TMEM16A (Woodward and Guggino, unpublished data). (c) Phylogenetic tree of human TMEM16 members. *(Reprinted from Schroeder, B. C., Cheng, T., Jan, Y. N., and Jan, L. Y. (2008). Expression cloning of TMEM16A as a calcium-activated chloride channel subunit. Cell* ***134****, 1019–1029, with permission from Elsevier.*[111]*)* (d) Typical ATP/Ca^{2+}-activated Cl^- and fluid secretion in secretory epithelium mediated by TMEM16A.

limiting, CaCC shows an outward rectifying I/V relationship, but as cytosolic Ca^{2+} increases the rectification diminishes.[45,85,138,139] The open probability appears to be voltage-dependent and the single channel conductance is small 1–3 pS, although a variety of conductance sizes has been reported.[45] Classic CaCCs, like other anion channels, are relatively non-selective, with Na^+ permeability being roughly 10% that of Cl^-. Among anions the selectivity sequence is $SCN^- > NO_3^- > I^- > Br^- > Cl^- > F^-$.[45]

The ubiquitous nature of CaCC channels makes describing their physiological function difficult; it plays different roles in each cell type. In *Xenopus* oocytes CaCC plays a major role in blocking polyspermy fertilization of the egg. Fertilization generates a Ca^{2+} wave across the membrane, activating the CaCC channels and depolarizing the egg.[45] In secretory epithelia Cl^- secretion is critical to draw Na^+ and water across the apical membrane, and CaCCs appear to contribute to the Cl^- conductance across the apical membrane, often in an ATP-dependent manner.[45]

Similar to many other epithelial cell types, kidney epithelia have demonstrated CaCC currents and channels, including rabbit distal convoluted tubules, proximal convoluted tubules, and cortical collecting duct. However, most of the work has been done on a mouse medullary collecting duct cell line, IMCD-K2.[15,99] Using the IMCD-K2 line, Qu et al.[99] described CaCC currents that they suggested were the same as those found endogenously in *Xenopus* oocytes. These currents can be activated by ATP and rely on intracellular Ca^{2+} store release for activation.[15] They are co-expressed in IMCD-K2 cells with CFTR, and while their specific function in the collecting duct is not known, it may be similar to the Cl^- secretory role they play in airway epithelium. Because CaCC currents may be controlled by hormones, the CaCC-mediated Cl^- secretion in the distal kidney may help fine-tune urine composition.[45]

The molecular identity of the CaCC channels was for decades an elusive dream, with a stream of potential candidates including the CLCAs and the bestrophins, whose biophysical characteristics matched some of the classic CaCC characteristics, but not all. Recently, a new family of genes has been proposed to represent the CaCCs, the TMEM16 or Anoctamin gene family which, unlike previous candidates, shares all of the biophysical characteristics of the classic CaCC channels. The confidence in this new family of proteins as CaCC comes from a number of factors, not the least of which was the methods used to discover their

identities. Three different research groups, using three totally different methodologies, each independently arrived at the conclusion that TMEM16A/Aco 1 was the classic CaCC. Schroeder et al.[111] took advantage of the unique property of Axolotl (*Ambystoma mexicanum*) salamander oocytes of not having any CaCC currents. They used these oocytes to screen a cDNA library from size fractionated RNA isolated from *Xenopus* oocytes resulting in the identification and cloning of a gene that coded for a 979 amino acid protein, the *Xenopus* ortholog to the human TMEM16A gene. Expression of TMEM16A in the Axolotl oocytes produced Cl^- currents identical in most of the biophysical properties that define the classic CaCCs. Schroeder et al.[111] also showed that TMEM16s are expressed in salivary glands, as expected if they are the CaCCs. A second group, Yang et al.[146] used a bioinformatic search targeting putative channel or transporter-like genes with more than two transmembrane domains. Their search turned up TMEM16A, which met their criteria but became their focus because it had no described function, and the TMEM16 family has 10 human homologs. They renamed the TMEM16s anoctamins because the channels appeared to be anion selective with eight (OCT) transmembrane domains.[47] Yang et al.[146] tested the biophysical properties of TMEM16A when expressed in HEK cells, and like Schroeder et al.[111] found their properties to be very similar to those described above for the classic CaCCs, although the pharmacological sensitivities of the overexpressed TMEM16A channels in HEK cells were far more sensitive to the classic anion channel blockers DIDS, NPPB, and NFA than their endogenous counterparts.[47] Yang et al.[146] went further, and showed that mutating the putative poor region, between TM5 and TM6, disrupted anion permeability markedly. Importantly, like Schroeder et al. they showed that TMEM16s were expressed in tissues where classic CaCCs have been described, and demonstrated that knocking-down TMEM16A in acinar cells of the salivary gland reduced the endogenous CaCC currents, and reduced saliva production upon pilocarpine application. And finally, a third group, Caputo et al.,[16] identified TMEM16s through a microarray screen of airway epithelial cells treated with IL-4, a treatment known to increase CaCC currents in these cells. They isolated a group of membrane proteins with no known function, including TMEM16A, then generated RNAi against each of the most likely candidates and attempted to knock-down the endogenous CaCC activity inCFPAC-1 and CFBE410 cells. Activity was assayed using a halide sensitive YFP protein and short-circuit currents, and siRNA TMEM16A was found to very effectively reduce the endogenous CaCC currents. Caputo et al.[16] went on to express TMEM16A in FRT cells, and again described their biophysical properties as being almost identical as those known for the classic CaCC currents.

The TMEM16 family of genes is well-conserved, with members found throughout eukaryotic phyla; however, there appears to be an increased representation in mammals.[47] Humans have 10 members of the TMEM16 family (A–H, J–K) or Ano 1–10, and their predicted topology has both N- and C-termini intracellular, eight transmembrane domains, and the pore region located between TM5 and TM6.[146] Interestingly, no clear Ca^{2+}-binding domain has yet been discovered in the TMEM16s. In TMEM16A there is no EF hand region or CaM-binding sites.[47] However, there does appear to be a Ca^{2+} bowl structure, similar to that found in BK Ca^{2+}-activated K^+ channels. This same structure was predicted by Hartzell et al.[45] for classical CaCCs before the identification of the TMEM16 genes based on the demonstrated μmolar range Ca^{2+} affinity.[45] The molecular diversity of the TMEM16 family could help explain the differences in described biophysical properties of endogenous CaCCs in different cell and tissue types. Members of the TMEM16 family may have different channel properties or they may heterodimerize to create chimera channels. The TMEM16s also exhibit multiple splice variants, TMEM16A has at least four,[16] and these variants were found to have different channel properties.[16] The likelihood that members of the TMEM16 family other than TMEM16A are anion channels is high, because of the close sequence homology among the members. And although most of the descriptive work has focused on TMEM16A, Cl^- currents have also been described for TMEM16B (Ano2) which is found in olfactory receptors,[27] and for TMEM16F and TMEM16K (Ano 6 and 10).[110] In each case, like TMEM16A they share many similarities with the classic CaCC, but each has some differences as well, supporting the idea that the diversity of the TMEM16 family corresponds to the diversity of CaCCs.

The TMEM16s are only now getting the in-depth attention necessary to discern how TMEM16s function as CaCCs, which ones are expressed in which cell and tissue type, and what role if any they may play in human disease. Even before TMEM16A was known to be a Cl^- channel it had been observed to be upregulated in tumors, but why is unknown.[27,47] Initial reports on the Cl^- channel functions of TMEM16A have focused on tissues and cells historically known to have large CaCC currents, including airway epithelial cells. In these cells CaCC currents have long been seen as a potential target in treating cystic fibrosis; by upregulating CaCC currents the lost anion conductance from dysfunctional CFTR could be replaced, and disease severity lessened. Mouse models of CF, strangely devoid of the debilitating lung systems found in

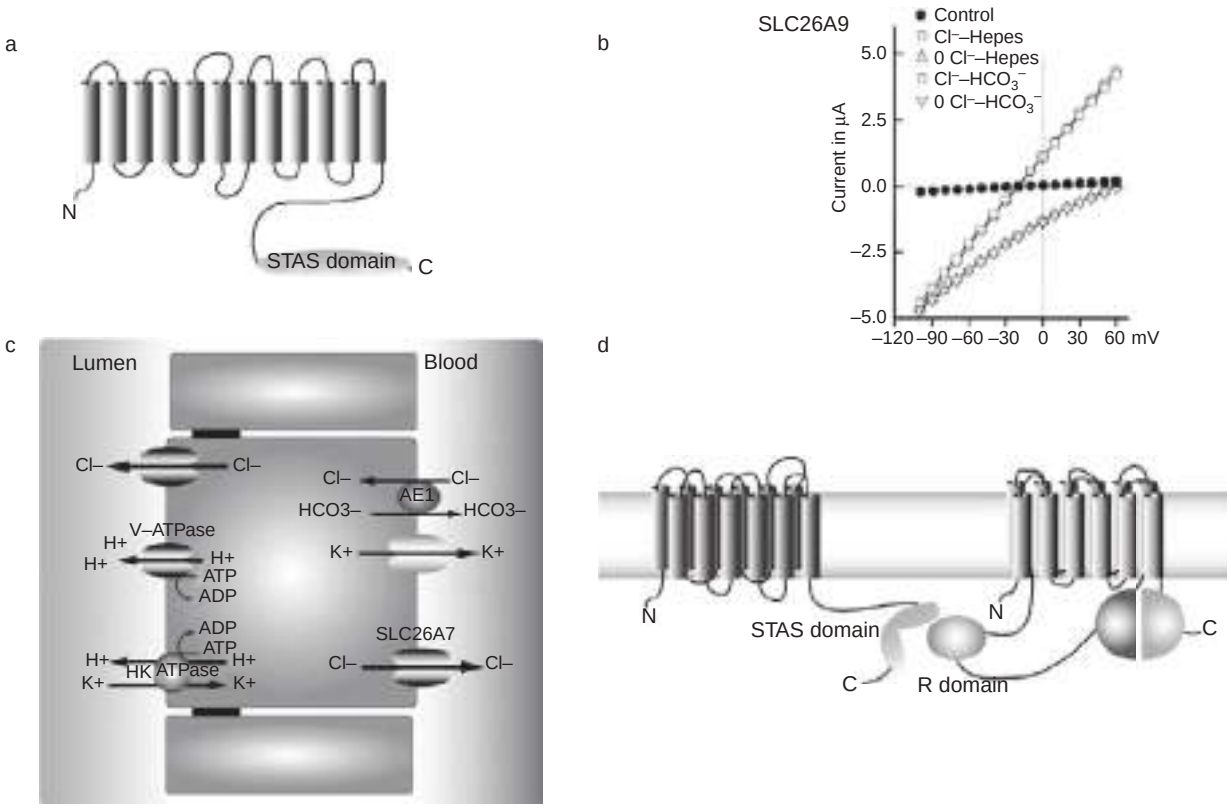

FIGURE 31.5 **Solute carrier (SLC) 26A7 and A9.** (a) Proposed, although not experimentally verified, topography of the SLC26 proteins. (b) I/V relationship from whole cell currents in *Xenopus* oocytes cells expressing SLC26A9. *(Reprinted with permission from Dorwart, M. R., Shcheynikon, N., Wang, Y., Stippec, S., and Muallem, S. (2007). SLC26A9 is a Cl⁻ channel regulated by the WNK kinases. J. Physiol. **584**(1), 333–345.[26a])* (c) SLC26A7 provides a pH sensitive basolateral Cl^- conductance in α-intercalated cells of the collecting duct. (d) SLC26A9 is regulated through direct interactions between the SLC26A9s STAS domain and the R domain of CFTR.

humans, have been shown to express TMEM16A at much higher levels than in wild-type airway epithelia, strongly supporting the targeting of TMEM16A in humans as a CF treatment.[62] It is not clear what functional role the TMEM16s play in the kidney. Presumably they underlie the known CaCC currents identified in the kidney, but which ones and how remains unknown. Yang et al.[146] showed specifically that TMEM16A is expressed in the epithelia of proximal tubules and the distal renal tubules. In mice TMEM16F mRNA was found in the kidney at high levels, as were slightly lower levels of TMEM16K and H. Going forward it will be exciting to learn more about the TMEM16 family, and specifically their role in anion regulation in the kidney and the role they play in diseases such as ADPKD.

Solute Carrier 26 Transporters

As discussed earlier, the distinction between Cl^- transporter and Cl^- channel can be the position of one or two amino acids, and just as recently resolved crystal structures revealed members of the CLC Cl^- channel family to be transporters, recent studies of the large SLC26 transporter family revealed at least two of its members bear the hallmarks of Cl^- channels, not transporters. Specifically, SLC26A9 and SLC26A7 appear to operate solely as Cl^- channels, and have little or no bicarbonate permeability.[89] The SLC26 family is large and very diverse, much like the CLC gene family, and many of its members still lack identified physiological function, including SLC26A7 and SLC26A9 (Figure 31.5). However, present work does suggest both may play important roles in secretory epithelia in areas of the lung and kidney. As discussed earlier, SLC26A9 is expressed highly in lung epithelia, and may be regulated by CFTR[13] via the highly-conserved SLC26 STAS domain.[17] When expressed in HEK cells or *Xenopus* oocytes, the SLC26A9 channel is constitutively active, with a linear to slight inward rectification I/V relation,[13,17,26,26a,89] is only slightly permeable to bicarbonate, and is not pH sensitive.[26,26a,89] And while SLC26A9 is most highly expressed in ciliated bronchial airway epithelial and alveolar cells, its expression is widespread.[26]

SLC26A7, on the other hand, is very highly expressed in the human kidney, including in the renal

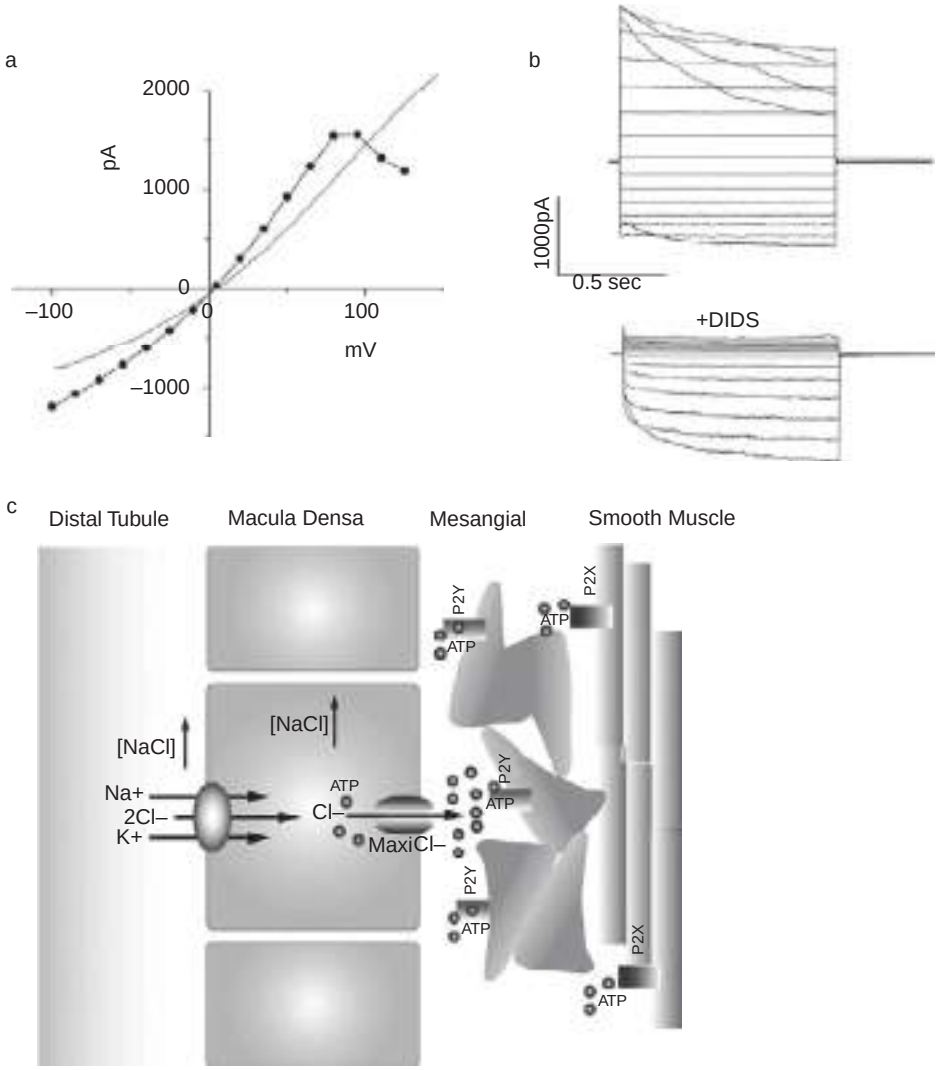

FIGURE 31.6 **Volume regulated anion channels (VRAC).** (a) Instantaneous and steady-state I/V relationships of VRAC currents in human bronchial epithelial cells (IB3-1 cells) (Woodward and Guggino, unpublished data). (b) Whole cell currents activated by a hypotonic extracellular bath and inhibited by DIDS (Woodward and Guggino, unpublished data). (c) Maxi-anion/Cl^- channels in macula densa cells secrete ATP in response to increases in intracellular NaCl. ATP may regulate the mesangial and smooth muscle responses to high tubular salt levels.

outer medullary collecting duct, the thick ascending limb, and the apical membrane of proximal tubule.[26] Like SLC26A9, SLC26A7 is constitutively active, has a linear I/V relation, is not permeable to bicarbonate,[58] but unlike SLC26A9, SLC26A7 is very sensitive to pH.[26,89] Acidic pHi increases the selectivity of SLC26A7 to Cl^-,[58] apparently through intracellular H^+ regulation of the channel. SLC26A7s pHi sensitivity has prompted the hypothesis that it may function as a pHi sensor[89] or function in Cl^--loading in parietal cells. The physiological function of SLC26A7 in the kidney remains unknown, although it is expressed on the basolateral membrane of the alpha-intercalated cells of the outer medullary collecting duct, cells that secrete acid[116,120] as part of the kidney's role in regulating the blood's acid–base balance (Figure 31.5). It would seem that the pHi sensitivity of SLC26A7 would make it an affective pHi sensor in alpha-intercalating cells just as in parietal cells, and it could again function as a Cl^--loading mechanism and therefore would be important in the apical secretion of H^+ from the cells. Currently no human diseases are associated with SLC26A7 or SLC27A9 dysfunction; however, it seems likely that further work will reveal their importance in human and kidney physiology.

Volume-Regulated Anion Channels

The recent success in discovering the molecular identity of the CaCC only highlights the need to identify the last remaining functional group of Cl^- channels, the volume-regulated anion channels (VRAC) (Figure 31.6). VRACs are found in every cell type as part of the normal housekeeping functions possessed by all cells. In mammalian cells when an osmotic imbalance occurs and water moves into the cell, threatening the integrity of the membrane, the cell initiates the regulatory volume decrease (RVD) response consisting of the efflux of K^+ and Cl^- ions, as well as bicarbonate and amino acids; through the loss of these

osmolites the osmotic balance can be regained and the cell shrinks. In the dynamic osmotic conditions along the mammalian nephron the VRAC channels may play a dominant role in the RVD response, protecting the cells from osmotic harm. In addition to cell volume regulation, VRAC channels are known to play roles in maintaining resting potentials, aiding in vectorial Cl^- transport, salt and fluid secretion, cell proliferation and differentiation,[85] cell migration,[92] apoptosis,[91] and ATP secretion.[85,92] In addition to VRACs role in RVD in kidney cells, another role has been described for the large conductance maxi-anion type of VRAC channels which appear concentrated in the macula densa cells of the thick ascending limb (TAL). Macular densa cells function to sense changes in the luminal NaCl concentration, and signal the regulator mechanism necessary to bring salt levels back to normal via tubuloglomerular feedback (TGF).[10] Bell et al.[10] found that maxi-anion channels in the macula densa cells could conduct ATP, and did so under conditions of experimentally high luminal NaCl. It is not yet clear how the maxi-anion channels are activated by the high luminal NaCl concentrations, nor is it clear exactly what role ATP plays in signaling as compared to NO and PGE2.[11] But it is clear that ATP is important, and that the maxi-anion channels are the only described mechanism for its secretion from the macula densa cells, implying a very important role for the VRAC channels in the TAL. Ultimately only the molecular identity of the VRAC channels will further our understanding of their function in the kidney.

The general biophysical characteristics of the VRAC channels are similar to other known anion channels, including its relative non-selectivity, and its outward rectification. The most unique characteristics of VRAC channels are their voltage-dependence: depolarization above $+60$ mV causes time and voltage inactivation, with negative potentials removing inactivation.[84,85] Intracellular Mg^{2+} and extracellular protons appear to accelerate this inactivation. The anion selectivity sequence is $SNC^- > I^- > NO_3^- > Br^- > Cl^- > F^-$, but VRAC channels are also permeable to amino acids like glutamate and aspartate, polyols, and ATP.[84,85] This promiscuity is in part due to the large calculated pore size of ~ 11 Å.[85] Pharmacologically, the usual nonspecific anion channel blockers also work on VRAC channels, NPPB > DIDS > NFA,[84] some, like DIDS, show a strong voltage-dependence to its block, demonstrating it can only block from one direction. The single channel properties suggest VRAC channels are a heterogeneous group consisting of mini-anion channels (0.1–8 pS), volume-sensitive outwardly rectifying channels (VSOR: 20–80 pS), and maxi-anion channels (100–400 pS), although most fall into either the VSOR or maxi-anion groups.

Because of their extremely important physiological role in TGF, a further look at the maxi-anion channel subclass of VRAC channels is deserved. As mentioned above, maxi-anion channels have very large single channel conductances that increase with saturating concentrations of Cl^- in excess of 640 pS.[107] In contrast to the characteristics described above for the classic VSOR type of VRAC channels, the maxi-anion channels have a much larger pore size of 1.16–1.42 nm, which again helps to explain its ability to conduct ATP. Like other VRAC channels, maxi-anion channels are voltage-dependent with inactivation at depolarizing potentials, but unlike other VRAC channels it also inactivates at hyperpolarizing potentials, resulting in a bell shaped voltage-dependence of open channel probability.[107] At potentials with little or no inactivation, the I/V relationship is linear. Further questions about maxi-anion channel structure and function in both the kidney and beyond will, as for the entire VRAC group, depend on resolving its molecular identity. This is perhaps the most pressing issue in all of anion channel research currently, and remains a gaping hole in our fundamental understanding of how anion conductances shape cellular function and life.

Other Cl^- Channels

GABA and Glycine Receptor Channels

The GABA (GABAA, GABAC) and glycine receptor (GlyR) Cl^- channels represent the only examples of anion channels within the cation channel gene families. Both GABA- and glycine-gated channels are members of the ligand-gated ion channel (LGIC) superfamily,[18] and share a large amount of structure homology with cation members of the same LGIC family, including the nicotinic acetylcholine (nACh) receptor channels and the 5HT3 receptors.[18] Like nACh channels, both the GABA and glycine receptor channels have a 5 subunit structure, with two alpha-, two beta-, and one gamma-subunit.[88] There are two GABA receptor channel groups that conduct anions, GABAA and GABAC, both are important for inhibitory synaptic transmission in the nervous system, and both have a $I^- > Cl^-$ permeability.[131] GABA receptors may play key roles in human disorders including epilepsy, multiple sleep disorders, and Alzheimer's.[18] GlyR channels are also important in synaptic inhibition in the nervous system, and have been linked to hyperekplexia[73,131] or human startle disease. GlyR channels have an ion selectivity sequence, $I^- > Br^- > Cl^- > F^-$, similar to the GABA channels, with a pore size around 5–6 Å,[88] slightly smaller than the other cation members of the LGIC family. The GlyR single channel conductance is variable depending on the arrangement and type of

subunits, but most frequently is around 90 ps.[88] Though the GABA and GlyR channels play significant roles in human disease and are very important in the function of the human nervous system, they have not been shown to express in the human kidney and therefore their discussion will remain superficial.

Voltage-Dependent Anion-Selective Channel (VDAC)

Often in a discussion of anion channels the voltage-dependent anion selective channels (VDAC) are omitted, because of their believed confinement to the outer membranes of the mitochondria (hence their alternative name of mitochondria porins),[24] loose anion selectivity, and giant poor size. Thus, the logic goes, the VDAC channels are not comparable to the Cl^- channels that inhabit the other cellular membranes. However, their recent localization to the plasma membrane has elevated them to Cl^- channel status, if just barely. VDACs were first discovered on the membrane in human B-lymphocytes, and the subsequent development of an antibody lead to the description of VDAC surface localization in numerous cell types including epithelium. Subsequent work confirmed VDAC1 to be located within caveolins, or plasma membrane subcompartments, and found VDAC in proteomic surveys of the plasma membrane of human cells.[24] Perhaps most convincingly, VDAC proteins have been purified from both the plasma membrane (using a NH-SS-biotin label) and from the mitochondria, and compared via electrophoretic mobility, antibodies, and electrophysiological recordings in reconstructed lipid bilayers.[8,9,52] The question remained, however, what were they doing there? In the mitochondria, the VDAC family of proteins resident in the outer mitochondrial membrane is responsible for a number of functions, but probably not the regulation of Cl^- conductance. The VDAC proteins are 30–35 kDa proteins that contain a single alpha helix and 13, 16 or 19 transmembrane beta sheets.[24,114] When reconstituted in a lipid bilayer VDAC forms a very large 2–3 nm pore,[114] and is loosely voltage-dependent (40% of the initial conductance persists in the "closed" state).[107] Its Cl^-/K^+ permeability ratio is an astoundingly low 1.7–1.9,[107] but its single channel conductance of Cl^- is linear up to 10 nS with no saturation.[107] However, its primary function in mitochondria is probably more related to metabolite flux (including ATP, cytochrome c, and superoxide anions),[105] membrane composition, and an important role in apoptosis.[40]

There are a number of hypotheses as to the nature of the VDAC function on the plasma membrane. The voltage-dependence of VDAC means that at most resting potentials the channel should be closed,[24] alleviating the obvious lethal potential of a large, relatively nonselective pore in the plasma membrane. There is some evidence that VDAC may be an ATP release channel,[90,114] although there is also evidence that VDAC may inhibit ATP release.[24] Other proposed functions include plasma membrane VDAC1 as a redox enzyme which reduces extracellular ferricyanide in the presence of NADH.[5] Its role as a redox enzyme is supported by evidence that transfection of COS-7 cells with a VDAC1 construct increased the plasma membrane NADH:ferricyanide reductase activity 40-fold.[5] This VDAC1 function may play a role in the reductive activation of the anticancer drug 2-methyl-furanonaphthoquinone.[115] Finally, plasma membrane VDAC has been long hypothesized to be the maxi-anion channel found in many tissue types including the kidney. There exist many superficial similarities in the biophysical properties of each, which has lead for years to the acceptance that VDAC was the molecular identity of maxi-anion channels, even though there appear to be some vast differences in characteristics and localization. For instance, surface VDAC has been shown in epithelium,[24] but not specifically in kidney. Recently this hypothesis was tested directly by Sabirov et al.,[106] where they either knocked-out or knocked-down expression of the three VDAC isoforms, and found the endogenous maxi-anion channel of mouse embryonic fibroblasts (MEFs) unaltered, strongly arguing against VDACs being the molecular identity of maxi-anion channels. However, it is worth noting that expression of surface VDAC channels is not universal and could be very cell type-specific, thus in cell types other than MEFs VDAC could still be the previously identified maxi-anion channels that are critical for renal salt balance in the human kidney (see discussion above).

Tweety (Human Homolog hTTYH3)

The VDAC proteins are not the only recent entrant in the race to win the title "identity of maxi-anion channel." Using a rather novel bioinformatic methodology Susuki[122] screened for *Drosophila* genes that coded for proteins with four or more predicted transmembrane domains and a described behavioral abnormality. Suzuki found a gene, *tweety*, within the *flightless* locus, which matched his criteria, and its knockout resulted in loss of normal flight. Suzuki further found that *tweety* has a human homology, hTTYH3, a gene encoding a 523 amino acid protein. mRNA expression of mouse TTYH3 is found in most excitable tissues as well as kidney, fat cells, thymus, and uterus, and also a number of cell lines including kidney epithelial cells (OK, HEK, and MDCK lines).[122] Using a c-terminal antibody, TTYH3 was positively localized in the glomerulus of the kidney.[122] Other *tweety* genes may also be important in the human kidney, hTTYH2 mRNA

has been shown to be upregulated in renal cell carcinoma.[48]

The electrophysiological characteristics of hTTYH3 do certainly show similarities to maxi-anion channels, but also to large conductance Ca^{2+}-activated Cl^- channels. Expression of hTTYH3 in CHO cells in the presence of ionomycin results in large linear Cl^- currents.[122] The ion selectivity for the hTTYH channel is $I^- > Br^- > Cl^-$, and the mutations of positively-charged amino acids in the pore region result in an appropriate reduction in the gluconate/Cl^- permeability ratio.[122] The large linear Cl^- currents of hTTYH3-expressing cells were not blocked by niflumic acid, DTT, ZnCl or SITS; however, the hTTYH3 currents were blocked by DIDS (10 μm).[122] Suzuki[122] also reports the single channels characteristic of the human *tweety* channel: large single channel conductance (250 pS) in the presence of high cytosolic Ca^{2+}; and a linear I–V relationship.

Although, like the VDAC channels, *tweety* channels share characteristics with the well-defined maxi-anion channels, but like the VDAC channels, recent experiments suggest they probably do not represent the molecular indentity of the maxi-anion channels.[107] They could, however, represent a novel class of large conductance CaCC channels or a prototype Cl^- channel based on its 6TMD topology and homology to other *Drosophila* cation channels.[122] Their localization to kidney epithelium and upregulation in renal cell carcinoma demands further exploration for this very interesting, newly discovered group of Cl^- channels.

CLCAs

Despite early promise, the possibility that the family of proteins called the Ca^{2+}-activated Cl^- channels (CLCAs) function as anion channels has become very remote. The CLCAs were the first cloned proteins to demonstrate CaCC characteristics under experimental conditions.[37] Specifically, expression of the bovine homolog, bCLCA1, in *Xenopus* oocytes resulted in an increase in CaCC current.[37] Single channel characteristics also seemed to fit with those previously described for CaCC channels: a single channel conductance of 25–30 pS; a mostly linear I–V relationship; and a selectivity profile of $I^- > Br^- > Cl^-$.[22,123] CLACs possible CaCC activity, its expression in airway epithelia, and its connection to airway inflammation in cystic fibrosis attracted a lot of research attention to the new family of proteins.[36] Unfortunately, the increased scrutiny brought with it increased evidence that the structure of the CLCA proteins made them unlikely candidates as integral channel proteins.[93] Newly performed structure and sequence analysis now predicts that CLCA are soluble proteins that may be secreted from the cell as signaling molecules.[93] More recent work has focused on the very real connection between the CLCAs and chronic obstructive disease (COPD), and CLCAs revised localization to the airway mucal cells, not epithelium. Specifically, mouse Clca3 expression was sufficient to drive mucin production *in vitro*, and in multiple animal models CLCAs were found to play an important role in mucal cell metaplasia and airway hyperactivity.[93] Thus, now yoked with an unfortunate name, it seems a consensus exists concluding that CLCAs do not function physiologically as anion channels.

Bestrophin

Until the discovery of the TMEM16/Anoctamin gene, the four mammalian bestrophin genes, Best 1–4, were the most obvious candidate for the CaCC channel. There is overwhelming evidence that bestrophins are Cl^- channels, and recent clear evidence that they are critical in a number of channelopathies. However, slight discrepancies in their characteristics and localization always created questions as to their identity[27] as the classic CaCC. The identification of this new family of Cl^- channels came from a study of the disease Best Vitelliform Macular Dystrophy (BVMD) within a large Swedish family.[86] Linkage analysis identified a region of chromosome 11 (11q13) as the locus for BVMD, which lead to the cloning of the VMD2 gene.[34,76,95,119] Subsequent syntax revision has renamed VMD2 as Best 1, and the other mammalian members of the gene family as Best 2, 3, and 4.

All the members of the Best gene family code for Cl^- channels. Early recordings done in HEK cells demonstrated novel Cl^- conductances in cells expressing the Best genes; however, the biophysical characteristics varied for each, strongly supporting the idea that each is a Cl^- channel and not a regulatory or support protein.[46] In HEK cells, Best 1 proved to be Ca^{2+}-dependent; removal and chelation of Ca^{2+} in the pipette substantially reduced current amplitudes. The currents showed some outward rectification, but were not time-dependent.[46] However, other Best channels display linear I–V (Best 2), strong inward rectification and time-dependence (Best 3), and linear I–V but with time-dependent inactivation.[46] The Best channels are weakly inhibited by niflumic acid and stilbenes[131] including DIDS (at 500 μM). The selectivity sequence is $I^- > Br^- > Cl^-$. Mutagenesis of the Best proteins provides further evidence that the Best proteins are Cl^- channels. A mutation W93H in mbest2 changes the channel gating, the I–V relation from linear to inwardly rectifying, and activates slowly upon hyperpolarization[100,126]; whereas an S79C mutation in mbest2 increases the IC_{50} of DIDS blockage by a factor of 5.[100] Regulation of the Best channels by calcium has also received recent attention. Extensive work has

demonstrated that Ca^{2+} can activate bestrophins with a KD of 200 nM without the need for any diffusible intermediate,[27] suggesting that Ca^{2+} can bind bestrophins directly. Structural analysis revealed an EF-hand region in the C-terminus of the bestrophin proteins, and mutation of the region reduces the channels Ca^{2+} affinity 20-fold.[27]

Clearly, bestrophins are Cl^- channels, but where they function and their role in human disease has become increasingly controversial. Best gene mutations were known from the beginning to cause the human disease BVMD, and were known to be expressed highly in the retinal pigment epithelium (RPE). BVMD results in increased fluid in the subretinal and sub-RPE spaces, and an abnormal electro-oculogram[46]; phenotypes that appeared to be related to the function of basolateral CaCC channels in the RPE cells. hBest1 seemed a logical candidate channel to mediate these important Cl^- currents. However, recent studies using mouse knockout models of mBest1 do not phenocopy the human disease, and the mice have no retinal dysfunction.[75] Further, it appears that the newly discovered TMEM16/Anoctamin CaCC channels are also expressed in the basolateral membrane of RPE cells, and are now thought more likely to mediate the CaCC currents of these cells.[27] So although hBest1 is a Cl^- channel, in this case it does not appear to be essential for the conductance of Cl^-. Subsequent work suggests that hBest1 may regulate other channels (voltage-gated Ca^{2+} channels) or be a HCO_3^- channel, and therefore be important in cellular pH regulation.[27]

The characteristics of the four hBest channels are similar to a number of Cl^- currents identified in the kidney, and mRNA expression of all four hBest genes has been demonstrated in large mRNA expression surveys. However, there is currently no specific evidence that hBest proteins are expressed in the kidney or have any involvement in kidney function.

Chloride Intracellular Channel (CLIC)

Chloride intracellular channels (CLICs) were initially discovered in an attempt to identify the elusive Cl^- channel responsible for cystic fibrosis. Landry et al.[64] affinity purified a 64 kDa protein from bovine kidney cortex membrane vesicles using a weak Cl^- channel inhibitor, IAA-94 (indanyloxyacetic acid), and found when reconstituted into a lipid bilayer it produced a novel Cl^- conductance. Using an antibody against the 64 kDa protein, they localized it to the apical membrane and to intracellular vesicles in CFPAC-1 cells.[102] Using the same antibody, the 64 kDa protein was cloned[63] from a kidney cDNA library, and subsequent work showed it to be a member of a large family of proteins that became known as the CLICs, with the original 64 kDa protein becoming CLIC5B. In humans, six homologs exist, each representative of a highly-conserved paralog; however, the most extensive research has been done on CLIC1 and CLIC4.

The early work on CLICB showed that it could insert into the membrane and can act as a Cl^- channel, but only in a reconstituted bilayer system, presumably because the protein was exclusively in intracellular membranes. Experiments overexpressing human CLIC1 in CHO-K1 cells managed to record a novel Cl^- current, and were able to measure some single channel characteristics.[4] The overexpressed CLIC1 localized to both the nuclear and plasma membrane, and patch recordings were done from both. CLIC1 demonstrated a slight inward rectification and voltage-dependent inactivation,[71] a selectivity sequence of $F^- > Cl^- > I^-$ (unfortunately from a single experiment), a single channel conductance of approximately 30 pS,[4,71] and was reversibly inhibited by 10 μM IAA-94.[4] Further work demonstrated that CLIC1 actually forms tetramers, each with a pore conductance of approximately 8 pS.[71] Importantly, a single point mutation in CLIC1 (C24A) changes the channel characteristics, demonstrating that CLIC1 is unambiguously a Cl^- channel when inserted into a membrane.[71] In contrast, overexpression of CLIC4 in HEK cells produces channels with a significantly smaller single channel conductance, 1 pS, but a similar selectivity sequence, $I^- > Cl^-$,[4] although CLIC4 appears to be poorly selective generally with K^+ and Cl^- having similar permeability.[71]

The most interesting recent CLIC protein discovery concerns their switch hitting life-style. It is clear that CLIC1 can be both a stable globular soluble protein, and an integral membrane protein. The solved crystal structure of CLIC1 demonstrated its nature as a soluble protein, and more importantly marked it as a member of the superfamily of glutathione s-transferase (GST) genes.[71] This revelation dramatically altered the hypothesized function of the CLICs; they may not act as Cl^- channels, but instead as soluble enzymes like the rest of the GST family. It appears their putative function depends on whether the CLIC proteins insert into the membrane or not, and recent work has concentrated on environmental factors that can manipulate CLIC tertiary structure. It turns out that, like other GST proteins, oxidation can drastically alter the structure of CLIC1, creating a second stable tertiary structure, marking it as a metamorphic protein.[71] This second oxidized stable state appears likely to insert into membranes, thus oxidation may control the function of CLIC1, channel or enzyme. Separate unfolding experiments on soluble CLIC1 suggest that low pH "primes" the protein for insertion into membranes.[33] These two environmental modulators of CLIC1 may point to its possible *in vivo* physiological function. The localization

of CLIC1 and CLIC4 to acidified intracellular vesicles and endosomes may imply a coupling of CLIC Cl^- channel activity to the acidification by a proton pump reminiscent of CLC5 or CFTR. A link between CFTR and CLIC1 is supported by work done by Edwards,[30] who demonstrated in *Xenopus* oocytes that the co-expression of CFTR and CLIC1 lead to a synergistic increase in cAMP-activated current, part of which was IAA-94 sensitive. A similar regulator relationship between CLIC1 and CFTR could be even further enhanced in the acidic environment of endosomes, where more of the CLIC1 protein would form Cl^- channels. As genetic tools continue to evolve, a number of mouse knockout models have been developed to test the physiological role of CLIC *in vivo*. Both the $CLIC1^{-/-}$ and $CLIC4^{-/-}$ showed very slight phenotypes; however, a study of the intracellular vesicles of the $CLC4^{-/-}$ mice revealed that the large intracellular vesicles were less acidic than wild-type, although the endosomes demonstrated no change in acidification.[129] The potential redundancy of the CLICs may have masked many phenotypic changes from single CLIC knockouts. To further grasp the role of the CLICs specifically in the intracellular vesicles, multiple knockout models are needed.

ANION CHANNELOPATHIES OF THE KIDNEY

Thus far, only a single anion channelopathy has been described in human kidney, dysfunction of ClC-Kb which causes type III and IV Bartter's syndrome. Recent evidence has shown that ClC-5 is a Cl^-/H^+ exchanger, and thus has removed Dent's disease from the ranks of anion channelopathies, so it will be discussed elsewhere. In fact, the dearth of anion channelopathies in the kidney does not suggest that Cl^- conductances are not important in the nephron, but perhaps instead is illustrative of our limited knowledge of Cl^- channels' functional roles. The physiological functions of the newly identified TMEM16 Cl^- channel family are only beginning to be understood, and the missing molecular identities of the vast collection of volume-sensitive Cl^- channels still represent a significant hole in our understanding. Learning more about Cl^- channels in the kidney will undoubtedly teach us more about the cause of human diseases and how to treat them.

Bartter's Syndrome

Bartter's syndrome is a collection of kidney diseases that result in mishandling of salts in the thick ascending limb (TAL), and result in renal salt-wasting, hypokalemic metabolic alkalosis, elevated rennin and aldosterone levels, normal or low blood pressure, and hypercalciuria.[50] Traditionally, Bartter's was divided into two classes based on the age of the onset of symptoms: either neonatal or classic Bartter's. More recent genetic analysis of Bartter's patients revealed that mutations in five separate genes could cause the symptoms associated with Bartter's, prompting a further division into five classes, each demonstrating a separate dysfunction in the NaCl absorption pathway of the TAL[55] (Figure 31.7). Na^+, K^+, and Cl^- anions are imported across the apical membrane from the tubule lumen in the cells of the TAL via the NKCC2 co-transporter; mutations causing dysfunction in the NKCC2 co-transporter result in type I Bartter's syndrome. The K^+ leaves the cell via apical ROMK K^+ channels to return to the lumen; mutations in the ROMK K^+ channels result in type II Bartter's. The Cl^- exits the cell across the basolateral membrane through the ClC-Kb/Barttin channel complex; mutations in the ClC-Kb channel cause type III Bartter's, and mutations in the ClC-Kb channel subunit Barttin cause type IV.[55] Type V Bartter's syndrome results from gain-of-function mutations in the calcium sensing receptor protein, CaSR, a member of the G-protein receptor superfamily.[50] CaSR is activated by high extracellular Ca^{2+}, and in turn inhibits salt transport, thus overactive CaSR inappropriately inhibits salt absorption, resulting in symptoms typical in Bartter's syndrome.[49]

Interestingly, type III and type IV Bartter's does not result in the same phenotype, which would be expected if only the ClC-Kb–Barttin complex was being affected. Patients with mutations in the Barttin subunit have more severe salt-wasting than those with type III, in addition to sensorineural deafness. The deafness is now known to be caused by dysfunction of both ClC-Ka and ClC-Kb channels in the inner ear (see previous CLC section), demonstrating that Barttin is a required subunit for both ClC-Ks. In humans, the increased severity of type IV Bartter's therefore suggests a role of ClC-Ka in salt absorption in the TAL, although dysfunction in ClC-Ka alone is not associated with any renal disease phenotype.[61]

Polycystic Kidney Disease

Unlike type III and IV Bartter's syndrome, autosomal dominant polycystic kidney disease (ADPKD) is not a Cl^- channelopathy; however, the progress of ADPKD depends directly on an inappropriate increase in Cl^- channel function. ADPKD is the most common genetic disorder found in humans, effecting 1 out of 800 births.[137] It results in the slow and progressive accumulation of fluid filled cysts in the kidney and the liver, which by adulthood can result in renal failure and necessitate kidney transplantation or result in patient death.[137] Two genes have been causally associated with ADPKD, the two polycystin genes, PKD1

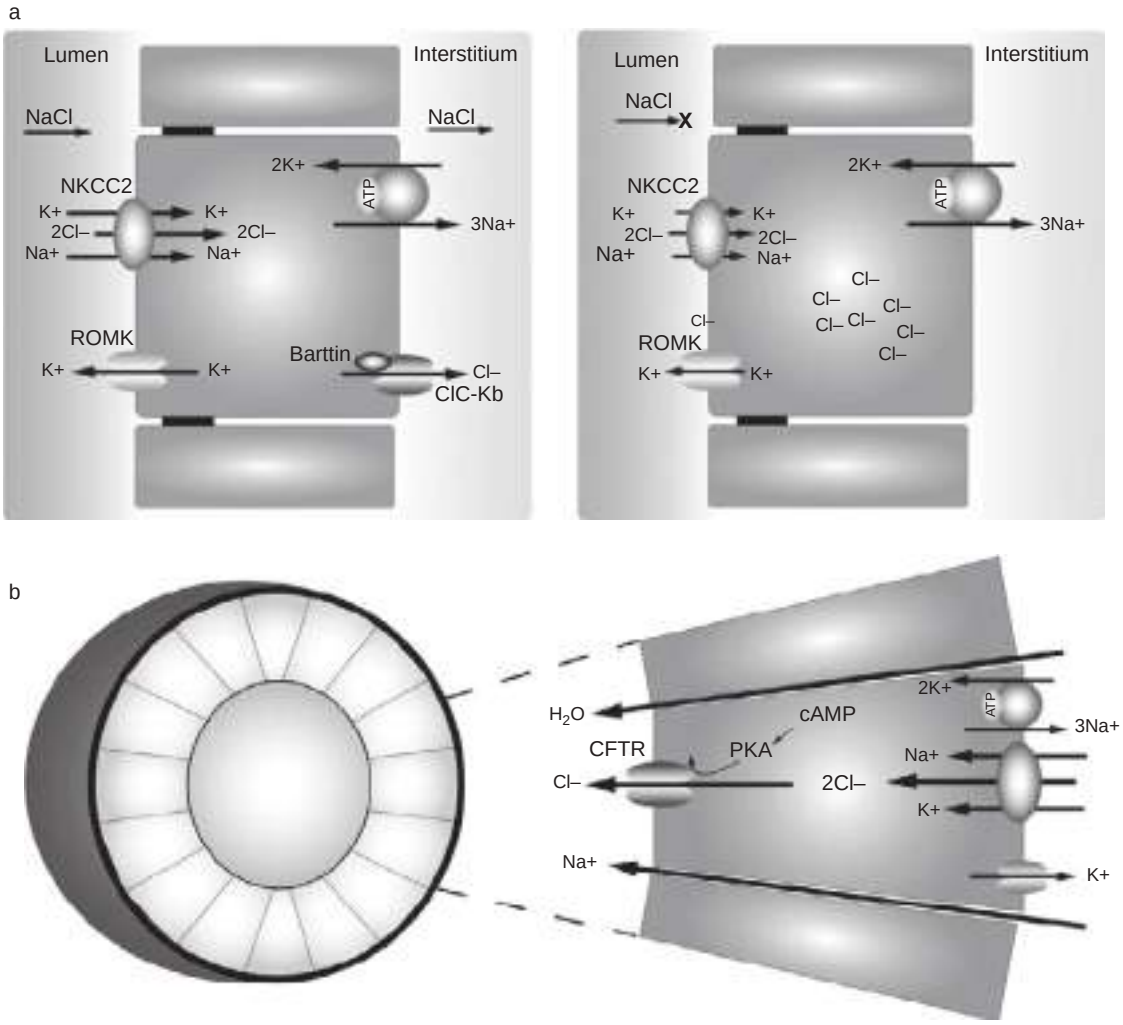

FIGURE 31.7 **Anion channelopathies of the kidney.** (a) Bartter's syndrome type III and IV. In normal cells of the thick ascending loop (TAL), NaCl is absorbed from the lumen and moved into the interstitium, a process that requires the transport of K^+, $2Cl^-$, and Na^+ across the apical membrane (NKCC2), and the subsequent efflux of Na^+ (Na^+/K^+-ATPase) and Cl^- (ClC-Kb) across the basolateral membrane. When either the ClC-Kb or its barttin subunit is dysfunctional, Cl^- builds within the cell, slowing apical transport of Na^+, Cl^-, and K^+. Without NaCl absorption in the TAL potentially severe salt-wasting will occur. (b) Mutations of either PKD1 or PKD2 genes causes tubule epithelial cells to form cysts and not tubules. Cyst growth and expansion, however, relies on fluid secretion into the cyst lumen driven by an apical CFTR Cl^- conductance that pulls paracellular Na^+ and H_2O along with it.

and PKD2[137]; how mutations in these genes and their gene products, PC1 and PC2/TRPP2 respectively, lead to cyst development remains unclear. PC1 is a large membrane protein that includes an extensive extracellular domain and may be part of focal adhesion complexes at the plasma membrane,[60] but it has also been shown to cleave into numerous functional products including P100, which has been shown to inhibit the ER Ca^{2+} sensor protein STIM1.[141] PC1 may also regulate the function of PC2. PC2 is a calcium channel that may reside on either the ER or plasma membranes. PC2 has been shown to be a key regulator of ER Ca^{2+} stores and ATP-mediated Ca^{2+} release.[60,69] A PC1–PC2 complex on an extended non-motile cilium has been proposed to detect intertubule flow, a key developmental signal during tubulogenesis. Under this hypothesis, a dysfunction in flow directionality may lead to abnormal tubule growth and the creation of cysts.[148] Alternative hypotheses have PC1 and PC2 playing key roles in regulating proliferation and apoptosis, both key elements in normal tubulogenesis, and being co-opted for cyst development.[121]

Although the mechanism that begins cytogenesis is not yet understood, the mechanisms contributing to cyst growth and enlargement are better understood. The development of ADPKD cysts requires the proliferation of epithelial cells and fluid accumulation within the cyst cavity.[67] Both of these are accelerated by the

cAMP signal transduction pathway.[68] In studies of primary cultures of ADPKD cells, apical cAMP-activated Cl^- conductances were identified using the patch-clamp technique. These currents were sensitive to glibenclamide and DPC, but not DIDS, and had a selectivity sequence of $Br^- > Cl^- > I^-$; these are all hallmark characteristics of the CFTR Cl^- channel.[44] Immunohistochemistry showed CFTR to be in the apical membranes of ADPKD cells and in cyst linings of ADPKD kidneys.[44] The movement of fluid, therefore, is believed to be facilitated by Cl^- secretion into the lumen of the cysts by apical CFTR channels, pulling both Na^+ and water along with it via paracellular pathways (Figure 31.7). This model of CFTR-mediated secretion is very similar to the role of CFTR in the airway, where it maintains the airway surface liquid (ASL). The apical Cl^- secretion in cyst epithelia is made possible by the accumulation of cytosolic Cl^- via the basolateral NKCC1 co-transporter, which transports in two Cl^- for every Na^+ and K^+ ion.[65] More recent work has also confirmed a more direct connection between CFTR and the polycystin proteins. Ikeda et al.[51] demonstrated in a MDCK model system that the expression of PC1 downregulated the amount of apical CFTR expression, concluding that mutant PC1 would promote increased CFTR plasma membrane expression, and increased Cl^- and fluid secretion into the cyst lumen. Thus, the increased function of CFTR may lead to fluid accumulation in the cysts; perhaps demonstrating better than any of the numerous experiments mentioned earlier in the CFTR section that CFTR is in the kidney and it functions there just as it does elsewhere: facilitating salt and fluid secretion.

To test the role CFTR plays in cyst growth in humans, researchers looked specifically at families with members who suffered from both ADPKD and CF. Although very few of these individuals have been studied, it does appear that ADPKD patients who also suffer from CF have fewer and smaller renal and hepatic cysts than do their age-matched siblings with ADPKD but not CF.[143] However, in another study where a single CF (Δ508CFTR) patient with ADPKD was compared to non-siblings with ADPKD but no CF, there appeared to be no difference in kidney volume or renal function.[94] Obviously, in humans it will require further accumulation of the very rare occurrence of families with both ADPKD and CF before we can really know whether CF patients receive some renal protection. Surprisingly, $CFTR^{-/-}$ knockout mice have not been crossed with any ADPKD mouse models to see if cytogenesis or cyst growth is diminished; this type of experiment could increase our understanding of CFTRs role in ADPKD.

Recent work has focused on CFTR as a target for a therapeutic approach to control ADPKD-mediated cyst growth and expansion using specific, high-affinity CFTR inhibitors. MDCK cells with endogenous CFTR and low levels of PC1 will form cysts when grown in a collagen matrix and given the cAMP agonist forskolin, but cyst growth is inhibited with the application of the specific CFTR inhibitor CFTRinh-172.[67] Similarly, when CFTR inhibitor compounds CFTRinh-172 and Ph-GlyH-101 were used to treat embryonic cystic mouse kidneys in a 4 day culture model system, they reduced cyst number and growth by more than 80%. Further, direct treatment of PKD1 knockout mice with the CFTR inhibitor slowed the normally fast development of kidney cysts and preserved kidney function.[144,131] These studies strongly support targeting CFTR as a therapy for ADPKD patients that may prove efficacious in decreasing cyst size and preserving kidney function.

SUMMARY

Recent years have marked an exciting time in the field of Cl^- channel research. More and more of the molecular identities of the functional Cl^- channel groups have been discovered, and this new knowledge has given us an expanded view of the importance of Cl^- channels in both kidney physiology and human physiology. So, too, we must acknowledge the shifting landscape that has redefined many anion channels as exchangers, and accept that perhaps that the characteristics that separate the two groups are far less significant than previously believed. But what hasn't changed is the importance of anion channels in kidney function. Each year increases our understanding of their role in secretion of waste, water retention, ionic balance, blood pressure regulation, and the recapture of essential solutes. We can now add the TMEM16 and SLC26a gene families to those expressed in the kidney that conduct anions, and look forward to what these newly discovered Cl^- channels can tell us. But not all recent discoveries have been on the large-scale, many incremental but significant discoveries have also been made that slowly progress our understanding of human diseases like Bartter's Syndrome and PKD, and bring us one step closer to developing more effective therapies. The same questions persist: how do anion channels work in the context of the human kidney? How does their dysfunction lead to human disease? Can we develop new or more effective pharmacologic therapies for human kidney disease? But we now have even greater tools, knockout animals, siRNA, vast drug libraries, and the ability for large-scale molecular screens with which to answer these fundamental questions.

References

[1] Accardi A, Miller C. Secondary active transport mediated by a prokaryotic homologue of ClC Cl^- channels. Nature 2004;427:803–7.

[2] Akrouh A, Halcomb SE, Nichols CG, Sala-Rabanal M. Molecular biology of K(ATP) channels and implications for health and disease. IUBMB Life 2009;61:971–8.

[3] Anderson MP, Gregory RJ, Thompson S, Souza DW, Paul S, Mulligan RC, et al. Demonstration that CFTR is a chloride channel by alteration of its anion selectivity. Science 1991;253: 202–5.

[4] Ashley RH. Challenging accepted ion channel biology: p64 and the CLIC family of putative intracellular anion channel proteins (Review). Mol Membr Biol 2003;20:1–11.

[5] Baker MA, Lane DJ, Ly JD, De Pinto V, Lawen A. VDAC1 is a transplasma membrane NADH-ferricyanide reductase. J Biol Chem 2004;279:4811–9.

[6] Bao HF, Liu L, Self J, Duke BJ, Ueno R, Eaton DC. A synthetic prostone activates apical chloride channels in A6 epithelial cells. Am J Physiol Gastrointest Liver Physiol 2008;295:G234–51.

[7] Barlassina C, Dal FC, Lanzani C, Manunta P, Guffanti G, Ruello A, et al. Common genetic variants and haplotypes in renal CLCNKA gene are associated to salt-sensitive hypertension. Hum Mol Genet 2007;16:1630–8.

[8] Bathori G, Parolini I, Tombola F, Szabo I, Messina A, Oliva M, et al. Porin is present in the plasma membrane where it is concentrated in caveolae and caveolae-related domains. J Biol Chem 1999;274:29607–12.

[9] Bathori G, Parolini I, Szabo I, Tombola F, Messina A, Oliva M, et al. Extramitochondrial porin: facts and hypotheses. J Bioenerg Biomembr 2000;32:79–89.

[10] Bell PD, Lapointe JY, Sabirov R, Hayashi S, Peti-Peterdi J, Manabe K, et al. Macula densa cell signaling involves ATP release through a maxi anion channel. Proc Natl Acad Sci USA 2003;100:4322–7.

[11] Bell PD, Komlosi P, Zhang ZR. ATP as a mediator of macula densa cell signalling. Purinergic Signal 2009;5:461–71.

[12] Berdiev BK, Qadri YJ, Benos DJ. Assessment of the CFTR and ENaC association. Mol Biosyst 2009;5:123–7.

[13] Bertrand CA, Zhang R, Pilewski JM, Frizzell RA. SLC26A9 is a constitutively active, CFTR-regulated anion conductance in human bronchial epithelia. J Gen Physiol 2009;133:421–38.

[14] Birkenhager R, Otto E, Schurmann MJ, Vollmer M, Ruf EM, Maier-Lutz I, et al. Mutation of BSND causes Bartter syndrome with sensorineural deafness and kidney failure. Nat Genet 2001;29:310–4.

[15] Boese SH, Aziz O, Simmons NL, Gray MA. Kinetics and regulation of a Ca^{2+}-activated Cl^- conductance in mouse renal inner medullary collecting duct cells. Am J Physiol Renal Physiol 2004;286:F682–92.

[16] Caputo A, Caci E, Ferrera L, Pedemonte N, Barsanti C, Sondo E, et al. TMEM16A, a membrane protein associated with calcium-dependent chloride channel activity. Science 2008;322:590–4.

[17] Chang MH, Plata C, Sindic A, Ranatunga WK, Chen AP, Zandi-Nejad K, et al. Slc26a9 is inhibited by the R-region of the cystic fibrosis transmembrane conductance regulator via the STAS domain. J Biol Chem 2009;284:28306–18.

[18] Chebib M. GABAC receptor ion channels. Clin Exp Pharmacol Physiol 2004;31:800–4.

[19] Chen TY. Structure and function of clc channels. Annu Rev Physiol 2005;67:809–39.

[20] Chillon M, Casals T, Mercier B, Bassas L, Lissens W, Silber S, et al. Mutations in the cystic fibrosis gene in patients with congenital absence of the vas deferens. N Engl J Med 1995;332:1475–80.

[21] Choudari CP, Lehman GA, Sherman S. Pancreatitis and cystic fibrosis gene mutations. Gastroenterol Clin North Am 1999;28:543–9 [vii-viii]

[22] Cunningham SA, Awayda MS, Bubien JK, Ismailov II, Arrate MP, Berdiev BK, et al. Cloning of an epithelial chloride channel from bovine trachea. J Biol Chem 1995;270:31016–26.

[23] Cuppoletti J, Malinowska DH, Tewari KP, Li QJ, Sherry AM, Patchen ML, et al. SPI-0211 activates T84 cell chloride transport and recombinant human ClC-2 chloride currents. Am J Physiol Cell Physiol 2004;287:C1173–83.

[24] De Pinto V, Messina A, Lane DJ, Lawen A. Voltage-dependent anion-selective channel (VDAC) in the plasma membrane. FEBS Lett 2010;584:1793–9.

[25] Devuyst O, Guggino WB. Chloride channels in the kidney: lessons learned from knockout animals. Am J Physiol Renal Physiol 2002;283:F1176–91.

[26] Dorwart MR, Shcheynikov N, Yang D, Muallem S. The solute carrier 26 family of proteins in epithelial ion transport. *Physiology* (Bethesda) 2008;23:104–14.

[26a] Dorwart MR, Shcheynikon N, Wang Y, Stippec S, Muallem S. SLC26A9 is a Cl^- channel regulated by the WNK kinases. J Physiol 2007;584(1):333–45.

[27] Duran C, Thompson CH, Xiao Q, Hartzell HC. Chloride channels: often enigmatic, rarely predictable. Annu Rev Physiol 2010;72:95–121.

[28] Dutzler R, Campbell EB, Cadene M, Chait BT, MacKinnon R. X-ray structure of a ClC chloride channel at 3.0 Å reveals the molecular basis of anion selectivity. Nature 2002;415:287–94.

[29] Dutzler R, Campbell EB, MacKinnon R. Gating the selectivity filter in ClC chloride channels. Science 2003;300:108–12.

[30] Edwards JC. The CLIC1 chloride channel is regulated by the cystic fibrosis transmembrane conductance regulator when expressed in *Xenopus* oocytes. J Membr Biol 2006;213:39–46.

[31] Embark HM, Bohmer C, Palmada M, Rajamanickam J, Wyatt AW, Wallisch S, et al. Regulation of CLC-Ka/barttin by the ubiquitin ligase Nedd4-2 and the serum- and glucocorticoid-dependent kinases. Kidney Int 2004;66:1918–25.

[32] Estevez R, Boettger T, Stein V, Birkenhager R, Otto E, Hildebrandt F, et al. Barttin is a Cl^- channel beta-subunit crucial for renal Cl^- reabsorption and inner ear K^+ secretion. Nature 2001;414:558–61.

[33] Fanucchi S, Adamson RJ, Dirr HW. Formation of an unfolding intermediate state of soluble chloride intracellular channel protein CLIC1 at acidic pH. Biochemistry 2008;47:11674–81.

[34] Forsman K, Graff C, Nordstrom S, Johansson K, Westermark E, Lundgren E, et al. The gene for Best's macular dystrophy is located at 11q13 in a Swedish family. Clin Genet 1992;42:156–9.

[35] Frey A, Lampert A, Waldegger S, Jeck N, Waldegger P, Artunc F, et al. Influence of gain of function epithelial chloride channel ClC-Kb mutation on hearing thresholds. Hear Res 2006;214:68–75.

[36] Fuller CM, Benos DJ. $Ca^{(2+)}$-activated $Cl^{(-)}$ channels: a newly emerging anion transport family. News Physiol Sci 2000;15:165–71.

[37] Fuller CM, Ji HL, Tousson A, Elble RC, Pauli BU, Benos DJ. $Ca^{(2+)}$-activated $Cl^{(-)}$ channels: a newly emerging anion transport family. Pflugers Arch 2001;443(Suppl. 1):S107–10.

[38] Gabriel SE, Clarke LL, Boucher RC, Stutts MJ. CFTR and outward rectifying chloride channels are distinct proteins with a regulatory relationship. Nature 1993;363:263–8.

[39] Gadsby DC, Vergani P, Csanady L. The ABC protein turned chloride channel whose failure causes cystic fibrosis. Nature 2006;440:477–83.

[40] Goncalves RP, Buzhysnskyy N, Scheuring S. Mini review on the structure and supramolecular assembly of VDAC. J Bioenerg Biomembr 2008;40:133–8.

[41] Guggino WB. The cystic fibrosis transmembrane regulator forms macromolecular complexes with PDZ domain scaffold proteins. Proc Am Thorac Soc 2004;1:28–32.
[42] Guggino WB, Stanton BA. New insights into cystic fibrosis: molecular switches that regulate CFTR. Nat Rev Mol Cell Biol 2006;7:426–36.
[43] Gunther W, Luchow A, Cluzeaud F, Vandewalle A, Jentsch TJ. ClC-5, the chloride channel mutated in Dent's disease, colocalizes with the proton pump in endocytotically active kidney cells. Proc Natl Acad Sci USA 1998;95:8075–80.
[44] Hanaoka K, Devuyst O, Schwiebert EM, Wilson PD, Guggino WB. A role for CFTR in human autosomal dominant polycystic kidney disease. Am J Physiol 1996;270:C389–99.
[45] Hartzell C, Putzier I, Arreola J. Calcium-activated chloride channels. Annu Rev Physiol 2005;67:719–58.
[46] Hartzell HC, Qu Z, Yu K, Xiao Q, Chien LT. Molecular physiology of bestrophins: multifunctional membrane proteins linked to Best disease and other retinopathies. Physiol Rev 2008;88:639–72.
[47] Hartzell HC, Yu K, Xiao Q, Chien LT, Qu Z. Anoctamin/TMEM16 family members are Ca^{2+}-activated Cl^- channels. J Physiol 2009;587:2127–39.
[48] He Y, Ramsay AJ, Hunt ML, Whitbread AK, Myers SA, Hooper JD. N-glycosylation analysis of the human Tweety family of putative chloride ion channels supports a penta-spanning membrane arrangement: impact of N-glycosylation on cellular processing of Tweety homologue 2 (TTYH2). Biochem J 2008;412:45–55.
[49] Hebert SC. Extracellular calcium-sensing receptor: implications for calcium and magnesium handling in the kidney. Kidney Int 1996;50:2129–39.
[50] Hebert SC. Bartter syndrome. Curr Opin Nephrol Hypertens 2003;12:527–32.
[51] Ikeda M, Fong P, Cheng J, Boletta A, Qian F, Zhang XM, et al. A regulatory role of polycystin-1 on cystic fibrosis transmembrane conductance regulator plasma membrane expression. Cell Physiol Biochem 2006;18:9–20.
[52] Jakob C, Gotz H, Hellmann T, Hellmann KP, Reymann S, Florke H, et al. Studies on human porin: XIII. The type-1 VDAC "porin 31HL" biotinylated at the plasmalemma of trypan blue excluding human B lymphocytes. FEBS Lett 1995;368:5–9.
[53] Jeck N, Waldegger S, Lampert A, Boehmer C, Waldegger P, Lang PA, et al. Activating mutation of the renal epithelial chloride channel ClC-Kb predisposing to hypertension. Hypertension 2004;43:1175–81.
[54] Jentsch TJ, Poet M, Fuhrmann JC, Zdebik AA. Physiological functions of CLC Cl^- channels gleaned from human genetic disease and mouse models. Annu Rev Physiol 2005;67:779–807.
[55] Jentsch TJ. CLC chloride channels and transporters: from genes to protein structure, pathology and physiology. Crit Rev Biochem Mol Biol 2008;43:3–36.
[56] Jouret F, Devuyst O. CFTR and defective endocytosis: new insights in the renal phenotype of cystic fibrosis. Pflugers Arch 2009;457:1227–36.
[57] Kerem B, Rommens JM, Buchanan JA, Markiewicz D, Cox TK, Chakravarti A, et al. Identification of the cystic fibrosis gene: Genetic analysis. Science 1989;245:1073–80.
[58] Kim KH, Shcheynikov N, Wang Y, Muallem S. SLC26A7 is a Cl^- channel regulated by intracellular pH. J Biol Chem 2005;280:6463–70.
[59] Ko SB, Zeng W, Dorwart MR, Luo X, Kim KH, Millen L, et al. Gating of CFTR by the STAS domain of SLC26 transporters. Nat Cell Biol 2004;6:343–50.
[60] Kottgen M. TRPP2 and autosomal dominant polycystic kidney disease. Biochim Biophys Acta 2007;1772:836–50.
[61] Kramer BK, Bergler T, Stoelcker B, Waldegger S. Mechanisms of disease: the kidney-specific chloride channels ClCKA and ClCKB, the Barttin subunit, and their clinical relevance. Nat Clin Pract Nephrol 2008;4:38–46.
[62] Kunzelmann K, Kongsuphol P, Aldehni F, Tian Y, Ousingsawat J, Warth R, et al. Bestrophin and TMEM16-$Ca(^{2+})$ activated Cl $(^-)$ channels with different functions. Cell Calcium 2009;46:233–41.
[63] Landry D, Sullivan S, Nicolaides M, Redhead C, Edelman A, Field M, et al. Molecular cloning and characterization of p64, a chloride channel protein from kidney microsomes. J Biol Chem 1993;268:14948–55.
[64] Landry DW, Akabas MH, Redhead C, Edelman A, Cragoe Jr EJ, al-Awqati Q. Purification and reconstitution of chloride channels from kidney and trachea. Science 1989;244:1469–72.
[65] Lebeau C, Hanaoka K, Moore-Hoon ML, Guggino WB, Beauwens R, Devuyst O. Basolateral chloride transporters in autosomal dominant polycystic kidney disease. Pflugers Arch 2002;444:722–31.
[66] Letz B, Korbmacher C. cAMP stimulates CFTR-like Cl^- channels and inhibits amiloride-sensitive Na^+ channels in mouse CCD cells. Am J Physiol 1997;272:C657–66.
[67] Li H, Findlay IA, Sheppard DN. The relationship between cell proliferation, Cl^- secretion, and renal cyst growth: a study using CFTR inhibitors. Kidney Int 2004;66:1926–38.
[68] Li H, Sheppard DN. Therapeutic potential of cystic fibrosis transmembrane conductance regulator (CFTR) inhibitors in polycystic kidney disease. BioDrugs 2009;23:203–16.
[69] Li Y, Santoso NG, Yu S, Woodward OM, Qian F, Guggino WB. Polycystin-1 interacts with inositol 1,4,5-trisphosphate receptor to modulate intracellular Ca^{2+} signaling with implications for polycystic kidney disease. J Biol Chem 2009;284:36431–41.
[70] Liantonio A, Picollo A, Carbonara G, Fracchiolla G, Tortorella P, Loiodice F, et al. Molecular switch for CLC-K Cl^- channel block/activation: Optimal pharmacophoric requirements towards high-affinity ligands. Proc Natl Acad Sci USA 2008;105:1369–73.
[71] Littler DR, Harrop SJ, Goodchild SC, Phang JM, Mynott AV, Jiang L, et al. The enigma of the CLIC proteins: Ion channels, redox proteins, enzymes, scaffolding proteins? FEBS Lett 2010;584:2093–101.
[71a] Lisal J, Maduke M. The ClC-0 chloride channel is a broken Cl^-/H^+ antiporter. Nat Struct Mol Bio 2008;15:805–10.
[72] Lu M, Dong K, Egan ME, Giebisch GH, Boulpaep EL, Hebert SC. Mouse cystic fibrosis transmembrane conductance regulator forms cAMP-PKA-regulated apical chloride channels in cortical collecting duct. Proc Natl Acad Sci USA 2010;107:6082–7.
[73] Lynch JW. Molecular structure and function of the glycine receptor chloride channel. Physiol Rev 2004;84:1051–95.
[74] Ma T, Thiagarajah JR, Yang H, Sonawane ND, Folli C, Galietta LJ, et al. Thiazolidinone CFTR inhibitor identified by high-throughput screening blocks cholera toxin-induced intestinal fluid secretion. J Clin Invest 2002;110:1651–8.
[75] Marmorstein LY, Wu J, McLaughlin P, Yocom J, Karl MO, Neussert R, et al. The light peak of the electroretinogram is dependent on voltage-gated calcium channels and antagonized by bestrophin (best-1). J Gen Physiol 2006;127:577–89.
[76] Marquardt A, Stohr H, Passmore LA, Kramer F, Rivera A, Weber BH. Mutations in a novel gene, VMD2, encoding a protein of unknown properties cause juvenile-onset vitelliform macular dystrophy (Best's disease). Hum Mol Genet 1998;7:1517–25.

[77] Matsumura Y, Uchida S, Kondo Y, Miyazaki H, Ko SB, Hayama A, et al. Overt nephrogenic diabetes insipidus in mice lacking the CLC-K1 chloride channel. Nat Genet 1999;21:95–8.
[78] Matulef K, Maduke M. The CLC "chloride channel" family: revelations from prokaryotes. *Mol Membr Biol* 2007;24:342–50.
[79] Miller C. ClC chloride channels viewed through a transporter lens. Nature 2006;440:484–9.
[80] Morales MM, Carroll TP, Morita T, Schwiebert EM, Devuyst O, Wilson PD, et al. Both the wild-type and a functional isoform of CFTR are expressed in kidney. Am J Physiol 1996;270:F1038–48.
[81] Morales MM, Falkenstein D, Lopes AG. The cystic fibrosis transmembrane regulator (CFTR) in the kidney. An Acad Bras Cienc 2000;72:399–406.
[82] Moyer BD, Denton J, Karlson KH, Reynolds D, Wang S, Mickle JE, et al. A PDZ-interacting domain in CFTR is an apical membrane polarization signal. J Clin Invest 1999;104:1353–61.
[83] Muanprasat C, Sonawane ND, Salinas D, Taddei A, Galietta LJ, Verkman AS. Discovery of glycine hydrazide pore-occluding CFTR inhibitors: Mechanism, structure–activity analysis, and *in vivo* efficacy. J Gen Physiol 2004;124:125–37.
[84] Nilius B, Eggermont J, Voets T, Buyse G, Manolopoulos V, Droogmans G. Properties of volume-regulated anion channels in mammalian cells. Prog Biophys Mol Biol 1997;68:69–119.
[85] Nilius B, Droogmans G. Amazing chloride channels: an overview. Acta Physiol Scand 2003;177:119–47.
[86] Nordstrom S, Barkman Y. Hereditary macular degeneration (HMD) in 246 cases traced to one gene-source in central Sweden. Hereditas 1977;84:163–76.
[87] Novarino G, Weinert S, Rickheit G, Jentsch TJ. Endosomal chloride–proton exchange rather than chloride conductance is crucial for renal endocytosis. Science 2010;328:1398–401.
[88] Nutt D. GABAA receptors: subtypes, regional distribution, and function. J Clin Sleep Med 2006;2:S7–11.
[89] Ohana E, Yang D, Shcheynikov N, Muallem S. Diverse transport modes by the solute carrier 26 family of anion transporters. J Physiol 2009;587:2179–85.
[90] Okada SF, O'Neal WK, Huang P, Nicholas RA, Ostrowski LE, Craigen WJ, et al. Voltage-dependent anion channel-1 (VDAC-1) contributes to ATP release and cell volume regulation in murine cells. J Gen Physiol 2004;124:513–26.
[91] Okada Y, Shimizu T, Maeno E, Tanabe S, Wang X, Takahashi N. Volume-sensitive chloride channels involved in apoptotic volume decrease and cell death. J Membr Biol 2006;209:21–9.
[92] Okada Y, Sato K, Numata T. Pathophysiology and puzzles of the volume-sensitive outwardly rectifying anion channel. J Physiol 2009;587:2141–9.
[93] Patel AC, Brett TJ, Holtzman MJ. The role of CLCA proteins in inflammatory airway disease. Annu Rev Physiol 2009;71:425–49.
[94] Persu A, Devuyst O, Lannoy N, Materne R, Brosnahan G, Gabow PA, et al. CF gene and cystic fibrosis transmembrane conductance regulator expression in autosomal dominant polycystic kidney disease. J Am Soc Nephrol 2000;11:2285–96.
[95] Petrukhin K, Koisti MJ, Bakall B, Li W, Xie G, Marknell T, et al. Identification of the gene responsible for Best macular dystrophy. Nat Genet 1998;19:241–7.
[96] Picollo A, Pusch M. Chloride/proton antiporter activity of mammalian CLC proteins ClC-4 and ClC-5. Nature 2005;436:420–3.
[97] Piwon N, Gunther W, Schwake M, Bosl MR, Jentsch TJ. ClC-5 Cl^--channel disruption impairs endocytosis in a mouse model for Dent's disease. Nature 2000;408:369–73.
[98] Plans V, Rickheit G, Jentsch TJ. Physiological roles of CLC Cl$(^-)$/H$(^+)$ exchangers in renal proximal tubules. Pflugers Arch 2009;458:23–37.
[99] Qu Z, Wei RW, Hartzell HC. Characterization of Ca^{2+}-activated Cl^- currents in mouse kidney inner medullary collecting duct cells. Am J Physiol Renal Physiol 2003;285:F326–35.
[100] Qu Z, Fischmeister R, Hartzell C. Mouse bestrophin-2 is a *bona fide* Cl$(^-)$ channel: identification of a residue important in anion binding and conduction. J Gen Physiol 2004;123:327–40.
[101] Reddy MM, Quinton PM. Functional interaction of CFTR and ENaC in sweat glands. Pflugers Arch 2003;445:499–503.
[102] Redhead CR, Edelman AE, Brown D, Landry DW, al-Awqati Q. A ubiquitous 64-kDa protein is a component of a chloride channel of plasma and intracellular membranes. Proc Natl Acad Sci USA 1992;89:3716–20.
[103] Riordan JR, Rommens JM, Kerem B, Alon N, Rozmahel R, Grzelczak Z, et al. Identification of the cystic fibrosis gene: cloning and characterization of complementary DNA. Science 1989;245:1066–73.
[104] Rommens JM, Iannuzzi MC, Kerem B, Drumm ML, Melmer G, Dean M, et al. Identification of the cystic fibrosis gene: Chromosome walking and jumping. Science 1989;245:1059–65.
[105] Roy SS, Ehrlich AM, Craigen WJ, Hajnoczky G. VDAC2 is required for truncated BID-induced mitochondrial apoptosis by recruiting BAK to the mitochondria. EMBO Rep 2009;10:1341–7.
[106] Sabirov RZ, Sheiko T, Liu H, Deng D, Okada Y, Craigen WJ. Genetic demonstration that the plasma membrane maxianion channel and voltage-dependent anion channels are unrelated proteins. J Biol Chem 2006;281:1897–904.
[107] Sabirov RZ, Okada Y. The maxi-anion channel: a classical channel playing novel roles through an unidentified molecular entity. J Physiol Sci 2009;59:3–21.
[108] Sanchez-Rodriguez JE, De Santiago-Castillo JA, Arreola J. Permeant anions contribute to voltage dependence of ClC-2 chloride channel by interacting with the protopore gate. J Physiol 2010;588:2545–56.
[109] Scheel O, Zdebik AA, Lourdel S, Jentsch TJ. Voltage-dependent electrogenic chloride/proton exchange by endosomal CLC proteins. Nature 2005;436:424–7.
[110] Schreiber R, Uliyakina I, Kongsuphol P, Warth R, Mirza M, Martins JR, et al. Expression and function of epithelial anoctamins. J Biol Chem 2010;285:7838–45.
[111] Schroeder BC, Cheng T, Jan YN, Jan LY. Expression cloning of TMEM16A as a calcium-activated chloride channel subunit. Cell 2008;134:1019–29.
[112] Schwiebert EM, Cid-Soto LP, Stafford D, Carter M, Blaisdell CJ, Zeitlin PL, et al. Analysis of ClC-2 channels as an alternative pathway for chloride conduction in cystic fibrosis airway cells. Proc Natl Acad Sci USA 1998;95:3879–84.
[113] Schwiebert EM, Benos DJ, Egan ME, Stutts MJ, Guggino WB. CFTR is a conductance regulator as well as a chloride channel. Physiol Rev 1999;79:S145–66.
[114] Shoshan-Barmatz V, Israelson A. The voltage-dependent anion channel in endoplasmic/sarcoplasmic reticulum: characterization, modulation and possible function. J Membr Biol 2005;204:57–66.
[115] Simamura E, Shimada H, Ishigaki Y, Hatta T, Higashi N, Hirai K. Bioreductive activation of quinone antitumor drugs by mitochondrial voltage-dependent anion channel 1. Anat Sci Int 2008;83:261–6.
[116] Sindic A, Chang MH, Mount DB, Romero MF. Renal physiology of SLC26 anion exchangers. Curr Opin Nephrol Hypertens 2007;16:484–90.
[117] Souza-Menezes J, Tukaye DN, Novaira HJ, Guggino WB, Morales MM. Small nuclear RNAs U11 and U12 modulate expression of TNR-CFTR mRNA in mammalian kidneys. Cell Physiol Biochem 2008;22:93–100.

[118] Steinmeyer K, Ortland C, Jentsch TJ. Primary structure and functional expression of a developmentally regulated skeletal muscle chloride channel. Nature 1991;354:301–4.
[119] Stone EM, Nichols BE, Streb LM, Kimura AE, Sheffield VC. Genetic linkage of vitelliform macular degeneration (Best's disease) to chromosome 11q13. Nat Genet 1992;1:246–50.
[120] Sun X, Petrovic S. Increased acid load and deletion of AE1 increase Slc26a7 expression. Nephron Physiol 2008;109:29–35.
[121] Sutters M, Germino GG. Autosomal dominant polycystic kidney disease: molecular genetics and pathophysiology. J Lab Clin Med 2003;141:91–101.
[122] Suzuki M. The *Drosophila* tweety family: molecular candidates for large-conductance Ca^{2+}-activated Cl^- channels. Exp Physiol 2006;91:141–7.
[123] Suzuki M, Morita T, Iwamoto T. Diversity of $Cl(^-)$ channels. Cell Mol Life Sci 2006;63:12–24.
[124] Tarran R, Button B, Boucher RC. Regulation of normal and cystic fibrosis airway surface liquid volume by phasic shear stress. Annu Rev Physiol 2006;68:543–61.
[125] Thiemann A, Grunder S, Pusch M, Jentsch TJ. A chloride channel widely expressed in epithelial and non-epithelial cells. Nature 1992;356:57–60.
[126] Tsunenari T, Sun H, Williams J, Cahill H, Smallwood P, Yau KW, et al. Structure–function analysis of the bestrophin family of anion channels. J Biol Chem 2003;278:41114–25.
[127] Uchida S, Sasaki S, Furukawa T, Hiraoka M, Imai T, Hirata Y, et al. Molecular cloning of a chloride channel that is regulated by dehydration and expressed predominantly in kidney medulla. J Biol Chem 1993;268:3821–4.
[128] Uchida S, Sasaki S. Function of chloride channels in the kidney. Annu Rev Physiol 2005;67:759–78.
[129] Ulmasov B, Bruno J, Gordon N, Hartnett ME, Edwards JC. Chloride intracellular channel protein-4 functions in angiogenesis by supporting acidification of vacuoles along the intracellular tubulogenic pathway. Am J Pathol 2009;174:1084–96.
[130] Vandewalle A. Expression and function of CLC and cystic fibrosis transmembrane conductance regulator chloride channels in renal epithelial tubule cells: pathophysiological implications. Chang Gung Med J 2007;30:17–25.
[131] Verkman AS, Galietta LJ. Chloride channels as drug targets. Nat Rev Drug Discov 2009;8:153–71.
[132] Waldegger S, Jentsch TJ. Functional and structural analysis of ClC-K chloride channels involved in renal disease. J Biol Chem 2000;275:24527–33.
[133] Waldegger S, Jeck N, Barth P, Peters M, Vitzthum H, Wolf K, et al. Barttin increases surface expression and changes current properties of ClC-K channels. Pflugers Arch 2002;444:411–8.
[134] Wang SS, Devuyst O, Courtoy PJ, Wang XT, Wang H, Wang Y, et al. Mice lacking renal chloride channel, CLC-5, are a model for Dent's disease, a nephrolithiasis disorder associated with defective receptor-mediated endocytosis. Hum Mol Genet 2000;9:2937–45.
[135] Wang Y, Soyombo AA, Shcheynikov N, Zeng W, Dorwart M, Marino CR, et al. Slc26a6 regulates CFTR activity *in vivo* to determine pancreatic duct HCO_3^- secretion: relevance to cystic fibrosis. EMBO J 2006;25:5049–57.
[136] Wilson PD. Polycystic kidney disease. N Engl J Med 2004;350:151–64.
[137] Woodward OM, Willows AO. Dopamine modulation of $Ca(^{2+})$ dependent $Cl(^-)$ current regulates ciliary beat frequency controlling locomotion in *Tritonia diomedea*. J Exp Biol 2006;209:2749–64.
[138] Woodward OM, Willows AO. Nervous control of ciliary beating by $Cl(^-)$, $Ca(^{2+})$ and calmodulin in *Tritonia diomedea*. J Exp Biol 2006;209:2765–73.
[139] Woodward OM, Kottgen A, Coresh J, Boerwinkle E, Guggino WB, Kottgen M. Identification of a urate transporter, ABCG2, with a common functional polymorphism causing gout. Proc Natl Acad Sci USA 2009;106:10338–42.
[140] Woodward OM, Li Y, Yu S, Greenwell P, Wodarczyk C, Boletta A, et al. Identification of a polycystin-1 cleavage product, P100, that regulates store operated Ca entry through interactions with STIM1. PLoS One 2010;5(8):e12305.
[141] Xu J, Song P, Nakamura S, Miller M, Barone S, Alper SL, et al. Deletion of the chloride transporter slc26a7 causes distal renal tubular acidosis and impairs gastric acid secretion. J Biol Chem 2009;284:29470–9.
[142] Xu N, Glockner JF, Rossetti S, Babovich-Vuksanovic D, Harris PC, Torres VE. Autosomal dominant polycystic kidney disease coexisting with cystic fibrosis. J Nephrol 2006;19:529–34.
[143] Yang B, Sonawane ND, Zhao D, Somlo S, Verkman AS. Small-molecule CFTR inhibitors slow cyst growth in polycystic kidney disease. J Am Soc Nephrol 2008;19:1300–10.
[144] Yang IC, Cheng TH, Wang F, Price EM, Hwang TC. Modulation of CFTR chloride channels by calyculin A and genistein. Am J Physiol 1997;272:C142–55.
[145] Yang YD, Cho H, Koo JY, Tak MH, Cho Y, Shim WS, et al. TMEM16A confers receptor-activated calcium-dependent chloride conductance. Nature 2008;455:1210–5.
[146] Zhou J. Polycystins and primary cilia: primers for cell cycle progression. Annu Rev Physiol 2009;71:83–113.

This page intentionally left blank

CHAPTER

32

Physiology and Pathophysiology of the NaCl Co-Transporters in the Kidney

Gerardo Gamba

Molecular Physiology Unit, Department of Nephrology and Mineral Metabolism, Instituto Nacional de Ciencias Médicas y Nutrición Salvador Zubirán, and Instituto de Investigaciones Biomédicas, Universidad Nacional Autónoma de México, Mexico City, Mexico

INTRODUCTION

There are four types of electroneutral co-transporter systems that have been identified: (1) the sulfamoylbenzoic (or bumetanide)-sensitive Na^+-K^+-$2Cl^-$ co-transporter; (2) the sulfamoylbenzoic (or bumetanide)-sensitive Na^+-Cl^- co-transporter; (3) the benzothiadiazine (or thiazide)-sensitive Na^+-Cl^- co-transporter; and (4) the dihydroindenyloxy-alkanoic acid (DIOA)-sensitive K^+-Cl^- co-transporter. All these possibilities are encoded by members of the family of solute carriers SLC12, according to the classification of the Human Genome Organization.[1] Two genes of this family, SLC12A1 encoding the apical Na^+:K^+:$2Cl^-$ co-transporter, NKCC2 (also known as BSC1), and SLC12A3, encoding the Na^+:Cl^- co-transporter, NCC (also known as TSC1), are particularly relevant to kidney physiology, pharmacology, and pathophysiology. NKCC2 and NCC play a key role in salt reabsorption of the thick ascending limb of Henle's loop and distal convoluted tubule, respectively, with consequent effects in potassium, calcium, and acid–base homeostasis. They also serve as receptors for the loop diuretics (furosemide, bumetanide, ethacrinic acid) and thiazide-type diuretics (chlortalidone, hydrochlorothiazide, metolazone), respectively, that are heavily used in the management of patients with arterial hypertension or edematous states, such a cardiac failure, chronic liver disease, chronic renal disease or nephrotic syndrome. Inactivating mutations of NKCC2 cause Bartter syndrome type I, and of NCC cause Gitelman's syndrome. Additionally, dysregulation of NCC is implicated in the genesis of pseudohypoaldosteronism type II, and it is proposed that both co-transporters belong to the hypertension susceptibility genes. In this chapter we will discuss the cation-coupled chloride co-transporters, with particular emphasis on NKCC2 and NCC.

The SLC12A family was identified in the early 1990s with the cloning of the thiazide-sensitive Na^+-Cl^- co-transporter,[2,3] followed by two genes encoding the Na^+-K^+-$2Cl^-$ co-transporters,[3–6] and is composed of nine related genes.[7,8] Later, the four genes encoding K^+:Cl^- co-tranporters that were named KCC1,[9] KCC2,[10] KCC3,[11,12] and KCC4[12] were identified.

Figure 32.1 depicts a phylogenetic tree of all members of the SLC12 family for which functional properties are known, as well as the chromosome to which each gene has been mapped in humans, the inherited disease that results from inactivating mutations of the gene, and the consequence of knocking-out each gene in the mouse. Two branches within the family are clearly identified. The Na^+-driven branch encompasses three genes: *SLC12A1* and *SLC12A2* encode the Na^+:K^+:$2Cl^-$ co-transporters, NKCC2 and NKCC1, respectively. NKCC2 is a kidney-specific gene, with expression restricted to the apical membrane of the thick ascending limb of Henle's loop (TAL).[3,5,13,14] In contrast, NKCC1 is a ubiquitously expressed protein that is located at the basolateral membrane of secretory epithelial cells, as well as in many non-epithelial cells (neurons, fibroblasts, erythrocytes, etc.).[15,16] *SCL12A3* is the third gene of the Na^+-driven branch, and encodes the thiazide-sensitive Na^+:Cl^- co-transporter,

Seldin and Giebisch's The Kidney, Fifth Edition.
DOI: http://dx.doi.org/10.1016/B978-0-12-381462-3.00032-X

© 2013 Elsevier Inc. All rights reserved.

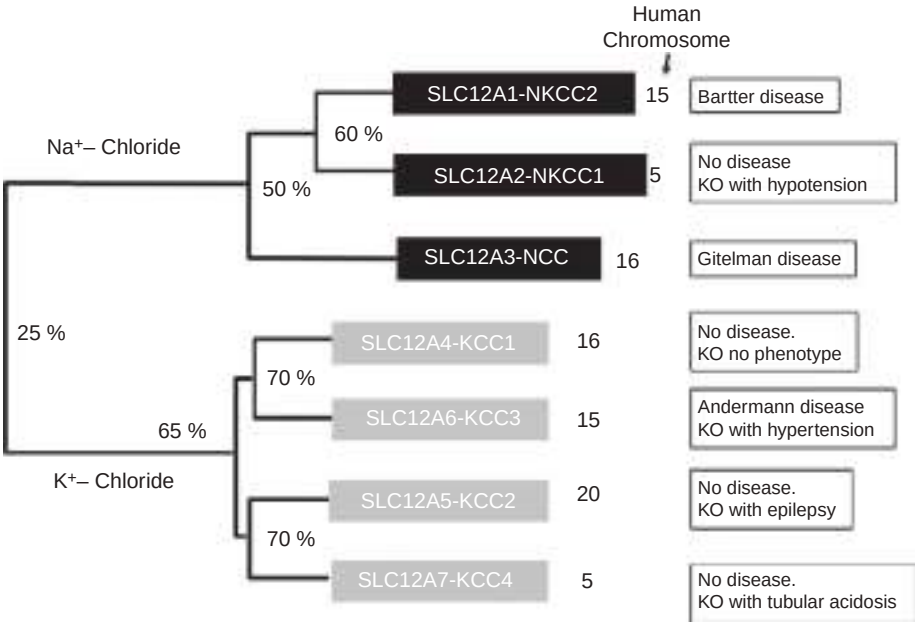

FIGURE 32.1 SLC12 phylogenetic tree. The family is divided in two branches: the Na-coupled and the K-coupled co-transporters. The degree of identity between members is shown in percentages. Chromosome location, inherited diseases, consequences in corresponding knockout mice, and the tissue specific expression is shown.

NCC.[2,3,17] It is mainly expressed in the apical membrane of the distal convoluted tubule (DCT). Initially it was thought that NCC is a gene with restrictive expression in the kidney; however, later it was demonstrated to be expressed at the protein level along the gut,[18] in bone,[19] and in the lens.[20] Although a thiazide-sensitive Na^+-Cl^- co-transporter has been postulated to exist in other tissues,[21] blood vessels,[22] pancreas,[23] peripheral blood mononuclear cells,[24] gallbladder[25] and heart,[26] its presence at the molecular level has not been demonstrated. In bone, NCC activity is associated with the rate of bone formation. Many clinical studies have shown that thiazide diuretics in elderly subjects promote an increase in bone mineral density and help to prevent pathological fractures.[27,28] Consistent with this beneficial effect of thiazides, NCC is expressed in osteoblasts of rat and human bones, and addition of thiazides to osteoblasts in culture increases the formation of mineralized nodules. This effect of thiazides was not present after NCC expression was reduced by transfecting cells with an NCC antisense plasmid.[19]

The degree of identity at the protein level between NKCC1 and NKCC2 is ~60%, and between NCC and the NKCCs is ~50%. The degree varies, however, within specific domains of the co-transporters. It is >80% in some of the central hydrophobic membrane spanning domains, ~50% in the carboxyl terminal domain, and <10% in the amino terminal domain and most of the interconnecting loops that are oriented toward the extracellular side.

The K^+-driven branch is composed of four genes, SLC12A4 to SLC12A7, encoding the K^+:Cl^- co-transporters KCC1 to KCC4, respectively. KCC1 is ubiquitously expressed, while KCC2 is only present in neurons. KCC3 and KCC4 are expressed in several tissues, including the kidney.[7,8,29] Along the nephron KCC3 has been shown to be present only in the proximal tubule, while KCC4 is also expressed in the basolateral membrane of TAL and the intercalated cells of collecting duct (CD).[30–32] The degree of identity is about 60% between KCCs and about 25% with the members of the Na^+-driven branch.

Two additional genes are classified within the SLC12A family (not shown in Figure 32.1) due to a degree of identity of ~20% with either the Na^+-driven or the K^+-driven branches. SLC12A8 gene (human chromosome 3) encodes a protein of 714 amino acid residues that has been identified as a psoriasis susceptibility gene by two independent groups.[33,34] One report suggests that this protein may translocate polyamines and amino acids across the plasma membrane.[35] SLC12A9 (human chromosome 7) encodes a 918 residue protein originally named as co-transporter interacting protein (CIP) for its ability to modulate the activity of NKCC1.[36] Its topological similarity and the 25% identity with other members of the family suggest that it is likely that CIP transports substrates that have not been identified.

THE PHYSIOLOGY OF NaCl CO-TRANSPORTERS IN THE KIDNEY

The electroneutral cation–chloride co-transporters translocate Cl^- ions together with a cation, which can be Na^+, K^+ or both, maintaining the requirement of

electroneutrality: $1Na^+$-$1Cl^-$, or $1K^+$-$1Cl^-$ or $1Na^+$-$1K^+$-$2Cl^-$ stoichiometry. The direction of the transport process is defined by the cation gradient. Therefore, NKCC1, NKCC2, and NCC move ions inward across the plasma membrane, while KCCs move ions outward. Because Na^+ and K^+ are returned to the steady-state by the Na^+:K^+-ATPase, the activity of the SLC12A co-transporters is considered to be primarily regulation of the intracellular chloride concentration $[Cl^-]_i$, a role that is critical to some physiological processes. One of these is cell volume regulation. During cell shrinking, due to increased osmolarity of the extracellular medium, the regulatory volume increase response stimulates transport mechanisms to enhance the intracellular osmolarity, including activation of NKCC1 > NKCC2 > NCC. In contrast, during cell swelling, the regulatory volume decrease promotes the activation of KCCs to reduce intracellular osmolarity. Because basically every cell expresses NKCC1 and KCC1, this cell volume regulatory mechanism is universal.[37]

Another major function of electroneutral cation–chloride co-transporters is the setting of the intraneuronal chloride concentration, either above or below its electrochemical equilibrium potential. For this reason, the activity of these co-transporters is critical in determining the polarity and magnitude of the effect of neurotransmitters that gate Cl^- channels in postsynaptic membranes, such as GABA.[16,38] It is known that before birth GABA behaves mostly as an excitatory neurotransmitter, in neurons in which intracellular chloride is above the electrochemical equilibrium due to more prominent expression of NKCC1 than KCC2. After birth, however, GABA becomes predominantly an inhibitor transmitter, due to the inversion of NKCC1/KCC2 ratio of expression that lowers intracellular chloride below equilibrium.[39]

A third major role of the SLC12A co-transporters that will occupy our interest for the rest of this chapter is the transepithelial movement of ions. NCC and NKCC2 are polarized to the apical membrane of DCT and TAL, respectively, where they participate in renal salt reabsorption. NKCC1 is expressed in the basolateral membrane of several chloride-secreting epithelia, where its activity is critical to provide the cell with chloride ions to be secreted in the apical membrane. The K^+:Cl^- co-transporters are also involved in epithelial movement of ions. One example is KCC4 that is expressed in the intercalated cells of the CD, where it plays a role in the chloride efflux required to maintain hydrogen secretion and thus, acid–base homeostasis.[31]

The Thiazide-Sensitive Na^--Cl^- Co-Transporter

NCC is the major salt transport pathway in the apical membrane of mammalian DCT cells[40–44] which mediates reabsorption of 5–10% of glomerular filtrate. In the early DCT (DCT1) NCC is fully in charge of salt reabsorption, while in the late DCT (DCT2) it shares the responsibility with the sodium channel ENaC.[45–49] This is an important difference, since DCT1 is not considered to be part of the aldosterone-sensitive distal nephron, due to the lack of 11β-hydroxysteroid dehydrogenase type 2 (11β-HSD2), which prevents illicit occupation of the mineralocorticoid receptor by cortisol.[46,49–52] Thus, NCC is susceptible to aldosterone regulation only in DCT2 cells. The molecular mechanism of salt reabsorption in DCT is illustrated in Figure 32.2. The Na^+ gradient that drives transport from the lumen to the interstitium is generated and maintained by the intense activity of Na^+/K^+-ATPase that is polarized to the basolateral membrane.[53] Potassium entering the cell through the Na^+/K^+ pump is secreted by the luminal membrane via K^+ channels[54] and by an apical K^+-Cl^- co-transporter.[55] Thus, potassium secretion rate is determined, at least in part, by the rate of Na^+-Cl^- reabsorption. In addition, NCC modulates magnesium and calcium reabsorption, the latter in an inverse relationship with sodium reabsorption. The lower the sodium reabsorption, the higher the calcium reabsorption, and *vice versa*.[42] As shown in Figure 32.2, NCC is the target for thiazide-type diuretics (metolazone, hydrochlorothiazide, chlortalidone, bendroflumethiazide).[3,43,56] Because thiazides are recommended for the treatment of arterial hypertension, some edematous states, and renal stone disease,[57,58] this group of drugs are among the most commonly prescribed medicines in the world.

The Loop-Diuretic-Sensitive Na^+-K^+-$2Cl^-$ Co-Transporter 2 (NKCC2)

NKCC2 is the major salt transport pathway in the apical membrane of the mammalian TAL, a nephron segment where 15–20% of glomerular filtrate is reabsorbed.[59–64] In addition to its role in salt reabsorption, NKCC2 activity also serves to keep the countercurrent multiplication mechanism by promoting salt concentration in the renal medulla and thus, the renal ability to concentrate urine. Divalent cation (Ca^{2+} and Mg^{2+}) and ammonium (NH_4^+) reabsorption in the TAL also requires the activity of NKCC2 (for reviews see [64–66]). As shown in Figure 32.2, in the case of Ca^{2+} and Mg^{2+} this is due to the fact that simultaneous

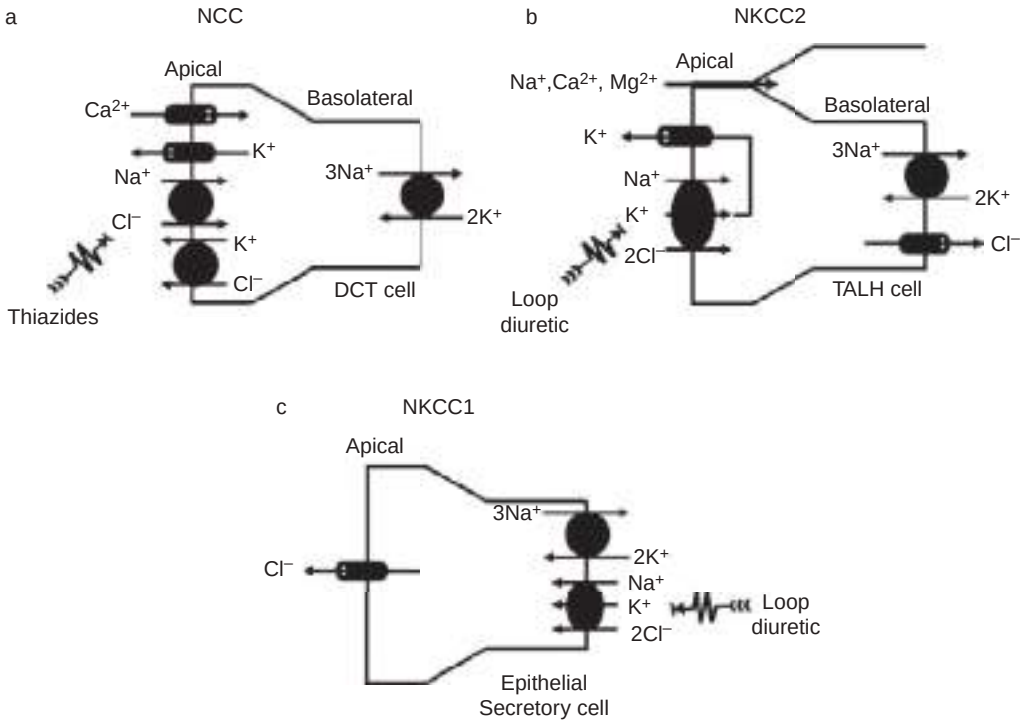

FIGURE 32.2 **Transepithelial ion transport by NCC, NKCC2, and NKCC1.** (a) Distal convoluted tubule. Expression of NCC is polarized towards the apical membrane. (b) Thick ascending limb of Henle's loop. NKCC2 expression is located to the apical membrane. (c) An example of secretory epithelial cell that could be from trachea, gills, intestine, salivary gland, etc. NKCC1 present in the basolateral membrane provides the cell with the chloride to be secreted through the apical membrane.

operation of NKCC2 with the basolateral chloride channels CLC-KB, the Na^+/K^+-ATPase, and the apical inwardly rectifying K^+ channel known as ROMK, promotes the generation of positive voltage within the TAL lumen, which in turn drives the reabsorption of a second cation via a paracellular pathway, which could be Na^+, Ca^{2+} or Mg^{2+}. Thus, in contrast to what occurs in DCT, in the TAL reducing salt reabsorption is associated with reducing calcium reabsorption. Because of this, loop diuretics are often used in the clinical setting for the management of life-threatening hypercalcemia. In the case of ammonium, this is due to the fact that NH_4 can use potassium transport pathways for its translocation through the plasma membrane. Thus, NKCC2 can also operate as the Na^+:NH_4^+:$2Cl^-$ co-transporter.[67,68]

NKCC2 is an important target in cardiovascular and renal pharmacology, because inhibition of this co-transporter is the base of the loop diuretic actions that are the most potent natriuretic agents available for clinical use (furosemide, ethacrinic acid, bumetanide). Loop diuretics decrease the salt reabsorption in TAL, producing significant natriuresis and diuresis. Because loop diuretics reduce interstitial osmolarity of the renal medulla, another mechanism of action is to reduce the concentration capacity of the kidney. Any increase in salt delivery to the macula densa is expected to be compensated by reducing the glomerular filtration rate due to the tubuloglomerular balance.[69] This compensation is absent, however, in the presence of loop diuretics, because the salt-sensing protein in macula densa is also NKCC2.[70] Since the B variant of NKCC2 is the most abundant variant in macula densa cells,[71] and it is not expressed in shark kidney, which also lacks a macula densa,[72] it has been proposed that NKCC2B is the Cl^- sensor in TAL cells. It has been difficult to prove this hypothesis because the variant-specific knockout mice lacking NKCC2B developed a compensatory increase in NKCC2A expression in the TAL cells, and only exhibited a very slight shift to the right of the tubuloglomerular feedback curve.[73] Similarly, the isoform-specific null mice for NKCC2A variant also showed slight changes in tubuloglomerular feedback.[74] These observations suggest that both isoforms working together compose the Cl^- sensor in the macula densa.

Increasing net NaCl reabsorption in TAL by hormones generating cAMP via Gs-coupled receptors such as vasopressin, glucagon, parathyroid hormone, β-adrenergic, and calcitonin is a fundamental mechanism for regulating salt transport in this nephron segment.[75,76] Of these hormones, the most important is the antidiuretic hormone vasopressin, which increases NaCl absorption by TAL through a mechanism that appears

to involve trafficking of NKCC2 to the apical plasma membrane.[77–79] Supporting this proposal it has been observed in medullary TAL that most NKCC2 protein is located in intracellular vesicles, and that addition of cAMP increases the expression of NKCC2 in the apical membrane by activating the exocytosis, rather than by inhibiting the endocytosis of NKCC2-containing vesicles.[80,81] Additionally, long-term increases in vasopressin are associated with increased expression of NKCC2 and maximal urinary concentration ability.[82,83]

The Loop-Diuretic Sensitive Na^+-K^+-$2Cl^-$ Co-Transporter 1 (NKCC1)

NKCC1 is the Na^+-K^+-$2Cl^-$ co-transporter that is present in secretory epithelium, as well as in many non-epithelial cells. At the cellular physiology level, NKCC1 is very important for cell volume and $[Cl^-]_i$ regulation.[7,15,37,84] The diverse phenotypes of NKCC1 knockout mice illustrate the role of this transporter in numerous physiological processes.[85-87] NKCC1 knockout mice feature deafness due to both disrupted epithelial secretion in the labyrinth and a sensorineural defect, infertility due to a deficiency in spermatocyte production, cecum bleeding and blockade of the colon due to impaired intestinal secretion, salivation impairment, and low blood pressure due to vascular and renal effects.[88] Blood pressure in NKCC1 null mice is decreased due to reduced vascular tone.[86,88–90] In this regard, the loop diuretic bumetanide decreased blood pressure in normal mice by inhibiting the activity of NKCC1 in vascular beds, and reduced the vascular smooth muscle cells' myogenic tone. Both effects are not present in the NKCC1 null mice, strongly suggesting that are the results of inhibiting NKCC1 in blood vessels.[91,92] Of note, however, one study using telemetry to monitor blood pressure day and night for several days failed to confirm hypotension in the NKCC1 knockout mice, and suggested a salt-sensitive component because a significant increase in blood pressure was produced by a high-salt diet.[93] Finally, NKCC1 is expressed in the basolateral membrane of the macula densa cells,[94] where it has been suggested that it modulates renin secretion.[95]

MOLECULAR BIOLOGY OF THE SODIUM-DEPENDENT CHLORIDE CO-TRANSPORTERS

The Thiazide-Sensitive Na^+-Cl^- Co-Transporter

Following an expression cloning strategy using the functional expression system of *Xenopus laevis* oocytes, NCC cDNA was first identified at the molecular level from the winter flounder (*Pseudopleuronectes americanus*) urinary bladder.[2] This clone was named as TSC (for thiazide-sensitive co-transporter), and later changed to NCC. The flounder's transcript produced a 3.7 kb cDNA clone containing a 3609 bp open reading frame that predicted a 1023 amino acid residues protein with a core molecular mass of 112 kDa. The computer-based analysis hydrophobicity/hydrophylicity[96] suggested the putative basic topology of the Na^+-coupled-Cl^- co-transporters shown in Figure 32.3a. The short amino terminal domain is followed by a central hydrophobic domain containing what appear to be 12 α-helices compatible with transmembrane-spanning segments. A long carboxyl terminal domain follows this. The amino and carboxyl terminal domains are predicted to be located within the cell. The long loop between transmembrane segments 7 and 8 is glycosylated in NCC[97,98] and NKCC2,[99] and thus presumably in all members of the SLC12A family. In flounder, a shorter 3.0 kb transcript due to alternative splicing is expressed in several tissues including the brain, eye, heart, intestine, gonads, and skeletal muscle.[2] The functional consequence of this variant remains elusive.[100] After the cloning of NCC from the flounder urinary bladder, cDNAs encoding NCC from a variety of mammalian sources were isolated, including rat (*Rattus norvegicus*),[3] mouse (*Mus musculus*),[177] rabbit (*Oryctolagus cuniculus*),[101] and human (*Homo sapiens*).[102,103] Additionally, the NCC cDNA sequence has been deposited in gene databases for at least another 10 species, mostly mammalians and one birth.[104] The degree of identity between mammalian NCCs is ~90%, and of any mammalian with flounder is ~60%. Molecular identification of putative NCC sequences in eel suggests the existence of two different NCC genes.[105] NCCα is expressed only in eel kidney, while NCCβ was observed in many tissues, but more abundantly in intestine. The amino acid residues of NCCα and NCCβ are 1027 and 1043, respectively. No functional expression was analyzed, but the extend of identity of NCCα or NCCβ with any NCC, NKCC1 or NKCC2 supports the proposition that these eel sequences probably correspond to NCC, since degree of identity of NCCα or NCCβ with any NCC sequence is higher than with any NKCC1 or NKCC2. In mammals, rabbit and human NCC is longer than other species due to the presence of 17–26 amino acid residues in the carboxyl terminal domain. These extra residues were shown to be encoded in humans by a separate exon (exon 20) which is not present in rodents.[7,104] It is noteworthy that in humans, there is a putative protein kinase A (PKA) site (RPS) within the extra fragment. No functional significance for this extra exon in humans has been reported, but an extensive proteomic analysis of human urinary

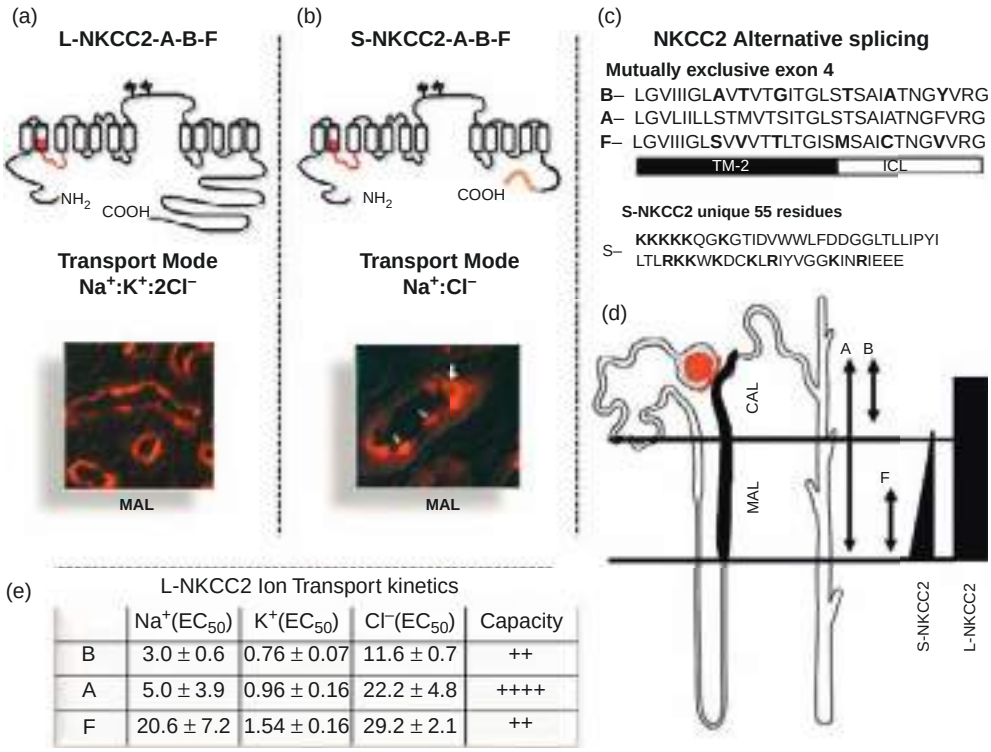

(e) L-NKCC2 Ion Transport kinetics

	$Na^+(EC_{50})$	$K^+(EC_{50})$	$Cl^-(EC_{50})$	Capacity
B	3.0 ± 0.6	0.76 ± 0.07	11.6 ± 0.7	++
A	5.0 ± 3.9	0.96 ± 0.16	22.2 ± 4.8	++++
F	20.6 ± 7.2	1.54 ± 0.16	29.2 ± 2.1	++

FIGURE 32.3 **Molecular physiology of the Na^+-K^+-$2Cl^-$ co-transporter, NKCC2.** (a) Proposed topology (similar to NCC and NKCC1), transport mode, and immunolocalization of the long isoform of NKCC2 (L-NKCC2). The intracellular short amino-terminal domain is followed by 12 transmembrane segments and a long carboxyl terminal domain. The long hydrophilic loop between TM segments 7 and 8 is gylcosylated.[97,99] Several threonines/serine residues in the amino-terminal domain are known to be critical for the regulation of the co-transporters. The mutually exclusive cassette exons A, B, and F are shown in red. (b) Proposed topology, transport mode, and immunolocalization of the short isoform of NKCC2 (L-NKCC2). Location of the mutually exclusive cassette exons is shown in red, and the unique 55 piece at the end is shown in orange. In the picture the white arrows points to positive cells. (c) Sequence and alignment of the exon cassettes A, B, and F. Swapping the red or green residues between B and F isoforms switches their ion transport kinetics between each other (TM-2: transmembrane domain 2; ICL: interconnecting segment between TM2 and TM3). The 55 unique fragment of the short NKCC2 is shown. Positively charged residues are shown in blue. (d) Distribution of L-NKCC2 and S-NKCC2, as well as exons A, B, and F along the limb of Henle, as stated. (e) Ion transport kinetics and capacity of transport for L-NKCC2 A, B, and F variants, as informed by Plata et al.[77] *(Modified from ref. [64].)*

exosomes revealed, among may proteins found, the presence of several fragments of NCC, some of which have the serine 811 phosphorylated, that correspond to the putative protein kinase A site RPS contained by the human exon 20.[106] The expression of NCC protein has been confirmed using specific antibodies in intestine,[18] bone cells,[19] and lens.[20] Additionally, *in silico* analysis of NCC expression revealed that NCC transcripts are abundantly present in sensory ganglia, such as trigeminal and dorsal root ganglion.[104] No report has confirmed the presence of NCC protein in this tissue, and its functional significance is unknown.

The Loop-Diuretic-Sensitive Na^+-K^+-$2Cl^-$ Co-Transporter 2 (NKCC2)

The product of SLC12A1 is the Na^+-K^+-$2Cl^-$ co-transporter known as NKCC2, and it has been located exclusively in the apical membrane of the TAL. Two groups simultaneously identified the cDNA encoding both Na^+:K^+:$2Cl^-$ co-transporter isoforms. Hebert and co-workers cloned the cDNA encoding NKCC2/BSC1 from rat renal outer medulla, and then NKCC1/BSC2 from a mouse inner medullary collecting cells cDNA library,[6] while Forbush and co-workers first identified NKCC1/BSC2 cDNA from a shark rectal gland cDNA library,[4] and later NKCC2/BSC1 from rabbit renal outer medulla.[5] Later, human and mouse NKCC2 sequences were reported.[14,107] Isolated cDNA clones were about 4.5 kb in size, with an open reading frame of 3285 bp encoding a 1095 residue protein. The predicted NKCC2 topology (Figure 32.3A) is highly similar to NCC, featuring the central hydrophobic domain with 12 putative membrane-spanning segments that is flanked by the predominantly hydrophilic amino terminal domain (~165 amino acids) and carboxyl terminal domain (~450 residues). Functional expression

analysis in *Xenopus laevis* oocytes demonstrated that NKCC2 encodes a bumetanide-sensitive Na^+-K^+-$2Cl^-$ co-transporter.[3] It was observed, in a tissue distribution analysis using Northern blot, that NKCC2 transcripts are exclusively present in the renal outer medulla. All other tissues were negative and, until today, no study has confirmed the presence of NKCC2 protein in any other tissue or culture cell. It was proposed that this is due to the presence of a tissue-specific promoter.[108] Interestingly, however, as shown for NCC, *in silico* distribution analysis suggests the existence of NKCC2 transcripts in the sensory ganglia, such as trigeminal and dorsal root ganglion.[104]

SLC12A1 gives rise to a number of alternative splicing variants. At least six isoforms have been suggested to be present in the mouse kidney. Two independent alternatively splicing mechanisms are responsible[7,13,109] (Figure 32.3a,b). One splicing event was first observed in rabbit,[5] and later also in mouse,[14] rat,[110] and human[107] kidney. Three isoforms or variants arise from this splicing mechanism that involve the existence of three mutually-exclusive cassette exons nominated as A, B, and F (Figure 32.3a). These cassettes are composed of 96 bp encoding a 32 amino acid that is part of the second part of the transmembrane segment 2 and the first part of the intracellularly-located interconnecting segment between TM2 and 3 (Figure 32.3c). Thus, three NKCC2 proteins are produced differing only in the 32 amino acid residues, and all three are present in the mammalian NKCC2s known to date.[104] Only variants A and F have been identified from *Squalus acanthias* (shark) kidney.[72]

Another splicing of *SLC12A1* gene that was observed in the mouse kidney is due to the presence of a poly-adenylation site located in the intron between exons 16 and 17, resulting in a shorter C-terminal domain with an extra 55 amino acid residues, not present in the long isoform (Figure 32.3b).[13] Thus, two NKCC2 proteins are produced. These are identical from the first residue in the amino terminal domain to residue 74 of the carboxyl terminal domain. After this point, the longer isoform contains 383 residues not present in the shorter isoform, while the shorter contains 55 residues not present in the longer variant (Figure 32.3c). The existence of the shorter isoform in mouse kidney was demonstrated by a specific polyclonal antibody directed against the 55 unique piece of the shorter isoform.[13] By means of RT-PCR, it was shown that mouse kidney exhibits transcripts of the three isoforms A, B, and F, combined with both possibilities for the carboxyl terminal domain, suggesting that both splicing mechanisms are independent of each other and thus, that a total of six isoforms are predicted to be produced in mouse kidney: three long NKCC2 isoforms (A, B, and F), and three short NKCC2 isoforms (A, B and F).[13] The possible functional significance of spliced isoforms is discussed below.

The Ubiquitous Bumetanide-Sensitive Na^+-K^+-$2Cl^-$ Co-Transporter (NKCC1)

The SLC12A2 gene encodes the ubiquitously expressed Na^+-K^+-$2Cl^-$ co-transporter. NKCC1 is expressed in the plasma membrane of both epithelial and non-epithelial cells. In the first case, it is limited to the basolateral membrane in which the activity NKCC1 serves to provide the cell with the potassium or chloride ions to be secreted through the apical membrane. The only exception is the choroid plexus, in which both the Na^+-K^+-ATPase and NKCC1 are expressed in the apical membrane.[111] NKCC1 has been identified at the molecular level in several species, including mouse,[6] rat,[112] human,[113] *Bos taurus* (bovine),[114] shark,[4] *Anguilla anguilla* (eel),[115] and *Dicentrarchus labrax* (sea bass),[116] and even from the plant *Arabidopsis thaliana*.[117] The existence of one alternatively-spliced isoform of NKCC1 has been suggested.[118] This is a slightly shorter splice variant present in mouse brain total RNA due to the lack of 48 bp corresponding to the entire exon 21. This exon contains a potential PKA phosphorylation site. The existence of a splice transcript was supported by an RNAse protection assay. Distribution analysis within the brain showed that an NKCC1 transcript lacking exon 21 is present in all areas examined except in the choroid plexus, where only the full-length isoform containing exon 21 is expressed. Functional expression in heterologous systems revealed that the shorter variant behaves as a Na^+-K^+-$2Cl^-$ co-transporter.[119] Interestingly, it was recently shown that exon 21 of NKCC1 is implicated in differential sorting in polarized epithelial cells.[120]

Genes, Promoters, and Phylogenetic Analysis

The location of *SLC12A1*, the gene encoding NKCC2 in humans is within chromosome 15,[107] in rat within chromosome 3,[121] and in mouse within chromosome 2.[122] *SLC12A1* is composed of more than 80 kb and 26 exons have been clearly described to encode for the full length 1095 amino acid residue protein.[104] Mouse is the only species from which the *SLC12A1* promoter region has been cloned.[108] The NKCC2 transcript starts with the first exon of 34 bp that is non-coding, followed by a first intron of 1101 bp and a second exon containing the translation start codon. The promoter is composed of 2255 bp. There is a TATA box located at position -29 and consensus recognition sites for several transcription factors, of which the most interesting could be a binding site for HNF-1 at -211 bp. In developing mouse

kidney, the expression of HNF-1 precedes the expression of NKCC2.[123] HNF-1 has been implicated in the regulation of tissue-specific expression of genes in liver, pancreas, kidney, and intestine. Deletion of −2255 to −1529 bp of the promoter resulted in a ~three-fold increase in gene transcription rate, suggesting the presence of negative regulatory elements in this segment. No further effect was observed by deleting −1529 to −469 bp, but a significant reduction in gene expression was obtained by elimination from −469 to −190, suggesting that this region contains positive regulatory elements. An HFN-1-binding site is located in this region. A cAMP response element-binding protein is located at nucleotide −1111, and this could be of major importance because it is known that NKCC2 expression is stimulated by vasopressin.[75,82,124]

The gene *SLC12A2* encodes NKCC1 and is located to chromosome 5q23 in humans,[113] and to chromosome 18 in mouse.[6] The complete gene encompasses a region of 75 kb[118] and is made up of 28 exons. Significant luciferase activity was produced by transfection of mouse IMDC3 cells with a 2063 bp promoter region, together with a luciferase reporter gene. Deletions of >1 kb that reduced the promoter region to 702 or 516 bp resulted in a significant increase in luciferase activity, suggesting the existence of silencer sequences in the deleted bases. Additional deletions resulted in progressive reduction of luciferase activity, suggesting the presence of enhancer elements. Expression of NKCC1 in vascular smooth muscle cells has been suggested to be associated with the development of hypertension in rat models of hypertension. In this regard, a recent report showed that SLC2A2 gene promoter hypomethylation upregulates NKCC1 expression in aorta and heart of spontaneously hypertensive rats.[125,126]

SLC12A3, the gene encoding the thiazide sensitive Na^+-Cl^- co-transporter, is located in humans to chromosome 16q13,[102,103] in rat to chromosome 19p12-14,[127] and in mouse to chromosome 8.[128] Human *SLC12A3* is 55 kb long and contains 26 exons.[102] Transcription initiation is confined to an area from -18 to -6 bp upstream of the translation start codon. The promoter activity observed in the mouse distal convoluted cell line (MDCT),[129] with a construct containing 1019 bp of the 5′ flanking region was reduced only 25% by eliminating the first 885 bp. Sequence analysis of the promoter revealed the presence of a TATA element, two Sp-binding sites, and potential binding sites for NF-1/CTF or NY-I/CP-I. Interestingly, the promoter activity of the rat NCC gene is inhibited by acidosis. This is consistent with a marked fall in renal cortical abundance of NCC protein assessed by Western blot,[130] and by [^{3}H] Metolazone-binding to plasma membranes from the renal cortex[131] of rats exposed to chronic NH_4Cl-loading.

FUNCTIONAL PROPERTIES

The member of the family that has been more extensively characterized is NKCC1. This is because it is expressed in many different cell types that, on one hand, made it accessible for functional characterization, even before the cDNA was identified, and on the other hand, it attracted the interest of many groups of researchers in a variety of fields such as neuroscience, cell volume regulation, red blood cell, and epithelial transport mechanism (for an in-depth review see [15]). In contrast, before identification of the corresponding genes, functional characterization of NKCC2 and NCC was relatively scarce,[57,132,133] and most of the knowledge came from analysis of renal outer medulla or cortical plasma membrane-binding of tracer [^{3}H] Bumetanide or [^{3}H]Metolazone, respectively.[134–136] With the cloning of cDNAs encoding the SLC12A co-transporter proteins and several variants, in-depth characterization of their major functional, pharmacologic, and some regulatory properties has been made possible.

The Thiazide-Sensitive-Na^+-Cl^- Co-Transporter

Heterologous expression of teleost, rat, mouse, and human NCC has been achieved in *Xenopus laevis* oocytes.[2,3,137–140] Oocytes are not epithelial cells; however, this expression system is a useful tool for robust and reproducible NCC expression. Unfortunately, expression of NCC in mammalian cells transfected with NCC cDNAs has been almost impossible to achieve, and so far has been reported only by two independent groups in MDCK[141] and HEK-293.[142] However, in both cases, the level of NCC expression was low, and not sufficient for that required to define the functional properties of the co-transporter. Thus, *Xenopus laevis* continued to be the best cells to assess NCC activity, and basically all of what is known today regarding the functional properties and regulation of NCC activity comes from studies performed in oocytes. Recent reports from Hoover and co-workers[143,144] showed that a subcloned version of the immortal mouse DCT cell line originally produced by Gesek, Friedman and co-workers[145] exhibit what appears to be a robust expression of endogenous NCC, promising an excellent tool for NCC functional analysis in a mammalian cell system.

As shown in Table 32.1, a number of interesting differences have been observed between fish (flounder) and mammalian (rat and mouse) NCC. The affinity for Na^+ and Cl^- in rat[137] or mouse NCC proteins[139] is significantly higher than the affinity observed in the

flounder NCC.[146] In addition, the Km values for Na^+ and Cl^- in mammalian NCCs are similar, whereas in flounder the Km value for extracellular Cl^- is lower than the value for Na^+. NCC activity is inhibited by thiazide-type diuretics with the following profile: polythiazide > metolazone > bendroflumethiazide > trichloromethiazide > chlorthalidone. However, for all thiazides, flounder's NCC exhibited lower affinity. At a concentration of 100 μM, the thiazides with lower potency, trichloromethiazide and chlorthalidone, reduced flounder NCC activity by only 68 and 46%, respectively,[146] whereas the same concentration of all thiazides inhibited rat NCC by >95% .[137]

Two proposals for the order of ion-binding to NCC have been suggested. By assessing the [^{3}H]metolazone-binding to membranes extracted from rat renal cortex, Tran and collaborators[147] observed that Na^+ increased tracer-binding to the putative thiazide-sensitive transport protein. In contrast, Cl^- decreased the affinity for metolazone. Thus, the model that was proposed included two binding sites within the thiazide receptor: one selective for Na^+; and the other that recognizes either Cl^- or metolazone in a competitive fashion. In this model, occupation of the Na^+ site increases the affinity of the second site for either Cl^- and/or metolazone.[148]

The second model was based on observations of functional properties of NCC as expressed in *Xenopus laevis* oocytes. Monroy et al.[137] observed that affinity for Na^+ or Cl^- changed as a function of counterion concentration. The lower the extracellular Na^+ concentration, the lower the Cl^- affinity, a relationship that supports the initial conclusions of Tran et al.[147] However, it was also observed that lower extracellular Cl^- concentrations coincided with lower Na^+ affinity. In addition, it was observed that the IC_{50} for metolazone inhibition increased when the thiazide dose–response curves were measured in lower Na^+ or Cl^- conditions, suggesting that both ions compete with metolazone for binding to the co-transporter. Thus, the proposed model included a random order of binding, with both ions affecting affinity for the counterion and competing with thiazide diuretics.[137] Supporting this model, data produced later that is discussed below suggest that affinity-defining domains or residues for Cl^-- and thiazide-binding are located in different parts of the protein.[98]

TABLE 32.1 Ion Transport and Thiazide-Sensitive Kinetics of Mammalian and Flounder NCC Expressed in *Xenopus laevis* Oocytes

	Rat NCC[98,137]	Mouse NCC[139]	Flounder NCC[98,137]
Na^+ Km (mM)	5.5 ± 1.0	7.2 ± 0.4	30.0 ± 6.0
Cl^- Km (mM)	2.6 ± 0.6	5.6 ± 0.6	15.2 ± 2.0
Metolazone IC_{50} μM	0.3 ± 0.001	0.4 ± 0.001	4.0 ± 0.08

Modified from references [98,137,139].

The Loop-Diuretic-Sensitive Na^+-K^+-2Cl^- Co-Transporter 2 (NKCC2)

Several NKCC2 splice variants in different species have been analyzed at tissue-specific expression and functional level, including shark,[72] rat,[3] mouse,[78] rabbit,[5] and human.[149] As previously discussed, there are three variants of NKCC2 named A, B, and F (Figure 32.3c). The three variants from mouse perform as Na^+-K^+-2Cl^-, suggesting that the difference between variants could be in the kinetic properties for ion transport and/or bumetanide affinity.[78] This hypothesis was supported by intrarenal localization studies that demonstrated axial distribution of these variants along TAL.[5,14,110] As shown in Figure 32.3d, the A isoform is present in both cortical and medullary TAL. In contrast, the B isoform is present only in cortical TAL, and the F variant is expressed only in the inner stripe of the outer medulla. Early studies[150–152] demonstrated that the NaCl transport rate in mTAL is significantly more rapid than in the cTAL, but with greater diluting power in the later segment. Thus, the possibility for heterogeneity of the transport process was suggested. Evidence supporting this hypothesis was obtained simultaneously by Plata et al. [153] and Gimenez et al.[71] using mouse and rabbit NKCC2 variants, respectively (Figure 32.3e). NKCC2F exhibits the lowest affinity for co-transported ions, and is more sensitive to changes in extracellular osmolarity. As shown in Figure 32.3d, NKCC2F is predominantly expressed in the inner stripe of the outer medulla, where the salt concentration is very high, and where greater changes in extracellular osmolarity occur. NKCC2A exhibits the highest transport capacity and is expressed along all TAL. Finally, NKCC2B, the variant that is expressed only the cTAL where ion concentration of the tubular fluid has decreased to values even below those in plasma, is the variant with the highest affinity for the co-transported ions. Thus, the dilution power along TAL is explained by the presence of three alternatively-spliced variants of NKCC2 with distinct functional characteristics. The NKCC2 influx data from Plata et al.[153] were later used to construct a mathematical model for the NKCC2 co-transporter isoforms.[154]

As discussed above, a shorter variant containing 55 amino acid residues at the end that are not present in the longer NKCC2 isoform has been described

(Figure 32.3b,c). This variant is only present in mTAL, not in cTAL[13] and performs as a K^+-independent, but nevertheless, loop diuretic-sensitive Na^+-Cl^- co-transporter that is activated by hypotonicity and inhibited by cAMP.[155] Therefore, the shorter NKCC2 variant may provide a molecular explanation for previous physiological studies that suggested a switch from Na^+-Cl^- to Na^+-K^+-Cl^- co-transporter mode in TAL by extracellular osmolarity or by the presence of vasopressin. Eveloff and co-workers[156,157] observed, in rabbit TAL cells, the existence of a K^+-independent, furosemide-sensitive Na^+-Cl^- co-transporter in hypotonic conditions that became K^+-dependent, constituting the Na^+-K^+-$2Cl^-$ co-transporter, when cells were changed to isotonic medium. In addition, Sun et al.[158] found that in mouse TAL cells, vasopressin (i.e., cAMP) shifts the mode of apical co-transport from Na^+-Cl^- (in its absence) to Na^+-K^+-$2Cl^-$ (in its presence). Consistent with these studies, the large NKCC2 is a Na^+-K^+-$2Cl^-$ co-transporter that is activated by increased tonicity or the presence of vasopressin, while the shorter NKCC2 is a Na^+-Cl^- co-transporter that is activated in hypotonicity or by inhibition of protein kinase A activity.

The shorter variant also exerts a dominant-negative effect upon the activity of the longer NKCC2 that can be abrogated by cAMP.[78] Using confocal microcopy, in oocytes injected with both the long (NKCC2F) and the short variant of mouse NKCC2, Meade et al.[79] observed that the short NKCC2 reduced the activity and surface expression of the long NKCC2. This effect could be prevented by cAMP, and correlated with the observation that the short NKCC2 variant prevented co-transporter trafficking and surface membrane expression of the long NKCC2. These studies thus suggested that in mouse medullary TAL, activation of Na^+-K^+-$2Cl^-$ co-transporter by hormones that increase intracellular cAMP (e.g., vasopressin, PTH) requires the presence of the short NKCC2 protein. The absence of cAMP allows the short form of NKCC2 to reduce co-transporter activity, whereas in the presence of cAMP, the negative effect of the short isoform on NKCC2 is inhibited. In this regard, Mount and collaborators[13] observed that expression of the short NKCC2 is axially distributed along TAL, as cortical TAL appears to lack this isoform. This heterogeneity may explain the observation that in mouse the vasopressin effect is present only in the medullary TAL.[63] Interestingly, the short isoform is also expressed in the thin ascending limb (Figure 32.3d), but its significance in this region is not known.

STRUCTURE–FUNCTION RELATIONSHIPS

The proposed topology for the Na-coupled chloride co-transporters NKCC1, NKCC2, and NCC is shown in Figure 32.3. There is only one study that has addressed the topology at the biochemical level. Gerelsaikhan and Turner[159] used an *in vitro* translation experiment with a variety of human NKCC1 constructs with the carboxyl-terminal reporter sequence containing multiple N-linked glycosylation sites located after each of the putative transmembrane domain. The authors concluded that the amino- and carboxyl-terminal domains are located intracellulary and flank the central hydrophobic domain in which the first eight TM segments are easily identifiable, exhibiting the classical ~20 residue α-helices. It was impossible to differentiate between TMs 9 and 10, and between TMs 11 and 12, and thus it was proposed that probably there are only two large TMs of ~36 residues in length that form tight hairpin-like structures in the membrane or take up either a non-helical or a partial-helical structure.

Ion or Diuretic Affinity Modifier Domains or Residues

Several attempts to begin to understand structure–function relationship issues in the Na^+-coupled Cl^--co-transporters have been made on NKCC1 (for review see [160]), NKCC2,[71,153,161–163] and NCC.[98] In most cases, functional differences in NKCC1 or NCC between fish and mammalian orthologs have been exploited to design chimeric proteins to begin to define domains, regions or individual residues that are defining the ion transport or diuretic-binding affinities and/or specificity. In the case of NKCC2, most of the structure–function information available comes from the functional analysis of alternatively spliced variants.

The identity degree between shark and human NKCC1 is 74%, and interesting functional differences occurs between these orthologs (Table 32.2). Several chimeric constructs were studied by interchanging fragments of NKCC1 between human and shark cDNAs. First, the amino- and carboxyl-terminal domains between both species were swapped, providing evidence that residues located within the central hydrophobic core define ion affinity.[164] Then, a variety of chimeras were constructed and analyzed by in-depth kinetic analysis.[164–166] The chimeric design took into account the transmembrane segments that are identical in NKCC1 of both species. According to the results,[160] the three TM segments playing an important

TABLE 32.2 Ion Transport Kinetics and Bumetanide Affinity of the Na^+-K^+-$2Cl^-$ Co-Transporter NKCC1 from Human and Shark

	Sodium Km (mM)	Rubidium Km (mM)	Chloride Km (mM)	Bumetanide Ki (μM)	Reference
hNKCC1	19.6 ± 4.9	2.68 ± 0.72	26.5 ± 1.3	0.16	113
hNKCC1	15.2 ± 1.5	1.6–2.5	31 ± 1.0	0.044–0.079	164
HEK-293	22	12	110	0.054	4
sNKCC1	42	12	110	0.54	4
sNKCC1	165 ± 34	14 ± 8.0	101 ± 24	0.57	113
sNKCC1	113 ± 11	9.6–11.6	102 ± 7	0.22–0.30	164

hNKCC1: human NKCC1; sNKCC1: shark NKCC1.

role in ion transport kinetics in NKCC1 are TM2, TM4, and TM7. TM2 is involved in Na^+ and Rb^+ kinetics, TM 4 in Rb^+ and Cl^- kinetics, and TM7 in Na^+, Rb^+, and Cl^- kinetics. Interestingly, the behavior of several chimeric proteins with respect to bumetanide inhibition was completely different from that observed in ion transport kinetics. In the case of bumetanide, data suggested that TM segments 2–6 and 10–12 play a role in defining affinity for loop diuretics. Thus, results from studies using shark and human NKCC1 chimeric co-transporters argued against a previous hypothesis that loop diuretics and Cl^- compete for the same binding site.[167]

Analysis of the spliced variants A, B, and F of NKCC2 revealed a clear role of the segments encoded by these exons (TM2) in transport kinetics properties, not only for Na^+ and Rb^+, but also for Cl^- and bumetanide[71,153] (Figure 32.3). Further studies[72] showed that NKCC2 variants A and F, but not B, are present in the shark kidney, and that also in shark, the affinity for transported ions of the NKCC2A variant is higher than the NKCC2F variant. Additional chimeric proteins were constructed: chimera A/F contained the TM2 sequence of variant A followed by an interconnecting sequence of variant F, and *vice versa*.[168] The results suggested that Cl^- transport affinity-defining domains between isoforms A and F were located within the predicted interconnecting segment between TM2 and TM3, rather than within the TM2 segment. The chimeras' behavior with respect to bumetanide affinity was opposite to that of Cl^- affinity, suggesting that residues located within TM2, and not within the TM2–TM3 interconnecting segment, play a role in defining bumetanide affinity. The most recent study regarding structure–function relationship on the NKCC2 variants included a series of single or multiple point mutations of rabbit NKCC2 variants B and F or A and B, in order to switch one or few residues between variants.[162] The results demonstrated that replacement of six residues in NKCC2B resulted in a variant with Na^+ and Cl^- affinities identical to those of NKCC2F. Interestingly, three of these residues are located within the TM2 segment (ATG in B isoform were switched to TAY), and the other three within the interconnecting segment between TM2 and TM3 (SVT in B isoform were changed to MCV). The six mutations (ATG-TAY/SVT-MCV) turned NKCC2B into the F variant (Figure 32.3c), suggesting that the interconnecting loop between TM2 and TM3 might actually be part of a membrane-embedded domain.

The domains or residues defining the affinity for co-transporter ions or inhibitors may not be the same as the residues critical for the specificity for certain ions or inhibitors. All studies discussed above were performed in native, chimeric, and/or mutant NKCC1 or NKCC2 that were expected to behave as Na^+-K^+-$2Cl^-$ co-transporters. Thus, no information was obtained concerning structural requirements to define specificity for ions or diuretics. In this regard, the short isoform of NKCC2 in mouse perform as a K^+-independent, but loop diuretic-sensitive, Na^+-Cl^- co-transporter,[155] suggesting that sequences within the carboxyl-terminal domain could be critical to endow NKCC2 with K^+ transport ability. However, a study in which chimeras were constructed by swapping the amino- and carboxyl-terminal domains between NCC and NKCC2F[161] showed that chimera with the central hydrophobic domain of NKCC2, flanked by amino- and carboxyl-terminal domains of rat NCC, exhibit NKCC2 behavior. That is, as a bumetanide-sensitive Na^+-K^+-$2Cl^-$ co-transporter, indicating that the residues that endow rat NKCC2F with its functional properties should be located within the central hydrophobic domain. Thus, the explanation on how the short NKCC2 variant performs as a bumetanide-sensitive Na^+-Cl^- co-transporter remains elusive. The unique 55 amino acid segment at the end of this isoform contains several negatively-charged residues, suggesting that this fragment could interact with the co-transporter core to prevent K^+ translocation, like the ball and chain mechanism proposed for some membrane channels.[169]

Similar chimera construction and directed point mutation approaches have been used to gain insight into the structure–function relationships of NCC. It was first observed that rat[137] and mouse[139] NCCs exhibit similar functional properties that are, however, significantly different from those shown for flounder NCC.[146] Differences in functional properties and primary sequences between rat and flounder NCCs were

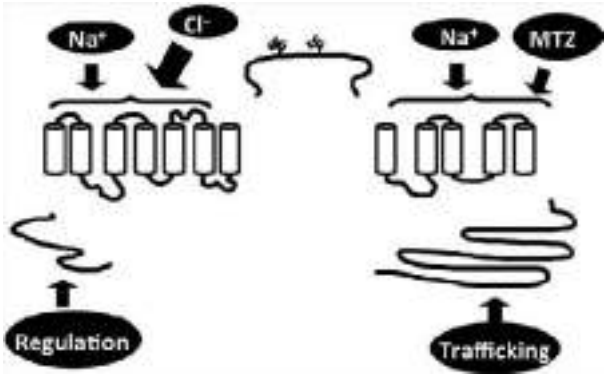

FIGURE 32.4 **Affinity modifying domains in the thiazide-sensitive Na^+-Cl^- co-transporter, NCC.** *(Modified from ref. [98].)*

exploited to define affinity-modifying domains and residues.[98,170] Figure 32.4 depicts what is known regarding the structure–function relationship of NCC. By means of silent restriction sites, NCC cDNAs from rat and flounder were divided into five fragments: amino terminal domain; TM segments 1–7; extracellular glycosylated loop; TM segments 8–12; and the entire carboxyl-terminal domain, and then fragments were swapped between them to obtain a variety of combinations. The results first indicated that the central hydrophobic domains define functional characteristics of NCC. Chimeras in which the TM segments 1–7 were interchanged between flounder and rat NCCs demonstrated that affinity-defining residues for Cl^- are located within these segments. Similarly, affinity-defining residues for thiazide inhibition are located within TM segments 8–12. The observation that Cl^- affinity is defined by residues located within TM segments 1–7 is supported by another study, in which functional consequences of single nucleotide polymorphisms (SNP) located within the exons of the human *SLC12A3* gene changed the primary structure of NCC.[171] The results revealed that a highly-conserved glycine within the fourth transmembrane domain plays a critical role in defining the level of co-transporter activity and the affinity for Cl^-. Accordingly, it was observed that a glycine-to-alanine SNP at position 264 resulted in decreased activity of the co-transporter by 50%, with increased affinity for Cl^- by one order of magnitude. Based on these observations, it was later observed that this SNP on NCC increases the response of humans to loop diuretics, probably because of the reduced capacity of DCT to compensate for the effect of inhibiting salt reabsorption in TAL.[172] The information that thiazide affinity-defining residues were located within TM8 to TM12 was further explored by site directed mutagenesis, revealing that a single residue in rNCC and flNCC is responsible for the differences in affinity for thiazides between mammalian and fish co-transporters. The serine 575 in rat NCC corresponds to the cysteine 576 in flounder NCC. By changing this residue, the affinity for thiazides can be transformed from mammalian to fish affinity, and *vice versa*.[170] It is worth noticing that the NCC mutants that changed the affinity for thiazides had no effect upon the co-transporter affinity for Cl^-, arguing against the proposal that thiazide diuretics and Cl^- compete for the same binding site.[147]

Analysis of the putative glycosylation sites in rat NCC by means of mutagenesis revealed that glycosylation itself is another component of the co-transporter that affects thiazide affinity. In one study, eliminating the glycosylation sites located within the extracellular loop between TM segments 7 and 8 has remarkable consequences in NCC transport activity and properties.[97] Elimination of one site (either N204 or N242) resulted in a 50% reduction of NCC activity, and elimination of both sites was associated with a 95% reduction. Interestingly, prevention of glycosylation was associated with increased affinity for extracellular Cl^- and metolazone. This effect of glycosylation on thiazide affinity seems to be unique to rat NCC, since it was not observed after preventing glycosylation of flounder NCC[98] or rat NKCC2F.[99] In this last co-transporter, elimination of glycosylation by means of site directed mutagenesis was associated with increased affinity for extracellular chloride, but no effect was observed on the affinity for the loop diuretic bumetanide.

The carboxyl terminal domain appears to have an important role in maturation and trafficking of the co-transporters. A region of 77 amino acid residues of NKCC2 (amino acid 708–884), that is not present in NKCC1, seems to be required for driving NKCC2 to the apical membrane in polarized cells,[120] while there is a dileucine motif NKCC1, not present in NKCC2, that directs this co-transporter to the basolateral membrane.[173] A LLV motif in NKCC2 was identified as an ER retaining signal.[174] A protein known as SCMP2 influences NKCC2 expression through recycling endosomes and interfering with its exocytotic trafficking.[175]

The Na-Coupled Chloride Co-Transporters Form Homodimers

Moore-Hoon and Turner[176] used rat parotid plasma membrane to analyze NKCC1 using the reversible chemical cross-linker DTSSP (3,3′-dithiobis-[sulfosuccinimidyl propionate]). They observed that NKCC1 migrates at ~335 kDa. After protein denaturation, single monomers of approximately ~170 kDa were obtained, in which the investigators were unable to detect the presence of any additional protein. Similar

results were later observed on human NKCC2 by Starremans et al.,[177] and on NCC by De Jong et al.[178] These studies were performed in *Xenopus laevis* oocytes injected with *in vitro*-transcribed cRNA from FLAG- and/or HA-tagged wild-type co-transporters and concatamer constructions. These experiments revealed that FLAG-NKCC2 and HA-NKCC2 are physically linked.[177] Similar observations were obtained for FLAG-NCC and HA-NCC constructs.[178] Thus, NKCC1, NKCC2, and NCC are able to form homodimers, and might be functional in this conformation. Because dimers are sensitive to reducing agents such as β-mercaptoethanol, it is likely that disulfide bonds between cysteines are involved.[170] Additionally, some data suggest that members of the *SLC12A* family can build heterocomplexes comprised of different members of the family. For example, an orphan gene of the family known as CIP appears to inhibit transport activity of NKCC1[36] or activate KCC2.[179] However, it does not affect the activity of other family members, raising the possibility that CIP may form an activating heterocomplex specifically with NKCC1.[36] A recent study has shown, by means of yeast two-hybrid and pull down assays, that K^+-Cl^- co-transporter isoforms can interact among themselves, and even with NKCC1.[180]

REGULATION OF SODIUM CATION-COUPLED CO-TRANSPORTERS

The activity of the sodium−cation coupled chloride co-transporters, as occurs with many other ion transport proteins, can be modulated at multiple levels. One is the level of expression of the protein, which in turn can be due to increase in the rate of gene transcription, in the stability of the messenger RNA or post-translationally by affecting the turnover rate of the protein. This level of regulation requires activation/deactivation of synthesis/degradation mechanisms that usually take time to install, and thus are preferred with increased or decreased activity of the co-transporters required for longer periods of time. Another level of regulation is the balance between endocytosis and exocytosis of the co-transporter containing vesicles into the plasma membrane, as only the fraction of co-transporters inserted in the membrane are able to translocate ions. Finally, a co-transporter that is already in the membrane can be regulated to increase or decrease its turnover rate due to conformational changes that affect their activity. The presence of a co-transporter in the cell surface and its intrinsic level of activity are often modulated by phosphorylation/dephosphorylation processes and thus, are subjected to a rapid regulation through cascades of second messengers induced by a variety of hormonal signals.

With the availability of cDNA probes, primers, and high-quality polyclonal antibodies against NCC or NKCC2, several strategies have been implemented to study patterns of these co-transporters abundance, and changes under several physiological and pathophysiological circumstances.[7,181] Discussion of each model is beyond the scope of this chapter, but Tables 32.3 and 32.4 summarize the several experimental, physiological or pathophysiological conditions in which the level of NCC or NKCC2 protein and/or mRNA expression has been analyzed. In general, increased expression of either NCC or NKCC2 is observed in models in which salt retention is induced, while decreased expression is observed by salt-wasting stimuli.

The knowledge of the cation-coupled chloride co-transporters regulation by phosphorylation/dephosphorylation processes has expanded enormously in the last few years, thanks to the discovery of a kinase network that works in conjunction to modulate the ion transport mechanisms. It is well-known that activity of NKCC1/2 and NCC is tightly regulated by means of phosphorylation/dephosphorylation processes, and several lines of evidence suggest that intracellular chloride concentration $[Cl^-]_i$ is a common pathway of NKCCs regulation. When $[Cl^-]_i$ falls, the co-transporters become phosphorylated and activated, whereas when $[Cl^-]_i$ rises, the co-transporters are dephosphorylated and inhibited.[182,183] These effects of $[Cl^-]_i$ on co-transporter activity have been demonstrated for NKCC1,[182,184,185] NKCC2,[186] and NCC.[142,187] In all cases, it was observed that activation of the co-transporter by intracellular Cl^- depletion is associated with increased phosphorylation of the co-transporter in several conserved threonine residues located within the amino-terminal domain.

A great tool to advance in our understanding of NKCC1, NKCC2, and NCC regulation came from the discovery that certain threonine/serine residues in the amino-terminal domain become phosphorylated in association with activation of the co-transporters. The first evidence was obtained for activation of the NKCC1 with phosphorylation of a threonine residue by Lytle and Forbush,[188] in suspensions of shark rectal gland tubules. The peptide FGHNTIDAVP, which became phosphorylated, was isolated and corresponds to amino acid residues 184−194, which are located within the amino-terminal domain of NKCC1.[4] It was later demonstrated by mass spectrophotometry that in phospho-acceptor amino acid sites within the co-transporter amino-terminal domain threonines located at positions 184, 189, and 202 of NKCC1 become phosphorylated in associated with the co-transporter's activation.[184] Of these, threonine 189 is absolutely required for NKCC1 to be functional. Then, analysis *in vivo* was performed using a specific antiphospho-NKCC1

TABLE 32.3 Analysis of NCC Expression in Different Experimental, Physiological or Pathophysiological Conditions

	mRNA	Protein	References
Low Na^+ diet	$\leftrightarrow^{****}\uparrow^{**}$	$\uparrow$	289–296
Loop diuretics	$\leftrightarrow^{*}\uparrow^{****}$	$\uparrow$	294,295,297
Spironolactone[&]	$\leftrightarrow^{*}$	$\uparrow$	297
Thiazide diuretics	–	$\uparrow$	298
Low-protein diet	–	$\uparrow^{+}$	299
L-NAME therapy	–	$\uparrow$	300
Aldosterone	–	$\uparrow$	293
Aldosterone + high-salt diet (4%)	$\uparrow$	$\uparrow$	296
Fludrocortisone		$\uparrow$	293
dDAVP	–	$\uparrow^{b}\leftrightarrow^{c}$	b:301; c:194
Vasopressin escape	–	$\uparrow^{\#}$	302
dDAVP + candesartan	–	$\uparrow^{d}\leftrightarrow^{c}$	d:303; c:194
Obesity	–	$\uparrow$	304
Angiotensin II	–	$\uparrow$	197
Metabolic acidosis	–	$\uparrow$	130,305
Estradiol	–	$\uparrow$	306
Prenatally programmed hypertension[a]	$\uparrow^{**}$	$\uparrow$	307
Chronic renal failure + dDAVP (surgical reduction of renal mass)	–	$\uparrow$	308
KS-WNK1 KO model	–	$\uparrow$	221
Dexamethasone	–	$\uparrow$	309
Tacroliums	–	$\uparrow$	310
Isoproterenol	–	$\uparrow$	311
WNK4 BAC transgenic mice. Two wild-type and two PHAII WNK4 alleles	–	$\uparrow$	214
PHAII WNK4 knockin mice ($WNK4^{+/D561A}$)	–	$\uparrow$	215
Conditional kidney-specific Nedd4-2 knockout mice	–	$\uparrow$	279
WNK1 knockout	–	$\uparrow$	312
Kidney specific OSR1 knockout	–	$\uparrow$	235
Gentamicin	–	$\leftrightarrow$	313
Water restriction	–	$\leftrightarrow$	301
Insulin	–	$\leftrightarrow$	314
Chronic noradrenaline infusion	–	$\leftrightarrow$	315
Lithium (low dose or high dose) 40 versus 60 mmol lithium/kg dry food	–	$\leftrightarrow$	316
Chronic renal failure (surgical reduction of renal mass)	–	$\leftrightarrow$	308
High-K^+ diet	–	$\downarrow$	290,317
High-K^+ diet and HS diet after unilateral nephrectomy	–	$\downarrow$	318
Low-K^+ diet	$\downarrow^{*}$	$\downarrow$	319,320
DOCA	–	$\downarrow$	321

(*Continued*)

TABLE 32.3 (*Continued*)

	mRNA	Protein	References
Candesartan	–	↓[e] ↔[c]	e:322; c:194
Chronic renal failure + candesartan	–	↓	323
Aldosterone escape	↔[****]	↓	324
L-NAME + aldosterone escape	–	↓	325
Bilateral ureteral obstruction	–	↓	326
Bilateral ureteral obstruction and release of obstruction (Day 14)	–	↓	327
Puromycin-induced nephrotic syndrome	–	↓	328
Spironolactone infusion in low-salt (0.7%) diet	↓	↓	296
SGK1 inducible knockout mouse model	↔	↓	329
Cyclosporine	–	↓	330
WNK4 BAC transgenic mice. Four wild-type WNK4 alleles	↓	↓	214
SPAK knockin mice ($SPAK^{T243A/T243A}$)	↓	↓	192
SPAK knockout mice	–	↓	234
Overexpression of WNK1	–	↓	312
Dehydration	↑[****]	–	294
High-Na^+ diet	↔[***] ↓[**]	↓	294–296
Saline-loading	↔[***]	–	294
Water-loading	↔[***]	–	294

[*] *Northern Blot.*
[**] *Real-time PCR.*
[***] *Semi-quantitative PCR.*
[****] *mRNA Protection Assay.*
[&] *in loop- diuretic treated animals.*
[+] *Associated with high plasma aldosterone levels.*
[#] *Increased NCC protein during days 1 and 2, no difference in days 3 or 7.*
[a] *Prenatal hypertension induced by low-protein diets in pregnant rats.*

antibody named R5, which was raised against a synthetic peptide of the amino-terminal domain containing threonines 212 and 217 of human NKCC1 (corresponding to threonines 184 and 189 of shark NKCC1).[185,189] The results demonstrated that activation of NKCC1 by intracellular Cl^- depletion is associated with phosphorylation of these threonines.

The same R5 phospho-antibody was used to demonstrate that activation of NKCC2 or NCC by cell volume changes or intracellular Cl^- depletion is associated with phosphorylation of the conserved threonines 96–101 in rat NKCC2 and 53–58 in rat NCC.[186,187,190] Later, specific phospho-antibodies for these and other threonine/serines in the amino-terminal domain were raised against each rat or human co-transporter, confirming the role of the residues detected by R5 antibody and suggesting other sites within the amino-terminal domain as potential residues to be involved.[142,191] Similar to NKCC1, threonine 60 of human NCC (corresponding to 189 from shark NKCC1) is required for NCC to be functional,[187] and when activated by phosphorylation it appears that T60 is the first to be phosphorylated; this opens the possibility to phosphorylate nearby threonine/serine residues.[191] None of these phospho-acceptor sites are individually required for NKCC2 to be functional, because elimination of each one at a time reduces, but does not prevent, the activity of the co-transporter.[186]

Figure 32.5 shows an alignment analysis of a region of the amino-terminal domain of NCC, NKCC2, and NKCC1 highlighting the conserved threonine/serine phosphorylation sites among species that have been implicated in activation of the co-transporters in different studies. Tables 32.5 and 32.6 contain detailed information on all the works in which phosphorylation of specific site or sites on NCC or NKCC2 have been studied. Several works *in vitro* and *in vivo* have shown that some of the amino-terminal domain phosphorylation

TABLE 32.4 Analysis of NKCC2 Expression in Different Experimental, Physiological or Pathophysiological Conditions

	mRNA	Protein	References
Low-Na^+ diet	↔*	↔,↑	289,292,294,295
Loop diuretics	↔*	↑	294,295,298
Low-protein diet	–	↑ +	299
Dexamethasone	↑****	↑	331,309
High-fat diet	–	↑	332
Lipopolysacharide injections	–	↑++	333
Candesartan	–	↑	322
Chronic renal failure + candesartan	–	↑	323
L-NAME therapy	–	↑	334
Diclofenac/indomethacin	–	↑	335
Growth hormone	–	↑$	201
Obesity	–	↓↑	336,304
Rosiglitazone	–	↑	336
Hyperosmolarity	–	↑	337
Bilateral ureteral obstruction and release of obstruction (Day 14)	–	↑	327
Angiotensin II	–	↑	338
dDAVP	–	↑	82,301,303
Water restriction	–	↑	82,301
Lithium	–	↑	339
Chronic noradrenaline infusion	–	↑	315
Prenatally programmed hypertensiona	↑**	↑	307
Lithium (high dose) 60 mmol lithium/kg dry food	–	↑	340
Sildenafil in the presence of lithium-induced DI	–	↑	341
Vasopressin escape	–	↑↓#	302
Chronic renal failure + dDAVP	–	↑	308
(Surgical reduction of renal mass.)			
Hypothyroid rat model	–	↑	342
Dahl salt-sensitive rats	–	↑##	343
SPAK knockout mice	–	↑	234,236
WNK1 knockout	–	↑	312,221
P2Y2 receptor KO mice with high-salt diet	–	↑	344
Aldosterone	–	↔	197
Candesartan	–	↔	345
Aldosterone escape	–	↔	324
dDAVP + candesartan	–	↔	303
Chronic metabolic acidosis	↑****	↔,↑	130,346–348
Lithium (low dose) 40 mmol lithium/kg dry food	–	↔	340

(*Continued*)

TABLE 32.4 (*Continued*)

	mRNA	Protein	References
Chronic renal failure (surgical reduction of renal mass)	–	↔	308
Low-K^+ diet	↓*	↓	319,320
DOCA	–	↓	321
Cyclosporine	–	↓	349
Parecoxib	↓***	↓	350
Gentamicin	–	↓	313
Bilateral ureteral obstruction	–	↓	326,351
17-Beta-estradiol	–	↓	352
L-NAME + aldosterone escape	↔**	↓	325
Puromycin-induced nephrotic syndrome	–	↓	328
SGK1 inducible knockout mouse model	–	↓	329
High-K^+ diet and high-salt diet after unilateral nephrectomy	–	↓#$	318
Dahl salt-resistant rats	–	↓###	343
P2Y2 receptor knockout mice with high-salt diet	–	↓	344
SPAK knockin mice ($SPAK^{T243A/T243A}$)	–	↓	192
Overexpression WNK1	–	↓	312
Kidney-specific OSR1 knockout	–	↓	235
High-Na^+ diet	↔*	–	294,295
Saline-loading	↔*	–	294
Dehydration	↔*	–	294
Water-loading	↔*	–	294

*Northern Blot.
**Real time PCR.
***Semi-quantitative PCR.
****RT PCR.
+ Associated with high plasma aldosterone levels.
++Increased in inner stripe of outer medulla.
$Increased total protein in outer stripe of outer medulla, increased phosphorylation with no change in NKCC2 total protein in inner stripe.
#Increased during day 2 of dDAVP and decreased by day 7. No change in days 1 or 3.
##Increase in surface NKCC2 with no change in total/G6PD.
###Decrease in surface NKCC2 with no change in total/G6PD.
[a]Prenatal hypertension induced by low protein diets in pregnant rats.
#$Change in NKCC2 after 3 wks, no change after 1 wk with HS + KCl diet. L-NAME - N-nitro-L-arginine-methyl esterase.

residues are involved in activation of NCC by intracellular chloride depletion,[142,187] low-salt diet,[192,193] vasopressin,[194,195] angiotensin II[196,197] or aldosterone[193,198]; and NKCC2 by hypertonicity,[199] intracellular chloride depletion,[186,200] vasopressin,[77] and growth hormone.[201] Thus, NKCC1, NKCC2 or NCC are activated by phosphorylation of particular amino-terminal domain threonine/serine residues by different stimuli and intracellular cascades such as Gαs receptor-cAMP-PKA (vasopressin), Gαq receptor-IP3-PKC (angiotensin II), tyrosine kinase-associated receptor (growth hormone) or activation of an intracellular soluble kinase by $[Cl^-]_i$ or changes in cell volume (see below). These data suggest that different cascades probably combine in activation of a particular kinase pathway that is responsible for the phosphorylation of these particular sites.

The kinase cascade that has been shown to be involved in the phosphorylation of the amino terminal threonine or serine residues of NKCC1, NKCC2 or NCC is the WNK-SPAK pathway. The WNK family of serine/threonine kinases is closely related to MAP kinases. Members of this family lack the conserved catalytic lysine (K) present in subdomain II of all the other serine/threonine kinases, hence the name WNK for "with no lysine (K)".[202] The crystal structure of the WNK1 catalytic domain later revealed that the catalytic lysine is present in subdomain I.[203] The family is

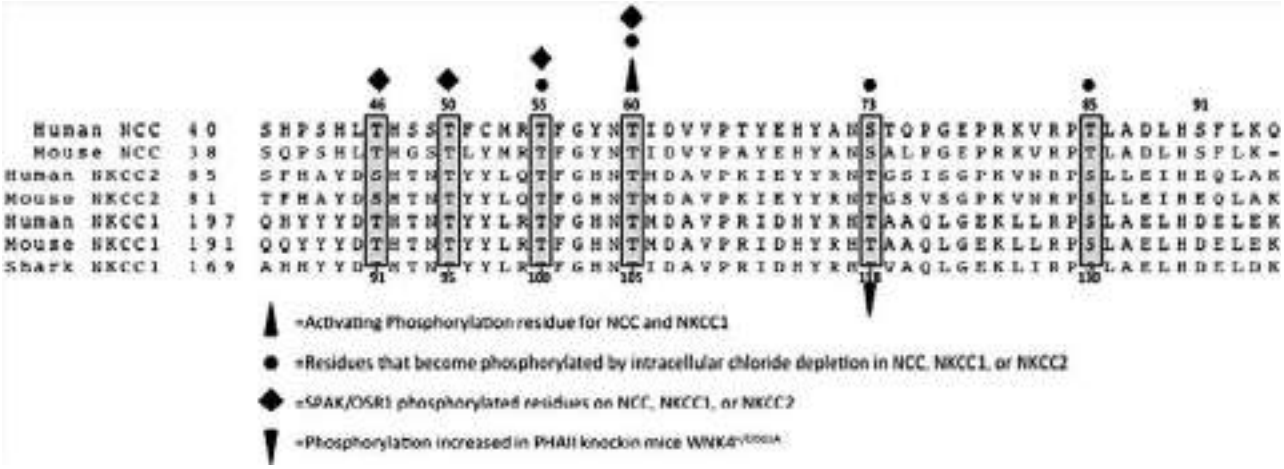
Human NCC 40
Mouse NCC 38
Human NKCC2 85
Mouse NKCC2 81
Human NKCC1 197
Mouse NKCC1 191
Shark NKCC1 169
=Activating Phosphorylation residue for NCC and NKCC1
=Residues that become phosphorylated by intracellular chloride depletion in NCC, NKCC1, or NKCC2
=SPAK/OSR1 phosphorylated residues on NCC, NKCC1, or NKCC2
=Phosphorylation increased in PHAII knockin mice WNK4

FIGURE 32.5 **Sequence alignment of a region of the amino-terminal domain containing the conserved residues (highlighted in gray) that have been associated with phosphorylation/activation of the co-transporters.** Numbering above alignment indicates residues in NCC. Numbering below alignment indicates numbering in NKCC2.

composed of four members, known as WNK1 to WNK4,[204] each containing a serine/threonine kinase domain of 294 residues flanked by a short amino-terminal domain (146 to 220 amino acid residues) and a long carboxyl terminal domain (796 to 1888 residues) exhibiting two coiled-coil domains for protein interaction, and a conserved auto-inhibitory motif shown to inhibit autophosphorylation in WNK1.[202,205] The degree of conservation among the four isoforms is high within the kinase domain (>80%), but low within the amino- or carboxyl-terminal domains (<15%).

The importance of WNKs to renal physiology and pathophysiology was highlighted by the demonstration that intronic deletions of WNK1 or missense mutations in an acidic conserved region of WNK4 are the cause of a human form of an inherited syndrome featuring arterial hypertension, hyperkalemia, and metabolic acidosis known as pseudohypoaldosteronism type II (PHAII), Familiar Hyperkalemic Hypertension (FHH) or Gordon's disease.[206–208] Because PHAII is a mirror image of Gitelman's disease and it is treatable with low doses of thiazides (see below), it was suspected that activity of NCC was implicated in the pathophysiology of the disease. This was first demonstrated using the heterologous expression system of *Xenopus laevis* oocytes.[209,210] WNK4 inhibits the activity of NCC, and this effect is prevented by either eliminating the catalytic activity of WNK4[209,211–213] or by the introduction of one of the PHAII-type mutations in WNK4,[209,213] thus suggesting that the activity of NCC in PHAII patients is increased due to elimination of the WNK4-induced inhibition of NCC. The activation/phosphorylation of NCC as the major mechanism for hypertension and hyperkalemia was confirmed in two animal models of PHAII[214,215] (Table 32.5). The mechanism for PHAII in families with intronic deletion of WNK1 is less-understood. WNK1 does not seem to have a direct effect upon NCC. Instead, it has been observed that WNK1 prevents the WNK4-induced inhibition of NCC.[210] Thus, if WNK1 expression is increased, as is suggested to occur as a consequence of WNK1 intronic 1 deletion,[206] the WNK4 inhibitory effect upon NCC will be prevented and thus, NCC activity will increase. Interestingly, there is a shorter variant of WNK1, lacking the entire amino and kinase domain that is exclusively expressed in the kidney, specifically in DCT.[216–218] The short WNK1 prevents the WNK1 effect on WNK4.[219] Thus, it is postulated that under physiological conditions the expression of the short WNK1 in DCT modulates the interaction between WNK1 and WNK4, regulating NCC activity. In PHAII, however, increased expression of the long WNK1 surpasses the regulatory capacity of short-WNK1, thus inhibiting WNK4 with the consequent activation of NCC. This model, however, awaits definitive confirmation by *in vivo* models.[220–222]

Two kinases related to the yeast Ste-20p family known as SPAK (Ste20p-related proline-alanine rich kinase) and OSR1 (oxidative stress response 1) have been shown to be located downstream of WNKs, at least for their effects on the cation-coupled chloride co-transporters.[223,224] The first evidence of the WNK-SPAK/OSR1 interaction was obtained in a study in which the K-Cl co-transporter, KCC3, was shown to interact with SPAK/OSR1 in a two-hybrid yeast system. The co-transporter interacting with SPAK/OSR1 using a specific binding domain was determined to be RFx(V/I).[225] One such binding site is located in the amino-terminal domain of NCC and NKCC2, two are present in NKCC1, and two or three sites in each

TABLE 32.5 Phosphorylation of NCC in Different Sites and Conditions

Experimental System/Model	Phospho-site*	Effect	Stimuli	Kinase Involved	Reference
In tube	T^{55},T^{60},S^{73}	–	SPAK	WNK1/SPAK	190
Xenopus oocytes	T^{55},T^{60},S^{73}	↑↑	Intracellular Cl^- depletion	¿?	187
Mouse	S^{73}	↑↑	WNK4 knockin	WNK4	215
HEK-293 cells	T^{46},T^{55},T^{60},S^{91}	↑↑	Intracellular Cl^- depletion	SPAK	142
Rat	T^{55},T^{60},S^{73}	↑↑	Low-salt diet	¿?	193
Human urine	S^{811}	↑	None	¿?	106
Xenopus oocytes/mpkDCT cells	T^{55},T^{60}	↑↑	Angiotensin II	WNK4-SPAK	196
Mouse	T^{55},T^{60},S^{73}	↑	Low-K^+ diet	SGK1	290
Mouse	T^{55},T^{60},S^{73}	↓	WNK4 hypomorphic	WNK4	280
Brattleboro rats	T^{55},S^{73}	↑↑	dDAVP	¿?	195
Brattleboro rats/wistar rats	T^{55},T^{60}	↑↑	dDAVP	SPAK	194
Mouse	T^{55},T^{60},S^{91}	↓↓	SPAK knockin	SPAK	192
mpkDCT cells/mouse	T^{55},T^{60},S^{73}	↑↑	Angiotensin II/aldosterone	SPAK	198
Adrenalectomized rats	T^{55},T^{60}	↑↑	Angiotensin II/aldosterone	WNK4-SPAK	197
Mouse	T^{45},T^{55},T^{60}, S^{73}	↑↑	KS-WNK1 knockout	WNK1/WNK4	221
In tube	T^{46},T^{55},T^{60},S^{91}	↑	Incubation with MO25	SPAK/OSR1	353
Mouse	T^{55},T^{60},S^{73}	↓↓	SPAK knockout	SPAK	234
Mouse	T^{55},S^{73}	↓↓	SPAK knockout	SPAK	236
mDCT cells/Rats	T^{55},T^{60},S^{73}	↑	Cyclosporine	¿?	354
Mouse	T^{55}	↑	Tacrolimus	WNK3/WNK4	310
Mouse	T^{55}	↔	NCC transgenic	¿?	355
Mouse	T^{60}	↓↓	WNK4 knockout	WNK4/SPAK	356
mpkDCT cells/mouse	T^{55},T^{60},S^{73}	↑	Insulin	WNK4/SPAK	357
Xenopus oocytes *Ex vivo* kidney	T^{60}	↑	Insulin	WNK4/SPAK	358
Mouse	T^{55}	↑	KS-OSR1 knockout	OSR1/SPAK	235
Mouse	T^{55},S^{73}	↑	Isoproterenol salt-sensitive hypertension	WNK4	311
Xenopus oocytes	T^{60}	↑↑	WNK3	WNK3/SPAK	226

*Numbers correspond to human NCC sequence.

WNKs support the interaction between WNKs and co-transporters with SPAK.[142,225,226] In fact, among all proteins in the human proteome, WNK1 and NKCC1 are the ones with higher numbers of SPAK-binding domains.[227] Functional and biochemical studies using NKCC1 demonstrated that both WNK1 or WNK4, as well as SPAK or OSR1, must be present to induce amino-terminal domain phosphorylation and activation of the co-transporter.[190,223,228] It was shown that WNKs lie upstream of SPAK/OSR1, and that WNK phosphorylates SPAK/OSR1 on two specific threonine and serine residues (T243 and S383 in SPAK), inducing activation of the kinase.[192,223] Thus, it is believed that SPAK/OSR1 are the kinases that actually phosphorylate the amino-terminal threonine residues of NKCC1, NKCC2 or NCC, and that WNKs modulate this effect by activating SPAK/OSR1.[191,229–232]

The interaction between SPAK and NCC has been confirmed, and also the requirement for the amino-terminal domain SPAK-binding site of NCC.[142,191,226] To find out the importance of the interaction and phosphorylation between SPAK and NCC *in vivo*, Rafiqui et al.[192] generated a mice knockin model by eliminating the threonine residue of the T-loop in SPAK (T243A) or OSR1 (T185A) that is phosphorylated by WNK1 or WNK4. The $OSR1^{185A/185A}$ mice died on embryonic

TABLE 32.6 Phosphorylation of NKCC2 in Different Sites and Conditions

Experimental System/Model	Phospho-site*	Effect	Stimuli	Kinase Involved	Reference
Mice	T^{100},T^{105}	↑↑	Vasopressin	¿?	77
Xenopus oocytes	T^{100},T^{105}	↑↑	Hypertonicity	¿?	199
In tube	Amino terminal fragment 1–181	–	SPAK/OSR1	WNK1/SPAK	190
Xenopus oocytes	T^{100},T^{105}	↑↑	WNK3	WNK3	239
Rat	T^{100},T^{105}	↑↑	Growth hormone	¿?	201
Xenopus oocytes/MMDD1 cells	S^{130}	↑	Hypertonicity	AMPK	359
Xenopus oocytes	T^{100},T^{105}	↑↑	Intracellular Cl^- depletion/WNK3	WNK3/SPAK	186
Mouse	T^{55},T^{60},S^{91}	↓↓	SPAK knockin	SPAK	192
Dahl TAL cells	T^{100},T^{105}	↔	High-salt diet	¿?	343
HEK-293 cells	T^{95}, T^{100},T^{105},S^{130}	↑↑	Intracellular Cl^- depletion	SPAK	200
In tube	T^{95},T^{100},T^{105}	↑	Incubation with MO25	SPAK/OSR1	353
HEK-293 cells	T^{100},T^{105}	↑↑	Ouabain Calyculin A	SPAK	360
Milan rats	T^{100},T^{105}	↑	–	SPAK	361
Mice/culture TAL	T^{118}	↑↑	dDAVP	¿?	362
THP knockout mice/culture TAL	T^{118}	↓	dDAVP	¿?	362
Mouse	T^{100},T^{105}	↑↑	SPAK knockout	SPAK	234
Mouse	T^{100},T^{105}	↓	KS-OSR1 knockout	OSR1/SPAK	235

Numbers correspond to human NKCC2 sequence.

day 17.5, while the $SPAK^{234A/234A}$ mice were viable, grew normally and thus were further analyzed. Along the nephron, SPAK is specifically expressed in TAL and DCT. The blood pressure of $SPAK^{234A/234A}$ mice is reduced and consistent with reduction in salt reabsorption as the mechanism of hypotension; blood pressure was normalized after feeding the $SPAK^{234A/234A}$ mice with a high-salt diet for several days. In fact, $SPAK^{234A/234A}$ mice developed a Gitelman-like syndrome, with hypomagnesemia and hypocalciuria. Hypokalemia was not observed in a normal-sodium diet, but became apparent with a low-sodium diet. Using specific phosphoantibodies for NCC amino-terminal threonine residues, it was shown that in $SPAK^{234A/234A}$ mice expression of NCC in the kidney was reduced by 30% and phosphorylation at residues T53, T58, and S89 were reduced by about 80% (Tables 32.3 and 32.5). Similar observations were obtained using specific antibodies against NKCC2 (Tables 32.4 and 32.6). All these observations together indicate that absence of SPAK activity resulted in decreased activity of NKCC2 and/or NCC. Because the phenotype resembles Gitelman's rather than Bartter's disease, it was suggested that the effect of SPAK inactivation upon NCC was stronger. Crossing the PHAII knockin mice generated by Yang et al.[215] with the $SPAK^{234A/234A}$ mice[192] demonstrated that hypertension and the whole PHAII syndrome were prevented, indicating the major role of SPAK-induced regulation of NCC in this syndrome.[233] Thus, the SPAK knockin mice model provided compelling evidence of the key role of SPAK in modulation of NKCC2 and NCC activity.

Interestingly, the complete elimination of SPAK in a SPAK knockout model also resulted in decreased expression and phosphorylation of NCC, but in contrast to the $SPAK^{234A/234A}$ mice, resulted in increased phosphorylation of NKCC2[234] (Tables 32.4 and 32.6). In contrast, a recent study in which a kidney tissue-specific elimination of OSR1 was achieved (KS-$OSR1^{-/-}$ mice) resulted in an incomplete form of Bartter's syndrome, with decreased expression and phosphorylation of NKCC2, together with increased expression of SPAK and NCC phosphorylation[235] (Tables 32.4 and 32.6). Thus, it is possible that NKCC2 is preferentially under the control of OSR1, while NCC is under the control of SPAK. Several SPAK splicing isoforms are expressed in the kidney that could serve to explain the different regulation of NKCC2 and NCC under different circumstances.[236]

WNK2 and WNK3 also exert effects on the cation-coupled chloride co-transporters that are of interest. WNK3 is expressed along the entire nephron, as well as in several epithelial and non-epithelial cells outside the kidney,[232,237] and strongly activates NKCC1, NKCC2, and NCC, while it inhibits all four KCCs.[238–240] Thus, WNK3 activates chloride influx pathways and inactivates chloride efflux pathways. Activation of NKCC1, NKCC2, and NCC by WNK3 is associated with phosphorylation of the same amino-terminal domain threonines in the several models discussed above[226,238,239] (Tables 32.5 and 32.6). WNK3 activation of NCC is associated with increased expression of NCC on the cell surface, suggesting that it promotes the trafficking of NCC vesicles into the plasma membrane.[239] One study suggests that the effect of WNK3 and WNK4 on NCC can be achieved by the carboxyl-terminal domain of the kinase alone, that is, in the complete absence of the kinase domain.[241] Other studies, however, have shown that the effect of WNK3 and WNK4 on NCC are kinase-dependent,[209,212,213,239,241] and unlike what occurs with WNK1 variants[216,217] there is no evidence that such truncated variants of WNK3 or WNK4 are expressed in the DCT. One study in which chimeric proteins between WNK3 and WNK4 domains were constructed suggested that the type of effect of WNK3 or WNK4 upon NCC resides within the amino-terminal domain.[211]

The WNK3-induced activation of NKCCs or inhibition of KCCs occurs even during cell swelling, which is a well-known inhibitor of NKCCs and activator of KCCs.[3,137,199] WNK3 catalytic activity can be prevented by the substitution of D294A. By doing this, the effect on the co-transporters is not only prevented, indicating the requirement for catalytic activity, but additionally, catalytically inactive WNK3 becomes an inhibitor of NKCC1, NKCC2, and NCC, and an activator of KCCs, even in isotonic conditions in which KCCs are non-functional. Because activation of KCCs by WNK3-D294A can be prevented with calyculin A and/or cyclosporine A, it is likely due to a catalytically inactive WNK3-induced activation of protein phosphatases.[240] Because the effect of WNK3 upon the sodium-coupled chloride co-transporters is associated with phosphorylation of the SPAK phospho-acceptor sites in the co-transporter's amino-terminal domain, it is likely that WNK3 also lies upstream of SPAK/OSR1 for its effect on the SLC12A co-transporters. Supporting this possibility, the positive effect of WNK3 on NKCC2 or NCC can be prevented by elimination of SPAK-binding sites located in WNK3.[186,226] Thus, WNK3 modulates the activity of all members of the SLC12 family and, in doing so, bypasses the changes in cell volume and/or intracellular chloride concentration that are usually required for their activation or inhibition. It is believed that WNK3/SPAK is the intracellular kinase pathway sensitive to cell volume and/or intracellular chloride concentration.[184,232,242] WNK2 is preferentially expressed in the central nervous system, and is apparently absent in kidney. Its effects on NKCC1 and KCCs are similar to those of WNK3.[243]

THE ROLE OF THE SODIUM-COUPLED CATION CHLORIDE CO-TRANSPORTERS IN INHERITED DISEASE

Given the major roles that NCC and NKCC2 play in renal physiology, it is of no surprise that inactivating mutations of these co-transporter genes are associated with monogenic disease, such as Gitelman's and type I Bartter's diseases, respectively. In addition, by affecting the modulation of NCC by certain kinases, increased activity of this co-transporter (and other ion transport protein in the distal nephron) is the mechanism behind another monogenic disease known as PHAII.

Gitelman's Disease

Gitelman's disease is an autosomal recessive monogenic disease featuring hypokalemic metabolic alkalosis, arterial hypotension, hypocalciuria, and hypomagenesemia. The clinical presentation usually becomes evident by the second decade of life. All these manifestations are due to a lack of salt transport capacity of the DCT, and resemble the clinical consequences of thiazide diuretic intoxication. Because of this, NCC became a strong candidate for the cause of the disease, and links between Gitelman's disease and the locus for *SLC12A3* in human chromosome 16 was found by several groups.[102,244–246] At present, nearly 350 different mutations of NCC have been reported to be associated with Gitelman's disease or with low blood pressure in an open population (see the human gene mutation data base at www.hgmd.or). Supporting the studies on genomic associations, phenotypes resembling Gitelman's disease have been obtained in mice by targeted disruption of NCC.[247,248] Interestingly, total knockout of NCC produces an incomplete Gitelman syndrome, while substituting the serine residue at the position 707 by a stop codon completely expunges the disease. Functional analysis of human or rat NCC containing some of the reported point mutations revealed that mutant NCC proteins are non-functional.[138–140]

Although Gitelman's disease is an autosomal recessive disorder, surprisingly, not all patients have shown mutations in both SLC12A3 alleles. About 30% of the Gitelman patients have been diagnosed with mutations in only one allele, another 45% are compound heterozygous; that is, they exhibit mutations in both alleles, but the mutation is different for each one, and near 20% are homozygous.[7,102,249–254] Because inheritance of Gitelman's disease is clearly recessive, and heterozygous relatives of patients with Gitelman's disease are clinically and metabolically asymptomatic, it is likely that undetected mutations in the other allele also exist. Most of the studies usually search for mutation within exons, but it is possible that mutations within the promoter or even in some introns or in the 3′ untranslated region affect expression of the protein. Most of the Gitelman's mutations are single point mutations in residues that are highly-conserved from fish to humans, and the mechanisms by which mutations reduce or abolish transporter activity are several, including impairment of protein synthesis, impairment of protein processing, impairment of insertion of an otherwise functional protein into the plasma membrane, impairment of functional properties of the co-transporter, and acceleration of protein removal from the membrane or degradation. Initial reports of missense mutations reported along the NCC protein revealed that the co-transporter is not glycosylated and thus, is not present at the plasma membrane.[138] It is known that preventing NCC glycosylation remarkably reduces the activity of the co-transporter due to deficient insertion into the plasma membrane.[97] Later studies of more mutants of NCC[139,140] showed that some missense mutations in NCC causing partially functional proteins are explained by a defect in the trafficking of the co-transporter to the plasma membrane which possesses normal functional and kinetic properties, but in which insertion into plasma membrane is seriously impaired.

Bartter's Disease

The characteristic clinical picture of Bartter's syndrome includes a salt-wasting state with low blood pressure due to dehydration, metabolic alkalosis with hypokalemia, hypercalciuira, hypereninemia, and secondary aldosteronism.[255] This picture is clearly due to a reduction in the salt transporting capacity of the TAL. The disease is usually apparent at birth or even earlier, due to excessive accumulation of amniotic fluid (polyhydramnios). A striking difference with Gitelman's disease is that Bartter's patients exhibit hypercalciuria and some develop nephrocalcinosis (Table 32.7), while in Gitelman's syndrome the expected presentation is hypocalciuria. Although Bartter's disease is monogenic, it is heterogeneous, because mutations in five different genes expressed in TAL can produce a very similar disease. Of these, three are directly involved in salt reabsorption in TAL and two other genes modulate the activity and/or trafficking of salt transporters. Thus, Bartter's disease is classified into five types. Types I to IV (Table 32.7) are the consequence of inactivating mutations of NKCC2 (type I), the potassium channel ROMK (type II), the basolateral Cl^- channel CLC-KB (type III), and the CLC-KB chaperon protein Barttin (type IV).[66,107,256–258] The absence of ROMK prevents NKCC2 activity, because recycling of potassium to the TAL lumen is prevented. Reduction of CLC-KB activity, due to mutations on the channel or because of the absence of barttin, probably decreases the activity of NKCC2, because the co-transporter is sensitive to intracellular chloride concentration.[186] Bartter's disease type V is the result of activating mutations in the calcium sensing receptor located in the basolateral membrane.[64,259–261] The

TABLE 32.7 Clinical Presentation of Patients with Bartter's Disease According To Genomic Classification in Types I to IV

	Type I	Type II	Type III	Type IV
Affected gene	SLC12A1	KCNJ1/ROMK	ClCNKB	BSND
Age of onset	Neonatal	Neonatal	First decade	Neonatal
Polyhydramnios	Yes	Yes	No	Yes
Sensorineural deafness	Rare	Rare	No	Yes
Poliuria	Yes	Yes	Uncommon	Yes
End-stage renal disease	No	No	No	Yes
Hypokalemia	Severe	Severe	Moderate	Severe
Metabolic alkalosis	Moderate	Moderate	Mild	Moderate
Nephrocalcinosis	Yes	Yes	No	Yes

stimulation of the calcium sensing receptor by extracellular calcium activates a second messenger cascade within the TAL that inhibits NKCC2 and ROMK. This way, an increase in extracellular calcium reduces salt reabsorption in the TAL that is followed by a reduction in calcium reabsorption, thus increasing calciuria. In patients with active mutations of the calcium sensing receptor, the receptor is activated with normal extracellular calcium concentration inducing a permanent reduction in NKCC2/ROMK activity. Bartter's disease in this case is usually a mild syndrome.

At present, nearly 75 different mutations of NKCC2 have been reported to be associated with Bartter's disease or with low blood pressure in an open population (see the human gene mutation data base at www.hgmd.or). It is possible to suggest the molecular nature of Bartter's syndrome just by analyzing the clinical picture, although a confirmation by specific gene sequencing is desirable (Table 32.7). For instance, all patients present hypokalemia and metabolic alkalosis, which are less severe in type III patients. Antenatal presentation and polyhydroamnios are much more often seen in Bartter's type I, II, and IV than in type III disease. Patients with type III disease do not develop nephrocalcinosis. Type IV is associated with deafness and development of chronic renal failure.[66,262] Therefore, age of clinical presentation and certain features such as nephrocalcinosis, deafness, and chronic renal failure help the clinician to identify of the appropriate molecular target.

Pseudohypoaldosteronism Type II/Familial Hypekalemia Hypertension

PHAII/FHH is the mirror image of Gitelman's disease. It is an autosomal dominant inherited disease featuring arterial hypertension with hyperkalemia, despite a normal glomerular filtration rate, and hyperchloremic metabolic acidosis as a consequence of decreased urinary H^+ excretion.[207,208] In addition, while Gitelman's patient's develop hypocalciuria, PHAII patients develop hypercalciuria.[263] This is translated into bone, because the first exhibit is increased bone mineral density,[264,265] whereas later a significant decrease in bone density develops.[266] As shown above, Gitelman's disease is the consequence of inactivating mutations of NCC. In contrast, all clinical features in PHAII patients are corrected by treatment with low dose, thiazide-type diuretics,[208,266] suggesting that increased activity of NCC is required for PHAII. No significant linkage was found between PHAII and the *SLC12A3* locus on chromosome 16,[267] eliminating the possibility that activating mutations of NCC are behind the development of this syndrome. Instead, four different genes have been shown to be the cause of PHAII. As discussed above, the gene responsible in families linked to chromosomes 12 and 17 have been observed to be WNK1 and WNK4, respectively.[206,268–274] Two other genes can be the cause of the disease: Kelch-like 3 (KLHL3) and cullin 3 (CUL3).[275] While KLHL3 mutations can be dominant or recessive, CUL3 are dominant and most of them are *de novo* mutations.

Extensive work has been done with WNKs regarding NCC modulation. Nothing is known yet regarding KLHK3 and CUL3 modulation of NCC activity. However, because most of the pathophysiology of PHAII seems to be explained by increased activity of NCC,[17,191,276,277] it is highly likely that these proteins modulate the activity of NCC. KLHL3 and CUL3 together form a protein complex that provides a RING-type of E3-ubiquitin ligase.[278] It has been demonstrated that the HECT-type of E3-ubiquitin ligase known as Nedd4-2 modulates NCC activity.[279] Thus, it is possible that the KLHL3–CUL3 complex regulates either NCC, some of the WNKs, or SPAK by ubiquitination or another known or unknown associated protein that in turn affects the activity of NCC.

WNK4 has been proposed to be a negative regulator of NCC activity that becomes a positive regulator when it harbors PHAII-type mutations.[209,210,212,213] A PHAII syndrome develops in BAC transgenic mice containing two wild-type WNK4 alleles and two PHAII-type mutant alleles,[214] indicating that haploinsufficiency does not explain the disease, because this model contains two wild-type WNK4 alleles. The disease is also present in a knockin mouse harboring WNK4 with a PHAII type mutation.[215] In these models, PHAII clinical features were rescued by treatment of mice with a thiazide-type diuretic, by crossing the mouse with the NCC null mice or with the SPAK knockin mice,[214,215,233] highlighting the importance of SPAK-NCC in producing the disease. Thus, it is possible that under certain conditions WNK4 inhibits NCC activity and in patients with PHAII mutations this inhibition is not present, leading to a chronic increase in the activity of NCC that produces arterial hypertension and hyperkalemia. One study proposed that PHAII mutations in WNK4 reconstitute the effect of angiotensin II upon the WNK4-SPAK-NCC cascade, suggesting that PHAII is a gain-of-function disease producing a state of hyperactivity of angiotensin II in the DCT.[17,196] There are, however, other proposals. One is that NCC activation is the result of altered interactions between the NCC activating WNK3 and the inhibitory WNK4.[241] The other, based on observations on hypomorphic WNK4 mice, is that WNK4 could be an activator of NCC that increases its potency by PHAII mutations.[280]

POTENTIAL ROLE IN POLYGENIC DISEASES

The physiological roles of sodium–chloride co-transporters and the diseases that are produced by their inactivating mutations or misregulation by WNKs support that they are implicated in the development of complex polygenic diseases, such as arterial hypertension. This is a highly prevalent disease (>20% of the adult population) with an important genetic component. NCC and NKCC2 are genes that clearly play a role in defining blood pressure levels, since inactivation of these transport proteins is associated with hypotension. Inhibition of NCC with thiazides is the base of the most recommended first line therapy for arterial hypertension.[281] Supporting the role of NCC or NKCC2 in defining blood pressure levels in an open population, a work based on genetic analysis of the Framingham Population Study sequenced the NCC, NKCC2, and ROMK genes in 3125 subjects. It was observed that 49 out of the 3125 exhibited a rare mutation in one allele of one these genes. This is 1.5% of the studied population. Subjects harboring such mutations have lower blood pressure, a reduced risk for developing hypertension, and a reduced risk of death due to cardiovascular disease.[282] Although several of the mutations detected in this study were not reported previously as causing Gitelman's or Bartter's disease, it was later shown that they indeed reduced the activity of NCC[283] or NKCC2.[283,284] A genome-wide association study in an Amish population revealed that SPAK or STK39 is a hypertension risk gene.[285] Thus, genome studies are beginning to reveal the role of SLC12A co-transporter genes in essential hypertension.

Osteoporosis is a polygenic disease of the skeleton that is secondary to a decrease in bone mineral density, with a disruption of the normal bone architecture and a consequent increase in the risk of fractures. Due to the functional interaction of NCC with calcium-transport mechanisms, this co-transporter is involved in renal calcium absorption. Inactivating mutations of NCC in Gitelman's disease are associated with high bone mineral density,[264,265] whereas activation of NCC in PHAII subjects is accompanied by decreased bone mineral density.[266] In addition, there is strong epidemiological evidence that hypertensive patients treated with thiazides are at a lower risk for osteoporosis.[27,28,286–288] In this regard, it has been shown that the NCC protein is expressed in osteoblasts in rat and human bones, and that addition of thiazides to osteoblast cells in culture increases the formation of mineralized nodules by a mechanism that may involve NCC.[19] Therefore, it is likely that osteoporosis is another polygenic disease in which this co-transporter could be implicated.

Acknowledgments

This chapter is dedicated with endless gratitude to the memory of my mentor Steven C. Hebert MD for his invaluable help and collaboration of over 20 years. Experimental work performed in the author's laboratory has been supported by The Mexican Council of Science and Technology (CONACYT), NIH grants DK36803 and DK064635, the Wellcome Trust, The Foundation Leducq for the Transatlantic Network on Hypertension–Renal Salt Handling in the Control of Blood Pressure.

References

[1] Hediger MA, Romero MF, Peng JB, Rolfs A, Takanaga H, Bruford EA. The ABCs of solute carriers: physiological, pathological and therapeutic implications of human membrane transport proteins. Introduction. Pflugers Arch 2004;447:465–8.

[2] Gamba G, Saltzberg SN, Lombardi M, Miyanoshita A, Lytton J, Hediger MA, et al. Primary structure and functional expression of a cDNA encoding the thiazide-sensitive, electroneutral sodium-chloride co-transporter. Proc Natl Acad Sci USA 1993;90:2749–53.

[3] Gamba G, Miyanoshita A, Lombardi M, Lytton J, Lee WS, Hediger MA, et al. Molecular cloning, primary structure and characterization of two members of the mammalian electroneutral sodium-(potassium)-chloride co-transporter family expressed in kidney. J Biol Chem 1994;269:17713–22.

[4] Xu J-C, Lytle C, Zhu TT, Payne JA, Benz Jr E, Forbush III B. Molecular cloning and functional expression of the bumetanide-sensitive Na-K-Cl co-transporter. Proc Natl Acad Sci USA 1994;91:2201–5.

[5] Payne JA, Forbush III B. Alternatively spliced isoforms of the putative renal Na-K-Cl co-transporter are differentially distributed within the rabbit kidney. Proc Natl Acad Sci USA 1994;91:4544–8.

[6] Delpire E, Rauchman MI, Beier DR, Hebert SC, Gullans SR. Molecular cloning and chromosome localization of a putative basolateral Na^+-K^+-$2Cl^-$ co-transporter from mouse inner medullary collecting duct (mIMCD-3) cells. J Biol Chem 1994;269:25677–83.

[7] Gamba G. Molecular physiology and pathophysiology of the electroneutral cation-chloride co-transporters. Physiol Rev 2005;85:423–93.

[8] Hebert SC, Mount DB, Gamba G. Molecular physiology of cation-coupled Cl(−) co-transport: the SLC12 family. Pflugers Arch 2004;447:580–93.

[9] Gillen CM, Brill S, Payne JA, Forbush III B. Molecular cloning and functional expression of the K-Cl co-transporter from rabbit, rat and human. A new member of the cation-chloride co-transporter family. J Biol Chem 1996;271:16237–44.

[10] Payne JA, Stevenson TJ, Donaldson LF. Molecular characterization of a putative K-Cl co-transporter in rat brain. A neuronal-specific isoform. J Biol Chem 1996;271:16245–52.

[11] Hiki K, D'Andrea RJ, Furze J, Crawford J, Woollatt E, Sutherland GR, et al. Cloning, characterization, and chromosomal location of a novel human K^+-Cl^- co-transporter. J Biol Chem 1999;274:10661–7.

[12] Mount DB, Mercado A, Song L, Xu J, George Jr AL, Delpire E, et al. Cloning and characterization of KCC3 and KCC4, new members of the cation-chloride co-transporter gene family. J Biol Chem 1999;274:16355–62.

[13] Mount DB, Baekgard A, Hall AE, Plata C, Xu J, Beier DR, et al. Isoforms of the Na-K-2Cl transporter in murine TAL I.

Molecular characterization and intrarenal localization. Am J Physiol (Renal Physiol) 1999;276:F347–58.
[14] Igarashi P, Vanden Heuver GB, Payne JA, Forbush III B. Cloning, embryonic expression, and alternative splicing of a murine kidney-specific Na-K-Cl co-transporter. Am J Physiol (Renal Fluid Electrolyte Physiol) 1995;269:F406–18.
[15] Russell JM. Sodium-potassium-chloride co-transport. Physiol Rev 2000;80:211–76.
[16] Kahle KT, Staley KJ, Nahed BV, Gamba G, Hebert SC, Lifton RP, et al. Roles of the cation-chloride co-transporters in neurological disease. Nat Clin Pract Neurol 2008;4:490–503.
[17] Gamba G. The thiazide-sensitive Na^+-Cl^- co-transporter: molecular biology, functional properties, and regulation by WNKs. Am J Physiol Renal Physiol 2009;297:F838–48.
[18] Bazzini C, Vezzoli V, Sironi C, Dossena S, Ravasio A, Debiasi S, et al. Thiazide-sensitive NaCl co-transporter in the intestine: possible role of HCTZ in the intestinal Ca^{2+} uptake. J Biol Chem 2005;280:19902–10.
[19] Dvorak MM, De Joussineau C, Carter DH, Pisitkun T, Knepper MA, Gamba G, et al. Thiazide diuretics directly induce osteoblast differentiation and mineralized nodule formation by interacting with a sodium chloride co-transporter in bone. J Am Soc Nephrol 2007;18:2509–16.
[20] Chee KN, Vorontsova I, Lim JC, Kistler J, Donaldson PJ. Expression of the sodium potassium chloride co-transporter (NKCC1) and sodium chloride co-transporter (NCC) and their effects on rat lens transparency. Mol Vis 2010;16:800–12.
[21] Deng L, Chen G. Cyclothiazide potently inhibits gamma-aminobutyric acid type a receptors in addition to enhancing glutamate responses. Proc Natl Acad Sci USA 2003;100:13025–9.
[22] Clader JA, Schacheter M, Sever PS. Direct vascular actions of hydrochlorothaizide and indapamide in isolated small vessels. Eur J Pharmacol 1992;220:19–26.
[23] Bernstein PL, Zawalach W, Bartiss A, Reilly R, Palcso M, Ellison DH. The thiazide-sensitive Na-Cl co-transporter is expressed in rat endocrine pancreas. J Am Soc Nephrol 1995;6:732.
[24] Abuladze N, Yanagawa N, Lee I, Jo OD, Newman D, Hwang J, et al. Peripheral blood mononuclear cells express mutated NCCT mRNA in Gitelman's syndrome: evidence for abnormal thiazide-sensitive NaCl co-transport. J Am Soc Nephrol 1998;9:819–26.
[25] Cremaschi D, Porta C, Botta G, Bazzini C, Baroni MD, Garavaglia M. Apical $Na(^+)$-$Cl(^-)$ symport in rabbit gallbladder epithelium: a thiazide- sensitive co-transporter (TSC). J Membr Biol 2000;176:53–65.
[26] Drewnowska K, Baumgarten CM. Regulation of cellular volume in rabbit ventricular myocytes: Bumetanide, chlorthiazide, and ouabain. *Am J Physiol* (*Cell Physiol*) 1991;260:C122–31.
[27] Jones G, Nguyen T, Sambrook PN, Eisman JA. Thiazide diuretics and fractures: can meta-analysis help? J Bone Miner Res 1995;10:106–11.
[28] Schoofs MW, van der KM, Hofman A, de Laet CE, Herings RM, Stijnen T, et al. Thiazide diuretics and the risk for hip fracture. Ann Intern Med 2003;139:476–82.
[29] Mount DB, Gamba G. Renal potassium-chloride co-transporters. Curr Opin Nephrol Hypertens 2001;10:685–91.
[30] Mercado A, Vazquez N, Song L, Cortes R, Enck AH, Welch R, et al. Amino-terminal heterogeneity in the KCC3 K^+-Cl^- co-transporter. Am J Physiol Renal Physiol 2005;289:F1246–61.
[31] Boettger T, Hubner CA, Maier H, Rust MB, Beck FX, Jentsch TJ. Deafness and renal tubular acidosis in mice lacking the K-Cl co-transporter Kcc4. Nature 2002;416:874–8.
[32] Jentsch TJ. Chloride transport in the kidney: lessons from human disease and knockout mice. J Am Soc Nephrol 2005;16:1549–61.
[33] Hewett D, Samuelsson L, Polding J, Enlund F, Smart D, Cantone K, et al. Identification of a psoriasis susceptibility candidate gene by linkage disequilibrium mapping with a localized single nucleotide polymorphism map. Genomics 2002;79:305–14.
[34] Huffmeier U, Lascorz J, Traupe H, Bohm B, Schurmeier-Horst F, Stander M, et al. Systematic linkage disequilibrium analysis of SLC12A8 at PSORS5 confirms a role in susceptibility to psoriasis vulgaris. J Invest Dermatol 2005;125:906–12.
[35] Daigle ND, Carpentier GA, Frenette-Cotton R, Simard MG, Lefoll MH, Noel M, et al. Molecular characterization of a human cation-Cl^- co-transporter (SLC12A8A, CCC9A) that promotes polyamine and amino acid transport. J Cell Physiol 2009;220:680–9.
[36] Caron L, Rousseau F, Gagnon E, Isenring P. Cloning and functional characterization of a cation C1-co-transporter interacting protein. J Biol Chem 2000;275:32027–36.
[37] Lang F, Busch GL, Ritter M, Volkl H, Waldegger S, Gulbins E, et al. Functional significance of cell volume regulatory mechanisms. Physiol Rev 1998;78:247–306.
[38] Mercado A, Mount DB, Gamba G. Electroneutral cation-chloride co-transporters in the central nervous system. Neurochem Res 2004;29:17–25.
[39] Blaesse P, Airaksinen MS, Rivera C, Kaila K. Cation-chloride co-transporters and neuronal function. Neuron 2009;61:820–38.
[40] Kunau RT, Weller DR, Webb HL. Clarification of the site of action of chlorothiazide in the rat nephron. J Clin invest 1975;56:401–7.
[41] Velazquez H, Good DW, Wright FS. Mutual dependence of sodium and chloride absorption by renal distal tubule. Am J Physiol (Renal Fluid Electrolyte Physiol) 1984;247:F904–11.
[42] Costanzo LS. Localization of diuretic action in microperfused rat distal tubules: Ca and Na transport. Am J Physiol (Renal Fluid Electrolyte Physiol) 1985;248:F527–35.
[43] Ellison DH, Velazquez H, Wright FS. Thiazide-sensitive sodium chloride co-transport in early distal tubule. Am J Physiol (Renal Fluid Electrolyte Physiol) 1987;253:F546–54.
[44] Plotkin MD, Kaplan MR, Verlander JM, Lee W-S, Brown D, Poch E, et al. Localization of the thiazide sensitive Na-Cl co-transporter, rTSC1, in the rat kidney. Kidney Int 1996;50:174–83.
[45] Loffing J, Kaissling B. Sodium and calcium transport pathways along the mammalian distal nephron: from rabbit to human. Am J Physiol Renal Physiol 2003;284:F628–43.
[46] Loffing J, Loffing-Cueni D, Valderrabano V, Klausli L, Hebert SC, Rossier BC, et al. Distribution of transcellular calcium and sodium transport pathways along mouse distal nephron. Am J Physiol Renal Physiol 2001;281:F1021–7.
[47] Obermuller N, Bernstein P, Velázquez H, Reilly R, Moser D, Ellison DH, et al. Expression of the thiazide-sensitive Na-Cl co-transporter in rat and human kidney. Am J Physiol (Renal Fluid Electrolyte Physiol) 1995;269:F900–10.
[48] Campean V, Kricke J, Ellison D, Luft FC, Bachmann S. Localization of thiazide-sensitive $Na(^+)$-$Cl(^-)$ co-transport and associated gene products in mouse DCT. Am J Physiol Renal Physiol 2001;281:F1028–35.
[49] Reilly RF, Ellison DH. Mammalian distal tubule: physiology, pathophysiology, and molecular anatomy. Physiol Rev 2000;80:277–313.
[50] Bostanjoglo M, Reeves WB, Reilly RF, Velazquez H, Robertson N, Litwack G, et al. 11 Beta-hydroxysteroid dehydrogenase, mineralocorticoid receptor, and thiazide-sensitive Na-Cl co-transporter expression by distal tubules. J Am Soc Nephrol 1998;9:1347–58.

[51] Bonvalet JP, Doignon I, Blot-Chabaud M, Pradelles P, Farman N. Distribution of 11 beta-hydroxysteroid dehydrogenase along the rabbit nephron. J Clin Invest 1990;86:832–7.
[52] Rusvai E, Naray-Fejes-Toth A. A new isoform of 11 beta-hydroxysteroid dehydrogenase in aldosterone target cells. J Biol Chem 1993;268:10717–20.
[53] Doucet A. Function and control of Na-K-ATPase in single nephron segments of the mammalian kidney. Kidney Int 1988;34:749–60.
[54] Xu JZ, Hall AE, Peterson LN, Bienkowski MJ, Eessalu TE, Hebert SC. Localization of the ROMK protein on apical membranes of rat kidney nephron segments. Am J Physiol Renal Physiol 1997;273:F739–49.
[55] Amorim JB, Bailey MA, Musa-Aziz R, Giebisch G, Malnic G. Role of luminal anion and pH in distal tubule potassium secretion. Am J Physiol Renal Physiol 2003;284:F381–8.
[56] Stokes JB, Lee I, D'Amico M. Sodium chloride absorption by the urinary bladder of the winter flounder. A thiazide-sensitive, electrically neutral transport system. J Clin invest 1984;74:7–16.
[57] Rose BD. Diuretics. Kidney Int 1991;39:336–52.
[58] Gamba G. Molecular biology of distal nephron sodium transport mechanisms. Kidney Int 1999;56:1606–22.
[59] Greger R. Chloride reabsorption in the rabbit cortical thick ascending limb of the loop of Henle. A sodium dependent process. Pflugers Arch 1981;390:38–43.
[60] Greger R, Schlatter E. Presence of luminal K^+, a prerequisite for active NaCl transport in the cortical thick ascending limb of Henle's loop of rabbit kidney. Pflugers Arch 1981;392:92–4.
[61] Greger R, Schlatter E, Lang F. Evidence for electroneutral sodium chloride co-transport in the cortical thick ascending limb of Henle's loop of rabbit kidney. Pflugers Arch 1983;396:308–14.
[62] Greger R, Schlatter E. Properties of the lumen membrane of the cortical thick ascending limb of Henle's loop of rabbit kidney. Pflugers Arch 1983;396:315–24.
[63] Hebert SC, Culpepper RM, Andreoli TE. NaCl transport in mouse medullary thick ascending limbs. I. Functional nephron heterogeneity and ADH-stimulated NaCl co-transport. Am J Physiol (Renal Fluid Electrolyte Physiol) 1981;241:F412–31.
[64] Gamba G, Friedman PA. Thick ascending limb: the $Na(^+)$:$K(^+)$:$2Cl(^-)$ co-transporter, NKCC2, and the calcium-sensing receptor, CaSR. Pflugers Arch 2009;458:61–76.
[65] Greger R. Ion transport mechanisms in thick ascending limb of Henle's loop of mammalian nephron. Physiol Rev 1985;65:760–97.
[66] Hebert SC. Bartter syndrome. Curr Opin Nephrol Hypertens 2003;12:527–32.
[67] Amlal H, Paillard M, Bichara M. $Cl(^-)$-dependent NH_4^+ transport mechanisms in medullary thick ascending limb cells. Am J Physiol 1994;267:C1607–15.
[68] Attmane-Elakeb A, Amlal H, Bichara M. Ammonium carriers in medullary thick ascending limb. Am J Physiol Renal Physiol 2001;280:F1–9.
[69] Schnermann J. Juxtaglomerular cell complex in the regulation of renal salt excretion. Am J Physiol (Regulatory Integrative Comp Physiol) 1998;274:R263–79.
[70] Nielsen S, Maunsbach AB, Ecelbarger CA, Knepper MA. Ultrastructural localization of Na-K-2Cl co-transporter in thick ascending limb and macula densa of rat kidney. Am J Physiol 1998;275:F885–93.
[71] Gimenez I, Isenring P, Forbush III B. Spatially distributed alternative splice variants of the renal Na-K-Cl co-transporter exhibit dramatically different affinities for the transported ions. J Biol Chem 2002;277:8767–70.
[72] Gagnon E, Forbush B, Flemmer AW, Gimenez I, Caron L, Isenring P. Functional and molecular characterization of the shark renal Na-K-Cl co-transporter: novel aspects. Am J Physiol Renal Physiol 2002;283:F1046–55.
[73] Oppermann M, Mizel D, Huang G, Li C, Deng C, Theilig F, et al. Macula densa control of renin secretion and preglomerular resistance in mice with selective deletion of the B isoform of the Na,K,2Cl co-transporter. J Am Soc Nephrol 2006;17:2143–52.
[74] Oppermann M, Mizel D, Kim SM, Chen L, Faulhaber-Walter R, Huang Y, et al. Renal function in mice with targeted disruption of the a isoform of the Na-K-2Cl co-transporter. J Am Soc Nephrol 2007;18:440–8.
[75] Hebert SC, Culpepper RM, Andreoli TE. NaCl transport in mouse medullary thick ascending limbs. II. ADH enhancement of transcellular NaCl cotrasport; origin of transepithelial voltage. Am J Physiol (Renal Fluid Electrolyte Physiol) 1981;241: F432–42.
[76] Hebert SC, Culpepper RM, Andreoli TE. NaCl transport in mouse medullary thick ascending limbs. III. Modulation of ADH efect by peritubular osmolality. Am J Physiol (Renal Fluid Electrolyte Physiol) 1981;241:F443–51.
[77] Gimenez I, Forbush B. Short-term stimulation of the renal Na-K-Cl co-transporter (NKCC2) by vasopressin involves phosphorylation and membrane translocation of the protein. J Biol Chem 2003;278:26946–51.
[78] Plata C, Mount DB, Rubio V, Hebert SC, Gamba G. Isoforms of the Na-K-2Cl co-transporter in murine TAL. II. Functional characterization and activation by cAMP. Am J Physiol (Renal Physiol) 1999;276:F359–66.
[79] Meade P, Hoover RS, Plata C, Vazquez N, Bobadilla NA, Gamba G, et al. cAMP-dependent activation of the renal-specific Na^+-K^+-$2Cl^-$ co-transporter is mediated by regulation of co-transporter trafficking. Am J Physiol Renal Physiol 2003;284: F1145–54.
[80] Ortiz PA. cAMP increases surface expression of NKCC2 in rat thick ascending limbs: role of VAMP. Am J Physiol Renal Physiol 2006;290:F608–16.
[81] Caceres PS, Ares GR, Ortiz PA. cAMP stimulates apical exocytosis of the renal Na-K-2Cl co-transporter NKCC2 in the thick ascending limb: Role of protein kinase A (PKA). J Biol Chem 2009;284:24965–71.
[82] Kim G-H, Ecelbarger CA, Mitchell C, Packer RK, Wade JB, Knepper MA. Vasopressin increases Na-K-2Cl co-transporter expression in thick ascending limb of Henle's loop. Am J Physiol (Renal Physiol) 1999;276:F96–103.
[83] Knepper MA, Kim GH, Fernandez-Llama P, Ecelbarger CA. Regulation of thick ascending limb transport by vasopressin. J Am Soc Nephrol 1999;10:628–34.
[84] Alvarez-Leefmans FJ. Intracellular chloride regulation. 3rd ed. 2001:301-318.
[85] Delpire E, Mount DB. Human and murine phenotypes associated with defects in cation-chloride co-transport. Annu Rev Physiol 2002;64:803–43.
[86] Flagella M, Clarke LL, Miller ML, Erway LC, Giannella RA, Andringa A, et al. Mice lacking the basolateral Na-K-2Cl co-transporter have impaired epithelial chloride secretion and are profoundly deaf. J Biol Chem 1999;274:26946–55.
[87] Delpire E, Lu J, England R, Dull C, Thorne T. Deafness and imbalance associated with inactivation of the secretory Na-K-2Cl co-transporter. Nat Genet 1999;22:192–5.
[88] Orlov SN, Tremblay J, Hamet P. NKCC1 and hypertension: a novel therapeutic target involved in the regulation of vascular tone and renal function. Curr Opin Nephrol Hypertens 2010;19:163–8.

[89] Meyer JW, Flagella M, Sutliff RL, Lorenz JN, Nieman ML, Weber CS, et al. Decreased blood pressure and vascular smooth muscle tone in mice lacking basolateral $Na(^+)$-$K(^+)$-2Cl $(^-)$ co-transporter. Am J Physiol Heart Circ Physiol 2002;283: H1846–55.

[90] Wall SM, Knepper MA, Hassell KA, Fischer MP, Shodeinde A, Shin W, et al. Hypotension in NKCC1 null mice: role of the kidneys. Am J Physiol Renal Physiol 2006;290:F409–16.

[91] Garg P, Martin CF, Elms SC, Gordon FJ, Wall SM, Garland CJ, et al. Effect of the Na-K-2Cl co-transporter NKCC1 on systemic blood pressure and smooth muscle tone. Am J Physiol Heart Circ Physiol 2007;292:H2100–5.

[92] Koltsova SV, Kotelevtsev SV, Tremblay J, Hamet P, Orlov SN. Excitation-contraction coupling in resistance mesenteric arteries: evidence for NKCC1-mediated pathway. Biochem Biophys Res Commun 2009;379:1080–3.

[93] Kim SM, Eisner C, Faulhaber-Walter R, Mizel D, Wall SM, Briggs JP, et al. Salt sensitivity of blood pressure in NKCC1-deficient mice. Am J Physiol Renal Physiol 2008;295:F1230–8.

[94] Kaplan MR, Plotkin MD, Brown D, Hebert SC, Delpire E. Expression of the mouse Na-K-2Cl co-transporter, mBSC2, in the terminal inner medullary collecting duct, the glomerular and extraglomerular masangium, and the glomerular afferent arteriole. J Clin invest 1996;98:723–30.

[95] Castrop H, Lorenz JN, Hansen P, Friis U, Mizel D, Oppermann M, et al. Contribution of the basolateral isoform of the Na, K,2Cl-co-transporter (NKCC1/BSC2) to renin secretion. Am J Physiol Renal Physiol 2005;289:F1185–92.

[96] Kyte J, Doolittle RF. A simple method for displaying the hydropathic character of a protein. J Mol Biol 1982;157:105–32.

[97] Hoover RS, Poch E, Monroy A, Vazquez N, Nishio T, Gamba G, et al. N-Glycosylation at two sites critically alters thiazide binding and activity of the rat thiazide-sensitive $Na(^+)$:$Cl(^-)$ co-transporter. J Am Soc Nephrol 2003;14:271–82.

[98] Moreno E, San Cristobal P, Rivera M, Vazquez N, Bobadilla NA, Gamba G. Affinity defining domains in the Na-Cl co-transporter: different location for Cl^- and thiazide binding. J Biol Chem 2006;281:17266–75.

[99] Paredes A, Plata C, Rivera M, Moreno E, Vazquez N, Munoz-Clares R, et al. Activity of the renal Na^+:K^+:$2Cl^-$ co-transporter is reduced by mutagenesis of N-glycosylation sites: role for protein surface charge in Cl^- transport. Am J Physiol Renal Physiol 2006;290:F1094–102.

[100] Merino A, Hebert SC, Gamba G. Correlation between water salinity and tissue expression of the thiazide-sensitive co-transporter (TSC) in teleost. J Am Soc Nephrol 1999;10:39A.

[101] Velazquez H, Naray-Fejes-Toth A, Silva T, Andujar E, Reilly RF, Desir GV, et al. Rabbit distal convoluted tubule coexpresses NaCl co-transporter and 11 beta-hydroxysteroid dehydrogenase II mRNA. Kidney Int 1998;54:464–72.

[102] Simon DB, Nelson-Williams C, Johnson-Bia M, Ellison D, Karet FE, Morey-Molina A, et al. Gitelman's variant of Bartter's syndrome, inherited hypokalaemic alkalosis, is caused by mutations in the thiazide-sensitive Na-Cl co-transporter. Nature Genetics 1996;12:24–30.

[103] Mastroianni N, DeFusco M, Zollo M, Arrigo G, Zuffardi O, Bettinelli A, et al. Molecular cloning, expression pattern, and chromosomal localization of the human Na-Cl thiazide-sensitive co-transporter (SLC12A3). Genomics 1996;35:486–93.

[104] Di Fulvio M, Alvarez-Leefmans FJ. The NKCC and NCC genes: an *in silico* view. In: Alvarez-Leefmans FJ, Delpire E, editors. Physiology and pathology of chloride transporters and channels in the nervous system. New York: Elsevier; 2009. p. 169–208.

[105] Cutler CP, Cramb G. Differential expression of absorptive cation-chloride-co-transporters in the intestinal and renal tissues of the European eel (*Anguilla anguilla*). Comp Biochem Physiol B Biochem Mol Biol 2008;149:63–73.

[106] Gonzales PA, Pisitkun T, Hoffert JD, Tchapyjnikov D, Star RA, Kleta R, et al. Large-scale proteomics and phosphoproteomics of urinary exosomes. J Am Soc Nephrol 2009;20:363–79.

[107] Simon DB, Karet FE, Hamdan JM, Di Pietro A, Sanjad SA, Lifton RP. Bartter's syndrome, hypokalaemic alkalosis with hypercalciuria, is caused by mutations in the Na-K-2Cl co-transporter NKCC2. Nature Genetics 1996;13:183–8.

[108] Igarashi P, Whyte DA, Kui L, Nagami GT. Cloning and kidney cell-specific activity of the promoter of the murine renal Na-K-Cl co-transporter gene. J Biol Chem 1996;271:9666–74.

[109] Gamba G. Alternative splicing and diversity of renal transporters. Am J Physiol Renal Physiol 2001;281:F781–94.

[110] Yang T, Huang YG, Singh I, Schnermann J, Briggs JP. Localization of bumetanide- and thiazide-sensitive Na-K-Cl co-transporters along the rat nephron. Am J Physiol (Renal Fluid Electrolyte Physiol) 1996;271:F931–9.

[111] Plotkin MD, Kaplan MR, Peterson LN, Gullans SR, Hebert SC, Delpire E. Expression of the Na^+-K^+-$2Cl^-$ co-transporter BSC2 in the nervous system. Am J Physiol (Cell Physiol) 1997;272: C173–83.

[112] Moore-Hoon ML, Turner RJ. Molecular and topological characterization of the rat parotid Na^+-K^+-$2Cl^-$ co-transporter1. Biochim Biophys Acta 1998;1373:261–9.

[113] Payne JA, Xu J-C, Haas M, Lytle CY, Ward D, Forbush III B. Primary structure, functional expression, and chromosomal localization of the bumetanide-sensitive Na-K-Cl co-transporter in human colon. J Biol Chem 1995;270:17977–85.

[114] Yerby TR, Vibat CRT, Sun D, Payne JA, O'Donnell ME. Molecular characterization of the Na-K-Cl co-transporter of bovine aortic endothelial cells. Am J Physiol (Cell Physiol) 1997;273:C188–97.

[115] Cutler CP, Cramb G. Two isoforms of the $Na^+/K^+/2Cl^-$ co-transporter are expressed in the European eel (*Anguilla anguilla*). Biochim Biophys Acta 2002;1566:92–103.

[116] Lorin-Nebel C, Boulo V, Bodinier C, Charmantier G. The $Na^+/K^+/2Cl^-$ co-transporter in the sea bass *dicentrarchus labrax* during ontogeny: involvement in osmoregulation. J Exp Biol 2006;209:4908–22.

[117] Colmenero-Flores JM, Martinez G, Gamba G, Vazquez N, Iglesias DJ, Brumos J, et al. Identification and functional characterization of cation-chloride co-transporters in plants. Plant J 2007;50:278–92.

[118] Randall J, Thorne T, Delpire E. Partial cloning and characterization of Slc12a2: the gene encoding the secretory Na^+-K^+-$2Cl^-$ co-transporter. Am J Physiol (Cell Physiol) 1997;273: C1267–77.

[119] Vibat CR, Holland MJ, Kang JJ, Putney LK, O'Donnell ME. Quantitation of Na^+-K^+-$2Cl^-$ co-transport splice variants in human tissues using kinetic polymerase chain reaction. Anal Biochem 2001;298:218–30.

[120] Carmosino M, Gimenez I, Caplan M, Forbush B. Exon loss accounts for differential sorting of Na-K-Cl co-transporters in polarized epithelial cells. Mol Biol Cell 2008;19:4341–51.

[121] Wang J, Pravenec M, Kren V, Kurtz TW. Linkage mapping of the Na-K-2Cl co-transporter gene (Slc12a1) to rat chromosome 3. Mamm Genome 1997;8:379.

[122] Quaggin SE, Payne JA, Forbush III B, Igarashi P. Localization of the renal Na-K-Cl co-transporter gene (Slc12a1) on mouse chromosome 2. Mamm Genome 1995;6:557–8.

[123] Lazzaro D, De SV, De Magistris L, Lehtonen E, Cortese R. LFB1 and LFB3 homeoproteins are sequentially expressed during kidney development. Development 1992;114:469–79.

[124] Molony DA, Reeves WB, Hebert SC, Andreoli TE. ADH increases apical Na^+,K^+,$2Cl^-$ entry in mouse medullary thick ascending limbs of Henle. Am J Physiol (Renal Fluid Electrolyte Physiol) 1987;252:F177–87.

[125] Lee HA, Baek I, Seok YM, Yang E, Cho HM, Lee DY, et al. Promoter hypomethylation upregulates Na^+-K^+-$2Cl^-$ co-transporter 1 in spontaneously hypertensive rats. Biochem Biophys Res Commun 2010;396:252–7.

[126] Cho HM, Lee HA, Kim HY, Han HS, Kim IK. Expression of Na^+-K^+-$2Cl^-$ co-transporter 1 is epigenetically regulated during postnatal development of hypertension. Am J Hypertens 2011;24:1286–93.

[127] Taniyama Y, Sato K, Sugawara A, Uruno A, Ikeda Y, Kudo M, et al. Renal tubule-specific transcription and chromosomal localization of rat thiazide-sensitive Na-Cl co-transporter gene. J Biol Chem 2001;276:26260–8.

[128] Pathak BG, Shaughnessy Jr JD, Meneton P, Greeb J, Shull GE, Jenkins NA, et al. Mouse chromosomal location of three epithelial sodium channel subunit genes and an apical sodium chloride co-transporter gene. Genomics 1996;33:124–7.

[129] MacKenzie S, Vaitkevicius H, Lockette W. Sequencing and characterization of the human thiazide-sensitive Na-Cl co-transporter (SLC12A3) gene promoter. Biochem Biophys Res Commun 2001;282:991–1000.

[130] Kim GH, Martin SW, Fernandez-Llama P, Masilamani S, Packer RK, Knepper MA. Long-term regulation of renal Na-dependent co-transporters and ENaC: response to altered acid–base intake. Am J Physiol Renal Physiol 2000;279:F459–67.

[131] Fanestil DD, Vaughan DA, Blakely P. Metabolic acid–base influences on renal thiazide receptor density. Am J Physiol (Regulatory Integrative Comp Physiol) 1997;272:R2004–8.

[132] O'Grady SM, Palfrey HC, Field M. Characteristics and function of Na-K-Cl co-transport in epithelial tissues. Am J Physiol (Cell Physiol) 1987;253:C177–92.

[133] Bachmann S, Bostanjoglo M, Schmitt R, Ellison DH. Sodium transport-related proteins in the mammalian distal nephron – distribution, ontogeny and functional aspects. Anat Embryol (Berl) 1999;200:447–68.

[134] Haas M. Properties and diversity of (Na-K-Cl) co-transporters. Annu Rev Physiol 1989;51:443–57.

[135] Haas M, Dunham PB, Forbush III B. [^{3}H]Bumetanide binding to mouse kidney membranes: identification of corresponding membrane proteins. Am J Physiol (Cell Physiol) 1991;260: C791–804.

[136] Fanestil DD, Tran JM, Vaughn DA, Maciejewski AR, Beaumont K. Investigation of the metolazone receptor 1990:195–204.

[137] Monroy A, Plata C, Hebert SC, Gamba G. Characterization of the thiazide-sensitive $Na(^+)$-$Cl(^-)$ co-transporter: a new model for ions and diuretics interaction. Am J Physiol Renal Physiol 2000;279:F161–9.

[138] Kunchaparty S, Palcso M, Berkman J, Velazquez H, Desir GV, Bernstein P, et al. Defective processing and expression of thiazide-sensitive Na-Cl co-transporter as a cause of Gitelman's syndrome. Am J Physiol 1999;277:F643–9.

[139] Sabath E, Meade P, Berkman J, De Los Heros P, Moreno E, Bobadilla NA, et al. Pathophysiology of functional mutations of the thiazide-sensitive Na-Cl co-transporter in Gitelman disease. Am J Physiol Renal Physiol 2004;287:F195–203.

[140] De Jong JC, Van Der Vliet WA, van den Heuvel LP, Willems PH, Knoers NV, Bindels RJ. Functional expression of mutations in the human NaCl co-transporter: evidence for impaired routing mechanisms in Gitelman's syndrome. J Am Soc Nephrol 2002;13:1442–8.

[141] De Jong JC, Willems PH, van den Heuvel LP, Knoers NV, Bindels RJ. Functional expression of the human thiazide-sensitive NaCl co-transporter in Madin–Darby canine kidney cells. J Am Soc Nephrol 2003;14:2428–35.

[142] Richardson C, Rafiqi FH, Karlsson HK, Moleleki N, Vandewalle A, Campbell DG, et al. Activation of the thiazide-sensitive Na^+-Cl^- co-transporter by the WNK-regulated kinases SPAK and OSR1. J Cell Sci 2008;121:675–84.

[143] Ko B, Joshi LM, Cooke LL, Vazquez N, Musch MW, Hebert SC, et al. Phorbol ester stimulation of RasGRP1 regulates the sodium-chloride co-transporter by a PKC-independent pathway. Proc Natl Acad Sci USA 2007;104:20120–5.

[144] Ko B, Kamsteeg EJ, Cooke LL, Moddes LN, Deen PM, Hoover RS. RasGRP1 stimulation enhances ubiquitination and endocytosis of the sodium-chloride co-transporter. Am J Physiol Renal Physiol 2010;299:F300–9.

[145] Gesek FA, Friedman PA. Mechanism of calcium transport stimulated by chlorothiazide in mouse distal convoluted tubule cells. J Clin Invest 1992;90:429–38.

[146] Vazquez N, Monroy A, Dorantes E, Munoz-Clares RA, Gamba G. Functional differences between flounder and rat thiazide-sensitive Na-Cl co-transporter. Am J Physiol Renal Physiol 2002;282:F599–607.

[147] Tran JM, Farrell MA, Fanestil DD. Effect of ions on binding of the thiazide-type diuretic metolazone to kidney membrane. Am J Physiol (Renal Fluid Electrolyte Physiol) 1990;258:F908–15.

[148] Chang H, Fujita T. A kinetic model of the thaizide-sensitive Na-Cl co-transporter. Am J Physiol (Renal Physiol) 1999;276: F952–9.

[149] Starremans PG, Kersten FF, Knoers NV, van den Heuvel LP, Bindels RJ. Mutations in the human Na-K-2Cl Co-transporter (NKCC2) identified in Bartter syndrome Type I consistently result in nonfunctional transporters. J Am Soc Nephrol 2003;14:1419–26.

[150] Burg MB. Thick ascending limb of Henle's loop. Kidney Int 1982;22:454–64.

[151] Rocha AS, Kokko JP. Sodium chloride and water transport in the medullary thick ascending limb of Henle. Evidence for active chloride transport. J Clin Invest 1973;52:612–23.

[152] Reeves WB, Molony DA, Andreoli TE. Diluting power of thick limbs of Henle. III. Modulation of *in vitro* diluting power. Am J Physiol 1988;255:F1145–54.

[153] Plata C, Meade P, Vazquez N, Hebert SC, Gamba G. Functional properties of the apical Na^+-K^+-$2Cl^-$ co-transporter isoforms. J Biol Chem 2002;277:11004–12.

[154] Marcano M, Yang HM, Nieves-Gonzalez A, Clausen C, Moore LC. Parameter estimation for mathematical models of NKCC2 co-transporter isoforms. Am J Physiol Renal Physiol 2009;296: F369–81.

[155] Plata C, Meade P, Hall AE, Welch RC, Vazquez N, Hebert SC, et al. Alternatively spliced isoform of the apical Na-K-Cl co-transporter gene encodes a furosemide sensitive Na-Cl co-transporter. Am J Physiol Renal Physiol 2001;280:F574–82.

[156] Eveloff J, Calamia J. Effect of osmolarity on cation fluxes in medullary thick ascending limb cells. Am J Physiol (Renal Fluid Electrolyte Physiol) 1986;250:F176–80.

[157] Alvo M, Calamia J, Eveloff J. Lack of potassium effect on Na-Cl co-transport in the medullary thick ascending limb. Am J Physiol (Renal Fluid Electrolyte Physiol) 1985;249:F34–9.

[158] Sun A, Grossman EB, Lombardi M, Hebert SC. Vasopressin alters the mechanism of apical Cl^- entry from Na^+:Cl^- to Na^+:K^+:$2Cl^-$ co-transport in mouse medullary thick ascending limb. J Membrane Biol 1991;120:83–94.

[159] Gerelsaikhan T, Turner RJ. Transmembrane topology of the secretory Na^+-K^+-$2Cl^-$ co-transporter (NKCC1) studied by *in vitro* translation. J Biol Chem 2000;275:40471–7.
[160] Isenring P, Forbush B. Ion transport and ligand binding by the Na-K-Cl co-transporter, structure–function studies. Comp Biochem Physiol A Mol Integr Physiol 2001;130:487–97.
[161] Tovar-Palacio C, Bobadilla NA, Cortes P, Plata C, De Los Heros P, Vazquez N, et al. Ion and diuretic specificity of chimeric proteins between apical Na^+:K + :$2Cl^-$ and Na^+:Cl^- co-transporters. Am J Physiol Renal Physiol 2004;287:F570–7.
[162] Gimenez I, Forbush B. The residues determining differences in ion affinities among the alternative splice variants F, A, and B of the mammalian renal Na-K-Cl co-transporter (NKCC2). J Biol Chem 2007;282:6540–7.
[163] Gagnon E, Bergeron MJ, Daigle ND, Lefoll MH, Isenring P. Molecular mechanisms of cation transport by the renal Na^+-K^+-Cl^- co-transporter: structural insight into the operating characteristics of the ion transport sites. J Biol Chem 2005;280:32555–63.
[164] Isenring P, Forbush III B. Ion and bumetanide binding by the Na-K-Cl co-transporter. Importance of transmembrane domains. J Biol Chem 1997;272:24556–62.
[165] Isenring P, Jacoby SC, Forbush III B. The role of transmembrane domain 2 in cation transport by the Na-K-Cl co-transporter. Proc Natl Acad Sci USA 1998;95:7179–84.
[166] Isenring P, Jacoby SC, Chang J, Forbush III B. Mutagenic mapping of the Na-K-Cl co-transporter for domains involved in ion transport and bumetanide binding. J Gen Physiol 1998;112:549–58.
[167] Forbush III B, Palfrey HC. [^{3}H]Bumetanide binding to membranes isolated from dog kidney outer medulla. Relationship to the Na,K,Cl co-transport system. J Biol Chem 1983;258:11787–92.
[168] Gagnon E, Bergeron MJ, Brunet GM, Daigle ND, Simard CF, Isenring P. Molecular mechanisms of Cl transport by the renal Na-K-Cl co-transporter: identification of an intracellular locus that may form part of a high affinity Cl-binding site. J Biol Chem 2003;279:5648–54.
[169] Malysiak K, Grzywna ZJ. On the possible methods for the mathematical description of the ball and chain model of ion channel inactivation. Cell Mol Biol Lett 2008;13:535–52.
[170] Castaneda-Bueno M, Vazquez N, Bustos-Jaimes I, Hernandez D, Rodriguez-Lobato E, Pacheco-Alvarez D, et al. A single residue in transmembrane domain 11 defines the different affinity for thiazides between mammalian and flounder NaCl transporter. Am J Physiol Renal Physiol 2010;299:F1111–9.
[171] Moreno E, Tovar-Palacio C, De Los Heros P, Guzman B, Bobadilla NA, Vazquez N, et al. A single nucleotide polymorphism alters the activity of the renal Na^+:Cl^- co-transporter and reveals a role for transmembrane segment 4 in chloride and thiazide affinity. J Biol Chem 2004;279:16553–60.
[172] Vormfelde SV, Sehrt D, Toliat MR, Schirmer M, Meineke I, Tzvetkov M, et al. Genetic variation in the renal sodium transporters NKCC2, NCC, and ENaC in relation to the effects of loop diuretic drugs. Clin Pharmacol Ther 2007;82:300–9.
[173] Nezu A, Parvin MN, Turner RJ. A conserved hydrophobic tetrad near the C terminus of the secretory Na^+-K^+-$2Cl^-$ co-transporter (NKCC1) is required for its correct intracellular processing. J Biol Chem 2009;284:6869–76.
[174] Zaarour N, Demaretz S, Defontaine N, Mordasini D, Laghmani K. A highly conserved motif at the C-terminus dictates ER exit and cell-surface expression of NKCC2. J Biol Chem 2009;284:21752–64.
[175] Zaarour N, Defontaine N, Demaretz S, Azroyan A, Cheval L, Laghmani K. Secretory carrier membrane protein 2 regulates exocytic insertion of NKCC2 into the cell membrane. J Biol Chem 2011;286:9489–502.
[176] Moore-Hoon ML, Turner RJ. The structural unit of the secretory Na^+-K^+-$2Cl^-$ co-transporter (NKCC1) is a homodimer. Biochemistry 2000;39:3718–24.
[177] Starremans PG, Kersten FF, van den Heuvel LP, Knoers NV, Bindels RJ. Dimeric architecture of the human bumetanide-sensitive Na-K-Cl Co-transporter. J Am Soc Nephrol 2003;14:3039–46.
[178] De Jong JC, Willems PH, Mooren FJ, van den Heuvel LP, Knoers NV, Bindels RJ. The structural unit of the thiazide-sensitive NaCl co-transporter is a homodimer. J Biol Chem 2003;278:24302–7.
[179] Wenz M, Hartmann AM, Friauf E, Nothwang HG. CIP1 is an activator of the K(+)-Cl(−) co-transporter KCC2. Biochem Biophys Res Commun 2009;381(3):388–92.
[180] Simard CF, Bergeron MJ, Frenette-Cotton R, Carpentier GA, Pelchat ME, Caron L, et al. Homooligomeric and heterooligomeric associations between K^+-Cl^- co-transporter isoforms and between K^+-Cl^- and Na^+-K^+-Cl^- co-transporters. J Biol Chem 2007;282:18083–93.
[181] Knepper MA, Brooks HL. Regulation of the sodium transporters NHE3, NKCC2 and NCC in the kidney. Curr Opin Nephrol Hypertens 2001;10:655–9.
[182] Lytle C, McManus T. Coordinate modulation of Na-K-2Cl co-transport and K-Cl co-transport by cell volume and chloride. Am J Physiol Cell Physiol 2002;283:C1422–31.
[183] McManus ML, Churchwell KB, Strange K. Regulation of cell volume in health and disease. N Engl J Med 1995;333:1260–6.
[184] Dowd BF, Forbush B. PASK (proline-alanine-rich STE20-related kinase), a regulatory kinase of the Na-K-Cl co-transporter (NKCC1). J Biol Chem 2003;278:27347–53.
[185] Flemmer AW, Gimenez I, Dowd BF, Darman RB, Forbush B. Activation of the Na-K-Cl cotransporter NKCC1 detected with a phospho-specific antibody. J Biol Chem 2002;277:37551–8.
[186] Ponce-Coria J, San Cristobal P, Kahle KT, Vazquez N, Pacheco-Alvarez D, De Los Heros P, et al. Regulation of NKCC2 by a chloride-sensing mechanism involving the WNK3 and SPAK kinases. Proc Natl Acad Sci USA 2008;105:8458–63.
[187] Pacheco-Alvarez D, San Cristobal P, Meade P, Moreno E, Vazquez N, Munoz E, et al. The Na-Cl co-transporter is activated and phosphorylated at the amino terminal domain upon intracellular chloride depletion. J Biol Chem 2006;281:28755–63.
[188] Lytle C, Forbush III B. The Na-K-Cl co-transport protein of shark rectal gland. II Regulation by direct phosphorylation. J Biol Chem 1992;267:25438–43.
[189] Darman RB, Forbush B. A regulatory locus of phosphorylation in the N terminus of the Na-K-Cl co-transporter, NKCC1. J Biol Chem 2002;277:37542–50.
[190] Moriguchi T, Urushiyama S, Hisamoto N, Iemura S, Uchida S, Natsume T, et al. WNK1 regulates phosphorylation of cation-chloride-coupled co-transporters via the STE20-related kinases, SPAK and OSR1. J Biol Chem 2005;280:42685–93.
[191] Richardson C, Alessi DR. The regulation of salt transport and blood pressure by the WNK-SPAK/OSR1 signalling pathway. J Cell Sci 2008;121:3293–304.
[192] Rafiqi FH, Zuber AM, Glover M, Richardson C, Fleming S, Jovanovic S, et al. Role of the WNK-activated SPAK kinase in regulating blood pressure. EMBO Mol Med 2010;2:63–75.
[193] Chiga M, Rai T, Yang SS, Ohta A, Takizawa T, Sasaki S, et al. Dietary salt regulates the phosphorylation of OSR1/SPAK kinases and the sodium chloride co-transporter through aldosterone. Kidney Int 2008;74:1403–9.

[194] Pedersen NB, Hofmeister MV, Rosenbaek LL, Nielsen J, Fenton RA. Vasopressin induces phosphorylation of the thiazide-sensitive sodium chloride co-transporter in the distal convoluted tubule. Kidney Int 2010;78:160–9.

[195] Mutig K, Saritas T, Uchida S, Kahl T, Borowski T, Paliege A, et al. Short-term stimulation of the thiazide-sensitive Na^+,Cl^--co-transporter by vasopressin involves phosphorylation and membrane translocation. Am J Physiol Renal Physiol 2010;298: F502–9.

[196] San Cristobal P, Pacheco-Alvarez D, Richardson C, Ring AM, Vazquez N, Rafiqi FH, et al. Angiotensin II signaling increases activity of the renal Na-Cl co-transporter through a WNK4-SPAK-dependent pathway. Proc Natl Acad Sci USA 2009;106:4384–9.

[197] van der LN, Lim CH, Fenton RA, Meima ME, Jan Danser AH, Zietse R, et al. Angiotensin II induces phosphorylation of the thiazide-sensitive sodium chloride co-transporter independent of aldosterone. Kidney Int 2011;79:66–76.

[198] Talati G, Ohta A, Rai T, Sohara E, Naito S, Vandewalle A, et al. Effect of angiotensin II on the WNK-OSR1/SPAK-NCC phosphorylation cascade in cultured mpkDCT cells and *in vivo* mouse kidney. Biochem Biophys Res Commun 2010;393:844–8.

[199] Gimenez I, Forbush B. Regulatory phosphorylation sites in the N-terminus of the renal Na-K-Cl co-transporter (NKCC2). Am J Physiol Renal Physiol 2005;289:F1341–5.

[200] Richardson C, Sakamoto K, De Los Heros P, Deak M, Campbell DG, Prescott AR, et al. Regulation of the NKCC2 ion co-transporter by SPAK-OSR1-dependent and -independent pathways. J Cell Sci 2011;124:789–800.

[201] Dimke H, Flyvbjerg A, Bourgeois S, Thomsen K, Frokiaer J, Houillier P, et al. Acute growth hormone administration induces antidiuretic and antinatriuretic effects and increases phosphorylation of NKCC2. Am J Physiol Renal Physiol 2007;292:F723–35.

[202] Xu B, English JM, Wilsbacher JL, Stippec S, Goldsmith EJ, Cobb MH. WNK1, a novel mammalian serine/threonine protein kinase lacking the catalytic lysine in subdomain II. J Biol Chem 2000;275:16795–801.

[203] Min X, Lee BH, Cobb MH, Goldsmith EJ. Crystal structure of the kinase domain of WNK1, a kinase that causes a hereditary form of hypertension. *Structure* (*Camb*) 2004;12:1303–11.

[204] Verissimo F, Jordan P. WNK kinases, a novel protein kinase subfamily in multi-cellular organisms. Oncogene 2001;20:5562–9.

[205] Lenertz LY, Lee BH, Min X, Xu BE, Wedin K, Earnest S, et al. Properties of WNK1 and implications for other family members. J Biol Chem 2005;280:26653–8.

[206] Wilson FH, Disse-Nicodeme S, Choate KA, Ishikawa K, Nelson-Williams C, Desitter I, et al. Human hypertension caused by mutations in WNK kinases. Science 2001;293:1107–12.

[207] Gordon RD. Syndrome of hypertension and hyperkalemia with normal glomerular filtration rate. Hypertension 1986;8:93–102.

[208] Gordon RD, Hodsman GP. The syndrome of hypertension and hyperkalaemia without renal failure: long term correction by thiazide diuretic. Scott Med J 1986;31:43–4.

[209] Wilson FH, Kahle KT, Sabath E, Lalioti MD, Rapson AK, Hoover RS, et al. Molecular pathogenesis of inherited hypertension with hyperkalemia: the Na-Cl co-transporter is inhibited by wild-type but not mutant WNK4. Proc Natl Acad Sci USA 2003;100:680–4.

[210] Yang CL, Angell J, Mitchell R, Ellison DH. WNK kinases regulate thiazide-sensitive Na-Cl co-transport. J Clin Invest 2003;111:1039–45.

[211] San Cristobal P, Ponce-Coria J, Vazquez N, Bobadilla NA, Gamba G. WNK3 and WNK4 amino terminal domain defines their effect on the renal Na^+:Cl^- co-transporter. Am J Physiol Renal Physiol 2008;295:F1199–206.

[212] Golbang AP, Cope G, Hamad A, Murthy M, Liu CH, Cuthbert AW, et al. Regulation of the expression of the Na/Cl co-transporter (NCCT) by WNK4 and WNK1: evidence that accelerated dynamin-dependent endocytosis is not involved. Am J Physiol Renal Physiol 2006;291:F1369–76.

[213] Cai H, Cebotaru V, Wang YH, Zhang XM, Cebotaru L, Guggino SE, et al. WNK4 kinase regulates surface expression of the human sodium chloride co-transporter in mammalian cells. Kidney Int 2006;69:2162–70.

[214] Lalioti MD, Zhang J, Volkman HM, Kahle KT, Hoffmann KE, Toka HR, et al. Wnk4 controls blood pressure and potassium homeostasis via regulation of mass and activity of the distal convoluted tubule. Nat Genet 2006;38:1124–32.

[215] Yang SS, Morimoto T, Rai T, Chiga M, Sohara E, Ohno M, et al. Molecular pathogenesis of pseudohypoaldosteronism type II: generation and analysis of a Wnk4(D561A/ +) knockin mouse model. Cell Metab 2007;5:331–44.

[216] Delaloy C, Lu J, Houot AM, Disse-Nicodeme S, Gasc JM, Corvol P, et al. Multiple promoters in the WNK1 gene: one controls expression of a kidney-specific kinase-defective isoform. Mol Cell Biol 2003;23:9208–21.

[217] Faure S, Delaloy C, Leprivey V, Hadchouel J, Warnock DG, Jeunemaitre X, et al. WNK kinases, distal tubular ion handling and hypertension. Nephrol Dial Transplant 2003;18:2463–7.

[218] O'Reilly M, Marshall E, Speirs HJ, Brown RW. WNK1, a gene within a novel blood pressure control pathway, tissue-specifically generates radically different isoforms with and without a kinase domain. J Am Soc Nephrol 2003;14:2447–56.

[219] Subramanya AR, Yang CL, Zhu X, Ellison DH. Dominant-negative regulation of WNK1 by its kidney-specific kinase-defective isoform. Am J Physiol Renal Physiol 2006;290:F619–24.

[220] Huang CL, Kuo E. Mechanisms of disease: WNK-ing at the mechanism of salt-sensitive hypertension. Nat Clin Pract Nephrol 2007;3:623–30.

[221] Hadchouel J, Soukaseum C, Busst C, Zhou XO, Baudrie V, Zurrer T, et al. Decreased ENaC expression compensates the increased NCC activity following inactivation of the kidney-specific isoform of WNK1 and prevents hypertension. Proc Natl Acad Sci USA 2010;107:18109–14.

[222] Delaloy C, Elvira-Matelot E, Clemessy M, Zhou XO, Imbert-Teboul M, Houot AM, et al. Deletion of WNK1 first intron results in misregulation of both isoforms in renal and extrarenal tissues. Hypertension 2008;52:1149–59.

[223] Vitari AC, Deak M, Morrice NA, Alessi DR. The WNK1 and WNK4 protein kinases that are mutated in Gordon's hypertension syndrome, phosphorylate and activate SPAK and OSR1 protein kinases. Biochem J 2005;391:17–24.

[224] Gamba G. WNK lies upstream of kinases involved in regulation of ion transporters. Biochem J 2005;391:e1–3.

[225] Piechotta K, Lu J, Delpire E. Cation chloride co-transporters interact with the stress-related kinases Ste20-related proline-alanine-rich kinase (SPAK) and oxidative stress response 1 (OSR1). J Biol Chem 2002;277:50812–9.

[226] Pacheco-Alvarez D, Vazquez N, Castaneda-Bueno M, de los Heros P, Cortes-Gonzalez C, Moreno E, et al. WNK3-SPAK interaction is required for the modulation of NCC and other members of the SLC12 family. Cell Physiol Biochem 2012;29:291–302.

[227] Delpire E, Gagnon KB. Genome-wide analysis of SPAK/OSR1 binding motifs. Physiol Genomics 2007;28:223–31.

[228] Gagnon KB, England R, Delpire E. Volume sensitivity of cation-Cl- co-transporters is modulated by the interaction of two kinases: Ste20-related proline-alanine-rich kinase and WNK4. Am J Physiol Cell Physiol 2006;290:C134–42.
[229] Delpire E. The mammalian family of sterile 20p-like protein kinases. Pflugers Arch 2009;458:953–67.
[230] Delpire E, Gagnon KB. SPAK and OSR1, key kinases involved in the regulation of chloride transport. Acta Physiol (Oxf) 2006;187:103–13.
[231] Delpire E, Gagnon KB. SPAK and OSR1: STE20 kinases involved in the regulation of ion homoeostasis and volume control in mammalian cells. Biochem J 2008;409:321–31.
[232] Kahle KT, Rinehart J, Ring A, Gimenez I, Gamba G, Hebert SC, et al. WNK protein kinases modulate cellular Cl^- flux by altering the phosphorylation state of the Na-K-Cl and K-Cl co-transporters. Physiology (Bethesda) 2006;21:326–35.
[233] Chiga M, Rafiqi FH, Alessi DR, Sohara E, Ohta A, Rai T, et al. Phenotypes of pseudohypoaldosteronism type II caused by the WNK4 D561A missense mutation are dependent on the WNK-OSR1/SPAK kinase cascade. J Cell Sci 2011;124:1391–5.
[234] Yang SS, Lo YF, Wu CC, Lin SW, Yeh CJ, Chu P, et al. SPAK-knockout mice manifest Gitelman syndrome and impaired vasoconstriction. J Am Soc Nephrol 2010;21:1868–77.
[235] Lin SH, Yu IS, Jiang ST, Lin SW, Chu P, Chen A, et al. Impaired phosphorylation of Na^+-K^+-$2Cl^-$ co-transporter by oxidative stress-responsive kinase-1 deficiency manifests hypotension and Bartter-like syndrome. Proc Natl Acad Sci USA 2011;108:17538–43.
[236] McCormick JA, Mutig K, Nelson JH, Saritas T, Hoorn EJ, Yang CL, et al. A SPAK isoform switch modulates renal salt transport and blood pressure. Cell Metab 2011;14:352–64.
[237] San Cristobal P, De Los Heros P, Ponce-Coria J, Moreno E, Gamba G. WNK kinases, renal ion transport and hypertension. Am J Nephrol 2008;28:860–70.
[238] Kahle KT, Rinehart J, De Los Heros P, Louvi A, Meade P, Vazquez N, et al. WNK3 modulates transport of Cl^- in and out of cells: implications for control of cell volume and neuronal excitability. Proc Natl Acad Sci USA 2005;102:16783–8.
[239] Rinehart J, Kahle KT, De Los Heros P, Vazquez N, Meade P, Wilson FH, et al. WNK3 kinase is a positive regulator of NKCC2 and NCC, renal cation-Cl^- co-transporters required for normal blood pressure homeostasis. Proc Natl Acad Sci USA 2005;102:16777–82.
[240] De Los Heros P, Kahle KT, Rinehart J, Bobadilla NA, Vazquez N, San Cristobal P, et al. WNK3 bypasses the tonicity requirement for K-Cl co-transporter activation via a phosphatase-dependent pathway. Proc Natl Acad Sci USA 2006;103:1976–81.
[241] Yang CL, Zhu X, Ellison DH. The thiazide-sensitive Na-Cl co-transporter is regulated by a WNK kinase signaling complex. J Clin Invest 2007;117:3403–11.
[242] Kahle KT, Ring AM, Lifton RP. Molecular physiology of the WNK kinases. Annu Rev Physiol 2008;70:329–55.
[243] Rinehart J, Vazquez N, Kahle KT, Hodson CA, Ring AM, Gulcicek EE, et al. WNK2 is a novel regulator of essential neuronal cation-chloride co-transporters. J Biol Chem 2011;286:30171–80.
[244] Pollak MR, Delaney VB, Graham RM, Hebert SC. Gitelman's syndrome (Bartter's variant) maps to the thiazide-sensitive co-transporter gene locus on chromosome 16q13 in a large kindred. J Am Soc Nephrol 1996;7:2244–8.
[245] Mastroianni N, Bettinelli A, Bianchetti M, Colussi G, de Fusco M, Sereni F, et al. Novel molecular variants of the Na-Cl co-transporter gene are responsible for Gitelman syndrome. Am J Hum Genet 1996;59:1019–26.
[246] Lemmink HH, van den Heuvel LP, van Dijk HA, Merkx GF, Smilde TJ, Taschner PE, et al. Linkage of Gitelman syndrome to the thiazide-sensitive sodium-chloride co-transporter gene with identification of mutations in Dutch families. Pediatr Nephrol 1996;10:403–7.
[247] Schultheis PJ, Lorenz JN, Meneton P, Nieman ML, Riddle TM, Flagella M, et al. Phenotype resembling Gitelman's syndrome in mice lacking the apical Na^+-Cl^- co-transporter of the distal convoluted tubule. J Biol Chem 1998;273:29150–5.
[248] Yang SS, Lo YF, Yu IS, Lin SW, Chang TH, Hsu YJ, et al. Generation and analysis of the thiazide-sensitive Na^+-Cl^- co-transporter (Ncc/Slc12a3) Ser707X knockin mouse as a model of Gitelman syndrome. Hum Mutat 2010;31:1304–15.
[249] Cruz DN, Shaer AJ, Bia MJ, Lifton RP, Simon DB. Gitelman's syndrome revisited: an evaluation of symptoms and health-related quality of life. Kidney Int 2001;59:710–7.
[250] Maki N, Komatsuda A, Wakui H, Ohtani H, Kigawa A, Aiba N, et al. Four novel mutations in the thiazide-sensitive Na-Cl co-transporter gene in Japanese patients with Gitelman's syndrome. Nephrol Dial Transplant 2004;19(7):1761–6.
[251] Lemmink HH, Knoers NV, Karolyi L, van Dijk H, Niaudet P, Antignac C, et al. Novel mutations in the thiazide-sensitive NaCl co-transporter gene in patients with Gitelman syndrome with predominant localization to the C-terminal domain. Kidney Int 1998;54:720–30.
[252] Lin SH, Cheng NL, Hsu YJ, Halperin ML. Intrafamilial phenotype variability in patients with Gitelman syndrome having the same mutations in their thiazide-sensitive sodium/chloride co-transporter. Am J Kidney Dis 2004;43:304–12.
[253] Syren ML, Tedeschi S, Cesareo L, Bellantuono R, Colussi G, Procaccio M, et al. Identification of fifteen novel mutations in the SLC12A3 gene encoding the Na-Cl Co-transporter in Italian patients with Gitelman syndrome. Hum Mutat 2002;20:78.
[254] Vargas-Poussou R, Dahan K, Kahila D, Venisse A, Riveira-Munoz E, Debaix H, et al. Spectrum of mutations in Gitelman syndrome. J Am Soc Nephrol 2011;22:693–703.
[255] Shaer AJ. Inherited primary renal tubular hypokalemic alkalosis: a review of Gitelman and Bartter syndromes. Am J Med Sci 2001;322:316–32.
[256] Simon DB, Karet FE, Rodriguez-Soriano J, Hamdan JH, DiPietro A, Trachtman H, et al. Genetic heterogeneity of Bartter's syndrome revealed by mutations in the K^+ channel, ROM. Nature Genetics 1996;14:152–6.
[257] Simon DB, Bindra RS, Mansfield TA, Nelson-Williamns C, Mendonca E, Stone R, et al. Mutations in the chloride channel gene, CLCNKB, cause Bartter's syndrome type III. Nature Genetics 1997;17:171–8.
[258] Estevez R, Boettger T, Stein V, Birkenhager R, Otto E, Hildebrandt F, et al. Barttin is a Cl^- channel beta-subunit crucial for renal Cl^- reabsorption and inner ear K^+ secretion. Nature 2001;414:558–61.
[259] Watanabe S, Fukumoto S, Chang H, Takeuchi Y, Hasegawa Y, Okazaki R, et al. Association between activating mutations of calcium-sensing receptor and Bartter's syndrome. Lancet 2002;360:692–4.
[260] Vargas-Poussou R, Huang C, Hulin P, Houillier P, Jeunemaitre X, Paillard M, et al. Functional characterization of a calcium-sensing receptor mutation in severe autosomal dominant hypocalcemia with a Bartter-like syndrome. J Am Soc Nephrol 2002;13:2259–66.
[261] Vezzoli G, Arcidiacono T, Paloschi V, Terranegra A, Biasion R, Weber G, et al. Autosomal dominant hypocalcemia with mild type 5 Bartter syndrome. J Nephrol 2006;19:525–8.

[262] Meade P, Sabath E, Gamba G. Fisiopatología molecular del sìndrome de Bartter. Rev Invest Clin 2003;55:74–83.
[263] Mayan H, Munter G, Shaharabany M, Mouallem M, Pauzner R, Holtzman EJ, et al. Hypercalciuria in familial hyperkalemia and hypertension accompanies hyperkalemia and precedes hypertension: description of a large family with the Q565E WNK4 mutation. J Clin Endocrinol Metab 2004;89:4025–30.
[264] Cruz DN. The renal tubular Na-Cl co-transporter (NCCT): a potential genetic link between blood pressure and bone density? Nephrol Dial Transplant 2001;16:691–4.
[265] Nicolet-Barousse L, Blanchard A, Roux C, Pietri L, Bloch-Faure M, Kolta S, et al. Inactivation of the Na-Cl co-transporter (NCC) gene is associated with high BMD through both renal and bone mechanisms: analysis of patients with Gitelman syndrome and Ncc null mice. J Bone Miner Res 2005;20:799–808.
[266] Mayan H, Vered I, Mouallem M, Tzadok-Witkon M, Pauzner R, Farfel Z. Pseudohypoaldosteronism type II: marked sensitivity to thiazides, hypercalciuria, normomagnesemia, and low bone mineral density. J Clin Endocrinol Metab 2002;87:3248–54.
[267] Simon DB, Farfel Z, Ellison D, Bia M, Tucci J, Lifton RP. Examination of the thiazide-sensitive Na-Cl co-transporter as a candidate gene in Gordon's syndrome. J Am Soc Nephrol 1995;6:632.
[268] Brooks AM, Owens M, Sayer JA, Salzmann M, Ellard S, Vaidya B. Pseudohypoaldosteronism type 2 presenting with hypertension and hyperkalaemia due to a novel mutation in the WNK4 gene. QJM 2011;: e-pub ahead of print
[269] Zhang C, Wang Z, Xie J, Yan F, Wang W, Feng X, et al. Identification of a novel WNK4 mutation in Chinese patients with pseudohypoaldosteronism type II. Nephron Physiol 2011;118:53–61.
[270] Gong H, Tang Z, Yang Y, Sun L, Zhang W, Wang W, et al. A patient with pseudohypoaldosteronism type II caused by a novel mutation in WNK4 gene. Endocrine 2008;33:230–4.
[271] Golbang AP, Murthy M, Hamad A, Liu CH, Cope G, Hoff WV, et al. A new kindred with pseudohypoaldosteronism type II and a novel mutation (564D > H) in the acidic motif of the WNK4 gene. Hypertension 2005;46(2):295–300.
[272] Kamide K, Takiuchi S, Tanaka C, Miwa Y, Yoshii M, Horio T, et al. Three novel missense mutations of WNK4, a kinase mutated in inherited hypertension, in Japanese hypertensives: implication of clinical phenotypes. Am J Hypertens 2004;17:446–9.
[273] Achard JM, Warnock DG, Disse-Nicodeme S, Fiquet-Kempf B, Corvol P, Fournier A, et al. Familial hyperkalemic hypertension: phenotypic analysis in a large family with the WNK1 deletion mutation. Am J Med 2003;114:495–8.
[274] Bergaya S, Vidal-Petiot E, Jeunemaitre X, Hadchouel J. Pathogenesis of pseudohypoaldosteronism type 2 by WNK1 mutations. Curr Opin Nephrol Hypertens 2012;21:39–45.
[275] Boyden LM, Choi M, Choate KA, Nelson-Williams CJ, Farhi A, Toka HR, et al. Mutations in kelch-like 3 and cullin 3 cause hypertension and electrolyte abnormalities. Nature 2012;482 (7383):98–102.
[276] Welling PA, Chang YP, Delpire E, Wade JB. Multigene kinase network, kidney transport, and salt in essential hypertension. Kidney Int 2010;77:1063–9.
[277] Huang CL, Yang SS, Lin SH. Mechanism of regulation of renal ion transport by WNK kinases. Curr Opin Nephrol Hypertens 2008;17:519–25.
[278] Zimmerman ES, Schulman BA, Zheng N. Structural assembly of cullin-RING ubiquitin ligase complexes. Curr Opin Struct Biol 2010;20:714–21.
[279] Arroyo JP, Lagnaz D, Ronzaud C, Vazquez N, Ko BS, Moddes L, et al. Nedd4-2 modulates renal Na^+-Cl^- co-transporter via the aldosterone-SGK1-Nedd4-2 pathway. J Am Soc Nephrol 2011;22:1707–19.
[280] Ohta A, Rai T, Yui N, Chiga M, Yang SS, Lin SH, et al. Targeted disruption of the Wnk4 gene decreases phosphorylation of Na-Cl co-transporter, increases Na excretion, and lowers blood pressure. Hum Mol Genet 2009;18:3978–86.
[281] Chobanian AV, Bakris GL, Black HR, Cushman WC, Green LA, Izzo Jr. JL, et al. The seventh report of the joint national committee on prevention, detection, evaluation, and treatment of high blood pressure: the JNC 7 Report. JAMA 2003;289:2560–71.
[282] Ji W, Foo JN, O'Roak BJ, Zhao H, Larson MG, Simon DB, et al. Rare independent mutations in renal salt handling genes contribute to blood pressure variation. Nat Genet 2008;40:592–9.
[283] Acuna R, Martinez-de-la-Maza L, Ponce-Coria J, Vazquez N, Ortal-Vite P, Pacheco-Alvarez D, et al. Rare mutations in SLC12A1 and SLC12A3 protect against hypertension by reducing the activity of renal salt co-transporters. J Hypertens 2011;29:475–83.
[284] Monette MY, Rinehart J, Lifton RP, Forbush B. Rare mutations in the human Na-K-Cl co-transporter (NKCC2) associated with lower blood pressure exhibit impaired processing and transport function. Am J Physiol Renal Physiol 2011;300:F840–7.
[285] Wang Y, O'Connell JR, McArdle PF, Wade JB, Dorff SE, Shah SJ, et al. Whole-genome association study identifies STK39 as a hypertension susceptibility gene. Proc Natl Acad Sci USA 2009;106:226–31.
[286] Ray WA, Griffin MR, Downey W, Melton III LJ. Long-term use of thiazide diuretics and risk of hip fracture. The Lancet 1989; I:687–90.
[287] Sebastian A. Thiazides and bone. Am J Med 2000;109:429–30.
[288] Reid IR, Ames RW, Orr-Walker BJ, Clearwater JM, Horne AM, Evans MC, et al. Hydrochlorothiazide reduces loss of cortical bone in normal postmenopausal women: a randomized controlled trial. Am J Med 2000;109:362–70.
[289] Frindt G, Palmer LG. Surface expression of sodium channels and transporters in rat kidney: effects of dietary sodium. Am J Physiol Renal Physiol 2009;297:F1249–55.
[290] Vallon V, Schroth J, Lang F, Kuhl D, Uchida S. Expression and phosphorylation of the Na-Cl-co-transporter NCC *in vivo* is regulated by dietary salt, potassium and SGK1. Am J Physiol Renal Physiol 2009;297:F704–12.
[291] Masilamani S, Kim GH, Mitchell C, Wade JB, Knepper MA. Aldosterone-mediated regulation of ENaC alpha, beta, and gamma subunit proteins in rat kidney. J Clin Invest 1999;104: R19–23.
[292] Masilamani S, Wang X, Kim GH, Brooks H, Nielsen J, Nielsen S, et al. Time course of renal Na-K-ATPase, NHE3, NKCC2, NCC, and ENaC abundance changes with dietary NaCl restriction. Am J Physiol Renal Physiol 2002;283:F648–57.
[293] Kim G-H, Masilamani S, Turner R, Mitchell C, Wade JB, Knepper MA. The thiazide-sensitive Na-Cl co-transporter is an aldosterone-induced protein. Proc Natl Acad Sci USA 1998;95:14552–7.
[294] Moreno G, Merino A, Mercado A, Herrera JP, González-Salazar J, Correa-Rotter R, et al. Electronuetral Na-coupled co-transporter expression in the kidney during variations of NaCl and water metabolism. Hypertension 1998;31:1002–6.
[295] Wolf K, Castrop H, Riegger GA, Kurtz A, Kramer BK. Differential gene regulation of renal salt entry pathways by salt load in the distal nephron of the rat. Pflugers Arch 2001;442:498–504.

[296] Lai L, Feng X, Liu D, Chen J, Zhang Y, Niu B, et al. Dietary salt modulates the sodium chloride co-transporter expression likely through an aldosterone-mediated WNK4-ERK1/2 signaling pathway. Pflugers Arch 2012;463:477–85.
[297] Abdallah JG, Schrier RW, Edelstein C, Jennings SD, Wyse B, Ellison DH. Loop diuretic infusion increases thiazide-sensitive Na^+/Cl^- co-transporter abundance: role of aldosterone. J Am Soc Nephrol 2001;12:1335–41.
[298] Na KY, Oh YK, Han JS, Joo KW, Lee JS, Earm JH, et al. Upregulation of Na^+ transporter abundance in response to chronic thiazide or loop diuretic treatment in rats. Am J Physiol Renal Physiol 2003;284:F133–43.
[299] Ruete MC, Carrizo LC, Bocanegra MV, Valles PG. Altered renal expression of $Na(^+)$ transporters and ROMK in protein-deprived rats. Nephron Physiol 2009;111:17–29.
[300] Kim JS, Choi KC, Jeong MH, Kim SW, Oh YW, Lee JU. Increased expression of sodium transporters in rats chronically inhibited of nitric oxide synthesis. J Korean Med Sci 2006;21:1–4.
[301] Ecelbarger CA, Kim GH, Wade JB, Knepper MA. Regulation of the abundance of renal sodium transporters and channels by vasopressin. Exp Neurol 2001;171:227–34.
[302] Ecelbarger CA, Knepper MA, Verbalis JG. Increased abundance of distal sodium transporters in rat kidney during vasopressin escape. J Am Soc Nephrol 2001;12:207–17.
[303] Kwon TH, Nielsen J, Knepper MA, Frokiaer J, Nielsen S. Angiotensin II AT1 receptor blockade decreases vasopressin-induced water reabsorption and AQP2 levels in NaCl-restricted rats. Am J Physiol Renal Physiol 2005;288: F673–84.
[304] Bickel CA, Verbalis JG, Knepper MA, Ecelbarger CA. Increased renal Na-K-ATPase, NCC, and beta-ENaC abundance in obese Zucker rats. Am J Physiol Renal Physiol 2001;281:F639–48.
[305] Faroqui S, Sheriff S, Amlal H. Metabolic acidosis has dual effects on sodium handling by rat kidney. Am J Physiol Renal Physiol 2006;291:F322–31.
[306] Verlander JM, Tran TM, Zhang L, Kaplan MR, Hebert SC. Estradiol enhances thiazide-sensitive NaCl co-transporter density in the apical plasma membrane of the distal convoluted tubule in ovariectomized rats. J Clin Invest 1998;101:1661–9.
[307] Manning J, Beutler K, Knepper MA, Vehaskari VM. Upregulation of renal BSC1 and TSC in prenatally programmed hypertension. Am J Physiol Renal Physiol 2002;283:F202–6.
[308] Kwon TH, kiaer J, ndez-Llama P, Maunsbach AB, Knepper MA, Nielsen S. Altered expression of Na transporters NHE-3, NaPi-II, Na-K-ATPase, BSC- 1, and TSC in CRF rat kidneys. Am J Physiol 1999;277:F257–70.
[309] Frindt G, Palmer LG. Regulation of epithelial Na^+ channels by adrenal steroids: Mineralocorticoid and glucocorticoid effects. Am J Physiol Renal Physiol 2012;302:F20–6.
[310] Hoorn EJ, Walsh SB, McCormick JA, Furstenberg A, Yang CL, Roeschel T, et al. The calcineurin inhibitor tacrolimus activates the renal sodium chloride co-transporter to cause hypertension. Nat Med 2011;17:1304–9.
[311] Mu S, Shimosawa T, Ogura S, Wang H, Uetake Y, Kawakami-Mori F, et al. Epigenetic modulation of the renal beta-adrenergic-WNK4 pathway in salt-sensitive hypertension. Nat Med 2011;17:573–81.
[312] Liu Z, Xie J, Wu T, Truong T, Auchus RJ, Huang CL. Downregulation of NCC and NKCC2 co-transporters by kidney-specific WNK1 revealed by gene disruption and transgenic mouse models. Hum Mol Genet 2011;20:855–66.
[313] Sassen MC, Kim SW, Kwon TH, Knepper MA, Miller RT, Frokiaer J, et al. Dysregulation of renal sodium transporters in gentamicin-treated rats. Kidney Int 2006;70:1026–37.
[314] Song J, Hu X, Riazi S, Tiwari S, Wade JB, Ecelbarger CA. Regulation of blood pressure, the epithelial sodium channel (ENaC), and other key renal sodium transporters by chronic insulin infusion in rats. Am J Physiol Renal Physiol 2006;290: F1055–64.
[315] Sonalker PA, Tofovic SP, Bastacky SI, Jackson EK. Chronic noradrenaline increases renal expression of NHE-3, NBC-1, BSC-1 and aquaporin-2. Clin Exp Pharmacol Physiol 2008;35:594–600.
[316] Kwon TH, Laursen UH, Marples D, Maunsbach AB, Knepper MA, Frokiaer J, et al. Altered expression of renal AQPs and Na $(^+)$ transporters in rats with lithium-induced NDI. Am J Physiol Renal Physiol 2000;279:F552–64.
[317] Frindt G, Palmer LG. Effects of dietary K on cell-surface expression of renal ion channels and transporters. Am J Physiol Renal Physiol 2010;299:F890–7.
[318] Jung JY, Kim S, Lee JW, Jung ES, Heo NJ, Son MJ, et al. Effects of potassium on expression of renal sodium transporters in salt-sensitive hypertensive rats induced by uninephrectomy. Am J Physiol Renal Physiol 2011;300:F1422–30.
[319] Amlal H, Wang Z, Soleimani M. Potassium depletion downregulates chloride-absorbing transporters in rat kidney. J Clin Invest 1998;101:1045–54.
[320] Elkjaer ML, Kwon TH, Wang W, Nielsen J, Knepper MA, Frokiaer J, et al. Altered expression of renal NHE3, TSC, BSC-1, and ENaC subunits in potassium-depleted rats. Am J Physiol Renal Physiol 2002;283:F1376–88.
[321] Bae EH, Kim IJ, Ma SK, Kim SW. Altered regulation of renal sodium transporters and natriuretic peptide system in DOCA-salt hypertensive rats. Regul Pept 2009;157:76–83.
[322] Madala H V, Tiwari S, Riazi S, Hu X, Ecelbarger CM. Chronic candesartan alters expression and activity of NKCC2, NCC, and ENaC in the obese Zucker rat. Am J Physiol Renal Physiol 2008;294:F1222–31.
[323] Kim EJ, Jung YW, Kwon TH. Angiotensin II AT1 receptor blockade changes expression of renal sodium transporters in rats with chronic renal failure. J Korean Med Sci 2005;20:248–55.
[324] Wang XY, Masilamani S, Nielsen J, Kwon TH, Brooks HL, Nielsen S, et al. The renal thiazide-sensitive Na-Cl co-transporter as mediator of the aldosterone-escape phenomenon. J Clin Invest 2001;108:215–22.
[325] Turban S, Wang XY, Knepper MA. Regulation of NHE3, NKCC2 and NCC abundance in kidney during aldosterone-escape phenomenon: role of NO. Am J Physiol Renal Physiol 2003;285:F841–3.
[326] Kim SW, Lee J, Jung K, Ma SK, Oh Y, Kim WY, et al. Diminished expression of sodium transporters in the ureteral obstructed kidney in rats. Nephron Exp Nephrol 2004;96:e67–76.
[327] Li C, Wang W, Kwon TH, Knepper MA, Nielsen S, Frokiaer J. Altered expression of major renal Na transporters in rats with bilateral ureteral obstruction and release of obstruction. Am J Physiol Renal Physiol 2003;285:F889–901.
[328] Kim SW, Wang W, Nielsen J, Praetorius J, Kwon TH, Knepper MA, et al. Increased expression and apical targeting of renal ENaC subunits in puromycin aminonucleoside-induced nephrotic syndrome in rats. Am J Physiol Renal Physiol 2004;286:F922–35.
[329] Faresse N, Lagnaz D, Debonneville A, Ismailji A, Maillard M, Fejes-Toth G, et al. Inducible kidney specific Sgk1 knock-out mice show a salt losing phenotype. Am J Physiol Renal Physiol 2012;302(8):F977–85.
[330] Ledeganck KJ, Boulet GA, Horvath CA, Vinckx M, Bogers JJ, Van Den BR, et al. Expression of renal distal tubule transporters TRPM6 and NCC in a rat model of cyclosporine nephrotoxicity and effect of EGF treatment. Am J Physiol Renal Physiol 2011;301:F486–93.

[331] Attmane-Elakeb A, Sibella V, Vernimmen C, Belenfant X, Hebert SC, Bichara M. Regulation by glucocorticoids of expression and activity of rBSC1, the Na^+-K^+(NH_4^+)-$2Cl^-$ co-transporter of medullary thick ascending limb. J Biol Chem 2000;275:33548–53.

[332] Riazi S, Tiwari S, Sharma N, Rash A, Ecelbarger CM. Abundance of the Na-K-2Cl co-transporter NKCC2 is increased by high-fat feeding in Fischer 344 X Brown Norway (F1) rats. Am J Physiol Renal Physiol 2009;296:F762–70.

[333] Olesen ET, de Seigneux S, Wang G, Lutken SC, Frokiaer J, Kwon TH, et al. Rapid and segmental specific dysregulation of AQP2, S256-pAQP2 and renal sodium transporters in rats with LPS-induced endotoxaemia. Nephrol Dial Transplant 2009;24:2338–49.

[334] Wangensteen R, Rodriguez-Gomez I, Moreno JM, Vargas F, Alvarez-Guerra M. Chronic nitric oxide blockade modulates renal Na-K-2Cl co-transporters. J Hypertens 2006;24:2451–8.

[335] Fernandez-Llama P, Ecelbarger CA, Ware JA, Andrews P, Lee AJ, Turner R, et al. Cyclooxygenase inhibitors increase Na-K-2Cl co-transporter abundance in thick ascending limb of Henle's loop. Am J Physiol 1999;277:F219–26.

[336] Riazi S, Khan O, Tiwari S, Hu X, Ecelbarger CA. Rosiglitazone regulates ENaC and Na-K-2Cl co-transporter (NKCC2) abundance in the obese Zucker rat. Am J Nephrol 2006;26:245–57.

[337] Li C, Wang W, Summer SN, Cadnapaphornchai MA, Falk S, Umenishi F, et al. Hyperosmolality *in vivo* upregulates aquaporin 2 water channel and Na-K-2Cl co-transporter in Brattleboro rats. J Am Soc Nephrol 2006;17:1657–64.

[338] Kwon TH, Nielsen J, Kim YH, Knepper MA, Frokiaer J, Nielsen S. Regulation of sodium transporters in the thick ascending limb of rat kidney: response to angiotensin II. Am J Physiol Renal Physiol 2003;285:F152–65.

[339] Blount MA, Sim JH, Zhou R, Martin CF, Lu W, Sands JM, et al. Expression of transporters involved in urine concentration recovers differently after cessation of lithium treatment. Am J Physiol Renal Physiol 2010;298:F601–8.

[340] Kwon TH, Laursen UH, Marples D, Maunsbach AB, Knepper MA, Frokiaer J, et al. Altered expression of renal AQPs and Na (+) transporters in rats with lithium-induced NDI. Am J Physiol Renal Physiol 2000;279:F552–64.

[341] Sanches TR, Volpini RA, Massola Shimizu MH, Braganca AC, Oshiro-Monreal F, Seguro AC, et al. Sildenafil reduces polyuria in rats with lithium-induced NDI. Am J Physiol Renal Physiol 2012;302:F216–25.

[342] Moreno JM, Perez-Abud R, Wangensteen R, Rodriguez G I, Lopez M I, Osuna A, et al. Function and expression of renal epithelial sodium transporters in rats with thyroid dysfunction. J Endocrinol Invest 2011;: e-pub ahead of print

[343] Haque MZ, Ares GR, Caceres PS, Ortiz PA. High salt differentially regulates surface NKCC2 expression in thick ascending limbs of Dahl salt-sensitive and salt-resistant rats. Am J Physiol Renal Physiol 2011;300:F1096–104.

[344] Zhang Y, Listhrop R, Ecelbarger CM, Kishore BK. Renal sodium transporter/channel expression and sodium excretion in P2Y2 receptor knockout mice fed a high-NaCl diet with/without aldosterone infusion. Am J Physiol Renal Physiol 2011;300:F657–68.

[345] Beutler KT, Masilamani S, Turban S, Nielsen J, Brooks HL, Ageloff S, et al. Long-term regulation of ENaC expression in kidney by angiotensin II. Hypertension 2003;41:1143–50.

[346] Attmane-Elakeb A, Mount DB, Sibella V, Vernimmen C, Micheli L, Hebert SC, et al. Chronic metabolic acidosis upregulates expression of mRNA and protein of the MTAL Na^+-K^+(NH_4^+)-$2Cl^-$ co-transporter BSC1 (NKCC2). J Am Soc Nephrol 1998;9:2A.

[347] Attmane-Elakeb A, Mount DB, Sibella V, Vernimmen C, Hebert SC, Bichara M. Stimulation by *in vivo* and *in vitro* metabolic acidosis of expression of rBSC-1, the Na^+-K^+(NH_4^+)-$2Cl^-$ co-transporter of the rat medullary thick ascending limb. J Biol Chem 1998;273:33681–91.

[348] Karim Z, Attmane-Elakeb A, Sibella V, Bichara M. Acid pH increases the stability of BSC1/NKCC2 mRNA in the medullary thick ascending limb. J Am Soc Nephrol 2003;14:2229–36.

[349] Lim SW, Ahn KO, Sheen MR, Jeon US, Kim J, Yang CW, et al. Downregulation of renal sodium transporters and tonicity-responsive enhancer binding protein by long-term treatment with cyclosporin A. J Am Soc Nephrol 2007;18:421–9.

[350] Norregaard R, Jensen BL, Topcu SO, Diget M, Schweer H, Knepper MA, et al. COX-2 activity transiently contributes to increased water and NaCl excretion in the polyuric phase after release of ureteral obstruction. Am J Physiol Renal Physiol 2007;292:F1322–33.

[351] Jensen AM, Li C, Praetorius HA, Norregaard R, Frische S, Knepper MA, et al. Angiotensin II mediates downregulation of aquaporin water channels and key renal sodium transporters in response to urinary tract obstruction. Am J Physiol Renal Physiol 2006;291:F1021–32.

[352] Riazi S, Maric C, Ecelbarger CA. 17-beta Estradiol attenuates streptozotocin-induced diabetes and regulates the expression of renal sodium transporters. Kidney Int 2006;69:471–80.

[353] Filippi BM, De Los Heros P, Mehellou Y, Navratilova I, Gourlay R, Deak M, et al. MO25 is a master regulator of SPAK/OSR1 and MST3/MST4/YSK1 protein kinases. EMBO J 2011;30:1730–41.

[354] Melnikov S, Mayan H, Uchida S, Holtzman EJ, Farfel Z. Cyclosporine metabolic side effects: association with the WNK4 system. Eur J Clin Invest 2011;41(10):1113–20.

[355] McCormick JA, Nelson JH, Yang CL, Curry JN, Ellison DH. Overexpression of the sodium chloride co-transporter is not sufficient to cause familial hyperkalemic hypertension. Hypertension 2011;58:888–94.

[356] Castaneda-Bueno M, Cervantes LG, Vazquez N, Bobadilla NA, Uribe N, Alessi D, et al. *In vivo* activation of NCC by angiotensin II requires integrity of the WNK4-SPAK pathway. J Am Soc Nephrol 2011;22:102A.

[357] Sohara E, Rai T, Yang SS, Ohta A, Naito S, Chiga M, et al. Acute insulin stimulation induces phosphorylation of the Na-Cl co-transporter in cultured distal mpkDCT cells and mouse kidney. PLoS One 2011;6:e24277.

[358] Chavez-Canales M, Vazquez N, Arroyo JP, Castaneda-Bueno M, Ko B, Bobadilla NA, et al. Insulin is a positive modulator of NCC activity through a PI3K dependent mechanism. J Am Soc Nephrol 2010;21:64A.

[359] Fraser SA, Gimenez I, Cook N, Jennings I, Katerelos M, Katsis F, et al. Regulation of the renal-specific Na^+-K^+-$2Cl^-$ co-transporter NKCC2 by AMP-activated protein kinase (AMPK). Biochem J 2007;405:85–93.

[360] Hannemann A, Flatman PW. Phosphorylation and transport in the Na-K-2Cl co-transporters, NKCC1 and NKCC2A, compared in HEK-293 cells. PLoS One 2011;6:e17992.

[361] Carmosino M, Rizzo F, Ferrari P, Torielli L, Ferrandi M, Bianchi G, et al. NKCC2 is activated in Milan hypertensive rats contributing to the maintenance of salt-sensitive hypertension. Pflugers Arch 2011;462:281–91.

[362] Mutig K, Kahl T, Saritas T, Godes M, Persson P, Bates J, et al. Activation of the bumetanide-sensitive Na^+,K^+,$2Cl^-$-co-transporter NKCC2 is facilitated by Tamm-Horsfall protein in a chloride-sensitive manner. J Biol Chem 2011;286:30200–10.

CHAPTER

33

Sodium and Chloride Transport: Proximal Nephron

Alan M. Weinstein

Department of Physiology and Biophysics, Weill Medical College of Cornell University, New York, NY, USA

INTRODUCTION

The principal function of the proximal tubule is the reabsorption of some two-thirds to three-quarters of the glomerular filtrate. This means, primarily, reabsorption of Na^+, Cl^-, HCO_3^-, and in smaller quantities potassium, phosphate, and various filtered organic compounds. In view of the copious glomerular filtrate, proximal reabsorption plays a crucial role in the maintenance of fluid and electrolyte balance of the body. In particular, modern hypertension research has considered it essential to identify proximal tubule Na^+ transporters, and understand the signals and second messengers that regulate these transporters. Proximal tubular transport is energized by the metabolic reactions within the proximal tubular epithelium, either directly by ATP-driven "ion pumps" (primary active transport) or indirectly by the coupling of solute fluxes to Na-transport (secondary active transport). The workload to this epithelium is prescribed by the glomerular filtration rate (GFR), which can vary several-fold within the course of a day, so that the ensemble of epithelial transport systems are also asked to modulate their function responsively, and in a coordinated manner.

All segments of isolated proximal tubules are capable of reabsorbing the same solutes when perfused *in vitro*. Quantitatively, however, marked differences exist along the tubule; reabsorption of sodium, water, glucose, and bicarbonate in the early proximal tubule is about three-fold greater than that in the mid-portion of the convoluted proximal tubule, and nearly ten times that of the straight segment of the tubule. Furthermore, *in vivo*, the transtubular concentration gradients of the luminal solutes, as well as the electrical potential of the lumen, change as one moves from early- to late-proximal tubule. In the earliest part of the proximal tubule, preferential reabsorption of organic solutes (glucose and amino acids, etc.) and of sodium bicarbonate, lactate, acetate, phosphate, and citrate occurs. Consequently, the luminal concentration of these solutes is reduced in the remaining portion of the proximal tubule. Alterations in solute reabsorption have been inferred in a number of disorders of proximal tubule, and have been of particular interest to workers seeking to understand how changes in urine composition alter the propensity to kidney stone formation.

Historically, *in vivo* micropuncture and microperfusion was the experimental method that delineated proximal tubule transport properties, namely transepithelial fluxes and permeabilities. The next investigative focus was identification of specific transporters within luminal and peritubular cell membranes, and the experimental techniques have been diverse. Assessment of the cellular compartment was first done electrophysiologically, using conventional and ion-selective microelectrodes, and subsequently with pH- or cation-sensitive fluorescent dyes. More direct information about the membrane transporters derived from vesicle preparations enriched in fractions from luminal (brush border) or peritubular cell membranes. Patch-clamp techniques (whole-cell or excised patch) allowed the study of single membrane ion channels, but have had limited application to proximal tubule. A major advance came with molecular identification of the transporters, expressing these transporters in cells that are convenient for study, developing antibodies for location and quantification within tubular cell membranes, and examination of tubules from mice in which the transporter has been knocked-out.

Seldin and Giebisch's The Kidney, Fifth Edition.
DOI: http://dx.doi.org/10.1016/B978-0-12-381462-3.00033-1

© 2013 Elsevier Inc. All rights reserved.

Central to its role in body fluid homeostasis is the responsiveness of proximal tubule sodium transport to changes in GFR, as well as to neural and hormonal signals. In large measure, changes in sodium reabsorption that accompany changes in GFR may be understood in terms of transepithelial oncotic and hydrodynamic forces which impact on the tubule cells or on the paracellular pathway. Neurohumoral regulation of proximal tubule transport begins with a cellular signal, followed by transduction steps, which ultimately produce changes in transporter densities or kinetics within the cell membranes. The signaling pathways for the important neurohumoral regulators have been an object of intense investigation, although the insights have come slowly. This research program has had to contend with a number of cellular second messenger molecules, with a number of kinases and phosphatases, with identification of anchoring proteins that secure the local action of a signal, and with the cytoskeletal elements responsible for transporter traffic. Although much information is available, a facile description of the path from neurohumoral signal to transporter flux is not yet at hand.

The organization of this chapter starts with the description of whole tubule function: fluxes and the associated driving forces; and tubule permeabilities. Historically, this is the section with the oldest data, and the section that has undergone the least revision from earlier chapter versions. The next two sections are devoted to the description of the epithelial components: luminal and peritubular cell membrane transporters; the tight junction; and the lateral intercellular space. In view of the copious transepithelial solute fluxes, special attention will be given to the problem of matching luminal and peritubular transport fluxes, in order to avoid catastrophic perturbation of cell volume and composition. The last section describes the regulation of proximal transport, with emphasis on physical factors, and on the action of the two key regulatory molecules, angiotensin and dopamine.

EPITHELIAL FUNCTION

Net Fluxes

The filtered load of a solute to the proximal tubule is the product of the single nephron glomerular filtration rate (SNGFR) and the ultrafilterable concentration of the solute. For small nonelectrolyte species the ultrafilterable concentration is that in plasma water. For electrolytes, negatively-charged serum proteins produce a Donnan potential, which acts to decrease ultrafilterable Na^+ and increase Cl^- concentration with respect to that of plasma water.[556] In amphibian and mammalian proximal tubules, the net effect of proximal tubule transport is the reabsorption of the luminal solution, resulting in a diminished axial flow rate as one proceeds along the tubules. The systemic infusion of a substance, such as inulin, which is filtered at the glomerulus, not reabsorbed (or secreted) by the proximal tubule, and which may be assayed in aliquots of tubular fluid, permits the calculation of the net volume reabsorption by the tubule from the glomerulus to the point of sampling. Thus, in the rat superficial cortical nephrons, the tubular fluid (TF) inulin concentration at the end of the convoluted proximal tubules is twice that of plasma (P), indicating that half of the filtrate is reabsorbed proximally.[242] In the amphibian, *Necturus*, the TF/P ratio suggests that about one-third of the filtrate is reabsorbed by the proximal tubule,[600] and in certain fish, the net effect of proximal tubule transport is secretion of fluid into the lumen[88]; however, in view of translational considerations, only the mammalian kidney is considered in this chapter.

With micropuncture sampling of fluid from the proximal tubule, if a complete collection of tubule fluid is made, then the absolute transport rate by the nephron segment is known and can be expressed as a flux per unit area of epithelium (Table 33.1). Alternatively, one may perfuse dissected segments of tubule to directly

TABLE 33.1 Net Fluxes across Proximal Tubules

		Rat PCT	References	Rabbit PCT	References	Rabbit PST	References
SNGFR	(nl/min)	30	(a)	20	(c)		
PT diameter	(μm)	20	(a)	26	(d)	22	(g)
Length	(mm)	5.5	(a)	5.4	(c)	3.3	(h)
J_v	(nl/s/cm^2)	65	(b)	30	(e)	9.8	(g)
J_{Na}	(nEq/s/cm^2)	9.4	(b)	4.5	(e)	1.5	(g)
J_{Cl}		5.1	(b)			1.3	(g)
J_{HCO3}		2.7	(b)	1.7	(f)	0.2	(g)

(a)[242]; (b)[757]; (c)[152]; (d)[15]; (e)[388]; (f)[214]; (g)[597]; (h)[43].

establish the epithelial fluxes under well-defined luminal and peritubular conditions. One must then obtain an independent measure of SNGFR to estimate the fractional reabsorption. The advantage of this approach is that proximal nephron segments not accessible to micropuncture may be examined. For the data from the perfused proximal convoluted tubule of the rabbit shown in Table 33.1, the measured sodium flux, referred to a 5.4 mm segment of tubule, implies sodium reabsorption of 1.2 nEq/min. With a SNGFR of 20 nl/min, the filtered load of sodium is 2.9 nEq/min, so that the fractional reabsorption is predicted to be about 40%. In the instances of successful micropuncture of rabbit proximal tubule, the observed fractional reabsorption of sodium has been 50[152] and 45%.[762] This type of comparison is particularly important, in that it suggests a reasonably well-maintained transport capacity for tubules examined *in vitro*. When examined carefully, however, conditions *in vitro* can produce subtle differences from the tubule *in vivo*. As might be expected, dissection conditions of isolated rabbit proximal tubules can decrease the peritubular membrane electrical potential and increase cytosolic Na^+ concentration; however, they can also engender a peritubular membrane K^+ channel, not seen *in vivo*, and change the Na^+ :HCO_3^- stoichiometry of the peritubular membrane co-transporter from 3:1 to 2:1.[490,492]

Unfortunately, attempts to present a concise tabulation of proximal transport (Table 33.1) must be tempered by an appreciation of internephron heterogeneity, and the structural changes along the individual tubule. In broad terms, two nephron populations have been identified: those with superficial cortical glomeruli, whose short loops of Henle turn at the outer–inner medullary border (about ⅔ of rat nephrons); and those with juxtamedullary glomeruli, whose long loops of Henle penetrate the inner medulla to variable extents. In many mammalian species, the juxtamedullary glomeruli are larger and have a greater SNGFR than the mid-cortical or superficial cortical nephrons.[556] In the rat, the filtration rate of juxtamedullary glomeruli has been measured by micropuncture collection of Henle limb fluid, and found to be about 1.5- to 2-fold that of superficial glomeruli.[286,344,512] In the rabbit, an indirect technique has given estimates confirming the disparity between superficial and juxtamedullary nephrons (e.g., 43 and 66 nl/min,[36]; 23 and 29 nl/min[43]). Comparisons of transport properties of superficial cortical and juxtamedullary proximal tubules are available.[78] Corresponding to the greater SNGFR of the juxtamedullary nephrons, there is a greater overall rate of volume and sodium reabsorption. Perfused tubule data from rabbit has indicated a relative magnitude of juxtamedullary-to-superficial Na^+ fluxes from 1.2-[341] to 2-fold[364] larger; the relative magnitude of HCO_3^- fluxes is 2-fold larger.[342] Beyond this quantitative distinction, the relative importance of specific transport mechanisms may also differ between the two nephron populations.[342,468,634]

The capacity for volume transport gradually diminishes as one proceeds along the mammalian proximal nephron.[352] This occurs in association with morphologic changes at the electron-microscopic level that have prompted the division of mammalian proximal tubule into three segments[455] (Figure 33.1). The early proximal convoluted tubule, S1, is characterized by tall, densely-packed apical microvilli, numerous mitochondria, and an intricate pattern of folding and

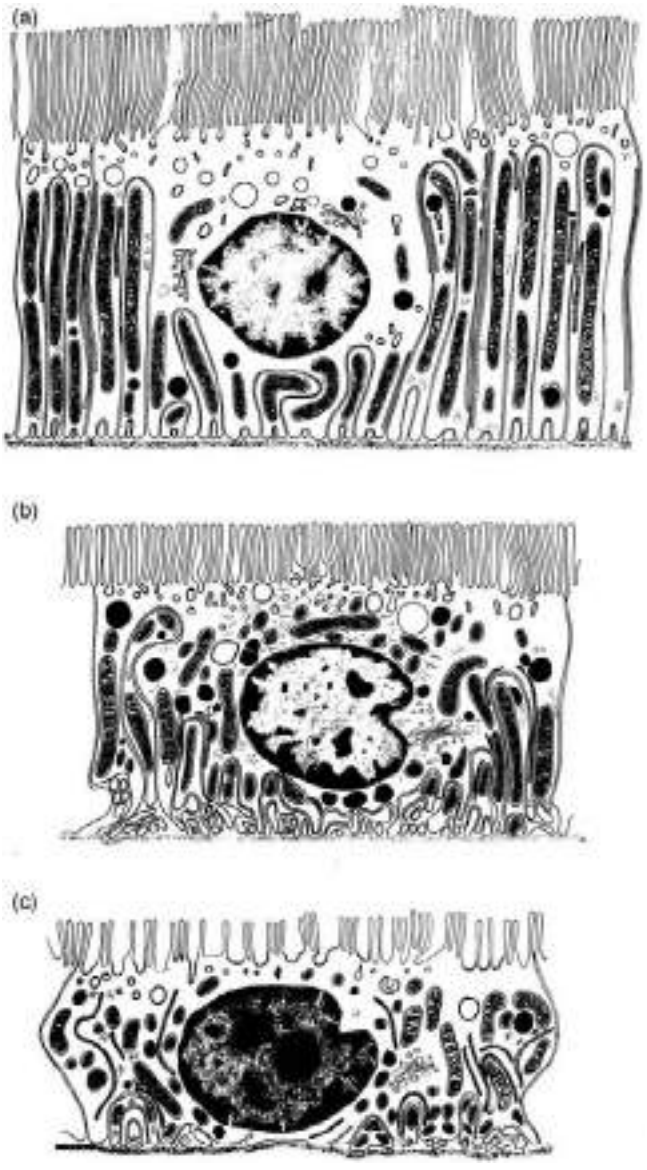

FIGURE 33.1 **Proximal tubule cells within the: (a) S1; (b) S2; and (c) S3 segments of the rabbit nephron.** *(From[352], with permission.)*

interdigitation of the lateral cell membranes.[739] There is a gradual transition to the S2 segment, which comprises the remainder of the proximal convoluted tubule and the very beginning of the proximal straight tubule. Here, there are fewer mitochondria and less amplification of membrane area. Finally, the proximal straight tubule, S3, shows a more cuboidal cell with fewer mitochondria and rare interdigitations. Welling and Welling[738] have compared the cell membrane areas in the S1 and S3 segments of rabbit proximal tubule, and found that for each segment, the apical and basolateral areas are nearly equal. In S1, however, the absorptive area of the cell is increased by membrane folding to 36 cm^2/cm^2 epithelium, whereas in S3 this value is 15 cm^2/cm^2 epithelium. The transport of solutes and water has been measured in dissected perfused segments of rabbit proximal tubule, and the spontaneous transport rate was substantially less in the proximal straight tubule than in convoluted segments[125,388] (Table 33.1). In the rat, microperfusion of proximal tubule segments *in vivo* (with comparable flow rates and luminal fluid composition) has demonstrated a lower volume reabsorption rate for segments more than 1–2 mm from the glomerulus.[165] Serial micropuncture along a single proximal tubule with filtered fluid flowing freely confirmed the sharp decline in reabsorptive flux of volume (sodium) and anions after the first 1–2 mm of tubule[426,427] (Figure 33.2). Comparison of Na^+ transport by perfused proximal straight tubules from superficial and juxtamedullary rabbit nephrons has demonstrated comparable reabsorptive rates. The respective convoluted tubule fluxes are two- and four-fold greater for Na^+,[45,364] with a similar proportionality for HCO_3^-.[708] Proximal convoluted tubule fluxes of glucose may be six-fold greater,[44] and of phosphate three-fold greater than those of proximal straight tubule.[530]

In rat and rabbit kidneys, the Na^+ concentration, and hence the total osmolality, remain relatively constant along the proximal tubule.[255,388] This constancy of tubule fluid osmolality implies "isotonic transport," and poses a special problem for rationalizing the forces at work in water reabsorption (*vide infra*). The fates of chloride and bicarbonate in the mammalian proximal tubule differ, however, in that the chloride rapidly rises to a level above that of the glomerular filtrate and the bicarbonate falls.[125,215,255,685] This shift in anion composition occurs early in the proximal tubule, that is to say, within the S1 segment. This is referred to as "preferential bicarbonate reabsorption," and has received much attention as a clue to transport activity at the cellular level. The key features of the compositional changes in tubular fluid during its passage through the mammalian proximal tubule are illustrated in Figure 33.3.[552] The tubular fluid/plasma (TF/P) concentration ratio of several solutes is plotted as a function of proximal tubular length. TF/P inulin rises to approximately 2.0, indicating water reabsorption. Glucose and amino acids are rapidly reabsorbed so that at 25% proximal tubular length their concentrations decline to some 10% of the filtrate concentration. Preferential bicarbonate reabsorption lowers the bicarbonate concentration of tubular fluid to approximately 5–8 mM. Along the initial portion of the proximal tubule, the chloride concentration is increased by reabsorption of water.[28] In the initial segment, the transepithelial voltage is lumen negative,[46,220] due to the electrogenic nature of co-transport of sodium with glucose or amino acids.[221,387] As the concentration of these solutes declines and that of chloride rises, the polarity of the transepithelial electrical potential difference changes to lumen positive values.[46,220] This voltage is, at least in part, a diffusion potential, generated by the chloride and bicarbonate concentration gradients, and the greater permeability of the tubular wall to chloride than to bicarbonate.

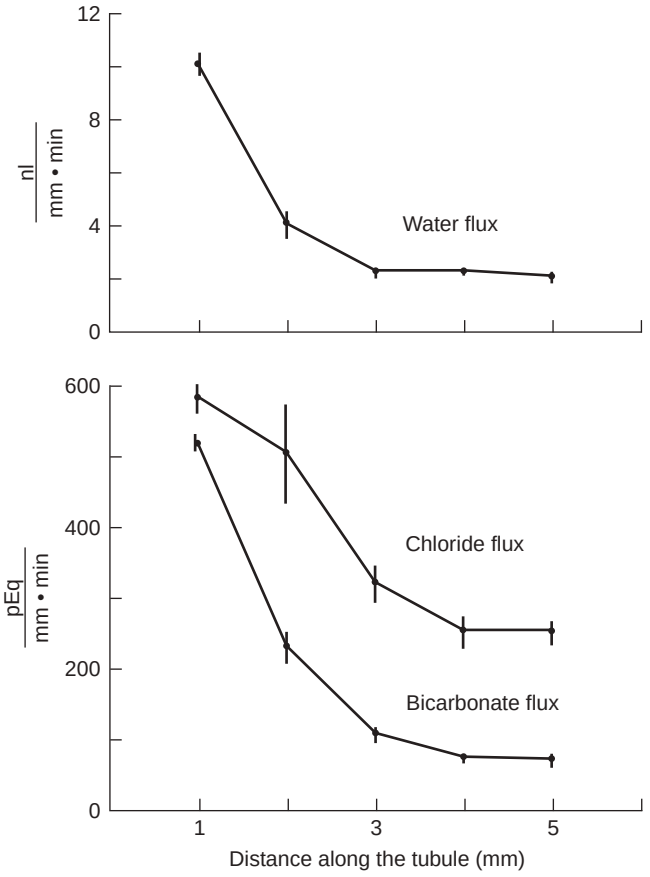

FIGURE 33.2 **Reabsorption of water, bicarbonate, and chloride along the rat proximal convoluted tubule.** *(From[427].)*

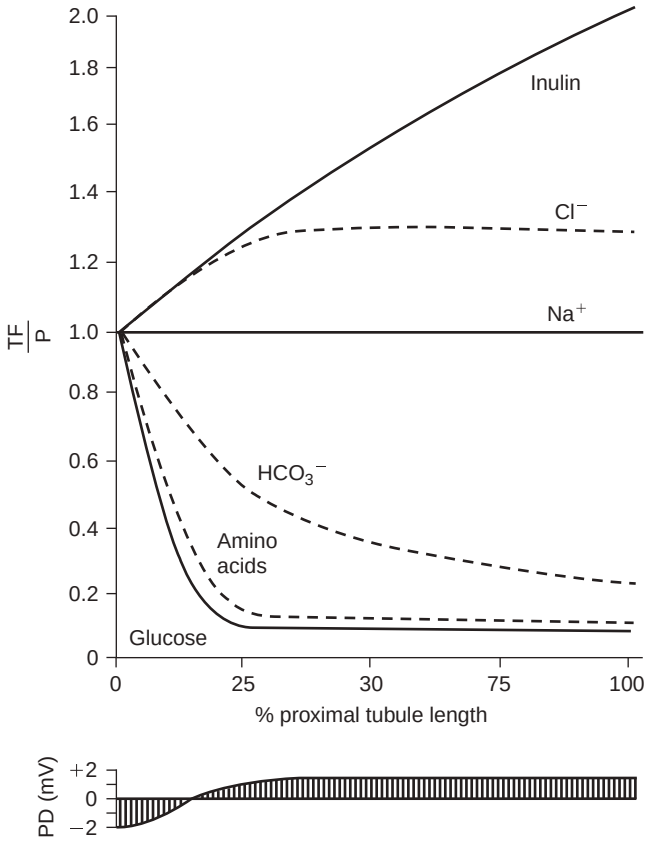

FIGURE 33.3 **Compositional changes in proximal tubule fluid along the mammalian nephron.** *(From[552], with permission.)*

Transport Forces

To attribute mechanisms to epithelial transport, fluxes must be resolved in terms of responsible driving forces, specifically hydrostatic or osmotic pressure, solute concentration gradients, electrical potential or metabolic energy. The transepithelial volume flow, J_v (ml/s · cm^2 epithelium), is a function of hydrostatic and osmotic driving forces:

$$J_v = L_p\left[\Delta p - RT\sum_1^n \sigma_i \Delta c_i\right] = (RTL_p)\left[\frac{\Delta p}{RT} - \sum_1^n \sigma_i \Delta c_i\right] = \overline{v}_w P_f\left[\frac{\Delta p}{RT} - \sum_1^n \sigma_i \Delta c_i\right] \tag{33.1}$$

Here the water permeability of the epithelium is represented either by the coefficient L_p (ml/s · cm^2 · mmHg), by RTL_p (ml/s · cm^2 · Osm) or by P_f (cm/s), where RT is the product of the gas constant and absolute temperature (1.93×10^4 mmHg/Osm at 37°C), and $\overline{v}_w$ is the partial molar volume of water (0.018 ml/mmol). In Eq. (33.1) the osmotic effect of any species is incorporated in the reflection coefficient, σ_i, ($0.0 \le \sigma_i \le 1.0$). For $\sigma_i = 1.0$, the species exerts a full osmotic effect, and the epithelium is an ideal semipermeable membrane. When $\sigma_i = 0.0$, the species exerts no osmotic force. To determine the reflection coefficient for a specific solute, the change in the transepithelial volume flow produced by a transepithelial concentration gradient, Δc_i, is compared to the volume flow produced by an equal concentration gradient of an impermeant species. The ratio of these two volume flows is just the reflection coefficient, σ_i.

To represent solute transport, J_i (mmol/s · cm^2), the epithelial flux equation is of the form:

$$J_i = J_v(1-\sigma_i)\,\overline{c}_i + \sum_{j=1}^n L_{ij}\Delta\overline{\mu}_j^c = J_v(1-\sigma_i)\,\overline{c}_i + \sum_{j=1}^n L_{ij}[RT\Delta\ln(c_j) + z_jF\Delta\psi] \tag{33.2}$$

in which the first term is a convective flux in which a mean concentration appears:

$$\overline{c}_i = \frac{\Delta c_i}{\Delta\ln(c_i)} \approx 0.5\cdot\left[c_i(l) + c_i(p)\right]$$

in which c_i(l) and c_i(p) designate luminal and plasma concentrations. It is a consequence of thermodynamic theory (Onsager symmetry) that the reflection coefficient, σ_i, from Eq. (33.1) also appears in Eq. (33.2) for convective solute drag. This formalizes the intuitive notion that the smaller solutes, which are least osmotically effective, are more likely to be entrained in the volume flow. The second term in Eq. (33.2) represents electrodiffusive solute flux, namely the flux of solute i as a function of the electrochemical potential differences, $\Delta\overline{\mu}_j^c$, of all of the solutes under consideration. Expansion of this potential is shown in the rightmost expression, in which RT is the product of gas constant and absolute temperature (2.57 J/mmol at 37°C), z_i is the valence of solute j, F is the Faraday (96.5 C/mEq), and $\Delta\psi$ is the electrical potential difference across the epithelium. It is also a consequence of Onsager symmetry that the coefficients $L_{ij} = L_{ji}$ (mmol^2/J · s cm^2). When the coefficient L_{ij} is positive (for i≠j), then a reabsorptive driving force on solute i will also promote reabsorption of solute j, so that this coefficient may be considered to represent co-transport of the two solutes. Such co-transport obviously arises when a common carrier transports the two species, but may also occur as a result of intraepithelial convective flows.[730]

Some of the most precise experimental measurements that can be made are those of electrical

potentials and currents. In the absence of solute-solute interaction, the transepithelial solute flux is written:

$$J_i = J_v(1-\sigma_i)\,\bar{c}_i + L_{ii}\,[RT\Delta\ln(c_i) + z_iF\Delta\psi] = J_v(1-\sigma_i)\,\bar{c}_i + P_i\left[\Delta c_i + \frac{z_iF}{RT}\bar{c}_i\Delta\psi\right] \quad (33.3)$$

where $RTL_{ii}/\bar{c}_i = P_i$ (cm/s) is the conventional solute permeability. Equation (33.3) has generally been the starting point for the application of electrophysiology to characterize proximal tubule. For example, if luminal and peritubular solutions have equal ionic concentrations ($\Delta c_i = 0$), and there is zero volume flow, then application of an electrical potential difference ($\Delta\psi$) produces a change in ionic current:

$$I_i = z_iFJ_i = P_i\left(\frac{z_i^2F^2}{RT}\right)\bar{c}_i\Delta\psi = g_i\Delta\psi \quad (33.4)$$

in which g_i (S/cm^2) is the partial ionic conductance of species i. The total epithelial electrical conductance, $g = \Sigma g_i$, or the epithelial electrical resistance, $R = 1/g$, thus provides a measure of the sum of the ionic permeabilities. When the luminal and peritubular solutions are unequal, the open-circuit potential, in the absence of net transepithelial volume flow ($J_v = 0$), gives useful information about the relative ionic permeabilities. In this case, the sum of all ionic currents is zero ($0 = \Sigma\, I_i$), so that the transepithelial electrical potential is:

$$\Delta\psi = -\sum_{i=1}^{n}\frac{g_i}{g}\frac{RT}{z_iF}\,\Delta\ln(c_i) \quad (33.5)$$

If, for example, the only concentration differences across the epithelium are equal and opposite anion gradients (such as chloride and bicarbonate), Eq. 33.5) shows that the difference in ionic conductances determines the magnitude of the transepithelial "diffusion potential."

Table 33.2 is a compilation of the permeability properties of the proximal tubules of rat and rabbit. Again, the inclination to present such tabulation must be tempered by acknowledgement of variation of the permeabilities along the nephron, and of differences between superficial and juxtamedullary nephrons. With respect to water permeability, it has been suggested that there is a decline in L_p from the S1 to the S2 segment of the rat tubule.[432] Nevertheless, the water permeability remains at least as large in the straight segment as in the convoluted segment.[598] With respect to solute permeabilities, an increase in the electrical conductance of the rat proximal tubule has been observed as one moves from the earliest to the latest accessible segments.[620] Experiments in perfused rabbit tubules suggest that the increase in total conductance is due to an increase in the chloride permeability.[343] Comparison of tubule permeabilities indicates that juxtamedullary proximal convoluted tubules[82,84,164,343] and proximal straight tubules[330,364,708,713] are more cation selective than the superficial proximal tubule segments. Comparison of permeabilities of K^+[764] and of Cl^-,[713] between rabbit juxtamedullary and superficial proximal straight tubules suggests that the increase in cation selectivity derives from an absolute increase in juxtamedullary nephron cation permeability, with little difference in anion permeability.

There is no doubt that proximal tubule metabolism is required for transport to proceed at its normal rate. In the absence of ionic concentration gradients across the epithelium, reabsorption still proceeds and cooling or poisoning with metabolic inhibitors

TABLE 33.2 Permeabilities of Proximal Tubules

	Rat PCT	References	Rabbit PCT	References	Rabbit PST	References
$L_p \times 10^8$ ml/s · cm^2 · mmHg	22.6	(a)	32.6		48.5	
P_f cm/s	0.24		0.35	(b)	0.52	(e)
σ(Na)	0.7	(a)			0.9– 1.0	(b)
σ(Cl)	0.43	(a)			0.78– 0.95	(b)
σ(HCO_3)	1.0	(a)			0.97	(b)
P(Na) $\times 10^5$ cm/s	24.7	(a)	4.0– 11.9	(b)	2.3– 2.6	(b)
P(K)	27.1	(a)				
P(Cl)	21.2	(a)	1.9– 6.5	(b)	5.6– 7.3	(b)
P(HCO_3)	6.7	(a)	1.3– 2.3	(c,d)	0.4– 2.0	(b)
Resistance ohm · cm^2	5	(a)	7.0	(b)	8.2	(b)

(a)[672]; (b)[595]; (c)[313]; (d)[713]; (e)[598].

abolishes transport. A generally accepted treatment of active transport by the proximal tubule has been that of Frömter[215] in which Eq. (33.2) is extended by inclusion of a term for metabolically driven transport, J_i^a:

$$J_i = J_v(1-\sigma_i)\,\bar{c}_i + \sum_{j=1}^{n} L_{ij}\Delta\bar{\mu}_j^c + J_i^a \qquad (33.6)$$

or in the absence of coupled fluxes

$$J_i = J_v(1-\sigma_i)\bar{c}_i + P_i\left[\Delta c_i + \frac{z_i F}{RT}\bar{c}_i\Delta\psi\right] + J_i^a \qquad (33.7)$$

It may also occur that water flux is linked to metabolic reactions in a way that reabsorption proceeds in the absence of transepithelial driving forces. This flux, J_v^a, has been termed "active water transport," and, by analogy with Eq. (33.6), Eq. (33.1) for transepithelial volume flow has been written[267,731]:

$$J_v = L_p\left[\Delta p - RT\sum_{1}^{n}\sigma_i\Delta c_i\right] + J_v^a \qquad (33.8)$$

A derivation of J_v^a from considerations of the internal structure of the tubule epithelium will be indicated in the section on the paracellular pathway.

THE TRANSCELLULAR PATHWAY

Cytosolic Concentrations

In the foregoing, proximal tubule transport has been treated from the perspective of the epithelium as a homogeneous entity, with reflection coefficients and permeabilities inferred from the transepithelial fluxes produced by changes in luminal and peritubular solutions. Over the last decades, however, a more microscopic view of proximal tubule transport has evolved. Crucial to this perspective were the observations that the intercellular tight junctions could serve as a low resistance route for transepithelial ion permeation.[223,758] This defines a "paracellular pathway" for fluxes, across the tight junction, into the lateral intercellular space, and out across the basement membrane to the peritubular capillaries. The "transcellular pathway" enters the cell cytosol via the luminal membrane and exits across the basal cell surface or across the lateral cell membrane into the lateral intercellular space. To discern solute transport across individual cell membranes, one must be able to monitor changes in intracellular concentrations.[110] Historically, the first estimates of cell ion content derived from chemical analysis of tissue. Difficulties with this method include the inaccuracy associated with the subtraction of the extracellular contribution to the total, as well as the limitation of examining the concentration at only a single point in time. An additional concern arises when one tries to estimate transmembrane chemical potential differences, if some of the cell ion content is bound or sequestered, and thus not available to the "transport pool." Somewhat akin to the chemical assay has been the application of the electron probe to determine cell solutes. With the small beam of this technique, true intracellular sampling can be ensured, although the estimate of cell water is indirect and an important source of uncertainty. Nuclear magnetic resonance (NMR) spectroscopy has been used as a nondestructive method for measuring intracellular sodium of proximal tubules in suspension.[278,396] Unfortunately, only a portion of the cell sodium is "visible" by NMR, and additional steps must be taken to estimate the total pool.[111] One fruitful technique for probing the cell interior has been the use of microelectrodes capable of penetrating the cell membrane, presumably without destroying the functional integrity of the cell. The electrodes may record the electrical potential of the cytosol or, when fashioned with a substance that reacts selectively with an ion, the cytosolic electrochemical potential of the selected ion species. Although technically challenging, these measurements provide precisely the information necessary for establishing the driving forces for ionic fluxes.[219,370] Subsequently, ion-sensitive fluorescent dyes were developed, and these could be loaded into proximal tubule cells and used to monitor continuous changes in pH,[7] calcium[174] or chloride.[329,395]

Despite the technical difficulty of studying the small cells of mammalian proximal tubules, a reasonably complete picture of the intracellular milieu is available (Table 33.3). In the rat, the intracellular potential has been found to be −76 mV.[189] Good agreement has been reported for the cell sodium concentration estimated electrophysiologically (17.5 mmol/l)[782] and with the electron probe (20.3 mmol/l).[61] Potassium is actively accumulated above its electrochemical equilibrium.[141,189]

TABLE 33.3a Ion Activities in Rat Proximal Tubule

	Cell Conc.	Cell Activity	Capillary Conc.	Electrochemical Potential Difference (cell-capillary)‡
	(mM)	(mM)	(mM)	(J/mmol)
Na^+	17.5	13 (a)	145	−12.8
K^+	113	82 (b)	4	1.3
Cl^-	18	13 (c)	118	2.5
HCO^{-3}	17 (d)	12	25	6.3
PD		−76 mV (b)		

‡*RT* = 2.57 J/mmol; (a)[781] (b)[189]; (c)[139]; (d)[7].

TABLE 33.3b Ion Activities in Rabbit Proximal Tubule

	Cell Conc.	Cell Activity	Capillary Conc.	Electrochemical Potential Difference (cell-capillary)‡
	(mM)	(mM)	(mM)	(J/mmol)
Na^+	44 (e)	32	145	−9.0
K^+	68	49 (f)	5	0.8
Cl^-	25	18 (g)	118	1.9
HCO^{-3}	16 (h)	12	25	4.7
PD		−61 mV (i)		

‡*RT = 2.57 J/mmol; (e)[278]; (f)[90]; (g)[335]; (h)[590]; (i)[70].*

Although an early investigation suggested passive distribution of chloride across the proximal tubule,[639] subsequent work established cellular chloride uptake against a potential gradient.[139] The mechanism underlying this elevation of cytosolic chloride will be considered below. At this point, it suffices to acknowledge that the potential hill for chloride is linked via several anion exchangers to the bicarbonate potential. In turn, the elevation of cytosolic bicarbonate is regulated and maintained well above the equilibrium value (1.4 mmol/L) by a number of transport processes, including Na^+/H^+ exchange and metabolically driven proton extrusion from the cell (H^+-ATPase).[9,576]

It has also been possible to impale cells of the isolated perfused rabbit proximal tubule. The intracellular potentials of the proximal convoluted and proximal straight tubules were first found to be −51 and −47 mV respectively,[89] and subsequent determinations have been confirmatory (−50 mV[590]; −61 mV,[70]). In the proximal straight tubule, the cell potassium activity is higher than its electrical equilibrium. Both the cell potassium activity and the cell potential fall (depolarize) with ouabain-inhibition of the peritubular Na^+, K^+-ATPase.[90] As in the rat, the chloride activity is elevated above equilibrium, and there is good agreement between the electrophysiologic determination (18 mmol/L)[335] and that found using a fluorescent dye (21 mmol/L).[395] The intracellular pH of rabbit proximal tubules in suspension was first investigated using a radiolabeled weak organic acid. Under control conditions, the cells were found to be alkaline, 7.51, becoming acid with the application of ouabain, 7.42.[96] Subsequent determinations have revealed the pH to be lower (7.22,[590]), and thus more akin to that found in the rat proximal tubule.

Luminal Membrane

General Properties

Important information about membrane permeabilities and species-species interactions has been obtained from studies in vesicle suspensions prepared from proximal tubule brush border. The water permeability of the luminal membrane was assessed by the response of vesicle volume (light scattering) to an osmotic shock.[682,683,688] Corresponding to the approximate doubling of transepithelial water permeability from proximal convoluted tubule to proximal straight tubule of the rabbit (Table 33.2), is the observation of a comparable increase in water permeability of luminal membranes from these two segments.[680] Critical insight into the mechanism of water transport came with the discovery of an integral membrane protein (designated AQP-1), which serves as a water channel, or aquaporin, and is the principal water pathway for luminal and peritubular membranes of proximal tubule (reviewed by [2]). Consistent with the membrane water permeability measurements, the abundance of AQP-1 along the proximal tubule doubles as one moves from S2 to S3 segments.[449] In mice, the importance of AQP-1 for proximal tubule water flux was demonstrated with the study of S2 segments from AQP-1 knockout mice, whose water permeability (P_f) was about 20% that of wild-type mice.[794] Additional vesicle studies indicated that across the luminal membrane, solute−water interaction appears to be minimal, with a reflection coefficient for NaCl of 1.0.[523,681,682] This is consistent with absence of solute permeation through AQP-1, when expressed and studied in oocytes.[2] Thus, in the application of Eq. (33.6) to the luminal membrane, the terms for convective solute flux may be ignored.

Electrophysiological investigation of proximal tubule revealed that luminal membrane electrical resistance (260 ohm · cm^2) is between one and two orders of magnitude greater than the total epithelial resistance[217,218] (Table 33.2). The impact of altering luminal ionic composition on intracellular potential suggested that the potassium permeability of the luminal cell membrane was much greater than the sodium permeability, and that the chloride permeability was negligible.[216] These observations provided strong evidence that sodium entry into proximal tubule cells is coupled to the entry or exit of other solute species. Direct examination of the conductive channels within this membrane using the patch-clamp technique has been possible only to a limited extent. In the first successful attempt, Gögelein and Greger[250] identified a channel in the luminal membrane of rabbit proximal convoluted tubule, which showed a greater conductance to K^+ than to Na^+. Luminal K^+ channels have also been identified in patch-clamp studies of primary culture of rabbit S1 proximal tubule.[471] Additional K^+ channels have been identified immunohistochemically in the luminal cell membrane of mammalian proximal tubule, including the voltage-gated channel KCNA10,[776] and the

voltage-dependent K^+ channel complex, KCNE1/KCNQ1.[678] Both are thought to play a role in stabilizing the membrane potential against the depolarizing effect of Na^+-dependent uptake of glucose and amino acids (*vide infra*). This role for luminal K^+ channels received confirmation in microperfusion and electrophysiological investigation of proximal tubules from homozygous kcnq1 knockout mice.[679]

Luminal membrane sodium channels ($P_{Na}/P_K \geq 19$ and blocked by amiloride) have been found in a patch-clamp study of the rabbit proximal straight tubule.[251] This result anticipated the observation of voltage-sensitive, amiloride-blockable sodium entry across luminal membrane vesicles of this tubule segment,[340] and across the luminal membrane of cultured LLC-PK1 cells.[132] The LLC-PK1 cell line is derived from pig kidney, and is thought to resemble S3 proximal tubule. A later study of the S3 segment of rat proximal tubule demonstrated a luminal membrane conductance which could be inhibited by micromolar concentrations of amiloride, and which could be enhanced by a low-sodium diet or mineralocorticoid injection.[756] Under conditions of enhanced channel expression, the mRNA which encodes for the ENaC sodium channel could be detected in these proximal tubule cells. It is natural to surmise that the capacity of the proximal straight tubule of the rabbit to reabsorb sodium in the absence of a co-transported solute[599] might be a consequence of such channels.

Chloride channels have also been identified within proximal tubule cell membranes. In the mammalian kidney, an interesting finding has been the appearance of a chloride conductance after addition of cyclic AMP[424] or by modulating cytosolic production of cyclic AMP.[425] These observations, made in a preparation of brush border membrane vesicles, were confirmed in a patch-clamp study of the luminal membrane of proximal tubule cells in primary culture,[168,577,653] and parallels observations in other epithelia. Under the cellular conditions of Table 33.3, one would expect such a channel to be a pathway for Cl^- secretion; however, in the presence of a lumen-to-blood chloride gradient, application of cyclic AMP induces a reabsorptive transcellular chloride flux, which can be inhibited by luminal application of a chloride channel blocker.[702] The physiologic role of this chloride channel in proximal tubule function remains to be delineated.

Sodium-Glucose Co-Transport

The first sodium entry pathway to receive intensive study was its coupled transport with glucose. Considerable insight had been derived from intestinal and renal preparations, and the description of co-transport that emerged received confirmation as molecular biology provided expression and study of these transporters in other cells.[305,765,766,767] The co-transport of glucose with sodium was demonstrated in vesicles prepared from luminal membranes of rabbit[23] and rat[372] proximal tubules. In the presence of a sodium gradient (medium to vesicle), vesicle glucose concentration rises to levels above that in the medium, and then slowly equilibrates with the ambient concentration. This glucose uptake, which carries a net positive current, can be enhanced by short-circuiting the vesicle membrane.[62] Conversely, glucose gradients (medium to vesicles) may be used to drive vesicle sodium concentration transiently well above that of the bathing solution.[310] In the intact epithelium, the presence of glucose and sodium in the luminal perfusate depolarizes the luminal cell membrane.[217,452,586] Examining rat proximal tubule *in vivo*, Samarzija et al.[586] observed that the magnitude of luminal membrane depolarization is diminished by lowering either the luminal glucose or sodium concentrations, by depolarizing the luminal membrane, or by elevating the cell glucose concentration. In short, reabsorptive flux of the Na^+-glucose pair is dependent upon the electrochemical potentials for each species across the luminal membrane. These qualitative features of Na^+-dependent glucose flux could be captured using a linear nonequilibrium thermodynamic model of the co-transporter.[729]

Kinetic studies of glucose uptake across luminal membrane have been presented within the framework of carrier-mediated transport, characterized by a maximal transport rate and a luminal glucose concentration for which transport is half-maximal (K_m). When Turner and Silverman examined sodium-dependent uptake of glucose into vesicles prepared from dog renal cortex, their data suggested the presence of two such carrier sites.[671] In their preparation a high-velocity, low-affinity site had a $K_m = 4.5$ mmol/L, while the second site had a low velocity and high affinity ($K_m = 0.2$ mmol/L). The possibility was suggested that these two carriers might correspond to different sites of glucose uptake along the nephron. In pursuit of this issue, Turner and Moran[638,668] prepared vesicles from both the outer cortex and outer medulla of rabbit kidney. Here, the low-affinity carrier localized to the outer cortical region (presumably containing S1 and S2 segments of the proximal tubule), and the high affinity carrier localized to the outer medullary vesicles (presumably containing S3 segments). Corresponding to the affinity difference is the determination of a 1:1 (glucose:Na^+) stoichiometry of the cortical co-transporter,[316,669] and a 1:2 stoichiometry of the high affinity carrier.[670] More direct studies, localizing glucose uptake, were performed in isolated segments of rabbit proximal tubule by Barfuss and Schafer.[44] Their data were compatible with a single high-capacity carrier in the proximal convoluted tubule ($J_{max} = 1800$ pmol/s · cm^2 and $K_m = 1.7$ mmol/L), and

low-capacity, high-affinity transporters in the proximal straight tubule ($J_{max} = 170-270\ pmol/s \cdot cm^2$ and $K_m = 0.35-0.70$). Thus, these experiments presented a coherent picture of a system of proximal glucose transport which would, under normal conditions, deliver only negligible quantities of glucose to the distal nephron. It should be noted that Na^+-glucose co-transport appears in cultured cell systems, and its identification was useful in establishing the similarity of the LLC-PK1 cell line to proximal tubule.[549] As in the straight tubule, the stoichiometry of glucose:Na^+ is 1:2.[417,476] Co-transport was also identified in primary cultures of proximal tubule cells,[153,777] again as high-affinity with 1:2 stoichiometry,[5,584] although electrophysiological study of one preparation suggested a lower affinity transporter.[74]

An important step in the study of Na^+-glucose co-transport came with the cloning of the gene for the intestinal co-transporter, SGLT1 (or, using the Human Genome Organization nomenclature, SoLute Carrier SLC5A1).[304] When this co-transporter was expressed in amphibian oocytes[328] or in mammalian cells,[102] it had high glucose affinity and kinetics indicating 1:2 stoichiometry. Early on, the availability of the intestinal transporter allowed identification of antigenic similarity with renal brush border proteins.[793] Subsequent *in situ* hybridization studies localized SGLT1 to the S3 segment of proximal tubule, precisely the site suggested by the kinetic data.[413] Prior to the cloning of this transporter, a number of detailed mathematical representations of Na^+ co-transport had been developed.[306,367,557,667] In each of these models, the co-transport of glucose and sodium was represented as a series of reactions: substrate binding to carrier; translocation of loaded carrier; unbinding at the opposite membrane face; and cycle completion by translocation of empty carrier. Expression of SGLT1 in oocytes enabled more extensive electrophysiological investigation and reformulation of a more secure model. Steady-state experiments revealed several salient features of the transporter: solute binding affinity is asymmetric, comparing inside and outside of the carrier; translocation of empty carrier is an important rate-limiting step and sensitive to the transmembrane PD; and solute-binding is not sufficiently rapid as to be considered at equilibrium with respect to translocation.[146,521,522] This expression system also enabled time-dependent studies to directly examine individual potential-dependent steps within the transport cycle. These have been useful in confirming charge of the unloaded carrier and identifying similarity in kinetics of SGLT1 from human, rat, and rabbit.[302,437,520] More recently, Loo and co-workers have focused on SGLT1 structure, and specifically characterization of the external sugar-binding domain.[311,439]

The cloning of SGLT1 also yielded insights not suspected from earlier studies, namely that protons could substitute for sodium in the transport of glucose,[312] and that in the translocation of two Na^+ and one glucose, SGLT1 also transports over 200 water molecules.[438,469] This degree of water transport may be important with respect to intestinal function, but in the kidney these fluxes through SGLT1 will be tiny. The discrepancy between the limited abundance of SGLT1 and the high capacity for glucose transport of cortical brush border membrane vesicles was readily apparent.[519] Homology screening revealed a gene which encoded for a second Na^+-glucose co-transporter, SGLT2 (SLC5A2), expressed in kidney, for which the stoichiometry is 1:1 and which, by *in situ* hybridization, localizes to the S1 segment of proximal tubule.[353] More detailed kinetic studies indicated that SGLT2 is the low-affinity, high-capacity system identified in kinetic studies.[784] When SGLT2 is expressed in oocytes and studied electrophysiologically, a kinetic scheme similar to that for SGLT1 could be developed to represent this transporter.[445] While still other sodium-glucose co-transporters have been identified, any significance with respect to renal transport remains to be established.

Sodium/Proton Exchange

From a quantitative perspective, the most important sodium flux across the luminal cell membrane is the Na^+/H^+ counter-transporter.[622] The Na^+/H^+ exchanger was securely established by Murer et al.,[494] using a suspension of vesicles composed predominately of luminal membrane. Their basic observation was that a sodium concentration gradient from suspension medium to vesicle interior resulted in acidification of the medium. This effect required the presence of intact vesicles, but was undisturbed when electrical potential differences between the vesicle interior and the medium were eliminated. Further, a suspension medium alkaline, with respect to vesicle interior, stimulated sodium uptake by the vesicles. These results were confirmed in rabbit proximal tubule vesicles by Kinsella and Aronson (Figure 33.4)[374], who further demonstrated alkalinization of the vesicle interior by the inwardly directed sodium gradient. This counter-transport is reversibly inhibited by amiloride,[375] and proceeds with a Na^+:H^+ stoichiometry of 1:1.[376] Following those early observations, kinetics of the proximal tubule luminal membrane Na^+/H^+ antiporter were studied intensively.[20,270,480] Vesicle preparations revealed a transport site that bound a single Na^+[714] with an affinity roughly one-tenth that of the external Na^+ concentration, and with competitive binding by H^+ or NH_4^+.[24,375] Studies of the antiporter at lower temperatures indicated that Na^+ uptake and H^+ extrusion occurred in a sequential ("ping-pong")

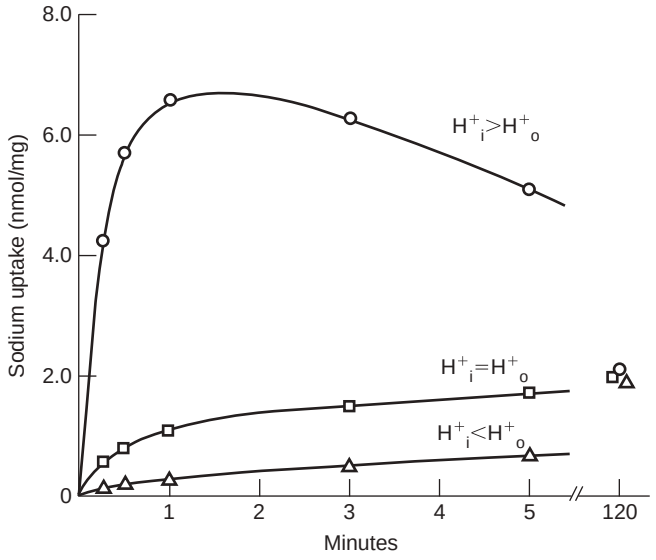

FIGURE 33.4 Effect of proton gradients on sodium uptake by luminal membrane vesicles prepared from rabbit renal cortex. Low internal pH ($H_i^+ > H_o^+$) enhances; and elevated internal pH; ($H_i^+ < H_o^+$) retards sodium entry, relative to the rate of entry in the absence of pH gradients. The vesicles were prepared in sodium-free medium and uptake was measured in solutions containing 1 mM Na^+. *(From[374], with permission.)*

fashion, with H^+ transport likely to be the rate-limiting step.[513,514] The effect of intracellular pH is more complex, with cytosolic alkalosis shutting off Na^+/H^+ exchange more sharply than a simple substrate depletion effect.[22] Cytosolic pH appears to have little impact on the Na^+ affinity of the antiporter,[377] but rather modifies the turnover rate.[514] With respect to the kinetic properties of this transporter, the information gained from renal brush border membrane vesicles has generally received confirmation in studies of isolated proximal tubule cell suspensions,[97,504] and in vesicles prepared from established cell lines[482] or from primary culture of proximal tubule cells.[209,652]

In mammalian proximal tubule, comparison of brush border and basolateral membrane vesicle showed that the Na^+/H^+ exchanger is primarily within the luminal cell membrane.[338] In the intact tubule, Schwartz[616] presented evidence for the direct coupling of Na^+ and H^+ fluxes, showing that ouabain inhibition of the peritubular Na,K-ATPase, presumably raising cell sodium concentration, could run the luminal Na^+/H^+ exchanger in reverse. Examination of vesicles from cortical and outer medullary regions of the kidney indicated that the Na^+/H^+ exchanger is present along both convoluted and straight segments of proximal tubule.[339,483] More direct evidence for the presence of the luminal membrane Na^+/H^+ exchanger in the S3 segment was offered by Kurtz.[400] Using tubules whose cells had been loaded with the pH-sensitive fluorescent dye, BCECF, he found acidification of the cell interior with removal of luminal sodium. Nevertheless, the vesicle studies indicated that the maximal Na^+/H^+ exchange rate was lower in the outer medullary population, suggesting a lower density of the transporter in straight proximal tubules.[339] This also received confirmation by Baum,[52] who perfused both convoluted and straight proximal tubules with BCECF-loaded cells. Comparing the impact of changes in luminal sodium on intracellular pH, he concluded that, relative to the convoluted segment, the straight tubule had a 30% capacity for Na^+/H^+ exchange.

In the molecular era, the Na^+/H^+ exchangers came to be recognized as a family of transport proteins, NHE-, with the luminal membrane exchanger of proximal tubule identified as NHE3 (SLC9A3). The gene for NHE3 was cloned and sequenced,[511,662] and the product identified immunocytochemically in the brush border membrane.[99] Kinetic studies of the NHE3 in expression systems generally confirmed the properties noted a decade earlier in the membrane preparations.[510,663] With respect to the Na^+/H^+ exchange activity of the peritubular membrane, the NHE1 isoform was identified in basolateral membrane vesicles and in immunohistochemical staining of rabbit proximal tubule.[100] Failure to detect NHE3 protein in proximal straight tubule prompted speculation that another NHE isoform may be operative in this segment.[12] More generally, even in tubule segments in which NHE3 was abundant, the magnitude of the Na^+/H^+ flux that actually traversed this isoform was uncertain. Based on the observation that the inhibitor profile of rat brush border vesicle Na^+/H^+ exchange was identical to the inhibitor profile of NHE3 in expression systems, it was concluded that NHE3 was the sole exchanger within the luminal cell membrane.[700] That view was quickly amended with the development of the NHE3 knockout mouse, in which proximal microperfusion revealed rates for Na^+ and HCO_3^- reabsorption of 25% and 40% compared with wild-type.[610] In subsequent *in vivo* microperfusion studies, residual Na^+ reabsorption was found to be slightly greater, 60%[443] and 45%.[703] When the proximal tubules from knockout mice were dissected, loaded with BCECF, and perfused *in vitro*, the magnitude of luminal Na^+/H^+ exchange could be assessed as the change in intracellular pH in response to restoration of luminal Na^+.[151] In those experiments, the Na^+-dependent proton secretion in knockout tubules was about 50% of the wild-type, and completely inhibitable by amiloride. The magnitude of NHE3 flux was also assessed in rat proximal tubules perfused *in vivo*, in which a specific NHE3 inhibitor reduced Na^+ reabsorption by 30%[676] and 40%.[700] These values are likely to be underestimates of

the NHE3 flux, in view of the fact that amiloride inhibition was only 50%.[700] In sum, it seems safe to attribute about half of the luminal membrane Na^+/H^+ exchange to NHE3. With respect to the molecular identity of the residual transport, both NHE2 knockout[151] and specific inhibitor studies[700] have eliminated NHE2 as a candidate. Goyal and co-workers identified NHE8, within kidney cortex[258] and expressed on proximal tubule brush border.[257] Its quantitative role in luminal Na^+/H^+ exchange remains to be defined.

Regarding the functional importance of the luminal membrane Na^+/H^+ exchanger in the proximal nephron, two caveats are in order. It is important to distinguish total HCO_3^- reabsorption from the Na^+-dependent portion of HCO_3^- reabsorption. The luminal membrane contains an H^+-ATPase,[120] and amiloride block of the Na^+/H^+ transporter has been used to identify a significant component of proton secretion via the H^+-ATPase.[41,319,400,537] The second caveat is that total Na^+-dependent proton secretion may be considerably greater than tubular HCO_3^- reabsorption. Preisig and Rector[538] microperfused rat proximal convoluted with a late proximal solution, low in bicarbonate and high in chloride. In this situation, where net bicarbonate absorption was virtually absent, amiloride still inhibited 44% of NaCl reabsorption. These findings were taken as evidence for the importance of parallel pathways through the luminal membrane for Na^+ (via the Na^+/H^+ exchanger) and for Cl^- (via a Cl^- base exchanger) in the net reabsorption of NaCl. The implication of such a scheme is that the net flux of Na^+ across the Na^+/H^+ transporter can well exceed the total reabsorptive bicarbonate flux. The first mathematical model of NHE3 was based on a scheme of Na^+-binding, translocation, and release, H^+-binding, translocation, and release, and also included competing NH_4^+-binding, translocation, and release.[734] In this model, all binding was assumed to be rapid (equilibrium), and affinity coefficients were assumed to be symmetric with respect to internal and external faces of the transporter. With one additional assumption, namely the inclusion of an internal modifier site which enhances translocation in response to cytosolic acidification, the kinetic behavior described in vesicle studies could be represented. When this simulation of NHE3 was incorporated into a mathematical model of rat proximal tubule, Na^+/H^+ exchange functioned directly to reabsorb luminal $NaHCO_3$, and in parallel with a luminal membrane Cl^-/base exchanger, yielded net NaCl reabsorption. An additional prediction of this kinetic model was that Na^+/NH_4^+ exchange via NHE3 is the most important mechanism for ammonia secretion by proximal tubule. This comported with conclusions from tubules *in vitro*, that ammonia secretion from cellular ammoniagenesis could be blocked by inhibition of NHE3.[496] Both experiment and model cast doubt on an earlier scheme of diffusive NH_3 secretion and trapping in acidic luminal fluid. With respect to NHE function, more sensitive experimental techniques have revealed nonlinearities. Fuster et al. used a pH-sensitive electrode to determine bath pH gradient in the immediate neighborhood of proton-transporting cells; from the gradient magnitude and the cell shape, they calculated the transmembrane proton flux.[231] When this methodology was applied to cells expressing NHE1 (and to a lesser extent NHE3), it was found that NHE turnover rate as a function of external Na^+ became sigmoidal.[232] Their observations were consistent with NHE schemes in which two "monomers" functioned cooperatively to yield a functional transport stoichiometry of $2Na^+$ for $2H^+$. The study demonstrated the power of an electrophysiological technique to examine an electroneutral transporter; whether the observations have a physiologic correlate in kidney tubule function, remains uncertain.

Chloride/Base Exchange

To enter the cell across the luminal membrane, chloride must be transported up an electrochemical potential gradient (Table 33.3); either co-transport with luminal Na^+ or exchange for cytosolic base, is energetically feasible. In the rat, Lucci and Warnock[444] found that furosemide inhibited two-thirds of the fluid transport when the luminal perfusion was a high-chloride, low-bicarbonate solution. In view of the ability of a known inhibitor of erythrocyte anion exchange (SITS) to also inhibit proximal volume reabsorption, Lucci and Warnock suggested that NaCl transport occurred via parallel luminal Na^+/H^+ and Cl^-/OH^- (or Cl^-/HCO_3^-) exchangers. Warnock and his colleagues supported this hypothesis with the demonstration of pH-gradient driven, electroneutral Cl^- fluxes across brush border membrane vesicles.[709,711,712] Similar conclusions were drawn by Liedtke and Hopfer,[421] whose study of luminal membrane vesicles from rat small intestine indicated that coupled Na^+-Cl^- co-transport was unlikely. Their work also indicated an inhibitory effect of furosemide on the Cl^-/OH^- exchanger.[422] Absence of Na^+-Cl^- co-transport was also a consistent finding in vesicles prepared from brush border membranes of the mammalian kidney.[493,623] In the straight proximal tubule of rabbit, a Cl^- microelectrode study has failed to detect Na^+-dependent luminal chloride entry.[335] Although a number of reports confirmed the presence of a Cl^-/OH^- exchanger in renal brush border membrane vesicles,[129,144,637] the absence of quantitatively significant flux through such an exchanger was indicated by others.[138,337,580,623] Methodological concerns relating to vesicle experiments were raised on both sides of this issue. When Schwartz[617] perfused rabbit proximal

convoluted tubules with a sodium-free acidic fluid, there was no significant effect of luminal Cl^- on the appearance of bicarbonate within the luminal fluid.

Critical insight into luminal chloride transport came with the work of Karniski and Aronson,[355] who demonstrated a chloride-formate (Cl^-/HCO_2^-) exchanger in brush border membrane vesicles from the rabbit. In their experiments, a formate gradient could drive transmembrane chloride flux, and a chloride gradient could drive formate flux. This process was electroneutral and could be blocked by the anion exchange inhibitor, DIDS. Most significantly, they found (Figure 33.5) that while a pH gradient only slightly enhanced chloride uptake, this same gradient in the presence of a physiologic concentration of formate could drive substantial chloride flux. To account for this formate effect, they suggested that a backflux of formic acid, down its concentration gradient, from the acidic bath to the alkaline vesicle interior, would serve to constantly resupply the Cl^-/HCO_2^- exchanger. Karniski and Aronson proposed that in the intact tubule, the concurrent operation of Cl^-/HCO_2^- and Na^+/H^+ exchangers, along with backdiffusion of formic acid, would yield a net flux of NaCl across the luminal cell membrane. Subsequently,

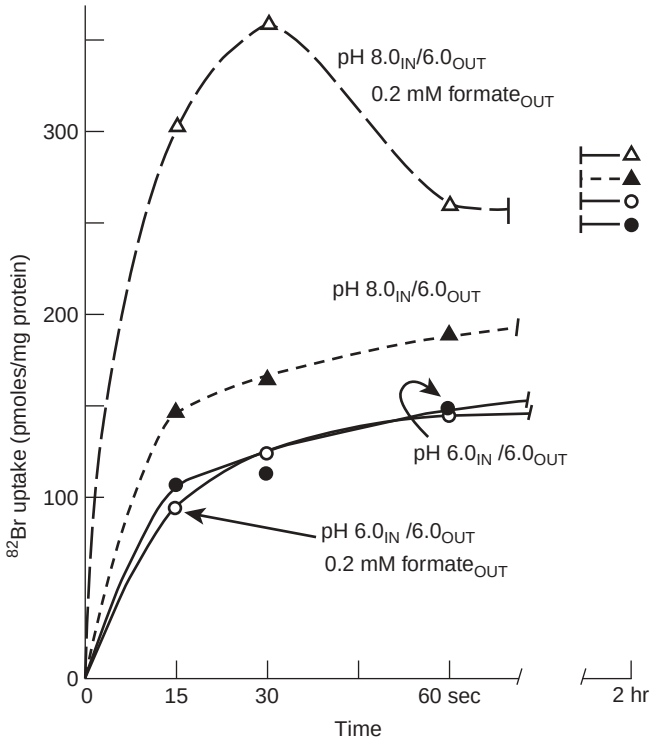

FIGURE 33.5 **Effect of formate and a pH gradient on $^{82}Br^-$ uptake by luminal membrane vesicles prepared from rabbit renal cortex.** While a pH gradient (8.0–6.0) only slightly enhances $^{82}Br^-$ transport, this same gradient in the presence of 0.2 mM formate produces a substantial increase in uptake, with an overshoot above the equilibrium concentration. *(From[355].)*

this mechanism was refined, with the identification of a luminal membrane HCO_2^-/OH^- exchanger, which could recycle secreted formate back into the cell.[585] (By virtue of its inhibitor profile, this anion exchanger is distinct from the Cl^-/HCO_2^- antiporter.) One point of difficulty with the overall scheme was the subsequent finding that the diffusional permeability of the luminal membrane to formic acid was far too low to sustain a flux comparable to the estimated chloride flux.[535] An effort was made to rationalize this discrepancy mathematically, by considering the possibility of formic acid accumulation within an unstirred layer defined by the brush border. It was found, however, that with realistic diffusion coefficients, the microvilli were sufficiently short that no significant differences of formic acid concentration could develop between the bulk luminal solution and that near the cell membrane.[393,394] At this time, the possibility of a microdomain of low pH adjacent to the luminal membrane in which the formic acid to formate concentration ratio is enhanced remains the least secure element of this proposed mechanism.

Acknowledging points of uncertainty, a scheme emerged in which Cl^-/base exchange in proximal tubule is effected by two or more anion exchangers functioning in parallel[21] (Figure 33.6). To pursue this scheme further, a candidate protein for the Cl^-/HCO_2^- antiporter was sought and purified from brush border membrane vesicles.[642] Of uncertain significance was the observation that when reconstituted into phospholipid vesicles, this protein could also mediate direct Cl^-/HCO_3^- exchange.[641] The effect of formate has been examined in intact tubules, with cells containing BCECF, in which luminal chloride is able to acidify the cell in the presence (but not the absence) of formate.[8,51] It must also be acknowledged that one protocol which could detect formate stimulation of Cl^-/base exchange in superficial proximal convoluted tubules failed to detect it in tubules from juxtamedullary nephrons.[634] There has also been the observation of a negative formate effect in a study of proximal straight tubule,[402] again raising the possibility of nephron heterogeneity with respect to the mechanism of chloride entry. In their search for chloride entry mechanisms, Karniski and Aronson[356] also demonstrated a Cl^-/oxalate exchanger within brush border vesicles, on a carrier distinct from that for Cl^-/HCO_2^-. The subsequent finding of luminal membrane pathways for oxalate recycling, either in exchange for SO_4^{2-} or OH^-,[398] supported the possibility that the Cl^-/oxalate exchanger may also be an important route for luminal membrane Cl^- entry (Figure 33.6). Aronson and colleagues[398,698] envisioned the possibility that three carriers in parallel, Cl^-/oxalate and oxalate/SO_4^{2-} antiporters plus the $2Na^+$–SO_4^{2-} co-transporter, would effect luminal entry of NaCl.

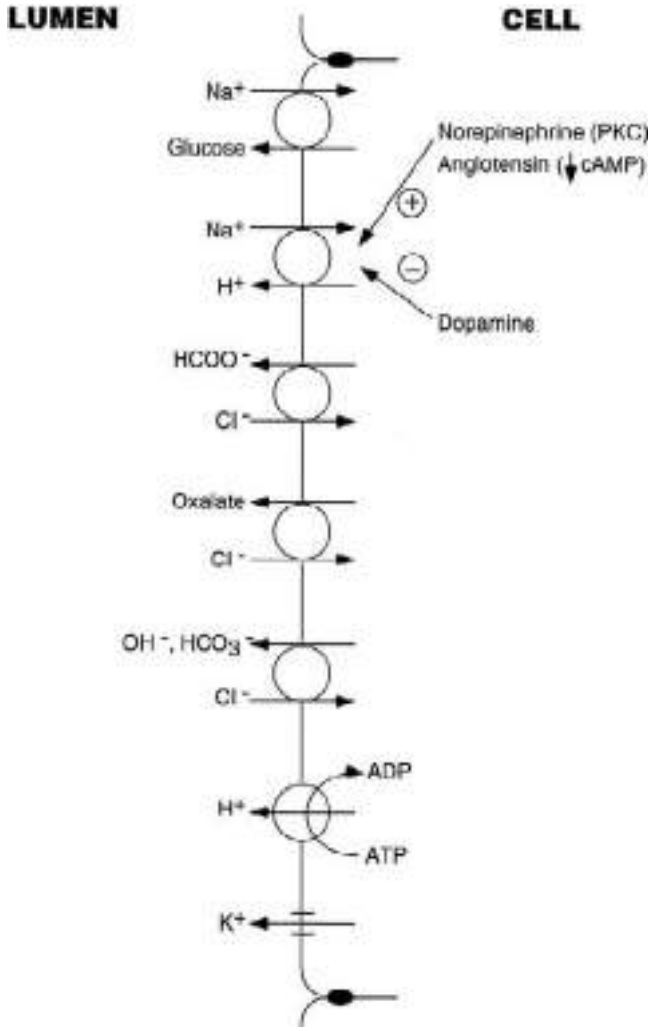

FIGURE 33.6 **Transport pathways across the luminal cell membrane of the mammalian proximal tubule.**

Confirmation of the importance of luminal chloride/base exchangers came with measurements of fluxes in intact proximal tubules. When any segment of rabbit proximal tubule (S1–S3) was perfused with an acidic (high Cl^-, low HCO_3^-) solution, there was a substantial impact of formate to stimulate volume (NaCl) reabsorption[603,604] In perfusions with a relatively alkaline solution (such as an ultrafiltrate of plasma) there was no such enhancement, presumably due to the limited recycling of formate. In reviewing these observations, Berry and Rector[83] pointed out that the pH-dependence of formic acid permeation effectively prioritizes proximal anion reabsorption along the tubule, HCO_3^- taking precedence over Cl^-. The increased volume reabsorption observed with formate was subsequently found to occur in association with an increase in cell volume, thus supporting the transcellular route for the increment in chloride flux.[601] With perfusion of proximal tubules of the intact rat kidney, both luminal formate and oxalate enhance NaCl reabsorption from an acidic, high-chloride, luminal solution.[698,699,706] The ability of a chloride channel blocker, DPC, within the peritubular perfusate, to block the formate and oxalate effects is additional evidence that the increment in NaCl flux is transcellular.

Molecular identification of luminal membrane anion transporters has focused attention on the SLC26 family of anion exchangers.[178,489] Of the members in this family, the SLC26A4 transporter (pendrin) was demonstrated to be a Cl^-/formate exchanger when expressed in *Xenopus* oocytes,[619] and its mRNA was identified in rat kidney cortex.[645] The protein, however, was not detected immunohistochemically in mouse proximal tubule brush border.[381] Furthermore, in pendrin knockout mice, Cl^-/formate exchange in brush border membrane vesicles was normal, and microperfusion of proximal tubules showed normal formate stimulation of volume reabsorption.[357] The transporter SLC26A6 (CFEX, PAT1) could also mediate Cl^-/formate exchange in oocytes, and the protein was expressed in brush border of mouse proximal tubules.[381] Further study of SCL26A6 revealed that it had a broad transport capacity, which included Cl^-/oxalate, Cl^-/HCO_3^-, and Cl^-/OH^-.[148,772] The observation that low concentrations of oxalate could inhibit Cl^-/HCO_3^- exchange led Jiang et al.[345] to surmise that the primary function of SLC26A6 in proximal tubule was as the luminal Cl^-/oxalate exchanger. This prediction was borne out in a study of mice deficient in SLC26A6.[705] The mice had normal serum electrolytes and normal proximal tubule volume reabsorption under control conditions; oxalate stimulation of proximal volume flux was absent. These knockout mice showed only a tendency toward deficient formate stimulation of volume reabsorption, so that at this time, the identity of the Cl^-/formate exchanger(s) remains uncertain.

Suspicion that formate may have other effects on proximal transport, beyond luminal anion exchange, was raised in a mathematical model of rat proximal convoluted tubule which included representation of luminal membrane Cl^-/HCO_2^- exchange.[733] Simulation of formate addition reproduced the observed cell swelling and increase in cytosolic chloride concentration; however, the density of the chloride/formate exchanger had virtually no effect on overall NaCl reabsorption along the tubule. In similar simulations, the density of the Na^+/H^+ exchanger had a powerful impact on NaCl reabsorption, indicating that for the model tubule, sodium reabsorption was rate-limiting for NaCl flux. Subsequent experimental examination of mice deficient in NHE3 found that formate stimulation of proximal sodium (volume) and chloride reabsorption was absent, although oxalate stimulation was entirely preserved.[704] These workers surmised that, in the normal tubule, there

might be a functional coupling between NHE3 and the Cl^-/formate exchanger. A direct study of the formate effect on NHE3 function was undertaken by Petrovic et al.[528] In the absence of CO_2/HCO_3^-, addition of formate to the bath and lumen of mouse microperfused kidney proximal tubule caused intracellular alkalinization, with cell pH increasing from baseline level 7.17 to 7.55. Removal of sodium from the lumen or addition of EIPA completely prevented the alkalinization. It was concluded that formate stimulates the apical Na^+/H^+ exchanger NHE3 in kidney proximal tubule, and that formate stimulation of chloride reabsorption could be indirect and secondary to activation of NHE3. An intriguing possibility is that the Cl^-/formate exchanger may be acting as a formate receptor to modulate NHE3.[528] In a subsequent study, deletion of the Slc26a6 anion exchanger from the S3 mouse proximal tubule diminished NHE3 activity, despite comparable protein abundance.[527]

Peritubular Membrane

General Properties

The cell sodium content reflects the balance among conductive, coupled, and metabolically driven fluxes across both luminal and peritubular cell membranes. In the rat, the potassium-to-sodium permeability ratio is about 20:1,[215] and the electrical resistance of this membrane is 90 ohm · cm^2, roughly a third of the luminal membrane.[217] A similar apportionment of electrical resistance appears in the proximal convoluted tubule of the rabbit, where the peritubular and luminal resistances are 39 and 118 ohm · cm^2.[410] In the straight proximal tubule of the rabbit, Bello-Reuss[70] has found the peritubular sodium conductance undetectable. In the first successful application of a patch pipette to the peritubular membrane of rabbit proximal tubule, only a potassium channel was clearly identified.[250] With respect to convective sodium fluxes across this membrane, all the data are negative with one exception. Welling et al.[740,742] applied an osmotic shock to the peritubular surface of isolated rabbit tubules and recorded the change in cell volume. A comparison of the effect of raffinose and NaCl indicated a reflection coefficient, $\sigma_{NaCl} = 0.5$, suggesting that water flow across this membrane would carry significant quantities of NaCl. This surprising result did not receive confirmation, however, in two subsequent studies of basolateral membrane vesicles. Using either light-scattering[682] or a fluorescent indicator[523] to assess vesicle volume, salt reflection coefficients of 1.0 were obtained. Subsequent experiments in whole tubule preparations, with optical measurement of cell volume[284] or using a fluorescent indicator[635] indicated $\sigma_{NaCl} = 1.0$, implying no NaCl flowed convectively across the peritubular membrane.

Sodium Bicarbonate Co-transport

Co-transport of sodium with bicarbonate is an important pathway for sodium and the principal pathway for bicarbonate exit across the peritubular membrane in both amphibian and mammalian proximal nephron.[9,109,534] The delineation of this coupled transport followed from the careful examination of bicarbonate exit from the salamander proximal tubule by Boron and Boulpaep.[108] Using pH and Na^+-sensitive microelectrodes, they observed that a reduction in peritubular bicarbonate concentration led to a decline in cytosolic pH, a peritubular depolarization, and a decline in cell sodium activity. Further, a reduction in peritubular sodium also led to a decline in cytosolic pH and, in contrast to the expectation from a conductive Na^+ pathway, peritubular depolarization. All of these effects could be blocked by the anion transport inhibitor, SITS. These results suggested the operation of a coupled Na^+ and HCO_3^- co-transporter, with the exit of at least two bicarbonate ions for each sodium. In the salamander, the electrochemical gradient of bicarbonate across the peritubular membrane was sufficient to drive sodium exit from the cell, if the stoichiometry were 2:1 or greater (HCO_3^-:Na^+). Subsequent study of the *Necturus* proximal tubule confirmed the presence of substantial voltage-sensitive HCO_3^- exit across the peritubular membrane,[454] which was later shown to be coupled to Na^+ and HCO_3^- transport.[441] Here, it was suggested that the stoichiometry might well be 3:1. With regard to the issue of HCO_3^-:Na^+ stoichiometry, one interesting set of observations in *Necturus* was the finding that when functioning in the normal reabsorptive direction, this ratio was 3:1, but when bath conditions were changed to reverse the flux direction, the ratio changed to 2:1.[531] This suggested an asymmetry with respect to the affinities of the substrates, perhaps secondary to the conformational changes of the transporter during the translocation step.

In rat proximal tubule, experiments using conventional microelectrodes indicated that elimination of bicarbonate from the perfused peritubular capillaries produced a large instantaneous depolarization.[225] In this early work, the investigators attributed the depolarization to a conductive bicarbonate pathway and estimated (Eq. (33.5)) that nearly half the peritubular membrane conductance might be mediated by bicarbonate. Electrophysiologic study of the perfused straight proximal tubule of the rabbit also disclosed a steady-state depolarization with removal of peritubular bicarbonate.[70,89] In that work, however, the depolarization was attributed to a pH-dependent decrease in peritubular membrane K^+ conductance, and thus

a decreased contribution of the K^+ potential to the overall membrane potential. The rat proximal tubule was then re-examined, and still the results indicated that the immediate depolarization produced by peritubular bicarbonate removal did not depend upon changes in membrane K^+ conductance.[123,124] This depolarization was inhibited by SITS, but a clear implication of Na^+ in the bicarbonate exit step was not confirmed. Within a short period of time, a number of investigators securely established the presence of Na^+—HCO_3^- co-transport in the peritubular membrane of the mammalian kidney. Sasaki et al.[590] using pH-sensitive microelectrodes, demonstrated that in the straight proximal tubule of rabbit, elimination of bath sodium resulted in cellular acidification and peritubular depolarization, an effect that was partially blocked by SITS. Biagi and Sohtell[91,92] used conventional microelectrodes to document a peritubular depolarization with sodium removal in both convoluted and straight proximal segments. The effect was substantially blocked by SITS, and attributed to coupled HCO_3^- transport. Yoshitomi et al.[781] re-examined the rat proximal tubule, now using both Na^+-sensitive and pH-sensitive microelectrodes. Removal of peritubular sodium or bicarbonate led to the expected depolarization, acidification, and decrease in cell sodium activity. When these investigators compared the (SITS-inhibitable) depolarization with either 10-fold reductions of peritubular Na^+ or HCO_3^- (equal changes in chemical potential) they found that the impact of the bicarbonate removal was three-fold greater. They concluded that the HCO_3^-:Na^+ stoichiometry was 3:1. In an independent set of experiments, sudden reduction in peritubular bicarbonate produced peritubular HCO_3^- and Na^+ fluxes (estimated from cell size and buffering power), which confirmed the 3:1 coupling ratio.[781]

The peritubular bicarbonate pathway in the rat proximal tubule was also investigated using fluorescence of intracellular BCECF to monitor changes in cytosolic pH.[7] In this first use of BCECF in the rat, Alpern was able to document SITS-inhibitable acidification of the cell with reduction of peritubular sodium. When BCECF was used to detect pH changes along the nephron, the transporter was identified in the S3 segment, but in clearly reduced capacity compared with S2.[52,238] Abuladze et al.,[1] used BCECF to quantify Na^+—HCO_3^- transport capacity in all three proximal tubule segments from both cortical and juxtamedullary rabbit kidneys. They reported S1 fluxes three- to five-fold greater than those of S2, and S2 fluxes eight-fold greater than those of S3. Examination of isolated basolateral membrane vesicles prepared from rabbit[4,263] and rat kidney[264] permitted the kinetics of the transporter to be studied in relative isolation. By determining driving force equilibrium across this transporter, Soleimani et al.[644] confirmed that three negative charges were carried for each sodium. Subsequently, the co-transported species were identified as one HCO_3^- plus one CO_3^{2-}.[640] Identification of the transported species was also pursued electrophysiologically. In rabbit proximal tubules *in vitro*, under "standard" conditions, the stoichiometry of peritubular HCO_3^-:Na^+ flux through this co-transporter was 2:1, and insensitive to carbonic anhydrase inhibition. However, with perfusion conditions more closely approximating those *in vivo*, the stoichiometry shifted to 3:1, and was sensitive to carbonic anhydrase inhibition. This change in transport was interpreted as a shift of the transported species from $2HCO_3^-$—Na^+ to CO_3^{2-}-HCO_3^-—Na^+, as *in vivo*[490,492,625] Gross and Hopfer[273] studied the Na^+—HCO_3^- co-transporter in a cell line derived from the S1 segment of rat proximal tubule, grown to confluence on filters. When the luminal cell membrane of this artificial epithelium was permeabilized with amphotericin, cytosolic solute concentrations were identified with those of the luminal solution, and the stilbene-sensitive transepithelial current with current through the Na^+—HCO_3^- co-transporter. Data from this preparation indicated a 3:1 flux stoichiometry,[273] and provided information with which to construct a detailed kinetic model for this transporter.[274,275]

The Na^+—HCO_3^- co-transporter (SLC4A4) was cloned first from *Ambystoma* kidney,[573] and then from human[127] and rat kidneys.[128,572] Denoted akNBC, hkNBC, and rkNBC respectively, all three co-transporters are comprised of 1035 amino acids, and structural comparisons have been presented.[571,643] Using antibody developed against rNBC, the protein was demonstrated in rat proximal tubule in an exclusively basolateral pattern, with intense staining in S1, rapid decline in S2, and no detectable staining in S3.[607] Staining in *Ambystoma* proximal tubule was also basolateral, but considerably weaker. Immunohistochemistry at the electron microscopic level confirmed these findings.[460] When rkNBC was expressed in *Xenopus* oocytes, transporter function could be studied electrophysiologically, and the stoichiometry of HCO_3^- to Na^+ fluxes was found to be 2:1.[184,618] It was concluded that the function of this transporter in mammalian cells *in vivo* was clearly different from its function in oocytes. The conundrum was sharpened with experiments in artificial epithelia derived from mouse proximal tubule or collecting duct, each deficient in NBC. In these two mammalian cells, transfected kNBC showed 3:1 or 2:1 stoichiometry for proximal and collecting duct cells, respectively.[271] Important insight came from, Müller-Berger et al.[491] who examined rkNBC in oocytes electrophysiologically, and found that with elevation of cytosolic calcium concentration, there was a relatively slow (30 second) activation of

the NBC conductance, plus a shift in stoichiometry from 2:1 to 3:1. They understood that such events in the proximal tubule *in vivo* would constitute a switch from zero (or secretory) peritubular HCO_3^- flux to brisk HCO_3^- reabsorption. This switch was deciphered by Gross et al.,[272] working with the artificial mouse proximal tubule epithelium transfected with kNBC. They found that addition of cAMP caused a shift in stoichiometry from the basal 3:1 to 2:1, and this was PKA-dependent. Replacing the single PKA phosphorylation site of the transfected transporter eliminated the stoichiometric shift.

Chloride Transporters

In early electrophysiologic investigation of both amphibian[276,636] and mammalian[70,124,133] proximal tubules, peritubular chloride conductance appeared to be virtually absent or at least negligible. In proximal convoluted tubules of the rabbit, perfused *in vitro*, peritubular application of a chloride channel blocker had no effect on NaCl reabsorption.[53] Welling and O'Neil[744] found that in rabbit proximal straight tubule the conductive chloride pathway in peritubular membrane could account for about 6% of the total membrane conductance. However, after cell swelling induced by a 150 mOsmol hypotonic osmotic shock, the chloride conductance increased to 20% of the total peritubular membrane conductance. Using quantitative video microscopy, the volume of rabbit proximal convoluted tubules was unaffected by changes in peritubular chloride concentration. However, prior hypotonic cell swelling rendered the cell volume sensitive to peritubular chloride concentration, and this effect was eliminated by application of a chloride channel blocker.[602] Peritubular chloride channel blockers have also been effective in blunting the changes in the membrane electrical potential following a change in peritubular chloride concentration.[626] Further electrophysiologic study of rabbit convoluted tubule during osmotic shock estimated the fractional chloride conductance to increase from 3% to a maximum of 16%, with relaxation to 8%. During these same experiments, the fractional conductance of the $Na^+-3HCO_3^-$ pathway declined from 41 to 16%, with little change in the absolute conductance through this pathway. Data from such experiments provide enough information to estimate the reabsorptive flux of chloride through the peritubular channels. If one assumes that the peritubular membrane has an electrical resistance of 100 ohm $\cdot$ cm^2,[410] equivalently a conductance of 10 mS/cm^2, then the conductance of the $Na^+-3HCO_3^-$ pathway is about 5 mS/cm^2, as is the maximal chloride conductance after the osmotic shock. With reference to Table 33.3b, the cytosolic chloride electrochemical potential across this channel is about 2 J/mmol or 20 mV. Multiplication by the steady-state chloride conductance of the swollen cell, 2.5 mS/cm^2, yields a chloride current of 50 nA or 0.5 nmol/s $\cdot$ cm^2. This estimate may be compared with the overall transepithelial sodium flux of late proximal convoluted tubule at 4.5 nmol/s $\cdot$ cm^2. Thus, the conductive chloride flux is not insignificant, and yet it cannot be the whole story. Further, concern over the magnitude of the osmotic shocks used in these experiments prompted re-examination with smaller perturbations by Breton et al.[117] When the cell volumes increased by only 20–25%, the peritubular chloride conductance increased by only 3–4-fold from control. Another important observation from the study of Breton et al.[117] was that the time course of chloride channel activation was delayed with respect to the time course of cell swelling, suggesting perhaps a chemical modification of the channel, rather than an immediate stretch-activated response. As in the luminal membrane, increases in cytosolic cAMP also activate a chloride channel within the peritubular membrane of rabbit[627,628] and rat.[702]

From the considerations above, peritubular chloride fluxes must also occur as electroneutral-coupled transport with other ions. Guggino and associates[277,436] examined chloride transport across the peritubular membrane of *Necturus* proximal tubule, using Cl^-- and pH-sensitive microelectrodes. They found that following either removal of peritubular Cl^- or increase of cytosolic Cl^-, exit of chloride from the cell was substantially blunted by removal of either peritubular Na^+ or HCO_3^-. This chloride exit was inhibited by SITS. In view of the electroneutral nature of the process, they proposed a coupled transport mechanism in which intracellular Cl^- was exchanged for Na^+ and 2 HCO_3^- from the peritubular side (Figure 33.7). Such coupled transport systems had been established in invertebrate neurons.[576] Other studies of chloride permeation of the peritubular membrane of amphibian proximal tubule suggested a Cl^-/HCO_3^- exchanger that was independent of sodium,[188,783] although such a transporter would mediate chloride uptake by the cell. In the mammalian proximal tubule, peritubular Cl^-/HCO_3^- exchange had been suspected from peritubular capillary perfusion studies in the rat.[119,673] More convincing evidence for the presence of Na^+-dependent Cl^-/HCO_3^- exchange in the peritubular membrane of rat proximal tubule came from experiments of Alpern and Chambers.[10] In these tubules loaded with BCECF, restoration of peritubular capillary chloride produced cellular acidification. This acidification did not occur in the absence of ambient (luminal and peritubular) Na^+, and was blocked by SITS. Consistent with these findings was the observation[264] that in basolateral membrane vesicles from rat renal cortex, an oppositely directed Cl^- gradient (inside to outside) stimulated

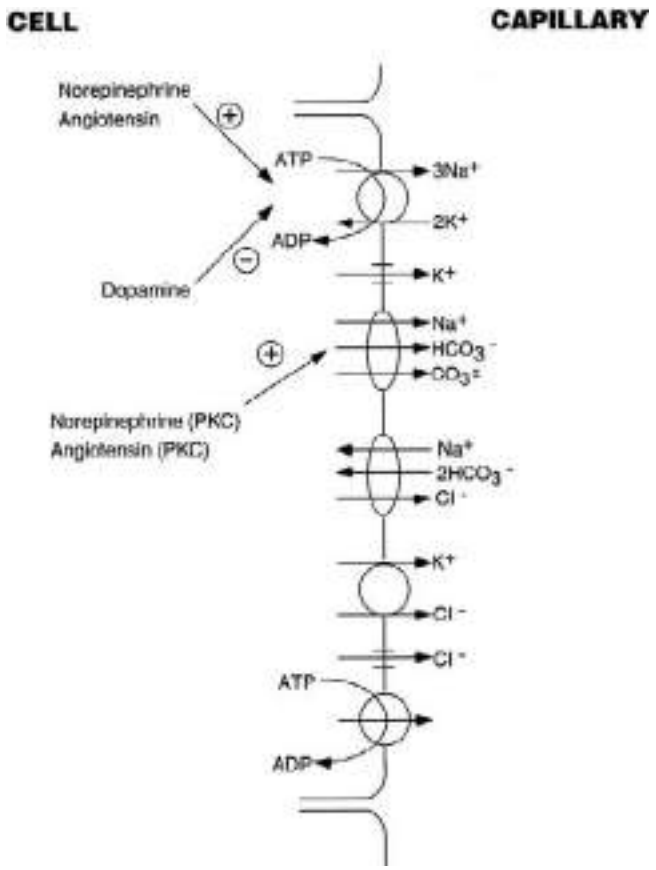

FIGURE 33.7 **Transport pathways across the basolateral cell membrane of the mammalian proximal tubule.**

HCO_3^--dependent Na^+ uptake. In vesicles from the rabbit, in which Cl^- uptake was assayed, it was found to be enhanced by an outwardly directed HCO_3^- gradient, and further stimulated by the addition of a Na^+ gradient.[145] In a Cl^- microelectrode study of rabbit proximal convoluted tubule, Ishibashi et al.[333] found that removal of either HCO_3^- or Na^+ from the peritubular bath increased cytosolic Cl^-, an effect inhibited by SITS, and which was interpreted as confirmation of Na^+-dependent Cl^-/HCO_3^- exchange. A subsequent examination of the rate of decline of cell Cl^- following perturbations of the peritubular bath suggested that this transporter was the dominant pathway for peritubular Cl^- exit.[334]

Examination of the straight proximal tubule of the rabbit has not yielded consistent findings regarding the Na^+-dependence of Cl^-/HCO_3^- exchange. Sasaki and his associates, using pH-sensitive microelectrodes, first found a small cellular alkalinization with the removal of peritubular chloride.[591] Subsequent study with a Cl^--sensitive electrode demonstrated a substantial increase in intracellular chloride with reduction of peritubular bicarbonate, an effect that was blunted by the complete removal of sodium and blocked by SITS.[593] Using straight proximal tubules containing BCECF, Kurtz[401] found a peritubular Cl^-/HCO_3^- exchanger that could function in the absence of Na^+. A basolateral Cl^-/HCO_3^- exchanger in this segment was also identified by Nakhoul et al.,[500] but its Na^+-dependence could not be defined. A microelectrode study of the S3 segment of the rabbit was performed by Kondo and Frömter,[390] who observed that removal of bath Cl^- decreased intracellular Cl^-, alkalinized the cell, and produced no change in cytosolic Na^+. This effect was blocked by peritubular SITS. Further, reduction of peritubular HCO_3^- increased cell Cl^-, so that a strong case was advanced for the presence of a Na^+-independent Cl^-/HCO_3^- exchanger in the peritubular membrane. With reference to Table 33.3b, this exchanger must mediate chloride uptake by the cell. A cycle of this exchanger in association with a cycle of a luminal or peritubular Na^+/H^+ transporter would yield net cellular uptake of NaCl, and could increase the volume of the tubule cell. Indeed, the peritubular Cl^-/HCO_3^- exchanger has been implicated in the recovery of cell volume after shrinkage in a hyperosmolar medium.[434,435,570]

Electrically silent chloride exit across the peritubular membrane may also occur as co-transport of KCl.[710] This transport mechanism had been proposed in connection with studies of *Necturus* gallbladder by Reuss and his associates[559,560] as a means of rationalizing the necessary Cl^- exit with the low membrane chloride conductance, and was confirmed with the demonstration that intracellular chloride activity could be made to vary with variation in the basolateral potassium concentration.[163,558] With respect to the mammalian proximal tubule, beyond the need for Cl^- exit, the brisk influx of K^+ via the Na-K-ATPase mandates substantial peritubular K^+ exit. For the rat proximal tubule, it was estimated that the conductive pathway was inadequate to account completely for this exit, so that in the construction of a mathematical model of this epithelium a peritubular KCl co-transporter was incorporated.[727] The first evidence for the proximal tubule KCl co-transporter came with the experiments of Eveloff and Warnock[198] on rabbit renal basolateral membrane vesicles. Here, K^+ or Cl^- gradients drove uptake of the other species in a voltage-independent manner. These findings received support with observations of furosemide-sensitive cell volume decrease in rabbit proximal straight tubule,[743] and furosemide-sensitive K^+ exit in proximal tubule suspensions.[30,391] In proximal straight tubule, Sasaki et al.[589] used both K^+- and Cl^--sensitive microelectrodes to demonstrate the mutual interaction of K^+ and Cl^- across the peritubular membrane. This interaction was independent of membrane electrical potential, and independent of Na^+. These findings received confirmation in the proximal convoluted tubule, examined with Cl^--sensitive microelectrodes by Ishibashi et al.,[333] although

in this work, coupled KCl exit appeared to be insensitive to furosemide. A subsequent electrophysiological investigation also failed to detect furosemide-sensitive coupled K^+ and Cl^- fluxes.[626] At the molecular level, four KCl co-transporters have been identified within the SLC12 family (SLC12A4-7), also known as KCC1-4.[303,487] Cloning and expression of KCC1 was achieved by Gillen et al.,[246] who reported that it was widely expressed; KCC3 and KCC4 were cloned by Mount et al.,[488] who noted a more selective expression, including kidney for both.

Na,K-ATPase

Metabolically driven sodium extrusion from the cell and potassium uptake are effected by the Na,K-ATPase situated exclusively within the peritubular cell membrane.[358,403] The biophysical properties of this pump were a key focus of early investigations of epithelial transport.[249,348–350] The functional transport unit of the Na,K-ATPase consists of an alpha-subunit bound to cytoplasmic structural proteins[485] and an externally protruding beta-subunit. Although there are three isoforms for the alpha-subunit, only a single isoform (α_1) appears to be expressed in proximal tubule.[467,666] The beta-subunit appears to function as a molecular chaperone, targeting insertion of the transporter.[237] Together the alpha–beta unit spans the peritubular membrane and contains, within its interior, cation-binding sites. A gamma-subunit to the Na,K-ATPase exists within kidney, and has been identified as one member of the FXYD family of proteins with wide ranging organ distribution.[27,234,237] The role of the gamma-subunit remains uncertain, although it has been suggested that it may function to limit transport during hypoxia or other tissue stress.[25,26] The most widely held scheme[350] for the operation of the pump envisions a cycle which begins with an E1 state, in which ATP is bound to the alpha-subunit and the cation-binding sites are open to the cytoplasmic surface for the binding of 3-Na^+ ions. With the binding of Na^+, ADP is released, leaving a phosphorylated unit in which the cations are initially inaccessible to either membrane face (occluded). A conformational change in the transport unit brings it to the E2 state, in which the cationic-binding sites are open to the external surface. At this point the release of Na^+ is followed by the binding of 2 K^+ ions, and with hydrolysis of the phosphate bond, these K^+ ions are occluded. Binding of ATP is associated with the conformational transition back to the E1 state, and release of K^+ into the cytoplasm. Stoichiometry of the Na,K-ATPase was first established in nonrenal systems,[249,379,503] and this was confirmed in oxygen utilization experiments in whole kidney[371] or in tubule suspensions.[298,299] A suspension of rabbit renal cortical tubules was examined, using NMR to monitor Na^+ transport from the cell and a K^+-electrode in the suspending medium to determine K^+ uptake, and it was demonstrated that over nearly an order of magnitude of Na,K-ATPase turnover, the Na:K stoichiometry remained 3:2.[29] By virtue of this stoichiometry, the Na,K-ATPase generates a net outward current across the peritubular membrane; pump inhibition with ouabain induces prompt depolarization of the peritubular membrane in rat proximal tubule.[222]

Development of a microassay system for Na, K-ATPase by Schmidt and Dubach[605,606] permitted the first estimate of enzyme activity within individual tubule segments. Subsequently, Morel and his colleagues developed a simpler assay and identified the distribution of Na,K-ATPase along the nephron.[180,360] They found comparable distribution in rat, rabbit, and mouse, with substantially greater concentration of ATPase in proximal convoluted tubule than in the straight segment. Garg et al.[233] found Na,K-ATPase activities of the S1, S2, and S3 segments of rabbit proximal tubule to be 17.5, 6.7, and 3.8 pmol ATP/s · cm tubule. Under conditions of the assay, maximal hydrolytic activity of the enzyme was determined, so that maximal Na^+ transport is three times these values. Corresponding to the transport activity of the Na, K-ATPase, there is a free energy change of 28.6 J/mmol (Table 33.3) or 6.8 cal/mmol, a figure compatible with the free energy of hydrolysis of ATP of 13–14 cal/mmol.[686] El Mernissi and Doucet[195] quantified ouabain-binding sites of rabbit PCT, and found 0.109 pmol/cm or 25×10^6 sites/cell. Thus, the ATPase activity of 10 pmol/s · cm would correspond to about 100 cycles/s of a single Na,K-ATPase unit. The actual rate of sodium transport by the Na,K-ATPase is usually less than maximal enzyme activity, and is dependent upon the levels of intracellular Na^+, peritubular K^+, and intracellular ATP. Of these three factors, in proximal tubule *in vivo*, cytosolic Na^+ concentration is the most important regulator of pump activity.[348,359] The half-maximal enzyme activation occurs at 31 mmol/l,[249,647] a level which is comparable to normal intracellular chemical concentrations. The physiological correlate to this biochemical data is the observation in *Necturus* proximal tubule that the rate of sodium transport responds to variations in the cytosolic sodium concentrations (Figure 33.8).[650] This suggested that under normal conditions the luminal cell membrane is the rate-limiting step for sodium transport. With respect to peritubular K^+, half-maximal ATPase activation occurs at concentrations under 1.0 mmol/l.[249,647] In lysed membrane preparations, the half-maximal saturation of ATPase activity, with respect to ATP, occurs at 0.4 mmol/l.[348,648] Thus, at normal levels of intracellular ATP (1–3 mmol/l) there should be little change in the rate of hydrolysis with variation of

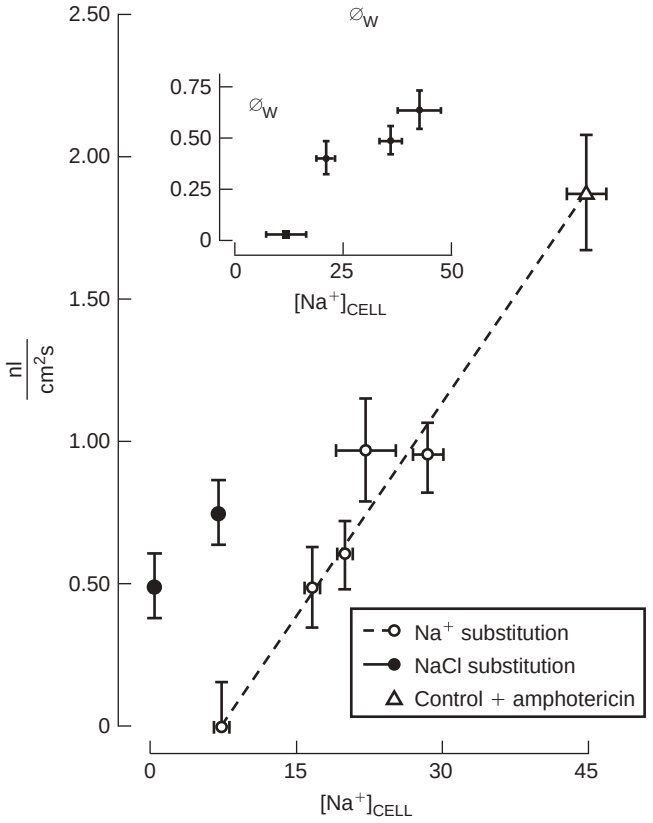

FIGURE 33.8 **Transepithelial water flow, Φ_w, (or, equivalently, transepithelial sodium flux) is plotted as a function of intracellular sodium concentration in *Necturus* proximal tubules. Intracellular sodium is decreased from the control value (30 mM) by substitution of luminal Na^+ with tetramethylammonium (or substitution of luminal NaCl with mannitol – see inset); sodium is increased above control by the luminal application of amphotericin.** *(From[650], with permission.)*

the ATP concentration. Nevertheless, in the intact tubule, partial inhibition of mitochondrial respiration produced proportional declines in cellular ATP and transport.[279] In a more extensive study, Soltoff and Mandel[646,648] found a linear correlation between cellular respiration and ion transport spanning a range of cellular ATP concentrations of 0–4 mmol/l. Thus, in the intact cell, it appears that ATP concentration can serve as an intermediary between transport and metabolism.

Coordination of Entry and Exit

Under normal circumstances, there may be several-fold variations in glomerular filtration rate to which the proximal tubule responds with nearly proportional changes in sodium reabsorption (*vide infra*). Although the mechanism underlying this glomerulotubular balance is not completely understood, the wide swings in the transcellular fluxes of sodium and bicarbonate pose a threat to the proximal tubule cell, with respect to maintaining a viable cell volume and pH. Such challenges are not unique to proximal tubule, but threaten all transporting epithelial cells, particularly the gastrointestinal epithelia, which experience swings in sodium-dependent glucose and amino acid uptake. In part, the kinetic response of Na,K-ATPase to cell Na^+ concentration will increase Na^+ exit (Figure 33.8), but this is generally insufficient to provide cellular homeostasis. Schultz and associates have emphasized the need for peritubular exit pathways to keep pace with luminal entry in order to preserve the integrity of cell composition and cell volume.[611,612,613] Beyond this, considerable attention has focused on the positive correlation between the potassium permeability of the peritubular membrane and the rate of epithelial sodium transport.[66,169] Increasing peritubular potassium conductance beyond enhancing potassium exit, should be expected to hyperpolarize the membrane, thus enhancing chloride and bicarbonate exit as well. The critical experimental observations were made in the epithelium of the small intestine of *Necturus*, from recordings with conventional and K^+-selective microelectrodes.[262,280] It was found that with the addition of alanine to the luminal solution there was a prompt depolarization of the cell interior in association with a doubling of sodium reabsorption. Over a period of several minutes the K^+ conductance of the basolateral membrane increased, repolarizing the cell and further enhancing sodium transport. The parallel response of peritubular K^+-conductance with reabsorptive Na^+ flux was subsequently documented in frog proximal tubule, following the application of phenylalanine to the tubule lumen,[473,474] and in the mammalian proximal tubule with luminal application of glucose and alanine.[67,408,409] Direct examination of the K^+ channel of the peritubular membrane via patch-clamp has shown that the increase in K^+-conductance with luminal application of organics is the result of an increase in the open probability of this channel.[65] Thus, attention focused on identifying the signal by which luminal solute entry could activate these channels. The two principal candidates for modulators of peritubular exit have been cell volume and coupling of the Na, K-ATPase activity with K^+-channel open probability (pump-leak parallelism) via cytosolic ATP concentration. The signaling and transport effectors for cell volume regulation have been extensively reviewed.[406,407]

Examination of *Necturus* small intestine indicated that both increased sodium transport and hypotonic cell swelling had similar impact on the basolateral membrane. These observations led to the proposal that a transport-associated increase in cell volume might mediate the enhanced K^+-conductance found with increased Na^+ reabsorption.[412] It had been known

since the experiments of MacRobbie and Ussing[446] that frog skin epithelium could volume-regulate. When the skin was placed in a hypotonic bathing solution, the initial swelling of the epithelial cells was followed by a gradual restoration of cell volume, presumably with the loss of cell solute. A critical observation was that hypotonic swelling of the toad urinary bladder was associated with increased basolateral membrane conductance.[210] In his analysis of cell volume regulation, Ussing[675] articulated the hypothesis that cell swelling was associated with the appearance or activation of both K^+ and Cl^- channels within the basolateral cell membrane, and loss of KCl via these pathways. With respect to proximal tubule, there has been considerable attention focused on the response of the peritubular membrane to increases in cell volume.[197,481,692] It was first noted in proximal tubules from the rabbit that exposure to a hypotonic solution was followed by a "volume regulatory decrease" (VRD).[170] This VRD was associated with a loss of cytosolic potassium.[261] In both *Necturus*[440] and rabbit tubules[378] cell swelling enhances peritubular K^+-conductance. Further, Kirk et al.[380] made the important observation that proximal tubule VRD occurred during isotonic swelling, where cell volume increased as a result of enhanced luminal Na^+ entry (rather than a hypotonic shock).

Proposed mechanisms of volume-induced K^+-conductance have included the direct effect of stretch on the K^+ channel or a volume-driven increase in cytosolic Ca^{2+}, with secondary channel activation. Patch-clamp studies have demonstrated stretch-activated K^+ channels within the peritubular membrane of amphibian proximal tubule,[362,582] as well as stretch-activated nonselective cation channels, which are permeable to Ca^{2+}.[207,208] In frog proximal tubule cells subjected to Na^+-alanine uptake, there is also evidence for stretch-activated anion channels.[475,567] In the mammalian tubule, stretch-activated K^+ channels have not been identified; however, it was observed that hypotonic cell swelling resulted in a rise in cytosolic calcium concentration.[462–464] This finding, in association with the appearance of Ca^{2+}-activated K^+ channels during hypotonic shock,[363] supplied a plausible mechanism for the increase in peritubular membrane K^+ permeability. In these studies (proximal straight tubules of the rabbit), blocking the rise in cytosolic calcium eliminated the hypotonic VRD. Questions were raised, however, by experiments in proximal convoluted tubule,[116] which indicated that VRD persists despite elimination of the rise in cell calcium. Most germane to the problem of coordinating entry and exit is the observation that when proximal convoluted tubules are exposed to luminal glucose and alanine, there is no significant increase in cytosolic calcium.[63] The importance of this result is the demonstration of differences in the cellular response to hypotonic swelling, and that due to enhanced luminal entry. Indeed, even in amphibian tubules, differences between hypotonic and isotonic VRD have been discerned, with Na^+-coupled alanine uptake the VRD is independent of external Ca^{2+}.[486] Critical insight into the coupling of transport to peritubular K^+ permeability came with the discovery that the peritubular K^+ channel open probability was decreased by increases in cytosolic ATP concentration in the physiological range.[664] With application of luminal glucose and alanine to rabbit proximal convoluted tubule, sodium transport increased, cytosolic ATP decreased, and peritubular K^+ conductance increased in proportion to the decrease in ATP.[64,664] When ATP was applied exogenously, this effect of luminal organics to increase peritubular K^+ conductance was eliminated.[664] Conversely, application of an inhibitor of the Na,K-ATPase increased cytosolic ATP concentration, and thus decreased the open probability of the peritubular K^+ channel.[322]

One question which received relatively little attention in these investigations, was whether the observed changes in peritubular membrane K^+ permeability were sufficient to rationalize the observed volume homeostasis. Contributing to this homeostatic effect is the impact of increased K^+ permeability to hyperpolarize the peritubular membrane, and thus augment chloride and bicarbonate exit. These events are complicated by the fact that peritubular hyperpolarization will also enhance luminal entry via the Na^+-glucose cotransporter, and cytosolic acidification (increased peritubular HCO_3^- exit) will enhance luminal entry via the Na^+/H^+ exchanger. The quantitative issue of the sufficiency of the documented pump-leak parallelism to maintain cell volume was examined in a mathematical model of proximal tubule.[735] In those calculations, it was found that with realistic bounds on the electrical conductance of the peritubular membrane, variation of K^+ permeability by itself does not provide adequate homeostasis for proximal tubule. Satisfactory volume regulation was achieved, however, when the activity of the peritubular $Na^+-3HCO_3^-$ co-transporter was allowed to vary directly in response to changes in the rate of luminal Na^+/H^+ exchange. Evidence for the coordination of these two transporters will be considered below. There are data regarding the anion lost in association with K^+ during cell swelling, and it appears to show some variability among species. In *Necturus*[440] and mouse tubules,[691] omission of bicarbonate impairs VRD and cell swelling is associated with enhanced peritubular HCO_3^- conductance.[690] In the straight proximal tubule of rabbit, however, removal of chloride impaired VRD, while omission of bicarbonate or the application of SITS had no inhibitory effect.[743] In the proximal convoluted tubule of the rabbit, hypotonic swelling increases both K^+-conductance and Cl^--conductance of

the peritubular cell membrane.[744,745] An intriguing examination of cell volume was undertaken in primary culture of mouse proximal tubule cells, comparing wild-type with knockouts of the peritubular K^+ channel, KCNE1.[47] The wild-type cells showed VRD with the appearance of swelling-induced K^+ and Cl^- channels; the knockouts showed neither K^+ nor Cl^- currents during swelling. When knockout cells were transfected with KCNE1, both swelling-activated K^+ and Cl^- currents were restored. These experiments demonstrated a close functional linkage between the two channels allowing a coordinated response to a volume challenge.

THE PARACELLULAR PATHWAY

The Lateral Intercellular Space

It had long been recognized that certain epithelia, such as gallbladder or small intestine, could transport water from lumen to blood against an adverse osmotic gradient. Curran[167] and Durbin[185] hypothesized that metabolically-driven salt transport into an intraepithelial compartment could drive transepithelial water flow, if the membranes bounding this compartment had suitable permeability properties. Subsequently, several groups of investigators[244,674,746] proposed that the space between the basolateral cell membrane and the basement membrane qualifies as the "middle compartment" within the epithelium. Salt transport into the interspace across the lateral cell membrane would induce an osmotic water flow across this membrane. Accumulation of salt and water within the interspace would then generate local hydrostatic pressure, sufficient to drive this solution out across the permeable basement membrane and connective tissue. This proposal identifies the lateral intercellular space as part of the pathway for the bulk of transepithelial water flow. Morphologic observations on gall bladder,[366,660] intestine,[752] *Necturus* proximal tubule,[76,456,457] and the isolated perfused rabbit proximal tubule[659] have all been confirmatory, showing interspace dilatation with reabsorptive flow and interspace collapse with cessation or reversal of flow.

It is also a secure finding that along the length of the proximal tubule the luminal sodium concentration differs little, if at all, from that in peritubular blood. This means that water reabsorption must occur in a constant proportion to sodium reabsorption. Windhager et al.[759] demonstrated that in *Necturus* proximal tubule the sodium flux drives the net water reabsorption. These investigators introduced into the tubule lumen solutions isosmotic with plasma, but with varying sodium concentration, in order to obtain a wide range of values for the sodium flux. Over the course of the experiment, the luminal osmolality did not change, indicating a negligible external driving force in the passive movement of water. Nevertheless, a plot of the net water flux as a function of the net sodium flux shows a line, the slope of which indicates that transport occurred isotonically (Figure 33.9a). A similar series of experiments was performed in rat proximal convoluted tubule by Morel and Murayama.[484] They again verified

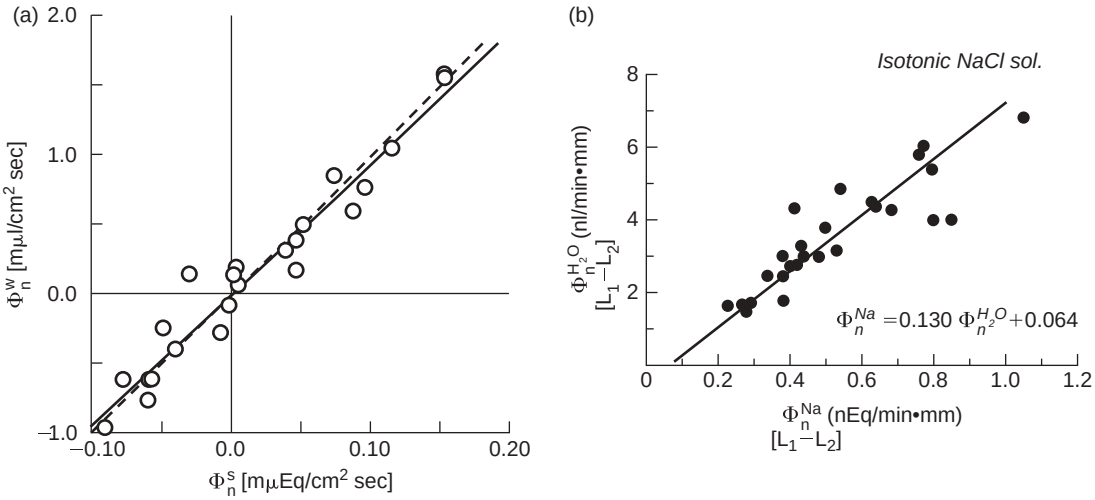

FIGURE 33.9 **(a) Correlation of net solute flux, Φ_n^s, and net water flux, Φ_n^w, across the perfused proximal tubule of *Necturus*. The least squares line of regression for the data points (solid line) is not statistically different from the line through the origin (dashed line), whose slope is that for isotonic water reabsorption. *(From[759], with permission.)* (b) Correlation of net sodium flux, Φ_n^{Na}, and net water flux, Φ_n^{H20}, occurring between two collection sites (L1 and L2) of a perfused rat proximal tubule. The line of regression for the data points (solid line) indicates isotonic transport of sodium.** *(From[484], with permission.)*

over a wide range of luminal sodium concentrations (and sodium fluxes) that the flux of sodium determined the flow of water. Further, the water flow occurred so as to maintain the lumen isotonic to plasma (Figure 33.9b).

The dependence of isotonic water reabsorption on sodium reabsorption has been referred to as "coupled water transport" to distinguish it from water flux referable to a demonstrable transepithelial osmotic gradient. This coupled water transport has been rationalized in an analysis of the lateral intercellular space as an intraepithelial middle compartment.[731,736,737] As in Figure 33.10, the lateral interspace is represented with a tight junction (J_A), basement membrane (J_B), and lateral cell membranes (J_L). A reference osmolality, C_0, is assumed (such as that of the blood), and the osmolalities of the interspace, $C_0 + C_E$, of the lumen and cell interior, $C_0 + C_M$, and of the peritubular solution, $C_0 + C_S$, are written in terms of increments above or below the reference. Each membrane, α, (α = A, B or L) has water and solute permeabilities $L_{p\alpha}$ and H_α, and a reflection coefficient σ_α. Transmembrane fluxes for volume and solute are denoted by $J_{v\alpha}$ and $J_{s\alpha}$. Assumptions may be made which simplify the analysis, but which maintain most of the important features of the lateral interspace model: (1) the tight junction is relatively impermeable, $L_{pA} = H_A = 0$; (2) the lateral cell membrane is relatively solute impermeable, $H_L = 0$, and $\sigma_L = 1$; but (3) there is fixed solute transport across the lateral membrane at a rate, N; and (4) the reflection coefficient for the interspace basement membrane and underlying tissue is zero, $\sigma_B = 0$. With these assumptions the transport equations for each membrane may be written, for volume and solute flows:

$$J_v = J_{vL} = L_{pL}[(P_M - P_E) + RT(C_E - C_M)] = J_{vB} = L_{pB}[(P_E - P_S)] \tag{33.9}$$

$$J_s = J_{sL} = N = J_{sB} = J_{vB}C_0 + H_B(C_E - C_S) \tag{33.10}$$

where P_M, P_E, and P_S are the hydrostatic pressures in the respective compartments. The equalities, $J_v = J_{vL} = J_{vB}$ and $J_s = J_{sL} = J_{sB}$, reflect the fact that in the steady-state, mass entry across the lateral membrane must be equal to that leaving the channel mouth. It may be noted that an additional approximation has been introduced into Eq. (33.10), in which the reference concentration, C_0, is identified as the mean basement membrane concentration.

When the mass balance relations are used to eliminate the unknowns P_E and C_E, from Eqs (33.10) and (33.11), one obtains an expression for transepithelial volume flow:

$$J_v = L_p(P_M - P_S) + RTL_p\left(C_S - C_M + \frac{N}{H_B}\right) \tag{33.11}$$

in which the epithelial water permeability, L_p, is given by the expression:

$$L_p = \frac{L_{pLB}H_B}{H_B + RTL_{pLB}C_0} \quad \text{where} \quad L_{pLB} = \frac{L_{pL}L_{pB}}{L_{pL} + L_{pB}} \tag{33.12}$$

Equation (33.12) describes the volume flow of the whole epithelial model in terms of the permeability parameters of the component membranes. It shows the volume flow to be a linear function of the pressure and osmolality of the bathing solutions. When there are exactly equal bathing media ($C_M = C_S = P_M = P_S = 0$), there is still transepithelial volume flow:

$$J_v^a = RTL_p\frac{N}{H_B} = RTL_p\hat{C} \tag{33.13}$$

This "active water transport," referenced in Eq. (33.9), thus arises naturally as a component of volume flow driven by intraepithelial solute–solvent coupling, i.e., the empirically described "coupled water transport." It increases with larger rates of solute transport and decreases when there is little solute trapping by the basement membrane (large H_B). The virtual concentration, $\hat{C} = N/H_B$, represents the strength of transport of the epithelium, in that volume flow just ceases when the osmolality of the luminal solution is raised by this amount. For a proximal tubule model one must also verify isotonic transport. In approximate terms, this means that only a small decrement in luminal osmolality is required for the reabsorbate tonicity to be equal to that of the peritubular fluid. Formally, one seeks the osmotic deviation, C*, such that if

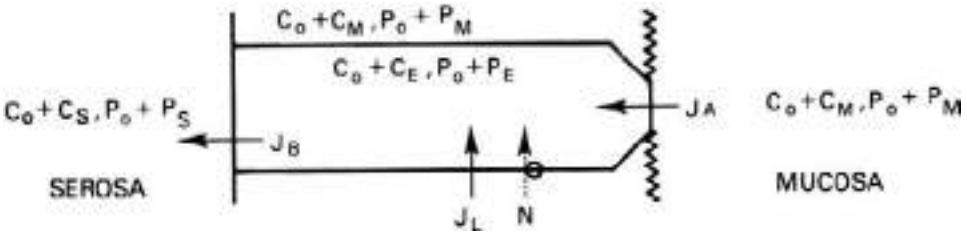

FIGURE 33.10 **Schematic representation of the lateral intercellular space**. The cell and mucosal medium are assumed to be at the same osmolality and pressure. *(From[736], with permission.)*

$C_S \approx C_0$, and $C_M \approx C_0 - C^*$, then $J_s/J_v \approx C_0$. This corresponds to solving the equation:

$$C_0 = \frac{J_s}{J_v} = \frac{N}{RTL_p(\hat{C} + C_s - C_M)} = \frac{N}{RTL_p(\hat{C} + C^*)} \quad (33.14)$$

which has the solution:

$$C^* = \frac{N}{RTL_{pLB}C_0} \quad (33.15)$$

When the luminal osmolality is decreased by the amount C*, transport is isotonic to plasma. Provided C* is at most a few mOsm/l, there will be no experimentally-detectable difference between lumen and blood. Transport is generally considered isotonic if C* is within 2% of C_0. It should also be noted that isotonic transport depends only upon the water permeabilities of the epithelial membranes. The notion of solute trapping within the interspace, which was crucial to uphill water transport, is really unimportant in the dynamics of isotonic transport.

Perhaps one of the confusing features of transport isotonicity is that the relevant membrane permeabilities may be quite different from the whole epithelial water permeability that is actually measured. The expression for L_p (Eq. (33.12)) shows that both water permeabilities and solute trapping effects are involved. Intuitively, this corresponds to the fact that water flow across the lateral membrane, driven by a hypotonic lumen, will tend to dilute the interspace and hence, negate some of the osmotic flow. The interspace dilution will be smaller for larger basement membrane permeabilities. This "intraepithelial solute polarization" effect is an inescapable feature of the lateral interspace. The expression for L_p may be rewritten:

$$\frac{L_p}{L_{pLB}} = \frac{1}{1 + \hat{C}/C^*} \quad (33.16)$$

which shows that to the extent that an epithelium can transport against a gradient (large $\hat{C}$), and yet reabsorb water isotonically (small C*), the observed epithelial L_p must be substantially smaller than the cell membrane water permeabilities.

In Table 33.4, this model is applied to the data of Tables 33.1 and 33.2 for proximal tubules of rat and rabbit. The upper panel shows rates of isotonic reabsorption, along with the measured water permeabilities. For the rat, two values for L_p are given, corresponding to the older[672] and later determinations.[536] A value for the equilibrium deviation from isotonicity (C*) has been assumed to be at 2% of the ambient osmolality. At least in the rat, this is comparable to experimental determinations.[265,432] The quantities in the lower panel of the table are derived from the experimental data using the model equations. The estimate of cell membrane water permeability required for isotonic transport, RTL_{pLB}, is just J_v/C^*. If the value of RTL_{pLB} computed for the rabbit tubule is referred to the luminal and lateral cell membranes in series, each of 36 cm^2/cm^2,[738] then one obtains a unit membrane water permeability, consistent with direct estimates, using rapid video techniques.[136,741] In theory, the AQP1 knockout mouse, deficient in water channels from both luminal and peritubular cell membranes, provides a pure decrease in the parameter RTL_{pLB}. The experimental observations in this knockout were an overall epithelial water permeability (L_p) about 22% that of wild-type (Schnermann et al., 1998), and luminal hypotonicity (C*) about four-fold greater than wild-type.[677] In terms of the model developed here, and with the assumption that active Na^+ transport is little changed in the knockout mouse, the change in C* should reflect a 78% reduction in L_{pLB}. The fact that the fractional change in overall L_p is comparable indicates that in the mouse, one would expect little intraepithelial solute polarization, and thus little capacity for water reabsorption against an adverse osmotic gradient. The discrepancy between the overall epithelial water permeability and that of the cell membranes in series, allows the calculation of the strength of transport, $\hat{C}$ in Eq. (33.13).

Williams and Schafer[754] have emphasized that the middle compartment need not be the true lateral interspace, but could actually be the cortical interstitial space. In their model of rat proximal tubule, the salt permeability of the peritubular capillary corresponds to the term H_B used here. With estimates of cell membrane water permeability and capillary solute permeability comparable to those of the first column in Table 33.4, they also predicted that solute polarization would reduce the epithelial L_p to about 50% of that of

TABLE 33.4 Application of the Interspace Model to Proximal Tubule

		Rat PCT	Rat PCT	Rabbit PCT
J_s	(nOsm/s · cm^2)	19	19	9.0
J_v	(nl/s · cm^2)	65	65	30
$RTL_p \times 10^4$	(cm/s · Osm)	44	22	63
P_f	(cm/s)	0.24	0.12	0.35
c*	(mOsm/L)	6	6	6
$RTL_{LB} \times 10^4$	(cm/s · Osm)	105	105	50
$\hat{c}$	(mOsm/L)	8	23	–
J_v[a]	(nl/s · cm^2)	35	51	
$H_B \times 10^4$	(cm/s)	24	8.3	–

the cell membranes. For the rat, the discrepancy between L_p and L_{pLB} requires that active water transport be substantial, i.e., from 55–80% of the isotonic flux (Table 33.4). In the more detailed models of proximal tubule epithelium which have been developed there is considerable disagreement in the estimates of coupled water flux, ranging from predominant[323,324,583,657] to negligible.[14,595,707,753] In a simulation of the rat proximal tubule, in which both isotonic transport and the whole epithelial L_p were reproduced faithfully, coupled water flux was estimated to be about two-thirds of the isotonic transport rate.[727] This corresponded to a strength of transport of 23 mOsm/l of NaCl. There are few experimental studies examining uphill water transport by the proximal tubule. Bomsztyk and Wright[105] reported that in rat tubules, microperfused with a low bicarbonate (10 mEq/l) luminal solution, an additional 30 mmol/L of mannitol was required within the lumen to nullify volume reabsorption. Although the interpretation of this experiment was complicated by the presence of several forces favoring water reabsorption (anion gradients and protein oncotic forces), the findings suggested a substantial component of solute-linked water reabsorption by the rat proximal tubule. Green et al.[267] examined the doubly perfused rat proximal tubule, specifically with the aim of determining the presence of active water transport. Using low bicarbonate solutions in both tubule and capillary perfusions, an isotonic luminal solution yielded reabsorptive water flux of 1 nl/mm · min. Varying only the luminal NaCl concentration allowed the determination of volume flux as a linear function of the transepithelial salt gradient (Figure 33.11). Regression analysis indicated that a luminal osmolality between 13 and 29 mosm/l (depending on peritubular protein concentration) greater than in peritubular blood would be required to null volume reabsorption. These experiments document active water transport by rat proximal tubule, quantitatively close to model predictions, and thus provide support for solute–solvent coupling within the lateral intercellular space.

The interspace outlet permeability, H_B, is a parameter of critical importance. It directly determines the strength of transport (Eq. (33.13)), and when this solute permeability is sufficiently small ($H_B < RTL_{pLB}C_0$) it is dominant in determining the epithelial L_p (Eq. (33.12)). Persson and Spring[525] examined the subepithelial tissue of *Necturus* gallbladder and found that it has only about twice the resistivity of free solution. They argue, therefore, that any important limitation to solute exit from the interspace must derive from the small area of the lateral interspace as it abuts the basement membrane. More recent experiments using photoactivation of caged fluorescent dyes have indicated that solute

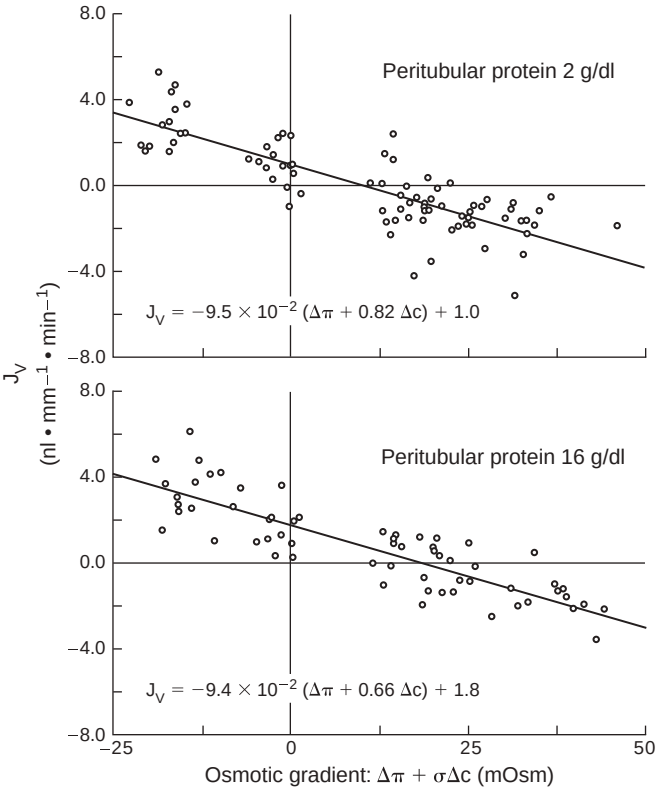

FIGURE 33.11 **Volume flux as a function of transepithelial osmotic driving force in rat proximal tubules, in which both lumen and peritubular capillaries have been perfused**. Each point corresponds to a single tubule perfusion. The abcissa is the transepithelial osmotic driving force, $\Delta\pi + \sigma\Delta C$; the ordinate is the measured volume flux, J_v. For each protein concentration, the line shown is the graph of Eq. (33.1), so that the ordinate intercept, J_v^a, is the coupled water transport (water flux in the absence of a transepithelial driving force.) The abcissa intercept is the concentration of the luminal impermeant required to null volume reabsorption. *(From[267], with permission.)*

diffusion within the lateral interspace is comparable to that in free solution.[770] Such had been the assumption in analytical estimates of the electrical resistance of the interspace fluid of proximal tubule from ultrastructural data. Mathias,[453] using data from the rabbit[739] estimated interspace resistance at about 4% that of tight junction, and Maunsbach and Boulpaep[458] calculated 4–21% of epithelial resistance may be attributed to the interspace. Welling et al.[740] have indicated that beyond the limitations of interspace width, interdigitating cellular elements at the base of the interspace may provide the most important barrier to mass exit. With reference to Table 33.4, Eq. (33.13) defines the outlet permeability required by the model ($H_B = N/\hat{C} = J_s/\hat{C}$). For the rat, H_B is predicted to be $8.3–24 \times 10^{-4}$ cm/s. When interpreted as an electrical resistance (Eq. (33.4)), this is 0.4–1.1 ohm · cm^2, and is not incompatible with the whole epithelial resistance of 5–10 ohm · cm^2.

The Tight Junction

The tight junction of the proximal tubule provides a low resistance pathway between the luminal solution and the lateral intercellular space. Morphologically, the tight junctions have been identified with the "zonula occludentes," visualized in electron microscopy, in which there is no detectable space between the epithelial cells. Freeze-fracture techniques indicated the fibrillar structure of these junctions, with relatively few fibrils present in the junctions of the proximal tubule.[156,539] In epithelia with greater electrical resistance, there are, correspondingly, a greater number of fibrils.[155,156] The TJ strands may be viewed as chains of particles, with typical spacing of these particles, as seen in freeze-fracture electron micrographs, being in the order of 20 nm.[509] The structural composition of these strands has been deciphered slowly.[477,608] Occludin was the first of the transmembrane proteins to be associated with the tight junction,[228] and to be implicated in a functional role in junctional permeability.[461] An important advance came with the identification of claudin-1 and claudin-2 within the junctional strands.[226,229] When claudin-2 was introduced into the Madin–Darby canine kidney (MDCK) cells, a conversion from a very "tight" junction to a "leaky" junction was observed.[227] This suggested that claudin-2 could be responsible for the leakiness of the MDCK epithelium and the formation of pores between apposing TJ strands. Indeed, when the claudins expressed in MDCK cells are selectively modified, the paracellular conductance of small electrolytes can be modulated, including the anion/cation selectivity preference.[159] The sodium conductance of tight junctions containing claudin-2 can also be modulated by changes in ambient calcium concentration.[785,786] Claudin-2 exists throughout the proximal tubule, and in a contiguous early segment of the thin descending limb of long-looped nephrons in mouse kidney.[196] In mice with deletion of the claudin-2 gene, the proximal tubules have a 2.5-fold increase in electrical resistance, due to a decrease in tight junctional Na^+ permeability.[495] Although these mice have normal renal function, they do excrete a Na^+ infusion more rapidly than wild-type mice. Of note, the high Na^+ permeability of proximal tubules appears as a maturational event, and is not present in the neonatal period in which natriuresis figures prominently.[57,546] Apparently, claudin-2 expression of proximal tubule is subject to modulation by changes in metabolic status, and in the rat is downregulated during metabolic acidosis.[37] If the impact of decreased claudin-2 is to increase distal NaCl delivery, this might be expected to enhance the distal nephron functions of K^+ and net acid excretion.

Like proximal tubule, other leaky epithelia (gallbladder, small intestine) also transport large volumes of salt solutions isotonically, and this encouraged speculation as to the function of the tight junction in isotonic water transport. A number of mathematical simulations of proximal tubule addressed this issue,[323,324,583,651,657,736,737] but have simply not provided an answer as to why electrical leakiness should correlate with the ability to transport isotonically. The fraction of reabsorptive water flow which actually traverses the tight junction is also unknown. Arguments in favor of transjunctional water flow in proximal tubules have included: substantial solvent drag of ionic species[16,106,224,266,308,361,596]; the appearance of streaming potentials with the application of an impermeant osmotic agent[164,221,661]; and ionic permeabilities roughly in proportion to their mobility in free solution.[392] None of these findings, however, provides proof of tight junctional water flow. Either streaming potentials or solvent drag can come as the result of a solute polarization effect within the interspace. With solute polarization, water flux across the cell and through the lateral interspace alters interspace ion concentrations, thus promoting either a diffusion potential or diffusive flux across the tight junction. For a true streaming potential, water flux across the tight junction must be present and carry either an anion or cation preferentially. This issue was addressed by Tripathi and Boulpaep[661] in their measurements of streaming potentials across the proximal tubule of *Ambystoma*. With the application of peritubular sucrose, a lumen-positive potential appeared, consistent with either a streaming potential or interspace NaCl depletion (and an anion-selective junction). When ambient chloride was replaced by cyclamate, the junction became cation-selective and its total conductance substantially decreased. Repeat application of peritubular sucrose produced the same lumen-positive potential, now inconsistent with a diffusion potential. With respect to the solvent drag measurements, it is undisputed that intraepithelial solute polarization may produce an overall reflection coefficient that is substantially less than that of the cell and tight junction, taken in parallel. The question is thus a quantitative one, as to whether one could construct a model of proximal tubule with just the right solute polarization to yield realistic reflection coefficients as well as a proper L_p. So far, this does not appear possible. For the rat, the data of Frömter et al.[224] were used to determine composite interspace models for this epithelium.[730] It was found that all of the acceptable interspace models required substantial tight junction convective chloride flux.

An apparently direct argument for tight junctional water flux in rabbit tubules came from Whittembury and associates,[135,253,748] whose estimate of the water permeability of the peritubular cell membrane

indicated a transcellular water permeability less than the overall epithelial L_p. The unit membrane water permeability obtained with this technique has received confirmation in a vesicle preparation,[687,689] although higher values have also been obtained.[683] Strong evidence for tight junction water flow was also obtained in the rat, with observation of substantial convective entrainment of sucrose, despite relatively small diffusional flux.[747] The small diffusive component effectively rules out interspace solute polarization as a confounding factor. Nevertheless, an objection had been raised by Rector and Berry,[80,553] who presented calculations based on pore theory which indicated that the tight junctions were not large enough to allow passage of a significant fraction of transepithelial water flow. Subsequently, Preisig and Berry[536] measured the permeation of sucrose and mannitol across the rat proximal tubule. Applying the Renkin equations to their data, they computed the dimensions of the "sucrose pore," and indicated that it could be responsible for at most 2% of the tubule water permeability. It was acknowledged, however, that a smaller paracellular pore that did not admit the sucrose molecule could account for up to one-third of the water permeability. An important contribution to this discussion came with the suggestion of Fraser and Baines[213] that the tight junction might be more realistically represented as a fiber matrix, rather than as a collection of pores. The critical feature of the fiber matrix equations is that for a given solute permeability, the water permeability can be substantially greater than that predicted from the Renkin equations. It was demonstrated that this formulation was compatible with the known permeabilities of rat proximal tubule.[213] Alternatively, Guo et al.[281] reproduced a pore-theoretic representation of the tight junction, utilizing two pores to fit the mannitol and sucrose data of Preisig and Berry.[536] In this model, the two pores were given anatomic correlates: the small pore was referred to gaps in the apposition of claudins molecules, while the large pore corresponded to breaks within a strand, occupying about 2% of its length. With these dimensions, tight junction water permeability was predicted to be about 21% of transepithelial water permeability.

With the tight junction established as a route for reabsorptive solute flux, a hypothesis was advanced that the junction might be an important site for the regulation of proximal sodium reabsorption. Lewy and Windhager found that in rats, both with and without acutely elevated renal venous pressure, there was a direct correlation between single nephron filtration fraction and proximal tubule sodium reabsorption.[418] Given that lower filtration fractions would result in reduced protein oncotic pressure within the peritubular capillaries, they surmised that this would lead to reduced capillary uptake of fluid from the renal interstitium and lateral intercellular space and, hence, elevated interspace pressure. This, in turn, would result in increased backflux of the sodium, already transported into the interspace, that is, backflux across the tight junction into the lumen. At the time of this proposal, attention had focused on intrarenal mechanisms responsible for the natriuresis of extracellular fluid volume expansion with saline.[187,383,384] Dirks et al.[173] had shown that proximal tubule sodium reabsorption was depressed following saline expansion. In the dog, the ability to reverse the natriuresis with infusion of hyperoncotic albumin indicated that peritubular oncotic pressure could influence sodium reabsorption, and Earley and his associates[186,451] had proposed that renal interstitial pressure might be an intermediate variable. Subsequent micropuncture experiments in the rat documented enhancement of proximal sodium reabsorption by peritubular protein.[113,114,385] In particular, the depression of proximal tubule sodium reabsorption which occurs with saline infusion could be reversed by perfusion of the efferent arteriole with a solution whose protein concentration is comparable to that under control conditions.[115,649] It has been well-documented that changes in the ambient protein concentration alter sodium reabsorption by the perfused proximal tubule. In the isolated perfused rabbit proximal tubule, Imai and Kokko found enhancement of sodium reabsorption with increasing concentrations of protein in the bathing solution.[331] In the absence of peritubular colloid, the permeability of the tubule to sucrose was increased. In the rat kidney, Green et al.[269] studied proximal tubule volume reabsorption when albumin was present in varying concentrations in luminal or peritubular capillary perfusates. Figure 33.12 shows the asymmetry (luminal versus peritubular protein) and the non-linearity of the reabsorptive enhancement by peritubular colloid. This implies that the colloid effect is not a simple oncotic force, such as might be reckoned using Eq. (33.1) and the known water permeability. It does suggest that the increase in peritubular capillary albumin changes the "state" of the epithelium to make active sodium transport more efficient at driving volume reabsorption. A comparable asymmetric effect of protein on salt reabsorption was also documented in rabbit proximal convoluted tubule *in vitro*.[332]

It is a tenet of the backflux hypothesis that the action of peritubular protein is mediated through an effect on renal interstitial pressure and hence, pressures within lateral intercellular spaces. In substantiation of this point, decreases in peritubular capillary oncotic pressure, which occur with saline volume expansion, result in increases in renal interstitial pressure (as least as assessed by renal subcapsular pressures).[515,516,548,629]

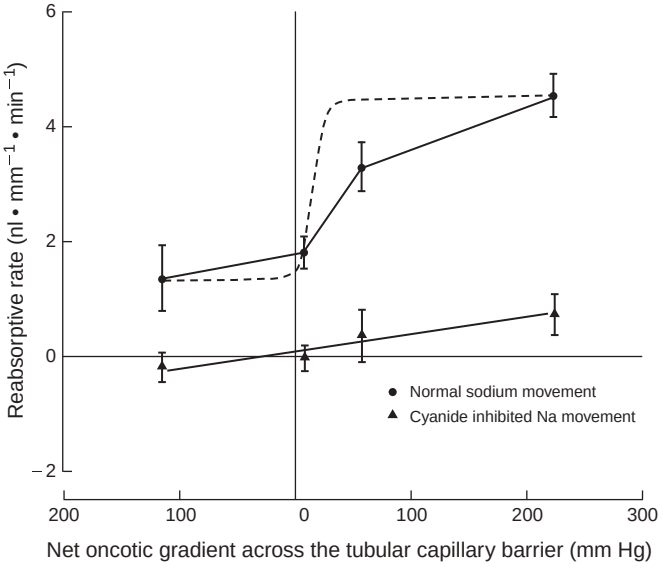

FIGURE 33.12 **Effects of transtubular oncotic pressure gradients on volume reabsorption by rat proximal tubule**. Both tubule lumen and peritubular capillaries are perfused with identical Ringer's solutions to which variable amounts of albumin have been added. In the tubules perfused with cyanide (lower curve) spontaneous sodium reabsorption has ceased and the effect of oncotic pressure is blunted. *(From[269], with permission.)* The dashed curve represents the prediction of an interspace model in which the tight junction is compliant. *(From[732].)*

Prevention of this rise in interstitial pressure by applying a renal artery clamp also prevents the fall in absolute proximal reabsorption associated with saline expansion.[212,327] Further, the deliberate increase of renal interstitial pressure by the instillation of fluid decreases proximal sodium reabsorption and produces a natriuresis.[260,287] Morphologic examination of the proximal tubule of the rat[75,140] has shown progressive dilation of the lateral intercellular space, as well as opening of the interspace at the tubule basement membrane, with increments of saline volume expansion. The precise mechanism of sodium "backflux" across the tight junction remains to be delineated. One possibility is that with increased interstitial pressure there is junctional widening and diffusion of sodium from interspace to lumen. A small decrease in epithelial electrical resistance has been documented with saline-loading in the rat.[621] In the rat, mannitol injected into the proximal tubule does not permeate and is completely recovered in the urine. However, with massive saline diuresis, as with renal venous constriction or elevated ureteral pressure, a significant fraction of the mannitol traversed the tubular epithelium into the systemic circulation.[442] Similarly, sucrose infused into the systemic circulation may permeate the proximal tubule epithelium during periods of renal vein constriction.[42] Perhaps the strongest objection to the view that sodium diffuses back across widened junctions is that, at least in the rat proximal tubule, the electrodiffusive force on sodium is likely to be in the reabsorptive direction. A second possibility is that backflux of sodium across the tight junction occurs by convective flow. The tight junctions of the leaky epithelia are very sensitive to hydrostatic pressures applied from the contraluminal side. In rabbit gallbladder[684] and *Necturus* proximal tubule,[259,301] contraluminal pressures drive substantially greater volume flow across the epithelium than an equal luminal pressure. In *Necturus*, volume expansion decreases the proximal tubule NaCl reflection coefficient.[77] In these experiments, it is likely that junctional structure is distorted, forming relatively large pores with negligible sieving of solute, as both salt and water return to the lumen. Indeed, in the meticulous study of van Os et al.[684] on the rabbit gallbladder, serosal pressures drove water back into the lumen at a rate 30-fold greater than would have been predicted from the osmotic water permeability of this epithelium. This occurred with little change in diffusional solute permeability. These investigators suggested that their results were most compatible with a serosal pressure effect of opening up relatively large water channels at a small number of junctional loci. Convective backflux across the tight junction of rat proximal tubule has been invoked by Ramsey et al.[550] to explain their observation that the luminal appearance of lanthanum deposited within the renal interstitium is enhanced during saline volume expansion.

The mathematical model of the lateral interspace, set out in the previous section, cannot represent the peritubular oncotic effects on sodium reabsorption considered above.[728] However, when this model is extended by inclusion of a compliant tight junction, a regulatory effect of peritubular Starling forces can be simulated.[732] In this case, tight junction "compliance" signifies that both junctional salt and water permeability increase, and the salt reflection coefficient decreases in response to small pressure differences from lateral interspace to tubule lumen. Although these compliance properties were completely empirical, they provided a model in which decreases in peritubular protein (which increased interspace hydrostatic pressure) opened the tight junction, and produced a secretory salt flux. This backflux was a combination of both diffusive and convective terms, and did not specifically require either component to dominate. When this model was used to simulate the experiments of, Green et al.[269] the model predictions were consistent with the observed reabsorption. The predicted fluxes appear as the dashed curve in Figure 33.12. In this model of the tight junction, once the interspace pressure falls below that of the lumen, the junction is closed and junctional properties are fixed. The consequence of junction closure in

the simulation of Figure 33.12 is that beyond a certain value of peritubular protein, one expects little influence of peritubular Starling forces on volume reabsorption. In this light, it is not surprising that a number of investigators found no significant influence of peritubular protein on proximal reabsorption,[40,161,315] and even interstitial Starling forces could correlate poorly with sodium transport.[103,472,665] Consistent with this view are the observations by Ott et al.[516] that in the dog, hyperoncotic albumin infusion increased proximal reabsorption only in the previously volume-expanded group. In the isolated perfused proximal tubule of the rabbit, several reports have indicated a lack of effect of peritubular bath protein on paracellular permeability.[79,82,410] Pirie and Potts[529] explored the influence of pressure gradients in this preparation. They found that elevations in intraluminal hydrostatic pressures abolished the effect of peritubular protein to enhance sodium reabsorption. Although they did not offer a specific explanation for their data, the present considerations might suggest that with higher luminal pressures, the tight junction always stayed closed.

REGULATION OF PROXIMAL NaCl TRANSPORT

Convergence on NHE3

Considerable attention has been given to understanding proximal sodium reabsorption in relation to neural and hormonal signals, and to changes in glomerular filtration rate. The luminal membrane Na^+/H^+ exchanger is responsible for both $NaHCO_3$ reabsorption and a substantial component of NaCl reabsorption. This, along with the fact that luminal entry is rate-limiting for transcellular sodium flux, renders the antiporter ideally suited as a regulatory site for proximal reabsorption. Indeed, a coherent picture has emerged in which every signal that regulates proximal Na^+ reabsorption converges on NHE3. A remarkable diversity of pathways has been identified as proximate modifiers of the antiporter.[176,177,243,270,300,478,717] Regulatory signals to NHE3 converge on the carboxy-terminal tail of the transporter, and Donowitz and Li[176] have organized the NHE3 binding partners and signals anatomically, according to their position on this tail (Figure 33.13). Of these, the most important is inhibition by cAMP-dependent phosphorylation of the antiporter by protein kinase A (PKA).[351,479,722] Liu and Cogan[430] examined bicarbonate reabsorption by the S1 segment of rat proximal tubule following a variety of maneuvers designed to affect cellular cAMP concentration. When luminal appearance of cAMP is used as a measure of cytosolic concentration, the correlation with bicarbonate transport over nearly a 10-fold range is striking (Figure 33.14). The acute nature of these experimental maneuvers must be emphasized, since the impact of chronic stimulation by cAMP is different.[131] Beyond cAMP effects, NHE3 activity is also phosphorylated acutely by the calcium−phospholipid-dependent protein kinase, PKC,[354,470,720,721,750] by direct signals from G-proteins,[6] and perhaps by a tyrosine kinase.[247] Beyond transporter phosphorylation, rapid regulation of sodium reabsorption via NHE3 is achieved through cellular machinery that makes NHE3 physically available within the brush border membrane, including insertion and retrieval of transporter from subapical vesicle pools.[104,199,307,790] Ultimately, chronic NHE3 regulation must be referable to the protein synthetic machinery.[317,130,248]

Of the signals that impact NHE3 flux, the first to be studied was the decrease in Na^+/H^+ exchange via cAMP-dependent phosphorylation, initially as a consequence of parathyroid hormone (PTH)-binding. This signal pathway is critical to the action of angiotensin II and dopamine, and will be considered below. The PTH effect was documented in isolated perfused proximal tubules,[171,293] and paralleled the effect of cAMP when examined in tubule suspensions[174] or brush border membrane vesicles.[351] A major advance came with the identification of a protein cofactor, NHERF-1 (NHE regulatory factor), which is required for cAMP phosphorylation of NHE3.[723,726,792] Ultimately, a number of such regulatory proteins have been identified whose role has come to be recognized as scaffolding molecules, for which transporter-binding occurs by virtue of their tertiary structure, termed PDZ domains.[93,175,176,716] The OK cell is a proximal tubule cell line from opossum kidney that expresses NHE3 and NHERF-1, and which displays cAMP-dependent inhibition of NHE3. This cell served as a preparation in which to demonstrate the physical link between NHE3 and NHERF-1, as well as a link between NHERF-1 and ezrin.[405] Ezrin is a protein kinase A (PKA) anchoring protein, as well as a linking molecule to the actin cytoskeleton. The scheme that emerged was that of a multiprotein signal complex, in which NHERF and ezrin brought PKA and NHE3 into proximity[718,724] (Figure 33.13). Supporting this picture in the intact kidney was immunocytochemical co-localization of NHE3, NHERF-1, and ezrin within the brush border of rat proximal tubule.[693] Although mice with homozygous deficiency of NHERF-1 show normal electrolytes, brush border membrane vesicles from these mice showed no effect of cAMP to inhibit NHE3 activity, despite normal protein levels of NHE3, PKA, and ezrin.[632,725] Cultured proximal tubule cells from these mice display absent regulation of NHE3 by

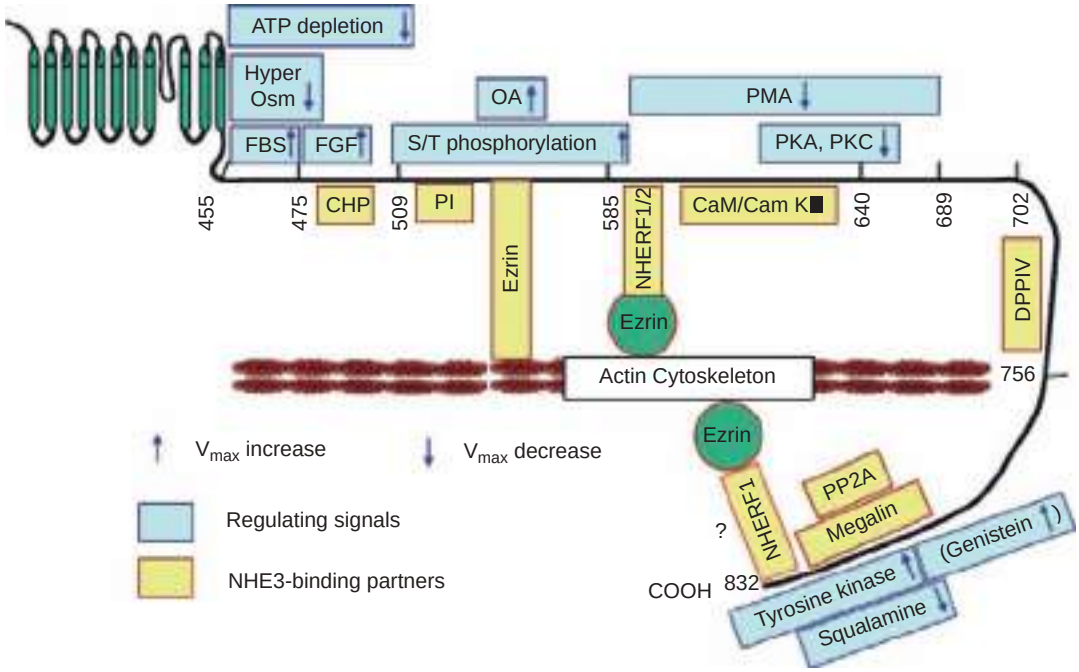

FIGURE 33.13 NHE3 organization, including COOH-terminal domains involved in acute regulation and binding partners. Shown above the COOH terminus in blue are sites of action of regulatory stimuli defined by the truncations, which abolish the specific regulatory effects. The direction of the arrow indicates acute stimulation or inhibition of NHE3 activity. Below the COOH terminus in yellow are listed associating proteins and the areas of their binding sites on NHE3. *(From[176].)*

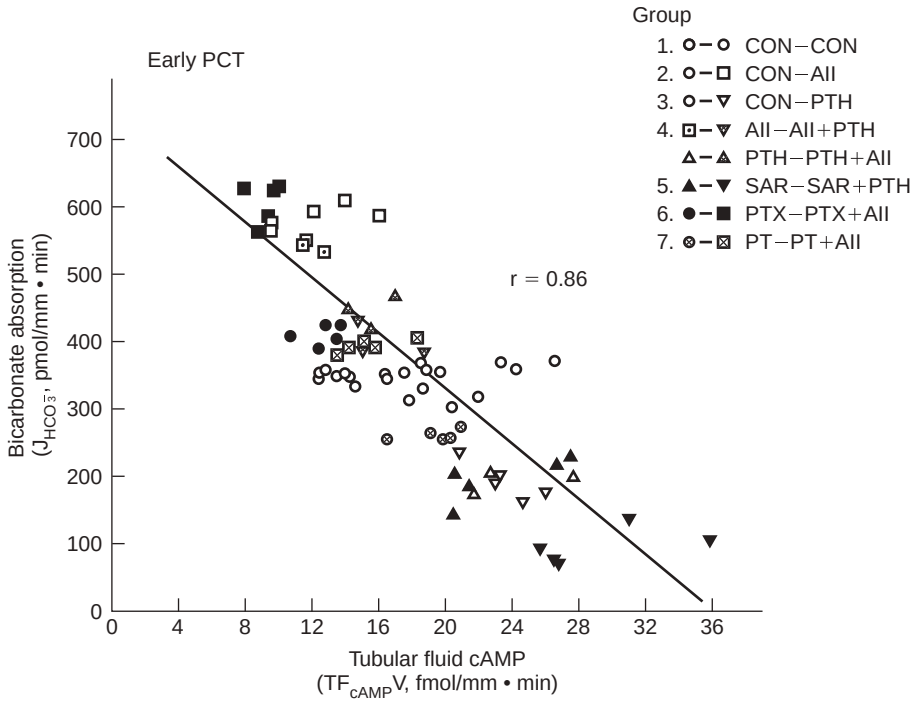

FIGURE 33.14 Relationship of bicarbonate absorption to tubular fluid cAMP delivery in the early S1 segment of PCT. A variety of maneuvers have been used to alter cellular content of cAMP, including parathyroidectomy (PTX) or infusion of angiotensin II (AII), parathyroid hormone (PTH), saralasin (SAR) or pertussis toxin (PT). *(From[430].)*

PTH, which could be restored via transfection with adenovirus containing the gene for NHERF-1.[166] Although NHERF-1 binds to the proximal tubule luminal membrane Na^+-phosphate co-transporter, NaPi-2a, and although NaPi-2a is downregulated by PTH, the NHERF-1 role in this context may be quite different from its NHE3 paradigm. In the case of NaPi-2a, NHERF-1 affects trafficking,[632] but there is no evidence that NHERF-1 is involved in the PTH-induced cAMP-dependent phosphorylation of this transporter.[93,94]

Beyond chemical modification of a fixed contingent of microvillous Na^+/H^+ exchangers, there is regulation of the NHE3 density within the luminal membrane.[466,633] An early observation in cultured proximal tubule cells was that PTH perturbed actin filament structure and caused microvillous shortening, events not replicated with application of cAMP alone.[252] Subsequently, density-gradient centrifugation of cell homogenates permitted examination of distinct membrane vesicle populations from rat proximal tubule suspension. It was found that PTH treatment resulted in migration of Na^+/H^+ exchange activity from one fraction to another, and then disappeared.[307] With the availability of NHE3-specific antibody, the distinction between Na^+/H^+ activity and NHE3 abundance could be made. Using vesicles prepared from the kidneys of parathyroidectomized rats treated acutely with PTH, it was found that within minutes of treatment Na^+/H^+ activity decreased, and phosphorylated NHE3 appeared. Over the course of hours, brush border NHE3 antigen declined, and this could be blocked by pretreating the animals with colchicine.[199] The ability of PTH to couple to adenylate cyclase appears to be critical to its ability to provoke NHE3 redistribution.[790] Events *in vivo* were mimicked in OK cells in which PTH induced a rapid phosphorylation of membrane-bound NHE3 and a parallel decrease in function, and then a slower retrieval of the cell surface transporter into an endocytic pathway.[160] Disruption of the actin cytoskeleton in proximal tubule suspension produced an increase in NHE3 abundance in luminal membrane vesicles prepared from these tubules.[142] A precise role, however, for the actin cytoskeleton in the regulation of NHE3 function has been elusive. Beyond transporter retrieval, the state of cellular actin fibers has been implicated in modulation of PKA phosphorylation of NHE3, consistent with its physical association with the NHERF–ezrin complex.[399,654] An additional complication is that the retrieval destination of apical transporters may be transporter-dependent. Whereas PTH *in vivo* produces transfer to endosomes of the luminal membrane sodium–phosphate transporter, the destination of NHE3 appears to be a reserve compartment at the base of the microvilli.[774] In addition, NHE3 is also internalized in association with megalin to a distinct vesicle compartment[98,101]; this appears to be critical to the action of the proximal tubule to reabsorb and process luminal proteins in OK cells and in mouse.[240,241] The kinetics of insertion and retrieval of NHE3 are clearly altered in consequence to demands for proximal Na^+ conservation (see below), although precise mechanisms remain uncertain, due in part to the uncertainty of extrapolation from cell culture preparations to tubules *in vivo*.

Modulation of the Na,K-ATPase

All of the regulatory signals that impact on the luminal Na^+/H^+ exchanger also modulate the Na,K-ATPase.[204] Early study of the action of PTH in OK cells identified the release of inositol triphosphate (IP3) and diacyl glycerol, along with an increase in cytosolic Ca^{2+}. In intact proximal tubule cells and basolateral membrane vesicles, it was possible to confirm the IP3 release.[320] With this information, it was natural to focus on the role of protein kinase C (PKC) in mediating the PTH-induced decrease in proximal Na^+ reabsorption. Baum and Hays[55] were first to examine the effect of PKC activation on PCT transport, and demonstrated inhibition of bicarbonate, chloride, and glucose transport by rabbit tubules *in vitro*. This global effect on multiple solutes was consistent with inhibition of the Na,K-ATPase, and this was the finding of Bertorello and Aperia,[85] who determined maximal Na,K-ATPase activity in rat proximal tubules preincubated with a PKC activator. The logical connection of these portions of the story was the demonstration that PTH inhibited maximal Na,K-ATPase activity in tubules in which cytosolic Na^+ was elevated by the ionophore, monensin.[562] This stimulation also occurred when a truncated PTH analog was used, which had no PKA activity, so that the Na,K-ATPase inhibition was dissociated from cAMP generation. These observations were supported by the finding in intact tubules that the PTH effect on Na,K-ATPase is eliminated by inhibition of PKC with staurosporine[594] or with calphostin.[508] Interest has focused on the structural correlates of Na,K-ATPase regulation, and these have been depicted by Feraille and Doucet[204] (Figure 33.15). The first observation is that regulatory phosphorylation occurs on the alpha-subunit, which can be phosphorylated by both PKA and PKC.[86] There is a single PKA phosphorylation site at a serine within the last cytoplasmic loop, while PKC phosphorylation occurs on the N-terminal cytoplasmic tail.[68,205] The rate of alpha chain phosphorylation by PKC was influenced by the ionic environment, enhancing with K^+ and diminishing with Na^+, suggesting preference for the E2 over the E1 conformation.[205] The converse of this observation has also been reported, namely that PKC phosphorylation impacts on the conformational equilibrium of the enzyme, favoring the E1-Na state.[433] Although an inhibitory effect of PKC phosphorylation had been reported[86], Feschenko and Sweadner[206] found no effect of alpha-subunit phosphorylation on Na,K-ATPase kinetics, neither on maximal velocity nor Na^+ affinity. They concluded that the regulatory impact of PKC must derive from the cellular environment, and other signals.

One complicating aspect of the PTH effect on proximal tubule Na,K-ATPase is the interaction with the

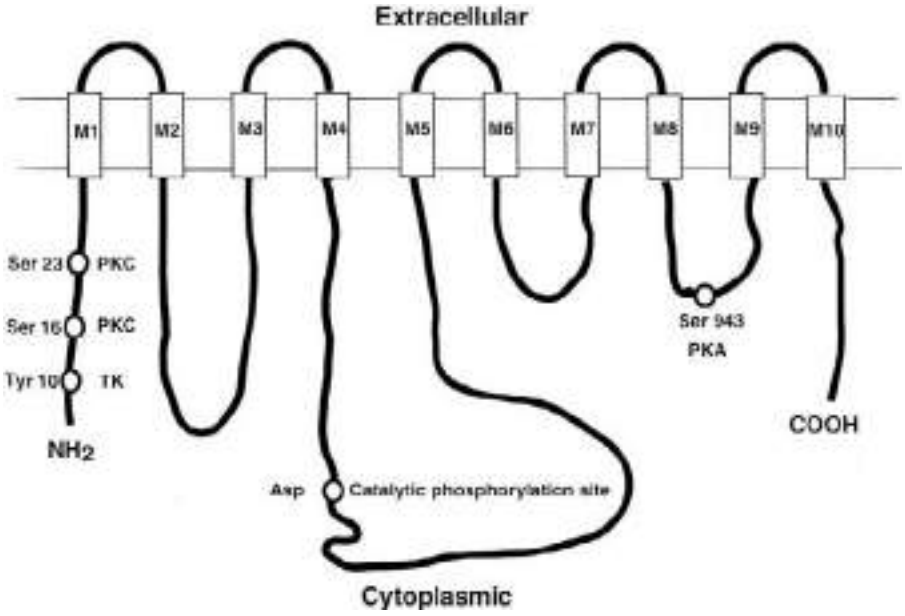

FIGURE 33.15 **Transmembrane looping of the alpha subunit of the Na, K-ATPase, with localization of phosphorylated amino acids**. The PKA site is located at serine-943; PKC sites are on the NH_2 cytoplasmic tail. The aspartate residue within the M4–M5 loop is phosphorylated during the catalytic cycle of the pump. *(From[204].)*

cytochrome P450 pathway. Ribeiro et al.[561] demonstrated that PTH released arachidonic acid in proximal tubule suspension, that a specific inhibitor of P450 prevented the inhibitory effect of PTH on the Na, K-ATPase, and that the effects of 20-hydroxyeicosatetraenoic acid (20-HETE) and PTH on the Na,K-ATPase were not additive. These observations were extended by Ominato et al.[508] working with rat proximal tubules, who showed that inhibition of cytochrome P450 not only blocked the PTH effect, but also Na,K-ATPase inhibition by activators of PKC, as well as inhibition by a PKC catalytic fragment. These workers drew the conclusion that the P450 product was an effector for PKC on the Na,K-ATPase. A slightly different conclusion was reached by Nowicki et al.[506] working in a cultured cell line (COS cells), who observed that 20-HETE had no effect on Na,K-ATPase in the absence of PKC, and that inhibitors of PKC (or mutation of the PKC catalytic site) eliminated the 20-HETE effect. These workers drew the conclusion that the P450 product was an effector for PKC on the Na,K-ATPase. A second complicating aspect of the regulation of Na,K-ATPase is the interaction with the cell's endocytic machinery. In proximal tubule cells in suspension, dopamine treatment caused phosphorylation of the alpha-subunit of Na,K-ATPase, decreasing its activity and resulting in its appearance in endosomes.[150] Dopamine-induced phosphorylation was blocked by PKC inhibition. In OK cells, phosphorylation of the alpha-subunit and its uptake into endosomes could be prevented with either PKC inhibition or by transfection with an alpha-subunit lacking the PKC phosphorylation site.[150]

Complexity of PKC modulation of the Na,K-ATPase became apparent with microperfusion studies of rat proximal tubules by Liu and Cogan, and their observation that Na^+ and HCO_3^- reabsorption was stimulated by PKC activation and depressed by PKC inhibition.[431] Wang and Chan[697] sharpened this picture with their report of a time-dependent effect of PKC activation on microperfused rat proximal tubules, with early stimulation (0 to 10 minutes) yielding to late inhibition after 25 to 35 minutes of perfusion. In rat proximal tubule cells in suspension, Feraille et al.[203] examined the effect of PKC activation on Na,K-ATPase activity, and reproduced prior observations that with standard incubation conditions PKC activation inhibited Na,K-ATPase activity. However, the thrust of their report was that in a well-oxygenated preparation, PKC was stimulatory due to an increase in Na^+-affinity. Enhancement of the transport activity occurred in parallel with phosphorylation of the alpha-subunit of the Na,K-ATPase.[137] In contrast to the findings of Chibalin et al.[150], Efendiev et al.[191] reported that in OK cells, PKC activation increased Na,K-ATPase activity by recruiting new transporters to the cell membrane. With regard to the inhibitory or stimulatory effect of PKC on the Na,K-ATPase, Efendiev et al.[192] have focused attention on cytosolic Na^+ concentration to act as a switch. Working in OK cells, they manipulated cell Na^+ using the ionophore monensin, and used rubidium uptake to assay Na,K-ATPase activity in intact tubules. They found that PKC activation stimulated the pump at low cell [Na^+], had no effect at estimated [Na^+] around 12 mM, and was inhibitory at cell [Na^+] greater than 16 mM. The inhibition, but not the stimulation, was abrogated with P450 inhibition. This work was extended by experiments in rat proximal tubules in which the phosphorylation of the PKC site of the

alpha-subunit was measured.[326] It was found that at the normally low cell Na^+, the sites were largely phosphorylated, and only at abnormally high cell Na^+ were they dephosphorylated and susceptible to the action of PKC. In more recent studies in OK cells, fluorescence microscopy of tagged alpha-subunits has demonstrated an impact of increased cytosolic Na^+ to traffic Na,K-ATPase to endosomes adjacent to the cell membrane.[154] Whether this represents trafficking of transporter to or from the plasma membrane may depend upon other neuro-humoral factors.

Neural and Humoral Factors

Renal Nerves

Renal sympathetic nerves have long been known to modulate proximal tubule sodium transport, and are perhaps the most important regulator.[172,256] Denervation of the rat kidney reduced proximal reabsorption by 40% in the absence of any change in single nephron glomerular filtration.[71] Stimulation of the sympathetic nerves can increase reabsorption by 30%, again without change in filtration.[73] In the isolated perfused convoluted proximal tubule of the rabbit (but not the straight portion) both alpha and beta catecholamines enhance sodium transport.[69] Similar stimulation by both adrenergic agonists is observed in the doubly microperfused rat tubule.[719] In the perfused mammalian tubule, norepinephrine increases both bicarbonate and chloride transport.[60] Nord and his associates[505] found that in a suspension of tubule cells from the rabbit, sodium uptake was enhanced by alpha agonists and blocked by ethylisopropylamiloride, thus suggesting alpha stimulation of brush border Na^+/H^+ exchange. Subsequently, Wong et al.[761] demonstrated that in the microperfused S1 segment of rat proximal tubule, both acute renal denervation or acute alpha-1 blockade reduce chloride reabsorption by 40%, while manipulation of alpha-2 activity had little impact. The effect of alpha-1 blockade could be eliminated by pre-activation of PKC, suggesting that the calcium–phospholipid-dependent kinase was the important signaling pathway for renal sympathetic activity. In view of the increase in cellular cAMP with beta adrenergic agonists, the mechanism by which beta agonists enhance proximal sodium reabsorption must be indirect, and the evidence implicates NHERF: activated beta-2 receptor binds NHERF, and thus prevents cAMP-dependent downregulation of NHE3. When binding was prevented with a mutated beta receptor, the PKA-dependent decrease in NHE3 flux was also prevented.[292] A coordinated effect of sympathetic activity on luminal and peritubular cell membranes was suggested by the observation that PKC activation also enhanced activity of the peritubular $Na^+-3HCO_3^-$ co-transporter.[578] Of greater significance with respect to luminal-peritubular coordination is the observation that norepinephrine also increases the activity of the Na,K-ATPase.[60,87] The effect on the sodium pump, however, is more likely mediated by a phosphatase, since PKC is inhibitory here.[19,314,419]

Angiotensin

Angiotensin II has been intensely studied as a regulator of proximal sodium transport.[158,295,296,541,614] In the intact animal, selective blockade of angiotensin II is diuretic, so it appears that under normal conditions there is tonic stimulation of the proximal tubule.[771] In physiologic doses, it enhances Na^+ reabsorption in rat[297] or rabbit tubules,[615] and the stimulatory effect appears to be more pronounced in the S1 segment.[429] Specific receptors for angiotensin exist on both luminal[121] and peritubular membranes,[122] and the hormone effect may be achieved from either side of the cell.[429] Distinguished on the basis of inhibitor binding, several distinct receptor types have been identified on proximal tubule, each with affinity for angiotensin in the nanomolar range.[181,190] In intact rat tubules, the most prominent effect of angiotensin, in picomolar concentrations, is the stimulation of $NaHCO_3$ reabsorption via Na^+/H^+ exchange,[429] and this is mediated by binding to AT1 receptors.[543,763] In a suspension of proximal tubule cells, angiotensin II enhances both Na^+ uptake and cell pH recovery after an acid-load.[581] The increase in tubular reabsorption due to angiotensin is correlated with the inhibition of cAMP generation,[430] and these findings are reproduced in cultured proximal tubule cells transfected with the AT1 angiotensin receptor.[656]

While systemic angiotensin concentrations may be in the 0.01–0.1 nM range, luminal concentrations are 100-fold higher[624] due to tubular synthesis and secretion of angiotensin.[112,532] Microperfusion studies, combining luminal perfusion of angiotensin with simultaneous inhibition of local synthesis, have confirmed the stimulation of transport starting in the picomolar range.[58,540] However, over a broad range of luminal concentrations (0.01–10.0 nM) these workers found the stimulatory effect of luminal angiotensin to be relatively flat. With respect to the peritubular action of angiotensin, inhibition of Na^+ transport becomes apparent at concentrations above 0.1 nM as an attenuation of the stimulation seen at lower doses. Inhibition may dominate at concentrations greater than 100 nM,[296] and may involve binding to an AT2 receptor.[291] *In vivo*, AT1 blockade has been used to reveal an effect of peritubular angiotensin II, metabolized to angiotensin III, which then binds to the AT2 receptor to decrease Na^+ reabsorption.[517,518] Pursuit of the signaling pathway underlying the inhibitory effect of angiotensin has

indicated formation (via phospholipase A2) of an epoxygenase metabolite of arachidonic acid.[181,294,318,448,575]

Microperfusion experiments have also revealed a coordinated action of luminal angiotensin and renal nerve activity. In volume-contracted animals, proximal reabsorption is brisk, additional luminal angiotensin adds little, and luminal AT1 antagonism has a dramatic inhibitory effect on reabsorption; in volume-expanded animals, there is only a small impact of luminal AT1 inhibition, while luminal angiotensin sharply increases volume reabsorption.[542] Quan and Baum[544] made the observation that when renal nerves were cut luminal perfusion of an angiotensin converting enzyme inhibitor (enalaprilat) failed to decrease proximal volume reabsorption, although the tubule remained sensitive to the stimulatory effect of directly applied luminal angiotensin. Conversely, stimulation of renal nerves conferred enalaprilat-sensitivity to proximal reabsorption.[545] These studies suggested that renal nerves amplified their signal to enhance proximal sodium reabsorption by switching on the local angiotensin synthetic machinery. A mysterious aspect of luminal angiotensin signaling is the luminal angiotensin concentration maintained well above that needed for maximal stimulation. One explanation that has been advanced is that in such a system, regulation of transport might be determined by AT1 receptor density.[389] Indeed, metabolic acidosis increases proximal tubule AT1 expression, and thus increases the effect of angiotensin to stimulate proximal ammoniagenesis.[498] In OK cells, both AT1 receptor expression[39] and NHE3 activity[230] are increased by insulin. The significance of the proximal AT1 receptor to total body Na^+ balance is suggested by the demonstration of Gurley et al.[283] that mice with AT1 knockout restricted to proximal tubule have decreased proximal tubule Na^+ reabsorption and are relatively hypotensive.

With respect to specific proximal tubule transporters, angiotensin is pleiotropic. Beyond the effect of decreasing cAMP to increase NHE3 flux, there is evidence that angiotensin can act to increase NHE3 membrane density in intact tubules.[415] It is likely that the increase in NHE3 activity contributes to the observed increase in NH_4^+ secretion by perfused mouse proximal tubule, although the increased NH_4^+ production in perfused S3 segments is evidence for a more global angiotensin action.[497] Within proximal tubules of rats with renovascular hypertension, there is increased expression of the Na^+-glucose co-transporter (SGLT2), which is blunted by AT1 inhibition.[59] Additionally, angiotensin augments proximal acidification by the luminal membrane H^+-ATPase, at least in part through transporter insertion.[694] Indeed *in vivo*, ACE inhibition produces translocation of an array of luminal transport proteins, including NHE3, NHERF, ezrin, and the H^+-ATPase, from tip to base of brush border microvilli,[414] and this translocation is reversed by direct infusion of angiotensin II.[564] In the picomolar to nanomolar concentration range, angiotensin stimulates HCO_3^- exit via the peritubular $Na^+-3HCO_3^-$ co-transporter,[162,193,239] perhaps via a pathway which activates PKC,[579] and perhaps by increasing the membrane content of this transporter.[565] Within the concentration range of angiotensin that stimulates proximal reabsorption, there is increased peritubular Na, K-ATPase[235]; this occurs promptly and with changes in the phosphorylation of the Na,K-ATPase.[778] There is also increased peritubular K^+ conductance.[162] Despite enhancement of peritubular exit pathways, the net effect of angiotensin on cytosolic Na^+ concentration is an increase.[555]

Dopamine

The proximal tubule is also the target of natriuretic signals, and dopamine is the most important.[17,134,787] Among the key early observations were findings that urinary dopamine could derive from circulating L-DOPA,[34] that on balance, the whole kidney synthesized dopamine (consuming DOPA), with tubular secretion providing the bulk of urinary dopamine,[38] and that proximal tubules could be a source for this excreted dopamine.[35] Within proximal tubule, conversion from DOPA to dopamine is due to the enzyme L-amino acid decarboxylase (L-AADC), and the importance of the local generation of dopamine was underscored by the demonstration that maximal L-AADC activity was modulated by dietary salt intake.[631] In mice, in which proximal tubule AADC has been knocked-out, urinary dopamine is dramatically reduced, and the animals show elevated blood pressure (compared with wild-type) when on a normal- or high-salt diet.[791] Proximal tubules are a target for the locally generated dopamine. Dopamine inhibits sodium reabsorption in the isolated perfused straight tubule,[72] and in tubule suspensions.[411] In proximal convoluted tubules (*in vitro*), however, dopamine decreased sodium reabsorption only in tubules in which transport had been stimulated by norepinephrine,[56] consistent with the observation *in vivo* that a DA-1 agonist is not natriuretic in a denervated kidney.[325] RNA message for the DA-1 dopamine receptor was demonstrated in proximal tubule,[773] and subsequently the protein was identified on both luminal and peritubular cell membranes.[507]

As with angiotensin, dopamine impacts on transporters of both luminal and peritubular cell membranes, most notably but not exclusively NHE3 and the Na, K-ATPase. Studies of dopamine action via the DA-1 receptor have implicated a number of second messenger systems, but principally cAMP-PKA targeting

NHE3 and Ca^{2+}-PKC targeting the Na,K-ATPase.[17] When renal cortical tissue was incubated with dopamine or DA-1 agonists, Na^+/H^+ exchange in brush border membrane vesicles decreased, and this could be blocked by inhibition of either adenylate cyclase or PKA.[200] Use of OK cells permitted direct demonstration that dopamine (via DA-1) and PKA phosphorylated NHE3 on identical sites.[749] In large measure, the decrease in Na^+/H^+ exchange reflects a dopamine-mediated decrease in NHE3 within the luminal cell membrane.[32] This conclusion was based on experiments in which mouse cortical slices were treated with dopamine, and brush border membrane vesicles assayed for NHE3 activity and antigen. A prior observation had been made in OK cells that dopamine produced endocytosis of NHE3 in a PKA-dependent manner.[321] Development of antibodies recognizing NHE3 phosphorylated at PKA target sites, confirmed the effect of dopamine to increase phosphorylation at those sites, and permitted the observation that in the rat *in vivo*, NHE3 phosphorylation shifted from microvilli to a subapical location.[386] With respect to other luminal transporters, dopamine also induces internalization of the Na^+-phosphate co-transporter,[31] and this effect involves participation of NHERF.[715] The impact of dopamine on the Na,K-ATPase was demonstrable as a decrease of enzyme activity in microdissected tubules[18] or as a decrease in oxygen consumption by proximal tubules in suspension in which cell Na^+ was kept high by nystatin permeabilization.[630] The dopamine-mediated decrease in proximal tubule cellular Na,K-ATPase activity has been shown to occur in association with endocytosis of the enzyme, and blocking the endocytosis with an actin stabilizer eliminated the decrease in enzyme activity.[149] An early event in the endocytic process is PKC-dependent phosphorylation of the alpha-subunit of the Na,K-ATPase.[150] An early observation in rat proximal tubule was that, like ouabain, dopamine produced an increase in tubule diameter.[18] Subsequent study of rabbit PST with Na^+-sensitive fluorescent dye demonstrated a prompt rise in cell Na^+ in response to dopamine.[397] This indicates that with inhibition of both Na^+ entry and exit pathways, on balance, the effect of dopamine on the Na,K-ATPase dominates. In an electrophysiologic study, dopamine also blunted peritubular HCO_3^- exit via the Na^+—$3HCO_3^-$ co-transporter.[397]

The DA-1 receptor density is regulated, and consistent with the physiology, there is an inverse relationship with AT1 angiotensin receptor density. Early observations included the findings that in cell culture (LLCPK) dopamine recruits its own DA-1 receptor to the cell membrane[118]; and in rats, dopamine downregulates the AT1 receptor.[147] In a primary culture of rat proximal tubule cells, application of a dopamine agonist increased DA-1 density, decreased AT1 density, and eliminated the angiotensin-elicited increase in cytosolic Ca^{2+} (Figure 33.16).[368] In these same cells, angiotensin decreased the DA-1 density, and blunted the dopamine-agonist-induced increase in cAMP. The dopaminergic decrease in AT1 density was also observed in a primary culture of human proximal tubule cells.[245] Complementing these observations, the proximal tubule AADC knockout mouse showed increased renal AT1 mRNA expression.[791] Another aspect of dopamine receptor physiology, which may have direct translational impact, is "desensitization" of the DA1 receptor by phosphorylation.[201] In proximal tubule, the G-protein-coupled receptor kinase 4 (GRK4) is the principal kinase to phosphorylate the DA1 receptor, thus diminishing the dopamine effect. The critical observation is that in primary cultures of human proximal tubule, cells derived from hypertensive patients show decreased responsiveness to dopamine agonists and increased DA-1 phosphorylation.[587] These observations may be understood in light of the later demonstration that cells from hypertensive patients have substantially greater GRK activity.[202] Furthermore, a GRK4 mutation identified in human hypertension produced hypertension in a transgenic mouse.[202] Renal interstitial infusion of GRK4 antisense oligonucleotides decreased GRK4 expression, decreased DA-1 phosphorylation, and mitigated the blood pressure rise of spontaneously hypertensive rats.[588]

Nitric Oxide (NO)

Nitric oxide provides a paracrine signal from renal nerves or renal endothelial cells to affect proximal tubule Na^+ transport.[420] Due to its short half-life and difficulty in measurement, the impact of NO has been assessed indirectly, in experiments in which NO synthase (NOS) has been inhibited or NO donors have been infused, so that renal tubular dose—response for NO is not available. In whole animals, infusion of a NOS inhibitor at a dose which does not increase arterial blood pressure or glomerular filtration, leads to a reduction in sodium excretion.[404,450] Majid et al.[450] found that with NOS inhibition, urinary Na^+ excretion failed to increase as a function of renal perfusion pressure, and this prompted them to propose that NO may be a mediator of the pressure-natriuresis response (see below). When the NO donor, sodium nitroprusside (SNP), was added to tubule lumen or to peritubular capillaries, it decreased proximal Na^+ reabsorption.[194] Wu et al.[768] added the observation that when NOS inhibition increased proximal sodium reabsorption, the effect could be abrogated by transection of renal nerves; the NOS inhibition effect was reproduced with specific inhibition of neuronal NOS. With renal nerve stimulation, proximal Na^+ reabsorption increased, but

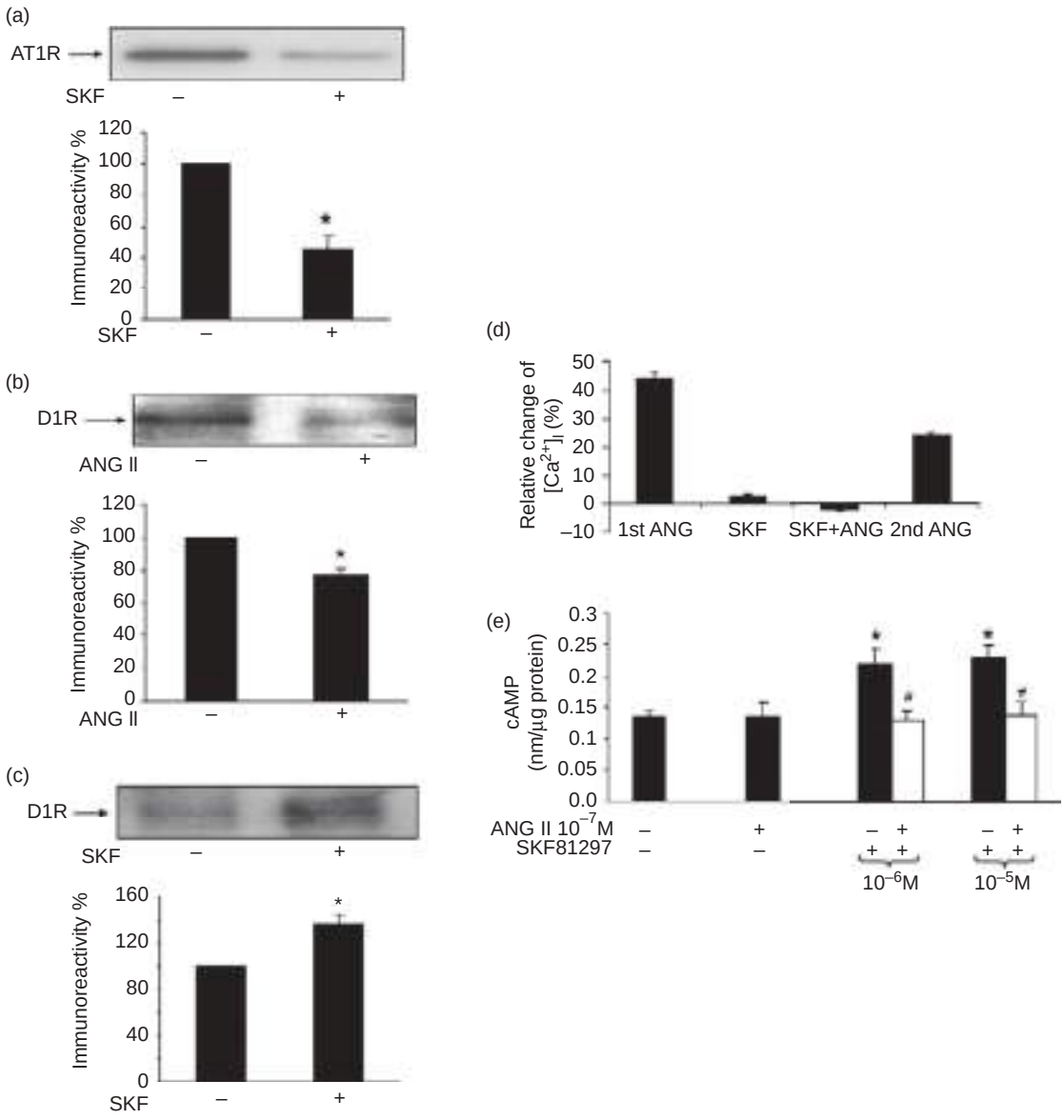

FIGURE 33.16 **Effects of ANG II and the DA-1 receptor (D1R) activating ligand, SKF81297, acting singly and in combination on renal proximal tubule (RPT) cells in culture**. (a)–(c): Cell surface expression of receptors was studied using biotinylation and densitometric quantification of bands. (a) Effect of SKF81297 on the abundance of cell surface membrane angiotensin receptor (AT1R); (b) effect of ANG II on the abundance of cell surface membrane D1R; (c) effect of SKF81297 on the abundance of cell surface membrane D1R. (d)–(e) SKF81297 abolishes the ANG II-mediated calcium response and ANG II abolishes the SKF81297-mediated cAMP response. (d) Treatment-induced change in the $[Ca^{2+}]$i level was calculated as the percent change in the $[Ca^{2+}]_i$ value before and after each treatment. (e) Renal cortical slices were exposed to ANG II alone or SKF81297 alone or pretreated with ANG II and then treated with both ANG II and SKF81297 and cAMP levels were measured in the tissue lysates. (*P 0.05 vs. control. #P 0.05 vs. respective SKF81297-treated groups.) *(From[368].)*

not in the presence of neuronal NOS inhibition.[769] At apparent odds with the natriuretic effect of NO are rat micropuncture findings that NOS inhibition decreased proximal sodium reabsorption (an effect blocked by renal nerve transection or infusion of an alpha 2 adrenergic blocker)[658] or the observation that peritubular capillary perfusion with agents promoting NO release increased Na^+-dependent luminal proton secretion.[13] Consistent with these results, mice with deficient neuronal NOS showed defective proximal $NaHCO_3$ reabsorption.[701] Pertinent to such discordant findings are the observations of Wang,[696] who observed a dose-dependent effect of tubule perfusion with SNP, in which low dose increased and high dose decreased proximal Na^+ and HCO_3^- reabsorption; perfusion with a NOS inhibitor decreased reabsorption, consistent with the enhancing effect of low-dose SNP. One possible reconciliation has been the suggestion that the

variable impact of NO on proximal tubule Na^+ transport may be contingent on cytosolic cAMP concentration.[236]

With respect to mechanism, proximal tubule epithelial cells do not contain RNA message for constitutive nitric oxide synthases (endothelial or neuronal NOS), but have abundant message for guanylate cyclase.[655] In primary culture, rat proximal tubule cells showed little cGMP production in response to NO inducers, but co-incubation with bovine pulmonary endothelial cells rendered the cells sensitive, and resulted in a sharp increase in cGMP, a decrease in Na,K-ATPase activity, and a decrease in vectorial Na^+ transport from apical to basal surfaces.[423] Carey and associates have offered the perspective that renal interstitial cGMP mediates the action of NO. Infusion of cGMP into the renal interstitium produces natriuresis in the whole kidney; infusion of an NO donor increases the interstitial cGMP concentration, and blocking the production of cGMP by administration of a soluble guanylate cyclase inhibitor completely blocked the natriureteic effect of NO.[346] In a follow-up to this observation, human proximal tubule cells in culture were found to contain soluble guanylate cyclase, and it was demonstrated that stimulation by NO produced cGMP that was secreted into the culture medium.[592] Of interest, in these experiments application of an NO donor resulted in a decrease in cell Na^+ content, consistent with a dominance of an inhibitory effect on Na^+ entry pathways.[592] A recent study has implicated a tyrosine kinase (Src) as a downstream mediator of the cGMP effect.[501]

Volume Expansion and Pressure Natriuresis

The influence of physical factors on the paracellular pathway does not preclude important effects of volume expansion on the cell itself. This was the supposition of, Robson et al.[566] who reported depression of glucose reabsorption in the kidney of the volume-expanded rat. This view found support in a whole organ tracer study, which failed to discern increased glucose backflux during volume expansion.[309] Proximal micropuncture documented decreased capacity for glucose reabsorption during volume expansion,[33] and a correlation of sodium and glucose reabsorption under the influence of albumin infusion.[365] The microperfusion study of Boonjarern et al.[107] demonstrated decreased reabsorptive flux of labeled glucose in the presence of volume expansion. The case for a cellular effect of peritubular protein has also been presented by Berry and associates, working with isolated tubules, and finding depression of chloride reabsorption with removal of bath protein.[81] The evidence was strengthened in subsequent experiments in which transepithelial concentration gradients were adjusted to virtually eliminate electro-diffusive forces across the epithelium. In that study, the increase of peritubular protein from 6 to 10 gm/dl still produced a 42% increase in NaCl reabsorption.[54] Consistent with these findings, micropuncture of the volume-expanded rat has also indicated a greater depression of proximal reabsorption of NaCl than $NaHCO_3$.[95,157] Pursuing this issue in another coupled transport system, Pitts et al. found that prior volume expansion of the rabbit depressed phosphate transport in straight proximal tubule removed and perfused over 90 minutes.[530] In the same study, prior volume expansion also depressed Na^+-coupled phosphate transport in brush border membrane vesicles.

There has been considerable effort to define the cellular impact of volume expansion. Electron probe analysis of rat kidney suggested that cell Na^+ concentration increases following saline infusion.[285] When the kidney from the volume-expanded rat is protected from physical factors using an arterial snare, the increase in cell Na^+ is eliminated.[554] These findings were interpreted as most consistent with a decrease in Na,K-ATPase activity during volume expansion. "Pressure natriuresis," in which systemic arterial pressure is increased, has been an important model with which to examine the acute impact of physical factors on proximal sodium reabsorption.[502,574] In these animals, renal autoregulation maintains a relatively constant renal blood flow and glomerular filtration rate, but renal sodium excretion increases in association with an increase in renal interstitial hydrostatic pressure.[369] In prior studies, Kinoshita and Knox[373] had shown that the decrease of proximal sodium reabsorption that normally follows increased renal interstitial pressure could be eliminated by blocking prostaglandin synthesis. In pressure natriuresis during block of prostaglandin synthesis with indomethacin, renal interstitial hydrostatic pressure still increases, but sodium and lithium reabsorption are no longer decreased.[254] Complementing this observation is the finding that with a directly applied increase in interstitial hydrostatic pressure, treatment with indomethacin eliminated the increase in tight junctional lanthanum permeability.[551] Although physical factors are involved, these results are best rationalized by an impact on the cell, rather than a direct tight junction effect.

To delineate cellular events following volume expansion, membrane fractions were obtained from kidneys undergoing pressure natriuresis, and examined for content of NHE3 and Na,K-ATPase.[789] This study revealed that acute hypertension prompted the retrieval of luminal membrane transporters (change in membrane fraction in which transport activity appeared), and a sharp reduction in the the activity of Na,K-ATPase. The retrieval of NHE3 was prompt

(within 5 minutes of acute hypertension), reversible (within 20 minutes), and concurrent with the acute changes in lithium clearance.[788] With respect to the Na, K-ATPase, the decrease in activity was not accompanied by any loss of immunoreactivity of its subunits within the membrane fractions. Immunohistochemical staining of NHE3 plus confocal microscopy permitted the visual demonstration that with acute hypertension NHE3 redistributed from the brush border into the base of the microvilli, confirming the inference from the membrane fraction analysis (Figure 33.17). Complementing these structural changes, functional changes in luminal membrane Na^+/H^+ exchange could be identified *in vivo*. When proximal tubule cells were loaded with BCECF, cytosolic pH could be monitored continuously during luminal microperfusion, specifically the time course of cellular acidification following luminal Na^+ removal. Within 20 minutes of acute hypertension, the Na^+-dependent change in cytosolic pH was reduced 52% from control.[780] When brush border membrane vesicles were examined both for NHE3 protein and for Na^+/H^+ exchange activity, it was found that despite retrieval (change in membrane fraction), the activity per transporter remained constant.[774] Thus, in contrast to the changes in Na, K-ATPase activity, the reduction in Na^+/H^+ activity could not be attributed to kinetic modification of the NHE3 transporter. The chronic analog to pressure natriuresis is a high-salt diet, and in this model there was reduction in Na,K-ATPase activity, with no change in α1-subunit density.[524] Following 3 weeks of high salt, young rats showed retrieval of luminal membrane NHE3 and NaPi2 and peritubular membrane Na,K-ATPase.[775] With acute volume contraction, however, transporter kinetics do appear to change, since the increase in lithium reabsorption is not accompanied by the appearance of new NHE3.[416] Over time, however, chronic volume contraction does increase NHE3 message in proximal tubule.[211] McDonough[465] has provided a summary scheme of the impact of extracellular fluid volume or blood pressure on proximal tubule transporter expression (Figure 33.18).

The signals from interstitium to tubule have also been pursued in more detail, and there is evidence that arachidonic acid metabolites of cytochrome P450 are implicated. Acknowledging the prior identification of eicosanoids (specifically 20-hydroxyeicosatetraenoic acid, 20-HETE) as inhibitors of Na,K-ATPase, Zhang et al.[788] sought evidence for their role as mediators of pressure natriuresis. They examined pressure natriuresis in rats pretreated with cobalt chloride to blunt cytochrome P450 metabolism, and found that this treatment blocked the pressure-associated increase in lithium clearance. This occurred in association with failure of NHE3 retrieval from brush border vesicles, and failure of Na,K-ATPase activity to decrease within its membrane fraction.[788] These findings received support with the observation that proximal convoluted tubule contains abundant cytochrome P450 4A isoforms.[336] Furthermore, rabbit proximal straight tubules in suspension produce 20-HETE, and when 20-HETE production is inhibited in an isolated perfused tubule, volume reabsorption is enhanced.[547] Using a specific inhibitor of eicosanoid formation, Dos Santos et al.[179] re-examined pressure natriuresis in pretreated rats. In these animals, 20-HETE excretion was nearly eliminated, and the pressure-induced increase in sodium excretion and lithium clearance was substantially blunted. This occurred in association with blunted retrieval of NHE3 from brush border and blunted decrease in Na,K-ATPase activity.[179] A more specific inhibitor of 20-HETE formation reproduced these results, although it was emphasized that about half of the increase in pressure-induced Na^+ excretion persisted.[755] It must be acknowledged that this work leaves unanswered the identity of the signal from

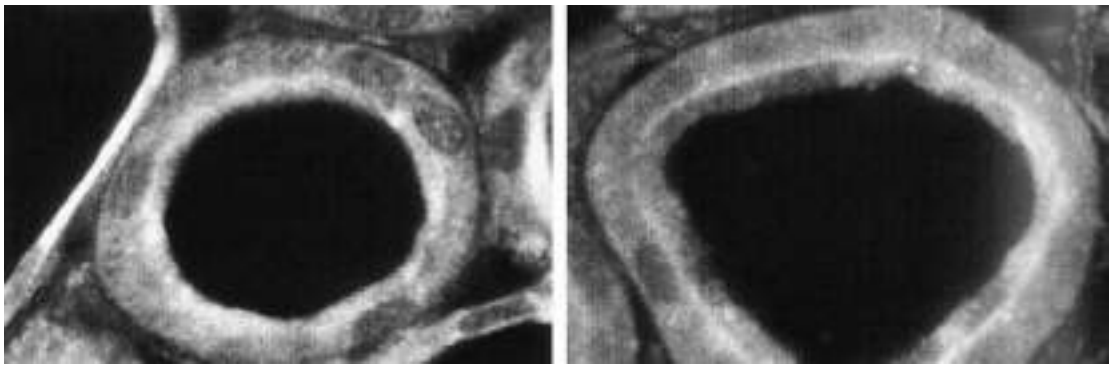

FIGURE 33.17 **Effect of acute hypertension on NHE3 distribution in rat proximal tubules**. Panels show NHE3 immunofluoresence under control conditions (left), and after 20 minutes of acute hypertension. Under control conditions, NHE3 appears along microvilli; with pressure natriuresis, there is redistribution of the exchanger to base of the brush border. *(From[779].)*

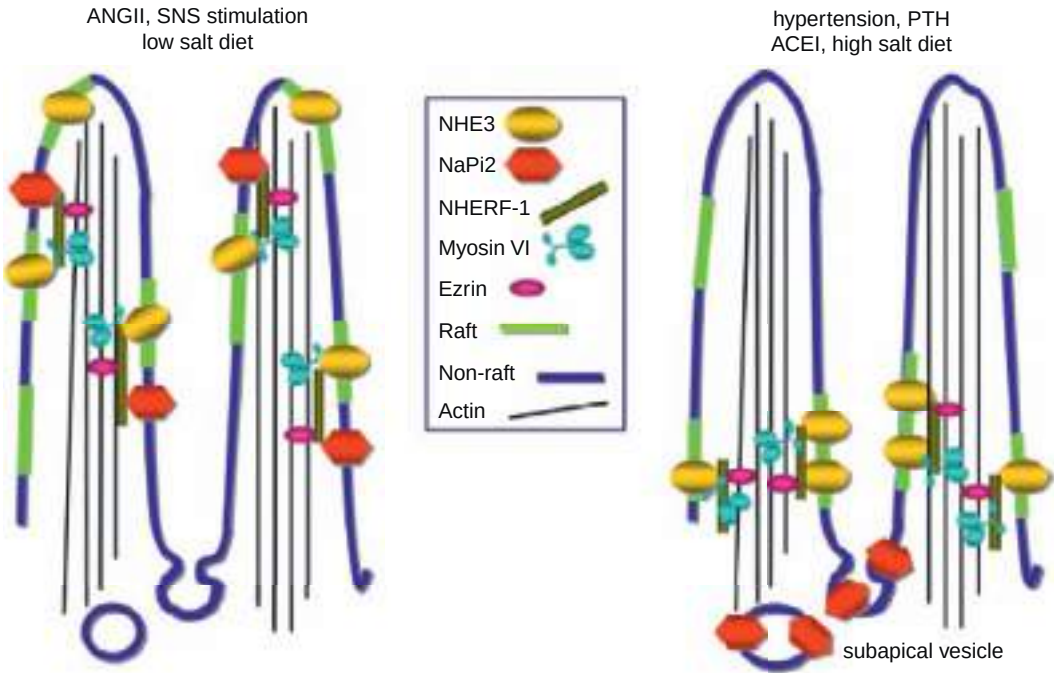

FIGURE 33.18 **Schematic representing response of renal PT sodium transporters NaPi2 and NHE3 to natriuretic and antinatriuretic stimuli**. With ANG II and sympathetic nerve stimulation, both NaPi2 and NHE3 are located in the body of the microvilli, NHE3 along with NHERF-1 and ezrin. With elevated perfusion pressure, ACEI or PTH, NHE3, and NaPi2 are translocated out of the body of the microvilli; NHE3 remains in a domain at the base of the microvilli, while NaPi2 moves to subabpical endosomes. *(From[465].)*

interstitial hydrostatic pressure to cell. A role for NO was examined in the rat, but NOS inhibition blunted transmission of renal perfusion pressure to the interstitium, so that the failure to observe pressure natriuresis may simply have been a consequence of low interstitial pressure.[499] More recently, renal interstitial cyclic GMP concentration was found to increase with renal perfusion pressure, and guanylyl cyclase inhibition blunted the pressure-associated decrease in proximal Na^+ reabsorption.[347] Leaving cGMP systhesis intact, but blocking cellular secretion of cGMP with intrarenal probenecid, also eliminated pressure natriuresis.[3] This action of extracellular cGMP to decrease Na^+ transport appeared to be tonic, in the sense that intrarenal infusion of phosphodiesterase decreased renal Na^+ excretion.[3]

Glomerulotubular Balance

In response to spontaneous variations in glomerular filtration rate, the rate of proximal tubule reabsorption varies proportionally. This "glomerulotubular balance" was apparent in the first micropuncture examination of mammalian kidney,[695] and was demonstrated elegantly by Schnermann et al.,[609] with their finding that over a four-fold change in GFR, the accessible rat proximal tubule reabsorbed roughly 40% of the filtered load (Figure 33.19). Although glomerulotubular balance may

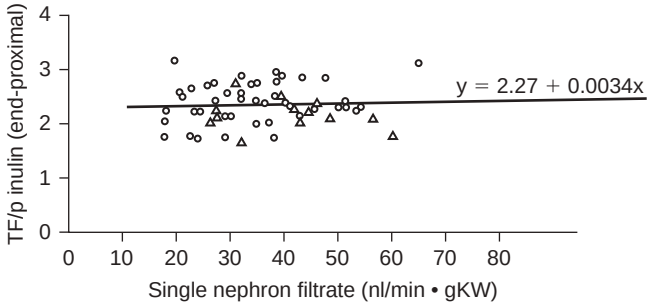

FIGURE 33.19 **End-proximal tubular fluid was sampled from rat nephrons and plotted as a function of SNGFR**. With spontaneous variation in SNGFR over a four-fold range there is virtually no change in the fractional water reabsorption. *(From[609], with permission.)*

prevent solute loss following GFR increases, perhaps its most important effect is to preserve distal delivery of sodium (permitting distal regulation of acid and potassium excretion) in times of low GFR. The mechanisms underlying balanced tubular reabsorption include both peritubular capillary effects and luminal factors.[242,290,751] Peritubular oncotic forces are generally recognized as a major force in the maintenance of balanced tubular reabsorption.[187] Any increase in filtration fraction must result in an increased peritubular protein concentration, and thus, enhanced proximal reabsorption. Experimental maneuvers which distort this oncotic force (such as saline infusion or albumin

administration) disrupt glomerulotubular balance. Nevertheless, in a mathematical model comprised of glomerulus, proximal tubule, peritubular capillary, and interstitium, simulation of only the filtration fraction effect on tubular transport failed to reproduce glomerulotubular balance.[732] In simulations of glomerular arteriolar resistance changes, it was found that fractional changes in proximal sodium reabsorption were smaller than the fractional changes in GFR. This derived from the fact that the variation in GFR came as a result of changes in glomerular plasma flow, as well as in filtration fraction. In order to achieve glomerulotubular balance, there must be a mechanism by which alterations in plasma flow, independent of peritubular Starling forces, can influence proximal reabsorption.

Perhaps the most important factor underlying perfusion–absorption balance is a direct effect of axial flow velocity on reabsorption.[751] Such "perfusion–absorption balance" has been found to influence the transport of glucose,[382] bicarbonate[11,143,428] and chloride.[268,760] One of the best illustrations of this phenomenon is the micropuncture data of Chan et al.[143] shown in Figure 33.20, in which a three-fold increase in luminal perfusion rate (with trivial changes in luminal HCO_3^- concentration)

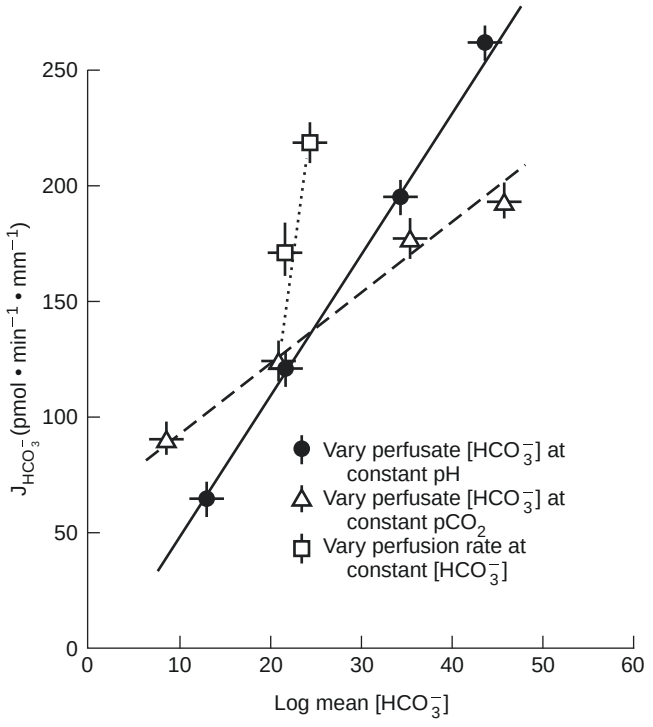

FIGURE 33.20 **Net bicarbonate reabsorption, J_{HCO3}, by perfused rat proximal tubule as a function of mean luminal bicarbonate concentration**. At a constant pCO_2, bicarbonate transport varies linearly with the transepithelial concentration gradient (dashed line). Elevation of pCO_2 enhances, and depression of pCO_2 diminishes, bicarbonate reabsorption (solid line). There is a steep dependence of J_{HCO3} on luminal flow rate. *(From[143], with permission.)*

produced a doubling of the rate of bicarbonate reabsorption. More pronounced effects have been reported with "native" tubular fluid, in comparison with artificial microperfusion solutions, suggesting the presence of a filtered, transport-promoting factor.[49,288] It may also be the case that reductions (rather than increases) in luminal flow are more faithfully followed by proportional changes in transport.[48,289,526,569] Nevertheless, the range over which modulation of luminal flow produces proportional changes in proximal reabsorption is broad.[568] The underlying mechanism for flow-dependent reabsorption has been a point of controversy. One perennial consideration is an unstirred layer effect within the brush border.[563] Morphological observations of Maunsbach et al.[459] demonstrated that lower tubule flow rates are associated with diminished tubule distention and a compaction of the brush border microvilli. Nevertheless, model calculations indicate it unlikely that there is any appreciable convective stirring within this pile,[50] neither should the diffusion barrier between the bulk luminal fluid and the cell membrane pose any significant hindrance to Na^+/H^+ exchange.[394] An intriguing mechanism for flow-dependent transport gained support from two studies, using very different methodologies, which both suggested that increases in axial flow velocity recruit new transporters into the luminal membrane. Preisig[533] loaded rat proximal tubule cells with the pH-indicator BCECF and examined recovery from an acute acid-load *in vivo* (ammonium pulse). With increases in luminal flow rate, the pH recovery mediated by Na^+/H^+ exchange was enhanced. Maddox et al.[447] subjected rats to acute changes in vascular volume in order to obtain hydropenic, euvolemic, and volume-expanded groups, with respective grouping according to decreased, normal, and increased GFR. When brush border membrane vesicles were prepared from each of these groups, and Na^+/H^+ kinetic parameters assessed, it was found that the V_{max} determinations stratified in parallel with GFR.

Guo et al.[282] proposed that the brush border microvilli serve as the sensor for axial flow along the proximal tubule. In that hypothesis, the drag force on each microvillus produces torque on an actin filament core, and this force is transmitted to the underlying cytoskeleton. The close spacing and uniform height of the microvilli allowed a precise calculation of that torque, and using the known bending moment for an actin filament, the Young's modulus for a microvillus was estimated. This yielded the prediction that for microvilli 2.5 μm in height, the tip deflection under axial flows of 30 nl/min would be about 4 nm, in effect depicting the microvilli as a set of stiff bristles that would retain their configuration through the physiological range of flows.[282] In a subsequent analysis, a simplified equation for microvillous torque was derived which has

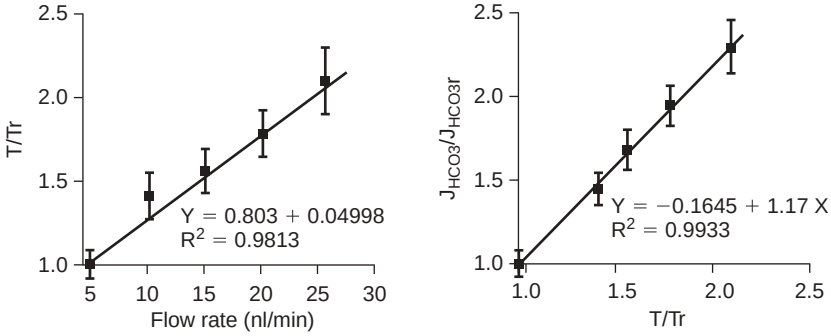

FIGURE 33.21 **Impact of luminal flow rate on bicarbonate reabsorption (J_{HCO3}) in mouse proximal tubules perfused *in vitro*.** The panel on the left shows the computed microvillous torque, T, at each flow, relative to the torque when perfusion is at 5 nl/min (T_r.) In the right panel, the observed J_{HCO3} is plotted as a function of the relative torque. *(From [183], with permission.)*

been useful for assessment of experimental data.[182] The essence of that derivation was identifying microvillous drag with the force on the tubular fluid:

$$D \cdot N = \frac{dp}{dz} \cdot \pi \cdot R^2 \tag{33.17}$$

where D is the drag per microvillus, N is the number of microvilli per unit length of tubule, p is luminal hydrostatic pressure, z is axial length, and R is the tubule radius from center-line to microvillus tip. Assuming Poiseuille flow:

$$\frac{dp}{dz} = 8\mu Q/\pi R^4 \tag{33.18}$$

where Q is luminal flow rate and μ is the tubule fluid viscosity. This provides the estimate of microvillous drag:

$$D \cdot N = 8\mu Q/R^2 \tag{33.19}$$

and for a microvillus of height, L, the torque, T, is:

$$T \cdot N = 8\mu QL/R^2 \tag{33.20}$$

Since the number of microvilli, N, is not easily obtained, Eq. (33.20) is most useful in comparing two experimental trials in which flow is varied and the assumption is made that neither N nor L change with the experimental conditions:

$$\frac{T}{T_r} = \left[\frac{\mu Q}{\mu_r Q_r}\right] \cdot \left[\frac{R_r^2}{R^2}\right] \tag{33.21}$$

in which the subscript "r" denotes a reference flow. This equation reveals the microvillous torque to vary directly with luminal flow and fluid viscosity, and inversely as the square of the luminal radius.

Du et al.[182] applied a slightly more detailed version of Eq. (33.21) to analyze the first experimental study of flow-dependent volume reabsorption, J_v, in isolated perfused mouse proximal tubules. The key finding of that work was that fractional changes in perfusion were greater than the fractional changes in J_v, but when changes in luminal diameter were included in the calculation, the fractional change in microvillous torque and J_v were identical. Furthermore, luminal fluid viscosity increased J_v at constant perfusion rate. And finally, disruption of the cytoskeleton with cytochalasin D eliminated the perfusion-dependent increase in J_v. Du et al.[183] subsequently re-examined flow-dependent transport in mouse proximal tubule, with measurement of HCO_3^- reabsorption, J_{HCO3}. Over a five-fold variation of luminal perfusion rate, there was a predicted two-fold variation in microvillous torque, which scaled identically with the reabsorption (Figure 33.21). Du et al.[182] also reconsidered the data of Burg and Orloff,[126] widely cited as a negative effect of flow on proximal sodium reabsorption in isolated perfused rabbit proximal convoluted tubule. Burg and Orloff had observed that a three-fold increase in tubule perfusion rate produced a 37% increase in volume reabsorption, a value that did not achieve statistical significance. However, they also noted that with the highest flow, there was a 41% increase in tubule diameter. Du et al. estimated that these changes of flow and diameter would yield a 43% increase in microvillous torque, certainly compatible with the observed impact on J_v. In sum, it appears that rabbit proximal tubules were more distensible than mouse tubules, so that perfusion-dependent changes in luminal diameter precluded large deviations in microvillous torque. At present, the cellular signals from torque to Na^+/H^+ exchange remain to be delineated.

PERSPECTIVE

Sodium reabsorption along the proximal tubule refers to a multiplicity of processes, occurring in series and in parallel along a heterogeneous epithelium. Sodium transport cannot be considered out of context of the secretion of protons or the reabsorption of chloride, bicarbonate, potassium, calcium, and organic solutes. Furthermore, the precise interrelationship of these coupled transport processes depends upon the location along the proximal tubule, as well as upon physiologic parameters external to the nephron, such as plasma composition or extracellular volume status of the organism.

One focus of this chapter has been on the biophysics of transport, namely identification of the transporters and the driving forces for their fluxes. The feasibility of such an approach was due to the development of experimental technology, which permitted examination of cell membranes and recording of intracellular composition. With these tools, the first order of business had been definition and localization of the transporters. More recent molecular methods enhanced this aspect of tubule physiology by providing means to visualize a transporter within proximal tubule, and to distinguish biochemical modifications or changes in membrane density. The ability to clone and express transporters in high density in otherwise quiet systems (in which flux through the pathway of interest dominates) has yielded advances in the definition of transport kinetics.

The second order of business has been identifying important regulatory factors. This means an understanding of how changes in cell volume or composition translate into alterations of sodium reabsorption, and of the key neurohumoral signals and physical factors which modulate transport. The complexity of this task is in part technical, insofar as cellular transport machinery may involve an assembly of interacting proteins that are not fully recovered in convenient expression systems. Furthermore, the overall impact on sodium transport by one hormone may depend upon the state of activation of the other systems. Nevertheless, one recurring theme in descriptions of transport regulation has been the targeting of both luminal and peritubular membranes in a coordinated fashion.

Enrichment of our perspective of proximal tubule function must ultimately confer a quantitative understanding of its roles in pathologic states of the organism. Traditionally, this has focused on secondary renal response to disorders of extracellular volume homeostasis, such as edema forming states. It is entirely likely, however, that a role for proximal tubule may come to be identified in primary pathogenesis, as perhaps in volume-dependent hypertension. One anticipates, as a consequence of such information, that therapeutic intervention, which seeks to alter renal sodium transport, will be achieved with greater accuracy and greater safety.

Acknowledgment

This work was supported by National Institute of Diabetes and Digestive and Kidney Disease Grant 1-RO1-DK-29857.

References

[1] Abuladze N, Lee I, Newman D, Hwang J, Pushkin A, Kurtz I. Axial heterogeneity of sodium-bicarbonate co-transporter expression in the rabbit proximal tubule. Am J Physiol 1998;274: F628–33.

[2] Agre P, Preston GM, Smith BL, Jung JS, Raina S, Moon C, et al. Aquaporin CHIP: the archetypal molecular water channel. Am J Physiol 1993;265:F463–76.

[3] Ahmed F, Kemp BA, Howell NL, Siragy HM, Carey RM. Extracellular renal guanosine cyclic 3′5′-monophosphate modulates nitric oxide- and pressure-induced natriuresis. Hypertension 2007;50:958–63.

[4] Akiba T, Alpern RJ, Eveloff J, Calamina J, Warnock DG. Electrogenic sodium/bicarbonate co-transport in rabbit renal cortical basolateral membrane vesicles. J Clin Invest 1986;78:1472–8.

[5] Alavi N, Spangler RA, Jung CY. Sodium-dependent glucose transport by cultured proximal tubule cells. Biochim Biophys Acta 1987;899:9–16.

[6] Albrecht FE, Xu J, Moe OW, Hopfer U, Simonds WF, Orlowski J, et al. Regulation of NHE3 activity by G protein subunits in renal brush-border membranes. Am J Physiol 2000;278:R1064–73.

[7] Alpern RJ. Mechanism of basolateral membrane $H^+/OH^-/HCO3^-$ transport in the rat proximal convoluted tubule. A sodium-coupled electrogenic process. J Gen Physiol 1985;86:613–36.

[8] Alpern RJ. Apical membrane chloride/base exchange in the rat proximal convoluted tubule. J Clin Invest 1987;79:1026–30.

[9] Alpern RJ. Cell mechanisms of proximal tubule acidification. Physiol Rev 1990;70:79–114.

[10] Alpern RJ, Chambers M. Basolateral membrane Cl/HCO3 exchange in the rat proximal convoluted tubule. Na-dependent and-independent modes. J Gen Physiol 1987;89:581–98.

[11] Alpern RJ, Cogan MG, Rector Jr FC. Flow dependence of proximal tubular bicarbonate absorption. Am J Physiol 1983;245: F478–84.

[12] Amemiya M, Loffing Lötscher M, Kaissling B, Alpern RJ, Moe OW. Expression of NHE-3 in the apical membrane of rat renal proximal tubule and thick ascending limb. Kid Int 1995;48:1206–15.

[13] Amorena C, Castro AF. Control of proximal tubule acidification by the endothelium of the peritubular capillaries. Am J Physiol 1997;272:R691–4.

[14] Andreoli TE, Schafer JA. Volume absorption in the pars recta. III Luminal hypotonicity as a driving force for isotonic volume absorption. Am J Physiol 1978;234:F349–55.

[15] Andreoli TE, Schafer JA, Troutman SL. Perfusion rate-dependence of transepithelial osmosis in isolated proximal convoluted tubules: estimation of the hydraulic conductance. Kidney Int 1978;14:263–9.

[16] Andreoli TE, Schafer JA, Troutman SL, Watkins ML. Solvent drag component of Cl^- flux in superficial proximal straight tubules: evidence for a paracellular component of isotonic fluid absorption. Am J Physiol 1979;237:F455–62.

[17] Aperia AC. Intrarenal dopamine: a key signal in the interactive regulation of sodium metabolism. Ann Rev Physiol 2000;62:621–47.

[18] Aperia A, Bertorello A, Seri I. Dopamine causes inhibition of Na^+-K^+-ATPase activity in rat proximal convoluted tubule segments. Am J Physiol 1987;252:F39–45.

[19] Aperia A, Ibarra F, Svensson L-B, Klee C, Greengard P. Calcineurin mediates alpha-adrenergic stimulation of Na^+-K^+-ATPase activity in renal tubule cells. Proc Natl Acad Sci 1992;89:7394–7.

[20] Aronson PS. Kinetic properties of the plasma membrane Na^+-H^+ exchanger. Ann Rev Physiol 1985;47:545–60.

[21] Aronson PS, Giebisch G. Mechanisms of chloride transport in the proximal tubule. Am J Physiol 1997;273:F179–92.

[22] Aronson PS, Nee J, Suhm MA. Modifier role of internal H in activating the Na^+-H^+ exchanger in renal microvillus membrane vesicles. Nature 1982;299:161–3.

[23] Aronson PS, Sacktor B. The Na^+ gradient-dependent transport of D-glucose in renal brush border membranes. J Biol Chem 1975;250:6032–9.
[24] Aronson PS, Suhm MA, Nee J. Interaction of external H^+ with the Na^+–H^+ exchanger in renal microvillus membrane vesicles. J Biol Chem 1983;258:6767–71.
[25] Arystarkhova E, Donnet C, Muñoz-Matta A, Specht SC, Sweadner KJ. Multiplicity of expression of FXYD proteins in mammalian cells: dynamic exchange of phospholemman and g-subunit in response to stress. Am J Physiol 2007;292: C1179–91.
[26] Arystarkhova E, Sweadner KJ. Splice variants of the gamma subunit (FXYD2) and their significance in regulation of the Na, K-ATPase in kidney. J Bioenerg Biomembr 2005;37:381–6.
[27] Arystarkhova E, Wetzel RK, Sweadner KJ. Distribution and oligomeric association of splice forms of Na^+-K^+-ATPase regulatory g-subunit in rat kidney. Am J Physiol 2002;282: F393–407.
[28] Atherton JC. Comparison of chloride concentration and osmolality in proximal tubular fluid peritubular capillary plasma and systemic plasma in the rat. J Physiol (Lond) 1977;273: 765–73.
[29] Avison MJ, Gullans SR, Ogino T, Giebisch G, Shulman RG. Measurement of Na^+-K^+ coupling ratio of Na^+-K^+-ATPase in rabbit proximal tubules. Am J Physiol 1987;253:C126–36.
[30] Avison MJ, Gullans SR, Ogino T, Giebisch G. Na^+ and K^+ fluxes stimulated by Na^+-coupled glucose transport: evidence for a Ba^{2+}-insensitive K^+ efflux pathway in rabbit proximal tubules. J Membr Biol 1988;105:197–205.
[31] Bacic D, Capuano P, Baum M, Zhang J, Stange G, Biber J, et al. Activation of dopamine D1-like receptors induces acute internalization of the renal Na^+/phosphate co-transporter NaPi-IIa in mouse kidney and OK cells. Am J Physiol Renal Physiol 2005;288:F740–7.
[32] Bacic D, Kaissling B, McLeroy P, Zou L, Baum M, Moe OW. Dopamine acutely decreases apical membrane Na/H exchanger NHE3 protein in mouse renal proximal tubule. Kidney Int 2003;64:2133–41.
[33] Baines AD. Effect of extracellular fluid volume expansion on maximum glucose reabsorption rate and glomerular tubular balance in single rat nephrons. J Clin Invest 1971;50: 2414–25.
[34] Baines AD, Chan W. Production of urine free dopamine from DOPA: a micropuncture study. Life Sci 1980;26:253–9.
[35] Baines AD, Drangova R, Hatcher C. Dopamine production by isolated glomeruli and tubules from rat kidneys. Can J Physiol Pharmacol 1985;63:155–8.
[36] Baines AD, deRouffignac C. Functional hetereogeneity of nephrons. II. Filtration rates, intraluminal flow velocities and fractional water reabsorption. Pf Arch 1969;308:260–76.
[37] Balkovetz DF, Chumley P, Amlal H. Downregulation of claudin-2 expression in renal epithelial cells by metabolic acidosis. Am J Physiol 2009;297:F604–11.
[38] Ball SG, Gunn IG, Douglas IHS. Renal handling of dopa dopamine norepinephrine and epinephrine in the dog. Am J Physiol 1982;242:F56–62.
[39] Banday AA, Siddiqui AH, Menezes MM, Hussain T. Insulin treatment enhances AT1 receptor function in OK cells. Am J Physiol 2005;288:F1213–9.
[40] Bank N, Aynedjian HS. Failure of changes in intracapillary pressures to alter proximal fluid reabsorption. Kidney Int 1984;26:275–82.
[41] Bank N, Aynedjian HS, Mutz BF. Proximal bicarbonate absorption independent of Na^+-H^+ exchange: effect of bicarbonate load. Am J Physiol 1989;256:F577–82.
[42] Bank N, Yarger WE, Aynedjian HS. A microperfusion study of sucrose movement across the rat proximal tubule during renal vein constriction. J Clin Invest 1971;50:294–302.
[43] Bankir L, de Rouffignac C. Anatomical and functional heterogeneity of nephrons in the rabbit: Microdissection studies and SNGFR measurements. Pflügers Arch 1976;366: 89–93.
[44] Barfuss DW, Schafer JA. Differences in active and passive glucose transport along the proximal nephron. Am J Physiol 1981;240:F322–32.
[45] Barfuss DW, Schafer JA. Rate of formation and composition of absorbate from proximal nephron segments. Am J Physiol 1984;247:F117–29.
[46] Barratt LJ, Rector Jr. FC, Kokko JP, Seldin DW. Factors governing the transepithelial potential difference across the proximal tubule of the rat kidney. J Clin Invest 1974;53:454–64.
[47] Barriere H, Rubera I, Belfodil R, Tauc M, Tonnerieux N, Poujeol C, et al. Swelling-activated chloride and potassium conductance in primary cultures of mouse proximal tubules. Implication of KCNE1 protein. J Membr Biol 2003;193 (3):153–70.
[48] Bartoli E, Conger JD, Earley LE. Effect of intraluminal flow on proximal tubular reabsorption. J Clin Invest 1973;52:843–9.
[49] Bartoli E, Earley LE. Importance of ultrafilterable plasma factors in maintaining tubular reabsorption. Kidney Int 1973;3:142–50.
[50] Basmadjian D, Dykes DS, Baines AD. Flow through brushborders and similar protuberant wall structures. J Membr Biol 1980;56:183–90.
[51] Baum M. Effect of luminal chloride on cell pH in rabbit proximal tubule. Am J Physiol 1988;254:F677–83.
[52] Baum M. Axial heterogeneity of rabbit proximal tubule luminal H^+ and basolateral HCO_3^- transport. Am J Physiol 1989;256: F335–41.
[53] Baum M, Berry CA. Evidence for neutral transcellular NaCl transport and neutral basolateral chloride exit in the rabbit proximal convoluted tubule. J Clin Invest 1984;74: 205–11.
[54] Baum M, Berry CA. Peritubular protein modulates neutral active NaCl absorption in rabbit proximal convoluted tubule. Am J Physiol 1985;248:F790–5.
[55] Baum M, Hays SR. Phorbol myristate acetate and dioctanoylglycerol inhibit transport in rabbit proximal convoluted tubule. Am J Physiol 1988;254:F9–14.
[56] Baum M, Quigley R. Inhibition of proximal convoluted tubule transport by dopamine. Kidney Int 1998;54:1593–600.
[57] Baum M, Quigley R. Maturation of rat proximal tubule chloride permeability. Am J Physiol 2005;289:R1659–64.
[58] Baum M, Quigley R, Quan A. Effect of luminal angiotensin II on rabbit proximal convoluted tubule bicarbonate absorption. Am J Physiol 1997;273:F595–600.
[59] Bautista R, Manning R, Martinez F, Avila-Casado M, Soto V, Medina A, et al. Angiotensin II-dependent increased expression of Na^+-glucose co-transporter in hypertension. Am J Physiol 2004;286:F127–33.
[60] Beach RE, Schwab SJ, Brazy PC, Dennis VW. Norepinephrine increases Na^+-K^+-ATPase and solute transport in rabbit proximal tubules. Am J Physiol 1987;252:F215–20.
[61] Beck FX, Dorge A, Rick R, Schramm M, Thurau K. Effect of potassium adaptation on the distribution of potassium sodium and chloride across the apical membrane of renal tubular cells. Pflügers Arch 1987;409:477–85.
[62] Beck JC, Sacktor B. Energetics of the Na^+-dependent transport of D-glucose in renal brush border membrane vesicles. J Biol Chem 1975;250:8674–80.

[63] Beck JS, Breton S, Laprade R, Giebisch G. Volume regulation and intracellular calcium in the rabbit proximal convoluted tubule. Am J Physiol 1991;260:F861–7.
[64] Beck JS, Breton S, Mairbäurl H, Laprade R, Giebisch G. Relationship between sodium transport and intracellular ATP in isolated perfused rabbit proximal convoluted tubule. Am J Physiol 1991;261:F634–9.
[65] Beck JS, Hurst AM, Lapointe J-Y, Laprade R. Regulation of basolateral K channels in proximal tubule studied during continuous microperfusion. Am J Physiol 1993;264:F496–501.
[66] Beck JS, Laprade R, Lapointe J-Y. Coupling between transepithelial Na transport and basolateral K conductance in renal proximal tubule. Am J Physiol 1994;266:F517–27.
[67] Beck JS, Potts DJ. Cell swelling, co-transport activation and potassium conductance in isolated perfused rabbit kidney proximal tubules. J Physiol 1990;425:369–78.
[68] Beguin P, Beggah AT, Chibalin AV, Burgener-Kairuz P, Jaisser F, Mathews PM, et al. Phosphorylation of the NaK-ATPase alpha-subunit by protein kinase A and C in vitro and in intact cells. J Biol Chem 1994;269(39):24437–45.
[69] Bello-Reuss E. Effect of catecholamines on fluid reabsorption by the isolated proximal convoluted tubule. Am J Physiol 1980;238:F347–52.
[70] Bello-Reuss E. Electrical properties of the basolateral membrane of the straight portion of the rabbit proximal renal tubule. J Physiol (Lond) 1982;326:49–63.
[71] Bello-Reuss E, Colindres RE, Pastoriza-Munoz E, Mueller RA, Gottschalk CW. Effects of acute unilateral renal denervation in the rat. J Clin Invest 1975;56:208–17.
[72] Bello-Reuss E, Higashi Y, Kaneda Y. Dopamine decreases fluid reabsorption in straight portions of rabbit proximal tubule. Am J Physiol 1982;242:F634–40.
[73] Bello-Reuss E, Trevino DL, Gottschalk CW. Effect of renal sympathetic nerve stimulation on proximal water and sodium reabsorption. J Clin Invest 1976;57:1104–7.
[74] Bello-Reuss E, Weber MR. Electrophysiological studies on primary cultures of proximal tubule cells. Am J Physiol 1986;251: F490–8.
[75] Bengele HH, Evan AP. The effects of Ringer-Locke or blood infusions on the lateral intercellular spaces of the rat proximal tubule. Anat Rec 1975;182:201–14.
[76] Bentzel CJ, Parsa B, Hare DK. Osmotic flow across proximal tubule of *Necturus*: correlation of physiologic and anatomic studies. Am J Physiol 1969;217:570–80.
[77] Bentzel CJ, Reczek PR. Permeability changes in *Necturus* proximal tubule during volume expansion. Am J Physiol 1978;234: F225–34.
[78] Berry CA. Heterogeneity of tubular transport processes in nephron. Ann Rev Physiol 1982;44:181–201.
[79] Berry CA. Lack of effect of peritubular protein on passive NaCl transport in the rabbit proximal tubule. J Clin Invest 1983;71:268–81.
[80] Berry CA. Water permeability and pathways in the proximal tubule. Am J Physiol 1983;245:F279–94.
[81] Berry CA, Cogan MG. Influence of peritubular protein on solute absorption in the rabbit proximal tubule. A specific effect on NaCl transport. J Clin Invest 1981;68:506–16.
[82] Berry CA, Rector Jr. FC. Relative sodium-to-chloride permeability in the proximal convoluted tubule. Am J Physiol 1978;235:F592–604.
[83] Berry CA, Rector Jr. FC. Electroneutral NaCl absorption in the proximal tubule: mechanisms of apical Na-coupled transport. Kidney Int 1989;36:403–11.
[84] Berry CA, Warnock DG, Rector Jr. FC. Ion selectivity and proximal salt reabsorption. Am J Physiol 1978;235:F234–45.
[85] Bertorello A, Aperia A. Na^+-K^+-ATPase is an effector protein for protein kinase C in renal proximal tubule cells. Am J Physiol 1989;256:F370–3.
[86] Bertorello A, Aperia A, Walaas SI, Nairn AC, Greengard P. Phosphorylation of the catalytic subunit of Na^+,K^+-ATPase inhibits the activity of the enzyme. Proc Natl Acad Sci 1991;88:11359–62.
[87] Bertorello AM, Katz AI. Short-term regulation of renal Na-K-ATPase activity: Physiological relevance and cellular mechanisms. Am J Physiol 1993;265:F743–55.
[88] Beyenbach KW. Secretory NaCl and volume flow in renal tubules. Am J Physiol 1986;250:R753–63.
[89] Biagi B, Kubota T, Sohtell M, Giebisch G. Intracellular potentials in rabbit proximal tubules perfused *in vitro*. Am J Physiol 1981;240:F200–10.
[90] Biagi B, Sohtell M, Giebisch G. Intracellular potassium activity in the rabbit proximal straight tubule. Am J Physiol 1981;241: F677–86.
[91] Biagi BA, Sohtell M. pH sensitivity of the basolateral membrane of the rabbit proximal tubule. Am J Physiol 1986;250: F261–6.
[92] Biagi BA, Sohtell M. Electrophysiology of basolateral bicarbonate transport in the rabbit proximal tubule. Am J Physiol 1986;250:F267–72.
[93] Biber J, Gisler SM, Hernando N, Murer H. Protein/protein interactions (PDZ) in proximal tubules. J Membr Biol 2005;203:111–8.
[94] Biber J, Gisler SM, Hernando N, Wagner CA, Murer H. PDZ interactions and proximal tubular phosphate reabsorption. Am J Physiol 2004;287:F871–5.
[95] Bichara M, Paillard M, Corman B, de-Rouffignac C, Leviel F. Volume expansion modulates $NaHCO_3$ and NaCl transport in the proximal tubule and Henle's loop. Am J Physiol 1984;247: F140–50.
[96] Bichara M, Paillard M, Leviel F, Gardin J-P. Hydrogen transport in rabbit kidney proximal tubules – Na:H exchange. Am J Physiol 1980;238:F445–51.
[97] Bidet M, Tauc M, Merot J, Vandewalle A, Poujeol P. Na^+-H^+ exchanger in proximal cells isolated from rabbit kidney. I Functional characteristics. Am J Physiol 1987;253:F935–44.
[98] Biemesderfer D, Nagy T, DeGray B, Aronson PS. Specific association of megalin and the Na^+/H^+ exchanger isoform NHE3 in the proximal tubule. J Biol Chem 1999;274(25):17518–24.
[99] Biemesderfer D, Pizzonia J, Abu-Alfa A, Exner M, Reilly R, Igarashi P, et al. NHE3: a Na^+/H^+ exchanger isoform of renal brush border. Am J Physiol 1993;265:F736–42.
[100] Biemesderfer D, Reilly RF, Exner M, Igarashi P, Aronson PS. Immunocytochemical characterization of Na^+-H^+ exchanger isoform NHE-1 in rabbit kidney. Am J Physiol 1992;263:F833–40.
[101] Biemesderfer D, DeGray B, Aronson PS. Active (9.6 S) and inactive (21 S) oligomers of NHE3 in microdomains of the renal brush border. J Biol Chem 2001;276:10161–7.
[102] Birnir B, Lee H-S, Hediger MA, Wright EM. Expression and characterization of the intestinal Na^+/glucose co-transporter in COS-7 cells. Biochim Biophys Acta 1990;1048:100–4.
[103] Blantz RC, Tucker BJ. Determinants of peritubular capillary fluid uptake in hydropenia and saline and plasma expansion. Am J Physiol 1975;228:1927–35.
[104] Bloch RD, Zikos D, Fisher KA, Schleicher L, Oyama M, Cheng J-C, et al. Activation of proximal tubular Na^+-H^+ exchange by angiotensin II. Am J Physiol 1992;263:F135–43.
[105] Bomsztyk K, Wright FS. Effects of transepithelial fluid flux on transepithelial voltage and transport of calcium sodium chloride and potassium by renal proximal tubule. Kidney Int 1982;21:269 [Abstr.]

[106] Bomsztyk K, Wright FS. Dependence of ion fluxes on fluid transport by rat proximal tubule. Am J Physiol 1986;250:F680–9.
[107] Boonjarern S, Leski ME, Kurtzman NA. Effects of extracellular volume expansion on the tubular reabsorption of glucose. Pflügers Arch 1976;366:67–71.
[108] Boron WF, Boulpaep EL. Intracellular pH regulation in the renal proximal tubule of the salamander: Basolateral HCO_3^- transport. J Gen Physiol 1983;81:53–94.
[109] Boron WF, Boulpaep EL. The electrogenic Na/HCO_3 co-transporter. Kidney Int 1989;36:392–402.
[110] Boron WF, Sackin H. Measurement of intracellular ionic composition and activities in renal tubules. Ann Rev Physiol 1983;45:483–96.
[111] Boulanger Y, Vinay P, Boulanger M. NMR monitoring of intracellular sodium in dog and rabbit kidney tubules. Am J Physiol 1987;253:F904–11.
[112] Braam B, Mitchell KD, Fox J, Navar LG. Proximal tubular secretion of angiotensin II in rats. Am J Physiol 1993;264: F891–8.
[113] Brenner BM, Falchuk KH, Keimowitz RI, Berliner RW. The relationship between peritubular capillary protein concentration and fluid reabsorption by the renal proximal tubule. J Clin Invest 1969;48:1519–31.
[114] Brenner BM, Troy JL. Postglomerular vascular protein concentration: evidence for a causal role in governing fluid reabsorption and glomerulotubular balance by the renal proximal tubule. J Clin Invest 1971;50:336–49.
[115] Brenner BM, Troy JL, Daugharty TM. On the mechanism of inhibition in fluid reabsorption by the renal proximal tubule of the volume-expanded rat. J Clin Invest 1971;50:1596–602.
[116] Breton S, Beck JS, Cardinal J, Giebisch G, Laprade R. Involvement and source of calcium in volume regulatory decrease of collapsed proximal convoluted tubule. Am J Physiol 1992;263:F656–64.
[117] Breton S, Marsolais M, Lapointe JY, Laprade R. Cell volume increases of physiologic amplitude activate basolateral K and Cl conductances in the rabbit proximal convoluted tubule. J Am Soc Nephrol 1996;7:2072–87.
[118] Brismar H, Asghar M, Carey RM, Greengard P, Aperia A. Dopamine-induced recruitment of dopamine D1 receptors to the plasma membrane. Proc Natl Acad Sci 1998;95:5573–8.
[119] Brisolla-Diuana A, Amorena C, Malnic G. Transfer of base across the basolateral membrane of cortical tubules of rat kidney. Pflügers Arch 1985;405:209–15.
[120] Brown D, Hirsch S, Gluck S. Localization of proton-pumping ATPase in rat kidney. J Clin Invest 1988;82:2114–26.
[121] Brown GP, Douglas JG. Angiotensin II binding sites on isolated rat renal brush border membranes. Endocrinology 1982;111:1830–6.
[122] Brown GP, Douglas JG. Angiotensin II binding sites in rat and primate isolated renal tubular basolateral membranes. Endocrinology 1983;112:2007–14.
[123] Burckhardt B-Ch, Cassola AC, Frömter E. Electrophysiological analysis of bicarbonate permeation across the peritubular cell membrane of rat kidney proximal tubule. II Exclusion of HCO_3^- effects on other ion permeabilities and of coupled electroneutral HCO_3^- transport. Pflügers Arch 1984;401:43–51.
[124] Burckhardt B-Ch, Sato K, Frömter E. Electrophysiological analysis of bicarbonate permeation across the peritubular cell membrane of rat kidney proximal tubule. I Basic observations. Pflügers Arch 1984;401:34–42.
[125] Burg MB, Green N. Bicarbonate transport by isolated perfused rabbit proximal convoluted tubules. Am J Physiol 1977;233: F307–14.
[126] Burg MB, Orloff J. Control of fluid absorption in the renal proximal tubule. J Clin Invest 1968;47:2016–24.
[127] Burnham CE, Amlal H, Wang Z, Shull GE, Soleimani M. Cloning and functional expression of a human kidney Na^+: HCO_3^- co-transporter. J Biol Chem 1997;272:19111–4.
[128] Burnham CE, Flagella M, Wang Z, Amlal H, Shull GE, Soleimani M. Cloning renal distribution and regulation of the rat Na^+ :HCO_3^- co-transporter. Am J Physiol 1998;274: F1119–26.
[129] Burnham C, Munzesheimer C, Rabon E, Sachs G. Ion pathways in renal brush border membranes. Biochem Biophys Acta 1982;685:260–72.
[130] Cano A, Baum M, Moe OW. Thyroid hormone stimulates the renal Na/H exchanger NHE3 by transcriptional activation. Am J Physiol 1999;276(1 Pt 1):C102–8.
[131] Cano A, Preisig P, Alpern RJ. Cyclic adenosine monophosphate acutely inhibits and chronically stimulates Na/H antiporter in OKP cells. J Clin Invest 1993;92:1632–8.
[132] Cantiello HF, Scott JA, Rabito CA. Conductive Na^+ transport in an epithelial cell line (LLC-PK\d1\u) with characteristics of proximal tubular cells. Am J Physiol 1987;252: F590–7.
[133] Cardinal J, Lapointe J-Y, Laprade R. Luminal and peritubular ionic substitutions and intracellular potential of the rabbit proximal convoluted tubule. Am J Physiol 1984;247: F352–64.
[134] Carey RM. Theodore Cooper Lecture. Renal dopamine system: Paracrine regulator of sodium homeostasis and blood pressure. Hypertension 2001;38:297–302.
[135] Carpi-Medina P, Gonzalez E, Whittembury G. Cell osmotic water permeability of isolated rabbit proximal convoluted tubules. Am J Physiol 1983;244:F554–63.
[136] Carpi-Medina P, Lindemann B, Gonzalez E, Whittembury G. The continuous measurement of tubular volume changes in response to step changes in contraluminal osmolality. Pflügers Arch 1984;400:343–8.
[137] Carranza ML, Feraille E, Favre H. Protein kinase C-dependent phosphorylation of Na^+-K^+-ATPase alpha-subunit in rat kidney cortical tubules. Am J Physiol 1996;271:C136–43.
[138] Cassano G, Stieger B, Murer H. Na/H and Cl/OH exchange in rat jejunal and rat proximal tubular brush border membrane vesicles. Pflügers Arch 1984;400:309–17.
[139] Cassola AC, Mollehauer M, Frömter E. The intracellular chloride activity of rat kidney proximal tubular cells. Pflügers Arch 1983;399:259–65.
[140] Caulfield JB, Trump BF. Correlation of ultrastructure with function in the rat kidney. Am J Pathol 1962;40:199–218.
[141] Cemerikic D, Wilcox CS, Giebisch G. Intracellular potential and K^+ activity in rat kidney proximal tubular cells in acidosis and K^+ depletion. J Membr Biol 1982;69:159–65.
[142] Chalumeau C, du Cheyron D, Defontaine N, Kellermann O, Paillard M, Poggioli J. NHE3 activity and trafficking depend on the state of actin organization in proximal tubule. Am J Physiol 2001;280:F283–90.
[143] Chan YL, Biagi B, Giebisch G. Control mechanisms of bicarbonate transport across the rat proximal convoluted tubule. Am J Physiol 1982;242:F532–43.
[144] Chen P-Y, Illsley NP, Verkman AS. Renal brush-border chloride transport mechanisms characterized using a fluorescent indicator. Am J Physiol 1988;254:F114–20.
[145] Chen P-Y, Verkman AS. Sodium-dependent chloride transport in basolateral membrane vesicles isolated from rabbit proximal tubule. Biochemistry 1988;27:655–60.
[146] Chen XZ, Coady MJ, Jackson F, Berteloot A, Lapointe JY. Thermodynamic determination of the Na^+:glucose coupling ratio for the human SGLT1 co-transporter. Biophys J 1995;69: 2405–14.

[147] Cheng H, Becker BN, Harris RC. Dopamine decreases expression of type-1 angiotensin II receptors in renal proximal tubule. J Clin Invest 1996;97:2745–52.
[148] Chernova MN, Jiang L, Friedman DJ, Darman RB, Lohi H, Kere J, et al. Functional comparison of mouse slc26a6 anion exchanger with human SLC26A6 polypeptide variants. J Biol Chem 2005;280(9):8564–80.
[149] Chibalin AV, Katz AI, Berggren PO, Bertorello AM. Receptor-mediated inhibition of renal Na^+-K^+-ATPase is associated with endocytosis of its alpha and beta subunits. Am J Physiol 1997;273:C1458–65.
[150] Chibalin AV, Pedemonte CH, Katz AI, Feraille E, Berggren PO, Bertorello AM. Phosphorylation of the catalyic alpha-subunit constitutes a triggering signal for Na^+,K^+-ATPase endocytosis. J Biol Chem 1998;273(15):8814–9.
[151] Choi JY, Shah M, Lee MG, Schultheis PJ, Shull GE, Muallem S, Baum M. Novel amiloride-sensitive sodium-dependent proton secretion in the mouse proximal convoluted tubule. J Clin Invest 2000;105:1141–6.
[152] Chonko AM, Osgood RW, Nickel AE, Ferris TF, Stein JH. The measurement of nephron filtration rate and absolute reabsorption in the proximal tubule of the rat kidney. J Clin Invest 1975;56:232–5.
[153] Chung SD, Alavi N, Livingston D, Hiller S, Taub M. Characterization of primary rabbit kidney cultures that express proximal tubule functions in a hormonally defined medium. J Cell Biol 1982;95:118–26.
[154] Cinelli AR, Efendiev R, Pedemonte CH. Trafficking of Na-K-ATPase and dopamine receptor molecules induced by changes in intracellular sodium concentration of renal epithelial cells. Am J Physiol 2008;295:F1117–25.
[155] Claude P. Morphological factors influencing transepithelial permeability: a model for the resistance of the zonula occludens. J Membr Biol 1978;39:219–32.
[156] Claude P, Goodenough DA. Fracture faces of zonulae occludentes from "tight" and "leaky" epithelia. J Cell Biol 1973;58:390–400.
[157] Cogan MG. Volume expansion predominantly inhibits proximal reabsorption of NaCl rather than $NaHCO_3$. Am J Physiol 1983;245:F272–5.
[158] Cogan MG. Angiotensin II: a powerful controller of sodium transport in the early proximal tubule. Hypertension 1990;15:451–8.
[159] Colegio OR, van Itallie CM, McCrea HJ, Rahner C, Anderson JM. Claudins create charge-selective channels in the paracellular pathway between epithelial cells. Am J Physiol 2002;283:C142–7.
[160] Collazo R, Fan L, Hu MC, Zhao H, Wiederkehr MR, Moe OW. Acute regulation of Na^+/H^+ exchanger NHE3 by parathyroid hormone via NHE3 phosphorylation and dynamin-dependent endocytosis. J Biol Chem 2000;275(41):31601–8.
[161] Conger JD, Bartoli E, Earley LE. A study *in vivo* of peritubular oncotic pressure and proximal tubular reabsorption in the rat. Clin Sci Mol Med 1976;51:379–92.
[162] Coppola S, Frömter E. An electrophysiological study of angiotensin II regulation of Na-HCO_3 co-transport and K conductance in renal proximal tubules. I. Effect of picomolar concentrations. Pflügers Arch 1994;427:143–50.
[163] Corcia A, Armstrong WMcD. KCl co-transport: a mechanism for basolateral chloride exit in *Necturus* gallbladder. J Membr Biol 1983;76:173–82.
[164] Corman B. Streaming potentials and diffusion potentials across rabbit proximal convoluted tubule. Pflügers Arch 1985;403:156–63.
[165] Corman B, Roinel N, de Rouffignac C. Water reabsorption capacity of the proximal convoluted tubule: a microperfusion study on rat kidney. J Physiol 1981;316:379–92.
[166] Cunningham R, Steplock D, Wang F, Huang H, Xiaofei E, Shenolikar S, et al. Defective parathyroid hormone regulation of NHE3 activity and phosphate adaptation in cultured NHERF-$1^{-/-}$ renal proximal tubule cells. J Biol Chem 2004;279(36):37815–21.
[167] Curran PF. Na Cl and water transport by rat ileum *in vitro*. J Gen Physiol 1960;43:1137–48.
[168] Darvish N, Winaver J, Dagan D. Diverse modulations of chloride channels in renal proximal tubules. Am J Physiol 1994;267:F716–24.
[169] Dawson DC, Richards NW. Basolateral K conductance: role in regulation of NaCl absorption and secretion. Am J Physiol 1990;259:C181–95.
[170] Dellasega M, Grantham JJ. Regulation of renal tubule cell volume in hypotonic media. Am J Physiol 1973;224:1288–94.
[171] Dennis VW. Influence of bicarbonate on parathyroid hormone-induced changes in fluid absorption by the proximal tubule. Kidney Int 1976;10:373–80.
[172] DiBona GF. Neural regulation of renal tubular sodium reabsorption and renin secretion. Fed Proc 1985;44:2816–22.
[173] Dirks JH, Cirksena WJ, Berliner RW. The effect of saline infusion on sodium reabsorption by the proximal tubule of the dog. J Clin Invest 1965;44:1160–70.
[174] Dolson GM, Hise MK, Weinman EJ. Relationship among parathyroid hormone cAMP, and calcium on proximal tubule sodium transport. Am J Physiol 1985;249:F409–16.
[175] Donowitz M, Cha B, Zachos NC, Brett CL, Sharma A, Tse CM, et al. NHERF family and NHE3 regulation. J Physiol 2005;567:3–11.
[176] Donowitz M, Li X. Regulatory binding partners and complexes of NHE3. Physiol Rev 2007;87:825–72.
[177] Donowitz M, Mohan S, Zhu CX, Chen T, Lin R, Cha B, et al. NHE3 regulatory complexes. J Exp Biol 2009;212:1638–46.
[178] Dorwart MR, Shcheynikov N, Yang D, Muallem S. The solute carrier 26 family of proteins in epithelial ion transport. Physiology 2008;23:104–14.
[179] Dos Santos EA, Dahly-Vernon AJ, Hoagland KM, Roman RJ. Inhibition of the formation of EETs and 20-HETE with 1-aminobenzotriazole attenuates pressure natriuresis. Am J Physiol 2004;287:R58–68.
[180] Doucet A, Katz AI, Morel F. Determination of Na-K-ATPase activity in single segments of the mammalian nephron. Am J Physiol 1979;237:F105–13.
[181] Douglas JG, Hopfer U. Novel aspect of angiotensin receptors and signal transduction in the kidney. Ann Rev Physiol 1994;56:649–69.
[182] Du Z, Duan Y, Yan Q, Weinstein AM, Weinbaum S, Wang T. Mechanosensory function of microvilli of the kidney proximal tubule. Proc Natl Acad Sci 2004;101:13068–73.
[183] Du Z, Yan Q, Duan Y, Weinbaum S, Weinstein AM, Wang T. Axial flow modulates proximal tubule NHE3 and H-ATPase activities by changing microvillous bending moments. Am J Physiol 2006;290:F289–96.
[184] Ducoudret O, Diakov A, Muller-Berger S, Romero MF, Frömter E. The renal Na-HCO_3-co-transporter expressed in *Xenopus laevis* oocytes: inhibition by tenidap and benzamil and effect of temperature on transport rate and stoichiometry. Pflügers Arch 2001;442:709–17.
[185] Durbin RP. Osmotic flow of water across permeable cellulose membranes. J Gen Physiol 1960;44:315–26.
[186] Earley LE, Martino JA, Friedler RM. Factors affecting sodium reabsorption by the proximal tubule as determined during blockade of distal sodium reabsorption. J Clin Invest 1966;45:1668–84.

[187] Earley LE, Schrier RW. Intrarenal control of sodium excretion by hemodynamic and physical factors. In: Orloff J, Berliner RW, editors. Handbook of physiology. section 8:renal physiology. Washington DC: American Physiological Society; 1973. p. 721–62.

[188] Edelman A, Bouthier M, Anagnostopoulos T. Chloride distribution in the proximal convoluted tubule of *Necturus* kidney. J Membr Biol 1981;62:7–17.

[189] Edelman A, Curci S, Samarzija I, Frömter E. Determination of intracellular K^+ activity in rat kidney proximal tubular cells. Pflügers Arch 1978;378:37–45.

[190] Edwards RM, Alyar N. Angiotensin II receptor subtypes in the kidney. J Am Soc Nephrol 1993;3:1643–52.

[191] Efendiev R, Bertorello AM, Pressley TA, Rousselot M, Feraille E, Pedemonte CH. Simultaneous phosphorylation of Ser11 and Ser18 in the alpha-subunit promotes the recruitment of $Na(^+)$,$K(^+)$-ATPase molecules to the plasma membrane. Biochemistry 2000;39:9884–92.

[192] Efendiev R, Bertorello AM, Zandomeni R, Cinelli AR, Pedemonte CH. Agonist-dependent regulation of renal Na^+, K^+-ATPase activity is modulated by intracellular sodium concentration. J Biol Chem 2002;277(13):11489–96.

[193] Eiam-Ong S, Hilden SA, Johns CA, Madias NE. Stimulation of basolateral Na^+–HCO_3^- co-transporter by angiotensin II in rabbit renal cortex. Am J Physiol 1993;265:F195–203.

[194] Eitle E, Hiranyachattada S, Wang H, Harris PJ. Inhibition of proximal tubular fluid absorption by nitric oxide and atrial natriuretic peptide in rat kidney. Am J Physiol 1998;274: C1075–80.

[195] El Mernissi G, Duocet A. Quantitation of [u^3dH]ouabain binding and turnover of Na-K-ATPase along the rabbit nephron. Am J Physiol 1984;247:F158–67.

[196] Enck AH, Berger UV, Yu AS. Claudin-2 is selectively expressed in proximal nephron in mouse kidney. Am J Physiol 2001;281:F966–74.

[197] Eveloff JL, Warnock DG. Activation of ion transport systems during cell volume regulation. Am J Physiol 1987;252: F1–10.

[198] Eveloff J, Warnock DG. K-Cl transport systems in rabbit renal basolateral membrane vesicles. Am J Physiol 1987;252:F883–9.

[199] Fan L, Wiederkehr MR, Collazo R, Wang H, Crowder LA, Moe OW. Dual mechanisms of regulation of Na/H exchanger NHE-3 by parathyroid hormone in rat kidney. J Biol Chem 1999;274(16):11289–95.

[200] Felder RA, Campbell T, Albrecht F, Jose PA. Dopamine inhibits Na^+-H^+ exchanger activity in renal BBMV by stimulation of adenylate cyclase. Am J Physiol 1990;259:F297–303.

[201] Felder RA, Jose PA. Mechanisms of disease: the role of GRK4 in the etiology of essential hypertension and salt sensitivity. Nature Clin Prac 2006;2:637–50.

[202] Felder RA, Sanada H, Xu J, Yu P, Wang Z, Watanabe H, et al. G protein-coupled receptor kinase 4 gene variants in human essential hypertension. Proc Natl Acad Sci 2002;99:3872–7.

[203] Feraille E, Carranza ML, Buffin-Meyer B, Rousselot M, Doucet A, Favre H. Protein kinase C-dependent stimulation of Na^+-K^+-ATPase in rat proximal convoluted tubule. Am J Physiol 1995;268:C1277–83.

[204] Feraille E, Doucet A. Sodium–potassium–adenosinetriphosphatase-dependent sodium transport in the kidney: hormonal control. Physiol Rev 2001;81:345–418.

[205] Feschenko MS, Sweadner KJ. Conformation-dependent phosphorylation of NaK-ATPase by protein kinase A and protein kinase C. J Biol Chem 1994;269(48):30436–44.

[206] Feschenko MS, Sweadner KJ. Phosphorylation of Na,K-ATPase by protein kinase C at Ser18 occurs in intact cells but does not result in direct inhibiton of ATP hydrolysis. J Biol Chem 1997;272:17726–33.

[207] Filipovic D, Sackin H. A calcium-permeable stretch-activated cation channel in renal proximal tubule. Am J Physiol 1991;260:F119–29.

[208] Filipovic D, Sackin H. Stretch- and volume-activated channels in isolated proximal tubule cells. Am J Physiol 1992;262: F857–70.

[209] Fine LG, Sakhrani LM. Proximal tubular cells in primary culture. Miner Electrolyte Metab 1986;12:51–7.

[210] Finn AL, Reuss L. Effects of changes in the composition of the serosal solution on the electrical properties of the toad urinary bladder epithelium. J Physiol 1975;250:541–58.

[211] Fisher KA, Lee SH, Walker J, Dileto-Fang C, Ginsberg L, Stapleton SR. Regulation of proximal tubule sodium/hydrogen antiporter with chronic volume contraction. Am J Physiol 2001;280:F922–6.

[212] Fitzgibbons JP, Gennari FJ, Garfinkel HB, Cortell S. Dependence of saline-induced natriuresis upon exposure of the kidney to the physical effects of extracellular fluid volume expansion. J Clin Invest 1974;54:1428–36.

[213] Fraser WD, Baines AD. Application of a fiber-matrix model to transport in renal tubules. J Gen Physiol 1989;94:863–79.

[214] Friedman PA, Figueiredo JF, Maack T, Windhager EE. Sodium–calcium interactions in the renal proximal convoluted tubule of the rabbit. Am J Physiol 1981;240:F558–68.

[215] Frömter E. Electrophysiology and isotonic fluid absorption of proximal tubules of mammalian kidney. In: Thurau K, editor. Kidney and urinary tract physiology MTP international reviews of science physiology series I, vol. 6. Baltimore: University Park Press; 1974. p. 1–38.

[216] Frömter E. Magnitude and significance of the paracellular shunt path in rat kidney proximal tubule. In: Kramer M, Lauterbach F, editors. Intestinal permeation, vol. 4. Amsterdam: Excerpta Medica; 1977. p. 393–405.

[217] Frömter E. Solute transport across epithelia: what can we learn from micropuncture studies on kidney tubules? J Physiol (Lond) 1979;288:1–31.

[218] Frömter E. Electrophysiological analysis of rat renal sugar and amino acid transport. Pflügers Arch 1982;393:179–89.

[219] Frömter E. Viewing the kidney through microelectrodes. Am J Physiol 1984;247:F695–705.

[220] Frömter E, Gessner K. Free-flow potential profile along rat kidney proximal tubule. Pflügers Arch 1974;351:69–83.

[221] Frömter E, Gessner K. Active transport potentials membrane diffusion potentials and streaming potentials across rat kidney proximal tubule. Pflügers Arch 1974;351:85–98.

[222] Frömter E, Gessner K. Effect of inhibitors and diuretics on electrical potential differences in rat kidney proximal tubule. Pflügers Arch 1975;357:209–24.

[223] Frömter E, Muller CW, Wick T. Permeability properties of the proximal tubular epithelium of the rat kidney studied with electrophysiological methods. In: Giebisch G, editor. Electrophysiology of epithelial cells. FK Schattauer Verlag Stuttgart; 1971. p. 119–48.

[224] Frömter E, Rumrich G, Ullrich KJ. Phenomenologic description of Na^+, Cl^- , and HCO_3^- absorption from proximal tubules. Pflügers Arch 1973;343:189–220.

[225] Frömter E, Sato K. Electrical events in active H^+/HCO_3^- transport across rat kidney proximal tubular epithelium. In: Kasbeker DK, Sachs G, Rehm WS, editors. Gastric hydrogen ion secretion. New York: Marcel Dekker; 1976. p. 382–403.

[226] Furuse M, Fujita K, Hiiragi T, Fujimoto K, Tsukita S. Claudin-1 and -2: novel integral membrane proteins localizing at tight

junctions with no sequence similarity to occludin. J Cell Biol 1998;141:1539–50.
[227] Furuse M, Furuse K, Sasaki H, Tsukita S. Conversion of zonulae occludentes from tight to leaky strand type by introducing claudin-2 into Madin–Darby canine kidney I cells. J Cell Biol 2001;153:263–72.
[228] Furuse M, Hirase T, Itoh M, Nagafuchi A, Yonemura S, Tsukita S, et al. Occludin: a novel integral membrane protein localizing at tight junctions. J Cell Biol 1993;123:1777–88.
[229] Furuse M, Sasaki H, Fujimoto K, Tsukita S. A single gene product claudin-1 or -2, reconstitutes tight junction strands and recruits occludin in fibroblasts. J Cell Biol 1998;43: 391–401.
[230] Fuster DG, Bobulescu IA, Zhang J, Wade J, Moe OW. Characterization of the regulation of renal Na^+/H^+ exchanger NHE3 by insulin. Am J Physiol 2007;292:F577–85.
[231] Fuster D, Moe OW, Hilgemann DW. Lipid- and mechanosensitivities of sodium/hydrogen exchangers analyzed by electrical methods. Proc Natl Acad Sci 2004;101:10482–7.
[232] Fuster D, Moe OW, Hilgemann DW. Steady-state function of the ubiquitous mammalian Na/H exchanger (NHE1) in relation to dimmer coupling models with 2Na/2H stoichiometry. J Gen Physiol 2008;132:465–80.
[233] Garg LC, Knepper MA, Burg MB. Mineralocorticoid effects on Na-K-ATPase in individual nephron segments. Am J Physiol 1981;240:F536–44.
[234] Garty H, Karlish SJD. Role of FXYD proteins in ion transport. Annu Rev Physiol 2006;68:431–59.
[235] Garvin JL. Angiotensin stimulates bicarbonate transport and Na^+/K^+-ATPase in rat proximal straight tubules. J Am Soc Nephrol 1991;1:1146–52.
[236] Garvin JL, Herrera M, Ortiz Pa. Clinical implications. Annu Rev Physiol 2011;73:359–76.
[237] Geering K. FXYD proteins: new regulators of Na-K-ATPase. Am J Physiol 2006;290:F241–50.
[238] Geibel J, Giebisch G, Boron WF. Basolateral sodium-coupled acid–base transport mechanisms of the rabbit proximal tubule. Am J Physiol 1989;257:F790–7.
[239] Geibel J, Giebisch G, Boron WF. Angiotensin II stimulates both Na^+/H^+ exchange and Na^+/HCO_3^- co-transport in the rabbit proximal tubule. Proc Natl Acad Sci 1990;87:7917–20.
[240] Gekle M, Serrano OK, Drumm K, Mildenberger S, Freudinger R, Gassner B, et al. NHE3 serves as a molecular tool for cAMP-mediated regulation of receptor-mediated endocytosis. Am J Physiol 2002;283:F549–58.
[241] Gekle M, Völker K, Mildenberger S, Freudinger R, Shull GE, Wiemann M. NHE3 Na^+/H^+ exchanger supports proximal tubular protein reabsorption *in vivo*. Am J Physiol 2004;287: F469–73.
[242] Gertz KH, Boylan JW. Glomerular-tubular balance. In: Orloff J, Berliner RW, editors. Handbook of physiology. section 8: renal physiology. Washington DC: American Physiological Society; 1973. p. 763–90.
[243] Gesek FA, Schoolwerth AC. Hormonal interactions with the proximal Na^+-H^+ exchanger. Am J Physiol 1990;258:F514–21.
[244] Giebisch G, Windhager EE. Renal tubular transfer of sodium chloride and potassium. Am J Med 1964;36:643–69.
[245] Gildea JJ, Wang X, Jose PA, Felder RA. Differential D1 and D5 receptor regulation and degradation of the angiotensin type 1 receptor. Hypertension 2008;51:360–6.
[246] Gillen CM, Brill S, Payne JA, Forbush III B. Molecular cloning and functional expression of the K-Cl co-transporter from rabbit, rat, and human. A new member of the cation-chloride co-transporter family. J Biol Chem 1996;271: 16237–44.
[247] Girardi AC, Knauf F, Demuth HU, Aronson PS. Role of dipeptidyl peptidase IV in regulating activity of Na^+/H^+ exchanger isoform NHE3 in proximal tubule cells. Am J Physiol 2004;287: C1238–45.
[248] Girardi AC, Titan SMO, Malnic G, Reboucas NA. Chronic effect of parathyroid hormone on NHE3 expression in rat renal proximal tubules. Kidney Int 2000;58:1623–31.
[249] Glynn IM, Karlish SJD. The sodium pump. Annu Rev Physiol 1975;37:13–55.
[250] Gögelein H, Greger R. Single channel recordings from basolateral and apical membranes of renal proximal tubules. Pflügers Arch 1984;401:424–6.
[251] Gögelein H, Greger R. Na^+ selective channels in the apical membrane of rabbit late proximal tubules (pars recta). Pflügers Arch 1986;406:198–203.
[252] Goligorsky MS, Menton DN, Hruska KA. Parathyroid hormone-induced changes of the brush border topography and cytoskeleton in cultured renal proximal tubular cells. J Membr Biol 1986;92:151–62.
[253] Gonzalez E, Carpi-Medina P, Whittembury G. Cell osmotic water permeability of isolated rabbit proximal straight tubules. Am J Physiol 1982;242:F321–30.
[254] Gonzalez-Campoy JM, Long C, Roberts D, Berndt TJ, Romero JC, Knox FG. Renal interstitial hydrostatic pressure and PGE_2 in pressure natriuresis. Am J Physiol 1991;260:F643–9.
[255] Gottschalk CW. Renal tubular function: lessons from micropuncture. The harvey lectures series 58. New York and London: Academic Press; 1963. p. 99–124
[256] Gottschalk CW. Renal nerves and sodium excretion. Ann Rev Physiol 1979;41:229–40.
[257] Goyal S, Mentone S, Aronson PS. Immunolocalization of NHE8 in rat kidney. Am J Physiol 2005;288:F530–8.
[258] Goyal S, Vanden Heuvel G, Aronson PS. Renal expression of novel Na^+/H^+ exchanger isoform NHE8. Am J Physiol 2003;284:F467–73.
[259] Grandchamp A, Boulpaep EL. Pressure control of sodium reabsorption and intercellular backflux across proximal kidney tubule. J Clin Invest 1974;54:69–82.
[260] Granger JP, Haas JA, Pawlowska D, Knox FG. Effect of direct increases in renal interstitial hydrostatic pressure on sodium excretion. Am J Physiol 1988;254:F527–32.
[261] Grantham JJ, Lowe CM, Dellasega M, Cole BR. Effect of hypotonic medium on K and Na content of proximal renal tubules. Am J Physiol 1977;232:F42–9.
[262] Grasset E, Gunter-Smith P, Schultz SG. Effects of Na-coupled alanine transport on intracellular K activities and the K conductance of the basolateral membranes of *Necturus* small intestine. J Memb Biol 1983;71:89–94.
[263] Grassl SM, Aronson PS. Na^+/HCO_3^- co-transport in basolateral membrane vesicles isolated from rabbit renal cortex. J Biol Chem 1986;261(19):8778–83.
[264] Grassl SM, Holohan PD, Ross CR. HCO_3^- transport in basolateral membrane vesicles isolated from rat renal cortex. J Biol Chem 1987;262:2682–7.
[265] Green R, Giebisch G. Luminal hypotonicity: a driving force for fluid absorption from the proximal tubule. Am J Physiol 1984;246:F167–74.
[266] Green R, Giebisch G. Reflection coefficients and water permeability in rat proximal tubule. Am J Physiol 1989;257:F658–68.
[267] Green R, Giebisch G, Unwin R, Weinstein AM. Coupled water transport by rat proximal tubule. Am J Physiol 1991;261: F1046–54.
[268] Green R, Moriarty RJ, Giebisch G. Ionic requirements of proximal tubular fluid reabsorption: flow dependence of fluid transport. Kidney Int 1981;20:580–7.

[269] Green R, Windhager EE, Giebisch G. Protein oncotic pressure effects on proximal tubular fluid movement in the rat. Am J Physiol 1974;226:265–76.
[270] Grinstein S, Rothstein A. Mechanisms of regulation of the Na^+/H^+ exchanger. J Membr Biol 1986;90:1–12.
[271] Gross E, Hawkins K, Abuladze N, Pushkin A, Cotton CU, Hopfer U, et al. The stoichiometry of the electrogenic sodium bicarbonate co-transporter NBC1 is cell-type dependent. J Physiol 2001;531:597–603.
[272] Gross E, Hawkins K, Pushkin A, Sassani P, Dukkipati R, Abuladze N, et al. Phosphorylation of Ser(982) in the sodium bicarbonate co-transporter kNBC1 shifts the HCO_3^-:Na^+ stoichiometry from 3:1 to 2:1 in murine proximal tubule cells. J Physiol 2001;537:659–65.
[273] Gross E, Hopfer U. Activity and stoichiometry of Na^+:HCO_3^- co-transport in immortalized renal proximal tubule cells. J Membr Biol 1996;152:245–52.
[274] Gross E, Hopfer U. Voltage and cosubstrate dependence of the Na-HCO_3 co-transporter kinetics in renal proximal tubule cells. Biophys J 1998;75:810–24.
[275] Gross E, Hopfer U. Effects of pH on kinetic parameters of the Na-HCO_3 co-transporter in renal proximal tubule. Biophys J 1999;76:3066–75.
[276] Guggino WB, Boulpaep EL, Giebisch G. Electrical properties of chloride transport across the *Necturus* proximal tubule. J Membr Biol 1982;65:185–96.
[277] Guggino WB, London R, Boulpaep EL, Giebisch G. Chloride transport across the basolateral cell membrane of the *Necturus* proximal tubule: dependence on bicarbonate and sodium. J Membr Biol 1983;71:227–40.
[278] Gullans SR, Avison MJ, Ogino T, Giebisch G, Shulman RG. NMR measurements of intracellular sodium in the rabbit proximal tubule. Am J Physiol 1985;249:F160–8.
[279] Gullans SR, Brazy PC, Soltoff SP, Dennis VW, Mandel LJ. Metabolic inhibitors: effects on metabolism and transport in the proximal tubule. Am J Physiol 1982;243:F133–40.
[280] Gunter-Smith PJ, Grasset E, Schultz SG. Sodium-coupled amino acid and sugar transport by *Necturus* small intestine. An equivalent electrical circuit analysis of a rheogenic co-transport system. J Memb Biol 1982;66:25–39.
[281] Guo P, Weinstein AM, Weinbaum S. A dual-pathway ultrastructural model for the tight junction of rat proximal tubule epithelium. Am J Physiol 2003;285:F241–57.
[282] Guo P, Weinstein AM, Weinbaum S. A hydrodynamic mechanosensory hypothesis for brush border microvilli. Am J Physiol 2000;279:F698–712.
[283] Gurley SB, Riquier-Brison ADM, Schnermann J, Sparks MA, Allen AM, Haase VH, et al. AT1A angiotensin receptors in the renal proximal tubule regulate blood pressure. Cell Metab 2011;13:469–75.
[284] Gutierrez AM, Gonzalez E, Echevarria M, Hernandez CS, Whittembury G. The proximal straight tubule (PST) basolateral cell membrane water channel: selectivity characteristics. J Membr Biol 1995;143:189–97.
[285] Györy AZ, Beck F, Rick R, Thurau K. Electron microprobe analysis of proximal tubule cellular Na Cl and K element concentrations during acute mannitol-saline volume expansion in rats: evidence for inhibition of the Na pump. Pflügers Arch 1985;403:205–9.
[286] Haas JA, Granger JP, Knox FG. Effect of renal perfusion pressure on sodium reabsorption from proximal tubules of superficial and deep nephrons. Am J Physiol 1986;250:F425–9.
[287] Haas JA, Granger JP, Knox FG. Effect of intrarenal volume expansion on proximal sodium reabsorption. Am J Physiol 1988;255:F1178–82.
[288] Häberle DA, Shiigai T. Flow-dependent volume reabsorption in the proximal convolution of the rat kidney – the role of glomerular-born tubular fluid for the maintenance of glomerulotubular balance. In: Vogel HG, Ullrich KJ, editors. New aspects of renal function. Amsterdam: Excerpta Medica; 1978. p. 198–206.
[289] Häberle DA, Shiigai TT, Maier G, Schiffl H, Davis JM. Dependency of proximal tubular fluid transport on the load of glomerular filtrate. Kidney Int 1981;20:18–28.
[290] Häberle DA, von Baeyer H. Characteristics of glomerulotubular balance. Am J Physiol 1983;244:F355–66.
[291] Haithcock D, Jiao H, Cui XL, Hopfer U, Douglas JG. Renal proximal tubular AT2 receptor: signaling and transport. J Am Soc Nephrol 1999;10(Suppl. 11):S69–74.
[292] Hall RA, Premont RT, Chow CW, Blitzer JT, Pitcher JA, Claing A, et al. The beta2-adrenergic receptor interacts with the Na^+/H^+-exchanger regulatory factor to control Na^+/H^+ exchange. Nature 1998;392(6676):626–30.
[293] Hamburger RJ, Lawson NL, Schwartz JH. Response to parathyroid hormone in defined segments of proximal tubule. Am J Physiol 1976;230:286–90.
[294] Han HJ, Park SH, Koh HJ, Taub M. Mechanism of regulation of Na^+ transport by angiotensin II in primary renal cells. Kidney Int 2000;57:2457–67.
[295] Harris PJ. Regulation of proximal tubule function by angiotensin. Clin Exp Pharmacol Physiol 1992;19:213–22.
[296] Harris PJ, Navar LG. Tubular transport responses to angiotensin. Am J Physiol 1985;248:F621–30.
[297] Harris PJ, Young JA. Dose-dependent stimulation and inhibition of proximal tubular sodium reabsorption by angiotensin II in the rat kidney. Pflügers Arch 1977;367:295–7.
[298] Harris SI, Balaban RS, Mandel LJ. Oxygen consumption and cellular ion transport: evidence for adenosine triphosphate to O_2 ratio near 6 in intact cell. Science 1980;208:1148–50.
[299] Harris SI, Patton L, Barrett L, Mandel LJ. (Na^+,K^+)-ATPase kinetics within the intact renal cell. J Biol Chem 1982;257:6996–7002.
[300] Hayashi H, Szaszi K, Grinstein S. Multiple modes of regulation of Na^+/H^+ exchangers. Ann NY Acad Sci 2002;976:248–58.
[301] Hayslett JP. Effect of changes in hydrostatic pressure in peritubular capillaries on the permeability of the proximal tubule. J Clin Invest 1973;52:1314–9.
[302] Hazama A, Loo DD, Wright EM. Presteady-state currents of the rabbit Na^+/glucose co-transporter (SGLT1). J Membr Biol 1997;155:175–86.
[303] Hebert SC, Mount DB, Gamba G. Molecular physiology of cation-coupled Cl^- co-transport: the SCL12 family. Pflügers Arch 2004;447:580–93.
[304] Hediger MA, Coady MJ, Ikeda TS, Wright EM. Expression cloning and cDNA sequencing of the Na^+/glucose co-transporter. Nature 1987;330:379–81.
[305] Hediger MA, Rhoads DB. Molecular physiology of sodium–glucose co-transporters. Physiol Rev 1994;74:993–1026.
[306] Heinz E, Weinstein AM. The overshoot phenomenon in co-transport. Biochim Biophys Acta 1984;776:83–91.
[307] Hensley CB, Bradley ME, Mircheff AK. Parathyroid hormone-induced translocation of Na-H antiporters in rat proximal tubules. Am J Physiol 1989;257:C637–45.
[308] Hierholzer K, Kawamura S, Seldin DW, Kokko JP, Jacobson HR. Reflection coefficients of various substrates across superficial and juxtamedullary proximal convoluted segments of rabbit nephrons. Mineral Electrolyte Metab 1980;3:172–80.
[309] Higgins Jr. JT, Meinders AE. Quantitative relationship of renal glucose and sodium reabsorption during ECF expansion. Am J Physiol 1975;229:66–71.

[310] Hilden SA, Sacktor B. D-glucose-dependent sodium transport in renal brush border membrane vesicles. J Biol Chem 1979;254:7090–6.
[311] Hirayama BA, Loo DDF, Díez-Sampedro A, Leung DW, Meinild A, Lai-Bing M, et al. Sodium-dependent reorganization of the sugar-binding site of SGLT1. Biochemistry 2007;46:13391–406.
[312] Hirayama BA, Loo DD, Wright EM. Protons drive sugar transport through the Na^+/glucose co-transporter (SGLT1). J Biol Chem 1994;269:21407–10.
[313] Holmberg C, Kokko JP, Jacobson HR. Determination of chloride bicarbonate permeabilities in proximal convoluted tubules. Am J Physiol 1981;241:F386–94.
[314] Holtback U, Eklof AC. Mechanism of FK 506/520 action on rat renal proximal tubular Na^+,K^+-ATPase activity. Kidney Int 1999;56:1014–21.
[315] Holzgreve H, Schrier RW. Variation of proximal tubular reabsorptive capacity by volume expansion and aortic constriction during constancy of peritubular capillary protein concentration in rat kidney. Pflügers Arch 1975;356:73–86.
[316] Hopfer J, Groseclose R. The mechanism of Na^+-dependent D-glucose transport. J Biol Chem 1980;255:4453–62.
[317] Horie S, Moe O, Tejedor A, Alpern RJ. Preincubation in acid medium increases Na/H antiporter activity in cultured renal proximal tubule cells. Proc Natl Acad Sci 1990;87:4742–5.
[318] Houillier P, Chambrey R, Achard JM, Froissart M, Poggioli J, Paillard M. Signaling pathways in the biphasic effect of angiotensin II on apical Na/H antiport activity in proximal tubule. Kid Int 1996;50:1496–505.
[319] Howlin KJ, Alpern RJ, Rector Jr. FC. Amiloride inhibition of proximal tubular acidification. Am J Physiol 1985;248:F773–8.
[320] Hruska KA, Moskowitz D, Esbrit P, Civitelli R, Westbrook S, Huskey M. Stimulation of inositol trisphosphate and diacylglycerol production in renal tubular cells by parathyroid hormone. J Clin Invest 1987;79:230–9.
[321] Hu MC, Fan L, Crowder LA, Karim-Jimenez Z, Murer H, Moe OW. Dopamine acutely stimulates Na^+/H^+ exchanger (NHE3) endocytosis via clathrin-coated vesicles: dependence on protein kinase A-mediated NHE3 phosphorylation. J Biol Chem 2001;276(29):26906–15.
[322] Hurst AM, Beck JS, Laprade R, Lapointe J-Y. Na^+ pump inhibition downregulates an ATP-sensitive K^+ channel in rabbit proximal convoluted tubule. Am J Physiol 1993;264:F760–4.
[323] Huss RE, Marsh DJ. A model of NaCl and water flow through paracellular pathways of renal proximal tubules. J Membr Biol 1975;23:305–47.
[324] Huss RE, Stephenson JL. A mathematical model of proximal tubule absorption. J Membr Biol 1979;47:377–99.
[325] Ibarra F, Aperia A, Svensson L-B, Eklöf A-C, Greengard P. Bidirectional regulation of Na^+,K^+-ATPase activity by dopamine and an alpha-adrenergic agonist. Proc Natl Acad Sci 1993;90:21–4.
[326] Ibarra FR, Cheng SX, Agren M, Svensson LB, Aizman O, Aperia A. Intracellular sodium modulates the state of protein kinase C phosphorylation of rat proximal tubule Na^+,K^+-ATPase. Acta Physiol Scand 2002;175:165–71.
[327] Ichikawa I, Brenner BM. Mechanism of inhibition of proximal tubule fluid reabsorption after exposure of the rat kidney to the physical effects of expansion of extracellular fluid volume. J Clin Invest 1979;64:1466–74.
[328] Ikeda TS, Hwang E-S, Coady MJ, Hirayama BA, Hediger MA, Wright EM. Characterization of a Na^+/glucose co-transporter cloned from rabbit small intestine. J Membr Biol 1989;110:87–95.
[329] Illsley NP, Verkman AS. Membrane chloride transport measured using a chloride-sensitive fluorescent probe. Biochemistry 1987;26:1215–9.
[330] Imai M. Functional heterogeneity of the descending limbs of Henle's loop. II. Interspecies differences among rabbits, rats, and hamsters. Pf Arch 1984;402:393–401.
[331] Imai M, Kokko JP. Effect of peritubular protein concentration on reabsorption of sodium and water in isolated perfused proximal tubules. J Clin Invest 1972;51:314–25.
[332] Imai M, Kokko JP. Transtubular oncotic pressure gradients and net fluid transport in isolated proximal tubules. Kidney Int 1974;6:138–45.
[333] Ishibashi K, Rector Jr. FC, Berry CA. Chloride transport across the basolateral membrane of rabbit proximal convoluted tubules. Am J Physiol 1990;258:F1569–78.
[334] Ishibashi K, Rector Jr. FC, Berry CA. Role of Na-dependent Cl/HCO_3 exchange in basolateral Cl transport of rabbit proximal tubules. Am J Physiol 1993;264:F251–8.
[335] Ishibashi K, Sasaki S, Yoshiyama N. Intracellular chloride activity of rabbit proximal straight tubule perfused *in vitro*. Am J Physiol 1988;255:F49–56.
[336] Ito O, Alonso-Galicia M, Hopp KA, Roman RJ. Localization of cytochrome P-450 4A isoforms along rat nephron. Am J Physiol 1998;274:F395–404.
[337] Ives HE, Chen P-Y, Verkman AS. Mechanism of coupling between Cl^- and OH^- transport in renal brush-border membranes. Biochim Biophys Acta 1986;863:91–100.
[338] Ives HE, Yee VJ, Warnock DG. Asymmetric distribution of the Na^+/H^+ antiporter in the renal proximal tubule epithelial cell. J Biol Chem 1983;258(22):13513–6.
[339] Jacobsen C, Kragh-Hansen U, Sheikh MI. Na^+-H^+ exchange in luminal-membrane vesicles from rabbit proximal convoluted and straight tubules in response to metabolic acidosis. Biochem J 1986;239:411–6.
[340] Jacobsen C, Rigaard-Petersen H, Sheikh MI. Demonstration of Na^+-selective channels in the luminal-membrane vesicles isolated from pars recta of rabbit proximal tubule. FEBS-Lett 1988;236:95–9.
[341] Jacobson HR. Characteristics of volume reabsorption in rabbit superficial and juxtamedullary proximal convoluted tubules. J Clin Invest 1979;63:410–8.
[342] Jacobson HR. Effects of CO_2 and acetazolamide on bicarbonate and fluid transport in rabbit proximal tubules. Am J Physiol 1981;240:F54–62.
[343] Jacobson HR, Kokko JP. Intrinsic differences in various segments of the proximal convoluted tubule. J Clin Invest 1976;57:818–25.
[344] Jamison RL. Intrarenal heterogeneity. The case for two functionally dissimilar populations of nephrons in the mammalian kidney. Am J Med 1973;54:281–9.
[345] Jiang Z, Grichtchenko II, Boron WF, Aronson PS. Specificity of anion exchange mediated by mouse slc26a6. J Biol Chem 2002;277(37):33963–7.
[346] Jin X, Siragy HM, Carey RM. Renal interstitial cGMP mediates natriuresis by direct tubule mechanism. Hypertension 2001;38:309–16.
[347] Jin XH, McGrath HE, Gildea JJ, Siragy HM, Felder RA, Carey RM. Renal interstitial guanosine cyclic 3′,5′-monophosphate mediates pressure-natriuresis via protein kinase G. Hypertension 2004;43:1133–9.
[348] Jorgensen PL. Sodium and potassium ion pump in kidney tubules. Physiol Rev 1980;60:864–917.
[349] Jorgensen PL. Structure, function and regulation of NaK-ATPase in the kidney. Kidney Int 1986;29:10–20.

[350] Jorgensen PL, Andersen JP. Structural basis for E_1-E_2 conformational transitions in NaK-pump and Ca-pump proteins. J Membr Biol 1988;103:95–120.

[351] Kahn AM, Dolson GM, Hise MK, Bennett SC, Weinman EJ. Parathyroid hormone and dibutyryl cAMP inhibit Na^+-H^+ exchange in renal brush border vesicles. Am J Physiol 1985;248:F212–8.

[352] Kaissling B, Kriz W. Structural analysis of the rabbit kidney. Berlin: Springer-Verlag; 1979. pp.1-121

[353] Kanai Y, Lee W, You G, Brown D, Hediger MA. The human kidney low affinity Na^+/glucose co-transporter SGLT2. Delineation of the major renal reabsorptive mechanism for D-glucose. J Clin Invest 1994;93:397–404.

[354] Karim ZG, Chambrey R, Chalumeau C, Defontaine N, Warnock DG, Paillard M, et al. Regulation by PKC isoforms of $Na(^+)/H(^+)$ exchanger in luminal membrane vesicles isolated from cortical tubules. Am J Physiol 1999;277:F773–8.

[355] Karniski LP, Aronson PS. Chloride/formate exchange with formic acid recycling: a mechanism of active chloride transport across epithelial membranes. Proc Natl Acad Sci USA 1985;82 (18):6362–5.

[356] Karniski LP, Aronson PS. Anion exchange pathways for Cl^- transport in rabbit renal microvillus membranes. Am J Physiol 1987;253:F513–21.

[357] Karniski LP, Wang T, Everett LA, Green ED, Giebisch G, Aronson PS. Formate-stimulated NaCl absorption in the proximal tubule is independent of the pendrin protein. Am J Physiol 2002;283:F952–6.

[358] Kashgarian M, Biemesderfer D, Caplan M, Forbush III B. Monoclonal antibody to NaK-ATPase: Immunocytochemical localization along nephron segments. Kidney Int 1985;28:899–913.

[359] Katz AI. Renal Na-K-ATPase: its role in tubular sodium and potassium transport. Am J Physiol 1982;242:F207–19.

[360] Katz AI, Doucet A, Morel F. Na-K-ATPase activity along the rabbit rat and mouse nephron. Am J Physiol 1979;237: F114–20.

[361] Kaufman JS, Hamburger RJ. Passive potassium transport in the proximal convoluted tubule. Am J Physiol 1985;248: F228–32.

[362] Kawahara K. A stretch-activated K^+ channel in the basolateral membrane of *Xenopus* kidney proximal tubule cells. Pflügers Arch 1990;415:624–9.

[363] Kawahara K, Ogawa A, Suzuki M. Hyposmotic activation of Ca-activated K channels in cultured rabbit kidney proximal tubule cells. Am J Physiol 1991;260:F27–33.

[364] Kawamura S, Imai M, Seldin DW, Kokko JP. Characteristics of salt and water transport in superficial and juxtamedullary straight segments of proximal tubules. J Clin Invest 1975;55: 1269–77.

[365] Kawamura J, Mazumdar DC, Lubowitz H. Effect of albumin infusion on renal glucose reabsorption in the rat. Am J Physiol 1977;232:F286–90.

[366] Kaye GI, Wheeler HO, Whitlock RT, Lane N. Fluid transport in the rabbit gallbladder. J Cell Biol 1966;30:237–68.

[367] Kessler M, Semenza G. The small intestinal Na^+-D-glucose co-transporter: an asymmetric gated channel (or pore) responsive to Dy. J Membr Biol 1983;76:27–56.

[368] Khan F, Zelenin SS, Holtbäck U, Scott L, Aperia A. Negative reciprocity between angiotensin II type 1 and dopamine D1 receptors in rat renal proximal tubule cells. Am J Physiol 2008;295:F1110–6.

[369] Khraibi AA, Haas JA, Knox FG. Effect of renal perfusion pressure on renal interstitial hydrostatic pressure in rats. Am J Physiol 1989;256:F165–70.

[370] Khuri RN. Electrochemistry of the nephron. In: Giebisch G, editor. Membrane transport in biology. Vol. IV: transport organs. Berlin: Springer-Verlag; 1979. p. 47–96.

[371] Kinne R. Metabolic correlates of tubular transport. In: Giebisch G, editor. Membrane transport in biology. Vol. IV: transport organs. Berlin: Springer-Verlag; 1979. p. 529–62.

[372] Kinne R, Murer H, Kinne-Saffran E, Thees M, Sachs G. Sugar transport by renal plasma membrane vesicles. J Membr Biol 1975;21:375–95.

[373] Kinoshita Y, Knox FG. Role of prostaglandins in proximal tubule sodium reabsorption: response to elevated renal interstitial hydrostatic pressure. Circ Res 1989;64:1013–8.

[374] Kinsella JL, Aronson PS. Properties of the Na^+-H^+ exchanger in renal microvillus membrane vesicles. Am J Physiol 1980;238: F461–9.

[375] Kinsella JL, Aronson PS. Amiloride inhibition of the Na^+-H^+ exchanger in renal microvillus membrane vesicles. Am J Physiol 1981;241:F374–9.

[376] Kinsella JL, Aronson PS. Determination of the coupling ratio for Na^+-H^+ exchange in renal microvillus membrane vesicles. Biochim Biophys Acta 1982;689:161–4.

[377] Kinsella JL, Cujdik T, Sacktor B. Kinetic studies on the stimulation of Na^+- H^+ exchange activity in renal brush border membranes isolated from thyroid hormone-treated rats. J Membrane Biol 1986;91:183–91.

[378] Kirk KL, DiBona DR, Schafer JA. Regulatory volume decrease in perfused proximal nephron: evidence for a dumping of cell K^+. Am J Physiol 1987;252:F933–42.

[379] Kirk KL, Halm DR, Dawson DC. Active sodium transport by turtle colon via an electrogenic Na-K exchange pump. Nature 1980;287:237–9.

[380] Kirk KL, Schafer JA, DiBona DR. Cell volume regulation in rabbit proximal straight tubule perfused *in vitro*. Am J Physiol 1987;252:F922–32.

[381] Knauf F, Yang CL, Thomson RB, Mentone SA, Giebisch G, Aronson PS. Identification of a chloride-formate exchanger expressed on the brush border membrane of renal proximal tubule cells. Proc Natl Acad Sci 2001;98:9425–30.

[382] Knight TF, Senekjian HO, Sansom SC, Weinman EJ. Proximal tubule glucose efflux in the rat as a function of delivered load. Am J Physiol 1980;238:F499–503.

[383] Knox FG, Haas JA. Factors influencing renal sodium reabsorption in volume expansion. Rev Physiol Biochem Pharm 1982;92:75–113.

[384] Knox FG, Mertz JI, Burnett Jr. JC, Haramati A. Role of hydrostatic and oncotic pressures in renal sodium reabsorption. Circ Res 1983;52:491–500.

[385] Knox FG, Schneider EG, Willis LR, Strandhoy JW, Ott CE. Effect of volume expansion on sodium excretion in the presence and absence of increased delivery from superficial proximal tubules. J Clin Invest 1973;52:1642–6.

[386] Kocinsky HS, Girardi ACC, Biemesderfer D, Nguyen T, Mentone S, Orlowski J, et al. Use of phosph-specific antibodies to determine the phosphorylation of endogenous Na^+/H^+ exchanger NHE3 at PKA consensus sites. Am J Physiol 2005;289:F249–58.

[387] Kokko JP. Proximal tubule potential difference: dependence on glucose HCO3- and amino acids. J Clin Invest 1973;52:1362–7.

[388] Kokko JP, Burg MB, Orloff J. Characteristics of NaCl and water transport in the renal proximal tubule. J Clin Invest 1971;50:69–76.

[389] Kolb RJ, Woost PG, Hopfer U. Membrane trafficking of angiotensin receptor type-1 and mechanochemical signal transduction in proximal tubule cells. Hypertension 2004;44:352–9.

[390] Kondo Y, Frömter E. Evidence of chloride/bicarbonate exchange mediating bicarbonate efflux from S3 segments of rabbit renal proximal tubule. Pflügers Arch 1990;415:726–33.
[391] Kone BC, Brady HR, Gullans SR. Coordinated regulation of intracellular K^+ in the proximal tubule: Ba^{2+} blockade down-regulates the Na^+,K^+-ATPase and up-regulates two K^+ permeability pathways. Proc Natl Acad Sci 1989;86:6431–5.
[392] Kottra G, Frömter E. Functional properties of the paracellular pathway in some leaky epithelia. J Exp Biol 1983;106:217–29.
[393] Krahn TA, Aronson PS, Weinstein AM. Weak acid permeability of a villous membrane: formic acid transport across rat proximal tubule. Bull Math Biol 1994;56:459–90.
[394] Krahn TA, Weinstein AM. Acid/base transport in a model of the proximal tubule brush border: impact of carbonic anhydrase. Am J Physiol 1996;270:F344–55.
[395] Krapf R, Berry CA, Verkman AS. Estimation of intracellular chloride activity in isolated perfused rabbit proximal convoluted tubules using a fluorescent indicator. Biophys J 1988;53:955–62.
[396] Kumar AM, Spitzer A, Gupta RK. 23Na NMR spectroscopy of proximal tubule suspensions. Kidney Int 1986;29:747–51.
[397] Kunimi M, Seki G, Hara C, Taniguchi S, Uwatoko S, Goto A, et al. Dopamine inhibits renal Na^+:HCO_3^- co-transporter in rabbits and normotensive rats but not in spontaneously hypertensive rats. Kid Int 2000;57:534–43.
[398] Kuo S-M, Aronson PS. Pathways for oxalate transport in rabbit renal microvillus membrane vesicles. J Biol Chem 1996;271:15491–7.
[399] Kurashima K, D'Souza S, Szaszi K, Ramjeesingh R, Orlowski J, Grinstein S. The apical Na^+/H^+ exchanger isoform NHE3 is regulated by the actin cytoskeleton. J Biol Chem 1999;274 (42):29843–9.
[400] Kurtz I. Apical Na^+/H^+ antiporter and glycolysis-dependent H^+-ATPase regulate intracellular pH in the rabbit S3 proximal tubule. J Clin Invest 1987;80:928–35.
[401] Kurtz I. Basolateral membrane Na^+/H^+ antiport Na^+/base co-transport and Na^+-independent Cl^-/base exchange in the rabbit S3 proximal tubule. J Clin Invest 1989;83:616–22.
[402] Kurtz I, Nagami G, Yanagawa N, Li L, Emmons C, Lee I. Mechanism of apical and basolateral Na^+-independent Cl^-/base exchange in the rabbit superficial proximal straight tubule. J Clin Invest 1994;94:173–83.
[403] Kyte J. Immunoferritin determination of the distribution of (Na^+,K^+) ATPase over the plasma membranes of renal convoluted tubules. II. Proximal segment. J Cell Biol 1976;68: 304–18.
[404] Lahera V, Salom MG, Miranda-Guardiola F, Moncada S, Romero JC. Effects of NG-nitro-L-arginine methyl ester on renal function and blood pressure. Am J Physiol 1991;261: F1033–7.
[405] Lamprecht G, Weinman EJ, Yun CH. The role of NHERF and E3KARP in the cAMP-mediated inhibition of NHE3. J Biol Chem 1998;273(45):29972–8.
[406] Lang F, Busch GL, Ritter M, Völkl H, Waldegger S, Gulbins E, et al. Functional significance of cell volume regulatory mechanisms. Physiol Rev 1998;78:247–306.
[407] Lang F, Busch GL, Völkl H. The diversity of volume regulatory mechanisms. Cell Physiol Biochem 1998;8:1–45.
[408] Lapointe J-Y, Duplain M. Regulation of basolateral membrane potential after stimulation of Na^+ transport in proximal tubules. J Membr Biol 1991;120:165–72.
[409] Lapointe J-Y, Garneau L, Bell PD, Cardinal J. Membrane cross-talk in the mammalian proximal tubule during alterations in transepithelial sodium transport. Am J Physiol 1990;258: F339–45.
[410] Lapointe J-Y, Laprade R, Cardinal J. Transepithelial and cell membrane electrical resistances of the rabbit proximal convoluted tubule. Am J Physiol 1984;247:F637–49.
[411] Laradi A, Sakhrani LM, Massry SG. Effect of dopamine on sodium uptake by renal proximal tubule cells of rabbit. Miner Electrolyte Metab 1986;12:303–7.
[412] Lau KR, Hudson RL, Schultz SG. Cell swelling increases a barium-inhibitable potassium conductance in the basolateral membrane of *Necturus* small intestine. Proc Natl Acad Sci 1984;81:3591–4.
[413] Lee WS, Kanai Y, Wells RG, Hediger MA. The high affinity Na^+/glucose co-transporter. Re-evaluation of function and distribution of expression. J Biol Chem 1994;269:12032–9.
[414] Leong PKK, Devillez A, Sandberg MB, Yang LE, Yip DKP, Klein JB, et al. Effect of ACE inhibition on proximal tubule sodium transport. Am J Physiol 2006;290:F854–63.
[415] Leong PK, Yang LE, Holstein-Rathlou NH, McDonough AA. Angiotensin II clamp prevents the second step in renal apical NHE3 internalization during acute hypertension. Am J Physiol 2002;283:F1142–50.
[416] Leong PK, Yang LE, Lin HW, Holstein-Rathlou NH, McDonough AA. Acute hypotension induced by aortic clamp vs. PTH provokes distinct proximal tubule Na^+ transporter redistribution patterns. Am J Physiol 2004;287:R878–85.
[417] Lever JE. A two sodium ion/D-glucose symport mechanism: Membrane potential effect on phlorizin binding. Biochemistry 1984;23:4697–702.
[418] Lewy JE, Windhager EE. Peritubular control of proximal tubular fluid reabsorption in the rat kidney. Am J Physiol 1968;214:943–54.
[419] Li D, Xian S, Cheng J, Fisone G, Caplan MJ, Ohtomo Y, et al. Effects of okadaic acid calyculin A, and PDBu on state of phosphorylation of rat renal Na^+-K^+-ATPase. Am J Physiol 1998;275:F863–9.
[420] Liang M, Knox FG. Production and functional roles of nitric oxide in the proximal tubule. Am J Physiol 2000;278: R1117–24.
[421] Liedtke CM, Hopfer U. Mechanism of Cl^- translocation across small intestinal brush-border membrane. I. Absence of Na^+–Cl^- co-transport. Am J Physiol 1982;242:G263–71.
[422] Liedtke CM, Hopfer U. Mechanism of Cl^- translocation across small intestinal brush-border membrane. II. Demonstration of Cl^{--} OH^- exchange and Cl^- conductance. Am J Physiol 1982;242:G272–80.
[423] Linas SL, Repine JE. Endothelial cells regulate proximal tubule epithelial cell sodium transport. Kidney Int 1999;55: 1251–8.
[424] Lipkowitz MS, Abramson RG. Modulation of the ionic permeability renal cortical brush-border membranes by cAMP. Am J Physiol 1989;257:F769–76.
[425] Lipkowitz MS, London RD, Beck JC, Abramson RG. Hormonal regulation of rat renal proximal tubule brush-border membrane ionic permeability. Am J Physiol 1992;263:F144–51.
[426] Liu F-Y, Cogan MG. Axial heterogeneity in the rat proximal convoluted tubule. I. Bicarbonate chloride and water transport. Am J Physiol 1984;247:F816–21.
[427] Liu F-Y, Cogan MG. Axial heterogeneity of bicarbonate chloride and water transport in the rat proximal convoluted tubule. J Clin Invest 1986;78:1547–57.
[428] Liu F-Y, Cogan MG. Flow dependence of bicarbonate transport in the early (S1) proximal convoluted tubule. Am J Physiol 1988;254:F851–5.
[429] Liu F-Y, Cogan MG. Angiotensin II stimulation of hydrogen ion secretion in the rat early proximal tubule. Modes of action mechanism and kinetics. J Clin Invest 1988;82:601–7.

[430] Liu F-Y, Cogan MG. Angiotensin II stimulates early proximal bicarbonate absorption in the rat by decreasing cyclic adenosine monophosphate. J Clin Invest 1989;84:83–91.
[431] Liu F, Cogan MG. Role of protein kinase C in proximal bicarbonate absorption and angiotensin signaling. Am J Physiol 1990;258:F927–33.
[432] Liu F-Y, Cogan MG, Rector Jr FC. Axial heterogeneity in the rat proximal convoluted tubule. II Osmolality and osmotic water permeability. Am J Physiol 1984;247:F822–6.
[433] Logvinenko NS, Dulubova I, Fedosova N, Larsson SH, Nairn AC, Esmann M, et al. Phosphorylation by protein kinase C of serine-23 of the alpha-1 subunit of rat Na^+,K^+-ATPase affects its conformational equilibrium. Proc Natl Acad Sci 1996;93:9132–7.
[434] Lohr JW, Grantham JJ. Isovolumetric regulation of isolated S2 proximal tubules in anisotonic media. J Clin Invest 1986;78:1165–72.
[435] Lohr JW, Sullivan LP, Cragoe Jr. EJ, Grantham JJ. Volume regulation determinants in isolated proximal tubules in hypertonic medium. Am J Physiol 1989;256:F622–31.
[436] London R, Cohen B, Guggino WB, Giebisch G. Regulation of intracellular chloride activity during perfusion with hypertonic solutions in the *Necturus* proximal tubule. J Membr Biol 1983;75:253–8.
[437] Loo DD, Hazama A, Supplisson S, Turk E, Wright EM. Relaxation kinetics of the Na^+/glucose co-transporter. Proc Natl Acad Sci 1993;90:5767–71.
[438] Loo DD, Zeuthen T, Chandy G, Wright EM. Co-transport of water by the Na^+/glucose co-transporter. Proc Natl Acad Sci 1996;93:13367–70.
[439] Loo DDF, Hirayama BA, Karakossian MH, Meinild A, Wright EM. Conformational dynamics of hSGLT1 during Na^+/glucose co-transport. J Gen Physiol 2006;128:701–20.
[440] Lopes AG, Guggino WB. Volume regulation in the early proximal tubule of the *Necturus* kidney. J Memb Biol 1987;97:117–25.
[441] Lopes AG, Siebens AW, Giebisch G, Boron WF. Electrogenic Na/HCO_3 co-transport across basolateral membrane of isolated perfused *Necturus* proximal tubule. Am J Physiol 1987;253:F340–50.
[442] Lorentz Jr. WB, Lassiter WE, Gottschalk CW. Renal tubular permeability during increased intrarenal pressure. J Clin Invest 1972;51:484–92.
[443] Lorenz JN, Schultheis PJ, Traynor T, Shull GE, Schnermann J. Micropuncture analysis of single-nephron function in NHE3-deficient mice. Am J Physiol 1999;277:F447–53.
[444] Lucci MS, Warnock DG. Effects on anion-transport inhibitors on NaCl reabsorption in the rat superficial proximal convoluted tubule. J Clin Invest 1979;64:570–9.
[445] Mackenzie B, Loo DDF, Panayotova-Heiermann M, Wright EM. Biophysical characteristics of the pig kidney Na^+/glucose co-transporter SGLT2 reveal a common mechanism for SGLT1 and SGLT2. J Biol Chem 1996;271:32678–83.
[446] MacRobbie EAC, Ussing HH. Osmotic behavior of the epithelial cells of frog skin. Acta Physiol Scand 1961;53:348–65.
[447] Maddox DA, Fortin SM, Tartini A, Barnes WD, Gennari FJ. Effect of acute changes in glomerular filtration rate on Na^+/H^+ exchange in rat renal cortex. J Clin Invest 1992;89:1296–303.
[448] Madhun ZT, Goldthwait DA, McKay D, Hopfer U, Douglas JG. An epoxygenase metabolite of arachidonic acid mediates angiotensin II-induced rises in cytosolic calcium in rabbit proximal tubule epithelial cells. J Clin Invest 1991;88:456–61.
[449] Maeda Y, Smith BL, Agre P, Knepper MA. Quantification of aquaporin-CHIP water channel protein in microdissected renal tubules by fluorescence-based ELISA. J Clin Invest 1995;95:422–8.
[450] Majid DSA, Williams A, Navar LG. Inhibition of nitric oxide synthesis attenuates pressure-induced natriuretic responses in anesthetized dogs. Am J Physiol 1993;264:F79–87.
[451] Martino JA, Earley LE. Demonstration of a role of physical factors as determinants of the natriuretic response to volume expansion. J Clin Invest 1967;46:1963–78.
[452] Maruyama T, Hoshi T. The effect of D-glucose on the electrical potential profile across the proximal tubule of newt kidney. Biochim Biophys Acta 1972;282:214–25.
[453] Mathias RT. Epithelial water transport in a balanced gradient system. Biophys J 1985;47:823–36.
[454] Matsumura Y, Cohen B, Guggino WB, Giebisch G. Electrical effects of potassium and bicarbonate on proximal tubule cells of *Necturus*. J Membr Biol 1984;79:145–52.
[455] Maunsbach AB. Ultrastructure of the proximal tubule. In: Orloff J, Berliner RW, editors. Handbook of physiology. section 8: renal physiology. Washington DC: American Physiological Society; 1973. p. 31–80.
[456] Maunsbach AB, Boulpaep EL. Hydrostatic pressure changes related to paracellular shunt ultrastructure in proximal tubule. Kidney Int 1980;17:732–48.
[457] Maunsbach AB, Boulpaep EL. Paracellular shunt ultrastructure and changes in fluid transport in *Necturus* proximal tubule. Kidney Int 1983;24:610–9.
[458] Maunsbach AB, Boulpaep EL. Quantitative ultrastructure and functional correlates in proximal tubule of *Ambystoma* and *Necturus*. Am J Physiol 1984;246:F710–24.
[459] Maunsbach AB, Giebisch GH, Stanton BA. Effects of flow rate on proximal tubule ultrastructure. Am J Physiol 1987;253:F582–7.
[460] Maunsbach AB, Vorum H, Kwon TH, Nielsen S, Simonsen B, Choi I, et al. Immunoelectron microscopic localization of the electrogenic Na/HCO_3 co-transporter in rat and *Ambystoma* kidney. J Am Soc Nephrol 2000;11:2179–89.
[461] McCarthy KM, Skare IB, Stankewich MC, Furuse M, Tsukita S, Rogers RA, et al. Occludin is a functional component of the tight junction. J Cell Sci 1996;109:2287–98.
[462] McCarty NA, O'Neil RG. Dihydropyridine-sensitive cell volume regulation in proximal tubule: the calcium window. Am J Physiol 1990;259:F950–60.
[463] McCarty NA, O'Neil RG. Calcium-dependent control of volume regulation in renal proximal tubule cells: i. Swelling-activated Ca^{2+} entry and release. J Membr Biol 1991;123:149–60.
[464] McCarty NA, O'Neil RG. Calcium-dependent control of volume regulation in renal proximal tubule cells: II. Roles of dihydropyridine-sensitive and -insensitive Ca^{2+} entry pathways. J Membr Biol 1991;123:161–70.
[465] McDonough AA. Mechanisms of proximal tubule sodium transport regulation that link extracellular fluid volume and blood pressure. Am J Physiol 2010;298:R851–61.
[466] McDonough AA, Biemesderfer D. Does membrane trafficking play a role in regulating the sodium/hydrogen exchanger isoform 3 in the proximal tubule? Curr Opin Nephrol Hypertens 2003;12:533–41.
[467] McDonough AA, Magyar CE, Komatsu Y. Expression of Na^+-K^+-ATPase alpha- and beta-subunits along rat nephron: isoform specificity and response to hypokalemia. Am J Physiol 1994;267:C901–8.
[468] McKeown J, Brazy PC, Dennis VW. Intrarenal heterogeneity for fluid phosphate and glucose absorption in the rabbit. Am J Physiol 1979;234:F312–8.
[469] Meinild AK, Klaerke DA, Loo DDF, Wright EM, Zeuthen T. The human Na^+-glucose co-transporter is a molecular water pump. J Physiol 1998;508:15–21.

[470] Mellas J, Hammerman MR. Phorbol ester-induced alkalinization of canine renal proximal tubular cells. Am J Physiol 1986;250:F451–9.
[471] Merot J, Bidet M, Le Maout S, Tauc M, Poujeol P. Two types of K^+ channels in the apical membrane of rabbit proximal tubule in primary culture. Biochem Biophys Acta 1989;978:134–44.
[472] Mertz JJ, Haas JA, Berndt TJ, Burnett Jr. JC, Knox FG. Effects of bradykinin on renal interstitial pressures and proximal tubule reabsorption. Am J Physiol 1984;247:F82–5.
[473] Messner G, Koller A, Lang F. The effect of phenylalanine on intracellular pH and sodium activity in proximal convoluted tubule cells of the frog kidney. Pflügers Arch 1985;404:145–9.
[474] Messner G, Oberleithner H, Lang F. The effect of phenylalanine on the electrical properties of proximal tubule cells in the frog kidney. Pflügers Arch 1985;404:138–44.
[475] Millar ID, Robson L. Na^+-alanine uptake activates a Cl^- conductance in frog renal proximal tubule cells via nonconventional PKC. Am J Physiol 2001;280:F758–67.
[476] Misfeldt DS, Sanders MJ. Transepithelial transport in cell culture: Stoichiometry of Na/phlorizin binding and Na/D-glucose co-transport. A two-step two-sodium model of binding and translocation. J Membr Biol 1982;70:191–8.
[477] Mitic LL, Anderson JM. Molecular architecture of tight junctions. Annu Rev Physiol 1998;60:121–42.
[478] Moe OW. Acute regulation of proximal tubule apical membrane Na/H exchanger NHE-3: role of phosphorylation protein trafficking and regulatory factors. J Am Soc Nephrol 1999;10:2412–25.
[479] Moe OW, Amemiya M, Yamaji Y. Activation of protein kinase A acutely inhibits and phosphorylates Na/H exchanger NHE-3. J Clin Invest 1995;96:2187–94.
[480] Montrose MH, Murer H. Kinetics of Na^+/H^+ exchange. In: Grinstein S, editor. Na^+-H^+ Exchange. Boca Raton FL: CRC Press; 1988. p. 57–75.
[481] Montrose-Rafizadeh C, Guggino WB. Cell volume regulation in the nephron. Ann Rev Physiol 1990;52:761–72.
[482] Moran A, Biber J, Murer H. A sodium–hydrogen exchange system in isolated apical membrane from LLC-PK1 epithelia. Am J Physiol 1986;251:F1003–8.
[483] Moran A, Stange G, Murer H. Sodium–hydrogen exchange system in brush border membranes from cortical and medullary regions of the proximal tubule. Biochem Biophys Res Commun 1989;163:269–75.
[484] Morel F, Murayama Y. Simultaneous measurement of unidirectional and net sodium fluxes in microperfused rat proximal tubules. Pflügers Arch 1970;320:1–23.
[485] Morrow JS, Cianci CD, Ardito T, Mann AS, Kashgarian M. Ankyrin links fodrin to the alpha subunit of NaK-ATPase in Madin–Darby canine kidney cells and in intact renal tubule cells. J Cell Biol 1989;108:455–65.
[486] Mounfield PR, Robson L. The role of Ca^{2+} in volume regulation induced by Na^+-coupled alanine uptake in single proximal tubule cells isolated from frog kidney. J Physiol 1998;510:145–53.
[487] Mount DB, Gamba G. Renal potassium–chloride co-transporters. Curr Opin Nephrol Hypertens 2001;10:685–91.
[488] Mount DB, Mercado A, Song L, Xu J, George Jr AL, Delpire E, et al. Cloning and characterization of KCC3 and KCC4, new members of the cation–chloride co-transporter gene family. J Biol Chem 1999;274:16355–62.
[489] Mount DB, Romero MF. The SLC26 gene family of multifunctional anion exchangers. Pflügers Arch 2004;447:710–21.
[490] Muller-Berger S, Coppola S, Samarzija I, Seki G, Frömter E. Partial recovery of *in vivo* function by improved incubation conditions of isolated renal proximal tubule. I. Change of amiloride-inhibitable K^+ conductance. Pflügers Arch 1997;434:373–82.
[491] Muller-Berger S, Ducoudret O, Diakov A, Frömter E. The renal Na-HCO_3-co-transporter expressed in *Xenopus laevis oocytes*: change in stoichiometry in response to elevation of cytosolic Ca^{2+} concentration. Pflügers Arch 2001;442:718–28.
[492] Muller-Berger S, Nesterov VV, Frömter E. Partial recovery of *in vivo* function by improved incubation conditions of isolated renal proximal tubule. II. Change of Na-HCO_3 co-transport stoichiometry and of response to acetazolamide. Pflügers Arch 1997;434:383–91.
[493] Murer H, Burckhardt G. Membrane transport of anions across epithelia of mammalian small intestine and kidney proximal tubule. Rev Physiol Biochem Pharmacol 1983;96:1–51.
[494] Murer H, Hopfer U, Kinne R. Sodium/proton antiport in brush-border-membrane vesicles isolated from rat small intestine and kidney. Biochem J 1976;154:597–604.
[495] Muto S, Hata M, Taniguchi J, Tsuruoka S, Moriwaki K, Saitou M, et al. Claudin-2-deficient mice are defective in the leaky and cation-selective paracellular permeability properties of renal proximal tubules. Proc Natl Acad Sci 2010;107:8011–6.
[496] Nagami GT. Luminal secretion of ammonia in the mouse proximal tubule perfused *in vitro*. J Clin Invest 1988;81:159–64.
[497] Nagami GT. Enhanced ammonia secretion by proximal tubules from mice receiving NH_4Cl: role of angiotensin II. Am J Physiol 2002;282:F472–7.
[498] Nagami GT, Chang JA, Plato ME, Santamaria R. Acid loading *in vivo* and low pH in culture increase angiotensin receptor expression: Enhanced ammoniagenic response to angiotensin II. Am J Physiol 2008;295:F1864–70.
[499] Nakamura T, Alberola AM, Salazar FJ, Saito Y, Kurashina T, Granger JP, et al. Effects of renal perfusion pressure on renal interstitial hydrostatic pressure and Na^+ excretion: role of endothelium-derived nitric oxide. Nephron 1998;78:104–11.
[500] Nakhoul NL, Chen LK, Boron WF. Intracellular pH regulation in rabbit S3 proximal tubule: Basolateral Cl-HCO_3 exchange and Na-HCO_3 co-transport. Am J Physiol 1990;258:F371–81.
[501] Nascimento NRF, Kemp BA, Howell NL, Gildea JJ, Santos CF, Harris TE, et al. Role of Src family kinase in extracellular renal cyclic guanosine 3′,5′-monophosphate- and pressure-induced natriuresis. Hypertension 2011;58:107–13.
[502] Navar LG, Majid DSA. Interactions between arterial pressure and sodium excretion. Curr Opin Nephrol Hyperten 1996;5:64–71.
[503] Nielsen R. A 3 to 2 coupling of the Na-K pump responsible for the transepithelial Na transport in frog skin disclosed by the effect of Ba. Acta Physiol Scand 1979;107:189–91.
[504] Nord EP, Goldfarb D, Mikhail N, Moradeshagi P, Hafezi A, Vaystub S, et al. Characteristics of the Na^+-H^+ antiporter in the intact renal proximal tubular cell. Am J Physiol 1986;250: F539–50.
[505] Nord EP, Howard MJ, Hafezi A, Moradeshagi P, Vaystub S, Insel PA. Alpha 2 adrenergic agonists stimulate Na^+-H^+ antiport activity in the rabbit renal proximal tubule. J Clin Invest 1987;80:1755–62.
[506] Nowicki S, Chen SL, Aizman O, Cheng XJ, Li D, Nowicki C, et al. 20-Hydroxyeicosa-tetraenoic acid (20-HETE) activates protein kinase C. Role in regulation of rat renal Na^+,K^+-ATPase. J Clin Invest 1997;99:1224–30.
[507] O'Connell DP, Botkin SJ, Ramos SI, Sibley DR, Ariano MA, Felder RA, et al. Localization of dopamine D1A receptor protein in rat kidneys. Am J Physiol 1995;268:F1185–97.
[508] Ominato M, Satoh T, Katz AI. Regulation of Na-K-ATPase activity in the proximal tubule: role of the protein kinase C pathway and of eicosanoids. J Membr Biol 1996;152:235–43.

[509] Orci L, Humbert F, Brown D, Perrelet A. Membrane ultrastructure in urinary tubules. In: Bourne GH, Danielli JF, Jeon KW, editors. International review of cytology, vol. 73. New York: Academic; 1981. p. 183–242.

[510] Orlowski J. Heterologous expression and functional properties of amiloride high affinity (NHE-1) and low affinity (NHE-3) isoforms of the rat Na/H exchanger. J Biol Chem 1993;268:16369–77.

[511] Orlowski J, Kandasamy RA, Shull GE. Molecular cloning of putative members of the Na/H exchanger gene family. cDNA cloning deduced amino acid sequence and mRNA tissue expression of the rat Na/H exchanger NHE-1 and two structurally related proteins. J Biol Chem 1992;267:9331–9.

[512] Osgood RW, Reineck HJ, Stein JH. Effect of hyperoncotic albumin on superficial and juxtamedullary nephron sodium transport. Am J Physiol 1979;237:F34–7.

[513] Otsu K, Kinsella JL, Koh E, Froehlich JP. Proton dependence of the partial reactions of the sodium-proton exchanger in renal brush border membranes. J Biol Chem 1992;267:8089–96.

[514] Otsu K, Kinsella JL, Sacktor B, Froehlich JP. Transient state kinetic evidence for an oligomer in the mechanism of Na^+-H^+ exchange. Proc Natl Acad Sci 1989;86:4818–22.

[515] Ott CE. Effect of saline expansion on peritubule capillary pressures and reabsorption. Am J Physiol 1981;240:F106–10.

[516] Ott CE, Haas JA, Cuche J-L, Knox FG. Effect of increased peritubule protein concentration on proximal tubule protein concentration on proximal tubule reabsorption in the presence and absence of extracellular volume expansion. J Clin Invest 1975;55:612–20.

[517] Padia SH, Howell NL, Siragy HM, Carey RM. Renal angiotensin type 2 receptors mediate natriuresis via angiotensin III in the angiotensin II type 1 receptor-blocked rat. Hypertension 2006;47:537–44.

[518] Padia SH, Kemp BA, Howell NL, Fournie-Zaluski M-C, Roques BP, Carey RM. Conversion of renal angiotensin II to angiotensin III is critical for AT2 receptor-mediated natriuresis in rats. Hypertension 2008;51:460–5.

[519] Pajor AM, Hirayama BA, Wright EM. Molecular evidence for two renal Na^+/glucose co-transporters. Biochim Biophys Acta 1992;1106:216–20.

[520] Panayotova-Heiermann M, Loo DD, Wright EM. Kinetics of steady-state currents and charge movements associated with the rat Na^+/glucose co-transporter. J Biol Chem 1995;270:27099–105.

[521] Parent L, Supplisson S, Loo DDF, Wright EM. Electrogenic properties of the cloned Na^+/glucose co-transporter: I. Voltage-clamp studies. J Membrane Biol 1992;125:49–62.

[522] Parent L, Supplisson S, Loo DDF, Wright EM. Electrogenic properties of the cloned Na^+/glucose co-transporter: II. A transport model under nonrapid equilibrium conditions. J Membrane Biol 1992;125:63–79.

[523] Pearce D, Verkman AS. NaCl reflection coefficients in proximal tubule apical and basolateral membrane vesicles. Measurement by induced osmosis and solvent drag. Biophys J 1989;55:1251–9.

[524] Periyasamy SM, Liu J, Tanta F, Kabak B, Wakefield B, Malhotra D, et al. Salt loading induces redistribution of the plasmalemmal Na/K-ATPase in proximal tubule cells. Kid Int 2005;67:1868–77.

[525] Persson B, Spring KR. Permeability properties of the subepithelial tissues of *Necturus* gallbladder. Biochim Biophys Acta 1984;772:135–9.

[526] Peterson OW, Gushwa LC, Blantz RC. An analysis of glomerular–tubular balance in the rat proximal tubule. Pflügers Arch 1986;407:221–7.

[527] Petrovic S, Barone S, Wang Z, McDonough AA, Amlal H, Soleimani M. Slc2616 (PAT1) deletion downregulates the apical Na^+/H^+ exchanger in the straight segment of the proximal tubule. Am J Nephrol 2008;28:330–8.

[528] Petrovic S, Barone S, Weinstein AM, Soleimani M. Activation of the apical Na^+/H^+ exchanger NHE3 by formate: a basis of enhanced fluid and electrolyte reabsorption by formate in the kidney. Am J Physiol 2004;287:F336–46.

[529] Pirie SC, Potts DJ. The effect of peritubular protein upon fluid reabsorption in rabbit proximal convoluted tubules perfused *in vitro*. J Physiol 1983;337:429–40.

[530] Pitts TO, McGowan JA, Chen TC, Silverman M, Rose ME, Puschett JB. Inhibitory effects of volume expansion performed *in vivo* on transport in the isolated rabbit proximal tubule perfused *in vitro*. J Clin Invest 1988;81:997–1003.

[531] Planelles G, Thomas SR, Anagnostopoulos T. Change of apparent stoichiometry of proximal-tubule $Na(^+)$-HCO_3^- co-transport upon experimental reversal of its orientation. Proc Natl Acad Sci 1993;90:7406–10.

[532] Pohl M, Kaminski H, Castrop H, Bader M, Himmerkus N, Bleich M, et al. Intrarenal renin angiotensin system revisited. Role of megalin-dependent endocytosis along the proximal nephron. J Biol Chem 2010;285:41935–46.

[533] Preisig PA. Luminal flow rate regulates proximal tubule H-HCO_3 transporters. Am J Physiol 1992;262:F47–54.

[534] Preisig PA, Alpern RJ. Basolateral membrane H-OH-HCO_3 transport in the proximal tubule. Am J Physiol 1989;256: F751–65.

[535] Preisig PA, Alpern RJ. Contributions of cellular leak pathways to net $NaHCO_3$ and NaCl absorption. J Clin Invest 1989;83:1859–67.

[536] Preisig PA, Berry CA. Evidence for transcellular osmotic water flow in rat proximal tubules. Am J Physiol 1985;249:F124–31.

[537] Preisig PA, Ives HE, Cragoe Jr. EJ, Alpern RJ, Rector Jr FC. Role of the Na^+/H^+ antiporter in rat proximal tubule bicarbonate absorption. J Clin Invest 1987;80:970–8.

[538] Preisig PA, Rector Jr FC. Role of Na^+-H^+ antiport in rat proximal tubule NaCl absorption. Am J Physiol 1988;255:F461–5.

[539] Pricam C, Humbert F, Perrelet A, Orci L. A freeze-etch study of the tight junctions of the rat kidney tubules. Lab Invest 1974;30:286–91.

[540] Quan A, Baum M. Endogenous production of angiotensin II modulates rat proximal tubule transport. J Clin Invest 1996;97:2878–82.

[541] Quan A, Baum M. Regulation of proximal tubule transport by angiotensin II Semin. Nephrol 1997;17:423–30.

[542] Quan A, Baum M. Endogenous angiotensin II modulates rat proximal tubule transport with acute changes in extracellular volume. Am J Physiol 1998;275:F74–8.

[543] Quan A, Baum M. Effect of luminal angiotensin II receptor antagonists on proximal tubule transport. Am J Hypertension 1999;12:499–503.

[544] Quan A, Baum M. The renal nerve is required for regulation of proximal tubule transport by intraluminally produced ANG II. Am J Physiol 2001;280:F524–9.

[545] Quan A, Baum M. Renal nerve stimulation augments effect of intraluminal angiotensin II on proximal tubule transport. Am J Physiol 2002;282:F1043–8.

[546] Quigley R, Baum M. Developmental changes in rabbit proximal straight tubule paracellular permeability. Am J Physiol 2002;283:F525–31.

[547] Quigley R, Baum M, Reddy KM, Griener JC, Falck JR. Effects of 20-HETE and 19(S)-HETE on rabbity proximal straight tubule volume transport. Am J Physiol 2000;278:F949–53.

[548] Quinn MD, Marsh DJ. Peritubular capillary control of proximal tubule reabsorption in the rat. Am J Physiol 1979;236:F478–87.

[549] Rabito CA, Ausiello DA. Na^+-dependent sugar transport in a cultured epithelial cell line from pig kidney. J Membr Biol 1980;54:31–8.
[550] Ramsey CR, Berndt T, Knox FG. Effect of volume expansion on the paracellular flux of lanthanum in the proximal tubule. J Am Soc Nephrol 1998;9:1147–52.
[551] Ramsey CR, Berndt TJ, Knox FG. Indomethacin blocks enhanced paracellular backflux in proximal tubules. J Am Soc Nephrol 2002;13:1449–54.
[552] Rector Jr FC. Sodium bicarbonate and chloride absorption by the proximal tubule. Am J Physiol 1983;244:F461–71.
[553] Rector Jr. FC, Berry CA. Role of the paracellular pathway in reabsorption of solutes and water by proximal convoluted tubule of the mammalian kidney. In: Bradley SE, Purcell EF, editors. The paracellular pathway. New York: Josiah Macy Jr. Foundation; 1982. p. 135–57.
[554] Reddy S, Gyory AZ, Bostrom T, Dyne M, Salipan-Moore N, Field MJ, et al. Proximal tubular cell electrolytes during volume expansion in the rat. J Physiol 1994;481:217–22.
[555] Reilly AM, Harris PJ, Williams DA. Am J Physiol 1995;269: F374–80.
[556] Renkin EM, Gilmore JP. Glomerular filtration. In: Orloff J, Berliner RW, editors. Handbook of physiology. section 8: renal physiology. Washington DC: American Physiological Society; 1973. p. 185–248.
[557] Restrepo D, Kimmich GA. Kinetic analysis of mechanism of intestinal Na^+-dependent sugar transport. Am J Physiol 1985;248:C498–509.
[558] Reuss L. Basolateral KCl co-transport in a NaCl-absorbing epithelium. Nature 1983;305:723–6.
[559] Reuss L. Electrical properties of the cellular transepithelial pathway in *Necturus* gallbladder. III. Ionic permeability of the basolateral cell membrane. J Membr Biol 1979;47: 239–59.
[560] Reuss L, Weinman SA, Grady TP. Intracellular K^+ activity and its relation to basolateral membrane ion transport in *Necturus* gallbladder epithelium. J Gen Physiol 1980;76:33–52.
[561] Ribeiro CMP, Dubay GR, Falck JR, Mandel LJ. Parathyroid hormone inhibits Na^+-K^+-ATPase through a cytochrome P-450 pathway. Am J Physiol 1994;266:F497–505.
[562] Ribeiro CP, Mandel LJ. Parathyroid hormone inhibits proximal tubule Na^+-K^+-ATPase activity. Am J Physiol 1992;262: F209–16.
[563] Richardson IW, Licko V, Bartoli E. The nature of passive flows through tightly folded membranes. J Membr Biol 1973;11:293–308.
[564] Riquier-Brison ADM, Leong PKK, Pihakaski-Maunsbach K, McDonough AA. Angiotensin II stimulates trafficking of NHE3, NaPi2, and associated proteins into the proximal tubule microvilli. Am J Physiol 2010;298:F177–86.
[565] Robey RB, Ruiz OS, Espiritu DJ, Ibanez VC, Kear FT, Noboa OA, et al. Angiotensin II stimulation of renal epithelial cell Na/HCO_3 co-transport activity: a central role for Src family kinase/classic MAPK pathway coupling. J Membr Biol 2002;187:135–45.
[566] Robson AM, Srivastava PL, Bricker NS. The influence of saline loading on renal glucose reabsorption in the rat. J Clin Invest 1968;47:329–35.
[567] Robson L, Hunter M. Stimulation of Na^+-alanine co-transport activates a voltage-dependent conductance in single proximal tubule cells isolated from frog kidney. J Physiol 1999;517:193–200.
[568] Romano G, Favret G, Damato R, Bartoli E. Proximal reabsorption with changing tubular fluid inflow in rat nephrons. Exp Physiol 1998;83:35–48.
[569] Romano G, Favret G, Federico E, Bartoli E. The effect of intraluminal flow rate on glomerulotubular balance in the proximal tubule of the rat kidney. Exp Physiol 1996;81:95–105.
[570] Rome L, Grantham J, Savin V, Lohr J, Lechene C. Proximal tubule volume regulation in hyperosmotic media: Intracellular K^+, Na^+, and Cl^-. Am J Physiol 1989;257:C1093–100.
[571] Romero MF, Boron WF. Electrogenic Na^+/HCO_3^- co-transporters: Cloning and physiology. Ann Rev Physiol 1999;61:699–723.
[572] Romero MF, Fong P, Berger UV, Hediger MA, Boron WF. Cloning and functional expression of rNBC, an electrogenic Na $(^+)$-$HCO_3(^-)$ co-transporter from rat kidney. Am J Physiol 1998;274:F425–32.
[573] Romero MF, Hediger MA, Boulpaep EL, Boron WF. Expression cloning and characterization of a renal electrogenic Na^+/HCO_3^- co-transporter. Nature 1997;387:409–13.
[574] Romero JC, Knox FG. Mechanisms underlying pressure-related natriuresis: the role of the renin–angiotensin and prostaglandin systems. Hypertension 1988;11:724–38.
[575] Romero MF, Hopfer U, Madhun ZT, Zhou J, Douglas JG. Angiotensin II mediated signaling mechanisms and electrolyte transport in the rabbit proximal tubule. Renal Physiol Biochem 1991;14:199–207.
[576] Roos A, Boron WF. Intracellular pH. Physiol Reviews 1981;61:296–434.
[577] Rubera I, Tauc M, Bidet M, Poujeol C, Cuiller B, Watrin A, et al. Chloride currents in primary cultures of rabbit proximal and distal convoluted tubules. Am J Physiol 1998;275:F651–63.
[578] Ruiz OS, Arruda JAL. Regulation of the renal $Na–HCO_3$ co-transporter by cAMP and Ca-dependent protein kinases. Am J Physiol 1992;262:F560–5.
[579] Ruiz OS, Qiu Y-Y, Wang L-J, Arruda JAL. Regulation of the renal $Na–HCO_3$ co-transporter: IV. Mechanisms of the stimulatory effect of angiotensin II. J Am Soc Nephrol 1995;6:1202–8.
[580] Sabolic J, Burckhardt G. Proton pathways in rat renal brush border and basolateral membranes. Biochim Biophys Acta 1983;734:210–20.
[581] Saccomani G, Mitchell KD, Navar LG. Angiotensin II stimulation of Na^+-H^+ exchange in proximal tubule cells. Am J Physiol 1990;258:F1188–95.
[582] Sackin H. Stretch-activated potassium channels in renal proximal tubule. Am J Physiol 1987;253:F1253–62.
[583] Sackin H, Boulpaep EL. Models for coupling of salt and water transport. J Gen Physiol 1975;66:671–733.
[584] Sakhrani LM, Badie-Dezfooly B, Trizna W, Mikhail N, Lowe AG, Taub M, et al. Transport and metabolism of glucose by renal proximal tubular cells in primary culture. Am J Physiol 1984;246:F757–64.
[585] Saleh AM, Rudnick H, Aronson PS. Mechanism of H^+-coupled formate transport in rabbit renal microvillus membranes. Am J Physiol 1996;271:F401–7.
[586] Samarzija I, Hinton BT, Frömter E. Electrophysiological analysis of rat renal sugar and amino acid transport. II. Dependence on various transport parameters and inhibitors. Pflügers Arch 1982;393:190–7.
[587] Sanada H, Jose PA, Hazen-Martin D, Yu P, Xu J, Bruns DE, et al. Dopamine-1 receptor coupling defect in renal proximal tubule cells in hypertension. Hypertension 1999;33:1036–42.
[588] Sanada H, Yatabe J, Midorikawa S, Katoh T, Hashimoto S, Watanabe T, et al. Amelioration of genetic hypertension by suppression of renal G protein-coupled receptor kinase type 4 expression. Hypertension 2006;47:1131–9.
[589] Sasaki S, Ishibashi K, Yoshiyama N, Shiigai T. KCl co-transport across the basolateral membrane of rabbit renal proximal straight tubules. J Clin Invest 1988;81:194–9.

[590] Sasaki S, Shiigai T, Takeuchi J. Intracellular pH in the isolated perfused rabbit proximal straight tubule. Am J Physiol 1985;249:F417–23.
[591] Sasaki S, Shiigai T, Yoshiyama N, Takeuchi J. Mechanism of bicarbonate exit across basolateral membrane of rabbit proximal straight tubule. Am J Physiol 1987;252:F11–8.
[592] Sasaki S, Siragy HM, Gildea JJ, Felder RA, Carey RM. Production and role of extracellular guanosine cyclic 3′,5′ monophosphate in sodium uptake in human proximal tubule cells. Hypertension 2004;43:286–91.
[593] Sasaki S, Yoshiyama N. Interaction of chloride and bicarbonate transport across the basolateral membrane of rabbit proximal straight tubule. Evidence for sodium coupled chloride/bicarbonate exchange. J Clin Invest 1988;81:1004–11.
[594] Satoh T, Cohen HT, Katz AI. Different mechanisms of renal Na-K-ATPase regulation by protein kinases in proximal and distal nephron. Am J Physiol 1993;265:F399–405.
[595] Schafer JA, Andreoli TE. Perfusion of isolated mammalian renal tubules. In: Giebisch G, editor. Membrane transport in biology. Vol. IV: transport organs. Berlin: Springer-Verlag; 1979. p. 473–528.
[596] Schafer JA, Patlak CS, Andreoli TE. A component of fluid absorption linked to passive ion flows in the superficial pars recta. J Gen Physiol 1975;66:445–71.
[597] Schafer JA, Patlak CS, Andreoli TE. Fluid absorption and active and passive ion flows in the rabbit superficial pars recta. Am J Physiol 1977;233:F154–67.
[598] Schafer JA, Patlak CS, Troutman SL, Andreoli TE. Volume absorption in the pars recta. II. Hydraulic conductivity coefficient. Am J Physiol 1978;234:F340–8.
[599] Schafer JA, Troutman SL, Watkins ML, Andreoli TE. Volume absorption in the pars recta. I. "Simple" active Na^+ transport. Am J Physiol 1978;234:F332–9.
[600] Schatzmann HJ, Windhager EE, Solomon AK. Single proximal tubules of the *Necturus* kidney. II. Effect of 2,4-dinitrophenol and ouabain on water reabsorption. Am J Physiol 1958;195: 570–4.
[601] Schild L, Aronson PS, Giebisch G. Effects of apical membrane Cl^--formate exchange on cell volume in rabbit proximal tubule. Am J Physiol 1990;258:F530–6.
[602] Schild L, Aronson PS, Giebisch G. Basolateral transport pathways for K^+ and Cl^- in rabbit proximal tubule: effects on cell volume. Am J Physiol 1991;260:F101–9.
[603] Schild L, Giebisch G, Karniski L, Aronson PS. Chloride transport in the mammalian proximal tubule. Pflügers Arch 1986;407(Suppl. 2):S156–9.
[604] Schild L, Giebisch G, Karniski LP, Aronson PS. Effect of formate on volume reabsorption in the rabbit proximal tubule. J Clin Invest 1987;79:32–8.
[605] Schmidt U, Dubach UC. Activity of (Na^+,K^+)-stimulated adenosinetriphosphatase in the rat nephron. Pflügers Arch 1969;306:219–26.
[606] Schmidt U, Schmid H, Funk B, Dubach UC. The function of Na-K-ATPase in single portions of the rat nephron. Ann NY Acad Sci 1974;242:489–500.
[607] Schmitt BM, Biemesderfer D, Romero MF, Boulpaep EL, Boron WF. Immunolocalization of the electrogenic Na^+–HCO_3^- cotransporter in mammalian and amphibian kidney. Am J Physiol 1999;276:F27–38.
[608] Schneeberger EE, Lynch RD. Structure, function and regulation of cellular tight junctions. Am J Physiol 1992;262:L647–61.
[609] Schnermann J, Wahl M, Liebau G, Fischbach H. Balance between tubular flow rate and net fluid reabsorption in the proximal convolution of the rat kidney. Pflügers Arch 1968;304:90–103.
[610] Schultheis PJ, Clarke LL, Meneton P, Miller ML, Soleimani M, Gawenis LR, et al. Renal and intestinal absorptive defects in mice lacking the NHE3 Na^+/H^+ exchanger. Nature Genetics 1998;19:2282–5.
[611] Schultz SG. Homocellular regulatory mechanisms in sodium-transporting epithelia: Avoidance of extinction by "flush-through". Am J Physiol 1981;241:F579–90.
[612] Schultz SG. Membrane cross-talk in sodium-absorbing epithelial cells. In: Seldin DW, Giebisch G, editors. Chap. 11 in the kidney. Physiology and pathophysiology. New York: Raven Press; 1992. p. 287–99.
[613] Schultz SG, Hudson RL, Lapointe JY. Electrophysiological studies of sodium co-transport in epithelia: toward a cellular model. Ann NY Acad Sci 1985;456:127–35.
[614] Schuster VL. Effects of angiotensin on proximal tubular reabsorption. Fed Proc 1986;45:1444–7.
[615] Schuster VL, Kokko JP, Jacobson HR. Angiotensin II directly stimulates sodium transport in rabbit proximal convoluted tubules. J Clin Invest 1984;73:507–15.
[616] Schwartz GJ. Na^+-dependent H^+ efflux from proximal tubule: evidence for reversible Na^+-H^+ exchange. Am J Physiol 1981;241:F380–5.
[617] Schwartz GJ. Absence of Cl^-–OH^- or Cl^-–HCO_3^- exchange in the rabbit renal proximal tubule. Am J Physiol 1983;245:F462–9.
[618] Sciortino CM, Romero MF. Cation and voltage dependence of rat kidney electrogenic $Na(^+)$–$HCO_3(^-)$ co-transporter rkNBC, expressed in oocytes. Am J Physiol 1999;277:F611–23.
[619] Scott DA, Karniski LP. Human pendrin expressed in *Xenopus laevis* oocytes mediates chloride/formate exchange. Am J Physiol 2000;278:C207–11.
[620] Seely JF. Variation in electrical resistance along length of rat proximal convoluted tubule. Am J Physiol 1973;225:48–57.
[621] Seely JF. Effects of peritubular oncotic pressure on rat proximal tubule electrical resistance. Kidney Int 1973;4:28–35.
[622] Seifter JL, Aronson PS. Properties and physiologic roles of the plasma membrane sodium–hydrogen exchanger. J Clin Invest 1986;78:859–64.
[623] Seifter JL, Knickelbein R, Aronson PS. Absence of Cl-OH exchange and NaCl transport in rabbit renal microvillus membrane vesicles. Am J Physiol 1984;247:F753–9.
[624] Seikaly MG, Arant Jr. BS, Seney Jr. FD. Endogenous angiotensin concentrations in specific intrarenal fluid compartments of the rat. J Clin Invest 1990;86:1352–7.
[625] Seki G, Coppola S, Yoshitomi K, Burckhardt BC, Samarzija I, Muller-Berger S, et al. On the mechanism of bicarbonate exit from renal proximal tubular cells. Kidney Int 1996;49: 1671–7.
[626] Seki G, Taniguchi S, Uwatoko S, Suzuki K, Kurokawa K. Evidence for conductive Cl^- pathway in the basolateral membrane of rabbit renal proximal tubule S3 segment. J Clin Invest 1993;92:1229–35.
[627] Seki G, Taniguchi S, Uwatoko S, Suzuki K, Kurokawa K. Activation of the basolateral Cl^- conductance by cAMP in rabbit renal proximal tubule S3 segments. Pflügers Arch 1995;430:88–95.
[628] Seki G, Yamada H, Taniguchi S, Uwatoko S, Suzuki K, Kurokawa K. Mechanism of anion permeation in the basolateral membrane of isolated rabbit renal proximal tubule S3 segment. Am J Physiol 1997;272:C837–46.
[629] Selen G, Persson AEG. Hydrostatic and oncotic pressures in the interstitium of dehydrated and volume expanded rats. Acta Physiol Scand 1983;117:75–81.
[630] Seri I, Kone BC, Gullans SR, Aperia A, Brenner BM, Ballerman BJ. Locally formed dopamine inhibits Na^+-K^+-ATPase activity in rat renal cortical tubule cells. Am J Physiol 1988;255: F666–73.

[631] Seri I, Kone BC, Gullans SR, Aperia A, Brenner BM, Ballerman BJ. Influence of Na^+ intake on dopamine-induced inhibition of renal cortical Na^+-K^+-ATPase. Am J Physiol 1990;258:F52–60.

[632] Shenolikar S, Voltz JW, Minkoff CM, Wade JB, Weinman EJ. Targeted disruption of the mouse NHERF-1 gene promotes internalization of proximal tubule sodium-phosphate co-transporter type IIa and renal phosphate wasting. Proc Natl Acad Sci 2002;99:11470–5.

[633] Shenolikar S, Weinman EJ. NHERF: targeting and trafficking membrane proteins. Am J Physiol 2001;280:F389–95.

[634] Sheu J-N, Quigley R, Baum M. Heterogeneity of chloride/base exchange in rabbit superficial and juxtamedullary proximal convoluted tubules. Am J Physiol 1995;268:F847–53.

[635] Shi L-B, Fushimi K, Verkman AS. Solvent drag measurement of transcellular and basolateral membrane NaCl reflection coefficient in kidney proximal tubule. J Gen Physiol 1991;98:379–98.

[636] Shindo T, Spring KR. Chloride movement across the basolateral membrane of proximal tubule cells. J Membr Biol 1981;58:35–42.

[637] Shiuan D, Weinstein SW. Evidence for electroneutral chloride transport in rabbit renal cortical brush border membrane vesicles. Am J Physiol 1984;247:F837–47.

[638] Silverman M. Glucose reabsorption in the kidney. Can J Physiol Pharmacol 1981;59:209–24.

[639] Sohtell M. Electrochemical forces for chloride transport in the proximal tubules of the rat kidney. Acta Physiol Scand 1978;103:363–9.

[640] Soleimani M, Aronson PS. Ionic mechanism of Na^+–HCO_3^- co-transport in rabbit renal basolateral membrane vesicles. J Biol Chem 1989;264(31):18302–8.

[641] Soleimani M, Bizal GL. Functional indentity of a purified proximal tubule anion exchange protein: Mediation of chloride/formate and chloride/bicarbonate exchange. Kid Int 1996;50:1914–21.

[642] Soleimani M, Bizal GL, Anderson CC. A protein with anion exchange properties found in the kidney proximal tubule. Kid Int 1993;44:565–73.

[643] Soleimani M, Burnham CE. Na^+:HCO_3^- co-transporters (NBC): cloning and characterization. J Membr Biol 2001;183:71–84.

[644] Soleimani M, Grassi SM, Aronson PS. Stoichiometry of Na^+–HCO_3^- co-transport in basolateral membrane vesicles isolated from rabbit renal cortex. J Clin Invest 1987;79:1276–80.

[645] Soleimani M, Greeley T, Petrovic S, Wang Z, Amlal H, Kopp P, et al. Pendrin: an apical $Cl^-/OH^-/HCO_3^-$ exchanger in the kidney cortex. Am J Physiol 2001;280:F356–64.

[646] Soltoff SP, Mandel LJ. Active ion transport in the renal proximal tubule. I. Transport and metabolic studies. J Gen Physiol 1984;84:601–22.

[647] Soltoff SP, Mandel LJ. Active ion transport in the renal proximal tubule. II. Ionic dependence of the Na pump. J Gen Physiol 1984;84:623–42.

[648] Soltoff SP, Mandel LJ. Active ion transport in the renal proximal tubule. III. The ATP dependence of the Na pump. J Gen Physiol 1984;84:643–62.

[649] Spitzer A, Windhager EE. Effect of peritubular oncotic pressure changes on proximal tubular fluid reabsorption. Am J Physiol 1970;218:1188–93.

[650] Spring KR, Giebisch G. Kinetics of Na^+ transport in *Necturus* proximal tubule. J Gen Physiol 1977;70:307–28.

[651] Spring KR. A parallel path model for *Necturus* proximal tubule. J Membr Biol 1973;13:323–52.

[652] Stanton RC, Mendrick DL, Rennke HG, Seifter JL. Use of monoclonal antibodies to culture rat proximal tubule cells. Am J Physiol 1986;251:C780–6.

[653] Suzuki M, Morita T, Hanaoka K, Kawaguchi Y, Sakai O. A Cl^- channel activated by parathyroid hormone in rabbit renal proximal tubule cells. J Clin Invest 1991;88:735–42.

[654] Szaszi K, Kurashima K, Kaibuchi K, Grinstein S, Orlowski J. Role of the cytoskeleton in mediating cAMP-dependent protein kinase inhibition of the epithelial Na^+/H^+ exchanger NHE3. J Biol Chem 2001;276(44):40761–8.

[655] Terada Y, Tomita K, Nonoguchi H, Marumo F. Polymerase chain reaction localization of constitutive nitric oxide synthase and soluble guanylate cyclase messenger RNAs in microdissected rat nephron segments. J Clin Invest 1992;90:659–65.

[656] Thekkumkara TJ, Cookson R, Linas SL. Angiotensin (AT1A) receptor-mediated increases in transcellular sodium transport in proximal tubule cells. Am J Physiol 1998;274:F897–905.

[657] Thomas SR, Mikulecky DC. A network thermodynamic model of salt and water flow across the kidney proximal tubule. Am J Physiol 1978;235:F638–48.

[658] Thomson SC, Vallon V. Alpha-2-adrenoceptors determine the response to nitric oxide inhibition in the rat glomerulus and proximal tubule. J Am Soc Nephrol 1995;6:1482–90.

[659] Tisher CC, Kokko JP. Relationship between peritubular oncotic pressure gradients and morphology in isolated proximal tubules. Kidney Int 1974;6:146–56.

[660] Tormey JM, Diamond JM. The ultrastructural route of fluid transport in rabbit gall bladder. J Gen Physiol 1967;50:2031–60.

[661] Tripathi S, Boulpaep EL. Cell membrane water permeabilities and streaming currents in *Ambystoma* proximal tubule. Am J Physiol 1988;255:F188–203.

[662] Tse C-M, Brant SR, Walker MS, Pouyssegur J, Donowitz M. Cloning and sequencing of a rabbit cDNA encoding an intestinal and kidney-specific Na^+/H^+ exchanger isoform (NHE-3). J Biol Chem 1992;267:9340–6.

[663] Tse C-M, Levine SA, Yun CHC, Brant SR, Pouyssegur J, Montrose MH, et al. Functional characteristics of a cloned epithelial Na^+/H^+ exchanger (NHE3): resistance to amiloride and inhibition by protein kinase C. Proc Natl Acad Sci 1993;90:9110–4.

[664] Tsuchiya K, Wang W, Giebisch G, Welling PA. ATP is a coupling modulator of parallel NaK-ATPase-K-channel activity in the renal proximal tubule. Proc Natl Acad Sci 1992;89:6418–22.

[665] Tucker BJ, Blantz RC. Determinants of proximal tubular reabsorption as mechanisms of glomerulotubular balance. Am J Physiol 1978;235:F142–50.

[666] Tumlin JA, Hoban CA, Medford RM, Sands JM. Expression of Na-K-ATPase alpha- and beta-subunit mRNA and protein isoforms in the rat nephron. Am J Physiol 1994;266:F240–5.

[667] Turner RJ. Quantitative studies of co-transport systems: models and vesicles. J Membr Biol 1983;76:1–15.

[668] Turner RJ, Moran A. Further studies of proximal tubular brush border membrane D-glucose transport heterogeneity. J Membr Biol 1982;70:37–45.

[669] Turner RJ, Moran A. Heterogeneity of sodium-dependent D-glucose transport sites along the proximal tubule: evidence from vesicle studies. Am J Physiol 1982;242:F406–14.

[670] Turner RJ, Moran A. Stoichiometric studies of the renal outer cortical brush border membrane D-glucose transporter. J Membr Biol 1982;67:73–80.

[671] Turner RJ, Silverman M. Sugar uptake into brush border vesicles from dog kidney. II. Kinetics. Biochim Biophys Acta 1978;511:470–86.

[672] Ullrich KJ. Permeability characteristics of the mammalian nephron. In: Geiger SR, Orloff J, Berliner RW, editors. Handbook of physiology. section 8: renal physiology. Washington DC: American Physiological Society; 1973. p. 377–98.

[673] Ullrich KJ, Papavassiliou F. Contraluminal bicarbonate transport in the proximal tubule of the rat kidney. Pflügers Arch 1987;410:501–4.
[674] Ullrich KJ, Rumrich G. Direkte Messung der Waserpermabilitat corticaler Nephronabschnitte bei Verschiedenen Diuresezustanden. Pflügers Arch 1963;351:35–48.
[675] Ussing HH. Volume regulation of frog skin epithelium. Acta Physiol Scand 1982;114:363–9.
[676] Vallon V, Schwark JR, Richter K, Hropot M. Role of $Na(^{+})/H(^{+})$ exchanger NHE3 in nephron function: Micropuncture studies with S3226, an inhibitor of NHE3. Am J Physiol 2000;278:F375–9.
[677] Vallon V, Verkman AS, Schnermann J. Luminal hypotonicity in proximal tubules of aquaporin-1-knockout mice. Am J Physiol 2000;278:F1030–3.
[678] Vallon V, Grahammer F, Richter K, Bleich M, Lang F, Barhanin J, et al. Role of KCNE1-dependent K^{+} fluxes in mouse proximal tubule. J Am Soc Nephrol 2001;12:2003–11.
[679] Vallon V, Grahammer F, Volkl H, Sandu CD, Richter K, Rexhepaj R, et al. KCNQ1-dependent transport in renal and gastrointestinal epithelia. Proc Natl Acad Sci 2005;102:17864–9.
[680] Van der Goot F, Corman B. Axial heterogeneity of apical water permeability along rabbit kidney proximal tubule. Am J Physiol 1991;260:R186–91.
[681] Van der Goot FG, Podevin RA, Corman BJ. Water permeabilities and salt reflection coefficients of luminal basolateral and intracellular membrane vesicles isolated from rabbit kidney proximal tubule. Biochim Biophys Acta 1989;986:332–40.
[682] Van der Goot F, Ripoche P, Corman B. Determination of solute reflection coefficients in kidney brush-border membrane vesicles by light scattering: influence of the refractive index. Biochim Biophys Acta 1989;979:272–4.
[683] van Heeswijk MPE, van Os CH. Osmotic water permeabilities of brush border and basolateral membrane vesicles from rat renal cortex and small intestine. J Membr Biol 1986;92:183–93.
[684] van Os CH, Wiedner G, Wright EM. Volume flows across gallbladder epithelium induced by small hydrostatic and osmotic gradients. J Membr Biol 1979;49:1–20.
[685] Vari RC, Ott CE. *In vivo* proximal tubular fluid-to-plasma chloride concentration gradient in the rabbit. Am J Physiol 1982;242:F575–9.
[686] Veech RL, Lawson JWR, Cornell NW, Krebs HA. Cytosolic phosphorylation potential. J Biol Chem 1979;254:6538–47.
[687] Verkman AS. Mechanisms of regulation of water permeability in renal epithelia. Am J Physiol 1989;257:C837–50.
[688] Verkman AS, Dix JA, Seifter JL. Water and urea transport in renal microvillus membrane vesicles. Am J Physiol 1985;248:F650–5.
[689] Verkman AS, Ives HE. Water permeability and fluidity of renal basolateral membranes. Am J Physiol 1986;250:F633–43.
[690] Völkl H, Lang F. Electrophysiology of cell volume regulation in proximal tubules of the mouse kidney. Pflügers Arch 1988;411:514–9.
[691] Völkl H, Lang F. Ionic requirement for regulatory cell volume decrease in renal straight proximal tubules. Pflügers Arch 1988;412:1–6.
[692] Völkl H, Paulmichl M, Lang F. Cell volume regulation in renal cortical cells. Renal Physiol Biochem 1988;11:158–73.
[693] Wade JB, Welling PA, Donowitz M, Shenolikar S, Weinman EJ. Differential renal distribution of NHERF isoforms and their colocalization with NHE3, ezrin and ROMK. Am J Physiol 2001;280:C192–8.
[694] Wagner CA, Giebisch G, Lang F, Geibel JP. Angiotensin II stimulates vesicular H^{+}-ATPase in rat proximal tubular cells. Proc Natl Acad Sci 1998;95:9665–8.
[695] Walker AM, Bott PA, Oliver J, MacDowell MC. The collection and analysis of fluid from single nephrons of the mammalian kidney. Am J Physiol 1941;134:580–95.
[696] Wang T. Nitric oxide regulates HCO_3^{-} and Na^{+} transport by a cGMP-mediated mechanism in the kidney proximal tubule. Am J Physiol 1997;272:F242–8.
[697] Wang T, Chan YL. Time- and dose-dependent effects of protein kinase C on proximal bicarbonate transport. J Membr Biol 1990;117:131–9.
[698] Wang T, Egbert Jr. AL, Abbiati T, Aronson PS, Giebisch G. Mechanisms of stimulation of proximal tubule chloride transport by formate and oxalate. Am J Physiol 1996;271:F446–50.
[699] Wang T, Giebisch G, Aronson PS. Effects of formate and oxalate on volume absorption in rat proximal tubule. Am J Physiol 1992;263:F37–42.
[700] Wang T, Hropot M, Aronson PS, Giebisch G. Role of NHE isoforms in mediating bicarbonate reabsorption along the nephron. Am J Physiol 2001;281:F1117–22.
[701] Wang T, Inglis FM, Kalb RG. Defective fluid and $HCO(_3)(^{-})$ absorption in proximal tubule of neuronal nitric oxide synthase-knockout mice. Am J Physiol 2000;279:F518–24.
[702] Wang T, Segal AS, Giebisch G, Aronson PS. Stimulation of chloride transport by cAMP in rat proximal tubules. Am J Physiol 1995;268:F204–10.
[703] Wang T, Yang CL, Abbiati T, Schultheis PJ, Shull GE, Giebisch G, et al. Mechanism of proximal tubule bicarbonate absorption in NHE3 null mice. Am J Physiol 1999;277:F298–302.
[704] Wang T, Yang CL, Abbiati T, Shull GE, Giebisch G, Aronson PS. Essential role of NHE3 in facilitating formate-dependent NaCl absorption in the proximal tubule. Am J Physiol 2001;281:F288–92.
[705] Wang Z, Wang T, Petrovic S, Tuo B, Riederer B, Barone S, et al. Renal and intestinal transport defects in Slc26a6-null mice. Am J Physiol 2005;288:C957–65.
[706] Wareing M, Green R. Effect of formate and oxalate on fluid reabsorption from the proximal convoluted tubule of the anaesthetized rat. J Physiol 1994;477:347–54.
[707] Warner RR, Lechene C. Isosmotic volume reabsorption in rat proximal tubule. J Gen Physiol 1980;76:559–86.
[708] Warnock DG, Burg MB. Urinary acidification: CO_2 transport by the rabbit proximal straight tubule. Am J Physiol 1977;232:F20–5.
[709] Warnock DG, Eveloff J. NaCl entry mechanisms in the luminal membrane of the renal tubule. Am J Physiol 1982;242:F561–74.
[710] Warnock DG, Eveloff J. K-Cl co-transport systems. Kidney Int 1989;36:412–7.
[711] Warnock DG, Yee VJ. Neutral NaCl co-transport in the proximal tubule: evidence for the parallel exchanger model. Clin Res 1981;29:479A [Abstr.]
[712] Warnock DG, Yee VJ. Chloride uptake by brush border membrane vesicles isolated from rabbit renal cortex. J Clin Invest 1981;67:103–15.
[713] Warnock DG, Yee VJ. Anion permeabilities of the isolated perfused rabbit proximal tubule. Am J Physiol 1982;242:F395–405.
[714] Warnock DG, Reenstra WW, Yee VJ. Na^{+}/H^{+} antiporter of brush border vesicles: studies with acridine orange uptake. Am J Physiol 1982;242:F733–9.
[715] Weinman EJ, Biswas R, Steplock D, Douglass TS, Cunningham R, Shenolikar S. Sodium-hydrogen exchanger regulatory factor 1 (NHERF-1) transduces signals that mediate dopamine inhibition of sodium–phosphate co-transport in mouse kidney. J Biol Chem 2010;285:13454–60.
[716] Weinman EJ, Cunningham R, Wade JB, Shenolikar S. The role of NHERF-1 in the regulation of renal proximal tubule

sodium-hydrogen exchanger 3 and sodium-dependent phosphate co-transporter 2a. J Physiol 2005;567:27–32.
[717] Weinman EJ, Dubinsky W, Shenolikar S. Regulation of the renal Na^+-H^+ exchanger by protein phosphorylation. Kidney Int 1989;36:519–25.
[718] Weinman EJ, Minkoff C, Shenolikar S. Signal complex regulation of renal transport proteins: NHERF and regulation of NHE3 by PKA. Am J Physiol 2000;279:F393–9.
[719] Weinman EJ, Sansom SC, Knight TF, Senekjian HO. Alpha and beta adrenergic agonists stimulate water absorption in the rat proximal tubule. J Membr Biol 1982;69:107–11.
[720] Weinman EJ, Shenolikar S. Protein kinase C activates the renal apical membrane Na^+/H^+ exchanger. J Membr Biol 1986;93:133–9.
[721] Weinman EJ, Shenolikar S. Regulation of the renal brush border membrane Na^+/H^+ exchanger. Ann Rev Physiol 1993;55:289–304.
[722] Weinman EJ, Shenolikar S, Kahn AM. cAMP-associated inhibition of Na^+-H^+ exchanger in rabbit kidney brush-border membranes. Am J Physiol 1987;252:F19–25.
[723] Weinman EJ, Steplock D, Shenolikar S. CAMP-mediated inhibition of the renal brush border membrane Na^+-H^+ exchanger requires a dissociable phosphoprotein cofactor. J Clin Invest 1993;92:1781–6.
[724] Weinman EJ, Steplock D, Shenolikar S. Acute regulation of NHE3 by protein kinase A requires a multiprotein signal complex. Kidney Int 2001;60(2):450–4.
[725] Weinman EJ, Steplock D, Shenolikar S. NHERF-1 uniquely transduces the cAMP signals that inhibit sodium–hydrogen exchange in mouse renal apical membranes. FEBS Lett 2003;536:141–4.
[726] Weinman EJ, Steplock D, Wang Y, Shenolikar S. Characterization of a protein cofactor that mediates protein kinase A regulation of the renal brush border membrane Na^+-H^+ exchanger. J Clin Invest 1995;95:2143–9.
[727] Weinstein AM. A nonequilibrium thermodynamic model of the rat proximal tubule epithelium. Biophys J 1983;44: 153–70.
[728] Weinstein AM. Transport by epithelia with compliant lateral intercellular spaces: Asymmetric oncotic effects across the rat proximal tubule. Am J Physiol 1984;247:F848–62.
[729] Weinstein AM. Glucose transport in a model of the rat proximal tubule epithelium. Math Biosci 1985;76:87–115.
[730] Weinstein AM. Convective paracellular solute flux: a source of ion–ion interaction in the epithelial transport equations. J Gen Physiol 1987;89:501–18.
[731] Weinstein AM. Modeling the proximal tubule: complications of the paracellular pathway. Am J Physiol 1988;254: F297–305.
[732] Weinstein AM. Glomerulotubular balance in a mathematical model of the proximal nephron. Am J Physiol 1990;258:F612–26.
[733] Weinstein AM. Chloride transport in mathematical model of the rat proximal tubule. Am J Physiol 1992;263:F784–98.
[734] Weinstein AM. Performance of a kinetically defined Na^+/H^+ antiporter within a mathematical model of the rat proximal tubule. J Gen Physiol 1995;105:617–41.
[735] Weinstein AM. Coupling of entry to exit by peritubular K^+-permeability in a mathematical model of the rat proximal tubule. Am J Physiol 1996;271:F158–68.
[736] Weinstein AM, Stephenson JL. Models of coupled salt and water transport across leaky epithelial. J Membr Biol 1981;60:1–20.
[737] Weinstein AM, Stephenson JL, Spring KR. The coupled transport of water. In: Bonting SL, de Pont JJHHM, editors. Membrane Transport. Amsterdam: Elsevier/North-Holland Biomedical Press; 1981. p. 311–51.
[738] Welling LW, Welling DJ. Surface areas of brush border and lateral cell walls in the rabbit proximal nephron. Kidney Int 1975;8:343–8.
[739] Welling LW, Welling DJ. Shape of epithelial cells and intracellular channels in the rabbit proximal nephron. Kidney Int 1976;9:385–94.
[740] Welling LW, Welling DJ, Holsapple JW, Evan AP. Morphometric analysis of distinct microanatomy near the base of proximal tubule cells. Am J Physiol 1987;22:F126–40.
[741] Welling LW, Welling DJ, Ochs TJ. Video measurement of basolateral membrane hydraulic conductivity in the proximal tubule. Am J Physiol 1983;245:F123–9.
[742] Welling LW, Welling DJ, Ochs TJ. Relative osmotic effects of raffinose KCl and NaCl across basolateral cell membrane. Am J Physiol 1990;259:F594–7.
[743] Welling PA, Linshaw MA. Importance of anion in hypotonic volume regulation of rabbit proximal straight tubule. Am J Physiol 1988;255:F853–60.
[744] Welling PA, O'Neil RG. Ionic conductive properties of rabbit proximal straight tubule basolateral membrane. Am J Physiol 1990;258:F940–50.
[745] Welling PA, O'Neil RG. Cell swelling activates basolateral membrane Cl and K conductances in rabbit proximal tubule. Am J Physiol 1990;258:F951–62.
[746] Whitlock RT, Wheeler HO. Coupled transport of solute and water across rabbit gallbladder epithelium. J Clin Invest 1964;48:2249–65.
[747] Whittembury G, Malnic G, Mello-Aires M, Amorena C. Solvent drag of sucrose during absorption indicates paracellular water flow in the rat kidney proximal tubule. Pflügers Arch 1988;412:541–7.
[748] Whittembury G, Pas-Aliaga A, Biondi A, Carpi-Medina P, Gonzalez E, Linares H. Pathways for volume flow and volume regulation in leaky epithelia. Pflügers Arch 1985;405:S17–22.
[749] Wiederkehr MR, Di Sole F, Collazo R, Quinones H, Fan L, Murer H, et al. Characterization of acute inhibition of Na/H exchanger NHE-3 by dopamine in opossum kidney cells. Kidney Int 2001;59:197–209.
[750] Wiederkehr MR, Zhao H, Moe OW. Acute regulation of Na/H exchanger NHE3 activity by protein kinase C: role of NHE3 phosphorylation. Am J Physiol 1999;276:C1205–17.
[751] Wilcox CS, Baylis C. Glomerular–tubular balance and proximal regulation. In: Seldin DW, Giebisch G, editors. The kidney. Physiology and pathophysiology. New York: Raven Press; 1985. p. 985–1012.
[752] Williams AW. Electron microscopic changes associated with water absorption in the jejunum. Gut 1963;4:1–7.
[753] Williams Jr. JC, Schafer JA. A model of osmotic and hydrostatic pressure effects on volume absorption in the proximal tubule. Am J Physiol 1987;253:F563–75.
[754] Williams JC, Schafer JA. Cortical interstitium as a site for solute polarization during tubular absorption. Am J Physiol 1988;254:F813–23.
[755] Williams JM, Sarkis A, Lopez B, Ryan RP, Flasch AK, Roman RJ. Elevations in renal interstitial hydrostatic pressure and 20-hydroxyeicosatetraenoic acid contribute to pressure natriuresis. Hypertension 2007;49:687–94.
[756] Willmann JK, Bleich M, Rizzo M, Schmidt-Hieber M, Ullrich KJ, Greger R. Amiloride-inhibitable Na^+ conductance in rat proximal tubule. Pflügers Arch 1997;434:173–8.
[757] Windhager EE. Sodium chloride transport. In: Giebisch G, editor. Membrane transport in biology. Vol. IV transport organs. Berlin: Springer-Verlag; 1979. p. 145–214.
[758] Windhager EE, Boulpaep EL, Giebisch G. Electrophysiological studies on single nephrons. Proceedings of the 3rd

international congress of nephrology. Washington: Karger Basel; 1967. pp. 35–47

[759] Windhager EE, Whittembury G, Oken DE, Schatzmann HJ, Solomon AK. Single proximal tubules of the *Necturus* kidney. III. Dependence of H_2O movement on NaCl concentration. Am J Physiol 1959;197:313–8.

[760] Wong KR, Berry CA, Cogan MG. Flow dependence of chloride transport in rat S1 proximal tubules. Am J Physiol 1995;269: F870–5.

[761] Wong KR, Berry CA, Cogan MG. Alpha-1 adrenergic control of chloride transport in the rat S1 proximal tubule. Am J Physiol 1996;270:F1049–56.

[762] Wong NL, Whiting SJ, Mizgala CL, Quamme GA. Electrolyte handling by the superficial nephron of the rabbit. Am J Physiol 1986;250:F590–5.

[763] Wong PS, Johns EJ. The receptor subtype mediating the action of angiotensin II on intracellular sodium in rat proximal tubules. Br J Pharm 1998;124:41–6.

[764] Work J, Troutman SL, Schafer JA. Transport of potassium in the rabbit pars recta. Am J Physiol 1982;242:F226–37.

[765] Wright EM. The intestinal Na^+/glucose co-transporter. Ann Rev Physiol 1993;55:575–89.

[766] Wright EM. Renal $Na(^+)$-glucose co-transporters. Am J Physiol 2001;280:F10–8.

[767] Wright EM, Loo DDF, Panayotova-Heiermann M, Lostao MP, Hirayama BH, Mackenzie B, et al. Active sugar transport in eukaryotes. J Exp Biol 1994;196:197–212.

[768] Wu XC, Harris PJ, Johns EJ. Nitric oxide and renal nerve-mediated proximal tubular reabsorption in normotensive and hypertensive rats. Am J Physiol 1999;277:F560–6.

[769] Wu XC, Johns EJ. Nitric oxide modulation of neurally induced proximal tubular fluid reabsorption in the rat. Hypertension 2002;39:790–3.

[770] Xia P, Bungay PM, Gibson CC, Kovbasnjuk ON, Spring KR. Diffusion coefficients in the lateral intercellular spaces of Madin–Darby canine kidney cell epithelium determined with caged compounds. Biophys J 1998;74:3302–12.

[771] Xie M-H, Liu F-Y, Wong PC, Timmermans PBMWM, Cogan MG. Proximal nephron and renal effects of DuP 753, a nonpeptide angiotensin II receptor antagonist. Kidney Int 1990;38:473–9.

[772] Xie Q, Welch R, Mercado A, Romero MF, Mount DB. Molecular characterization of the murine Slc26a6 anion exchanger: functional comparison with Slc26a1. Am J Physiol 2002;283:F826–38.

[773] Yamaguchi I, Jose PA, Mouradian MM, Canessa LM, Monsma Jr. FJ, Sibley DR, et al. Expression of dopamine D1A receptor gene in proximal tubule of rat kidneys. Am J Physiol 1993;264: F280–5.

[774] Yang LE, Maunsbach AB, Leong PK, McDonough AA. Differential traffic of proximal tubule Na^+ transporters during hypertension or PTH: NHE3 to base of microvilli vs. NaPi2 to endosomes. Am J Physiol 2004;287:F896–906.

[775] Yang LE, Sandberg MB, Can AD, Pihakaski-Maunsbach K, McDonough AA. Effects of dietary salt on renal Na + transporter subcellular distribution, abundance, and phosphorylation status. Am J Physiol 2008;295:F1003–16.

[776] Yao X, Tian S, Chan HY, Biemesderfer D, Desir GV. Expression of KCNA10, a voltage-gated K channel in glomerular endothelium and at the apical membrane of the renal proximal tubule. J Am Soc Nephrol 2002;13:2831–9.

[777] Yau C, Rao L, Silverman M. Sugar uptake into a primary culture of dog kidney proximal tubular cells. Can J Physiol Pharmacol 1985;63:417–26.

[778] Yingst DR, Massey KJ, Rossi NF, Mohanty MJ, Mattingly RR. Angiotensin II directly stimulates activity and alters the phosphorylation of Na-K-ATPase in rat proximal tubule with a rapid time course. Am J Physiol 2004;287:F713–21.

[779] Yip KP, Tse CM, McDonough AA, Marsh DJ. Redistribution of Na^+/H^+ exchXer isoform NHE3 in proximal tubules induced by acute and chronic hypertension. Am J Physiol 1998;275:F565–75.

[780] Yip KP, Wagner AJ, Marsh DJ. Detection of apical $Na(^+)/H(^+)$ exchanger activity inhibition in proximal tubules induced by acute hypertension. Am J Physiol 2000;279: R1412–8.

[781] Yoshitomi K, Burckhardt BC, Frömter E. Rheogenic sodium-bicarbonate co-transport in the peritubular cell membrane of rat renal proximal tubule. Pflügers Arch 1985;405:360–6.

[782] Yoshitomi K, Frömter E. How big is the electrochemical potential difference of Na^+ across rat renal proximal tubular cell membranes *in vivo*?. Pflügers Arch 1985;405(Suppl. 1):S121–6.

[783] Yoshitomi K, Hoshi T. Intracellular Cl^- activity of the proximal tubule of *Triturus* kidney: dependence on extracellular ionic composition and transmembrane potential. Am J Physiol 1983;245:F359–66.

[784] You G, Lee W, Barros EJG, Kanai Y, Huo T, Khawaja S, et al. Molecular characterization of Na^+-coupled glucose transporters in adult and embryonic rat kidney. J Biol Chem 1995;270:29365–71.

[785] Yu AS, Cheng MH, Angelow S, Günzel D, Kanzawa SA, Schneeberger EE, et al. Molecular basis for cation selectivity in claudin-2-based paracellular pores: identification of an electrostatic interaction site. J Gen Physiol 2009;133:111–27.

[786] Yu ASL, Cheng MH, Coalson RD. Calcium inhibits paracellular sodium conductance through claudin-2 by competitive binding. J Biol Chem 2010;285:37060–9.

[787] Zeng C, Jose PA. Dopamine receptors. Important antihypertensieve counterbalance agains hypertensive factors. Hyptertension 2011;57:11–7.

[788] Zhang Y, Magyar CE, Norian JM, Holstein-Rathlou NH, Mircheff AK, McDonough AA. Reversible effects of acute hypertension on proximal tubule sodium transporters. Am J Physiol 1998;274:C1090–100.

[789] Zhang Y, Mircheff AK, Hensley CB, Magyar CE, Warnock DG, Chambrey R, et al. Rapid redistribution and inhibition of renal sodium transporters during acute pressure natriuresis. Am J Physiol 1996;270:F1004–14.

[790] Zhang Y, Norian JM, Magyar CE, Holstein-Rathlou NH, Mircheff AK, McDonough AA. *In vivo* PTH provokes apical NHE3 and NaPi2 redistribution and Na-K-ATPase inhibition. Am J Physiol 1999;276:F711–9.

[791] Zhang M, Yao B, Wang S, Fan X, Wu G, Yang H, et al. Intrarenal dopamine deficiency leads to hypertension and decreased longevity in mice. J Clin Invest 2011;121:2845–54.

[792] Zizak M, Lamprecht G, Steplock D, Tariq N, Shenolikar S, Donowitz M, et al. cAMP-induced phosphorylation and inhibition of Na^+/H^+ exchanger 3 (NHE3) are dependent on the presence but not the phosphorylation of NHE regulatory factor. J Biol Chem 1999;274:24753–8.

[793] Hirayama BA, Wong HC, Smith CD, Hagenbuch BA, Hediger MA, Wright EM. Intestinal and renal Na^+/glucose cotransporters share common structures. Am J Physiol 1991;261: C296–304.

[794] Schnermann J, Chou C, Ma T, Traynor T, Knepper MA, Verkman AS. Defective proximal tubular fluid reabsorption in transgenic aquaporin-1 null mice. Proc Natl Acad Sci 1998;95:9660–4.

This page intentionally left blank

CHAPTER

34

Sodium Chloride Transport in the Loop of Henle, Distal Convoluted Tubule, and Collecting Duct

Gerardo Gamba[1], *Wenhui Wang*[2] *and Laurent Schild*[3]

[1]Molecular Physiology Unit, Department of Nephrology and Mineral Metabolism, Instituto Nacional de Ciencias Médicas y Nutrición Salvador Zubirán, and Instituto de Investigaciones Biomédicas, Universidad Nacional Autónoma de México, Mexico City, Mexico

[2]Department of Pharmacology, New York Medical College, Valhalla, NY, USA

[3]Département de Pharmacologie et de Toxicologie, Université de Lausanne, Lausanne, Switzerland

INTRODUCTION

In this chapter we review the transport of ions by the loop of Henle, distal convoluted tubule, the connecting tubule, and the collecting duct. We will place special emphasis on the cellular and molecular mechanisms responsible for Na^+ transport in these regions, as well as the factors that regulate Na^+ transport.

ANATOMIC CONSIDERATIONS

The mammalian loop of Henle contains the descending thin limb, the ascending thin limb, and the thick ascending limb. The thin descending segment begins in the outer medulla after a gradual transition from the pars recta, and ends at the hairpin turn at the tip of Henle's loop. The thin ascending limb begins at the tip of Henle's loop and ends with its abrupt transition to the thick ascending limb. Loops of Henle that arise from superficial or midcortical nephrons may lack a thin ascending limb. In these short loops, thick limbs generally begin at, or slightly before, the hairpin turn (for a detailed discussion see Chapter 20).

The thick ascending limbs of Henle (TAL) of long looped nephrons begin at the boundary between the inner and outer medulla. The TAL of short looped nephrons does not extend as far into the medulla and may, in fact, be entirely cortical. The TAL extends up into the cortex, where it abuts the glomerulus of origin for that nephron and forms the macula densa part of the juxtaglomerular apparatus. The TAL is composed of two parts: a medullary portion and a cortical portion. The ratio of medullary to cortical TAL for a given nephron is a function of the depth of the glomerulus of the nephron such that superficial nephrons have primarily cortical thick limbs, while juxtamedullary nephrons possess primarily medullary thick limbs.

The distal nephron is divided into three segments: the distal convoluted tubule (DCT); the connecting tubule (CNT); and the collecting duct (CD). These segments are clearly delineated in the rabbit, but in many species the transition between segments is gradual. Therefore, distal tubule segments are most accurately defined by their respective cell types. The DCT begins about 50–100 μm beyond the macula densa, and is lined by a single type of cell: the DCT cell. Na^+-K^+-ATPase activity is particularly high in the basolateral membrane of this segment. The CNT forms a transition zone between the DCT and the cortical CD (CCD). In superficial nephrons, a single CNT drains the DCT into the collecting duct. The CNTs of deep nephrons, however, form arcades that ascend through the cortex draining several DCTs into a CCD. The CNT contains two types of cells: the CNT cell, exclusive to the CNT; and the intercalated cell, also found in the CD.

Seldin and Giebisch's The Kidney, Fifth Edition.
DOI: http://dx.doi.org/10.1016/B978-0-12-381462-3.00034-3

© 2013 Elsevier Inc. All rights reserved.

The collecting duct begins at or slightly before the confluence of two or more connecting tubules, and may be divided into three main parts: the CCD; the outer medullary collecting duct (OMCD); and the inner medullary collecting duct (IMCD). The CCD consists of at least three cell types: principal cells, responsible for Na^+ and K^+ transport; and two types of intercalated cells, responsible for H^+ and HCO_3^- transport. In the rabbit, principal cells account for 65–75% of cells in the CCD. The OMCD can be divided into two regions based on location: the outer stripe and the inner stripe. Approximately 80–90% of cells within the OMCD are principal cells. However, as will be discussed later, the functional properties of principal cells in the OMCD differ from those of the CCD. The IMCD extends from the junction between the inner and outer medulla to the tip of the papilla. The IMCD has been divided into three subsegments based on functional differences, including Na^+ transport. Intercalated cells account for about 10% of all cells in the initial portion of the IMCD, but are absent from the terminal IMCD.

Na^+ TRANSPORT IN THE LOOP OF HENLE

The loop of Henle is responsible for absorbing 25 to 40% of the filtered sodium load. Moreover, the dissociation of salt and water absorption by the loop of Henle is ultimately responsible for the capacity of the kidney either to concentrate or to dilute the urine. The active absorption of NaCl in the water-impermeable TAL serves both to dilute the urine and supply the energy for the single effect of countercurrent multiplication.

Salt Transport by Thin Descending and Thin Ascending Segments

There is morphologic and functional evidence of interspecies and inter- and intranephron heterogeneity in the thin loop segments. The morphologic characteristics of the loop of Henle are covered in detail in Chapter 20 of this volume. Generally, loops of Henle can be divided into two groups: long loops and short loops.[150] The thin descending limb of short loop nephrons is a simple, flat epithelium with few organelles and deep junctional complexes. The thin descending limbs of long loop nephrons are heterogeneous. The upper segment of these thin limbs has a larger diameter and thicker epithelium than short loops. The cells in this region have complicated basolateral interdigitations and apical microvilli, but shallow junctional complexes consist of a single junctional strand. These characteristics are most pronounced in rodents, while in rabbits and humans the upper portion of the thin descending limb has a simpler organization with less extensive interdigitation and deeper junctional complexes.

The lower portion of the thin descending limb consists of flat, noninterdigitating cells with a few apical microvilli and with junctional complexes of intermediate depth. There is little interspecies variability in this portion of the descending limb. The thin ascending limb, present only in long loop nephrons, consists of very flat cells connected by very shallow junctional complexes.

According to the passive models for urinary concentration (see Chapter 40), the thin descending limb should have very high water permeability such that the tubular fluid is concentrated by water abstraction rather than solute entry. *In vitro* microperfusion studies have confirmed that upper and lower portions of mammalian descending limbs are very permeable to water[149,150,176,219] (Table 34.1). The passive models also require the thin ascending limb to be rather impermeable to water, highly permeable to sodium chloride, and only modestly permeable to urea. As indicated in Table 34.1, *in vitro* microperfusion studies of thin ascending limb segments have demonstrated that these requirements are, in fact, satisfied.

The permeability of thin descending limb segments to sodium and chloride has been measured in hamsters, rats, and rabbits. In hamsters and rats, the upper portion of long looped descending limbs has a higher sodium permeability and higher P_{Na}/P_{Cl} ratio than do descending limbs of short looped nephrons. In contrast, there is little difference in P_{Na}/P_{Cl} between long and short loop nephrons in rabbits.[149,150] These results are consistent with the morphologic evidence of greater heterogeneity in rats and hamsters than in rabbits. The pathways for transepithelial movement of sodium and chloride in the descending limb are not defined.

The formation of dilute urine begins in the thin ascending limb of Henle. Fluid from the thin ascending limb is more dilute than fluid obtained from the descending limb at the same level. The decrease in osmolality is due primarily to a fall in the NaCl content of the luminal fluid. The mechanism for NaCl transport across the thin ascending limb epithelium is incompletely understood. Measurements of salt dilution potentials in microperfused thin ascending limb segments reveal them to be chloride selective, with P_{Cl}/P_{Na} ratios of 2.2 to 3.5 in rats and hamsters; segments perfused and bathed with symmetric solutions do not generate a spontaneous transepithelial voltage and do not show net transport of solute (reviewed in [150]). These observations have been interpreted to indicate that salt transport *in vivo* results from passive electrodiffusion rather than active transport. Although driven by passive electrochemical gradients, Cl^- movement across the TAL proceeds through a transcellular, and regulated, pathway. $^{36}Cl^-$ flux ratios and salt dilution voltages indicate that the Cl^- pathway discriminates among anions and is saturable.[150]

TABLE 34.1 Permeability Properties of Thin Limb of Henle Segments

	P_f (10^{-3}cm/sec)	P_{Na} (10^{-5}cm/sec)	P_{Cl} (10^{-5}cm/sec)	P_{Na}/P_{Cl}		P_{urea}(10^{-5}cm/sec)
				SDL	LDL_u	
DESCENDING LIMB						
Rabbit	240–250	1.61	–	0.75	0.76	1.5
Rat	227	34–47	–	0.61	5.0	
Hamster SDL	285	4.2	1.3	0.68	–	7.4
Hamster LDL_u	403	45.6	4.2	–	4–6	1.5
ASCENDING LIMB						
Rabbit	0	25.5	117	0.29		6.7
Rat	2.5	67.9	183.7	0.43		23.0
Hamster	3	87.6	196	0.47		18.5

Table from Reeves, W. B., and Andreoli, T. E. (2008). Sodium chloride transport in the loop of Henle, distal convoluted tubule, and collecting duct. In "The Kidney: Physiology and Pathophysiology," 4th edn, 849–888, Alpern, R. J., and Hebert, S. C. (eds.). Elsevier.
Note: P_{Na} and P_{Cl} determined from isotope flux measurements. P_{Na}/P_{Cl} determined from salt dilution voltages.
LDL_u: upper portion of long loop descending limb; P_f: osmotic water permeability; SDL: short loop descending limb.

NaCl Absorption in Thick Ascending Limb

General Features

Rocha and Kokko[257] and Burg and Green[33] first demonstrated the salient characteristics of salt absorption in rabbit medullary and cortical TAL segments, respectively. First, net salt absorption resulted in a lumen-positive transepithelial voltage (Ve, mV), which could be abolished by furosemide, and in dilution of the luminal fluid. Second, the transport of Cl^- under these circumstances occurred against both electrical and chemical gradients, and hence involved an active transport process. Third, both net chloride absorption and the transepithelial voltage depended on (Na^+, K^+)-ATPase activity, present in large amounts along the basolateral membrane of this segment. A final curious feature of the TAL is that this segment is a "hybrid epithelium" possessing a very low permeability to water, yet a high ionic conductance (Table 34.2). The ionic conductance determined from the fluxes of $^{22}Na^+$ and $^{36}Cl^-$ is approximately 20–50 mS/cm^2, and is cation selective ($P_{Na}/P_{Cl} = 2–6$). This high electrical conductance is unusual among epithelia with low water permeabilities.

Table 34.2 presents a summary of the important transport properties of the rabbit, mouse, and rat TAL which are relevant to the concentrating and diluting functions of this nephron segment. A low permeability to water is required for the TAL to function as a diluting segment. Hebert et al.,[138,140] and subsequently Hebert[132] demonstrated that the apical cell membrane constitutes the major barrier to transcellular water flow in this segment.

Studies of the electrophysiologic (Table 34.3) and biochemical properties of intact, isolated, perfused thick limb segments, and of apical and basolateral membranes of thick limb cells have provided insights into the specific transport mechanisms involved in salt absorption, and the origin of the lumen-positive transepithelial voltage in this nephron segment.[107,108,110–113,135,138–140] A model for salt absorption by the TAL, which integrates the results of these studies, is shown in Figure 34.1. Net Cl^- absorption by the TAL is a secondary active transport process. Luminal Cl^- entry into the cell is mediated by an electroneutral Na^+-K^+-$2Cl^-$ co-transport process driven by the favorable electrochemical gradient for sodium entry. More specifically, the net driving force for the entry of Cl^- into the cell is determined by the sum of the chemical gradients for Na^+, K^+, and Cl^-. Since the Na^+ gradient is maintained by the continuous operation of the basolateral membrane (Na^+,K^+)-ATPase pump, apical entry of Cl^- via the co-transporter ultimately depends on the operation of the basolateral (Na^+,K^+)-ATPase. Accordingly, maneuvers that inhibit ATPase activity, such as removal of K^+ from or addition of ouabain to, peritubular solutions leads to dissipation of the Na^+ gradient and subsequent inhibition of apical membrane Cl^- entry.[138,257]

In contrast to the electroneutral entry of Cl^- across the apical membrane, the majority of Cl^- efflux across the basolateral membrane proceeds through conductive pathways.[135,142,276] A favorable electrochemical gradient for Cl^- efflux through dissipative pathways has been demonstrated by Greger et al.[110] in the rabbit cTAL. In this study, an intracellular Cl^- activity of 22 mM, measured using single Cl^--selective microelectrodes, was substantially above the equilibrium value (5 mM) predicted from the intracellular voltage. Intracellular Cl^- is maintained at concentrations above electrochemical

TABLE 34.2 Transport Properties of Cortical and Medullary Thick Ascending Limb of Henle

	VTe (mV)	Pf (μm/sec)	PNa (μm/sec)	PCl (μm/sec)	JCl (pEq/cm2/sec)
RABBIT					
cTAL	3–10	11	0.28	0.14	2500
mTAL	3–7	0	0.63	0.11	5600
MOUSE					
cTAL	8–12		0.63	0.51	5200
mTAL					
−ADH	5	6–23	0.23	0.10	3000
+ADH	10	6–23	0.25	0.12	10,900
RAT					
cTAL	7–8	0			8405
mTAL	5–6	0			9300

Table from Reeves, W. B., and Andreoli, T. E. (2008). Sodium chloride transport in the loop of Henle, distal convoluted tubule, and collecting duct. In "The Kidney: Physiology and Pathophysiology," 4th edn, 849–888, Alpern, R. J., and Hebert, S. C. (eds.). Elsevier.
Note: Values of J_{Cl} for rat were calculated assuming an inner tubule diameter of 20 μm.
J_{Cl}: chemically determined net rate of Cl^- absorption; P_f: osmotic water permeability; P_{Na}, P_{Cl}: isotopically determined Na^+ and Cl^- permeabilities; V_{Te}: transepithelial voltage (lumen positive).

TABLE 34.3 Basal Electrophysiologic Parameters of Thick Ascending Limb Segments

	Ve (mV)	Ge	Gc (mS/cm^2)	Gs	Va (mV)	Vbl	Ra/Rb
Rabbit cTAL	4–8	33	12	21	76	−69	2.0
Mouse mTAL	3–7	70–100	45–50	40–60	55.4	−50.7	1.2
Mouse cTAL	7–14	88	39	49			
Hamster mTAL	4.0	934				−72	

Table from Reeves, W. B., and Andreoli, T. E. (2008). Sodium chloride transport in the loop of Henle, distal convoluted tubule, and collecting duct. In "The Kidney: Physiology and Pathophysiology," 4th edn, 849–888, Alpern, R. J., and Hebert, S. C. (eds.). Elsevier.
G_c: transcellular conductance; G_e: transepithelial conductance; G_s: paracellular conductance; V_a: apical membrane voltage; V_{bl}: basolateral membrane voltage; V_c: transepithelial voltage; R_a/R_b: apical to basolateral membrane resistance.

equilibrium by the continued entry of Cl^- via the apical Na^+-K^+-$2Cl^-$ co-transporter. Blocking Cl^- entry through this pathway with furosemide or substitution of extracellular Cl^- by gluconate, caused the intracellular Cl^- activity to fall to a value close to its equilibrium.[110] In addition to electrodiffusive efflux of Cl^- across the basolateral membrane, a component of electroneutral KCl co-transport has been proposed in some species,[112] and the the K^+-Cl^- co-transporter, KCC4, has been shown to be present at the TAL basolateral membrane.[25]

In addition, according to the model in Figure 34.1, the potassium that enters TAL cells via the Na^+-K^+-Cl^- co-transporter recycles, to a large extent, across the apical membrane by way of a K^+ conductive pathway. This apical K^+ recycling serves several purposes. First, it ensures a continued supply of luminal potassium in order to sustain Na^+-K^+-Cl^- co-transport. Without recycling, the luminal K^+ concentration would fall rapidly as a consequence of K^+ entry via Na^+-K^+-Cl^- co-transport, and would limit net NaCl absorption. Second, the apical membrane potassium current provides a pathway for net potassium secretion by the TAL, which is an active process, ultimately driven by the (Na^+,K^+)-ATPase, proceeding in the face of a lumen-positive transepithelial potential. Third, under open circuit conditions, the transcellular and paracellular pathways form a current loop in which the currents traversing the two pathways are of equal size but opposite direction. The potassium current from cell to lumen polarizes the lumen and causes an equivalent current to flow from lumen to bath through the paracellular pathway.[113] Since the paracellular pathway is cation-selective ($P_{Na}/P_{Cl} = 2–6$), the majority of the current through the paracellular pathway is carried by sodium moving from the lumen to the interstitium. This paracellular absorption of sodium increases the efficiency of sodium transport by the TAL. With reference to Figure 34.1, for each

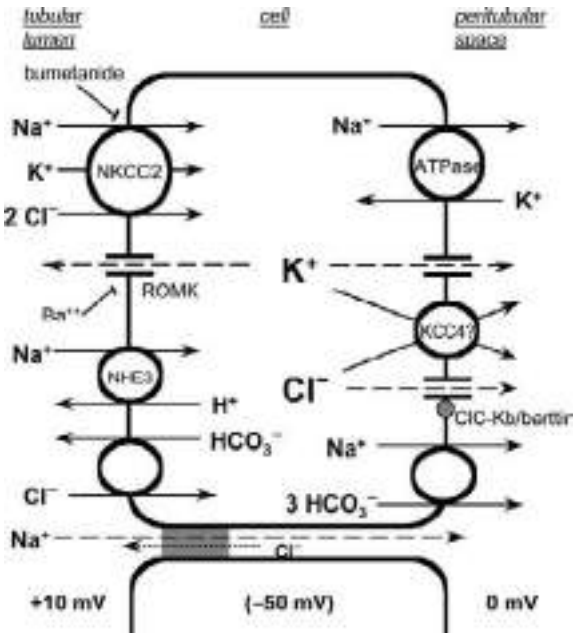

FIGURE 34.1 **A model depicting the major pathways involve in NaCl absorption mechanism by the thick ascending limb.** Dashed lines indicate passive movements down electrochemical gradient. *From Reeves, W. B., and Andreoli, T. E. (2008). Sodium chloride transport in the loop of Henle, distal convoluted tubule, and collecting duct. In "The Kidney: Physiology and Pathophysiology," 4th edn, 849–888, Alpern, R. J., and Hebert, S. C. (eds.). Elsevier.*

Na^+ transported through the cell – and requiring utilization of ATP – one Na^+ is transported through the paracellular pathway without any additional expenditure of energy. Finally, the apical K^+ current satisfies the continuity requirement imposed by a high degree of conductive Cl^- efflux across basolateral membranes.[135,214] A small component of sodium transport by the TAL (5–10%) is accounted for by sodium bicarbonate absorption.[105] Sodium bicarbonate absorption is thought to be mediated by an apical membrane amiloride-sensitive Na^+/H^+ exchanger and a basolateral membrane electrogenic $3Na^+/(HCO_3^-)$ co-transporter.[105] The following sections will describe the individual components of the mechanism for TAL salt transport (Figure 34.1) in greater detail.

Apical Na^+-K^+-Cl^- Co-Transport

The predominant mode for Cl^- entry into the TAL cell is via a Na^+-K^+-$2Cl^-$ co-transporter.[107,135,138] A characteristic feature of this transporter is its sensitivity to inhibition by furosemide, bumetanide, and other 5-sulfamoylbenzoic acid derivatives.[253] The first demonstration of dependence on luminal sodium for Cl^- absorption was reported by Greger in isolated perfused rabbit cortical TAL segments.[107] Moreover, a requirement for luminal potassium has been demonstrated for sodium and chloride absorption in both mouse medullary[135] and rabbit[111] cortical thick ascending segments perfused *in vitro*. As a result of these studies, it is now recognized that Cl^- absorption in the TAL generally depends on the simultaneous presence of Na^+ and K^+ (or NH_4) in the lumen.

Measurement of isotope flux into TAL cells or membrane vesicles prepared from the inner stripe of outer medulla have delineated further the ionic requirements and stoichiometry of $1Na^+$-$1K^+$-$2Cl^-$ co-transport.[34,171,174] There is a general agreement that the co-transporter in the thick ascending limb conforms to this stoichiometry under most experimental conditions. However, under certain circumstances, which will be discussed below, apical membrane NaCl entry may be independent of luminal potassium. Early work suggested differences in apparent affinity constant for chloride along TAL[71,108,147,174] which suggested axial heterogeneity in the properties of the Na^+-K^+-$2Cl^-$ co-transporter, because Greger,[108] and Hus-Citharel and Morel[147] examined the cortical TAL, while Koenig et al.[174] and Burnham et al.[34] prepared membranes from the medulla. An axial heterogeneity in the regulation of co-transporter activity as the thick limb ascends from the medulla into the cortex might be anticipated. This is explained by differences in affinity constant for ions of axially distributed along TAL of alternatively spliced variants of the Na^+-K^+-$2Cl^-$ co-transporter.

SLC12A1 gene encodes for the absorptive form of the co-transporter, referred to as BSC1 or NKCC2, located exclusively at the apical membrane of TAL, simultaneously cloned by Gamba et al.[94] and Payne et al.[241] Molecular biology of this gene is extensively discussed in Chapter 32. Inactivating mutations in the *SLC12A1* gene is the cause of Bartter syndrome type I. This syndrome, characterized by hypokalemia, metabolic alkalosis, hyperaldosteronism, and low blood pressure, results from a defect in salt absorption by the TAL, providing strong support for the conclusion that NKCC2 is responsible for apical Na^+-K^+-$2Cl^-$ co-transport in the thick ascending limb.[92] The NKCC2 cDNA encodes a protein containing ~1100 amino acids and having a predicted molecular weight of 115–120 kDa.[92] The observed molecular weight, however, is approximately 150 kDa due to extensive glycosylation. Hydropathy analysis of the amino acid sequence predicts a protein having 12 putative transmembrane spanning domains (TM). Six isoforms of NKCC2 have been identified that are results of alternative splicing in the 5′ and 3′ regions of the NKCC2 gene. Three 5′ splice products, termed A, B, and F, are expressed in all mammalian species.[92] These variants differ only in a 96 bp region, which encodes the amino acids forming half of the second TM and interconnecting segment between TM2 and 3. The isoforms show differential expression within the thick ascending limb. Using RT-PCR, Yang et al.[345] examined

the distribution of NKCC2 isoforms in single nephron segments. The A isoform was found in both the cortical and medullary TAL, the B isoform was restricted to the cortical TAL, while the F isoform was present in the medullary, but not cortical, TAL and, to a lesser extent, in the outer medullary collecting duct. Altough the three variants mediate Na^+-K^+-$2Cl^-$ co-transport, they have different transport properties. The A and B isoforms have higher affinities for Na^+, K^+, and Cl^- than the F isoform. The A isoform appears to have a greater transport capacity than the other isoforms[244] (see Figure 32.3 of Chapter 32). Thus, the presence of the A and F isoform in the medullary thick ascending limb could account for the observed high rates of NaCl transport relative to the cortical segment (Table 34.2), while the expression of the A and B isoforms in the cortical thick ascending limb may subserve the ability to achieve lower luminal NaCl concentrations in that segment. As discussed with detail in Chapter 32, difference in affinity for ions among the NKCC2 variants B and F has been attributed to only six residues within these exons.

There is experimental evidence that the apical co-transporter in TAL might operate as a simple NaCl symporter under certain conditions. Eveloff and coworkers have reported potassium-independent, furosemide-sensitive NaCl transport in isolated rabbit TAL cells and membrane vesicles prepared from TAL cells.[71] Potassium dependence of the co-transporter might be subject to physiologic regulation. Eveloff and Calamia[72] have shown that under isotonic conditions the chloride-dependent, furosemide-sensitive component of sodium uptake is independent of potassium, but that under hypertonic conditions the sodium uptake becomes K^+-dependent. Sun et al.[301] have also reported that, in perfused mouse medullary TAL segments, basal sodium chloride transport was K^+-independent, but that upon stimulation of salt transport by ADH NaCl transport became dependent on luminal K^+. The NKCC2 variants at the carboxyl terminal domain help to explain this discrepancy. Alternative splicing at the 3′ end of NKCC2 produces additional isoforms with either long (C9) or short (C4) carboxy-termini.[221] Under isotonic conditions, the truncated (C4) isoforms do not mediate Na^+-K^+-$2Cl^-$ co-transport. Under hypotonic conditions, however, the C4 isoforms mediate K^+-independent NaCl co-transport, which is inhibited by cAMP[243] and may account for the K^+-independent NaCl transport noted in earlier studies.[72,301] Of note, the C4 isoform inhibit the transport activity of the full-length (C9) isoforms when the two are co-expressed,[245] and this inhibition is relieved by cAMP.[245] The inhibition of C9 NKCC2 isoforms by C4 isoforms suggests a physical interaction between these proteins. Biochemical studies have established that NKCC2 exists as a dimer.[295] Thus, it is possible that different combinations of NKCC2 isoforms within the dimer could produce transporters with a wide variety of functional properties. Moreover, the subunit composition of the dimers may be a point of physiologic regulation. Alternatively, the C4 isoform could alter membrane trafficking or stability of the C9 isoform. The C4 isoform resides predominantly in subapical vesicles rather than the cell membrane.[245] Meade et al.[209] found that co-expression of the C4 isoform reduced the abundance of C9 isoform in *Xenopus* oocyte membranes. The reduction in cell surface C9 isoform was reflected by a commensurate reduction in bumetanide-sensitive Rb uptake. The inhibitory effect of C4 on C9 cell surface localization could be prevented by cAMP or by disruption of microtubules, suggesting that C4 alters the trafficking of C9 in or out of the apical membrane.

Evidence for a model of two distinct binding sites for Cl^- with differing affinities follows from studies of Forbush and Palfrey[80] on ^{3}H-bumetanide binding to renal medullary membranes. In these studies, Na^+, K^+, and Cl^- were all required for bumetanide to bind to canine renal medullary membranes. The K_a values for sodium and potassium were 2 mM and 1 mM, respectively. The effect of Cl^- concentration on bumetanide binding was biphasic. At low concentrations (<5 mM), Cl^- enhanced ^{3}H-bumetanide-binding. These data are consistent with a model in which the binding of Cl^- to a high-affinity site exposes a second lower-affinity site that may be occupied either by bumetanide or by the second Cl^-. However, functional studies using chimeras constructed between the ubiquitously expressed Na^+-K^+-$2Cl^-$ co-transporter NKCC1 encoded by *SLC12A2* gene and NKCC2, as well as in wild-type and mutant variants A, B, and F of NKCC2, revealed that changes in chloride affinity are not paralleled by changes in bumetanide affinity, and *vice versa*, questioning the competition of chloride and bumetanide for a single-binding site (see Chapter 32 on NaCl co-transporters).

The binding of ions to the co-transporter is thought to be ordered and cooperative.[185] Thus, sodium binds to the co-transporter first, and promotes binding of a Cl^- and then K^+. Binding of K^+ to its site, in turn, promotes binding of the second Cl^- to the co-transporter. Once fully occupied, the co-transporter–ion complex translocates to the internal surface of the cell membrane, where debinding occurs in the same order. The full reaction sequence of binding and debinding results in inward $Na^+/K^+/2Cl^-$ transport. Partial reactions permit K^+/K^+ and Na^+/Na^+ exchange.

Apical Potassium (K) Channels

Studies of isolated, perfused, thick limb segments have established that the predominant, and perhaps

only, conductance across the apical membrane is to potassium.[113,136] Blockade of the apical K conductance by luminal barium in mouse medullary thick ascending limb (mTAL) decreases the transepithelial electrical conductance (G_e) by roughly 50%, while increasing the apical-to-basolateral membrane resistance ratio (Ra/Rb) from 1.9 to 12.9.[135] Moreover, changes in the luminal K^+ concentration produce essentially Nernstian changes in the apical membrane electrical potential.[135] Electrophysiological studies demonstrated that the apical membrane K^+ conductance is sufficient to recycle the potassium uptake via the Na^+-K^+-$2Cl^-$ co-transporter.

The properties of the apical membrane K^+ conductance have been studied in plasma membrane vesicles prepared from outer renal medulla.[34,252] Conductive K^+ fluxes in these vesicles can be measured by loading the vesicles with a high concentration of potassium, and then removing the potassium from the external solutions. Tracer amounts of $^{86}Rb^+$ are then added to the extravesicular solutions to begin uptake. Under these conditions, the outwardly directed K^+ gradient creates an inside-negative diffusion potential that drives $^{86}Rb^+$ uptake into the vesicles. Burnham et al.[34] and Reeves et al.[252] were thus able to demonstrate barium-sensitive $^{86}Rb^+$ flux in membranes from rabbit outer medulla. The Rb^+ flux was conductive as judged by its inhibition via collapse of the intravesicular voltage or by measurement of intravesicular voltage using voltage-sensitive dyes. The $K_{0.5}$ value for barium inhibition of Rb^+ flux was 50−100 μM.[34] The barium-sensitive Rb^+ flux was also dependent on the calcium activity within the vesicles.[34] Moreover, in reconstituted proteoliposomes prepared from porcine outer medulla, the calcium dependence of the K^+ conductance was modulated by a high-affinity ($K_{0.5}$ = 0.1 nM) calmodulin-binding site.[173]

The patch-clamp technique has identified two types of apical K^+ channels in the TAL, a low-conductance (35 pS) K^+ channel and an intermediate-conductance (70 pS) K^+ channel in the apical membrane of the TAL. The 35 pS K^+ channel is observed in the apical membrane of rabbit,[327] rat,[325] and mouse.[202] Moreover, exposure of the cytoplasmic surface of the patch to ATP inhibited channel activity. In addition to the 35 pS K^+ channel, Bleich et al.[23] and Wang[325] described an intermediate conductance (60−70 pS) K^+ channel in rat TAL segments. Like the low conductance K^+ channel, the 70 pS K^+ channel was inhibited by ATP and barium.[325] In addition, the channel activity was voltage-dependent with depolarization increasing its activity; the channel could be blocked by quinine, verapamil, and diltiazem, and was inhibited at low cytosolic pH. The activities of both the intermediate and low conductance K^+ channels are increased by high dietary potassium.[200] An overview regarding regulation of

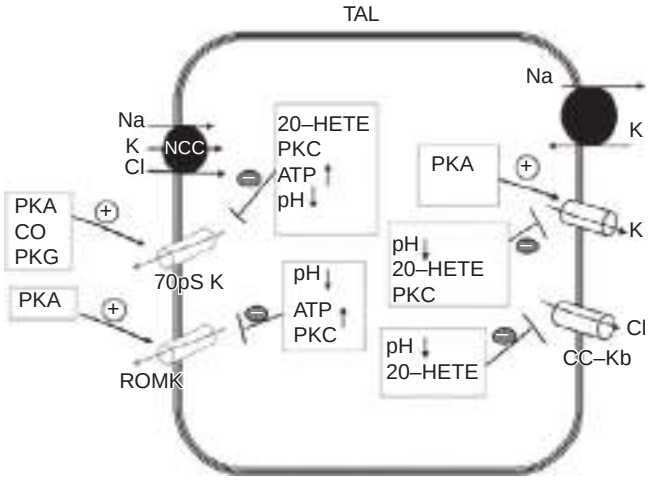

FIGURE 34.2 **A cell scheme illustrating the inhibitory and stimulatory factors for regulation of apical and basolateral ion channels.**

apical K^+ channels in the TAL is summarized in Figure 34.2, and detailed information can also be found in the review articles.[141,329]

An ATP-dependent K^+ channel was cloned from rat kidney by Ho et al.[143] This channel, termed ROMK (Renal Outer Medullary K^+ channel), is the prototype for a large family of inward rectifying K^+ channels (K_{IR} channels). K_{IR} channels have two transmembrane spanning domains, intracellular N- and C-termini, and an extracellular helical domain between the two transmembrane domains. Structural studies of other K_{IR} channels have established that the channels exist as heteromers of four K_{IR} subunits.[230,231,307] The extracellular helical domain appears to form the outer vestibule and selectivity filter of the channel, while the second transmembrane domain lines the pore cavity.

$ROMK^+$ channels have three alternatively spliced forms and they are ROMK2 (Kir1.1b), ROMK3 (Kir1.1c),[26,350] and ROMK6 (Kir1.1d).[178] The encoded ROMK proteins differ at the beginning of the N-terminus; ROMK2 has the shortest N-terminus[177] and splicing adds either 19 or 26 amino acids for ROMK1 or ROMK3, respectively. Relative ROMK mRNA abundance measured by competitive PCR has shown that ROMK2 and ROMK3 are much more abundant than ROMK1 or ROMK6 in rat kidney.[17] Moreover, single-nephron PCR analysis indicated that ROMK1 is expressed in the collecting duct, while both ROMK2 and ROMK3 are expressed in the medullary and cortical thick ascending limb.[26] Immunolocalization of ROMK proteins, using antibodies that recognized all three isoforms, revealed apical membrane localization in the medullary and cortical thick ascending limb, the late distal tubule, the connecting tubule, and the cortical collecting duct.[210,341] Oddly, the expression of ROMK in the thick limb was

heterogeneous, with some cells lacking demonstrable staining. In contrast, the expression of the Na^+-K^+-$2Cl^-$ co-transporter was uniform within the TAL.[341] This implies that apical K^+ recycling by the ROMK-positive cells may be sufficient to supply K^+ for Na^+-K^+-$2Cl^-$ transport in the ROMK-negative cells.

The 35 pS channel conductance of ROMK corresponds to the low conductance K^+ channel described by Wang et al.[325] The current−voltage relations exhibit weak inward rectification, which is due to blocking of the channel by intracellular Mg^{2+} or polyamines.[177] The activity of this channel is modulated by intracellular pH and by intracellular ATP, through both phosphorylation-dependent and phosphorylation-independent pathways.[141] The maintenance of $ROMK^+$ channel activity requires protein kinase A (PKA)-mediated phosphorylation and deletion of any two of three PKA-phosphorylation sites inactivates ROMK.[203] Phosphorylation of ROMK affects both channel activity (P_o) and the number of functional channels in the plasma membrane.[346] In addition, PKA-induced phosphorylation of ROMK enhances the sensitivity of the $ROMK^+$ channel to phosphatidylinositol phosphates (PIP2).[189]

Nucleotides have both inhibitory and stimulatory effects on ROMK activity. At micromolar concentrations, ATP stimulates ROMK activity via PKA-mediated phosphorylation and production of PIP_2.[329] Millimolar concentrations of ATP inhibit ROMK activity.[326,328] The inhibition by ATP can be relieved by increasing concentrations of ADP or by PIP_2.[198] Certain other members of the K_{IR} family are also inhibited by ATP. The ATP sensitivity of these channels—for example, $K_{IR}6.2$—is endowed by the association of regulatory subunits.[51] These regulatory subunits, such as the sulfonylurea receptor (SUR) and CFTR,[3,151] belong to the ABC gene family which is characterized by nucleotide-binding domains. The sulfonylurea receptor, together with $K_{IR}6.2$, forms the glibenclamide-sensitive, ATP-sensitive K^+ channel that controls insulin secretion by pancreatic β-cells.[151] The K_{IR}/SUR channels are more sensitive to inhibition by ATP than those of heterologously expressed $ROMK^+$ channels. In addition, the native 35 pS K^+ channel, but not the heterologously expressed $ROMK^+$ channel, is inhibited by glibenclamide.[324] These observations have prompted the search for regulatory subunits for the $ROMK^+$ channel. Both SUR2B[18] and CFTR[216] are expressed in the thick ascending limb and collecting duct, making them candidates for ROMK regulation. In transfection studies, co-expression of ROMK with either SUR2B[305] or CFTR[208,264] dramatically increases both the nucleotide dependence and glibenclamide sensitivity of ROMK. Immunoprecipitation studies confirmed that one of the ROMK isoforms, ROMK2, physically interacts with SUR2B.[305] The role of CFTR in regulating the native $ROMK^+$ channels has been further suggested by the finding that PKA-induced regulation of ATP sensitivity of the native 35 pS K^+ channel is compromised in CFTR knockout mice.[199] Figure 34.3 is a cartoon illustrating the current view regarding the composition of the native ATP-sensitive K^+ channel in the apical membrane of the TAL.

The electrophysiologic properties of the ROMK channels have strongly suggested that ROMK is the native 35 pS K^+ channel expressed in the thick ascending limb.[47,233,329] In support of this view, no low-conductance K^+ channels were detected by patch-clamp analysis in ROMK knockout mice.[201] Moreover, deleting the gene product encoding ROMK also abolished the expression of intermediate conductance K^+ channels in the thick ascending limb.[200] It has been proposed that the intermediate conductance channel may be a heteromeric protein containing ROMK and other, as yet unidentified, subunits. The notion that one of the ROMK channels is the predominant channel responsible for apical K^+ recycling in the thick ascending limb is strongly supported by the finding of mutations in the ROMK gene in some families with Bartter syndrome.[290] Thus, the presence of ROMK mutations as a cause of Bartter syndrome indicates the important role of ROMK in net salt absorption by the thick ascending limb.

Basolateral Potassium (K) Channels

Basolateral K^+ channels in the TAL play an important role in the regulation of transepithelial transport.[98,141] They are responsible for generating basolateral membrane potential which is essential for Cl diffusion across the basolateral membrane in the TAL. Activation of basolateral K^+ channels in the TAL is expected to hyperpolarize the basolateral cell membrane, thereby augmenting the driving force for Cl exit across the basolateral membrane. In contrast, decreasing basolateral K^+ channel activity depolarizes the cell membrane potential, thereby diminishing the driving force for Cl^- exit across the basolateral membrane. Consequently, inhibition of Cl^- exit leads to an increase in intracellular Cl^- concentration which decreases the activity of NKCC2, probably via inhibiting WNK3-SPAK.[247]

The physiological importance of the basolateral K^+ channels in maintaining transepithelial membrane transport in the TAL and distal nephron is best demonstrated in SeSAME disease (Seizures, Sensorineural deafness, Ataxia, Mental retardation, and Electrolyte imbalance). This disease is the result of defective gene product encoding KCNJ10, an inwardly-rectifying K^+ channel,[281] which is also expressed in the basolateral membrane of TAL and distal nephron.[183] The renal phenotypes of SeSAME disease are hypokalemia, metabolic alkalosis, and hypomagnesemia. Presumably, defective basolateral K^+ channels cause membrane potential depolarization,

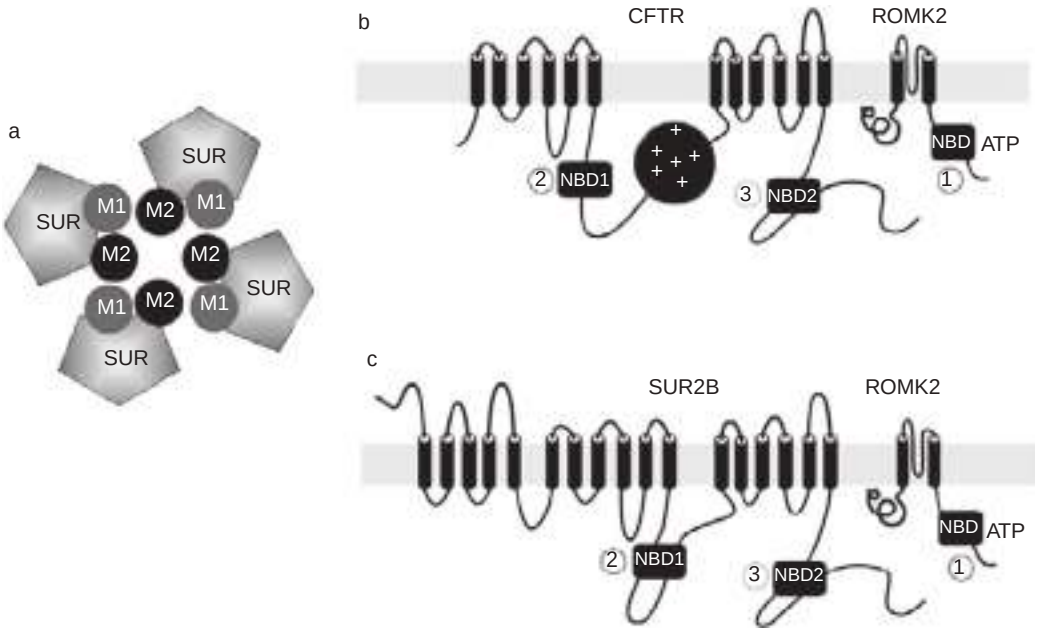

FIGURE 34.3 **Assembly of the native ATP-sensitive K channels in the TAL with ATP-binding cassette [ABC] proteins.** (a) The proposed hetero-octameric complex forming the native ATP-sensitive K channels in the TAL with four K_{IR} subunits and four sulfonylurea receptor [SUR] subunits. (b) The topology of CFTR and ROMK channels proposed to form kidney K_{ATP} channels. A single nucleotide-binding domain [NBD, 1] is present on the C-terminus of ROMK while two NBDs [numbered 2 and 3] are found on CFTR. (c) The topology of the sulfonylurea receptor, SUR2B, and ROMK proposed to form kidney K_{ATP} channels.

thereby decreasing Cl^- diffusion across the basolateral membrane. Consequently, an increase in intracellular Cl^- concentrations results in the inhibition of the apical Na entry through NKCC2, thereby suppressing Na absorption and diminishing the lumen-positive potential in the TAL. A decrease in the lumen-positive potential results in inhibition of magnesium absorption through the paracellular pathway in the TAL.[134] Also, the inhibition of Na absorption in the TAL increases Na delivery to the distal nephron, accordingly stimulating Na absorption in the expanse of K^+ in the connecting tubule and causing K^+-wasting. Therefore, an alteration in the basolateral K^+ channel activity in the TAL has a significant effect on transepithelial transport not only in the TAL, but also in the distal nephron segment.

Patch-clamp experiments demonstrated that an inwardly-rectifying 50 pS K^+ channel[119,238] and a Na^+ and Cl^- activated 140−180 pS K^+ channel[240] are present in the basolateral membrane of the TAL. The 50 pS K^+ channel is highly-expressed, and may be the main K^+ channel in the basolateral membrane of the TAL. The regulation of the 50 pS K^+ channels has been intensively studied and several factors, including protein kinase A (PKA), 20-hydroxyeicosatetraenoic acid (20-HETE), and external Ca^{2+}, have been identified to modulate the 50 pS K^+ channels (Figure 34.2). Arachidonic acid inhibits the basolateral 50 pS K^+ channels in the TAL through the CYP-omega-hydroxylase-dependent metabolism, and 20-HETE mediates the effect of arachidonic acid on the K^+ channel.[115,119] Also, raising the external Ca^{2+} inhibited the basolateral 50 pS K^+ channels in the TAL by a PKC-dependent mechanism.[179] Two lines of evidence suggest that the effect of the external Ca^{2+} on the basolateral 50 pS K^+ channels was the result of stimulating the Ca^{2+}-sensing receptor (CaSR) which is expressed in the TAL[133]: (1) the inhibitory effect of raising the external Ca^{2+} on the 50 pS K^+ channels was observed only in cell-attached patches, but not in excised patches; (2) the effect of raising external Ca^{2+} on the 50 pS K^+ channel was absent in the presence of the CaSR antagonist. It is possible that the CaSR might directly interact with the basolateral 50 pS K^+ channels in the TAL. This speculation is supported by reports from several studies. First, the basolateral 50 pS K^+ channels in the TAL might represent heterotetramers made of Kir4.1/Kir5.1, because the basolateral K^+ channels in the distal tubules with similar biophysical properties to those of the 50 pS K^+ channel in the TAL are composed of Kir4.1 and Kir5.1.[183,197] Second, immunostaining experiments demonstrated that Kir4.1 and Kir5.1 were expressed in the basolateral membrane of the TAL.[254,306] Finally, the study using immunoprecipitation performed in the cells transiently transfected with Kir4.1 and the CaSR has demonstrated that Kir4.1 was associated with the CaSR.[144] The regulation of the basolateral 50 pS K^+ channel by the external Ca^{2+} should play a role in the

modulation of transepithelial Na transport and concentrating ability in the TAL. Since the active reabsorption of $NaCl^-$ in the water-impermeable TAL is essential for urinary concentrating mechanism, inhibition of $NaCl^-$ reabsorption in the TAL should result in a decrease in concentrating ability. Indeed, it has been reported that hypercalcemia impairs urinary concentrating ability.[99]

Because the activity of the basolateral K^+ channels is regulated by the external Ca^{2+}/Mg^{2+} concentrations at a physiologically relevant range (1 to 2 mM), the CaSR-mediated regulation of the membrane transport in the TAL is mainly through controlling the basolateral K^+ channel activity. Figure 34.4 is a cell scheme illustrating the role of basolateral K^+ channels in mediating the effect of stimulation of the CaSR on Na^+ and divalent cation transport in the TAL. Under physiological conditions, the basolateral K^+ channels maintain the cell membrane potential such that it could sustain a constant Cl^- diffusion across the basolateral membrane. An increase in the external Ca^{2+} (hypercalcemia) activates the CaSR, thereby inhibiting basolateral K^+ channels and decreasing the driving force for Cl^- diffusion across the basolateral membrane. Inhibition of Cl^- exit is expected to lead to hyperpolarization of transepithelial voltage (V_{te}). A less positive V_{te} would diminish the reabsorption of Na^+ and divalent cations such as Ca^{2+} and Mg^{2+}. Indeed, it has been reported that an increase in plasma Ca^{2+}/Mg^{2+} level enhanced urinal Ca^{2+}/Mg^{2+} excretion.[249,250]

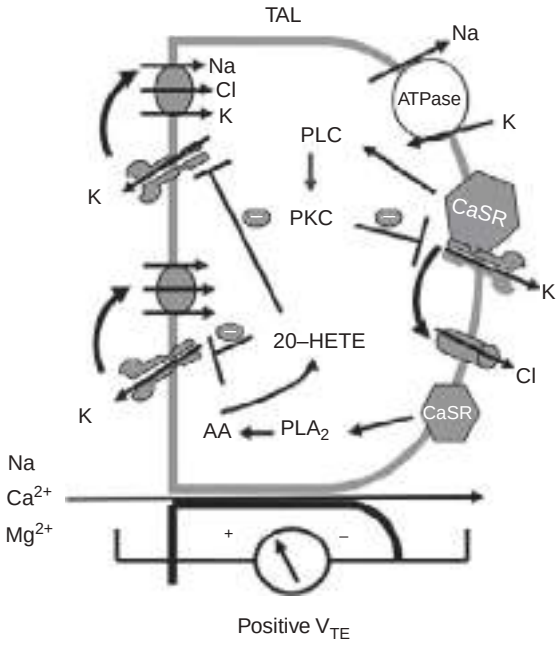

FIGURE 34.4 **A cell scheme illustrating the role of stimulation of Ca^{2+} ensing receptor (CaSR) in regulation of apical and basolateral K channels, thereby affecting the transepithelial transport of Na and divalent cations.** (Abbreviations: PLC: phospholipase C; PLA2: phospholipase A2; PKC: protein kinase C; 20-HETE: 20-hydroxyeicosatetraenoic acid.)

Basolateral Membrane Cl^- Channel and Transporter

Cl^- CHANNEL

Cl^- exit across the basolateral membrane of TAL cells is largely conductive, proceeding down its electrochemical gradient through Cl^--selective channels in the basolateral membrane. The notion that basolateral Cl^- transport is electrogenic first derived from observations that, in the mouse medullary TAL and rabbit cTAL,[138] net Cl^- absorption accounts for about 90% of the equivalent short-circuit current. Measurements of the basolateral membrane voltage by Greger and Schlatter[112] confirmed that reductions in bath chloride concentration depolarized the basolateral membrane, while reductions in intracellular chloride concentration produced by blocking Cl^- entry with furosemide hyperpolarized the basolateral membrane. Both sets of observations are consistent with the presence of a Cl^- conductance in the basolateral membrane. Consistent with the view that basolateral Cl^- transport is via chloride channels, a variety of compounds known to block Cl^- channels also inhibit salt absorption in TAL segments. Wangemann et al.[121] have catalogued the electrophysiologic effects, relative potencies, and structure–function relations of over 200 such compounds. The major effects of these agents, when present in the peritubular bathing solutions, are inhibition of transepithelial voltage, inhibition of the equivalent short circuit current, and hyperpolarization of the basolateral membrane.

Application of the patch-clamp technique to the TAL has established that Cl^- channels are present in the basolateral membrane of TAL cells. Paulais and Teulon detected a 40 pS anion selective channel ($P_{Cl}/P_{Na} = 20$) in the basolateral membrane of collagenase treated mouse cortical TAL segments.[121] The I–V relations of the channel were linear in both the cell-attached and excised configurations. The open probability of the channel in the cell-attached state was voltage-dependent, increasing as the membrane was depolarized. In the excised patch configuration, the open probability was no longer voltage-dependent. Greger et al. described a Cl^- channel in the basolateral membrane of rat TAL segments.[109] This channel also has a conductance of about 40 pS, but rather than having a linear I–V relation, this channel exhibits outward rectification. The open probability increases with depolarization in both the cell-attached and -excised patch configuration. A low conductance Cl^- channel (8–10 pS) having linear I–V relations has also been detected in the basolateral membrane of TAL cells.[121,120,118] The activity of this channel is

increased following incubation with cAMP-dependent protein kinase and ATP,[120] and is inhibited by 20-HETE acid, a Cyp-ω-hydroxylase-dependent metabolite of arachidonic acid.[118]

Evidence for Cl^- channels in the TAL also comes from studies of Cl^- flux in renal medullary membrane vesicles. Since TALs comprise approximately 70% of the volume in the inner stripe of outer medulla, vesicles prepared from this region should be predominantly derived from this segment. $^{36}Cl^-$ flux into vesicles from rabbit outer medulla[16] is electrogenic, cation-independent, inhibitable by chloride channel blockers, and has a low activation energy ($E_a = 6.4$ kcal/mole), characteristic of transport through a channel. Moreover, when vesicles from rabbit outer medulla were incorporated into planar lipid bilayers, chloride channel activity was demonstrated.[251] These channels were anion selective ($P_{Cl}/P_K = 10$) and had a single-channel conductance of 80−90 pS in 320 mM KCl solution. The I−V relations in symmetric solution were linear, and in asymmetric solutions the I−V relations conformed to the Goldman−Hodgkin−Katz equation. The open probability of this channel was voltage-dependent, increasing activity with depolarizing voltages. These channels are also seen in vesicles made from highly purified suspensions of mouse thick ascending limb.[337]

Molecular cloning has demonstrated the basolateral Cl^- channels are composed of ClC-K1 and ClC-K2,[2,166,311] members of a large number of the ClC family of channels.[155] ClC-K1 and ClC-K2 are expressed exclusively within the rat kidney. In the human, the two corresponding channels are denoted hCLC-Ka and hCLC-Kb, and are located contiguously on chromosome 1.[265] Due to the high degree of sequence similarity between hCLC-Ka and hCLC-Kb, it is not certain which of the human channels correspond to CLC-K1 versus CLC-K2, although the distribution of ClC-K2 along the nephron most closely matches that of hClC-Kb.[304] Zimniak and colleagues[351] have cloned cDNA from rabbit renal outer medulla, named rbClC-Ka, which shares 80% homology to the rat CLC-K1 and CLC-K2. The distribution of rbClC-Ka along the nephron resembles that of CLC-K2 rather than ClC-K1.[351] Several lines of evidence support the view that CLC-K2 (or the probable human homolog hCLC-Kb) is the channel that mediates chloride efflux across the basolateral membrane of the thick ascending limb. First, using polymerase chain reaction amplification of single tubule segments, the ClC-K2 and rbClC-Ka channels were shown to be expressed primarily in the thick ascending limb and the collecting duct.[2,351] Second, immunohistochemical studies using an antibody against the rbClC-Ka channel revealed predominantly basolateral staining in the medullary and cortical thick ascending limb.[338] Similar results were obtained by Vandewalle and colleagues using an antibody that recognized both CLC-K1 and CLC-K2.[314] Finally, and most compelling, is the identification of mutations in hCLC-Kb in patients with neonatal Bartter syndrome.[289] Thus, as was the case for the NKCC2 and ROMK proteins, linkage of ClC-Kb to Bartter syndrome establishes the importance of its gene product in transepithelial NaCl transport. Activating mutations of CLC-Kb have also been reported.[153] Specifically, substitution of threonine by serine at position 481 of CLC-Kb results in a dramatic increase in Cl^- currents, without a change in channel selectivity or cell surface expression. The T481S polymorphism is relatively common in the general population, particularly in African populations. Among Caucasians, the presence of the T481S polymorphism was associated with higher systolic and diastolic blood pressures, and a higher prevalence of hypertension.[154] Thus, ClC-Kb is an attractive candidate gene for certain forms of essential hypertension, particularly salt-sensitive hypertension. Additional studies in different populations will be required to determine the significance of these ClC-Kb polymorphisms.

To form functional Cl^- channels in thick ascending limb requires not only CLC-K2/hCLC-Kb, but also a subunit, named barttin.[21] Lost function of mutation of barttin is responsible for a form of Bartter syndrome accompanied by sensorineural deafness.[21] Barttin is believed to act, at least in part, by increasing the cell surface expression of ClC-Kb.[70]

KCl SYMPORTER

Some uncertainty remains regarding the role of basolateral electrochemical KCl symport in net Cl^- efflux across that membrane. In the rabbit cortical TAL, Greger and Schlatter[239] concluded that KCl symport accounted for about one-third of basolateral Cl^- efflux. This conclusion is based on the following observations: an increase in the K^+ concentration or decrease in the Cl^- concentration of the basolateral solution depolarized the basolateral membrane; bath barium depolarized the basolateral membrane and abolished the K^+-induced changes in V_bl; and barium had no discernible effect on the transepithelial resistance or fractional resistance of the basolateral membrane. The lack of an effect of barium on resistance persuaded the investigators to propose that a barium-sensitive KCl co-transporter was present.[112] Alternatively, these data are compatible with parallel conductive pathways for K^+ and Cl^-. The absence of a barium effect on transepithelial resistance could be due to an offsetting increase in basolateral Cl^- conductance or to changes in basolateral membrane resistance below the experimental limits of detection. A cloned KCl co-transporter, KCC4, is present in the basolateral

membrane of the thick ascending limb.[316] However, its physiologic role in thick ascending limb function is not known.

Synchronous Na^+/H^+: Cl^-/HCO_3^- Exchange

An additional form of apical membrane NaCl entry has been observed in the mouse cTAL. Friedman and Andreoli[83] found that net Cl^- absorption and the transepithelial voltage were doubled when CO_2 and HCO_3^- were added to the external solutions bathing cTAL segments. Since the (CO_2 HCO_3^-)-stimulated rate of NaCl absorption did not result in net CO_2 transport, and could be abolished by the lipophilic carbonic anhydrase inhibitor ethoxyzolamide or by the luminal addition of the anion exchange inhibitor SITS or DIDS, it was proposed that the apical membrane of the mouse cTAL contains parallel, near-synchronous Na^+/H^+: Cl^-/HCO_3^- exchangers in addition to a Na^+-K^+-Cl^- co-transporter. Subsequent studies have shown that, like the mouse mTAL, the apical membrane of the mouse cTAL contains a potassium conductance, and that both the (CO_2 HCO_3^-)-dependent and (CO_2 HCO_3^-)-independent components of NaCl absorption require luminal potassium.[84,82] Thus, the cation exchange process may proceed as (Na^+, K^+)/2 H^+. Both the (CO_2 HCO_3^-)-dependent and -independent components of NaCl absorption in mouse cTAL segments were equally susceptible to inhibition by luminal bumetanide ($K_i = 5-8 \times 10-7$ M).[82] Addition of CO_2 and HCO_3^- to the bathing solutions has no effect on net NaCl transport in either rabbit cTAL or mouse mTAL. Both the rat and mouse mTAL do contain Na^+/H^+ exchangers in their apical membranes. However, in these segments, Na^+/H exchange plays a role in net HCO_3^- transport and cell pH regulation, rather than transcellular NaCl absorption.[104,168]

Bicarbonate and Ammonium Transport

Medullary and cortical TAL segments from the rat absorb bicarbonate and acidify the luminal fluid.[105] The rates of bicarbonate absorption measured in *in vitro* perfused TAL segments account for most of the filtered bicarbonate that is reabsorbed by the loop of Henle *in vivo*.[104] The rate of sodium bicarbonate absorption in the rat TAL is, however, only a small fraction (5–10%) of total sodium absorption by this segment. Thus, while bicarbonate transport by the TAL may play an important role in urinary acidification in some species, bicarbonate transport has little impact on net salt balance or free water excretion. There is considerable species variation in the rates of bicarbonate absorption by the TAL. No significant bicarbonate transport was detected in mouse and rabbit TAL.[83,105] In the rabbit, this correlates with the absence of carbonic anhydrase activity in the TAL.[95]

The mechanism of bicarbonate absorption by the rat TAL has been reviewed.[105,38] Transcellular bicarbonate absorption results from proton secretion across the apical membrane and bicarbonate reabsorption across the basolateral membrane. The apical proton secretion occurs primarily by NaH exchange. Evidence for functional apical Na^+/H^+ exchange has been presented for the rat[104,180] and mouse TAL.[83,167] In these segments, acidification of luminal fluid is sodium-dependent and amiloride-sensitive. Moreover, removal of luminal sodium or luminal amiloride results in cytoplasmic acidification. As noted above, the NHE3 isoform of the Na^+/H^+ exchanger is expressed in the apical membrane of the thick ascending limb.[6] NHE3 expression in the TAL is increased by chronic metabolic acidosis, providing a mechanism for enhanced HCO_3^- absorption in this setting. An apical membrane H-ATPase may also contribute to bicarbonate absorption in the TAL.[105] Inhibition of the Na^+-K^+-Cl^- co-transporter by furosemide stimulates bicarbonate absorption in the rat TAL. Thus, this transporter is not directly involved in bicarbonate absorption. Rather, the reduction in cell Na^+ activity that attends inhibition of Na^+-K^+-Cl^- co-transport provides a greater driving force for apical Na^+/H^+ exchange.

Krapf[180] has demonstrated that base efflux across the basolateral membrane of perfused rat TAL segments occurs as $Na^+(HCO_3^-)$ co-transport. This process is electrogenic (probable stoichiometry $1Na^+:3HCO_3^-$), sodium-dependent, Cl^--independent, and SITS-sensitive. $Na^+(HCO_3^-)$ co-transport has been demonstrated in mouse medullary TAL as well. In the mouse, the apical Na^+/H^+ exchanger and basolateral $Na^+(HCO_3^-)$ co-transporter play a role in cell pH regulation, rather than transcellular bicarbonate transport.

Origin of Transepithelial Voltage

The spontaneous, lumen-positive transepithelial potential that accompanies net NaCl absorption is, in principle, the sum of at least two terms: an electrogenic voltage arising from rheogenic cellular pathways; and a zero-current dilution voltage referable to salt accumulation in intercellular spaces during salt absorption. Given the cation selectivity of the paracellular pathway (P_{Na}/P_{Cl} ~2–6), an accumulation of Na^+ in the lateral intracellular space mediated by the (Na^+, K^+)-ATPase could create a lumen-positive diffusion potential across the junctional complex. As discussed earlier, the lumen-positive potential arising from rheogenic cellular transport serves to drive a proportion of net sodium reabsorption through the paracellular pathway.

However, this paracellular sodium absorption will be diminished by the extent to which paracellular diffusion potential accounts for the spontaneous transepithelial voltage, V_e. Thus, it is pertinent to consider the relative contributions of both electrogenic and diffusion potentials to the total transepithelial voltage.

Hebert and Andreoli[136] assessed the possible contributions of a paracellular diffusion potential to V_e in the mouse TAL. The conductance of the paracellular pathway, G_s, was measured by blocking the transcellular conductance with 20 mM Ba^{2+} in the lumen. The junctional complexes were then disrupted by the imposition of large osmotic gradients produced by the addition of urea to the luminal perfusate. Using the value of G_s in the presence of 800 mM luminal urea as an estimate of the ionic conductance of the lateral interspace, exclusive of the junctional complex, Hebert and Andreoli[136] calculated that, during net NaCl transport, the maximal rise in NaCl concentration in the lateral interspace was 10 mEq/liter, and that the resulting dilution potential was less than 1 mV. These results are consistent with the notion that virtually all of the transepithelial voltage is the result of rheogenic transcellular processes.

Specifically, because the apical membrane is exclusively conductive to potassium, and because the $Na^+K^+2Cl^-$ co-transporter is electroneutral, the apical membrane voltage, V_a, will approximate the K^+ equilibrium voltage, E_K. The basolateral membrane voltage, V_{bl}, in contrast, is a function of several conductive pathways; examples include K^+ and Cl^- channels, $Na^+HCO_3^-$ symport, (Na^+, K^+)-ATPase. Of these, Cl^- is likely the most important conductive species across the basolateral membrane. V_{bl}, therefore, will be greater than E_{Cl}, but less that E_K, and hence less than V_a (Table 34.3). The lumen-positive V_e then is the result of differing conductance characteristics of the apical and basolateral membranes. The exact value of V_e will be determined by the relative magnitude of the basolateral K^+ and Cl^- conductances, and the currents passing through the apical and basolateral membranes.

According to these arguments, the electrogenic nature of V_e should allow for a significant fraction of net sodium absorption to proceed via the paracellular pathway. Indeed, for a constant stoichiometry of the Na^+K^+-$2Cl^-$ entry, the ratio of net Cl^- absorption to paracellular sodium absorption should have a value of 2. The rate of net paracellular Na^+ absorption depends on a variety of factors, such as V_e, G_s, and P_{Na}/P_{Cl}, which vary considerably from tubule to tubule. When each of these variables was measured in the same tubule, however, the ratio of net Cl^- absorption to paracellular Na^+ absorption was reasonably constant at 2.4 ± 0.3.[136] Thus, the stoichiometry of Na^+K^+-$2Cl^-$ entry may be constant under those experimental conditions, that is, ADH stimulated mTAL segments, and the variables G_e, G_s, and P_{Na}/P_{Cl} are related in a given tubule in such a way as to maintain the net Cl^- to paracellular Na^+ ratio at 2.

Coupling of Substrate Utilization to Ion Transport

Transepithelial NaCl absorption accounts for the single largest expenditure of energy by TAL cells. Inhibition of the (Na^+,K^+)-ATPase by ouabain reduces O_2 consumption by rabbit,[42,71] rat,[309] and mouse[168] TAL segments by 50%. The effect of ouabain on O_2 consumption can be mimicked by either furosemide or by removal of Na^+ or Cl^- from the bath solutions.[42,71] This suggests that about one-half of the total cellular ATP supply is consumed by the basolateral membrane (Na^+,K^+)-ATPase pump, and that this pump operates almost exclusively for the purpose of transepithelial NaCl transport.

TAL segments utilize a variety of metabolic substrates including D-glucose, D-mannose, butyrate, β-OH-butyrate, acetoacetate, lactate, acetate, and pyruvate to support the high ATP requirement imposed by salt transport.[339] Uchida and Endou[310] determined the ability of various substrates to maintain cellular ATP concentrations in microdissected mouse TAL segments. In mTAL segments, glucose, lactate, and β-hydroxybutyrate all conserved cellular ATP content equally well. In the cTAL, lactate and β-hydroxybutyrate increased cellular ATP more than did glucose. Wittner et al. reported that in the absence of exogenous substrate, NaCl transport fell by 73% in 10 minutes in rabbit cTAL.[339] Chamberlin and Mandel[43] assessed the ability of various endogenous and exogenous substrates to support oxidative metabolism in suspensions of rabbit mTAL segments. Unlike the findings in rabbit cTAL, the mTAL suspensions maintained 85% of their basal O_2 consumption in the absence of exogenous substrates. Inhibitors of glycolysis, fatty acid oxidation, and amino acid oxidation reduced O_2 consumption, indicating that glucose, fatty acids, and amino acids all serve as endogenous substrates capable of supporting oxidative metabolism when the availability of exogenous substrate is limited.[43]

Therefore, the TAL, particularly the medullary portion, relies almost exclusively on oxidative metabolism as its source of energy. However, the mTAL resides in an oxygen-poor environment. The oxygen tension in the outer medulla is about 10 mmHg.[186] Apparently, like the cTAL, the O_2 affinity of the mTAL is sufficiently high that oxidative metabolism is maintained even at low oxygen pressures. Nonetheless, the high oxygen requirement in an oxygen-poor environment

might predispose the mTAL to injury if oxygen delivery falls or salt transport requirements increase. Brezis and co-workers have shown that the medullary TAL is, in fact, exquisitely susceptible to hypoxic injury.[30] Maneuvers that diminish TAL salt transport, such as furosemide, exert a marked protective effect against hypoxic injury.[31]

Regulation of Salt Absorption in TAL

The rate of salt absorption by the thick ascending limb is modulated by physical factors, such as luminal flow rate and the composition and osmolality of luminal and peritubular fluids, and hormones, such as vasopressin and glucagon, which exert their effects through interactions with specific cellular receptor proteins. The regulation of TAL salt transport is characterized by considerable interspecies variation, as well as intranephron heterogeneity. It is worth noting, again, that the cortical and medullary portions of the TAL have different transport properties (Table 34.2) and subserve different functions. Salt absorption in both segments creates luminal fluid dilution and the potential for free water excretion; however, only salt absorption by the medullary TAL enriches the medullary interstitial osmolality and enhances urinary concentrating power. Given these differences, it is not surprising that the rates of transport in the medullary and cortical TAL are modulated quite differently. A good example of both species and intranephronal heterogeneity is the effect of antidiuretic hormone on TAL transport.

Antidiuretic Hormone

The ADH affects NaCl absorption in the ascending limb of Henle, and thereby regulates the countercurrent multiplication process. Support for this contention was provided by the demonstration, in some species, of an ADH-induced increase in adenylate cyclase activity[40,55] and protein kinase activity[65] in the medullary, but not cortical, portions of the TAL.

Table 34.4 summarizes the effects of ADH on salt transport in *in vitro* microperfused medullary TAL segments of mouse, rat, and rabbit. Hall and Varney[123] established that ADH increased the lumen-positive transepithelial voltage and the net rate of tracer Cl^- absorption in the mouse medullary TAL. Several laboratories have confirmed these effects of ADH on the transepithelial voltage and unidirectional Cl^- flux in the mouse, and have demonstrated that the effect of ADH on NaCl transport was restricted to the medullary portion of this segment.[138,270,276,338] Moreover, the maximal stimulation of the transepithelial voltage in the mouse medullary TAL occurred at hormone concentrations of approximately 20 pg/ml or 10 μU/ml, found during states of antidiuresis.[138] A similar increase in transepithelial voltage can be obtained in the mouse medullary TAL, but not the cortical TAL, by the addition of cAMP analogs or forskolin, a nonhormonal activator of adenylate cyclase to the peritubular media.[138] In contrast, ADH, even at peritubular concentrations of 250 μU/ml, has no effect on V_e in the mouse cortical TAL.[138] Taken together, these results indicate that the mouse medullary TAL and cortical TAL are functionally heterogeneous with respect to the effect of ADH on net NaCl absorption, and that stimulation of net NaCl absorption in the mouse medullary TAL by ADH is mediated by cAMP. The effect of ADH in TAL does not seem to be contant in all species. ADH causes a variable increase in cyclic AMP production in the rabbit TAL, but pharmacologic concentrations of ADH had no effects on either the transepithelial voltage or tracer Cl^- efflux in this species.[270] ADH or the V_2 selective analog dDAVP increased NaCl absorption from the TAL on homozygous Brattleboro (central diabetes insipidus) rats.[340] In humans evidence is limited. Studies in pump-perfused human kidneys rejected for transplantation have shown ADH-sensitive adenylate cyclase activity in collecting ducts, but not in TAL segments.[40,263] Since the ability of humans to elaborate concentrated urine is limited compared to the mouse, the failure of ADH to increase cAMP in the human TAL is consistent with Morel's suggestion that the response of medullary TAL segments to ADH correlates directly with urinary concentrating ability.[217]

TABLE 34.4 Effects of ADH on NaCl Transport by Thick Ascending Limb Segments

Species	ADH	V_e (mV)	J_{NaCl} (pmol/sec/cm^2)
Mouse	−	5	2600
	+	11	10,800
Rat	−	2.4–3.3	4825
	+	3.6–4.7	7770
Rabbit	−	3–7	6400
	+	3–7	Unchanged

Table from Reeves, W. B., and Andreoli, T. E. (2008). Sodium chloride transport in the loop of Henle, distal convoluted tubule, and collecting duct. In "The Kidney: Physiology and Pathophysiology," 4th edn, 849–888, Alpern, R. J., and Hebert, S. C. (eds.). Elsevier.

Mechanisms of ADH Affect on TAL

The mechanism whereby ADH stimulates salt transport in the medullary TAL has been studied most extensively in the mouse. The effects of ADH in this segment are mediated predominantly through interaction of the hormone with the vasopressin V_2 receptor coupled to adenylate cyclase. Thus, ADH stimulates

adenylate cyclase activity in the TAL,[217] and cAMP analogs and forskolin[139] mimic the effects of ADH on transport in this segment. Cholera toxin stimulates salt transport in the TAL, indicating that the V_2 receptor is coupled to the catalytic subunit of adenylate cyclase by a stimulatory guanine nucleotide-binding protein, G_s. The catalytic subunit of adenylate cyclase may, in turn, be influenced by calmodulin. Takaichi and Kurokawa[302] have shown that calmodulin inhibitors inhibited ADH-sensitive cAMP production in isolated mouse medullary TAL segments. Likewise, Ausiello and Hall[13] showed that the addition of exogenous calmodulin stimulated ADH-sensitive cAMP production by LLC PK_1 cells.

Table 34.5 lists the effects of ADH on several electrophysiologic parameters of mouse medullary TAL segments perfused *in vitro*. The approximate doubling of the equivalent short-circuit current results from an increase in the transepithelial voltage[135,138,214] and an increase of roughly 20% in the transepithelial conductance. Moreover, the ADH-induced increase in transepithelial conductance, G_e, is referable to an increase in the barium-sensitive or transcellular conductance, Gc. ADH has no effect on the magnitude or permselectivity of the paracellular conductance, G_s (Table 34.5).

ADH increases both the apical and basolateral membrane conductance.[135,214] The apical membrane of TAL cells is, as noted previously, predominantly K^+ conductive. In the presence of luminal furosemide to block K^+ uptake via the Na^+-K^+-$2Cl^-$ co-transporter, mouse TAL segments exhibit net K^+ secretion that is increased by ADH.[135] Because the electrochemical driving force for K^+ secretion is presumably constant in the presence of furosemide, it was suggested that the increase in K^+ secretion was due to an increase in apical membrane K^+ conductance.[135] In support of this notion, using membrane vesicles prepared from rabbit outer medulla, Reeves et al.[252] demonstrated that *in vitro* exposure to cAMP-dependent protein kinase and ATP specifically enhanced barium-sensitive rates of $^{86}Rb^+$ uptake. This finding has been confirmed in subsequent work that examined the effects of phosphorylation on the activity of ROMK channels. ROMK is phosphorylated by cAMP-dependent protein kinase at a number of sites,[342] and this phosphorylation increases the activity of the channel.[208]

The ADH-induced increase in transepithelial NaCl absorption can be blocked by luminal furosemide, and therefore represents an increase in apical Na^+-K^+-$2Cl^-$ co-transport activity. The mechanism whereby ADH increases apical co-transport activity is unclear. Sun et al.[301] demonstrated that in isolated perfused mouse TAL segments, ADH changed the stoichiometry of NaCl entry from $1Na^+$:$1Cl^-$ to $1Na^+$:$1\ K^+$:$2Cl^-$. This change in stoichiometry, accompanied by apical K^+ recycling, could create a lumen-positive potential to drive Na^+ reabsorption via the paracellular pathway. Phosphorylation of the cloned Na^+-K^+-$2Cl^-$ co-transporter NKCC2 by cAMP-dependent protein kinase does not appear to directly increase co-transporter activity. However, phosphorylation may influence co-transporter activity by modulating the interactions between NKCC2 isoforms. As noted above, an isoform with a truncated C-terminus, denoted C4, can inhibit the activity of the full-length NKCC2.[245] However, the inhibition by the C4 isoform can be relieved by phosphorylation by cAMP-dependent protein kinase.[245,209] Thus, ADH may increase apical Na^+-K^+-$2Cl^-$ entry by releasing NKCC2 from tonic inhibition by truncated isoforms. Of note, the short C4 variant is expressed in medullary TAL, but not in cortical TAL,[221] providing a potential explanation for the lack of ADH effect on cortical TAL discussed above. Chronic exposure to ADH may increase apical Na^+-K^+-$2Cl^-$ entry by increasing the abundance of NKCC2.[64]

The predominant portion of the ADH-induced increase in cellular conductance is accounted for by an increase in the basolateral membrane Cl^- conductance.[135,214] Two mechanisms have been suggested for the hormone-dependent increase in basolateral Cl^- conductance. Schlatter and Greger[276] proposed that the ADH-induced increase in intracellular cAMP results in a direct increase in chloride channel activity. Such a mechanism has been amply demonstrated in Cl^- secreting epithelia, such as the trachea and intestine. In support of their proposal, Schlatter and Greger demonstrated that cAMP and ADH elicited a fall in the fractional resistance of the basolateral membrane in mouse medullary TAL segments, even when cell Cl^- activity was kept at low levels by blocking apical Cl^- entry with furosemide.[276] Likewise, using patch-clamp analysis, Paulais and Teulon[239] found that preincubation of mouse cortical TAL segments with forskolin or cAMP analogs increased the number of Cl^-

TABLE 34.5 Effects of ADH on Electrophysiologic Parameters in Mouse Medullary TAL Segments

ADH (μU/ml)	V_e (mV)	G_e (mS/cm^2)	G_c (mS/cm^2)	G_s (mS/cm^2)	V_a (mV)	V_{bl} (mV)	R_a/R_b
0	5.6	103.7	45.1	58.6	54.4	− 50.7	1.2
250	10.3	121.3	60.2	61.0	47.3	− 38.9	2.2

Table from Reeves, W. B., and Andreoli, T. E. (2008). Sodium chloride transport in the loop of Henle, distal convoluted tubule, and collecting duct. In "The Kidney: Physiology and Pathophysiology," 4th edn, 849–888, Alpern, R. J., and Hebert, S. C. (eds.). Elsevier.

channels observed in basolateral membrane patches. It is now known that NKCC2 is sensitive to intracellular chloride concentration: chloride depletion activates the co-transporter by inducing phosphorylation of key amino terminal domain threonines of the co-transporter by a pathway involving the soluble kinases WNK3 and SPAK.[247] Additionaly, elimination of TAL basolateral chloride channels in Bartter's type III and IV reduces salt reabsorption by TAL, producing the disease. Thus, one mode of regulation of NKCC2 can be achieved by modulating intracellular chloride concentration in TAL.

Alternatively, ADH might enhance Cl^- conductance indirectly by increasing apical membrane Cl^- entry.[135] According to this proposal, an ADH-dependent activation of apical membrane Na^+-K^+-$2Cl^-$ co-transporter and K^+ channels leads to an increase in intracellular Cl^- activity, and a subsequent increase in basolateral Cl^- conductance. In support of this view, Molony et al.[214] found, also in mouse medullary TAL, that the ADH-dependent rise in cellular and basolateral conductance were much lower when Cl^- entry was inhibited by furosemide than in control conditions. Studies of Cl^- channels incorporated from basolaterally enriched renal medullary membrane vesicles into planar lipid bilayers have demonstrated several properties of these channels that may account for an intracellular Cl^- concentration-dependent rise in basolateral Cl^- conductance.[251,336] First, the activity of the Cl^- channels is increased with membrane depolarization evidently due to the basolateral membrane depolarization that follows ADH stimulation of TAL segments.[251] Second, Cl^- channels in the vesicles behave like Goldman rectifiers, so that increases in intracellular Cl^- cause an increase in the outward single-channel conductance.[251] Third, channel activity is dependent on the intracellular Cl^- concentration, such that increases in Cl^- over the range 2−50 mM result in large increases in the open time probability of these Cl^- channels.[336] In this respect, it should be recognized that the time-averaged conductance of a basolateral Cl^- channel is given by the product $g_{Cl}P_o$, where g_{Cl} is unit channel conductance and P_o is open time probability.

Thus, an ADH-dependent increase in apical Cl^- entry could stimulate basolateral Cl^- conductance to a far greater extent than expected from simple Goldman rectification. In that connection, at least two laboratories have found, in mTAL segments, that reducing intracellular Cl^- with luminal furosemide produced a three-fold reduction in basolateral Cl^- conductance.[214,276]

Modulation of ADH Effect on TAL Segments

Several factors, such as prostaglandins, peritubular calcium concentration, and peritubular osmolality, have been demonstrated to modulate the actions of ADH on NaCl absorption in the TAL (see the review articles by Hebert and Molony).[135,212] In isolated mouse and rabbit TAL segments, increases in peritubular osmolality, induced by adding urea or impermeant solutes such as mannitol, rapidly and reversibly inhibit the ADH-stimulated rate of net Cl^- absorption. Peritubular hypertonicity results in a prompt reduction in the transepithelial voltage and in the cellular conductance.[213] Molony and Andreoli determined that hypertonicity inhibits the basolateral membrane chloride conductance.[212] The antagonizing effect on ADH-induced stimulation of net Cl transport is not due to decreasing cAMP, because application of either ADH or cAMP is unable to reverse the hypertonicity-mediated effect. Thus, increasing the absolute magnitude of interstitial osmolality provides a negative feedback signal that can reduce ADH-dependent salt absorption by the mTAL.

PGE_2 also plays a role in modulating the effect of ADH on NaCl absorption in the mTAL (see Molony's review article [212]). In the mouse mTAL, PGE_2 abolished the effect of ADH on transepithelial voltage and on net NaCl absorption, while it had no effect on NaCl salt absorption in the absence of ADH. Likewise, reported biochemical studies in the mTAL[226] indicate that PGE_2 has no effect on cellular cAMP concentrations in the absence of ADH, and that PGE_2 markedly inhibits the ADH-dependent stimulation of cytosolic cAMP concentrations. The TAL, particularly in the macula densa, expresses COX-2.[130] COX-2 expression in these cells may be coupled to renin secretion. Thus, COX-2 expression is increased by salt restriction, diuretics, and in Bartter syndrome all conditions characterized by hyperreninemia.[46] In addition to PGE_2, 20-HETE may also modulate the effect of cAMP on Na^+ transport in the TAL. McGiff and co-workers[207] demonstrated that 20-HETE inhibits NaCl transport in the TAL by a mechanism involving inhibition of the apical K^+ channel[323] and the Na^+-K^+-$2Cl^-$ co-transporter.[69] Moreover, high 20-HETE concentration inhibits the effect of cAMP on the apical K^+ channels in the rat TAL.[116]

Hypercalcemia often results in an ADH-resistant urinary concentrating defect, that is, nephrogenic diabetes insipidus. At least part of this concentrating defect results from the inhibition of ADH-stimulated cAMP production in the TAL by calcium. Takaichi and Kurokawa demonstrated that high ambient calcium inhibited cAMP production stimulated by forskolin, indicating that the inhibition probably involved the catalytic subunit of adenylate cyclase. Preincubation of tubule segments with pertussis toxin abolishes the effect of hypercalcemia on cAMP generation, indicating that the inhibition of cAMP generation is mediated through activation of G_i.[303] The effects of hypercalcemia on cAMP production are mediated by a G-protein-coupled CaSR present on the basolateral membrane of

TAL cells.[133] As discussed above, stimulation of CaSR also inhibits the apical 70 pS and basolateral 50 pS K channels.[117,179] Consequently, activation of CaSR is expected to alter NaCl absorption, thereby affecting the concentrating mechanism.[137]

Intracellular Mechanisms for NKCC2 modulation in TAL

The physiological pathways for NKCC2 regulation have begun to be uncovered. The rate of salt reabsorption by TAL depends on the amount of NKCC2 protein expressed in the apical membrane at any given time; that is, the protein half-life in the plasma membrane. As shown in Figure 34.5, the amount of NKCC2 is the result of a dynamic process involving exocytosis and endocytosis mechanisms. Stimulators of NKCC2, such as cAMP (vasopressin, PTH, glucagon or β-adrenergic stimulation) promote exocytosis over endocytosis. Electron microscopy analysis of mouse TAL[100] and biotinylation of rat TAL apical membrane[232] demonstrated that only between 3–5% of total NKCC2 is present in the apical membrane in basal conditions. Vasopressin stimulates trafficking of NKCC2 towards the plasma membrane in *Xenopus* oocytes,[209] in mouse TAL,[100] and in rat TAL,[232] by a process that is modulated by the vesicle-associated membrane proteins VAMP2 and VAMP3. Exocytosis of NKCC2 is a continuous dynamic process that is further activated by cAMP, via protein kinase A (PKA).[9] Because PKA inhibition does not completely prevent cAMP-induced increase of NKCC2 presence in the apical membrane, it is possible that cAMP also inhibits endocytosis. Two amino acid residues of NKCC2 become phosphorylated by PKA, Ser126 and Ser874, but the exact consequence of this is not known.[122] Endocytosis of NKCC2 occurs also constitutively in TAL. A fraction recycles toward the apical membrane and another fraction undergoes degradation. Inhibition of endocytosis by cholesterol depletion completely block NKCC2 retrieval from the membrane, increasing NKCC2 presence and chloride transport by TAL.[9] Supporting this view, it has been shown that part of NKCC2 is associated with lipid rafts.[331]

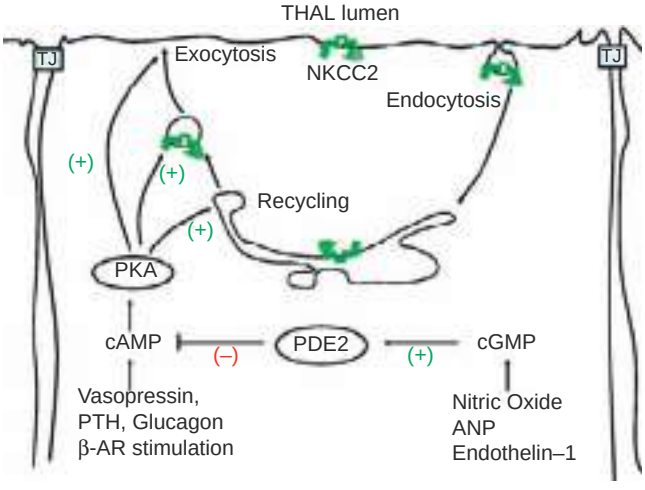

FIGURE 34.5 **Physiological regulatory pathways of NKCC2 in thick ascending limbs of Henle's loop (TALs).** *From ref. [8].*

Inhibitors of NKCC2 such as nitric oxide, through the eNOS synthase,[246] atrial natriuretic peptide, and endothelin affect trafficking of the co-transporter, mainly through a cGMP-dependent activation of phosphodiestarese 2 (PDE2) that in turn degradates cAMP (Figure 34.5). The intracellular mechanism for other NKCC2 inhibitors such as 20-HETE and PGE_2 is not extensively known,[8] but can be achieved at least in part by modulating the ADH effect in TAL. PGE_2 for instance, in the *in vitro* mouse mTAL PGE_2 has no effect on NaCl salt absorption when ADH is absent.[246] In the presence of ADH, PGE_2 reduces the ADH-dependent values for transepithelial voltage and net NaCl absorption to ADH-independent values, by what appears to be inhibition of ADH-stimulated generation of cAMP in the mTAL by activating G_i. Hypercalcemia reduces TAL salt reabsorption by a calcium-induced inhibition of NKCC2 and ROMK vía calcium sensing receptor activation of G_i.[93]

Adrenergic Agents

Adenylate cyclase activity stimulated by β-adrenergic receptors is present in the rat, but not rabbit, TAL.[41] Likewise, β-adrenoceptors have been detected along the rat TAL by autoradiographic localization. The physiologic effects of adrenergic agents have been tested in micropunctures and *in vitro* microperfusion studies. DiBona and Sawin[58] demonstrated an enhancement of loop NaCl absorption during low-frequency renal nerve stimulation. Acute renal denervation, on the other hand, depressed NaCl absorption by the loop of Henle.[19]

Mineralocorticoids

There is controversy regarding mineralocorticoid effects on TAL. Some evidence suggests that aldosterone influences NaCl transport in the TAL (reviewed in [59]). First, clearance studies indicate that aldosterone increases free water clearance in adrenalectomized animals, consistent with an increase in NaCl absorption by the TAL. Second, nuclear mineralocorticoid receptors are present in both the medullary and cortical portions of the TAL of rat and rabbit, although it is known that the presence of mineralocorticoid receptors is no guarantee of being a specific target site of aldosterone. The mechanisms of aldosterone actions are discussed in Chapter 35. Third, aldosterone appears to modulate the

activity of certain transport-related enzymes in the TAL. Specifically, adrenalectomy reduces the activity of (Na^+,K^+)-ATPase in the rabbit TAL. The activity of these enzymes can be restored to almost normal by aldosterone, but not by dexamethasone. In the adrenal-intact mouse, pharmacologic doses of mineralocorticoid increased (Na^+,K^+)-ATPase activity of mTAL segments by 25%. Finally, *in vivo* and *in vitro* microperfusion studies have demonstrated effects of aldosterone on TAL sodium transport. Adrenalectomy inhibited loop of Henle sodium absorption by 33−50%. Aldosterone, but not dexamethasone, increased sodium transport to control levels. Also in the rat medullary TAL, adrenalectomy decreases $NaHCO_3$ absorption by 33%. However, other studies have failed to show an effect of mineralocorticoids on (Na^+,K^+)-ATPase activity in the TAL (also reviewed in [59]). Additionally, a recent study shows that aldosterone administration on adernalectomized rats had no effect on NKCC2 expression.[313]

Na^+ TRANSPORT IN DISTAL CONVOLUTED TUBULE

General Characteristics

The DCT absorbs roughly 10% of the filtered sodium load.[255] Fluid enters the DCT with a sodium concentration of 25−30 mM, but salt is added along the initial 20% of the DCT, so that the sodium concentration averages 50 mM at a point 200−300 μm from the macula densa. From there, tubular sodium concentration decreases along the DCT to a value of approximately 30 mM at the end.[279] Tubular fluid to plasma sodium ratios as low as 0.10 have been observed during stationary microperfusion.[255] This finding, together with the presence of the lumen-negative potential difference (see subsequent discussion), establishes clearly the active nature of sodium absorption in this segment.

Sodium absorption by the DCT is load-dependent. That is, over a wide range of delivery rates, the proportion of sodium absorbed by the DCT remains constant at 80%.[255] At high tubular fluid flow rates, the fall in luminal sodium concentration along the tubule is attenuated; thus, more sodium is available to distal sodium absorptive sites at high flow rates than at low flow rates. Sodium absorption in the rat DCT has been reported to be 25−30 pEq/mm^2/sec, that is, about one-third of the rate occurring in the PCT. However, rates comparable to those in the PCT have been reported in isolated perfused DCT.[52,53,66]

Electophysiologic Considerations

The electrophysiologic and transport properties of the DCT and CNT are summarized in Table 34.6. The transepithelial voltage in the earliest loops of the DCT, measured with fine tip electrodes, ranges from 9 to 19 mV, lumen-negative. Small lumen-positive voltages, 3.7 to 5.7 mV, have been measured both in micropuncture experiments, by using low resistance micropuncture electrodes, and in isolated, perfused early DCT segments (reviewed in [255]). When the composition of the luminal perfusate resembled distal tubular fluid, i.e., having a low NaCl concentration (see earlier discussion), the lumen voltage tended to be slightly positive, whereas when tubules were perfused with solutions resembling plasma, i.e., high NaCl concentration, the lumen voltage was negative. The lumen-negative potential measured with high NaCl solutions was abolished by luminal amiloride, an inhibitor of epithelial sodium channels. The positive voltage under *in vivo* conditions is a salt dilution potential arising from the differential permeability of the DCT to Na^+ and Cl^-, while the lumen-negative potential under symmetric solutions reflects active Na^+ reabsorption via amiloride-sensitive sodium channels (see subsequent discussion).

The transepithelial electrical potential in the late DCT of rats measured *in vivo* ranges from 37 to 60 mV. Values in isolated rabbit DCT and CNT segments perfused with symmetric solutions are less negative, 5 to 30 mV.[114,286,347] The voltage can be inhibited by peritubular ouabain or luminal amiloride,[347] and is quite sensitive to changes in perfusion pressure and flow rate, decreasing with high pressures or flow rates.

The transepithelial resistance of the rat DCT decreases from 337 Ω-cm^2 in the early DCT to 135 Ω-cm^2 in the late DCT.[255] Hypotonic luminal fluids increase, and hypertonic perfusates decrease, the transepithelial resistance with respect to isotonic luminal fluid. Somewhat lower electrical resistances have been found in isolated perfused rabbit DCT[114,347] and CNT.[4]

Intracellular microelectrode analysis of rabbit DCT cells has yielded conflicting results. Yoshitomi et al.[347] found evidence for both K^+ and Na^+ conductive pathways in the apical membrane and K^+ and Cl^- conductive pathways in the basolateral membrane. The apical membrane accounted for 80% of the total cellular resistance. In contrast, Velazquez et al.[319] found the apical membrane to comprise over 99% of the cellular resistance, and could not detect any Na^+ or K^+ conductances in that membrane. Perhaps some of this discrepancy could have arisen from the examination of different portions of the DCT in the two laboratories. Ellison et al. have demonstrated that sodium reabsorption in the early DCT is largely mediated by a thiazide-sensitive, neutral NaCl co-transporter, while sodium absorption in the late DCT involves an amiloride-sensitive electrogenic pathway.[66] Thus, Yoshitomi et al.[347] may have described the late DCT and Velazquez et al.[319] the early DCT.

TABLE 34.6 Electrophysiologic and Transport Properties of DCT

	V_t (mV)	Rt ($\Omega - cm^2$)	V_{bl} (mV)	fRa	J_{Na} (pmol/mm/min)	J_{Cl} (pmol/mm/min)
Rat DCT	+8 to −19	81–382	−57 to −65		128–258	285
Rabbit DCT	−2 to −40	22–116	−78 to −84	0.78–0.99	82	
Rabbit CNT	−4 to −27	29–31	−71 to −83		62–121	405

Table from Reeves, W. B., and Andreoli, T. E. (2008). Sodium chloride transport in the loop of Henle, distal convoluted tubule, and collecting duct. In "The Kidney: Physiology and Pathophysiology," 4th edn, 849–888, Alpern, R. J., and Hebert, S. C. (eds.). Elsevier.

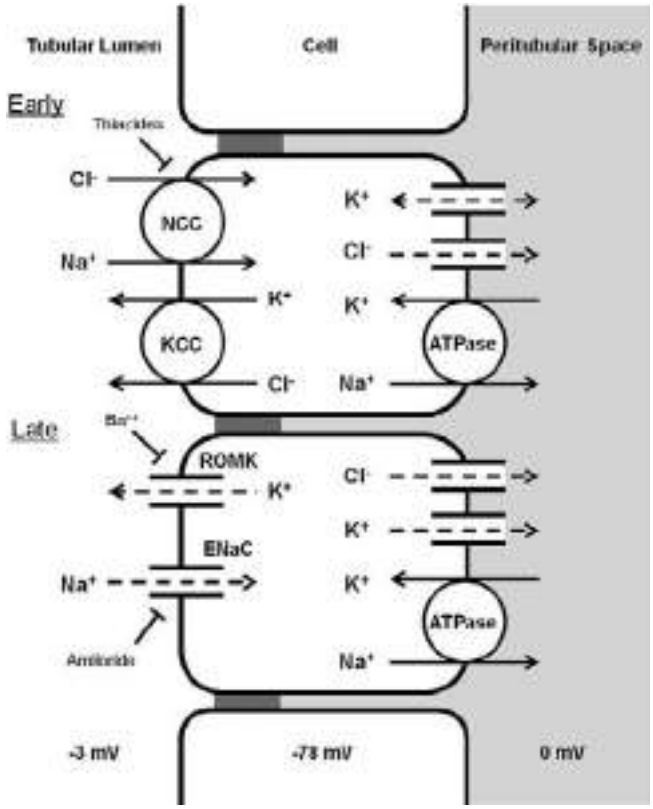

FIGURE 34.6 **Model of NaCl absorption by cells of the early (DCT1) and late (DCT2) convoluted tubule.** *Modified from Reeves, W. B., and Andreoli, T. E. (2008). Sodium chloride transport in the loop of Henle, distal convoluted tubule, and collecting duct. In "The Kidney: Physiology and Pathophysiology," 4th edn, 849–888, Alpern, R. J., and Hebert, S. C. (eds.). Elsevier.*

Mechanism of Na^+ Absorption

The available evidence permits the delineation of certain facets of Na^+ absorption in the DCT. A general model for these mechanisms is presented in Figure 34.6. Central among these are the characteristics discussed in the following subsections.

APICAL NaCl CO-TRANSPORT

The absorption of sodium and chloride in the early DCT is mutually dependent.[319] Sodium absorption is a function of the luminal chloride concentration, and chloride absorption is a function of the luminal sodium concentration. The half-maximal concentrations of both sodium and chloride are 10 mM.[319] Furthermore, the intracellular Cl^- activity is above its electrochemical equilibrium, such that Cl^- entry into the cell must involve active transport. The early distal tubule is the site of action of thiazide diuretics.[53,66,286]

A thiazide-sensitive neutral NaCl co-transporter (TSC) was cloned from the flounder urinary bladder using an expression cloning strategy.[95] A homologous transporter, NCC (SLC12A3) was subsequently cloned from the mammalian kidney.[94] NCC and NKCC2 are members of the same family of solute transporters and share considerable sequence homology (see Chapter 32). NCC transports NaCl with a 1:1 stoichiometry, is K-independent, and is inhibited by thiazide diuretics.[215] NCC is expressed in the apical membrane of early DCT cells (or DCT1) and extends, in most species, into the late DCT (or DCT2) (reviewed in [92,255,278]). In addition, mutations in the NCC gene are the cause of Gitelman syndrome that mimics the effects of thiazide diuretics.[92] Full discussion on NCC molecular physiology is presented in Chapter 32.

APICAL CONDUCTIVE SODIUM CHANNELS

The entry of sodium into the late rat DCT cell[52] is inhibited by amiloride, a sodium channel blocker. A sodium channel in the apical membrane would serve to depolarize the membrane and create the observed lumen-negative transepithelial potential. This transepithelial voltage, in turn, is a driving force for passive chloride reabsorption. Sodium channel subunits have been found by immunolocalization in the late DCT in mouse and rat kidney.[255,278]

BASOLATERAL ELECTROGENIC Na^+ PUMP

The voltage (V_{bl}) across the basolateral membrane of the *Amphiuma*[333] and rabbit[114,347] DCT is 60 to 90 mV. A reduction in the luminal sodium concentration causes V_{bl} to depolarize, while increases in the sodium concentration hyperpolarize V_{bl}. In addition, V_{bl} depolarizes after ouabain treatment. These observations are consistent with the notion that apical sodium

entry stimulates the electrogenic (Na^+,K^+)-ATPase system in the basolateral membrane.

BASOLATERAL POTASSIUM CHANNELS

The basolateral membrane of DCT cells contains a large, barium-sensitive potassium conductance.[114] Patch-clamp studies of the basolateral membrane of DCT cells have identified three different potassium channels. Two of the channels have similar conductances (50−60 pS) and kinetics, and both are blocked by barium. The third channel is seen less frequently, has a conductance of 80 pS, and is not blocked by barium. A basolateral potassium channel Kir4.1/KCNJ10 which has been localized to the basolateral membrane of DCT when mutated causes the SeSAME/EAST syndrome characterized by epilepsy, ataxia, sensorineural deafness, and renal salt-losing nephropathy similar to Gitelman's disease.[254,281] Inactivating mutations of this channel prevent the K^+ efflux of the basolateral membrane, presumably increasing the intracellular K^+ concentration that inhibits the basolateral Na^+,K^+-ATPase.

BASOLATERAL CHLORIDE CHANNELS

Microelectrode studies by Yoshitomi et al.[347] provided evidence for a chloride conductive pathway in the basolateral membrane of rabbit DCT cells. Likewise, Gesek and Friedman[97] found evidence for basolateral membrane Cl^- channels in cultured mouse DCT cells. Specifically, inhibition of apical Cl^- entry with thiazide diuretics resulted in a fall in intracellular Cl^- activity and a hyperpolarization of the membrane voltage.[97] The thiazide-induced hyperpolarization could be abolished by either a reduction in the extracellular Cl^- concentration or by NPPB, a Cl^- channel blocker,[97] suggesting that a Cl^- channel accounts for the basolateral Cl^- conductance. The single-channel properties of Cl^- channels in DCT cells have not been reported, but now it is known that CLC-Kb chloride channels are present in DCT basolateral membrane.[283] The basolateral Cl^- conductance was increased by parathyroid hormone, presumably acting via cAMP.[97]

Regulation of NaCl Transport in DCT

Na^+ DELIVERY

As noted earlier, NaCl reabsorption in the DCT is dependent on the delivered load of NaCl. Chronic increases in the delivery of NaCl to the DCT can be achieved using furosemide to inhibit NaCl reabsorption in the thick ascending limb. The DCT responds to such a maneuver with an increase in the capacity for NaCl transport,[67] and increased expression of NCC,[1] as well as marked ultrastructural changes in the DCT cell. These morphologic changes include an increase in the size of the DCT cell, an increase in the basolateral membrane surface area, and an increase in the size of mitochondria.[67,159] Hypertrophy of DCT is also seen in Bartter's mice due to knockout of ROMK,[37] and in BAC transgenic mice harboring two alleles of WNK4 containing the pseudohypoaldosteronism type II (PHAII) type mutation Q562E.[184] Thus, it is likely that DCT hypertrophy is due to either an increase in sodium entry into the DCT cell or activation of the renin−angiotensin system (see discussion below). In addition, an increase in dietary sodium alone, which increases distal NaCl delivery but not distal Na^+ absorption or activation of the renin−angiotensin−aldosterone system, does not, in the rat, result in an increase in cell height.[67] Moreover, inhibition of NaCl entry into DCT cells with chronic thiazide treatment resulted in a loss of cell height, loss of normal polarity, and apoptosis of the DCT cells.[191]

STEROID HORMONES

The presence of both mineralocorticoid and glucocorticoid receptors in the DCT has been demonstrated by immunohistochemistry and by hormone-binding. In addition, adrenalectomy resulted in a decrease in (Na^+,K^+)-ATPase activity in the DCT.[59] Microperfusion studies of superficial distal tubules (containing both DCT and CNT), however, demonstrated an increase in sodium transport in animals receiving aldosterone infusions.[59,317] Both the thiazide-sensitive and thiazide-insensitive components of sodium transport were increased by aldosterone.[317] The former may reflect neutral NaCl co-transport in the DCT, while the latter reflects electrogenic sodium absorption in the late DCT or CNT. Aldosterone infusion also resulted in large increases in NCC protein,[1,169,258,317] and phosphorylation in amino-terminal domain regulatory threonines[313] (see Chapter 32). These findings establish NCC as an aldosterone-regulated transporter, a situation that occurs in DCT2 that is considered to be part of the aldosterone sensitive distal nephron.[11] Aldosterone increases of NCC expression do not seem to be due to an increased transcription rate of the SLC12A3 gene encoding NCC.[1,218] Instead, it has been observed that NCC expression in the plasma membrane is regulated by ubiquitylation via the HECT-E3 ubiquitin ligase Nedd4-2, which in turn is modulated by phosphorylation by the serum glucocorticoid kinase 1 (Sgk1),[10] similar to what occurs with ENaC. Thus, aldosterone regulation of NCC appears to be, at least in part, through the Sgk1-Nedd4-2 pathway. Interestingly, in some families with PHAII, an inherited form of salt-sensitive hypertension in humans also known as Familial Hyperkalemic Hypertension or Gordon's syndrome, it results from mutations in Cullin 3 and KLHL3 proteins, which are part of a RING-type E3 ubiquitin ligase complex which presumably modulates NCC activity by ubiquitilation processes.[29,196]

Glucocorticoids increase (Na^+,K^+)-ATPase activity following adrenalectomy in the DCT. This effect was not blocked by spironolactone, a mineralocorticoid receptor antagonist, suggesting that glucocorticoids were acting via glucocorticoid receptors rather than mineralocorticoid receptors.[59] In addition, dexamethasone infusions increased thiazide-sensitive NaCl transport and [^{3}H]metolazone-binding sites in adrenalectomized rats.[317] Nonetheless, the role of glucocorticoids in the physiologic regulation of sodium transport in the DCT remains unclear.

Gonadal steroid hormones may also influence NaCl transport in the DCT. Chen et al.[45] first reported gender differences in the density of thiazide receptors, and in the natriuretic response to thiazides in rats. Female rats had higher levels of thiazide-binding sites in the renal cortex than males. The levels in females fell following ovariectomy, while levels rose in males following orchiectomy. Moreover, the increase in urinary sodium excretion caused by thiazides was greater in females than in males, suggesting that the differences in thiazide-binding sites were reflective of differences in thiazide-sensitive salt transport *in vivo*. Likewise, using antibodies against the cloned thiazide-sensitive NaCl co-transporter (NCC), Verlander et al.[320] found that estrogen treatment increased NCC expression in the DCT. These results are consistent with the view that male sex hormones (e.g., testosterone) may downregulate NCC expression and salt transport, while estrogens increase NCC expression and salt transport in the DCT.

PROTEIN KINASES

Studies of PHAII have yielded additional insights into the regulation of NCC function. PHAII is the phenotypic opposite of Gitelman syndrome, and is characterized by hypertension, hyperkalemia, and metabolic acidosis. The disorder is largely corrected by thiazide diuretics. These features suggested that an increase in NCC activity may be involved in the pathogenesis of PHAII. Positional cloning demonstrated that PHAII in some families is caused by mutations in either of two serine-threonine kinases, WNK1 and WNK4,[334] and more recently the whole exomes sequencing strategy revealed that Cullin 3 and KLHL3[29,196] are responsible for the disease in WNK-negative families. Subsequent studies have shown that WNK4 acts to inhibit NCC-mediated NaCl transport, likely by reducing cell surface expression of NCC[35,334,343] and that effect of WNK4 turns into activation by the PHAII type mutations,[184,334,344] resulting in higher rates of NaCl transport. It has been observed that a switch of WNK4 from inhibiting to activating NCC can be achieved by angiotensin II,[266] suggesting that NCC activation by angiotensin II,[267] which is independent of the presence of aldosterone,[313] is a WNK4-dependent process. In this regard, it has been shown that WNK4-induced phosphorylation of the downstream kinase SPAK/OSR1 is modulated by calcium concentration,[225] and that phosphorylation of SPAK and NCC in the presence of a low-salt diet or angiotensin II infusion is abrogated in WNK4 total knockout mice,[39] supporting the proposal that angiotensin II signaling via the $G\alpha_q$-coupled AT1 receptor that increases intracellular calcium could be a modulator of the WNK4 type of effect on NCC. WNK4 also affects the activity of apical ROMK channels: wild-type WNK4 inhibits ROMK and the PHAII mutant WNK4 further reduces the activity of the channels, helping to explain the hyperkalemia of PHAII patients.[157] Recent observation also shows that angiotensin II-induced inhibition of ROMK channels[330] is at least in part dependent on the presence of WNK4.[349] Thus, it is possible that PHAII type mutations in WNK4 are of the gain-of-function type, mimicking the effect of angiotensin II on NCC and ROMK activity on DCT-CD. WNK4 also affects the Cl^- permeability of the paracellular pathway.[156] The mechanism whereby WNK1 produces PHAII is less well-defined. Yang et al.[343] found that WNK1 does not directly affect NCC activity, but modulates the inhibition of NCC by WNK4. They propose that mutations that increase the activity of WNK1 prevent WNK4 from inhibiting NCC-mediated transport. Although not causing disease, WNK3 is also a powerful modulator of NCC activity. Wild-type WNK3 activates NCC, while the catalytically inactive WNK3 inhibits NCC.[256] Activity of NCC is also modulated by protein phosphatase 4.[101] (For an extensive review on NCC regulation see Chapter 32.)

Na^+ TRANSPORT IN THE CONNECTING TUBULE AND COLLECTING DUCT

The transport of Na^+ in the connecting tubule and the collecting duct is responsible for the final adjustments of renal Na^+ excretion. These tubular segments share in common an electrogenic Na^+ transport mediated by the epithelial sodium channel (ENaC), and sensitivity to aldosterone.

The Connecting Tubule

The connecting tubule connects the distal convoluted tubule (DCT) with the cortical collecting duct (CCD). Developmentally, the DCT originates from the metanephric blastema, whereas the CCD arises from the ureteric bud. The origin of the CNT is not clear, since the CNT shares some transport characteristics with both the late DCT and the downstream CCD.[14] This suggests that the CNT is a hybrid tubular segment

that develops at the border of the two adjoining segments, the DCT and the CCD.[278] The transition between the late distal convoluted tubule (DCT2) and the CNT is gradual in the mouse, rat, and human kidney.[190] In the mouse kidney, the CNT represents more than 8% of the fractional renal tubular volume, compared to 12% for the DCT and 4% for the CCD.[194]

The distal convolutions of superficial nephrons comprising the late DCT, the CNT, and the initial collecting tubule, are accessible by micropuncture. The importance of the CNT in Na^+ absorption was evaluated in a number of *in vivo* experiments. Microperfusion studies of the late distal convoluted tubule show that more than 90% of the Na^+ delivery in the DCT is reabsorbed in the DCT2 and the CNT by an amiloride-sensitive Na^+ transport.[52,205] In the rabbit isolated and perfused CNT, Na^+ absorption measured by net ^{22}Na fluxes is 3–4-fold higher than in the CCD under similar conditions.[4] Furthermore, patch-clamp studies in microdissected CNTs from the cortical labyrinth show that the amiloride-sensitive current was 4–5-fold higher than that measured in the CCD of the same animal.[88] From these experiments it was estimated that the maximal Na^+ transport capacity of the CNT allows the reabsorption of 10% of the filtered load of Na^+. Thus, the CNT represents a major site for the regulation of distal Na^+ reabsorption. Recent genetic experiments using homologous recombination in the mouse to invalidate ENaC specifically in the DCT2 and the CNT, provided direct evidence that the CNT plays a critical role for the maintenance of the Na^+ and K^+ homeostasis.[50]

In the CNT, a significant fraction of Na^+ absorption is associated with K^+ secretion. Patch-clamp and immunolocalization studies identified the presence of the inward rectifier Kir1 channel ROMK at the apical membrane as the major channel.[87,210,318] The density of active ROMK channels was found to be higher in the CNT compared to CCD, consistent with the idea that the CNT is an important site for K^+ secretion in the distal nephron. However, the density of active ROMK channels in the CNT was independent of the K^+ diet. This suggests that the increased K^+ secretion under a high-K^+ diet is primarily due to an increase in the driving force for K^+ efflux across the apical membrane, due to the upregulation of the apical Na^+ conductance.

The connecting tubule contains CNT-specific cells and intercalated cells; the specific CNT cells represent 70–80% of the epithelial lining in the CNT, and are the site for Na^+ absorption and K^+ secretion; the remainder of the epithelial lining consists of the intercalated cells that mediate acid–base balance.[61,158,170,204] Under a standard Na^+ diet, the epithelial sodium channel (ENaC) is detected by immunohistochemistry at the apical membrane of CNT specific cells.[193] ENaC is highly selective for Na^+ ions with a $P_{Na}/P_K > 100$, and a single channel conductance g_{Na} of 4 to 5 pS.[36] ENaC is blocked by submicromolar concentrations of amiloride, and by triamterene at higher concentrations. ENaC is expressed in other epithelial tissues such as the lungs, the colon, salivary glands, and sweat ducts. The channel is constitutively open; analysis of the ENaC gating kinetics suggests two different gating modes, one with a high (> 0.75), the other with low (< 0.25) open probability.[236] Transitions between these gating modes are influenced by factors such as membrane voltage or Na ions; hyperpolarization or a low extracellular Na favors the high open probability gating mode. By contrast, an acute increase in extracellular or intracellular Na^+ reduces the ENaC openings and channel current.[234,235,236] These regulatory mechanisms, termed self-inhibition and feedback inhibition respectively, are likely important to prevent a massive entry of Na^+ ions into the cell when luminal Na^+ concentration is high.[7,48] Other intracellular factors associated with cellular stress such as a decrease in pH, an increase in oxidative stess or a rise in Ca^{2+} ions decrease channel open probability.[48,162,234] ENaC is not mechanosensitive.[236]

Cloning by functional expression revealed that the ENaC channel consists of three homologous α-, β-, and γ-subunits that all are required for the full expression and activity of the channel at the cell surface.[36] The ENaC subunits share 30% homology at the amino acid level; each subunit is made of two transmembrane α helices and a large extracellular domain that represents more than half of the mass of the protein; the amino- and carboxy-termini are facing the cytosolic side of the membrane. The recent crystalization of an ortholog of ENaC, the Acid Sensing Ion Channel 1 (ASIC1), confirms this membrane topology and provides a high-resolution structure of the homologous subunits that constitute the channel core.[152] Based on homology models and functional data, the second transmembrane α helix is lining the ENaC pore and comprises important functional domains controlling ion flux through the pore: they include sequentially from outside, an extracellular gate, the amiloride- and triamterene-binding site, and further downstream the selectivity filter.[102,163,164,165] The cytosolic N-terminus of ENaC comprises a functional domain made of conserved cysteines that control ENaC gating; the C-terminus of ENaC subunits is characterized by conserved proline residues involved in ENaC interactions with cytosolic regulatory proteins.[242,296]

ENaC is activated by soluble proteases including trypsin, chymotrypsin, kallicrein or elastase. In addition, ENaC activity is significantly increased *in vitro* when co-expressed with membrane-attached serine proteases, such as the GPI-anchored proteases CAP-1

(an ortholog of the human prostasin) or CAP-2 (an ortholog of the human transmembrane protease serine 4 (TRPMSS4)).[49,129,312,322] In heterologous expression systems and in the kidney, the α and the γ ENaC subunit are found as a high and a low molecular weight forms, the latter resulting from ENaC cleavage by endogenous proteases.[89,68,89,129,145,206] The active α and γ ENaC at the cell surface is predominantly in its cleaved form. The α and γ ENaC have both canonical cleavage sequences for furin-like proteases in their extracellular domain. Furin is an endoprotease, a member of the subtilisin-like proprotein convertase family that cleaves precursor proteins along their secretory pathway from the trans-Golgi network to the apical surface. The molecular mechanism of ENaC maturation and activation by endoproteases is not yet completely understood.

The ROMK are expressed at the apical membrane of specific CNT cells.[15,87,210] Big K channels (BK channels) or maxi-K channels have been shown to account for K^+ secretion in the late distal tubule; the co-expression of these high-conductance Ca^{2+}-activated K channels (BK channels) with ENaC in CNT cells remains controversial.[15] From patch-clamp studies it seems that BK channels are restricted to the apical membrane of the intercalated cells.[237]

At the basolateral membrane, the Na/K-ATPase is responsible for pumping Na^+ out of the cell in exchange with K^+; the Na/K-ATPase activity as measured by pump current and ATP hydrolysis is higher in the CNT than in the CCD, consistent with the idea that the CNT transports more Na^+ and K^+ than the downstream segments.[161]

These membrane transporters provide a transcellular route for electrogenic Na^+ reabsorption and K^+ secretion in the CNT cells. ENaC at the apical membrane represents the entry step for Na^+ ions along a favorable electrochemical gradient; the resulting depolarization of the apical membrane provides a favorable driving force for K^+ secretion. The electrical coupling in the Na^+ and K^+ transport across the apical membrane, and the direct coupling of the Na^+ and K^+ transport by the basolateral Na/K pump, indicates that Na^+ absorption in the CNT directly affects K^+ secretion, and that these two ion transports are closely linked.

The Collecting Ducts

THE CORTICAL COLLECTING DUCT

The Na^+ and the K^+ transports in the CCD have been largely studied and differ from those in the CNT, more quantitatively than qualitatively. Table 34.7 summarizes the electrophysiologic and transport properties of CCD. The electrogenic Na^+ absorption mediated by ENaC generates a lumen-negative transepithelial voltage (V) in the CCD that varies widely according to the mineralocorticoid status of animals.[106,269] This lumen-negative voltage in mammalian CCD segments is abolished by ouabain,[106,125] luminal amiloride,[300] and luminal sodium deletion.[300] However, the lumen-negative transepithelial potential in the rabbit CCD is seven times less negative compared with the CNT.[148]

The membrane transporters involved in Na^+ absorption and K^+ secretion in the CCD principal cells are essentially the same as in the CNT cells (see Figure 34.7). Immunohistochemical studies have shown that, under standard salt diet, the abundance of ENaC at the apical membrane decreases from the late DCT and CNT to the CCD, further supporting the idea that the CNT is a major site for ENaC-mediated Na^+ absorption in the aldosterone distal nephron.[192,193] By contrast to the CNT, the selective invalidation of ENaC in the mouse CCD using homologous recombination does not result in any alteration in Na^+ and K^+ homeostasis, even under restricted dietary Na^+ intake.[261] This suggests that the absence of ENaC in the CD can be compensated, at least in part, by an increase in ENaC activity in the CNT.

From isolated and perfused rat CCD, the major fraction of Na^+ absorption in the CCD is electrogenic and mediated by ENaC; no evidence was found supporting the contribution of a thiazide-sensitive electroneutral NaCl co-transport in Na^+ absorption.[260] Recent studies, however, have reported that a significant fraction of Na^+ absorption in the mouse and rat CCD is electroneutral, insensitive to luminal amiloride, but sensitive to thiazides.[187] Microperfusion studies in different

TABLE 34.7 Electrophysiologic and Transport Properties of CCD

	V_t (mV)	R_t (Ω/cm^2)	V_{bl} (mV)	fRa	J_{Na} (pmol/mm/min)	J_{Cl} (pmol/mm/min)
Rabbit CCD	−2 to −27	86–133	−73 to −85	0.31–0.53	5.7–24.3	− 3.4 to 4.0
Rat CCD	−1 to −5	51–64	−77 to −83	0.76–0.84	− 2.3 to 0.2	

Table from Reeves, W. B., and Andreoli, T. E. (2008). Sodium chloride transport in the loop of Henle, distal convoluted tubule, and collecting duct. In "The Kidney: Physiology and Pathophysiology," 4th edn, 849–888, Alpern, R. J., and Hebert, S. C. (eds.). Elsevier.
Note: Intracellular data from principal cells only.

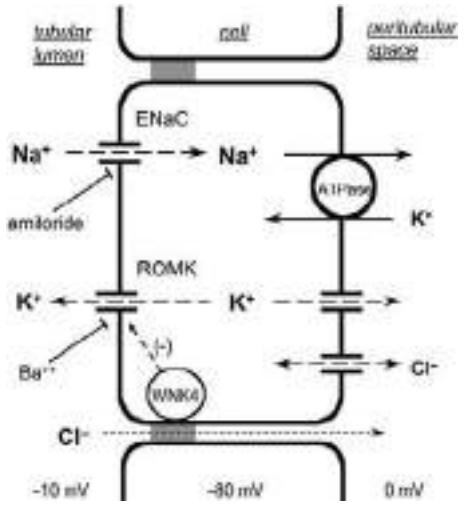

FIGURE 34.7 **Model of salt transport by the principal cell of the cortical collecting duct.** *From Reeves, W. B., and Andreoli, T. E. (2008). Sodium chloride transport in the loop of Henle, distal convoluted tubule, and collecting duct. In "The Kidney: Physiology and Pathophysiology," 4th edn, 849–888, Alpern, R. J., and Hebert, S. C. (eds.). Elsevier.*

genetically-engineered mouse models under a low-Na^+ diet concluded that this electroneutral Na^+ and Cl^- absorption results from the parallel operation of two bicarbonate transporters, a Na^+-dependent Cl/HCO_3^- exchanger and the anion exchanger pendrin. This amiloride-insensitive Na^+ transport pathway likely occurs through the intercalated cells.

THE OUTER MEDULLARY COLLECTING DUCT

The transport properties of the outer medullary collecting duct (OMCD) have been studied by *in vitro* perfusion of isolated tubule segments. The functional properties of the OMCD differ depending on the location of the segment within the outer medulla. Table 34.8 summarizes the electrophysiologic and transport properties of OMCD. Segments within the outer stripe of the outer medulla ($OMCD_o$) exhibit electrophysiologic properties resembling those of the cortical collecting duct, with an electrogenic apical Na^+ entry and a lumen-negative transepithelial voltage.[175] Compared to the CCD, the $OMCD_o$ displays a less-negative transepithelial voltage, much lower ionic permeabilities, and a lower rate of active reabsorption of Na^+.[298,299] In the collecting ducts extending into the medulla, principal cells that mediate Na^+ and K^+ transport in the CCD are progressively replaced by cells with electrical properties similar to intercalated cells of the CCD lacking a demonstrable Na^+ or K^+ conductance in the apical membrane.[175] Within the inner stripe of outer medulla ($OMCD_i$), principal cells are virtually absent and no net Na^+ absorption occurs.[298,299]

THE INNER MEDULLARY COLLECTING DUCT

The analysis of salt transport by the IMCD has been confounded by problems of axial tubule heterogeneity, species variability, and differences in experimental approaches. Studies examining IMCD function *in vivo* have yielded markedly different results than *in vitro* studies of isolated perfused tubules. Table 34.9 summarizes the electrophysiologic and transport properties of IMCD. *In vivo* microcatheterization studies and microperfusion studies have demonstrated that the IMCD reabsorbs about 80% of the sodium delivered to it[182,293] while, with one exception,[182] little sodium transport could be observed in IMCD tubules perfused *in vitro*.[268,294]

ENaC AND THE MAINTENANCE OF Na^+ BALANCE

ENaC represents the main transport pathway for Na^+ absorption in the CNT and the collecting duct. The role of ENaC in the maintenance of Na^+ homeostasis and extracellular body fluid is supported by genetic studies of rare monogenic diseases that identified functional mutations of ENaC associated with changes in Na^+ and K^+ balance, in plasma levels of aldosterone, and in blood pressure.

The pseudohypoaldosteronism type 1 (PHA-1) is characterized in the first week of life by severe dehydration, hyponatremia, hyperkalemia, and acidosis.[44] There are two clinically distinct forms of PHA-1: an autosomal recessive form that affects multiple organs (systemic form), including kidneys, colon, salivary glands, and sweat ducts (but not the skin or inner ear, for instance); and an autosomal dominant form that is restricted to the kidneys. Patients with the systemic form of PHA-1 have mutations in α, β, and γ ENaC subunits.[44] Mutations in the α, β or γ ENaC genes include nonsense, frameshift or missense mutations leading to different degrees of channel loss-of-function; the severity of the syndrome correlates usually with the extent to which ENaC activity is reduced. The autosomal dominant form of PHA-1 is caused by mutations of the mineralocorticoid receptors.[96] A variety of genetic mouse models recapitulate PHA-1 in which the constitutive inactivation of the genes encoding either the α, β or γ ENaC subunits leads to a severe renal phenotype of increased sodium excretion, hyperkalemia, metabolic acidosis, and elevated plasma aldosterone levels.[146]

Pseudoaldosteronism or Liddle's syndrome is an autosomal dominant form of salt-sensitive hypertension with early onset of elevated blood pressure during adolescence; the elevated blood pressure is usually associated with hypokalemia, metabolic alkalosis, low plasma aldosterone, and suppressed plasma renin activity.[28] The elevated blood pressure in Liddle's

TABLE 34.8 Electrophysiologic and Transport Properties of Rabbit OMCD

	V_t (mV)	R_t (Ω/cm^2)	V_{bl} (mV)	fRa	J_{Na} (pmol/mm/min)	J_{Cl} (pmol/mm/min)
Outer OMCD	−2 to −11	233–272	−65	0.81	7.9	−1.4
Inner OMCD	+2 to +48	294–534	−24 to −36	0.96–0.99	1.5	−9.8

Table from Reeves, W. B., and Andreoli, T. E. (2008). Sodium chloride transport in the loop of Henle, distal convoluted tubule, and collecting duct. In "The Kidney: Physiology and Pathophysiology," 4th edn, 849–888, Alpern, R. J., and Hebert, S. C. (eds.). Elsevier.

TABLE 34.9 Electrophysiologic and Transport Properties of Rat IMCD

	V_t (mV)	R_t (Ω/cm^2)	V_{bl} (mV)	fRa	J_{Na} (pmol/mm/min)	J_{Cl} (pmol/mm/min)
Initial IMCD	−2 to 0	73	−51	0.94	10	
Terminal IMCD	0	148	−81	0.99	54–92	72

Table from Reeves, W. B., and Andreoli, T. E. (2008). Sodium chloride transport in the loop of Henle, distal convoluted tubule, and collecting duct. In "The Kidney: Physiology and Pathophysiology," 4th edn, 849–888, Alpern, R. J., and Hebert, S. C. (eds.). Elsevier.

syndrome can be normalized under salt restriction and amiloride treatment. Based on these clinical evidences, G.W. Liddle postulated that the syndrome was "*a disorder in which the renal tubules transport ions with such abnormal facility that the end result simulates that of a mineralocorticoid excess*".[188] The mutation identified in the index case is a 45 amino acid deletion in the cytosolic C-terminus of the β ENaC subunit.[287] Subsequent genetic analysis of other Liddle's syndrome families revealed corresponding missense or deletion mutations in the C-terminus of the γ ENaC subunit, but none in the α-subunit.[127,128] These mutations allowed the identification of a conserved proline-rich motif (a canonical PxxY motif) in the C-termini β and γ ENaC subunits as the common target for the mutations causing Liddle'syndrome.[275,292]

ENaC channels carrying mutations associated with Liddle's syndrome exhibit an increased ENaC activity *in vitro* and *in vivo*, consistent with Liddle's hypothesis.[12,54,274] These ENaC gain of function mutations result in both, an increased number of active channels at the cell surface, and a higher open probability.[79]

REGULATION OF Na^+ TRANSPORT

The regulation of Na^+ absorption mediated by ENaC is quite similar in the CNT and the collecting duct. Factors that directly modulate ENaC activity at the cell surface include extracellular or intracellular Na^+, membrane potential, serine proteases, as already mentioned. Certainly the most relevant ENaC regulation for the fine tuning of Na^+ absorption in the CNT and CCD is the control of ENaC activity by hormones such as aldosterone and vasopressin.

ALDOSTERONE

The effects and the mechanisms of action of aldosterone are reviewed in detail in Chapter 35, and are discussed here briefly. The major renal target for aldosterone action is ENaC in the DCT2, in the CNT-specific cells, and in the principal cells of the CCD.[62,75] The DCT2, CNT, and CCD are renal tubular segments that share the expression of the mineralocorticoid receptor (MR) and the enzyme 11β-steroid dehydrogenase type 2 (11βHSD2).[14,181,332] Aldosterone, but also glucocorticoids like cortisol, bind[5] with high affinity the cytoplasmic mineralocorticoid receptor. *In vivo* the specificity of aldosterone versus cortisol for the mineralocorticoid effects is due to the selective degradation of glucocorticoids, but not mineralocorticoids, by the 11βHSD2.[91] Which is high in CCD segments, and protects the MR from being activated by glucocorticoids[27,227] (see Figure 34.8). Illustrating the important role of this enzyme in preventing the activation of the mineralocorticoid receptor by glucocorticoids, the genetic deficiency of 11βHSD2 produces a syndrome of apparent mineralocorticoid excess (AME), which resembles hyperaldosteronism (hypertension, hypokalemia, metabolic alkalosis), except for the fact that aldosterone levels are low.[222,335] The clinical manifestations result from the stimulation of mineralocorticoid receptors by circulating cortisol.

Aldosterone increases the rates of Na^+ absorption and K^+ secretion in these nephron segments[269,273,282] (see Figure 34.8). An increase in the Na^+ permeability of the apical membrane occurs within a few hours of exposure. In the aldosterone-sensitive distal nephron (DCT2, CNT) and the CCD, aldosterone increases the

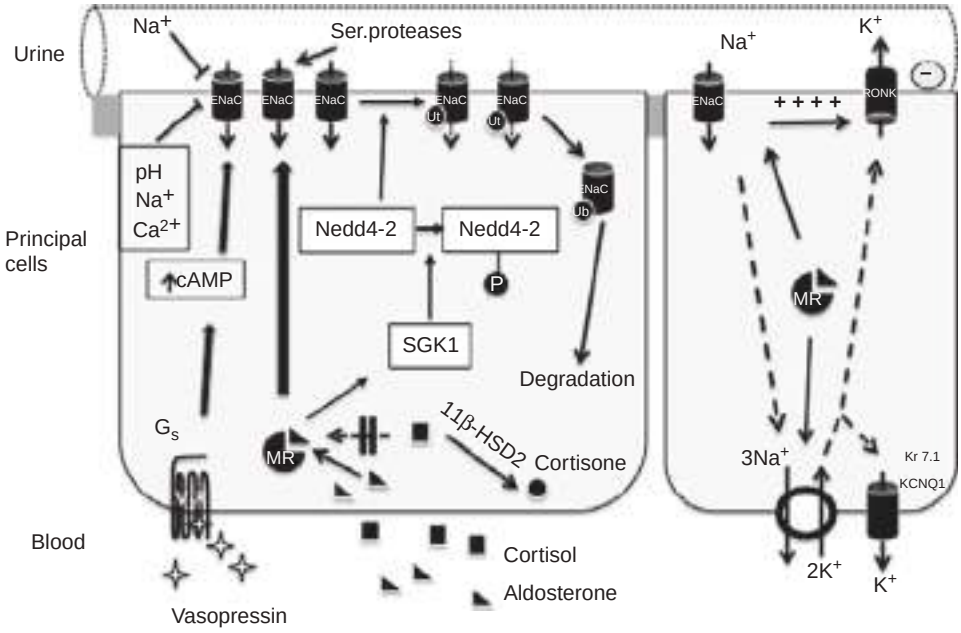

FIGURE 34.8 **ENaC regulation and Na^+ absorption in the connecting tubule and the collecting duct.** Na^+ absorption and K^+ secretion mediated by ENaC and ROMK, respectively, are coupled electrically at the apical membrane, and by the Na/K-ATPase at the basolateral membrane. Aldosterone regulates both ENaC and the Na/K-ATPase. Aldosterone and vasopressin increase the number of newly synthesized ENaC at the cell surface. The ubiquitin ligase Nedd4-2 controls the stability of ENaC at the cell surface. ENaC is activated by serine proteases.

biosynthesis of αENaC whereas the β and γ ENaC subunits are constitutively expressed.[86,195] The upregulation of the synthesis of αENaC by aldosterone leads to an increase in the expression of active, cleaved forms of ENaC channels at the cell surface.[85]

It is not clear whether the increase in the biosynthesis of αENaC is sufficient for triggering the trafficking of the multimeric αβγ ENaC channels at the cell surface or whether specific aldosterone-induced regulators of ENaC trafficking and stabilization at the apical membrane are required. For a constitutively active channel such as ENaC, the stability and the density of active channels at the cell surface is the most important determinant in the regulation of Na^+ absorption in the distal nephron. Measured by patch-clamp techniques in the amphibian distal nephron cell line A6, the half-life of ENaC activity at the cell surface was estimated at around three hours.[348] The molecular determinants of the ENaC half-life at the cell surface are not completely understood. Ubiquitylation is an important post-translational modification that determines ENaC stability at the cell surface. Ubiquitylation is a general process that labels proteins with ubiquitin to target the ubiquitylated proteins for endocytosis and/or degradation. Nedd4-2 is a protein ubiquitin ligase that catalyses the monoubiquitylation of β and γ ENaC subunits after binding specifically of the enzyme to conserved PY motifs in their cytosolic C-terminus of ENaC[259,296] (see Figure 34.8). The ubiquitylated ENaC at the cell surface undergoes clathrin-mediated endocytosis and degradation. *In vitro*, Nedd4-2 efficiently suppresses ENaC activity. Mutations in the cytosolic PY motifs of ENaC subunits are associated with Liddle's syndrome and prevent the interaction between Nedd4-2 and ENaC; the resulting defect in ENaC ubiquitylation leads to the retention of active channels at the cell surface.[274,79] Deubiquitylation enzymes such as Usp2-45 increase ENaC activity *in vitro*.[262]

In vitro experiments support the idea that aldosterone stabilizes ENaC at the cell surface by inhibiting ENaC ubiquitylation and endocytosis.[297] A number of ENaC regulatory proteins are induced by aldosterone, such as the phosphatidylinositide 3′-kinase(PI3K)-dependent kinase SGK-1 (serum- and glucocorticoid-regulated kinase 1) or the 14-3-3 scafolding protein.[56,73] The SGK-1 kinase (serum- and glucocorticoid-regulated kinase 1), increases the abundance of the active ENaC at the cell surface.[321,346] SGK-1 was shown to phosphorylate Nedd4-2, promoting the interaction between Nedd4-2 and the 14-3-3 scafolding protein; this interaction prevents the Nedd4-2 dependent ubiquitylation of ENaC[56] (Figure 34.8). These studies, performed *in vitro* in heterologous expression systems or in cortical collecting duct cell lines, identify Nedd4-2 as a critical convergence point for the regulation of ENaC at the cell surface. In addition to the SGK1/Nedd4-2 pathway, a number of kinases have been reported to

modulate ENaC activity *in vitro*. Activation of the Raf-1-MAPK/ERK kinases inhibits the cell surface expression of ENaC by stimulating the interaction between Nedd4-2 and ENaC.[74,229,284]

Mouse models in which genes contributing to the aldosterone-signaling pathway have been invalidated, only partially confirm the data obtained *in vitro* in heterologous expression systems. Mice deficient in the mineralocorticoid receptor (MR) have a normal prenatal development, but die soon after birth from dehydration and hyperkalemia. This severe PHA-1 phenotype confirms the roles of the MR, and the Na^+ transporters ENaC and NCC, in maintaining Na^+ and K^+ homeostasis.[20] However, the severity of the MR knockout phenotype contrasts with the mild renal phenotype of the mice lacking the aldosterone-induced protein SGK1.[76] The SGK1 deficient mice show a higher natriuresis compared to wt mice only under a low-Na^+ diet, and this higher natriuresis is not related to decreased ENaC activity.[76] Furthermore, under chronic aldosterone treatment, ENaC activity is identical in the SGK1 deficient mice and the wt littermates. This suggests that *in vivo* SGK1 is not central for the long-term regulation of ENaC by aldosterone; in addition, SGK1 could regulate other Na^+ transporters such as NCC located upstream of ENaC.[10]

Mice carrying Liddle's mutation in the SCNN1B gene encoding a deletion of the C-terminus of β ENaC recapitulate Liddle's syndrome under a high-salt diet.[248] These mice with a defective interaction between ENaC and Nedd4-2 represent an informative model to evaluate the contribution of Nedd4-2 in the regulation of ENaC by aldosterone. In addition to the Liddle's phenotype including hypervolemia, elevated blood pressure, hypokalemia, metabolic alkalosis, these mice retain their ability to respond to aldosterone.[54] The knockout of the Nedd4-2 gene in mice results in an elevated blood pressure associated with low plasma aldosterone levels; these effects correlate with an increase in the expression of α and β ENaC, but also NCC.[24,285] These mice also remain sensitive to aldosterone. From these *in vivo* data it appears that neither SGK1 nor Nedd4-2 appear to be limiting in the signaling pathway of aldosterone for stimulating ENaC at the cell surface.

VASOPRESSIN

Exposure of rat CCD *in vitro* to antidiuretic hormone results in a sustained stimulation of a apical electrogenic Na^+ transport,[272] as shown by the increase in the transepithelial potential, a depolarization of the apical membrane, and an increase the apical Na^+ conductance of the tubule.[277] These changes are entirely reversed by luminal amiloride, consistent with Na^+ absorption mediated by ENaC. These effects of ADH on ENaC are mediated by binding to vasopressin type 2 receptors (V2R) expressed in the CCD and CNT, activation of the adenylate cyclase, and by the generation of intracellular cAMP[32,77,220,224,272] (see Figure 34.8). In humans, a reduction in renal Na^+ excretion starts to be observed when the urine osmolality reaches a certain threshold.[223] This suggest that the effect of vasopressin on Na^+ reabsorption likely requires higher concentrations than for the effect on water reabsorption.[273] The effects of ADH on Na^+ transport in the rat CCD are synergistic to aldosterone.[131]

It is not clear how vasopressin and the generation of intracellular c-AMP upregulate ENaC and stimulate ENaC-mediated Na^+ absorption *in vivo* in the CCD. *In vivo* ADH increases both the number of active channels and the open probability.[32] In MDCK cells, c-AMP increases the amiloride-sensitive short-circuit current (I_{SC}) proportionally with the number of ENaC channels at the cell surface, indicating that an increase in active ENaC density can account for the upregulation of the ENaC-mediated Na^+ absorption by vasopressin.[220] In COS cells, c-AMP-dependent phosphorylation and inhibition of Nedd4-2 could be demonstrated that would lead to an increased ENaC stability at the cell surface.[291] Of course, the Nedd4-2 pathway mediating both the vasopressin and aldosterone effects on ENaC cannot explain their synergistic stimulation of Na^+ transport in the distal nephron and the collecting duct.

In addition to its short-term regulation of water and Na^+ absorption in the CCD, vasopressin has long-term transcriptional effects. Chronic vasopressin treatment increases the expression of β and γ ENaC expression in the CCD, with a concommittent increase in Na^+ transport.[63,228] However, no detectable change in the surface expression of the ENaC subunits could be observed.[271] An increase in the Isc and Na^+ transport could be demonstrated after long-term treatment with vasopressin, which was only partially inhibited by amiloride.[60] Thus, the contribution of ENaC in mediating the chronic effects of vasopressin remains unclear, and probably does not simply result from effects on ENaC transcription or trafficking at the cell surface.

INSULIN

The direct effects of insulin on renal Na^+ excretion is difficult to evaluate, because of its secondary effects on plasma glucose or potassium that are difficult to control precisely.

In humans and rats maintained euglycemic, insulin decreased urinary Na^+ excretion.[57,172] This effect on Na^+ excretion was abrogated when K^+ was infused to correct for hypokalemia.[81] Using a euglycemic insulin-clamp technique, insulin does not change renal Na^+ excretion[258] in rats when both plasma glucose and K^+ levels are precisely controlled.

However, insulin and IGF-1 receptors are expressed in the mammalian renal tubular system including the collecting duct.[124] The effect of insulin on Na^+ transport appears tissue-specific. Insulin stimulates ENaC-mediated Na^+ transport in the frog skin,[280] toad urinary bladder[288] or *in vitro* in A6 cells[22] or in a mammalian CCD cell line.[103] In mammalian isolated and perfused CCD, insulin failed to increase Na^+ transport.[315] IGF-1 is under the control of growth hormone (GH). Both GH and IGF-1 induces fluid and Na^+ retention in humans.[126,211] In acromegalic rats, evidence supports that the IGF1-induced increase amiloride-sensitive Na^+ absorption accounts for renal Na^+ retention.[160]

Insulin increases Na/K-ATPase pump activity.[78] Evidence supporting upregulation of ENaC-mediated Na^+ absorption after acute insulin treatment has been reported.[308] However, a patch-clamp study failed to demonstrate an effect of insulin on whole cell amiloride-sensitive Na^+ conductance in rat CCD, whereas ROMK conductance and Na^+-pump current were clearly increased.[90] It is conceivable that under both euglycemic and normokalemic conditions insulin primarily increases K^+ secretion via ROMK; the resulting hyperpolarization of the apical membrane increases the driving force for Na^+ absorption through ENaC channels. This effect is expected to be small and can be compensated by other Na^+ transporters along the nephron so that Na excretion remains unchanged.

References

[1] Abdallah JG, Schrier RW, Edelstein C, Jennings SD, Wyse B, Ellison DH. Loop diuretic infusion increases thiazide-sensitive Na^+/Cl^- co-transporter abundance: role of aldosterone. J Am Soc Nephrol 2001;12:1335–41.

[2] Adachi S, Uchida S, Ito H, Hata M, Hiroe M, Marumo F, et al. Two isoforms of a chloride channel predominantly expressed in thick ascending limb of Henle's loop and collecting ducts of rat kidney. J Biol Chem 1994;269:17677–83.

[3] Aguilar-Bryan L, Nichols CG, Wechsler SW, Clement IV JP, Boyd III AE, Gonzalez G, et al. Cloning of the b cell high-affinity sulfonylurea receptor: a regulator of insulin secretion. Science 1995;268:423–6.

[4] Almeida AJ, Burg MB. Sodium transport in the rabbit connecting tubule. Am J Physiol 1982;243:F330–4.

[5] Alvarez dlR ZP, Naray-Fejes-Toth A, Fejes-Toth G, Canessa CM. The serum and glucocorticoid kinase sgk increases the abundance of epithelial sodium channels in the plasma membrane of *Xenopus* oocytes. J Biol Chem 1999;274:37834–9.

[6] Amemiya M, Loffing J, Lotscher M, Kaissling B, Alpern RJ, Moe OW. Expression of NHE-3 in the apical membrane of rat renal proximal tubule and thick ascending limb. Kidney Int 1995;48:1206–15.

[7] Anantharam A, Tian Y, Palmer LG. Open probability of the epithelial sodium channel is regulated by intracellular sodium. J Physiol 2006;574:333–47.

[8] Ares GR, Caceres PS, Ortiz PA. Molecular regulation of NKCC2 in the thick ascending limb. Am J Physiol Renal Physiol 2011;301:F1143–59.

[9] Ares GR, Ortiz PA. Constitutive endocytosis and recycling of NKCC2 in rat thick ascending limbs. Am J Physiol Renal Physiol 2010;299:F1193–202.

[10] Arroyo JP, Lagnaz D, Ronzaud C, Vazquez N, Ko BS, Moddes L, et al. Nedd4-2 modulates renal Na^+-Cl^- Co-transporter via the aldosterone-SGK1-Nedd4-2 pathway. J Am Soc Nephrol 2011;22:1707–19.

[11] Arroyo JP, Ronzaud C, Lagnaz D, Staub O, Gamba G. Aldosterone paradox: differential regulation of ion transport in distal nephron. Physiology (Bethesda) 2011;26:115–23.

[12] Auberson M, Hoffmann-Pochon N, Vandewalle A, Kellenberger S, Schild L. Epithelial Na^+ channel mutants causing Liddle's syndrome retain ability to respond to aldosterone and vasopressin. Am J Physiol Renal Physiol 2003;285:F459–71.

[13] Ausiello DA, Hall D. Regulation of vasopressin-sensitive adenylate cyclase by calmodulin. J Biol Chem 1981;256:9796–8.

[14] Bachmann S, Bostanjoglo M, Schmitt R, Ellison DH. Sodium transport-related proteins in the mammalian distal nephron – distribution, ontogeny and functional aspects. Anat Embryol (Berl) 1999;200:447–68.

[15] Bailey MA, Cantone A, Yan Q, MacGregor GG, Leng Q, Amorim JB, et al. Maxi-K channels contribute to urinary potassium excretion in the ROMK-deficient mouse model of Type II Bartter's syndrome and in adaptation to a high-K diet. Kidney Int 2006;70:51–9.

[16] Bayliss JM, Reeves WB, Andreoli TE. Cl^- transport in basolateral renal medullary vesicles: I. Cl^- transport in intact vesicles. J Membr Biol 1990;113:49–56.

[17] Beesley AH, Hornby D, White SJ. Regulation of distal nephron K^+ channels (ROMK) mRNA expression by aldosterone in rat kidney. J Physiol 1998;509:629–34.

[18] Beesley AH, Qureshi IZ, Giesberts AN, Parker AJ, White SJ. Expression of sulphonylurea receptor protein in mouse kidney. Pflugers Arch 1999;438:1–7.

[19] Bencsath P, Szenasi G, Takacs L. Water and electrolyte transport in Henle's loop and distal tubule after renal sympathectomy in the rat. Am J Physiol 1985;249:F308–14.

[20] Berger S, Bleich M, Schmid W, Cole TJ, Peters J, Watanabe H, et al. Mineralocorticoid receptor knockout mice: pathophysiology of Na^+ metabolism. Proc Natl Acad Sci USA 1998;95:9424–9.

[21] Birkenhager R, Otto E, Schurmann MJ, Vollmer M, Ruf EM, Maier-Lutz I, et al. Mutation of BSND causes bartter syndrome with sensorineural deafness and kidney failure. Nat Genet 2001;29:310–4.

[22] Blazer-Yost BL, Esterman MA, Vlahos CJ. Insulin-stimulated trafficking of ENaC in renal cells requires PI 3-kinase activity. Am J Physiol Cell Physiol 2003;284:C1645–53.

[23] Bleich M, Schlatter E, Greger R. The luminal K^+ channel of the thick ascending limb of Henle's loop. Pfl_gers Arch 1990;415:449–60.

[24] Boase NA, Rychkov GY, Townley SL, Dinudom A, Candi E, Voss AK, et al. Respiratory distress and perinatal lethality in Nedd4-2-deficient mice. Nat Commun 2011;2:287.

[25] Boettger T, Hubner CA, Maier H, Rust MB, Beck FX, Jentsch TJ. Deafness and renal tubular acidosis in mice lacking the K-Cl co-transporter Kcc4. Nature 2002;416:874–8.

[26] Boim MA, Ho K, Shuck ME, Bienkowski MJ, Block JH, Slightom JL, et al. ROMK inwardly rectifying ATP-sensitive K^+ channel. II. Cloning and distribution of alternative forms. Am J Physiol 1995;268:F1132–40.

[27] Bonvalet JP, Doignon I, Blot-Chabaud M, Pradelles P, Farman N. Distribution of 11 beta-hydroxysteroid dehydrogenase along the rabbit nephron. J Clin Invest 1990;86:832–7.

[28] Botero-Velez M, Curtis JJ, Warnock DG. Brief report: Liddle's syndrome revisited. A disorder of sodium reabsorption in the distal tubule. N Engl J Med 1994;330:178–81.
[29] Boyden LM, Choi M, Choate KA, Nelson-Williams CJ, Farhi A, Toka HR, et al. Mutations in kelch-like 3 and cullin 3 cause hypertension and electrolyte abnormalities. Nature 2012;482:98–102.
[30] Brezis M, Rosen S, Silva P, Epstein FH. Selective vulnerability of the medullary thick ascending limb to anoxia in the isolated perfused rat kidney. J Clin Invest 1984;73:182–90.
[31] Brezis M, Rosen S, Silva P, Epstein FH. Transport activity modifies thick ascending limb damage in the isolated perfused kidney. Kidney Int 1984;25:65–72.
[32] Bugaj V, Pochynyuk O, Stockand JD. Activation of the epithelial Na^+ channel in the collecting duct by vasopressin contributes to water reabsorption. Am J Physiol Renal Physiol 2009;297: F1411–8.
[33] Burg MB, Green N. Function of the thick ascending limb of Henle's loop. Am J Physiol 1973;224:659–68.
[34] Burnham C, Karlish SJD, Jorgensen PL. Identification and reconstitution of a $Na^+/K^+/Cl^-$ co-transporter and K^+ channel from lumninal membranes of red outer medulla. Biochim Biophys Acta 1985;821:461–9.
[35] Cai H, Cebotaru V, Wang YH, Zhang XM, Cebotaru L, Guggino SE, et al. WNK4 kinase regulates surface expression of the human sodium chloride co-transporter in mammalian cells. Kidney Int 2006;69:2162–70.
[36] Canessa CM, Schild L, Buell G, Thorens B, Gautshi I, Horisberger JD, et al. Amiloride-sensitive epithelial Na^+ channel is made of three homologous subunits. Nature 1994;367:463–7.
[37] Cantone A, Yang X, Yan Q, Giebisch G, Hebert SC, Wang T. Mouse model of type II Bartter's syndrome. I. Upregulation of thiazide-sensitive Na-Cl co-transport activity. Am J Physiol Renal Physiol 2008;294:F1366–72.
[38] Capasso G, Unwin R, Rizzo M, Pica A, Giebisch G. Bicarbonate transport along the loop of Henle: molecular mechanisms and regulation. J Nephrol 2002;15(Suppl. 5):S88–96.
[39] Castaneda-Bueno M, Cervantes LG, Vazquez N, Bobadilla NA, Uribe N, Alessi D, et al. *In vivo* activation of NCC by angiotensin II requires integrity of the WNK4-SPAK pathway. J Am Soc Nephrol 2011;22:102A.
[40] Chabardes D, Gagnan-Brunette M, Imbert-Teboul M, Gontcharevskaia O, Montegut M, Clique A, et al. Adenylate cyclase responsiveness to hormones in various portions of the human nephron. J Clin Invest 1980;65:439–48.
[41] Chabardes D, Imbert-Teboul M, Montegut M, Clique A, Morel F. Catecholamine sensitive adenylate cyclase activity in different segments of the rabbit nephron. Pflugers Arch 1975;361:9–15.
[42] Chamberlin ME, LeFurgey A, Mandel LJ. Suspension of medullary thick ascending limb tubules from the rabbit kidney. Am J Physiol 1984;247:F955–64.
[43] Chamberlin ME, Mandel LJ. Substrate support of medullary thick ascending limb oxygen consumption. Am J Physiol 1986;251(Renal. 20):F758–63.
[44] Chang SS, Grunder S, Hanukoglu A, Rosler A, Mathew PM, Hanukoglu I, et al. Mutations in subunits of the epithelial sodium channel cause salt wasting with hyperkalaemic acidosis, pseudohypoaldosteronism type 1. Nat Genet 1996;12: 248–53.
[45] Chen Z, Vaughn DA, Fanestil DD. Influence of gender on renal thiazide diuretic receptor density and response. J Am Soc Nephrol 1994;5:1112–9.
[46] Cheng HF, Harris RC. Cyclooxygenases, the kidney, and hypertension. Hypertension 2004;43:525–30.
[47] Choe H, Zhou H, Palmer LG, Sackin H. A conserved cytoplasmic region of ROMK modulates pH sensitivity, conductance, and gating. Am J Physiol (Renal Physiol) 1997;273: F516–29.
[48] Chraibi A, Horisberger JD. Na self inhibition of human epithelial Na channel: temperature dependence and effect of extracellular proteases. J Gen Physiol 2002;120:133–45.
[49] Chraibi A, Vallet V, Firsov D, Hess SK, Horisberger JD. Protease modulation of the activity of the epithelial sodium channel expressed in *Xenopus* oocytes. J Gen Physiol 1998;111: 127–38.
[50] Christensen BM, Perrier R, Wang Q, Zuber AM, Maillard M, Mordasini D, et al. Sodium and potassium balance depends on alphaENaC expression in connecting tubule. J Am Soc Nephrol 2010;21:1942–51.
[51] Clement JP, Kunjilwar K, Gonzalez G, Schwanstecher M, Panten U, Aguilar-Bryan L, et al. Association and stoichiometry of K_{ATP} channel subunits. Neuron 1997;18:827–38.
[52] Costanzo LS. Comparison of calcium and sodium transport in early and late rat distal tubules: effect of amiloride. Am J Physiol (Renal Fluid Electrolyte Physiol) 1984;246:F937–45.
[53] Costanzo LS. Localization of diuretic action in microperfused rat distal tubules: Ca and Na transport. Am J Physiol (Renal Fluid Electrolyte Physiol) 1985;248:F527–35.
[54] Dahlmann A, Pradervand S, Hummler E, Rossier BC, Frindt G, Palmer LG. Mineralocorticoid regulation of epithelial Na^+ channels is maintained in a mouse model of Liddle's syndrome. Am J Physiol Renal Physiol 2003;285:F310–8.
[55] de Rouffignac C, Elalouf JM. Hormonal regulation of chloride transport in the proximal and distal nephron. Annu Rev Physiol 1988;50:123–40.
[56] Debonneville C, Flores SY, Kamynina E, Plant PJ, Tauxe C, Thomas MA, et al. Phosphorylation of Nedd4-2 by Sgk1 regulates epithelial Na(+) channel cell surface expression. EMBO J 2001;20:7052–9.
[57] DeFronzo RA, Cooke CR, Andres R, Faloona GR, Davis PJ. The effect of insulin on renal handling of sodium, potassium, calcium, and phosphate in man. J Clin Invest 1975;55:845–55.
[58] DiBona GF, Sawin LL. Effect of renal nerve stimulation on NaCl and H_2O transport in Henle's loop of the rat. Am J Physiol 1982;243:F576–80.
[59] Dietl P, Good D, Stanton B. Adrenal corticosteroid action on the thick ascending limb. Semin Nephrol 1990;10:350–64.
[60] Djelidi S, Fay M, Cluzeaud F, Escoubet B, Eugene E, Capurro C, et al. Transcriptional regulation of sodium transport by vasopressin in renal cells. J Biol Chem 1997;272:32919–24.
[61] Dorup J. Ultrastructure of distal nephron cells in rat renal cortex. J Ultrastruct Res 1985;92:101–18.
[62] Doucet A, Katz AI. Mineralcorticoid receptors along the nephron: [^{3}H]aldosterone binding in rabbit tubules. Am J Physiol 1981;241:F605–11.
[63] Ecelbarger CA, Kim GH, Terris J, Masilamani S, Mitchell C, Reyes I, et al. Vasopressin-mediated regulation of epithelial sodium channel abundance in rat kidney. Am J Physiol Renal Physiol 2000;279:F46–53.
[64] Ecelbarger CA, Kim GH, Wade JB, Knepper MA. Regulation of the abundance of renal sodium transporters and channels by vasopressin. Exp Neurol 2001;171:227–34.
[65] Edwards RM, Jackson BA, Dousa TP. Protein kinase activity in isolated tubules of rat renal medulla. Am J Physiol 1980;238: F269–78.
[66] Ellison DH, Velazquez H, Wright FS. Thiazide-sensitive sodium chloride co-transport in early distal tubule. Am J Physiol (Renal Fluid Electrolyte Physiol) 1987;253:F546–54.

[67] Ellison DH, Velazquez H, Wright FS. Adaptation of the distal convoluted tubule of the rat. Structural and functional effects of dietary salt intake and chronic diuretic infusion. J Clin Invest 1989;83:113–26.
[68] Ergonul Z, Frindt G, Palmer LG. Regulation of maturation and processing of ENaC subunits in the rat kidney. Am J Physiol Renal Physiol 2006;291:F683–93.
[69] Escalante B, Erlij D, Falck JR, McGiff JC. Effect of cytochrome P450 arachidonate metabolites on ion transport in rabbit kidney loop of Henle. Science 1991;251:799–802.
[70] Estevez R, Boettger T, Stein V, Birkenhager R, Otto E, Hildebrandt F, et al. Barttin is a Cl^- channel b-subunit crucial for renal Cl^- reabsorption and inner ear K^+ secretion. Nature 2001;414:558–61.
[71] Eveloff J, Bayerdorffer E, Silva P, Kinne R. Sodium–chloride transport in the thick ascending limb of Henle's looop. Oxygen consumption studies in isolated cells. Pfl_gers Arch 1981;389: 263–70.
[72] Eveloff J, Calamia J. Effect of osmolarity on cation fluxes in medullary thick ascending limb cells. Am J Physiol (Renal Fluid Electrolyte Physiol) 1986;250:F176–80.
[73] Fakitsas P, Adam G, Daidie D, van Bemmelen MX, Fouladkou F, Patrignani A, et al. Early aldosterone-induced gene product regulates the epithelial sodium channel by deubiquitylation. J Am Soc Nephrol 2007;18:1084–92.
[74] Falin RA, Cotton CU. Acute downregulation of ENaC by EGF involves the PY motif and putative ERK phosphorylation site. J Gen Physiol 2007;130:313–28.
[75] Farman N, Bonvalet JP. Aldosterone binding in isolated tubules. III. Autoradiography along the rat nephron. Am J Physiol 1983;245:F606–14.
[76] Fejes-Toth G, Frindt G, Naray-Fejes-Toth A, Palmer LG. Epithelial Na^+ channel activation and processing in mice lacking SGK1. Am J Physiol Renal Physiol 2008;294:F1298–305.
[77] Fenton RA, Brond L, Nielsen S, Praetorius J. Cellular and subcellular distribution of the type-2 vasopressin receptor in the kidney. Am J Physiol Renal Physiol 2007;293:F748–60.
[78] Feraille E, Rousselot M, Rajerison R, Favre H. Effect of insulin on Na^+,$K(^+)$-ATPase in rat collecting duct. J Physiol 1995;488 (Pt 1):171–80.
[79] Firsov D, Schild L, Gautschi I, Merillat AM, Schneeberger E, Rossier BC. Cell surface expression of the epithelial Na channel and a mutant causing Liddle syndrome: a quantitative approach. Proc Natl Acad Sci USA 1996;93:15370–5.
[80] Forbush IB, Palfrey HC. [^{3}H]Bumetanide binding to membranes isolated from dog kidney outer medulla. Relationship to the Na,K,Cl co-transport system. J Biol Chem 1983;258: 11787–92.
[81] Friedberg CE, Koomans HA, Bijlsma JA, Rabelink TJ, Dorhout Mees EJ. Sodium retention by insulin may depend on decreased plasma potassium. Metabolism 1991;40:201–4.
[82] Friedman PA. Bumetanide inhibition of $[CO_2 + HCO_3]$-dependent and -independent equivalent electrical flux in renal cortical thick ascending limbs. J Pharmacol Exp Ther 1986;238:407–14.
[83] Friedman PA, Andreoli TE. CO_2-stimulated NaCl absorption in the mouse renal cortical thick ascending limb of Henle. Evidence for synchronous Na^+/H^+ and Cl^-/HCO_3^- exchange in apical plasma membranes. J Gen Physiol 1982;80:683–711.
[84] Friedman PA, Andreoli TE. Effects of $(CO_2 + HCO_3^-)$ on electrical conductance in cortical thick ascending limbs. Kidney Int 1986;30:325–31.
[85] Frindt G, Ergonul Z, Palmer LG. Surface expression of epithelial Na channel protein in rat kidney. J Gen Physiol 2008;131:617–27.
[86] Frindt G, Masilamani S, Knepper MA, Palmer LG. Activation of epithelial Na channels during short term Na deprivation. Am J Physiol Renal Physiol 2001;280:F112–8.
[87] Frindt G, Palmer LG. Apical potassium channels in the rat connecting tubule. Am J Physiol Renal Physiol 2004;287: F1030–7.
[88] Frindt G, Palmer LG. Na channels in the rat connecting tubule. Am J Physiol Renal Physiol 2004;286:F669–74.
[89] Frindt G, Palmer LG. Surface expression of sodium channels and transporters in rat kidney: effects of dietary sodium. Am J Physiol Renal Physiol 2009;297:F1249–55.
[90] Frindt G, Palmer LG. Effects of insulin on Na and K transporters in the rat CCD. Am J Physiol Renal Physiol 2012;302(10): F1227–33.
[91] Funder JW, Pearce PT, Smith R, Smith AI. Mineralocorticoid action: target tissue specificity is enzyme, not receptor, mediated. Science 1988;242:583–5.
[92] Gamba G. Molecular physiology and pathophysiology of the electroneutral cation-chloride co-transporters. Physiol Rev 2005;85:423–93.
[93] Gamba G, Friedman PA. Thick ascending limb: the $Na(^+)$:$K(^+)$:$2Cl(^-)$ co-transporter, NKCC2, and the calcium-sensing receptor, CaSR. Pflugers Arch 2009;458:61–76.
[94] Gamba G, Miyanoshita A, Lombardi M, Lytton J, Lee WS, Hediger MA, et al. Molecular cloning, primary structure and characterization of two members of the mammalian electroneutral sodium-(potassium)-chloride co-transporter family expressed in kidney. J Biol Chem 1994;269:17713–22.
[95] Gamba G, Saltzberg SN, Lombardi M, Miyanoshita A, Lytton J, Hediger MA, et al. Primary structure and functional expression of a cDNA encoding the thiazide-sensitive, electroneutral sodium-chloride co-transporter. Proc Natl Acad Sci USA 1993;90:2749–53.
[96] Geller DS, Rodriguez-Soriano J, Vallo BA, Schifter S, Bayer M, Chang SS, et al. Mutations in the mineralocorticoid receptor gene cause autosomal dominant pseudohypoaldosteronism type I. Nat Genet 1998;19:279–81.
[97] Gesek FA, Friedman PA. Mechanism of calcium transport stimulated by chlorothiazide in mouse distal convoluted tubule cells. J Clin Invest 1992;90:429–38.
[98] Giebisch G. Physiological roles of renal potassium channels. Semin Nephrol 1999;19:458–71.
[99] Gill Jr JR, Bartter FC. On the impairment of renal concentrating ability in prolonged hypercalcemia and hypercalciuria in man. J Clin Invest 1961;40:716–22.
[100] Gimenez I, Forbush B. Short term stimulation of the renal Na-K-Cl co-transporter (NKCC2) by vasopressin involves phosphorylation and membrane translocation of the protein. J Biol Chem 2003;278:26946–51.
[101] Glover M, Mercier ZA, Figg N, O'Shaughnessy KM. The activity of the thiazide-sensitive $Na(^+)$-Cl co-transporter is regulated by protein phosphatase PP4. Can J Physiol Pharmacol 2010;88:986–95.
[102] Gonzales EB, Kawate T, Gouaux E. Pore architecture and ion sites in acid-sensing ion channels and P2X receptors. Nature 2009;460:599–604.
[103] Gonzalez-Rodriguez E, Gaeggeler HP, Rossier BC. IGF-1 vs insulin: respective roles in modulating sodium transport via the PI-3 kinase/Sgk1 pathway in a cortical collecting duct cell line. Kidney Int 2007;71:116–25.
[104] Good DW. Sodium-dependent bicarbonate absorption by cortical thick ascending limb of rat kidney. Am J Physiol (Renal Fluid Electrolyte Physiol) 1985;248-17:F821–9.
[105] Good DW. Bicarbonate absorption by the thick ascending limb of Henle's loop. Semin Nephrol 1990;10:132–8.

[106] Grantham JJ, Kurg MB, Obloff J. The nature of transtubular Na and K transport in isolated rabbit renal collecting tubules. J Clin Invest 1970;49:1815–26.
[107] Greger R. Chloride reabsorption in the rabbit cortical thick ascending limb of the loop of Henle. A sodium dependent process. Pflugers Arch 1981;390:38–43.
[108] Greger R. Coupled transport of Na^+ and Cl^- in the thick ascending limb of Henle's loop of rabbit nephron. Scand Audiol Suppl 1981;14(Suppl):1–15.
[109] Greger R, Bleich M, Schlatter E. Ion channels in the thick ascending limb of Henle's loop. Renal Physiol Biochem 1990;13:37–50.
[110] Greger R, Oberleithner H, Schlatter E, Cassola AC, Weidtke C. Chloride activity in cells of isolated perfused cortical thick ascending limbs of rabbit kidney. Pflugers Arch 1983;399: 29–34.
[111] Greger R, Schlatter E. Presence of luminal K^+, a prerequisite for active NaCl transport in the cortical thick ascending limb of Henle's loop of rabbit kidney. Pflugers Arch 1981;392:92–4.
[112] Greger R, Schlatter E. Properties of the basolateral membrane of the cortical thick ascending limb of Henle's loop of rabbit kidney. A model for secondary active chloride transport. Pflugers Arch 1983;396:325–34.
[113] Greger R, Schlatter E. Properties of the lumen membrane of the cortical thick ascending limb of Henle's loop of rabbit kidney. Pflugers Arch 1983;396:315–24.
[114] Greger R, Velazquez H. The cortical thick ascending limb and early distal convoluted tubule in the urinary concentrating mechanism. Kidney Int 1987;31:590–6.
[115] Gu RM, Wang WH. Arachidonic acid inhibits K channels in basolateral membrane of the thick ascending limb. Am J Physiol Renal Physiol 2002;283:F407–14.
[116] Gu RM, Wei Y, Jiang H, Balazy M, Wang WH. The role of 20-HETE in mediating the effect of dietary K intake on the apical K channels in the mTAL. Am J Physiol Renal Physiol 2001;280: F223–30.
[117] Gu RM, Wei Y, Jiang HL, Lin DH, Sterling H, Bloom P, et al. K depletion enhances the extracellular Ca^{2+}-induced inhibition of the apical K channels in the mTAL of rat kidney. J Gen Physiol 2002;119:33–44.
[118] Gu RM, Yang L, Zhang Y, Wang L, Kong S, Zhang C, et al. CYP-omega-hydroxylation-dependent metabolites of arachidonic acid inhibit the basolateral 10 pS chloride channel in the rat thick ascending limb. Kidney Int 2009;76:849–56.
[119] Gu R, Wang J, Zhang Y, Li W, Xu Y, Shan H, et al. Adenosine stimulates the basolateral 50 pS K channels in the thick ascending limb of the rat kidney. AJP-Renal Physiol 2007;293: F299–305.
[120] Guinamard R, Chraibi A, Teulon J. A small-conductance Cl^- channel in the mouse thick ascending limb that is activated by ATP and protein kinase A. J Physiol 1995;485:97–112.
[121] Guinamard R, Paulais M, Teulon J. Inhibition of a small-conductance cAMP-dependent Cl^- channel in the mouse thick ascending limb at low internal pH. J Physiol 1996;490:759–65.
[122] Gunaratne R, Braucht DW, Rinschen MM, Chou CL, Hoffert JD, Pisitkun T, et al. Quantitative phosphoproteomic analysis reveals cAMP/vasopressin-dependent signaling pathways in native renal thick ascending limb cells. Proc Natl Acad Sci USA 2010;107:15653–8.
[123] Hall DA, Varney DM. Effect of vasopressin on electrical potential difference and chloride transport in mouse medullary thick ascending limb of Henle's loop. J Clin Invest 1980;66:792–802.
[124] Hammerman MR, Miller SB. The growth hormone insulin-like growth factor axis in kidney revisited. Am J Physiol 1993;265: F1–14.
[125] Hanley MJ, Kokko JP, Gross JB, Jacobson HR. Electrophysiologic study of the cortical collecting tubule of the rabbit. Kidney Int 1980;17:74–81.
[126] Hansen TK, Moller J, Thomsen K, Frandsen E, Dall R, Jorgensen JO, et al. Effects of growth hormone on renal tubular handling of sodium in healthy humans. Am J Physiol Endocrinol Metab 2001;281:E1326–32.
[127] Hansson JH, Nelson-Williams C, Suzuki H, Schild L, Shimkets R, Lu Y, et al. Hypertension caused by a truncated epithelial sodium channel gamma subunit: genetic heterogeneity of Liddle syndrome. Nat Genet 1995;11:76–82.
[128] Hansson JH, Schild L, Lu Y, Wilson TA, Gautschi I, Shimkets R, et al. A *de novo* missense mutation of the beta subunit of the epithelial sodium channel causes hypertension and Liddle syndrome, identifying a proline-rich segment critical for regulation of channel activity. Proc Natl Acad Sci USA 1995;92:11495–9.
[129] Harris M, Firsov D, Vuagniaux G, Stutts MJ, Rossier BC. A novel neutrophil elastase inhibitor prevents elastase activation and surface cleavage of the epithelial sodium channel expressed in *Xenopus laevis* oocytes. J Biol Chem 2007;282:58–64.
[130] Harris RC, McKanna JA, Akai Y, Jacobson HR, Dubois RN, Breyer MD. Cyclooxygenase-2 is associated with the macula densa of rat kidney and increases with salt restriction. J Clin Invest 1994;94:2504–10.
[131] Hawk CT, Li L, Schafer JA. AVP and aldosterone at physiological concentrations have synergistic effects on Na^+ transport in rat CCD. Kidney Int Suppl 1996;57:S35–41.
[132] Hebert SC. Hypertonic cell volume regulation in mouse thick limbs. I. ADH dependency and nephron heterogeneity. Am J Physiol 1986;250:C907–19.
[133] Hebert SC. Extracellular calcium-sensing receptor: implications for calcium and magnesium handling in the kidney. Kidney Int 1996;50:2129–39.
[134] Hebert SC. Bartter syndrome. Curr Opin Nephrol Hypertens 2003;12:527–32.
[135] Hebert SC, Andreoli TE. Effects of antidiuretic hormone on cellular conductive pathways in mouse medullary thick ascending limbs of Henle: II. Determinants of the ADH-mediated increases in transepithelial voltage and in net Cl^- absorption. J Membr Biol 1984;80:221–33.
[136] Hebert SC, Andreoli TE. Ionic conductance pathways in the mouse medullary thick ascending limb of Henle. The paracellular pathway and electrogenic Cl^- absorption. J Gen Physiol 1986;87:567–90.
[137] Hebert SC, Brown EM. The scent of an ion: calcium-sensing and its roles in health and disease. Curr Opin Nephrol Hypertens 1996;5:45–53.
[138] Hebert SC, Culpepper RM, Andreoli TE. NaCl transport in mouse medullary thick ascending limbs. I. Functional nephron heterogeneity and ADH-stimulated NaCl co-transport. Am J Physiol (Renal Fluid Electrolyte Physiol) 1981;241:F412–31.
[139] Hebert SC, Culpepper RM, Andreoli TE. NaCl transport in mouse medullary thick ascending limbs. II. ADH enhancement of transcellular NaCl cotrasport; origin of transepithelial volatge. Am J Physiol (Renal Fluid Electrolyte Physiol) 1981;241:F432–42.
[140] Hebert SC, Culpepper RM, Andreoli TE. NaCl transport in mouse medullary thick ascending limbs. III. Modulation of ADH efect by peritubular osmolality. Am J Physiol (Renal Fluid Electrolyte Physiol) 1981;241:F443–51.
[141] Hebert SC, Desir G, Giebisch G, Wang W. Molecular diversity and regulation of renal potassium channels. Physiol Rev 2005;85:319–71.

[142] Hebert SC, Friedman PA, Andreoli TE. Effects of antidiuretic hormone on cellular conductive pathways in mouse medullary thick ascending limbs of Henle: I. ADH increases transcellular conductance pathways. J Membr Biol 1984;80:201–19.

[143] Ho K, Nichols CG, Lederer WJ, Lytton J, Vassilev PM, Kanazirska MV, et al. Cloning and expression of an inwardly rectifying ATP-regulated potassium channel. Nature 1993;362:31–8.

[144] Huang C, Sindic A, Hill CE, Hujer KM, Chan KW, Sassen M, et al. Interaction of the Ca^{2+}-sensing receptor with the inwardly rectifying potassium channels Kir4.1 and Kir4.2 results in inhibition of channel function. AJP–Renal Physiol 2007;292:F1073–81.

[145] Hughey RP, Mueller GM, Bruns JB, Kinlough CL, Poland PA, Harkleroad KL, et al. Maturation of the epithelial Na^+ channel involves proteolytic processing of the alpha- and gamma-subunits. J Biol Chem 2003;278:37073–82.

[146] Hummler E, Barker P, Talbot C, Wang Q, Verdumo C, Grubb R, et al. A mouse model for the renal salt-wasting syndrome pseudohypoaldosteronism. Proc Natl Acad Sci USA 1997;94:11710–5.

[147] Hus-Citharel A, Morel F. Coupling of metabolic CO_2 production to ion transport in isolated rat thick ascending limbs and collecting tubules. Pflugers Arch 1986;407:421–7.

[148] Imai M. The connecting tubule: a functional subdivision of the rabbit distal nephron segments. Kidney Int 1979;15:346–56.

[149] Imai M, Hayashi M, Araki M. Functional heterogeneity of the descending limbs of Henle's loop. I. Internephron heterogeneity in the hamster kidney. Pflugers Arch 1984;402:385–92.

[150] Imai M, Taniguchi J, Tabei K. Function of thin loops of Henle. Kidney Int 1987;31:565–79.

[151] Inagaki N, Gonoi T, Clement IV JP, Namba N, Inazawa J, Gonzalez G, et al. Reconstitution of I_{ATP}: an inward rectifier subunit plus the sulfonylurea receptor. Science 1995;270:1166–70.

[152] Jasti J, Furukawa H, Gonzales EB, Gouaux E. Structure of acid-sensing ion channel 1 at 1.9 A resolution and low pH. Nature 2007;449:316–23.

[153] Jeck N, Waldegger P, Doroszewicz J, Seyberth H, Waldegger S. A common sequence variation of the CLCNKB gene strongly activates ClC-Kb chloride channel activity. Kidney Int 2004;65:190–7.

[154] Jeck N, Waldegger S, Lampert A, Boehmer C, Waldegger P, Lang PA, et al. Activating mutation of the renal epithelial chloride channel ClC-Kb predisposing to hypertension. Hypertension 2004;43:1175–81.

[155] Jentsch TJ, Stein V, Weinreich F, Zdebik AA. Molecular structure and physiological function of chloride channels. Physiol Rev 2002;82:503–68.

[156] Kahle KT, MacGregor GG, Wilson FH, Van Hoek AN, Brown D, Ardito T, et al. Paracellular Cl^- permeability is regulated by WNK4 kinase: insight into normal physiology and hypertension. Proc Natl Acad Sci USA 2004;101:14877–82.

[157] Kahle KT, Wilson FH, Leng Q, Lalioti MD, O'Connell AD, Dong K, et al. WNK4 regulates the balance between renal NaCl reabsorption and K^+ secretion. Nat Genet 2003;35:372–6.

[158] Kaissling B. Ultrastructural characterization of the connecting tubule and the different segments of the collecting duct system in the rabbit kidney. Curr Probl Clin Biochem 1977;8:435–46.

[159] Kaissling B, Stanton BA. Adaptation of distal tubule and collecting duct to increased sodium delivery. I. Ultraestructure. Am J Physiol (Renal Fluid Electrolyte Physio) 1988;255:F1256–68.

[160] Kamenicky P, Viengchareun S, Blanchard A, Meduri G, Zizzari P, Imbert-Teboul M, et al. Epithelial sodium channel is a key mediator of growth hormone-induced sodium retention in acromegaly. Endocrinology 2008;149:3294–305.

[161] Katz AI, Doucet A, Morel F. Na-K-ATPase activity along the rabbit, rat, and mouse nephron. Am J Physiol 1979;237:F114–20.

[162] Kellenberger S, Gautschi I, Pfister Y, Schild L. Intracellular thiol-mediated modulation of epithelial sodium channel activity. J Biol Chem 2005;280:7739–47.

[163] Kellenberger S, Gautschi I, Schild L. A single point mutation in the pore region of the epithelial Na^+ channel changes ion selectivity by modifying molecular sieving. Proc Natl Acad Sci USA 1999;96:4170–5.

[164] Kellenberger S, Gautschi I, Schild L. An external site controls closing of the epithelial Na^+ channel ENaC. J Physiol 2002;543:413–24.

[165] Kellenberger S, Gautschi I, Schild L. Mutations in the epithelial Na^+ channel ENaC outer pore disrupt amiloride block by increasing its dissociation rate. Mol Pharmacol 2003;64: 848–56.

[166] Kieferle S. Two highly homologous members of the CIC chloride channel family in both rat and human kidney. Proc Natl Acad Sci USA 1994;91:6943–7.

[167] Kikeri D, Azar S, Sun A, Zeidel ML, Hebert SC. $Na(^+)$-H^+ antiporter and $Na(^+)$-(HCO_3^-)n symporter regulate intracellular pH in mouse medullary thick limbs of Henle. Am J Physiol 1990;258:F445–56.

[168] Kikeri D, Azar S, Sun A, Zeidel ML, Hebert SC. Na^+-H^+ antiporter and Na^+-$(HCO_3^-)_n$ symporter regulate intracellular pH in mouse medullary thick limbs of Henle. Am J Physiol (Renal Fluid Electrolyte Physiol) 1990;258-27:F445–56.

[169] Kim GH, Masilamani S, Turner R, Mitchell C, Wade JB, Knepper MA. The thiazide-sensitive Na-Cl co-transporter is an aldosterone-induced protein. Proc Natl Acad Sci USA 1998;95:14552–7.

[170] Kim J, Kim YH, Cha JH, Tisher CC, Madsen KM. Intercalated cell subtypes in connecting tubule and cortical collecting duct of rat and mouse. J Am Soc Nephrol 1999;10:1–12.

[171] Kinne R, Kinne-Saffran E, Scholermann B, Schutz H. The anion specificity of the sodium-potassium-chloride co-transporter in rabbit kidney outer medulla: studies on medullary plasma membranes. Pflugers Arch 1986;407(Suppl. 2):S168–73.

[172] Kirchner KA. Insulin increases loop segment chloride reabsorption in the euglycemic rat. Am J Physiol 1988;255:F1206–13.

[173] Klaerke DA, Petersen J, Jorgensen PL. Purification of Ca^{2+}-activated K^+ channel protein on calmodulin affinity columns after detergent solubilization of luminal membranes from outer medulla. FEBS Lett 1987;216:211–6.

[174] Koenig B, Ricapito S, Kinne R. Chloride transport in the thick ascending limb of Henle's loop: potassium dependence and stoichiometry of the NaCl co-transport system in plasma membrane vesicles. Pflugers Arch 1983;399:173–9.

[175] Koeppen BM. Conductive properties of the rabbit outer medullary collecting duct: inner stripe. Am J Physiol 1985;248:F500–6.

[176] Kokko JP. Sodium chloride and water transport in the descending limb of Henle. J Clin Invest 1970;49:1838–46.

[177] Kondo C, Isomoto S, Matsumoto S, Yamada M, Horio Y, Yamashita S, et al. Cloning and functional expression of a novel isoform of ROMK inwardly rectifying ATP-dependent K^+ channel, ROMK6 (Kir1.1f). FEBS Lett 1996;399:122–6.

[178] Kondo C, Isomoto S, Matsumoto S, Yamada M, Horio Y, Yamashita S, et al. Cloning and functional expression of a novel isoform of ROMK inwardly rectifying ATP-dependent K^+ channel, ROMK6 (Kir1.1f). FEBS Lett 1996;399:122–6.

[179] Kong S, Zhang C, Li W, Wang L, Luan H, Wang WH, et al. Stimulation of Ca^{2+}-sensing receptor inhibits the basolateral 50-pS K channels in the thick ascending limb of rat kidney.

Biochimica et Biophysica Acta (BBA)—Mol Cell Res 2012;1823: 273—81.
[180] Krapf R. Basolateral membrane H/OH/HCO_3 transport in the rat cortical thick ascending limb. Evidence for an electrogenic Na/HCO_3 co-transporter in parallel with a Na/H antiporter. J Clin Invest 1988;82:234—41.
[181] Krozowski Z, MaGuire JA, Stein-Oakley AN, Dowling J, Smith RE, Andrews RK. Immunohistochemical localization of the 11 beta-hydroxysteroid dehydrogenase type II enzyme in human kidney and placenta. J Clin Endocrinol Metab 1995;80:2203—9.
[182] Kudo LH, van Baak AA, Rocha AS. Effect of vasopressin on sodium transport across inner medullary collecting duct. Am J Physiol 1990;258:F1438—47.
[183] Lachheb S, Cluzeaud F, Bens M, Genete M, Hibino H, Lourdel S, et al. Kir4.1/Kir5.1 channel forms the major K^+ channel in the basolateral membrane of mouse renal collecting duct principal cells. AJP—Renal Physiol 2008;294:F1398—407.
[184] Lalioti MD, Zhang J, Volkman HM, Kahle KT, Hoffmann KE, Toka HR, et al. Wnk4 controls blood pressure and potassium homeostasis via regulation of mass and activity of the distal convoluted tubule. Nat Genet 2006;38:1124—32.
[185] Lauf PK, McManus TJ, Haas M, Forbush IB, Duhm J, Flatman PW, et al. Physiology and biophysics of chloride and cation co-transport across cell membranes. Fed Proc 1987;46:2377—94.
[186] Leichtweiss HP, Lubbers DW, Weiss CH, Baumgartl H, Reschke W. The oxygen supply of the rat kidney: measurement of intrarenal pO_2. Pflugers Arch 1969;309:328—49.
[187] Leviel F, Hubner CA, Houillier P, Morla L, El Moghrabi S, Brideau G, et al. The Na^+-dependent chloride-bicarbonate exchanger SLC4A8 mediates an electroneutral Na^+ reabsorption process in the renal cortical collecting ducts of mice. J Clin Invest 2010;120:1627—35.
[188] Liddle GW, Bledsoe T, Coppage Jr WS. A familial renal disorder simulating primary aldosteronism but with negligible aldosterone secretion. Trans Assoc Am Phys 1963;76:199—213.
[189] Liou HH, Zhou SS, Huang CL. Regulation of ROMK1 channel by protein kinase A via a phosphatidylinositol 4,5-bisphosphate-dependent mechanism. Proc Natl Acad Sci USA 1999;96:5820—5.
[190] Loffing J, Kaissling B. Sodium and calcium transport pathways along the mammalian distal nephron: from rabbit to human. Am J Physiol Renal Physiol 2003;284:F628—43.
[191] Loffing J, Loffing-Cueni D, Hegyi I, Kaplan MR, Hebert SC, Hir ML, et al. Thiazide treatment of rats provokes apoptosis in distal tubule cells. Kidney Int 1996;50:1180—90.
[192] Loffing J, Loffing-Cueni D, Macher A, Hebert SC, Olson B, Knepper MA, et al. Localization of epithelial sodium channel and aquaporin-2 in rabbit kidney cortex. Am J Physiol Renal Physiol 2000;278:F530—9.
[193] Loffing J, Pietri L, Aregger F, Bloch-Faure M, Ziegler U, Meneton P, et al. Differential subcellular localization of ENaC subunits in mouse kidney in response to high- and low-Na diets. Am J Physiol Renal Physiol 2000;279:F252—8.
[194] Loffing J, Vallon V, Loffing-Cueni D, Aregger F, Richter K, Pietri L, et al. Altered renal distal tubule structure and renal Na^+ and Ca^{2+} handling in a mouse model for Gitelman's syndrome. J Am Soc Nephrol 2004;15:2276—88.
[195] Loffing J, Zecevic M, Feraille E, Kaissling B, Asher C, Rossier BC, et al. Aldosterone induces rapid apical translocation of ENaC in early portion of renal collecting system: possible role of SGK. Am J Physiol Renal Physiol 2001;280:F675—82.
[196] Louis-Dit-Picard H, Barc J, Trujillano D, Miserey-Lenkei S, Bouatia-Naji N, Pylypenko O, et al. KLHL3 mutations cause familial hyperkalemic hypertension by impairing ion transport in the distal nephron. Nat Genet 2012;44:456—60.
[197] Lourdel S, Paulais M, Cluzeaud F, Bens M, Tanemoto M, Kurachi Y, et al. An inward rectifier K^+ channel at the basolateral membrane of the mouse distal convoluted tubule: similarities with Kir4-Kir5.1 heteromeric channels. J Physiol 2002;538:391—404.
[198] Lu M, Hebert SC, Giebisch G. Hydrolyzable ATP and PIP_2 modulate the small conductance K^+ channel in apical membranes of rat cortical collecting duct (CCD). J Gen Physiol 2002;120:603—15.
[199] Lu M, Leng Q, Egan ME, Caplan MJ, Boulpaep E, Giebisch G, et al. CFTR is required for PKA-regulated ATP sensitivity of Kir1.1 potassium channels in mouse kidney. J Clin Invest 2006;116:797—807.
[200] Lu M, Wang T, Yan Q, Wang W, Giebisch G, Hebert SC. ROMK is required for expression of the 70pS K channel in the thick ascending limb. Am J Physiol Renal Physiol 2004;286: F490—5.
[201] Lu M, Wang T, Yan Q, Yang X, Dong K, Knepper MA, et al. Absence of small-conductance K^+ channel (SK) activity in apical membranes of thick ascending limb and cortical collecting duct in ROMK (Bartter's) knockout mice. J Biol Chem 2002;277:37881—7.
[202] Lu M, Wang W. Two types of K^+ channels are present in the apical membrane of the thick ascending limb of the mouse kidney. Kidney Blood Press Res 2000;23:75—82.
[203] MacGregor GG, Xu J, McNicholas CM, Giebisch G, Hebert SC. Partially active channels produced by PKA site mutation of the cloned renal K^+ channel ROMK2. Am J Physiol (Renal Physiol) 1998;275:F415—22.
[204] Madsen KM, Verlander JW, Tisher CC. Relationship between structure and function in distal tubule and collecting duct. J Electron Microsc Tech 1988;9:187—208.
[205] Malnic G, Klose RM, Giebisch G. Microperfusion study of distal tubular potassium and sodium transfer in rat kidney. Am J Physiol 1966;211:548—59.
[206] Masilamani S, Kim GH, Mitchell C, Wade JB, Knepper MA. Aldosterone-mediated regulation of ENaC alpha, beta, and gamma subunit proteins in rat kidney. J Clin Invest 1999;104: R19—23.
[207] McGiff JC. Cytochrome P-450 metabolism of arachidonic acid. Annu Rev Pharmacol Toxicol 1991;31:339—69.
[208] McNicholas CM, Guggino WB, Schwiebert EM, Hebert SC, Giebisch G, Egan ME. Sensitivity of a renal K^+ channel (ROMK2) to the inhibitory sulfonylurea compound, glibenclamide, is enhanced by co-expression with the ATP-binding cassette transporter cystic fibrosis transmembrane regulator. Proc Natl Acad Sci USA 1996;93:8083—8.
[209] Meade P, Hoover RS, Plata C, Vazquez N, Bobadilla NA, Gamba G, et al. cAMP-dependent activation of the renal-specific Na^+-K^+-$2Cl^-$ co-transporter is mediated by regulation of co-transporter trafficking. Am J Physiol Renal Physiol 2003;284:F1145—54.
[210] Mennitt PA, Wade JB, Ecelbarger CA, Palmer LG, Frindt G. Localization of ROMK channels in the rat kidney. J Am Soc Nephrol 1997;8:1823—30.
[211] Moller J, Jorgensen JO, Marqversen J, Frandsen E, Christiansen JS. Insulin-like growth factor I administration induces fluid and sodium retention in healthy adults: possible involvement of renin and atrial natriuretic factor. Clin Endocrinol (Oxf) 2000;52:181—6.
[212] Molony DA, Reeves WB, Andreoli TE. Na^+:K^+:$2Cl^-$ co-transport and the thick ascending limb. Kidney Int 1989;36:418—26.

[213] Molony DA, Reeves WB, Andreoli TE. Na^+:K^+:2Cl^- co-transport and the thick ascending limb. Kidney Int 1989;36:418–26.
[214] Molony DA, Reeves WB, Hebert SC, Andreoli TE. ADH increases apical Na^+,K^+,2Cl^- entry in mouse medullary thick ascending limbs of Henle. Am J Physiol (Renal Fluid Electrolyte Physiol) 1987;252:F177–87.
[215] Monroy A, Plata C, Hebert SC, Gamba G. Characterization of the thiazide-sensitive $Na(^+)$-$Cl(^-)$ co-transporter: a new model for ions and diuretics interaction. Am J Physiol Renal Physiol 2000;279:F161–9.
[216] Morales MM, Carroll TP, Morita T, Schwiebert EM, Devuyst O, Wilson PD, et al. Both the wild type and a functional isoform of CFTR are expressed in kidney. Am J Physiol (Renal Fluid Electrolyte Physiol) 1996;270:F1038–48.
[217] Morel F, Imbert-Teboul M, Chabardes D. Distribution of hormone-dependent adenylate cyclase in the nephron and its physiological significance. Annu Rev Physiol 1981;43:569–81.
[218] Moreno G, Merino A, Mercado A, Herrera JP, Gonzalez-Salazar J, Correa-Rotter R, et al. Electronuetral Na-coupled co-transporter expression in the kidney during variations of NaCl and water metabolism. Hypertension 1998;31:1002–6.
[219] Morgan T, Berliner RW. Permeability of the loop of Henle, vasa recta, and collecting duct to water, urea, and sodium. Am J Physiol 1968;215:108–15.
[220] Morris RG, Schafer JA. cAMP increases density of ENaC subunits in the apical membrane of MDCK cells in direct proportion to amiloride-sensitive $Na(^+)$ transport. J Gen Physiol 2002;120:71–85.
[221] Mount DB, Baekgard A, Hall AE, Plata C, Xu J, Beier DR, et al. Isoforms of the Na-K-2Cl transporter in murine TAL: I. Molecular characterization and intrarenal localization. Am J Physiol (Renal Physiol) 1999;276:F347–58.
[222] Mune T, Rogerson FM, Nikkila H, Agarwal AK, White PC. Human hypertension caused by mutations in the kidney isozyme of 11 beta-hydroxysteroid dehydrogenase. Nat Genet 1995;10:394–9.
[223] Musch W, Hedeshi A, Decaux G. Low sodium excretion in SIADH patients with low diuresis. Nephron Physiol 2004;96:11–8.
[224] Mutig K, Paliege A, Kahl T, Jons T, Muller-Esterl W, Bachmann S. Vasopressin V2 receptor expression along rat, mouse, and human renal epithelia with focus on TAL. Am J Physiol Renal Physiol 2007;293:F1166–77.
[225] Na T, Wu G, Peng JB. Disease-causing mutations in the acidic motif of WNK4 impair the sensitivity of WNK4 kinase to calcium ions. Biochem Biophys Res Commun 2012;419:293–8.
[226] Nakao A, Allen ML, Sonnenberg WK, Smith WL. Regulation of cAMP metabolism by PGE_2 in cortical and medullary thick ascending limb of Henle's loop. Am J Physiol (Cell Physiol) 1989;256-25:C652–7.
[227] Naray-Fejes-Toth A, Watlington CO, Fejes-Toth G. 11 beta-Hydroxysteroid dehydrogenase activity in the renal target cells of aldosterone. Endocrinology 1991;129:17–21.
[228] Nicco C, Wittner M, diStefano A, Jounier S, Bankir L, Bouby N. Chronic exposure to vasopressin upregulates ENaC and sodium transport in the rat renal collecting duct and lung. Hypertension 2001;38:1143–9.
[229] Nicod M, Michlig S, Flahaut M, Salinas M, Fowler JN, Horisberger JD, et al. A novel vasopressin-induced transcript promotes MAP kinase activation and ENaC downregulation. EMBO J 2002;21:5109–17.
[230] Nishida M, MacKinnon R. Structural basis of inward rectification. cytoplasmic pore of the G protein-gated inward rectifier GIRK1 at 1.8 Å resolution. Cell 2002;111:957–65.
[231] Nishida M, Cadene M, Chait BT, MacKinnon R. Crystal structure of a Kir3.1-prokaryotic Kir channel chimera. EMBO J 2007;26:4005–15.
[232] Ortiz PA. cAMP increases surface expression of NKCC2 in rat thick ascending limbs: role of VAMP. Am J Physiol Renal Physiol 2006;290:F608–16.
[233] Palmer LG, Choe H, Frindt G. Is the secretory K channel in the rat CCT ROMK? Am J Physiol (Renal Fluid Electrolyte Physiol) 1997;273:F404–10.
[234] Palmer LG, Frindt G. Effects of cell Ca and pH on Na channels from rat cortical collecting tubule. Am J Physiol 1987;253:F333–9.
[235] Palmer LG, Frindt G. Conductance and gating of epithelial Na channels from rat cortical collecting tubule. Effects of luminal Na and Li. J Gen Physiol 1988;92:121–38.
[236] Palmer LG, Frindt G. Gating of Na channels in the rat cortical collecting tubule: effects of voltage and membrane stretch. J Gen Physiol 1996;107:35–45.
[237] Palmer LG, Frindt G. High-conductance K channels in intercalated cells of the rat distal nephron. Am J Physiol Renal Physiol 2007;292:F966–73.
[238] Paulais M, Lourdel S, Teulon J. Properties of an inwardly rectifying K^+ channel in the basolateral membrane of mouse TAL. Am J Physiol Renal Physiol 2002;282:F866–76.
[239] Paulais M, Teulon J. cAMP-activated chloride channel in the basolateral membrane of the thick ascending limb of the mouse kidney. J Membr Biol 1993;113:253–60.
[240] Paulais M, Lachheb S, Teulon J. A Na^+- and Cl^--activated K^+ channel in the thick ascending limb of mouse kidney. J Gen Physiol 2006;127:205–15.
[241] Payne JA, Forbush IB. Alternatively spliced isoforms of the putative renal Na-K-Cl co-transporter are differentially distributed within the rabbit kidney. Proc Natl Acad Sci USA 1994;91:4544–8.
[242] Pfister Y, Gautschi I, Takeda AN, van Bemmelen M, Kellenberger S, Schild L. A gating mutation in the internal pore of ASIC1a. J Biol Chem 2006;281:11787–91.
[243] Plata C, Meade P, Hall AE, Welch RC, Vazquez N, Hebert SC, et al. Alternatively spliced isoform of the apical Na-K-Cl co-transporter gene encodes a furosemide sensitive Na-Cl co-transporter. Am J Physiol Renal Physiol 2001;280:F574–82.
[244] Plata C, Meade P, Vazquez N, Hebert SC, Gamba G. Functional properties of the apical Na^+-K^+-2Cl^- co-transporter isoforms. J Biol Chem 2002;277:11004–12.
[245] Plata C, Mount DB, Rubio V, Hebert SC, Gamba G. Isoforms of the Na-K-2Cl co-transporter in murine TAL. II. Functional characterization and activation by cAMP. Am J Physiol (Renal Physiol) 1999;276:F359–66.
[246] Plato CF, Stoods BA, Wang D, Garvin JL. Endogenous nitric oxide inhibits chloride transport in the thick ascending limb. Am J Physiol (Renal Physiol) 1999;276:F159–63.
[247] Ponce-Coria J, San Cristobal P, Kahle KT, Vazquez N, Pacheco-Alvarez D, los Heros P, et al. Regulation of NKCC2 by a chloride-sensing mechanism involving the WNK3 and SPAK kinases. Proc Natl Acad Sci 2008;105:8458–63.
[248] Pradervand S, Wang Q, Burnier M, Beermann F, Horisberger JD, Hummler E, et al. A mouse model for Liddle's syndrome. J Am Soc Nephrol 1999;10:2527–33.
[249] Quamme GA. Effect of hypercalcemia on renal tubular handling of calcium and magnesium. Can J Physiol Pharmacol 1982;60:1275–80.
[250] Quamme GA, de Rouffignac C. Epithelial magnesium transport and regulation by the kidney. Front Biosci 2000;5:D694–711.

[251] Reeves WB, Andreoli TE. Cl^- transport in basolateral renal medullary vesicles: II. Cl^- channels in planar lipid bilayers. J Membr Biol 1990;113:57–65.
[252] Reeves WB, McDonald GA, Mehta P, Andreoli TE. Activation of K^+ channels in renal medullary vesicles by cAMP-dependent protein kinase. J Membr Biol 1989;109:65–72.
[253] Reeves WB, Molony DA. The physiology of loop diuretic action. Semin Nephrol 1988;8:225–33.
[254] Reichold M, Zdebik AA, Lieberer E, Rapedius M, Schmidt K, Bandulik S, et al. KCNJ10 gene mutations causing EAST syndrome (epilepsy, ataxia, sensorineural deafness, and tubulopathy) disrupt channel function. Proc Natl Acad Sci 2010;107:14490–5.
[255] Reilly RF, Ellison DH. Mammalian distal tubule: physiology, pathophysiology, and molecular anatomy. Physiol Rev 2000;80:277–313.
[256] Rinehart J, Kahle KT, De Los HP, Vazquez N, Meade P, Wilson FH, et al. WNK3 kinase is a positive regulator of NKCC2 and NCC, renal cation-Cl^- co-transporters required for normal blood pressure homeostasis. Proc Natl Acad Sci USA 2005;102:16777–82.
[257] Rocha AS, Kokko JP. Sodium chloride and water transport in the medullary thick ascending limb of Henle. Evidence for active chloride transport. J Clin Invest 1973;52:612–23.
[258] Rossetti L, Klein-Robbenhaar G, Giebisch G, Smith D, DeFronzo R. Effect of insulin on renal potassium metabolism. Am J Physiol 1987;252:F60–4.
[259] Rotin D, Schild L. ENaC and its regulatory proteins as drug targets for blood pressure control. Curr Drug Targets 2008;9:709–16.
[260] Rouch AJ, Chen L, Troutman SL, Schafer JA. Na^+ transport in isolated rat CCD: effects of bradykinin, ANP, clonidine, and hydrochlorothiazide. Am J Physiol 1991;260:F86–95.
[261] Rubera I, Loffing J, Palmer LG, Frindt G, Fowler-Jaeger N, Sauter D, et al. Collecting duct-specific gene inactivation of alphaENaC in the mouse kidney does not impair sodium and potassium balance. J Clin Invest 2003;112:554–65.
[262] Ruffieux-Daidie D, Poirot O, Boulkroun S, Verrey F, Kellenberger S, Staub O. Deubiquitylation regulates activation and proteolytic cleavage of ENaC. J Am Soc Nephrol 2008;19:2170–80.
[263] Ruggles BT, Murayama N, Werness JL, Gapstur SM, Bentley MD, Dousa TP. The vasopressin-sensitive adenylate cyclase in collecting tubules and in thick ascending limb of Henle's loop of human and canine kidney. J Clin Endocrinol Metab 1985;60:914–21.
[264] Ruknudin A, Schulze DH, Sullivan SK, Lederer WJ, Welling PA. Novel subunit composition of a renal epithelial K_{ATP} channel. J Biol Chem 1998;273:14165–71.
[265] Saito-Ohara F. Assignment of the genes encoding the human chloride channels, CLCNKA and CLCNKB, to 1p36 and of CLCN3 to 4q32[ndash]q33 by *in situ* hybridization. Genomics 1996;36:372–4.
[266] San Cristobal P, Pacheco-Alvarez D, Richardson C, Ring AM, Vazquez N, Rafiqi FH, et al. Angiotensin II signaling increases activity of the renal Na-Cl co-transporter through a WNK4-SPAK-dependent pathway. Proc Natl Acad Sci USA 2009;106:4384–9.
[267] Sandberg MB, Maunsbach AB, McDonough AA. Redistribution of distal tubule Na^+-Cl^- co-transporter (NCC) in response to a high-salt diet. Am J Physiol Renal Physiol 2006;291:F503–8.
[268] Sands JM, Nonoguchi H, Knepper MA. Hormone effects on NaCl permeability of rat inner medullary collecting duct. Am J Physiol 1988;255:F421–8.
[269] Sansom SC, O'Neil RG. Mineralocorticoid regulation of apical cell membrane Na^+ and K^+ transport of the cortical collecting duct. Am J Physiol 1985;248:F858–68.
[270] Sasaki S, Imai M. Effects of vasopressin on water and NaCl transport across the *in vitro* perfused medullary thick ascending limb of Henle's loop of mouse, rat, and rabbit kidneys. Pflugers Arch 1980;383:215–21.
[271] Sauter D, Fernandes S, Goncalves-Mendes N, Boulkroun S, Bankir L, Loffing J, et al. Long term effects of vasopressin on the subcellular localization of ENaC in the renal collecting system. Kidney Int 2006;69:1024–32.
[272] Schafer JA, Troutman SL. cAMP mediates the increase in apical membrane Na^+ conductance produced in rat CCD by vasopressin. Am J Physiol 1990;259:F823–31.
[273] Schafer JA, Troutman SL, Schlatter E. Vasopressin and mineralocorticoid increase apical membrane driving force for K^+ secretion in rat CCD. Am J Physiol 1990;258:F199–210.
[274] Schild L, Canessa CM, Shimkets RA, Gautschi I, Lifton RP, Rossier BC. A mutation in the epithelial sodium channel causing Liddle disease increases channel activity in the *Xenopus laevis* oocyte expression system. Proc Natl Acad Sci USA 1995;92:5699–703.
[275] Schild L, Lu Y, Gautschi I, Schneeberger E, Lifton RP, Rossier BC. Identification of a PY motif in the epithelial Na channel subunits as a target sequence for mutations causing channel activation found in Liddle syndrome. EMBO J 1996;15:2381–7.
[276] Schlatter E, Greger R. cAMP increases the basolateral Cl^- conductance in the isolated perfused medullary thick ascending limb of Henle's loop of the mouse. Pflugers Arch 1985;405:367–76.
[277] Schlatter E, Schafer JA. Electrophysiological studies in principal cells of rat cortical collecting tubules. ADH increases the apical membrane Na^+-conductance. Pflugers Arch 1987;409:81–92.
[278] Schmitt R, Ellison DH, Farman N, Rossier BC, Reilly RF, Reeves WB, et al. Developmental expression of sodium entry pathways in rat nephron. Am J Physiol 1999;276:F367–81.
[279] Schnermann J, Briggs J, Schubert G. *In situ* studies of the distal convoluted tubule in the rat. I. Evidence for NaCl secretion. Am J Physiol 1982;243:F160–6.
[280] Schoen HF, Erlij D. Insulin action on electrophysiological properties of apical and basolateral membranes of frog skin. Am J Physiol 1987;252:C411–7.
[281] Scholl UI, Choi M, Liu T, Ramaekers VT, Usler MG, Grimmer J, et al. Seizures, sensorineural deafness, ataxia, mental retardation, and electrolyte imbalance (SeSAME syndrome) caused by mutations in KCNJ10. Proc Natl Acad Sci 2009;106:5842–7.
[282] Schwartz GJ, Burg MB. Mineralocorticoid effects on cation transport by cortical collecting tubules *in vitro*. Am J Physiol 1978;235:F576–85.
[283] Seyberth HW. An improved terminology and classification of Bartter-like syndromes. Nat Clin Pract Nephrol 2008;4:560–7.
[284] Shi H, Asher C, Chigaev A, Yung Y, Reuveny E, Seger R, et al. Interactions of beta and gamma ENaC with Nedd4 can be facilitated by an ERK-mediated phosphorylation. J Biol Chem 2002;277:13539–47.
[285] Shi PP, Cao XR, Sweezer EM, Kinney TS, Williams NR, Husted RF, et al. Salt-sensitive hypertension and cardiac hypertrophy in mice deficient in the ubiquitin ligase Nedd4-2. Am J Physiol Renal Physiol 2008;295:F462–70.
[286] Shimizu T, Yoshitomi K, Nakamura M, Imai M. Site and mechanism of action of trichlormethiazide in rabbit distal nephron segments perfused *in vitro*. J Clin Invest 1988;82:721–30.
[287] Shimkets RA, Warnock DG, Bositis CM, Nelson-Williamns C, Hansson JH, Schambelan M, et al. Liddle's syndrome:

heritable human hypertension caused by mutations in the beta subunit of the epithelial sodium channel. Cell 1994;79:407–14.
[288] Siegel B, Civan MM. Aldosterone and insulin effects on driving force of Na^+ pump in toad bladder. Am J Physiol 1976;230:1603–8.
[289] Simon DB, Bindra RS, Mansfield TA, Nelson-Williams C, MendonOa E, Stone R, et al. Mutations in the chloride channel gene, *CLCNKB*, cause Bartter's syndrome type III. Nat Genet 1997;17:171–8.
[290] Simon DB, Karet FE, Rodriguez-Soriano J, Hamdan JH, DiPietro A, Trachtman H, et al. Genetic heterogeneity of Bartter's syndrome revealed by mutations in the K^+ channel, ROMK. Nat Genet 1996;14:152–6.
[291] Snyder PM, Olson DR, Kabra R, Zhou R, Steines JC. cAMP and serum and glucocorticoid-inducible kinase (SGK) regulate the epithelial $Na(^+)$ channel through convergent phosphorylation of Nedd4-2. J Biol Chem 2004;279:45753–8.
[292] Snyder PM, Price MP, McDonald FJ, Adams CM, Volk KA, Zeiher BG, et al. Mechanism by which Liddle's syndrome mutations increase activity of a human epithelial Na^+ channel. Cell 1995;83:969–78.
[293] Sonnenberg H, Honrath U, Wilson DR. Effects of amiloride in the medullary collecting duct of rat kidney. Kidney Int 1987;31:1121–5.
[294] Stanton BA. Characterization of apical and basolateral membrane conductances of rat inner medullary collecting duct. Am J Physiol 1989;256:F862–8.
[295] Starremans PG, Kersten FF, van den Heuvel LP, Knoers NV, Bindels RJ. Dimeric architecture of the human bumetanide-sensitive Na-K-Cl Co-transporter. J Am Soc Nephrol 2003;14:3039–46.
[296] Staub O, Abriel H, Plant P, Ishikawa T, Kanelis V, Saleki R, et al. Regulation of the epithelial Na^+ channel by Nedd4 and ubiquitination. Kidney Int 2000;57:809–15.
[297] Staub O, Gautschi I, Ishikawa T, Breitschopf K, Ciechanover A, Schild L, et al. Regulation of stability and function of the epithelial Na^+ channel (ENaC) by ubiquitination. EMBO J 1997;16:6325–36.
[298] Stokes JB. Ion transport by the cortical and outer medullary collecting tubule. Kidney Int 1982;22:473–84.
[299] Stokes JB. Na and K transport across the cortical and outer medullary collecting tubule of the rabbit: evidence for diffusion across the outer medullary portion. Am J Physiol 1982;242:F514–20.
[300] Stoner LC, Burg MB, Orloff J. Ion transport in cortical collecting tubule; effect of amiloride. Am J Physiol 1974;227:453–9.
[301] Sun A, Grossman EB, Lombardi M, Hebert SC. Vasopressin alters the mechanism of apical Cl^- entry from Na^+:Cl^- to Na^+:K^+:$2Cl^-$ co-transport in mouse medullary thick ascending limb. J Membr Biol 1991;120:83–94.
[302] Takaichi K, Kurokawa K. AVP-sensitive cAMP production is dependent on calmodulin in both MTAL and MCT. Am J Physiol 1988;255:F834–40.
[303] Takaichi K, Kurokawa K. Inhibitory guanosine triphophate-binding protein-mediated regulation of vasopressin action in isolated single medullary of mouse kidney. J Clin Invest 1988;82:1437–44.
[304] Takeuchi Y, Uchida S, Marumo F, Sasaki S. Cloning, tissue distribution, and intrarenal localization of ClC chloride channels in human kidney. Kidney Int 1995;48:1497–503.
[305] Tanemoto M, Vanoye CG, Dong K, Welch R, Abe T, Hebert SC, et al. Rat homolog of sulfonylurea receptor 2B determines glibenclamide sensitivity of ROMK2 in *Xenopus laevis* oocyte. Am J Physiol Renal Physiol 2000;278:F659–66.
[306] Tanemoto M, Abe T, Onogawa T, Ito S. PDZ binding motif-dependent localization of K^+ channel on the basolateral side in distal tubules. Am J Physiol-Renal Physiol 2004;287:F1148–53.
[307] Tao X, Avalos JL, Chen J, MacKinnon R. Crystal structure of the eukaryotic strong inward-rectifier K^+ channel Kir2.2 at 3.1 Å resolution. Science 2009;326:1668–74.
[308] Tiwari S, Nordquist L, Halagappa VK, Ecelbarger CA. Trafficking of ENaC subunits in response to acute insulin in mouse kidney. Am J Physiol Renal Physiol 2007;293:F178–85.
[309] Trinh-Trang-Tan MM, Bouby MM, Coutaud C, Bankir L. Quick isolation of rat medullary thick ascending limbs. Pflugers Arch 1986;407:228–34.
[310] Uchida S, Endou H. Substrate specificity to maintain cellular ATP along the mouse nephron. Am J Physiol (Renal Fluid Electrolyte Physiol) 1988;255-24:F977–83.
[311] Uchida S, Sasaki S, Nitta K, Uchida K, Horita S, Nihei H, et al. Localization and functional characterization of rat kidney-specific chloride channel, ClC-K1. J Clin Invest 1995;95:104–13.
[312] Vallet V, Chraibi A, Gaeggeler HP, Horisberger JD, Rossier BC. An epithelial serine protease activates the amiloride-sensitive sodium channel. Nature 1997;389:607–10.
[313] van der LN, Lim CH, Fenton RA, Meima ME, Jan Danser AH, Zietse R, et al. Angiotensin II induces phosphorylation of the thiazide-sensitive sodium chloride co-transporter independent of aldosterone. Kidney Int 2011;79:66–76.
[314] Vandewalle A, Cluzeaud F, Bens M, Kieferle S, Steinmeyer K, Jentsch TJ. Localization and induction by dehydration of ClC-K chloride channels in the rat kidney. Am J Physiol (Renal Fluid Electrolyte Physiol) 1997;272:F678–88.
[315] Vehaskari VM, Hering-Smith KS, Moskowitz DW, Weiner ID, Hamm LL. Effect of epidermal growth factor on sodium transport in the cortical collecting tubule. Am J Physiol 1989;256:F803–9.
[316] Velazquez H, Silva T. Cloning and localization of KCC4 in rabbit kidney: expression in distal convoluted tubule. Am J Physiol-Renal Physiol 2003;285:F49–58.
[317] Velazquez H, Bartiss A, Bernstein P, Ellison DH. Adrenal steroids stimulate thiazide-sensitive NaCl transport by rat renal distal tubules. Am J Physiol (Renal Fluid Electrolyte Physiol) 1996;270:F211–9.
[318] Velazquez H, Ellison DH, Wright FS. Chloride-dependent potassium secretion in early and late renal distal tubules. Am J Physiol 1987;253:F555–62.
[319] Velazquez H, Good DW, Wright FS. Mutual dependence of sodium and chloride absorption by renal distal tubule. Am J Physiol (Renal Fluid Electrolyte Physiol) 1984;247:F904–11.
[320] Verlander JM, Tran TM, Zhang L, Kaplan MR, Hebert SC. Estradiol enhances thiazide-sensitive NaCl co-transporter density in the apical plasma membrane of the distal convoluted tubule in ovariectomized rats. J Clin Invest 1998;101:1661–9.
[321] Verrey F, Fakitsas P, Adam G, Staub O. Early transcriptional control of ENaC (de)ubiquitylation by aldosterone. Kidney Int 2008;73:691–6.
[322] Vuagniaux G, Vallet V, Jaeger NF, Pfister C, Bens M, Farman N, et al. Activation of the amiloride-sensitive epithelial sodium channel by the serine protease mCAP1 expressed in a mouse cortical collecting duct cell line. J Am Soc Nephrol 2000;11:828–34.
[323] Wang MH, Brand-Schieber E, Zand BA, Nguyen X, Falck JR, Balu N, et al. Cytochrome P450-derived arachidonic acid metabolism in the rat kidney: characterization of selective inhibitors. J Pharmacol Exp Ther 1998;284:966–73.
[324] Wang T, Wang WH, Klein-Robbenhaar G, Giebisch G. Effects of a novel K_{ATP} channel blocker on renal tubule function and K channel activity. J Pharmacol Exp Ther 1995;273:1382–9.

[325] Wang W. Two types of K^+ channel in TAL of rat kidney. Am J Physiol (Renal Fluid Electrolyte Physiol) 1994;267-36: F599–605.

[326] Wang W, Giebisch G. Dual effect of adenosine triphosphate on the apical small conductance K^+ channel of the rat cortical collecting duct. J Gen Physiol 1991;98:35–61.

[327] Wang W, White S, Geibel J, Giebisch G. A potassium channel in the apical membrane of rabbit thick ascending limb of Henle's loop. Am J Physiol (Renal Fluid Electrolyte Physiol) 1990;258-27:F244–53.

[328] Wang WH, Giebisch G. Dual modulation of renal ATP-sensitive K^+ channel by protein kinases A and C. Proc Natl Acad Sci USA 1991;88:9722–5.

[329] Wang WH, Hebert SC, Giebisch G. Renal K channels: structure and function. Ann Rev Physiol 1997;59:413–36.

[330] Wei Y, Zavilowitz B, Satlin LM, Wang WH. Angiotensin II inhibits the ROMK-like small conductance K channel in renal cortical collecting duct during dietary potassium restriction. J Biol Chem 2007;282:6455–62.

[331] Welker P, Boehlick A, Mutig K, Salanova M, Kahl T, Schlueter H, et al. Renal Na-K-Cl co-transporter activity and vasopressin-induced trafficking are lipid raft-dependent. Am J Physiol Renal Physiol 2008;295:F789–802.

[332] Whorwood CB, Ricketts ML, Stewart PM. Epithelial cell localization of type 2 11 beta-hydroxysteroid dehydrogenase in rat and human colon. Endocrinology 1994;135:2533–41.

[333] Wiederholt M, Hansen LL. *Amphiuma* kidney as a model for distal tubular transport studies. Contrib Nephrol 1980;19: 28–32.

[334] Wilson FH, Kahle KT, Sabath E, Lalioti MD, Rapson AK, Hoover RS, et al. Molecular pathogenesis of inherited hypertension with hyperkalemia: the Na-Cl co-transporter is inhibited by wild-type but not mutant WNK4. Proc Natl Acad Sci USA 2003;100:680–4.

[335] Wilson RC, Krozowski ZS, Li K, Obeyesekere VR, Razzaghy-Azar M, Harbison MD, et al. A mutation in the HSD11B2 gene in a family with apparent mineralocorticoid excess. J Clin Endocrinol Metab 1995;80:2263–6.

[336] Winters CJ, Reeves WB, Andreoli TE. Cl^- channels in basolateral renal medullary membranes: III. Determinants of single-channel activity. J Membr Biol 1990;118:269–78.

[337] Winters CJ, Reeves WB, Andreoli TE. Cl^- channels in basolateral renal medullary vesicles: V. Comparison of basolateral mTALH Cl^- channels with apical Cl^- channels from jejunum and trachea. J Membr Biol 1992;128:27–39.

[338] Winters CJ, Zimniak L, Reeves WB, Andreoli TE. Cl^- channels in basolateral renal medullary membranes XII. Anti-rbClC-Ka antibody blocks MTAL Cl^- channels. AJP–Renal Physiol 1997;273:F1030–8.

[339] Wittner M, Weidtke C, Schlatter E, diStefano A, Greger R. Substrate utilization in the isolated perfused cortical thick ascending limb of rabbit nephron. Pflugers Arch 1984;402: 52–62.

[340] Work J, Galla JH, Booker BB, Schafer JA, Luke RG. Effect of ADH on chloride reabsorption in the loop of Henle of the Brattleboro rat. Am J Physiol 1985;249:F698–703.

[341] Xu JZ, Hall AE, Peterson LN, Bienkowski MJ, Eessalu TE, Hebert SC. Localization of the ROMK protein on apical membranes of rat kidney nephron segments. Am J Physiol (Renal Physiol) 1997;273:F739–48.

[342] Xu ZC, Yang Y, Hebert SC. Phosphorylation of the ATP-sensitive, inwardly rectifying K^+ channel, ROMK, by cyclic AMP-dependent protein kinase. J Biol Chem 1996;271:9313–9.

[343] Yang CL, Angell J, Mitchell R, Ellison DH. WNK kinases regulate thiazide-sensitive Na-Cl co-transport. J Clin Invest 2003;111:1039–45.

[344] Yang SS, Morimoto T, Rai T, Chiga M, Sohara E, Ohno M, et al. Molecular pathogenesis of pseudohypoaldosteronism Type II: generation and analysis of a Wnk4(D561A/ +) knockin mouse model. Cell Metab 2007;5:331–44.

[345] Yang T, Huang YG, Singh I, Schnermann J, Briggs JP. Localization of bumetanide- and thiazide-sensitive Na-K-Cl cotransporters along the rat nephron. Am J Physiol (Renal Fluid Electrolyte Physiol) 1996;271:F931–9.

[346] Yoo D, Kim BY, Campo C, Nance L, King A, Maouyo D, et al. Cell surface expression of the ROMK (Kir 1.1) channel is regulated by the aldosterone-induced kinase, SGK-1, and protein kinase A. J Biol Chem 2003;278:23066–75.

[347] Yoshitomi K, Shimizu T, Taniguchi J, Imai M. Electrophysiological characterization of rabbit distal convoluted tubule cell. Pflugers Arch 1989;414:457–63.

[348] Yu L, Helms MN, Yue Q, Eaton DC. Single-channel analysis of functional epithelial sodium channel (ENaC) stability at the apical membrane of A6 distal kidney cells. Am J Physiol Renal Physiol 2008;295:F1519–27.

[349] Yue P, Sun P, Lin DH, Pan C, Xing W, Wang W. Angiotensin II diminishes the effect of SGK1 on the WNK4-mediated inhibition of ROMK1 channels. Kidney Int 2011;79:423–31.

[350] Zhou H, Chepilko S, Schutt W, Choe H, Palmer LG, Sackin H. Mutations in the pore region of ROMK enhance Ba^{2+} block. Am J Physiol 1996;271:C1949–56.

[351] Zimniak L, Winters CJ, Reeves WB, Andreoli TE. Cl^- channels in basolateral renal medullary vesicles X. Cloning of a Cl^- channel from rabbit outer medulla. Kidney Int 1995;48:1828–36.

This page intentionally left blank

CHAPTER

35

Mineralocorticoid Action in the Aldosterone Sensitive Distal Nephron

Olivier Staub[1] *and Johannes Loffing*[2]

[1]Department of Pharmacology & Toxicology, University of Lausanne, Lausanne, Switzerland
[2]Institute of Anatomy, University of Zurich, Zurich, Switzerland

INTRODUCTION

The kidney of vertebrates plays a major role in the homeostasis of the extracellular fluid. Despite large changes in water and salt intake, the kidney is able to maintain the extracellular osmolarity and volume within very narrow margins. Such fine control requires specific factors or hormones. In 1952, Simpson and Tait identified aldosterone as the most potent Na^+-retaining factor in mammals. When the Na^+-retaining activity of the newly identified steroid hormone was compared to that of cortisol (or corticosterone), aldosterone was found to be 3000-fold more potent *in vivo*. Aldosterone differs from cortisol (or corticosterone) by the presence of an aldehyde group in position 18 on the second ring. Thus, an apparently minimal change in the structure of the steroid confers on the molecule a strikingly different biological activity (see review in [1]). During the evolution of vertebrates, aldosterone appeared about 300 million years ago with amphibians, which were the first vertebrates to adapt to a dry, terrestrial environment.[2] The three most important and conserved functions of aldosterone are to promote Na^+ reabsorption and K^+ and H^+ secretion across certain "tight" epithelia – that is, epithelia which display a high transepithelial electrical resistance and an amiloride-sensitive, electrogenic Na^+ transport. In mammals, such epithelia are found in the distal part of the nephron, the bladder, the distal part of the intestine (mainly the surface epithelium of distal colon and rectum), and the ducts of exocrine glands (salivary, mammary, and sweat glands). In the mammalian kidney, the Na^+ and K^+ responses are localized in the segment-specific cells of the aldosterone-sensitive distal nephron (ASDN), while acid secretion is mediated via intercalated cells. The main goal of this chapter is to provide an overview on the renal tubular sites that respond to aldosterone, and to highlight the underlying cellular and molecular mechanisms by which aldosterone controls sodium, potassium, and extracellular fluid homeostasis. The chapter is revised and updated from its previous version established by our colleagues François Verrey, Edith Hummler, Laurent Schild, and Bernard Rossier that appeared in the fourth edition of this book.

The Aldosterone Sensitive Distal Nephron (ASDN)

Each day, the glomeruli of the human kidney filter about 1.5 kg of NaCl out of the blood into the primary urine. However, usually less than 1% of the filtered NaCl is finally excreted. Thus, most of it is reabsorbed along the renal tubular system, which is composed by serial arrangement of the proximal tubule (PCT and PST), the thin limb (TL), the thick ascending limb (TAL), the distal convoluted tubule (DCT), the connecting tubule (CNT), and the collecting duct (CD) (Figure 35.1). While the bulk of Na^+ reabsorption occurs in the proximal tubule (PT) and the TAL, the final regulation of Na^+ excretion takes place in the so-called Aldosterone-Sensitive Distal Nephron (ASDN) which extends from the late portion of the DCT (also called DCT-2) to the end of the collecting duct (IMCD) in the renal papilla.[3] The three ASDN segments differ in their histotopographical localization and epithelial structure. The DCT and CNT are located in the cortical labyrinth, while the CD extends from the

Seldin and Giebisch's The Kidney, Fifth Edition.
DOI: http://dx.doi.org/10.1016/B978-0-12-381462-3.00035-5

© 2013 Elsevier Inc. All rights reserved.

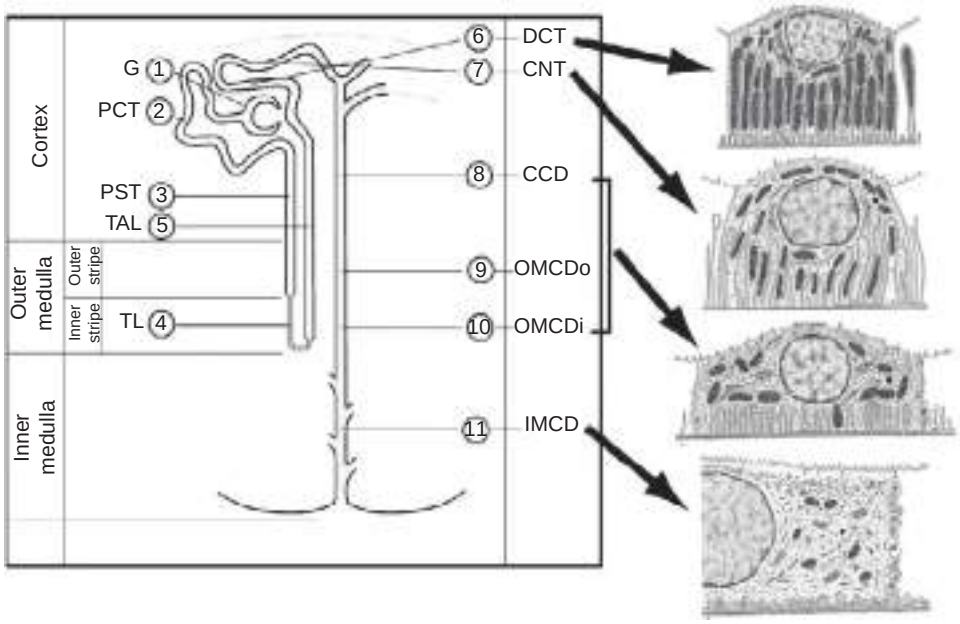

FIGURE 35.1 **Schematic representation of the renal tubule system.** On the right (see arrows): a distal convoluted tubule (DCT) cell, a connecting tubule (CNT) cell, a principal cell of the cortical and outer medullary collecting duct, and a principal cell of the inner medullary collecting duct (G: glomerulus; PCT: proximal convoluted tubule; PST: proximal straight tubule; TL: thin limb; TAL: thick ascending limb; DCT: distal convoluted tubule; CNT: connecting tubule; CCD: cortical collecting duct; OMCD: outer medullary collecting duct; IMCD: inner medullary collecting duct). The aldosterone-sensitive distal nephron (ASDN) comprises the late DCT, the CNT and the collecting duct. *(Adapted from Kriz, R. W., and Kaissling, B. (2000). Structural organization of the mammalian kidney. In "The Kidney," Vol. 1, 3rd edn, 587–654, Seldin, D. W., and Giebisch, G. (eds.). Lippincott Williams & Wilkins, Philadelphia.)*

medullary rays in the renal cortex down to the renal medulla until its opening on the tip of the renal papilla. DCT cells have an apical localized cell nucleus and numerous mitochondria that are densely stuffed into the interdigitating basolateral membrane infoldings. The CNT cells are usually less tall than the DCT cells, have less mitochondria and a basal membranous labyrinth that is predominantly formed by membrane infoldings. The CCD cells are even smaller, and are characterized by a basal thin rim of mitochondria-free membrane infoldings. The medullary CD is formed by cuboidal cells that have few cell organelles (Figure 35.1). Membrane infoldings and mitochondrial density progressively decrease from DCT to CCD, in parallel with a reduction in the abundance and activity of the Na^+,K^+-ATPase,[4] suggesting different ion transport rates along the ASDN. In fact, recordings of transepithelial Na^+ fluxes in isolated rabbit CNTs[5,6] and rat CCDs,[7,8] indicate at least a 10-fold higher Na^+ transport rate in the CNT than in the CCD (600–120 versus 0.2 to 24 pmoles Na^+/min/mm). The rates of Na^+ transport in OMCD and IMCD are generally low,[9] but Na^+ channels are also expressed in the OMCD and IMCD, and can be activated, at least to some extent, by aldosterone.[10]

Although the sequence of tubule portions appears to be quite similar in mammals, subtle species differences in the structural and functional organization of the ASDN have to be taken into account if functional data from different nephron portions and species are compared.[11] For example, rabbits have morphologically well-defined sharp transitions from DCT to CNT and from CNT to CD, while the segment transitions in rats, mice, and humans are gradual. These morphological differences are reflected by the distribution pattern of ion- and water-transporting proteins. In rabbits, the sharp transitions from DCT to CNT and from CNT to CCD coincide with the immediate replacement of the DCT-specific NaCl co-transporter (NCC) by the epithelial Na^+ channel (ENaC), and the abrupt onset of aquaporin-2 (AQP2) expression.[12] In contrast, in rats, mice, and humans NCC and ENaC overlap in the late DCT (DCT2), and AQP2 extends into the connecting tubule.[11,13]

Despite the above-mentioned segmental and species differences, all ASDN cells in common express high levels of the mineralocorticoid receptor (MR), the glucocorticoid receptor (GR), the enzyme 11-beta-hydroxysteroid-dehydrogenase type 2 (11β-HSD2), and the epithelial Na^+ channel (ENaC)[3] (Figure 35.2). The MR and the GR are hormone-activated transcription factors that can bind both mineralocorticoid and glucocorticoid hormones, although with different affinities. While the MR is a high-affinity receptor (K_d for

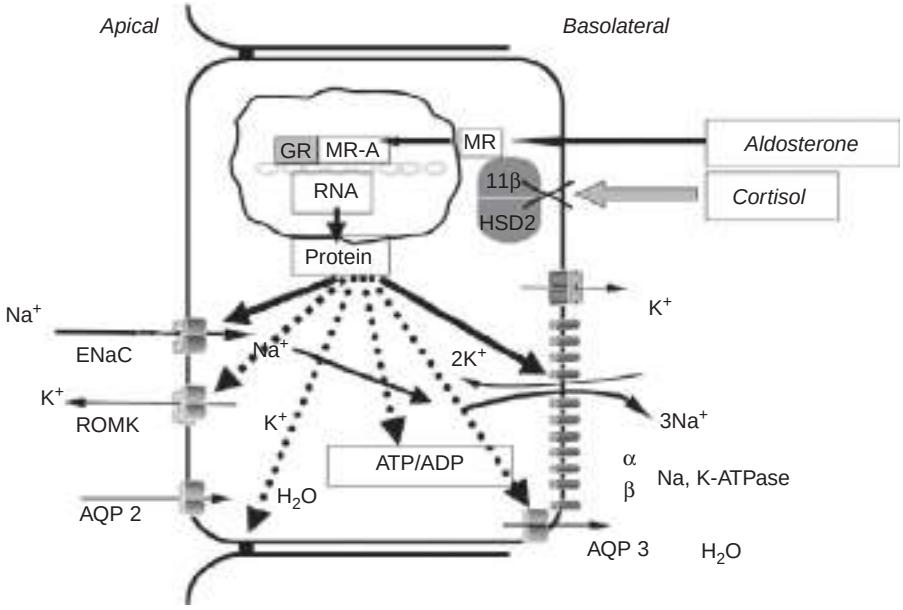

FIGURE 35.2 Model of the mechanism of aldosterone action in an epithelial target cell. Aldosterone crosses the plasma membrane and binds to its high affinity mineralocorticoid receptor (MR) and/or the low affinity glucocorticoid receptor (GR). Cortisol is metabolized by the 11βHSD-2 into inactive metabolites with a very low affinity for MR and GR. The complex translocates to the nucleus, where it undergoes interaction with promoter regions of target genes, activating or repressing their transcriptional activity. Induced or repressed proteins mediate an increase in transepithelial sodium transport by the activation of pre-existing transport proteins (ENaC, Na,K-ATPase), and a further accumulation of transport proteins and other elements of the sodium transport machinery. Possible effects on ROMK, tight junction proteins, mitochondria, and water transport proteins (AQP 3) are indicated with dotted arrows. *(From Verrey, F., Hummler, E., Schild, L., and Rossier, B. C. (2008). Mineralocorticoid action in the aldosterone-sensitive distal nephron. In "Seldin and Giebisch's The Kidney," Vol. 1, 4th edn., 889–924. Elsevier Inc.)*

aldosterone and cortisol in the range from 0.5 to 3 nM), the GR has a more than 10 times lower affinity for these steroids (K_d in the range from 20 to 65 nM).[14] The corticosteroid levels in the plasma (cortisol in humans and corticosterone in rats) are usually far above these K_d values, and exceed the plasma concentrations of aldosterone 100–1000-fold. Under these conditions, mineralocorticoid specificity is thought to be conferred to the ASDN cells by their high expression of 11β-HSD2 that rapidly hydrolyzes the physiological corticosteroids to inactive metabolites.[15] Upon hormone binding, the receptors are thought to homo- or heterodimerize and to translocate to the cell nucleus, where they modulate a transcriptional program that modulates the expression of ENaC, the Na^+,K^+-ATPase, and of regulatory proteins that control the activity of these Na^+-reabsorbing proteins.

Na^+ transport across the ASDN cells occurs in two steps. Na^+ uptake from the lumen into the cells is mediated by ENaC, while Na^+ exit across the basolateral plasma membrane depends on the Na^+,K^+-ATPase. The activity of ENaC and the Na^+,K^+-ATPase is electrogenic, and generates a transepithelial electrochemical gradient that drives paracellular Cl^- reabsorption and transcellular K^+ secretion. The apical K^+ secretion is thought to occur via secretory K^+ channels such as the renal outer medulla K^+ channel (ROMK) and the flow-dependent maxi-K (BK) channel.[16–19] Immunohistochemical studies revealed that ROMK is highly abundant in the DCT, CNT, and CD cells,[20,21] where it becomes activated and redistributed to the apical plasma membrane in response to an increased dietary K^+ intake.[22] Likewise, a high-K^+ diet appears to stimulate the BK channel. In rabbits, it increases the mRNA expression of the α-, β2-, and β4-subunits,[23] and in rats it elevates the electrical activity in CCD cells.[24] In contrast to ROMK, the BK channel is not only present in the segment-specific ASDN cells, but also in intercalated cells.[17] Intercalated cells may not only secrete but also reabsorb K^+ via their apical H^+,K^+-ATPase.[25] Thereby, intercalated cells may help to modulate the interdependence of ENaC-mediated Na^+ reabsorption and K^+ secretion via apical K^+ channels. A close link between the function of intercalated and segment-specific ASDN cells is also indicated by the fact that, in all species investigated so far, the appearance of intercalated cells in the early ASDN coincides precisely with the onset of functional ENaC expression.[11] Moreover, several recent studies on various rodent models further supported the idea of a functional cooperation between ASDN and intercalated cells. The ASDN has at least two types of intercalated

cells.[26,27] The acid-secreting type-A intercalated cells have the vacuolar H^+-ATPase in the apical plasma membrane and the Cl^-/HCO_3^- anion exchanger AE1 in the basolateral plasma membrane, whereas the bicarbonate-excreting type-B intercalated cells have the H^+-ATPase in the basolateral plasma membrane, and are characterized by the abundance of the Cl^-/HCO_3^- exchanger pendrin in the apical membrane, which may contribute to a combined transcellular reabsorption of Na^+ (via ENaC) and Cl^- (via pendrin). In fact, experiments in pendrin-deficient mice indicated that bicarbonate secretion via the type-B intercalated cells is necessary for normal ENaC expression and activity.[28,29] Consistent with this view, the mice are prone to develop arterial hypotension when placed on an NaCl-deficient diet, and they are protected from hypertension under mineralocorticoid treatment.[30,31] Pendrin may not only cooperate with ENaC, but also with the Na^+-dependent chloride-bicarbonate exchanger SLC4A8,[32] which may account for the previously reported thiazide-sensitive NaCl reabsorption in the renal collecting system. Experiments in SLC4A8- and NCC-deficient mice indicated that about 40–70% of collecting duct Na^+-absorption involve SLC4A8.[32] Similar to ENaC, the thiazide-sensitive electroneutral Na^+ reabsorption, as well as SLC4A8, appear to be stimulated by aldosterone.[27] Na^+ reabsorption via ENaC may not only interfere with K^+, H^+, and Cl^- handling of the ASDN cells, but also with transepithelial water reabsorption. The ENaC activity generates an osmotic gradient that likely favors the vasopressin-dependent transepithelial water reabsorption via the water channels AQP2 in the apical and AQP3 and AQP4 in the basolateral plasma membrane of the segment-specific ASDN cells. Although there are some indications that aldosterone directly controls the expression and activity of ROMK,[33–35] BK,[36] pendrin,[31,37] SLC4A8,[32] AQP2,[38,39] and AQP3,[40] the functional significance of these regulations compared with the indirect effects mediated via enhanced activity of ENaC and Na^+,K^+-ATPase are still unclear. Nevertheless, the various cell types and ion transport pathways with manifold possible interactions likely contribute significantly to the complexity of ion handling along the ASDN which may allow adaptation of urinary ion excretion precisely to homeostatic needs. Details on the regulation of K^+ channels, pendrin, SLC4A8, and aquaporins are given in several excellent recent reviews.[16,17,26,27,37,41–43]

Aldosterone Action in Non-ASDN Cells

A huge variety of studies have been aimed at localizing MR and GR along the mammalian nephron. Ligand-binding studies and RNAase protection assays on microdissected nephron portions, as well as autoradiography, *in situ* hybridization and immunohistochemistry on kidney sections, revealed a very high abundance of MR and GR along the classical ASDN.[44] Moreover, these studies indicated that the MR, the GR, and 11β-HSD2 are expressed in nephron segments and cell types that are considered not to be classical targets for aldosterone, including glomerular mesangial cells, podocytes, and proximal tubules (reviewed in [15]). Using a set of highly specific MR antibodies,[45] Ackerman et al. recently confirmed that the MR is expressed along the entire distal tubule, including the TAL and the entire DCT.[46] MR expression in the TAL is in line with studies describing a profound stimulatory effect of aldosterone on TAL Na^+ transport,[47] but contrasts with other reports that did not reveal any effect of the mineralocorticoid on the expression and activity of the Na^+,K^+-ATPase and K^+ transport in the TAL of adrenalectomized rabbits and rats, respectively.[48–50] Likewise, there is considerable evidence that aldosterone stimulates NaCl co-transport in the DCT. Velazquez et al. demonstrated that adrenalectomy lowers the electroneutral Na^+ transport activity (corresponding to NCC activity) in the DCT, and that this effect can be fully restored to normal when aldosterone and/or glucocorticoids are replaced.[51] Consistent with a stimulatory role of aldosterone on the DCT, immunoblotting and immunohistochemistry on rat kidneys showed that dietary Na^+ restriction, which stimulates endogenous aldosterone production, as well as exogenous aldosterone application, increases the abundance and phosphorylation of NCC in the DCT.[52–56] Frindt and Palmer used *in vivo* cell surface biotinylation to show in the rat that dietary Na^+ restriction does also increase the cell surface abundance of NCC.[57] Conversely, dietary Na^+-loading removes NCC from the plasma membrane, indicating that aldosterone may affect the trafficking of NCC as well.[58] Interestingly, the increase in NCC protein abundance and phosphorylation was significantly lower when MR was blocked by spironolactone.[53,59] Although the effect of spironolactone points to an MR-mediated transcriptional response, changes in plasma aldosterone do not appear to directly affect NCC mRNA expression, indicating that mineralocorticoids elicit their effects on NCC abundance via enhanced translation and/or reduced degradation of the protein.[55] In fact, there is increasing evidence that NCC protein abundance might be controlled by ubiquitylation, and hence by altered protein stability.[60–63] Aldosterone is also known to stimulate renal H^+ excretion. The intercalated cells in the ASDN play an important role for renal acid–base handling. However, so far it is unclear whether aldosterone directly affects renal acid

secretion via activation of the H^+-ATPase in intercalated cells or indirectly via activation of ENaC-dependent Na^+ transport in principal cells, which increases the electrochemical driving force for H^+secretion by intercalated cells. Functional studies on isolated collecting ducts indicated that aldosterone rapidly stimulates intercalated cells via non-genomic pathways that may involve PKC and PKA signaling,[64] and perhaps require the vasopressin V1 receptor.[65] Nevertheless, it is uncertain whether the observed effects depend on a yet-unknown putative membrane-bound corticosteroid-binding receptor or the classical MR. Although expression of the MR in intercalated cells was long disputed, a recent immunohistochemical study established rather strong expression of the MR, not only in the ASDN segment-specific cells, but also in all subtypes of intercalated cells.[46] However, this study did also provide evidence that the rather low expression levels of the 11β-HSD2 in TAL, early DCT, and intercalated cells, makes it unlikely that aldosterone has significant direct genomic effects on these cell types in the physiological context of several-fold higher plasma levels of corticosterone than aldosterone. Nevertheless, mineralocorticoid-selectivity might be conferred to the MR also in an 11β-HSD2-independent way by a functional preference of the receptor to aldosterone, as indicated in cell culture assays[66] and *in vivo* experiments.[67] Moreover, MR expression in TAL, early DCT, and intercalated cells may become relevant in patients with pharmacological (e.g., by spironolactone) or genetic (i.e., PHA-1) MR inactivation. Under these conditions, the loss of MR function in these cells may contribute to the salt-losing phenotype with hyperkalemia and metabolic acidosis.[68]

SODIUM TRANSPORT REGULATION BY ALDOSTERONE: PHYSIOLOGICAL AND BIOPHYSICAL MECHANISMS

Epithelial Na^+ transport is a two-step process that comprises: (1) facilitated transport – driven by an electrochemical potential difference – across the apical membrane (from urine to cell); and (2) active transport – driven by metabolic energy – across the basolateral membrane (from cell to interstitium).[69] In the ASDN, the apical-membrane entry step is mediated by Na^+-selective amiloride-sensitive ion channels,[70] while the exit step is catalyzed by Na^+, K^+-ATPase, the ouabain-sensitive Na^+ pump.[71,72] The aldosterone-dependent electrogenic transepithelial Na^+ transport has been studied in a great variety of *in vitro*, *ex vivo*, and *in vivo* models.[73,74] The different models revealed different baseline and maximal transport rates in response to aldosterone. In the *toad urinary bladder*, "basal" transport rates, measured by the short-circuit current method, are around 5–10 $\mu A/cm^2$[75] and aldosterone produces a 2- to 5-fold increase in transport. In the *rat colon*, basal transport rates through amiloride-sensitive channels are very low, while tissues stimulated *in vivo* by adrenal steroids can have rates of 500–1000 $\mu A/cm^2$.[76] *Isolated, perfused rat cortical collecting ducts* express no measurable net Na^+ fluxes when the animals are maintained on normal diets. When animals are placed on a low-Na^+ diet (to elevate endogenous aldosterone levels) or injected with mineralocorticoids, Na^+ reabsorption is as high as 30 pmoles/min-mm, which corresponds to ~100 $\mu A/cm^2$.[7,8] These values match well the amiloride-sensitive current measured by cell attached patches of mouse CCD cells.[77]

Aldosterone and the Epithelial Sodium Channel ENaC

The apical entry of Na^+ involves the low conductance, highly selective (Na^+ over K^+), and amiloride-sensitive epithelial Na^+ channel[78,79] (ENaC). ENaC was cloned from rat distal colon by functional expression in *Xenopus* oocytes. The channel is composed of three homologous subunits denoted α-, β-, and γ-EnaC, which share 30 to 40% identity at the level of their amino acid sequences. In addition to these three well-characterized ENaC subunits, a fourth EnaC subunit, δ-ENaC, has been cloned from a human kidney cDNA library.[80] However, this subunit has been described so far only in humans, and its relevance for transepithelial Na^+ reabsorption in the ASDN is unclear. When the three classical α-, β-, and γ-ENaC subunits are co-expressed in *Xenopus laevis* oocytes, the subunits form a channel with functional characteristics similar to the channel identified by Palmer in the rat CCD, with a low 5 pS conductance (for Na^+), a high selectivity ratio of Na^+ over K^+ (>20), and a high sensitivity for amiloride with a K_i in the submicromolar range. In the *Xenopus* oocyte expression system, the co-expression of all three ENaC subunits is required for maximal cell surface abundance and activity of the channel.[81] The subunit stoichiometry of the active channel is not finally resolved. Various technical approaches suggested models with four, eight or nine subunits.[82] Recently, the crystal structure of the closely related acid-sensing ion channel isoform $ASIC1_A$ has been reported, and points to a trimeric oligomerization of the channel.[83,84] However, this trimeric model still awaits further confirmation by establishing the crystal structure of ENaC itself.

ENaC is expressed in several organs including the kidney, the colon, the salivary and sweat glands.

ENaC-mediated Na^+ transport helps to adjust Na^+ excretion in the urine, feces, and sweat. In lung and airways, ENaC activity is important for alveolar liquid clearance and regulation of mucous fluidity. In the taste buds of the tongue, ENaC is likely involved in salt tasting, whereas ENaC expression in the eye and inner ear may help to control the ionic composition of the aqueous humor and the endolymph, respectively.[82] In the kidney the distribution of ENaC is fully compatible with its involvement in aldosterone-dependent Na^+ transport. Morphological and functional studies on rodent and human kidneys[11,13] clearly showed that the ENaC subunits are highly abundant along the entire ASDN, starting in the late DCT (DCT2), and extending through the CNT down to the medullary CD. In the ASDN cells, increased plasma aldosterone levels induced either by dietary Na^+ restriction or by exogenous application appear to stimulate ENaC mainly by three mechanisms. First, aldosterone increases the abundance of the α-ENaC mRNA and protein, without much affecting the mRNAs encoding for the β- and γ-subunits.[85–87] In contrast, the β- and γ-subunit mRNAs are upregulated in the colon by aldosterone, while the α-subunit mRNA is expressed constitutively.[85,86,88] Second, aldosterone induces the appearance of low molecular weight forms of α- and γ-ENaC, which are thought to represent proteolytically activated channel subunits.[89–91] Recently, Frindt and co-workers performed cell surface biotinylation experiments on rat kidneys perfused with biotin *in situ*. These experiments showed that feeding a low-Na^+ diet or the infusion of aldosterone for one week increases the cell surface pool of cleaved α- and γ-ENaC, but not β-ENaC subunits at the cell surface.[92] Third, aldosterone causes a redistribution of ENaC channel subunits from intracellular storage compartments to the apical plasma membrane. In fact, the subcellular localization of ENaC along the axis of the ASDN changes drastically with altered plasma aldosterone levels in response to altered dietary Na^+ intake.[90,93] In rodents kept under a high dietary Na^+ intake with low plasma aldosterone levels, ENaC subunits are barely detectable at the luminal membrane, and are found almost exclusively at intracellular sites. On a standard dietary Na^+ intake with moderate plasma aldosterone levels, ENaC subunits are traceable at the luminal membrane in the late DCT and the early CNT, but in downstream segments (i.e., late CNT and CD), particularly β- and γ-ENaC are found almost exclusively at intracellular sites.[93] Only the α-EnaC-subunit was reported to have a more pronounced apical localization and can be found at the apical plasma membrane in CNT and CD.[94] In response to dietary Na^+ restriction, the apical abundance of ENaC subunits drastically increases due to a translocation of channel subunits from intracellular compartments to the apical plasma membrane.[59,90,93,95,96] Nevertheless, the axial gradient for apical ENaC prevails, and the apical localization of ENaC subunits remains more prominent in early ASDN than in late ASDN.[12,97] The activation and apical translocation of ENaC occurs rapidly (within hours), suggesting that they are relevant for the renal adaptation to day-to-day variations of Na^+ intake.[3,89,98] Likewise, injection of aldosterone in adrenalectomized rats induces a rapid (within 2 hours) induction of α-ENaC-subunit expression along the ASDN which is followed by a translocation of all three ENaC subunits to the apical plasma membrane (Figure 35.3). Again, the apical shift occurs predominantly in the early and not in the late ASDN, although the induction of α-ENaC was seen to be similar along the entire segment.[3] Based on previous studies in *Xenopus laevis* A6 cells, it has been proposed that the induction of α-ENaC might be a prerequisite for full assembly of ENaC in the ER and its subsequent delivery to the cell surface.[99] However, in the kidney *in vivo* the induction of α-ENaC protein by aldosterone is rather small[90] and, at least in the CCD, not necessarily followed by an apical redistribution of all three ENaC subunits.[3] Moreover, apical targeting of ENaC apparently occurs even without previous α-ENaC induction.[100] Likewise, when ENaC activity was assessed as whole-cell amiloride-sensitive current, ENaC activity in rat CCD was drastically increased within 15 hours of salt restriction, and thus in a timeframe in which no changes in the abundance of ENaC mRNA or protein could be detected.[89] Thus, the induction of α-ENaC alone cannot account for the apical targeting of ENaC. Other co-stimulatory factors are needed. One of these factors was proposed to be the serum- and glucocorticoid-regulated kinase (Sgk1). Sgk1 is a member of the PKB/Akt family of serine/threonine kinases, and is rapidly induced by aldosterone in ASDN model epithelia *in vitro*, as well as in the kidney *in vivo*.[3,101–103] Likewise, prolonged dietary Na^+ restriction increases Sgk1 mRNA expression in the kidney.[104] Co-expression of ENaC with Sgk1 in heterologous expression systems profoundly increases ENaC-mediated Na^+-currents, most likely by an accelerated insertion-rate of ENaC into the plasma membrane.[105] Consistently, the induction of Sgk1 by aldosterone precedes the apical translocation of ENaC in ASDN cells *in vitro* and Sgk1-deficient mice (Table 35.1) show mild urinary Na^+-wasting that becomes aggravated on dietary Na^+ restriction.[106] At least part of the effects of Sgk1 on ENaC cell surface abundance is mediated by an Sgk1-dependent phosphorylation of the ubiquitin-protein ligase Nedd4-2. Nedd4-2 phosphorylation blocks the interaction of this ligase with the C-terminus of ENaC subunits, and thereby presumably prevents

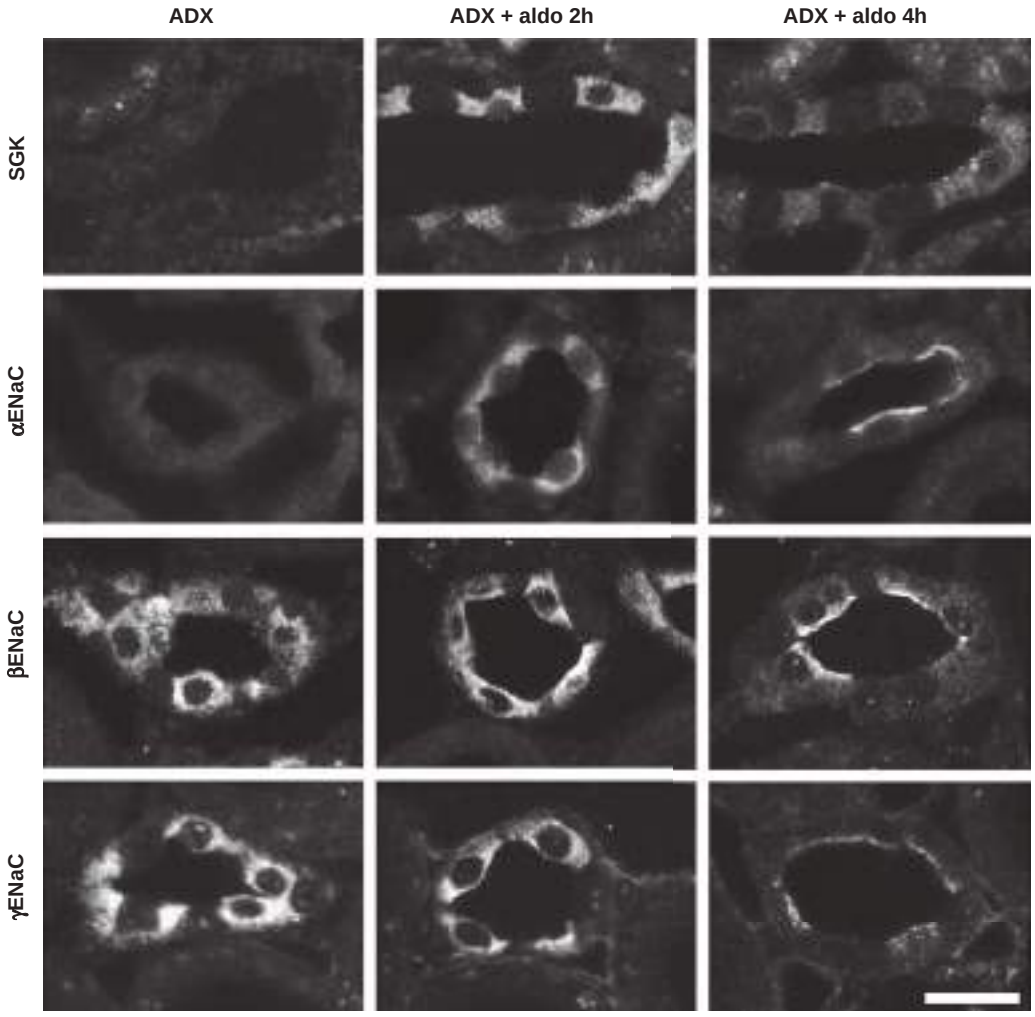

FIGURE 35.3 **CNT profiles in kidney from ADX rats, 2 and 4 hours after aldosterone injection.** Immunofluorescence with rabbit antisera against α-, β-, and γ-ENaC, and the serum-and-glucocorticoid-induced kinase (SGK1) on cryostat sections is shown. Unstained cells in the CNT epithelium are intercalated cells. Aldosterone induces a rapid induction of SGK1 and α-ENaC (at 2 hours) that precedes the apical translocation of all three ENaC subunits from intracellular sites towards the apical plasma membrane (at 4 hours). *(Adapted from Loffing, J., et al. (2001).[3])*

Nedd4-2-induced ubiquitylation and subsequent endocytosis and degradation of ENaC subunits.[107–109] Interestingly, immunohistochemical studies showed that the Nedd4-2 abundance increases along the ASDN, which is inverse to the axial gradient of apical ENaC abundance, and further supports the idea that Nedd4-2 is a negative regulator of ENaC cell surface abundance.[110]

Patch-clamp studies corroborated the immunohistochemically traceable axial gradient of the apical localization of ENaC.[111] The ASDN segments isolated from rats kept on a standard lab chow exhibited no amiloride-sensitive currents at the single channel level, whereas CNTs and CDs isolated from rats with elevated plasma aldosterone levels revealed significant single channel ENaC currents (Figure 35.4). Mice appear to have sizeable ENaC whole-cell currents already on a standard diet, which further increase when animals are kept on low dietary Na^+ intake.[112] In general, amiloride-sensitive currents decrease in the following order: CNT > initial CD > CD.[113] These findings on apical ENaC localization and activity are consistent with previous studies on microperfused rat tubules,[7] and on isolated rabbit tubules[5] that established several times higher Na^+ transport rates in early ASDN (i.e., DCT and CNT) than in further downstream ASDN segments (i.e., CD). The axial gradient of ENaC also parallels the progressive decrease of the basolateral Na^+,K^+-ATPase activity along the ASDN.[4] Taken together, these data clearly indicate that the aldosterone-dependent adaptation of renal Na^+ excretion to dietary Na^+ intake occurs through ENaC, predominantly in the early ASDN, while the late ASDN gets recruited only under high plasma

TABLE 35.1 Transgenic Mouse Models Used to Elucidate Mechanisms of Aldosterone-Dependent Sodium/Potassium Transport

Strain	Phenotype	References
	Signaling Cascade	
MR − / −	Severe PHA-1	187,189
MR − / − , CNT/CD-specific (MRlox/lox AQP2Cre)	Mild PHA-1	116
MR − / − , CNT/CD-specific, inducible (MRlox/lox AQP2CreERT2)	Mild PHA-1	190
GR − / −	Not viable due to perturbed lung development	192
GR − / − , distal tubule-specific (GRlox/lox KspCre)	Slightly elevated blood pressure	194
GR overexpression, CD-specific (hGR Hoxb7-tetON2)	Mild renal sodium retention	193
Mutation GR knockin (hGRM604L)	Increased sensitivity to glucocorticoids	276
11-b HSD2 − / −	Severe AME	199
11-b HSD2 + / −	Salt-sensitive hypertension	277
Sgk1 − / −	Mild PHA1	106,278,279
Sgk1 − / − (Sgk1lox/lox c-TgCMVcre)	Mild PHA1	232
Sgk1 − / − , renal tubule-specific (Sgk1lox/lox Pax8/LC1)	Mild PHA1	233
Nedd4-2 − / −	Salt-sensitive hypertension	229
Nedd4-2 − / −	Not viable due to respiratory distress	231
Nedd4-2 − / −	Cystic fibrosis-like lung phenotype	230
Nedd4-2 − / − , renal tubule-specific (Nedd4-2lox/lox Pax8/LC1)	NCC upregulation	60
CHIF − / −	Mild renal and colon defect in Na/K transport	264
	ENaC	
α-ENaC − / −	Not viable due to respiratory distress	132
α-ENaC − / − , CD-specific (α-ENaClox/lox Hoxb7Cre)	No obvious phenotype	95
α-ENaC − / − , CNT/CD-specific (α-ENaClox/lox AQP2Cre)	Mild PHA-1	115
Transgenic α-ENaC − / − Tg	Mild PHA-1	133
Mutation β-ENaCm/m	Mild PHA-1	139
Mutation γ-ENaCL/L	Liddle's syndrome, salt-sensitive hypertension	77,127,128,280
β-ENaC − / −	Severe PHA-1	136
β-ENaC + / −	Very mild PHA-1	281
γ-ENaC − / −	Severe PHA-1	135

aldosterone levels. Using whole-cell current data, and considering the anatomical length of the two segments, Frindt and Palmer estimated that the Na^+ transport capacity of the CNT is at least 10 times higher than that of the CD.[113]

The importance of the early ASDN versus late ASDN for the maintenance of Na^+ balance was highlighted by the development of a mouse model with targeted inactivation of α-ENaC in the collecting duct.[95] These mice survive well and are able to maintain Na^+ and K^+ balance, even when challenged by salt restriction or K^+-loading (Figure 35.5a). Moreover, these mice show a normal urinary acidification in response to furosemide and thiazide treatment,[114] suggesting that functional expression of ENaC in the CNT is sufficient for maintaining ion homeostasis. In contrast, mice with targeted inactivation of α-ENaC in CD and CNT show symptoms of renal salt-wasting (Figure 35.5b). Already under control conditions, the mice have significantly higher urinary Na^+ excretion and increased plasma aldosterone levels. With dietary Na^+ restriction, the mice start to decompensate and exhibited at day 15 a more than 12% reduction in body weight and exceedingly high plasma aldosterone levels (∼20,000 pg/ml in knockout

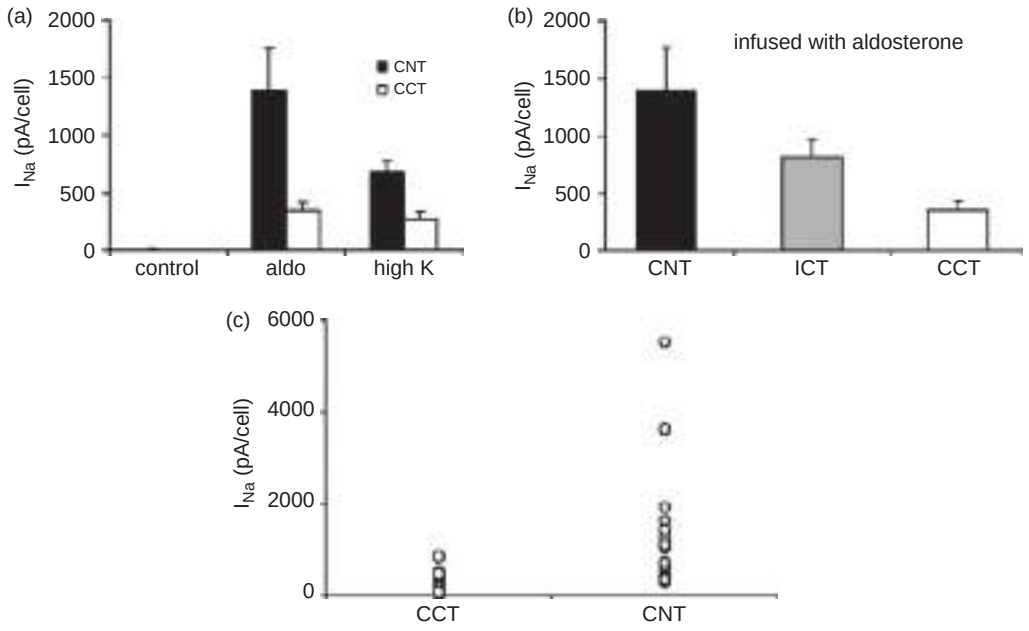

FIGURE 35.4 **Sodium transport in CNT and principal cells of the ASDN (I_{Na}).** (a) I_{Na} in CNT and cortical collecting tubule (CCT) of control rats fed a normal (control) diet, aldosterone treated rats fed a normal diet or rats fed a high-K diet. (b) I_{Na} in cells of CNT, initial collecting tubule (ICT), and CCT of aldosterone-treated rats. (c) Individual values of I_{Na} in CCT and CNT cells of aldosterone-treated rats. *(From Frindt, G., and Palmer, L.G. (2004).*[113]*)*

mice versus ~1200 pg/ml in control mice). Moreover, the mice show hyperkalemia, that worsens with dietary K^+-loading. Furthermore, the mice are polyuric, consistent with the idea that ENaC is important not only for renal Na^+ and K^+ handling, but also for the control of water reabsorption.[115]

Similar to this CNT and CD α-ENaC knockout model, mice with targeted deletion of the MR in the CD and CNT, but intact MR expression and ENaC regulation in early CNT and DCT2, show impaired Na^+ balance (Figure 35.6). Although these mice develop normally under a standard diet, they continuously lose body weight and show signs of severe extracellular volume contraction under a low-Na^+ diet.[116] These studies did also show that the MR is crucial for the increased expression of αENaC and apical targeting of all three ENaC subunits in response to dietary Na^+ restriction. Interestingly, these observations in mice with genetic deletion of the MR contrast with findings in rodents with pharmacological inhibition of the MR. In rats, blockade of the MR by spironolactone does not prevent the apical translocation of ENaC in response to dietary Na^+ restriction.[100] Likewise, the combined inhibition of the MR and GR by spironolactone and RU486 does not block the induction of αENaC and ENaC trafficking induced by aldosterone-infusion.[117] Together with the observation that the severe symptoms of pseudohypoaldosteronism in MR-deficient mice can be improved by glucocorticoid treatment,[118] and that mice with CNT/CD-specific MR-deficiency have a milder phenotype than mice with CNT/CD-specific deletion of αENaC, the data point to some redundancies in the MR and GR-dependent signaling pathways that control ENaC function.

ENaC-Related Genetic Diseases Underline Pathophysiological Relevance

The discovery that rare monogenic diseases caused by mutations in the genes encoding the ENaC subunits cause defects in the control of Na^+ balance and blood pressure provided direct evidence for the implication of this channel in these processes.[119] Remarkably, these diseases represent on the one hand, a gain-of-function phenotype (Liddle's syndrome), and on the other hand a loss-of-function disease (pseudohypoaldosteronism type I or PHAI).

LIDDLE'S SYNDROME

Liddle's syndrome is a rare disorder (pseudoaldosteronism) described first by G. W. Liddle in a family in which multiple siblings had early onset of severe hypertension associated with hypokalemia.[120] Urinary excretion of aldosterone was low in these patients, and no effects of spironolactone on blood pressure could be demonstrated. By contrast, administration of the Na^+ channel-blocker triamterene, together with restriction of salt intake, tended to normalize blood pressure. These clinical features suggested that hypertension was due to excessive aldosterone-independent Na^+ reabsorption in the distal nephron, due to the constitutive

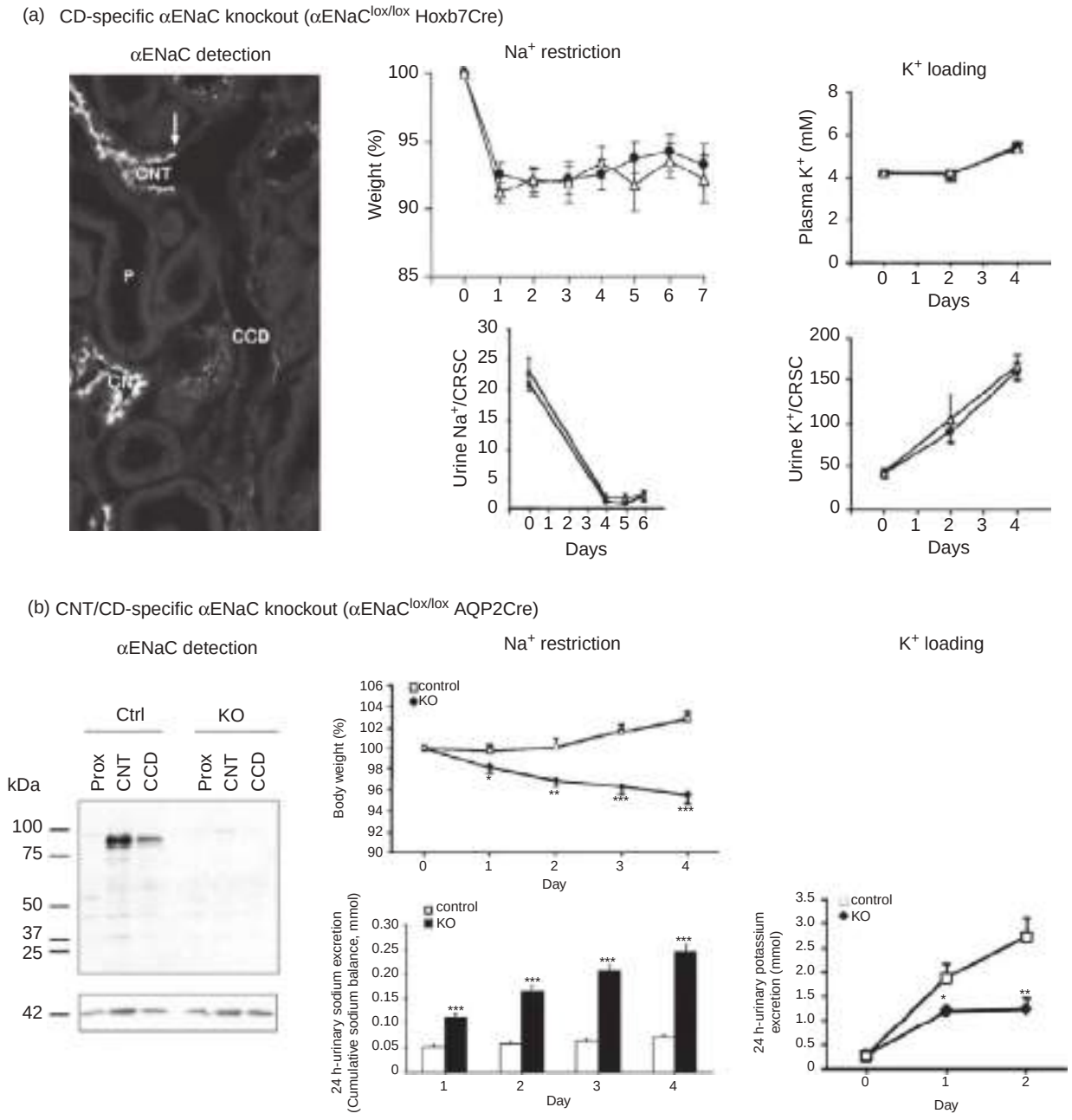

FIGURE 35.5 **Different phenotype of mice with targeted deletion of α-ENaC in the CD only (a) or in the CD and CD (b).** Left panels (a) and (B): Detection of α-ENaC by immunohistochemistry (a) or immunoblotting (b) confirms the efficient deletion of α-ENaC in the targeted segments in the mouse models. Middle panels (a) and (b): On dietary Na^+ restriction, $MR^{lox/lox}$ Hoxb7Cre mice do not lose more body weight than control mice, while $MR^{lox/lox}$ AQP2Cre mice lose more body weight than controls. Moreover, $MR^{lox/lox}$ AQP2Cre mice do not retain Na^+ from the urine as efficently as control mice. Right panels (a) and (b): $MR^{lox/lox}$ Hoxb7Cre mice tolerate dietary K^+-loading without any differences from control mice with respect to plasma K^+ levels and fractional urinary K^+ excretion. In contrast, $MR^{lox/lox}$ AQP2Cre mice become hyperkalemic (Serum K^+ 7.7 ± 0.8 mM vs. 5.2 ± 0.2 mM in controls) and excrete less K^+ with their urine than control mice. *(Adapted from (a) Rubera, I., et al. (2003).[95]; and (b) from Christensen, B. M., et al. (2010)[115].)*

activation of ENaC. Despite the low plasma aldosterone in these patients, they still responded to aldosterone injections by further decreasing their renal Na^+ excretion.

The pedigree of the original kindred described by Liddle was in the meantime extended, clearly demonstrating the autosomal dominant inheritance of the disease.[121] A candidate gene approach was used to

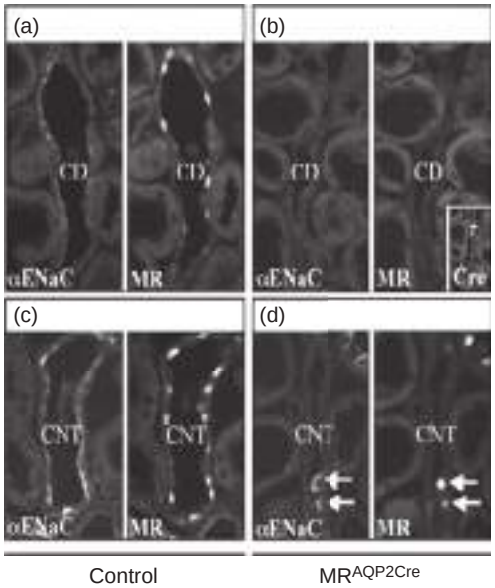

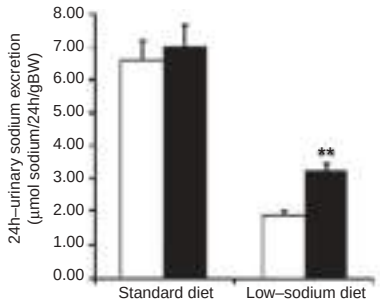

Diet	Plasma Aldosterone (pg/ml)	
	Controls	$MR^{AQP2Cre}$
Standard	430 ± 82 (7)	5195 ± 701 (11)[b]
Low-sodium (3 d)	1083 ± 154 (10)[c]	10500 ± 990 (9)[b,c]
Low-sodium (10 d)	3167 ± 423 (3)[c]	19719 ± 1667 (8)[b,c]

FIGURE 35.6 **Renal sodium wasting in transgenic mice with CNT- and CD-specific deletion of the MR (MR^{AQPcre} mice).** (a)–(d) Immunofluorescent detection of α-ENaC and MR in collecting ducts (CD) and connecting tubules (CNT) of control mice and of MR^{AQPcre} mice kept for 10 days on a low-NaCl diet. Deletion of the MR goes along with a loss of detectable α-ENaC levels. In only a few CNT cells with inefficient MR-targeting, does α-ENaC remain detectable at the cell surface (arrows). Insert in panel (b) shows expression of the Cre recombinase in the CCD of the transgenic mouse. While the rate of urinary Na^+ excretion does not differ between the groups on a standard diet, MR^{AQPcre} mice cannot lower their urinary Na^+ excretion as efficiently as control mice when kept for 9 days on dietary Na^+ restriction (white bars: control mice; black bars: MR^{AQPcre} mice). Consistent with mild pseudohypoaldosteronism type 1, MR^{AQPcre} mice have higher plasma aldosterone levels than control mice on standard and low-sodium diets. *(Adapted from Ronzaud, C., et al. (2007).[116])*

identify mutations causing this rare Mendelian form of hypertension.[122] Complete linkage of the Liddle's syndrome to a locus encoding the β-subunit of ENaC, and analysis of the β gene revealed various mutations in the cytoplasmic C-terminus: deletion or frameshift mutations leading to truncation of a major portion of the C-terminus; and missense mutations in a highly-conserved proline-rich domain.[122–124] A deletion of the C-terminus in the γ-subunit has also been identified as a cause of Liddle's syndrome, whereas no mutations in the α-subunit have been linked to this disorder.[125] Expression of these β- and γ-ENaC variants, together with α-subunits in the *Xenopus* oocyte system, revealed a significant increase in ENaC channel activity at the cell surface, consistent with the initial postulate that these hyperactive channel mutants lead to an excessive Na^+ reabsorption and hypertension.[126]

To elucidate the causal relationship between dietary salt intake, genetically-determined salt handling by the kidney, and hypertension, a mouse model for Liddle's syndrome was developed by introducing the R566stop mutation at the β-ENaC allele ("knockin" strategy).[127] Interestingly, with a normal-salt diet, mice carrying the β-ENaC mutated L/L allele remain normotensive, despite evidence of hypervolemia and increased Na^+ reabsorption in the large intestine. Moreover, plasma pH, Na^+, K^+, Cl^- or HCO_3^- concentrations were not significantly affected.[127] However, these mice manifested the classical Liddle's phenotype with higher blood pressure, metabolic alkalosis, and hypokalemia, accompanied by cardiac and renal hypertrophy in response to a high-salt diet. Moreover, evidence for impaired ENaC internalization was demonstrated *in vivo*, as the increase in urinary Na^+ excretion upon short time (6–12 hours) salt repletion following 1 week of a low-salt diet is significantly delayed in Liddle mice, despite the presence of lower circulating aldosterone concentrations.[128] Isolated perfused CCDs from Liddle mice exhibit higher transepithelial potential differences, and confluent primary cultures of CCDs microdissected from their kidneys exhibit significant lower transepithelial electrical resistance and higher negative potential differences, consistent with an overall increased ENaC activity.[128] Interestingly, mineralocorticoid upregulation of ENaC expression and function is still maintained in Liddle mice that show a remarkable high sensitivity to aldosterone *in vitro*[129] and *in vivo*.[77] Renal CD cells from Liddle mice exhibit hyperactive apical vasopressin-regulated CFTR Cl^- conductance that could contribute to the enhanced NaCl reabsorption observed in the distal nephron of patients with Liddle's syndrome. In

summary, in the Liddle mouse, dysfunction of ENaC in the kidney is demonstrated before onset of arterial hypertension that argues in favor of the kidney hypothesis proposed by Liddle.[120]

PSEUDOHYPOALDOSTERONISM TYPE 1

Pseudohypoaldosteronism type 1 (PHA-1) is characterized by dehydration, hyponatremia, hyperkalemia and metabolic acidosis, despite elevated plasma aldosterone concentration and plasma renin activity. The association of renal Na^+-wasting, hyperkalemia, and failure to respond to mineralocorticoids suggest a defective Na^+ reabsorption in the distal nephron. There are two forms of PHA-1, an inherited recessive disease characterized by a culminant clinical presentation in the neonatal period persisting in adulthood,[130] and an autosomal dominant or sporadic form which is milder and remits with age.[68] Genetic investigations of kindred with the recessive PHA-1 revealed deletion or missense mutations in each of the three ENaC subunits, resulting in decreased channel function when expressed in Xenopus oocytes. Linkage of PHA-1 to loss-of-function ENaC variants further supports the critical role ENaC in aldosterone regulation of Na^+ reabsorption.

Constitutive gene inactivation studies for all three subunits of ENaC (α-, β-, and γ-, encoded by *Scnn1a*, *Scnnn1b*, and *Scnn1g*, respectively) revealed a crucial role for each subunit in the survival of the animal (see for review [131]). Constitutive inactivation of the mouse αENaC gene locus leads to severe respiratory distress with neonatal death, demonstrating the crucial role of ENaC in lung liquid clearance at birth.[132] The αENaC knockout neonates died so rapidly from their lung phenotype that they did not manifest any electrolyte disturbances. However, mice with a genetic rescue by reintroducing the αENaC-subunit under the control of a heterologous (cytomegalovirus) promoter demonstrated the importance of precise regulation of ENaC in the kidney.[133] The transgenic rescued mice had sufficient basal Na^+ absorptive capacity to clear lung liquid and survive the early neonatal period, but developed a severe PHA-1 like phenotype with renal salt-wasting, metabolic acidosis, high aldosterone levels, growth retardation, and increased early mortality.[134] In contrast to the αENaC knockout mice, mice with constitutive inactivation of βENaC and γENaC revealed severe early renal dysfunction.[135,136] Urinary Na^+-wasting, K^+ retention, and increased plasma aldosterone concentrations go along with failure to thrive and early postnatal deaths (see for review [137,138]). It seems that low residual ENaC activity in these mice is sufficient to circumvent the neonatal lung phenotype, consistent with the assumption that αβ- and αγ-subunit combinations can establish some ENaC activity in airway epithelia. Inactivation of the γ-ENaC-subunit in mice resulted in early death (at 36 hours after birth) of the mice, mainly due to disturbed total body electrolyte balance.[135] In the course of generating a mouse model for Liddle's syndrome by the insertion of a stop codon corresponding to residue R566 in human β-ENaC, together with the selection marker neomycin, mice were obtained with a partial disruption of the β-ENaC gene locus (β-ENaCm/m).[139] Under a normal-salt diet, these mice show a mild PHA-1 phenotype with reduced ENaC activity and elevated plasma aldosterone levels, but develop an acute PHA-1 with continuous weight loss, hyperkalemia, and decreased blood pressure when kept under a low-salt diet.

In summary, although the onset and severity of PHA-1 symptoms vary in these models, the renal phenotype of these mice corresponds well to the human PHA-1 phenotype (with salt-wasting, hyperkalemia, and metabolic acidosis), revealing the important implication of ENaC in Na^+, K^+ homeostasis.

Aldosterone and K^+ Secretion

The ASDN of mammals also plays a critical role in the maintenance of K^+ homeostasis. In this nephron segment, Na^+ reabsorption through ENaC is electrically coupled with K^+ secretion: increasing the Na^+ influx depolarizes the apical membrane and increases the driving force for K^+ secretion into the lumen, and *vice versa* (see Figure 35.2). Pathophysiological conditions where Na^+ absorption is increased in the ASDN (hyperaldosteronism, pseudoaldosteronism) are associated with hypokalemia; conversely, ENaC loss-of-function in PHA-1 results in a loss of Na^+ absorption in the ASDN and hyperkalemia (see above). Consistently, mice with constitutive inactivation of β- and γ-ENaC show renal Na^+-wasting and elevated plasma aldosterone level that goes along with renal K^+ retention and hyperkalemia.[135,136] While mice lacking the α-ENaC subunit die soon after birth due to respiratory insufficiency related to impaired alveolar fluid clearance,[132] mice with targeted inactivation of α-ENaC in the CNT and CD survive, and show not only renal salt-wasting, but also hyperkalemia,[115] further confirming the critical role of ENaC for Na^+ and K^+ homeostasis.

The K^+ secretion in the ASDN is mediated by a K^+ conductive pathway in the apical membrane of principal cells. Small conductance inwardly rectifying K^+ channels, termed SK channels, account for most of the apical conductance of principal cells.[140–142] These SK channels have been identified at the molecular level and are the product of the ROMK channel gene. Moreover, the large, Ca^{2+}-activated K^+ channel (BK), present in intercalated and/or principal cells, is thought to contribute to K^+ secretion along the ASDN.[17]

Experiments in mice deficient for either ROMK or the α-subunit of BK suggest that the channels may compensate for each other.[143,144] The functional role and the regulation of these channels in the kidney have been the topic of several recent reviews,[16,18,19,145] and are also extensively addressed in a separate chapter in this book. Therefore, we will here only briefly touch the possible impact of aldosterone on renal K^+ secretion via these channels.

High dietary K^+ intake and elevated plasma K^+ concentrations increase aldosterone secretion by the zona glomerulosa of the adrenal gland and stimulate urinary K^+ excretion. This raises the question of whether aldosterone has a primary effect on K^+ secretion, via genomic effects on principal cells of the ASDN. However, although some studies indicated that aldosterone may directly affect the activity of the renal secretory K^+ channels,[33–36] there is no strong evidence that aldosterone at physiological concentrations increases the apical K^+ conductance of principal cells in the CCD *in vivo*.[146] In fact, rats fed with a low-Na^+ diet have a high plasma level of aldosterone and show a large increase in the density of active ENaC channels in the apical membrane of principal cells, but the density of ROMK channels remains unchanged.[147] Recently, Fodstad and co-workers described that the established mouse CCD cell line (mCCD(cl1)) expresses ROMK mRNA and a robust Ba^{2+}- and tertiapin-Q sensitive K^+ conductance in the apical membrane.[148] Overnight exposure to 100 nM aldosterone did not significantly change the K^+ conductance, but it increased the amiloride-sensitive Na^+ transport. Surprisingly, in this cell model the mRNA levels of all ROMK isoforms measured by qRT-PCR were even decreased by 15–45%, further supporting the idea that aldosterone does not directly stimulate ROMK.

Nevertheless, a high dietary K^+ intake increases both the activity of ENaC and of ROMK (Figure 35.4). Interestingly, the kaliuretic response to dietary K^+ occurs very rapidly, and even before plasma K^+ and aldosterone levels are elevated. Moreover, renal kaliuresis can be clearly dissociated from renal Na^+ handling (for review see [145,149]). In a recent study, Frindt and Palmer addressed the question of whether the concomitant activation of ENaC is required for enhanced urinary K^+ excretion. Rats were kept on different K^+ diets, and then infused via osmotic minipumps with a constant dose of amiloride which was supposed to block more than 98% of Na^+ transport through ENaC. Measurements of urinary K^+ excretion indicated that on a control diet (0.6% KCl), distal nephron K^+ secretion completely depends on ENaC, while on a high-K^+ diet (10% KCl) an increasing fraction of K^+ excretion is independent of Na^+ channels.[150]

Taken together, the current evidence suggests that the activation of ENaC by aldosterone is sufficient to increase the driving force for K^+ secretion, leading to an increase in kaliuresis, without upregulating K^+ channels. In contrast, a high-K^+ diet increases the density of active ROMK channels, suggesting the presence of kaliuretic factors that control K^+ secretion, independently of aldosterone.[145,149]

Aldosterone and the Na^+,K^+-ATPase

For efficient transepithelial sodium reabsorption, apical Na^+ entry via ENaC has to be matched by Na^+ extrusion across the basolateral plasma membrane via the Na^+,K^+-ATPase. Consistently, the activity of the Na^+,K^+-ATPase is also regulated by aldosterone (for a review see [151,152]). Briefly, it was already shown 30 years ago that aldosterone induced augmentation of Na^+,K^+-ATPase in the CCD of adrenalectomized rats after 1 to 3 hours of aldosterone infusion.[153,154] In non-adrenalectomized animals, aldosterone also induced the Na^+ pump, but the response was delayed and observable between 2 days and 1 week.[48] In the rabbit CCD, Sansom and O'Neil observed a doubling in the basolateral membrane conductance after 24 hours of the mineralocorticoid DOCA (deoxycorticosterone acetate) treatment, which could be accounted for by a rise in basolateral K^+ and Cl^- conductance.[155] Moreover, morphometric studies revealed a significant increase in the basal side surface area of the rabbit CCD principal cells, which can be correlated with an increase in single cell capacitance.[156,157] However, these changes in cell surface area could only partially account for the increase in basolateral membrane conductance. It is not clear in these cases whether the mineralocorticoid-induced increase in basolateral membrane conductance is a direct effect of the hormone or secondary to an increase in Na^+ entry into the cell.

As discussed in,[151] it is likely that the early effects involve activation and/or translocation to the basolateral membrane of pre-existing Na^+,K^+-ATPases, whereas the late effects are caused by *de novo* synthesis of the Na^+,K^+-ATPase. Indeed, it has been shown both in adrenalectomized rats and in mpkCCD_{cl4} cells that infusion or treatment for 2 to 3 hours with aldosterone strongly increases the cell surface abundance of Na^+,K^+-ATPase, whereas the total cellular pool was only affected later.[152,158,159] It was shown by the same researchers that Sgk1 is able to increase the cell surface expression of Na^+,K^+-ATPase,[160] providing a potential mechanism of how aldosterone may regulate the pump. However, it remains open if the kinase regulates Na^+,K^+-ATPase by direct phosphorylation or not.

Hence, aldosterone is able to modify Na^+,K^+-ATPase activity by increasing the number of Na^+,K^+-ATPase at the basolateral membrane, likely by translocating pre-existing pumps to the surface (short-term regulation), and by increasing the *de novo*

synthesis of Na^+,K^+-ATPases. Moreover, aldosterone is also able to increase the basolateral membrane surface. The cellular and molecular mechanisms that are involved in this regulation are only vaguely known, and may involve Sgk1.

SODIUM TRANSPORT REGULATION BY ALDOSTERONE: CELLULAR AND MOLECULAR MECHANISMS

Non-Genomic Actions of Aldosterone

Aldosterone, similar to many other steroid hormones, has two fundamentally different mechanisms of action, namely rapid, non-genomic effects that are different from the classical and delayed genomic effects, involving MR and GR and the induction of a complex translational/transcriptional response.[161,162] The non-genomic effects of aldosterone on intracellular signaling pathways have been demonstrated in a variety of animal and human cell types, including those localized in the classical mineralocorticoid target organs.[161,162] These effects are characterized by short latencies of seconds or minutes, and do not involve changes in gene expression mediated by the transcriptional role of the MR.[163] They may involve MR itself and being sensitive to MR antagonists such as spironolactone or eplerenone or being independent of MR. The existence of an alternative receptor with high affinity for aldosterone has been postulated, which may be membrane-bound or representing a signaling molecule within the cell. Recently it has been shown that aldosterone signals independently of MR through GPR-30, an intracellular G-protein-coupled receptor localized in the endoplasmic reticulum, leading to extracellular related kinase (ERK) activation and apoptosis, and to myosin light chain phosphorylation.[164,165] It will be important to determine the role of GPR-30 in the ASDN, where its presence has been reported.[166]

The non-genomic effects involve the activation of protein kinase pathways, including mitogen activated protein (MAP) kinases, protein kinase D1 (PKD1), and protein kinase C (PKC).[162] Interestingly, PKCα (a PKC isoform) directly binds *in vitro* aldosterone via its C2 domain, leading to its autophosphorylation. Hence, PKCα may represent an intracellular aldosterone receptor distinct from the classical MR. PKC signaling is an illustrative example of cross-talk between non-genomic and genomic pathways, as demonstrated in cultured rat cortical collecting duct cells, in which transepithelial Na^+ transport may be stimulated in the early phase by PKCα and independent of MR, whereas the late phase requires genomic action via MR.[167] Also involved in short non-genomic activation of ENaC may be PKD1 that appears to regulate subcellular localization of αENaC in M1 CCD cells.[168] Together, the number of different non-genomic effects of aldosterone that have been described, the lack of physiological targets in many cases, as well as the potentially diverse modes of action, do not allow us to draw a unifying conclusion. However, it is likely that non-genomic actions and genomic actions of aldosterone interfere in some instances with each other for the control of physiological functions.

Genomic Actions of Aldosterone

Mineralocorticoid Receptor (MR) and Glucocorticoid Receptor (GR)

As discussed above, both MR and GR act as aldosterone receptors, having different affinities to aldosterone. MR is the high-affinity type 1 receptor (K_d approximately 0.5 to 2 nmol/l), and GR is the low-affinity type 2 receptor (K_d approximately 14 to 60 nmol/l).[169] On the other hand, the glucocorticosteroid hormone cortisol (corticosterone in rodents) binds to MR with high affinity similar to that of aldosterone, and with a higher affinity to GR.[14,170] Cell-specific hormone and receptor specificity-conferring mechanisms discussed below are necessary to explain the differences in the response to mineralocorticoids and glucocorticoids at the systemic and organ levels.[161,171,172] It is important to note that the precise role of these two receptors (MR versus GR), the extent of their functional overlap, and the role of specificity-conferring mechanism are not fully-understood, and the analysis of MR/GR-modified animals may help to clarify these issues.

The clinical importance of the MRs was demonstrated in patients carrying mutations in the gene leading to an autosomal dominant form of pseudohypoaldosteronism, a disease that remits with age.[68] Moreover, various heterozygous loss-of-function mutations in the human MR (hMR) gene have been identified and characterized, including frameshift, nonsense, and missense mutations, and gene deletions.[173,174] In contrast, a constitutive active mutation in MR (S810L) has been found in patients with an early-onset hypertension that is markedly exacerbated in females during pregnancy.[175] This mutation alters the receptor specificity, and renders progesterone and other steroids lacking 21-hydroxyl groups, normally MR antagonists, to potent agonists of the receptor. Biochemical studies revealed that the S810L mutation induces a change in the receptor conformation, which increases the steroid−receptor complex stability, contributing to the agonistic action.[176,177]

MR and GR belong to the nuclear receptor superfamily that includes other steroid hormone receptors,

including the thyroid hormone, retinoic acid, vitamin D. These nuclear receptors are modulary proteins harboring different conserved domains.[178] The N-terminal domain is the less conserved among nuclear receptors, both in size and sequence, and represents in the case of MR almost half of the protein. This region contains a ligand-independent activation function, which is important for interaction with transcriptional co-regulators, and for intramolecular interactions with the ligand-binding domain (LBD) that lies at the C-terminus.[14,172] This latter domain is complex, as it harbors regions involved in formation of the ligand-binding pocket, interaction with heat shock proteins, dimerization, and a ligand-dependent activation function, which interacts with transcriptional co-regulators. The centrally located DNA-binding domain (DBD) is the most conserved region of the receptor. It folds into two zinc fingers, in which one zinc atom is tetra-coordinated by four cysteines. The core DBD contains two α-helices; the first one, or recognition helix, binds to the major groove of DNA making contacts with specific bases. This domain also contains segments involved in receptor homo- and heterodimerization. Putative nuclear localization signals are localized in the C-terminal part of the DBD and the beginning of the hinge region. Acting as enhancers or repressors of transcription, steroid receptors target specific DNA sequences; these hormone-responsive elements (HREs) then confer inducibility/repressibility to the genes by the corresponding hormone.[172]

In the absence of a ligand, the corticosteroid receptors and possibly all other members of the steroid receptor gene family are primarily localized in the cytosol and associated to a heat shock protein complex, which includes Hsp90, Hsp70, p23, p48, FK-binding protein 51, 52, 59 immunophilins or cyclophillin 40[171,179] (Figure 35.7). This maintains the receptors in an inactive, but ligand binding-competent and stable conformation. Recently it was suggested that this complex also binds via FKB52 to the motor protein dynein, promoting MR translocation into the nucleus.[180] Thereby, the classical concept that MR dissociates from the complex in order to translocate through the nuclear pore was challenged by showing that MR-Hsp90 cross-linked complexes accumulate in the nucleus in an aldosterone-dependent fashion (Figure 35.7). Hsp90 also stabilizes the MR, as inhibition of Hsp90 with the geldanamycin analog 17-AAG (17-Allylamino-17-demethoxygeldanamycin) promotes rapid ubiquitylation by the CHIP (carboxyl terminus of Hsc70-interacting protein) ubiquitin-protein ligase and consequent proteasomal degradation.[181] It was suggested that treatment with 17-AAG may represent an interesting and alternative pharmacological tool to interfere with MR activation. Activation of the receptor by the binding of an agonist or some antagonists results in receptor dimerization. After nuclear translocation, the dimerized receptors will bind to the corresponding hormone-responsive elements and alter the transcription of target gene(s), as do classical sequence-specific transcription factors.[171]

Once activated and translocated to the nucleus, MR and GR associate with and recruit a complex co-activator and co-repressor machinery, involving numerous proteins[171,179] (Figure 35.7). In the case of MR, these include the transcription co-activators SRC-1, SRC-1e, and PGC-1, the histone acetylase CBP/p300, the helicase RHA, and the Pol II elongation factor ELL. The latter one represents an MR-specific transcriptional co-regulator of MR. Similar complexes are also recruited by the GR.[182] Moreover, co-repressors of the steroid receptors are recruited as well. They include SMRT and NCoR, the apoptosis-controlling DAXX and the sumo ligase PIAS that has been shown to sumoylate MR, causing inhibition of transcription activation of MR.[179] Besides sumoylation, both MR and GR become modified by numerous post-translational modifications (PTMs). These modifications involve phosphorylation, ubiquitylation, and acetylation at various sites. For many of these PTMs the functional consequences have not yet been clearly established, nor have the specific sites been determined.

There are, beside aldosterone, other high-affinity ligands for MR which do not produce the same effects, including progesterone, spironolactone, and other antagonists.[183,184] The working hypothesis to explain this specific differential response is the following: (1) agonists bind to and produce a conformational change which fully activates the receptor and elicits the maximal biologic response; (2) partial agonists fully occupy the receptor, but afford incomplete activation and thus a partial response; and (3) antagonists fully occupy the receptor, but are not able to induce a conformational change necessary for binding to target DNA and transactivation.[185] In the latter case it is assumed that MR (or GR), upon antagonist binding, translocates into the nucleus and recruit instead of the transactivation a transrepression machinery, including the co-repressors described above.[172,186]

Specific aldosterone binding, immunochemical staining, and messenger RNA detection have identified MR in classical mineralocorticoid target tissues such as kidney, gut, and sweat glands, and also in skin, brain, pituitary, and heart.[171,172] In kidney, aldosterone appears to control Na^+ reabsorption across the entire distal nephron from DCT to the IMCD. Indeed, presence of MR and GR protein in the distal nephron has been demonstrated.[46] Both MR and GR are expressed in the TAL, DCT, CNT, CD, and in intercalated cells.[46] The GR is found additionally in proximal tubule cells. In the study by Ackermann et al.,[46] the concept of ligand-dependent translocation into the nucleus of GR and MR

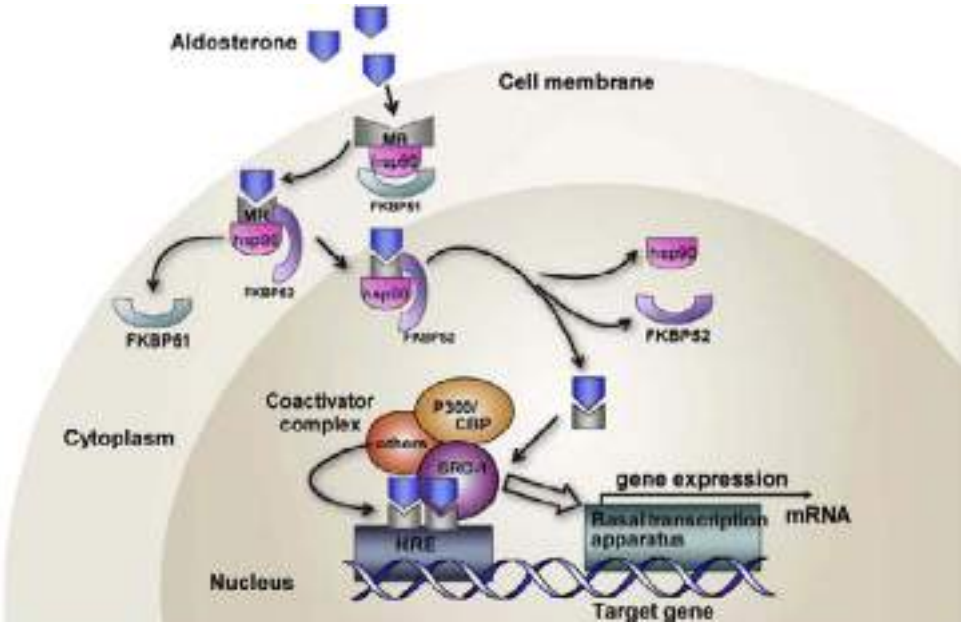

FIGURE 35.7 **Model of MR transcriptional activation.** In the non-stimulated state, MR is localized to the cytosol, where it is compexed to a number of proteins, including Hsp90, FKB51, FKB52, and other proteins. Upon binding to aldosterone, FKB51 dissociates, and MR/Hsp90/FKB52 translocate into the nucleus. There the complex dissociates, and MR will associate with a co-activator complex including SRC-1/P300/CBP and other proteins, and stimulate a complex transcriptional response. *(Reproduced with permission from Yang, J., and Fuller, P. J., (2012).[179])*

was nicely confirmed, although important differences between GR and MR were revealed (see below).

KO and Transgenic Mouse Models of MR and GR

Several mouse models have been generated to study the role of the MR and the GR for ENaC regulation and the control of ion homeostasis (Table 35.1). Mice in which the mineralocorticoid receptor (MR) was inactivated developed severe symptoms of pseudohypoaldosteronism with failure to thrive, weight loss, severe Na^+ and water loss, and highly stimulated renin–angiotensin system.[187] At day 10 after birth, these $MR^{-/-}$ mice die, since they are not able to compensate for Na^+ loss. Interestingly, amiloride-sensitive Na^+ reabsorption is reduced, but the abundance of the mRNAs encoding ENaC and Na^+,K^+-ATPase is unchanged in the kidney, indicating that regulation of Na^+ reabsorption via MR may not be achieved by transcriptional control of ENaC and Na^+,K^+-ATPase. In $MR^{-/-}$ mice, expression of the renin–angiotensin–aldosterone system (RAAS) is highly stimulated. The changes in mRNA levels of the components of the RAAS in 8-day-old $MR^{-/-}$ mice were not apparent in the heterozygous $MR^{+/-}$ mice. However, these animals have an increased urinary Na^+ loss, three-fold increase in Na^+ fractional excretion, and a modest compensatory stimulation of the circulating RAAS, revealed by a three-fold increase in renin, angiotensin II, and aldosterone levels compared with those in $MR^{+/+}$. This suggests a modest neonatal Na^+ loss, compatible with survival in the $MR^{+/-}$ mice. This mild Na^+ loss exhibited by these heterozygous mice is similar to the phenotype observed in patients with autosomal dominant pseudohypoaldosteronism type I.[68] In patients with a heterozygous defect in the MR gene, a modest form of neonatal renal salt-wasting, with hyperkalemia and acidosis, was observed. The disease remits with age, indicating the crucial importance of aldosterone-dependent Na^+ reabsorption in the postnatal period, and its decreasing role with age.[188] Daily injections of β methasone, a synthetic glucocorticoid, from day 5 after birth onward prolonged the survival of $MR^{-/-}$ mice, suggesting that an activated GR can partially but not completely compensate for the loss of MR function.[188] Daily subcutaneous injections of NaCl from day 5 after birth until weaning and continued oral NaCl supply lead to the survival of MR knockout mice.[189] This NaCl rescue proves that neonatal MR knockout mice die because they are not able to compensate for their renal Na^+ loss. Injections of isotonic NaCl solution enabled the animals to live through a critical phase of life, after which they adapt their salt and water intake to their persisting renal salt-wasting. Mice in which tissue-specific deletion of the MR has been achieved in the late CNT and CD by Cre recombinase under the control of the AQP2 promotor (either constitutive or inducible by tamoxifen), develop normally and show unchanged Na^+ balance under standard conditions and highly elevated aldosterone levels. When kept under low Na^+ diet, mice

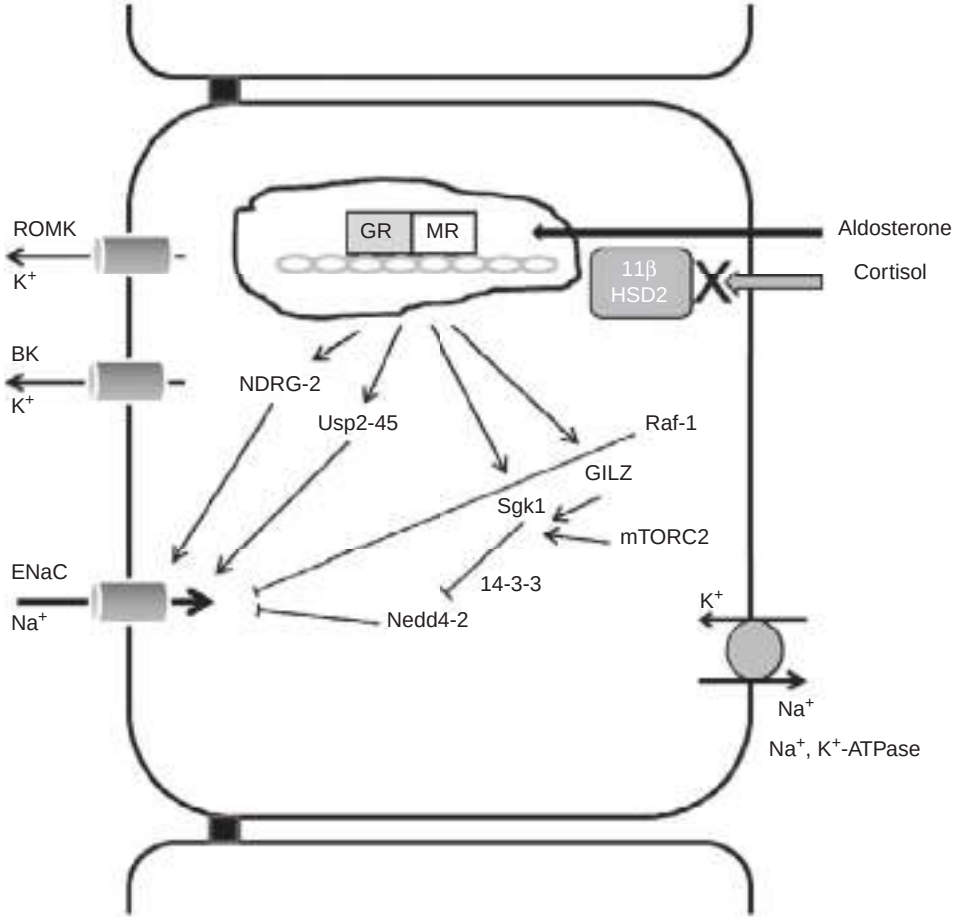

FIGURE 35.8 **Model of the aldosterone-signaling cascade in the principal cells of CD/CCD.** Upon binding of MR to the promotor regions of aldosterone-induced proteins (e.g., Sgk1, Usp2-45, NDRG-2, GILZ, 14-3-3β), transcription/translation leads to increased levels of these proteins. Sgk1, which is part of the ERC complex (comprising also Nedd4-2, GILZ and Raf-1), is activated by PI-3 kinase/mTORC2, stabilized by GILZ, and phosphorylates the ubiquitin-protein ligase Nedd4-2 on specific sites. 14-3-3β binds to these sites and interferes with binding and ubiquitylation of ENaC by Nedd4-2, causing reduced internalization and degradation of ENaC.

lose bodyweight due to Na^+ and water loss. The data indicate that the loss of MR in the late CNT and CD can be compensated by increased aldosterone levels, likely causing an increased MR-dependent Na^+ reabsorption in the DCT 2 and early CNT and/or activation of MR-independent sodium-retaining mechanisms in late CNT and CD.[116,190]

Constitutive hMR overexpression in all MR-expressing tissues, notably the kidney and heart, led to both renal and mild cardiac alterations compatible with hypokalemic nephropathies, despite normal K^+ serum levels.[191]

Inactivation of the GR *in vivo* resulted in perinatal death due to respiratory failure.[192] Lung maturation was severely retarded and RNA encoding ENaC was diminished, which may cause insufficient fluid clearance of the lung at birth. That the GR may play a role in the control of Na^+ handling along the ASDN can be deduced from the observation that mice with a conditional overexpression of the human GR in the CD show some signs of enhanced ENaC activation with renal Na^+ retention.[193] However, mice with targeted deletion of the GR in the entire distal nephron do not reveal any overt phenotype, suggesting that the MR can largely compensate for the loss of the GR along the ASDN.[194]

11β-HSD2 and Molecular Determinants of Mechanisms Conferring Specificity

Aldosterone is present at low concentration in the extracellular fluid (in the order of 10^{-10}–10^{-8} mol/l). It can diffuse (or eventually be transported) through the plasma membrane of all cells, but may encounter a specific receptor only in target cells. The free MR and GR are localized mostly in the cytosol.[46] At the cellular level, the action of aldosterone is initiated by its binding to the MR, and under certain conditions also to the GR. However, the major glucocorticoid in humans is cortisol; in the plasma, 95% is bound to plasma proteins, in particular to the corticosteroid-binding globulin (CBG).[195] In comparison, the plasma level of aldosterone, the main mineralocorticoid hormone, is much lower (two orders

of magnitude) than that of cortisol or corticosterone. Thus, the glucocorticoids, which have a similar high affinity for the MR as aldosterone, would be expected to occupy the high-affinity type I sites of MR. Indeed, even the "effective" free concentration of aldosterone, which in contrast to the natural glucocorticoids has no specific carrier plasma protein, is lower than that of glucocorticoids. However, glucocorticoids do normally not occupy MR or GR at a significant extent in aldosterone target epithelia. As described below, this is essentially due to the expression of a crucial protection mechanism represented by the 11β-hydroxysteroid dehydrogenase type 2 (11β-HSD2), which catalyzes the conversion of the active 11-hydroxycorticosteroids (cortisol and corticosterone) to 11-oxocorticosteroids (cortisone or 11-dehydrocorticosterone) that have a much lower affinity for the corticosteroid receptors.[15,196] Consequently, this mechanism allows aldosterone to occupy MR but also GR. Along the ASDN, 11β-HSD2 and MR may not only share the cellular, but also the subcellular localization. The 11β-HSD2 is thought to be restricted to the endoplasmic reticulum[197] that spans as a membranous labyrinth throughout almost the entire cytoplasm of the cells. In the non-activated state, MR may localize in direct vicinity to the 11β-HSD2, either outside or even inside the ER.[198] This close co-localization likely contributes to the efficient protection from cortisol activation. The crucial role of 11β-HSD2 for preventing the occupation of the MR by endogenous glucocorticoids is underlined by the fact that mutations of its gene or inhibition of its function by licorice (glycyrrhenetic acid) produces a syndrome of apparent mineralocorticoid excess (AME) with salt retention, arterial hypertension, and hypokalemic alkalosis.[196] Genetic inactivation of 11β-HSD2s in the mouse confirmed the crucial role of the enzyme in the protection of the MR (and GR) from circulating glucocorticoids, and allowed further study of the molecular and cellular mechanisms leading to the characteristic pathophysiology of AME.[199] About 50% of the 11β-HSD2 knockout mice die early after birth, showing muscle weakness, reduced suckling, intestinal ileus, and possible cardiac arrest, which are all likely due to the severe hypokalemia.[200] Also, the surviving knockouts exhibit hypokalemia with hypochloremia, hypotonic polyuria, and marked arterial hypertension. They further show striking histological changes, with marked hyperplasia and hypertrophy of the distal nephron, consistent with persistent MR activation, leading to the AME disease phenotype with severe electrolyte imbalances.[199] The structural changes to the ASDN cells might be irreversible, and hence may explain why suppression of endogenous glucocorticoid production does not always reverse the phenotype in AME patients.[200,201]

The utmost importance of 11β-HSD2 for the regulation of the renal corticosteroid receptors was also demonstrated by immunohistochemical studies on rat kidneys.[46] In the 11β-HSD2-positive cells of the ASDN, the MR and GR were found to be localized to the cell nuclei under control conditions. Under a high dietary Na^+ intake, when aldosterone plasma levels are low, the GR but not the MR was removed from the cell nuclei. The differential response was suggested to be the result of the different affinities of both receptors to corticosteroids. In the presence of low plasma aldosterone levels, the activity of the 11β-HSD2 is likely high enough to lower the intracellular corticosterone levels sufficiently to protect the low-affinity GR, but not the high-affinity MR, from glucocorticoid-binding and nuclear translocation. Consistently in adrenalectomized rats (having no endogenous gluco- and mineralocorticoids), any nuclear localization of the MR and GR was lacking. Infusion of low dose of corticosterone translocated the MR to the cell nucleus of all distal tubules cells, but the GR only translocated in those cells that have little or no 11β-HSD2 expression. Only when corticosterone was infused at high level, were both MR and GR located to the cell nuclei in all ASDN cells. These findings were interpreted to indicate that the 11β-HSD2 protects primarily the GR, and not the MR, from activation and translocation to the cell nuclei in the ASDN cells.[46] The separate regulation of MR and GR trafficking may allow for a differential control of MR and GR homo- and heterodimerization, which might be decisive for the induced and/or repressed transcriptional program,[44] and hence may contribute to the complexity of corticosteroid effects along the ASDN.

Other Specificity-Conferring Mechanisms

Two distinct molecular mechanisms are widely accepted to define the actions of nuclear receptors on gene expression: (1) the classic mechanisms involving transactivation and transrepression via interaction with cognate DNA-binding sites (e.g., HREs); and (2) mechanisms of transcription interference and synergy mediated by protein−protein interactions between corticosteroid receptors and other transacting factors. Transcriptional synergy, functionally defined as a more-than-additive increase in gene transcription conferred by multiple transacting factors or multiple linked cis-acting DNA response elements, can result from cooperative binding of transacting factors to linked enhancers, cooperative recruitment of transcription initiation complexes, and regulation of sequential steps in transcription initiation.[183] The relevance of the distinct properties of synergy of MR and GR is highlighted by the fact that in the MR, the N-terminal domain NTD and the ligand-binding domain (LBD) do interact in an aldosterone-dependent manner. This interaction is not observed in the GR, and

is antagonized by the antagonists spironolactone and eplerenone, and surprisingly, by cortisol.[172] The precise regions involved in this interaction are not known. However, the N-terminal region of MR contains so-called synergy control (SC) motifs whose disruption selectively increased MR activity at GRE multimers.[202] Possibly of relevance, the SCs correspond also to sites that are modified by sumoylation. Although mutations of the sumoylation sites do not interfere with the NTD/LBD interaction, direct and distinguishable inhibitory roles for SUMO isoforms in the control of transcriptional synergy have been demonstrated,[203] although the mechanistic basis for SUMO1 synergy inhibition remains to be determined (see for review[172,204]).

In addition to the major role played by the prereceptor protective mechanisms, the nature of the cellular responses to aldosterone or glucocorticoid is determined to a large extent by the type and the state of the target cell. Indeed, the set of genes regulated by a given activated receptor is cell-specific. This is due to the fact that much more than a single regulatory protein has to bind to a gene to activate its transcription. An intracellular receptor can activate a gene only if an appropriate cell type-specific combination of other gene regulatory proteins is expressed. This opens the possibility of interaction at several levels. As mentioned above, protein−protein interactions play a central role in the establishment of pre-initiation complexes. Thus, the structural differences of the MR and GR, in particular at the level of their amino-terminal domains, certainly allow them to undergo receptor-specific interactions. These interactions, in turn, might selectively modulate the transregulatory action of the receptors, independent of their common DNA-binding properties. Considerable efforts have been made to identify ligand-specific interacting and/or transactivation proteins. RNA helicase A (RHA) has been found to mediate transactivation of MR only in the presence of aldosterone, but not of cortisol; it was speculated that the NTD/LBD interaction may be affected.[172] On the other hand, differential expression and regional distribution of steroid receptor co-activators SRC-1 and SRC-2 in brain and pituitary have been found, and two splice variants of the steroid receptor co-activator-1 (SRC-1), 1a and 1e, can differ significantly in certain cell populations.[205,206] Thus, each cell might have its specific pattern of co-activators which might be involved in cell-specific responses to corticosteroids in a promoter- and ligand-dependent way. Finally, PTMs may also modify the transcriptional effects of MR. Recently it has been shown that cyclin-dependent kinase 5 does modify the MR transcriptional response. However, it is not known to date if aldosterone and cortisol induce different modifications of MR, which might contribute to the differential effects of the two corticosteroids.[172]

How Does Transcriptional Regulation Lead to Transport Regulation?

This question has interested many scientists over the last five decades. Until recently, the epithelial Na^+ channel (ENaC) and the Na^+ pump (Na^+,K^+-ATPase) were recognized as the two main transport proteins mediating Na^+ reabsorption in the ASDN, although the thiazide-sensitive Na^+,Cl^--co-transporter NCC may also be involved (see discussion above). Here we will focus on ENaC and the pump, which were primarily investigated in this context. Starting at the level of Na^+ transport effectors, this approach has permitted definition of different phases of aldosterone action: an early phase, characterized by an activation of pre-existing proteins; and a late phase, during which new structural proteins are accumulated. Another approach to the mechanism of aldosterone action starts from the transcriptional event, with the identification of aldosterone-regulated gene products.[207,208] These are then further investigated at the level of their potential involvement in the physiological action of the hormone. Using new powerful techniques to analyze differential gene expression, aldosterone-regulated gene products were identified, as discussed below. It is believed that there are still many important aldosterone-regulated gene products that remain to be identified.

ENaC Activation: Transcriptional Induction and Regulation

Aldosterone directly controls ENaC transcription at the level of the α-subunit gene.[209] The mRNA of this subunit was correspondingly shown to increase in the ASDN of adrenalectomized rats within 2 hours of aldosterone treatment, and on long-term treatment.[3,210] This effect can account for the accumulation of the α-subunit in ASDN cells that was also observed within 2 hours of aldosterone treatment and in the long-term.[3,90] Interestingly, at the protein level aldosterone not only increases the amount of α-ENaC, but also induces a cleavage of γ-ENaC.[90]

Although the induction of αENaC and the apical translocation of all three ENaC-subunits are well visible 2 and 4 hours after aldosterone treatment, transepithelial Na^+ reabsorption and K^+ secretion start earlier, being measurable already within 30 min of treatment.[211] Thus, the early aldosterone response must also involve the activation of pre-existing but previously silent channels. In this regard, ubiquitylation of ENaC (i.e., the modification with ubiquitin[212]) is an

important aldosterone-regulated mechanism that has been shown to control channel surface expression and function.[213] Indeed, experiments have indicated that the ubiquitin-protein ligase Nedd4-2 ubiquitylates ENaC on Lys residues in the NH_2-terminal tails of ENaC-subunits.[214–217] The enzyme binds to PY motifs of the COOH-terminal tails of β- and γ-ENaC via WW protein–protein interaction domains,[214,215,218] and ubiquitylates the channel.[217] Interestingly, missense mutations causing deletion of the PY motifs in β- and γ-ENaC characteristic of Liddle's syndrome lead to an increase in cell surface ENaC expression, and also to an increase in its open probability (P_o), a condition leading to Na^+ retention, low K^+, and hypertension.[119,137,219] The control of ENaC by ubiquitylation appears to be regulated at several levels. First, dietary Na^+, likely via aldosterone action, controls Nedd4-2 expression in the ASDN. A high-salt diet increases Nedd4-2 expression, whereas a low-salt diet decreases it,[110] likely by interfering with excess Na^+ uptake via ENaC. Second, aldosterone has been shown to induce the expression of Sgk1 kinase[220] and the deubiquitylating enzyme Usp2-45.[221,222] In the former case, Sgk1 phosphorylates Nedd4-2, creating a binding site for 14-3-3 proteins.[107,216] By binding to Nedd4-2, 14-3-3 proteins mask the ENaC interacting motif of Nedd4-2, and thus prevent ENaC ubiquitylation and downregulation. This short cascade represents the first direct link between the aldosterone-regulated transcriptional activity of the MR and the function of ENaC that was demonstrated[220,223] (Figure 35.8). Besides acting via Nedd4-2, Sgk1 has been shown to act in concert via other mechanisms: (1) it may phosphorylate a consensus phosphorylation site on the C-terminus of α-ENaC close to the second transmembrane domain.[224] It is noteworthy, though, that this site is not conserved in *Xenopus laevis* ENaC, indicating that this mode of regulation has evolved lately in evolution; (2) it relieves the transcriptional repression by Dot1a-Af9 of the channel subunit,[225] consequently stimulating aldosterone-induced transcription of α-ENaC.

Usp2-45 was identified in a microarray screen of aldosterone early induced transcripts of the CCD.[221] This deubiquitylating enzyme was then shown to deubiquitylate ENaC, to interact both with ENaC and Nedd4-2, and to promote ENaC activity, activation by cleavage and cell surface expression.[226–228] The *in vivo* physiological relevance of Usp2-45 in ENaC regulation, however, remains to be demonstrated. Moreover, it is important to note that the Sgk1-Nedd4-2 pathway is not the only link between aldosterone and ENaC function. This has been indicated by results of experiments performed with mpkCCD cells expressing Liddle's-type ENaC that cannot bind Nedd4-2 and still responds to aldosterone, as did mutant mice expressing an ENaC β-subunit with the Liddle's mutation.[77,129]

Several mouse models deficient for Nedd4-2[60,229–231] and Sgk1[106,232,233] have been created (Table 35.1). Nedd4-2 knockout models have a relatively mild renal phenotype. They show normal Na^+ and K^+ balance, normal[229] or decreased[60] aldosterone, and salt-sensitive hypertension (Figure 35.9). They display increased ENaC protein levels, and in at least one model there were significantly increased NCC levels.[60] Therefore it is likely that Nedd4-2 is not only involved in ENaC regulation, but also in regulation of NCC. Two Nedd4-2 KO models have been shown to have a lung phenotype, with defective ENaC regulation.[230,231] The Sgk1 knockout mice generated by Wulff et al. and Fejes-Toth et al. are total knockouts, whereas the third model by Faresse et al. is an inducible, nephron-specific inactivation of Sgk1. They all display normal Na^+ and K^+ balance when kept under normal-salt diet, but have higher aldosterone levels, indicating a problem in the handling of Na^+ and K^+ (Figure 35.10). Under a low-salt diet, the knockout mice were unable to sufficiently upregulate NaCl reabsorption, despite excessive elevation of plasma aldosterone concentrations, and reduced and maintained apical ENaC translocation.[106,233] Intriguingly, although I_{Na} (measured by whole cell patch-clamping in the CD) was elevated, the proteolytic processing of γENaC is reduced in Sgk1 KO mice, even under conditions were aldosterone is induced.[232] These findings suggest that Sgk1 is required for processing of ENaC, but is not necessary for aldosterone-induced ENaC activation. The Sgk1 knockout models also revealed that Sgk1 is not only involved in ENaC regulation, but also controls the expression of NCC.[232,233] This control of NCC by Sgk1 appears to involve different regulatory pathways, and may act via Nedd4-2 phosphorylation[60,233] or via WNK kinases.[234–237]

Nedd4-2 has been associated through genome-wide studies with essential hypertension (for a recent review see [238]). On the other hand, the contribution of Sgk1 and Usp2-45 to hypertension has remained uncertain.[239–241]

The major part of the ENaC protein faces the extracellular milieu like a receptor, and evidence has accumulated during recent years that furin-mediated cleavage within the extracellular loop appears to be part of the maturation process of α- and γ-ENaC.[242] Yet luminal protease-mediated ENaC activation systems have also been suggested to play an important regulatory role in the function of ENaC. Originally this hypothesis was formulated from the model kidney cell line A6, when a cDNA that encodes a protease that activates ENaC by increasing its P_o was identified.[243] This channel-activating protease (CAP-1) and related

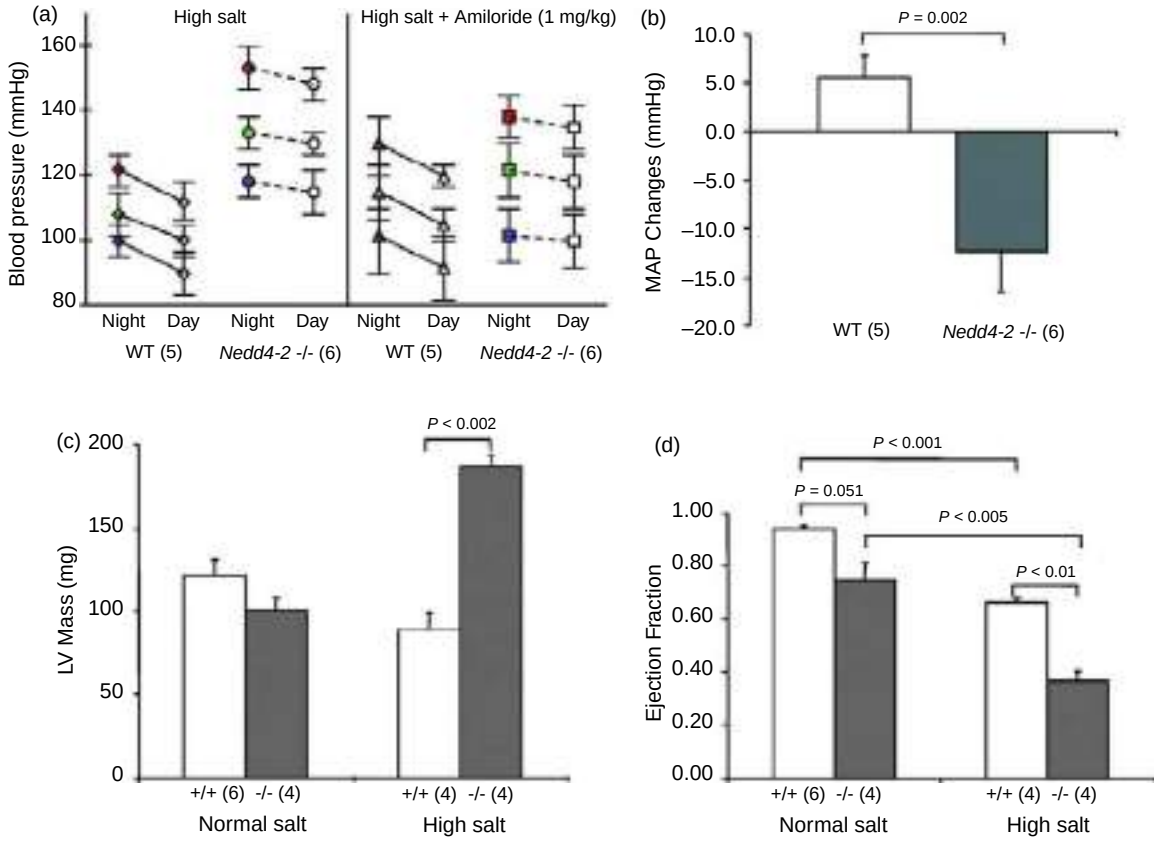

FIGURE 35.9 **Salt-sensitive arterial hypertension, cardiac hypertrophy, and reduced cardiac function in Nedd4-2$^{-/-}$ mice.** Top: Arterial blood pressure (bp) was recorded continuously by radiotelemetry in wild-type (WT) and Nedd4-2$^{-/-}$ mice that were kept for at least two weeks on a high-salt diet (Systolic bp: red symbols; diastolic bp: blue symbols; mean Bp: green symbols). Subsequent daily injections of amiloride for 12 days lowered arterial blood pressure in Nedd4-2$^{-/-}$, but not in WT mice (a), which was most evident when mean arterial pressure (MAP) values before and after amiloride treatment were plotted (b). Bottom: Left ventricular (LV) mass and cardiac ejection fraction in Nedd4-2$^{+/+}$ and Nedd4-2$^{-/-}$ mice kept for 8 to 10 months on normal or a high-salt diet. Heart weights and cardiac ejection fraction were determined by postmortem gravimetry and intravital echocardiography, respectively. *(Adapted from Shi, P. P., et al. (2008).*[229]*)*

proteases have been shown to be highly-expressed in ENaC expressing tissues, like kidney and intestine, in which protease inhibitors have also been shown to decrease Na^+ channel activity (for a review see [244]). The finding that proteolytic events modulate ENaC activity from the extracellular side is supported by the observation made in different cell lines that the application of protease inhibitors decreases, and the addition of proteases increases, Na^+ channel activity. As of yet, the actual mechanism by which this pathway leads to channel activation has not been elucidated. One report suggests that this ENaC-activating mechanism is induced by aldosterone. It was observed that urinary CAP1/prostasin was augmented by aldosterone in rats and humans.[245] Interestingly, proteolysis of ENaC by furin/extracellular proteases may be regulated by ubiquitylation of Nedd4-2. Indeed, it has been shown in transfected cells that ENaC channels with Liddle's mutations (inactivation of PY-motifs, the binding motifs for Nedd4-2) display a higher degree of proteolytic cleavage,[246] similar to co-expression of the deubiquitylating enzyme Usp2-45.[226,227] In view of the fact that proteases have been shown to primarily affect P_o, these observations may explain the observed effect of Liddle's mutations on both cell surface expression and P_o.[219] These observations have to be confirmed *in vivo*. It is noteworthy, however, that in Sgk1 knockout mice, the proteolytic processing of γ-ENaC appears to be defective, compatible with the role of Sgk1 in Nedd4-2-dependent ENaC regulation.[232]

ENaC has also been found to be regulated by lipid-based signaling pathways involving phosphoinositides, such as phosphatidylinositol 4,5-biphosphate (PIP_2), and phosphatidylinositol 3,4,5-triphosphate (PIP_3).[247] PIP_2 is required for ENaC-gating, and is likely to bind directly to the channel. It is important to note that $P2Y_2$ receptors interfere with ENaC activity by stimulating the metabolism of PIP_2. Evidence for such regulation is

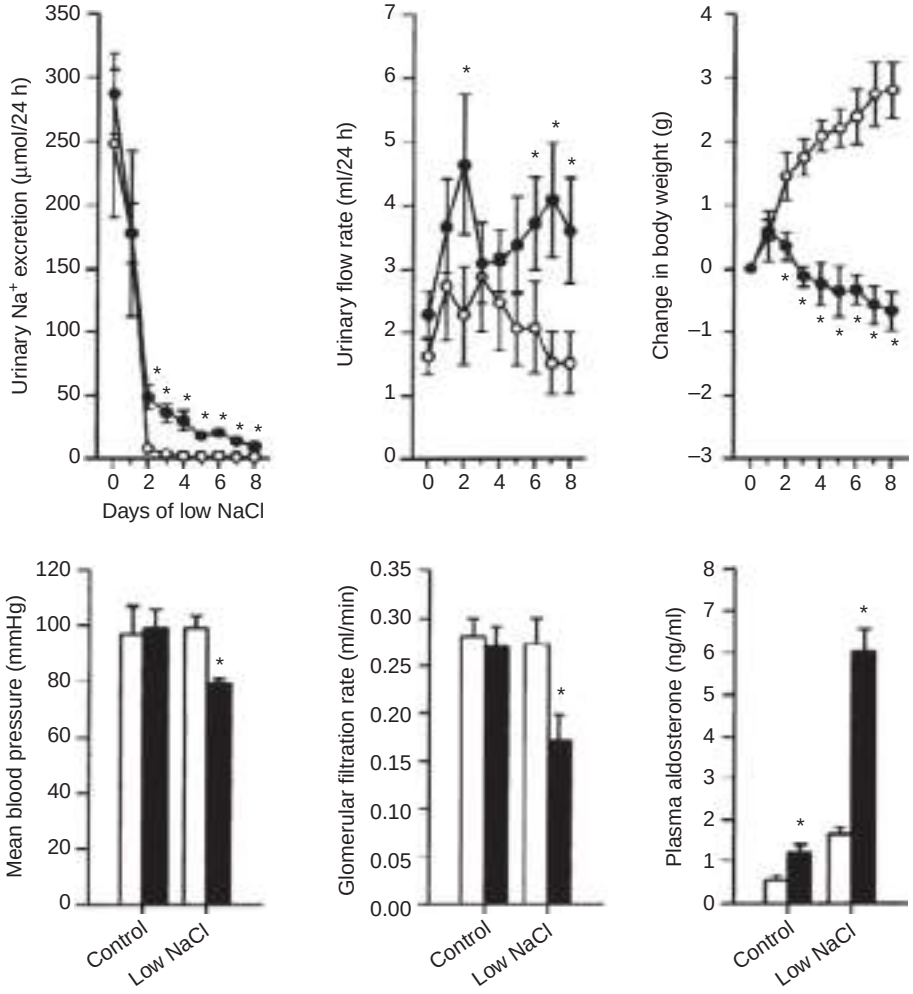

FIGURE 35.10 **Deficient adaptive response to low-Na intake in Sgk1$^{-/-}$ mice.** (Top) Urinary excretion of Na^+ and water, and change in body weight in response to a low-NaCl diet assessed in metabolic cages. (Bottom) Mean arterial blood pressure, glomerular filtration rate, and plasma aldosterone concentration in mice on the control diet and after feeding 3 days of a low-NaCl diet. Filled circles and bars indicate Sgk1$^{+/+}$ mice, open circles and bars indicate Sgk1$^{-/-}$ mice (*p 0.05 vs Sgk1$^{+/+}$mice). *(Adapted from Wulff, P., et al. (2002).[106])*

provided by $P2Y_2$ receptor null mice that are hypertensive with increased ENaC activity.[248] PIP_3 is thought to affect ENaC by several mechanisms: (1) PIP_3 may directly increase the P_o of ENaC expressed in CHO cells, and the aldosterone-induced protein K-Ras[249,250] may act by localizing the PIP_3-producing enzyme phosphatidylinositol-3OH kinase PI3-K close to the channel[251,252]; (2) PI-3K and PIP_3 may acutely stimulate ENaC open probability, likely by direct binding to ENaC[247,253]; (3) another important role for PIP_3 in this context is its role as activator of the PDK kinases (e.g., mSIN1/mTORC2 complex) that in turn activate aldosterone-inducible Sgk1.[220,254] As discussed above, Sgk1 positively affects ENaC by the inhibition of the ubiquitin-protein ligase Nedd4-2, and eventually also by direct phosphorylation of α-ENaC.[220]

Identification of Aldosterone-Regulated RNAs by Gene Expression Profiling

The aim of this section is to mention additional aldosterone-regulated gene products that support the pleiotropic action of aldosterone. Some of these gene products were identified because they were considered as candidates for aldosterone regulation, and therefore the impact of the hormone on their expression was directly tested. Others were identified in the context of screening procedures for aldosterone-regulated mRNAs.[208] This was the case for the two gene products discussed above, Sgk1 and Usp2-45.[222]

Besides ENaC and Na^+,K^+-ATPase, three gene products clearly involved in NaCl reabsorption were identified due to their role in controlling the ion balance in the ASDN. First, two epithelial transporters were shown to be upregulated *in vivo* by mineralocorticoids in the long-term: the thiazide-sensitive Na^+,Cl^--co-transporter NCC of DCT segment-specific cells; and the Cl^-/HCO_3-exchanger pendrin expressed in type B-intercalated cells.[31,52] Both transporters participate at the NaCl reabsorption, and might be upregulated by indirect mechanisms. The third candidate involved in NaCl transport and shown to be induced by aldosterone is the regulatory protein WNK1. This latter effect was shown in a cell culture model to be mediated rapidly by activated MR.[255] It will be interesting to verify

the *in vivo* regulation of WNK1, the role of which appears to be the control of the balance between partially overlapping Na^+, K^+, and Cl^- reabsorption.[256,257] The EGF receptor is an additional regulatory protein, the expression of which was shown in kidney cells to be induced by aldosterone. Interestingly, this receptor has been implicated in the signaling of non-genomic actions of aldosterone, and might play a role in the pathological actions of aldosterone.[258]

Progressively, molecular biology methods have become available that have started to allow the identification of regulated gene products. First, the group of Garty cloned a cDNA-encoding CHIF, a protein that is induced by aldosterone in the colon and belongs to the FXYD family of small Na^+,K^+-ATPase regulatory proteins.[259–261] Interestingly, CHIF is also localized to the distal part of the ASDN, and increases the apparent affinity of the Na^+,K^+-ATPase for Na^+.[262,263] CHIF-deficient mice have a rather mild phenotype pointing to some defects in renal and colonic Na^+ and K^+ transport when stressed by low-Na^+ or high-K^+ intake. The findings were consistent with a dysregulation of the Na^+-K^+-ATPase as the common denominator.[264]

Moreover, Spindler and colleagues used a differential display PCR approach to compare cDNA fragments generated from RNA of control and aldosterone-treated A6 epithelia.[249] They showed that only a small proportion of the mRNA ($<0.5\%$) was significantly regulated within the lag period of aldosterone action, and hence potentially involved in its early effect. One of the regulated gene products was a splice variant of a *Xenopus* K-*ras*. Functional experiments in *Xenopus* oocytes showed that this small G-protein activates ENaC at the cell surface.[250] The connection of K-*Ras* with PIP_3-mediated ENaC activation has been described above.

Another aldosterone-regulated gene product that has been identified by subtractive hybridization is NDRG2.[265] When co-expressed with ENaC, it has been shown to potentiate ENaC activity.[266] Moreover, it is a potential target of Sgk1.[267] Its potential physiological role in the context of Na^+ transport remains to be established.

Some gene screens were performed by SAGE (Serial Analysis of Gene Expression) or gene array analysis on kidney-derived cultured cells.[208] The major limitation of these studies was the large number of genes normally repressed *in vivo* that are expressed in cultured cells, some of which are sensitive to corticosteroids. Nonetheless, some interesting gene products were identified. One of them is the strongly upregulated GILZ, a gene product identified in mpkCCD cells by SAGE analysis.[268] Its induction has been verified in kidney, but its functional role has not yet been unraveled.[269] Interestingly, GILZ has been shown recently to be part of the ENaC regulatory complex (ERC), which also comprises the ENaC inhibitory proteins Raf-1 and Nedd4-2, as well as Sgk1.[270] In this context, GILZ is able to regulate ENaC via Sgk1 stabilization by decreasing its endoplasmic reticulum-mediated degradation.[271] Moreover, GILZ deficient mice show subtle deficiencies in water and Na^+ handling.[272]

In IMCD-3 cells, a series of aldosterone-regulated gene products (1 hour treatment) was identified. Sgk1 was one of the most highly-regulated ones. Moreover, genes involved in circadian rhythm were identified, and it was then shown that the circadian rhythm plays an essential role in ion and water homeostasis, and that Per1, part of the basic circadian regulatory machinery, is involved in α-ENaC regulation.[273–275] It will be timely to obtain a more complete list of the gene products regulated by aldosterone in target cells. It can be envisaged that most of them participate in signaling cascades, directly affecting the function of the cellular machinery for Na^+ reabsorption and K^+ secretion.

CONCLUSION

Since the identification of aldosterone as a major hormone that controls extracellular Na^+, K^+ and fluid homeostasis, tremendous progress has been made in the identification of the cellular and molecular mechanisms by which this hormone mediates its actions, in particular in the kidney. Structural and functional studies allowed us to define the renal tubule segments forming the aldosterone-sensitive distal nephron (ASDN) and to address their contribution to the adaptation of the kidneys to varying functional needs. The main receptors (e.g., MR, GR), specificity conferring mechanisms (e.g., 11-α-HSD2), and effectors (e.g., ENaC, NCC, and Na^+,K^+-ATPase) have been cloned and studied in various *in vitro* and *in vivo* settings. Rare human genetic diseases related to mutations in these proteins were unraveled, and mouse models mimicking the human phenotypes have been generated. Together, these studies further underlined the utmost importance of the ASDN for ion homeostasis and blood pressure control. However, we have just started to identify the homeostatic signals and mechanisms that ensure the efficient cooperation of the different ASDN segments and cell types, which ensure an independent regulation of renal Na^+, K^+, proton, and fluid excretion. Co-expression of the MR, the GR, and additional alternative receptors in the same ASDN cells may add significantly to the complexity of genomic and non-genomic corticosteroid actions along the ASDN. The mild phenotype of Sgk1, Nedd4-2, and CHIF deficient mice points to a rather extensive and redundant signaling cascade. The rapid advancement

of molecular and physiological techniques, together with the increasing availability of genetic mouse models with conditional deletion or overexpression of the receptors and certain regulatory molecules will allow us to further unravel the complex control of the aldosterone-dependent control of renal ion homeostasis. As even subtle dysfunction within the underlying regulatory cascades may already predispose to human diseases such as salt-sensitive hypertension, further research is needed.

Acknowledgment

We are grateful to Drs. Edith Hummler, Bernard Rossier, Laurent Schild, and François Verrey for having established with the previous edition(s) of this chapter a solid base to build on. Moreover, we thank Drs. Dominique Loffing-Cueni, Caroline Ronzaud, and Nourdine Faresse for critically reading the manuscript. We also thank Mr. Jean-Claude Broillet for having established the Reference Databank.

References

[1] Simpson ER, Mason JI. Molecular Aspects of Biosynthesis of Adrenal Steroids. Oxford: Pergamon; 1979.

[2] Studer RA, Person E, Robinson-Rechavi M, Rossier BC. Evolution of the epithelial sodium channel and the sodium pump as limiting factors of aldosterone action on sodium transport. Physiol Genomics 2011;43:844–54.

[3] Loffing J, Zecevic M, Feraille E, Kaissling B, Asher C, Rossier BC, et al. Aldosterone induces rapid apical translocation of ENaC in early portion of renal collecting system: possible role of SGK. Am J Physiol Renal Physiol 2001;280:F675–82.

[4] Katz AI, Doucet A, Morel F. Na-K-ATPase activity along the rabbit, rat, and mouse nephron. Am J Physiol 1979;237:F114–20.

[5] Almeida AJ, Burg MB. Sodium transport in the rabbit connecting tubule. Am J Physiol 1982;243:F330–4.

[6] Shareghi GR, Stoner LC. Calcium transport across segments of the rabbit distal nephron *in vitro*. Am J Physiol 1978;235: F367–75.

[7] Tomita K, Pisano JJ, Knepper MA. Control of sodium and potassium transport in the cortical collecting duct of the rat. Effects of bradykinin, vasopressin, and deoxycorticosterone. J Clin Invest 1985;76:132–6.

[8] Reif MC, Troutman SL, Schafer JA. Sodium transport by rat cortical collecting tubule. Effects of vasopressin and desoxycorticosterone. J Clin Invest 1986;77:1291–8.

[9] Stokes JB. Ion transport by the cortical and outer medullary collecting tubule. Kidney Int 1982;22:473–84.

[10] Frindt G, Ergonul Z, Palmer LG. Na channel expression and activity in the medullary collecting duct of rat kidney. Am. JPhysiolRenal Physiol 2007;292:F1190–6.

[11] Loffing J, Kaissling B. Sodium and calcium transport pathways along the mammalian distal nephron: from rabbit to human. Am J Physiol Renal Physiol 2003;284:F628–43.

[12] Loffing J, Loffing-Cueni D, Macher A, Hebert SC, Olson B, Knepper MA, et al. Localization of epithelial sodium channel and aquaporin-2 in rabbit kidney cortex. Am J Physiol Renal Physiol 2000;278:F530–9.

[13] Bachmann S, Bostanjoglo M, Schmitt R, Ellison DH. Sodium transport-related proteins in the mammalian distal nephron – distribution, ontogeny and functional aspects. Anat Embryol 1999;200:447–68.

[14] Arriza JL, Weinberger C, Cerelli G, Glaser TM, Handelin BL, Housman DE, et al. Cloning of human mineralocorticoid receptor complementary DNA: structural and functional kinship with the glucocorticoid receptor. Science 1987;237:268–75.

[15] Odermatt A, Kratschmar DV. Tissue-specific modulation of mineralocorticoid receptor function by 11beta-hydroxysteroid dehydrogenases: an overview. Mol Cell Endocrinol 2012;350:168–86.

[16] Wang WH, Giebisch G. Regulation of potassium (K) handling in the renal collecting duct. Pflug Arch Eur J Phy 2009;458:157–68.

[17] Holtzclaw JD, Grimm PR, Sansom SC. Role of BK channels in hypertension and potassium secretion. Curr Opin Nephrol Hypertens 2011;20:512–7.

[18] Rodan AR, Cheng CJ, Huang CL. Recent advances in distal tubular potassium handling. Am J Physiol Renal Physiol 2011;300:F821–7.

[19] Welling PA, Ho K. A comprehensive guide to the ROMK potassium channel: form and function in health and disease. Am J Physiol Renal Physiol 2009;297:F849–63.

[20] Mennitt PA, Wade JB, Ecelbarger CA, Palmer LG, Frindt G. Localization of ROMK channels in the rat kidney. J Am Soc Nephrol: JASN 1997;8:1823–30.

[21] Xu JZ, Hall AE, Peterson LN, Bienkowski MJ, Eessalu TE, Hebert SC. Localization of the ROMK protein on apical membranes of rat kidney nephron segments. Am J Physiol 1997;273: F739–48.

[22] Wade JB, Fang L, Coleman RA, Liu J, Grimm PR, Wang T, et al. Differential regulation of ROMK (Kir1.1) in distal nephron segments by dietary potassium. Am J Physiol Renal Physiol 2011;300(6):F1385–93.

[23] Najjar F, Zhou H, Morimoto T, Bruns JB, Li HS, Liu W, et al. Dietary K^+ regulates apical membrane expression of maxi-K channels in rabbit cortical collecting duct. Am J Physiol Renal Physiol 2005;289:F922–32.

[24] Li D, Wei Y, Babilonia E, Wang Z, Wang WH. Inhibition of phosphatidylinositol 3-kinase stimulates activity of the small-conductance K channel in the CCD. Am J Physiol Renal Physiol 2006;290:F806–12.

[25] Gumz ML, Lynch IJ, Greenlee MM, Cain BD, Wingo CS. The renal H^+-K^+-ATPases: Physiology, regulation, and structure. Am J Physiol Renal Physiol 2010;298:F12–21.

[26] Wagner CA, Mohebbi N, Capasso G, Geibel JP. The anion exchanger pendrin (SLC26A4) and renal acid–base homeostasis. Cell Physiol Biochem 2011;28:497–504.

[27] Eladari D, Hubner CA. Novel mechanisms for NaCl reabsorption in the collecting duct. Curr Opin Nephrol Hypertens 2011;20:506–11.

[28] Kim YH, Pech V, Spencer KB, Beierwaltes WH, Everett LA, Green ED, et al. Reduced ENaC protein abundance contributes to the lower blood pressure observed in pendrin-null mice. Am J Physiol Renal Physiol 2007;293:F1314–24.

[29] Pech V, Pham TD, Hong S, Weinstein AM, Spencer KB, Duke BJ, et al. Pendrin modulates ENaC function by changing luminal HCO3. J Am Soc Nephrol: JASN 2010;21:1928–41.

[30] Wall SM, Kim YH, Stanley L, Glapion DM, Everett LA, Green ED, et al. NaCl restriction upregulates renal Slc26a4 through subcellular redistribution: role in Cl^- conservation. Hypertension 2004;44:982–7.

[31] Verlander JW, Hassell KA, Royaux IE, Glapion DM, Wang ME, Everett LA, et al. Deoxycorticosterone upregulates PDS (Slc26a4) in mouse kidney: role of pendrin in mineralocorticoid-induced hypertension. Hypertension 2003;42:356–62.

[32] Leviel F, Hubner CA, Houillier P, Morla L, El Moghrabi S, Brideau G, et al. The Na^+-dependent chloride-bicarbonate

exchanger SLC4A8 mediates an electroneutral Na^+ reabsorption process in the renal cortical collecting ducts of mice. J Clin Invest 2010;120:1627–35.

[33] Yoo D, Kim BY, Campo C, Nance L, King A, Maouyo D, et al. Cell surface expression of the ROMK (Kir 1.1) channel is regulated by the aldosterone-induced kinase, SGK-1, and protein kinase A. J Biol Chem 2003;278:23066–75.

[34] Beesley AH, Hornby D, White SJ. Regulation of distal nephron K^+ channels (ROMK) mRNA expression by aldosterone in rat kidney. J Physiol 1998;509(Pt 3):629–34.

[35] Wald H, Garty H, Palmer LG, Popovtzer MM. Differential regulation of ROMK expression in kidney cortex and medulla by aldosterone and potassium. Am J Physiol 1998;275:F239–45.

[36] Estilo G, Liu W, Pastor-Soler N, Mitchell P, Carattino MD, Kleyman TR, et al. Effect of aldosterone on BK channel expression in mammalian cortical collecting duct. Am J Physiol Renal Physiol 2008;295:F780–8.

[37] Rozenfeld J, Efrati E, Adler L, Tal O, Carrithers SL, Alper SL, et al. Transcriptional regulation of the pendrin gene. Cell Physiol Biochem 2011;28:385–96.

[38] de Seigneux S, Nielsen J, Olesen ET, Dimke H, Kwon TH, Frokiaer J, et al. Long-term aldosterone treatment induces decreased apical but increased basolateral expression of AQP2 in CCD of rat kidney. Am J Physiol Renal Physiol 2007;293: F87–99.

[39] Hasler U, Mordasini D, Bianchi M, Vandewalle A, Feraille E, Martin PY. Dual influence of aldosterone on AQP2 expression in cultured renal collecting duct principal cells. J Biol Chem 2003;278:21639–48.

[40] Kwon TH, Nielsen J, Masilamani S, Hager H, Knepper MA, Frokiaer J, et al. Regulation of collecting duct AQP3 expression: response to mineralocorticoid. Am J Physiol Renal Physiol 2002;283:F1403–21.

[41] Wang WH, Yue P, Sun P, Lin DH. Regulation and function of potassium channels in aldosterone-sensitive distal nephron. Curr Opin Nephrol Hypertens 2010;19:463–70.

[42] Kwon TH, Nielsen J, Moller HB, Fenton RA, Nielsen S, Frokiaer J. Aquaporins in the kidney. Handb Exp Pharmacol 2009;95–132.

[43] Boone M, Deen PM. Physiology and pathophysiology of the vasopressin-regulated renal water reabsorption. Pflug Arch Eur J Phy 2008;456:1005–24.

[44] Farman N, Rafestin-Oblin ME. Multiple aspects of mineralocorticoid selectivity. Am J Physiol Renal Physiol 2001;280:F181–92.

[45] Gomez-Sanchez CE, de Rodriguez AF, Romero DG, Estess J, Warden MP, Gomez-Sanchez MT, et al. Development of a panel of monoclonal antibodies against the mineralocorticoid receptor. Endocrinology 2006;147:1343–8.

[46] Ackermann D, Gresko N, Carrel M, Loffing-Cueni D, Habermehl D, Gomez-Sanchez C, et al. *In vivo* nuclear translocation of mineralocorticoid and glucocorticoid receptors in rat kidney: differential effect of corticosteroids along the distal tubule. Am J Physiol Renal Physiol 2010;299:F1473–85.

[47] Stanton BA. Regulation by adrenal corticosteroids of sodium and potassium transport in loop of Henle and distal tubule of rat kidney. J Clin Invest 1986;78:1612–20.

[48] El Mernissi G, Chabardes D, Doucet A, Hus-Citharel A, Imbert-Teboul M. Le Bouffant F, Montegut M, Siaume S, and Morel F. Changes in tubular basolateral membrane markers after chronic DOCA treatment. Am J Physiol 1983;245:F100–9.

[49] Garg LC, Knepper MA, Burg MB. Mineralocorticoid effects on Na-K-ATPase in individual nephron segments. Am J Physiol 1981;240:F536–44.

[50] Tsuruoka S, Muto S, Taniguchi J, Suzuki M, Imai M. Effects of glucocorticoid and mineralocorticoid on potassium transport in the rat medullary thick ascending limb of Henle's loop. Kidney Int 1995;47:802–10.

[51] Velazquez H, Bartiss A, Bernstein P, Ellison DH. Adrenal steroids stimulate thiazide-sensitive NaCl transport by rat renal distal tubules. Am J Physiol 1996;270:F211–9.

[52] Kim GH, Masilamani S, Turner R, Mitchell C, Wade JB, Knepper MA. The thiazide-sensitive Na-Cl co-transporter is an aldosterone-induced protein. P Natl Acad Sci USA 1998; 95:14552–7.

[53] Chiga M, Rai T, Yang SS, Ohta A, Takizawa T, Sasaki S, et al. Dietary salt regulates the phosphorylation of OSR1/SPAK kinases and the sodium chloride co-transporter through aldosterone. Kidney Int 2008;74(11):1403–9.

[54] Vallon V, Schroth J, Lang F, Kuhl D, Uchida S. Expression and phosphorylation of the Na^+-Cl^- co-transporter NCC *in vivo* is regulated by dietary salt, potassium, and SGK1. Am J Physiol Renal Physiol 2009;297:F704–12.

[55] Masilamani S, Wang X, Kim GH, Brooks H, Nielsen J, Nielsen S, et al. Time course of renal Na-K-ATPase, NHE3, NKCC2, NCC, and ENaC abundance changes with dietary NaCl restriction. Am J Physiol Renal Physiol 2002;283:F648–57.

[56] van der Lubbe N, Lim CH, Fenton RA, Meima ME, Jan Danser AH, Zietse R, et al. Angiotensin II induces phosphorylation of the thiazide-sensitive sodium chloride co-transporter independent of aldosterone. Kidney Int 2011;79:66–76.

[57] Frindt G, Palmer LG. Surface expression of sodium channels and transporters in rat kidney: effects of dietary sodium. Am J Physiol Renal Physiol 2009;297:F1249–55.

[58] Sandberg MB, Maunsbach AB, McDonough AA. Redistribution of distal tubule Na^+-Cl^- co-transporter (NCC) in response to a high-salt diet. Am J Physiol Renal Physiol 2006;291:F503–8.

[59] Nielsen J, Kwon TH, Frokiaer J, Knepper MA, Nielsen S. Maintained ENaC trafficking in aldosterone-infused rats during mineralocorticoid and glucocorticoid receptor blockade. Am J Physiol Renal Physiol 2007;292:F382–94.

[60] Arroyo JP, Lagnaz D, Ronzaud C, Vazquez N, Ko BS, Moddes L, et al. Nedd4-2 modulates renal Na^+-Cl^- co-transporter via the aldosterone-SGK1-Nedd4-2 pathway. J Am Soc Nephrol: JASN 2011;22:1707–19.

[61] Ko B, Kamsteeg EJ, Cooke LL, Moddes LN, Deen PM, Hoover RS. RasGRP1 stimulation enhances ubiquitination and endocytosis of the sodium-chloride co-transporter. Am J Physiol Renal Physiol 2010;299:F300–9.

[62] Louis-Dit-Picard H, Barc J, Trujillano D, Miserey-Lenkei S, Bouatia-Naji N, Pylypenko O, et al. KLHL3 mutations cause familial hyperkalemic hypertension by impairing ion transport in the distal nephron. Nat Genet 2012;44:456–60.

[63] Boyden LM, Choi M, Choate KA, Nelson-Williams CJ, Farhi A, Toka HR, et al. Mutations in kelch-like 3 and cullin 3 cause hypertension and electrolyte abnormalities. Nature 2012; 482:98–102.

[64] Winter C, Kampik NB, Vedovelli L, Rothenberger F, Paunescu TG, Stehberger PA, et al. Aldosterone stimulates vacuolar H(+)-ATPase activity in renal acid-secretory intercalated cells mainly via a protein kinase C-dependent pathway. Am J Physiol Cell Physiol 2011;301:C1251–61.

[65] Izumi Y, Hori K, Nakayama Y, Kimura M, Hasuike Y, Nanami M, et al. Aldosterone requires vasopressin V1a receptors on intercalated cells to mediate acid-base homeostasis. J Am Soc Nephrol JASN 2011;22:673–80.

[66] Lombes M, Kenouch S, Souque A, Farman N, Rafestin-Oblin ME. The mineralocorticoid receptor discriminates aldosterone from glucocorticoids independently of the 11 beta-hydroxysteroid dehydrogenase. Endocrinology 1994;135:834–40.

[67] Gomez-Sanchez EP, Venkataraman MT, Thwaites D, Fort C. ICV infusion of corticosterone antagonizes ICV-aldosterone hypertension. Am J Physiol 1990;258:E649–53.
[68] Geller DS, Rodriguezsoriano J, Boado AV, Schifter S, Bayer M, Chang SS, et al. Mutations in the mineralocorticoid receptor gene cause autosomal dominant pseudohypoaldosteronism type I. Nat Genet 1998;19:279–81.
[69] Koefoed-Johnson V, Ussing HH. The nature of the frog skin potential. Acta Physiol Scand 1958;42:298–308.
[70] Lindemann B, Van Driessche W. Sodium-specific membrane channels of frog skin are pores: current fluctuations reveal high turnover. Science 1977;195:292–4.
[71] Horisberger JD. The Na,K-ATPase: Structure-Function Relationship. Austin,TX: R.G. Landes Company; 1994.
[72] Jorgensen PL. Structure, function and regulation of Na,K-ATPase in the kidney. Kidney Int 1986;29:10–20.
[73] Rossier BC. Mechanisms of action of mineralocorticoid hormones. Endocr Res 1989;15:203–26.
[74] Handler JS. Use of cultured epithelia to study transport and its regulation. J Exp Biol 1983;106:55–69.
[75] Geering K, Claire M, Gaeggeler H-P, Rossier BC. Receptor occupancy vs induction of Na-K-ATPase and Na^+ transport by aldosterone. Am J Physiol 1985;248:C102–8.
[76] Will PC, Cortright RN, DeLisle RC, Douglas JG, Hopfer U. Regulation of amiloride-sensitive electrogenic sodium transport in the rat colon by steroid hormones. Am J Physiol 1985;248:G124–32.
[77] Dahlmann A, Pradervand S, Hummler E, Rossier BC, Frindt G, Palmer LG. Mineralocorticoid regulation of epithelial Na^+ channels is maintained in a mouse model of Liddle's syndrome. Am J Physiol Renal Physiol 2003;285:F310–8.
[78] Canessa CM, Horisberger J-D, Rossier BC. Epithelial sodium channel related to proteins involved in neurodegeneration. Nature 1993;361:467–70.
[79] Canessa CM, Schild L, Buell G, Thorens B, Gautschi I, Horisberger J-D, et al. Amiloride-sensitive epithelial Na^+ channel is made of three homologous subunits. Nature 1994; 367:463–7.
[80] Waldmann R, Champigny G, Bassilana F, Voilley N, Lazdunski M. Molecular cloning and functional expression of a novel amiloride- sensitive Na^+ channel. J Biol Chem 1995; 270:27411–4.
[81] Firsov D, Gautschi I, Mérillat A-M, Rossier BC, Schild L. The heterotetrameric architecture of the epithelial sodium channel (ENaC). EMBO J 1998;17:344–52.
[82] Loffing J, Schild L. Functional domains of the epithelial sodium channel. J Am Soc Nephrol: JASN 2005;16:3175–81.
[83] Jasti J, Furukawa H, Gonzales EB, Gouaux E. Structure of acid-sensing ion channel 1 at 1.9 Å resolution and low pH. Nature 2007;449:316–23.
[84] Gonzales EB, Kawate T, Gouaux E. Pore architecture and ion sites in acid-sensing ion channels and P2X receptors. Nature 2009;460:599–604.
[85] Asher C, Wald H, Rossier BC, Garty H. Aldosterone-induced increase in the abundance of Na^+ channel subunits. Am J Physiol 1996;271:C605–11.
[86] Escoubet B, Coureau C, Bonvalet JP, Farman N. Noncoordinate regulation of epithelial Na channel and Na pump subunit mRNAs in kidney and colon by aldosterone. Am J Physiol 1997;272:C1482–91.
[87] Ono S, Kusano E, Muto S, Ando Y, Asano Y. A low-Na^+ diet enhances expression of mRNA for epithelial Na^+ channel in rat renal inner medulla. Pflug Arch Eur J Phy 1997;434:756–63.
[88] Renard S, Voilley N, Bassilana F, Lazdunski M, Barbry P. Localization and regulation by steroids of the alpha, beta and gamma subunits of the amiloride-sensitive Na^+ channel in colon, lung and kidney. Pflug Arch Eur J Phy 1995;430:299–307.
[89] Frindt G, Masilamani S, Knepper MA, Palmer LG. Activation of epithelial Na channels during short-term Na deprivation. Am J Physiol Renal Physiol 2001;280:F112–8.
[90] Masilamani S, Kim GH, Mitchell C, Wade JB, Knepper MA. Aldosterone-mediated regulation of ENaC alpha, beta, and gamma subunit proteins in rat kidney. J Clin Invest 1999;104: R19–23.
[91] Ergonul Z, Frindt G, Palmer LG. Regulation of maturation and processing of ENaC subunits in the rat kidney. Am J Physiol Renal Physiol 2006;291:F683–93.
[92] Frindt G, Ergonul Z, Palmer LG. Surface expression of epithelial Na channel protein in rat kidney. J Gen Physiol 2008;131:617–27.
[93] Loffing J, Pietri L, Aregger F, Bloch-Faure M, Ziegler U, Meneton P, et al. Differential subcellular localization of ENaC subunits in mouse kidney in response to high- and low-Na diets. Am J Physiol 2000;279:F252–8.
[94] Hager H, Kwon TH, Vinnikova AK, Masilamani S, Brooks HL, Frokiaer J, et al. Immunocytochemical and immunoelectron microscopic localization of alpha-, beta-, and gamma-ENaC in rat kidney. Am J Physiol Renal Physiol 2001;280:F1093–106.
[95] Rubera I, Loffing J, Palmer LG, Frindt G, Fowler-Jaeger N, Sauter D, et al. Collecting duct-specific gene inactivation of aENaC in the mouse kidney does not impair sodium and potassium balance. J Clin Invest 2003;112:554–65.
[96] Dijkink L, Hartog A, Deen PM, van Os CH, Bindels RJ. Time-dependent regulation by aldosterone of the amiloride-sensitive Na^+ channel in rabbit kidney. Pflug Arch Eur J Phy 1999;438:354–60.
[97] Sauter D, Fernandes S, Goncalves-Mendes N, Boulkroun S, Bankir L, Loffing J, et al. Long-term effects of vasopressin on the subcellular localization of ENaC in the renal collecting system. Kidney Int 2006;69:1024–32.
[98] Frindt G, McNair T, Dahlmann A, Jacobs-Palmer E, Palmer LG. Epithelial Na channels and short-term renal response to salt deprivation. Am J Physiol Renal Physiol 2002;283:F717–26.
[99] May A, Puoti A, Gaeggeler H-P, Horisberger J-D, Rossier BC. Early effect of aldosterone on the rate of synthesis of the epithelial sodium channel a subunit in A6 renal cells. J Am Soc Nephrol 1997;8:1813–22.
[100] Nielsen J, Kwon TH, Masilamani S, Beutler K, Hager H, Nielsen S, et al. Sodium transporter abundance profiling in kidney: effect of spironolactone. Am J Physiol Renal Physiol 2002;283:F923–33.
[101] Chen S, Bhargava A, Mastroberardino L, Meijer OC, Wang J, Buse P, et al. Epithelial sodium channel regulated by aldosterone-induced protein sgk. P Natl Acad Sci USA 1999;96:2514–9.
[102] Shigaev A, Asher C, Latter H, Garty H, Reuveny E. Regulation of sgk by aldosterone and its effects on the epithelial Na(+) channel. Am J Physiol 2000;278:F613–9.
[103] Naray-Fejes-Toth A, Canessa CM, Cleaveland ES, Aldrich G, Fejes-Toth G. sgk is an aldosterone-induced kinase in the renal collecting duct. J Biol Chem 1999;274:16973–8.
[104] Hou J, Speirs HJ, Seckl JR, Brown RW. Sgk1 gene expression in kidney and its regulation by aldosterone: spatio-temporal heterogeneity and quantitative analysis. J Am Soc Nephrol: JASN 2002;13:1190–8.
[105] Alvarez de la Rosa D, Zhang P, Naray-Fejes-Toth A, Fejes-Toth G, Canessa CM. The serum and glucocorticoid kinase sgk increases the abundance of epithelial sodium channels in the plasma membrane of *Xenopus* oocytes. J Biol Chem 1999;274:37834–9.

[106] Wulff P, Vallon V, Huang DY, Volkl H, Yu F, Richter K, et al. Impaired renal Na(+) retention in the sgk1-knockout mouse. J Clin Invest 2002;110:1263–8.
[107] Debonneville C, Flores SY, Kamynina E, Plant PJ, Tauxe C, Thomas MA, et al. Phosphorylation of Nedd4-2 by Sgk1 regulates epithelial Na(+) channel cell surface expression. EMBO J 2001;20:7052–9.
[108] Snyder PM, Olson DR, Thomas BC. Serum and glucocorticoid-regulated kinase modulates Nedd4-2-mediated inhibition of the epithelial Na^+ channel. J Biol Chem 2002;277:5–8.
[109] Rauh R, Dinudom A, Fotia AB, Paulides M, Kumar S, Korbmacher C, et al. Stimulation of the epithelial sodium channel (ENaC) by the serum- and glucocorticoid-inducible kinase (Sgk) involves the PY motifs of the channel but is independent of sodium feedback inhibition. Pflug Arch Eur J Phy 2006;452 (3):290–9.
[110] Loffing-Cueni D, Flores SY, Sauter D, Daidie D, Siegrist N, Meneton P, et al. Dietary sodium intake regulates the ubiquitin-protein ligase nedd4-2 in the renal collecting system. J Am Soc Nephrol: JASN 2006;17:1264–74.
[111] Frindt G, Silver RB, Windhager EE, Palmer LG. Feedback regulation of Na channels in rat CCT. II. Effects of inhibition of Na entry. Am J Physiol 1993;264:F565–74.
[112] Nesterov V, Dahlmann A, Bertog M, Korbmacher C. Trypsin can activate the epithelial sodium channel (ENaC) in microdissected mouse distal nephron. Am J Physiol Renal Physiol 2008;295(4):F1052–62.
[113] Frindt G, Palmer LG. Na channels in the rat connecting tubule. Am J Physiol Renal Physiol 2004;286:F669–74.
[114] Kovacikova J, Winter C, Loffing-Cueni D, Loffing J, Finberg KE, Lifton RP, et al. The connecting tubule is the main site of the furosemide-induced urinary acidification by the vacuolar H(+)-ATPase. Kidney Int 2006;70(10):1706–16.
[115] Christensen BM, Perrier R, Wang Q, Zuber AM, Maillard M, Mordasini D, et al. Sodium and potassium balance depends on alphaENaC expression in connecting tubule. J Am Soc Nephrol: JASN 2010;21:1942–51.
[116] Ronzaud C, Loffing J, Bleich M, Gretz N, Grone HJ, Schutz G, et al. Impairment of sodium balance in mice deficient in renal principal cell mineralocorticoid receptor. J Am Soc Nephrol: JASN 2007;18:1679–87.
[117] Nielsen J, Kwon TH, Frokiaer J, Knepper MA, Nielsen S. Lithium-induced NDI in rats is associated with loss of alpha-ENaC regulation by aldosterone in CCD. Am J Physiol Renal Physiol 2006;290:F1222–33.
[118] Schulz-Baldes A, Berger S, Grahammer F, Warth R, Goldschmidt I, Peters J, et al. Induction of the epithelial Na^+ channel via glucocorticoids in mineralocorticoid receptor knockout mice. Pflug Arch Eur J Phy 2001;443:297–305.
[119] Lifton RP, Gharavi AG, Geller DS. Molecular mechanisms of human hypertension. Cell 2001;104:545–56.
[120] Liddle GW, Bledsoe T, Coppage Jr. WS. A familial renal disorder simulating primary aldosteronism but with negligible aldosterone secretion. Trans Assoc Am Physicians 1963;76:199–213.
[121] Botero-Velez M, Curtis JJ, Warnock DG. Brief report: Liddle's syndrome revisited – a disorder of sodium reabsorption in the distal tubule. N Engl J Med 1994;330:178–81.
[122] Shimkets RA, Warnock DG, Bositis CM, Nelson-Williams C, Hansson JH, Schambelan M, et al. Liddle's syndrome: Heritable human hypertension caused by mutations in the b subunit of the epithelial sodium channel. Cell 1994;79:407–14.
[123] Hansson JH, Schild L, Lu Y, Wilson TA, Gautschi I, Shimkets R, et al. A *de novo* missense mutation of the beta subunit of the epithelial sodium channel causes hypertension and Liddle syndrome, identifying a proline-rich segment critical for regulation of channel activity. P Natl Acad Sci USA 1995;92:11495–9.
[124] Tamura H, Schild L, Enomoto N, Matsui N, Marumo F, Rossier BC, et al. Liddle disease caused by a missense mutation of beta subunit of the epithelial sodium channel gene. J Clin Invest 1996;97:1780–4.
[125] Hansson JH, Nelson-Williams C, Suzuki H, Schild L, Shimkets RA, Lu Y, et al. Hypertension caused by a truncated epithelial sodium channel gamma subunit: Genetic heterogeneity of Liddle syndrome. Nat Genet 1995;11:76–82.
[126] Schild L, Canessa CM, Shimkets RA, Warnock DG, Lifton RP, Rossier BC. A mutation in the epithelial sodium channel causing Liddle's disease increases channel activity in the *Xenopus laevis* oocyte expression system. Proc Nat Acad Sci USA 1995;92:5699–703.
[127] Pradervand S, Wang Q, Burnier M, Beermann F, Horisberger JD, Hummler E, et al. A mouse model for Liddle's syndrome. J Am Soc Nephrol 1999;10:2527–33.
[128] Pradervand S, Vandewalle A, Bens M, Gautschi I, Loffing J, Hummler E, et al. Dysfunction of the epithelial sodium channel expressed in the kidney of a mouse model for Liddle syndrome. J Am Soc Nephrol 2003;14:2219–28.
[129] Auberson M, Hoffmann-Pochon N, Vandewalle A, Kellenberger S, Schild L. Epithelial Na^+ channel mutants causing Liddle's syndrome retain ability to respond to aldosterone and vasopressin. Am J Physiol 2003;285:F459–71.
[130] Chang SS, Grunder S, Hanukoglu A, Rosler A, Mathew PM, Hanukoglu I, et al. Mutations in subunits of the epithelial sodium channel cause salt wasting with hyperkalaemic acidosis, pseudohypoaldosteronism type 1. Nat Genet 1996; 12:248–53.
[131] Hummler E. Implication of ENaC in salt-sensitive hypertension. J Steroid Biochem Mol Biol 1999;69:385–90.
[132] Hummler E, Barker P, Gatzy J, Beermann F, Verdumo C, Schmidt A, et al. Early death due to defective neonatal lung liquid clearance in aENaC-deficient mice. Nat Genet 1996; 12:325–8.
[133] Hummler E, Barker P, Talbot C, Wang Q, Verdumo C, Grubb BR, et al. A mouse model for the renal salt-wasting syndrome pseudohypoaldosteronism. P Natl Acad Sci USA 1997; 94:11710–5.
[134] Kerem E, Bistritzer T, Hanukoglu A, Hofmann T, Zhou ZQ, Bennett W, et al. Pulmonary epithelial sodium-channel dysfunction and excess airway liquid in pseudohypoaldosteronism. Nengl J Med 1999;341:156–62.
[135] Barker PM, Nguyen MS, Gatzy JT, Grubb B, Norman H, Hummler E, et al. Role of gammaENaC subunit in lung liquid clearance and electrolyte balance in newborn mice. Insights into perinatal adaptation and pseudohypoaldosteronism. J Clin Invest 1998;102:1634–40.
[136] McDonald FJ, Yang B, Hrstka RF, Drummond HA, Tarr Jr DE, Stokes MP, et al. Disruption of the beta subunit of the epithelial Na^+ channel in mice: Hyperkalemia and neonatal death associated with a pseudohypoaldosteronism phenotype. Proc Nat Acad Sci USA 1999;96:1727–31.
[137] Bonny O, Hummler E. Dysfunction of epithelial sodium transport: from human to mouse. Kidney Int 2000;57:1313–8.
[138] Bonny O, Rossier BC. Disturbances of Na/K balance: Pseudohypoaldosteronism revisited. J Am Soc Nephrol: JASN 2002;13:2399–414.
[139] Pradervand S, Barker PM, Wang Q, Ernst SA, Beerman F, Grubb BR, et al. Salt restriction induces pseudohypoaldosteronism type 1 in mice expressing low levels of the a-subunit of the amiloride-sensitive epithelial sodium channel. Proc Natl Acad Sci USA 1999;96:1732–7.

[140] Frindt G, Palmer LG. Apical potassium channels in the rat connecting tubule. Am J Physiol Renal Physiol 2004;287:F1030–7.
[141] Frindt G, Palmer LG. Low-conductance K channels in apical membrane of rat cortical collecting tubule. Am J Physiol 1989;256:F143–51.
[142] Wang WH, Schwab A, Giebisch G. Regulation of small-conductance K^+ channel in apical membrane of rat cortical collecting tubule. Am J Physiol 1990;259:F494–502.
[143] Rieg T, Vallon V, Sausbier M, Sausbier U, Kaissling B, Ruth P, et al. The role of the BK channel in potassium homeostasis and flow-induced renal potassium excretion. Kidney Int 2007; 72:566–73.
[144] Bailey MA, Cantone A, Yan Q, MacGregor GG, Leng Q, Amorim JB, et al. Maxi-K channels contribute to urinary potassium excretion in the ROMK-deficient mouse model of Type II Bartter's syndrome and in adaptation to a high-K diet. Kidney Int 2006;70:51–9.
[145] Youn JH, McDonough AA. Recent advances in understanding integrative control of potassium homeostasis. Annu Rev Physiol 2009;71:381–401.
[146] Palmer LG, Frindt G. Aldosterone and potassium secretion by the cortical collecting duct. Kidney Int 2000;57:1324–8.
[147] Gray DA, Frindt G, Palmer LG. Quantification of K^+ secretion through apical low-conductance K channels in the CCD. Am J Physiol Renal Physiol 2005;289:F117–26.
[148] Fodstad H, Gonzalez-Rodriguez E, Bron S, Gaeggeler H, Guisan B, Rossier BC, et al. Effects of mineralocorticoid and K^+ concentration on K^+ secretion and ROMK channel expression in a mouse cortical collecting duct cell line. Am J Physiol Renal Physiol 2009;296:F966–75.
[149] Palmer LG, Frindt G. Na^+ and K^+ transport by the renal connecting tubule. Curr Opin Nephrol Hypertens 2007;16:477–83.
[150] Frindt G, Palmer LG. K + secretion in rat kidney: Na^+-channel-dependent and independent mechanisms. Am J Physiol Renal Physiol 2009;297(2):F389–96.
[151] Feraille E, Doucet A. Sodium-potassium-adenosinetriphosphatase-dependent sodium transport in the kidney: Hormonal control. Physiol Rev 2001;81:345–418.
[152] Feraille E, Mordasini D, Gonin S, Deschenes G, Vinciguerra M, Doucet A, et al. Mechanism of control of Na,K-ATPase in principal cells of the mammalian collecting duct. Ann N Y Acad Sci 2003;986:570–8.
[153] El Mernissi G, Doucet A. Short-term effects of aldosterone and dexamethasone on Na-K-ATPase along the rabbit nephron. Pflug Arch Eur J Phy 1983;399:147–51.
[154] El Mernissi G, Doucet A. Specific activity of Na-K-ATPase after adrenalectomy and hormone replacement along the rabbit nephron. Pflug Arch Eur J Phy 1984;402:258–63.
[155] Sansom SC, O'Neil RG. Effects of mineralocorticoids on transport properties of cortical collecting duct basolateral membrane. Am J Physiol 1986;251:F743–57.
[156] Kashgarian M, Ardito T, Hirsch DJ, Hayslett JP. Response of collecting tubule cells to aldosterone and potassium loading. Am J Physiol 1987;253:F8–14.
[157] Wade JB, O'Neil RG, Pryor JL, Boulpaep EL. Modulation of cell membrane area in renal collecting tubules by corticosteroid hormones. J Cell Biol 1979;81:439–45.
[158] Summa V, Mordasini D, Roger F, Bens M, Martin PY, Vandewalle A, et al. Short term effect of aldosterone on Na,K-ATPase cell surface expression in kidney collecting duct cells. J Biol Chem 2001;276:47087–93.
[159] Verrey F, Summa V, Heitzmann D, Mordasini D, Vandewalle A, Feraille E, et al. Short-term aldosterone action on Na,K-ATPase surface expression: role of aldosterone-induced SGK1? Ann N Y Acad Sci 2003;986:554–61.
[160] Zecevic M, Heitzmann D, Camargo SM, Verrey F. SGK1 increases Na,K-ATP cell-surface expression and function in Xenopus laevis oocytes. Pflug Arch Eur J Phy 2004;448:29–35.
[161] Funder JW. Minireview: Aldosterone and mineralocorticoid receptors: past, present, and future. Endocrinology 2010;151:5098–102.
[162] Dooley R, Harvey BJ, Thomas W. Non-genomic actions of aldosterone: from receptors and signals to membrane targets. Mol Cell Endocrinol 2012;350:223–34.
[163] Thomas W, Harvey BJ. Mechanisms underlying rapid aldosterone effects in the kidney. Annu Rev Physiol 2011;73:335–57.
[164] Gros R, Ding Q, Sklar LA, Prossnitz EE, Arterburn JB, Chorazyczewski J, et al. GPR30 expression is required for the mineralocorticoid receptor-independent rapid vascular effects of aldosterone. Hypertension 2011;57:442–51.
[165] Wendler A, Albrecht C, Wehling M. Nongenomic actions of aldosterone and progesterone revisited. Steroids 2012; 77:1002–6.
[166] Hofmeister MV, Damkier HH, Christensen BM, Olde B, Fredrik Leeb-Lundberg LM, Fenton RA, et al. 17beta-Estradiol induces nongenomic effects in renal intercalated cells through G protein-coupled estrogen receptor 1. Am J Physiol Renal Physiol 2012;302:F358–68.
[167] Le Moellic C, Ouvrard-Pascaud A, Capurro C, Cluzeaud F, Fay M, Jaisser F, et al. Early nongenomic events in aldosterone action in renal collecting duct cells: PKCalpha activation, mineralocorticoid receptor phosphorylation, and cross-talk with the genomic response. J Am Soc Nephrol: JASN 2004;15:1145–60.
[168] McEneaney V, Dooley R, Yusef YR, Keating N, Quinn U, Harvey BJ, et al. Protein kinase D1 modulates aldosterone-induced ENaC activity in a renal cortical collecting duct cell line. Mol Cell Endocrinol 2010;325:8–17.
[169] Hellal-Levy C, Couette B, Fagart J, Souque A, Gomez-Sanchez C, Rafestin-Oblin M. Specific hydroxylations determine selective corticosteroid recognition by human glucocorticoid and mineralocorticoid receptors. FEBS Lett 1999;464:9–13.
[170] Arriza JL, Simerly RB, Swanson LW, Evans RM. The neuronal mineralocorticoid receptor as a mediator of glucocorticoid response. Neuron 1988;1:887–900.
[171] Viengchareun S, Le Menuet D, Martinerie L, Munier M, Pascual-Le Tallec L, Lombes M. The mineralocorticoid receptor: insights into its molecular and (patho)physiological biology. Nucl Recept Signal 2007;5:e012.
[172] Fuller PJ, Yao Y, Yang J, Young MJ. Mechanisms of ligand specificity of the mineralocorticoid receptor. J Endocrinol 2012;213:15–24.
[173] Hubert EL, Teissier R, Fernandes-Rosa FL, Fay M, Rafestin-Oblin ME, Jeunemaitre X, et al. Mineralocorticoid receptor mutations and a severe recessive pseudohypoaldosteronism Type 1. J Am Soc Nephrol: JASN 2011;22(11):1997–2003.
[174] Riepe FG. Clinical and molecular features of type 1 pseudohypoaldosteronism. Horm Res 2009;72:1–9.
[175] Geller DS, Farhi A, Pinkerton N, Fradley M, Moritz M, Spitzer A, et al. Activating mineralocorticoid receptor mutation in hypertension exacerbated by pregnancy. Science 2000;289:119–23.
[176] Fagart J, Huyet J, Pinon GM, Rochel M, Mayer C, Rafestin-Oblin ME. Crystal structure of a mutant mineralocorticoid receptor responsible for hypertension. Nat Struct Mol Biol 2005;12:554–5.
[177] Huyet J, Pinon GM, Fay MR, Rafestin-Oblin ME, Fagart J. Structural determinants of ligand binding to the mineralocorticoid receptor. Mol Cell Endocrinol 2012;350:187–95.

[178] McKenna NJ. Discovery-driven research and bioinformatics in nuclear receptor and coregulator signaling. Biochim Biophys Acta 2011;1812:808–17.
[179] Yang J, Fuller PJ. Interactions of the mineralocorticoid receptor – within and without. Mol Cell Endocrinol 2012;350:196–205.
[180] Galigniana MD, Erlejman AG, Monte M, Gomez-Sanchez C, Piwien-Pilipuk G. The hsp90-FKBP52 complex links the mineralocorticoid receptor to motor proteins and persists bound to the receptor in early nuclear events. Mol Cell Biol 2010; 30:1285–98.
[181] Faresse N, Ruffieux-Daidie D, Salamin M, Gomez-Sanchez CE, Staub O. Mineralocorticoid receptor degradation is promoted by Hsp90 inhibition and the ubiquitin-protein ligase CHIP. Am J Physiol Renal Physiol 2010;299:F1462–72.
[182] Revollo JR, Cidlowski JA. Mechanisms generating diversity in glucocorticoid receptor signaling. Ann N Y Acad Sci 2009; 1179:167–78.
[183] Rupprecht R, Arriza JL, Spengler D, Reul JM, Evans RM, Holsboer F, et al. Transactivation and synergistic properties of the mineralocorticoid receptor: relationship to the glucocorticoid receptor. Mol Endocrinol 1993;7:597–603.
[184] Yang J, Chang CY, Safi R, Morgan J, McDonnell DP, Fuller PJ, et al. Identification of ligand-selective peptide antagonists of the mineralocorticoid receptor using phage display. Mol Endocrinol 2011;25:32–43.
[185] Fagart J, Wurtz JM, Souque A, Hellal-Levy C, Moras D, Rafestin-Oblin ME. Antagonism in the human mineralocorticoid receptor. EMBO J 1998;17:3317–25.
[186] Pascual-Le Tallec L, Lombes M. The mineralocorticoid receptor: a journey exploring its diversity and specificity of action. Mol Endocrinol 2005;19:2211–21.
[187] Berger S, Bleich M, Schmid W, Cole TJ, Peters J, Watanabe H, et al. Mineralocorticoid receptor knockout mice – pathophysiology of Na + metabolism. P Natl Acad Sci USA 1998; 95:9424–9.
[188] Berger S, Bleich M, Schmid W, Greger R, Schutz G. Mineralocorticoid receptor knockout mice: lessons on Na^+ metabolism. Kidney Int 2000;57:1295–8.
[189] Bleich M, Warth R, Schmidt-Hieber M, Schulz-Baldes A, Hasselblatt P, Fisch D, et al. Rescue of the mineralocorticoid receptor knock-out mouse. Pflug Arch Eur J Phy 1999; 438:245–54.
[190] Ronzaud C, Loffing J, Gretz N, Schutz G, Berger S. Inducible renal principal cell-specific mineralocorticoid receptor gene inactivation in mice. Am J Physiol Renal Physiol 2011;300: F756–60.
[191] Le Menuet D, Viengchareun S, Muffat-Joly M, Zennaro MC, Lombes M. Expression and function of the human mineralocorticoid receptor: lessons from transgenic mouse models. Mol Cell Endocrinol 2004;217:127–36.
[192] Cole TJ, Blendy JA, Monaghan AP, Krieglstein K, Schmid W, Aguzzi A, et al. Targeted disruption of the glucocorticoid receptor gene blocks adrenergic chromaffin cell development and severely retards lung maturation. Genes Dev 1995; 9:1608–21.
[193] Nguyen Dinh Cat A, Ouvrard-Pascaud A, Tronche F, Clemessy M, Gonzalez-Nunez D, Farman N, et al. Conditional transgenic mice for studying the role of the glucocorticoid receptor in the renal collecting duct. Endocrinology 2009; 150:2202–10.
[194] Goodwin JE, Zhang J, Velazquez H, Geller DS. The glucocorticoid receptor in the distal nephron is not necessary for the development or maintenance of dexamethasone-induced hypertension. Biochem Biophys Res Commun 2010;394:266–71.
[195] Hammond GL, Smith CL, Goping IS, Underhill DA, Harley MJ, Reventos J, et al. Primary structure of human corticosteroid binding globulin, deduced from hepatic and pulmonary cDNAs, exhibits homology with serine protease inhibitors. P Natl Acad Sci USA 1987;84:5153–7.
[196] Ferrari P. The role of 11beta-hydroxysteroid dehydrogenase type 2 in human hypertension. Biochim Biophys Acta 2010;1802:1178–87.
[197] Naray-Fejes-Toth A, Fejes-Toth G. Extranuclear localization of endogenous 11beta-hydroxysteroid dehydrogenase-2 in aldosterone target cells. Endocrinology 1998;139:2955–9.
[198] Odermatt A, Arnold P, Frey FJ. The intracellular localization of the mineralocorticoid receptor is regulated by 11beta-hydroxysteroid dehydrogenase type 2. J Biol Chem 2001; 276:28484–92.
[199] Kotelevtsev Y, Brown RW, Fleming S, Kenyon C, Edwards CR, Seckl JR, et al. Hypertension in mice lacking 11beta-hydroxysteroid dehydrogenase type 2. J Clin Invest 1999;103:683–9.
[200] Holmes MC, Kotelevtsev Y, Mullins JJ, Seckl JR. Phenotypic analysis of mice bearing targeted deletions of 11beta-hydroxysteroid dehydrogenases 1 and 2 genes. Mol Cell Endocrinol 2001;171:15–20.
[201] Paterson JM, Seckl JR, Mullins JJ. Genetic manipulation of 11beta-hydroxysteroid dehydrogenases in mice. Am J Physiol Regul Integr Comp Physiol 2005;289:R642–52.
[202] Iniguez-Lluhi JA, Pearce D. A common motif within the negative regulatory regions of multiple factors inhibits their transcriptional synergy. Mol Cell Biol 2000;20:6040–50.
[203] Holmstrom S, Van Antwerp ME, Iniguez-Lluhi JA. Direct and distinguishable inhibitory roles for SUMO isoforms in the control of transcriptional synergy. P Natl Acad Sci USA 2003;100:15758–63.
[204] Bhargava A, Pearce D. Mechanisms of mineralocorticoid action: determinants of receptor specificity and actions of regulated gene products. Trends Endocrinol Metab 2004;15:147–53.
[205] Meijer OC, Kalkhoven E, van der Laan S, Steenbergen PJ, Houtman SH, Dijkmans TF, et al. Steroid receptor coactivator-1 splice variants differentially affect corticosteroid receptor signaling. Endocrinology 2005;146:1438–48.
[206] Meijer OC, Steenbergen PJ, De Kloet ER. Differential expression and regional distribution of steroid receptor coactivators SRC-1 and SRC-2 in brain and pituitary. Endocrinology 2000;141:2192–9.
[207] Verrey F. Transcriptional control of sodium transport in tight epithelial by adrenal steroids. J Membr Biol 1995;144:93–110.
[208] Firsov D. Revisiting sodium and water reabsorption with functional genomics tools. Curr Opin Nephrol Hypertens 2004;13:59–65.
[209] Mick VE, Itani OA, Loftus RW, Husted RF, Schmidt TJ, Thomas CP. The alpha-subunit of the epithelial sodium channel is an aldosterone-induced transcript in mammalian collecting ducts, and this transcriptional response is mediated via distinct cis-elements in the 5′-flanking region of the gene. Mol Endocrinol 2001;15:575–88.
[210] MacDonald P, MacKenzie S, Ramage LE, Seckl JR, Brown RW. Corticosteroid regulation of amiloride-sensitive sodium-channel subunit mRNA expression in mouse kidney. J Endocrinol 2000;165:25–37.
[211] Horisberger JD, Diezi J. Effects of mineralocorticoids on Na + and K + excretion in the adrenalectomized rat. Am J Physiol 1983;245:F89–99.
[212] Weissman AM, Shabek N, Ciechanover A. The predator becomes the prey: regulating the ubiquitin system by ubiquitylation and degradation. Nat Rev Mol Cell Biol 2011;12:605–20.

[213] Staub O, Gautschi I, Ishikawa T, Breitschopf K, Ciechanover A, Schild L, et al. Regulation of stability and function of the epithelial Na^+ channel (ENaC) by ubiquitination. EMBO J 1997;16:6325–36.

[214] Abriel H, Loffing J, Rebhun JF, Pratt JH, Horisberger J-D, Rotin D, et al. Defective regulation of the epithelial Na^+ channel (ENaC) by Nedd4 in Liddle's syndrome. J Clin Invest 1999;103:667–73.

[215] Kamynina E, Debonneville C, Bens M, Vandewalle A, Staub O. A novel mouse Nedd4 protein suppresses the activity of the epithelial Na^+ channel. FASEB J 2001;15:204–14.

[216] Bhalla V, Daidie D, Li H, Pao AC, Lagrange LP, Wang J, et al. Serum- and glucocorticoid-regulated kinase 1 regulates ubiquitin ligase neural precursor cell-expressed, developmentally down-regulated protein 4-2 by inducing interaction with 14-3-3. Mol Endocrinol 2005;19:3073–84.

[217] Rotin D, Staub O. Role of the ubiquitin system in regulating ion transport. Pflug Arch Eur J Phy 2010;461:1–21.

[218] Staub O, Dho S, Henry P, Correa J, Ishikawa T, McGlade J, et al. WW domains of Nedd4 bind to the proline-rich PY motifs in the epithelial Na^+ channel deleted in Liddle's syndrome. EMBO J 1996;15:2371–80.

[219] Firsov D, Schild L, Gautschi I, Mérillat A-M, Schneeberger E, Rossier BC. Cell surface expression of the epithelial Na^+ channel and a mutant causing Liddle syndrome: a quantitative approach. Proc Nat Acad Sci Usa 1996;93:15370–5.

[220] Loffing J, Flores SY, Staub O. Sgk kinases and their role in epithelial transport. Annu Rev Physiol 2006;68:461–90.

[221] Fakitsas P, Adam G, Daidie D, van Bemmelen MX, Fouladkou F, Patrignani A, et al. Early aldosterone-induced gene product regulates the epithelial sodium channel by deubiquitylation. J Am Soc Nephrol: JASN 2007;18:1084–92.

[222] Verrey F, Fakitsas P, Adam G, Staub O. Early transcriptional control of ENaC (de)ubiquitylation by aldosterone. Kidney Int 2008;73:691–6.

[223] Staub O, Verrey F. Impact of Nedd4 proteins and serum and glucocorticoid-induced kinases on epithelial Na^+ transport in the distal nephron. J Am Soc Nephrol: JASN 2005;16:3167–74.

[224] Diakov A, Korbmacher C. A novel pathway of epithelial sodium channel activation involves a serum- and glucocorticoid-inducible kinase consensus motif in the C terminus of the channel's alpha-subunit. J Biol Chem 2004;279:38134–42.

[225] Zhang W, Xia X, Reisenauer MR, Rieg T, Lang F, Kuhl D, et al. Aldosterone-induced Sgk1 relieves Dot1a-Af9-mediated transcriptional repression of epithelial Na channel alpha. J Clin Invest 2007;117:773–83.

[226] Ruffieux-Daidie D, Poirot O, Boulkroun S, Verrey F, Kellenberger S, Staub O. Deubiquitylation regulates activation and proteolytic cleavage of ENaC. J Am Soc Nephrol: JASN 2008;19:2170–80.

[227] Ruffieux-Daidie D, Staub O. Intracellular ubiquitylation of the epithelial Na^+ channel controls extracellular proteolytic channel activation via conformational change. J Biol Chem 2011;286:2416–24.

[228] Oberfeld B, Ruffieux-Daidie D, Vitagliano JJ, Pos KM, Verrey F, Staub O. Ubiquitin-specific protease 2-45 (Usp2-45) binds to epithelial Na^+ channel (ENaC)-ubiquitylating enzyme Nedd4-2. Am J Physiol Renal Physiol 2011;301: F189–96.

[229] Shi PP, Cao XR, Sweezer EM, Kinney TS, Williams NR, Husted RF, et al. Salt-sensitive hypertension and cardiac hypertrophy in mice deficient in the ubiquitin ligase Nedd4-2. Am J Physiol Renal Physiol 2008;295:F462–70.

[230] Kimura T, Kawabe H, Jiang C, Zhang W, Xiang YY, Lu C, et al. Deletion of the ubiquitin ligase Nedd4L in lung epithelia causes cystic fibrosis-like disease. P Natl Acad Sci USA 2011;108(8):3216–21.

[231] Boase NA, Rychkov GY, Townley SL, Dinudom A, Candi E, Voss AK, et al. Respiratory distress and perinatal lethality in Nedd4-2-deficient mice. Nat Commun 2011;2:287.

[232] Fejes-Toth G, Frindt G, Naray-Fejes-Toth A, Palmer LG. Epithelial Na^+ channel activation and processing in mice lacking SGK1. Am J Physiol Renal Physiol 2008;294:F1298–305.

[233] Faresse N, Lagnaz D, Debonneville A, Ismailji A, Maillard M, Fejes-Toth G, et al. Inducible kidney-specific Sgk1 knockout mice show a salt-losing phenotype. Am J Physiol Renal Physiol 2012;302:F977–85.

[234] Ring AM, Leng Q, Rinehart J, Wilson FH, Kahle KT, Hebert SC, et al. An SGK1 site in WNK4 regulates Na^+ channel and K^+ channel activity and has implications for aldosterone signaling and K^+ homeostasis. Proc Nat Acad Sci Usa 2007;104:4025–9.

[235] Rozansky DJ, Cornwall T, Subramanya AR, Rogers S, Yang YF, David LL, et al. Aldosterone mediates activation of the thiazide-sensitive Na-Cl co-transporter through an SGK1 and WNK4 signaling pathway. J Clin Invest 2009;119:2601–12.

[236] Xu BE, Stippec S, Chu PY, Lazrak A, Li XJ, Lee BH, et al. WNK1 activates SGK1 to regulate the epithelial sodium channel. P Natl Acad Sci USA 2005.

[237] Heise CJ, Xu BE, Deaton SL, Cha SK, Cheng CJ, Earnest S, et al. Serum and glucocorticoid-induced kinase (SGK) 1 and the epithelial sodium channel are regulated by multiple with no lysine (WNK) family members. J Biol Chem 2010;285:25161–7.

[238] Rossier BC, Schild L. Epithelial sodium channel: Mendelian versus essential hypertension. Hypertension 2008;52:595–600.

[239] Vallon V, Lang F. New insights into the role of serum- and glucocorticoid-inducible kinase SGK1 in the regulation of renal function and blood pressure. Curr Opin Nephrol Hypertens 2005;14:59–66.

[240] Riepe FG, Holterhus PM. Exclusion of serum- and glucocorticoid-induced kinase 1 (SGK1) as a candidate gene for genetically heterogeneous renal pseudohypoaldosteronism Type I in eight families. Am J Nephrol 2007;27:164–9.

[241] Jin HS, Hong KW, Lim JE, Hwang SY, Lee SH, Shin C, et al. Genetic variations in the sodium balance-regulating genes ENaC, NEDD4L, NDFIP2 and USP2 influence blood pressure and hypertension. Kidney Blood Press Res 2010;33:15–23.

[242] Hughey RP, Bruns JB, Kinlough CL, Harkleroad KL, Tong Q, Carattino MD, et al. Epithelial sodium channels are activated by furin-dependent proteolysis. J Biol Chem 2004;279:18111–4.

[243] Vallet V, Chraibi A, Gaeggeler H-P, Horisberger J-D, Rossier BC. An epithelial serine protease activates the amiloride-sensitive sodium channel. Nature 1997;389:607–10.

[244] Rossier BC, Stutts MJ. Activation of the epithelial sodium channel (ENaC) by serine proteases. Annu Rev Physiol 2009;71:361–79 [250]

[245] Narikiyo T, Kitamura K, Adachi M, Miyoshi T, Iwashita K, Shiraishi N, et al. Regulation of prostasin by aldosterone in the kidney. J Clin Invest 2002;109:401–8.

[246] Knight KK, Olson DR, Zhou R, Snyder PM. Liddle's syndrome mutations increase Na^+ transport through dual effects on epithelial Na^+ channel surface expression and proteolytic cleavage. P Natl Acad Sci USA 2006;103:2805–8.

[247] Pochynyuk O, Bugaj V, Stockand JD. Physiologic regulation of the epithelial sodium channel by phosphatidylinositides. Curr Opin Nephrol Hypertens 2008;17:533–40.

[248] Rieg T, Bundey RA, Chen Y, Deschenes G, Junger W, Insel PA, et al. Mice lacking P2Y2 receptors have salt-resistant hypertension and facilitated renal Na^+ and water reabsorption. FASEB J 2007;21(13):3717–26.

[249] Spindler B, Mastroberardino L, Custer M, Verrey F. Characterization of early aldosterone-induced RNAs identified in A6 kidney epithelia. Pflügers Arch 1997;434:323–31.
[250] Mastroberardino L, Spindler B, Forster I, Loffing J, Assandri R, May A, et al. Ras pathway activates epithelial Na^+ channel and decreases its surface expression in Xenopus oocytes. Mol Biol Cell 1998;9:3417–27.
[251] Staruschenko A, Pochynyuk OM, Tong Q, Stockand JD. Ras couples phosphoinositide 3-OH kinase to the epithelial Na^+ channel. Biochim Biophys Acta 2005;1669:108–15.
[252] Staruschenko A, Patel P, Tong Q, Medina JL, Stockand JD. Ras activates the epithelial Na(+) channel through phosphoinositide 3-OH kinase signaling. J Biol Chem 2004;279: 37771–8.
[253] Staruschenko A, Pochynyuk O, Vandewalle A, Bugaj V, Stockand JD. Acute regulation of the epithelial Na^+ channel by phosphatidylinositide 3-OH kinase signaling in native collecting duct principal cells. J Am Soc Nephrol: JASN 2007;18: 1652–61.
[254] Lu M, Wang J, Ives HE, Pearce D. mSIN1 protein mediates SGK1 protein interaction with mTORC2 protein complex and is required for selective activation of the epithelial sodium channel. J Biol Chem 2011;286:30647–54.
[255] Naray-Fejes-Toth A, Snyder PM, Fejes-Toth G. The kidney-specific WNK1 isoform is induced by aldosterone and stimulates epithelial sodium channel-mediated Na^+ transport. P Natl Acad Sci USA 2004;101:17434–9.
[256] Hoorn EJ, Nelson JH, McCormick JA, Ellison DH. The WNK kinase network regulating sodium, potassium, and blood pressure. J Am Soc Nephrol: JASN 2011;22:605–14.
[257] Arroyo JP, Ronzaud C, Lagnaz D, Staub O, Gamba G. Aldosterone paradox: differential regulation of ion transport in distal nephron. Physiology (Bethesda) 2011;26:115–23.
[258] Grossmann C, Gekle M. Interaction between mineralocorticoid receptor and epidermal growth factor receptor signaling. Mol Cell Endocrinol 2012;350:235–41.
[259] Attali B, Latter H, Rachamim N, Garty H. A corticosteroid-induced gene expressing an "IsK-like" K^+ channel activity in Xenopus oocytes. Proceedings of the National Academy of Sciences of the Unites States of America 1995;92:6092–6.
[260] Geering K, Beguin P, Garty H, Karlish S, Fuzesi M, Horisberger JD, et al. FXYD proteins: new tissue- and isoform-specific regulators of Na,K-ATPase. Ann N Y Acad Sci 2003;986:388–94.
[261] Sweadner KJ, Arystarkhova E, Donnet C, Wetzel RK. FXYD proteins as regulators of the Na,K-ATPase in the kidney. Ann N Y Acad Sci 2003;986:382–7.
[262] Beguin P, Crambert G, Guennoun S, Garty H, Horisberger JD, Geering K. CHIF, a member of the FXYD protein family, is a regulator of Na,K-ATPase distinct from the gamma-subunit. EMBO J 2001;20:3993–4002.
[263] Capurro C, Coutry N, Bonvalet JP, Escoubet B, Garty H, Farman N. Cellular localization and regulation of CHIF in kidney and colon. Am J Physiol 1996;271:C753–62.
[264] Goldschmidt I, Grahammer F, Warth R, Schulz-Baldes A, Garty H, Greger R, et al. Kidney and colon electrolyte transport in CHIF knockout mice. Cell Physiol Biochem 2004;14:113–20.
[265] Boulkroun S, Fay M, Zennaro MC, Escoubet B, Jaisser F, Blot-Chabaud M, et al. Characterization of rat NDRG2 (N-Myc downstream regulated gene 2), a novel early mineralocorticoid-specific induced gene. J Biol Chem 2002;277: 31506–15.
[266] Wielputz MO, Lee IH, Dinudom A, Boulkroun S, Farman N, Cook DI, et al. (NDRG2) stimulates amiloride-sensitive Na + currents in Xenopus laevis oocytes and fisher rat thyroid cells. J Biol Chem 2007;282:28264–73.
[267] Murray JT, Campbell DG, Morrice N, Auld GC, Shpiro N, Marquez R, et al. Exploitation of KESTREL to identify NDRG family members as physiological substrates for SGK1 and GSK3. Biochem J 2004;384:477–88.
[268] Robert-Nicoud M, Flahaut M, Elalouf JM, Nicod M, Salinas M, Bens M, et al. Transcriptome of a mouse kidney cortical collecting duct cell line: effects of aldosterone and vasopressin. P Natl Acad Sci USA 2001;98:2712–6.
[269] Muller OG, Parnova RG, Centeno G, Rossier BC, Firsov D, Horisberger JD. Mineralocorticoid effects in the kidney: correlation between alphaENaC, GILZ, and Sgk-1 mRNA expression and urinary excretion of Na(+) and K(+). J Am Soc Nephrol 2003;14:1107–15.
[270] Soundararajan R, Melters D, Shih IC, Wang J, Pearce D. Epithelial sodium channel regulated by differential composition of a signaling complex. P Natl Acad Sci USA 2009;106:7804–9.
[271] Soundararajan R, Wang J, Melters D, Pearce D. Glucocorticoid-induced Leucine zipper 1 stimulates the epithelial sodium channel by regulating serum- and glucocorticoid-induced kinase 1 stability and subcellular localization. J Biol Chem 2010;285:39905–13.
[272] Suarez PE, Rodriguez EG, Soundararajan R, Merillat AM, Stehle JC, Rotman S, et al. The glucocorticoid-induced leucine zipper (gilz/tsc22d3-2) gene locus plays a crucial role in male fertility. Mol Endocrinol 2012;26(6):1000–13.
[273] Gumz ML, Stow LR, Lynch IJ, Greenlee MM, Rudin A, Cain BD, et al. The circadian clock protein Period 1 regulates expression of the renal epithelial sodium channel in mice. J Clin Invest 2009;119:2423–34.
[274] Nikolaeva S, Pradervand S, Centeno G, Zavadova V, Tokonami N, Maillard M, et al. The circadian clock modulates renal sodium handling. J Am Soc Nephrol: JASN 2012; 23:1019–26.
[275] Firsov D, Tokonami N, Bonny O. Role of the renal circadian timing system in maintaining water and electrolytes homeostasis. Mol Cell Endocrinol 2012;349:51–5.
[276] Zhang J, Ge R, Matte-Martone C, Goodwin J, Shlomchik WD, Mamula MJ, et al. Characterization of a novel gain of function glucocorticoid receptor knock-in mouse. J Biol Chem 2009;284:6249–59.
[277] Bailey MA, Craigie E, Livingstone DE, Kotelevtsev YV, Al-Dujaili EA, Kenyon CJ, et al. Hsd11b2 haploinsufficiency in mice causes salt sensitivity of blood pressure. Hypertension 2011;57:515–20.
[278] Huang DY, Wulff P, Volkl H, Loffing J, Richter K, Kuhl D, et al. Impaired regulation of renal K^+ elimination in the sgk1-knockout mouse. J Am Soc Nephrol: JASN 2004;15:885–91.
[279] Lang F, Vallon V. Serum- and glucocorticoid-inducible kinase 1 in the regulation of renal and extrarenal potassium transport. Clin Exp Nephrol 2012;16:73–80.
[280] Pradervand S, Wang Q, Burnier M, Beermann F, Horisberger JD, Hummler E, et al. A mouse model for Liddle's syndrome. J Am Soc Nephrol: JASN 1999;10:2527–33.
[281] Cao XR, Shi PP, Sigmund RD, Husted RF, Sigmund CD, Williamson RA, et al. Mice heterozygous for beta-ENaC deletion have defective potassium excretion. Am J Physiol Renal Physiol 2006;291:F107–15.

This page intentionally left blank

CHAPTER

36

Inherited Disorders of Renal Salt Homeostasis: Insights from Molecular Genetics Studies

Ute I. Scholl and Richard P. Lifton

Departments of Genetics and Internal Medicine, Howard Hughes Medical Institute, Yale University School of Medicine, New Haven, CT, USA

INTRODUCTION

Approaches to Identify Genes and Mutations that Contribute to Human Disease

The regulation of blood pressure is fantastically complex, with contributions from the brain, heart, vasculature, adrenal, and kidney. In the face of such complexity, it has been very difficult to identify the rate-limiting steps in the determination of long-term blood pressure from physiologic analysis alone. In this setting, human genetics has proven highly informative, because the finding of mutations in specific genes that result in significant effects on blood pressure can establish a causal link between specific genes, their biochemical pathways, and blood pressure.[1]

There are a number of approaches to the discovery of human disease genes. One approach is to search for rare mutations with large effects on the trait. In the most extreme form these are so-called Mendelian traits, in which the presence of rare mutations produces a distinctive trait, and the transmission of that trait can be followed through families based on the clinical features. These traits generally follow a few simple patterns of inheritance. Autosomal dominant traits are produced by the inheritance of one mutated copy of a gene. As a result, such traits are commonly transmitted from an affected parent to half of their offspring, and multigenerational pedigrees with many affected subjects can sometimes be found. Dominant mutations can either be gain-of-function – in which the mutant gene has function not present in the normal gene – or less often loss of biochemical function, with a large effect produced by a 50% reduction in gene dosage. Dominant mutations that drastically impair reproductive fitness are commonly found as *de novo* mutations; new mutations found in affected index cases that are absent in their biological parents. Autosomal recessive traits require the inheritance of mutations in the genes on both chromosomes. Typical recessive pedigrees show affected subjects among a single sibship in a family, with parents being clinically unaffected and one in four of their offspring being affected. The mutations that cause autosomal recessive traits typically result in loss of biochemical function. Mutations on the X-chromosome produce distinctive patterns of transmission, since males have only one copy of this chromosome. As a result, these traits are never transmitted from affected fathers to their sons, and loss-of-function traits are found far more frequently among males than females. Other patterns of Mendelian transmission are much less frequent.

The development of complete genetic maps of the human genome identified extensive variations in DNA sequence, allowing the comparison of the inheritance of every segment of every chromosome to the inheritance of the Mendelian trait in families. With sufficient numbers of informative individuals and families, the chromosomal location of disease genes can be mapped, and genes in the linked interval can be searched for mutations. The finding of independent mutations that show specificity for the trait, and which significantly segregate with the trait in pedigrees, provides evidence that a gene responsible for the trait has been identified.

Seldin and Giebisch's The Kidney, Fifth Edition.
DOI: http://dx.doi.org/10.1016/B978-0-12-381462-3.00036-7

© 2013 Elsevier Inc. All rights reserved.

To date, genes and their corresponding mutations that underlie more than 3000 human disease traits have been identified by this approach. The strength of Mendelian genetics has been that the identified mutations directly identify the gene whose function is altered, and is causal to the trait. A second strength is that because the effect size is typically very large, robust inferences about the effect of implicated genes on the trait are possible.

A second general approach to genetic analysis is genetic association. This approach has historically sought to determine whether specific common variants are found with significantly different frequency among cohorts of patients contrasting for specific phenotypes. Early efforts typically used candidate gene approaches, and commonly produced false-positive results. The development of dense maps containing millions of common variants called single nucleotide polymorphisms (SNPs) across the human genome, coupled with the ability to genotype these inexpensively, has led to large-scale genome-wide association studies (GWAS). These studies have allowed careful matching of genetic backgrounds of cases and controls, as well as rigorous statistical thresholds for significance. More than 1200 robust associations of common sequence variations with disease have been established using this approach. Strengths of the approach are the ability to find effects that are common in the population. These have been highly informative in diseases for which Mendelian forms have not been found. Weaknesses are that the common variants are most often not in genes, and consequently identifying the genes whose expression might be altered can be difficult to establish. Also, effect sizes are typically very small, changing disease risk by ~20%. As a result, new biological inferences are frequently difficult to immediately discern from these studies. Nonetheless, these studies can provide leads for diseases that have not yielded productive results from Mendelian studies.

Most recently, the ability to inexpensively sequence whole genomes or whole exomes (all the exons of protein-coding genes) has provided new opportunities for disease gene discovery. Classes of Mendelian traits that were previously intractable, such as diseases caused predominantly by *de novo* mutations, can now be solved. Moreover, one can anticipate that searches for rare variants with moderate effect size – less than typical Mendelian traits, but much larger than GWAS signals – are likely to be discovered by sequencing large cohorts of cases and controls.

Insight into Human Blood Pressure Variation from Genetic Studies

In the past 20 years, molecular genetic studies of rare Mendelian diseases featuring extreme forms of hyper- and hypotension have greatly contributed to our understanding of renal salt handling, and its role in blood pressure regulation.[1] Despite the complexity of blood pressure regulation, which is influenced by diverse mechanisms including the neuronal, cardiovascular, and endocrine systems, many if not all of the genes thus far identified ultimately directly or indirectly affect renal salt reabsorption. Specifically, genes whose products increase renal salt reabsorption cause hypertension, while genes diminishing renal salt reabsorption result in hypovolemia, and sometimes life-threatening hypotension. Increased salt reabsorption is accompanied by water reabsorption to maintain normal concentrations of Na^+, leading to increased intravascular volume, increased venous blood return to the heart, and increased cardiac output via the Frank–Starling mechanism. Blood pressure then rises according to Ohm's law. These findings have implicated renal salt handling as a key element of long-term blood pressure homeostasis.

Nonetheless, hemodynamic patterns among hypertensive patients, even among those with primary increases in renal salt homeostasis, show increased systemic vascular resistance (SVR) with normal cardiac output. An explanation for this has been provided by Hall and Guyton, who have shown that tissues regulate their perfusion by increasing or decreasing vascular resistance according to metabolic demand. Dogs given aldosterone initially show expanded intravascular volume and increased cardiac output, but within weeks evolve to a state of high SVR and normal cardiac output.[2] These findings establish that one cannot infer the initiating cause of hypertension from steady-state hemodynamic profiles.

Overview of Renal Salt Homeostasis

The kidneys filter about 180 liters of plasma per day, containing ~1.5 kg of salt; ~99.5% of the filtered salt load must be reabsorbed on a typical Western diet to maintain sodium homeostasis (Figure 36.1). The bulk of this reabsorption (50–60%) occurs in the proximal tubule, driven by the basolateral Na^+/K^+-ATPase and apical Na^+/H^+ exchanger, as well as co-transporters that couple uptake of glucose, amino acids, and other solutes to the favorable gradient for Na^+ reabsorption. Approximately 30% of the filtered load is reabsorbed in the thick ascending limb of Henle (TAL) via the $Na^+/K^+/2Cl^-$ co-transporter NKCC2, the target of loop diuretics, and ~7–10% in the distal convoluted tubule (DCT) via the thiazide-sensitive Na-Cl co-transporter NCC. The fine-tuning of renal salt reabsorption (~2–5%) occurs in the connecting tubule (CNT) and cortical collecting duct (CCD), and is predominantly mediated by the epithelial sodium channel

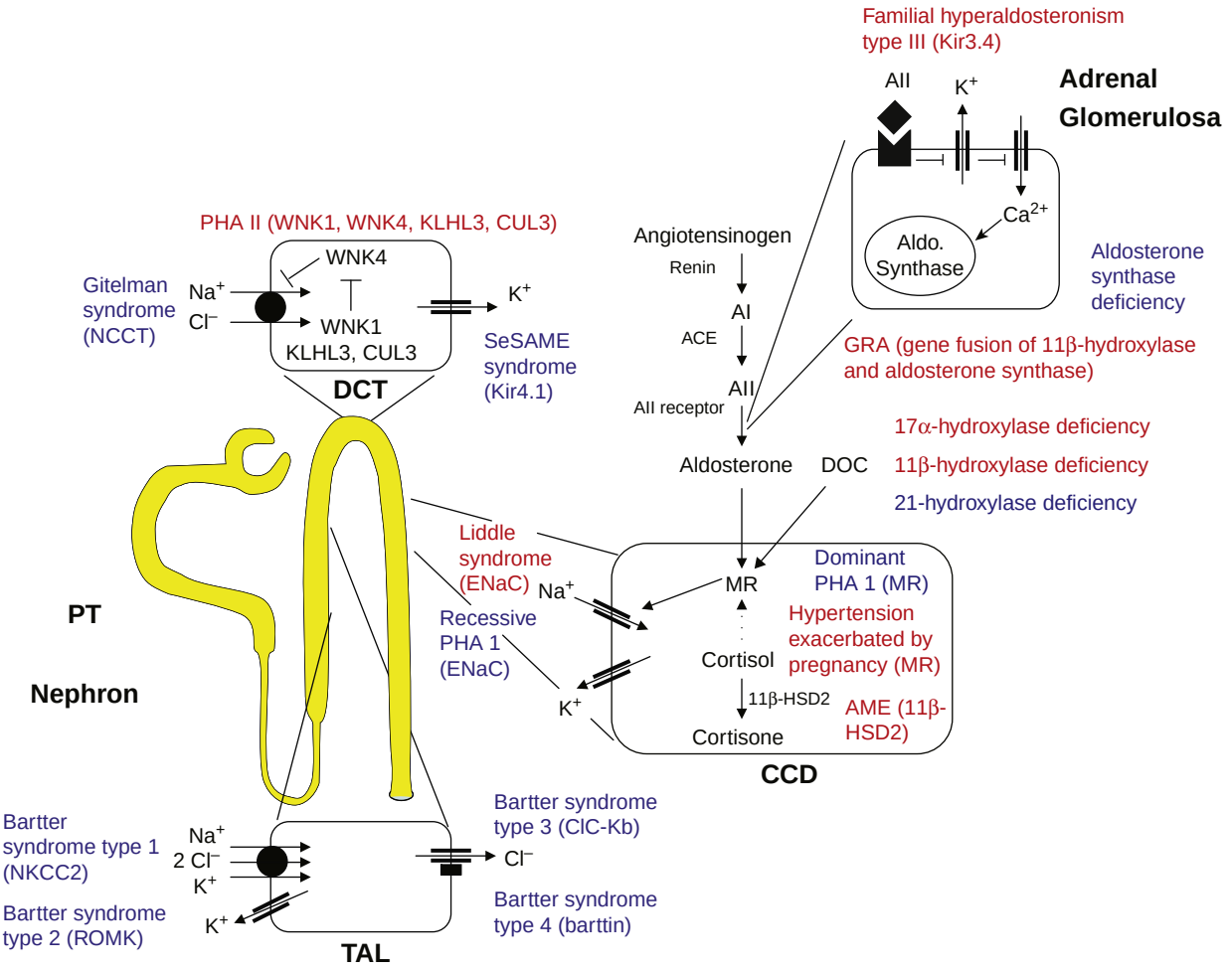

FIGURE 36.1 **Diagram of the nephron and the renin–angiotensin–aldosterone system.** Shown are key molecular pathways mutated in Mendelian forms of hypertension (red) and hypotension (blue). See text for details (AI: angiotensin I; AII: angiotensin II; ACE: angiotensin converting enzytme; Aldo. Synthase: aldosterone synthase; AME: apparent mineralocorticoid excess; CCD: cortical collecting duct; DOC: desoxycortisone; GRA: glucocorticoid remediable aldosteronism; MR: mineralocorticoid receptor; 11β-HSD2: 11β-hydroxysteroid dehydrogenase-2; PHAI: pseudohypoaldosteronism type 1; PHA II: pseudohypoaldosteronism type II; PT: proximal tubule; TAL: thick ascending limb of Henle). *(adapted from ref. [1]).*

(ENaC), the target of the potassium-sparing diuretic amiloride. Many of the tubular channels, transporters, and regulators involved in these processes of salt reabsorption are affected by loss- and/or gain-of-function mutations that will be discussed in this chapter.

A major regulatory pathway that modulates renal salt reabsorption is the renin–angotensin–aldosterone system (Figure 36.1). In response to intravascular volume depletion or reduced delivery of salt to the thick ascending limb of Henle, the juxtaglomerular apparatus of the kidney secretes the active form of the aspartyl protease renin. Active renin cleaves angiotensinogen that is produced by the liver and constitutively circulates in the blood; this cleavage produces the decapeptide angiotensin I (AI), which is then cleaved by the angiotensin-converting enzyme (ACE), resulting in the octapeptide angiotensin II (AII). Angiotensin II binds to a specific G-protein-coupled receptor in adrenal glomerulosa (the type 1 angiotensin II receptor or AT1 receptor). This binding results in the activation of signaling cascades leading to adrenal glomerulosa membrane depolarization, activation of voltage-gated calcium channels, calcium influx, and increased synthesis of the steroid hormone aldosterone. Aldosterone, an effector of this pathway, communicates a signal for increased salt reabsorption to the kidney: it binds to the mineralocorticoid receptor (MR), a nuclear hormone receptor located in cells of the DCT, CNT, and principal cells of the CCD (the so-called aldosterone-sensitive distal nephron), leading to increased salt reabsorption via ENaC, and also the NCC (see above). The renin–angiotensin–aldosterone (RAA) pathway is not only

mutated in genetic disorders of salt homeostasis, but is also the target of multiple pharmacologic approaches in the treatment of hypertension, including renin inhibitors, ACE inhibitors, angiotensin receptor blockers, and aldosterone antagonists.

This chapter covers the genetic disorders that modulate blood pressure by altering renal salt reabsorption, as well as the insights into physiological mechanisms of blood pressure regulation derived from these discoveries.

GENETIC DISORDERS CAUSING HYPERTENSION

Mendelian forms of hypertension are rare among the general hypertensive population. Clues to the deduction that a patient may have an underlying Mendelian cause of hypertension generally come from the age of onset, the family history, and distinctive biochemical features. Hypertension is very uncommon in the first decade of life, and unusual before the age of 18; however, this is a typical finding among subjects with Mendelian hypertension. Consequently, Mendelian diseases should be considered in patients with early onset hypertension, and should be ruled out if there is also a family history of early onset hypertension. Other diseases that can cause hypertension in young subjects, such as structural renal defects and other causes of renal insufficiency, should be ruled out as well. Hypertension can be very severe, but this is not invariably the case. Biochemical findings that are most helpful in pointing to a diagnosis are plasma renin activity, aldosterone levels (best measured in 24 hour urine specimens), and serum/plasma electrolyte values. It is important to note that patients with aldosteronism need not have hypokalemia, and the absence of this finding should not be taken to exclude a disorder caused by increased aldosterone or increased activity of the mineralocorticoid receptor. An algorithm that is helpful in the evaluation of these patients is shown in Figure 36.2.

Disorders of the Renin–Angiotensin–Aldosterone System

Mutations that Increase Activation of the Mineralocorticoid Receptor

A number of genes have been identified in which mutation results in hypertension due to increased activation of the mineralocorticoid receptor (MR). These include diseases caused by mutations that lead to renin-independent production of aldosterone, as well as diseases in which steroids other than aldosterone can activate MR.

MUTATIONS RESULTING IN INCREASED ALDOSTERONE SECRETION

GLUCOCORTICOID-REMEDIABLE ALDOSTERONISM (FAMILIAL HYPERALDOSTERONISM TYPE I) Glucocorticoid-Remediable Aldosteronism (GRA) is an autosomal dominant disease featuring hypertension with inappropriate aldosterone secretion despite suppression of the renin–angiotensin system.[3] Patients typically present with hypertension in the first two decades of life, and are found to have elevated

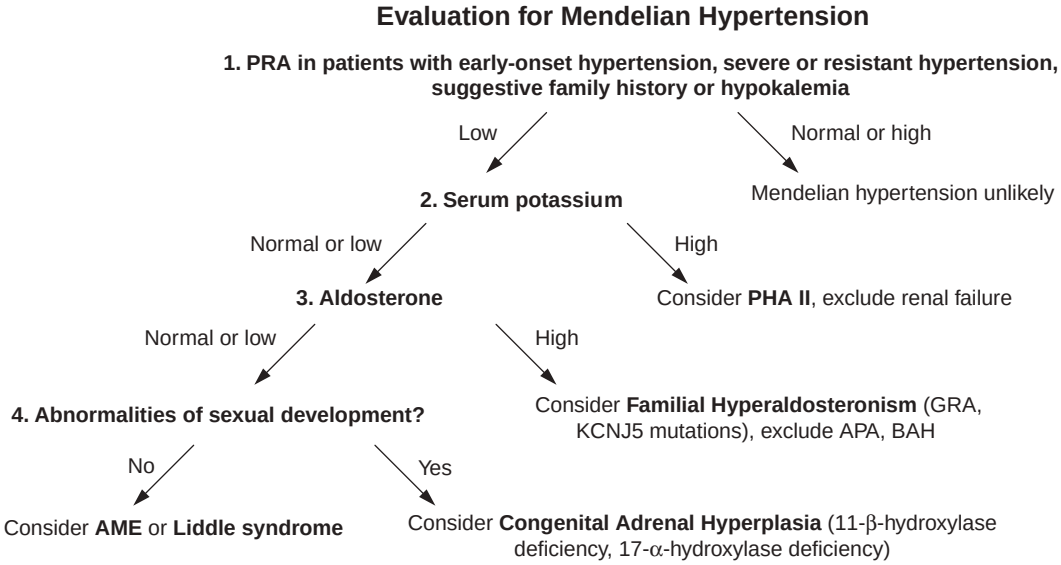
Evaluation for Mendelian Hypertension
1. PRA in patients with early-onset hypertension, severe or resistant hypertension, suggestive family history or hypokalemia
Low
Normal or high
Mendelian hypertension unlikely
2. Serum potassium
Normal or low
High
3. Aldosterone
Consider PHA II, exclude renal failure
Normal or low
High
4. Abnormalities of sexual development?
Consider Familial Hyperaldosteronism (GRA, KCNJ5 mutations), exclude APA, BAH
No
Yes
Consider AME or Liddle syndrome
Consider Congenital Adrenal Hyperplasia (11-β-hydroxylase deficiency, 17-α-hydroxylase deficiency)

FIGURE 36.2 **A diagnostic approach to Mendelian hypertension.** (PRA: plasma renin activity; PHAII: pseudohypoaldosteronism type II; GRA: glucocorticoid remediable aldosteronism; APA: aldosterone-producing adenoma; BAH: bilateral adrenal hyperplasia; AME: apparent mineralocorticoid excess.)

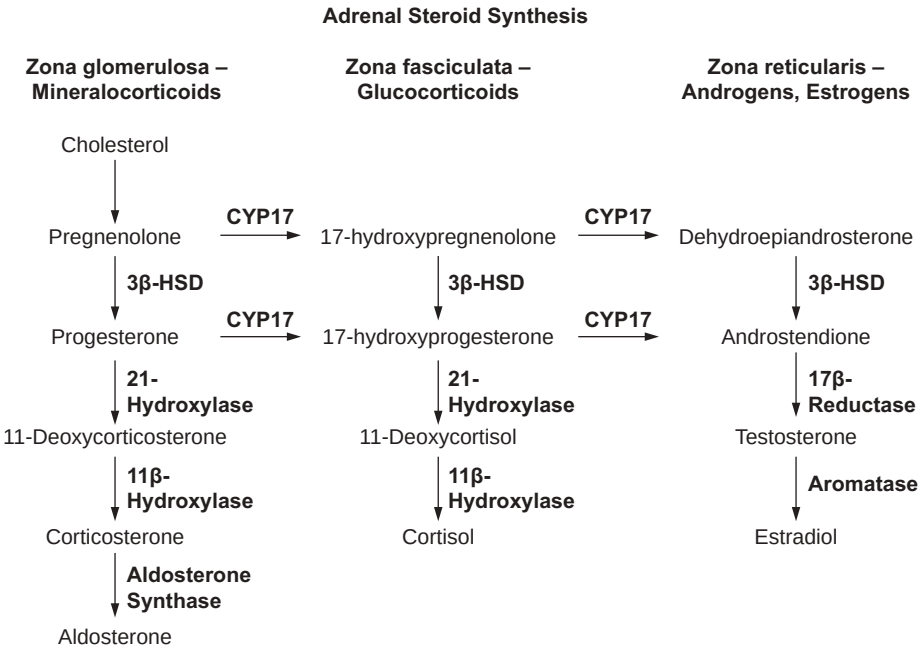

FIGURE 36.3 **Adrenal steroid synthesis.** Hormone synthesis in the adrenal cortex occurs in distinct compartments: aldosterone is synthesized in the outermost zona glomerulosa; cortisol in adrenal fasciculata; and sexual steroids in the innermost zona reticularis. Enzymes required for biosynthesis are noted (3β-HSD: 3β-hydroxysteroid dehydrogenase).

aldosterone secretion despite suppressed plasma renin activity, indicating autonomous production of aldosterone. Hypertension is often severe, and affected subjects are at a markedly increased risk of cerebral hemorrhage at young ages.[4] Hypokalemia and metabolic alkalosis are variable associated findings.[5,6] Consistent with autosomal dominant transmission, the family history is usually positive, with one parent and about half of siblings and offspring having early diagnosis of hypertension, and there is a frequent history of early cerebral hemorrhage.

Unlike normal individuals, aldosterone secretion in GRA shows sustained increase with administration of the cortisol secretagogue ACTH. Moreover, affected subjects produce so-called hybrid steroids, 18-hydroxy- and 18-oxocortisol, which are present in negligible amounts in normal subjects. These hybrid steroids have hydroxylation at C-17, characteristic of metabolism by 17-alpha hydroxylase (CYP17 gene) in the adrenal fasciculata, and oxidation at C-18, characteristic of metabolism by aldosterone synthase, which is normally confined to the adrenal glomerulosa[7,8] (Figure 36.3). Suppression of cortisol secretion from the adrenal gland by administration of exogenous glucocorticoids also causes rapid and sustained suppression of aldosterone secretion, a finding that does not occur in normal individuals.[3] These features suggest that aldosterone in GRA is produced in the adrenal fasciculata under the control of ACTH, rather than in adrenal glomerulosa under the control of the normal secretagogue angiotensin II (Ang II).

Analysis of linkage in a large GRA kindred demonstrated complete linkage of early hypertension to

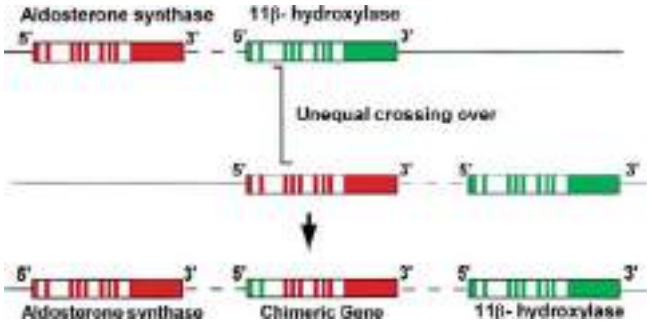

FIGURE 36.4 **Unequal crossing-over recombination between aldosterone synthase and 11-β hydroxylase causes GRA.** Shown is the segment of chromosome 8 that contains the two highly homologous genes. Unequal crossing-over between these two genes produces a chromosome with normal copies of aldosterone synthase and 11-β hydroxylase, and a third chimeric gene between them that fuses 5′ regulatory sequences from 11-β hydroxylase to coding sequences of aldosterone synthase, conferring aldosterone synthase function on the encoded gene product *(reproduced with permission from ref. [1]).*

chromosome 8q, which contains the gene aldosterone synthase (CYP11B2) and the closely related gene steroid 11-β hydroxylase (CYP11B1). These two genes recently evolved from a common ancestor, and are highly similar at the DNA sequence level. Patients with GRA prove uniformly to have mutations that result from unequal crossing-over recombination between these two homologous genes (Figure 36.4). This recombination event produces two mutant chromosomes, one with normal copies of aldosterone synthase and 11-β hydroxylase, and a third chimeric gene between them that fuses 5′ regulatory sequences from 11-β hydroxylase to coding sequences of aldosterone

synthase.[9,10] This is the mutation uniformly found in patients with GRA. The other mutant chromosome has no normal gene, and only a single hybrid gene that fuses 5′ sequences from aldosterone synthase to a coding sequence that produces 11-β hydroxylase enzymatic activity. This mutation is found in some patients with 11-β hydroxylase deficiency. These events occur in pre-meiotic germ cell development, hence only one is transmitted to a zygote. All of these recombination events seen in GRA occur upstream of exon 5,[10] with the result that the hybrid genes in patients with GRA include the two amino acids in exons 5 and 6 that are critical for the resulting enzyme having aldosterone synthase rather than 11-β hydroxylase activity.[11] These hybrid genes bear the 5′ regulatory elements of 11-β hydroxylase, and are consequently expressed in adrenal fasciculata under the control of ACTH, but encode aldosterone synthase enzymatic activity. As a consequence, aldosterone secretion in these patients is constitutive, driven by ACTH and the maintenance of normal cortisol levels. The renin−angiotensin system is suppressed, but this fails to turn off aldosterone production. These mutations thus account for the ectopic production of aldosterone in adrenal fasciculata and its control by ACTH, and explain the resulting hypertension.

GRA should be suspected by the finding of hypertension in young individuals with elevated aldosterone level (best measured in 24 hour urine samples), despite suppressed plasma renin activity, particularly if there is a history of early hypertension among first degree relatives. Hypokalemia and metabolic alkalosis are common but by no means invariant, and the absence of these findings should not be used to exclude the diagnosis.[5] Molecular genetic testing by either Southern blotting[9] or PCR[12] provides a sensitive and specific means for establishing the diagnosis. Because of the autosomal dominant transmission, there are frequently many affected members among extended families of index cases, and case finding can be performed by sequential sampling, testing all first degree relatives of affected subjects, then all first degree relatives of positive cases in subsequent rounds. Sampling in these families is likely to prevent morbidity and mortality from uncontrolled hypertension and early cerebral hemorrhage. Because of the availability of genetic screening, determination of urinary levels of hybrid steroids or dexamethasone suppression test is no longer recommended.[13] Of note, family screening has demonstrated that not all individuals carrying the gene fusion are hypertensive,[14] and first degree relatives of patients with confirmed GRA should be genetically screened even in the absence of hypertension.[15]

Treatment options for GRA include use of mineralocorticoid receptor antagonists (spironolactone or eplerenone), amiloride or triamterene (which inhibit the epithelial sodium channel that drives both hypertension and hypokalemic alkalosis in GRA). Exogenous glucocorticoids can be used to shut down aldosterone production from the adrenal fasciculata. Careful attention to dosage in children is essential to maintain normal growth and to avoid glucocorticoid side-effects. Potassium-wasting diuretics such as hydrochlorothiazide and furosemide should be used with caution, because of the risk of severe hypokalemia.[13,15]

ALDOSTERONE-PRODUCING ADRENAL ADENOMA AND FAMILIAL HYPERALDOSTERONISM DUE TO KCNJ5 MUTATIONS Aldosterone-producing adenoma, also known as Conn's syndrome,[16] is a common cause of severe hypertension, found in about 5% of patients in hypertension referral clinics worldwide, and in about half of patients diagnosed with primary aldosteronism.[17] Patients typically present with worsening hypertension, and are found to have elevated serum and 24 hour urinary aldosterone levels in conjunction with suppressed plasma renin activity, consistent with these tumors having renin-independent aldosterone secretion. Hypokalemia and metabolic alkalosis are frequent, but not invariant findings. The finding of an adrenal mass by CT scan with increased aldosterone levels in ipsilateral adrenal vein plasma is considered diagnostic, and removal of these tumors corrects or improves blood pressure in the large majority of patients.[13]

Exome sequencing of four aldosterone-producing adrenal adenomas (APAs) and matched blood DNA enabled identification of somatic mutations in the tumors.[18] The results showed a low somatic mutation rate, with only 2−5 somatic mutations per tumor. Surprisingly, the K^+ channel encoded by KCNJ5 was mutated in two of these tumors. Examination of this channel in 22 tumors identified somatic KCNJ5 mutations in 8 tumors, and either of the same two mutations were found in all, substituting arginine for glycine at position 151 or arginine for leucine at position 168. These two positions lie in or abut the highly conserved K^+ channel selectivity filter that enables these channels to allow passage of K^+ but not other ions through the channel pore.[19,20] Electrophysiologic studies demonstrated that these mutations cause markedly increased Na^+ conductance of the mutant channel, sufficient to depolarize the cell.

These findings explain the pathogenesis of APA in these tumors. The normal adrenal glomerulosa cell is hyperpolarized owing to constitutively open K^+ channels.[21,22] Angiotensin II signaling results in closure of these channels,[23,24] resulting in depolarization and activation of voltage-gated calcium channels, which raises

intracellular calcium. Hyperkalemia produces the same results, potentially via increased frequency of depolarizing membrane potential oscillations.[25] Increased intracellular Ca^{2+} is the acute signal for increased expression of aldosterone synthase and other rate-limiting steps in aldosterone biosynthesis. Chronic signaling provides the stimulus for increased cell replication.[26] Thus, these single mutations can explain both the cell-autonomous aldosterone secretion and cell proliferation that are the hallmarks of these benign tumors.

Subsequent work has confirmed these findings. The study of 287 tumors by Björklund et al. found the G151R or L168R mutations in 47% of APAs, and a markedly higher prevalence of these mutations among women with APA (63%) than men (22%). Only one additional mutation (E145Q) was found in two cases.[26a] Similar findings were observed by Boulkroun et al., who found either of these two mutations in 34% of all APAs with a similar bias for female subjects.[27] These tumors are more prevalent among younger individuals, and tend to be slightly larger compared to non-KCNJ5-mutant tumors.

In addition to these mutations causing APAs, they also account for a rare inherited form of primary aldosteronism. In 2008, Geller et al. reported a father and two daughters with a new familial form of severe early-onset hypertension due to primary aldosteronism.[28] Hypertension in these patients was diagnosed between the ages of 4 and 7 years; it was resistant to aggressive antihypertensive therapy, including spironolactone and amiloride. There was massive adrenocortical hyperplasia. Hybrid steroids 18-oxocortisol and 18-hydroxycortisol were elevated, however, in clear contrast to patients with GRA, there was a significant increase in aldosterone levels upon dexamethasone administration, and affected subjects did not have the gene fusion characteristic of GRA. Due to unrelenting hypertension, all three subjects underwent bilateral adrenalectomy in childhood, demonstrating massive adrenal hyperplasia (with paired adrenal weights up to 81 g, normal is less than 12 g) and diffuse hyperplasia of the zona fasciculata by light microscopy (with transitional zone morphology by electron microscopy). Screening of candidate genes revealed no pathogenic mutations.

Affected members of this family proved to have a T158A mutation in KCNJ5 which also modified channel selectivity, resulting in Na^+ conductance.[18] In this case, since the mutation is present in every cell, rather than acquired somatically by a single cell, every cell in the adrenal glomerulosa is receiving the signal for aldosterone production and cell proliferation, accounting for the massive adrenal hyperplasia and severe aldosteronism at young ages. This Mendelian form of disease provides strong evidence that these single mutations are sufficient for cell proliferation and constitutive aldosterone secretion.

Subsequent studies have identified additional families with early severe aldosteronism and mutations in KCNJ5. Most interestingly, these include two different mutations at the same amino acid – G151 – that result in markedly different phenotypes. One of these inherited mutations is G151R, the same mutation found as a somatic mutation in APA. Patients with inherited G151R[29] mutations develop massive adrenocortical hyperplasia, have difficult-to-control hypertension, and virtually invariably come to bilateral adrenalectomy for control of hypertension, similar to the T158A mutation described above. The other mutation is G151E. Patients with this mutation also present with early hypertension and aldosteronism; however, they do not develop adrenal hyperplasia, are typically responsive to antihypertensive therapy, and do not come to adrenalectomy.[29–31] Most interestingly, the milder human phenotype resulting from G151E is associated with a much more severe electrophysiologic phenotype. G151E results in dramatically greater Na^+ conductance than G151R. The consequence of this is markedly increased sodium-dependent lethality. This suggests a model in which cells expressing the G151E mutation differentiate from a stem cell pool, produce aldosterone as they are born, but die rapidly, preventing development of hyperplasia. Their continuous renewal from a stem cell pool provides a long-term source for excessive aldosterone production, and a milder hypertension than in subjects with the G151R mutation.

This phenotype of primary aldosteronism without adrenal hyperplasia due to KCNJ5 mutation is as yet unique to the G151E mutation, while massive adrenal hyperplasia requiring adrenalectomy has also been reported with another KCNJ5 mutation, I157S.[32]

While KCNJ5 mutations unequivocally explain the pathogenesis of a large fraction of APAs and a rare form of familial hypertension, the role of the wild-type channel in human adrenal function is less clear. Its activation by dopamine, an inhibitor of aldosterone secretion,[18,33] suggests that the normal role of this channel might be to hyperpolarize cells, contributing to inhibition of aldosterone secretion.

Primary aldosteronism due to mutations in aldosterone synthase and KCNJ5 both produce constitutive secretion of aldosterone and hypertension. Patients with KCNJ5 mutations tend to present in the first several years of life with severe hypertension, while those with GRA are more frequently, though not exclusively, diagnosed later in the first or second decade. Consistent with greater disease severity among KCNJ5 families and impaired reproductive fitness, no families

with more than four affected members have been reported to date, while a number of large, multigenerational families with more than 20 members with GRA have been studied.

MUTATIONS CAUSING IMPAIRED CORTISOL BIOSYNTHESIS AND INCREASED MINERALOCORTICOIDS

CONGENITAL ADRENAL HYPERPLASIA DUE TO 11-β-HYDROXYLASE DEFICIENCY Congenital adrenal hyperplasia (CAH) is a recessive disease, featuring cortisol deficiency caused by inherited defects of enzymes required for cortisol biosynthesis in the adrenal gland. Affected patients have increased ACTH levels due to impaired feedback inhibition, which stimulates excessive production of steroids proximal to the impaired step in cortisol biosynthesis. Precursor steroids can have androgenic effects, and female patients may present with virilization. In the most common form of CAH (21-hydroxylase deficiency), impaired synthesis of mineralocorticoids leads to salt-wasting (see below), while other defects can result in accumulation of precursors which have mineralocorticoid effects, leading to hypertension.

The most common form of congenital adrenal hyperplasia associated with hypertension is 11-β-hydroxylase deficiency[34] (Figure 36.3). Affected females may present with ambiguous genitalia at birth or with menstrual irregularities and hirsutism in adolescence or adulthood, while male subjects may present with penile enlargement or precocious puberty. Hypertension and hypokalemia are variable associated features, and are thought to occur due to the accumulation of 11-deoxycorticosterone, a moderately potent mineralocorticoid. However, there is no clear correlation between 11-deoxycorticosterone levels, the degree of virilization and the presence of hypertension. Renin and aldosterone are typically low.[35–37]

In most cases, 11-β-hydroxylase deficiency is caused by recessive point mutations that cause loss-of-function of CYP11B1, although loss-of-function mutations due to the reciprocal product of unequal crossing-over between aldosterone synthase and 11-β-hydroxylase found in GRA (see above) can also produce loss-of-function mutations (in this case there is a chromosome that only expresses 11-β hydroxylase in adrenal glomerulosa).[38]

11-β-hydroxylase deficiency should be suspected in female infants with ambiguous genitalia and male infants with penile enlargement. In the late onset form, hirsutism and menstrual irregularities in female patients and precocious puberty in boys may be the only signs of presentation. The abnormal hormone profile, in particular the finding of elevated basal and ACTH-stimulated 11-deoxycortisol concentrations, is diagnostic. Treatment with exogenous glucocorticoids suppresses ACTH secretion and the accumulation of precursor steroids. Precursor steroids should be monitored, and glucocorticoid dosage has to be carefully adjusted to avoid growth inhibition in children and exogenous Cushing's syndrome. Persistent hypertension may require additional treatment with aldosterone antagonists or amiloride.

CONGENITAL ADRENAL HYPERPLASIA DUE TO 17-α-HYDROXYLASE DEFICIENCY 17-α-hydroxylase deficiency[39] is a rare cause of congenital adrenal hyperplasia. Patients typically present in adolescence with lack of pubertal development. Genetic females have primary amenorrhea and do not develop secondary sexual characteristics; genetic males typically have complete pseudohermaphroditism with female external genitalia and intra-abdominal testes, although ambiguous genitalia have been reported. Hypertension is a common finding, and may be associated with hypokalemia.[40]

17-α-hydroxylase deficiency is caused by mutations in CYP17.[41] The encoded enzyme is expressed in adrenal gland and gonads, and has both 17-hydroxylase and 17,20-lyase activities (Figure 36.3). Most patients with CYP17 mutations thus have combined deficiencies of both enzymatic functions, although isolated deficiency of 17,20-lyase activity has been reported.[42] Hydroxylation at carbon 17 of the steroid nucleus is required for cortisol production, and in its absence normal activation of the glucocorticoid receptor is not achieved. In addition, 17,20-lyase activity is needed for the generation of androgen and estrogen precursors from cortisol precursors.

Patients with CYP17 mutations consequently have cortisol deficiency leading to elevated ACTH levels, as well as androgen and estrogen deficiency, accounting for sexual infantilism and pseudohermaphroditism. Hypertension is caused by activation of the mineralocorticoid receptor (MR) due to increased levels of 11-deoxysteroids (corticosterone, 11-deoxycorticosterone, and 18-hydroxy-deoxycorticosterone), similar to the mechanism of hypertension in 11-β-hydroxylase deficiency. As a result, renin and aldosterone are typically suppressed.

The diagnosis is based on the clinical presentation and characteristic hormone profile, and treatment relies on replacement of glucocorticoids and sex steroids, the latter starting in adolescence.

Mutations that Impair Conversion of Cortisol to Cortisone: Syndrome of Apparent Mineralocorticoid Excess

The syndrome of apparent mineralocorticoid excess (AME)[43] is an autosomal recessive disease featuring severe hypertension presenting in the first decade of

life. It is associated with suppression of both the renin–angiotensin system and aldosterone secretion. Hypokalemia and metabolic alkalosis are common associated findings. The hypertension can be mitigated with antagonists of the mineralocorticoid receptor, which suggested the presence of a new circulating mineralocorticoid; however, such a molecule was not found. Instead, a defect in cortisol metabolism was identified in affected patients, causing reduced conversion of cortisol to cortisone, with a consequently increased half-life of cortisol.[44]

How this defect in cortisol metabolism resulted in hypertension remained unclear until the cloning and subsequent purification of the mineralocorticoid receptor (MR).[45] *In vitro*, cortisol binds and activates MR as well as aldosterone does,[46] while cortisol is normally a weak mineralocorticoid *in vivo*. This discrepancy is explained by the presence in many aldosterone-responsive cells of an enzyme, steroid 11-β hydroxysteroid dehydrogenase type 2 (11βHSD2), that "protects" MR from cortisol by converting cortisol to cortisone. Cortisone has negligible ability to activate MR. The finding of homozygous loss-of-function mutations in 11βHSD2 in AME provided proof of the relevance of this mechanism *in vivo*.[47] These findings fully explain the pathophysiology of AME, and are confirmed by the recapitulation of AME in mice deficient for 11βHSD2.[48]

AME should be suspected in young individuals with hypertension, suppressed PRA, and low aldosterone levels. AME shares these clinical features with Liddle syndrome (see below); however, Liddle syndrome is autosomal dominant, and affected subjects consequently commonly have one parent with early severe hypertension, and may have other relatives in earlier generations or other branches of the pedigree with similar findings. In contrast, AME is suggested by the absence of disease in earlier generations and the presence of parental consanguinity. The diagnosis of AME can typically be made by genetic testing involving sequencing of 11βHSD2. Abnormal cortisol:cortisone ratios can also establish the diagnosis.[49]

Inhibitors of the mineralocorticoid receptor, such as spironolactone or eplerenone, or inhibitors of the epithelial sodium channel, such as amiloride or triamterene, are treatment options in AME. Eplerenone has recently been suggested for prevention of strokes even in the absence of hypertension; however, the utility of this approach is not established.[50]

Intriguingly, exuberant ingestion of natural licorice produces a clinically similar syndrome owing to the effects of a metabolite of glycyrrhetinic acid – derived from glycyrrhizic acid in licorice – which inhibits 11βHSD2.[51] Carbenoxolone, a drug once used for peptic/gastric ulcer disease, has similar effects.

In the presence of 11βHSD2, elevated levels of cortisol are required to achieve activation of the mineralocorticoid receptor (by exceeding the capacity of 11βHSD2 to metabolize cortisol).[1] Hypertension can therefore occur in states of glucocorticoid excess, such as ectopic ACTH syndrome, Cushing's disease due to a pituitary tumor, iatrogenic Cushing's syndrome or cortisol-producing adenomas.

Mutations in the Mineralocorticoid Receptor

HYPERTENSION EXACERBATED IN PREGNANCY

As discussed above, binding of aldosterone to the mineralocorticoid receptor causes increased renal salt reabsorption by raising the activity of the epithelial sodium channel ENaC, which results in elevated blood pressure. Geller and colleagues identified an as-yet unique family with early onset of typically severe hypertension associated with suppressed PRA, negligible aldosterone levels, and variable hypokalemia and alkalosis; this trait segregated as an autosomal dominant trait in a large extended family.[52,53] A striking clinical feature among affected women was marked exacerbation of hypertension in pregnancy, requiring early delivery for poorly controlled hypertension and marked hypokalemia. Analysis of linkage in this large kindred localized the disease gene to the segment of chromosome 4 that harbors the mineralocorticoid receptor. This gene proved to have a novel missense mutation in the ligand-binding domain, S810L, which precisely co-segregated with the disease phenotype in the kindred.

The clinical features suggested that this mutation results in an activated receptor, despite the absence of aldosterone. *In vitro* studies demonstrated that this is the case: the mutant receptor shows partial constitutive activity in the absence of ligand. In addition, however, the mutation altered the specificity of the receptor such that some steroids lacking 21-hydroxyl groups, which normally fail to activate MR, are now potent agonists. One of these new agonists is progesterone, a steroid whose level increases dramatically in pregnancy. Cortisone is another molecule that can more weakly activate the mutant receptor, suggesting that this cortisol metabolite may play a constitutive role. The crystal structure of the mutant mineralocorticoid receptor was solved,[54] suggesting that progesterone-induced MR S810L activation is caused by a network of contacts at the A-ring, created by L810.

Mutations that Cause Hypertension without Activation of MR

Mineralocorticoids impart their renal effects by modulating the expression and activity of ion

transporters and channels. Mutations in several genes have been identified that cause hypertension without activation of MR.

LIDDLE SYNDROME Liddle syndrome[55] is an autosomal dominant trait featuring hypertension with variable hypokalemia and alkalosis. While these features recapitulate the phenotype of the diseases with mineralocorticoid excess discussed above, there are no circulating mineralocorticoids in patients with Liddle syndrome. Hypertension is responsive to treatment with blockers of the epithelial sodium channel ENaC (amiloride or triamterene), but not to spironolactone.

Genetic studies identified rare mutations in subunits of ENaC as the cause of Liddle syndrome[56,57] (Figures 36.5 and 36.6). ENaC is composed of subunits encoded by three homologous genes, alpha, beta, and gamma[58]; each has cytoplasmic amino and carboxy termini, and traverses the plasma membrane twice.[59] Virtually all mutations that cause Liddle syndrome eliminate a sequence required for removal of the channel from the cell surface by clathrin-coated pit-mediated endocytosis. This internalization sequence, PPPXY (where X is variable among different ENaC subunits) is present in the carboxy terminus of each subunit. Disease causing mutations introduce premature termination codons after the second transmembrane domain and before the PPPXY sequence, or alternatively produce missense mutations at one of the cognate positions of the internalization motif.[56,57,60] These mutations result in reduced clearance and prolonged half-life of the channel at the cell surface[61–63] (Figure 36.6). Nedd4 was subsequently identified as having domains that specifically bind the PPPXY domains in ENaC, and contribute to its clearance from the cell surface.[64] This protein contains ubiquitin-ligase domains, suggesting that ubiquitination and subsequent degradation plays a role in ENaC regulation. The likely candidate for this regulation in human kidney is Nedd4-2.[65] Together, these findings suggest that mutations in ENaC in Liddle syndrome impair binding of Nedd4 to the mutant channel, and prevent ubiquitination and degradation. In addition to the mutations deleting or altering the PY motif, a mutation in the extracellular domain of γ-ENaC has been reported as causing an increased open probability of the channel.[66] Consistent with these genetic findings, renal transplantation can cure the hypertension of Liddle syndrome.[67]

A mouse model of Liddle syndrome[68] does not develop hypertension or hypokalemic alkalosis on a standard diet, despite increased ENaC activity. However, a Liddle phenotype develops when these animals are fed a high-salt diet.

Liddle syndrome should be suspected in patients with early hypertension and suppressed PRA and aldosterone levels; hypokalemia and metabolic alkalosis are supportive, but not essential findings. As discussed above, these features are shared with AME. A family history of hypertension consistent with

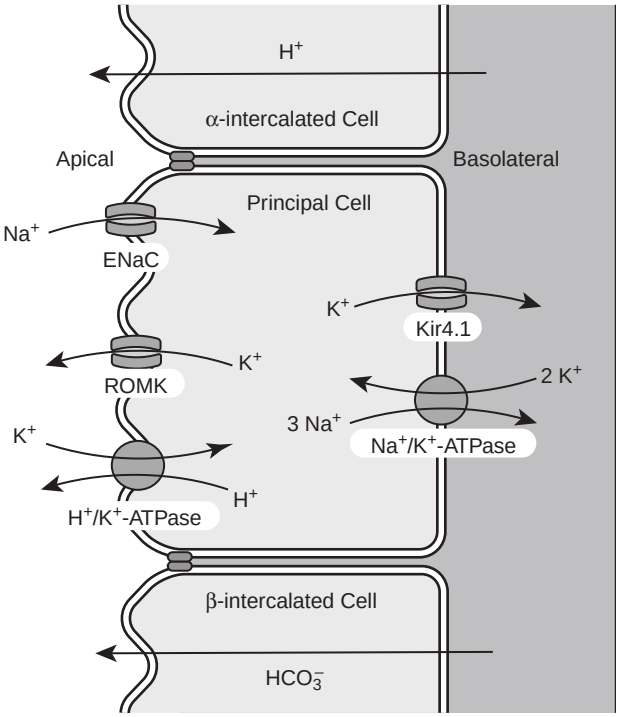

FIGURE 36.5 **Salt reabsorption in the cortical collecting duct.** Na^+ reabsorption in the principal cells of the cortical collecting duct is dependent on aldosterone and happens via ENaC. The resulting lumen-negative potential promotes K^+ secretion via ROMK and H^+ secretion.

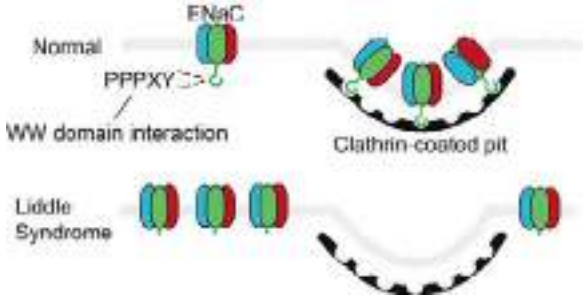

FIGURE 36.6 **Increased surface expression of the epithelial sodium channel ENaC causes Liddle syndrome.** The β- and γ-subunits of the channel contain a PPPXY motif in the cytoplasmic C-terminus. In normal individuals, binding of Nedd4-2 (not shown) leads to internalization in clathrin-coated pits. Channels are then either degraded or recycled back to the membrane. ENaC lacking the PPPXY motif in Liddle syndrome does not interact with Nedd4-2, and as a result is retained at the membrane. This causes increased Na^+ reabsorption and hypertension in affected individuals *(reproduced with permission from ref. [1]).*

autosomal dominant transmission, however, is suggestive of Liddle syndrome. Genetic testing is recommended. Treatment with amiloride or triamterene can correct hypertension and hypokalemia.

THE SYNDROME OF HYPERTENSION WITH HYPERKALEMIA (PSEUDOHYPOALDOSTERONISM TYPE II) Aldosterone is secreted in two distinct physiologic conditions: volume depletion and hyperkalemia. Restoration of normal intravascular volume in the former condition requires increased salt and water reabsorption, while K^+ secretion must be increased in the latter state. How the kidney achieves these alternative results has been obscure. Classical explanations have suggested that this is a result of alterations in fluid flow and/or delivery of salt to the distal nephron. The notion that this is an incomplete explanation comes from a disease in which the kidney appears to be unable to use aldosterone to direct K^+ secretion, but instead constitutively activates salt reabsorption. This disease, referred to as pseudohypoaldosteronism type II (also known as syndrome of hyperkalemia with hypertension, Gordon syndrome) invariably features hyperkalemia, and has variable levels of hypertension and distal renal tubular acidosis. Aldosterone levels are normal to slightly elevated, and plasma renin activity is suppressed. Serum K^+ levels are virtually always greater than 5.0 mM without therapy, and can be greater than 7.0 mM. The disease was first described in 1964 by Paver and Pauline, who reported a 15-year-old boy with blood pressure 180/120 mmHg, serum potassium 7.0–8.2 mM, but normal glomerular filtration, and suppressed PRA and normal aldosterone.[69] Since early descriptions, the disease has been recognized to be familial, initially described as an autosomal dominant trait.[70–72]

Subsequent studies have demonstrated that K^+ cannot be corrected by supplemental aldosterone; however, both hypertension and hyperkalemia can be corrected by elimination of chloride intake or by low doses of thiazide diuretics.[70,73] These findings have suggested that increased activity of the thiazide-sensitive Na-Cl co-transporter may play a role in this disease.

Analysis of genetic linkage in families followed by molecular studies identified mutations in two members of a novel family of serine-threonine kinases, PRKWNK1 and PRKWNK4, as causes of PHAII[74] (Figure 36.7). Mutations in WNK4 were novel missense mutations that predominantly clustered in a short acidic domain of unknown function in the protein. Mutations in WNK1 were large deletions of 20,000 to 40,000 base pairs in the first intron of WNK1 that caused increased expression of WNK1 mRNA. These genes were both found to be expressed in the distal convoluted tubule and collecting duct of the kidney.

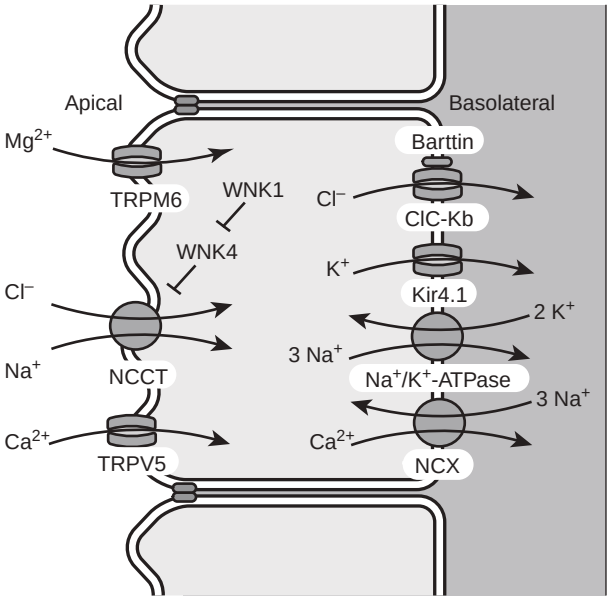

FIGURE 36.7 Salt reabsorption in the distal convoluted tubule. Salt reabsorption is driven by the activity of the Na^+/K^+-ATPase on the basolateral suface. K^+ entering the cell via the sodium pump recirculates through Kir4.1 ("pump leak coupling"). NaCl enters the cell via NCCT following the favorable Na^+ gradient, and Cl^- exits via basolateral ClC-Kb channels. The basolateral NCX transporter uses the Na^+ gradient for Ca^{2+} reabsorption. Ca^{2+} enters on the apical site via the TRPV5 channel. On the apical surface, Mg^{2+} enters the cell via TRPM6. The molecular identity of a putative basolateral Mg^{2+} transporter is unknown. NCCT activity is regulated by the WNK1 and WNK4 protein kinases.

At the time of this discovery, the normal and disease-related functions of WNK1 and WNK4 were entirely unknown. Much subsequent work has been done to determine the roles these WNK kinases play in physiology.[74–82] It appears that both play a role in coordinating the functions of diverse electrolyte flux pathways, and that a key function in the kidney is to regulate the balance between Na-Cl reabsorption and K^+ secretion. The WNK kinases regulate ion transport by several mechanisms, among them phosphorylation via intermediary kinases (SPAK, OSR1, and SGK1), and regulation of protein trafficking.[81]

Early studies addressed the role of WNK4 in the regulation of NCCT using the oocyte expression system.[75,83] Co-expression of NCCT with WT-WNK4 resulted in inhibition of thiazide-sensitive Na^+ uptake due to reduced surface expression. This effect was completely abrogated when a mutation seen in PHA II (Q562E) or kinase-dead WNK4 was used, suggesting that NCCT inhibition is lost in patients with PHA II, causing hypertension. Subsequent studies in mammalian cells suggested that this inhibitory WNK4 effect is

mediated by suppression of membrane delivery via lysosomal accumulation.[84]

Co-expression with WNK4 also dramatically reduces ROMK activity in oocytes,[76] by interaction with an endocytic scaffold protein, intersectin.[85] However, in contrast to the effect on NCCT, PHA II-mutant WNK4 produces increased inhibition of ROMK, accounting for hyperkalemia in PHA II. While WT WNK4 led to a modest increase of paracellular chloride permeability in MDCK cells, this effect was greatly augmented in PHA II-mutant WNK4, which may contribute to the chloride retention observed in PHA II.[77,78] In addition, WNK4 inhibited ENaC activity in oocytes, and this inhibition was relieved by PHA II mutations.[86] The inhibitory effect of WNK4 on ENaC and ROMK appears to require phosphorylation of WNK4 by SGK1, a kinase which translates aldosterone effects in the kidney.[87]

Similar studies as for WNK4 were performed for WNK1. While a direct effect of WNK1 on NCCT was not identified, a long isoform of WNK1 (L-WNK1) inhibits WNK4 (which inhibits NCCT, see above), and a kidney-specific isoform (KS-WNK1) inhibits L-WNK1.[75] In addition, L-WNK1 inhibits ROMK, an effect reversed by KS-WNK1 and synergistic with, but not dependent on, the WNK4 effect on ROMK[88]; L-WNK1 also activates ENaC.[89] Finally, similar to WNK4, WNK1 increases paracellular chloride flux.[90] ATII, which is produced in volume depletion, appears to be an upstream regulator of WNK4, attenuating its inhibitory effect on NCCT and thus stimulating salt reabsorption via NCCT. In contrast, the inhibitory effect of WNK4 of ROMK is retained. These findings suggest that PHA II mutations mimic a state of volume depletion with increased angiotensin II levels.[91]

Regulation of several additional proteins (e.g., TRP channels, SLC26A6) by WNK1 and WNK4 kinases has been reported, and studies of the related kinase WNK3 has revealed a role in regulation of NKCC, as well as KCC co-transporters.[92]

Taken together, *in vitro* studies suggest a key role of the WNK kinases in a functional switch among three states governing the balance between salt reabsorption and K^+ secretion. In a basal equilibrium state, both NaCl reabsorption and K^+ secretion are inhibited by the WNK kinases. In the setting of low intravascular volume, AII signaling inhibits WNK4's inhibition of NCC, but increases inhibition of ROMK; this effect is mimicked by PHA II mutations, accounting for constitutive NaCl reabsorption and hyperkalemia seen in affected patients. In a third state, hyperkalemia leads to increased aldosterone production by the adrenal gland and, potentially via SGK, to increased ROMK activity and increased ENaC activity, with sustained inhibition of electroneutral salt reabsorption via NCCT.[80]

Animal models have confirmed the role of WNK1 and WNK4 in generating hyperkalemia and hypertension. A transgenic mouse model carrying an additional copy of PHA II-mutant WNK4 shows hypertension, hyperkalemia, and hypercalciuria and, in addition, increased mass of the distal convoluted tubule and increased NCCT expression. In contrast, an additional copy of WT WNK4 leads to decreased DCT mass and reduced NCCT abundance.[79] A knockout mouse model of WNK4 displays a phenotype similar to Gitelman syndrome (see below), with increased plasma renin activity, and decreased NCC activity.[93] Deletion of the first WNK1 intron as found in PHA II in mice leads to ubiquitous ectopic KS-WNK1 expression, as well as overexpression of L-WNK1 in the DCT,[94] which explains increased activity of NCCT through alleviation of WNK4 inhibition.

Importantly, mutations in WNK1 and WNK4 explained only about 15% of families with PHA II. Exome sequencing of unrelated PHA II cases led to the identification of two additional genes for PHA II, which together account for nearly all of the remaining cases.[95,96] These two genes are partners in a ubiquitin ligase complex. Cullin 3 (CUL3) is a scaffold that serves to assemble a complex containing a RING E-3 ubiquitin ligase and one of many BTB domain-containing proteins that target specific proteins for ubiquitination. One of these BTB domain proteins is Kelch-like 3 (KLHL3). KLHL3 has a C-terminal BTB domain, and an N-terminal kelch domain, a six-bladed propeller that is likely used to bind and target proteins for ubiquitination. Surprisingly, different families showed either autosomal dominant or autosomal recessive transmission of mutations in KLHL3. Recessive mutations are distributed throughout the protein, and include typical loss-of-function mutations such as premature termination mutations. In contrast, dominant mutations cluster at positions in the kelch domain that are clustered at parts of the domain inferred to be involved in target binding. Because these dominant mutations produce a phenotype very similar to that caused by homozygous loss-of-function mutations in KLHL3, the dominant mutations likely have a dominant-negative effect.

The mutations in CUL3 that cause PHA II all cause skipping of exon 9, resulting in an in-frame deletion of 57 amino acids between the BTB-binding and RING-binding domains. These mutations are all dominant, and nearly all appear to be *de novo* mutations. Because these mutations phenocopy recessive loss-of-function mutations in KLHL3, it is inferred that these CUL3 mutations selectively prevent ubiquitination at targets bound by KLHL3. While CUL3 is ubiquitously expressed, KLHL3 is selectively expressed in the distal nephron.

Comparison of the phenotypes of patients with mutations in these different genes reveals strong genotype–phenotype correlations. Patients with CUL3 mutations have the most severe hyperkalemia, are nearly always hypertensive at young ages, and commonly have acidosis. Patients with recessive and dominant KLHL3 mutations have intermediate phenotypic severity, and those with WNK1 and WNK4 mutations often have only hyperkalemia without hypertension at early ages, and do not uniformly develop hypertension at later ages. The molecular mechanisms that link mutations in KLHL3 and CUL3 to PHA II are presently unknown; however, it is highly likely that these mutations will intersect with the WNK/NCC/ROMK pathway.

GENETIC DISORDERS CAUSING RENAL SALT LOSS

Several Mendelian disorders can cause renal salt loss, leading to signs and symptoms ranging from mild polyuria and salt craving to life-threatening hypotension and shock. A diagnostic approach to these diseases is suggested in Figure 36.8.

Disorders of the Renin–Angiotensin–Aldosterone System

Mutations Affecting Circulating Mineralocorticoid Levels

MUTATIONS RESULTING IN CONGENITAL HYPOALDOSTERONISM

Congenital hyper-reninemic hypoaldosteronism is a rare autosomal recessive disorder.[97,98] Affected patients present in infancy with salt-wasting, leading to severe dehydration, failure to thrive and growth retardation, as well as hyponatremia and hyperkalemia. Aldosterone is low despite elevated renin. These features are a clinical mirror image of the states of primary aldosteronism described above.

Genetic studies identified mutations in the aldosterone synthase gene (CYP11B2) as the cause of congenital hypoaldosteronism.[99,100] Aldosterone synthase catalyzes both 18-hydroxylation of corticosterone, and the subsequent conversion of the 18-hydroxyl group to an aldehyde (Figure 36.3). Several mutations, including nonsense, missense, and frameshift mutations, affect the 18-hydroxylase activity of the enzyme; as a result, levels of 18-hydroxycorticosterone are low in these patients. In other cases, specific missense mutations can abolish 18-oxidase activity, while 18-hydroxylase activity remains intact or is only slightly reduced. These patients consequently have elevated levels of 18-hydroxycortisone.[99]

Not all patients with hyper-reninemic hypoaldosteronism, however, have mutations at the CYP11B2 locus. Kayes-Wandover et al.[101] described four unrelated kindreds (two consanguineous) without evidence of such mutations; linkage to the CYP11B2 locus could be excluded in the two consanguineous families, suggesting genetic heterogeneity. The underlying gene defect of this disorder, termed familial hyper-reninemic hypoaldosteronism type 2, remains to be established.

CONGENITAL ADRENAL HYPERPLASIA DUE TO STEROID 21-HYDROXYLASE DEFICIENCY

Steroid 21-hydroxylase deficiency is an autosomal recessive disease. It accounts for the vast majority of the cases of congenital adrenal hyperplasia (CAH), and is one of the most common Mendelian diseases.

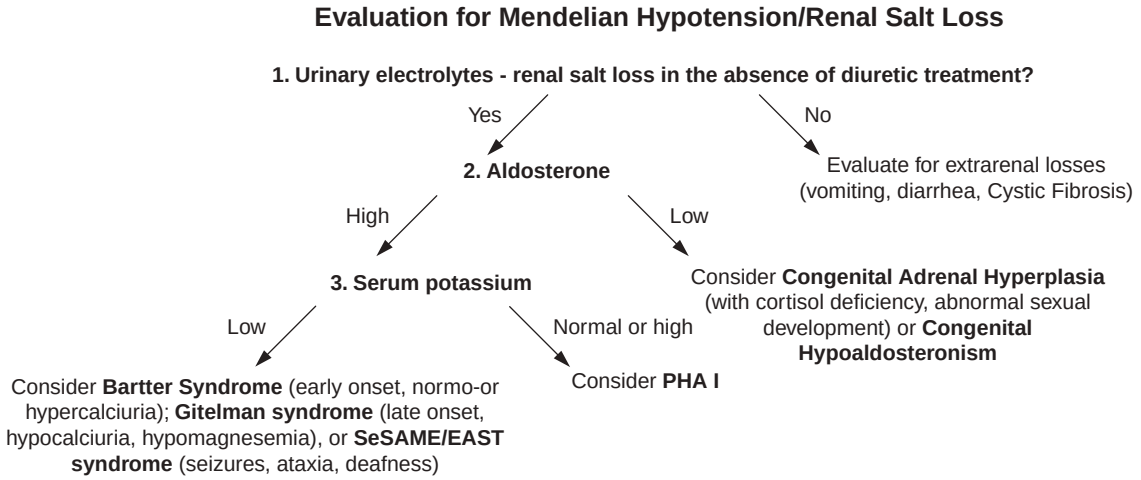
Evaluation for Mendelian Hypotension/Renal Salt Loss
1. Urinary electrolytes - renal salt loss in the absence of diuretic treatment?
Yes
No
2. Aldosterone
Evaluate for extrarenal losses (vomiting, diarrhea, Cystic Fibrosis)
High
Low
3. Serum potassium
Consider Congenital Adrenal Hyperplasia (with cortisol deficiency, abnormal sexual development) or Congenital Hypoaldosteronism
Low
Normal or high
Consider Bartter Syndrome (early onset, normo-or hypercalciuria); Gitelman syndrome (late onset, hypocalciuria, hypomagnesemia), or SeSAME/EAST syndrome (seizures, ataxia, deafness)
Consider PHA I

FIGURE 36.8 **A diagnostic approach to Mendelian hypotension and renal salt loss.** (PHA I: pseudohypoaldosteronism type I.)

21-hydroxylase catalyzes the 21-hydroxylation of progesterone, and is a required step in the biosynthesis of both cortisol and aldosterone (Figure 36.3).

Three subforms of the disease are recognized: patients with the salt-losing form of classic CAH are severely affected and present at birth or in infancy with cortisol and mineralocorticoid deficiency; females typically have ambiguous genitalia and virilization. In the simple virilizing form of classic CAH, high ACTH levels are sufficient to produce adequate levels of glucocorticoids and mineralocorticoids at the expense of increased adrenal androgen synthesis, resulting in virilization. Finally, patients with the late-onset or non-classic form may present in childhood, adolescence or even adulthood with premature pubarche and accelerated bone age; female patients develop hirsutism, infertility or irregular menstrual cycles.

The salt-losing form of classic CAH has an estimated incidence of ~1/23,000 live births, and is due to mutations in 21-hydroxylase (CYP21A gene) in almost all cases.[102] Girls with this condition present as neonates with masculinization. Salt-losing adrenal crisis, with vomiting, dehydration, hypotension, hypoglycemia, and electrolyte abnormalities (hyponatremia and hyperkalemia) typically occurs in the first or second week of life, and these can be the only presenting symptoms in boys. When untreated, adrenal crisis can lead to shock, cardiac arrhythmia, and neonatal death.[103]

CYP21A mutations causing salt-losing CAH often arise from unequal crossing-over between the functional CYP21A gene and a non-functional pseudogene located in close proximity[104]; the mutated enzyme typically shows complete loss-of-function. 21-hydroxylase deficiency is recognized clinically in patients with ambiguous genitalia or adrenal crisis, or in newborn screening programs; the diagnosis is based on elevated levels of 17-hydroxyprogesterone. Genetic testing is available, and can be supplemental for prenatal diagnosis, genetic counseling or ambiguous cases. Prenatal therapy with exogenous glucocorticoids can prevent or ameliorate virilization in female children, but is only recommended in a research setting due to potential side-effects.[105] If the child is known to be at risk, treatment is started as early as the mother knows she is pregnant, and stopped if the child is found to be male or unaffected by prenatal screening. Treatment after birth includes glucocorticoid and mineralocorticoid replacement, as well as salt supplementation in infants, and potentially feminizing surgery.[105]

RARE CAUSES OF SALT-WASTING CONGENITAL ADRENAL HYPERPLASIA

Very rare causes of salt-wasting congenital adrenal hyperplasia include 3-β-HSD 2 deficiency[106] and StAR deficiency[107] in lipoid adrenal hyperplasia. In both diseases, severe adrenal insufficiency with deficiency of gluco- and mineralocorticoids occurs at neonatal age or in infancy; genetically male patients typically have abnormalities of sexual development at birth, with female external genitalia in StAR deficiency.

Mutations in Genes Expressed in the Kidney that Cause Salt-Wasting

PSEUDOHYPOALDOSTERONISM TYPE I

Pseudohypoaldosteronism Type I (PHA I) is a rare genetic syndrome whose features include renal salt-wasting, hyperkalemia, hyponatremia, and metabolic acidosis despite elevated renin and aldosterone levels.[52,108] The disease presents as either an autosomal dominant or autosomal recessive trait. The recessive form appears to be uniformly severe, and requires life-long salt supplementation. The dominant form is clinically more variable at birth, and typically largely resolves after the first years of life with the ability to self-select a high-salt diet.

AUTOSOMAL RECESSIVE PSEUDOHYPOALDOSTERONISM TYPE I (PHAI) Infants with autosomal recessive PHA I frequently present with life-threatening episodes of hypovolemia, sometimes leading to neonatal death. Affected subjects have marked renal salt-wasting and striking hyperkalemia (as high as 12 mM), and renal tubular acidosis despite drastic elevations of PRA and aldosterone. There is also salt-wasting from salivary and sweat glands, as well as the colon. These patients require life-long sodium supplementation and often chronic treatment with resin-binding agents for hyperkalemia. Frequent pulmonary infections somewhat reminiscent of cystic fibrosis have been reported in some patients,[109] and markedly increased ciliary clearance of lung water has been reported.[110]

Genetic studies led to identification of recessive loss-of-function mutations in the alpha, beta or gamma subunits of the epithelial Na^+ channel (ENaC) in virtually all affected subjects.[111,112] Functional studies in *Xenopus* oocytes confirmed loss of channel activity. In summary, these findings demonstrated that mutations in all ENaC subunits can cause PHA I. All the features of this disease are explained by loss of ENaC function. Loss of ENaC function results in dramatic salt-wasting, leading to activation of the renin–angiotensin system; however, because ENaC is absent, this fails to adequately augment salt reabsorption in the kidney. Impaired salt absorption in the colon may also contribute to disease severity. K^+ and H^+ secretion are also markedly impaired, owing to loss the lumen-negative

potential resulting from loss of ENaC, causing hyperkalemia and acidosis.

These findings have been confirmed in animal studies. Mice deficient for the β- and γ-subunits show a phenotype characteristic of PHA I, with early death due to Na^+-wasting and K^+ retention,[113,114] and a PHA I-like phenotype is observed in α-ENaC knockout mice with transgenic expression of rat α-ENaC for rescue.[115] α-ENaC knockout mice show early postnatal demise with a mean survival of 24 hours postnatally due to respiratory distress,[116] suggesting a role of the mouse channel in pulmonary liquid clearance after birth that is apparently not observed at birth in humans but is found later in life.[110,117]

AUTOSOMAL DOMINANT PHA I Autosomal dominant PHA I has a milder phenotype that typically largely resolves in the early years of life. Patients may be asymptomatic or can present with renal salt-wasting and mild-to-moderate hyperkalemia and acidosis.[118,119] NaCl supplementation can typically be discontinued after early childhood, as the disease remits with age. Geller et al.[118] identified heterozygous mutations in the mineralocorticoid receptor gene in five kindreds with autosomal dominant PHA I. All mutations were inferred to be loss-of-function, inferred to cause diminished ENaC activity, with resulting salt loss. Since Na^+ reabsorption via ENaC is required for the lumen-negative potential that drives K^+ and H^+ secretion in the cortical collecting duct, diminished ENaC activity can cause hyperkalemic acidosis in these kindreds. The improvement with age is consistent with a decreasing requirement for aldosterone action in older children, presumably due to increasing salt intake and a self-selected high-salt diet after infancy. Adult carriers show no abnormalities of serum and urinary electrolytes or blood pressure, but consistently demonstrate markedly elevated serum aldosterone levels, consistent with homeostasis being achieved by compensating for the reduced level of MR by increased aldosterone levels.[119]

A case of autosomal recessive PHA I due to mutations in the mineralocorticoid receptor was recently reported – a newborn with very severe PHA I who was compound heterozygous for S166X and W806X deletions.[120] Within her family, carriers of the S166X mutation had typical autosomal dominant PHA I, while carriers of the W806X mutation were clinically asymptomatic, but had elevated renin and aldosterone levels.

A mouse model of PHA 1 shows increased renin and aldosterone, but develops normally in the heterozygous state. The homozygous knockout is lethal,[121] but can be rescued by subcutaneous NaCl injection before weaning.[122]

Mutations Affecting Renal Ion Channels, Transporters and their Regulators

Thick Ascending Limb of Henle

BARTTER SYNDROME

Bartter syndrome is a rare autosomal recessive disorder.[123] Patients may present at various ages with a variety of signs and symptoms. Renal salt-wasting is the key underlying primary problem, causing polyuria and subsequent polydipsia. In severe cases, patients present antenatally with polyhydramnios[124] (due to intrauterine polyuria), and affected subjects are often born prematurely. Renal salt-wasting, typically severe, leads to volume depletion, activation of the renin–angiotensin–aldosterone system and subsequent hypokalemic alkalosis; growth and mental development are impaired in some patients.[125] Hypercalciuria and nephrocalcinosis[126] are frequently found and can cause end-stage renal disease; deafness has been observed in a subset of patients.[127]

Early physiologic studies localized defective salt reabsorption in patients with Bartter syndrome to the loop of Henle[128] (Figure 36.9), and the finding of elevated levels of prostaglandins enabled treatment with inhibitors of prostaglandin synthesis.[129–131] The spectrum of clinical presentations and the underlying

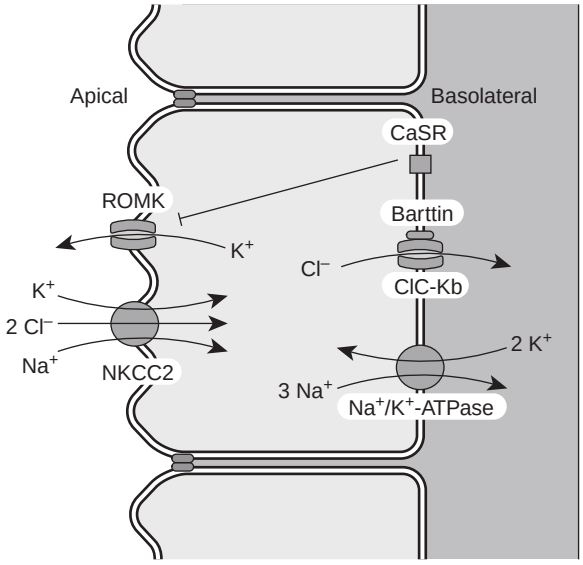

FIGURE 36.9 **Salt reabsorption in the thick ascending limb of Henle's loop.** Salt reabsorption is driven by the activity of the Na^+/K^+-ATPase on the basolateral suface. Na^+, Cl^-, and K^+ enter the cell on the apical surface via NKCC2 following the favorable gradient established by the sodium pump. While K^+ recirculates through ROMK, Cl^- is reabsorbed on the basolateral surface via ClC-Kb and its accessory subunit barttin. ROMK is inhibited by the calcium-sensing receptor (CaSR).

pathophysiology of this disorder was elucidated by the identification of the underlying genetic defects.

MUTATIONS IN NKCC2 CAUSE BARTTER SYNDROME TYPE I Recessive loss-of-function mutations in NKCC2, the bumetanide-sensitive Na-K-2Cl co-transporter (product of the SLC12A1 gene) were identified among a subset of patients with Bartter syndrome[132] (now Bartter syndrome type I). Affected index cases had all been born prematurely with polyhydramnios, and presented as neonates with hypokalemia and hyper-reninemic hyperaldosteronism; all had hypercalciuria. These clinical findings were consistent with the observation that pharmacologic inhibitors of NKCC2 produce similar electrolyte abnormalities. Loss of Na-Cl reabsorption in the TAL leads to massive salt-wasting, with activation of the renin–angiotensin system, and defense of intravascular volume by increased ENaC activity, which causes increased K^+ loss via increased lumen-negative potential in the connecting tubule and collecting duct. NCKK2 activity leads to reabsorption of two Cl^- and one Na^+ ions; the K^+ that enters across the apical membrane returns to the lumen via the K^+ channel ROMK. This results in a lumen-positive potential, which provides the electrical driving force for paracellluar calcium and magnesium reabsorption in the TAL. It is thus not surprising that loss of NKCC2 function results in hypercalciuria. Surprisingly, however, Mg^{2+} levels remain normal with little renal Mg^{2+} loss, suggesting compensation in other nephron segments. A knockout mouse model of NKCC2[133] generally recapitulated the features of Bartter syndrome (salt loss, dehydration, failure to thrive, response to treatment with indomethacin, and hypercalciuria).

MUTATIONS IN ROMK CAUSE BARTTER SYNDROME TYPE II Following the discovery of mutations in NKCC2, Simon et al. identified nine additional kindreds with Bartter syndrome without mutations in NKCC2, and excluded genetic linkage to this locus in several, providing strong evidence of genetic heterogeneity and indicating that additional loci accounted for many cases of Bartter syndrome.[134]

In the TAL, NKCC2 mediates apical sodium, potassium, and chloride influx using the favorable sodium gradient established by the basolateral Na^+/K^+-ATPase. Because luminal K^+ levels are low in the TAL compared to Na^+ and Cl^-, a role for the apical "recycling" of K^+ was speculated to be important for normal salt reabsorption in the TAL.[135,136] This was proven to be true by the finding of recessive loss-of-function mutations in the renal outer medullary K^+ channel (ROMK, product of the KCNJ1 gene), the apical K^+ channel of the TAL, in a subset of patients with Bartter syndrome (now referred to as Bartter syndrome type II).[134] These findings not only identified ROMK as a second disease locus in Bartter syndrome, but also established a key role of this apical potassium channel in renal salt reabsorption. Interestingly, ROMK is not only expressed in the thick ascending limb, but also in the cortical collecting duct, where it mediates apical potassium secretion (see above) driven by the lumen-negative potential established by reabsorption of Na^+ via ENaC. As found by Simon et al.,[134] and further elaborated by Peters et al.[137] and Finer et al.,[138] due to this defect in apical potassium secretion, serum potassium levels in patients with mutations in ROMK are significantly higher than in patients with NKCC2 mutations. Moreover, these patients typically present with hyperkalemia at birth. The development of relatively mild hypokalemia later in life indicates the presence of an alternative potassium-secreting channel with delayed maturation, likely the BK potassium channel.[139,140] A mouse model of Bartter syndrome with mutation in ROMK generally recapitulates the human phenotype.[141]

These findings define ROMK as a very promising target for the development of saluretic or antihypertensive agents with an adverse effect profile preferable over that of the common loop diuretics, limiting hypokalemia; such agents are currently under development.

MUTATIONS IN CLCNKB CAUSE BARTTER SYNDROME TYPE III Screening of 66 Bartter syndrome kindreds found mutations in NKCC2 and ROMK in only 22 kindreds.[142] This suggested the presence of at least one additional disease gene, supported by exclusion of linkage to either of the known genes by homozygosity mapping in 10 of 11 consanguineous kindreds. In the model of channels and transporters mediating salt reabsorption in the TAL outlined above, sodium enters via NKCC2 and exits via the Na^+/K^+-ATPase, while K^+ enters the cell via NKCC2 and returns to the lumen via ROMK. However, for net NaCl reabsorption, a basolateral exit pathway for chloride entering via NKCC2 is required. This exit had been suggested to be mediated by the chloride channels ClC-K1 and ClC-K2 in rat kidney[143,144] and their human homologs ClC-Ka (CLCNKA gene) and ClC-Kb (CLCNKB gene).[145] These two genes are closely linked, with CLCNKA located at 5′ of CLCNKB. Genetic analysis revealed linkage to this chromosome interval among Bartter syndrome families without mutation in NKCC2 and ROMK. Further analysis revealed deletions, missense, splice site, and premature termination mutations in the CLCNKB gene in affected members of 17 kindreds. Several of the deletions arose via unequal crossing-over between CLCNKB and CLCNKA. No point mutations were identified in the CLCNKA gene.

In contrast to the findings in patients with NKCC2 and ROMK mutations, hypercalciuria was variable, and none of the kindreds initially reported demonstrated nephrocalcinosis. Strikingly, there is a wide range of presentations in these patients, from severe volume depletion in the neonatal period to late-onset presentation. Hypomagnesemia[146] (see below) has been described in a few of these kindreds, but not to the extent generally seen in Gitelman syndrome. A possible explanation for this overlapping phenotype may be found in the expression of ClC-Kb, which is not restricted to the thick ascending limb of Henle, but extends into the distal convoluted tubule; the milder phenotype in some kindreds may be due to residual function of the mutant channel or partially compensating activity of the ClC-Ka channel in the thick ascending limb.

MUTATIONS IN BSND OR COMBINED MUTATIONS IN CLCNKA AND CLCNKB CAUSE BARTTER SYNDROME WITH SENSORINEURAL DEAFNESS (TYPE IV) Patients with Bartter syndrome type IV[127] typically present early with polyhydramnios and prematurity, as well as polyuria and renal saltloss after birth. This subtype is clinically distinguished from other forms of Bartter syndrome by the presence of sensorineural deafness. Genetic studies[147,148] led to the identification of a novel gene, named BSND (Bartter syndrome with sensorineural deafness), which had recessive loss-of-function mutations in 11 kindreds with this phenotype.[148] The novel disease gene and its product, named barttin, were found to be expressed in human and mouse kidney, as well as stria vascularis of the cochlea and dark cells of the vestibular organ. In stria vascularis, a set of channels and transporters highly similar to that mediating salt reabsorption in the thick ascending limb is responsible for potassium secretion into the endolymph and generation of the endocochlear potential, effects that are essential for normal hearing. Barttin was found to be an accessory subunit of ClC-Ka and ClC-Kb chloride channels required for surface insertion of the channel.[149] Most BSND missense mutations reduced current compared to WT when co-expressed with the chloride channels. Barttin co-localized with ClC-K channels on the basolateral surface of thin and thick ascending limb of Henle and more distal segments, including intercalated cells of the cortical collecting duct. The more severe renal phenotype of patients with BSND mutations compared to patients with CLCNKB mutation is likely caused by an additional effect on the ClC-Ka channel. In the inner ear, ClC-Ka can compensate for loss of ClC-Kb function in patients with CLCNKB mutations, while mutations in BSND abrogate basolateral chloride conductance in this epithelium, leading to sensorineural deafness. Accordingly, combined CLCNKA and CLCNKB mutations can cause Bartter syndrome and sensorineural deafness[150,151]; a condition sometimes referred to as Bartter syndrome type IVb. Isolated mutations in CLCNKA have not been described so far; a knockout ClC-K1 mouse model has diabetes insipidus,[152] which may clinically be less apparent than the salt loss observed with CLCNKB mutations. A constitutional BSND knockout mouse model manifests severe dehydration and early postnatal lethality, while inner-ear-specific disruption causes profound congenital hearing loss and subtle vestibular symptoms.[153]

MUTATIONS IN THE CALCIUM-SENSING RECEPTOR CAUSE BARTTER SYNDROME TYPE V The calcium-sensing receptor (CaSR) is a G-protein-coupled receptor, which, by sensing extracellular calcium, regulates both PTH secretion from the parathyroid and renal calcium reabsorption. Activating mutations in CaSR cause the syndrome of autosomal dominant hypoparathyroidism,[154] characterized by hypocalcemia, hypomagnesemia, and low serum PTH. A small number of these patients demonstrate features of Bartter syndrome (hyper-reninemic hyperaldosteronism and hypokalemia due to volume depletion),[155,156] potentially due to inhibition of apical ROMK channels[157] and inhibition of paracellular Na^+, Ca^{2+}, and Mg^{2+} reabsorption in the thick ascending limb. Although this disease clearly differs from Bartter syndrome, and the primary manifestation is hypocalcemia rather than salt loss, it is sometimes referred to as Bartter syndrome type V.

In summary, the identification of the genes mutated in subsets of Bartter syndrome has suggested a detailed classification, including clinically relevant features such as transient hyperkalemia in patients with Bartter syndrome type II that had not been recognized previously. This classification is now preferred over the the traditional distinction of "hyperprostaglandin E syndrome" in patients with early onset, severe salt loss, and increased urinary prostaglandin production, and "classic Bartter syndrome" with later onset and milder phenotype.[158]

The clinical diagnosis of Bartter syndrome is based on the presence of renal salt loss in infancy or childhood (high urinary chloride excretion in the absence of diuretic treatment), hyperaldosteronism, and hypokalemic alkalosis in the absence of hypertension. Urinary calcium is typically elevated, but can be normal in some patients with Cl^- channel mutations. Serum Mg^{2+} may be normal or slightly low, but does not typically reach the extremely low values seen in Gitelman syndrome (see below). Other causes of hypokalemia, such as vomiting and treatment with diuretics, should be excluded. Genetic testing is available.

Genotype–phenotype correlations can suggest the underlying mutant gene from the clinical presentation. Patients with ROMK mutations are distinguished by typically having hyperkalemia in the neonatal period, and evolve to hypokalemia that is less severe than that seen in other patients. Patients with CLCNKB mutations are least likely to have hypercalciuria and nephrocalcinosis, and account for most patients with mild disease, as can be seen with a few particular mutations.[159] Patients with sensorineural deafness have either BSND or combined CLCNKA/CLCNKB mutations. Patients without these distinguishing features are enriched for NKCC2 mutations.

Prostaglandin synthesis inhibitors (NSAIDs) are an important part of the therapeutic regimen in Bartter syndrome. While the exact mechanism of increased prostaglandin synthesis in these patients remains unclear, prostaglandin E2 can exacerbate renal salt-wasting.[160] Monitoring for nephrotoxicity and gastrointestinal side-effects is important. Severe volume depletion requires intravenous fluids, and a life-long high-salt diet is encouraged. Potassium supplementation is often needed, and magnesium supplementation is occasionally also needed. Potassium-sparing diuretics to limit renal K^+ loss can be used if necessary; however, these must be used with caution as they will exacerbate renal salt loss in these patients. Therapy with growth hormone can be considered in patients with growth retardation. As expected for a genetic disease affecting the kidney, renal transplantation is curative. Transplantation is usually limited to patients who proceed to end-stage renal failure, although preemptive transplantation has been reported.[161]

Salt-Wasting Due to Mutations Affecting Salt Reabsorption in the Distal Convoluted Tubule

GITELMAN SYNDROME

Gitelman syndrome is an autosomal recessive disorder. The clinical features typically include renal salt-wasting, elevated levels of PRA and aldosterone, hypokalemia, metabolic alkalosis, hypomagnesemia, and hypocalciuria.[162,163] The clinical distinction from Bartter syndrome is usually obvious. While Bartter syndrome patients typically present in the first year of life (mean age 0.8 years), often with severe volume depletion, Gitelman patients typically present later (mean age 10.5 years) with symptoms that are less obviously due to volume depletion, but often related to hypokalemia and/or hypomagnesemia. The urinary calcium: creatinine ratio in Bartter syndrome is typically ≥ 0.4 mmol/mmol, hypocalciuria is characteristic of Gitelman syndrome (ratio ≤ 0.1 mmol/mmol). Mean plasma magnesium is considerably lower in Gitelman patients (mean 0.54 mmol/L versus 0.82 mmol/L in Bartter syndrome), and seizures or tetanic episodes have been described in several cases.[163] While adult patients with Bartter syndrome are very uncommon, adult Gitelman syndrome patients are not rare, and women with Gitelman syndrome successfully complete pregnancy in many cases.

Clinical studies localized salt loss in Gitelman syndrome to the distal convoluted tubule (Figure 36.7), and demonstrated a reduced response to intravenous administration of a thiazide diuretic.[164] The thiazide-sensitive carrier, NCC, had been cloned from flounder bladder and rat kidney,[165,166] but not from human. To study NCC as a disease gene in Gitelman syndrome, Simon et al.[167] cloned and characterized the human gene; they isolated DNA from members of 12 kindreds with Gitelman syndrome and genotyped markers spanning the NCC locus, demonstrating linkage of Gitelman syndrome and NCC. Affected kindred members all had mutations in NCC, including splice site mutations and premature termination codons. The findings demonstrated that Gitelman syndrome is caused by mutations in NCCT. Many additional patients and mutations have been reported since; for example Ji et al. found 91 different mutations in 246 alleles among 123 patients with Gitelman syndrome.[168] In a single large kindred comprising more than 200 subjects segregating mutations in NCC, virtually complete penetrance of hypokalemia, alkalosis, and hypocalciuria was seen among subjects with two mutant NCC alleles, and these subjects had lower blood pressure than others in the pedigree, despite consuming significantly more salt.[206] Heterozygotes were intermediate in salt consumption and blood pressure.

While Gitelman syndrome is a much milder disease than Bartter syndrome, these patients are not asymptomatic – common complaints include salt craving, musculoskeletal symptoms such as cramps, muscular weakness, and aches, as well as fatigue, generalized weakness, polydipsia, and polyuria.[169]

The finding of mutations in NCC clearly explains renal salt loss in patients with Gitelman syndrome – apical NaCl entry in DCT is impaired, leading to reduced salt reabsorption with concomitant water loss, activation of the renin–angiotensin–aldosterone system and upregulation of ENaC activity in the collecting duct. This again accounts for hypokalemic alkalosis in these patients. It is less clear, however, why these patients develop hypomagnesemia and hypocalciuria, similar to patients treated with thiazide diuretics. Hypocalciuria has been attributed to increased proximal calcium reabsorption[170]; however, the exact physiologic mechanism of this effect is still a matter of debate. Hypomagnesemia was linked to decreased expression of the apical TRPM6 channel in DCT,[171] which mediates magnesium reabsorption and is mutated in another

rare Mendelian syndrome, hypomagnesemia with secondary hypocalcemia. This may be due to the decreased mass of the distal convoluted tubule observed with NCC deficiency or thiazide treatment.[172,173]

The above results from human studies have been confirmed in a knockout mouse model of NCCT[172] featuring hypomagnesemia and hypocalciuria. While hypokalemia and hyperaldosteronism were absent on a normal rodent diet, a marked reduction in plasma potassium occured upon low-potassium diet, and was accompanied by polyuria, polydipsia, and hyperaldosteronism.[174]

Although genetic testing is available, the diagnosis of Gitelman syndrome can be made reliably in typical cases in adolescents and adults on the basis of elevated PRA and aldosterone with hypokalemic alkalosis, hypomagnesemia, hypocalciuria, and evidence of renal salt loss in the absence of diuretic treatment or abuse. Because this clinical picture is virtually identical to that seen with use of thiazide diuretics, affected patients are often suspected of surreptitiously taking these medications. Genetic studies can be helpful in this situation.

Therapeutic options include electrolyte supplements (although magnesium supplementation can be particularly challenging) and potassium-sparing diuretics, although the latter can worsen volume depletion. Treatment with NSAIDs is generally not recommended, because these patients typically do not show elevated prostaglandin production.

SeSAME/EAST SYNDROME

A novel autosomal-recessive genetic disorder featuring renal salt loss was recently independently described as SeSAME (seizures, sensorineural deafness, ataxia, mental retardation, and electrolyte imbalance)[175] and EAST (epilepsy, ataxia, sensorineural deafness, tubulopathy)[176] syndrome. The renal features of this disorder resemble Gitelman syndrome, with persistent hypokalemic alkalosis due to activation of the renin–angiotensin–aldosterone system and variable hypomagnesemia, as well as hypocalciuria. Patients typically present in infancy with recurrent seizures; brain MRI is normal. More severe sensorineural hearing loss may be apparent in neonatal screening, while milder cases may go unnoticed until late childhood. Speech and motor delay are associated features, and may in part be due to ataxia. Genome-wide linkage analysis in three informative kindreds demonstrated complete linkage of SeSAME to a single segment on chromosome 1q23, and the Kir4.1 inward rectifier potassium channel (encoded by the *KCNJ10* gene) was identified as a candidate gene within the interval. Kir4.1 is expressed in kidney, inner ear, and brain; a knockout mouse model shows seizures, sensorineural deafness, and ataxia.[177–179] Screening of five affected subjects from four kindreds revealed homozygous or compound heterozygous mutations that segregated with the disease; this included a nonsense mutation and five missense mutations at conserved residues, which were inferred to be loss-of-function.[175] Similar findings were reported by Böckenhauer et al.[176] in two consanguineous families. In addition, they demonstrated electrophysiologic loss of channel function in mutant channels, and confirmed expression of Kir4.1 in the distal convoluted tubule, connecting tubule, and early cortical collecting duct. Analysis of the previously established knockout mouse model revealed polyuria, elevated urinary sodium concentration, and low urinary calcium concentration.

Seizures in patients with KCNJ10 mutations are likely due to loss of the channel's function in "spatial buffering",[180,181] i.e., glial uptake of excess potassium ions released during neuronal activity, followed by release at domains with low extracellular potassium concentration, a process that normally prevents neuronal hyperexcitability. Likewise, deafness is accounted for by expression of the channel in the stria vascularis, where it is essential for the generation of the endocochlear potential.[182]

The renal abnormalities in SeSAME/EAST syndrome are likely due to loss of basolateral potassium recycling which is required for maximal activity of the sodium pump ("pump leak coupling"[183]). Na^+/K^+-ATPase activity, which drives NaCl reabsorption via NCC, increases K^+ entry, which is inferred to be mitigated by return across the basolateral membrane via Kir4.1 activity. In the absence of this function, the accumulation of potassium in the cell limits Na^+/K^+-ATPase activity, and hence NaCl reabsorption in the DCT, and is inferred to cause hypomagnesemia and hypocalciuria due to impaired NCC function, analogous to Gitelman syndrome (see above). Subsequent studies have identified several additional families with SeSAME/EAST syndrome.[184–186] The diagnosis of this syndrome is based on the unique clinical findings. Genetic testing is available.

Treatment options include anticonvulsives and hearing aids to prevent further language delay. Potassium and, where required, magnesium supplementation and potassium-sparing diuretics are used to treat the electrolyte abnormalities in SESAME/EAST syndrome.

GENETIC STUDIES OF ESSENTIAL HYPERTENSION IN THE GENERAL POPULATION

The above considerations largely focus on rare genetic diseases with extreme phenotypes. The identification of the underlying defects had made an

invaluable contribution to our current concept of renal salt handling, and to the identification of novel physiological pathways. The results of these studies unequivocally link increased renal salt reabsorption to hypertension, and renal salt loss to sometimes life-threatening hypotension.

While Mendelian diseases of blood pressure homeostasis are extremely rare, hypertension affects more than one billion people worldwide[187] and contributes to more than seven million deaths each year.[188,189] However, despite the early recognition from twin and family studies that blood pressure is influenced by genetic mechanisms,[190,191] with ~60% heritability of hypertension,[192] the genes involved are still largely unknown.

The genetic contribution to common diseases could, in theory, be based on common genetic variants (defined by an allelic frequency of more than 5%). Such variants are identified in genome-wide association studies (GWAS), where a large number of polymorphic markers is genotyped in affected subjects and controls to identify those associated with the disease. Many large GWAS studies on hypertension have been reported,[193,194] with the most recent large meta-analysis evaluating 2.5 million single nucleotide polymorphisms (SNPs) in 69,395 individuals, with replication in up to 133,661 individuals, all of European ancestry.[15] The authors identified 29 independent SNPs at 28 loci that were significantly associated with systolic blood pressure (SBP), diastolic blood pressure (DBP) or both. However, these variants are typically of very small effect size, less than 1 mmHg on systolic blood pressure, and the 29 SNPs reported collectively account for only 0.9% of the phenotypic variance for SBP and DBP. Even including an estimated another 116 variants with similar effect size that did not achieve statistical significance, only ~2.2% of the variance could be explained.

These considerations suggest that only a small fraction of heritability of blood pressure in the general population is explained by common variants, and raise the possibility that a greater fraction of heritability is based on rare variants with larger effect size. Such hypothetical variants are not amenable to analysis by GWAS due to their small allelic frequency. However, their proposed larger effect could well be due to alterations in similar pathways as in Mendelian diseases of blood pressure regulation, i.e., genes involved in renal salt homeostasis. To test this hypothesis, Ji et al. resequenced three target genes, encoding NCC, NKCC2, and ROMK implicated in Bartter and Gitelman syndrome, respectively (see above) in 3125 members of the Framingham Heart Study population (1985 unrelated subjects and 1140 kindred members), all with careful and systematic blood pressure measurements at regular intervals.[168] From the frequency of the homozygous recessive state for Gitelman and Bartter syndrome, it was expected that heterozygous loss-of-function mutations should be present in about 1−2% of the population. Sequencing of these three genes in this cohort identified 23 subjects with 10 mutations that were previously known loss-of-function mutations or null alleles. Another 19 variants in 25 subjects were found at positions that are completely conserved from flies and worms to humans, strongly suggesting that these are functionally significant. Importantly, these functional mutations are all rare in the population, with allele frequencies less than 1 in 2000. Blood pressure in carriers of mutations in any of the three genes was significantly reduced at ages 40, 50, and 60 years compared to either non-carrier members of the cohort or non-carrier siblings, with a mean 9 mmHg reduction in systolic blood pressure at age 60. Mutation carriers were significantly protected from hypertension (59% risk reduction compared to non-carriers at age 60).

The development of next generation sequencing techniques and the dropping cost of this technology now enables genome-wide and unbiased analysis of rare variants by means of whole genome sequencing or, for reasons of cost effectiveness, whole exome sequencing, in large cohorts. It is expected that ongoing studies will provide new insights into the contribution of rare variants to blood pressure homeostasis, although large sample sizes will be required.[195]

NEW INSIGHTS INTO BASIC PHYSIOLOGY, PREVENTION, AND THERAPEUTICS FROM GENETIC STUDIES

The molecular genetic studies described above have collectively made a number of tangible contributions to our understanding of electrolyte homeostasis and blood pressure regulation. One element in renal physiology that was difficult to predict *a priori* was the physiologic consequence of eliminating specific transport pathways. For example, it was known that ENaC mediates the reabsorption of only a few percent of the filtered sodium load, and clinically used inhibitors of this channel have modest effects on salt balance and blood pressure. It consequently came as a surprise that genetic deficiency of any of the ENaC subunits results in profound renal salt-wasting with severe hyperkalemia and acidosis.[111,112] Affected subjects are extremely ill from birth onward, and typically require massive salt supplementation as well as treatment for hyperkalemia. These findings indicate that ENaC is constitutively active in the absence of an activated renin−angiotensin system, and is required for

maintenance of normal salt balance; its absence cannot be reasonably compensated by increasing the activity of other nephron segments. These findings also left no doubt that ENaC activity is absolutely required for normal K^+ and H^+ ion secretion, since severe hyperkalemia and acidosis results in the absence of ENaC activity. In contrast, loss of activity of the target for thiazide diuretics, NCC, has a far more subtle effect on salt balance, despite the fact that NCC normally accounts for reabsorption of a far greater fraction of the filtered salt load.[167] Similarly, the effects of loss of ROMK on net salt and K^+ balance were quite unpredictable from physiologic studies alone.[134] Would loss of ROMK produce hyperkalemia owing to its normal role in K^+ secretion in the distal nephron or hypokalemia due to K^+-wasting from the TAL? The finding that loss of ROMK results in dramatic salt-wasting but only mild hypokalemia, much less severe than that seen with loss of NKCC2, suggests that inhibitors of ROMK might be of particular clinical benefit as antihypertensive diuretic agents.

Second, this work has firmly established the key role of altered renal salt balance in the determination of long-term blood pressure in humans. All mutations that increase salt reabsorption raise blood pressure, while those that reduce salt reabsorption lower blood pressure. Despite diverse effects on K^+, pH, Mg^{2+}, and Ca^{2+} handling, the vector for salt reabsorption dictates the direction of blood pressure. This has implications for control of blood pressure in the general population (see below). These findings underscore the observation that other known sufficient causes of hypertension also modulate renal salt handling. Renovascular hypertension caused by stenosis of one or both renal arteries decreases renal blood flow and thereby causes activation of the RAA system and increased renal salt reabsorption; renal blood flow is likewise reduced in aortic coarctation and pheochromocytoma, again leading to increased renal renin secretion. The same final common pathway is activated by primary aldosteronism with increased aldosterone production from the adrenal gland and by licorice intoxication. Finally, in ESRD, the kidney is unable to eliminate excess volume, leading to hypertension.

Third, this work has uncovered entirely new physiology that was not previously anticipated. Specifically, the role of the WNK kinases in the regulation of the balance between salt reabsorption and K^+ secretion, revealed by genetic studies,[74] has identified a new layer of regulatory physiology in which these kinases are orchestrating the activity of diverse flux pathways to allow appropriate responses to diverse environmental perturbations. Moreover, the realization of the yin and yang relationship between Na-Cl reabsorption and K^+ secretion produced by the WNK kinase pathway provides an explanation for the long-recognized blood pressure-lowering effect of increased dietary potassium—increased K^+ secretion must occur at the expense of reduced Na-Cl reabsorption, accounting for the observed reduction in blood pressure.[196–199] The recent identification of the CUL3-KLHL3 ubiquitin ligase pathway[95,96] will extend this developing paradigm in the coming years.

Perhaps the most important implication of this work is the recognition that modulation of salt balance can modulate blood pressure across the entire spectrum seen in the human population. For example, genetic loss of ENaC function results in life-threatening hypotension, while gain of ENaC function results in early and often severe hypertension. The finding that modulation of activity of single genes in this pathway can dial blood pressure across the entire spectrum seen in the human population reveals the power of this system. These findings provide the basic science foundation that suggests that reduction of dietary salt intake might be beneficial in lowering blood pressure in the general population. This idea has been supported by recent studies showing that even a modest 25% reduction in dietary salt results in clinically significant blood pressure reduction, and that larger reductions in salt intake have proportionately larger effects.[196,200] Goldman and colleagues[201] have estimated that such a 25% reduction in dietary salt intake would be expected to dramatically reduce the number of strokes, myocardial infarctions, all cause deaths, and healthcare costs. The Institute of Medicine has released a study suggesting that such a 25% reduction in salt intake could be approached by reducing salt in processed foods and restaurant meals.[202] Programs to reduce dietary salt have been implemented in a number of countries worldwide.

These insights also have implications for the control of hypertension among patients with end-stage renal disease (ESRD), who have a particularly high prevalence of hypertension. Interestingly, a retrospective cross-sectional study in patients on hemodialysis suggested that a traditional treatment protocol lowering "dry weight" (weight at the end of dialysis) until optimal blood pressure is achieved and limiting dietary salt intake to 5–6 g per day may lead to similar control of hypertension as treatment with antihypertensive drugs, yet better outcome in terms of left ventricular (LV) hypertrophy, LV function, and intradialytic hypotension.[203] Other studies demonstrated that longer, slower dialysis to remove more salt and volume enabled drastic reduction in the prevalence of hypertension.[204,205]

Lastly, these findings provide insight into the potential for new antihypertensive diuretic agents and rational combination therapy. It is striking that patients

genetically deficient for the thiazide target (NCC) dramatically increase their dietary salt intake.[206] This suggests that activation of the renin–angiotensin system secondary to salt-wasting contributes to the drive to eat more salt as an adaptive response to volume depletion. Thus, the effects of diuretics are inherently blunted without blockade of compensatory activation of the renin–angotensin system.

The effects of loss-of-function mutations in specific genes provide an excellent proxy for both the magnitude of effect that could be achieved by pharmacologic inhibition of a target, as well as insight into potential mechanism-based adverse effects. It is interesting that loss of the thiazide target, NCC, has a modest effect on blood pressure compared to the effect of loss-of-function mutation in many other genes in the salt reabsorption pathway. The largest loss-of-function effects on blood pressure are seen with targets in the thick ascending limb and collecting duct. Among these, hyper- and hypokalemia are quite severe with most targets, including hypokalemia with mutations in NKCC2, CLCNKB, and BSND, and severe hyperkalemia with loss-of-function mutations in ENaC. These findings might limit the ability to push inhibition at these targets to high enough levels to achieve desired blood pressure lowering. In contrast, ROMK, which produces salt-wasting similar to that seen with mutations in NKCC2, the target of furosemide, produces much less hypokalemia, suggesting that one might achieve very large reductions in salt balance with little effect on K^+. Moreover, heterozygotes for ROMK mutations show significant reductions in blood pressure,[168] suggesting that graded effects can be achieved with dose modification. These findings suggest that ROMK inhibitors, plus inhibition of the renin–angiotensin system, could provide greater blood pressure lowering with fewer side-effects than current treatment regimens, and that ROMK inhibitors may also be of benefit in congestive heart failure. This speculation will require substantial empiric validation to determine the potential value of such agents.

References

[1] Lifton RP, Gharavi AG, Geller DS. Molecular mechanisms of human hypertension. Cell 2001;104:545–56.

[2] Montani JP, Mizelle HL, Adair TH, Guyton AC. Regulation of cardiac output during aldosterone-induced hypertension. J Hypertens Suppl 1989;7:S206–7.

[3] Sutherland DJ, Ruse JL, Laidlaw JC. Hypertension, increased aldosterone secretion and low plasma renin activity relieved by dexamethasone. Can Med Assoc J 1966;95:1109–19.

[4] Litchfield WR, Anderson BF, Weiss RJ, Lifton RP, Dluhy RG. Intracranial aneurysm and hemorrhagic stroke in glucocorticoid-remediable aldosteronism. Hypertension 1998;31:445–50.

[5] Rich GM, Ulick S, Cook S, Wang JZ, Lifton RP, Dluhy RG. Glucocorticoid-remediable aldosteronism in a large kindred: clinical spectrum and diagnosis using a characteristic biochemical phenotype. Ann Intern Med 1992;116:813–20.

[6] Litchfield WR, Coolidge C, Silva P, Lifton RP, Fallo F, Williams GH, et al. Impaired potassium-stimulated aldosterone production: a possible explanation for normokalemic glucocorticoid-remediable aldosteronism. J Clin Endocrinol Metab 1997;82:1507–10.

[7] Chu MD, Ulick S. Isolation and identification of 18-hydroxycortisol from the urine of patients with primary aldosteronism. J Biol Chem 1982;257:2218–24.

[8] Ulick S, Chu MD, Land M. Biosynthesis of 18-oxocortisol by aldosterone-producing adrenal tissue. J Biol Chem 1983;258:5498–502.

[9] Lifton RP, Dluhy RG, Powers M, Rich GM, Cook S, Ulick S, et al. A chimaeric 11 beta-hydroxylase/aldosterone synthase gene causes glucocorticoid-remediable aldosteronism and human hypertension. Nature 1992;355:262–5.

[10] Lifton RP, Dluhy RG, Powers M, Rich GM, Gutkin M, Fallo F, et al. Hereditary hypertension caused by chimaeric gene duplications and ectopic expression of aldosterone synthase. Nat Genet 1992;2:66–74.

[11] Pilon C, Mulatero P, Barzon L, Veglio F, Garrone C, Boscaro M, et al. Mutations in CYP11B1 gene converting 11beta-hydroxylase into an aldosterone-producing enzyme are not present in aldosterone-producing adenomas. J Clin Endocrinol Metab 1999;84:4228–31.

[12] Jonsson JR, Klemm SA, Tunny TJ, Stowasser M, Gordon RD. A new genetic test for familial hyperaldosteronism type I aids in the detection of curable hypertension. Biochem Biophys Res Commun 1995;207:565–71.

[13] Funder JW, Carey RM, Fardella C, Gomez-Sanchez CE, Mantero F, Stowasser M, et al. Case detection, diagnosis, and treatment of patients with primary aldosteronism: an endocrine society clinical practice guideline. J Clin Endocrinol Metab 2008;93:3266–81.

[14] Fallo F, Pilon C, Williams TA, Sonino N, Morra Di Cella S, Veglio F, et al. Coexistence of different phenotypes in a family with glucocorticoid-remediable aldosteronism. J Hum Hypertens 2004;18:47–51.

[15] Ehret GB, Munroe PB, Rice KM, Bochud M, Johnson AD, Chasman DI, et al. Genetic variants in novel pathways influence blood pressure and cardiovascular disease risk. Nature 2011;478:103–9.

[16] Conn JW, Louis LH. Primary aldosteronism: a new clinical entity. Trans Assoc Am Physicians 1955;68:215–31, discussion, 231–213.

[17] Rossi GP, Bernini G, Caliumi C, Desideri G, Fabris B, Ferri C, et al. A prospective study of the prevalence of primary aldosteronism in 1,125 hypertensive patients. J Am Coll Cardiol 2006;48:2293–300.

[18] Choi M, Scholl UI, Yue P, Bjorklund P, Zhao B, Nelson-Williams C, et al. K^+ channel mutations in adrenal aldosterone-producing adenomas and hereditary hypertension. Science 2011;331:768–72.

[19] Heginbotham L, Lu Z, Abramson T, MacKinnon R. Mutations in the K^+ channel signature sequence. Biophys J 1994;66:1061–7.

[20] Tao X, Avalos JL, Chen J, MacKinnon R. Crystal structure of the eukaryotic strong inward-rectifier K^+ channel Kir2.2 at 3.1 Å resolution. Science 2009;326:1668–74.

[21] Enyeart JJ, Xu L, Danthi S, Enyeart JA. An ACTH- and ATP-regulated background K^+ channel in adrenocortical cells is TREK-1. J Biol Chem 2002;277:49186–99.

[22] Czirjak G, Enyedi P. TASK-3 dominates the background potassium conductance in rat adrenal glomerulosa cells. Mol Endocrinol 2002;16:621–9.
[23] Lotshaw DP. Characterization of angiotensin II-regulated K^+ conductance in rat adrenal glomerulosa cells. J Membr Biol 1997;156:261–77.
[24] Brauneis U, Vassilev PM, Quinn SJ, Williams GH, Tillotson DL. ANG II blocks potassium currents in zona glomerulosa cells from rat, bovine, and human adrenals. Am J Physiol 1991;260:E772–9.
[25] Hu C, Rusin CG, Tan Z, Guagliardo NA, Barrett PQ. Zona glomerulosa cells of the mouse adrenal cortex are intrinsic electrical oscillators. J Clin Invest 2012;122(6):2046–53.
[26] Spat A, Hunyady L. Control of aldosterone secretion: a model for convergence in cellular signaling pathways. Physiol Rev 2004;84:489–539.
[26a] Akerström T, Crona J, Delgado Verdugo A, Starker LF, Cupisti K, Willenberg HS, et al. Comprehensive Re-Sequencing of Adrenal Aldosterone Producing Lesions Reveal Three Somatic Mutations near the KCNJ5 Potassium Channel Selectivity Filter. PLoS One 2012;7:e41926.
[27] Boulkroun S, Beuschlein F, Rossi GP, Golib-Dzib JF, Fischer E, Amar L, et al. Prevalence, clinical, and molecular correlates of KCNJ5 mutations in primary aldosteronism. Hypertension 2012;59:592–8.
[28] Geller DS, Zhang J, Wisgerhof MV, Shackleton C, Kashgarian M, Lifton RP. A novel form of human Mendelian hypertension featuring nonglucocorticoid-remediable aldosteronism. J Clin Endocrinol Metab 2008;93:3117–23.
[29] Scholl UI, Nelson-Williams C, Yue P, Grekin R, Wyatt RJ, Dillon MJ, et al. Hypertension with or without adrenal hyperplasia due to different inherited mutations in the potassium channel KCNJ5. Proc Natl Acad Sci USA 2012;109:2533–8.
[30] Mulatero P, Tauber P, Zennaro MC, Monticone S, Lang K, Beuschlein F, et al. KCNJ5 mutations in European families with nonglucocorticoid remediable familial hyperaldosteronism. Hypertension 2012;59:235–40.
[31] Mussa A, VCamilla R, Monticone S, Porta F, Tessaris D, Verna F, et al. Polyuric-polydipsic syndrome in a pediatric case of nonglucocorticoid remediable familial hyperaldosteronism. Endocr J 2012;59:497–502.
[32] Charmandari E, Sertedaki A, Kino T, Merakou C, Hoffman DA, Hatch MM, et al. A novel point mutation in the KCNJ5 gene causing primary hyperaldosteronism and early-onset autosomal dominant hypertension. J Clin Endocrinol Metab 2012;97: E1532-9.
[33] Pivonello R, Ferone D, de Herder WW, de Krijger RR, Waaijers M, Mooij DM, et al. Dopamine receptor expression and function in human normal adrenal gland and adrenal tumors. J Clin Endocrinol Metab 2004;89:4493–502.
[34] Tannin GM, Agarwal AK, Monder C, New MI, White PC. The human gene for 11 beta-hydroxysteroid dehydrogenase. Structure, tissue distribution, and chromosomal localization. J Biol Chem 1991;266:16653–8.
[35] Zachmann M, Tassinari D, Prader A. Clinical and biochemical variability of congenital adrenal hyperplasia due to 11 beta-hydroxylase deficiency. A study of 25 patients. J Clin Endocrinol Metab 1983;56:222–9.
[36] Rosler A, Leiberman E, Sack J, Landau H, Benderly A, Moses SW, et al. Clinical variability of congenital adrenal hyperplasia due to 11 beta-hydroxylase deficiency. Horm Res 1982;16:133–41.
[37] Cerame BI, New MI. Hormonal hypertension in children: 11beta-hydroxylase deficiency and apparent mineralocorticoid excess. J Pediatr Endocrinol Metab 2000;13:1537–47.
[38] Portrat S, Mulatero P, Curnow KM, Chaussain JL, Morel Y, Pascoe L. Deletion hybrid genes, due to unequal crossing over between CYP11B1 (11beta-hydroxylase) and CYP11B2(aldosterone synthase) cause steroid 11beta-hydroxylase deficiency and congenital adrenal hyperplasia. J Clin Endocrinol Metab 2001;86:3197–201.
[39] Biglieri EG, Herron MA, Brust N. 17-hydroxylation deficiency in man. J Clin Invest 1966;45:1946–54.
[40] Costa-Santos M, Kater CE, Auchus RJ. Two prevalent CYP17 mutations and genotype-phenotype correlations in 24 Brazilian patients with 17-hydroxylase deficiency. J Clin Endocrinol Metab 2004;89:49–60.
[41] Kagimoto M, Winter JS, Kagimoto K, Simpson ER, Waterman MR. Structural characterization of normal and mutant human steroid 17 alpha-hydroxylase genes: molecular basis of one example of combined 17 alpha-hydroxylase/17,20 lyase deficiency. Mol Endocrinol 1988;2:564–70.
[42] Geller DH, Auchus RJ, Mendonca BB, Miller WL. The genetic and functional basis of isolated 17,20-lyase deficiency. Nat Genet 1997;17:201–5.
[43] New MI, Levine LS, Biglieri EG, VPareira J, Ulick S. Evidence for an unidentified steroid in a child with apparent mineralocorticoid hypertension. J Clin Endocrinol Metab 1977;44:924–33.
[44] Ulick S, Levine LS, Gunczler P, Zanconato G, Ramirez LC, Rauh W, et al. A syndrome of apparent mineralocorticoid excess associated with defects in the peripheral metabolism of cortisol. J Clin Endocrinol Metab 1979;49:757–64.
[45] Arriza JL, Weinberger C, Cerelli G, Glaser TM, Handelin BL, Housman DE, et al. Cloning of human mineralocorticoid receptor complementary DNA: structural and functional kinship with the glucocorticoid receptor. Science 1987;237:268–75.
[46] Krozowski ZS, Funder JW. Renal mineralocorticoid receptors and hippocampal corticosterone-binding species have identical intrinsic steroid specificity. Proc Natl Acad Sci USA 1983;80:6056–60.
[47] Mune T, Rogerson FM, Nikkila H, Agarwal AK, White PC. Human hypertension caused by mutations in the kidney isozyme of 11 beta-hydroxysteroid dehydrogenase. Nat Genet 1995;10:394–9.
[48] Kotelevtsev Y, Brown RW, Fleming S, Kenyon C, Edwards CR, Seckl JR, et al. Hypertension in mice lacking 11beta-hydroxysteroid dehydrogenase type 2. J Clin Invest 1999;103:683–9.
[49] Palermo M, Delitala G, Mantero F, Stewart PM, Shackleton CH. Congenital deficiency of 11beta-hydroxysteroid dehydrogenase (apparent mineralocorticoid excess syndrome): diagnostic value of urinary free cortisol and cortisone. J Endocrinol Invest 2001;24:17–23.
[50] Knops NB, Monnens LA, Lenders JW, Levtchenko EN. Apparent mineralocorticoid excess: time of manifestation and complications despite treatment. Pediatrics 2011;127:e1610–4.
[51] Stewart PM, Wallace AM, Valentino R, Burt D, Shackleton CH, Edwards CR. Mineralocorticoid activity of liquorice: 11-beta-hydroxysteroid dehydrogenase deficiency comes of age. Lancet 1987;2:821–4.
[52] Geller DS. Pseudohypoaldosteronism Type 1 and Hypertension Exacerbated in Pregnancy. In: Lifton RP, Somlo S, Giebisch GH, Seldin DW, editors. *Genetic diseases of the kidney*. burlingon. London, San Diego, New York: Elsevier; 2009. p. 301–12.
[53] Geller DS, Farhi A, Pinkerton N, Fradley M, Moritz M, Spitzer A, et al. Activating mineralocorticoid receptor mutation in hypertension exacerbated by pregnancy. Science 2000;289:119–23.
[54] Fagart J, Huyet J, Pinon GM, Rochel M, Mayer C, Rafestin-Oblin ME. Crystal structure of a mutant mineralocorticoid receptor responsible for hypertension. Nat Struct Mol Biol 2005;12:554–5.
[55] Liddle GW, Bledsoe T, Coppage WS. A familial renal disorder stimulating primary aldosteronism but with negligible aldosterone secretion. Trans Assoc Am Physicians 1963;76:199–213.

[56] Shimkets RA, Warnock DG, Bositis CM, Nelson-Williams C, Hansson JH, Schambelan M, et al. Liddle's syndrome: heritable human hypertension caused by mutations in the beta subunit of the epithelial sodium channel. Cell 1994;79:407–14.
[57] Hansson JH, Nelson-Williams C, Suzuki H, Schild L, Shimkets R, Lu Y, et al. Hypertension caused by a truncated epithelial sodium channel gamma subunit: genetic heterogeneity of Liddle syndrome. Nat Genet 1995;11:76–82.
[58] Canessa CM, Schild L, Buell G, Thorens B, Gautschi I, Horisberger JD, et al. Amiloride-sensitive epithelial Na^+ channel is made of three homologous subunits. Nature 1994;367:463–7.
[59] Canessa CM, Merillat AM, Rossier BC. Membrane topology of the epithelial sodium channel in intact cells. Am J Physiol 1994;267:C1682–90.
[60] Hansson JH, Schild L, Lu Y, Wilson TA, Gautschi I, Shimkets R, et al. A *de novo* missense mutation of the beta subunit of the epithelial sodium channel causes hypertension and Liddle syndrome, identifying a proline-rich segment critical for regulation of channel activity. Proc Natl Acad Sci USA 1995;92:11495–9.
[61] Snyder PM, Price MP, McDonald FJ, Adams CM, Volk KA, Zeiher BG, et al. Mechanism by which Liddle's syndrome mutations increase activity of a human epithelial Na^+ channel. Cell 1995;83:969–78.
[62] Schild L, Canessa CM, Shimkets RA, Gautschi I, Lifton RP, Rossier BC. A mutation in the epithelial sodium channel causing Liddle disease increases channel activity in the *Xenopus laevis* oocyte expression system. Proc Natl Acad Sci USA 1995;92:5699–703.
[63] Firsov D, Schild L, Gautschi I, Merillat AM, Schneeberger E, Rossier BC. Cell surface expression of the epithelial Na channel and a mutant causing Liddle syndrome: a quantitative approach. Proc Natl Acad Sci USA 1996;93:15370–5.
[64] Staub O, Dho S, Henry P, Correa J, Ishikawa T, McGlade J, et al. WW domains of Nedd4 bind to the proline-rich PY motifs in the epithelial Na^+ channel deleted in Liddle's syndrome. EMBO J 1996;15:2371–80.
[65] Kamynina E, Debonneville C, Bens M, Vandewalle A, Staub O. A novel mouse Nedd4 protein suppresses the activity of the epithelial Na^+ channel. FASEB J 2001;15:204–14.
[66] Hiltunen TP, Hannila-Handelberg T, Petajaniemi N, Kantola I, Tikkanen I, Virtamo J, et al. Liddle's syndrome associated with a point mutation in the extracellular domain of the epithelial sodium channel gamma subunit. J Hypertens 2002;20:2383–90.
[67] Botero-Velez M, Curtis JJ, Warnock DG. Brief report: liddle's syndrome revisited – a disorder of sodium reabsorption in the distal tubule. N Engl J Med 1994;330:178–81.
[68] Pradervand S, Wang Q, Burnier M, Beermann F, Horisberger JD, Hummler E, et al. A mouse model for Liddle's syndrome. J Am Soc Nephrol 1999;10:2527–33.
[69] Paver WK, Pauline GJ. Hypertension and hyperpotassaemia without Renal disease in a young male. Med J Aust 1964;2:305–6.
[70] Farfel Z, Iaina A, Rosenthal T, Waks U, Shibolet S, Gafni J. Familial hyperpotassemia and hypertension accompanied by normal plasma aldosterone levels: possible hereditary cell membrane defect. Arch Intern Med 1978;138:1828–32.
[71] Farfel Z, Rosenthal T, Shibolet S, Iaina A, Gafni J. Familial hyperkalemia and hypertension. Harefuah 1976;90:468–70.
[72] Lee MR, Morgan DB. Familial hyperkalaemia responsive to benzothiadiazine diuretic. Lancet 1980;1:879.
[73] Schambelan M, Sebastian A, Rector Jr FC. Mineralocorticoid-resistant renal hyperkalemia without salt wasting (type II pseudohypoaldosteronism): role of increased renal chloride reabsorption. Kidney Int 1981;19:716–27.
[74] Wilson FH, Disse-Nicodeme S, Choate KA, Ishikawa K, Nelson-Williams C, Desitter I, et al. Human hypertension caused by mutations in WNK kinases. Science 2001;293:1107–12.
[75] Yang CL, Angell J, Mitchell R, Ellison DH. WNK kinases regulate thiazide-sensitive Na-Cl co-transport. J Clin Invest 2003;111:1039–45.
[76] Kahle KT, Wilson FH, Leng Q, Lalioti MD, O'Connell AD, Dong K, et al. WNK4 regulates the balance between renal NaCl reabsorption and K^+ secretion. Nat Genet 2003;35:372–6.
[77] Kahle KT, Macgregor GG, Wilson FH, Van Hoek AN, Brown D, Ardito T, et al. Paracellular Cl^- permeability is regulated by WNK4 kinase: insight into normal physiology and hypertension. Proc Natl Acad Sci USA 2004;101:14877–82.
[78] Yamauchi K, Rai T, Kobayashi K, Sohara E, Suzuki T, Itoh T, et al. Disease-causing mutant WNK4 increases paracellular chloride permeability and phosphorylates claudins. Proc Natl Acad Sci USA 2004;101:4690–4.
[79] Lalioti MD, Zhang J, Volkman HM, Kahle KT, Hoffmann KE, Toka HR, et al. Wnk4 controls blood pressure and potassium homeostasis via regulation of mass and activity of the distal convoluted tubule. Nat Genet 2006;38:1124–32.
[80] Kahle KT, Ring AM, Lifton RP. Molecular physiology of the WNK kinases. Annu Rev Physiol 2008;70:329–55.
[81] Hoorn EJ, Nelson JH, McCormick JA, Ellison DH. The WNK kinase network regulating sodium, potassium, and blood pressure. J Am Soc Nephrol 2011;22:605–14.
[82] Kahle KT, Wilson FH, Lifton RP. The Syndrome of Hypertension and Hyperkalemia (Pseudohypoaldosteronism Type II): WNK Kinases regulate the balance between renal salt reabsorption and potassium secretion. In: Lifton RP, Somlo S, Giebisch G, Seldin DW, editors. Genetic diseases of the kidney. Burlington, London, San Diego, New York: Elsevier; 2009. p. 313–29.
[83] Wilson FH, Kahle KT, Sabath E, Lalioti MD, Rapson AK, Hoover RS, et al. Molecular pathogenesis of inherited hypertension with hyperkalemia: the Na-Cl co-transporter is inhibited by wild-type but not mutant WNK4. Proc Natl Acad Sci USA 2003;100:680–4.
[84] Subramanya AR, Liu J, Ellison DH, Wade JB, Welling PA. WNK4 diverts the thiazide-sensitive NaCl co-transporter to the lysosome and stimulates AP-3 interaction. J Biol Chem 2009;284:18471–80.
[85] He G, Wang HR, Huang SK, Huang CL. Intersectin links WNK kinases to endocytosis of ROMK1. J Clin Invest 2007;117:1078–87.
[86] Ring AM, Cheng SX, Leng Q, Kahle KT, Rinehart J, Lalioti MD, et al. WNK4 regulates activity of the epithelial Na^+ channel *in vitro* and *in vivo*. Proc Natl Acad Sci USA 2007;104:4020–4.
[87] Ring AM, Leng Q, Rinehart J, Wilson FH, Kahle KT, Hebert SC, et al. An SGK1 site in WNK4 regulates Na^+ channel and K^+ channel activity and has implications for aldosterone signaling and K^+ homeostasis. Proc Natl Acad Sci USA 2007;104:4025–9.
[88] Lazrak A, Liu Z, Huang CL. Antagonistic regulation of ROMK by long and kidney-specific WNK1 isoforms. Proc Natl Acad Sci USA 2006;103:1615–20.
[89] Xu BE, Stippec S, Chu PY, Lazrak A, Li XJ, Lee BH, et al. WNK1 activates SGK1 to regulate the epithelial sodium channel. Proc Natl Acad Sci USA 2005;102:10315–20.
[90] Ohta A, Yang SS, Rai T, Chiga M, Sasaki S, Uchida S. Overexpression of human WNK1 increases paracellular chloride permeability and phosphorylation of claudin-4 in MDCKII cells. Biochem Biophys Res Commun 2006;349:804–8.
[91] San-Cristobal P, Pacheco-Alvarez D, Richardson C, Ring AM, Vazquez N, Rafiqi FH, et al. Angiotensin II signaling increases activity of the renal Na-Cl co-transporter through a WNK4-SPAK-dependent pathway. Proc Natl Acad Sci USA 2009;106:4384–9.

[92] McCormick JA, Ellison DH. The WNKs: atypical protein kinases with pleiotropic actions. Physiol Rev 2011;91:177–219.
[93] Castaneda-Bueno M, Cervantes-Perez LG, Vazquez N, Uribe N, Kantesaria S, Morla L, et al. Activation of the renal Na^+:Cl^- co-transporter by angiotensin II is a WNK4-dependent process. Proc Natl Acad Sci USA 2012;109:7929–34.
[94] Delaloy C, Elvira-Matelot E, Clemessy M, Zhou XO, Imbert-Teboul M, Houot AM, et al. Deletion of WNK1 first intron results in misregulation of both isoforms in renal and extrarenal tissues. Hypertension 2008;52:1149–54.
[95] Boyden LM, Choi M, Choate KA, Nelson-Williams CJ, Farhi A, Toka HR, et al. Mutations in kelch-like 3 and cullin 3 cause hypertension and electrolyte abnormalities. Nature 2012;482:98–102.
[96] Louis-Dit-Picard H, Barc J, Trujillano D, Miserey-Lenkei S, Bouatia-Naji N, Pylypenko O, et al. KLHL3 mutations cause familial hyperkalemic hypertension by impairing ion transport in the distal nephron. Nat Genet 2012;44:456–60.
[97] Peter M, Fawaz L, Drop SL, Visser HK, Sippell WG. Hereditary defect in biosynthesis of aldosterone: aldosterone synthase deficiency 1964-1997. J Clin Endocrinol Metab 1997;82:3525–8.
[98] Ulick S, Gautier E, Vetter KK, Markello JR, Yaffe S, Lowe CU. An aldosterone biosynthetic defect in a salt-losing disorder. J Clin Endocrinol Metab 1964;24:669–72.
[99] Pascoe L, Curnow KM, Slutsker L, Rosler A, White PC. Mutations in the human CYP11B2 (aldosterone synthase) gene causing corticosterone methyloxidase II deficiency. Proc Natl Acad Sci USA 1992;89:4996–5000.
[100] Mitsuuchi Y, Kawamoto T, Miyahara K, Ulick S, Morton DH, Naiki Y, et al. Congenitally defective aldosterone biosynthesis in humans: inactivation of the P-450C18 gene (CYP11B2) due to nucleotide deletion in CMO I deficient patients. Biochem Biophys Res Commun 1993;190:864–9.
[101] Kayes-Wandover KM, Tannin GM, Shulman D, Peled D, Jones KL, Karaviti L, et al. Congenital hyperreninemic hypoaldosteronism unlinked to the aldosterone synthase (CYP11B2) gene. J Clin Endocrinol Metab 2001;86:5379–82.
[102] White PC, New MI, Dupont B. HLA-linked congenital adrenal hyperplasia results from a defective gene encoding a cytochrome P-450 specific for steroid 21-hydroxylation. Proc Natl Acad Sci USA 1984;81:7505–9.
[103] Bongiovanni AM, Root AW. The adrenogenital syndrome. N Engl J Med 1963;268:1283–9 contd
[104] Higashi Y, Yoshioka H, Yamane M, Gotoh O, Fujii-Kuriyama Y. Complete nucleotide sequence of two steroid 21-hydroxylase genes tandemly arranged in human chromosome: a pseudogene and a genuine gene. Proc Natl Acad Sci USA 1986;83:2841–5.
[105] Speiser PW, Azziz R, Baskin LS, Ghizzoni L, Hensle TW, Merke DP, et al. Congenital adrenal hyperplasia due to steroid 21-hydroxylase deficiency: an Endocrine Society clinical practice guideline. J Clin Endocrinol Metab 2010;95:4133–60.
[106] Rheaume E, Simard J, Morel Y, Mebarki F, Zachmann M, Forest MG, et al. Congenital adrenal hyperplasia due to point mutations in the type II 3 beta-hydroxysteroid dehydrogenase gene. Nat Genet 1992;1:239–45.
[107] Lin D, Sugawara T, Strauss JF 3rd, Clark BJ, Stocco DM, Saenger P, et al. Role of steroidogenic acute regulatory protein in adrenal and gonadal steroidogenesis. Science 1995;267:1828–31.
[108] Cheek DB, Perry JW. A salt wasting syndrome in infancy. Arch Dis Child 1958;33:252–6.
[109] Hanukoglu A, Bistritzer T, Rakover Y, Mandelberg A. Pseudohypoaldosteronism with increased sweat and saliva electrolyte values and frequent lower respiratory tract infections mimicking cystic fibrosis. J Pediatr 1994;125:752–5.
[110] Kerem E, Bistritzer T, Hanukoglu A, Hofmann T, Zhou Z, Bennett W, et al. Pulmonary epithelial sodium-channel dysfunction and excess airway liquid in pseudohypoaldosteronism. N Engl J Med 1999;341:156–62.
[111] Chang SS, Grunder S, Hanukoglu A, Rosler A, Mathew PM, Hanukoglu I, et al. Mutations in subunits of the epithelial sodium channel cause salt wasting with hyperkalaemic acidosis, pseudohypoaldosteronism type 1. Nat Genet 1996;12:248–53.
[112] Strautnieks SS, Thompson RJ, Gardiner RM, Chung E. A novel splice-site mutation in the gamma subunit of the epithelial sodium channel gene in three pseudohypoaldosteronism type 1 families. Nat Genet 1996;13:248–50.
[113] McDonald FJ, Yang B, Hrstka RF, Drummond HA, Tarr DE, McCray Jr PB, et al. Disruption of the beta subunit of the epithelial Na^+ channel in mice: hyperkalemia and neonatal death associated with a pseudohypoaldosteronism phenotype. Proc Natl Acad Sci USA 1999;96:1727–31.
[114] Barker PM, Nguyen MS, Gatzy JT, Grubb B, Norman H, Hummler E, et al. Role of gammaENaC subunit in lung liquid clearance and electrolyte balance in newborn mice. Insights into perinatal adaptation and pseudohypoaldosteronism. J Clin Invest 1998;102:1634–40.
[115] Hummler E, Barker P, Talbot C, Wang Q, Verdumo C, Grubb B, et al. A mouse model for the renal salt-wasting syndrome pseudohypoaldosteronism. Proc Natl Acad Sci USA 1997;94:11710–5.
[116] Hummler E, Barker P, Gatzy J, Beermann F, Verdumo C, Schmidt A, et al. Early death due to defective neonatal lung liquid clearance in alpha-ENaC-deficient mice. Nat Genet 1996;12:325–8.
[117] Huppmann S, Lankes E, Schnabel D, Buhrer C. Unimpaired postnatal respiratory adaptation in a preterm human infant with a homozygous ENaC-alpha unit loss-of-function mutation. J Perinatol 2011;31:802–3.
[118] Geller DS, Rodriguez-Soriano J, Vallo Boado A, Schifter S, Bayer M, Chang SS, et al. Mutations in the mineralocorticoid receptor gene cause autosomal dominant pseudohypoaldosteronism type I. Nat Genet 1998;19:279–81.
[119] Geller DS, Zhang J, Zennaro MC, Vallo-Boado A, Rodriguez-Soriano J, Furu L, et al. Autosomal dominant pseudohypoaldosteronism type 1: mechanisms, evidence for neonatal lethality, and phenotypic expression in adults. J Am Soc Nephrol 2006;17:1429–36.
[120] Hubert EL, Teissier R, Fernandes-Rosa FL, Fay M, Rafestin-Oblin ME, Jeunemaitre X, et al. Mineralocorticoid receptor mutations and a severe recessive pseudohypoaldosteronism type 1. J Am Soc Nephrol 2011;22:1997–2003.
[121] Berger S, Bleich M, Schmid W, Cole TJ, Peters J, Watanabe H, et al. Mineralocorticoid receptor knockout mice: pathophysiology of Na^+ metabolism. Proc Natl Acad Sci USA 1998;95:9424–9.
[122] Bleich M, Warth R, Schmidt-Hieber M, Schulz-Baldes A, Hasselblatt P, Fisch D, et al. Rescue of the mineralocorticoid receptor knock-out mouse. Pflugers Arch 1999;438:245–54.
[123] Bartter FC, Pronove P, Gill Jr JR, Maccardle RC. Hyperplasia of the juxtaglomerular complex with hyperaldosteronism and hypokalemic alkalosis. A new syndrome. Am J Med 1962;33:811–28.
[124] Rodrigues Pereira R, Hasaart T. Hydramnios and observations in Bartter's syndrome. Acta Obstet Gynecol Scand 1982;61:477–8.
[125] Simopoulos AP. Growth characteristics in patients with Bartter's syndrome. Nephron 1979;23:130–5.

[126] Matsumoto J, Han BK, Restrepo de Rovetto C, Welch TR. Hypercalciuric Bartter syndrome: resolution of nephrocalcinosis with indomethacin. AJR Am J Roentgenol 1989;152:1251–3.
[127] Landau D, Shalev H, Ohaly M, Carmi R. Infantile variant of Bartter syndrome and sensorineural deafness: a new autosomal recessive disorder. Am J Med Genet 1995;59:454–9.
[128] Chaimovitz C, Levi J, Better OS, Oslander L, Benderli A. Studies on the site of renal salt loss in a patient with Bartter's syndrome. Pediatr Res 1973;7:89–94.
[129] Fichman MP, Telfer N, Zia P, Speckart P, Golub M, Rude R. Role of prostaglandins in the pathogenesis of Bartter's syndrome. Am J Med 1976;60:785–97.
[130] Verberckmoes R, van Damme BB, Clement J, Amery A, Michielsen P. Bartter's syndrome with hyperplasia of renomedullary cells: successful treatment with indomethacin. Kidney Int 1976;9:302–7.
[131] Gill Jr JR, Frolich JC, Bowden RE, Taylor AA, Keiser HR, Seyberth HW, et al. Bartter's syndrome: a disorder characterized by high urinary prostaglandins and a dependence of hyperreninemia on prostaglandin synthesis. Am J Med 1976;61:43–51.
[132] Simon DB, Karet FE, Hamdan JM, DiPietro A, Sanjad SA, Lifton RP. Bartter's syndrome, hypokalaemic alkalosis with hypercalciuria, is caused by mutations in the Na-K-2Cl co-transporter NKCC2. Nat Genet 1996;13:183–8.
[133] Takahashi N, Chernavvsky DR, Gomez RA, Igarashi P, Gitelman HJ, Smithies O. Uncompensated polyuria in a mouse model of Bartter's syndrome. Proc Natl Acad Sci USA 2000;97:5434–9.
[134] Simon DB, Karet FE, Rodriguez-Soriano J, Hamdan JH, DiPietro A, Trachtman H, et al. Genetic heterogeneity of Bartter's syndrome revealed by mutations in the K^+ channel, ROMK. Nat Genet 1996;14:152–6.
[135] Hebert SC. An ATP-regulated, inwardly rectifying potassium channel from rat kidney (ROMK). Kidney Int 1995;48:1010–6.
[136] Giebisch G. Renal potassium channels: an overview. Kidney Int 1995;48:1004–9.
[137] Peters M, Jeck N, Reinalter S, Leonhardt A, Tonshoff B, Klaus GG, et al. Clinical presentation of genetically defined patients with hypokalemic salt-losing tubulopathies. Am J Med 2002;112:183–90.
[138] Finer G, Shalev H, Birk OS, Galron D, Jeck N, Sinai-Treiman L, et al. Transient neonatal hyperkalemia in the antenatal (ROMK defective) Bartter syndrome. J Pediatr 2003;142:318–23.
[139] Satlin LM. Postnatal maturation of potassium transport in rabbit cortical collecting duct. Am J Physiol 1994;266:F57–65.
[140] Satlin LM, Palmer LG. Apical K^+ conductance in maturing rabbit principal cell. Am J Physiol 1997;272:F397–404.
[141] Lorenz JN, Baird NR, Judd LM, Noonan WT, Andringa A, Doetschman T, et al. Impaired renal NaCl absorption in mice lacking the ROMK potassium channel, a model for type II Bartter's syndrome. J Biol Chem 2002;277:37871–80.
[142] Simon DB, Bindra RS, Mansfield TA, Nelson-Williams C, Mendonca E, Stone R, et al. Mutations in the chloride channel gene, CLCNKB, cause Bartter's syndrome type III. Nat Genet 1997;17:171–8.
[143] Vandewalle A, Cluzeaud F, Bens M, Kieferle S, Steinmeyer K, Jentsch TJ. Localization and induction by dehydration of ClC-K chloride channels in the rat kidney. Am J Physiol 1997;272:F678–88.
[144] Adachi S, Uchida S, Ito H, Hata M, Hiroe M, Marumo F, et al. Two isoforms of a chloride channel predominantly expressed in thick ascending limb of Henle's loop and collecting ducts of rat kidney. J Biol Chem 1994;269:17677–83.
[145] Kieferle S, Fong P, Bens M, Vandewalle A, Jentsch TJ. Two highly homologous members of the ClC chloride channel family in both rat and human kidney. Proc Natl Acad Sci USA 1994;91:6943–7.
[146] Jeck N, Konrad M, Peters M, Weber S, Bonzel KE, Seyberth HW. Mutations in the chloride channel gene, CLCNKB, leading to a mixed Bartter–Gitelman phenotype. Pediatr Res 2000;48:754–8.
[147] Brennan TM, Landau D, Shalev H, Lamb F, Schutte BC, Walder RY, et al. Linkage of infantile Bartter syndrome with sensorineural deafness to chromosome. Am J Hum Genet 1998;62:355–61.
[148] Birkenhager R, Otto E, Schurmann MJ, Vollmer M, Ruf EM, Maier-Lutz I, et al. Mutation of BSND causes Bartter syndrome with sensorineural deafness and kidney failure. Nat Genet 2001;29:310–4.
[149] Estevez R, Boettger T, Stein V, Birkenhager R, Otto E, Hildebrandt F, et al. Barttin is a Cl^- channel beta-subunit crucial for renal Cl- reabsorption and inner ear K^+ secretion. Nature 2001;414:558–61.
[150] Schlingmann KP, Konrad M, Jeck N, Waldegger P, Reinalter SC, Holder M, et al. Salt wasting and deafness resulting from mutations in two chloride channels. N Engl J Med 2004;350:1314–9.
[151] Nozu K, Inagaki T, Fu XJ, Nozu Y, Kaito H, Kanda K, et al. Molecular analysis of digenic inheritance in Bartter syndrome with sensorineural deafness. J Med Genet 2008;45:182–6.
[152] Matsumura Y, Uchida S, Kondo Y, Miyazaki H, Ko SB, Hayama A, et al. Overt nephrogenic diabetes insipidus in mice lacking the CLC-K1 chloride channel. Nat Genet 1999;21:95–8.
[153] Rickheit G, Maier H, Strenzke N, Andreescu CE, De Zeeuw CI, Muenscher A, et al. Endocochlear potential depends on Cl^- channels: mechanism underlying deafness in Bartter syndrome IV. EMBO J 2008;27:2907–17.
[154] Pearce SH, Williamson C, Kifor O, Bai M, Coulthard MG, Davies M, et al. A familial syndrome of hypocalcemia with hypercalciuria due to mutations in the calcium-sensing receptor. N Engl J Med 1996;335:1115–22.
[155] Vargas-Poussou R, Huang C, Hulin P, Houillier P, Jeunemaitre X, Paillard M, et al. Functional characterization of a calcium-sensing receptor mutation in severe autosomal dominant hypocalcemia with a Bartter-like syndrome. J Am Soc Nephrol 2002;13:2259–66.
[156] Watanabe S, Fukumoto S, Chang H, Takeuchi Y, Hasegawa Y, Okazaki R, et al. Association between activating mutations of calcium-sensing receptor and Bartter's syndrome. Lancet 2002;360:692–4.
[157] Hebert SC, Brown EM, Harris HW. Role of the $Ca^{(2+)}$-sensing receptor in divalent mineral ion homeostasis. J Exp Biol 1997;200:295–302.
[158] Seyberth HW, Koniger SJ, Rascher W, Kuhl PG, Schweer H. Role of prostaglandins in hyperprostaglandin E syndrome and in selected renal tubular disorders. Pediatr Nephrol 1987;1:491–7.
[159] Rodriguez-Soriano J, Vallo A, Perez de Nanclares G, Bilbao JR, Castano L. A founder mutation in the CLCNKB gene causes bartter syndrome type III in Spain. Pediatr Nephrol 2005;20:891–6.
[160] Reinalter SC, Jeck N, Brochhausen C, Watzer B, Nusing RM, Seyberth HW, et al. Role of cyclooxygenase-2 in hyperprostaglandin E syndrome/antenatal Bartter syndrome. Kidney Int 2002;62:253–60.
[161] Chaudhuri A, Salvatierra Jr O, Alexander SR, Sarwal MM. Option of pre-emptive nephrectomy and renal transplantation for Bartter's syndrome. Pediatr Transplant 2006;10:266–70.

[162] Gitelman HJ, Graham JB, Welt LG. A new familial disorder characterized by hypokalemia and hypomagnesemia. Trans Assoc Am Physicians 1966;79:221–35.
[163] Bettinelli A, Bianchetti MG, Girardin E, Caringella A, Cecconi M, Appiani AC, et al. Use of calcium excretion values to distinguish two forms of primary renal tubular hypokalemic alkalosis: bartter and Gitelman syndromes. J Pediatr 1992;120:38–43.
[164] Sutton RA, Mavichak V, Halabe A, Wilkins GE. Bartter's syndrome: evidence suggesting a distal tubular defect in a hypocalciuric variant of the syndrome. Miner Electrolyte Metab 1992;18:43–51.
[165] Gamba G, Miyanoshita A, Lombardi M, Lytton J, Lee WS, Hediger MA, et al. Molecular cloning, primary structure, and characterization of two members of the mammalian electroneutral sodium-(potassium)-chloride co-transporter family expressed in kidney. J Biol Chem 1994;269:17713–22.
[166] Gamba G, Saltzberg SN, Lombardi M, Miyanoshita A, Lytton J, Hediger MA, et al. Primary structure and functional expression of a cDNA encoding the thiazide-sensitive, electroneutral sodium-chloride co-transporter. Proc Natl Acad Sci USA 1993;90:2749–53.
[167] Simon DB, Nelson-Williams C, Bia MJ, Ellison D, Karet FE, Molina AM, et al. Gitelman's variant of Bartter's syndrome, inherited hypokalaemic alkalosis, is caused by mutations in the thiazide-sensitive Na-Cl co-transporter. Nat Genet 1996;12:24–30.
[168] Ji W, Foo JN, O'Roak BJ, Zhao H, Larson MG, Simon DB, et al. Rare independent mutations in renal salt handling genes contribute to blood pressure variation. Nat Genet 2008;40:592–9.
[169] Cruz DN, Shaer AJ, Bia MJ, Lifton RP, Simon DB. Gitelman's syndrome revisited: an evaluation of symptoms and health-related quality of life. Kidney Int 2001;59:710–7.
[170] Nijenhuis T, Vallon V, van der Kemp AW, Loffing J, Hoenderop JG, Bindels RJ. Enhanced passive Ca^{2+} reabsorption and reduced Mg^{2+} channel abundance explains thiazide-induced hypocalciuria and hypomagnesemia. J Clin Invest 2005;115:1651–8.
[171] Schlingmann KP, Weber S, Peters M, Niemann Nejsum L, Vitzthum H, Klingel K, et al. Hypomagnesemia with secondary hypocalcemia is caused by mutations in TRPM6, a new member of the TRPM gene family. Nat Genet 2002;31:166–70.
[172] Schultheis PJ, Lorenz JN, Meneton P, Nieman ML, Riddle TM, Flagella M, et al. Phenotype resembling Gitelman's syndrome in mice lacking the apical Na^+-Cl^- co-transporter of the distal convoluted tubule. J Biol Chem 1998;273:29150–5.
[173] Loffing J, Loffing-Cueni D, Hegyi I, Kaplan MR, Hebert SC, Le Hir M, et al. Thiazide treatment of rats provokes apoptosis in distal tubule cells. Kidney Int 1996;50:1180–90.
[174] Morris RG, Hoorn EJ, Knepper MA. Hypokalemia in a mouse model of Gitelman's syndrome. Am J Physiol Renal Physiol 2006;290:F1416–20.
[175] Scholl UI, Choi M, Liu T, Ramaekers VT, Hausler MG, Grimmer J, et al. Seizures, sensorineural deafness, ataxia, mental retardation, and electrolyte imbalance (SeSAME syndrome) caused by mutations in KCNJ10. Proc Natl Acad Sci USA 2009;106:5842–7.
[176] Bockenhauer D, Feather S, Stanescu HC, Bandulik S, Zdebik AA, Reichold M, et al. Epilepsy, ataxia, sensorineural deafness, tubulopathy, and KCNJ10 mutations. N Engl J Med 2009;360:1960–70.
[177] Djukic B, Casper KB, Philpot BD, Chin LS, McCarthy KD. Conditional knock-out of Kir4.1 leads to glial membrane depolarization, inhibition of potassium and glutamate uptake, and enhanced short-term synaptic potentiation. J Neurosci 2007;27:11354–65.
[178] Kofuji P, Ceelen P, Zahs KR, Surbeck LW, Lester HA, Newman EA. Genetic inactivation of an inwardly rectifying potassium channel (Kir4.1 subunit) in mice: phenotypic impact in retina. J Neurosci 2000;20:5733–40.
[179] Neusch C, Rozengurt N, Jacobs RE, Lester HA, Kofuji P. Kir4.1 potassium channel subunit is crucial for oligodendrocyte development and *in vivo* myelination. J Neurosci 2001;21:5429–38.
[180] Olsen ML, Sontheimer H. Functional implications for Kir4.1 channels in glial biology: from K^+ buffering to cell differentiation. J Neurochem 2008;107:589–601.
[181] Chever O, Djukic B, McCarthy KD, Amzica F. Implication of Kir4.1 channel in excess potassium clearance: an *in vivo* study on anesthetized glial-conditional Kir4.1 knock-out mice. J Neurosci 2010;30:15769–77.
[182] Rozengurt N, Lopez I, Chiu CS, Kofuji P, Lester HA, Neusch C. Time course of inner ear degeneration and deafness in mice lacking the Kir4.1 potassium channel subunit. Hear Res 2003;177:71–80.
[183] Koefoed-Johnsen V, Ussing HH. The nature of the frog skin potential. Acta Physiol Scand 1958;42:298–308.
[184] Reichold M, Zdebik AA, Lieberer E, Rapedius M, Schmidt K, Bandulik S, et al. KCNJ10 gene mutations causing EAST syndrome (epilepsy, ataxia, sensorineural deafness, and tubulopathy) disrupt channel function. Proc Natl Acad Sci USA 2010;107:14490–5.
[185] Freudenthal B, Kulaveerasingam D, Lingappa L, Shah MA, Brueton L, Wassmer E, et al. KCNJ10 mutations disrupt function in patients with EAST syndrome. Nephron Physiol 2011;119:40–8.
[186] Thompson DA, Feather S, Stanescu HC, Freudenthal B, Zdebik AA, Warth R, et al. Altered electroretinograms in patients with KCNJ10 mutations and EAST syndrome. J Physiol 2011;589:1681–9.
[187] Kearney PM, Whelton M, Reynolds K, Muntner P, Whelton PK, He J. Global burden of hypertension: analysis of worldwide data. Lancet 2005;365:217–23.
[188] WHO. Global health risks - mortality and burden of disease attributable to selected major risks. Geneva: WHO; 2009.
[189] Chobanian AV, Bakris GL, Black HR, Cushman WC, Green LA, Izzo Jr JL, et al. The seventh report of the joint national committee on prevention, detection, evaluation, and treatment of high blood pressure: the jnc 7 report. Jama 2003;289:2560–72.
[190] Feinleib M, Garrison RJ, Fabsitz R, Christian JC, Hrubec Z, Borhani NO, et al. The NHLBI twin study of cardiovascular disease risk factors: methodology and summary of results. Am J Epidemiol 1977;106:284–5.
[191] Longini Jr IM, Higgins MW, Hinton PC, Moll PP, Keller JB. Environmental and genetic sources of familial aggregation of blood pressure in Tecumseh, Michigan. Am J Epidemiol 1984;120:131–44.
[192] Kupper N, Willemsen G, Riese H, Posthuma D, Boomsma DI, de Geus EJ. Heritability of daytime ambulatory blood pressure in an extended twin design. Hypertension 2005;45:80–5.
[193] Newton-Cheh C, Johnson T, Gateva V, Tobin MD, Bochud M, Coin L, et al. Genome-wide association study identifies eight loci associated with blood pressure. Nat Genet 2009;41:666–76.
[194] Levy D, Ehret GB, Rice K, Verwoert GC, Launer LJ, Dehghan A, et al. Genome-wide association study of blood pressure and hypertension. Nat Genet 2009;41:677–87.
[195] Tennessen JA, Bigham AW, O'Connor TD, Fu W, Kenny EE, Gravel S, et al. Evolution and functional impact of rare coding variation from deep sequencing of human exomes. Science 2012;337:64–9.
[196] Sacks FM, Svetkey LP, Vollmer WM, Appel LJ, Bray GA, Harsha D, et al. Effects on blood pressure of reduced dietary

sodium and the dietary approaches to stop hypertension (dash) diet. Dash-sodium collaborative research group. N Engl J Med 2001;344:3–10.

[197] Cappuccio FP, MacGregor GA. Does potassium supplementation lower blood pressure? A meta-analysis of published trials. J Hypertens 1991;9:465–73.

[198] Whelton PK, He J, Cutler JA, Brancati FL, Appel LJ, Follmann D, et al. Effects of oral potassium on blood pressure. Meta-analysis of randomized controlled clinical trials. Jama 1997;277:1624–32.

[199] Geleijnse JM, Kok FJ, Grobbee DE. Blood pressure response to changes in sodium and potassium intake: a metaregression analysis of randomised trials. J Hum Hypertens 2003;17:471–80.

[200] He FJ, Marciniak M, Visagie E, Markandu ND, Anand V, Dalton RN, et al. Effect of modest salt reduction on blood pressure, urinary albumin, and pulse wave velocity in white, black, and Asian mild hypertensives. Hypertension 2009;54:482–8.

[201] Bibbins-Domingo K, Chertow GM, Coxson PG, Moran A, Lightwood JM, Pletcher MJ, et al. Projected effect of dietary salt reductions on future cardiovascular disease. N Engl J Med 2010;362:590–9.

[202] McGuire S. Institute of Medicine. Strategies to reduce sodium intake in the United States. Adv Nutr, 1. Washington, DC: The National Academies Press 2010;49–50.

[203] Kayikcioglu M, Tumuklu M, Ozkahya M, Ozdogan O, Asci G, Duman S, et al. The benefit of salt restriction in the treatment of end-stage renal disease by haemodialysis. Nephrol Dial Transplant 2009;24:956–62.

[204] Chazot C, Charra B, Laurent G, Didier C, Vo Van C, Terrat JC, et al. Interdialysis blood pressure control by long haemodialysis sessions. Nephrol Dial Transplant 1995;10:831–7.

[205] Culleton BF, Walsh M, Klarenbach SW, Mortis G, Scott-Douglas N, Quinn RR, et al. Effect of frequent nocturnal hemodialysis vs conventional hemodialysis on left ventricular mass and quality of life: a randomized controlled trial. Jama 2007;298:1291–9.

[206] Cruz DN, Simon DB, Nelson-Williams C, Farhi A, Finberg K, Burleson L, et al. Mutations in the Na-Cl co-transporter reduce blood pressure in humans. Hypertension 2001;37:1458–64.

CHAPTER

37

Natriuretic Hormones

David L. Vesely

University of South Florida Cardiac Hormone Center, and James A. Haley Veterans Medical Center, Tampa, FL, USA

INTRODUCTION

Cardiac, Renal, Intestinal, and Adrenal Hormones which Enhance Sodium Excretion

Hormones which enhance sodium excretion, i.e., natriuretic peptide hormones, are very important for the maintenance of extracellu/lar fluid volume within a narrow range, despite wide variations in dietary sodium intake. This regulation occurs through a complex interplay of the antinatriuretic renin–angiotensin–aldosterone system and the antinatriuretic renal sympathetic system, which help to conserve sodium when sodium intake is low, and the natriuretic hormones, which enhance sodium excretion whenever sodium excess occurs. Several of the cardiac natriuretic hormones (Figure 37.1) directly inhibit aldosterone secretion[14,46,124,195,214,354,375] and/or indirectly inhibit aldosterone secretion by inhibiting renin release from the kidney to help regulate extracellular fluid volume.[39,104,149,197,214,404] This chapter will concentrate on the natriuretic hormones (cardiac, intestinal, renal, and adrenal) in normal renal physiology, their synthesis, secretion, biologic effects, pathophysiological changes with hypertension and renal diseases, and potential for treating diseases such as acute renal failure.

HISTORY OF ATRIAL (CARDIAC) NATRIURETIC PEPTIDE HORMONES

In 1628, Harvey[147] first correctly described the heart as a pump or a muscular organ that contracts in rhythm, pushing blood first to the lungs for oxygenation and then through the peripheral vascular system, bringing oxygen and nutrients to every cell in the body. It was another 350 years before the heart was established as an endocrine gland with its main physiologic targets being the kidney and vasculature.[366] The history of experimentation leading to defining the cardiac natriuretic peptide hormonal system (the first of the natriuretic hormonal systems) has followed two pathways: anatomical and physiological.

History of Cardiac Hormones: Anatomical Studies

Atrial Granule Structure

Shortly before Henry and colleagues[150] reported their observation that balloon distention of atria caused a diuresis, in 1955 Kisch,[188] utilizing electron microscopy, described dense granules that were located in the atria, but not in the ventricles of mammals. The presence of these dense granules in the cytoplasm of atrial cardiac myocytes, but not in the ventricles of the heart, was rapidly confirmed by others utilizing electron microscopy.[28,156,268] Jamieson and Palade[164] demonstrated that such granules are present in cardiocytes of the atria of all mammals, including humans, and were the first, in 1964, to suggest that these granules resemble other granules that release polypeptide hormones.[164] These granules are usually adjacent to one or occasionally both poles of the nucleus, and are interspersed among the voluminous elements of the Golgi complex and within close proximity to the mitochondria,[164] and are influenced by salt intake reduction.[218,269]

Ultrastructural cytochemistry has shown that these granules consist of proteins.[151] They incorporate both [^{3}H]-leucine and [^{3}H]-fructose in a pattern identical to other endocrine-secreting cells, with protein synthesis

Seldin and Giebisch's The Kidney, Fifth Edition.
DOI: http://dx.doi.org/10.1016/B978-0-12-381462-3.00037-9

© 2013 Elsevier Inc. All rights reserved.

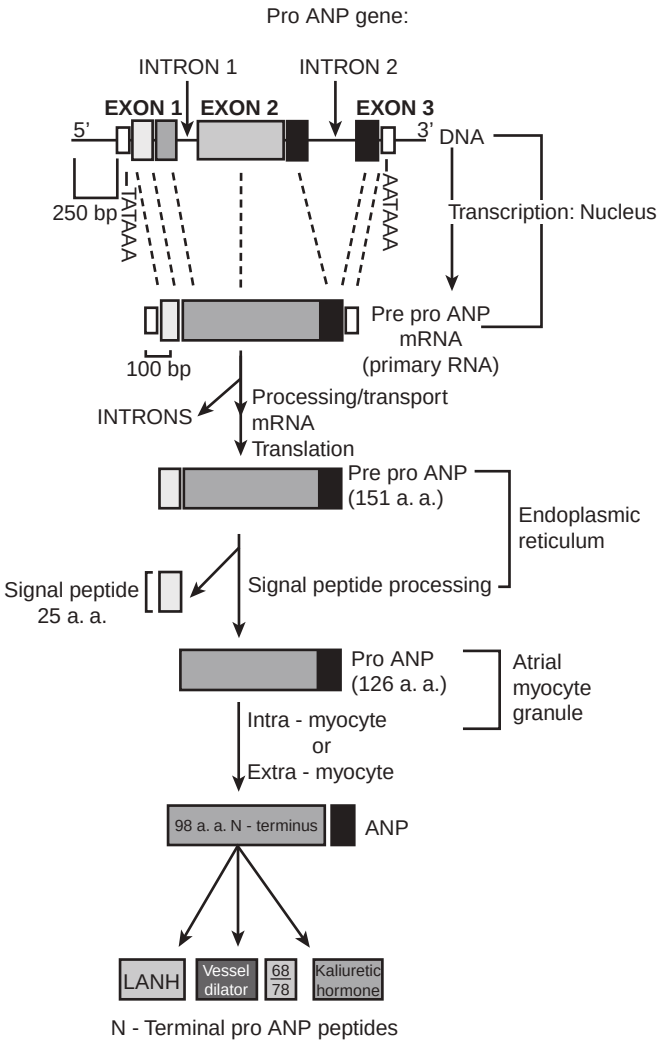

FIGURE 37.1 **Structure of the atrial natriuretic peptide prohormone (proANP) gene.** Four peptide hormones (e.g., atrial natriuretic peptide (ANP), long-acting natriuretic peptide (LANP), vessel dilator, and kaliuretic peptide) are synthesized by this gene. Each of these peptide hormones have biological effects, such as natriuresis and diuresis, mediated via the kidney[24,72,73,124,126,201,329,350,376,437] (a.a.: amino acids; LANH: long-acting natriuretic hormone (a different nomenclature for LANP). *(With permission, from ref. [366].)*

occurring in the Golgi complex.[155] The ultrastructural features of the specific granules of different species are similar, in that they display an amorphous core and a limiting membrane, and generally measure 300–500 nm.[68,70,164] The size and number of these granules vary among species, and generally are inversely related to size. Thus, atrial myocytes from large animals such as cows contain fewer and smaller granules than myocytes from small rodents such as rats.[70] In the rat there are up to 600 spherical, electron-opaque granules per cell.[70,164]

Atrial Extracts and Natriuresis

In 1922, Banting and Best[20] utilized what is now considered a classic endocrinological technique in their discovery of insulin. They pulverized pancreas with buffer, filtered the crude tissue extract, and found that it produced hypoglycemia in an experimental dog.[20] In 1981, deBold and colleagues,[69] utilizing a similar approach, infused the supernatants of extracts of rat cardiac atria and rat ventricles into other rats, and found that the rat atria extracts, but not the extracts from the rat ventricles, caused dramatic diuresis and natriuresis, with urine flow increasing 10-fold, and sodium and chloride excretion increasing 30-fold. This simple but elegant experiment led to the discovery of atrial peptides that have the most potent endogenous natriuretic activity of any substance yet described.[349] Atrial natriuretic peptide(s) isolated from these atrial extracts has been found to be a two-fold stronger natriuretic producing agent than furosemide (Lasix®, which is one of the most potent natriuretic producing drugs utilized in clinical medicine today.)[349] Other investigators quickly confirmed this natriuretic action,[110] as well as the ability of atrial extracts to cause vasodilation.[63,419] It was rapidly demonstrated that these effects were at least partially due to a peptide(s).[70,349] Further investigation revealed that the atrial extracts have significantly more natriuresis and diuresis than pure synthetic ANP, suggesting that other peptide hormones with natriuretic properties were in these atrial extracts.[75,123,140]

History of Cardiac Hormones: Physiological Studies

Association of Heart and Renal Function

In 1847, Harthshorne suggested that the heart possessed volume receptors capable of sensing the "fullness of bloodstream" induced by whole-body immersion, which he clearly recognized had a diuretic effect.[146] This observation received little further notice until 1935, when John Peters of Yale University made the same proposal that "the fullness of the bloodstream may provoke the diuretic response on the part of the kidney".[262] This concept then received experimental verification when it was shown that expansion of blood volume increases urine flow.[29,118,263,264,441] Peters also suggested that the diuretic response was secondary to the ability of the heart, or something very near the heart, to "sense the fullness of the bloodstream".[262]

Balloon Distention of Atria

Experimental evidence of an association between cardiac atria and renal function was provided in

1956 by Henry et al.,[150] who observed that balloon distention of the left atrium in anesthetized dogs was associated with an increase in urine flow. Because the renal response to left atrial distention could not be elicited after the cervical vagi had been cooled to block nerve conduction, Henry and colleagues[150,151] concluded that stretch receptors in the left atrium must be present. This finding was later extended to the right atrium.[117] In their reports, Henry et al.[150,151] noted the diuresis, but did not investigate whether it was associated with increased salt excretion (natriuresis). It is well-established now, however, that balloon distention of the cardiac atria causes natriuresis as well as diuresis.[121,123,213] Evidence that animals with denervated hearts or denervated kidneys may also respond to an atrial pressure increase to produce diuresis[209] suggests a hormonal pathway between the heart and the kidney. At least part of this hormonal pathway involves hormones made in the heart.

The "Third Factor"

With respect to a possible hormonal agent causing natriuresis and diuresis, de Wardener and colleagues[73] demonstrated in 1961 that saline infusion produced an increase in urine flow and sodium excretion in anesthetized dogs independent of changes in glomerular filtration rate (GFR), which was decreased, and even in the presence of high circulating levels of aldosterone. These experiments gave rise to the popular concept of an unidentified "third factor," a term coined by Levinsky and Lalone.[206] The other two factors were aldosterone and GFR-affected sodium excretion. The search for this third factor soon focused on a possible hormonal mediator that came to be known as "natriuretic hormone." Although this mediator (or mediators) from plasma or urine of volume-expanded humans or animals that causes natriuresis when injected into animals[37] was never chemically identified, the evidence points toward this third factor having a peptide structure(s), because acid hydrolysis characteristically inactivated this substance.[149] The "third factor" that was sought for decades now appears to be a family of peptide hormones termed "atrial natriuretic peptides" (ANPs), so named since they are found in their highest concentrations in the atria of the heart, have natriuretic properties, and are peptides. The third factor(s) also has the ability to inhibit Na^+,K^+-ATPase in the kidney.[149] Some of the natriuretic peptide hormones synthesized in the heart fill all of the criteria of being the "third factor(s)." Atrial natriuretic peptide (ANP) does not inhibit Na^+,K^+-ATPase,[51,139,270] so it would not fulfill the criteria of being the "third factor." Three of the other peptide hormones synthesized by the ANP prohormone gene (Figure 37.1), namely long-acting natriuretic peptide, vessel dilator, and kaliuretic peptide, however, do inhibit renal Na^+, K^+-ATPase[51,139] and fill all of the criteria of being the "third factor(s)" that researchers have sought since the 1960s.

Family of Cardiac Natriuretic Peptide Hormones

At first it was thought that a single peptide was found in atrial extracts, but further investigation revealed a sophisticated endocrine system in the atria (and other tissues including the kidney) in which the atrial natriuretic peptide (ANP) prohormone gene synthesized four peptide hormones[23,368,369,370] (Figure 37.1), and two other genes were present, as reviewed below. The three other peptide hormones synthesized by the ANP prohormone gene – long-acting natriuretic peptide, vessel dilator, and kaliuretic peptide – were first demonstrated to have biologic effects in 1987,[389] and one of their mechanisms of action, via intracellular messenger cyclic GMP, was also elucidated in 1987.[373] Fifth and sixth members of the natriuretic peptide family were identified in 1988, i.e., brain natriuretic peptide (BNP) isolated from a porcine brain cDNA library,[332] and urodilatin, a peptide formed by differential processing of ANP prohormone in the kidney, which was first found in opossum urine.[205,240,315] A seventh member of this family was identified in 1990 in brain tissue and termed C-type natriuretic peptide (CNP).[333] A possible eighth member, DNP, was first described in 1992 from the venom of the green mamba snake.[316]

FAMILY OF CARDIAC NATRIURETIC HORMONES: SYNTHESIS OF THREE PROHORMONES

This family of cardiac peptide hormones has been designated atrial natriuretic peptides (ANPs), also known as atrial natriuretic hormones (ANHs). These peptide hormones are synthesized by three different genes,[94,116,205,216,240,290,426] and then stored as three different prohormones (126 amino acid (a.a.) ANP, 108 a.a. BNP, and 103 a.a. CNP prohormones).[205,366] In healthy adults, the main site of ANP prohormone synthesis is the atrial myocyte with its mRNA being 30–50-fold higher in the atria than that observed in the ventricle,[114] but it is also synthesized in a variety of other tissues including the kidney.[114,393] The different organs that synthesize the ANPs in the approximate order that they contribute to the synthesis of ANPs are listed in Table 37.1.

TABLE 37.1 Site of Synthesis, Molecular Weight, and Hemodynamic and Natriuretic Properties of Natriuretic Peptides

	Molecular Weight (kDa)	Site of Synthesis	MAP	Diuresis	Natriuresis
LANP	3508	Atria, ventricle, GI, lung, kidney, brain, adrenal	↓	↑	↑
Vessel dilator	3878	Atria, ventricle, GI, lung, kidney, brain, adrenal	↓	↑	↑
Kaliuretic peptide	2184	Atria, ventricle, GI, lung, brain, adrenal	↓	↑	–[a]
ANP	3078	Atria, ventricle, GI, lung, kidney, brain, adrenal	↓	↑	↑
Urodilatin	3503	Kidney	↓	↑	↑
BNP	3462	Atria, ventricle, brain, adrenal	↓	↑	↑
CNP	2198	Endothelium, CNS	↓	↑	–
DNP	4191	Atria, ventricle	↓	↑	↑
Adrenomedullin	6029	Adrenal, kidney	↓	↑	↑

[a]*No significant effect.*
Note: The sites of synthesis are listed in approximate order in which they contribute to synthesis.
ANP: atrial natriuretic peptide; BNP: brain natriuretic peptide; CNP: C-type natriuretic peptide; CNS: central nervous system; DNP: *Dendroaspis* natriuretic peptide; GI:, gastrointestinal tract; ANP: long-acting natriuretic peptide; MAP: mean arterial pressure.
(*With permission, from ref. [368].*)

CARDIAC PEPTIDE HORMONES ORIGINATING FROM ATRIAL NATRIURETIC PEPTIDE PROHORMONE

Within the 126 a.a. ANP prohormone encoded by a single gene are four peptide hormones (Figure 37.1) with blood pressure lowering, natriuretic, diuretic, and/or kaliuretic (i.e., potassium excreting) properties in both animals[24,77,78,140,141,220,389,405,433,434] and humans.[379–382] These peptide hormones, numbered by their a.a. sequences beginning at the N-terminal end of the ANP prohormone, consist of the first 30 a.a. of the prohormone (proANP 1–30, long-acting natriuretic peptide [LANP]); a.a. 31–67 (proANP 31–67, vessel dilator); a.a. 79–98 (proANP 79–98, kaliuretic peptide); and a.a. 99–126 (ANP) (Figure 37.1). These peptide hormones which were each discovered before BNP and CNP were named for their most prominent biologic effects rather than the tissue they were first found in, because these peptides are synthesized in many tissues.[114,369,393] Brain natriuretic peptide, so named because it was first found in porcine brain cDNA, for example, is actually present in the heart in 10-fold higher concentrations than in the brain.[52,140,212,344] Each of the four peptide hormones from the ANP prohormone circulate in healthy humans, with LANP and vessel dilator concentrations in plasma being 15–20-fold higher than ANP and 100-fold higher than BNP.[18,72,102,103,160,391,420,421]

BNP and CNP Prohormones

The BNP and CNP genes, on the other hand, appear to synthesize only one peptide hormone each within their respective prohormones, that is, BNP and CNP.[22,93,116,199,200,428] The pro BNP gene and its regulation are reviewed in the section on BNP prohormone gene. The biologic effects of BNP and CNP are reviewed in sections on BNP, "Biologic Effects" and CNP, "Circulating Concentrations and Biologic Effects."

ORIGINATION OF PEPTIDE HORMONES FROM PROHORMONES

More than one peptide hormone originating from the same prohormone is common with respect to the synthesis of hormones.[366] Adrenocorticotropin (ACTH), for example, is derived from a prohormone that contains four known peptide hormones.[366] α-MSH, which has natriuretic properties,[157,158] originates from this same prohormone. ACTH, similar to vessel dilator, originates from the middle of its prohormone. The middle of their respective prohormones is the most common origin of hormones with calcitonin, glucagon, vasoactive intestinal peptide, gastrin, cholecystokinin, and substance P, as well as ACTH and vessel dilator.[366] Several hormones, such as vasopressin (antidiuretic hormone (ADH)), oxytocin, pancreatic polypeptide, angiotensin, and gastrin-releasing peptide, originate from the N-terminus of their respective prohormones,[366] as does long-acting natriuretic peptide (proANF 1–30). The origin of hormones from the C-terminus of their respective prohormones like ANP, BNP, and CNP is less common, with somatostatin, inhibin, and parathyroid hormone (PTH) being the only known C-terminal prohormone-derived peptides.[366] In the case of PTH, 84 of the 90 a.a. in its

prohormone are considered to be the C-terminal "active" hormone; thus, it is not a small C-terminal-derived prohormone peptide, but rather nearly the intact PTH prohormone that serves as the actual peptide hormone.

MOLECULAR BIOLOGY OF THE CARDIAC NATRIURETIC HORMONAL SYSTEM

ProANP Gene

The gene encoding the synthesis of atrial natriuretic peptide prohormone (proANP) consists of three exon (coding) sequences separatedby two intron (intervening) sequences which encode for a mature mRNA transcript approximately 900 bases long[135,171,172,244,251,275,321,440] (Figure 37.1). Translation of human ANP prohormone mRNA results in a 151 a.a. preprohormone.[135,244,251,321] Exon 1 encodes the 5′-untranslated region, the hydrophobic signal peptide (leader segment), and the first 16 a.a. of the ANP prohormone (first 16 a.a. of long-acting natriuretic peptide).[133,135,244,251,321] The signal peptide, which is important for the translocation of the precursor peptide from the ribosome into the rough endoplasmic reticulum,[244,249] is cleaved from the preprohormone (151 a.a.) in the endoplasmic reticulum (Figure 37.1). The resulting 126 a.a. prohormone is the storage form for the four atrial natriuretic peptide hormones in tissues and the major constituent of the atrial granules.[27,135,244,251] The first 16 a.a. of this prohormone encoded by exon 1 are, after proteolytic processing of the ANP prohormone, also the first 16 a.a. of long-acting natriuretic peptide (LANP) (Figure 37.1). Exon 3 encodes for the terminal tyrosine (a.a. 126 of the ANP prohormone) in humans, and terminal three a.a. (Try-Arg-Arg) in rat, rabbit, cow, and mouse.[133,135,244,251,321] Deletion of this terminal tyrosine residue encoded by exon 3 does slightly affect the binding of ANP, but does not appear to contribute to biologic activity, as there is no apparent decrease in biologic activity when this terminal tyrosine is not present.[313] Exon 2 encodes for the rest of the prohormone (a.a. 17−125 in humans).[135,244,251,321]

There is considerable homology in the proANP gene among species, particularly in the encoding and 5′ flanking sequences.[93,251,406] The proANP gene has many features common to all eukaryotic genes,[27,33,242,276,382] including a TATTA box (T=thymine; A=adenine), intervening sequences bounded by GT-AG splicing signals (G=guanine), and a consensus sequence found in promoted regions. An interesting feature of the human proANP gene is a consensus sequence for a putative glucocorticoid hormone regulatory element in the second intron.[115,260,321]

The amino acid sequence of the whole ANP prohormone synthesized by the above gene is strikingly homologous among many species with differences clustered at the extreme carboxy terminal end of the prohormone, i.e., where ANP is formed.[15,120,148,173,175,183,202,216,242,244,251,252,406,450] In each species, the C-terminus is distinguished from the rest of the prohormone by forming a 17 a.a. ring structure via the joining by a disulfide bond between two cysteine residues (105 and 121 of the prohormone), as schematically shown in Figure 37.2. The ring structure originally was believed to be absolutely necessary for biologic activity,[64,152] but linear forms (same amino acids in linear form) without a ring structure have since been shown also to have biologic activity.[30] For full natriuretic and vasorelaxant activity, the Phe-Arg-Tyr (a.a. 124−126) at the COOH-terminus[64] and a.a. 99−104 of the NH_2-terminus of ANP are necessary.[34] In the dog, it appears that deletion of a.a. 99−102 of prohormone does not affect natriuresis, but deletion of a.a. 103 and 104 decreases natriuretic activity 10-fold.[34] Twenty of 30 a.a. in long-acting natriuretic peptide (Figure 37.2) are exactly the same in the five above species, and another six of the remaining 10 amino acids are exactly the same in four out of the five species.[15,93,94,119,321] Only three a.a. (33, 42, and 43 of the prohormone) are not the same in vessel dilator (Figure 37.2) in the majority of the five species.[119,174,251,321,406] Kaliuretic peptide has a highly-conserved sequence among the aforementioned five species, with 16 of its 20 a.a. (Figure 37.2) being the same in all five.[15,93,94,119,174,321]

BNP

This extraordinary conservation among species of LANP, vessel dilator, and kaliuretic peptide is not observed in the BNP prohormone, where there is a marked difference in amino acid sequence homology among species.[93,113,199,290,332]

Tissue-Specific Expression of ProANP Gene

In healthy adult animals and humans, the atrial myocyte is the main site of the ANP prohormone synthesis, but it is also synthesized in a variety of other tissues.[114,128,129,271,273] ProANP gene expression is 30−50 times higher in the atria of the heart than in extra-atrial tissues.[114] The expression of this gene has been found in kidney, gastrointestinal tract (antrum of stomach, small and large intestine), lung, aorta, central nervous system, anterior pituitary, and hypothalamus.[114,128,129,272,273] An example of where the

FIGURE 37.2 **Amino acid sequences of the natriuretic peptides.** Each of the sequences are human sequences except for *Dendroaspis* natriuretic peptide (DNP), whose sequence is only known in the snake. The brackets illustrate the location of cysteine bridges that help to form a ring structure in a number of these peptides (BNP: brain natriuretic peptide; CNP: C-type natriuretic peptide). *(With permission, from ref. [370.])*

proANP gene synthesized peptides localized in the kidney is illustrated in Figure 37.3.

Mechanisms of Action of Gene Products (i.e., Cardiac Hormones and Urodilatin) of ProANP Gene

Part of the intracellular mechanism of action(s) of the four peptide hormones encoded by the proANP gene is that after they bind to their specific receptors they enhance membrane-bound guanylyl cyclase to cause an increase in the intracellular messenger cyclic GMP[50,409,429](Figure 37.4). Cyclic GMP then stimulates a cyclic GMP-dependent, protein kinase that phosphorylates protein(s) in the cell, producing physiologic effects (Figure 37.4). Cyclic GMP mediates the vasodilation of each of the cardiac hormones.[250,373,419] The receptors for ANP that mediate ANPs biologic effects (e.g., ANP-A and -B receptors) are interesting, in that they contain guanylyl cyclase and a protein kinase in the receptors themselves[82,194,369](Figure 37.5). The NPR-A receptor has a 441 a.a. extracellular portion that binds ANP which, in turn, activates the catalytic portion of guanylyl cyclase in the cell (Figure 37.5). The protein kinase in this receptor has an inhibitory influence on guanylyl cyclase until this receptor is activated by ANP or BNP.[82,369] There is a 21 a.a. portion of this receptor which attaches this receptor to the membrane (Figure 37.5). The natriuresis secondary to the ANP is thought to also be mediated by cyclic GMP.[34] Vessel dilator, LANP, and kaliuretic peptide's mechanisms of action of producing a natriuresis is via enhancing the synthesis of prostaglandin E_2, which in turn inhibits Na^+-K^+-ATPase in the kidney,[51,139] which ANP does not do.[45,51,270] Vessel dilator and kaliuretic peptide's homodynamic effects via vasodilation of blood vessels are, however, mediated by cyclic GNP.

PROCESSING OF ATRIAL NATRIURETIC PEPTIDE PROHORMONE IN KIDNEY

ANP prohormone processing is different in the kidney compared to other tissues, resulting in an additional four a.a. added to the N-terminus of ANP (proANP 95–126, urodilatin (Figure 37.2)), a peptide first identified in opossum urine.[315] Thus, in the kidney, the identical four a.a. from the C-terminus of kaliuretic peptide are added to ANP to form the peptide urodilatin (Figure 37.2). At first, urodilatin was thought not to circulate,[231,315] and that it was not a

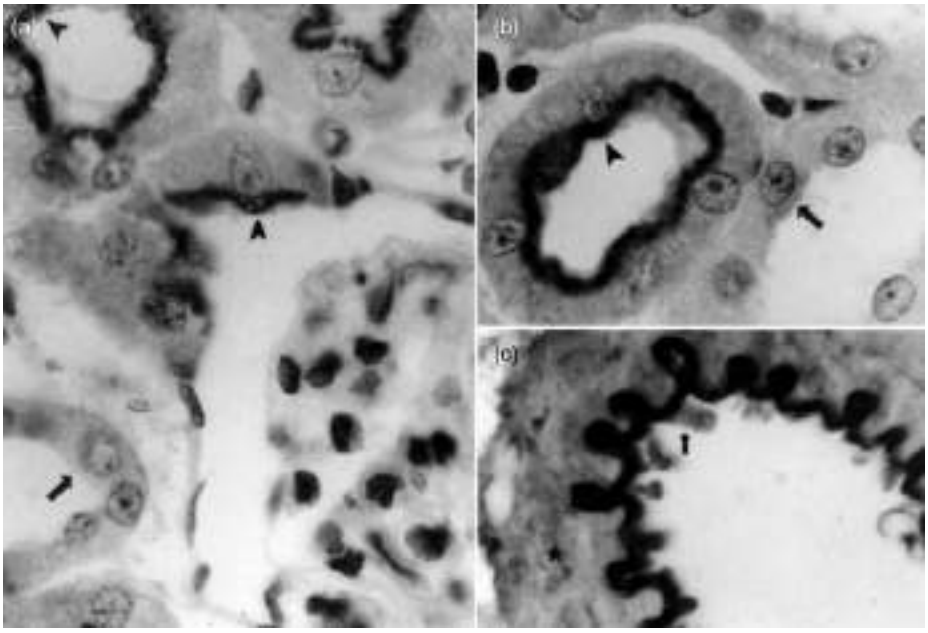

FIGURE 37.3 Vessel dilator immunoperoxidase staining in the rat kidney reveals strong staining of the sub-brush border of proximal convoluted tubules (arrowheads in a and b), including a proximal tubule in (a) originating directly from the top left portion of the glomerulus. The interstitial artery (c) had strong proANF (31–67) staining of the elastica with moderate staining of endothelial cells (arrow) and media (*). The distal tubules and collecting ducts (arrows in a and b) had weak staining with no demonstrable staining in some of the collecting ducts cells (Magnification× 940). *(With permission, from ref. [281].)*

hormone. To be defined as a hormone, a given protein has to be synthesized in a tissue or organ, circulate in the bloodstream, and have biologic effects in another tissue or organ.[366] With a very sensitive radioimmunoassay, it appears that urodilatin does circulate, but in such low concentrations (9–12 pg/ml) that it may not be physiologically relevant.[392] Since urodilatin constitutes less than 1% of the circulating natriuretic hormones, its physiologic importance as a circulating hormone is very limited, with over 99% of the physiologic natriuretic effects being from the other natriuretic hormones. Urodilatin, however, may have paracrine functions, and may mediate the effects of one of the other natriuretic hormones (ANP).[392] Infusion of ANP increases the circulating concentration of urodilatin, suggesting that some ANP effects may be mediated by urodilatin.[392] Infusion of long-acting natriuretic peptide, vessel dilator, and kaliuretic peptide, on the other hand, do not affect the circulating concentration of urodilatin in healthy humans.[392]

REGULATION OF ATRIAL NATRIURETIC PEPTIDE PROHORMONE GENE

Enhancement of ProANP Gene Expression

Stretch

Mechanical stretch, or more specifically tension, delivered across the atrial wall is a potent activator of proANP gene expression and/or secretion.[74,76,408] In animals, an increase of sodium intake results in an increased release of the ANP prohormone peptides.[78,80,403]

Thyroid Hormones

Thyroid hormones thyroxine (T_4) and triiodothyronine (T_3) increase proANP gene expression.[13,198] The increase in proANP mRNA in hypothyroidism when treated with thyroid hormone is paralleled by the increase in circulating concentrations of the gene products of this synthesis – vessel dilator, LANP, and ANP – in persons with hypothyroidism treated with thyroid hormone.[400]

The changes in proANP mRNA in both hypothyroidism and hyperthyroidism parallel very closely the circulating concentrations of vessel dilator, LANP, and ANP in humans, which are decreased in hypothyroidism and increased in hyperthyroidism.[400,438,439] When the hyperthyroid subjects were treated with the antithyroid drug propylthiouracil (PTU) the circulating concentrations of LANP, vessel dilator, and ANP decreased 50% after one week of treatment, with a simultaneous 50% decrease in serum triiodothyronine (T_3) levels.[400]

Glucocorticoids

Dexamethasone, at a dose of 1 mg/day, increases proANP mRNA levels in both atria and ventricles of the rat approximately two-fold.[115] There is negative feedback between cortisol and the gene products of proANP gene expression in that the cardiac hormones vessel dilator, LANP, kaliuretic hormone, and ANP decrease the circulating concentration of

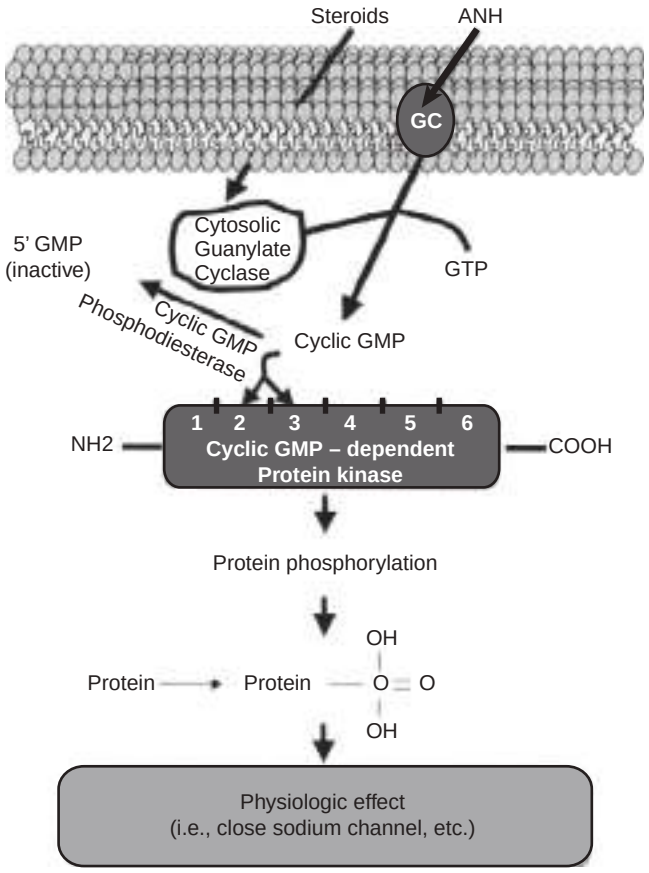

FIGURE 37.4 **Atrial natriuretic hormone (ANH) stimulates a membrane-bound guanylate cyclase.** Steroid hormones, on the other hand, diffuse through the cell to enhance the activity of a cytosolic guanylate cyclase. When either membrane-bound or soluble guanylate cyclase is activated, the intracellular messenger, cyclic 3′5′-guanosine monophosphate (cyclic GMP) is generated from guanosine triphosphate (GTP). Cyclic GMP then stimulates cyclic GMP-dependent protein kinase, which, in turn, phosphorylates proteins within the cell producing a biologic effect. Cyclic GMP is metabolized to an inactive 5′-GMP within the cell by cyclic GMP phosphodiesterase. *(With permission, from ref. [366].)*

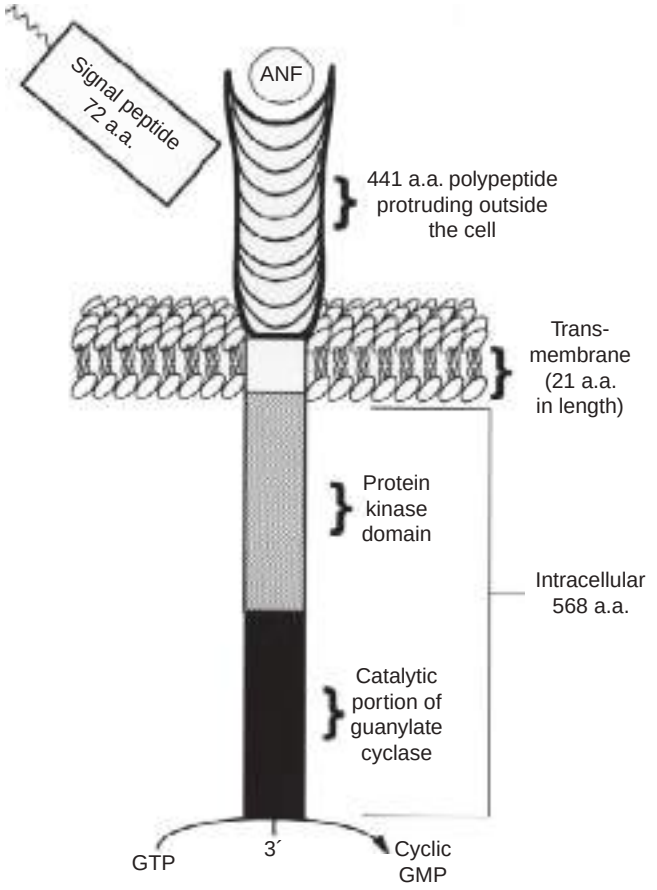

FIGURE 37.5 **Structure of atrial natriuretic peptide (ANP or NPR)-A (active) receptor.** The 441 amino acid (a.a.) extracellular portion of the receptor binds ANP, which activates the catalytic prrtion of guanylate cyclase within the cell. The protein kinase within this receptor has an inhibitory influence on guanylate cyclase until the receptor is activated by ANP. *(With permission, from ref. [366].)*

cortisol.[398] This decrease in cortisol is due, at least in part, to these cardiac hormones decreasing the circulating concentration of the hypothalamic peptide corticotrophin-releasing hormone (CRH), with a resultant decrease in ACTH, which stimulates the production of cortisol.[398]

Mineralocorticoids

Administration of mineralocorticoids to animals causes transient fluid and sodium retention. Despite continued administration of a mineralocorticoid, animals return to sodium balance within a few days, a phenomenon termed "mineralocorticoid escape." To investigate the role of ANP in mineralocorticoid escape, Ballerman et al.[19] administered DOCA to rats in sodium balance, and found plasma ANP levels and atrial proANP mRNA content increased in rats retaining sodium in response to DOCA. After "escape" from the mineralocorticoid-induced sodium retention, plasma ANP levels returned to baseline and relative atrial proANP mRNA content remained moderately elevated.[19] This increase in proANP mRNA probably resulted from the secondary cardiovascular effects of the steroids (e.g., increased intravascular volume), rather than from a direct effect of the mineralocorticoids on the ANP-secreting cell, as DOCA has no direct effect on proANP mRNA in ANP-expressing neonatal cardiocytes.[113,115]

Vasoconstrictive Peptides

Several vasoconstrictive peptides, including endothelin, norepinephrine, and angiotensin II, stimulate

proANP transcription and secretion.[290,294,295] The cardiac hormones, in turn, affect endothelin in a negative-feedback manner.[376]

Calcium

Primary cultures of neonatal rat cardiocytes exposed for 24 hours to 2 mM $CaCl_2$ in the culture media increase proANP messenger RNA three-fold, and increase secretion of ANP prohormone into the media three-fold.[201] When these cardiocytes were treated with the calcium channel-blocking agents diltiazem, nifedipine or verapamil, both proANP synthesis and secretion decreased to 25–40% of control values.[201]

TRANSGENIC KNOCKOUT AND/OR MICE OVEREXPRESSING ATRIAL NATRIURETIC PEPTIDE PROHORMONE GENE

Transgenic mice with an 11 base-pair deletion in exon 2 of the proANP gene (Figure 37.1) have increased blood pressure in homologous ($^{-/-}$) mice of 8–23 mmHg compared to wild-type ($^{+/+}$) mice.[168] Exon 2 of the proANP gene encodes for vessel dilator, kaliuretic peptide, and ANP (Figure 37.2). Exon 2 homozygote mutants have no circulating ANP, and they become hypertensive when fed a standard diet.[168] Heterozygotes ($^{+/-}$) with this base pair deletion in exon 2 are salt-sensitive and become hypertensive (systolic blood pressure increases 27 mmHg) on a high-salt (8%) diet.[168] Mice that overexpress the proANP gene, on the other hand, become hypotensive.[331]

HUMAN DISEASES WITH UPREGULATION OF ATRIAL NATRIURETIC PEPTIDE PROHORMONE GENE

Cerebrovascular Disease (Stroke and Hypertension)

A genetic linkage study followed 22,071 male physicians, all of whom had no history of stroke, from 1982 to 1999.[293] DNA extracted from peripheral white blood cells of those individuals who had a subsequent stroke revealed that, when compared to those without strokes, these individuals had a molecular variant in exon 1 of the proANP gene that was associated with a two-fold ($p < 0.01$) increased risk of stroke.[293] The individuals who had cerebrovascular accident (stroke) had significantly ($p < 0.001$) higher systolic and diastolic blood pressures than the persons who did not have a stroke.[293] This molecular variant of the proANP gene was found to be an independent risk factor (in addition to hypertension) for a cerebrovascular accident. This molecular variant was found to be responsible for a valine-to-methionine transposition in long-acting natriuretic peptide (LANP), i.e., the only peptide hormone synthesized by exon 1.[366] (Exon 1 does not encode for ANP.) In the 16 a.a. of LANP encoded by exon 1 there is only one valine, which is at position 7 of LANP (Figure 37.2).[370] Residue #7 (amino acid #7 of the ANP prohormone) is highly-conserved among different species.[15,93,94,119,321] In this human study there was no defect in the structure or expression of the proBNP gene.[293] In humans, blood pressure and the cardiac hormones correlate throughout the 24-hour period in a circadian relationship.[329,330] There is evidence to suggest that long-acting natriuretic peptide reflects salt sensitivity in hypertension-prone individuals, even before they develop hypertension.[228]

LANP and Stroke

Long-acting natriuretic peptide (LANP) has potent vasodilatory properties in both animals[389] and humans.[381,382] Antisera to LANP (to block the biologic activity of this peptide hormone) results in a significant increase in mean arterial pressure from 112 ± 12 mmHg to 131 ± 9 mmHg in normotensive animals, and exacerbates hypertension in spontaneously hypertensive rats (SHR) from 140 ± 10 mmHg to 159 ± 9 mmHg.[79] These antisera data indicate an important physiological role for long-acting natriuretic peptide in the regulation of arterial pressure.[79] In the brain of stroke-prone rats, the expression ANP prohormone gene (which synthesizes LANP) is significantly reduced.[291] There were no mutations in the BNP gene, and no differences in BNP gene expression between stroke-prone and stroke-resistant animals.[291,292]

Further evidence of the importance of the peptide hormones synthesized by the ANP prohormone gene derives from studies in mice with the ANP prohormone gene knocked-out: all develop salt-sensitive hypertension within one week leading to stroke.[168] The BNP gene does not upregulate to prevent hypertension and/or stroke when the proANP gene is knocked-out.[168] Downregulation of the proANP gene in the brain in stroke-prone SHRs has further been found to co-segregate with the occurrence of early strokes in their F_2 descendants.[291]

Natriuretic Peptide Hormones and Hypertension

The original hypothesis for hypertension was that there was a defect in the production of the

blood pressure-lowering cardiac hormones.[12,334] Experimental evidence revealed that, rather than being decreased, these blood pressure lowering cardiac hormones are elevated in the circulation in an apparent attempt to overcome the elevated blood pressure.[12,227,334,371] ANP increases in essential hypertension[12,334] and in persons with pheochromocytomas.[371] The hypertension associated with pheochromocytomas is characterized by increased circulating concentrations of vessel dilator and long-acting natriuretic peptide (LANP), as well as ANP.[372] Each of these blood pressure lowering hormones increase further with surgical manipulation-induced increases in blood pressure, and then these peptides return to normal after surgical removal of the pheochromocytomas and lowering of blood pressure.[371,372] The hypertension of obesity also is associated with increased circulating concentrations of ANP which decreases into the normal range with weight reduction-induced decrease in high blood pressure.[227]

In pregnancy, cardiac hormones increase in each trimester with the plasma volume expansion which accompanies a normal pregnancy.[229] ANP, vessel dilator, and LANP increase dramatically with the hypertension of pre-eclampsia, compared to their circulating concentrations in healthy pregnant women.[230] If one knocks-out the ANP prohormone gene that synthesizes the four cardiac hormones (Figure 37.1), within one week the animals develop salt-sensitive hypertension[168] while, on the other hand, transgenic mice overexpressing the ANP prohormone gene develop hypotension.[331] In addition to directly vasodilating vasculature, kaliuretic peptide and ANP inhibit the release of the potent vasoconstrictive peptide endothelin which is produced by the vascular endothelium.[376]

Congestive Heart Failure

In congestive heart failure (CHF), proANP gene expression is upregulated.[83,274,350] The increase in proANP gene expression is, however, not in the atria of the heart, but rather in the ventricle of the heart.[83,273,274,350] In persons with CHF, there is no defect in the production of the peptides from the ANP prohormone, but rather each are increased in the bloodstream in an attempt by the heart to overcome abnormal sodium and water retention by releasing more of these peptides that cause sodium and water excretion.[379,380,420] Vessel dilator and LANP increase in direct proportion to the severity of CHF, as classified by the New York Heart Association (NYHA).[420] The ANP-clearance receptor pathway is not linked to the avid sodium retention and/or to the renal ANP resistance observed in CHF.[32]

Cirrhosis with Ascites

Another salt- and water-retaining state, cirrhosis with ascites, is characterized by increased circulating concentration of the cardiac hormones, and with a 4.1-fold ventricular (but not atrial) increased steady-state proANP messenger RNA.[273] Although the liver expresses proANP messenger RNA, there is no upregulation of proANP gene expression in the liver when ascites develops.[272] Rather, the upregulation of this gene is only in the ventricle of the heart.[272]

LOCALIZATION OF ATRIAL NATRIURETIC PEPTIDE PROHORMONE GENE ON CHROMOSOMES

The proANP gene is located on the distal short arm of chromosome 1 in band 1P36 in humans and on chromosome 4 in mice.[366]

BRAIN NATRIURETIC PEPTIDE PROHORMONE GENE

The BNP gene is comprised of three exons separated by two introns, similar to the proANP gene in Figure 37.1.[113,345] Regulation of the BNP gene is controlled at the transcriptional level by several cis-acting regulatory elements in the proximal promoter, and the transcription factors that associate with them.[26,44,138,345] The cardiac specific transcription factor GATA 4 plays a major role directing basal activity of the BNP gene promoter.[44,138] GATA 4 is a nuclear mediator of mechanical stretch-activated BNP gene,[266] and might function as a central integrator of regulatory activity controlled by other transcription factors, such as GATA 6,[44] the neuron restricted silencer element-binding factor,[249] and YY1 the embryonic development protein.[26] Several of these factors interact synergistically with GATA 4, in both a physical and a functional sense, to stimulate BNP gene transcription.[44,249] Both the proANP and proBNP genes are activated in cardiac hypertrophy.[113,138] The GATA 4 transcription factor activates the proANP gene, as well as the proBNP gene.[113,138,266]

In healthy animals, cardiac BNP mRNA is mainly of atrial origin, that is, 10−50-fold more abundant than in ventricles.[52,140,212,344] In early left ventricular (LV) dysfunction, BNP mRNA markedly increases in the left atrium, but remains below or just barely at the level of detection in the ventricles.[212] The majority of investigations have found no increase in BNP mRNA in the ventricles in congestive heart failure,[140,212] which is exactly the opposite of ANP prohormone gene expression

which increases in the ventricle but not in the atria in sodium and water-retaining states.[83,274,350] Likewise, with streptotocin-induced diabetes BNP mRNA doubles in atria, without any change in ventricular myocardium BNP mRNA.[52] BNP gene knockout mice do not develop hypertension or hypertrophy[343] as ANP prohormone knockout mice do.[168] BNP knockout mice exhibit cardiac fibrosis as the only known effect of the BNP gene being knocked-out.[343] These knockout studies suggest that regulation of blood pressure is contributed to by the cardiac hormones synthesized by the proANP gene, but not by BNP.

SECRETION OF CARDIAC NATRIURETIC PEPTIDES

The main physiological stimulus to secretion of these peptide hormones to control blood volume appears to be an increase in pressure in the atria.[74,76,264,294,295,408] An increase of 4 to 6 mmHg in the atria releases the four cardiac hormones from the ANP prohormone.[76] These peptide hormones, in turn, decrease the volume returning to the heart secondary to their causing a diuresis and natriuresis.[76,220,405] Rapid heart rates at 125 beats/min and higher release the cardiac hormones into the circulation.[247] Both atrial and ventricular arrhythmias with heart rates of 125 beats/min and higher release these peptide hormones and increase the circulating concentrations of these cardiac hormones in humans.[246] Hypoxia and a variety of humoral factors (endothelin, glucocorticoids, acetylcholine, adrenergic agonists) have been suggested as contributing to release, but the majority of these humoral factors' effects are to increase the ANP prohormone gene synthesis, as outlined previously, rather than release *per se*.[294,295] With respect to hyperosmolarity, the threshold for ANP release is as low as 10 mOsmol/kg H_2O and this is regulated by a cross-talk between sarcolemmal L-type Ca^2 channel and the sarcoplasmic Ca^2 release.[167] ANP, vessel dilator, LANP, and kaliuretic peptide have a feedback mechanism whereby they inhibit their own and each other's release.[381] CNP also inhibits ANP release.[203]

BIOLOGIC EFFECTS OF THE CARDIAC NATRIURETIC HORMONES AND THEIR MECHANISMS OF ACTION

ANP

Vasodilation

The original report by deBold et al.[69] where crude atrial extracts cause diuresis and natriuresis also indicated that these extracts could decrease mean arterial pressure. Crude atrial extracts were then shown to possess vasorelaxant activity in isolated aortic segments.[5,63,111] When synthetic ANP became available, it was demonstrated that the pure form of ANP could also cause vasodilation *in vitro*.[112,191,312,374,419] Both crude[5] and synthetic[107] ANP decrease total peripheral resistance. Large central arteries (aorta and renal) relax, whereas more distal (ear and basilar) arteries are refractory to nanomalor concentrations of ANP.[283,366] Pulmonary, femoral, and iliac arteries are intermediate in their response to ANP.[366] One exception to small arteries not responding well upon the addition of ANP is the carotid arteries, which respond well.[283] In general, veins do not appear to vasodilate with the addition of ANP as well as arteries do, but ANP has been shown to relax peripheral veins in addition to aortic rings.[312]

ANP produces a dose-dependent reduction in systemic blood pressure in humans.[413] The immediate blood pressure lowering of 5.5 mmHg in 2 minutes with 100 μg ANP intravenously has been associated with a sensation of facial flushing in four of six human subjects, suggesting acute vasodilation of skin.[366] ANP elicits greater blood pressure-lowering properties in spontaneously hypertensive rats than in normotensive rats.[366] A greater response in hypertensive versus normotensive subjects is also true for most, if not all, antihypertensive agents.

MECHANISM OF ANP-INDUCED VASODILATION

The vasodilation observed with ANP is endothelium-independent.[317,373,419] It is mediated by cyclic GMP, which is increased after enhancement of membrane-bound guanylyl cyclase by ANP.[250,373,419] Cyclic GMP itself has been demonstrated to cause vasodilation.[282,317,419] The vasorelaxation with ANP appears to be independent of calcium[373,419] and cyclic AMP, with no change in cyclic AMP occurring during the same period of time that cyclic GMP increases.[373,419] With respect to calcium, ANP can increase cyclic GMP and cause vasodilation with no calcium in the incubation media,[250,373,409,419] but possible shifts of calcium already in the vasculature are still being debated. The ANP-induced relaxation of contracted vasculature is not blocked by adrenergic antagonists,[111] cholinergic antagonists[111] or indomethacin,[111] the latter suggesting that this vasodilation is not mediated by prostaglandins.

Natriuresis

ANP-induced natriuresis[8,105,259,327] appears to have a dependence on renal vasodilation, since ligation of the renal artery eliminates ANP-induced natriuresis.[328]

ANP has been shown to directly increase renal blood flow in dogs.[39] Redistribution of renal blood flow to the proximal[144] and distal[181] tubules has been reported as contributing to the natriuretic effects. The proximal tubule contains guanylyl cyclase, and cyclic GMP produced by this enzyme increases amiloride-sensitive ^{22}Na uptake in the phosphorylated brush border membranes of the proximal tubule, suggesting that the ANP intracellular mediator, cyclic GMP, directly stimulates the Na−H antiporter in the proximal tubule.[134]

ANP and Site of Action in Kidney

The renal actions of ANP are complex. Hemodynamic effects of pharmacologic doses of exogenous ANP constrict efferent and dilate afferent arterioles[219]; the resultant increase in glomerular capillary hydrostatic pressure could increase the glomerular filtration rate (GFR).[56,105] Physiologic doses of ANP, however, do not increase GFR.[105,259,327] The circulating physiological concentration of ANP is below the concentration of ANP that has been found necessary to increase GFR.[259,327] Early micropuncture and microcatheterization studies suggested a late distal nephron site of action, but functional studies of ANP in the inner medullary collecting duct (IMCD) indicate that it is a major target site of ANP action in the tubule.[433,435] Binding studies indicated specific binding sites for ANP on IMCD cells.[366] ANP increases cGMP accumulation in isolated cells from this segment in a concentration-dependent manner.[433] ANP also inhibits oxygen consumption in IMCD cells, indicative of inhibition of sodium transport.[435] This inhibition occurs through a cGMP-mediated effect on an amiloride-sensitive sodium channel.[433,435]

A proximal tubular site of action has been suggested from studies showing that ANP inhibits angiotensin II-stimulated proximal sodium reabsorption at very low concentrations (as low as 10^{-12} mol/L).[109,145] In the cortical collecting ducts, ANP inhibits tubular water transport by antagonizing the action of vasopressin.[81] ANP has been localized by immunoperoxidase and immunofluorescence methods to the sub-brush border of the pars convuluta and pars recta proximal tubule, as well as the distal tubule.[281,297] These studies indicate that ANP may have widespread actions on tubular function.

ANP Inhibits the Renin–Aldosterone System

Atrial natriuretic peptide has been found to be a potent *in vivo* and *in vitro* inhibitor of aldosterone secretion via a direct effect on aldosterone secretion from the zona glomerular cells of adrenal cortex,[14,46,124,195,214,354,375] and indirectly through inhibition of renin release from the juxtaglomerular cells of the kidney.[39,104,149,197,214,404] The mechanism of the inhibition of renin release by ANP appears to involve cyclic GMP, as this inhibition is duplicated by permeable analogs of cyclic GMP.[149,197]

Cardiac Peptide Hormones: LANP, Vessel Dilator, and Kaliuretic Peptide

Vasodilation

LANP, vessel dilator, and kaliuretic peptide cause vasodilation of vasculature that is endothelium-independent,[373] and similar to ANP endothelium-independent vasodilation of vasculature.[317,374,419] The amount of vasodilation *in vitro* with these cardiac peptide hormones is similar to that observed with addition of ANP.[373] When infused over 2 hours at the same 100 ng/kg of body weight/per minute concentration, vessel dilator and ANP were found to decrease blood pressure from an average of 145 to 124 mmHg ($p<0.05$), and from 143 to 123 mmHg ($p<0.05$), respectively.[220] Long-acting natriuretic peptide lowered blood pressure from a mean of 138 to 122 mmHg ($p<0.05$), whereas kaliuretic peptide decreased blood pressure from a mean of 155 to 138 mmHg ($p<0.05$).[220] Blood pressure did not change in the control animals throughout the 120-minute pre-experimental period or during the 120-minute experimental period.[220] Similar to ANP, the mechanism of vasodilating vasculature for these hormones is mediated by cyclic GMP.[373] The enhancement of guanylyl cyclase by the cardiac hormones is calcium-independent in vasculature.[373]

Cardiac Hormones: LANP, Vessel Dilator, and Kaliuretic Peptide

Natriuresis Mechanism of Action

Comparison of the relative natriuretic and diuretic potencies of the same dose in 100 ng/kg of body weight per minute of vessel dilator, revealed that LANP and ANP have significant natriuretic properties in healthy humans, but kaliuretic peptide enhancement of the urinary sodium excretion rate was not significant.[382] The natriuretic properties of vessel dilator are especially impressive in light of the fact that ANP has been found to be a more potent natriuretic and diuretic agent than furosemide,[349] and that vessel dilator has equally potent natriuretic effects[376,380,382] and circulates normally at a 17-fold higher concentration than ANP and 100-fold higher than BNP.[72,102,103,113,126,145,160,390,391,420] This 17-fold higher circulating concentration is found both during unstimulated conditions and with release secondary to

physiological stimuli, such as head-out water immersion where the atria are stretched releasing these peptides.[390,391] Vessel dilator's biologic effects also last significantly longer than ANP (greater than 6 hours versus 30 minutes).[376,380,382] Vessel dilator and ANP, with nearly equal abilities to enhance sodium excretion, are markedly different, however, with respect to potassium excretion.[382] Vessel dilator is the only one of the four cardiac peptide hormones from the ANP prohormone that does not significantly enhance potassium excretion.[220,382] This potassium-sparing effect of vessel dilator makes it distinctly different from ANP, LANP, and kaliuretic peptide. Kaliuretic peptide does not significantly enhance the fractional excretion of sodium (FE_{Na}), but it is the only natriuretic peptide that significantly enhances the fractional excretion of potassium (FE_k) in healthy humans. (Fractional excretion of sodium or potassium is the percentage of glomerular-filtered sodium or potassium that is excreted into the urine.[382])

The natriuretic effects of long-acting natriuretic peptide, kaliuretic peptide, and vessel dilator have different mechanism(s) of action from ANP, in that they inhibit renal Na^+,K^+-ATPase secondary to their ability to enhance the synthesis of prostaglandin E_2,[51,139] which ANP does not do.[51,139,270] ANP, BNP, and CNP effects in the kidney are thought to be mediated by cyclic GMP.[34,140,294,368]

Cardiac Hormones: Localization within the Kidney

Immunohistochemical studies have localized vessel dilator (Figure 37.3) and long-acting natriuretic peptide as well as ANP to the sub-brush border of the pars convuluta and pars recta of the proximal tubules of animal[281] and human[297] kidneys. Immunofluorescent studies reveal that each of these peptides has a strong inclination for the perinuclear region in both the proximal and distal tubules.[281,297]

LANP, Vessel Dilator, and Kaliuretic Peptide: Renin–Aldosterone System

Kaliuretic hormone and long-acting natriuretic peptide (LANP) are potent inhibitors of the circulating concentrations of aldosterone in healthy humans.[375] Kaliuretic peptide and LANP effects on decreasing plasma aldosterone levels last for at least 3 hours after their infusions have stopped, while ANP no longer has any effect on plasma aldosterone concentrations within 30 minutes of infusion cessation.[375] Vessel dilator does not appear to have direct effects on aldosterone synthesis, but is a potent inhibitor (66%) of plasma renin activity.[404] Thus, the four cardiac hormones from the ANP prohormone gene act as endogenous antagonists of the vasoconstrictor and salt-and-water-retaining systems (e.g., the renin–angiotensin–aldosterone system, vasopressin,[81] and endothelin[351,376]) in the body's defense against blood pressure elevation and plasma volume expansion via direct vasodilator, diuretic, and natriuretic properties. These four cardiac hormones' multiple biologic effects are illustrated in Figure 37.6. It is important to note in this illustration with respect to the kidney, that these peptide hormones also increase protein excretion (albumin, B2 microglobulin)[226,394,395] and phosphate reabsorption,[144] as well as cause a natriuresis and diuresis.

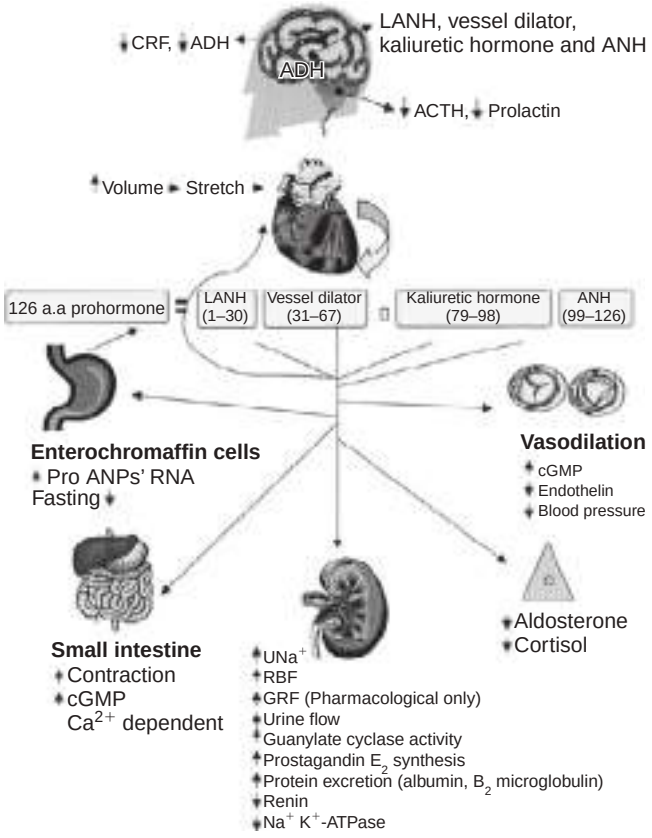

FIGURE 37.6 **Long-acting natriuretic hormone (LANH or LANP), vessel dilator, kaliuretic hormone, and atrial natriuretic hormone (ANH or ANP) are released with increased volume, which causes stretching of the atrium of the heart.** The biological effects of these peptide hormones include vasodilation mediated via enhancing guanylate cyclase activity with a resultant increase in the intracellular messenger cyclic GMP and inhibiting the vasoconstrictive peptide endothelin. ANPs cause a natriuresis mediated (except for ANH) by their enhancing the synthesis of prostaglandin E2, which, in turn, inhibits renal Na^+,K^+-ATPase. These peptide hormones also reduce circulating cortisol, aldosterone, and/or plasma renin activity. ANPs decrease corticotrophin-releasing factor (CRF) and antidiuretic hormone (ADH) from the hypothalamus as well as decrease the circulating concentration of adenocorticotropin (ACTH) and prolactin from the anterior pituitary. They increase protein excretion by the kidney.[394,395] *(With permission, from ref. [369].)*

Kidney Hormone: Urodilatin

Vasodilation

Urodilatin has vasodilatory effects similar to those of ANP.[309,315] This would be expected, since the ANP prohormone post-translational processing in the kidney results in an additional four a.a. from kaliuretic peptide being added to the N-terminus of ANP (proANP 95–126, urodilatin)[205,240,315] (Figure 37.2). The rest of the amino acids in urodilatin are identical, and in the same sequence as those in ANP (Figure 37.2). Urodilatin and ANP have identical ring structures formed with cysteine-to-cysteine bonding (Figure 37.2). The four a.a. added to form urodilatin are the same four a.a. present in the C-terminus of kaliuretic peptide in other tissues, but in the kidney the ANP prohormone is cleaved between a.a. 94 and 95 rather than between a.a. 98 and 99 to form urodilatin.[315] Urodilatin is not formed in the heart or in other tissues except the kidney.[205] Urodilatin at first was thought not to be a hormone, in that it was thought that it did not circulate,[315] but sensitive assays revealed that it circulates at very low concentrations (9–12 pg/ml).[392] Infusion of ANP increases the circulating concentration of urodilatin, suggesting that some ANP effects may be mediated by urodilatin.[392] Infusion of long-acting natriuretic peptide, vessel dilator, and kaliuretic peptide, on the other hand, do not affect the circulating concentration of urodilatin in healthy humans.[392]

Urodilatin: Natriuresis

Urodilatin has natriuretic and diuretic effects similar to ANP,[309] and since it has an identical amino acid sequence and ring structure as ANP one would expect it to bind to the same receptors and have similar biologic effects as ANP. It does bind to the same receptor and has similar biologic effects as ANP.

Localization of Urodilatin in Kidney

Immunohistochemical studies have localized urodilatin to the distal tubule with no evidence of urodilatin in the proximal tubule.[281] ANP messenger-RNA studies have confirmed that the ANP prohormone is synthesized in the kidney.[137] The amount of the ANP prohormone present in the kidney, however, is only 1/190th of that produced in the atria of the heart.[274] These studies taken together suggest that since urodilatin is found mainly in the distal nephron,[137,281,288] and since it is part of the ANP prohormone,[278,315,369] synthesis of the ANP prohormone may take place in the distal nephron.[137,281,288] The ANP prohormone gene is present and can be expressed in the kidney.[137,274] This gene is upregulated within the kidney in early renal failure in diabetic animals,[324] and in the remnant kidney of rats with 5/6 reduced renal mass.[347] Within the kidney, in addition to urodilatin, the ANP prohormone gene synthesizes LANP, vessel dilator, and a shortened form of kaliuretic peptide, but not ANP *per se*.[130,369]

Urodilatin and Renin–Aldosterone System

Urodilatin does not affect renin or aldosterone concentrations.[88]

BNP and CNP

BNP: Biologic Effects

Brain natriuretic peptide (BNP) is a 32 a.a. peptide in humans (45 a.a. in rat) with similar diuretic and natriuretic effects and a short half-life as ANP[332] (Figure 37.2). BNP half-life is 100-fold shorter than the half-lives of vessel dilator and LANP.[4,199,332,333,366] BNP has remarkable sequence homology to ANP with only four a.a. being different in the 17 a.a. ring structure formed by a disulfide bond common to both peptides[199,200,290,294,332] (Figure 37.2). Although BNP was named[332] for where it was first isolated (porcine brain), the main source of its synthesis and secretion is the heart (10-fold greater than brain)[65,140,199,205,294,344] (Table 37.1). As with ANP, the highest levels of BNP are found in the atria of the heart.[140,344] BNP levels in the atria, however, are less than 1% of ANP levels.[344] The immunoreactive level of BNP in the ventricles is only 1% of BNP concentration in the atria; in brief, 99% of BNP is found in the atria.[344] BNP, however, has been termed a "ventricular" peptide, based on ventricular BNP mRNA levels being similar to those in the atria with ventricles being much larger than the atria,[240] but as above, 99% of BNP is in the atria rather than the ventricles.[344]

The 108 a.a. BNP prohormone is processed in the heart to yield a biologic functioning BNP consisting of a.a. 77–108 of the BNP prohormone (in humans) and a biologically inactive N-terminus of the BNP prohormone (a.a. 1–76 of prohormone), both of which circulate.[199] BNP circulating concentration is less than 20% of ANP.[140] The sequence homology of BNP differs appreciably across species (both in size and a.a. sequence).[93,199,240,344] The major circulating form varies substantially among species, being 26, 45, and 32 a.a. in pig, rat, and human, respectively.[113,199] The marked sequence variability of BNP explains in part variations in its biologic activity in different species. The peptide hormones from the ANP prohormone, on the other hand, have remarkable homology across different species.[15,93,94,116,120,321] Mice overexpressing the BNP gene, where the circulating concentration of BNP is 10- to 100-fold higher than in healthy mice, have less glomerular hypertrophy and mesangial expansion with

intraglomerular cells than healthy mice 16 weeks after both received renal ablation.[179] This mouse model of subtotal renal ablation, however, also has significantly increased ANP concentrations,[254,303,378] which may also have contributed to the effects attributed to BNP in the BNP-gene overexpressing mice.[179]

CNP: Circulating Concentrations and Biologic Effects

C-type natriuretic peptide (CNP) is a 22 a.a. peptide with remarkable similarity to ANP and BNP in its amino acid sequence, but lacks the carboxy-terminal tail of ANP and BNP[21,22,333] (Figure 37.2). CNP was found originally in the brain, but more recent studies suggest that it is also present in the heart[176] and kidney.[222,223,342] The amount of CNP in the heart, however, is very low and only small amounts are present in plasma.[176] Two CNP molecules, 22 and 53 a.a. in length, have been identified in plasma.[22,55] Each is derived from a single CNP prohormone, with the 22 a.a. form contained in the carboxy-terminal portion of the 53 a.a. form. The 22 a.a. form predominates in plasma, and is more potent than the 53 a.a. form in humans.[21,22,55,333] The plasma concentration of CNP is very low, with some authors reporting that CNP is not normally detectable but becomes detectable only in renal failure[304] and congestive heart failure.[176] CNP is present in the human kidney.[223,342] CNP has been found to have little effect on renal vasoconstriction.[430] Although CNP has been reported to have natriuretic effects in some animals, when infused in humans at physiological concentrations and in concentrations that reached four- to ten-fold above those observed in disease states, CNP did not affect renal function.[21] Thus, in healthy humans CNP had no effect on renal hemodynamics, systemic hemodynamics, intrarenal sodium handling, sodium excretion or plasma levels of renin and aldosterone.[21] Even when CNP was increased 60-fold in human plasma there were no significant hemodynamic or natriuretic effects.[159] The authors of this study concluded that it is unlikely that CNP has any endocrine role in circulatory physiology.[159] There is one study in humans where infusion of CNP to increase CNP plasma levels 550-fold above normal caused a 1.5-fold increase in urine volume and sodium excretion.[161] With this very high plasma concentration of CNP, both ANP and BNP also increased 2.4-fold,[161] which may have been the cause of the natriuresis and diuresis observed that was not observed in any other study with CNP.[21,159] Each of these studies suggests that CNP does not contribute physiologically to any natriuresis or diuresis in healthy humans.[21,159,161] The main site of CNP synthesis is vascular endothelium, and CNP acts as a paracrine endothelium-derived hyperpolarizing factor (EDHF) via activation of NPR-C receptor and the opening of a G-protein-gated inwardly rectifying K channel (GIRK) in mesenteric resistance arteries to mediate vasodilation.[47] In conduit vessels, on the other hand, CNP induces relaxation via a cyclic GMP-dependent mechanism.[47]

Adrenal Natriuretic Peptides, Adrenomedullin and Proadrenomedullin N-Terminal 20 Peptide: Biologic Effects

Adrenomedullin (ADM), a 52 a.a. peptide with one intramolecular disulfide bond (Figure 37.2) originally isolated from an extract of a pheochromocytoma,[189] also has a range of biologic properties similar to the cardiac hormones, but these properties are less pronounced than those of the cardiac hormones[170,189,190,301] (Table 37.1). Infusion of ADM lowers blood pressure and produces diuresis and natriuresis.[170,189,301] Adrenomedullin causes a long-lasting hypotension accompanied by increased heart rate as a side-effect.[257] ANP, but not LANP, vessel dilator or kaliuretic hormone, increases the circulating concentration of adrenomedullin three- to four-fold, suggesting that some of the reported effects of ANP may be mediated via adrenomedullin.[374] However, the natriuresis and diuresis secondary to ANP were much larger than has ever been observed with adrenomedullin,[374] suggesting that ADM does not mediate all of the natriuretic and diuretic effects of ANP. Adrenomedullin is a larger peptide than any of the cardiac hormones, with its main site of synthesis being in the adrenal (Table 37.1), but isolated renal cells also have the ability to synthesize adrenomedullin secondary to stimulation by vasopressin via V2 receptors.[301,306] Since vasopressin (antidiuretic hormone, ADH) inhibits a diuresis these findings are opposed to findings that ADM causes a diuresis.[170,189,301] Adrenomedullin is part of a peptide family that shares structural similarity with calcitonin gene-related peptides and amylin, which share biologic effects and some cross-reactivity between receptors.[89,301,305] The adrenomedullin prohormone at its N-terminal end contains another biologically active peptide with vasodilating properties known as proadrenomedullin N-terminal 20 peptide (PAMP).[90,302] Whether more PAMP or adrenomedullin is produced depends on alternate splicing of its prohormone by the enzyme peptidylglycine C-amidating monoxygenase.[53,170,190,301,302] Adrenomedullin exerts its actions through G-protein-coupled membrane receptors linked to adenylyl cyclase, resulting in an increase in cellular cyclic AMP[301] as opposed to the cardiac hormones (ANP, BNP, LANP, vessel dilator, and kaliuretic peptide) whose second messenger is cyclic GMP.[373,409,419] Proadrenomedullin is thought not to act via either

cyclic AMP or cyclic GMP, but rather via potassium channels, which eventually exert a presympathetic inhibition of sympathetic nerves innervating blood vessels.[302]

Dendroaspis Natriuretic Peptide: Biologic Effects

Dendroaspis natriuretic peptide (DNP) is the newest of the natriuretic peptides (Figure 37.2). This peptide was isolated from the venom of the green mamba snake *Dendroaspis angusticeps*.[316] This venom also contains several polypeptide toxins that block cholinergic receptors to cause paralysis.[316] DNP-like peptide has been reported to be present in human plasma and in heart atria.[310] In plasma, DNP concentration is very low at 6 pg/ml, which is 0.5% of the circulating cardiac hormones.[310] This peptide has a 17 a.a. disulfide ring structure similar to ANP, BNP, and CNP (Figure 37.2), and causes a natriuresis and diuresis in dogs.[210] Infusion of DNP does not cause any significant change in the circulating levels of ANP, BNP, or CNP.[210]

Richards et al.[286] have questioned whether DNP actually exists in humans and mammals, since it has not been characterized by high-pressure liquid chromatography linked to immunoassay, followed by purification and analysis to establish the human amino acid sequence, as has been done with the aforementioned cardiac hormones. The gene for DNP has not been cloned in the snake or in any mammal as has been done for each of the other natriuretic peptides.[286] Richards et al.[286] suggest that DNP may be "snake BNP," since BNP varies markedly in amino acid sequence among species (and the BNP sequence in this snake is unknown). The peptides from the ANP prohormone are markedly conserved among species,[15,93,94,116,119,321] and one would not suspect that DNP is one of these peptides as their amino acid sequences are markedly different from DNP. Further experimentation with the studies discussed previously suggested by Richards et al.[286] should give one more insight with respect to this peptide.

Guanylin, Lymphoguanylin, Renoguanylin, and Uroguanylin: Biologic Effects

Guanylin, a 15 a.a. peptide,[62] isolated from rat intestine, and uroguanylin, a 16 a.a. peptide originally isolated from opossum urine,[99,143] are peptides which are structurally and functionally similar to bacterial heat-stable enterotoxins produced by strains of pathogenic *Escherichia coli* intestinal bacteria.[82] Traveler's diarrhea is the result of these enterotoxins interacting with a membrane-bound guanylyl cyclase-C (GC-C receptor) on the luminal surface of enterocytes.[82] The resulting increase in cyclic GMP phosphorylates the cystic fibrosis transmembrane conductance regulator (CFTR), leading to an efflux of chloride into the intestinal lumen.[287] Cyclic GMP in the intestine inhibits Na^+ absorption mediated by apical Na^+/H^+ exchange, and activates protein kinase G II.[326] Guanylin and uroguanylin, which have similar structures to this enterotoxin, have a similar mechanism of action in the intestine via the same GC-C receptor.[100,101] These peptides have been identified in the intestine in different locations, with guanylin in the colon but not the proximal intestine, and uroguanylin expressed in the proximal intestine but not in the colon.[91,97,99,142] These intestinal peptides have natriuretic properties.[62,99] The observation of renal expression of guanylin and uroguanylin mRNA[62,99] suggests renal synthesis and a local paracrine action of these peptides in a manner analogous to the ANP prohormone gene products. Wang et al.[412] showed that intravenous and intraluminal administration of uroguanylin in the kidney affects tubuloglomerular feedback, but it failed to cause a natriuresis and diuresis in rats at up to 100 nmol/kg/h intravenously, which was less than other supraphysiologic concentrations used previously[41,136] to cause a natriuresis. The uroguanylin dose used by Wang et al.[412] was still, however, a pharmacologic dose which resulted in higher uroguanylin concentrations in rat blood and urine than physiological concentrations which are in the femtomolar range.[106] Rats fed a high-salt diet had higher uroguanylin and cGMP concentrations in the urine; however, the plasma concentration of uroguanylin was not increased, which argues against uroguanylin being an endocrine hormone in the kidney.[106]

Renoguanylin is a peptide hormone similar to guanylin and uroguanylin that has, thus far, been only found in Japanese eels.[432] In the eel it has been proposed that renoguanylin may be involved in osmol regulation, but this has not been proven at present.[432] Renoguanylin was not as prominent in the kidney and intestine of the eel as guanylin and uroguanylin.[432] Renoguanylin has not been found in mammals or humans and may be unique to the Japanese eel and fish.[432] Lymphoguanylin is a 109 a.a polypeptide expressed in spleen and lymphoid tissues of opossum.[98] The 109 a.a polypeptide shares 84% and 40% of its residues with prouroguanylin and proguanylin, respectively.[98] Lymphoguanylin is less potent than uroguanylin or guanylin in intestinal bioassay, and has reduced efficacy for activation of OK-GC receptor in the kidney.[98] 100 μM of lymphoguanylin stimulates cGMP production in renal cells only five-fold, compared to 206-fold with uroguanylin and 88-fold with guanylin.[98] A serine-7 analog of lymphoguanylin has

natriuretic properties in *ex vivo* rat kidneys and increases cyclic GMP 1000-fold more than the native lymphoguanylin.[96]

The inactive precursor of uroguanylin, i.e., prouroguanylin, is delivered to the kidney as an unprocessed propeptide,[277] and is processed to its active natriuretic form exclusively within the renal tubules.[277] The proximal convoluted tubule is thought to be the target for the uroguanylin natriuretic response.[87] Renal uroguanylin messenger RNA expression is also highest in proximal tubules, while guanylin is expressed mainly in the collecting ducts.[271] Salt-loading (1% NaCl in drinking water) for three days increases uroguanylin mRNA expression by 1.8-fold, but has no effect on guanylin expression.[271] The synthesis of these peptides by renal tubule epithelium may contribute to local control of renal function and adaptation to dietary salt.[271]

Both guanylin and uroguanylin elicit natriuretic responses from the kidney.[40,95,136] Both guanylin and uroguanylin exist in conformationally distinct A and B type topoisomers.[222,238,239] Topoisomer uroguanylin B has natriuretic activity in the kidney,[239] while the uroguanylin A in high concentration antagonizes the natriuretic action of the B form.[239] Uroguanylin knockout mice have an impaired ability to excrete an enteral load of NaCl, primarily due to an inappropriate increase in renal Na^+ reabsorption.[211] Further, there appears to be an interaction between guanylin, uroguanylin, and the cardiac hormone natriuretic peptide system, in that pretreatment with ANP (0.03 nM) enhances guanylin and uroguanylin's natriuretic activity when ANP is present in low dose.[304] When pharmacological doses of ANP or urodilatin are utilized they clearly inhibit uroguanylin-induced natriuresis.[304]

The GC-C receptor with which the heat-stable enterotoxin, uroguanylin, and guanylin interact in the intestine was cloned from intestinal cDNA libraries.[82] It exhibits 55% identity to NPR-A and NPR-B receptors in the catalytic region, 39% identity in the protein kinase domain, but only 10% identity in the extracellular region.[82] Within the kidneys, heat-stable enterotoxin, uroguanylin, and guanylin bind chiefly to apical membranes of proximal tubule cells,[91,100] also a site of CFTR expression.[60]

Two different guanylyl cyclase signaling receptors have been identified, one in kidney (OK-GC) and one in the intestine (GC-C), that are activated by the guanylin peptides.[101] Uroguanylin and guanylin regulate transport in mouse renal cortical collecting ducts independent of guanylyl cyclase C receptor,[325] and in guanylyl cyclase C-receptor deficient mice renal effects are retained,[325] strongly suggesting that GC-C is not the mediator of uroguanylin or guanylin effects in the kidney.

ANP Prohormone System and Expression in Gastrointestinal Tract

Almost 37 years ago it was noted that an oral load of sodium resulted in a natriuresis that was greater than the same amount of sodium chloride given intravenously, suggesting that the gastrointestinal tract monitors and responds to oral sodium-load.[204] Guanylin and uroguanylin may respond to this oral sodium-load in the colon and proximal intestine, respectively, but the stomach is an earlier monitor of this sodium-load. Immunoreactive cardiac hormones, ANP prohormone, and mRNA are present in the proximal stomach and antrum.[84,128,129,132] ANP prohormone gene expression and gene products LANP and ANP have been localized to the enterochromaffin cells in the lower portion of antropyloric glands of the stomach.[129] Fasting for 72 hours in adult rats results in a significant ($p < 0.05$) decrease in the levels of ANP prohormone messenger RNA, and a decrease in immunoreactive long-acting natriuretic peptide and ANP to <33% of that of fed rats.[129] In humans, food intake increases the excretion of LANP, vessel dilator, and ANP into the urine, suggesting an interaction between the cardiac hormones synthesized in the gastrointestinal tract and the kidneys.[384] A fluid load of Coca-Cola© rapidly (in 15 minutes) decreases the excretion of LANP, vessel dilator, and ANP into the urine, allowing more of these peptides which cause a diuresis to be present to respond to the fluid load.[384] In the stomach, cholinergic neurons inhibit, and pituitary adenylate cyclase-activating polypeptide neurons stimulate, ANP secretion, suggesting that there is also neuronal control of their secretion from the stomach.[127] ANPs are present not only in the stomach, but throughout the gastrointestinal tract (small intestine) and colon,[122,393,407] as opposed to guanylin and uroguanylin, which are present only in specific portions of the gastrointestinal tract.[91,97,99,142] Guanylyl cyclases A and B, which ANP, BNP, and CNP interact with, are present in the gastrointestinal tract,[280] as well as guanylyl cyclase-C which guanylin and uroguanylin enhance.[100] ANPs also appear to have effects within the gastrointestinal track itself.[17] ANP increases the spontaneous phasic contractions of longitudinal music two- to four-fold over a concentration range of 10 pm to 1000 mM, which was associated with a three-fold increase in cyclic GMP.[17] Vessel dilator and LANP also increase these spontaneous place contractions, which are additive with ANP.[17] The ANPs appear to act as neurotransmitters in the gastrointestinal tract to move water and feces through the gastrointestinal tract via increased force of contraction of the longitudinal muscles[17] until feces reaches the anal sphincter which ANP has been shown to relax to expel the contents of the gastrointestinal tract.[17,63]

Melanocyte-Stimulating Hormones

Melanocyte-stimulating hormones (MSHs) are small peptides of three different primary sequences (α-, β-, and γ-MSH), derived from the precursor prohormone pro-opiomelanocortin (POMC), which also gives rise to ACTH. Thus, MSHs, like ANPs, are from a prohormone containing four peptide hormones when proteolytically processed.[157,158] Each of the MSH peptides is natriuretic when infused in experimental animals.[49,157,158,253] The mechanisms of action of the MSHs are different from those of the cardiac hormones, in that MSH works via intracellular cyclic AMP rather than cyclic GMP.[388] The MSH-induced natriuresis does not appear to be a direct effect on the kidney, but rather via an interaction with renal nerves to inhibit sodium reabsorption, as prior renal denervation completely prevents the natriuresis secondary to MSH.[49]

Ouabain-Like Factors

Ouabain-like factors (factors that circulate and by definition inhibit Na^+,K^+-ATPase) have been sought for decades. Utilizing a very sensitive radioimmunoassay to ouabain, E. P. Gomez-Sanchez et al. determined that ouabain itself does not circulate in human or rat plasma, as a peak corresponding to ouabain was not found on high pressure liquid chromatography.[125] In most samples, they found only very low levels of an ouabain-like substance was present.[125] As outlined previously, vessel dilator, long-acting natriuretic peptide, and kaliuretic peptide are circulating peptide hormones[72,102,103,160,391,420,421] that inhibit the ouabain site on renal $Na^+ - K^+$-ATPase.[51,139] ANP does not inhibit renal $Na^+ - K^+$-ATPase,[51,139,270] and therefore would not be the "third factor" or an ouabain-like factor. Since the other three peptide hormones fulfill all the characteristic of the "third factor," they may actually be the "ouabain-like factors" that have been sought. Since LANP, vessel dilator, and kaliuretic peptide circulate at 100-fold higher levels than this substance, the volume-expanded substance(s) that do the majority of inhibiting of Na^+-K^+-ATPase at the ouabain site on the Na^+-K^+-ATPase are LANP, vessel dilator, and kaliuretic peptide, rather than some substance structurally similar to ouabain which, if it circulates, is present in extremely low levels in the circulation.[125]

NATRIURETIC PEPTIDE RECEPTORS A, B, AND C

Atrial natriuretic peptides, after moving via the circulation to their respective target tissues, mediate their action(s) at the cellular level by first binding to high-affinity specific receptors on the cell surface (Figure 37.4), which results in the intracellular generation of cyclic GMP via activation of the enzyme guanylyl cyclase which resides in the cytosolic domain of these membrane receptors as an integral part of these receptors.[50,82,194] Guanylyl cyclase (also termed guanylate cyclase) catalyzes the formation of the intracellular messenger cyclic 3′,5′-guanosine monophosphate (cyclic GMP).[373,409,419]

The area in the kidney with the most ANP-binding sites is the glomeruli, followed by proximal tubules and then inner medullary collecting ducts.[194] With respect to ANP, BNP, and CNP receptors, cDNA cloning has shown three types of natriuretic peptide receptors (NPR): NPR-A; NPR-B; and NPR-C.[50,82,194,199,240] Only NPR-A and NPR-B exhibit the intracellular guanylyl cyclase (GC) catalytic domain (Figure 37.4), whereas the third receptor, NPR-C, contains no guanylyl cyclase domain.[82,194,240] NPR-A and NPR-B, which bind ANP, BNP, and CNP, are structurally similar and contain a ligand-binding extracellular domain,[194] a protein kinase-like domain, and a guanylyl cyclase domain[50,82,194] (Figure 37.4). Upon ligand biding, a change in receptor conformation allows cytosolic factors to interact with the kinase-like domain, leading to activation of guanylyl cyclase and the consequent generation of cGMP, the second messenger of the cardiac hormones. The NPR-A receptor binds ANP, BNP, CNP, and urodilatin with a rank order of selectivity being ANP = urodilatin > BNP > CNP.[50,82,194,240] The order is reversed for NPR-B receptor (CNP >> ANP > BNP). NPR-B is structurally similar to the NPR-A receptor, with 74% homology at the cytoplasmic domain, but only 44% homology in the extracellular-binding domain, which may explain the difference in ligand specificities of the two guanylyl cyclase receptors.[50,194]

NPR-A mRNA is expressed mainly in the kidney, in the glomeruli, renal vasculature, proximal tubules, and in the IMCD.[19,50,194] The distribution of NPR-B overlaps to some extent with that of the NPR-A, and is found in the kidney, vasculature, and brain. In vascular endothelium and smooth muscle, NPR-B is more abundant than NPR-A. Compared to the NPR-A receptor, low levels of the NPR-B receptor are present in the kidney.[34,221]

Number of ANP Receptors per Cell

The number of ANP receptors per cell varies with the cell type.[19,71,152] Smooth muscle vasculature appears to be the target cell most richly endowed with ANP receptors.[152] The reported number of receptors in

vascular smooth muscle cells has ranged from 18,400 binding sites per cell to 500,000.[366] Comparison of a variety of cultured cells revealed 310,000, 80,000, 50,000, 14,000, and 3,000 sites per cell for vascular smooth muscle, lung fibroblasts, adrenal cortex, aortic endothelial cells, and Leydig cells of the testis, respectively.[366] Twelve thousand ANP-binding sites per cell have been found in kidney glomerular mesangial cells; markedly less than in other vascular areas, but the receptors in the mesangial cells exhibited as high affinity as other vascular areas for ANP.[19]

Inverse Relationship of Change in Number of ANP Receptors with Circulating ANP Concentrations

The number of ANP receptors varies with fluid status, and inversely with the circulating ANP concentration.[366] Deprivation of water decreases the circulating ANP concentration and augments receptor number in both kidney and adrenal gland.[366] Rats fed a low-salt diet for 2 weeks exhibit "upregulation" of glomerular ANP receptor density, whereas animals fed a high-salt diet have a decreased receptor density.[366] The decrease in total ANP receptors, at least after salt-loading, is due exclusively to a decrease in the NPR-C receptor, rather than the NPR-A receptor.[366]

Structure of NPR-A Receptor

The structure of the NPR-A receptor is illustrated in Figure 37.5. This structure was elucidated using complimentary DNA (cDNA) encoding a 115 kDa human natriuretic peptide receptor (NPR)-active (A or functional) receptor that possesses guanylyl cyclase activity.[50,82,194] The NPRA receptor has 1029 a.a., a 32 a.a. signal sequence followed by at 441 a.a. extracellular domain (i.e., projecting from the cell).[50,82,194] This extracellular portion of the NPR-A receptor is 33% homologous to the 60 kDa NPR-C receptor.[82,194] This extracellular portion of the receptor is the binding site for ANP, BNP, and CNP. A 21 a.a. transmembrane portion of the receptor "anchors" the receptor to the membrane. Inside the cell (intracellular domain) there is a 568 a.a. cytoplasmic portion of the receptor with homology (23%) to the protein kinase family (protein kinase domain) being next to the membrane,[50,82,194] followed by a large guanylyl cyclase catalytic portion of the receptor (Figure 37.5) that is 42% homologous to cytoplasmic guanylyl cyclase.[50,82,194] The kinase domain binds ATP, but lacks true kinase activity. Rather, it functions to inhibit the guanylyl cyclase domain. If the kinase domain is "knocked-out," guanylyl cyclase continuously functions. The molecular weight of this receptor is 114,426.[50]

The guanylyl cyclase portion of human and rat NPR-A receptors are 90% identical throughout their sequences.[50,82] The similar amino acid sequence between the NPR-C receptor[82,194,240] and the extracellular portion of the NPR-A receptor reflect a common function shared between them – they both bind ANP, BNP, and CNP.

NPR-C (Clearance) Receptor

Cross-linking studies revealed that in addition to the high molecular weight receptors for ANP, BNP, and CNP there was also a low molecular weight 60 kDa receptor that appeared to be a subunit of the high molecular weight receptor.[82,194,240] This 60 kDa receptor was found not to contain guanylyl cyclase or to mediate any of the known effects of ANP, such as natriuresis or diuresis.[82,194,215]

Structure of NPR Clearance Receptor

The NPR-C receptor is similar structurally outside the cell to the NPR-A receptor, with 496 a.a. compared to the 441 a.a. projecting from the cell for the NPR-A receptor.[82,194,215] They have a similar single short transmembrane-spanning region, but where the two receptors markedly differ is inside the cell. The NPR-C receptor has only a very short 37 a.a. tail into the cytoplasm of the cell as compared to the large 568 a.a. portion in the cell for the NPR-A receptor.[50,82,194,215] Neither the protein kinase domain nor the guanylyl cyclase catalytic site is present in the NPR-C receptor. That the NPR-C receptor is not linked to a second messenger system explains its inability to cause vasodilation, diuresis or natriuresis.[50,82,194,215] The order of binding to the NPR-C receptor is ANP > CNP > BNP. The NPR-C receptor is the most abundant receptor of the natriuretic receptors, accounting for more than 95% of the total receptor population, and is located at high density in kidney, vascular endothelium, smooth muscle cells, and the heart.[82,194,215]

Vessel Dilator and LANP Receptors

Vessel dilator and long-acting natriuretic peptide do not bind to the NPR-A, B or C receptors, but rather have their own specific receptors.[365,372,378,397] Vessel dilator, LANP, and kaliuretic peptide, on the other hand, are linear peptide hormones, and one would not expect binding to the above NPR-A, -B, and -C receptors which require a ring structure for binding[50,82,194,215,240] which ANP, BNP, and CNP have.[372,378]

LANP Receptor

Long-acting natriuretic peptide (LANP), as well as ANP, binds specifically to smooth muscle membranes,[378] placental membranes,[365] distal nephrons,[397] proximal tubules,[397] and renal cortical and medullary membranes.[397] ANP and vessel dilator inhibit ^{125}I-labeled LANP-binding somewhat at concentrations above which these peptide hormones are known to circulate, i.e., 10^{-6} M for ANP and 10^{-7} M for vessel dilator. Scatchard analysis of the LANP-binding data resulted in a straight line,[378] suggesting that these smooth muscle cells contain a single class of high-affinity binding sites for LANP with an equilibrium dissociation constant (K_d) of 0.11 nM. The binding capacity (maximal binding, B_{max}) for LANP was 2.57 fmol/10^6 cells, and the number of binding sites was calculated to be 1548 per cell.[378]

Vessel Dilator Receptor

Vessel dilator also binds specifically to smooth muscle membranes,[378] proximal tubules,[397] distal nephrons,[397] placental membranes,[365] and renal cortical and medullary membranes[397] at a site distinct from the binding of ANP to membranes. The binding of this peptide hormone could be inhibited by concentrations (10^{-4} to 10^{-7} M) of ANP, LANP, insulin, and ACTH, which are far in excess of their respective circulating concentrations.[378] Scatchard analysis of the vessel dilator-binding data resulted in a straight line,[378] suggesting that smooth muscles contain a single class of high-affinity binding sites for vessel dilator with an equilibrium dissociation constant (K_d) of 4 nM. B_{max} for vessel dilator was 59.9 fmol/10^6 cells, and the number of binding sites was calculated to be 36,087 per cell.[378]

DEGRADATION OF NATRIURETIC PEPTIDES BY KIDNEY

The inactivation of the ANP, BNP, and CNP occurs via two pathways: binding to clearance receptors and enzymatic degradation. The clearance receptor (NPR-C)[32,50,82,194,240] clears ANP, BNP, and CNP through receptor-mediated uptake, internalization, and lysosomal hydrolysis with rapid and efficient recycling of internalized receptors to the cell surface. Enzymatic degradation of ANP, BNP, and CNP takes place in the lung, liver, and kidney, and the main enzyme responsible for this degradation is neutral endopeptidase (NEP-24.11).[34,411] NEP, originally referred to as enkephalinase because of its ability to degrade opioid peptides in the brain, was subsequently shown to be identical to a well-characterized zinc metallopeptidase present in the kidney.[411] This zinc metalloproteinase hydrolyzes internal peptide bonds of polypeptides, rather than those adjacent to their N- or C-terminal ends. NEP has a ubiquitous tissue distribution and multiple functions, sharing structural similarities with various metallopeptidases, including aminopeptidase ACE, and carboxypeptidases A, B, and E.[411] NEP is most abundant in the brush borders of the proximal tubules of the kidney, where it rapidly degrades filtered ANP, thus preventing ANP from reaching more distal luminal receptors.[411] In the case of ANP, NEP-24.11 cleaves the Cys^{105}–Phe^{106} bond to disrupt the ring structure and inactivate the peptide. NEP 24.11 is a nonspecific enzyme that also cleaves enkephalins, endothelin, substance P, kinins, neurotensin, insulin B chain, angiotensin, calcitonin gene-related peptide, and adrenomedullin, as well as ANP, BNP, and CNP. With respect to ANPs in humans,[411] ANP and CNP are preferred substrates for NEP as opposed to BNP with the Cys–Phe bond of human BNP being relatively insensitive to enzymatic cleavage.[411]

INFLUENCE OF ACUTE RENAL FAILURE ON CIRCULATING CONCENTRATION OF CARDIAC HORMONES

Each of the cardiac hormones from the ANP prohormone (vessel dilator, ANP, LANP, and kaliuretic peptide),[12,18,48,56,103,160,193,243,300,395,396,420,421] BNP,[39,43,58,108,199,200] and CNP[22,159,161,348] increase in the circulation (mainly from the heart ventricle[83,115,271]) in salt- and water-retaining states such as renal failure and congestive heart failure, compared to their concentrations in healthy individuals, in an apparent attempt to overcome the salt and water retention via their natriuretic and diuretic properties.[379,380] The disease state associated with the highest circulating concentrations of the cardiac natriuretic peptides is renal failure.[102,103,307,417,421] One would suspect that cardiac natriuretic peptides are higher in renal failure versus Class IV New York Heart Association congestive heart failure patients, because of the added pathophysiology of decreased degradation of these peptides with the decreased functioning renal parenchyma.[421] Franz et al.,[103] however, have shown that there is an increased excretion of the cardiac natriuretic peptides in renal failure, and that the increase in vessel dilator excretion occurs even before serum creatinine levels begin to rise. The circulating concentrations of the cardiac hormones in chronic renal failure appear to reflect volume status.[193,236,284,422] Despite increased circulating concentrations of cardiac hormones in sodium-retaining disease states, the kidney retains sodium and is hyporesponsive to ANP, LANP, and BNP.[35,199,277,352,379] The mechanism for the attenuated

renal response to these natriuretic peptides is multifactoral and includes renal hypoperfusion, activation of the renin–angiotensin–aldosterone and the sympathetic nervous systems.[34,140,235]

Influence of Renal Failure on other Natriuretic Peptides

Adrenomedullin,[90,305,346] guanylin,[187] and uroguanylin[185,186] increase in renal failure and/or experimental nephrotic syndrome.

HEMODIALYSIS

Cardiac Hormones Synthesized by ANP Prohormone Gene

The circulating concentrations of the cardiac hormones have been suggested as possible indicators of when to perform dialysis in persons with chronic renal failure.[193,236,284,307,422] Other data, however, suggest that ANPs are not useful to predict when hemodialysis is necessary.[29] Hemodialysis lowers the circulating concentration of cardiac hormones by 34%–42%, with the amount of decrease appearing to be related to volume status of the patients.[193,417,422] Hemodialysis does not return the levels of ANP to those of healthy adults,[193,416,417,422] and it does not reduce circulating concentrations of vessel dilator and LANP.[422] Part of the reason for the difference in hemodialysis effects on the cardiac hormones is that less than 1.5% of vessel dilator and LANP cross the dialysis membrane, compared to 15% to 25% of ANP crossing hemodialysis membranes.[422] Hemodialysis using cellulose-triacetate dialyzers reduces plasma levels of these peptides in acute renal failure more than hemodialysis therapy with polysulfone dialyzers.[102]

BNP

Hemodialysis has been reported both to lower,[200] and to have no effect on circulating BNP levels.[49] Before dialysis in persons with chronic renal failure (CRF), plasma BNP levels have no relationship to serum creatinine or mean blood pressure.[192] In CRF patients whose plasma BNP levels decrease with dialysis, this decrease correlates with the degree of postural blood pressure drop, but there is no correlation with the fall in serum creatinine.[200] In none of the studies of BNP and dialysis[39,58,192,200] has BNP ever returned its circulating concentration to that of healthy individuals. With volume repletion after hemodialysis there is an exaggerated release of ANP, but changes in BNP are small and without any correlation with either atrial or ventricular volume.[58]

Adrenomedullin and Proadrenomedullin N-Terminal 20 Peptide

Both adrenomedullin and proadrenomedullin N-terminal 20 peptide (PAMP) increase in chronic renal failure.[90,305,346] Hemodialysis decreases these peptides to near-control levels, with PAMP being 2.17 ± 0.18 fmol/ml versus 1.64 ± 0.12 fmol/ml for controls.[346]

Guanylin and Uroguanylin

Both guanylin and uroguanylin are increased in persons with impaired renal function.[168,169] Hemodialysis with EVAL membranes decreases guanylin concentrations after one hour of dialysis, but the plasma levels after hemodialysis with PC membranes show no change.[187]

RENAL TRANSPLANTATION

Successful transplantation of functioning kidneys decreases the markedly elevated circulating levels of cardiac hormones in persons with acute renal failure to those of healthy individuals.[265,279] Nonfunctioning renal allografts continue to have elevated circulating concentrations of the cardiac hormones.[265,279] Post renal transplant, it takes seven days for ANP and 10 days for vessel dilator to return to normal.[265] This suggests that the allograft kidney does not fully function immediately with respect to clearing these peptides. The half-life of ANP in healthy persons is only 2.5–3.5 minutes.[4,366] If the transplanted kidneys began to function immediately, one would have expected the circulating concentration of ANP to have decreased to the normal range within 24 hours (360 half-lives). Vessel dilator has a 20-fold longer half-life compared to that of ANP,[4,366] which may explain why it takes three more days for this peptide hormone to normalize in the circulation after successful renal transplantation. If one gives ANP (via infusion) at the time of renal transplant, this does not appear to have any beneficial effect on the outcome of the renal allograft.[303] It is important to note that the elevated circulating cardiac hormones in heart failure also normalize with successful heart transplantation.[416]

ATRIAL NATRIURETIC PEPTIDE PROHORMONE GENE EXPRESSION IN INVERTEBRATES AND PLANTS

In addition to proANP gene being present in mammals and vertebrates, where lower vertebrates such as

the frog have an identical proANP gene,[296] blue crabs and oysters have been demonstrated to have the proANP gene in their hearts.[273,367] The proANP gene in oysters and blue crabs can be upregulated by increasing salinity in the external environment, such as when the animal moves from freshwater to seawater.[273,402] This change in environmental salinity also modulates end-product concentrations of this gene expression, that is, the cardiac hormones.[256] Environmental salinity also modulates ANP in the teleost fish *Gila atraria*.[415] Seawater trout have higher concentrations of ANP, vessel dilator, and LANP than freshwater trout to help them maintain volume homeostasis in a higher salt environment.[59] Even the most primitive heart in the animal kingdom contains the atrial natriuretic peptide hormonal system.[386] Diving is a modulator of ANP in lower animals, with diving increasing ANP in freshwater diving turtles[16] similar to whole body immersion in humans.[390,391,396]

Although a gene in the animal kingdom expressing a peptide hormonal system in plants had never been demonstrated previously, there is now evidence for a proANP-like gene in plants.[401] Southern blots of English ivy (*Hedera helix*) genomic DNA revealed that the proANP gene sequence was present in its roots, stems, and leaves.[401] In plants, ANPs enhance the flow of water up stems to flowers and leaves, a process that is at least partially due to increasing the rate of transpiration (loss of water from the leaves) via opening the stomatal pores in leaves.[367,387] These peptides are present even in *Euglena*, a single-cell, flagellated, chlorophyll-containing plant without leaves, stems or roots.[387] The oldest existing trees on Earth, the *Metasequoia*, which exist only in China, contain the ANP prohormone and ANP.[427] These peptide hormones are also found in single-cell animals, such as paramecium.[385] In single cell organisms, these peptides appear to help maintain the internal volume of the cell.[385] The demonstration of the proANP gene sequences and expression of the ANP-like gene in plants suggests that plants and animals may have evolved much more similarly than previously thought.[387]

PROTECTIVE AND THERAPEUTIC EFFECTS OF CARDIAC AND RENAL HORMONES IN ACUTE RENAL FAILURE

ANP and Urodilatin

Animals

Acute renal failure (ARF) develops in 2–5% of all patients admitted to tertiary care hospitals.[154,423] The underlying cause is a renal insult (acute tubular necrosis) in 60% of patients.[154,423] When dialysis was introduced in the mid-1940s, the mortality resulting from severe ARF was approximately 50%.[154] This poor prognosis has not improved, with mortality now in the 40–80% range in oliguric ARF.[9,31,66,153,154,308,423] The occurrence of ARF in the hospital increases the relative risk of dying by 6.2-fold, and the length of hospitalization by 10 days.[277]

Several of the cardiac hormones have been investigated as possible treatment(s) for ARF. Atrial natriuretic peptide (ANP) had encouraging results in early studies of ARF in animals.[57,208] The infusion of ANP[57,208,219,236,240,245,254,278,308,322,378,379] or urodilatin[232,314,323] in rat models of ischemic ARF attenuated renal tissue damage and preserved glomerular filtration rate. Nakamoto et al.[241] and Shaw et al.[322] were able to shorten the course of renal artery cross-clamping-induced ARF in rats with ANP. Conger et al.[57] found marked improvement in GFR in a rat renal artery-clamp model when ANP-III (0.2 μg/kg/min) was given intravenously immediately after clamp release in combination with dopamine sufficient to maintain mean arterial pressure above 100 mmHg. In the rat, ANP had no effect on GFR when given intravenously, but did have a GFR effect when given directly into the renal artery for four hours.[322] The inability of ANP to increase GFR when given intravenously could be restored if dopamine was given simultaneously.[57] In the dog, the improvement in renal perfusion only lasted for a short period after a 180-minute infusion of ANP.[245] When ANP was given by intra-aortic bolus on days 1 and 2 after the above infusion, there was no significant improvement in renal perfusion on those days.[245] Thus, in animals the improvement in renal failure with ANP was only of short duration and depended upon whether ANP was given intravenously or directly into the artery.[57,245,322]

Humans

The administration of 0.2 μg of ANP/kg of body weight^{-1}/min^{-1} for 24 hours to humans with ARF revealed that ANP did not cause significant improvement, and did not reduce the need for dialysis or reduce mortality.[7,207] ANP infusions were associated with decreased survival in the nonoliguric ARF subjects (75% of subjects).[7] The usefulness of ANP for treatment is hampered by its short half-life of 2.5 minutes,[4,366] and by its very short duration of action.[57,208,214,220,278,382] Of 504 ARF patients treated with ANP, 46% developed hypotension, which would further limit its usefulness in ARF.[7] Urodilatin has also been associated with severe hypotension and bradycardia, when given as a potential treatment of congestive heart failure.[184] ANP is now considered more harmful than helpful with respect to the treatment of acute renal failure.[35] When ANP was given before and

during radiocontrast study in 247 patients with chronic renal failure, no beneficial effect was found.[196] Urodilatin has been suggested as a possible treatment of renal failure,[231,314,315] but in double-blind phase II trials in acute renal failure patients, urodilatin has been found to have no beneficial effect.[232]

Vessel Dilator

Vessel dilator appears to be the cardiac hormone with the most promising therapeutic potential in ARF. Vessel dilator ($0.3\,\mu g/kg^{-1}/min^{-1}$ via intraperitoneal pump) decreases blood urea nitrogen (BUN) and serum creatinine from 162 ± 4 mg/dl and 8.17 ± 0.5 mg/dl, respectively, to 53 ± 17 mg/dl and 0.98 ± 0.12 mg/dl in acute renal failure animals, where ARF was established for 2 days (after vascular clamping) before vessel dilator was given.[54] At day 6 of ARF, mortality decreased to 14% with vessel dilator from 88% without vessel dilator.[54] The ARF animals that did not receive vessel dilator had moderate (25%–75% of all tubules involved) to severe (>75% of all tubules necrotic) acute tubular necrosis by day 8 after their ischemic event (Figure 37.7b). As shown in Figure 37.7b, the nuclei in the tubules of these animals were almost completely destroyed, and the tubules were filled with sludge. The destruction of the tubules included both the proximal and distal tubules, with the proximal tubules being more severely affected (Figure 37.7b). The glomerulus of the ARF animals was spared compared to the renal tubules, with glomerulus appearing to be normal in the ARF animals (Figure 37.7a and 37.7b).

The addition of vessel dilator after renal failure had been present for two days resulted in a marked improvement in the renal histology (Figure 37.7c), with scores ranging from 0 (no tubular necrosis) to 1+ (<5% of the tubules involved).[54] The nuclei of the ischemic tubules regenerated secondary to vessel dilator (Figure 37.7c). When the kidneys were examined at day 8 of renal failure, the brush borders of the proximal tubules of the ARF animals treated with vessel dilator were present (Figure 37.7c), which was similar to the proximal tubules of healthy animals (Figure 37.7a). In the ARF animals not treated with vessel dilator, the brush borders of the tubules were destroyed (Figure 37.7b). The glomeruli of vessel dilator-treated ARF animals also appeared normal (Figure 37.7c). It is important to note that the animals treated with vessel dilator who had a significant increase in survival had nonoliguric renal failure.[54] As noted previously, nonoliguric renal failure subjects treated with ANP had a decreased survival and it was the nonoliguric renal failure subjects who did not respond to ANP.[7] Vessel dilator, LANP, and kaliuretic peptide, as opposed to ANP, BNP, and urodilatin, have never caused a hypotensive episode when given to either healthy animals or humans[220,381,382] or when given to humans with sodium and water retention.[243,379,380]

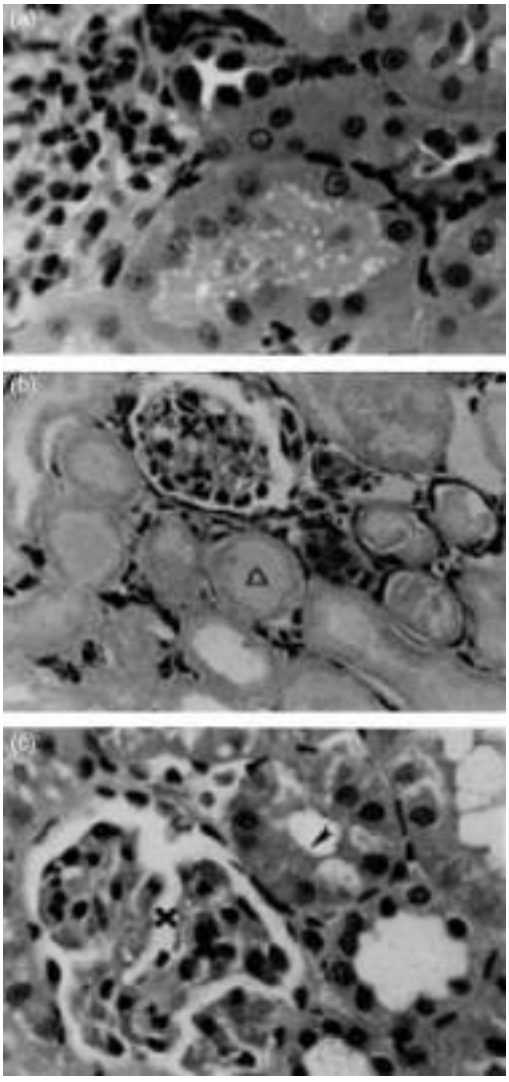

FIGURE 37.7 **Renal histology of healthy Sprague–Dawley rat.** (a) with intact proximal tubular brush border (arrowhead). (b) ARF rat at day 8 with marked tubular necrosis (open triangle) and without intact brush border present (>75% of tubules are necrotic). The glomerulus (x) appears to be normal. (c) ARF rat treated with vessel dilator from days 2 to 5 of ARF with kidney examined after day 8 of ARF reveals brush border to be present in proximal tubule (arrowhead). No tubules are necrotic in this ARF animal treated with vessel dilator. The glomerulus (x) is intact (Magnification of hematoxylin and eosin: ×426 (a) and (c); and ×320 (b); ARF: acute renal failure). *(With permission, from ref. [54].)*

The ability of vessel dilator to reverse ischemic ARF is consistent with the important concept that the pathophysiology of ischemic ARF is due to a sublethal and reversible injury to renal tubular cells.[31,234] Part of the improvement by vessel dilator may be due to its ability to cause intrarenal vasodilation, as it is a strong vasodilator.[389] The reason why vessel dilator has greater beneficial effects than ANP, BNP, CNP, and urodilatin in acute renal failure appears due, at least in part, to its ability to cause the endogenous synthesis of renoprotective prostaglandin E_2 (PGE_2)[6,180,414] which ANP, BNP, CNP, and urodilatin do not do.[51,139]

A suggestion that PGE_2 is renoprotective (by maintaining glomerular hemodynamics) is reinforced by the observation that cyclooxygenase inhibitors in congestive heart failure and volume depletion states augment the reduction in RBF and GFR.[92,410] There is a dramatic decrease with prostaglandins in the outer medulla perfusion following ischemic injury,[178] a region of renal tissue which normally operates "on the verge of ischemia".[36] Prostaglandins have a favorable effect on blood flow distribution to this region.[237] In addition, prostaglandins have distinct cytoprotective effects and improve microvascular permeability in ischemic ARF.[42,180] Prostaglandins are not stored in the kidney, but rather have to be synthesized acutely secondary to a stimulating agent such as vessel dilator[51,139] in order for prostaglandins to have a positive beneficial effect in renal failure.

Adrenomedullin

There is evidence that ADM is renoprotective in Dahl salt-sensitive rats, in that when perfused for seven days the glomerular injury score is 54% less ($p < 0.05$) than in untreated Dahl salt-sensitive rats.[248] The adrenomedullin treated salt-sensitive rats, however, had considerably more ($p < 0.01$) glomerular sclerosis and anteriolar sclerosis and atrophic tubules after treatment than the control Dahl salt-resistant rats.[248]

BNP

BNP has not been investigated as a treatment of acute renal failure, but one would expect that BNP, similar to ANP, will have blunted or no effects in ARF compared to its effects in healthy animals.[7,207,245]

CNP

CNP increases in the circulation in ARF,[348] but its effects in acute renal failure are unknown. As discussed above, CNP has no natriuretic effects in healthy humans.[21,47,161]

DNP

DNP has been evaluated in persons with end-stage renal disease on dialysis and was found not to correlate ($p = 0.62$) with echocardiographic left ventricular mass index (LVMI), while ANP and BNP did correlate with LVMI of these end-stage renal patients.[43] DNP has not been investigated with respect to its possible therapeutic effects in renal failure.

TREATMENT OF OTHER DISEASES WITH ABNORMAL BLOOD VOLUME

Congestive Heart Failure

As part of the adaptive response to the pathophysiology of congestive heart failure, cardiac hormones increase in circulation.[32,38,83,108,176,177,273,350,368,379,380,418] The rationale for treatment of the pathophysiology of CHF with cardiac hormones (which are already increased in the circulation) is based upon other hormonal systems, where if one gives pharmacological rather than physiological concentrations of a hormone one often can overcome a defect in the target organ with respect to a particular hormone. In congestive heart failure, the pathophysiology with respect to atrial natriuretic peptides appears to be in the target organ(s) – the kidney has a diminished response to some of the atrial peptides – rather than the heart not producing enough of the respective hormones.[366] When ANP was investigated for possible treatment of CHF pathophysiology, it was found to have a markedly attenuated natriuretic response.[56,104,255,318] High-dose administration of ANP produces little or no diuresis or natriuresis in humans with CHF.[56] Synthetic brain natriuretic peptide (Nesteride®) in CHF individuals causes a small increase in urine volume (90 ± 38 versus 67 ± 27 ml/hr).[217] There is no significant natriuresis[3] or diuresis[166,233] with Nesteride® infusion in humans with CHF. In CHF animals, BNP has had no significant natriuretic or diuretic effects.[199] BNP can cause significant hypotension, however, in CHF subjects[3,233] with an incidence of 27% reported with 0.06 μg/kg/min dose.[233] Urodilatin infusion in CHF animals, likewise, causes significantly less natriuresis and diuresis compared to healthy animals.[1]

Vessel dilator, when given intravenously for 60 minutes to NYHA Class III CHF subjects, increases urine flow two- to 13-fold, which is still increased three hours after its infusion is stopped.[380] In CHF subjects, vessel dilator infusion enhances sodium excretion levels three- to four-fold, and the fractional excretion of sodium (FE_{Na}) six-fold, which are still

significantly ($p < 0.01$) elevated 3 hours later.[380] Vessel dilator simultaneously decreases systemic vascular resistance 24%, pulmonary vascular resistance 25%, pulmonary capillary wedge pressure 33%, and central venous pressure 27%, while simultaneously increasing cardiac output 34%, cardiac index 35%, and stroke volume index 24% in individuals with CHF.[380] There were no side-effects with infusion of vessel dilator in CHF subjects, and specifically none of the CHF subjects became hypotensive as with BNP and ANP.[380] The natriuretic and diuretic effects of vessel dilator to help reverse the pathophysiology of CHF are as potent (not decreased or blunted) in persons with CHF as those observed in healthy persons.[380]

Long-acting natriuretic peptide (LANP) maximally increases urine flow and natriuresis only two-fold in persons with CHF[379] compared to four- to five-fold increase in urine flow and three- to eight-fold increase in natriuresis in healthy individuals.[382]

ANTIPROLIFERATIVE AND ANTI-CANCER PROPERTIES OF CARDIAC NATRIURETIC HORMONES

In blood vessels, ANP inhibits smooth muscle cell proliferation (hyperplasia) as well as smooth muscle cell growth (hypertrophy).[2,162,163,431] Atrial natriuretic peptide has growth-regulatory properties in a variety of other tissues including brain, bone, myocytes, red blood cell precursors, and endothelial cells.[10,11,143,169,261,431] In the kidney, ANP causes antimitogenic and antiproliferative effects in glomerular mesangial cells via inhibiting DNA synthesis.[10,11,169] The newest discovered property of the cardiac hormones, urodilatin, CNP, and DNP is their ability to inhibit the growth of cancers *in vitro* and *in vivo*.[361,362,377] The first cancer studied both *in vitro* and *in vivo* was human pancreatic adenocarcinomas, which have the lowest five-year survival rate of all common cancers.[267,424] The five-year survival rate of persons with adenocarcinoma of the pancreas is 1%.[267,424] The median survival is four months.[267,424] Current cancer chemotherapy and surgery prolong survival by a few months, but the abovementioned survival rates are for persons treated with surgery and/or currently available cancer chemotherapeutic agents.[267,424]

The four cardiac hormones from the ANP prohormone (Figure 37.1) decrease the number, i.e., eliminate up to 97% of human pancreatic, kidney, prostate, colon, breast, and ovarian adenocarcinoma cells,[131,355,356,357,361,362] angiosarcoma of the heart cells,[363] melanomas,[358] medullary thyroid carcinomas,[85] glioblastomas of brain,[359] as well as small-cell,[364] and squamous cell lung carcinoma cells[360] within 24 hours. There was a 97.4%, 87%, 88%, and 89% ($p < 0.001$ for each) decrease (i.e., elimination) of human prostate adenocarcinoma cells secondary to vessel dilator, long-acting natriuretic peptide, kaliuretic peptide, and ANP, respectively, within 24 hours at their 1 mM concentrations, without any proliferation in the three days following this decrease.[355] When utilized with these four cardiac hormones respective antibodies, their ability to decrease the number of prostate cancer cells was completely blocked, indicating that their effects were specific, i.e., not due to some other hormone or substance.[355] Atrial natriuretic peptide reduces the number of hepatoblastoma cells in culture.[285]

BRAIN NATRIURETIC PEPTIDE AND C-NATRIURETIC HAVE LESS SIGNIFICANT ANTI-CANCER EFFECTS

Dose–response investigations indicate that brain natriuretic peptide (BNP) has no anti-cancer effects at any concentration.[131,355–357,364] The addition of BNP for 24 hour results in a 1%, 2%, and 4% (all non-significant) decrease in renal carcinoma cell numbers at its 1, 10, and 100 μM concentrations.[356] C-natriuretic peptide (CNP) has anti-cancer effects, but only at 100-fold higher concentrations than that observed for the four cardiac hormones synthesized by the proANP gene.[356,364] With exposure to CNP for 24 hours there was a 1% (n.s.), 7% (n.s.), and 10% ($p = 0.04$) decrease in renal carcinoma cell numbers at its 1, 10, and 100 μM concentrations.[356] Similar results were found at 48, 72, and 96 hours exposure to BNP and CNP.[356]

THE KIDNEY HORMONE URODILATIN ALSO HAS ANTI-CANCER EFFECTS

One might expect that urodilatin may have anti-cancer effects, as this peptide has identical a.a. to ANP and identical a.a. to the four terminal a.a. of kaliuretic peptide, both of which have anti-cancer effects. Urodilatin decreases the number of renal carcinoma cells by 66% at its 100 μM concentration, while ANP and kaliuretic peptide with the same amino acids at this same concentration eliminated 70% and 74% of the renal carcinoma cells in 24 hours.[356] Urodilatin, vessel dilator, LANP, kaliuretic peptide, and ANP each at their 1 μM concentrations inhibit DNA synthesis when incubated with the human renal carcinoma cells for 24 hours by 65%, 84%, 70%, 74%, and 77%, respectively ($p < 0.001$).[356]

CARDIAC NATRIURETIC HORMONES ELIMINATE UP TO 80% OF HUMAN PANCREATIC ADENOCARCINOMAS *IN VIVO*

When the four cardiac hormones from the proANP gene each at 3 nM min^{-1} kg^{-1} body weight were infused subcutaneously for 28 days in athymic mice bearing human pancreatic adenocarcinomas, ANP eliminated 80% of the human pancreatic cancers.[383] Vessel dilator, LANP, and kaliuretic peptide eliminated the primary pancreatic cancers in 33%, 20%, and 14% of their respective treatment groups.[383] In none of the animals in which the pancreatic adenocarcinomas were eliminated in the primary site did a single animal ever have a recurrence in the primary site during its normal lifespan.[383] One ANP-treated animal developed a metastatic lesion, and this lesion was eliminated with treatment with vessel dilator.[383] Even in the treated animals which did not have total elimination of their human pancreatic adenocarcinoma, their tumor volume decreased to less than 10% (and with vessel dilator to less than 2%) of that of the untreated animals both during treatment and in a 12-month follow-up period.[383]

CARDIAC HORMONES ELIMINATE TWO-THIRDS OF HUMAN BREAST CANCERS *IN VIVO* WITHOUT ANY SURGERY

It was estimated that in 2009 there were 194,280 new cases of breast cancer and 40,610 deaths from breast cancer in the United States.[165] Breast cancer is the second leading cause of death from cancer in women, and the leading cause of death in women aged 40 to 55 in the United States.[258] Breast cancer is the leading cause of cancer death in women worldwide.[258] The number of new cases of breast cancer worldwide was estimated to be 1.05 million, with 370,000 deaths in 2000.[258]

Vessel dilator, LANP, kaliuretic peptide, and ANP eliminated 67%, 50%, 67%, and 33% of the human breast adenocarcinomas in athymic mice when infused subcutaneously for 28 days 3 nM min^{-1} kg^{-1} body weight.[399] There was no recurrence of the breast cancers in the primary site, and no metastasis except in the ANP-treated group[399] (Table 37.2).

TABLE 37.2 Cardiac Hormones Ability to Eliminate Human Cancer Growing in Athymic Mice

	Breast Cancer	Pancreatic Adenocarcinoma	Small-cell Lung Cancer
VDL	67%	33%	71%
LANP	50%	20%	86%
ANP	33%	80%	43%
KP	67%	14%	57%

The numbers in each column are the percentages of human cancers which are eliminated and never recur in the primary site in athymic mice when treated with each of the cardiac hormones for 28 days at 3 nM/kg body weight/minute. Abbreviations: VDL: vessel dilator; LANP: long acting natriuretic peptide; ANP: atrial natriuretic peptide; KP: kaliuretic peptide.

CARDIAC AND KIDNEY HORMONES ELIMINATE UP TO 86% OF HUMAN SMALL-CELL LUNG CANCERS IN MICE *IN VIVO*

Cancer of the lung and bronchus is the leading cause of cancer death in both men and women in the United States, with an estimated 88,900 deaths in men and 70,490 deaths in women in 2009.[165] The same trend is seen in many other countries.[353] In the current management of small-cell lung cancers, the majority of patients are treated first with chemotherapy plus radiotherapy, but with this combination survival is only 20% with limited disease and 0% survival with more extensive disease at three years.[182,353]

Long-acting natriuretic peptide, vessel dilator, kaliuretic peptide, ANP, and urodilatin eliminated 86%, 71%, 57%, 43% ($p < 0.001$ for each of the cardiac hormones), and 25% ($p < 0.05$; urodilatin) of the human small-cell lung carcinomas.[86] One vessel dilator-treated small-cell lung carcinoma animal developed a large tumor (8,428 mm^3 volume) on treatment, and this tumor was eliminated utilizing atrial natriuretic peptide and then long-acting natriuretic peptide each for four weeks sequentially.[86]

ANTI-CANCER MECHANISM WITHIN CANCER CELLS OF THE CARDIAC HORMONES

The Ras mitogen-activated protein kinase (MAPK)/extracellular signal-related kinase (ERK) kinase-(MEK)-ERK cascade (Figure 37.8), hereafter referred to as the Ras-MAPK pathway, is the prototypical signal transduction pathway in cancer.[224,313] This pathway is aberrantly activated in many types of neoplasms, including prostate and breast cancer, with this activation being associated with a poor prognosis.[224,313] The integral role of the Ras-MEK-ERK pathway in mediating multiple hallmarks of cancer has suggested that the different kinases in this pathway may be targets for the treatment of cancer.[225,289,319,320]

Ras

Structural alteration in the GTPase Ras occur in 25 to 30% of human cancers, which allows them to relay

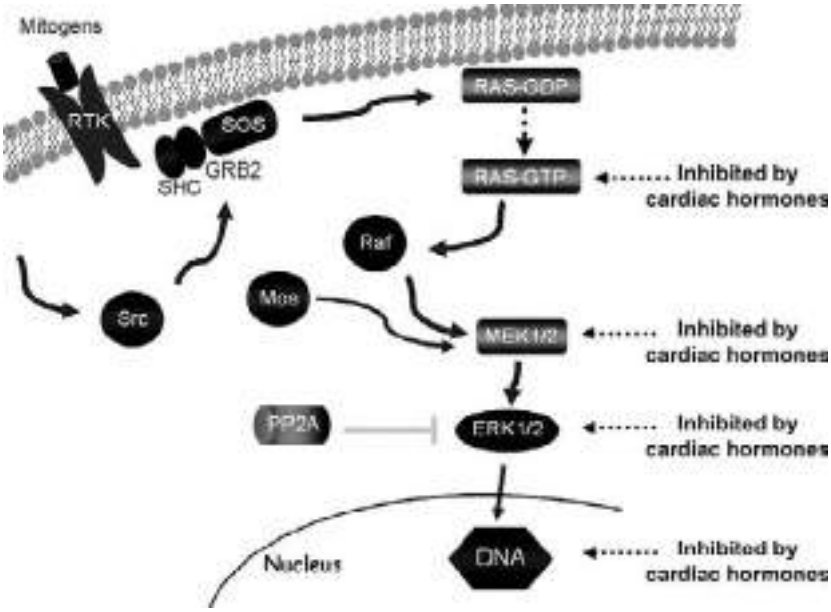

FIGURE 37.8 **Mitogens such as epidermal growth factor bind to their tyrosine kinase receptor (RTK) to convert inactive Ras-GTP mainly via SHC to active Ras-GTP.** Cardiac hormones inhibit up to 98% of 5 metabolic targets (kinases) important in cancer cell growth, i.e., Ras-GTP, MEK 1/2 kinases, and ERK 1/2 kinases of the Ras-MEK 1/2-ERK 1/2 kinase cascade in cancer cells. They are also strong inhibitors (up to 91%) of DNA synthesis within cancer cells. The cardiac hormones also block mitogens such as epidermal growth factor's ability to stimulate the conversion of Ras-GDP to Ras-GTP. [442]

mitogen signals in a ligand-independent manner, thereby obviating the need for ligand activation of growth factor receptors that occurs in normal cells.[225,319] Attempts to target Ras by perturbing its interaction with either Son of Sevenless gene (SOS) or growth factor receptor-bound 2 (GRB2) (Figure 37.8) have not yielded viable drug development candidates, largely because of the inherent difficulties of disrupting protein−protein interactions with drug-like molecules.[319] Several drug discovery programs have also been devoted to finding inhibitors of farnesyltransferase as a means to prevent the membrane localization of Ras.[319] Despite the successful identification of several chemical leads that effectively inhibited this prenylation enzyme, tumor cells, however, have proved generally to be impervious to the action of this class of inhibitors.[319]

Vessel dilator and kaliuretic peptide decrease the activation of Ras-GTP over a concentration range of 0.01 μM to 1 μM.[335] Vessel dilator and kaliuretic peptide (each 1 μM) inhibit the activation of Ras by 95% ($p < 0.001$) and 90% ($p < 0.001$), respectively. At 0.01 μM of kaliuretic peptide, the maximal inhibition was 95%. The inhibition of Ras lasted for 48 to 72 hours secondary to both peptides.[335] Their ability to inhibit Ras was inhibited by cyclic GMP antibody, and cyclic GMP itself inhibited Ras phosphorylation (89%; $p = 0.0015$).[335]

ANP and long-acting natriuretic peptide (each 0.1 μM) inhibited the phosphorylation of Ras 90% ($p < 0.0001$) and 83% ($p < 0.0001$), respectively.[336] At 0.01 μM of long-acting natriuretic peptide, the maximal inhibition was 89%, which occurred within 5 minutes. Both peptide hormones inhibited the activation of Ras for 3 to 4 hours.[336] Their ability to inhibit Ras was inhibited by cyclic GMP antibody and cyclic GMP itself inhibited Ras phosphorylation (72%; $p = 0.009$).[336] Thus, ANP, vessel dilator, kaliuretic peptide, and long-acting natriuretic peptide inhibit the activation of Ras via cyclic GMP as part of their anti-cancer mechanism(s) of action.[335,336]

MEK 1/2 Kinases

The prototype member of the MEK kinases, designated MAP kinase kinase (MKK-1)/or MEK-1, specifically phosphorylates the MAP kinase regulatory threonine and tyrosine residues present in the Thr-Glu-Tyr motif of ERK 1/2[61,425] (Figure 37.8). A second MEK family member, i.e., MEK-2, resembles MEK-1 at its substrate specificity, but is seven residues longer than MEK-1 with the amino acid sequence of MEK-2 being 81% identical to MEK-1.[425]

Vessel dilator and kaliuretic peptide decrease the activation of MEK 1/2 (Figure 37.8) over a concentration range of 0.01 μM to 10 μM.[339] Vessel dilator and kaliuretic peptide (each 10 μM) inhibited the phosphorylation of MEK 1/2 kinase 98% ((Figure 37.9, $p < 0.0001$) and 81% ($p < 0.001$), respectively.[339] The inhibition of MEK 1/2 lasted for at least two hours, where it was maximal, secondary to both peptides.[339] Their ability to inhibit MEK 1/2 was inhibited by cyclic GMP antibody, and cyclic GMP itself inhibited MEK 1/2 phosphorylation, indicating that cyclic GMP is important for mediating these cardiac hormones' effects.[339]

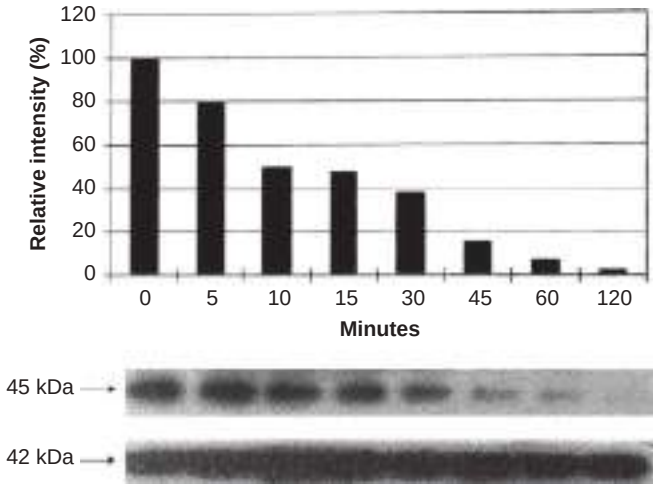

FIGURE 37.9 **Vessel dilator at 10 μM inhibits 98% of the phosphorylation of mitogen-activated protein kinase kinase (MEK 1/2), which was maximal at two hours and significant at $p < 0.00001$ when evaluated by analysis of variance (ANOVA). MEK 1/2 is at 45 kDa while B-actin (loading control) is at 42 kDa.** The relative intensity in the bar graphs is a comparison against untreated MEK 1/2 (100% intensity). *(Reprinted from Anticancer Res.* ***27****, 1387–1392, 2007.)*

ANP and long-acting natriuretic peptide decreased the activation of MEK 1/2 over a concentration range of 0.01 μM to 10 μM.[340] Long-acting natriuretic peptide and atrial natriuretic peptide (each 10 μM) inhibited the phosphorylation of MEK 1/2 kinase 97% ($p < 0.00001$) and 88% ($p < 0.00001$), respectively.[340] The inhibition of MEK 1/2 was maximal at two hours, and ceased by four hours secondary to both peptides.[340] The ability of peptides to inhibit MEK 1/2 was inhibited by cyclic GMP antibody, and cyclic GMP itself inhibited MEK 1/2 phosphorylation by 93%,[340] indicating that cyclic GMP is an important mediator of the cardiac natriuretic peptides' effects on MEK 1/2 kinase.

Cardiac Hormones Inhibit Activation of ERK 1/2 Kinases

Extracellular-signal regulated kinase (ERK) 1/2 is a mitogen-activated protein kinase (MAP kinase) important for the growth of cancer(s).[67,311] Growth factors such as epidermal growth factor (EGF), fibroblast growth factor, platelet derived growth factor, and vascular endothelial growth factor (VEGF) after binding to their specific receptor tyrosine kinases work via ERK 1/2 kinase to cause proliferation.[311]

Vessel dilator and kaliuretic peptide decrease the activation of ERK 1/2 over a concentration range of 0.01 μM to 1 μM. Vessel dilator and kaliuretic peptide (each 1 μM) inhibit the phosphorylation of ERK 1/2 kinases 96 and 70% ($p < 0.001$), respectively.[337] Both have significant effects within five minutes at their 0.01 μM concentrations.[337] The inhibition of ERK 1/2 lasted for at least two hours secondary to both. Their ability to inhibit ERK 1/2 was inhibited by cyclic GMP antibody, and cyclic GMP itself inhibited ERK 1/2 phosphorylation.[337]

ANP and LANP, likewise, decrease the activation of ERK 1/2 over a concentration range of 0.01 μM to 10 μM[(297d)]. ANP and LANP's maximal inhibition of the phosphorylation of ERK 1/2 kinase were 94 and 88% ($p < 0.0001$), respectively.[338] Their ability to inhibit ERK 1/2 was inhibited by cyclic GMP antibody, and cyclic GMP itself inhibited ERK 1/2 phosphorylation, suggesting that cyclic GMP mediates their effects of inhibition the phosphorylation of ERK 1/2.[338]

Growth promoting hormones such as insulin and epidermal growth factor (EGF) work as mitogens via ERK 1/2 (mitogen-activated) protein kinase (MAP kinase) to cause growth.[67,311] Insulin (1 μM) and EGF (10 ng/ml) each enhance the phosphorylation of ERK 1/2 by 66%.[341] This enhanced phosphorylation of ERK 1/2 by EGF and insulin was decreased down to 10%, 8%, 27%, and 13% above non-stimulated ERK 1/2 by vessel dilator, kaliuretic peptide, LANP, and ANP.[341]

CARDIAC HORMONES' MECHANISM OF ACTION: INHIBITION OF DNA SYNTHESIS

Vessel dilator, LANP, kaliuretic peptide, and ANP each at their 1 μM concentrations inhibit DNA synthesis when incubated with pancreatic adenocarcinoma cells for 24 hours by 91%, 84%, 86%, and 83%, respectively ($p < 0.001$ for each).[361] One of the known mediators[369,409] of these peptide hormones' mechanism(s) of action, i.e., cyclic GMP, inhibited DNA synthesis in these adenocarcinoma cells by 51%.[361] These four cardiac hormones inhibit DNA synthesis by 80–91% in all human cancer cell lines.[85,131,355–359,361,364] Thus, after inhibiting ERK 1/2, DNA synthesis (a further or final step in the Ras-ERK 1/2 pathway) is inhibited within the nucleus. The ability of these peptide hormones to inhibit DNA synthesis is specifically mediated by the intracellular mediator cyclic GMP, as when a cyclic GMP antibody is incubated with the cardiac hormones they are unable to inhibit DNA synthesis.[131]

LOCALIZATION OF CARDIAC HORMONES TO THE NUCLEUS OF PANCREATIC ADENOCARCINOMAS

All four of these cardiac hormones synthesized by the ANP gene localize to the nucleus of human

pancreatic adenocarcinomas by immunocytochemical evaluation, where they can inhibit DNA synthesis.[298,299] These are the first antigrowth peptide hormones that have been demonstrated to localize to the nucleus of cancers, and all four cardiac hormones localized to the nucleus.[298,299] These four cardiac hormones also localize to the capillaries growing into the human cancers, and the cytoplasm and fibroblasts within the tumors.[298,299]

SUMMARY AND FUTURE DIRECTIONS

Cardiac natriuretic peptides are synthesized both in the kidney and the heart,[130,271,347] and have some of their most potent biologic effects, such as natriuresis and diuresis, in the kidney.[24,27,78,139,141,220,405,434] Vessel dilator, via its ability to ameliorate acute renal failure and enhance tubule regeneration in acute tubular necrosis,[54] may prove useful in the future for the treatment of acute renal failure. BNP and adrenomedullin, with their effects in glomerular hypertrophy[179] and glomerular injury,[248] respectively, may be useful for the treatment of renal glomerular diseases. Since BNP, ANP, and adrenomedullin do not appear to help tubular diseases such as acute tubular necrosis, the major cause of acute renal failure,[154,423] their therapeutic potential in acute tubular necrosis appears limited. Future studies with these peptide hormones in humans with acute renal failure and/or glomerular diseases are necessary to determine whether the findings in animal models of ARF are applicable to the treatment of humans with acute renal failure.

Future research will concentrate on these cardiac hormones in humans with acute renal failure and renal cancer. With respect to side-effects, there have been no side-effects when infused for 28 days in athymic mice.[86,399] These cardiac hormones have been infused for one hour in 50 healthy humans and 50 humans with congestive heart failure, and one person had a marked decrease in blood pressure with ANP which was immediately corrected with 0.9% saline.[380,382] There have been no side-effects with the other three cardiac hormones in humans,[380,382] suggesting that they will be safe to treat persons with acute tubular necrosis and renal cancer and other cancers.

References

[1] Abassi ZA, Powell JR, Golomb E, Keiser HR. Renal and systemic effects of urodilatin in rats with high-output heart failure. Am J Physiol 1992;262:F615–21.

[2] Abell TJ, Richards AM, Ikram H, Espiner EA, Yandle T. Atrial natriuretic factor inhibits proliferation of vascular smooth muscle cells stimulated by platelet derived growth factor. Biochem Biophys Res Commun 1989;160:1392–6.

[3] Abraham WT, Lowes BD, Ferguson DA, Odom J, Kim JK, Robertson AD, et al. Systemic hemodynamic, neurohormonal, and renal effects of a steady-state infusion of human brain natriuretic peptide in patients with hemodynamically decompensated heart failure. J Card Fail 1998;4:37–44.

[4] Ackerman BH, Overton RM, McCormick MT, Schocken DD, Vesely DL. Disposition of vessel dilator and long-acting natriuretic peptide in healthy humans after a one-hour infusion. J Pharmacol Exp Therap 1997;282:603–8.

[5] Ackermann U, Irizawa TG, Milojevie S, Sonnennberg H. Cardiovascular effects of atrial extracts in anesthetized rats. Can J Physiol Pharmacol 1984;62:819–26.

[6] Agmon Y, Peleg H, Greenfeld Z, Rosen S, Brezis M. Nitric oxide and prostanoids protect the renal outer medulla from radiocontrast toxicity in the rat. J Clin Invest 1994;94:1069–75.

[7] Allgren RL, Marbury TC, Rahman SN, Weisberg LS, Fenves AZ, Lafayette RA, et al. Anaritide in acute tubular necrosis. N Engl J Med 1997;336:828–34.

[8] Anderson JV, Donckier J, Payne NN, Beacham H, Stater JDH, Bloom SR. Atrial natriuretic peptide: evidence as a natriuretic hormone at physiological plasma concentrations in man. Clin Sci 1987;72:305–12.

[9] Anderson RJ, Schrier RW. Acute renal failure. In: Schrier RW, editor. Diseases of the Kidney and Urinary Tract. 7th ed. Philadelphia: Lippincott, Williams & Wilkins; 2001. p. 1093–136.

[10] Appel RG. Growth inhibitory activity of atrial natriuretic factor in rat glomerular mesangial cells. FEBS Lett 1988;238:135–8.

[11] Appel RG. Growth-regulatory properties of atrial natriuretic factor. Am J Physiol 1992;262:F911–8.

[12] Arendt R, Gerbes A, Ritter D, Stangl E, Bach P, Zahringer J. Atrial natriuretic factors in plasma of patients with arterial hypertension, heart failure or cirrhosis of the liver. J Hypertens 1986;4(Suppl. 2):131–5.

[13] Argentin S, Drouin J, Nemer M. Thyroid hormone stimulates rat pro-natriodilatin mRNA levels in primary cardiocyte cultures. Biochem Biophys Res Commun 1987;146:1336–41.

[14] Atarashi K, Mulrow PJ, Franco-Saenz R, Snajdar R, Rapp J. Inhibition of aldosterone production by an atrial extract. Science 1984;224:992–4.

[15] Atlas SA, Kleinert HD, Camargo MJ, Januszewicz A, Sealey JE, Laragh JH, et al. Purification, sequencing and synthesis of natriuretic and vasoactive rat atrial peptide. Nature 1984;309:717–9.

[16] Baeyens DA, Price E, Winters CJ, Vesely DL. Diving increases atrial natriuretic factor-like peptide in fresh water diving turtles. Comp Physiol Biochem 1989;94 A:515–8.

[17] Baeyens DA, Walters JM, Vesely DL. Atrial natriuretic factor increases the magnitude of duodenal spontaneous phasic contractions. Biochem Biophys Res Commun 1988;155:1437–43.

[18] Baker BJ, Wu WL, Winters CJ, Dinh H, Wyeth R, Sallman AL, et al. Exercise increases the circulating concentration of the N-terminus of the atrial natriuretic factor prohormone in normal humans. Am Heart J 1991;122:1395–402.

[19] Ballerman BJ, Bloch KD, Seidman JG, Brenner BM. Atrial natriuretic peptide transcription, secretion and glomerular receptor activity during mineralocorticoid escape in the rat. J Clin Invest 1986;78:840–3.

[20] Banting FG, Best CH. The internal secretion of the pancreas. J Lab Clin Med 1922;7:251–61.

[21] Barletta G, Lazzeri C, Vecchiarino S, Del Bene R, Messeri G, Dello Sbarba A, et al. Low-dose C-type natriuretic peptide does not affect cardiac and renal function in humans. Hypertension 1988;31:802–8.

[22] Barr CS, Rhodes P, Struthers AD. C-type natriuretic peptide. Peptides 1996;17:1243–51.

[23] Beltowski J, Wojcicka G. Regulation of renal tubular transport by cardiac natriuretic peptides: two decades of research. Med Sci Monit 2002;8:RA39–52.
[24] Benjamin BA, Peterson TV. Effects of proANF-(31-67) on sodium excretion in conscious monkeys. Am J Physiol Regul Integr Comp Physiol 1995;269:R1351–5.
[25] Benoist C, Chambon P. *In vivo* sequence requirements of the SV40 early promoter region. Nature 1981;290:304–10.
[26] Bhalla SS, Robitaille L, Nemer M. Cooperative activation by GATA-4 and YY1 of the cardiac B-type natriuretic peptide promoter. J Biol Chem 2001;276:11439–45.
[27] Bloch KD, Scott JA, Zisfein JB, Fallon JT, Margolis NN, Seidman CE, et al. Biosynthesis and secretion of proatrial natriuretic factor by cultured rat cardiocytes. Science 1985;230:1168–71.
[28] Bompiani GD, Rouiller CH, Hatt PY. Le tissue de conduction du coeur chez le rat. Etude au microscope electronique. I. Le tronc commun du faisceau de His et les cellules claires de L'oreillette droite. Arch Mal Coeur 1959;52:1257–74.
[29] Borst JGG. The maintenance of an adequate cardiac output by the regulation of the urinary excretion of water and sodium chloride; an essential factor in the genesis of edema. Acta Med Scand 1948;130(Suppl. 207):1–71.
[30] Bovy PR, O'Neal JM, Olins GM, Patton DR, Mehta PP, McMahon EG, et al. A synthetic linear decapeptide binds to the atrial natriuretic peptide receptors and demonstrates cyclase activation and vasorelaxant activity. J Biol Chem 1989;264: 20309–13.
[31] Brady HR, Brenner BM, Clarkson MR, Lieberthal W. Acute renal failure. In: Brenner M, editor. Brenner & Rector's the kidney. 6th ed. Philadelphia: WB Saunders; 2000. p. 1201–62.
[32] Brandt RB, Redfield MM, Aarhus LL, Lewicki JA, Burnett Jr JC. Clearance receptor-mediated control of atrial natriuretic factor in experimental congestive heart failure. Am J Physiol 1994;266: R936–43.
[33] Breathnach R, Chambon P. Organization and expression of eukaryotic split genes coding for proteins. Am Rev Biochem 1981;50:349–83.
[34] Brenner BM, Ballermann BJ, Gunning ME, Zeidel ML. Diverse biological actions of atrial natriuretic peptide. Physiol Rev 1990;70:665–99.
[35] Brenner RM, Chertow GM. The rise and fall of atrial natriuretic peptide for acute renal failure. Curr Opin Nephrol Hypertens 1997;6:474–6.
[36] Brezis M, Rosen S, Silva P, Epstein FH. Renal ischemia: a new perspective. Kidney Int 1984;26:375–83.
[37] Bricker NS, Klahr S, Purkerson M, Schultze RG, Avioli LV, Binge SJ. *In vitro* assay for a humoral substance present during volume expansion and uremia. Nature 1968;219:1058–9.
[38] Buckley MG, Sethi D, Markandu ND, Sagnella GA, Singer DR, MacGregor GA. Plasma concentrations and comparisons of brain natriuretic peptide and atrial natriuretic peptide in normal subjects, cardiac transplant recipients and patients with dialysis-independent or dialysis-dependent chronic renal failure. Clin Sci 1992;83:437–44.
[39] Burnett Jr JC, Granger JP, Opgenorth TJ. Effects of synthetic atrial natriuretic factor on renal function and renin release. Am J Physiol 1984;247:F863–6.
[40] Carrithers SL, Ott CE, Hill MJ, Johnson BR, Cai W, Chang JJ, et al. Guanylin and uroguanylin induce natriuresis in mice lacking guanylyl cyclase-C receptor. Kidney Int 2004;65: 40–53.
[41] Carrithers SL, Hill MJ, Johnson BR, O'Hara SM, Jackson BA, Ott CE, et al. Renal effects of uroguanylin and guanylin *in vivo*. Braz J Med Biol Res 1999;32:1137–44.
[42] Casey KF, Machiedo GW, Lyons MJ, Slotman GJ, Novak RT. Alteration of postischemic renal pathology by prostaglandin infusion. J Surg Res 1980;29:1–10.
[43] Cataliotti A, Malatino LS, Jougasaki M, Zoccali C, Castellino P, Giacone G, et al. Circulating natriuretic peptide concentrations in patients with end-state renal disease: role of brain natriuretic peptide as a biomarker for ventricular remodeling. Mayo Clin Proc 2001;76:1111–9.
[44] Charron F, Paradis P, Bronchain O, Nemer G, Nemer M. Cooperative interaction between GATA-4 and GATA-6 regulates myocardial gene expression. Mol Cell Biol 1999;19: 4355–65.
[45] Charlton JA, Baylis PH. Lack of inhibition of vasopressin-stimulated Na^+K^+-ATPase by atrial natriuretic factor in rat renal medullary thick ascending limb of Henle's loop. Cell Biochem Funct 1990;8:25–9.
[46] Chartier L, Schiffrin E, Thibault G. Effect of atrial natriuretic factor (ANF)-related peptides on aldosterone secretion by adrenal glomerulosa cells: critical role of the intramolecular disulphide bond. Biochem Biophys Res Commun 1984;122: 171–4.
[47] Chauhan SD, Nilsson H, Ahluwalia A, Hobbs AJ. Release of C-type natriuretic peptide accounts for the biological activity of endothelium-derived hyperpolarizing factor. Proc Natl Acad Sci USA 2003;100:1426–31.
[48] Chen JH, Tsai JH, Lai YH, Hwang SJ. Plasma atrial natriuretic peptide in patients with chronic renal failure. J Formos Med Assoc 1990;89:645–50.
[49] Chen XW, Ying WZ, Valentin JP, Ling KT, Lin SY, Wiedemann E, et al. Mechanism of the natriuretic action of γ-melanocyte-stimulating hormone. Am J Physiol 1997;272: R1946–53.
[50] Chinkers M, Garbers DL, Chang MS, Lowe DG, Chin HM, Goeddel DV, et al. A membrane form of guanylate cyclase is an atrial natriuretic peptide receptor. Nature 1989;338:78–83.
[51] Chiou S, Vesely DL. Kaliuretic peptide: the most potent inhibitor of Na^+-K^+-ATPase of the atrial natriuretic peptides. Endocrinology 1995;136:2033–9.
[52] Christoffensen C, Goetz JP, Bartles ED, Larsen MD, Ribel U, Rehfeld JF, et al. Chamber-dependent expression of brain natriuretic peptide and its mRNA in normal and diabetic pig heart. Hypertension 2002;40:54–60.
[53] Chun TH, Itoh H, Ogawa Y, Tamura N, Takaya K, Igaki T, et al. Shear stress augments expression of C-type natriuretic peptide and adrenomedullin. Hypertension 1997; 29:1296–302.
[54] Clark LC, Farghaly H, Saba SR, Vesely DL. Amelioration with vessel dilator of acute tubular necrosis and renal failure established for 2 days. Am J Physiol 2000;278:H1555–64.
[55] Clavell AL, Stingo AJ, Wei CM, Heublein DM, Burnett Jr. JC. C-type natriuretic peptide: a selective cardiovascular peptide. Am J Physiol 1993;264:R290–5.
[56] Cody RJ, Atlas SA, Laragh JH, Kubo SH, Covit AB, Ryman KS, et al. Atrial natriuretic factor in normal subjects and heart failure patients: plasma levels and renal, hormonal, and hemodynamic responses to peptide infusion. J Clin Invest 1986;78: 1362–74.
[57] Conger JD, Falk SA, Yuan BH, Schrier RW. Atrial natriuretic peptide and dopamine in a rat model of ischemic acute renal failure. Kidney Int 1989;35:1126–32.
[58] Corboy JC, Walker RJ, Simmonds MB, Wilkins GT, Richards AM, Espiner EA. Plasma natriuretic peptides and cardiac volume during acute changes in intravascular volume in haemodialysis patients. Clin Sci 1994;87:679–84.
[59] Cousins KL, Farrell AP, Sweeting RM, Vesely DL, Keen JE. Release of atrial natriuretic factor prohormone peptides 1-30,

31-67, and 99-126 from fresh-water and sea-water acclimated perfused trout (*Oncorhynchus mykiss*) hearts. J Exp Biol 1997;200:1351–62.

[60] Crawford I, Maloney PC, Zeitlin PL, Guggino WB, Hyde SC, Turley H, et al. Immunocytochemical localization of the cystic fibrosis gene product CFTR. Proc Natl Acad Sci USA 1991;88:9262–6.

[61] Crews CM, Alessandrini A, Erikson RL. The primary structure of MEK, a protein kinase that phosphorylates the ERK gene product. Science 1992;258:478–80.

[62] Currie MG, Fok KF, Kato J, Moore RJ, Hamra FK, Duffin KL, et al. Guanylin: an endogenous activator of intestinal guanylate cyclase. Proc Natl Acad Sci USA 1992; 89:947–51.

[63] Currie MG, Geller DM, Cole BR, Boylan JG, Yu Sheng W, Holmberg SW, et al. Bioactive cardiac substances: potent vasorelaxant activity in mammalian atria. Science 1983;221: 71–3.

[64] Currie MG, Geller DM, Cole BR, Siegel NR, Fox KF, Adams SP, et al. Purification and sequence analysis of bioactive atrial peptides. Science 1984;223:67–9.

[65] Dagnino L, Lavigne JP, Nemer M. Increased transcripts for B-type natriuretic peptide in spontaneously hypertensive rats: quantitative polymerase chain reaction for atrial and brain natriuretic peptide transcripts. Hypertension 1992;20: 690–700.

[66] Davidman M, Olson P, Kohen J, Leither T, Kjellstrand C. Iatrogenic renal disease. Arch Intern Med 1991;151:1809–12.

[67] Davis RJ. Signal transduction by the JNK group of Map kinases. Cell 2000;103:239–52.

[68] Debold AJ. Heart atria granularity effects changes in water–electrolyte balance. Proc Soc Exp Biol Med 1979;161:508–11.

[69] Debold AJ, Borenstein HB, Veress AT, Sonnenberg H. A rapid and potent natriuretic response to intravenous injections of atrial myocardial extracts in rats. Life Sci 1981;28: 89–94.

[70] DeBold AJ, Salerno TA. Natriuretic activity of extracts obtained from hearts of different species and from various rat tissues. Can J Physiol Pharmacol 1983;61:127–30.

[71] De Lean A, Gutkowska J, McNicoll N, Schiller PW, Cantin M, Genest J. Characterization of specific recepors for atrial natriuretic factor in bovine adrenal zona glomerulosa. Life Sci 1984;35:2311–8.

[72] De Palo EF, Woloszczuk W, Meneghetti M, DePalo CB, Nielsen HB, Secher NH. Circulating immunoreactive proANP (1-30) and proANP (31-67) in sedentary subjects and athletes. Clin Chem 2000;46:843–7.

[73] de Wardener HE, Mills IH, Clapham WF, Hayter CJ. Studies on the efferent mechanism of sodium diuresis which follows administration of intravenous saline in the dog. Clin Sci 1961;21:249–58.

[74] Dietz JR. Release of natriuretic factor from rat heart–lung preparation by atrial distension. Am J Physiol 1984;247: R1093–6.

[75] Dietz JR, Landon CS, Nazian SJ, Vesely DL, Gower Jr. WR. Effects of cardiac hormones on arterial pressure and sodium excretion in NPRa knockout mice. Exp Biol Med 2004;229: 813–8.

[76] Dietz JR, Nazian SJ, Vesely DL. Release of ANF, proANF 1-98, and proANF 31-67 from isolated rat atria by atrial distention. Am J Physiol 1991;260:H1774–8.

[77] Dietz JR, Scott DY, Landon CS, Nazian SJ. Evidence supporting a physiological role for pro ANP (1-30) in the regulation of renal excretion. Am J Physiol 2001;280:R1510–7.

[78] Dietz JR, Vesely DL, Gower Jr WR, Nazian SJ. Secretion and renal effects of ANF prohormone peptides. Clin Exp Pharmacol Physiol 1995;22:115–20.

[79] Dietz JR, Vesely DL, Gower Jr WR, Landon CS, Lee S, Nazian SJ. Neutralization of proANP 1-30 exacerbates hypertension in spontaneously hypertensive rat (SHR). Clin Exp Pharm Physiol 2003;30:627–31.

[80] Dietz JR, Vesely DL, Nazian SJ. The effect of changes in sodium intake on atrial natriuretic factor (ANF) and peptides derived from the N-terminus of the ANF prohormone in the rat. Proc Soc Exp Biol Med 1992;200:44–8.

[81] Dillingham MA, Anderson RJ. Inhibition of vasopressin action by atrial natriuretic factor. Science 1986;250:F963–6.

[82] Drewett JG, Garbers DL. The family of guanylyl cyclase receptors and their ligands. Endocr Rev 1994;15:135–62.

[83] Edwards BS, Ackerman DM, Lee ME, Reeder GS, Wold LE, Burnett JC. Identification of atrial natriuretic factor within ventricular tissue in hamsters and humans with congestive heart failure. J Clin Invest 1988;81:82–6.

[84] Ehrenreich H, Sinowatz R, Schulz RM, Arendt RM, Goebel FD. Immunoreactive atrial natriuretic peptide (ANP) in endoscopic biopsies of human gastrointestinal tract. Res Exp Med 1989;189:421–5.

[85] Eichelbaum EJ, Vesely BA, Alli AA, Sun Y, Gower Jr WR, Vesely DL. Four cardiac hormones decrease up to 82% of human medullary thyroid carcinoma cells within 24 hours. Endocrine 2006;30:325–32.

[86] Eichelbaum EJ, Sun Y, Alli AA, Gower Jr WR, Vesely DL. Cardiac hormones and urodilatin eliminate up to 86% of human small-cell lung carcinomas in mice. Eur J Clin Invest 2008;38:562–70.

[87] Elitsur N, Lorenz JN, Hawkins JA, Rudolph JA, Witte D, Yang LE, et al. The proximal convoluted tubule is a target for the uroguanylin-regulated natriuretic response. J Pediatr Gastroenterol Nutr 2006;43:S74–81.

[88] Elsner D, Muders F, Muntze A, Kromer EP, Forssmann WG, Riegger G. Efficacy of prolonged infusion of urodilatin [ANP 95-126] in patients with congestive heart failure. Am Heart J 1995;129:766–73.

[89] Entzeroth M, Doods HN, Wieland HA, Wiene W. Adrenomedullin mediates vasodilation via CGRP1 receptors. Life Sci 1995;56:PL19–25.

[90] Eto T, Washimine H, Kato J, Kitamura K, Yamamoto Y. Adrenomedullin and proadrenalmedullin N-terminal 20 peptide in impaired renal function. Kidney Int Suppl 1996;55:S148–9.

[91] Fan X, Hamra FK, Freeman RH, Eber SL, Krause WJ, Lin RW, et al. Uroguanylin: cloning of preprouroguanylin cDNA, mRNA expression in the intestine and heart and isolation of uroguanylin and prouroguanylin from plasma. Biochem Biophys Res Commun 1996;219:457–62.

[92] Fink MP, Mac Vittie TJ, Casey LC. Effects of nonsteroidal anti-inflammatory drugs on renal function in septic dogs. J Surg Res 1984;36:516–25.

[93] Flynn TG. Past and current perspectives on the natriuretic peptides. Proc Soc Exp Biol Med 1996;213(2):98–104.

[94] Flynn TG, deBold ML, deBold AJ. The amino acid sequence of an atrial peptide with potent diuretic and natriuretic properties. Biochem Biophys Res Commun 1983;117:859–65.

[95] Fonteles MC, Greenberg RN, Monteiro HAS, Currie MG, Forte LR. Natriuretic and kaliuretic activities of guanylin and uroguanylin in the isolated perfused rat kidney. Am J Physiol 1998;44: F191–7.

[96] Fonteles MC, Carrithers SL, Monteiro HSA, Carvalho AF, Coelho GR, Greenberg RN, et al. Renal effects of serine-7 analog of lymphoguanylin in *ex vivo* rat kidney. Am J Physiol Renal Physio 2001;280:F207–13.

[97] Forte LR. Uroguanylin: cloning of preprouroguanylin cDNA, mRNA expression in intestine and heart and isolation of

uroguanylin and prouroguanylin from plasma. Biochem Biophys Res Commun 1996;219:457–62.
[98] Forte LR, Eber SL, Fan X, London RM, Rowland LM, Chin DT, et al. Lymphoguanylin: cloning characterization of a unique member of the guanylin peptide family. Endocrinology 1999;140:1800–6.
[99] Forte LR, Fan S, Hamra FK. Salt and water homeostasis: uroguanylin is a circulating peptide hormone with natriuretic activity. Am J Kidney Dis 1996;28:296–304.
[100] Forte LR, Krause WJ, Freeman RH. *Escherichia coli* enterotoxin receptors: localization in opossum kidney, intestine, and testis. Am J Physiol 1989;257:F874–81.
[101] Forte LR, London RM, Freeman RH, Krause WJ. Guanylin peptides: renal actions mediated by cyclic GMP. Am J Physiol Renal Physiol 2000;278:F180–91.
[102] Franz M, Woloszczuk W, Horl WH. N-terminal fragments of the proatrial natriuretic peptide in patients before and after hemodialysis treatment. Kidney Int 2000;58:374–8.
[103] Franz M, Woloszczuk W, Horl WH. Plasma concentration and urinary excretion of N-terminal proatrial natriuretic peptides in patients with kidney diseases. Kidney Int 2001;59: 1928–34.
[104] Freeman RH, David JO, Vari RC. Renal response to atrial natriuretic factor in conscious dogs with caval constriction. Am J Physiol 1985;248:R495–500.
[105] Freid TA, Osgood RW, Stein JH. Tubular site(s) of action of atrial natriuretic peptide in rat. Am J Physiol 1988;255:F313–6.
[106] Fukae H, Kinoshita H, Fujimoto S, Kita T, Nakazato M, Eto T. Changes in urinary levels and renal expression of uroguanylin on low or high salt diets in rats. Nephron 2002;92: 373–8.
[107] Fukioka S, Tamaki T, Fukui K, Ikahara T, Abe Y. Effects of a synthetic human atrial natriuretic polypeptide on regional blood flow in rats. Eur J Pharmacol 1985;109:301–4.
[108] Fyhrquist F, Tikkanen I, Totterman KJ, Hynynen M, Tikkanen T, Andersson S. Plasma atrial natriuretic peptide in health and disease. Eur Heart J 1987;8(Suppl. B):117–22.
[109] Garcia NH, Garvin JL. ANF and angiotensin II interact via kinases in the proximal straight tubule. Am J Physiol 1995;268: F730–5.
[110] Garcia R, Cantin M, Thibault G, Ong H, Genest J. Relationship of specific granules to the natriuretic and diuretic activity of rat atria. Experientia 1982;38:1071–3.
[111] Garcia R, Thibault G, Cantin M, Genest J. Effect of a purified atrial natriuretic factor on rat and rabbit vascular strips and vascular beds. Am J Physiol 1984;247:R34–9.
[112] Garcia R, Thibault G, Nutt RF, Cantin M, Genest J. Comparative vasoactive effects of native and synthetic atrial natriuretic factor (ANF). Biochem Biophys Res Commun 1984;119:685–8.
[113] Gardner DG. Natriuretic peptides: markers or modulators of cardiac hypertrophy. Trends Endo Metab 2003;14:411–6.
[114] Gardner DG, Deschepper CT, Ganong WF, Hane S, Fiddes J, Baxter JD, et al. Extra-atrial expression of the gene for atrial natriuretic factor. Proc Natl Acad Sci USA 1986;83:6697–701.
[115] Gardner DG, Gertz BJ, Deschepper CF, Kim DY. Gene for the rat atrial natriuretic peptide is regulated by glucocorticoids *in vitro*. J Clin Invest 1988;82:1275–81.
[116] Gardner DG, Kovacic-Milivojevic BK, Garmai M. Molecular biology of the natriuretic peptides. In: Vesely DL, editor. Atrial natriuretic peptides. Trivandrum, India: Research Signpost; 1997. p. 15–38.
[117] Gauer OH, Henry JP, Seiker HO. Cardiac receptors and fluid volume control. Progr Cardiovasc Dis 1961;4:1–26.
[118] Gauer OH, Henry JP. Circulatory basis of fluid volume control. Physiol Rev 1963;43:423–81.
[119] Geller DM, Currie MG, Siegel NR, Fok KF, Adams SP, Needleman P. The sequence of an atriopeptigen: a precursor of the bioactive atrial peptides. Biochem Biophys Res Commun 1984;121:802–7.
[120] Geller DM, Currie MG, Wakitani K, Cole BR, Adams SP, Fok KF, et al. Atriopeptins: a family of potent biologically active peptides derived from mammalian atria. Biochem Biophys Res Commun 1984;120:333–8.
[121] Gillespie DJ, Sandberg RL, Koike TI. Dual effect of left atrial receptors on the excretion of sodium and water in the dog. Am J Physiol 1973;255:706–10.
[122] Godellas CV, Gower Jr WR, Fabri PJ, Knierim TH, Giordano AT, Vesely DL. Atrial natriuretic factor (ANF) – a possible new gastrointestinal regulatory peptide. Surgery 1991;110: 1022–7.
[123] Goetz KL, Bond GC, Bloxham DD. Atrial receptors and renal function. Physiol Rev 1975;55:157–205.
[124] Goodfriend TL, Elliott ME, Atlas SA. Actions of synthetic atrial natriuretic factor on bovine adrenal glomerulosa. Life Sci 1984;35:1675–82.
[125] Gomez-Sanchez EP, Foecking MF, Sellers D, Blankenship MS, Gomez-Sanchez CE. Is circulating ouabain-like compound quabain? Am J Hypertens 1994;7:647–50.
[126] Gower Jr WR, Chiou S, Skolnick K, Vesely DL. Molecular forms of circulating atrial natriuretic peptides in human plasma and their metabolites. Peptides 1994;15:861–7.
[127] Gower WR, Dietz JR, McCuen RW, Fabri PJ, Lerner EA, Schubert ML. Regulation of atrial natriuretic peptide secretion by cholinergic and PACAP neurons of the gastric antrum. Am J Physiol 2003;284:G68–74.
[128] Gower Jr WR, Dietz JR, Vesely DL, Finley CL, Skolnick KA, Fabri PJ, et al. Atrial natriuretic peptide gene expression in the rat gastrointestinal tract. Biochem Biophys Res Commun 1994;202:562–70.
[129] Gower Jr WR, Salhab KF, Foulis WL, Pillai N, Bund JR, Vesely DL, et al. Regulation of atrial natriuretic peptide gene expression in gastric antrum by fasting. Am J Physiol 2000;278: R770–80.
[130] Gower Jr WR, San Miguel GI, Carter GM, Hassan I, Farese RV, Vesely DL. Atrial natriuretic prohormone gene expression in cardiac and extracardiac tissues of diabetic Goto-Kakizaki rats. Mol Cell Biochem 2003;252:263–71.
[131] Gower Jr WR, Vesely BA, Alli AA, Vesely DL. Four peptides decrease human colon adenocarcinoma cell number and DNA synthesis via guanosine 3′,5′-cyclic monophosphate. Int J Gastrointestinal Cancer 2005;36:77–87.
[132] Gower Jr WR, Vesely DL. The gastrointestinal natriuretic peptide system. Trends Comp Biochem Physiol 2000;6:125–38.
[133] Grammer RT, Fukumi H, Inagami T, Misono KS. Rat atrial natriuretic factor. Purification and vasorelaxant activity. Biochem Biophys Res Commun 1983;116:696–703.
[134] Green M, Ruiz OS, Kear F, Arruda JA. Dual effect of cyclic GMP on renal brush border Na-H antiporter. Proc Soc Exp Biol Med 1991;198:846–51.
[135] Greenberg BD, Bencen GH, Seilhamer JJ, Lewicki JA, Fiddes JC. Nucleotide sequence of the gene encoding human ANF precursor. Nature 1984;312:656–8.
[136] Greenberg RN, Hill M, Crytzer J, Krause WJ, Eber SL, Hamra FK, et al. Comparison of effects of uroguanylin, guanylin, and *Escherichia coli* heat-stable entertoxin STa in mouse intestine and kidney: evidence that uroguanylin is an intestinal natriuretic hormone. J Invest Med 1997;45:276–82.

[137] Greenwald JE, Needleman P, Wilkins MR, Schreiner GF. Renal synthesis of atriopeptin-like protein in physiology and pathophysiology. Am J Physiol 1991;260:F602–7.
[138] Grepin C, Dagino L, Robitaille L, Haberstroh L, Antakly T, Nemer M. A hormone-encoding gene identifies a pathway for cardiac but not skeletal muscle gene transcription. Mol Cell Biol 1994;14:3115–29.
[139] Gunning ME, Brady HR, Otuechere G, Brenner BM, Zeidel ML. Atrial natriuretic peptide (31–67) inhibits Na^+ transport in rabbit inner medullary collecting duct cells: role of prostaglandin E_2. J Clin Invest 1992;89:1411–7.
[140] Gunning ME, Brenner BM. Natriuretic peptides and the kidney: current concepts. Kidney Int 1992;42(Suppl. 38): S127–33.
[141] Habibullah AA, Villarreal D, Freeman RH, Dietz JR, Vesely DL, Simmons JC. Atrial natriuretic peptide fragments in dogs with experimental heart failure. Clin Exp Pharmacol Physiol 1995;22:130–5.
[142] Hamra FK, Forte LR, Eber SL, Pidhorodeckyj NV, Krause WJ, Freeman RH, et al. Uroguanylin: structure and activity of a second endogenous peptide that stimulates intestinal guanylate cyclase. Proc Natl Acad Sci USA 1993;90:10464–8.
[143] Harma F, Hagiwara H, Inoue A, Yamaguchi A, Yokose S, Furuya M, et al. cGMP produced in response to ANP and CNP regulates proliferation and differentiation of osteoblastic cells. Am J Physiol 1996;270:C1311–8.
[144] Hammond TG, Haramati A, Knox FG. Synthetic atrial natriuretic factor decreases renal tubular phosphate reabsorption in rats. Am J Physiol 1985;249:F315–8.
[145] Harris PJ, Thomas D, Morgan TO. Atrial natriuretic peptide inhibits angiotensin-stimulated proximal tubular sodium and water reabsorption. Nature 1987;326:697–8.
[146] Harthshorne H. Water versus hydrotherapy. Philadelphia: Lloyd P. Smith Press; 1847.
[147] Harvey W. Exercitatio de motu cordis et sanguinis animalibus. Leake CD [trans], Francofurti guilielem fitzeri, 1628. Springfield, IL: Charles C. Thomas; 1928.
[148] Hayashida H, Miyata T. Sequence similarity between epidermal growth factor precursor and atrial natriuretic factor precursor. FEBS Lett 1985;185:125–8.
[149] Henrich WL. Southwestern Internal Medicine Conference: renal sodium excretion and atrial natriuretic factor. Am J Med Sci 1986;291:199–208.
[150] Henry JP, Gauer OH, Reeves JL. Evidence of the atrial location of receptors influencing urine flow. Circ Res 1956;4:85–90.
[151] Henry JP, Pearce JW. The possible role of cardiac atrial stretch receptors in the induction of changes in urine flow. J Physiol 1956;131:572–85.
[152] Hirata Y, Tomita M, Takada S, Yoshimi H. Vascular receptor binding activities and cyclic GMP responses by synthetic human and rat atrial natriuretic peptides (ANP) and receptor down-regulation by ANP. Biochem Biophys Res Commun 1985;128:538–46.
[153] Hock R, Anderson RJ. Prevention of drug-induced nephrotoxicity in the intensive care unit. J Crit Care 1995;10:33–43.
[154] Hou SH, Bushinsky DA, Wish JB, Cohen JJ, Harrington JT. Hospital acquired renal insufficiency: a prospective study. Am J Med 1983;74:243–8.
[155] Huet M, Benchimol S, Berlinguet JC, Castonguay Y, Cantin M. Cytochimie ultrastructurale des cardiocytes de l'oreillette humaine. IV. Digestion des granules specifiques par less proteases. J Microsc 1974;21:147–58.
[156] Huet M, Cantin M. Ultrastructural cytochemistry of atrial muscle cells. II. Characterization of the protein content of specific granules. Lab Invest 1974;30:525–32.
[157] Humphreys MH. Gamma-MSH, sodium metabolism, and salt sensitive hypertension. Am J Physiol 2004;286:R417–30.
[158] Humphreys MH, Lin SY. Peptide hormones and the control of sodium excretion. Hypertension 1988;11:397–410.
[159] Hunt PJ, Richards AM, Espiner EA, Nicholls ME, Yandle TG. Bioactivity and metabolism of C-type natriuretic peptide in normal man. J Clin Endocrinol Metab 1994;78:1428–35.
[160] Hunter EFM, Kelly PA, Prowse C, Woods FJ, Lowry PJ. Analysis of peptides derived from pro atrial natriuretic peptide that circulate in man and increase in heart disease. Scand J Clin Lab Invest 1998;58:205–16.
[161] Igaki T, Itoh H, Suga S, Hama N, Ogawa Y, Komatsu Y, et al. C-type natriuretic peptide in chronic renal failure and its action in humans. Kidney Int 1996;49(Suppl. 55):S144–7.
[162] Itoh H, Pratt RE, Dzau VJ. Atrial natriuretic polypeptide inhibits hypertrophy of vascular smooth muscle cells. J Clin Invest 1990;86:1690–7.
[163] Itoh H, Pratt RE, Ohno M, Dzau VJ. Atrial natriuretic polypeptide as a novel antigrowth factor of endothelial cells. Hypertension 1992;19:758–61.
[164] Jamieson JD, Palade GE. Specific granules in atrial muscle cell. J Cell Biol 1964;23:151–62.
[165] Jemal A, Siegel R, Ward E, Hao Y, Xu J, Thun MJ. Cancer Statistics, 2009. Ca Cancer J Clin 2009;59:225–49.
[166] Jensen KT, Eiskjaer H, Carstens J, Pedersen EB. Renal effects of brain natriuretic peptide in patients with congestive heart failure. Clin Sci 1999;96:5–15.
[167] Jin JY, Wen JF, Li D, Cho KW. Osmoregulation of atrial myocytic ANP release: osmotransduction via cross-talk between L-type Ca^2 channel and SR Ca^2 release. Am J Physiol 2004;287: R1101–9.
[168] John SWM, Krege JH, Oliver PM, Hagaman JR, Hodgkin JB, Pang SC, et al. Genetic decreases in atrial natriuretic peptide and salt-sensitive hypertension. Science 1995;267:679–81.
[169] Johnson A, Lermioglu F, Garg UC, Morgan-Boyd R, Hassid A. A novel biological effect of atrial natriuretic hormone: inhibition of mesangial cell mitogenesis. Biochem Biophys Res Commun 1988;152:893–7.
[170] Jougasaki M, Burnett Jr JC. Adrenomedullin: potential in physiology and pathophysiology. Life Sci 2000;66:855–72.
[171] Kangawa K, Fukuda A, Kubota I, Hayashi Y, Matsuo H. Identification in rat atrial tissue of multiple forms of natriuretic polypeptides of about 3,000 daltons. Biochem Biophys Res Commun 1984;121:585–91.
[172] Kangawa K, Fukuda A, Matsuo H. Purification and complete amino acid sequence of rat atrial natriuretic polypeptides of 5,000 daltons. Biochem Biophys Res Commun 1984;119: 933–40.
[173] Kangawa K, Fukuda A, Matsuo H. Structural identification of beta- and gamma-human atrial natriuretic polypeptides (β- and γ-ANP). Nature 1985;313:397–400.
[174] Kangawa K, Matsuo H. Purification and complete amino acid sequence of alpha-human atrial natriuretic polypeptide (alpha-hANP). Biochem Biophys Res Commun 1984;118:131–9.
[175] Kangawa K, Tawaragi Y, Oikawa S, Mizuno A, Sakuragawa Y, Nakazato M, et al. Identification rat gamma atrial natriuretic polypeptide and characterization of the cDNA encoding its precursor. Nature 1984;312:152–5.
[176] Karla PR, Anker SD, Struthers AD, Coats AJS. The role of C-natriuretic peptide in cardiovascular medicine. Eur Heart J 2001;22:997–1007.
[177] Kalra PR, Clague JR, Bolger AP, Anker SD, Poole-Wilson PA, Struthers AD, et al. Myocardial production of C-type natriuretic peptide in chronic heart failure. Circulation 2003;107: 571–3.

[178] Karlberg L, Norlen BJ, Ojteg G, Wolgast M. Impaired medullary circulation in postischemic acute renal failure. Acta Physiol Scand 1983;118:11–7.
[179] Kasahara M, Mukoyama M, Sugawara A, Makino H, Suganami T, Ogawa Y, et al. Ameliorated glomerular injury in mice over expressing brain natriuretic peptide with renal ablation. J Am Soc Nephrol 2000;11:1691–701.
[180] Kaufman Jr RP, Anner H, Kobzik L, Valeri CR, Shepro D, Hechtman HB. Vasodilator prostaglandins (PG) prevent renal damage after ischemia. Ann Surg 1987;205:195–8.
[181] Keeler R. Atrial natriuretic factor has a direct, prostaglandin-independent action on kidneys. Can J Physiol Pharmacol 1982;60:1078–82.
[182] Kelley MJ, Johnson BE. Molecular biology of lung cancer. In: Mendelsohn J, Howley PM, Israel MA, Liotta LA, editors. The molecular basis of cancer. 2nd ed. Philadelphia: W.B. Saunders Company; 2001. p. 260–87.
[183] Kennedy BP, Marsden JJ, Flynn TG, DeBold AJ, Davies PL. Isolation and nucleotide sequence of a cloned cardionatrin cDNA. Biochem Biophys Res Commun 1984;122:1076–82.
[184] Kentsch M, Drummer C, Gerzer R, Muller-Esch G. Severe hypotension and bradycardia after continuous intravenous infusion of urodilatin (ANP 95-126) in a patient with congestive heart failure. Eur J Clin Invest 1995;25:281–3.
[185] Kikuchi M, Fujimoto S, Fukae H, Kinoshita H, Kita T, Nakazato M, et al. Role of uroguanylin, a peptide with natriuretic activity, in rats with experimental nephrotic syndrome. J Am Soc Nephrol 2005;16(2):392–7.
[186] Kinoshita H, Fujimoto S, Fukae H, Yokota N, Hisanaga S, Nakazato M, et al. Plasma and urine levels of uroguanylin, a new natriuretic peptide, in nephrotic syndrome. Nephron 1999;81:160–4.
[187] Kinoshita H, Nakazato M, Yamaguchi H, Matsukura S, Fujimoto S, Eto T. Increased plasma guanylin levels in patients with impaired renal function. Clin Nephrol 1997;47:28–32.
[188] Kisch B. Studies in comparative electron microscopy of the heart. II. Guinea pig and rat. Exp Med Surg 1955;13:404–28.
[189] Kitamura K, Kangawa K, Kawamoto M, Ichiki Y, Nakamura S, Matsuo H, et al. Adrenomedullin: a novel hypotensive peptide isolated from human pheochromocytoma. Biochem Biophys Res Commun 1993;192:553–60.
[190] Kitamura K, Kangawa K, Matsuo H, Eto T. Adrenomedullin: implications for hypertension research. Drugs 1995;49:485–95.
[191] Kleinert HD, Maack T, Atlas SA, Januszewicz A, Sealey JE, Laragh JH. Atrial natriuretic factor inhibits angiotensin-, norepinephrine-, and potassium-induced vascular contractility. Hypertension 1984;6(Suppl. I):I143–7.
[192] Kohse KP, Feifel K, Mayer-Wehrstein R. Differential regulation of brain and atrial natriuretic peptides in hemodialysis patients. Clin Nephrol 1993;40:83–90.
[193] Kojima S, Inoue I, Hirata Y, Kimura G, Saito F, Kawano Y, et al. Plasma concentrations of immunoreactive-atrial natriuretic polypeptide in patients on hemodialysis. Nephron 1987;46:45–8.
[194] Koller KJ, Goeddel DV. Molecular biology of natriuretic peptides and their receptors. Circulation 1992;86:1081–8.
[195] Kudo T, Baird A. Inhibition of aldosterone production in the adrenal glomerulosa by atrial natriuretic factor. Nature 1984;312:756–7.
[196] Kurnik BR, Allgren RL, Genter FC, Solomon RJ, Bates ER, Weisberg LS. Prospective study of atrial natriuretic peptide for the prevention of radiocontrast-induced nephropathy. Am J Kidney Dis 1998;31:674–80.
[197] Kurtz A, Della Bruna R, Pfeilschifter J, Taugner R, Bauer C. Atrial natriuretic peptide inhibits renin release from juxtaglomerular cells by cGMP-mediated process. Proc Natl Acad Sci USA 1986;83:4769–73.
[198] Ladenson PW, Bloch KD, Seidman JG. Modulation of atrial natriuretic factor by thyroid hormone: messenger ribonucleic acid and peptide levels in hypothyroid, euthyroid, and hyperthyroid rat atria and ventricles. Endocrinology 1988;123:652–7.
[199] Lainchbury J, Richards AM, Nicholls MG. Brain natriuretic peptide in heart failure. In: Vesely DL, editor. Atrial natriuretic peptides. Trivandrum, India: Research Signpost; 1997. p. 151–8.
[200] Lang CC, Choy AM, Henderson IS, Coutie WJ, Struthers AD. Effect of haemodialysis on plasma levels of brain natriuretic peptide in patients with chronic renal failure. Clin Sci 1992;82:127–31.
[201] La Pointe MC, Deschepper CF, Wu J, Gardner DG. Extracellular calcium regulates expression of the gene for atrial natriuretic factor. Hypertension 1990;15:20–8.
[202] Lazure C, Seidah NG, Chretien M, Thibault G, Garcia R, Cantin M, et al. Atrial pronatriodilatin: a precursor for natriuretic factor and cardiodilatin. FEBS Lett 1984;172:80–6.
[203] Lee SJ, Kim SZ, Cui X, Kim SH, Lee KS, Chung YJ, et al. C-type natriuretic peptide inhibits ANP secretion and atrial dynamics in perfused atria: NPR-B-cGMP signaling. Am Heart J 2000;278:H208–21.
[204] Lennane RJ, Peart WS, Carey RM, Shaw J. A comparison on natriuresis after oral and intravenous sodium loading in sodium-depleted rabbits: evidence for a gastrointestinal or portal monitor of sodium intake. Clin Sci Mol Med 1975;49:433–6.
[205] Levin ER, Gardner DG, Samson WK. Natriuretic peptides. N Engl J Med 1998;339:321–8.
[206] Levinsky NG, Lalone RC. Mechanism of sodium diuresis after saline infusion in the dog. J Clin Invest 1963;42:1261–8.
[207] Lewis J, Salem MM, Chertow GM, Weisberg LS, McGrew F, Marbury TC, et al. Atrial natriuretic factor in oliguric acute renal failure. Anaritide Acute Renal Failure Study Group. Am J Kidney Dis 2000;36:767–74.
[208] Lieberthal W, Sheridan AM, Valeri CR. Protective effect of atrial natriuretic factor and mannitol following renal ischemia. Am J Physiol 1990;258:F1266–72.
[209] Linden RJ, Sreeharan N. Humoral nature of the urine response to stimulation of atrial receptors. Q J Exp Physiol 1981;66:431–8.
[210] Lisy O, Jougasaki M, Heublein DM, Schirger JA, Chen HH, Wennberg PW, et al. Renal actions of synthetic dendroaspis natriuretic peptide. Kidney Int 1999;56:502–8.
[211] Lorenz JN, Nieman M, Sabo J, Sanford LP, Hawkins JA, Elitsur N, et al. Uroguanylin knockout mice have increased blood pressure and impaired natriuretic response to enteral NaCl load. J Clin Invest 2003;112:1244–54.
[212] Luchner A, Stevens TL, Borgeson DD, Redfield M, Wei CM, Porter JG, et al. Differential atrial and ventricular expression of myocardial BNP during evaluation of heart failure. Am J Physiol 1998;274:H1684–9.
[213] Lydtin H, Hamilton WF. Effect of acute changes in left atrial pressure on urine flow in unanesthetized dogs. Am J Physiol 1964;207:503–36.
[214] Maack T, Marion DN, Camargo MJ, Kleinert HD, Laragh JH, Vaughan Jr ED, et al. Effects of auriculin (atrial natriuretic factor) on blood pressure, renal function, and the renin–aldosterone system in dogs. Am J Med 1984;77: 1069–75.
[215] Maack T, Suzuki M, Almedida FA, Nussenzveig D, Scarborough RW, McEnroe GA, et al. Physiological role of silent receptors of atrial natriuretic factor. Science 1987;238:675–8.

[216] Maki M, Takayanagi R, Misono KS, Pandy KN, Tibbetts C, Inagami T. Structure of rat atrial natriuretic factor precursor deduced for cDNA sequence. Nature 1984;309:722–4.

[217] Marcus LS, Hart D, Packer M, Yushak M, Medina N, Danziger RS, et al. Hemodynamic and renal excretory effects of human brain natriuretic peptide infusions in patients with congestive heart failure. A double-blind, placebo-controlled, randomized crossover trial. Circulation 1996;94:3184–9.

[218] Marie JP, Guillemont H, Hatt PY. Le degree de granulation des cardiocytes auriculaires. Etude planimetrique au cours de differents apports d'eau et de sodium chez le rat. Pathol Biol 1976;24:549–54.

[219] Marin-Grez M, Fleming JT, Steinhausen M. Atrial natriuretic peptide causes pre-glomerular vasodilatation and post-glomerular vasoconstriction in rat kidney. Nature 1986;324:473–6.

[220] Martin DR, Pevahouse JB, Trigg DJ, Vesely DL, Buerkert JE. Three peptides from the ANF prohormone NH_2-terminus are natriuretic and/or kaliuretic. Am J Physiol 1990;258: F1401–8.

[221] Marttila M, Puhakka J, Luodonpaa M, Vuolteenaho O, Ganten L, Ruskoaho H. Augmentation of BNP gene expression in atria by pressure overload in transgenic rats harboring human renin and angiotensinogen genes. Blood Press 1999;8:308–16.

[222] Marx UC, Klodt J, Meyer M, Gerlach H, Rosch P, Forsmann WG, et al. One peptide, two topologies: structure and interconversion dynamics of human uroguanylin isomers. J Pept Res 1998;2:229–40.

[223] Mattingly MT, Brandt RR, Heublein DM, Wei CM, Nir A, Burnett Jr JC. Presence of C-type natriuretic peptide in human kidney and urine. Kidney Int 1994;46:744–7.

[224] McCubrey JA, Steelman LS, Chappell WH, Abrams SL, Wong EWT, Chang F, et al. Roles of the Raf/MEK/ERK pathway in cell growth, malignant transformation and drug resistance. Biochim Biophys Acta 2007;1773:1263–84.

[225] McCubrey JA, Milella M, Tafuri A, Martelli AM, Lunghi P, Bonati A, et al. Targeting the Raf/MEK/ERK pathway with small-molecule inhibitors. Curr Opin Investig Drugs 2008;9:614–30.

[226] McMurray J, Seidenlin PH, Howey JEA, Balfour DJ, Struthers AD. The effect of atrial natriuretic factor on urinary albumin and beta-2-microglobulin excretion in man. Hypertension 1988;6:783–6.

[227] McMurray RW, Vesely DL. Weight reduction decreases atrial natriuretic factor and blood pressure in obese patients. Metabolism 1989;38:1231–7.

[228] Melander O, Frandsen E, Groop L, Hulthen UL. Plasma proANP 1-30 reflects salt sensitivity in subjects with hereditary for hypertension. Hypertension 2002;39:996–9.

[229] Merkouris RW, Miller FC, Catanzarite V, Rigg LA, Quirk Jr JG, Vesely DL. Increase in the plasma levels of the N-terminal and C-terminal portions of the prohormone of atrial natriuretic factor in normal pregnancy. Am J Obstet Gynecol 1990;162: 859–64.

[230] Merkouris RW, Miller FC, Catanzarite V, Quirk Jr JG, Rigg LA, Vesely DL. The N-terminal and C-terminal portions of the atrial natriuretic factor prohormone increase during preeclampsia. Am J Obstet Gynecol 1991;164:1197–202.

[231] Meyer M, Richter R, Forssmann WG. Urodilatin a natriuretic peptide with clinical implications. Eur J Med Res 1998;3: 103–10.

[232] Meyer M, Pfarr E, Schirmer G, Uberbacher HJ, Schope K, Bohm E, et al. Therapeutic use of the natriuretic peptide ularitide in acute renal failure. Ren Fail 1999;21:85–100.

[233] Mills RM, LeJemtel TH, Horton DP, Liang C, Lang R, Silver MA, et al. Sustained hemodynamic effects of an infusion of nesiritide (human b-type natriuretic peptide) in heart failure: a randomized, double-blind, placebo-controlled clinical trial. Natrecor Study Group. J Am Coll Cardiol 1999;34: 155–62.

[234] Molitoris BA, Meyer C, Dahl R, Geerdes A. Mechanism of ischemia-enhanced aminoglycoside binding and uptake by proximal tubule cells. Am J Physiol 1993;264:F907–16.

[235] Morgan DA, Peuler JD, Koepke JP, Mark AL, DiBona GF. Renal sympathetic nerves attenuate the natriuretic effects of atrial peptide. J Lab Clin Med 1989;114:538–44.

[236] Morrissey EC, Wilner KD, Barager RR, Ward DM, Ziegler MG. Atrial natriuretic factor in renal failure and posthemodialytic postural hypotension. Am J Kidney Dis 1988;12: 510–5.

[237] Moskowitz PS, Korobkin M, Rambo ON. Diuresis and improved renal hemodynamics produced by prostaglandin E_1 in the dog with norepinephrine-induced acute renal failure. Invest Radiol 1975;10:284–99.

[238] Moss NG, Fellner RC, Qian X, Yu SJ, Li Z, Nakazato M, et al. Uroguanylin, an intestinal natriuretic peptide, is delivered to the kidney as an unprocessed propeptide. Endocrinology 2008;149:4486–98.

[239] Moss NG, Riguera DA, Solinga RM, Kessler MM, Zimmer DP, Arendshorst WJ, et al. The natriuretic peptide uroguanylin elicits physiologic actions through 2 distinct topoisomers. Hypertension 2009;53:867–76.

[240] Nakao K, Ogawa Y, Suga S, Imura H. Molecular biology and biochemistry of the natriuretic peptide system. I. Natriuretic peptides. J Hypertens 1992;10:907–12.

[241] Nakamoto M, Shapiro JI, Shanley PF, Chan L, Schrier RW. *In vitro* and *in vivo* protective effect of atriopeptin III on ischemic acute renal failure. J Clin Invest 1987;80:698–705.

[242] Nakayama K, Ohkubo H, Hirose T, Inayama S, Nakanishi S. mRNA sequence for human cardiodilatin-atrial natriuretic factor precursor and regulation of precursor mRNA in rat atria. Nature 1984;310:699–701.

[243] Nasser A, Dietz JR, Siddique M, Patel H, Khan N, Antwi EK, et al. Effects of kaliuretic peptide on sodium and water excretion in persons with congestive heart failure. Am J Cardiol 2001;88:23–9.

[244] Nemer M, Chamberland M, Sirois D, Argentin J, Drouin RA, Dixon RA, et al. Gene structure of human cardiac hormone precursor, pronatriodilatin. Nature 1984;312:654–6.

[245] Neumayer HH, Blossei N, Seherr-Thohs U, Wagner K. Amelioration of postischaemic acute renal failure in conscious dogs by human atrial natriuretic peptide. Nephrol Dial Transplant 1990;5:32–8.

[246] Ngo L, Bissett JK, Winters CJ, Vesely DL. Plasma prohormone atrial natriuretic peptides 1-98 and 31-67 increase with supraventricular and ventricular arrhytmias. Am J Med Sci 1990;300:71–7.

[247] Ngo L, Wyeth RP, Bissett JK, Hester WL, Newton MT, Sallman AL, et al. Prohormone atrial natriuretic peptides 1-30, and 99-126 increase in proportion to right ventricular pacing rate. Am Heart J 1989;118:893–900.

[248] Nishikimi T, Mori Y, Kobayashi N, Tadokoro K, Wang X, Akimoto K, et al. Renoprotective effect of chronic adrenomedullin infusion in Dahl salt-sensitive rats. Hypertension 2002;39:1077–82.

[249] Ogawa E, Saito Y, Kuwahara K, Harada M, Miyamoto Y, Hamana I, et al. Fibronectin signaling stimulates BNP gene transcription by inhibiting neuron-restrictive silencer element-dependent repression. Cardiovasc Res 2002;53:451–9.

[250] Ohlstein EH, Berkowitz BA. Cyclic guanosine monophosphate mediates vascular relaxation induced by atrial natriuretic factor. Hypertension 1985;7:306–10.

[251] Oikawa S, Imai M, Inuzuka C, Tawaragi Y, Nakazato H, Matsuo H. Structure of dog and rabbit precursors of atrial natriuretic polypeptides deduced from nucleotide sequence of cloned cDNA. Biochem Biophys Res Commun 1985;132:892–9.
[252] Oikawa S, Imai M, Ueno A, Tanaka S, Noguchi T, Nakazato H, et al. Cloning and sequence analysis of cDNA encoding a precursor for human atrial natriuretic peptide. Nature 1984;309: 724–6.
[253] Orias R, McCann SM. Natriuresis induced by alpha and beta melanocyte stimulating hormones in rats. Endocrinology 1972;90:700–6.
[254] Ortola FV, Ballermann BJ, Brenner BM. Endogenous ANP augments fractional excretion of Pi, Ca, and Na in rats with reduced renal mass. Am J Physiol 1988;255:F1091–7.
[255] Palmer BF, Alpern RJ. Pathogenesis of edema formation in the nephrotic syndrome. Kidney Int 1997;59:521–7.
[256] Palmer PA, Friedl FE, Giordano AT, Vesely DL. Alteration of environmental salinity modulates atrial natriuretic peptides' concentrations in heart, and hemolymph of the oyster, *Crassostrea virginica*. Comp Biochem Physiol 1994;108A: 589–97.
[257] Parkes DG. Cardiovascular actions of adrenomedullin in conscious sheep. Am J Physiol 1995;268:H2574–8.
[258] Parkin DM. Global cancer statistics in the year 2000. Lancet Oncol 2001;2:533–43.
[259] Paul RV, Kirk KA, Navar LG. Renal autoregulation and pressure natriuresis during ANF-induced diuresis. Am J Physiol 1987;253:F424–31.
[260] Payvar F, DeFranco D, Firestone G, Edgar B, Wrange O, O'Kret S, et al. Sequence specific binding of glucocorticoid receptor to MMTV DNA at sites within and upstream of the transcribed region. Cell 1983;35:381–92.
[261] Pedram A, Razandi M, Hu RM, Levin ER. Vasoactive peptides modulate vascular endothelial cell growth factor production and endothelial cell proliferation and invasion. J Biol Chem 1997;272:17097–103.
[262] Peters JP. Body water: the exchange of fluids in man. Springfield, IL: Charles C Thomas; 1935.
[263] Pettersson A, Hedner J, Hedner T. Renal interaction between sympathetic activity and ANP in rats with chronic heart failure. Acta Physiol Scand 1989;135:487–92.
[264] Pettersson A, Hedner J, Ricksten SE, Towle AC, Hedner T. Acute volume expansion as a physiological stimulus for the release of atrial natriuretic peptides in the rat. Life Sci 1986;38:1127–33.
[265] Pevahouse JB, Flanigan WJ, Winters CJ, Vesely DL. Normalization of elevated circulating N-terminal and C-terminal atrial natriuretic factor prohormone concentrations by renal transplantation. Transplantation 1992;53:1375–7.
[266] Pikkarainen S, Tokola H, Majalahti-Palviainen T, Kerkela R, Hautala N, Bahalla SS, et al. GATA-4 is a nuclear mediator of mechanical stretch-activated hypertrophic program. J Biol Chem 2003;278:23807–16.
[267] Pitchumoni CS. Pancreatic disease. In: Stein JH, editor. Internal Medicine. St. Louis, MO: Mosby; 1998. p. 2233–47.
[268] Poche R. Electronenmikroskopische untersuchuwgen des liopfuscin im herzmuskel des menschen. Zbl Allg Path Anat 1957;96:395.
[269] Poche R. Submikroskopische beitrage zur pathologie der herzmuskelzelle bei phosphorvergiftung. Hypertrophie, atrophie und kaliummangel. Virchows Arch 1958;331:165–248.
[270] Pollock DM, Mullins MM, Banks RO. Failure of atrial myocardial extract to inhibit renal Na^+-K^+-ATPase. Renal Physiol 1983;6:295–9.
[271] Potthast R, Ehler E, Sheving LA, Sindic A, Schlatter E, Kuhn M. High salt intake increases uroguanylin expression in mouse kidney. Endocrinology 2001;142:3087–97.
[272] Poulos JE, Gower Jr WR, Fontanet HL, Kalmus GW, Vesely DL. Cirrhosis with ascites: increased atrial natriuretic peptide gene expression in rat ventricle. Gastroenterology 1995;108: 1496–503.
[273] Poulos JE, Gower Jr WR, Friedl FE, Vesely DL. Atrial natriuretic peptide gene expression within invertebratic hearts. Gen Comp Endocrinol 1995;100:61–8.
[274] Poulos JE, Gower Jr WR, Sullebarger JT, Fontanet HL, Vesely DL. Congestive heart failure: increased cardiac and extracardiac atrial natriuretic peptide gene expression. Cardiovasc Res 1996;32:909–19.
[275] Proudfoot N. The end of the message. Nature 1982;298:516–7.
[276] Proudfoot NT, Brownlee GG. 3′ non-coding region sequences in eukaryotic messenger RNA. Nature 1976;263:211–4.
[277] Qian X, Moss NG, Fellner RC, Goy MF. Circulating prouroguanylin is processed to its active natriuretic form exclusively within the renal tubules. Endocrinology 2008;149: 4499–509.
[278] Rahman SN, Kim GE, Mathew AS, Goldberg CA, Allgren R, Schrier RW, et al. Effects of atrial natriuretic peptide in clinical acute renal failure. Kidney Int 1994;45:1731–8.
[279] Raine AE, Anderson JV, Bloom SR, Morris PJ. Plasma atrial natriuretic factor and graft function in renal transplant recipients. Transplantation 1989;48:796–800.
[280] Rambotti MG, Giambanco I, Spreca A. Detection of guanylate cyclases A and B stimulated by natriuretic peptides in gastrointestinal tract of rat. Histochem J 1996;29:117–26.
[281] Ramirez G, Saba SR, Dietz JR, Vesely DL. Immunocytochemical localization of proANF1-30, proANF 31-67, and atrial natriuretic factor in the kidney. Kidney Int 1992;41:334–41.
[282] Rapoport RM. Cyclic guanosine monophosphate inhibition of contraction may be mediated through inhibition of phosphatidylinositol hydrolysis in rat aorta. Circ Res 1986;58:407–10.
[283] Rapoport RM, Ginsburg R, Waldman SA, Murad F. Effects of atriopeptins on relaxation and cyclic GMP levels in human coronary artery *in vitro*. Eur J Pharmacol 1986;124:193–6.
[284] Rascher W, Tulassay T, Lang RE. Atrial natriuretic peptide in plasma of volume-overloaded children with chronic renal failure. Lancet 1985;2:303–5.
[285] Rashed HM, Su H, Patel TB. Atrial natriuretic peptide inhibits growth of hepatoblastoma (HEP G2) cells by means of activation of clearance receptors. Hepatology 1993;17:677–84.
[286] Richards AM, Lainchbury JG, Nicholls MG, Cameron AV, Yandle TG. *Dendroaspis* natriuretic peptide: endogenous or dubious? Lancet 2002;359:5–6.
[287] Riordan JR. The cystic fibrosis transmembrane conductance regulator. Annu Rev Physiol 1993;55:609–30.
[288] Ritter D, Chao J, Needleman P, Tetens E, Greenwald JE. Localization, synthetic regulation, and biology of renal atriopeptin-like prohormone. Am J Physiol 1992;263:F503–9.
[289] Roberts PJ, Der CJ. Targeting the RAF-MEK-ERK mitogen-activated protein kinase cascade for the treatment of cancer. Oncogene 2007;26:3291–310.
[290] Rosenzweig A, Seidman CE. Atrial natriuretic factor and related peptide hormones. Annu Rev Biochem 1991;60:229–55.
[291] Rubattu S, Gilberti R, Ganten U, Volpe M. A differential brain atrial natriuretic peptide expression co-segregates with occurrence of early strokes in the stroke prone phenotype of spontaneously hypertensive rat. J Hypertens 1999;17:1849–52.
[292] Rubattu S, Lee-Kirsch MA, DePaolis P, Giliberti R, Gigante B, Lombardi A, et al. Altered structure, regulation, and function

of the gene encoding the atrial natriuretic peptide in stroke prone spontaneously hypertensive rat. Cir Res 1999;85:900–5.
[293] Rubattu S, Ridker P, Stampfer MJ, Volpe M, Henekens CH, Lindpaintner K. The gene encoding atrial natriuretic peptide and the risk of human stroke. Circulation 1999;100:1722–6.
[294] Ruskoaho H. Atrial natriuretic peptide: synthesis, release, and metabolism. Pharmacol Rev 1992;44:479–602.
[295] Ruskoaho H, Leskinen H, Magga J, Tashinen P, Mantymaa P, Vuolteenaho O, et al. Mechanisms of mechanical load-induced atrial natriuretic peptide secretion: role of endothelin, nitric oxide, and angiotensin II. J Mol Med 1997;75:876–85.
[296] Ryu H, Cho KW, Kim SH, Kim SZ, Oh SH, Hwang YH, et al. Frog lymph heart synthesizes and stores immune reactivate atrial natriuretic peptide. Gen Comp Endocrinol 1992;87: 171–7.
[297] Saba SR, Ramirez G, Vesely DL. Immunocytochemical localization of ProANF 1-30, ProANF 31-67, atrial natriuretic factor and urodilatin in the human kidney. Am J Nephrol 1993;13: 85–93.
[298] Saba SR, Garces AH, Clark LC, Gower Jr WR, Vesely DL. Immunocytochemical localization of atrial natriuretic peptide, vessel dilator, long acting natriuretic peptide, and kaliuretic peptide in human pancreatic adenocarcinomas. J Histochem Cytochem 2005;53:989–95.
[299] Saba SR, Vesely DL. Cardiac natriuretic peptides: hormones with anti-cancer effects that localize to nucleus, cytoplasm, endothelium and fibroblasts of human cancers. Histol Hitopathol 2006;21:775–83.
[300] Sagnella GA, Saggar-Malik AK, Buckley MG, Markandu ND, Eastwood JB, MacGregor GA. Association between atrial natriuretic peptide and cyclic GMP in hypertension and in chronic renal failure. Clin Chem Acta 1998;275:9–18.
[301] Samson WK. Adrenomedullin and the control of fluid and electrolyte homeostasis. Annu Rev Physiol 1999;61:363–89.
[302] Samson WK. Proadrenomedullin-derived peptides. Front Neuroendocrinol 1998;19:100–17.
[303] Sands JM, Neylan JF, Olson RA, O'Brien DP, Whelchel JD, Mitch WE. Atrial natriuretic factor does not improve the outcome of cadaveric renal transplantation. J Am Soc Nephrol 1991;1:1081–6.
[304] Santos-Neto MS, Carvalho AF, Monteiro HS, Forte LR, Fonteles MC. Interaction of atrial natriuretic peptide, urodilatin, guanylin and uroguanylin in the isolated perfused rat kidney. Regul Pept 2006;136:14–22.
[305] Sato K, Hirata Y, Imai T, Iwashita M, Mariuo F. Characterization of immunoreactive adrenomedullin in human plasma and urine. Life Sci 1995;57:189–94.
[306] Sato K, Imai T, Iwashina M, Marumo F, Hirata Y. Secretion of adrenomedullin by renal tubular cell lines. Nephron 1998;78:9–14.
[307] Saxenhofer H, Gnadinger MP, Weidmann P, Shaw S, Schohn D, Hess C, et al. Plasma levels and dialysance of atrial natriuretic peptide in terminal renal failure. Kidney Int 1987;32:554–61.
[308] Schafferhans K, Heidbreder E, Grimm D, Heidland A. Norepinephrine-induced acute renal failure: beneficial effects of atrial natriuretic factor. Nephron 1986;44:240–4.
[309] Schermuly RT, Weissmann N, Enke B, Ghofrani HA, Forssmann WG, Grimminger F, et al. Urodilatin, a natriuretic peptide stimulating guanylate cyclase, and the phosphodiesterase five inhibitor dipyridamole attenuate experimental pulmonary hypertension. Am J Respir Cell Mol Biol 2001;25: 219–25.
[310] Schirger JA, Heublein DM, Chen HH, Lisy O, Jougasaki M, Wennberg PW, et al. Presence of *Dendroaspis* natriuretic peptide-like immunoreactivity in human plasma and its increase during human heart failure. Mayo Clin Proc 1999;74:126–30.
[311] Schlessinger J. Cell signaling by receptor tyrosine kinases. Cell 2000;103:211–25.
[312] Schnermann J, Marin-Grez M, Briggs JP. Filtration pressure response to infusion of atrial natriuretic peptides. Pflugers Arch 1986;406:237–9.
[313] Scholl FA, Dumesic PA, Khavan PA. Effects of active MEK 1 expression *in vivo*. Cancer Lett 2005;230:1–8.
[314] Schramm L, Heidbreder E, Schaar J, Lopau K, Zimmermann J, Gotz R, et al. Toxic acute renal failure in the rat: effects of diltiazem and urodilatin on renal function. Nephron 1994;68: 454–61.
[315] Schulz-Knappe P, Forssmann K, Herbst F, Hock D, Pipkorn R, Forssmann WG. Isolation and structural analysis of "urodilatin," a new peptide of the cardiodilatin-(ANP)-family, extracted from human urine. Klin Wochenschr 1988;66: 752–9.
[316] Schweitz H, Vigne P, Moinier D, Frelin C, Lazdunski M. A new member of the natriuretic peptide family is present in the venom of the green mamba (*Dendroaspis augusticeps*). J Biol Chem 1992;267:13928–32.
[317] Scivoletto R, Carcalho MHC. Cardionatrin causes vasodilation *in vitro* which is not dependent on the presence of endothelial cells. Eur J Pharmacol 1984;101:143–5.
[318] Scriven TA, Burnett Jr JC. Effects of synthetic atrial natriuretic peptide on renal function and renin release in acute experimental heart failure. Circulation 1985;72:892–7.
[319] Sebolt-Leopold JS. Advances in the development of cancer therapeutics directed against the Ras mitogen-activated protein kinase pathway. Clin Can Res 2008;14:3651–6.
[320] Sebolt-Leopold JS, Herrera R. Targeting the mtogen-activated protein kinase casecade to treat cancer. Nature Rev Cancer 2004;4:937–47.
[321] Seidman C, Bloch KD, Klein KA, Smith JA, Seidman JG. Nucleotide sequences of the human and mouse atrial natriuretic factor genes. Science 1984;226:1206–9.
[322] Shaw SG, Weidmann P, Hodler J, Zimmermann A, Paternostro A. Atrial natriuretic peptide protects against ischemic renal failure in the rat. J Clin Invest 1987;80:1232–7.
[323] Shaw SG, Weidmann P, Zimmermann A. Urodilatin not nitroprusside, combined with dopamine reverses ischemic acute renal failure. Kidney Int 1992;42:1153–9.
[324] Shin SJ, Lee YJ, Tan MS, Hsieh TJ, Tsai JH. Increased atrial natriuretic peptide mRNA expression in the kidney of diabetic rats. Kidney Int 1997;51:1100–5.
[325] Sindic A, Velic A, Basoglu C, Hirsch JR, Edemir B, Kuhn M, et al. Uroguanylin and guanylin regulate transport of mouse cortical collecting duct independent of guanylate cyclase C. Kidney Int 2005;68:1008–17.
[326] Sindic A, Schlatter E. Mechanisms of action or uroguanylin and guanylin and their role in salt handling. Nephrol Dial Transplant 2006;21:3007–12.
[327] Soejima H, Grekin RJ, Briggs JP, Schnermann J. Renal response of anesthetized rats to low-dose infusion of atrial natriuretic peptide. Am J Physiol 1988;255:R449–55.
[328] Sosa RE, Volpe M, Marion DN, Atlas SA, Laragh JH, Vaughn Jr ED, et al. Relationship between renal hemodynamic and natriuretic effects of atrial natriuretic factor. Am J Physiol 1986;250:F520–4.
[329] Sothern RB, Vesely DL, Kanabrocki EL, Bremner FW, Third JLAC, Boles MA, et al. Blood pressure and atrial natriuretic peptides correlate throughout the day. Am Heart J 1995;129:907–16.

[330] Sothern RB, Vesely DL, Kanabrocki EL, Hermida RC, Bremner FW, Third JLAC, et al. Temporal (circadian) and functional relationship between atrial natriuretic peptides and blood pressure. Chronobiol Int 1995;12:106–20.
[331] Steinhelper ME, Cochrane KL, Field LJ. Hypotension in transgenic mice expressing atrial natriuretic factor fusion genes. Hypertension 1990;16:301–7.
[332] Sudoh T, Kangawa K, Minamino W, Matsuo H. A new natriuretic peptide in porcine brain. Nature 1988;332:78–81.
[333] Sudoh T, Minamino N, Kangawa K, Matsuo H. C-type natriuretic peptide (CNP): a new member of the natriuretic peptide family identified in porcine brain. Biochem Biophys Res Commun 1990;168:863–70.
[334] Sugawara A, Nakao K, Sakamoto M, Morii N, Yamada T, Itoh H, et al. Plasma concentration of atrial natriuretic polypeptide in essential hypertension. Lancet 1985;2:1426–7.
[335] Sun Y, Eichelbaum EJ, Skelton IV WP, Lenz A, Regales N, Wang H, et al. Vessel dilator and kaliuretic peptide inhibit Ras in human prostate cancer cells. Anticancer Res 2009;29: 971–5.
[336] Sun Y, Eichelbaum EJ, Lenz A, Skelton IV WP, Wang H, Vesely DL. Atrial natriuretic peptide and long-acting natriuretic peptide inhibit Ras in human prostate cancer cells. Anticancer Res 2009;29:1889–93.
[337] Sun Y, Eichelbaum EJ, Wang H, Vesely DL. Vessel dilator and kaliuretic peptide inhibit activation of ERK 1/2 in human prostate cancer cells. Anticancer Res 2006;26:3217–22.
[338] Sun Y, Eichelbaum EJ, Wang H, Vesely DL. Atrial natriuretic peptide and long acting natriuretic peptide inhibit ERK 1/2 in prostate cancer cells. Anticancer Res 2006;26: 4143–8.
[339] Sun Y, Eichelbaum EJ, Wang H, Vesely DL. Vessel dilator and kaliuretic peptide inhibit MEK 1/2 activation in human prostate cancer cells. Anticancer Res 2007;27:1387–92.
[340] Sun Y, Eichelbaum EJ, Wang H, Vesely DL. Atrial natriuretic peptide and long acting natriuretic peptide inhibit MEK 1/2 activation in human prostate cancer cells. Anticancer Res 2007;27:3813–8.
[341] Sun Y, Eichelbaum EJ, Wang H, Vesely DL. Insulin and epidermal growth factor activation of ERK 1/2 and DNA synthesis is inhibited by four cardiac hormones. J Cancer Mol 2007;3: 113–20.
[342] Suzuki E, Hirata Y, Hayakawa H, Omata M, Kojima M, Kangawa K, et al. Evidence for C-type natriuretic peptide production in the rat kidney. Biochem Biophys Res Commun 1993;192:532–8.
[343] Tamura N, Ogawa Y, Chusho H, Nakamura K, Nakao K, Suda M, et al. Cardiac fibrosis in mice lacking brain natriuretic peptide. Proc Natl Acad Sci USA 2000;97:4239–44.
[344] Tateyama H, Hino J, Minamino N, Kangawa K, Ogihara T, Matsuo H. Characterization of immunoreactive brain natriuretic peptide in human cardiac atrium. Biochem Biophys Res Commun 1990;166:1080–7.
[345] Thuerauf DJ, Hanford DS, Glembotski CC. Regulation of rat brain natriuretic peptide transcription. Potential role for GATA-related transcription factors in myocardial gene expression. J Biol Chem 1994;269:17772–5.
[346] Tokura T, Kinoshita H, Fujimoto S, Kitamura K, Eto T. Plasma levels of proadrenomedullin N-terminal 20 peptide and adrenomedullin in patients undergoing hemodialysis. Nephron Clin Pract 2003;95:C67–72.
[347] Totsune K, Mackenzie HS, Totsune H, Troy JL, Lytton J, Brenner BM. Upregulation of atrial natriuretic peptide gene expression in remnant kidney of rats with reduced renal mass. J Am Soc Nephrol 1998;9:1613–7.
[348] Totsune K, Takahashi, Murakami O, Satoh F, Sone M, Mouri T. Elevated plasma C-type natriuretic peptide concentrations in patients with chronic renal failure. Clin Sci 1994;87:319–22.
[349] Trippodo NC, MacPhee AA, Cole FE, Blakesley HL. Partial chemical characterization of a natriuretic substance in rat atrial heart tissue. Proc Soc Exp Biol Med 1982;170:502–8.
[350] Tsuchimochi H, Yazaki Y, Ohno H, Takanashi R, Takaku F. Ventricular expression of atrial natriuretic peptide. Lancet 1987;2:336–7.
[351] Valentin JP, Gardner DG, Wiedemann E, Humphreys MH. Modulation of endothelin effects on blood pressure and hematocrit by atrial natriuretic peptide. Hypertension 1991;17:864–9.
[352] Valentin JP, Ying WZ, Couser WG, Humphreys MH. Extra renal resistance to atrial natriuretic peptide in rats with experimental nephrotic syndrome. Am J Physiol 1998;274:F556–63.
[353] Vaporciyan AA, Kies M, Stevens C, Komaki R, Roth JA. Cancer of the lung. In: Kufe DW, Pollock RE, Weichselbaum RR, Bast RC, Gansler TS, Holland JR, Frei III E, editors. Cancer medicine. 6th ed. Hamilton, Ontario, BC: Decker Inc.; 2003. p. 1385–445.
[354] Vari RC, Freeman RH, Davis JO, Villarreal D, Verburg KM. Effect of synthetic atrial natriuretic factor on aldosterone secretion in the rat. Am J Physiol 1986;251:R48–52.
[355] Vesely BA, Alii AA, Song S, Gower Jr WR, Sanchez-Ramos J, Vesely DL. Four peptide hormones specific decrease (up to 97%) of human prostate carcinoma cells. Eur J Clin Invest 2005;35:700–10.
[356] Vesely BA, Eichelbaum EJ, Alli AA, Sun Y, Gower Jr WR, Vesely DL. Urodilatin and four cardiac hormones decrease human renal carcinoma cell number. Eur J Clin Invest 2006;36:810–9.
[357] Vesely BA, Eichelbaum EJ, Alii AA, Sun Y, Gower Jr WR, Vesely DL. Four cardiac hormones cause cell death in 81% of human ovarian adenocarcinoma cells. Cancer Therapy 2007;5:97–104.
[358] Vesely BA, Eichelbaum EJ, Alii AA, Sun Y, Gower Jr WR, Vesely DL. Four cardiac hormones cause cell death of melanoma cells and inhibit their DNA synthesis. Am J Med Sci 2007;334:342–9.
[359] Vesely BA, Eichelbaum EJ, Alii AA, Sun Y, Gower Jr WR, Vesely DL. Four cardiac hormones eliminate 4-fold more human glioblastoma cells than green mamba snake peptide. Cancer Lett 2007;254:94–101.
[360] Vesely BA, Fitz SR, Gower Jr WR, Vesely DL. Vessel dilator: most potent of the atrial natriuretic peptides in decreasing the number and DNA synthesis of squamous lung cancer cells. Cancer Lett 2006;232:226–31.
[361] Vesely BA, McAfee Q, Gower Jr WR, Vesely DL. Four peptides decrease the number of human pancreatic adenocarcinoma cells. Eur J Clin Invest 2003;33:998–1005.
[362] Vesely BA, Song S, Sanchez-Ramos J, Fitz SR, Solivan SM, Gower Jr WR, et al. Four peptide hormones decrease the number of human breast adenocarcinoma cells. Eur J Clin Invest 2005;35:60–9.
[363] Vesely BA, Alli A, Song S, Sanchez-Ramos J, Fitz SR, Gower Jr WR, et al. Primary malignant tumors of the heart: four cardiovascular hormones decrease the number and DNA synthesis of human angiosarcoma cells. Cardiology 2006;105:226–33.
[364] Vesely BA, Song S, Sanchez-Ramos J, Fitz SR, Alli A, Solivan SM, et al. Five cardiac hormones decrease the number of human small-cell cancer cells. Eur J Clin Invest 2005;35: 388–98.
[365] Vesely DL. Aprotinin blocks the binding of pro atrial natriuretic peptides 1–30, 31–67, and 99–126 to human placental membranes. Am J Obstet Gynecol 1991;165:567–73.

[366] Vesely DL. Atrial natriuretic hormones. Englewood Cliffs, NJ: Prentice Hall; 1992.
[367] Vesely DL. Atrial natriuretic peptides within invertebrates and plants. Trends Comp Biochem Physiol 1998;4:89–103.
[368] Vesely DL. Atrial natriuretic peptides in pathophysiological diseases. Cardiovasc Res 2001;51:647–58.
[369] Vesely DL. Atrial natriuretic peptide prohormone gene expression: hormones and diseases that upregulate its expression. IUBMB Life 2002;53:153–9.
[370] Vesely DL. Natriuretic peptides and acute renal failure. Am J Physiol 2003;285:F167–77.
[371] Vesely DL, Arnold WC, Winters CJ, Sallman AL, Rico DM. Increased circulating concentration of atrial natriuretic factor in persons with pheochromocytomas. Clin Exp Hypertens [A] 1989;11:353–69.
[372] Vesely DL, Arnold WC, Winters CJ, Sallman AL, Rico DM. Increased circulating concentration of the N-terminus of the atrial natriuretic prohormone in persons with pheochromocytomas. J Clin Endocrinol Metab 1990;71:1138–46.
[373] Vesely DL, Bayliss JM, Sallman AL. Human prepro atrial natriuretic factors 26–55 56–92 and 104–123 increase renal guanylate cyclase activity. Biochem Biophys Res Commun 1987;143:186–93.
[374] Vesely DL, Blankenship M, Douglass MA, McCormick MT, Rodriguez-Paz G, Schocken DD. Atrial natriuretic peptide increases adrenomedullin in the circulation of healthy humans. Life Sci 1996;59:243–54.
[375] Vesely DL, Chiou S, Douglass MA, McCormick MT, Rodriguez-Paz G, Schocken DD. Kaliuretic peptide and long acting natriuretic peptide as well as atrial natriuretic factor inhibit aldosterone secretion. J Endocrinol 1995;146: 373–80.
[376] Vesely DL, Chiou S, Douglass MA, McCormick MT, Rodriguez-Paz G, Schocken DD. Atrial natriuretic peptides negatively and positively modulate circulating endothelin in humans. Metabolism 1996;45:315–9.
[377] Vesely DL, Clark LC, Garces AH, McAfee QW, Soto J, Gower Jr. WR. Novel therapeutic approach for cancer using four cardiovascular hormones. Eur J Clin Invest 2004;34: 674–82.
[378] Vesely DL, Cornett LE, McCleod SL, Nash AA, Norris JS. Specific binding sites for prohormone atrial natriuretic peptides 1–30, 31–67, and 99–126. Peptides 1990;11:193–7.
[379] Vesely DL, Dietz JR, Parks JR, Antwi EA, Overton RM, McCormick MT, et al. Comparison of vessel dilator and long acting natriuretic peptide in the treatment of congestive heart failure. Am Heart J 1999;138:625–32.
[380] Vesely DL, Dietz JR, Parks JR, Baig M, McCormick MT, Cintron G, et al. Vessel dilator enhances sodium and water excretion and has beneficial hemodynamic effects in persons with congestive heart failure. Circulation 1998;98: 323–9.
[381] Vesely DL, Douglass MA, Dietz JR, Giordano AT, McCormick MT, Rodriguez-Paz G, et al. Negative feedback of atrial natriuretic peptides. J Clin Endocrinol Metab 1994;78:1128–34.
[382] Vesely DL, Douglass MA, Dietz JR, Gower Jr WR, McCormick MT, Rodriguez-Paz G, et al. Three peptides from the atrial natriuretic factor prohormone amino terminus lower blood pressure and produce diuresis, natriuresis, and/or kaliuresis in humans. Circulation 1994;90:1129–40.
[383] Vesely DL, Eichelbaum EJ, Sun Y, Alli AA, Vesely BA, Luther SL, et al. Elimination of up to 80% of human pancreatic adenocarcinomas in athymic mice by cardiac hormones. In Vivo 2007;21:445–52.
[384] Vesely DL, Giordano AT. Food intake and body positional change alter the circadian rhythm of atrial natriuretic peptides excretion into human urine. Chronobiol Int 1991;8: 373–84.
[385] Vesely DL, Giordano AT. Atrial natriuretic factor-like peptide and its prohormone within single cell organisms. Peptides 1992;13:177–82.
[386] Vesely DL, Giordano AT. The most primitive heart in the animal kingdom contains the atrial natriuretic peptide hormonal system. Comp Biochem Physiol 1992; 101C:325–9.
[387] Vesely DL, Gower Jr WR, Giordano AT. Atrial natriuretic peptides throughout the plant kingdom: enhancement of solute flow by peptides from the N-terminus of the atrial natriuretic factor prohormone. Am J Physiol 1993;265:E465–77.
[388] Vesely DL, Hadley ME. Calcium requirements for melanophore-stimulating hormone action on melanophores. Science 1971;173:923–5.
[389] Vesely DL, Norris JS, Walters JM, Jespersen RR, Baeyens DA. Atrial natriuretic prohormone peptides 1–30, 31–67 and 79–98 vasodilate the aorta. Biochem Biophys Res Commun 1987;148:1540–8.
[390] Vesely DL, Norsk P, Gower Jr WR, Chiou S, Epstein M. Release of kaliuretic peptide during immersion-induced central hypervolemia in healthy humans. Proc Soc Exp Biol Med 1995;209:20–6.
[391] Vesely DL, Norsk P, Winters CJ, Rico DM, Sallman AL, Epstein M. Increased release of the N-terminal and C-terminal portions of the prohormone of atrial natriuretic factor during immersion-induced central hypervolemia in normal humans. Proc Soc Exp Biol Med 1989;192:230–5.
[392] Vesely DL, Overton RM, Blankenship M, McCormick MT, Schocken DD. Atrial natriuretic peptide increases urodilatin in the circulation. Am J Nephrol 1998;18:204–13.
[393] Vesely DL, Palmer PA, Giordano AT. Atrial natriuretic factor prohormone peptides are present in a variety of tissues. Peptides 1992;13:165–70.
[394] Vesely DL, Perez-Lamboy GI, Schocken DD. Long acting natriuretic peptide, vessel dilator, and kaliuretic peptide enhance urinary excretion of β_2 microglobulin. Metabolism 2000;49: 1592–7.
[395] Vesely DL, Perez-Lamboy GI, Schocken DD. Long acting natriuretic peptide, vessel dilator, and kaliuretic peptide enhance urinary excretion rate of β_2 microglobulin in congestive heart failure patients. J Cardiac Failure 2001;7:55–63.
[396] Vesely DL, Preston R, Gower Jr WR, Chiou S, Epstein M. Increased release of kaliuretic peptide during immersion-induced central hypervolemia in cirrhotic humans. Am J Nephrol 1996;16:128–37.
[397] Vesely DL, Sallman AL, Bayliss JM. Specific binding sites for pro atrial natriuretic factors 1–30, 31–67, and 99–126 on distal nephrons, proximal tubules, renal cortical and medullary membranes. Renal Physiol Biochem 1992;15:23–32.
[398] Vesely DL. San Miguel GI, Hassan I, Schocken DD. Atrial natriuretic hormone, vessel dilator, long acting natriuretic hormone, and kaliuretic hormone decrease the circulating concentrations of corticotropin releasing hormone, corticotropin and cortisol. J Clin Endocrinol Metab 2001;86:4244–9.
[399] Vesely DL, Vesely BA, Eichelbaum EJ, Sun Y, Alli AA, Gower Jr. WR. Four cardiac hormones eliminate up to two-thirds of human breast cancers in athymic mice. In Vivo 2007;21:973–8.
[400] Vesely DL, Winters CJ, Sallman AL. Prohormone atrial natriuretic peptides 1–30 and 31–67 increase in hyperthyroidism and decrease in hypothyroidism. Am J Med Sci 1989;297: 209–15.

[401] Vesely MD, Gower Jr WR, Perez-Lamboy GI, Overton RM, Graddy L, Vesely DL. Evidence for an atrial natriuretic peptide-like gene in plants. Exp Biol Med 2001;226:61–5.
[402] Vesely MD, Vesely DL. Environmental upregulation of atrial natriuretic peptide gene in the living fossil, *Limulus polyphemus*. Biochem Biophys Res Commun 1999;254:751–6.
[403] Villarreal D, Freeman RH, Reams GP. Natriuretic peptides and salt sensitivity: endocrine cardiorenal integration in heart failure. Congest Heart Fail 2002;8:29–36.
[404] Villarreal D, Freeman RH, Taraben A, Reams GP. Modulation of renin secretion by atrial natriuretic factor prohormone fragment 31–67. Am J Med Sci 1999;318:330–5.
[405] Villarreal D, Reams GP, Taraben A, Freeman RH. Hemodynamic and renal effects of proANF 31-67 in hypertensive rats. Proc Soc Exp Biol Med 1999;221:166–70.
[406] Vlasuk G, Miller J, Beneen G, Lewicki J. Structure and analysis of the bovine atrial natriuretic peptide precursor gene. Biochem Biophys Res Commun 1986;136:396–403.
[407] Vuolteenaho O, Arjama O, Vakkuri O, Madsniemi T, Nikkila L, Kangas J, et al. Atrial natriuretic peptide (ANP) in rat gastrointestinal tract. FEBS Lett 1988;233:79–82.
[408] Vuolteenaho O, Leskinen H, Magga J, Taskinen P, Mantymaa P, Leppaluoto J, et al. Regulation of atrial natriuretic peptide synthesis and secretion. In: Vesely DL, editor. Atrial natriuretic peptides. Trivandrum, India: Research Signpost; 1997. p. 39–52.
[409] Waldman SA, Rapoport RM, Murad F. Atrial natriuretic factor selectively activates particulate guanylate cyclase and elevates cyclic GMP in rat tissues. J Biol Chem 1984;259: 14332–4.
[410] Walshe JJ, Venuto RC. Acute oliguric renal failure induced by indomethacin: possible mechanism. Ann Intern Med 1979;91:47–9.
[411] Walter T, Stepan H, Pankow K, Becker M, Schultheiss HP, Sein WE. Biochemical analysis of neutral endopeptidase activity reveals independent catabolism of atrial and brain natriuretic peptide. J Biol Chem 2004;385:179–84.
[412] Wang T, Kawabata M, Haneda M, Takabatake T. Effects of uroguanylin, an intestinal natriuretic peptide, on ubuloglomerular feedback. Hypertens Res 2003;26:557–82.
[413] Weidmann P, Hasler L, Gnadinger MP, Lang RE, Uehlinger DE, Shaw S, et al. Blood levels and renal effects of atrial natriuretic peptide in normal man. J Clin Invest 1986;77: 734–42.
[414] Werb R, Clark WF, Lindsay RM, Jones EO, Turnbull DI, Linton AL. Protective effect of prostaglandin [PGE_2] in glycerol-induced acute renal failure in rats. Clin Sci Mol Med 1978;55: 505–7.
[415] Westenfelder C, Birch FM, Baranowski RL, Rosenfeld MJ, Shiozawa DK, Kablitz C. Atrial natriuretic factor and salt adaptation in the teleost fish *Gila atraria*. Am J Physiol 1988;255: F1281–6.
[416] Weston MW, Cintron GB, Giordano AT, Vesely DL. Normalization of circulating atrial natriuretic peptides in cardiac transplant recipients. Am Heart J 1994;127: 129–42.
[417] Wilkins MR, Wood JA, Adu D, Lote CJ, Kendall MJ, Michael J. Change in plasma immunoreactive atrial natriuretic peptide during sequential ultrafiltration and haemodialysis. Clin Sci 1986;71:157–60.
[418] Williamson JR, Holmberg SW, Chang K, Marvel J, Sutera SP, Needleman P. Mechanisms underlying atriopeptin-induced increases in hematocrit and vascular permeation in rats. Circ Res 1989;64:890–9.
[419] Winquist RJ, Faison EP, Waldman SA, Schwartz K, Murad F, Rapoport RM. Atrial natriuretic factor elicits an endothelium independent relaxation and activates particulate guanylate cyclase in vascular smooth muscle. Proc Natl Acad Sci USA 1984;81:7661–4.
[420] Winters CJ, Sallman AL, Baker BJ, Meadows J, Rico DM, Vesely DL. The N-terminus and a 4000 molecular weight peptide from the mid portion of the N-terminus of the atrial natriuretic factor prohormone each circulate in humans and increase in congestive heart failure. Circulation 1989;80: 438–49.
[421] Winters CJ, Sallman AL, Meadows J, Rico DM, Vesely DL. Two new hormones: prohormone atrial natriuretic peptides 1–30 and 31–67 circulate in man. Biochem Biophys Res Commun 1988;150:231–6.
[422] Winters CJ, Vesely DL. Change in plasma immunoreactive N-terminus, C-terminus, and 4000 dalton mid portion of atrial natriuretic factor prohormone with hemodialysis. Nephron 1991;58:17–22.
[423] Woolf AS, Mansell MA, Hoffbrand BI, Cohen SL, Moult PJ. The effect of low dose intravenous 99–126 atrial natriuretic factor infusion in patients with chronic renal failure. Postgrad Med J 1989;65:362–6.
[424] Wolff RA, Abbruzzese JL, Evans DB. Neoplasms of the exocrine pancreas. In: Holland JF, Frei III E, editors. Cancer medicine. London: BC Decker Inc; 2000. p. 1436–74.
[425] Wu J, Harrison JK, Dent P, Lynch KR, Weber MJ, Sturgill TW. Identification and characterization of a new mammalian mitogen-activated protein kinase kinase MKK-2. Mol Cell Biol 1993;13:4539–48.
[426] Yamanaka M, Greenberg B, Johnson L, Seilhamer J, Brewer M, Friedemann T, et al. Cloning and sequence analysis of the cDNA for the rat atrial natriuretic factor precursor. Nature 1984;309:719–22.
[427] Yang Q, Gower Jr WR, Li C, Chen P, Vesely DL. Atrial natriuretic-like peptide and its prohormone within Metasequoia. Proc Soc Exp Biol Med 1999;221:188–92.
[428] Yokota N, Bruneau BG, Fernandez BE, Kuroski de Bold ML, Piazza LA, Eid H, et al. Dissociation of cardiac hypertrophy, myosin heavy chain isoform expression, and natriuretic peptide production in DOCA-salt rats. Am J Hypertens 1995;8:301–10.
[429] Yonemaru M, Ishii K, Murad F, Raffin TA. Atriopeptin-induced increases in endothelial permeability are associated with elevated cGMP levels. Am J Physiol 1992;263:L363–9.
[430] Yoshida K, Yamagata T, Tomura Y, Suzuki-Kusaba M, Yoshida M, Hisa H, et al. Effects of c-type natriuretic peptide on vasoconstriction in dogs. Eur J Pharmacol 1997;338: 131–4.
[431] Yu SM, Hung LM, Lin CC. CGMP-elevating agents suppress proliferation of vascular smooth muscle cells by inhibiting the activation of epidermal growth factor signaling pathway. Circulation 1997;95:1269–77.
[432] Yuge S, Inoue K, Hyodo S, Takei Y. A novel guanylin family (guanylin, uroguanylin, and renoguanylin) in eels: possible osmoregulartory hormones in intestine and kidney. J Biol Chem 2003;278:22726–33.
[433] Zeidel ML. Renal actions of atrial natriuretic peptide: regulation of collecting duct sodium and water transport. Annu Rev Physiol 1990;52:747–59.
[434] Zeidel ML. Regulation of collecting duct Na^+ reabsorption by ANP 31–67. Clin Exp Pharmacol Physiol 1995;22:121–4.
[435] Zeidel ML, Kikeri D, Silva P, Burrowes M, Brenner BM. Atrial natriuretic peptides inhibit conductive sodium uptake by

rabbit inner medullary collecting duct cells. J Clin Invest 1988;82:1067–74.

[436] Zhang PL, Mackenzie HS, Troy KL, Brenner BM. Effects of natriuretic peptide receptor inhibition on remnant kidney function in rats. Kidney Int 1994;46:414–20.

[437] Zietse R, Schalekamp MA. Effect of synthetic human atrial natriuretic peptide (102–126) in nephrotic syndrome. Kidney Int 1988;34:717–24.

[438] Zimmerman RS, Gharib H, Zimmerman D, Heublein D, Burnett Jr JC. Atrial natriuretic peptide in hypothyroidism. J Clin Endocrinol Metab 1987;64:353–5.

[439] Zimmerman RS, Trippodo NC, MacPhee AA, Martinez AZ, Barbee RW. High-dose atrial natriuretic factor enhances albumin escape from the systemic but not the pulmonary circulation. Circ Res 1990;67:461–8.

[440] Zivin RA, Condra JH, Dixon R, Seidah NG, Chreitien M, Nemer M, et al. Molecular cloning and characterization of DNA sequences encoding rat and human ANF. Proc Natl Acad Sci USA 1984;81:6325–9.

[441] Zuidema GD, Clarke NP, Reeves JL, Gauer OH, Henry JP. Influence of moderate changes in blood volume on urine flow. Am J Physiol 1956;186:89–92.

[442] Ying Sun, Ehrentraud J. Eichelbaum, Anne Lenz, Hai Wang, David L. Vesely. Epidermal growth factor's activation of Ras is inhibited by four cardiac hormones. European Journal of Clinical Investigation, 2010;40(5):408–13.

This page intentionally left blank

CHAPTER

38

Pathophysiology of Sodium Retention and Wastage

Biff F. Palmer[1], *Robert J. Alpern*[2] *and Donald W. Seldin*[1]

[1]Department of Internal Medicine, Division of Nephrology, University of Texas Southwestern Medical Center, Dallas, TX, USA

[2]Office of the Dean, Yale University School of Medicine, New Haven, CT, USA

INTRODUCTION

Extracellular fluid (ECF) volume is determined by the balance between sodium intake and renal excretion of sodium. Under normal circumstances, wide variations in salt intake lead to parallel changes in renal salt excretion, such that ECF volume is maintained within narrow limits. This relative constancy of ECF volume is achieved by a series of afferent sensing systems, central integrative pathways, and renal and extrarenal effector mechanisms acting in concert to modulate sodium excretion by the kidney.

In the major edematous states, effector mechanisms responsible for sodium retention behave in a more-or-less nonsuppressible manner, resulting in either subtle or overt expansion of ECF volume. In some instances, an intrinsic abnormality of the kidney leads to primary retention of sodium, resulting in expansion of ECF volume. In other instances, the kidney retains sodium secondarily as a result of an actual or sensed reduction in effective circulatory volume.

Renal sodium wastage can be defined as the inability of the kidney to conserve sodium to such an extent that continued loss of sodium into the urine leads to contraction of intravascular volume and hypotension. Renal sodium wastage occurs in circumstances where renal sodium transport is pharmacologically interrupted (administration of diuretics), where the integrity of renal tubular function is breached (tubulointerstitial renal disease) or when mineralocorticoid activity or tubular responsiveness are diminished or absent.

SODIUM INTAKE AND SODIUM BALANCE

Under normal circumstances, renal excretion of sodium is regulated so that balance is maintained between intake and output, and ECF volume is stabilized. A subject maintained on a normal-sodium diet is in balance when body weight is constant, and sodium intake and output are equal. When the diet is abruptly decreased, a transient negative sodium balance ensues. A slight contraction of ECF volume signals activation of sodium-conserving mechanisms, which lead to decreases in urinary sodium excretion. After a few days, sodium balance is achieved and ECF volume and weight are stabilized, albeit at a lower value. If sodium intake is increased to the previous normal values, transient positive sodium balance leads to expansion of ECF volume, thereby suppressing those mechanisms that enhanced sodium reabsorption. A new steady-state is reached when ECF volume has risen sufficiently so that sodium excretion now equals intake (Figure 38.1). In both directions a steady-state is achieved, whereby sodium intake equals output, while ECF volume is expanded during salt loads and shrunk during salt restriction. The kidney behaves as though ECF volume is the major regulatory element modulating sodium excretion.

The major edematous states – congestive heart failure, cirrhosis of the liver, and nephrotic syndrome – depart strikingly from those constraints. These states are characterized by persistent renal salt retention despite progressive expansion of ECF volume.

Seldin and Giebisch's The Kidney, Fifth Edition.
DOI: http://dx.doi.org/10.1016/B978-0-12-381462-3.00038-0

© 2013 Elsevier Inc. All rights reserved.

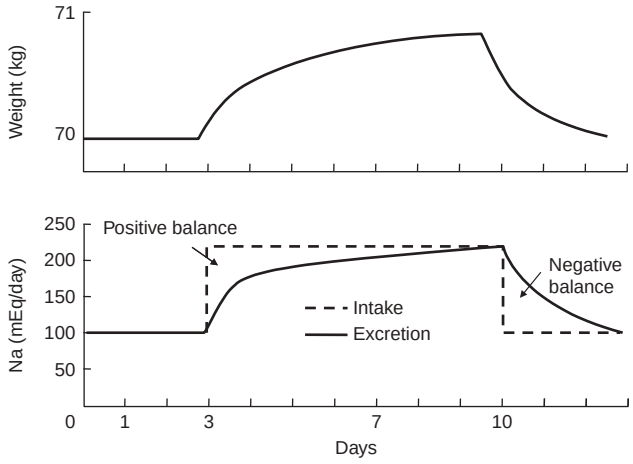

FIGURE 38.1 **Changes in body weight in response to abrupt changes in dietary salt demonstrating the ability of a normal subject to maintain salt balance with only minimal changes in extracellular fluid volume.**

Unrelenting sodium reabsorption is not the result of diminished sodium intake or even in most cases diminished plasma volume, as dietary salt is adequate and total ECF and plasma volumes are expanded. Renal sodium excretion no longer parallels changes in ECF volume; rather, the kidney behaves as if sensing a persistent low-volume stimulus. Some critical component of ECF volume remains underfilled.

PRIMARY AND SECONDARY EDEMA

A common feature of the major edematous states is persistent renal salt retention despite progressive expansion of both plasma and ECF volume. Two themes have been proposed to explain the persistent salt retention that characterizes the major edematous states: salt retention may be a primary abnormality of the kidney or a secondary response to some disturbance in circulation.

Primary edema (overflow, overfill, nephritic) refers to expansion of ECF volume and subsequent edema formation consequent to a primary defect in renal sodium excretion. Increased ECF volume and expansion of its subcompartments result in manifestations of a well-filled circulation. Hypertension and increased cardiac output are commonly present. The mechanisms normally elicited in response to an underfilled circulation are suppressed (↓renin–angiotensin–aldosterone,↓antidiuretic hormone (ADH),↓activity of sympathetic nerves,↓circulating catecholamines). Acute post-streptococcal glomerulonephritis and acute or advanced chronic kidney disease are disorders in which edema formation is primary in origin.

Secondary edema (underfill) results from the response of normal kidneys to actual or sensed underfilling of the circulation. In this form of edema, a primary disturbance within the circulation secondarily triggers renal mechanisms for sodium retention. Those systems that normally serve to defend the circulation are activated (rises in renin–angiotensin–aldosterone, ADH, activity of sympathetic nerves, and circulating catecholamines). The renal response in underfill edema is similar to that in normal subjects placed on a low-salt diet, that is, low fractional excretion of sodium, increased filtration fraction, and prerenal azotemia. Despite these similarities, a number of critical features distinguish these two states: (1) sodium balance is positive in underfill edema while salt-restricted normal subjects are in balance; and (2) administration of salt to sodium-restricted normals transiently expands ECF volume, after which sodium excretion equals intake, whereas in underfill edema, ECF volume expands progressively consequent to unyielding salt retention; and features of an underfilled circulation persist in underfill edema, while the circulation is normalized in normals.

The circulatory compartment that signals persistent activation of sodium-conserving mechanisms in secondary edema is not readily identifiable. Cardiac output may be high (arteriovenous shunts) or low (dilated cardiomyopathy). Similarly, plasma volume may be increased (arteriovenous shunts and heart failure) or decreased (some cases of nephrotic syndrome). The body fluid compartment ultimately responsible for signaling a volume-regulatory reflex leading to renal sodium retention is effective arterial blood volume (EABV). EABV identifies that critical component of arterial blood volume, actual or sensed, that regulates sodium reabsorption by the kidney.[184] In both normal circumstances and the major edematous states, the magnitude of EABV is the major determinant of renal salt and water handling.

CONCEPT OF EFFECTIVE ARTERIAL BLOOD VOLUME

In order to explain adequately persistent sodium retention in underfill edema, two cardinal features must exist. First, there must be a persistent low-volume stimulus sensed by the kidney that is then translated into persistent, indeed often unrelenting, retention of sodium despite adequate salt intake and overexpansion of ECF volume. Second, there must be a disturbance in those forces that partition retained fluid into the various subcompartments of the ECF space, resulting in an inability to terminate the low-volume stimulus. The first feature can be ascribed to a shrunken EABV, a

feature common to all major edematous states. The second feature can be attributed to a disruption in Starling forces, which normally dictate the distribution of fluid within the extracellular compartment. A disturbance in the circulation exists such that retained fluid is unable to restore EABV but rather is sequestered, resulting in edema formation.

Fluctuations in EABV are modulated by two key determinants: (1) filling of the arterial tree (normally determined by venous return and cardiac output); and (2) peripheral resistance (a factor influenced by compliance of the vasculature and degree of arteriolar runoff). A reduction in EABV can be the result of decreased arterial blood volume owing to low cardiac output, as in congestive heart failure. Conversely, EABV can be reduced in the face of increased arterial blood volume when there is excessive peripheral runoff, as seen in arteriovenous shunting and vasodilation. Increased compliance of the arterial vasculature in which arterial blood volume is reduced relative to the holding capacity of the vascular tree results in decreased EABV. For example, administration of salt to a subject with a highly compliant or "slack" circulation (as in pregnancy or cirrhosis) results in a sluggish natriuretic response, in contrast to a high resistance or "tight" circulation (as in primary aldosteronism or accelerated hypertension) in which salt administration causes prompt natriuresis.

Under normal circumstances, EABV is well-correlated with ECF volume. Figure 38.1 depicts the relationship between subcompartments of ECF volume and renal sodium excretion in both normal and edematous states. Under normal circumstances, subcompartments of ECF volume freely communicate in response to changes in dietary sodium, such that expansion or shrinkage of these compartments occurs in concert (Figure 38.2, states 1A and 1B). In steady-state conditions, sodium intake and output are in balance; the set point at which balance is attained is dictated by salt intake.

By contrast, major edematous states are characterized by a shrunken EABV, which cannot be filled despite expansion of one or more subcompartments. No longer is EABV well-correlated with total ECF volume and salt intake. Due to a disturbance in the forces that normally partition fluid into the various subcompartments of ECF space, EABV remains contracted even though total ECF volume is greatly expanded. Activation of sodium-conserving mechanisms persists, despite plentiful salt intake. Such derangements in fluid distribution can be categorized as disturbances in Starling forces within the interstitial space, between interstitial space and vascular tree, and disturbances within the circulation. These disturbances are summarized next.

1. *Trapped fluid* (Figure 38.2, state 2A). In the first type of disturbance, fluid is trapped within a pathologic compartment such that it cannot contribute to effective extracellular volume, that is, volume capable of filling interstitial and vascular spaces. Decrease in effective extracellular volume leads to decreases in total blood volume, arterial blood volume, and EABV, and renal sodium retention is stimulated. Retention of salt and water cannot re-expand effective extracellular volume, as fluid is sequestered into an abnormal fluid compartment behind the "Starling block" within the interstitial space. Such spacing of fluid into inflamed tissue, vesicles and bullae, peritonitis, necrotizing pancreatitis, rhabdomyolysis, and burns functionally behaves as if lost from the body.
2. *Reduced oncotic pressure.* A reduction in the circulating level of albumin can lead to a second type of fluid maldistribution. Decreased plasma oncotic pressure allows fluid to translocate from the vascular compartment to the interstitial space. Reductions in total blood volume, arterial blood volume, and EABV lead to sodium retention. The retained salt and water, owing to a "Starling block" across the capillary bed, leaks into the interstitial space.
3. *Vascular disturbances* (Figure 38.2, states 2B and 2C). A third type of fluid distributory disturbance results from abnormalities within the circulation, and can be of two types. The prototypical example of the first type is congestive heart failure. A failing ventricle results in decreased cardiac output and high diastolic intraventricular pressures. Venous return is impeded, with consequent reductions in arterial blood volume and EABV. Sodium retention is stimulated, but arterial blood volume and EABV remain contracted due to a circulatory block across the heart. In consequence, venous volume expands and leads to transudation of fluid into the interstitial space. The second type of circulatory abnormality that leads to fluid maldistribution is exemplified by arteriovenous shunting (e.g., Paget's disease, beriberi, thyrotoxicosis, anemia, cirrhosis). Widespread shunting through multiple small arteriovenous communications results in increased venous return, thereby augmenting cardiac output and arterial filling. However, arterial runoff and vasodilation lead to underperfusion of some critical area in the microcirculation. The circulatory block lies between the arterial blood volume and EABV.

What distinguishes secondary edematous states from the normal circumstance is an inability to expand EABV owing to Starling or circulatory blocks within the extracellular space. Normally, the system of

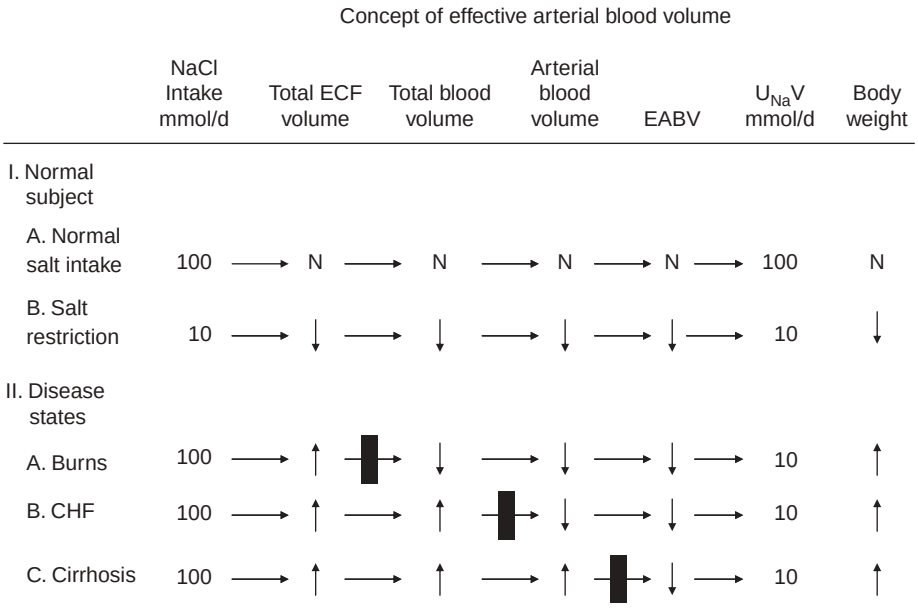

FIGURE 38.2 Concept of effective arterial blood volume and effect of fluid distributory disturbances on sodium balance and sodium excretion.

volume regulation behaves as an open system, such that fluctuations in one compartment are quickly translated into parallel changes in other compartments; total ECF volume and EABV are closely related. In contrast, volume regulation in underfill edema can be regarded as clamped; EABV remains shrunken despite expansion of the subcompartments of the extracellular space. EABV becomes dissociated from total ECF volume; salt retention becomes unrelenting and salt administration cannot re-expand the contracted EABV.

The reader is referred to the fourth edition of this book, in which a comprehensive discussion is provided on the afferent and efferent mechanisms involved in the regulation of extracellular fluid volume under normal circumstances. An overview of renal sodium handling in each segment of the nephron was also provided in that discussion. In this edition, the chapter will focus exclusively on the pathophysiology of the major edematous and salt-wasting states.

CONGESTIVE HEART FAILURE

The fundamental abnormality underlying congestive heart failure is an inability of the heart to maintain its function as a pump. As a result, a series of complex compensatory reflexes are initiated that serve to defend the circulation. The renal response to a failing myocardium is retention of salt and water resulting in expansion of ECF volume. If myocardial dysfunction is mild, expansion of ECF volume leads to increased left ventricular end-diastolic volume, which raises cardiac output according to the dictates of the Frank–Starling principle. In this state of compensated congestive heart failure, salt intake and output come into balance, but at the expense of an expanded ECF volume. Further deterioration in ventricular function leads to further renal retention of salt and water. There is progressive expansion of ECF volume and features of a congested circulation become manifest: peripheral edema, engorged neck veins, and pulmonary edema. Despite massive overexpansion of ECF volume, the kidneys behave as though they were responding to a low-volume stimulus. In subsequent sections, a detailed analysis of the afferent and efferent regulatory limbs in congestive heart failure will be provided.

Afferent Sensing Mechanisms in Congestive Heart Failure

Low and High Pressure Baroreceptors

A characteristic feature in many forms of congestive heart failure is increased stretch and transmural pressure within the cardiac atria. These alterations would normally provide afferent signals that suppress sympathetic outflow and decrease the release of renin and ADH, and ultimately result in a diuretic and natriuretic response. In congestive heart failure, this afferent signaling mechanism is markedly perturbed. Despite the presence of venous congestion and elevated cardiac filling pressures, sympathetic nervous activity and serum concentrations of renin and ADH are increased and urinary salt excretion is blunted. Both clinical and experimental studies are consistent with a decrease in sensitivity of the pressure-sensitive receptors in the cardiac atria.

Increased renal sympathetic nerve activity in cardiac failure has also been attributed to impaired arterial

baroreceptor function. High pressure baroreceptors in the carotid sinus and aortic arch normally exert a tonic inhibitory effect on central nervous system sympathetic outflow. Although the precise mechanism for the sympathoexcitation is not known, a sustained reduction in arterial pressure is unlikely to be the sole explanation, since arterial pressure is usually normal in congestive heart failure. Rather, sympathetic tone becomes insensitive to manipulations that normally suppress or enhance its activity. For example, infusion of nitroprusside increases both the heart rate and the circulating norepinephrine levels in normal subjects, whereas equivalent hypotensive doses in subjects with congestive heart failure elicit a blunted response.[149] Similarly, patients with heart failure show less bradycardia when arterial pressure is raised by infusion of phenylephrine. Such alterations in baroreflex function may result from abnormalities peripherally or alterations in central autonomic regulatory centers.

Several observations suggest angiotensin II may contribute to the depressed baroreflex sensitivity in heart failure. Angiotensin II has been shown to upwardly reset the arterial baroreflex control of heart rate in the rabbit, independent of a change in arterial pressure.[20] In the rat, increased levels of endogenous angiotensin II produced by changes in dietary salt intake tonically increase the basal level of renal sympathetic nerve activity, and upwardly reset the arterial baroreflex control of renal sympathetic nerve activity.[36] In experimental models, administration of an angiotensin II receptor blocker can reverse these changes and improve the sensitivity of the arterial baroreflex mechanism. Interestingly, captopril administered to patients with congestive heart failure restores the normal hemodynamic response to postural tilt and infusion of vasoconstrictive agents.[30]

Cardiac Output

A reduction in cardiac output has been suggested as the afferent signal that leads to Na retention in heart failure. When cardiac output is reduced by constriction of the abdominal or thoracic vena cava, urinary sodium excretion is typically decreased.[166,186] Restoring cardiac output to normal by autologous blood transfusion ameliorates renal salt retention, despite persistently elevated venous and hepatic pressures.[166] By contrast, rats with small-to-moderate myocardial infarctions have normal capacities to increase cardiac output in response to volume loads, and yet renal sodium excretion remains blunted in these animals. Even when cardiac output is increased above normal, as with the creation of an arteriovenous fistula in dogs, clinical findings of ascites and peripheral and pulmonary edema develop.[218] Despite increased cardiac output, levels of renin, aldosterone, and ANP are high.[202] Thus, the signal which initiates renal salt retention in congestive heart failure cannot originate solely from a decrease in cardiac output.

Other Sensors

Other afferent sensing mechanisms potentially active in congestive heart failure include intrahepatic baroreceptors and mechanoreceptors within the kidney. Chemosensitive receptors that respond to changing levels of metabolic breakdown products may participate in sensing of ECF volume. One such sensing mechanism may relate to the cardiac sympathetic afferent reflex. The reflex begins with sympathetic afferent fibers that respond to changes in cardiac pressure and dimension or substances that may accumulate in ischemia or heart failure. The reflex is excitatory in nature, such that activation of the afferent fibers leads to increased central sympathetic outflow. In summary, a contracted EABV serves as the afferent signal that elicits activation of effector mechanisms resulting in sodium retention. As with other edematous disorders, the exact volume compartment that comprises EABV has not been elucidated (Figure 38.3).

Effector Mechanisms in Congestive Heart Failure

Nephron Sites of Renal Sodium Retention

Renal sodium handling in the setting of congestive heart failure is similar to that which occurs in an otherwise normal individual who is volume-depleted. Activation of effector mechanisms lead to alterations in renal hemodynamics and tubular transport mechanisms that culminate in renal salt retention.

Renal hemodynamics in congestive heart failure are characterized by reduced renal plasma flow and a well-preserved glomerular filtration rate, such that filtration fraction is typically increased. In a rat model of myocardial infarction, Hostetter et al.[75] found a positive correlation between the decline in renal plasma flow and the degree to which left ventricular function was impaired. The glomerular filtration rate remained well-preserved as a result of an increased filtration fraction, except in animals with a severely compromised left ventricle. When examined at the level of the single nephron, these hemodynamic changes were found to be the result of a disproportionate increase in efferent arteriolar vasoconstriction and increased glomerular capillary hydraulic pressure.[76] Treatment with an angiotensin-converting enzyme inhibitor caused a decline in filtration fraction and efferent arteriolar resistance, suggesting an important role for angiotensin II in mediating efferent arteriolar constriction.

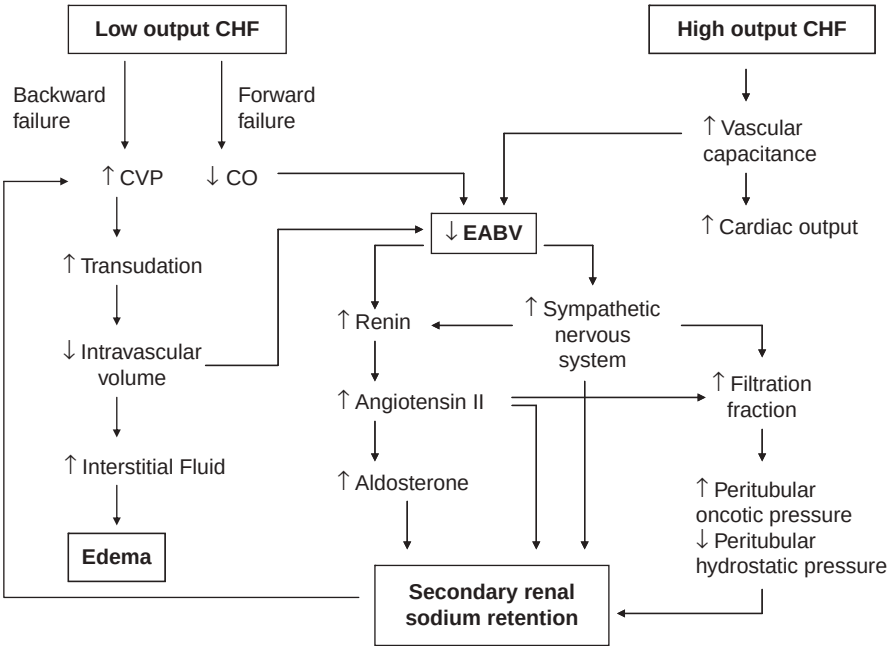

FIGURE 38.3 **Summary of pathways leading to renal sodium retention in low- and high-output congestive heart failure** (CO: cardiac output; EABV: effective arterial blood volume; CVP: central venous pressure).

Changes in glomerular and proximal tubular function in heart failure are similar to those that result from infusion of angiotensin II or norepinephrine. Angiotensin II, catecholamines, and renal nerves are all capable of increasing both the afferent and the efferent arteriolar tone, but predominantly act on the latter. These changes serve to maintain glomerular filtration rate near normal as renal plasma flow declines secondary to impaired cardiac function. As cardiac function progressively declines and the reduction in renal plasma flow becomes severe, the glomerular filtration rate will begin to fall. At this point there is an inadequate rise in filtration fraction, because efferent arteriolar vasoconstriction can no longer offset the intense afferent arteriolar constriction. Higher plasma catecholamines and further increases in sympathetic nerve activity acting to provide circulatory stability result in greater constriction of the afferent arteriole, such that glomerular plasma flow and transcapillary hydraulic pressure are reduced. In this setting, the glomerular filtration rate becomes dependent on afferent arteriolar flow.

These observations are similar to what has been observed in human subjects with varying degrees of left ventricular function.[119] As left ventricular function declines, the glomerular filtration rate is initially maintained by an increased filtration fraction. However, in patients with severely depressed left ventricular function, a progressive decline in renal blood flow becomes associated with a fall in glomerular filtration rate due to an inadequate rise in filtration fraction. In this setting, administration of an ACE inhibitor can result in a further lowering of the glomerular filtration rate, even though systemic arterial pressure remains fairly constant.[151]

Both experimental and clinical studies support the proximal nephron as a major site of increased sodium reabsorption in the setting of congestive heart failure. In human subjects, clearance techniques have primarily been employed to demonstrate the contribution of the proximal nephron. For example, infusion of mannitol was shown to increase free water excretion to a greater extent in patients with congestive heart failure as compared to normal controls. Since mannitol inhibits fluid reabsorption proximal to the diluting segment, it was inferred that enhanced free water clearance was reflective of augmented delivery of Na from the proximal tubule to the diluting segment.[10] In dogs with an arteriovenous fistula, there is a failure to escape from the Na-retaining effects of deoxycorticosterone acetate. In addition, these animals do not develop hypokalemia in contrast to normal controls.[82] The absence of hypokalemia in the setting of mineralocorticoid excess is best explained by decreased delivery of Na to the distal nephron due to enhanced proximal Na reabsorption. Alterations in peritubular hydrostatic and oncotic forces, as well as direct effects of various neurohormonal effectors, account for enhanced proximal sodium and water absorption in this setting.[76]

Clearance and micropuncture studies are also consistent with enhanced sodium reabsoption in the distal tubule in states of congestive heart failure. The loop of Henle has been identified as a site of enhanced sodium reabsoption in dogs with chronic vena cava obstruction[112] and rats with an arteriovenous fistula.[193]

Renin–Angiotensin–Aldosterone System

The renin–angiotensin–aldosterone system is activated when the heart fails as a pump.[139] Components of this system serve to compensate for decreased cardiac output by stabilizing the circulation and expanding ECF volume.

Several mechanisms are activated in the setting of a failing myocardium which serve to increased renin release. Diminished pressure in the afferent arteriole enhances renin release via a baroreceptor mechanism, the sensitivity of which is heightened consequent to augmented baseline sympathetic nerve activity.[94] Enhanced salt and water reabsorption in the proximal tubule and loop of Henle diminishes sodium chloride concentration at the macula densa, providing a stimulatory signal for renin release by way of the tubuloglomerular feedback mechanism. Finally, increased sympathetic nerve activity directly enhances renin release via stimulation of β-adrenergic receptors on the juxtaglomerular cells.

Renin acts on angiotensinogen synthesized in the liver and elsewhere to produce the decapeptide, angiotensin I. Angiotensin I is converted to angiotensin II by the angiotensin-converting enzyme present in the lungs, kidney, and blood vessels throughout the circulation.

Angiotensin II plays a pivotal role in glomerular and proximal tubule function in models of congestive heart failure (Figure 38.4). By selectively increasing efferent arteriolar tone, adjustments in the glomerular and postglomerular circulatory network favor net reabsorption in the proximal tubule. Increased filtration fraction leads to increased peritubular oncotic pressure, and in combination with decreased peritubular hydrostatic pressure net sodium reabsorption is enhanced. Angiotensin II also stimulates salt and water reabsorption through a direct effect on proximal tubular cells.[70,187] Increased efferent arteriolar resistance increases glomerular capillary hydrostatic pressure, mitigating any fall in GFR that would otherwise occur from decreased renal blood flow. In clinical, as well as experimental, models of heart failure, administration of ACE inhibitors improves renal blood flow and increases urinary sodium excretion, consistent with important angiotensin II-mediated effects on the renal microvasculature.[44]

Angiotensin II also contributes to renal salt and water retention through effects mediated by increased renal sympathetic nerve activity. As previously mentioned, angiotensin II decreases the sensitivity of the baroreflex mechanism such that a higher pressure is required to decrease central sympathetic outflow. In addition, angiotensin II directly stimulates sympathetic outflow at the level of the central nervous system. Chronic administration of an ACE inhibitor to patients with congestive heart failure reduces central sympathetic outflow and improves the sympathoinhibitory response to baroreflex stimulation.[65]

Angiotensin II also influences renal salt and water handling in the distal nephron, primarily through stimulatory effects on aldosterone release in the adrenal gland.[183] Aldosterone acts primarily on the collecting duct to promote tubular reabsorption of sodium. Aldosterone-stimulated sodium reabsorption generates a luminal-negative voltage that secondarily enhances excretion of hydrogen and potassium ions. The magnitude of potassium secretion will depend on the volume and composition of filtrate reaching the collecting duct. In this regard, patients with heart failure rarely manifest hypokalemia and alkalosis, despite oversecretion of mineralocorticoid, unless distal sodium delivery is increased by use of a diuretic. In the absence of diuretic therapy, distal delivery of sodium is low due to enhanced proximal reabsorption mediated by angiotensin II, sympathetic nerves, and peritubular physical factors. Thus, although plasma renin and aldosterone levels are frequently elevated in heart failure, there is conflicting data as to the importance of aldosterone in mediating renal salt retention.[43,71,206]

Conflicting data regarding the importance of the renin–angiotensin–aldosterone system in the generation of cardiac edema is best resolved when analyzed with respect to severity of heart failure. The initial response to constriction of the pulmonary artery or thoracic inferior vena cava in dogs is a reduction in blood pressure, and increases in renin and aldosterone levels. During this acute phase there is avid renal sodium retention,[206] and stability of blood pressure is critically dependent on circulating angiotensin II. Over several days plasma volume and body weight increase, while renin, aldosterone, and sodium balance return to control values. During the acute phase, administration of a converting enzyme inhibitor results in hypotension, while no effect on blood pressure is observed during this chronic phase. If plasma renin and aldosterone fail to decrease due to severe impairment of cardiac output, then converting enzyme inhibitor-induced hypotension persists.

A similar pattern is seen in dogs with an arteriovenous fistula.[202] In the early phase of this high-output cardiac failure model, significant elevations in renin and aldosterone levels occur, and renal sodium retention is marked. Several days later, after development of peripheral edema and ascites, renin and aldosterone levels return to baseline and daily sodium excretion begins to match dietary intake.

A similar relationship between the renin–angiotensin–aldosterone system and stage and

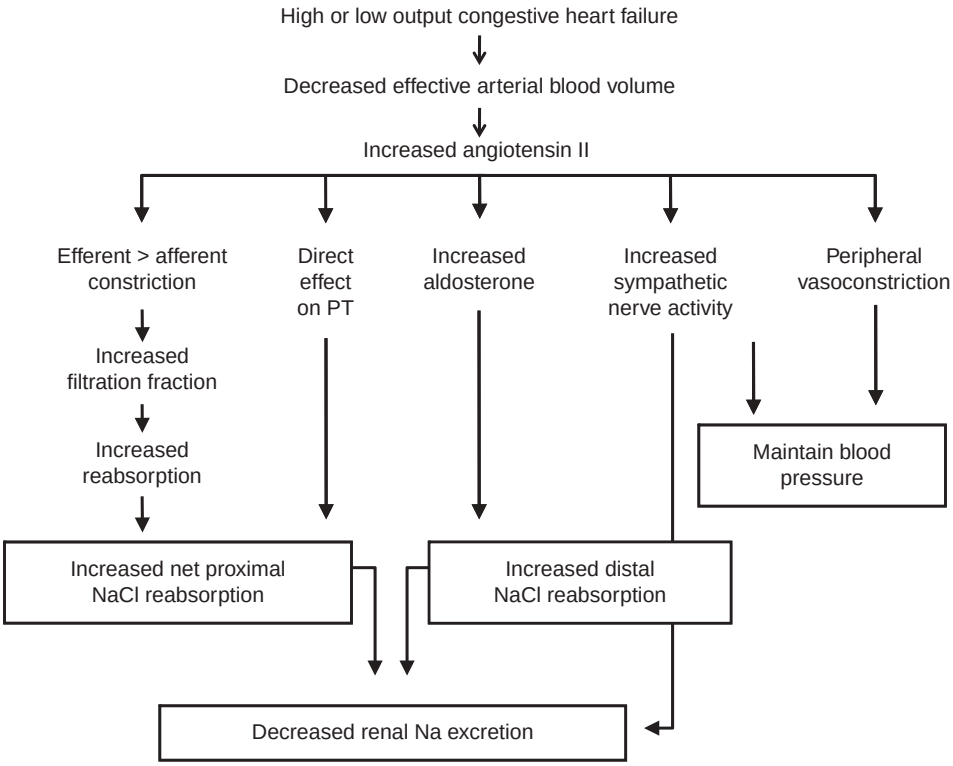

FIGURE 38.4 **Pathways by which angiotensin II regulates renal sodium excretion in response to a decrease in effective arterial blood volume.**

severity of congestive heart failure exists in humans.[43] This relationship may explain why renal function improves in some patients treated with ACE inhibitors, whereas renal function deteriorates in others.[152] In subjects whose renal function worsens after administration of the drug, there is a greater fall in mean right atrial pressure, left ventricular filling pressure, mean arterial pressure, and systemic vascular resistance as compared to subjects with stable renal function. In addition, plasma renin activity increases to a greater extent. These changes suggest a more contracted EABV and greater dependency of systemic vascular resistance on circulating angiotensin II in patients with ACE inhibitor-induced renal dysfunction.

In summary, during severe decompensated left ventricular failure, decreased EABV elicits release of renin with consequent activation of angiotensin II and aldosterone. Acutely, increased circulating levels of angiotensin II serve to maintain systemic blood pressure and augment renal sodium reabsorption. Salt retention is the result of hemodynamic and direct effects of angiotensin II at the level of the proximal tubule, and enhanced sodium reabsorption in the distal nephron primarily mediated by increased aldosterone. As ECF volume expands, renin, angiotensin II, and aldosterone become suppressed, although not necessarily to normal levels. Maintenance of systemic blood pressure is more dependent on volume rather than angiotensin II. Sodium balance is now achieved, but at the expense of increased steady-state ECF volume. ACE inhibitor therapy is not associated with deleterious effects on renal function at this stage of the disease. Should further deterioration in cardiac function ensue, persistent activation of the renin–angiotensin–aldosterone system may result, such that systemic blood pressure remains dependent on circulating angiotensin II despite expansion of ECF volume. In this setting, ACE inhibitor therapy can precipitate hypotension and significant reductions in the glomerular filtration rate. One has to consider this sequential change in renin to volume dependency of mean arterial blood pressure in attempting to predict net renal and hemodynamic effects of converting enzyme inhibition.[156,194]

Sympathetic Nervous System

The sympathetic nervous system is activated in congestive heart failure. Plasma norepinephrine levels are elevated, and concentrations correlate with the degree of left ventricular dysfunction.[111] Direct nerve recordings demonstrate a direct relationship between central sympathetic nerve outflow and left ventricular filling pressures.[109]

Increased sympathetic tone influences renal reabsorption of salt and water by indirect, as well as direct, mechanisms (Figure 38.5). Glomerular hemodynamics are affected similarly to that produced by angiotensin II. In addition, sympathetic nerves directly stimulate

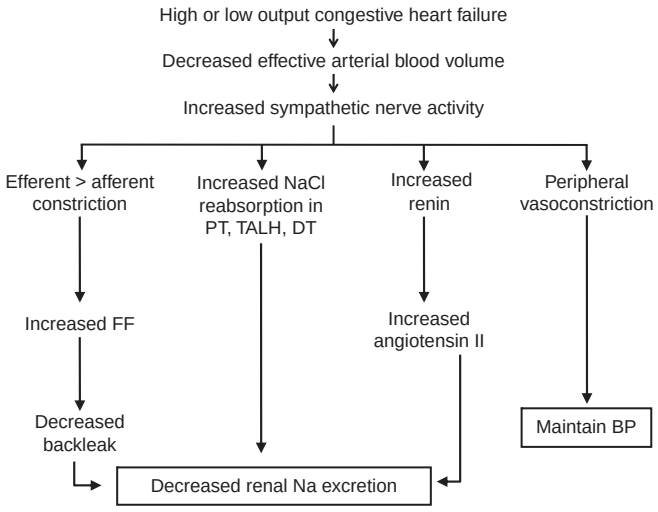

FIGURE 38.5 **Pathways by which sympathetic nerves regulate renal sodium excretion in response to a decrease in effective arterial blood volume.**

tubular reabsorption of salt and water in both the proximal and the distal nephron.

Increased sympathetic nerve activity stimulates renin release. The subsequent formation of angiotensin II provides a positive feedback loop leading to further increases in sympathetic nerve activity. Angiotensin II sensitizes tissues to the actions of catecholamines, and acts synergistically with renal nerves in modulating renal blood flow.[158]

Arginine Vasopressin

Increased circulating levels of AVP is a characteristic finding in patients with congestive heart failure.[172] The nonosmotic release of AVP plays an important role in the development of hyponatremia, which in turn is a well-defined predictor of mortality in heart failure patients. In experimental heart failure, there is upregulation of the mRNA for vasopressin in the hypothalamus.[91] In addition, there is increased expression of the mRNA and the protein for the aquaporin-2 water channel.[216] In a rat model of heart failure, selective antagonism of the V-2 receptor is associated with a significant improvement in free water clearance.[216] Administration of a V-2 receptor antagonist to patients with congestive heart failure is associated with a significant reduction in body weight and improvement in dyspnea, but has not been shown to reduce mortality.[173]

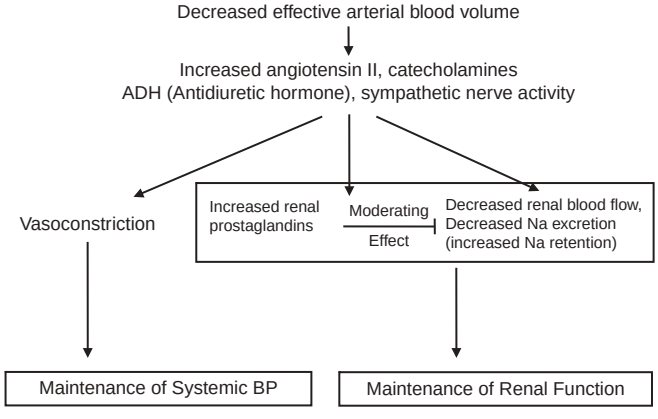
Decreased effective arterial blood volume
Increased angiotensin II, catecholamines
ADH (Antidiuretic hormone), sympathetic nerve activity
Vasoconstriction
Increased renal prostaglandins
Moderating Effect
Decreased renal blood flow, Decreased Na excretion (increased Na retention)
Maintenance of Systemic BP
Maintenance of Renal Function

FIGURE 38.6 **Renal prostaglandins moderate the effect of various effector mechanisms, thereby allowing renal function to be well-maintained in the setting of increased systemic vasoconstrictor input.**

Prostaglandins

Increased production of prostaglandins plays an important role in maintaining circulatory homeostasis in congestive heart failure. In response to decreases in cardiac output, neurohumoral vasoconstrictor forces (i.e., the renin–angiotensin–aldosterone system, the neurosympathoadrenal axis) participate in the maintenance of systemic arterial pressure, and result in increased total peripheral vascular resistance. These same vasoconstrictors stimulate the renal production of vasodilatory prostaglandins, such that the rise in renal vascular resistance is less than that seen in the periphery. Vasodilatory prostaglandins function in a counterregulatory role, attenuating the fall in renal blood flow and glomerular filtration rate that would otherwise occur if vasoconstrictor forces were left unopposed.[154]

Renal prostaglandins also serve to moderate salt and water retention that would otherwise occur in the setting of unopposed activation of effector mechanisms such as angiotensin II, aldosterone, renal sympathetic nerves, and ADH.[154] The importance of prostaglandins in modulating renal hemodynamics, sodium excretion, and circulatory homeostasis progressively increases in proportion to the severity of the heart failure (Figure 38.6).

Natriuretic Peptides

Circulating atrial natriuretic peptide (ANP) and brain natriuretic peptide (BNP) are circulating hormones which are primarily synthesized in the cardiac atria and ventricles respectively. The synthesis and release of these peptides provide a mechanism whereby cardiac atria and ventricles serve both an afferent and efferent function in the control of ECF volume. Levels of ANP are elevated and correlate with the severity of disease in humans and experimental animals with heart failure.[29,168]

The natriuretic and vasodilatory properties of ANP suggest that this peptide plays an important counterregulatory role in congestive heart failure. However, attempts to use ANP therapeutically in congestive heart failure have produced disappointing results.[29,95] ANP infused in patients with heart failure causes only

a minimal change in fractional sodium excretion and urine flow rates, as compared to the robust response in normal controls.[29] The mechanism of renal nonresponsiveness in heart failure is not entirely clear. A downregulation of receptors due to sustained exposure to high levels of ANP or altered intrarenal hemodynamics are possibilities. Decreased delivery of sodium to the distal nephron where ANP normally exerts its natriuretic effect is also a likely cause of resistance. While ANP levels are uniformly elevated in congestive heart failure, potentially beneficial natriuretic properties are overwhelmed by more powerful antinatriuretic effector mechanisms.

Similar to ANP, plasma levels of BNP are elevated in congestive heart failure, and in proportion to the severity of systolic and diastolic dysfunction.[153] Infusion of BNP is associated with a significant reduction in pulmonary capillary wedge pressure, pulmonary artery pressure, right atrial pressure, and mean arterial pressure, as well as an increase in cardiac index. These hemodynamic benefits are accompanied by significant increases in urinary volume and sodium excretion, in some but not all studies.[131,133] Infusion of BNP can be associated with hypotension, particularly when given with other vasodilators. Measurement of plasma BNP levels is often utilized as a diagnostic tool to differentiate between cardiac versus other causes of pulmonary congestion. In addition, BNP levels can be used as a prognostic indicator and a marker reflecting the degree of cardiac dysfunction.

Endothelin and Nitric Oxide

Circulating levels of endothelin are increased in congestive heart failure, and correlate positively with the degree of myocardial dysfunction. Studies in which endothelin antagonists have been administered suggest this substance may play a role in the pathophysiology of cardiac failure.[130,172] In a randomized, double-blind study of human subjects with heart failure, infusion of an ETa and ETb receptor blocker (bosentan) was associated with a reduction in right atrial pressure, pulmonary artery pressure, pulmonary capillary wedge pressure, and mean arterial pressure.[93] In a dog model of heart failure,[204] ETa blockade alone lead to a reduction in cardiac filling pressures and increased cardiac output. These hemodynamic changes were associated with an increase in GFR and renal plasma flow, as well as increased urinary sodium excretion. By contrast, administration of an ETb receptor blocker caused an increase in cardiac filling pressures and a decrease in cardiac output, suggesting endogenous endothelins adversely effect cardiac hemodynamics and cause fluid retention, primarily through ETa receptors.

Nitric oxide production is increased in congestive heart failure.[210] Increased release of nitric oxide from resistance vessels may partly antagonize neurohumoral vasoconstrictor forces. Inhibiting nitric oxide production in heart failure patients causes a significant increase in pulmonary and systemic vascular resistance, as well as a decline in cardiac output. In the renal vasculature, nitric oxide production is also increased; however, the renal vasodilatory response to nitric oxide is impaired.[2] Administration of an angiotensin receptor antagonist restores nitric oxide-mediated renal vasodilation, suggesting angiotensin II plays a contributory role in this defect.[1]

CIRRHOSIS

Renal sodium excretion is normally regulated so that extracellular fluid (ECF) volume is maintained within normal limits. Any maneuver that increases ECF volume will lead to a prompt and sustained natriuresis until the volume returns to normal. In patients with cirrhosis, this homeostatic mechanism becomes deranged such that large increases in ECF volume are accompanied by continued renal salt retention, resulting in edema and ascites formation.

Presinusoidal Versus Postsinusoidal Obstruction and Ascites Formation

In patients with cirrhosis, the kidneys are normal but are signaled to retain salt in an unrelenting manner. The critical event in the generation of this signal is development of hepatic venous outflow obstruction. In the normal state, the portal circulation is characterized by high flow, low pressure, and low resistance. The imposition of a resistance into this high-flow vasculature will uniformly raise portal pressure, but development of ascites is critically dependent on location of the resistance. Conditions associated with presinusoidal vascular obstruction, such as portal vein thrombosis and schistosomiasis, raise portal pressure but are not generally associated with ascites. By contrast, hepatic diseases such as Laennec's cirrhosis and Budd Chiari syndrome cause early postsinusoidal vascular obstruction, and are associated with marked degrees of salt retention, anasarca, and ascites. Thus, during the development of the cirrhotic process, ascites will accumulate primarily when the pathologic process is associated with hepatic venous outflow obstruction and sinusoidal hypertension.

This distinction between presinusoidal and postsinusoidal obstruction can best be explained by comparing the characteristics of fluid exchange in capillaries of the splanchnic bed versus those in the hepatic sinusoids. The intestinal capillaries are similar to those in the peripheral tissues, in that they have continuous

membranes with small pores such that a barrier exists, preventing plasma proteins from moving into the interstitial space. An increase in capillary hydrostatic pressure will cause the movement of a protein-poor fluid to enter the interstitial compartment and decrease the interstitial protein concentration. Interstitial protein concentration is further reduced by an acceleration in lymph flow that is stimulated by the fluid movement. As a result, the interstitial oncotic pressure falls, and the plasma oncotic pressure remains unchanged. The net oncotic force therefore rises and offsets the increase in hydrostatic force, providing a buffer against excessive fluid filtration. The fall in intestinal lymph protein concentration is maximal at relatively low pressures, and is much greater than that observed from the cirrhotic liver.[8,213] Thus, the increase in net oncotic force associated with dilution of the interstitial protein and accelerated lymph flow contribute to the protection against ascites in patients whose only abnormality is portal hypertension.

The situation across the liver sinusoids is quite different. Hepatic sinusoids, unlike capillaries elsewhere in the body, are extremely permeable to protein. As a result, colloid osmotic pressure exerts little influence on movement of fluid. Rather, direction of fluid movement is determined almost entirely by changes in sinusoidal hydraulic pressure. Thus, efflux of protein-rich filtrate into the space of Disse is critically dependent on hepatic venous pressures. Obstruction to hepatic venous outflow will lead to large increments in the formation of hepatic lymph and flow through the thoracic duct. Unlike the intestinal capillaries, there is little or no restriction in the movement of protein into the interstitium, such that the protein concentration of hepatic lymph will quickly approach that of plasma.[64] As a result, no significant oncotic gradient develops between plasma and the interstitium at high sinusoidal pressures and flow.

When sinusoidal pressure increases to such a degree that hepatic lymph formation exceeds the capacity of the thoracic duct to return fluid to the circulation, interstitial fluid weeps off the liver into the peritoneal space and forms ascites. Lymph formation in the setting of cirrhosis can be more than 20-fold greater than that which occurs under normal circumstances.[213] Whereas in normal humans 1−1.5 liters/day of lymph are returned to the circulation, subjects with cirrhosis, even without ascites, may have lymph flow through the thoracic duct as high as 15−20 liters/day.[212] The predominance of hepatically-produced lymph to overall lymph production is illustrated by studies in experimental animals with cirrhosis. Barrowman and Granger[8] found a 29-fold increase in hepatic lymph flow, while only a three-fold increase was noted in the splanchnic lymphatics. Eleven of 19 animals had normal flows of intestinal lymph, while all the cirrhotic animals had increased flows in liver lymph.

Conditions associated with the rapid onset of postsinusoidal obstruction, such as acute right-sided congestive heart failure and Budd−Chiari syndrome, initially give rise to ascitic fluid that has a high protein concentration that may even approach that of plasma. This high protein concentration is reflective of the liver being the predominant source of the ascitic fluid. However, over time the protein content of ascites in these conditions begins to decrease. Witte et al.[214] measured the total protein in ascitic, pleural, and peripheral edema fluid in acute and chronic heart failure patients. In the setting of acute heart failure, the mean concentration of protein in ascitic fluid was approximately 5 g/dl. By contrast, the protein concentration in ascitic fluid of chronic congestive heart failure patients was 2.7 g/dl. A lower protein concentration is also typical of conditions such as Laennec's cirrhosis, in which postsinusoidal obstruction develops slowly.

Two phenomena contribute to this change in ascitic fluid protein concentration. If the hepatic sinusoids are subject to an increased hydrostatic pressure for a long period of time, they begin to assume the anatomic and functional characteristics of capillaries found elsewhere in the body, a process referred to as capillarization.[181] This change leads to a decrease in albumin permeability, such that oncotic forces begin to play some role in hepatic lymph formation. At the same time, hypoalbuminemia develops secondary to decreased hepatic synthesis, as well as dilution secondary to ECF volume expansion. As a result, the protein content of hepatic lymph, although still high, falls to approximately 50−55% of plasma values.[213]

The second factor contributing to the lower ascitic protein concentration is the superimposition of portal hypertension. Early in the development of portal hypertension when plasma protein concentration is normal only minimal amounts of ascitic fluid are derived from the splanchnic bed, due to the buffering effect of increased net oncotic force opposing fluid filtration. Extremely high hydrostatic pressures are required to produce significant amounts of ascitic fluid in the setting of normal plasma protein concentrations. By contrast, less and less hydrostatic pressure is required for the formation of ascitic fluid, as the plasma albumin concentration decreases and the net osmotic force declines. In this setting, the splanchnic bed begins to make a greater contribution to the generation of ascites, and the fluid is characterized by a low protein concentration.[9]

The development of portal hypertension is also associated with changes in the splanchnic circulation that secondarily lead to increased lymph production in the splanchnic bed. The importance of the splanchnic

lymphatic pool in the generation of ascites is reflected by the fact that in most instances ascitic fluid is transudative and characterized by a protein concentration of approximately 2.5 g/dl. Classically, portal hypertension was considered to be the sole result of increased resistance to portal venous flow. However, studies in experimental models suggest that increased portal venous flow resulting from generalized splanchnic arteriolar vasodilation also plays a role in the genesis of increased portal pressure.[19,203] This vasodilation leads to changes in the splanchnic microcirculation that may predispose to increased filtration of fluid. For example, an acute elevation of venous pressure in the intestine normally elicits a myogenic response that leads to a reduction in blood flow. This decrease in flow is thought to serve a protective role against the development of bowel edema. However, in chronic portal hypertension this myogenic response is no longer present. In this setting, arteriolar resistance is reduced, such that capillary pressure and filtration are increased.[12,174] The loss of this autoregulatory mechanism may account for the greater increase in intestinal capillary pressure and lymph flow seen under conditions of chronic portal hypertension when compared to acute increases in portal pressure of the same magnitude.[102] The potential causes of splanchnic arteriolar vasodilation are discussed below.

The importance of portal hypertension in the pathogenesis of ascites is highlighted by several observations. First, patients with ascites have significantly higher portal pressures as compared to those without ascites.[143] Although the threshold for ascites development is not clearly defined, it is unusual for ascites to develop with a pressure below 12 mmHg. Gines found that only 4 of 99 cirrhotic patients with ascites had a portal pressure <12 mmHg, as estimated by hepatic venous wedged pressure.[63] Second, portal pressure correlates inversely with urinary sodium excretion.[143] Third, maneuvers designed to reduce portal pressure are known to have a favorable effect on the development of ascites. For example, surgical portosystemic shunts used in the treatment of variceal bleeding reduce portal pressure, and are associated with a lower probability of developing ascites during follow-up.[29] Both side-to-side and end-to-side portocaval anastomosis have been shown effective in the management of refractory ascites in cirrhosis. Recent studies also suggest that reducing portal pressure with a transjugular intrahepatic portasystemic shunt has a beneficial effect on ascites.[148]

In summary, ascites develops when the production of lymph from either or both the hepatic sinusoids and the splanchnic circulation exceeds the transport capacity of the lymphatics. In this setting, fluid will begin to weep from the surface of the liver and the splanchnic capillary bed, and accumulate as ascites. The final protein concentration measured in the peritoneal fluid is determined by the sum of the two contributing pools of fluid; one relatively high in protein originating in the liver and the other, a low protein filtered across splanchnic capillaries. Hepatic venous outflow obstruction leading to increased sinusoidal pressure and portal hypertension are the major determinants of whether lymph production will be of a magnitude sufficient for ascitic fluid to accumulate. Increased sinusoidal pressure is also related to the subsequent development of renal salt retention. The mechanism by which sinusoidal hypertension signals the kidney to retain sodium is discussed in the following section.

Afferent Limb of Sodium Retention: Overfill Versus Underfill Mechanisms

Classical Underfill Mechanism for Renal Salt Retention

The mechanism by which hepatic venous outflow obstruction leads to sufficiently high sinusoidal pressures for ascites formation is controversial. The classical (underfill) theory predicts that the degree of hepatic venous outflow obstruction is sufficient in the presence of normal splanchnic perfusion to perturb the balance between rates of hepatic lymph formation and thoracic duct flow, thereby resulting in the formation of ascites. Both increased sinusoidal and portal venous pressures, in conjunction with hypoalbuminemia, cause formation of ascites in the presence of normal splanchnic perfusion. The formation of ascites, however, occurs at the expense of decreased intravascular volume. In consequence, a low venous filling pressure and a low cardiac output activate baroreceptor mechanisms, resulting in renal salt retention. According to this formulation, development of ascites is the primary event that leads to an underfilled circulation and subsequent renal salt retention.

The failure of measured hemodynamic parameters to satisfy predictions of the classical theory has raised questions regarding its validity. As originally conceived, it was predicted that extrasplanchnic plasma volume would be decreased, and that cardiac output would be low. When measured, however, these values have rarely been low. In fact, measurements have indicated that total plasma volume is usually elevated in cirrhotic patients. Similarly, cardiac output is rarely low, but tends to vary from normal to very high. In addition, studies performed in animal models of cirrhosis have found that sodium retention precedes the formation of ascites, suggesting that salt retention is a cause and not a consequence of ascites formation.

Overfill Mechanism for Renal Salt Retention

The incompatibility of measured hemodynamic parameters and timing of renal salt retention with the classical theory of ascites has led others to propose the overflow theory.[118] Once again, hepatic disease with venous outflow obstruction is viewed as a prerequisite for development of increased sinusoidal and portal pressures. In contrast to the classical theory, however, normal splanchnic perfusion fails to raise sinusoidal pressure sufficiently to cause ascites formation. Rather, venous outflow obstruction signals renal sodium retention independent of diminished intravascular volume. Salt retention, in turn, increases plasma volume, cardiac output, and splanchnic perfusion, thus raising sinusoidal and portal pressures sufficiently to culminate in translocation of fluid into the interstitial space and eventually the peritoneum. The combination of portal hypertension and increased arterial volume would lead to overflow ascites formation. This hypothesis is supported by the positive correlation between plasma volume and hepatic venous pressure, and the persistence of increased plasma volume after portacaval anastomosis. Moreover, patients with ascites have significantly higher portal pressure than patients without ascites, and portal pressure correlates inversely with urinary sodium excretion.[63]

Additional evidence linking hepatic venous outflow obstruction directly to renal sodium retention comes from studies performed in dogs fed the potent hepatotoxin dimethylnitrosamine.[115–117] The pathophysiologic disturbances and histologic changes that develop over a 6–8-week period are similar in nature to those seen in Laennec's cirrhosis. In this model, sodium retention and increases in plasma volume precede formation of ascites by about 10 days.[115] In order to exclude the possibility that the increase in plasma volume was solely due to an increased splanchnic plasma volume, repeat measurements were obtained after ligation of the superior and inferior mesenteric arteries, the celiac axis, and portal vein. In this way, any contribution of the splanchnic circulation could be excluded. These studies clearly showed that extrasplanchnic plasma volume was elevated at a time when dogs were in positive sodium balance. To further prove that extrasplanchnic plasma volume was increased, end-to-side portacaval shunts were placed prior to inducing cirrhosis.[117] This maneuver was designed to prevent any increase in splanchnic plasma volume. In these studies, evidence of salt retention preceded the formation of ascites, and was accompanied by a parallel increase in plasma volume.

In another series of studies using this same model, hemodynamic parameters were monitored during control, precirrhotic, and postcirrhotic sodium balance periods.[116] Sodium retention was found to precede any detectable change in cardiac output or peripheral vascular resistance. Once ascites developed, plasma volume increased further, and this was associated with increased cardiac output and a fall in peripheral vascular resistance. It was concluded that initiation of sodium retention and plasma volume expansion was not dependent on alterations in systemic hemodynamics. This conclusion has been corroborated in the canine model of hepatic cirrhosis induced by bile duct ligation,[197] as well as in rats made cirrhotic with carbon tetrachloride inhalation and oral phenobarbital.[123]

The pathway by which primary renal sodium retention would be linked to venous outflow obstruction in the overfill theory is not clear. Convincing evidence does exist for the presence of an intrahepatic sensory network composed of osmoreceptors, ionic receptors, and baroreceptors. Studies in which hepatic venous pressure is raised have demonstrated increases in hepatic afferent nerve activity.[113,114,197] Furthermore, a neural reflex pathway linking hepatic venous congestion and augmented sympathetic nerve activity has been identified.[104] In addition, acute constriction of the portal vein in dogs results in renal sodium and water retention in the innervated unilateral kidney, while these effects are abolished in the contralateral denervated kidney.[2] In addition to a neural mechanism, there may also be a hormonal system by which the liver and kidney can communicate. Hepatically-produced cAMP has been proposed to be a component of such a system.[6] Circulating cAMP is known to inhibit proximal salt and water absorption, as well as to contribute to the regulation of glomerular filtration rate. According to this hypothesis, decreased circulating cAMP levels as a result of liver disease could secondarily lead to renal salt retention and impaired renal function.

In summary, the overfill hypothesis is supported by a number of observations that indicate sodium retention precedes development of ascites in the absence of hemodynamic factors known to lead to salt retention. Moreover, high cardiac output coupled with increased plasma volume argues strongly for increased arterial blood volume, a finding seemingly incompatible with the underfill theory. Against such an analysis, however, is that mechanisms that sense arterial volume physiologically may be more sensitive than methods used to measure it. It should be noted that while statistically insignificant, there was a fall in blood pressure at the time of positive sodium balance in the dimethylnitrosamine model. This decrease may have been of sufficient magnitude to signal renal salt retention.[116] Since cardiac output was unchanged, total peripheral resistance may have decreased. Similarly, patients with hepatic cirrhosis and ascites behave as if they are effectively volume-depleted. Despite an increase in cardiac

output and plasma volume, arterial pressure is typically low. This fall in systemic blood pressure is consistent with an underfilled arterial vascular compartment. Thus, the distinction between classical and overflow theories better rests on the measurement of effective arterial blood volume (EABV).

Use of EABV to Distinguish Underfill and Overfill Mechanisms of Renal Salt Retention

The classical (underfill) theory predicts that EABV is low in patients with ascites, and is the afferent mechanism signaling renal salt retention. The overflow theory predicts that EABV is expanded due to primary salt retention. While EABV cannot be measured directly, assessing the level of activation of neurohumoral effectors known to be regulated by EABV can be considered a measure of it. In this regard, levels of renin, aldosterone, ADH, and norepinephrine can serve as markers reflective of the magnitude of the EABV.

When renin and aldosterone values have been measured in patients with cirrhosis, values have varied from low to high. It is important, however, to consider these levels in the context of whether ascites is present or not. In the absence of ascites, subjects are in sodium balance, and renin and aldosterone levels are normal.[171] In the presence of ascites, mean renin and aldosterone levels are elevated, but individual values are often still normal.[4,63] This observation seems in conflict with the classical theory, as all patients with ascites who are in positive sodium balance should have decreased EABV and high aldosterone levels. However, not all patients with ascites are retaining sodium. In fact, some patients are in balance such that sodium intake equals output. Thus, in examining the mechanism of sodium retention in cirrhosis with ascites, neurohumoral effectors such as renin, aldosterone, ADH, and sympathetic nerve activity should be considered with respect to the rate of sodium excretion. When examined in this fashion, a significant inverse relationship is found between urinary sodium excretion and neurohumoral markers, suggesting the presence of a contracted EABV.

One component of the circulation that appears to be contributing to the overall decrease in EABV is the central circulation. Indirect measurements demonstrate that central blood volume is reduced, while noncentral blood volume is expanded.[140] In fact, the size of central and arterial blood volume is inversely correlated with sympathetic nervous system activity, suggesting that unloading of central arterial baroreceptors is responsible for enhanced sympathetic activity. This conclusion is supported by studies using the technique of head-out water immersion (HWI).[49,50] In this technique, subjects are seated and immersed in a water bath up to their necks. This technique results in redistribution of ECF volume from the interstitial space into the vasculature, with a sustained increase in central blood volume. The central volume expansion is comparable to that induced by infusion of 2 liters of isotonic saline.[50] Such a maneuver would be expected to raise both the EABV and the hepatic sinusoidal pressure. The classical theory would predict that HWI would lead to decreases in renin, aldosterone, ADH, and norepinephrine concentrations in response to expansion of EABV. Since renin levels correlate with wedged hepatic vein pressures, the overfill theory would predict further rises in renin and other hormonal systems consequent to initiation of a sinusoidal pressure-sensitive hepatorenal reflex. When HWI was performed in a heterogeneous group of patients with cirrhosis, the natriuretic response was variable, but suppression of renin and aldosterone levels was uniform.[52] In a more homogenous group of patients characterized by impaired ability to excrete water and sodium, HWI was shown consistently to suppress plasma AVP, renin, aldosterone, and norepinephrine, as well as to increase sodium and water excretion.[17,146]

Taken together, the multiplicity of data support the presence of decreased EABV in patients with decompensated cirrhosis, and is most consistent with an underfill mechanism of renal salt retention (Figure 38.7). Since blockade of endogenous vasoconstrictor systems in patients with cirrhosis and ascites leads to marked arterial hypotension, activation of these systems function to contribute to the maintenance of arterial pressure. At least one component of the decrease in EABV may be due to an underfilled central circulation. As discussed in the following paragraphs, increased perfusion of arteriovenous communications, systemic vasodilation, and increased perfusion of the splanchnic bed are important factors in the genesis of an underfilled circulation. In addition, these factors play a major role in the hyperdynamic circulation that is typical of patients with chronic liver disease.

Hyperdynamic Circulation in Cirrhosis

Arteriovenous Communications

The characteristic circulatory changes observed in animal, as well as clinical, studies of cirrhosis consist of increased cardiac output, low mean arterial pressures, and low peripheral vascular resistance. The most attractive explanation for a contracted EABV in the setting of such a hyperdynamic circulation assigns a pivotal role to increased vascular capacitance.[92] An increased vascular holding capacity out of proportion to plasma volume results in an underfilled circulation and decreased EABV. One factor that may account for increased vascular capacitance and a hyperdynamic

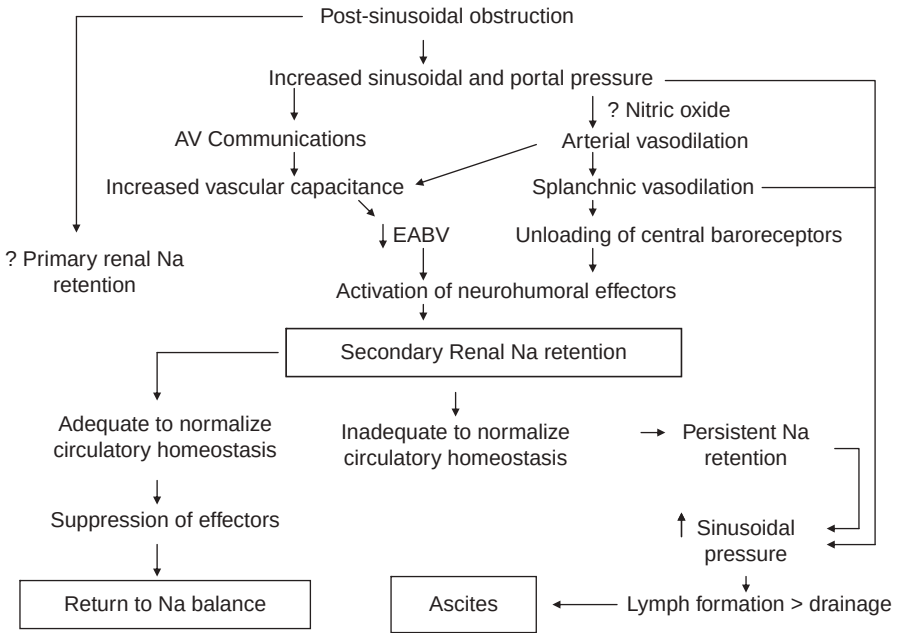

FIGURE 38.7 **Unified theory of ascites formation: a modified underfill mechanism.**

circulation is the formation of widespread arteriovenous communications.[15] In cirrhotics, arteriovenous fistula formation has been identified in the pulmonary, mesenteric, and upper and lower extremity circulations. In addition, increased blood flow has been measured in muscle and skin of the upper extremity not attributable to increased oxygen consumption, anemia or thiamine deficiency.[97] Postmortem injection demonstrated intense proliferation of small arteries in the splenic vasculature of patients with cirrhosis.[129]

The hemodynamic changes and salt retention that occur with an arteriovenous fistula are reminiscent of what occurs in cirrhotic humans.[48] With an open fistula, peripheral vascular resistance falls, cardiac output increases, and diastolic and mean blood pressures fall. The proportionately greater increase in vascular capacitance over cardiac output results in a contracted EABV. Consequent sodium retention expands ECF volume, raises venous filling pressure, and further increases cardiac output until balance is achieved between cardiac output and lowered peripheral resistance. At this point, sodium intake equals excretion, EABV is normalized, and the patient is in balance.

In cirrhosis, a similar imbalance occurs between plasma volume and vascular capacitance, such that EABV remains contracted and renal sodium retention is stimulated. In contrast to a simple arteriovenous fistula, however, several factors are present in cirrhosis that make sodium balance more difficult to achieve. First, these patients often have impaired cardiovascular function.[15] Diminished venous return consequent to tense ascites or cardiomyopathy from alcohol or malnutrition may limit increases in cardiac output. Furthermore, depression of left ventricular function in response to increased afterload suggests subclinical cardiac disease, despite elevated forward output.[120] Second, retained sodium does not remain in the vascular space and lead to increased venous return. Rather, retained sodium becomes sequestered within the abdomen as ascites. Third, increased vascular permeability may further impair the ability of retained sodium to expand EABV. Peripheral arterial vasodilation in cirrhotic rats is associated with increased vasopermeability to albumin, electrolytes, and water.[25] Examination of interstitial fluid dynamics by means of a subcutaneous plastic capsule reveals substantial increases in interstitial fluid volume early in cirrhosis before the appearance of ascites or peripheral edema.[179] Such capillary leakage impedes filling of the intravascular compartment and prevents replenishment of a contracted EABV.

Primary Arterial Vasodilation

Arteriovenous fistulas and formation or hyperdynamic perfusion of pre-existing capillary beds are changes that develop as cirrhosis progresses. Nevertheless, salt retention occurs early in the cirrhotic process before these anatomic changes are fully-established. Since sodium retention antedates the formation of overt ascites and portosystemic shunting, peripheral arterial vasodilation has been proposed to be a primary event in the initiation of sodium and water retention in cirrhosis.[185] In this manner, a decreased EABV and increased vascular capacitance could still be the signal for renal salt retention, even in the earliest stages of liver injury. The peripheral arterial vasodilation

hypothesis is supported by several studies in animal models.[209] In rats with partial ligation of the portal vein, evidence of a reduced systemic vascular resistance precedes the onset of renal salt retention. In addition, a direct correlation has been found between the onset of decreased arterial pressure and renal sodium retention in spontaneously hypertensive rats with experimental cirrhosis.[123] As opposed to the classical underfilling theory, the arterial vascular underfilling would not be the result of a reduction in plasma volume, which in fact is increased, but rather to a disproportionate enlargement of the arterial tree secondary to arterial vasodilation. In the rat with carbon tetrachloride-induced cirrhosis, the fall in peripheral vascular resistance and hyperdynamic circulatory state precede ascites formation, suggesting that generalized vasodilation is indeed an early finding with hepatic injury.[56]

Perhaps the best evidence to date in support of an underfilled circulation due to arterial vasodilation comes from human studies of HWI accompanied by infusion of a vasoconstrictor. HWI is associated with increased perfusion of the central circulation, however, urinary excretion rates of salt and water improve, but do not normalize with this procedure alone.[17] Since systemic vascular resistance falls during HWI, it was proposed that further vasodilation may prevent complete restoration of EABV in subjects already peripherally vasodilated. Infusion of a vasoconstrictor will increase peripheral vascular resistance, but will do little to improve an underfilled central circulation. Predictably, infusion of norepinephrine alone into cirrhotic subjects fails to significantly increase urinary sodium excretion.[188] By contrast, when norepinephrine is infused during HWI so as to increase central perfusion and at the same time attenuate the fall in systemic vascular resistance, sodium excretion increases significantly. In six subjects with decompensated cirrhosis, this combined maneuver was found to increase urinary sodium excretion to an amount that when extrapolated over a 24-hour period was greater than sodium intake.[188] These results are consistent with the hypothesis that arterial vasodilation causes an abnormal distribution of the total blood volume, such that effective central blood volume is reduced.

SPLANCHNIC ARTERIAL VASODILATION

As alluded to earlier, arterial vasodilation is particularly marked in the splanchnic arteriolar bed.[80,180,203] Increasing degrees of splanchnic vasodilation contribute to the fall in mean arterial pressure and unloading of baroreceptors in the central circulation.[32,135] As a result, central afferent sensors signal the activation of neurohumoral effectors, which in turn decrease perfusion of other organs, but in particular in the kidney. The importance of splanchnic vasodilation in the genesis of renal ischemia has been indirectly illustrated by the response to ornipressin, an analog of AVP that is a preferential splanchnic vasoconstrictor.[67,110] The administration of ornipressin to patients with advanced cirrhosis leads to correction of many of the systemic and renal hemodynamic abnormalities that are present. These include an elevation in mean arterial pressure, reductions in plasma renin activity and norepinephrine concentration, and increases in renal blood flow, glomerular filtration rate, and urinary sodium excretion and volume. Similar benefits have been reported with the combined use of octreotide and midodrine.[85]

ROLE OF NITRIC OXIDE IN ARTERIAL VASODILATION

The underlying cause of arterial vasodilation, particularly in the early stages of cirrhosis, has not been fully-elucidated, but a great deal of attention has been focused on humoral factors.[79] There is an increasing body of experimental and preliminary human evidence suggesting that increased nitric oxide production may be an important factor in this process. In both experimental models and in human subjects with cirrhosis, increased production of nitric oxide can be demonstrated.[176,192,207] In the cirrhotic rat, evidence of increased production is already present when the animals begin to retain sodium, and antedates the appearance of ascites.[11] Administration of nitric oxide synthase inhibitor L-NMMA to cirrhotic human subjects improves the vasoconstrictor response to noradrenaline, suggesting that overproduction of nitric oxide is an important mediator of the impaired responsiveness of the vasculature to circulating vasoconstrictors.[24] In addition, this same inhibitor administered in low doses has been shown to correct the hyperdynamic circulation in cirrhotic rats.[147] In a more recent study utilizing this same model, normalization of nitric oxide production was associated with a marked natriuretic and diuretic response, as well as a reduction in the degree of ascites in cirrhotic rats.[132]

The precise mechanism for increased nitric oxide production in cirrhosis is not known, but may be mediated at least in part via the release of tumor necrosis factor-alpha.[121] In experimental models of hepatic disease, for example, the administration of anti-TNF-alpha antibodies or an inhibitor of nitric oxide synthesis results in increases in splanchnic and total vascular resistance, an elevation in the mean arterial pressure, and a reduction in cardiac output toward or, with nitric oxide inhibition, to normal.[121,147] Similarly, blocking the signaling events induced by TNF and nitric oxide production, via inhibition of protein tyrosine kinase, ameliorates the hyperdynamic abnormalities in rats with cirrhosis and portal hypertension.[122] Studies in

cirrhotic humans with an increased cardiac output and systemic vasodilatation have shown evidence of enhanced nitric oxide production, a finding compatible with the experimental observations. Portosystemic shunts and decreased reticuloendothelial cell function may allow intestinal bacteria and endotoxin to enter the systemic circulation, providing a potential stimulus for tumor necrosis factor-alpha and/or nitric oxide production.

It is not yet known with certainty whether the endothelial (eNOS) or the inducible (iNOS) isoform is primarily responsible for increased production of nitric oxide. The hyperdynamic circulatory state of cirrhosis may impose a shear stress on the vascular endothelium, thus providing a stimulus for the upregulation of eNOS.[134,207] On the other hand, increased activity of nitric oxide synthase in polymorphonuclear cells and monocytes (cells that primarily contain iNOS) in cirrhotic human subjects suggest the inducible isoform may also play a role in increased production.[134]

In summary, an underfill mechanism appears to explain the bulk of experimental, as well as clinical, findings in established cirrhosis (Figure 38.7). Less certain are mechanisms responsible for sodium retention that precede the development of ascites. The overfill theory invokes the presence of a hepatorenal reflex sensitive to subtle rises in intrahepatic pressure mediating initiation of renal salt retention. However, the finding of decreased peripheral vascular resistance, even at this early stage, suggests diminished arterial filling.[116] Early peripheral arterial vasodilation and later formation of anatomic shunts lead to disproportionate increases in vascular capacitance with subsequent contraction of EABV, thereby signaling renal salt retention.[59,103,141] While it is conceivable that both overfill mechanisms and underfill mechanisms may be operative at different stages of disease, the multiplicity of data both clinical and experimental can be assimilated into an underfill theory.

Concept of Balance in Cirrhosis

In the earliest stages of cirrhosis when arterial vasodilation is moderate and the lymphatic system is able to return increased lymph production to the systemic circulation, renal sodium and water retention are sufficient to restore EABV and thereby suppress neurohumoral effectors. Balance is re-established such that sodium intake equals sodium excretion, but at the expense of an increased ECF volume. As liver disease progresses, this sequence of arterial underfilling followed by renal salt retention is repeated. As long as the EABV can be restored to near normal levels the activation of effector mechanisms will be moderated, and balance will be achieved albeit at ever-increasing levels of ECF volume (Figure 38.8). Eventually, lymph production will begin to exceed the drainage capacity of the lymphatic system. At this stage of the disease renal salt retention becomes less efficient at restoring EABV, as retained fluid is sequestered in the peritoneal cavity as ascites. At the same time arterial underfilling is more pronounced, particularly as splanchnic arteriolar vasodilation becomes more prominent. Activation of neurohumoral effectors is magnified, resulting in more intense renal salt retention. Even at this stage of the disease cirrhotic patients with ascites eventually re-establish salt balance. The terminal stages of the cirrhotic process are characterized by extreme arterial underfilling. At this time there is intense and sustained activation of neurohumoral effectors. As a result, renal salt retention is nearly complete as the urine becomes virtually devoid of sodium. The vasoconstrictor input focused in on the kidney is of such a degree that renal failure begins to develop.

Effector Mechanisms in Cirrhosis

Nephron Sites of Renal Sodium Retention

Salt retention and impaired free water clearance are characteristic disturbances in renal function in cirrhotic patients. Evidence is available to support an important role for proximal and distal nephron segments in mediating enhanced sodium reabsorption.

PROXIMAL NEPHRON

Indirect evidence supporting enhanced proximal salt reabsorption comes from studies in human cirrhotic subjects in which infusion of mannitol or saline improves free water clearance.[27,182] Increased proximal

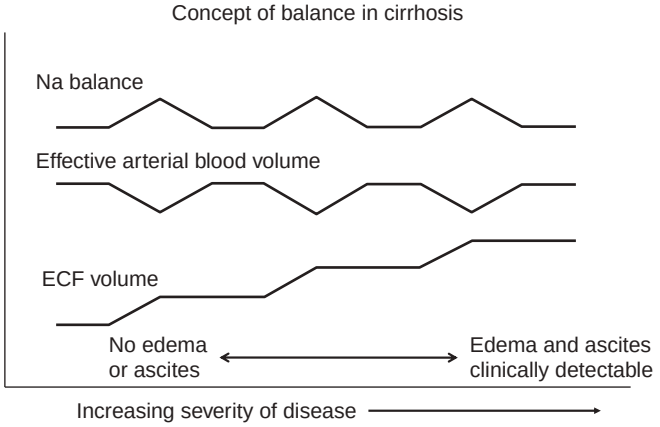

FIGURE 38.8 **As liver disease progressively worsens, salt balance is continually re-established as total extracellular fluid (ECF) volume increases.** Early in the disease process the increase in ECF volume is not clinically detectable. With more severe disease, peripheral edema and ascites are readily apparent.

tubular salt reabsorption leads to decreased delivery of filtrate to the distal diluting segments, thereby impairing free water formation. Presumably, by restoring distal delivery of filtrate, mannitol and saline infusions result in increased solute free water formation. Similar increases in free water clearance occur when central hypervolemia is induced by HWI. The increase in urine sodium is accompanied by increased K excretion, suggesting enhanced distal delivery of sodium. Increased water excretion seen in response to HWI, combined with simultaneous infusion of norepinephrine, is also consistent with baseline enhanced proximal sodium reabsorption in decompensated cirrhotics.[188]

Experimental models of cirrhosis have provided more direct assessment of nephron function. Micropuncture studies in rats made cirrhotic by ligation of the common bile duct demonstrated increases in both the proximal tubule solute reabsorption and filtration fraction.[5] Enhanced proximal reabsorption was attributed to increased peritubular oncotic pressure. In a dog model of cirrhosis,[136] intrarenal administration of the vasodilator acetylcholine was found to ameliorate the blunted natriuretic response to saline infusion. In this model, sodium reabsorption was enhanced in both the proximal and the diluting segments of the nephron.[16]

DISTAL NEPHRON

Clinical and experimental evidence also supports an important role for distal nephron sodium retention in cirrhosis. In cirrhotic patients manifesting a sluggish natriuretic response to HWI, phosphate clearance was found similar to a group who demonstrated an appropriate increase in urinary sodium excretion.[53] Since phosphate clearance was used as a marker of proximal sodium reabsorption, it was concluded that distal sodium reabsorption contributed importantly to renal sodium retention in patients with a sluggish natriuretic response. The results of a prospective, double-blind study comparing the diuretic response of furosemide to spironolactone in cirrhotic patients with ascites suggest that salt absorption in the cortical collecting tubule is enhanced.[161] When administered furosemide, only 11 of 21 patients exhibited a diuresis, while 18 of 19 patients responded to spironolactone. Furthermore, 10 patients who failed to respond to furosemide demonstrated a diuretic response to spironolactone. Furosemide inhibits sodium reabsorption in the loop of Henle, thereby increasing delivery to the collecting duct. All patients treated with furosemide had increases in the rate of potassium excretion, including the 11 patients who failed to increase urinary sodium excretion. These results, combined with the clinical effectiveness of spironolactone in treatment of cirrhotic ascites, suggest enhanced salt absorption in the aldosterone-sensitive cortical collecting tubule.[7]

In summary, clinical and experimental studies suggest an important role for proximal, as well as distal, nephron sites mediating renal salt retention in cirrhosis. The relative contribution of different nephron sites to impaired salt and water excretion may depend on the degree to which systemic hemodynamics are altered. With each stage of advancing liver disease there becomes a greater contraction of the EABV. In the earliest stages of liver disease, enhanced proximal reabsorption limits distal delivery of solute in a manner analogous to a nonedematous subject with intravascular volume depletion. If distal delivery can be normalized at this early stage, distal nephron sites may continue to reabsorb sodium avidly, and therefore appear as the primary site responsible for ECF volume expansion. With severe reductions in EABV, presumably the proximal nephron becomes the dominant site of fluid reabsorption, such that the contribution of the distal nephron becomes much less apparent.

Sympathetic Nervous System

The sympathetic nervous system has been shown to contribute importantly to abnormalities in body fluid homeostasis in cirrhosis. Studies in rats made cirrhotic by ligating the common bile duct suggest that increased renal nerve activity is a major factor in the progressive salt retention that occurs in these animals.[35,37] In this model, baseline renal nerve activity is increased, and fails to decrease appropriately in response to intravenous saline. Renal denervation significantly improves the impaired ability to excrete an oral or intravenous salt-load. In addition, renal denervation has been shown to normalize the attenuated diuretic and natriuretic response to the intravenous administration of ANP.[96] In chronic metabolic studies, renal denervation also leads to a significant improvement in the positive cumulative sodium balance. The cause of increased renal nerve activity is multifactorial. Impaired aortic and cardiopulmonary baroreceptor regulation, as well as[175] abnormalities in hepatic NaCl-sensitive receptors and their immediate intrahepatic afferent connections, have been implicated as a cause of heightened autonomic activity.

Studies in human cirrhotic subjects are more indirect, but also suggest an important role for the sympathetic nervous system. Levels of norepinephrine in patients with cirrhosis are high, and are inversely correlated with urinary sodium excretion.[18] In addition, direct measurement of peripheral nerve firing rates show evidence of increased central sympathetic activity. Patients characterized by impaired ability to excrete water loads have plasma levels of norepinephrine that

correlate positively with levels of ADH, aldosterone, and plasma renin activity.[18]

Decreased EABV leads to baroreceptor-mediated activation of sympathetic nerve activity, with subsequent enhancement of proximal salt reabsorption. The subsequent decrease in sodium delivery to the diluting segment, in addition to nonosmotic release of ADH, contributes to the inability to maximally excrete water-loads. Increased renal nerve activity also contributes to enhanced distal sodium reabsorption through activation of the renin–angiotensin–aldosterone system.

In addition to stimulating renal salt and water retention, activation of the sympathetic nervous system serves as a compensatory response to cirrhosis-induced vasodilation. Increased renal nerve activity contributes to increased renal vascular resistance, and is one of several factors responsible for the progressive decline in renal function which occurs as patients develop the hepatorenal syndrome.[38,51]

In summary, the sympathetic nervous system is activated under conditions of decompensated cirrhosis. Overactivity of this system is the result of a contracted EABV. In addition, there is impaired regulation of sympathetic outflow due to abnormalities in several afferent sensing mechanisms. Increased renal nerve activity contributes to the cumulative salt retention that accompanies advancing liver disease. In addition, activation of sympathetic outflow plays an important compensatory role in maintaining vascular tone in the setting of decreased vascular resistance.

Aldosterone

In patients with cirrhosis and ascites, plasma concentrations of aldosterone are frequently elevated. Although aldosterone metabolism is impaired in liver disease, secretion rates are greatly elevated, and are the major cause of elevated levels.[177] The relationship between hyperaldosteronism and sodium retention is not entirely clear. Several studies have provided evidence that argues against an important role of aldosterone in mediating salt retention in cirrhosis. For example, patients treated with an aldosterone synthesis inhibitor do not necessarily exhibit a natriuretic response.[177] In one study, renal salt excretion and changes in plasma renin and aldosterone levels were examined in 11 patients with ascites subjected to 5 days of high-salt intake. In patients with normal suppression of renin and aldosterone, salt retention and weight gain occurred to the same extent as patients who had persistent hypersecretion of renin and aldosterone.[28] In addition, cirrhotic patients in positive sodium balance, as compared to controls with matched sodium excretion, have increased fractional distal sodium reabsorption despite lower plasma aldosterone levels. In 16 cirrhotic patients subjected to HWI, plasma renin activity and plasma aldosterone levels were found to decrease promptly. Despite suppression of the hormones, however, half of the patients manifested a blunted or absent natriuretic response.[52] In another group of cirrhotic patients with ascites and edema, HWI induced a significant natriuresis despite acute administration of desoxycorticosterone, suggesting that enhanced sodium reabsorption can occur independently of increased mineralocorticoid activity.

By contrast, other studies suggest aldosterone is an important factor in the pathogenesis of sodium retention in patients with cirrhosis. For example, adrenalectomy or administration of a competitive inhibitor of aldosterone increases urinary sodium excretion.[45] Patients who fail to manifest a diuretic response to furosemide tend to have higher renin and aldosterone levels and lower urinary sodium concentrations prior to treatment.[16] Inability of furosemide to increase urinary sodium in these patients may result from reabsorption of delivered sodium in the collecting tubule under the influence of aldosterone. Similarly, patients with the highest renin and aldosterone levels are those who fail to diurese in response to HWI.[52,144,145]

As with the conflicting data regarding the role of the proximal and distal nephron in salt retention discussed previously, the degree to which systemic hemodynamics and EABV are impaired may explain some of the conflicting data noted above. It is possible that in patients with the greatest contraction of EABV, intense proximal sodium reabsorption limits distal delivery to such an extent that the contribution of aldosterone to increase salt absorption is difficult to detect. By contrast, with less impairment in EABV, distal delivery is better maintained, and the contribution of aldosterone to renal sodium retention is more obvious.

Alternatively, acquired inhibition of 11β-hydroxysteroid dehydrogenase type 2 may be of importance in the salt retention that occurs in some patients with cirrhosis of the liver. Bile acids which can accumulate in the setting of chronic liver disease have been shown to inhibit the activity of 11β-hydroxysteroid dehydrogenase type 2.[195] Such an effect would allow cortisol-mediated stimulation of the mineralocorticoid receptor, and potentially explain aldosterone-independent salt retention in the distal nephron in liver cirrhosis. Studies in the bile duct ligation and carbon tetrachloride models of chronic liver disease are consistent with a component of cortisol-mediated stimulation of the mineralocorticoid receptor.[195] In these models there is decreased activity of 11β-hydroxysteroid dehydrogenase type 2 that is temporally related to increased ENaC abundance in the apical membrane of the cortical collecting duct. These changes are most pronounced in the sodium-retaining stage of disease.

Prostaglandins

Prostaglandins function in a protective role in decompensated cirrhosis. Similar to other hypovolemic states, prostaglandins act to maintain renal blood flow and GFR by ameliorating pressor effects of angiotensin II and sympathetic nerves.[154] These agents counterbalance the salt retaining effects of these effectors and mitigate the impairment in free water clearance mediated by AVP. Administration of prostaglandin inhibitors can partially correct excessive hyperreninemia and hyperaldosteronism, and restore the pressor response to angiotensin II.

Kallikrein–Kinin System

Urinary kallikrein activity is increased in cirrhotic patients with ascites and preserved GFR, while urinary activity decreases in association with impaired renal function.[160] The correlation between renal plasma flow and GFR suggests that the renal kallikrein–kinin system may contribute to maintenance of renal hemodynamics in cirrhosis.

At the level of the renal tubule, bradykinin has been shown to exhibit a natriuretic effect. However, bradykinin also is a potent peripheral vasodilator, and can cause microvascular leakage. In cirrhosis, these later effects could exacerbate an already contracted EABV, and cause further salt retention. MacGilchrist et al.[127] studied the effects of kinin inhibition by systemically infusing aprotinin (a strong inhibitor of tissue kallikrein) into a group of patients with cirrhosis. This infusion was associated with a doubling of urinary sodium excretion, and an increase in renal plasma flow and GFR. This beneficial effect on renal function in the setting of kinin inhibition was attributed to an improvement in systemic hemodynamics as systemic vascular resistance increased. Similarly, administration of a bradykinin receptor antagonist to cirrhotic rats normalized renal sodium retention, and reduced the activity of the renin–angiotensin–aldosterone system.[211] Inhibiting bradykinin-induced microvascular leakage and lessening the degree of vascular underfilling was felt to be the mechanism of the beneficial effect.

Natriuretic Peptides

The role of ANP in the pathogenesis of edema in hepatic cirrhosis remains undefined. While atrial ANP content was reduced in cirrhotic rats, most data indicate ANP levels are either normal or elevated in cirrhotic humans.[81,190] Elevated levels are the result of increased cardiac release rather than just impaired clearance. The cause of the high levels is not understood, because atrial pressure is normal and central blood volume is reduced. Stimulating the endogenous release of ANP induces a natriuretic response in some patients with cirrhosis, while other patients are insensitive.[190] However, both groups of patients exhibited an increase in urinary cGMP, suggesting that the kidney is still capable of responding to ANP even in the absence of a natriuretic effect.[190]

Several potential mechanisms may account for ANP resistance in cirrhosis. This resistance could be the result of a defect intrinsic to the kidney or could be the result of altered systemic hemodynamics leading to activation of more potent sodium-retaining mechanisms.[128] With regards to the first possibility, an altered density of glomerular ANP-binding sites has been demonstrated in the bile duct-ligated rat model of cirrhosis.[62] In addition, ANP resistance was found in the isolated perfused kidney taken from sodium avid rats with cirrhosis induced by carbon tetrachloride.[157] In the chronic caval dog model of cirrhosis, intrarenal infusion of bradykinin restored ANP responsiveness to previously resistant animals, suggesting that an intrarenal deficiency of kinins could be a contributing factor.[108]

Other studies have focused on systemic hemodynamics as a cause of ANP resistance. With each stage of advancing liver disease there becomes a greater reduction in EABV. Since ANP resistance tends to occur with more severe and advanced disease, it is possible that ANP resistance is directly related to the impairment in EABV. Decreased EABV is associated with enhanced proximal reabsorption of solute. As a result, ANP resistance may be due to decreased delivery of salt to the site where ANP exerts its natriuretic effect. In support of this possibility, ANP resistance could be restored in cirrhotic rats by infusions of vasopressors so as to normalize arterial pressure, and presumably improve the decrease in EABV.[124] In human cirrhotics, ANP responsiveness can be markedly improved when distal sodium delivery is increased by administration of mannitol.[143]

Circulating brain natriuretic peptide (BNP) levels are also increased in patients with cirrhosis.[107] Infusion of BNP at a dose that elicits an increase in GFR, renal plasma flow, and urinary sodium excretion in normal controls has no effect in cirrhotic humans. The infusion is associated with an increase in urinary cGMP, as well as a fall in plasma aldosterone levels, suggesting that the peptide is capable of interacting with its receptor in these patients. As with ANP, the lack of natriuretic response to BNP may be due to overactivity of other antinatriuretic factors, as well as decreased delivery of sodium to its tubular site of action.

Adrenomedullin is a peptide with vasodilatory properties that is highly expressed in cardiovascular tissues. Increased circulating levels that correlate with severity of disease have been described in patients with cirrhosis.[57] Urodilatin is a natriuretic factor that is

exclusively synthesized within the kidney. Unlike other natriuretic factors, levels are not increased in patients with cirrhosis.[178]

Endothelin

Increased circulating levels of endothelin have been reported in cirrhosis.[142] The stimulus and pathophysiologic significance of these levels is not known with certainty. The peptide may play a role in the renal vasoconstriction seen in the hepatorenal syndrome.[63,142]

Therapeutic Implications for Treatment of Salt Retention in Cirrhosis

Renal salt retention is the most common abnormality of renal function in chronic liver disease. Whenever urinary sodium excretion falls to an amount less than dietary salt intake ECF volume will begin to expand and eventually lead to the development of ascites and peripheral edema. The approach to the treatment of the cirrhotic patient with ascites is to alter sodium balance in such a way that urinary sodium excretion exceeds dietary salt intake.

In the earliest stages of the disease, urinary sodium excretion is plentiful and negative salt balance can be achieved by simply lowering dietary sodium intake. As the disease advances, neurohumoral effectors become more activated, initially resulting in more intense renal salt retention and later in a progressive decline in renal function. Eventually, the filtered load of sodium becomes completely reabsorbed by the tubule, such that the final urine becomes virtually devoid of salt. If some component of the filtered load reaches the collecting duct or beyond spironolactone will be effective in increasing urinary sodium excretion. Once sodium reabsorption is complete proximal to the collecting duct then thiazides, and later loop diuretics, will have to be added to spironolactone in order to increase urinary sodium excretion. Eventually, the filtered load is completely reabsorbed proximal to the thick ascending loop of Henle. At this point the patient is resistant to the effects of diuretics, and requires more invasive procedures such as repetitive large-volume paracentesis in order to remain in salt balance. In the terminal stages of the disease, the glomerular filtration rate falls to such a degree that oliguria, azotemia, and eventually uremia are present, and the patient is clinically diagnosed with hepatorenal syndrome (Figure 38.9). Vasoconstrictive input focused on the kidney is severe. The renal failure is functional in nature, however, since restoration of near normal renal function can be obtained following a liver transplant.

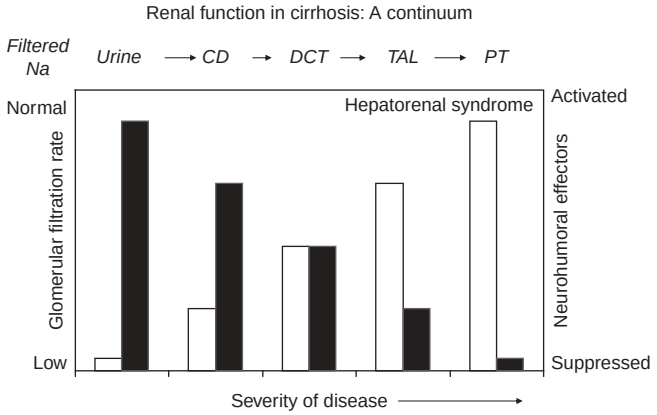

FIGURE 38.9 **The fall in glomerular filtration rate (solid bars) and activation of neurohumoral effectors (open bars) can be viewed as a continuum that varies according to severity of the underlying cirrhotic process.** As the disease advances, the urinary Na concentration falls. The filtered load of Na is completely reabsorbed at progressively more proximal sites along the nephron. A patient with hepatorenal syndrome is merely at the end of this continuum, when the glomerular filtration rate has fallen sufficiently to cause significant azotemnia.

NEPHROTIC SYNDROME

The development of edema is one of the cardinal features of nephrotic syndrome. The mechanism of its formation is not entirely understood. The classical view of edema formation in nephrotic syndrome describes the process as an underfill mechanism. According to this theory, urinary loss of protein results in hypoalbuminemia and decreased plasma oncotic pressure. As a result, plasma water translocates from the intravascular space into the interstitial space. When the magnitude of this transudation is sufficiently great, clinically detectable edema develops. Reduction in intravascular volume elicits activation of effector mechanisms that signal renal salt and water retention in an attempt to restore plasma volume. The renal response leads to further dilution of plasma protein concentration, thereby exaggerating the already reduced plasma oncotic pressure and further enhancing edema formation. In order for this formulation of edema genesis to be true, three critical predictions must be satisfied: (1) blood and plasma volume must be reduced during accumulation of edema; (2) measurement of neurohumoral effectors should reflect activation consequent to contraction of effective arterial blood volume; and (3) maneuvers that increase plasma volume into the normal range should result in a natriuretic response. As discussed below, these predictions are satisfied in some patients, especially those with minimal-change nephrotic syndrome, whereas the majority of nephrotic patients fail to conform to this conceptual model.

Blood and Plasma Volume in Nephrotic Syndrome

The classical view of edema formation assigns a pivotal role to decreased plasma volume serving as the afferent mechanism signaling renal salt and water retention. When measured directly, plasma volume has indeed been low in a variable proportion of patients with nephrotic syndrome.[106,138,198] Even in patients judged to be normovolemic, an exaggerated fall in plasma volume has been observed when nephrotic patients go from the recumbent to the standing position.[46,84] This orthostatic reduction in plasma volume can be profound and may, in part, explain the development of acute oliguric renal failure and hypovolemic shock that has been reported in patients with nephrotic syndrome.[191]

Most studies, however, have failed to find a consistent reduction in blood and plasma volume in patients with nephrotic syndrome.[39,47,61,100] In a survey of 10 studies, plasma volume measurements were analyzed in 217 nephrotic patients.[40] In only one-third of patients was plasma volume reduced, whereas it was normal in 42% and increased in 25%. It has been suggested that conflicting measurements of plasma volume in patients with nephrotic syndrome can be reconciled by separating patients according to histologic class.[137] In this regard, one study compared the volume status of four patients with minimal change disease to that in five patients with membranous or membranoproliferative lesions.[137] In patients with minimal change disease, plasma volume was decreased and plasma renin activity and aldosterone levels were increased. By contrast, plasma volume was either normal or increased and plasma renin activity was suppressed in the latter group. These authors concluded that edema formation in minimal change disease was primarily the result of decreased effective circulatory volume inciting secondary renal salt retention. By contrast, patients with more distorted glomerular architecture were felt to have a primary defect in renal salt excretion, leading secondarily to an expanded plasma volume and eventually formation of edema.

Other studies have failed to find such a correlation between histology and plasma volume measurements. Even in patients with untreated minimal change disease, plasma volume has been found to be increased.[40] In order to avoid potential methodologic problems, a recent study first established a reference frame for blood volume that was normalized to lean body mass, and measured directly from plasma volume and red cell volume in otherwise normal children.[205] Blood volume measurements in children with nephrotic syndrome due to minimal change disease, as well as other histologic lesions, were all found to be within this defined normal range. Following successful therapy with steroids, patients with minimal change disease demonstrate a fall in plasma volume and blood pressure, and an increase in plasma renin activity.[40] These changes are exactly the opposite of what one would expect if arterial underfilling were the proximate cause of renal salt retention. Finally, a large study of nephrotic patients, including 35 patients with minimal change disease, found virtually all patients have normal or increased plasma and blood volume.[60]

Neurohumoral Markers of Effective Circulatory Volume

Measurements of plasma renin activity and aldosterone concentration have been utilized as a method to indirectly differentiate primary sodium retention from an underfill mechanism of edema formation in nephrotic patients. Elevated values would be expected if blood volume was decreased, while suppressed values would occur in the setting of primary renal sodium retention and blood volume expansion. In this regard, plasma renin activity values collated from nine studies were found to be normal or low in 64 of 123 patients investigated.[39] Plasma aldosterone levels were also decreased in the majority of these patients. When measured with respect to salt intake or urinary sodium excretion, no consistent relationship was found. While some studies have found elevated plasma renin activity and aldosterone concentrations in patients with minimal change diseases, others have not.[69,137] In a study examining plasma renin activity with respect to blood volume, no relationship was found in either patients with minimal change disease or those with histologic lesions on light microscopy.[61] Although a higher proportion of patients with minimal change disease have elevated plasma renin and aldosterone levels as compared to those with histologic glomerular lesions, these values tend to overlap.[61,69] Thus, measurement of various elements of the renin–angiotensin–aldosterone axis suggests that an underfill mechanism may mediate renal sodium retention in some but not all patients with nephrotic syndrome.

Effects of Manipulations to Expand Central Blood Volume

Another approach utilized to investigate the pathogenesis of sodium retention in the nephrotic syndrome has been to examine renal sodium handling and hormonal indices of effective circulatory volume in response to expansion of the intravascular blood volume. This has been primarily achieved by infusing albumin or expanding central blood volume

by head-out body water immersion (HWI).[34,87] The classical view of nephrotic edema would predict that expansion of the intravascular volume should correct renal salt and water retention. In children with minimal change disease, infusion of albumin has been reported to decrease plasma renin activity, arginine vasopressin (AVP), aldosterone, and catecholamines.[169,196] In association with these hormonal changes, there was a significant increase in the glomerular filtration rate, urine flow, and sodium excretion. In a less homogenous group of adult patients with nephrotic syndrome, baseline blood volumes were found to be low when expressed per kilogram wet weight.[199] Plasma AVP was inversely correlated with blood volume and failed to decrease in response to a water-load. When blood volume was expanded with 20% albumin, plasma levels of AVP fell, accompanied by an augmented water diuresis. It was concluded that a contracted blood volume was responsible for the non-osmotic release of AVP. By contrast, other studies have found either no or only a minimal increase in urinary sodium excretion in response to infusion of albumin. In one study, infusion of hyperoncotic albumin in quantities sufficient to expand blood volume by 35% resulted in only a modest natriuretic response.[100] In order to exclude the possibility that the blunted natriuretic response was due to an increase in peritubular colloid osmotic pressure, similar studies have been performed utilizing a prolonged infusion of iso-oncotic albumin. This maneuver was similarly accompanied by only a modest increase in sodium excretion, such that the patients remained in positive salt balance.[167] Studies utilizing HWI to expand blood volume have likewise produced conflicting results. Expansion of central blood volume by HWI in children with minimal change disease resulted in decreased levels of AVP, aldosterone, noradrenaline and plasma renin activity.[169,170] These changes were accompanied by significant increases in urine flow and sodium excretion. Similarly, adult patients with a variety of histologic lesions subjected to HWI were found to have significant increases in urinary sodium excretion.[13,105] By contrast, a more recent study in 10 patients with a variety of underlying glomerular diseases found only a blunted natriuretic response to HWI.[165] While ANP levels rose to the same extent in control and nephrotic subjects, suggesting equivalent degrees of volume expansion, peak urinary sodium excretion and urine flow in the nephrotic patients were one-third that in the control group.

A number of other observations also question the pivotal role assigned to hypoalbuminemia and reduced plasma oncotic pressure in the initiation of edema formation.[3,83,84] For example, reducing plasma protein concentration in humans[3] or experimental animals[83,84] with plasmapheresis results in either no change or actually increases plasma volume. In addition, patients with congenital analbuminemia demonstrate no disturbance in water and electrolyte balance, and do not necessarily develop edema. Despite the reduction in plasma oncotic pressure, these patients exhibit an exaggerated natriuretic response when administered isotonic saline.

In summary, available data would argue for a contracted plasma volume as the afferent mechanism initiating sodium retention in some but not all patients with nephrotic syndrome. Rather, some component of primary renal sodium retention appears to be operative in nephrotic syndrome with histologic glomerular lesions, as well as in many patients with minimal change disease (Table 38.1). Studies in experimental animals also suggest a defect intrinsic to the nephrotic kidney as the mechanism responsible for salt retention in nephrotic syndrome. In the rat model of unilateral proteinuric renal disease induced by infusing puromycin aminonucleoside (PAN) into one kidney, diminished urinary sodium excretion was confined to the proteinuric kidney, despite the fact that each kidney shared the same systemic milieu.[77] In kidneys taken from rats previously exposed to PAN and then perfused *in vitro*, less sodium was excreted as compared to kidneys taken from control rats. Utilizing this experimental design, the defect in renal salt excretion was found to be localized to the kidney, as systemic and circulating factors were eliminated.

In some patients, primary salt retention and an underfill mechanism of edema formation may coexist. For example, in the earliest stages of a glomerular disease salt retention by the kidney may be primary in origin. As hypoalbuminemia develops and becomes progressively severe, plasma volume may fall and result in an element of superimposed secondary salt retention. The coexistence of these two mechanisms

TABLE 38.1 Evidence for Primary Renal Sodium Retention in the Nephrotic Syndrome

Blood volume is often normal or increased.
Blood pressure is often increased.
Renin activity and aldosterone levels are not uniformly increased.
Onset of natriuresis during recovery precedes rise in plasma protein concentration.
Sodium excretion is modest in response to HWI or albumin infusion.
Experimental models.
Sodium retention in a unilateral nephrosis model is confined to the diseased kidney.
Kidneys taken from nephrotic animals and perfused *in vitro* retain Na.

may account for the lack of uniformity in hemodynamic, as well as hormonal and neurocirculatory, profiles in patients with nephrotic syndrome.

Peripheral Capillary Mechanisms of Edema Formation

The presence of normal or increased plasma volume in the setting of a decreased serum albumin concentration is difficult to reconcile with the classical view of edema formation in the nephrotic syndrome. These findings can best be explained by examining the alterations that are known to occur in transcapillary exchange mechanisms in the setting of hypoproteinemia. Fluid movement within the capillary bed between intravascular and interstitial spaces is determined by the balance of Starling forces between these two compartments:

$$J_v = K_f[(P_c\text{-}P_i)\text{-}(\Pi_c\text{-}\Pi_i)]$$

where J_v is fluid flux along the length of a capillary, K_f is the ultrafiltration coefficient, P_c is capillary hydrostatic pressure, P_i is interstitial hydrostatic pressure, Π_c is capillary oncotic pressure, and Π_i is interstitial oncotic pressure. On the arterial side of the capillary, the net hydrostatic pressure gradient $P_c - P_i$ (ΔP) exceeds the net colloid osmotic pressure gradient $\Pi_c - \Pi_i$ ($\Delta\Pi$), resulting in net filtration of fluid into the interstitial space. Due to an axial fall in capillary hydrostatic pressure, the balance of Starling forces at the venous end of the capillary ($\Delta\Pi > \Delta P$) favors net reabsorption of fluid back into the capillary. In some tissues, net hydrostatic pressure exceeds opposing net colloid osmotic pressure throughout the length of the capillary, such that filtration occurs along its entire length. Net ultrafiltrate is returned to the circulation via lymphatic flow, such that in steady-state conditions total body capillary flux is equal to lymph flow; interstitial and intravascular volume remain stable and edema formation does not occur.

Absence of compensatory mechanisms would predict that small changes in ΔP, $\Delta\Pi$ or K_f would lead to increased fluid transudation and result in clinically detectable edema. However, the poor correlation between plasma albumin concentration and the presence or absence of edema suggests that counter-regulatory adjustments do occur in those forces that govern fluid exchange between the intravascular and interstitial space (Table 38.2). One such factor relates to compliance characteristics of the interstitium.[68] Under normal circumstances, interstitial pressure ranges from 6 mmHg to 10 mmHg. Due to the noncompliant nature of this compartment, small increases in interstitial volume result in large increases in interstitial pressure.

TABLE 38.2 Edema Defense Mechanisms which Limit Excessive Capillary Fluid Filtration

Increased interstitial hydrostatic pressure.
Increased lymph flow.
Decreased interstitial oncotic pressure.
Decreased permeability of the capillary to protein.

Such increases in P_i act to oppose further transudation of fluid, and provide an initial defense against the formation of edema. Increased interstitial pressure leads to the development of a second factor that also protects against edema formation, namely, increased lymphatic flow. Lymph flow can increase many-fold under conditions of augmented net capillary fluid filtration. In patients with edema resulting from heart failure or nephrosis, the disappearance rate of a subcutaneous injection of ^{131}I-albumin is markedly enhanced consistent with increased lymphatic flow.[73]

A third factor that minimizes fluid filtration is a reduction in interstitial oncotic pressure.[54] In normal human plasma, colloid oncotic pressure (COP) is about 24 mmHg, and interstitial COP is about 12 mmHg, creating a transcapillary COP gradient of about 12 mmHg.[84] Since transcapillary fluid flux consists primarily of a protein-free ultrafiltrate, interstitial protein concentration tends to become diluted. In addition, increased lymphatic flow removes fluid and protein from the interstitial space, and returns both to the vascular compartment thereby further reducing interstitial oncotic pressure. Body albumin pools are redistributed such that a greater fraction than normal is located in the vascular compartment.[84] As hypoalbuminemia develops in the nephrotic syndrome, the COP of the interstitial fluid space falls in parallel with the COP of plasma.[74,99,101] Nephrotic patients studied both in remission and in relapse demonstrate almost equivalent changes in the COP of plasma and the interstitium at all levels of serum albumin.[101] The maintenance of the net COP gradient within the normal range mitigates this potential driving force for transudation of fluid into the interstitial space. A final factor that favors decreased fluid filtration is a change in the permeability of the capillary. Under conditions of hypoalbuminemia, the intrinsic permeability of the capillary to protein tends to decrease, thereby increasing Π_c along the capillary.[215]

In summary, the reduction in serum oncotic pressure that accompanies the nephrotic syndrome would be predicted to alter Starling forces in a direction favoring net flux of fluid across the capillary bed. Despite this alteration, however, fluid tends not to accumulate within the interstitium in response to

hypoalbuminemia, because of the activation of a series of defense mechanisms that serve to oppose those forces favoring fluid movement from the intravascular space. These edema-preventing factors include increased interstitial hydrostatic pressure, accelerated lymphatic flow, a parallel decline in plasma and interstitial oncotic pressure, and decreased capillary permeability to protein. However, in the setting of ongoing primary renal salt retention, these buffering mechanisms become exhausted and clinically apparent edema may become evident. This occurs because salt retention leads to increases in capillary hydrostatic pressure at the very time defense mechanisms normally employed to prevent edema have been maximized. In the hypoproteinemic patient without salt retention, edema-preventing factors may be sufficient to protect against the development of edema. Thus, edema formation in the nephrotic syndrome results from the combined effects of primary salt retention coupled with exhausted defenses against edema (Figure 38.10).

The changes in mean arterial pressure and blood volume as a function of varying extracellular fluid volume in hypoalbuminemic nephrotic patients as compared to normoalbuminemic chronic renal-failure patients illustrate these principles.[98] In hypoalbuminemic patients with nephrotic syndrome, expansion of the extracellular fluid volume leads to immediate translocation of fluid into the extravascular space, as evidenced by little change in mean arterial pressure or blood volume. Presumably, factors that serve to prevent edema are already maximized, and are overwhelmed by increases in capillary hydrostatic pressure that occur as a result of extracellular fluid volume expansion. By contrast, normoalbuminemic patients with chronic renal failure develop an increase in mean arterial pressure and blood volume as extracellular fluid volume expands. In these patients, more of the fluid is retained in the vascular tree due to activation of edema preventing factors. At some point of extracellular fluid volume expansion, these factors would also become overwhelmed and clinically detectable edema would develop.

Mechanism of Salt Retention in Nephrotic Syndrome

The bulk of experimental and clinical data implicate a tubular mechanism as the primary cause of salt retention in the nephrotic syndrome. Both experimental and clinical studies implicate the distal nephron as the site responsible for sodium retention. Utilizing clearance techniques, proximal sodium handling was assessed during diuretic-induced distal tubular blockade using chlorothiazide and ethacrynic acid.[66] Nephrotic patients exhibited a greater natriuretic response than controls, suggesting that distal nephron sites were responsible for enhanced sodium reabsorption. Measurement of tubular glucose handling has been used as a marker of proximal sodium reabsorption.[198] In a group of nephrotic patients, glucose titration curves revealed a reduced threshold for glucose reabsorption, further suggesting diminished proximal sodium reabsorption.

In volume-expanded rats with autologous immune complex nephritis, a model that resembles membranous nephropathy, micropuncture, and clearance methodology were used to study the site of sodium retention.[14] Absolute proximal sodium reabsorption was decreased in nephrotic rats, while sodium delivery to the late distal tubule of superficial nephrons was comparable in control as well as nephrotic animals. Since fractional excretion of sodium was significantly lower in nephrotic versus control rats, the collecting duct was suggested as a possible site of altered handling of sodium. Enhanced sodium reabsorption in juxtamedullary nephrons not accessible to micropuncture could not be excluded. In the rat model of unilateral proteinuric renal disease induced by infusing PAN into one kidney, diminished urinary sodium excretion was confined to the proteinuric kidney.[77] Since sodium delivery to the initial portion of the collecting duct was similar to the control kidney, increased sodium reabsorption at the collecting duct must have been the primary site of salt retention.

Studies using immunocytochemical analysis are consistent with the distal nephron being a major site for sodium retention in nephrotic syndrome.[33,41,89,90,125] The activity of the $Na^+ - K^+$-ATPase is increased in the colleting duct in the puromycin aminonucleoside rat model of nephrosis. There is also increased expression and targeting of the epithelial sodium channel (ENaC) in the connecting tubule and collecting duct in these animals, as well as those made nephrotic through injection of $HgCl_2$.

Neurohumoral Control of Enhanced Tubular Sodium Excretion

Renin–Angiotensin–Aldosterone

Studies demonstrating increased sodium retaining activity in the urine of nephrotic patients lead early investigators to suggest that aldosterone might play an important role in mediating sodium retention in the nephrotic syndrome.[126] In rats made nephrotic with PAN, juxtaglomerular cell granularity was found to vary directly with the degree of sodium retention. In this same model, prior adrenalectomy prevented sodium retention that otherwise occurred in nephrotic

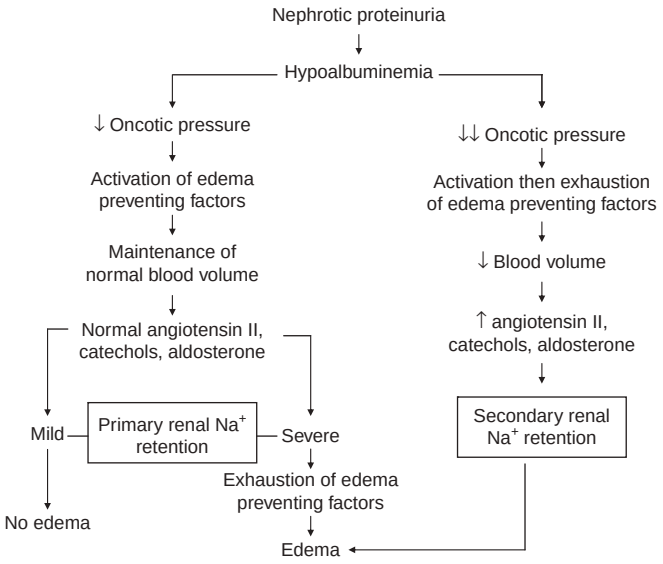

FIGURE 38.10 **The left side of the figure depicts the mechanism of edema formation in most patients with nephrotic syndrome.** An important variable that helps to explain the poor correlation between serum albumin concentration and the presence or absence of edema is the degree of primary renal Na retention. With severe Na retention by the kidney, edema-preventing factors become exhausted and edema becomes clinically apparent, even when the serum albumin concentration is only mildly depressed. In the setting of mild renal Na retention, these factors remain adequate to prevent edema formation, even in the presence of severe hypoalbuminemia. **The right side of the figure depicts the classical view of edema formation in which low blood volume serves as the signal for secondary renal Na retention.** This mechanism of edema formation is most commonly present in children with minimal change disease. In some patients, both mechanisms of edema formation may be operative. For example, early in the nephrotic syndrome, blood volume is normal and only primary renal Na retention is present. With worsening hypoalbuminemia, blood volume may begin to fall and result in a component of superimposed secondary renal Na retention.

controls with intact capacity to secrete aldosterone.[86] When plasma renin activity and aldosterone concentrations were measured in a large group of nephrotic patients placed on a low-sodium diet values varied widely, although a negative correlation was found between urinary sodium and plasma aldosterone concentration.[61] In a study of five nephrotic patients placed on a high-salt diet for 8 days, plasma renin activity and plasma aldosterone levels were similar in both nephrotic subjects and control subjects.[189] Administration of the aldosterone antagonist, spironolactone, on day 4 of the study resulted in an increase in urinary sodium excretion in the nephrotic patients, while no change was observed in the control group. Since aldosterone exerts salt-retaining effects on the distal nephron, a site implicated in formation of nephrotic edema, excess aldosterone activity is an attractive explanation for observed salt retention.

Most data, however, fail to confirm an important role for aldosterone. In patients spontaneously retaining sodium, measurements of plasma renin activity and aldosterone concentration may be either low or high.[21,23] This disassociation is also seen during steroid-induced remission of nephrotic syndrome. In four patients with minimal change disease, plasma renin and aldosterone concentrations fell during steroid-induced diuresis, but once in remission these hormones returned to the same plasma concentrations observed when edema was present.[137] Studies involving administration of either saralasin or converting enzyme inhibitors also fail to support an important role for the renin–angiotensin–aldosterone system in mediating salt retention.[22,23,42] In nephrotic patients selected for high plasma renin activity, captopril administration also failed to prevent sodium retention, despite producing marked reductions in plasma aldosterone.[22] In the unilateral model of PAN-induced nephrosis, infusion of saralasin led to substantial increases in total kidney and single-nephron GFR of the perfused kidney, but urinary sodium excretion remained unchanged.[77] This observation lends support for an intrarenal mechanism of salt retention independent of changes in GFR or activation of the renin–angiotensin–aldosterone system.

Sympathetic Nervous System

Increased plasma and urinary catecholamine concentrations have been found in patients with nephrotic syndrome.[88,150] The role of renal sympathetic nerve activity in mediating salt retention in nephrotic syndrome has been studied in rats made nephrotic by injection of adriamycin. An impaired ability to excrete an acute oral or intravenous isotonic saline-load was improved by bilateral renal denervation.[35] In response to acute infusion of saline, efferent renal sympathetic-nerve activity decreased to a lesser extent than that in control rats. Metabolic balance studies carried out over 26 days revealed an overall decrease in cumulative sodium balance only in those nephrotic rats with bilateral renal denervation.[72] Given the evidence for a distal nephron site of sodium reabsorption in nephrotic syndrome, it is noteworthy that beta-adrenergic stimulation of rabbit cortical collecting tubules enhances chloride transport.[78]

Other studies show enhanced sodium retention in nephrotic syndrome cannot be entirely explained by sympathetic nervous system activity. In kidneys taken from rats previously exposed to puromycin aminonucleoside and perfused *in vitro* so as to remove extrinsic neural factors, urinary sodium excretion is decreased as compared to kidneys taken from control animals.[58] Similarly, bilateral renal denervation does not correct

the blunted natriuretic response to volume expansion in the adriamycin model of nephrosis.[200]

Atrial Natriuretic Peptide

Levels of ANP are reported to be normal or slightly elevated in patients with nephrotic syndrome.[196] In animal models of nephrotic syndrome, renal responsiveness to ANP has generally been found to be blunted.[162] In contrast, infusion of synthetic human ANP to nephrotic patients results in increased sodium and water excretion, similar to that in normal subjects. Infusion of albumin in children with nephrotic syndrome resulted in a rise in ANP levels that closely correlated with urinary sodium excretion. However, other studies have found a blunted natriuretic response to ANP in nephrotic patients.[162] It has been proposed that enhanced distal sodium reabsorption in the nephrotic syndrome may, in part, be due to resistance of the collecting duct to the natriuretic actions of ANP.[159,163] The cellular basis of this resistance does not appear to be an abnormality in ANP binding to its receptor. Rather, the mechanism appears to be an inability to generate adequate amounts of the intracellular cGMP as a result of heightened activity of intracellular cGMP phosphodiesterase.[201]

In summary, edema formation in the majority of patients with nephrotic syndrome can best be explained by an overfill mechanism. The maintenance of a normal plasma volume in the setting of hypoalbuminemia is the result of a series of edema preventing factors that act to both oppose fluid filtration across the capillary wall, and to return fluid back into the vascular tree. The single most important variable in determining whether these factors are sufficient to prevent edema formation is the degree of renal salt retention. The variability in renal salt retention explains the poor correlation between the presence or absence of edema and the serum albumin concentration. In patients with severe hypoalbuminemia and no edema, renal salt retention is likely to be minimal, such that edema preventing factors are sufficient in preventing excessive fluid filtration across the capillary wall. By contrast, edematous patients with near normal serum albumin concentration are more likely to have avid renal salt retention, such that the factors opposing fluid filtration become exhausted. The defect in renal salt excretion has not been precisely localized, but appears to reside in the distal nephron. The exact mechanism underlying this defect is unknown.

SODIUM-WASTAGE

Renal salt-wastage may be defined as persistent inappropriate renal loss of sodium from the body sufficient in magnitude to result in shrinkage of extracellular fluid volume causing azotemia, hypotension, and when extreme, circulatory collapse. When evaluating the relationship between urine sodium excretion and dietary intake, the initial status of the extracellular fluid volume must be taken into consideration before concluding renal salt-wasting is present. For example, renal salt-wasting should not be considered present when urine sodium excretion greatly exceeds dietary intake in edematous patients placed on a low salt diet. In this instance, negative salt balance is an appropriate response to correct the volume-expanded state. As extracellular fluid volume normalizes, the natriuresis will stop and sodium balance will be re-established. By contrast, the imposition of a salt-restricted diet to a euvolemic patient with chronic kidney disease may result in negative salt balance, and contraction of extracellular fluid volume below normal limits. Even though the cumulative amount of sodium lost from the body may be far less than in the diuresing edematous patient, renal salt-wasting is considered present since the reduction of extracellular fluid volume has fallen below normal. In this setting, worsening azotemia and hypotension may be present. The critical feature of renal salt-wasting is the continued shrinkage of extracellular fluid volume below the lower limit of normal as a result of ongoing natriuresis. Disorders of renal salt-wasting can be divided into intrinsic disorders of the kidney and disorders of efferent mechanisms that regulate renal sodium handling.

Intrinsic Renal Disease

Chronic Kidney Disease

Patients with advanced chronic kidney disease may exhibit mild renal salt-wastage when subjected to rigid dietary sodium restriction. The pathogenesis of salt-wastage is related to the adaptive increase in perfusion of remaining viable nephrons, as total nephron mass progressively declines. Accompanying nephron hyperperfusion is a large increase in solute-load. This solute-load exceeds the reabsorptive capacity of remaining nephrons, resulting in increased excretion of salt and water. The nephrons of patients with chronic kidney disease are continuously undergoing an osmotic diuresis of solutes, including urea and the sodium salts of acids.

Studies by Coleman et al.[31] support an important role of osmotic diuresis in hyperfiltering nephrons in the genesis of salt-wastage in chronic kidney disease. In these experiments, patients with chronic kidney disease are placed on a low sodium diet and then subjected to a water diuresis. As urine volume increases, the urine sodium concentration falls to a minimum

value and thereafter remains fixed. At this point, urine sodium excretion increases in parallel with further increases in urine flow rates. In salt-restricted normal participants subjected to a water diuresis combined with mannitol diuresis, the urine sodium concentration at which flow dependence of urine sodium excretion commences is greater compared to the level during water diuresis alone. These data indicate that an osmotic diuresis is at least in part responsible for the mild salt-wastage observed in patients with chronic kidney disease.

Clinical evidence of salt-wastage in most patients with chronic kidney disease is typically only found when dietary salt restriction is extreme. Patients ingesting dietary sodium of 10–15 mEq/day require a much longer period of time to establish salt balance compared to normals, and in many patients salt balance is never achieved. A persistent negative sodium balance leads to volume depletion, weight loss, relative hypotension, and worsening azotemia. In most instances, these findings are seen during the course of an intercurrent illness when salt intake is abruptly stopped or markedly reduced.

There are several reports in the literature in which renal salt-wastage is more severe.[26] Most of these cases have been described in patients with what appears to be chronic tubulointerstitial disease accompanied by cystic transformation of the renal medulla. In these unusual cases, urine sodium excretion is of such a magnitude that contraction of extracellular fluid volume develops in the setting of normal salt intake. Medullary cystic disease is an autosomal recessive disorder with cystic changes in corticomedullary and medullary regions of the kidney in which renal salt-wastage can be severe.

Acute Renal Failure

Transient renal salt-wastage is often seen in patients during the recovery phase of acute tubular necrosis. The magnitude of the natriuresis is a function of the amount of salt and water retained as the renal failure developed. Massive salt-wasting leading to volume-depletion and cardiovascular collapse is not a feature of this disorder. Some degree of salt-wastage is often seen following the relief of urinary obstruction. The excretion of retained urea and other solutes contribute to an osmotic diuresis and account for the natriuresis. However, persistent salt-wastage after these solutes are cleared does not typically occur.

Renal Tubular Disorders

Proximal or type II renal tubular acidosis is associated with renal salt-wastage owing to the loss of sodium bicarbonate into the urine. Defective proximal acidification leads to a large increase in distal sodium bicarbonate delivery that is subsequently lost into the urine. The bicarbonaturic effect will continue until the serum bicarbonate concentration falls to a level that matches the reabsorptive capacity of the proximal nephron, at which point sodium-wastage will cease. As a result, salt-wastage is transient in this disorder, but nevertheless causes mild volume-depletion from inappropriate renal salt loss.

Distal or type I renal tubular acidosis is also characterized by a mild form of renal salt-wastage. The defect in distal acidification leads to the development of a hyperchloremic metabolic acidosis. Systemic acidosis impairs proximal salt reabsorption, resulting in mild sodium-wastage.[55]

Bartter's and Gitelman's syndromes are characterized by renal salt-wastage due to genetic defects in ion transporters involved in sodium reabsorption. In Bartter's syndrome, impaired salt transport is localized to the thick ascending limb, while in Gitelman's syndrome the defect is localized to the distal convoluted tubule.

A variety of drugs can cause renal salt-wastage as a result of tubular injury. This injury can be due to direct toxic effects of the drug, as with Cis-platinum, aminoglycosides, and amphotericin B or be the result of acute tubulointerstitial nephritis, as reported with methicillin and trimethoprim/sulfamethoxazole.

Disorders of Effector Mechanisms that Regulate Renal Sodium Transport

Decreased Mineralocorticoid Activity

Mineralocorticoid activity plays an important role in renal sodium conservation. Decreased activity and renal resistance to mineralocorticoids are causes of renal sodium-wastage.[217] The most clinically relevant form of mineralocorticoid deficiency results from primary diseases of the adrenal cortex. These diseases may either be acquired or congenital in origin. Subnormal aldosterone secretory rates lead to decreased reabsorption of sodium chloride in the cortical collecting tubule of the kidney. The kidney is fundamentally intact and the cortical collecting tubule cell responds normally to exogenously administered mineralocorticoids.

Renal salt-wastage is a hallmark of Addison's disease, in which patients may demonstrate severe volume-depletion and cardiovascular collapse. Addison's disease results from progressive adrenocortical destruction, leading to deficiencies in glucocorticoid and mineralocorticoid activity. These patients present with anorexia, vomiting, abdominal pain, weight loss, weakness, and salt craving. Physical examination reveals generalized hyperpigmentation, particularly in

skin folds and the axillae, as well as bluish-grey hyperpigmentation of the lingual and buccal mucosa. Orthostatic hypotension is very common, indicative of volume depletion. Laboratory examination reveals increased blood urea nitrogen-to-creatinine ratio characteristic of prerenal azotemia and elevated urinary sodium concentration. Hyponatremia, hyperkalemia, and hyperchloremic metabolic acidosis are the characteristic electrolyte abnormalities.

Isolated aldosterone deficiency accompanied by normal glucocorticoid production occurs in association with hyporeninism, as an inherited biosynthetic defect, during protracted heparin administration, and postoperatively following the removal of an aldosterone secreting adenoma. These patients have an inadequate ability to release aldosterone during salt restriction. In severe cases, salt-wastage may be present on a normal salt intake.

Mineralocorticoid Unresponsiveness

Defective transport of sodium may also result from abnormalities in tubular responsiveness to aldosterone. Disorders in which there is a resistance to aldosterone have been localized to abnormalities in the mineralocorticoid receptor, and to postreceptor defects in the epithelial sodium channel (ENaC).[217]

Pseudohypoaldosteronism type I is an inherited disorder of salt-wasting that presents in infancy. The autosomal dominant form of this disease has been linked to functional mutations in the mineralocorticoid receptor. Renal salt-wasting in these patients tends to be mild, and spontaneously improves as patient's age. A second form of the disease is inherited in an autosomal recessive fashion, and is caused by inactivating mutations in either the alpha- or beta-subunits of the epithelial sodium channel in the collecting duct. The clinical manifestations are more severe in this form of the disease. Patients present in infancy with severe unrelenting salt-wasting, hyperkalemia, and hyperchloremic metabolic acidosis, and a failure to survive syndrome. In addition to renal manifestations, patients also display frequent respiratory tract illnesses caused by an increase in the volume of airway secretions.

Cerebral Salt-Wasting

The concept of a CSW syndrome was first introduced by Peters and colleagues in 1950 in a report describing three patients with neurological disorders who presented with hyponatremia, clinical evidence of volume depletion, and renal sodium-wasting without an obvious disturbance in the pituitary–adrenal axis.[164] These findings were subsequently confirmed in additional patients with widely varying forms of cerebral disease.[208] The mechanism by which cerebral disease leads to renal salt-wasting is poorly-understood. The most probable process involves disruption of neural input into the kidney and/or central elaboration of a circulating natriuretic factor (Figure 38.11).

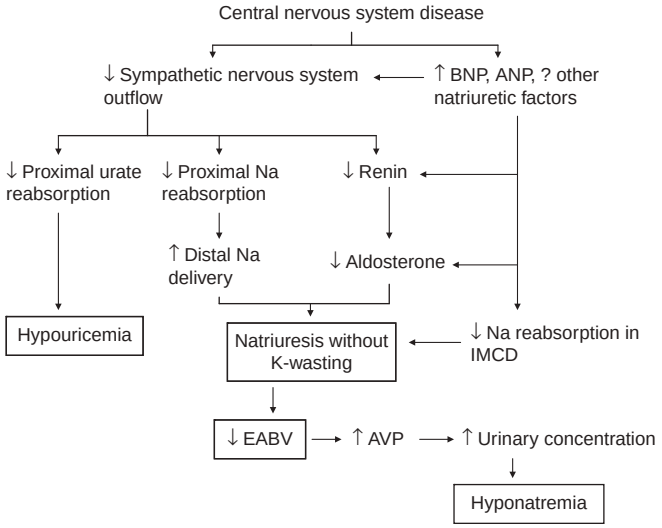

FIGURE 38.11 **The pathophysiology of cerebral salt-wasting.** Conditions associated with increased urinary sodium excretion in the setting of volume contraction would be expected to result in renal potassium-wasting, because of increased delivery of sodium to the cortical collecting duct in the setting of increased aldosterone levels. The lack of renal potassium-wasting in CSW can be accounted for by the failure of aldosterone to increase in spite of low extracellular fluid volume (ANP: atrial natriuretic peptide; AVP: arginine vasopressin; BNP: brain natriuretic peptide; CSW: cerebral salt-wasting; EABV: effective arterial blood volume; IMCD: inner medullary collecting duct).

CSW should be considered in patients with central nervous system disease who develop hyponatremia and otherwise meet the clinical criteria for a diagnosis of SIADH, but have a volume status that is inconsistent with that diagnosis. Unlike patients with SIADH who are volume-expanded, patients with CSW show evidence of negative salt balance and reductions in plasma, as well as total blood volume.[155] The onset of this disorder is typically seen within the first 10 days following a neurosurgical procedure or after a definable event, such as a subarachnoid hemorrhage or stroke. CSW has been described in other intracranial disorders, such as carcinomatous or infectious meningitis and metastatic carcinoma.

References

[1] Abassi ZA, Gurbanov K, Mulroney SE, Potlog C, Opgenorth TJ, Hoffman A, et al. Impaired nitric oxide–mediated renal vasodilation in rats with experimental heart failure: role of angiotensin II. Circulation 1997;96:3655–64.

[2] Anderson RJ, Cronin RE, McDonald KM, Schrier RW. Mechanisms of portal hypertension-induced alterations in renal hemodynamics, renal water excretion, and renin secretion. J Clin Invest 1976;58:964–70.

[3] Anderson SB, Rossing N. Metabolism of albumin and G-globulin during albumin infusions and plasmapheresis. Scand J Clin Lab Invest 1967;20:183–4.
[4] Arroyo V, Bosch J, Mauri M, et al. Renin, aldosterone and renal hemodynamics in cirrhosis with ascites. Eur J Clin Invest 1979;9:69–73.
[5] Bank N, Aynedjian HS. A micropuncture study of renal salt and water retention in chronic bile duct obstruction. J Clin Invest 1975;55:994–1002.
[6] Bankir L, Martin H, Dechaux M, Ahloulay M. Plasma Camp: a hepatorenal link influencing proximal reabsorption and renal hemodynamics? Kidney Int 1997;51(Suppl. 59):S50–6.
[7] Bansal S, Lindenfeld J, Schrier RW. Sodium retention in heart failure and cirrhosis: potential role of natriuretic doses of mineralocorticoid antagonist? Circ Heart Fail 2009;2:370–6.
[8] Barrowman JA, Granger DN. Effects of experimental cirrhosis on splanchnic microvascular fluid and solute exchange in the rat. Gastroenterology 1984;87:165–72.
[9] Battin DL, Ali S, Shahbaz AU, Massie JD, Munir A, Davis Jr RC, et al. Hypoalbuminemia and lymphocytopenia in patients with decompensated biventricular failure. Am J Med Sci 2010;339:31–5.
[10] Bell NH, Schedl HP, Bartter FC. An explanation for abnormal water retention and hypoosmolality in congestive heart failure. Am J Med 1964;36:351–60.
[11] Bennett WM, Bagby GC, Antonovic JN, Porter GA. Influence of volume expansion on proximal tubular sodium reabsorption in congestive heart failure. Am Heart 1973;85:55–64.
[12] Benoit JN, Granger DN. Intestinal microvascular adaptation to chronic portal hypertension in the rat. Gastroenterology 1988;94:471–6.
[13] Berlyne GM, Sutton J, Brown C, Feinroth M, Adler AJ, Friedman EA. Renal salt and water handling in water immersion in the nephrotic syndrome. Clin Sci 1981;61:605–10.
[14] Bernard DB, Alexander EA, Couser WG, Levinsky NG. Renal sodium retention during volume expansion in experimental nephrotic syndrome. Kidney Int 1978;14:478–85.
[15] Better O. Renal and cardiovascular dysfunction in liver disease. Kidney Int 1986;29:598–607.
[16] Better OS, Massry SG. Effect of chronic bile duct obstruction on renal handling of salt and water. J Clin Invest 1972;51:402–11.
[17] Bichet DG, Groves BM, Schrier RW. Mechanisms of improvement of water and sodium excretion by immersion in decompensated cirrhotic patients. Kidney Int 1983;24:788–94.
[18] Bichet DG, Van Putten VJ, Schrier RW. Potential role of increased sympathetic activity in impaired sodium and water excretion in cirrhosis. N Engl J Med 1982;307:1552–7.
[19] Bosch J, Enriquez R, Groszmann RJ, Storer EH. Chronic bile duct ligation in the dog: hemodynamic characterization of a portal hypertensive model. Hepatology 1983;3:1002–7.
[20] Brooks VL, Ell KR, Wright RM. Pressure-independent baroreflex resetting produced by chronic infusion of angiotensin II in rabbits. Am J Physiol 1993;265:H1275–82.
[21] Brown EA, Markandu ND, Roulston JE, Jones BE, Squires M, MacGregor GA. Is the renin–angiotensin–aldosterone system involved in the sodium retention in the nephrotic syndrome. Nephron 1982;32:102–7.
[22] Brown EA, Markandu ND, Sagnella GA, Jones BE, MacGregor GA. Lack of effect of captopril on the sodium retention of the nephrotic syndrome. Nephron 1984;37:43–8.
[23] Brown EA, Markandu ND, Sagnella GA, Squires M, Jones BE, MacGregor GA. Evidence that some mechanism other than the rennin system causes sodium retention in nephrotic syndrome. Lancet 1982;2:1237–9.
[24] Campillo B, Chabrier P-E, Pelle G, Sediame S, Altan G, Fouet P, et al. Inhibition of nitric oxide synthesis in the forearm arterial bed of patients with advanced cirrhosis. Hepatology 1995;22:1423–9.
[25] Caramelo C, Fernandez-Munoz D, Santos JC, Blanchart A, Rodriguez-Puyol D, Lopez-Novoa JM, et al. Effect of volume expansion on hemodynamics, capillary permeability and renal function in conscious, cirrhotic rats. Hepatology 1986;6:129–34.
[26] Chagnac A, Zevin D, Weinstein T, Hirsh J, Levi J. Combined tubular dysfunction in medullary cystic disease. Arch Intern Med 1986;146:1007–9.
[27] Chiandussi L, Bartoli E, Arras S. Reabsorption of sodium in the proximal renal tubule in cirrhosis of the liver. Gut 1978;19:497–503.
[28] Chonko AM, Bay WH, Stein J, Ferris TF. The role of renin and aldosterone in the salt retention of edema. Am J Med 1977;63:881–9.
[29] Cody RJ, Atlas SA, Laragh JH, Kubo SH, Covit AB, Ryman KS, et al. Atrial natriuretic factor in normal subjects and heart failure patients. J Clin Invest 1986;78:1362–74.
[30] Cody RJ, Franklin KW, Kluger J, Laragh JH. Mechanisms governing the postural response and baroreceptor abnormalities in chronic congestive heart failure: effect of acute and long-term converting enzyme inhibition. Circulation 1982;66:135–42.
[31] Coleman AJ, Arias M, Carter NW, Rector FC, Seldin DW. The mechanism of salt wastage in chronic renal disease. J Clin Invest 1966;45:1116–25.
[32] Colombato L, Albillos A, Groszmann R. The role of blood volume in the development of sodium retention in portal hypertensive rats. Gastroenterology 1996;110:193–8.
[33] de Seigneux S, Kim SW, Hemmingsen SC, Frokiaer JNielsen S. Increased expression but not targeting of ENaC in adrenalectomized rats with PAN-induced nephrotic syndrome. Am J Physiol Renal Physiol 2006;291:F208–17.
[34] Dharmaraj R, Hari P, Bagga A. Randomized cross-over trial comparing albumin and furosemide infusions in nephrotic syndrome. Pediatr Nephrol 2009;24:775–82.
[35] DiBona GF, Herman PJ, Sawin LL. Neural control of renal function in edema-forming states. Am J Physiol 1988;254:R1017–24.
[36] DiBona GF, Jones SY, Sawin LL. Effect of endogenous angiotensin II on renal nerve activity and its arterial baroreflex regulation. Am J Physiol 1996;271:R361–7.
[37] DiBona GF, Sawin LL. Role of renal nerves in sodium retention of cirrhosis and congestive heart failure. Am J Physiol 1991;260: R298–305.
[38] DiBona GF. Renal neural activity in hepatorenal syndrome. Kidney Int 1984;25:841–53.
[39] Dorhout Mees EJ, Geers AB, Koomans HA. Blood volume and sodium retention in the nephrotic syndrome: a controversial pathophysiological concept. Nephron 1984;36:201–11.
[40] Dorhout Mees EJ, Roos JC, Boer P, Yoe EH, Simatupang TA. Observations on edema formation in the nephrotic syndrome in adults with minimal lesions. Am J Med 1979;67:378–84.
[41] Doucet A, Favre G, Deschenes G. Molecular mechanism of edema formation in nephrotic syndrome: therapeutic implications. Pediatr Nephrol 2007;22:1983–90.
[42] Dusing R, Vetter H, Kramer HJ. The renin–angiotensin–aldosterone system in patients with nephrotic syndrome: effects of 1-sar-8 ala-angiotensin II. Nephron 1980;25: 187–92.
[43] Dzau VJ, Colucci WS, Hollenberg NK, Williams GH. Relation of the renin–angiotensin–aldosterone system to clinical state in congestive heart failure. Circulation 1981;63:645–51.
[44] Dzau VJ, Colucci WS, Williams GH, Curfman G, Meggs L, Hollenberg NK. Sustained effectiveness of converting enzyme

inhibition in patients with severe congestive heart failure. N Engl J Med 1980;302:1373–9.
[45] Eggert RC. Spironolactone diuresis in patients with cirrhosis and ascites. BMJ 1970;4:401–3.
[46] Eisenberg S. Postural changes in plasma volume in hypoalbuminemia. Arch Intern Med 1963;112:544–9.
[47] Eisenberg S. Blood volume in persons with the nephrotic syndrome. Am J Med Sci 1968;255:320–6.
[48] Epstein FH, Post RS, McDowell M. The effect of an arteriovenous fistula on renal hemodynamics and electrolyte excretion. J Clin Invest 1953;32:233–41.
[49] Epstein M. Cardiovascular and renal effects of head-out water immersion in man. Circ Res 1976;39:619–28.
[50] Epstein M. Deranged sodium homeostasis in cirrhosis. Gastroenterology 1979;76:622–35.
[51] Epstein M, Berk DP, Hollenberg NK, Adams DF, Chalmers TC, Abrams HL, et al. Renal failure in the patient with cirrhosis. The role of active vasoconstriction. Am J Med 1970;49:175–85.
[52] Epstein M, Levinson R, Sancho J, Haber E, Re R. Characterization of the renin–aldosterone system in decompensated cirrhosis. Circ Res 1977;41:818–29.
[53] Epstein M, Ramachandran M, De Nunzio AG. Interrelationship of renal sodium and phosphate handling in cirrhosis. Miner Electrolyte Metab 1982;7:305–15.
[54] Fadnes HO, Pape JF, Sundsfjord JA. A study on oedema mechanism in nephrotic syndrome. Scand J Clin Lab Invest 1986;46:533–8.
[55] Faroqui S, Sheriff S, Amlal H. Metabolic acidosis has dual effects on sodium handling by rat kidney. Am J Physiol Renal Physiol 2006;291:F322–31.
[56] Fernandez-Munoz D, Caramelo C, Santos JC, Blanchart A, Hernando L, Lopez-Novoa JM. Systemic and splanchnic hemodynamic disturbances in conscious rats with experimental liver cirrhosis without ascites. Am J Physiol 1985;249:G316–20.
[57] Fernandez-Rodriguez C, Prada I, Prieto J, Montuenga LM, Elssasser T, Quiroga J, et al. Circulating adrenomedullin in cirrhosis: relationship to hyperdynamic circulation. J Hepatol 1998;98:250–6.
[58] Firth JD, Raine AEG, Ledingham JGG. Abnormal sodium handling occurs in the isolated perfused kidney of the nephrotic rat. Clin Sci 1989;76:387–95.
[59] Garcia-Tsao G, Bosch J. Management of varices and variceal hemorrhage in cirrhosis. N Engl J Med 2010;362:823–32.
[60] Geers AB, Koomans HA, Boer P, Dorhout Mees EJ. Plasma and blood volumes in patients with the nephrotic syndrome. Nephron 1984;38:170–3.
[61] Geers AB, Koomans HA, Roos JC, Boer P, Dorhout Mees EJ. Functional relationships in the nephrotic syndrome. Kidney Int 1984;26:324–30.
[62] Gerbes AL, Kollenda MC, Vollmar AM, Reichen J, Vakil N, Scarborough RM. Altered density of glomerular binding sites for atrial natriuretic factor in bile duct-ligated rats with ascites. Hepatology 1991;13:562–6.
[63] Gines P, Fernandez-Esparrach G, Arroyo V, Rodes J. Pathogenesis of ascites in cirrhosis. Semin Liver Dis 1997;17:175–89.
[64] Granger DN, Miller T, Allen R, Parker RE, Parker JC, Taylor AE. Permselectivity of cat liver blood–lymph barrier to endogenous macromolecules. Gastroenterology 1979;77:103–9.
[65] Grassi G, Cattaneo BM, Seravalle G, Lanfranchi A, Pozzi M, Morganti A, et al. Effects of chronic ACE inhibition on sympathetic nerve traffic and baroreflex control of circulation in heart failure. Circulation 1997;96:1173–9.
[66] Grausz H, Lieberman R, Earley LE. Effect of plasma albumin on sodium reabsorption in patients with nephrotic syndrome. Kidney Int 1972;1:47–54.
[67] Guevara M, Gines P, Fernandez-Esparrach G, Sort P, Salmeron JM, Jimenez W, et al. Reversibility of hepatorenal syndrome by prolonged administration of ornipressin and plasma volume expansion. Hepatology 1988;27:35–41.
[68] Guyton AC. Interstitial fluid pressure II. Pressure volume curves of the interstitial space. Circ Res 1965;16:452–60.
[69] Hammond TG, Whitworth JA, Saines D, Thatcher R, Andrews J, Kincaid-Smith P. Renin–angiotensin–aldosterone system in nephrotic syndrome. Am J Kidney Dis 1984;4:18–23.
[70] Harris PJ, Young JA. Dose-dependent stimulation and inhibition of proximal tubular sodium reabsorption by angiotensin II in the rat kidney. Pflugers Arch 1977;367:295–7.
[71] Hensen J, Abraham WT, Durr JA, Schrier RW. Aldosterone in congestive heart failure: analysis of determinants and role in sodium retention. Am J Nephrol 1991;11:441–6.
[72] Herman PJ, Sawin LL, DiBona GF. Role of renal nerves in renal sodium retention of nephrotic syndrome. Am J Physiol 1989;256:F823–9.
[73] Hollander W, Reilly P, Burrows BA. Lymphatic flow in human subjects as indicated by the disappearance of 131I-labeled albumin from the subcutaneous tissue. J Clin Lab Invest 1989;40:222–3.
[74] Hommel E, Mathiesen ER, Aukland K, Parving HH. Pathophysiological aspects of edema formation in diabetic nephropathy. Kidney Int 1990;38:1187–92.
[75] Hostetter TH, Pfeffer JM, Pfeffer MA, Dworkin LD, Braunwald E, Brenner BM. Cardiorenal hemodynamics and sodium excretion in rats with myocardial infarction. Am J Physiol 1983;245:H98–103.
[76] Ichikawa I, Pfeffer JM, Pfeffer MA, Hostetter TH, Brenner BM. Role of angiotensin II in the altered renal function of congestive heart failure. Circ Res 1984;55:669–75.
[77] Ichikawa I, Rennke HG, Hoyer JR, Badr KF, Schor N, Troy JL, et al. Role for intrarenal mechanisms in the impaired salt excretion of experimental nephrotic syndrome. J Clin Invest 1983;71:91–103.
[78] Iino Y, Troy JL, Brenner BM. Effects of catecholamines on electrolyte transport in cortical collecting tubule. J Membr Biol 1981;61:67–73.
[79] Iwakiri Y. The molecules: mechanisms of arterial vasodilatation observed in the splanchnic and systemic circulation in portal hypertension. J Clin Gastroenterol 2007;41(Suppl. 3):S288–94.
[80] Iwao T, Toyonaga A, Sato M, Oho K, Sakai T, Tayama C, et al. Effect of posture-induced blood volume expansion on systemic and regional hemodynamics in patients with cirrhosis. J Hepatol 1997;27:484–91.
[81] Jimenez W, Martinez-Pardo A, Arroyo V, Gaya J, Rivera F, Rodes J. Atrial natriuretic factor: reduced cardiac content in cirrhotic rats with ascites. Am J Physiol 1986;250:F749–52.
[82] Johnston CI, Davis JO, Robb CA, Mackenzie JW. Plasma renin in chronic experimental heart failure and during renal sodium "escape" from mineralocorticoids. Circ Res 1968;22:113–25.
[83] Joles JA, Koomans HA, Kortlandt W, Boer P, Dorhout Mees EJ. Hypoproteinemia and recovery from edema in dogs. Am J Physiol 1988;254:F887–94.
[84] Joles J, Rabelink T, Braam B, Koomans HA. Plasma volume regulation: defenses against edema formation (with special emphasis on hypoproteinemia). Am J Nephrol 1993;13:399–412.
[85] Kalambokis G, Economou M, Fotopoulos A, Al Bokharhii J, Pappas C, Katsaraki A, et al. The effects of chronic treatment with octreotide versus octreotide plus midodrine on systemic hemodynamics and renal hemodynamics and function in nonazotemic cirrhotic patients with ascites. Am J Gastroenterol 2004;99:1–7.

[86] Kalant N, Das Gupta D, Despointes R, Giroud CJP. Mechanisms of edema in experimental nephrosis. Am J Physiol 1962;202:91–6.
[87] Kapur G, Valentini RP, Imam AA, Mattoo TK. Treatment of severe edema in children with nephrotic syndrome with diuretics alone: a prospective study. Clin J Am Soc Nephrol 2009;4:907–13.
[88] Kelsch RC, Light GS, Oliver WJ. The effect of albumin infusion upon plasma norepinephrine concentration in nephrotic children. J Lab Clin Med 1972;79:516–25.
[89] Kim SW, Frokiaer J, Nielsen S. Pathogenesis of oedema in nephrotic syndrome: role of epithelial sodium channel. Nephrology (Carlton) 2007;12(Suppl. 3):S8–10.
[90] Kim SW, de Seigneux S, Sassen MC, Lee J, Kim J, Knepper MA, et al. Increased apical targeting of renal ENaC subunits and decreased expression of 11betaHSD2 in HgCl2-induced nephrotic syndrome in rats. Am J Physiol Renal Physiol 2006;290:F674–87.
[91] Kim JK, Michel J-B, Soubrier F, Durr J, Corvol P, Schrier RW. Arginine vasopressin gene expression in chronic cardiac failure in rats. Kidney Int 1990;38:818–22.
[92] Kim MY, Baik SK. Hyperdynamic circulation in patients with liver cirrhosis and portal hypertension. Korean J Gastroenterol 2009;54:143–8.
[93] Kiowski W, Sutsch G, Hunziker P, Müller P, Kim J, Oechslin E, et al. Evidence for endothelin-1-mediated vasoconstriction in severe chronic heart failure. Lancet 1995;346:732–6.
[94] Kirchheim HR, Finke R, Hackenthal E, Lowe W, Persson P. Baroreflex sympathetic activation increases threshold pressure for the pressure-dependent renin release in conscious dogs. Pflugers Arch 1985;405:127–35.
[95] Koepke JP, DiBona GF. Blunted natriuresis to atrial natriuretic peptide in chronic sodium-retaining disorders. Am J Physiol 1987;252:F865–71.
[96] Koepke JP, Jones S, DiBona GF. Renal nerves mediate blunted natriuresis to atrial natriuretic peptide in cirrhotic rats. Am J Physiol 1987;252:R1019–23.
[97] Kontos HA, Shapiro W, Mauck HP, Patterson Jr JL. General and regional circulatory alterations in cirrhosis of the liver. Am J Med 1964;37:526–35.
[98] Koomans HA, Braam B, Geers AB, Roos JC, Dorhout Mees EJ. The importance of plasma protein for blood volume and blood pressure homeostasis. Kidney Int 1986;30:730–5.
[99] Koomans HA, Geers AB, Dorhout Mees EJ, Kortland W. Lowered tissue-fluid oncotic pressure protects the blood volume in the nephrotic syndrome. Nephron 1986;42:317–22.
[100] Koomans HA, Geers AB, Meiracker AH, Roos JC, Boer P, Dorhout Mees EJ. Effects of plasma volume expansion on renal salt handling in patients with the nephrotic syndrome. Am J Nephrol 1984;4:227–34.
[101] Koomans HA, Kortlandt W, Geers AB, Dorhout Mees EJ. Lowered protein content of tissue fluid in patients with the nephrotic syndrome: observations during disease and recovery. Nephron 1985;40:391–5.
[102] Korthuis RJ, Kinden DA, Brimer GE, Slattery KA, Stogsdill P, Granger DN. Intestinal capillary filtration in acute and chronic portal hypertension. Am J Physiol 1988;254:G339–45.
[103] Kashani A, Landaverde C, Medici V, Rossaro L. Fluid retention in cirrhosis: pathophysiology and management. QJM 2008;101:71–85.
[104] Kostreva DR, Castaner A, Kampine JP. Reflex effects of hepatic baroreceptors on renal and cardiac sympathetic nerve activity. Am J Physiol 1980;238:R390–4.
[105] Krishna GG, Danovitch K, Danovitch GM. Effects of water immersion on renal function in the nephrotic syndrome. Kidney Int 1982;21:395–401.
[106] Kumagai H, Onoyama K, Iseki K, Omae T. Role of renin angiotensin aldosterone on minimal change nephrotic syndrome. Clin Nephrol 1985;23:229–35.
[107] La Villa G, Riccardi D, Lazzeri C, Cassini Raggi V, Dello Sbarba A, Tosti Guerra C, et al. Blunted natriuretic response to low-dose brain natriuretic peptide infusion in nonazotemic cirrhotic patients with ascites and avid sodium retention. Hepatology 1995;22:1745–50.
[108] Legault L, Cernacek P, Levy M, Maher E, Farber D. Renal tubular responsiveness to atrial natriuretic peptide in sodium-retaining chronic caval dogs: a possible role for kinins and luminal actions of the peptide. J Clin Invest 1992;90:1425–35.
[109] Leimbach WN, Wallin BG, Victor RG, Aylward PE, Sundlof G, Mark AL. Direct evidence from intraneural recordings for increased central sympathetic outflow in patients with heart failure. Circulation 1986;73:913–9.
[110] Lenz K, Hortnagl H, Druml W, Reither H, Schmid R, Schneewiess B, et al. Ornipressin in the treatment of functional renal failure in decompensated liver cirrhosis. Gastroenterology 1991;101:1060–7.
[111] Levine TB, Francis GS, Goldsmith SR, Simon AB, Cohn JN. Activity of the sympathetic nervous system and renin–angiotensin system assessed by plasma hormone levels and their relation to hemodynamic abnormalities in congestive heart failure. Am J Cardiol 1982;49:1659–66.
[112] Levy M. Effects of acute volume expansion and altered hemodynamics on renal tubular function in chronic caval dogs. J Clin Invest 1972;51:922–34.
[113] Levy M, Wexler MJ. Sodium excretion in dogs with low-grade caval constriction: role of hepatic nerves. Am J Physiol 1987;253:F672–8.
[114] Levy M, Wexler MJ. Hepatic denervation alters first-phase urinary sodium excretion in dogs with cirrhosis. 1987;253: F664–71.
[115] Levy M. Sodium retention and ascites formation in dogs with experimental portal cirrhosis. Am J Physiol 1977;233:F572–85.
[116] Levy M, Allotey JB. Temporal relationships between urinary salt retention and altered systemic hemodynamics in dogs with experimental cirrhosis. J Lab Clin Med 1978;92:560–9.
[117] Levy M, Wexler MJ. Renal sodium retention and ascites formation in dogs with experimental cirrhosis but without portal hypertension or increased splanchnic vascular capacity. J Lab Clin Med 1978;91:520–36.
[118] Lieberman FL, Denison EK, Reynolds TB. The relationship of plasma volume, portal hypertension, ascites, and renal sodium retention in cirrhosis: the overflow theory of ascites formation. Ann NY Acad Sci 1978;170:202–11.
[119] Ljungman S, Laragh JH, Cody RJ. Role of the kidney in congestive heart failure: relationship of cardiac index to kidney function. Drugs 1990;39(Suppl. 4):10–21.
[120] Limas CJ, Guiha NH, Lekagul O, Cohn JN. Impaired left ventricular function in alcoholic cirrhosis with ascites. Circulation 1974;69:755–60.
[121] Lopez-Talavera JC, Merrill WM, Groszmann RJ. Tumor necrosis factor a: a major contributor to the hyperdynamic circulation in prehepatic portal-hypertensive rats. Gastroenterology 1995;108:761–7.
[122] Lopez-Talavera JC, Levitzki A, Martinez M, Gazit A, Esteban R, Guardia J. Tyrosine kinase inhibition ameliorates the hyperdynamic state and decreases nitric oxide production in cirrhotic rats with portal hypertension and ascites. J Clin Invest 1997;100:664–70.
[123] Lopez C, Jimenez W, Arroyo V, Claria J, La Villa G, Asbert M, et al. Temporal relationship between the decrease in arterial pressure and sodium retention in conscious spontaneously

hypertensive rats with carbon tetrachloride-induced cirrhosis. Hepatology 1991;13:585–9.
[124] Lopez C, Jimenez W, Arroyo V, La Villa G, Gaya J, Claria J, et al. Role of altered systemic hemodynamics in the blunted renal response to atrial natriuretic peptide in rats with cirrhosis and ascites. J Hepatology 1989;9:217–26.
[125] Lourdel S, Loffing J, Favre G, Paulais M, Nissant A, Fakitsas P, et al. Hyperaldosteronemia and activation of the epithelial sodium channel are not required for sodium retention in puromycin-induced nephrosis. J Am Soc Nephrol 2005;16:3642–50.
[126] Luetscher JA, Johnson BB. Observations on the sodium-retaining corticoid (aldosterone) in the urine of children and adults in relation to sodium balance and edema. J Clin Invest 1954;33:1441–6.
[127] MacGilchrist A, Craig KJ, Hayes PC, Cumming AD. Effect of the serine protease inhibitor, aprotinin, on systemic haemodynamics and renal function in patients with hepatic cirrhosis and ascites. Clin Sci 1994;87:329–35.
[128] Maher E, Cernacek P, Levy M. Heterogeneous renal responses to atrial natriuretic factor II. Cirrhotic dogs. Am J Physiol 1989;257:R1068–74.
[129] Manenti F, Williams R. Injection studies of the splenic vasculature in portal hypertension. Gut 1966;7:175–80.
[130] Mann JF, Green D, Jamerson K, Ruilope LM, Kuranoff SJ, Littke T, et al. Avosentan for overt diabetic nephropathy. J Am Soc Nephrol 2010;21:527–35.
[131] Marcus LS, Hart D, Packer M, Yushak M, Medina N, Danziger RS, et al. Hemodynamic and renal excretory effects of human brain natriuretic peptide infusion in patients with congestive heart failure: a double-blind, placebo-controlled, randomized crossover trial. Circulation 1996;94:3184–9.
[132] Martin P-Y, Ohara M, Gines P, Xu DL, St John J, Niederberger M, et al. Nitric oxide synthase (NOS) inhibition for one week improves renal sodium and water excretion in cirrhotic rats with ascites. J Clin Invest 1998;101:235–42.
[133] Martin P-Y, Schrier RW. Sodium and water retention in heart failure: pathogenesis and treatment. Kidney Int 1997;51(Suppl. 59):S57–61.
[134] Martin P, Gines P, Schrier R. Nitric oxide as a mediator of hemodynamic abnormalities and sodium and water retention in cirrhosis. N Engl J Med 1998;339:533–41.
[135] Mejias M, Garcia-Pras E, Tiani C, Miquel R, Bosch J, Fernandez M. Beneficial effects of sorafenib on splanchnic, intrahepatic, and portocollateral circulations in portal hypertensive and cirrhotic rats. Hepatology 2009;49:1245–56.
[136] Melman A, Massry SG. Role of renal vasodilation in the blunted natriuresis of saline infusion in dogs with chronic bile duct obstruction. J Lab Clin Med 1977;89:1053–65.
[137] Meltzer J, Keim HJ, Laragh JH, Sealey JE, Jan KM, Chien S. Nephrotic syndrome: vasoconstriction and hypervolemic types indicated by renin-sodium profiling. Ann Intern Med 1979;91:688–96.
[138] Metcoff J, Janeway CA. Studies on the pathogenesis of nephrotic edema. J Pediatr 1961;58:640–85.
[139] Metlauer B, Rouleau JL, Bichet D, Juneau C, Kortas C, Barjon JN, et al. Sodium and water excretion abnormalities in congestive heart failure. Ann Intern Med 1986;105:161–7.
[140] Moller S, Henriksen JH. Circulatory abnormalities in cirrhosis with focus on neurohumoral aspects. Semin Nephrol 1997;17:505–19.
[141] Moller S, Henriksen JH, Bendtsen F. Ascites: pathogenesis and therapeutic principles. Scand J Gastroenterol 2009;44:902–11.
[142] Moore K, Wendon J, Frazer M, Karani J, Williams R, Badr K. Plasma endothelin immunoreactivity in liver disease and the hepatorenal syndrome. N Engl J Med 1992;327:1774–8.
[143] Morali GA, Tobe SW, Skorecki KL, Blendis LM. Refractory ascites: modulation of atrial natriuretic factor unresponsiveness by mannitol. Hepatology 1992;16:42–8.
[144] Nicholls KM, Shapiro MD, Groves BS, Schrier RW. Factors determining renal response to water immersion in nonexcretor cirrhotic patients. Kidney Int 1986;30:417–21.
[145] Nicholls KM, Shapiro MD, Kluge R, Chung HM, Bichet DG, Schrier RW. Sodium excretion in advanced cirrhosis: effect of expansion of central blood volume and suppression of plasma aldosterone. Hepatology 1986;6:235–8.
[146] Nicholls KM, Shapiro MD, Van Putten VJ, Kluge R, Chung HM, Bichet DG, et al. Elevated plasma norepinephrine concentrations in decompensated cirrhosis. Circ Res 1985;56:457–61.
[147] Niederberger M, Martin P-Y, Gines P, Morris K, Tsai P, Xu DL, et al. Normalization of nitric oxide production corrects arterial vasodilation and hyperdynamic circulation in cirrhotic rats. Gastroenterology 1995;109:1624–30.
[148] Ochs A, Rossle M, Haag K, Hauenstein KH, Deibert P, Siegerstetter V, et al. The transjugular intrahepatic portosystemic stent-shunt procedure for refractory ascites. N Engl J Med 1995;332:1192–7.
[149] Olivari MT, Levine TB, Cohn JN. Abnormal neurohormonal response to nitroprusside infusion in congestive heart failure. J Am Coll Cardiol 1983;2:411.
[150] Oliver WJ, Kelsch RC, Chandler JP. Demonstration of increased catecholamine excretion in the nephrotic syndrome. Proc Soc Exp Biol Med 1967;125:1176–80.
[151] Packer M, Lee WH, Kessler PD. Preservation of glomerular filtration in human heart failure by activation of the renin–angiotensin system. Circulation 1986;74:766–74.
[152] Packer M, Lee WH, Medina N, Yushak M, Kessler PD. Functional renal insufficiency during long-term therapy with captopril and enalapril in severe chronic heart failure. Ann Intern Med 1987;106:346–54.
[153] Palazzuoli A, Gallotta M, Quatrini I, Nuti R. Natriuretic peptides (BNP and NT-proBNP): measurement and relevance in heart failure. Vasc Health Risk Manag 2010;6:411–8.
[154] Palmer BF. Renal complications associated with use of nonsteroidal anti-inflammatory agents. J Invest Med 1995;43:516–33.
[155] Palmer BF. Hyponatremia in patients with central nervous system disease: SIADH or CSW. Trends Endocrinol Metab 2003;14:182–743.
[156] Palmer BF. Renal dysfunction complicating treatment of hypertension. N Engl J Med 2002;347:1256–61.
[157] Panos MZ, Gove C, Firth JD, Raine AE, Ledingham JG, Westaby D, et al. Impaired natriuretic response to atrial natriuretic peptide in the isolated kidney of rats with experimental cirrhosis. Clin Sci 1990;79:67–71.
[158] Pelayo JC, Ziegler MG, Blantz RC. Angiotensin II in adrenergic-induced alterations in glomerular hemodynamics. Am J Physiol 1984;247:F799–807.
[159] Pelayo JC, Ziegler MG, Jose PA, Blantz RC. Renal denervation in the rat: analysis of glomerular and proximal tubular function. Am J Physiol 1983;244:F70–7.
[160] Perez-Ayuso RM, Arroyo V, Camps J, Rimola A, Costa J, Gaya J, et al. Renal kallikrein excretion in cirrhosis with ascites: relationship to renal hemodynamics. Hepatology 19844:247–252.
[161] Perez-Ayuso RM, Arroyo V, Planas R, Gaya J, Bory F, Rimola A, et al. Randomized comparative study of efficacy of furosemide versus spironolactone in nonazotemic cirrhosis with ascites. Gastroenterology 1983;84:961–8.
[162] Perico N, Remuzzi G. Edema of the nephrotic syndrome: the role of the atrial peptide system. Am J Kidney Dis 1993;22:355–66.

[163] Perico N, Remuzzi G. Renal handling of sodium in the nephrotic syndrome. Am J Nephrol 1993;13:413–21.
[164] Peters JP, Welt LG, Sims EA, Orloff J, Needham J. Salt-wasting syndrome associated with cerebral disease. Trans Assoc Am Physicians 1950;63:57–64.
[165] Peterson C, Madson B, Perlman A, Chan AY, Myers BD. Atrial natriuretic peptide and the renal response to hypervolemia in nephrotic humans. Kidney Int 1988;34:825–31.
[166] Priebe HJ, Heimann JC, Hedley-White J. Effects of renal and hepatic venous congestion on renal function in the presence of low and normal cardiac output in dogs. Circ Res 1980;47:883–90.
[167] Rabelink T, Bijlsma J, Koomans H. Iso-oncotic volume expansion in the nephrotic syndrome. Clin Sci 1993;84:627–32.
[168] Raine AE, Erne P, Burgisser E, Muller FB, Bolli P, Burkart F, et al. Atrial natriuretic peptide and atrial pressure in patients with congestive heart failure. N Engl J Med 1986;315:533–7.
[169] Rascher W, Tulassay T. Hormonal regulation of water metabolism in children with nephrotic syndrome. Kidney Int 1987;32:583–9.
[170] Rascher W, Tulassay T, Seyberth HW, Himbert U, Lang U, Scharer K. Diuretic and hormonal response to head-out water immersion in nephrotic syndrome. J Pediatr 1986;109:609–14.
[171] Rector WG, Hossack KF. Pathogenesis of sodium retention complicating cirrhosis: is there room for diminished "effective" arterial blood volume? Gastroenterology 1988;95:1658–63.
[172] Rehsia NS, Dhalla NS. Potential of endothelin-1 and vasopressin antagonists for the treatment of congestive heart failure. Heart Fail Rev 2010;15:85–101.
[173] Reilly T, Schork MR. Vasopressin antagonists: pharmacotherapy for the treatment of heart failure. Ann Pharmacother 2010;44:680–7.
[174] Resch M, Wiest R, Moleda L, Fredersdorf S, Stoelcker B, Schroeder JA, et al. Alterations in mechanical properties of mesenteric resistance arteries in experimental portal hypertension. Am J Physiol Gastrointest Liver Physiol 2009;297: G849–57.
[175] Rodriguez-Martinez M, Sawin LL, DiBona GF. Arterial and cardiopulmonary baroreflex control of renal nerve activity in cirrhosis. Am J Physiol 1995;268:R117–29.
[176] Ros J, Jimenez W, Lamas S, Claria J, Arroyo V, Rivera F, et al. Nitric oxide production in arterial vessels of cirrhotic rats. Hepatology 1995;21:554–60.
[177] Rosoff L, Zia P, Reynolds T, Horton R. Studies of renin and aldosterone in cirrhotic patients with ascites. Gastroenterology 1975;69:698–705.
[178] Salo J, Jimenez W, Kuhn M, Ginès A, Ginès P, Fernández-Esparrach G, et al. Urinary excretion of urodilatin in patients with cirrhosis. Hepatology 1996;24:1428–32.
[179] Sanz E, Caramelo C, Lopez-Novoa JM. Interstitial dynamics in rats with early stage experimental cirrhosis of the liver. Am J Physiol 1989;256:F497–503.
[180] Sato S, Ohnishi K, Sugita S, Okuda K. Splenic artery and superior mesenteric artery blood flow: nonsurgical Doppler US measurement in healthy subjects and patients with chronic liver disease. Radiology 1987;164:347–52.
[181] Schaffner F, Popper H. Capillarization of hepatic sinusoids in man. Gastroenterology 1963;44:239–42.
[182] Schedl HP, Bartter FC. An explanation for an experimental correction of the abnormal water diuresis in cirrhosis. J Clin Invest 1960;39:248–61.
[183] Schrier RW, Masoumi A, Elhassan E. Aldosterone: role in edematous disorders, hypertension, chronic renal failure, and metabolic syndrome. Clin J Am Soc Nephrol 2010;5:1132–40.
[184] Schrier RW. Decreased effective blood volume in edematous disorders: what does this mean? J Am Soc Nephrol 2007;18:2028–31.
[185] Schrier RW. Pathogenesis of sodium and water retention in high-output and low-output cardiac failure, nephrotic syndrome, cirrhosis, and pregnancy. N Engl J Med 1988;319 (1065–1072):1127–34.
[186] Schrier RW, Humphreys MH, Ufferman RC. Role of cardiac output and the autonomic nervous system in the antinatriuretic response to acute constriction of the thoracic superior vena cava. Circ Res 1971;29:490–8.
[187] Schuster VL, Kokko JP, Jacobson HR. Angiotensin II directly stimulates sodium transport in rabbit proximal convoluted tubules. J Clin Invest 1984;73:507–15.
[188] Shapiro MD, Nicholls KM, Groves BM, Kluge R, Chung HM, Bichet DG, et al. Interrelationship between cardiac output and vascular resistance as determinants of effective arterial blood volume in cirrhotic patients. Kidney Int 1985;28:206–11.
[189] Shapiro MD, Hasbargen J, Hensen J, Schrier RW. Role of aldosterone in the sodium retention of patients with nephrotic syndrome. Am J Nephrol 1990;10:44–8.
[190] Skorecki KL, Leung WM, Campbell P, Warner LC, Wong PY, Bull S, et al. Role of atrial natriuretic peptide in the natriuretic response to central volume expansion induced by head-out water immersion in sodium-retaining cirrhotic subjects. Am J Med 1988;85:375–82.
[191] Smith JD, Hayslett JP. Reversible renal failure in the nephrotic syndrome. Am J Kidney Dis 1992;19:201–13.
[192] Sogni P, Garnier P, Gadano A, Moreau R, Dall'Ava-Santucci J, Dinh-Xuan AT, et al. Endogenous pulmonary nitric oxide production measured from exhaled air is increased in patients with severe cirrhosis. J Hepatol 1995;23:471–3.
[193] Stumpe KO, Solle H, Klein H, Kruck . Mechanism of sodium and water retention in rats with experimental heart failure. Kidney Int 1973;4:309–17.
[194] Suki WN. Renal hemodynamic consequences of angiotensin-converting enzyme inhibition in congestive heart failure. Arch Intern Med 1989;149:669–73.
[195] Thiesson HC, Jensen B, Bistrup C, Ottosen PD, McNeilly AD, Andrew R, et al. Renal sodium retention in cirrhotic rats depends on glucocorticoid-mediated activation of mineralocorticoid receptor due to decreased renal beta 11beta-HSD-2 activity. Ann J Physiol Integr Comp Physiol 2007;292:R625–36.
[196] Tulassay T, Rascher W, Lang RE, Seyberth HW, Scharer K. Atrial natriuretic peptide and other vasoactive hormones in nephrotic syndrome. Kidney Int 1987;31:1391–5.
[197] Unikowsky B, Wexler MJ, Levy M. Dogs with experimental cirrhosis of the liver but without intrahepatic hypertension do not retain sodium or form ascites. J Clin Invest 1983;72:1594–604.
[198] Usberti M, Federico S, Cianciaruso B, Costanzo R, Russo D, Andreucci VE. Relationship between serum albumin concentration and tubular reabsorption of glucose in renal disease. Kidney Int 1983;16:546–51.
[199] Usberti M, Federico S, Meccariello S, Cianciaruso B, Balletta M, Pecoraro C, et al. Role of plasma vasopressin in the impairment of water excretion in nephrotic syndrome. Kidney Int 1984;25:422–9.
[200] Valentin J, Qiu C, Muldowney WP, Ying WZ, Gardner DG, Humphreys MH. Cellular basis for blunted volume expansion natruresis in experimental nephrotic syndrome. J Clin Invest 1992;90:1302–12.
[201] Valentin J, Ying W, Sechi LA, Ling KT, Qiu C, Couser WG, et al. Phosphodiesterase inhibitors correct resistance to

natriuretic peptides in rate with Heymann nephritis. J Am Soc Nephrol 1996;7:582–93.
[202] Villareal D, Freeman RH, Davis JO, Verburg KM, Vari RC. Atrial natriuretic factor secretion in dogs with experimental high-output heart failure. Am J Physiol 1987;252:H692–6.
[203] Vorobioff J, Bredfeldt JE, Groszmann RJ. Increased blood flow through the portal system in cirrhotic rats. Gastroenterology 1984;87:1120–6.
[204] Wada A, Tsutamoto T, Fukai D, Ohnishi M, Maeda K, Hisanaga T, et al. Comparison of the effects of selective endothelin ETA and ETB receptor antagonists in congestive heart failure. J Am Coll Cardiol 1997;30:1385–92.
[205] Walle J, Donckerwolcke R, Boer P, van Isselt HW, Koomans HA, Joles JA. Blood volume, colloid osmotic pressure and F-cell ratio in children with the nephrotic syndrome. Kidney Int 1996;49:1471–7.
[206] Watkins L, Burton JA, Haber E, Cant JR, Smith FW, Barger AC. The renin–angiotensin–aldosterone system in congestive heart failure in conscious dogs. J Clin Invest 1976;57:1606–17.
[207] Weigert AL, Martin P-Y, Schrier RW. Vascular hyporesponsiveness in cirrhotic rats: role of different nitric oxide synthase isoforms. Kidney Int 1997;52(Suppl. 61):S41–4.
[208] Welt LG, Seldin DW, Nelson WP, German WJ, Peters JP. Role of the central nervous system in metabolism of electrolytes and water. Arch Intern Med 1952;90:355–78.
[209] Wiest R. Splanchnic and systemic vasodilation: the experimental models. J Clin Gastroenterol 2007;41(Suppl. 3):S272–87.
[210] Winlaw DS, Smythe GA, Keogh AM, Schwens CG, Spratt PM, Macdonald PS. Increased nitric oxide production in heart failure. Lancet 1994;344:373–4.
[211] Wirth KJ, Bickel M, Hropot M, Gunzler V, Heitsch H, Ruppert D, et al. The bradykinin B2 receptor antagonist Icatibant (HOE 140) corrects avid Na retention in rats with CCL4-induced liver cirrhosis: possible role of enhanced microvascular leakage. Eur J Pharmacol 1997;337:45–53.
[212] Witte MH, Witte CL, Dumont AE. Progress in liver disease: physiological factors involved in the causation of cirrhotic ascites. Gastroenterology 1971;61:742–50.
[213] Witte MH, Witte CL, Dumont AE. Estimated net transcapillary water and protein flux in the liver and intestine of patients with portal hypertension from hepatic cirrhosis. Gastroenterology 1981;80:265–72.
[214] Witte CL, Witte MH, Dumont AE, Cole WR, Smith JR. Protein content in lymph and edema fluids in congestive heart failure. Circulation 1969;40:623–30.
[215] Wraight EP. Capillary permeability of protein as a factor in the control of plasma volume. J Physiol 1974;237:39.
[216] Xu D-L, Martin P-Y, Ohara St M, John J, Pattison T, Meng X, et al. Upregulation of aquaporin-2 water channel expression in chronic heart failure rat. J Clin Invest 1997;99:1500–5.
[217] Zennaro M-C, Lombes M. Mineralocorticoid resistance. Trends Endocrinol Metab 2004;15:264–70.
[218] Zucker IH, Earle AM, Gilmore JP. The mechanism of adaptation of left atrial stretch receptors in dogs with chronic congestive heart failure. J Clin Invest 1977;60:323–31.

This page intentionally left blank

CHAPTER

39

Physiology and Pathophysiology of Hypertension

John E. Hall[1], *Joey P. Granger*[2] *and Michael E. Hall*[2]

[1]Department of Physiology and Biophysics, University of Mississippi Medical Center, MS, USA

[2]Department of Physiology and Biophysics and Department of Medicine, University of Mississippi Medical Center, MS, USA

INTRODUCTION

Hypertension is the leading risk factor for cardiovascular deaths, causing approximately 7.6 million premature deaths per year worldwide.[1] Over 1 billion people including more than 50 million Americans have hypertension, making it the most common chronic disease.[1,2] Blood pressure (BP) typically rises with age and in the United States, approximately 50% of people 60–69 years old and 75% of people 70 years and older have hypertension.[1] In non-industrialized populations, however, BP does not rise with aging and only a small fraction of the population develops hypertension. This suggests that environmental factors play a major role in causing hypertension, and that a rise in BP with aging is not inevitable when these conditions are absent.

A direct positive relationship between BP and cardiovascular disease CVD risk has been observed in men and women of all ages, races, ethnic groups, and countries, regardless of other risk factors for CVD.[2] Observational studies indicate that death from CVD increases progressively as BP rises above 115 mmHg systolic and 75 mmHg diastolic pressure.[2] For every 20 mmHg systolic or 10 mmHg diastolic increase in BP there is a doubling of mortality from ischemic heart disease and stroke in all age groups from 40 to 89 years old.[3]

Despite major advances in our understanding of its pathophysiology, and the availability of many drugs that can effectively reduce BP in most hypertensive subjects, hypertension is still poorly-controlled in most countries, including the United States, and continues to be the most important modifiable risk factor for CVD.

BLOOD PRESSURE CLASSIFICATION FOR HYPERTENSION TREATMENT

BP is a variable, quantitative trait with a normal distribution slightly skewed toward higher BPs. Although there is no clear level of BP where cardiovascular or renal disease begins to occur, a definition of hypertension is useful for treatment decisions. A commonly used BP classification was proposed in 2003 by the Seventh Report of the United States Joint National Committee on Prevention, Detection, Evaluation, and Treatment of High BP JNC 7 and is now widely used.[4]

According to these criteria, normal BP is defined as a systolic BP <120 mmHg and a diastolic BP <80 mmHg. Persons with a systolic BP between 120–139 mmHg or diastolic BP between 80–89 mmHg are designated as having *prehypertension*. Hypertension is further characterized by two stages: Stage 1, the milder (systolic 140–159 mmHg and/or diastolic 90–99 mmHg) and most common form of hypertension, accounts for approximately 80% of hypertension. Stage 2 hypertension includes those with systolic BP ≥160 mmHg and/or diastolic BP ≥100 mmHg. Isolated systolic hypertension is defined as systolic BP of ≥140 mmHg and diastolic BP <90 mmHg.

Using these definitions, and including those taking antihypertensive medications, approximately 24% of the adult population in the United States has hypertension.[4] This percentage varies with: 1) race, being higher in blacks 32% and lower in whites 23% and Mexican Americans 23%; 2) age, because systolic BP rises throughout life in the United States, as well as in most

Seldin and Giebisch's The Kidney, Fifth Edition.
DOI: http://dx.doi.org/10.1016/B978-0-12-381462-3.00039-2

© 2013 Elsevier Inc. All rights reserved.

industrialized countries, whereas diastolic BP rises until age 55–60 years; 3) gender, with hypertension being more prevalent in men than in premenopausal women, after menopause women have BPs that are nearly the same as in men; 4) geographic patterns, with hypertension being more prevalent in the Southeastern United States; and 5) socioeconomic status, which is inversely related to the prevalence of hypertension.

Primary hypertension accounts for about 95% of all cases of hypertension, and is usually defined as elevated BP for which an obvious secondary cause (e.g., renovascular disease, aldosteronism, pheochromocytoma or gene mutations) cannot be determined. Although primary hypertension is a heterogeneous disorder, some of the main risk factors are known. For example, overweight and obesity may account for as much as 65–75% of the risk for primary hypertension. Other factors, such as sedentary lifestyle, excess consumption of alcohol or sodium chloride, and low potassium intake are also thought to contribute to increased BP in many patients.[5] This review discusses basic concepts of BP control and pathophysiological changes that may cause primary hypertension, as well as selected forms of genetic and secondary hypertension.[5,6]

BASIC PHYSIOLOGY OF BLOOD PRESSURE REGULATION

BP regulation depends on integrated actions of multiple cardiovascular, renal, neural, endocrine, and local tissue control systems. Although hypertension is usually considered as a disorder of the average level at which BP is regulated, there is increasing interest in other measures of BP, including peak arterial pressure, BP variability, nighttime and daytime BP, and responses of BP to stress, which may affect cardiovascular risk.

The complex local control, hormonal, neural, and renal systems that regulate BP are often discussed in terms of how they influence cardiac function or vascular resistance because of the well-known formula: *mean arterial pressure = cardiac output × total peripheral resistance*. This conceptual framework, with the addition of factors that influence vascular capacity and transcapillary fluid exchange, is adequate to explain short-term BP regulation, but not chronic hypertension.[5,7] Two additional concepts are useful when considering chronic BP regulation: 1) BP control mechanisms are time-dependent; and 2) renal excretion of water and electrolytes play a key role in long-term BP regulation.

Blood Pressure Control Systems are Time-Dependent

Figure 39.1 shows the maximum feedback gains of major BP controllers following a sudden disturbance,

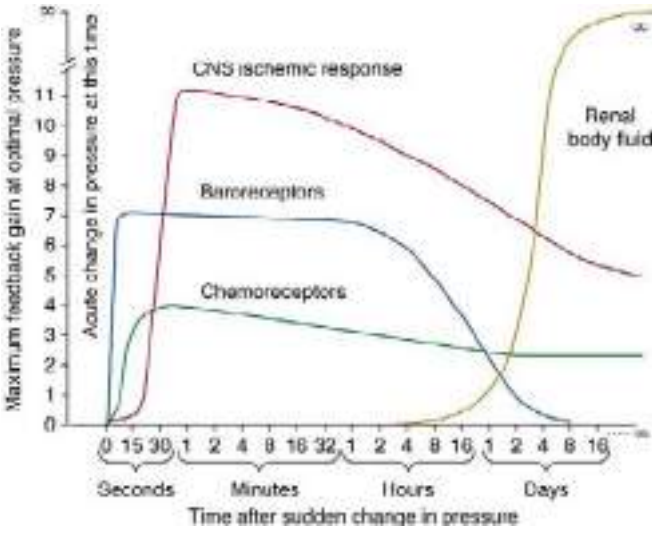
Maximum feedback gain at optimal pressure
Acute change in pressure at this time
CNS ischemic response
Renal body fluid
Baroreceptors
Chemoreceptors
0 15 30 1 2 4 8 16 32 1 2 4 8 16 1 2 4 8 16
Seconds
Minutes
Hours
Days
Time after sudden change in pressure

FIGURE 39.1 **Time-dependency of blood pressure control mechanisms.** Approximate maximum feedback gains of various blood pressure control mechanisms at different time intervals after the onset of a disturbance to arterial pressure.

as might occur with rapid blood loss. Three important neural control systems begin to function powerfully within a few seconds: 1) the arterial baroreceptors, which detect changes in BP and send appropriate autonomic reflex signals back to the heart and blood vessels to return the BP toward normal; 2) the chemoreceptors, which detect changes in oxygen or carbon dioxide in the blood and initiate autonomic feedback responses that influence BP; and 3) the central nervous system, which responds within a few seconds to ischemia of the vasomotor centers in the medulla, especially when BP falls below about 50 mmHg. Each of these nervous control mechanisms works rapidly and has potent effects on BP. Also note, however, that the feedback gains of these systems decrease with time, as disturbances of BP are maintained.

Within a few minutes or hours after a BP disturbance, additional control systems react, including: 1) a shift of fluid from the interstitial spaces into the blood in response to decreased BP or a shift of fluid out of the blood into the interstitial spaces in response to increased BP; 2) the renin–angiotensin–aldosterone system RAAS which is activated when BP falls too low and is suppressed when BP increases above normal; 3) multiple vasodilator systems not shown in the figure that are suppressed when BP decreases and stimulated when BP rises above normal.

Most of the BP regulators are *proportional* control systems. This means that they can correct a BP abnormality only part of the way back toward the normal level, but never all the way back. The arterial baroreceptor reflex system, for example, has a feedback gain of approximately 2.0 during acute changes in BP, and

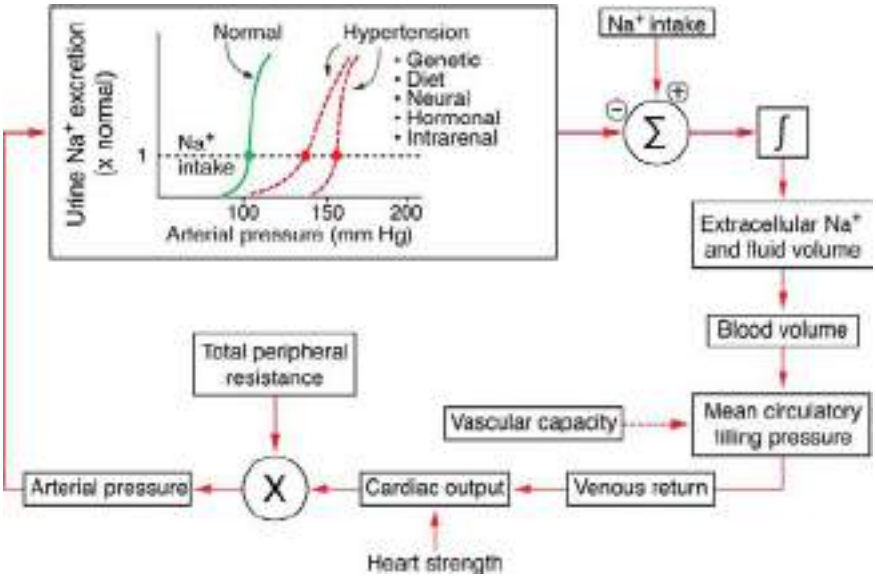

FIGURE 39.2 **Block diagram showing the basic elements of the renal–body fluid feedback mechanism for long-term regulation of arterial pressure.**

therefore buffers about two-thirds of a sudden change in the BP. The renal–body fluid feedback system, however, is the one BP control system with *near infinite feedback gain* if it is given enough time to operate.[7]

The Renal–Body Fluid Feedback Mechanism for Long-Term BP Regulation

Figure 39.2 shows the basic components of the renal–body fluid feedback mechanism. Extracellular fluid volume is determined by the balance between intake and excretion of salt and water by the kidneys. Even a temporary imbalance between intake and output can lead to a change in extracellular volume, and potentially a change in BP. Under steady-state conditions there must be a precise balance between intake and output of salt and water; otherwise, there would be continued accumulation or loss of fluid leading to circulatory collapse within a few days. A key component of this mechanism for regulating salt and water balance is *pressure natriuresis*—the effects of increased BP to raise sodium excretion.[5] Under many conditions this mechanism stabilizes BP. For example, when BP is increased above the renal set-point, because of increased TPR or increased cardiac pumping ability, this also tends to increase sodium excretion, via pressure natriuresis, if the effectiveness of pressure natriuresis is not impaired (Figure 39.3). As long as fluid excretion exceeds intake, extracellular fluid volume will continue to decrease, reducing venous return and cardiac output, until BP returns to normal and fluid balance is re-established.

An important feature of pressure natriuresis is that it continues to operate until BP returns to the original set-point. Another key aspect of pressure natriuresis is that various neurohumoral systems can amplify or blunt the pressure natriuresis mechanism.[5] For example, increases in sodium intake are associated with only small changes in BP in many people. One reason for this insensitivity of BP to changes in salt intake is decreased formation of antinatriuretic hormones such as angiotensin II and aldosterone, which enhance the effectiveness of pressure natriuresis and allow sodium balance to be maintained with minimal increases in BP. On the other hand, excessive activation of these antinatriuretic systems reduces the effectiveness of pressure natriuresis, necessitating greater increases in BP to maintain sodium balance.

In all forms of human or experimental hypertension studied thus far, there is a shift of pressure natriuresis toward higher BPs. In some cases, impaired pressure natriuresis is caused by *intrarenal* disturbances that reduce glomerular filtration rate GFR or increase tubular reabsorption. In other instances, impaired pressure natriuresis is caused by *extrarenal* factors, such as increased activity of the SNS or antinatriuretic hormones that reduce the kidney's ability to excrete sodium and eventually raise BP.

Vasoconstrictors May Decrease Extracellular Volume Despite Impairing Renal-Pressure Natriuresis

Some forms of hypertension, especially those associated with increased levels of vasoconstrictors such as norepinephrine, are associated with reduced rather than increased extracellular fluid volume. How can the hypertension in these instances be attributed to impaired renal pressure natriuresis when there is no evidence of sodium retention? Consider the physiological changes caused by infusion of a powerful

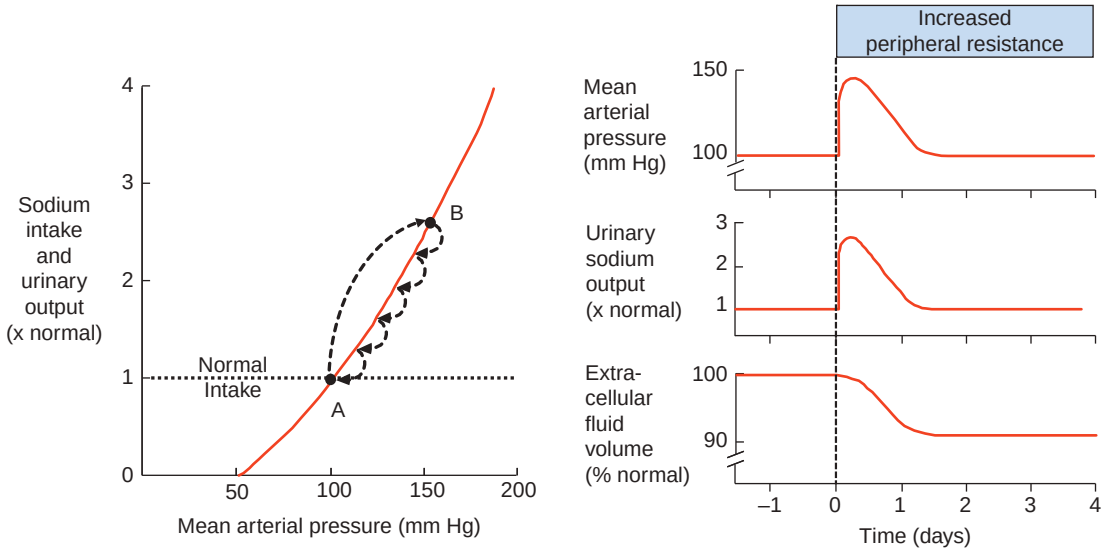

FIGURE 39.3 **Long-term effects of increased total peripheral resistance (TPR), such as that caused by closure of a large arteriovenous fistula, with no change in the renal pressure natriuresis relationship**. BP is initially increased from point A to point B, but elevated BP cannot be sustained because sodium excretion exceeds intake, reducing extracellular fluid volume until BP returns to normal and sodium balance is re-established.[10]

vasoconstrictor such as norepinephrine. Chronic iv infusion of norepinephrine causes mild hypertension associated with an initial increase in sodium excretion as BP rises.[8] After several days, sodium excretion returns to normal but extracellular fluid volume is reduced. On the other hand, if norepinephrine is infused directly into the renal artery at a low dose so that its effect on other vascular beds is minimal or if renal perfusion pressure is servo-controlled and prevented from increasing during iv norepinephrine infusion there is significant sodium retention, demonstrating a direct antinatriuretic effect on the kidneys, as well as development of hypertension.[5,8]

Figure 39.4 shows the relationship between BP and sodium excretion caused by a powerful vasoconstrictor, such as norepinephrine, which has a relatively weak antinatriuretic action. The antinatriuretic effect shifts pressure natriuresis to higher BPs, but because norepinephrine has a weak antinatriuretic effect, compared to its peripheral vasoconstrictor effect, BP initially increases above the renal set-point for sodium balance and causes transient natriuresis. After a few days, extracellular fluid volume decreases and BP stabilizes at a point where sodium intake and output are balanced. The sodium retaining actions are obscured by peripheral vasoconstriction which raises BP above the renal set-point at which sodium balance is maintained, causing increased renal excretion and decreased extracellular fluid volume. However, the maintenance of high BP chronically depends on the changes in renal function that shift pressure natriuresis to higher BPs.

RENAL MECHANISMS OF HYPERTENSION

Commonly used measurements of kidney function, such as GFR, renal blood flow, serum creatinine, and sodium excretion, are often within the normal range in hypertensive patients, at least prior to renal damage due to prolonged high BP. On the other hand, increased TPR is found in many hypertensive patients, leading to emphasis on peripheral vasoconstriction as a cause of increased BP. However, increased TPR may be an autoregulatory response to increased BP, and may not cause sustained hypertension in the absence of impaired pressure natriuresis.

Almost all forms of experimental hypertension and all monogenic forms of human hypertension discovered thus far are caused by insults to the kidneys that alter renal hemodynamics or tubular reabsorption. For example, constriction of the renal arteries e.g., Goldblatt hypertension, compression of the kidneys e.g., perinephritic hypertension or administration of sodium-retaining hormones (e.g., mineralocorticoids or angiotensin II) are all associated with either initial reductions in renal blood flow and GFR or increases in renal tubular reabsorption prior to development of hypertension. Likewise, in all known monogenic forms of human hypertension there is impaired renal excretory function caused by mutations that increase renal sodium reabsorption or activity of antinatriuretic hormones. As BP rises, the initial changes are obscured by compensations that restore kidney function toward

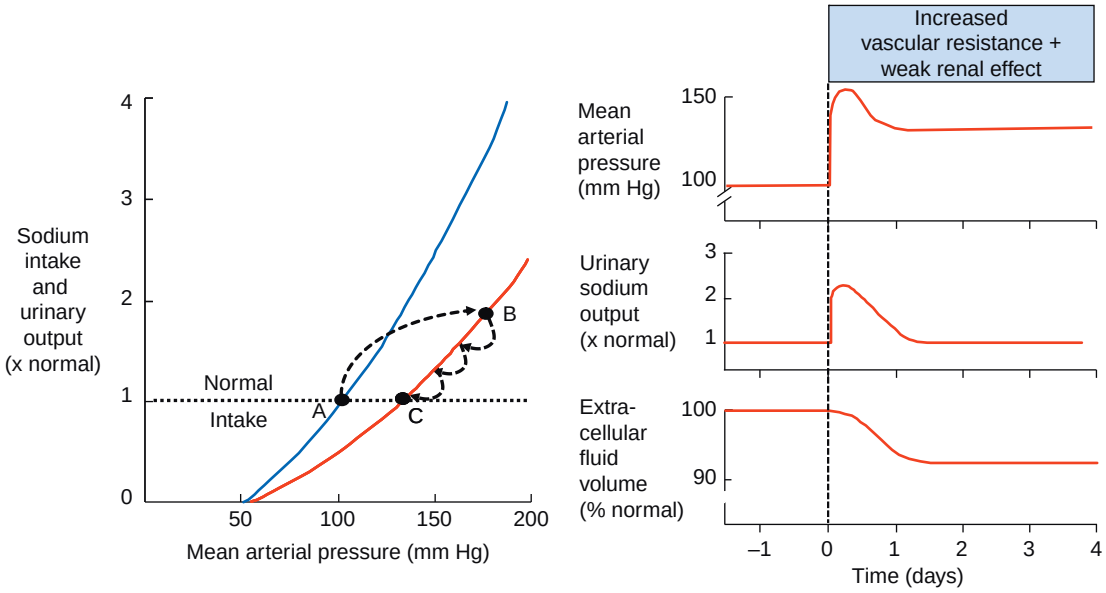

FIGURE 39.4 **Long-term effects of norepinephrine, a vasoconstrictor that has a relatively weak effect to impair pressure natriuresis**. The normal curve (blue) is compared with the vasoconstrictor curve (red line). Initially the vasoconstrictor raises BP (from point A to point B) above the renal set point for sodium balance. Increased BP, however, causes a transient natriuresis and decreases extracellular fluid volume until BP eventually stabilizes at a level (point C) at which sodium intake and output are balanced at a reduced extracellular fluid volume.[10]

normal. The rise in BP then initiates a cascade of cardiovascular changes, including increased TPR that may be more striking than the initial kidney disturbance. For this reason, the importance of renal dysfunction in causing hypertension has often been underestimated.

Although specific abnormalities of kidney function are difficult to identify in most patients with primary hypertension, one aspect of kidney function that is invariably abnormal is renal pressure natriuresis.[9,10] Maintenance of a normal sodium excretion equal to sodium intake despite elevated BP, which would normally cause natriuresis and diuresis, indicates that pressure natriuresis is reset in hypertensive subjects.

Some types of renal abnormalities that cause chronic hypertension include: 1) increased preglomerular resistance; 2) decreased glomerular capillary filtration coefficient; 3) reduced numbers of functional nephrons; and 4) increased tubular reabsorption (Figure 39.5). As discussed below, some of these abnormalities cause blood pressure to be more sensitive to changes in dietary salt intake (salt-sensitive), whereas other renal abnormalities may cause hypertension that is relatively insensitive to changes in salt intake (salt-insensitive).

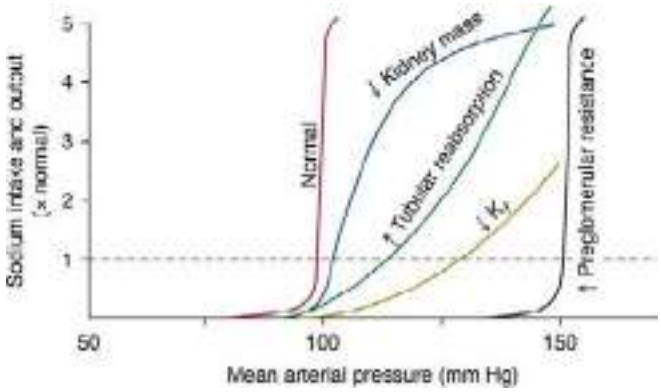

FIGURE 39.5 **Steady-state relationships between BP, sodium excretion, and sodium intake for subjects with normal kidneys and four general types of renal dysfunction that cause hypertension: decreased kidney mass; increased reabsorption in distal and collecting tubules; reductions in glomerular capillary filtration coefficient (K_f); and increased preglomerular resistance**. Note that increased preglomerular resistance causes *salt-insensitive* hypertension, whereas the other renal abnormalities cause *salt-sensitive* hypertension.

Generalized Increases in Preglomerular Resistance Cause Salt-Insensitive Hypertension

Examples of a generalized increase in preglomerular resistance are those caused by suprarenal aortic coarctation or constriction of one renal artery and removal of the contralateral kidney (e.g., 1-kidney, 1-clip Goldblatt hypertension). After renal artery constriction or aortic coarctation, renal blood flow, GFR, and sodium excretion are initially reduced, and there is a rapid rise in renin secretion. Renal blood flow and GFR may return to near normal if autoregulatory mechanisms are not impaired, and if constriction is not so severe that it reduces renal perfusion pressure

below the autoregulatory range ~65–70 mmHg. Even if GFR is not fully autoregulated, sodium excretion returns to normal and sodium balance is re-established within a few days. If sodium and fluid intakes are normal, renin secretion also returns to normal in the established phase of hypertension. At this point, most indices of renal function are nearly normal, including BP distal to the stenosis if the constriction is not too severe.[11]

Homogeneous increases in preglomerular resistance typically cause salt-insensitive rather than salt-sensitive hypertension. One of the main reasons that increased salt intake does not greatly exacerbate this form of hypertension is that after BP increases sufficiently to restore renal perfusion pressure and renin secretion to nearly normal, the RAAS is fully capable of appropriate suppression during high salt intake. As discussed later, the ability to effectively modulate RAAS activity is critical for preventing salt-sensitivity of BP.

Functional or pathologic increases in preglomerular resistance at other sites besides the main renal arteries, such as the interlobular arteries or afferent arterioles, could also increase BP through the same mechanisms activated by clipping the renal artery. For example, structural increases in afferent arteriolar resistance (e.g., nephrosclerosis or functional increases in resistance caused by excessive activation of the SNS) could also cause hypertension through the same mechanisms as constriction of the main renal artery. Some patients with primary hypertension have essentially the same characteristics seen in 1-kidney, 1-clip Goldblatt hypertension, including nearly normal GFR and plasma renin activity, a parallel shift of pressure natriuresis to higher BP, and a relatively salt-insensitive form of hypertension.[5,11] Also, drug therapies that decrease preglomerular resistance, such as calcium channel blockers, cause a parallel shift of pressure natriuresis toward lower BP.[6] Thus, primary hypertension in some patients may be caused by functional or pathologic increases in preglomerular resistance. This is almost certainly the case in patients who have severe atherosclerotic lesions in the renal blood vessels.

Non-Homeogeneous Increases in Preglomerular Resistance Cause Salt-Sensitive Hypertension

In 2-kidney, 1-clip Goldblatt hypertension or in patients with a stenosis in only one renal artery, there is a non-homogeneous increase in preglomerular resistance, with ischemia occurring in nephrons of the clipped/stenotic kidney, while nephrons in the contralateral nonstenotic kidney have normal or increased single-nephron blood flow and GFR. The underperfused clipped kidney secretes large amounts of renin, whereas the untouched kidney secretes little renin.[6,12]

In the 2-kidney, 1-clip model, the glomeruli of the untouched kidney are subject to the full effects of increased BP. With prolonged hypertension, pathologic changes in the untouched kidney may further impair renal function. At this stage, removal of the clipped kidney only partially normalizes BP. However, removal of the contralateral untouched kidney and unclipping the stenotic kidney usually normalizes BP if the underperfusion of the clipped kidney is not too severe and ischemic injury has not occurred. Thus, chronic exposure to high BP in the untouched kidney may cause pathological changes that increase the severity of hypertension.

Non-homogeneous increases in preglomerular resistance may also cause salt-sensitivity of BP. The main reason is that the underperfused nephrons secrete large amounts of renin, whereas the remaining nephrons are overperfused and have reduced renin secretion.[5,6] In both cases, the nephrons have impaired ability to adequately suppress renin secretion during high salt intake, and BP becomes more salt-sensitive.

Some patients with essential hypertension may have non-homogenous nephrosclerosis within each kidney, providing another clinical counterpart to the 2-kidney, 1-clip Goldblatt model of hypertension. In these instances, the combined effects of hypertension and hyperfiltration in non-ischemic nephrons may eventually damage the nephrons that were not initially ischemic, leading to progressive nephron loss.

Reduced Glomerular Capillary Filtration Coefficient

Decreased glomerular capillary filtration coefficient K_f initially lowers GFR and sodium excretion, while stimulating renin release and causing vasodilation of afferent arterioles via macula densa feedback.[5,6] The sodium retention and increased angiotensin II formation raise BP, which helps to normalize GFR and renin release. After these compensations, the main persistent abnormalities of kidney function are reduced filtration fraction, increased glomerular hydrostatic pressure, and increased renal blood flow. Unfortunately, compensatory increases in BP and glomerular hydrostatic pressure, which offset a fall in K_f and restore sodium excretion to normal, may also cause further glomerular injury, loss of glomeruli, further reductions in K_f, and additional increases in BP.

The clinical counterparts of this sequence may be found in hypertension caused by glomerulonephritis or by other conditions that cause thickening and damage to the glomerular capillary membranes, such as chronic diabetes mellitus.

Nephron Loss Increases Salt-Sensitivity

Surgical removal of large amounts of the kidney, to the point that uremia occurs, rarely cause much hypertension as long as sodium intake is normal.[6,9,13] In this case, GFR and tubular reabsorption capability are proportionally reduced so that balance between filtration and reabsorption are maintained without major changes in BP. Reducing the number of nephrons, however, makes the kidneys susceptible to additional challenges of sodium homeostasis. For example, hypertension associated with excess mineralocorticoids is more severe after reducing kidney mass. Likewise, high sodium intake is accompanied by larger BP increases when kidney mass is reduced.[6]

Nephron loss also initiates compensatory changes that may damage the surviving nephrons. For example, renal vasodilation and increased single nephron GFR, over long periods of time, may lead to glomerulosclerosis and reductions in K_f. These pathologic changes, in addition to loss of functional nephrons, may further impair pressure natriuresis and cause hypertension. Thus, even though hypertension may not begin with nephron loss, chronic elevations in glomerular pressure and other metabolic abnormalities often associated with hypertension may cause progressive nephron loss that amplifies the hypertension and makes BP salt-sensitive.

Partial renal infarction causes high renin hypertension. In contrast to the effects of surgical removal of kidney mass, loss of nephrons because of ischemia or infarction of renal tissue usually causes marked hypertension, even with normal salt intake. The so-called *5/6 ablation* model is produced by removing one kidney and obstructing two of the three branches of the renal artery of the remaining kidney. In this model, hypertension develops even without high salt intake because of ischemia of the surviving nephrons, activation of the RAAS, and immune-mediated renal injury.[14] This hypertension model has non-homogeneous areas of renal ischemia with characteristics similar to that described for the 2-kidney, 1-clip Goldblatt model. The clinical counterpart of this model occurs with partial renal infarction caused by septic emboli, thrombus, trauma or sometimes after corrective surgery for renal artery stenosis.

Increased Renal Tubular Sodium Reabsorption

Hypertension caused by increased *distal* or *collecting tubular reabsorption* is exacerbated by increased salt intake. Increased reabsorption at sites beyond the macula densa elicits increased sodium chloride delivery to the macula densa which, in turn, suppresses renin secretion,[5,10] sometimes to very low levels, which prevents further suppression of angiotensin II formation during high sodium intake, making BP salt-sensitive.

An increase in *proximal* or *loop of Henle* tubular reabsorption, however, may result in a salt-insensitive hypertension. Increased proximal tubular reabsorption tends to increase renin secretion, and elicits a compensatory renal vasodilation that raises GFR and renal plasma flow in response to reduced macula densa NaCl delivery. However, as hypertension develops, macula densa NaCl delivery and renin secretion return to nearly normal, and the RAAS may be fully capable of responding to increased salt intake. Therefore, high salt intake may be accompanied by appropriate suppression of angiotensin II formation, which permits sodium balance to be maintained with only small increases in BP.[10] Nevertheless, pressure natriuresis is shifted to higher BP.

A feature of hypertension caused by increased tubular reabsorption is that it may initially be associated with extracellular volume-expansion. However, volume-expansion and increased cardiac output usually subside because of pressure natriuresis, and TPR increases secondarily to increased BP. When increased tubular reabsorption is also associated with marked peripheral vasoconstriction, such as occurs with very high levels of angiotensin II, the degree of volume-expansion depends on the relative effects of the vasoconstrictor on peripheral and renal blood vessels.[5] With severe peripheral vasoconstriction and decreased vascular capacitance, relatively small amounts of volume retention can lead to substantial hypertension.

Significance of Salt-Sensitive Hypertension

Many factors are associated with salt-sensitivity of BP. Older individuals are usually more salt-sensitive than young people, and African Americans are often more salt-sensitive than whites. However, there are exceptions to these generalizations and considerable heterogeneity exists in the BP responses to increased salt intake.

Genetic factors independent of ethnicity have been linked to salt-sensitivity of BP, especially monogenic disorders that increase distal and collecting tubule sodium reabsorption or that increase secretion of sodium-retaining hormones.[15] Also, diabetes mellitus, renal diseases that cause nephron loss, and abnormalities of the RAAS are associated with increased salt-sensitivity of BP.[5] Many of these examples share two common pathways to salt-sensitivity: 1) loss of functional nephrons as discussed previously or 2) reduced responsiveness of the RAAS.

Figure 39.6 shows the importance of changes in angiotensin II formation in maintaining BP relatively constant during wide variations in salt intake. In dogs with a fully-functional RAAS, only small increases in

BP were associated with a 100-fold increase in sodium intake.[16,17] However, when angiotensin II was prevented from being suppressed as sodium intake was raised, BP became salt-sensitive. After blockade of angiotensin II formation, BP was also salt-sensitive, although maintained at lower levels.[17] Thus, a major function of the RAAS is to permit wide variations in sodium intake and excretion without large fluctuations in BP.

As discussed previously, focal nephrosclerosis or patchy preglomerular vasoconstriction, as occurs with renal infarction, leads to increased renin secretion in ischemic nephrons and very low levels of renin release by overperfused nephrons.[6] Thus, in ischemic and overperfused nephrons, the ability to suppress renin secretion during high salt intake is impaired. Another cause of reduced responsiveness of the RAAS is increased distal and collecting tubular sodium reabsorption, as occurs with mineralocorticoid excess or mutations that increase distal and collecting tubule reabsorption (e.g., Liddle syndrome). In these conditions, excess sodium retention causes almost complete suppression of renin secretion, resulting in an inability to further decrease renin release during high sodium intake. Consequently, BP becomes very salt-sensitive.

Salt-Sensitive Subjects May Have Greater Target Organ Injury

Some studies suggest that salt-sensitivity predicts hypertensive target organ injury. Salt-sensitive hypertension may be associated with glomerular hyperfiltration and increased glomerular hydrostatic pressure that is further amplified by the hypertension[5]; together the hypertension and renal hyperfiltration may promote glomerular injury and cause loss of nephron function. Clinical studies support this concept, and demonstrate that salt-sensitive individuals typically have increased glomerular pressure and albumin excretion when given a salt-load, whereas salt-resistant individuals have lower glomerular pressure and less urinary albumin excretion.[18]

There is also evidence that salt-sensitive subjects may die earlier than individuals who are salt-resistant. Weinberger et al. studied individuals for more than 20 years and found that normotensive individuals with increased salt-sensitivity died almost at the same rate as hypertensive individuals, and much faster than salt-resistant individuals who were normotensive.[19] Whether this increased mortality was related to BP effects of salt or to other effects is still unclear. It is also not known whether long-term high salt intake may cause a person who is initially salt-insensitive to become salt-sensitive as a consequence of gradual renal injury.

NEURAL AND HORMONAL MECHANISMS OF HYPERTENSION

The following sections discuss the multiple neural, hormonal, and autacoid mechanisms that alter renal pressure natriuresis, and their potential roles in hypertension.

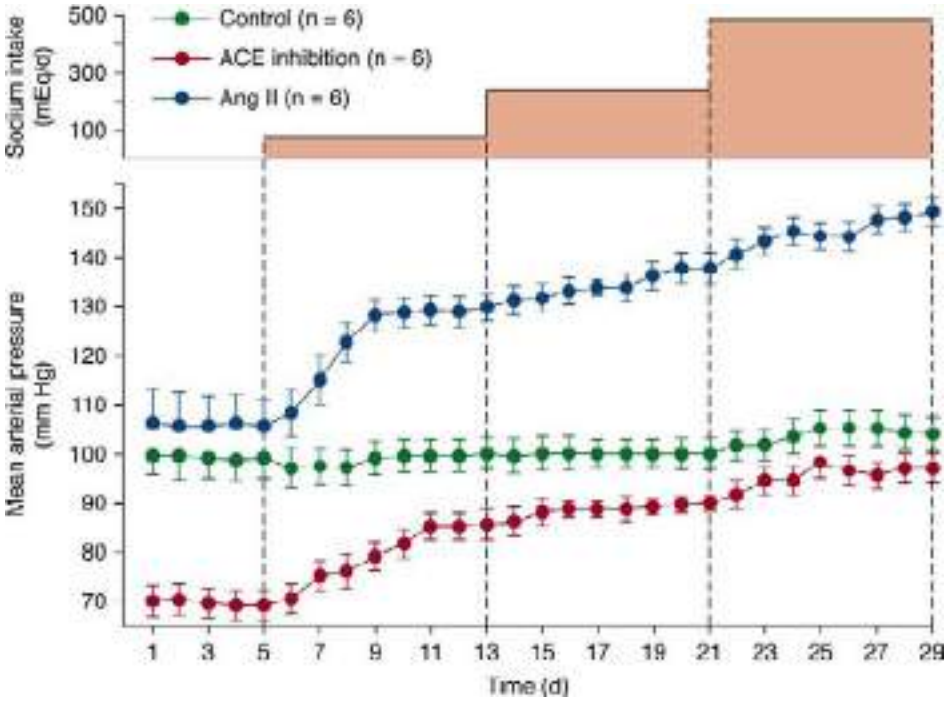

FIGURE 39.6 **Changes in mean arterial pressure during chronic changes in sodium intake in normal control dogs, after ACE inhibition, or after angiotensin II infusion (5 ng/kg/min) to prevent angiotensin II from being suppressed when sodium intake was raised ref. [17].**

The Sympathetic Nervous System SNS

Activation of the SNS can raise BP within a few seconds by causing vasoconstriction, increased cardiac pumping capability, and increased heart rate. Conversely, sudden inhibition of SNS activity can decrease BP to as low as half normal in less than a minute. Therefore, changes in SNS activity, caused by various reflex mechanisms, central nervous system ischemia or by activation of higher centers in the brain, provide powerful and rapid moment-to-moment regulation of BP.

The SNS also plays an important role in long-term regulation of BP and in the pathogenesis of hypertension by activation of the renal sympathetic nerves.[20] There is extensive innervation of the renal blood vessels, the juxtaglomerular apparatus, and the renal tubules, and overactivation of these nerves causes sodium retention, increased renin secretion, and impaired renal pressure natriuresis.[20] Even mild increases of the renal sympathetic nerve activity (RSNA) stimulate renin secretion and sodium reabsorption in multiple segments of the nephron, including the proximal tubule, the loop of Henle, and more distal segments.[20] Thus, the renal nerves provide a mechanism by which the various autonomic reflexes and central nervous system (CNS) centers contribute to long-term BP regulation.

Multiple studies have shown that renal denervation reduces BP in some experimental models of hypertension.[20] For example, renal denervation attenuates hypertension in (SHR)[20] as well as in obese hypertensive dogs.[21] Renal denervation also delays or attenuates increased BP in other forms of experimental hypertension, although some studies have not found an important role for the renal nerves in various forms of secondary hypertension.[5]

Human primary hypertension, especially when associated with obesity, is often associated with increased RSNA.[22] Bilateral renal denervation in humans, using a percutaneous, catheter-based radiofrequency method to selectively ablate the nerves that run along the renal arteries, reduced BP in patients who were resistant to the usual antihypertensive drugs.[23,24] Moreover, reductions in BP were sustained for up to two years of follow-up, suggesting the absence of substantial nerve fiber regrowth. However, longer follow-up periods will be needed to determine if the renal nerves eventually regrow and reinitiate increased BP, as observed in experimental animal models of renal denervation.

Although the mechanisms that activate renal sympathetic nerves in primary hypertension or in most experimental models are still unclear, we will briefly discuss two that have attracted the interest of many researchers.

Resetting of Baroreceptor Reflexes in Hypertension

The importance of the arterial baroreceptors in buffering moment-to-moment changes in BP is clearly evident in baroreceptor-denervated animals in which there is extreme BP variability associated with normal daily activities.[25] After baroreceptor denervation, BP increases to very high levels or falls to low levels with normal daily activities, although the average 24-hour BP is not markedly altered. However, some studies suggest that the baroreceptors are relatively unimportant in chronic regulation of BP, because they tend to reset within a few days after a change in BP.[25] To the extent that resetting of baroreceptors occurs, this would attenuate their potency in long-term control of BP.

Other experimental studies suggest that the baroreceptors do not completely reset and may contribute to chronic BP regulation. With prolonged increases in BP, the baroreflexes may contribute to *reductions* in renal sympathetic activity, and promote sodium and water excretion.[26] This, in turn, may attenuate the rise in BP. Thus, impairment of baroreflexes may cause increased lability of BP in hypertension, and fail to attenuate the rise in BP caused by other disturbances.

Currently, there is little evidence that primary disturbances of baroreceptor function play a major role in *causing* chronic hypertension. However, experimental studies in dogs indicate that chronic electrical stimulation of carotid sinus baroreceptors reduces BP in some forms of experimental hypertension.[26] In humans with hypertension resistant to drug treatment, electrical stimulation of baroreceptors also reduced BP.[26] These observations are consistent with the hypothesis that strong activation of baroreceptors can have long-term influences on BP. However, this finding does not necessarily imply that impaired baroreflexes actually *cause* chronic hypertension. The primary role of arterial baroreceptors in hypertension, as in normotension, appears to be buffering of rapid deviations in BP from the set-point determined by renal pressure natriuresis.

Obesity Causes Chronic SNS Activation

Excess weight gain appears to be a major cause of human primary hypertension, and one key mechanism that links obesity with increased BP is SNS activation.[10] Obese persons have elevated SNS activity in various tissues, including the kidneys.[10,22] Studies in experimental animals and humans indicate that combined α-and β-adrenergic blockade markedly attenuates obesity-associated hypertension.[10] Moreover, renal sympathetic efferent nerves mediate much of the chronic effects of SNS activation on BP in obesity, as bilateral renal denervation greatly attenuates sodium retention and hypertension in obese dogs.[10] Thus, obesity

increases renal sodium reabsorption, impairs pressure natriuresis, and causes hypertension in part by increasing RSNA. The mechanisms for SNS activation in obesity have not been fully-elucidated, as discussed in more detail later in this chapter.

The Renin–Angiotensin–Aldosterone System (RAAS)

The RAAS is perhaps the body's most powerful hormone system for regulating BP, as evidenced by the effectiveness of various RAAS blockers in treating hypertension. Although the RAAS has many components, its most important effects on BP are exerted by angiotensin II, a powerful vasoconstrictor that maintains BP in conditions associated with blood volume depletion, sodium depletion or circulatory depression e.g., heart failure. The long-term effects of angiotensin II on BP, however, are closely intertwined with volume homeostasis through direct and indirect effects on the kidneys.

Blockade of the RAAS, with angiotensin II receptor blockers ARBs, angiotensin converting enzyme ACE inhibitors or mineralocorticoid receptor MR antagonists, increases renal excretory capability so that sodium balance is maintained at reduced BP.[5,6] However, blockade of the RAAS also makes BP salt-sensitive.[16] Thus, effectiveness of RAAS blockers in lowering BP is greatly diminished by high salt intake; conversely, reducing sodium intake or addition of a diuretic improves effectiveness of RAAS blockers in reducing BP.

Inappropriately high levels of angiotensin II reduce renal excretory capability and impair pressure natriuresis, thereby necessitating increased BP to maintain sodium balance. The mechanisms that mediate the potent antinatriuretic effects of angiotensin II include direct and indirect effects to increase tubular reabsorption, as well as renal hemodynamic effects.[16]

Angiotensin II Stimulates Renal Sodium Reabsorption

Angiotensin II increases renal sodium reabsorption through stimulation of aldosterone secretion, by direct effects on epithelial transport, and by hemodynamic effects. Angiotensin II-mediated constriction of efferent arterioles reduces renal blood flow and peritubular capillary hydrostatic pressure, and increases peritubular colloid osmotic pressure as a result of increased filtration fraction.[16] These changes, in turn, increase the driving force for fluid reabsorption across tubular epithelial cells. Reductions in renal medullary blood flow caused by efferent arteriolar constriction or by direct effects of angiotensin II on the vasa recta may also enhance reabsorption in the loop of Henle and collecting ducts.[16]

Angiotensin II also directly stimulates tubular sodium reabsorption. This effect occurs at low angiotensin II concentrations, and is mediated by actions on the luminal and basolateral membranes.[16,27] In proximal tubules, angiotensin II stimulates the Na^+–H^+ exchanger on luminal membranes and increases sodium–potassium ATPase activity, as well as sodium bicarbonate co-transport on basolateral membranes[13,27] (Figure 39.7). These effects are partly mediated by inhibition of adenyl cyclase and increased phospholipase C activity.

Angiotensin II also stimulates sodium reabsorption in the loop of Henle, macula densa, and distal nephron segments. At physiologic concentrations, angiotensin II increases loop of Henle bicarbonate reabsorption and stimulates Na^+–K^+–2Cl transport in the medullary thick ascending loop of Henle.[5,16] In the distal parts of the nephron, angiotensin II stimulates multiple ion transporters, including H^+-ATPase activity, as well as epithelial sodium channel activity in the cortical collecting ducts.[5,16]

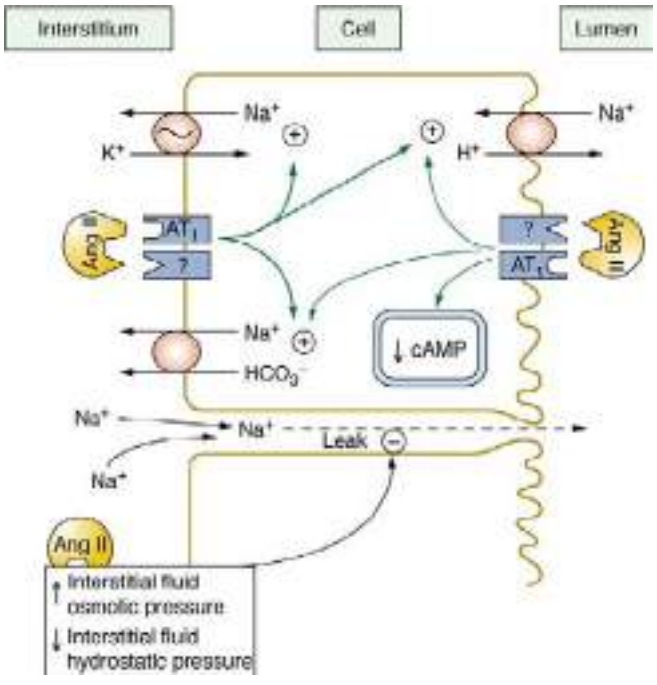

FIGURE 39.7 **Angiotensin II increases proximal tubular reabsorption by binding to receptors on the luminal and basolateral membranes and stimulating Na^+/H^+ antiporter, Na^+/HCO_3 co-transport, and Na^+/K^+ adenosine triphosphatase (ATPase) activity**. Angiotensin II also increases reabsorption by increasing interstitial fluid colloid osmotic pressure and decreasing interstitial fluid hydrostatic pressure.

Renal hemodynamic Effects of Angiotensin II

Angiotensin II is a powerful renal vasoconstrictor, but in most physiological conditions the constriction is confined mainly to postglomerular efferent arterioles. For example, efferent arteriolar constriction by angiotensin II acts in concert with other autoregulatory mechanisms, such as tubuloglomerular feedback (TGF) and myogenic activity, to prevent excessive reductions in GFR when kidney perfusion is threatened.[16] In these cases, administration of ARBs or ACE inhibitors may reduce GFR further, even though renal blood flow is preserved. Impairment of GFR after RAS blockade is caused, in part, by inhibition of the constrictor effects of angiotensin II on efferent arterioles, as well as reduced BP.[16]

The relatively weak constrictor action of angiotensin II on preglomerular vessels is due partly to protection of these vessels by autacoid mechanisms, such as prostaglandins or endothelial-derived nitric oxide NO.[16] When the ability of the kidney to produce these autacoids is impaired by treatment with nonsteroidal anti-inflammatory drugs (NSAIDS) or by chronic vascular disease (e.g., atherosclerosis) angiotensin II may reduce GFR by constricting afferent arterioles.

ANGIOTENSIN II MAY CONTRIBUTE TO GLOMERULAR INJURY IN OVERPERFUSED KIDNEYS

Although blockade of angiotensin II vasoconstrictor of efferent arterioles may cause a further decline of GFR in ischemic nephrons, RAAS blockade may be beneficial when nephrons are hyperfiltering, especially if angiotensin II is not appropriately suppressed. For example, in diabetes mellitus and in certain forms of hypertension associated with glomerulosclerosis and nephron loss, angiotensin II blockade, by decreasing efferent arteriolar resistance and BP, lowers glomerular hydrostatic pressure and attenuates glomerular hyperfiltration.[16] Thus, RAAS blockers are more effective than other antihypertensive agents in preventing glomerular injury, even with similar reductions in BP.[28,29]

DOES ANGIOTENSIN II CAUSE TARGET ORGAN INJURY INDEPENDENT OF INCREASED BP?

Angiotensin II has been suggested to cause injury to the kidneys and other organs through direct actions, in addition to its hemodynamic effects. Although RAAS blockers may provide greater renal protection than other antihypertensive drugs, decreases in glomerular hydrostatic pressure because of efferent arteriolar vasodilation may have contributed to these beneficial effects. In studies where BP was measured accurately, using 24-hour telemetry, the renal protective effects of angiotensin II blockade appeared to be largely a result of reduced BP.[30]

An observation that is difficult to reconcile with the concept that ANG II directly mediates target organ injury, independent of BP, is the finding that physiologic activation of the RAAS is not associated with vascular or renal injury as long as the BP is not elevated. For example, sodium depletion does not cause renal, cardiac or vascular injury, despite marked increases in renal angiotensin II levels. Also, the clipped kidney in 2-kidney, 1-clip Goldblatt hypertension is exposed to high angiotensin II levels, but is protected from increased BP by the clip on the renal artery and has no visible injury as long as the stenosis is not too severe. However, the nonclipped kidney, exposed to lower angiotensin II concentrations but higher BP, has marked focal segmental glomerular sclerosis, as well as tubulointerstitial changes characteristic of hypertension.[31]

Convincing evidence in this controversial area of research comes from the observations of Coffman and colleagues who studied the effects of chronic angiotensin II infusion in normal wild-type mice, in wild-type mice that received transplanted kidneys from AT1 receptor knockout mice, and in AT1 receptor knockout mice that received transplanted kidneys from normal wild-type mice.[32] Chronic angiotensin II infusion in normal wild-type mice increased BP and caused cardiac hypertrophy and fibrosis. However, in wild-type mice that received transplanted kidneys from AT1 receptor knockout mice (i.e., AT1 receptors were present in the heart and other organs, but not in the kidneys), angiotensin II infusion did not chronically raise BP or cause cardiac hypertrophy and fibrosis. In AT1 receptor knockout mice that received transplanted kidneys from normal wild-type mice (i.e., AT1 receptors were present only in the kidneys and not in the heart or other organs), angiotensin II infusion caused chronic hypertension, as well as cardiac hypertrophy and fibrosis.[32] These observations indicate that: 1) the renal effects of angiotensin II, and not the peripheral vascular or other non-renal effects, mediate chronic increases in BP; and 2) in the absence of hypertension, angiotensin II does not cause cardiac hypertrophy or fibrosis. Thus, the hemodynamic effects appear to account for most of the target organ injury that occurs in angiotensin II-dependent hypertension, and the effects of angiotensin II to raise BP are due to its renal actions, not to extrarenal effects, such as peripheral vasoconstriction or central nervous system effects.

Aldosterone

Aldosterone is also a powerful sodium-retaining hormone, and consequently has important effects on renal pressure natriuresis and BP regulation. The

primary sites of actions of aldosterone on sodium reabsorption are the principal cells of the distal tubules, cortical collecting tubules, and collecting ducts where aldosterone stimulates sodium reabsorption and potassium secretion. Aldosterone binds to intracellular mineralocorticoid receptors (MRs) and activates transcription by target genes which, in turn, stimulate synthesis or activation of the Na^+—K^+-ATPase pump on the basolateral epithelial membrane and activation of amiloride-sensitive sodium channels on the luminal epithelial membrane.[33] These effects are termed *genomic*, because they are mediated by gene transcription and require 60—90 minutes to occur after aldosterone administration.

Aldosterone also exerts rapid *nongenomic* effects on the cardiovascular and renal systems.[33] Aldosterone increases the sodium current in principal cells of the cortical collecting tubule through activation of the amiloride-sensitive channel, and stimulates the Na^+—H^+ exchanger a few minutes after application.[33] In vascular smooth muscle cells, aldosterone stimulates sodium influx by activating the Na^+—H^+ exchanger in less than 4 minutes. Acute aldosterone administration may rapidly reduce forearm blood flow in humans, although some investigators have found no change or an increase in blood flow.[33] The putative membrane receptor and the cell-signaling mechanisms responsible for these rapid actions of aldosterone have not been identified, especially with physiologic levels of aldosterone. Thus, the importance of the nongenomic effects of aldosterone on long-term regulation of BP is still unclear.

The overall effects of aldosterone on pressure natriuresis are similar to those observed for angiotensin II. With low sodium intake, increased aldosterone helps prevent sodium loss and reductions in BP. Conversely, during high sodium intake, suppression of aldosterone prevents excessive sodium retention and attenuates increased BP. Excess aldosterone secretion reduces the slope of pressure natriuresis so that BP becomes salt-sensitive. Consequently, increasing plasma aldosterone six-to ten-fold causes marked hypertension when sodium intake is normal or elevated, but there is very little effect on BP when sodium intake is low.[5]

The role of aldosterone and MR activation in human hypertension is a topic of renewed interest in recent years. Hyperaldosteronism may be more common than previously believed, especially in patients with hypertension that are resistant to treatment with the usual antihypertensive medications. For example, the prevalence of primary aldosteronism is reported to be almost 20% among patients referred to specialty clinics for resistant hypertension. Many of these patients, however, are overweight or obese.[34]

There is also emerging evidence that MR antagonism may provide an important therapeutic tool for reducing BP and preventing target organ injury in hypertension[34]; for example, antagonism of MR attenuated sodium retention, hypertension, and glomerular hyperfiltration in obese dogs fed a high-fat diet even though plasma aldosterone concentration was only slightly elevated.[35] However, even mild increases of plasma aldosterone may increase BP when accompanied by high sodium intake and volume-expansion, because aldosterone greatly enhances salt-sensitivity of BP.

In obese, insulin-resistant patients there may be enhanced sensitivity to the effects of aldosterone because of increased abundance of epithelial sodium channels ENaCs, which would amplify the effects of MR activation on sodium reabsorption and BP. It is also possible that glucocorticoids may contribute to MR activation in obese, insulin-resistant patients.

Endothelin

Endothelin-1 ET-1 is derived from a 203 amino acid peptide precursor, preproendothelin, which is cleaved after translation to form proendothelin. A converting enzyme cleaves proendothelin to produce the 21 amino acid peptide, endothelin. ET-1 receptor-binding sites have been identified throughout the body, with the greatest numbers of receptors in the kidneys and lungs.[36,37] ET-1 can either elicit a hypertensive effect by activating endothelin type A (ET_A) receptors or an antihypertensive effect via endothelin type B (ET_B) receptor activation in the kidneys.[36,37] Thus, the ability of ET-1 to influence BP regulation is highly dependent on where ET-1 is produced, and which ET receptor type is activated (Figure 39.8).

ET-1 Elicits a Hypertensive Effect by Activating ET_A Receptors in the Kidneys

Endothelin-1 produces renal and systemic vasoconstriction, impairs renal pressure natriuresis, and increases BP via ET_A receptor activation.[36,37] ET-1 exerts multiple actions via ET_A receptor activation that, if sustained chronically, could contribute to the development of hypertension and progressive renal injury. ET-1 decreases GFR and renal plasma flow through stimulation of vascular smooth muscle and mesangial cell contraction.[36,37] Long-term effects of ET-1 on the kidneys include stimulation of mesangial cell proliferation and extracellular matrix deposition, as well as vascular smooth muscle hypertrophy in renal resistance vessels.[36,37] Expression of ET-1 is greatly enhanced in several animal models of severe hypertension with renal vascular hypertrophy, and in models of

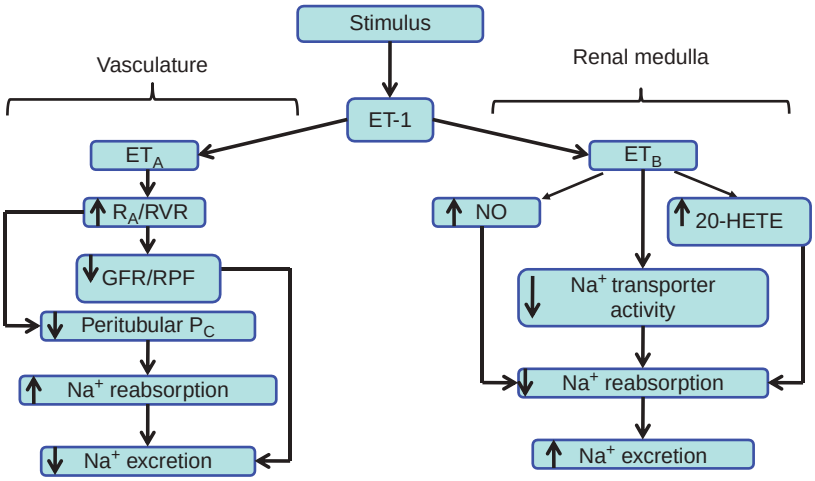

FIGURE 39.8 **Summary of the pro- and antihypertensive actions of endothelin-1 (ET-1).** The ability of ET-1 to influence blood pressure and renal pressure natriuresis is highly dependent on where ET-1 is produced, and which renal ET receptor type is activated. ET-1 can elicit a prohypertensive anti-natriuretic effect by activating ET_A receptors in the kidneys. Activation of renal ET_A receptors increases renal vascular resistance (RVR), which decreases renal plasma flow (RPF) and glomerular filtration rate (GFR), and enhances sodium reabsorption by decreasing peritubular capillary hydrostatic pressure (Pc). The net effect of renal ET_A receptor activation is decreased sodium excretion and increased BP. Conversely, ET-1 can elicit an antihypertensive natriuretic effect via ET_B receptor activation. Activation of the renal ET_B receptor leads to enhanced synthesis of nitric oxide (NO) and 20-HETE, and suppression of the renin–angiotensin system. The net effect of renal ET_B receptor activation is increased sodium excretion and decreased BP.

progressive renal injury.[36,37] Treatment with endothelin receptor antagonists attenuated the hypertension and small artery morphologic changes, and improved kidney function in these models.[36,37]

ET-1 Elicits an Antihypertensive Effect by Activating ET_B Receptors in the Kidneys

ET_B receptor activation by ET-1 causes vasodilation, enhances renal pressure natriuresis, and decreases BP. While much attention has been given to ET_A receptor activation, several studies indicate an important antihypertensive role for ET_B receptor.[37] The most compelling evidence comes from reports that transgenic mice deficient in ET_B receptors develop salt-sensitive hypertension, and that pharmacologic antagonism of ET_B receptors produces hypertension in rats.[36–38]

Because ET_B receptors are located on multiple cell types throughout the body, including endothelial cells and renal epithelial cells, both intrarenal and extrarenal mechanisms could theoretically mediate the hypertension produced by chronic disruption of ET_B receptors. Bagnall et al. reported that ablation of ET_B receptors exclusively from endothelial cells produced endothelial dysfunction, but did not cause hypertension.[39] In contrast to models of total ET_B receptor ablation, the BP response to a high-salt diet was unchanged in endothelial cell-specific $ET_{A/B}$ receptor knockouts compared to control mice.[37,40,41] These findings suggest that ET_B receptors in non-endothelial cells are important for BP regulation. Supporting this concept are the findings that collecting duct ET_B knockout mice on a normal-sodium diet were hypertensive and a high-sodium diet worsened the hypertension.[40,41] Moreover, collecting duct ET_B knockout mice on a normal-sodium diet were hypertensive, and a high-sodium diet worsened the hypertension.[37,40,41] These findings provide strong evidence that the intrarenal effect of ET_B receptor activation on the collecting duct is an important physiologic regulator that increases renal sodium excretion and reduces BP.

ET-1 Plays an Important Role in Experimental Salt-Sensitive Hypertension

Dahl salt-sensitive (DS) rats placed on a high-sodium diet have impaired pressure natriuresis and develop hypertension and progressive renal injury. ET-1, acting via an ET_A receptor, may play a role in mediating renal injury in DS hypertension. Prepro-ET-1 mRNA and vascular responsiveness to ET-1 are increased in the renal cortex of DS rats compared with Dahl salt-resistant (DR) rats, and a positive correlation between ET-1 generation in the renal cortex and the extent of glomerulosclerosis has been reported in DS hypertensive rats.[42] Acute infusion of a nonselective ET_A-ET_B receptor antagonist directly into the renal interstitium improved renal hemodynamic and excretory function in DS rats, but not in DR rats.[43] Moreover, chronic blockade of ET_A receptors attenuated hypertension and proteinuria, and ameliorated glomerular and tubular damage associated with high-salt intake in DS rats. An important unanswered question is whether these beneficial effects of ET_A blockade

are mediated through lower BP or through direct renal mechanisms.

Role of Endothelin in Human Hypertension

Bosentan, a combined ET_A-ET_B receptor antagonist, lowered BP in a large, double-blind, clinical trial, indicating that the endothelin system helps maintain BP in human hypertension.[44,45] However, the magnitude of the BP reduction by bosentan was almost the same as that observed in normotensive humans. This observation suggests that endothelin probably may not play a major role in raising BP in most patients with essential hypertension, although bosentan blocks both ET_A and ET_B receptors and antagonism of the antihypertensive ET_B receptor may have masked an important role of endothelin on BP via ET_A receptor activation. In another study, six weeks of darusentan, a selective ET_A receptor antagonist, lowered systolic and diastolic BP.[44] Bakris et al.[46] and Weber et al.[47] also showed that darusentan reduced mean 24 hour systolic BP more than placebo in patients with treatment-resistant hypertension. There are currently no clinical studies that directly compare selective and mixed ET receptor antagonism in the treatment of hypertension, although both approaches clearly reduce BP. Moreover, clinical studies examining the effect of selective ET_A receptor antagonism in humans with salt-sensitive hypertension are lacking. Therefore, the importance of ET-1 in human essential hypertension deserves further investigation.[37,45]

Nitric Oxide

Release of nitric oxide NO by the vascular endothelium and renal tubular cells plays a major role in regulating renal hemodynamics and tubular function.[48–50] Long-term inhibition of NO synthase causes impaired renal pressure natriuresis and sustained hypertension.[48–50] The renal mechanisms whereby reduction in NO synthesis impairs pressure natriuresis can be divided into hemodynamic and tubular components, each of which may be modulated by processes that are intrinsic or extrinsic to the kidneys Figure 39.9. For example, reduced NO synthesis may decrease renal sodium excretory function by increasing renal vascular resistance directly or by enhancing responsiveness to vasoconstrictors such as angiotensin II or norepinephrine.[49,50] Reductions in NO synthesis also increase renal sodium reabsorption via direct effects on tubular transport, and through changes in intrarenal physical factors, such as renal interstitial hydrostatic pressure (RIHP) and medullary blood flow. Inhibition of NO synthesis reduces RIHP and urinary sodium excretion.[49,50] Stimulation of NO production normalizes the blunted pressure natriuretic response in DS rats as a result of improvement in the kidney's ability to generate increased RIHP in response to increased BP.[49,50]

Impaired NO Production Produces Salt-Sensitive Hypertension

Increased renal NO production, as evidenced by increased urinary excretion of NO metabolites or the NO second messenger, cyclic guanosine mono-phosphate, has been reported to be essential for the maintenance of normotension during a dietary salt challenge. Prevention of this increase in renal NO production resulted in salt-sensitive hypertension.[48–51]

There is also evidence that NO-induced vasodilation is impaired in many models of hypertension, and in some vascular beds in human essential hypertension.[52,53] The extent to which these effects are secondary to hypertension or reflect important mechanisms for the etiology of hypertension remains unclear. NO activity does not increase with increasing dietary salt-loading in the Dahl salt-sensitive DS hypertensive rats as it does in normotensive Dahl salt-resistant DR rats; furthermore, chronic administration of L-arginine prevents hypertension during dietary salt-loading in the DS rat, but has no effect on BP in DR rats.[54] We have shown that injections of L-arginine will prevent the development of hypertension in DS rats, even during prolonged exposure to an 8% sodium diet.[49,50] This is

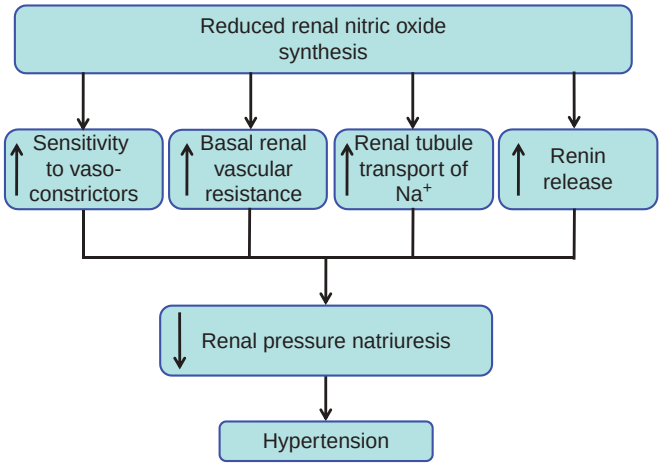

FIGURE 39.9 **Renal mechanisms whereby reduced nitric oxide (NO) synthesis decreases pressure natriuresis and increases BP.** Decreased endothelial-derived nitric oxide (EDNO) synthesis impairs renal sodium excretory function by increasing basal renal vascular resistance, enhancing the renal vascular responsiveness to vasoconstrictors such as angiotensin II or norepinephrine, or activating the renin–angiotensin system. Reductions in NO synthesis also impair sodium excretory function, either by directly increasing tubular reabsorption or by altering intrarenal physical factors, such as renal interstitial hydrostatic pressure or medullary blood flow.

not the case in all models of hypertension, even when individual tissues from these animals show impaired NO responses. Thus, in 2-kidney, 1-clip renovascular hypertension, inhibitors of NO synthesis result in an exaggerated increase in BP and vascular resistance compared to normotensive rats, but L-arginine does not prevent hypertension. Similarly, in the DOCA salt-hypertensive model, L-arginine administration improves agonist-induced NO release, but has no effect on BP.[48–50]

Because of the central role of the kidney in sustaining changes in BP, it is reasonable to postulate that the long-term increases in BP induced by inhibition of NO synthase in normal animals, as well as the reduction in blood pressure induced by NO agonists in DS rat, should be associated with changes in the relationship between renal perfusion pressure and urinary sodium excretion. This has been confirmed in several studies.[48–50] In normal animals, the acute intrarenal administration of the NO synthesis inhibitor NG nitro L-arginine methyl ester L-NAME significantly reduces the natriuresis and diuresis usually induced by increases in renal perfusion pressure. Chronic NO synthase inhibition also blunts the chronic renal function curve measured during changes in sodium intake.[48–50] Stimulation of NO production by L-arginine supplementation has also been reported to alter BP and enhance renal pressure natriuresis. Chronic L-arginine supplementation in DS rats maintained on a high-sodium diet normalizes the blunted pressure natriuresis relationship which usually characterizes these hypertensive-prone animals.[48–50,54] Thus, alterations in NO production or release can have important effects on renal pressure natriuresis.

Role of NO in Human Hypertension

There is also evidence that NO synthesis is impaired in vascular beds in human primary hypertension.[52] The extent to which these changes are secondary to increased BP or reflect important mechanisms for the pathogenesis of hypertension, however, remains unclear. NO deficiency can occur by multiple mechanisms, including altered NOS enzyme expression, NO scavenging or NOS enzyme inhibition by endogenous inhibitors. Recent studies have implicated the endogenous NO synthase inhibitor asymmetric dimethylarginine ADMA in the pathogenesis of hypertension.[55,56] While there is a strong correlation between ADMA levels and severe cardiovascular events and mortality, only a few clinical studies have shown a relationship between high BP and high plasma ADMA concentrations.[55,56] However, when hypertension and renal disease are present, increased plasma ADMA is observed. Thus, it appears that the observed increase in ADMA during hypertension may be secondary to chronic kidney disease.[52,54–56]

Oxidative Stress

Recent studies suggest that reactive oxygen species (ROS) may play a role in the initiation and progression of cardiovascular dysfunction associated with hypertension.[57–59] In many forms of hypertension, increased ROS appear to be derived mainly from nicotinamide adenine dinucleotide phosphate (NADPH) oxidases, which could serve as a trigger for uncoupling endothelial nitrous oxide synthase NOS by oxidants. Four members of the NADPH oxidase Nox enzyme family have been identified as important sources of ROS in the vasculature: Nox1, Nox2, Nox4, and Nox5.[57,59] Multiple factors control the expression and activity of these enzymes and of their regulatory subunits, such as p22phox, p47phox, Noxa1, and p67phox.[57,59] Several physical, hormonal, and local autocoid factors are known to be important stimuli for the production of ROS. For example angiotensin II, aldosterone, ET-1, and sodium intake all enhance production of ROS.[57,59] Moreover, BP-induced endothelial damage is also associated with increased production of ROS. Thus, in many forms of hypertension, the elevation in ROS production may be secondary to the increased BP.

ROS produced by migrating inflammatory cells and/or vascular cells cause endothelial dysfunction, increased renal tubule sodium transport, cell growth and migration, inflammatory gene expression, and stimulation of extracellular matrix formation.[57,59] ROS, by affecting vascular and renal tubule function, can also impair renal pressure natriuresis, alter systemic hemodynamics, and raise BP[60–62] (Figure 39.10).

There is growing evidence that supports a role for ROS in various animal models of hypertension, especially salt-sensitive models.[60–62] The DS rat, for example, has increased vascular and renal superoxide production, and increased levels of H_2O_2. Renal expression of superoxide dismutase is decreased in the kidneys of DS rats, and long-term administration of Tempol, a superoxide dismutase mimetic, significantly decreases BP and attenuates renal damage.[62] Another salt-sensitive model, the stroke-prone SHR, has elevated levels of superoxide and decreased plasma antioxidant capacity.[60–62] Superoxide production is also increased in the deoxycorticosterone acetate (DOCA)-salt hypertensive rat, and treatment with apocynin, a nicotinamide adenine dinucleotide phosphate NADPH oxidase inhibitor, decreases BP.[60–62] ROS also appears to play an important role in chronic angiotensin II hypertension. Angiotensin II is a potent stimulator of

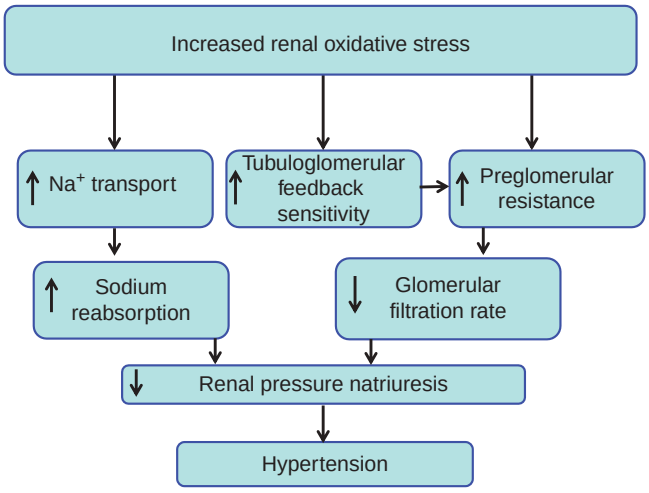

FIGURE 39.10 **Renal mechanisms whereby ROS impair pressure natriuresis and increase BP.** An increase in renal oxidative stress impairs renal pressure natriuresis by increasing renal vascular resistance or enhancing tubuloglomerular feedback, both of which decrease the glomerular filtration rate. Renal oxidative stress also reduces sodium excretion by direct effects to increase renal tubular reabsorption.

NADPH oxidase, and long-term administration of Tempol significantly decreases the chronic BP response to angiotensin II.[60–62]

Despite the fact that elevated ROS plays an important role in many experimental models of hypertension, antioxidant therapy has failed to lower BP in clinical studies.[63] An imbalance between total oxidant production and the antioxidant capacity in human primary hypertension has been reported to occur in some, but not all, studies. Equivocal findings in humans are partly due to the difficulty of assessing oxidative stress in clinical studies. Measurement of ROS in tissues represents a challenge, because of their low levels and relatively short half-lives.[64] Most human studies have found that chronic antioxidant therapy with vitamin E and C supplementation has little effect on BP. However, a major shortcoming of clinical trials using vitamin E and C is the lack of verification that antioxidant treatment actually decreased ROS.[63]

Inflammatory Cytokines and the Immune System

While inflammation and the immune system activation were first associated with hypertension over four decades ago, it has become increasingly evident over the last few years that inflammatory cytokines and the immune system play an important role in the progression of various models of experimental and genetic hypertension.[65–68]

Increased Inflammatory Cytokines in Hypertension

Plasma levels of proinflammatory cytokines correlate with increased BP in human hypertension, and in some experimental animal models of hypertension.[65,67] Moreover, several studies have demonstrated that chronic increases in plasma cytokines, comparable to concentrations observed in hypertension associated with pre-eclampsia, cause significant increases in BP.[69,70] A two-fold elevation in the plasma levels of Tumor Necrosis Factor alpha (TNF-α) significantly increased BP and renal vascular resistance in pregnant rats.[69,70] These studies are consistent with the hypothesis that increasing plasma levels of cytokines may contribute to pregnancy-induced hypertension. Etanercept, a selective TNF-α inhibitor, was not only effective in lowering BP, but also in dampening the ET-1 transcript that is typically observed in response to placental ischemia in pregnant rats.[69,70] Whether etanercept and other cytokine inhibitors would have beneficial effects in pre-eclamptic women remains unknown, because elevated levels of cytokines and exaggerated inflammatory responses have been reported in some studies.

Lee and co-workers[71] found that hypertension caused by chronic angiotensin II excess may depend, at least in part, on the presence of Interleukin-6 (IL-6). Mice with knockout of IL-6 had significantly lower BP than wild-type mice during two weeks of angiotensin II infusion. Although these findings demonstrate a significant role for IL-6 in mediating the chronic hypertensive response to angiotensin II in mice, the importance of inflammatory cytokines in the pathogenesis and progression of the various forms of human hypertension is unclear, and is currently an area of active investigation.

Several recent studies have demonstrated that T-cells play an important role in the progression of hypertension. Harrison and colleagues proposed that hypertensive stimuli lead to renal injury, neoantigen formation, and eventual T-cell activation within the kidney.[67,68,72] T-cell-derived signals promote entry of other inflammatory cells such as macrophages, which result in renal vasoconstriction and increased sodium reabsorption, thereby increasing the severity of the hypertension.[68] Supporting this concept is a recent report that RAG-$1^{-/-}$ mice, which lack T-cells and B-cells, do not develop the degree of hypertension in response to angiotensin II infusion as the wild-type mice, an observation that was attributed to lack of T-cells. Moreover, chronic angiotensin II infusion was associated with a greater number of activated T-cells, as well as increased Rantes, a chemotaxic protein, in the vasculature and perivascular fat.[67,68,72] These observations were confirmed by Crowley et al.[73] using a model very similar to the RAG-$1^{-/-}$ mice. They reported that angiotensin II hypertension, renal injury,

left ventricular hypertrophy, and cardiac fibrosis were prevented in mice lacking T-cells. While these findings in experimental models of hypertension are intriguing, the importance of the immune system in the pathogenesis of essential hypertension in humans remains to be determined.

Eicosanoids

The kidneys produce several types of prostaglandins with multiple functions, including prostacyclin, thromboxane, 20-hydroxyeicosatetraenoic acid 20-HETE, and epoxyeicosatetraenoic acids (EETs), all of which have been reported to influence renal pressure natriuresis and BP. However, the major renal prostaglandin controlling sodium excretion is probably PGE_2.[74] The largest production of PGE_2 occurs in the renal medulla, with decreasing synthesis in the cortex. PGE_2 is synthesized and released, not stored. Once released, PGE_2 inhibits sodium reabsorption by several mechanisms, including direct effects on the renal tubules.

Even though long-term administration of PG synthesis inhibitors has very little effect on volume and/or BP regulation under normal physiologic conditions, renal PGs may be important in pathophysiologic states associated with enhanced activity of the RAAS. *In vitro* and *in vivo* studies indicate that renal PGs protect the preglomerular vessels from excessive angiotensin II-induced vasoconstriction. In the absence of this protective mechanism, the renal vasculature could be exposed to the potent vasoconstrictor actions of angiotensin II in various conditions, such as sodium and volume depletion. This could, in turn, lead to significant impairment of renal hemodynamics and excretory function.

Inhibitors of the COX-2 enzyme reduce pressure natriuresis, cause vasoconstriction, and increase BP.[74–76] There are at least two distinct cyclooxygenases—COX-1 and COX-2. COX-1 is called the *constitutive enzyme*, because of its wide tissue distribution, whereas COX-2 has been termed as *inducible*, because of its more restricted basal expression and its upregulation by inflammatory and/or proliferative stimuli. Based on the concept that COX-1 performs cellular housekeeping functions for normal physiologic activity and COX-2 acts at inflammatory sites, it was initially hypothesized that the BP and renal effects of nonsteroidal anti-inflammatory drugs might be linked to COX-1 inhibition.[74] However, experimental and clinical evidence indicates that COX-2 metabolites may also play a role in the regulation of vascular and renal function under various physiologic and pathophysiologic conditions.[74–76]

Selective COX-2 inhibitors were designed to minimize gastrointestinal complications of traditional NSAIDs—adverse effects attributed to suppression of COX-1-derived PGE_2 and prostacyclin. However, randomized controlled clinical trials of inhibitors of COX-2 indicate that such compounds may elevate the risk of hypertension, myocardial infarction, and stroke, possibly by removing the protective action of prostacyclin in counteracting thrombogenesis, hypertension, and atherogenesis.[75,76]

Eicosanoids produced by cytochrome P450 monooxygenase metabolism of arachidonic acid alter vascular function and renal pressure natriuresis. In addition to the PGs generated via the COX pathway, other eicosanoids that affect vascular function and/or renal sodium transport are produced by cytochrome P450 CYP monooxygenase metabolism of arachidonic acid. CYP enzymes metabolize arachidonic acid primarily to 20-HETE and EETs. 20-HETE is a potent vasoconstrictor that may regulate vascular tone and contribute to the autoregulation of renal blood flow. 20-HETE also inhibits sodium reabsorption in the proximal tubule and thick ascending limb of the loop of Henle.[77,78] Therefore, the ability of 20-HETE to influence BP regulation and renal pressure natriuresis is highly dependent on where 20-HETE is produced. The effect of 20-HETE to inhibit sodium transport tends to lower BP, whereas its vasoconstrictor effects on the renal vasculature and glomerulus tend to lower glomerular filtration rate, promote sodium retention, and increase BP (Figure 39.11).

Compelling evidence suggests that the renal production of CYP metabolites of arachidonic acid is altered in genetic and experimental models of hypertension, and contributes to the resetting of pressure natriuresis and increased BP.[77,78] Studies in humans also suggest that CYP metabolites may play a role in sodium homeostasis. Urinary 20-HETE excretion is regulated by salt intake, and is differentially regulated in salt-sensitive versus salt-resistant individuals.[79,80] Moreover, there appears to be a strong negative relationship between 20-HETE excretion and body mass index BMI, suggesting that some factor related to obesity may be responsible for decreased synthesis or excretion of this eicosanoid.[79,80] These observations support the possibility that attenuated renal production of 20-HETE could impair pressure natriuresis in human hypertension, especially when associated with obesity. However, further mechanistic studies are needed to test the importance of 20-HETE in human hypertension.

Atrial Natriuretic Peptide (ANP)

ANP is a 28 amino acid peptide synthesized and released from atrial cardiocytes in response to stretch.

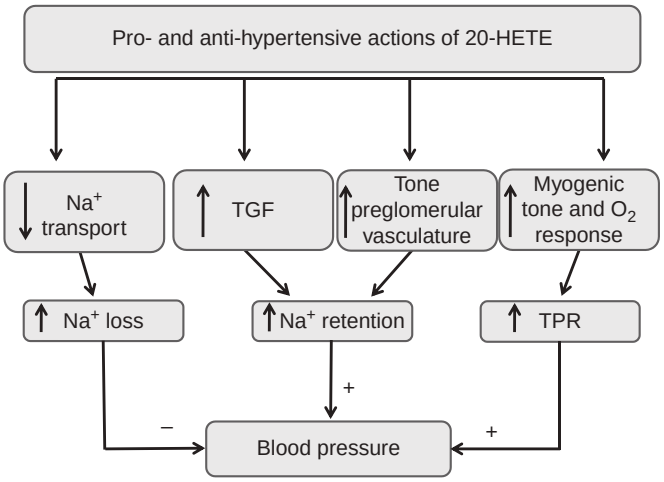

FIGURE 39.11 **Summary of the pro- and antihypertensive actions of 20-HETE. 20-HETE produced in the renal tubules which inhibits sodium transport and lowers BP.** In the renal vasculature and glomerulus, 20-HETE is a constrictor that lowers glomerular filtration rate, promotes sodium retention, and increases BP. In the peripheral circulation, 20-HETE increases vascular tone and increases BP (TGF: tubuloglomerular feedback; TPR: total peripheral resistance).

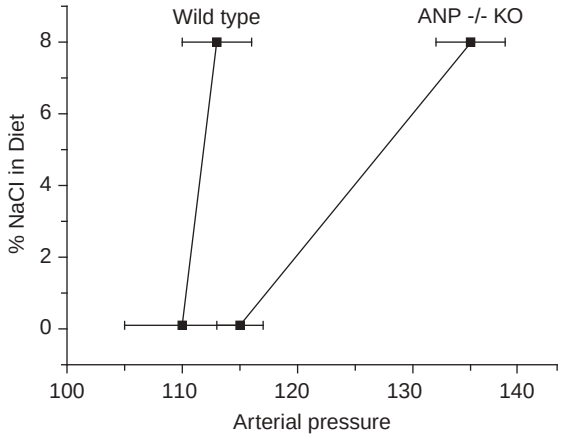

FIGURE 39.12 **Effect of atrial natriuretic peptide (ANP) receptor knockout on the chronic pressure natriuresis relationship.**[83]

ANP reduces vascular resistance, while enhancing sodium excretion through extrarenal and intrarenal mechanisms. ANP increases GFR, but has little effect on renal blood flow. However, an increase in GFR is not a prerequisite for ANP to enhance sodium excretion. ANP may also inhibit renal tubular sodium reabsorption directly by inhibiting active tubular sodium transport or indirectly via alterations in medullary blood flow, physical factors, and inhibiting formation of antinatriurectic hormones such as angiotensin II and aldosterone.

Plasma levels of ANP are elevated in numerous physiologic conditions associated with enhanced sodium excretion. Acute blood volume expansion consistently elevates circulating ANP. Some investigators report that chronic increases in dietary sodium intake also raise circulating levels of ANP.[81] Infusions of exogenous ANP at rates that result in physiologically relevant plasma concentrations, comparable to those observed during volume-expansion, elicit significant natriuresis, especially in the presence of other natriuretic stimuli, such as high renal perfusion pressure. Long-term physiologic elevations in plasma ANP also enhance pressure natriuresis and reduce BP.[82]

Transgenic mice overexpressing ANP are hypotensive relative to their wild-type littermates, whereas mice harboring functional disruptions of the ANP or NPR-A genes are hypertensive.[81,83] ANP gene knockout mice develop a salt-sensitive form of hypertension (Figure 39.12) in association with failure to adequately suppress the RAAS.[83] While these findings suggest that genetic deficiencies in ANP or its receptors could play a role in the pathogenesis of salt-sensitive hypertension, the importance of this system in the pathogenesis of human hypertension remains unclear.

PRIMARY ESSENTIAL HYPERTENSION

Human primary essential hypertension appears to be largely a modern disorder associated with industrialization and the ready availability of food. Nearly all studies of Westernized, industrialized populations have demonstrated that BP, and therefore the prevalence of hypertension, rises with age.[84] Hunter-gatherers living in non-industrialized societies, however, rarely develop hypertension or age-related increases in systolic and mean pressures.[84] Thus, environmental factors appear to play a major role in raising BP in most patients with primary hypertension. However, it is likely that genetic variation contributes to differences in baseline BP that result in the normal distribution of BP in a population. When hypertension-producing environmental factors are added to the population baseline BP, the normal distribution is shifted toward higher BP; variations in the impact of environmental factors appear to flatten the BP curve and cause greater variability in BP of the population.

What elements of industrialized societies cause BP to increase in the majority of people as they age? How do they affect the physiologic controllers of BP? One factor that is clearly important is resetting of renal pressure natriuresis to higher BPs.[10] In some cases, this resetting may be related to increased renal sodium reabsorption, because of abnormalities intrinsic to the kidneys or altered neurohumoral control of the

kidneys.[10] In other instances, resetting of pressure natriuresis may be associated with renal vasoconstriction and reductions in GFR, as a result of intrarenal mechanisms or nervous and hormonal mechanisms.[10] However, many of these initial changes in kidney function are difficult to discern after hypertension is established, because increased BP often returns renal function to normal. Experimental, clinical, and population studies suggest one of the key factors that affect BP is excess weight gain.

Overweight and Obesity are Major Risk Factors for Primary Hypertension

The prevalence of obesity has risen dramatically in the past 2–3 decades, and is now the most important public health problem in many industrialized countries, including the United States. Current estimates indicate that more than 1 *billion* people in the world are overweight or obese.[85] In the United States, more than 65% of adults are overweight, and one-third of the adult population is obese with a BMI greater than 30.[86] Population studies show that the relationship between BMI and systolic and diastolic BP is nearly linear in diverse populations throughout the world. Risk estimates from the Framingham Heart Study, for example, suggest that approximately 78% of primary hypertension in men and 65% in women can be ascribed to excess weight gain.[87] Clinical studies also indicate that weight loss is effective in reducing BP in most hypertensive subjects, and that weight loss, if it can be achieved, is effective in primary prevention of hypertension.[88]

If excess weight gain is a major cause of hypertension, why are some obese persons not hypertensive (i.e., BP greater than 140/90 mmHg)? Perhaps this is not so surprising if one considers that excess weight gain shifts the normal frequency distribution of BP toward higher levels. Although obesity increases the probability that a person's BP will register in the hypertensive range, not all obese people will have BPs greater than 140/90 mmHg. However, obese individuals who are classified as "normotensive" have higher BP than they would at a lower body weight. Thus, weight loss lowers BP in "normotensive" as well as "hypertensive" obese subjects.[5] Although the importance of obesity as a cause of hypertension is well-established, the physiologic mechanisms by which excess weight gain alters renal function and raises BP are only beginning to be elucidated.

Obesity is associated with extracellular fluid volume expansion, as well as increased tissue blood flow and cardiac output.[10] Studies in experimental animals and in humans indicate that blood flow is increased in many tissues, including the heart, kidneys, gastrointestinal tract, and skeletal muscles.[10] Some of the increased flow is caused by growth of skeletal muscle and organs in response to increased workload and the metabolic demands associated with obesity. However, obesity also causes functional vasodilation, perhaps as a consequence of an increased metabolic rate, higher oxygen consumption, and accumulation of vasodilator metabolites. This vasodilation occurs despite mild activation of the RAAS and SNS. Although resting blood flows are increased in many tissues, there appears to be reduced blood flow "reserve" during exercise or during reactive hyperemia in obese, compared to lean, individuals.[10] Cardiac reserve is also reduced in obesity, despite higher resting cardiac outputs.

Increased renal tubular sodium reabsorption and impaired pressure natriuresis play a major role in initiating the rise in BP associated with excess weight gain. At least three mechanisms are important in altering renal function in obesity hypertension (Figure 39.13): 1) increased SNS activity; 2) activation of the RAAS; and 3) physical compression of the kidneys by fat accumulation within and around the kidneys, and by increased abdominal pressure.

SNS Activation in Obesity Hypertension

Several observations indicate that increased SNS activity contributes to obesity hypertension[10]: 1) SNS activation, especially renal sympathetic activity, is increased in obese subjects; 2) pharmacologic blockade of adrenergic activity lowers BP to a greater extent in obese, compared to lean, individuals; and 3) renal denervation markedly attenuates sodium retention and hypertension associated with a high-fat diet in experimental animals.

Administration of α-and β-adrenergic blockers or clonidine, a drug that stimulates central α-2 receptors and reduces SNS activity, prevents most of the rise in BP in obese dogs fed a high-fat diet.[10,89] In obese hypertensive patients, combined α-and β-adrenergic blockade for one month reduced ambulatory BP significantly more in obese than in lean essential hypertensive patients.[10] These findings suggest that increased adrenergic activity contributes importantly to the development and maintenance of obesity hypertension in experimental animals and in humans.[10,89] The renal sympathetic nerves mediate most, if not all, of the chronic effects of SNS activation on BP in obesity. Bilateral renal denervation greatly attenuated sodium retention and hypertension in obese dogs fed a high-fat diet.[10]

Obesity does not cause mass activation of the SNS. Instead, increased SNS activity in various tissues is modest, and appears to be differentially controlled in obesity. For example, cardiac sympathetic activity does

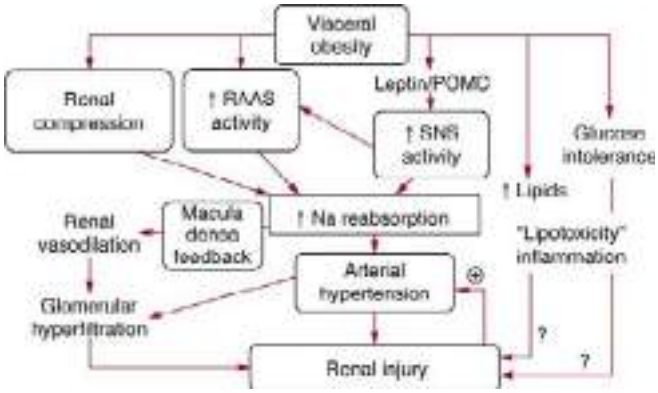

FIGURE 39.13 **Summary of mechanisms by which obesity causes hypertension and renal injury.** Visceral obesity increases BP by activation of the sympathetic nervous system (SNS), the renin–angiotensin–aldosterone system (RAAS), and by physical compression of the kidneys from the fat surrounding the kidneys. SNS activation may be caused by, in large part, the effects of leptin, which acts on proopiomelanocortin (POMC) neurons in the hypothalamus and brainstem. Obesity-induced hypertension and glomerular hyperfiltration may cause renal injury, especially when combined with dyslipidemia and hyperglycemia. Renal injury then exacerbates the hypertension and makes it more difficult to control.

not appear to be substantially elevated, whereas renal and skeletal muscle SNS activity is usually increased in obese subjects.[90–92] Obesity-induced SNS activation is usually not sufficient to cause vasoconstriction in most tissues, such as skeletal muscle or the kidneys, but does contribute to renin secretion and increased renal tubular sodium reabsorption.[60]

Several potential mediators of SNS activation in obesity have been suggested, including: 1) hyperinsulinemia; 2) angiotensin II; 3) increased levels of free fatty acids; 4) impaired baroreceptor reflexes; 5) activation of chemoreceptor-mediated reflexes associated with sleep apnea; and 6) cytokines released from adipocytes i.e., "adipokines" such as leptin, TNF-α and IL-6. Although these mechanisms have been reviewed previously,[5,6,10] there is little direct evidence to support cause-and-effect relationships for most of these factors and obesity-induced SNS activation.

Leptin–Melanocortin Activation May Mediate SNS Activation in Obesity

A promising candidate for linking obesity with hypertension is hyperleptinemia (Figure 39.14). Leptin, released from adipocytes in proportion to the degree of adiposity, acts on the hypothalamus and other regions of the brain to reduce appetite and increase SNS activity. In rodents, leptin increases sympathetic activity and BP.[10,93] Moreover, the hypertensive effects of leptin are enhanced when NO synthesis is inhibited,[10] as often occurs in obese subjects with endothelial dysfunction.

Additional support for leptin as a potential mechanism of obesity hypertension is the finding that leptin-deficient, obese mice and obese mice with mutations of the leptin receptor usually have little or no increase in BP compared to their lean controls.[89] Similar results have been found in obese children with leptin gene mutations who have early onset morbid obesity, but normal BP and impaired SNS activity.[94] Furthermore, children with leptin gene mutations did not have hypertension, despite having many other characteristics of the metabolic syndrome, including severe insulin resistance, hyperinsulinemia, and hyperlipidemia.[94] These observations suggest that the functional effects of leptin may be critical in linking obesity with SNS activation and hypertension.[89]

Leptin's stimulatory effect on SNS activity appears to be mediated by interactions with other hypothalamic factors, especially the proopiomelanocortin POMC pathway (Figure 39.14). In mice with leptin receptors deleted specifically in POMC neurons, leptin's hypertensive effects were completely abolished.[95] Also, pharmacological antagonism of melanocortin 3/4 receptors MC3/4R completely prevented leptin's chronic BP effects,[89] and the chronic hypertensive effects of leptin were absent in MC4R knockout mice.[89] These observations indicate that leptin's chronic BP effects are mediated almost entirely by activation of POMC neurons which, in turn, release α-melanocyte-stimulating hormone α-MSH, leading to activation of MC4R and increased SNS activity.[89]

A study in humans also suggests that MC4R activation may contribute to obesity-induced hypertension. The prevalence of hypertension is lower in MC4R-deficient humans compared to obese control subjects, despite severe obesity and associated metabolic disorders.[96] Moreover, subcutaneous administration of an MC4R agonist for seven days significantly increased BP. Thus, in humans and rodents, chronic activation of MC4R raises BP, and the presence of a functional MC4R system appears to be necessary for obesity and hyperleptinemia to increase SNS activity and BP.[96]

RAAS Activation in Obesity

Obese subjects, especially those with visceral obesity, often have mild-to-moderate increases in plasma renin activity PRA, angiotensinogen, ACE activity, angiotensin II, and aldosterone levels.[5] Activation of the RAAS occurs despite sodium retention, volume expansion, and hypertension, all of which normally tend to suppress renin secretion and angiotensin II formation.

An important role for angiotensin II in stimulating renal sodium reabsorption and in mediating obesity hypertension is supported by studies in experimental animals demonstrating that angiotensin II receptor blockade or ACE inhibition markedly attenuates

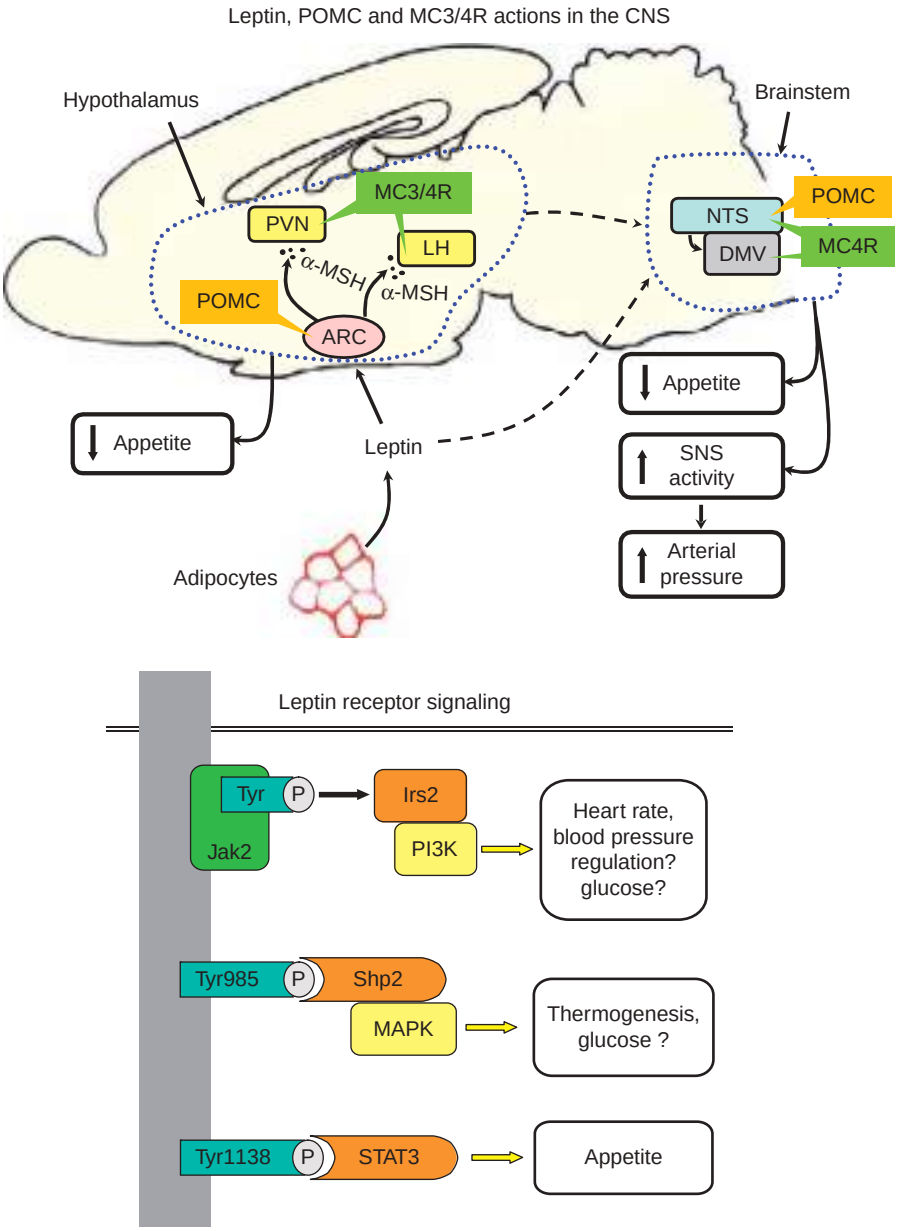

FIGURE 39.14 **Possible links among leptin and its effects on the hypothalamus, sympathetic activation, and hypertension.** Within the hypothalamus, one of the key pathways of leptin's action on appetite, SNS activity, and BP is stimulation of the proopiomelanocortin (POMC) neurons in the arcuate nucleus (ARC). These neurons send projections to the paraventricular nucleus (PVN) and lateral hypothalamus, releasing α-melanocyte-stimulating hormone (α-MSH), which then acts as an agonist for melanocortin 4 receptors (MC4R). These neurons, in turn, send projections to the nucleus of the solitary tract (NTS) to effect changes in appetite, SNS activity, and blood pressure. Leptin also suppresses the NPY/AGRP neurons, but their role in controlling SNS activity and BP are still unclear. Leptin–melanocortin activation in distinct areas of the brain and through multiple intracellular signaling pathways may differentially regulate appetite, energy expenditure, and BP (LH: lateral hypothalamus; RSNA: renal sympathetic nerve activity).

sodium retention, volume expansion, and increased BP during the development of obesity.[5,6,97] Whether the effects of angiotensin II to raise BP in obesity are due primarily to direct actions on the kidneys or stimulation of aldosterone secretion is unclear. The direct renal sodium-retaining effects of angiotensin II are well-known, as are the effects of angiotensin II to stimulate aldosterone secretion.

Although smaller clinical trials have clearly shown that both ARBs and ACE inhibitors are effective in lowering BP in obese hypertensive patients, there have been no large-scale clinical studies comparing the effectiveness of RAAS blockers in obese and lean hypertensive patients.

Activation of the RAAS may also contribute to the glomerular injury and nephron loss associated with obesity. By constricting efferent arterioles, increased angiotensin II formation exacerbates the rise in glomerular hydrostatic pressure caused by systemic arterial hypertension.[5] Studies in type II diabetic patients, who are usually overweight or obese, clearly indicate that ACE inhibitors or ARBs slow the progression of renal disease.[28,98] Thus, ARBs and ACE inhibitors may be particularly useful in obese patients, especially those with diabetes and renal disease.

Mineralocorticoid Receptor (MR) Activation in Obesity Hypertension

Studies in experimental animals and in humans suggest that antagonism of MR may provide an important therapeutic tool not only for lowering BP, but also for

attenuating target organ injury in obesity hypertension. Antagonism of MR in obese dogs markedly attenuated sodium retention, hypertension, and glomerular hyperfiltration.[35] The observation that MR antagonism attenuated glomerular hyperfiltration may also have important implications for renal protection in obesity, although there are no studies, to our knowledge, that have directly tested this in non-diabetic obese humans. Administration of MR antagonists also provides significant antihypertensive benefit in resistant obese patients.[34] Reductions in BP caused by MR antagonism in obese patients with resistant hypertension occurred despite concurrent therapy with ACE inhibitor or ARB, calcium channel blocker, and thiazide diuretic, suggesting that MR activation in obesity can occur independently of angiotensin II-mediated stimulation of aldosterone secretion.

Visceral Obesity May Cause Renal Compression

Visceral obesity initiates several changes that lead to compression of the kidneys, increased intrarenal pressures, impaired renal pressure natriuresis, and hypertension.[10] Intra-abdominal pressure rises in proportion to abdominal diameter, reaching levels as high as 35–40 mmHg in some individuals.[5] In addition, retroperitoneal adipose tissue often encapsulates the kidney and penetrates the renal hilum into the renal medullary sinuses in obese dogs as well as in obese humans, causing additional compression and increased intrarenal pressures.[99]

Obesity also causes changes in renal medullary histology and increased extracellular matrix that exacerbate intrarenal compression and hypertension.[97] Increased intrarenal hydrostatic pressure may, in turn, cause compression of the loops of Henle and vasa recta, thereby increasing tubular sodium and water reabsorption. Although these physical changes in the kidneys cannot account for the initial increase in BP that occurs with rapid weight gain, they may help to explain why abdominal obesity is much more closely associated with hypertension than subcutaneous obesity.[97]

Kidney Injury in Obesity Hypertension

Obesity has not been widely recognized as a major risk factor for ESRD, and is not included as a cause of kidney failure in renal data registries. However, the impact of obesity on renal disease is clear when one considers that diabetes and hypertension, both of which are closely associated with excess weight gain, account for more than 70% of ESRD. Moreover, the rapid rise in the prevalence of ESRD in the past two decades has paralleled increasing obesity and diabetes.[97] Although most of the increasing prevalence of ESRD has been attributed to the increase in type II diabetes, patients with diabetes are usually hypertensive, and the increased BP likely contributes to renal injury.

Population studies indicate that obesity is a major cause of renal disease, even after adjustment for hypertension, diabetes or pre-existing renal disease. In a retrospective analysis of adults who were followed for 15–35 years, the rate of ESRD increased in a stepwise manner as BMI increased.[100] This relationship was not affected by BP or diabetes, and the analysis was adjusted for age, sex, race, education level, smoking status, history of myocardial infarction, serum cholesterol level, proteinuria, hematuria, and serum creatinine level. Thus, observational studies suggest that obesity may be an important risk factor for renal disease through other mechanisms in addition to hypertension and diabetes.

Obesity may also amplify the effect of other primary renal insults, even those that are usually considered to be relatively benign, such as unilateral nephrectomy. Praga and co-workers[101] reported that of patients with a BMI greater than 30 who had undergone unilateral nephrectomy, 92% developed proteinuria or renal insufficiency, whereas only 12% of patients with a BMI less than 30 developed these disorders. Similar findings have also been reported for patients with immunoglobulin A nephropathy.[102] These observations suggest that obesity exacerbates the loss of kidney function in patients with pre-existing glomerulopathies, and that weight loss may lessen the impact of renal injury from other causes.

Animals placed on a high-fat diet for only a few weeks also have significant structural changes in the kidneys, including enlargement of the Bowman space, glomerular cell proliferation, increased mesangial matrix, and increased expression of glomerular TGF-β.[103] These early changes occur with only modest hypertension, only mild metabolic abnormalities, and may be the precursors of more severe renal injury as obesity is sustained. Obese patients often develop proteinuria, frequently in the nephrotic range, that is followed by progressive loss of kidney function.[97] The most common types of renal lesions observed in renal biopsies of obese subjects are focal and segmental glomerular sclerosis and glomerulomegaly.

The gradual loss of kidney function, as well as the hypertension and diabetes that commonly coexist with obesity, may lead to progressive impairment of pressure natriuresis, salt-sensitivity, and greater increases in BP. Thus, renal injury in obese subjects not only exacerbates the hypertension, but also makes BP more difficult to control with antihypertensive drugs. The mechanisms of obesity-induced renal injury are not fully-understood, but likely involve a combination of hemodynamic and metabolic abnormalities.

As discussed previously, obesity causes marked glomerular hyperfiltration and preglomerular vasodilation that permits greater transmission of the increased BP to the glomerular capillaries. These renal hemodynamic changes, along with the metabolic abnormalities, such as hyperglycemia and hyperlipidemia, exacerbate the effects of increases in BP to cause renal injury. A synergistic relationship may exist between the metabolic abnormalities and increased glomerular pressure in causing chronic renal vascular disease and nephron loss, similar to the synergistic effects of hypertension, diabetes, and dyslipidemia in increasing the risk for coronary artery disease and myocardial infarction. However, there are no large-scale studies that have tested this idea.

How Does "Metabolic Syndrome" Relate to Primary Hypertension?

Dyslipidemia, hyperinsulinemia, and hyperglycemia often occur concurrently with hypertension, leading to the proposal of a unique pathophysiologic condition that is often called the *metabolic syndrome*. Definitions of the metabolic syndrome have been proposed by the World Health Organization WHO,[104] the Third Report of the National Cholesterol Education Program's Adult Treatment Panel ATP III,[105] and other organizations.[104] All of these definitions include disordered glucose homeostasis or measures of insulin resistance, dyslipidemia, hypertension, and obesity.

Recent analyses of the metabolic syndrome have questioned whether insulin resistance and hyperinsulinemia are the underlying causes of this complex cluster of cardiovascular risk factors.[104,106] Chronic hyperinsulinemia, in the absence of obesity, does not raise BP in dogs or humans.[107] Multiple studies in humans have also shown that chronic insulin treatment does not raise BP in patients with type 1 or type 2 diabetes, and patients with severe hyperinsulinemia as a result of insulinoma are not hypertensive.[107] Taken together, these observations suggest that hyperinsulinemia *per se* is insufficient to cause chronic hypertension.

Insulin resistance has been proposed to cause hypertension independent of hyperinsulinemia. However, there are several disorders associated with severe insulin resistance and hyperinsulinemia in humans and experimental animal models that are not linked with hypertension. In mice, mutations of the leptin gene or the leptin receptor or mutations of the MC4-R, cause severe insulin resistance and many characteristics of the metabolic syndrome, but BP is not increased compared to wild-type controls.[5,89] Likewise, humans with leptin gene or MC4R mutations have severe insulin resistance, but no indication of SNS activation or hypertension.[94,96] These observations do not support a direct role for insulin resistance in causing hypertension.

Several reports indicate that agents that increase insulin sensitivity, such as the thiazolidinediones, also lower BP. However, these drugs influence expression of multiple genes by binding to the peroxisome proliferator-activated receptor-γ (PPARγ), a nuclear receptor. Thiazolidinediones may also inhibit L-type calcium channels, and they reduce BP in renovascular hypertension that is not associated with insulin resistance or hyperinsulinemia.[5,108] Therefore, it appears that the BP-lowering effects of these drugs are related to other actions besides improvement of insulin sensitivity.

Abnormalities of glucose and lipid metabolism associated with insulin resistance may, over many years, lead to athereosclerosis and vascular injury, and in this way contribute indirectly to increased BP, especially if the renal blood vessels and glomeruli are damaged. Progressive loss of kidney function could contribute to salt-sensitivity of BP and gradual development of hypertension. Thus, the metabolic disturbances associated with severe insulin resistance may exacerbate hypertension by causing renal injury, although the importance of these effects, in the absence of diabetes, is still unclear.

Although insulin resistance and hypertension are often closely correlated, much of the available evidence suggests that this association is largely a consequence of obesity which causes both insulin resistance and high BP through parallel mechanisms. There is little doubt that obesity, especially visceral obesity, is a major cause of the entire cluster of CVD risk factors associated with the metabolic syndrome.[104,107] Importantly, all of the disorders associated with the metabolic syndrome can usually be reversed by weight loss.

GENETIC CAUSES OF HYPERTENSION

Success in identifying genes that contribute importantly to human primary hypertension has been limited mainly to identification of monogenic forms of hypertension. When one considers the complexity of the multiple neural, hormonal, renal, and vascular mechanisms that contribute to short-term and long-term BP regulation, it is perhaps not surprising that finding a few variant genes alleles to account for a major portion of BP variation has been challenging. The complexity of the problem is compounded by the likelihood that BP variation is caused not only by single-gene variants, but also by polymorphic genetic differences, complex interactions among several genes, and interaction among genetic and environmental factors. The finding that

hypertension does not often occur in populations living in non-industrialized regions of the world suggests that environmental influences play a major role in common forms of hypertension.

What is the evidence that gene variants play a major role in human primary hypertension? Multiple studies provide evidence that the closer the genetic relatedness, the greater the similarity of BP.[109] For monozygotic twins (with genetic similarity of 100%), the correlation coefficient for systolic BP has ranged from 0.5 to 0.8 (average: 0.6), for dizygotic twins it has ranged from 0.19 to 0.46 (average: 0.35), and for non-twin siblings (genetic similarity of around 50%) the correlation coefficient has averaged around 0.23. There is also a better correlation of BP values in biologic children than in adopted children. However, the importance of shared family environment is also evident from the BP correlations observed in genetically unrelated adopted siblings.

Comprehensive familial analyses that include other relatives in addition to twins suggest that environment may contribute to as much as 30% of BP variance, and genetic factors may contribute 40 to 50% of BP variance.[109] However, despite the use of sophisticated mathematical models for these calculations, the possibility of nonlinear gene−environmental interactions makes it difficult to quantify the precise roles of genes and environment in BP variation.

Hypertension has been suggested to result from additive effects of multiple variant genes acting in concert to elevate BP. Each gene variant is presumed to have a relatively weak impact on BP, but may produce significant hypertension when they act together in the presence of the necessary environmental conditions. This *polygenic* model also applies to other complex diseases such as diabetes or cancer, where multiple genes and environmental factors may play a role in the development of the disease.

Although the hypertension research literature is replete with studies showing associations of gene polymorphisms and BP, the genetic alterations that contribute to primary hypertension remain unknown.[109] Most of these genetic studies have produced mixed results, even for widely studied polymorphisms such as the ACE insertion/deletion and angiotensinogen polymorphisms.[110] Polymorphisms and mutations in other genes such as α-adducin, atrial natriuretic factor, the insulin receptor, β_2-adrenergic receptor, calcitonin gene-related peptide, angiotensinase C, renin-binding protein, endothelin-1 precursor, G-protein β_3-subunit have also been associated with the development of hypertension in some studies[110]; however, all of these polymorphisms show weak associations, if any, with BP, and many of the early studies showing statistically significant associations have not been confirmed. Large-scale genome-wide association studies (GWAS) in which hundreds of thousands of common genetic variants are genotyped and analyzed for blood pressure association have shown limited success in identifying genes that contribute to hypertension. At best, the gene variations discovered thus far explain only a tiny part of the BP variation found in humans.[111]

Monogenic Disorders that Cause Hypertension

Table 39.1 shows some of the monogenic disorders that are associated with high BP. An interesting feature of these genetic disorders is that they all affect electrolyte transport in the renal tubule or the synthesis and/or activity of RAAS hormones. In all monogenic hypertensive disorders thus far, the final common pathway to hypertension appears to be increased sodium reabsorption and volume expansion. Monogenic hypertension, however, is rare, and all of the known forms together account for less than 1% of human hypertension.

Familial Hyperaldosteronism Type I

Also called *glucocorticoid remediable aldosteronism (GRA)*, familial hyperaldosteronism type I (FH-I) is inherited as an autosomal dominant trait caused by a chimeric gene derived from a meiotic mismatch and unequal crossing between the promoter of the 11β-hydroxylase *CYP11B1* controlled by the structural portion of the aldosterone synthase gene *CYP11B2*.[15] This causes aldosterone secretion to be abnormally regulated by adrenocorticotrophic hormone (ACTH). Because ACTH is suppressed by glucocorticoids, administration of excess glucocorticoids is effective in reducing aldosterone secretion in patients with FH-I.

Patients with FH-I exhibit many of the same characteristics as those with primary aldosteronism, including high aldosterone, hypokalemia, volume expansion, metabolic alkalosis, and low renin. Although some patients with FH-I have severe hypertension, others have only moderate hypertension or may even be normotensive. This wide range of BP could be related to variable expression of the chimeric gene or to other differences in genetic background that would place the inherited BP in the low or normal range in the absence of the FH-I mutation. The final BP could therefore be the combined result of the low or normal inherited BP, the hypertensive effect of the FH-I mutation, and other environmental factors, such as salt intake. Patients with FH-I respond well to thiazide diuretics, as well as spironolactone.

TABLE 39.1 Known Genetic Causes of Hypertension

Genetic Disorder	Age of Onset	Pattern of Inheritance	Aldosterone Level	Serum Potassium Level	Treatment[a]
FH-I (GRA)[b]	2nd or 3rd decade	Autosomal dominant	High	Decreased in 50% of cases; marked decrease with thiazides	Glucocorticoids
FH-II[c]	Middle age	Autosomal dominant	High	Low to normal	Spironolactone, eplerenone
DOC oversecretion due to CAH[c,d]	Childhood	Autosomal recessive	Low	Low to normal	Glucocorticoids
Activating MR mutation exacerbated by pregnancy[e]	2nd or 3rd decade	Unknown	Low	Low to normal	Delivery of fetus
AME2[c,f]	Childhood	Autosomal recessive	Low	Low to normal	Spironolactone, dexamethasone
Liddle's syndrome[g]	3rd decade	Autosomal dominant	Low	Low to normal	Amiloride, triamterene
Gordon's syndrome[h]	2nd or 3rd decade	Autosomal dominant	Low	High	Thiazide diuretic, low-sodium diet

[a]*Treatment for underlying mechanisms; other forms of treatment, including different antihypertensive medications, might be needed to adequately control BP.*
[b]*Familial hyperaldosteronism.*
[c]*Excess production of non-aldosterone mineralocorticoids.*
[d]*Congential adrenal hyperplasia, DOC-producing tumors.*
[e]*Increased activity of MR*
[f]*Apparent mineralocorticoid excess caused by either licorice ingestion or ectopic ACTH secretion.*
[g]*Increased activity of sodium channels.*
[h]*Increased activity of NaCl co-transporter in the distal tubule.*
ACTH: adrenocorticotropic hormone; AME: apparent mineralocorticoid excess; CAH: congenital adrenal hyperplasia; DOC: deoxycorticosterone; FH-I: familial hyperaldosteronism type I; FH-II: familial hyperaldosteronism type II; GRA: glucocorticoid-remediable aldosteronism; MR: mineralocorticoid receptor.

Familial Hyperaldosteronism Type II

Familial hyperaldosteronism type II (FH-II) is a rare disease in which hypertension is caused by excessive aldosterone secretion that is not suppressed by glucocorticoid administration, distinguishing it from FH-I.[112] Patients with FH-II have the same clinical symptoms as patients with primary hyperaldosteronism caused by bilateral adrenal hyperplasia. The genetic abnormality causing FH-II has been localized to chromosome 7p22.[112] Although hypertension in FH-II is unresponsive to glucocorticoids, spironolactone is effective in reducing BP and correcting the metabolic disturbances.

Congenital Adrenal Hyperplasia and Excess Deoxycorticosterone Secretion

This disorder describes a group of syndromes caused by defects in cortisol biosynthesis. Congenital adrenal hyperplasia is an autosomal recessive disorder. When 21-hydroxylase *CYP21A2* is deficient, the most common cause of congenital adrenal hyperplasia, patients are normotensive.[112] When 11β-hydroxylase *CYP11B1* and 17β-hydroxylase *CYP17* are deficient, production of deoxycorticosterone, which has mineralocorticoid activity, is increased, leading to hypertension. Defects in *CYP11B1* and *CYP17* cause inhibition of cortisol production with a subsequent reduction in feedback inhibition of ACTH secretion by the anterior pituitary and hypothalamus. Increased ACTH secretion then stimulates production of steroid precursors proximal to the blocked step, leading to excessive levels of deoxycorticosterone.

Both forms of congenital adrenal hyperplasia are associated with early-onset hypertension and hypokalemia. Signs of androgen excess distinguish the two disorders: 11β-hydroxylase deficiency causes virilization in girls and precocious puberty in boys, whereas 17α-hydroxylase deficiency causes sex hormone deficiency, primary amenorrhea, and delayed sexual development in girls, and ambiguous genitalia in boys. Genetic diagnosis of both conditions relies on testing for mutations that either severely depress or abolish enzyme activity. Both conditions can be effectively treated by administering glucocorticoids that normalize ACTH secretion and ACTH-mediated build-up of cortisol precursors proximal to the enzymatic deficiency, including deoxycorticosterone.

Liddle's Syndrome

This is an autosomal dominant form of monogenic hypertension that results from mutations in the amiloride-sensitive ENaC. Several mutations that result in the elimination of 45–75 amino acids from the cytoplasmic carboxyl terminus of β- or γ-subunits of the channel

have been reported. Mutations that increase ENaC activity, in turn, cause excessive distal and collecting tubule sodium reabsorption and hypertension.[15,112]

Liddle's syndrome is characterized by early-onset hypertension with hypokalemia and suppression of renin and aldosterone. Decreased aldosterone and lack of responsiveness to MR antagonists differentiates this syndrome from primary aldosteronism. Both hypertension and hypokalemia vary in severity, depending on salt intake, and can be treated with amiloride or triamterene, specific inhibitors of ENaC.

Apparent Mineralocorticoid Excess (AME)

AME is an autosomal recessive form of monogenic hypertension that results from a mutation in the renal-specific isoform of the 11β-hydroxysteroid dehydrogenase 2 gene.[15,112] This enzyme normally converts cortisol to the inactive metabolite cortisone and "protects" the MR from being activated by cortisol. This is important, because the renal epithelial MR receptor in the distal and collecting tubules has a similar affinity for aldosterone and cortisol, while cortisol concentrations are normally much higher than aldosterone. Deficiency of 11β-hydroxysteroid dehydrogenase 2 allows the tubular MR to be occupied and activated by cortisol, causing sodium retention and volume expansion, low renin, low aldosterone, and a form of hypertension that is salt-sensitive.

A non-genetic form of the AME syndrome is found in persons ingesting large amounts of licorice which contains glycyrrhetinic acid, an inhibitor of the enzyme 11β-hydroxysteroid dehydrogenase. Both forms of apparent mineralocorticoid excess are effectively treated with MR antagonists, such as spironolactone or eplerenone.

Pseudohypoaldosteronism Type II

Also called *Gordon's syndrome*, pseudohypoaldosteronism type II is a rare Mendelian form of hypertension that is salt-sensitive and associated with hyperkalemia, hyperchloremia, metabolic acidosis, and suppressed renin and aldosterone levels. The disorder is caused by mutations in two genes encoding the serine/threonine protein kinases, WNK1 and WNK4.[113]

The phenotypes of excessive salt retention and hypertension are caused by loss of normal inhibition or constitutive activation of the renal tubular NaCl co-transporter by mutant WNK1 or WNK4 genes. WNK4 normally inhibits NaCl co-transporter activity, and loss-of-function mutations therefore increase NaCl reabsorption and cause hypertension. WNK1 does not regulate NaCl co-transporter activity directly, but exerts an indirect effect through suppression of WNK4 inhibition of the NaCl transporter. Therefore, gain-of-function mutations of WNK1 result in highly active NaCl co-transporter, volume expansion, and hypertension with characteristics similar to those caused by loss-of-function mutations of WNK4.[113]

Hyperkalemia is a major feature of pseudohypoaldosteronism type II[112] and may be due, in part, to decreased NaCl delivery to the cortical collecting tubules, which limits their secretion of potassium. Mutant WNKs may also cause hyperkalemia by inhibiting activity of renal outer medullary potassium (ROMK) channels, the major potassium secretory channels in the distal nephron. The fact that hyperkalemia is invariably present in pseudohypoaldosteronism type II is often used to distinguish it from other monogenic forms of hypertension.

Thiazide diuretics, which inhibit distal nephron NaCl reabsorption, are especially effective in reducing BP and correcting hyperkalemia in patients with pseudohypoaldosteronism type II. Because NaCl co-transporter activity is regulated by luminal salt delivery, decreased NaCl intake also reduces activity of the transporter, and therefore attenuates volume-expansion and hypertension in patients with pseudohypoaldosteronism type II syndrome. Therefore, BP in Gordon's syndrome is highly salt-sensitive.

Mineralocorticoid Receptor Activating Mutation

This monogenic disorder is caused by a substitution of leucine for serine at codon 810 of the MR.[15] This mutation alters the shape and specificity of the MR, and eliminates the usual requirement for the 21-hydroxyl group of aldosterone to interact with the MR. This explains why other steroids, such as progesterone, activate the MR and why spironolactone, which is normally an antagonist of the MR, acts as an agonist for the MR in this disorder. Thus, treatment of these patients with spironolactone or increased levels of progesterone worsens the sodium retention, hypokalemia, and hypertension.

SECONDARY CAUSES OF HYPERTENSION

In a small fraction of patients, the clinical features, history, and physical examination point to a specific cause of increased BP, and the hypertension is therefore said to be *secondary*. Some types of secondary hypertension have a genetic basis, whereas others are caused by cardiovascular diseases and target organ injury associated with various disorders such as diabetes and kidney disease, and in some instances hypertension can be caused by drugs or treatments that patients receive. Table 39.2 lists some of the most frequently-diagnosed causes of secondary hypertension, although we discuss only a few of the more common types.

TABLE 39.2 Some Secondary Causes of Hypertension

- **A.** Renal parenchymal disease
  - Acute and chronic glomerulonephritis
  - Chronic nephritis e.g., pyelonephritis, radiation
  - Polycystic disease
  - Diabetic nephropathy
  - Hydronephrosis
  - Neoplasms
- **B.** Renovascular
  - Renal artery stenosis/compression
  - Intrarenal vasculitis
  - Suprarenal aortic coarctation
- **C.** Renoprival renal failure, loss of kidney tissue
- **D.** Endocrine disorders
  - Renin-producing tumors
  - Cushing syndrome
  - Primary aldosteronism
  - Pheochromocytoma adrenal or extraadrenal chromaffin tumors
  - Acromegaly
- **E.** Pregnancy-induced hypertension
- **F.** Sleep apnea
- **G.** Increased intracranial pressure brain tumors, encephalitis
- **H.** Hormones and drugs (partial list)
  - Glucocorticoids
  - Mineralocorticoids
  - Sympathomimetics
  - Tyramine-containing foods and monoamine oxidase inhibitors
  - Estrogen (e.g., oral contraceptive pills)
  - Apparent mineralocorticoid excess (e.g., licorice)
  - Nonsteroidal anti-inflammatory drugs
  - Cyclosporine
  - Excess alcohol use
  - Drug abuse (e.g., amphetamines, cocaine)

Renovascular Hypertension

Renovascular hypertension, although accounting for only 2–3% of all hypertension, is one of the most common causes of secondary hypertension. The pathophysiology of renovascular hypertension is due to an initial reduction in renal perfusion that occurs as a result of stenosis of the main renal artery, one of its branches or stenosis/injury of other smaller preglomerular blood vessels and glomeruli. The majority of renal vascular lesions reflect either fibromuscular dysplasia or atherosclerosis.[114] The predominant lesion found in the main renal artery or its branches in patients older than 50 years of age is atherosclerotic disease. More subtle functional constriction or structural changes in smaller blood vessels (e.g., afferent arterioles, glomeruli) are difficult to detect clinically, but can contribute to increased BP.

Renovascular hypertension can be unilateral or bilateral, and can result in a homogeneous or nonhomogeneous ischemia of nephrons. As discussed earlier in the chapter, there are some important differences in the pathophysiology of homogeneous compared to non-homogenous impairments of renal perfusion. Experimental counterparts of these two clinical forms of renovascular hypertension can be found in the 1-kidney, 1-clip and the 2-kidney, 1-clip models of Goldblatt hypertension, respectively.

Renal Artery Stenosis in a Single Remaining Kidney or Aortic Coarctation above Both Renal Arteries

Renal artery constriction or aortic coarctation, if severe enough to reduce renal perfusion pressure below the range of autoregulation (approximately 70 mmHg), initially decreases renal blood flow, GFR, and sodium excretion, while increasing renin secretion. However, if the stenosis is not too severe, sodium excretion returns to normal, and if sodium intake is normal and adequate volume is available, renin secretion also returns to nearly normal in the established phase of hypertension.[9,115] At this point, the hypertension is stable, and most indices of renal function are relatively normal, including pressure distal to the stenosis.

Increased angiotensin II accounts for much of the rapid increase in BP after stenosis of the renal artery or suprarenal aortic coarctation. However, even after blocking the RAAS, BP still increases although more slowly until renal perfusion pressure returns to nearly normal. This increase in renal perfusion pressure, at the expense of systemic arterial hypertension, permits normal excretion of sodium and water to be maintained. As long as the sodium intake is normal, activation of the RAAS serves mainly to increase the rate at which BP is elevated. In the established phase of hypertension, blockade of the RAAS causes only small reductions in BP, similar to the decreases observed in normal subjects after angiotensin II blockade.[5]

The importance of volume-expansion in elevating BP in 1-kidney, 1-clip Goldblatt hypertension or suprarenal aortic coarctation depends on the sodium intake. With normal-or high-sodium intake, significant volume-expansion occurs, whereas a low-sodium diet converts this model of hypertension to one that is highly angiotensin II-dependent. When the stenosis is severe and adequate renal perfusion cannot be restored even with increased systemic BP, renin secretion continues to increase, as does BP, leading eventually to malignant hypertension and renal failure. Thus, the ability to return renal perfusion pressure to normal or nearly normal, by volume retention or activation of the RAAS, is critical to maintaining homeostasis when there is stenosis of a single remaining kidney. The same sequence occurs when there are widespread homogeneous increases in preglomerular resistance caused by bilateral renal artery stenosis or aortic coarctation above both renal arteries.[11]

Non-Homogeneous Increases in Renal Vascular Resistance or Unilateral Renal Artery Stenosis in Patients with two Kidneys

As discussed previously, non-homogeneous increases in preglomerular resistance can occur as a result of stenosis of one renal artery and normal perfusion of the contralateral kidney. Also, patchy increases in preglomerular resistance within the kidneys, with some nephrons being underperfused and others having normal or increased blood flow, can cause hypertension with characteristics similar to those found in the 2-kidney, 1-clip form of Goldblatt hypertension. These forms of hypertension all have underperfusion of some nephrons, and normal or increased blood flow in adjacent nephrons or in the nonstenotic kidney.

In experimental models with unilateral renal artery stenosis, the increase in BP is less predictable if the contralateral kidney does not become injured because of the hypertension. In this situation, underperfused nephrons or the entire underperfused kidney in the case of a unilateral renal artery stenosis are exposed to reduced perfusion pressure, secrete increased amounts of renin, and excrete less sodium and water than kidneys with normal blood flow. In contrast, the non-ischemic nephrons or nonstenotic kidney are exposed to increased renal perfusion pressure, causing renin secretion to fall to low levels and increasing sodium excretion above normal. However, even with increased perfusion pressure, the function of the non-ischemic nephrons or unclipped, nonstenotic kidney is impaired because of high circulating angiotensin II, which exerts an antinatriuretic effect and helps to sustain hypertension.

The higher BPs experienced by the nonstenotic kidney may eventually cause nephron damage which then maintains increased BP, even after correction of the stenosis in the other kidney. However, correction of the stenosis plus nephrectomy of the non-stenotic kidney may normalize BP if the stenosis is not so severe that it causes vascular rarefaction and permanent injury to the stenotic kidney.[5,6]

Administration of ACE inhibitors or ARBs as a treatment for renovascular hypertension may improve the structure and function of the non-stenotic kidney, but can in severe cases produce serious reductions in GFR and shrinkage of the stenotic kidney, resulting in fibrosis and further deterioration of its function. This is partly a result of the fall in BP, which may reduce renal perfusion pressure distal to the lesion to below the range of autoregulation. Blockade of angiotensin II also causes vasodilation of efferent arterioles which contributes to a decline in GFR in the stenotic kidney. In some patients with severe renal vascular lesions, administration of ACE inhibitors or ARBs may cause severe decreases in renal function, especially when there is also volume-depletion because of concomitant use of diuretics. Therefore, renal function should be monitored frequently after administration of RAS inhibitors in patients suspected of having renovascular hypertension. Fortunately, these effects appear to be reversible upon cessation of ACE inhibition or ARB, and in many patients the beneficial effects of angiotensin II blockade to reduce BP can be achieved without precipitating further loss of kidney function.

Adrenal Cortex Hypertension

Aldosterone normally exerts nearly 90% of the mineralocorticoid activity of the adrenocortical secretions. However, cortisol can also provide a significant amount of mineralocorticoid activity in some conditions. Aldosterone's mineralocorticoid activity is about 3000 times greater than that of cortisol, but the plasma concentration of cortisol is nearly 2000 times that of aldosterone. Normally, the renal MR is protected from activation by cortisol by 11β-HSD2, which converts active cortisol into inactive cortisone. However, when activity of this enzyme is reduced or when cortisol levels are very high, the MR can be activated by cortisol.

Primary Aldosteronism (Conn Syndrome)

Primary aldosteronism, also called *Conn Syndrome*, results from hypersecretion of aldosterone in the absence of a known stimulus. The excess aldosterone secretion almost always comes from the adrenal cortex, and is usually associated with a solitary adenoma or bilateral hyperplasia of the adrenal cortex. *Secondary aldosteronism* refers to increased aldosterone secretion caused by a known stimulus, such as high levels of angiotensin II. This is the most common form of aldosteronism, and occurs in various conditions associated with increased renin secretion and angiotensin II formation, such as congestive heart failure, sodium depletion or renal artery stenosis.[116]

Primary aldosteronism can occur as a result of an aldosterone-producing adenoma (APA) or because of unilateral or bilateral adrenal hyperplasia.[117] The effects of excess aldosterone were discussed earlier, but the most important actions with regard to BP regulation are increased sodium reabsorption and increased potassium secretion by the renal tubules. This leads to extracellular fluid volume-expansion, hypertension, decreased renin secretion, hypokalemia, and metabolic alkalosis. Most of these effects are highly salt-sensitive, and low sodium intake can greatly attenuate the hypertension and hypokalemia.

Adrenal adenomas and bilateral adrenal hyperplasia account for more than 95% of primary aldosteronism. However, in most studies of unselected patients, the classic form of primary aldosteronism was found in less than 1% of hypertensive patients. Some adrenal glands in patients with primary aldosteronism may have varying degrees of hyperplasticity, and the term *idiopathic hyperaldosteronism* (IHA) was coined to describe this condition. Clinically, APA and IHA are difficult to distinguish, although patients with APA often have more severe hypertension and hypokalemia compared to those with IHA.

The measurement of the aldosterone−renin ratio has been used in an attempt to define more subtle cases of primary aldosteronism.[34,117] This approach has led to the suggestion that excess aldosterone secretion may account for as much as 5 to 10% of essential hypertension. However, there is still debate about whether patients with increased aldosterone−renin ratio truly have primary aldosteronism. In many of these patients, the main reason for the increased aldosterone−renin ratio is the low level of renin, rather than excess aldosterone secretion.[116]

"ESCAPE" FROM SODIUM RETENTION DURING HYPERALDOSTERONISM

Although aldosterone is a powerful sodium-retaining hormone, sodium excretion eventually returns to match sodium intake, even in patients with very high levels of aldosterone. This "escape" from sodium retention is secondary to increased extracellular fluid volume and pressure natriuresis.[118] Thus, after the extracellular fluid volume increases 5−15% above normal, BP also increases 15−25 mmHg, and the elevated BP returns the renal output of salt and water to normal, despite the excess aldosterone. The importance of pressure natriuresis in permitting aldosterone escape has been demonstrated experimentally by servo-controlling renal perfusion pressure; when renal perfusion pressure was servo-controlled, aldosterone infusion caused continued sodium retention and progressive increases in cumulative sodium balance and extracellular fluid volume, resulting in severe circulatory congestion and edema.[118] Failure of the kidneys to escape from aldosterone-induced sodium retention also occurs in patients with heart failure who, because of a severely weakened heart, cannot increase BP sufficiently to re-establish salt and water balance.

Cushing Syndrome Glucocorticoid Excess

Cushing syndrome is characterized by excess secretion of glucocorticoids, with hypertension occuring in approximately 80% of patients.[119] The hypertension with cortisol excess is often difficult to control, morbidity is substantial, and risk for death is largely a result of cardiovascular events, including heart attack and stroke.

Cushing syndrome can be caused by administration of excess cortisol (e.g., for treatment of various inflammatory disorders) or by oversecretion of endogenous cortisol. The most common cause of endogenous cortisol excess is overproduction of ACTH from a pituitary adenoma, a condition referred to as *Cushing disease*. The increased ACTH causes adrenal hyperplasia and stimulates cortisol secretion. Cushing disease can also occur as a result of ectopic secretion of ACTH by tumors outside the pituitary, such as an abdominal carcinoma.

ACTH-independent hypercortisolism can also occur as a result of adenomas of the adrenal cortex. Primary overproduction of cortisol by the adrenal glands, independent of ACTH, accounts for approximately 20−25% of Cushing syndrome, and is usually associated with suppressed ACTH caused by cortisol-induced feedback inhibition of ACTH secretion by the anterior pituitary gland. Administration of large doses of dexamethasone, a synthetic glucocorticoid, can distinguish between ACTH-dependent and ACTH-independent Cushing syndrome. In patients with overproduction of cortisol because of an ACTH-secreting pituitary adenoma or hypothalamic−pituitary dysfunction, even large doses of dexamethasone usually do not suppress ACTH secretion. In contrast, patients with primary adrenal overproduction of cortisol ACTH-independent usually have low or undetectable levels of ACTH. However, the dexamethasone test may occasionally give an incorrect diagnosis, because some ACTH-secreting pituitary tumors respond to dexamethasone with suppression of ACTH secretion.

Glucocorticoids modulate many cell processes, and the precise mechanisms by which hypercortisolism causes hypertension are incompletely-understood. One potential mechanism is activation of the MR; the high levels of cortisol in Cushing syndrome may simply overwhelm the ability of renal 11β-HSD2 to convert active cortisol into inactive cortisone at the MR receptor, so that cortisol stimulates the MR and causes sodium retention, volume-expansion, hypertension, and hypokalemia. High levels of cortisol may also increase the responsiveness to various pressor stimuli, including angiotensin II and norepinephrine.[120]

Studies in experimental animals suggest that excess cortisol may also raise BP through mechanisms that may be at least partially independent of activation of classical glucocorticoid receptor or MR.[120] Most of the available evidence, however, suggests that sodium retention may play a key role, although the precise mechanisms that lead to sodium retention are incompletely-understood.

Pheochromocytoma

Pheochromocytoma is a rare form of secondary hypertension occurring in approximately 0.05% of hypertensive patients.[116] Although rare, pheochromocytoma can provoke fatal hypertensive crises if unrecognized and untreated. Pheochromocytoma can arise from neuroectodermal chromaffin cells, which are part of the sympathoadrenal system. The chromaffin cells have the capacity to synthesize and store catecholamines, and are normally found mainly in the adrenal medulla. Although most chromaffin cell tumors are found in the adrenal medulla, as many as 15 to 30% may be extra-adrenal, located along the sympathetic chain or, rarely, in other sites.[116]

The symptoms and severity of hypertension associated with pheochromocytoma vary depending on the secretory pattern and amount of catecholamines released.[121] With tumors that continuously release large amounts of catecholamines, there may be sustained hypertension with few paroxysms or sudden bursts of very high BP. Tumors that are less active may have cyclical release of catecholamine stores that induce paroxysms of hypertension.

The clinical presentation also depends on whether the predominant catecholamine secreted is norepinephrine or epinephrine. Norepinephrine produces α-adrenergically-mediated vasoconstriction with diastolic hypertension, whereas epinephrine produces β-adrenergically-mediated systolic hypertension and tachycardia, along with sweating, tremors, and flushing. Patients with predominantly epinephrine-secreting tumors sometimes have hypertension alternating with hypotension, and approximately 5% of patients with pheochromocytoma remain normotensive.[116]

Pheochromocytoma patients often have decreased blood volume, consistent with the potent vasoconstrictor effects of norepinephrine. This observation, and the finding that chronic excess catecholamines often increase sodium excretion, could be interpreted as evidence that the hypertensive effects of catecholamines are unrelated to any impairment of renal function. However, the natriuretic effect of catecholamines and volume contraction appear to be secondary to peripheral vasoconstriction, decreased vascular capacitance, and increased BP, which causes pressure natriuresis.[10] Chronic intrarenal infusion of norepinephrine causes sodium retention and sustained hypertension, indicating important direct effects of catecholamines on the kidney to cause hypertension.

Although a high level of circulating catecholamine is the ultimate cause of hypertension in pheochromocytoma, BP is often only modestly correlated with the level of plasma catecholamines. However, the periodic burst of catecholamine release may cause moderate-to-severe hypertension, and lead to target organ injury. Consequently, diagnosis and effective treatment of pheochromocytoma are essential.

Pre-eclampsia

Pre-eclampsia occurs in approximately 5–7% of all pregnancies, with significantly higher rates in certain subpopulations. It remains one of the leading causes of maternal and fetal morbidity and mortality.[122,123] Disease manifestations, including hypertension, proteinuria, and edema, typically occur after 20 weeks of gestation.[69,123–126]

Pre-eclampsia is postulated to occur in two distinct phases: an early maternally asymptomatic phase in which abnormalities of vascular remodeling lead to placental insufficiency and hypoxia; and a later symptomatic phase characterized by widespread maternal endothelial dysfunction. The direct result of the failure to remodel the maternal arteries is that the placenta becomes severely hypoxic. In response, the placenta produces several factors that are released into the maternal circulation, and elicit many of the symptoms characteristic of pre-eclampsia. Several pathways which have been recently elucidated include altered angiogenic balance, increased maternal inflammation/immunological dysfunction, suppression of NO production, enhanced endothelin-1 production, and the creation of harmful ROS, as shown in Figure 39.15.

Multiple Placental Factors Cause Endothelial Dysfunction

One of the most intensely studied pathways activated by placental ischemia is abnormal circulating levels of pro-and antiangiogenic factors. Experimental reductions in vascular endothelial growth factor (VEGF), a protein necessary for the maintenance of endothelial cell health, result in hypertension, proteinuria, and glomerular endotheliosis, all common symptoms of pre-eclampsia.[123] In pre-eclampsia, VEGF and placental growth factor (PLGF) are antagonized by soluble fms-like tyrosine kinase-1 (sFlt-1), an inducible splice variant of the VEGF receptor flt-1 which binds to circulating VEGF and renders it unavailable for receptor binding.[123] Thus, sFlt-1 effectively acts as a competitive inhibitor of VEGF. In pre-eclamptic patients, circulating sFlt-1 levels increase significantly, sometimes well before pre-eclampsia symptoms develop. Furthermore, several models of experimental pre-eclampsia demonstrate elevated production of sFlt-1, and concomitant decreases in the amount of bioavailable VEGF.[123] Finally, administration of VEGF in these models has been shown to attenuate the associated hypertension.[123–126]

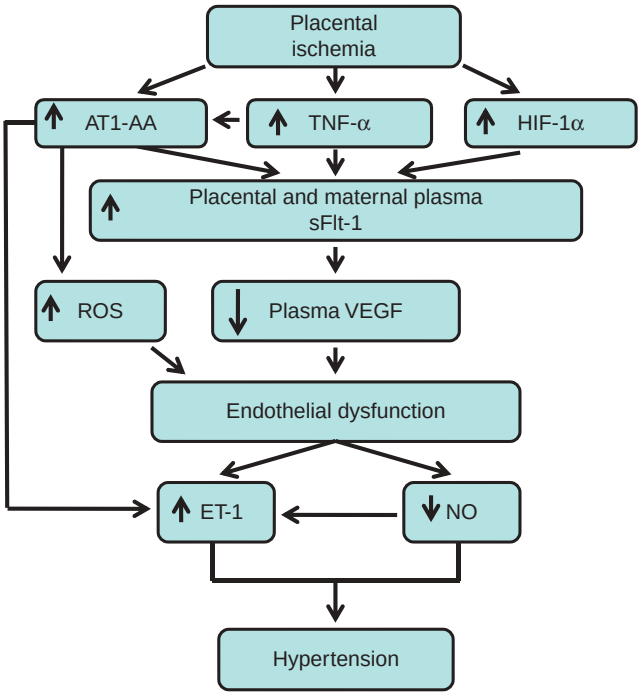

FIGURE 39.15 **Mechanisms linking placental ischemia and hypertension during pre-eclampsia.** (AT1-AA: angiotensin 1 receptor auto antibody; TNF-α: tumor necrosis factor-α; HIF-1α: hypoxia inducible factor-1α; ROS: reactive oxygen species; VEGF: vascular endothelial growth factor; sFlt-1: soluble fms-like tyrosine kinase-1; PlGF: placental growth factor; sEng: soluble endoglin; ET-1: endothelin-1; NO: nitric oxide.)

Another major pathway activated by the ischemic placenta is maternal inflammation. Even during normal pregnancy there is a heightened maternal inflammatory response. In pre-eclampsia, however, this seems to be exaggerated.[70] Inflammatory cytokines, such as IL-6 and TNF-α, are increased in pre-eclamptic women. Administration of either cytokine in pregnant rodents induces a gestational hypertension, similar to that seen in placental ischemia models. Administration of the soluble TNF-α receptor Etanercept in a rodent model of placental ischemia blunted the hypertension through ET-1 suppression, implicating TNF-α as an important link between placental ischemia and endothelial dysfunction.[70]

The maternal immune component of pre-eclampsia also includes circulating agonistic autoantibodies to the angiotensin type 1 receptor AT1-AA.[124] Besides its proposed role in the activation of the AT1 receptor, there appears to be a significant correlation between AT1-AA levels and the production of sFlt-1. Infusion of the purified antibody into pregnant rodents leads to gestational hypertension similar to that seen in placental ischemia models. This effect can be blocked by concurrent infusion of a synthetic heptapeptide which mimics the antibody's natural epitope on the AT1 receptor.[124]

Another important factor implicated in the characteristic maternal endothelial dysfunction associated with pre-eclampsia is elevated levels of the signaling peptide endothelin-1 ET-1.[126] The preponderance of published studies indicate that there is no significant increase in circulating endothelin in pre-eclamptic women compared to non-pregnant controls; however, local tissue levels of preproET-1 are elevated in women with pre-eclampsia.[126] One interesting aspect of ET-1 in pre-eclampsia is that increased vascular and renal ET-1 production have been shown to result from several independent mechanistic pathways, suggesting that it is a central connecting agent in the pathologies associated with these models.[126]

While an effective treatment for pre-eclampsia remains elusive, improved understanding of the mechanisms underlying the disease pathology offer new targets for intervention. Continued research into these molecular and physiological pathways should prove illuminating in the search for a treatment for pre-eclampsia.

Acknowledgments

Our research was supported by grants from the National Heart, Lung and Blood Institute. We thank Stephanie Lucas for expert assistance in preparing this chapter.

References

[1] Lloyd-Jones D, Adams R, Carnethon M, De SG, Ferguson TB, Flegal K, et al. Heart disease and stroke statistics—2009 update: a report from the American Heart Association Statistics Committee and Stroke Statistics Subcommittee. Circulation 2009;119:e21—181.

[2] Lawes CM, Vander HS, Rodgers A. Global burden of blood-pressure-related disease, 2001. Lancet 2008;371:1513—8.

[3] Lewington S, Clarke R, Qizilbash N, Peto R, Collins R. Age-specific relevance of usual blood pressure to vascular mortality: a meta-analysis of individual data for one million adults in 61 prospective studies. Lancet 2002;360:1903—13.

[4] Chobanian AV, Bakris GL, Black HR, Cushman WC, Green LA, Izzo Jr JL, et al. Seventh report of the joint national committee on prevention, detection, evaluation, and treatment of high blood pressure. Hypertension 2003;42:1206—52.

[5] Hall JE, Granger JP, Jones DW, Hall ME. Pathophysiology of hypertension. In: Fuster V, Walsh RA, Harrington RA, editors. Hurst's the heart. McGraw-Hill, Inc; 2011. p. 1549—84.

[6] Hall JE, Granger JP, do Carmo JM, da Silva AA, Dubinion J, George E, et al. Hypertension: physiology and pathophysiology. In: Pollock DM, Garvin JL, editors. Comprehensive physiology-renal physiology; 2012. [In Press].

[7] Guyton AC, Coleman TG, Granger HJ. Circulation: overall regulation. Annu Rev Physiol 1972;34:13—46.

[8] Hall JE, Mizelle HL, Woods LL, Montani JP. Pressure natriuresis and control of arterial pressure during chronic norepinephrine infusion. J Hypertens 1988;6:723—31.

[9] Guyton AC. Arterial pressure and hypertension. Circulatory physiology III. Philadelphia: WB Saunders; 1980.

[10] Hall JE. The kidney, hypertension, and obesity. Hypertension 2003;41:625–33.
[11] Hall JE. Renal function in one-kidney, one-clip hypertension and low renin essential hypertension. Am J Hypertens 1991;4:523S–33S.
[12] Hall JE, Guyton AC, Brands MW. Pressure–volume regulation in hypertension. Kidney Int Suppl 1996;55:S35–41.
[13] Hall JE, Granger JP. Regulation of fluid and electrolyte balance in hypertension: role of hormones and peptides. In: Battegay EJ, Lip GHY, Bakris GL, editors. Hypertension: principles and practice. Boca Raton: Taylor & Francis; 2005. p. 121–42.
[14] Norman Jr. RA, Galloway PG, Dzielak DJ, Huang M. Mechanisms of partial renal infarct hypertension. J Hypertens 1988;6:397–403.
[15] Lifton RP, Gharavi AG, Geller DS. Molecular mechanisms of human hypertension. Cell 2001;104:545–56.
[16] Hall JE. Control of sodium excretion by angiotensin II: intrarenal mechanisms and blood pressure regulation. Am J Physiol 1986;250:R960–72.
[17] Hall JE, Guyton AC, Smith Jr MJ, Coleman TG. Blood pressure and renal function during chronic changes in sodium intake: role of angiotensin. Am J Physiol 1980;239:F271–80.
[18] Campese VM. Salt sensitivity in hypertension. Renal and cardiovascular implications. Hypertension 1994;23:531–50.
[19] Weinberger MH, Fineberg NS, Fineberg SE, Weinberger M. Salt sensitivity, pulse pressure, and death in normal and hypertensive humans. Hypertension 2001;37:429–32.
[20] DiBona GF. Neural control of the kidney: past, present,and future. Hypertension 2003;41:621–4.
[21] Kassab S, Kato T, Wilkins FC, Chen R, Hall JE, Granger JP. Renal denervation attenuates the sodium retention and hypertension associated with obesity. Hypertension 1995;25:893–7.
[22] Esler M, Straznicky N, Eikelis N, Masuo K, Lambert G, Lambert E. Mechanisms of sympathetic activation in obesity-related hypertension. Hypertension 2006;48:787–96.
[23] DiBona GF, Esler M. Translational medicine: the antihypertensive effect of renal denervation. Am J Physiol Regul Integr Comp Physiol 2010;298:R245–53.
[24] Krum H, Sobotka P, Mahfoud F, Bohm M, Esler M, Schlaich M. Device-based antihypertensive therapy: therapeutic modulation of the autonomic nervous system. Circulation 2011;123:209–15.
[25] Cowley Jr AW. Long-term control of arterial blood pressure. Physiol Rev 1992;72:231–300.
[26] Lohmeier TE, Iliescu R. Chronic lowering of blood pressure by carotid baroreflex activation: mechanisms and potential for hypertension therapy. Hypertension 2011;57:880–6.
[27] Hall JE, Brands MW, Henegar JR. Angiotensin II and long-term arterial pressure regulation: the overriding dominance of the kidney. J Am Soc Nephrol 1999;10(Suppl. 12):S258–65.
[28] Brenner BM, Cooper ME, de ZD, Keane WF, Mitch WE, Parving HH, et al. Effects of losartan on renal and cardiovascular outcomes in patients with type 2 diabetes and nephropathy. N Engl J Med 2001;345:861–9.
[29] Lewis EJ, Hunsicker LG, Bain RP, Rohde RD. The effect of angiotensin-converting-enzyme inhibition on diabetic nephropathy. The collaborative study group. N Engl J Med 1993;329:1456–62.
[30] Griffin KA, Abu-Amarah I, Picken M, Bidani AK. Renoprotection by ACE inhibition or aldosterone blockade is blood pressure-dependent. Hypertension 2003;41:201–6.
[31] Eng E, Veniant M, Floege J, Fingerle J, Alpers CE, Menard J, et al. Renal proliferative and phenotypic changes in rats with two-kidney, one-clip Goldblatt hypertension. Am J Hypertens 1994;7:177–85.
[32] Crowley SD, Gurley SB, Herrera MJ, Ruiz P, Griffiths R, Kumar AP, et al. Angiotensin II causes hypertension and cardiac hypertrophy through its receptors in the kidney. Proc Natl Acad Sci USA 2006;103:17985–90.
[33] Fuller PJ, Young MJ. Mechanisms of mineralocorticoid action. Hypertension 2005;46:1227–35.
[34] Calhoun DA. Is there an unrecognized epidemic of primary aldosteronism? Pro. Hypertension 2007;50:447–53.
[35] de Paula RB, da Silva AA, Hall JE. Aldosterone antagonism attenuates obesity-induced hypertension and glomerular hyperfiltration. Hypertension 2004;43:41–7.
[36] Granger JP, Abram S, Stec D, Chandler D, LaMarca B. Endothelin, the kidney, and hypertension. Curr Hypertens Rep 2006;8:298–303.
[37] Kohan DE, Rossi NF, Inscho EW, Pollock DM. Regulation of blood pressure and salt homeostasis by endothelin. Physiol Rev 2011;91:1–77.
[38] Gariepy CE, Ohuchi T, Williams SC, Richardson JA, Yanagisawa M. Salt-sensitive hypertension in endothelin-B receptor-deficient rats. J Clin Invest 2000;105:925–33.
[39] Bagnall AJ, Kelland NF, Gulliver-Sloan F, Davenport AP, Gray GA, Yanagisawa M, et al. Deletion of endothelial cell endothelin B receptors does not affect blood pressure or sensitivity to salt. Hypertension 2006;48:286–93.
[40] Ge Y, Bagnall A, Stricklett PK, Strait K, Webb DJ, Kotelevtsev Y, et al. Collecting duct-specific knockout of the endothelin B receptor causes hypertension and sodium retention. Am J Physiol Renal Physiol 2006;291:F1274–80.
[41] Ge Y, Bagnall A, Stricklett PK, Webb D, Kotelevtsev Y, Kohan DE. Combined knockout of collecting duct endothelin A and B receptors causes hypertension and sodium retention. Am J Physiol Renal Physiol 2008;295:F1635–40.
[42] Kassab S, Miller MT, Novak J, Reckelhoff J, Clower B, Granger JP. Endothelin-A receptor antagonism attenuates the hypertension and renal injury in Dahl salt-sensitive rats. Hypertension 1998;31:397–402.
[43] Kassab S, Novak J, Miller T, Kirchner K, Granger J. Role of endothelin in mediating the attenuated renal hemodynamics in Dahl salt-sensitive hypertension. Hypertension 1997;30:682–6.
[44] Krum H, Viskoper RJ, Lacourciere Y, Budde M, Charlon V. The effect of an endothelin-receptor antagonist, bosentan, on blood pressure in patients with essential hypertension. Bosentan hypertension investigators. N Engl J Med 1998;338:784–90.
[45] Prasad VS, Palaniswamy C, Frishman WH. Endothelin as a clinical target in the treatment of systemic hypertension. Cardiol Rev 2009;17:181–91.
[46] Weber MA, Black H, Bakris G, Krum H, Linas S, Weiss R, et al. A selective endothelin-receptor antagonist to reduce blood pressure in patients with treatment-resistant hypertension: a randomised, double-blind, placebo-controlled trial. Lancet 2009;374:1423–31.
[47] Bakris GL, Lindholm LH, Black HR, Krum H, Linas S, Linseman JV, et al. Divergent results using clinic and ambulatory blood pressures: report of a darusentan-resistant hypertension trial. Hypertension 2010;56:824–30.
[48] Cowley Jr. AW, Mori T, Mattson D, Zou AP. Role of renal no production in the regulation of medullary blood flow. Am J Physiol Regul Integr Comp Physiol 2003;284:R1355–69.
[49] Granger JP, Alexander BT. Abnormal pressure-natriuresis in hypertension: role of nitric oxide. Acta Physiol Scand 2000;168:161–8.
[50] Schnackenberg C, Patel AR, Kirchner KA, Granger JP. Nitric oxide, the kidney and hypertension. Clin Exp Pharmacol Physiol 1997;24:600–6.

[51] O'Conner PM, Cowley Jr AW. Modulation of pressure-natriuresis by renal medullary reactive oxygen species and nitric oxide. Curr.Hypertens.Rep 2010;12:86–92.
[52] Baylis C. Nitric oxide deficiency in chronic kidney disease. Am J Physiol Renal Physiol 2008;294:F1–9.
[53] Rajapakse NW, Mattson DL. Role of L-arginine in nitric oxide production in health and hypertension. Clin Exp Pharmacol Physiol 2009;36:249–55.
[54] Chen PY, Sanders PW. L-arginine abrogates salt-sensitive hypertension in Dahl/Rapp rats. J Clin Invest 1991;88:1559–67.
[55] Boger RH. Asymmetric dimethylarginine ADMA and cardiovascular disease: insights from prospective clinical trials. Vasc Med 2005;10(Suppl. 1):S19–25.
[56] Matsuoka H, Itoh S, Kimoto M, Kohno K, Tamai O, Wada Y, et al. Asymmetrical dimethylarginine, an endogenous nitric oxide synthase inhibitor, in experimental hypertension. Hypertension 1997;29:242–7.
[57] Lassegue B, Griendling KK. NADPH oxidases: functions and pathologies in the vasculature. Arterioscler Thromb Vasc Biol 2010;30:653–61.
[58] Rodrigo R, Gonzalez J, Paoletto F. The role of oxidative stress in the pathophysiology of hypertension. Hypertens Res 2011;34:431–40.
[59] Taniyama Y, Griendling KK. Reactive oxygen species in the vasculature: molecular and cellular mechanisms. Hypertension 2003;42:1075–81.
[60] Cowley Jr AW. Renal medullary oxidative stress, pressure-natriuresis, and hypertension. Hypertension 2008;52:777–86.
[61] Garvin JL, Ortiz PA. The role of reactive oxygen species in the regulation of tubular function. Acta Physiol Scand 2003;179:225–32.
[62] Manning Jr. RD, Meng S, Tian N. Renal and vascular oxidative stress and salt-sensitivity of arterial pressure. Acta Physiol Scand 2003;179:243–50.
[63] Pechanova O, Simko F. Chronic antioxidant therapy fails to ameliorate hypertension: potential mechanisms behind. J Hypertens Suppl 2009;27:S32–6.
[64] Dikalov S, Griendling KK, Harrison DG. Measurement of reactive oxygen species in cardiovascular studies. Hypertension 2007;49:717–27.
[65] Chae CU, Lee RT, Rifai N, Ridker PM. Blood pressure and inflammation in apparently healthy men. Hypertension 2001;38:399–403.
[66] Dzielak DJ. Immune mechanisms in experimental and essential hypertension. Am J Physiol 1991;260:R459–67.
[67] Harrison DG, Guzik TJ, Goronzy J, Weyand C. Is hypertension an immunologic disease? Curr Cardiol Rep 2008;10:464–9.
[68] Harrison DG, Guzik TJ, Lob HE, Madhur MS, Marvar PJ, Thabet SR, et al. Inflammation, immunity, and hypertension. Hypertension 2011;57:132–40.
[69] LaMarca BD, Gilbert J, Granger JP. Recent progress toward the understanding of the pathophysiology of hypertension during preeclampsia. Hypertension 2008;51:982–8.
[70] LaMarca BD, Ryan MJ, Gilbert JS, Murphy SR, Granger JP. Inflammatory cytokines in the pathophysiology of hypertension during preeclampsia. Curr Hypertens Rep 2007;9:480–5.
[71] Lee DL, Sturgis LC, Labazi H, Osborne Jr JB, Fleming C, Pollock JS, et al. Angiotensin II hypertension is attenuated in interleukin-6 knockout mice. Am J Physiol Heart Circ Physiol 2006;290: H935–40.
[72] Guzik TJ, Hoch NE, Brown KA, McCann LA, Rahman A, Dikalov S, et al. Role of the T cell in the genesis of angiotensin II induced hypertension and vascular dysfunction. J Exp Med 2007;204:2449–60.
[73] Crowley SD, Song YS, Lin EE, Griffiths R, Kim HS, Ruiz P. Lymphocyte responses exacerbate angiotensin II-dependent hypertension. Am J Physiol Regul Integr Comp Physiol 2010;298:R1089–97.
[74] Cheng HF, RC. Harris. Cyclooxygenases, the kidney, and hypertension. Hypertension 2004;43:525–30.
[75] Grosser T, Fries S, FitzGerald GA. Biological basis for the cardiovascular consequences of COX-2 inhibition: therapeutic challenges and opportunities. J Clin Invest 2006;116:4–15.
[76] Snowden S, Nelson R. The effects of nonsteroidal anti-inflammatory drugs on blood pressure in hypertensive patients. Cardiol Rev 2011;19:184–91.
[77] Roman RJ. P-450 metabolites of arachidonic acid in the control of cardiovascular function. Physiol Rev 2002;82:131–85.
[78] Williams JM, Murphy S, Burke M, Roman RJ. 20-hydroxyeicosatetraeonic acid: a new target for the treatment of hypertension. J Cardiovasc Pharmacol 2010;56:336–44.
[79] Laffer CL, Laniado-Schwartzman M, Wang MH, Nasjletti A, Elijovich F. 20-HETE and furosemide-induced natriuresis in salt-sensitive essential hypertension. Hypertension 2003;41:703–8.
[80] Laffer CL, Laniado-Schwartzman M, Wang MH, Nasjletti A, Elijovich F. Differential regulation of natriuresis by 20-hydroxyeicosatetraenoic acid in human salt-sensitive versus salt-resistant hypertension. Circulation 2003;107:574–8.
[81] Melo LG, Steinhelper ME, Pang SC, Tse Y, Ackermann U. ANP in regulation of arterial pressure and fluid-electrolyte balance: lessons from genetic mouse models. Physiol Genomics 2000;3:45–58.
[82] Granger JP, Opgenorth TJ, Salazar J, Romero JC, Burnett Jr JC. Long-term hypotensive and renal effects of atrial natriuretic peptide. Hypertension 1986;8:II112–6.
[83] Melo LG, Veress AT, Chong CK, Pang SC, Flynn TG, Sonnenberg H. Salt-sensitive hypertension in ANP knockout mice: potential role of abnormal plasma renin activity. Am J Physiol 1998;274:R255–61.
[84] Whelton PK. Epidemiology of hypertension. Lancet 1994;344:101–6.
[85] Yach D, Stuckler D, Brownell KD. Epidemiologic and economic consequences of the global epidemics of obesity and diabetes. Nat Med 2006;12:62–6.
[86] Ogden CL, Carroll MD, Curtin LR, McDowell MA, Tabak CJ, Flegal KM. Prevalence of overweight and obesity in the United States, 1999–2004. JAMA 2006;295:1549–55.
[87] Garrison RJ, Kannel WB, Stokes III J, Castelli WP. Incidence and precursors of hypertension in young adults: the framingham offspring study. Prev Med 1987;16:235–51.
[88] Stevens VJ, Obarzanek E, Cook NR, Lee IM, Appel LJ, Smith WD, et al. Long-term weight loss and changes in blood pressure: results of the Trials of hypertension prevention, phase II. Ann Intern Med 2001;134:1–11.
[89] Hall JE, da Silva AA, do Carmo JM, Dubinion J, Hamza S, Munusamy S, et al. Obesity-induced hypertension: role of sympathetic nervous system, leptin, and melanocortins. J Biol Chem 2010;285:17271–6.
[90] Esler M. The sympathetic system and hypertension. Am J Hypertens 2000;13:99S–105S.
[91] Grassi G, Seravalle G, Cattaneo BM, Bolla GB, Lanfranchi A, Colombo M, et al. Sympathetic activation in obese normotensive subjects. Hypertension 1995;25:560–3.
[92] Rumantir MS, Vaz M, Jennings GL, Collier G, Kaye DM, Seals DR, et al. Neural mechanisms in human obesity-related hypertension. J Hypertens 1999;17:1125–33.
[93] Shek EW, Brands MW, Hall JE. Chronic leptin infusion increases arterial pressure. Hypertension 1998;31:409–14.

[94] Ozata M, Ozdemir IC, Licinio J. Human leptin deficiency caused by a missense mutation: multiple endocrine defects, decreased sympathetic tone, and immune system dysfunction indicate new targets for leptin action, greater central than peripheral resistance to the effects of leptin, and spontaneous correction of leptin-mediated defects. J Clin Endocrinol Metab 1999;84:3686–95.

[95] do Carmo JM, da Silva AA, Cai Z, Lin S, Dubinion JH, Hall JE. Control of blood pressure, appetite, and glucose by leptin in mice lacking leptin receptors in proopiomelanocortin neurons. Hypertension 2011;57:918–26.

[96] Greenfield JR, Miller JW, Keogh JM, Henning E, Satterwhite JH, Cameron GS, et al. Modulation of blood pressure by central melanocortinergic pathways. N Engl J Med 2009;360:44–52.

[97] Hall JE, Crook ED, Jones DW, Wofford MR, Dubbert PM. Mechanisms of obesity-associated cardiovascular and renal disease. Am J Med Sci 2002;324:127–37.

[98] Lewis EJ, Hunsicker LG, Clarke WR, Berl T, Pohl MA, Lewis JB, et al. Renoprotective effect of the angiotensin-receptor antagonist irbesartan in patients with nephropathy due to type 2 diabetes. N Engl J Med 2001;345:851–60.

[99] Hall JE, Henegar JR, Dwyer TM, Liu J, da Silva AA, Kuo JJ, et al. Is obesity a major cause of chronic kidney disease? Adv Ren Replace Ther 2004;11:41–54.

[100] Hsu CY, McCulloch CE, Iribarren C, Darbinian J, Go AS. Body mass index and risk for end-stage renal disease. Ann Intern Med 2006;144:21–8.

[101] Praga M, Hernandez E, Herrero JC, Morales E, Revilla Y, Diaz-Gonzalez R, et al. Influence of obesity on the appearance of proteinuria and renal insufficiency after unilateral nephrectomy. Kidney Int 2000;58:2111–8.

[102] Bonnet F, Deprele C, Sassolas A, Moulin P, Alamartine E, Berthezene F, et al. Excessive body weight as a new independent risk factor for clinical and pathological progression in primary IgA nephritis. Am J Kidney Dis 2001;37:720–7.

[103] Hall JE, Jones DW, Henegar J, Dwyer TW, Kuo J. Obesity hypertension, and renal disease. In: Eckel RH, editor. Obesity: mechanisms and clinical management. Philadelphia: Lippincott, Williams & Wilkins; 2003. p. 273–300.

[104] Alberti KG, Eckel RH, Grundy SM, Zimmet PZ, Cleeman JI, Donato KA, et al. Harmonizing the metabolic syndrome: a joint interim statement of the International diabetes federation task force on epidemiology and prevention; national heart, lung, and blood institute; american heart association; world heart federation; international atherosclerosis society; and international association for the study of obesity. Circulation 2009;120:1640–5.

[105] Executive summary of the third report of the national cholesterol education program ncep expert panel on detection, evaluation, and treatment of high blood cholesterol in adults adult treatment panel III. JAMA 2001;285:2486–97.

[106] Kahn R, Buse J, Ferrannini E, Stern M. The metabolic syndrome: time for a critical appraisal–joint statement from the american diabetes association and the european association for the study of diabetes. Diabetes Care 2005;28:2289–304.

[107] Hall JE, Summers RL, Brands MW, Keen H, Alonso-Galicia M. Resistance to metabolic actions of insulin and its role in hypertension. Am J Hypertens 1994;7:772–88.

[108] Kurtz TW, Gardner DG. Transcription-modulating drugs: a new frontier in the treatment of essential hypertension. Hypertension 1998;32:380–6.

[109] Cui J, Hopper JL, Harrap SB. Genes and family environment explain correlations between blood pressure and body mass index. Hypertension 2002;40:7–12.

[110] Luft FC. Geneticism of essential hypertension. Hypertension 2004;43:1155–9.

[111] Kurtz TW. Genome-wide association studies will unlock the genetic basis of hypertension: con side of the argument. Hypertension 2010;56:1021–5.

[112] Garovic VD, Hilliard AA, Turner ST. Monogenic forms of low-renin hypertension. Nat Clin Pract Nephrol 2006;2:624–30.

[113] McCormick JA, Ellison DH. The WNKs: atypical protein kinases with pleiotropic actions. Physiol Rev 2011;91:177–219.

[114] Garovic VD, Textor SC. Renovascular hypertension and ischemic nephropathy. Circulation 2005;112:1362–74.

[115] Bianchi G, Tenconi LT, Lucca R. Effect in the conscious dog of constriction of the renal artery to a sole remaining kidney on haemodynamics, sodium balance, body fluid volumes, plasma renin concentration and pressor responsiveness to angiotensin. Clin Sci 1970;38:741–66.

[116] Kaplan NM. Clinical hypertension. Philadelphia: Lippincott, William & Wilkins; 2002, p. 89–92.

[117] Young Jr WF. Minireview: primary aldosteronism–changing concepts in diagnosis and treatment. Endocrinology 2003;144:2208–13.

[118] Hall JE, Granger JP, Smith Jr MJ, Premen AJ. Role of renal hemodynamics and arterial pressure in aldosterone "escape". Hypertension 1984;6:I183–92.

[119] Fallo F, Paoletta A, Tona F, Boscaro M, Sonino N. Response of hypertension to conventional antihypertensive treatment and/or steroidogenesis inhibitors in Cushing's syndrome. J Intern Med 1993;234:595–8.

[120] Whitworth JA, Mangos GJ, Kelly JJ. Cushing, cortisol, and cardiovascular disease. Hypertension 2000;36:912–6.

[121] Goldstein DS, Eisenhofer G, Flynn JA, Wand G, Pacak K. Diagnosis and localization of pheochromocytoma. Hypertension 2004;43:907–10.

[122] Ilekis JV, Reddy UM, Roberts JM. Preeclampsia–a pressing problem: an executive summary of a National Institute of Child Health and Human Development workshop. Reprod Sci 2007;14:508–23.

[123] Powe CE, Levine RJ, Karumanchi SA. Preeclampsia, a disease of the maternal endothelium: the role of antiangiogenic factors and implications for later cardiovascular disease. Circulation 2011;123:2856–69.

[124] George EM, Granger JP. Recent insights into the pathophysiology of preeclampsia. Expert Rev Obstet Gynecol 2010;5:557–66.

[125] George EM, Granger JP. Mechanisms and potential therapies for preeclampsia. Curr Hypertens Rep 2011;13:269–75.

[126] George EM, Palei AC, Granger JP. Endothelin as a final common pathway in the pathophysiology of preeclampsia: therapeutic implications. Curr Opin Nephrol Hypertens 2012;21:157–62.

CHAPTER

40

Physiology and Pathophysiology of Diuretic Action

David H. Ellison

Oregon Health & Science University & VA Medical Center, Portland, OR, USA

INTRODUCTION

The term *diuretic* derives from the Greek *diouretikos*, meaning "to promote urine." Although infusion of saline or ingestion of water would therefore qualify as being diuretic, the term *diuretic* usually connotes a drug that can reduce the extracellular fluid (ECF) volume by increasing urinary solute or water excretion. The term aquaretic has sometimes been applied to drugs that increase excretion of solute free water, distinguishing them from traditional diuretics, which increase solute and water together. The clinical picture of ECF volume expansion leading to edema or "dropsy" (from the Latin, *hydrops*) has been recognized since the earliest days of recorded history. Ancient Egyptians referred to "flooding of the heart," and the Hippocratic Corpus later suggested specific remedies for dropsical patients, although their results are not noted. In 1553, Paracelsus recorded the first truly effective form of therapy for dropsy, inorganic mercury (Calomel). Inorganic mercury remained the mainstay of diuretic treatment until the beginning of this century.

In 1919, the ability of organic mercurial antisyphilitics to effect diuresis was discovered by Vogl, then a medical student. This observation led to the development of effective organic mercurial diuretics, drugs that were used commonly until the 1960s. In 1937, the antimicrobial, sulfanilamide, was found to cause metabolic acidosis in patients. Carbonic anhydrase had been discovered in 1932; it was know that sulfanilamide inhibited this enzyme. Pitts demonstrated that sulfanilamide inhibited Na bicarbonate reabsorption in dogs, and Schwartz showed that sulfanilamide could induce diuresis in patients with congestive heart failure who were resistant to organic mercurial diuretics. Soon, more potent sulfonamide-based carbonic anhydrase inhibitors were developed, but these drugs suffered from side-effects and limited potency. Nevertheless, a group at Sharp & Dohme Inc. was stimulated by these developments to explore the possibility that modification of sulfonamide-based drugs could lead to drugs that enhanced Na *chloride* rather than Na *bicarbonate* excretion. The result of this program was the synthesis of chlorothiazide and its marketing in 1957. This drug ushered in the modern era of diuretic therapy, and revolutionized the clinical treatment of edema.

The search for more potent classes of diuretics continued, based on the structure of chlorothiazide and sulonamyl derivatives. This led to the development of ethacrynic acid and furosemide in the United States and Germany, respectively. The safety and efficacy of these drugs led them to replace the organic mercurials as drugs of first choice for severe and resistant edema. Spironolactone, marketed in 1961, was developed after the properties and structure of aldosterone had been established, and steroidal analogs of aldosterone were found to have aldosterone-blocking activity. Triamterene was initially synthesized as a folic acid antagonist, but was found to have diuretic and K-sparing activity.

The availability of safe, effective, and relatively inexpensive diuretic drugs has made it possible to treat edematous disorders and hypertension effectively. Driven by clinical need, however, the development of effective diuretic drugs generated specific ligands that interact with Na and Cl transport proteins in the kidney. In the 1990s, these ligands were used to identify and clone the Na and Cl transport proteins that mediate the bulk of renal Na and Cl reabsorption.

Seldin and Giebisch's The Kidney, Fifth Edition.
DOI: http://dx.doi.org/10.1016/B978-0-12-381462-3.00040-9

© 2013 Elsevier Inc. All rights reserved.

The diuretic-sensitive transport proteins that have been cloned include the sodium hydrogen exchanger (NHE) family of proteins, the bumetanide-sensitive Na-K-2Cl co-transporters, the thiazide-sensitive Na-Cl co-transporter, and the epithelial Na channel. The information derived from molecular cloning has also permitted identification of inherited human diseases that are caused by mutations in these transport proteins. The phenotypes of several of these disorders resemble the manifestations of chronic diuretic administration. The recognition, for example, that Gitelman's syndrome results from mutation of the thiazide-sensitive Na-Cl co-transporter, has spurred interest in determining how blockade or dysfunction of this transport protein leads to magnesium-wasting. Thus, the development of clinically useful diuretics permitted identification, and later cloning, of specific ion transport pathways. The molecular cloning then helped to define mechanisms of diuretic action and diuretic side-effects, permitting the development of specific antibodies and probes, and of animals in which diuretic-sensitive transport pathways have been "knocked-out." Many primarily historical references included in prior editions of this book have been omitted here. The interested reader is referred to prior editions for more complete references and details.[1]

Diuretic-Sensitive Salt Transport

In a normal human kidney, approximately 23 moles of NaCl are filtered in 150 liters of fluid each day. Approximately 6–10 grams of salt (102–170 mEq NaCl) are consumed each day by individuals on a typical Western diet. To maintain balance, renal NaCl excretion must be approximately 92–160 mmol/day (the difference owing to nonrenal losses). Such calculations imply that 99.2% of the filtered NaCl load is reabsorbed by kidney tubules each day (the fractional sodium excretion, FE_{Na}, is 0.8%). Sodium, chloride, and water reabsorption along the nephron is driven by the metabolic energy in ATP. The ouabain-sensitive Na/K-ATPase is expressed at the basolateral cell membrane of nearly all Na transporting epithelial cells along the nephron. This pump maintains large ion gradients across the plasma membrane, with the intracellular Na concentration maintained low and the intracellular K concentration maintained high. Because the pump is electrogenic, and because it is associated with a K channel, renal epithelial cells have a voltage across the plasma membrane oriented with the inside negative relative to the outside.

The combination of the low intracellular Na concentration and the plasma membrane voltage generates a large electrochemical gradient favoring Na entry from lumen or interstitium. Specific diuretic-sensitive Na transport pathways are expressed at the apical surface of cells along the nephron, permitting vectorial transport of Na from lumen to blood (see Figure 40.1). Along the proximal tubule, where approximately two-thirds of filtered Na is reabsorbed, a major component of Na reabsorption is exchanged for H^+ via an isoform of the Na/H exchanger (NHE3) at the apical membrane. Along the thick ascending limb, where approximately 20–25% of filtered Na is reabsorbed, an isoform of the Na-K-2Cl co-transporter (NKCC2) is expressed at the apical membrane. Along the distal convoluted tubule (DCT), where approximately 5% of filtered Na is reabsorbed, the thiazide-sensitive Na-Cl co-transporter (NCC) is expressed. The DCT comprises two subsegments, the DCT1 (or "early DCT") and the DCT2 (or "late DCT"). Along the DCT1, the NCC is the predominant Na transporter. Along the connecting tubule and cortical collecting duct, where approximately 3% of filtered Na is reabsorbed, isoforms of the amiloride-sensitive epithelial Na channel are expressed (ENaC). DCT2 cells express both NCC and ENaC. Together, these apical Na transport pathways along the nephron form the molecular targets for diuretic action.

This chapter will discuss the physiological and pharmacological bases for diuretic action in the kidney. Although some aspects of clinical diuretic usage will be discussed, we have emphasized physiological principles and mechanisms of action. Several recent texts provide detailed discussions of diuretic treatment of clinical conditions.[2] Extensive discussions of diuretic pharmacokinetics are also available.[3] The influence of renal disease on diuretic drug usage is discussed in the following chapter of this volume.

One classification of diuretic drugs is based on the primary nephron site of action. Such a scheme emphasizes that drugs of more than one chemical class can affect the same ion transport mechanism. Although most diuretic drugs have actions on more than one nephron segment, most owe their clinical effects primarily to their ability to inhibit Na transport by one particular nephron segment. An exception is the osmotic diuretics. Although these drugs were initially believed to inhibit solute and water flux primarily along the proximal tubule, subsequent studies have revealed effects in multiple segments. Other diuretics, however, will be classified according to their primary site of action.

OSMOTIC DIURETICS

Osmotic diuretics are substances that are freely filtered at the glomerulus, but are poorly reabsorbed (see Figure 40.2). The pharmacological activity of drugs in

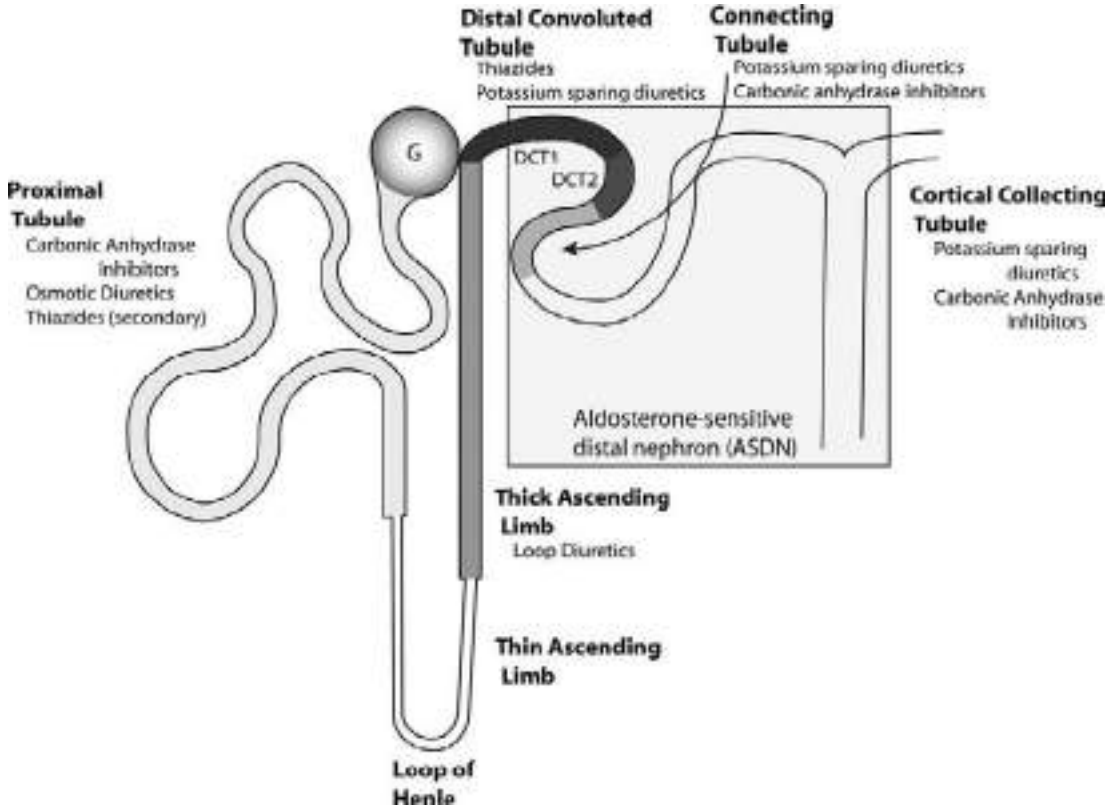

FIGURE 40.1 **Sites of diuretic action along the nephron.** Carbonic anhydrase inhibitors reduce Na reabsorption along the proximal tubule (light gray). Loop diuretics inhibit Na and Cl transport along the thick ascending limb of the Loop of Henle (medium gray). Distal convoluted tubule diuretics (thiazides and others) inhibit Na and Cl transport primarily along the distal convoluted tubule (DCT1 and the DCT2, as shown), with a secondary effect along the collecting duct, under some conditions. Potassium-sparing diuretics inhibit electrogenic Na transport along the aldosterone-sensitive distal nephron, which is indicated by the gray box.

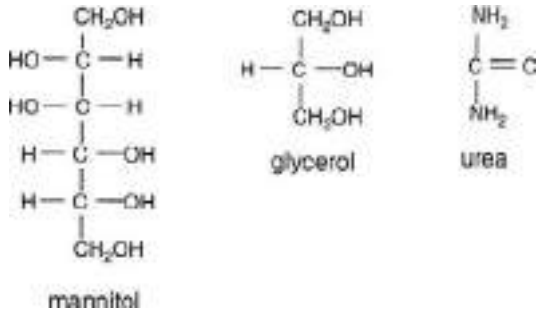

FIGURE 40.2 **Structures of osmotic diuretics.**

this group depends entirely on the osmotic pressure exerted by the drug molecules in solution, and not on interaction with specific transport proteins or enzymes. Mannitol is the prototypical osmotic diuretic. Its diuretic effect is not due to interactions with receptors or renal transporters, but rather it is due to more complex mechanisms that involve osmotic effects on tubule epithelium and reduction of the medullary interstitial osmolality. Because the relationship between the magnitude of effect and concentration of osmotic diuretic in solution is linear, all agents used clinically are small molecules. Other agents considered in this class include urea, sorbitol, and glycerol.

Urinary Electrolyte Excretion

Although osmotic agents do not act directly on transport pathways, the rate of transport of ions is affected. Following the infusion of mannitol, the excretion of sodium, potassium, calcium, magnesium, bicarbonate, and chloride is increased (see Table 40.1). The fractional reabsorption rates for sodium and water are reduced substantially following the infusion of mannitol. Reabsorption of magnesium and calcium are also reduced in the proximal tubule and loop of Henle, and phosphate reabsorption is inhibited slightly along the proximal tubule. In addition to increasing electrolyte excretion, mannitol infusion increases cortical and medullary blood flow, and has a variable effect on GFR. The most pronounced effect observed with mannitol is a brisk diuresis and natriuresis.

TABLE 40.1 Effects of Diuretics on Electrolyte Excretion

	Na	Cl	K	Pi	Ca	Mg
Osmotic diuretics	↑(10–25%)	↑(15–30%)	↑(6%)	↑(5–10%)	↑(10–20%)	↑(>20%)
Carbonic anhydrase inhibitors	↑(6%)	↑(4%)	↑(60%)	↑(>20%)	↑ or ⇔ (<5%)	↑(<5%)
Loop diuretics	↑(30%)	↑(40%)	↑(60–100%)	↑(>20%)	↑(>20%)	↑(>20%)
DCT diuretics	↑(6–11%)	↑(10%)	↑(200%)	↑(>20%)	↓	↑(5–10%)
Na channel blockers	↑(3–5%)	↑(6%)	↓(8%)	⇔	⇔	↓
Spironolactone	↑(3%)	↑(6%)	↓	⇔	⇔	↓

Figures indicate approximate maximal fractional excretions of ions following acute diuretic administration in maximally effective doses. ↑ indicates that the drug increases excretion; ↓ indicates that the drug decreases excretion; ⇔ indicates that the drug has little or no direct effect on excretion. During chronic treatment, effects often wane (Na excretion), may increase (K excretion during DCT diuretic treatment) or may reverse as with uric acid (not shown).
For references that support this table, please see[1].

Mechanism of Action

The mechanisms by which mannitol produces a diuresis are thought to be secondary to: (1) an increase in osmotic pressure in the proximal tubule fluid and loop of Henle, thereby retarding the passive reabsorption of water; and (2) an increase in renal blood flow and washout of the medullary tonicity.

Mannitol is freely filtered at the glomerulus, and its presence in the tubule fluid minimizes passive water reabsorption primarily by the proximal tubule and by the thin limbs of the loop of Henle. Normally, within the proximal tubule, sodium reabsorption creates an osmotic gradient for water reabsorption. When an osmotic diuretic is administered, however, the osmotic force of the nonreabsorbable solute in the lumen opposes the osmotic force produced by sodium reabsorption. Isoosmolality of the tubule fluid is preserved, because molecules of mannitol replace sodium ions reabsorbed. Sodium reabsorption eventually stops, however, because the luminal sodium concentration is reduced to a point where a limiting gradient is reached. Surprisingly, mincropuncture experiments showed that mannitol has a greater effect on inhibiting Na and water reabsorption in the loop of Henle than in the proximal tubule. Within the loop of Henle the site of action of mannitol appears to be restricted to the thin descending limb, resulting in a decrease in reabsorption of Na and water. In the thick ascending limb, reabsorption of Na will continue in proportion to its delivery to this segment. The sum of net transport in the thin and thick limbs will determine the net effect of mannitol in the loop of Henle. Further downstream in the collecting duct, mannitol also reduces sodium and water reabsorption.

Renal Hemodynamics

During the administration of mannitol, its molecules diffuse from the bloodstream into the interstitial space. In the interstitial space, the increased osmotic pressure draws water from the cells to increase ECF volume. This effect increases total renal plasma flow. Cortical blood flow and medullary blood flow are both increased following mannitol infusion. Single nephron GFR, on the other hand, increases in the cortex and decreases in the medulla, this action on the medulla washes out the medullary osmotic gradient by reducing papillary sodium and urea content. The mechanisms that contribute to the increase in renal blood flow include a decrease in hematocrit and blood viscosity, and the release of vasoactive agents. Experimental studies indicate that the osmotic effect of mannitol to increase water movement from intracellular to extracellular space leads to a decrease in hematocrit and in blood viscosity. This fact contributes to a decrease in renal vascular resistance and increase in renal blood flow. Both prostacyclin (PGI_2) synthesis and atrial natriuretic peptide could mediate the effect of mannitol on renal blood flow. The vasodilatory effect of mannitol is reduced when the recipient is pretreated with indomethacin or meclofenamate, suggesting that PGI_2 is involved in the vasodilatory effect.

The effect of mannitol on GFR has been variable, but most studies indicate that the overall effect of mannitol is to increase GFR.[4] Whereas mannitol increased cortical and medullary blood flow, it increased cortical but decreased medullary single nephron GFR. The mechanisms by which mannitol reduces the GFR of deep nephrons are not known, but it has been postulated that mannitol reduces efferent arteriolar pressure. Micropuncture studies examining the determinants of GFR in superficial nephrons have demonstrated that the increase in single nephron GFR is owing to an increase in single nephron plasma flow, and a decrease in oncotic pressure. Alterations in renal hemodynamics contribute to the diuresis observed following administration of mannitol. An increase in medullary blood flow rate reduces medullary tonicity primarily by

decreasing papillary sodium and urea content, and increasing urine flow rate.

Pharmacokinetics

Mannitol is not readily absorbed from the intestine;[4] therefore it is routinely administered intravenously. Following infusion, mannitol distributes in ECF with a volume of distribution of approximately 16 liters; its excretion is almost entirely by glomerular filtration.[5] Of the filtered load, less than 10% is reabsorbed by the renal tubule, and a similar quantity is metabolized, probably in the liver. With normal GFR, plasma half-life is approximately 2.2 hours.

Clinical Use

Mannitol is often used prophylactically to help prevent acute kidney injury (AKI) in the setting of rhabdomyolysis,[4] although some controlled studies have not confirmed benefit.[6] It was previously used for prophylaxis from contrast-induced nephropathy, but appears of no benefit here, and is of potential harm.[7] In the past, it was also used to treat established AKI, but its use here has also fallen from favor, as convincing evidence of benefit has been lacking.

Mannitol is used for short-term reduction of intraocular pressure. By increasing the osmotic pressure, mannitol reduces the volume of aqueous humor and the intraocular pressure by extracting water. Mannitol also decreases cerebral edema and the increase in intracranial pressure associated with trauma, tumors, and neurosurgical procedures, where its benefits are most clearly established.[8] Mannitol is used perioperatively in patients undergoing cardiopulmonary bypass surgery. The beneficial effects may be related to its osmotic activity reducing intravenous fluid requirement,[9] and its ability to act as a free radical antioxidant.[10] Mannitol and other osmotic agents have been used in the treatment of dialysis disequilibrium syndrome.[11,12] This syndrome is characterized acute symptoms immediately following hemodialysis. Most significant symptoms are attributable to disorders of the central nervous system, such as headache, nausea, blurred vision, confusion, seizure, coma, and death. Rapid removal of small solutes such as urea during dialysis of patients who are markedly azotemic is associated with the development of an osmotic gradient for water movement into brain cells producing cerebral edema and neurologic dysfunction. Dialysis disequilibrium syndrome can be minimized by slow solute removal and raising plasma osmolality with saline or mannitol.

Adverse Effects

In patients with reduced cardiac output, an increase in extracellular volume induced by mannitol infusion may lead to pulmonary edema. Intravenous administration of mannitol increases cardiac output and pulmonary capillary wedge pressures. Acute and prolonged administration of mannitol leads to different electrolyte disturbances. Acute overzealous use or the accumulation of mannitol leads to dilutional metabolic acidosis and hyponatremia. Accumulation of mannitol also produces hyperkalemia, as a result of an increase in plasma osmolality. An increase in plasma osmolality increases potassium movement from intracellular to extracellular fluid from bulk solute flow, and increases the electrochemical gradient for potassium secretion. Prolonged administration of mannitol can lead to urinary losses of sodium and potassium, leading to volume-depletion, hypernatremia (as urinary loss of sodium is invariably less than water), and hypokalemia. Marked accumulation of mannitol in patients can lead to reversible AKI that appears to be due to vasoconstriction and tubular vacuolization. Mannitol-induced AKI usually occurs when large cumulative doses of $\sim$295 g are given to patients with previously compromised renal function.[6]

PROXIMAL TUBULE DIURETICS

(Carbonic Anhydrase Inhibitors)

Through the development of carbonic anhydrase inhibitors, important compounds were discovered that have utility as therapeutic agents, and as research tools. Carbonic anhydrase inhibitors (CAI) have a limited therapeutic role as diuretic agents, because of weak natriuretic properties. They are used primarily to reduce intraocular pressure in glaucoma, and to enhance bicarbonate excretion in metabolic alkalosis. CAIs have been useful in the development of other diuretic agents, such as thiazide and loop diuretics, and have been instrumental in elucidating transport function in proximal and distal nephron segments. Structures of carbonic anhydrase inhibitors are shown in Figure 40.3.

Urinary Electrolyte Excretion

Through their effects on carbonic anhydrase in the proximal tubule, CAIs increase bicarbonate excretion by 25–30% (see Table 40.1). Chronic CAI administration, however, causes only a modest natriuresis, despite the magnitude of carbonic anhydrase-dependent proximal Na reabsorption. Several factors account for this. First, carbonic anhydrase is required for reabsorption of HCO_3^-, whereas about two thirds of the proximal Na^+ reabsorption is accompanied by Cl^-. Second, some proximal HCO_3^- reabsorption persists

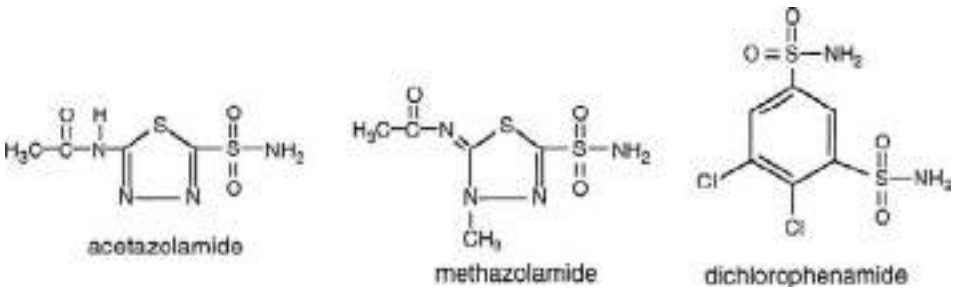

FIGURE 40.3 **Structures of carbonic anhydrase inhibitors.**

even after apparently full inhibition of carbonic anhydrase. Third, some of the HCO_3^- that is delivered from the proximal tubule can be reabsorbed at more distal sites. Fourth, the metabolic acidosis that develops limits the filtered load to HCO_3^-, and thereby curtails the natriuresis. Fifth, the increased delivery of filtered Na^+ to the macula densa elicits a tubuloglomerular feedback (TGF)-induced reduction in the GFR. Micropuncture studies of mice with deletion of the proximal Na^+/H^+ exchanger, NHE3, also show that inhibition of proximal Na reabsorption is largely balanced by reduced GFR,[13] suggesting that the reduction of GFR with CAI use contributes importantly to limiting their natriuretic potency.

The effecs of CAI on calcium excretion are complex. Proximal tubule calcium and phosphate reabsorption are inhibited by acetazolamide, partly because sodium and calcium reabsorption are closely linked within this segment.[14] Yet fractional calcium excretion is often unchanged or reduced, because distal calcium reabsorption is stimulated[15] and because luminal bicarbonate promotes calcium reabsorption. Over the longer-term, however, CAI can increase urinary calcium excretion and predispose to nephrocalcinosis and kidney stone formation.[16] In contrast, phosphate appears to escape distal reabsorption following acetazolamide administration, resulting in an increase in fractional excretion of phosphate by ~3%.[17] Although proximal tubule magnesium transport is inhibited by CAI, fractional excretion is either unchanged or is increased as a result of variable distal reabsorption.[17]

Acetazolamide increases potassium excretion.[17] Although a direct effect of acetazolamide has not been established, it is likely that several indirect effects could contribute to the observed kaliuresis. Carbonic anhydrase inhibition could block proximal tubule potassium reabsorption and increase delivery to the distal tubule, but the reported effects of carbonic anhydrase inhibition on proximal tubule transport have been conflicting. Whereas CAI decreases proximal tubule sodium, bicarbonate, and water absorption during both free flow micropuncture and microperfusion, the effects of CAI on *proximal* tubule potassium transport have been less consistent. In free flow micropuncture studies, carbonic anhydrase inhibition did not affect proximal tubule potassium reabsorption, whereas net potassium transport was reduced during proximal perfusion *in vivo*.[18] The effect of acetazolamide on the proximal tubule ion transport does, however, facilitate an increase in tubular fluid flow rate and delivery to the distal nephron of sodium bicarbonate. This effect is thought to increase the concentration of nonreabsorbable anions, creating an increase in lumen-negative voltage and an increase in flow rate,[19] factors known to increase potassium secretion by the distal tubule.

Most diuretics have some CAI action.[20] This contributes to the weak inhibition of proximal reabsorption by furosemide and chlorothiazide, and to the relaxation of vascular smooth muscle cells by high-dose furosemide Goldfarb diuretics.[20]

Mechanism of Action

In the kidney, CAI likely acts via three distinct, but related mechanisms (see Figure 40.4). First, they inhibit the hydration of CO_2 within cells, thereby reducing the generation of substrate for H^+ and HCO_3^- transporters; second, they reduce the dehydration of carbonic acid to CO_2 and H_2O in the luminal compartment, thereby inhibiting continued H^+ secretion; finally, intracellular CA appears to associate with several membrane transport proteins, and may affect their activity more directly. These actions take place along the nephron, but actions along the proximal tubule and collecting duct are especially important. The biochemical, morphological, and functional properties of carbonic anhydrase have been reviewed previously.[21] Carbonic anhydrase (CA), a metalloenzyme containing one zinc atom per molecule, is important in sodium bicarbonate reabsorption and hydrogen ion secretion by renal epithelial cells.

CA is expressed by many tissues, including erythrocytes, kidney, gut, ciliary body, choroid plexus, and glial cells. Although at least 15 isoforms of CA have been identified,[21] two play predominant roles in renal acid–base homeostasis: CAII and CAIV. CAII is widely expressed, comprising the enzyme expressed by red blood cells and a variety of secretory and absorptive

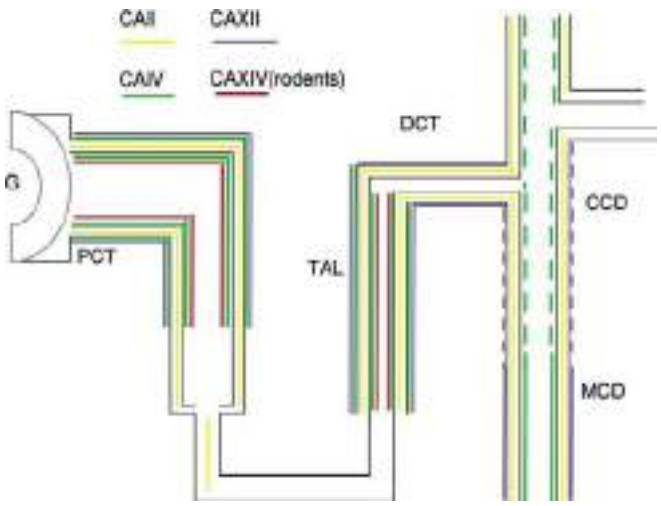

FIGURE 40.4 **Localization of CA isoforms along the nephron.** CAII (yellow stripe) is expressed within the cytoplasm of virtually all nephron segments with the exception of the loop of Henle and the thin ascending limb. CAIV (green stripe) is both apically and basolaterally expressed in the S1 and S2 segments of the proximal tubule and the thick ascending limb. In the distal nephron CAIV is expressed exclusively on the luminal (apical) surface of a-intercalated cells of the CCD and acid secreting cells of the medullary collecting duct. CAXII (blue stripe) is found on the basolateral membrane of S1and S2 segments of the proximal tubule and the thick ascending limb. In the distal nephron, CAXII is located in distal convoluted tubules, principal cells of the CCD, and the medullary collecting duct of some species. In rodent species CAXIV is expressed on the luminal surface of cells in the S1 and S2 segments of the proximal tubule and the thick ascending limb. *(Figure 40 from ref. [21], with permission.)*

epithelia. In the kidney, CAII is a cytoplasmic protein expressed, comprising 95% of renal CA.[21] It is present in proximal tubule cells and intercalated cells of the aldosterone-sensitive distal nephron (ASDN)[21](see Figure 40.4). In rodents, carbonic anhydrase XIV is expressed at the luminal border of the cells of the proximal tubule, thick ascending limb (TAL) of the loop of Henle, and α-intercalated cells of the ASDN,[22] but its role in other species is not as clear.[21]

Carbonic anhydrase (CA) catalyzes the reversible hydration of CO_2 according to the reaction:

$$H^+ + HCO_2^- \leftrightarrow H_2CO_2 \leftrightarrow CO_2 + H^+$$

CO_2 gas dissolves in water and is in equilibrium with the acid H_2CO_3. The Henderson–Hasselbalch equation relates pH, HCO_3^- concentration, and partial pressure of CO_2 gas in physiologic solutions:

$$pH = 6.1 + \log_{10}\frac{(HCO_3^-)}{0.03 \times pCO_2}$$

The uncatalyzed hydration of CO_2 is relatively slow, whereas the turnover number for CAII is in the order of $10^6\ s^{-1}$.

Type IV carbonic anhydrase is bound to renal cortical membranes, comprising up to 5% of the overall activity in kidney, and is sensitive to sulfonamides.[23,24] Type IV carbonic anhydrase, expressed on basolateral and luminal plasma membranes of proximal tubule cells and luminal membrane of intercalated cells,[25] catalyzes the dehydration of intraluminal carbonic acid generated from secreted protons.

Evidence for the physiological importance of carbonic anhydrase is apparent, as a deficiency of CAII leads to a renal acidification defect resulting in renal tubular acidosis.[26] Furthermore, metabolic acidosis leads to an adaptive increase in both CAII and CAIV mRNA expression in kidney,[27] suggesting the importance of both carbonic anhydrase isoforms in this disorder.

Carbonic anhydrase, which is associated with the brush border, prevents H^+ from accumulating in tubule fluid, and secondarily permits the continued secretion of H^+ (see Figure 40.5). Carbon dioxide rapidly diffuses from the lumen into the cell across the apical membrane. Within the cell, H is secreted into the tubule lumen via Na/H exchange, and perhaps other pathways such as H-ATPase. Following H secretion, OH^- formed combines with CO_2, forming HCO_3, which exits the basolateral membrane via $Na(HCO_3)_3$ co-transport.[28] Thus, in the early proximal tubule, the net effect of the process described results in the isosmotic reabsorption of $NaHCO_3$. The lumen chloride concentration increases, because water continues to be reabsorbed producing a lumen-positive potential. These axial changes provide an electrochemical gradient for transport of chloride via paracellular and transcellular pathways. The latter pathway for chloride likely involves a chloride–base exchanger operating in parallel with a Na/H proton exchanger.[29] The dual operation of these parallel exchangers results in net transepithelial NaCl absorption.

The participation of a membrane-bound component of carbonic anhydrase was first suggested by Rector, Carter, and Seldin.[30] The observation that carbonic anhydrase inhibitors produced an acid disequilibrium pH in the proximal tubule suggested that luminal fluid was normally in contact with carbonic anhydrase. Disequilibrium pH refers to the difference between the pH of tubule fluid *in situ* (in this case during infusion of carbonic anhydrase inhibitors), and the pH achieved after the tubule fluid is allowed to reach chemical equilibrium at known pCO_2. Thus, when carbonic anhydrase is present, the pH measured *in situ* should be the same as the pH measured at equilibrium (in other words, CA should make the HCO_3 dissociate into CO_2 and H_2O very rapidly). When carbonic anhydrase is inhibited by the administration of CAI, the dissociation of HCO_3 to OH and CO_2 is slow, allowing H to accumulate in the lumen, and reducing pH.

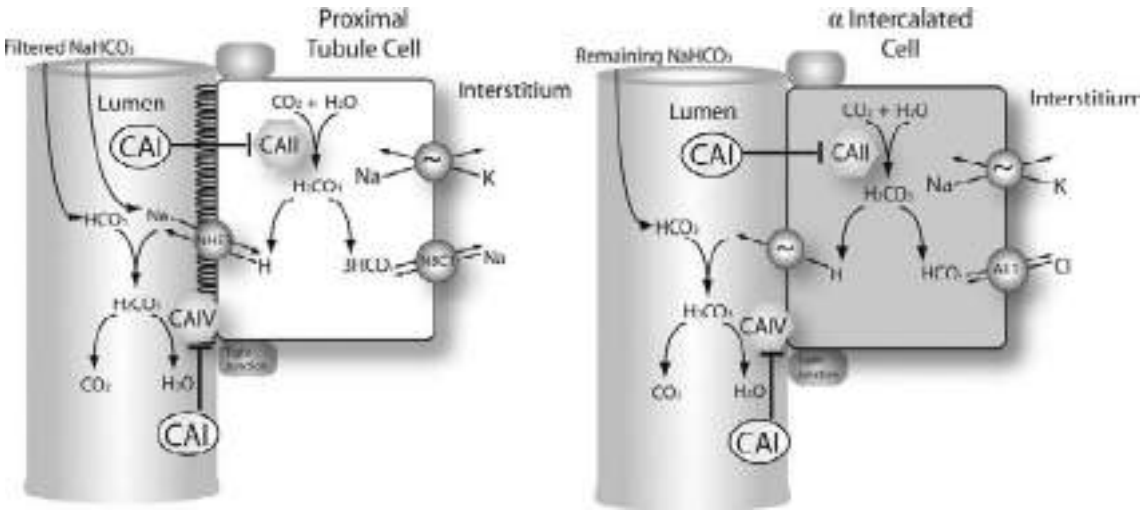

FIGURE 40.5 **Mechanisms of carbonic anhydrase inhibitors in the proximal tubule.** Water and CO_2 form carbonic acid (H_2CO_3) inside proximal cells. Carbonic anhydrase inside the cell (isoform II, CAII) catalyzes the formation of HCO_3 from OH and CO_2. Bicarbonate leaves the cell via the Na,HCO_3 co-transporter (see text). A second pool of carbonic anhydrase (isoform IV, CAIV) is located in the brush border. This participates in disposing of luminal carbonic acid, formed by the combination of filtered bicarbonate and secreted protons. Both pools of carbonic anhydrase are inhibited by acetazolamide and other carbonic anhydrase inhibitors (see text for details).

The demonstration of an acid disequilibrium pH provided physiological evidence in support of previous histochemical findings that a fraction of enzymatic activity was present in the tubule lumen. Although the cytoplasmic carbonic anhydrase constitutes the majority of enzyme activity in kidney, it is believed that the membrane bound carbonic anhydrase plays a significant role in bicarbonate reabsorption by the proximal tubule. Studies addressing this question have employed CAIs that differ in their ability to penetrate proximal tubule cell membranes. Benzolamide is charged at normal pH and is relatively impermeant, whereas acetazolamide enters the cell relatively easily. Both intravenous and intratubular administration of benzolamide resulted in an acid disequilibrium pH, indicating that luminal carbonic anhydrase inhibition contributes to bicarbonate absorption. Furthermore, proximal tubular perfusion of benzolamide resulted in 90% inhibition of bicarbonate reabsorption. Despite near equal efficacy in inhibiting proximal tubule bicarbonate reabsorption, benzolamide lowered tubular fluid pH, whereas acetazolamide increased tubular fluid pH. These results suggest that the site of action of benzolamide is at the luminal membrane, whereas the site of action of acetazolamide is within the cell. Inhibition of luminal carbonic anhydrase causes lumen pH to decrease, because of the continued secretion of hydrogen ions and its accumulation in the tubular lumen. In contrast, acetazolamide does not produce an acid disequilibrium pH.[31] The conclusion that tubular fluid was in direct contact with membrane carbonic anhydrase was substantiated by the use of dextran-bound carbonic anhydrase inhibitor. In proximal tubules perfused *in vivo*, Lucci et al.[32] determined that dextran-bound inhibitors, which inhibit only luminal carbonic anhydrase, decreased proximal tubule bicarbonate absorption by approximately 80%, and reduced lumen pH. Although these studies establish the importance of luminal carbonic anhydrase, they also support a role for intracellular carbonic anhydrase, and as acetazolamide is the only CAI used for its renal properties, suggesting that cytoplasmic CA is the predominant drug target in humans.

Following administration of carbonic anhydrase inhibitors, proximal tubule bicarbonate reabsorption is inhibited variably between 35 and >85%. As suggested from the sites of expression along the nephron (see Figure 40.4), however, additional sites of action of carbonic anhydrase inhibitors include proximal straight tubule or loop of Henle, distal tubule, collecting tubule, and papillary collecting duct.

As noted, CAII may participate more directly in facilitating net bicarbonate and, perhaps, NaCl reabsorption. CAII has been shown to associate with several proximal tranpsporters, including the basolateral bicarbonate exit transport system, kNBC1,[33] the apical Cl/base exchanger, SCL26A6,[34] and the basolateral Na/H exchanger, NHE1,[35] by binding to their respective carboxyl-terminal tails, associations that may be physiologically relevant.[36] Thus, CAIs may act both directly on transporters and via inhibition of substrate production.[37,38]

In α-intercalated cells (see Figure 40.5) within the DCT2, connecting tubule, and collecting duct, CA

facilitates acid secretion that is mediated by a vacuolar H adenosinetriphosphatase (H-ATPase)[39] H-K-ATPase, and the blood group protein RhCG at the apical membrane;[40] RhCG is now known to be an important contributor to renal ammonia secretion.[41–43] The anion exchanger (AE3) at the basolateral cell membrane participates importantly in bicarbonate reabsorption. As for the proximal tubule, both membrane-associated and cytosolic forms of CA likely contribute to distal acidification. Individuals with CAII deficiency display both proximal and distal acidification defects,[44] confirming a role for this enzyme in the distal nephron. Yet, luminal administration of acetazolamide produced an acid disequilibrium pH in the outer medullary collecting duct, suggesting contribution a of luminal carbonic anhydrase as well.[45] In subsequent studies, a membrane-impermeant carbonic anhydrase inhibitor reduced bicarbonate absorption, thus confirming the presence of membrane-bound carbonic anhydrase in the outer medullary collecting duct.[46] The K_i for inhibition of bicarbonate absorption was 5 μM, consistent with the inhibition of Type IV carbonic anhydrase.

Like the proximal tubule, where CAII association with solute transporters may contribute to their regulation and activity, CAII has been shown to associate with CAII at the basolateral membrane,[47,48] and inhibition of CA nearly completely blocked the bicarbonate transport induced by transfection of cells with AE1.

Effects of CAI on renal calcium transporters have also been examined. In mice, acetazolamide increased urinary pH and urinary calcium excretion, in association with a reduced TRPV5 abundance. Similar changes were induced by loading with NH_4Cl, but not by treatment with $NaHCO_3$, suggesting that they were the result of systemic acidosis, and not high urine pH. The importance of TRPV5 in these processes was confirmed by showing that acetazolamide did not alter urinary calcium excretion in TRPV5 knockout mice.[49] These studies suggest that the hypercalciuria and tendency to stone formation induced by CAI is the result of systemic acidosis.

Renal Hemodynamics

Inhibition of carbonic anhydrase produces an acute decrease in GFR by activating TGF.[18] Systemic infusion of acetazolamide resulted in a 30% decrease in GFR. Distally measured single nephron glomerular filtration rate (SNGFR) was reduced by 23% during acetazolamide infusion, whereas proximally measured SNGFR was not affected. These results indicated that acetazolamide blocked activated TGF, which in turn reduced GFR. Similar results were observed following infusion of benzolamide.[50] Sar-ala8-angiotensin I, an angiotensin II antagonist, prevented the decrease in SGNFR, suggesting the involvement of local angiotensin II in response to benzolamide.[50]

Pharmacokinetics

Acetazolamide is well-absorbed from the gastrointestinal (GI) tract. More than 90% of the drug is plasma protein-bound. The highest concentrations are found in tissues that contain large amounts of carbonic anhydrase (e.g., renal cortex, red blood cells). Renal effects are noticeable within 30 minutes, and are usually maximal at 2 hours. Acetazolamide is not metabolized, but is excreted rapidly by glomerular filtration and proximal tubular secretion. The half-life is approximately 5 hours, and renal excretion is essentially complete in 24 hours.[5] In comparison, methazolamide is absorbed more slowly from the GI tract, and its duration of action is long, with a half-life of approximately 14 hours.

Adverse Effects

Generally, carbonic anhydrase inhibitors are well-tolerated, with infrequent serious adverse effects. Side-effects of carbonic anhydrase inhibitors may arise from the continued excretion of electrolytes. Significant hypokalemia and metabolic acidosis may develop. In elderly patients with glaucoma treated with acetazolamide (250 mg to 1000 mg/day), metabolic acidosis was a frequent finding in comparison to a control group.[51] Acetazolamide is also associated with nephrocalcinosis and nephrolithiasis, due to its effects on urine pH facilitating stone formation.[52] Premature infants treated with furosemide and acetazolamide are particularly susceptible to nephrocalcinosis, presumably due to the combined effect of an alkaline urine and hypercalciuria.[53] Other adverse effects include drowsiness, fatigue, CNS depression, and parathesias. Bone marrow suppression has been reported.[51,54]

Clinical Use

The popularity of carbonic anhydrase inhibitors as diuretics has waned, principally because more effective agents are available, but in specific settings these drugs remain useful. In general, tolerance to the natriuretic effects of CAI develops rapidly, and renders them relatively ineffective in treatment of edema. Daily use produces systemic acidemia from an increase in urinary excretion of bicarbonate. Nevertheless, acetazolamide can be administered for short-term therapy, usually in combination with other diuretics to patients who are resistant or who do not respond adequately to other agents. The rationale for using a combination of diuretic agents is based on the summation of their effect at different sites along the nephron.[55]

The major indication for the use of acetazolamide as a diuretic agent is in the treatment of patients with metabolic alkalosis that is accompanied by edematous states or chronic obstructive lung disease.[56] In patients with cirrhosis, congestive heart failure or nephrotic syndrome, aggressive diuresis with loop diuretics promotes intravascular chloride and volume-depletion, secondary hyperaldosteronism, and renal insufficiency, conditions that promote metabolic alkalosis. Administration of sodium chloride to correct the metabolic alkalosis may exacerbate edema. Acetazolamide can improve metabolic alkalosis by decreasing proximal tubule bicarbonate reabsorption and distal proton secretion, thereby increasing the fractional excretion of bicarbonate. An increase in urinary pH (>7.0) indicates enhanced bicarbonaturia. However, it should be noted that potassium-depletion should be corrected prior to acetazolamide use, as acetazolamide will increase potassium excretion. The time-course of acetazolamide effect is rapid. In critically ill patients on ventilators, following the correction of fluid and electrolyte disturbances, intravenous acetazolamide produced an initial effect within 2 hours, and a maximum effect in 15 hours.[57]

Acetazolamide was used to treat chronic open-angle glaucoma, but its popularity has been limited by side-effects and limited efficacy. The high bicarbonate concentration in aqueous humor is carbonic anhydrase-dependent, and oral carbonic anhydrase inhibition can be used to reduce aqueous humor formation. Dorzolamide is a topical CAI that is in clinical use to treat glaucoma.

Acute mountain sickness usually occurs in sojourners who ascend to heights greater than 2500−3000 feet. Symptoms occur within the 12−72 hours, and are characterized by a symptom complex consisting of headache, nausea, dizziness, and breathlessness. Carbonic anhydrase inhibitors improve symptoms and arterial oxygenation.[58−60]

The administration of acetazolamide has been used in the treatment of familial hypokalemic periodic paralysis,[61,62] a disorder characterized by intermittent episodes of muscle weakness and flaccid paralysis. Its efficacy may be related to a decrease in influx of potassium as a result of a decrease in plasma insulin and glucose[63] or to metabolic acidosis. Carbonic anhydrase inhibitors can also be used as an adjunct treatment of epilepsy,[64] pseudotumor cerebri,[65] and central sleep apnea.[66]

By increasing urinary pH, acetazolamide has been used effectively in certain clinical conditions. Acetazolamide is used to treat cystine and uric acid stones by increasing their solubility in urine. Acetazolamide, in combination with sodium bicarbonate infusion, is also used to treat salicylate toxicity. Salicylates are weak acids (pK_a 3.0), therefore their ionic and nonionic forms exist in equilibrium. They are excreted primarily by the kidney through secretion via the organic anion transport pathway in the proximal tubule. Acetazolamide and sodium bicarbonate infusions increase urinary pH, thereby favoring formation of a nondiffusible nonionic form of salicylate, thus increasing excretion of salicylates.[67]

LOOP DIURETICS

The loop diuretics inhibit sodium and chloride transport along the loop of Henle. Although these drugs also impair ion transport by proximal and distal tubules under some conditions, these effects probably contribute little to their action clinically. Although the predominant natriuretic effects result from blockade of NKCC2, the apical transporter of the TAL, other effects may result from blockade of NKCC1, the more widely-expressed form. The affinity of loop diuretics for the two classes of transporter appears to be similar;[68] differential selectivity for the renal isoform during topical use is likely the result of the concentration of secreted drug within the tubule lumen, leading to a higher concentration adjacent to TAL cells. The role of NKCC1 inhibition in pharmacological actions of loop diuretics is discussed below. The loop diuretics available in the United States include furosemide, bumetanide, torsemide, and ethacrynic acid (see Figure 40.6). Organic mercurial diuretics also inhibit ion transport along the loop of Henle, but these drugs are of historical interest, as they are no longer available for clinical use.

Urinary Electrolyte and Water Excretion

Loop diuretics increase the excretion of water, Na, K, Cl, phosphate, magnesium, and calcium (see Table 40.1). The dose−response relationship between loop diuretic and urinary Na and Cl excretion is sigmoidal (see Figure 40.7). The steep dose−response relationship in the therapeutic range has led many to refer to these as "threshold" drugs.[3] Loop diuretics have the highest natriuretic and chloriuretic potency of any class of diuretics; they can increase Na and Cl excretion to more than 25% of the filtered load. Following oral water-loading, the administration of a loop diuretic decreases free water clearance (C_{H2O}) and increases osmolar clearance, although the urine always remains dilute. This effect contrasts with that of osmotic diuretics, in which increases in osmolar clearance are associated with increase in C_{H2O}. During water deprivation, loop diuretics impair the reabsorption of solute free water (T^C_{H2O}). Loop diuretics may induce a "negative"

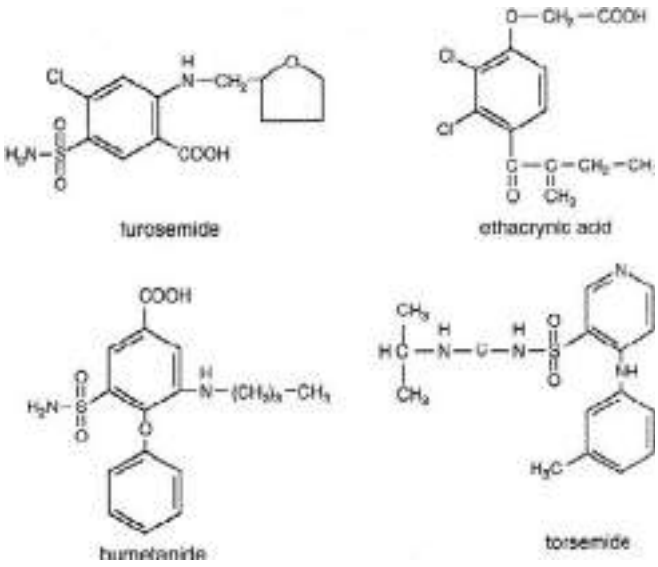

FIGURE 40.6 **Structures of loop diuretics.**

T^{C}_{H2O}, even during water deprivation. During maximal loop diuretic action, the urinary Na concentration is usually between 75−100 mM.[69] Because urinary K concentrations during furosemide-induced natriuresis remain low, the clearance of electrolyte free water (C_{H2O}) is increased when loop diuretics are administered during conditions of water diuresis or water deprivation.[69]

Mechanisms of Action

Na and Cl Transport

The predominant effect of loop diuretic drugs is to inhibit the electroneutral Na-K-2Cl co-transporter at the apical surface of thick ascending limb cells. The loop of Henle, defined as the region between the last surface proximal segment and the first surface distal segment, reabsorbs from 20−50% of the filtered Na- and Cl-load (see Figure 40.1); approximately 10−20% is reabsorbed by thick ascending limb cells. The model in Figure 40.8 shows key components of Na, K, and Cl transport pathways in a thick ascending limb cell. Although mechanisms of Na and Cl transport are discussed more thoroughly in other chapters in this volume, some important points deserve emphasis. First, as in other nephron segments, the Na/K-ATPase at the basolateral cell membrane maintains the intracellular Na concentration low (approximately 10-fold lower than interstitial) and the K concentration high (approximately 20-fold higher than interstitial). Potassium channel(s) in the basolateral cell membrane permit K to diffuse out of the cell, rendering the cell membrane voltage oriented with the intracellular surface negative, relative to extracellular fluid.[70] A chloride channel in the basolateral cell membrane[71] and a barium-sensitive K channel permit Cl to exit the cell.

The transporter inhibited by loop diuretics is one member of the cation-chloride co-transporter family.[72] The cation-chloride co-transporters are part of the amino acid, polyamine, organocation (APC) superfamily.[73] This Na-K-2Cl co-transporter of the thick ascending limb, NKCC2 (formerly called the bumetanide-sensitive co-transporter, BSC1), is encoded by the gene *SLC12A1*. It is a protein with 12 putative membrane-spanning domains that is expressed at the apical membrane of thick ascending limb[74] and macula densa (MD) cells.[75] It lies in parallel with a K channel (ROMK, Kir 1.1) that permits potassium to recycle from the cell to the lumen.[76] Along the thick ascending limb, the asymmetrical orientation of channels (apical versus basolateral), and the action of the Na/K-ATPase and Na-K-2Cl co-transporter, combine to create a transepithelial voltage oriented with the lumen-positive, with respect to the interstitium. This lumen-positive potential drives paracellular absorption of Na, Ca, and Mg. The paracellular component of Na reabsorption comprises as much as 50% of the total transepithelial Na transport by thick ascending limb cells[77]; it should be noted, however, that both the transcellular and the paracellular components of Na transport are inhibited by loop diuretics, the former directly and the latter indirectly; this is because loop diuretics reduce the magnitude of the transepithelial voltage, which normally drives paracellular transport. The thick ascending limb is virtually impermeable to water. The combination of solute absorption and water impermeability leads to dilution of tubule fluid.

Until recently, models of ion- and diuretic-binding to NKCC2 were largely inferential. One model of Na-K-2Cl co-transport, based on the ionic requirements for transport, postulates that ion-binding sites on the transporter must be occupied sequentially, first by Na, then by chloride, then by potassium, and finally by a second chloride.[78] Loop diuretics are organic anions that bind to the NKCC2 from the luminal surface. Early studies showed that [^{3}H] bumetanide binds to membranes that express the NKCC proteins. Optimal binding requires the presence of all three transported species, and binding and inhibition is competed by Cl^-.[79] Binding of bumetanide is also known to be a relatively slow process, and bumetanide becomes "occluded" with Na, K, and Cl.[80] Studies using chimeric NKCC molecules investigated sites of bumetanide-binding and interactions with ions by determining effects on ion transport of heterologously expressed NKCC proteins. Using this approach, it was shown that changes in amino acids that affected bumetanide-binding are not the same as those affecting the kinetics of ion translocation, and it

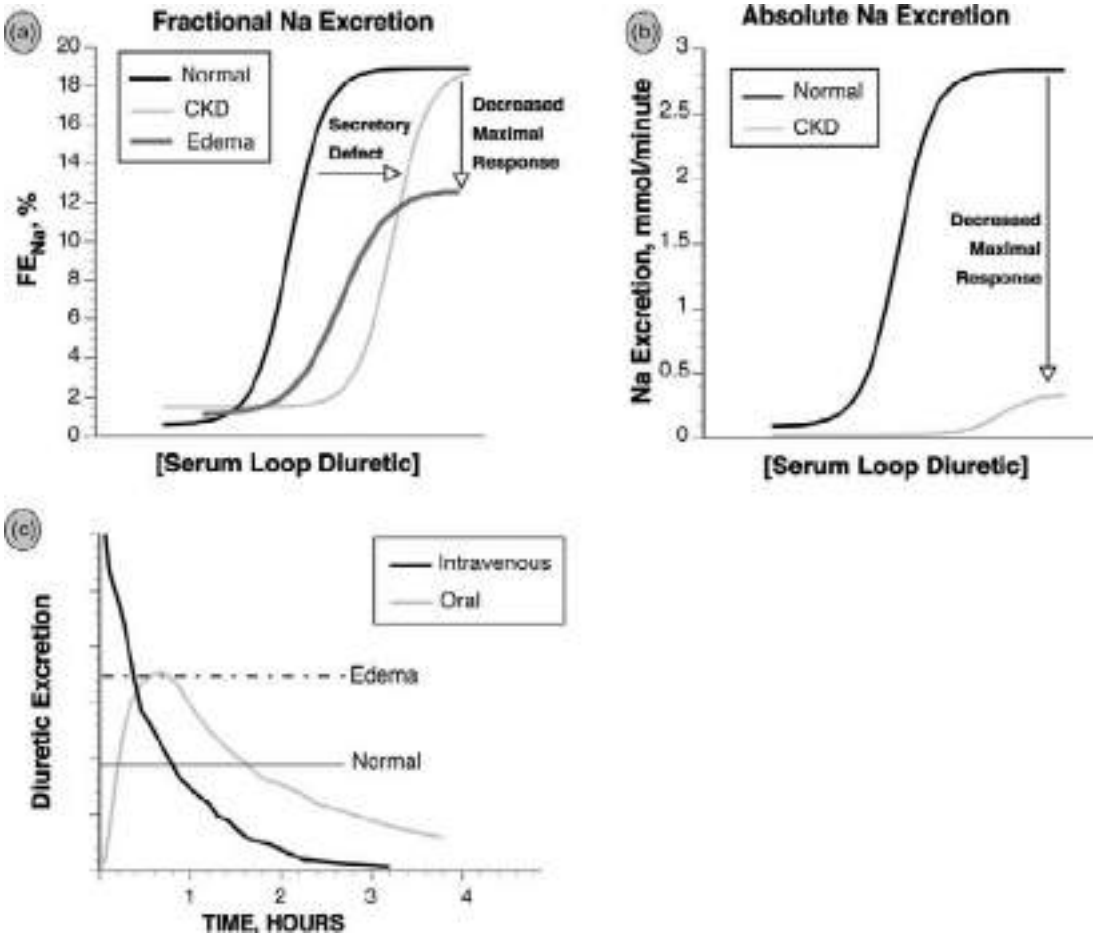

FIGURE 40.7 **Dose–response curve for loop diuretics.** Panel a shows the fractional Na excretion (FE_{Na}) as a function of loop diuretic concentration. Compared with normal patients, patients with chronic renal failure (CKD) show a rightward shift in the curve, owing to impaired diuretic secretion. The maximal response is preserved when expressed as FE_{Na}, but when expressed as absolute Na excretion, (Panel b), maximal natriuresis is reduced in patients with CKD. Patients with edema demonstrate a rightward and downward shift, even when expressed as FE_{Na} (Panel a). Panel c compares the response to intravenous and oral doses of loop diuretics. In a normal individual (Normal), an oral dose may be as effective as an intravenous dose, because the time above the natriuretic threshold (indicated by the "normal" line) is approximately equal. If the natriuretic threshold increases (as indicated by the dashed line, from an edematous patient), then the oral dose may not provide a high enough serum level to elicit natriuresis.

was suggested that bumetanide- and Cl-binding did not occur to the same site.[81,82]

More recently, however, a substantial advance in understanding mechanisms of ion transport and diuretic action has been made possible by solution of the crystal structure of two members of the APC superfamily.[83–86] The insights derived recently permitted Forbush and colleagues[73] to perform homology-based modeling of NKCC1, and to use cysteine mutagenesis of putative pore and binding regions to investigate function. While the work utilized NKCC1, the ubiquitous form, rather than NKCC2, the apical form from TAL, it is likely that the structural insights apply, at least in part. The results suggest that functionally important residues in transmembrane segment 3 (TM3) face the translocation pathway; in contrast to past results in which effects of mutations on affinity were modest, mutations of residues in TM3 led to large changes in inhibitor affinities. Three mutations led to dramatic alterations, one (M382) at the extracellular entry port, and two (F372 and I371) at the inner end of the proposed pore. The investigators suggested, therefore, that loop diuretics bind within the translocating pore, and that the binding site may be near its inner surface. The work also identified a mutation that produces a virtually bumetanide-insensitive NKCC, but which retains some furosemide sensitivity. This work appears to help resolve some discrepancies, and confirm that loop diuretics interact with vital ion transporting segments of the protein.

Although direct inhibition of ion transport is the most important natriuretic action of loop diuretics,

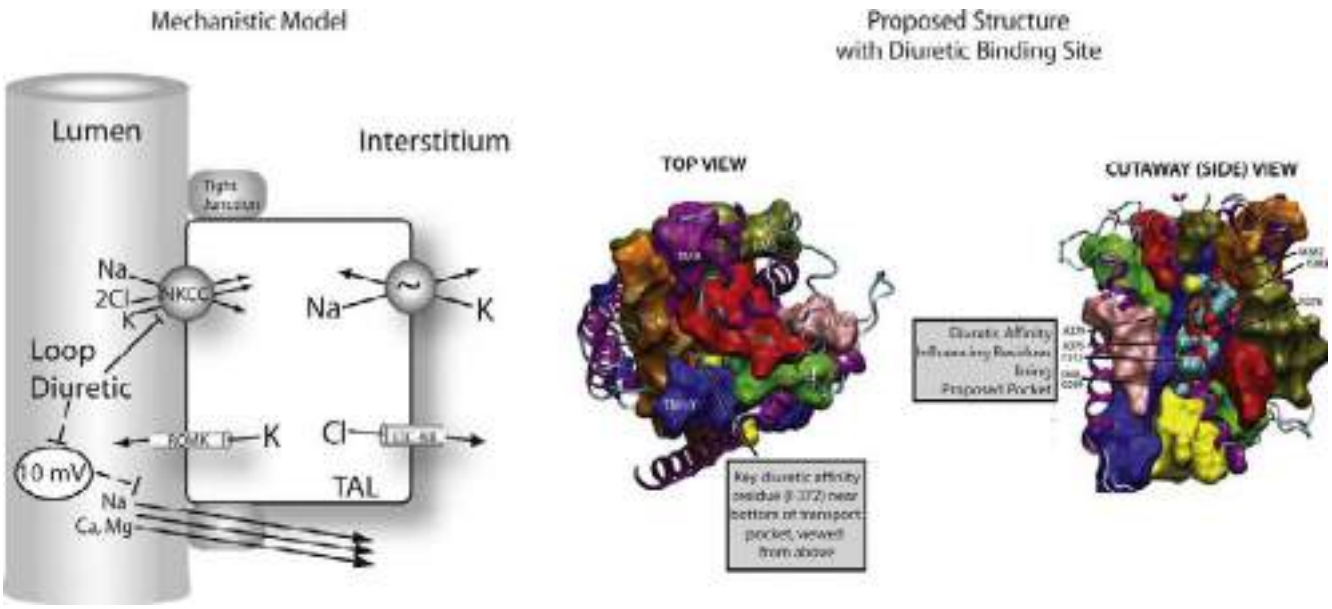

FIGURE 40.8 **Mechanisms of loop diuretic action and proposed NKCC1 structure.** Left panel: Na and Cl are reabsorbed across the apical membrane via the loop diuretic-sensitive Na-K-2Cl co-transporter, NKCC2. Note that the transepithelial voltage along the thick ascending limb is oriented with the lumen-positive relative to interstitium. This transepithelial voltage drives a component of Na (and calcium and magnesium) reabsorption via the paracellular pathway (the "tight junction," shown). Loop diuretics block the NKCC2 directly, thereby reducing the magnitude of the transepithelial voltage, and reducing Na, K, Cl, Mg, and Ca reabsorption. Right panel: Proposed structure of NKCC1. On the left, a view from above shows the translocation pocket, where residue F372, which lies nears its bottom, can be seen through the open pocket. On the right, a cutaway view into transmembrane segment 3, showing pore-lining residues colored blue and labeled. *(Structural models are adapted from J. Biol. Chem. (2012). Mar 21. (Epub ahead of print) PMID: 22437837, with permission.)*

other actions may contribute to natriuresis. Thick ascending limb cells have been shown to produce prostaglandin E_2 following stimulation with furosemide[87] or low luminal NaCl concentration.[88] Blockade of cyclooxygenase reduces the effects of furosemide to inhibit loop segment chloride transport in rats[89]; prostaglandin E_2, but not I_2, can restore this effect.[90] Animals defective in PGE_2 receptors also demonstrate blunted natriuresis, compared with wild-type animals,[91] indicating an important role for PGE_2 in loop diuretic-induced natriuresis. Increases in renal prostaglandins may contribute to the hemodynamic effects of loop diuretics, described below.

Ca and Mg Transport

Loop diuretics increase the excretion of the divalent cations, calcium and magnesium. This effect to increase calcium excretion is used to advantage when furosemide is added to saline to treat hypercalcemia,[92] although this approach is no longer recommended routinely[93] (see below). Although a component of magnesium and calcium absorption by thick ascending limbs may be active (especially when circulating PTH levels are high[94]), a large component of their absorption is passive and paracellular, driven by the transepithelial voltage. As described above, active NaCl transport by thick ascending limb cells leads to a transepithelial voltage, oriented in the lumen-positive direction. The paracellular pathway in the thick ascending limb is cation selective; expression of claudins 16 and 19 appear to play dominant roles.[95–97] The positive voltage in the lumen, relative to interstitium, drives calcium and magnesium absorption through the paracellular pathway; because these are divalent cations, the electrical driving force is double that for Na. Loop diuretics, by blocking the activity of the Na-K-2Cl co-transporter at the apical membrane of thick ascending limb cells, reduce the transepithelial voltage, impairing passive calcium and magnesium absorption.

Renin Secretion

In addition to enhancing Na and Cl excretion, effects that result directly from inhibiting Na and Cl transport, loop diuretics also stimulate renin secretion. A portion of this effect results from contraction of the ECF volume and a reduction of blood pressure (see below), but loop diuretics also stimulate renin secretion by inhibiting NaCl uptake by macula densa cells (see Figure 40.9). Macula densa cells sense the NaCl concentration in the lumen of the thick ascending limb, because NaCl enters the cell across the apical membrane.[98] High luminal NaCl concentrations in the

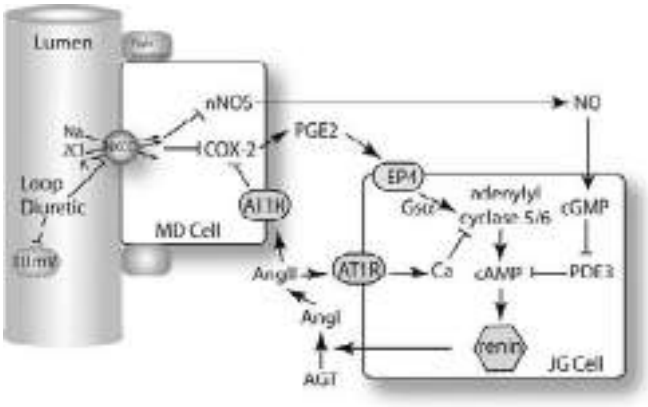

FIGURE 40.9 **Regulation of renin secretion by diuretics**. A macula densa (MD) cell is shown expressing NKCC2 at its apical surface, in parallel with a K channel. Movement of NaCl across the apical membrane inhibits production of nitric oxide (NO) via nitric oxide synthase I (nNOS). When loop diuretics inhibit NaCl uptake, nitric oxide is produced and diffuses to the extraglomerular mesangium or directly to juxtaglomerular (JG) cells, where it increases cGMP. cGMP inhibits phosphodiesterase 3 (PDE_3) which metabolizes cAMP to 5″ AMP. cAMP stimulates renin secretion. NaCl entry across the apical membrane also inhibits cyclooxygenase (COX-2). When loop diuretics block NaCl entry, COX-2 produces prostaglandin E_2 (PGE_2), which acts via Gsα to stimulate adenylyl cyclase, thereby increasing cAMP and renin.

region of the macula densa lead to two distinct but related effects. First they activate the TGF response, which suppresses the GFR. Second, they inhibit renin secretion. The relation between these two effects is complex and has been reviewed,[98] but both appear to be controlled, at least in part, by NaCl movement across the apical membrane.

The pathways mediating Na and Cl uptake into macula densa cells are similar to those expressed by adjacent TAL cells. These include the loop diuretic-sensitive Na-K-2Cl co-transporter at the apical surface. Under normal conditions, an increase in luminal NaCl concentration in the thick ascending limb raises the NaCl concentration inside macula densa cells. Because the activity of the basolateral Na/K-ATPase is lower in macula densa cells than in surrounding thick ascending limb cells,[99] the cell NaCl concentration is much more dependent on luminal NaCl concentration than in TAL cells.[100] When luminal and macula densa cell NaCl concentrations decline, COX-2 activity and expression are induced; this leads to the production of PGE_2, which diffuses to juxtaglomerular cells. There, PGE_2 activates EP4 receptors, resulting in Gsα-mediated activation of adenylyl cyclase. This process, in turn, increases the concentration of cyclic AMP, which eventually stimulates renin secretion.[98]

The constitutive (neuronal) isoform of nitric oxide synthase (NOS I) is expressed by macula densa cells, but not substantially by other cells in the kidney. Nitric oxide produced by macula densa cells has a paracrine effect to increase cAMP in adjacent juxtaglomerular cells (Figure 40.9). In these cells, nitric oxide increases cellular concentrations of cGMP, which inhibit phosphodiesterase 3.[101] Inhibition of phosphodiesterase 3 permits cAMP accumulation. Renin secretion induced by dietary NaCl depletion or furosemide is dependent on an intact nitric oxide system,[102] although it appears that basal renin secretion is not.

The second isoform of cyclooxygenase, COX-2, is also highly expressed by macula densa cells; its expression is increased by loop diuretic treatment.[88,103–105] Blockade of prostaglandin synthesis either by nonspecific cyclooxygenase inhibitors or by specific COX-2 blockers[106] reduces the renin secretory response to loop diuretics. Current views suggest that loop diuretics, like low luminal NaCl delivery, stimulate renin secretion by macula densa cells by activating COX-2, leading to PGE_2 production. PGE_2 stimulates EP4 receptors leading to renin synthesis.[107]

RENAL HEMODYNAMICS AND OXYGENATION

Most classes of diuretic reduce glomerular filtration; in contrast, loop diuretics tend to preserve GFR and renal blood flow, although GFR and RPF can decline when ECF volume contracts. NKCC1 is expressed by many cells, including vascular smooth muscle cells,[108] where it appears to contribute to vasoconstriction. The ability of loop diuretics to inhibit NKCC1, therefore, would suggest that the hemodynamic effect of loop diuretics in the kidney should consist of vasodilatation. In addition, a reduction of renal vascular resistance should result from the well-known blockade of TGF mechanism by loop diuretics, discussed below. In several species, an effect of loop diuretics to increase renal blood flow and dilate renal vessels has been observed in studies in humans[69] and dogs.[109,110] In contrast, in the majority of studies in the rat, furosemide led to a ~10–20% reduction of RBF.[111,112] In the rodent, the renal hemodynamic effects of NKCC inhibition may be unrelated to the primary actions of the diuretic on tubular and vascular functions, but to result from secondary effects on RBF activated by the diuretic. In addition, loop diuretics are known to rapidly stimulate renin secretion and prostaglandin formation, so that differences in the response of these regulatory systems to the diuretic could cause species-specific responses. Oppermann and colleagues[112] found that furosemide dilated glomerular afferent arterioles, when perfused *in vitro*, as expected from a direct effect to inhibit NKCC1, but rather led to a 50% reduction in total renal

blood flow and a 27% reduction in superficial blood flow. Notably, mice in which NKCC1 was knocked-out responded with qualitatively similar reductions in renal blood flow. These workers suggested that the effects on renal blood flow may have resulted from increased angiotensin II production, production of vasoconstrictor prostaglandins or intrarenal pressure changes consequent to diuresis.

Changes in renal hemodynamics are associated with changes in renal oxygen consumption and tissue oxygenation. Most studies in animals show that renal oxygen consumption declines and renal oxygen tension increases, especially in the medulla.[113,114] This information was used to suggest that loop diuretics might be beneficial in preventing or treating AKI; although this prediction was not borne out by clinical trials (see below), it is clear that loop diuretics do increase renal medullary oxygen tension, both in animals and in humans, as detected by BOLD MRI.[115,116]

Another factor that may contribute to the tendency of loop diuretics to maintain GFR and renal plasma flow despite volume contraction is their effect on the TGF system. The sensing mechanism that activates TGF involves NaCl transport across the apical membrane of macula densa cells by NKCC2 (see Figure 40.9). Under normal conditions when the luminal concentration of NaCl reaching the macula densa rises (as during volume expansion) GFR decreases via TGF. To a large degree, the TGF-mediated decrease in GFR results from afferent arteriolar constriction.[98] Although the mechanisms by which ion transport across the apical membrane of macula densa cells translates to afferent arteriolar vasoconstriction are unclear, they appear to involve the production of adenosine (an afferent arteriolar vasoconstrictor) and an increase in mesangial and smooth muscle cell calcium concentrations.[98] ATP release from macula densa cells[117] leads to the extracellular formation of adenosine by ecto-5′-nucleotidase. The fact that TGF is blunted in animals where ecto-5′-nucleotidase and A1 receptors are pharmacologically inhibited, and in A1 receptor and ecto-5′-nucleotidase knockout mice, supports the importance of adenosine formation and activation of adenosine A1 receptors in mediating TGF.[118–121] In a manner analogous to the effects on renin secretion, loop diuretic drugs block TGF by blocking the sensing step. In the absence of direct effects to inhibit NaCl uptake by macula densa cells, loop diuretics would be expected to suppress GFR and RPF, because they increase NaCl delivery (this action explains the effects of CAI and distal convoluted tubule diuretics on TGF[18]). Instead, blockade of NaCl uptake actually inhibits the TGF, despite increased delivery, permitting GFR and RPF to be maintained.

Systemic Hemodyanamics

Acute intravenous administration of loop diuretics tends to increase venous capacitance.[122] Most studies suggest that this effect results from stimulation of prostaglandin synthesis by the kidney.[123,124] Other studies, however, suggest that loop diuretics have effects in peripheral vascular beds as well[125] or may stimulate nitric oxide production.[126] Pickkers and co-workers examined the local effects of furosemide in the human forearm. Furosemide had no effect on arterial vessels, but did cause dilation of veins, an effect that was dependent on local prostaglandin production.[127] As noted above, there is increasing interest in the role of NKCC1 in maintaining vascular smooth muscle tone. Some,[128,129] but not other,[130] investigators have reported that NKCC1 knockout leads to basal hypotension; although NKCC1 inhibition may contribute to vasodilation under some circumstances, the plasma diuretic concentration needed for this effect is probably rare in clinical practice, for reasons noted above.

Although venodilation and improvements in cardiac hemodynamics frequently result from intravenous therapy with loop diuretics, the hemodynamic response to intravenous loop diuretics is more complex. Johnston et al. reported that low-dose furosemide increased venous capacitance, but that higher doses did not.[131] It was suggested that furosemide-induced renin secretion may generate angiotensin II-induced vasoconstriction. This vasoconstrictor might overwhelm the prostaglandin-mediated vasodilatory effects in some patients. In two series, 1–1.5 mg/kg furosemide boluses, administered to patients with chronic congestive heart failure, resulted in transient *deteriorations* in hemodyanamics (during the first hour), with a decline in stroke volume index, an increase in left ventricular filling pressure,[132,133] and exacerbation of congestive heart failure symptoms. These changes were attributed to activation of both the sympathetic nervous system and the renin–angiotensin system by the diuretic drug. Evidence for a role of the renin–angiotensin system in the furosemide-induced deterioration in systemic hemodynamics includes the temporal association between its activation and hemodynamic deterioration,[132,133] and the ability of angiotensin I-converting enzyme inhibitors to prevent much of the pressor effect.[132,133] Other studies have shown that acute loop diuretic administration frequently produces a transient decline in cardiac output; whether diuretic administration increases or decreases left atrial pressure acutely may depend primarily on the state of underlying sympathetic nervous system and renin–angiotensin axis activation. Interestingly, these complex interactions between prior physiological state and hemodynamic response to loop diuretics in humans parallel the

TABLE 40.2 Pharmacokinetics of Loop Diuretics

	Bioavailability, % Oral Dose Absorbed	Healthy	Kidney Disease	Liver Disease	HF
Furosemide	50% (range: 10–100%)	1.5–2	2.8	2.5	2.7
Bumetanide	80–100%	1	1.6	2.3	1.3
Torsemide	80–100%	3–4	4–5	8	6

Data from ref. [72].
Elimination half-life: h; HF: heart failure.

complex interactions postulated to explain the paradoxical effects of loop diuretics in mice.[112]

Pharmacokinetics

The three loop diuretics that are used most commonly, furosemide, bumetanide, and torsemide, are absorbed quickly after oral administration, reaching peak concentrations within 0.5–2 hours (see Table 40.2). Furosemide absorption is slower than the rate of elimination in normal subjects; thus, the time to reach peak serum level is slower for furosemide than for bumetanide and torsemide. This phenomenon is called "absorption-limited kinetics".[3] The bioavailability of loop diuretics varies from 50 to 90% (Table 40.2), with furosemide having the lowest, and most variable oral bioavailability. For this reason, when changing a patient from intravenous to oral furosemide, the dose is frequently doubled to account for its limited oral bioavailability.[3] The half-lives of the loop diuretics available in the United States vary, but all are relatively short (ranging from approximately 1 hour for bumetanide to 3–4 hours for torsemide). The half-lives of muzolimine, xipamide, and ozolinone, none of which is available in the United States, are 6–15 hours.

Loop diuretics are organic anions that circulate tightly bound to albumin (>95%); thus their volumes of distribution are small, except during extreme hypoproteinemia.[134] Approximately 50% of an administered dose of furosemide is excreted unchanged into the urine. The remainder appears to be eliminated by glucuronidation, probably by the kidney. Bumetanide and torsemide are both metabolized by the liver, and also excreted unchanged by the kidney. These differences mean that furosemide kinetics are affected by renal disease, whereas bumetanide and torsemide kinetics tend not to be; this has clinical implications, discussed below.[135]

Clinical Use

Indications for loop diuretic use are given in Table 40.3. They are used commonly to treat the edematous conditions, heart failure, cirrhosis of the liver, and nephrotic syndrome. In addition, a variety of other electrolyte, fluid, and acid–base disorders can respond to loop diuretic therapy. Essentials of diuretic treatment of disease are the focus of other reviews, and will not be discussed here. The interested reader is referred to other sources for information.[2,55,136]

Loop diuretics are commonly used in the treatment of AKI. Diuretics might be thought to reduce the severity of AKI by preventing tubule obstruction and decreasing oxygen consumption,[114] as discussed above, but studies have failed to demonstrate convincingly that diuretics affect rates of renal recovery rate of patients with established AKI.[137]

Adverse Effects

There are at least three types of adverse effects of loop diuretics. The first and most common effects result directly from the effects of these drugs on renal electrolyte and water excretion. The second are toxic effects of the drugs that are dose-related and predictable. The third are idiosyncratic allergic drug reactions.

Loop diuretics are frequently administered to treat edematous expansion of the ECF volume. Edema usually results from a decrease in the "effective" arterial blood volume. Thus, zealous diuretic usage or the development of complicating illnesses can lead to excessive contraction of the ECF volume. This can be manifested by orthostatic hypotension, renal dysfunction or evidence of sympathetic overactivity. Although patients suffering from heart failure usually require diuretic therapy, the combination of diuretics and angiotensin-converting enzyme inhibitors can exacerbate prerenal azotemia. High diuretic doses or extreme dietary NaCl restriction may predispose to renal dysfunction during therapy with diuretics and angiotensin-converting enzyme inhibitors or angiotensin-receptor blockers for heart failure.[138,139] In this case, renal failure often abates when the diuretic dose is reduced or the dietary NaCl intake is liberalized, permitting continued administration of the ACE inhibitor.

Other patients at increased risk for relative contraction of the ECF volume during loop diuretic therapy include elderly patients,[140] patients with pre-existing renal insufficiency,[141] patients with right-sided heart failure or pericardial disease, and concomitant use of non-steroidal anti-inflammatory drugs.[142,133]

Disorders of Na and K concentration are among the most frequent adverse effects of loop diuretics. Hyponatremia may be less common with loop diuretics than with distal convoluted tubule diuretics (DCT diuretics; see below), but it still may occur. Its pathogenesis is usually multifactorial, but involves the effect of loop diuretics to impair the clearance of solute-free water. Additional factors that may contribute include

TABLE 40.3 Indications for Diuretic Drugs

I. INDICATIONS FOR OSMOTIC DIURETICS
A. Prevention of rhabdomyolysis
B. To reduce intraocular or intracranial pressure
II. INDICATIONS FOR CARBONIC ANHYDRASE INHIBITORS
A. Glaucoma
B. Acute mountain sickness
C. Metabolic alkalosis
D. Cystinuria
E. Resistant Edema (used in combination with other diuretics)
F. Pseudotumor cerebri
III. INDICATIONS FOR LOOP DIURETICS
A. Edematous Conditions
1. Congestive Heart Failure
2. Cirrhotic Ascites
3. Nephrotic Syndrome
B. Hypercalcemia (now recommended only as second line treatment)
C. Hyperkalemia
D. Hyponatremia (with saline)
E. Hyperkalemic, hyperchloremic metabolic acidosis (Type 4 RTA)
F. Hypermagnesemia
G. Intoxications
H. Hypertension
I. AKI
IV. INDICATIONS FOR DISTAL CONVOLUTED TUBULE DIURETICS
A. Hypertension
B. Edematous Conditions
1. Heart Failure
2. Cirrhotic Ascites
3. Nephrotic Syndrome
C. Prevention of recurrent nephrolithiasis
D. Nephrogenic Diabetes Insipidus
E. Osteoporosis
F. Hypoparathyroidism
G. Diuretic Resistance (used in combination with other diuretics)
V. INDICATIONS FOR POTASSIUM-SPARING DIURETICS
A. Cirrhotic Ascites
B. Lithium-induced diabetes insipidus
C. Prevention of hypokalemia (owing to potassium-wasting diuretics)
D. Prevention of hypomagnesemia (owing to potassium-wasting diuretics)
E. Diuretic Resistance (used in combination with other diuretics
F. Heart Failure with systolic dysfunction
G. Resistant hypertension
H. Aldosteronism
VI. INDICATIONS FOR AQUARETICS
A. Euvolemic hyponatremia
B. Hypervolemic hyponatremia

the non-osmotic release of arginine vasopressin,[144] hypokalemia, and hypomagesemia.[145] Conversely, loop diuretics have been used to treat hyponatremia when combined with hypertonic saline, in the setting of the syndrome of inappropriate ADH secretion.[146,147] In contrast, the combination of loop diuretics and angiotensin I-converting enzyme inhibitors has been reported to correct hyponatremia in the setting of heart failure, presumably in part owing to improved cardiac function.[148]

Hypokalemia occurs commonly during therapy with loop diuretics, although the magnitude is smaller than the magnitude of hypokalemia induced by diuretics that act in the DCT (loop diuretics, 0.3 mM versus DCT diuretics, 0.5–0.9 mM[149,150]). Loop diuretics increase the delivery of potassium to the distal tubule, because they block potassium reabsorption via the Na-K-2Cl co-transporter. In rats, approximately half the excreted potassium is delivered to the "early" distal tubule. During furosemide infusion, the delivery of potassium to the "early" distal tubule rose to 28% of the filtered load.[151] Thus, it appears that a large component of the effect of loop diuretics to increase potassium excretion acutely reflects their ability to block potassium reabsorption by the thick ascending limb. By increasing flow to the aldosterone-sensitive distal nephron, loop diuretics will also stimulate potassium secretion by activating flow-dependent maxi-K (BK) channels.[152] Nevertheless, during chronic diuretic therapy, when urinary flow has returned to or close to baseline, the degree of potassium-wasting correlates best with volume contraction and serum aldosterone levels.[153] These data suggest that, under chronic conditions, the predominant effect of loop diuretics to stimulate potassium excretion results from their tendency to increase mineralocorticoid hormones, while simultaneously increasing distal Na and water delivery.

Metabolic alkalosis is very common during chronic treatment with loop diuretics. Loop diuretics cause metabolic alkalosis via several mechanisms. First, they increase urine volume; the elaborated urine is bicarbonate-free, but contains Na and Cl. This leads to contraction of the ECF around a fixed amount of bicarbonate buffer; a phenomenon known as "contraction alkalosis." This probably contributes only slightly to the metabolic alkalosis that commonly accompanies chronic loop diuretic treatment. Loop diuretics directly inhibit transport of Na and Cl into thick ascending limb cells. In some species, these cells also express an isoform of the Na/H exchanger at the apical surface. When Na entry via the Na-K-2Cl co-transporter is blocked by a loop diuretic, the decline in intracellular Na activity will stimulate H secretion via the Na/H exchanger.[154–156] Loop diuretics also stimulate the renin–angiotensin–aldosterone pathway, both directly

and indirectly, as discussed above. Aldosterone directly stimulates H secretion by the medullary collecting tubule,[157] but more importantly increases the magnitude of the transepithelial voltage in the cortical collecting duct. This effect stimulates H secretion via the electrogenic H-ATPase present at the apical membrane of α-intercalated cells. Loop diuretics frequently cause hypokalemia, which may contribute to metabolic alkalosis by increasing ammonium production,[158] stimulating bicarbonate reabsorption by proximal tubules,[159] and increasing the activity of the H/K-ATPase in the distal nephron.[160] Finally, contraction of the ECF volume stimulates Na/H exchange in the proximal tubule, and may reduce the filtered load of bicarbonate. All of these factors may contribute to the metabolic alkalosis observed during chronic loop diuretic treatment.

Ototoxicity is the most common toxic effect of loop diuretics that is unrelated to their effects on the kidney. Deafness, which is usually temporary but can be permanent, was reported shortly after the introduction of loop diuretics.[161] It appears likely that all loop diuretics cause ototoxicity, because ototoxicity can occur during use of chemically dissimilar drugs, such as furosemide and ethacrynic acid. The mechanism of ototoxicity remains unclear, although the stria vascularis, which is responsible for maintaining endolymphatic potential and ion balance, appears to be a primary target for toxicity.[162] Loop diuretics reduce the striatal potential from +80 mV to −10 to −20 mV within minutes of application.[163] A characteristic finding in loop diuretic ototoxicity is strial edema. This suggests that toxicity involves inhibition of ion fluxes.[162] Ikeda and Morizono detected functional evidence for the presence of a Na-K-2Cl co-transporter in the basolateral membrane of marginal cells.[164] According to the model proposed by these investigators, marginal cells resemble secretory cells in other organ systems, with a Na-K-2Cl co-transporter and Na/K-ATPase at the basolateral cell membrane and channels for K and Cl at the apical surface. According to this model, loop diuretic-induced shrinkage of marginal cells results from inhibition of cell Na, K, and Cl uptake across the basolateral cell membrane.

The ototoxic effects of loop diuretics appear to be related to their ability to inhibit NKCC1. This protein has been localized in the lateral wall of the cochlea, using specific antibodies[165] and RT-PCR.[166] Mice lacking the secretory isoform of the Na-K-2Cl co-transporter are profoundly deaf.[167,168] Loop diuretics cause loss of outer hair cells in the basal turn of the cochlea, rupture of endothelial layers, cystic formation in the stria vascularis, and marginal cell edema in the stria vascularis.[163]

Ototoxicity appears to be related to the peak serum concentration of loop diuretic, and therefore tends to occur during rapid drug infusion of high doses. This is likely to be related to the need to attain levels in the plasma that typically are only achieved in the renal tubule, for inhibition of NKCC1 to occur. For this reason, this complication is most common in patients with uremia,[169] where higher loop diuretic doses are frequently administered. It is recommended that furosemide infusion be no more rapid than 4 mg/minute, to avoid this complication.[169] In addition to renal failure, infants, patients with cirrhosis, and patients receiving aminoglycosides or cisplatin may be at increased risk.[169]

DISTAL CONVOLUTED TUBULE DIURETICS

The first orally active drug that inhibited Na and Cl transport along the DCT was chlorothiazide. Chlorothiazide was developed when chemical modification of sulfonamide-based CA inhibitors resulted in substances that increased NaCl, rather than $NaHCO_3$, excretion. The development of modified CA inhibitors that increased NaCl excretion preferentially was recognized immediately as significant, because ECF contains predominantly NaCl rather than $NaHCO_3$, and acidosis limited the effectiveness of CA inhibitors. Subsequent development led to a wide variety of benzothiadiazide (thiazide) diuretics (see Figure 40.10); all are analogs of 1,2,4-benzothiadiazine-1,1-dioxide. Other structurally related non-thiazide diuretics include the quinazolinones (such as metolazone) and substituted benzopehenone sulfonamide (such as chlorthalidone). Although there was some confusion initially about the site of their action along the nephron, molecular identification of their target ion transporter permitted delineation of their predominant site of action as the DCT. Recent studies, however, suggest an additional site of action along the collecting duct. Based upon the common site at which both true thiazide and "thiazide-like" diuretics inhibit ion transport, it is reasonable to refer to this class of drugs as *distal convoluted tubule diuretics*, in analogy with the *loop diuretics*.

Urinary Electrolyte and Water Excretion

Acute administration of these drugs increases the excretion of Na, K, Cl, HCO_3, phosphate, and urate, although the increases in HCO_3, phosphate, and urate excretion are probably related primarily to CA inhibition (see below). As such, the effects of DCT diuretics to increase HCO_3, phosphate, and urate excretion may vary, depending on the CA inhibiting potency of the

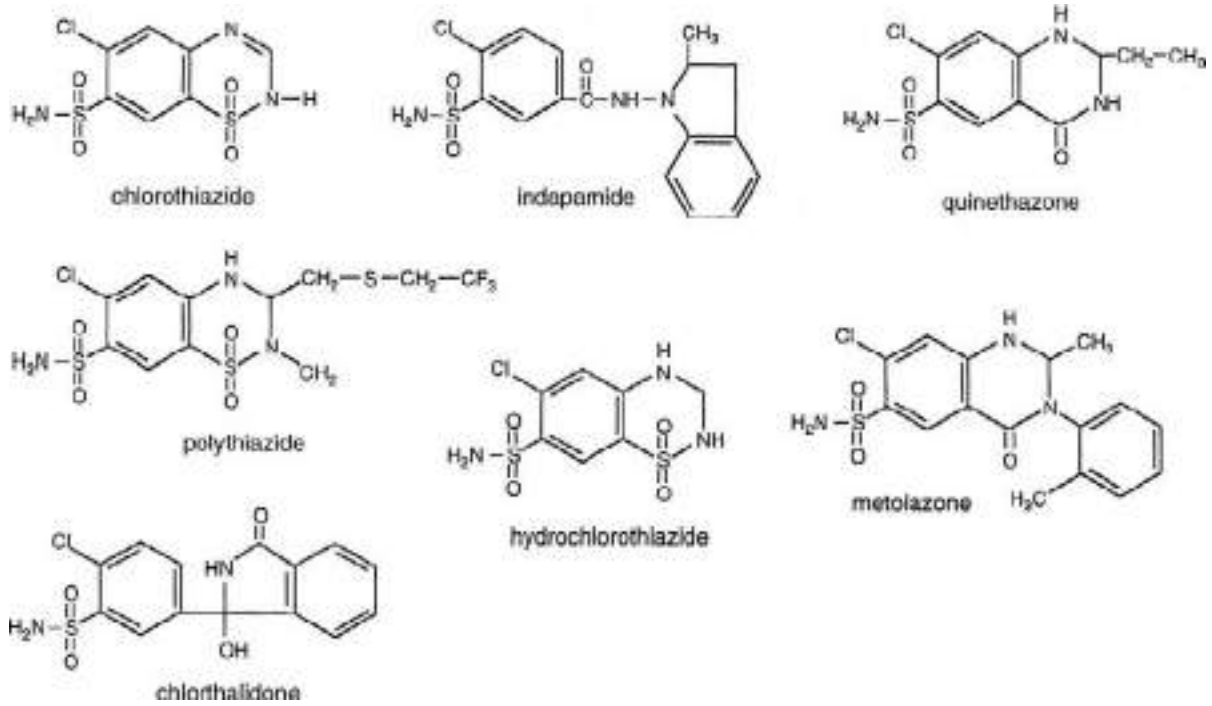

FIGURE 40.10 **Structures of DCT diuretics.**

DCT diuretic. Chronically, as contraction of the ECF volume occurs, uric acid excretion declines and hyperuricemia can occur. Further, any initial excretion of bicarbonaturia ceases, whereas continuing losses of chloride without bicarbonate and ECF volume contraction may lead to metabolic alkalosis. In contrast to loop and proximally acting diuretics, DCT diuretics tend to reduce urinary calcium excretion. Although the effects on urinary calcium excretion can be variable during acute administration,[170] these drugs uniformly lead to calcium retention when administered chronically, and also lead to positive calcium balance in humans.[171]

DCT diuretics inhibit the clearance of solute-free water (C_{H2O}) when administered during water diuresis. This effect is similar to that of loop diuretics, and originally led to the mistaken inference that they act along the thick ascending limb. In contrast to loop diuretics, however, DCT diuretics do not limit free water reabsorption during antidiuresis.

Mechanism of Action

Na AND WATER TRANSPORT IN THE PROXIMAL TUBULE

DCT diuretics are related chemically to CA inhibitors, and most retain significant CA-inhibiting potential. As discussed above, CA inhibitors interfere indirectly with the activity of NHE3 in the proximal tubule. Although this effect of DCT diuretics may be useful when these drugs are administered acutely (as during intravenous chlorothiazide administration), it probably contributes little to the overall natriuresis during chronic use. Yet this effect may play a role in the tendency for DCT diuretics to reduce the GFR and activate the TGF mechanism.[18] The relative CA inhibiting potency (shown in parentheses, compared with hydrochlorothiazide) of some commonly used DCT diuretics is chlorthalidone (67) >benthiazide (50) >polythiazide (40) >chlorothiazide (14) >hydrochlorothiazide (1) >bendroflumethiazide (0.07).[172]

NaCl ABSORPTION IN THE DISTAL NEPHRON

The predominant site at which DCT diuretics inhibit ion transport is the DCT. Although clearance studies had identified one site of thiazide action as the cortical diluting segment, and a second site as the proximal tubule, micropuncture studies pinpointed the primary site of action as the superficial "distal tubule".[173] This region of the nephron, which lies between the macula densa and the confluence with another nephron to form the cortical collecting duct, is morphologically heterogenous. It comprises a short stretch of post macula densa thick ascending limb, the DCT, the connecting tubule, and the initial portion of the cortical collecting duct. When this morphological heterogeneity became evident, experiments were designed to determine the site of thiazide action more precisely. Microperfusion experiments in rats indicated that thiazide diuretics inhibit Na and Cl transport along the

"early" portion of the distal tubule,[174,175] a segment known to contain predominantly DCT cells.[176]

Although microperfusion data from rats indicated that thiazide diuretics inhibit Na transport in the DCT, the transition along the distal nephron segments in rats is gradual. For several years, therefore, it was impossible to attribute thiazide-sensitive Na-Cl transport to a specific cell type in the rat. In contrast, rabbit distal nephron segments have abrupt transitions. *In vitro* studies suggested that thiazide-sensitive Na-Cl co-transport is present in connecting tubules instead of DCTs,[177,178] but Velázquez and Greger obtained indirect evidence for thiazide-sensitive transport in rabbit DCTs.[179] Molecular cloning[180] permitted definitive identification of DCT cells as the only sites of thiazide-sensitive Na-Cl co-transporter expression in both rat and rabbit.[181–183] Friedman and colleagues developed a clonal cell line from immunodissected mouse thick ascending limb and DCT cells that expresses thiazide-sensitive transport.[184] Molecular studies identified the DCT as the site of thiazide-sensitive Na-Cl co-transport in this species, as well.[185]

In 1984, Velázquez and colleagues reported the mutual dependence of Na and Cl transport in the superficial rat distal tubule.[186] The same year, Stokes reported evidence that a directly-coupled thiazide-sensitive Na-Cl co-transporter is expressed in the urinary bladder of the Winter Flounder.[187] Gamba et al. cloned this protein[180] and detected homologous mRNA in mammalian kidney. The same group cloned a rat form of the thiazide-sensitive Na-Cl co-transporter.[188] Mouse, human, and rabbit forms were cloned shortly thereafter;[189–191] the gene is *SLC12A3*; it is a member of the cation-chloride co-transporter family, which includes NKCC1 and NKCC2. This transport protein was previously termed the TSC (thiazide-sensitive co-transporter), and the NCCT (sodium chloride co-transporter), but most investigators prefer the term NCC (sodium chloride co-transporter), for its analogy with NKCC. At the molecular level, the NCC is expressed only by DCT cells in all mammalian species examined to date. In humans, rats, and mice, expression of NCC also extends into a transitional segment, referred to as the "late" DCT or DCT-2, which shares properties of the distal convoluted and connecting tubules.[181,185]

Evidence for thiazide action in other nephron segments has also been obtained, however. *In vivo* catheterization experiments demonstrated a component of thiazide-sensitive Na transport in medullary collecting tubules of rats.[192] Some,[193] but not other[194] investigators have detected thiazide-sensitive Na-Cl transport in rat cortical collecting ducts perfused *in vitro*. In those experiments, pretreatment of animals with mineralocorticoid hormones was necessary to elicit the thiazide-sensitive Na and Cl transport. Eladari and colleagues[195] detected an effect of DCT diuretics on NaCl excretion in NCC knockout mice; these mice lack NCC entirely, and therefore the observed effect must be related to NCC-independent pathways. They also found that collecting ducts from animals exposed to aldosterone reabsorbed Na and Cl in a thiazide-sensitive manner. They went on to show that this transport was dependent on the Na-dependent chloride bicarbonate transporter (NDCBE) and on pendrin (SLC26A4), transport proteins expressed by intercalated cells. While this work deserves verification, it strongly suggests that DCT diuretics may have important effects on net NaCl transport within segments other than the DCT. A model of NaCl transport by DCT cells and a proposed model for NaCl transport by intercalated cells in the collecting duct are shown in Figure 40.11.

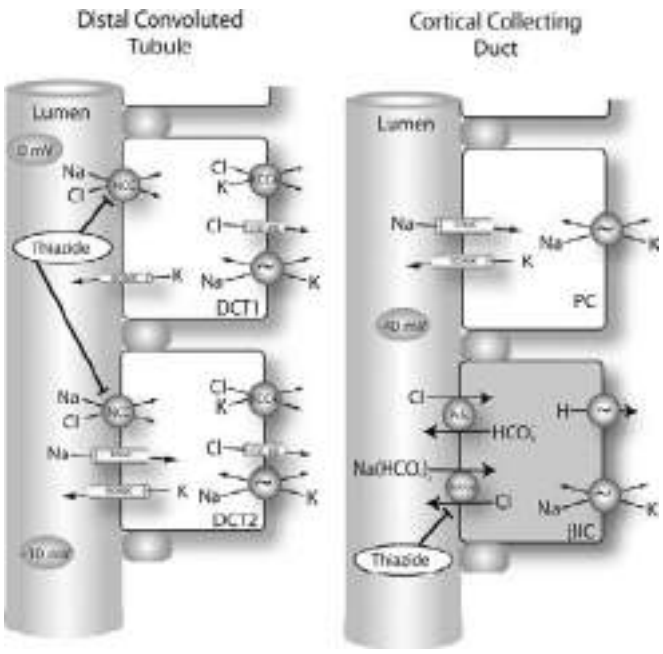

FIGURE 40.11 **Mechanisms of thiazide diuretics.** The left panel shows the mechanism of action of thiazide diuretics in the DCT. Two types of DCT cells have been identified; referred to here as DCT1 and DCT2. Na and Cl are reabsorbed across the apical membrane of DCT1 cells only via the thiazide-sensitive Na-Cl co-transporter. This transport protein is also expressed by DCT2 cells, where Na can also cross through the epithelial Na channel, ENaC (see text for details). Thus, the transepithelial voltage along the DCT-1 is near to 0 mV, whereas it is lumen-negative along the DCT-2. The right panel shows recently established mechanisms of action of thiazide diuretics along the collecting duct, in the presence of aldosterone stimulation. Here Na is reabsorbed in exchange for K by principal cells (PC), but in beta type intercalated cells (βIC) Na reabsorption occurs via a Na-dependent chloride bicarbonate exchanger (Ndcbe). This occurs in parallel with the action of pendrin (Pds) to achieve net NaCl reabsorption. The Ndcbe appears to be sensitive to thiazide diuretics.

Like loop diuretics, DCT diuretics, including the thiazides, are organic anions that bind to the transport

protein from the luminal surface. Results of studies to determine the mechanism by which DCT diuretics interact with the transport protein have varied, depending on the methods employed, and in a manner that resembles those described above concerning loop diuretics and NKCC. Before the transport protein was identified at the molecular level, Fanestil and colleagues showed that [^{3}H] metolazone binds avidly to kidney membrane proteins; its binding is inhibited competitively by Cl^-, suggesting that Cl^- and diuretic compete for the same binding site.[196,197] These results are reminiscent of those that utilized [^{3}H] bumetanide to study properties of the NKCC proteins and were used to develop a kinetic model for the NCC.[198] More recently, Gamba and colleagues have expressed chimeras of the NCC in *Xenopus* oocytes and determined thiazide affinity based on transport inhibition. The results suggest a more complicated picture. They conclude that thiazide diuretic affinity is conferred by transmembrane segments 8–12, whereas transmembrane segments 1–7 affect chloride affinity. Both segments are involved in determining Na^+ affinity.[199] These data suggest that that the affinity of thiazide diuretics for binding to the transport protein is in a region distinct from that which participates in Cl^- transport. As was the case for NKCC, however, it seems likely that the recent data concerning the crystal structure of APC transporters, coupled with molecular modeling, will provide new information concerning potential binding sites that can then be tested empirically.[73]

Calcium and Magnesium Transport

When administered chronically, DCT diuretics reduce calcium excretion. This effect has been utilized clinically to reduce the risk of recurrent calcium nephrolithiasis (see below). As noted above, acute administration of DCT diuretics has a variable effect on calcium excretion, sometimes leading to increases in calcium excretion. This probably reflects the CA-inhibiting capacity of these drugs, because CA inhibitors increase urinary calcium excretion acutely. Ca reabsorption by proximal tubules is functionally coupled to sodium reabsorption (see Figure 40.12); drugs that inhibit proximal Na reabsorption also inhibit proximal calcium reabsorption. During chronic treatment, however, the filtered calcium-load decreases, owing to the hemodynamic effects discussed below, and the proximal calcium reabsorption increases, owing to ECF volume contraction.

Mechanisms and sites responsible for the hypocalciuric effects of DCT diuretics have been quite controversial.[200] Early micropuncture and microperfusion studies showed that DCT diuretics stimulate Ca reabsorption along the DCT costanzo.[201,202] Three potential

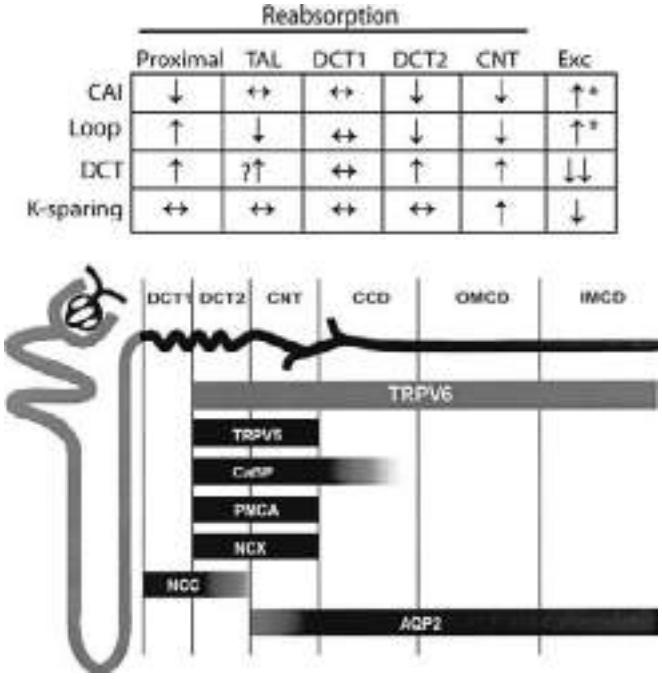

FIGURE 40.12 **Summary of diuretic effects on calcium excretion and sites of calcium transport protein expression.** Top panel: Effects of diuretics, including carbonic anhydrase inhibitors (CAI), loop diuretics (Loop), distal convoluted tubule diuretics (DCT), and K-sparing diuretics on calcium reabsorption along the proximal tubule, the thick ascending limb (TAL), the distal convoluted tubule (segments 1, DCT1, and 2, DCT2), and connecting tubule (CNT). Also shown are effects of these diuretics on urinary excretion (Exc). As noted by *, effects of CAI and loop diuretics to increase urinary calcium excretion may be inhibited when moderate depletion of the ECF volume increases reabsorption further along the proximal tubule. CAIs have been shown to reduce the abundance of TRPV5, as discussed in text. Effects of DCT diuretics on transport along TAL are speculative.[212] Bottom panel: Sites of expression of calcium-transporting proteins, including TRPV5 and -6, the calcium-binding proteins (CaBP), the plasma membrane Ca ATPase (PMCA), the Na/Ca exchanger (NCX). It also shows sites of NCC and AQP expression. Note the concurrence of expression within the DCT2 and CNT. *(Bottom panel from Nijenhuis, T., et al. (2003). J. Am. Soc. Nephrol.* ***14*** *(11); 2731–2740, with permission.)*

and non-redundant mechanisms were postulated to account for this.[203] First, blockade of luminal NaCl entry should reduce the tubule cell [Na^+] sufficiently to enhance the basolateral Na^+/Ca^{2+} exchange.[202] A low cellular Na concentration provides part of the driving force for basolateral calcium exit via the 3Na/Ca exchanger. Second, thiazides reduce cell [Cl^-] concentration, which should hyperpolarize the membrane voltage (making the interior of the cell more negative, electrically). Hyperpolarization should enhance calcium absorption, because the 3Na/Ca exchanger is electrogenic, so transport (in the reabsorptive direction) should be stimulated, and the transient receptor potential channel subfamily V, member 5 (TRPV5) channel,

which is expressed at the apical membrane of DCT and connecting tubule cells, may be stimulated.[204,205]

More recently, the role of proximal tubular processes has been re-emphasized. In one study[206] thiazides were found to reduce Ca^2 excretion, even when the major calcium reabsorptive pathway of the distal nephron, TRPV5, was deleted genetically. TRPV5 deletion produced a marked rise in urinary calcium excretion at baseline, but hydrochlorothiazide still reduced urine calcium excretion in these animals, albeit to levels which were quite high. A prominent role for ECF volume contraction and enhanced proximal reabsorption is consistent with older data suggesting that thiazides stimulate proximal reabsorption of Ca^2.[207] Yet, there are several reasons to consider that a distal effect also contributes importantly. First, HCTZ induced a profound hypocalciuria in parvalbumin knockout mice, without increasing NaCl excretion.[208] This argues that ECF volume depletion is not a prerequisite for DCT diuretic-induced hypocalciuria. Second, saline infusion does not normalize urinary calcium excretion, either in humans with Gitelman syndrome,[209] in whom NCC is dysfunctional or in mice with the kinase SPAK deleted, in whom the abundance and phosphorylation of NCC is missing.[210] One difference may be related to species and dose. Animals such as the TRPV5 knockout animals, often display evidence of marked ECF volume-depletion in response to thiazide treatment (as indicated by hemoconcentration and weight loss), whereas ECF volume, at least at steady-state, is typically normal in people treated with DCT diuretics clinically. Most recently, it was shown that individuals with Gitelman syndrome have evidence of activated NaCl transport along the TAL.[211] It has been suggested on this basis that increased solute transport along the TAL might then contribute to increased calcium reabsorption there, as transepithelial voltage should vary directly with solute transport.[212]

DCT diuretics also increase urinary magnesium excretion when administered chronically, and can cause hypomagnesemia,[213,214] although the acute effects of DCT diuretics are more variable. Magnesium transport across the apical membrane of DCT cells is mediated, largely, by the transient receptor potential channel, TRPM6.[215] Chronic treatment of rats with hydrochlorothiazide reduced the abundance of this transport protein, a finding that is mimicked by genetic disruption of the NCC.[206] Thus, thiazides may induce magnesium-wasting, at least in part, by reducing the abundance of the apical magnesium channel. These data are consistent with findings from NCC knockout animals, and from results of chronic thiazide treatment of rats. In NCC knockout animals, the DCT1 is atrophic,[216] an effect that appears to be mimicked by chronic thiazide infusion.[217] Inasmuch as this segment normally expresses TRPM6 at high levels, such atrophy may explain the reduced TRPM6 expression and magnesium-wasting. This finding, however, may also account for the relatively mild effects of DCT diuretics on magnesium homeostasis in humans. The effects of DCT diuretics to cause apoptosis and atrophy of parts of the DCT may be a species-specific phenomenon[218]; thiazide treatment of humans has not been reported to cause substantial tubule disruption.

Other effects of DCT diuretics have been suggested to contribute to magnesium-wasting. Dai et al. proposed that magnesium is transported across the apical membrane of DCT cells by a hyperpolarization-activated magnesium channel.[219] They found that DCT diuretics stimulated magnesium uptake into DCT cells by reducing the intracellular activity of chloride, hyperpolarizing the membrane voltage, and activating magnesium channels. These magnesium channels are sensitive to dihydropyridines, but appear to be distinct from calcium channels. Amiloride was found to have similar effects on magnesium uptake.[220] The importance of these channels in renal magnesium homeostasis, however, is unclear, as molecular and genetic studies have suggested the key role played by TRPM6.[221]

Quamme proposed that magnesium-wasting in Gitelman"s syndrome (and by analogy during DCT diuretic treatment) results from hypokalemia and from hyperaldosteronism.[222] Ellison suggested that distal magnesium transport is dependent on the transepithelial voltage. In this case, thiazide diuretics, by increasing aldosterone concentrations and blocking electroneutral Na reabsorption, would enhance the luminal negativity. This would inhibit magnesium reabsorption.[203] The mechanisms of drugs that cause distal depolarization, such as amiloride magnesium,[223–225] or that block mineralocorticoid receptors (MR), such as spironolactone,[226,227] remain to be defined.

Renal Hemodynamics

DCT diuretics increase renal vascular resistance and decrease the GFR when given acutely. Okusa et al.[18] showed that intravenous chlorothiazide reduced the GFR by 16% when measured as whole kidney clearance or by micropuncture of a superficial distal tubule. In contrast, however, when flow to the macula densa was blocked and the SNGFR was measured by micropuncture of a proximal tubule, intravenous chlorothiazide had no effect on GFR. These data indicate that diuretic-induced stimulation of the TGF system mediates the effect of DCT diuretics on GFR; DCT diuretics are known to increase the concentration of Na in luminal fluid entering the superficial distal tubule. It is

assumed that a change in the tubule fluid ion concentration mediates this effect.

During chronic treatment with DCT diuretics, contraction of the ECF volume develops, thereby increasing solute and water reabsorption by the proximal tubule. This effect reduces the distal Na delivery to levels that are lower than under control conditions. In view of the fact that the initial suppression of GFR resulted from TGF, initiated by distal NaCl delivery, the GFR usually returns close to control values during chronic treatment with DCT diuretics.[228,229] Thus, when used chronically, DCT diuretics lead to a state of very mild ECF volume contraction, increased fractional proximal reabsorption, and relatively preserved glomerular filtration.

When administered acutely, the effect of DCT diuretics on renin secretion is variable. If urinary NaCl losses are replaced, these drugs tend to suppress renin secretion, probably by increasing NaCl delivery to the macula densa.[18] In contrast, during chronic administration, renin secretion increases both because solute delivery to the macula densa declines, and because volume-depletion activates the vascular mechanism for renin secretion.[102]

Pharmacokinetics

DCT diuretics are organic anions that circulate in a highly protein-bound state. As with loop diuretics, the amount reaching the tubule fluid by filtration across the glomerular basement membrane is small; the predominant route of entry into tubule fluid is by secretion via the organic anion secretory pathway in the proximal tubule. DCT diuretics are rapidly absorbed, reaching peak concentrations within 1.5 to 4 hours.[3] The amount of administered drug that reaches the urine varies greatly (for a review see [3]), as does the half-life. Short-acting DCT diuretics include bendroflumethiazide, hydrochlorothiazide, tizolemide, and trichlormethiazide. Medium-acting DCT diuretics include chlorothiazide, hydroflumethiazide, indapamide, and mefruside. Long-acting DCT diuretics include chlorthalidone, metolazone, and polythiazide.[3] The clinical effects of the differences in half-life are increasingly being appreciated. The incidence of hypokalemia may be higher in patients taking the longer-acting drugs such as chlorthalidone,[149,230] but it also appears that longer-acting drugs, and especially chlorthalidone, have greater antihypertensive efficacy.[231]

Clinical Use

Indications for the use of DCT diuretics are listed in Table 40.3. Many details of DCT diuretic use are available in other reviews[2,55,232] and will not be discussed here. DCT diuretics are used most commonly to treat essential hypertension. Despite a great deal of recent debate about their potential complications in the setting of essential hypertension, DCT diuretics continue to be recommended as drugs of first choice in the treatment of hypertension.[233] DCT diuretics are also used commonly to treat edematous conditions, although they are frequently perceived as being less effective than loop diuretics. Although the maximal effect of loop diuretics to increase urinary Na, Cl, and water excretion is greater than that of DCT diuretics, Leary and colleagues have shown that the cumulative effects of DCT diuretics on urinary Na and Cl excretion are greater than those of once daily furosemide.[234] Although these studies were conducted in normal volunteers, they may extend to patients with mild cases of edema. In addition, DCT diuretics have proved useful to treat edematous patients who have become resistant to loop diuretics. In this case, the addition of a DCT diuretic to a regimen that includes a loop diuretic frequently increases urinary Na and Cl excretion dramatically (see below).

DCT diuretics have become drugs of choice to reduce the recurrence of risk for kidney stones in patients with idiopathic hypercalciuria.[235] As noted, these drugs decrease urine calcium excretion, and in randomized controlled trials they significantly reduced recurrence rates of calcium stones by more than 50% during three-year periods, as compared with placebo. Long-acting agents like chlorthalidone and indapamide are effective with once-daily doses, whereas twice-daily doses are recommended for hydrochlorothiazide.

The ability of DCT diuretics to reduce urinary calcium excretion suggests that these drugs may prevent bone loss. Some,[236,237] but not all,[238,239] epidemiological studies suggested that DCT diuretics reduce the risk of hip fracture and osteoporosis. Clinical trials have confirmed that thiazide diuretics reduce the loss of cortical bone and may prevent hip fracture, although the effect seems modest, and does not persist once the drug has been discontinued.[240–242]

DCT diuretics are also employed to treat nephrogenic diabetes insipidus, causing a paradoxical decrease in urinary volume flow rate. This action of DCT diuretics results from the combination of actions. The best-studied effects include the induction of mild ECF volume contraction, owing to diuretic-induced natriuresis, suppression of GFR, owing largely to diuretic-induced activation of the TGF, and reduced distal water delivery. Such a mechanism would require depletion of the ECF volume, a requirement that has been documented in several studies.[229,243] The human DCT, like the thick ascending limb, is nearly impermeable to water.[244] Solute reabsorption by the thiazide-sensitive Na-Cl co-transporter therefore contributes directly to urinary dilution; thus, blocking Na-Cl co-transport reduces urinary diluting capacity. More

recently, DCT diuretics have been shown to alter the abundance of water and salt transport pathways in the distal nephron. Kim and colleagues used a rat model of lithium-induced diabetes insipidus. They showed a lithium-induced decrease in aquaporin expression that could be reversed, partially, by DCT diuretics.[245] Another report showed that DCT diuretics enhance water absorption in IMCD from normal rats (in the absence of ADH) and from Brattleboro rats, and that HCTZ-stimulated water permeability was blocked partially by PGE_2.[246]

Adverse Effects

Electrolyte disorders, such as hypokalemia, hyponatremia, and hypomagnesemia, are common side-effects of DCT diuretics. A measurable fall in serum K concentration is nearly universal in patients given DCT diuretics, but most patients do not become frankly hypokalemic.[230] In the Allhat study, the largest controlled antihypertensive trial, mean plasma K concentrations were 0.3 mM lower in patients randomized to cholorthalidone, compared with amoldipine (which has little effect on K metabolism). The clinical significance of diuretic-induced hypokalemia continues to be debated.[247,248] Unlike the loop diuretics, DCT diuretics do not influence K transport directly.[249,250] Instead, they increase K excretion indirectly. DCT diuretics increase tubule fluid flow in the connecting tubule and collecting duct, the predominant sites of K secretion along the nephron. Increased flow stimulates K secretion both via flow-dependent potassium channels[152] and by diluting luminal potassium.[251] In addition, DCT diuretic-induced ECF volume contraction activates the renin−angiotensin−aldosterone system, further stimulating K secretion. Evidence for the central role of aldosterone in diuretic-induced hypokalemia includes the observation that hypokalemia is somewhat more common during treatment with long-acting DCT diuretics, such as chlorthalidone, than with short-acting DCT diuretics, such as hydrochlorothiazide or with the very-short-acting loop diuretics.[149] Another reason that DCT diuretics may produce more potassium-wasting than loop diuretics is the differences in effects on calcium transport. As discussed above, loop diuretics inhibit calcium transport by the thick ascending limb, increasing distal calcium delivery. In contrast, DCT diuretics stimulate calcium transport, reducing calcium delivery to sites of potassium secretion. Okusa and colleagues[252,253] showed that high luminal concentrations of calcium inhibit ENaC in the distal nephron, thereby inhibiting potassium secretion. DCT diuretics also increase urinary magnesium excretion and can lead to hypomagnesemia, as discussed above. Hypomagnesemia may cause or contribute to the hypokalemia observed under these conditions.[254] Some studies suggest that maintenance magnesium therapy can prevent or attenuate the development of hypokalemia,[255,256] but this has not been supported universally.

Diuretics have been reported to contribute to more than 50% of all hospitalizations for serious hyponatremia. Hyponatremia is especially common during treatment with DCT diuretics,[257] compared with other classes of diuretics, and the disorder is potentially life-threatening. Several factors contribute to DCT diuretic-induced hyponatremia. First, as discussed above, DCT diuretics inhibit solute transport in the terminal portion of the "diluting segment," the DCT. This impairs the ability to excrete free water. Second, DCT diuretics can reduce the GFR, primarily by activating the TGF system. This limits solute delivery to the diluting segment, and impairs free water clearance. Third, DCT diuretics lead to volume-contraction, which increases proximal tubule solute and water reabsorption, further restricting delivery to the "diluting segment." Fourth, hyponatremia has been correlated with the development of hypokalemia in patients receiving DCT diuretics,[258] suggesting total cation depletion. Finally, susceptible patients may be stimulated to consume water during therapy with DCT diuretics; although the mechanisms are unclear, this may contribute importantly to the sudden appearance of hyponatremia that can occur during DCT diuretic therapy. Of note, one report suggests that patients who are predisposed to develop hyponatremia during treatment with DCT diuretics will demonstrate an acute decline in serum sodium concentration in response to a single dose of the drug.[259] Recent studies suggest that female gender, advanced age, and low body mass are risk factors for thiazide-induced hyponatremia.[260,261]

DCT diuretics frequently cause metabolic alkalosis. The mechanisms are similar to those described above for loop diuretics, except that DCT diuretics do not stimulate Na/H exchange in the TAL.

DCT diuretics cause several disturbances of endocrine glands. Glucose intolerance has been a recognized complication of DCT diuretic use since the 1950s. This complication appears to be dose-related.[262,263] The pathogenesis of DCT diuretic-induced glucose intolerance remains unclear, but several factors have been suggested to contribute. First, diuretic-induced hypokalemia may alter insulin secretion by the pancreas, via effects on the membrane voltage of pancreatic β-cells. When hypokalemia was prevented by oral potassium supplementation, the insulin response to hyperglycemia normalized, suggesting an important role for hypokalemia.[264] Hypokalemia may also interfere with insulin-mediated glucose uptake by muscle, but most patients demonstrate relatively normal insulin sensitivity.[265] Yet others have suggested that hypokalemia is not likely the only factor, as individuals with familial

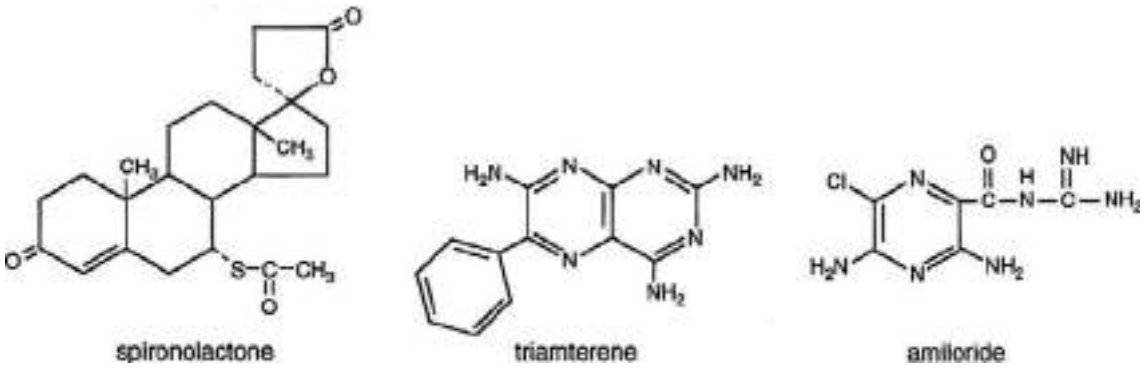

FIGURE 40.13 **Structure of collecting duct diuretics.**

hyperkalemic hypertension who are treated with DCT diuretics can manifest impaired glucose tolerance, despite normal-to-high serum potassium.[218] Other factors may contribute to glucose intolerance as well. Volume-depletion may stimulate catecholamine secretion, but volume-depletion during therapy with DCT diuretics is usually very mild. DCT diuretics directly activate calcium-activated potassium channels that are expressed by pancreatic β-cells, perhaps contributing to the hyperglycemia.[266] Activation of these channels is known to inhibit insulin secretion.

DCT diuretics increase levels of total cholesterol, total triglyceride, and LDL cholesterol. These drugs reduce the HDL.[265] Definitive information about the mechanisms by which DCT diuretics alter lipid metabolism is not available, but many of the mechanisms that affect glucose homeostasis have been suggested to contribute. Hyperlipidemia, like hyperglycemia, is a dose-related side-effect, and one that wanes with chronic diuretic use. In several recent large clinical studies, the effect of low-dose DCT diuretic treatment on serum LDL was not significantly different from placebo.[267] In the ALLHAT study, mean cholesterol concentrations were higher in the group randomized to chlorthalidone, but the absolute differences at two and four years were 2–3 mg/dl.

POTASSIUM-SPARING DIURETICS

Diuretic drugs that act primarily along the aldosterone-sensitive distal nephron (which includes the DCT2, the connecting tubule, and the collecting duct) comprise three pharmacologically distinct groups: aldosterone antagonists (spironolactone); pteridines (triamterene); and pyrazinoylguanidines (amiloride, see Figure 40.13). The site of action for all diuretics of this class is the segment of the nephron that begins within the DCT. It has been recognized increasingly that the DCT2 and the connecting tubule play especially important roles in modulating renal Na and K balance in response to aldosterone.[268] Because of the ability to minimize the normal tendency of diuretic drugs to increase potassium excretion, these drugs are considered "potassium-sparing." Acute diuretic activity is weak, because fractional sodium reabsorption in the collecting tubule usually does not exceed 3% of the filtered load. For this reason, potassium-sparing drugs are ordinarily used in combination with thiazides or loop diuretics, often in a single preparation, to restrict potassium losses and sometimes augment diuretic action. However, in certain conditions potassium-sparing diuretics are used as first line agents (see Table 40.2). For example, spironolactone is used in the treatment of edema in patients with cirrhosis,[269] and amiloride or triamterene is used as a first line treatment of Liddle's syndrome.[270]

Urinary Electrolyte Excretion

Amiloride, triamterene, and spironolactone are weak natriuretic agents (see Table 40.1). Their major effect is to diminish potassium excretion. Additionally, these three diuretic agents decrease hydrogen ion secretion by the ASDN. Evidence that spironolactone decreases hydrogen ion excretion comes from the finding of metabolic acidosis associated with mineralocorticoid deficiency, and the finding that spironolactone produces metabolic acidosis in patients with cirrhosis who have mineralocorticoid excess. In rats, the administration of amiloride and triamterene has been shown to inhibit urinary acidification. A common mechanism is likely to be involved in mediating the effects of all three diuretic agents on hydrogen ion secretion. These drugs reduce the voltage across the distal epithelium, which is oriented in the lumen-negative direction; they thus decrease the gradient for hydrogen ion secretion (see Figure 40.14).

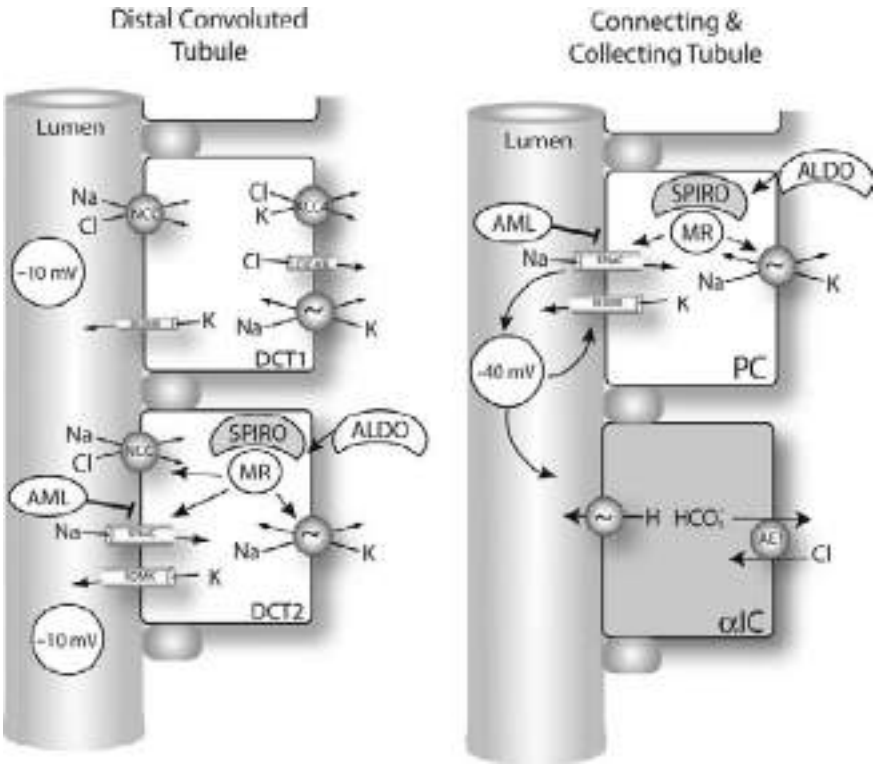

FIGURE 40.14 **Mechanisms of potassium-sparing diuretics.** Amiloride (AML, and triamterene, not shown) block ENaC directly, as discussed in the text. This occurs in the DCT2 and in the connecting and collecting tubules. Blockade reduces the magnitude of the transepithelial voltage, which secondarily inhibits K secretion and H secretion. Spironolactone (and eplerenone, not shown) act by blocking mineralocorticoid receptors (MR), impeding aldosterone's (ALDO) ability to bind. These drugs, therefore, only act when aldosterone levels are elevated. DCT1 and DCT2 cells are shown (PC: principal cell; βIC: beta intercalated cell).

Clearance studies in rats have demonstrated that amiloride produces a decrease in calcium excretion.[202] In these studies, amiloride produced both a decrease in the calcium clearance/Na clearance ratio (C_{Ca}/C_{Na}), as well as a decrease in the fractional excretion of calcium. The effect of triamterene on clearance of calcium was less clear, although it did decrease the C_{Ca}/C_{Na} ratio. *In vivo* microperfusion of rat distal tubules demonstrated that the effect of chlorothiazide on calcium absorption was enhanced when amiloride was added, suggesting that amiloride also increased calcium absorption by the distal tubule.[175] Furthermore, *in vitro* perfusion of connecting tubules has shown that amiloride stimulates calcium absorption.[271] Amiloride is believed to stimulate calcium absorption through its ability to block sodium channels, thereby hyperpolarizing the apical membrane.[94] Hyperpolarization of the apical membrane stimulates calcium entry through epithelial calcium channels TRPV5 (see DCT diuretics, above). Amiloride has also been reported to reduce magnesium excretion,[214,272] and to prevent the development of hypomagesemia during therapy with a DCT diuretic (see above).

Mechanism of Action

The site of action of potassium-sparing diuretics is ASDN (see Figure 40.1 and above). The ASDN comprises the second part of the DCT, the DCT2, where amiloride-sensitive Na channels intermingle with NCC at the apical membrane.[176] It also includes the connecting tubule, a segment that may play the dominant role in regulating urinary K excretion. Finally, it comprises the cortical and medullary collecting tubules. The connecting and collecting tubules are composed of two cell types; although they appear to have separate functions, some information has suggested that the view that principal cells are responsible for the transport of sodium, potassium, and water, whereas intercalated cells are primarily responsible for the secretion of hydrogen or bicarbonate ions, is oversimplified. The apical membrane of principal cells expresses separate channels that permit selective conductive transport of sodium and potassium (Figure 40.14). The mechanism by which sodium reabsorption occurs is through conductive sodium channels (for a review see [273]). The low intracellular sodium concentration as a result of the basolateral Na,K-ATPase generates a favorable electrochemical gradient for sodium entry through sodium channels. Because sodium channels are present only in the apical membrane of principal cells, sodium conductance depolarizes the apical membrane, resulting in an asymmetric voltage profile across the cell. This effect produces a lumen-negative transepithelial potential difference. The lumen-negative potential difference, together with a high intracellular-to-lumen potassium concentration gradient, provides the driving force for potassium secretion.

Sodium is the principal extracellular cation whose conductance across the principal cell of the collecting duct is amiloride-sensitive, and is regulated by the activity and apical membrane expression of the epithelial sodium channel (ENaC).[274,275] The functional channel comprises at least three homologous subunits, α, β, γ. The biophysical characteristics of ENaC include a low single channel conductance of ~5 pS, long open and closed times, a high Na^+ to K^+ selectivity ratio of >100:1, and it is inhibited by submicromolar concentrations of amiloride.[276] Although inferential work suggested several different stoichiometries,[277,278] the crystal structure of the structurally-related acid sensing channel, ASIC, provides strong support for a heterotrimeric model, in which one of each subunit is present.[279,280,283]

Although the crystal structure should permit clearer insights into the site of ENaC blockade by amiloride, a great deal of information has already accumulated. Amiloride and other large cations block apical Na^+ channels in a voltage-dependent manner, suggesting that amiloride block occurs within the pore of these channels.[281] Schild et al.[282] found that mutations at equivalent positions in all three subunits reduce the efficacy of amiloride block. When cysteine residues were introduced at these sites, they were susceptible to chemical modification by methanethiosulfonate compounds from the extracellular space,[283] suggesting that amiloride gains entry to and binds within the channel pore. If this is confirmed, it is strikingly similar to the new model for loop diuretic binding to NKCC1.[73]

Kleyman and colleagues[283] describe two potential models for ENaC structure. Mutation of sites within the proposed selectivity tract and an upstream site one helical turn away alters the efficacy of amiloride block. In one model, these sites face the pore lumen, but lie on the cytosolic side of the most constricted part. The selectivity tract lies one turn further toward the cytosol. In the other model, these sites lie near the extracellular entry of the most constricted part of the pore. It was suggested that the requirement for amiloride addition to the extracellular side of the membrane for inhibition is more consistent with the latter configuration, but these issues should be clarified now that relevant crystal structures are becoming available.

This group further suggested that the glycines at β525 and γ537 (the greek letters correspond to the ENaC subunits), and the tolerance of a wide variety of substitutions for serine α583, indicate that these residues probably do not interact directly with amiloride, but instead affect the shape of the amiloride-binding pocket. They proposed a model for amiloride-binding where the pyrazine ring is positioned at the αSer583/βGly525/γGly537 site, and the guanidinium group is positioned at the outer mouth of the selectivity tract.[284] As the ASIC crystal structure is not in the open-state likely to bind to the diuretic, it is not surprising that the pore models do not allow for amiloride to interact with the channel at these sites, and that neither model is fully consistent with functional data. Both models are based on structures of ASIC1 in a nonconducting state, and amiloride blocks ENaC in the open state. It is likely, however, that progress in unraveling what has been a difficult question concerning the mechanisms of amiloride association with the channel will now be more rapid, and should resolve these confusing issues.

The amount of sodium and potassium present in the final urine is tightly controlled by aldosterone action on cells of the ASDN. Extensive studies have demonstrated that, in epithelia, aldosterone produces an early increase in sodium conductance,[285,286] followed by a sustained increase in transepithelial sodium transport. As a result, transepithelial sodium transport is increased, an effect that depolarizes the apical membrane (see Figure 40.14). An increase in the lumen negative potential in turn enhances potassium secretion through conductive potassium channels located in the apical membrane. The cellular mechanisms that are responsible for these events have been extensively studied and reviewed.[287,288] The effects of aldosterone are largely mediated through a classical genomic effect through action on MR. Nongenomic actions in extrarenal tissues are likely to occur, but appear less prominent in the kidney.[287–289] Genomic actions of aldosterone are initiated by penetration of the hormone through the basolateral membrane of principal cells and attachment to a cytosolic MR, a heterotrimeric 8–9 s complex of proteins. This receptor complex includes the steroid-binding protein and heat shock proteins (HSP). Binding of aldosterone to this complex stimulates the release of HSPs, leading to the translocation of the receptor-aldosterone complex to the nucleus. The function of HSPs is not clear. It is thought that they facilitate anchoring of unbound steroid receptors to the cytoskeleton, maintaining a high-affinity conformation.[290] Evidence also indicates that released HSP90 stimulates calcineurin, a protein phosphatase that regulates sodium transport, in a transcription-independent process.[291] This binding and translocation sequence leads to production of proteins called *aldosterone-induced proteins* (AIPs)[292] that regulate sodium flux.[293] These AIPs regulate channel activity.[292,294] Although signaling pathways for aldosterone in the ASDN remain incompletely understood, a central role for serum and glucocorticoid-regulated kinase (sgk1) is generally inferred.[289] Sgk is regulated at the level of transcription by corticosteroids, including aldosterone,[295,296] and in turn is known to phosphorylate Nedd4 ubiquitin ligases.[297] Serum and glucocorticoid-regulated kinase modulates Nedd4–2-mediated

inhibition of the epithelial Na^+ channel. Nedd4−2 phosphorylation induces serum and glucocorticoid-regulated kinase (SGK) ubiquitination and degradation,[298] and prolongs the surface expression and activity of ENac. The reader is referred to other chapters in these volumes for a more thorough discussion of aldosterone signaling.

SPIRONOLACTONE AND EPLERENONE

Spirolactones are compounds that have the principal effect of blocking aldosterone action.[299,300] One of these, spironolactone (Figure 40.13), is an analog of aldosterone that is extensively metabolized. Spironolactone is converted by deacylation to 7α-thiospironolactone or by diethioacetylation to canrenone.[300] The appearance of active metabolites means that the physiological effects of spironolactone outlast the half-life of the parent drug (see below). In the kidney, spironolactone and its metabolites enter target cells from the peritubular side, and compete for binding to cytosolic MRs. In studies using radiolabeled spironolactone or aldosterone, [^{3}H]-spironolactone-receptor complexes were found to be excluded from the nucleus. In contrast, [^{3}H]-aldosterone-receptor complexes were detected in the nucleus.[301] These results are consistent with the proposal that aldosterone antagonists block the translocation of MRs to the nucleus. The mechanism by which aldosterone antagonists block nuclear localization of antagonist-receptor complexes is not known, however, it has been suggested that they destabilize MRs, facilitating proteolysis.[302] As discussed previously MRs, like other steroid receptors, contain a steroid-binding unit associated with other cellular components including HSP90, in its inactive state. Steroid-binding produces dissociation of HSP90 from the steroid-binding unit, uncapping the DNA-binding sites. Spironolactone facilitates the release of HSP90, and in combination with rapid dissociation of ligand, could lead to degradation of the receptor.[302]

A newer aldosterone receptor antagonist, eplerenone, is also a competitive antagonist of the aldosterone receptor. Replacing the 17alpha-thoacetyl group of spironolactone with a carbomethoxy group confers improved selectivity for aldosterone receptors, and negligible activity at the cytochrome P450 enzyme,[303] but 10−20-fold lower affinity for its receptor.[304] Eplerenone has a slightly longer half-life of 3.5 hours compared to spironolactone, but it does not produce important metabolites; thus, the apparent effective half-life of eplerenone is shorter than that of spironolactone, in clinical use. *In vitro* receptor-binding studies have revealed that the affinity of eplerenone is approximately 10- to 20-fold less than the affinity of spironolactone for the MR.

Spironolactone induces a mild increase in sodium excretion (1−2%), and a decrease in potassium and hydrogen ion excretion.[305,306] Its effect depends on the presence of aldosterone, as spironolactone is ineffective in adrenalectomized animals, and in patients with Addison"s disease or patients on a high-salt diet. In cortical collecting tubules perfused *in vitro*, spironolactone added to the bath solution reduced the aldosterone-induced lumen-negative transepithelial voltage. By blocking sodium absorption in the collecting tubule, a decrease in lumen-negative potential reduces the driving force for passive sodium and hydrogen ion secretion (see Figure 40.14). It is likely that the mechanism of eplerenone action on Na and K transport along the ASDN is identical.

AMILORIDE AND TRIAMTERENE

Amiloride and triamterene (see Figure 40.13) differ structurally, but both are organic cations that use the same primary site of action (see Figure 40.14). Triamterene is an aminopteridine chemically related to folic acid, and amiloride is a pyrazinoylguanidine. Systemically administered amiloride results in an increase in sodium excretion and a decrease in potassium excretion.[151] Their actions on sodium and potassium transport, unlike spironolactone, are independent of aldosterone. Systemically administered amiloride produced a small increase in sodium excretion, and a much larger decrease in potassium excretion. Sampling of tubule fluid from the distal tubule demonstrated an inhibition of the normal rise in the tubule fluid-to-plasma potassium ratio. These results indicated that amiloride decreased distal tubule potassium secretion. Experiments employing *in vivo* microperfusion of distal tubules[250,307] and *in vitro* perfusion of isolated cortical collecting tubules[308,309] demonstrated that luminally administered amiloride reduced sodium absorption and potassium secretion. Similar results were obtained following *in vivo* microperfusion with benazamil,[253] a more potent amiloride analog that is not available for use clinically. The mechanism by which amiloride decreases potassium secretion is due to its effect in blocking sodium conductance in the apical membrane of distal tubule and collecting tubule cells (see Figure 40.14), thereby decreasing the electrochemical gradient for potassium secretion.

In high concentrations (>100 μM), amiloride interacts nonspecifically with different transporters, enzymes, and receptors, however, at concentrations of 0.05 to 0.5 μM, amiloride interacts specifically with sodium channels. Furthermore, aromatic substitutions on the guanidinium moiety render the molecule even more potent (IC_{50} 10−20-fold lower than amiloride).[310,311]

Clearance and free-flow micropuncture studies using triamterene demonstrated results similar to studies with amiloride,[151] although the mechanism of action is not as clearly defined. In earlier studies of rabbit cortical collecting tubules perfused *in vitro*, triamterene produced a gradual, reversible inhibition of the potential difference after a latent period of 10 minutes, suggesting a mechanism different from amiloride. Recent studies, however, suggest that triamterene binds to the epithelial sodium channel, and thus has a mechanism of action similar to amiloride.[312]

Pharmacokinetics

Spironolactone is poorly soluble in aqueous fluids. Bioavailability of an oral dose is approximately 90% in some, but not all, commercial preparations. The drug is rapidly metabolized in the liver into a number of metabolites. Until recently, canrenone was thought to be the major metabolite of spironolactone.[299,313] This conclusion was based on fluorometric assays. Assays of spironolactone and its metabolites by the use of high performance liquid chromatography (HPLC), however, demonstrated that fluorometrically measured levels of canrenone overestimated true canrenone levels.[314] Using HPLC, the predominant metabolite, 7α-methylspironolactone,[315] is responsible for roughly 80% of the potassium-sparing effect. Spironolactone and its metabolites are extensively bound to plasma protein (98%). In normal volunteers, taking spironolactone (100 mg/day) for 15 days, the mean half-lives for spironolactone, canrenone, 7-thiomethylspironolactone, and 6β-hydroxy-7α-thiomethylspironolactone were 1.4, 16.5, 13.8, and 15 hours, respectively. Thus, although unmetabolized spironolactone is present in serum, it has a rapid elimination time. The onset of action is extremely slow, with peak response sometimes occurring 48 hours or more after the first dose; effects gradually wane over a period of 48 to 72 hours. Spironolactone is used in cirrhotic patients to induce a natriuresis. In these patients, pharmacokinetic studies indicate that the half-lives of spironolactone and its metabolites are increased. The half-lives for spironolactone, canrenone, 7α-thiomethylspironolactone, and 6β-hydroxy-7α-thiomethylspironolactone are 9, 58, 24, and 126 hours respectively.[316]

Less information concerning pharmacokinetics is available for amiloride and triamterene. Amiloride is rapidly absorbed, and reaches peak serum concentrations after approximately 4 hours. Its elimination half-life is 17–26 hours, with 40–60% appearing in the urine unchanged.[3] Both amiloride and triamterene are organic cations that are secreted into proximal tubule fluid by an organic cation transporter, in a manner analogous to secretion of loop and DCT diuretics by the organic anion transporter.

Clinical Use

The uses of potassium-sparing diuretics are broadening, as negative effects of aldosterone in human disease are discovered. Traditionally, an important indication for potassium-sparing diuretics is to prevent or attenuate K losses that are consequent to administration of DCT or loop diuretics.[317]

MR antagonists become effective natriuretics in patients with high circulating aldosterone levels, such as in primary (adrenal adenoma or bilateral adrenal hyperplasia)[318] or secondary hyperaldosteronism (congestive heart failure, cirrhosis, nephrotic syndrome). Spironolactone is especially appropriate for the treatment of cirrhosis with ascites, a condition invariably associated with secondary hyperaldosteronism. In comparison to loop or thiazide diuretics, spironolactone is equivalent or more effective.[319] The reason for this observation could be related to the differences in the mechanism of drug action, including the fact that MR antagonists do not require secretion by transporters to reach their sites of action. A combination of loop diuretic in addition to spironolactone is considered to be the best combination between safety and efficacy in cirrhotic patients with resistant edema (ratio of 40 mg furosemide to 100 mg spironolactone[320]).

Although its acute natriuretic action is weak, MR antagonists lower blood pressure and are often quite effective in the control of resistant hypertension.[321] Spironolactone or eplerenone is also indicated for the treatment of mineralocorticoid hypertension. Several controlled randomized studies have shown benefits of MR blockade on outcomes in patients with heart failure. A discussion of these indications is beyond the scope of this chapter, but it has been suggested that these beneficial effects are independent of effects of these drugs on the kidney.[322]

Triamterene or amiloride is generally used in combination with potassium-wasting diuretics (thiazide or loop diuretics), especially when maintenance of normal serum potassium concentrations is clinically important. In addition, amiloride (or triamterene) has also been used as initial therapy in potassium-wasting states, such as primary hyperaldosteronism,[323,324] Liddle's[325] or Gitelman's syndrome.[326] Amiloride has been used in the treatment of lithium-induced nephrogenic diabetes insipidus. The efficacy of amiloride in this disorder relates to the ability of amiloride to block collecting duct sodium channels, a pathway which lithium uses to gain entry into cells.[327]

Adverse Effects

The most serious adverse reaction encountered during therapy with spironolactone and eplerenone is hyperkalemia.[328] Serum potassium should be monitored

periodically, even when the drug is administered with a potassium-wasting diuretic. Patients at highest risk are those with low GFRs, and those individuals who take potassium supplements concurrently. In patients with cirrhosis and ascites treated with spironolactone, hyperchloremic metabolic acidosis can develop independent of changes in renal function. Unwanted antiandrogenic and progestational side-effects of spironolactone include gynecomastia, decreased libido, and impotence in men. Women may develop menstrual irregularities, hirsutism or swelling and tenderness of the breast. These troublesome side-effects were the impetus for developing eplerenone. In subjects receiving eplerenone for heart failure, the incidence of gynecomastia and impotence among men was similar to placebo.[329] These differences in side-effects are likely related to eplerenone's greater selectivity for the MR versus androgen and progesterone receptors. Spironolactone-induced agranulocytosis has also been reported.[330]

Triamterene and amiloride may cause hyperkalemia. The risk of hyperkalemia is highest in patients with limited renal function (e.g., renal insufficiency, diabetes, and elderly patients). Additional complications included elevated blood urea nitrogen and uric acid, glucose intolerance, and GI disturbances. Triamterene induces crystalluria or cylinduria,[331] and may contribute to or initiate formation of renal stones[332] and AKI when combined with nonsteroidal anti-inflammatory agents.[333,334] The drugs are contraindicated in patients with hyperkalemia, individuals taking potassium supplements in any form, and in patients with severe renal failure with progressive oliguria.

AQUARETICS (VASOPRESSIN RECEPTOR ANTAGONISTS)

Urinary Electrolyte Excretion

Vasopressin-receptor antagonists are nonpeptide molecules that competitively inhibit one or more of the human vasopressin receptors V1a, V1b or V2. Conivaptan is a combined V1a/V2-receptor antagonist for intravenous use, whereas tolvaptan, mozavaptan, and lixivaptan are orally active V2-selective receptor antagonists. All of these agents cause a free water diuresis without appreciable natriuresis or kaliuresis, and they are therefore sometimes referred to as "aquaretics." This effect is mainly attributed to inhibition of the V2-receptor in the collecting duct, which prevents vasopressin from recruiting AQP2 water channels to increase water reabsorption. Therefore, vasopressin-receptor antagonists can be used to treat hypervolemic or euvolemic hyponatremia, in which increased vasopressin is considered "inappropriate."

Mechanism of Action

The effects of arginine vasopressin (AVP, also called antidiuretic hormone, ADH) are mediated by two major receptor subtypes: V_1- and V_2. V_1 receptors are expressed in many cell types, including vascular smooth muscle (V_{1a}) and adenohypophysis (V_{1b}). V_2-vasopressin receptors are expressed in kidney and seminal vesicles. V_2 receptors have been localized to principal cells of the connecting tubule, cortical and medullary collecting duct. Binding of AVP to V_2-vasopressin receptors in collecting duct cells results in water reabsorption. Many clinical disorders such as cirrhosis, congestive heart failure, and syndrome of inappropriate antidiuretic hormone secretion (SIADH) are associated with high levels of AVP that prevent appropriate water excretion, resulting in hyponatremia.

Nonpeptide vasopressin receptor antagonists (conivaptan and tolvaptan) are now available for clinical use in the United States; they are indicated to treat euvolemic and hypervolemic hyponatremia. Conivaptan is a benzazepine derivative and the first combined vasopressin V1aR/V2R antagonist.[335] This agent displaces a selective vasopressin V1aR antagonist in a dose-dependent manner from rat liver membranes; the IC_{50} was 2.2 ± 0.1 nmol/L. The agent also caused a concentration-dependent displacement of a vasopressin V2R antagonist from renal medullary membranes, and the IC_{50} of the binding affinity was 0.4 ± 0.1 nmol/L.[336] Oral conivaptan given for seven days in normotensive rats caused a dose-dependent aquaresis, with no effect on specific blood pressure.[337] When administered to healthy volunteers orally, conivaptan effects were observed after two hours including a seven-fold increase in the urinary flow rate, and a decrease in urinary osmolality from 600 mOsm/kg to $<$100 mOsm/kg. Plasma osmolality increased from 283 ± 1.3 mOsm/kg to 289 ± 1.7 mOsm/kg.[336]

Clinical Use

In double-blind, randomized, placebo-controlled clinical trials conivaptan was shown to increase serum Na concentrations in a variety of settings.[336] Although conivaptan was originally discovered as an orally active V1a/V2 antagonist, it was developed for intravenous application. In one study it was given intravenously by continuous infusion over four days at doses of 40 mg/day and 80 mg/day following a loading dose of 20 mg intravenously on the first day. During the study, patients adhered to fluid restriction of 2 L/day. In the group of patients receiving high-dose conivaptan (80 mg/day), the treatment increased the serum sodium concentration significantly from a baseline of 125 mmol/L to 134 mmol/L.[336] These data suggest that conivaptan is an efficient therapy of hyponatremia and

is safe. Unfortunately, infusion side-effects, including infusion site reactions are quite common.

At present, some 20 clinical trials have tested these agents against placebo or conventional therapy in patients with liver cirrhosis, heart failure or hyponatremia secondary to SIADH.[338] In all trials, vasopressin-receptor angatonists effectively raised serum sodium and helped to correct hyponatremia. In addition, a positive effect on some secondary endpoints was observed, including improved mental condition and reductions in body weight, dyspnea, and ascites.[339–341] Unfortunately, these effects have not led to improvements in most hard endpoints. The Efficacy of Vasopressin Antagonist in Heart Failure Outcome Study with Tolvaptan (EVEREST), which included 4133 patients hospitalized for heart failure, did not show a beneficial effect on the primary outcomes of death or rehospitalization for heart failure.[339] Thus, vasopressin-receptor antagonists appear effective in the correction of hyponatremia, but have not yet shown an effect on primary outcomes.

GENERAL PRINCIPLES OF DIURETIC ACTION

When a diuretic drug (other than an aquaretic) is first administered to a normal individual, urinary sodium and chloride excretion rates increase. The magnitude of the increase is determined by the nature of the drug, the dose, the gastrointestinal absorption, the delivery to the kidney, entry into tubule fluid (for diuretics that act from the tubule lumen), and the physiological state of the individual. Except for diuretics that act predominantly in the proximal tubule, such as the CA inhibitors, the maximal natriuretic potency of a diuretic can be predicted from its site of action. Table 40.1 shows that loop diuretics can increase fractional Na excretion to 30%, DCT diuretics can increase it to 9%, and Na channel blockers can increase it to 3% of the filtered load. Because CA inhibitors enhance excretion of Na with bicarbonate rather than chloride, and because they induce adaptive processes that are described more fully below, the maximal natriuretic potency of CA inhibitors is much lower than would be predicted from their site of action. The dose–response curve for diuretic action has been best characterized for loop diuretics. In this case, the relationship is sigmoidal (see Figure 40.7), when the fractional Na excretion is plotted versus the urinary diuretic concentration.[136] Most diuretics act from the luminal surface. Therefore, the best external indicator of diuretic drug concentration at the active site is the urinary diuretic concentration.

The bioavailability of diuretic drugs varies widely, between classes of drugs, between different drugs of the same class, and even between days of the week with the same drug. The bioavailability of loop diuretics ranges from 10–100% (mean of 50% for furosemide, 80–100% for bumetanide and torsemide (see Table 40.2). Limited bioavailability can usually be overcome by appropriate dosing, but some drugs, such as furosemide, are variably absorbed, making precise titration difficult.[136] Although the bioavailability predicts that oral furosemide should be half as potent as intravenous furosemide, the relationship is not simple, and depends on the clinical state of the individual. For example, the amount of Na excreted during 24 hours is similar when furosemide is administered to a normal individual by mouth or by vein (see Figure 40.7). Yet the total amount of furosemide excreted in the urine during the same period is approximately half as great following oral compared with intravenous administration.[342,343] This paradox results from the fact that oral furosemide absorption is slower than its clearance, leading to "absorption-limited" kinetics. Thus, effective serum furosemide concentrations persist longer when the drug is given by mouth, because a reservoir in the gastrointestinal tract continues to supply furosemide to the body. This relationship holds for a normal individual (Figure 40.7), but not necessarily for a patient who suffers from an edematous disorder. In this case, a higher serum drug level may be needed to elicit natriuresis, and the lower serum drug level achieved by oral treatment may be inadequate to reach the natriuretic threshold. For this reason, it is customary to double the furosemide dose when changing from intravenous to oral therapy.[136] Variations in bioavailability may lead to increased hospitalizations for patients with congestive heart failure treated with furosemide, compared to a drug such as torsemide that is more completely absorbed, but this remains to be established in larger studies.[344]

A third factor that determines the maximal natriuresis following diuretic drug administration is drug delivery to its active site. Most diuretics, including the loop diuretics, DCT diuretics, and amiloride, act from the luminal surface. Thus, to be effective, these drugs must be delivered into tubule fluid by glomerular filtration or by tubular secretion. Although most diuretics are small molecules, most circulate tightly bound to protein and reach tubule fluid primarily by secretion. When serum albumin concentrations are very low, the volume of diuretic distribution increases,[134] but this factor may not be as important in causing diuretic resistance as believed previously.[345] Nevertheless, when serum albumin concentrations are less than 2 g/L, reduced diuretic delivery to the kidney may play a role in resistance.[346–349]

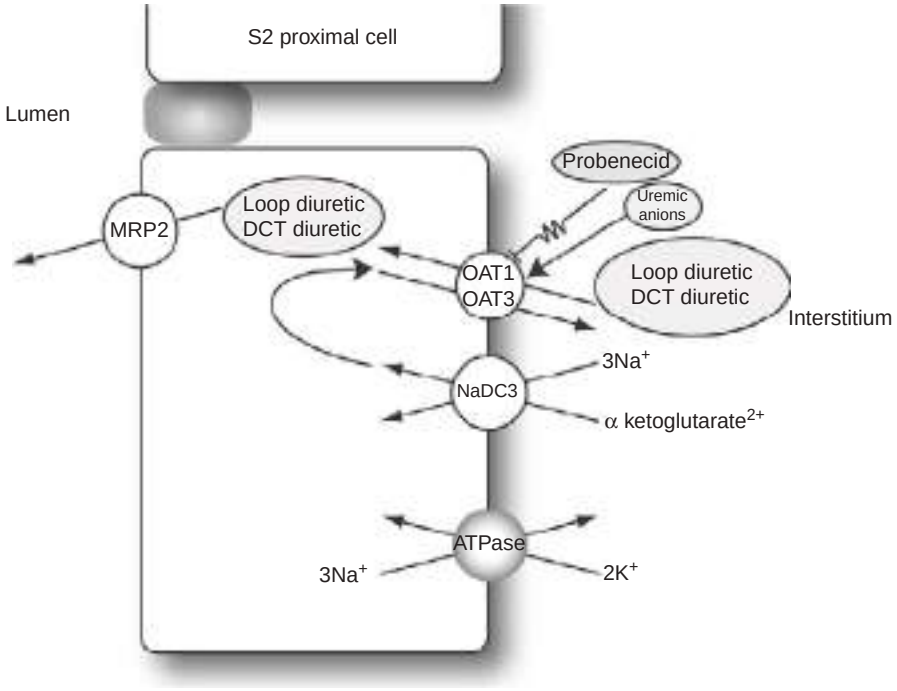

FIGURE 40.15 Mechanisms of diuretic secretion by proximal tubule cells. Cell diagram of the S2 segment of the proximal tubule, showing secretion of anionic diuretic, including loop diuretics and DCT diuretics. Peritubular uptake by an organic anion transporter (primarily OAT1, although OAT3 may play a smaller role) is in exchange for α-ketoglutarate. α-Ketoglutarate is brought into the cell by the Na-dependent cation transporter, NaDC-3. Luminal secretion can be via a voltage-dependent pathway or in exchange for luminal hydroxyl (OH^-) or urate. A portion of the luminal transport traverses the multidrug resistance protein-2 (MRP-2).[412]

Loop and DCT diuretics are organic anions that circulate bound to albumin, and reach tubule fluid primarily via organic anion secretory pathways in the proximal tubule.[350] Four isoforms of organic anion transporters (OATs) have been cloned and are expressed in the kidney.[351,352] Peritubular uptake by an OAT is a tertiary active process (see Figure 40.15). Energy derives from the basolateral Na^+,K^+-ATPase that provides a low intracellular [Na^+] that drives an uptake of Na^+ coupled to a-ketoglutarate (aKG^-) to maintain a high intracellular level of aKG^-. This, in turn, drives a basolateral OA^-/aKG^- countertransporter. OAT translocates diuretics into the proximal tubule cell where they can be sequestered in intracellular vesicles. They are secreted across the luminal membrane by a voltage-driven OAT,[353] and by a countertransporter in exchange for urate or OH^-.[352] OAT1 is expressed on the basolateral membrane of the S2 segment of the proximal tubule. Genetic OAT1 causes dramatically impaired renal organic anion secretion, and also furosemide resistance.[354] Thus, OAT1 plays a central role in mediating loop diuretic secretion by proximal cells. Albumin has been reported to stimulate renal organic anion secretion directly, in a dose-dependent manner, up to a maximum when the concentration reaches 1 g/dl.[355]

Endogenous and exogenous substances may compete with diuretics for secretion into tubule fluid and affect diuretic response. Uremic anions,[356] non-steroidal anti-inflammatory drugs,[357] probenecid,[358] and penicillins all inhibit loop and DCT diuretic secretion into tubule fluid. Under some conditions, this may predispose to diuretic resistance, because the concentration of drug achieved in tubule fluid does not exceed the diuretic threshold. For example, in chronic kidney disease, diuretic delivery into the urine is reduced. This shifts the diuretic dose–response curve to the right, requiring a higher dose to achieve maximal effect (see Figure 40.7). Surprisingly, however, probenecid *increases* the natriuretic effects of chlorothiazide and furosemide when administered to normal individuals.[358,359] This effect results from the probenecid-induced impairment in renal diuretic clearance, which prolongs the effective half-life, permitting diuresis to continue over a longer period of time. Thus, achieving sufficient levels, the effect of a secretory inhibitor will be to increase the natriuretic response, owing to a prolonged half-life. In contrast, in a patient whose dose is near to the diuretic threshold, impairments of secretion can lead to achievement of sub-threshold levels in tubule fluid, and to diuretic resistance.

Amiloride and triamterene are organic cations that reach tubule fluid via organic cation secretory pathways in the proximal tubule. Movement of cationic diuretics from cell to lumen occurs, at least in part, via an organic cation/H exchanger, which is coupled functionally to the apical Na/H exchanger.[350] Creatinine, cimetidine, trimethoprim, quinidine, quinine, atropine, ofloxacin, morphine, and paraquat are all secreted by this pathway.[350] Cimetidine has been shown to inhibit the secretion of amiloride.[360]

A fourth factor that may influence diuretic effectiveness is protein-binding in tubule fluid. Diuretic drugs are normally bound to proteins in the plasma, but not once they are secreted into tubule fluid. This reflects the normally low protein concentrations in tubule fluid. In contrast, when serum proteins such as albumin are filtered in appreciable quantities, diuretic drugs will interact with them.[361] This protein−drug interaction appears to inhibit the ability of the diuretic to interact with luminal transport proteins. Kirchner and colleagues showed that adding albumin to diuretic-containing fluid used to perfuse rat loops of Henle reduced the effects of the loop diuretic by approximately 50%. This effect was specific for albumin, since IgG did not mimic it,[362] and the effect could be prevented by adding inhibitors of protein-binding such as warfarin or sulfisoxizole.[363] The role of this process in human diuretic resistance, however, has been questioned, as protein-binding inhibitors do not increase diuretic efficacy in proteinurinc humans.[364] Although the reasons for the discrepant results between animal models and humans are unclear, it seems unlikely that urinary albumin-binding to diuretics is an important contributor to diuretic resistance.

Patients given diuretic drugs to treat edematous conditions all manifest some diuretic resistance (see Figure 40.7). This is evident in the shift to the right and downward in the dose−response curve for a loop diuretic.

DIURETIC ADAPTATIONS AND DIURETIC RESISTANCE

Although the clinically useful diuretic drugs all increase urinary solute and water excretion, the goal of diuretic therapy of edema is to reduce the ECF volume. This usually requires an increase in urinary solute and water excretion, but such an increase is not sufficient to effect ECF volume contraction by itself. Furthermore, any initial increase in daily urinary NaCl and water excretion begins to wane after several days of diuretic treatment. That is because of specific renal adaptations that occur during diuretic therapy. When diuretic adaptation becomes manifest once the desired ECF volume has been attained, it is clinically useful and prevents progressive ECF volume contraction. When these same processes develop prior to achieving the desired ECF volume, they would be viewed as contributing to diuretic resistance. Because specific therapeutic approaches can be devised to overcome these adaptations, an understanding of renal adaptations to diuretic treatment is crucial for understanding diuretic treatment of edema. For the purposes of this discussion, diuretic adaptations will be classified as *immediate*, *short-term*, and *chronic*. Immediate adaptations limit the intrinsic potency of diuretic drugs; these occur during the initial diuretic-induced natriuresis, and generally result from intrinsic renal processes. Short-term adaptations occur after the initial effect of the diuretic drug has worn off, and may result from both systemic and intrarenal processes. Chronic adaptations occur only when diuretic drugs have been administered during a long period of time (days to weeks). Because diuretic resistance is most commonly observed in patients who have received high doses of loop diuretics during long periods of time, these chronic adaptations may be especially relevant to the phenomenon of diuretic resistance in patients.

Immediate Adaptations

About 25 moles of sodium are filtered every day by the kidneys in a normal human. Because dietary salt intake on a Western diet is typically 110−260 mmol daily, approximately 3 pounds of salt (17 moles = 1 kg NaCl) must be reabsorbed every day by the renal tubules to maintain salt balance. As discussed above, all sodium chloride reabsorption along the mammalian nephron is driven by the action of Na/K-ATPase, which is present along the basolateral cell membrane of most renal epithelial cells. Transepithelial sodium transport occurs because apical transport pathways permit Na to move down its electrochemical gradient from tubule lumen to cell, often coupled to the movement of other ions across the same membrane. Most diuretics drugs act by inhibiting apical Na transport pathways. Because apical Na transport pathways are nephron segment-specific, each class of diuretic inhibits Na transport *predominantly* along a single segment of the nephron (see Figure 40.1). The axial organization of renal tubules, and the nephron segment-specific inhibition of salt transport by diuretics, means that diuretics have both direct effects and indirect effects on solute transport along the nephron.

When NaCl reabsorption along the thick ascending limb is inhibited by loop diuretics, the NaCl concentration in fluid that enters the distal tubule is greatly increased. In one study, the Na concentration in fluid entering the distal tubule of rats rose from 42 to 140 mM during acute loop diuretic infusion.[151] The higher luminal NaCl concentration increased Na absorption along the distal tubule (from 148 to 361 pmol/minute), because NaCl transport varies directly with the luminal NaCl concentration. Further, loop diuretics have little or no effect on ion transport along the distal tubule.[250] The bulk of the increased NaCl transport along the distal tubule appears to result from enhanced transcellular transport via the thiazide-

sensitive Na-Cl co-transporter. In microperfused rat distal tubules, raising the luminal NaCl concentration two-fold increased transepithelial Na transport by a factor of 3; this increase could be blocked entirely by luminal chorothiazide.[365] The dependence of transepithelial NaCl transport on luminal NaCl concentration probably results from a dependence of the thiazide-sensitive Na-Cl co-transporter on extracellular Na and Cl concentrations,[180] although effects to increase the abundance of NCC may also be involved.

This first level of adaptation to diuretic drugs occurs *during* the period of diuretic-induced natriuresis; this is the compensatory increase in NaCl reabsorption along segments that are not targets of diuretic action. The *net* effect of acute diuretic administration on urinary Na and Cl excretion, therefore, reflects the sum of effects in the diuretic-sensitive segment (inhibition of NaCl reabsorption) and in diuretic-insensitive segments (secondary stimulation of NaCl reabsorption). Although the most clinically important example of this form of adaptation involves loop diuretics, these compensatory processes occur during administration of most classes of diuretics. The importance of compensatory processes to blunt the acute effects of diuretics is exemplified by CA inhibitors, which inhibit Na transport across cells of the proximal tubule. Because a large portion of the Na that is rejected by the proximal tubule during CA inhibitor administration is reabsorbed along the loop of Henle and distal tubule, only a fraction escapes into the urine. CA inhibitors, therefore, are drugs of only modest potency. Blockade of immediate adaptive processes enhances the effects of the administered diuretic, as when loop diuretics are combined with CA inhibitors, acutely. A similar phenomenon has been observed in animals lacking NHE3, the apical Na/H exchanger of the proximal tubule.[13] These animals exhibit minimal salt-wasting, owing to compensatory processes.

Short-Term Adaptations (Post-Diuretic NaCl Retention)

The half-life of most diuretics (especially the loop diuretics) is relatively short. Thus, serum diuretic concentrations are often below the natriuretic threshold during a portion of each day, except when the drugs are infused constantly. This second type of adaptive response to diuretic administration occurs after the peak natriuresis has occurred, and is most prominent when the drug concentration in plasma and tubular fluid declines below the diuretic threshold. In this situation, diuretic is no longer present in tubule fluid to inhibit renal Na reabsorption and a period of NaCl retention, often termed "post-diuretic NaCl retention" begins (see Figure 40.16). The net effect of the diuretic drug during 24 hours, therefore, results from a period of natriuresis (when NaCl transport is inhibited by the diuretic), and a period of anti-natriuresis (when the drug concentration is low, before the next dose is given).

Mechanisms that contribute to post-diuretic NaCl retention have been investigated intensively and may be grouped into three classes: first, factors that result from changes in ECF volume; second, factors that result from diuretic-induced increases in distal sodium, chloride, and fluid delivery; and third, factors that result from direct effects of diuretic drugs on tubule transport processes. One signal initiating NaCl retention in the post-diuretic period is the change in ECF volume and the change in "effective" arterial blood volume. Evidence indicating a central role for changes in ECF volume includes the observation that post-diuretic NaCl retention can be prevented by administering Na, K, and Cl at rates sufficient to equal diuretic induced losses.[366] This observation does not, however, exclude a contributory role for mechanisms that occur independent of changes in ECF volume, as will be discussed below.

Diuretic drugs have effects on vascular and ECF volume within minutes of administration, both because of their ability to increase renal Na and Cl excretion, and because they have direct vascular effects. These changes activate a number of physiological control systems, which tend to favor NaCl retention and act to attenuate further NaCl loss. Important contributors to ECF volume-dependent NaCl retention have been discussed above, and include changes in the GFR, activation of the renin−angiotensin−aldosterone system, stimulation of efferent renal sympathetic nerves, suppression of atrial natriuretic peptide secretion, and suppression of renal prostaglandin secretion. Post-diuretic NaCl retention has been shown to occur in humans whether dietary NaCl intake is high or low, suggesting that true ECF volume *depletion* may not be essential. Some *decline* in ECF volume, however, was shown to be necessary for secondary NaCl retention during furosemide-induced natriuresis in rats. In rats given furosemide continuously, the secondary decline in NaCl excretion was associated with a 25% decline in GFR, suggesting that decreases in filtered NaCl-load contribute to short-term adaptations to diuretic treatment.[367] In normal humans, changes in GFR were reported to be statistically insignificant during post-diuretic NaCl retention, suggesting a decline in filtered Na does not contribute.[368] Although a statistically significant decline in GFR can be observed in the post-diuretic period when the data from several subgroups are pooled,[368] the magnitude of this effect is small, and increases in NaCl reabsorption rather than declines in GFR probably play the larger role.

One mechanism that may mediate a decline in GFR after loop diuretic drug concentrations decline may be

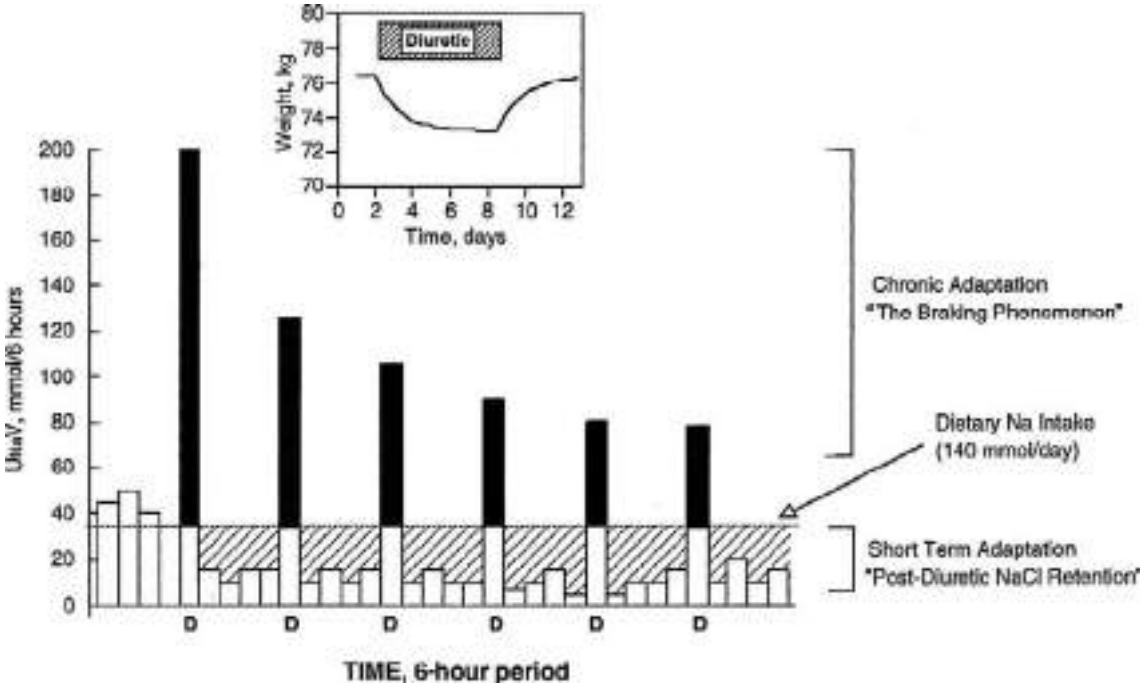

FIGURE 40.16 **Effects of diuretics on urinary Na excretion and ECF volume.** Inset: Effect of diuretic on body weight, an index of ECF volume. Note that steady-state is reached within 6–8 days, despite continued diuretic administration. Main graph: Effects of loop diuretic on urinary Na excretion. Bars represent six-hour periods before (in Na balance) and after doses of loop diuretic (D). The dotted line indicates dietary Na intake. The solid portion of bars indicates the amount by which Na excretion exceeds intake during natriuresis. The hatched areas indicate the amount of positive Na balance after the diuretic effect has dissipated. Net Na balance during 24 hours is the difference between the hatched area (post-diuretic NaCl retention) and the solid area (diuretic-induced natriureisis). Chronic adaptation is indicated by progressively smaller peak natriuretic effects (the "braking phenomenon"), and is mirrored by a return to neutral balance, as indicated in the inset, where the solid and hatched areas are equal. As discussed in the text, chronic adaptation requires ECF volume depletion.

activation of the TGF system. Loop diuretics block this system directly by interfering with Na and Cl uptake by macula densa cells, as discussed above. Thus, loop diuretics tend to maintain the GFR higher than would be expected in the absence of diuretic action. When the diuretic concentration declines, and the inhibitory effects at the macula densa wane, the TGF system is poised to respond again to NaCl delivery and to suppress the GFR, thus contributing to post-diuretic NaCl retention.

Diuretic drugs stimulate the renin–angiotensin–aldosterone axis via mechanisms described above and in Figure 40.9. The renin–angiotensin–aldosterone axis contributes importantly to renal NaCl homeostasis, but evidence for an important role of these hormones in post-diuretic NaCl retention has been mixed. In normal volunteers, post-diuretic NaCl retention was unaffected by the angiotensin-converting enzyme inhibitor captopril[369] given in doses sufficient to block furosemide-induced changes in angiotensin II and aldosterone levels. Further, in those studies, diuretic-induced changes in blood pressure were similar with or without captopril, suggesting that hypotension did not mediate the NaCl retention in the ACE inhibitor group. These data indicate that post-diuretic NaCl retention *can* occur without activation of the renin–angiotensin–aldosterone system; they do not indicate, however, that stimulation of the renin–angiotensin–aldosterone axis has no role in post-diuretic NaCl retention when it occurs. An important role for the renin–angiotensin–aldosterone axis is implied by comparing the effects of volume removal via loop diuretics and hemofiltration. In one study, diuresis of patients with heart failure led to a larger increase in renin than did removal of the same fluid using an ultrafiltration device.[370,371] Yet this effect was not supported by more recent studies.[372]

Stimulation of alpha adrenergic renal nerves enhances NaCl reabsorption. Petersen et al. showed that systemic α-1 blockade attenuated the secondary reduction in NaCl excretion that occurs during short-term furosemide-induced volume-depletion in rats.[373] They concluded that stimulation of α-1 adrenoceptors on proximal tubules contributed to the compensatory response to short-term furosemide infusion. In humans, however, administration of prazosin, in doses that block the pressor response to α-adrenergic agonists, does not prevent post-diuretic NaCl retention. Even when both prazosin and captopril are

administered concurrently, to block both the renin–angiotensin–aldosterone axis and the effects of renal nerve activity, post-diuretic NaCl retention may occur ([374]; although in this case, furosemide did reduce mean arterial pressure significantly). Thus, ECF volume-dependent stimulation of α-1 adrenergic receptors, especially along the proximal tubule, may contribute to post-diuretic NaCl retention.

Diuretic-induced decrements in ECF volume have been shown to be associated with suppression of atrial natriuretic peptide secretion. These changes occur following diuretic administration in both normal individuals, and in patients with nephrotic syndrome,[375] chronic glomerulonephritis, and essential hypertension. In some studies, atrial natriuretic peptide concentrations have declined before significant changes in extracellular or blood volume occur; in these cases it has been suggested that furosemide-induced changes in venous capacitance may underlie the effect.

The studies discussed above in which post-diuretic NaCl retention occurred despite blockade of several effector mechanisms raise the possibility that changes in ECF volume are not required for post-diuretic NaCl retention to occur. Wilcox and colleagues investigated acute effects of the loop diuretic bumetanide in the absence of ECF volume-depletion. Na, K, Cl, and water were administered to volunteers during loop diuretic administration to balance electrolyte losses completely. When changes in ECF volume were prevented, post-diuretic NaCl retention did not occur, indicating that decrements in ECF volume do play a critical role in post-diuretic NaCl retention. A volume-independent component of adaptation may also contribute to NaCl retention, however. When volunteers were challenged with a 100 mmol NaCl-load with or without prior diuretic treatment, differences were observed. The NaCl-load was excreted fully within two days under control conditions; after pretreatment with bumetanide, however, much less of the administered load was excreted during the subsequent two days.[366] This result occurred despite complete replacement of water and electrolyte losses induced by the loop diuretic. These results suggest that there are subtle but physiologically significant effects of diuretic administration, even in the short-term, that favor NaCl retention in the absence of changes in ECF volume status (see below).

In normal individuals, diuretic administration strongly activates the control systems discussed above; in edematous individuals, however, one or more of these control systems may be active at baseline, having contributed to the pathological accumulation of extracellular volume. The role of these control systems in the adaptive response to diuretic may, therefore, be different in normal and edematous individuals.

One mechanism by which diuretic drugs may increase the tendency for NaCl retention directly without changes in ECF volume involves diuretic-induced *activation* of ion transporters within the diuretic sensitive nephron segment. The cation chloride co-transporters, such as the NKCC2, are phosphorylated and activated by low intracellular chloride concentrations[376]; because loop diuretics reduce the Cl concentration in cells of the thick ascending limb, pre-existing transporters should be activated leading to increased NaCl transport capacity. This increase will be unmasked once the luminal concentration of loop diuretic declines. Ecelbarger et al.[377] reported evidence that furosemide administration activates NKCC2 via more than one mechanism. Five days of furosemide infusion led to a 50–100% increase in abundance of NKCC2, and also to an upward mobility shift of 9 kDa in apparent molecular mass. These results were interpreted as suggesting that furosemide blockade of apical NaCl uptake led to both increased expression and "modification" of NKCC2. As phosphorylation of NKCC2 regulates its activity, one possibility is that loop diuretic blockade activates the transporter via phosphorylation.

A similar mechanism has been reported to occur along the distal tubule during short-term administration of thiazide diuretics. Within 60 minutes of thiazide administration, the number of thiazide-sensitive Na-Cl co-transporters in kidney cortex (measured as the number of [^{3}H]metolazone binding sites) increases substantially.[378] The techniques used to estimate the number of transporters in these experiments do not permit one to determine whether the increased number reflects insertion of pre-existing transporters from a subapical storage pool or activation of transporters that are present but inactive in the apical membrane. It is now clear that a subapical pool of NCC shuttles to and from the apical membrane in response to physiological perturbation.[379] An increase in the number of activated ion transporters at the apical membrane would be expected to increase the transport capacity, so that when diuretic concentrations decline, increased Na and Cl transport would result.

Another mechanism by which diuretic drugs may enhance the tendency to NaCl retention directly involves stimulation of transport pathways in nephron segments that lie distal to the target of diuretic action (segments that are insensitive to the diuretic drug). For example, the number of metolazone-binding sites increases within 60 minutes after a loop diuretic has been administered.[378] Because NCC is expressed by nephron segments that do not express loop diuretic-sensitive pathways, the increased NCC is believed to result from increases in salt and water delivery to DCT cells (discussed in more detail below).

Post-diuretic NaCl retention can have major effects on the clinical efficacy of diuretic drugs. The half-life of most loop diuretics is short, so that NaCl retention can occur during 18 hours per day, if the drug is administered once daily (see Figure 40.16). If dietary NaCl intake is low, then post-diuretic NaCl retention does not compensate for the drug-induced NaCl losses, and NaCl balance becomes negative (the desired therapeutic response). If, on the other hand, dietary NaCl intake is high, then post-diuretic NaCl retention can compensate entirely for the initial NaCl losses during the period of drug action. When dietary NaCl intake is high, therefore, salt balance may be neutral, even from the first day of diuretic therapy,[368] despite impressive increases in urine volume after each dose of diuretic. This is one reason that dietary NaCl intake is a key determinant of diuretic efficacy, especially for the short-acting loop diuretics.

Chronic Adaptations (The "Braking" Phenomenon)

When diuretics reduce ECF volume effectively, NaCl balance gradually returns to neutral, despite continued diuretic administration[368,380] (see Figure 40.16). This "braking phenomenon" occurs when the magnitude of natriuresis following each diuretic dose declines. Several factors, acting in concert, may participate in chronic adaptation. A critical factor that is necessary for the braking phenomenon to occur is a decline in the ECF volume. Wilcox and co-workers showed that the magnitude of each diuretic-induced natriuresis declined during ECF volume-depletion of humans consuming a low-NaCl diet. In contrast, when dietary NaCl intake was high, ECF volume-depletion did not occur, and the magnitude of diuretic-induced natriuresis did not decline.[368,380] Relative or absolute ECF volume contraction limits NaCl excretion by reducing the amount of NaCl that is filtered, and by increasing the amount of NaCl that is reabsorbed. In experimental animals, declines in renal blood flow occur during chronic diuretic treatment. Declines in GFR are usually modest, however, unless volume depletion is extreme or unles renal perfusion is compromised by drugs or physical factors such as renal artery stenosis. The effects of diuretics on glomerular filtration and renal blood flow are not caused primarily by changes in mean arterial pressure, as the renal autoregulatory response tends to maintain GFR and renal blood flow relatively constant when arterial pressure changes. Instead, ECF volume contraction itself leads to decrements in renal blood flow and GFR; because renal blood flow declines proportionately more than GFR, ECF volume-contraction increases the filtration fraction (GFR/RPF).

The role of the proximal tubule in diuretic adaptation has been documented clearly in rats treated chronically with thiazide diuretics, and in animals and humans treated with loop diuretics. In the case of thiazide treatment, micropuncture studies showed that hydrochlorothiazide initially inhibited Na and Cl absorption along both the proximal tubule (by inhibiting CA) and the distal tubule (by inhibiting Na-Cl co-transport) of rats.[228] After 7−10 days of treatment, however, ECF volume-contraction led to increases in proximal solute reabsorption, thereby limiting delivery of Na and Cl to the distal sites of thiazide action. During the chronic phase of treatment, inhibition of NaCl transport along the distal nephron (the predominant site of thiazide action) counterbalanced the reduction in distal NaCl delivery; under these conditions, at steady-state, urinary NaCl was equal to dietary NaCl intake.[228] Loop diuretics such as furosemide have also been shown to inhibit Na and Cl absorption by the proximal tubule, although the mechanism is unclear. But, as with DCT diuretics, chronic treatment with loop diuretics leads to ECF volume-contraction and enhanced proximal NaCl reabsorption.[381] That effects on proximal absorption require decrements in ECF volume was shown by comparing NaCl delivery out of the proximal tubule during furosemide administration, with and without volume replacement. Only when the ECF volume was permitted to decline was proximal absorption stimulated.[367] Many of the same effector systems that participate in post-diuretic NaCl retention also may participate in chronic adaptations to diuretic drugs.

Physical Factors

A rise in filtration fraction increases the protein oncotic pressure in peritubular capillaries (more protein free filtrate is formed per ml of blood flow, thereby contracting the plasma volume around a constant amount of serum protein). The increased peritubular oncotic pressure increases solute and fluid reabsorption, especially in the proximal tubule. ECF volume contraction also enhances proximal solute and fluid reabsorption by decreasing the renal interstitial pressure during chronic diuretic treatment.

Sympathetic Renal Nerve Activity

Efferent sympathetic nerves innervate the renal vasculature, the macula densa, and essentially all segments of the nephron. Stimulation of sympathetic nerves reduces urinary NaCl excretion by reducing renal blood flow, by stimulating renin release at the macula densa, by stimulating tubule NaCl reabsorption along the nephron, and by interacting with hormonal modulators of NaCl transport. Renal nerves may contribute to NaCl retention in edematous disorders, and renal nerve activity is stimulated when furosemide is administered either to normal or volume-depleted

animals.[382] Yet experimental models of chronic diuretic administration have failed to substantiate a central role for renal nerve activity in adaptive processes. Chronic sympathectomy or blockade of α-1 receptors inhibits the compensatory increase in proximal NaCl reabsorption that occurs during furosemide-induced ECF volume-depletion, but these maneuvers did not enhance the natriuretic response to furosemide.[383] This indicates that the inhibition of proximal solute reabsorption which occurs secondary to adrenergic blockade is compensated by increased reabsorption distally. Use of systemic pharmacological sympathetic blockade to study the role of renal nerves in diuretic adaptation is limited because of drug-induced systemic hypotension, but Petersen and DiBona showed that even anatomical renal denervation in normal rats does not abrogate the compensatory response to chronic furosemide administration.[384] Although it seems clear that renal nerves do not play a critical role in mediating compensation to chronic diuretic use in normal humans and animals, the consistent observation that diuretics do stimulate renal nerve activity suggests that renal nervous activity may contribute to diuretic adaptation in some patients. In patients suffering from edematous disorders, distal Na reabsorption may already be stimulated; denervation in this situation might lead to significant impairment in adaptation to diuretic drugs.

Renin–Angiotensin–Aldosterone

A third factor participating in chronic adaptation to diuretic drugs is the renin–angiotensin–aldosterone system. Renin acts on angiotensinogen to generate angiotensin I, which is converted to angiotensin II by converting enzyme. Angiotensin II stimulates aldosterone secretion from the adrenal cortex; aldosterone stimulates salt reabsorption by the distal nephron. Recent studies indicate that, in addition to stimulating Na transport by ENaC of the collecting duct, as discussed above, mineralocorticoid hormones stimulate Na transport by the thiazide-sensitive Na-Cl co-transporter of the DCT.[191,385–387] In addition, however, angiotensin II directly stimulates Na reabsorption along both the proximal and distal tubule by stimulating Na/H exchange activity.[388] Thus, diuretic drugs frequently result in stimulation of the renin–angiotensin–aldosterone system, and the Na retention that occurs during diuretic treatment may result in part from this. As is the case with renal nerves, it has been difficult to show conclusively that the renin–angiotensin–aldosterone system plays a critical role in chronic adaptation to diuretic drugs. Yet as with renal nerves, the systemic effects of inhibition of the system, either with angiotensin I-converting enzyme inhibitor, angiotensin II receptor blockers or competitive aldosterone blockers make it difficult to exclude a role for this hormonal system in the compensation to diuretic therapy.

Epithelial Hypertrophy and Hyperplasia

Other factors that can enhance renal NaCl reabsorptive capacity are structural and functional changes in the nephron itself. When a diuretic is administered, solute delivery to segments that lie distal to the site of diuretic action increase, leading to load-dependent increases in solute reabsorption, as discussed above.[389] When solute delivery and solute reabsorption increase chronically, epithelial cells undergo both hypertrophy and hyperplasia (see Figure 40.17). Infusion of furosemide into rats continuously for seven days increased the percentage of renal cortical volume occupied by distal nephron cells. DCT cell volume increased by nearly 100%, with accompanying increases in luminal membrane area per length of tubule, in basolateral membrane area per length of tubule, and in mitochondrial volume per cell.[365,390,391] Chronic loop diuretic administration increases the Na/K-ATPase activity in the distal convoluted and cortical collecting tubules[392,393](see Figure 40.17), and increases the number of thiazide-sensitive Na-Cl co-transporters, measured as the maximal number of binding sites for [^{3}H] metolazone.[181,385] In one study, chronic furosemide treatment increased expression of mRNA encoding the thiazide-sensitive Na-Cl co-transporter, as detected by *in situ* hybridization[181](see Figure 40.18). In another study, however, mRNA expression of the thiazide-sensitive Na-Cl co-transporter, as well as ouabain-sensitive Na/K-ATPase, were not affected by chronic furosemide infusion, when detected by Northern analysis.[394] Distal tubule cells that express high levels of transport proteins and are hypertrophic have a higher Na and Cl transport capacity than normal tubules. Compared with tubules from normal animals, tubules of animals treated chronically with loop diuretics can absorb Na and Cl up to three times more rapidly than control animals, even when salt and water delivery are fixed by microperfusion (Figure 40.18). When distal tubules are presented with high NaCl-loads, as occurs during loop diuretic administration *in vivo*, Na and Cl absorption rates approach those commonly observed only in the proximal tubule.[365] Chronic treatment of rats with loop diuretics also results in significant hyperplasia of cells along the distal nephron. Whereas mitoses of renal tubule epithelial cells are infrequent in adult kidneys, distal tubules from animals treated with furosemide chronically demonstrate prominent mitoses; increased synthesis of DNA in these cells was confirmed by showing increases in labeling of DCT cells with bromodeoxyurindine and proliferating cell nuclear antigen.[395]

The diuretic-induced signals that initiate changes in distal nephron structure and function are poorly-

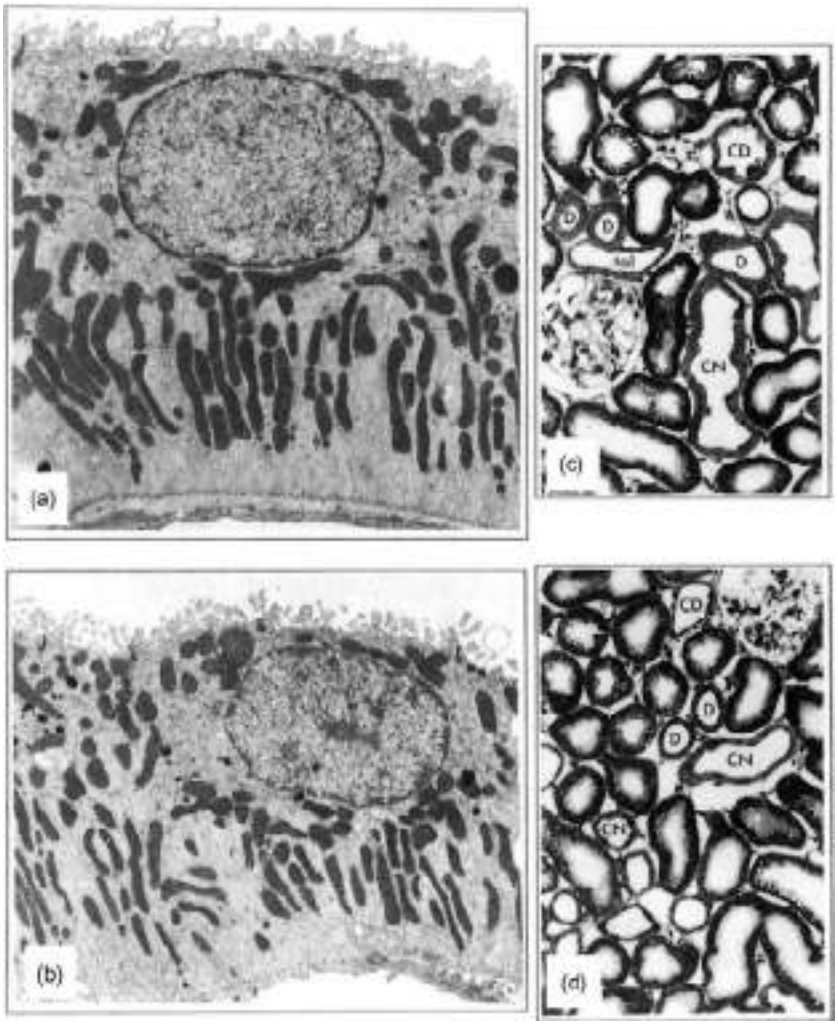

FIGURE 40.17 **Effects of chronic loop diuretic administration on distal convoluted tubule cells of rats.** Rats received furosemide continuously for seven days. Panels (a) and (b): Electron micrographs (×10,000) of distal convoluted tubule cells from control- and furosemide-infused animals respectively. Note that furosemide increases the size of the cell, the size of the nucleus, the amount of mitochondrial volume, and the amount of basolateral membrane area. Panels (c) and (d): Photomicrographs of kidney cortices from control and furosemide infused animals respectively (×480) (*D*: distal convoluted tubule; *CN*: connecting tubule; *CD*: cortical collecting duct: *tal*: thick ascending limb). Note thickening of the epithelium in all distal segments. *(Photomicrographs are used with permission from ref. [365].)*

understood.[389] Several factors, acting in concert, may contribute to these changes; these include diuretic-induced increases in Na and Cl delivery to distal segments, effects of ECF volume depletion on systemic hormone secretion and renal nerve activity, and local effects of diuretics on autocrine and paracrine secretion. Increased production of angiotensin II or increased secretion of aldosterone resulting from increases in renin activity may contribute to hypertrophy and hyperplasia. Angiotensin is a potent mitogen; angiotensin II receptors have not been localized definitively to DCT cells, but recent functional studies do suggest that DCT cells express angiotensin II receptors.[396] Beck et al.[397] showed that angiotensin I-converting enzyme inhibitors do not prevent loop diuretic-induced hypertrophy of DCT cells. Yet the hypertrophy during angiotensin I-converting enzyme inhibition is one that results from lengthening of kidney tubules; in their absence the hypertrophy results from thickening of the tubular cells.

Aldosterone also promotes growth of responsive tissues under some circumstances[398]; when salt delivery to the collecting duct is increased in the presence of high levels of circulating aldosterone, principal cell hypertrophy develops; when salt delivery is high in the absence of aldosterone secretion, hypertrophy is absent. This indicates that aldosterone plays a permissive role in the development of cellular hypertrophy in this aldosterone-responsive renal epithelium. Aldosterone does affect ion transport by cells of the DCT,[185,190,399,400] and aldosterone almost certainly contributes to adaptations along the cortical collecting tubule. Yet hypertrophy of DCT cells has been shown to occur during chronic loop diuretic infusion, even when changes in circulating mineralocorticoid, glucocorticoid, and vasopressin levels are prevented.[391]

One intriguing hypothesis is that cellular ion concentrations regulate epithelial cell growth directly.[401] Increases in Na uptake across the apical plasma

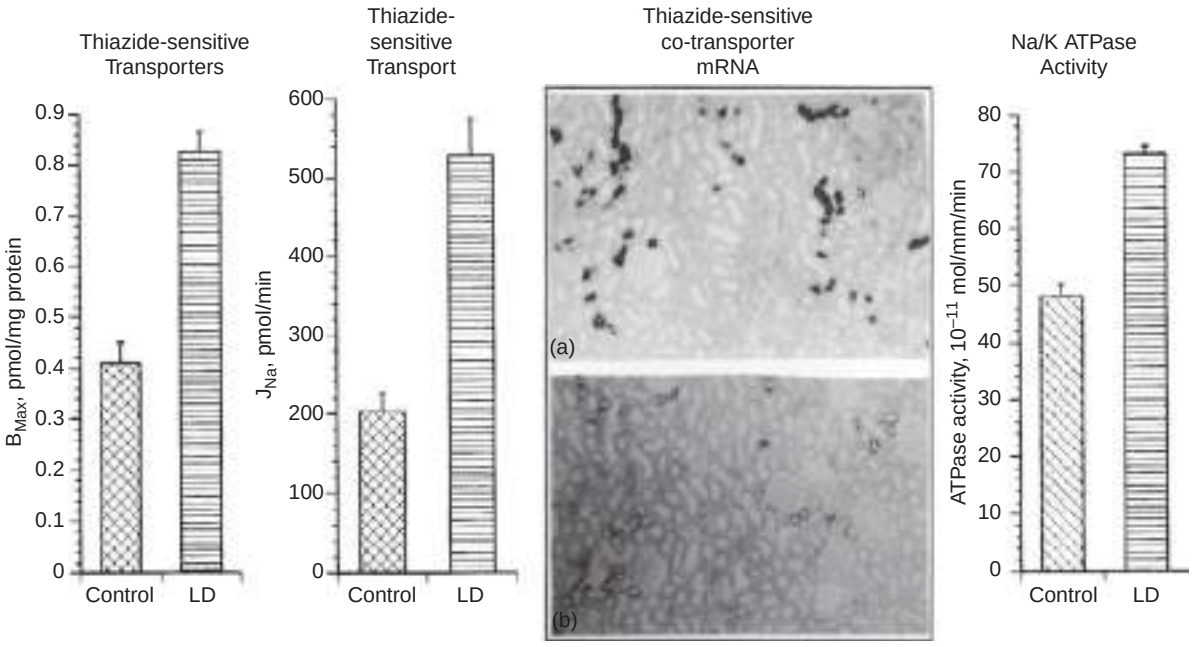

FIGURE 40.18 **Effects of continuous loop diuretic infusion on rat kidney.** Loop diuretic infusion increased the number of thiazide-sensitive Na-Cl co-transporters,[378] the rate of thiazide-sensitive Na transport along the distal tubule,[365] the abundance of thiazide-sensitive Na-Cl co-transporter mRNA (a: furosemide-treated kidney cortex; b: control kidney cortex). *(Ref. [181], used with permission),* and Na/K-ATPase activity along the distal convoluted tubule. *(Data from ref. [392].)*

membrane precede cell growth in the TAL during treatment with ADH,[402] in principal cells of the CCT during treatment with mineralocorticoid hormones,[403,404] and in the DCT during treatment with loop diuretics.[365,398] Although the cause of the increased Na uptake varies, changes in the intracellular Na concentration appear to precede growth in each example. This hypothesis predicts that blockade of apical Na entry would lead to atrophy of epithelial cells. Chronic treatment of rats with DCT diuretics reduces activity of Na/K-ATPase and Na transport capacity of DCT segments,[405,406] but these experiments are complicated by other structural effects of chronic DCT diuretic treatment, discussed below. Regardless of the proximate stimulus for DCT cell growth, recent experiments have shown that immunoreactivity for insulin-like growth factor-1 (IGF-1), and for an IGF-binding protein (IGFBP-1), increases during chronic treatment of rats with loop diuretics.[407] The changes in IGF-1 expression appeared not to result from changes in IGF-1 mRNA expression, but rather appeared to reflect post-transcriptional events. IGFBP-1 mRNA was increased by three-fold 18 hours after loop diuretic treatment was initiated. IGF-1 has been shown to participate in regeneration of injured or ischemic renal tissue, and promotes cell proliferation and differentiation *in vitro*; whether these changes in IGF expression mediate the effects of diuretics on distal nephron structure remains to be established.

Morphological changes in the distal nephron during loop diuretic administration are not restricted to Na reabsorbing cells. Chronic diuretic infusion stimulates selective hypertrophy of type-B intercalated-cells.[408] Type-B intercalated-cells secrete bicarbonate and express apical Cl/HCO_3 exchangers and basolateral H-ATPase pumps; chronic bumetanide infusion increased the number of apical microvilli in Type-B cells, increased the basolateral cell membrane area, and led to marked cytoplasmic and basolateral labeling for H-ATPase. Type-A cells, which normally mediate acid secretion, were small; H-ATPase was distributed primarily within intracellular tubulovesicles in the tubules of treated animals. The authors concluded that the structural changes in intercalated cells resulted from increased distal chloride delivery, because serum pH and electrolyte concentrations were not affected by the diuretic treatment. Increased distal chloride delivery might be expected to enhance Cl/HCO_3 exchange, increasing transepithelial solute transport, stimulating cell growth via mechanisms similar to those discussed above. These effects are likely to contribute to the profound metabolic alkalosis that can complicate aggressive treatment with loop diuretics.

Chronic diuretic administration has structural effects not only on nephron segments that lie distal to the site of diuretic action, but also on the nephron segments that are directly inhibited by the drugs themselves.

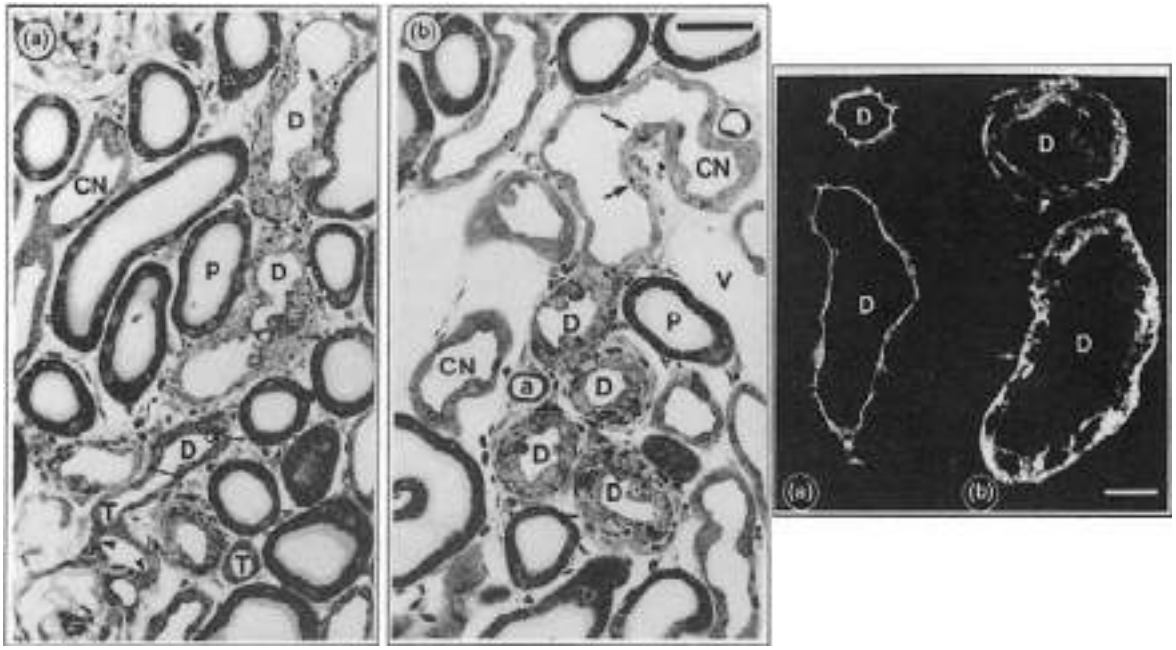

FIGURE 40.19 **Effects of continuous DCT diuretic treatment on the structure of distal convoluted tubules.** Panels a and b at the left show photomicrograph of kidney cortex from animals treated chronically with thiazide diuretics; note extreme hyperplasia and dysmorphology of distal segments (compare normal distal convoluted tubules in Figure 40.16, above) (T: thick ascending limb; D: distal convoluted tubule; CN: connecting tubule; CD: collecting duct; P: proximal tubule; a: arteriole). Double arrow indicates transition from thick ascending limb to distal convoluted tubule; note normal morphology of the thick ascending limb. Panels a and b on the right show immunostaining for the thiazide-sensitive Na-Cl co-transporter from control rats (a) and rats infused with a thiazide continuously for 10 days (b). Note that the normal apical localization of the transporter immunoreactivity (a) is distributed throughout the cytoplasm in animals exposed to diuretics chronically (b). *(From ref. [217]. Used with permission.)*

Within hours of furosemide administration to rats, autophagocytic vacuoles develop in thick ascending limb cells.[409] Following seven days of furosemide treatment of rats, the cell height of thick ascending limb cells was significantly reduced.[365] Chronic treatment of rabbits with loop diuretics decreased Na/K-ATPase activity in medullary thick ascending limb cells by approximately one-third.[410] These results are consistent with an effect of transepithelial ion transport to stimulate "work hypertrophy" and blockade of transepithelial transport to stimulate "disuse atrophy." When DCT diuretics are administered chronically, Na/K-ATPase activity in the DCT is reduced,[406] and the capacity of DCT cells to reabsorb Na and Cl declines.[405] Yet chronic administration of DCT diuretics, like genetic disruption of the thiazide-sensitive Na-Cl co-transporter,[216] to rats leads to profound changes in cellular morphology; the DCT epithelium becomes disordered, DCT cells undergo apoptosis and necrosis, and interstitial fibrosis occurs (see Figure 40.19). Chronic treatment also leads to the disappearance of normal polarization of thiazide-sensitive Na-Cl co-transporter proteins. Under normal conditions, immunoreactivity for the thiazide-sensitive Na-Cl co-transporter is restricted to the apical membrane and to a small subapical pool of vesicles (see Figure 40.19**)**. During chronic treatment with DCT diuretics, the protein is distributed uniformly throughout the cell. Surprisingly, based on the severe morphological degenerative changes in tubular morphology, chronic thiazide administration results in an *increase* in the density of [^{3}H] metolazone-binding sites (functional thiazide-sensitive transporters) in kidney cortex,[406] despite a decline in mRNA expression for the transporter.[395] These results demonstrate that chronic thiazide administration regulates the thiazide-sensitive transporter in a complex way. Further studies are necessary to determine the mechanisms involved.

Although experimental data concerning structural and functional responses of the distal nephron to chronic treatment with diuretic drugs come predominantly from studies employing experimental animals, Loon et al.[411] reported that chronic treatment with loop diuretics in humans enhanced ion transport rates in the distal tubule. They estimated the transport capacity of the DCT as the portion of Na and Cl reabsorption that could be inhibited by thiazide diuretics. When furosemide was administered to volunteers for one month, the enhancement in sodium excretion that occurred resulting from dose of a thiazide diuretic was

significantly larger. Although these data are necessarily indirect, they are entirely consistent with the data derived from experimental animals given loop diuretics chronically. The ECF volume-independent component of NaCl retention that occurs following loop diuretic administration[366] may also reflect changes in distal nephron structure and function.

Acknowledgments

Work in the author's laboratory has been supported by a Merit Review from the Department of Veterans Affairs, by a Grand-In-Aid from American Heart Association, by a Scherbenske Award from the American Society of Nephrology, and by an RO1 from the National Institutes of Health. The author thanks Mark Okusa, the coauthor of the previous version of this text, for much of the research that led to this update.

References

[1] Okusa MD, Ellison DH. Physiology and pathophysiology of diuretic action. In: Alpern RJ, Hebert SC, editors. The kidney: physiology and pathophysiology. 4th ed. Amsterdam: Elsevier; 2008. p. 1051–984.

[2] Ellison DH, Hoorn EJ, Wilcox CS. Diuretics. In: Taal MW, Chertow GM, Marsden PA, Skorecki K, Yu AS, Brenner BM, editors. Brenner and Rector's the kidney. 9th ed. Philadelphia: Elsevier; 2012. p. 1879–916.

[3] Brater DC. Diuretic pharmacokinetics and pharmacodynamics. In: Seldin DW, Giebisch G, editors. Diuretic agents: clinical physiology and pharmacology. San Diego: Academic Press; 1997. p. 189–208.

[4] Better OS, Rubinstein I, Winaver JM, Knochel JP. Mannitol therapy revisited (1940–1997). Kidney Int 1997;51:886–94.

[5] Weiner IM. Diuretics and other agents employed in the mobilization of edema fluid. In: Gilman AG, Rall TW, Nies AS, Taylor AS, editors. The pharmacological basis of therapuetics. 8th ed. New York: Pergamon Press; 1990. p. 713–42.

[6] Homsi E, Barreiro MF, Orlando JM, Higa EM. Prophylaxis of acute renal failure in patients with rhabdomyolysis. Ren Fail 1997;19(2):283–8.

[7] Majumdar SR, Kjellstrand CM, Tymchak WJ, Hervas-Malo M, Taylor DA, Teo KK. Forced euvolemic diuresis with mannitol and furosemide for prevention of contrast-induced nephropathy in patients with CKD undergoing coronary angiography: a randomized controlled trial. Am J Kidney Dis 2009;54(4):602–9.

[8] Hinson HE, Stein D, Sheth KN. Hypertonic saline and mannitol therapy in critical care neurology. J Intensive Care Med. 2011; epub ahead of print.

[9] Jenkins IR, Curtis AP. The combination of mannitol and albumin in the priming solution reduces positive intraoperative fluid balance during cardipulmonary bypass. Perfusion 1995;10:301–5.

[10] England MD, Cavaroocchi NC, O'Brien JF, Solis E, Pluth JR, Orszulak TA, et al. Influence of antioxidants (mannitol and allopurinol) on oxygen free radical generation during and after cardiopulmonary bypass. Circulation 1986;74:134–7.

[11] Arieff AI. Dialysis disequilibrium syndrome: current concepts on pathogenesis and prevention. Kidney Int 1994;45:629–35.

[12] Gong G, Lindberg J, Abrams J, Whitaker WR, Wade CE, Gouge S. Comparison of hypertonic saline solutions and dextran in dialysis-induced hypotension. J Am Soc Nephrol 1993;3: 1808–12.

[13] Lorenz JN, Schultheis PJ, Traynor T, Shull GE, Schnermann J. Micropuncture analysis of single-nephron function in NHE3-deficient mice. Am J Physiol 1999;277(3 Pt 2):F447–53.

[14] Bomsztyk K, George JP, Wright FS. Effects of luminal fluid anions on calcium transport by proximal tubule. Am J Physiol 1984;246:F600–8.

[15] Beck LH, Goldberg M. Effects of acetazolamide and parathyroidectomy on renal transprot of sodium, calcium and phosphate. Am J Physiol 1973;224:1136–42.

[16] Higashihara E, Nutahara K, Takeuchi T, Shoji N, Araie M, Aso Y. Calcium metabolism in acidotic patients induced by carbonic anhydrase inhibitors: responses to citrate. J Urol 1991;145(5): 942–8.

[17] Puschett JB, Winaver J. Efects of diuretics on renal function. In: Windhager EE, editor. Handbook of physiology section 8: renal physiology. New York: Oxford University Press; 1992. p. 2335–406.

[18] Okusa MD, Erik A, Persson G, Wright FS. Chlorothiazide effect on feedback-mediated control of glomerular filtration rate. Am J Physiol 1989;257:F137–44.

[19] Good DW, Wright FS. Luminal influences on potassium secretion: sodium concentration and fluid flow rate. Am J Physiol 1979;236:F192–205.

[20] Puscas I, Coltau M, Baican M, Pasca R, Domuta G. The inhibitory effect of diuretics on carbonic anhydrases. Res Commun Mol Pathol Pharmacol 1999;105(3):213–36.

[21] Purkerson JM, Schwartz GJ. The role of carbonic anhydrases in renal physiology. Kidney Int 2007;71(2):103–15.

[22] Kaunisto K, Parkkila S, Rajaniemi H, Waheed A, Grubb J, Sly WS. Carbonic anhydrase XIV: luminal expression suggests key role in renal acidification. Kidney Int 2002;61(6):2111–8.

[23] Eveloff J, Swenson ER, Maren TH. Carbonic anhydrase activity of brush border and plasma membraens prepared from rat kidney cortex. Biochem Pharmacol 1979;28:1434–7.

[24] Maren TH. Current status of membrane-bound carbonic anhydrase. Ann NY Acad Sci 1980;341:246–58.

[25] Lonnerholm G, Wistrand PJ. Membrane-bound carbonic anhydrase CA IV in the human kidney. Acta Physiol Scand 1991;141: 231–4.

[26] Sly WS, Whyte MP, Sundaram V, Tashian RE, Hewett-Emmett D, Guibaud P, et al. Carbonic anhydrase II deficiency in 12 families with the autosomal recessive syndrome of osteopetrosis with renal tubular acidosis and cerebral calcification. N Engl J Med 1985;313:139–45.

[27] Tsuruoka S, Kittelberger AM, Schwartz GJ. Carbonic anhydrase II and IV mRNA in rabbit nephron segments: stimulation during metabolic acidosis. Am J Physiol 1998;274(2 Pt 2): F259–67.

[28] Moe OW, Preisig PA, Alpern RJ. Cellular model of proximal tubule NaCl and $NaHCO_3$ absorption. Kidney Int 1990;38: 605–11.

[29] Aronson PS. Role of SLC26A6-mediated Cl–oxalate exchange in renal physiology and pathophysiology. J Nephrol 2010;23 (Suppl. 16):S158–64.

[30] Rector Jr. FC, Carter NW, Seldin DW. The mechanism of bicarbonate reabsorption in the proximal and distal tubules of the kidney. J Clin Invest 1965;44:278–90.

[31] Lucci MS, Pucacco LR, DuBose Jr. TD, Kokko JP, Carter NW. Direct evaluation of acidification by rat proximal tubule: role of carbonic anhydrase. Am J Physiol 1980;238:F372–9.

[32] Lucci MS, Tinker JP, Weiner I, DuBose Jr. TD. Function of proximal tubule carbonic anhydrase defined by selective inhibition. Am J Physiol 1983;245:F443–9.

[33] Gross E, Pushkin A, Abuladze N, Fedotoff O, Kurtz I. Regulation of the sodium bicarbonate co-transporter kNBC1

function: role of Asp(986), Asp(988) and kNBC1-carbonic anhydrase II binding. J Physiol 2002;544(Pt 3):679–85.
[34] Alvarez BV, Kieller DM, Quon AL, Markovich D, Casey JR. Slc26a6: a cardiac chloride-hydroxyl exchanger and predominant chloride-bicarbonate exchanger of the mouse heart. J Physiol 2004;561(Pt 3):721–34.
[35] Li X, Alvarez B, Casey JR, Reithmeier RA, Fliegel L. Carbonic anhydrase II binds to and enhances activity of the Na^+/H^+ exchanger. J Biol Chem 2002;277(39):36085–91.
[36] Soleimani M, Xu J. SLC26 chloride/base exchangers in the kidney in health and disease. Semin Nephrol 2006;26(5):375–85.
[37] Soleimani M, Aronson PS. Effects of acetazolamide on Na^+-HCO_3^- co-transport in basolateral membrane vesicles isolated from rabbit renal cortex. J Clin Invest 1989;83:945–51.
[38] Sasaki S, Marumo F. Effects of carbonic anhydrase inhibitors on basolateral base transport of rabbit proximal straight tubule. Am J Physiol 1989;257:F947–52.
[39] Brown D, Hirsch S, Gluck S. An H^+-ATPase in opposite plasma membrane domains in kidney epithelial cell subpopulations. Nature 1988;331:622–4.
[40] Wagner CA, Devuyst O, Bourgeois S, Mohebbi N. Regulated acid–base transport in the collecting duct. Pflugers Arch: Eur J Phy 2009;458(1):137–56.
[41] Biver S, Belge H, Bourgeois S, Van Vooren P, Nowik M, Scohy S, et al. A role for Rhesus factor Rhcg in renal ammonium excretion and male fertility. Nature 2008;456(7220):339–43.
[42] Lee HW, Verlander JW, Bishop JM, Igarashi P, Handlogten ME, Weiner ID. Collecting duct-specific Rh C glycoprotein deletion alters basal and acidosis-stimulated renal ammonia excretion. Am J Physiol Renal Physiol 2009;296(6):F1364–75.
[43] Weiner ID, Verlander JW. Role of NH_3 and NH_4^+ transporters in renal acid–base transport. Am J Physiol Renal Physiol 2011;300(1):F11–23.
[44] Sato S, Zhu XL, Sly WS. Carbonic anhydrase isozymes IV and II in urinary membranes from carbonic anhydrase II-deficient patients. Proc Natl Acad Sci USA 1990;87(16):6073–6.
[45] Star RA, Burg MB, Knepper MA. Luminal disequilibrium pH and ammonia transport in outer medullary collecting duct. Am J Physiol 1987;29984:26980–8021.
[46] Shuichi T, Schwartz GJ. HCO_3^- absorption in rabbit outer medullary collecting duct: role of luminal carbonic anhydrase. Am J Physiol 1998;274:F139–47.
[47] Sterling D, Reithmeier RA, Casey JR. Carbonic anhydrase: in the driver's seat for bicarbonate transport. Jop 2001;2(4 Suppl.): 165–70.
[48] Sterling D, Reithmeier RA, Casey JR. A transport metabolon. functional interaction of carbonic anhydrase II and chloride/bicarbonate exchangers. J Biol Chem 2001;276(51):47886–94.
[49] Nijenhuis T, Renkema KY, Hoenderop JG, Bindels RJ. Acid–base status determines the renal expression of Ca^{2+} and Mg^{2+} transport proteins. J Am Soc Nephrol 2006;17(3):617–26.
[50] Tucker BJ, Blantz RC. Studies on the mechanism of reduction in glomerular filtration rate after benzolamide. Pflugers Arch 1980;388:211–6.
[51] Johnson T, Kass MA. Hematologic reactions to carbonic anhydrase inhibitors. Am J Opthal 1986;101:410–8.
[52] Paisley KE, Tomson CR. Calcium phosphate stones during long-term acetazolamide treatment for epilepsy. Postgrad Med J 1999;75(885):427–8.
[53] Stafstrom CE, Gilmore HE, Kurtin PS. Nephrocalcinosis complicating medical treatment of posthemorrhagic hydrocephalus. Pediatr Neurol 1992;8:179–82.
[54] Werblin TP, Pollack IP, Liss RA. Blood dyscrasias in patients suing methazolamide (Neptazane) for glaucoma. Opthalmology 1980;87:350–4.
[55] Ellison DH, Wilcox CS. Diuretics: use in edema and the problem of resistance. In: Brady HR, Wilcox CS, editors. Therapy in nephrology and hypertension. London: Saunders; 2003. p. 955–76.
[56] Kassamali R, Sica DA. Acetazolamide: a forgotten diuretic agent. Cardiol Rev 2011;19(6):276–8.
[57] Marik PE, Kussman BD, Lipman J, Kraus P. Acetazolamide in the treatment of metabolic alkalosis in critically ill patients. Heart Lung 1991;20:455–9.
[58] Fiore DC, Hall S, Shoja P. Altitude illness: risk factors, prevention, presentation, and treatment. Am Fam Physician 2010;82(9): 1103–10.
[59] Gertsch JH, Lipman GS, Holck PS, Merritt A, Mulcahy A, Fisher RS, et al. Prospective, double-blind, randomized, placebo-controlled comparison of acetazolamide versus ibuprofen for prophylaxis against high altitude headache: the Headache Evaluation at Altitude Trial (HEAT). Wilderness Environ Med 2010;21(3):236–43.
[60] Seupaul RA, Welch JL, Malka ST, Emmett TW. Pharmacologic prophylaxis for acute mountain sickness: a systematic shortcut review. Ann Emerg Med 2011;59(4):307–17.
[61] Resnick JS, Engle WK, Griggs RC, Stam AC. Acetazolamide prophylaxis in hypokalemic periodic paralysis. N Engl J Med 1968;278:582–6.
[62] Grissom CK, Roach RC, Sarnquist FH, Hackett PH. Acetazolamide in the treatment of acute mountain sickenss: clinical efficacy and effect on gas. Ann Intern Med 1992;116: 461–5.
[63] Johnsen T. Effect upon serum insulin, glucose and potassium concentrations of acetazolamide during attacks of familial periodic hypokalemic paralysis. Acta Neurol Scand 1977;56: 533–41.
[64] Reiss WG, Oles KS. Acetazolamide in the treatment of seizures. Ann Pharmacother 1996;30:514–9.
[65] Shoeman JF. Childhood pseudotumor cerebri: clinical and intracranial pressure response to acetazolamide and furosemide treatment in a case series. J Child Neurol 1994;9:130–4.
[66] Shore ET, Millman EP. Central sleep apnea and acetazolamide therapy. Arch Intern Med 1983;143:1278–80.
[67] Prescott LF, Balali-Mood M, Critchley JA, Johnstone AF, Proudfoot AT. Diuresis or urinary alkalinization for salicylate poisoning? British Med J 1982;285:1383–6.
[68] Hannaert P, Alvarez-Guerra M, Pirot D, Nazaret C, Garay RP. Rat NKCC2/NKCC1 co-transporter selectivity for loop diuretic drugs. Naunyn–Schmiedeberg's Arch Pharmacol 2002;365(3): 193–9.
[69] Puschett JB, Goldberg M. The acute effects of furosemide on acid and electrolyte excretion in man. J Lab Clin Med 1968;71: 666–77.
[70] Paulais M, Lachheb S, Teulon JA. Na^+- and Cl^--activated K^+ channel in the thick ascending limb of mouse kidney. J Gen Physiol 2006;127(2):205–15.
[71] Vandewalle A, Cluzeaud F, Bens M, Kieferle S, Steinmeyer K, Jentsch TJ. Localization and induction by dehydration of ClC-K chloride channels in the rat kidney. Am J Physiol 1997;272 (5 Pt 2):F678–88.
[72] Shankar SS, Brater DC. Loop diuretics: from the Na-K-2Cl transporter to clinical use. Am J Physiol 2003;284(1):F11–21.
[73] Somasekharan S, Tanis J, Forbush B. Loop diuretic and ion binding residues revealed by scanning mutagenesis of transmembrane helix 3 (TM3) of the Na-K-Cl Co-transporter (NKCC1). J Biol Chem 2012.
[74] Kaplan MR, Plotkin MD, Lee WS, Xu ZC, Lytton J, Hebert SC. Apical localization of the Na-K-Cl co-transporter, rBSC1, on rat thick ascending limbs. Kidney Int 1996;49:40–7.

[75] Obermuller N, Kunchaparty S, Ellison DH, Bachmann S. Expression of the Na-K-2Cl co-transporter by macula densa and thick ascending limb cells of rat and rabbit nephron. J Clin Invest 1996;98(3):635–40.
[76] Ho K, Nichols CG, Lederer WJ, Lytton J, Vassilev PM, Kanazirska MV, et al. Cloning and expression of an inwardly rectifying ATP-regulated potassium channel. Nature 1993;362(6415):31–8.
[77] Hebert SC, Reeves WB, Molony DA, Andreoli TE. The medullary thick limb: function and modulation of the single-effect multiplier. Kidney Int 1987;31:580–8.
[78] Lytle C, McManus TJ, Haas M. A model of Na-K-2Cl co-transport based on ordered ion binding and glide symmetry. Am J Physiol 1998;274:C299–309.
[79] Haas M, McManus TJ. Bumetanide inhibits (Na + K + 2Cl) co-transport at a chloride site. Am J Physiol 1983;245:C235–40.
[80] Moore ML, George JN, Turner RJ. Anion dependence of bumetanide binding and ion transport by the rabbit parotid $Na^{(+)}$-$K^{(+)}$-$2Cl^{-}$ co-transporter: evidence for an intracellular anion modifier site. Biochem J 1995;309(Pt 2):637–42.
[81] Isenring P, Jacoby SC, Chang J, Forbush B. Mutagenic mapping of the Na-K-Cl co-transporter for domains involved in ion transport and bumetanide binding. J Gen Physiol 1998;112(5):549–58.
[82] Gagnon E, Bergeron MJ, Brunet GM, Daigle ND, Simard CF, Isenring P. Molecular mechanisms of Cl^{-} transport by the renal $Na^{(+)}$-$K^{(+)}$-Cl^{-} co-transporter. Identification of an intracellular locus that may form part of a high affinity $Cl^{(-)}$-binding site. J Biol Chem 2004;279(7):5648–54.
[83] Kowalczyk L, Ratera M, Paladino A, Bartoccioni P, Errasti-Murugarren E, Valencia E, et al. Molecular basis of substrate-induced permeation by an amino acid antiporter. Proc Natl Acad Sci USA 2011;108(10):3935–40.
[84] Gao X, Zhou L, Jiao X, Lu F, Yan C, Zeng X, et al. Mechanism of substrate recognition and transport by an amino acid antiporter. Nature 2010;463(7282):828–32.
[85] Fang Y, Jayaram H, Shane T, Kolmakova-Partensky L, Wu F, Williams C, et al. Structure of a prokaryotic virtual proton pump at 3.2 Å resolution. Nature 2009;460(7258):1040–3.
[86] Shaffer PL, Goehring A, Shankaranarayanan A, Gouaux E. Structure and mechanism of a Na^{+}-independent amino acid transporter. Science 2009;325(5943):1010–4.
[87] Miyanoshita A, Terada M, Endou H. Furosemide directly stimulates prostaglandin E2 production in the thick ascending limb of Henle's loop. J Pharmacol Exp Ther 1989;251:1155–9.
[88] Peti-Peterdi J, Komlosi P, Fuson AL, Guan Y, Schneider A, Qi Z, et al. Luminal NaCl delivery regulates basolateral PGE2 release from macula densa cells. J Clin Invest 2003;112(1):76–82.
[89] Kirchner KA. Prostaglandin inhibitors alter loop segment chloride uptake during furosemide diuresis. Am J Physiol 1985;248:F698–704.
[90] Kirchner KA, Martin CJ, Bower JD. Prostaglandin E2 but not I2 restores furosemide response in indomethacin-treated rats. Am J Physiol 1986;250:F980–5.
[91] Nusing RM, Treude A, Weissenberger C, Jensen B, Bek M, Wagner C, et al. Dominant role of prostaglandin E2 EP4 receptor in furosemide-induced salt-losing tubulopathy: a model for hyperprostaglandin E syndrome/antenatal Bartter syndrome. J Am Soc Nephrol 2005;16(8):2354–62.
[92] Bilezikian JP. Management of hypercalcemia. J Clin Endocrin Metab 1993;77:1445–9.
[93] LeGrand SB, Leskuski D, Zama I. Narrative review: furosemide for hypercalcemia: an unproven yet common practice. Ann Intern Med 2008;149(4):259–63.
[94] Friedman PA. Codependence of renal calcium and sodium transport. Annu Rev Physiol 1998;60:179–97.
[95] Hou J, Renigunta A, Gomes AS, Hou M, Paul DL, Waldegger S, et al. Claudin-16 and claudin-19 interaction is required for their assembly into tight junctions and for renal reabsorption of magnesium. Proc Natl Acad Sci USA 2009;106(36):15350–5.
[96] Hou J, Goodenough DA. Claudin-16 and claudin-19 function in the thick ascending limb. Curr Opin Nephrol Hypertens 2010;19(5):483–8.
[97] Hou J, Shan Q, Wang T, Gomes AS, Yan Q, Paul DL, et al. Transgenic RNAi depletion of claudin-16 and the renal handling of magnesium. J Biol Chem 2007;282(23):17114–22.
[98] Schnermann J, Homer W. Smith Award lecture. The juxtaglomerular apparatus: from anatomical peculiarity to physiological relevance. J Am Soc Nephrol 2003;14(6):1681–94.
[99] Schnermann J. Juxtaglomerular cell complex in the regulation of renal salt excretion. Am J Physiol 1998;274:R263–79.
[100] Lapointe J-Y, Laamarti A, Hurst AM, Fowler BC, Bell PD. Activation of Na:2Cl:K co-transport by luminal chloride in macula densa cells. Kidney Int 1995;47:752–7.
[101] Kurtz A, Gotz KH, Hamann M, Wagner C. Stimulation of renin secretion by nitric oxide is mediated by phosphodiesterase 3. Proc Natl Acad Sci USA 1998;95:4743–7.
[102] Schnermann J, Briggs JP. Synthesis and secretion of renin in mice with induced genetic mutations. Kidney Int 2012;81(6):529–38.
[103] Harris RC, McKanna JA, Akai Y, Jacobson HR, Dubois RN, Breyer MD. Cyclooxygenase-2 is associated with the macula densa of rat kidney and increases with salt restriction. J Clin Invest 1994;94(6):2504–10.
[104] Komhoff M, Jeck ND, Seyberth HW, Grone HJ, Nusing RM, Breyer MD. Cyclooxygenase-2 expression is associated with the renal macula densa of patients with Bartter-like syndrome [In Process Citation]. Kidney Int 2000;58(6):2420–4.
[105] Mann B, Hartner A, Jensen BL, Kammerl M, Kramer BK, Kurtz A. Furosemide stimulates macula densa cyclooxygenase-2 expression in rats. Kidney Int 2001;59(1):62–8.
[106] Harding P, Sigmon DH, Alfie ME, Huang PL, Fishman MC, Beierwaltes WH, et al. Cyclooxygenase-2 mediates increased renal renin content induced by low-sodium diet. Hypertension 1997;29:297–302.
[107] Facemire CS, Nguyen M, Jania L, Beierwaltes WH, Kim HS, Koller BH, et al. A major role for the EP4 receptor in regulation of renin. Am J Physiol Renal Physiol 2011;301(5):F1035–41.
[108] Orlov SN. NKCC1 as a regulator of vascular tone and a novel target for antihypertensive therapeutics. Am J Physiol Heart Circ Physiol 2007;292(5):H2035–6.
[109] Gerber JG, Nies AS. Furosemide-induced vasodilation: importance of the state of hydration and filtration. Kidney Int 1980;18(4):454–9.
[110] Patak RV, Fadem SZ, Rosenblatt SG, Lifschitz MD, Stein JH. Diuretic-induced changes in renal blood flow and prostaglandin E excretion in the dog. Am J Physiol 1979;236(5):F494–500.
[111] Dobrowolski L, Bdzynska B, Sadowski J. Differential effect of frusemide on renal medullary and cortical blood flow in the anaesthetised rat. Exp Physiol 2000;85(6):783–9.
[112] Oppermann M, Hansen PB, Castrop H, Schnermann J. Vasodilatation of afferent arterioles and paradoxical increase of renal vascular resistance by furosemide in mice. Am J Physiol Renal Physiol 2007;293(1):F279–87.
[113] Brezis M, Agmon Y, Epstein FH. Determinants of intrarenal oxygenation. I. Effects of diuretics. Am J Physiol Renal, Fluid Electrolyte Physiol 1994;267:F1059–62.

[114] Heyman SN, Rosen S, Epstein FH, Spokes K, Brezis ML. Loop diuretics reduce hypoxic damage to proximal tubules of the isolated perfused rat kidney. Kidney Int 1994;45(4):981–5.
[115] Kusakabe Y, Matsushita T, Honda S, Okada S, Murase K. Using BOLD imaging to measure renal oxygenation dynamics in rats injected with diuretics. Magn Reson Med Sci 2010;9(4): 187–94.
[116] Warner L, Glockner JF, Woollard J, Textor SC, Romero JC, Lerman LO. Determinations of renal cortical and medullary oxygenation using blood oxygen level-dependent magnetic resonance imaging and selective diuretics. Invest Radiol 2011;46(1):41–7.
[117] Bell PD, Lapointe JY, Sabirov R, Hayashi S, Peti-Peterdi J, Manabe K, et al. Macula densa cell signaling involves ATP release through a maxi anion channel. Proc Natl Acad Sci U S A 2003;100(7):4322–7.
[118] Sun D, Samuelson LC, Yang T, Huang Y, Paliege A, Saunders T, et al. Mediation of tubuloglomerular feedback by adenosine: evidence from mice lacking adenosine 1 receptors. Proc Natl Acad Sci U S A 2001;98(17):9983–8.
[119] Thomson S, Bao D, Deng A, Vallon V. Adenosine formed by 5′-nucleotidase mediates tubuloglomerular feedback. J Clin Invest 2000;106(2):289–98.
[120] Vallon V, Richter K, Huang DY, Rieg T, Schnermann J. Functional consequences at the single-nephron level of the lack of adenosine A1 receptors and tubuloglomerular feedback in mice. Pflugers Arch 2004;448(2):214–21.
[121] Brown R, Ollerstam A, Johansson B, Skott O, Gebre-Medhin S, Fredholm B, et al. Abolished tubuloglomerular feedback and increased plasma renin in adenosine A1 receptor-deficient mice. Am J Physiol Regul Integr Comp Physiol 2001;281(5): R1362–7.
[122] Dikshit K, Vyden JK, Forrester JS, Chatterjee K, Prakash R, Swan HJC. Renal and extrarenal hemodynamic effects of furosemide in congestive heart failure after acute myocardial infarction. N Engl J Med 1973;288:1087–90.
[123] Mukherjee SK, Katz MA, Michael UF, Ogden DA. Mechanisms of hemodynamic actions of furosemide: differentiation of vascular and renal effects on blood pressure in functionally anephric hypertensive patients. Am Heart J 1981;101:313–8.
[124] Bourland WA, Day DK, Williamson HE. The role of the kidney in the early nondiuretic action of furosemide to reduce elevated left atrial pressure in the hypervolemic dog. J Pharmacol Exp Ther 1977;202:221–9.
[125] Schmieder RE, Messerli FH, deCarvalho JGR, Husserl FE. Immediate hemodynamic response to furosemide in patients undergoing chronic hemodialysis. Am J Kidney Dis 1987;9: 55–9.
[126] Costa MA, Loria A, Elesgaray R, Balaszczuk AM, Arranz C. Role of nitric oxide pathway in hypotensive and renal effects of furosemide during extracellular volume expansion. J Hypertens 2004;22(8):1561–9.
[127] Pickkers P, Dormans TP, Russel FG, Hughest AD, Thien T, Schaper N, et al. Direct vascular effects of furosemide in humans. Circulation 1997;96:1847–52.
[128] Meyer JW, Flagella M, Sutliff RL, Lorenz JN, Nieman ML, Weber CS, et al. Decreased blood pressure and vascular smooth muscle tone in mice lacking basolateral $Na^{(+)}$-$K^{(+)}$-2$Cl^{(-)}$ co-transporter. Am J Physiol Heart Circ Physiol 2002;283(5): H1846–55.
[129] Wall SM, Knepper MA, Hassell KA, Fischer MP, Shodeinde A, Shin W, et al. Hypotension in NKCC1 null mice: role of the kidneys. Am J Physiol Renal Physiol 2006;290(2):F409–16.
[130] Kim SM, Eisner C, Faulhaber-Walter R, Mizel D, Wall SM, Briggs JP, et al. Salt sensitivity of blood pressure in NKCC1-deficient mice. Am J Physiol Renal Physiol 2008;295(4): F1230–8.
[131] Johnston GD, Nicholls DP, Leahey WJ. The dose–response characteristics of the acute non-diuretic peripheral vascular effects of frusemide in normal subjects. Br J Clin Pharmacol 1984;18:75–81.
[132] Francis GS, Siegel RM, Goldsmith SR, Olivari MT, Levine B, Cohn JN. Acute vasoconstrictor response to intravenous furosemide in patients with chronic congestive heart failure. Ann Intern Med 1985;103:1–6.
[133] Goldsmith SR, Francis G, Cohn JN. Attenuation of the pressor response to intravenous furosemide by angiotensin converting enzyme inhibition in congestive heart failure. Am J Cardiol 1989;64:1382–5.
[134] Inoue M, Okajima K, Itoh K, Ando Y, Watanabe N, Yasaka T, et al. Mechanism of furosemide resistance in analbuminemic rats and hypoalbuminemic patients. Kidney Int 1987;32: 198–203.
[135] Brater DC. Disposition and response to bumetanide and furosemide. Am J Cardiol 1986;57(2):20A–5A.
[136] Brater DC. Diuretic therapy. N Engl J Med 1998;339:387–95.
[137] Nigwekar SU, Waikar SS. Diuretics in acute kidney injury. Semin Nephrol 2011;31(6):523–34.
[138] Packer M, Lee WH, Medina N, Yushak M, Kessler PD. Functional renal insufficiencey during long-term therapy with captopril and enalapril in severe congestive heart failure. Ann Intern Med 1987;106:346–54.
[139] Packer M. Identification of risk factors predisposing to the development of functional renal insufficiency during treatment with converting-enzyme inhibitors in chronic heart failure. Cardiology 1989;76(Suppl. 2):50–5.
[140] Smith WE, Steele TH. Avoiding diuretic related complications in older patients. Geriatrics 1983;38:117–9.
[141] Kaufman AM, Levitt MF. The effect of diuretics on systemic and renal hemodynamics in patients with renal insufficiency. Am J Kidney Dis 1985;5:A71–8.
[142] Heerdink ER, Leufkens HG, Herrings RMC, Ottervanger JP, Stricker BHC, Bakker A. NSAIDs associated with increased risk of congestive heart failure in elderly patients taking diuretics. Arch Intern Med 1998;158:1108–12.
[143] Huerta C, Castellsague J, Varas-Lorenzo C, Garcia Rodriguez LA. Nonsteroidal anti-inflammatory drugs and risk of ARF in the general population. Am J Kidney Dis 2005;45(3): 531–9.
[144] Bichet DG, Van Putten VJ, Schrier RW. Potential role of increased sympathetic activity in impaired sodium and water excretion in cirrhosis. N Engl J Med 1982;307:1552–7.
[145] Dyckner T, Webster PO. Magnesium treatment of diuretic-induced hyponatremia with a preliminary report on a new aldosterone antagonist. J Am Coll Nutr 1982;1:149–53.
[146] Schrier RW. New treatments for hyponatremia. N Engl J Med 1978;298:214–5.
[147] Hantman D, Rossier B, Zohlman R, Schrier RW. Rapid correction of hyponatremia in the syndrom of inappropriate secretion of antidiuretic hormone: an alternative treatment to hypertonic saline. Ann Intern Med 1973;78:870–5.
[148] Dzau VJ, Hollenberg NK. Renal response to captopril in severe heart failure: role of furosemide in natriuresis and reversal of hyponatremia. Ann Intern Med 1984;100: 777–82.
[149] Ram CV, Garrett BN, Kaplan NM. Moderate sodium restriction and various diuretics in the treatment of hypertension. Arch Intern Med 1981;141(8):1015–9.
[150] Palmer BF. Potassium disturbances associated with the use of diuretics. San Diego: Academic Press; 1997. p. 571–583.

[151] Hropot M, Fowler NB, Karlmark B, Giebisch G. Tubular action of diuretics: distal effects on electrolyte transport and acidification. Kidney Int 1985;28:477–89.
[152] Sansom SC, Welling PA. Two channels for one job. Kidney Int 2007;72(5):529–30.
[153] Wilcox CS, Mitch WE, Kelly RA, Freidman PA, Souney PF, et al. Factors affecting potassium balance during frusemide administration. Clin Sci 1984;67:195–203.
[154] Good DW. Sodium-dependent bicarbonate absorption by cortical thick ascending limb of rat kidney. Am J Physiol 1985;248: F821–9.
[155] Knepper MA, Good DW, Burg MB. Ammonia and bicarbonate transport by rat cortical collecting ducts perfused *in vitro*. Am J Physiol 1985;249:F870–7.
[156] Oberleithner H, Lang F, Messner G, Wang W. Mechanism of hydrogen ion transport in the diluting segment of frog kidney. Pflügers Arch 1984;402:272–80.
[157] Stone DK, Seldin DW, Kokko JP, Jacobson HR. Mineralocorticoid modulation of rabbit medullary collecting duct acidification. J Clin Invest 1983;72:77–83.
[158] Han KH. Mechanisms of the effects of acidosis and hypokalemia on renal ammonia metabolism. Electrolyte Blood Press 2011;9(2):45–9.
[159] Aronson PS, Giebisch G. Effects of pH on potassium: new explanations for old observations. J Am Soc Nephrol 2011;22 (11):1981–9.
[160] Wingo CS, Straub SG. Active proton secretion and potassium absorption in the rabbit outer medullary collecting duct. Functional evidence for proton-potassium-activated adenosine triphosphatase. J Clin Invest 1989;84:361–5.
[161] Maher JF, Schreiner GF. Studies on ethacrynic acid in patients with refractory edema. Ann Intern Med 1965;62:15–29.
[162] Ikeda K, Oshima T, Hidaka H, Takasaka T. Molecular and clinical implications of loop diuretic ototoxicity. Hear Res 1997;107:1–8.
[163] Ryback LP. Ototoxicity of loop diuretics. Otolaryngol Clin N Am 1993;26:829–44.
[164] Ikeda K, Morizono T. Electrochemical profiles for monvalent ions in the stria vascularis: cellular model of ion transport mechanisms. Hear Res 1989;39:279–86.
[165] Mizuta K, Adachi M, Iwasa KH. Ultrastructural localization of the Na-K-Cl co-transporter in the lateral wall of the rabbit cochlear duct. Hear Res 1997;106(1–2):154–62.
[166] Hidaka H, Oshima T, Ikeda K, Furukawa M, Takasaka T. The Na-K-Cl co-transporters in the rat cochlea: RT-PCR and partial sequence analysis. Biochem Biophys Res Comm 1996;220: 425–30.
[167] Flagella M, Clarke LL, Miller ML, Erway LC, Giannella RA, Andringa A, et al. Mice lacking the basolateral Na-K-2Cl co-transporter have impaired epithelial chloride secretion and are profoundly deaf. J Biol Chem 1999;274(38):26946–55.
[168] Delpire E, Lu J, England R, Dull C, Thorne T. Deafness and imbalance associated with inactivation of the secretory Na-K-2Cl co-transporter. Nat Genet 1999;22(2):192–5.
[169] Star RA. Ototoxicity. San Diego: Academic Press; 1997 [p. 637642]
[170] Eknoyan G, Suki WN, Martinez-Maldonado M. Effect of diuretics on urinary excretion of phosphate, calcium, and magnesium in thyroparathyroidectomized dogs. J Lab Clin Med 1970;76:257–66.
[171] Bolland MJ, Ames RW, Horne AM, Orr-Walker BJ, Gamble GD, Reid IR. The effect of treatment with a thiazide diuretic for 4 years on bone density in normal postmenopausal women. Osteoporos Int 2007;18(4):479–86.
[172] Friedman PA, Hebert SC. Site and mechanism of diuretic action. San Diego: Academic Press; 1997 [p. 75-111]
[173] Kunau Jr. RT, Weller DR, Webb HL. Clarification of the site of action of chlorothiazide in the rat nephron. J Clin Invest 1975;56(2):401–7.
[174] Ellison DH, Velázquez H, Wright FS. Thiazide sensitive sodium chloride co-transport in the early distal tubule. Am J Physiol 1987;253:F546–54.
[175] Costanzo LS. Localization of diuretic action in microperfused rat distal tubules: Ca and Na transport. Am J Physiol 1985;248: F527–35.
[176] Reilly RF, Ellison DH. Mammalian distal tubule: physiology, pathophysiology, and molecular anatomy. Physiol Rev 2000;80 (1):277–313.
[177] Imai M, Nakamura R. Function of distal convoluted and connecting tubules studied by isolated nephron fragments. Kidney Int 1982;22:465–72.
[178] Shimizu T, Yoshitomi K, Nakamura M, Imai M. Site and mechanism of action of trichlormethiazide in rabbit distal nephron segments perfused *in vitro*. J Clin Invest 1988;82:721–30.
[179] Velázquez H, Greger R. Electrical properties of the early distal convoluted tubules of the rabbit kidney. Renal Physiol 1986;55.
[180] Gamba G, Saltzberg SN, Lombardi M, Miyanoshita A, Lytton J, Hediger MA, et al. Primary structure and functional expression of a cDNA encoding the thiazide-sensitive, electroneutral sodium-chloride co-transporter. Proc Natl Acad Sci USA 1993;90:2749–53.
[181] Obermuller N, Bernstein P, Velazquez H, Reilly R, Moser D, Ellison DH, et al. Expression of the thiazide-sensitive Na-Cl co-transporter in rat and human kidney. Am J Physiol 1995;269 (6 Pt 2):F900–10.
[182] Bachmann S, Velazquez H, Obermuller N, Reilly RF, Moser D, Ellison DH. Expression of the thiazide-sensitive Na-Cl co-transporter by rabbit distal convoluted tubule cells. J Clin Invest 1995;96(5):2510–4.
[183] Plotkin MD, Kaplan MR, Verlander JW, Lee W-S, Brown D, Poch E, et al. Localization of the thiazide sensitive Na-Cl co-transporter, rTSC1, in the rat kidney. Kidney Int 1996;50: 174–83.
[184] Pizzonia JH, Gesek FA, Kennedy SM, Coutermarsh BA, Bacskai BJ, Friedman PA. Immunomagnetic separation, primary culture, and characterization of cortical thick ascending limb plus distal convoluted tubule cells from mouse kidney. In Vitro Cell Dev Biol 1991;27A:409–16.
[185] Campean V, Kricke J, Ellison D, Luft FC, Bachmann S. Localization of thiazide-sensitive $Na(^{+})$-$Cl(^{-})$ co-transport and associated gene products in mouse DCT. Am J Physiol 2001;281(6):F1028–35.
[186] Velázquez H, Good DW, Wright FS. Mutual dependence of sodium and chloride absorption by renal distal tubule. Am J Physiol 1984;247:F904–11.
[187] Stokes JB. Sodium chloride absorption by the urinary bladder of the winter flounder: a thiazide-sensitive electrically neutral transport system. J Clin Invest 1984;74:7–16.
[188] Miyanoshita A, Gamba G, Lytton J, Lombardi M, Brenner BM, Hebert SC. Primary structure and functional expression of the rat renal thiazide-sensitive Na^{+}:Cl^{-} co-transporter. Proc 12th Int Congr Nephrol 1993:110.
[189] Simon DB, Nelson-Williams C, Bia MJ, Ellison D, Karet FE, Molina AM, et al. Gitelman's variant of Bartter's syndrome, inherited hypokalaemic alkalosis, is caused by mutations in the thiazide-sensitive Na-Cl co-transporter. Nat Genet 1996;12(1):24–30.

[190] Velázquez H, Naray-Fejes-Toth A, Reilly RF, Ellison DH. NaCl co-transporter and 11-b- hydroxysteroid dehydrogenase are coexpressed in rabbit distal convoluted tubule. FASEB J 1996;: A368.

[191] Bostanjoglo M, Reeves WB, Reilly RF, Velazquez H, Robertson N, Litwack G, et al. 11Beta-hydroxysteroid dehydrogenase, mineralocorticoid receptor, and thiazide-sensitive Na-Cl co-transporter expression by distal tubules. J Am Soc Nephrol 1998;9(8):1347–58.

[192] Wilson DR, Honrath U, Sonnenberg H. Thiazide diuretic effect on medullary collecting duct function in the rat. Kidney Int 1983;23:711–6.

[193] Terada Y, Knepper MA. Thiazide-sensitive NaCl absorption in rat cortical collecting duct. Am J Physiol Renal, Fluid Electrolyte Physiol 1990;259:F519–28.

[194] Rouch AJ, Chen L, Troutman SL, Schafer JA. Na^+ transport in isolated rat CCD: effects of bradykinin, ANP, clonidine, and hydrochlorothiazide. Am J Physiol Renal, Fluid Electrolyte Physiol 1991;260:F86–95.

[195] Leviel F, Hubner CA, Houillier P, Morla L, El Moghrabi S, Brideau G, et al. The Na^+-dependent chloride-bicarbonate exchanger SLC4A8 mediates an electroneutral Na^+ reabsorption process in the renal cortical collecting ducts of mice. J Clin Invest 2010;120(5):1627–35.

[196] Beaumont K, Vaughn DA, Fanestil DD. Thiazide diuretic drug receptors in rat kidney: identification with [^{3}H]Metolazone. Proc Natl Acad Sci 1988;85:2311–4.

[197] Tran JM, Farrell MA, Fanestil DD. Effect of ions on binding of the thiazide-type diuretic metolazone to kidney membrane. Am J Physiol 1990;258:F908–15.

[198] Chang H, Fujita T. A kinetic model of the thiazide-sensitive Na-Cl co-transporter. Am J Physiol 1999;:276.

[199] Moreno E, San Cristobal P, Rivera M, Vazquez N, Bobadilla NA, Gamba G. Affinity defining domains in the Na-Cl co-transporter: different location for Cl^- and thiazide binding. J Biol Chem 2006;281(25):17266–75.

[200] Reilly RF, Huang CL. The mechanism of hypocalciuria with NaCl co-transporter inhibition. Nat Rev Nephrol 2011;7(11): 669–74.

[201] Costanzo LS, Weiner IM. On the hypocalciuric action of chlorothiazide. J Clin Invest 1974;54:628–37.

[202] Costanzo LS, Windhager EE. Calcium and sodium transport by the distal convoluted tubule of the rat. Am J Physiol 1978;235:F492–506.

[203] Ellison DH. Divalent cation transport by the distal nephron: insights from Bartter's and Gitelman's syndromes. Am J Physiol 2000;279(4):F616–25.

[204] den Dekker E, Hoenderop JG, Nilius B, Bindels RJ. The epithelial calcium channels, TRPV5 & TRPV6: from identification towards regulation. Cell Calcium 2003;33(5-6):497–507.

[205] Friedman PA. Calcium transport in the kidney. Curr Opin Nephrol Hypertens 1999;8(5):589–95.

[206] Nijenhuis T, Vallon V, van der Kemp AW, Loffing J, Hoenderop JG, Bindels RJ. Enhanced passive Ca^{2+} reabsorption and reduced Mg^{2+} channel abundance explains thiazide-induced hypocalciuria and hypomagnesemia. J Clin Invest 2005;115(6):1651–8.

[207] Porter RH, Cox BG, Heaney D, Hostetter TH, Stinebaugh BJ, Suki WN. Treatment of hypoparathyroide patients with chlorthalidone. N Engl J Med 1978;298:577–81.

[208] Belge H, Gailly P, Schwaller B, Loffing J, Debaix H, Riveira-Munoz E, et al. Renal expression of parvalbumin is critical for NaCl handling and response to diuretics. Proc Natl Acad Sci U S A 2007;104(37):14849–54.

[209] Cheng CJ, Shiang JC, Hsu YJ, Yang SS, Lin SH. Hypocalciuria in patients with Gitelman syndrome: role of blood volume. Am J Kidney Dis 2007;49(5):693–700.

[210] McCormick JA, Mutig K, Nelson JH, Saritas T, Hoorn EJ, Yang C-L, et al. A SPAK isoform switch modulates renal salt transport and blood pressure. Cell Metab 2011;14(3):352–64.

[211] Favre GA, Nau V, Kolb I, Vargas-Poussou R, Hannedouche T, Moulin B. Localization of tubular adaptation to renal sodium loss in Gitelman syndrome. Clin J Am Soc Nephrol 2012;7(3): 472–8.

[212] Ellison DH. Adaptation in gitelman syndrome: "we just want to pump you up.". Clin J Am Soc Nephrol 2012;7(3):379–82.

[213] Dai LJ, Ritchie G, Kerstan D, Kang HS, Cole DE, Quamme GA. Magnesium transport in the renal distal convoluted tubule. Physiol Rev 2001;81(1):51–84.

[214] Douban S, Brodsky MA, Whang DD. Significance of magnesium in congestive heart failure. Am Heart J 1996;132:664–71.

[215] Voets T, Nilius B, Hoefs S, van der Kemp AW, Droogmans G, Bindels RJ, et al. TRPM6 forms the Mg^{2+} influx channel involved in intestinal and renal Mg^{2+} absorption. J Biol Chem 2004;279(1):19–25.

[216] Loffing J, Vallon V, Loffing-Cueni D, Aregger F, Richter K, Pietri L, et al. Altered renal distal tubule structure and renal $Na(^+)$ and $Ca(^{2+})$ handling in a mouse model for Gitelman's syndrome. J Am Soc Nephrol 2004;15(9):2276–88.

[217] Loffing J, Loffing-Cueni D, Hegyi I, Kaplan MR, Hebert SC, Le Hir M, et al. Thiazide treatment of rats provokes apoptosis in distal tubule cells. Kidney Int 1996;50(4):1180–90.

[218] Ellison DH, Loffing J. Thiazide effects and adverse effects: insights from molecular genetics. Hypertension 2009;54(2): 196–202.

[219] Dai LJ, Friedman PA, Quamme GA. Cellular mechanisms of chlorothiazide and potassium depletion on Mg^{2+} uptake in mouse distal convoluted tubule cells. Kidney Int 1997;51: 1008–17.

[220] Dai LJ, Friedman PA, Quamme GA. Mechanisms of amiloride stimulation of Mg^{2+} uptake in immortalized mouse distal convoluted tubule cells. Am J Physiol 1997;F249–56.

[221] Dimke H, Hoenderop JG, Bindels RJ. Molecular basis of epithelial Ca^{2+} and Mg^{2+} transport: insights from the TRP channel family. J Physiol 2011;589(Pt 7):1535–42.

[222] Quamme GA. Renal magnesium handling: new insights in undertsanding old problems. Kidney Int 1997;52:1180–95.

[223] Dyckner T, Wester P-O, Widman L. Amiloride prevents thiazide-induced intracellular potassium and magnesium losses. Acta Med Scand 1988;224:25–30.

[224] Murdoch DL, Forrest G, Davies DL, McInnes GT. A comparison of the potassium and magnesium-sparing properties of amiloride and spironolactone in diuretic-treated normal subjects. Br J Clin Pharmacol 1993;35(4):373–8.

[225] Wazny LD, Brophy DF. Amiloride for the prevention of amphotericin B-induced hypokalemia and hypomagnesemia. Ann Pharmacother 2000;34(1):94–7.

[226] Stergiou GS, Mayopoulou-Symvoulidou D, Mountokalakis TD. Attenuation by spironolactone of the magnesiuric effect of acute frusemide administration in patients with liver cirrhosis and ascites. Miner Electrolyte Metab 1993;19(2):86–90.

[227] Gao X, Peng L, Adhikari CM, Lin J, Zuo Z. Spironolactone reduced arrhythmia and maintained magnesium homeostasis in patients with congestive heart failure. J Card Fail 2007;13(3): 170–7.

[228] Walter SJ, Shirley DG. The effect of chronic hydrochlorothiazide administration on renal function in the rat. Clin Sci (Lond) 1986;70(4):379–87.

[229] Earley LE, Orloff J. The mechanism of antidiuresis associated with the administration of hydrochlorothiazide to patients with vasopressin-resistant diabetes insipidus. J Clin Invest 1962;41:1988–97.
[230] Siegel D, Hulley SB, Black DM, Cheitlin MD, Sebastian A, Seeley DG, et al. Diuretics, serum and intracellular electrolyte levels, and ventricular arrhythmias in hypertensive men. JAMA 1992;267:1083–9.
[231] Kountz DS, Goldman A, Mikhail J, Ezer M. Chlorthalidone: the forgotten diuretic. Postgrad Med 2012;124(1):60–6.
[232] Ellison DH, Wilcox CS. Diuretics. In: Brenner BM, editor. Brenner and Rector's the kidney. 2008. p. 1646–78.
[233] Appel LJ. The verdict from ALLHAT – thiazide diuretics are the preferred initial therapy for hypertension. JAMA 2002;288 (23):3039–42.
[234] Leary WP, Reyes AJ. Renal excretory actions of diuretics in man: correction of various current errors and redefinition of basic concepts. In: Reyes AJ, Leary WP, editors. Clinical pharmacology and therapeutic uses of diuretics. 153rd ed. Stuttgart: GustavFischer Verlag; 1988. p. 153–66.
[235] Worcester EM, Coe FL. Clinical practice. Calcium kidney stones. N Engl J Med 2010;363(10):954–63.
[236] Ray WA, Griffin MR, Downey W, Melton III LJ. Long-term use of thiazide diuretics and risk of hip fracture. Lancet 1989;1: 687–90.
[237] Felson DT, Sloutskis D, Anderson JJ, Anthony JM, Kiel DP. Thiazide diuretics and the risk of hip fracture. Results from the Framingham study. JAMA 1991;265:370–3.
[238] Cauley JA, Cummings SR, Seeley DG, Black D, Browner W, Kuller LH, et al. Effects of thiazide diuretic therapy on bone mass, fractures, and falls. Ann Intern Med 1993;118:666–73.
[239] Heidrich FE, Stergachis A, Gross KM. Diuretic drug use and the risk for hip fracture. Ann Intern Med 1991;115:1–6.
[240] Reid IR, Ames RW, Orr-Walker BJ, Clearwater JM, Horne AM, Evans MC, et al. Hydrochlorothiazide reduces loss of cortical bone in normal postmenopausal women: a randomized controlled trial. Am J Med 2000;109(5):362–70.
[241] Rejnmark L, Vestergaard P, Pedersen AR, Heickendorff L, Andreasen F, Mosekilde L. Dose-effect relations of loop- and thiazide-diuretics on calcium homeostasis: a randomized, double-blinded Latin-square multiple cross-over study in postmenopausal osteopenic women. Eur J Clin Invest 2003;33(1): 41–50.
[242] Schoofs MW, van der Klift M, Hofman A, de Laet CE, Herings RM, Stijnen T, et al. Thiazide diuretics and the risk for hip fracture. Ann Intern Med 2003;139(6):476–82.
[243] Janjua NR, Jonassen TE, Langhoff S, Thomsen K, Christensen S. Role of sodium depletion in acute antidiuretic effect of bendroflumethiazide in rats with nephrogenic diabetes insipidus. J Pharmacol Exp Ther 2001;299(1):307–13.
[244] Biner HL, Arpin-Bott MP, Loffing J, Wang X, Knepper M, Hebert SC, et al. Human cortical distal nephron: distribution of electrolyte and water transport pathways. J Am Soc Nephrol 2002;13(4):836–47.
[245] Kim GH, Lee JW, Oh YK, Chang HR, Joo KW, Na KY, et al. Antidiuretic effect of hydrochlorothiazide in lithium-induced nephrogenic diabetes insipidus is associated with upregulation of aquaporin-2, Na-Cl co-transporter, and epithelial sodium channel. J Am Soc Nephrol 2004;15(11):2836–43.
[246] Cesar KR, Magaldi AJ. Thiazide induces water absorption in the inner medullary collecting duct of normal and Brattleboro rats. Am J Physiol 1999;277(5 Pt 2):F756–60.
[247] Moser M. Diuretics should continue to be one of the preferred initial therapies in the management of hypertension: the argument for. J Clin Hypertens (Greenwich) 2005;7(2):111–6 [quiz 21-2].
[248] Sica DA. Diuretics should continue to be one of the preferred initial therapies in the management of hypertension: the argument against. J Clin Hypertens (Greenwich) 2005;7(2):117–20 [quiz 21-2].
[249] Velázquez H, Wright FS. Control by drugs of renal potassium handling. Ann Rev Pharmacol Toxicol 1986;26:293–309.
[250] Velázquez H, Wright FS. Effects of diuretic drugs on Na, Cl, and K transport by rat renal distal tubule. Am J Physiol 1986;250:F1013–23.
[251] Wright FS. Flow-dependent transport processes: filtration, absorption, secretion. Am J Physiol 1982;243:F1–11.
[252] Okusa MD, Velazquez H, Ellison DH, Wright FS. Luminal calcium regulates potassium transport by the renal distal tubule. Am J Physiol 1990;258(2 Pt 2):F423–8.
[253] Okusa MD, Velazquez H, Wright FS. Effect of Na-channel blockers and lumen Ca on K secretion by rat renal distal tubule. Am J Physiol 1991;260(3 Pt 2):F459–65.
[254] Huang CL, Kuo E. Mechanism of hypokalemia in magnesium deficiency. J Am Soc Nephrol 2007;18(10):2649–52.
[255] Odvina CV, Mason RP, Pak CY. Prevention of thiazide-induced hypokalemia without magnesium depletion by potassium-magnesium-citrate. Am J Ther 2006;13(2):101–8.
[256] Dorup I, Skajaa K, Thybo NK. Oral magnesium supplementation restores the concentrations of magnesium, potassium and sodium-potassium pumps in skeletal muscle of patients receiving diuretic treatment. J Intern Med 1993;233:117–23.
[257] Leung AA, Wright A, Pazo V, Karson A, Bates DW. Risk of thiazide-induced hyponatremia in patients with hypertension. Am J Med 2011;124(11):1064–72.
[258] Fichman MP, Vorherr H, Kleeman CR, Telfer N. Diuretic-induced hyponatremia. Ann Intern Med 1971;75:853–63.
[259] Friedman E, Shadel M, Halkin H, Farfel Z. Thiazide-induced hyponatremia: reproducibility by single dose rechallenge and an analysis of pathogenesis. Ann Intern Med 1989;110:24–30.
[260] Chow KM, Szeto CC, Wong TY, Leung CB, Li PK. Risk factors for thiazide-induced hyponatraemia. QJM 2003;96(12):911–7.
[261] Chow KM, Kwan BC, Szeto CC. Clinical studies of thiazide-induced hyponatremia. J Natl Med Assoc 2004;96(10):1305–8.
[262] Harper R, Ennis CN, Heaney AP, Sheridan B, Gormley M, Atkinson AB, et al. A comparison of the effects of low- and conventional-dose thiazide diuretic on insulin action in hypertensive patients with NIDDM. Diabetologia 1995;38:853–9.
[263] Carlsen JE, Kober L, Torp-Pedersen C, Johansen P. Relation between dose of bendrofluazide, antihypertensive effect, and adverse biochemical effects. BMJ (Clinical Research Ed.) 1990;300:975–8.
[264] Helderman JH, Elahi D, Andersen DK, Raizes GS, Tobin JD, Shocken D, et al. Prevention of the glucose intolerance of thiazide diuretics by maintenance of body potassium. Diabetes 1983;32(2):106–11.
[265] Toto RA. Metabolic derangements associated with diuretic use: insulin resistance, dyslipidemia, hyperuricemia, and anti-adronergic effects. In: Seldin DW, Giebisch G, editors. Diuretic agents: clinical physiology and pharmacology. San Diego: Academic Press; 1997. p. 621–36.
[266] Pickkers P, Schachter M, Hughes AD, Feher MD, Sever PS. Thiazide-induced hyperglycaemia: a role for calcium-activated potassium channels? Diabetologia 1996;39:861–4.
[267] Grimm Jr RH, Flack JM, Granditis GA. Treatment of Mild Hypertension Study (TOMHS) Research Group. Long-term effects on plasma lipids of diet and drugs to treat hypertension. JAMA 1996;275:1549–56.

[268] Meneton P, Loffing J, Warnock DG. Sodium and potassium handling by the aldosterone-sensitive distal nephron: the pivotal role of the distal and connecting tubule. Am J Physiol Renal Physiol 2004;287(4):F593–601.

[269] Perez-Ayuso RM, Arroyo V, Planas R, Gaya J, Bory F, Rimola A, et al. Randomized comparative study of efficacy of furosemide versus spironolactone in nonazotemic cirrhosis with ascites. Relationship between the diuretic response an the activity of the renin–aldosterone system. Gastroenterology 1983;84: 961–8.

[270] Casavola V, Guerra L, Reshkin SJ, Jacobson KA, Verrey F, Murer H. Effect of adenosine on Na^+ and Cl^- curents in A6 monolayers. Receptor localization and messenger involvement. J Membrane Biol 1996;151:237–45.

[271] Shimizu T, Nakamura M, Yoshitomi K, Imai M. Interaction of trichlormethiazide or amiloride with PTH in stimulating Ca^{2+} absorption in rabbit CNT. Am J Physiol 1991;261:F36–43.

[272] Bundy JT, Connito D, Mahoney MD, Pontier PJ. Treatment of idiopathic renal magesium wasting with amiloride. Am J Nephrol 1995;15:75–7.

[273] Schild L. The epithelial sodium channel: from molecule to disease. Rev Physiol Biochem Pharmacol 2004;151:93–107.

[274] Canessa CM, Horisberger J-D, Rossier BC. Epithelial sodium channel related to proteins involved in neurodegeneration. Nature 1993;361:467–70.

[275] Canessa CM, Schild L, Buell G, Thorens B, Gatuschi I, Horisberger J-D, et al. Amiloride-sensitive epithelial Na^+ channel is made of three homologous subunits. Nature 1994;367:463–7.

[276] Kellenberger S, Schild L. Epithelial sodium channel/degenerin family of ion channels: a variety of functions for a shared structure. Physiol Rev 2002;82(3):735–67.

[277] Kosari F, Sheng S, Li J, Mak DO, Foskett JK, Kleyman TR. Subunit stoichiometry of the epithelial sodium channel. J Biol Chem 1998;273(22):13469–74.

[278] Firsov D, Gautschi I, Merillat AM, Rossier BC, Schild L. The heterotetrameric architecture of the epithelial sodium channel (ENaC). EMBO J 1998;17(2):344–52.

[279] Jasti J, Furukawa H, Gonzales EB, Gouaux E. Structure of acid-sensing ion channel 1 at 1.9 Å resolution and low pH. Nature 2007;449(7160):316–23.

[280] Canessa CM. Structural biology: unexpected opening. Nature 2007;449(7160):293–4.

[281] Palmer LG. Voltage-dependent block by amiloride and other monovalent cations of apical Na channels in the toad urinary bladder. J Membr Biol 1984;80(2):153–65.

[282] Grunder S, Jaeger NF, Gautschi I, Schild L, Rossier BC. Identification of a highly conserved sequence at the N-terminus of the epithelial Na^+ channel alpha subunit involved in gating. Pflugers Arch 1999;438(5):709–15.

[283] Kashlan OB, Kleyman TR. ENaC structure and function in the wake of a resolved structure of a family member. Am J Physiol Renal Physiol 2011;301(4):F684–96.

[284] Sheng S, Perry CJ, Kashlan OB, Kleyman TR. Side chain orientation of residues lining the selectivity filter of epithelial Na^+ channels. J Biol Chem 2005;280(9):8513–22.

[285] Verrey F, Pearce D, Pfeiffer R, Spindler B, Mastroberardino L, Summa V, et al. Pleiotropic action of aldosterone in epithelia mediated by transcription and post-transcription mechanisms. Kidney Int 2000;57(4):1277–82.

[286] Loffing J, Zecevic M, Feraille E, Kaissling B, Asher C, Rossier BC, et al. Aldosterone induces rapid apical translocation of ENaC in early portion of renal collecting system: possible role of SGK. Am J Physiol 2001;280(4):F675–82.

[287] Gründer S, Rossier BC. A reappraisal of aldosterone effects on kidney: new insights provided by epithelial sodium channel cloning. Curr Opin Nephrol Hypertens 1997;6:35–9.

[288] Funder JW. The nongenomic actions of aldosterone. Endocr Rev 2005;26(3):313–21.

[289] Fourkiotis VG, Hanslik G, Hanusch F, Lepenies J, Quinkler M. Aldosterone and the kidney. Horm Metab Res 2012;44 (3):194–201.

[290] Pratt WB. The role of heat shock proteins in regulating the function, folding, and trafficking of the glucocorticoid receptor. J Biol Chem 1993;268:21455–8.

[291] Tumlin JA, Lea JP, Swanson CE, Smith CL, Edge SS, Someren JS. Aldosterone and dexamethasone stimulate calcineurin activity through a transcription-independent mechanism involving steroid receptor-associated heat shock proteins. J Clin Invest 1997;99(6):1217–23.

[292] Verrey F. Transcriptional control of sodium transport in tight epithelia by adrenal steroids. J Membrane Biol 1995;144: 93–110.

[293] Rogerson FM, Brennan FE, Fuller PJ. Mineralocorticoid receptor binding, structure and function. Mol Cell Endocrinol 2004;217(1-2):203–12.

[294] Rokaw MD, Benos DJ, Palevsky PM, Cunningham SA, West ME, Johnson JP. Regulation of a sodium channel-associated G-protein by aldosterone. J Biol Chem 1996;271(8):4491–6.

[295] Chen SY, Bhargava A, Mastroberardino L, Meijer OC, Wang J, Buse P, et al. Epithelial sodium channel regulated by aldosterone-induced protein sgk. Proc Natl Acad Sci U S A 1999;96 (5):2514–9.

[296] Naray-Fejes-Toth A, Canessa C, Cleaveland ES, Aldrich G, Fejes-Toth G. sgk is an aldosterone-induced kinase in the renal collecting duct. Effects on epithelial Na^+ channels. J Biol Chem 1999;274(24):16973–8.

[297] Snyder PM, Olson DR, Thomas BC. Serum and glucocorticoid-regulated kinase modulates Nedd4-2-mediated inhibition of the epithelial Na^+ channel. J Biol Chem 2002;277(1):5–8.

[298] Zhou R, Snyder PM. Nedd4-2 phosphorylation induces serum and glucocorticoid-regulated kinase (SGK) ubiquitination and degradation. J Biol Chem 2005;280(6):4518–23.

[299] Shackleton CR, Wong NLM, Sutton RA. Distal (potassium-sparing) diuretics. In: Dirks JH, Sutton RAL, editors. Diuretics physiology, pharmacology and clinical use. 1st ed. Philadelphia: W.B. Saunders; 1986. p. 117–34.

[300] Fanestil DD. Mechanism of action of aldosterone blockers. Sem Nephrol 1988;8:249–63.

[301] Marver D, Stewart J, Funder JW, Feldman D, Edelman IS. Renal aldosterone receptors: studies with [^{3}H]adlosterone and the antimineralocorticoid [^{3}H]spirolactone (SC26304). Proc Natl Acad Sci 1974;71:1431–5.

[302] Couette B, Lombes M, Baulieu E-E, Rafestin-Oblin M-E. Aldosterone antagonists destablilize the mineralocorticoid receptor. Biochem J 1992;282:697–702.

[303] Delyani JA. Mineralocorticoid receptor antagonists: the evolution of utility and pharmacology. Kidney Int 2000;57(4): 1408–11.

[304] de Gasparo M, Joss U, Ramjoue HP, Whitebread SE, Haenni H, Schenkel L, et al. Three new epoxy-spirolactone derivatives: characterization *in vivo* and *in vitro*. J Pharmacol Exp Ther 1987;240(2):650–6.

[305] Liddle GW. Aldosterone antagonists and triamterene. Ann NYAcad Sci 1966;134:466–70.

[306] Kagawa CM. Blocking the renal electrolyte effects of mineralocorticoids with an orally active steroidal spirolactone. Endocrinology 1960;65:125–32.

[307] Costanzo LS. Comparison of calcium and sodium transport in early and late rat distal tubules: effect of amiloride. Am J Physiol 1984;246:F937–45.
[308] Stokes JB. Ion transport by the cortical and outer medullary collecting tubule. Kidney Int 1982;22:473–84.
[309] Stoner LC, Burg MB, Orloff J. Ion transport in cortical collecting tubule; effect of amiloride. Am J Physiol 1974;227: 453–9.
[310] Garty H, Benos D. Characteristics and regulatory mechanisms of the amiloride-blockable Na^+ channel. Physiol Reviews 1988;68:309–73.
[311] Cassin S, Vogh B. Effect of Hydrochlorothiazide on renal blood flow and clearance of para-aminohippurate and creatinine. Proc Soc Exp Biol Med 1966;122:970–3.
[312] Busch AE, Suessbrich H, Kunzelmann K, Hipper A, Greger R, Waldegger S, et al. Blockade of epithelial Na^+ channels by triamterene-underlying mechanisms and molecular basis. Pflugers Arch 1996;432:760–6.
[313] Karim A. Spironolactone: disposition, metabolism, pharmacodynamics and bioavailability. Drug Metab Rev 1978;8:151–88.
[314] Merkus FWHM, Overdiek JWPM, Cilissen J, Zuidema J. Pharmacokinetics of spironolactone after a single dose: evaluation of the true canrenone serum concentrations during 24 hours. Clin Exp Hypertens 1983;([[A]5):249–69.
[315] Gardiner P, Schrode K, Quinlan D, Martin BK, Boreham DR, Rogers MS, et al. Spironolactone metabolism: steady-state serum levels of the sulfur-containing metabolites. J Clin Pharmacol 1989;29:342–7.
[316] Sungaila I, Bartle WR, Walker SE, DeAngelis C, Uetrecht J, Pappas C, et al. Spironolactone pharmacokinetics and pharmacodynamics in patients with cirrhotic ascites. Gastroenterology 1992;102:1680–5.
[317] Widmer P, Maibach R, Kunzi UP, Capaul R, Mueller U, Galeazzi R, et al. Diuretic-related hypokalaemia: the role of diuretics, potassium supplements, glucocorticoids and beta 2-adrenoceptor agonists. Results from the comprehensive hospital drug monitoring programme, Berne (CHDM). Eur J Clin Pharmacol 1995;49(1-2):31–6.
[318] Brown JJ, Davies DL, Ferriss JB, Fraser R, Haywood E, Lever AF, et al. Comparison of surgery and prolonged spironolactone therapy in patients with hypertension, aldosterone excess, and low plasma renin. Br Med J 1972;2:729–34.
[319] Laffi G, La Villa G, Carloni V, Foschi M, Bartoletti L, Quartini M, et al. Loop diuretic therapy in liver cirrhosis with ascites. J Cardiovasc Pharmacol 1993;22(Suppl. 3):S51–8.
[320] Runyon BA. Practice Guidelines Committee AAftSoLD. Management of adult patients with ascites due to cirrhosis. Hepatology 2004;39(3):841–56.
[321] Chapman N, Dobson J, Wilson S, Dahlof B, Sever PS, Wedel H, et al. Effect of spironolactone on blood pressure in subjects with resistant hypertension. Hypertension 2007;49(4):839–45.
[322] Rossignol P, Menard J, Fay R, Gustafsson F, Pitt B, Zannad F. Eplerenone survival benefits in heart failure patients post-myocardial infarction are independent from its diuretic and potassium-sparing effects. Insights from an EPHESUS (Eplerenone Post-Acute myocardial infarction heart failure efficacy and survival study) substudy. J Am Coll Cardiol 2011;58 (19):1958–66.
[323] Griffing GT, Cole AG, Aurecchia SA, Sindler BH, Komanicky P, Melby JC. Amiloride for primary hyperaldosteronism. Clin Pharmacol Ther 1982;31:56–61.
[324] Ganguly A, Weinberger MH. Triamteren-thiazide combination: alternative therapy for primary aldosteronism. Clin Pharmacol Ther 1981;30:246–50.
[325] Botero-Velez M, Curtis JJ, Warnock DG. Brief report: Liddle's syndrome revisited – a disorder of sodium reabsorption in the distal tubule. N Engl J Med 1994;174:178–8078.
[326] Okusa MD, Bia MJ. Bartter's syndrome. In: Foa PP, Cohen MP, editors. Endocrinology and metabolism. 1st ed. New York: Springer-Verlag; 1987. p. 231–63.
[327] Kortenoeven ML, Li Y, Shaw S, Gaeggeler HP, Rossier BC, Wetzels JF, et al. Amiloride blocks lithium entry through the sodium channel thereby attenuating the resultant nephrogenic diabetes insipidus. Kidney Int 2009;76(1):44–53.
[328] Juurlink DN, Mamdani MM, Lee DS, Kopp A, Austin PC, Laupacis A, et al. Rates of hyperkalemia after publication of the Randomized Aldactone Evaluation Study. N Engl J Med 2004;351(6):543–51.
[329] Pitt B, Remme W, Zannad F, Neaton J, Martinez F, Roniker B, et al. Eplerenone, a selective aldosterone blocker, in patients with left ventricular dysfunction after myocardial infarction. N Engl J Med 2003;348(14):1309–21.
[330] Whitling AM, Pergola PE, Sang JL, Talbert RL. Spironolactone-induced agranulocytosis. Ann Pharmacother 1997;31:582–5.
[331] Perazella MA. Crystal-induced acute renal failure. Am J Med 1999;106(4):459–65.
[332] Carr MC, Prien Jr. EL, Babayan RK. Triamterene nephrolithiasis: renewed attention is warranted. J Urol 1990;144:1339–40.
[333] Weinberg MS, Quigg RJ, Salant DJ, Bernard DB. Anuric renal failure precipitated by indomethacin and triamterene. Nephron 1985;40:216–8.
[334] Favre L, Glasson P, Vallotton MB. Reversible acute renal failure from combined triamterene and indomethacin: a study in healthy subjects. Ann Intern Med 1982;96:317–20.
[335] Tahara A, Tomura Y, Wada KI, Kusayama T, Tsukada J, Takanashi M, et al. Pharmacological profile of YM087, a novel potent nonpeptide vasopressin V1A and V2 receptor antagonist, *in vitro* and *in vivo*. J Pharmacol Exp Ther 1997;282(1): 301–8.
[336] Palm C, Pistrosch F, Herbrig K, Gross P. Vasopressin antagonists as aquaretic agents for the treatment of hyponatremia. Am J Med 2006;119(7 Suppl. 1):S87–92.
[337] Risvanis J, Naitoh M, Johnston CI, Burrell LM. *In vivo* and *in vitro* characterisation of a nonpeptide vasopressin V(1 A) and V(2) receptor antagonist (YM087) in the rat. Eur J Pharmacol 1999;381(1):23–30.
[338] Hoorn EJ, Zietse R. Hyponatremia and mortality: how innocent is the bystander? Clin J Am Soc Nephrol 2011;6(5):951–3.
[339] Konstam MA, Gheorghiade M, Burnett Jr. JC, Grinfeld L, Maggioni AP, Swedberg K, et al. Effects of oral tolvaptan in patients hospitalized for worsening heart failure: the EVEREST Outcome Trial. Jama 2007;297(12):1319–31.
[340] Schrier RW, Gross P, Gheorghiade M, Berl T, Verbalis JG, Czerwiec FS, et al. Tolvaptan, a selective oral vasopressin V2-receptor antagonist, for hyponatremia. N Engl J Med 2006;355 (20):2099–112.
[341] Cardenas A, Gines P, Marotta P, Czerwiec F, Oyuang J, Guevara M, et al. Tolvaptan, an oral vasopressin antagonist, in the treatment of hyponatremia in cirrhosis. J Hepatol 2012;56 (3):571–8.
[342] Kelly MR, Cutler RE, Forrey AW, Kimpel BM. Pharmacokinetics of orally administered furosemide. Clin Pharmacol Ther 1973;15:178–86.
[343] Branch RA, Roberts CJC, Homeida M, Levine D. Determinants of response to frusemide in normal subjects. Br J Clin Pharmacol 1977;4:121–7.
[344] Murray MD, Deer MM, Ferguson JA, Dexter PR, Bennett SJ, Perkins SM, et al. Open-label randomized trial of torsemide

compared with furosemide therapy for patients with heart failure. Am J Med 2001;111(7):513–20.
[345] Brater DC, Chalasani N, Gorski JC, Horlander JCS, Craven R, Hoen H, et al. Effect of albumin-furosemide mixtures on response to furosemide in cirrhotic patients with ascites. Trans Am Clin Climatol Assoc 2001;112:108–15 [discussion 16]
[346] Fliser D, Zurbruggen I, Mutschler E, Bischoff I, Nussberger J, Franek E, et al. Coadministration of albumin and furosemide in patients with the nephrotic syndrome [In Process Citation]. Kidney Int 1999;55(2):629–34.
[347] Blendis L, Wong F. Intravenous albumin with diuretics: protean lessons to be learnt? [editorial; comment] J Hepatol 1999;30(4):727–30.
[348] Gentilini P, Casini-Raggi V, Di Fiore G, Romanelli RG, Buzzelli G, Pinzani M, et al. Albumin improves the response to diuretics in patients with cirrhosis and ascites: results of a randomized, controlled trial. J Hepatol 1999;30(4):639–45.
[349] Na KY, Han JS, Kim YS, Ahn C, Kim S, Lee JS, et al. Does albumin preinfusion potentiate diuretic action of furosemide in patients with nephrotic syndrome? J Korean Med Sci 2001;16 (4):448–54.
[350] Kirchner KA. Impairment of diuretic secretion. In: Seldin DW, Giebisch G, editors. Diuretic agents: clinical physiology and pharmacology. San Diego: Academic Press; 1997. p. 259–70.
[351] Uwai Y, Saito H, Hashimoto Y, Inui KI. Interaction and transport of thiazide diuretics, loop diuretics, and acetazolamide via rat renal organic anion transporter rOAT1. J Pharmacol Exp Ther 2000;295(1):261–5.
[352] Sweet DH, Bush KT, Nigam SK. The organic anion transporter family: from physiology to ontogeny and the clinic. Am J Physiol 2001;281(2):F197–205.
[353] Krick W, Wolff NA, Burckhardt G. Voltage-driven p-aminohippurate, chloride, and urate transport in porcine renal brush-border membrane vesicles. Pflugers Arch 2000;441(1): 125–32.
[354] Eraly SA, Vallon V, Vaughn DA, Gangoiti JA, Richter K, Nagle M, et al. Decreased renal organic anion secretion and plasma accumulation of endogenous organic anions in OAT1 knockout mice. J Biol Chem 2006;281(8):5072–83.
[355] Beseghir K, Mosig D, Roch-Ramel F. Facilitation by serum albumin of renal tubular secretion of organic anions. Am J Physiol 1989;256:F475–84.
[356] Rose H, O'Malley K, Pruitt A. Depression of renal clearance of furosemide in man by azotemia. Clin Pharmacol Ther 1976;21:141–6.
[357] Chennavasin P, Seiwell R, Brater DC. Pharmacokinetic-dynamic analysis of the indomethacin-furosemide interaction in man. J Pharmacol Exp Ther 1980;215:77–81.
[358] Brater DC. Increase in diuretic effect of chlorothiazide by probenecid. Clin Pharmacol Ther 1978;23:259–65.
[359] Chennavasin P, Seiwell R, Brater DC, Liang WM. Pharmacodynamic analysis of the furosemide-probenecid interaction in man. Kidney Int 1979;16:187–95.
[360] Somogyi AA, Hovens CM, Muirhead MR, Bochner F. Renal tubular secretion of amiloride and its inhibition by cimetidine in humans and in an animal model. Drug Metab Dispos 1989;17(2):190–6.
[361] Voelker JR, Jameson DM, Brater DC. *In vitro* evidence that urine composition affects the fraction of active furosemide in the nephrotic syndrome. J Pharmacol Exp Ther 1989;250: 772–8.
[362] Kirchner KA, Voelker JR, Brater DC. Intratubular albumin blunts the response to furosemide: a mechanism for diuretic resistance in the nephrotic syndrome. J Pharmacol Exp Ther 1990;252:1097–101.
[363] Kirchner KA, Voelker JR, Brater DC. Binding inhibitors restore furosemide potency in tubule fluid containing albumin. Kidney Int 1991;40:418–24.
[364] Agarwal R, Gorski JC, Sundblad K, Brater DC. Urinary protein binding does not affect response to furosemide in patients with nephrotic syndrome. J Am Soc Nephrol 2000;11(6): 1100–5.
[365] Ellison DH, Velazquez H, Wright FS. Adaptation of the distal convoluted tubule of the rat. Structural and functional effects of dietary salt intake and chronic diuretic infusion. J Clin Invest 1989;83(1):113–26.
[366] Almeshari K, Ahlstrom NG, Capraro FE, Wilcox CS. A volume-independent component to postdiuretic sodium retention in humans. J Am Soc Nephrol 1993;3:1878–83.
[367] Christensen S, Steiness E, Christensen H. Tubular sites of furosemide natriuresis in volume-replaced and volume-depleted conscious rats. J Pharmacol Exp Ther 1986;239:211–8.
[368] Wilcox CS, Mitch WE, Kelly RA, Skorecki K, Meyer TW, Friedman PA, et al. Response of the kidney to furosemide: I. Effects of salt intake and renal compensation. J Lab Clin Med 1983;102:450–8.
[369] Kelly RA, Wilcox CS, Mitch WE, Meyer TW, Souney PF, Rayment CM, et al. Response of the kidney to furosemide. II. Effect of captopril on sodium balance. Kidney Int 1983;24: 233–9.
[370] Agostoni P, Marenzi G, Lauri G, Perego G, Schianni M, Sganzerla P, et al. Sustained improvement in functional capacity after removal of body fluid with isolated ultrafilration in chronic cardiac insufficiency: failure of furosemide to provide the same result. Am J Med 1994;96:191–9.
[371] Marenzi G, Lauri G, Grazi M, Assanelli E, Campodonico J, Agostoni P. Circulatory response to fluid overload removal by extracorporeal ultrafiltration in refractory congestive heart failure. J Am Coll Cardiol 2001;38(4):963–8.
[372] Costanzo MR, Guglin ME, Saltzberg MT, Jessup ML, Bart BA, Teerlink JR, et al. Ultrafiltration versus intravenous diuretics for patients hospitalized for acute decompensated heart failure [See comment] J Am Coll Card 2007;49(6): 675–83.
[373] Petersen JS, Shalmi M, Abildgaard U, Christensen S. Alpha-1 blockade inhibits compensatory sodium reabsorption in the proximal tubules during furosemide-induced volume contraction. J Pharmacol Exp Ther 1991;258:42–8.
[374] Wilcox CS, Guzman NJ, Mitch WE, Kelly RA, Maroni BJ, Souney PF, et al. Na^+,K^+ and BP homeostasis in man during furosemide: effects of prozosin and captopril. Kidney Int 1987;31:135–41.
[375] Jespersen B, Jensen L, Sorensen SS, Pedersen EB. Atrial natriuretic factor, cyclic 3′,5′-guanosine monophosphate and prostaglandin E2 in liver cirrhosis: relation to blood volume and changes in blood volume after furosemide. Eur J Clin Invest 1990;20:632–41.
[376] Isenring P, Jacoby SC, Payne JA, Forbush III B. Comparison of Na-K-Cl co-transporters. J Biol Chem 1998;273:11295–301.
[377] Ecelbarger CA, Terris J, Hoyer JR, Nielsen S, Wade JB, Knepper MA. Localization and regulation of the rat renal Na^+-K^+-$2Cl^-$ co-transporter, BSC-1. Am J Physiol Renal, Fluid Electrolyte Physiol 1996;271:F619–28.
[378] Chen ZF, Vaughn DA, Beaumont K, Fanestil DD. Effects of diuretic treatment and of dietary sodium on renal binding of 3H-metolazone. J Am Soc Nephrol 1990;1:91–8.
[379] Sandberg MB, Maunsbach AB, McDonough AA. Redistribution of distal tubule Na^+-Cl^- co-transporter (NCC) in response to a high-salt diet. Am J Physiol Renal Physiol 2006;291(2):F503–8.

[380] Ellison DH. Diuretic resistance: physiology and therapeutics. Sem Nephrol 1999;19(6):581–97.
[381] Stein JH, Osgood RW, Boonjarern S, Cox JW, Ferris TF. Segmental sodium reabsorption in rats with mild and severe volume depletion. Am J Physiol 1974;227:351–9.
[382] DiBona GF, Sawin LL. Renal nerve activity in conscious rats during volume expansion and depletion. Am J Physiol 1985;248:F15–23.
[383] Petersen JS, Shalmi M, Lam HR, Christensen S. Renal response to furosemide in conscious reats: effects of acute instrumentation and peripheral sympathectomy. J Pharmacol Exp Ther 1991;258:1–7.
[384] Petersen JS, DiBona GF. Effects of renal denervation on sodium balance and renal function during chronic furosemide administration in rats. J Pharmacol Exp Ther 1992;262:1103–9.
[385] Chen Z, Vaughn DA, Blakeley P, Fanestil DD. Adrenocortical steroids increase renal thiazide diuretic receptor density and response. J Am Soc Nephrol 1994;5:1361–8.
[386] Bernstein PL, Velázquez H, Bartiss A, Reilly RF, Desir GV, Kunchaparty S, et al. Adrenal steroids stimulate thiazide-sensitive Na-Cl co-transport by rat distal tubules. J Am Soc Nephrol 1994:282.
[387] Velázquez H, Náray-Fejes-Tóth A, Silva T, Andújar E, Reilly RF, Desir GV, et al. The distal convoluted tubule of the rabbit coexpresses NaCl co-transporter and 11b-hydroxysteroid dehydrogenase. Kidney Int 1998;54:464–72.
[388] Wang T, Giebisch G. Angiotensin II regulates bicarbonate and fluid transport in the early and late distal tubule in rat kidney. J Am Soc Nephrol 1994:673.
[389] Kim GH. Long-term adaptation of renal ion transporters to chronic diuretic treatment. Am J Nephrol 2004;24(6):595–605.
[390] Kaissling B, Bachmann S, Kriz W. Structural adaptation of the distal convoluted tubule to prolonged furosemide treatment. Am J Physiol 1985;248:F374–81.
[391] Kaissling B, Stanton BA. Adaptation of distal tubule and collecting duct to increased sodium delivery. I. Ultrastructure. Am J Physiol 1988;255:F1256–68.
[392] Scherzer P, Wald H, Popovtzer MM. Enhanced glomerular filtration and Na^+-K^+-ATPase with furosemide administration. Am J Physiol 1987;252:F910–5.
[393] Wald H, Scherzer P, Popovtzer MM. Na, K-ATPase in isolated nephron segments in rats with experimental heart failure. Circ Res 1991;68:1051–8.
[394] Moreno G, Merino A, Mercado A, Herrera JP, Gonzalez-Salazar J, Correa-Rotter R, et al. Electroneutral Na-coupled cotransporter expression in the kidney during variations of NaCl and water metabolism. Hypertension 1998;31(4):1002–6.
[395] Loffing J, Le Hir M, Kaissling B. Modulation of salt transport rate affects DNA synthesis *in vivo* in rat renal tubules. Kidney Int 1995;47:1615–23.
[396] Wang T, Giebisch G. Effects of angiotensin II on electrolyte transport in the early and late distal tubule in rat kidney. Am J Physiol Renal, Fluid Electrolyte Physiol 1996;271:F143–9.
[397] Beck FX, Ohno A, Muller E, Seppi T, Pfaller W. Inhibition of angiotensin-converting enzyme modulates structural and functional adaptation to loop diuretic-induced diuresis. Kidney Int 1997;51:36–43.
[398] Kaissling B, Stanton BA. Structure-function correlation in electrolyte transporting epithelia. In: Seldin DW, Giebisch G, editors. The kidney: physiology and pathophysiology. 2nd ed. New York: Raven Press, Ltd; 1992. p. 779–801.
[399] Kim GH, Masilamani S, Turner R, Mitchell C, Wade JB, Knepper MA. The thiazide-sensitive Na-Cl co-transporter is an aldosterone-induced protein. Proc Natl Acad Sci U S A 1998;95 (24):14552–7.
[400] Velazquez H, Bartiss A, Bernstein P, Ellison DH. Adrenal steroids stimulate thiazide-sensitive NaCl transport by rat renal distal tubules. Am J Physiol 1996;270(1 Pt 2):F211–9.
[401] Stanton BA, Kaissling B. Regulation of renal ion transport and cell growth by sodium. Am J Physiol 1989;257:F1–10.
[402] Bouby N, Bankir L, Trinh-Trang-Tan MM, Minuth WW, Kriz W. Selective ADH-induced hypertrophy of the medullary thick ascending limb in Brattleboro rats. Kidney Int 1985;28: 456–66.
[403] Petty KJ, Kokko JP, Marver D. Secondary effect of aldosterone on Na-K ATPase activity in the rabbit cortical collecting tubule. J Clin Invest 1981;68:1514–21.
[404] Kaissling B. Structural adaptation to altered electrolyte metabolism by cortical distal segments. Fed Proc 1985;44:2710–6.
[405] Morsing P, Velazquez H, Wright FS, Ellison DH. Adaptation of distal convoluted tubule of rats. II. Effects of chronic thiazide infusion. Am J Physiol 1991;261(1 Pt 2):F137–43.
[406] Garg LC, Narang N. Effects of hydrochlorothiazide on Na-K-ATPase activity along the rat nephron. Kidney Int 1987;31: 918–22.
[407] Kobayashi S, Clemmons DR, Nogami H, Roy AK, Venkatachalam MA. Tubular hypertrophy due to work load induced by furosemide is associated with increses of IGF-1 and IGFBP-1. Kidney Int 1995;47:818–28.
[408] Kim J, Welch WJ, Cannon JK, Tisher CC, Madsen KM. Immunocytochemical response of type A and type B intercalated cells to increased sodium chloride delivery. Am J Physiol Renal, Fluid Electrolyte Physiol 1992;262:F288–302.
[409] Bahro M, Gertig G, Pfeifer U. Short-term stimulation of cellular autophagy by furosemide in the thick ascending limb of Henle's loop in the rat kidney. Cell Tissue Res 1988;253:625–9.
[410] Grossman EB, Hebert SC. Modulation of Na-K-ATPase activity in the mouse medullary thick ascending limb of Henle: effects of mineralocorticoids and sodium. J Clin Invest 1988;81: 885–92.
[411] Loon NR, Wilcox CS, Unwin RJ. Mechanism of impaired natriuretic response to furosemide during prolonged therapy. Kidney Int 1989;36:682–9.
[412] Burckhardt BC, Burckhardt G. Transport of organic anions across the basolateral membrane of proximal tubule cells. Rev Physiol Biochem Pharmacol 2003;146:95–158.

CHAPTER

41

Aquaporin Water Channels in Mammalian Kidney

Søren Nielsen[1], *Tae-Hwan Kwon*[2], *Henrik Dimke*[3], *Martin Skott*[4] *and Jørgen Frøkiær*[5]

[1]Water and Salt Research Center, Department of Biomedicine, University of Aarhus, Aarhus, Denmark
[2]Department of Biochemistry and Cell Biology, School of Medicine, Kyungpook National University, Taegu, Korea
[3]Department of Biomedicine, University of Aarhus, Aarhus, Denmark; The Samuel Lunenfeld Research Institute, Mt. Sinai Hospital, Toronto, Ontario, Canada
[4]Department of Biomedicine, University of Aarhus, Aarhus, Denmark
[5]Water and Salt Research Center, Department of Clinical Physiology, Aarhus University Hospital-Skejby, Aarhus, Denmark

INTRODUCTION

Water is the most abundant component of all cells, and the ability to absorb and release water is considered a fundamental process of life. Plasma membranes serve as selective barriers that control the solute composition of the cell and regulate the entry of ions, small uncharged solutes, and even water. Epithelial tissues have apical and basolateral plasma membranes that constitute serial barriers that regulate the transepithelial movement of solutes and water, thereby contributing to the homeostasis of multicellular organisms. Identification and characterization of the molecular entities responsible for the function of biologic membranes have been long-standing goals of physiologists; however, the molecular identity of water transporters remained unknown until less than two decades ago.

Because water can slowly diffuse through lipid bilayers, all biologic membranes exhibit some degree of water permeability. Nevertheless, observations made in multiple laboratories indicated that specialized membrane water-transport molecules must exist in tissues with distinctively high water permeability (see review [1]). For example, the water permeability of red cell membranes is higher than that of many other cell types or artificial lipid bilayers, and the activation energy of this process is equivalent to the diffusion of water in solution, E_a <5 kcal/mol.[2] In addition, reversible inhibition by $HgCl_2$ and a subset of organomercurials suggested that the water transporter is a membrane protein (see review [3]). Further evidence that a membrane protein is involved in water transport was provided by the observation that some epithelial tissues exhibit changes in water permeability on a timescale that is not compatible with changes in lipid composition.

Kidneys are the major determinant of body water and electrolyte composition. Thus, comprehending the mechanisms of water transport is essential to understanding mammalian kidney physiology and water balance. Because of its importance to human health, water permeability has been particularly well-characterized in the mammalian kidney (see review [4]). Approximately 180 L/day of glomerular filtrate is generated in an average adult human, the majority of this is reabsorbed by the highly water-permeable proximal tubules and descending thin limbs of Henle's loop. The ascending thin limbs and thick limbs are relatively impermeable to water, and empty into renal distal tubules and ultimately into the collecting ducts. The collecting ducts are extremely important clinically in water-balance disorders, because they are the chief site

Seldin and Giebisch's The Kidney, Fifth Edition.
DOI: http://dx.doi.org/10.1016/B978-0-12-381462-3.00041-0

© 2013 Elsevier Inc. All rights reserved.

of regulation of water reabsorption. Basal epithelial water permeability in collecting duct principal cells is low, but the water permeability can become exceedingly high when stimulated with vasopressin (also known as ADH, antidiuretic hormone). In this regard, the toad urinary bladder behaves like the collecting duct, and it has served as an important model of vasopressin-regulated water permeability. Stimulation of this epithelium with vasopressin produces an increase in water permeability in the apical membrane, which coincides with the redistribution of intracellular particles to the cell surface.[5–8] These particles were believed to contain water channels.

DISCOVERY OF AQUAPORIN-1 (AQP1)

The molecular identity of membrane water channels long proved elusive. Attempts to purify water channel proteins from native tissues or to isolate water channel cDNAs by expression cloning, were unproductive (see review [9]). This may be explained by the physical characteristics of water, a simple molecule not amenable to chemical modification such as introduction of chemical cross-linking groups or labels. In addition, $HgCl_2$ was known to inhibit membrane water channels, a property potentially useful in the identification of the water channel proteins. However, because the agent reacts with free sulfhydryls in other proteins, its inhibitory effect on water channels is not specific. This circumstance led to the mistaken identification of the band 3 anion exchanger as a molecular water channel.[10] In addition, the diffusional permeability of all biologic membranes results in high background permeability, and frustrated efforts to clone cDNAs for water channels by functional expression.

The recognized characteristics of membrane water channels led to chance identification of the first known water channel. In the process of isolating the 32 kDa bilayer-spanning polypeptide component of the red cell Rh blood group antigen,[11] a 28 kDa polypeptide was partially co-purified.[12] Initial studies demonstrated that the 28 kDa polypeptide comprised hydrophobic amino acids and exhibited an unusual detergent solubility, which facilitated purification and biochemical characterization. The 28 kDa polypeptide was found to exist as an oligomeric protein with physical dimensions of a tetramer; a unique N-terminal amino acid sequence was identified[13] which permitted cDNA cloning.[14] Also of note, radiation inactivation studies of water permeability by renal vesicles yielded a target size of 30 kDa.[15] Because the 28 kDa polypeptide was found to be abundant in red cells, renal proximal tubules, and descending thin limbs,[12] it was suggested that this protein might be the sought-after water channel. Although this protein was first known as "CHIP28" (channel-like integral protein of 28 kDa), the need for a functionally relevant name was recognized. The name "aquaporin" was coined. After recognition of related proteins with similar functions, this name was formally proposed for the emerging family of water channels now known as the aquaporins.[16] Thus, CHIP28 was designated aquaporin-1 (symbol AQP1). The Human Genome Nomenclature Committee has embraced this nomenclature for all related proteins,[17] and presently a total of 13 such related proteins have been identified in mammals.

The measurement of the movement of water across cell membranes poses a unique experimental challenge. Unlike ion conductances, which may be measured electrophysiologically, or solute transport, which may be measured with radioactive substrates, transmembrane water movement in cells relies on determination of changes in cell volume in response to an osmotic driving force. The *Xenopus laevis* oocyte expression system was used to search for water channel RNAs, because these cells are known to exhibit remarkably low membrane water permeability.[18,19] Oocytes injected with cRNA encoding AQP1 exhibit remarkably high osmotic water permeability ($P_f \sim 200 \times 10^{-17}$ cm/s), causing the cells to swell rapidly and eventually rupture in hyposmotic buffer.[20] In contrast, control oocytes not injected with AQP1 cRNA exhibited less than one tenth of this permeability.

Oocyte studies demonstrated that AQP1 behaves like the water channels in native cell membranes.[20] Osmotically-induced swelling of oocytes expressing AQP1 occurs with a low activation energy, and is reversibly inhibited by $HgCl_2$. Moreover, AQP1 oocytes fail to demonstrate any measurable increase in membrane current. Although these early studies demonstrated only swelling of oocytes, it was predicted that the direction of water flow through AQP1 is determined by the orientation of the osmotic gradient. Thus, AQP1 oocytes swell in hyposmolar buffers but shrink in hyperosmolar buffers.[21]

To confirm that the interpretation of the oocyte studies was correct, highly purified AQP1 protein from human red cells was reconstituted with pure phospholipids into proteoliposomes, which were compared with simple vesicles (liposomes) by rapid transfer to hyperosmolar buffer.[22] These studies permitted determination of the unit water permeability, which had an astonishingly high value ($P_f \sim 3 \times 10^9$ water molecules subunit^{-111} sec^{-111}). Moreover, the water permeability is reversibly inhibited by $HgCl_2$, and exhibits low activation energy. Several of these studies have been confirmed by using red cell membranes partially depleted of other proteins,[23] and attempts to demonstrate permeation by other small solutes or even

protons showed that AQP1 is water selective.[24] Together, these studies indicated that AQP1 is both necessary and sufficient to explain the well-recognized membrane water permeability of the red cell, and suggested that AQP1 or similar proteins could be the long-sought-after epithelial water channels of the nephron and collecting ducts.

STRUCTURE AND FUNCTION OF AQUAPORINS

General Structure of AQP1

The availability of pure AQP1 protein in milligram quantities and the simple functional assay in oocytes led to rapid advances in the understanding of the molecular structure of AQP1. Hydropathy analysis of the deduced amino acid sequence of AQP1 predicted that the protein resides primarily within the lipid bilayer,[14] a feature in agreement with initial studies of red cell AQP1.[12,13] As previously described for the homolog major intrinsic protein from lens (MIP, now referred to as AQP0), the polypeptide contains an internal repeat (Figure 41.1), with the N- and C-terminal halves being sequence-related, and each containing the signature motif Asn-Pro-Ala (NPA),[25,26] suggesting ancestral gene duplication.[14] When evaluated by hydropathy analysis, six bilayer-spanning domains, five connecting loops (A–E), and intracellular N-and C-termini are predicted. Attenuated total reflection-FTIR (Fourier Transform InfraRed spectroscopy) of highly-purified red cell AQP1 reconstituted into membrane crystals demonstrated a lack of beta structure in AQP1, indicating the existence of tilted alpha helices.[27]

The two homologous domains equivalent to the N-and C-termini halves of the protein each consist of three transmembrane helices that are thought to be oppositely orientated in the lipid bilayer.[28] A system was adapted for analyzing the structure of AQP1 after minimally perturbing the molecule by adding peptide epitopes at various sites. It was important that the epitope did not destroy function, and could be localized to intracellular or extracellular sites with antibodies and by selective proteolysis of intact membranes or inside-out membrane vesicles. These studies demonstrated that loop C resides at the extracellular surface of the oocytes and the intracellular location of loop D as well as the N-and C-termini. Moreover, the obverse symmetry of the N-and C-terminal halves of the molecule was confirmed[29] (Figure 41.1).

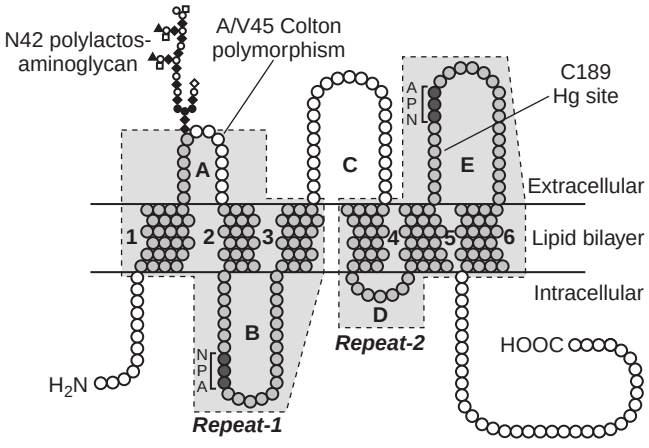

FIGURE 41.1 **Proposed membrane topology of AQP1 subunit.** Each molecule subunit spans the plasma membrane six times with the N- and C-termini in the cytoplasmic space. Extracellular and intracellular loops are labeled A–E.[32] Loop A contains an attachment site for a polylactosaminoglycan at asparagine-42 and the Co blood group polymorphism at alanine/valine-45.[100] The aquaporin signature motif asparagine-proline-alanine (NPA) is present in the loop Band E. Loop E also contains the site of mercury inhibition at cysteine-189. The amino acid sequences of C-termini of the known aquaporins are not conserved, and are sufficiently immunogenic to permit preparation of specific polyclonal antibodies to each aquaporin (see text) *(reproduced and modified from ref. [370], with permission).*

Loops B and E

Loops B and E encompass the two NPA motifs, and are the most conserved regions in the major intrinsic protein family. The loops exhibit significant hydrophobicity, suggesting association with the lipid bilayer.[14] Subsequent studies implicated loops B and E as a structural component of the aqueous pathway. Experiments expressing AQP1 in *Xenopus* oocytes led to the observation that Cys^{189} in loop E is the site of mercurial inhibition.[30,31] Site-directed mutagenesis experiments in oocytes revealed that substitution of Cys^{189} with a serine residue eliminates $HgCl_2$ sensitivity and increases osmotic water permeability, while substitution with larger amino acids residues prevents facilitated water transport.[30] These results suggest that water transport and selectivity in AQP1 is somehow dependent on the steric properties of Cys^{189}. In accordance with the internal repeat theory, Ala^{73} located in loop B, the equivalent to Cys^{189} in loop E, was investigated. By creating double mutants expressing Cys^{189} as a serine and Ala^{73} as a cysteine, the $HgCl_2$ sensitivity and osmotic water permeability were restored.[32] These results suggested that loops B and E were arranged in a symmetrical fashion, and underlined that these loops were functionally essential for water permeability. This line of inquiry lead to the "hourglass" model,[32] in which these domains overlap midway between the leaflets of the bilayer, creating a constitutively open, narrow aqueous pathway (Figure 41.2).

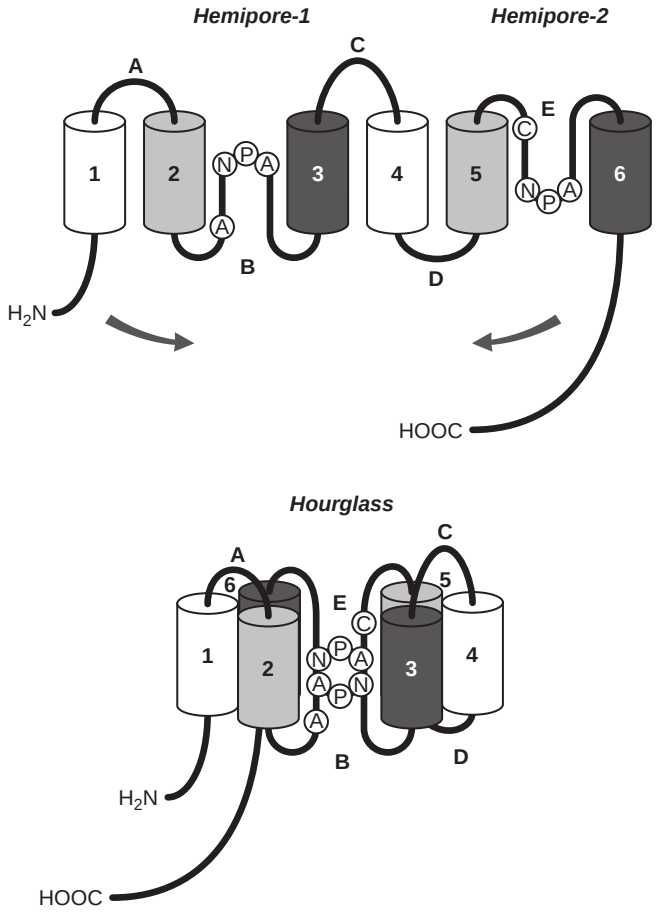

FIGURE 41.2 **Hourglass model of aquaporin-l (AQP1) structure.** Bilayer spans 1–3 (Repeat-l) and spans 4–6 (Repeat-2) are sequence-related, and are oriented in obverse symmetry. Loop B and loop E are believed to dip into the bilayer and emerge from the same side (top). When folded together, loops B and E form a single aqueous pathway (the "hourglass"), flanked by the site of mercury inhibition at cysteine189 (bottom) *(reproduced and modified from ref. [32], with permission).*

Tetrameric Organization

Early biophysical characterization of AQP1 suggested that the protein formed multisubunit oligomers.[13] Rotary and unidirectionally shadowed freeze-fracture electron microscopic analyses of AQP1 protein from human red cell membranes reconstituted in proteoliposomes provided detailed molecular insights. AQP1 had an oligomeric structure, consisting of four subunits surrounding a central depression. These tetrameric structures were also seen in highly water-permeable nephron segments expressing native AQP1.[33] Although the oligomerization of AQP1 is still not understood in detail, all studies indicate that the protein is a tetramer composed of functionally-independent aqueous pores.[15,30,32,34]

Structural Analyses and Molecular Dynamics of Aquaporins

By reconstituting the highly-purified red cell AQP1 into membranes under controlled conditions, membrane crystals were produced with AQP1 in highly uniform lattices. These membranes appeared as flat sheets or as large, resealed vesicles in which the AQP1 protein was found to fully retain water permeability.[35] Thus, the opportunity to define the structure of AQP1 in a biologically-active state became possible. Electron microscopic studies by multiple groups permitted the elucidation of the protein at increasing levels of resolution. By performing high-resolution electron microscopic evaluation of negatively-stained membranes at a series of tilts, a three-dimensional view was obtained.[36] Image projections revealed the presence of multiple bilayer-spanning domains, and atomic force microscopy further defined the orientation and extramembranous dimensions of AQP1.[37] Electron crystallographic analysis of cryopreserved specimens has been undertaken at tilts of up to 60°. These analyses revealed the three-dimensional structure of AQP1 at increasing resolutions, down to 3.8 Å.[38–46] X-ray crystallographic analysis has added further information about the structure of AQP1. Using the above method, the structure of AQP1 has been determined down to a resolution of 2.2 Å.[47] In contrast to the previous studies, the high resolution enables observation of water molecules in transit through the channel. Based on combined efforts, a detailed picture of AQP1s tertiary structure could be formed.

As earlier studies indicated, the AQP1 monomers form a tetrameric cluster. The model shows an extension of the tetramer from the extracellular plane, while the intracellular surfaces form a shallow depression. The N-termini from one monomer is closely situated near the C-termini of the neighboring monomer. The gap formed by the four monomers narrows from 8.5 Å down to 3.5 Å. The residues surrounding the gap are hydrophobic, suggesting an interaction with a hydrophobic molecule.[43] So, despite the monomeric formation of a central cavity, the tetrameric structure does not support the transport of water. This is in agreement with earlier observations, suggesting that each monomer is capable of facilitating water transport.

The dimensions of each monomer are 40 Å across and 60 Å long, as reported by Sui et al.[47] (Figure 41.3). The monomer is composed of six bilayer-spanning alpha helices surrounding a central density. The C loop located on the extracellular surface connects the N-and C-termini halves of the protein. Part of the central density represents the B and E loops, which appear as two short α-helix structures not permeating the

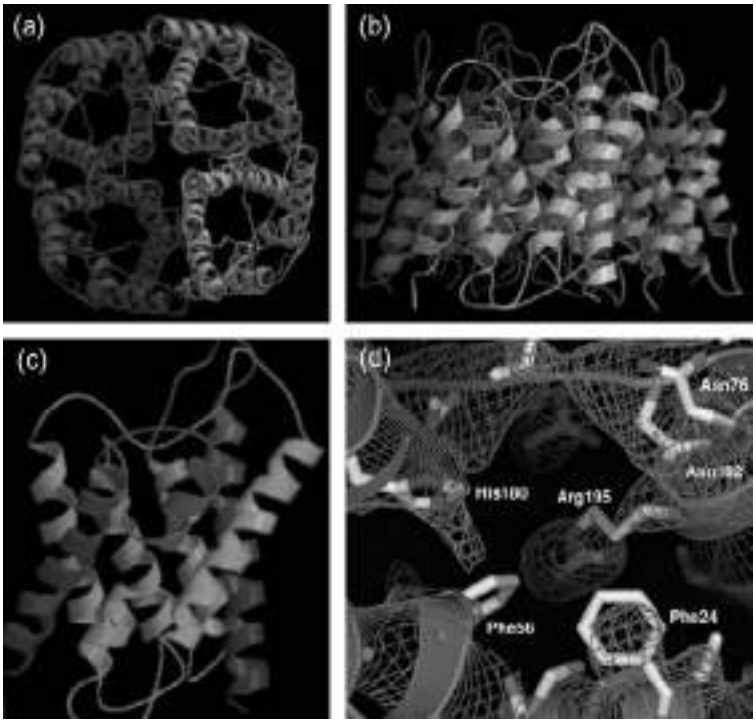

FIGURE 41.3 (a)–(b): Structure of the human AQP1 tetramer, viewed from the top (a) and side (b). (c): Structure of the human AQP1 monomer. (d): Model of the central pore region of human AQP1-EM3 structure (pdb code 1H6I [371] together with the 3.8 Å resolution EM potential map rendered at 1.0s.[43] Several residues critical for AQP1 facilitated water transport are marked *(reproduced and modified with permission from ref. [372]).*

membrane[42] (Figure 41.3). This organization is strikingly similar to the proposed hourglass arrangement of the B and E loops.[32] The NPA containing loops are located on opposite sides of the membrane, juxtapositional to each other, interacting through their NPA motifs. The central density is composed of an extracellular and intracellular vestibule, separated by a narrow pore. The extracellular vestibule is approximately 15 Å at its widest.[47] Following the extracellular vestibule towards the lipid bilayer, a decrease in diameter occurs and the pore becomes exceedingly small.[43,47] The constriction site (also referred to as the aromatic/arginine constriction) is located 20 Å from the beginning of the extracellular vestibule, and is composed of several highly-conserved residues in conventional aquaporins. The constriction site is approximately 2.8 Å wide, about the diameter of a water molecule.[47] After the constriction site the pore continues for 20 Å, a region termed the "selectivity filter".[47] The selectivity filter is slightly wider and part of the region is formed by the helical loops B and E.[43,47] This locates the asparagine residues in the NPA motifs within the selectivity filter.[43,47] Additionally, Cys^{189} in loop E protrudes into the pore, confirming earlier studies, suggesting that $HgCl_2$ sensitivity was due to steric hindrance of water movement through the pore.[32,43,47] Following the pore towards the intracellular vestibule, the diameter increases again, reaching 15 Å[47] (Figure 41.3).

Using molecular dynamic simulations, de Groot and Grubmüller obtained time-resolved, atomic resolution models of water transport through AQP1.[48] From the extracellular vestibule, water molecules enter the constriction site, composed of side chains from the aromatic Phe^{56} and His^{180}, and the charged Arg^{195}. This conformation situates the water molecule, allowing hydrogen bonding with the polar residues, thereby reducing hydrogen bonding between water molecules. In addition, electrostatic repulsion by Arg^{195} suggests that the constriction site is the main site for exclusion of protons (hydronium ions) and other ions.[48] This is further supported by mutagenic analysis of the residues in the constriction site, showing permeation of urea, glycerol, and ammonia in AQP1 when altered. Moreover, replacing Arg^{195} with a valine residue appears to facilitate proton transport.[49] Passing onward through the hydrophobic selectivity filter, exposed polar moieties mainly consisting of backbone carbonyls, lead the water molecules towards the NPA motifs. The water molecule transiently reorientates to bond with the two asparagines residues of the NPA motifs, and is led out of the selectivity filter towards the intracellular vestibule, again by hydrogen bonding with a few selected backbone carbonyls. Hence, the selectivity filter encompassing the highly-conserved NPA motifs appears to serve mainly as a filter for size,[48] while the ar/R constriction is a major checkpoint for solute amd ion permeability. The *Escherichia coli* aquaglyceroporin (GlpF) selectively facilitates glycerol transport over that of water.[50] Evaluation of differences between AQP1 and GlpF using molecular dynamic

simulations revealed a larger selectivity filter in GlpF. Moreover, the preference for glycerol could be explained by what de Groot and Grubmüller describe as a glycerol-mediated "induced fit" gating motion (i.e., glycerol transport serves as the prime mechanism for water exclusion).[48]

Structural characterizations of crystallized human AQP2 in two-dimensional protein–lipid arrays by atomic force microscopy and electron crystallography have revealed the structure of AQP2 at a resolution of 4.5 Å in the membrane plane.[51] As with AQP1, AQP2 is found in a tetrameric assembly in the lipid bilayer.[51,52] The AQP2 monomer shows structural features similar to those earlier reported for AQP1,[51] while structural variation is found around the tetramer's axis.[51,53]

The structure of AQP0 has also been determined down to a resolution of 2.2 Å.[54,55] The water conductance of AQP0 is much lower than that reported for AQP1,[56] possibly due to highly-conserved tyrosine residues in AQP0 imposing further constriction on the channel.[55] The constriction site is smaller than that in AQP1, and the selectivity filter is also narrower.[54,55] Molecular dynamics studies suggest that water movement is facilitated by AQP0 due to thermal motions of certain side chains, although this builds up a free energy barrier, possibly contributing to the lower permeability of AQP0.[57] The extensive analyses of the structure of various AQP isoforms have provided detailed insight into the molecular basis for transmembrane water transport. Future studies aimed at defining the distinct structure of other members, including aquaglyceroporins such as AQP7 and AQP9 that appear to be involved in metabolism rather than water transport may provide further insights. Several studies have also been aimed at identifying novel aquaporin blockers. Although some progress has been reported so far, only a few compounds, including related tetraammonium compounds, have shown selective effects on AQPs.[58–60] Copper[61] and nickel[62] also significantly block aquaporins. Over the past five years the overall structural concepts of aquaporins have been confirmed.[63–74]

DISTRIBUTION OF AQP1 IN KIDNEY AND OTHER TISSUES

Well before recognition of its function, the red cell AQP1 protein was known to be expressed at high levels in the proximal convoluted tubules and descending thin limbs of kidney.[12] This was confirmed with polyclonal rabbit antiserum,[75] and was defined in rat and human kidney with affinity-purified immunoglobulin specific for the N- and C-terminal domains of

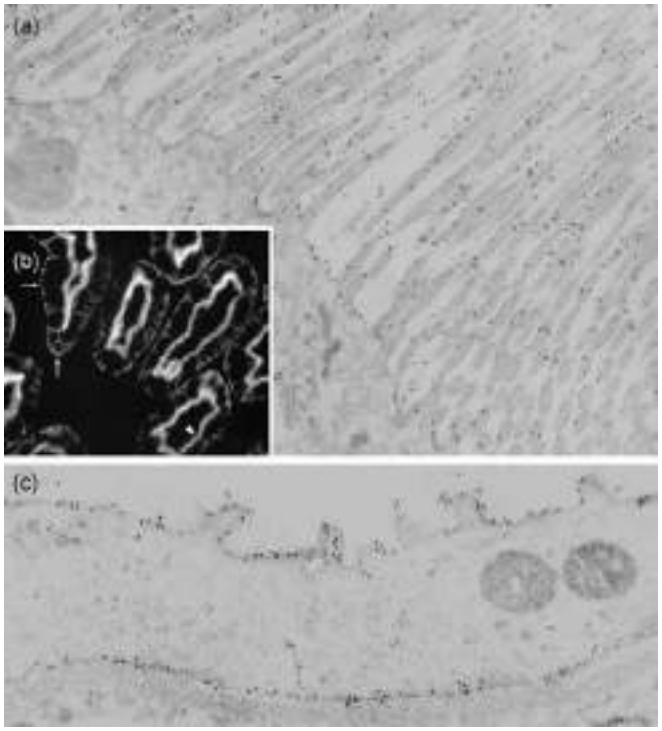

FIGURE 41.4 **Distribution of aquaporin 1 (AQP1) in kidney.** Ultrathin cryosections of rat renal cortex and inner medulla stained with anti-immunogold AQP1. (a): Strong labeling is present over the apical brush border of S3 section of proximal tubule. (b): Strong labeling is present over apical and basolateral membrane of thin descending limb of Henle's loop *(reproduced and modified from ref. [77], with permission).*

AQP1.[76,77] In all studies, AQP1 was demonstrated to be constitutively present in the apical plasma membranes (i.e., the brush borders), and in basolateral membranes of S2 and S3 segment proximal tubules (Figure 41.4). Quantitative immunoblotting indicated that AQP1 makes up 0.9% of total membrane protein from rat renal cortex and 4% of brush border proteins.[77] Enzyme-Linked Immunosorbent Assay (ELISA) measurements of microdissected tubules revealed that proximal tubules contain approximately 20 million copies of AQP1 per cell.[78] Additionally, AQP1 is found in the plasma membrane of glomerular mesangial cells in humans, although not in rat.[76,77,79] Other immunohistochemical and immunogold electron microscopic studies have demonstrated AQP1 in multiple capillary endothelia throughout the body,[80–82] including the renal vasa recta.[83] AQP1 is also abundant in peribronchiolar capillary endothelium, where expression is induced by glucocorticoids,[80,84] apparently acting through the classic glucocorticoid response elements in the *AQP1* gene.[85] In addition, AQP1 has been defined in multiple water-permeable epithelia including choroid plexus, peritoneal mesothelial cells,[86] fetal

membranes,[87] at multiple locations in eye, including ciliary epithelium, lens epithelium, and corneal endothelium,[81,88,89] and in hepatobiliary epithelium,[90] pancreatic interlobular ducts,[91] heart and skeletal muscle,[92] gall bladder,[93] salivary glands,[94] inner ear,[95] and several other organs including the nervous system (see review [96]). AQP1 has also been localized in tumor cells and their vasculature.[97] Developmental expression of AQP1 is complex: transient expression occurs in some tissues before birth; expression in other tissues is subsequent to birth; constitutive life-long expression is found in other tissues.[84,98,99]

AQP1 DEFICIENCY

Humans have been identified who totally lack the AQP1 protein. The human *AQP1* gene was localized to chromosome 7p14 and the Co blood group antigens were previously linked to 7p, suggesting a molecular relationship. It was determined that the Co blood group antigen results from an Ala/Val polymorphism at the extracellular surface of red cell AQP1[100] (Figure 41.1). Although the International Blood Group Referencing Laboratory in Bristol, England, has detailed phenotyping information on millions of donors worldwide, only six individuals had been shown to lack Co. Most of these Co-null individuals are women who developed anti-Co during pregnancy. Three of these Co-null individuals were found to have mutations in the *AQP1* gene.[101] Although the exceedingly rare blood group phenotype makes them impossible to match for blood transfusion, it was surprising that none of them exhibited any other obvious severe clinical phenotype. The extreme rarity of the Co-null state may reflect an important developmental role, resulting in reduced fetal survival; however, the frequency of the heterozygous state is unknown. Detailed studies of the urinary concentrating ability of Co-null individuals revealed a marked inability of the individuals to concentrate urine to more than 400 mOsm/l, even in the presence of dehydration or dDAVP treatment, revealing a significant urinary concentrating defect.[102] Moreover, Co-null individuals display reduced pulmonary vascular permeability.[103]

The development of *AQP1* gene knockout mice has provided further insights into the role of AQP1 in renal water homeostasis. AQP1-null ($AQP1^{-/-}$) mice appeared moderately polyuric under basal conditions. However, $AQP1^{-/-}$ animals exhibited an extreme degree of polyuria and polydipsia when undergoing water deprivation, including rapid hyperosmolar extracellular fluid volume depletion.[104] Additionally, $AQP1^{-/-}$ mice failed to respond appropriately to vasopressin, suggesting that renal water conservation and urinary concentration is highly dependent on AQP1 protein.[104] Detailed classic *in vivo* and *in vitro* physiological evaluation of proximal tubules from the $AQP1^{-/-}$ mice established that transepithelial water permeability was reduced by 80%, and led to an approximate 50% decrease in proximal tubule fluid reabsorption.[105] The apparent differences in transepithelial water permeability and proximal tubule fluid reabsorption are likely dependent on the generation of a hypotonic filtrate in proximal tubules of $AQP1^{-/-}$ mice.[106] Despite these observations, distal fluid delivery in $AQP1^{-/-}$ remained unchanged, due to a compensatory reduction in single nephron glomerular filtration.[105] When blunting the TGF response, and thereby the compensatory reduction in glomerular filtration observed in $AQP1^{-/-}$ mice, ambient urine osmolalities and urinary flow rates appeared no different from normal $AQP1^{-/-}$ mice, probably due to distal tubular compensatory mechanisms.[107] The impaired proximal fluid reabsorption observed in $AQP1^{-/-}$ mice, albeit with normal distal fluid delivery, suggests that the polyuric phenotype largely depends on a concentrating defect impairing collecting duct water reabsorption

Studies using isolated perfused thin descending limbs have revealed that the osmotic water permeability of the type II thin descending limbs (outer medullary thin descending limbs from long loop nephron) is decreased by 90% relative to wild-type values in kidneys from AQP1 knockout mice.[108] Additionally, earlier observations using freeze-fracture electron microscopic techniques showed a remarkably high density of intramembrane particles in the thin descending limb of rat, which has been attributed to the tetrameric assembled AQP1 subunits.[33] In the thin descending limb of $AQP1^{-/-}$ mice, the abundance and size of these intramembrane particles was markedly reduced.[108] Moreover, the distribution of AQP1 in the vasa recta suggests a role in microvascular exchange, hence affecting urinary concentration. In the presence of a NaCl gradient, osmotic water permeability was almost eliminated in the descending vasa recta of $AQP1^{-/-}$ mice, leading to a predicted reduction in medullary interstitial osmolality and likely an impairment of countercurrent multiplication.[109] Additional studies using adenoviral gene delivery restored AQP1 protein expression in the proximal tubule epithelia and renal microvessels of $AQP1^{-/-}$ knockout mice, albeit not in the descending thin limbs. The adenovirus-treated mice showed slight restoration of the concentrating defect during water deprivation, probably due to reinsertion of AQP1 water channels in the vasa recta, although urinary concentrating ability was still highly insufficient in comparison to wild-type mice.[110] In conclusion, the severe concentrating defect seen in the $AQP1^{-/-}$ mice primarily results from impaired water

absorption in the thin descending limb, underlining the necessity for a constitutively high water permeability in this segment for a functional countercurrent multiplication system.

ADDITIONAL FUNCTIONS OF AQP1

AQP1 is generally believed to be a constitutively active, water-selective pore. Nonetheless, some observations contradict this. A small degree of permeation by glycerol has been seen in oocytes which may represent opening of an unidentified leak pathway,[111] and the biologic significance remains unclear.[21] Forskolin was reported to induce a cation current in AQP1-expressing oocytes,[112] but multiple other scientific groups have failed to reproduce this effect.[113] Although small changes in water permeability by oocytes expressing a bovine homolog of AQP1 have also been ascribed to vasopressin and atrial natriuretic peptide, the significance is uncertain.[114] Likewise, secretin-induced membrane trafficking has been noted in isolated cholangiocytes[115,116]; however, this awaits confirmation by immunoelectron microscopy. Permeation of AQP1 by CO_2 has also been evaluated. Rates of pH change are about 40% higher in oocytes expressing AQP1[117] than in control oocytes. Although the background permeation of lipid bilayers by CO_2, as well as oxygen, ammonia, nitric oxide, and other gases, may be high,[118] the potential physiological relevance of AQP1 permeation by gases warrants more study (see review [119]). Additionally, AQP1 appears to play a role in cell migration.[120] $AQP1^{-/-}$ mice implanted with tumor cells show reduced tumor vascularity and growth, thus leading to improved survival in comparison to wild-type mice. Moreover, *in vitro* analysis of endothelial cells isolated from $AQP1^{-/-}$ mice showed marked impairment in cell migration.[120] In primary cultures of proximal tubule cells from $AQP1^{-/-}$ mice, *in vitro* cell migration was impaired compared to $AQP1^{+/+}$ mice. Furthermore, in an ischemia–reperfusion model of acute renal tubular injury, $AQP1^{-/-}$ mice showed more severe pathological changes, including more prominent tubule degeneration.[121] Thus, although the evidence that AQP1 functions as a water channel is incontrovertible, the possibility of yet undiscovered transport functions cannot be excluded.

AQUAPORINS IN KIDNEY

The first functional definition of one member of a protein family often prompts a search for related proteins. This has certainly been the case for the aquaporins, and the homology cloning approach has been undertaken by multiple laboratories whose combined efforts have expanded the aquaporin family membership list. Homology cloning has most frequently been undertaken by using polymerase chain amplification with degenerate oligonucleotide primers.[122] Thirteen mammalian aquaporins are now known, and they form at least two subgroups: water-selective channels (orthodox aquaporins) and channels permeated by water, glycerol, and other small molecules (aquaglyceroporins). Given the large potential for confusion, the Human Genome Organization has established an Aquaporin Nomenclature System,[117] accessible by internet (http://www.gene.ucl.ac.uk/nomenclature). Of the known aquaporins, eight are expressed in mammalian kidney (Table 41.1). Soon after AQP1 was discovered to be a water channel, AQP2 was identified in renal collecting duct,[123] where it is regulated by vasopressin and is involved in multiple clinical disorders (Table 41.2). AQP3 was identified in kidney and other tissues, and was found to be permeated by glycerol and water.[124–126] AQP4, a $HgCl_2$-insensitive water channel is most abundantly expressed in brain, and is present in kidney collecting duct in the basolateral plasma membrane of principal and IMCD cells and in other tissues, but it is not inhibited by mercury.[127,128] AQP6 was identified at the cDNA level and found to be localized in intracellular vesicles in the collecting duct intercalated cells in the kidney.[129–131] AQP7 is permeated by water and glycerol.[132,133] First cloned from testis,[132] AQP7 is present in segment 3 proximal tubule brush border membranes, where it facilitates glycerol and water transport.[134] AQP8 is a $HgCl_2$-sensitive water channel found in intracellular domains of proximal tubule and collecting duct cells[135,136]; however, its function remains unclear. AQP11 is found in the cytoplasm of renal proximal tubule cells.[137] The exact function is not established, although deletion of the *AQP11* gene produces a severe phenotype with renal vacuolization and cyst formation.[137]

Localization and Function of AQP2, AQP3, AQP4, AQP6, AQP7, AQP8, and AQP11 in Kidney

The amino acid sequences of the N-and C-termini of the different aquaporins are not closely related, and specific polyclonal antibodies can be raised in rabbits immunized with synthetic peptides conjugated to carrier proteins such as keyhole limpet hemocyanin. As with AQP1, these antibodies have permitted localization of the other aquaporins in kidney by immunocytochemistry, immunoelectron microscopy, and single

TABLE 41.1 Aquaporins in Kidney

AQP	Localization (renal)	Subcellular Distribution	Regulation	Localization (extrarenal)
AQP1	S2, S3 segments of proximal tubules	Apical and basolateral plasma membranes	Glucocorticoids (peribronchiolar capillary endothelium)	Multiple tissues, including capillary endothelia, choroids plexus, ciliary and lens epithelium, etc.
AQP2	Collecting duct principal cells	Intracellular vesicles, apical plasma membrane	Vasopressin stimulates short-term exocytosis long-term biosynthesis	Epididymis
AQP3	Collecting duct principal cells	Basolateral plasma membrane	Vasopressin stimulates long-term biosynthesis	Multiple tissues, including airway basal epithelia, conjunctiva, colon
AQP4	Collecting duct principal cells	Basolateral plasma membrane	Dopamine, protein kinase C	Multiple tissues, including central nervous system astroglia, ependyma, airway surface epithelia
AQP6	Collecting duct intercalated	Intracellular vesicles	Rapidly gated	Unknown
AQP7	S3 proximal tubules	Apical plasma membrane	Insulin (adipose tissue)	Multiple tissues, including adipose tissue, testis, and heart
AQP8	Proximal tubule, collecting duct cells	Intracellular domains	Unknown	Multiple tissues, including gastronintestinal tract, testis, and airways
AQP11	Proximal tubule	Intracellular domains	Unknown	Multiple tissues, including liver, testes, and brain

AQP, aquaporin.

tubule microdissection combined with ELISA (Figure 41.5).

Three aquaporins (AQP2, AQP3, and AQP4) are expressed in the collecting duct principal cells and the connecting tubule segment, sites where vasopressin regulates epithelial water permeability. AQP2 is located in the apical plasma membrane and small intracellular vesicles of collecting duct principal cells[138] (Figure 41.6). ELISA measurements of microdissected rat collecting ducts have revealed that AQP2 is an extremely abundant protein in the collecting duct, with more than six million copies per cell throughout the collecting duct system.[139] Additional studies using the single-tubule ELISA method and immunocytochemistry demonstrated co-localization of AQP2 and V2 vasopressin receptor expression on connecting tubule arcades, suggesting that regulated water transport may occur in the arcades of the cortical labyrinth in addition to the collecting duct.[139,140] Additionally, AQP2 has been identified in the basolateral membranes of connecting tubules and inner medullary collecting ducts.[141]

The apical plasma membrane is the rate-limiting barrier for transepithelial water transport across the collecting duct principal cell, and is the site where vasopressin regulates water permeability.[142] Localization of AQP2 in the apical plasma membrane suggested that it is the target for vasopressin-regulated collecting duct water permeability (Figure 41.6). This conclusion was firmly established by multiple studies. A direct correlation between AQP2 expression and collecting duct water permeability has been demonstrated in Brattleboro rats, which lack circulating vasopressin owing to a mutation in the gene encoding vasopressin precursor protein.[143] Likewise, human patients with mutations in the *AQP2* gene manifest severe vasopressin-resistant nephrogenic diabetes insipidus,[144] demonstrating the requirement for AQP2 in collecting duct water transport. Lack of functional AQP2 expression in mice, by generation of *AQP2* gene knockouts, produces a severe concentration defect, resulting in early postnatal death.[145,146] Moreover, morphological changes including renal medullary atrophy and dilation of the collecting ducts is observed in these mice.[145,146] Generation of $AQP2^{-/-}$ knockouts selectively in the collecting ducts, but not in the connecting tubule segments, rescues mice from the lethal phenotype; however, body weight, urinary production, and the response to water deprivation is still severely impaired.[145] Additionally, in a tamoxifen-inducible mouse model of AQP2 gene deletion, adult mice present with severe polyuria, a marked urinary concentration defect, and develop mild renal damage.[147] Together these studies demonstrate the pivotal role of AQP2 in urinary concentration.

AQP3 is localized in a large variety of organs and highly-expressed in the kidney. AQP3 was originally cloned from rat kidney,[124–126] and when expressed in *Xenopus* oocytes it facilitated glycerol transport (discussed below) and increased $HgCl_2$-sensitive osmotic water permeability.[148–150] Moreover, channel-gating is

TABLE 41.2 Water-balance Disorders Associated with Aquaporin Abnormalities

Congenital defects
Central diabetes insipidus
Mutation in gene encoding vasopressin (Brattleboro rat)
Nephrogenic diabetes insipidus
Mutations in gene encoding V_2 receptor (human, X-linked)
Mutations in gene encoding aquaporin-2 (human, dominant and recessive)
Partial concentration defects
Targeted disruption of gene encoding aquaporin-1 (mouse)
Targeted disruption of gene encoding aquaporin-4 (mouse)
Acquired defects
Lithium treatment
Hypokalemia
Hypercalcemia
Postobstructive nephropathy, unilateral or bilateral
Conditions with water retention
Congestive heart failure
Hepatic cirrhosis
Nephritic syndrome
Pregnancy
Other conditions
Syndrome of inappropriate vasopressin secretion
Primary polydipsia
Chronic renal failure
Acute renal failure
Low-protein diet
Age-induced reduction in renal concentration

regulated by protons and copper.[61,150] AQP4 was found to be expressed in several tissues with high abundance in the brain. In oocyte expression studies, the protein increased osmotic water permeability in a $HgCl_2$-insensitive manner.[127,149]

AQP3 and AQP4 are also present in the connecting tubule and collecting duct principal cells; however, the sites where they are expressed do not overlap with the expression of AQP2 in most portions of the collecting duct.[140,151–153] AQP3 and AQP4 are restricted to the basolateral plasma membranes of collecting duct principal cells, where they are presumed to permit water entry into the interstitium. Although both are basolateral water channels, they are distributed differently along the collecting duct system, with the greatest abundance of AQP3 in cortical and outer medullary collecting ducts, and the greatest abundance of AQP4 in inner medullary collecting duct.[153] AQP4 is also found in basolateral membranes of proximal tubule S3 segments, although only in mice.[154] Using freeze-fracture electron microscopy, orthogonal arrays of intramembrane particles (OAP) were demonstrated in the basolateral membranes of the proximal tubule S3 segment in $AQP4^{+/+}$, but not in $AQP4^{-/-}$, mice.[154] AQP4 is expressed in two splice isoforms, the M1 and M23 splice variants. The M23-AQP4 appears to be the OAP-forming water channel when expressed in LLC-PK1 cells. When organized in OAPs, a significantly higher single-channel water permeability coefficient is observed in comparison to the non-AOP forming M1-AQP4.[141,155] Shuttling of AQP3 or AQP4 is not expected to occur, as the predominant fraction is found in the plasma membrane (short- and long-term regulation of these aquaporins will be discussed later). Sodium restriction or aldosterone infusion in normal and Brattleboro rats greatly increases the abundance of AQP3, while AQP3 abundance is markedly reduced during aldosterone deficiency, suggesting a direct effect of aldosterone on collecting duct AQP3 expression.[156] AQP4 appears to be regulated by PKC and dopamine, where stimulation by these factors decreases water permeability in AQP4 transfected cells.[157]

Deletion of the *AQP3* gene induces polyuria and polydipsia and a marked reduction in osmotic water permeability in the basolateral plasma membrane of the cortical collecting duct.[148] Moreover, urinary osmolality is reduced in $AQP3^{-/-}$ mice and they fail to respond appropriately to dDAVP, thus presenting with a urinary concentrating defect.[148] Targeted disruption of AQP4 in mice results in a 75% reduction in the osmotic water permeability of the inner medullary collecting duct.[158] However, phenotypically the $AQP4^{-/-}$ mice appeared grossly normal, presenting with a very mild urinary concentrating defect.[159] In double $AQP3^{-/-}/AQP4^{-/-}$-knockout mice, concentrating ability was only slightly more impaired than in the $AQP3^{-/-}$ mice.[148] It should be noted that the localization of AQP2 in basolateral membranes in both the connecting tubule and inner medullary collecting duct raises the possibility that the observed effect is partly compensated by this mechanism.[141]

AQP6 vesicles reside in subapical vesicles within intercalated cells of the collecting duct, where it is co-expressed with the V-type H^+-ATPase.[131,160] AQP6 appears functionally distinct from other known aquaporins. Oocyte expression studies have revealed low water permeability of AQP6 during basal conditions, while in the presence of $HgCl_2$ a rapid increase in water permeability and ion conductance is observed.

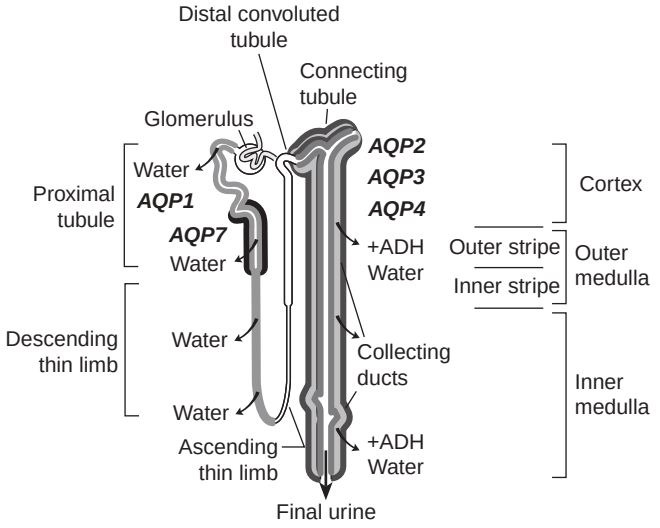

FIGURE 41.5 **Sites of aquaporin (AQP1) expression in kidney and segmental water-transport function.** Proximal nephron: AQP1 is present in apical and basolateral plasma membranes of proximal tubules and thin descending limbs. AQP6 is present in intracellular vesicles of collecting duct intercalated cells. AQP7 is present in proximal tubules. Distal nephron: aquaporins are not present in ascending limbs. Collecting duct: AQP2 is present in intracellular vesicles and apical plasma membranes of principal cells; AQP3 and AQP4 are present in basolateral membranes. AQP6 is present in intracellular vesicles in type A intercalated cells.

Additionally, reductions in pH (below 5.5) quickly and reversibly increase anion conductance and water permeability in AQP6 expressing oocytes.[160] Subsequent studies have shown that the channel is permeable to halides, with the highest permeability to NO_3^-,[160,161] while the ionic selectivity becomes less specific after the addition of $HgCl_2$.[162] Moreover, when Asn^{60}, a residue unique in mammalian AQP6, is converted to glycine, a highly-conserved residue in other mammalian aquaporins, anionic permeability is abolished and osmotic water permeability is increased during basal conditions.[163]

AQP7 is a member of the aquaglyceroporin family, and was originally cloned from rat testis.[132] Additionally, AQP7 is expressed in several organs, including adipose tissue and kidney.[132,164] In the kidney, AQP7 localizes to the brush border membrane of the proximal tubule S3 segment.[165,166] Expression of AQP7 in *Xenopus* oocytes showed that AQP7 facilitated the transport of glycerol and urea in addition to water.[132] The development of AQP7 knockout mice has aided understanding of the physiological role of AQP7. Glycerol excretion is markedly increased in $AQP7^{-/-}$ mice, suggesting a role for AQP7 in facilitating proximal tubular glycerol transport, and possibly renal gluconeogenesis (discussed below).[134] In terms of water transport, $AQP7^{-/-}$ mice experience only a slight reduction in proximal tubule membrane water permeability, and AQP7/AQP1 double knockout mice showed only a slightly more severe urinary concentrating defect than $AQP1^{-/-}$ mice during water deprivation.[134] Additionally, evaluation of the channels' permeability to urea in $AQP7^{-/-}$ mice revealed no change in urinary urea excretion or urea accumulation in the papilla, indicating a less prominent physiological role in urea transport.[134] Expression of AQP7 in *Xenopus* oocytes increases the permeability to arsenite, thereby providing a possible route for arsenite uptake in mammalian cells[167]; the physiological role of these observations awaits further investigation.

Cloning of the murine AQP8 water channel[136,168,169] revealed its presence in many organs, including the kidney.[135,136,168,169] In kidney, AQP8 localizes to intracellular domains of proximal tubule and collecting duct cells.[135] Expression of AQP8 in *Xenopus* oocytes increased $HgCl_2$-sensitive osmotic water permeability. Additionally, oocyte expression of AQP8 showed permeability to urea.[136] Targeted deletion of the *AQP8* gene produced a mild phenotype in $AQP8^{-/-}$ mice, with no obvious changes in renal parameters.[170] Subsequent studies have suggested that AQP8 facilitates NH_3 transport in *Xenopus* oocytes[171,172] and in ammonia transport-deficient yeast.[173] In $AQP8^{-/-}$ mice, ammonia-loading mildly reduced hepatic ammonia accumulation and increased renal ammonia excretion,[174] indicating that AQP8 does not play a significant physiological role in facilitated NH_3 transport.

Recently a new aquaporin was cloned from rat testis, namely AQP11.[168] This AQP has only one NPA motif, and shares low similarity with the conventional aquaporins. AQP11 is most abundantly expressed in the testis, kidney, and liver.[168] In the kidney, the AQP11 protein localizes to the cytoplasm of the renal proximal tubules.[137] While lack of plasma membrane expression of the AQP11 protein in *Xenopus* oocytes greatly impaired measurements of transport,[137] targeted deletion of the *AQP11* gene in mice resulted in a severe phenotype with vacuolization and cyst formation in the proximal tubule. The $AQP11^{-/-}$ mice died of renal failure and kidneys were polycystic. The cyst epithelia contained vacuoles, and the $AQP11^{-/-}$ mice also presented with a proximal tubular endosomal acidification defect.[137]

AQUAGLYCEROPORINS

AQP3, AQP7, and AQP9 constitute a subgroup of aquaporins with a broader permeation range that includes glycerol, hence the name "aquaglyceroporins." AQP3, which transports water and glycerol, was cloned by three groups at the same time.[124–126] The

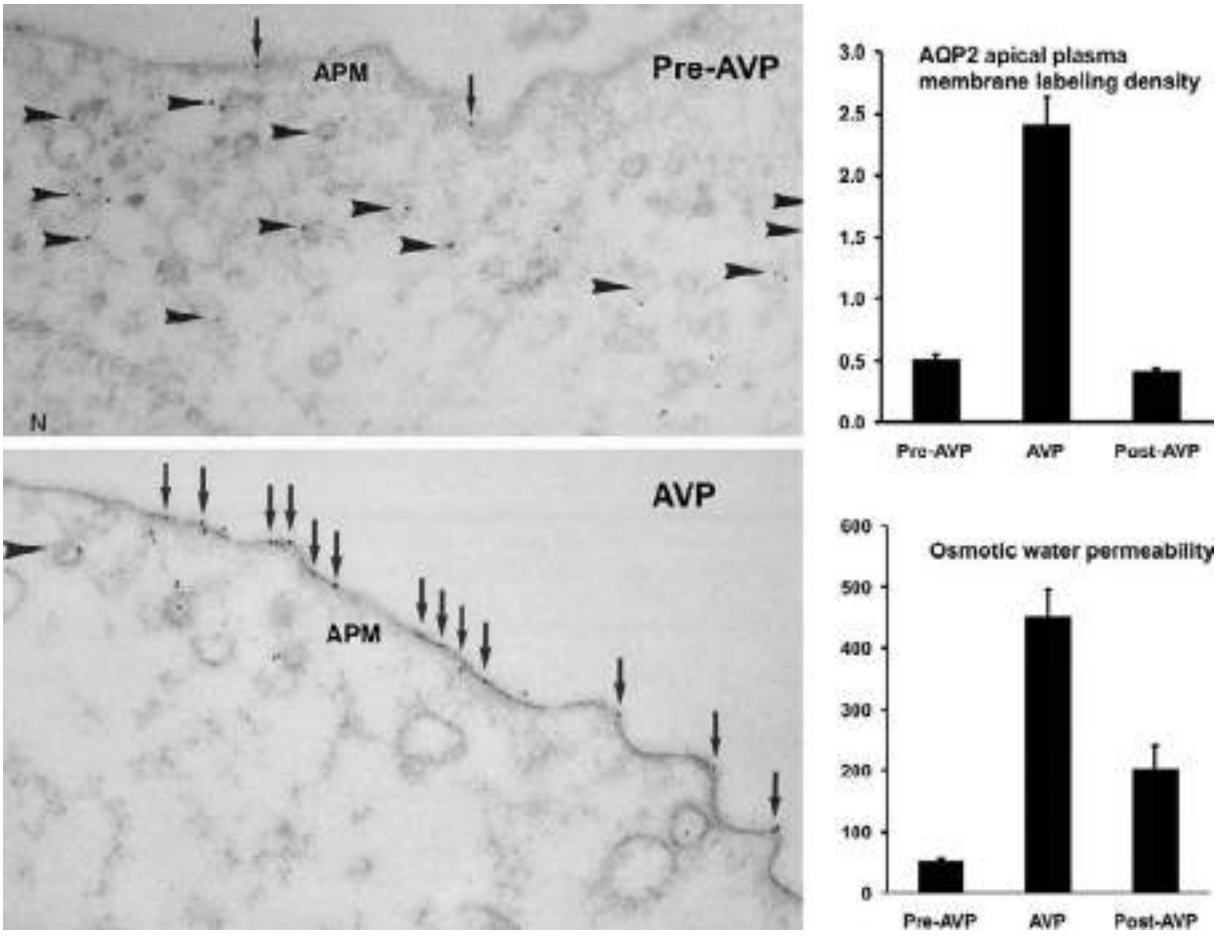

FIGURE 41.6 **Vasopressin-induced trafficking of aquaporin 2 (AQP2) in isolated, perfused rat collecting duct and resulting changes in water permeability.** Anti-AQP2 immunogold electron microscopy of ultrathin cryosections of isolated rat collecting duct fixed before exposure to arginine vasopressin (pre-AVP, top left), and after exposure (AVP, bottom left). Note intracellular AQP2 (arrowheads) and plasma membrane AQP2 (small arrows). Quantification of AQP2 labeling density before, during or after vasopressin exposure (top right). Quantification of osmotic water permeability of isolated collecting duct (bottom right) (Nucleus: N; mitochondrion: M; × 50,000) *(reproduced and modified from ref. [182], with permission).*

distribution at multiple sites, including the kidney collecting duct principal cells, airway epithelia, skin, urinary bladder, and secretory glands, suggests several functions.[151,152,175] AQP3-null mice exhibit a nephrogenic diabetes insipidus phenotype; however, human mutants have not yet been reported. AQP7 is also permeated by water and glycerol, and is localized to the apical brush border of the proximal tubules, especially to the S3 segment. Recent studies have indicated that AQP7 may play a role in glycerol metabolism by showing adaptation to fasting by glycerol transport through AQP7 in adipose tissue.[176] AQP7$^{-/-}$ mice have a significantly lower plasma glycerol concentration than wild-type mice, and impaired adipocytic glycerol release in response to a β3 receptor stimulation.[176] Moreover, AQP7$^{-/-}$ mice experience severe hypoglycemia, but show normal hepatic gluconeogenesis during fasting, indicative of defective adipocytic glycerol transport in these mice.[176] Glycerol excretion is also markedly increased in AQP7$^{-/-}$ mice, suggesting a role for AQP7 in facilitating proximal tubular glycerol transport.[134] AQP9, which is expressed in the liver but not in kidney,[177–179] is permeated by a range of solutes including glycerol and urea.[180] Recently, it has been demonstrated that expression of AQP9 in liver was induced up to 20-fold in rats fasted for 24–96 hours, and that AQP9 levels gradually declined after re-feeding.[181] This indicates that the liver takes up glycerol for gluconeogenesis through AQP9 during starvation.

VASOPRESSIN REGULATION OF KIDNEY AQUAPORINS

Of all the aquaporins, AQP2 has invoked the largest interest by nephrologists, because it is expressed

in principal cells of the renal collecting duct, where it is the primary target for short-term regulation of collecting duct water permeability.[182–184] AQP2 and AQP3 are also regulated either directly or indirectly by vasopressin through long-term effects that alter the abundance of these water-channel proteins in collecting duct cells.[138,143,151,185–187]

Short- and Long-Term Regulation of Water Permeability in the Collecting Duct

Two modes of vasopressin-mediated regulation of water permeability have been identified in the renal collecting duct. Both involve regulation of the AQP2 water channel. Short-term regulation is the widely recognized process by which vasopressin rapidly increases water permeability of principal cells by binding to vasopressin V2-receptors at the basolateral membranes, a response measurable within 5 to 30 minutes after increasing peritubular vasopressin concentration.[188,189] It is believed that vasopressin, acting through a cyclic adenosine monophosphate (cAMP) cascade, causes intracellular AQP2 vesicles to fuse with the apical plasma membrane, which increases the number of water channels in the apical plasma membrane (Figures 41.6 and 41.7). Long-term regulation of collecting duct water permeability is seen when circulating vasopressin levels are increased for 24 hours or more, resulting in an increase in the maximal water permeability of the collecting duct epithelium.[185] This response is a consequence of an increase in the abundance of AQP2 water channels per cell in the collecting duct,[138,143] apparently due to increased transcription of the *AQP2* gene (Figure 41.7).

Short-Term Regulation of AQP2 by Vasopressin-Induced Trafficking

The final concentration of the urine depends on the medullary osmotic gradient built up by the loop of Henle, and the water permeability of the collecting ducts through the cortex and medulla (see review [190]). Collecting duct water permeability is regulated by vasopressin, and it has been suspected for many years on the basis of indirect biophysical evidence that the vasopressin-induced increase in water permeability depended on the appearance of specific water channels in the apical plasma membrane of the vasopressin-responsive cells. Molecular actions of vasopressin to increase epithelial water permeability were first demonstrated in the 1950s and early 1960s in the skin and urinary bladder of amphibia.[191,192] Direct demonstrations that vasopressin rapidly increases water permeability of isolated collecting ducts were made during the next few years.[193,194] These studies, undertaken with *in vitro* preparations, showed that vasopressin applied to the basolateral aspect of the collecting duct cells directly increased transepithelial osmotic water permeability within minutes. Kinetic studies in isolated perfused inner medullary collecting ducts revealed an increase in osmotic water permeability after only 40 seconds of incubation at 37°C, and half of the maximal water permeability was reached within 10 minutes.[189,195] cAMP has been implicated in the regulatory process, because direct application of cAMP analogs to the collecting duct was found to mimic the short-term effects of vasopressin.[193]

Multiple studies with affinity-purified polyclonal antibodies to AQP2 have unequivocally established that AQP2 is specifically involved in vasopressin-induced increases of renal collecting duct water permeability. Soon after isolation of the AQP2 cDNA and generation of specific antibodies,[123] immunoperoxidase microscopy and immunoelectron microscopy clearly demonstrated that principal cells within renal collecting ducts contain abundant AQP2 in the apical plasma membranes and in subapical vesicles.[138,143] These studies strongly supported the "shuttle hypothesis" originally proposed more than a decade earlier.[196] This hypothesis proposed that water channels can shuttle between an intracellular reservoir in subapical vesicles and the apical plasma membrane, and that vasopressin alters water permeability by regulating the shuttling process.[8] Shuttling of AQP2 was directly demonstrated in isolated perfused tubule studies.[182] In these studies, water permeability of isolated perfused collecting ducts was measured before or after stimulation with vasopressin, and the tubules were fixed directly for immunoelectron microscopic examination (Figure 41.6). Vasopressin stimulation resulted in a markedly decreased immunogold labeling of intracellular AQP2, accompanied by a five-fold increase in the appearance of AQP2 immunogold particles in the apical plasma membrane. This redistribution was associated with an increase in osmotic water permeability of similar magnitude. These findings were reproduced *in vivo* by injecting rats with vasopressin, which also caused redistribution of AQP2 to the apical plasma membrane of collecting duct principal cells.[183,197] In contrast to the effect of vasopressin treatment, removal of vasopressin led to a reappearance of AQP2 in intracellular vesicles, and a decline in osmotic water permeability in the isolated perfused collecting duct system[182,186] (Figure 41.6). Moreover, the off-set response to vasopressin has been examined *in vivo* by acute treatment of rats with vasopressin-V_2-receptor antagonist[198,199] or acute water-loading (to reduce endogenous vasopressin levels[200]). These treatments (both reducing

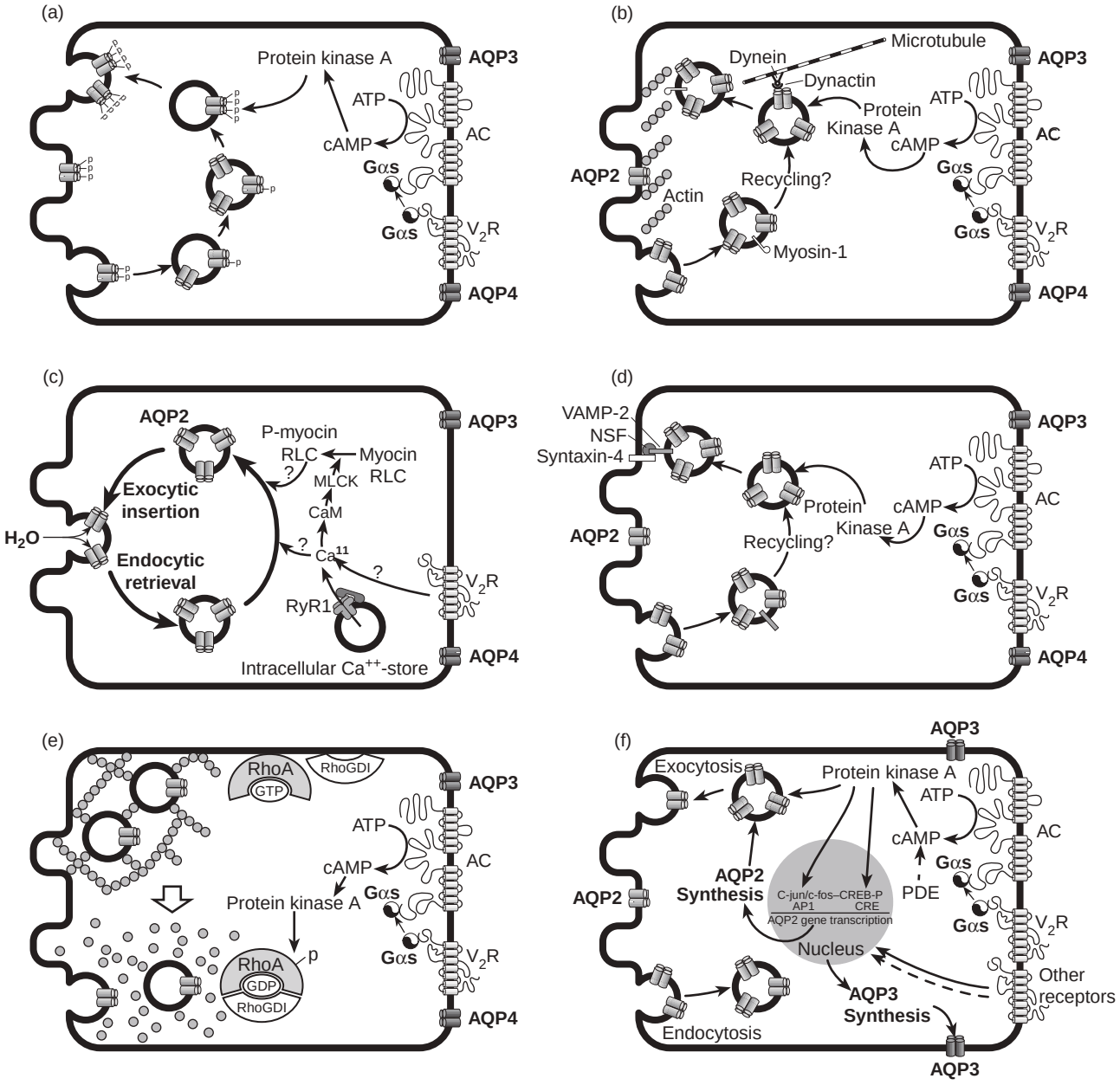

FIGURE 41.7 **Regulation of AQP2 trafficking (Panels a–e), and expression (Panel F) in collecting duct principal cells.** (a):Vasopressin binding to basolateral G-protein-linked V2-receptor stimulates adenylyl cyclase (AC); cyclic adenosine monophosphate (cAMP) activates protein kinase A to phosphorylate AQP2 in intracellular vesicles; phosphorylated AQP2 is exocytosed to the apical plasma membrane, resulting in increased apical membrane water permeability. (b): Overview of cytoskeletal elements, which may be involved in AQP2-trafficking. AQP2-containing vesicles may be transported along microtubules by dynein/dynactin. The cortical actin web may act as a barrier to fusion with the plasma-membrane. (c): Intracellular calcium signaling and AQP2-trafficking. Increases in intracellular Ca^{2+} concentration may arise from stimulation of the V2 receptor. The existence and potential role of other receptors and pathways, e.g., VACM-1, in Ca^{2+} mobilization is still uncertain. The downstream targets of the calcium signal are unknown, and conflicting data exist on the importance of a rise in intracellular Ca^{2+} for the hydrosmotic response to vasopressin. (d): Vesicle-targeting receptors and AQP2-trafficking. AQP2 vesicles dock at the apical membrane by association of VAMP-2 with syntaxin-4 targets in the presence of NSF; the exact role of these remains to be established. (e): Changes in the actin cytoskeleton associated with AQP2-trafficking to the plasma membrane. Inactivation of RhoA by phosphorylation and increased formation of RhoARhoGDI complexes seem to control the dissociation of actin fibers seen after vasopressin stimulation. (f): Specifically, cAMP participates in the long-term regulation of AQP2 by increasing the levels of the catalytic subunit of PKA in the nuclei, which is thought to phosphorylate transcription factors such as CREB-P (Cyclic AMP Responsive Element Binding Protein) and C-Jun/c-Fos. Binding of these factors are thought to increase gene transcription of AQP2, resulting in synthesis of AQP2 protein which in turn enters the regulated trafficking system. In parallel, AQP3 and AQP4 synthesis and trafficking to the basolateral plasma membrane takes place. Importantly, AQP2 regulation can be modified by a number of hormones including dopamine, ANP, PGE2, and adrenergic hormones. See text for details (Vasopressin-V2-receptors: V2R; adenylyl cyclase: AC; cAMP and protein kinase A: PKA) *(redrawn and modified from ref. [190]).*

vasopressin action) resulted in a prominent internalization of AQP2 from the apical plasma membrane to intracellular subapical vesicles, further underscoring the role of AQP2 trafficking in the regulation of collecting duct water permeability and the reversibility of AQP2 trafficking to the plasma membrane.

The quantity of AQP2 in the apical plasma membrane is determined by the relative rates of exocytosis and endocytosis. Both processes occur continuously, and their relative rates are regulated to effect changes in water permeability. Kinetic evidence indicates that vasopressin regulates both endocytosis and exocytosis of apical water channels.[195,201] These conclusions are supported by multiple earlier experiments with fluid-phase markers, which assessed rates of internalization of the apical plasma membrane.[202–204] Intravenous injection of horseradish peroxidase was followed by uptake of the material into intracellular vesicles and multivesicular bodies by collecting duct principal cells.[202] When compared with normal rats, the rate of uptake by vasopressin-deficient Brattleboro rats was much lower; however, this difference was lost after administration of vasopressin, presumably reflecting an effect of vasopressin in accelerating exocytosis, followed by a secondary increase in the rate of endocytosis to re-establish the steady-state. These observations were supported by studies with fluorescein-labeled dextrans,[203] which confirmed that vasopressin enhances the rate of endocytosis of the apical plasma membrane under steady-state conditions. In apparent contrast, removal of vasopressin from isolated perfused rabbit cortical collecting ducts also was accompanied by increased endocytosis of horseradish peroxidase from the lumen, and it was suggested that water channels would also be internalized at an increased rate.[204] Similar results were obtained in isolated rat inner medullary collecting duct, which showed that vasopressin washout was associated with increased appearance of albumin-gold or cationic ferritin in small apical vesicles and multivesicular bodies.[205] Presumably this response reflects a direct effect of vasopressin to decrease the intrinsic rate of endocytosis and is reversed on vasopressin removal. Therefore, it appears that two factors affect the rate of endocytosis of the apical plasma membrane of collecting duct principal cells: (1) vasopressin directly decelerates endocytosis by unknown mechanisms; and (2) vasopressin indirectly accelerates the rate of endocytosis by stimulating exocytosis and increasing the total amount of apical plasma membrane. The latter effect is believed to be slower than the former, resulting in a biphasic decline in water permeability on vasopressin removal.[195,201] Other studies have demonstrated that apical endocytosis is most rapid at about 3 to 5 minutes after vasopressin washout from isolated perfused inner medullary collecting ducts,[205] corresponding to the period of the most rapid decrease in transepithelial water permeability.[195,201] Thus, the results taken together strongly suggest that vasopressin directly regulates both endocytosis and exocytosis of AQP2. Presumably the net increase in water permeability seen in response to vasopressin is due both to direct stimulation of exocytosis and to direct inhibition of endocytosis.

Several groups have now successfully reconstituted the AQP2 delivery system using cultured cells transfected with either wild-type AQP2 or AQP2 tagged with a marker protein or a fluorescent protein.[206–211] Using such cultured cells stably transfected with AQP2, it has been shown that AQP2 trafficking occurs from vesicles to the apical plasma membrane, albeit in some cases to the basolateral plasma membrane, as well as retrieval and subsequent trafficking back to the surface upon repeated stimulation. This recycling of AQP2 also occurs in LLC-PK1 cells in the continued presence of cycloheximide, preventing *de novo* AQP2 synthesis. Despite remaining uncertainties, a working model for collecting duct water permeability permits molecular insight into this process (Figure 41.7). The short-term effects of vasopressin-enhanced water permeability are explained by the redistribution of AQP2 to the apical plasma membrane in collecting duct principal cells. Acting through the V2 receptor, vasopressin stimulates adenylyl cyclase; the elevated levels of intracellular cAMP activate protein kinase A (PKA), causing a redistribution of AQP2 from intracellular vesicles to the apical plasma membrane by inducing exocytosis of AQP2 vesicles, and by inhibiting endocytosis of AQP2 from the apical membrane. The net increase of AQP2 in the apical plasma membrane increases the water permeability. In the pre-antidiuretic state, the apical membrane is the rate-limiting barrier for transepithelial water transport, because AQP3 and AQP4 are abundant in the basolateral plasma membrane. Thus, increasing the water permeability of the apical plasma membrane by insertion of AQP2 water channels results in an increase in transepithelial osmotic water permeability. Whereas the general model is now well-established, the molecular details explaining how an elevation in intracellular cAMP levels regulates trafficking of AQP2 to the apical plasma membrane and back remain uncertain. Serine at position 256, in the carboxyl-terminal tail of AQP2, is apparently a substrate for protein kinase A, and regulation of exocytosis and endocytosis of AQP2 is expected to involve phosphorylation and dephosphorylation of AQP2,[208,212,213] and of ancillary proteins involved in the trafficking processes. This

question will likely be a major focus of future research.

Signal Transduction Pathways Involved in Vasopressin Regulation of AQP2 Trafficking

The signal transduction pathways have been described thoroughly in previous reviews.[190,214–217] cAMP levels in collecting duct principal cells are increased by binding of vasopressin to V_2-receptors.[218,219] The synthesis of cAMP by adenylate cyclase is stimulated by a V_2-receptor coupled heterotrimeric GTP-binding protein, G_s. G_s interconverts between an inactive GDP-bound form and an active GTP-bound form, and the vasopressin-V_2-receptor complex catalyzes the exchange of GTP for bound GDP on the ∀-subunit of G_s. This causes release of the ∀-subunit, G_s∀-GTP, which subsequently binds to adenylate cyclase, thereby increasing cAMP production. Protein kinase A is a multimeric protein which is activated by cAMP, and consists in its inactive state of two catalytic subunits and two regulatory subunits. When cAMP binds to the regulatory subunits, these dissociate from the catalytic subunits, resulting in activation of the kinase activity of the catalytic subunits.

AQP2 contains a consensus site for PKA phosphorylation (RRQS) in the cytoplasmic COOH terminus at Ser^{256}.[123] Recent studies using ^{32}P labeling or using an antibody specific for phosphorylated AQP2 showed a very rapid phosphorylation of AQP2 (within 1 minute) in response to vasopressin-treatment of slices of the kidney papilla.[220] This is compatible with the time-course of vasopressin-stimulated water permeability of kidney collecting ducts.[189] As described above, PKA-induced phosphorylation of AQP2 apparently does not change the water conductance of AQP2 significantly. Importantly, it was recently demonstrated that vasopressin or forskolin treatment failed to induce translocation of AQP2 when Ser^{256} was substituted by an alanine (S256A) in contrast to a significant regulated trafficking of wild-type AQP2 in LLC-PK1 cells.[208] A parallel study by Sasaki and colleagues also demonstrated the lack of cAMP-mediated exocytosis of mutated (S256A) AQP2 transfected into LLC-PK1 cells.[221] Thus, these studies indicate a specific role of PKA-induced phosphorylation of AQP2 for regulated trafficking. To explore this further, an antibody was designed that exclusively recognizes AQP2 which is phosphorylated in the PKA consensus site (Ser256). In normal rats phosphorylated AQP2 (Ser256) is present in intracellular vesicles and apical plasma membrane, indicating that it is constitutively phosphorylated even in low circulating vasopressin states.[222,223] In contrast, phosphorylated AQP2 is mainly located in intracellular vesicles in Brattleboro rats, as shown by immunocytochemistry and immunoblotting using membrane fractionation.[222] Importantly, dDAVP treatment of Brattleboro rats caused a marked redistribution of phosphorylated AQP2 (Ser256) to the apical plasma membrane, which is in agreement with an important role of PKA phosphorylation in this trafficking.[222] Conversely, treatment with V_2-receptor antagonist induced a marked decrease in the abundance of phosphorylated AQP2 (Ser256),[222] likely due to reduced PKA activity and/or increased dephosphorylation of AQP2, e.g., by increased phosphatase activity. Moreover, the necessity for the Ser^{256} phosphorylation in AQP2-regulated urine concentration is underlined by the recent identification of this site as being spontaneously mutated in congenital progressive hydronephrosis (cph).[224] The spontaneous conversion of the serine phosphorylated site (Ser 256) to leucine in the cytoplasmic tail of the AQP2 protein in cph-mice prevents its phosphorylation at Ser^{256}, and inhibits the subsequent accumulation of AQP2 on the apical membrane of the collecting duct principal cells. This causes polydipsia, polyuria, and a severe urinary concentration defect leading to hydronephrosis and obstructive nephropathy in these mice. Recently, three previously unknown phosphorylation sites in the C-terminus of AQP2 were identified (S261, S264, and S269) by using liquid chromatography coupled to mass spectrometry neutral loss scanning.[225] During basal conditions, AQP2 phosphorylated on Ser^{261} is approximately 24-fold more abundant than Ser^{256} phosphorylated AQP2. During administration of dDAVP a decrease in Ser261 phosphorylation was observed, while AQP2 phosphorylated on Ser256, Ser264, and Ser269 increased.[225,226] It is clear that phosphorylation of AQP2 is required for cell surface expression; however, it is still unclear how phosphorylation of AQP2 (S256, S261, S264, S269) induces apical trafficking of AQP2. One possibility is that phosphorylation of AQP2 directly influences an interaction between AQP2-containing vesicles and the cell cytoskeleton, microtubules or accessory cross-linking proteins. Indeed, S256 is important for a direct interaction of AQP2 with 70 kDa heat-shock proteins.[227] Alternatively, phosphorylation could prevent endocytosis of AQP2, leading to accumulation at the cell surface.

Prostaglandin E_2 (PGE_2) has been known to inhibit vasopressin-induced water permeability by reducing cAMP levels. Zelenina et al.[228] investigated the effect of PGE_2 on PKA phosphorylation of AQP2 in rat kidney papilla, and the results suggest that the action of prostaglandins are associated with retrieval of AQP2 from the plasma membrane, but this appears to be independent of AQP2 phosphorylation by PKA.[228] In contrast, a recent study revealed the effect of selective

E-prostanoid receptor agonists on the vasopressin-independent targeting of AQP2.[229] *In vitro*, PGE2 and selective agonists for the E-prostanoid receptors EP2 or EP4 all increased trafficking and AQP2 phosphorylation (Ser264) in MDCK cells. *In vivo*, a V2R antagonist caused a severe urinary concentrating defect in rats, which was greatly alleviated by treatment with a selective agonist for the EP2 receptor.[229] Further studies are still needed on the effects of PGE2 on urine concentration.

Phosphorylation of AQP2 by other kinases, e.g., protein kinase C or casein kinase II, may potentially participate in regulation of AQP2 trafficking. Angiotensin II-induced activation of protein kinase C could be, at least in part, involved in the AQP2 trafficking/expression.[207,230,231] S256 is also a substrate for Golgi casein kinase 2, which is required for the Golgi transition of AQP2.[232] Additionally, the phosphatase inhibitor okadaic acid induces increased AQP2 expression at the cell surface, even in the presence of the PKA inhibitor H89 and S256A AQP2 mutants (that lack S256 phosphorylation) which are able to accumulate at the cell surface after treatment with cholesterol-depleting agents.[233] Phosphorylation of other cytoplasmic or vesicular regulatory proteins may also be involved. These issues remain to be investigated directly.

Involvement of the Cytoskeleton and Ca^{2+} in AQP2 Trafficking

The cytoskeleton has been shown to be involved in AQP2 trafficking in the kidney collecting duct. In particular, the microtubular network has been implicated in this process, since chemical disruption of microtubules inhibits the increase in permeability both in the toad bladder and in the mammalian collecting duct.[234,235] Thus, AQP2 vesicles may be transported along microtubules on their way to the apical plasma membrane. The microtubule-based motor protein dynein and the associated protein Arp1, which is part of the protein complex dynactin, were found by immunoblotting to be among the proteins associated with AQP2 vesicles from rat inner medulla. Immunoelectron microscopy further supported the presence of both AQP2 and dynein on the same vesicles.[236] Moreover, both vanadate (a non-specific inhibitor of ATPases) and EHNA (a specific inhibitor of dynein) inhibit the antidiuretic response in toad bladder[237,238] and kidney collecting duct.[239] Thus, it is likely that dynein may drive the microtubule-dependent delivery of AQP2-containing vesicles to the apical plasma membrane.

Actin filaments are also involved in the hydrosmotic response.[240–245] Recently evidence was provided that the myosin light chain kinase (MLCK) pathway, through calmodulin-mediated calcium activation of MLCK, leads to phosphorylation of myosin regulatory light chain and non-muscle myosin 2 motor activity.[246] Studies in isolated perfused rat inner medullary collecting ducts showed the MLCK inhibitors ML-7 and ML-9 reduce the vasopressin-induced increase in water permeability,[246] indicating that MLCK may be a downstream target for the vasopressin-induced Ca^{2+} signal.

The intracellular Ca^{2+} concentration has been shown to increase upon stimulation of isolated perfused rat inner medullary collecting ducts with vasopressin or dDAVP.[247] These observations have been followed by a number of studies on the role of Ca^{2+} in the vasopressin-induced increase in water permeability. Vasopressin or 8−4-chlorophenylthio-cAMP induced a marked increase in intracellular [Ca^{2+}] in isolated perfused IMCD, and BABTA blocked the rise in intracellular [Ca^{2+}] and co-contaminantly led to inhibition of the vasopressin-induced increase in tubular water permeability.[248] Moreover, blocking calmodulin with W7 or trifluoperazine also inhibited the effect of vasopressin on tubular water permeability, and inhibited the vasopressin-induced AQP2 plasma membrane targeting in primary cultured IMCD cells.[248] Removing Ca^{2+} from both bath and lumen in isolated perfused tubules did not affect the vasopressin-induced Ca^{2+} signal, indicating that Ca^{2+} was released from an intracellular source. This was further supported by the observations that ryanodine inhibited the Ca^{2+} signal in perfused IMCDs and inhibited AQP2 accumulation in the plasma membrane in primary cultured IMCD cells. In addition, RyR1 ryanodine receptor was localized to rat IMCD by immunohistochemistry.[248] Ryanodine receptors are generally known to mediate a positive feedback and release Ca^{2+} from intracellular stores in response to an initial rise in intracellular [Ca^{2+}]. Thus, it is likely that another mechanism is responsible for the initialization of the rise in intracellular [Ca^{2+}]. Further studies revealed that vasopressin or dDAVP elicited oscillations in intracellular [Ca^{2+}] in isolated perfused rat IMCD.[249] The results on isolated perfused IMCDs indicate that an intracellular increase in [Ca^{2+}] is an obligate component of the vasopressin response leading to increased AQP2 expression in the apical plasma membrane. However, it should be mentioned that there is a discrepancy between the results from primary cultured IMCD cells[250] and isolated perfused IMCD tubules[248] with regard to the role of intracellular [Ca^{2+}] in vasopressin-induced AQP2 trafficking. Consistent with this, Lorenz et al.[250] demonstrated that AQP2 shuttling is evoked neither by AVP-dependent increase of [Ca^{2+}] nor by AVP-independent increase of [Ca^{2+}] in primary cultured IMCD cells from rat kidney, although clamping of intracellular [Ca^{2+}] below resting levels inhibits AQP2 exocytosis. Further studies are

required to clarify this discrepancy, which may be related to altered expression levels of vasopressin receptors and/or AQP2 or other elements in the AQP2 trafficking system.

Mechanism of AQP2 Trafficking by Targeting Receptors

The mechanism by which AQP2 vesicles are targeted to the apical plasma membrane and the mechanism by which cAMP controls docking and fusion of vesicles is a current area of active investigation. Considerable insight into this problem has been obtained from previous studies of regulated exocytosis of synaptic vesicles, which involve the actions of multiple proteins.[251,252] Vesicle-targeting receptors (often referred to as "SNAREs") are believed to induce specific interaction of vesicles with membrane sites. Vesicle-targeting receptors associated chiefly with translocating vesicles are known as "VAMPs" (vesicle associated membrane proteins, also referred to as "synaptobrevins") and "synaptotagmins." Two other families of membrane proteins are believed to serve as receptors in target membranes: the "syntaxins" and SNAP-25 homologs. Several of these SNAREs have been found in the renal collecting duct.[253–260]

Syntaxins are 30 to 40 kDa integral membrane proteins. Syntaxins have a one bilayer-spanning domain near the C-terminus, so the majority of the protein resides in the cytoplasm. Syntaxins are widely distributed among mammalian tissues. It has been established that syntaxin-4 is expressed in the mammalian collecting duct by studies using polyclonal antibodies raised to conjugated peptides specific for individual syntaxins, and this has been confirmed by reverse transcription polymerase chain reaction.[258] Immunolocalization studies have demonstrated that syntaxin-4 is predominantly located in the apical plasma membrane of collecting duct principal cells, where AQP2 is targeted in response to vasopressin.

VAMPs are believed to induce specific docking of vesicles by interacting directly with syntaxins in the target plasma membrane (Figure 41.7). Although their primary amino acid sequences are not related to syntaxins, VAMPs also have a single bilayer-spanning domain near the C-terminus, and the majority of the protein resides in the cytoplasm. Three VAMP isoforms were initially identified[261]: VAMP-1; VAMP-2; and VAMP-3 (also referred to as "cellubrevin"), and subsequently several additional homologs have been cloned.[262] VAMP-2 and VAMP-3 have been localized in principal cells of renal collecting duct.[253–260] Double-labeling immunoelectron microscopy revealed that AQP2 and VAMP-2 reside in the same intracellular vesicles in collecting duct principal cells.[260] Furthermore, AQP2 vesicles isolated by differential centrifugation were found to contain VAMP-2.[254,257]

At this time, several putative vesicle-targeting proteins are known to reside in collecting duct principal cells. VAMP-2 resides in AQP2 intracellular vesicles, and syntaxin-4 resides in the apical plasma membrane. *In vitro* binding assays have documented that VAMP-2 binds syntaxin-4 with high affinity, but VAMP-2 has not been shown to interact with syntaxin-3 or syntaxin-2.[263,264] Thus, VAMP-2 and syntaxin-4 are likely participants in the targeting of AQP2 vesicles to the apical plasma membrane; however, a functional role for these targeting proteins remains to be formally demonstrated. A third SNARE protein, SNAP-23, has also been identified in principal cells of the collecting duct.[255] Although considered a target-membrane SNARE (t-SNARE), SNAP-23 is present both in AQP2-containing vesicles and in the apical plasma membrane of principal cells. VAMP-2, syntaxin-4, and SNAP-23 may potentially form a complex with the N-ethylmaleimide-sensitive factor (NSF). Finally, synaptotagmin VIII, a calcium-insensitive homolog, was identified in collecting duct principal cells,[256] and may potentially also play a role in vesicle targeting.

Recently, LC-MS/MS-based proteomic analysis of immunoisolated AQP2-containing intracellular vesicles from rat inner medullary collecting duct revealed that AQP2-containing vesicles are heterogeneous, and that intracellular AQP2 resides chiefly in endosomes, trans-Golgi network, and rough endoplasmic reticulum.[265] Vasopressin-stimulated exocytosis of AQP2 vesicles involves several steps including: (1) translocation of vesicles from a diffuse distribution throughout the cell to the apical region of the cell; (2) translocation of AQP2 across the apical part of the cell composed of a dense filamentous actin network; (3) priming of vesicles for docking; (4) docking of vesicles; and (5) fusion of vesicles with the apical plasma membrane. Theoretically, each of these steps could be a target for regulation by vasopressin. If the SNARE proteins are involved in the vasopressin-induced trafficking of AQP2 to the apical plasma membrane, the regulatory mechanism might involve selective phosphorylation of one of the SNARE proteins or an ancillary protein that binds to them, possibly via protein kinase A or calmodulin-dependent kinase II. Although the SNARE proteins are recognized as potential targets for phosphorylation,[266–268] there is presently no evidence for phosphorylation in the collecting duct. As noted above, however, AQP2 itself appears to be a target for PKA-mediated phosphorylation at a serine in position 256.[212] The phosphorylation does not modify the single channel water permeability of AQP2,[213] and instead the phosphorylation is believed to play a critical role in

regulation of AQP2 trafficking to the plasma membrane.[208,221] The establishment of a role for these SNARE proteins in regulated trafficking of AQP2 will most likely depend on the preparation of targeted knockouts for each of these genes in the collecting duct.

Long-Term Regulation of Aquaporin Expression

It has been known for more than 40 years that urinary concentrating ability is regulated through a long-term conditioning effect of sustained increases in vasopressin levels exerted over a period of days.[269] The physiological and molecular basis for long-term conditioning of urinary concentrating ability is still being investigated. Water restriction causes a large, stable increase in water permeability of inner medullary collecting ducts dissected from rat kidneys and perfused *in vitro*.[185] Thus, water permeability of the tubules from water-restricted rats became five-fold greater than that measured in well-hydrated rats by a mechanism independent of the short-term action of vasopressin. Other studies confirmed that water restriction enhances the vasopressin-independent water permeability of collecting ducts,[270,271] and increases vasopressin-stimulated water permeability.[272] This contrasts with the lack of an observed increase in urea permeability in water-restricted rats.[185] These studies provided the firm conclusion that restriction of water intake for 24 hours or longer leads to a marked increase in the water-reabsorbing capacity of the renal collecting duct epithelium.

Further studies with anti-peptide antibodies have documented that the conditioned increase in water permeability is associated with increased expression of aquaporin proteins in collecting duct principal cells. Specifically, the increased water permeability that occurs in response to water restriction is accompanied by significant increases in the levels of AQP2 and AQP3 proteins in rat collecting ducts.[138,151,195] Water restriction for 24 to 48 hours resulted in an approximately five-fold increase in AQP2 protein in the rat renal inner medulla when measured by immunoblotting[138,195] and by immunostaining.[199] This increase paralleled the increase in water permeability in response to water restriction.[185]

A direct role for vasopressin in AQP2 expression has been established by multiple studies. Continuous infusion of arginine vasopressin into Brattleboro rats for 5 days resulted in a three-fold increase in AQP2 expression and a three-fold increase in water permeability of inner medullary collecting ducts.[143] When the time-course of AQP2 expression in inner medullary collecting duct was studied, it was found that 5 days of vasopressin infusion were required to reach maximal AQP2 levels in Brattleboro rats.[139]

Vasopressin is believed to be essential for evoking AQP2 expression, because Brattleboro rats totally lack circulating vasopressin fail to exhibit increased expression of AQP2 protein after long-term water restriction.[273] Moreover, administration of a selective V2-receptor antagonist blocked the increase in AQP2 expression usually seen with thirsting in normal rats,[199] whereas administration of the V2-selective agonist dDAVP (1-desamino-8-D-arginine vasopressin) to rats elicited a large increase in renal AQP2 mRNA[274] and AQP2 protein abundance.[275] The question of hyperosmolar induction of AQP2 during thirsting has been raised; however, five-day infusion of arginine vasopressin increased AQP2 comparably in renal cortex and medulla. This indicates that the vasopressin-induced expression of AQP2 is not critically dependent on increased osmolality or ionic strength in the tissue surrounding the collecting ducts.[187] Thus, it has been clearly established that the major increase in AQP2 water channel expression elicited by restriction of water intake is due to vasopressin binding to the V2 receptor in collecting duct principal cells. However, studies of the mechanism of escape from the antidiuretic effects of vasopressin[275,276] make it clear that AQP2 expression is regulated by other factors in addition to vasopressin (see later).

AQP3 protein expression also has been found to parallel AQP2 expression. A marked increase in AQP3 protein expression was observed in rats in response to restriction of water intake[151] and after a five-day infusion of arginine vasopressin.[187] These conditions did not lead to observed changes in AQP1 or AQP4 protein expression.[153,187] Thus, it is concluded that long-term circulation of high vasopressin levels is associated with an adaptive increase in maximal water permeability in collecting ducts, apparently due a selective increase in the expression of both AQP2 and AQP3 in the principal cells of the collecting duct. However, immunoelectron microscopy has demonstrated that AQP3 is predominantly present in the basolateral plasma membranes with little labeling of intracellular vesicles.[151] This suggests that AQP3 is not regulated by vesicular trafficking (in contrast to the findings with AQP2[182]). Moreover, there are several examples where there is a decoupling of AQP2 and AQP3 expression, suggesting that other factors in addition to vasopressin may regulate one or other of the aquaporins. This is seen in conditions such as hepatic cirrhosis,[277] vasopressin-escape,[275] low-protein diet,[278] and restriction of NaCl intake.[156]

The adaptive changes in AQP2 and AQP3 expression are believed to be due to transcriptional regulation of these genes. Increased AQP2 mRNA was found in the inner medullae of water-restricted rats,[279] and in response to infusion of dDAVP.[274,275] All of these

studies indicate that the long-term upregulation of AQP2 expression in the rat kidney is due to elevation of the levels of AQP2 mRNA. Vasopressin-induced increase in AQP2 mRNA expression could reflect either increased gene transcription or reduced transcript degradation. Examination of the 3′-untranslated region of the AQP2 mRNA has not revealed the presence of recognizable mRNA stabilization motifs, and it is presumed that vasopressin directly increases *AQP2* gene transcription; however, no direct evidence supports this presumption. Transcriptional regulation would most likely occur through the vasopressin-induced increases in intracellular cyclic AMP that activates protein kinase A in collecting duct cells. Examination of the 5′-flanking region of the *AQP2* gene revealed a putative cAMP-response element (CRE), which may play a role in the vasopressin-induced increase in AQP2 expression.[280] Attempts to demonstrate expression of AQP2 promoter-luciferase reporter constructs have been undertaken in cultured renal epithelial cells and suggest that the putative CRE can drive increased expression of the *AQP2* gene; however, the inability of the cell line to express AQP2 protein limits the interpretation.[281–283]

As with AQP2, AQP3 mRNA levels were induced by infusion with the selective V2 agonist dDAVP.[275] Examination of the 5′-flanking DNA of AQP3 failed to reveal a CRE; however, Sp1 and AP2 cis-regulatory elements are present,[284] and these are known to be associated with cyclic AMP-mediated transcriptional regulation of other genes. A previous study revealed that AQP2 is ubiquitinated with one UbLys63-linked poly-Ub chain at K270 of AQP2 and lysosomal degradation was extensive for ubiquitinated AQP2.[285] The degradation pathways, therefore, balance the abundance of proteins which play an important role in body water homeostasis.[186]

DYSREGULATION OF RENAL AQUAPORINS IN WATER BALANCE DISORDERS

In a variety of conditions renal water handling is disturbed. Over the past decade, the role of changes in the expression and/or function of aquaporins have been investigated in a range of these conditions, including genetic defects or acquired defects showing a decreased renal responsiveness to vasopressin (acquired nephrogenic diabetes insipidus). The importance of aquaporins playing an essential role for regulation of renal water balance has been established (Table 41.2), and the following text represents extracted and updated information reported in previous reviews by the authors or other investigators.[190,286–288]

URINARY CONCENTRATING DEFECTS

Inherited Diabetes Insipidus

There are two significant inherited forms of diabetes insipidus (DI): central and nephrogenic. In central (or neurogenic) DI, there is a defect of vasopressin production. Central DI is rarely hereditary in man, but usually occurs as a consequence of head trauma or diseases in the hypothalamus or pituitary gland. The Brattleboro rat provides an excellent model of this condition. These animals have a total or near-total lack of vasopressin production.[289,290] Consequently, Brattleboro rats have substantially decreased expression levels of vasopressin-regulated AQP2 compared with the parent strain (Long Evans), and the AQP2 deficit was reversed by chronic vasopressin infusion, suggesting that patients lacking vasopressin are likely to have decreased AQP2 expression.[143] The subsequent work showing that expression of AQP3 is also regulated by vasopressin implies that the expression levels of these water channels will also be decreased in patients with CDI. The most important denominator is the deficiency of AQP2 trafficking to the apical membrane. These deficits are likely to be the most important causes of the polyuria from which these patients suffer, which will be reversed by desmopressin treatment. The second form of DI is called nephrogenic diabetes insipidus (NDI), and is caused by the inability of the kidney to respond to vasopressin stimulation. The most common hereditary cause (in 95% of cases) is an X-linked disorder associated with mutations of the V2 vasopressin receptor (AVPR2) making the collecting duct cells insensitive to vasopressin.[291] Although there is no direct evidence, it is likely that this form of NDI will be associated with decreased expression of AQP2, since the cells are unable to respond to circulating vasopressin.[292] This will compound the lack of AQP2 trafficking. Consistent with this, urinary AQP2 levels are very low in patients with X-linked NDI.[196,293] However, since the amount of AQP2 in the urine appears to be determined largely by the response of the collecting duct cells to vasopressin[294] rather than their content of AQP2, the data must be interpreted with caution with respect to predicting AQP2 expression levels. More rarely (in 5% of cases), congenital diabetes insipidus (CNDI) is inherited in an autosomal recessive fashion which is not due to mutations in the gene encoding the V2 vasopressin receptor, but these patients have been found to possess mutations in both alleles of the *AQP2* gene, and the sites of point mutations were observed at functionally important sites in the water transport pathway.[144,295–298] Since these patients manifest a particularly severe form of diabetes insipidus, the critical role of AQP2 in renal water conservation was

established. It is believed that these mutations lead to abnormal intracellular routing of the expressed protein.[299] More than 155 mutations in the vasopressin receptor gene have been recognized to cause CNDI. Functional analysis has been carried out for over 79 of these mutations.[300] The analyses have revealed four different types of mutant receptors. The most common is impaired intracellular trafficking, which is seen in up to 70% of cases.[300] The remaining types include reduced ligand-binding capacity, failure to generate cAMP, and defects in the synthesis of stable mRNA.[301] Only five of the 155 known mutations cause partial CNDI (D85N, R104C, G201D, P322S, and S329R). Recently, a different kindred was identified with a dominant form of nephrogenic diabetes insipidus, and biochemical evaluations revealed that the mutation in the cytoplasmic C-terminus blocked the trafficking of AQP2 vesicles to the cell surface.[302] Thus, intracellular trafficking of vesicles containing products of the mutant allele and the product of the normal allele may be misdirected. It is not known if these individuals suffer a more or less severe clinical defect, and recently it was shown that the ligand-binding and signal transduction capability are dependent on localization of the amino acid variation, suggesting that striking divergences at the level of receptor functionality may thus underlie similar clinical phenotypes in CNDI.[303–305]

Acquired Nephrogenic Diabetes Insipidus

Acquired abnormalities of AQP2 expression have been implicated in multiple clinical disorders associated with abnormal water balance (Table 41.2). The role of vasopressin-regulated AQP2 has been established in a number of rat models with acquired NDI. In many of these conditions the kidney is unable to handle water, due to an impaired responsiveness to vasopressin; in the following text the most important of these condtions are described.

Lithium-Induced NDI

Lithium is a major therapeutic agent used to treat bipolar disorder (also referred to as "manic depressive disease") which affects approximately 1% of the US population.[306] However, lithium treatment is associated with a variety of renal side-effects, including nephrogenic diabetes insipidus (NDI, i.e., a pronounced vasopressin-resistant polyuria and inability to concentrate urine),[307,308] increased urinary sodium excretion,[309] and distal renal tubular acidosis.[310] Patients who have been treated with lithium manifest a slow recovery of urinary concentrating ability when treatment is discontinued. In rats treated with lithium for 4 weeks, AQP2 and AQP3 levels were progressively reduced to approximately 5% of levels in control rats.[307,308] AQP2 downregulation was paralleled by a progressive development of severe polyuria.[307,308] Quantitative immunoelectron microscopy of AQP2 labeling in the inner medullary collecting duct principal cells showed that there was a reduction of AQP2 in the apical plasma membrane, as well as in the basolateral plasma membrane and intracellular vesicles. Reduction in AQP2 (and AQP3) expression may be induced by a lithium-dependent impairment in the production of cAMP in collecting duct principal cells,[309,311] indicating that inhibition of cAMP production may in part be responsible for the reduction in AQP2 expression, as well as the inhibition of targeting to the plasma membrane in response to lithium treatment. This is consistent with the presence of a cAMP-responsive element in the 5′-untranslated region of the AQP2 gene,[281,282] and with the demonstration that mice with inherently low cAMP levels have low expression of AQP2 ($DI^{+/+}$ severe mouse).[312] Lithium treatment is also associated with a concomitant increase in urinary sodium excretion, which is likely to play a role in the polyuria. It has also been demonstrated that chronic lithium treatment induces a marked decrease in protein abundance of epithelial sodium channel β- and γ-ENaC in the cortex and outer medulla, whereas the other renal sodium transporters upstream from the connecting tubule are unchanged.[313] This was also revealed by immunocytochemistry showing an almost complete absence of β-ENaC and γ-ENaC labeling in cortical and outer medullary collecting duct. This suggests a reduced responsiveness to aldosterone and vasopressin in these specific renal tubule segments, and that dysregulation of ENaC subunits is likely to play a role in the development of natriuresis and partly in the decreased urinary concentrating ability in rats with lithium-induced NDI.[314] Additional studies have identified proteins with altered abundance in the inner medullary collecting ducts (IMCD) of lithium-treated rats and their possible cellular function.[315,316] Moreover, it has been shown that prostaglandins, in lithium-treated mpkCCD cells, dcreases APQ2 protein stability by increasing its lysosomal degradation, indicating that *in vivo* paracrine-produced prostaglandins might have a role in lithium-induced NDI via this mechanism.[317]

Hypokalemia and Hypercalcemia

Hypokalemia and hypercalcemia are also associated with polyuria due to a vasopressin-resistant urinary concentrating defect. Rat models of these conditions are valuable tools to study the molecular defects. Treating rats with a potassium-deficient diet for 4 days

induced a significant hypokalemia which was associated with downregulation of AQP2 expression and polyuria.[318] Likewise, hypercalcemia induced in rats by oral treatment for 7 days with dihydrotachysterol produced a urinary concentrating defect and polyuria which was also associated with downregulaion of AQP2.[319,320] Thus, both hypokalemia and hypercalcemia are associated with downregulation of AQP2 expression, and immunolocalization studies of AQP2 demonstrated similar features. In addition to the downregulation of AQP2, expression of Na-K-2Cl co-transporter in the thick ascending limb was decreased in both conditions,[321,322] suggesting that reduced sodium and chloride reabsorption in the thick ascending limb, and hence decreased medullary hyperosmolality, could also partly contribute to the polyuria and decreased urinary concentration in hypokalemia and hypercalcemia. Thus, these studies in part describe the underlying molecular defects involved in the development of the polyuria in these conditions.

Urinary Tract Obstruction

Another serious condition seen in both children and adults is urinary tract obstruction which is associated with complex changes in renal function involving marked alterations in both glomerular and tubular function and bilateral urinary tract obstruction (BUO) which may result in long-term impairment of the ability to concentrate urine.[323] BUO for 24 hours in rats is associated with markedly reduced expression of AQP2, AQP3, AQP4, and AQP1.[324–327] In addition, BUO is associated with marked downregulation of key sodium transporters and urea transporters.[328] Following release of the obstruction, there is a marked polyuria, during which period AQP2 and AQP3 levels remain downregulated up to two week after release, providing an explanation at the molecular level for the observed post-obstructive polyuria. In a number of studies BUO has been demonstrated to be associated with COX2 induction and cellular infiltration of the renal medulla.[292,329–331] Using specific COX2 inhibition to rats subjected to BUO it was demonstrated that this treatment prevents downregulation of AQP2 and several sodium transporters located to the proximal tubule and mTAL.[329,330] Also, increased expression and activity of the P2Y2, EP1, and EP3 receptors have been suggested to play important roles in post-obstructive polyuria.[332] Moreover, specific inhibition of the AT1 receptor in rats subjected to BUO prevented AVP2R downregulation of NaPi2 in the PT, BSC-1 in the mTAL, and AQP2/pS256-AQP2 in the CD three days after release of BUO,[134,333] confirming that the renin–angiotensin system plays an important role for the pathophysiological changes in urinary tract obstruction.

In contrast to BUO conditions, unilateral ureteral obstruction is not associated with changes in the absolute excretion of sodium and water since the non-obstructed kidney compensates for the reduced ability of the obstructed kidney to excrete solutes.[328,334] These studies demonstrated a profound downregulation of AQP1, AQP2, AQP3, and AQP4, and pAQP2 levels in the obstructed kidney, suggesting that 1ocal factors play a major role.

Renal Failure

Renal failure, both acute and chronic, is associated with polyuria and a urinary concentrating defect, and in both cases there is a wide range of glomerular and tubular abnormalities that contribute to the overall renal dysfunction. Ischemia and reperfusion (I/R)-induced experimental acute renal failure (ARF) in rats is a model that is widely used. In this model there are structural alterations in the renal tubule, in association with an impaired urinary concentration.

ARF is associated with defects both in collecting duct water reabsorption and proximal tubule water reabsorption, as well as defects in solute handling.[335–337] Using the isolated tubule microperfusion model, it was demonstrated that water reabsorption in the proximal tubule and cortical collecting duct was significantly reduced following ischemia,[335] and no differences in either basal or vasopressin-induced cAMP levels in outer or inner medulla in rats with ARF were demonstrated,[338] supporting the view that there are defects in collecting duct water reabsorption. Consistent with these findings, it was demonstrated that AQP2 and AQP3 expression in the collecting duct, as well as AQP1 expression in the proximal tubule, are significantly reduced in response to ARF.[339,340] The decreased levels of aquaporins were associated with impaired urinary concentration in rats with both oliguric or nonoliguric ARF. The reduced expression of AQP1–3 and the reduced urinary concentration capacity was significantly prevented by co-treatment with alpha-melanocyte-stimulating hormone (α-MSH), which is an anti-inflammatory cytokine that inhibits both neutrophil and nitric oxide pathways.[340] This finding indicates that decreased levels of aquaporins in both the proximal tubule and collecting duct in post-ischemic kidneys may play a significant role in the impaired urinary concentration. Recently it was also demonstrated that hemorrhagic shock-induced acute renal failure is associated with decreased expression of collecting duct water channel AQP2 and AQP3,[341] and that erythropoietin treatment (single or combined with

α-MSH) in rats with I/R-induced ARF, which is known to prevent caspase-3, -8, and -9 activation *in vivo* and reduces apoptotic cell death,[342] prevents or reduces the urinary concentrating defects and downregulation of AQP expression levels.[341] Consistent with this, it was demonstrated that NF-kappaB activation is of importance for the downregulation of AQP2 channel and vasopressin V2-receptor expression during sepsis in a cecal ligation and puncture (CLP) mouse model of ARF, and that NF-kappaB inhibition ameliorates sepsis-induced ARF in the CLP model.[343]

Patients with advanced chronic renal failure (CRF) have urine which remains hypotonic to plasma despite the administration of supramaximal doses of vasopressin.[344] This vasopressin-resistant hyposthenuria specifically implies abnormalities in collecting duct water reabsorption in CRF patients. Recent observations demonstrated virtual absence of V2 receptor mRNA in the inner medulla of CRF rat kidneys,[345] providing evidence for significant defects in the collecting duct water permeability. Consistent with these observations, it has shown both decreased collecting duct water channel AQP2 and AQP3 expression and a vasopressin-resistant downregulation of AQP2 in a 5/6 nephrectomy-induced CRF rat model.[346]

WATER RETENTION

Congestive Heart Failure

Retention of sodium and water is a common and clinically important complication of congestive heart failure (CHF). Two studies have examined the changes in renal AQP expression in rats with CHF induced by ligation of the left coronary artery[347,348] to test if upregulation of AQP2 expression and targeting may play a role in the water retention in CHF. Both studies demonstrated that renal water retention in severe CHF in rats is associated with dysregulation of AQP2 in the renal collecting duct principal cells, involving both an increase in the AQP2 expression and a marked redistribution of AQP2 to the apical plasma membrane.[347,348] Rats with severe CHF had significantly elevated left ventricular end-diastolic pressures (LVEDP), and had reduced plasma sodium concentrations.[347] Immunoblotting revealed a three-fold increase in AQP2 expression compared with sham operated animals. These changes were associated with elevated LVEDP or hyponatremia, since animals with normal LVEDP and plasma sodium did not have increased AQP2 levels compared with sham operated controls.[347] Furthermore, this study showed an increased plasma membrane targeting, providing an explanation for the increased permeability of the collecting duct and an increase in water reabsorption. This may provide an explanation for excess free water retention in severe CHF, and for the development of hyponatremia. In parallel, the other study showed upregulation of both AQP2 protein and AQP2 mRNA levels in kidney inner medulla and cortex in rats with CHF.[348] These rats had significantly decreased cardiac output and, importantly, increased plasma vasopressin levels. Furthermore, in this study administration of V2 antagonist OPC 31260 was associated with a significant increase in diuresis, a decrease in urine osmolality, a rise in plasma osmolality, and a significant reduction in AQP2 protein and AQP2 mRNA levels compared with untreated rats with CHF. Consistent with this, treatment of V2-receptor antagonist in human patients and rats with heart failure is associated with a dose-related increase in water excretion and a decrease in urinary AQP2 excretion.[349,350] Moreover, it has been shown in patients with CHF that treatment with furosemide increases the urinary excretion of AQP2, free water clearance, and sodium exceretion.[351]

Hepatic Cirrhosis

Hepatic cirrhosis is another chronic condition associated with water retention.[352] It has been suggested that an important pathophysiological factor in the impaired ability to excrete water could be increased levels of plasma vasopressin. However, unlike CHF, the changes in expression of AQP2 protein levels vary considerably between different experimental models of hepatic cirrhosis. Several studies have examined the changes in renal AQP expression in rats with cirrhosis induced by common bile duct ligation (CBDL).[277,353,354] The rats displayed impaired vasopressin-regulated water reabsorption despite normal plasma vasopressin levels. Consistent with this, semiquantitative immunoblotting showed a significant decrease in AQP2 expression in rats with hepatic cirrhosis.[277,353] In addition, the expression levels of AQP3 and AQP4 were downregulated in CBDL rats. This may predict a reduced water permeability of the collecting duct in this model[277]; hence, renal water reabsorption in the collecting duct is decreased in rats with compensated liver cirrhosis. In contrast, Fujita et al.[274] demonstrated that hepatic cirrhosis induced by intraperitoneal administration of carbon tetrachloride (CCl_4) was associated with a significant increase in both AQP2 protein levels and AQP2 mRNA expression. Interestingly, AQP2 mRNA expression correlated with the amount of ascites, suggesting that AQP2 may play a role in the abnormal water retention followed by the development of ascites in hepatic cirrhosis.[355] In a different model of CCl_4-induced cirrhosis, using CCl_4 inhalation, AQP2

expression was not increased.[356] There was, however, evidence for increased trafficking of AQP2 to the plasma membrane, consistent with the presence of elevated levels of vasopressin in the plasma. Interestingly, there was a marked increase in AQP3 expression that is likely to be due to increased vasopressin levels. The pattern of increased AQP3 expression without upregulation of AQP2 is consistent with previous findings observed in the vasopressin escape,[276] suggesting that the lack of increase in AQP2 expression could be a result of a normal compensatory response related to the escape phenomenon. Although the explanation for the differences between cirrhosis induced by CBDL and CCl_4 administration remains to be determined, it is well-known that the dysregulation of body water balance depends on the severity of cirrhosis.[357–360] CBDL results in a compensated cirrhosis characterized by peripheral vasodilation and increased cardiac output, whereas cirrhosis induced by 12 weeks of CCl_4 administration may be associated with the late state of decompensated liver cirrhosis characterized by sodium retention, edema, and ascites.[358,359,361] Thus, the downregulation of AQP2 observed in milder forms of cirrhosis (i.e., in a compensated stage without water retention) may represent a compensatory mechanism to prevent development of water retention. In contrast, the increased levels of vasopressin seen in severe "non-compensated" cirrhosis with ascites may induce an inappropriate upregulation of AQP2 that would in turn participate in the development of water retention. Recent studies have shown a prominent role for AQP1 in angiogenesis, fibrosis, and portal hypertension after bile duct ligation in wild-type and AQP1 knockout mice.[362]

Experimental Nephrotic Syndrome

Nephrotic syndrome is characterized by extracellular volume expansion with excessive renal salt and water reabsorption. The underlying mechanisms of salt and water retention are poorly-understood; however, they can be expected to be associated with dysregulation of solute transporters and water channels.[359] In contrast to congestive heart failure and liver cirrhosis, a marked downregulation of AQP2 and AQP3 expression was demonstrated in rats with PAN-induced and adriamycin-induced nephrotic syndrome.[363–365] The reduced expression of collecting duct water channels could represent a physiologically appropriate response to extracellular volume expansion. The signal transduction involved in this process is not clear, but circulating vasopressin levels are high in rats with PAN-induced nephrotic syndrome. Thus, the marked downregulation of AQP2 in experimental nephrotic syndrome may share similarities with the downregulation of AQP2 in water-loaded dDAVP-treated rats that escape from the action of vasopressin.[275,276]

SIADH and Vasopressin Escape

Hyponatremia, defined as a serum sodium less than 135 mmol/L, is one of the most commonly encountered electrolyte disorders of clinical medicine.[366] The predominant cause of hyponatremia is an inappropriate secretion of vasopressin relative to serum osmolality or the "syndrome of inappropriate antidiuretic hormone secretion" (SIADH).[367] SIADH occurs most frequently in association with vascular, infectious or neoplastic abnormalities in the lung or central nervous system. In an experimental rat model of SIADH it was shown that AQP2 mRNA expression and AQP2 protein expression were increased in the collecting duct.[274] Thus, increased expression of AQP2 in the collecting duct accounts for the water retention and hyponatremia in SIADH.

The degree of hyponatremia is limited by a process that counters the water-retaining action of vasopressin, namely "vasopressin escape." Vasopressin escape is characterized by a sudden increase in urine volume with a decrease in urine osmolality independent of high circulating vasopressin levels. The onset of escape coincided temporally with a marked decrease in renal AQP2 protein, as measured by immunoblotting, as well as decreased mRNA expression, as assessed by Northern blotting.[276] In contrast to AQP2, there were no decreases in renal expression of AQP1, AQP3, and AQP4.[276] These results suggest that escape from vasopressin-induced antidiuresis is attributable, at least in part, to a selective vasopressin-independent decrease in AQP2 expression in the renal collecting duct.[368,369]

Acknowledgments

Support for this chapter was partially provided by funds from the Danish National Research Foundation, The European Commission, the Danish Medical Research Council, Novo Nordic Foundation, Karen Elise Jensen Foundation and the National Institutes of Health. Portions of the text were previously published in abridged form and are reproduced and modified with permission.[122] Moreover, the authors gratefully acknowledge the major contributions from Peter Agre and Mark Knepper, who together with SN authored a previous version of this chapter.

References

[1] Finkelstein A. Water movement through lipid bilayers, pores, and plasma membranes: theory and reality. New York: John Wiley & Sons; 1987.
[2] Solomon AK. Characterization of biological membranes by equivalent pores. J Gen Physiol 1968;51(Suppl).

[3] Macey RI. Transport of water and urea in red blood cells. Am J Physiol 1984;246:C195–203.
[4] Knepper MA, Wade JB, Terris J, Ecelbarger CA, Marples D, Mandon B, et al. Renal aquaporins. Kidney Int 1996;49:1712–7.
[5] Bourguet J, Chevalier J, Hugon JS. Alterations in membrane-associated particle distribution during antidiuretic challenge in frog urinary bladder epithelium. Biophys J 1976;16:627–39.
[6] Brown D, Orci L. Vasopressin stimulates formation of coated pits in rat kidney collecting ducts. Nature 1983;302:253–5.
[7] Kachadorian WA, Wade JB, DiScala VA. Vasopressin: induced structural change in toad bladder luminal membrane. Science 1975;190:67–9.
[8] Wade JB, Stetson DL, Lewis SA. ADH action: evidence for a membrane shuttle mechanism. Ann N.Y Acad Sci 1981;372: 106–17.
[9] Agre P, Preston GM, Smith BL, Jung JS, Raina S, Moon C, et al. The archetypal molecular water channel. Am J Physiol 1993;265: F463–76.
[10] Solomon AK, Chasan B, Dix JA, Lukacovic MF, Toon MR, Verkman AS. The aqueous pore in the red cell membrane: band 3 as a channel for anions, cations, nonelectrolytes, and water. Ann NY Acad Sci 1983;414:97–124.
[11] Agre P, Saboori AM, Asimos A, Smith BL. Purification and partial characterization of the Mr 30,000 integral membrane protein associated with the erythrocyte Rh(D) antigen. J Biol Chem 1987;262:17497–503.
[12] Denker BM, Smith BL, Kuhajda FP, Agre P. Identification, purification, and partial characterization of a novel Mr 28,000 integral membrane protein from erythrocytes and renal tubules. J Biol Chem 1988;263:15634–42.
[13] Smith BL, Agre P. Erythrocyte Mr 28,000 transmembrane protein exists as a multisubunit oligomer similar to channel proteins. J Biol Chem 1991;266:6407–15.
[14] Preston GM, Agre P. Isolation of the cDNA for erythrocyte integral membrane protein of 28 kilodaltons: member of an ancient channel family. Proc Natl Acad Sci USA 1991;88:11110–4.
[15] Van Hoek AN, Hom ML, Luthjens LH, de J, Dempster JA, van Os CH. Functional unit of 30 kDa for proximal tubule water channels as revealed by radiation inactivation. J Biol Chem 1991;266:16633–5.
[16] Agre P, Sasaki S, Chrispeels MJ. Aquaporins: a family of water channel proteins. Am J Physiol 1993;265:F461.
[17] Agre P. Molecular physiology of water transport: aquaporin nomenclature workshop. Mammalian aquaporins. Biol Cell 1997;89:255–7.
[18] Fischbarg J, Kuang KY, Vera JC, Arant S, Silverstein SC, Loike J, et al. Glucose transporters serve as water channels. Proc Natl Acad Sci USA 1990;87:3244–7.
[19] Zhang RB, Logee KA, Verkman AS. Expression of mRNA coding for kidney and red cell water channels in *Xenopus* oocytes. J Biol Chem 1990;265:15375–8.
[20] Preston GM, Carroll TP, Guggino WB, Agre P. Appearance of water channels in *Xenopus* oocytes expressing red cell CHIP28 protein. Science 1992;256:385–7.
[21] Meinild AK, Klaerke DA, Zeuthen T. Bidirectional water fluxes and specificity for small hydrophilic molecules in aquaporins 0–5. J Biol Chem 1998;273:32446–51.
[22] Zeidel ML, Ambudkar SV, Smith BL, Agre P. Reconstitution of functional water channels in liposomes containing purified red cell CHIP28 protein. Biochemistry 1992;31:7436–40.
[23] Van Hoek AN, Verkman AS. Functional reconstitution of the isolated erythrocyte water channel CHIP28. J Biol Chem 1992;267:18267–9.
[24] Zeidel ML, Nielsen S, Smith BL, Ambudkar SV, Maunsbach AB, Agre P. Ultrastructure, pharmacologic inhibition, and transport selectivity of aquaporin channel-forming integral protein in proteoliposomes. Biochemistry 1994;33:1606–15.
[25] Pao GM, Wu LF, Johnson KD, Hofte H, Chrispeels MJ, Sweet G, et al. Evolution of the MIP family of integral membrane transport proteins. Mol Microbiol 1991;5:33–7.
[26] Wistow GJ, Pisano MM, Chepelinsky AB. Tandem sequence repeats in transmembrane channel proteins. Trends Biochem Sci 1991;16:170–1.
[27] Cabiaux V, Oberg KA, Pancoska P, Walz T, Agre P, Engel A. Secondary structures comparison of aquaporin-1 and bacteriorhodopsin: a fourier transform infrared spectroscopy study of two-dimensional membrane crystals. Biophys J 1997;73:406–17.
[28] Reizer J, Reizer A, Saier Jr MH. The MIP family of integral membrane channel proteins: sequence comparisons, evolutionary relationships, reconstructed pathway of evolution, and proposed functional differentiation of the two repeated halves of the proteins. Crit Rev Biochem Mol Biol 1993;28:235–57.
[29] Preston GM, Jung JS, Guggino WB, Agre P. Membrane topology of aquaporin CHIP. Analysis of functional epitope-scanning mutants by vectorial proteolysis. J Biol Chem 1994;269:1668–73.
[30] Preston GM, Jung JS, Guggino WB, Agre P. The mercury-sensitive residue at cysteine 189 in the CHIP28 water channel. J Biol Chem 1993;268:17–20.
[31] Zhang R, Van Hoek AN, Biwersi J, Verkman AS. A point mutation at cysteine 189 blocks the water permeability of rat kidney water channel CHIP28k. Biochemistry 1993;32:2938–41.
[32] Jung JS, Preston GM, Smith BL, Guggino WB, Agre P. Molecular structure of the water channel through aquaporin CHIP. The hourglass model. J Biol Chem 1994;269:14648–54.
[33] Verbavatz JM, Brown D, Sabolic I, Valenti G, Ausiello DA, Van Hoek AN, et al. Tetrameric assembly of CHIP28 water channels in liposomes and cell membranes: a freeze-fracture study. J Cell Biol 1993;123:605–18.
[34] Shi LB, Skach WR, Verkman AS. Functional independence of monomeric CHIP28 water channels revealed by expression of wild-type mutant heterodimers. J Biol Chem 1994;269:10417–22.
[35] Walz T, Smith BL, Zeidel ML, Engel A, Agre P. Biologically active two-dimensional crystals of aquaporin CHIP. J Biol Chem 1994;269:1583–6.
[36] Walz T, Smith BL, Agre P, Engel A. The three-dimensional structure of human erythrocyte aquaporin CHIP. EMBO J 1994;13:2985–93.
[37] Walz T, Tittmann P, Fuchs KH, Muller DJ, Smith BL, Agre P, et al. Surface topographies at subnanometer-resolution reveal asymmetry and sidedness of aquaporin-1. J Mol Biol 1996;264:907–18.
[38] Cheng A, Van Hoek AN, Yeager M, Verkman AS, Mitra AK. Three-dimensional organization of a human water channel. Nature 1997;387:627–30.
[39] Jap BK, Li H. Structure of the osmo-regulated H_2O-channel, AQP-CHIP, in projection at 3.5 Å resolution. J Mol Biol 1995;251:413–20.
[40] Li H, Lee S, Jap BK. Molecular design of aquaporin-1 water channel as revealed by electron crystallography. Nat Struct Mol Biol 1997;4:263–5.
[41] Mitra AK, Van Hoek AN, Wiener MC, Verkman AS, Yeager M. The CHIP28 water channel visualized in ice by electron crystallography. Nat Struct Biol 1995;2:726–9.
[42] Mitsuoka K, Murata K, Walz T, Hirai T, Agre P, Heymann JB, et al. The structure of aquaporin-1 at 4.5-Å resolution reveals short [alpha]-helices in the center of the monomer. J Struct Biol 1999;128:34–43.
[43] Murata K, Mitsuoka K, Hirai T, Walz T, Agre P, Heymann JB, et al. Structural determinants of water permeation through aquaporin-1. Nature 2000;407:599–605.

[44] Ren G, Cheng A, Reddy V, Melnyk P, Mitra AK. Three-dimensional fold of the human AQP1 water channel determined at 4 Å resolution by electron crystallography of two-dimensional crystals embedded in ice. J Mol Biol 2000;301: 369–87.
[45] Ren G, Reddy VS, Cheng A, Melnyk P, Mitra AK. Visualization of a water-selective pore by electron crystallography in vitreous ice. Proc Natl Acad Sci USA 2001;98:1398–403.
[46] Walz T, Hirai T, Murata K, Heymann JB, Mitsuoka K, Fujiyoshi Y, et al. The three-dimensional structure of aquaporin-1. Nature 1997;387:624–7.
[47] Sui H, Han BG, Lee JK, Walian P, Jap BK. Structural basis of water-specific transport through the AQP1 water channel. Nature 2001;414:872–8.
[48] de Groot BL, Grubmuller H. Water permeation across biological membranes. mechanism and dynamics of aquaporin-1 and GlpF. Science 2001;294:2353–7.
[49] Beitz E, Wu B, Holm LM, Schultz JE, Zeuthen T. Point mutations in the aromatic/arginine region in aquaporin 1 allow passage of urea, glycerol, ammonia, and protons. Proc Nat Acad Sci 2006;103:269–74.
[50] Maurel C, Reizer J, Schroeder JI, Chrispeels MJ, Saier Jr. MH. Functional characterization of the *Escherichia coli* glycerol facilitator, GlpF, in *Xenopus* oocytes. J Biol Chem 1994;269:11869–72.
[51] Schenk AD, Werten PJL, Scheuring S, de Groot BL, Muller SA, Stahlberg H, et al. The 4.5 Å structure of human AQP2. J Mol Biol 2005;350:278–89.
[52] Werten PJL, Hasler L, Koenderink JB, Klaassen CHW, de Grip WJ, Engel A, et al. Large-scale purification of functional recombinant human aquaporin-2. FEBS Lett 2001;504:200–5.
[53] Fotiadis D, Suda K, Tittmann P, Jeno P, Philippsen A, Muller DJ, et al. Identification and structure of a putative Ca^{2+}-binding domain at the C terminus of AQP1. J Mol Biol 2002;318: 1381–94.
[54] Gonen T, Sliz P, Kistler J, Cheng Y, Walz T. Aquaporin-0 membrane junctions reveal the structure of a closed water pore. Nature 2004;429:193–7.
[55] Harries WEC, Akhavan D, Miercke LJW, Khademi S, Stroud RM. The channel architecture of aquaporin 0 at a 2.2-Å resolution. Proc Nat Acad Sci 2004;101:14045–50.
[56] Mulders SM, Preston GM, Deen PMT, Guggino WB, Os CH, Agre P. Water channel properties of major intrinsic protein of lens. J Biol Chem 1995;270:9010–6.
[57] Han BG, Guliaev AB, Walian PJ, Jap BK. Water transport in AQP0 aquaporin. Molecular dynamics studies. J Mol Biol 2006;360:285–96.
[58] Brooks HL, Regan JW, Yool AJ. Inhibition of Aquaporin-1 water permeability by tetraethylammonium: involvement of the loop E pore region. Mol Pharmacol 2000;57:1021–6.
[59] Detmers FJM, de Groot BL, Muller EM, Hinton A, Konings IBM, Sze M, et al. Quaternary ammonium compounds as water channel blockers. Specificity, potency, and site of action. J Biol Chem 2006;281:14207–14.
[60] Verkman AS. Applications of aquaporin inhibitors. Drug News Perspect 2001;14:412.
[61] Zelenina M, Tritto S, Bondar AA, Zelenin S, Aperia A. Copper inhibits the water and glycerol permeability of aquaporin-3. J Biol Chem 2004;279:51939–43.
[62] Zelenina M, Bondar AA, Zelenin S, Aperia A. Nickel and extracellular acidification inhibit the water permeability of human aquaporin-3 in lung epithelial cells. J Biol Chem 2003;278: 30037–43.
[63] Agemark M, Kowal J, Kukulski W, Norden K, Gustavsson N, Johanson U, et al. Reconstitution of water channel function and 2D-crystallization of human aquaporin 8. Biochim Biophys Acta 2012;1818:839–50.
[64] Berthaud A, Manzi J, Perez J, Mangenot S. Modeling detergent organization around aquaporin-0 using small angle X-ray scattering. J Am Chem Soc 2012;134(24):10080–8.
[65] Crane JM, Rossi A, Gupta T, Bennett JL, Verkman AS. Orthogonal array formation by human aquaporin-4: examination of neuromyelitis optica-associated aquaporin-4 polymorphisms. J Neuroimmunol 2011;236:93–8.
[66] Fischer G, Kosinska-Eriksson U, ponte-Santamaria C, Palmgren M, Geijer C, Hedfalk K, et al. Crystal structure of a yeast aquaporin at 1.15 angstrom reveals a novel gating mechanism. PLoS Bio 2009;7:e1000130.
[67] Fujiyoshi Y. Electron crystallography for structural and functional studies of membrane proteins. *J Electron Microsc* (Tokyo) 2011;60(Suppl. 1):S149–59.
[68] Ho JD, Yeh R, Sandstrom A, Chorny I, Harries WE, Robbins RA, et al. Crystal structure of human aquaporin 4 at 1.8 Å and its mechanism of conductance. Proc Natl Acad Sci USA 2009;106:7437–42.
[69] Horsefield R, Norden K, Fellert M, Backmark A, Tornroth-Horsefield S, Terwisscha van Scheltinga AC, et al. High-resolution x-ray structure of human aquaporin 5. Proc Natl Acad Sci USA 2008;105:13327–32.
[70] Jiang Y. Expression and functional characterization of NPA motif-null aquaporin-1 mutations. IUBMB Life 2009;61: 651–7.
[71] Strand L, Moe SE, Solbu TT, Vaadal M, Holen T. Roles of aquaporin-4 isoforms and amino acids in square array assembly. Biochemistry 2009;48:5785–93.
[72] Wolburg H, Wolburg-Buchholz K, Fallier-Becker P, Noell S, Mack AF. Structure and functions of aquaporin-4-based orthogonal arrays of particles. Int Rev Cell Mol Biol 2011;287:1–41.
[73] Wree D, Wu B, Zeuthen T, Beitz E. Requirement for asparagine in the aquaporin NPA sequence signature motifs for cation exclusion. FEBS J 2011;278:740–8.
[74] Yakata K, Tani K, Fujiyoshi Y. Water permeability and characterization of aquaporin-11. J Struct Biol 2011;174:315–20.
[75] Sabolic I, Valenti G, Verbavatz JM, Van Hoek AN, Verkman AS, Ausiello DA, et al. Localization of the CHIP28 water channel in rat kidney. Am J Physiol 1992;263:C1225–33.
[76] Maunsbach AB, Marples D, Chin E, Ning G, Bondy C, Agre P, et al. Aquaporin-1 water channel expression in human kidney. J Am Soc Nephrol 1997;8:1–14.
[77] Nielsen S, Smith B, Christensen EI, Knepper MA, Agre P. CHIP28 water channels are localized in constitutively water-permeable segments of the nephron. J Cell Biol 1993;120: 371–83.
[78] Maeda Y, Smith BL, Agre P, Knepper MA. Quantification of aquaporin-CHIP water channel protein in microdissected renal tubules by fluorescence-based ELISA. J Clin Invest 1995;95: 422–8.
[79] Bedford JJ, Leader JP, Walker RJ. Aquaporin expression in normal human kidney and in renal disease. J Am Soc Nephrol 2003;14:2581–7.
[80] King LS, Nielsen S, Agre P. Aquaporin-1 water channel protein in lung: ontogeny, steroid-induced expression, and distribution in rat. J Clin Invest 1996;97:2183–91.
[81] Nielsen S, Smith BL, Christensen EI, Agre P. Distribution of the aquaporin CHIP in secretory and resorptive epithelia and capillary endothelia. Proc Natl Acad Sci USA 1993;90:7275–9.
[82] Schnitzer JE, Oh P. Aquaporin-1 in plasma membrane and caveolae provides mercury-sensitive water channels across lung endothelium. Am J Physiol 1996;270:H416–22.

[83] Pallone TL, Kishore BK, Nielsen S, Agre P, Knepper MA. Evidence that aquaporin-1 mediates NaCl-induced water flux across descending vasa recta. Am J Physiol 1997;272:F587–96.
[84] King LS, Nielsen S, Agre P. Aquaporins in complex tissues. I. Developmental patterns in respiratory and glandular tissues of rat. Am J Physiol 1997;273:C1541–8.
[85] Moon C, King LS, Agre P. Aqp1 expression in erythroleukemia cells: genetic regulation of glucocorticoid and chemical induction. Am J Physiol 1997;273:C1562–70.
[86] Lai, KN., Li, FG., Yui, LH., Tang, S., Tsang, AWL., Chan, DTM, et al., Expression of aquaporin-1 in human peritoneal mesothelial cells and its upregulation by glucose in vitro. J Am Soc Nephrol 12:1036–45.
[87] Mann SE, Ricke EA, Yang BA, Verkman AS, Taylor RN. Expression and localization of aquaporin 1 and 3 in human fetal membranes. Am J Obstet Gynecol 2002;187:902–7.
[88] Hasegawa H, Lian SC, Finkbeiner WE, Verkman AS. Extrarenal tissue distribution of CHIP28 water channels by *in situ* hybridization and antibody staining. Am J Physiol 1994;266:C893–903.
[89] Stamer WD, Snyder RW, Smith BL, Agre P, Regan JW. Localization of aquaporin CHIP in the human eye: implications in the pathogenesis of glaucoma and other disorders of ocular fluid balance. Invest Ophthalmol Vis Sci 1994;35:3867–72.
[90] Roberts SK, Yano M, Ueno Y, Pham L, Alpini G, Agre P, et al. Cholangiocytes express the aquaporin CHIP and transport water via a channel-mediated mechanism. Proc Natl Acad Sci USA 1994;91:13009–13.
[91] Ko SBH, Naruse S, Kitagawa M, Ishiguro H, Furuya S, Mizuno N, et al. Aquaporins in rat pancreatic interlobular ducts. AJP-Gastrointest Liver Physiol 2002;282:G324–31.
[92] Au CG, Cooper ST, Lo HP, Compton AG, Yang N, Wintour EM, et al. Expression of aquaporin 1 in human cardiac and skeletal muscle. J Mol Cell Cardiol 2004;36:655–62.
[93] Calamita G, Ferri D, Bazzini C, Mazzone A, Botta G, Liquori G, et al. Expression and subcellular localization of the AQP8 and AQP1 water channels in the mouse gall-bladder epithelium. Biol Cell 2005;97(6):415–23.
[94] Gresz V, Kwon TH, Hurley PT, Varga G, Zelles T, Nielsen S, et al. Identification and localization of aquaporin water channels in human salivary glands. AJP-Gastrointest Liver Physiol 2001;281:G247–54.
[95] Huang D, Chen P, Chen S, Nagura M, Lim DJ, Lin X. Expression patterns of aquaporins in the inner ear: evidence for concerted actions of multiple types of aquaporins to facilitate water transport in the cochlea. Hear Res 2002;165:85–95.
[96] Takata K, Matsuzaki T, Tajika Y. Aquaporins: water channel proteins of the cell membrane. Prog Histochem Cytochem 2004;39:1–83.
[97] Endo M, Jain RK, Witwer B, Brown D. Water channel (aquaporin 1) expression and distribution in mammary carcinomas and glioblastomas. Microvasc Res 1999;58:89–98.
[98] Bondy C, Chin E, Smith BL, Preston GM, Agre P. Developmental gene expression and tissue distribution of the CHIP28 water-channel protein. Proc Natl Acad Sci USA 1993;90:4500–4.
[99] Smith BL, Baumgarten R, Nielsen S, Raben D, Zeidel ML, Agre P. Concurrent expression of erythroid and renal aquaporin CHIP and appearance of water channel activity in perinatal rats. J Clin Invest 1993;92:2035–41.
[100] Smith BL, Preston GM, Spring FA, Anstee DJ, Agre P. Human red cell aquaporin CHIP. I. Molecular characterization of ABH and Colton blood group antigens. J Clin Invest 1994;94:1043–9.
[101] Preston GM, Smith BL, Zeidel ML, Moulds JJ, Agre P. Mutations in aquaporin-1 in phenotypically normal humans without functional CHIP water channels. Science 1994;265: 1585–7.
[102] King LS, Choi M, Fernandez PC, Cartron JP, Agre P. Defective urinary concentrating ability due to a complete deficiency of aquaporin-1. N Engl J Med 2001;345:175–9.
[103] King LS, Nielsen S, Agre P, Brown RH. Decreased pulmonary vascular permeability in aquaporin-1-null humans. Proc Natl Acad Sci 2002;99:1059–63.
[104] Ma T, Yang B, Gillespie A, Carlson EJ, Epstein CJ, Verkman AS. Severely impaired urinary concentrating ability in transgenic mice lacking aquaporin-1 water channels. J Biol Chem 1998;273:4296–9.
[105] Schnermann J, Chou CL, Ma T, Traynor T, Knepper MA, Verkman AS. Defective proximal tubular fluid reabsorption in transgenic aquaporin-1 null mice. Proc Natl Acad Sci USA 1998;95:9660–4.
[106] Vallon V, Verkman AS, Schnermann J. Luminal hypotonicity in proximal tubules of aquaporin-1-knockout mice. AJP-Renal Physiol 2000;278:F1030–3.
[107] Hashimoto S, Huang Y, Mizel D, Briggs J, Schnermann J. Compensation of proximal tubule malabsorption in AQP1-deficient mice without TGF-mediated reduction of GFR. Acta Physiol Scand 2004;181:455–62.
[108] Chou CL, Knepper MA, Hoek AN, Brown D, Yang B, Ma T, et al. Reduced water permeability and altered ultrastructure in thin descending limb of Henle in aquaporin-1 null mice. J Clin Invest 1999;103:491–6.
[109] Pallone TL, Edwards A, Ma T, Silldorff EP, Verkman AS. Requirement of aquaporin-1 for NaCl-driven water transport across descending vasa recta. J Clin Invest 2000;105:215–22.
[110] Yang B, Tonghui MA, Dong JY, Verkman AS. Partial correction of the urinary concentrating defect in aquaporin-1 null mice by adenovirus-mediated gene delivery. Human Gene Therapy 2000;11:567–75.
[111] Abrami L, Tacnet F, Ripoche P. Evidence for a glycerol pathway through aquaporin 1 (CHIP28) channels. Pflugers Arch 1995;430:447–58.
[112] Yool AJ, Stamer WD, Regan JW. Forskolin stimulation of water and cation permeability in aquaporin 1 water channels. Science 1996;273:1216–8.
[113] Agre P, Lee MD, Devidas S, Guggino WB. Aquaporins and ion conductance. Science 1997;275:1490.
[114] Patil RV, Saito I, Yang X, Wax MB. Expression of aquaporins in the rat ocular tissue. Exp Eye Res 1997;64:203–9.
[115] Marinelli RA, Pham L, Agre P, LaRusso NF. Secretin promotes osmotic water transport in rat cholangiocytes by increasing aquaporin-1 water channels in plasma membrane. Evidence for a secretin-induced vesicular translocation of aquaporin-1. J Biol Chem 1997;272:12984–8.
[116] Marinelli RA, Tietz PS, Pham LD, Rueckert L, Agre P, LaRusso NF. Secretin induces the apical insertion of aquaporin-1 water channels in rat cholangiocytes. AJP-Gastrointest Liver Physiol 1999;276:G280–6.
[117] Nakhoul NL, Davis BA, Romero MF, Boron WF. Effect of expressing the water channel aquaporin-1 on the CO_2 permeability of *Xenopus* oocytes. Am J Physiol 1998;274:C543–8.
[118] Reuss L. Focus on "Effect of expressing the water channel aquaporin-1 on the CO_2 permeability of *Xenopus* oocytes". Am J Physiol 1998;274:C297–8.
[119] Cooper GJ, Zhou Y, Bouyer P, Grichtchenko II, Boron WF. Transport of volatile solutes through AQP1. J Physiol Online 2002;542:17–29.

[120] Saadoun S, Papadopoulos MC, Hara-Chikuma M, Verkman AS. Impairment of angiogenesis and cell migration by targeted aquaporin-1 gene disruption. Nature 2005;434:786–92.
[121] Hara-Chikuma M, Verkman AS. Aquaporin-1 facilitates epithelial cell migration in kidney proximal tubule. J Am Soc Nephrol 2006;17:39–45.
[122] Agre P, Bonhivers M, Borgnia MJ. The aquaporins, blueprints for cellular plumbing systems. J Biol Chem. 1998;273: 14659–62.
[123] Fushimi K, Uchida S, Hara Y, Hirata Y, Marumo F, Sasaki S. Cloning and expression of apical membrane water channel of rat kidney collecting tubule. Nature 1993;361:549–52.
[124] Echevarria M, Windhager EE, Tate SS, Frindt G. Cloning and expression of AQP3, a water channel from the medullary collecting duct of rat kidney. Proc Natl Acad Sci USA 1994;91:10997–1001.
[125] Ishibashi K, Sasaki S, Fushimi K, Uchida S, Kuwahara M, Saito H, et al. Molecular cloning and expression of a member of the aquaporin family with permeability to glycerol and urea in addition to water expressed at the basolateral membrane of kidney collecting duct cells. Proc Natl Acad Sci USA 1994;91:6269–73.
[126] Ma T, Frigeri A, Hasegawa H, Verkman AS. Cloning of a water channel homolog expressed in brain meningeal cells and kidney collecting duct that functions as a stilbene-sensitive glycerol transporter. J Biol Chem 1994;269:21845–9.
[127] Hasegawa H, Ma T, Skach W, Matthay MA, Verkman AS. Molecular cloning of a mercurial-insensitive water channel expressed in selected water-transporting tissues. J Biol Chem. 1994;269:5497–500.
[128] Jung JS, Bhat RV, Preston GM, Guggino WB, Baraban JM, Agre P. Molecular characterization of an aquaporin cDNA from brain: candidate osmoreceptor and regulator of water balance. Proc Natl Acad Sci USA 1994;91:13052–6.
[129] Ma T, Frigeri A, Skach W, Verkman AS. Cloning of a novel rat kidney cDNA homologous to CHIP28 and WCH-CD water channels. Biochem Biophys Res Commun 1993;197: 654–9.
[130] Ma T, Yang B, Kuo WL, Verkman AS. cDNA cloning and gene structure of a novel water channel expressed exclusively in human kidney: evidence for a gene cluster of aquaporins at chromosome locus 12q13. Genomics 1996;35:543–50.
[131] Yasui M, Kwon TH, Knepper MA, Nielsen S, Agre P. Aquaporin-6. An intracellular vesicle water channel protein in renal epithelia. Proc Natl Acad Sci 1999;96:5808–13.
[132] Ishibashi K, Kuwahara M, Gu Y, Kageyama Y, Tohsaka A, Suzuki F, et al. Cloning and functional expression of a new water channel abundantly expressed in the testis permeable to water, glycerol, and urea. J Biol Chem. 1997;272:20782–6.
[133] Kuriyama H, Kawamoto S, Ishida N, Ohno I, Mita S, Matsuzawa Y, et al. Molecular cloning and expression of a novel human aquaporin from adipose tissue with glycerol permeability. Biochem Biophys Res Commun 1997;241:53–8.
[134] Sohara E, Rai T, Miyazaki Ji, Verkman AS, Sasaki S, Uchida S. Defective water and glycerol transport in the proximal tubules of AQP7 knockout mice. AJP-Renal Physiol 2005;289: F1195–200.
[135] Elkjar ML, Nejsum LN, Gresz V, Kwon TH, Jensen UB, Frokiar J, et al. Immunolocalization of aquaporin-8 in rat kidney, gastrointestinal tract, testis, and airways. AJP-Renal Physiol 2001;281:F1047–57.
[136] Ma T, Yang B, Verkman AS. Cloning of a novel water and urea-permeable aquaporin from mouse expressed strongly in colon, placenta, liver, and heart. Biochem Biophys Res Commun 1997;240:324–8.
[137] Morishita Y, Matsuzaki T, Hara-chikuma M, Andoo A, Shimono M, Matsuki A, et al. Disruption of aquaporin-11 produces polycystic kidneys following vacuolization of the proximal tubule. Mol Cell Biol 2005;25:7770–9.
[138] Nielsen S, DiGiovanni SR, Christensen EI, Knepper MA, Harris HW. Cellular and subcellular immunolocalization of vasopressin- regulated water channel in rat kidney. Proc Natl Acad Sci USA 1993;90:11663–7.
[139] Kishore BK, Terris JM, Knepper MA. Quantitation of aquaporin-2 abundance in microdissected collecting ducts: axial distribution and control by AVP. Am J Physiol 1996;271: F62–70.
[140] Coleman RA, Wu DC, Liu J, Wade JB. Expression of aquaporins in the renal connecting tubule. AJP-Renal Physiol 2000;279: F874–83.
[141] Christensen BM, Wang W, Frokiar J, Nielsen S. Axial heterogeneity in basolateral AQP2 localization in rat kidney: effect of vasopressin. AJP-Renal Physiol 2003;284:F701–17.
[142] Flamion B, Spring KR. Water permeability of apical and basolateral cell membranes of rat inner medullary collecting duct. Am J Physiol 1990;259:F986–99.
[143] DiGiovanni SR, Nielsen S, Christensen EI, Knepper MA. Regulation of collecting duct water channel expression by vasopressin in Brattleboro rat. Proc Natl Acad Sci USA 1994;91:8984–8.
[144] Deen PM, Verdijk MA, Knoers NV, Wieringa B, Monnens LA, van Os CH, et al. Requirement of human renal water channel aquaporin-2 for vasopressin-dependent concentration of urine. Science 1994;264:92–5.
[145] Rojek A, Fuchtbauer EM, Kwon TH, Frokiar J, Nielsen S. Severe urinary concentrating defect in renal collecting duct-selective AQP2 conditional-knockout mice. Proc Natl Acad Sci 2006;103(15):6037–42.
[146] Yang B, Gillespie A, Carlson EJ, Epstein CJ, Verkman AS. Neonatal mortality in an aquaporin-2 knock-in mouse model of recessive nephrogenic diabetes insipidus. J Biol Chem 2001;276:2775–9.
[147] Yang B, Zhao D, Qian L, Verkman AS. Mouse model of inducible nephrogenic diabetes insipiduc produced by floxed aquaporin-2 gene deletion. AJP-Renal Physiol 2006;291(2): F465–72.
[148] Ma T, Song Y, Yang B, Gillespie A, Carlson EJ, Epstein CJ, et al. Nephrogenic diabetes insipidus in mice lacking aquaporin-3 water channels. Proc Natl Acad Sci 2000;97: 4386–91.
[149] Yang B, Verkman AS. Water and glycerol permeabilities of aquaporins 1–5 and MIP determined quantitatively by expression of epitope-tagged constructs in *Xenopus* oocytes. J Biol Chem 1997;272:16140–6.
[150] Zeuthen T, Klaerke DA. Transport of water and glycerol in aquaporin 3 is gated by H^+. J Biol Chem 1999;274:21631–6.
[151] Ecelbarger CA, Terris J, Frindt G, Echevarria M, Marples D, Nielsen S, et al. Aquaporin-3 water channel localization and regulation in rat kidney. Am J Physiol 1995;269:F663–72.
[152] Frigeri A, Gropper MA, Turck CW, Verkman AS. Immunolocalization of the mercurial-insensitive water channel and glycerol intrinsic protein in epithelial cell plasma membranes. Proc Natl Acad Sci USA 1995;92:4328–31.
[153] Terris J, Ecelbarger CA, Marples D, Knepper MA, Nielsen S. Distribution of aquaporin-4 water channel expression within rat kidney. Am J Physiol 1995;269:F775–85.
[154] van Hoek AN, Ma T, Yang B, Verkman AS, Brown D. Aquaporin-4 is expressed in basolateral membranes of proximal tubule S3 segments in mouse kidney. AJP-Renal Physiol 2000;278:F310–6.

[155] Silberstein C, Bouley R, Huang Y, Fang P, Pastor-Soler N, Brown D, et al. Membrane organization and function of M1 and M23 isoforms of aquaporin-4 in epithelial cells. AJP-Renal Physiol 2004;287:F501–11.

[156] Kwon TH, Nielsen J, Masilamani S, Hager H, Knepper MA, Frokiar J, et al. Regulation of collecting duct AQP3 expression: response to mineralocorticoid. AJP-Renal Physiol 2002;283: F1403–21.

[157] Zelenina M, Zelenin S, Bondar AA, Brismar H, Aperia A. Water permeability of aquaporin-4 is decreased by protein kinase C and dopamine. AJP-Renal Physiol 2002;283:F309–18.

[158] Chou CL, Ma T, Yang B, Knepper MA, Verkman AS. Fourfold reduction of water permeability in inner medullary collecting duct of aquaporin-4 knockout mice. Am J Physiol 1998;274: C549–54.

[159] Ma T, Yang B, Gillespie A, Carlson EJ, Epstein CJ, Verkman AS. Generation and phenotype of a transgenic knockout mouse lacking the mercurial-insensitive water channel aquaporin-4. J Clin Invest 1997;100:957–62.

[160] Yasui M, Hazama A, Kwon TH, Nielsen S, Guggino WB, Agre P. Rapid gating and anion permeability of an intracellular aquaporin. Nature 1999;402:184–7.

[161] Ikeda M, Beitz E, Kozono D, Guggino WB, Agre P, Yasui M. Characterization of aquaporin-6 as a nitrate channel in mammalian cells. Requirement of pore-lining residue threonine 63. J Biol Chem 2002;277:39873–9.

[162] Hazama A, Kozono D, Guggino WB, Agre P, Yasui M. Ion permeation of AQP6 water channel protein. Single-channel recordings after Hg^{2+} activation. J Biol Chem 2002;277: 29224–30.

[163] Liu K, Kozono D, Kato Y, Agre P, Hazama A, Yasui M. From the cover. Conversion of aquaporin 6 from an anion channel to a water-selective channel by a single amino acid substitution. Proc Natl Acad Sci 2005;102:2192–7.

[164] Kishida K, Kuriyama H, Funahashi T, Shimomura I, Kihara S, Ouchi N, et al. Aquaporin adipose, a putative glycerol channel in adipocytes. J Biol Chem 2000;275:20896–902.

[165] Ishibashi K, Imai M, Sasaki S. Cellular localization of aquaporin 7 in the rat kidney. Nephron Exp Nephrology 2000;8:252–7.

[166] Nejsum LN, Elkjaer M-L, Hager H, Frokiaer J, Kwon TH, Nielsen S. Localization of aquaporin-7 in rat and mouse kidney using RT-PCR, immunoblotting, and immunocytochemistry. Biochem Biophys Res Commun 2000;277:164–70.

[167] Liu Z, Shen J, Carbrey JM, Mukhopadhyay R, Agre P, Rosen BP. Arsenite transport by mammalian aquaglyceroporins AQP7 and AQP9. Proc Natl Acad Sci 2002;99:6053–8.

[168] Ishibashi K, Kuwahara M, Kageyama Y, Tohsaka A, Marumo F, Sasaki S. Cloning and functional expression of a second new aquaporin abundantly expressed in testis. Biochem Biophys Res Commun 1997;237:714–8.

[169] Koyama Y, Yamamoto T, Tani T, Nihei K, Kondo D, Funaki H, et al. Expression and localization of aquaporins in rat gastrointestinal tract. Am J Physiol 1999;276:C621–7.

[170] Yang B, Song Y, Zhao D, Verkman AS. Phenotype analysis of aquaporin-8 null mice. AJP-Cell Physiol 2005;288:C1161–70.

[171] Holm LM, Jahn TP, Moller AL, Schjoerring JK, Ferri D, Klaerke DA, et al. NH_3 and NH_4^+ permeability in aquaporin-expressing *Xenopus* oocytes. Pflugers Arch 2005;450:415–28.

[172] Liu KF, Nagase HF, Huang CG, Calamita G, Agre P. Purification and functional characterization of aquaporin-8. Biol Cell 2006;98(3):153–61.

[173] Jahn TP, Moller ALB, Zeuthen T, Holm LM, Klaerke DA, Mohsin B, et al. Aquaporin homologues in plants and mammals transport ammonia. FEBS Lett 2004;574:31–6.

[174] Yang B, Zhao D, Solenov E, Verkman AS. Evidence from knockout mice against physiologically significant aquaporin-8 facilitated ammonia transport. AJP-Cell Physiol 2006;291(3): C417–423.

[175] Nielsen S, King LS, Christensen BM, Agre P. Aquaporins in complex tissues. II. Subcellular distribution in respiratory and glandular tissues of rat. AJP-Cell Physiol 1997;273:C1549–61.

[176] Maeda N, Funahashi T, Hibuse T, Nagasawa A, Kishida K, Kuriyama H, et al. Adaptation to fasting by glycerol transport through aquaporin 7 in adipose tissue. Proc Natl Acad Sci 2004;101:17801–6.

[177] Ishibashi K, Kuwahara M, Gu Y, Tanaka Y, Marumo F, Sasaki S. Cloning and functional expression of a new aquaporin (AQP9) abundantly expressed in the peripheral leukocytes permeable to water and urea, but not to glycerol. Biochem Biophys Res Commun 1998;244:268–74.

[178] Ko SB, Uchida S, Naruse S, Kuwahara M, Ishibashi K, Marumo F, et al. Cloning and functional expression of rAOP9L a new member of aquaporin family from rat liver. Biochem Mol Biol Int 1999;47:309–18.

[179] Tsukaguchi H, Weremowicz S, Morton CC, Hediger MA. Functional and molecular characterization of the human neutral solute channel aquaporin-9. AJP-Renal Physiol 1999;277: F685–96.

[180] Tsukaguchi H, Shayakul C, Berger UV, Mackenzie B, Devidas S, Guggino WB, et al. Molecular characterization of a broad selectivity neutral solute channel. J Biol Chem 1998;273: 24737–43.

[181] Carbrey JM, Gorelick-Feldman DA, Kozono D, Praetorius J, Nielsen S, Agre P. Aquaglyceroporin AQP9. Solute permeation and metabolic control of expression in liver. Proc Natl Acad Sci 2003;100:2945–50.

[182] Nielsen S, Chou CL, Marples D, Christensen EI, Kishore BK, Knepper MA. Vasopressin increases water permeability of kidney collecting duct by inducing translocation of aquaporin-CD water channels to plasma membrane. Proc Natl Acad Sci USA 1995;92:1013–7.

[183] Sabolic I, Katsura T, Verbavatz JM, Brown D. The AQP2 water channel: effect of vasopressin treatment, microtubule disruption, and distribution in neonatal rats. J Membr Biol 1995;143: 165–75.

[184] Yamamoto T, Sasaki S, Fushimi K, Ishibashi K, Yaoita E, Kawasaki K, et al. Vasopressin increases AQP-CD water channel in apical membrane of collecting duct cells in Brattleboro rats. AJP-Cell Physiol 1995;268:C1546–51.

[185] Lankford SP, Chou CL, Terada Y, Wall SM, Wade JB, Knepper MA. Regulation of collecting duct water permeability independent of cAMP-mediated AVP response. Am J Physiol 1991;261: F554–66.

[186] Lee YJ, Lee JE, Choi HJ, Lim JS, Jung HJ, Baek MC, et al. E3 ubiquitin-protein ligases in rat kidney collecting duct: response to vasopressin stimulation and withdrawal. Am J Physiol-Renal Physiol 2011;301:F883–96.

[187] Terris J, Ecelbarger CA, Nielsen S, Knepper MA. Long-term regulation of four renal aquaporins in rats. Am J Physiol 1996;271:F414–22.

[188] Kuwahara M, Verkman AS. Pre-steady-state analysis of the turn-on and turn-off of water permeability in the kidney collecting tubule. J Membr Biol 1989;110:57–65.

[189] Wall SM, Han JS, Chou CL, Knepper MA. Kinetics of urea and water permeability activation by vasopressin in rat terminal IMCD. Am J Physiol 1992;262:F989–98.

[190] Nielsen S, Frokiar J, Marples D, Kwon TH, Agre P, Knepper MA. Aquaporins in the Kidney. From molecules to medicine. Physiol Rev 2002;82:205–44.

[191] Hays RM, Leaf A. Studies on the movement of water through the isolated toad bladder and its modification by vasopressin. J Gen Physiol 1962;45:905–19.
[192] Koefoed-Johnsen V, Ussing HH. The contributions of diffusion and flow to the passage of D2O through living membranes; effect of neurohypophyseal hormone on isolated anuran skin. Acta Physiol Scand 1953;28:60–76.
[193] Grantham JJ, Burg MB. Effect of vasopressin and cyclic AMP on permeability of isolated collecting tubules. Am J Physiol 1966;211:255–9.
[194] Morgan T, Berliner RW. Permeability of the loop of Henle, vasa recta, and collecting duct to water, urea, and sodium. Am J Physiol 1968;215:108–15.
[195] Nielsen S, Knepper MA. Vasopressin activates collecting duct urea transporters and water channels by distinct physical processes. Am J Physiol 1993;265:F204–13.
[196] Kanno K, Sasaki S, Hirata Y, Ishikawa S, Fushimi K, Nakanishi S, et al. Urinary excretion of aquaporin-2 in patients with diabetes insipidus. N Eng J Med 1995;332:1540–5.
[197] Marples D, Knepper MA, Christensen EI, Nielsen S. Redistribution of aquaporin-2 water channels induced by vasopressin in rat kidney inner medullary collecting duct. Am J Physiol 1995;269:C655–64.
[198] Christensen BM, Marples D, Jensen UB, Frokiaer J, Sheikh-Hamad D, Knepper M, et al. Acute effects of vasopressin V2-receptor antagonist on kidney AQP2 expression and subcellular distribution. AJP-Renal Physiol 1998;275:F285–97.
[199] Hayashi M, Sasaki S, Tsuganezawa H, Monkawa T, Kitajima W, Konishi K, et al. Expression and distribution of aquaporin of collecting duct are regulated by vasopressin V2 receptor in rat kidney. J Clin Invest 1994;94:1778–83.
[200] Saito T, Ishikawa SE, Sasaki S, Fujita N, Fushimi K, Okada K, et al. Alteration in water channel AQP-2 by removal of AVP stimulation in collecting duct cells of dehydrated rats. AJP-Renal Physiol 1997;272:F183–91.
[201] Knepper MA, Nielsen S. Kinetic model of water and urea permeability regulation by vasopressin in collecting duct. Am J Physiol 1993;265:F214–24.
[202] Brown D, Weyer P, Orci L. Vasopressin stimulates endocytosis in kidney collecting duct principal cells. Eur J Cell Biol 1988;46:336–41.
[203] Lencer WI, Brown D, Ausiello DA, Verkman AS. Endocytosis of water channels in rat kidney: cell specificity and correlation with *in vivo* antidiuresis. Am J Physiol 1990; 259:C920–32.
[204] Strange K, Willingham MC, Handler JS, Harris Jr HW. Apical membrane endocytosis via coated pits is stimulated by removal of antidiuretic hormone from isolated, perfused rabbit cortical collecting tubule. J Membr Biol 1988;103:17–28.
[205] Nielsen S, Muller J, Knepper MA. Vasopressin- and cAMP-induced changes in ultrastructure of isolated perfused inner medullary collecting ducts. Am J Physiol 1993;265:F225–38.
[206] Deen PM, van Aubel RA, Van Lieburg AF, van Os CH. Urinary content of aquaporin 1 and 2 in nephrogenic diabetes insipidus. J Am Soc Nephrol 1996;7:836–41.
[207] Katsura T, Ausiello DA, Brown D. Direct demonstration of aquaporin-2 water channel recycling in stably transfected LLC-PK1 epithelial cells. AJP-Renal Physiol 1996;270:F548–53.
[208] Katsura T, Gustafson CE, Ausiello DA, Brown D. Protein kinase A phosphorylation is involved in regulated exocytosis of aquaporin-2 in transfected LLC-PK1 cells. Am J Physiol 1997;272:F817–22.
[209] Katsura T, Verbavatz J, Farinas J, Ma T, Ausiello DA, Verkman AS, et al. Constitutive and regulated membrane expression of aquaporin 1 and aquaporin 2 water channels in stably transfected LLC-PK1 epithelial cells. Proc Natl Acad Sci 1995;92:7212–6.
[210] Valenti G, Frigeri A, Ronco PM, D'Ettorre C, Svelto M. Expression and functional analysis of water channels in a stably AQP2-transfected human collecting duct cell line. J Biol Chem 1996;271:24365–70.
[211] Frische S, Kwon TH, Frokiaer J, Nielsen S. Aquaporin-2 trafficking. In: Boles E, Kramer R, editors. Molecular mechanisms controlling transmembrane transport. Berlin: Springer; p. 353–77.
[212] Kuwahara M, Fushimi K, Terada Y, Bai L, Marumo F, Sasaki S. cAMP-dependent phosphorylation stimulates water permeability of aquaporin-collecting duct water channel protein expressed in *Xenopus* oocytes. J Biol Chem 1995;270:10384–7.
[213] Lande MB, Jo I, Zeidel ML, Somers M, Harris Jr. HW. Phosphorylation of aquaporin-2 does not alter the membrane water permeability of rat papillary water channel-containing vesicles. J Biol Chem 1996;271:5552–7.
[214] Knepper M, Nielsen S, Chou CL, DiGiovanni, SR, Mechanism of vasopressin action in the renal collecting duct. Semin Nephrol 14:302–21.
[215] Kwon TH, Nielsen J, Moller HB, Fenton RA, Nielsen S, Frokiaer J. Aquaporins in the kidney. Handb Exp Pharmacol 2009;190:95–132.
[216] Moeller HB, Olesen ET, Fenton RA. Regulation of the water channel aquaporin-2 by posttranslational modification. AJP-Renal Physiol 2011;300:F1062–73.
[217] Nedvetsky PI, Tamma G, Beulshausen S, Valenti G, Rosenthal W, Klussmann E. Regulation of aquaporin-2 trafficking. Handb Exp Pharmacol 2009;190:133–57.
[218] Edwards RM, Jackson BA, Dousa TP. ADH-sensitive cAMP system in papillary collecting duct: effect of osmolality and PGE2. Am J Physiol 1981;240:F311–8.
[219] Kurokawa K, Massry SG. Interaction between catecholamines and vasopressin on renal medullary cyclic AMP of rat. Am J Physiol 1973;225:825–9.
[220] Nishimoto G, Zelenina M, Li D, Yasui M, Aperia A, Nielsen S, et al. Arginine vasopressin stimulates phosphorylation of aquaporin-2 in rat renal tissue. Am J Physiol 1999;276:F254–9.
[221] Fushimi K, Sasaki S, Marumo F. Phosphorylation of serine 256 is required for cAMP-dependent regulatory exocytosis of the aquaporin-2 water channel. J Biol Chem 1997;272:14800–4.
[222] Christensen BM, Zelenina M, Aperia A, Nielsen S. Localization and regulation of PKA-phosphorylated AQP2 in response to V (2)-receptor agonist/antagonist treatment. Am J Physiol Renal Physiol 2000;278:F29–42.
[223] Moeller HB, Praetorius J, Rutzler MR, Fenton RA. Phosphorylation of aquaporin-2 regulates its endocytosis and protein–protein interactions. Proc Natl Acad Sci USA 2010;107:424–9.
[224] McDill BW, Li SZ, Kovach PA, Ding L, Chen F. Congenital progressive hydronephrosis (cph) is caused by an S256L mutation in aquaporin-2 that affects its phosphorylation and apical membrane accumulation. Proc Natl Acad Sci 2006;103:6952–7.
[225] Hoffert JD, Pisitkun T, Wang G, Shen RF, Knepper MA. Quantitative phosphoproteomics of vasopressin-sensitive renal cells. Regulation of aquaporin-2 phosphorylation at two sites. Proc Natl Acad Sci 2006;103:7159–64.
[226] Hoffert JD, Fenton RA, Moeller HB, Simons B, Tchapyjnikov D, McDill BW, et al. Vasopressin-stimulated increase in phosphorylation at Ser269 potentiates plasma membrane retention of aquaporin-2. J Biol Chem 2008;283:24617–27.
[227] Lu HAJ, Sun TX, Matsuzaki T, Yi XH, Eswara J, Bouley R, et al. Heat shock protein 70 interacts with aquaporin-2 and regulates its trafficking. J Biol Chem 2007;282:28721–32.

[228] Zelenina M, Christensen BM, Palmer J, Nairn AC, Nielsen S, Aperia A. Prostaglandin E(2) interaction with AVP: effects on AQP2 phosphorylation and distribution. Am J Physiol Renal Physiol 2000;278:F388–94.

[229] Olesen ET, Rutzler MR, Moeller HB, Praetorius HA, Fenton RA. Vasopressin-independent targeting of aquaporin-2 by selective E-prostanoid receptor agonists alleviates nephrogenic diabetes insipidus. Proc Natl Acad Sci USA 2011;108: 12949–54.

[230] Kwon TH, Nielsen J, Knepper MA, Frokiaer J, Nielsen S. Angiotensin II AT1 receptor blockade decreases vasopressin-induced water reabsorption and AQP2 levels in NaCl-restricted rats. AJP-Renal Physiol 2005;288:F673–84.

[231] Lee YJ, Song IK, Jang KJ, Nielsen J, Frokiaer J, Nielsen S, et al. Increased AQP2 targeting in primary cultured IMCD cells in response to angiotensin II through AT1 receptor. Am J Physiol-Renal Physiol 2007;292:F340–50.

[232] Procino G, Carmosino M, Marin O, Brunanti AM, Contri A, Pinna LA, et al. Ser-256 phosphorylation dynamics of aquaporin 2 during maturation from the endoplasmic reticulum to the vesicular compartment in renal cells. FASEB J 2003;17(13): 1886–8.

[233] Lu H, Sun TX, Bouley R, Blackburn K, McLaughlin M, Brown D. Inhibition of endocytosis causes phosphorylation (S256)-independent plasma membrane accumulation of AQP2. AJP-Renal Physiol 2004;286:F233–43.

[234] Phillips ME, Taylor A. Effect of nocodazole on the water permeability response to vasopressin in rabbit collecting tubules perfused *in vitro*. J Physiol 1989;411:529–44.

[235] Phillips ME, Taylor A. Effect of colcemid on the water permeability response to vasopressin in isolated perfused rabbit collecting tubules. J Physiol 1992;456:591–608.

[236] Marples D, Schroer TA, Ahrens N, Taylor A, Knepper MA, Nielsen S. Dynein and dynactin colocalize with AQP2 water channels in intracellular vesicles from kidney collecting duct. Am J Physiol 1998;274:F384–94.

[237] de Sousa RC, Grosso A. Vanadate blocks cyclic AMP-induced stimulation of sodium and water transport in amphibian epithelia. Nature 1979;279:803–4.

[238] Marples D, Barber B, Taylor A. Effect of a dynein inhibitor on vasopressin action in toad urinary bladder. J Physiol 1996;490 (Pt 3):767–74.

[239] Shaw S, Marples D. N-ethylmaleimide causes aquaporin-2 trafficking in the renal inner medullary collecting duct by direct activation of protein kinase A. Am J Physiol Renal Physiol 2005;288:F832–9.

[240] Dibona DR. Cytoplasmic involvement in ADH-mediated osmosis across toad urinary bladder. Am J Physiol 1983;245: C297–307.

[241] Ding GH, Franki N, Condeelis J, Hays RM. Vasopressin depolymerizes F-actin in toad bladder epithelial cells. Am J Physiol 1991;260:C9–16.

[242] Kachadorian WA, Ellis SJ, Muller J. Possible roles for microtubules and microfilaments in ADH action on toad urinary bladder. Am J Physiol 1979;236:F14–20.

[243] Muller J, Kachadorian WA. Aggregate-carrying membranes during ADH stimulation and washout in toad bladder. Am J Physiol 1984;247:C90–8.

[244] Pearl M, Taylor A. Actin filaments and vasopressin-stimulated water flow in toad urinary bladder. Am J Physiol 1983;245: C28–39.

[245] Wade JB, Kachadorian WA. Cytochalasin B inhibition of toad bladder apical membrane responses to ADH. Am J Physiol. 1988;255:C526–30.

[246] Chou CL, Christensen BM, Frische S, Vorum H, Desai RA, Hoffert JD, et al. Non-muscle myosin II and myosin light chain kinase are downstream targets for vasopressin signaling in the renal collecting duct. J Biol Chem 2004;279:49026–35.

[247] Star RA, Nonoguchi H, Balaban R, Knepper MA. Calcium and cyclic adenosine monophosphate as second messengers for vasopressin in the rat inner medullary collecting duct. J Clin Invest 1988;81:1879–88.

[248] Chou CL, Yip KP, Michea L, Kador K, Ferraris JD, Wade JB, et al. Regulation of aquaporin-2 trafficking by vasopressin in the renal collecting duct. Roles of ryanodine-sensitive Ca^{2+} stores and calmodulin. J Biol Chem 2000;275:36839–46.

[249] Yip KP. Coupling of vasopressin-induced intracellular Ca^{2+} mobilization and apical exocytosis in perfused rat kidney collecting duct. J Physiol 2002;538:891–9.

[250] Lorenz D, Krylov A, Hahm D, Hagen V, Rosenthal W, Pohl P, et al. Cyclic AMP is sufficient for triggering the exocytic recruitment of aquaporin-2 in renal epithelial cells. EMBO Rep 2003;4:88–93.

[251] Bajjalieh SM, Scheller RH. The biochemistry of neurotransmitter secretion. J Biol Chem 1995;270:1971–4.

[252] Sollner T, Whiteheart SW, Brunner M, Erdjument-Bromage H, Geromanos S, Tempst P, et al. SNAP receptors implicated in vesicle targeting and fusion. Nature 1993;362:318–24.

[253] Franki N, Macaluso F, Schubert W, Gunther L, Hays RM. Water channel-carrying vesicles in the rat IMCD contain cellubrevin. Am J Physiol 1995;269:C797–801.

[254] Harris Jr HW, Zeidel ML, Jo I, Hammond TG. Characterization of purified endosomes containing the antidiuretic hormone-sensitive water channel from rat renal papilla. J Biol Chem 1994;269:11993–2000.

[255] Inoue T, Nielsen S, Mandon B, Terris J, Kishore BK, Knepper MA. SNAP-23 in rat kidney: colocalization with aquaporin-2 in collecting duct vesicles. Am J Physiol 1998;275:F752–60.

[256] Kishore BK, Wade JB, Schorr K, Inoue T, Mandon B, Knepper MA. Expression of synaptotagmin VIII in rat kidney. Am J Physiol 1998;275:F131–42.

[257] Liebenhoff U, Rosenthal W. Identification of Rab3-, Rab5a- and synaptobrevin II-like proteins in a preparation of rat kidney vesicles containing the vasopressin-regulated water channel. FEBS Lett 1995;365:209–13.

[258] Mandon B, Chou CL, Nielsen S, Knepper MA. Syntaxin-4 is localized to the apical plasma membrane of rat renal collecting duct cells: possible role in aquaporin-2 trafficking. J Clin Invest 1996;98:906–13.

[259] Mandon B, Nielsen S, Kishore BK, Knepper MA. Expression of syntaxins in rat kidney. Am J Physiol 1997;273:F718–30.

[260] Nielsen S, Marples D, Birn H, Mohtashami M, Dalby NO, Trimble M, et al. Expression of VAMP-2-like protein in kidney collecting duct intracellular vesicles. Colocalization with aquaporin-2 water channels. J Clin Invest 1995;96: 1834–44.

[261] Sudhof TC, De CP, Niemann H, Jahn R. Membrane fusion machinery: insights from synaptic proteins. Cell 1993;75:1–4.

[262] Advani RJ, Bae HR, Bock JB, Chao DS, Doung YC, Prekeris R, et al. Seven novel mammalian SNARE proteins localize to distinct membrane compartments. J Biol Chem 1998;273: 10317–24.

[263] Calakos N, Bennett MK, Peterson KE, Scheller RH. Protein–protein interactions contributing to the specificity of intracellular vesicular trafficking. Science 1994;263:1146–9.

[264] Pevsner J, Hsu SC, Braun JE, Calakos N, Ting AE, Bennett MK, et al. Specificity and regulation of a synaptic vesicle docking complex. Neuron 1994;13:353–61.

[265] Barile M, Pisitkun T, Yu MJ, Chou CL, Verbalis MJ, Shen RF, et al. Large scale protein identification in intracellular aquaporin-2 vesicles from renal inner medullary collecting duct. Mol Cell Proteomics 2005;4:1095–106.

[266] Foster LJ, Yeung B, Mohtashami M, Ross K, Trimble WS, Klip A. Binary interactions of the SNARE proteins syntaxin-4, SNAP23, and VAMP-2 and their regulation by phosphorylation. Biochemistry 1998;37:11089–96.

[267] Risinger C, Bennett MK. Differential phosphorylation of syntaxin and synaptosome-associated protein of 25 kDa (SNAP-25) isoforms. J Neurochem 1999;72:614–24.

[268] Shimazaki Y, Nishiki T i, Omori A, Sekiguchi M, Kamata Y, Kozaki S, et al. Phosphorylation of 25-kDa synaptosome-associated protein. Possible involvement in protein kinase c-mediated regulation of neurotransmitter release. J Biol Chem 1996;271:14548–53.

[269] Jones RV, De Wardener HE. Urine concentration after fluid deprivation or pitressin tannate in oil. Br Med J 1956;1 (4961):271–4.

[270] Han JS, Maeda Y, Ecelbarger C, Knepper MA. Vasopressin-independent regulation of collecting duct water permeability. Am J Physiol 1994;266:F139–46.

[271] Wade JB, Nielsen S, Coleman RA, Knepper MA. Long-term regulation of collecting duct water permeability: freeze-fracture analysis of isolated perfused tubules. Am J Physiol 1994;266:F723–30.

[272] Flamion B, Spring KR, Abramow M. Adaptation of inner medullary collecting duct to dehydration involves a paracellular pathway. Am J Physiol 1995;268:F53–63.

[273] Chou CL, DiGiovanni SR, Mejia R, Nielsen S, Knepper MA. Oxytocin as an antidiuretic hormone. I. Concentration dependence of action. Am J Physiol 1995;269:F70–7.

[274] Fujita N, Ishikawa SE, Sasaki S, Fujisawa G, Fushimi K, Marumo F, et al. Role of water channel AQP-CD in water retention in SIADH and cirrhotic rats. Am J Physiol 1995;269: F926–31.

[275] Ecelbarger CA, Nielsen S, Olson BR, Murase T, Baker EA, Knepper MA, et al. Role of renal aquaporins in escape from vasopressin-induced antidiuresis in rat. J Clin Invest 1997;99:1852–63.

[276] Ecelbarger CA, Chou CL, Lee AJ, DiGiovanni SR, Verbalis JG, Knepper MA. Escape from vasopressin-induced antidiuresis: role of vasopressin resistance of the collecting duct. Am J Physiol 1998;274:F1161–6.

[277] Fernandez-Llama P, Turner R, Dibona G, Knepper MA. Renal expression of aquaporins in liver cirrhosis induced by chronic common bile duct ligation in rats. J Am Soc Nephrol 1999;10:1950–7.

[278] Sands JM, Naruse M, Jacobs JD, Wilcox JN, Klein JD. Changes in aquaporin-2 protein contribute to the urine concentrating defect in rats fed a low-protein diet. J Clin Invest 1996;97:2807–14.

[279] Ma T, Hasegawa H, Skach WR, Frigeri A, Verkman AS. Expression, functional analysis, and *in situ* hybridization of a cloned rat kidney collecting duct water channel. Am J Physiol 1994;266:C189–97.

[280] Uchida S, Sasaki S, Fushimi K, Marumo F. Isolation of human aquaporin-CD gene. J Biol Chem 1994;269:23451–5.

[281] Hozawa S, Holtzman EJ, Ausiello DA. cAMP motifs regulating transcription in the aquaporin 2 gene. Am J Physiol 1996;270: C1695–702.

[282] Matsumura Y, Uchida S, Rai T, Sasaki S, Marumo F. Transcriptional regulation of aquaporin-2 water channel gene by cAMP. J Am Soc Nephrol 1997;8:861–7.

[283] Yasui M, Zelenin SM, Celsi G, Aperia A. Adenylate cyclase-coupled vasopressin receptor activates AQP2 promoter via a dual effect on CRE and AP1 elements. Am J Physiol 1997;272: F443–50.

[284] Inase N, Fushimi K, Ishibashi K, Uchida S, Ichioka M, Sasaki S, et al. Isolation of human aquaporin 3 gene. J Biol Chem 1995;270:17913–6.

[285] Kamsteeg EJ, Hendriks G, Boone M, Konings IBM, Oorschot V, van der Sluijs P, et al. Short-chain ubiquitination mediates the regulated endocytosis of the aquaporin-2 water channel. Proc Natl Acad Sci 2006;103:18344–9.

[286] Agre P, King LS, Yasui M, Guggino WB, Ottersen OP, Fujiyoshi Y, et al. Aquaporin water channels–from atomic structure to clinical medicine. J Physiol Online 2002;542:3–16.

[287] Nielsen S, Knepper MA, Kwon T-H, Frokiaer J. Regulation of water balance. Urine concentration and dilution. In: Schrier RW, editor. Diseases of the Kidney and Urinary Tract. Philadelphia, Lippincott Willialms & Wilkins; 2004. p. 109–34.

[288] Robben JH, Knoers NV, Deen PM. Cell biological aspects of the vasopressin type-2 receptor and aquaporin 2 water channel in nephrogenic diabetes insipidus. AJP-Renal Physiol 2006;291: F257–70.

[289] Babey M, Kopp P, Robertson GL. Familial forms of diabetes insipidus: clinical and molecular characteristics. Nat Rev Endocrinol 2011;7:701–14.

[290] Schmale H, Ivell R, Breindl M, Darmer D, Richter D. The mutant vasopressin gene from diabetes insipidus (Brattleboro) rats is transcribed but the message is not efficiently translated. EMBO J 1984;3(13):3289–93.

[291] Bichet DG. Vasopressin receptors in health and disease. Kidney Int 1996;49:1706–11.

[292] Jensen AM, Bae EH, Fenton RA, Noregaard R, Nielsen S, Kim SW, et al. Angiotensin II regulates V2 receptor and pAQP2 during ureteral obstruction. Am J Physiol-Renal Physiol 2009;296:F127–34.

[293] Deen PM, van Aubel RA, Van Lieburg AF, van Os CH. Urinary content of aquaporin 1 and 2 in nephrogenic diabetes insipidus. J Am Soc Nephrol 1996;7(6):836–41.

[294] Wen H, Frokiaer J, Kwon TH, Nielsen S. Urinary excretion of aquaporin-2 in rat is mediated by a vasopressin-dependent apical pathway. J Am Soc Nephrol 1999;10:1416–29.

[295] Moon SS, Kim HJ, Choi YK, Seo HA, Jeon JH, Lee JE, et al. Novel mutation of aquaporin-2 gene in a patient with congenital nephrogenic diabetes insipidus. Endocrine J 2009;56: 905–10.

[296] Mulders SM, Knoers NV, Van Lieburg AF, Monnens LA, Leumann E, Wuhl E, et al. New mutations in the AQP2 gene in nephrogenic diabetes insipidus resulting in functional but misrouted water channels. J Am Soc Nephrol 1997;8:242–8.

[297] Oksche A, Moller A, Dickson J, Rosendahl W, Rascher W, Bichet DG, et al. Two novel mutations in the aquaporin-2 and the vasopressin V2 receptor genes in patients with congenital nephrogenic diabetes insipidus. Hum Genet 1996;98:587–9.

[298] Van Lieburg AF, Verdijk MA, Knoers VV, van Essen AJ, Proesmans W, Mallmann R, et al. Patients with autosomal nephrogenic diabetes insipidus homozygous for mutations in the aquaporin 2 water-channel gene. Am J Hum Genet 1994;55: 648–52.

[299] Deen PM, Croes H, van Aubel RA, Ginsel LA, van Os CH. Water channels encoded by mutant aquaporin-2 genes in nephrogenic diabetes insipidus are impaired in their cellular routing. J Clin Invest 1995;95:2291–6.

[300] Morello JP, Salahpour A, Petaja-Repo UE, Laperriere A, Lonergan M, Arthus MF, et al. Association of calnexin with

wild type and mutant AVPR2 that cause nephrogenic diabetes insipidus. Biochemistry 2001;40:6766–75.

[301] Knoers NV, van Os CH. Molecular and cellular defects in nephrogenic diabetes insipidus. Curr Opin Nephrol Hypertens 1996;5:353–8.

[302] Mulders SM, Bichet DG, Rijss JP, Kamsteeg EJ, Arthus MF, Lonergan M, et al. An aquaporin-2 water channel mutant which causes autosomal dominant nephrogenic diabetes insipidus is retained in the Golgi complex. J Clin Invest 1998;102:57–66.

[303] Faerch M, Christensen JH, Corydon TJ, Kamperis K, de ZF, Gregersen N, et al. Partial nephrogenic diabetes insipidus caused by a novel mutation in the AVPR2 gene. Clin Endocrinol(Oxf) 2008;68:395–403.

[304] Faerch M, Christensen JH, Rittig S, Johansson JO, Gregersen N, de ZF, et al. Diverse vasopressin V2 receptor functionality underlying partial congenital nephrogenic diabetes insipidus. AJP-Renal Physiol 2009;297:F1518–25.

[305] Faerch M, Corydon TJ, Rittig S, Christensen JH, Hertz JM, Jendle J. Skewed X-chromosome inactivation causing diagnostic misinterpretation in congenital nephrogenic diabetes insipidus. Scand J Urol Nephrol 2010;44:324–30.

[306] Timmer RT, Sands JM. Lithium intoxication. J Am Soc Nephrol 1999;10:666–74.

[307] Kwon T-H, Laursen UH, Marples D, Maunsbach AB, Knepper MA, Frokiaer J, et al. Altered expression of renal AQPs and Na (+) transporters in rats with lithium-induced NDI. Am J Physiol Renal Physiol 2000;279:F552–64.

[308] Marples D, Christensen S, Christensen EI, Ottosen PD, Nielsen S. Lithium-induced downregulation of aquaporin-2 water channel expression in rat kidney medulla. J Clin Invest 1995;95:1838–45.

[309] Christensen S, Kusano E, Yusufi AN, Murayama N, Dousa TP. Pathogenesis of nephrogenic diabetes insipidus due to chronic administration of lithium in rats. J Clin Invest 1985;75:1869–79.

[310] Kim YH, Kwon TH, Christensen BM, Nielsen J, Wall SM, Madsen KM, et al. Altered expression of renal acid–base transporters in rats with lithium-induced NDI. AJP-Renal Physiol 2003;285:F1244–57.

[311] Wilting I, Baumgarten R, Movig KL, Laarhoven J, Apperloo AJ, Nolen WA, et al. Urine osmolality, cyclic AMP and aquaporin-2 in urine of patients under lithium treatment in response to water loading followed by vasopressin administration. Eur J Pharmacol 2007;566:50–7.

[312] Frokiaer J, Marples D, Valtin H, Morris JF, Knepper MA, Nielsen S. Low aquaporin-2 levels in polyuric $DI^{+/+}$ severe mice with constitutively high cAMP-phosphodiesterase activity. AJP-Renal Physiol 1999;276:F179–90.

[313] Nielsen J, Kwon TH, Praetorius J, Kim YH, Frokiaer J, Knepper MA, et al. Segment-specific ENaC downregulation in kidney of rats with lithium-induced NDI. AJP-Renal Physiol 2003;285: F1198–209.

[314] Christensen BM, Zuber AM, Loffing J, Stehle JC, Deen PM, Rossier BC, et al. ENaC-mediated lithium absorption promotes nephrogenic diabetes insipidus. J Am Soc Nephrol 2011;22: 253–61.

[315] Nielsen J, Hoffert JD, Knepper MA, Agre P, Nielsen S, Fenton RA. Proteomic analysis of lithium-induced nephrogenic diabetes insipidus. Mechanisms for aquaporin 2 downregulation and cellular proliferation. Proc Natl Acad Sci 2008;105:3634–9.

[316] Nielsen J, Kwon TH, Christensen BM, Frokiaer J, Nielsen S. Dysregulation of renal aquaporins and epithelial sodium channel in lithium-induced nephrogenic diabetes insipidus. Seminars Nephrol 2008;28(3):227–44.

[317] Kortenoeven ML, Schweer H, Cox R, Wetzels JF, Deen PM. Lithium reduces aquaporin-2 transcription independent of prostaglandins. Am J Physiol-Cell Physiol 2012;302: C131–40.

[318] Marples D, Frokiaer J, Dorup J, Knepper MA, Nielsen S. Hypokalemia-induced downregulation of aquaporin-2 water channel expression in rat kidney medulla and cortex. J Clin Invest 1996;97:1960–8.

[319] Earm JH, Christensen BM, Frokiaer J, Marples D, Han JS, Knepper MA, et al. Decreased aquaporin-2 expression and apical plasma membrane delivery in kidney collecting ducts of polyuric hypercalcemic rats. J Am Soc Nephrol 1998;9: 2181–93.

[320] Sands JM, Flores FX, Kato A, Baum MA, Brown EM, Ward DT, et al. Vasopressin-elicited water and urea permeabilities are altered in IMCD in hypercalcemic rats. AJP-Renal Physiol 1998;274:F978–85.

[321] Elkjar ML, Kwon TH, Wang W, Nielsen J, Knepper MA, Frokiar J, et al. Altered expression of renal NHE3, TSC, BSC-1, and ENaC subunits in potassium-depleted rats. AJP-Renal Physiol 2002;283:F1376–88.

[322] Wang W, Li C, Kwon TH, Miller RT, Knepper MA, Frokiaer J, et al. Reduced expression of renal Na^+ transporters in rats with PTH-induced hypercalcemia. AJP-Renal Physiol 2004;286: F534–45.

[323] Zeidel M, Pirtskhalaishvili G. Urinary tract obstruction. In: Brenner BM, editor. The kidney. Philadelphia: Saunders; 2004. p. 1867–94.

[324] Frokiaer J, Marples D, Knepper MA, Nielsen S. Bilateral ureteral obstruction downregulates expression of vasopressin-sensitive AQP-2 water channel in rat kidney. Am J Physiol 1996;270:F657–68.

[325] Kim SW, Cho SH, Oh BS, Yeum CH, Choi KC, Ahn KY, et al. Diminished renal expression of aquaporin water channels in rats with experimental bilateral ureteral obstruction. J Am Soc Nephrol 2001;12:2019–28.

[326] Li C, Wang W, Kwon TH, Isikay L, Wen JG, Marples D, et al. Downregulation of AQP1, -2, and -3 after ureteral obstruction is associated with a long-term urine-concentrating defect. AJP-Renal Physiol 2001;281:F163–71.

[327] Stodkilde L, Norregaard R, Fenton RA, Wang G, Knepper MA, Frokiar J. Bilateral ureteral obstruction induces early downregulation and redistribution of AQP2 and phosphorylated AQP2. Am J Physiol-Renal Physiol 2011;301:F226–35.

[328] Li C, Wang W, Knepper MA, Nielsen S, Frokiar J. Downregulation of renal aquaporins in response to unilateral ureteral obstruction. AJP-Renal Physiol 2003;284:F1066–79.

[329] Cheng X, Zhang H, Lee HL, Park JM. Cyclooxygenase-2 inhibitor preserves medullary aquaporin-2 expression and prevents polyuria after ureteral obstruction. J Urol 2004.

[330] Norregaard R, Jensen BL, Li C, Wang W, Knepper MA, Nielsen S, et al. COX-2 inhibition prevents downregulation of key renal water and sodium transport proteins in response to bilateral ureteral obstruction. AJP-Renal Physiology 2005;289: F322–33.

[331] Norregaard R, Jensen BL, Topcu SO, Diget M, Schweer H, Knepper MA, et al. COX-2 activity transiently contributes to increased water and NaCl excretion in the polyuric phase after release of ureteral obstruction. Am J Physiol-Renal Physiol 2007;292:F1322–33.

[332] Zhang Y, Kohan DE, Nelson RD, Carlson NG, Kishore BK. Potential involvement of P2Y2 receptor in diuresis of

postobstructive uropathy in rats. AJP-Renal Physiol 2010;298: F634–42.

[333] Jensen AM, Li C, Praetorius HA, Norregaard R, Frische S, Knepper MA, et al. Angiotensin II mediates downregulation of aquaporin water channels and key renal sodium transporters in response to urinary tract obstruction. AJP-Renal Physiol 2006;291(5):F1021–32.

[334] Frokiaer J, Christensen BM, Marples D, Djurhuus JC, Jensen UB, Knepper MA, et al. Downregulation of aquaporin-2 parallels changes in renal water excretion in unilateral ureteral obstruction. Am J Physiol 1997;273:F213–23.

[335] Hanley MJ. Isolated nephron segments in a rabbit model of ischemic acute renal failure. Am J Physiol 1980;239: F17–23.

[336] Tanner GA, Sloan KL, Sophasan S. Effects of renal artery occlusion on kidney function in the rat. Kidney Int 1973;4: 377–89.

[337] Venkatachalam MA, Bernard DB, Donohoe JF, Levinsky NG. Ischemic damage and repair in the rat proximal tubule: differences among the S1, S2, and S3 segments. Kidney Int 1978;14: 31–49.

[338] Anderson RJ, Gordon JA, Kim J, Peterson LM, Gross PA. Renal concentration defect following nonoliguric acute renal failure in the rat. Kidney Int 1982;21:583–91.

[339] Fernandez-Llama P, Andrews P, Turner R, Saggi S, Di Mari J, Kwon T-H, et al. Role of collecting duct aquaporins in polyuria of post-ischemic acute renal failure in rats. J Am Soc Nephrol 1999;10:1658–68.

[340] Kwon T-H, Frokiaer J, Fernandez-Llama P, Knepper MA, Nielsen S. Reduced abundance of aquaporins in rats with bilateral ischemia-induced acute renal failure: prevention by alpha-MSH. Am J Physiol 1999;277:F413–27.

[341] Gong H, Wang W, Kwon TH, Jonassen T, Frokiaer J, Nielsen S. Reduced renal expression of AQP2, p-AQP2 and AQP3 in haemorrhagic shock-induced acute renal failure. Nephrol Dialysis Transplant 2003;18:2551–9.

[342] Sharples EJ, Patel N, Brown P, Stewart K, Mota-Philipe H, Sheaff M, et al. Erythropoietin protects the kidney against the injury and dysfunction caused by ischemia-reperfusion. J Am Soc Nephrol 2004;15:2115–24.

[343] Hocherl K, Schmidt C, Kurt B, Bucher M. Inhibition of NF-kappaB ameliorates sepsis-induced downregulation of aquaporin-2/V2 receptor expression and acute renal failure *in vivo*. AJP-Renal Physiol 2010;298:F196–204.

[344] Tannen RL, Regal EM, Dunn MJ, Schrier RW. Vasopressin-resistant hyposthenuria in advanced chronic renal disease. N Engl J Med 1969;280:1135–41.

[345] Teitelbaum I, McGuinness S. Vasopressin resistance in chronic renal failure. Evidence for the role of decreased V2 receptor mRNA. J Clin Invest 1995;96:378–85.

[346] Kwon T-H, Frokiaer J, Knepper MA, Nielsen S. Reduced AQP1, -2, and -3 levels in kidneys of rats with CRF induced by surgical reduction in renal mass. Am J Physiol 1998;275: F724–41.

[347] Nielsen S, Terris J, Andersen D, Ecelbarger C, Frokiaer J, Jonassen T, et al. Congestive heart failure in rats is associated with increased expression and targeting of aquaporin-2 water channel in collecting duct. Proc Natl Acad Sci USA 1997;94: 5450–5.

[348] Xu DL, Martin PY, Ohara M, St.John J, Pattison T, Meng X, et al. Upregulation of aquaporin-2 water channel expression in chronic heart failure rat. J Clin Invest 1997;99: 1500–5.

[349] Lutken SC, Kim SW, Jonassen T, Marples D, Knepper MA, Kwon TH, et al. Changes of renal AQP2, ENaC, and NHE3 in experimentally induced heart failure: response to angiotensin II AT1 receptor blockade. Am J Physiol-Renal Physiol 2009;297: F1678–88.

[350] Martin PY, Abraham WT, Lieming X, Olson BR, Oren RM, Ohara M, et al. Selective V2-receptor vasopressin antagonism decreases urinary aquaporin-2 excretion in patients with chronic heart failure. J Am Soc Nephrol 1999;10: 2165–70.

[351] Starklint J, Bech JN, Nyvad O, Jensen P, Pedersen EB. Increased urinary aquaporin 2 excretion in response to furosemide in patients with chronic heart failure. Scandinavian J Clinical Lab Invest 2006;66:55–66.

[352] Portincasa P, Palasciano G, Svelto M, Calamita G. Aquaporins in the hepatobiliary tract. Which, where and what they do in health and disease? European J Clin Invest 2008;38:1–10.

[353] Jonassen TE, Nielsen S, Christensen S, Petersen JS. Decreased vasopressin-mediated renal water reabsorption in rats with compensated liver cirrhosis. Am J Physiol 1998;275: F216–25.

[354] Jonassen TE, Promeneur D, Christensen S, Petersen JS, Nielsen S. Decreased vasopressin-mediated renal water reabsorption in rats with chronic aldosterone-receptor blockade. Am J Physiol Renal Physiol 2000;278:F246–56.

[355] Asahina Y, Izumi N, Enomoto N, Sasaki S, Fushimi K, Marumo F, et al. Increased gene expression of water channel in cirrhotic rat kidneys. Hepatology 1995;21: 169–73.

[356] Fernandez-Llama P, Jimenez W, Bosch-Marce M, Arroyo V, Nielsen S, Knepper MA. Dysregulation of renal aquaporins and Na-Cl co-transporter in CCl4-induced cirrhosis. Kidney Int 2000;58:216–28.

[357] Esteva-Font C, Baccaro ME, Fernández-Llama P, Sans L, Guevara M, Ars E, et al. Aquaporin-1 and aquaporin-2 urinary excretion in cirrhosis: relationship with ascites and hepatorenal syndrome. Hepatology 2006;44:1555–63.

[358] Gines P, Berl T, Bernardi M, Bichet DG, Hamon G, Jimenez W, et al. Hyponatremia in cirrhosis: from pathogenesis to treatment. Hepatology 1998;28:851–64.

[359] Kim SW, Schou UK, Peters CD, de Seigneux S, Kwon TH, Knepper MA, et al. Increased apical targeting of renal epithelial sodium channel subunits and decreased expression of type 2 11beta-hydroxysteroid dehydrogenase in rats with CCl4-induced decompensated liver cirrhosis. J Am Soc Nephrol 2005;16:3196–210.

[360] Wood LJ, Massie D, McLean AJ, Dudley FJ. Renal sodium retention in cirrhosis: tubular site and relation to hepatic dysfunction. Hepatology 1988;8:831–6.

[361] Levy M, Wexler MJ. Hepatic denervation alters first-phase urinary sodium excretion in dogs with cirrhosis. Am J Physiol 1987;253:F664–71.

[362] Huebert RC, Jagavelu K, Hendrickson HI, Vasdev MM, Arab JP, Splinter PL, et al. Aquaporin-1 promotes angiogenesis, fibrosis, and portal hypertension through mechanisms dependent on osmotically sensitive microRNAs. Am J Pathol 2011;179:1851–60.

[363] Apostol E, Ecelbarger CA, Terris J, Bradford AD, Andrews P, Knepper MA. Reduced renal medullary water channel expression in puromycin aminonucleoside: induced nephrotic syndrome. J Am Soc Nephrol 1997;8:15–24.

[364] Fernandez-Llama P, Andrews P, Ecelbarger CA, Nielsen S, Knepper M. Concentrating defect in experimental nephrotic syndrome: altered expression of aquaporins and thick ascending limb Na^+ transporters. Kidney Int 1998;54: 170–9.

[365] Fernandez-Llama P, Andrews P, Nielsen S, Ecelbarger CA, Knepper MA. Impaired aquaporin and urea transporter expression in rats with adriamycin-induced nephrotic syndrome. Kidney Int 1998;53:1244–53.

[366] Flear CT, Gill GV, Burn J. Hyponatraemia: mechanisms and management. Lancet 1981;2:26–31.

[367] Bartter FC, Schwartz WB. The syndrome of inappropriate secretion of antidiuretic hormone. Am J Med 1967;42: 790–806.

[368] Ishikawa S, Saito T, Saito T, Kasono K, Funayama H. Pathophysiological role of aquaporin-2 in impaired water excretion. In: Neumann ID, editor. Progress in brain research advances in vasopressin and oxytocin–from genes to behaviour to disease. Elsevier; 2008. p. 581–8.

[369] Verbalis JG. Whole-body volume regulation and escape from antidiuresis. Am J Med 2006;119:S21–9.

[370] Heymann JB, Agre P, Engel A. Progress on the structure and function of aquaporin 1. J Struct Biol 1998;121:191–206.

[371] de Groot BL, Engel A, Grubmuller H. A refined structure of human aquaporin-1. FEBS Lett 2001;504:206–11.

[372] de Groot BL, Engel A, Grubmuller H. The structure of the aquaporin-1 water channel. A comparison between cryo-electron microscopy and X-ray crystallography. J Mol Biol 2003;325:485–93.

This page intentionally left blank

CHAPTER

42

Thirst and Vasopressin

Gary L. Robertson

The Feinberg School of Medicine, Northwestern University, Chicago, IL, USA

INTRODUCTION

Thirst and the antidiuretic hormone, arginine vasopressin, are the principal elements of a powerful homeostatic system that regulates the "effective" osmotic pressure of body fluids. This variable, usually referred to as "tonicity," must be important for survival since mechanisms to regulate it are found throughout the animal kingdom, and abnormalities in humans can have adverse effects, especially on central nervous function. However, it is less clear why it is important. It may be that regulating the *tonicity* of body fluids is mainly an indirect way to minimize changes in the *volume* of water within cells, particularly those of the brain.[1] It may also be that tight control of intracellular water and solute concentrations is necessary for optimum function of the cell.[2]

The tonicity of body fluids is regulated primarily by raising or lowering total body water to keep it in balance with solute. In a healthy adult, about 55 to 60% of body weight is water.[3] It is slightly lower in women than men, owing to differences in body fat. About two-thirds of body water is intracellular. The rest is in the extracellular space, where it is subdivided further between the interstitial and intravascular (plasma) compartments in a ratio of about 3:1. Thus, a human weighing 70 kg contains about 39 L of water, of which 26 L is intracellular, 10 L is interstitial fluid, and 3 L is plasma.

A change in total body water results in a proportionate change in the volume of all compartments, providing the solute content of the compartments does not also change. The reason is that almost all cell membranes are penetrated by channels composed of aquaporin proteins[4] that permit the passive diffusion of water selectively in response to an osmotic gradient. In contrast, these membranes resist the passage of sodium, potassium, and most other solutes by actively pumping them in or out of the cell (see Chapter 2). Thus, a change in the amount of water in one compartment creates an osmotic gradient that results in a rapid flow of water from one compartment to the other, thereby restoring osmotic equilibrium and redistributing the change in volume in a similar proportion to each compartment. Thus, a reduction in the water content of the extracellular compartment due, for example, to increased perspiration, increases the tonicity and reduces the volume of the intracellular and extracellular compartments in equal proportion. A rise in total body water has the opposite but equivalent effect on the tonicity and volume of the two compartments.

In contrast, the volume of extracellular and intracellular water changes in opposite directions if the *amount* of osmotically effective solute in either compartment changes, but total body water does not. Osmotically effective solutes are those, such as sodium and its anions, which do not equilibrate readily across cell membranes. Thus, if the *amount* of sodium and its anions in extracellular fluid increases, the effective osmotic pressure or "tonicity" of this fluid also increases, resulting in a rapid osmotically-driven inflow of water from the intracellular compartment until osmotic equilibrium is re-established. The net effect is again an increase in the osmotic pressure of both compartments, but at a level lower than if the shift of water had not occurred. In fact, because of this shift, the effect on plasma sodium *concentration* of adding a given amount of sodium to the extracellular compartment is the same as if the sodium was distributed throughout total body water. In this circumstance, however, the volume of extracellular fluid increases, while that of intracellular fluid decreases. A reduction in the amount of sodium in extracellular fluid has opposite effects.

Because sodium and its anions normally make up 95% of all solutes, and nearly 100% of osmotically effective solute in extracellular fluid, the measurement of either plasma sodium or osmolarity probably

Seldin and Giebisch's The Kidney, Fifth Edition.
DOI: http://dx.doi.org/10.1016/B978-0-12-381462-3.00042-2

© 2013 Elsevier Inc. All rights reserved.

provides an accurate estimate of the "tonicity" or effective osmotic pressure of both the intracellular and extracellular fluids. Urea and glucose contribute little if anything because, normally, they are present in relatively low molar concentrations, and can enter or leave cells very rapidly. In the absence of insulin, however, glucose becomes osmotically effective because it enters cells much more slowly. In that situation, hyperglycemia induces a shift of water from the intracellular to extracellular space, and the tonicity of body fluids is determined much more reliably by measuring plasma osmolarity than plasma sodium. In intracellular fluid (ICF), the major solutes are potassium and its anions, but others including proteins, polyols, and some as yet unidentified solutes are also present.[2]

Body water is in a constant state of flux, owing to obligatory unregulated losses and gains produced by physical activity, the environment, diet, and the metabolism of fat. The rate of evaporative water loss from skin and lungs can vary markedly, depending on ambient temperature and physical activity, but it amounts to at least 10 mL/kg a day (0.7 L in a 70 kg human), even at rest in a comfortably cool environment.[5] The rate of solute-free water loss in urine is tightly regulated by vasopressin but, in humans, it cannot be reduced below a certain minimum required to excrete the load of sodium, chloride, potassium, urea, and other waste solutes derived from the diet and metabolism. This load varies with the diet, but is usually about 700 mosmols a day. Since humans cannot increase their urine osmolarity much above 1400 mosmols/L, the amount of urine required to carry this solute load is at least 7 ml/kg a day (0.5 L a day in a 70 kg human) even under conditions of maximum antidiuresis. The total daily obligatory water loss in a healthy adult is, therefore, at least 17 mL/kg (1.2 L in a 70 kg human), and may be much more at times depending on diet, activity, and temperature. Normally, this loss does not result in dehydration because it is replaced by an equivalent intake of water. Much of the intake is incidental to other physiological needs. About 7 mL/kg (0.5 L in a 70 kg human) comes from water in food, and about 4 mL/kg (0.3 L/day in a 70 kg human) is derived from metabolism of fat. The rest is consumed as beverages with meals in response to various influences,[6] including a slight increase in plasma osmolarity and thirst induced by adsorption of salt and other solutes in food. Thus, water balance is usually maintained at relatively low levels of urine output and discretionary fluid intake. Alterations in this basic state bring into play corrective changes in water excretion and/or intake under control of the antidiuretic and thirst mechanisms.

VASOPRESSIN AND RELATED PEPTIDES

Chemistry

Arginine vasopressin (AVP) is a nonapeptide containing an intrachain disulfide bridge and a tripeptide tail on which the terminal-carboxyl is amidated[7] (Figure 42.1). Substitution of lysine for arginine in position 8 yields lysine vasopressin (LVP), the antidiuretic hormone found exclusively in pigs and other members of the suborder Suina.[8] Vasopressin is structurally similar to oxytocin, another nonapeptide hormone found in the posterior pituitary of all mammals Oxytocin differs chemically from vasopressin by the substitution of isoleucine for

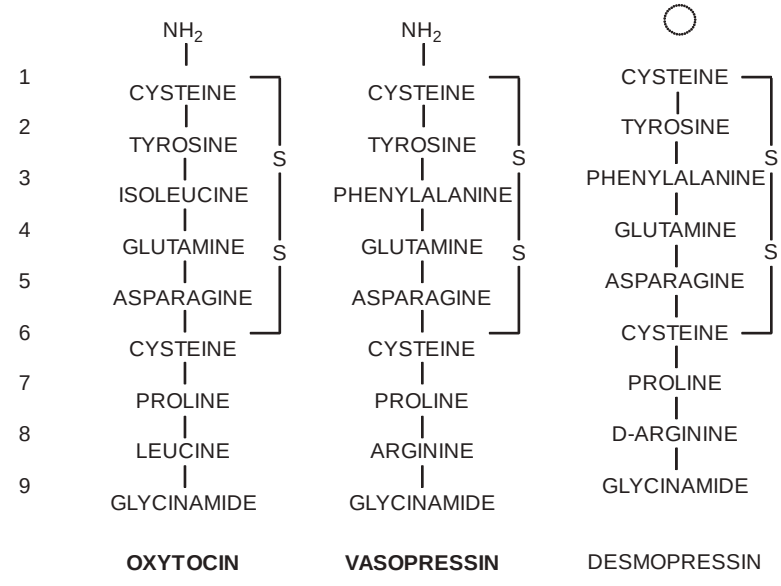

FIGURE 42.1 **The primary amino acid structures of oxytocin, vasopressin and desmopressin.**

phenylalanine at position 3, and of leucine for arginine at position 8.[7] Desmopressin is a potent synthetic analog of vasopressin used therapeutically because of its longer half-life and reduced effects on smooth muscle.

ANATOMY

Vasopressin and oxytocin are produced and stored in large amounts by magnocellular neurons in the hypothalamic neurohypophyseal tract.[9–14] These neurons arise bilaterally in the supraoptic and paraventricular nuclei of the hypothalamus, project medially to merge in the pituitary stalk, and continue through the diaphragm sella into the sella turcica, where they form the posterior lobe of the pituitary (Figure 42.2). Microscopically, the posterior pituitary appears as a densely interwoven network of capillaries, pituicytes, and large nonmyelinated neurons containing many electron-dense secretory granules. The neurons terminate as bulbous enlargements on capillary networks at many different levels throughout the stalk and body of the neurohypophysis. In healthy adults and children, the posterior pituitary usually appears as a hyperintense signal or "bright spot" on T-l weighted magnetic resonance images (MRI) of the brain.[15] The origin of this signal is still unknown, but it appears to be closely related to the content or turnover of vasopressin, and is almost invariably absent not only in patients with the pituitary form of diabetes insipidus, but also in many of those with nephrogenic diabetes insipidus (unpublished data). Vasopressin is also present in the suprachiasmatic nucleus and parvocellular neurons that originate in the paraventricular nucleus and project to the portal veins, anterior pituitary, and many other areas of the brain.[11,13] Oxytocin is also present in

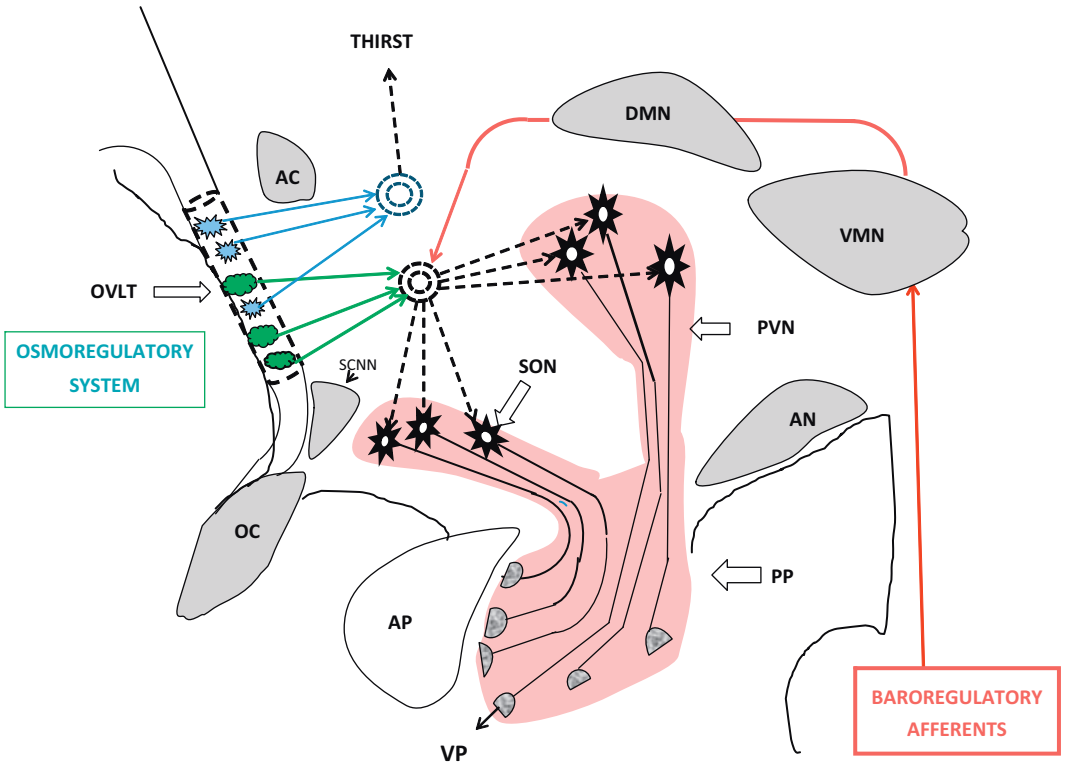

FIGURE 42.2 **Schematic diagram of the hypothalamic–neurohypophyseal tract and areas that osmoregulate thirst and vasopressin secretion.** The supraoptic nucleus (SON), paraventricular nucleus (PVN) and posterior pituitary are shaded red. The origin and course of the magnocellular neurons that form the tract and posterior pituitary are indicated in black. The green and blue icons represent the osmoreceptors that regulate vasopressin secretion and thirst, respectively. They appear to be in distinct but overlapping areas within in the organum vasculosum of the lamina terminalis (OVLT). The vasopressin osmoreceptors probably do not project directly to the SON or PVN but, as indicated by the black concentric circle with broken borders, appear to interact somewhere with ascending input from the baroregulatory system before the integrated signal is relayed to the magnocellular neurons in the SON and PVN. Signals from the thirst osmoreceptors probably follow a similar path to integration with baroregulatory input before projecting onwards to of the cerebral cortex. Other nearby landmarks shown include the anterior commissure (AC), optic chiasm (OC), suprachiasmatic nucleus (SCM), anterior pituitary (AP) and arcuate nucleus (AC). The ventral medial nucleus (VMN) and dorsal medial nucleus (DMN) probably transmit afferent input from the baroregulatory system. Not shown are the parvocellular vasopressinergic neurons which project to many other areas of brain including the SCM and portal venous system of the AP.

many parvocellular neurons of brain,[11–14] as well as in the uterus, prostate, and other peripheral tissues.[16]

The hypothalamic neurohypophyseal tract is supplied with blood by branches of the superior and inferior hypophyseal arteries that arise from the posterior communicating and intracavernous portions of the internal carotids.[9] In the body of the neurohypophysis, the arterioles break up into the aforementioned capillary networks that drain directly into the jugular vein by way of the sellar, cavernous, and lateral venous sinuses. In the stalk or infundibulum, the primary capillary networks coalesce into another system, the portal veins, which perfuse the anterior pituitary before discharging into the systemic circulation.

BIOSYNTHESIS

Vasopressin is synthesized as part of a protein precursor composed of a signal peptide at its amino terminus, vasopressin, the vasopressin-binding protein, neurophysin II, and a glycosylated peptide, copeptin, at its carboxyl-terminus[17,18] (Figure 42.3). During or after translocation to the endoplasmic reticulum, the signal peptide is removed and the N-terminus of the vasopressin moiety binds to a pocket in the neurophysin moiety. The prohormone then folds, forms a number of intrachain disulfide bridges, and dimerizes, before moving through the Golgi and into the neurosecretory granules where it is transported down the axon and further processed to yield amidated vasopressin, neurophysin, and copeptin.[19] Vasopressin and its neurophysin are stored in nerve terminals as insoluble complexes which dissociate completely after release into the systemic circulation.[20] Biosynthesis of vasopressin appears to be accelerated by stimuli, such as dehydration or hypertonic saline infusion,[21] which increase secretion. However, this compensatory response develops slowly, and may not completely offset the increased rate of release because pituitary stores of the hormone are severely depleted by a strong, sustained secretory stimulus such as prolonged water deprivation.[22]

The gene encoding the vasopressin–neurophysin precursor in humans is located distally on the short arm of chromosome 20 (20p13).[23] It contains three exons which code, respectively, for: (1) the signal peptide, vasopressin, a dipeptide link, and the N-terminal variable portion of neurophysin; (2) the middle, highly-conserved part of neurophysin; and (3) the C-terminal, variable portion of neurophysin, a peptide link and the glycopeptide, copeptin[24] (Figure 42.3). The 5′ untranslated region upstream of the transcription start site also has many conserved sequences, suggesting a role in regulation of gene expression.[25,26] Dehydration or osmotic stimulation increases expression of the vasopressin gene in the supraoptic nucleus,[27,28] whereas adrenal insufficiency or febrile stress does so in parts of the paraventricular nucleus.[28] In contrast, sustained hypoosmolarity inhibits expression.[29] The vasopressin genes in rats,[30] cows,[31] and mice[32] are similar to those in humans, but have several substitutions at either end of the highly-conserved central portion of the neurophysin moiety.

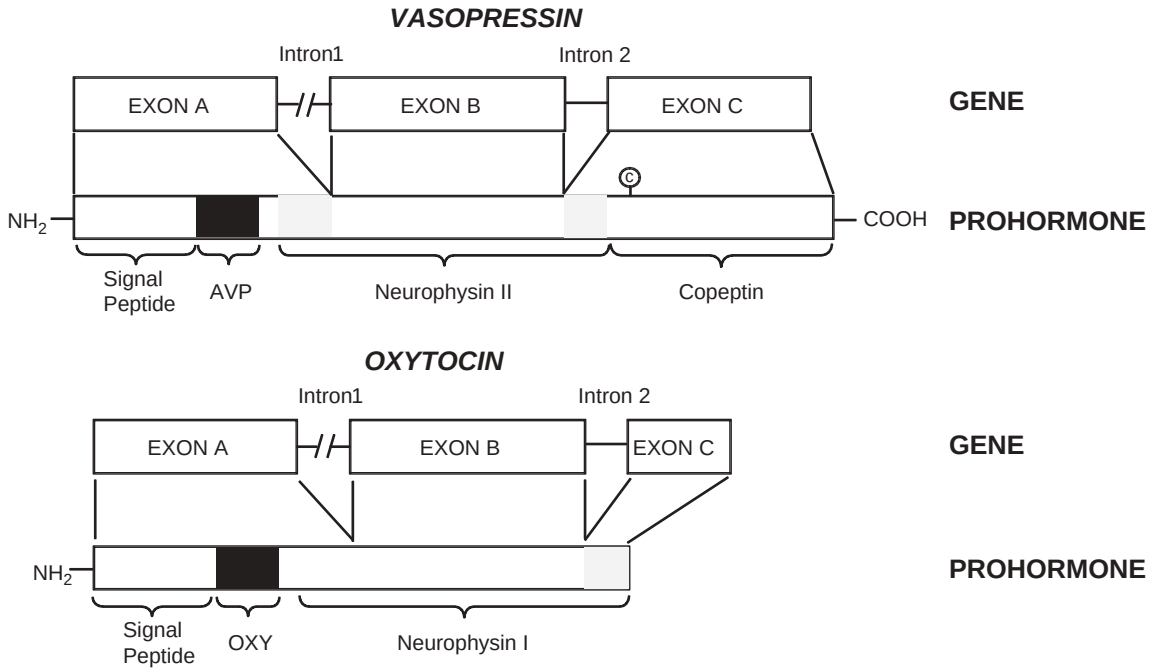

FIGURE 42.3 **Structure of the genes and the protein prohormones of vasopressin and oxytocin.**

The oxytocin gene is closely linked to the vasopressin gene on chromosome 20 with an intergenic region of only 11 kilobases.[24,33] However, the two genes are transcribed from opposite DNA strands, implying a tail-to-tail orientation, differ significantly in putative regulatory regions,[25] and are expressed in mutually-exclusive sets of neurons.[34] The oxytocin gene also differs significantly from the vasopressin gene, in that it does not contain a copeptin encoding sequence in exon 3.[25] Expression of the oxytocin gene in brain and some peripheral tissues is promoted by gonadal steroids.[16]

SECRETION

Vasopressin- and oxytocin-containing secretory granules are released from the terminals of magnocellular neurohypophysial neurons by a process of calcium-mediated exocytosis that is triggered by action potentials generated in the cell bodies of the supraoptic or paraventricular nucleus.[35] Many different neurotransmitters or neuromodulators including, possibly, vasopressin itself, can stimulate or inhibit this activity.[36,37] However, it is not yet known which, if any, of them are important in the regulation of secretion in health or disease. Secretory activity may also be influenced by the many glial cells in close proximity to the dendrites of the vasopressin cell bodies in the supraoptic nucleus.[38]

Vasopressin as well as the neurophysin and copeptin moieties with which it is associated are released into capillaries scattered throughout all levels of the posterior pituitary.[39–41] From there, they travel via the cavernous sinus to the subclavian vein, and thence to the inferior vena cava, heart, and general circulation. Neurophysin, which binds vasopressin in magnocellular neurons, dissociates from the hormone at the concentrations and pH present in plasma.[42] Binding of vasopressin to other plasma proteins has not been demonstrated. However, it does attach to platelets.[43] It is unclear whether or not the platelet-bound vasopressin represents a store of the hormone in equilibrium with free plasma vasopressin. However, the bound and unbound fractions of vasopressin do not appear to track together, at least during acute changes in secretion.[44] Oxytocin is also co-secreted with its neurophysin.[16]

ASSAY

The measurement of vasopressin at physiologic levels in plasma presents an unusual combination of concerns that must be addressed with exceptional care.[45] One problem is the large amount of hormone bound to platelets (see above). Because of it, vasopressin must be assayed not in serum, but in plasma that has been harvested very carefully to avoid contamination with platelets or fragments thereof.

A second problem is the fastidious requirements of the vasopressin assay itself. It must be unusually sensitive, because the hormone normally circulates and acts at very low concentrations. In healthy, normally hydrated, recumbent humans, the plasma concentration of "free" vasopressin is usually between 0.5 and 2.5 pg/mL ($\sim 10^{-12}$ M), an amount sufficient to concentrate the urine (Figure 42.4a). Basal levels in other mammals are similar. The assay must also be very specific, because plasma also contains oxytocin, a nonapeptide that is structurally similar to vasopressin but has different biologic effects. The only practical method now available

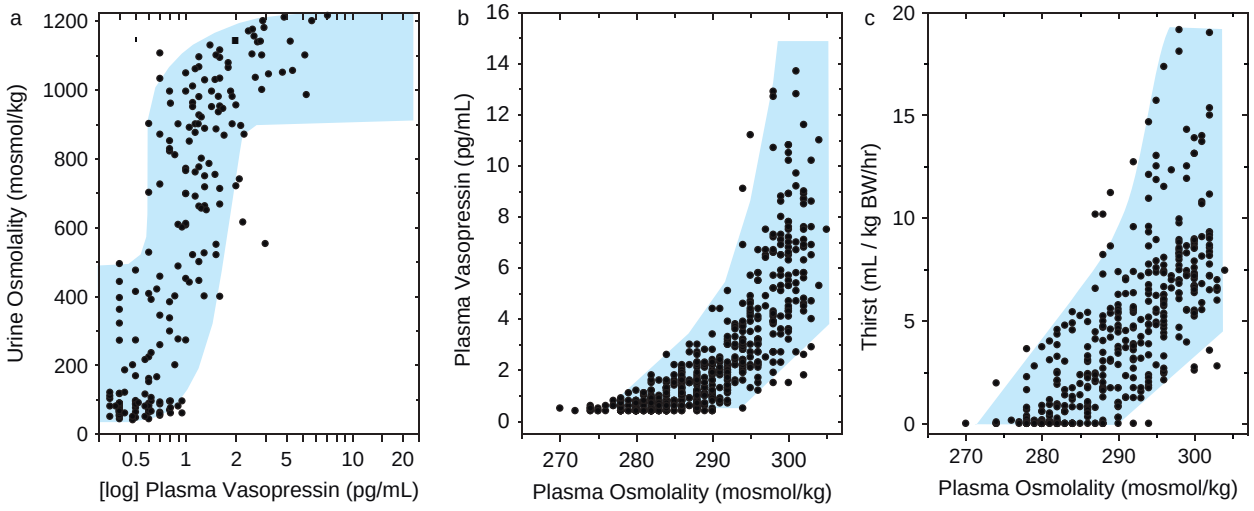

FIGURE 42.4 **Relationship of urine osmolality to plasma vasopressin (a), plasma vasopressin to plasma osmolality (b), and thirst to plasma osmolality (c) in healthy adults in various states of water balance.**

that can meet both requirements is radioimmunoassay. However, it too presents unusual problems, because vasopressin is relatively small and weakly antigenic. To complicate matters, most, if not all, the vasopressin antisera generated to date are susceptible to non-specific interference by one or more other unidentified components of plasma. Moreover, the characteristics and abundance of this interference can vary with the antiserum and type of anticoagulant used to prevent the blood from clotting. Consequently, vasopressin must be extracted from plasma, even if the antiserum employed is sensitive enough to detect the hormone at physiologic levels in unconcentrated extracts. Unfortunately, there is no one extraction method that is suitable for all assays. Therefore, the extraction method, as well as the anticoagulant, must be selected and tailored for the particular antiserum being used.

A third problem for vasopressin assays is the lack of a universal reference standard. Judging from the advertised biologic potencies, those available vary by as much as two-fold in purity, and unknown values reported in weight usually are not corrected for these differences. Therefore, unless the purity or potency of the standards is specified, it is impossible to compare absolute values reported by different laboratories unless they use the same standard, antiserum, and extraction technique.

The radioimmunoassay of vasopressin in urine would appear to be much easier than plasma, because the concentrations in urine are usually much higher, and interference by other substances is much less. However, urine samples must usually be diluted or concentrated to a constant solute concentration (preferably hypotonic), because some antisera are affected by high concentrations of salt or urea. Also, to adjust for the effect of changes in antidiuresis *per se*, the total amount of vasopressin in a urine sample must be expressed as a function of the length of time over which the sample was collected or of the amount of a solute such as creatinine that is excreted at a relatively constant rate. Finally, although changes in urinary excretion of vasopressin usually parallel the changes in plasma, this relationship can be distorted by changes in glomerular filtration or solute clearance.[45]

REGULATION

Osmotic

The most important determinant of vasopressin secretion under physiologic conditions is the "tonicity" or effective osmotic pressure of body water.[46] This influence is mediated by a group of cells known collectively as osmoreceptors,[47] that are located near but separate from the supraoptic nucleus, in or near a part of the anterior hypothalamus known as the organum vasculosum lamina terminalis[48–54] (Figure 42.2). Unlike the neurohypophysis, which receives its blood supply from a branch of the internal carotic artery, the area containing the osmoreceptors is supplied by small perforating branches of the anterior cerebral or communicating arteries.[9] Thus, the interruption of these perforators (or damage to the anterior hypothalamus by other diseases or experimental lesions) can eliminate the osmoregulation of vasopressin secretion, without affecting the neurohypophysis or its response to hemodynamic or other nonosmotic stimuli.[55,56] This dissociation indicates that the osmoregulation of vasopressin is mediated not by the magnocellular neurons that make the hormone, but by afferent inputs from osmosensitive cells located in other, anatomically discrete areas of the anterior hypothalamus. It is not yet known exactly how many such areas there are, whether they contain inhibitory as well as stimulatory elements, how they integrate with other regulatory afferents or how they communicate with vasopressin-producing neurons. Therefore, it may be more appropriate to refer to them as an osmoregulatory system.

The functional properties of the system that osmoregulates vasopressin resemble those of a discontinuous or "set-point" receptor (Figure 42.4b). Thus, in healthy adults and children, plasma vasopressin is very low or undetectable (<0.5 pg/mL) when plasma osmolarity is below a certain minimum or threshold level. Above that "set-point," plasma vasopressin increases steeply in direct proportion with the increase in plasma osmolality. The slope of the line describing this relationship indicates that, on average, a rise in plasma osmolality of 1% increases plasma vasopressin by 1 pg/mL, an amount sufficient to significantly alter urinary concentration and flow (Figure 42.4).

The functional properties of the osmoregulatory system are similar in men and non-pregnant women,[57,58] as well as in blacks and whites.[59] Within each group, however, they vary considerably from person to person.[58] Individual differences in the slope or sensitivity of the response are particularly large, varying as much as 10-fold. Differences in the apparent threshold or set-point are smaller, but still range from 274 to 293 mosmoles/L. These individual differences are constant over time, and appear to be determined largely by genetic factors.[58] However, neither the sensitivity or the set-point is totally immutable, because they can be altered by a variety of conditions, drugs, and hormones (see below).

It is uncertain whether the threshold concept accurately represents the operation of the osmoreceptor at

its most fundamental level. The relation of plasma vasopressin to plasma osmolarity in the population as a whole appears to be slightly curvilinear[60–62] (Figure 42.4). This curvilinearity could be due simply to individual variation, since there as a positive correlation between slope and threshold, i.e., the higher the threshold the steeper the slope. It is also possible, however, that the stimulation of vasopressin secretion is self-amplifying.[44] At present, however, the precision and reproducibility of the vasopressin assays at the low levels present under basal conditions are insufficient to determine if the best fit of the relationship is linear or exponential. It is also possible that vasopressin secretion reflects the balance of inhibitory as well as stimulatory inputs from a bimodal osmoregulatory system, because patients and animals with adipsic hypernatremia due to destruction of the osmoreceptors may lose the capacity to osmotically suppress, as well as to stimulate, vasopressin secretion.[54,55,57,63] As a practical matter, however, the concept of an osmotic threshold remains, for the present, a valid and useful way of describing many aspects of normal and abnormal osmoregulatory function in the intact animal.

It is also uncertain whether vasopressin is secreted continuously or episodically in response to osmotic stimulation. When nonosmotic stimuli such as posture, activity, and blood pressure are controlled, infusion of hypertonic saline in humans almost always produces a smooth progressive increase in systemic venous plasma vasopressin that correlates very closely with the increase in plasma osmolality.[45,58,64–67] However, samples obtained from experimental animals nearer the source of the hormone, for example, from the internal jugular vein, exhibit large fluctuations in plasma vasopressin during osmotic stimulation.[68] Whether these fluctuations reflect an intrinsic property of the neurohypophysis or the osmoreceptors, or are artifacts of the experimental conditions is unknown. Irregular phasic firing of the neurosecretory neurons has been observed by unit recording techniques during stimulation,[69] but this activity is unlikely to be related to episodic fluctuations in plasma vasopressin because the discharge cycles have a much shorter periodicity and are not synchronized from cell to cell.

The system that osmoregulates vasopressin secretion is not equally sensitive to all the solutes in plasma and extracellular fluid.[70–72] The most potent stimuli are sodium and its anions, the solutes that ordinarily account for more than 95% of measured plasma osmolarity. However, certain sugars, such as mannitol and sucrose, are also very effective when infused intravenously. In fact, particle-for-particle, mannitol is as potent as sodium chloride.[72] In contrast, an increase in plasma osmolarity produced by infusion of urea or glucose causes little or no increase in plasma vasopressin in healthy adults.[70–72] Thus, the concentration of sodium and its anions is the principal, if not the only, determinant of osmotically-mediated vasopressin secretion under normal conditions. The basic mechanism by which the osmoregulatory system senses changes in the plasma concentration of sodium and its anions has not been completely established. On the basis of studies in dogs, Verney proposed that the osmoreceptor is stimulated when its intracellular volume is reduced by an osmotically driven efflux of water.[47] If so, solutes that enter the osmoreceptor cells slowly or not at all would be "effective" stimuli, whereas those that penetrate rapidly would have little or no effect. This theory is consistent with the observations that vasopressin secretion is stimulated similarly by infusing hypertonic saline or mannitol, both of which are excluded from cells. In addition, vasopressin is not stimulated by a rise in plasma osmolarity produced by rapid infusion of hypertonic glucose, a solute which enters cells rapidly in the presence of insulin. If anything, the hyperglycemic hyperosmolarity produced by infusion of hypertonic glucose suppresses plasma vasopressin, probably because it also lowers the plasma concentration of sodium salts by inducing an osmotically driven efflux of water from the intracellular to the extracellular compartment. This disparity suggests that, in the presence of insulin, glucose enters osmoreceptor cells even more rapidly than many other cells of the body.

Another theory posits that the osmoreceptors are actually sodium receptors located on the brain side of the blood–brain barrier.[70,73] It is consistent with the observed effects of hypertonic mannitol infusion, because this solute does not cross the blood–brain barrier and, as a consequence, causes an osmotically driven efflux of water from brain that probably raises the extracellular concentration of sodium in that organ. However, the sodium receptor theory is not consistent with the relatively small rise in plasma vasopressin produced by an acute rise in plasma urea,[72] because this solute also crosses the blood–brain barrier slowly and, as a consequence, reduces brain water and raises brain extracellular sodium concentration much like mannitol. This singular disparity indicates that most, if not all, of the osmoreceptors are probably located outside the blood–brain barrier, and that another factor, most likely the solute permeability of the osmoreceptor cell itself, determines the solute-specificity of the system. This concept is also consistent with two other observations: (1) the osmoregulatory system appears to be located in or near the organum vasculosum lamina terminalis, a region of the anterior hypothalamus that is known to lack a blood–brain barrier; and (2) a severe deficiency of insulin sensitizes the osmoreceptors to stimulation by hyperglycemia,[74] presumably by

decreasing its permeability to glucose. It is not yet known, however, what distinguishes the cells of the osmoregulatory system from all the others whose volume and solute concentrations are similarly affected by changes in the extracellular concentration of sodium and its anions.

NON-OSMOTIC

Hemodynamic

An acute decrease of blood pressure or blood volume increases plasma vasopressin by an amount that is roughly proportional to the degree of hypotension or hypovolemia.[75–77] However, the stimulus–response relationship follows a distinctly exponential pattern (Figure 42.5). Small decreases in blood pressure or volume of 5 to 10% usually have little or no perceptible effect on plasma vasopressin, whereas decreases of 20 to 30% result in plasma hormone levels many times those required to produce maximum antidiuresis. Acute orthostasis, which decreases "effective" blood volume by 10 to 15%, usually doubles plasma vasopressin. In rats, chronic or sustained hypovolemia of 24 to 48 hours duration has even less effect on vasopressin, even though pituitary stores of the hormone

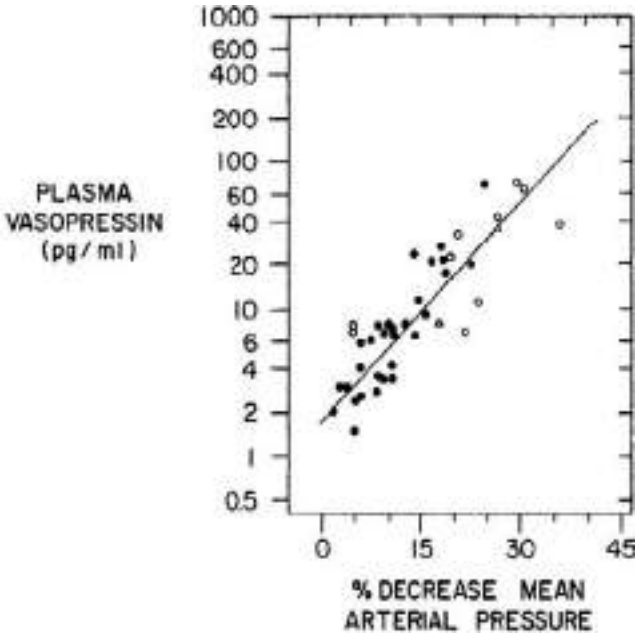

FIGURE 42.5 **Relationship between plasma vasopressin and percentage decrease in arterial pressure in healthy adults.** Hypotension was produced by infusion of a ganglionic blocker (filled symbols) or phlebotomy followed by orthostasis (open symbols). Note that plasma vasopressin is plotted on a log scale.

are undiminished.[78] This suggests that chronic stimulation selectively desensitizes the volume control mechanism.

The effects of acute hypovolemia on vasopressin secretion appear to be mediated largely by neuronal afferents that arise in pressure-sensitive receptors in the left side of the heart[79] and project by way of the vagus and glossopharyngeal nerves to primary synapses on the nuclei of the solitary tracts in the medulla. From there, signals ascend to the hypothalamus via postsynaptic pathways that appear to be mediated in part by a highly selective opioid neurotransmitter of the kappa subclass in the lateral parabrachial nucleus.[80–83] The vasopressin response to acute hypotension is mediated by neurogenic afferents that arise in high-pressure receptors in the aorta and carotid sinus, and project via the vagus and glossopharyngeal nerves, presumably, to the nuclei of the solitary tracts.[84,85] From there, pathways that are at least partly noradrenergic[86] ascend to the hypothalamus. At least for part of their length, these ascending pathways are separate from those that mediate the vasopressin response to hypovolemia, because they are not blocked by opioid antagonists that abolish the response to hypovolemia.[80,81,83]

Acute hypervolemia or hypertension can inhibit vasopressin secretion.[87–90] However, the increase in blood volume or pressure required is relatively large, and the inhibition of AVP is slight. The pathways that mediate the hemodynamic inhibition have not been fully-elucidated, and they may be the same as those that mediate stimulation. Interruption of primary vagal afferents eliminates the effect of hemodynamic stimuli, but also results in an acute rise in basal vasopressin secretion.[91,92] This suggests that the baroregulatory afferents tonically inhibit vasopressin secretion under basal, normovolemic, and normotensive conditions. If so, the slight decrease in vasopressin produced by acute hypervolemia and hypertension may be simply enhancement of this tonic inhibitory effect. Likewise, the increase in vasopressin produced by acute hypovolemia or hypotension could result from a reduction in basal inhibition of secretion. The effect of a *chronic* increase in blood volume or pressure is largely undefined. The osmoregulation of vasopressin secretion appears to be normal in patients with uncomplicated essential hypertension,[93,94] but may be inhibited slightly in primary hyperaldosteronism,[95] suggesting that chronic expansion of the blood volume has an effect opposite to that of hypovolemia.

Changes in blood volume or pressure large enough to affect vasopressin secretion do not interfere with osmoregulation of the hormone. Instead, they appear to act by shifting the set of the system in such a way as

to increase or decrease the effect on vasopressin of a given osmotic stimulus.[46,75,96–98] This means that the osmoregulatory and baroregulatory systems, although different in location and function, ultimately converge and act upon the same population of neurosecretory neurons[46,99] (Figure 42.2). Exactly how and where this integration occurs is unknown.

Emetic

Nausea is an extremely potent stimulus for vasopressin secretion in humans.[100] The pathways that mediate this effect have not been defined, but they probably involve the chemoreceptor trigger zone in the area postrema of the medulla. The effect on vasopressin is instantaneous and extremely potent. Increases of 100 to 500 times basal levels are not unusual, even when the nausea is transient and unaccompanied by vomiting or changes in blood pressure. Pretreatment with fluphenazine, haloperidol or promethazine in doses sufficient to prevent nausea completely abolish the vasopressin response.[100] The inhibitory effect of these dopamine antagonists is specific for emetic stimuli, because they do not alter the vasopressin response to osmotic or hemodynamic stimuli. Water-loading blunts, but does not abolish, the effect of nausea on vasopressin release, suggesting that osmotic and emetic influences interact in a manner similar to osmotic and hemodynamic pathways. The effect of emetic stimuli is also species-dependent. Whereas emetics such as apomorphine, cholecystokinin, lithium chloride, and copper sulfate stimulate the secretion of vasopressin but not oxytocin in humans[100,101] and monkeys,[102] they increase the secretion of oxytocin but have little effect on vasopressin in rodents.[103]

Emetic stimuli probably mediate many pharmacologic and pathologic effects on vasopressin secretion. These include not only apomorphine,[100] but also high doses of morphine,[104] nicotine,[105] alcohol,[100] cholecystokinin,[101,102] and motion sickness.[106] They may also be responsible, at least in part, for the increases in vasopressin secretion that have been observed with intravenous cyclophosphamide,[107] acute hypoxia,[108] diabetic ketoacidosis,[109] vasovagal syncope,[110] and hyperemesis gravidarum.[111] Because nausea and vomiting are frequent side-effects of many other drugs and diseases, additional examples of nausea-induced vasopressin secretion doubtlessly will be observed. The potency and ubiquity of emetic stimuli create special problems for research studies of vasopressin secretion in animals and unconscious subjects, because the occurrence of nausea is difficult to ascertain except by verbal report.

OTHER INFLUENCES

Glucopenia

Acute insulin-induced hypoglycemia also stimulates vasopressin release in proportion to the decrease in plasma glucose.[112] The rate of decrease in glucose is probably the critical determinant, however, because the increase in plasma vasopressin is not sustained even when the hypoglycemia persists.[113] The receptor and pathway that mediate this effect are unknown. They are probably separate from those that mediate the effects of other recognized stimuli, because hypoglycemia stimulates vasopressin secretion in patients who have selectively lost the capacity to respond to osmotic, hemodynamic or emetic stimuli.[112] However, the vasopressin response is accentuated by dehydration and abolished by water-loading,[113] indicating that hypoglycemic stimuli probably act in concert with osmotic influences even though the osmoreceptors *per se* are unnecessary for the response. The effect of hypoglycemia is not due to nonspecific stress, because it can occur in the absence of symptoms and is more pronounced in rats, a species in which vasopressin secretion appears to be unaffected by pain and other noxious stimuli. The variable that actually triggers the release of vasopressin may be an intracellular deficiency of glucose or one of its metabolites, because 2-deoxyglucose is also an effective stimulus.[114,115]

Angiotensin

The renin–angiotensin system has also been implicated in the control of vasopressin secretion.[116] The precise site and mechanism of action have not been defined, but one or more central receptors seem likely, because angiotensin II is most effective when injected directly into brain ventricles or cranial arteries.[117] The magnitude of the vasopressin response may depend on the concurrent osmotic stimulus.[118,119] This dependency may account for the failure of some investigators to demonstrate stimulation by peripherally administered angiotensin.[120] However, if angiotensin is directly involved in the physiologic control of vasopressin, it is more likely that produced by the renin–angiotensin system of the brain.[121]

Stress

Nonspecific stress caused by pain, emotion or physical exercise has long been thought to release vasopressin.[122] However, it has never been determined whether this effect is mediated by a specific pathway or is secondary to other stress-induced stimuli, such as the severe hypotension and/or nausea that often

accompanys the vasovagal reaction to pain or fear. In rats and humans, stresses severe enough to activate the pituitary adrenal axis and sympathetic nervous system do not stimulate an increase in plasma vasopressin unless they also lower blood pressure or alter blood volume.[123,124] If anything, stress seems to transiently suppress plasma vasopressin, possibly as a consequence of an acute rise in blood pressure or activation of other inhibitory input.[125] However, stresses of various types have been found to stimulate the release of vasopressin (as well as corticotropin releasing hormone) from parvocellular neurons which project to portal veins of the anterior pituitary and appear to play a role in the regulation of ACTH secretion.[126]

Temperature

Environmental temperature can also influence plasma vasopressin. In healthy adults, exposure to cold for a relatively short period of time depresses plasma vasopressin, and heat has the opposite effect.[127,128] These changes are independent of changes in plasma osmolality, but they cannot as yet be divorced from changes in effective blood volume or blood pressure. Experimentally-induced hypothermia or fever in animals is also associated with changes in plasma vasopressin,[129–131] but the effects seem to vary, possibly as a function of the species, the dose of endotoxin administered or the time interval. Thus, it is still uncertain how exogenous or endogenous changes in temperature effect vasopressin secretion by magnocellular neurons.

Oropharynx

Drinking can also inhibit vasopressin secretion, even before it produces a detectable decrease in plasma osmolarity or sodium.[132–134] This effect does not depend on the water reaching the stomach, and is unrelated to changes in blood pressure or blood volume. It may depend on the volume or temperature of the fluid ingested because, in humans at least, small volumes of water (100 mL) at room temperature are less inhibitory than larger volumes (700–1200 mL) or small amounts of ice. Thus, the inhibition may be mediated by neural afferents that originate in taste, temperature or other sensory receptors in the oropharynx. Inhibition of vasopressin by oropharyngeal receptors is rapid and transient. This may explain why it is not associated with a concurrent decrease in urine concentration. The rapidity of the decrease is also unexplained, since it appears to exceed the rate at which vasopressin is cleared from plasma under steady-state conditions (see below).

Age

Normal aging also appears to alter the osmoregulation of vasopressin secretion in humans, but the nature of the change is controversial.[135–138] Some find that the vasopressin response to an osmotic stimulus is enhanced, but others report no change or a decreased response. These differences are unexplained, and may represent individual variation in the impact of aging on various components of the osmoregulatory and other interacting control systems. Histologic studies of the human brain show variable changes in the suprachiasmitic nucleus and other vasopressin-containing parvocellular pathways, but no decrease in the number of large cell bodies in the supraoptic and paraventricular nucleus.[12,139] MRI studies indicate that the posterior pituitary bright spot is diminished or absent more often in the elderly than in the young,[140] but this decrease can be due either to atrophy of the gland or to more rapid turnover of vasopressin due, for example, to decreased fluid intake or decreased renal effect of the hormone. Aging does not seem to impair the ability to osmotically suppress vasopressin secretion and dilute the urine, but it does diminish the capacity to excrete a water-load, because of the large age-related reduction in glomerular filtration rate.[141] The capacity to maximally concentrate the urine also diminishes with age, but this may also be due largely to renal factors.[142]

Gender, Pregnancy, the Menstrual Cycle, and Gonadal Hormones

The effects of gender on the osmoregulation of vasopressin secretion are complex and unsettled. There appears to be little or no difference between adult human males and non-gravid females,[57,58] but pregnancy results in a relatively large reduction in the osmotic threshold for vasopressin release in rats as well as in humans.[143,144] Downward resetting of the osmostat also occurs during the luteal phase of the human menstrual cycle,[66,145] but the shift is small relative to that in pregnancy and is smaller even than the range of individual variation in men and non-gravid women.[58] The cause of the resetting is uncertain, but it may be mediated by relaxin,[144] an increase in estrogens[67] or chorionic gonadotropin,[65] since they also lower the set of the osmostat in humans. Progesterone appears to have no effect.[146] In rats, large doses of estrogen seem to have a different effect than in humans, since they enhance the slope or sensitivity of the vasopressin response to plasma osmolality, but do not significantly alter its set-point.[143]

TABLE 42.1 Drugs and Hormones that Affect Vasopressin Secretion

Stimulatory	Inhibitory
Acetycholine	Fluphenazine
Morphine (high doses)	Haloperidol
Epinephrine	Promethazine
Histamine	Oxilorphan
Bradykinin	Butorphanol
Prostaglandins	Opiods (κ and δ agonists)
β-Endorphin	Morphine (low doses)
Cyclophosphamide	Alcohol
Vincristine	Carbamazepine
Lithium	? Glucocorticoids
? Chlorpropamide	? Phenytoin
? Clofibrate	
? Corticotropin-releasing factor	

Drugs and Other Hormones

Many drugs and hormones also influence vasopressin secretion (Table 42.1). Those that stimulate, such as histamine, bradykinin, prostaglandin, β-endorphin, and high doses of morphine, have not been studied sufficiently to define their mechanisms of action, but may act by decreasing blood pressure or producing nausea. Vincristine may have a direct toxic effect on the neurohypophysis or peripheral neurons involved in the regulation of vasopressin secretion. Lithium, which antagonizes the antidiuretic effect of vasopressin, also increases secretion of the hormone. This effect is independent of changes in water balance, and appears to result from an increase in sensitivity of the osmoregulatory system.[147] The stimulatory effects of chlorpropamide and clofibrate are still controversial, and a mechanism of action has not been proposed.

Inhibitors such as the dopaminergic antagonists fluphenazine, haloperidol, and promethazine probably act by suppressing the emetic center, because they inhibit the vasopressin response to nausea but not to osmotic or hemodynamic stimuli. Antihistamines inhibit the vasopressin response to dehydration[148] which is largely an osmotic stimulus, indicating that some part of the osmoregulatory afferents may be histaminergic. Many opiates are also inhibitory. They include oxilorphan and butorphanol, the KAPPA agonists U50488[149] leu-morphin and U62066E, as well as low doses of morphine. In the case of morphine and butorphanol,[150] the inhibition is due to an increase in the osmotic threshold for vasopressin release, and is independent of changes in blood volume or pressure. The mechanism of the resetting has not been completely defined. However, it would appear to be due to the agonist properties of these opiates, because it can be blocked by naloxone.[150,151] The inhibitory effect of alcohol[136] may also be mediated in part by endogenous opiates, because it is also due to upward resetting of the osmostat and can be partly reversed by treatment with naloxone.[152] Carbamazepine inhibits vasopressin secretion by diminishing the sensitivity of the osmoregulatory system.[153] This effect is not dependent on changes in blood volume or blood pressure, and suggests that the ability of carbamazepine to produce antidiuresis in patients with neurogenic (pituitary) diabetes insipidus is due to an independent action on the kidney. The regulation of oxytocin secretion has not been studied extensively, partly because of the limited availability of reliable assays. However, it appears to be stimulated by gonadal steroids, as well as by labor and parturition.[16]

DISTRIBUTION AND CLEARANCE

After release into the systemic circulation, vasopressin distributes quickly into a space approximating extracellular fluid volume.[45,154] The mixing phase is followed by a second, slower decline that presumably reflects the metabolic or irreversible phase of clearance. It has a half-life of 10 to 30 minutes. Thus, the total clearance rate of vasopressin ranges from about 10 to 20 mL/kg body weight per minute. The metabolic clearance rate increases markedly during pregnancy, reaching a level three- to four-fold greater than normal by the third trimester.[155] Smaller animals, such as rats, also clear vasopressin much more rapidly because their cardiac output is much higher relative to body weight and surface area.[154] Although many tissues have the capacity to inactivate vasopressin *in vitro*, most metabolism *in vivo* appears to occur in liver and kidney.[154] In pregnancy, vasopressin is also degraded by a vasopressinase produced by the placenta.[155]

Some vasopressin is excreted intact in the urine. The amount can vary considerably depending on the overall rate of solute excretion,[45] but it is never more than a fraction of total irreversible clearance. In healthy, normally hydrated adults, the urinary clearance of vasopressin ranges from 0.1 to 0.6 mL/kg/min. The mechanisms involved in the excretion of vasopressin have not been defined, but the hormone is probably filtered at the glomerulus and variably reabsorbed at one or more sites along the tubule. The latter process seems to be influenced by the reabsorption of sodium and chloride in the proximal nephron, because the urinary clearance rate of vasopressin varies by as much as

20-fold in direct relationship to the clearance rate of total solute.[45] Thus, changes in urinary vasopressin excretion do not provide a reliable guide to changes in plasma vasopressin unless glomerular filtration or solute clearance rates are constant and normal.

ACTIONS

The biologic effects of vasopressin are mediated by three subtypes of a heptahelical transmembranous receptor coupled to guanine nucleotide-binding (GNB) proteins. Two of the receptors, V1a and V1b, activate phospholipase via GBN−protein coupling. The third, V2, activates adenyl cyclase and increases cyclic-AMP, also via GBN−protein coupling.[156,157] The genes encoding these receptors are located on different chromosomes: V1a on 12q14−15; V1b on 1q32; and V2 on Xq28. Among humans of different ethnic backgrounds, the gene encoding V1a receptors shows considerable polymorphism in the upstream regulatory regions and intron−exon junctions.[158] The anatomic distribution and sensitivity of the three receptors also differs. V1a receptors are found mainly in liver, platelets, the central nervous system, and vascular/gastrointestinal smooth muscle. V1b receptors are found mainly in the ACTH-producing cells of the anterior pituitary, but may also be in other areas of the brain. The V2 receptors are expressed in the distal and collecting tubules of the kidney. The V2 receptors bind vasopressin at very low plasma concentrations (10^{-12} M), and mediate the effect of the hormone on urinary concentration and flow. The V1 receptors, in contrast, are stimulated by vasopressin only at concentrations much higher than those found in plasma under physiological conditions. Thus, their role in other possible physiological functions of this hormone in the periphery is uncertain but unlikely. However, the relative insensitivity of the V1 receptors may not prevent them from acting as neurotransmitters in the brain, the anterior pituitary or other areas where locally high concentrations of the hormone may be produced in synapses with little or no dilution.

The biologic effects of oyxtocin are also mediated by a 7-transmembrane domain receptor coupled to GNB protein.[157] It is encoded by a gene on chromosome 3p25-26 and expressed in uterine smooth muscle, as well as other sites that vary according to the species and the effect of gonadal steroids. The oxytocin receptor is less specific than those for vasopressin, and can be activated by the latter at concentrations only tenfold higher than oxytocin.

Numerous peptide and non-peptide agonists and antagonists of the vasopressin and oxytocin receptors have been, and are still being, developed.[159] One peptide, a V2-selective agonist known generically as desmopressin, has been used for decades to treat the vasopressin-deficient form of diabetes insipidus, and recently also enuresis in children and nocturia in adults. Several non-peptides, antagonists with variable specificity for the V2 receptor, are now being used to treat certain types of hyponatremia resulting from osmotically inappropriate antidiuresis.[160] Non-peptide antagonists for the V1 or oxytocin receptors are now in various stages of development and testing. They may prove to be very helpful in determining if these receptors play a significant role in physiology or pathophysiology. The results of such studies should be interpreted with caution, however, because the receptor specificity and activity of many agonists and antagonists differ considerably, especially between species.[159]

RENAL ACTIONS

The principal, if not the only, clearly documented physiological role of peripherally secreted vasopressin in humans is to decrease urine output by increasing urine concentration. This antidiuretic effect is achieved by binding to G-protein-coupled V2 receptors located on the basal surface of principal cells in the distal and collecting tubules of the kidney (Figure 42.6). Binding to these receptors activates adenyl cyclase and increases intracellular cyclic AMP which, in turn, results in phosphorylation of aquaporin-2, one of a large family of proteins that self-associate to form water channels in other tissues of the body.[4] Aquaporin-2 is encoded by a gene on chromosome 12q13, and expressed almost exclusively in the collecting ducts of the cortex and inner/outer medulla of the kidney. It self-associates to form homotetramers that when phosphorylated are routed to the apical (luminal) surface of the principal cells and inserted through the membrane. There, they function as channels that selectively permit some of the water in dilute tubular fluid to back-diffuse across the membrane into the cell, and then out again into the body through channels formed on the basolateral side by aquaporin 3 and aquaporin 4.[161−164] This process of reabsorption is driven by the hyperosmolar gradient created in the renal medulla by the countercurrent mechanism of the kidney (see Chapter 43). Since water is reabsorbed without solute, the fluid that remains is decreased in volume and increased in concentration, by an amount proportional to the level of vasopressin stimulation and the number of water channels inserted through the apical surface of the cell.

The maximum antidiuresis achievable in healthy adult humans usually occurs at a plasma vasopressin concentration of about 2 to 3 pg/mL (Figure 42.4).

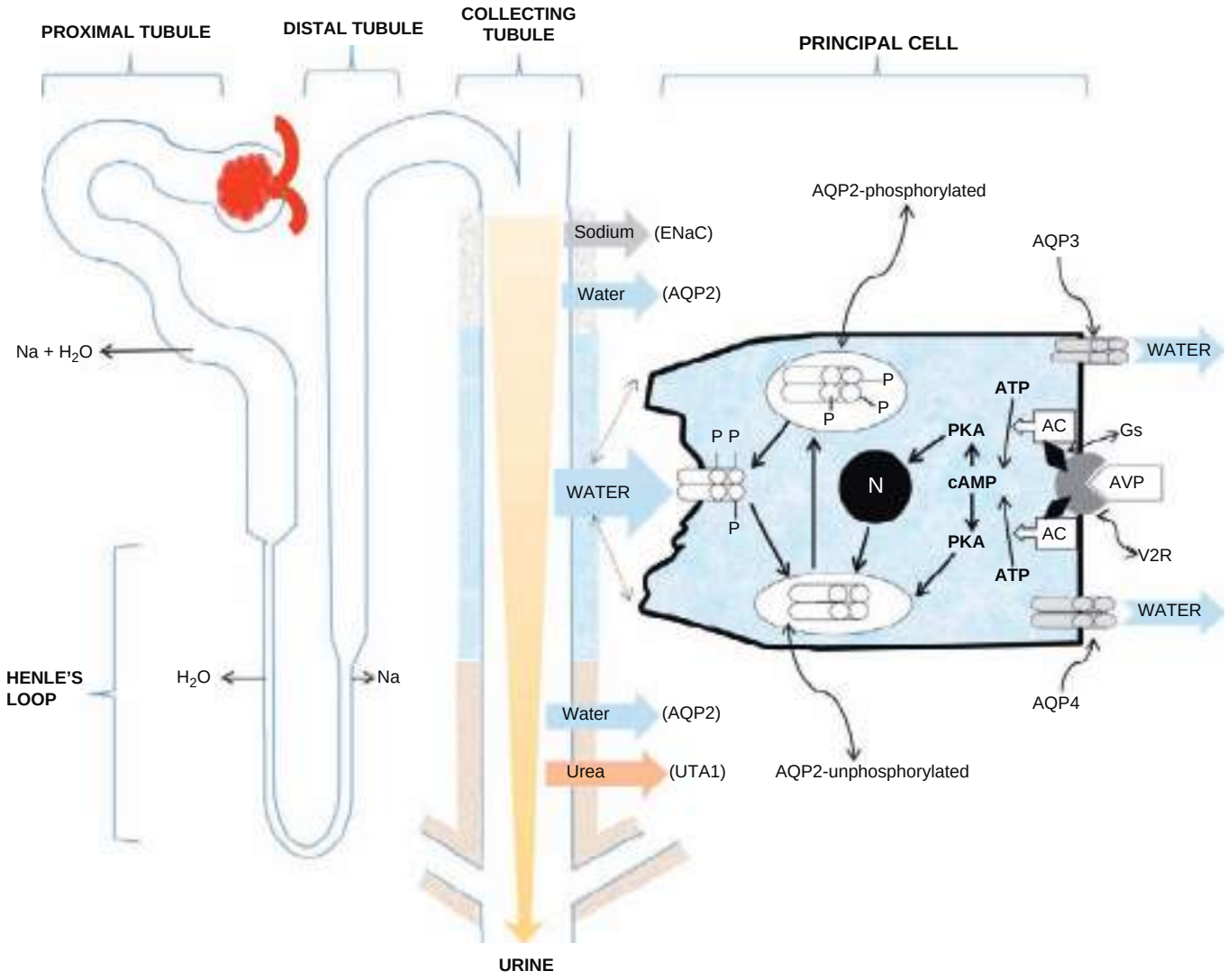

FIGURE 42.6 **Schematic diagram of renal nephron and a principal cell of the collecting tubule.** In healthy adults, the glomerulus filters about 180 L a day of ultrafiltrate with an osmolarity and sodium concentration approximating that of plasma. Water and sodium chloride are reabsorbed from the filtrate in the proximal tubule, Henle's loop, and the distal tubule, reducing the volume and the osmolarity of the fluid that enters the collecting tubules to about 15 L/day and 60 mosmols/L, respectively. In the absence of vasopressin action most, if not all, of this dilute fluid passes unmodified through the collecting tubules and is excreted as urine because the luminal (apical) surface of the principal cells that line the collecting tubules are impermeable to water and solute. This condition is known as a water diuresis. In the presence of vasopressin (AVP), the apical and basal lateral surfaces of the principal cells become permeable to water, allowing it to back-diffuse through the cell down the hyperosmotic gradient formed by the countercurrent mechanism in the renal medulla. As a consequence, the fluid that remains in the collecting tubules to be excreted as urine is more concentrated and less voluminous. Under conditions of maximal antidiuresis, the osmolarity can reach 1200–1400 mosmols/L, and the volume can be as low as 0.5 to 0.7 L/day. The increase in water permeability of the principal cell occurs by a series of intracellular reactions that begin with binding of AVP to a V2 receptor (V2R) on the basal surface, activation of adenyl cyclase (AC) via coupling of G-protein (◇) and conversion of adenosine triphosphate (ATP) to cyclic adenosine monophosphate (cAMP), which activates protein kinase A (PKA). The PKA has two effects. First, it causes the phosphorylation of preformed tetramers of aquaporin-2 (AQP2) which are stored in vesicles just below the apical surface of the cell. This phosphorylation, indicated in the diagram by −P, directs the tetramers to the apical surface of the cell, where they are inserted and function as channels allowing the passage of water into the cells and out the basolateral side through water channels formed by aquaporin 3 and 4 (AQP3 and AQP4). This process of reabsorption of water is driven by the hyperosmotic gradient created in the renal medulla by the countercurrent system.

It usually results in a urine osmolality of 1000 to 1200 mosmols/L, and a rate of excretion as low as 0.5 to 0.7 ml/min. By reducing the amount of urine needed to excrete urea and other waste solutes, this antidiuretic mechanism serves to minimize the amount of water that must be ingested to prevent dehydration. Rats and many other mammals are capable of even greater levels of antidiuresis, largely because their renal papilla are longer and, consequently, able to generate greater levels of hypertonicity in the medulla. The level of

antidiuresis produced in humans by a given level of plasma vasopressin also varies considerably, depending on the rate of solute excretion as well as, probably, the abundance of aquaporin channels available for insertion, and the rate at which they are removed from the membrane and recycled for later use. The factors that determine the abundance of water channels remain to be fully-defined, but probably include the level of prior vasopressin stimulation because the hormone also stimulates the synthesis of aquaporin-2. This may partly explain why antidiuretic response to vasopressin or desmopressin observed after a prolonged deficiency of the hormone (e.g., in pituitary diabetes insipidus or primary polydipsia) is blunted for several hours.[165] The variables that influence the removal of water channels from the membrane have not been fully-defined, but may include prostaglandin, dopamine, and hypertonicity itself.[163]

Vasopressin also has two other effects on the kidney that enhance its antidiuretic effects. One is to stimulate the activity of a urea transporter (UTA1) in the inner medullary collecting duct.[166,167] This effect, which is also mediated by V2 receptors and cyclic AMP, replenishes the concentration of urea in the renal medulla, thereby helping to maintain the hypertonic gradient generated by the countercurrent mechanism. The other renal effect of vasopressin is to stimulate the readsorption of sodium through an epithelial sodium channel (ENaC) in the collecting duct.[168] This also helps to reinforce the medullary concentration gradient. It does not appear to result in a sustained increase in total body sodium, probably because there is a compensatory decrease in proximal readsorption of sodium.

In the absence of vasopressin stimulation, the apical surfaces of the principal cells, as well as the tight junctions between them, are impermeable to water because the aquaporin-2 water channels remain in vesicles within the cell. As a consequence, the large volume of dilute filtrate that normally issues from the ascending limb of Henle's loop passes unmodified through the collecting ducts to be excreted as urine. In this condition, known as a water diuresis, the osmolarity of urine approximates 40 to 60 mosmols/L (Figure 42.4a), and the rate of excretion may be as high 10–15 mL/min. The excretion of water at this rate normally provides an effective barrier to over-hydration, since it suffices to offset all but the most pathologically excessive rates of water intake.

EXTRARENAL ACTIONS

Apart from its actions on the kidney, vasopressin has been investigated extensively for other effects that might be mediated via V1a or V1b receptors in the periphery or brain. These studies have yet to provide convincing evidence for a significant role in human physiology. However, they suggest that the V1 receptors may mediate certain pharmacologic or *in vitro* effects of the hormone on vascular resistance[169,170] or platelet aggregation,[171] and may also mediate the effects of parvocellular vasopressinergic neurons in brain to modulate various types of complex social behavior[172–174] or the effect of stress on ACTH secretion.[126,175]

The actions attributed to oxytocin are numerous,[16] but their role in human physiology or pathophysiology is not yet fully-defined. Most relate to sexual activity or reproduction, earning oxytocin the sobriquet of "the hormone of love." In the periphery, it stimulates contraction of smooth muscle in reproductive tissues, especially the uterus and mammary glands. However, it is not yet clear whether those effects are essential or only supportive for birth and nursing. In the brain, it has also been implicated in the genesis of various sexual behaviors and social bonding, in addition to regulation of temperature and cardiovascular function.

THIRST

The regulation of fluid intake is an indispensable part of the homeostatic system that regulates the tonicity of body fluids. It ensures that obligatory losses of water through urination, perspiration, and respiration are always replaced promptly and completely. This protection is provided by the thirst mechanism. Thirst may be defined as the subjective sensation of a desire or need for water. It is sometimes associated with feelings of dry mouth, headache or irritability, but these symptoms are not specific to thirst since they also have other causes. It must also be distinguished from cultural, social, psychological, medical, and other motivations to drink. Its vital importance is shown dramatically by the episodes of severe and sometimes fatal hypertonic dehydration that occur in patients who lack the sensation of thirst due to pathology in the anterior hypothalamus.[54] The opposite risk – that of hypotonic overhydration due to too much fluid intake – is not as great, because the mechanisms for suppressing vasopressin and excreting excess water can normally offset all but the most pathologically extreme polydipsia. However, excretory capacity can be impaired by a decrease in urinary solute load or a non-osmotic stimulus to vasopressin secretion. Therefore, the mechanism for regulating fluid intake also seems to include an inhibitory component that operates by producing a sense of satiation or distaste for water.

ANATOMY

The parts of the brain that mediate the conscious awareness of thirst and satiation have not been fully-defined. Studies using functional magnetic resonance imaging or positron emission tomography of the brain in healthy adults have shown that thirst is associated with activation in several areas, including the anterior wall of the third ventricle, anterior cingulate cortex, parahippocampal gyrus, inferior and middle frontal gyrus, insula, and cerebellum.[176] The difficulty with such findings, however, is that the sensation of thirst probably activates many brain areas involved in secondary feelings, thoughts or responses such as anxiety, discomfort or physical movement induced by feelings of thirst. To differentiate these secondary areas of arousal from those that mediate the consciousness of thirst *per se*, it will be necessary to employ a variety of other unpleasant stimuli as controls[177] or study the effect of discrete strokes or other ablative lesions in different brain areas.

REGULATION

Osmotic

Like the secretion of vasopressin, thirst is regulated primarily by the tonicity or effective osmotic pressure of body fluids.[54] This effect is also mediated via hypothalamic osmoreceptors that appear to be anatomically distinct from, but intermingled with, those that regulate vasopressin[178–180] (Figure 42.2). Their functional properties also seem to be similar to the vasopressin osmoreceptors, in that the intensity of thirst increases steeply in direct proportion to plasma osmolarity (Figure 42.4). The only difference is that the threshold for initiation of thirst seems to be set slightly higher than that for the initiation of vasopressin secretion.[54,58] In healthy adults, the level of plasma osmolality at which thirst begins averages about 287 mosmols/L, but varies from person to person over a range from 277 to 294 mosmols/L. In each individual, the the osmotic threshold for thirst tends to be about 4 mosmols/kg higher than that for vasopressin release. Therefore, thirst is not experienced until plasma osmolality rises to a level at which plasma vasopressin is high enough to maximally concentrate the urine. In other respects, the thirst osmoreceptors behave much like those for vasopressin secretion. They have the same solute specificity, since increases in plasma osmolality produced by infusion of hypertonic saline or mannitol are dipsogenic, whereas those resulting from infusions of hypertonic urea or glucose are not.[71,72] Their sensitivity – that is, the intensity of the thirst produced by a given rise in plasma osmolality – also differs significantly from person to person, and these differences also appear to be genetically determined.[58] However, one or both properties also can be altered by changes in blood volume,[181] pregnancy,[144] the menstrual cycle,[66] and human chorionic gonadotrophin.[65]

OTHER INFLUENCES

Hemodynamic

Anecdotal evidence indicates that thirst can also be stimulated by severe reductions in blood volume or blood pressure. The pathways that mediate this effect have not been defined, but are probably the same as those that mediate the effects on vasopressin (see above). In rats, a hypovolemia-induced increase in angiotensin II may also play an important role (see below), but such an effect has not been convincingly documented in humans. Also like vasopressin, moderate reductions in blood volume lower the osmotic threshold for thirst, but do not otherwise interfere with continued operation of the osmoregulatory system.[181]

Angiotensin

In rats and some other animals, angiotensin II stimulates water intake, particularly when injected into the lateral ventricles or other areas of brain.[180] Presumably, the increased intake is due to thirst, although some other type of inducement cannot be excluded. In humans, the dipsogenic effect of angiotensin II has not been investigated.

Glucopenia

Although anecdotal evidence suggests that thirst can also be induced by acute, insulin-induced hypoglycemia, controlled studies are lacking. However, it is clear that an intracellular deficiency of glucose produced by administration of 2-deoxy-glucose stimulates thirst as well as vasopressin release.[115]

Oropharynx

Like vasopressin secretion, thirst is also inhibited rapidly and transiently by the act of drinking *per se*.[182] The characteristics of this effect are similar to those for vasopressin (see above). They appear to be independent of osmotic and hemodynamic influences as well as the solute content of the fluid, but may be influenced by its volume or temperature. The inhibition of thirst is extremely rapid and nearly complete, decreasing the sensation to near zero in a matter of minutes.

However, it is also transient, lasting no more than 10 to 15 minutes, well short of the time required to absorb enough water to begin reducing the osmotic stimulus. Thus, thirst begins to increase again before undergoing a second decline due to absorption of the water and lowering of plasma osmolality. This timing is consistent with the temporal dissociation between the drinking-induced decrease of PET and MRI activity in the anterior cingulated cortex and the anterior hypothalamus (organum vasculosum lamina terminalis).[176] It may also explain why drinking in response to a strong osmotic stimulus often occurs in two or more bouts separated by 15 to 30 minutes.

Eating

It is common knowledge documented by observational studies that most of the water ingested each day is drunk in association with meals.[183] The finding that the amount of liquid drunk with each meal correlates with its estimated protein and carbohydrate content, and not with its estimated sodium content, lead to a theory that eating *per se* is a major independent stimulus to thirst unrelated to osmotic stimulation.[184] However, in healthy adults allowed to eat, drink, and ambulate at will, there appear to be slight increases in plasma osmolality and decreases in plasma protein during meals. Thus, it is not yet certain if drinking with meals is due to osmotically-induced thirst or to some other stimulus, such as taste or cultural habit.

Aging

In contrast to vasopressin secretion, the sensation of thirst and the drinking response to dehydration is diminished among the elderly.[185] The reason, however, is controversial. One theory holds that the sensitivity of the response is decreased due to loss of the potentiating effect of the mild volume depletion that occurs during dehydration. Others find that the decrease in thirst is due largely to upward resetting of the thirst osmostat, with little or no decrease in sensitivity. Compared to healthy young adults, however, there does not appear to be any change in the amount of fluid consumed in response to a given level of thirst or in the rapidity and extent of thirst suppression by oropharyngeal influences.

EFFECTS

Thirst induces the ingestion of water or other fluids in amounts proportional to the strength of the osmotic stimulus.[58] The water is absorbed from the gastrointestinal tract within 30 to 45 minutes, and is carried by blood throughout the body, distributing rapidly between ECF and ICF in a ratio of about 1:2. Thus, it dilutes all body fluid equally. The total amount of fluid drunk at one time, commonly referred to as a "bout" of drinking, is usually less than the amount required to restore tonicity to normal. This pause in drinking may be due to rapid inhibition of thirst by neural pathways arising in oropharyngeal receptors (see above). However, the inhibition is of short duration (10 to 15 minutes), and soon gives way to a return of thirst and drinking until enough water is absorbed to lower plasma osmolality to basal levels. These bouts may be repeated 2 or 3 times for up to 2 to 3 hours, until the hypertonicity is completely eliminated.

Hypotonicity often induces feelings of satiation which help to prevent further overhydration by producing a conscious aversion to drinking water. In humans, it occurs less often and less strongly than the sensation of thirst, but seems to result in negative "thirst" ratings and a marked reduction of spontaneous fluid intake after induction of plasma hypotonicity either by water-loading or repeat administration of high doses of the V2 agonist, desmopressin.[186]

VASOPRESSIN AND THIRST IN OSMOREGULATION

Vasopressin and thirst act in concert to control the tonicity of body fluids by raising or lowering body water to keep the concentration of osmotically effective solutes within a very narrow range. This control must be exerted largely, if not completely, by the osmoregulatory system because fluctuations in plasma osmolarity rarely exceed 1−2%, a change in body water too small to activate the baroregulatory system. The upper and lower limits of plasma osmolarity and sodium are determined by the osmotic thresholds for thirst and vasopressin secretion, because the very large increases in water intake or excretion that normally occur at these thresholds present almost insurmountable barriers to further dehydration or overhydration. Thus, even patients with a severe polyuria due to a deficiency of vasopressin maintain plasma osmolarity and sodium within normal limits simply by drinking more, while those with severe polydipsia do the same by rapidly increasing urine output. However, because the set of the thirst and vasopressin osmostats differs appreciably from person to person, the level at which plasma osmolarity is maintained also differs among healthy adults. This difference is reflected in the normal laboratory values for plasma osmolarity and sodium concentration which, depending on the laboratory methods employed, range from about 270 to 295 mosmols/L

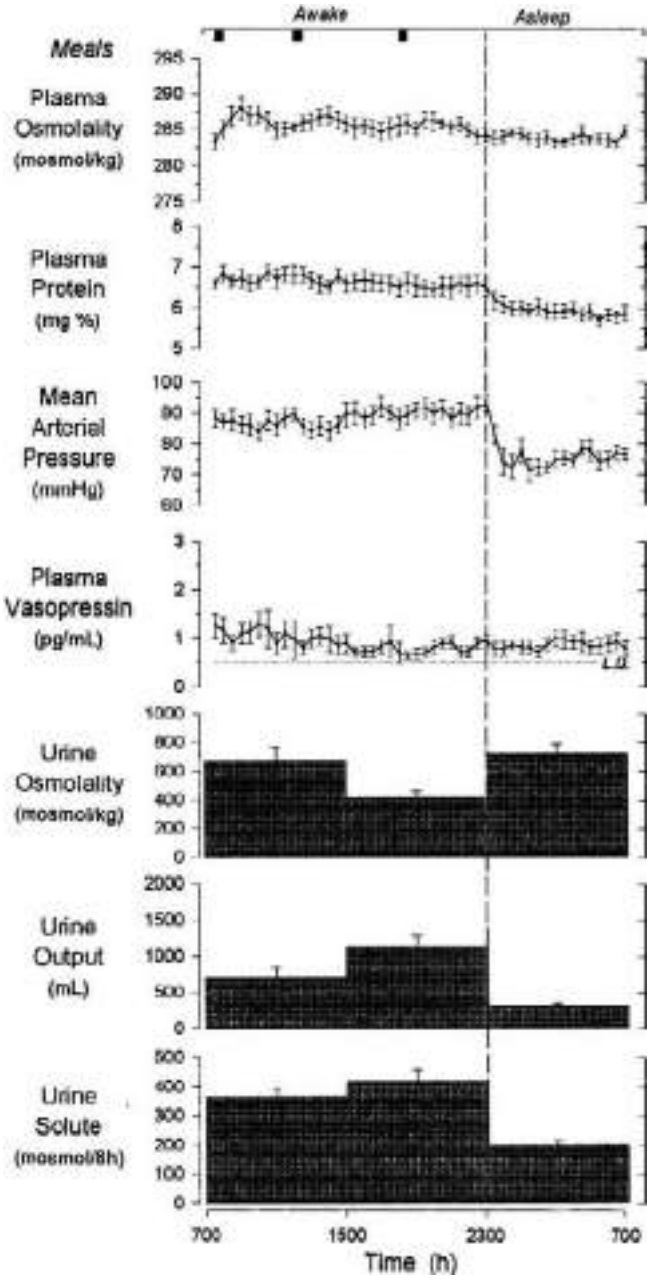

FIGURE 42.7 **Circadian variations in antidiuretic function and related variables in healthy young adults.** Each value is the mean ± SEM of 9 subjects (4 females and 5 males) on *ad libitum* intake of food and water. The three closed squares at the top indicate meals. Fluid intake, which is not shown, averaged 3.1 liters a day. It occurred in equal amounts during the two periods of the day (7 am to 3 pm, and 3 pm to 11 pm), usually with meals. *(From Robertson, G. L., Rittig, S., and Kovacs, L. (1993). Unpublished.)*

and 133 to 145 mmols/L, respectively. Within each person, however, these values are maintained even more tightly about half-way between his or her own set-point for thirst and vasopressin secretion. From that point, even a tiny increase or decrease in tonicity resulting from a change in water or sodium balance elicits a prompt change in vasopressin secretion and urine production, as well as in thirst and water intake. Consequently, the osmolality of plasma and other body fluids within each person rarely deviates by more than 3 to 5 mosmols/kg (1−1.5%), even in the face of large variations in insensible water loss and dietary solute load. In humans, the operation of this elegant osmoregulatory system is subject to changes in blood pressure or volume induced by posture and sleep. However, these influences do not seen to affect osmoregulation, probably because the system that mediates hemodynamic influences on thirst and/or vasopressin is relatively insensitive to normal fluctuations in blood pressure and volume, and even large changes produce only transient small changes in the set of the osmoregulatory system. Thus, plasma osmolarity, plasma vasopressin and urine osmolarity are relatively constant in the course of a normal day (Figure 42.7).

References

[1] Verbalis JG. Brain volume regulation in response to changes in osmolality. Neuroscience 2010;168:862−70.
[2] Ho SN. Intracellular water homeostasis and the mammalian cellular osmotic stress response. J Cell Phsiol 2006;206(1):9−15.
[3] Jaffrin MY, Morel H. Body fluid volume measurements by impedance: a review if bioimpedance spectroscopy (BIS) and bioempedance analysis (BIA) methods. Med Eng Phys 2008;30 (10):1257−69.
[4] Kruse E, Uehlein N, Kaldenhoff R. The Aquaporins. Genome Biol 2006;7:206.
[5] Adolph EF. In: Visscher MB, Bronk DW, Landis EM, et al., editors. Physiology of man in the desert. New York: Hafner; 1969.
[6] Kraly FS. Effects of eating on drinking. In: Ramsay DJ, Booth DA, editors. Thirst. London, UK: Springer-Verlag; 1991. p. 296−312.
[7] Du Vigneaud V. Hormones of the posterior pituitary gland: oxytocin and vasopressin. In: Du Vigneaud V, Bing RJ, Oncley JL, editors. The harvey lectures 1954−55. Orlando: Academic Press; 1956. p. 1−24.
[8] Sawyer W. Evolution of antidiuretic hormones and functions. Am J Med 1967;42:678−86.
[9] Haymaker W. Hypothalamo−pituirary neural pathways and the circulatory systems of the pituitary. In: Haymaker W, et al., editors. The hypothalamus. Springfield, IL: Charles C Thomas; 1969. p. 219.
[10] Scharrer E, Scharrer B. Hormones produced by neurosecretory cells. Recent Prog Horm Res 1954;10:183−240.
[11] Schwaab DE. Neurohypophysial peptides in the human hypothalamus in relation to development, sexual differentiation, aging and disease. Regul Pept 1993;45:143−7.
[12] Schwaab DE. Aging of the human hypothalamus. Horm Res 1995;43:8−11.
[13] Sofroniew MY, Weindl A, Schrell U, Wetzstein R. Immunohistochemistry of vasopressin, oxytocin and neurophysin in the hypothalamus and extrahypothalamic regions of the human and primate brain. Acta Histochem 1981;34(Suppl.):79−95.
[14] Zimmerman EA. The organization of oxytocin and vasopressin pathways. In: Martin JB, Reichlin S, Bick KL, editors. Neurosecretion and brain peptides. New York: Raven Press; 1981. p. 63−75.

[15] Fujisawa I. Magnetic resonance imaging of the hypothalamic–neurohypophyseal system. J Neuroendocrinol 2004;16:297–302.
[16] Tom JN, Assinder SJ. Oxytocin in health and disease. Internat J Biochem Cell Biol 2010;42(2):202–5.
[17] Schmale H, Fehr S, Richter D. Vasopressin synthesis: from gene to peptide hormone. Kidney Int Suppl 1987;21:S8–13.
[18] Brownstein MJ, Russell JT, Gainer H. Synthesis, transport and release of posterior pituitary hormones. Science 1980;207:373–8.
[19] Breslow E. The conformation and functional domains of neurophysins. In: Gross P, Richter D, Robertson GL, editors. Vasopressin. Paris: John Libbey Eurotext; 1993. p. 143–55.
[20] Breslow E. The neurophysins. Adv Enzymol 1974;40:271–333.
[21] Sachs H, Fawcett P, Takabatake Y, Portanova R. Biosynthesis and release of vasopressin and neurophysin. Recent Prog Horm Res 1969;25:447–91.
[22] Moses AM, Miller M. Accumulation and release of pituitary vasopressin in rats heterozygous for hypothalamic diabetes insipidus. Endocrinology 1970;86:34–41.
[23] Rao VV, Loffler C, Battey J, Hansmann I. The human gene for oxytocin neurophysin I (OXT) is physically mapped to chromosome 20p13 by *in situ* hybridization. Cytogenet Cell Genet 1992;61:271–3.
[24] Sausville E, Carney D, Battey J. The human vasopressin gene is linked to the oxytocin gene and is selectively expressed in a cultured lung cancer cell line. J Biol Chem 1985;260:10236–41.
[25] Richter D. Molecular events in expression of vasopressin and oxytocin and their cognate receptors. Am J Physiol 1988;255:F207.
[26] Iwasaki Y, Oiso Y, Saito H, Majzoub JA. Positive and negative regulation of the rat vasopressin gene promoter. Endocrinology 1997;138(12):5266–74.
[27] Zingg HH, Lefebvre D, Almazang G. Regulation of vasopressin gene expression in rat hypothalamic neurons; response to osmotic stimulation. J Biol Chem 1986;261(28):12956–9.
[28] Ueta Y, Fujihara H, Dayanithi G, Kawata M, Murphy D. Specific Expression of optically active reporter gene in arginine vasopressin-secreting neurosecretory cells in the hypothalamic–neurohypophyseal system. J Neuroendocrinol 2008;20 (6):660–4.
[29] Robinson AG, Roberts MM, Evron WA, Verbalis JG, Sherman TG. Hyponatremia in rats induces downregulation of vasopressin synthesis. J Clin Invest 1990;86:1023–9.
[30] Ivell R, Richter D. Structure and comparison of the oxytocin and vasopressin genes from rat. Proc Nat Acad Sci USA 1984;81:2006–10.
[31] Ruppert S, Scherer G, Schutz G. Recent gene conversion involving bovine vasopressin and oxytocin precursor genes suggested by the nucleotide sequence. Nature 1984;308:554–7.
[32] Hara Y, Battey J, Gainer H. Structure of mouse vasopressin and oxytocin genes. Mol Brain Res 1990;8:319–24.
[33] Mohr E, Schmitz E, Richter D. A single rat genomic DNA fragment encodes both the oxytocin and vasopressin genes separated by 11 kilobases and oriented in opposite transcriptional directions. Biochimie 1988;70:649–54.
[34] Mohr E, Bahnsen U, Kiessling C, Richter D. Expression of the vasopressin and oxytocin genes in rats occurs in mutually exclusive sets of hypothalamic neurons. FEBS Lett 1988;242:144–8.
[35] Dayanithi G, Viero C, Shibuya I. The role of calcium in the action and release of vasopressin and ocytocin from CNS neurons/terminals to the heart. J Physiol Pharmacol 2008;59 (S8):7–26.
[36] McDonald NA, Kuzmiski JB, Naderi N, SDchwab Y, Pittman QJ. Endogenous modulators of synaptic transmission: cannabinoid regulation in the supraoptic nucleus. Prog Brain Res 2008;170:129–36.
[37] Engel PA, Rowe JW, Minnaker KL, Robertson GL. Effect of exogenous vasopressin on vasopressin release. Am J Physiol 1984;246(9):E202–7.
[38] Panatier A. Glial cells: indispensable partners of hypothalamic magnocellular neurone. J Neuroendocrinol 2009;21:665–72.
[39] Jochberger S, Dorler J, Luckner G, Mayr VD, Wenzel V, Ulmer H, et al. The vasopressin and copeptin response to infection, severe sepsis and septic shock. Crit Care Med 2009;37(2):476–82.
[40] Szinnai G, Morgenthaler NG, Berneis K, Struck J, Muller B, Keller U, et al. Changes in plasma copeptin, the C-terminal portion of arginine vasopressin during water deprivation and excess in healthy subjects. J Clin Endocrinol Metab 2007;92 (10):3973–8.
[41] Seif SM, Robinson AG. Localization and release of neurophysins. Ann Rev Physiol 1978;40:45–76.
[42] Breslow E. Chemistry and biology of the neurophysins. Ann Rev Biochem 1979;48:251–74.
[43] Preibisz JJ, Sealey JE, Laragh JH, Cody RJ, Weksler BB. Plasma and platelet vasopressin in essential hypertension and congestive heart failure. Hypertension 1983;5(SI):I1129–38.
[44] Bichet DG, Arthus MF, Barjon JM, Lonergan M, Kortas C. Human platelet fraction arginine vasopressin. Potential physiologic role. J Clin Invest 1987;79(3):881–7.
[45] Robertson GL. Vasopressin function in health and disease. Recent Prog Horm Res 1977;33:333–85.
[46] Robertson GL, Athar S, Shelton RL. Osmotic control of vasopressin function. In: Andreoli TE, Grantham JJ, Rector Jr RC, editors. Disturbances in body fluid osmolality. Bethesda, MD: American Physiological Society; 1977. p. 125–48.
[47] Verney EB. The antidiuretic hormone and the factors which determine its release. Proc R Soc Lond (Biol) 1947;135:25–106.
[48] Gardiner TW, Verbalis G, Stricker EM. Impaired secretion of vasopressin and oxytocin in rats after lesions of nucleus medianus. Am J Physiol 1985;249:R681–8.
[49] Jewell PA, Verney EB. An experimental attempt to determine the site of the neurohypophyseal osmoreceptors in the dog. Philos Trans R Soc Lond (Biol) 1957;240:197–324.
[50] Mangiapane ML, Thrasher TN, Keil LC, Simpson JB, Ganong WF. Deficits in drinking and vasopressin secretion after lesions of the nucleus medianus. Neuroendocrinology 1983;37:73–7.
[51] Peck JW, Blass EM. Localization of thirst and antidiuretic osmoreceptors by intracranial injections in rats. Am Physiol 1975;228:1501–9.
[52] McKinley MJ, Mathai ML, McAllen RM, McClear RC, Miselis RR, Pennington GL, et al. Vasopressin secretion: osmotic and hormonal regulation by the lamina terminalis. J Neuroendocrinol 2004;16:340–7.
[53] Van Germert M, Miller M, Carey RJ, Moses AM. Polyuria and impaired ADH release following medial preoptic lesioning in the rat. Am Physiol 1975;228:1293–7.
[54] Robertson GL. Disorders of thirst in man. In: Ramsay D, editor. Thirst: physiological and psychological aspects. London: Springer-Verlag; 1991. p. 453–75.
[55] Robertson GL. Physiopathology of ADH secretion. In: Tolis G, Labrie F, Martin JB, et al., editors. Clinical neuroendocrinology: a pathophysiological approach. New York: Raven Press; 1979. p. 247–60.
[56] Halter JB, Goldberg AP, Robertson GL, Porte Jr. D. Selective osmoreceptor dysfunction in the syndrome of chronic hypernatremia. J Clin Endo Metab 1977;44:609–16.
[57] Robertson GL, Shelton RL, Athar S. The osmoregulation of vasopressin. Kidney Int 1976;10:25–37.
[58] Zerbe RL, Miller JZ, Robertson GL. The reproducibility and heritability of individual differences in osmoregulatory function in normal humans. J Lab Clin Med 1991;117:51–9.

[59] Hancock ML, Bichet DG, Eckert JG, Bankir L, Wagner MA, Pratt JH. Race, sex and the redulation of urine osmolarity: observations made during water deprivation. Am J Physiol Regul Integr Comp Phsiol 2010;299:R977–80.
[60] Moses AM. Is there an osmotic threshold for vasopressin release? Am J Physiol 1978;234:E339–40.
[61] Rodbard D, Munson PJ. Editorial comment. Am J Physiol 1978;234:E340–2.
[62] Weitzman RE, Fisher DA. Log–linear relationship between plasma arginine vasopressin and plasma osmolality. Am J Physiol 1977;233:E37–40.
[63] Robertson GL. Physiology of ADH secretion. Kidney Int 1987;32:S20–6.
[64] Baylis PH, Robertson GL. Plasma vasopressin response to hypertonic saline infusion to assess posterior pituitary function. J Roy Soc Med 1980;73:255–60.
[65] Evbuomwan IO, Davison JM, Baylis PH, Murdoch AP. Altered osmotic thresholds for arginine vasopressin secretion and thirst during superovulation and in the ovarian hyperstimulation syndrome (OHSS): relevance to the pathophysiology of OHSS. Fertil Steril 2001;75:933–41.
[66] Vokes TJ, Weiss NM, Schreiber J, Gaskill MB, Robertson GL. Osmoregulation of thirst and vasopressin during normal menstrual cycle. Am J Physiol 1988;254:R641–7.
[67] Stachenfeld NS, Keefe DL. Estrogen effects on osmotic regulation of AVP and fluid balance. Am J Physiol 2002;283(4):E711–21.
[68] Weitzman RE, Fisher DA, DiStefano III JH, Bennett CM. Episodic secretion of arginine vasopressin. Am J Physiol 1977;233:E32–6.
[69] Armstrong W. Morphological and electrophysiological classification of hypothalamic supraoptic neurons. Prog Neurobiol 1995;47(4–5):291–339.
[70] McKinley MJ, Denton DA, Weisinger RS. Sensors for antidiuresis and thirst – osmoreceptors or CSF sodium detectors? Brain Res 1978;141:89–103.
[71] Thrasher TN, Brown CJ, Keil LC, Ramsay DJ. Thirst and vasopressin release in the dog: an osmoreceptor or sodium receptor mechanism? Am J Physiol 1980;238:R333–9.
[72] Zerbe RL, Robertson GL. Osmoregulation of thirst and vasopressin secretion in human subjects: effect of various solutes. Am J Physiol 1983;224:E607–14.
[73] Olsson K, Kolmodin R. Dependence of basic secretion of antidiuretic hormone on cerebrospinal fluid (Na). Acta Physiol Scand 1974;91:286–8.
[74] Vokes T, Aycinena PR, Robertson GL. Effect of insulin on osmoregulation of vasopressin. Am J Physiol 1987;252:E538–48.
[75] Robertson GL. Thirst and vasopressin function in normal and disordered states of water balance. J Lab Clin Med 1983;101 (3):351–71.
[76] Wade CE, Keil LC, Ramsay DJ. Role of volume and osmolality in the control of plasma vasopressin in dehydrated dogs. Neuroendocrinology 1983;37:349–53.
[77] Zerbe RL, Henry D, Robertson GL. Vasopressin response to orthostatic hypotension: etiological and clinical implications. Am J Med 1983;74:265–71.
[78] Iwasaki Y, Gaskill MB, Robertson GL. Adaptive resetting of the volume control of vasopressin secretion during sustained hypovolemia. Am J Physiol 1995;268:R349–57.
[79] Goetz KL, Wang BC, Sundet WD. Comparative effects of cardiac receptors and sinoaortic baroreceptors on elevations of plasma vasopressin and renin activity elicited by haemorrhage. J Physiol (Lond) 1984;879:440–5.
[80] Iwasaki Y, Gaskill MB, Robertson GL. The effect of selective opioid antagonists on vasopressin secretion in the rat. Endocrinology 1994;134:55–62.
[81] Iwasaki Y, Gaskill MB, Boss CA, Robertson GL. The effect of the non-selective opioid antagonist diprenorphine on vasopressin secretion in the rat. Endocrinology 1994;134:48–54.
[82] Iwasaki Y, Gaskill MB, Fu R, Saper CB, Robertson GL. Opioid antagonist diprenorphine microinjected in parabrachial nucleus selectively inhibits vasopressin response ro hypovolemic stimuli in the rat. J Clin Invest 1993;92:2230–9.
[83] Robertson GL, Oiso Y, Vokes TP, Gaskill MB. Diprenorphine inhibits selectively the vasopressin response to hypovolemic stimuli. Trans Assoc Am Physicians 1985;98:322–33.
[84] Kirchheim HR. Systemic arterial baroreceptor reflexes. Physiol Rev 1976;56:100–76.
[85] Lee M, Thrasher TN, Keil LC, Ramsay DJ. Cardiac receptors, vasopressin, and corticosteroid release during arterial hypotension in dogs. Am J Physiol 1986;251:R614–20.
[86] Sawchenko PE, Swanson LW. Central noradrenergic pathways for the integration of hypothalamic neuroendocrine and autonomic responses. Science 1981;214:685–7.
[87] Berl T, Cadnapaphornachai P, Harbottle JA, Schrier RW. Mechanism of suppression of vasopressin during alpha-adrenergic stimulation with norepinephrine. J Clin Invest 1974;53:219–27.
[88] Billman GE, Keyl MJ, Dickey DT, Kern DC, Keil LC, Stone HL. Hormonal and renal response to plasma volume expansion in the primate *Macaca mulatta*. Am J Physiol 1983;244:H201–5.
[89] Jhamandas JH, Renaud LP. Neurophysiology of a central baroreceptor pathway projecting to hypothalamic vasopressin neurons. Can J Neurol Sci 1987;14:17–24.
[90] Shimamoto K, Miyahara M. Effect of norepinephine infusion on plasma vasopressin levels in normal human subjects. Clin Endocrinol Metab 1976;43:201–4.
[91] Schrier RW, Bed T, Harbottle JA. Mechanism of the antidiuretic effect associated with interruption of parasympathetic pathways. J Clin Invest 1972;51:2613–20.
[92] Thames MD, Schmid PG. Cardiopulmonary receptors with vagal afferents tonically inhibit ADH release in the dog. Am J Physiol 1979;237:H299–304.
[93] Ando T, Shimamoto K, Nakahashi Y, Nishitani T, Hosoda S, Ishida H, et al. Plasma antidiuretic hormone levels in patients with normal and low renin essential hypertension and secondary hypertension. Endocrinol Jpn 1983;30(4):567–70.
[94] Robertson GL, Ganguly A. Osmoregulation and baroregulation of plasma vasopressin in essential hypertension. J Cardiovasc Pharmacol 1986;8:S87–91.
[95] Ganguly A, Robertson GL. Elevated threshold for vasopressin release in primary aldosteronism. Clin Res 1980;28:330A (abstr).
[96] Moses AM, Miller M, Streeten DHP. Quantitative influence of blood volume expansion on the osmotic threshold for vasopressin release. Clin Endocrinol Metab 1967;27:655–62.
[97] Robertson GL, Athar S. The interaction of blood osmolality and blood volume in regulating plasma vasopressin in man. J Clin Endocrinol Metab 1976;42:613–20.
[98] Stricker EM, Verbalis JG. Interaction of osmotic and volume stimuli in regulation of neurohypophyseal secretion in rats. Am J Physiol 1986;250:R267–75.
[99] Kannan H, Yagi K. Supraoptic neurosecretory neurons: evidence for the existence of converging inputs both from carotid baroreceptors and osmoreceptors. Brain Res 1978;145:385–90.
[100] Rowe JW, Shelton RL, Helderman JH, Vestal RE, Robertson GL. Influence of the emetic reflex on vasopressin release in man. Kidney Int 1979;16:729–35.
[101] Miaskiewicz SL, Stricker EM, Verbalis JG. Neurohypophyseal secretion in response to cholecystokinin but not meal-induced

gastric distension in humans. J Clin Endocrinol Metab 1989;68:837–43.
[102] Verbalis JG, Richardson DW, Stricker EM. Vasopressin release in response to nausea-producing agents and cholecystokinin ip monkeys. Am J Physiol 1987;252:R749–53.
[103] McCann MJ, Verbalis JG, Stricker EM. LiCI and CCK inhibit gastric emptying and feeding and stimulate OT secretion in rats. Am J Physiol 1989;256:R463–8.
[104] Duke HN, Pickford M, Watt JA. The antidiuretic effect of morphine: its site and mode of action in the hypothalamus of the dog. Q J Exp Physiol 1951;36:149–58.
[105] Cates JE, Garrod O. The effect of nicotine on urinary flow in diabetes insipidus. Clin Sci 1951;10:145–60.
[106] Eversmann T, Guttsmann M, Uhlich E, Ulbrecht G, von Werder K, Scriba PC. Increased secretion of growth hormone, prolactin, antidiuretic hormone and cortisol induced by the stress of motion sickness. Aviat Space Environ Med 1978;49:53–7.
[107] Steele TH, Serpick AA, Block JB. Antidiuretic response to cyclophosphamide in man. J Pharmacol Exp Ther 1973;185:245–53.
[108] Heyes M, Farber MO, Manfredi F, Robertson GL, Fineberg NS, Manfredi F. Acute effects of hypoxia on renal and endocrine function in normal man. Am J Physiol 1982;243:R265–70.
[109] Zerbe RL, Vinicor F, Robertson GL. Plasma vasopressin in uncontrolled diabetes mellitus. Diabetes 1979;28:503–8.
[110] Wiggins RC, Basar I, Slater JD, Forsling M, Ramage CM. Vasovagal hypotension and vasopressin release. Clin Endocrinol 1977;6:387–93.
[111] Coutinho EM. Oxytocic and antidiuretic effects of nausea in women. Am J Obstet Gynecol 1969;105:127–31.
[112] Baylis PH, Zerbe RL, Robertson GL. Arginine vasopressin response to insulin-induced hypoglycemia in man. J Clin Endocrinol Metab 1981;53:935–40.
[113] Baylis PH, Robertson GL. Rat vasopressin response to insulin induced hypoglycemia. Endocrinology 1980;107:1975–9.
[114] Baylis PH, Robertson GL. Vasopressin response to 2-deoxy-d-glucose in the rat. Endocrinology 1980;107:1970–4.
[115] Thompson DA, Cambell RG, Lilavivat U, Welle SL, Robertson GL. Increased thirst and plasma arginine vasopressin levels during 2-deoxy_d-glucose-induced glucoprivation in humans. J Clin Invest 1981;67:1083–93.
[116] Mouw D, Bonjour JP, Malvin RL, Vander A. Central action of angiotensin in stimulating ADH release. Am J Physiol 1971;220:239–42.
[117] Keil Le, Summy-Long J, Severs WE. Release of vasopressin by angiotensin II. Endocrinology 1975;96:1063–5.
[118] Shimizu K, Share L, Claybaugh JR. Potentiation of angiotensin II of the vasopressin response to an increasing plasma osmolality. Endocrinology 1973;93:42–50.
[119] Yamaguchi K, Koike M, Hama H. Plasma vasopressin response to peripheral administration of angiotensin in conscious rats. Am J Physiol 1985;248:R249–56.
[120] Cadnapaphornachai P, Boykin J, Harbottle JA, McDonald KM, Schrier RW. Effect of angiotensin II on renal water excretion. Am J Physiol 1975;228:155–9.
[121] McKinley MJ, Allen AM, Mathai ML, May C, McCallen RM. Brain angiotensin and body fluid homeostasis. Jpn J Physiol 2001;51:281–9.
[122] Rydin H, Verney EB. The inhibition of water-diuresis by emotional stress and by muscular exercise. Q J Exp Physiol 1938;27:373–4.
[123] Edelson JT, Robertson GL. The effect of the cold pressor test on vasopressin secretion in man. Psychoneuroendocrinology 1986;11:307–16.
[124] Keil LC, Severs WE. Reduction of plasma vasopressin levels of dehydrated rats following acute stress. Endocrinology 1977;100:30–8.
[125] Engelmann M, Ludwig M. The activity of the hypothalamo–eurohypophysial system in response to acute stressor exposure: neuroendocrine and electrophysiological observations. Stress 2004;7(2):91–6.
[126] Aguilera G, Subburaju S, Young S, Chen J. The parvocellular vasopressinergic system and responsiveness of the hypothalamic pituitary adrenal axis during chronic stress. Prog Brain Res 2008;170:29–39.
[127] Segar WE, Moore WW. The regulation of antidiuretic hormone release in man. J Clin Invest 1968;47:2143–51.
[128] Takamata A, Mack GW, Stachenfeld MS, Nadel ER. Body temperature modification of osmotically induced vasopressin secretion and thirst in humans. Am J Physiol 1995;269:R874–80.
[129] Kasting NW, Mazurek MF, Martin JB. Endotoxin increases vasopressin release independently of known phsysiologic stimuli. Am J Physiol 1985;248:E420–4.
[130] Parrott RF, Vellucci SV, Goode JA, Lloyd DM, Forsling ML. Interrelated adrenocortical and neurohypophyseal responses associated with fever in endotoxin treated pigs. Am J Physiol 1997;273:R1046–52.
[131] Giusti-Piava A, Branco LGS, deCastro M, Autunes-Rodriguez J, Carnio EC. Role of nitric oxide in thermoregulation during septic shock: involvement of vasopressin. Pflugers Archiv-European J Physiol 2003;447(2):175–80.
[132] Davison JM, Shiells EA, Philips PR, Lindheimer MD. Suppression of AVP release by drinking despite hypertonicity during and after gestation. Am J Physiol 1988;254:F588–92.
[133] Geelen G, Keil LC, Kravik SE, Wade CE, Thrasher TN, Barnes PR, et al. Inhibition of plasma vasopressin after drinking in dehydrated humans. Am J Physiol 1984;247:R968–71.
[134] Thompson CJ, Burd JM, Baylis PH. Acute suppression of plasma vasopressin and thirst after drinking in hypernatremic humans. Am J Physiol 1987;252:RI138–42.
[135] Bevilacqua M, Norbiato G, Chebat E, Raggi U, Cavaiani P, Guzzetti R, et al. Osmotic and nonosmotic control of vasopressin release in the elderly: effect of metoclopramide. J Clin Endocrinol Metab 1987;65(6):1243–7.
[136] Helderman JH, Vestal RE, Rowe JW, Tobin JD, Andres R, Robertson GL. The response of arginine vasopressin to intravenous ethanol and hypertonic saline in man: the impact of aging. J Gerontol 1978;33:39–47.
[137] Ledingham JGG, Crowe MJ, Forsling ML, Phillips PA, Rolls BJ. Effects of aging on vasopressin secretion, water excretion and thirst in man. Kidney Int 1987;32(Suppl. 21):S90–2.
[138] Miller M. Fluid and electrolyte homeostasis in the elderly: physiological changes of ageing and clinical consequences. Baillieres Clin Endocrinol Metab 1997;11:367–87.
[139] Hofman MA. Lifespan changes in the human hypothalamus. Exp Gerontol 1997;32(4–5):559–75.
[140] Terano T, Seya A, Tamura Y, Yoshida S, Hirayama T. Characteristics of the pituitary gland in elderly subjects from magnetic resonance images: relationship to pituitary hormone secretion. Clin Endocrinol 1996;45:273–9.
[141] Crowe MJ, Forsling MJ, Rolls BJ, Phillips PA, Ledingham JG, Smith RF. Altered water excretion in healthy elderly men. Age Ageing 1987;16:285–93.
[142] Rowe JW, Andres R, Tobin JD, Norris AH, Shock NW. The effect of age on creatinine clearance in men: a cross-sectional and longitudinal study. J Geront 1976;31:155–63.
[143] Barron WM. Water metabolism and vasopressin secretion during pregnancy. Baillieres Clin Obstet GynaecoI 1987;1: 853–71.

[144] Lindheimer MD, Davison JM. Osmoregulation, the secretion of arginine vasopressin and its metabolism during pregnancy. Eur J Endocrinol 1995;132:133–43.
[145] Spruce BA, Baylis PH, Burd J, Watson MJ. Variation of osmoregulation of arginine vasopressin during the human menstrual cycle. Clin Endocrinol 1985;22:37–42.
[146] Calzone WL, Silva C, Keefe DL. Progesterone does not alter osmotic regulation of AVP. Am J Physiol 2001;281(6): R2011–20.
[147] Gold PW, Robertson GL, Post RM, Stachenfeld NS. The effect of lithium on the osmoregulation of arginine vasopressin secretion. J Clin Endocrinol Metab 1983;56:295–9.
[148] Kjaer A, Knigge U, Jorgensen H, Warberg J. Dehydration induced vasopressin secretion in humans: involvement of the histaminergic system. Am J Physiol 2000;279(6):E1305–10.
[149] Oiso Y, Iwasaki Y, Kondo K, Takatsuki K, Tomita A. Effect of the opioid kappa-receptor agonist U50488H on the secretion of arginine vasopressin. Neuroendocrinology 1988;48:658–62.
[150] Miller M. Role of endogenous opioids in neurohypophyseal function of man. J Clin Endocrinol Metab 1980;50:1016–20.
[151] van Wimersma Greidanus TB, Thody TJ, Verspaget H, de Rotte GA, Goedemans HJ, Croiset G, et al. Effects of morphine and β endorphin on basal and elevated plasma levels of alpha-MSH and vasopressin. Life Sci 1979;24:579–86.
[152] Oiso Y, Robertson GL. Role of endogenous opiates in mediating ethanol-induced suppression of vasopressin. Endocrinology 1982;751:267 (abstr)
[153] Gold PW, Robertson GL, Ballenger JC, Kaye W, Chen J, Rubinow DR, et al. Carbamazepine diminishes the sensitivity of the plasma arginine vasopressin response to osmotic stimulation. J Clin Endocrinol Metab 1983;57:952–7.
[154] Lausen HD. Metabolism of the neurohypophysial hormones. In: Geige SR, editor. Handbook of physiology, section 7. Endocrinology Vol. IV, Part 1. Bethesda, MD: American Physiological Society; 1974. p. 287–393.
[155] Davison JM, Sheills EA, Barron WM, Robinson AG, Lindheimer MD. Changes in the metabolic clearance of vasopressin and in plasma vasopressinase throughout human pregnancy. J Clin Invest 1989;83:1313–8.
[156] Birnbaumer M. Vasopressin receptors. Trends Endocrinol Metab 2000;11(1):406–10.
[157] Maybauer MO, Maybauer DM, Enkhbaatar P, Traber DL. Physiol Vasopressin Recept 2008;22(2):253–63.
[158] Thibonnier M. Genetics of vasopressin receptors. Curr Hypertens Rep 2004;6:21–6.
[159] Manning M, Stoev S, Chini B, Durroux T, Mouillac B, Guillon G. Peptide and non-peptide agonists and antagonists for the vasopressin and oxytocin V1a, V1b, V2 and OT receptors: research tools and potential therapeutic agents. Prog Brain Res 2008;170:473–512.
[160] Robertson GL. Vaptans for the treatment of hyponatremia. Nat Rev Endocrinol 2011;7(3):151–61.
[161] Sasaki S, Noda Y. Aquaporin-2 protein dynamics within the cell. Curr Opin Nephrol Hypertens 2007;16:348–52.
[162] Fenton RA, Moeller HB. Recent discoveries in vasopressin-regulated aquaporin-2 trafficking. Prog Brain Res 2008;170: 571–9.
[163] Brown D, Hasler U, Nunes P, Bouley R, Lu HAJ. Phosphorylation events and modulation of aquaporin 2 cell surface expression. Curr Opin Nephrol Hypertens 2008;17:491–8.
[164] Hoffert JD, Chou C, Knepper MA. Aquaporin-2 in the "-omics" era. J Biol Chem 2009;284(22):14683–7.
[165] Zerbe RL, Robertson GL. A comparison of plasma vasopressin measurements with a standard indirect test in the differential diagnosis of polyuria. N Engl J Med 1981;305:1539–46.
[166] Yang B, Bankir L. Urea and urine concentrating ability: new insights from studies in mice. Am J Physiol 2005;288: F881–96.
[167] Fenton RA. Essential role of vasopressin regulated urea transport processes in the mammalian kidney. Pfluger Arch-Eur J Physiol 2009;458:169–77.
[168] Bankir L, Bichet DG, Bouby N. Vasopressin V2 receptors, ENaC and sodium reabsorption: a risk factor for hypertension. Am J Physiol Renal Physiol 2010;299:F917–28.
[169] Voelckel WG, Covertino VA, Lurie KG, Karlbauer A, Schochl H, Lindner KH, et al. Vasopressin for hemorrhagic shock management: revisiting the potential value in civilian and combat casualty care. J Trauma 2010;69:S69–74.
[170] Oliver JA, Landry DW. Endogenous and exogenous vasopressin in shock. Curr Opin Crit Care 2007;13:376–82.
[171] Tomasiak M, Stelmach H, Rusak T, Ciborowski M, Radziwon P. Vasopressin acts on platelets to generate procoagulant activity. Blood Coagul Fibrinolysis 2008;19:615–24.
[172] Caldwell HK, Lee HJ, Macbeth AH, Young WH. Vasopressin: behavioral roles of an "original" neuropeptide. Prog Neurobiol 2008;84(1):1–24.
[173] Heinrichs M, Domes G. Neuropeptides and social behavior: effects of oxytocin and vasopressin in humans. Prog Brain Res 2008;170:337–50.
[174] Donaldson ZR, Young LJ. Oxytocin, vasopressin and the neurogenetics of sociality. Science 2008;322(5903):900–4.
[175] Serradeil-Le Gal C, Wagnon J, Tonnerre B, Roux R, Garcia G, Griebel G, et al. An overview of SSR149415, a selective nonpeptide vasopressin V1b receptor antagonist for the treatment of stress related disorders. CNS Drug Rev 2005;11(1):53–68.
[176] Egan G, Silk T, Zamarripa F, Williams J, Federico P, Cunnington R, et al. Neural correlates of the emergence of consciousness of thirst. Proc Nat Acad Sci USA 2003;100 (25):15241–6.
[177] Farrel MJ, Egan GF, Zamarripa F, Shade R, Blair-West J, Fox P, et al. Unique, common and interacting cortical correlates of thirst and pain. Proc Soc Nat Acad Sci USA 2006;103(7):2416–21.
[178] Andersson B. Regulation of water intake. Physiol Rev 1978;58:582–603.
[179] Erickson S, Simon-Oppermann C, Simon E, Gray DA. Occlusion of rostroventral 3rd ventricle abolishes drinking but not AVP release in response to central osmotic stimulation. Brain Res 1988;448(1):121–7.
[180] McKinley MJ, Cairns MJ, Denton DA, Egan C, Mathai ML, Uschakov A, et al. Physiological and pathophysiological influences on thirst. Physiol Behav 2004;81(5):795–803.
[181] Weiss NM, Conder ML, Robertson GL. The effect of hypovolemia on the osmoregulation of thirst and AVP. Clin Res 1984;32:786A.
[182] Figaro MK, Mack GW. Control of fluid intake in dehydrated humans: role of oropharyngeal stimulation. Am J Physiol 1997;272:R1740–6.
[183] DeCastro JM. A microregulatory analysis of spontaneous fluid intake by humans: evidence that the amount of fluid ingestion and its timing is governed by feeding. Physiol Behav 1988;43:705–14.
[184] DeCastro JM. The relation of spontaneous macronutrient and sodium intake with fluid ingestion and thirst in humans. Physiol Behav 1991;49:513–9.
[185] Kenney WL, Chiu P. Influence of age on thirst and fluid intake. Med Sci Sports Exerc 2001;33(9):1524–32.
[186] Kovacs L, Rittig S, Robertson GL. Effects of sustained antidiuretic treatment on plasma sodium concentration and body water homeostasis in healthy humans on *ad libitum* fluid intake. Clin Res 1991;40:165A (abst).

This page intentionally left blank

CHAPTER

43

The Urine Concentrating Mechanism and Urea Transporters

Jeff M. Sands[1] *and Harold E. Layton*[2]

[1]Renal Division, Department of Medicine, Emory University School of Medicine, Atlanta, GA, USA
[2]Department of Mathematics, Duke University, Durham, NC, USA

The ability to vary water excretion is essential for mammals, which generally do not have continuous access to water, but must maintain a nearly constant blood plasma osmolality. Mammals, therefore, need a mechanism that allows them to regulate water loss to closely match water intake. In addition, because sodium and its anions are the principal osmotic constituents of blood plasma, and plasma sodium concentration must be kept nearly constant, water loss must be regulated by a mechanism that decouples water and sodium. These critical regulatory capabilities are provided by the kidney's urine concentrating mechanism: when water intake is large enough to dilute blood plasma, urine more dilute than plasma is produced to concentrate the plasma; when water intake is so small that blood plasma is concentrated, urine more concentrated than plasma is produced to dilute the plasma. In both cases, the rate of sodium excretion is small and varies little; indeed, the total solute excretion rate varies little (Figure 43.1).

Urine osmolality varies widely in response to changes in water intake. Following a prolonged period without water intake, such as occurs when an individual sleeps, human urine osmolality may rise to ~1200 mOsm/kg H_2O, about four times plasma osmolality (~290 mOsm/kg H_2O). However, following the ingestion of large quantities of water, such as commonly occurs at breakfast, urine osmolality may decrease rapidly. Humans (and other mammalian species) are able to dilute their urine to ~50 mOsm/kg H_2O. Such large and rapid changes in osmolality require that the cells of the inner medulla have adaptive mechanisms (e.g., osmolytes) to protect them from osmotic damage.

Maximum urine osmolality varies widely among mammalian species. The long-nosed bat *Leptonycteris sanborni* can concentrate only to about 350 mOsm/kg H_2O, while the Australian hopping mouse *Notomys alexis* can concentrate to nearly 9400 mOsm/kg H_2O.[1] Primates can typically concentrate their urines from ~1000 to 2000 mOsm/kg H_2O.[1–3] Beluga whales and bottle-nosed dolphins, which have access only to hypertonic ocean water (~1000 mOsm/kg H_2O), can concentrate urine up to ~1800 mOsm/kg H_2O.[4] Most laboratory data relevant to the urine concentrating mechanism have been obtained from rabbits or rodents that can achieve higher maximum urine osmolalities than humans: the European rabbit can concentrate to ~1400 mOsm/kg H_2O, whereas the eastern cotton tail can concentrate to ~3300 mOsm/kg H_2O; rats to ~3000 mOsm/kg H_2O; mice and hamsters to ~4000 mOsm/kg H_2O; and chinchillas to ~7600 mOsm/kg H_2O.[1,4,5]

Regardless of maximum concentrating ability, the kidneys of all mammals maintain an osmotic gradient that increases from the cortico-medullary boundary to the tip of the medulla (papillary tip). This osmotic gradient is sustained even in diuresis, although it is diminished in magnitude relative to antidiuresis.[6,7] The major constituent of the osmotic gradient in the outer medulla is NaCl; in the inner medulla, the major constituents are NaCl and urea.[6,7] The cortex is nearly isotonic to plasma, while the papillary tip is hypertonic to plasma and, in antidiuresis, has osmolality similar to urine.[5] The major urinary solutes are sodium and potassium accompanied by univalent anions and by urea; urea is the predominant solute in urine during antidiuresis.[6,7] The sodium, potassium, and urea concentrations in rat plasma, papillary tissue, and urine,

Seldin and Giebisch's The Kidney, Fifth Edition.
DOI: http://dx.doi.org/10.1016/B978-0-12-381462-3.00043-4

© 2013 Elsevier Inc. All rights reserved.

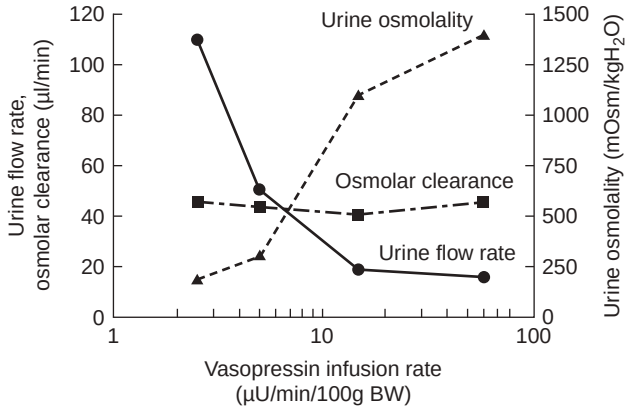

FIGURE 43.1 **Independent control of water and solute excretion.** Rats were infused with exogenous vasopressin and given a water-load (4% of body weight) to suppress endogenous vasopressin secretion. Vasopressin infusion causes a significant decrease in urine flow rate (left axis, circles) and increase in urine osmolality (right axis, triangles), but has little effect on osmolar clearance (left axis, squares). *(Figure is modified, with permission, from reference [232], using data from reference [450].)*

TABLE 43.1 Plasma, Papilla, and Urine Composition During Diuresis and Antidiuresis in Rats

A. Diuresis (urine flow/animal = 192:l/min)			
Component	Plasma	Papilla	Urine
Na^+ (mEq/l)	138	159	5.4
K^+ (mEq/l)	6.0	66.0	5.9
Urea (mM)	4.5	34.1	22.6
Osmolality (mOsm/kg H_2O)	304	572	59
B. Antidiuresis (urine flow/animal = ~5:l/min)			
Component	Plasma	Papilla	Urine
Na^+ (mEq/l)	145	417	148
K^+ (mEq/l)	6.7	102	140
Urea (mM)	4.4	605	946
Osmolality (mOsm/kg H_2O)	314	1832	1805

The data given in this table is from tables and figures in references [6,36,454].

during both diuresis and antidiuresis, are given in Table 43.1.

The mechanisms responsible for the separate control of water and sodium excretion are largely located in the renal medulla, where the nephron segments and vasa recta are arranged in complex but specific anatomic relationships, both in terms of which segments connect to which segments, and in terms of three-dimensional configuration. The production of concentrated urine involves complex interactions among the nephron segments and vasculature. In the outer medulla, thick ascending limbs of the loop of Henle actively absorb NaCl, diluting the luminal fluid and providing NaCl to increase the osmolality of the medullary interstitium, pars recta, descending limbs, collecting ducts, and vasculature. The countercurrent configuration of nephron segments and vessels allows the generation of a medullary osmolality gradient along the cortico-medullary axis. In the inner medulla, osmolality continues to increase, but the source of the concentrating effect remains controversial. However, the most widely accepted mechanism remains passive absorption of NaCl, in excess of solute secretion, from thin ascending limbs of the loops of Henle.[8,9]

KIDNEY STRUCTURE

The structural organization of the mammalian kidney is discussed in detail elsewhere in this book. This section, based in large measure on key studies (e.g., [10–12]), summarizes features that are pertinent to the urine concentrating mechanism.

In most mammals studied, the kidney contains short looped and long-looped nephrons; both have loops of Henle that are arranged in a hairpin configuration (Figure 43.2). They differ in two important aspects: the loops of short-looped nephrons turn near the inner-outer medullary border and lack a thin ascending limb, whereas the loops of long-looped nephrons extend into the inner medulla and contain a thin ascending limb. Thin ascending limbs are found only in the inner medulla, and their transition to thick ascending limbs defines the inner–outer medullary border. Thus, only thick ascending limbs are found in the outer medulla, regardless of the type of loop. Some mammalian kidneys, e.g., human kidneys, have nephrons whose loops of Henle do not reach into the medulla; these nephrons are called cortical nephrons. Tubular fluid flows from thick ascending limbs of both short and long looped nephrons to distal convoluted tubules. Several distal tubules merge to form cortical collecting ducts that descend through the cortex and then become medullary collecting ducts that pass through the outer medulla. The collecting ducts merge along the entire length of the inner medulla, ultimately forming the ducts of Bellini, which open into the renal pelvis at the papillary tip.

Small mammals, such as rodents, have unipapillate kidneys. In these mammals, the papilla is an inverted pyramid-shaped portion of the innermost inner medulla; the papilla descends into the renal pelvis. Larger mammals (including humans) have multipapillate kidneys in which each papilla descends into a renal calyx. The renal pelvis is formed from the merging of these calyces. In all mammals, urine exits through the ducts of Bellini into the renal pelvis.

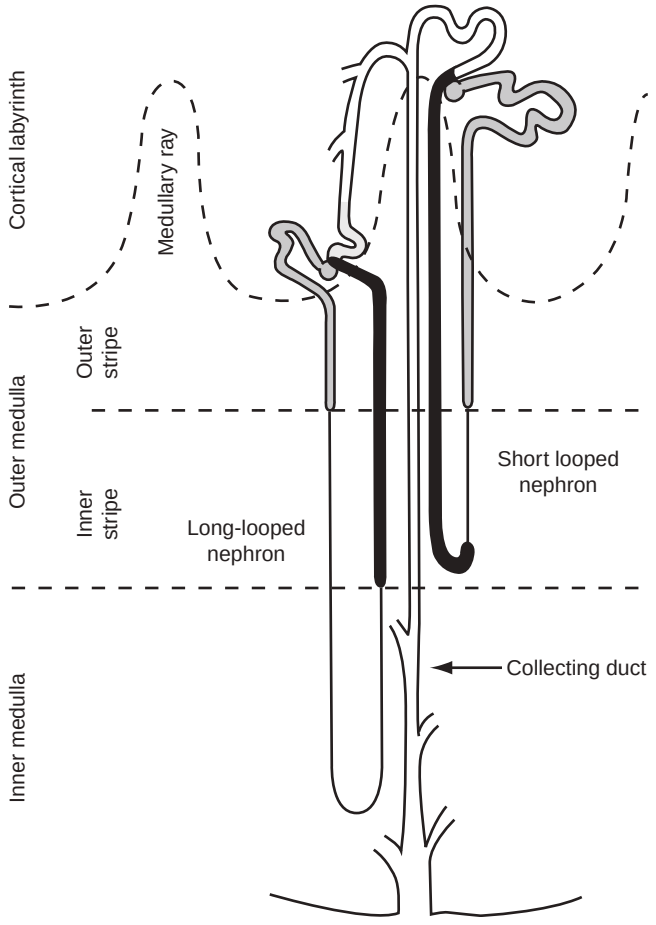

FIGURE 43.2 **Basic structure of mammalian kidney.** Diagram shows both a long-looped and a short-looped nephron. Glomeruli are shown as circles, proximal tubules are hatched, thin limbs of Henle's loop are lines, thick ascending limbs of Henle's loops are solid, distal convoluted tubules are stippled, and collecting duct system is open. *(Reproduced with permission, from reference [232].)*

The pelvis, which connects to the ureter, is bounded by two epithelia: the papillary surface epithelium lining the surface of the papilla, and a ureteral-type epithelium extending from the ureter up into the renal pelvic fornices.[13–16]

The descending and ascending vasa recta, which provide the blood supply for the medulla, are arranged roughly in parallel. Although their configuration is similar to the hair-pin configuration of the loops of Henle, there is an important anatomic difference: the tubular segments that make up the loops of Henle are contiguous, whereas the descending and ascending vasa recta are separated by capillary plexuses. Blood enters the medulla through descending vasa recta, passes through capillary plexuses located at various depths within the medulla, and then enters ascending vasa recta. Vascular bundles, which are aggregations of both descending and ascending vasa recta, form in the outer stripe, but become much more prominent in the inner stripe. Lemley and Kriz have proposed using the vascular bundle (see detail, Figure 43.3) as the histotopographical core around which the various outer medullary tubule structures are arranged.[10–12,17]

Studies of inner medullary structure by Kriz and co-workers,[10–12,17] and recent studies by Pannabecker and Dantzler,[18,19] found that the inner medullary collecting ducts (IMCDs) in the inner medullary base form clusters that coalesce along the cortico–medullary axis. Using immunohistochemical labeling and computer-assisted reconstruction, Pannabecker, Dantzler, and colleagues have elucidated new detail of the functional architecture of the rat inner medulla (see recent review [20]). A computerized reconstruction of the inner medullary portion of several long-looped nephrons from rats is shown in Figure 43.4, in which antibodies to the water channel aquaporin-1 (AQP1, shown in red) and the chloride channel ClC-K1 (shown in green)[18] are used to label the thin descending and ascending limbs of the loops of Henle, respectively (reviewed in [20]). In the base of the inner medulla, thin descending limbs are predominantly present at the periphery of these clusters, and appear to form an asymmetric ring around each collecting duct cluster. In thin descending limbs of loops of Henle that turn within the upper first millimeter of the inner medulla, no AQP1 was detected. In contrast, there are three discernible functional subsegments in thin descending limbs of loops of Henle that turn below the first millimeter: the upper 40% expresses AQP1, whereas the lower 60% do not. ClC-K1, a marker of the thin ascending limb-type epithelium, is first detected in the final ~165 micrometers of the thin descending limb, as well as in the contiguous thin ascending limb. Thus, ClC-K1 is detected before the bend of the loops of Henle. This finding is consistent with previous morphological studies demonstrating that the descending limb to ascending limb transition occurs before the loop bend. In addition, a substantial portion of the inner medullary thin descending limbs of long-looped nephrons did not express either AQP1 or ClC-K1, as indicated in gray in Figure 43.4a.

In contrast, thin ascending limbs are distributed relatively uniformly among collecting ducts and thin descending limbs. In Munich-Wistar rats, Pannabecker and Dantzler[19] identified three population groups of loops of Henle, distinguished by thin ascending limb position at the base of the inner medulla and by differing loop length. Group 1 loops, having thin ascending limbs that are interposed between collecting ducts, reach a mean length of 700 μm into the inner medulla; Group 2 loops, having thin ascending limbs that are adjacent to just one collecting duct, reach 1500 μm and Group 3 loops, having thin ascending limbs that lie more than a half-tubule diameter from a collecting

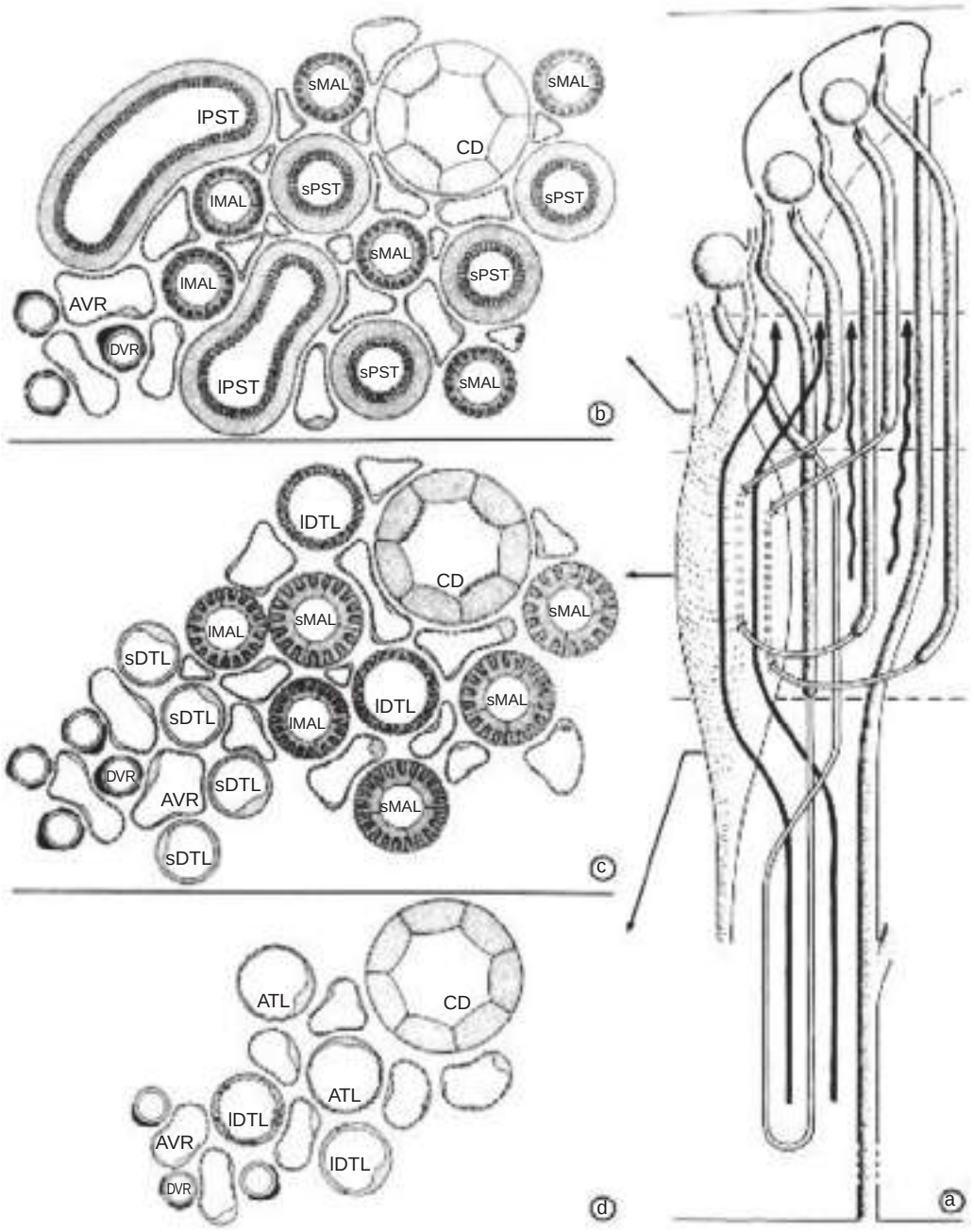

FIGURE 43.3 **Lemley and Kriz model of the architectural organization of the rat renal medulla.** Shown are a schematic longitudinal section (a); and cross-sections through the outer stripe of the outer medulla (b); inner stripe of the outer medulla (c); and the inner medulla (IM) (d). In (a) 1 long and 2 short loops of Henle, the collecting duct, and a vascular bundle (shown in three-dimensional solid form) are shown. The vascular bundle contains ascending vasa recta (AVR) originating from the inner medulla (AVRIM, long, bold-face arrows) and the descending limbs of the short-looped nephrons (sDTL). Ascending vasa recta originating from the inner stripe (AVRIS, bold, wavy arrows) ascend directly within the interbundle region. In the cross-sections (b)–(d), the relationships of 4 short and 2 long loops of Henle are shown with the collecting duct (CD) and vasa recta. (b) In the outer stripe, the proximal straight tubules (PST) and medullary thick ascending limbs of long-looped nephrons (lMAL) are located among the AVRIM near the vascular bundle. Located at a distance from the vascular bundle are the collecting ducts (CD) and the PSTs, and thick ascending limbs from short looped nephrons (sMAL). These structures are surrounded by AVRIS and the true capillaries (smaller unlabeled structures). (c) In the inner stripe, the core of a vascular bundle contains AVR and descending vasa recta (DVR), whereas sDTL are found among the AVRIM in the periphery. In the interbundle region, the thin descending limbs of long looped nephrons (lDTL) and CD run together with thick ascending limbs of short looped nephrons (sMAL); the lMAL are found bordering the vascular bundle. (d) In this section through the upper IM, a vascular bundle is still discernible, but AVR are already present throughout the cross-section. The CD is distant from the vascular bundle. Between the bundle and the CD are lDTL (with different wall structures corresponding to upper and lower part epithelia) and ascending limbs of long looped nephrons (ATL) (Abbreviations: AVR and DVR: ascending and descending vasa recta; CD: collecting duct; DTL: descending thin limb; MAL: medullary thick ascending limb; PST: proximal straight tubule (pars recta); subscripts s and l: short-looped and long-looped nephrons, respectively; OS, IS, and IM: outer and inner stripe of the outer medulla and inner medulla, respectively). *(Reproduced with permission, from reference [12].)*

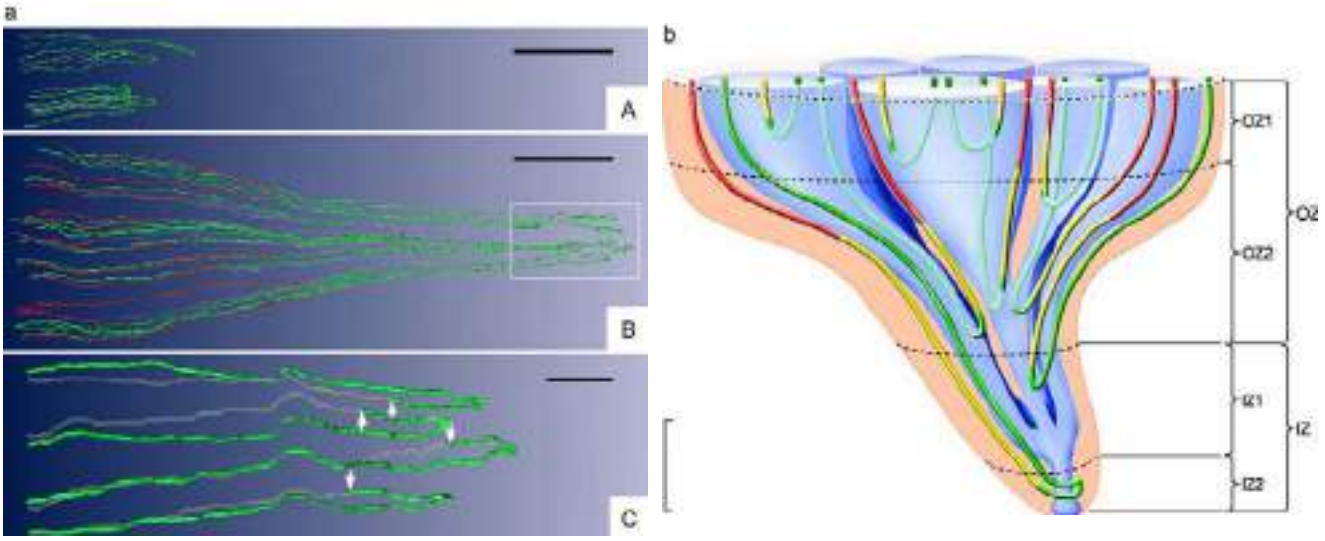

FIGURE 43.4 (a) Computer-assisted reconstruction of loops of Henle from rat inner medulla showing expression of aquaporin-1 (AQP1; red) and ClC-K1 (green); gray regions (B-crystallin) express undetectable levels of AQP1 and ClC-K1. Loops are oriented along the corticopapillary axis, with the left edge of each image nearer the base of the inner medulla. Panel A: Thin limbs that have their bends within the first millimeter beyond the outer–inner medullary boundary. Descending segments lack detectable AQP1. ClC-K1 is expressed continuously along the prebend segment and the thin ascending limb. Panel B: Loops that have their bends beyond the first millimeter of the inner medulla. AQP1 is expressed along the initial 40% of each thin descending limb, and is absent from the remainder of each loop. ClC-K1 is expressed continuously along the prebend segment and the thin ascending limb. Boxed area is enlarged in panel C. Panel C: Enlargement of near-bend regions of 4 thin limbs from box in panel B. ClC-K1 expression, corresponding to thin descending limb prebend segment, begins, on average, 165 μm before the loop bend (arrows). Scale bars, 500 μm (panels A and B); and 100 μm (panel C). *(Reproduced with permission, from reference [20].)* (b) Based on computer-assisted functional anatomy reconstructions that included immunolabeling of key transporters along the limbs of long loops of Henle, Pannabecker et al.[21] have proposed that the inner medulla of the rat can be considered to have four four zones (or subsections): (1) an outer-most zone (OZ1), about 1 mm thick, that lies just below the OM and in which loops labeling for little or no AQP1 have their bends; (2) a larger outer zone (OZ2), 2 to 2.5 mm in thickness that lies just below OZ1 that has well-organized CD clusters and tubules where loop bends turn within central portions of the clusters; (3) an outer inner zone (IZ1) where the organization of CD clusters diminishes, and all vasa recta are fenestrated; and (4) an inner-most zone (IZ2) where CD clusters can no longer be distinguished, where all vasa recta are fenestrated, and where many loops of Henle have transversely-running segments that wrap alongside CDs. The two inner zones combined are 1.5 to 2 mm thick. Representative collecting duct clusters are shown in blue; intercluster tissue is orange. AQP1-positive and AQP1-negative descending thin limbs are shown in red and yellow, respectively. Prebend segments and ascending thin limbs are shown in green. This color scheme differs from that of Figure 43.4A only by the use of yellow rather than gray for AQP-1 negative descending thin limbs. *(Reproduced with permission from [21].)*

duct, reach 2200 μm. As collecting ducts coalesce and shorter loops disappear, the originating portions of longer thin ascending limbs run alongside the collecting ducts for substantial distances (a more detailed description of inner medullary loop subgroups was given in [20]).

Moreover, Pannabecker et al.[20,21] proposed that the inner medulla has at least four distinguishable zones (axial subsections) that can be differentiated by the variable characteristics of vasa recta and loops of Henle. The four zones are illustrated in Figure 43.4b. Three countercurrent systems were hypothesized to exist within these zones: (1) an intercluster system within the CD clusters where most of the work of concentrating is conducted in and around nodal spaces that are surrounded by IMCDs, thin ascending limbs, and AVR; (2) an extracluster system in the outerzones (outer 3 to 3.5 mm) that serves to carry water absorbed from water-permeable portions of descending limbs back to the OM via AVR; and (3) a papillary system in the inner zones where the highest concentrations are attained with the aid of direct interactions between transversely-running segments of loops of Henle and collecting ducts.

Distinct types of interstitium are found in the vascular bundle in the outer medulla, in the interbundle region of the outer medulla, and in the inner medulla.[12] These interstitia may play an important role in medullary solute and water transfer, especially in the inner medulla, where interstitial cells are interspersed in a gelatinous matrix of acid mucopolysaccharides, which is largely devoid of any capillary plexuses, laterally flowing capillaries or lymphatics.[12,22,23] Thus, the inner medullary interstitium should greatly slow lateral bulk flow of solutes and water.

The number of nephrons found in mammals, and thus the number of loops of Henle, varies over many

orders of magnitude, increasing sub-linearly with increasing body mass.[24] The mouse has about 12,400 nephrons per kidney[24]; rat, 30,000–40,000[24,25]; rabbit, 230,000[24,25]; human, 0.3–1.4 million[26,27]; elephant, 7.5 million[24]; and fin whale, 192 million.[27] In contrast, medullary thickness in mammals varies from 3 to 25 mm, thus indicating that maximum loop of Henle length varies over about an order of magnitude[4]; proximal tubule diameter changes little from rat to fin whale, increasing by a factor of about 1.3.[27,28]

Although loops of Henle of variable length are found in all mammals, most mammals are thought to have both short- and long-looped nephrons. Exceptions include the dog, with all long loops,[29] and the mountain beaver *Aplodontia rufa*, which has thick ascending limbs only, and has a renal medulla that corresponds to the outer medulla of other mammals.[30] Generally, however, there are more short-looped than long looped nephrons, and the long-looped nephrons tend to exhibit substantial variation in the depth reached within the inner medulla. Measurements in the rabbit[31] and rat[25,32] indicate that the decrease in loop of Henle and collecting duct population in the inner medulla is approximately exponential, with most loops of Henle turning back in the outer portion of the inner medulla, and with collecting ducts converging to a few ducts of Bellini. A similar pattern is seen in the medullary cones of the avian kidney[33] which, like the mammalian kidney, is able to produce a concentrated urine, although only to osmolalities of about twice that of blood plasma.[34]

The pattern of decrease in the tubule populations of the rat renal medulla[25,32] is portrayed in Figure 43.5, which gives curves approximating loop and collecting duct population as a function of normalized medullary depth. About 38,000 loops and 7300 collecting ducts extend through most of the outer medulla.[25] About 28–33% of the loops of Henle in rat have thin ascending limbs and reach into the inner medulla.[10,29] The populations of loops of Henle and collecting ducts both decline rapidly, but the loop population decreases more rapidly, so that the loop and collecting duct populations are more nearly equal in the papilla. In human, about $\frac{1}{7}$ of the loops of Henle reach into the inner medulla.[27]

Figure 43.5 also portrays the concentration of urea, the sum of the concentrations of sodium and its anions, and the osmolality, as a function of medullary depth, as determined in tissue slices harvested from vasopressin-treated Wistar rats.[6,35,36] The experimental data points indicated in Figure 43.5 are connected by natural cubic splines which generate smooth curves; these curves have shapes supported by other studies in rat.[37,38] Osmolality increases by a factor of about 2 in the outer medulla, and by an additional factor of 3 in the inner medulla, where urea makes a substantive contribution. As can be inferred from the values for urine (U) in Figure 43.5, sodium is largely carried by flow in the loops of Henle and vasculature, while urea makes up a large portion of the solute in collecting duct flow. Potassium has a tissue concentration of

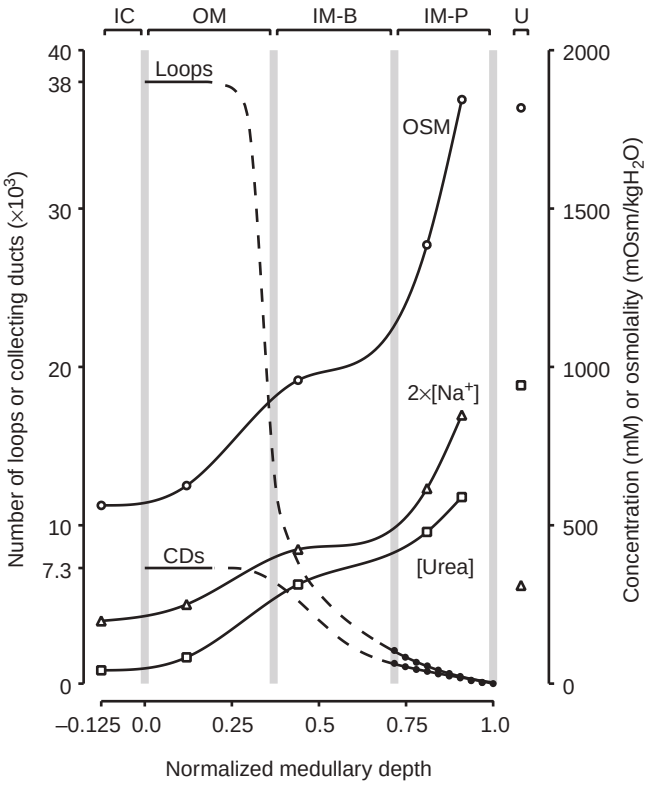

FIGURE 43.5 **Loop of Henle and collecting duct population in rat (scale at left) as a function of normalized medullary depth; also, tissue osmolality, concentration of urea, and concentration of sodium plus its anion (scale at right).** Loop of Henle and collecting duct populations decrease in inner medulla because loops turn back and collecting ducts merge. The osmolality gradient is larger in the outer medulla and papilla than in the outer part of the inner medulla. The gradient is largest in the papilla, where the osmolality and concentration profiles appear to increase exponentially. The shape of the sodium profile has been corroborated by electron microprobe measurements [38] (Key: IC: inner cortex; OM: outer medulla; IM: outer part (base) of inner medulla; P: papilla or inner part (tip) of inner medulla; U: urine). Figure based on published data. Curves connecting data points are natural cubic splines, computed by standard algorithms.[451] Dashed curve segments are interpolations without supporting measurements. Tubule populations in papilla are from reference [32]; tubule populations in outer medulla are based on estimates in reference.[25] Concentrations and osmolalities are from tissue slices and urine samples collected 4.5 hours after onset of vasopressin infusion at 15 μU/min/100 g body weight. Data is from Figure 5 in reference [36] and Figures 1, 3, and 9 in reference [6]; slice locations were given in reference.[35] The osmolality reported in the inner cortex seems high relative to the reported plasma concentration of 314 mOsm/kg H_2O. The osmolality and concentration profiles, as drawn in reference [6], apparently do not take into account relative distances between tissue sample sites.

about 80–100 mM along the medulla, but it makes a larger contribution (~150 mM) to urine.[6,36]

The osmolality increase along the outer medulla arises from the vigorous transepithelial transport of NaCl from thick ascending limbs into the surrounding interstitium. This effect is believed to be augmented by a process of countercurrent multiplication, described in a subsequent section (*vide infra*). However, as shown in Figure 43.5, the osmolality gradient is largest in the papilla, even though only a small fraction of the loops, tubules, and vasa recta reach into the papilla, and even though the population of tubules and vessels is rapidly decreasing there. The remarkable capacity for generating high osmolalities in so small a volume (~0.5% of total kidney volume[22]) has thus far resisted a generally satisfactory explanation.

TRANSPORT PROPERTIES OF INDIVIDUAL NEPHRON SEGMENTS

This section will review the water, urea, and sodium permeability values measured in isolated perfused tubules in nephron segments involved in producing concentrated or dilute urine. Thin limb segments are difficult to perfuse, and most measurements involving different species have been made by different laboratories. Thus, some caution must be used in comparing these values. Tables 43.2–43.5 contain values obtained from animals receiving food and water *ad libitum*; representative values were chosen since space does not permit citing every original manuscript.

In the past two decades, many of the proteins which mediate water, urea, and sodium transport in nephron segments important for urinary concentration and dilution have been cloned (Figure 43.6). The water channels (called aquaporins) and sodium transporters are discussed in detail elsewhere in this book. The urea transport proteins and their role in the long-term regulation of the urine concentrating mechanism are discussed later in this chapter.

In general, the water, urea, and sodium transport proteins are highly specific. Reflection coefficients are not included in Tables 43.2–43.5, since the specificity of these transport proteins appears to eliminate a molecular basis for solvent drag and suggests that the reflection coefficients should be 1.

THIN DESCENDING LIMB

Thin descending limbs are conventionally divided into types I, II, and III: types I and II are located in the outer medulla in short and long looped nephrons, respectively, while type III limbs are located in the inner medulla.[39,40] The osmotic water permeability of thin descending limb subtypes that express aquaporin 1 (AQP1) water channels[41] is extremely high in all species studied[42–45] (Table 43.2). AQP1, a constitutively active water channel, is present in both the apical and basolateral plasma membranes in sufficient abundance to account for the measured rates of transepithelial water transport.[46] Transgenic mice lacking the AQP1 channel (which is also found in proximal tubule and descending vasa recta), were found to have greatly impaired urine concentrating capability, which was attributed in large measure to defective water absorption from the proximal tubules and descending limbs, which may lead to an overloading of available concentrating capacity.[47,48]

The chinchilla has an additional inner medullary subsegment (type II distal) in the deepest 20% of the

TABLE 43.2 Permeability Properties in Thin Descending Limb Nephron Segments[a]

	Species			
	Chinchilla	Rat	Rabbit	Hamster
THIN DESCENDING LIMB TYPE I				
Na[b]			0–2 [65;64;66c]	4.8[58]
Urea[b]		13[63c]	1–2[60,62c]	8[58]
Water[d]		2295[44c]	2420[64c]	3257[58]
Na^+/K^+-ATPase[e]		2–5[67,68c]	2–4[67c]	
THIN DESCENDING LIMB TYPE II				
Na[b]			1[64–66c]	23–66[58,59]
Urea[b]	3[57]	0[61]	1[60,62c]	3[58,59]
Water[d]	2600[42,49]	2295[79c]	2315[64c]	5378[58]
Na^+/K^+-ATPase[e]		2–5[67,68c]	2–4[67c]	
THIN DESCENDING LIMB TYPE III				
Na[b]	29[57]			4[59]
Urea[b]	17–29[52,57]	13[63c]		13[59]
Water[d]	1550[42,49]	2295[79c]		1693[59]
Na^+/K^+-ATPase[e]		3[68]		
THIN DESCENDING LIMB TYPE III DISTAL (PAPILLARY SUBSEGMENT)				
Na[b]	74[57]			
Urea[b]	48[57]			
Water[d]	60[42,49]			

[a] *References are in supercripted.*
[b] *units: 10^{-5} cm/sec.*
[c] *Subsegment not specified, thus cannot differentiate between thin descending limb subtypes.*
[d] *units: μm/sec.*
[e] *units: pmol/mm/min.*

TABLE 43.3 Permeability Properties in Ascending Limb Nephron Segments[a]

	Species			
	Chinchilla	Rat	Rabbit	Mouse
THIN ASCENDING LIMB				
Na[b]	238[57]	80[79]	26[80]	55–88[79,82]
Urea[b]	171[57]	14–23[63,79]	7[80]	19[79]
Water[c]	0–8[42,49]	25[79]	13[80]	29[79]
Na^+/K^+-ATPase[d]		2–4[67,68]	3[67]	
MEDULLARY THICK ASCENDING LIMB				
Na[b]			6[94,430]	2[455]
Cl[b]			1[94]	1[455]
Urea[b]		1.4 (outer stripe)[98]	1[99]	
		0.6–0.9 (inner stripe)[98]		
Water[c]			0[94]	23[456]
K[b]			1[457]	
PD[e]		2–3[458]	3–7[94,459,460]	
Na^+/K^+-ATPase[d]		41–139 (outer stripe)[95]	41–124[67]	62[67]
		260 (inner stripe)[95]		
CORTICAL THICK ASCENDING LIMB				
Na[b]		1[461]	3[462]	
Cl[b]		1[461]	1[462]	
Urea[b]		1.5[98]	2[463]	
Water[c]			0[94]	23[456]
PD[e]			3–7[92,462]	
Na^+/K^+-ATPase[d]		83–133[95]	16–31[67]	61[67]

[a] *References are superscripted.*
[b] *units: 10^{-5} cm/sec.*
[c] *units: μm/sec.*
[d] *units: pmol/mm/min.*
[e] *PD: transepithelial potential difference, mV.*

TABLE 43.4 Permeability Properties in Cortical and Outer Medullary Collecting Duct Segments[a]

	Species	
	Rat	Rabbit
CORTICAL COLLECTING DUCT		
Na[b]		0.1[464]
K[b]		1–2[464,465]
Cl[b]		2–5[108,464]
Urea[b] ± [c] AVP	1[98,104]	0–1[100,466]
Water[d] − AVP	17–43[101,102]	4–13[225,467,468]
+ AVP	389–994[101,102,469]	166–280[225,467,468,470]
Na^+/K^+-ATPase[e]	13–81[67,68,95]	12–23[67,471–474]
OUTER MEDULLARY COLLECTING DUCT		
Na[b]		0.39[465]
K[b]		0.59[465]
Cl[b]		0.5[475]
Urea[b]	3.5[102]	0.3[99]
Water[d] −AVP		14[99,110]
+ AVP		445[99,110]
Na^+/K^+-ATPase[e]	11–41[95,68]	8–19[67,471,472,474]

[a] *References are superscripted;*
[b] *units: 10^{-5} cm/sec.*
[c] *± AVP: value unchanged by AVP; − AVP: no vasopressin; + AVP: with vasopressin.*
[d] *units: μm/sec;*
[e] *units: pmol/mm/min.*

longest loops of Henle.[42] This subsegment has low osmotic water permeability[42,49] and lacks AQP1.[50] The Munich-Wistar rat has a similar subsegment in the deepest 60% of the longest loops[51,52] and also a prebend segment of ~164 μm in length that labels for the ClC-K1 chloride transporter, but not for AQP1.[18] Avian loops of Henle appear to have similar pre-bend segments.[53] The pre-bend segments may be functionally important as a site of NaCl absorption.[52,54–56]

Urea permeability varies in different portions of the thin descending limb (Table 43.2). Urea permeability is relatively low in types I and II thin descending limbs.[57–62] Urea permeability is higher in type III thin descending limbs,[52,57,59,63] and is quite high in the chinchilla type III distal thin descending limb.[57] The reflection coefficient for urea is close to 1 in thin descending limbs.[58,64]

Sodium permeability is relatively low in rabbit types I and II[64–66] and hamster types I and III thin descending limbs,[58,59] but is relatively high in hamster type II and chinchilla types III and III distal thin descending limbs.[57–59] Na^+/K^+-ATPase activity is very low in all thin descending limb segments in which it has been measured.[67,68] Rabbit types I and II thin descending limbs have a NaCl reflection coefficient that is close to 1.[64] However, the measured NaCl reflection coefficient is heterogeneous in hamster: 0.83 in type II and 0.99 in type III thin descending limbs.[58,69]

The perfused tubule studies reviewed above provide important information about the transport properties of

TABLE 43.5 Permeability Properties in Inner Medullary Collecting Duct Subsegments[a]

	Species		
	Rat	**Rabbit**	**Hamster**
INITIAL INNER MEDULLARY COLLECTING DUCT – IMCD$_1$			
Urea[b] ± [c]AVP	2–5[102,104,114,118]	1[104]	8–9[116]
Sodium-Urea[d]	0[115,118]		
Water[e] − AVP	16–81[102,117,476]		
+AVP	148–460[102,117,476]		534[116]
Na^+/K^+-ATPase[f]	18–42[68]		
TERMINAL INNER MEDULLARY COLLECTING DUCT – IMCD$_2$			
Na[b]	1[124]		2[116]
K[b]	4[123]		
Cl[b]	1–2[123,124]		
Urea[b] −AVP	15–46[102,104,114,120,476]	12[104]	12[116]
+AVP	69–93[102,114,120]		32[116]
+Hypertonic bath:	120–143[119,121]		
+Hypertonic bath and AVP:	163–190[119,121]		
Sodium-Urea[g]	0–1[115,118]		
Water[e] − AVP	70–333[102,117,476]		
+AVP	208–749[102,117,476]		646[116]
Na^+/K^+-ATPase[f]	12–40[68]		
TERMINAL INNER MEDULLARY COLLECTING DUCT - IMCD$_3$			
Na[b]	1[124]		
Urea[b] − AVP	39–49[104,114]	13[104]	
+AVP	110[114]		
Sodium-Urea[g]	−9[115]		
Water[e] − AVP	43–145[102,117]		
+AVP	389–749[102,117]		
Na^+/K^+-ATPase[f]	8–17[68]		
PAPILLARY SURFACE EPITHELIUM			
Chloride[b] ± AVP	2–3[127]		
Urea[b] ± AVP	1[104]		
Water[d] ± AVP	14[127]		

[a] *References are superscripted.*
[b] *units: 10^{-5} cm/sec.*
[C] *± AVP: value unchanged by AVP; − AVP: no vasopressin; + AVP: with vasopressin.*
[d] *sodium-urea co-transport, units: pmol/mm/min.*
[e] *units: μm/sec.*
[f] *units: pmol/mm/min.*
[g] *sodium-urea counter-transport, units: pmol/mm/min; + : urea absorption; − : urea secretion.*

the individual nephron segments comprising the descending limb of the loop of Henle. In contrast, micropuncture studies provide *in vivo* information about the concentrations of solute within the portions of the descending limb that are accessible to micropuncture: comparisons can be made between the composition of tubular fluid near the ends of those proximal convoluted tubules that are accessible on the cortical surface and the composition of fluid in the bends of the longest loops of Henle near the papillary tip. Since proximal tubules on the surface of the kidney originate from superficial glomeruli, and the loops of Henle which reach the papillary tip generally originate from juxtamedullary nephrons, it is not possible, currently, to compare fluid samples taken from cortical and medullary sites in a single nephron. Thus, the validity of this comparison depends upon the assumption that the composition and delivery of solute and water to the beginning of the superficial and juxtamedullary descending limbs are similar. In addition, papillary micropuncture requires the removal of the ureter, which also reduces maximum urinary concentrating ability by a mechanism that is not completely understood.[70–72] Thus, micropuncture studies are limited to studies performed during moderate, not maximal, antidiuretic conditions.

In the rat, osmolality increases along the length of the descending limb. Water removal accounts for 90% of this increase in osmolality in Brattleboro rats that are not treated with vasopressin.[73] When Brattleboro rats are treated with vasopressin, there is an increase in the osmotic pressure of the descending limb fluid and in the volume of water absorbed from the descending limb.[73] This rise in descending limb fluid osmolality results from water extraction (60%), and from urea addition (40%).[72,73] The delivery of urea to the end of the thin descending limb averages 550% of the filtered load of urea.[72] Thus, urea is either secreted into the descending limb fluid[74] or there is a major difference between the filtered load of urea in superficial versus juxtamedullary glomeruli. When urea is infused into rats fed a low-protein diet, both water extraction from the descending limb and urinary concentrating ability are significantly increased.[75]

In hamster, ~65% of the osmotically active solute in fluid obtained near the bend of the loop of Henle is due to sodium (plus a univalent anion), while ~20% is due to urea.[70] Since only ~10% of the filtered load of water reaches the bend of the loop of Henle, the high luminal fluid sodium concentration results primarily from water extraction from the descending limb.[70] Both sodium and inulin concentrations increase along the length of the hamster descending limb, showing that water is extracted from the descending limb fluid.[76,77] As in the rat, significant amounts of urea are added to the descending limb fluid.

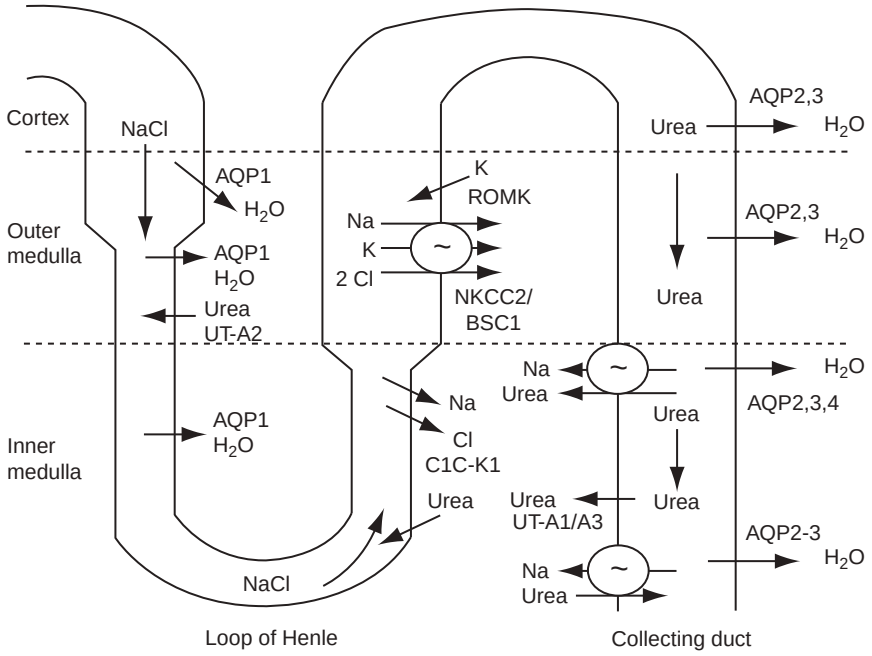

FIGURE 43.6 **Location and identities of the water, urea, and sodium transport proteins involved in the passive mechanism hypothesis for countercurrent multiplication in the inner medulla.**[8,9] The major kidney regions are shown on the left. NaCl is actively absorbed across the thick ascending limb by the apical membrane Na^+-K^+-$2Cl^-$ co-transporter (NKCC2, BSC1), and the basolateral membrane Na^+/K^+-ATPase (not shown). K^+ is recycled through an apical membrane ROMK channel. Water is absorbed across the descending limb by AQP1 water channels in both apical and basolateral plasma membranes. In the presence of vasopressin, water is absorbed across the apical plasma membrane of the collecting duct by AQP2 water channels. Water is absorbed across the basolateral plasma membrane by AQP3 water channels in the cortical and outer medullary collecting duct, and by both AQP3 and AQP4 water channels in the inner medullary collecting duct (IMCD). Urea is concentrated within the collecting duct lumen (by water absorption) until it reaches the terminal IMCD where it is absorbed by the UT-A1 and UT-A3 urea transporters. According to the passive mechanism hypothesis (see text), the fluid which enters the thin ascending limb from the contiguous thin descending limb has a higher NaCl and a lower urea concentration than the inner medullary interstitium, resulting in passive NaCl absorption and dilution of the fluid within the thin ascending limb. Also shown are 2 active urea transport pathways: a Na^+-urea counter-transporter is expressed in the terminal IMCD of normal rats and is upregulated by water diuresis[115]; a Na^+-urea co-transporter is expressed in the initial IMCD of hypercalcemic rats or rats fed a low-protein diet but not from rats fed a normal protein diet[423,118,358] (Abbreviations: AQP: aquaporin; UT: urea transporter).

Psammomys obesus, a desert rodent, feeds on halophilic plants which provide water along with large quantities of NaCl. In these animals, tubular fluid flow rate decreases by 1.7-fold along the descending limb, while osmotic pressure increases four-fold.[37,78] Water removal accounts for 40% of the increase and solute addition accounts for 60% under moderate NaCl-loading conditions.[37] Unlike the rat, NaCl is the principal solute added to descending limb fluid[37]; urea is added but is much less important than in the rat. In *Psammomys* which are producing more highly concentrated urine (although still less concentrated than can be achieved by the intact animal), NaCl addition accounts for nearly 80% of the rise in osmolality.[37]

Thin Ascending Limb

The thin ascending limb (Table 43.3) has an extremely low osmotic water permeability in all species studied,[42,49,79,80] and no aquaporin proteins have been detected (reviewed in [81]). Although the thin ascending limb has a urea permeability that is lower than its NaCl permeability,[57,63,79,82] it is significantly higher than the value that mathematical models indicate is required for the effective operation of the hypothesized passive mechanism (*vide infra*). While this is true in all species, it is especially true in chinchilla.[52,57]

The thin ascending limb has a very low level of Na^+/K^+-ATPase activity[67,68] that would not support a significant rate of active sodium transport.[83] However, some *in vivo* studies have found evidence for active sodium transport in thin ascending limbs.[72,77] The thin ascending limb has a high passive NaCl permeability.[57,63,79,80,82] Chloride transport occurs transcellularly via the ClC-K1 chloride channel, which is present in both the apical and basolateral plasma membranes.[84] Vasopressin increases chloride transport in thin ascending limbs,[85] and water deprivation increases the mRNA abundance of ClC-K1.[86] Transgenic mice lacking the ClC-K1 transporter were found to have greatly

reduced urine concentrating capability, which was attributed to defective chloride transport in the thin ascending limb.[87] Sodium transport is thought to occur paracellularly, since no apical plasma membrane sodium transport pathway has been demonstrated.[88,89]

When rabbit thin ascending limbs are perfused *in vitro* with concentration gradients of NaCl and urea that simulate *in vivo* conditions (NaCl gradient from lumen-to-bath and a urea gradient from bath-to-lumen), they are able to dilute their luminal fluid by purely passive means. Perfusing rabbit thin ascending limbs *in vitro* with solutions whose osmolality is increased from 290 to 600 mOsm/kg H_2O by adding NaCl to the perfusate and urea to the bath (to mimic the higher concentration of NaCl in the tubule lumen and the higher urea concentration in the medullary interstitium) reduces collected fluid osmolality to 70% of perfusate osmolality, suggesting that it may be possible to dilute the luminal fluid within thin ascending limbs without active transport *in vivo*.[80]

Heterogeneity in Thin Limbs of Long Loops

Pannabecker et al.[18] investigated inner medullary functional structure in Munich-Wistar rats by means of computer-assisted three-dimensional reconstructions of cross-sections in which tubules were identified and labeled by direct immunofluorescence of antibodies raised against specific transport proteins. The reconstructions indicate that thin descending limbs of Henle's loops that have bends within the first millimeter below the outer–inner medullary boundary lack the water transporter AQP1. Thin descending limbs of loops that have bends beyond the first millimeter express AQP1 for about the first 40% of their length below the outer–inner medullary boundary, but beyond that point lack AQP1 expression. Expression of ClC-K1 chloride channels begins abruptly with a prebend segment of length ~165 μm, and ClC-K1 expression continues uniformly along the entire length of thin ascending limbs. Co-localization of AQP1 and ClC-K1 was not found in any loop of Henle segment. Preliminary sections show no evidence of expression of the urea transporters UT-A1, UT-A2 or UT-A4 in thin limbs below the first millimeter of the inner medulla.[54] These observations are generally consistent with expression patterns indicated in other immunocytochemical studies in rat.[43,90] However, Mejia and Wade[91] found in Sprague-Dawley rats that ~30% of thin descending limbs that reached deep into the papilla labeled for AQP1 (in Brattleboro rats, ~11%); and Wade et al.[90] found co-labeling of a UT-A urea transport protein and AQP1 in thin descending limbs in the base of the inner medulla of Brattleboro rats (these limbs may correspond to the longer population identified by Pannabecker et al.[18]).

Thick Ascending Limb

Both the medullary and cortical portions of the thick ascending limb (Table 43.3) have osmotic water permeabilities that are essentially zero, and neither subsegment expresses aquaporin proteins (reviewed in [81]). Thus, the primary mechanism for diluting the luminal fluid in thick ascending limbs is net absorption of solute, particularly NaCl. NaCl is actively absorbed by the Na^+-K^+-$2Cl^-$ co-transporter (NKCC2, BSC1) in the apical plasma membrane, and the sodium pump (Na^+/K^+-ATPase) in the basolateral plasma membrane. The thick ascending limb from short looped nephrons can lower the concentration of NaCl in the luminal fluid at loop bend from ~300 to ~117–40 mM at the cortico–medullary border,[92,93] while the cortical thick ascending limb can lower the concentration of NaCl to ~32 mM.[94] However, the medullary portion has the capacity to absorb more NaCl than the cortical portion, as evidenced by the higher Na^+/K^+-ATPase activity in the medullary thick ascending limb.[67,95] The regulation of NaCl absorption in the thick ascending limb is discussed in detail in Chapter 34.

Vasopressin increases NaCl absorption in medullary and cortical thick ascending limbs in mouse.[96,97] This response is consistent with vasopressin's role in urinary concentration, and suggests that vasopressin can increase or maintain concentrating ability by increasing NaCl absorption across thick ascending limbs. However, vasopressin does not increase NaCl absorption in human and canine, and only weakly stimulates absorption in rabbit medullary thick ascending limbs.[96]

Urea permeability in the medullary thick ascending limb is lower than in the cortical thick ascending limb.[98,99] In rat, the transition to a higher urea permeability occurs between the inner and outer stripe portions of the medullary thick ascending limb, while in rabbit it occurs between outer medulla and cortex.[98] Urea permeability in the thick ascending limb could permit dilution of tubular fluid by passive urea absorption or increase urea concentration in the thick ascending limb by secretion.

Cortical Collecting Duct

The cortical collecting duct has an extremely low osmotic water permeability (Table 4) in the absence of vasopressin.[100–102] Vasopressin significantly increases the osmotic water permeability by a factor of 10 to 100 in both rat[101,102] and rabbit.[100] Arachidonic acid metabolites, produced by cytochrome P450, inhibit vasopressin-stimulated osmotic water permeability by a post-cyclic AMP (cAMP) mechanism[103]; the mechanism by which vasopressin increases osmotic water permeability is discussed in detail in Chapter 41 on Water Channels.

The cortical collecting duct has a low urea permeability that is unaffected by vasopressin.[98,104] Thus, vasopressin-induced water absorption will increase the urea concentration within the lumen of the cortical collecting duct, and also the osmolality, provided that there is no significant net absorption of solutes.

The cortical collecting duct is the major site for aldosterone-mediated sodium absorption and potassium secretion.[105] Vasopressin also stimulates sodium absorption in the cortical collecting duct.[106] Sodium is actively absorbed via the epithelial sodium channel (ENaC) in the apical plasma membrane of principal cells,[107] and sodium absorption is responsible for the generation of a lumen-negative voltage.[105] Sodium exits the principal cell via Na^+/K^+-ATPase in the basolateral plasma membrane.[67,95] Chloride is transported by both paracellular and transcellular pathways. Chloride absorption is primarily passive in rabbit, although some evidence for chloride absorption against an electrochemical gradient exists.[108] Active chloride absorption occurs in rat, and is stimulated by vasopressin and inhibited by bradykinin.[109]

Outer Medullary Collecting Duct

Few permeability measurements exist for the rat outer medullary collecting duct (Table 43.4). In rabbit, the outer medullary collecting duct has a low osmotic water permeability which is increased 20- or 30-fold by vasopressin.[99,110] The urea permeability is low in the outer medullary collecting duct in both rat and rabbit.[98,99]

Inner Medullary Collecting Duct

The inner medullary collecting duct (IMCD) was originally divided into three subsegments: $IMCD_1$; $IMCD_2$; and $IMCD_3$.[111] Subsequent studies showed that the inner medullary collecting duct could generally be viewed as consisting of two morphologically and functionally distinct subsegments: the initial IMCD (corresponding to the $IMCD_1$) and the terminal IMCD (corresponding to the $IMCD_2$ and $IMCD_3$).[102,104,112,113] However, some recent studies have found functional differences between the $IMCD_2$ and $IMCD_3$.[114,115] Histologically, the rat initial IMCD (or $IMCD_1$) contains 90% principal cells and 10% intercalated cells[112]; the rat terminal IMCD (or $IMCD_2$ and $IMCD_3$) contains a unique cell type, the IMCD cell.[113] Most of the permeability values available for IMCD subsegments are from the rat (Table 43.5).

In the absence of vasopressin, the initial IMCD has a low osmotic water permeability which is increased 10- to 30-fold by vasopressin.[102,116,117] Urea permeability is low in the initial IMCD, and is unaffected by vasopressin.[102,104,114,116,118] The initial IMCD from normal rats does not show any active urea transport.[115,118,119]

The terminal IMCD has a higher basal (no vasopressin) osmotic water permeability than other portions of the collecting duct.[102,116,117] Vasopressin can rapidly increase osmotic water permeability by a factor of 10.[102,117] The terminal IMCD also has a higher basal urea permeability than other portions of the collecting duct.[102,104,114,116,120] Vasopressin and hypertonicity can each increase urea permeability by a factor of 4–6, and together they can increase urea permeability by a factor of 10.[102,116,119–121] Although early studies suggested a urea reflection coefficient of less than 1, more recent studies which re-measured the urea reflection coefficient and explicitly measured the dissipation of the imposed urea gradient, showed that the urea reflection coefficient equals 1.[50,122] The $IMCD_2$ subsegment from normal rats does not show any active urea transport.[115,118] However, active urea secretion, which is completely dependent upon luminal sodium, is present in the $IMCD_3$ from normal rats, suggesting that sodium absorption may be coupled to urea secretion.[115]

Sodium and chloride permeabilities are low in the terminal IMCD.[116,123,124] Micropuncture studies indicate substantial rates of NaCl absorption from the IMCD, but perfused tubule studies have been unable to detect it.[124–126]

Papillary Surface Epithelium

Only a few permeability coefficients have been measured across the papillary surface epithelium, and these have been measured only in rabbit (Table 43.5). The urea and osmotic water permeabilities are low and unaffected by vasopressin.[104,127] The basal chloride permeability is higher than that of the terminal IMCD, and is inhibited by vasopressin.[127] The apical membrane of the papillary surface epithelial cell, which faces the urinary space, expresses a $Na^+–K^+–Cl^-$ co-transporter that is stimulated by vasopressin and inhibited by bumetanide.[15] The basolateral membrane contains a potassium conductive pathway in rat and rabbit.[128,129]

GENERAL FEATURES OF URINARY CONCENTRATION AND DILUTION

Countercurrent Multiplication Hypothesis

Since the late 1950s, the countercurrent multiplication hypothesis has been the generally accepted explanation for the generation of the osmolality gradient along the cortico–medulary axis in both the outer and inner medullas.[130] This hypothesis holds that, at each

level of the medulla, a small osmolality difference between tubular fluid flows in ascending and descending limbs is multiplied by the countercurrent flow configuration to establish a large axial osmolality difference. The principle of countercurrent multiplication is illustrated in Figure 43.7. The loop shown in the figure panels may be identified with a short loop of Henle: the left channel is analogous to the descending limb, whereas the right channel is analogous to the thick ascending limb. The channels are separated by a water-impermeable barrier. Vertical arrows indicate flow down the left channel and flow up the right channel. Left-directed horizontal arrows indicate active transport of solute from the right channel to the left channel. The numbers within channels indicate local fluid osmolality. Successive panels represent the time course of the multiplication process.

Panel (a) of Figure 43.7 illustrates a loop with isosmolar fluid throughout. In panel (b), an active transport mechanism has pumped enough solute to establish a 20 mOsm/kg H_2O osmolality difference between the ascending and descending flows at each level. This small difference, transverse to the flow, is called the "single effect." Panel (c) illustrates the osmolality values after the fluid has advected (or carried) the solute half-way down the left channel and half-way up the right channel. In panel (d), the active transport mechanism has re-established a 20 mOsm/kg H_2O osmolality difference, and the luminal fluid near the bend of the loop has attained a higher osmolality than in panel (a). By successive iterations of this process, a progressively higher osmolality is attained at the loop bend, and a large osmolality difference is generated along the flow direction. This is illustrated in panel (e), where the osmolality at the loop bend is nearly 300 mOsm/kg H_2O above the osmolality of the fluid entering the loop. Thus, the "single effect" of a 20 mOsm/kg H_2O difference has been multiplied axially down the length of the loop by the process of countercurrent multiplication.

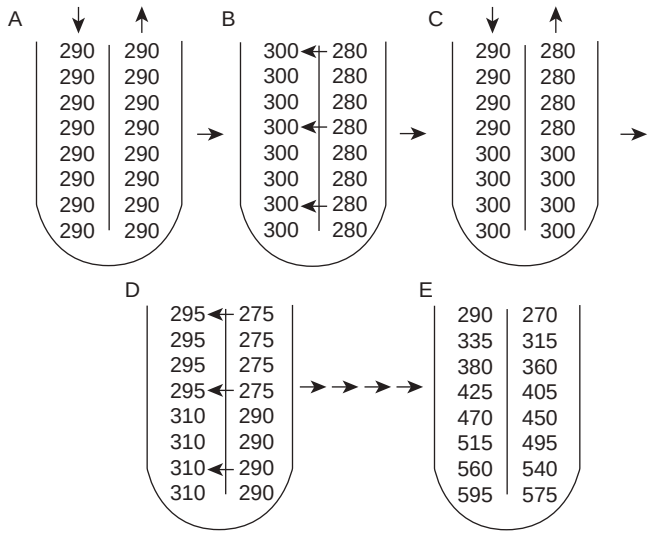

FIGURE 43.7 **Countercurrent multiplication of a single effect.** Panel (a): Process begins with isosmolar fluid throughout both channels. Panel (b): Active solute transport establishes a 20 mOsm/kg H_2O transverse gradient (single effect) across the boundary separating the channels. Panel (c): Fluid flows half-way down the descending limb and up the ascending limb. Panel (d): Active transport reestablishes a 20 mOsm/kg H_2O transverse gradient. Note that the luminal fluid near the bend of the loop achieves a higher osmolality than loop-bend fluid in panel (b). Panel (e): As the processes in (c) and (d) are repeated, the bend of the loop achieves a progressively higher osmolality so that the final axial osmotic gradient far exceeds the transverse 20 mOsm/kg H_2O gradient generated at any level.

In the outer medulla, countercurrent multiplication is believed to occur in the short loops of Henle by a process that is similar to that shown in Figure 43.7. The tubular fluid of the proximal tubule that enters the outer medulla is isotonic to plasma (about 290 mOsm/kg H_2O). That fluid is concentrated, as it passes through the pars recta and the thin desending limb, by osmotically driven water absorption; the absorption is driven by vigorous active transport of NaCl from the thick ascending limbs. At the bend of the loop of Henle, the tubular fluid osmolality attains an osmolality about twice that of blood plasma. Because the thick ascending limbs are nearly impermeable to water, its tubular fluid is diluted by NaCl absorption as it flows toward the cortex, so that the fluid emerging from this segment is hypoosmotic to blood plasma.

Countercurrent multiplication in the outer medulla, however, differs in important ways from the process illustrated in Figure 43.7. In some of the most completely studied mammals, the descending and ascending limbs do not abut one another[131]; therefore, solute is not directly transported from ascending limbs to descending limbs. Rather, NaCl is pumped from thick ascending limbs to the interstitium, raising the osmolality of the interstitial fluid and the blood flowing through the vasa recta and capillaries. The increased interstitial osmolality withdraws water from thin descending limbs, and some NaCl may diffuse into thin descending limbs, thus raising the osmolality of descending limb fluid. The NaCl absorbed from ascending limbs and the water absorbed from descending limbs is carried to the cortex by the vasa recta, which, somewhat like the loops of Henle, are arranged in a countercurrent configuration. Thus, a large axial osmolality difference, from the cortico–medullary boundary to the boundary of the inner and outer medulla, is established in the loops of Henle, the vasculature, and the interstitium.

In addition, Figure 43.7 does not represent the flow in the collecting ducts. Some of the water and solute in thick ascending limb tubular fluid delivered to the

cortex re-enters the outer medulla in the collecting ducts, and in the presence of vasopressin, sufficient water is absorbed from the collecting ducts, as a consequence of the hyperosmotic medullary interstitium, to bring collecting duct flow to near osmotic equilibrium with the surrounding interstitium. Thus, a large axial osmolality difference, similar to that in the thin descending limb, is established in collecting duct fluid.

Finally, the discrete, sequential process represented in Figure 43.7 does not arise under normal physiological conditions. Rather, the axial osmolality difference, or gradient, is sustained in near steady-state, much as indicated in panel (e), with a bend osmolality that is limited primarily by the rate of active transport, the diffusive back-leak of NaCl into the thick ascending limb, the length of the loop, the rate of water absorption from collecting duct flow, and the dissipative effects of the vasculature.

In recent years, some reasons have emerged for skepticism of the countercurrent multiplication hypothesis as the explanation for the axial osmolality gradient in the outer medulla. Several laboratories have reported evidence for the absence of AQP1 in significant portions of the terminal thin desending limbs of short loops of Henle.[43,90,132] Moreover, two modeling studies[55,133] have suggested that the osmotic load that is put on the concentrating mechanism in the outer medulla may be increased by water-permeable descending limbs, relative to water-impermeable limbs, and thus may reduce or eliminate the hypothesized concentration advantage of water absorption from descending limbs of short loops.

The axial osmolality gradient in the inner medulla has also been generally believed to be generated by the countercurrent multiplication of a small transverse osmolality difference, presumably between thin ascending and thin descending limbs. However, evidence for significant active transport from thin ascending limbs is lacking, and experiments indicate that the thin ascending limbs are highly permeable to both NaCl and urea. Thus, the inner medullary single effect must arise from a mechanism different from that found in the outer medulla. The roles of the vasculature and collecting duct are considered below; a more detailed treatment of countercurrent multiplication, and in particular, the concentrating mechanism of the inner medulla, is given in a subsequent section (*vide infra*).

Countercurrent Exchange

The descending and ascending vasa recta are arranged in a counter-flow configuration connected by a capillary plexus. Vasa recta are freely permeable to water, sodium, and urea, and achieve osmotic equilibration through a combination of water absorption and solute secretion.[134] Descending vasa recta gain solute and lose water, while ascending vasa recta lose solute and gain water. The exchange of solute and water between the descending and ascending vasa recta and the surrounding interstitium is called "countercurrent exchange."

Efficient countercurrent exchange is essential for producing concentrated urine, because hypotonic fluid carried into the medulla and hypertonic fluid carried away from the medulla both tend to dissipate the cortico−medullary gradient of countercurrent multiplication. Thus, to minimize wasted work, fluid flowing through the vasa recta must achieve near osmotic equilibrium with the surrounding interstitium at each medullary level, and fluid entering the cortex from the ascending vasa recta must have an osmolality close to that of blood plasma. Conditions which decrease medullary blood flow, such as volume depletion, improve the efficiency of countercurrent exchange and urine concentrating ability by allowing more time for blood in the ascending vasa recta to lose solute and achieve osmotic equilibration.[134] Conversely, conditions which increase medullary blood flow, such as osmotic diuresis, impair the efficiency of countercurrent exchange and decrease urine concentrating ability.[134] For a detailed treatment of countercurrent exchange, see Chapter 24.

Role of the Collecting Duct

The collecting duct, under the control of vasopressin and other factors, is the nephron segment responsible for final control of water excretion. Whereas the osmolality gradient along the cortico−medullary axis, in both the outer and inner medulla, presumably arises from mechanisms that principally involve participation of the loops of Henle, and countercurrent exchange in the vasa recta minimizes the dissipative effect of vascular flow, the excretion of water requires another structural component, the collecting duct system, which starts in the cortex and ends at the papillary tip. In the absence of vasopressin, the cortical, outer medullary, and initial inner medullary portions of the collecting duct are nearly water-impermeable. (The terminal IMCD has a moderate water-permeability even in the absence of vasopressin (*vide supra*).) Since the fluid that leaves the thick ascending limb and enters the cortical collecting duct is dilute relative to plasma, excretion of dilute urine only requires that not much water be absorbed nor much solute be secreted along the collecting duct.

In the presence of vasopressin, the entire collecting duct becomes highly water-permeable. This process

takes place in the following way. Plasma osmolality increases when a person or an animal becomes water depleted. Osmoreceptors in the hypothalamus, which can sense an increase of only 2 mOsm/kg H_2O, stimulate vasopressin secretion from the posterior pituitary. Vasopressin binds to V_2-receptors in the basolateral plasma membrane of principal and IMCD cells in the collecting duct, stimulates adenylyl cyclase to produce cAMP, activates protein kinase A (PKA), phosphorylates aquaporin-2 (AQP2) at serines 256, 261, 264, and 269, inserts AQP2 water channels into the apical plasma membrane, and increases water absorption across the collecting duct ([135–138] and reviewed in [81]). This regulated trafficking of AQP2 between subapical vesicles and the apical plasma membrane is the major mechanism for acute regulation of water absorption by vasopressin (reviewed in [81]). Wade and colleagues originally proposed the "membrane shuttle hypothesis," which proposes that water channels are stored in vesicles and inserted exocytically into the apical plasma membrane in response to vasopressin.[139] Since the cloning of AQP2, the shuttle hypothesis has been proven experimentally in rat inner medulla (reviewed in [81]). Subsequent studies have elucidated several signal transduction pathways that are involved in regulating AQP2 trafficking (insertion and retrieval of AQP2), the role of vesicle targeting proteins (SNAP/SNARE system), and the cytoskeleton (reviewed in [81]); these processes are discussed in more detail in Chapter 41.

Vasopressin-induced water permeability allows water to be absorbed across the collecting ducts at a sufficiently high rate for collecting duct tubular fluid to attain near osmotic equilibration with the hyperosmotic medullary interstitium; the absorbed water is returned to the systemic circulation via the ascending vasa recta. The majority of water is absorbed from collecting ducts in the cortex and outer medulla. Although the inner medulla has a higher osmolality than the outer medulla, its role in absorbing water from the collecting duct is important only when maximal water conservation is required. More water is actually absorbed across the IMCD during diuresis than antidiuresis, owing to the large transepithelial osmolality difference.[140]

URINE CONCENTRATING MECHANISM: HISTORY AND THEORY

Overview

The conceptual history of the urine concentrating mechanism may be divided into three periods. The first period, extending from 1942 through 1971, was inaugurated by the publication of a study by Kuhn and Ryffel,[141] who proposed that concentrated urine is produced by the countercurrent multiplication of a "single effect," and who constructed a working apparatus that exemplified the principles of countercurrent multiplication. During this first period, the theory of the countercurrent multiplication hypothesis was developed further, and experimental evidence accumulated that supported the hypothesis as the explanation for the concentrating mechanism of the outer medulla. In particular, active transport of NaCl from thick ascending limbs was identified as the source of the outer medullary single effect.[94,142]

The second period of conceptual history, extending from 1972 through 1992, was inaugurated by the simultaneous publication, by Kokko and Rector and by Stephenson, of papers proposing that a "passive mechanism" provides the single effect for countercurrent multiplication in the inner medulla.[8,9] According to the passive mechanism hypothesis, a net solute efflux from thin ascending limbs results from favorable transepithelial NaCl and urea gradients; these gradients arise from the separation of NaCl and urea, which is largely driven by the outer medullary concentrating mechanism. Although initially much experimental evidence appeared to support the passive mechanism, findings from many subsequent studies are difficult to reconcile with this hypothesis.[22,143,144] Moreover, mathematical models incorporating measured transepithelial permeabilities failed to predict a significant inner medullary concentrating effect.[52,145,146] The discrepancy between the consistently negative results from mathematical modeling studies and the very effective inner medullary concentrating effect has persisted through more than three decades. The discrepancy has helped to stimulate research on the transport properties of the renal tubules of the inner medulla and the formulation of several highly sophisticated mathematical models (notably,[147]), but no model study has resolved the discrepancy to the general satisfaction of experimentalists and modelers.

In the early 1990s, new hypotheses for the inner medullary concentrating mechanism began to receive serious consideration, and a third period of conceptual thought may be considered to have begun in 1993: in that year, Knepper and colleagues proposed a key role for the peristalsis of the papilla,[143,148] and in 1994 Jen and Stephenson[149] examined the principle of "externally driven" countercurrent multiplication, arising, e.g., by the net production of osmotically active particles in the interstitium. At about the same time, perfused tubule studies in chinchilla, which can produce very highly concentrated urine, provided evidence that the passive mechanism, as originally proposed, cannot explain the inner medullary concentrating mechanism.[57] Recent studies have sought

to further develop hypotheses involving peristalsis,[150] the potential generation of osmotically active particles, especially lactate,[151,152] and the role of complex inner medullary anatomy and detailed transporter localization.[21,54,153] In 2004, evidence suggesting an absence of significant urea transport proteins in loops of Henle reaching deep into the medulla led to a reconsideration of hypotheses related to the passive mechanism.[54]

Countercurrent Multiplication Hypothesis

In 1942, Kuhn and Ryffel proposed that urine is concentrated by means of multiplication (or augmentation) of a single effect ("Vervielfältigung des Einzeleffektes").[141] More precisely, they suggested that a small osmotic pressure difference between flows in parallel renal tubules (the single effect) was multiplied by means of the countercurrent principle ("Gegenstromprinzip"), resulting in a large increase in osmotic pressure along the cortico−medullary axis (*vide supra*: Figure 43.7 and accompanying discussion). Kuhn and Ryffel, however, made no specific conjectures regarding which tubules or what transport properties were involved. To test their hypothesis, Kuhn and Ryffel constructed an apparatus that, by embodying the countercurrent principle and by employing phenol and sucrose solutions separated by selectively permeable membranes, was able to increase the concentration of the sucrose solution by a factor of 3.5. This apparatus suggested that three fundamental components are needed for a physiologically plausible mechanism for generating concentrated urine: (1) countercurrent flow; (2) a source of energy to sustain a single effect (in this case, potential energy in the form of the differing solutions); and (3) specific membrane permeability characteristics.

In a 1951 study, Hargitay and Kuhn[154] proposed the basic framework for the modern conception of the urine concentrating mechanism. They hypothesized that the loop of Henle is a biological realization of a hairpin counterflow system, that the loops of Henle would generate a cortico−medullary osmolality gradient, and that final urine concentration would be achieved by the osmotic withdrawal of water from collecting ducts. Their study, which included both a working apparatus and a mathematical model, confirmed that countercurrent multiplication could generate a significant axial concentration gradient. However, their apparatus relied on the transport of water across the separating membrane, and they employed a mechanical pressure as a driving force to sustain the single effect. The pressure required for a significant axial gradient (estimated at 550 mmHg) was judged by the authors to far exceed a pressure likely to be found *in vivo* (~120 mmHg). They proposed, as an alternative, a single effect arising from water transport driven by a process of electro-osmosis ("Electroosmose"), which was hypothesized to arise from metabolic processes in epithelial cells. In 1959, a mathematical analysis by Kuhn and Ramel showed that active NaCl transport from ascending limbs could serve to provide the required single effect.[155]

The countercurrent multiplier hypothesis was bolstered by a 1951 study in which Wirz, Hargitay, and Kuhn used slices of renal tissue from hydropenic rats to demonstrate an osmotic pressure gradient, starting at approximately the cortico−medullary boundary, and increasing along the cortico−medullary axis to the papillary tip. In subsequent experimental studies, active transport of NaCl from thick ascending limbs was established as the driving force required to sustain the transepithelial osmolality difference needed for countercurrent multiplication in the outer medulla,[94,142] and the osmotic absorption of water from collecting ducts into the hypertonic interstitium was established as the ultimate process by which collecting duct fluid is concentrated in antidiuresis.[156] However, investigation of the inner medullary renal tubules revealed no active transport process that could generate a significant transepithelial osmolality difference.[63,130]

Concentrating Mechanism of the Outer Medulla

In the presence of vasopressin, the outer medullary concentrating mechanism is believed to operate as follows. Transepithelial active transport of NaCl, from the tubular fluid of thick ascending limbs and into the surrounding interstitium, raises the osmolality of interstitial fluid and promotes the osmotic absorption of water from the tubular fluid of nearby descending limbs and collecting ducts. Because of the absorption of fluid from descending limbs, the fluid delivered to the ascending limbs has a high NaCl concentration that favors the transepithelial transport of NaCl from ascending limb fluid. (There may also be some diffusion of NaCl into descending limb fluid.) NaCl transport dilutes the tubular fluid of thick ascending limbs, so that at each medullary level the fluid osmolality is less than that in the other tubules and in the vessels, and so that the fluid delivered to the cortex is dilute relative to blood plasma. The ascending limb fluid that enters the cortex is further diluted by active NaCl transport from cortical thick ascending limbs, so that its osmolality is less than the osmolality of blood plasma. In cortical collecting ducts, which are water-permeable in the presence of vasopressin, sufficient water is absorbed to return the collecting duct tubular fluid to isotonicity with blood plasma. This water absorption greatly reduces the load that is placed on

the concentrating mechanism by the fluid that re-enters the medulla. In the absence of vasopressin, the collecting duct system, both in the cortex and outer medulla, is much less water-permeable, and even though some water is absorbed due to the very large osmotic pressure gradient, fluid that is dilute relative to plasma is delivered by the collecting ducts to the border of the outer and inner medulla.

This modern conceptual formulation of the outer medullary concentrating mechanism (which is very similar to the proposal of Hargitay and Kuhn as modified by Kuhn and Ramel[154,155]) is supported by recent mathematical modeling studies using parameters compatible with micropuncture and perfused tubule experiments.[52,133,157–160] In particular, the osmotic gradients in the outer medulla predicted by simulations are consistent with the gradients reported in tissue slice experiments, where osmolality is increased by a factor of 2–3.[37,161]

Mass Balance in the Renal Medulla

For the outer medullary gradient to be sustained in a steady-state, the water and solute flows in the tubules and vessels of the outer medulla and, therefore, the spatial distribution of water and solute, must remain nearly fixed (provided there are no significant metabolic solute sources or sinks). Thus, for any transverse slice of the medulla, say of a thickness extending from location X_1 to X_2, the directed sum of water flow rates in all tubules and vessels at X_1 must equal that at level X_2, and the directed sum of solute flow rates in all tubules and vessels at level X_1 must equal that at level X_2. This is the principle of steady-state mass balance (for an explicit mathematical formulation see reference [7]).

Global mass balance for the outer medulla is thought to be preserved as follows (the relatively small effects of long looped nephrons, of vasa recta reaching into the inner medulla, and of solutes other than NaCl are ignored here for simplicity). At the cortico–medullary boundary, the water flowing in ascending vasa recta exceeds that flowing in descending vasa recta, owing to water absorption from thin descending limbs and collecting ducts. In contrast, the water flow emerging from thick ascending limbs is significantly reduced relative to the flow entering descending limbs at the cortico–medullary boundary. The directed sum of these flows, plus flow entering collecting ducts at the cortico–medullary boundary results in a small net flow from the cortex into the outer medulla that nearly equals net water flow at the outer–inner medullary boundary.

Similarly, solute flows must be balanced. At the cortico–medullary boundary, the solute emerging from ascending vasa recta exceeds that flowing in descending vasa recta, owing to NaCl absorption from thick ascending limbs. In contrast, the solute flow emerging from thick ascending limbs is reduced (relative to flow entering descending limbs) by a larger fraction than the thick ascending limb fluid flow. The directed sum of these solute flows at the cortico–medullary boundary, plus solute flow entering collecting ducts at that boundary, results in a small net solute flow nearly equal to net solute flow at the inner–outer medullary boundary.

The ratio of NaCl to water in net flow across the cortico–medullary boundary, and the ratio of NaCl to water in collecting duct flow at the inner–outer medullary boundary, both depend on whether the animal is in a diuretic or antidiuretic state. In either case, a greater fraction of loop of Henle solute flow is absorbed, relative to water flow, in the outer medulla and, consequently, a greater fraction of water is delivered to the cortex, relative to solute. Consequently, dilute fluid is delivered by the thick ascending limbs to the cortex, and this fluid is further diluted by NaCl transport from the cortical thick ascending limb.

In diuresis, little water is absorbed from the cortical collecting ducts. Consequently, the net fluid absorbed into the cortical circulation (taking into account NaCl absorption from cortical thick ascending limbs) is concentrated relative to blood plasma, and the fluid re-entering the outer medulla in collecting ducts remains dilute relative to blood plasma. The low water permeability of the outer medullary collecting duct in diuresis will prevent any significant dilution of vasa recta flow, and thus prevent any significant reduction in the concentrating capacity of the countercurrent mechanism. Thus, combined with slightly concentrated flow from ascending vasa recta, the ultimate effect of fluid absorbed in the cortex will be to raise the osmolality of the systemic circulation. Moreover, owing to the dominating effect of hypotonic fluid flowing from the cortical collecting ducts into the outer medullary collecting ducts, the net fluid flow from the cortex to the outer medulla will be dilute relative to systemic plasma, and as a consequence of mass balance, the net fluid flow across the inner–outer medullary boundary will be dilute relative to blood plasma.

In antidiuresis, much water is absorbed from the water-permeable cortical collecting ducts. Consequently, the net fluid absorbed in the cortex, from fluid entering the cortex via the thick ascending limbs, is dilute relative to plasma, and its diluting effect on the cortex outweighs the concentrating effect of slightly hypertonic ascending vasa recta flow. Collecting duct fluid entering the outer medulla is isotonic to blood plasma, and relative to the case of diuresis, reduced in flow rate, so that the fluid absorbed from the now-permeable outer medullary collecting duct

does not significantly reduce the concentrating capacity of the countercurrent mechanism. Thus, the ultimate effect of dilute fluid absorbed from the cortical collecting duct is to lower the osmolality of the systemic circulation. Moreover, owing to the dominating effect of dilute fluid emerging from the outer medullary thick ascending limbs into the cortex, the net flow from the cortex to the outer medulla will be concentrated relative to systemic blood plasma, and as a consequence of mass balance, the net flow of collecting duct fluid across the inner–outer medullary boundary will be concentrated relative to blood plasma.

Because the inner medullary concentrating effect remains elusive, and because the net generation of osmotically active molecules has been suggested as a possible source of the single effect for the inner medulla,[149,151,162] the role of the inner medullary concentrating mechanism has been ignored in our description of mass balance. However, a mass balance analysis similar to that given above for the outer medulla would apply to the inner medulla separately, and thus also to the whole medulla, according to most hypotheses for the inner medullary concentrating mechanism. (In the presence of oscillations in tubular flow mediated by the tubuloglomerular feedback mechanism[163] or in the presence of peristalsis of the papilla,[164] mass balance would have to be reformulated for time-averaged flows.) In any case, the overall effect of mass balance in the renal medulla, in diuresis, is that systemic blood plasma is concentrated by the production of urine that is dilute relative to plasma; in antidiuresis, blood plasma is diluted by the production of urine that is concentrated relative to plasma.

The Passive Mechanism Hypothesis for the Inner Medulla

Although active NaCl transport from thick ascending limbs was identified as the fundamental source of the outer medullary concentrating mechanism, isolated perfused tubule experiments in rabbits demonstrated that the thin ascending limb had no significant active NaCl transport,[63,94] but instead had relatively high permeabilities to sodium and urea, while being impermeable to water.[80] The inner medullary thin descending limb in rabbit, in contrast, was found to be highly water-permeable, but to have low sodium and urea permeabilities.[60,64] Moreover, evidence from some species showed that urea tended to accumulate in the inner medulla, with concentrations similar to those of NaCl,[6] and it had long been known that urea administration enhances maximum urine concentration in protein-deprived rats and humans.[165,166] Several models were published that sought to explain the inner medullary concentrating mechanism,[167–171] but they failed to gain general acceptance.

In 1972, independent papers by Kokko and Rector and by Stephenson (appearing in the same volume of *Kidney International*) proposed that the concentrating effect in the inner medulla arises from a "passive mechanism".[8,9] The key components of the passive mechanism are represented in Figure 43.6. Active absorption of NaCl from the thick ascending limb, and the subsequent absorption of water from the cortical and outer medullary collecting ducts work together to increase the urea concentration of collecting duct fluid. Urea diffuses down its transepithelial concentration gradient from the highly urea-permeable terminal IMCD into the inner medullary interstitium; urea is trapped in the inner medulla by countercurrent exchange in the vasa recta (*vide supra*). The fluid entering the thin ascending limb has a high NaCl concentration relative to urea, and the thin ascending limb is hypothesized to have a high NaCl permeability relative to urea. In addition, due to accumulation of urea in the interstitium, the NaCl concentration in the thin ascending limb exceeds the NaCl concentration in the interstitium, and consequently NaCl diffuses down its concentration gradient into the interstitium. If the thin ascending limb has sufficiently low urea permeability, the rate of NaCl efflux from the ascending limb will exceed the rate of urea influx, resulting in the dilution of thin ascending limb fluid, and the flow of relatively dilute fluid up the thin ascending limb at each medullary level and into the thick ascending limb. Thus, dilute fluid is removed from the inner medulla, and mass balance requires that the osmolality of the inner medulla be progressively elevated along the tubules of the inner medulla. The elevated osmolality will draw water from the thin descending limbs, thus raising the NaCl concentration of the descending limb flow that enters thin ascending limbs. In addition, the elevated osmolality of the inner medulla will draw water from the water-permeable IMCD, raising the concentration of urea in collecting duct flow; accumulation of NaCl in the interstitium will tend to sustain a transepithelial urea concentration gradient favorable to urea absorption from the terminal IMCD.

Several matters are worthy of note. First, this process, described above in step-wise fashion, should be thought of as a continuous, steady-state process. Second, although the mechanism is characterized as "passive," it depends on the separation of NaCl and urea that is sustained by the active absorption of NaCl by thick ascending limbs. The separated high concentration flows of NaCl (in the loop of Henle) and of urea (in the collecting duct) constitute a source of potential energy that is used to effect a net transport of solute from the thin ascending limb. Thus, the laws of

thermodynamics are not violated. Third, the description above speaks rather loosely of NaCl and urea as solutes having equal standing, but the atoms of NaCl are nearly completely dissociated, so that each NaCl molecule has nearly twice the osmotic effect of each urea molecule. This distinction must be represented in formal mathematical descriptions. Fourth, the passive mechanism hypothesis is very similar to the concentrating mechanism of the outer medulla, inasmuch as it depends on net solute absorption from the thin ascending limb to dilute thin ascending limb fluid and raise the osmolality of adjacent flows and structures. Finally, the concentrating effect is balanced, as in the outer medulla, by the dissipative effects of vascular flows, and by the production of a small amount of highly concentrated urine. These dissipative effects limit the achievable urine osmolality.

The passive mechanism hypothesis, as described above, closely follows the Kokko and Rector formulation,[8] which made use of key ideas set forth by Kokko in a largely experimental study.[60] Kokko and Rector acknowledged Niesel and Rosenbleck[169] for the proposal that urea absorbed from the IMCD contributes to the inner medullary osmolality gradient. Kokko and Rector presented the passive mechanism hypothesis conceptually, and although it was accompanied by a plausible set of solute fluxes, concentrations, and fluid flow rates that are consistent with the requirements of mass balance, their presentation did not include a mathematical treatment, and it did not demonstrate that measured loop of Henle permeabilities were consistent with the hypothesis. Stephenson's presentation of the passive hypothesis[9] included a more mathematical treatment, and it introduced the highly influential central core assumption (*vide infra*), but it also did not contain a mathematical reconciliation of tubular transport properties with the hypothesis.

The crucial test needed to confirm the passive mechanism hypothesis was an adequate mathematical representation of all the major components of the hypothesized mechanism, including tubular and vascular flows, transepithelial transport, tubular and vascular interactions, and medullary anatomy. The mathematical representation was needed to show that the magnitudes and distributions of the flow rates, transport rates, interactions, and structures, could produce a medullary gradient consistent with tissue slice experiments and measured urine osmolalities.

The Central Core Assumption

In the same paper that set forth the passive mechanism hypothesis,[9] Stephenson introduced the central core assumption, in which the interstitium and the vasculature are merged into a single compartment through which the renal tubules interact. Stephenson argued that if the vasa recta were sufficiently permeable to solutes and water, the vasa recta would serve as a nearly perfect countercurrent exchanger, in nearly complete osmotic equilibrium with each other, and with the interstitium, at each medullary level. In such a case, a very substantial simplification in conceptual and mathematical analysis could be obtained: the central core could be treated very much as an additional species of tubule, but serving a special role as the medium through which other tubules interact. Using the central core assumption, Stephenson was able to derive simplified mathematical expressions that not only aided the model analysis of the passive mechanism, but which were also general enough to permit extensive analysis in terms of fundamental quantities.[9,172–175]

The central core assumption, as illustrated by Stephenson, is represented in Figure 43.8. The upper panel depicts the interaction of the renal tubules with the central core. The lower panels show that the central core may be conceptualized as a single tubule through which the other tubules interact. The central core may be considered to carry, from the medulla to the cortex, the net water and solutes absorbed from the tubules.

The central core assumption has been examined in several theoretical studies,[176–178] all of which concluded that the assumption is a good approximation provided that vasa recta permeabilities are sufficiently high; experiments on vasa recta have tended to confirm the high permeabilities that are required for nearly ideal countercurrent exchange (see Chapter 24). The central core assumption has been used in a number of mathematical models and computer simulations.[10–12,17,23,52,54,55,159,178–181] However, models based on the central core assumption cannot incorporate the effects of the radial organization of medullary structures with respect to the vascular bundles in the outer medulla or with respect to the collecting duct clusters in the inner medulla, because that organization is likely to result in differing solute concentrations in the various interstitial spaces, tubules, and vessels as a function of their positions.[12,147]

Computer Simulations

Computer simulations of the urine concentrating mechanism are based on detailed mathematical models; the models consist of differential equations and algebraic relations that embody transepithelial transport processes and the requirements of water and solute mass balance. The degree of sophistication of these models has varied substantially in the number of molecular species represented, the degree of detail in

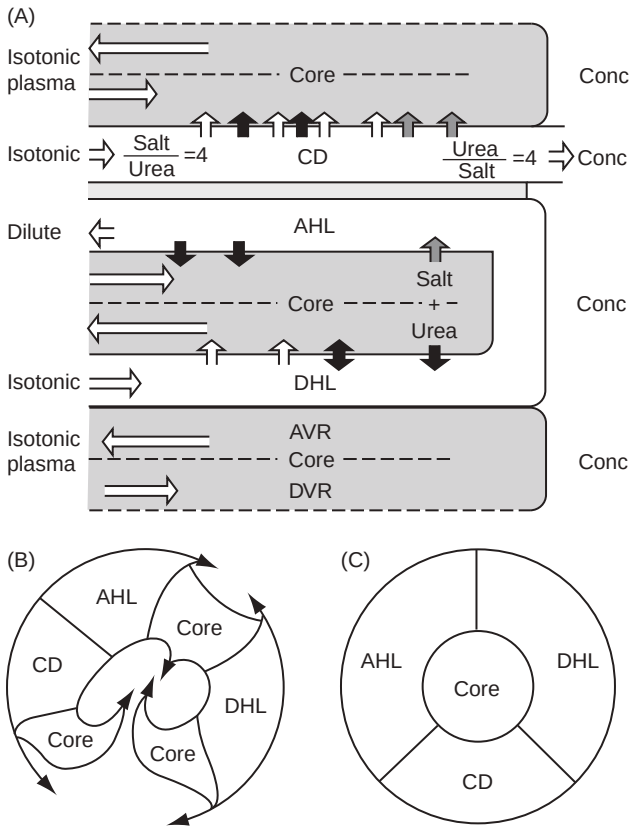

FIGURE 43.8 **Schematic representation of central core assumption, in which the interstitium and vasa recta (AVR, DVR) are merged into a single compartment (Core).** Upper panel (a) shows interaction of tubules with Core. Vertical arrows indicate transepithelial fluxes of NaCl (black), urea (hatched), and water (white); horizontal arrows indicate relative fluid flow. Water is absorbed from descending limb (DHL) into Core, urea enters DHL from Core, and NaCl may move in either direction. NaCl is absorbed from ascending limb (AHL) into Core, while urea enters AHL. Water, NaCl, and urea are absorbed from collecting duct (CD) into Core; as a result of differential absorption, salt/urea concentration reverses. Panel (b) shows Core from (a) being consolidated into a final cross-section (c), in which a single Core compartment interacts with AHL, DHL, and CD. *(Reproduced with permission, from reference [9].)*

the formulation of epithelial transport, the numbers of loops of Henle and collecting ducts, the representation of the vasculature, and the representation of three-dimensional connectivity. Because the mathematical models involve a large number of nonlinear equations, explicit solutions in terms of elementary functions cannot be obtained, and approximate solutions must be found by the methods of numerical analysis. Owing to the very large permeabilities measured in some renal tubules, and to orders-of-magnitude changes in the water and solute flow rates along the nephron, model solutions are difficult to approximate, and consequently a large amount of effort has been expended in the development of suitable numerical methods (see, e.g.,[20,133,153,157,182–186]). For comprehensive reviews of models and simulations of the concentrating mechanism, including substantial mathematical detail, see[187,188].

The passive mechanism hypothesis was developed at about the same time that it was becoming practical for large-scale simulations to be conducted on digital computers. Indeed, a computer simulation by Stewart and collaborators[189,190] appeared in the same issue of *Kidney International* that contained the papers that set forth the passive mechanism hypothesis.[8,9] In the absence of active NaCl transport from thin ascending limbs, a significant inner medullary osmolality gradient was generated when loop urea permeabilities were set to 0.1×10^{-5} cm/s. But the gradient was greatly diminished when thin descending limb urea permeability was increased to 0.3×10^{-5} cm/s, a small value compared to measurements in all species examined (see Table 43.2). Thus, the addition of a small amount of urea to thin descending limb fluid resulted in a marked decrease in the inner medullary gradient. Moreover, the authors reported that: "Computer simulation confirmed that low sodium or high urea permeability in ascending limb or high sodium or urea permeability in descending limb, singly or in combination, virtually abolished the osmotic gradient in the inner medulla." These results were difficult to reconcile with experiments that had shown significant net urea addition to both thin descending and ascending limbs in the hamster.[76]

This early simulation immediately cast doubt on the passive mechanism hypothesis, and it reported a result that was confirmed in many subsequent simulations: the addition of urea to the loops of Henle reaching into the inner medulla tends to dissipate the transepithelial NaCl and urea gradients that are required for the successful operation of the passive mechanism (see, e.g.,[145,146,179,180,191,192]). Thus, for example, if the thin ascending limb is significantly urea-permeable, diffusion of urea from the interstitium into thin ascending limb fluid counterbalances the diluting effect of the diffusion of NaCl from ascending limb fluid into the interstitium. Consequently, fluid in the ascending limb tends to osmotic equilibrium with respect to surrounding interstitial fluid. Because thin ascending limb fluid is not dilute relative to fluid in tubules and vessels at the same level, there is no inner medullary single effect to be multiplied by means of the countercurrent flow configuration.

Figure 43.9, based on data from a simulation published in 1996,[52] shows results that are representative of most simulation studies. Medullary osmolality and concentrations of electrolytes and urea are given as flow-weighted averages, taken across all tubules at each medullary level. Figure 43.9 has been drawn so that it may be easily compared with Figure 43.5.

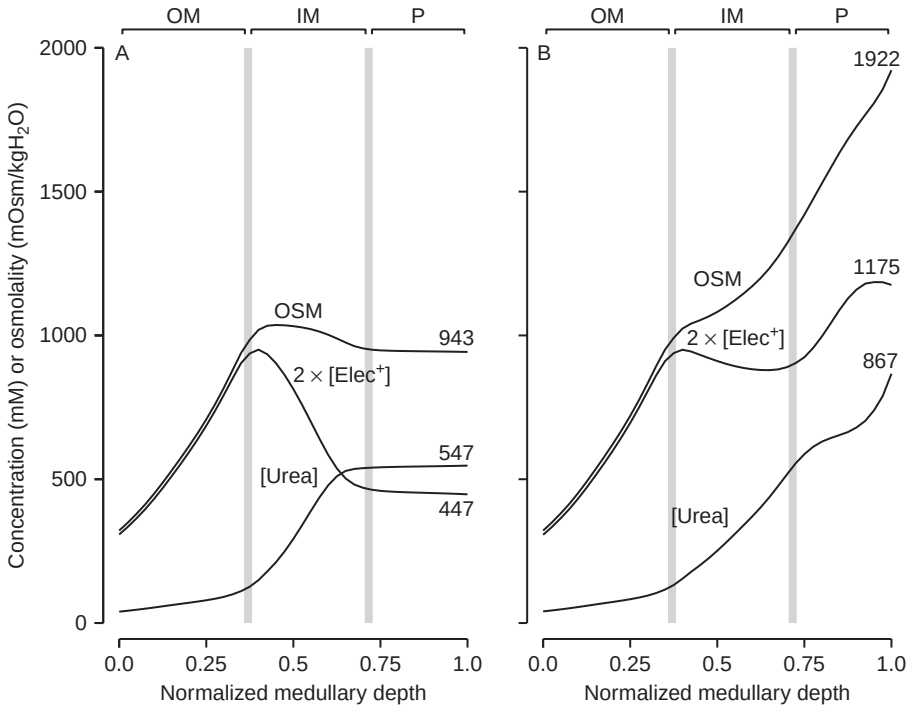

FIGURE 43.9 **Concentration and osmolality profiles as a function of medullary depth from computer simulation by Layton et al.**[52] Profiles represent flow-weighted averages across all tubules. Cation concentration [$Elec^+$] arose from Na^+, except in collecting ducts, where both Na^+ and K^+ were represented. Urine values are given at right of each panel. Profiles in panel (a) were computed from loop of Henle permeabilities based on measurements in chinchilla ([57]; see Tables 43.2 and 43.3). The non-increasing osmolality profile in the inner medulla is similar to that computed with lower permeability values from rabbit, rat, and hamster in a number of model studies (e.g., references[191,179,180,145,146]). Profiles in panel (b) were obtained when urea permeability ($\times 10^{-5}$ cm/s) was reduced from 16.8 to 1 in inner medullary descending limbs and from 170 to 1 in thin ascending limbs. Resulting profiles compare favorably with data from rat (cf. Figure 43.4), but despite greatly reduced urea permeabilities, model urine osmolality falls far short of 7600 mOsm/kg H_2O, the maximum concentrating capability of chinchilla.[1] Note that while tubular electrolytes (principally Na^+ and accompanying anions) account for most of the simulated osmolality in the outer medulla (in both panels (a) and (b)), the experimental results in Figure 43.4 show a large osmotic gap; this gap is mostly accounted for by large intracellular concentrations of K^+. *(The profiles in panels (a) and (b) were computed from data generated for cases designated V and I, respectively, in reference [52].)*

The simulation used loop and collecting duct distributions that are similar to those displayed in Figure 43.5, and the flow-weighted profiles in Figure 43.9 are roughly comparable to the tissue-slice profiles in Figure 43.5, although it must be kept in mind that Figure 43.5 includes the effects of intracellular fluid.

Panel (a) in Figure 43.9 shows results obtained using NaCl and urea permeabilities based on values measured in inner medullary thin descending and ascending limbs of chinchilla (see Tables 43.2 and 43.3). Owing to the significant entry of urea into descending and ascending limbs, no inner medullary gradient is generated. Moreover, the profile labeled as $2 \times [Elec^+]$, arising mostly from sodium and its anions, fails to show an exponential rise as it does in Figure 43.5 and in electron microprobe experiments.[106] Parameter studies showed that loop urea permeabilities and descending limb NaCl permeability must all be reduced to the range of $1-5 \times 10^{-5}$ cm/s to elicit a significant concentrating effect.[52]

Panel (b) in Figure 43.9 shows profiles obtained when loop urea permeability and descending limb NaCl permeability were reduced to 1×10^{-287} cm/s. Ascending limb NaCl permeability remains high, 294×10^{-5} cm/s. With these parameters, simulation profiles are remarkably similar to those reported for the rat in Figure 43.5. However, the greatly reduced permeabilities used for urea and NaCl in descending limbs, and for urea in ascending limbs, are much smaller than those measured in rat (see Tables 43.2 and 43.3), and the urine osmolality obtained, 1922 mOsm/kg H_2O, is far smaller than the maximum urine osmolality obtained in chinchilla, 7600 mOsm/kg H_2O.[1,4,5]

In recent years, mathematical simulations of the urine concentrating mechanism have become increasingly comprehensive and sophisticated in the representation of tubular transport (e.g.,[158,159,162]) and medullary architecture.[52,55,133,147,153,157,193,194] This evolution is a consequence of the increasing body of experimental knowledge, faster computers with

increased computational capacity, and the sustained failure of simulations to exhibit a significant inner medullary concentration gradient.

Stephenson and collaborators re-examined the passive mechanism hypothesis in a two-nephron central core model, in which the electrolyte concentrations for sodium, potassium, and chloride were represented, along with urea.[159] In a simulation using transport parameters from rabbit inner medulla, a significant inner medullary gradient could only be obtained when the urea permeabilities in both descending and ascending limbs had been reduced to less than 10^{-6} cm/s. For permeability values obtained from the hamster, both urea and electrolyte permeabilities needed to be greatly reduced, especially in thin descending limbs. Although it has been frequently suggested that a reduction in the urea reflection coefficient for the collecting duct epithelium could augment collecting duct osmolality by retaining urea in excess of fluid, this study showed that such a reduction was ineffective without a mechanism for generating a salt gradient in the core.

Layton and collaborators, in a series of papers, have sought to elucidate the role of the distributed loops of Henle.[52,55,180,195–197] These studies employ a model representation of the loops of Henle that allows the simulation of loops turning back at all levels of the inner medulla, while also representing the fluid flow and concentrations in individual loops.[195] Previously, models had typically used a small number of discrete loops (see, e.g.,[184]) or had employed shunts between a merged descending and ascending flow to represent the decreasing number of loops of Henle as a function of inner medullary depth (e.g.,[145]).

The distributed loop representation has been used to obtain several theoretical results. If solute is mostly absorbed near loop bends, then the loop distribution may allow a cascade effect that tends to increase the achievable concentration, provided, of course, that a net solute absorption can be obtained.[55,195] The concentrating effect can be further enhanced if solute is absorbed from a short, prebend segment of the descending limb with low water permeability[55] as has been detected in chinchilla,[42] and which may be present in other species (*vide supra*). Layton hypothesized that a cascade effect could allow the generation of an inner medullary osmolality gradient, despite large loop urea permeabilities, provided that the passive mechanism could operate near loop bends.[196,180] Average flow, taken over all thin ascending limbs at each medullary level, would be hypoosmotic relative to the flows in the surrounding tubules and vessels, due to the effect of more and more loops turning, as one proceeds from the papillary tip to the outer medulla. However, simulations using reported permeabilities in rat or chinchilla failed to support this hypothesis.[52,180]

Studies by Wexler and collaborators have sought to assess the role of preferential interactions among tubules and vessels.[147,160,162,194,198,199] Wexler, Kalaba, and Marsh introduced what has become known as the WKM model,[147,199] which was based on the organization of tubules around vascular bundles (Figure 43.3), and which therefore allowed both axial and radial concentration gradients. The preferential interaction of collecting ducts with both thick and thin ascending limbs was proposed as the key principle that allowed the generation of an inner medullary osmolality gradient. The preferential interaction with thick ascending limbs allowed highly concentrated collecting duct fluid to pass from the outer medulla to the inner medulla. The preferential interaction with thin ascending limbs allowed the passive mechanism to operate, since a urea-rich environment could be sustained around thin ascending limbs, and dissipative interaction of collecting ducts with thin descending limbs was diminished.

The WKM model drew criticism for some of its structural and transport assumptions.[32,176,200,201] Subsequent studies responded to these criticisms (with modified model assumptions), and acknowledged that preferential interactions are not sufficient to explain the inner medullary concentrating effect in the papilla.[160,162,198] Nonetheless, results from the WKM model and its successors have provided persuasive evidence that preferential interactions can be a significant factor in the degree of the outer and inner medullary concentrating effects. Moreover, the model structure permitted sensitivity testing as a function of interaction strength, and compared to other model studies, it allowed for a more accurate assessment of solute and water recycling pathways.

Two hypotheses closely related to the passive mechanism have been recently proposed by Layton et al.[54]; these hypotheses were motivated by the implications of recent studies in rat by Pannabecker et al..[18,19] One hypothesis is based directly on the principles of the passive mechanism: low urea permeabilities in thin limbs of Henle were assumed because no significant labeling for urea transport proteins was found in loops reaching deep into the inner medulla.[54] A second, more innovative hypothesis assumed very high urea loop of Henle permeabilities, but limited NaCl-permeability and zero water-permeability in thin descending limbs reaching deep into the inner medulla. Thus, in the innermost inner medulla, tubular fluid urea concentration in loops of Henle would nearly equilibrate with the local interstitial urea concentration; thin descending limb fluid osmolality would be raised by urea secretion; and substantial NaCl absorption would occur in the prebend segment and early thin ascending limb. Both hypotheses emphasize the role of the decreasing loop of Henle population, which facilitates

a spatially distributed NaCl absorption along the inner medulla, from prebend segments and early thin ascending limbs. A distinctive aspect of both hypotheses is an emphasis on NaCl transport from the IMCDs as an important active transport process that separates NaCl from tubular fluid urea, and that indirectly drives water and urea absorption from the collecting ducts. Computer simulations for both hypotheses predicted urine osmolalities, flow, and concentrations consistent with urine from moderately antidiuretic rats. The critical dependence of the first hypothesis on low loop urea permeabilities is subject to the criticism that urea transport may be paracellular rather than transepithelial: that hypothesis depends on more conclusive experiments to determine urea transport properties in rat. The second hypothesis may contribute to understanding the concentrating mechanism in chinchilla, in which high loop urea permeabilities have been measured.[57]

Subsequently, a modeling study by Marcano et al.,[181] which was based on the principles of the passive mechanism, produced somewhat higher osmolalities than reported by Layton et al.,[54] but did not reach osmolalities as large as those found in highly-concentrating rats. A modeling study by Layton et al.[153] that sought to represent the interactions among tubules and vessels hypothesized by Pannabecker et al.[20] exhibited concentrating capability similar to that found by Marcano et al.[181] A second modeling study by Layton et al.[202] that represented the interactions hypothesized by Pannabecker et al.[20] set forth the hypothesis that plentiful urine flow rates in rats accompanied by high urine concentrations may arise, in some cases, from altered boundary conditions at the boundary of the inner and outer medulla. Such altered conditions may arise from hyperfiltration and from inner stripe hypertrophy that result from feeding urea (thus providing, in part, an explanation for for findings by Gamble et al.[166]) or from a high-protein diet, water restriction or the administration of antidiuretic hormone.[203]

Steady-State Alternatives to the Passive Mechanism

The passive mechanism hypothesis is a comprehensive explanation for a large body of experimental findings, including the dilution of thin ascending limb fluid without active transport,[80,204,205] a role for urea in the concentrating mechanism,[166] and the NaCl and urea permeabilities measured in loops of Henle from rabbit inner medulla (see Tables 43.2 and 43.3). However, the larger permeabilities measured in rat, hamster, and chinchilla, in conjunction with the results of numerous simulation studies, have provided little support for the hypothesis. Significant concentrations of urea measured in long loops of Henle from rat and hamster[72,73,76] are generally consistent with studies reporting high loop urea permeabilities. In addition, some animals with high urine-concentrating ability, e.g., *Psammomys*, generate a medullary gradient that depends mostly on NaCl, with little medullary urea accumulation,[206] a result which suggests that, at least in some species, a mechanism differing from the passive mechanism is involved. Thus, while the passive mechanism hypothesis remains highly influential in both experimental and theoretical research, the accumulated evidence, from both experimental and mathematical studies, indicates that crucial elements are missing in our understanding of the inner medullary concentrating effect.

Alternatives to the original passive mechanism hypothesis have taken three forms. First, many simulation studies have attempted to show that a better representation of transepithelial transport or of medullary anatomy is required for the effective operation of the passive mechanism; some of these studies were summarized in the preceding section. Second, a number of steady-state mechanisms involving a single effect generated in either thin descending limbs or collecting ducts have been proposed. Third, several hypotheses which depend on the peristaltic contractions of the pelvic wall and their impact on the papilla have been proposed. The steady-state alternatives involving descending limbs or collecting ducts are considered directly below, within a general context of possible steady-state mechanisms; mechanisms involving peristalsis are considered in the subsequent subsection.

Based on the principle of mass balance, Knepper and colleagues have provided a systematic classification of possible steady-state concentrating models for the inner medulla.[7,148] The classification shows that a single effect for countercurrent multiplication can exist in any structure having axial flow. Thus, a single effect could be present in thin descending limbs, thin ascending limbs, collecting ducts, descending vasa recta or ascending vasa recta. The classification also shows that a concentrating single effect in an upward flowing stream (toward the cortex) would require a luminal osmolality less than that of the surrounding interstitium, whereas a single effect in a downward flowing stream would require a luminal osmolality exceeding that of the interstitium. Thus, for example, the active transport of NaCl from the thick ascending limbs of the outer medulla lowers the osmolality of the upward flowing luminal fluid relative to the surrounding interstitium; similarly the passive mechanism hypothesis proposes that diffusion of NaCl from thin ascending limbs renders luminal fluid hypoosmotic relative to the interstitium.

Several investigators have proposed a single effect in descending limbs arising from flow that is

hyperosmotic relative to the interstitium. Bonventre and Lechene proposed that the equilibration of descending limb flow with a compartment rendered hyperosmotic by active NaCl transport from ascending limbs or active secretion of solute into descending limb produces a relatively hyperosmotic descending flow from the outer medulla into the inner medulla.[207] In a mathematical simulation, Lory showed that an inwardly-directed NaCl transport combined with a loop of Henle cascade could produce a significant concentrating effect.[208] Jen and Stephenson performed a general mathematical analysis of mechanisms involving a hyperosmotic descending limb flow, and concluded that such mechanisms, in theory, could generate a potent single effect.[149] Their claim was supported by a subsequent simulation study by Thomas and Wexler,[162] which represented an external osmotic driving force to extract water from descending limbs and collecting ducts; the driving force was hypothesized to arise from the accumulation of osmotically active particles in local vessels or capillaries as a consequence of osmolyte production. Layton and colleagues[52] suggested that a descending limb single effect is consistent with the high NaCl and urea permeabilities of chinchilla ascending limb: the ascending limb could function as an equilibrating segment in which high permeabilities reduce dissipative osmotic lag. However, despite the attractive features of a descending limb single effect, experimental support for a relatively hypertonic descending limb is lacking. Moreover, in most species examined, the NaCl and urea permeabilities in thin descending limbs are too high to sustain a significant transepithelial osmolality gradient in the papilla, where the concentrating effect is most pronounced.

A single effect in the IMCD would require that the osmolality of luminal flow exceed the osmolality of the surrounding interstitium. Rabinowitz proposed such a single effect, based on the assumption that the urea reflection coefficient for the collecting duct is significantly less than unity.[209] He showed that the resulting reduction in the osmotic effect of urea in the collecting duct could, in theory, result in a water flux from collecting duct to interstitium that would significantly raise the osmolality of collecting duct fluid. A number of investigators have proposed or analyzed this hypothesis, including Sanjana et al.,[210] Bonventre and Lechene,[207] Chandhoke et al.,[211] and Imai et al.[39] However, experimental studies indicate that the urea reflection coefficient in rat does not differ significantly from unity.[50,122]

Thomas[152] and Hervy and Thomas[151] have investigated the hypothesis that the concentrating mechanism of the inner medulla may be driven or aided by lactate accumulation in the rat papilla. Anaerobic glycolysis in the hypoxic inner medulla is a net source of osmoles, because two lactates are produced for each glucose molecule. The rate of production, however may not be sufficient to produce a general concentrating effect. Modeling studies[151] indicate that lactate produced from glucose by anaerobic glycolysis could concentrate tubular fluid in thin descending limbs and collecting ducts (thus producing descending flows in these tubules that are relatively hyperosmotic to flows in other structures at each medullary level), provided that the descending limbs and collecting ducts are impermeable to lactate, as appears to be the case from low lactate levels in urine. However, several conditions require experimental verification: sufficient lactate production, impermeability of thin descending limbs to lactate, and sufficient intramedullary lactate cycling by vascular countercurrent exchange. The lactate-based mechanism is attractive because it appears to be insensitive to thin descending limb urea permeability, and independent of a necessary role for urea. However, modeling results for this mechanism appear to produce subphysiological urine flow, and do not explain the experimentally observed urea gradient in rat.

Hypotheses Based on the Peristalsis of the Papilla

Regular, sustained peristaltic contractions of the smooth muscles of the renal pelvic wall have been observed in a number of mammalian species. In the unipapillate kidneys of hamsters and rats, peristaltic contractions are propagated from the fornices to the lower pelvis, and continue in synchrony down the ureter. In the multipapillate kidneys of both humans and pigs, peristaltic contractions pass from the fornices down the calyces surrounding each papilla, but contractions in calyces are not synchronized with each other or with the peristalsis of the ureter. For a comprehensive review of the anatomy, physiology, and peristalsis of the renal pelvic region, see [212].

In hamsters and rats, the rates of pelvic contractions are about 13/min and 25/min, respectively.[164,213] The contractions interrupt fluid flow by forcing the collecting ducts, loops of Henle, and capillaries of the papilla to collapse. In hamster, the contractions induce bolus flow down the papillary collecting duct, with a bolus speed of about 1.6 mm/second. At the low urine flow rates characteristic of antidiuresis, boluses are so short that, 1 mm from the papillary tip, collecting ducts may be collapsed up to 94% of the time.[164] Even so, large quantities of urea, electrolytes, and, especially, water are absorbed in the final millimeters of the collecting duct system. Indeed, about 50% of the water in a bolus passing through the final millimeter of the collecting duct is absorbed.[214]

The blood in the capillaries of the papilla undergoes complicated motion during a pelvic contraction.[213] As a peristaltic wave approaches, blood is trapped in the capillaries closest to the papillary tip, which are full and expanded. As the wave passes over, the capillaries empty, with blood moving up both the descending and ascending *vasa recta*; after the wave has passed, the capillaries refill. The fluid motion in the loops of Henle is much like that of blood in the capillaries: fluid is trapped at the turns of the loops, and may move retrograde up the descending and ascending limbs as the peristaltic wave passes.[215] A net orthograde flow through the capillaries and loops of Henle is ensured by glomerular filtration pressure.

During the rising urine flow rates that accompany the onset of diuresis, the peristalsis in hamsters and rats induces refluxes of urine over the papilla and up into the fornices.[213] These refluxes, called full refluxes, may bathe the papillary surface epithelium with urine that is hypoosmotic and that has a low urea concentration, relative to the medullary structures; thus, water may diffuse into the medulla, and urea may diffuse out. Experiments in hamsters suggest that full refluxes accelerate the transition to the diuretic state.[216] When urine flow is constant or decreasing, refluxes are sporadic and limited to the lower 50–100 μm of the papilla.[213]

Experiments have shown that the excision of the pelvic wall results in a substantial reduction in urine osmolality[217–219]; the reduction has been attributed to the disruption of pelvic urea recycling[219–221] or to the dissipative effect of medullary blood flow, increased by continuous flow[164] or by prostaglandin release.[217] However, no significant change in osmolality was found in urine samples from rats 5–40 minutes after the smooth muscles of the pelvic wall were paralyzed with a topical application of verapamil and dimethylsulfoxide.[218] In the same study, the excision of the pelvic wall dramatically reduced the osmolality gradient in the papilla, and the gradient was substantially reduced when the ureter was severed just beyond the papillary tip, a procedure that preserved pelvic peristalsis (and intermittent urine flow), but eliminated urine reflux.[218] These results were interpreted to mean that while an intact pelvic wall, continuous with the ureter, is required for the production of maximally concentrated urine, the pelvic contractions are not. However, some experiments suggest that the peristaltic contractions do play a direct role in the concentrating mechanism. When the pelvic wall in rats was removed, causing a 10% decrease/hour in urine osmolality, and peristalsis was then simulated by a mechanical system, the decrease was reduced to 5%/hour.[222] When the muscles of the pelvic wall in hamster were paralyzed by cauterization or by xylocaine, urine osmolality was reduced by about 20% after one hour,[223] through a reduction in papillary sodium content.

Several studies have provided evidence of solute and water transport across the papillary surface epithelium. When the papillae of rats and gerbils were bathed in a solution containing ^{14}C-urea and ^{3}H-water, there was a marked tissue label for urea, increasing from cortex to inner medulla, and a smaller effect for water.[226] When the papilla was bathed *in vivo* with artificial solutions containing varying concentrations of urea, higher concentration of urea in the superfusate led to a higher osmolality in the urine that was collected as it emerged from the terminal IMCD.[220] Fluid collected from small catheters inserted far up into the fornices of the rat pelvis extracted fluid with concentrations of inulin and total solutes that were significantly lower than the concentrations in urine collected at the papillary tip.[227]

Recycling of urea from urine across the papillary surface epithelium has been proposed as a component of the inner medullary concentrating mechanism.[207,228] However, a comparison of ureteral urine and urine collected from the ducts of Bellini of hydropenic hamsters showed no significant differences in filtered water and urea,[229] and an analysis based on measured urea permeability and papillary surface area in rabbits suggests that urea transport across the papillary surface epithelium is negligible.[104]

The lack of a satisfactory explanation for the inner medullary concentrating effect has led to the formulation of hypotheses based on the peristaltic contractions of the smooth muscles of the pelvic wall. Layton proposed that the NaCl and urea concentrations in the tubular cells and interstitium undergo oscillations in tandem with the contractions.[196] Urea absorbed from boluses advancing down the collecting duct system would transiently, and substantially, increase urea concentration in collecting duct cells and in the interstitium. Immediately following passage of the peristaltic wave, NaCl absorbed from restored orthograde loop of Henle flow would significantly raise the interstitial NaCl concentration. The very large urea concentration encountered by loop flow would, perhaps, be sufficient to result in the transient operation of the passive mechanism near loop bends, raising interstitial osmolality. Consequently, water, in excess of solute, would be absorbed from the next bolus passing down the collecting duct, and a large urea gradient, resulting from increased interstitial NaCl, would favor urea absorption. However, as in the case of the steady-state formulation of the passive mechanism, the large permeabilities measured in chinchilla[57] suggest that rapid equilibration of NaCl and urea concentrations across thin ascending limbs would compromise this hypothesis.

Knepper and collaborators proposed that water may be driven out of thin descending limbs by the advancing peristaltic wave, thus concentrating tubular fluid and generating a single effect in descending limbs.[143,148] A sufficient net water flux might be achieved if the compliance of the papillary surface epithelium exceeds that of the thin descending limb, and if large enough pressures are attained by the compression wave. After the passage of the wave, solute would be absorbed in the relatively water-impermeable prebend segment, and in the early portion of the thin ascending limb, where NaCl and urea permeabilities are high. This hypothesis provides no explanation for the special role of urea in the production of high urine concentrations.[166]

Schmidt-Nielsen proposed that the contraction–relaxation cycle creates negative pressures in the interstitium that act to transport water, in excess of solute, from the collecting duct system.[230] According to this hypothesis, the compression wave would raise hydrostatic pressure in the collecting duct lumen, promoting a water flux into collecting duct cells. Because pressure would induce water flow through aquaporin water channels, without a commensurate solute flux, the remaining luminal fluid would be concentrated, relative to the contents of collecting duct cells and the surrounding interstitium. After the peristaltic wave had passed, the collecting ducts would be collapsed. The papilla, transiently lengthened and narrowed by the wave, would rebound, and a negative hydrostatic pressure would develop in the elastic interstitium, which is rich in glycosamine glycans and hyaluronic acid. The negative pressure would withdraw water from the collecting duct cells (through aquaporins) and into the vasa recta, which re-open during the relaxation phase of the contraction and carry reabsorbate toward the cortex. This hypothesis appears to provide no role for long loops of Henle, and it does not explain the large NaCl gradient generated in the papilla[6,106] or the special role of urea in producing concentrated urine.[166]

Knepper and colleagues[150] have recently hypothesized that hyaluronic acid, which is plentiful in the interstitium of the rat papilla, could serve as a mechano-osmotic transducer, i.e., that the intrinsic viscoelastic properties of hyaluronic acid could be utilized to transform the mechanical work of papillary peristalsis into osmotic work that could be used to concentrate urine. Three distinct concentrating mechanisms arising from peristalsis are proposed: (1) in the contraction phase, interstitial sodium activity would be reduced through the immobilization of cations by their pairing with fixed negative charges on hyaluronic acid. This would result in a lowered NaCl concentration in fluid that can be expressed from the interstitium, and that relatively dilute fluid would enter the ascending vasa recta. In the relaxation phase, water would be absorbed from descending thin limbs: (2) as a result of decreased interstitial pressure (previously proposed by Knepper and co-workers[143,148]); and (3) as a result of elastic forces exerted by the expansion of the elastic interstitial matrix arising from hyaluronic acid. If water is so absorbed, without proportionate solute, then the descending limb tubular fluid would be relatively concentrated relative to other flows.

All of the hypotheses summarized above involve complex, highly coordinated cycles, with critical combinations of permeabilities, flow rates, compliances, pressures, and frequencies of peristalsis. Moreover, a determination of the adequacy of these hypotheses would appear to require a comprehensive knowledge of the physical properties of the renal papilla, and a demonstration that the energy input of the contractions, plus any other sources of harnessed energy, is sufficient to account for the osmotic work performed. Thus, the evaluation of these hypotheses, whether by means of experiments or mathematical models, presents a daunting technical challenge.

OSMOPROTECTIVE OSMOLYTES

Since the osmolality in the renal medulla is able to vary rapidly over a wide range, medullary cells must be able to adapt to this unusual osmotic environment in order to survive.[207,231] One way for medullary cells to achieve osmotic balance would be for these cells to accumulate intracellularly the major osmotically active compounds (osmolytes) that are found extracellularly in the medullary interstitium and urine, i.e., NaCl and urea.[232] The problem with this approach is that NaCl and urea can perturb protein function.[231] If medullary cells accumulated such perturbing osmolytes to achieve osmotic balance, then it is likely that these cells would need to develop special mechanisms that would allow their proteins to function over a wide range of intracellular ionic compositions and/or in high concentrations of urea.

An alternative mechanism would be for medullary cells to accumulate osmotically active substances that do not alter protein function, i.e., non-perturbing osmolytes.[231,233,234] This second approach is actually employed by medullary cells (Figure 43.10). Medullary cells accumulate non-perturbing or "organic" osmolytes such as sorbitol, glycerophosphocholine, betaine, inositol, and taurine.[232,235–238] These organic osmolytes are divided into two general categories: compatible and counteracting osmolytes. Sorbitol, inositol, and taurine are the major compatible osmolytes, and have no effect on protein function. They are accumulated intracellularly to osmotically balance extracellular

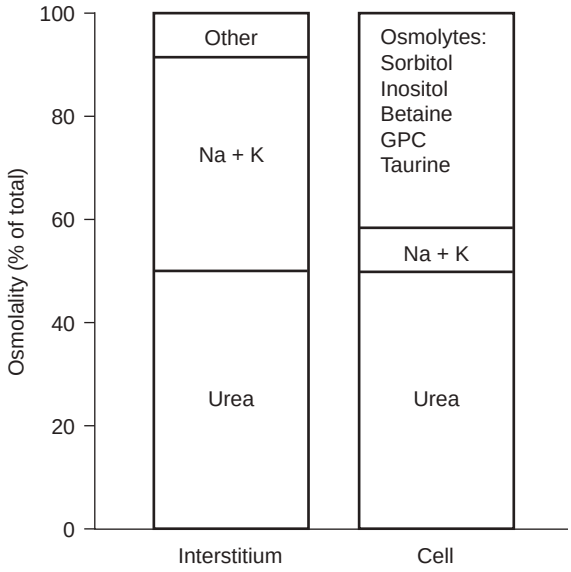

FIGURE 43.10 **Comparison of osmotic composition of the inner medullary interstitium and of cells in the inner medulla.** Sodium and potassium salts in the interstitium are balanced by compatible osmolytes (sorbitol, inositol, taurine). The denaturing effect of urea is balanced by counteracting osmolytes (betaine, glycerophosphocholine (GPC)). Data from references [452,453]. *(Figure is modified, with permission, from reference [232].)*

NaCl.[236,237,239] Glycerophosphocholine and betaine are the major counteracting osmolytes: in addition to being osmotically active, they have stabilizing effects on protein function and counteract the destabilizing effects of urea when they are accumulated intracellularly at a ratio of 1 mole of counteracting osmolyte to 2 moles of urea.[231,233,234,239,240,241]

In the medulla, organic osmolytes are regulated to respond to prolonged periods without water ingestion followed by short periods in which water is ingested.[236] During periods of antidiuresis, medullary cells maintain high intracellular concentrations of organic osmolytes to match extracellular osmolality. When water is ingested, these cells respond by rapidly losing osmolytes into the urine by increasing their cell membrane permeability to these osmolytes, thus decreasing intracellular osmolality.[236,237] However, the medullary cells continue osmolyte production during these short periods of diuresis. Although this continued osmolyte production may appear inefficient, it enables the cell to respond rapidly to the cessation of water ingestion. When water ingestion ceases, the cell's permeability to osmolyte efflux decreases, and intracellular osmolyte concentration is rapidly restored, since osmolyte production is maintained.[236,237] However, if the diuresis is prolonged (days), then osmolyte production is decreased in addition to the increase in cell permeability.[236,237] In this case, osmolyte concentration cannot be restored rapidly, since the upregulation of osmolyte production requires an increase in the transcription of osmolyte genes and new protein synthesis.[236]

ROLE OF UREA

Urea plays a unique role in the urine concentrating mechanism. Its importance to the generation of a concentrated urine has been appreciated since 1934, when Gamble and colleagues described "an economy of water in renal function referable to urea".[166] Several studies show that maximal urine concentrating ability is decreased in protein-deprived animals and humans, and is restored by urea infusion.[75,165,166,242–246] This is the mechanism that has been proposed to explain why protein-restricted and malnourished humans are unable to concentrate their urine maximally. Recently, a UT-A1/UT-A3 knockout mouse,[144] a UT-A2 knockout mouse,[247] and a UT-B knockout mouse[248–250] were each shown to have urine concentrating defects. Thus, any solution to the question of how the inner medulla concentrates urine needs to take into account some effect derived from urea.

Facilitated Urea Transporters

Several early studies in dog and rat suggested that vasopressin could increase urea permeability across the IMCD.[63,251–253] Direct evidence was obtained in the 1980s, when three groups showed that vasopressin could increase passive urea permeability in isolated perfused rat IMCDs.[102,120,123] A specific facilitated or carrier-mediated urea transport process in rat and rabbit terminal IMCDs was first proposed in 1987.[102] The physiologic studies provided a functional characterization for a vasopressin-regulated urea transporter (reviewed in [254–258]). Two urea transporter genes have been cloned: the UT-A (*Scl14A2*) gene encodes 6 protein and 9 cDNA isoforms; the UT-B (*Scl14A1*) gene encodes two protein isoforms[259] (and reviewed in[260]) (Table 43.6). The UT-A gene was initially cloned from rat,[261] then from human and mouse.[262,263] It has two promoter elements: promoter I is upstream of exon 1 and drives the transcription of UT-A1, UT-A1b, UT-A3, UT-A3b, and UT-A4; promoter II is located within intron 12 and drives the transcription of UT-A2 and UT-A2b.[224,261]

The mouse UT-A promoter α, equivalent to the rat UT-A promoter I, has been further studied by the creation of transgenic mice in which 4.2 kb of the 5′-flanking region of the UT-A gene is linked to a β-galactosidase reporter gene.[264] This transgene is sufficient to drive IMCD-specific expression of β-galactosidase in terminal IMCDs.[264] The β-galactosidase transgene is regulated by both water restriction and

TABLE 43.6 Cloned Mammalian Urea Transporters

Gene	Isoform	Tissue Localization
Slc14A1	UT-B1	red blood cells, endothelial cells, descending vasa recta
	UT-B2	bovine rumen
Slc14A2	UT-A1/UT-A1b	inner medullary collecting duct, apical membrane
	UT-A2/UT-A2b	thin descending limb (also heart and liver)
	UT-A3/UT-A3b	inner medullary collecting duct, apical and basolateral membranes
	UT-A4	rat medulla (not detected in mouse)
	UT-A5	mouse testis (not expressed in kidney)
	UT-A6	human colon (not expressed in kidney)

The original references can be found in the following reviews or references: [254,255,257–259,477–479].

glucocorticoids, similar to the regulation of the endogenous UT-A promoter α.[263–266]

UT-A1 is the largest UT-A protein and is expressed in the apical plasma membrane of cells in the IMCD.[262,267,268] Urea transport by UT-A1 is stimulated by cAMP when expressed in *Xenopus* oocytes,[269–271] and by vasopressin in cells that are stably transfected with UT-A1, UT-A1-MDCK cells,[272–274] and UT-A1-mIMCD3 cells.[275] Western blots of inner medullary tip proteins show bands at both 117 and 97 kDa; both bands represent glycosylated versions of a non-glycosylated 84 kDa UT-A1 protein.[276] UT-A1 protein is most abundant in the inner medullary tip; only the 97 kDa protein is detected in the inner medullary base, and it is not detected in outer medulla or cortex.[268,277,278]

UT-A3 is also expressed in the IMCD,[279] although reports of its location have varied in different studies. Initial studies performed in rat detected UT-A3 staining in the apical plasma membrane and intracellular cytoplasmic vesicles of terminal IMCDs, but none in the basolateral plasma membrane.[268,280] Subsequent studies detected UT-A3 staining only in the IMCD basolateral plasma membrane in mouse IMCD, and in mUT-A3-MDCK cells.[281,282] The most recent study detected UT-A3 staining in the basolateral plasma membrane in rats, but in both the apical and basolateral plasma membranes in rats following vasopressin administration.[283] UT-A3 expression in the basolateral plasma membrane provides a mechanism for transepithelial urea transport in the IMCD, with UT-A1 in the apical plasma membrane and UT-A3 in the basolateral plasma membrane.

Urea transport by UT-A3 is stimulated by cAMP analogs when expressed in human embryonic kidney (HEK) 293 cells or *Xenopus* oocytes in three studies,[269,279,284] but not in a fourth.[285] Vasopressin also stimulates urea transport via a PKA-dependent pathway in cells that are stably transfected with mouse UT-A3, mUT-A3-MDCK cells.[282]

UT-A2, the first urea transporter cloned,[286] is expressed in thin descending limbs.[90,267,268] Urea transport by UT-A2 is not stimulated by cAMP analogs when expressed in either *Xenopus* oocytes or human embryonic kidney HEK-293 cells.[270,271,279,286–289] UT-A4 is expressed in rat kidney medulla, although its exact location is unknown, and it has not been detected in mouse kidney.[248,263,269] Urea transport by UT-A4 is stimulated by cAMP analogs when expressed in HEK-293 cells.[279] UT-A5 and UT-A6 are expressed in testis and colon, respectively, but not in kidney.[284,290] In addition, there are three UT-A cDNA variants with alternative 3′-untranslated regions, but no difference in coding region, named UT-A1b, UT-A2b, and UT-A3b, respectively.[224]

The UT-B1 cDNA was initially cloned from a human erythroid cell line,[291] then from rodents.[249,292–294] UT-B1 protein is the Kidd antigen (in humans), and several mutations of the UT-B1/Kidd antigen gene exist[295–299]; red blood cells from these individuals also lack phloretin-sensitive facilitated urea transport.[300] The human UT-B gene encodes a single cDNA and a single protein[295]; both the N- and C-termini are located intracellularly.[296] However, in rat, two cDNA sequences that differ by only a few nucleotides at their 3′ end have been reported.[292,294] Whether the two cDNAs truly represent different rat UT-B1 isoforms, a polymorphism or a sequencing artifact is uncertain, since humans have only a single isoform. UT-B1 protein is detected as a broad band between 45–65 kDa in human red blood cells and 35–55 kDa in rodent red blood cells and kidney medulla.[249,301,302] UT-B1 protein and phloretin-inhibitable urea transport are present in descending vasa recta.[61,249,301–306]

Several studies have addressed the question of whether UT-B1 transports urea only, or water and urea.[249,307,308] Although red blood cells from a UT-B1/AQP1 double-knockout mouse show that UT-B1 can function as a water channel, the amount of water transported through UT-B1 under physiologic conditions is small (in comparison to AQP1), and is probably not physiologically significant to the urine concentrating mechanism.[250]

Rapid Regulation of Facilitated Urea Transport

The primary method for investigating the rapid regulation of urea transport has been perfusion of rat IMCDs. This method provides physiologically relevant

functional data, although it cannot determine which urea transporter isoform is responsible for a specific functional effect in rat terminal IMCDs, since both UT-A1 and UT-A3 are expressed in this nephron segment. Vasopressin addition to the basolateral membrane of a rat terminal IMCD results in binding to V_2-vasopressin receptors, stimulating adenylyl cyclase, generating cAMP, and ultimately increasing facilitated urea permeability.[63,102,120,121,253,309,310] This effect occurs within minutes of adding vasopressin to the bath.[311] Oxytocin also increases urea permeability by binding to V_2-receptors and increasing cAMP production in rat terminal IMCDs.[312] Functional studies show that phloretin-inhibitable urea transport is present in both the apical and basolateral plasma membranes, with the apical membrane being the rate-limiting barrier for vasopressin-stimulated urea transport.[313] As discussed above, it is unclear whether UT-A3 is the basolateral membrane urea transporter.[280,281]

The acute stimulation of urea permeability by vasopressin occurs by an increase in the number of functional urea transporters (V_{max}), without a change in the transporter's affinity (K_m) for urea.[314] Adding vasopressin to the lumen of a perfused rat terminal IMCD also increases urea permeability by binding to luminal V_2-receptors.[315] However, when vasopressin is first added to the bath, adding vasopressin to the lumen inhibits urea permeability, suggesting that luminal vasopressin is a negative modulator of basolateral vasopressin on urea permeability in rat terminal IMCDs.[315]

One mechanism for rapid regulation is a vasopressin-stimulated increase in UT-A1 phosphorylation.[316] The deduced amino acid sequence for UT-A1 contains several consensus sites for phosphorylation by PKA, as well as by protein kinase C (PKC) and tyrosine kinase.[279] UT-A1 and UT-A3 have been identified in proteomic and cDNA array approaches as proteins that are phosphorylated by vasopressin in the inner medulla.[137,317–322] Vasopressin increases the phosphorylation of both the 117 and 97 kDa UT-A1 proteins in freshly isolated suspensions of rat IMCDs within 2 minutes,[316] and of the 67 and 44 kDa UT-A3 proteins.[283] Vasopressin also increases UT-A1 phosphorylation in UT-A1-MDCK cells[273,274] and UT-A1-mIMCD3 cells.[275] The time-course and dose–response for vasopressin-stimulated increases in UT-A1 phosphorylation is similar to the time-course and dose–response for vasopressin-stimulated increases in urea permeability in perfused rat terminal IMCDs.[309–311,316] Cyclic AMP, dDAVP (a V_2-selective agonist), and forskolin also increase UT-A1 phosphorylation, and PKA inhibitors block vasopressin or forskolin-stimulated UT-A1 phosphorylation in rat IMCD suspensions[316] and UT-A1-MDCK cells.[274] Vasopressin/cAMP can stimulate Epac, exchange protein activated by cAMP,[323–328] in addition to stimulating PKA. Epac activation increases urea permeability in perfused rat terminal IMCDs, and increases UT-A1 phosphorylation in IMCD suspensions.[329]

Serine 486 was identified in a phosphoproteomic analysis as a potential vasopressin-stimulated phosphorylation site in UT-A1.[137] Serine 486 was identified in a second study, which also identified serine 499 as a second potential PKA phosphorylation site.[330] Using site-directed mutagenesis and transient transfection in heterologous expression systems, PKA was shown to phosphorylate UT-A1 at both serine 486 and serine 499.[330] Phospho-specific antibodies to serine 486 show that vasopressin increases UT-A1 phosphorylation at serine 486.[275,331] Phospho-serine 486-UT-A1 is detected primarily in the apical plasma membrane in rat IMCDs.[275] Recent work with chimera proteins of UT-A that attached the loop region of UT-A1 (aa 460–532) containing serines 486 and 499 to the UT-A2 protein, which normally lacks these amino acids, showed that this section conferred vasopressin sensitivity to UT-A2.[332]

A subsequent phosphoproteomic analysis showed that purified PKA could phosphorylate UT-A1 at serines 486 and 499; that analysis also showed that serine 84, which is present in both UT-A1 and UT-A3, could be phosphorylated by PKA.[317] In rat, vasopressin phosphorylates both UT-A1 and UT-A3 at serine 84, based upon studies utilizing a phospho-specific antibody to serine 84.[331] However, the equivalent site in mouse UT-A3, serine 85, was shown not to be a PKA phosphorylation site, based on site-directed mutagenesis.[284] The latter study also showed that serine 92 was not a PKA phosphorylation site.[284]

Another mechanism by which vasopressin rapidly increases urea transport is regulated trafficking or redistribution of UT-A1 between an intracellular compartment and the apical plasma membrane. In freshly isolated suspensions of rat IMCDs from normal rats, vasopressin increases the plasma membrane accumulation of UT-A1 and UT-A3.[283,333] However, in IMCDs from Brattleboro rats or two week water diuretic rats, vasopressin does not increase the plasma membrane accumulation of UT-A1.[333,334] (Brattleboro rats have central diabetes insipidus due to a congenital absence of vasopressin production in the hypothalamus.) When forskolin is used as the agonist, rather than vasopressin, it does increase the plasma membrane accumulation of UT-A1 in IMCDs from two week water diuretic rats.[333] Since chronically diuretic animals have a blunted cAMP response to vasopressin,[335–337] directly stimulating adenylyl cyclase with forskolin[337] may result in higher levels of cAMP production, which may result in an increase in UT-A1 accumulation in the

plasma membrane.[333] Epac activation also increases UT-A1 plasma membrane accumulation in rat IMCD suspensions.[329]

Either vasopressin or forskolin increases UT-A1 apical plasma membrane accumulation in UT-A1-MDCK cells[272,333] and UT-A1-mIMCD3 cells.[275] Mutation of both serines 486 and 499, but not either one alone, eliminates the stimulation of UT-A1 apical plasma membrane accumulation and urea transport by vasopressin, indicating that at least one of these serines must be phosphorylated in order to increase apical plasma membrane accumulation and urea flux.[330] A phospho-specific antibody to S486-UT-A1 also showed that vasopressin increases UT-A1 accumulation in the apical plasma membrane, and that the S486-phospho-UT-A1 form is primarily detected in the apical plasma membrane.[275]

Vasopressin also increases UT-A3 accumulation in both the basolateral and apical plasma membranes in rat IMCDs.[283] In mUT-A3-MDCK cells, vasopressin stimulation for 10 minutes increases urea flux through transporters already in the basolateral plasma membrane.[338] Vasopressin stimulation for one hour increases UT-A3 localization in the basolateral plasma membrane and further increases urea flux in mUT-A3-MDCK cells.[338] The basal expression of UT-A3 in the basolateral plasma membrane involves PKC and calmodulin, while UT-A3 regulation by vasopressin involves a casein-kinase II-dependent pathway.[338]

UT-A1 is linked to the SNARE machinery via snapin in rat IMCDs, suggesting that the SNARE-SNAP vesicle trafficking mechanism may be functionally important for regulating urea transport.[339] UT-A1 also interacts with caveolin-1 in lipid rafts, providing another mechanism for UT-A1 regulation of UT-A1 activity within the plasma membrane.[340] Both UT-A1 and UT-A3 proteins can be ubiquitinated.[341,342] However, only UT-A1 has been rigorously shown to express ubiquitinated higher molecular weight forms by immunoprecipitation and Western analysis.[341] The ubiquitin ligase MDM2 mediates UT-A1 ubiquitination and degradation, providing another regulatory mechanism for UT-A1.[341] Finally, mutation of the two N-linked glycosylation sites in UT-A1 that are predicted to reside in extracellular domains, Asn 279 and Asn 742, reduces urea flux by reducing UT-A1 half-life and apical plasma membrane accumulation in MDCK cells.[272]

Increasing osmolality to high physiological values, either by adding NaCl or mannitol, in the absence of vasopressin, acutely increases urea permeability in rat terminal IMCDs,[119,121,343] suggesting that hyperosmolality is an independent stimulator of urea transport. When osmolality is increased and vasopressin is present, they have additive stimulatory effects on urea permeability.[119,121,343,344] Hyperosmolality-stimulated urea permeability is inhibited by phloretin and the urea analog thiourea.[119] Kinetic studies show that hyperosmolality, like vasopressin, stimulates urea permeability by increasing V_{max} rather than reducing K_m.[119] However, hyperosmolality stimulates urea permeability via increases in intracellular calcium and activation of PKC,[345,346] whereas vasopressin stimulates urea permeability via increases in adenylyl cyclase.[310] Hypersomolality increases the phosphorylation and the plasma membrane accumulation of both UT-A1 and UT-A3, similar to vasopressin.[283,316,333,347] Thus, both hyperosmolality and vasopressin increase urea permeability by increasing V_{max}, but they do so via different second messenger pathways.

Active Urea Transporters

Functional evidence exists for two types of active urea transport in the rat collecting duct: sodium-urea co-transport and sodium-urea countertransport (reviewed in [255,256]). Although no sodium-dependent active urea transporter has been cloned to date, several sodium-coupled co-transporters (rabbit sodium-glucose co-transporters 1 and 3, human sodium-chloride-GABA co-transporter 1) behave as urea channels when expressed in *Xenopus* oocytes.[348,349]

LONG-TERM REGULATION OF UREA TRANSPORTERS

Vasopressin

Administering vasopressin to Brattleboro rats (which lack vasopressin) for 5 days decreases UT-A1 protein abundance in the inner medulla.[350,351] However, administering vasopressin for 12 days increases UT-A1 protein abundance.[350] This delayed increase in UT-A1 protein is consistent with the time-course for the increase in inner medullary urea content in Brattleboro rats following vasopressin administration.[352] In normal rats, suppressing endogenous vasopressin levels by two weeks of water diuresis also decreases UT-A1 protein abundance.[350] This time-course may be explained by analysis of UT-A promoter I, since the 1.3 kb that has been cloned does not contain a cAMP response element (CRE), and cAMP does not increase promoter activity.[261,265] However, promoter I does contain a tonicity enhancer (TonE) element, and hyperosmolality increases promoter activity.[261,265] Thus, vasopressin may increase UT-A1 indirectly after directly increasing the transcription of other genes, such as the Na-K-2Cl co-transporter NKCC2/BSC1 and the AQP2 water channel, which begin to increase inner

medullary osmolality.[353,354] Consistent with this hypothesis, water restricting rats with primary polydipsia results in an increase in plasma vasopressin, but no increase in medullary osmolality or UT-A1 protein abundance.[355]

In Brattleboro rats, UT-A2 mRNA increases at both 4 and 72 hours after administering dDAVP, while UT-A1 mRNA is unchanged.[318] The dDAVP-stimulated increase in UT-A2 mRNA is consistent with the presence of a CRE in UT-A promoter II, and the stimulation of promoter II activity by cAMP.[261]

Administering either vasopressin or dDAVP for 6 hours reduces UT-B mRNA abundance in both the outer and inner medulla of Brattleboro rats.[356] In contrast, administering vasopressin or dDAVP for 5 days increases UT-B mRNA abundance in the inner stripe of the outer medulla and the inner medullary base, while it is still decreased in the inner medullary tip.[356] Administering dDAVP for 7 days to normal rats decreases UT-B protein abundance in the inner medulla.[302]

Low-Protein Diet

Feeding rats a low-protein diet for at least 2 weeks results in a decrease in the fractional excretion of urea,[246] induces the functional expression of vasopressin-stimulated urea permeability in the initial IMCD,[118,287,357] increases basal urea permeability in the $IMCD_3$,[358] and increases the abundance of the 117 kDa glycoprotein form of UT-A1 in the inner medulla.[351] The vasopressin-stimulated urea permeability in the initial IMCD from low-protein fed rats is stimulated by hyperosmolality and inhibited by phloretin and thiourea.[118,287] Thus, it has the same functional characteristics as the vasopressin-stimulated urea permeability which is normally expressed in the terminal IMCD.[287] Whether the mRNA abundance of UT-A1 or UT-A2 changes in the inner medulla of low-protein fed rats is controversial.[287,289,359] Varying dietary protein between 10 and 40% has no effect on UT-B mRNA abundance in any portion of the medulla in either normal or Brattleboro rats.[359]

Glucocorticoids

Glucocorticoids (dexamethasone) increase the fractional excretion of urea[360] and decrease UT-A promoter I activity, UT-A1 and UT-A3 mRNA abundances, UT-A1 protein abundance, and facilitated urea transport.[266,361,362] Mineralocorticoids (aldosterone) also decrease UT-A1 protein abundance in the inner medulla of adrenalectomized rats, and this decrease can be blocked by spironolactone, a mineralocorticoid-receptor antagonist.[361] In contrast, spironolactone does not block the decrease due to dexamethasone,[361] indicating that each steroid hormone works through its own receptor. Aldosterone-induced volume-expansion (with a high-NaCl diet) decreases both UT-A1 and UT-A3 protein abundance.[363]

Dahl salt-sensitive rats have increased abundances of UT-A1 and UT-A3 proteins in the inner medulla, and of facilitated urea transport in the terminal IMCD.[364] They also have an increased level of the corticosterone-inactivating enzyme 11-hydroxysteroid dehydrogenase type II.[364] Inactivating glucocorticoids by increasing 11-hydroxysteroid dehydrogenase type II would lessen the repression of UT-A promoter I activity, thereby increasing UT-A1 and UT-A3 transcription and abundance.

Diabetes Mellitus

Uncontrolled diabetes mellitus (induced by streptozotocin) causes an osmotic diuresis and increases urea excretion, corticosterone production, and plasma vasopressin levels.[365–367] UT-A1 protein abundance decreases at 3–5 days after inducing diabetes mellitus in the rat inner medulla, but not in adrenalectomized diabetic rats.[336,368] The decrease in UT-A1 protein abundance is restored by giving dexamethasone to adrenalectomized diabetic rats, indicating that glucocorticoids mediate the decrease in UT-A1 protein.[368]

In contrast, UT-A1 mRNA and protein are increased 10–21 days after diabetes mellitus is induced in normal rats.[336,369] UT-A1 protein did not increase in diabetic Brattleboro rats, indicating that vasopressin is necessary for this increase in UT-A1.[350] In addition, vasopressin did not increase UT-A1 phosphorylation in either Brattleboro rats or diabetic Brattleboro rats, indicating that vasopressin is necessary for the increase in UT-A1 protein abundance and phosphorylation that occurs at 10–21 days after diabetes is induced.[350] UT-A2 is also decreased in the streptozotocin-induced diabetic rat. The reason for the decrease is not known, but it appears to result from a post-translational alteration in protein abundance, since the message for UT-A2 in control and diabetic rats is not different.[369]

The increase in UT-A1 protein abundance in the inner medulla from diabetic rats is accompanied by a shift in the glycoprotein forms expressed in inner medullary tip versus base.[336,370,371] The base of the inner medulla, which normally expresses only the 97 kDa glycoprotein form of UT-A1, shows both 97 kDa and 117 kDa forms in the diabetic rat.[336,370,371] Vasopressin sensitivity is also changed in the diabetic rat inner medulla. In the normal rat, only urea transport in the inner medullary tip is subject to stimulation by

vasopressin, whereas in the diabetic kidney, urea permeability in both the tip and the base are increased by vasopressin.[372] In addition, both UT-A1 and UT-A3 protein abundance increases in response to treatment of the diabetic rat with the angiotensin receptor-blocker candesartan, apparently to reduce the loss of solute during uncontrolled diabetes.[370]

A model of type 2 diabetes is the obese Zucker rat, which has a genetic mutation of the leptin-receptor gene that leads to obesity, insulin resistance, hypertension, and diabetes.[373] UT-A1 protein abundance is decreased in the obese Zucker rat when compared to the lean Zucker (non-diabetic) rat.[374] The decrease in UT-A1 protein abundance may be a response to the hypertension present in the obese Zucker rat, similar to the decrease in UT-A1 observed in normal Sprague-Dawley rats made hypertensive with angiotensin II.[375]

Angiotensin II

Angiotensin II does not affect basal (no vasopressin) facilitated urea permeability in rat terminal IMCDs.[346] However, it increases both vasopressin-stimulated urea permeability and UT-A1 phosphorylation via a PKC-mediated effect.[346] Thus, angiotensin II may play a physiologic role in the urine concentrating mechanism by augmenting the maximal urea permeability response to vasopressin. In the inner medulla of mice that lack tissue angiotensin-converting enzyme, and hence lack angiotensin II, UT-A1 protein abundance is decreased to 25% of the level in wild-type mice.[376,377] Administering angiotensin II to these mice for 2 weeks did not correct the reduction in UT-A1 protein, nor in urine concentrating ability.[377]

Osmolality

Renal medullary osmolality varies between diuresis and antidiuresis. The major solutes contributing to inner medullary osmolality are urea and NaCl. Urea-specific signaling pathways are present in mIMCD3 cells (reviewed in [378,379]). When the percentage of urea in total urinary solute is low, UT-A1 protein abundance increases.[380–383] The increase in UT-A1 may occur in order to restore inner medullary interstitial urea and urine concentrating ability.[380] In the outer medulla, UT-A2 and UT-B1 protein abundance increases when medullary interstitial urea concentration is high, such as during a urea-induced osmotic diuresis, but not during a NaCl- or glucose-induced osmotic diuresis.[380–383] During osmotic diuresis, the urinary urea and NaCl concentrations regulate UT-A1 and UT-A3 protein abundances, but in opposite directions.[384] This regulation involves the tonicity enhancer-binding protein, Ton EBP, and appears to be an attempt to minimize changes in plasma osmolality and maintain water homeostasis.[384]

TonEBP, which is also named OREBP (osmotic response element binding protein) or NFAT5, is an essential regulator of urine concentrating ability.[385,386] Transgenic mice that overexpress a dominant-negative form of TonEBP have reduced urine osmolality, and UT-A1 and UT-A2 mRNA abundance.[386] In these mice, water deprivation or vasopressin administration increases urine osmolality and UT-A1 mRNA abundance, but not UT-A2 mRNA abundance.[386] TonEBP also stimulates the transcription of genes whose products drive cellular accumulation of organic osmolytes, such as aldose reductase.[385] Mice with genetic deletion of aldose reductase have a urine osmolality below 1000 mOsm/kg H_2O.[387] The urine concentrating defect was largely corrected in bitransgenic mice in which an aldose reductase transgene was knocked-in. These mice displayed a tendency toward increased UT-A1 expression that might contribute to the restoration of urine concentration.[387]

Electrolye Abnormalities

Hypercalcemia or hypokalemia reduce urine concentrating ability.[278,388–390] Basal urea permeability is increased in terminal IMCDs from hypercalcemic rats compared to normocalcemic control rats.[278] Consistent with this functional increase, the abundance of UT-A1 protein is also increased.[278] These changes may be regulated by a calcium-sensing receptor in the apical plasma membrane of cells in the terminal IMCD.[391] In a mouse model of autosomal dominant polycystic kidney disease (ADPKD) or a rat model of autosomal recessive PKD (ARPKD), treatment with a type 2 calcimimetic, R-568, results in hypocalcemia, polyuria, and minimal changes in UT-A1 protein abundance, with significant increases in UT-A1 seen only in the female ARPKD rats.[392]

A low-potassium diet reduces the abundance of UT-A1, UT-A3, and UT-B proteins in the inner medulla, but increases UT-A2 protein abundance in the outer medulla.[389] TonEBP protein abundance and nuclear distribution in the medulla are reduced by hypokalemia.[393] TonEBP downregulation contributes to the reduced expression of UT-A1 and UT-A2, although UT-A2 expression is transcriptionally reduced whereas UT-A1 is reduced post-transcriptionally.[393] In addition, UT-B1 expression is reduced, along with a decrease in mRNA abundance in response to hypokalemia.[393] Another study also found that feeding rats a low-potassium diet reduces the abundance of UT-A1, UT-A3, and UT-B1 proteins in the inner medulla.[389] However,

this latter study found that hypokalemia increases UT-A2 protein abundance in the outer medulla.[389] The reason for the differing findings regarding UT-A2 in these studies is unclear.

Hypothyroidism

Hypothyroidism reduces urine concentrating ability, but does not alter UT-A1 or UT-A2 protein abundance in rats.[394] Water-restricting hypothyroid rats alters neither UT-A1 nor UT-A2 abundance.[394] Urine concentrating ability is reduced in normal aging (reviewed in [395]). UT-A1, UT-A3, and UT-B1 proteins are reduced in kidneys of aged rats.[396–398] A supra-physiologic dose of dDAVP increases UT-A1 and UT-B1 protein abundance and urine osmolality in aged rats, but not to the levels observed in younger rats.[399]

Purinergic P2Y2 Receptor

P2Y2 receptor activation in the IMCD tends to oppose the actions of vasopressin.[400] Urine concentrating ability, and UT-A1 and UT-A2 protein abundances, are higher in P2Y2-receptor knockout mice than in wild-type mice.[400] Vasopressin administration for 45 minutes or 5 days increases UT-A1 protein abundance in P2Y2-receptor knockout mice.[400] Vasopressin administration for 5 days increases UT-A2 protein abundance in both control and P2Y2 purinergic receptor-null mice,[400] suggesting a role for cAMP in the regulation of UT-A2. While acute treatment with PKA agonists did not increase UT-A2,[269] longer treatment times did upregulate UT-A2 protein abundance,[90,401] suggesting that cAMP may be involved in the long-term regulation, rather than in the acute response, for UT-A2.

Ureteral Obstruction

UT-A1, UT-A3, and UT-B1 protein abundances are reduced by bilateral or unilateral ureteral obstruction in rat inner medulla.[402] The abundance of all three urea transporters remained reduced at 2 weeks after release of bilateral ureteral obstruction.[402]

Lithium

Lithium causes nephrogenic diabetes insipidus and an inability to concentrate urine (reviewed in [403]). Lithium causes a marked reduction in inner medullary interstitial osmolality due to reductions in interstitial urea and NaCl concentrations.[404] Lithium-treated rats have marked reductions in AQP2, UT-A1, UT-A3, and UT-B1 proteins, and vasopressin-stimulated UT-A1 phosphorylation.[405–408] UT-A1 and UT-A3 protein abundances return to control levels 14 days after stopping lithium therapy.[405] A proteomic analysis shows that several proteins involved in various signaling cascades that have been implicated in urea transporter function and/or trafficking are altered after 14 days of lithium treatment.[409] However, immunohistochemistry shows that UT-A1 localization appears normal after recovery from lithium treatment,[405] indicating that the trafficking machinery remains intact. Surprisingly, lithium stimulates urea flux in UT-A1-MDCK cells, despite suppressing cAMP formation.[410] Lithium does not increase UT-A1 biotinylation, which suggests that the increased urea flux in UT-A1-MDCK cells is due to an alteration in cellular signaling, rather than the trafficking of UT-A1.[410]

Genetic Knockout of UT-B

Humans with genetic loss of Kidd antigen (UT-B1) are unable to concentrate their urine above 800 mOsm/kg H_2O, even following overnight water deprivation and exogenous vasopressin administration.[411] Mice with a genetic knockout of UT-B1 also have mildly reduced urine concentrating ability, which is not improved by urea loading.[249,412] UT-A1 and UT-A3 abundance unchanged in UT-B1 knockout mice, but UT-A2 protein abundance is increased.[248] Since UT-A2 mediates urea recycling through the thin descending limb, it may be upregulated to partially compensate for the loss of urea recycling through UT-B1, thereby contributing to the mild phenotype observed in humans lacking UT-B1/Kidd antigen, and in UT-B1 knockout mice.

Mathematical models of microcirculatory exchange between the descending and ascending vasa recta predict that the absence of UT-B1 will decrease the efficiency of small solute trapping within the renal medulla, thereby decreasing the efficiency of countercurrent exchange and urine concentrating ability.[413,414] Thus, UT-B1 protein expression in red blood cells and/or descending vasa recta is necessary for the production of maximally concentrated urine.[411–416]

UT-B1 knockout mice have an impaired ability to concentrate their urine, achieving a maximal urine osmolality of 2400 mOsm/kg H_2O, compared to 3400 in a wild-type mouse.[249] This is similar to the phenotype in humans lacking UT-B1, the Kidd antigen, who are unable to concentrate their urine above 800 mOsm/kg H_2O, even following overnight water deprivation and exogenous vasopressin administration.[411] These findings support the concept that urea transport in red blood cells is necessary to preserve the efficiency of countercurrent exchange.[415] Both red blood cells and perfused rat descending vasa recta exhibit phloretin-inhibitable urea transport and express

UT-B1 protein,[61,301,303–306] suggesting that UT-B1 mediates urea transport in red blood cells and descending vasa recta.

UT-A2 protein abundance is increased, while UT-A1 and UT-A3 abundance is unchanged in UT-B1 knockout mice.[248] UT-A2 may be upregulated to compensate for the loss of UT-B1, since both UT-A2 and UT-B1 are involved in urea recycling.[248] This may account for the mild phenotype observed in UT-B1 knockout mice, and in humans lacking UT-B1/Kidd antigen.

Genetic Knockout of UT-A1 and UT-A3

Genetic knockout of both UT-A1 and UT-A3 in mice results in reduced urine concentrating ability, reduced inner medullary interstitial urea content, and a lack vasopressin-stimulated or phloretin-inhibitable urea transport in the IMCD.[144,417] When these mice are fed a low-protein diet, they are able to concentrate their urine almost as well as wild-type mice fed a low-protein diet,[144,417] supporting the concept that IMCD urea transport contributes to urine concentrating ability by preventing urea-induced osmotic diuresis.[418] Inner medullary tissue urea content was markedly reduced following water restriction, but there was no measurable difference in NaCl content between UT-A1/UT-A3 knockout mice and wild-type mice.[144,417] This finding was initially interpreted as being inconsistent with the predictions of the passive mechanism hypothesis.[8,9,144,417,419,420] However, a mathematical modeling analysis of these same data concludes that the results found in the UT-A1/UT-A3 knockout mice are exactly what one would predict for the passive mechanism hypothesis.[20]

The UT-A1/UT-A3 knockout mice were used to revisit Gamble's classic study from 1934.[166] Urea and NaCl each induce an osmotic diuresis when given in large amounts, supporting the concept that the decrease in water excretion with mixtures of urea and NaCl added to the diet results from the separate abilities of these two solutes to induce osmotic diuresis, rather than to any specific interaction of urea and NaCl transport at the epithelial level.[421]

Genetic Knockout of UT-A2

UT-A2 knockout mice also have an impaired ability to concentrate urine.[247,419,422] The reduction in urine concentrating ability results from an impairment of urea recycling.[247,419,422]

Active Urea Transport

When urine concentrating ability is reduced, there are changes in active urea transport that follow one of two patterns.[115,118,357,358,423,424] The first pattern, which occurs in response to water diuresis, is upregulation of active urea secretion in the $IMCD_3$ and its induction in the $IMCD_2$. This increase in urea secretion will directly decrease urea content in the deep inner medulla. The second pattern, which occurs in response to a low-protein diet, hypercalcemia, and furosemide, is induction of active urea absorption in the $IMCD_1$ and inhibition of active urea secretion in the $IMCD_3$. This second pattern will increase urea delivery to the inner medullary base, thereby decreasing urea delivery to the inner medullary tip; the accompanying inhibition of active urea secretion in the $IMCD_3$ may prevent an even greater reduction in urea content in the deep inner medulla.

UREA RECYCLING

Several urea recycling pathways are believed to contribute to high urea concentrations within the inner medulla.[418,425,426] The major recycling pathway involves urea absorption from the terminal IMCD, mediated by UT-A1 and UT-A3, secretion into the thin descending limb, and, especially, the thin ascending limb (Figure 43.11). Collecting ducts and thin ascending limbs are nearly adjoining within much of the inner medulla.[12] The urea that enters the thin ascending limb is carried distally as the luminal fluid moves through several nephron segments having very low urea permeability until it reaches the urea-permeable terminal

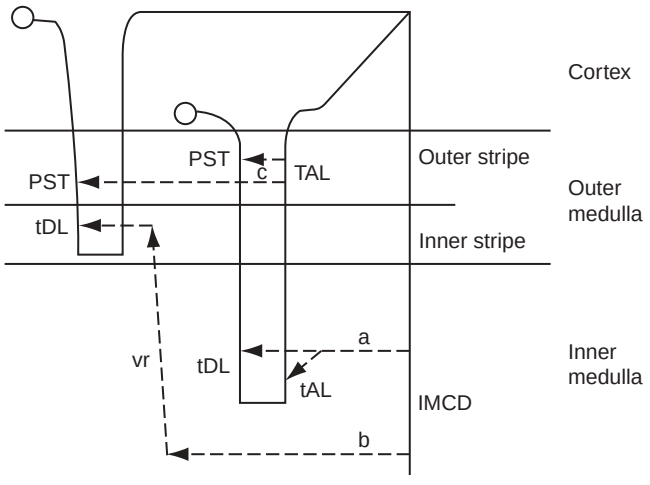

FIGURE 43.11 **Urea recycling pathways in mammalian kidney.** Diagram shows a short looped nephron (left) and a long looped nephron (right). Dashed lines labeled a, b, and c show urea recycling pathways (Abbreviations: PST: proximal straight tubule; tDL: thin descending limb of Henle's loop; tAL: thin ascending limb of Henle's loop; TAL: thick ascending limb of Henle's loop; IMCD: inner medullary collecting duct; vr: vasa recta). *(Figure is modified, with permission, from reference [425].)*

IMCD. Thus, urea is recycled from the terminal IMCD through the interstitium into the thin ascending limb, and back to the terminal IMCD.

Two other pathways for urea recycling may exist in the kidney.[425] One pathway is urea absorption from terminal IMCDs through ascending vasa recta and secretion into thin descending limbs of short looped nephrons[427] mediated by UT-A2[90] or into descending vasa recta mediated by UT-B1. The other pathway is urea absorption from cortical thick ascending limbs and secretion into proximal straight tubules.[425] All three urea recycling pathways would limit urea dissipation from the inner medulla where it is needed to increase interstitial osmolality.[425]

It must be emphasized that the terminal IMCD is the only portion of the collecting duct in which vasopressin increases urea permeability, even though the entire collecting duct is permeable to water when vasopressin is present. Water absorption from the cortical, outer medullary, and initial inner medullary collecting ducts concentrates urea within the collecting duct lumen. When the luminal fluid finally reaches the urea-permeable terminal IMCD, the luminal urea concentration is very high and exceeds that in vasa recta,[72,75,428,429] allowing urea to be rapidly absorbed into the deepest portion of the inner medullary interstitium where, in many studied mammals, it is needed to concentrate urine maximally.[102,192] This pattern of urea and water permeabilities separates the primary sites of urea and water absorption (Figure 43.6); water is primarily absorbed in the cortex and outer medulla where there is extensive vascularization with high blood flow, and the absorbed water can be returned to the circulation without diluting the deep inner medulla. Urea is principally absorbed in the deep inner medulla.[102,192]

Urea serves a second function in the medulla: it is the major source for excretion of nitrogenous waste; large quantities of urea need to be excreted daily. The kidney's ability to concentrate urea reduces the need to excrete water simply to remove nitrogenous waste. In addition, a high interstitial urea concentration is able to osmotically balance urea within the collecting duct lumen. If interstitial urea were unavailable to offset the osmotic effect of luminal urea destined for excretion, then the interstitial NaCl concentration would have to be much higher.[144,430]

DEVELOPMENT OF URINE CONCENTRATING ABILITY

Newborn mammals and birds are unable to concentrate their urine.[431–435] Rats and rabbits do not develop the ability to concentrate their urine maximally until 14–21 days after birth.[434,436–439] In rats, the increase in urine osmolality is paralleled by an increase in both medullary sodium and urea content.[440] In 10-day-old rats, neither urea- nor NaCl-loading enhances urine concentrating ability.[441] However, in 20-day-old rats, urea-loading significantly increases urine osmolality following water deprivation; NaCl loading has no effect.[441] The development of urine concentrating ability can be hastened by giving glucocorticoids to 10–17-day-old rats, but not to older rats.[440,442] Conversely, adrenalectomizing 16-day-old rats slows the development of urine concentrating ability and abolishes the increase in inner medullary sodium and urea concentrations that normally occurs at this age.[440]

In 1-day-old rats, the thin descending limb, thin ascending limb, and IMCD are all nearly water-impermeable.[433] At day 4, AQP1 mRNA is detected in the thin descending limb and water-permeability increases, however, it does not reach adult levels until day 14.[433] Even though AQP2 protein is detected starting at day 1, water-permeability remains low in the IMCD at day 7, but reaches adult levels at day 14.[368,433,443] However, AQP2 trafficking in the immature kidney responds normally to vasopressin[443] and AQP2 mRNA, and protein levels increase 24 hours after a single dose of betamethasone.[442]

In fetal rat kidney, UT-A protein is not detected and UT-B1 protein is weakly detected at embryonic age 20 days.[267] In 1-day-old rats, UT-A1, UT-A2, and UT-B1 proteins appear,[267] but the IMCD has a low urea permeability that is not stimulated by vasopressin.[433] At day 14, urea permeability becomes vasopressin-stimulatable and UT-A1 mRNA is detected, although the values are only one-third of adult levels.[433] UT-A1, UT-A2, and UT-B1 proteins increase progressively until adult levels are achieved at 21 days of age.[267] Thus, the time-course for the increases in UT-A1, UT-A2, and UT-B1 proteins coincides with the development of urine concentrating ability. On the basis of the functional implications of these findings, Lui et al.[433] proposed that the concentrating mechanism in newborn rats is similar to that in the avian kidney, which has very low descending limb water permeability, does not utilize urea, and can concentrate urine to only moderate levels; however, within about 14 days, the neonatal rat kidney more closely resembles the adult rat kidney.

In rabbits, the sodium concentration in cortex and medulla is similar regardless of age.[437] However, the medullary/cortical urea concentration ratio increases markedly between 14 and 21 days of age, coincident with the development of concentrated urine.[437] This increase in medullary/cortical urea concentration is primarily due to a reduction in cortical urea concentration, rather than an increase in medullary urea content.[437] However, in dogs, the developmental increase

in urinary concentrating ability is due predominantly to an increase in the medullary sequestration of urea.[444]

Newborn humans also have an inability to concentrate their urine.[445] Infants fed a high-protein diet are able to increase their urine osmolality following water deprivation; infants given a diet in which the extra protein is replaced by NaCl achieve a lower urine osmolality.[445] Thus, even in infants, urea has a special role in the production of concentrated urine.[166,445]

Aldose reductase enzyme activity is absent in IMCDs from newborn rat pups (<12 hours old), but is present in 3-day-old pups and increases progressively up to 20 days of age; enzyme activity then decreases to adult levels.[434] Consistent with these functional measurements, aldose reductase mRNA cannot be detected, even by RT-PCR, in inner medullas from newborn rats (<12 hours old), but can be detected in 3-day-old pups.[434] Aldose reductase mRNA abundance peaks between 8–20 days after birth, then decreases to levels found in adult rats.[434,446] Thus, aldose reductase mRNA and enzyme activity are induced prior to urine concentrating ability during development.

TonEBP is detected in the kidney at fetal day 16, and its expression increases at fetal day 20 and at postnatal day 1.[447] At day 21, the adult pattern of TonEBP expression is achieved, along with the development of urine concentrating ability.[434,447] Thus, TonEBP expression precedes the expression of its target genes, UT-A1 and UT-A3, and UT-A promoter I is under the transcriptional control of TonEBP.[265,447] In mouse kidney, NKCC2/BSC1 is first detected at fetal day 14, TonEBP at day 15, UT-A at day 16–18, and UT-A immunoreactivity increases markedly after birth.[448] Neonatal mice treated with furosemide have reduced expression of both TonEBP and UT-A.[448] These findings support the hypothesis that hypertonicity produced by NKCC2/BSC1 activates TonEBP, which in turn increases the transcription of UT-A during development and early postnatal life in mice,[448] consistent with UT-A promoter I containing a TonE.[224,261]

KLF12 is a transcription factor that is expressed in the fetal kidney starting at day 15.[449] KLF12 is able to increase UT-A promoter I activity by binding to a CACCC motif.[449] Thus, UT-A1 is a target gene of KLF12, which may be involved in collecting duct maturation after birth.[449]

SUMMARY

Concentrated urine is produced in the renal medulla through the generation of an osmotic gradient extending from the cortico–medullary boundary to the papillary tip. In the outer medulla, the gradient is generated by active NaCl transport from the thick limbs, and the resulting increase in osmolality in the interstitium and in water-permeable tubules and vessels; the effectiveness of this transport is widely believed to be augmented by a countercurrent multiplication mechanism involving interactions between descending and ascending limbs of Henle. Although the passive mechanism, proposed by Kokko and Rector[8] and by Stephenson,[9] remains the most widely-accepted hypothesis for the generation of the inner medullary osmolality gradient, much of the evidence from perfused tubule and micropuncture studies, and from the UT-A1/UT-A3 knockout mouse[144] is either inconclusive or at variance with the passive mechanism. Moreover, the passive mechanism has not been supported by mathematical simulations using measured transepithelial transport parameters.

Nonetheless, there have been important recent advances in the understanding of key components of the urine concentrating mechanism, notably the identification and localization of key transport proteins for water, urea, and sodium, and the elucidation of the role and regulation of osmoprotective osmolytes. Continued experimental investigation of transepithelial transport and its regulation, both in normal animals and in genetically-engineered mice, a more complete understanding of the interaction of anatomy and transmural transport among tubules and vessels, and incorporation of the resulting information into mathematical simulations, may help to more fully elucidate the inner medullary concentrating mechanism.

Acknowledgments

This work was supported by National Institutes of Health grants R01-DK41707 (to JM Sands) and R01-DK42091 (to HE Layton).

References

[1] Beuchat CA. Body size, medullary thickness, and urine concentrating ability in mammals. Am J Physiol 1990;258:R298–308.
[2] Tisher CC. Relationship between renal structure and concentrating ability in the rhesus monkey. Am J Physiol 1971;220:1100–6.
[3] Tisher CC, Schrier RW, McNeil JS. Nature of urine concentrating mechanism in the macaque monkey. Am J Physiol 1972;223:1128–37.
[4] Beuchat CA. Structure and concentrating ability of the mammalian kidney: correlations with habitat. Am J Physiol 1996;271: R157–79.
[5] Knepper MA. Measurement of osmolality in kidney slices using vapor pressure osmometry. Kidney Int 1982;21:653–5.
[6] Hai MA, Thomas S. The time-course of changes in renal tissue composition during lysine vasopressin infusion in the rat. Pfluegers Arch 1969;310:297–319.
[7] Knepper MA, Stephenson JL. Urinary concentrating and diluting processes. In: Andreoli TE, Hoffman JF, Fanestil DD, Schultz SG, editors. Physiology of membrane disorders. 2nd ed. New York: Plenum; 1986. p. 713–26.

[8] Kokko JP, Rector FC. Countercurrent multiplication system without active transport in inner medulla. Kidney Int 1972;2:214–23.
[9] Stephenson JL. Concentration of urine in a central core model of the renal counterflow system. Kidney Int 1972;2:85–94.
[10] Kriz W. Der architektonische und funktionelle Aufbau der Rattenniere. Z Zellforsch 1967;82:495–535.
[11] Kriz W, Schnermann J, Koepsell H. The position of short and long loops of Henle in the rat kidney. Z Anat Entwicklungsgesch 1972;138:301–19.
[12] Lemley KV, Kriz W. Cycles and separations: the histotopography of the urinary concentrating process. Kidney Int 1987;31:538–48.
[13] Khorshid MR, Moffat DB. The epithelia lining the renal pelvis in the rat. J Anat 1974;118:561–9.
[14] Lacy ER, Schmidt-Nielsen B. Anatomy of the renal pelvis in the hamster. Am J Anat 1979;154:291–320.
[15] Sands JM, Knepper MA, Spring KR. Na-K-Cl co-transport in apical membrane of rabbit renal papillary surface epithelium. Am J Physiol 1986;251:F475–84.
[16] Silverblatt FJ. Ultrastructure of the renal pelvic epithelium of the rat. Kidney Int 1974;5:214–20.
[17] Kriz W, Bankir L. Structural organization of the renal medullary counterflow system. Fed Proc 1983;42:2379–85.
[18] Pannabecker TL, Abbott DE, Dantzler WH. Three-dimensional functional reconstruction of inner medullary thin limbs of Henle's loop. Am J Physiol Renal Physiol 2004;286:F38–45.
[19] Pannabecker TL, Dantzler WH. Three-dimensional lateral and vertical relationships of inner medullary loops of Henle and collecting ducts. Am J Physiol Renal Physiol 2004;287:F767–74.
[20] Pannabecker TL, Dantzler WH, Layton HE, Layton AT. Role of three-dimensional architecture in the urine concentrating mechanism of the rat renal inner medulla. Am J Physiol Renal Physiol 2008;295:F1271–85.
[21] Layton AT, Layton HE, Dantzler WH, Pannabecker TL. The mammalian urine concentrating mechanism: hypotheses and uncertainties. Physiology (Bethesda) 2009;24:250–6.
[22] Jamison RL, Kriz W. Urinary concentrating mechanism. Structure and function. New York: Oxford University Press; 1982.
[23] Kriz W, Lever AF. Renal countercurrent mechanisms: structure and function. Am Heart J 1969;78:101–18.
[24] Rytand DA. The number and size of mammalian glomeruli as related to kidney and body weight, with methods for their enumeration and measurement. Am J Anat 1938;62:507–20.
[25] Knepper MA, Danielson RA, Saidel GM, Post RS. Quantitative analysis of renal medullary anatomy in rats and rabbits. Kidney Int 1977;12:313–23.
[26] Nyengaard JR, Bendtsen TF. Glomerular number and size in relation to age, kidney weight, and body surface in normal man. AR 1992;232:194–201.
[27] Oliver J. Nephrons and kidneys: a quantitative study of developmental and evolutionary mammalian renal architectonics. New York: Harper and Row; 1968.
[28] Calder WAI, Braun EJ. Scaling of osmotic regulation in mammals and birds. Am J Physiol Regul Integr Comp Physiol 1983;244:R601–6.
[29] Sperber I. Studies on the mammalian kidney. Zool Bidrag Uppsala 1944;22:249–437.
[30] Pfeiffer EW, Nungesser WC, Iverson DA, Wallerius JF. The renal anatomy of the primitive rodent, *Aplodontia rufa*, and a consideration of its functional significance. AR 1960;137:227–35.
[31] Sasaki Y, Takahashi T, Suwa N. Quantitative structural analysis of the inner medulla of rabbit kidney. Tohoku J Exp Med 1969;98:21–32.
[32] Han JS, Thompson KA, Chou C-L, Knepper MA. Experimental tests of three-dimensional model of urinary concentrating mechanism. J Am Soc Nephrol 1992;2:1677–88.
[33] Casotti G, Lindberg KK, Braun EJ. Functional morphology of the avian medullary cone. Am J Physiol Regul Integr Comp Physiol 2000;279:R1722–30.
[34] Williams JB, Pacelli MM, Braun EJ. The effect of water deprivation on renal function in conscious unrestrained Gambel's quail (*Callipepla gambelli*). Physiol Zool 1991;64:1200–16.
[35] Atherton JC, Hai MA, Thomas S. The time course of changes in renal tissue composition during mannitol diuresis in the rat. J Physiol 1968;197:411–28.
[36] Atherton JC, Hai MA, Thomas S. Acute effects of lysine vasopressin injection (single and continuous) on urinary composition in the conscious water diuretic rat. Pfluegers Arch 1969;310:281–96.
[37] de Rouffignac C. The urinary concentrating mechanism. In: Kinne RKH, editor. Urinary concentrating mechanisms. comparative physiology. Basel: Karger; 1990. p. 31–102.
[38] Koepsell H, Nicholson WAP, Kriz W, Hohling HJ. Measurements of exponential gradients of sodium and chlorine in the rat kidney medulla using the electron microprobe. Pfluegers Arch 1974;350:167–84.
[39] Imai M, Taniguchi J, Tabei K. Function of thin loops of Henle. Kidney Int 1987;31:565–79.
[40] Kriz W, Bankir L. A standard nomenclature for structures of the kidney. Am J Physiol Renal Physiol 1988;254:F1–8.
[41] Preston GM, Carroll TP, Guggino WB, Agre P. Appearance of water channels in *Xenopus* oocytes expressing red cell CHIP28 protein. Science 1992;256:385–7.
[42] Chou C-L, Nielsen S, Knepper MA. Structural–functional correlation in chinchilla long loop of Henle thin limbs: a novel papillary subsegment. Am J Physiol Renal, Fluid Electrolyte Physiol 1993;265:F863–74.
[43] Nielsen S, Pallone T, Smith BL, Christensen EI, Agre P, Maunsbach AB. Aquaporin-1 water channels in short and long loop descending thin limbs and in descending vasa recta in rat kidney. Am J Physiol Renal,Fluid Electrolyte Physiol 1995;268: F1023–37.
[44] Nielsen S, Smith BL, Christensen EI, Knepper MA, Agre P. CHIP28 water channels are localized in constitutively water-permeable segments of the nephron. J Cell Biol 1993;120:371–83.
[45] Sabolic I, Valenti G, Verbavatz J-M, Van Hoek AN, Verkman AS, Ausiello DA, et al. Localization of the CHIP28 water channel in rat kidney. Am J Physiol Cell Physiol 1992;263: C1225–33.
[46] Maeda Y, Smith BL, Agre P, Knepper MA. Quantification of Aquaporin-CHIP water channel protein in microdissected renal tubules by fluorescence-based ELISA. J Clin Invest 1995;95:422–8.
[47] Ma TH, Yang BX, Gillespie A, Carlson EJ, Epstein CJ, Verkman AS. Severely impaired urinary concentrating ability in transgenic mice lacking aquaporin-1 water channels. J Biol Chem 1998;273:4296–9.
[48] Schnermann J, Chou CL, Ma TH, Traynor T, Knepper MA, Verkman AS. Defective proximal tubular fluid reabsorption in transgenic aquaporin-1 null mice. Proc Natl Acad Sci USA 1998;95:9660–4.
[49] Chou C-L, Knepper MA. *In vitro* perfusion of chinchilla thin limb segments: segmentation and osmotic water permeability. Am J Physiol Renal Physiol 1992;263:F417–26.
[50] Chou C-L, Sands JM, Nonoguchi H, Knepper MA. Urea-gradient associated fluid absorption with $s_{urea} = 1$ in rat terminal collecting duct. Am J Physiol 1990;258:F1173–80.

[51] Dantzler WH, Evans KE, Pannabecker TL. Osmotic water permeabilities in specific segments of rat inner medullary thin limbs of Henle's loops (Abstract). FASEB J 2009;23: [970.3]
[52] Layton HE, Knepper MA, Chou C-L. Permeability criteria for effective function of passive countercurrent multiplier. Am J Physiol 1996;270:F9–20.
[53] Braun EJ, Reimer PR. Structure of avian loop of Henle as related to countercurrent multiplier system. Am J Physiol 1988;255: F500–12.
[54] Layton AT, Pannabecker TL, Dantzler WH, Layton HE. Two modes for concentrating urine in rat inner medulla. Am J Physiol Renal Physiol 2004;287:F816–39.
[55] Layton HE, Davies JM. Distributed solute and water reabsorption in a central core model of the renal medulla. Math Biosci 1993;116:169–96.
[56] Layton HE, Davies JM, Casotti G, Braun EJ. Mathematical model of an avian urine concentrating mechanism. Am J Physiol Renal Physiol 2000;279:1139–60.
[57] Chou C-L, Knepper MA. *In vitro* perfusion of chinchilla thin limb segments: urea and NaCl permeabilities. Am J Physiol Renal Physiol 1993;264:F337–43.
[58] Imai M, Hayashi M, Araki M. Functional heterogeneity of the descending limbs of Henle's loop. I. internephron heterogeneity in the hamster kidney. Pfluegers Arch 1984;402:385–92.
[59] Imai M, Taniguchi J, Yoshitomi K. Transition of permeability properties along the descending limb of long-loop nephron. Am J Physiol 1988;254:F323–8.
[60] Kokko JP. Urea transport in the proximal tubule and the descending limb of Henle. J Clin Invest 1972;51:1999–2008.
[61] Pallone TL, Work J, Myers RL, Jamison RL. Transport of sodium and urea in outer medullary descending vasa recta. J Clin Invest 1994;93:212–22.
[62] Stoner LC, Roch-Ramel F. The effects of pressure on the water permeability of the descending limb of Henle's loops of rabbits. Pfluegers Arch 1979;382:7–15.
[63] Morgan T, Berliner RW. Permeability of the loop of Henle, vasa recta, and collecting duct to water, urea, and sodium. Am J Physiol 1968;215:108–15.
[64] Kokko JP. Sodium chloride and water transport in the descending limb of Henle. J Clin Invest 1970;49:1838–46.
[65] Abramow M, Orci L. On the "tightness" of the rabbit descending limb of the loop of Henle-physiological and morphological evidence. Int J Biochem 1980;12:23–7.
[66] Rocha AS, Kokko JP. Membrane characteristics regulating potassium transport out of the isolated perfused descending limb of Henle. Kidney Int 1973;4:326–30.
[67] Katz AI. Distribution and function of classes of ATPases along the nephron. Kidney Int 1986;29:21–31.
[68] Terada Y, Knepper MA. Na^+-K^+-ATPase activities in renal tubule segments of rat inner medulla. Am J Physiol 1989;256: F218–23.
[69] Tabei K, Imai M. K transport in upper portion of descending limbs of long-loop nephron from hamster. Am J Physiol 1987;252:F387–92.
[70] Gottschalk CW, Mylle M. Micropuncture study of composition of loop of Henle fluid in desert rodents. Am J Physiol 1959;204:532–5.
[71] Horster M, Thurau K. Micropuncture studies on the filtration rate of single superficial and juxtamedullary glomeruli in the rat kidney. Pfluegers Arch 1968;301:162–81.
[72] Pennell JP, Lacy FB, Jamison RL. An *in vivo* study of the concentrating process in the descending limb of Henle's loop. Kidney Int 1974;5:337–47.
[73] Jamison RL, Buerkert J, Lacy FB. A micropuncture study of Henle's thin loop in brattleboro rats. Am J Physiol 1973;224:180–5.
[74] Bankir L, Trinh-Trang-Tan M-M. Urea and the kidney. In: Brenner BM, editor. Brenner and Rector's the kidney. 6th ed. Philadelphia: Saunders; 2000. p. 637–79.
[75] Pennell JP, Sanjana V, Frey NR, Jamison RL. The effect of urea infusion on the urinary concentrating mechanism in protein-depleted rats. J Clin Invest 1975;55:399–409.
[76] Marsh DJ. Solute and water flows in thin limbs of Henle's loop in the hamster kidney. Am J Physiol 1970;218:824–31.
[77] Marsh DJ, Azen SP. Mechanism of NaCl reabsorption by hamster thin ascending limb of Henle's loop. Am J Physiol 1975;228:71–9.
[78] Ito M, Oiso Y, Murase T, Kondo K, Saito H, Chinzei T, et al. Possible involvement of inefficient cleavage of preprovasopressin by signal peptidase as a cause for familial central diabetes insipidus. J Clin Invest 1993;91:2565–71.
[79] Imai M. Function of the thin ascending limbs of Henle of rats and hamsters perfused *in vitro*. Am J Physiol 1977;232:F201–9.
[80] Imai M, Kokko JP. Sodium, chloride, urea, and water transport in the thin ascending limb of Henle. J Clin Invest 1974;53:393–402.
[81] Nielsen S, Frokiaer J, Marples D, Kwon ED, Agre P, Knepper M. Aquaporins in the kidney: from molecules to medicine. Physiol Rev 2002;82:205–44.
[82] Kondo Y, Imai M. Effect of glutaraldehyde on renal tubular function. II. Selective inhibition of Cl^- transport in the hamster thin ascending limb of Henle's loop. Pfluegers Arch 1987;408:484–90.
[83] Kondo Y, Abe K, Igarashi Y, Kudo K, Tada K, Yoshinaga K. Direct evidence for the absence of active Na^+ reabsorption in hamster ascending thin limb of Henle's loop. J Clin Invest 1993;91:5–11.
[84] Uchida S, Sasaki S, Nitta K, Uchida K, Horita S, Nihei H, et al. Localization and functional characterization of rat kidney-specific chloride channel, ClC-K1. J Clin Invest 1995;95:104–13.
[85] Takahashi N, Kondo Y, Ito O, Igarashi Y, Omata K, Abe K. Vasopressin stimulates Cl^- transport in ascending thin limb of Henle's loop in hamster. J Clin Invest 1995;95:1623–7.
[86] Uchida S, Sasaki S, Furukawa T, Hiraoka M, Imai T, Hirata Y, et al. Molecular cloning of a chloride channel that is regulated by dehydration and expressed predominantly in kidney medulla. J Biol Chem 1993;268:3821–4.
[87] Akizuki N, Uchida S, Sasaki S, Marumo F. Impaired solute accumulation in inner medulla of *Clcnk1*$^{-/-}$ mice kidney. Am J Physiol Renal Physiol 2001;280:F79–87.
[88] Koyama S, Yoshitomi K, Imai M. Effect of protamine on ion conductance of ascending thin limb of Henle's loop from hamsters. Am J Physiol 1991;261:F593–9.
[89] Takahashi N, Kondo Y, Fujiwara I, Ito O, Igarashi Y, Abe K. Characterization of Na^+ transport across the cell membranes of the ascending thin limb of Henle's loop. Kidney Int 1995;47:789–94.
[90] Wade JB, Lee AJ, Liu J, Ecelbarger CA, Mitchell C, Bradford AD, et al. UT-A2: A 55 kDa urea transporter protein in thin descending limb of Henle's loop whose abundance is regulated by vasopressin. Am J Physiol 2000;278:F52–62.
[91] Mejia R, Wade JB. Immunomorphometric study of rat renal inner medulla. Am J Physiol Renal Physiol 2002;282:F553–7.
[92] Burg MB, Green N. Function of the thick ascending limb of Henle's loop. Am J Physiol 1973;224:659–68.
[93] Horster M. Loop of Henle functional differentiation: *in vitro* perfusion of the isolated thick ascending segment. Pfluegers Arch 1978;378:15–24.
[94] Rocha AS, Kokko JP. Sodium chloride and water transport in the medullary thick ascending limb of Henle. Evidence for active chloride transport. J Clin Invest 1973;52:612–23.

[95] Garg LC, Mackie S, Tisher CC. Effect of low potassium-diet on Na-K-ATPase in rat nephron segments. Pfluegers Arch 1982;394:113–7.
[96] Morel F, Imbert-Teboul M, Chabardes D. Distribution of hormone-dependent adenylate cyclase in the nephron and its physiologic significance. Annual Rev Physiol 1981;43:569–81.
[97] Wittner M, Di Stefano A, Mandon B, Roinel N, de Rouffignac C. Stimulation of NaCl reabsorption by antidiuretic hormone in the cortical thick ascending limb of Henle's loop of the mouse. Pfluegers Arch 1991;419:212–4.
[98] Knepper MA. Urea transport in isolated thick ascending limbs and collecting ducts from rats. Am J Physiol 1983;245:F634–9.
[99] Rocha AS, Kokko JP. Permeability of medullary nephron segments to urea and water: effect of vasopressin. Kidney Int 1974;6:379–87.
[100] Grantham JJ, Burg MB. Effect of vasopressin and cyclic AMP on permeability of isolated collecting tubules. Am J Physiol 1966;211:255–9.
[101] Reif MC, Troutman SL, Schafer JA. Sustained response to vasopressin in isolated rat cortical collecting tubule. Kidney Int 1984;26:725–32.
[102] Sands JM, Nonoguchi H, Knepper MA. Vasopressin effects on urea and H_2O transport in inner medullary collecting duct subsegments. Am J Physiol 1987;253:F823–32.
[103] Badr KF. Kidney and endocrine system. Part1: eicosanoids. In: Massry SG, Glassock RJ, editors. Book of nephrology. 3rd ed. Baltimore: Williams and Wilkins Co.; 1995. p. 182–91.
[104] Sands JM, Knepper MA. Urea permeability of mammalian inner medullary collecting duct system and papillary surface epithelium. J Clin Invest 1987;79:138–47.
[105] Grantham JJ, Burg MB, Orloff J. The nature of transtubular Na and K transport in isolated rabbit renal collecting tubules. J Clin Invest 1970;49:1815–26.
[106] Tomita K, Pisano JJ, Knepper MA. Control of sodium and potassium transport in the cortical collecting duct of the rat. Effects of bradykinin, vasopressin, and deoxycorticosterone. J Clin Invest 1985;76:132–6.
[107] Palmer LG, Frindt G. Amiloride-sensitive Na channels from the apical membrane of the rat cortical collecting tubule. Proc Natl Acad Sci USA 1986;83:2767–70.
[108] Hanley MJ, Kokko JP. Study of chloride transport across the rabbit cortical collecting tubule. J Clin Invest 1978;62:39–44.
[109] Tomita K, Pisano JJ, Burg MB, Knepper MA. Effects of vasopressin and bradykinin on anion transport by the rat cortical collecting duct. Evidence for an electroneutral sodium chloride transport pathway. J Clin Invest 1986;77:136–41.
[110] Horster MF, Zink H. Functional differentiation of the medullary collecting tubule: influence of vasopressin. Kidney Int 1982;22:360–5.
[111] Madsen KM, Tisher CC. Structural–functional relationship along the distal nephron. Am J Physiol 1986;250:F1–15.
[112] Clapp WL, Madsen KM, Verlander JW, Tisher CC. Intercalated cells of the rat inner medullary collecting duct. Kidney Int 1987;31:1080–7.
[113] Clapp WL, Madsen KM, Verlander JW, Tisher CC. Morphologic heterogeneity along the rat inner medullary collecting duct. Lab Invest 1989;60:219–30.
[114] Kato A, Naruse M, Knepper MA, Sands JM. Long-term regulation of inner medullary collecting duct urea transport in rat. J Am Soc Nephrol 1998;9:737–45.
[115] Kato A, Sands JM. Evidence for sodium-dependent active urea secretion in the deepest subsegment of the rat inner medullary collecting duct. J Clin Invest 1998;101:423–8.
[116] Imai M, Taniguchi J, Yoshitomi K. Osmotic work across inner medullary collecting duct accomplished by difference in reflection coefficients for urea and NaCl. Pfluegers Arch 1988;412:557–67.
[117] Sands JM, Naruse M, Jacobs JD, Wilcox JN, Klein JD. Changes in aquaporin-2 protein contribute to the urine concentrating defect in rats fed a low-protein diet. J Clin Invest 1996;97:2807–14.
[118] Isozaki T, Verlander JW, Sands JM. Low protein diet alters urea transport and cell structure in rat initial inner medullary collecting duct. J Clin Invest 1993;92:2448–57.
[119] Gillin AG, Sands JM. Characteristics of osmolarity-stimulated urea transport in rat IMCD. Am J Physiol 1992;262:F1061–7.
[120] Kondo Y, Imai M. Effects of glutaraldehyde fixation on renal tubular function. I. Preservation of vasopressin-stimulated water and urea pathways in rat papillary collecting duct. Pfluegers Arch 1987;408:479–83.
[121] Sands JM, Schrader DC. An independent effect of osmolality on urea transport in rat terminal IMCDs. J Clin Invest 1991;88:137–42.
[122] Knepper MA, Sands JM, Chou C-L. Independence of urea and water transport in rat inner medullary collecting duct. Am J Physiol 1989;256:F610–21.
[123] Rocha AS, Kudo LH. Water, urea, sodium, chloride, and potassium transport in the *in vitro* perfused papillary collecting duct. Kidney Int 1982;22:485–91.
[124] Sands JM, Nonoguchi H, Knepper MA. Hormone effects on NaCl permeability of rat inner medullary collecting duct subsegments. Am J Physiol 1988;255:F421–8.
[125] Ullrich KJ, Papavassiliou F. Sodium reabsorption in the papillary collecting ducts of rats. Pfluegers Arch 1979;379:49–52.
[126] Weinstein AM. A mathematical model of the inner medullary collecting duct of the rat: pathways for Na and K transport. Am J Physiol Renal Physiol 1998;274:F841–55.
[127] Packer RK, Sands JM, Knepper MA. Chloride and osmotic water permeabilities of isolated rabbit renal papillary surface epithelium. Am J Physiol 1989;257:F218–24.
[128] Reeves WB. Conductive properties of papillary surface epithelium. Am J Physiol 1994;266:F259–65.
[129] Sands JM, Ivy EJ, Beeuwkes III R. Transmembrane potential difference of renal papillary epithelial cells. Effect of urea and DDAVP. Am J Physiol 1985;248:F762–6.
[130] Smith HW. The fate of sodium and water in the renal tubules. Bull NY Acad Med 1959;35:293–316.
[131] Kriz W. Structural organization of the renal medulla: comparative and functional aspects. Am J Physiol Regul Integr Comp Physiol 1981;241:R3–16.
[132] Zhai XY, Fenton RA, Andreasen A, Thomsen JS, Christensen AE. Aquaporin-1 is not expressed in descending thin limbs of short-loop nephrons. J Am Soc Nephrol 2007;18:2937–44.
[133] Layton AT, Layton HE. A region-based mathematical model of the urine concentrating mechanism in the rat outer medulla. I. Formulation and base-case results. Am J Physiol Renal Physiol 2005;289:F1346–66.
[134] Zimmerhackl BL, Robertson CR, Jamison RL. The medullary microcirculation. Kidney Int 1987;31:641–7.
[135] Fenton RA, Moeller HB, Hoffert JD, Yu MJ, Nielsen S, Knepper MA. Acute regulation of aquaporin-2 phosphorylation at Ser-264 by vasopressin. PNAS 2008;105:3134–9.
[136] Hoffert JD, Fenton RA, Moeller HB, Simons B, Tchapyjnikov D, McDill BW, et al. Vasopressin-stimulated increase in phosphorylation at Ser269 potentiates plasma membrane retention of aquaporin-2. J Biol Chem 2008;283:24617–27.
[137] Hoffert JD, Pisitkun T, Wang G, Shen R-F, Knepper MA. Quantitative phosphoproteomics of vasopressin-sensitive renal cells: regulation of aquaporin-2 phosphorylation at two sites. Proc Natl Acad Sci USA 2006;103:7159–64.

[138] Hoffert JD, Pisitkun T, Wang GH, Shen RF, Knepper MA. Dynamics of aquaporin-2 serine-261 phosphorylation in response to short-term vasopressin treatment in collecting duct. Am J Physiol Renal Physiol 2007;292:F691–700.
[139] Wade JB, Stetson DL, Lewis SA. ADH action: evidence for a membrane shuttle mechanism. Annals NY Acad Sci 1981;372:106–17.
[140] Jamison RL, Buerkert J, Lacy FB. A micropuncture study of collecting tubule function in rats with hereditary diabetes insipidus. J Clin Invest 1971;50:2444–52.
[141] Kuhn W, Ryffel K. Herstellung konzentrierrter Lösungen aus verdünnten durch blosse Membranwirkung: ein Modellversuch zur Funktion der Niere. Hoppe-Seylers Z Physiol Chem 1942;276:145–78.
[142] Ullrich KJ, Schmidt-Nielsen B, O'Dell R, Pehling G, Gottschalk CW, Lassiter WE, et al. Micropuncture study of composition of proximal and distal tubular fluid in rat kidney. Am J Physiol 1963;204:527–31.
[143] Chou C-L, Knepper MA, Layton HE. Urinary concentrating mechanism: the role of the inner medulla. Semin Nephrol 1993;13:168–81.
[144] Fenton RA, Chou C-L, Stewart GS, Smith CP, Knepper MA. Urinary concentrating defect in mice with selective deletion of phloretin-sensitive urea transporters in the renal collecting duct. Proc Natl Acad Sci USA 2004;101:7469–74.
[145] Moore LC, Marsh DJ. How descending limb of Henle's loop permeability affects hypertonic urine formation. Am J Physiol 1980;239:F57–71.
[146] Wexler AS, Kalaba RE, Marsh DJ. Passive, one-dimensional countercurrent models do not simulate hypertonic urine formation. Am J Physiol 1987;253:F1020–30.
[147] Wexler AS, Kalaba RE, Marsh DJ. Three-dimensional anatomy and renal concentrating mechanism. I. Modelling results. Am J Physiol 1991;260:F368–83.
[148] Knepper MA, Chou C-L, Layton HE. How is urine concentrated by the renal inner medulla? Contrib Nephrol 1993;102:144–60.
[149] Jen JF, Stephenson JL. Externally driven countercurrent multiplication in a mathematical model of the urinary concentrating mechanism of the renal inner medulla. Bull Math Biol 1994;56:491–514.
[150] Knepper MA, Saidel GM, Hascall VC, Dwyer T. Concentration of solutes in the renal inner medulla: interstitial hyaluronan as a mechano-osmotic transducer. Am J Physiol Renal Physiol 2003;284:F433–46.
[151] Hervy S, Thomas SR. Inner medullary lactate production and urine-concentrating mechanism: a flat medullary model. Am J Physiol Renal Physiol 2003;284:F65–81.
[152] Thomas SR. Inner medullary lactate production and accumulation: a vasa recta model. Am J Physiol Renal Physiol 2000;279: F468–81.
[153] Layton AT, Pannabecker TL, Dantzler WH, Layton HE. Functional implications of the three-dimensional architecture of the rat renal inner medulla. Am J Physiol Renal Physiol 2010;298:F973–87.
[154] Hargitay B, Kuhn W. Das Multiplikationsprinzip als Grundlage der Harnkonzentrierung in der Niere. Z Elektrochem 1951;55:539–58.
[155] Vehaskari VM, Hering-Smith KS, Moskowitz DW, Weiner ID, Hamm LL. Effect of epidermal growth factor on sodium transport in the cortical collecting tubule. Am J Physiol 1989;256: F803–9.
[156] Morel F, Mylle M, Gottschalk CW. Tracer microinjection studies of effect of ADH on renal tubular diffusion of water. Am J Physiol 1965;209:179–87.
[157] Layton AT, Layton HE. A region-based mathematical model of the urine concentrating mechanism in the rat outer medulla. II. Parameter sensitivity and tubular inhomogeneity. Am J Physiol Renal Physiol 2005;289:F1367–81.
[158] Stephenson JL, Zhang Y, Eftekhari A, Tewarson RP. Electrolyte transport in a central core model of the renal medulla. Am J Physiol 1989;253:F982–97.
[159] Stephenson JL, Zhang Y, Tewarson RP. Electrolyte, urea, and water transport in a two-nephron central core model of the renal medulla. Am J Physiol 1989;257:F388–413.
[160] Wang X, Thomas SR, Wexler AS. Outer medullary anatomy and the urine concentrating mechanism. Am J Physiol 1998;274:F413–24.
[161] Macri P, Breton S, Marsolais M, Lapointe JY, Laprade R. Hypertonicity decreases basolateral K^+ and Cl^- conductances in rabbit proximal convoluted tubule. J Membr Biol 1997;155:229–37.
[162] Thomas SR, Wexler AS. Inner medullary external osmotic driving force in a 3D model of the renal concentrating mechanism. Am J Physiol 1995;269:F159–71.
[163] Holstein-Rathlou N-H, Marsh DJ. Oscillations of tubular pressure, flow, and distal chloride concentration in rats. Am J Physiol 1989;256:F1007–14.
[164] Reinking LN, Schmidt-Nielsen B. Peristaltic flow of urine in the renal papillary collecting ducts of hamsters. Kidney Int 1981;20:55–60.
[165] Epstein FH, Kleeman CR, Pursel S, Hendrikx A. The effect of feeding protein and urea on the renal concentrating process. J Clin Invest 1957;36:635–41.
[166] Gamble JL, McKhann CF, Butler AM, Tuthill E. An economy of water in renal function referable to urea. Am J Physiol 1934;109:139–54.
[167] Lever AF. The vasa recta and countercurrent multiplication. Acta Med Scand 1965;178:1–43.
[168] Niesel W, Röskenbleck H. Moglichkeiten der Konzentrierung von Stoffen biologischen Gegenstromsystemen. Pfluegers Arch 1963;276:555–67.
[169] Niesel W, Röskenbleck H. Konzentrierung von Lösungen unterschiedlicher Zusammensetzung durch alleinige Gegenstromdiffusion und Geggenstromosmose als möglicher Mechanismus der Harnkonzentrierung. Pfluegers Arch 1965;283:230–41.
[170] Niesel W, Röskenbleck H, Hanke P, Specht N, Heure L. Die gegenseitige Beeinflussung von Harnstoff, NaCl, KCl und Harnfluss bei der Bildung eines maximal konzentrierten Harns. Pfluegers Arch 1970;315:308–20.
[171] Pinter GG, Shohet JL. Origin of sodium concentration profile in the renal medulla. Nature 1963;200:955–8.
[172] Stephenson JL. Concentrating engines and the kidney. II. Multisolute central core systems. Biophys J 1973;13:546–67.
[173] Stephenson JL. Concentrating engines and the kidney. I. Central core model of the renal medulla. Biophys J 1973;13:512–45.
[174] Stephenson JL. Concentrating engines and the kidney. III. Canonical mass balance equation for multinephron models of the renal medulla. Biophys J 1976;16:1273–86.
[175] Stephenson JL. Concentrating engines and the kidney. IV. Mass balance in a single stage of a multistage model of the renal medulla. Math Biosci 1981;55:265–78.
[176] Jen JF, Wang H, Tewarson RP, Stephenson JL. Comparison of central core and radially separated models of renal inner medulla. Am J Physiol 1995;268:F693–7.
[177] Kellogg RB. Some singular perturbation problems in renal models. J Math Anal Appl 1987;128:214–40.
[178] Stephenson JL, Tewarson RP, Mejia R. Quantitative analysis of mass and energy balance in non-ideal models of the renal

counterflow system. Proc Natl Acad Sci USA 1974;71: 1618–22.
[179] Foster DM, Jacquez JA. Comparison using central core model of renal medulla of the rabbit and rat. Am J Physiol 1978;234: F402–14.
[180] Layton HE. Urea transport in a distributed loop model of the urine-concentrating mechanism. Am J Physiol 1990;258: F1110–24.
[181] Marcano M, Layton AT, Layton HE. Maximum urine concentrating capability in a mathematical model of the inner medulla of the rat kidney. Bull Math Biol 2010;72:314–39.
[182] Layton AT, Layton HE. An efficient numerical method for distributed-loop models of the urine concentrating mechanism. Math Biosci 2003;118:111–32.
[183] Layton HE, Pitman EB, Knepper MA. A dynamic numerical method for models of the urine concentrating mechanism. SIAM J Appl Math 1995;55:1390–418.
[184] Mejia R, Stephenson JL. Solution of a multinephron, multisolute model of the mammalian kidney by Newton and continuation methods. Math Biosci 1984;68:279–98.
[185] Tewarson RP, Wang H, Stephenson JL, Jen JF. Efficient computer algorithms for kidney modeling. Math Model Sci Comput 1993;1:164–71.
[186] Wexler AS, Marsh DJ. Numerical methods for three-dimensional models of the urine concentrating mechanism. Appl Math Comput 1991;45:219–40.
[187] Layton HE. Mathematical models of the mammalian urine concentrating mechanism. In: Layton HE, Weinstein AM, editors. Membrane transport and renal physiology. New York: Springer-Verlag; 2002. p. 233–72.
[188] Stephenson JL. Urinary concentration and dilution: models. In: Windhager EE, editor. Handbook of physiology: renal physiology. Bethesda: American Physiological Society; 1992. p. 1349–408.
[189] Stewart J, Luggen ME, Valtin H. A computer model of the renal countercurrent system. Kidney Int 1972;2:253–63.
[190] Stewart J, Valtin H. Computer simulation of osmotic gradient without active transport in renal inner medulla. Kidney Int 1972;2:264–70.
[191] Barrett GL, Packer JS, Davies JM. Sodium chloride, water and urea handling in the rat renal medulla: a computer simulation. Renal Physiol , Basel 1986;9:223–40.
[192] Chandhoke PS, Saidel GM. Mathematical model of mass transport throughout the kidney. Effects of nephron heterogeneity and tubular-vascular organization. Ann Biomed Eng 1981;9:263–301.
[193] Thomas SR. Cycles and separations in a model of the renal medulla. Am J Physiol Renal Physiol 1998;275:F671–90.
[194] Wang X, Wexler AS, Marsh DJ. The effect of solution non-ideality on membrane transport in three-dimensional models of the renal concentrating mechanism. Bull Math Biol 1994;56:515–46.
[195] Layton HE. Distribution of Henle's loops may enhance urine concentrating capability. Biophys J 1986;49:1033–40.
[196] Layton HE. Concentrating urine in the inner medulla of the kidney. Comments Theor Biol 1989;1:179–96.
[197] Layton HE. Distributed loops of Henle in a central core model of the renal medulla: where should the solute come out? Math Comput Modelling 1990;14:533–7.
[198] Wang XQ, Wexler AS. The effects of collecting duct active NaCl reabsorption and inner medulla anatomy on renal concentrating mechanism. Am J Physiol Renal, Fluid Electrolyte Physiol 1996;270:F900–11.
[199] Wexler AS, Kalaba RE, Marsh DJ. Three-dimensional anatomy and renal concentrating mechanism. II. Sensitivity results. Am J Physiol 1991;260:F384–94.
[200] Stephenson JL, Jen JF, Wang H, Tewarson RP. Convective uphill transport of NaCl from ascending thin limb of loop of Henle. Am J Physiol 1995;268:F680–92.
[201] Stephenson JL, Wang H, Tewarson RP. Effect of vasa recta flow on concentrating ability of models of renal inner medulla. Am J Physiol 1995;268:F698–709.
[202] Layton AT, Pannabecker TL, Dantzler WH, Layton HE. Hyperfiltration and inner stripe hypertrophy may explain findings by Gamble and co-workers. Am J Physiol Renal Physiol 2010;298:F962–72.
[203] Bankir L, Kriz W. Adaptation of the kidney to protein intake and to urine concentrating activity: similar consequences in health and CRF. Kidney Int 1995;47:7–24.
[204] Jamison RL. Micropuncture study of segments of thin loop of Henle in the rat. Am J Physiol 1968;215:236–42.
[205] Jamison RL, Bennett CM, Berliner RW. Countercurrent multiplication by the thin loops of Henle. Am J Physiol 1967;212:357–66.
[206] de Rouffignac C, Morel F. Micropuncture study of water, electrolytes and urea movements along the loop of Henle in *Psammomys*. J Clin Invest 1969;48:474–86.
[207] Bonventre JV, Lechene C. Renal medullary concentrating process: an integrative hypothesis. Am J Physiol 1980;239:F578–88.
[208] Lory P. Effectiveness of a salt transport cascade in the renal medulla: computer simulations. Am J Physiol 1987;252: F1095–102.
[209] Rabinowitz L. Discrepancy between experimental and theoretical urine-to-papilla osmotic gradient. J Appl Physiol 1970;29:389–90.
[210] Sanjana VF, Robertson CR, Jamison RL. Water extraction from the inner medullary collecting tubule system: a role for urea. Kidney Int 1976;10:139–48.
[211] Chandhoke PS, Saidel GM, Knepper MA. Role of inner medullary collecting duct NaC1 transport in urinary concentration. Am J Physiol 1985;18:F688–97.
[212] Schmidt-Nielsen B. Function of the pelvis. In: Kinne RKH, editor. Urinary concentrating mechanisms. Basel: Karger; 1990. p. 103–40.
[213] Schmidt-Nielsen B, Churchill M, Reinking LN. Occurrence of renal pelvic refluxes during rising urine flow rate in rats and hamsters. Kidney Int 1980;18:419–31.
[214] Schmidt-Nielsen B, Reinking LN. Morphometry and fluid reabsorption during peristaltic flow in hamster renal papillary collecting ducts. Kidney Int 1981;20:789–98.
[215] Schmidt-Nielsen B, Graves B. Changes in fluid compartments in hamster renal papilla due to peristalsis in the pelvic wall. Kidney Int 1982;22:613–25.
[216] Schmidt-Nielsen B. The renal pelvis. Kidney Int 1987;31:621–8.
[217] Chuang EL, Reineck HJ, Osgood RW, Kunau RT, Stein JH. Studies on the mechanism of reduced urinary osmolality after exposure of the renal papilla. J Clin Invest 1978;61:633–9.
[218] Oliver RE, Roy DR, Jamison RL. Urinary concentration in the papillary collecting duct of the rat. J Clin Invest 1982;69:157–64.
[219] Schütz W, Schnermann J. Pelvic urine composition as a determinant of inner medullary solute concentration and urine osmolality. Pfluegers Arch 1972;334:154–66.
[220] Bonventre JV, Karnovsky MJ, Lechene CP. Renal papillary epithelial morphology in antidiuresis and water diuresis. Am J Physiol 1978;235:F69–76.
[221] Bonventre JV, Roman RJ, Lechene C. Effect of urea concentration of pelvic fluid on renal concentrating ability. Am J Physiol 1980;239:F609–18.
[222] Reinking LN, Veale MC. Mechanical stimulation of renal pelvic wall peristalsis in the rat. Experientia 1984;40:540–1.

[223] Schmidt-Nielsen B, Graves B, MacDuffie H. Effect of peristaltic contractions of the renal papilla in hamsters, *Misocricetus auratus*. Bull MDIBL 1985;25:70–2.
[224] Bagnasco SM, Peng T, Nakayama Y, Sands JM. Differential expression of individual UT-A urea transporter isoforms in rat kidney. J Am Soc Nephrol 2000;11:1980–6.
[225] Ando Y, Jacobson HR, Breyer MD. Phorbol myristate acetate, dioctanoylglycerol, and phosphatidic acid inhibit the hydroosmotic effect of vasopressin on rabbit cortical collecting tubule. J Clin Invest 1987;80:590–3.
[226] Paxton WG, Runge M, Horaist C, Cohen C, Alexander RW, Bernstein KE. Immunohistochemical localization of rat angiotensin II AT_1 receptor. Am J Physiol Renal Physiol 1993;264:F989–95.
[227] Bargman J, Leonard SL, McNuly E, Robertson CR, Jamison RL. Examination of transepithelial exchange of water and solute in the rat renal pelvis. J Clin Invest 1984;74:1860–70.
[228] Lory P, Gilg A, Horster M. Renal countercurrent system: role of collecting duct convergence and pelvic urea predicted from a mathematical model. J Math Biol 1983;16:281–304.
[229] Marsh DJ, Martin CM. Lack of water or urea movement from pelvic urine to papilla in hydropenic hamsters. Miner Electrolyte Metab 1980;3:81–6.
[230] Schmidt-Nielsen B. The renal concentrating mechanism in insects and mammals: a new hypothesis involving hydrostatic pressures. Am J Physiol 1995;268:R1087–100.
[231] Yancey PH, Clark ME, Hand SC, Bowlus RD, Somero GN. Living with water stress: evolution of osmolyte systems. Science 1982;217:1214–22.
[232] Knepper MA, Rector Jr FC. Urinary concentration and dilution. In: Brenner BM, editor. The kidney. 5th ed. Philadelphia: W.B. Saunders Co.; 1996. p. 532–70.
[233] Burg MB. Role of aldose reductase and sorbitol in maintaining the medullary intracellular milieu. Kidney Int 1988;33:635–41.
[234] Burg MB, Kador PF. Sorbitol, osmoregulation, and the complications of diabetes. J Clin Invest 1988;81:635–40.
[235] Bagnasco SM, Balaban RS, Fales HM, Yang YM, Burg MB. Predominantly osmotically active organic solutes in rat and rabbit renal medullas. J Biol Chem 1986;261:5872–7.
[236] Garcia-Perez A, Burg MB. Renal medullary organic osmolytes. Physiol Rev 1991;71:1081–115.
[237] Sands JM. Regulation of intracellular polyols and sugars in response to osmotic stress. In: Strange K, editor. Cellular and molecular physiology of cell volume regulation. 1st ed. Boca Raton, FL: CRC Press, Inc; 1994. p. 133–44.
[238] Yancey PH, Burg MB. Distribution of major organic osmolytes in rabbit kidneys in diuresis and antidiuresis. Am J Physiol 1989;257:F602–7.
[239] Yancey PH. Osmotic effectors in kidneys of xeric and mesic rodents: corticomedullary distribution and changes with water availability. J Comp Physiol B 1988;158:369–80.
[240] Yancey PH, Burg MB. Counteracting effects of urea and betaine in mammalian cells in culture. Am J Physiol 1990;258: R198–204.
[241] Yancey PH, Somero GN. Methylamine osmoregulatory solutes of elasmobranch fishes counteract urea inhibition of enzymes. J Exp Zool 1980;212:205–13.
[242] Crawford JD, Doyle AP, Probst H. Service of urea in renal water conservation. Am J Physiol 1959;196:545–8.
[243] Hendrikx A, Epstein FH. Effect of feeding protein and urea on renal concentrating ability in the rat. Am J Physiol 1958;195:539–42.
[244] Klahr S, Alleyne GAO. Effects of chronic protein-calorie malnutrition on the kidney. Kidney Int 1973;3:129–41.
[245] Levinsky NG, Berliner RW. The role of urea in the urine concentrating mechanism. J Clin Invest 1959;38:741–8.
[246] Peil AE, Stolte H, Schmidt-Nielsen B. Uncoupling of glomerular and tubular regulations of urea excretion in rat. Am J Physiol Renal, Fluid Electrolyte Physiol 1990;258:F1666–74.
[247] Uchida S, Sohara E, Rai T, Ikawa M, Okabe M, Sasaki S. Impaired urea accumulation in the inner medulla of mice lacking the urea transporter UT-A2. Mol Cell Biol 2005;25:7357–63.
[248] Klein JD, Sands JM, Qian L, Wang X, Yang B. Upregulation of urea transporter UT-A2 and water channels AQP2 and AQP3 in mice lacking urea transporter UT-B. J Am Soc Nephrol 2004;15:1161–7.
[249] Yang B, Bankir L, Gillespie A, Epstein CJ, Verkman AS. Urea-selective concentrating defect in transgenic mice lacking urea transporter UT-B. J Biol Chem 2002;277:10633–7.
[250] Yang B, Verkman AS. Analysis of double knockout mice lacking aquaporin-1 and urea transporter UT-B. J Biol Chem 2002;277:36782–6.
[251] Jaenike JR. The influence of vasopressin on the permeability of the mammalian collecting duct to urea. J Clin Invest 1961;40:144–51.
[252] Morgan T. Permeability of the nephron to urea. In: Schmidt-Nielsen B, Kerr DWS, editors. Urea and the kidney. 1st ed. Amsterdam: Excerpta Medica Foundation; 1970. p. 186–92.
[253] Morgan T, Sakai F, Berliner RW. *In vitro* permeability of medullary collecting duct to water and urea. Am J Physiol 1968;214:574–81.
[254] Bagnasco SM. Gene structure of urea transporters. Am J Physiol Renal Physiol 2003;284:F3–10.
[255] Sands JM. Mammalian urea transporters. Annu Rev Physiol 2003;65:543–66.
[256] Sands JM. Molecular mechanisms of urea transport. J Membr Biol 2003;191:149–63.
[257] Sands JM. Renal urea transporters. Curr Opin Nephrol Hypertens 2004;13:525–32.
[258] Shayakul C, Hediger MA. The SLC14 gene family of urea transporters. Pfluegers Arch 2004;447:603–9.
[259] Stewart GS, Graham C, Cattell S, Smith TPL, Simmons NL, Smith CP. UT-B is expressed in bovine rumen: potential role in ruminal urea transport. Am J Physiol Regul Integr Comp Physiol 2005;289:R605–12.
[260] Sands JM, Layton HE. The urine concentrating mechanism and urea transporters. In: Alpern RJ, Hebert SC, editors. The kidney: physiology and pathophysiology. 4th ed. San Diego: Academic Press; 2008. p. 1143–78.
[261] Nakayama Y, Naruse M, Karakashian A, Peng T, Sands JM, Bagnasco SM. Cloning of the rat Slc14a2 gene and genomic organization of the UT-A urea transporter. Biochim Biophys Acta 2001;1518:19–26.
[262] Bagnasco SM, Peng T, Janech MG, Karakashian A, Sands JM. Cloning and characterization of the human urea transporter UT-A1 and mapping of the human *Slc14a2* gene. Am J Physiol Renal Physiol 2001;281:F400–6.
[263] Fenton RA, Cottingham CA, Stewart GS, Howorth A, Hewitt JA, Smith CP. Structure and characterization of the mouse UT-A gene (*Slc14a2*). Am J Physiol Renal Physiol 2002;282:F630–8.
[264] Fenton RA, Shodeinde A, Knepper MA. UT-A urea transporter promoter, UT-Aalpha, targets principal cells of the renal inner medullary collecting duct. Am J Physiol Renal Physiol 2006;290:F188–95.
[265] Nakayama Y, Peng T, Sands JM, Bagnasco SM. The TonE/TonEBP pathway mediates tonicity-responsive regulation of UT-A urea transporter expression. J Biol Chem 2000;275:38275–80.
[266] Peng T, Sands JM, Bagnasco SM. Glucocorticoids inhibit transcription and expression of the rat UT-A urea transporter gene. Am J Physiol Renal Physiol 2002;282:F853–8.

[267] Kim Y-H, Kim D-U, Han K-H, Jung JY, Sands JM, Knepper MA, et al. Expression of urea transporters in the developing rat kidney. Am J Physiol Renal Physiol 2002;282:F530–40.
[268] Nielsen S, Terris J, Smith CP, Hediger MA, Ecelbarger CA, Knepper MA. Cellular and subcellular localization of the vasopressin-regulated urea transporter in rat kidney. Proc Natl Acad Sci USA 1996;93:5495–500.
[269] Fenton RA, Stewart GS, Carpenter B, Howorth A, Potter EA, Cooper GJ, et al. Characterization of the mouse urea transporters UT-A1 and UT-A2. Am J Physiol Renal Physiol 2002;283: F817–25.
[270] Promeneur D, Rousselet G, Bankir L, Bailly P, Cartron JP, Ripoche P, et al. Evidence for distinct vascular and tubular urea transporters in the rat kidney. J Am Soc Nephrol 1996;7:852–60.
[271] Shayakul C, Steel A, Hediger MA. Molecular cloning and characterization of the vasopressin-regulated urea transporter of rat kidney collecting ducts. J Clin Invest 1996;98:2580–7.
[272] Chen G, Fröhlich O, Yang Y, Klein JD, Sands JM. Loss of N-linked glycosylation reduces urea transporter UT-A1 response to vasopressin. J Biol Chem 2006;281:27436–42.
[273] Fröhlich O, Klein JD, Smith PM, Sands JM, Gunn RB. Urea transport in MDCK cells that are stably transfected with UT-A1. Am J Physiol Cell Physiol 2004;286:C1264–70.
[274] Fröhlich O, Klein JD, Smith PM, Sands JM, Gunn RB. Regulation of UT-A1-mediated transepithelial urea flux in MDCK cells. Am J Physiol Cell Physiol 2006;291:C600–6.
[275] Klein JD, Blount MA, Fröhlich O, Denson CE, Tan X, Sim JH, et al. Phosphorylation of UT-A1 on serine 486 correlates with membrane accumulation and urea transport activity in both rat IMCDs and cultured cells. Am J Physiol Renal Physiol 2010;298:F935–40.
[276] Bradford AD, Terris J, Ecelbarger CA, Klein JD, Sands JM, Chou CL, et al. 97 and 117 kDa forms of the collecting duct urea transporter UT-A1 are due to different states of glycosylation. Am J Physiol Renal Physiol 2001;281:F133–43.
[277] Sands JM. Urea transport: it's not just "freely diffusible" anymore. NIPS 1999;14:46–7.
[278] Sands JM, Flores FX, Kato A, Baum MA, Brown EM, Ward DT, et al. Vasopressin-elicited water and urea permeabilities are altered in the inner medullary collecting duct in hypercalcemic rats. Am J Physiol Renal Physiol 1998;274:F978–85.
[279] Karakashian A, Timmer RT, Klein JD, Gunn RB, Sands JM, Bagnasco SM. Cloning and characterization of two new mRNA isoforms of the rat renal urea transporter: UT-A3 and UT-A4. J Am Soc Nephrol 1999;10:230–7.
[280] Terris JM, Knepper MA, Wade JB. UT-A3: localization and characterization of an additional urea transporter isoform in the IMCD. Am J Physiol Renal Physiol 2001;280:F325–32.
[281] Stewart GS, Fenton RA, Wang W, Kwon TH, White SJ, Collins VM, et al. The basolateral expression of mUT-A3 in the mouse kidney. Am J Physiol Renal Physiol 2004;286:F979–87.
[282] Stewart GS, King SL, Potter EA, Smith CP. Acute regulation of the urea transporter mUT-A3 expressed in a MDCK cell line. Am J Physiol Renal Physiol 2007;292:F1157–63.
[283] Blount MA, Klein JD, Martin CF, Tchapyjnikov D, Sands JM. Forskolin stimulates phosphorylation and membrane accumulation of UT-A3. Am J Physiol Renal Physiol 2007;293: F1308–13.
[284] Smith CP, Potter EA, Fenton RA, Stewart GS. Characterization of a human colonic cDNA encoding a structurally novel urea transporter, UT-A6. Am J Physiol Cell Physiol 2004;287: C1087–93.
[285] Shayakul C, Tsukaguchi H, Berger UV, Hediger MA. Molecular characterization of a novel urea transporter from kidney inner medullary collecting ducts. Am J Physiol Renal Physiol 2001;280:F487–94.
[286] You G, Smith CP, Kanai Y, Lee W-S, Stelzner M, Hediger MA. Cloning and characterization of the vasopressin-regulated urea transporter. Nature 1993;365:844–7.
[287] Ashkar ZM, Martial S, Isozaki T, Price SR, Sands JM. Urea transport in initial IMCD of rats fed a low-protein diet: functional properties and mRNA abundance. Am J Physiol 1995;268:F1218–23.
[288] Shayakul C, Knepper MA, Smith CP, DiGiovanni SR, Hediger MA. Segmental localization of urea transporter mRNAs in rat kidney. Am J Physiol 1997;272:F654–60.
[289] Smith CP, Lee W-S, Martial S, Knepper MA, You G, Sands JM, et al. Cloning and regulation of expression of the rat kidney urea transporter (rUT2). J Clin Invest 1995;96: 1556–63.
[290] Fenton RA, Howorth A, Cooper GJ, Meccariello R, Morris ID, Smith CP. Molecular characterization of a novel UT-A urea transporter isoform (UT-A5) in testis. Am J Physiol Cell Physiol 2000;279:C1425–31.
[291] Olives B, Neau P, Bailly P, Hediger MA, Rousselet G, Cartron JP, et al. Cloning and functional expression of a urea transporter from human bone marrow cells. J Biol Chem 1994;269:31649–52.
[292] Couriaud C, Ripoche P, Rousselet G. Cloning and functional characterization of a rat urea transporter: expression in the brain. Biochim Biophys Acta Gene Struct Expression 1996;1309:197–9.
[293] Sands JM, Timmer RT, Gunn RB. Urea transporters in kidney and erythrocytes. Am J Physiol 1997;273:F321–39.
[294] Tsukaguchi H, Shayakul C, Berger UV, Tokui T, Brown D, Hediger MA. Cloning and characterization of the urea transporter UT3. Localization in rat kidney and testis. J Clin Invest 1997;99:1506–15.
[295] Lucien N, Sidoux-Walter F, Olivès B, Moulds J, Le Pennec PY, Cartron JP, et al. Characterization of the gene encoding the human Kidd blood group urea transporter protein: evidence for splice site mutations in Jk_{null} individuals. J Biol Chem 1998;273:12973–80.
[296] Lucien N, Sidoux-Walter F, Roudier N, Ripoche P, Huet M, Trin-Trang-Tan MM, et al. Antigenic and functional properties of the human red blood cell urea transporter hUT-B1. J Biol Chem 2002;277:34101–8.
[297] Olivès B, Martial S, Mattei MG, Matassi G, Rousselet G, Ripoche P, et al. Molecular characterization of a new urea transporter in the human kidney. FEBS Lett 1996;386:156–60.
[298] Olivès B, Mattei M-G, Huet M, Neau P, Martial S, Cartron JP, et al. Kidd blood group and urea transport function of human erythrocytes are carried by the same protein. J Biol Chem 1995;270:15607–10.
[299] Sidoux-Walter F, Lucien N, Nissinen R, Sistonen P, Henry S, Moulds J, et al. Molecular heterogeneity of the Jk_{null} phenotype: expression analysis of the Jk(S291P) mutation found in Finns. Blood 2000;96:1566–73.
[300] Kimoto Y, Constantinou CE. Effects of [1-desamino-8-D-arginine]vasopressin and papaverine on rabbit renal pelvis. Eur J Pharmacol 1990;175:359–62.
[301] Timmer RT, Klein JD, Bagnasco SM, Doran JJ, Verlander JW, Gunn RB, et al. Localization of the urea transporter UT-B protein in human and rat erythrocytes and tissues. Am J Physiol Cell Physiol 2001;281:C1318–25.
[302] Trinh-Trang-Tan M-M, Bouby N, Kriz W, Bankir L. Functional adaptation of thick ascending limb and internephron heterogeneity to urine concentration. Kidney Int 1987;31:549–55.

[303] Hu MC, Bankir L, Michelet S, Rousselet G, Trinh-Trang-Tan M-M. Massive reduction of urea transporters in remnant kidney and brain of uremic rats. Kidney Int 2000;58:1202–10.
[304] Pallone TL. Characterization of the urea transporter in outer medullary descending vasa recta. Am J Physiol 1994;267: R260–7.
[305] Pallone TL, Nielsen S, Silldorff EP, Yang S. Diffusive transport of solute in the rat medullary microcirculation. Am J Physiol Renal,Fluid Electrolyte Physiol 1995;269:F55–63.
[306] Xu Y, Olives B, Bailly P, Fischer E, Ripoche P, Ronco P, et al. Endothelial cells of the kidney vasa recta express the urea transporter HUT11. Kidney Int 1997;51:138–46.
[307] Sidoux-Walter F, Lucien N, Olivès B, Gobin R, Rousselet G, Kamsteeg EJ, et al. At physiological expression levels the Kidd blood group/urea transporter protein is not a water channel. J Biol Chem 1999;274:30228–35.
[308] Yang BX, Verkman AS. Urea transporter UT3 functions as an efficient water channel: direct evidence for a common water/urea pathway. J Biol Chem 1998;273:9369–72.
[309] Nielsen S, Knepper MA. Vasopressin activates collecting duct urea transporters and water channels by distinct physical processes. Am J Physiol Renal,Fluid Electrolyte Physiol 1993;265: F204–13.
[310] Star RA, Nonoguchi H, Balaban R, Knepper MA. Calcium and cyclic adenosine monophosphate as second messengers for vasopressin in the rat inner medullary collecting duct. J Clin Invest 1988;81:1879–88.
[311] Wall SM, Suk Han J, Chou C-L, Knepper MA. Kinetics of urea and water permeability activation by vasopressin in rat terminal IMCD. Am J Physiol Renal Fluid Electrolyte Physiol 1992;262:F989–98.
[312] Chou C-L, DiGiovanni SR, Luther A, Lolait SJ, Knepper MA. Oxytocin as an antidiuretic hormone. II. Role of V_2 vasopressin receptor. Am J Physiol Renal Fluid Electrolyte Physiol 1995;269:F78–85.
[313] Star RA. Apical membrane limits urea permeation across the rat inner medullary collecting duct. J Clin Invest 1990;86:1172–8.
[314] Chou C-L, Knepper MA. Inhibition of urea transport in inner medullary collecting duct by phloretin and urea analogues. Am J Physiol 1989;257:F359–65.
[315] Nonoguchi H, Owada A, Kobayashi N, Takayama M, Terada Y, Koike J, et al. Immunohistochemical localization of V_2 vasopressin receptor along the nephron and functional role of luminal V_2 receptor in terminal inner medullary collecting ducts. J Clin Invest 1995;96:1768–78.
[316] Zhang C, Sands JM, Klein JD. Vasopressin rapidly increases the phosphorylation of the UT-A1 urea transporter activity in rat IMCDs through PKA. Am J Physiol Renal Physiol 2002;282: F85–90.
[317] Bansal AD, Hoffert JD, Pisitkun T, Hwang S, Chou CL, Boja ES, et al. Phosphoproteomic profiling reveals vasopressin-regulated phosphorylation sites in collecting duct. J Am Soc Nephrol 2010;21:303–15.
[318] Brooks HL, Ageloff S, Kwon TH, Brandt W, Terris JM, Seth A, et al. cDNA array identification of genes regulated in rat renal medulla in response to vasopressin infusion. Am J Physiol Renal Physiol 2003;284:F218–28.
[319] Hoorn EJ, Hoffert JD, Knepper MA. Combined proteomics and pathways analysis of collecting duct reveals a protein regulatory network activated in vasopressin escape. J Am Soc Nephrol 2005;16:2852–63.
[320] Uawithya P, Pisitkun T, Ruttenberg BE, Knepper MA. Transcriptional profiling of native inner medullary collecting duct cells from rat kidney. Physiol Genomics 2008;32:229–53.
[321] Yu MJ, Pisitkun T, Wang G, Aranda JF, Gonzales PA, Tchapyjnikov D, et al. Large-scale quantitative LC-MS/MS analysis of detergent-resistant membrane proteins from rat renal collecting duct. Am J Physiol Cell Physiol 2008;295: C661–78.
[322] Yu MJ, Pisitkun T, Wang G, Shen RF, Knepper MA. LC-MS/MS analysis of apical and basolateral plasma membranes of rat renal collecting duct cells. Mol Cell Proteomics 2006;5:2131–45.
[323] Bos JL. Epac: a new cAMP target and new avenues in cAMP research. Nat Rev Mol Cell Biol 2003;4:733–8.
[324] Helms MN, Chen X-J, Ramosevac S, Eaton DC, Jain L. Dopamine regulation of amiloride-sensitive sodium channels in lung cells. Am J Physiol Lung Cell Mol Physiol 2006;291: L610–8.
[325] Honegger KJ, Capuano P, Winter C, Bacic D, Stange G, Wagner CA, et al. Regulation of sodium-proton exchanger isoform 3 (NHE3) by PKA and exchange protein directly activated by cAMP (EPAC). Proc Natl Acad Sci USA 2006;103:803–8.
[326] Laroche-Joubert N, Marsy S, Michelet S, Imbert-Teboul M, Doucet A. Protein kinase A-independent activation of ERK and H,K-ATPase by cAMP in native kidney cells. Role of Epac I. J Biol Chem 2002;277:18598–604.
[327] Li Y, Konings IBM, Zhao J, Price LS, de Heer E, Deen PMT. Renal expression of exchange protein directly activated by cAMP (Epac) 1 and 2. Am J Physiol Renal Physiol 2008;295: F525–33.
[328] Yip KP. Epac-mediated Ca^{2+} mobilization and exocytosis in inner medullary collecting duct. Am J Physiol Renal Physiol 2008;291:F882–90.
[329] Wang Y, Klein JD, Blount MA, et al. Epac regulation of the UT-A1 urea transporter in rat IMCDs. J Am Soc Nephrol 2009;20:2018–24.
[330] Blount MA, Mistry AC, Fröhlich O, Price SR, Chen G, Sands JM, et al. Phosphorylation of UT-A1 urea transporter at serines 486 and 499 is important for vasopressin-regulated activity and membrane accumulation. Am J Physiol Renal Physiol 2008;295:F295–9.
[331] Hwang S, Gunaratne R, Rinschen MM, Yu MJ, Pisitkun T, Hoffert JD, et al. Vasporessin increases phosphorylation of ser84 and ser486 in Slc14a2 collecting duct urea transporters. Am J Physiol Renal Physiol 2010;299:F559–67.
[332] Mistry AC, Mallick R, Klein JD, Sands JM, Froehlich O. Functional characterization of the central hydrophilic linker region of the urea transporter UT-A1: cAMP activation and snapin binding. Am J Physiol Cell Physiol 2010;298: C1431–7.
[333] Klein JD, Fröhlich O, Blount MA, Martin CF, Smith TD, Sands JM. Vasopressin increases plasma membrane accumulation of urea transporter UT-A1 in rat inner medullary collecting ducts. J Am Soc Nephrol 2006;17:2680–6.
[334] Inoue T, Terris J, Ecelbarger CA, Chou C-L, Nielsen S, Knepper MA. Vasopressin regulates apical targeting of aquaporin-2 but not of UT1 urea transporter in renal collecting duct. Am J Physiol 1999;276:F559–66.
[335] Cotte N, Balestre MN, Phalipou S, Hibert M, Manning M, Barberis C, et al. Identification of residues responsible for the selective binding of peptide antagonists and agonists in the V2 vasopressin receptor. J Biol Chem 1998;273:29462–8.
[336] Kim D-U, Sands JM, Klein JD. Changes in renal medullary transport proteins during uncontrolled diabetes mellitus in rats. Am J Physiol Renal Physiol 2003;285:F303–9.
[337] Seamon KB, Padgett W, Daly JW. Forskolin: unique diterpene activator of adenylate cyclase in membranes and intact cells. Proc Natl Acad Sci USA 1981;87:3363–7.

[338] Stewart GS, Thistlethwaite A, Lees H, Cooper GJ, Smith C. Vasopressin regulation of the renal UT-A3 urea transporter. Am J Physiol Renal Physiol 2009;296:F642–9.
[339] Mistry AC, Mallick R, Fröhlich O, Klein JD, Rehm A, Chen G, et al. The UT-A1 urea transporter interacts with snapin, a snare-associated protein. J Biol Chem 2007;282:30097–106.
[340] Feng X, Huang H, Yang Y, Fröhlich O, Klein JD, Sands JM, et al. Caveolin-1 directly interacts with UT-A1 urea transporter: the role of caveolae/lipid rafts in UT-A1 regulation at the cell membrane. Am J Physiol Renal Physiol 2009;296:F1514–20.
[341] Chen G, Huang H, Fröhlich O, Yang Y, Klein JD, Price SR, et al. MDM2 E3 ubiquitin ligase mediates UT-A1 urea transporter ubiquitination and degradation. Am J Physiol Renal Physiol 2008;295:F1528–34.
[342] Stewart GS, O'Brien JH, Smith CP. Ubiquitination regulates the plasma membrane expression of renal UT-A urea transporters. Am J Physiol Cell Physiol 2008;295:C121–9.
[343] Kudo LH, César KR, Ping WC, Rocha AS. Effect of peritubular hypertonicity on water and urea transport of inner medullary collecting duct. Am J Physiol Renal Fluid Electrolyte Physiol 1992;262:F338–47.
[344] Chou C-L, Sands JM, Nonoguchi H, Knepper MA. Concentration dependence of urea and thiourea transport pathway in rat inner medullary collecting duct. Am J Physiol 1990;258:F486–94.
[345] Gillin AG, Star RA, Sands JM. Osmolarity-stimulated urea transport in rat terminal IMCD: role of intracellular calcium. Am J Physiol 1993;265:F272–7.
[346] Kato A, Klein JD, Zhang C, Sands JM. Angiotensin II increases vasopressin-stimulated facilitated urea permeability in rat terminal IMCDs. Am J Physiol Renal Physiol 2000;279: F835–40.
[347] Blessing NW, Blount MA, Sands JM, Martin CF, Klein JD. Urea transporters UT-A1 and UT-A3 accumulate in the plasma membrane in response to increased hypertonicity. Am J Physiol Renal Physiol 2008;295:F1336–41.
[348] Leung DW, Loo DDF, Hirayama BA, Zeuthen T, Wright EM. Urea transport by co-transporters. J Physiol (Lond) 2000;528:251–7.
[349] Panayotova-Heiermann M, Wright EA. Mapping the urea channel through the rabbit Na^+-glucose co-transporter SGLT1. J Physiol (Lond) 2001;535:419–25.
[350] Kim D-U, Sands JM, Klein JD. Role of vasopressin in diabetes mellitus-induced changes in medullary transport proteins involved in urine concentration in Brattleboro rats. Am J Physiol Renal Physiol 2004;286:F760–6.
[351] Terris J, Ecelbarger CA, Sands JM, Knepper MA. Long-term regulation of collecting duct urea transporter proteins in rat. J Am Soc Nephrol 1998;9:729–36.
[352] Harrington AR, Valtin H. Impaired urinary concentration after vasopressin and its gradual correction in hypothalamic diabetes insipidus. J Clin Invest 1968;47:502–10.
[353] Igarashi P, Whyte DA, Nagami GT. Cloning and kidney cell-specific activity of the promoter of the murine renal Na-K-Cl co-transporter gene. J Biol Chem 1996;271:9666–74.
[354] Yasui M, Zelenin SM, Celsi G, Aperia A. Adenylate cyclase-coupled vasopressin receptor activates AQP2 promoter via a dual effect on CRE and AP1 elements. Am J Physiol Renal Physiol 1997;272:F443–50.
[355] Cadnapaphornchai MA, Summer SN, Falk S, Thurman JM, Knepper MA, Schrier RW. Effect of primary polydipsia on aquaporin and sodium transporter abundance. Am J Physiol Renal Physiol 2003;285:F965–71.
[356] Promeneur D, Bankir L, Hu MC, Trinh-Trang-Tan M-M. Renal tubular and vascular urea transporters: influence of antidiuretic hormone on messenger RNA expression in Brattleboro rats. J Am Soc Nephrol 1998;9:1359–66.
[357] Isozaki T, Gillin AG, Swanson CE, Sands JM. Protein restriction sequentially induces new urea transport processes in rat initial IMCDs. Am J Physiol 1994;266:F756–61.
[358] Kato A, Sands JM. Urea transport processes are induced in rat IMCD subsegments when urine concentrating ability is reduced. Am J Physiol 1999;276:F62–71.
[359] Hu MC, Bankir L, Trinh-Trang-Tan MM. mRNA expression of renal urea transporters in normal and Brattleboro rats: effect of dietary protein intake. Exp Nephrol 1999;7:44–51.
[360] Knepper MA, Danielson RA, Saidel GM, Johnston KH. Effects of dietary protein restriction and glucocorticoid administration on urea excretion in rats. Kidney Int 1975;8:303–15.
[361] Gertner R, Klein JD, Bailey JL, Kim DU, Luo XH, Bagnasco SM, et al. Aldosterone decreases UT-A1 urea transporter expression via the mineralocorticoid receptor. J Am Soc Nephrol 2004;15:558–65.
[362] Naruse M, Klein JD, Ashkar ZM, Jacobs JD, Sands JM. Glucocorticoids downregulate the rat vasopressin-regulated urea transporter in rat terminal inner medullary collecting ducts. J Am Soc Nephrol 1997;8:517–23.
[363] Wang X-Y, Beutler K, Nielsen J, Nielsen S, Knepper MA, Masilamani S. Decreased abundance of collecting duct urea transporters UT-A1 and UT-A3 with ECF volume expansion. Am J Physiol Renal Physiol 2002;282:F577–84.
[364] Fenton RA, Chou C-L, Ageloff S, Brandt W, Stokes III JB, Knepper M. Increased collecting duct urea transporter expression in Dahl salt-sensitive rats. Am J Physiol Renal Physiol 2003;285:F143–51.
[365] Brooks DD, Nutting DF, Crofton JT, Share L. Vasopressin in rats with genetic and streptozotocin-induced diabetes. Diabetes 1989;38:54–7.
[366] Mitch WE, Bailey JL, Wang X, Jurkovitz C, Newby DN, Price SR. Evaluation of signals activating ubiquitin-proteasome proteolysis in a model of muscle wasting. Am J Physiol Cell Physiol 1999;276:C1132–8.
[367] Trinder D, Phillips PA, Stephenson JM, Risvanis J, Aminian A, Adam W, et al. Vasopressin V_1 and V_2 receptors in diabetes mellitus. Am J Physiol Endocrinol Metab 1994;266:E217–23.
[368] Klein JD, Price SR, Bailey JL, Jacobs JD, Sands JM. Glucocorticoids mediate a decrease in the AVP-regulated urea transporter in diabetic rat inner medulla. Am J Physiol 1997;273:F949–53.
[369] Bardoux P, Ahloulay M, Le Maout S, Bankir L, Trinh-Trang-Tan MM. Aquaporin-2 and urea transporter-A1 are up-regulated in rats with type I diabetes mellitus. Diabetologia 2001;44:637–45.
[370] Blount MA, Sands JM, Kent KJ, Smith TD, Price SR, Klein JD. Candesartan augments compensatory changes in medullary transport proteins in the diabetic rat kidney. Am J Physiol Renal Physiol 2008;285:F1448–52.
[371] Klein JD, Kozlowski SD, Abi Antooun T, Sands JM. Adrenalectomy blocks the compensatory increases in UT-A1 and AQP2 in diabetic rat kidney. J Membr Biol 2006;212 (2):139–44.
[372] Pech V, Klein JD, Kozlowski SD, Wall SM, Sands JM. Vasopressin increases urea permeability in initial IMCDs from diabetic rats. Am J Physiol Renal Physiol 2005;289:F531–5.
[373] Van Zwieten PA, Kam KL, ijl AJ, Hendriks MGC, Beenen OHM, Pfaffendorf M. Hypertensive diabetic rats in pharmacological studies. Pharmacol Res 1996;33:95–105.
[374] Bickel CA, Knepper MA, Verbalis JG, Ecelbarger CA. Dysregulation of renal salt and water transport proteins in diabetic Zucker rats. Kidney Int 2002;61:2099–110.

[375] Klein JD, Murrell BP, Tucker S, Kim Y-H, Sands JM. Urea transporter UT-A1 and aquaporin-2 proteins decrease in response to angiotensin II or norepinephrine-induced acute hypertension. Am J Physiol Renal Physiol 2006;291:F952–9.

[376] Esther Jr CR, Marrero MB, Howard TE, Machaud A, Corvol P, Capecchi MR, et al. The critical role of tissue angiotensin-converting enzyme as revealed by gene targeting in mice. J Clin Invset 1997;99:2375–85.

[377] Klein JD, Quach DL, Cole JM, Disher K, Mongiu AK, Wang X, et al. Impaired urine concentration and the absence of tissue ACE: the involvement of medullary transport proteins. Am J Physiol Renal Physiol 2002;283:F517–24.

[378] Berl T. On the adaptation of renal cells to hypertonicity. Am J Kidney Dis 2000;35:XLVII–L.

[379] Tian W, Cohen DM. Signaling and gene regulation by urea in cells of the mammalian kidney medulla. Comp Biochem Physiol A 2001;130:429–36.

[380] Kim D-U, Klein JD, Racine S, Murrell BP, Sands JM. Urea may regulate urea transporter protein abundance during osmotic diuresis. Am J Physiol Renal Physiol 2005;288:F188–97.

[381] Lam AK, Ko BC, Tam S, Morris R, Yang JY, Chung SK, et al. Osmotic response element-binding protein (OREBP) is an essential regulator of the urine concentrating mechanism. J Biol Chem 2004;279:48048–54.

[382] Leroy C, Basset G, Gruel G, Ripoche P, Trinh-Trang-Tan M-M, Rousselet G. Hyperosmotic NaCl and urea synergistically regulate the expression of the UT-A2 urea transporter *in vitro* and *in vivo*. Biochem Biophys Res Commun 2000;271:368–73.

[383] Lim SW, Han KH, Jung JY, Kim WY, Yang CW, Sands JM, et al. Ultrastructural localization of UT-A and UT-B in rat kidneys with different hydration status. Am J Physiol Regul Integr Comp Physiol 2006;290:R479–92.

[384] Kim YM, Kim WY, Lee HW, Kim J, Kwon HM, Klein JD, et al. Urea and NaCl regulate UT-A1 urea transporter in opposing directions via TonEBP pathway during osmotic diuresis. Am J Physiol Renal Physiol 2009;296:F67–77.

[385] Jeon US, Kim JA, Sheen MR, Kwon HM. How tonicity regulates genes: story of TonEBP transcriptional activator. Acta Physiol Scand 2006;187:241–7.

[386] Lam AKM, Ko BCB, Tam S, Morris R, Yang JY, Chung SK, et al. Osmotic response element-binding protein (OREBP) is an essential regulator of the urine concentrating mechanism. J Biol Chem 2004;279:48048–54.

[387] Yang JY, Tam WY, Tam S, Guo H, Wu X, Li G, et al. Genetic restoration of aldose reductase to the collecting tubules restores maturation of the urine concentrating mechanism. Am J Physiol Renal Physiol 2006;291:F186–95.

[388] Galla JH, Booker BB, Luke RG. Role of the loop segment in the urinary concentrating defect of hypercalcemia. Kidney Int 1986;29:977–82.

[389] Jung JY, Madsen KM, Han KH, Yang CW, Knepper MA, Sands JM, et al. Expression of urea transporters in potassium-depleted mouse kidney. Am J Physiol Renal Physiol 2003;285:F1210–24.

[390] Levi M, Peterson L, Berl T. Mechanism of concentrating defect in hypercalcemia. Role of polydipsia and prostaglandins. Kidney Int 1983;23:489–97.

[391] Sands JM, Naruse M, Baum M, Jo I, Hebert SC, Brown EM, et al. An apical extracellular calcium/polyvalent cation-sensing receptor regulates vasopressin-elicited water permeability in rat kidney inner medullary collecting duct. J Clin Invest 1997;99:1399–405.

[392] Wang X, Harris PC, Somlo S, Batlle D, Torres VE. Effect of calcium-sensing receptor activation in models of autosomal recessive or dominant polycystic kidney disease. Nephrol Dial Transplant 2009;24:526–34.

[393] Jeon US, Han K-H, Park SH, Lee SD, Sheen MR, Jung JY, et al. Downregulation of renal TonEBP in hypokalemic rats. Am J Physiol Renal Physiol 2007;293:F408–15.

[394] Cadnapaphornchai MA, Kim Y-W, Gurevich AK, Summer SN, Falk S, Thurman JM, et al. Urinary concentrating defect in hypothyroid rats: role of sodium, potassium, 2-chloride co-transporter, and aquaporins. J Am Soc Nephrol 2003;14:566–74.

[395] Sands JM. Urine-concentrating ability in the aging kidney. Sci Aging Knowledge Environ 2003;:24 [pe15]

[396] Combet S, Teillet L, Geelen G, Pitrat B, Gobin R, Nielsen S, et al. Food restriction prevents age-related polyuria by vasopressin-dependent recruitment of aquaporin-2. Am J Physiol Renal Physiol 2001;281:F1123–31.

[397] Preisser L, Teillet L, Aliotti S, Gobin R, Berthonaud V, Chevalier J, et al. Downregulation of aquaporin-2 and-3 in aging kidney is independent of V_2 vasopressin receptor. Am J Physiol Renal Physiol 2000;279:F144–52.

[398] Trinh-Trang-Tan MM, Geelen G, Teillet L, Corman B. Urea transporter expression in aging kidney and brain during dehydration. Am J Physiol Regul Integr Comp Physiol 2003;285: R1355–65.

[399] Combet S, Geffroy N, Berthonaud V, Dick B, Teillet L, Verbavatz JM, et al. Correction of age-related polyuria by dDAVP: molecular analysis of aquaporins and urea transporters. Am J Physiol Renal Physiol 2003;284:F199–208.

[400] Zhang Y, Sands JM, Kohan DE, Nelson RD, Martin CF, Carlson NG, et al. Potential role of purinergic signaling in urinary concentration in inner medulla: insights from P2Y2 receptor gene knockout mice. Am J Physiol Renal Physiol 2008;295: F1715–24.

[401] Verkman AS, Yang BX, Song YL, Manley GT, Ma TH. Role of water channels in fluid transport studied by phenotype analysis of aquaporin knockout mice. Exp Physiol 2000;85:233S–41S.

[402] Li C, Klein JD, Wang W, Knepper MA, Nielsen S, Sands JM, et al. Altered expression of urea transporters in response to ureteral obstruction. Am J Physiol Renal Physiol 2004;286: F1154–62.

[403] Timmer RT, Sands JM. Lithium intoxication. J Am Soc Nephrol 1999;10:666–74.

[404] Christensen S, Kusano E, Yusufi ANK, Murayama N, Dousa TP. Pathogenesis of nephrogenic diabetes insipidus due to chronic administration of lithium in rats. J Clin Invest 1985;75:1869–79.

[405] Blount MA, Sim JH, Zhou R, Martin CF, Lu W, Sands JM, et al. The expression of transporters involved in urine concentration recover differently after ceasing lithium treatment. Am J Physiol Renal Physiol 2010;298:F601–8.

[406] Klein JD, Gunn RB, Roberts BR, Sands JM. Down-regulation of urea transporters in the renal inner medulla of lithium-fed rats. Kidney Int 2002;61:995–1002.

[407] Marples D, Christensen S, Christensen EI, Ottosen PD, Nielsen S. Lithium-induced downregulation of Aquaporin-2 water channel expression in rat kidney medulla. J Clin Invest 1995;95:1838–45.

[408] Okusa MD, Crystal LJT. Clinical manifestations and management of acute lithium intoxication. Am J Med 1994;97:383–9.

[409] Nielsen J, Hoffert JD, Knepper MA, Agre P, Nielsen S, Fenton RA. Proteomic analysis of lithium-induced nephrogenic diabetes insipidus: mechanisms for aquaporin 2 down-regulation and cellular proliferation. PNAS 2008;105:3634–9.

[410] Fröhlich O, Aggarwal D, Klein JD, Kent KJ, Yang Y, Gunn RB, et al. Stimulation of UT-A1-mediated transepithelial urea flux in MDCK cells by lithium. Am J Physiol Renal Physiol 2008;294:F518–24.

[411] Sands JM, Gargus JJ, Fröhlich O, Gunn RB, Kokko JP. Urinary concentrating ability in patients with Jk(a-b-) blood type who lack carrier-mediated urea transport. J Am Soc Nephrol 1992;2:1689–96.
[412] Bankir L, Chen K, Yang B. Lack of UT-B in vasa recta and red blood cells prevents urea-induced improvement of urinary concentrating ability. Am J Physiol Renal Physiol 2004;286: F144–51.
[413] Edwards A, Pallone TL. Facilitated transport in vasa recta: theoretical effects on solute exchange in the medullary microcirculation. Am J Physiol Renal Physiol 1997;272:F505–14.
[414] Edwards A, Pallone TL. A multiunit model of solute and water removal by inner medullary vasa recta. Am J Physiol Heart Circ Physiol 1998;274:H1202–10.
[415] Macey RI. Transport of water and urea in red blood cells. Am J Physiol 1984;246:C195–203.
[416] Macey RI, Yousef LW. Osmotic stability of red cells in renal circulation requires rapid urea transport. Am J Physiol 1988;254:C669–74.
[417] Fenton RA, Flynn A, Shodeinde A, Smith CP, Schnermann J, Knepper MA. Renal phenotype of UT-A urea transporter knockout mice. J Am Soc Nephrol 2005;16:1583–92.
[418] Berliner RW, Levinsky NG, Davidson DG, Eden M. Dilution and concentration of the urine and the action of antidiuretic hormone. Am J Med 1958;24:730–44.
[419] Fenton RA, Knepper MA. Urea and renal function in the 21st century: insights from knockout mice. J Am Soc Nephrol 2007;18:679–88.
[420] Sands JM. Critical role of urea in the urine-concentrating mechanism. J Am Soc Nephrol 2007;18:670–1.
[421] Fenton RA, Chou CL, Sowersby H, Smith CP, Knepper MA. Gamble's "economy of water" revisited: studies in urea transporter knockout mice. Am J Physiol Renal Physiol 2006;291: F148–54.
[422] Fenton RA. Urea transporters and renal function: lessons from knockout mice. Curr Opin Nephrol Hypertens 2008;17: 513–8.
[423] Isozaki T, Lea JP, Tumlin JA, Sands JM. Sodium-dependent net urea transport in rat initial IMCDs. J Clin Invest 1994;94:1513–7.
[424] Kato A, Sands JM. Active sodium-urea counter-transport is inducible in the basolateral membrane of rat renal initial inner medullary collecting ducts. J Clin Invest 1998;102:1008–15.
[425] Knepper MA, Roch-Ramel F. Pathways of urea transport in the mammalian kidney. Kidney Int 1987;31:629–33.
[426] Lassiter WE, Gottschalk CW, Mylle M. Micropuncture study of net transtubular movement of water and urea in nondiuretic mammalian kidney. Am J Physiol 1961;200:1139–46.
[427] Valtin H. Structural and functional heterogeneity of mammalian nephrons. Am J Physiol 1977;233:F491–501.
[428] Imbert M, de Rouffignac C. Role of sodium and urea in the renal concentrating mechanism in *Psammomys obesus*. Pfluegers Arch 1976;361:107–14.
[429] Ullrich KJ, Rumrich G, Schmidt-Nielsen B. Urea transport in the collecting duct of rats on normal and low protein diet. Pfluegers Arch 1967;295:147–56.
[430] Aoshima T, Kajita M, Sekido Y, Kikuchi S, Yasuda I, Saheki T, et al. Novel mutations (H337R and 238-362del) in the *CPS1* gene cause carbamoyl phosphate synthetase I deficiency. Hum Hered 2001;52:99–101.
[431] Calcagno PL, Rubin MI, Weintraub DH. Studies on the renal concentrating and diluting mechanisms in the premature infant. J Clin Invest 1954;33:91–6.
[432] Edelmann Jr CM, Barnett HL, Troupkou V. Renal concentrating mechanisms in newborn infants. Effect of dietary protein and water content, role of urea, and responsiveness to antidiuretic hormone. J Clin Invest 1960;39:1062–9.
[433] Liu W, Morimoto T, Kondo Y, Iinuma K, Uchida S, Imai M. "Avian-type" renal medullary tubule organization causes immaturity of urine-concentrating ability in neonates. Kidney Int 2001;60:680–93.
[434] Schwartz GJ, Zavilowitz BJ, Radice AD, Garcia-Perez A, Sands JM. Maturation of aldose reductase expression in the neonatal rat inner medulla. J Clin Invest 1992;90:1275–83.
[435] Winberg J. Determination of renal concentrating capacity in infants and children without renal disease. Acta Paediatr 1959;48:318–28.
[436] Falk G. Maturation of renal function in infant rats. Am J Physiol 1955;181:157–70.
[437] Forrest Jr JN, Stanier MW. Kidney composition and renal concentrating ability in young rabbits. J Physiol 1966;187:1–4.
[438] Heller H. Effects of dehydration on adult and newborn rats. J Physiol 1949;108:303–14.
[439] McCrory Jr WW. Developmental nephrology. Cambridge, MA: Harvard University Press; 1972.
[440] Rane S, Aperia A, Neroth P, Lundin S. Development of urinary concentrating capacity in weaning rats. Pediatr Res 1985;19:472–5.
[441] Trimble ME. Renal response to solute loading in infant rats: relation to anatomical development. Am J Physiol 1970;219:1089–97.
[442] Yasui M, Marples D, Belusa R, Eklof AC, Celsi G, Nielsen S, et al. Development of urinary concentrating capacity: role of aquaporin-2. Am J Physiol Renal, Fluid Electrolyte Physiol 1996;271:F461–8.
[443] Bonilla-Felix M, Jiang W. Aquaporin-2 in the immature rat: expression, regulation, and trafficking. J Am Soc Nephrol 1997;8:1502–9.
[444] Horster M, Valtin H. Postnatal development of renal function: micropuncture and clearance studies in the dog. J Clin Invest 1971;50:779–95.
[445] Edelmann Jr CM, Barnett HL, Troupkou V. Renal concentrating mechanisms in newborn infants. Effect of dietary protein and water content, role of urea, and responsiveness to antidiuretic hormone. J Clin Invset 1960;39:1062–9.
[446] Bondy CA, Lightman SL. Developmental and physiological regulation of aldose reductase mRNA expression in renal medulla. Mol Endocrinol 1989;3:1409–16.
[447] Han KH, Woo SK, Kim WY, Park SH, Cha JH, Kim J, et al. Maturation of TonEBP expression in developing rat kidney. Am J Physiol Renal Physiol 2004;287:F878–85.
[448] Lee HW, Kim WY, Song HK, Yang CW, Han KH, Kwon HM, et al. Sequential expression of NKCC2, TonEBP, aldose reductase, and urea transporter-A in developing mouse kidney. Am J Physiol Renal Physiol 2007;292:F269–77.
[449] Suda S, Rai T, Sohara E, Sasaki S, Uchida S. Postnatal expression of KLF12 in the inner medullary collecting ducts of kidney and its trans-activation of UT-A1 urea transporter promoter. Biochem Biophys Res Commun 2006;344:246–52.
[450] Atherton JC, Green R, Thomas S. Influence of lysine-vasopressin dosage on the time course of changes in renal tissue and urinary composition in the conscious rat. J Physiol 1971;213:291–309.
[451] Press WH, Teukolsky SA, Vetterling WT, Flannery BP. Numerical recipes in FORTRAN: the art of scientific computing. 2nd ed. New York: Cambridge University Press; 1992.
[452] Beck F, Dorge A, Rick R, Thurau K. Intra- and extracellular element concentrations of rat renal papilla in antidiuresis. Kidney Int 1984;25:397–403.

[453] Beck F, Dorge A, Rick R, Thurau K. Osmoregulation of renal papillary cells. Pfluegers Arch 1985;405(Suppl. 1):S28–32.
[454] Atherton JC, Hai MA, Thomas S. The time course of changes in renal tissue composition during water diuresis in the rat. J Physiol 1968;197:429–43.
[455] Hebert SC, Culpepper RM, Andreoli TE. NaCl transport in mouse medullary thick ascending limbs. I. Functional nephron heterogeneity and ADH-stimulated NaCl co-transport. Am J Physiol 1981;241:F412–31.
[456] Hall DA, Varney DM. Effect of vasopressin on electrical potential differences and chloride transport in mouse medullary thick ascending limb of Henle's loop. J Clin Invest 1980;66:792–802.
[457] Shareghi GR, Agus ZS. Magnesium transport in the cortical thick ascending limb of Henle's loop of the rabbit. J Clin Invest 1982;69:759–69.
[458] Nonoguchi H, Tomita K, Marumo F. Effects of atrial natriuretic peptide and vasopressin on chloride transport in long- and short-looped medullary thick ascending limbs. J Clin Invest 1992;90:349–57.
[459] Imai M. Effect of bumetanide and furosemide on the thick ascending limb of Henle's loop of rabbits and rats perfused *in vitro*. Eur J Pharmacol 1977;41:409–16.
[460] Stokes JB. Effect of prostaglandin E_2 on chloride transport across the rabbit thick ascending limb of Henle. J Clin Invest 1979;64:495–502.
[461] Mason J, Gutsche H-U, Moore L, Müller-Suur R. The early phase of experimental acute renal failure. IV. The diluting ability of the short loops of Henle. Pfluegers Arch 1979;379:11–8.
[462] Burg MB, Bourdeau JE. Function of the thick ascending limb of Henle's loop. In: Vogel HG, Ullrich KJ, editors. New aspects of renal function. Amsterdam: Excerpta Medica; 1978. p. 91–102.
[463] Knepper MA. Urea transport in nephron segments from medullary rays of rabbits. Am J Physiol 1983;244:F622–7.
[464] Stoner LC, Burg MB, Orloff J. Ion transport in cortical collecting tubule effect of amiloride. Am J Physiol 1974;227:453–9.
[465] Stokes JB. Sodium and potassium transport across the cortical and outer medullary collecting tubule of the rabbit: evidence for diffusion across the outer medullary portion. Am J Physiol 1982;242:F514–20.
[466] Schafer JA, Andreoli TE. The effect of antidiuretic hormone on solute flows in mammalian collecting tubules. J Clin Invest 1972;51:1279–86.
[467] Kuwahara M, Berry CA, Verkman AS. Rapid development of vasopressin-induced hydroosmosis in kidney collecting tubules measured by a new fluorescence technique. Biophys J 1988;54:595–602.
[468] Schafer JA, Andreoli TE. Cellular constraints to diffusion. The effect of antidiuretic hormone on water flows in isolated mammalian collecting tubules. J Clin Invest 1972;51:1264–78.
[469] Nonoguchi H, Sands JM, Knepper MA. Atrial natriuretic factor inhibits NaCl and fluid absorption in cortical collecting duct of rat kidney. Am J Physiol 1989;256:F179–86.
[470] Lorenzen M, Frindt G, Taylor A, Windhager EE. Quinidine effect on hydrosmotic response of collecting tubules to vasopressin and cAMP. Am J Physiol 1987;252:F1103–11.
[471] Garg LC, Knepper MA, Burg MB. Mineralocorticoid effects on Na-K-ATPase in individual nephron segments. Am J Physiol 1981;240:F536–44.
[472] Katz AI, Doucet A, Morel F. Na-K-ATPase activity along the rabbit, rat and mouse nephron. Am J Physiol 1979;237: F114–20.
[473] O'Neil RG, Dubinsky WP. Micromethodology for measuring ATPase activity in renal tubules: mineralocorticoid influence. Am J Physiol 1984;247:C314–20.
[474] Schmidt U, Horster M. Na-K-activated ATPase: activity maturation in rabbit nephron segments dissected *in vitro*. Am J Physiol 1977;233:F55–60.
[475] Stokes JB, Ingram MJ, Williams AD, Ingram D. Heterogeneity of the rabbit collecting tubule: localization of mineralocorticoid hormone action to the cortical portion. Kidney Int 1981;20:340–7.
[476] Lankford SP, Chou C-L, Terada Y, Wall SM, Wade JB, Knepper MA. Regulation of collecting duct water permeability independent of cAMP-mediated AVP response. Am J Physiol Renal, Fluid Electrolyte Physiol 1991;261:F554–66.
[477] Sands JM, Layton HE. The physiology of urinary concentration: an update. Semin Nephrol 2009;29:178–95.
[478] Tickle P, Thistlethwaite A, Smith CP, Stewart GS. Novel bUT-B2 urea transporter isoform is constitutively activated. Am J Physiol Regul Integr Comp Physiol 2009;297:R323–9.
[479] Zhao HY, Tian W, Cohen DM. Rottlerin inhibits tonicity-dependent expression and action of TonEBP in a PKCd-independent fashion. Am J Physiol Renal Physiol 2002;282: F710–7.

CHAPTER

44

Hyponatremia

Richard H. Sterns[1], *Stephen M. Silver*[2] *and J. Kevin Hix*[3]

[1]Chief of Medicine, Rochester General Hospital, Professor of Medicine, University of Rochester School of Medicine and Dentistry, Rochester, New York, USA

[2]Clinical Professor of Medicine, University of Rochester School of Medicine and Dentistry, Rochester, New York, USA

[3]Clinical Assistant Professor of Medicine, University of Rochester School of Medicine and Dentistry, Rochester, New York, USA

THE PLASMA SODIUM CONCENTRATION AND BODY FLUID TONICITY

Sodium and its accompanying anions are the principle osmotically active solutes in extracellular fluid.[1,2] When extracellular osmolality is low, intracellular osmolality is equally low. Therefore, although there are exceptions (Table 44.1), hyponatremia is usually associated with hypoosmolality and dilution of all body fluids.[1,2,3]

When (as is usually the case) the concentration of non-permeant extracellular solutes other than sodium is very low, the plasma sodium concentration is a function of three variables, as indicated by the following equation:

$$\text{Plasma}[Na^+] \cong \frac{\text{Exchangeable } Na^+ + \text{Exchangeable } K^+}{\text{Total body water}} \quad (44.1)$$

Only the exchangeable fractions of sodium and potassium are included in the equation, because one-third of body sodium is bound to bone and osmotically inactive.[1] This relationship, which has been validated empirically,[3,4] indicates that the plasma (or serum) sodium concentration can be reduced by depletion of body cations, by an increase in body water or by a combination of these processes.[5] Recently, it has been emphasized that the original equation describing the relationship between the plasma sodium concentration, exchangeable sodium, exchangeable potassium, and total body water has an intercept that can be explained theoretically.[6] The simplified form of the relationship Eq. (44.1), which omits the intercept, is useful conceptually, but should not be considered a completely accurate basis for predicting the effect of therapy on the plasma sodium concentration.

It is intuitively obvious that the extracellular sodium concentration should be proportional to the body's content of water and soluble sodium. The sodium concentration falls when the body retains water (without solute) or when there are net external losses of sodium (without water). The importance of intracellular potassium stores to the plasma sodium concentration is less obvious.[7,8] In potassium depletion, sodium ions move intracellularly as intracellular potassium is lost, balancing negative charges on intracellular macromolecules. Thus, external loss of exchangeable potassium causes an internal loss of extracellular sodium. Similarly, when intracellular potassium is replaced by hydrogen ions, rather than sodium or when it is lost with phosphate (an intracellular anion), the loss of osmotically active intracellular solute causes a redistribution of water from the intracellular to the extracellular fluid compartments, diluting extracellular sodium ions.

PHYSIOLOGIC CONTROL OF WATER EXCRETION

Osmotic Regulation

Controlled by changes in water intake, vasopressin secretion, and water excretion, the plasma sodium

Seldin and Giebisch's The Kidney, Fifth Edition.
DOI: http://dx.doi.org/10.1016/B978-0-12-381462-3.00044-6

© 2013 Elsevier Inc. All rights reserved.

TABLE 44.1 Causes of Non-Hypotonic Hyponatremia

Plasma Osmolality	Disorder	Pathogenesis
Normal	Pseudohyponatremia	Excess non-aqueous material decreases plasma water content; no change in ECF or ICF volume
	Hyperlipidemia	
	Multiple myeloma	
	Exogenous solutes	Expansion of ECF volume with non-sodium solutes and water; no change in ICF volume
	Isotonic IV mannitol	
	Irrigant absorption	
Increased	Hyperglycemia, hypertonic IV mannitol, and maltose containing IgG solutions	Initial expansion of ECF volume and shift of water out of cells; decrease in ICF volume

concentration is normally prevented from rising above 142 mEq/L or falling below 135 mEq/L. When the plasma sodium concentration changes by as little as 1% (with a corresponding change in plasma osmolality), cell volume receptors ("osmoreceptors") in the hypothalamus respond, relaying signals to vasopressin-secreting neurons located in the supraoptic and paraventricular nuclei whose axons terminate in secretory bulbs in the neurohypophysis.[9–11] The antidiuretic hormone, arginine vasopressin, which is released into the systemic circulation by the neurohypophysis, controls water excretion by the kidneys. The hormone activates V_2 receptors on the basolateral membrane of principal cells in the renal collecting duct, initiating a cyclic AMP-dependent process that culminates in increased production of water channels (aquaporin 2), and their insertion into the cells' luminal membranes.[12] The effect of vasopressin on water flow is inhibited by locally produced prostaglandin E_2, which is stimulated by vasopressin action on V_1 receptors.[13] Vasopressin's short half-life in the circulation and continuous shuttling of aquaporins between the collecting duct's cell membrane and cytosol allow rapid changes in urinary water excretion in response to changes in body fluid tonicity.

Vasopressin levels are normally unmeasurable when the plasma sodium concentration falls to approximately 135 mEq/L. Low levels of the hormone allow the excretion of large volumes of a maximally dilute urine ($\approx$50 mOsm/kg) which reduces body water content and restores the plasma sodium concentration to normal. At higher plasma sodium levels, plasma vasopressin is directly related to the plasma sodium concentration, reaching levels that are high enough to promote the excretion of maximally concentrated urine ($\approx$1200 mOsm/kg) at a plasma sodium concentration of approximately 142 mEq/L. A rising plasma sodium concentration also stimulates thirst. Ingested water is retained, returning the plasma sodium concentration back towards normal.

Hemodynamic Regulation

Under day-to-day conditions, vasopressin secretion, urinary free water excretion, and thirst respond primarily to changes in body fluid tonicity. Under pathologic conditions, osmotic control of vasopressin secretion and thirst can be overridden by hemodynamic stimuli.[14] In addition to input from osmoreceptors, the hypothalamic neurons that secrete vasopressin also receive neural input from baroreceptors in the great vessels, and volume receptors in the atria. When these receptors are stimulated by hypotension or by a major reduction in plasma volume, impulses are carried via cranial nerves IX and X to the hypothalamus. The thirst center in the hypothalamus responds to similar non-osmotic stimuli. Vasopressin and thirst responses to hypovolemia and hypotension lead to water retention, despite hypotonicity of body fluids. These hemodynamic responses can be regarded as back-up systems that serve to maintain arterial blood volume under emergency conditions, sacrificing tonicity to tissue perfusion. Although high levels of vasopressin occur in response to hypovolemia, under experimental conditions, a rather large stimulus is required; while plasma vasopressin is measurably increased by a 1% change in plasma osmolality, a 10% change in extracellular fluid volume is required to elicit the same response. However, these experimental findings are difficult to reconcile with clinical observations, suggesting that non-osmotic vasopressin secretion occurs with more subtle volume depletion.

HYPOTONIC HYPONATREMIA: CLASSIFICATION AND PATHOGENESIS

Traditionally, patients with hyponatremia are divided into categories according to their body sodium content and/or intravascular volume: low body sodium content (volume depletion); high body sodium content (edematous conditions) or normal body sodium content (euvolemic hyponatremia or SIADH).[15] Although this time-honored approach is often helpful to clinicians, intravascular volume and body sodium content do not always change in parallel (e.g.,

self-induced water intoxication), and some causes of hyponatremia (e.g., diuretic-induced and cerebral salt-wasting) may be difficult to classify by intravascular volume. Moreover, physiologic responses to extracellular volume expansion and contraction often create ambiguities in volume status. Thus, secondary water retention in response to volume depletion and secondary natriuresis in response to water overload may ultimately yield similar values for total body sodium and water (Figure 44.1).

Table 44.2 classifies hyponatremia by the physiologic mechanism underlying the electrolyte disturbance. As the plasma sodium concentration is proportional to the ratio of exchangeable cations and total body water, it follows that changes in sodium concentration are related to external balances of sodium, potassium, and water. However, because the plasma sodium concentration is normally maintained within a narrow physiologic range by control systems which regulate water balance, hypotonic hyponatremia can only occur if water excretion is impaired or overwhelmed. The various causes of hyponatremia are therefore divided according to the status of urinary water excretion. Disordered water balance is often accompanied by changes in cation balance, which also play a pivotal role in the pathogenesis of hyponatremia.

TABLE 44.2 Pathophysiologic Classification of Hypotonic Hyponatremia

Urine Diluting Ability	Cause of Hyponatremia
Unimpaired	Psychotic polydipsia
	Beer potomania
	Infantile water intoxication
Impaired: vasopressin-independent	Oliguric renal failure
	Tubular interstitial renal disease
	Diuretics
	Nephrogenic syndrome of antidiuresis[a]
Impaired: vasopressin-dependent	Hemodynamically-mediated
	Volume-depletion
	Spinal cord disease
	Congestive heart failure
	Cirrhosis
	Addison's disease[b]
	Cerebral salt-wasting[b]
	SIADH (see Table 44.3)

[a]*Hereditary disorder of the V2 receptor with clinical features of SIADH, but with undetectable plasma vasopressin levels.*
[b]*Disorders with both hemodynamic and non-hemodynamic bases for vasopressin release.*

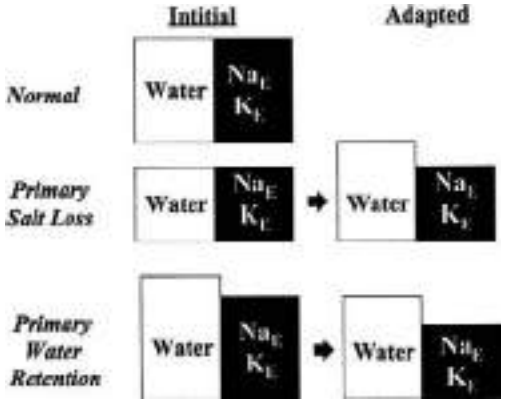

FIGURE 44.1 **Body water and cation content in hyponatremia.** When the primary disturbance is loss of salt water (middle figures), compensatory mechanisms are triggered—hemodynamically mediated thirst and vasopressin secretion—which result in secondary water retention. When the primary disturbance is pathologic secretion of vasopressin and water retention (bottom figures), compensatory mechanisms are triggered—increased secretion of atrial natriuretic peptide, decreased secretion of aldosterone, and pressure natriuresis—which result in secondary salt loss. Because of these adaptations, primary salt loss and primary water retention both result in near normal values for total body water and decreased body cation stores.

WATER INTOXICATION WITH MAXIMALLY DILUTE URINE

Pathophysiology

Rarely, fluid intake can overwhelm normal mechanisms for water excretion. In the absence of vasopressin, urine osmolality falls to approximately 50 mOsm/kg. A typical American diet provides a daily load of 600 to 900 milliosmoles of solute (electrolytes and urea) that must be excreted. At this rate of solute excretion, the volume of maximally dilute urine equals 12 to 18 liters per day or 500 to 750 ml/hour. Water intake can occasionally exceed this large excretory capacity. Patients with severe acute water intoxication are truly "waterlogged," and susceptible to pulmonary edema due to retained water.

Self-Induced Water Intoxication in Psychotic Polydipsia

Polydipsia and polyuria are extremely common among institutionalized patients with mental illness.[16–20] Many patients with polydipsia have frequent

episodes of hyponatremia, which may present with seizures. About half the reported cases have had maximally dilute urine (urine osmolalities below 100 mOsm/kg) at presentation. In others, inappropriately concentrated urine was present immediately following seizures or in association with nausea,[19] but the rate of correction of hyponatremia indicates that the urine became dilute soon afterwards.

In most psychotic water drinkers, hyponatremia can be ascribed to a generalized dilution of body solutes by retained water; thus, body weight increases in proportion to the severity of hyponatremia. Patients gain weight and become hyponatremic during the course of the day, and then spontaneously diurese, normalizing their plasma sodium concentration and body weight during the night. Caregivers in psychiatric hospitals routinely monitor weight changes in patients who are habitual water drinkers to determine when access to water must be rigidly restricted to avoid severe symptomatic hyponatremia.

Agents that interfere with the ability to maximally dilute the urine (e.g., diuretics or carbamazepine) should be avoided in polydipsic patients, as they can precipitate a rapid onset of life-threatening hyponatremia.[21,22]

Water Intoxication in Infants

Acute water intoxication is common among infants who are given excessively dilute formula.[23,24] The hungry infant ingests large volumes of fluid leading to water retention, despite the excretion of maximally dilute urine. Once water is restricted, the plasma sodium concentration self-corrects as large volumes of urine are excreted.

Beer Drinkers Potomania

Alcoholics who eat little and subsist on large volumes of beer may also become hyponatremic while excreting maximally dilute urine.[25–27] Beer's low protein content and the protein-sparing effect of its carbohydrate result in profoundly reduced blood urea nitrogen concentrations and urinary urea excretion. The total daily excretion of urinary solute may be only 200 to 300 milliosmoles. Thus, even at a urine osmolality of 50 mOsm/kg, urine output is limited to 4 to 6 liters per day, an amount that fails to match the enthusiastic beer drinker's intake of electrolyte free water. A similar phenomenon has been reported in non-beer drinkers with a high fluid and low protein intake.[27,28] Volume-depletion from gastrointestinal losses, and transient vasopressin release caused by nausea or alcohol withdrawal, may further limit the beer drinker's ability to excrete free water, contributing to the development and persistence of hyponatremia.[29]

VASOPRESSIN-INDEPENDENT DEFECTS IN WATER EXCRETION

Pathophysiology

Maximal free water excretion depends on adequate delivery of glomerular filtrate to the renal diluting segments (the ascending limb of the loop of Henle and the distal tubule), reabsorption of salt without water by the diluting segments to create hypotonic fluid within the tubular lumen, and a collecting duct that is relatively impermeable to water, so that the dilute tubular fluid formed "upstream" can be eliminated in the final urine. Hyponatremia occurs when water is taken in at a time when these mechanisms are not functioning normally.

Renal Failure

The most obvious cause of impaired water excretion is oliguric renal failure. Even when nonoliguric, patients with advanced renal failure have fixed isosthenuria, and are unable to excrete dilute urine despite normally suppressed vasopressin secretion. In the absence of renal failure, urinary dilution can still be impaired, despite low levels of vasopressin, by two mechanisms: (1) enhanced proximal reabsorption of the glomerular filtrate, limiting fluid delivery to the renal diluting segments (as in volume depletion, congestive heart failure, and cirrhosis)[30]; and (2) impaired sodium reabsorption in the renal diluting segments (by diuretics or tubular interstitial disease).[31]

Diuretic-Induced Hyponatremia

Both thiazides and loop diuretics interfere with the ability to maximally dilute the urine.[32] Thus, both classes of diuretic can lead to water intoxication in patients who habitually ingest extremely large volumes of water. Diuretics are one of the most important causes of hyponatremia.[33–37] Most cases are caused by thiazide or thiazide-like agents; loop diuretics are implicated much less commonly. Thiazides may be the sole factor responsible for causing hyponatremia, and they may also exacerbate hyponatremia in patients with disorders associated with SIADH.[36,38] The mechanism of thiazide-induced hyponatremia remains somewhat unclear; however, as for all causes of hyponatremia, water retention and/or cation depletion must be responsible. There is evidence that thiazides have a

direct antidiuretic effect mediated by upregulation of aquporin 2 (AQP2).[39]

Most cases of thiazide-induced hyponatremia have occurred in elderly small women who have been prescribed diuretics for the treatment of hypertension.[35,40–42] The impairment of renal diluting ability caused by thiazides is more pronounced in elderly people, especially those who have previously experienced thiazide-induced hyponatremia.[43] The predisposition of elderly women to severe hyponatremia may be explained by body size, in that small changes in body water and electrolyte content can lead to marked changes in serum sodium.

In susceptible individuals, the serum sodium may fall within hours of diuretic ingestion, and severe hyponatremia can develop in less than two days.[41,44–46] While in many cases the diuretic had been recently prescribed, in others thiazides had been used chronically without incident until, for some reason, water intake increased, dietary salt and protein intake decreased or an intercurrent illness led to "inappropriate" antidiuretic hormone secretion.[33,47] Mild hyponatremia often persists for a few weeks when diuretic therapy is withdrawn from patients with diuretic-induced hyponatremia,[48] apparently reflecting temporary "resetting" of the osmostat[49] or alternatively, slow restoration of depleted cation stores.

Although thiazide diuretics do not inhibit the ability to concentrate the urine, they do impair diluting ability in several ways[31,39,50–52]: inhibition of electrolyte transport at the cortical diluting sites; direct stimulation of vasopressin release; direct upregulation of AQP2; reduction of glomerular filtration; and enhancement of fractional proximal water reabsorption, reducing delivery to diluting sites.

Positive water balance during the onset of thiazide-induced hyponatremia and negative balance during its correction have been documented.[22,44,46] Some patients with thiazide-induced hyponatremia have low serum uric acid levels and high uric acid clearances (markers of volume expansion) which return to normal as the serum sodium normalizes.[36,53] Most affected patients drink large amounts of water, and the superimposed diuretic prevents urine output from keeping pace with water intake.[44]

Although increased total body water often contributes to the pathogenesis of thiazide-induced hyponatremia, there are many cases in which body weight decreased or remained the same during the fall in serum sodium.[41,54,55] In others, direct measurements of total body water in affected patients have been normal.[41] In these cases, other explanations for hyponatremia must be sought.

Negative cation balance plays a major role in the pathogenesis of diuretic-induced hyponatremia. Rejected cations may be excreted at a total concentration which exceeds that of plasma, directly "desalinating" the plasma even in the absence of water intake.[44] Potassium depletion is an important factor in many cases; treatment of hypokalemia has been shown to increase the plasma sodium concentration with no change in body weight.[41] Magnesium repletion may act similarly, presumably through an effect on skeletal muscle Na-K-ATPase.[56] Surprisingly, despite negative cation balance, many patients appear to be euvolemic. Apparently, enough water is retained to offset the initial tendency toward hypovolemia. Once diuretics are withdrawn, urinary sodium excretion falls to very low levels.[41,46]

VASOPRESSIN-DEPENDENT DEFECTS IN WATER EXCRETION

Pathophysiology

Normally, in response to hypotonicity, vasopressin secretion is suppressed, the collecting duct is impermeable to water, and a maximally dilute urine is formed. In two large surveys of hospitalized patients with hyponatremia, over 90% of cases were associated with elevated vasopressin levels.[57,58] Vasopressin levels are rarely elevated into pathologic ranges, even in cases associated with ectopic secretion by tumors. Rather, vasopressin levels are inappropriately high relative to the plasma osmolality. Non-osmotic vasopressin secretion may be an adaptive response driven by hemodynamic stimuli or it may be "inappropriate" and independent of any of the usual physiologic mechanisms which regulate water excretion. Persistent vasopressin secretion despite hypoosmolality allows ingested or infused free water to be retained, causing hypotonic hyponatremia. Vasopressin-mediated hyponatremia is characterized by urine which is more concentrated (usually much more) than 100 mOsm/kg and which becomes more dilute after administration of a V2 receptor antagonist (see section "V_2-Receptor Antagonists").

Patients with inappropriate vasopressin secretion must take in water to become hyponatremic. In some cases, hyponatremia develops when electrolyte-free water is administered parenterally. More commonly, patients become hyponatremic while ingesting water. Theoretically, osmotic inhibition of thirst should prevent water ingestion when the ability to excrete water is impaired. However, patients with SIADH continue to drink despite plasma osmolalities below the normal osmotic threshold for thirst. Formal testing has shown that there is downward resetting of the osmotic threshold for thirst in SIADH, but that thirst responds to

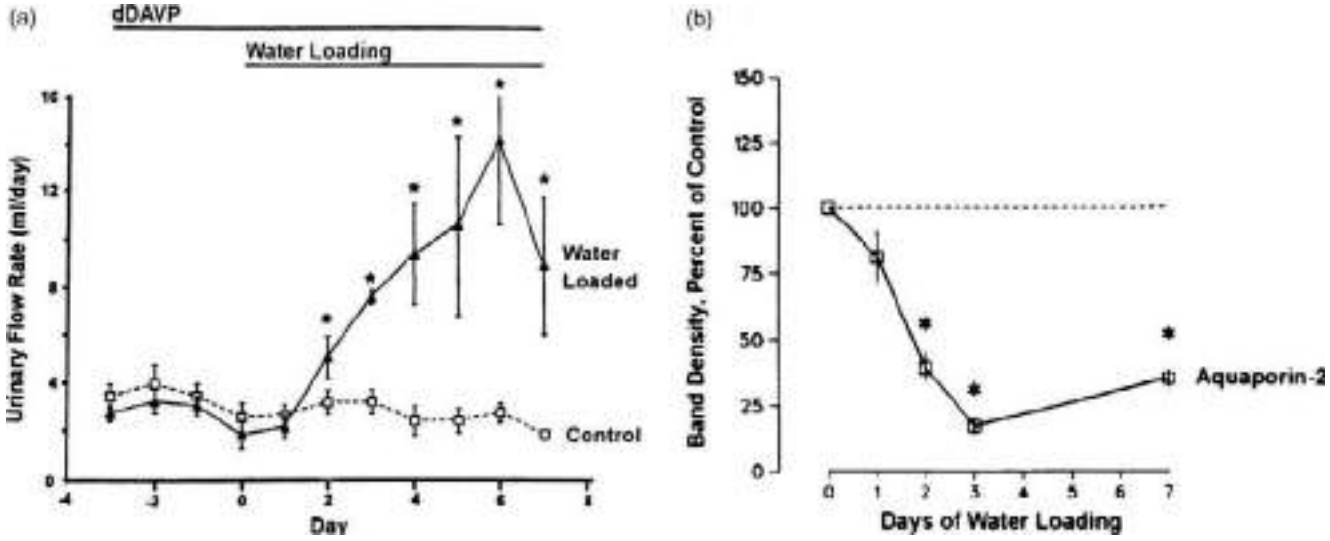

FIGURE 44.2 **Vasopressin escape.**[64] Panel (a) illustrates the gradual increase in urine flow rate (accompanied by a decrease in urine osmolality) that occurs when rats treated continuously with dDAVP are made hyponatremic with water-loading. The escape from the antidiuretic effect of vasopressin begins on the second day of water-loading. Panel (b) illustrates the levels of acquaporin 2 protein levels from kidney homogenates taken on each day of water-loading. Levels of acquaporin 2 protein decrease despite continued administration of vasopressin, and correlate with changes in urine volume.

osmotic stimulation and is suppressed by drinking around the lowered set-point.[59]

Escape from Vasopressin-Induced Water Retention

Experimentally, after several days of constant vasopressin infusion and constant water intake, there is an escape from the antidiuretic effect of vasopressin. With the onset of vasopressin escape, the urine becomes less concentrated, allowing water balance to be re-established at a new steady-state in which the plasma sodium concentration stabilizes at a level lower than normal. In experimental models, escape is temporally associated with a marked decrease in renal aquaporin-2 protein, accompanied by suppression of aquaporin-2 mRNA levels (Figure 44.2).[60] V2-receptor mRNA expression and binding are decreased, as is c-AMP production in response to vasopressin,[61] Plasma and urine aldosterone and mean arterial pressure are increased as are thiazide-sensitive Na-Cl co-transporter and ENaC proteins in the distal nephron that are known to be upregulated by aldosterone.[62] Inhibition of nitric oxide synthase or prostaglandin synthesis synergistically inhibit the escape phenomenon, supporting a role for nitric oxide and prostaglandins in mediating vasopressin escape.[63]

In conditions characterized by vasopressin-mediated water retention, (e.g., SIADH, congestive heart failure), renal escape from vasopressin-induced antidiuresis (along with decreased water intake in some cases) permits patients with vasopressin-mediated hyponatremic states to manifest a relatively stable level of hyponatremia, despite continued water intake and continued presence of vasopressin.

HEMODYNAMIC CAUSES OF VASOPRESSIN-MEDIATED HYPONATREMIA

Pathophysiology

Hypovolemia, heart failure, and cirrhosis are the most common non-osmotic stimuli for antidiuretic hormone secretion.[64] In a series of 100 consecutive hospitalized patients with hypotonic hyponatremia, volume contraction (29%), advanced heart failure (25%), and liver cirrhosis (16%) were identified as the cause of hyponatremia in a high percentage of cases.[58] The hemodynamic abnormalities that stimulate vasopressin release in these conditions also promote sodium reabsorption by the renal tubules (mediated by aldosterone, increased sympathetic nervous system activity, peritubular Starling forces, etc.), causing both sodium and water retention. In volume-depletion, sodium retention serves to replace a sodium deficit; in heart failure and cirrhosis, sodium retention serves to compensate for the circulatory abnormality, but it also causes edema.

Volume-Depletion

Sodium and potassium losses associated with gastrointestinal fluids (or with urinary losses caused by osmotic or loop diuretics) do not directly lower the plasma sodium concentration, because these fluids are either hypotonic or isotonic. However, the intravascular volume-depletion caused by such losses is a hemodynamic stimulus for thirst and vasopressin secretion; as a result, ingested water is retained, lowering the plasma sodium concentration. Thus, hyponatremia in these conditions is associated with a reduced content of both total body cations and water. However, in many patients, compensatory water retention makes it difficult to detect the underlying volume depletion. Laboratory clues, including a low urine sodium concentration and elevated serum uric acid levels, can be helpful diagnostically.[65]

Spinal Cord Disease

Hyponatremia is very common after spinal cord injury, particularly among patients with complete quadriplegia.[66,67] Contributing factors include a large water intake (reflecting physician recommendations, angiotensin II-mediated thirst, and loss of pharyngeal and gastric satiety signals), and baroreceptor-mediated vasopressin release. One study showed normal osmoregulation of vasopressin secretion and excretion of a water-load when subjects were supine, but with the subjects in a sitting position, there was a reduced osmotic threshold and increased sensitivity for vasopressin release, and urine diluting ability and free water clearance were markedly impaired.[68]

Edematous Conditions

Severe hyponatremia can occur despite increased body sodium content if retained sodium is offset by a disproportionate increase in body water.

Congestive Heart Failure

Hyponatremia in heart failure stems from reduced cardiac output and blood pressure which stimulate vasopressin, catecholamines, and the renin–angiotensin–aldosterone axis.[64,69–71] Increased vasopressin levels have even been documented in patients with impaired left ventricular function before the onset of symptomatic heart failure.[72] Hyponatremic patients with congestive heart failure have higher levels of plasma renin activity, norepinephrine, epinephrine, and lower renal and hepatic plasma flows than normonatremic patients with an apparently similar degree of heart disease. Hyponatremia in heart failure is associated with a poor prognosis.[73]

Hepatic Cirrhosis

Cirrhosis is characterized by a hyperdynamic circulation with low blood pressure, low systemic vascular resistance, and high cardiac output.[74] Systemic vasodilatation causes relative underfilling of the arterial vascular compartment and neurohumoral responses similar to those that occur in response to a low cardiac output.[75] Activation of the renin–angiotensin–aldosterone axis and the sympathetic system, combined with non-osmotic release of vasopressin, results in renal water and sodium retention.[76,77] Escape from the sodium-retaining effect of aldosterone does not occur, and there is renal resistance to atrial natriuretic peptide. Although the pathogenesis of the peripheral arterial vasodilation is incompletely understood, increased vascular nitric oxide by the endothelium may play a role. In a rat model of cirrhosis, normalization of vascular nitric oxide production with a nitric oxide synthetase inhibitor corrects the hyperdynamic circulation, improves sodium and water excretion, and decreases neurohumoral activation.[74]

Peritoneovenous shunting of hyponatremic cirrhotic patients with refractory ascites improves cardiac output, renal plasma flow, and creatinine clearance, and results in an immediate diuresis and natriuresis with a decrease in urine osmolality and an increase in plasma sodium concentration associated with a small but significant decrease in plasma vasopressin levels.[74]

INAPPROPRIATE VASOPRESSIN SECRETION (SIADH)

Pathophysiology

Definitions

Non-osmotic release of vasopressin without a hemodynamic stimulus to account for it is considered "inappropriate".[78] When Bartter and Schwarz first described the syndrome of inappropriate antidiuretic hormone secretion (SIADH), they defined clinical criteria for the disorder which are still generally accepted: hypoosmolality and clinical euvolemia with a sodium-containing urine (>30 mmol/L) that is less than maximally dilute (>100 mOsm/kg) without recent diuretic use or impaired renal function. Schwarz and Bartter also excluded endocrine disorders—primary and secondary adrenal insufficiency and hypothyroidism—from this designation. We have not made this exclusion, because patients with undiagnosed endocrine disturbances may present with all the clinical features of SIADH. Indeed, the discovery of SIADH is often the presenting feature of a clinically important systemic disease. Abnormal vasopressin secretion may be caused by ectopic

production of the hormone by tumors, from disordered secretion by the neurohypophysis or from increased sensitivity to the hormone (Table 44.3).

Patients with the syndrome of inappropriate antidiuretic hormone secretion (SIADH) retain ingested water, but they have no evidence of volume depletion and no tendency to form edema. Because of water retention, SIADH causes mild, subclinical volume-expansion, which is reflected by high uric acid clearance, a low plasma uric acid concentration, and urine sodium excretion which matches or exceeds sodium intake.[79,80] Clinicians make use of these characteristics to distinguish SIADH from hyponatremia caused by volume-depletion. The recently described syndrome of nephrogenic inappropriate antidiuresis (see section "Common Causes of SIADH") is discussed in this section because it exhibits clinical features of SIADH; in physiological terms, however, it is a cause of hyponatremia that is independent of vasopressin, as plasma vasopressin levels are undetectable (Table 44.2).[81]

TABLE 44.3 Causes of SIADH

Major Classification	Common Examples
Tumors	Small-cell lung cancer
	Head and neck tumors
Lung diseases	Pulmonary infection
	Hypoxia and hypercarbia
	Severe asthma
Neurologic disorders	Subarachnoid hemorrhage[a]
	Guillain-Barre syndrome[a]
	CNS infections
	Cerebral hemorrhage and infarction
	Brain tumors
Endocrine diseases	Hypothyroidism[a]
	Hypopituitarism
	Isolated ACTH deficiency
Medications	Arginine vasopressin and desmopressin acetate
	Amiodarone
	Chlorpropamide
	Carbamazepine and oxcarbazepine
	Cyclophosphamide
	Nonsteroidal anti-inflammatory agents; serotonin reuptake inhibitors
	Tricyclic antidepressants
	Vincristine
	3,4-methylenedioxymethamphetamine (ecstasy)
Hereditary	Nephrogenic syndrome of antidiuresis[b]
Miscellaneous, transitory causes	Surgery
	Pain and stress
	Nausea
	Alcohol withdrawal

[a]*Disorders with both hemodynamic and non-hemodynamic bases for vasopressin release.*
[b]*Hereditary disorder of the V2 receptor with clinical features of SIADH, but with undetectable plasma vasopressin levels.*

Patterns of Vasopressin Secretion

In most patients with SIADH, vasopressin secretion has followed one of two basic patterns: "reset osmostat" or "vasopressin leak".[11,82] In the reset osmostat variant of SIADH, seen in patients with chronic, debilitating illness and in normal pregnancy, the urine can be diluted maximally, but at a lower set-point than normal.[49] Such patients are thus mildly hyponatremic, but unlike other patients with SIADH, their plasma sodium concentration is very stable and they do not require dietary water restriction or other measures used to treat chronic hyponatremia. In the vasopressin leak variant, the basal level of vasopressin is elevated and unresponsive to osmotic stimuli when the plasma osmolality is low, but the levels increase appropriately when the plasma osmolality increases above a threshold level. Less commonly, patients exhibit erratic vasopressin secretion which is unrelated to osmotic stimuli. In about 10% of patients who present with typical clinical manifestations of SIADH, plasma vasopressin levels are at a low basal level that fails to increase as plasma osmolality increases. Such a pattern would be expected if an antidiuretic factor other than vasopressin were produced or if the collecting tubules were hypersensitive to normal hormone levels.

Interplay of Water Retention and Cation Depletion in SIADH

In SIADH, increased intravascular volume decreases renin secretion and increases release of atrial natriuretic peptide. These volume and hormonal changes promote sodium excretion, despite a low serum sodium concentration. Natriuresis in SIADH blunts the increase in extracellular volume caused by water retention (Figure 44.1),[80,83] but it also exacerbates hyponatremia (Eq. (44.1)). Balance studies in a group of patients with SIADH showed that during a period of high water and low sodium intake, the plasma sodium concentration decreased by 8 mEq/L with no gain in weight and no increase in chloride space (a measure of extracellular fluid volume).[84] Negative sodium and potassium balances accounted for the stability of

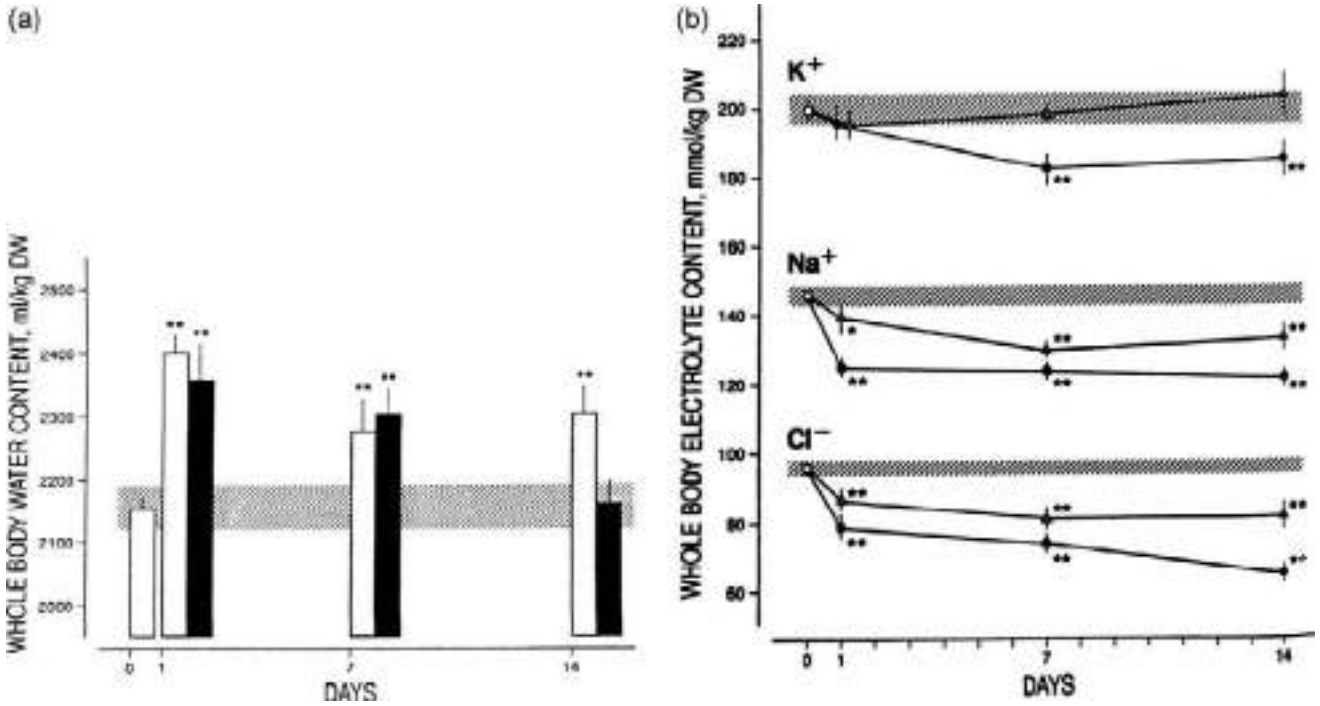

FIGURE 44.3 **Body water content in experimental SIADH.**[88] Panel (a) depicts measurements of body water content in rats made hyponatremic with dDAVP and a liquid diet. The open bar at the far left of the figure represents measurements obtained in normonatremic controls given no dDAVP. The black bars represent measurements obtained in animals made severely hyponatremic (plasma sodium 106 to 112 mmol/l) by giving dDAVP at 5 ng/hr; the gray bars represent measurements obtained in animals made less hyponatremic (plasma sodium 119 to 124 mmol/l) by giving dDAVP at 1 ng/hr. Body water content initially increases after the first day of hyponatremia at both doses of dDAVP, but falls to control levels after 14 days of severe hyponatremia. Panel (b) depicts whole body Na, K, and Cl measurements in the same experiment. Cation and chloride losses occur, beginning on the first day of hyponatremia, and are more severe in animals given the higher dose of dDAVP (with lower plasma sodium levels). Depletion of Na and Cl most likely represent adaptive responses to extracellular fluid volume expansion caused by retained water. Depletion of body K most likely represents a cell volume adaptive response.

extracellular volume, and for over 80% of the calculated solute loss. During a period of high sodium intake, over 600 mEq of sodium was retained (with only a small increase in weight and chloride space), fully accounting for the 11 mEq/L increase in serum sodium concentration.[84] In this study, there was a strong negative correlation between water intake and sodium balance, and between water intake and aldosterone secretory rate. Similar findings have been reported in studies in which pituitary extract was administered chronically to normal subjects.[83,85,86]

In an experimental model of SIADH produced by DDAVP and half-isotonic saline in the rat, hyponatremia was caused exclusively by negative balances of sodium and potassium; water balance, which was slightly negative, did not contribute to the decrease in sodium concentration.[87] Despite negative balances for sodium, chloride, and water, the extracellular volume (measured by inulin space) was not contracted, suggesting that water shifted from the intracellular to the extracellular space in response to the loss of intracellular solute (potassium and phosphate).

Similarly, direct measurements of body composition in a rat model of chronic SIADH showed that after 14 days of severe hyponatremia, body water content had returned to control levels[88] (Figure 44.3). Body sodium and chloride levels were reduced after one day of hyponatremia and were sustained for 14 days, and body potassium was significantly decreased after 7 days. Acutely, water retention was the major cause of hyponatremia, but solute depletion was primarily responsible when the electrolyte disturbance was sustained.

Urinary losses can directly lower the plasma sodium concentration when the concentration of sodium plus potassium in the urine is higher than the plasma sodium concentration. This can occur when high vasopressin levels (which concentrate the urine) and high rates of sodium and potassium excretion occur together. The excretion of hypertonic urine generates free water, in essence "desalinating" the plasma.[89]

Serum Bicarbonate Concentration in SIADH

In SIADH, the serum sodium and chloride concentrations are lowered by dilution, but the serum

bicarbonate concentration is typically normal.[90,91] This finding has been explained by a direct effect of hyponatremia on the adrenal gland to increase aldosterone secretion, which then augments renal net acid excretion.[92] Patients with hyponatremia due to hypopituitarism have many features in common with patients with non-endocrine SIADH, but their serum bicarbonate concentrations are about 5 mmol/l lower. Consistent with the hypothesis that hyponatremia-induced hyperaldosteronism is responsible for the normal serum bicarbonate in classic SIADH, aldosterone levels are much lower in patients with ACTH deficiency than in patients with non-endocrine SIADH.[90]

Common Causes of SIADH

Tumors

The first cases of SIADH were described in patients with lung cancer.[78] Small-cell carcinoma of the lung remains a common cause of the syndrome; approximately 10 to 15% of these patients present with SIADH, whereas fewer than 1% of patients with non-small-cell lung cancer become hyponatremic.[93,94] Ectopic production of vasopressin appears to be responsible for most cases hyponatremia associated with small-cell carcinoma.[95,96] Arginine vasopressin, oxytocin, and neurophysins have been found by radioimmunoassay in tumors, and are produced by the vast majority of small-cell lung cancers; the quantity of vasopressin peptide is closely correlated with the presence of hyponatremia.[97–99] Atrial natriuretic peptide mRNA has also been detected in a high percentage of cell lines from patients with small-cell cancer.[100] Hyponatremia develops in approximately 3 to 7% of patients with head and neck cancer[94,101]; the mechanism for SIADH associated with these tumors is unknown. Although a number of other tumors can produce vasopressin, there are very few reports of hyponatremia associated with them.[94] SIADH may also emerge in patients with acute tumor lysis syndrome.[102,103]

Pulmonary Disease

Mild hyponatremia has long been recognized in patients with tuberculosis.[104,105] The mechanism for vasopressin release has not been determined, but hormone levels fall in response to water-loading, reflecting the reset osmostat variant of SIADH. Ectopic secretion of antidiuretic hormone was the presumptive cause of SIADH in a patient with central diabetes insipidus who developed pulmonary tuberculosis.[106] Tuberculosis-associated hyponatremia resolves within days to weeks of antituberculous therapy. Plasma vasopressin levels are typically elevated on admission in patients with bacterial pneumonia, and fall rapidly during treatment.[107] Hyponatremia is common,[108,109] and usually self-corrects relatively rapidly after a few days.[110] Abnormal vasopressin secretion in simple pneumonia is not attributable to hypovolemia, hypotension or abnormal PO_2 or PCO_2. An antidiuretic decapeptide ("pneumadin"), which rapidly increases arginine vasopressin (AVP) levels, has been isolated from rat and human lung.[111,112] Further study is needed to determine if the decapeptide mediates SIADH associated with pneumonia and other lung disorders. Acute respiratory failure (hypoxia and hypercarbia) and severe asthma are also associated with SIADH.[113,114]

Endocrine Disease

Hyponatremia is present in up to 88% of patients with Addison's disease, and in 28% of patients with isolated ACTH deficiency.[115] In Addison's disease, vasopressin is released in response to volume-depletion caused by mineralocorticoid deficiency, and altered hemodynamics caused by glucocorticoid deficiency. Glucocorticoids may also directly inhibit vasopressin release. Unlike Addison's disease, impaired water excretion in hypopituitarism is not associated with hyperkalemia, and it does not respond to volume replacement with isotonic saline so that hyponatremia in this condition has all the features of SIADH.[116–119] However, hyponatremia in patients with hypopituitarism is associated with a lower serum bicarbonate concentration than in patients with hyponatremia from other causes of SIADH (see section "Serum Bicarbonate Concentration in SIADH").[90] Impaired water excretion in hypopituitarism and in adrenalectomized mineralocorticoid replaced subjects is associated with elevated vasopressin levels; administration of a vasopressin V2 receptor-antagonist normalizes urinary water excretion in adrenalectomized mineralocorticoid replaced rats.[120] Inhibitory glucocorticoid receptors have been identified in the magnocellular neurons which secrete vasopressin, and these receptors are markedly increased under hypoosmolar conditions.[121–123] Hyponatremia with clinical features of SIADH has been described frequently in hypothyroidism; impaired water excretion can be corrected rapidly by the administration of thyroid hormone. However, it is unclear whether hemodynamic or intrarenal factors, rather than vasopressin, is responsible for impaired water excretion in this condition.[124,125]

Non-Diuretic Drugs

Arginine vasopressin used therapeutically in the treatment of gastrointestinal bleeding or in the management of septic shock, and the vasopressin analog desmopressin acetate (DDAVP), a pure V2

receptor-agonist used to treat diabetes insipidus, enuresis, and von Willebrand disease, may cause hyponatremia.[126,127] In addition, a growing number of drugs that are unrelated to vasopressin have been reported to cause hyponatremia. Most published reports involve thiazide and thiazide-like diuretics, chlorpropamide, carbamazepine, oxcarbantipsychotics, antidepressants, and nonsteroidal anti-inflammatory drugs.[128–130] Vincristine and vinblastine increase vasopressin release by unknown mechanisms, and hyponatremia associated with these agents is dose related.[128]

Several drugs associated with hyponatremia appear to increase the response of the collecting duct to circulating vasopressin.[128,131] Chlorpropamide has been the most thoroughly studied.[132] In addition to augmenting release of vasopressin from the neurohypophysis, chlorpropamide increases the number of vasopressin receptors on collecting tubule cells[133] and inhibits renal medullary synthesis of prostaglandin E_2, an agent which blunts the hydroosmotic effect of vasopressin by diminishing adenylate cyclase activity.[134–136] Inhibition of PGE_2 permits increased cAMP formation, enhancing the effect of the hormone. Nonsteroidal anti-inflammatory agents increase the hydroosmotic effect of vasopressin by a similar mechanism. Hyponatremia attributable solely to nonsteroidals has been rarely reported, but these commonly used drugs may exacerbate other causes of hyponatremia.[137,138]

Carbamazepine most commonly causes hyponatremia when it is given to subjects who habitually drink large volumes of water.[130,139] Carbamazepine increases water permeability of the distal inner medulary collecting duct in the absence of vasopressin, an effect that is cAMP-dependent and negated by a vasopressin V2 receptor-antagonist, implying an action on the V2 receptor–protein G complex.[140] Oxcarbazepine, which is enjoying increased use because of fewer drug interactions than carbamazepine, causes hyponatremia in 9% of patients with epiliepsy who are treated with the drug.[141]

Hyponatremia caused by cyclophosphamide may also be due to enhanced vasopressin action, but the mechanism for this effect has not yet been elucidated.[130] Cyclophosphamide's antidiuretic effect is delayed, with a time-course which parallels excretion of active metabolites of the drug.[142] Cyclophosphamide's antidiuretic effect may be enhanced by indomethacin.[143] There are many reports of SIADH associated with psychotropic drugs, including phenothiazines, monoamine oxidase inhibitors, and tricyclic antidepressants; causality has been most convincingly demonstrated with tricyclics.[144] More recently, a large number of cases of SIADH have been reported in patients taking serotonin reuptake inhibitors (SSRIs).[145–147] Prospective series in elderly patients have shown that 12 to 40% became hyponatremic within two weeks of starting therapy with paroxetine.[147–149] All of these agents act centrally, and could conceivably affect vasopressin release directly. There is evidence that SSRIs may have a direct effect on water permeability of the inner medullary collecting duct, increasing AQP2 without changing vasopressin levels.[150] The recreational drug, 3,4-methylenedioxymethamphetamine ("Ecstasy") has been associated with severe, and sometimes fatal, acute hyponatremia.[151] Ecstasy induces vasopressin secretion, and users of the drug who become hyponatremic typically manifest marked polydipsia.[152,153] Many cases of SIADH associated with amiodarone have been reported.[154–157]

Post-Operative SIADH

Vasopressin levels are elevated after operative procedures, and remain elevated for several days.[158] Administration of hypotonic fluid during this period of antidiuresis causes acute hyponatremia, with potentially disastrous consequences.

Urinary cation loss has been shown to play an important role in the pathogenesis of hyponatremia in patients with post-operative SIADH. In the post-operative period, it is common for physicians to infuse several liters of isotonic or hypotonic saline solutions, exceeding the intended replacement of third-space and external losses, and actually causing extracellular fluid volume-expansion. A balance study in women undergoing uncomplicated gynecological surgery showed that sodium plus potassium concentrations in the urine peaked at 295 ± 9 mEq/L, and remained hypertonic to plasma for the first 16 hours after induction of anesthesia[89](Figure 44.4). Because of the action of vasopressin and the natriuretic response to saline-induced volume-expansion, electrolyte-free water was generated, lowering the plasma sodium concentration despite infusion of isotonic saline. The infused saline was, in effect, "desalinated." A similar phenomenon occurs when patients with subarachnoid hemorrhage and "cerebral salt-wasting" are given large volumes of isotonic saline to protect cerebral perfusion.[159]

Neurologic Disorders and Cerebral Salt-Wasting

An association between hyponatremia and intracranial disease has been recognized since the 1950s, and hyponatremia has been reported in a wide variety of systemic diseases involving the CNS, including systemic lupus erythematosus, Guillain-Barre syndrome, meningitis, encephalitis, brain tumors, and brain abscesses.[160] Noting increased urinary sodium excretion in hyponatremic patients with neurologic disorders, Peters referred to the condition as "cerebral salt-wasting".[161] Once it was recognized that high rates

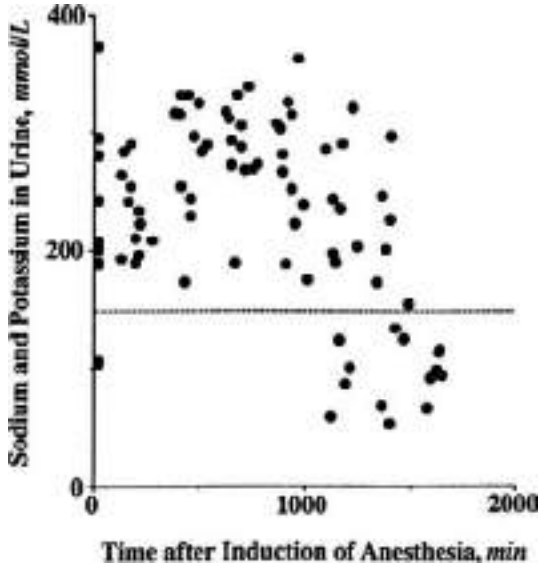

FIGURE 44.4 **Urine electrolytes in post-operative SIADH.**[89] The figure depicts the sum of urine sodium and potassium concentrations obtained post-operatively in 22 women undergoing uncomplicated gynecologic surgery and receiving infusions of 0.9% saline (sodium concentration 154 mmol/l) or lactated Ringer's solution (sodium concentration 130 mmol/l). The dotted line represents a urine cation concentration of 150 mmol/l, isotonic to normal plasma water. During the first 1000 minutes after the induction of anesthesia, urine cation concentrations were uniformly hypertonic to plasma, contributing to the genesis of hyponatremia. In samples obtained after 1000 minutes (from 16 to 24 hours), the urine remained hypertonic in some patients and became hypotonic in others. Hypotonic urine (below the dotted line) contributes to the correction of hyponatremia.

of urinary sodium excretion could be caused by unregulated secretion of antidiuretic hormone, most investigators ascribed hyponatremia in brain disease to SIADH, a syndrome which has been associated a wide array of central nervous system disorders, consistent with the multiple anatomic pathways leading to vasopressin secretion by hypothalamic neurons (Table 44.3).[162]

Cerebral salt-wasting was generally a forgotten term until the early 1980s, when a more concerted effort was made to understand the pathogenesis of hyponatremia in patients with intracranial disease (especially subarachnoid hemorrhage).[163,164] Reduced blood and plasma volume were found in most patients with intracranial disease who were presumed to have hyponatremia secondary to SIADH.[165–167] Prospective studies of patients with subarachnoid hemorrhage given maintenance fluids documented negative sodium balance, decreasing plasma volume, and increasing BUN among patients who became hyponatremic within a week of presentation.[164,168,169] A course consistent with cerebral salt-wasting was also observed in patients with head injury, brain metastases, and hydrocephalus.[170–172]

Maintaining an adequate circulatory volume has important clinical implications, especially in subarachnoid hemorrhage, where volume depletion and fluid restriction have been reported to predispose to cerebral ischemia and infarction.[173,174] This finding, and evidence that volume-expansion protects against cerebral ischemic events in subarachnoid hemorrhage, has led to a general acceptance of "hypertensive, hypervolemic, hemodilutional" therapy for the disorder.[175–177] When such treatment is given, a high urine sodium concentration and hyponatremia are not reliable indicators of salt-wasting, because hyponatremia may be due to SIADH and the natriuresis may be a response to iatrogenic volume-expansion. In one study, a positive balance for sodium could be documented in most patients believed to have cerebral salt-wasting when calculations included all infusions from the time of first contact with medical or paramedical personnel.[178] High levels of catecholamines which are often associated with brain injury decrease venous capacitance and raise blood pressure, potentially increasing "effective arterial blood volume," and promoting a physiological natriuresis.[179]

A valid diagnosis of cerebral salt-wasting requires proof of urinary sodium losses, despite reduced effective arterial blood volume. Attempts to establish a diagnosis of hypovolemia have included clinical impressions, central venous pressure, and measurements of plasma and blood volume; none of these can define hypovolemia definitively.[180]

As in patients with SIADH, plasma vasopressin levels are increased and urine sodium concentrations are elevated, but the increased vasopressin secretion in cerebral salt-wasting has been attributed to volume-depletion caused by the primary salt-wasting. Investigation into the pathogenesis of cerebral salt-wasting has focused primarily on the relative roles of natriuretic hormones and vasopressin after subarachnoid hemorrhage.[181–183] Atrial natriuretic peptide (ANP) and brain natriuretic peptide (BNP) are both derived from cardiac tissue, and have natriuretic and aldosterone-inhibiting properties. Although BNP has been localized to the hypothalamus, it is primarily of cardiac origin. Cardiac release of ANP and BNP is regulated in part by the CNS, and brain injury may induce their release from cardiac tissue. Plasma ANP levels generally correlate with the presence and severity of blood in the ventricles and increased intracranial pressure.[182] In one study, however, plasma levels of BNP, but not ANP or vasopressin, were correlated with urinary sodium excretion,[184] and in a rat model of cerebral salt-wasting, ANP levels decreased and BNP levels did not change.[185] Jugular venous sampling in

suspected cerebral salt-wasting did not support cerebral release of BNP.[186] It is thus unclear whether elevated natriuretic peptide levels are responsible for natriuresis in subarachnoid hemorrhage, and other factors, such altered sympathetic tone, depressed aldosterone levels, ouabain-like compound, and endothelin may contribute.[160,167,181,187] In fact, several studies have indicated that fludrocortisone may be effective in the treatment of cerebral salt-wasting.[188–191]

Regardless of the pathogenesis of renal salt-wasting in patients with subarachnoid hemorrhage, hyponatremia appears to be caused by vasopressin release that is independent of volume-depletion, and is thus "inappropriate." In a large prospective study of acute aneurysmal subarachnoid hemorrhage treated aggressively with isotonic saline (between 3 and 8 liters daily), hyponatremia developed in one-third of the patients within 4 to 6 days, despite positive fluid balance, increased blood volume, and suppressed plasma renin and aldosterone levels.[159] Plasma vasopressin was measured at concentrations of 1 to 4 pg/ml, despite plasma osmolalities at which the hormone should have been undetectable. Although plasma ANP levels were also increased in most patients, they did not correlate with serum sodium concentration. Thus, it is likely that both salt loss and SIADH contribute in varying degrees to the pathogenesis of hyponatremia after subarachnoid hemorrhage.

The true incidence of cerebral salt-wasting among patients with subarachnoid hemorrhage is probably low, and a clear distinction between this entity and SIADH in neurosurgical patients may not be important, because in either case the most effective treatment is intravenous hypertonic saline.[180]

Nephrogenic Syndrome of Inappropriate Antidiuresis

A gain-of-function mutation of the V2 receptor gene, named nephrogenic syndrome of antidiuresis (NSIAD), was first described in 2005.[81] Patients with this X-linked disease present with clinical and laboratory evaluations typical of SIADH, with undetectable plasma vasopressin levels. Missense mutations substituting cysteine or leucine for arginine on codon 137 cause constitutive activation of the vasopressin receptor, analogous to loss-of-function mutations found in patients with X-linked nephrogenic diabetes insipidus. Infants with NSIAD are at high risk for hyponatremia, because their diet consists primarily of liquid with little solute. However, the disease can escape detection until adulthood, and it should be suspected in young patients with a clinical diagnosis of idiopathic SIADH, especially if there is unresponsiveness to vasopressin antagonists. Female heterozygotes with skewed X-inactivation may develop spontaneous hyponatremia or an abnormal water-loading test.[192,193]

ADAPTATIONS TO HYPOTONIC HYPONATREMIA

Organic Osmolytes and Cell Volume Regulation

The osmotic challenges faced by hyponatremic patients are analogous to those faced by invertebrate organisms when they are exposed to a hypotonic environment. Throughout nature, cells respond to water stress in a similar manner. Water crosses cell membranes in response to osmotic forces, equalizing the activities of intracellular and extracellular solute. Cell volume is determined by the amount and concentration of intracellular solute. Since at equilibrium intracellular and extracellular osmolalities are equal, the relationship between cell volume and extracellular osmolality can be described by the following equation:

$$\text{Cell water} \approx \frac{\text{Cell solute content}}{\text{Extracellular osmolality}} \qquad (44.2)$$

Hypotonicity causes cells to swell initially as water diffuses into them, equalizing the osmolality of intracellular and extracellular fluids. Almost immediately, however, most cells begin to adjust their volume back towards normal.[194–196] This "volume regulatory decrease," is explained by reductions in cell solute content. The first response to osmotic stress is a loss of potassium. With time, loss of organic solutes dominate the response.

Most cells maintain relatively high concentrations of small, osmotically-active organic molecules known as "organic osmolytes." The major organic osmolytes found in nature are limited to a few classes of compounds—polyols, methylamines, and free amino acids—that are shared by diverse species. Organic osmolytes are non-perturbing solutes; unlike sodium and potassium, their intracellular concentrations may vary widely without affecting tertiary protein structure. Cells accumulate organic osmolytes under hypertonic conditions and lose them when confronted with hypotonicity. Several organic osmolytes are exported from swollen cells through a common channel, the volume-sensitive organic osmolyte/anion channel (VSOAC).[196,197] Osmolytes are transported into the cell by specific transporters, such as the sodium-myoinositol transporter (SMIT)[198] and the taurine transporter (TAUT).[199]

Cell volume control mechanisms could modify the relationship between the plasma sodium concentration and body water, sodium, and potassium content

shown in Eq. (44.1). For example, if the intracellular fluid compartment were to lose 15% of its solute (exclusive of potassium) in response to cell swelling, the amount of water needed to lower the plasma sodium concentration would be reduced by one-third. Some balance studies in patients with very low plasma sodium concentrations have failed to fully account for the severity of hyponatremia, a finding that would be expected if there were substantial losses of organic osmolytes from body cells.

Brain Adaptations to Hyponatremia

The need for cell volume regulation is greatest in the brain, where the rigid calvarium limits the degree of tissue swelling that can be tolerated.[200,201] An increase in brain water content of more than about 5 to 10% is incompatible with life. Although the capillary endothelium that forms the blood–brain barrier has a limited permeability to ions and other solutes, it allows relatively rapid water movement into the brain. Therefore, an osmotic gradient between the brain and plasma can exist only transiently, and it is dissipated by water movement in less than one hour. Hydraulic conductivity of the capillaries which form the blood–brain barrier decreases in response to hypotonicity.[202] However, because the brain and plasma must eventually come into osmotic equilibrium, this adaptation can only postpone brain swelling. The brain's interstitial fluid compartment communicates with the spinal fluid through a series of extracellular channels. Bulk flow of fluid between the brain's interstitial space and the cerebrospinal fluid provides a rapid defense against osmotic brain swelling. Ultimately, protection against lethal cerebral edema depends on the ability of brain cells to reduce their solute content.

In experimental hyponatremia in the rat, depletion of brain sodium, potassium, and chloride accounts for about two-thirds of the adaptive decrease in brain osmolality, while approximately one-third is contributed by organic osmolyte losses. Within 24 hours of the onset of hyponatremia, diminished brain concentrations of myoinositol, glutamate, creatine/phosphocreatine, and taurine can be detected.[203] During sustained hyponatremia, these compounds, plus glycerophosphorylcholine and glutamine, continue to be lost from the brain for approximately three days.[204,205] Reduced concentrations of these solutes persist when animals are kept severely hyponatremic for as long as two weeks. The loss of organic osmolytes contributes substantially to both the early and late adaptations to hyponatremia. In rats whose serum sodium concentrations were reduced to 96 mmol/L in one day, brain water content increased by less than 5%; it was estimated that the increase would have been 11% had there been no losses of organic osmolytes.[203] After three days of hyponatremia, additional losses of brain solute further decrease the severity of brain edema; animals exhibit minimal neurologic findings despite serum sodium concentrations of 95 to 100 mmol/L.[206]

Magnetic resonance spectroscopy has provided evidence of reduced concentrations of organic osmolytes in the brains of patients with hyponatremia.[207] One study showed that the peak associated with inositol remained depressed for at least two weeks after correction of hyponatremia (Figure 44.5).[208] An adaptive response of the brain is evident among patients with chronic hyponatremia. Computed axial tomography and magnetic resonance images do not show evidence of brain edema, and neurologic symptoms may be subtle even in patients with serum sodium concentrations less than 110 mEq/L. Most patients with hyponatremia of this severity survive, and the few neurologic sequelae that occur appear to be caused by overzealous correction of hyponatremia, rather than the electrolyte disturbance itself.[36,209]

In contrast to chronic hyponatremia, patients who become severely hyponatremic in less than 48 hours develop headaches, vomiting, agitated delirium, and eventually stupor, seizures, and coma. The clinical syndrome in both humans and experimental animals is associated with cerebral edema which can be reversed by the administration of hypertonic saline. On occasion, acute hyponatremia can lead to respiratory arrest, transtentorial herniation, and death.[210–214] When large volumes of water are retained in a short period of time, the arterial sodium concentration (to which the brain is exposed) may be up to 4 mmol/l lower than the venous concentration (which is most commonly sampled for clinical sodium measurements).[215]

Age, Sex, and the Adaptation to Hyponatremia

Recently, a single group of investigators have reported on over 100 previously healthy patients who became hyponatremic 1–2 days after routine elective surgery, and who subsequently died or suffered permanent brain damage. Individual patients had serum sodium concentrations as high as 129 mEq/L when they developed respiratory arrest and brain herniation.[212–214] The most recent reports emphasize the frequent association of hyponatremic encephalopathy with neurogenic pulmonary edema[213] and terminal diabetes insipidus.[216] Remarkably, virtually all of the reported patients were women, usually of child-bearing age[214] or prepubescent children.[212] These findings led these authors to suggest that sex hormones alter

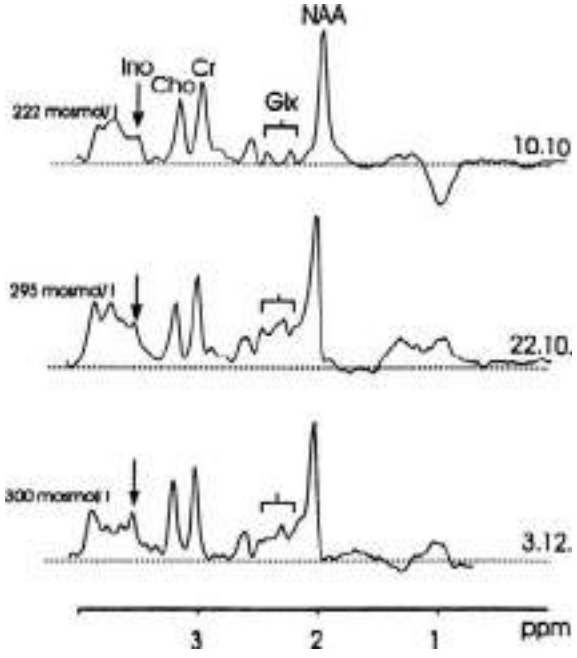

FIGURE 44.5 **Brain organic osmolytes in human hyponatremia.**[208] The figure depicts the results of magnetic resonance spectroscopy of the brain of a single patient before and after treatment of severe hyponatremia (plasma sodium 101 mmol/l, plasma osmolality 222 mosm/kg). The spectroscopy tracings were obtained on three different dates. The top tracing, taken on October 10, when the plasma osmolality was 222 mosm/l, shows an extremely low inositol peak (arrow). The middle tracing, taken on October 22, ten days after treatment of hyponatremia when the plasma osmolality was 295 mosm/l, shows an inositol peak that is still depressed. The bottom tracing, taken on December 3, 7 weeks after correction of hyponatremia shows a much higher inositol peak.

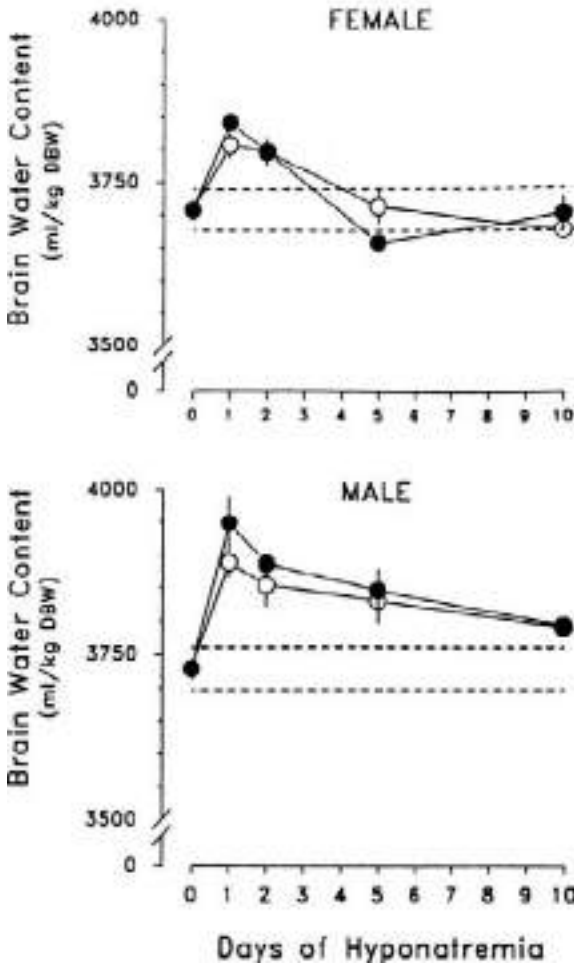

FIGURE 44.6 **Brain water content in hyponatremic male and female rats.**[219] The figure depicts measurements of brain water content obtained in male and female rats made hyponatremic with a liquid diet and either arginine vasopressin (solid circles) or dDAVP (open circles). Brain water contents are comparable in the two sexes, returning to or toward control values after ten days of hyponatremia.

the adaptive mechanisms that protect against brain edema in hyponatremia.[217]

The same investigators have used experimental models to test their hypothesis that hyponatremia causes more severe brain swelling in females than in males. The results of these studies are inconclusive. The investigators initially found that mortality from hyponatremia was markedly increased in adult female rats[218] (a finding that has not been reproduced by other laboratories[219]). They attributed excess mortality in females to lower levels of brain Na-K-ATPase (and thus a decreased ability to extrude brain sodium), and to increased susceptibility to vasopressin-induced vasoconstriction of the cerebral vasculature. *In vitro* studies showed that estrogens inhibit volume regulation in rat brain astrocyte culture.[220] However, measurements of brain water and solutes in whole brain by these and other investigators show comparable responses to hyponatremia in male and female animals[219] (Figure 44.6).

More recently, Arieff and co-workers reported that although brain water and electrolyte contents in hyponatremic adult male and female rats do not differ, the brains of newborn rats paradoxically accumulate excess sodium in response to hyponatremia, unless the animals are pretreated with testosterone.[221] Silver and co-workers were unable to reproduce this provocative finding.[222]

Hypoxia and the Adaptation to Hyponatremia

Some investigators have emphasized the adverse effects of hypoxia in hyponatremic patients. According to this view, when brain damage complicates symptomatic hyponatremia, an hypoxic episode can usually be implicated.[223] Although it is likely that hypoxia is an important factor among patients with acute hyponatremia who die of cerebral edema, the role of hypoxia in the demyelinating brain lesions which

complicate the treatment of chronic hyponatremia has not been proven (see section "Rapid Correction of Hyponatremia and Osmotic Demyelination").[224,225] Despite recurrent episodes of acute hyponatremia, hyponatremic seizures, respiratory arrests requiring endotracheal intubation, and rapid correction of hyponatremia (due to spontaneous diuresis), infants and psychotic patients with acute water intoxication rarely develop neurologic sequelae.[209]

Hyponatremic animals are more likely to die when exposed to hypoxia than normonatremic animals, and ischemic brain injury impairs the adaptive loss of brain sodium which protects against brain swelling in hyponatremia.[226] In addition, hyponatremia has been shown to lower levels of the antioxidants taurine, glutathione, and ascorbate in brain tissue, which could predispose to oxidant injury when a period of hypoxia is followed by reoxygenation.[227,228]

RAPID CORRECTION OF HYPONATREMIA AND OSMOTIC DEMYELINATION

Biochemical Effects of Rapid Correction of Hyponatremia

Adaptations that protect against brain swelling also predispose to injury when sustained hypotonicity is suddenly corrected. When the plasma sodium is returned to normal, cellular solutes lost in the adaptive phase must be recovered to prevent cellular dehydration. Electrolytes and glutamate quickly return to the brain after correction, but reaccumulation of other organic osmolytes requires several days, because it requires upregulation of sodium-dependent transport proteins.[229,230] The taurine transporter, SNAT2, may be particularly important because of its preferential localization on oligodendrocytes, the cells that are selectively damaged and lost when chronic hyponatremia is rapidly corrected.[231] After rapid correction of hyponatremia, solute-depleted brain cells are initially dehydrated. Brain electrolyte content then "overshoots," increasing to supernormal levels, possibly in compensation for the deficit in organic osmolyte content[225,232] (Figure 44.7).

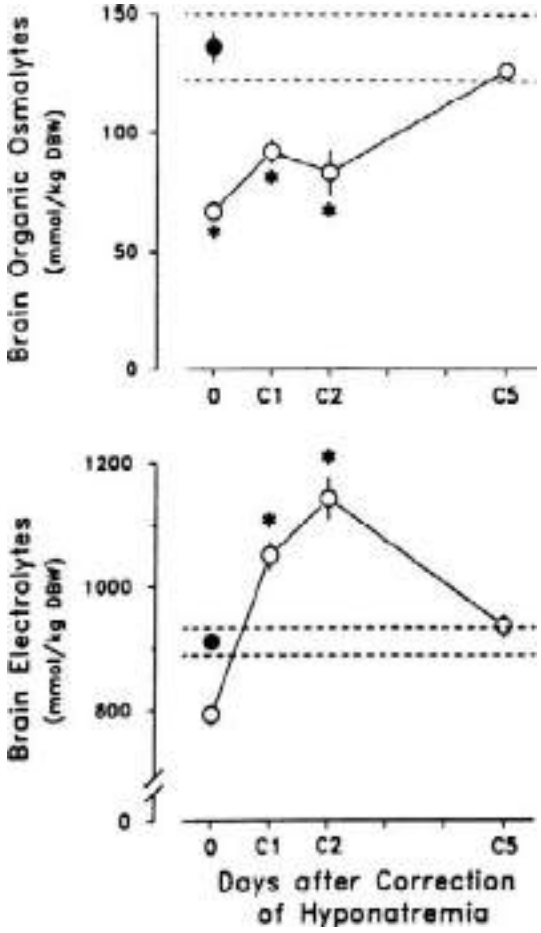

FIGURE 44.7 **Brain organic osmolytes and brain electrolytes after rapid correction of experimental hyponatremia.**[232] The figure depicts measurements of brain organic osmolytes (top panel) and brain electrolytes (bottom panel) made in rats made hyponatremic with dDAVP and a liquid diet and then corrected by withdrawal of dDAVP. Brain organic osmolytes remain significantly below normonatremic control levels (solid circle and dotted lines) on the first two days after correction (C1 and C2), and have not reached normal levels until five days after correction (C5). During the first two days after correction, brain electrolyte content "overshoots" exceeding control levels.

Clinical Effect of Rapid Correction of Hyponatremia

In humans, correction of severe chronic hyponatremia by more than 10 mEq/L in 24 hours or 18 mEq/L in less than 48 hours is associated with a distinctive clinical disorder known as the "osmotic demyelination syndrome".[210,233–236] In typical cases of the syndrome, improvement of hyponatremic symptoms during correction of hyponatremia is followed within one to several days by gradual neurologic deterioration. Behavioral disturbances, seizures, movement disorders or akinetic mutism may emerge, and severe cases develop clinical features of a pontine disorder (pseudobulbar palsy, quadriparesis, and pseudocoma).

The clinical symptoms are associated with demyelinating brain lesions which can be demonstrated by magnetic resonance images.[237,238] The most characteristic lesions are located in the center of the pons ("central pontine myelinolysis"),[239,240] but histologically similar lesions are often found in a symmetrical distribution in extrapontine areas of the brain where there is a close

admixture of gray and white matter.[234] The lesions are distinctly different from those caused by hypoxia, and they may develop without a preceding hypoxic insult.[209,235,236,241]

Patients with acute hyponatremia (e.g., infants and psychotic patients) usually tolerate rapid correction of hyponatremia without developing complications, and patients with liver disease (a disorder characterized by low levels of brain myoinositol,[242]) alcoholism, malnutrition, and potassium depletion[243] seem to be particularly susceptible to osmotic demyelination.

Experimental Models of Osmotic Demyelination

The osmotic demyelination syndrome has been reproduced in animal models in three different species by multiple laboratories.[206,244–248] These studies have confirmed the strong clinical impression that the disorder is caused by treatment of hyponatremia, rather than hyponatremia itself. Osmotic demyelination does not develop in animals with uncorrected or slowly-corrected hyponatremia. Rapid correction of chronic (three days), but not acute, hyponatremia produces a delayed onset of neurologic symptoms and brain lesions that are histologically similar to those seen in the human disease. Neurologic deterioration and histologic brain damage are preceded by pathologic evidence of blood–brain barrier disruption which can be demonstrated ultrastructurally as early as three hours, and by magnetic resonance imaging one day after rapid correction of hyponatremia.[249–251] After excessive correction of chronic hyponatremia, re-induction of hyponatremia when neurologic findings begin to appear improves survival and prevents the subsequent appearance of myelinolysis in rats, and this strategy has been successfully employed in isolated clinical case reports.[252–254]

Depletion of brain organic osmolytes is felt to play a key role in the blood–brain barrier disruption and demyelination that occurs after rapid correction of hyponatremia. In rats, measurements of organic osmolyte content in different areas of the brain after rapid correction of hyponatremia has shown that areas with the most severe demyelinating lesions are those with the least recovery of organic osmolytes.[255] It has been suggested that blood–brain barrier disruption can be explained by loss of organic osmolytes from brain capillary endothelial cells during the adaptation to hyponatremia with subsequent endothelial cell shrinkage after rapid correction. Blood–brain barrier disruption permits complement, and possibly other toxic plasma constituents, to enter the brain, which may explain the occurrence of progressive myelinolysis even after blood–brain integrity is restored.[249] Re-induction of hyponatremia following rapid correction prevents blood–brain barrier opening and microglial activation, and this can also be achieved by administering glucocorticoids; however, while therapeutic re-lowering of the serum sodium concentration reduced mortality after rapid correction, glucocorticoids did not, suggesting that the increased permeability seen in osmotic demyelination syndrome may not be a primary pathophysiological insult in this syndrome.[252]

Hyponatremic animals with uremia are relatively tolerant of rapid correction, with a lower incidence and severity of myelinolysis than non-uremic animals.[225,256] Resistance to myelinolysis in uremia is associated with more rapid reuptake of organic osmolytes, in particular myoinositol, following rapid correction of hyponatremia. In addition, rapidly corrected uremic animals do not exhibit the "overshoot" in brain sodium content seen in non-uremic animals. Normalization of brain myoinositol can be accelerated in non-uremic hyponatremic rats by administering myoinositol exogenously during rapid correction of the electrolyte disturbance.[257] Exogenous myoinositol improves survival and reduces mortality from rapid correction of chronic hyponatremia in rats.[258]

BONE DISEASE IN HYPONATREMIA

Even mild hyponatremia is associated with gait instability and an increased incidence of falls and fractures.[259,260] Hyponatremia-induced bone loss amplifies the risk of fracture. Three months of severe hyponatremia reduces bone mineral density by 30% in the rat, and is associated with decreased bone formation and increased bone resorption; cross-sectional human data showing that mild hyponatremia is associated with significantly increased odds of osteoporosis are consistent with the experimental data in rodents.[261]

TREATMENT OF HYPOTONIC HYPONATREMIA

Treatment Modalities

Water Restriction

Even with maximally-concentrated urine, evaporative water losses from the skin and lungs will lead to negative water balance and gradual correction of hyponatremia, regardless of the cause of the electrolyte disturbance. In patients whose ability to dilute the urine is intact (e.g., self-induced water intoxication) or can be restored to normal (e.g., by saline infusion in volume-depleted subjects), restriction of free water leads to a steady and sometimes rapid increase in the plasma sodium concentration. In patients with persistent

defects in water excretion (e.g., SIADH caused by tumors), water restriction alone increases the plasma sodium concentration extremely slowly, and it will be totally ineffective if the concentrations of sodium plus potassium in the urine exceed that of plasma.[262]

Sodium Chloride

Assuming that free water intake is restricted, sodium chloride solutions increase the plasma sodium concentration as long as the electrolyte concentration of the solution exceeds that of the urine. As urine cation concentrations rarely exceed 400 mEq/L, 3% sodium chloride (513 mEq/L) is always an effective treatment for hyponatremia. Isotonic saline itself does little to increase the plasma sodium concentration, unless it provokes a water diuresis by eliminating a hemodynamic stimulus for vasopressin secretion caused by volume-depletion. In fact, large volumes of isotonic saline can exacerbate hyponatremia in patients with SIADH who excrete highly concentrated urine.[89] The rate of hypertonic saline infusion must be adjusted frequently in response to the observed increase in serum sodium concentration; predictive formulas are unreliable, because urinary water losses often increase during therapy, even in patients who appear to have euvolemic hyponatremia.[263,264]

Potassium Chloride

Given the relationship between the plasma sodium concentration and exchangeable sodium and potassium,[3,8] it follows that potassium repletion of hypokalemic hyponatremic subjects should increase the plasma sodium concentration. There is limited published experience validating this expectation in patients with diuretic-induced hyponatremia,[41] and in the authors' experience (unpublished observations) potassium effectively corrects hyponatremia, regardless of the cause of potassium depletion.

Loop Diuretics

By blocking sodium reabsorption in the ascending limb of the loop of Henle, loop diuretics impair the ability to maximally concentrate the urine, even in the presence of high levels of plasma vasopressin. Used alone or in combination with angiotensin-converting enzyme inhibitors, loop diuretics are effective in treating hyponatremia associated with edematous conditions.[265–267] In patients with SIADH, loop diuretics can be combined with 3% saline for the treatment of hyponatremic emergencies.[268] Traditionally, in this maneuver, urinary sodium losses are matched with infused saline. However, given the adaptive loss of sodium that occurs in SIADH, it may be more appropriate to allow sodium intake to exceed urinary losses. In patients with SIADH who require chronic outpatient therapy, loop diuretics combined with oral salt tablets and potassium replacement (or concurrent therapy with a potassium sparing diuretic) are effective.

Demeclocycline

Demeclocycline is a tetracycline antibiotic which blocks the effect of vasopressin in the collecting duct. After a few days of therapy, demeclocycline induces a state of nephrogenic diabetes insipidus, which resolves within several days when the drug is stopped.[269] This side-effect of the antibiotic has been exploited in the long-term treatment of SIADH.[270,271] Demeclocycline is nephrotoxic in patients with heart failure and liver disease.[272,273]

Urea

Urea, administered orally in a daily dose of 0.5 g/kg body weight per day, increases urinary electrolyte free water losses, allowing liberalized fluid intake in patients with chronic hyponatremia due to SIADH, and other disorders such as congestive heart failure.[274,275] However, it tastes poorly and is contraindicated in liver and renal failure. Intravenous urea has also been effective in treating acute hyponatremia.[276] In experimental models, Soupart and Decaux have demonstrated that acute correction of chronic hyponatremia with urea decreases the risk of myelinolysis.[277] Although the mechanism of this protection is unknown, it has been speculated that urea enters the brain and then is cleared from the plasma more slowly than it is cleared from brain tissue,[278,279] thereby protecting against brain cell shrinkage after rapid correction. Experience with urea is much more extensive in Europe than in the United States.

V_2-Receptor Antagonists

Vasopressin antagonists, called "vaptans" because of the suffix applied to their generic names, block the binding of vasopressin to its renal receptor, preventing water reabsorption, decreasing urine osmololality, and increasing urine output. These agents induce a dose-related water diuresis lasting approximately six hours without a significant increase in urinary sodium or potassium excretion; therefore, vasopressin receptor-antagonists are sometimes called "aquaretics"[280–282] (Figure 44.8).

Tolvaptan (OPC-41061), and conivaptan (YM-087) have been approved by the United States Food and Drug Administration for the treatment of hyponatremia. Tolvaptan is selective for the vasopressin-2 (V2) receptor responsible for the antidiuretic actions of arginine vasopressin, conivaptan is active at both the V2 receptor and the V1a receptor responsible for the vasoconstricting properties of arginine vasopressin. Selective V2-antagonists have been shown to be

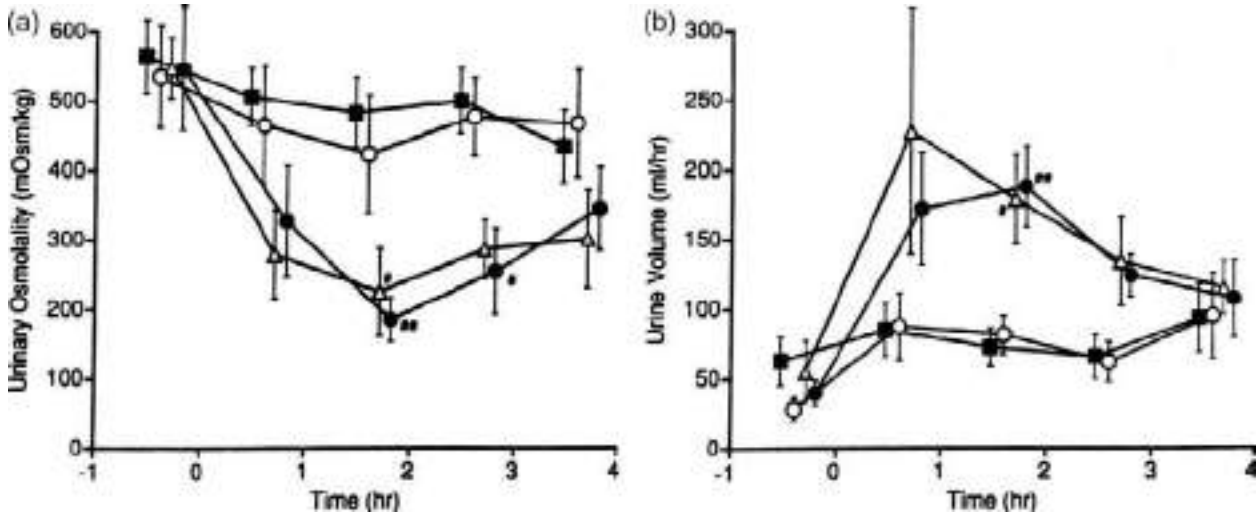

FIGURE 44.8 **Response to V2 receptor blocker in patients with SIADH.**[321] The figure depicts urine osmolality (panel a) and volume (panel b) in control subjects (closed squares) and in patients with SIADH given OPC-31260 intravenously in three doses: 0.1 mg/kg (open circles); 0.25 mg/kg (open triangles); 0.5 mg/kg (closed circles). The urine osmolality falls significantly below control values and urine volume increases significantly above control values after one hour at the two higher doses of the drug.

effective in correcting hyponatremia due to SIADH, cirrhosis, and heart failure in humans.[283–285] Conivaptan corrects hyponatremia in animal models of cirrhosis,[286] but it may be contraindicated in the human disease, because blockade of the V1a receptor may potentially provoke the hepatorenal syndrome. However, the dual receptor activity may be particularly useful in patients with CHF, because of load reduction from V1a receptor-blockade combined with reduced cardiac preload and increased sodium concentrations induced by V2 receptor antagonism.[287,288]

Because these agents cause a brisk and relatively prolonged water diuresis, V_2-receptor antagonists may risk overly rapid correction and osmotic demyelinization if they are used to treat severe chronic hyponatremia. Indeed, in an experimental model of chronic hyponatremia, increasing the plasma sodium concentration with a V_2-receptor antagonist was comparable to hypertonic saline in causing osmotic demyelination.[289]

Therapeutic Guidelines

The proper treatment of hyponatremia has been a controversial topic that has been extensively reviewed.[210,290,291] There is a general consensus that the dangers of cerebral edema and seizures mandate prompt and definitive treatment with one of the above modalities to ensure that the plasma sodium concentration begins to return to normal. Initial therapy in patients with acute hyponatremia or severe symptoms should probably begin with a bolus infusion of 1 to 2 ml/kg body weight of 3% saline, aiming for an increase of 1 to 2 mEq/L.[291–293] Therapy in all patients should be limited to avoid iatrogenic injury. Most investigators now agree that correction should not exceed 10 mEq/L in a single day or 18 mEq/L in two days, because these rates are sometimes harmful in susceptible patients, and have no proven advantage over more limited correction.[291,294] It should be emphasized that these are limits and not therapeutic goals; given the risks of severe neurological injury, and the danger of inadvertently "overshooting the mark" owing to an unexpected water diuresis, therapeutic regimens should be targeted at an increase of 6 to 8 mEq/L/day, with adjustments based on frequent measurements of the serum sodium concentration.[210,264,295]

Managing Unintentional Overcorrection

If a water diuresis occurs during therapy, sodium administration should be discontinued and, to avoid overcorrection, water losses should either be replaced or halted with the administration of desmopressin.[296,297] Alternatively, particularly in patients likely to have reversibly impaired ability to excrete dilute urine, desmopressin can be administered prophylactically, thereby maintain relatively constant urinary water losses while raising the serum sodium concentration with a concurrent infusion of 3% saline.[298]

Even with careful management, many patients experience a greater than intended increase in sodium concentration.[264,299] If this occurs, therapeutic re-lowering

of the serum sodium concentration with a brief infusion of 5% dextrose in water, using desmopressin to prevent further water losses, has been shown to be well-tolerated in a small series and a few case reports.[296,297] As discussed previously, this strategy prevents osmotic demyelination and mortality in experimental models.[252]

NON-HYPOTONIC HYPONATREMIA

Pseudohyponatremia

Plasma is normally 93% water. Thus, a sodium concentration of 143 mEq/L in a sample of whole plasma reflects a sodium concentration of 154 mEq/L in plasma water (143/0.93 = 154). Physiologic saline solutions (e.g., 0.9% NaCl) were designed to reproduce the sodium concentration in plasma water.

Pseudohyponatremia is an exaggeration of the physiologic dilution of plasma sodium by non-aqueous material.[300] High concentrations of intravascular protein (as in multiple myeloma) or lipid "dilute" the plasma sodium concentration, but do not alter the solute concentrations of the intracellular or interstitial fluid compartments. Because the "diluent" in these conditions is non-aqueous, the sodium concentration of the aqueous portion of a plasma sample, as determined by an ion-specific electrode in undiluted serum or plasma, is normal.[301,302] Plasma osmolality, as measured by an osmometer, is also normal. Thus, hyponatremia associated with hyperlipidemia or hyperproteinemia can be considered artifactual, and is called "pseudo-hyponatremia." Laboratory determinations which depend on a diluting step yield artifactually low sodium concentrations in samples taken from patients with severe hyperlipidemia or plasma cell dyscrasias, even if the instrument employs an ion-specific electrode.[301,303] In these disorders, the plasma aliquot obtained for dilution contains less plasma water (and therefore less sodium) than normal; the sodium concentration in the diluted sample is thus artifactually reduced.

Hypertonic and Isotonic Hyponatremia

Pathophysiology

If non-permeant solutes other than sodium salts accumulate in the extracellular space, the extracellular fluid volume expands, reducing the concentration of the sodium normally present in this fluid compartment. Plasma osmolality varies, depending on the cause of the syndrome.

Retention of a sodium-free isotonic solution (e.g., infusion of isotonic mannitol in a patient with renal insufficiency who excretes the solute slowly) causes isotonic hyponatremia. Mannitol, a solute that is unable to permeate cell membranes, is confined to the extracellular space; the fluid infused with the solute is similarly confined.[304] Thus, the extracellular fluid expands, and the intracellular compartment is unaffected. Sodium-free hypotonic solutions containing impermeant solutes can be considered isotonic solutions to which water has been added; hyponatremia caused by these solutions is primarily extracellular, but plasma osmolality is slightly reduced and the intracellular compartment is slightly diluted.

Retention of a sodium-free hypertonic solution (e.g., infusion of hypertonic mannitol) causes hypertonic hyponatremia.[305] In this case, intracellular water is osmotically drawn to the extracellular fluid compartment, compounding the dilution of extracellular sodium caused by the infused diluent. Thus, the sodium concentration of the extracellular space is reduced, while the osmolality of both extracellular and intracellular fluid compartments is increased.[306] A similar phenomenon has been described after administration of IgG solutions containing maltose or sucrose.[307]

Hyperglycemia

Glucose normally contributes only 5 milliosmoles per liter to plasma osmolality. The osmotic importance of glucose increases dramatically in patients with diabetic hyperglycemia. As glucose cannot permeate most cell membranes without insulin, hyperglycemia attracts intracellular water to the extracellular space, causing hyponatremia despite hyperosmolality of both extracellular and intracellular fluid compartments. Several correction factors have been offered to quantify this relationship.[308] However, a precise correction factor is probably unobtainable, because in practice hyperglycemia develops, in part, from the ingestion of glucose with water and resolves, in part, from the urinary excretion of glucose with water.[309] In patients with oliguric kidney failure, whose hyperglycemia is corrected solely by metabolism, the change in serum sodium during correction of hyperglycemia averages 1.6 mEq/L per 100 mg/dl change in blood glucose, but with considerable variability.[310]

Irrigant Absorption Syndrome

Until recently, fluid used to irrigate the operative field during transurethral resection of the prostate (TURP) and hysteroscopy had to be electrolyte free.[311] To avoid hemolysis, isosmotic to slightly hypoosmotic solutions of mannitol, sorbitol or glycine have been utilized. Several liters of irrigant may be absorbed systemically during these procedures, causing profound hyponatremia.[312–314] There are fundamental

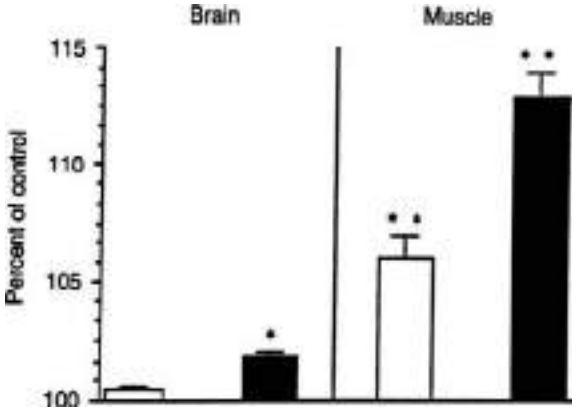

FIGURE 44.9 **Muscle and brain water contents in experimental irrigant absorption syndrome.**[318] The figure depicts measurements of brain and skeletal muscle tissue water contents, expressed as a percentage of normonatremic controls, made in ureter-ligated rats, two hours after infusion of intravenous infusion of isotonic mannitol (open bars) or glycine (black bars). Brain water content is only slightly higher after infusion of glycine than after infusion of mannitol (reflecting minimal but statistically significant penetration of the blood-brain barrier by glycine), and muscle water content is markedly higher in glycine infused animals, reflected the diffusion of glycine into muscle cells.

differences between irrigant absorption hyponatremia and post-operative hypotonic hyponatremia.

The most commonly used irrigant is 1.5% (200 mOsm/kg) glycine. Unlike patients dying of water intoxication, cerebral edema is not a prominent finding after systemic absorption of glycine irrigant and, in contrast to water intoxication, plasma osmolality is only mildly decreased despite severe hyponatremia.[315,316] Glycine and its metabolites, primarily serine and glucose, remain in the plasma for hours after absorption, contributing to plasma osmolality.[315,317]

Studies in experimental animals indicate that isosmotic (2.2%) glycine is initially confined to the extracellular space, markedly diluting the plasma sodium concentration without changing plasma osmolality.[318] As the amino acid enters skeletal muscle cells, carrying water with it, the plasma sodium concentration increases, but plasma osmolality remains constant, owing to increased plasma levels of glycine, serine, and other amino acids, urea, and glucose; in the absence of hypoosmolality brain water content increased only slightly because glycine did not enter the brain[318] (Figure 44.9). Toxicity from glycine or its metabolites, rather than hyponatremia, may contribute to the neurologic symptoms that develop after irrigant absorption. Glycine is a major inhibitory transmitter in retina, and visual hallucinations and transient blindness may occur even in the absence of hyponatremia after prostatectomy using glycine irrigant.[319] Plasma ammonia levels increase in glycine-infused animals and in humans who have absorbed glycine irrigant.[315,320] In brain, ammonia is metabolized by glutamine synthase to form glutamine, which may serve to protect the brain from the effects of hyperammonemia in liver failure.[242] In animals infused with isosmotic glycine, increased brain glutamine may contribute to the small increase in brain water content which occurs.[318] Levels of ammonia, a major metabolite of glycine, have correlated with neurologic symptoms in some, but not all, studies.

Recently, new resectoscopes have become available which permit endoscopic surgery using isotonic saline. As their use becomes more widespread, it is likely that irrigant absorption syndromes, although fascinating, will be relegated to historical interest.[311]

Hyperosmolality without Hyponatremia

Increased concentrations of permeant solutes like urea or ethanol do not affect the distribution of water in body fluid compartments, and do not cause hyponatremia. However, these solutes increase the plasma osmolality and may cause diagnostic confusion if they are present in patients with hypotonic hyponatremia from other causes.

References

[1] Edelman IS, Leibman J. Anatomy of body water and electrolytes. Am J Med 1959;27:256–77.
[2] Gennari FJ. Current concepts. Serum osmolality. Uses and limitations. N Engl J Med 1984;310(2):102–5.
[3] Edelman IS, Leibman J, O'Meara MW, Birkenfeld LW. Interrelations between serum sodium concentrations, serum osmolality and total exchangeable sodium, total exchangeable potassium and total body water. J Clin Invest 1958;37:1236–56.
[4] Overgaard-Steensen C, Larsson A, Bluhme H, Tonnesen E, Frokiaer J, Ring T. Edelman's equation is valid in acute hyponatremia in a porcine model: plasma sodium concentration is determined by external balances of water and cations. Am J Physiol Regul Integr Comp Physiol 2010;298(1):R120–9.
[5] Rose BD. New approach to disturbances in the plasma sodium concentration. Am J Med 1986;81(6):1033–40.
[6] Nguyen MK, Kurtz I. New insights into the pathophysiology of the dysnatremias: a quantitative analysis. Am J Physiol Renal Physiol 2004;287(2):F172–80.
[7] Gowrishankar M, Chen CB, Mallie JP, Halperin ML. What is the impact of potassium excretion on the intracellular fluid volume: importance of urine anions. Kidney Int 1996;50(5):1490–5.
[8] Nguyen MK, Kurtz I. Role of potassium in hypokalemia-induced hyponatremia: lessons learned from the Edelman equation. Clin Exp Nephrol 2004;8(2):98–102.
[9] Antunes-Rodrigues J, de Castro M, Elias LL, Valenca MM, McCann SM. Neuroendocrine control of body fluid metabolism. Physiol Rev 2004;84(1):169–208.
[10] Baylis PH, Thompson CJ. Osmoregulation of vasopressin secretion and thirst in health and disease. Clin Endocrinol (Oxf) 1988;29(5):549–76.
[11] Robertson GL, Aycinena P, Zerbe RL. Neurogenic disorders of osmoregulation. Am J Med 1982;72(2):339–53.

[12] Kwon TH, Hager H, Nejsum LN, Andersen ML, Frokiaer J, Nielsen S. Physiology and pathophysiology of renal aquaporins. Semin Nephrol 2001;21(3):231–8.
[13] Raymond KH, Lifschitz MD. Effect of prostaglandins on renal salt and water excretion. Am J Med 1986;80(1A):22–33.
[14] Robertson GL, Ganguly A. Osmoregulation and baroregulation of plasma vasopressin in essential hypertension. J Cardiovasc Pharmacol 1986;8(Suppl. 7):S87–91.
[15] Narins RG, Jones ER, Stom MC, Rudnick MR, Bastl CP. Diagnostic strategies in disorders of fluid, electrolyte and acid–base homeostasis. Am J Med 1982;72(3):496–520.
[16] Illowsky BP, Kirch DG. New information on polydipsia and hyponatremia in psychiatric patients. Am J Psychiatry 1988;145 (8):1039.
[17] de Leon J. Polydipsia–a study in a long-term psychiatric unit. Eur Arch Psychiatry Clin Neurosci 2003;253(1):37–9.
[18] Illowsky BP, Kirch DG. Polydipsia and hyponatremia in psychiatric patients. Am J Psychiatry 1988;145(6):675–83.
[19] Kawai N, Baba A, Suzuki T, Shiraishi H. Roles of arginine vasopressin and atrial natriuretic peptide in polydipsia-hyponatremia of schizophrenic patients. Psychiatry Res 2001;101(1):39–45.
[20] Mercier-Guidez E, Loas G. Polydipsia and water intoxication in 353 psychiatric inpatients: an epidemiological and psychopathological study. Eur Psychiatry 2000;15(5):306–11.
[21] Beresford HR. Polydipsia, hydrochlorothiazide, and water intoxication. Jama 1970;214(5):879–83.
[22] Kennedy RM, Earley LE. Profound hyponatremia resulting from a thiazide-induced decrease in urinary diluting capacity in a patient with primary polydipsia. N Engl J Med 1970;282 (21):1185–6.
[23] Bruce RC, Kliegman RM. Hyponatremic seizures secondary to oral water intoxication in infancy: association with commercial bottled drinking water. Pediatrics 1997;100(6):E4.
[24] Keating JP, Schears GJ, Dodge PR. Oral water intoxication in infants. An American epidemic. Am J Dis Child 1991;145(9): 985–90.
[25] Fenves AZ, Thomas S, Knochel JP. Beer potomania: two cases and review of the literature. Clin Nephrol 1996;45(1):61–4.
[26] Harrow AS. Beer potomania. South Med J. 1995;88(5):602.
[27] Thaler SM, Teitelbaum I, Berl T. "Beer potomania" in non-beer drinkers: effect of low dietary solute intake. Am J Kidney Dis 1998;31(6):1028–31.
[28] Steiner RW. Physiology of beer or non-beer potomania. Am J Kidney Dis 1998;32(6):1123.
[29] Taivainen H, Laitinen K, Tahtela R, Kilanmaa K, Valimaki MJ. Role of plasma vasopressin in changes of water balance accompanying acute alcohol intoxication. Alcohol Clin Exp Res 1995;19(3):759–62.
[30] Harrington AR. Hyponatremia due to sodium depletion in the absence of vasopressin. Am J Physiol 1972;222(3):768–74.
[31] Loffing J. Paradoxical antidiuretic effect of thiazides in diabetes insipidus: another piece in the puzzle [comment]. J Am Soc Nephrol 2004;15(11):2948–50.
[32] Beermann B. Thiazides and loop-diuretics therapeutic aspects. Acta Med Scand Suppl 1986;707:75–8.
[33] Chow KM, Kwan BC, Szeto CC. Clinical studies of thiazide-induced hyponatremia. J Natl Med Assoc 2004;96(10):1305–8.
[34] Kone B, Gimenez L, Watson AJ. Thiazide-induced hyponatremia. South Med J. 1986;79(11):1456–7.
[35] Sonnenblick M, Friedlander Y, Rosin AJ. Diuretic-induced severe hyponatremia. Review and analysis of 129 reported patients. Chest 1993;103(2):601–6.
[36] Sterns RH. Severe symptomatic hyponatremia: treatment and outcome. A study of 64 cases. Ann Intern Med 1987;107(5): 656–64.
[37] Clayton JA, Rodgers S, Blakey J, Avery A, Hall IP. Thiazide diuretic prescription and electrolyte abnormalities in primary care. Br J Clin Pharmacol 2006;61(1):87–95.
[38] Jiang JY, Wong MC, Ali MK, Griffiths SM, Mercer SW. Association of antihypertensive monotherapy with serum sodium and potassium levels in Chinese patients. Am J Hypertens 2009;22(3):243–9.
[39] Kim GH, Lee JW, Oh YK, Chang HR, Joo KW, Na KY, et al. Antidiuretic effect of hydrochlorothiazide in lithium-induced nephrogenic diabetes insipidus is associated with upregulation of aquaporin-2, Na-Cl co-transporter, and epithelial sodium channel. J Am Soc Nephrol 2004;15(11):2836–43.
[40] Chow KM, Szeto CC, Wong TY, Leung CB, Li PK. Risk factors for thiazide-induced hyponatraemia. Qjm 2003;96(12):911–7.
[41] Fichman MP, Vorherr H, Kleeman CR, Telfer N. Diuretic-induced hyponatremia. Ann Intern Med. 1971;75(6):853–63.
[42] Greenberg A. Diuretic complications. Am J Med Sci. 2000;319 (1):10–24.
[43] Clark BA, Shannon RP, Rosa RM, Epstein FH. Increased susceptibility to thiazide-induced hyponatremia in the elderly. J Am Soc Nephrol 1994;5(4):1106–11.
[44] Ashraf N, Locksley R, Arieff AI. Thiazide-induced hyponatremia associated with death or neurologic damage in outpatients. Am J Med 1981;70(6):1163–8.
[45] Fadel S, Karmali R, Cogan E. Safety of furosemide administration in an elderly woman recovered from thiazide-induced hyponatremia. Eur J Intern Med 2009;20(1):30–4.
[46] Friedman E, Shadel M, Halkin H, Farfel Z. Thiazide-induced hyponatremia. Reproducibility by single dose rechallenge and an analysis of pathogenesis. Ann Intern Med 1989;110(1): 24–30.
[47] Booker JA. Severe symptomatic hyponatremia in elderly outpatients: the role of thiazide therapy and stress. J Am Geriatr Soc 1984;32(2):108–13.
[48] Hamburger S, Koprivica B, Ellerbeck E, Covinsky JO. Thiazide-induced syndrome of inappropriate secretion of antidiuretic hormone. Time course of resolution. Jama 1981;246(11):1235–6.
[49] DeFronzo RA, Goldberg M, Agus ZS. Normal diluting capacity in hyponatremic patients. Reset osmostat or a variant of the syndrome of inappropriate antidiuretic hormone secretion. Ann Intern Med 1976;84(5):538–42.
[50] Earley LE, Kahn M, Orloff J. The effects of infusions of chlorothiazide on urinary dilution and concentration in the dog. J Clin Invest 1961;40:857–66.
[51] Sonnenblick M, Algur N, Rosin A. Thiazide-induced hyponatremia and vasopressin release. Ann Intern Med 1989;110(9):751.
[52] Spital A. Diuretic-induced hyponatremia. Am J Nephrol. 1999;19(4):447–52.
[53] Sonnenblick M, Rosin AJ. Significance of the measurement of uric acid fractional clearance in diuretic induced hyponatraemia. Postgrad Med J 1986;62(728):449–52.
[54] Fuisz RE, Lauler DP, Cohen P. Diuretic-induced hyponatremia and sustained antidiuresis. Am J Med 1962;33:783–91.
[55] Januezewicz W, Heinemann H, Demartini F, Laragh J. A clinical study of the effects of hydrochlorothiazide on the renal excretion of electrolytes and free water. N Engl J Med 1959;261: 264–9.
[56] Dyckner T, Wester PO. Effects of magnesium infusions in diuretic induced hyponatraemia. Lancet 1981;1(8220 Pt 1): 585–6.
[57] Anderson RJ, Chung HM, Kluge R, Schrier RW. Hyponatremia: a prospective analysis of its epidemiology and the pathogenetic role of vasopressin. Ann Intern Med 1985;102(2):164–8.
[58] Gross PA, Pehrisch H, Rascher W, Schomig A, Hackenthal E, Ritz E. Pathogenesis of clinical hyponatremia: observations of

vasopressin and fluid intake in 100 hyponatremic medical patients. Eur J Clin Invest 1987;17(2):123–9.
[59] Smith D, Moore K, Tormey W, Baylis PH, Thompson CJ. Downward resetting of the osmotic threshold for thirst in patients with SIADH. Am J Physiol Endocrinol Metab 2004;287 (5):E1019–23.
[60] Ecelbarger CA, Nielsen S, Olson BR, Murase T, Baker EA, Knepper MA, et al. Role of renal aquaporins in escape from vasopressin-induced antidiuresis in rat. J Clin Invest 1997;99(8): 1852–63.
[61] Ecelbarger CA, Murase T, Tian Y, Nielsen S, Knepper MA, Verbalis JG. Regulation of renal salt and water transporters during vasopressin escape. Prog Brain Res 2002;139:75–84.
[62] Song J, Hu X, Khan O, Tian Y, Verbalis JG, Ecelbarger CA. Increased blood pressure, aldosterone activity, and regional differences in renal ENaC protein during vasopressin escape. Am J Physiol Renal Physiol 2004;287(5):F1076–83.
[63] Murase T, Tian Y, Fang XY, Verbalis JG. Synergistic effects of nitric oxide and prostaglandins on renal escape from vasopressin-induced antidiuresis. Am J Physiol Regul Integr Comp Physiol 2003;284(2):R354–62.
[64] Schrier RW, Gurevich AK, Cadnapaphornchai MA. Pathogenesis and management of sodium and water retention in cardiac failure and cirrhosis. Semin Nephrol 2001;21(2): 157–72.
[65] Chung HM, Kluge R, Schrier RW, Anderson RJ. Clinical assessment of extracellular fluid volume in hyponatremia. Am J Med 1987;83(5):905–8.
[66] Peruzzi WT, Shapiro BA, Meyer Jr PR, Krumlovsky F, Seo BW. Hyponatremia in acute spinal cord injury. Crit Care Med 1994;22(2):252–8.
[67] Sica DA, Midha M, Zawada E, Stacy W, Hussey R. Hyponatremia in spinal cord injury. J Am Paraplegia Soc 1990;13(4):78–83.
[68] Williams HH, Wall BM, Horan JM, Presley DN, Crofton JT, Share L, et al. Nonosmotic stimuli alter osmoregulation in patients with spinal cord injury. J Clin Endocrinol Metab 1990;71(6):1536–43.
[69] Oren RM. Hyponatremia in congestive heart failure. Am J Cardiol 2005;95(9A):2B–7B.
[70] Schrier RW. Pathogenesis of sodium and water retention in high-output and low-output cardiac failure, nephrotic syndrome, cirrhosis, and pregnancy (2). N Engl J Med 1988;319 (17):1127–34.
[71] Sica DA. Hyponatremia and heart failure: pathophysiology and implications. Congest Heart Fail 2005;11(5):274–7.
[72] Francis GS, Benedict C, Johnstone DE, Kirlin PC, Nicklas J, Liang CS, et al. Comparison of neuroendocrine activation in patients with left ventricular dysfunction with and without congestive heart failure. A substudy of the studies of left ventricular dysfunction (SOLVD). Circulation 1990;82(5):1724–9.
[73] Packer M, Lee WH, Kessler PD, Gottlieb SS, Bernstein JL, Kukin ML. Role of neurohormonal mechanisms in determining survival in patients with severe chronic heart failure. Circulation 1987;75(5 Pt 2):IV80–92.
[74] Martin PY, Gines P, Schrier RW. Nitric oxide as a mediator of hemodynamic abnormalities and sodium and water retention in cirrhosis. N Engl J Med 1998;339(8):533–41.
[75] Martin PY, Schrier RW. Pathogenesis of water and sodium retention in cirrhosis. Kidney Int Suppl 1997;59:S43–9.
[76] Epstein M. Derangements of renal water handling in liver disease. Gastroenterology 1985;89(6):1415–25.
[77] Gines P, Berl T, Bernardi M, Bichet DG, Hamon G, Jiminez W, et al. Hyponatremia in cirrhosis: from pathogenesis to treatment. Hepatology 1998;28(3):851–64.
[78] Schwartz WB, Bennett W, Curelop S, Bartter FC. A syndrome of renal sodium loss and hyponatremia probably resulting from inappropriate secretion of antidiuretic hormone. Am J Med 1957;23(4):529–42.
[79] Beck LH. Hypouricemia in the syndrome of inappropriate secretion of antidiuretic hormone. N Engl J Med 1979;301 (10):528–30.
[80] Maesaka JK, Batuman V, Yudd M, Salem M, Sved AF, Venkatesan J. Hyponatremia and hypouricemia: differentiation from SIADH. Clin Nephrol. 1990;33(4):174–8.
[81] Feldman BJ, Rosenthal SM, Vargas GA, Fenwick RG, Huang EA, Matsuda-Abedini M, et al. Nephrogenic syndrome of inappropriate antidiuresis [see comment] N Engl J Med 2005;352 (18):1884–90.
[82] Zerbe R, Stropes L, Robertson G. Vasopressin function in the syndrome of inappropriate antidiuresis. Annu Rev Med 1980;31:315–27.
[83] Wrong O. The relationship between water retention and electrolyte excretion following administration of anti-diuretic hormone. *Clin Sci* (*Lond*) 1956;15(3):401–8.
[84] Cooke CR, Turin MD, Walker WG. The syndrome of inappropriate antidiuretic hormone secretion (SIADH): pathophysiologic mechanisms in solute and volume regulation. Medicine (Baltimore) 1979;58(3):240–51.
[85] Jaenike JR, Waterhouse C. The renal response to sustained administration of vasopressin and water in man. J Clin Endocrinol Metab 1961;21:231–42.
[86] Leaf A, Bartter FC, Santos RF, Wrong O. Evidence in man that urinary electrolyte loss induced by pitressin is a function of water retention. J Clin Invest 1953;32(9):868–78.
[87] Gowrishankar M, Chen CB, Cheema-Dhadli S, Steele A, Halperin ML. Hyponatremia in the rat in the absence of positive water balance. J Am Soc Nephrol 1997;8(4):524–9.
[88] Verbalis JG. Pathogenesis of hyponatremia in an experimental model of the syndrome of inappropriate antidiuresis. Am J Physiol 1994;267(6 Pt 2):R1617–25.
[89] Steele A, Gowrishankar M, Abrahamson S, Mazer CD, Feldman RD, Halperin ML. Postoperative hyponatremia despite near-isotonic saline infusion: a phenomenon of desalination. Ann Intern Med 1997;126(1):20–5.
[90] Decaux G, Musch W, Penninckx R, Soupart A. Low plasma bicarbonate level in hyponatremia related to adrenocorticotropin deficiency. J Clin Endocrinol Metab 2003;88(11): 5255–7.
[91] Graber M, Corish D. The electrolytes in hyponatremia. Am J Kidney Dis 1991;18(5):527–45.
[92] Cohen JJ, Hulter HN, Smithline N, Melby JC, Schwartz WB. The critical role of the adrenal gland in the renal regulation of acid–base equilibrium during chronic hypotonic expansion. Evidence that chronic hyponatremia is a potent stimulus to aldosterone secretion. J Clin Invest 1976;58(5):1201–8.
[93] List AF, Hainsworth JD, Davis BW, Hande KR, Greco FA, Johnson DH. The syndrome of inappropriate secretion of antidiuretic hormone (SIADH) in small-cell lung cancer. J Clin Oncol 1986;4(8):1191–8.
[94] Sorensen JB, Andersen MK, Hansen HH. Syndrome of inappropriate secretion of antidiuretic hormone (SIADH) in malignant disease. J Intern Med 1995;238(2):97–110.
[95] Johnson BE, Chute JP, Rushin J, Williams J, Le PT, Venzon D, et al. A prospective study of patients with lung cancer and hyponatremia of malignancy. Am J Respir Crit Care Med 1997;156(5):1669–78.
[96] Moses AM, Scheinman SJ. Ectopic secretion of neurohypophyseal peptides in patients with malignancy. Endocrinol Metab Clin North Am 1991;20(3):489–506.

[97] Legros JJ, Geenen V, Carvelli T, Martens H, Andre M, Corhay JL, et al. Neurophysins as markers of vasopressin and oxytocin release. A study in carcinoma of the lung. Horm Res 1990;34(3-4):151–5.
[98] Maurer LH, O'Donnell JF, Kennedy S, Faulkner CS, Rist K, North WG. Human neurophysins in carcinoma of the lung: relation to histology, disease stage, response rate, survival, and syndrome of inappropriate antidiuretic hormone secretion. Cancer Treat Rep 1983;67(11):971–6.
[99] North WG, Friedmann AS, Yu X. Tumor biosynthesis of vasopressin and oxytocin. Ann N Y Acad Sci 1993;689:107–21.
[100] Gross AJ, Steinberg SM, Reilly JG, Bliss Jr DP, Brennan J, Le PT, et al. Atrial natriuretic factor and arginine vasopressin production in tumor cell lines from patients with lung cancer and their relationship to serum sodium. Cancer Res 1993;53(1): 67–74.
[101] Ferlito A, Rinaldo A, Devaney KO. Syndrome of inappropriate antidiuretic hormone secretion associated with head neck cancers: review of the literature. Ann Otol Rhinol Laryngol 1997;106(10 Pt 1):878–83.
[102] Saintigny P, Chouahnia K, Cohen R, Pallier MC, Brechot JM, Morere JF, et al. Tumor lysis associated with sudden onset of syndrome of inappropriate antidiuretic hormone secretion. Clin Lung Cancer 2007;8(4):282–4.
[103] Vanhees SL, Paridaens R, Vansteenkiste JF. Syndrome of inappropriate antidiuretic hormone associated with chemotherapy-induced tumour lysis in small-cell lung cancer: case report and literature review. Ann Oncol 2000;11(8):1061–5.
[104] Hill AR, Uribarri J, Mann J, Berl T. Altered water metabolism in tuberculosis: role of vasopressin. Am J Med 1990;88(4): 357–64.
[105] Sims EA, Welt LG, Orloff J, Needham JW. Asymptomatic hyponatremia in pulmonary tuberculosis. J Clin Invest 1950;29 (11):1545–57.
[106] Lee P, Ho KK. Hyponatremia in pulmonary TB: evidence of ectopic antidiuretic hormone production. Chest 2010;137(1): 207–8.
[107] Dreyfuss D, Leviel F, Paillard M, Rahmani J, Coste F. Acute infectious pneumonia is accompanied by a latent vasopressin-dependent impairment of renal water excretion. Am Rev Respir Dis 1988;138(3):583–9.
[108] Kennedy PG, Mitchell DM, Hoffbrand BI. Severe hyponatraemia in hospital inpatients. Br Med J 1978;2(6147):1251–3.
[109] Thomas TH, Morgan DB, Swaminathan R, Ball SG, Lee MR. Severe hyponatraemia. A study of 17 patients. Lancet 1978;1 (8065):621–4.
[110] Dixon BS, Anderson RJ. Pneumonia and the syndrome of inappropriate antidiuretic hormone secretion: don't pour water on the fire. Am Rev Respir Dis 1988;138(3):512–3.
[111] Kosowicz J, Miskowiak B, Konwerska A, Tortorella C, Nussdorfer GG, Malendowicz LK. Tissue distribution of pneumadin immunoreactivity in the rat. Peptides 2003;24 (2):215–20.
[112] Watson JD, Jennings DB, Sarda IR, Pang SC, Lawson B, Wigle DA, et al. The antidiuretic effect of pneumadin requires a functional arginine vasopressin system. Regul Pept 1995;57(2): 105–14.
[113] Farber MO, Weinberger MH, Robertson GL, Fineberg NS, Manfredi F. Hormonal abnormalities affecting sodium and water balance in acute respiratory failure due to chronic obstructive lung disease. Chest 1984;85(1):49–54.
[114] Valli G, Fedeli A, Antonucci R, Paoletti P, Palange P. Water and sodium imbalance in COPD patients. Monaldi Arch Chest Dis 2004;61(2):112–6.
[115] Verbalis J. Hyponatremia: endocrinologic causes and consequences of therapy. Trends Endocrinol Metab 1992;3:1–7.
[116] Boykin J, DeTorrente A, Erikson A, Robertson G, Schrier R. Role of vasopressin in impaired water excretion of glucocorticoid deficiency. J Clin Invest 1978;62:738–44.
[117] Diederich S, Franzen NF, Bahr V, Oelkers W. Severe hyponatremia due to hypopituitarism with adrenal insufficiency: report on 28 cases. Eur J Endocrinol 2003;148(6):609–17.
[118] Oelkers W. Hyponatremia and inappropriate secretion of vasopressin (antidiuretic hormone) in patients with hypopituitarism. N Engl J Med 1989;321(8):492–6.
[119] Olchovsky D, Ezra D, Vered I, Hadani M, Shimon I. Symptomatic hyponatremia as a presenting sign of hypothalamic-pituitary disease: a syndrome of inappropriate secretion of antidiuretic hormone (SIADH)-like glucocorticosteroid responsive condition. J Endocrinological Invest 2005;28(2): 151–6.
[120] Ishikawa S, Schrier R. Effect of arginine vasopressin antagonist on renal water excretion in glucocorticoid and mineralocorticoid deficient rats. Kidney Int 1982;22:587–93.
[121] Berghorn KA, Knapp LT, Hoffman GE, Sherman TG. Induction of glucocorticoid receptor expression in hypothalamic magnocellular vasopressin neurons during chronic hypoosmolality. Endocrinology 1995;136(2):804–7.
[122] Kiss JZ, Van Eekelen JA, Reul JM, Westphal HM, De Kloet ER. Glucocorticoid receptor in magnocellular neurosecretory cells. Endocrinology 1988;122(2):444–9.
[123] Papanek PE, Sladek CD, Raff H. Corticosterone inhibition of osmotically stimulated vasopressin from hypothalamic-neurohypophysial explants. Am J Physiol 1997;272(1 Pt 2): R158–62.
[124] Hanna FW, Scanlon MF. Hyponatraemia, hypothyroidism, and role of arginine-vasopressin. Lancet 1997;350(9080):755–6.
[125] Iwasaki Y, Oiso Y, Yamauchi K, Takatsuki K, Kondo K, Hasegawa H, et al. Osmoregulation of plasma vasopressin in myxedema. J Clin Endocrinol Metab 1990;70(2):534–9.
[126] Callreus T, Ekman E, Andersen M. Hyponatremia in elderly patients treated with desmopressin for nocturia: a review of a case series. Eur J Clin Pharmacol 2005;61(4):281–4.
[127] Kristeller JL, Sterns RH. Transient diabetes insipidus after discontinuation of therapeutic vasopressin. Pharmacotherapy 2004;24(4):541–5.
[128] Brater DC. Drug-induced electrolyte disorders and use of diuretics. In: Kokko JP, Tannen RL, editors. Fluids and electrolytes. 3rd ed. Philadelphia: WB Saunders; 1996. p. 693–728.
[129] Chan TY. Drug-induced syndrome of inappropriate antidiuretic hormone secretion. Causes, diagnosis and management. Drugs Aging 1997;11(1):27–44.
[130] Van Amelsvoort T, Bakshi R, Devaux CB, Schwabe S. Hyponatremia associated with carbamazepine and oxcarbazepine therapy: a review. Epilepsia 1994;35(1):181–8.
[131] Moses AM, Miller M. Drug-induced dilutional hyponatremia. N Engl J Med 1974;291(23):1234–9.
[132] Weissman PN, Shenkman L, Gregerman RI. Chlorpropamide hyponatremia: drug-induced inappropriate antidiuretic-hormone activity. N Engl J Med 1971;284(2):65–71.
[133] Hensen J, Haenelt M, Gross P. Water retention after oral chlorpropamide is associated with an increase in renal papillary arginine vasopressin receptors. Eur J Endocrinol 1995;132(4): 459–64.
[134] Mendoza SA, Brown CFJ. Effect of chlorpropamide on osmotic water flow across toad bladder and the response to vasopressin, theophylline and cyclic AMP. J Clin Endocrinol Metab 1974;38:883–9.

[135] Webster B, Bain J. Antidiuretic effect and complications of chlorpropamide therapy in diabetes insipidus. J Clin Endocrinol Metab 1970;30(2):215–27.
[136] Zusman RM, Keiser HR, Handler JS. Inhibition of vasopressin-stimulated prostaglandin E biosynthesis by chlorpropamide in the toad urinary bladder. Mechanism of enhancement of vasopressin-stimulated water flow. J Clin Invest 1977;60:1348–53.
[137] Clive DM, Stoff JS. Renal syndromes associated with nonsteroidal anti-inflammatory drugs. N Engl J Med 1984;310:563–72.
[138] Petersson I, Nilsson G, Hansson BG, Hedner T. Water intoxication associated with non-steroidal anti-inflammatory drug therapy. Acta Med Scand 1987;221(2):221–3.
[139] Yassa R, Iskandar H, Nastase C, Camille Y. Carbamazepine and hyponatremia in patients with affective disorder. Am J Psychiatry 1988;145(3):339–42.
[140] de Braganca AC, Moyses ZP, Magaldi AJ. Carbamazepine can induce kidney water absorption by increasing aquaporin 2 expression. Nephrol Dial Transplant 2010;25(12):3840–5.
[141] Ortenzi A, Paggi A, Foschi N, Sabbatini D, Pistoli E. Oxcarbazepine and adverse events: impact of age, dosage, metabolite serum concentrations and concomitant antiepileptic therapy. Funct Neurol 2008;23(2):97–100.
[142] Spital A, Ristow S. Cyclophosphamide induced water intoxication in a woman with Sjogren's syndrome. J Rheumatol 1997;24(12):2473–5.
[143] Webberley MJ, Murray JA. Life-threatening acute hyponatraemia induced by low dose cyclophosphamide and indomethacin. Postgrad Med J 1989;65(770):950–2.
[144] Spigset O, Hedenmalm K. Hyponatremia in relation to treatment with antidepressants: a survey of reports in the world health organization data base for spontaneous reporting of adverse drug reactions. Pharmacotherapy 1997;17(2):348–52.
[145] Liu BA, Mittmann N, Knowles SR, Shear NH. Hyponatremia and the syndrome of inappropriate secretion of antidiuretic hormone associated with the use of selective serotonin reuptake inhibitors: a review of spontaneous reports. Cmaj 1996;155 (5):519–27.
[146] Spigset O. Adverse reactions of selective serotonin reuptake inhibitors: reports from a spontaneous reporting system. Drug Saf 1999;20(3):277–87.
[147] Woo MH, Smythe MA. Association of SIADH with selective serotonin reuptake inhibitors. Ann Pharmacother 1997;31 (1):108–10.
[148] Fabian TJ, Amico JA, Kroboth PD, Mulsant BH, Corey SE, Begley AE, et al. Paroxetine-induced hyponatremia in older adults: a 12-week prospective study. Arch Intern Med 2004;164 (3):327–32.
[149] Fabian TJ, Amico JA, Kroboth PD, Mulsant BH, Reynolds III CF, Pollock BG. Paroxetine-induced hyponatremia in the elderly due to the syndrome of inappropriate secretion of antidiuretic hormone (SIADH). J Geriatr Psychiatry Neurol 2003;16 (3):160–4.
[150] Moyses ZP, Nakandakari FK, Magaldi AJ. Fluoxetine effect on kidney water reabsorption. Nephrol Dial Transplant 2008;23 (4):1173–8.
[151] Hartung TK, Schofield E, Short AI, Parr MJ, Henry JA. Hyponatraemic states following 3,4-methylenedioxymethamphetamine (MDMA, "ecstasy") ingestion. QJM 2002;95(7): 431–7.
[152] Brvar M, Kozelj G, Osredkar J, Mozina M, Gricar M, Bunc M. Polydipsia as another mechanism of hyponatremia after "ecstasy" (3,4 methyldioxymethamphetamine) ingestion. Eur J Emerg Med 2004;11(5):302–4.
[153] Henry JA, Fallon JK, Kicman AT, Hutt AJ, Cowan DA, Forsling M. Low-dose MDMA ("ecstasy") induces vasopressin secretion. Lancet 1998;351(9118):1784.
[154] Aslam MK, Gnaim C, Kutnick J, Kowal RC, McGuire DK. Syndrome of inappropriate antidiuretic hormone secretion induced by amiodarone therapy. Pacing Clin Electrophysiol 2004;27(6 Pt 1):831–2.
[155] Ikegami H, Shiga T, Tsushima T, Nirei T, Kasanuki H. Syndrome of inappropriate antidiuretic hormone secretion (SIADH) induced by amiodarone: a report on two cases. J Cardiovasc Pharmacol Ther 2002;7(1):25–8.
[156] Odeh M, Schiff E, Oliven A. Hyponatremia during therapy with amiodarone. Arch Intern Med 1999;159(21):2599–600.
[157] Shavit E, Sherer Y. Hyponatremia induced by amiodarone therapy. Isr Med Assoc J 2007;9(7):564–5.
[158] Thomas TH, Morgan DB. Post-surgical hyponatraemia: the role of intravenous fluids and arginine vasopressin. Br J Surg 1979;66(8):540–2.
[159] Diringer MN, Wu KC, Verbalis JG, Hanley DF. Hypervolemic therapy prevents volume contraction but not hyponatremia following subarachnoid hemorrhage. Ann Neurol 1992;31(5): 543–50.
[160] Palmer BF. Hyponatremia in patients with central nervous system disease: SIADH versus CSW. Trends Endocrinol Metab 2003;14(4):182–7.
[161] Peters JP, Welt LG, Sims EA, Orloff J, Needham J. A salt-wasting syndrome associated with cerebral disease. Trans Assoc Am Physicians 1950;63:57–64.
[162] Kroll M, Juhler M, Lindholm J. Hyponatraemia in acute brain disease. J Intern Med 1992;232(4):291–7.
[163] Nelson PB, Seif S, Gutai J, Robinson AG. Hyponatremia and natriuresis following subarachnoid hemorrhage in a monkey model. J Neurosurg 1984;60(2):233–7.
[164] Nelson PB, Seif SM, Maroon JC, Robinson AG. Hyponatremia in intracranial disease: perhaps not the syndrome of inappropriate secretion of antidiuretic hormone (SIADH). J Neurosurg 1981;55(6):938–41.
[165] Nelson RJ. Blood volume measurement following subarachnoid haemorrhage. Acta Neurochir Suppl (Wien) 1990;47: 114–21.
[166] Solomon RA, Post KD, McMurtry III JG. Depression of circulating blood volume in patients after subarachnoid hemorrhage: implications for the management of symptomatic vasospasm. Neurosurgery 1984;15(3):354–61.
[167] Yamaki T, Tano-oka A, Takahashi A, Imaizumi T, Suetake K, Hashi K. Cerebral salt wasting syndrome distinct from the syndrome of inappropriate secretion of antidiuretic hormone (SIADH). Acta Neurochir (Wien) 1992;115(3-4):156–62.
[168] Kurokawa Y, Uede T, Ishiguro M, Honda O, Honmou O, Kato T, et al. Pathogenesis of hyponatremia following subarachnoid hemorrhage due to ruptured cerebral aneurysm. Surg Neurol 1996;46(5):500–7 [discussion 507-508]
[169] Wijdicks EF, Vermeulen M, ten Haaf JA, Hijdra A, Bakker WH, van Gijn J. Volume depletion and natriuresis in patients with a ruptured intracranial aneurysm. Ann Neurol 1985;18(2): 211–6.
[170] Ganong CA, Kappy MS. Cerebral salt wasting in children. The need for recognition and treatment. Am J Dis Child 1993;147 (2):167–9.
[171] Oster JR, Perez GO, Larios O, Emery WE, Bourgoignie JJ. Cerebral salt wasting in a man with carcinomatous meningitis. Arch Intern Med 1983;143(11):2187–8.
[172] Tanneau RA, Pennec YL, Jouquan J, Le Menn G. Cerebral salt wasting in elderly persons. Ann Intern Med 1987;107(1):120.

[173] Hasan D, Wijdicks EF, Vermeulen M. Hyponatremia is associated with cerebral ischemia in patients with aneurysmal subarachnoid hemorrhage. Ann Neurol 1990;27(1):106–8.
[174] Wijdicks EF, Vermeulen M, Hijdra A, van Gijn J. Hyponatremia and cerebral infarction in patients with ruptured intracranial aneurysms: is fluid restriction harmful? Ann Neurol 1985;17(2):137–40.
[175] Oropello JM, Weiner L, Benjamin E. Hypertensive, hypervolemic, hemodilutional therapy for aneurysmal subarachnoid hemorrhage. Is it efficacious? No. Crit Care Clin 1996;12 (3):709–30.
[176] Sivakumar V, Rajshekhar V, Chandy MJ. Management of neurosurgical patients with hyponatremia and natriuresis. Neurosurgery 1994;34(2):269–74 [discussion 274]
[177] Ullman JS, Bederson JB. Hypertensive, hypervolemic, hemodilutional therapy for aneurysmal subarachnoid hemorrhage. Is it efficacious? Yes. Crit Care Clin 1996;12(3):697–707.
[178] Carlotti AP, Bohn D, Rutka JT, Singh S, Berry WA, Sharman A, et al. A method to estimate urinary electrolyte excretion in patients at risk for developing cerebral salt wasting. J Neurosurg 2001;95(3):420–4.
[179] Singh S, Bohn D, Carlotti AP, Cusimano M, Rutka JT, Halperin ML. Cerebral salt wasting: truths, fallacies, theories, and challenges. Crit Care Med. 2002;30(11):2575–9.
[180] Sterns RH, Silver SM. Cerebral salt wasting versus SIADH: what difference? J Am Soc Nephrol 2008;19(2):194–6.
[181] Diringer MN. Neuroendocrine regulation of sodium and volume following subarachnoid hemorrhage. Clin Neuropharmacol 1995;18(2):114–26.
[182] Diringer MN, Lim JS, Kirsch JR, Hanley DF. Suprasellar and intraventricular blood predict elevated plasma atrial natriuretic factor in subarachnoid hemorrhage. Stroke 1991;22(5):577–81.
[183] McGirt MJ, Blessing R, Nimjee SM, Friedman AH, Alexander MJ, Laskowitz DT, et al. Correlation of serum brain natriuretic peptide with hyponatremia and delayed ischemic neurological deficits after subarachnoid hemorrhage. Neurosurgery 2004;54 (6):1369–73 discussion 1373–1364.
[184] Berendes E, Walter M, Cullen P, Prien T, Van Aken H, Horsthemke J, et al. Secretion of brain natriuretic peptide in patients with aneurysmal subarachnoid haemorrhage. Lancet 1997;349(9047):245–9.
[185] Kojima J, Katayama Y, Moro N, Kawai H, Yoneko M, Mori T. Cerebral salt wasting in subarachnoid hemorrhage rats: model, mechanism, and tool. Life Sci. 2005;76(20):2361–70.
[186] Powner DJ, Hergenroeder GW, Awili M, Atik MA, Robertson C. Hyponatremia and comparison of NT-pro-BNP concentrations in blood samples from jugular bulb and arterial sites after traumatic brain injury in adults: a pilot study. Neurocrit Care 2007;7(2):119–23.
[187] Wijdicks EF, Schievink WI, Burnett Jr. JC. Natriuretic peptide system and endothelin in aneurysmal subarachnoid hemorrhage. J Neurosurg 1997;87(2):275–80.
[188] Celik US, Alabaz D, Yildizdas D, Alhan E, Kocabas E, Ulutan S. Cerebral salt wasting in tuberculous meningitis: treatment with fludrocortisone. Ann Trop Paediatr 2005;25(4):297–302.
[189] Ishikawa SE, Saito T, Kaneko K, Okada K, Kuzuya T. Hyponatremia responsive to fludrocortisone acetate in elderly patients after head injury. Ann Intern Med 1987;106(2):187–91.
[190] Lee P, Jones GR, Center JR. Successful treatment of adult cerebral salt wasting with fludrocortisone. Arch Intern Med 2008;168(3):325–6.
[191] Papadimitriou DT, Spiteri A, Pagnier A, Bayle M, Mischalowski MB, Bourdat G, et al. Mineralocorticoid deficiency in post-operative cerebral salt wasting. J Pediatr Endocrinol Metab 2007;20(10):1145–50.
[192] Levtchenko EN, Monnens LA. Nephrogenic syndrome of inappropriate antidiuresis. Nephrol Dial Transplant 2010;25 (9):2839–43.
[193] Ranchin B, Boury-Jamot M, Blanchard G, Dubourg L, Hadj-Aissa A, Morin D, et al. Familial nephrogenic syndrome of inappropriate antidiuresis: dissociation between aquaporin-2 and vasopressin excretion. J Clin Endocrinol Metab 2010;95(9): E37–43.
[194] Hoffmann EK, Lambert IH, Pedersen SF. Physiology of cell volume regulation in vertebrates. Physiol Rev 2009;89(1): 193–277.
[195] McManus ML, Churchwell KB, Strange K. Regulation of cell volume in health and disease. N Engl J Med 1995;333(19): 1260–6.
[196] Strange K. Cellular volume homeostasis. Adv Physiol Educ 2004;28(1–4):155–9.
[197] Emma F, McManus M, Strange K. Intracellular electrolytes regulate the volume set point of the organic osmolyte/anion channel VSOAC. Am J Physiol 1997;272(6 Pt 1):C1766–75.
[198] Ibsen L, Strange K. *In situ* localization and osmotic regulation of the $Na(^{+})$-myoinositol co-transporter in rat brain. Am J Physiol 1996;271(4 Pt 2):F877–85.
[199] Benrabh H, Bourre JM, Lefauconnier JM. Taurine transport at the blood–brain barrier: an *in vivo* brain perfusion study. Brain Res 1995;692(1-2):57–65.
[200] Gullans SR, Verbalis JG. Control of brain volume during hyperosmolar and hypoosmolar conditions. Annu Rev Med 1993;44:289–301.
[201] Mount DB. The brain in hyponatremia: both culprit and victim. Semin Nephrol 2009;29(3):196–215.
[202] Olson JE, Banks M, Dimlich RV, Evers J. Blood–brain barrier water permeability and brain osmolyte content during edema development. Acad Emerg Med 1997;4(7):662–73.
[203] Sterns RH, Baer J, Ebersol S, Thomas D, Lohr JW, Kamm DE. Organic osmolytes in acute hyponatremia. Am J Physiol 1993;264(5 Pt 2):F833–6.
[204] Thurston JH, Hauhart RE, Nelson JS. Adaptive decreases in amino acids (taurine in particular), creatine, and electrolytes prevent cerebral edema in chronically hyponatremic mice: rapid correction (experimental model of central pontine myelinolysis) causes dehydration and shrinkage of brain. Metab Brain Dis 1987;2(4):223–41.
[205] Verbalis JG, Gullans SR. Hyponatremia causes large sustained reductions in brain content of multiple organic osmolytes in rats. Brain Res 1991;567(2):274–82.
[206] Sterns RH, Thomas DJ, Herndon RM. Brain dehydration and neurologic deterioration after rapid correction of hyponatremia. Kidney Int 1989;35(1):69–75.
[207] Videen JS, Michaelis T, Pinto P, Ross BD. Human cerebral osmolytes during chronic hyponatremia. A proton magnetic resonance spectroscopy study. J Clin Invest 1995;95(2):788–93.
[208] Haussinger D, Laubenberger J, vom Dahl S, Ernst T, Bayer S, Langer M, et al. Proton magnetic resonance spectroscopy studies on human brain myoinositol in hypo-osmolarity and hepatic encephalopathy. Gastroenterology 1994;107(5): 1475–80.
[209] Sterns RH, Clark EC, Silver SM. Clinical consequences of hyponatremia and its correction. In: Seldin DW, Giebisch G, editors. Clinical disorders of water metabolism. New York: Raven Press; 1993. p. 225–36.
[210] Adrogue HJ, Madias NE. Hyponatremia. N Engl J Med 2000;342(21):1581–9.
[211] Arieff AI. Hyponatremia, convulsions, respiratory arrest, and permanent brain damage after elective surgery in healthy women. N Engl J Med 1986;314(24):1529–35.

[212] Arieff AI, Ayus JC, Fraser CL. Hyponatraemia and death or permanent brain damage in healthy children. Bmj 1992;304 (6836):1218–22.
[213] Ayus JC, Arieff AI. Pulmonary complications of hyponatremic encephalopathy. Noncardiogenic pulmonary edema and hypercapnic respiratory failure. Chest 1995;107(2):517–21.
[214] Ayus JC, Wheeler JM, Arieff AI. Postoperative hyponatremic encephalopathy in menstruant women. Ann Intern Med 1992;117(11):891–7.
[215] Shafiee MA, Charest AF, Cheema-Dhadli S, Glick DN, Napolova O, Roozbeh J, et al. Defining conditions that lead to the retention of water: the importance of the arterial sodium concentration. Kidney Int 2005;67(2):613–21.
[216] Fraser CL, Arieff AI. Fatal central diabetes mellitus and insipidus resulting from untreated hyponatremia: a new syndrome. Ann Intern Med 1990;112(2):113–9.
[217] Ayus JC, Achinger SG, Arieff A. Brain cell volume regulation in hyponatremia: role of sex, age, vasopressin, and hypoxia. Am J Physiol Renal Physiol 2008;295(3):F619–24.
[218] Fraser CL, Kucharczyk J, Arieff AI, Rollin C, Sarnacki P, Norman D. Sex differences result in increased morbidity from hyponatremia in female rats. Am J Physiol 1989;256(4 Pt 2): R880–5.
[219] Verbalis JG. Hyponatremia induced by vasopressin or desmopressin in female and male rats. J Am Soc Nephrol 1993;3(9): 1600–6.
[220] Fraser CL, Swanson RA. Female sex hormones inhibit volume regulation in rat brain astrocyte culture. Am J Physiol 1994;267 (4 Pt 1):C909–14.
[221] Arieff AI, Kozniewska E, Roberts TP, Vexler ZS, Ayus JC, Kucharczyk J. Age, gender, and vasopressin affect survival and brain adaptation in rats with metabolic encephalopathy. Am J Physiol 1995;268(5 Pt 2):R1143–52.
[222] Silver SM, Schroeder BM, Bernstein P, Sterns RH. Brain adaptation to acute hyponatremia in young rats. Am J Physiol 1999;276(6 Pt 2):R1595–9.
[223] Knochel JP. Hypoxia is the cause of brain damage in hyponatremia. Jama 1999;281(24):2342–3.
[224] Soupart A, Penninckx R, Stenuit A, Decaux G. Lack of major hypoxia and significant brain damage in rats despite dramatic hyponatremic encephalopathy. J Lab Clin Med 1997;130(2): 226–31.
[225] Soupart A, Silver S, Schrooeder B, Sterns R, Decaux G. Rapid (24-hour) reaccumulation of brain organic osmolytes (particularly myoinositol) in azotemic rats after correction of chronic hyponatremia. J Am Soc Nephrol 2002;13(6):1433–41.
[226] Ayus JC, Armstrong D, Arieff AI. Hyponatremia with hypoxia: effects on brain adaptation, perfusion, and histology in rodents. Kidney Int 2006;69(8):1319–25.
[227] Clark EC, Thomas D, Baer J, Sterns RH. Depletion of glutathione from brain cells in hyponatremia. Kidney Int 1996;49(2): 470–6.
[228] Siushansian R, Dixon SJ, Wilson JX. Osmotic swelling stimulates ascorbate efflux from cerebral astrocytes. J Neurochem 1996;66(3):1227–33.
[229] Lien YH, Shapiro JI, Chan L. Study of brain electrolytes and organic osmolytes during correction of chronic hyponatremia. Implications for the pathogenesis of central pontine myelinolysis. J Clin Invest 1991;88(1):303–9.
[230] Spector R, Lorenzo AV. Myoinositol transport in the central nervous system. Am J Physiol 1975;228(5):1510–8.
[231] Maallem S, Mutin M, Gonzalez-Gonzalez IM, Zafra F, Tappaz ML. Selective tonicity-induced expression of the neutral amino-acid transporter SNAT2 in oligodendrocytes in rat brain following systemic hypertonicity. Neuroscience 2008;153(1): 95–107.
[232] Verbalis JG, Gullans SR. Rapid correction of hyponatremia produces differential effects on brain osmolyte and electrolyte reaccumulation in rats. Brain Res 1993;606(1):19–27.
[233] Karp BI, Laureno R. Pontine and extrapontine myelinolysis: a neurologic disorder following rapid correction of hyponatremia. Medicine (Baltimore) 1993;72(6):359–73.
[234] Laureno R, Karp BI. Myelinolysis after correction of hyponatremia. Ann Intern Med 1997;126(1):57–62.
[235] Martin RJ. Central pontine and extrapontine myelinolysis: the osmotic demyelination syndromes. J Neurol Neurosurg Psychiatry 2004;75(Suppl. 3):iii22–8.
[236] Sterns RH, Riggs JE, Schochet Jr. SS. Osmotic demyelination syndrome following correction of hyponatremia. N Engl J Med 1986;314(24):1535–42.
[237] Miller GM, Baker Jr. HL, Okazaki H, Whisnant JP. Central pontine myelinolysis and its imitators: MR findings. Radiology 1988;168(3):795–802.
[238] Ruzek KA, Campeau NG, Miller GM. Early diagnosis of central pontine myelinolysis with diffusion-weighted imaging. AJNR Am J Neuroradiol 2004;25(2):210–3.
[239] Adams RD, Victor M, Mancall EL. Central pontine myelinolysis: a hitherto undescribed disease occurring in alcoholic and malnourished patients. AMA Arch Neurol Psychiatry 1959;81 (2):154–72.
[240] Norenberg MD, Leslie KO, Robertson AS. Association between rise in serum sodium and central pontine myelinolysis. Ann Neurol 1982;11(2):128–35.
[241] Sterns RH, Cappuccio JD, Silver SM, Cohen EP. Neurologic sequelae after treatment of severe hyponatremia: a multicenter perspective. J Am Soc Nephrol 1994;4(8):1522–30.
[242] Restuccia T, Gomez-Anson B, Guevara M, Alessandria C, Torre A, Alayrach ME, et al. Effects of dilutional hyponatremia on brain organic osmolytes and water content in patients with cirrhosis. Hepatology 2004;39(6):1613–22.
[243] Lohr JW. Osmotic demyelination syndrome following correction of hyponatremia: association with hypokalemia. Am J Med 1994;96(5):408–13.
[244] Illowsky BP, Laureno R. Encephalopathy and myelinolysis after rapid correction of hyponatraemia. Brain 1987;110(Pt 4): 855–67.
[245] Kleinschmidt-DeMasters BK, Norenberg MD. Rapid correction of hyponatremia causes demyelination: relation to central pontine myelinolysis. Science 1981;211(4486):1068–70.
[246] Kleinschmidt-DeMasters BK, Norenberg MD. Neuropathologic observations in electrolyte-induced myelinolysis in the rat. J Neuropathol Exp Neurol 1982;41(1):67–80.
[247] Laureno R. Central pontine myelinolysis following rapid correction of hyponatremia. Ann Neurol 1983;13(3):232–42.
[248] Verbalis JG, Martinez AJ. Neurological and neuropathological sequelae of correction of chronic hyponatremia. Kidney Int 1991;39(6):1274–82.
[249] Adler S, Martinez J, Williams DS, Verbalis JG. Positive association between blood–brain barrier disruption and osmotically-induced demyelination. Mult Scler 2000;6(1):24–31.
[250] Rojiani AM, Cho ES, Sharer L, Prineas JW. Electrolyte-induced demyelination in rats. 2. Ultrastructural evolution. Acta Neuropathol (Berl) 1994;88(4):293–9.
[251] Rojiani AM, Prineas JW, Cho ES. Electrolyte-induced demyelination in rats. 1. Role of the blood–brain barrier and edema. Acta Neuropathol (Berl) 1994;88(4):287–92.
[252] Gankam Kengne F, Soupart A, Pochet R, Brion JP, Decaux G. Re-induction of hyponatremia after rapid overcorrection of

hyponatremia reduces mortality in rats. Kidney Int 2009;76 (6):614–21.
[253] Oya S, Tsutsumi K, Ueki K, Kirino T. Reinduction of hyponatremia to treat central pontine myelinolysis. Neurology 2001;57 (10):1931–2.
[254] Soupart A, Ngassa M, Decaux G. Therapeutic relowering of the serum sodium in a patient after excessive correction of hyponatremia. Clin Nephrol 1999;51(6):383–6.
[255] Lien YH. Role of organic osmolytes in myelinolysis. A topographic study in rats after rapid correction of hyponatremia. J Clin Invest 1995;95(4):1579–86.
[256] Soupart A, Penninckx R, Stenuit A, Decaux G. Azotemia (48 h) decreases the risk of brain damage in rats after correction of chronic hyponatremia. Brain Res 2000;852(1):167–72.
[257] Silver SM, Schroeder BM, Sterns RH. Brain uptake of myoinositol after exogenous administration. J Am Soc Nephrol 2002;13(5):1255–60.
[258] Silver SM, Schroeder BM, Sterns RH, Rojiani A. Myoinositol administration improves survival and reduces myelinolysis after rapid correction of hyponatremia in rats. J Neuropathol Exp Neurol 2006;65:1–8.
[259] Gankam Kengne F, Andres C, Sattar L, Melot C, Decaux G. Mild hyponatremia and risk of fracture in the ambulatory elderly. QJM 2008;101(7):583–8.
[260] Renneboog B, Musch W, Vandemergel X, Manto MU, Decaux G. Mild chronic hyponatremia is associated with falls, unsteadiness, and attention deficits. Am J Med 2006;119(1):71.e71–8.
[261] Verbalis JG, Barsony J, Sugimura Y, Tian Y, Adams DJ, Carter EA, et al. Hyponatremia-induced osteoporosis. J Bone Miner Res. 2010;25(3):554–63.
[262] Chen S, Jalandhara N, Batlle D. Evaluation and management of hyponatremia: an emerging role for vasopressin receptor antagonists. Nat Clin Pract Nephrol 2007;3(2):82–95.
[263] Bhaskar E, Kumar B, Ramalakshmi S. Evaluation of a protocol for hypertonic saline administration in acute euvolemic symptomatic hyponatremia: a prospective observational trial. Indian J Crit Care Med 2010;14(4):170–4.
[264] Mohmand HK, Issa D, Ahmad Z, Cappuccio JD, Kouides RW, Sterns RH. Hypertonic saline for hyponatremia: risk of inadvertent overcorrection. Clin J Am Soc Nephrol 2007;2 (6):1110–7.
[265] Dzau VJ, Hollenberg NK. Renal response to captopril in severe heart failure: role of furosemide in natriuresis and reversal of hyponatremia. Ann Intern Med 1984;100(6):777–82.
[266] Elisaf M, Theodorou J, Pappas C, Siamopoulos K. Successful treatment of hyponatremia with angiotensin-converting enzyme inhibitors in patients with congestive heart failure. Cardiology 1995;86(6):477–80.
[267] Packer M, Medina N, Yushak M. Correction of dilutional hyponatremia in severe chronic heart failure by converting-enzyme inhibition. Ann Intern Med 1984;100(6):782–9.
[268] Hantman D, Rossier B, Zohlman R, Schrier R. Rapid correction of hyponatremia in the syndrome of inappropriate secretion of antidiuretic hormone. An alternative treatment to hypertonic saline. Ann Intern Med 1973;78(6):870–5.
[269] De Troyer A. Demeclocycline. Treatment for syndrome of inappropriate antidiuretic hormone secretion. Jama 1977;237 (25):2723–6.
[270] Forrest Jr JN, Cox M, Hong C, Morrison G, Bia M, Singer I. Superiority of demeclocycline over lithium in the treatment of chronic syndrome of inappropriate secretion of antidiuretic hormone. N Engl J Med 1978;298(4):173–7.
[271] Trump DL. Serious hyponatremia in patients with cancer: management with demeclocycline. Cancer 1981;47(12): 2908–12.
[272] Miller PD, Linas SL, Schrier RW. Plasma demeclocycline levels and nephrotoxicity. Correlation in hyponatremic cirrhotic patients. Jama 1980;243(24):2513–5.
[273] Perez-Ayuso RM, Arroyo V, Camps J, Jimenez W, Rodamilans M, Rimola A, et al. Effect of demeclocycline on renal function and urinary prostaglandin E2 and kallikrein in hyponatremic cirrhotics. Nephron 1984;36(1):30–7.
[274] Cauchie P, Vincken W, Decaux G. Urea treatment for water retention in hyponatremic congestive heart failure. Int J Cardiol 1987;17(1):102–4.
[275] Decaux G, Genette F. Urea for long-term treatment of syndrome of inappropriate secretion of antidiuretic hormone. Br Med J (Clin Res Ed) 1981;283(6299):1081–3.
[276] Reeder RF, Harbaugh RE. Administration of intravenous urea and normal saline for the treatment of hyponatremia in neurosurgical patients. J Neurosurg 1989;70(2):201–6.
[277] Soupart A, Stenuit A, Perier O, Decaux G. Limits of brain tolerance to daily increments in serum sodium in chronically hyponatraemic rats treated with hypertonic saline or urea: advantages of urea. Clin Sci (Lond) 1991;80 (1):77–84.
[278] Silver SM, DeSimone Jr. JA, Smith DA, Sterns RH. Dialysis disequilibrium syndrome (DDS) in the rat: role of the "reverse urea effect". Kidney Int 1992;42(1):161–6.
[279] Silver SM, Sterns RH, Halperin ML. Brain swelling after dialysis: old urea or new osmoles? Am J Kidney Dis 1996;28 (1):1–13.
[280] Costello-Boerrigter LC, Smith WB, Boerrigter G, Ouyang J, Zimmer CA, Orlandi C, et al. Vasopressin-2 receptor antagonism augments water excretion without changes in renal hemodynamics or sodium and potassium excretion in human heart failure. Am J Physiol Renal Physiol 2005.
[281] Rozen-Zvi B, Yahav D, Gheorghiade M, Korzets A, Leibovici L, Gafter U. Vasopressin receptor antagonists for the treatment of hyponatremia: systematic review and meta-analysis. Am J Kidney Dis 2010;56(2):325–37.
[282] Verbalis JG. Vasopressin V2 receptor antagonists. J Mol Endocrinol 2002;29(1):1–9.
[283] Gerbes AL, Gulberg V, Gines P, Decaux G, Gross P, VPA study group, et al. Therapy of hyponatremia in cirrhosis with a vasopressin receptor antagonist: a randomized double-blind multicenter trial. Gastroenterology 2003;124(4):933–9.
[284] Gheorghiade M, Gattis WA, O'Connor CM, Adams Jr KF, Elkayam U, Barbagelata A, et al. Effects of tolvaptan, a vasopressin antagonist, in patients hospitalized with worsening heart failure: a randomized controlled trial. Jama 2004;291 (16):1963–71.
[285] Wong F, Blei AT, Blendis LM, Thuluvath PJ. A vasopressin receptor antagonist (VPA-985) improves serum sodium concentration in patients with hyponatremia: a multicenter, randomized, placebo-controlled trial. Hepatology 2003;37(1): 182–91.
[286] Fernandez-Varo G, Ros J, Cejudo-Martin P, Cano C, Arroyo V, Rivera F, et al. Effect of the V1a/V2-AVP receptor antagonist, Conivaptan, on renal water metabolism and systemic hemodynamics in rats with cirrhosis and ascites. J Hepatol 2003;38(6): 755–61.
[287] Goldsmith SR. Current treatments and novel pharmacologic treatments for hyponatremia in congestive heart failure. Am J Cardiol 2005;95(9A):14B–23B.
[288] Udelson JE, Smith WB, Hendrix GH, Painchaud CA, Ghazzi M, Thomas I, et al. Acute hemodynamic effects of conivaptan, a dual V(1A) and V(2) vasopressin receptor antagonist, in patients with advanced heart failure. Circulation 2001;104(20): 2417–23.

[289] Verbalis JG, Martinez AJ. Determinants of brain myelinolysis following correction of chronic hyponatremia in rats. In: Jamison RL, Jaid S, editors. Vasopressin. Paris: John Libby; 1991. p. 539–47.
[290] Sterns RH. The treatment of hyponatremia: first, do no harm. Am J Med 1990;88(6):557–60.
[291] Sterns RH, Nigwekar SU, Hix JK. The treatment of hyponatremia. Semin Nephrol 2009;29(3):282–99.
[292] Hew-Butler T, Almond C, Ayus JC, et al. Consensus statement of the 1st international exercise-associated hyponatremia consensus development conference, cape town, South Africa 2005. Clin J Sport Med 2005;15(4):208–13.
[293] Hew-Butler T, Ayus JC, Kipps C, et al. Statement of the Second International Exercise-Associated Hyponatremia Consensus Development Conference, New Zealand, 2007. Clin J Sport Med 2008;18(2):111–21.
[294] Verbalis JG, Goldsmith SR, Greenberg A, Schrier RW, Sterns RH. Hyponatremia treatment guidelines 2007: expert panel recommendations. Am J Med 2007;120(11 Suppl. 1):S1–21.
[295] Sterns RH, Hix JK, Silver S. Treating profound hyponatremia: a strategy for controlled correction. Am J Kidney Dis 2010;56 (4):774–9.
[296] Perianayagam A, Sterns RH, Silver SM, Grieff M, Mayo R, Hix J, et al. DDAVP is effective in preventing and reversing inadvertent overcorrection of hyponatremia. Clin J Am Soc Nephrol 2008;3(2):331–6.
[297] Sterns RH, Hix JK. Overcorrection of hyponatremia is a medical emergency. Kidney Int 2009;76(6):587–9.
[298] Sterns RH, Hix JK, Silver S. Treating profound hyponatremia: a strategy for controlled correction. Am J Kidney Dis 2010.
[299] Pham PC, Chen PV, Pham PT. Overcorrection of hyponatremia: where do we go wrong? Am J Kidney Dis 2000;36(2):E12.
[300] Nguyen MK, Ornekian V, Butch AW, Kurtz I. A new method for determining plasma water content: application in pseudohyponatremia. Am J Physiol Renal Physiol 2007;292(5): F1652–6.
[301] Turchin A, Seifter JL, Seely EW. Clinical problem-solving. Mind the gap. N Engl J Med 2003;349(15):1465–9.
[302] Weisberg LS. Pseudohyponatremia: a reappraisal. Am J Med. 1989;86(3):315–8.
[303] Ladenson JH, Apple FS, Koch DD. Misleading hyponatremia due to hyperlipemia: a method-dependent error. Ann Intern Med 1981;95(6):707–8.
[304] Nissenson AR, Weston RE, Kleeman CR. Mannitol. West J Med. 1979;131(4):277–84.
[305] Yun JJ, Cheong I. Mannitol-induced hyperosmolal hyponatraemia. Int Med J. 2008;38(1):73.
[306] Spital A, Sterns RH. The paradox of sodium's volume of distribution. Why an extracellular solute appears to distribute over total body water. Arch Int Med 1989;149(6):1255–7.
[307] Palevsky PM, Rendulic D, Diven WF. Maltose-induced hyponatremia. Ann Int Med 1993;118(7):526–8.
[308] Roscoe JM, Halperin ML, Rolleston FS, Goldstein MB. Hyperglycemia-induced hyponatremia: metabolic considerations in calculation of serum sodium depression. Can Med Assoc J 1975;112(4):452–3.
[309] Davids MR, Edoute Y, Stock S, Halperin ML. Severe degree of hyperglycaemia: insights from integrative physiology. QJM 2002;95(2):113–24.
[310] Tzamaloukas AH, Ing TS, Siamopoulos KC, Rohrscheib M, Elisaf MS, Raj DS, et al. Body fluid abnormalities in severe hyperglycemia in patients on chronic dialysis: review of published reports. J Diabetes Complications 2008;22(1):29–37.
[311] Issa MM, Young MR, Bullock AR, Bouet R, Petros JA. Dilutional hyponatremia of TURP syndrome: a historical event in the 21st century. Urology 2004;64(2):298–301.
[312] Gonzales R, Brensilver JM, Rovinsky JJ. Posthysteroscopic hyponatremia. Am J Kidney Dis. 1994;23(5):735–8.
[313] Hahn RG. The transurethral resection syndrome. Acta Anaesthesiol Scand 1991;35(7):557–67.
[314] Henderson DJ, Middleton RG. Coma from hyponatremia following transurethral resection of prostate. Urology 1980;15(3): 267–71.
[315] Agarwal R, Emmett M. The post-transurethral resection of prostate syndrome: therapeutic proposals. Am J Kidney Dis 1994;24(1):108–11.
[316] Campbell HT, Fincher ME, Sklar AH. Severe hyponatremia without severe hypoosmolality following transurethral resection of the prostate (TURP) in end-stage renal disease. Am J Kidney Dis 1988;12(2):152–5.
[317] Agraharkar M, Agraharkar A. Posthysteroscopic hyponatremia: evidence for a multifactorial cause. Am J Kidney Dis 1997;30(5):717–9.
[318] Silver SM, Kozlowski SA, Baer JE, Rogers SJ, Sterns RH. Glycine-induced hyponatremia in the rat: a model of postprostatectomy syndrome. Kidney Int 1995;47(1):262–8.
[319] Mizutani AR, Parker J, Katz J, Schmidt J. Visual disturbances, serum glycine levels and transurethral resection of the prostate. J Urol 1990;144(3):697–9.
[320] Istre O, Jellum E, Skajaa K, Forman A. Changes in amino acids, ammonium, and coagulation factors after transcervical resection of the endometrium with a glycine solution used for uterine irrigation. Am J Obstet Gynecol 1995;172(3): 939–45.
[321] Saito T, Ishikawa S, Abe K, Kamoi K, Yamada K, Shimizu K, et al. Acute aquaresis by the nonpeptide arginine vasopressin (AVP) antagonist OPC-31260 improves hyponatremia in patients with syndrome of inappropriate secretion of antidiuretic hormone (SIADH). J Clin Endocrinol Metab 1997;82(4):1054–7.

This page intentionally left blank

CHAPTER

45

Hypernatremic States

Christopher J. Rivard, Wei Wang and Laurence Chan

University of Colorado Denver, Aurora, Colorado, USA

Hypernatremia can occur with normal, increased or decreased total body sodium content. In healthy individuals and in normal conditions, the plasma concentration of sodium ranges between 136 and 143 mEq/l of plasma, despite large individual variations in the intake of salt and water. The concentration is maintained at constant levels because of the homeostatic mechanism in the body. Claude Bernard was the first to appreciate that higher animals: "have really two environments: a *milieu exterieur* in which the organism is situated, and a *milieu interieur* in which the tissue elements live." The latter is the extracellular fluid (ECF) that bathes the cells of the body.[1,2,3] Maintenance of this consistency of plasma sodium and solute activity is the function of the thirst–neurohypophyseal–renal axis.[4,5] Thirst and urinary concentration are the main defenses against hyperosmolality, and hence hypernatremia. Hypernatremia is a relatively common problem, with prevalence in hospitalized patients of 0.5 to 2%. It is defined as plasma Na^+ concentration ($[Na^+]$) greater than 145 mEq/l. It can be produced by the administration of hypertonic sodium solutions or in almost all cases, by the loss of free water. Since $[Na^+]$ is an effective osmole, the increase in the plasma osmolality (P_{osm}) induced by hypernatremia creates an osmotic gradient that results in water movement out of the cells into the ECF. It is this cellular dehydration, particularly in the brain, that is primarily responsible for the neurologic symptoms associated with hypernatremia. A similar syndrome can be produced when the plasma osmolality is elevated by hyperglycemia. However, when hyperosmolality is due to the accumulation of cell-permeable solute, such as urea or ethanol, there is no water shift in the steady-state because osmotic equilibrium is reached by solute entering the cell.

REGULATION OF WATER HOMEOSTASIS

Significance of the Plasma Sodium Concentration

The total body water (about 60% of body weight in males and 50% in females) is distributed between the intracellular fluid (ICF, 60% of body water) and extracellular fluid (ECF, 40% of body water) spaces.[6–9] Flame photometry and, more recently, ion selective electrode technology have made the plasma sodium concentration one of the simplest and most frequently measured constituents of the body fluids. It is not always appreciated that a given concentration of the plasma sodium may be consistent with different functional states.[10,11] The plasma sodium is simply a concentration term, and as such reflects only the relative amounts of sodium and water present in the sample. The concentration is not a measure of total body sodium content.[12] It is determined empirically by the following relationship:

$$\text{Plasma } [Na^+] = \frac{\text{Total-body } Na^+ + \text{Total-body } K^+}{\text{Total-body water}} \quad \text{(Eq.45.1)}$$

The relationship indicates the fact that hypernatremia can occur as a consequence of a decrease in total body water, an increase in total body sodium or a combination of these events. It gives no information regarding replacement or removal of sodium. When flame spectrophotometry is used to measure the amount of sodium in a plasma sample, substances such as plasma proteins, abnormally high glucose, and lipid can occupy a large fraction of the plasma volume and underestimate the actual sodium concentration. The

Seldin and Giebisch's The Kidney, Fifth Edition.
DOI: http://dx.doi.org/10.1016/B978-0-12-381462-3.00045-8

© 2013 Elsevier Inc. All rights reserved.

ionic composition of the plasma is measured as milliequivalents per liter of plasma. Only about 930 ml of each liter of plasma is water. The remaining 70 ml is occupied by the plasma proteins and, to a lesser degree, lipids. In the presence of hyperlipidemia or hyperproteinemia, the plasma water content may be less than 93%.

Generation of Hypernatremia

Since Na^+ and its accompanying anions are the major effective ECF osmoles, hypernatremia is a state of hyperosmolality. As a result of the fixed number of ICF particles, maintenance of osmotic equilibrium in hypernatremia results in ICF volume-contraction. The increase in the plasma osmolality induced by hypernatremia creates an osmotic gradient that results in water movement out of the cells into the ECF. A similar syndrome can be produced when plasma osmolality is elevated by hyperglycemia. When hyperosmolality is due to the accumulation of a cell-permeable solute, such as urea or ethanol, there is no water shift because osmotic equilibrium is reached by solute entry into cells. Therefore, both urea and ethanol are ineffective osmoles. Plasma osmolality can be measured directly by determining freezing point depression or vapor pressure.[13,14] Variable changes in the plasma sodium concentration occur with hyperglycemia. Since glucose enters cells slowly, an increase in the plasma glucose concentration raises effective plasma osmolality and causes water to move from the cells into the ECF. By dilution, this lowers the plasma Na^+ concentration. In theory, every 62 mg/dl increment in the plasma glucose concentration should draw enough water out of the cells to reduce the plasma Na^+ concentration by 1 mEq/l.[15,16]

The number of particles per gram of water determines the osmolality of a solution. Since sodium salts (particularly NaCl and $NaHCO_3$), glucose, and urea are primary extracellular osmoles, the plasma osmolality can be approximated from:

$$\text{Plasma osmolality } (P_{osm}) = 2 \times \text{Plasma } [Na^+] + \frac{[\text{Glucose}]}{18} + \frac{\text{BUN}}{2.8} \quad \text{(Eq.45.2)}$$

where 2 reflects the osmotic contribution of the anion accompanying Na^+, and 18 and 2.8 represent the conversion of the plasma glucose concentration and blood urea nitrogen (BUN) from units of milligrams per deciliter (mg/dl) into millimoles per liter (mmol/l).

Although urea contributes to the absolute value of the P_{osm}, it does not act to hold water within the extracellular space because of its membrane permeability. Therefore, urea is an ineffective osmole and does not contribute to the effective P_{osm}.

In general, the effective plasma osmolality can be calculated from or estimated from:

$$\text{Effective plasma osmolality} = \text{Measured plasma osmolality} - \frac{\text{BUN}}{2.8}$$

or estimated from

$$\text{Effective plasma osmolality} = 2 \times \text{Plasma } [Na^+] + \frac{[\text{Glucose}]}{18} \quad \text{(Eq.45.3)}$$

Under normal circumstances, glucose and urea contribute less than 10 mOsm/kg H_2O, and the plasma Na^+ concentration is the main determinant of the plasma osmolality, the osmolality of body fluids can be estimated to be twice the plasma sodium concentration.[14]

The major ECF particles are Na^+ and its accompanying anions Cl^- and HCO_3^-; a high plasma sodium concentration is always associated with a high osmolality. This indicates that water is needed to restore isotonicity. The water deficit can be estimated from the plasma sodium level. The percentage increase in sodium concentration approximates the percentage decrease in total body water. The water deficit can be estimated by the equation:

$$\text{Water deficit} = \text{Total-body Water} \times \left(\frac{\text{Plasma } [Na^+]}{140} - 1 \right) \quad \text{(Eq.45.4)}$$

Total body water varies with body size and fat content. It is approximately 60% of body weight in young men, 50% of body weight in old men and young women, and only 40% in elderly women.

DEFENSE MECHANISMS AGAINST WATER DEPLETION

Two primary mechanisms defend the body against water depletion and hyperosmolality of extracellular fluid space. These two defense mechanisms are the capacity of the kidney to excrete a concentrated urine, and stimulation of thirst to increase water intake. Each pathway is very effective and disturbance of the urinary concentrating mechanism alone generally does not cause hyperosmolality if the thirst mechanism is intact.

Control of ADH Secretion

Hypernatremia results in the stimulation of both the antidiuretic hormone (ADH) release and thirst by the

hypothalamic osmoreceptors (Figure 45.1). Argenine vasopressin is the ADH in humans.[17] Argenine vasopressin binds to specific receptors on collecting ducts (V_2 receptors), which are coupled to cyclic AMP (cAMP) formation. The regulation of ADH release from the posterior pituitary is dependent primarily on two mechanisms: osmotic and nonosmotic pathways (Figure 45.2). The osmotic regulation of ADH is dependent on osmoreceptor cells in the anterior hypothalamus.[18] These cells, most likely by altering their volume, recognize changes in ECF osmolality. Cell volume is decreased readily by substances that are restricted to the ECF, such as hypertonic saline or hypertonic mannitol. These substances are effective in stimulating ADH release. In contrast, urea moves readily into cells, and therefore does not alter cell volume and does not effectively stimulate ADH release. A similar response pattern is evident when vasopressin release is studied in the hypothalamo–neurohypophyseal complex in organ culture. Specifically, sodium chloride, sucrose, and mannitol at 310 mOsm/kg H_2O cause a three-fold increase in argenine vasopressin release, while urea and glucose fail to stimulate vasopressin. These studies also support the view that the receptor responds to changes in osmolality rather than sodium. The effects of increased osmolality on vasopressin release are associated with a measurable increase in vasopressin precursor messenger RNA (mRNA) in the hypothalamus[19,20] and salt-loading increases vasopressin RNA in the pituitary.[21,22] Vasopressin release can also occur in the absence of changes in plasma osmolality.[23] Physical pain, emotional stress, hypoglycemia, and a decrease in blood pressure or blood volume are important nonosmotic stimuli for vasopressin release. A 7 to 10% decrement in blood pressure or blood volume causes the prompt release of vasopressin (Figure 45.2). Although there are considerable genetically-determined individual variations in both the threshold and sensitivity, a close correlation between argenine vasopressin and plasma osmolality has been demonstrated in subjects with various states of hydration (Figure 45.3).

The secretion of ADH generally begins when the plasma osmolality exceeds 275 to 285 mOsm/kg H_2O.

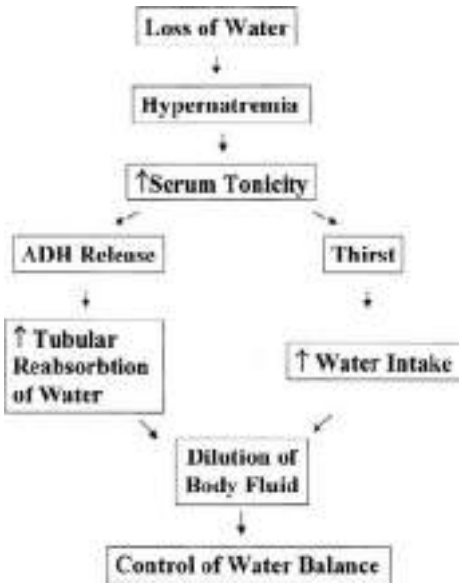

FIGURE 45.1 **Regulation of water homeostasis: feedback loop for the stimulation of antidiuretic hormone (ADH) release and thirst. Hypernatremia results in an increase in the plasma osmolality, which enhances ADH secretion and thirst, resulting in water retention and a reduction in the plasma osmolality toward normal.**

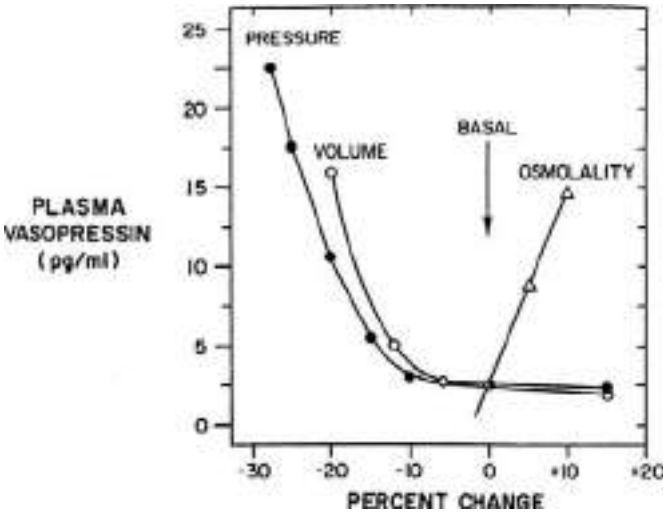

FIGURE 45.2 **Osmotic and nonosmotic stimulation of arginine vasopressin release.** *(from ref. [90]).*

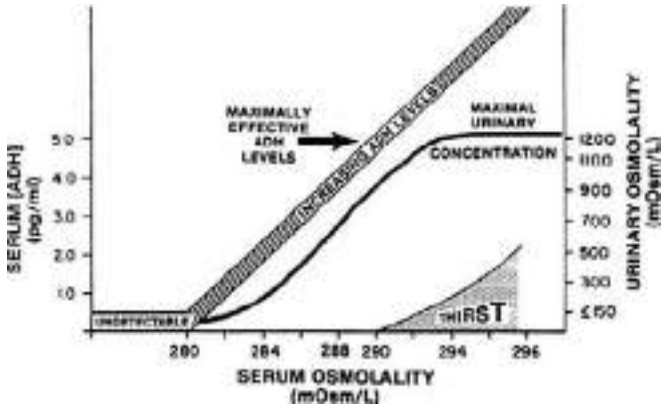

FIGURE 45.3 **Antidiuretic hormone (ADH) levels, urinary osmolality, and thirst as functions of serum osmolality.** *(from ref. [188]).*

The threshold for thirst appears to be approximately 10 mOsm/kg H_2O above that of vasopressin release. Prevention of a total body water deficit is thus largely dependent on water intake as modulated by thirst. The thirst center appears to be closely associated anatomically with the osmoreceptors in the region of the hypothalamus. Defects in thirst response may involve either organic or generalized central nervous system lesions, and can lead to severe water deficit even in the presence of a normal concentrating mechanism. The water deficit will occur more promptly if renal concentrating ability is also impaired.[24]

Thirst and the Maintenance of Hypernatremia

Thirst is, in fact, so effective that even patients with complete diabetes insipidus avoid hypernatremia by fluid intake in excess of 10 l/day.[25–27] Hypernatremia supervenes, therefore, only when hypotonic fluid losses occur in combination with a disturbance in water intake. This is most commonly seen in the aged with an alteration in level of consciousness, in the very young with inadequate access to water or in a rare subject with a primary disturbance in thirst.[28,29] Prevention of a total body water deficit is thus largely dependent on water intake as modulated by thirst. The thirst center appears to be closely associated anatomically with the osmoreceptors in the region of the hypothalamus. Defects in thirst response may involve either organic or generalized central nervous system lesions, and can lead to severe water deficit even in the presence of a normal concentrating mechanism.

In summary, persistent hypernatremia does not occur in normal subjects, because the ensuing rise in plasma osmolality stimulates both the releases of ADH, thereby minimizing further water loss and, more importantly, thirst. The associated increase in water intake then lowers the plasma sodium concentration back to normal. This regulatory system is so efficient that the plasma osmolality is maintained within a range of 1% to 2%, despite wide variations in sodium and water intake. Even patients with diabetes insipidus, who often have marked polyuria due to diminished ADH effect, maintain a near-normal plasma sodium concentration by appropriately increasing water intake. The net effect is that hypernatremia primarily occurs in those patients who cannot express thirst normally: infants and adults with impaired mental status.[30] The latter most often occurs in the elderly, who also appear to have diminished osmotic stimulation of thirst. A patient with a plasma sodium concentration of 150 mEq/l or more who is alert but not thirsty has, by definition, a hypothalamic lesion affecting the thirst center.

CELLULAR RESPONSE TO HYPERNATREMIA

Volume Regulation

When exposed to a change in extracellular osmolality, a cell shrinks or swells and subsequently exhibits either a regulatory volume increase or a regulatory volume decrease.[31–33] When exposed to hypertonicity, a cell loses water until the intracellular and extracellular osmolality are equal. Recovery of water is mediated by accumulation of inorganic and organic solutes known as osmolytes.[31,34] The principle inorganic osmolytes are Na^+, K^+, and Cl^-. The principle organic osmolytes may be classified into three general groups: polyols; methylamines; and amino acids.[35] A comparison of major and minor organic osmolytes for the kidney and brain are depicted in Table 45.1.

While hypernatremia in mammals affects all tissues, the greatest potential for harm is to the brain and kidney. Of these two organs, even modest changes in serum osmolality can have severe consequences to the brain, resulting in volume changes.[36] In the brain, acute hypernatremia is associated with a rapid decrease in water content and a corresponding increase in solute concentration.[32] In a study of rats by Cserr and co-workers,[37,38] acute hypernatremia (plasma $Na^+ = 180$ mEq/l) was accompanied by a prompt

TABLE 45.1 Organic Osmolytes in Kidney and Brain

Organic Osmolyte	Kidney [252–254]	Brain [32,33]
Major	Glutamate	Glutamate
	Glutamine	Glutamine
	Taurine	Taurine
	Myoinositol	Myoinositol
	Urea	Urea
	Alanine	Alanine
	Sorbitol	Aspartate
	GPC	Glycine
	Betaine	GABA
Minor	Val/Leu/Isoleu	Theonine
	Phosphocreatine	GPC
	Creatine	Betaine
		Choline
		Phosphocreatine
		Lysine
		Serine

GABA: γ-aminobutyric acid; GPC: glycerophosphorylcholine.

TABLE 45.2 Proposed Hypothesis for Cellular Osmoregulation in the Kidney

Name	Details	Reference
Compatible osmolyte principle	Cells accumulate high levels of polyols or certain amino acids that do not affect protein function in contrast to NaCl or KCl	255
Counteracting osmolyte principle	Cells accumulate methylamines (i.e., GPC or betaine) to attenuate the destabilizing effect of urea on protein structure	256,257
Constant transmembrane gradient	Cells maintain constant transmembrane gradients for sodium and potassium, thus the driving force for sodium gradient-coupled transport systems for organic and inorganic solutes	258,259

TABLE 45.3 Effect of Early Hypertonic Stress on Kidney Cell Function

General Function	Reference
DNA: Damage, inhibition of repair, dissociation of protein from chromatin, induction of p53	44,58,260,261,262
Metabolism, cell growth: Disruption of mitochondria function, cell cycle arrest, growth factor-dependent signaling inhibition, alteration in cytoskeletal structure, inhibition of protein translation	261,263–272
Secondary stress, apoptosis: Induction of secondary oxidative stress, apoptosis	261,265,273

decrease (7%) in total brain water content. The fall in water content was less than expected for simple osmotic behavior, indicating significant volume regulation had occurred. Moreover, the decrease in total brain water was the result of a fall in extracellular volume. Intracellular volume was not significantly changed at 30 and 90 minutes. The rapid regulatory volume increase was mediated by increases in Na^+, K^+, and Cl^-.[38] Most of these ions were derived from bulk flow of NaCl from cerebral spinal fluid (CSF). There was also a lesser contribution of electrolytes from the blood. During experimental hypernatremia in rabbits, intracellular brain water content also decreased by 12% at 1 hour and by 17% at 4 hours, accompanied by a corresponding increase in intracellular osmolality.[39] Most of the acute increase in brain osmolality was due to an increase in intracellular sodium and potassium concentration.[40] Although a substantial component of the increase in electrolyte concentration resulted from transcellular water loss, whole brain electrolyte content also increased, with the sodium content increasing from 268 ± 9 mm/kg dry weight in control animals to 321 ± 19 mmol/kg dry weight after 4 hours of hypernatremia. After sustained hypernatremia of 7 days duration, brain water and volume values were restored to normal. More prolonged hypernatremia results in accumulation of organic osmolytes to restore total brain water content to normal levels.[41–43]

In the kidney, the general mechanism for cellular osmoregulation in the face of hypertonic conditions involves the accumulation of organic rather than inorganic osmolytes. This strategy for the transport of organic rather than inorganic osmolytes across the cellular membrane has been explained in at least three hypothesized mechanisms, as detailed in Table 45.2. However, before mounting a coordinated osmoresponse, cells experience a "molecular mayhem"[44] due to the initial decrease in cellular volume, resulting in crowding of macromolecules and an increase in ionic osmolytes. These early changes in the cellular status, as well as the loss of water which can affect a variety of biochemical processes, can result in a variety of deleterious effects on normal cellular functions and viability, as depicted in Table 45.3.

Osmolytes

Organic molecules serve an important biologic function in the process of cellular osmoregulation.[4] When extracellular osmolality increases, organic molecules accumulate in the cells, thus maintaining cell volume and counteracting the perturbation of enzyme function and protein structure by high concentrations of inorganic ions and other molecules such as urea.[45] Lien and his co-workers[32] studied the effect of varying degrees and duration of hypernatremia on the concentrations of substances believed to be important idiogenic brain osmoles in rats using conventional biochemical assays, nuclear magnetic resonance spectroscopy, and high performance liquid chromatography. Idiogenic osmoles have been postulated to develop in the brain cells of patients suffering from chronic elevations in the osmolality of ECF. Moreover, the rapid correction of the osmolality in such patients is associated with the development of cerebral edema.

It has been known for more than 35 years that changes in intracellular brain sodium and potassium concentrations cannot account for all of the observed changes in brain osmolality that occur during chronic exposure to extracellular hypernatremia. The solutes that develop to maintain equality between extracellular and intracellular brain osmolality during this adaptation to hyperosmotic stress have been investigated by several groups. Arieff and his associates[46,47] have demonstrated that osmoles accumulated in the brain of chronic hypernatremic, but not in acute hypernatremic,

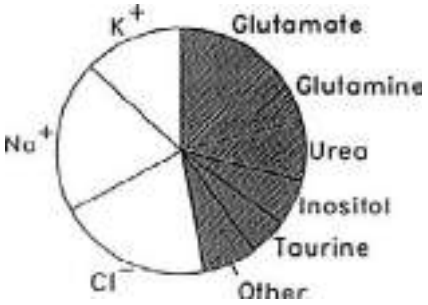

FIGURE 45.4 **Relative changes in brain osmolytes in chronic hypernatremia.** *(from ref. [32]).*

rabbits. Other investigators have shown that the level of amino acids and their derivatives, such as glutamine, taurine, and urea, rise in the brain of chronic hypernatremic animals, and account for about half of the increment of brain osmoles.[48] However, many of the idiogenic osmoles have not yet been characterized in brain tissue. Polyols and trimethylamines accumulate intracellularly in marine animals, plants, and bacteria when extracellular or environmental osmolality is significantly increased. In this study, it was found that the inorganic osmolytes account for 50% to 60% of the increase in solute content, whereas organic osmolytes account for the remainder during adaptation to chronic hypernatremia (Figure 45.4).

Recovery from chronic hypernatremia involves a small transient rise in brain water, which is restored to normal within 48 hours. With the exception of myoinositol, all the electrolytes and organic osmoles fall to normal levels within 24 to 48 hours. The cellular mechanisms responsible for the loss of intracellular organic osmolytes are poorly understood. *In vitro* studies of brain tissue found that cell swelling causes rapid loss of electrolytes and organic osmolytes. The losses of cellular K^+ and Cl^- are likely mediated by swelling-activated ion channels. Characterization of the organic osmolyte efflux pathways suggests that they represent pores or channels in the membrane that are permeable to Cl^-, as well as small organic salts. Roy and Banderali described a chloride channel that can transport small organic solutes, such as taurine and amino acids.[5] No specific inhibitors of the pathways are known. However, inhibitors of arachidonic acid metabolism are able to prevent activation of the efflux pathway, implicating eicosanoids in the signal transduction mechanism.

Lien et al. [32,33] reviewed previous studies to estimate the percentage of the osmolality that is still idiogenic. The contributions of electrolytes and other solutes to the changes in brain osmolality for various durations and degrees of hypernatremia were reported in different studies (Table 45.4).

As a group, amino acids represent the major pool of brain organic osmolytes (20−30%); polyols and methylamines represent 7 to 10%. Taurine, a sulfonated amino acid, appears to be very important in neonatal brain volume regulation. Urea (8%−9%), unlike other osmolytes, is not preferentially accumulated intracellularly. Therefore, the vast majority of the total change in brain osmolality can be accounted for by changes in the concentrations of measured solutes. In other words, there are no significant idiogenic brain osmoles.[49,50]

Response to hypertonic conditions in the kidney depends on the cell type, as determined by presence along the nephron. Microdissection of kidney nephron segments for study is difficult; however, data may be obtained from *in vitro* studies of stable cell lines derived from specific nephron segments. An example of the heterogeneous nature of osmolyte accumulation in response to hypertonic stress in cells along the nephron is depicted in Figure 45.5.

While these data only summarize the changes in selected organic osmolytes, the data indicate that different cells accumulate different osmolytes when challenged to increasing extracellular tonicity. Proximal and distal tubule cells accumulate more myoinositol compared with inner medullary collecting duct cells, and the reverse is true for glycerophosphorylcholine (GPC) in collecting duct cells. The cells located in the inner medullary collecting duct (IMCD) cells are exposed to the greatest range in tonicity, and are therefore valuable in studying the effects of chronic hypertonicity on cellular accumulation of organic osmolytes. Figure 45.6 demonstrates that $IMCD_3$ cells accumulate varying amounts of different organic osmolytes in response to increasing levels of tonicity.

Of interest in these cells is the substantial accumulation of sorbitol at substantially high hypertonic conditions. Sorbitol plays an important role in the osmotic response, especially at high tonicity, because it is not required to be transported across the membrane in the face of a substantial concentration gradient, but rather is metabolized from glucose by the cellular protein aldose reductase (AR). Thus, within the same cell line of the kidney, substantial changes in the accumulation of specific osmolytes occur with increasing tonicity. In the kidney, further metabolism of sorbitol by sorbitol dehydrogenase (SDH) produces fructose (polyol pathway). Studies show that $IMCD_3$ cells chronically adapted to increasing levels of tonicity increase AR message, while at the same time decreasing message for SDH (Figure 45.7). This allows cells to accumulate the organic osmolyte sorbitol. During a reduction in tonicity, cells can export sorbitol from the cell via

TABLE 45.4 Published Experimental Models of Animals with Hypernatremia.

Duration	Animal Species	Changes of Osmolality (mmol/kg)	Contribution to Osmolality Change				Reference
			Na^+	K^+	Cl^+	Other Solutes	
ACUTE HYPERNATREMIA (HOURS)							
1	Rat	139	24	24	ND	Amino acids Urea	106
1	Rabbit	60	38	32	18	ND	47
2	Rat	101	ND	ND	ND	Urea	32,33
3	Rat	117	30	19	30	ND	43
4	Rat	55	ND	ND	ND	Amino acids	274
4	Rabbit	96	21	26	24	Amino acids	47
9	Rabbit	118	29	19	25	ND	49
CHRONIC HYPERNATREMIA (DAYS)							
3	Rat	74	ND	ND	ND	Polyols	275
4	Rat	83	ND	ND	ND	Amino acids	274
4	Mouse	80	19	26	ND	Amino acids Urea	48
5	Rat	50	ND	ND	ND	Amino acids Methylamines polyols	34
7	Rat	80	25	1	25	ND	43
7	Rabbit	80	8	5	15	Amino acids	47
		58	28	21	19	ND	
7	Rat	102	ND	ND	ND	Amino acids Methylamines Polyols urea	32,33

ND: no data.

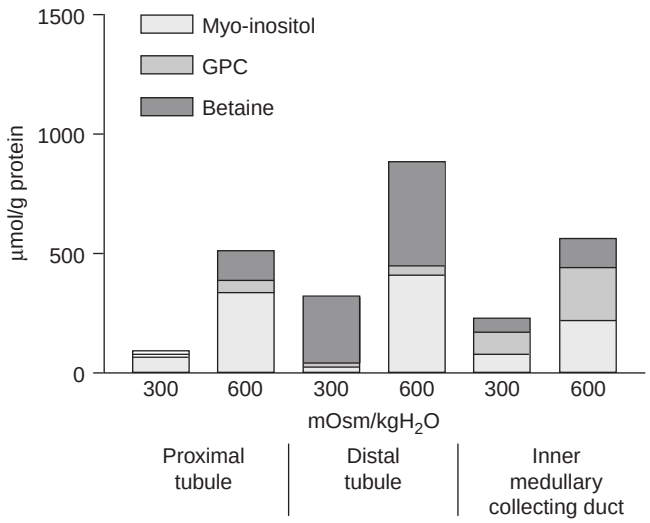

FIGURE 45.5 **Comparison of typical organic osmolytes accumulated in cell lines derived from the proximal tubule (LLC-PK1), distal tubule (thick ascending loop of Henle [TALH]), and inner medullary collecting duct (IMCD).** *(From ref. [250, 251]).*

sorbitol permease or by upregulation of SDH, thereby converting sorbitol to fructose with eventual recycling to glucose in the cell.

Accumulations of minor organic osmolytes in the kidney are similar to major organic osmolytes in demonstrating differential accumulation with increasing levels of hypertonicity. Figure 45.8 shows that, similar to major organic osmolytes, IMCD cells accumulate various amino acids as minor organic osmolytes to different levels in response to increasing extracellular tonicity. Glutamate and glutamine constitute the greatest level of accumulation.

Adaptation to Hypertonicity: *in Vivo* versus *in Vitro*

Interestingly, osmotic tollerance and adaptation is quite different in kidney tissues compared to cells grown *in vitro*. In the medulla of the kidney, cells routinely are bathed in hypertonic interstitum which

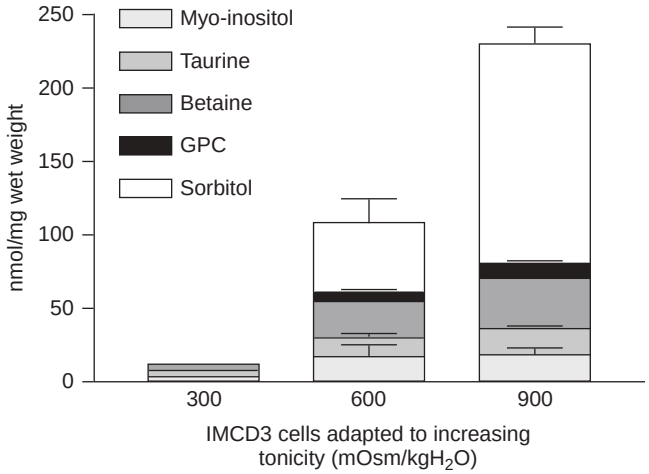

FIGURE 45.6 **Comparison of relative changes in common organic osmolyte concentration in IMCD3 cells chronically adapted to increasing tonicity.** *(from ref. [254]).*

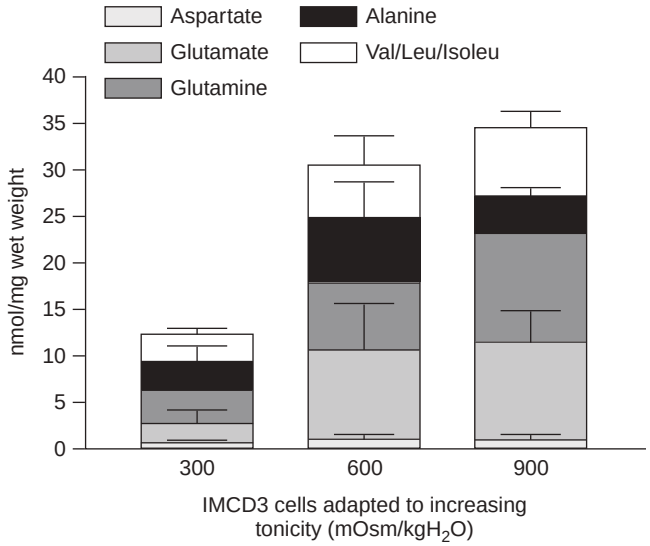

FIGURE 45.8 **Selective accumulation of amino acids as minor organic osmolytes in inner medullary collecting duct cells at increasing extracelluar tonicity.** *(from ref. [254]).*

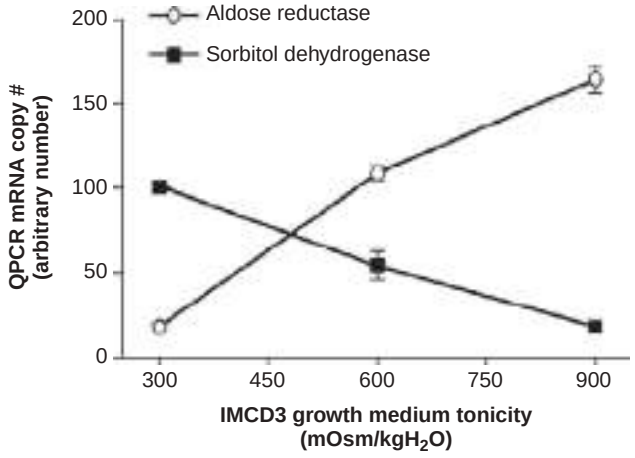

FIGURE 45.7 **Changes in cellular message levels for aldose reductase and sorbitol dehydrogenase in IMCD3 cells in response to chronic adaptation to increasing tonicity.**

reaches 1000 mOsm/kgH_2O or more during antidiuresis[51] without signs of cell injury.[52,53] However, cultured kidney cells including mouse IMCD3[54] and inner medullary epithelial cells[53,55] demonstrate substantial cell death with acute changes in media tonicity. For cultured cells, the rate at which cells are exposed to increases in tonicity plays an important role in adaptation and survival. Capasso and co-workers demonstrated that small increases of 50–100 mOsm/KgH_2O allow IMCD3 cells to be adapted to levels of 900 mOsm/KgH_2O or greater.[56,57] Extensive studies by Cai and co-workers determined a similar finding for mIM cells, in that a linear increase in culture tonicity allowed for better adaptation and survival.[53,55] Furthermore, they demonstrated that hormone additions, including insulin-like growth factor I, epidermal growth factor or vasopressin, and use of growth supports including porous media, collagen I, collagen IV, fibronectin, laminin or fibrillar collagen I, have no significant effect on cellular adaptation to acute increases in tonicity.[55] Rather, these researchers suggested that cells which demonstrate greater proliferative rates, and thus increased DNA replication, are more sensitive to acute changes in tonicity.[53,58] This level of sensitivity to acute changes in tonicity can be blunted if cells in culture are preadapted to moderate levels of tonicity.[53]

Regulation of Transcription in Response to Hypertonicity

Hypertonicity-induced stimulation of transcription plays an important role in the adaptation of renal cells to hypertonicity.[59,60] The regulatory sequence element named tonicity-responsive enhancer (TonE) has been found in the promoter region of a large number of osmotic response genes identified in Table 45.5. The TonE-binding protein (TonEBP) mediates the transcriptional stimulation in response to hypertonicity. These sequences have been found in the 52 flanking region of the aldose reductase gene in several species, suggesting a common mechanism by which tonicity response genes are regulated.[59,60] The TonEBP protein has been cloned by a number of researchers naming this protein nuclear factor of activated T-cell 5 (NFAT5),[61] NFAT-like protein 1 (NFATL1),[62] and osmotic response

TABLE 45.5 Tonicity Enhancer Binding Protein (TonEBP) Target Genes

Target Gene			
Gene Name	**Abbreviation**	**Function**	**Reference**
Aldose reductase	AR	Conversion of glucose to sorbitol	78,276
Sodium/myoinositol co-transporter	SMIT	Transports myoinositol	78,277
Sodium/chloride/ betaine co-transporter	BGT1	Transport betaine	60,78
Urea transporter	UT-A	Vasopressin-regulated urea transporter	278
Taurine transporter	TauT	Specific amino acid transporter	279
Heat shock protein 70	HSP70−2	Molecular chaperone	77,280
Sodium-coupled neutral amino acid transporter-2	ATA2, SNAT2	Neutral amino acid transporter	281
Osmotic stress protein 94	Osp94	Putative molecular chaperone	282
Aquaporin 2	AQP2	Water channel	78,283

element-binding protein (OREBP).[63] TonEBP/NFAT5 belongs to the Rel family of transcription factors which includes NF-kB and the calcineurin binding NFATs.[64] This family is defined by the conserved Rel DNA-binding domain.[65] The DNA-binding domain of TonEBP/NFAT5 has the ability to encircle the DNA, which may allow for greater kinetic stability.[66] The TonEBP/NFAT5 DNA-binding domain requires dimerization similar to NF-kB proteins to bind to DNA. In addition, TonEBP/NFAT5 forms dimers only with itself and not with other members of the Rel family. It also has a stricter recognition sequence (TGGAAAC/A/T) as compared to other Rel proteins.

Regulation of TonEBP/NFAT5 transcriptional activity in response to hypertonicity involves: (1) nuclear translocation; (2) upregulation of transcriptional activity; and (3) enhanced synthesis. Under unstimulated conditions, TonEBP/NFAT5 proteins shuttle in and out of the nucleus. However, following exposure of cells to hypertonic conditions, essentially all of the TonEBP/NFAT5 protein is translocated to the nucleus. This trafficking of TonEBP/NFAT5 to the nucleus is regulated by both specific nuclear localization sequences (NLS) and specific nucleoporin complexes.[67] Under hypertonic conditions, Nucleoporin 88 is upregulated in IMCD3 cells, and acts in concert with other nucleoporins to form a complex which retains TonEBP/NFAT5 to the nucleus. Transcriptional activation of TonEBP/NFAT5 is via the hypertonicity-responsive C-terminal domain.[68,69] While TonEBP/NFAT5 is phosphorylated in response to hypertoncity, and phosphorylation correlates with increased transactivation activity, activation can also occur in the presence of increased tonicity without phosphorylation.[68] Various studies have identified a number of kinases to be involved in phosphorylation of TonEBP/NFAT5 including p38, Fyn, PKA, ATM, and PI3K.[70−73] Finally, TonEBP/NFAT5 is also regulated by increased synthesis, resulting in substantial increases in protein under hypertonic conditions.[69,74] Increased levels of TonEBP/NFAT5 mRNA under hypertonic conditions are in part due to enhanced stabilization of pre-existing mRNA mediated by the 5′UTR of the message.[75]

An alternative role for TonEBP/NFAT5 has slowly emerged as additional transcriptional targets are identified. Lee and co-workers have used microarray analysis to identify greater than 100 genes in which transcription was upregulated two-fold or greater under a moderate increase in tonicity.[76] While the conventional osmotic response targets were identified (see Table 45.5), non-osmolyte accumulating genes were identified including asporin, insulin-like growth factor-binding protein 5 and 7, and extracellular lysophospholipase D. While mice lacking TonEBP/NFAT5 demonstrate reduced embryo survival and substantial perinatal death, implicating renal defects,[77,78] embryonic lethality may not be renal in nature as the maintenance of the extracellular milieu of the developing embryo is dependent on the placenta, and not the developing kidney.[64] In fact, TonEBP/NFAT5 has been shown to be expressed in most developing organs of the mouse embryo.[79] Furthermore, Dressler and co-workers have shown that Pax-2 knockout mice, which fail to develop kidneys, do not suffer from embryonic lethality.[80] While the exact nature of TonEBP/NFAT5 involvement in embryonic organ development is still unknown, it is likely extremely important to embryo development.

Nuclear Magnetic Resonance Spectroscopy

Nuclear magnetic resonance (NMR) is a physical phenomenon of atomic nuclei that has many biochemical and biophysical applications.[81−83] The methodologies derived from NMR imaging enable the chemical identification of different molecules, kinetic analysis of suitable chemical reactions, studies of secondary and tertiary protein structure, and analysis of receptor−ligand interactions. It is this latter application that has become an important clinical tool. The application

of spectroscopy, in concert with different imaging methods, ultimately may prove even more valuable than imaging alone in our understanding of the pathogenesis of different diseases. Bloch and Purcell first demonstrated NMR as a physical phenomenon, independently, in 1946. The fundamental basis of the NMR phenomenon is that nuclei have a quantum characteristic called spin, which because of the charged nature of the nucleus results in these nuclei having magnetic moments, and the net biological samples having magnetic moment in the direction of an applied external magnetic field (Bo). Transitions between the spin state aligned with and against the Bo field can be induced by a radiofrequency pulse, and sampled by radiofrequency antenna as free induction decay (FID). The FID can be transformed from a plot of magnetization-versus-time to a plot of magnetization-versus-frequency, also called an NMR spectrum, by a mathematical manipulation called a Fourier transformation. The frequency of the FID (υ) can be predicted by the knowledge of the nucleus under study and its gyromagnetic ratio (τ), and the magnitude of the Bo field by the following relationship:

$$\upsilon = \tau \mathrm{Bo}/2\pi \tag{45.5}$$

The area under the resultant spectral peak is directly proportional to the quantity of nuclei existing free in solution in the sample being studied. This, in fact, is the basis of NMR imaging experiments. Spectroscopic methodologies make use of the fact that the chemical environment of a given nucleus placed in a Bo field will affect the effective magnetic field of a given nucleus (B_{eff}). This can be described by the chemical environment of a nucleus defining the density of the electron cloud about that nucleus, which tends to appose the Bo field. We can, therefore, describe a shielding constant σ that results from this electron cloud apposing the Bo field in the following equation:

$$\mathrm{B_{eff}} = \mathrm{Bo}\ \ (1 - \sigma) \tag{45.6}$$

The magnitude of σ is usually small, and it is expressed in the dimensionless term of parts per million (ppm). This means that the spectrum acquired from a sample, containing the same nucleus in different chemical environments, will have multiple spectral peaks corresponding to these different chemical environments, allowing for chemical identification on the basis of the shielding constants of these nuclei, also known as chemical shift. Chemical shift, expressed in parts per million, is independent of the strength of the Bo field. Although other physical phenomena may be used in chemical identification (e.g., spin coupling, nuclear Overhauser effect), chemical shift is the primary method of chemical identification that has been used in NMR of living tissues.[81,82]

Figure 45.9 shows the H-1 NMR spectra of brain extract from normal and hypernatremic rats. The most prominent peaks represent N-acetylaspartate (2.02 ppm) and phosphocreatine (3.03 and 3.93 ppm). The peaks in the range of 2.0 to 2.5 ppm represent primarily amino acids, which have not been completely characterized yet. But it was evident that the peak area was larger in severe chronic hypernatremia than normal rat. The major peaks of polyols and trimethylamines were located between 3.1 and 3.9 ppm; GPC, 3.23; betaine, 3.26; myoinositol, 3.27, 3.57, 3.59, 3.61, and 4.06; and sorbitol, 3.85 ppm. We observed the increase of GPC, betaine, and myoinositol in severe chronic hypernatremia compared with normal rats. Sorbitol peak was not visualized in normal rats with severe chronic hypernatremia. The spectra of brain extracts from acute hypernatremia were similar to those of normal rats, and thus are not shown.[32]

Using clinical magnetic resonance imaging (MRI) and spectroscopy, Lee and his co-workers[84] examined an 18-month-old girl with severe dehydration and hypernatremia (plasma sodium concentration 195 mEq/l). A conventional 1.5 Tesla (1.5 T) Sigma General Electric magnetic resonance scanner was used. After MRI, quantitative proton NMR spectroscopy was performed in the parietal and occipital regions of the patient's cerebral cortex, revealing primarily white matter and gray matter, respectively. Spectra from the same regions in 50 healthy infants were also acquired. MRI revealed partial haloprosencephaly. Proton NMR spectroscopy of occipital gray matter and parietal white matter revealed several striking abnormalities (Figure 45.10). The principle abnormality was a reversal of the normal ratio of peak intensities between the neuronal metabolite N-acetylaspartate and the putative osmolyte myoinositol. The principle change was in the concentration of myoinositol, which was three times normal, whereas that of N-acetylaspartate was normal. Concentrations of choline and glutamine (plus glutamate) were also increased. The sequential spectra obtained during correction of the dehydration are shown (Figure 45.10).

The calculated concentrations of the five principle metabolites shown in the spectra of the infant's brain on days 4 to 36 are shown in Table 45.6. The direct determination of patterns of disordered cerebral organic osmolytes by proton NMR spectroscopy may be valuable in guiding therapy.[84,85]

NMR analyses of metabolic changes in the kidney in response to hypertonic stress have focused on specific cell lines and, in particular, the inner medullary collecting duct. Analysis of changes in organic osmolytes with respect to chronic adaptation of $IMCD_3$ cells to increasing tonicity from 300 to 900 mOsm/kg H_2O were studied by proton NMR, as shown in

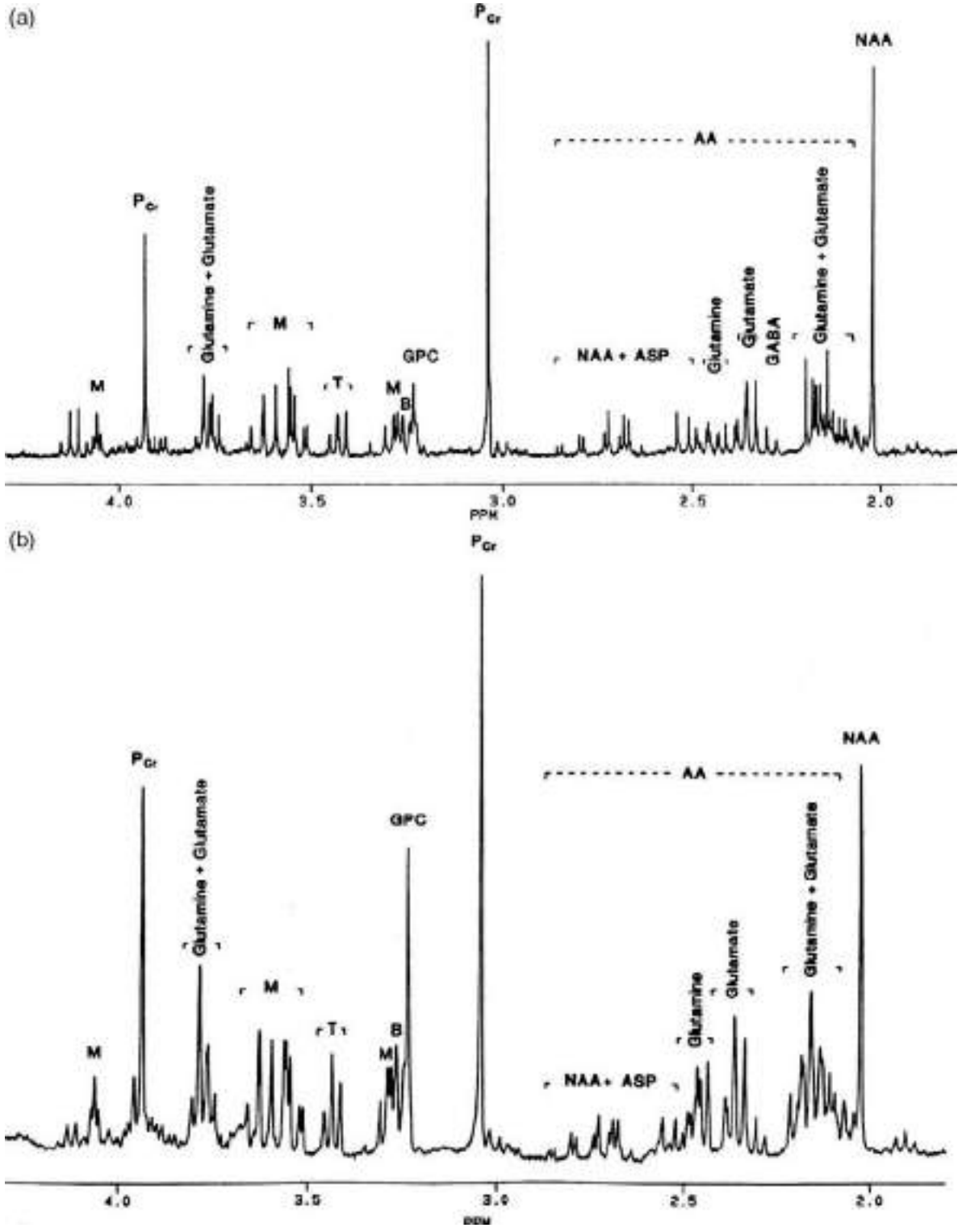

FIGURE 45.9 **Proton nuclear magnetic resonance (NMR) spectra of brain extracts from normal rat (a) and severe chronic hypernatremic rat (b).** These spectra are the sum of 128 transients and are referenced to trimethylsilylproprionate (TSP). Only peaks derived from glycerophosphoryl choline (GPC), betaine 67, myoinositol (M), amino acids (AA), phosphocreatine (PCr), and N-acetylaspartate (NAA) have been labeled. *(from ref. [32]).*

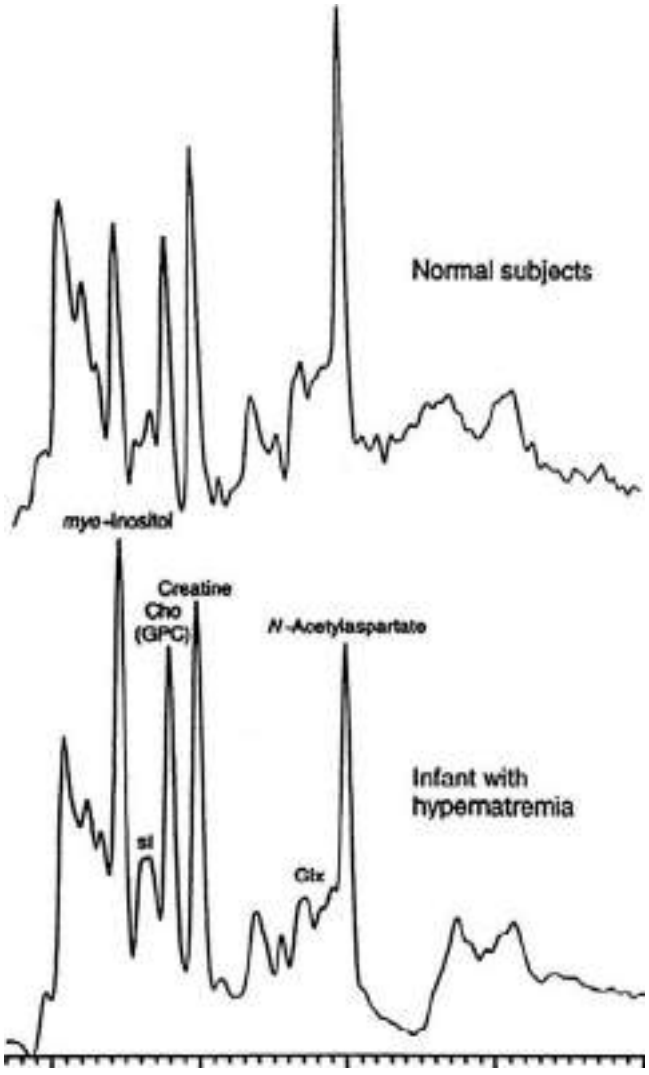

FIGURE 45.10 **Short-echo-time proton nuclear magnetic resonance (NMR) spectrum of cortical gray matter in an infant with severe dehydration.** The striking differences from normal in this patient were the apparent increase in myoinositol and the decrease in N-acetylaspartate. The increase in myoinositol was accompanied by increases in the concentrations of its stereoisomer, scyllo-inositol (sl), and choline-containing compounds (ho), especially glycerophosphoryl choline (GPC), glutamine plus glutamate (Glx), and creatine. *(from ref. [84]).*

Figure 45.11. Gross examination of NMR spectra demonstrates profound changes in nearly all organic osmolytes. Analysis of phosphorylated compounds can be determined by ^{86}P NMR, as shown in Figure 45.12. In a similar fashion, initial reflection indicates a substantial increase in GPC with more minor changes in GPE and PCr. While ^{86}P NMR has been used for analysis of nucleotide triphosphates (NTPs), possibly improved techniques involving HPLC-MS appear to provide for higher sensitivity, greater reproducibility, and throughput for analytical measurements.

ETIOLOGY OF HYPERNATREMIC STATES

Hypernatremia may be due to primary Na^+ gain or water deficit (Table 45.7). The two components of an appropriate response to hypernatremia are increased water intake stimulated by thirst, and the excretion of the minimum volume of maximally-concentrated urine reflecting ADH secretion in response to an osmotic stimulus.[87,88] Most cases of hypernatremia result from the loss of water. Since water is distributed between the ICF and the ECF in a 2:1 ratio, a given amount of solute-free water loss will result in a two-fold greater reduction in the ICF compartment than the ECF compartment. Sodium overload will result in hypernatremia with an increase in total body sodium, and the patient will have an increase in ECF. Water deficit, however, may occur with low or normal total body sodium.

Water deficit in excess of sodium deficit is associated with hypovolemic hypernatremia, and the patient will have low total body sodium. When hypernatremia is caused by pure water loss, the patient is euvolemic and the total body sodium remains normal. The causes of water losses in both of these settings may be renal or extrarenal. Renal losses of water may be a consequence of diabetes insipidus or osmotic diuresis. Diabetes insipidus will be discussed in more detail later in this chapter, in hypernatremia associated with normal total body sodium.

In the absence of increased water losses, hypernatremia can still develop (with normal total body sodium) if there is primary hypothalamic disease impairing thirst (called *hypodipsia*). Two different syndromes have been described, which are most often due to tumors, granulomatous diseases (such as sarcoidosis) or vascular disease. In the first, there is a defect in thirst, with or without concomitant diabetes insipidus. In this disorder, forced water intake is usually sufficient to maintain a normal plasma sodium concentration.[89,90] Other hypodipsic patients will not respond to water-loading, as the excess water will be excreted in the urine with little change in the plasma sodium concentration.[91,92]

Transient hypernatremia (in which the plasma sodium concentration can rise by 10 to 15 mEq/l within a few minutes) can be induced by severe exercise or seizures, which are also associated with the development of lactic acidosis. In this setting, the breakdown of glycogen into smaller, more osmotically active molecules (such as lactate) can increase the cell osmolality, thereby causing the osmotic movement of water into the cells. The plasma sodium concentration returns to normal within 5 to 15 minutes after the cessation of exertion.

TABLE 45.6 Results of Clinical Proton NMR Specteroscopy for Cerebral Osmometry of the Brain of an Infant with Hypernatremia and Normal Subjects

		Study Patients (mmol)				
Metabolite	**Normal Subjects**	**Day 4**	**Day 7**	**Day 11**	**Day 22**	**Day 36**
Myoinositol	6	18	13	13	11	10
Choline	1.5	3.3	2.6	2.7	2.7	2.5
Creatine	8	10	8	9	8	8
Glutamine plus glutamate	15	18	15	15	15	10
N-acetylaspartate	8	6	6	7	7	7
Total	38.5	55.3	44.6	46.7	43.7	37.5
Excess metabolite	0	+ 16.8	+ 6.1	+ 8.2	+ 5.2	− 1.0

From Lee, J.H., Arcinue, E., and Ross, B. D. (1994). Brief report: Organic osmolytes in the brain of an infant with hypernatremia (see comments). N. Engl. J. Med. ***331****, 439–442, with permission.*

Peak areas were converted to concentrations as previously described .[266] The T1 and T2 relaxation times of water and each metabolite were within the normal range given in that report, except for myoinositol, for which the value obtained in this study was 209 msec. As compared with a mean (± SD) of 301 ± 33 in the study by Ernst et al.[266]

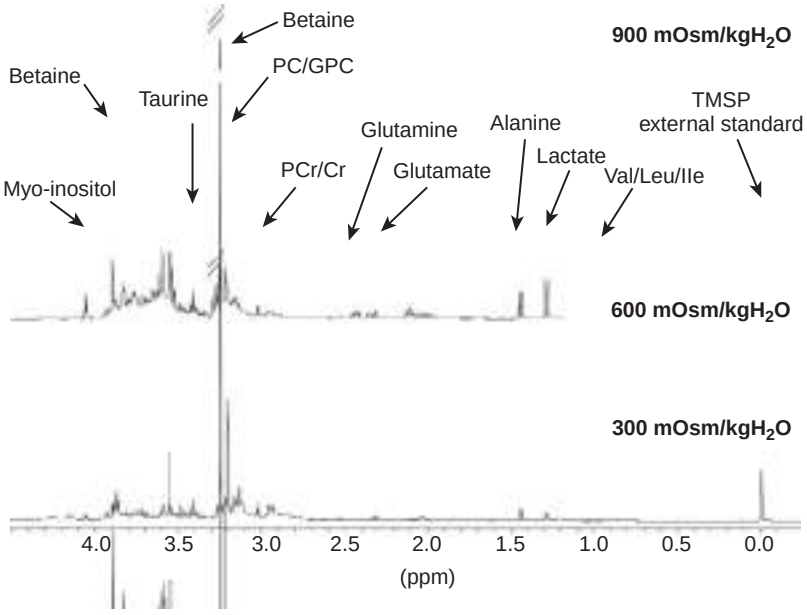

FIGURE 45.11 ^{1}H-nuclear magnetic resonance (NMR) spectra of PCA cell extracts. These spectra show the differences between cells cultivated in media containing 300 (bottom), 600 (middle), and 900 mOsm/kg H_2O (upper spectrum) (GPC: glycerophosphocholine; PC: phosphocholine; Cr: creatine; PCr: phosphocreatine; TMSP: trimethylsilyl propionic-2,2,3,3,-d4 acid).

CLASSIFICATION OF HYPERNATREMIA BASED ON TOTAL BODY SODIUM

Another clinical approach to the hypernatremic patient is based on the assessment of the ECF volume status and the total body sodium.

Hypernatremia in Patients with Low Total Body Sodium

Patients who sustain losses of both sodium and water, but with a relatively greater loss of water, are classified as having hypernatremia with low total body sodium. Signs of hypovolemia include orthostatic hypotension, tachycardia, flat neck veins, poor skin turgor, and dry mucous membranes. Isotonic sodium chloride should be given until systemic hemodynamics are stabilized.

The sources of free water loss that can lead to hypernatremia if intake is not increased include insensible water loss from the skin by evaporation and sweat, the loss of which is increased by fever, exercise, and exposure to high temperatures. Burns and infections will also increase the water loss. Some gastrointestinal losses, particularly osmotic diarrheas, will promote the

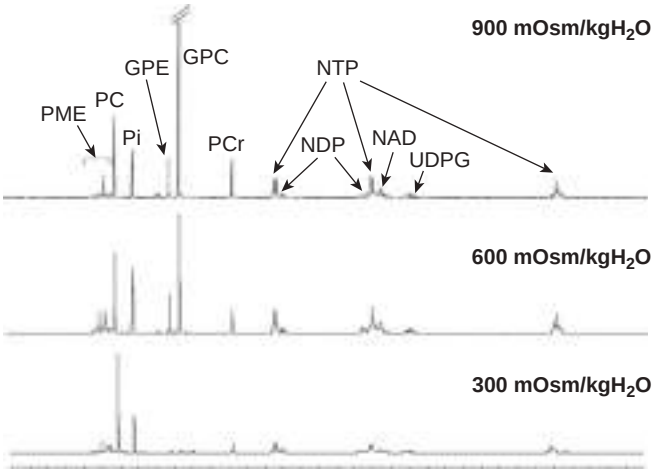

FIGURE 45.12 **^{31}P-nuclear magnetic resonance (NMR) spectra of PCA cell extracts.** These spectra show the differences between cells cultivated in media containing 300 (bottom), 600 (middle), and 900 mOsm/kg H_2O (upper spectrum) (PME: phosphomonoester; PC: phophocholine; Pi: inorganic phosphate; GPE: glycerophophoethanolamine; GPC: glycerophophocholine; PCr: phosphocreatine; NTP: nucleotide triphosphates; NDP: nucleotide diphosphates; NAD: nicotinamide adenine dinucleotide; UDPG: uridine diphosphosphate glucose).

TABLE 45.7 Etiology of Hypernatremic States

Water loss
Insensible
Increased sweating
Burns
Respiratory infections
Renal
Central diabetes insipidus
Nephrogenic diabetes insipidus
Osmotic diuresis
Gastrointestinal
Osmotic diarrhea
Hypothalamic
Primary hypodipsia
Reset osmostat due to volume expansion in primary mineralocorticoid excess
Water loss into cells
Seizures or severe exercise
Rhabdomyoluiss
Sodium overload
Administration of hypertonic NaCl or $NaHCO_3$
Ingestion of sodium

development of hypernatremia, because the sodium plus potassium concentration is less than that in the plasma.[93] Although primarily recognized in children, lactulose-induced diarrhea leading to hypernatremia appears to be common. Since the renal water- and sodium-conserving mechanisms operate normally in these patients, urinary osmolality is high (usually >800 mOsm/kg H_2O), and urinary sodium concentration is low (<10 mEq/l). An elevation in the plasma sodium concentration with diarrhea illness is particularly common in infants in whom fluid replacement with a relatively dilute solution can minimize the risk of hypernatremia. Decreased release of ADH or renal resistance to its effect causes the excretion of relatively dilute urine.[94,95] Most of these patients have a normal thirst mechanism. As a result, they typically present with polyuria and polydipsia, and at most a high-normal plasma sodium concentration. However, marked and symptomatic hypernatremia can occur if a central lesion impairs both ADH release and thirst, thereby preventing replacement of the urinary water losses.

An osmotic diuresis due to glucose, mannitol or urea causes an increase in urine output in which the sodium plus potassium concentration is well below that in the plasma, because of the presence of the nonreabsorbed organic solute. Patients with diabetic ketoacidosis or nonketotic hyperglycemia typically present with marked hyperosmolality, although the plasma sodium concentration may not be elevated due to hyperglycemia-induced water movement out of the cells. Hypotonic losses can also occur by the renal route during a loop diuretic-induced hypotonic diuresis or an osmotic diuresis with mannitol, glucose, glycerol or, more rarely, urea. Elderly patients with partial urinary tract obstruction can excrete large volumes of hypotonic urine.[96] The urine in these cases is hypotonic or isotonic, and the urinary sodium concentration is greater than 20 mEq/l. Since glucose and mannitol enhance osmotic water movement from the intracellular fluid to the ECF compartment, some of these patients may have a normal or even low serum sodium concentration, in spite of serum hypertonicity.

Hypernatremia in Patients with Normal Total Body Sodium

When hypernatremia is caused by pure water loss, total body sodium remains normal. Patients are usually euvolemic. The extrarenal sources of such water losses are the skin and the respiratory tract. A high environmental temperature, as well as a febrile or hypermetabolic states, can cause considerable water losses. If such hypotonic losses are not accompanied by appropriate water intake, hypernatremia supervenes. Urine osmolality is very high, reflecting an intact osmoreceptor–vasopressin–renal response. Urinary sodium concentration will vary according to the patient's sodium intake. This kind of hypernatremia has been reported in hepatic failure.[97] It was believed to occur due to total body water loss. The possible mechanisms include

increased insensible losses, decreased access to water secondary to hepatic encephalopathy, and increased hypotonic losses in stool secondary to osmotic cathartics used for treatment of encephalopathy. Chronic alcoholic subjects with end-stage liver disease who present with fulminant liver failure and hepatic encephalopathy have a high mortality rate.[97,98] Patients with liver disease who develop hypernatremia are particularly susceptible to the development of cerebral demyelinating lesions.

Diabetes insipidus is a polyuric disorder characterized by high rates of electrolyte-free water excretion.[99] When these are not appropriately replaced, hypernatremia supervenes. The causes of central neurogenic diabetes insipidus are listed in Table 45.8. If the thirst mechanism is intact and water is available, patients with central diabetes insipidus do not develop hypernatremia, and thus have no symptoms except for the inconvenience associated with the marked polyuria and polydipsia. With concomitant hypodipsia, no access to water or an illness that precludes adequate water intake, however, severe and even life-threatening hypernatremia can supervene.

Hypernatremia secondary to nonosmotic urinary water loss is usually due to central or neurogenic diabetes insipidus characterized by impaired argenine vasopressin secretion or nephrogenic diabetes insipidus resulting from end-organ (renal) resistance to the actions of AVP. The most common cause of central diabetes insipidus is destruction of the neurohypophysis. This may occur as a result of trauma, neurosurgery, granulomatous disease, neoplasms, vascular accidents or infection. In many cases, central diabetes insipidus is idiopathic and may occasionally be hereditary. The familial form of the disease is inherited in an autosomal dominant fashion, and has been attributed to mutations in the propressophysin (argenine vasopressin precursor) gene.[100–104] Nephrogenic diabetes insipidus may be either inherited or acquired. Congenital nephrogenic diabetes insipidus I is an X-linked recessive trait due to mutations in the V2 receptor gene.[105–112] Mutations in the autosomal aquaporin-2 gene may also result in NDI.[113–118] The aquaporin-2 gene encodes the water channel protein whose membrane insertion is stimulated by AVP. The causes of sporadic nephrogenic diabetes insipidus are numerous, and include drugs (especially lithium),[119–126] hypercalcemia, hypokalemia, and conditions that impair medullary hypertonicity (e.g., papillary necrosis or osmotic diuresis).[127–131] Pregnant women, in the second or third trimester, may develop nephrogenic diabetes insipidus as a result of excessive elaboration of vasopressinase by the placenta.[132,133]

TABLE 45.8 Causes of Central Diabetes Insipidus (CDI)

Hereditary
Autosomal dominant
Autosomal recessive (Wolfram syndrome)
Acquired
Head trauma, skull fracture, and orbital trauma
Posthypophysectomy
Suprasellar and intrasellar tumors
Primary (suprasellar cyst, craniopharyngioma, pinealoma, meningioma, and glioma)
Metastatic (breast or lung cancer, leukemia, and lymphomas)
Granulomas
Sarcoid
Wegener granulomatosis
Tuberculosis
Syphilis
Histiocytosis
Eosinophilic granuloma
Hand–Schuller–Christian disease
Infections
Encephalitis
Meningitis
Guillain-Barre syndrome
Vascular
Cerebral aneurysm
Cerebral thrombosis or hemorrhage
Sickle cell disease
Postpartum necrosis (Sheehan syndrome)
Pregnancy (transient)

Congenital nephrogenic diabetes insipidus is a rare hereditary disorder in which the renal tubule is insensitive to vasopressin.[134] The disease manifests itself in the complete clinical form only in males and in a subclinical form in females, suggesting a sex-linked dominant inheritance with variable penetrance in the female. The gene responsible for the defect has, in fact, been mapped to region 28 on the long arm of the X-chromosome (Xq28). Although the disease is most probably inborn, the diagnosis is usually not made until the infant has hyposmolar urine with severe dehydration, hypernatremia, vomiting, and fever. Unlike some of the females, who have partial responsiveness to vasopressin, the male with the full-blown complete form of this disorder will not have hypertonic urine even in the face of severe dehydration. The impaired growth and occasional mental retardation that supervene in these cases are most likely due to repeated episodes of dehydration and hypernatremia, rather than being integral components of the disease. Hydronephrosis is also common in these patients, perhaps because of voluntary retention of large volumes of urine, with subsequent vesicoureteral reflux.[135]

Neither vasopressin nor other pharmacologic agents that potentiate its action or stimulate its release, such as chlorpropamide, are effective in concentrating the urine of patients with nephrogenic diabetes insipidus. An intact thirst mechanism is, therefore, indispensable for the maintenance of good hydration in children with this disorder, as is careful monitoring of fluid balance.

Since the excretion of solute requires further water losses, children with this disorder who need rehydration should receive hypotonic (2.5%) rather than isotonic (5%) glucose solutions. Glucosuria may occur with the latter solution, and thus aggravate fluid losses.

Limitation of oral solute intake (low-sodium diet) may also lead to a decrease in urine flow in patients with nephrogenic diabetes insipidus. Thiazide diuretics, which inhibit sodium reabsorption in the cortical diluting segment of the nephron, have met with some success in the management of these patients. The ability of thiazides to diminish sodium reabsorption in this water-impermeable portion of the nephron would itself decrease C_{H2O}, but not urine flow. It seems most likely that the decrease in urine flow is secondary to the sodium loss and ECF volume-contraction. ECF volume-depletion in turn decreases glomerular filtration rate (GFR), and increases proximal tubular sodium and water reabsorption. These secondary effects of the diuretic agent then decrease urine flow. The ECF volume-contraction can be maintained with a low sodium intake after discontinuance of the diuretic, so that the therapy still remains effective. The addition of amiloride to hydrochlorothiazide may provide added benefit.[136–139] Nonsteroidal anti-inflammatory agents have been found to be effective.

The acquired form of nephrogenic diabetes insipidus is much more common than the congenital form of the disease, but it is rarely severe.[140] While maximal concentrating ability is impaired in this disorder, the ability to elaborate a hypertonic urine is usually preserved. Nocturia, polyuria, and polydipsia may occur in this acquired form of nephrogenic diabetes insipidus, but the urine volumes are generally less ($<3–4$ l/day) than those observed with complete central diabetes insipidus, psychogenic water-drinking or congenital nephrogenic central diabetes insipidus. The more common causes of acquired nephrogenic diabetes insipidus are listed in Table 45.9.

A defect in renal concentrating capacity is a consistent accompaniment of most forms of advanced renal failure.[141,142] Thus, chronic renal failure constitutes a form of acquired nephrogenic diabetes insipidus. Advanced renal insufficiency of any cause can cause a vasopressin resistance associated with hypotonic urine. In some forms of kidney disease vasopressin unresponsiveness can occur at a stage when GFR is not markedly diminished. The occurrence of a profound diuresis in association with a concentrating defect in glomerular diseases of the kidney is rare and, in general, a close correlation exists between GFR and maximal urinary osmolality. The causes of the defect in renal concentrating capacity associated with chronic renal failure are probably multiple.[143–145] These include: (1) a disruption of inner medullary structures or local alterations in medullary blood flow, as is seen in tubulointerstitial diseases, sickle cell disease,[146,147] and analgesic nephropathy; (2) impairment in sodium chloride transport out of the thick ascending limb of Henle's loop, a process that limits maximal interstitial tonicity; and (3) increase in solute excretion in the remaining few functioning nephrons, an adaptive response to the need to excrete the same solute load as the normal kidney.

TABLE 45.9 Causes of Acquired Nephrogenic Diabetes Insipidus (NDI)

Chronic renal disease
Polycystic disease
Medullary cystic disease
Ureteral obstruction
Amyloidosis
Advanced renal failure of any etiology
Electrolyte disorders
Hypokalemia
Hypercalcemia
Drugs
Alcohol
Lithium
Demeclocycline
Glyburide
Amphotericin
Foscarnet
Sickle cell disease
Dietary abnormalities
Excessive water intake
Decreased sodium chloride intake
Decreased protein intake
Miscellaneous
Gestational diabetes insipidus

Hypokalemia has long been known to cause polyuria as a consequence of a vasopressin-resistant renal concentrating defect.[40] A direct effect of hypokalemia on the collecting tubule is supported by studies in the toad bladder which show a decrease in cyclic AMP and vasopressin-stimulated water flow when potassium is removed from the bathing solution.[148] These findings suggest both a precyclic AMP and postcyclic AMP defect. The hypokalemia-induced resistance to vasopressin is associated with decreased cyclic AMP accumulation, apparently due to decreased adenylyl cyclase activity. Hypokalemia from any cause, such as diarrhea, chronic diuretic use or primary aldosteronism, may be associated with a urinary concentrating defect. The defect is generally reversible, but requires a longer time (1–3 months) than would be expected from a purely functional defect.

Hypercalcemia is another well-recognized cause of impaired urinary concentrating ability.[149–151] A decrement in medullary interstitial tonicity is clearly present

with hypercalcemia, which may be related to diminished solute reabsorption in the thick ascending limb. This defect is associated with a decrement in AVP-stimulated adenylate cyclase in this nephron segment. The concentrating defect is, however, multifactorial, as the elaboration of hypotonic urine implies an intrinsic defect in the collecting tubule. In this regard, studies in isolated toad bladders, as well as papillary collecting ducts, reveal a decreased response to vasopressin in hypercalcemia.

Various pharmacologic agents have been found to impair the renal capacity to concentrate urine (Table 45.9). Ethanol and phenytoin (Dilantin) seem to exert their action by a central effect on vasopressin release.[152] Some hypoglycemic agents cause a diuresis by a mechanism probably unrelated to suppression of vasopressin release. The renal toxicity of amphotericin can manifest in the form of a concentrating defect.[153] Foscarnet, an agent increasingly employed in the treatment of cytomegalovirus (CMV) infection in patients with acquired immune deficiency syndrome (AIDS), has been described to cause a nephrogenic diabetes insipidus.[91,154]

The drugs most commonly associated with nephrogenic diabetes insipidus are demeclocycline and lithium.[119,120,122,123,125,155] Since it was first recognized as a cause of nephrogenic diabetes insipidus, demeclocycline has become the drug of choice for the treatment of the syndrome of inappropriate ADH secretion (SIADH). It has yet to be determined if demeclocycline reduces argenine vasopressin secretion. It is clear, however, that demeclocycline induces dose-dependent decreases in human renal medullary adenylate cyclase activity. Since the drug decreases not only vasopressin but also cyclic AMP-stimulated water flow, a postcyclic AMP defect may be operant.[156]

Lithium is the most common cause of nephrogenic diabetes insipidus. There is no evidence that lithium impairs vasopressin release. In terms of the mechanism of its renal action, lithium does not interfere with accumulation of medullary solutes. Thus, an intrinsic tubular defect is postulated. In this regard, lithium decreases vasopressin-stimulated water transport in the perfused cortical collecting duct. An inhibition in adenylate cyclase or in cyclic AMP generation is observed in human tissue and cultured cells exposed to the cation, as well as in animals chronically treated with lithium. More recently, a downregulation of the vasopressin-regulated water channel (aquaporin) has been described in lithium-treated rats.[157] It is of interest that the urinary aquaporin levels remained low after removal of lithium, in line with the slow recovery of concentrating ability seen in man.

A renal concentrating defect is a common accompaniment of sickle cell anemia and sickle cell trait.[146,158,159] Sickling of red blood cells in the hypertonic medullary interstitium with occlusion of the vasa recta appears to cause inner medullary and papillary damage. Microradioangiographic studies have failed to demonstrate vasa recta blood flow in patients with sickle cell disease. The resultant medullary ischemia may impair sodium chloride transport in the ascending limb, and thus diminish medullary tonicity. Transfusions of normal blood have been shown to restore renal concentrating capacity in children, thus indicating that the sickled red blood cells have a role in the defect. With more prolonged disease, medullary infarcts occur and the concentrating defect is no longer reversible with transfusions.

The syndrome of essential hypernatremia and hypodipsia has been described in patients with normal total body sodium. A partial list of causes of this hypodipsia-hypernatremia syndrome is shown in Table 45.10. These patients exhibit persistent hypernatremia not explained by any volume loss. There is absence or attenuation of thirst. The patient may also have partial diabetes insipidus and a normal renal response to ADH. This is due to a primary hypothalamic disease impairing thirst (called *hypodipsia*). Two different syndromes have been described, which are most often due to tumors, granulomatous diseases (such as sarcoidosis) or vascular disease. In the first, there is a defect in thirst, with or without concomitant diabetes insipidus. In this disorder, forced water intake is usually sufficient to maintain a normal plasma sodium concentration.[89,160] Other hypodipsic patients will not respond to water-loading, as the excess water will be excreted in the urine with little change in the plasma sodium concentration.[91,92] It had been postulated that these

TABLE 45.10 Causes of the Hypodipsia–Hypernatremia Syndrome

Ectopic pinealoma
Dysgerminoma/germinoma
Craniopharyngioma
Teratoma
Meningioma
Metastatic bronchial carcinoma
Eosinophilic granuloma
Hand–Schuller–Christian disease
Ganulomatous tumor
Hypothalamic neuronal degeneration
Subarachnoid hemorrhage
Posttraumatic carotid cavernous fistula
Microcephaly
Occult hydrocephalus
Head trauma
Aneurysectomy (anterior communicating artery)
Sarcoidosis

From Levi, M., and Berl, T. (1982). Water metabolism In "Current Nephrology," Vol 5, 37, Gonick, H. C. (ed.). Year Book Medical, Chicago.[130]

patients had a reset osmostat upward (called *essential hypernatremia*), so that the new high plasma sodium concentration was recognized as normal.[161,162] Thus, giving water will decrease ADH release, and the excess water will be excreted in dilute urine. It is now clear, however, that these patients have selective injury to the osmoreceptors, with ADH secretion being primarily governed by changes in volume.[163] Thus, the suppression of ADH release by water-loading in this setting is due to the associated mild volume expansion, rather than a fall in plasma osmolality. True resetting of the osmostat upwards has been described only in patients with primary mineralocorticoid excess (such as primary hyperaldosteronism). The plasma sodium concentration in these patients is usually between 143 and 147 mEq/l. It is presumed that the suppressive effect of chronic mild volume expansion on ADH release is responsible for the resetting. This appears to be due to a specific osmoreceptor defect resulting in nonosmotic regulation of argenine vasopressin release. These patients are characterized by persistent hypernatremia not explained by any apparent extracellular volume loss with a normal response to AVP. It has been proposed that these patients have a "resetting" of the osmoreceptor, since these patients tend to concentrate and dilute urine at inappropriately high levels of plasma osmolality.[164–169] However, using the regression analysis of plasma argenine vasopressin level versus plasma osmolality, it has been shown that in some of these patients the tendency to concentrate and dilute urine at inappropriately high levels of plasma osmolality is due solely to a marked reduction in sensitivity or gain of the osmoregulatory mechanism. In other patients, however, plasma argenine vasopressin levels fluctuate in a random manner, bearing no apparent relationship to changes in plasma osmolality. Such patients frequently display large swings in serum sodium concentration. It appears that most patients with essential hypernatremia fit one of these two patterns.[88,170] Hypodipsia can also occur in elderly patients without overt hypothalamic lesions, and can culminate in severe hypernatremia.[168,171] It has been suggested that a decrement in angiotensin II-mediated thirst existed in the elderly.[29,172]

Hypernatremia in Patients with Increased Total Body Sodium

Hypernatremia with increased total body sodium is the least common type of hypernatremia, and is usually due to exogenous administration of hypertonic sodium containing solutes (Table 45.11).[13] Acute and often marked hypernatremia (in which the plasma sodium concentration can exceed 175–200 mEq/l) can be induced by the administration of hypertonic sodium-containing solutions. Hypernatremia supervenes during resuscitative efforts with hypertonic sodium bicarbonate,[46,173] inadvertent intravascular infusion of hypertonic saline in therapeutic abortions, inadvertent dialysis against a high sodium concentration dialysate, sea water drowning, and even after ingestion of large quantities of sodium chloride tablets.[174–178] Accidental or nonaccidental salt poisoning has been reported in infants and young children, and in patients taking highly concentrated saline emetic or gargle.[174,179,180] The hypernatremia in this setting will correct spontaneously if renal function is normal, since the excess sodium will be rapidly excreted in the urine. This process can be facilitated by inducing a sodium and water diuresis with a loop diuretic, and then replacing the urine output with water. Too rapid correction should be avoided if the patient is asymptotic. Since the hypernatremia is generally very acute with little time for cerebral adaptation, these patients are less likely to develop cerebral edema during correction.[181,182] The degree of hyperosmolality is typically mild, unless the thirst mechanism is abnormal or access

TABLE 45.11 Therapeutic Hypertonic Solutions

Solute	Molecular Weight	Concentration (mg/dL%)	Osmolality (mosm/kg water)	Typical Container Size (ML)	Use
Sodium chloride	58.5	3	1026	500	Emergency teatment of hypotonic states; intra-amniotic instillation for therapeutic abortion
		5	1711	500	
		20	6845	250	
Sodium bicarbonate	84.0	5	1190	500	Treatment of metaboliuc acidosis, hyperkalemia, cardiopulmonary arrest
		7.5	1786	50	

From Morrison, G., and Singer, L. (1994). Hyperosmolal states. In "Clinical Disorders of Fluid and Electrolyte Metabolism," 646, Narins, R. G., (ed.). McGraw-Hill, New York.[187]

to water is limited. This occurs in infants, the physically handicapped, patients with impaired mental status, in the postoperative state, and in patients on ventilators. Patients with primary hyperaldosteronism and Cushing syndrome have slight, clinically unimportant elevations in serum sodium concentration. As expected, patients with hypernatremia and high total body sodium excrete generous quantities of the cation in the urine.

CLINICAL FEATURES IN HYPERNATREMIA

A complete history and physical examination will often provide clues as to the underlying cause of hypernatremia.[183,184] Relevant symptoms and signs include the absence or presence of thirst, diaphoresis, diarrhea, polyuria, and the features of ECF volume contraction.[185–188] The major symptoms of hypernatremia are neurologic and include altered mental status, weakness, neuromuscular irritability, focal neurologic deficits, and occasionally coma or seizures (Table 45.12). As a consequence of hypertonicity, water shifts out of cells, leading to a contracted ICF volume. A decreased brain cell volume is associated with an increased risk of subarachnoid or intracerebral hemorrhage.[189–192] Patients may also complain of polyuria or thirst. For unknown reasons, patients with polydipsia from CDI tend to prefer ice-cold water. The signs and symptoms of volume depletion are often present in patients with a history of excessive sweating, diarrhea or an osmotic diuresis.[132,183,193–197]

The severity of the clinical manifestations is related to the acuity and magnitude of the rise in plasma Na^+ concentration. Chronic hypernatremia is generally less symptomatic as a result of adaptive mechanisms designed to defend cell volume. Brain cells initially take up Na^+ and K^+ salts, later followed by accumulation of organic osmolytes, such as inositol. This serves to restore the brain ICF volume towards normal.

The signs and symptoms of hypernatremia are most likely related to a variety of anatomic derangements.

TABLE 45.12 Signs and Symptoms of Hypernatremia

Intense thirst
Irritability
Signs of volume depletion (variable)
Nausea or vomiting
Depression of sensorium
Seizures (unusual in adults)
Focal neurologic deficits
Muscle spasticity (unusual in adults)
Fever
Labored respiration

The most prominent manifestations of hyperosmolar disorders are of a neurologic nature.[198–204] The loss of volume and the shrinkage of brain cells associated with the hyperosmolar states causes tearing of cerebral vessels. In addition to these gross anatomic changes, the brain sustains alterations in the composition of water and solutes that may be of great importance in the pathophysiology of the symptoms of hypernatremia. These are responses designed to regulate volume and restore cell size. Thus, the water losses are not as severe as would be predicted. In the early phase, the entry of sodium and chloride into brain cells greatly mitigates the loss of water that would otherwise occur from ideal osmotic behavior. After 7 days of hypernatremia, brain water has returned to control levels as brain osmolality remains elevated. At this time idiogenic osmoles account for as much as 60% of the increase in intracellular osmolality. It now seems possible that some of these idiogenic osmoles are due to an increase in intracellular amino acids, particularly taurine. In addition, accumulation of osmolytes such as urea, glutamine, glycerolphosphorylcholine, and myoinositol has been documented in hypernatremic rats, as well as in human using NMR spectroscopy.

Measurement of urine volume and osmolality are essential in the evaluation of hypernatremia. The appropriate renal response to hypernatremia is the excretion of the minimum volume (500 ml/d) of maximally-concentrated urine (urine osmolality greater than 800 mOsm/kg H_2O). These findings suggest extrarenal or remote renal water loss or administration of hypertonic Na^+ salt solutions. The presence of a primary Na^+ excess can be confirmed by the presence of ECF volume expansion and natriuresis (urine Na^+ concentration usually greater than 100 mmol/l). Many causes of hypernatremia are associated with polyuria and a submaximal urine osmolality. The product of the urine volume and osmolality, i.e., the solute excretion rate, is helpful in determining the basis of the polyuria. To maintain a steady-state, total solute excretion must equal solute production. Individuals eating a normal diet generate approximately 600 mOsm/d. Therefore, daily solute excretion in excess of 750 mOsm/d defines an osmotic diuresis. This can be confirmed by measuring the urine glucose and urea. In general, both CDI and NDI present with polyuria and hypotonic urine (urine osmolality less than 250 mOsm/kg H_2O). The degree of hypernatremia is usually mild unless there is an associated thirst abnormality.

THERAPY FOR HYPERNATREMIA

The therapeutic goals are to stop ongoing water loss by treating the underlying cause, and to correct the

TABLE 45.13 Diagnosis and Therapeutic Approach to the Hypernatremic Patient

		Urinary		
	Causes	Tonicity	Na^+ (mEq/L)	Therapies
Hypovolemia	Renal loss	Iso-	>20	Hypotonic saline
Low total body Na^+, H_2O loss	Osmotic or loop diuretics	Hypo-		
	Postobstruction			
	Intrinsic renal disease			
	Extrarenal loss	Hyper-	<10	
	Dermal			
	Sweating			
	Burns			
	Gastrointestinal			
	Diarrhea			
	Fistulas			
Euvolemia	Renal loss	Hypo-	Variable	Water replacement
Normal total body Na^+	Diabetes insipidus	Iso-		
H_2O loss	Nephrogenic	Hyper-		
	Central			
	Partial			
	Gestational			
	Hypodispsia			
	Extrarenal loss	Hyper-	Variable	
	Insensible losses			
	Respiratory			
	Dermal			
Hypervolemia	Primary hyperaldosteronism	Iso-	>20	Diuretics and water replacement
Increased total body Na^+	Cushing syndrome	Hyper-		
Na^+ addition	Hypertonic dialysate			
	Hypertonic sodium bicarbonate			
	Sodium chloride tablets			

water deficit. The specific approach depends on the patient's ECF volume (Table 45.13). Reversal of hypernatremic state must be undertaken slowly to prevent neurological complications. Rapid correction may result in cerebral edema, seizure, and death.[183,205–211]

When the patient has low total body sodium, as evidenced by circulatory manifestations (e.g., orthostatic hypotension), isotonic sodium chloride should be given until systemic hemodynamics are stabilized. Thereafter, the hypernatremia can be treated with 0.45% sodium chloride or 5% dextrose. When the patient is hypervolemic and hypernatremic, the removal of excess sodium is the goal, which can be achieved either by administration of diuretics along with 5% dextrose or, if renal function is impaired, by dialysis. The euvolemic hypernatremic patient who has sustained pure water losses requires water replacement as a 5% dextrose infusion. The water deficit in this setting can be calculated based on the current sodium concentration and body weight, using the assumption that total body water is approximately 50 or 60% of body weight:

$$\text{Water deficit} = \text{Total-body water} \times \left(\frac{\text{Plasma } [Na^+]}{140}\right) \quad (45.7)$$

In addition to replacing the calculated water deficit, ongoing fluid losses should be replaced. In acute hypernatremia, repletion of the water deficit may be faster. The electrolytes accumulated in the brain during hypernatremia are rapidly extruded into the extracellular space during treatment, minimizing the risk of cerebral edema.[206] In contrast, rapid correction in chronic hypernatremia is potentially dangerous. In this case, a sudden decrease in osmolality could potentially cause a rapid shift of water into cells that have undergone osmotic adaptation. This would result in swollen brain cells, and increase the risk of seizures or permanent neurologic damage.[212] A slower rate of correction probably can prevent this sequence of events by allowing idiogenic osmoles time to be dissipated.

The plasma Na^+ concentration should be lowered by 0.5 mmol/L per hour, and by no more than 12 mmol/L over the first 24 hours. The safest route of administration of water is by mouth or via a nasogastric tube (or other feeding tube). Alternatively, 5% dextrose in water or half-isotonic saline can be given intravenously. The patient's neurological status should be monitored carefully throughout treatment. Deterioration of neurological status after an initial improvement suggests the development of cerebral

edema, and mandates temporary discontinuation or slowing the rate of water replacement.

In patients with essential hypernatremia and the elderly with hypodipsia, 1 to 2 liters of water per day may need to be administered as a prescription. Chlorpropamide itself augments thirst, and its use with desmopressin in patients with adipsia has been proposed.

Patients with central diabetes insipidus do not develop hypernatremia if the thirst mechanism is intact and water is available. Hormonal replacement and pharmacologic agents are available for the treatment of central diabetes insipidus. In acute settings, such as after hypophysectomy, the aqueous vasopressin (Pitressin) preparation is preferable. Its short duration of action allows for more careful monitoring, and decreases the likelihood of complications such as water intoxication. In chronic settings, vasopressin tannate in oil (Pitressin Tannate) is potent and effective for 24 to 72 hours. It requires a deep subcutaneous or intramuscular injection by a fairly large-gauge needle, because of the viscosity of the oil vehicle. This material can cause sterile abscesses in some subjects, and on occasion be associated with resistance due to development of antibodies.[213–215] A modification of the natural vasopressin molecule to form desmopressin acetate (dDAVP) has resulted in a compound with prolonged antidiuretic activity (6–24 hours) and virtual elimination of vasopressor activity (antidiuretic to pressor ratio of approximately 2000:1) compared with the natural hormone argenine vasopressin (duration of action of 2–4 hours and antidiuretic to pressor ratio of 1:1[216–220]). Substitution of D-argenine for L-argenine at position 8 resulted in a peptide DAVP with diminished vasopressor activity, and deamination of the hemicysteine at position 1 gave rise to a second peptide, with enhanced antidiuretic to pressor activity and prolonged duration of action. dDAVP is administered intranasally in the dosage ranging from 10 to 20 μg every 8 to 12 hours.[221,222] Intranasal dDAVP is now the treatment of choice for central diabetes insipidus.

In some patients with partial central diabetes insipidus, drugs that stimulate argenine vasopressin secretion or enhance its action on the kidney have been useful. These include chlorpropamide, clofibrate, carbamazepine, and nonsteroidal anti-inflammatory drugs (NSAIDs).[223–226] Since, with very dilute urine of fixed osmolality, the urine volume is determined by the solute-load requiring excretion, a reduction of salt and protein in the diet will reduce the major urinary solutes, and thus the volume of urine necessary to accommodate their excretion.[14] A number of pharmacologic agents with antidiuretic properties are also used. Chlorpropamide (Diabinese) is the most commonly used. Its antidiuretic effects are manifested only if some vasopressin is present, and it is therefore useful only in partial diabetes insipidus. In Brattleboro rats with diabetes insipidus, chlorpropamide augmented the antidiuretic responses to dDAVP. A trial of 250 mg every day or twice a day may be offered to patients with partial central diabetes insipidus and at least 7 days allowed for an effect to occur. The anticonvulsant carbamazepine (Tegretol) has also caused antidiuresis in subjects with diabetes insipidus. A combination of chlorpropamide and carbamazepine has been found to provide an effect that could be synergistic.[227,228] Clofibrate also has been used to treat partial central diabetes insipidus.

In patients with nephrogenic diabetes insipidus, the concentrating defect may be reversible by treating the underlying disorder or eliminating the offending drug. Symptomatic polyuria can be treated with a low-sodium diet and thiazide diuretics.[136] This induces mild volume-depletion, which leads to enhanced proximal reabsorption of salt and water, and decreased delivery to the site of action of AVP, the collecting duct. By impairing renal prostaglandin synthesis, NSAIDs potentiate argenine vasopressin action, and thereby increase urine osmolality and decrease urine volume.[229] Amiloride may be useful in patients with nephrogenic diabetes insipidus who need to be on lithium.[126,230] The nephrotoxicity of lithium requires the drug to be taken up into collecting duct cells via the amiloride-sensitive Na^+ channel.

CLINICAL STUDIES AND OUTCOME

The clinical outcome of patients with hypernatremia depends on the age of the patient and the rapidity with which the hypernatremic state was attained.[231–233] Acute hypernatremia is associated with a 40% mortality, whereas the mortality for chronic hypernatremia is about 10%. In children, the mortality of acute hypernatremia ranges between 10 and 70%, with a mean of approximately 45%. Unfortunately, even in survivors, neurologic sequelae are common, affecting as many as two-thirds of the children.[30,234–237] In adults, acute elevation of serum sodium above 160 mEq/l is associated with a 75% mortality, while the mortality in chronic cases is approximately 60%. Note, however, that in the adult, hypernatremia frequently occurs in the setting of serious underlying diseases, which may be the primary cause of the high mortality.[153,238–240]

Table 45.14 summarizes clinical studies of hypernatremia in adults that have been published over the past two decades. From these varied studies,[232,233,241–246] it is apparent that hypernatremia is a common disturbance, with an incidence ranging from less than 1% to more than 3%. The variation in incidence is, in part, a

TABLE 45.14 Published Clinical Series of Patients with Hypernatremia

Series reference	Definition [Na], mmol/L	*N*	Incidence	Age years, mean ± SD	Etiologic Factors	Mortality
Daggett et al. [242]	>154	20	0.12%	N/A	Diabetes mellitus (57%)	40%
					CNS disease (57%)	
Mahowald and Himmelstein [245]	>150	23	N/A	72 ± 12	Infection (224%)	52%
Himmelstein et al. [243]	>150	56	0.65–2.25	73 ± 15	Infection (174%)	46%
					Nursing home care (265%)	
Snyder et al. [246]	>148 age	162	1.1%	78 ± 9	Febrile illness infirmity	42%
	>205 years				Nutritional supplementation post-operative state	
Bhatnagar and Weinkove [241]	>160	27	N/A	71.4	Poor intake (55%)	79%
					Increased insensible losses	
					Diuresis (100%)	
					Increased GI losses (241%)	
Long et al. [244]	>150	160	0.3%	76 median	Diuretics (193%)	54%
					Depressed sensorium 80%	
					Febrile illness (205%)	
					Mechanical ventilation (221%)	
Borra et al. [86]	>150	111	3.5%	On admission	Infection (267%)	49%
				83 ± 11	Malignancy (158%)	
				Hospital-acquired	Diabetes mellitus (67%)	
				76 ± 15		
Palevsky [232]	>150	103	On admission	On admission	On admission	41%
			0.2%	77 ± 17	infection (190%)	
			Hospital-acquired	Hospital-acquired	Hospital-acquired	
			1.0%	59 ± 19	fever (222%)	
					Mechanical ventilation (99%)	
					Enteral fluid loss (57%)	
					Mental status changes (255%)	

CNS: central nervous system; GI: gastrointestinal.

function of the populations at risk and the definition of hypernatremia used in various studies. The patient groups at increased risk for development of severe hypernatremia are listed in Table 45.15. Hypernatremia developing in nonhospitalized adults is predominantly a disease of the elderly,[86,245,247–249] is commonly a manifestation of underlying infection, and may reflect inadequate nursing care of patients in chronic care facilities. However, hospital-acquired hypernatremia occurs in a wider range of patients with an age distribution more similar to the general hospitalized population. The main factor contributing to the development of hypernatremia is the inability to control water intake in the setting of increased water losses. Pure water loss from diabetes insipidus rarely contributes to its development; more common etiologies of water loss include diuretic administration, solute diuresis, enteral fluid loss, and fever. The results from these clinical series

TABLE 45.15 Patient Groups at Increased Risk for Development of Severe Hypernatremia

Elderly patients
Hospitalized patients
Hypertonic infusions
Tube feedings
Osmotic diuretics
Lactulose
Mechanical ventilation
Patients with decreased baseline levels of consciousness
Patients with uncontrolled diabetes
Patients with underlying polyuric disorders

support the recommendation that the serum sodium concentration be corrected promptly, but gradually, over 48 to 72 hours.

References

[1] Peters JP. Water exchange. Physiol Rev 1944;24:40.
[2] Rose BD. New approach to disturbances in the plasma sodium concentration. Am J Med 1986;81:1033–40.
[3] Smith HW. From fish to philosopher. Boston: Little; 1953. p. 264
[4] Robertson GL, Aycinena P, Zerbe RL. Neurogenic disorders of osmoregulation. Am J Med 1982;72:339–53.
[5] Roy G, Banderali U. Channels for ions and amino acids in kidney cultured cells (MDCK) during volume regulation. J Exp Zool 1994;268:121–6.
[6] Abraham WT, Schrier RW. Body fluid volume regulation in health and disease. Adv Intern Med 1994;39:23–47.
[7] Berl T. The cAMP system in vasopressin-sensitive nephron segments of the vitamin D-treated rat. Kidney Int 1987;31:1065–71.
[8] Berl T, Anderson RJ, McDonald KM, Schrier RW. Clinical disorders of water metabolism. Kidney Int 1976;10:117–32.
[9] Gamble JL. Chemical anatomy, physiology and pathology of extracellular fluid: a lecture syllabus. Cambridge, Massachusetts: Harvard University Press; 1947.
[10] De Wardener HE, Herxheimer A. The effect of a high water intake on the kidney's ability to concentrate the urine in man. J Physiol 1957;139:42–52.
[11] Edelman IS, Leibman J, O'Meara MP, Birkenfeld LW. Interrelations between serum sodium concentration, serum osmolarity and total exchangeable sodium, total exchangeable potassium and total body water. J Clin Invest 1958;37:1236–56.
[12] Gault MH, Dixon ME, Doyle M, Cohen WM. Hypernatremia, azotemia, and dehydration due to high-protein tube feeding. Ann Intern Med 1968;68:778–91.
[13] Feig PU, McCurdy DK. The hypertonic state. N Engl J Med 1977;297:1444–54.
[14] Gennari FJ. Current concepts. Serum osmolality. Uses and limitations. N Engl J Med 1984;310:102–5.
[15] Shoker AS. Application of the clearance concept to hyponatremic and hypernatremic disorders: a phenomenological analysis. Clin Chem 1994;40:1220–7.
[16] Smithline N, Gardner Jr KD. Gaps–anionic and osmolal. JAMA 1976;236:1594–7.
[17] Verbalis JG. Disorders of body water homeostasis. Best Pract Res Clin Endocrinol Metab 2003;17:471–503.
[18] Gines P, Abraham WT, Schrier RW. Vasopressin in pathophysiological states. Semin Nephrol 1994;14:384–97.
[19] Majzoub JA, Rich A, van Boom J, Habener JF. Vasopressin and oxytocin mRNA regulation in the rat assessed by hybridization with synthetic oligonucleotides. J Biol Chem 1983;258:14061–4.
[20] Uhl GR, Zingg HH, Habener JF. Vasopressin mRNA *in situ* hybridization: localization and regulation studied with oligonucleotide cDNA probes in normal and Brattleboro rat hypothalamus. Proc Natl Acad Sci USA 1985;82:5555–9.
[21] Goldsmith C, Beasley HK, Whalley PJ, Rector Jr FC, Seldin DW. The effect of salt deprivation on the urinary concentrating mechanism in the dog. J Clin Invest 1961;40:2043–52.
[22] Murphy D, Levy A, Lightman S, Carter D. Vasopressin RNA in the neural lobe of the pituitary: dramatic accumulation in response to salt loading. Proc Natl Acad Sci USA 1989;86: 9002–5.
[23] Zerbe RL, Robertson GL. A comparison of plasma vasopressin measurements with a standard indirect test in the differential diagnosis of polyuria. N Engl J Med 1981;305:1539–46.
[24] Kumar S, Berl T. Sodium. Lancet 1998;352:220–8.
[25] Andersson B. Regulation of water intake. Physiol Rev 1978;58:582.
[26] Fitzsimons JT. Angiotensin, thirst, and sodium appetite: retrospect and prospect. Fed Proc 1978;37:2669–75.
[27] Fitzsimons JT. Thirst. Physiol Rev 1972;52:468–561.
[28] Phillips PA, Bretherton M, Johnston CI, Gray L. Reduced osmotic thirst in healthy elderly men. Am J Physiol 1991;261: R166–171.
[29] Phillips PA, Rolls BJ, Ledingham JG, Forsling ML, Morton JJ, Crowe MJ, et al. Reduced thirst after water deprivation in healthy elderly men. N Engl J Med 1984;311:753–9.
[30] Papadimitriou A, Kipourou K, Manta C, Tapaki G, Philippidis P. Adipsic hypernatremia syndrome in infancy. J Pediatr Endocrinol Metab 1997;10:547–50.
[31] Gullans SR, Verbalis JG. Control of brain volume during hyperosmolar and hypoosmolar conditions. Annu Rev Med 1993;44:289–301.
[32] Lien YH, Shapiro JI, Chan L. Effects of hypernatremia on organic brain osmoles. J Clin Invest 1990;85:1427–35.
[33] Lien YH, Shapiro JI, Chan L. Study of brain electrolytes and organic osmolytes during correction of chronic hyponatremia. Implications for the pathogenesis of central pontine myelinolysis. J Clin Invest 1991;88:303–9.
[34] Heilig CW, Stromski ME, Blumenfeld JD, Lee JP, Gullans SR. Characterization of the major brain osmolytes that accumulate in salt-loaded rats. Am J Physiol 1989;257:F1108–1116.
[35] Fishman RA, Chan PH. Changes in ammonia and amino acid metabolism induced by hyperosmolality *in vivo* and *in vitro*. Trans Am Neurol Assoc 1976;101:34–9.
[36] Verbalis JG. Brain volume regulation in response to changes in osmolality. Neuroscience 2010;168:862–70.
[37] Cserr HF, DePasquale M, Patlak CS. Regulation of brain water and electrolytes during acute hyperosmolality in rats. Am J Physiol 1987;253:F522–529.
[38] Cserr HF, DePasquale M, Patlak CS. Volume regulatory influx of electrolytes from plasma to brain during acute hyperosmolality. Am J Physiol 1987;253:F530–537.
[39] Ayus JC, Armstrong DL, Arieff AI. Effects of hypernatraemia in the central nervous system and its therapy in rats and rabbits. J Physiol 1996;492(Pt 1):243–55.
[40] Relman AS, Schwartz WB. The kidney in potassium depletion. Am J Med 1958;24:764–73.
[41] Chan PH, Fishman RA. Elevation of rat brain amino acids, ammonia and idiogenic osmoles induced by hyperosmolality. Brain Res 1979;161:293–301.
[42] Hochstenbach SL, Ciriello J. Plasma hypernatremia induces c-fos activity in medullary catecholaminergic neurons. Brain Res 1995;674:46–54.

[43] Holliday MA, Kalayci MN, Harrah J. Factors that limit brain volume changes in response to acute and sustained hyper- and hyponatremia. J Clin Invest 1968;47:1916–28.
[44] Proft M, Struhl K. MAP kinase-mediated stress relief that precedes and regulates the timing of transcriptional induction. Cell 2004;118:351–61.
[45] Yancey PH, Clark ME, Hand SC, Bowlus RD, Somero GN. Living with water stress: evolution of osmolyte systems. Science 1982;217:1214–22.
[46] Arieff AI, Guisado R. Effects on the central nervous system of hypernatremic and hyponatremic states. Kidney Int 1976;10:104–16.
[47] Arieff AI, Guisado R, Lazarowitz VC. The pathophysiology of hyperosmolar states. In: Andreoli TE, Grantham JJ, Rector FC, editors. Disturbances in body fluid osmolality. Baltimore: Williams & Wilkins; 1977. p. 227.
[48] Thurston JH, Hauhart RE, Dirgo JA. Taurine: a role in osmotic regulation of mammalian brain and possible clinical significance. Life Sci 1980;26:1561–8.
[49] Sotos JF, Dodge PR, Talbot NB. Studies in experimental hypertonicity. II. Hypertonicity of body fluids as a cause of acidosis. Pediatrics 1962;30:180–93.
[50] Soupart A, Penninckx R, Namias B, Stenuit A, Perier O, Decaux G. Brain myelinolysis following hypernatremia in rats. J Neuropathol Exp Neurol 1996;55:106–13.
[51] Beck FX, Burger-Kentischer A, Muller E. Cellular response to osmotic stress in the renal medulla. Pflugers Arch 1998;436: 814–27.
[52] Terada Y, Inoshita S, Hanada S, Shimamura H, Kuwahara M, Ogawa W, et al. Hyperosmolality activates Akt and regulates apoptosis in renal tubular cells. Kidney Int 2001;60:553–67.
[53] Zhang Z, Cai Q, Michea L, Dmitrieva NI, Andrews P, Burg MB. Proliferation and osmotic tolerance of renal inner medullary epithelial cells *in vivo* and in cell culture. Am J Physiol Renal Physiol 2002;283:F302–308.
[54] Rauchman MI, Nigam SK, Delpire E, Gullans SR. An osmotically tolerant inner medullary collecting duct cell line from an SV40 transgenic mouse. Am J Physiol 1993;265:F416–424.
[55] Cai Q, Michea L, Andrews P, Zhang Z, Rocha G, Dmitrieva N, et al. Rate of increase of osmolality determines osmotic tolerance of mouse inner medullary epithelial cells. Am J Physiol Renal Physiol 2002;283:F792–798.
[56] Capasso JM, Rivard CJ, Berl T. Long-term adaptation of renal cells to hypertonicity: role of MAP kinases and Na-K-ATPase. Am J Physiol Renal Physiol 2001;280:F768–776.
[57] Capasso JM, Rivard CJ, Enomoto LM, Berl T. Adaptation of murine inner medullary collecting duct (IMCD3) cell cultures to hypertonicity. Ann N Y Acad Sci 2003;986:410–5.
[58] Dmitrieva N, Michea L, Burg M. p53 Protects renal inner medullary cells from hypertonic stress by restricting DNA replication. Am J Physiol Renal Physiol 2001;281:F522–530.
[59] Miyakawa H, Woo SK, Chen CP, Dahl SC, Handler JS, Kwon HM. Cis- and trans-acting factors regulating transcription of the BGT1 gene in response to hypertonicity. Am J Physiol 1998;274: F753–761.
[60] Miyakawa H, Woo SK, Dahl SC, Handler JS, Kwon HM. Tonicity-responsive enhancer binding protein, a rel-like protein that stimulates transcription in response to hypertonicity. Proc Natl Acad Sci USA 1999;96:2538–42.
[61] Lopez-Rodriguez C, Aramburu J, Rakeman AS, Rao A. NFAT5, a constitutively nuclear NFAT protein that does not cooperate with Fos and Jun. Proc Natl Acad Sci USA 1999;96:7214–9.
[62] Trama J, Lu Q, Hawley RG, Ho SN. The NFAT-related protein NFATL1 (TonEBP/NFAT5) is induced upon T cell activation in a calcineurin-dependent manner. J Immunol 2000;165:4884–94.
[63] Ko BC, Turck CW, Lee KW, Yang Y, Chung SS. Purification, identification, and characterization of an osmotic response element binding protein. Biochem Biophys Res Commun 2000;270: 52–61.
[64] Aramburu J, Drews-Elger K, Estrada-Gelonch A, Minguillon J, Morancho B, Santiago V, et al. Regulation of the hypertonic stress response and other cellular functions by the rel-like transcription factor NFAT5. Biochem Pharmacol 2006;72:1597–604.
[65] Hogan PG, Chen L, Nardone J, Rao A. Transcriptional regulation by calcium, calcineurin, and NFAT. Genes Dev 2003;17:2205–32.
[66] Stroud JC, Lopez-Rodriguez C, Rao A, Chen L. Structure of a TonEBP-DNA complex reveals DNA encircled by a transcription factor. Nat Struct Biol 2002;9:90–4.
[67] Andres-Hernando A, Lanaspa MA, Rivard CJ, Berl T. Nucleoporin 88 (Nup88) is regulated by hypertonic stress in kidney cells to retain the transcription factor tonicity enhancer-binding protein (TonEBP) in the nucleus. J Biol Chem 2008;283:25082–90.
[68] Lee SD, Colla E, Sheen MR, Na KY, Kwon HM. Multiple domains of TonEBP cooperate to stimulate transcription in response to hypertonicity. J Biol Chem 2003;278:47571–7.
[69] Lopez-Rodriguez C, Aramburu J, Jin L, Rakeman AS, Michino M, Rao A. Bridging the NFAT and NF-kappaB families: NFAT5 dimerization regulates cytokine gene transcription in response to osmotic stress. Immunity 2001;15:47–58.
[70] Ferraris JD, Persaud P, Williams CK, Chen Y, Burg MB. cAMP-independent role of PKA in tonicity-induced transactivation of tonicity-responsive enhancer/ osmotic response element-binding protein. Proc Natl Acad Sci USA 2002;99:16800–5.
[71] Irarrazabal CE, Liu JC, Burg MB, Ferraris JD. ATM, a DNA damage-inducible kinase, contributes to activation by high NaCl of the transcription factor TonEBP/OREBP. Proc Natl Acad Sci USA 2004;101:8809–14.
[72] Ko BC, Lam AK, Kapus A, Fan L, Chung SK, Chung SS. Fyn and p38 signaling are both required for maximal hypertonic activation of the osmotic response element-binding protein/ tonicity-responsive enhancer-binding protein (OREBP/ TonEBP). J Biol Chem 2002;277:46085–92.
[73] Woo SK, Maouyo D, Handler JS, Kwon HM. Nuclear redistribution of tonicity-responsive enhancer binding protein requires proteasome activity. Am J Physiol Cell Physiol 2000;278: C323–330.
[74] Dahl SC, Handler JS, Kwon HM. Hypertonicity-induced phosphorylation and nuclear localization of the transcription factor TonEBP. Am J Physiol Cell Physiol 2001;280:C248–253.
[75] Cai Q, Ferraris JD, Burg MB. High NaCl increases TonEBP/ OREBP mRNA and protein by stabilizing its mRNA. Am J Physiol Renal Physiol 2005;289:F803–807.
[76] Lee SD, Choi SY, Lim SW, Lamitina ST, Ho SN, Go WY, et al. TonEBP stimulates multiple cellular pathways for adaptation to hypertonic stress: Organic osmolyte-dependent and -independent pathways. Am J Physiol Renal Physiol 2011.
[77] Go WY, Liu X, Roti MA, Liu F, Ho SN. NFAT5/TonEBP mutant mice define osmotic stress as a critical feature of the lymphoid microenvironment. Proc Natl Acad Sci USA 2004;101:10673–8.
[78] Lopez-Rodriguez C, Antos CL, Shelton JM, Richardson JA, Lin F, Novobrantseva TI, et al. Loss of NFAT5 results in renal atrophy and lack of tonicity-responsive gene expression. Proc Natl Acad Sci USA 2004;101:2392–7.
[79] Maouyo D, Kim JY, Lee SD, Wu Y, Woo SK, Kwon HM. Mouse TonEBP-NFAT5: expression in early development and alternative splicing. Am J Physiol Renal Physiol 09, 2002;282:F802–8.
[80] Dressler GR, Wilkinson JE, Rothenpieler UW, Patterson LT, Williams-Simons L, Westphal H. Deregulation of Pax-2

expression in transgenic mice generates severe kidney abnormalities. Nature 1993;362:65–7.
[81] Chan L. The current status of magnetic resonance spectroscopy–basic and clinical aspects. West J Med 1985;143:773–81.
[82] Chan L, Shapiro JI. Contributions of nuclear magnetic resonance to study of acute renal failure. Ren Fail 1989;11:79–89.
[83] Ross B, Freeman D, Chan L. Contributions of nuclear magnetic resonance to renal biochemistry. Kidney Int 1986;29:131–41.
[84] Lee JH, Arcinue E, Ross BD. Brief report: organic osmolytes in the brain of an infant with hypernatremia. N Engl J Med 1994;331:439–42.
[85] Schulman M. Organic osmolytes in the brain of an infant with hypernatremia. N Engl J Med 1994;331:1776–7.
[86] Borra SI, Beredo R, Kleinfeld M. Hypernatremia in the aging: causes, manifestations, and outcome. J Natl Med Assoc 1995;87:220–4.
[87] Perez GO, Oster JR, Robertson GL. Severe hypernatremia with impaired thirst. Am J Nephrol 1989;9:421–34.
[88] Robertson G. The physiopathology of ADH secretion. In: Tolis G, Labrie F, Martin J, editors. Clinical neuroendocrinology: a pathophysiological approach. New York: Ravens Press; 1979. p. 247.
[89] Robertson G. Disorders of thirst in man. In: Ramsay D, Booth D, editors. Thirst: physiological and psychological aspects. London: Springer-Verlag; 1991. p. 453.
[90] Robertson GL. Pathophysiology of water metabolism. In: Brenner BM, Rector FC, editors. The kidney. Philadelphia: Saunders; 1991. p. 677.
[91] Keuneke C, Anders HJ, Schlondorff D. Adipsic hypernatremia in two patients with AIDS and cytomegalovirus encephalitis. Am J Kidney Dis 1999;33:379–82.
[92] McIver B, Connacher A, Whittle I, Baylis P, Thompson C. Adipsic hypothalamic diabetes insipidus after clipping of anterior communicating artery aneurysm. BMJ 1991;303:1465–7.
[93] Shiau YF, Feldman GM, Resnick MA, Coff PM. Stool electrolyte and osmolality measurements in the evaluation of diarrheal disorders. Ann Intern Med 1985;102:773–5.
[94] Pollock AS, Arieff AI. Abnormalities of cell volume regulation and their functional consequences. Am J Physiol 1980;239: F195–205.
[95] Robertson GL. Antidiuretic hormone. Normal and disordered function. Endocrinol Metab Clin North Am 2001;30:671–94 vii
[96] Visser L, Devuyst O. Physiopathology of hypernatremia following relief of urinary tract obstruction. Acta Clin Belg 1994;49:290–5.
[97] Warren SE, Mitas JA, Swerdlin AH. Hypernatremia in hepatic failure. Jama 1980;243:1257–60.
[98] Kleeman CR, Rubini ME, Lamdin E, Epstein FH. Studies on alcohol diuresis. II. The evaluation of ethyl alcohol as an inhibitor of the neurohypophysis. J Clin Invest 1955;34:448–55.
[99] Chu HI, Liu SH, Yu TF. Water and electrolyte metabolism in diabetes insipidus. Proc Soc Exp Biol Med 1941;46:682.
[100] Birnbaumer M. The V2 vasopressin receptor mutations and fluid homeostasis. Cardiovasc Res 2001;51:409–15.
[101] Kinoshita K, Miura Y, Nagasaki H, Murase T, Bando Y, Oiso Y. A novel deletion mutation in the arginine vasopressin receptor 2 gene and skewed X chromosome inactivation in a female patient with congenital nephrogenic diabetes insipidus. J Endocrinol Invest 2004;27:167–70.
[102] McLeod JF, Kovacs L, Gaskill MB, Rittig S, Bradley GS, Robertson GL. Familial neurohypophyseal diabetes insipidus associated with a signal peptide mutation. J Clin Endocrinol Metab 1993;77:599AG.
[103] Merendino Jr JJ, Speigel AM, Crawford JD, O'Carroll AM, Brownstein MJ, Lolait SJ. Brief report: a mutation in the vasopressin V2-receptor gene in a kindred with X-linked nephrogenic diabetes insipidus. N Engl J Med 1993;328:1538–41.
[104] Miyakoshi M, Kamoi K, Murase T, Sugimura Y, Oiso Y. Novel mutant vasopressin-neurophysin II gene associated with familial neurohypophyseal diabetes insipidus. Endocr J 2004;51: 551–6.
[105] Bichet DG, Birnbaumer M, Lonergan M, Arthus MF, Rosenthal W, Goodyer P, et al. Nature and recurrence of AVPR2 mutations in X-linked nephrogenic diabetes insipidus. Am J Hum Genet 1994;55:278–86.
[106] Chan Seem CP, Dossetor JF, Penney MD. Nephrogenic diabetes insipidus due to a new mutation of the arginine vasopressin V2 receptor gene in a girl presenting with non-accidental injury. Ann Clin Biochem 1999;3(Pt 6):779–82.
[107] Holtzman EJ, Harris Jr HW, Kolakowski Jr LF, Guay-Woodford LM, Botelho B, Ausiello DA. Brief report: a molecular defect in the vasopressin V2-receptor gene causing nephrogenic diabetes insipidus. N Engl J Med 1993;328: 1534–7.
[108] Holtzman EJ, Kolakowski Jr LF, Geifman-Holtzman O, O'Brien DG, Rasoulpour M, Guillot AP, et al. Mutations in the vasopressin V2 receptor gene in two families with nephrogenic diabetes insipidus. J Am Soc Nephrol 1994;5:169–76.
[109] Kambouris M, Dlouhy SR, Trofatter JA, Conneally PM, Hodes ME. Localization of the gene for X-linked nephrogenic diabetes insipidus to Xq28. Am J Med Genet 1988;29:239–46.
[110] Knoers N, Monnens LA. A variant of nephrogenic diabetes insipidus: V2 receptor abnormality restricted to the kidney. Eur J Pediatr 1991;150:370–3.
[111] Knoers N, van der Heyden H, van Oost BA, Ropers HH, Monnens L, Willems J. Nephrogenic diabetes insipidus: close linkage with markers from the distal long arm of the human X chromosome. Hum Genet 1988;80:31–8.
[112] Rosenthal W, Seibold A, Antaramian A, Lonergan M, Arthus MF, Hendy GN, et al. Molecular identification of the gene responsible for congenital nephrogenic diabetes insipidus. Nature 1992;359:233–5.
[113] Asai T, Kuwahara M, Kurihara H, Sakai T, Terada Y, Marumo F, et al. Pathogenesis of nephrogenic diabetes insipidus by aquaporin-2 C-terminus mutations. Kidney Int 2003;64:2–10.
[114] Boccalandro C, De Mattia F, Guo DC, Xue L, Orlander P, King TM, et al. Characterization of an aquaporin-2 water channel gene mutation causing partial nephrogenic diabetes insipidus in a Mexican family: evidence of increased frequency of the mutation in the town of origin. J Am Soc Nephrol 2004;15:1223–31.
[115] de Mattia F, Savelkoul PJ, Kamsteeg EJ, Konings IB, van der Sluijs P, Mallmann R, et al. Lack of arginine vasopressin-induced phosphorylation of aquaporin-2 mutant AQP2-R254L explains dominant nephrogenic diabetes insipidus. J Am Soc Nephrol 2005;16(10):2872–80.
[116] Kamsteeg EJ, Bichet DG, Konings IB, Nivet H, Lonergan M, Arthus MF, et al. Reversed polarized delivery of an aquaporin-2 mutant causes dominant nephrogenic diabetes insipidus. J Cell Biol 2003;163:1099–109.
[117] Marr N, Bichet DG, Hoefs S, Savelkoul PJ, Konings IB, De Mattia F, et al. Cell-biologic and functional analyses of five new aquaporin-2 missense mutations that cause recessive nephrogenic diabetes insipidus. J Am Soc Nephrol 2002;13: 2267–77.
[118] Nielsen S, Frokiaer J, Marples D, Kwon TH, Agre P, Knepper MA. Aquaporins in the kidney: from molecules to medicine. Physiol Rev 2002;82:205–44.

[119] Baylis PH, Heath DA. Water disturbances in patients treated with oral lithium carbonate. Ann Intern Med 1978;88:607–9.
[120] Boton R, Gaviria M, Batlle DC. Prevalence, pathogenesis, and treatment of renal dysfunction associated with chronic lithium therapy. Am J Kidney Dis 1987;10:329–45.
[121] Christensen S, Kusano E, Yusufi AN, Murayama N, Dousa TP. Pathogenesis of nephrogenic diabetes insipidus due to chronic administration of lithium in rats. J Clin Invest 1985;75:1869–79.
[122] Cogan E, Abramow M. Inhibition by lithium of the hydroosmotic action of vasopressin in the isolated perfused cortical collecting tubule of the rabbit. J Clin Invest 1986;77:1507–14.
[123] Dousa TP. Interaction of lithium with vasopressin-sensitive cyclic AMP system of human renal medulla. Endocrinology 1974;95:1359–66.
[124] Forrest Jr JN, Cohen AD, Torretti J, Himmelhoch JM, Epstein FH. On the mechanism of lithium-induced diabetes insipidus in man and the rat. J Clin Invest 1974;53:1115–23.
[125] Goldberg H, Clayman P, Skorecki K. Mechanism of Li inhibition of vasopressin-sensitive adenylate cyclase in cultured renal epithelial cells. Am J Physiol 1988;255:F995–1002.
[126] Walker RG. Lithium nephrotoxicity. Kidney Int Suppl 1993;42: S93–98.
[127] Berl T, Linas SL, Aisenbrey GA, Anderson RJ. On the mechanism of polyuria in potassium depletion. The role of polydipsia. J Clin Invest 1977;60:620–5.
[128] Gutsche HU, Peterson LN, Levine DZ. *In vivo* evidence of impaired solute transport by the thick ascending limb in potassium-depleted rats. J Clin Invest 1984;73:908–16.
[129] Kim JK, Summer SN, Berl T. The cyclic AMP system in the inner medullary collecting duct of the potassium-depleted rat. Kidney Int 1984;26:384–91.
[130] Levi M, Peterson L, Berl T. Mechanism of concentrating defect in hypercalcemia. Role of polydipsia and prostaglandins. Kidney Int 1983;23:489–97.
[131] Peterson LN. Vitamin D-induced chronic hypercalcemia inhibits thick ascending limb NaCl reabsorption *in vivo*. Am J Physiol 1990;259:F122–129.
[132] Barron WM, Cohen LH, Ulland LA, Lassiter WE, Fulghum EM, Emmanouel D, et al. Transient vasopressin-resistant diabetes insipidus of pregnancy. N Engl J Med 1984;310:442–4.
[133] Siristatidis C, Salamalekis E, Iakovidou H, Creatsas G. Three cases of diabetes insipidus complicating pregnancy. J Matern Fetal Neonatal Med 2004;16:61–3.
[134] Robertson GL, McLeod JF, Zerbe RL. Vasopressin function in heritable forms of diabetes insipidus. In: Gross P, Richter D, Robertson GL, editors. Vasopressin. Paris: John Libbey Eurotext; 1993. p. 493–502.
[135] Carter RD, Goodman AD. Nephrogenic diabetes insipidus accompanied by massive dilatation of the kidneys, ureters and bladder. J Urol 1963;89:366–9.
[136] Alon U, Chan JC. Hydrochlorothiazide-amiloride in the treatment of congenital nephrogenic diabetes insipidus. Am J Nephrol 1985;5:9–13.
[137] Kirchlechner V, Koller DY, Seidl R, Waldhauser F. Treatment of nephrogenic diabetes insipidus with hydrochlorothiazide and amiloride. Arch Dis Child 1999;80:548–52.
[138] Konoshita T, Kuroda M, Kawane T, Koni I, Miyamori I, Tofuku Y, et al. Treatment of congenital nephrogenic diabetes insipidus with hydrochlorothiazide and amiloride in an adult patient. Horm Res 2004;61:63–7.
[139] Pattaragarn A, Alon US. Treatment of congenital nephrogenic diabetes insipidus by hydrochlorothiazide and cyclooxygenase-2 inhibitor. Pediatr Nephrol 2003;18:1073–6.
[140] Bichet DG. Nephrogenic diabetes insipidus. Am J Med 1998;105:431–42.
[141] Tannen RL, Regal EM, Dunn MJ, Schrier RW. Vasopressin-resistant hyposthenuria in advanced chronic renal disease. N Engl J Med 1969;280:1135–41.
[142] Teitelbaum I, McGuinness S. Vasopressin resistance in chronic renal failure. Evidence for the role of decreased V2 receptor mRNA. J Clin Invest 1995;96:378–85.
[143] Fine LG, Salehmoghaddam S. Water homeostasis in acute and chronic renal failure. Semin Nephrol 1984;4:289.
[144] Fine LG, Schlondorff D, Trizna W, Gilbert RM, Bricker NS. Functional profile of the isolated uremic nephron. Impaired water permeability and adenylate cyclase responsiveness of the cortical collecting tubule to vasopressin. J Clin Invest 1978;61:1519–27.
[145] Gabow PA, Kaehny WD, Johnson AM, Duley IT, Manco-Johnson M, Lezotte DC, et al. The clinical utility of renal concentrating capacity in polycystic kidney disease. Kidney Int 1989;35:675–80.
[146] Buckalew Jr VM, Someren A. Renal manifestations of sickle cell disease. Arch Intern Med 1974;133:660–9.
[147] Statius van Eps LW, Pinedo-Veels C, de Vries GH, de Koning J. Nature of concentrating defect in sickle-cell nephropathy. Microradioangiographic studies. Lancet 1970;1:450–2.
[148] Finn AL, Handler JS, Orloff J. Relation between toad bladder potassium content and permeability response to vasopressin. Am J Physiol 1966;210:1279–84.
[149] Beck N, Singh H, Reed SW, Murdaugh HV, Davis BB. Pathogenic role of cyclic AMP in the impairment of urinary concentrating ability in acute hypercalcemia. J Clin Invest 1974;54:1049–55.
[150] Goldfarb S, Agus ZS. Mechanism of the polyuria of hypercalcemia. Am J Nephrol 1984;4:69–76.
[151] Lins LE. Renal function in hypercalcemia. A clinical and experimental study. Acta Med Scand Suppl 1979;632:1–46.
[152] Gabow PA. Ethylene glycol intoxication. Am J Kidney Dis 1988;11:277–9.
[153] Douglas JB, Healy JK. Nephrotoxic effects of amphotericin B, including renal tubular acidosis. Am J Med 1969;46:154–62.
[154] Farese Jr RV, Schambelan M, Hollander H, Stringari S, Jacobson MA. Nephrogenic diabetes insipidus associated with foscarnet treatment of cytomegalovirus retinitis. Ann Intern Med 1990;112:955–6.
[155] Christensen S. Acute and chronic effects of vasopressin in rats with lithium-polyuria. Acta Pharmacol Toxicol (Copenh) 1976;38:241–53.
[156] Quintanilla AP. Pathophysiology of renal concentrating defects. Ann Clin Lab Sci 1981;11:300–7.
[157] Kanno K, Sasaki S, Hirata Y, Ishikawa S, Fushimi K, Nakanishi S, et al. Urinary excretion of aquaporin-2 in patients with diabetes insipidus. N Engl J Med 1995;332:1540–5.
[158] Ataga KI, Orringer EP. Renal abnormalities in sickle cell disease. Am J Hematol 2000;63:205–11.
[159] Pham PT, Pham PC, Wilkinson AH, Lew SQ. Renal abnormalities in sickle cell disease. Kidney Int 2000;57:1–8.
[160] Robertson G. Pathophysiology of water metabolism. In: Brenner B, editor. The kidney. Philadelphia: WB Saunders; 1996. p. 873–928.
[161] Hollenberg NK. Set point for sodium homeostasis: surfeit, deficit, and their implications. Kidney Int 1980;17:423–9.
[162] Hollenberg NK. Surfeit, deficit, and the set point for sodium homeostasis. Kidney Int 1982;21:883–4.
[163] Halter JB, Goldberg AP, Robertson GL, Porte Jr D. Selective osmoreceptor dysfunction in the syndrome of chronic hypernatremia. J Clin Endocrinol Metab 1977;44:609–16.
[164] Brezis M, Weiler-Ravell D. Hypernatremia, hypodipsia and partial diabetes inspipidus: a model for defective osmoregulation. Am J Med Sci 1980;279:37–45.

[165] DeRubertis FR, Michelis MF, Beck N, Field JB, Davis BB. "Essential" hypernatremia due to ineffective osmotic and intact volume regulation of vasopressin secretion. J Clin Invest 1971;50:97–111.
[166] DeRubertis FR, Michelis MF, Davis BB. "Essential" hypernatremia. Report of three cases and review of the literature. Arch Intern Med 1974;134:889–95.
[167] Hammond DN, Moll GW, Robertson GL, Chelmicka-Schorr E. Hypodipsic hypernatremia with normal osmoregulation of vasopressin. N Engl J Med 1986;315:433–6.
[168] Miller PD, Krebs RA, Neal BJ, McIntyre DO. Hypodipsia in geriatric patients. Am J Med 1982;73:354–6.
[169] Moder KG, Hurley DL. Fatal hypernatremia from exogenous salt intake: report of a case and review of the literature. Mayo Clin Proc 1990;65:1587–94.
[170] Thompson CJ, Baylis PH. Thirst in diabetes insipidus: clinical relevance of quantitative assessment. Q J Med 1987;65: 853–62.
[171] Silver AJ. Aging and risks for dehydration. Cleve Clin J Med 1990;57:341–4.
[172] Yamamoto T, Harada H, Fukuyama J, Hayashi T, Mori I. Impaired arginine-vasopressin secretion associated with hypoangiotensinemia in hypernatremic dehydrated elderly patients. Jama 1988;259:1039–42.
[173] Mattar JA, Weil MH, Shubin H, Stein L. Cardiac arrest in the critically ill. II. Hyperosmolal states following cardiac arrest. Am J Med 1974;56:162–8.
[174] Ellis RJ. Severe hypernatremia from sea water ingestion during near-drowning in a hurricane. West J Med 1997;167: 430–3.
[175] Meadow R. Non-accidental salt poisoning. Arch Dis Child 1993;68:448–52.
[176] Reid DE, Frigoletto Fd J, Goodlin RC. Hypernatremia from intravascular saline infusion during therapeutic abortion. Jama 1972;220:1749.
[177] Sanderson NA, Katz MA. The fate of hypertonic saline administered during hemodialysis. Anna J 1994;21:162–9 [discussion 170].
[178] Williams DJ, Jugurnauth J, Harding K, Woolfson RG, Mansell MA. Acute hypernatraemia during bicarbonate-buffered haemodialysis. Nephrol Dial Transplant 1994;9:1170–3.
[179] Allerton JP, Strom JA. Hypernatremia due to repeated doses of charcoal-sorbitol. Am J Kidney Dis 1991;17:581–4.
[180] Peskind ER, Jensen CF, Pascualy M, Tsuang D, Cowley D, Martin DC, et al. Sodium lactate and hypertonic sodium chloride induce equivalent panic incidence, panic symptoms, and hypernatremia in panic disorder. Biol Psychiatry 1998;44: 1007–16.
[181] Ishikawa S, Sakuma N, Fujisawa G, Tsuboi Y, Okada K, Saito T. Opposite changes in serum sodium and potassium in patients in diabetic coma. Endocr J 1994;41:37–43.
[182] Kahn T. Hypernatremia with edema. Arch Intern Med 1999;159:93–8.
[183] Lin M, Liu SJ, Lim IT. Disorders of water imbalance. Emerg Med Clin North Am 2005;23:749–70, ix.
[184] Richman RA, Post EM, Notman DD, Hochberg Z, Moses AM. Simplifying the diagnosis of diabetes insipidus in children. Am J Dis Child 1981;135:839–41.
[185] Milles JJ, Spruce B, Baylis PH. A comparison of diagnostic methods to differentiate diabetes insipidus from primary polyuria: a review of 21 patients. Acta Endocrinol (Copenh) 1983;104:410–6.
[186] Moses AM, Streeten DH. Differentiation of polyuric states by measurement of responses to changes in plasma osmolality induced by hypertonic saline infusions. Am J Med 1967;42:368–77.
[187] Narins RG, Krishna GC. Disorders of water balance. In: Stein JH, editor. Internal Medicine. Boston: Little, Brown; 1987. p. 794.
[188] Narins RG, Riley Jr LJ. Polyuria: simple and mixed disorders. Am J Kidney Dis 1991;17:237–41.
[189] AlOrainy IA, O'Gorman AM, Decell MK. Cerebral bleeding, infarcts, and presumed extrapontine myelinolysis in hypernatraemic dehydration. Neuroradiology 1999;41:144–6.
[190] Finberg L, Luttrell C, Redd H. Pathogenesis of lesions in the nervous system in hypernatremic states. II. Experimental studies of gross anatomic changes and alterations of chemical composition of the tissues. Pediatrics 1959;23:46–53.
[191] Fiordalisi I. Central nervous system complications during hypernatremia and its repair. Arch Pediatr Adolesc Med 1994;148:539–40.
[192] Korkmaz A, Yigit S, Firat M, Oran O. Cranial MRI in neonatal hypernatraemic dehydration. Pediatr Radiol 2000;30:323–5.
[193] Dunger DB, Broadbent V, Yeoman E, Seckl JR, Lightman SL, Grant DB, et al. The frequency and natural history of diabetes insipidus in children with langerhans-cell histiocytosis. N Engl J Med 1989;321:1157–62.
[194] Durr JA, Hoggard JG, Hunt JM, Schrier RW. Diabetes insipidus in pregnancy associated with abnormally high circulating vasopressinase activity. N Engl J Med 1987;316:1070–4.
[195] Ford Jr SM. Transient vasopressin-resistant diabetes insipidus of pregnancy. Obstet Gynecol 1986;68:288–9.
[196] Weiss NM, Robertson GL. Water metabolism in endocrine disorders. Semin Nephrol 1984;4:303.
[197] Yap HY, Tashima CK, Blumenschein GR, Eckles N. Diabetes insipidus and breast cancer. Arch Intern Med 1979;139:1009–11.
[198] Hartfield DS, Loewy JA, Yager JY. Transient thalamic changes on MRI in a child with hypernatremia. Pediatr Neurol 1999;20:60–2.
[199] Hilliard TN, Marsh MJ, Malcolm P, Murdoch IA, Wood BP. Radiological case of the month. Sagittal sinus thrombosis in hypernatremic dehydration. Arch Pediatr Adolesc Med 1998;152:1147 [discussion 1148].
[200] Hochstenbach SL, Ciriello J. Effects of plasma hypernatremia on nucleus tractus solitarius neurons. Am J Physiol 1994;266: R1916–1921.
[201] Manelfe C, Louvet JP. Computed tomography in diabetes insipidus. J Comput Assist Tomogr 1979;3:309–16.
[202] Marks SL, Taboada J. Hypernatremia and hypertonic syndromes. Vet Clin North Am Small Anim Pract 1998;28:533–43.
[203] Riggs JE. Neurologic manifestations of electrolyte disturbances. Neurol Clin 2002;20:227–39, vii.
[204] Tareen N, Martins D, Nagami G, Levine B, Norris KC. Sodium disorders in the elderly [Erratum appears in J Natl Med Assoc. 2005 apr;97(4):446] J Natl Med Assoc 2005;97:217–24.
[205] De Petris L, Luchetti A, Emma F. Cell volume regulation and transport mechanisms across the blood–brain barrier: implications for the management of hypernatraemic states. Eur J Pediatr 2001;160:71–7.
[206] Meyers A. Fluid and electrolyte therapy for children. Curr Opin Pediatr 1994;6:303–9.
[207] Miller NL, Finberg L. Peritoneal dialysis for salt poisoning. Report of a case. N Engl J Med 1960;263:1347–50.
[208] Sterns RH, Baer J, Ebersol S, Thomas D, Lohr JW, Kamm DE. Organic osmolytes in acute hyponatremia. Am J Physiol 36, 1993;264:F833–8.
[209] Sterns RH, Riggs JE, Schochet Jr SS. Osmotic demyelination syndrome following correction of hyponatremia. N Engl J Med 1986;314:1535–42.
[210] Verbalis JG, Gullans SR. Rapid correction of hyponatremia produces differential effects on brain osmolyte and electrolyte reaccumulation in rats. Brain Res 1993;606:19–27.

[211] Vexler ZS, Ayus JC, Roberts TP, Fraser CL, Kucharczyk J, Arieff AI. Hypoxic and ischemic hypoxia exacerbate brain injury associated with metabolic encephalopathy in laboratory animals. J Clin Invest 1994;93:256–64.
[212] Hogan GR, Dodge PR, Gill SR, Pickering LK, Master S. The incidence of seizures after rehydration of hypernatremic rabbits with intravenous or ad libitum oral fluids. Pediatr Res 1984;18:340–5.
[213] Scherbaum WA, Bottazzo GF. Autoantibodies to vasopressin cells in idiopathic diabetes insipidus: evidence for an autoimmune variant. Lancet 1983;1:897–901.
[214] Seckl JR, Dunger DB. Diabetes insipidus. Current treatment recommendations. Drugs 1992;44:216–24.
[215] Vokes TJ, Gaskill MB, Robertson GL. Antibodies to vasopressin in patients with diabetes insipidus. Implications for diagnosis and therapy. Ann Intern Med 1988;108:190–5.
[216] Harris AS. Clinical experience with desmopressin: efficacy and safety in central diabetes insipidus and other conditions. J Pediatr 1989;114:711–8.
[217] Moses AM, Coulson R. Augmentation by chlorpropamide of 1-deamino-8-D-arginine vasopressin-induced antidiuresis and stimulation of renal medullary adenylate cyclase and accumulation of adenosine 3′,5′-monophosphate. Endocrinology 1980;106:967–72.
[218] Rado JP, Marosi J, Borbely L, Tako J. Individual differences in the antidiuretic response induced by DDAVP in diabetes insipidus. Horm Metab Res 1976;8:155–6.
[219] Redmond GP, Rothner AD, Hahn JF, Schumacher OP. Combined desmopressin (DDAVP) and chlorpropamide therapy for diabetes insipidus with absent thirst. Cleve Clin Q 1983;50:351–2.
[220] Robertson GL, Harris A. Clinical use of vasopressin analogues. Hosp Pract (Off Ed) 1989;24:114–8 126–118, 133 passim.
[221] Bichet DG, Razi M, Lonergan M, Arthus MF, Papukna V, Kortas C, et al. Hemodynamic and coagulation responses to 1-desamino[8-D-arginine] vasopressin in patients with congenital nephrogenic diabetes insipidus. N Engl J Med 1988;318:881–7.
[222] Cunnah D, Ross G, Besser GM. Management of cranial diabetes insipidus with oral desmopressin (DDAVP). Clin Endocrinol (Oxf) 1986;24:253–7.
[223] Becker DJ, Foley Jr TP. 1-deamino-8-D-arginine vasopressin in the treatment of central diabetes insipidus in childhood. J Pediatr 1978;92:1011–5.
[224] Durr JA, Hensen J, Ehnis T, Blankenship MS. Chlorpropamide upregulates antidiuretic hormone receptors and unmasks constitutive receptor signaling. Am J Physiol Renal Physiol 2000;278:F799–808.
[225] Froyshov I, Haugen HN. Chlorpropamide treatment in diabetes insipidus. Acta Med Scand 1968;183:397–400.
[226] Wales JK. Treatment of diabetes insipidus with carbamazepine. Lancet 1975;2:948–51.
[227] Orloff J, Burn MB. Vasopressin-resistant diabetes insipidus. In: Stanbury J, Wyngaarden JB, BFrederickson NS, editors. The metabolic basis of inherited disease. New York: McGraw-Hill; 1972. p. 1567.
[228] Rado JP. Combination of carbamazepine and chlorpropamide in the treatment of "hyporesponder" pituitary diabetes insipidus. J Clin Endocrinol Metab 1974;38:1–7.
[229] Libber S, Harrison H, Spector D. Treatment of nephrogenic diabetes insipidus with prostaglandin synthesis inhibitors. J Pediatr 1986;108:305–11.
[230] Finch CK, Kelley KW, Williams RB. Treatment of lithium-induced diabetes insipidus with amiloride. Pharmacotherapy 2003;23:546–50.
[231] Finberg L. Hypernatremic (hypertonic) dehydration in infants. N Engl J Med 1973;289:196–8.
[232] Palevsky PM. Hypernatremia. Semin Nephrol 1998;18:20–30.
[233] Palevsky PM, Bhagrath R, Greenberg A. Hypernatremia in hospitalized patients. Ann Intern Med 1996;124:197–203.
[234] Chilton LA. Prevention and management of hypernatremic dehydration in breast-fed infants. West J Med 1995;163:74–6.
[235] Cooper WO, Atherton HD, Kahana M, Kotagal UR. Increased incidence of severe breastfeeding malnutrition and hypernatremia in a metropolitan area. Pediatrics 1995;96:957–60.
[236] Crook M, Robinson R, Swaminathan R. Hypertriglyceridaemia in a child with hypernatraemia due to a hypothalamic tumour. Ann Clin Biochem 1995;32(Pt 2):226–8.
[237] Dunn K, Butt W. Extreme sodium derangement in a paediatric inpatient population. J Paediatr Child Health 1997;33:26–30.
[238] Bacic A, Gluncic I, Gluncic V. Disturbances in plasma sodium in patients with war head injuries. Mil Med 1999;164:214–7.
[239] Gowrishankar M, Sapir D, Pace K, Halperin ML. Profound natriuresis, extracellular fluid volume contraction, and hypernatremia with hypertonic losses following trauma. Geriatr Nephrol Urol 1997;7:95–100.
[240] Vullo-Navich K, Smith S, Andrews M, Levine AM, Tischler JF, Veglia JM. Comfort and incidence of abnormal serum sodium, BUN, creatinine and osmolality in dehydration of terminal illness. Am J Hosp Palliat Care 1998;15:77–84.
[241] Bhatnagar D, Weinkove C. Serious hypernatraemia in a hospital population. Postgrad Med J 1988;64:441–3.
[242] Daggett P, Deanfield J, Moss F, Reynolds D. Severe hypernatraemia in adults. Br Med J 1979;1:1177–80.
[243] Himmelstein DU, Jones AA, Woolhandler S. Hypernatremic dehydration in nursing home patients: an indicator of neglect. J Am Geriatr Soc 1983;31:466–71.
[244] Long CA, Marin P, Bayer AJ, Shetty HG, Pathy MS. Hypernatraemia in an adult in-patient population. Postgrad Med J 1991;67:643–5.
[245] Mahowald JM, Himmelstein DU. Hypernatremia in the elderly: relation to infection and mortality. J Am Geriatr Soc 1981;29:177–80.
[246] Snyder NA, Feigal DW, Arieff AI. Hypernatremia in elderly patients. A heterogeneous, morbid, and iatrogenic entity. Ann Intern Med 1987;107:309–19.
[247] Ayus JC, Arieff AI. Abnormalities of water metabolism in the elderly. Semin Nephrol 1996;16:277–88.
[248] Kugler JP, Hustead T. Hyponatremia and hypernatremia in the elderly. Am Fam Physician 2000;61:3623–30.
[249] Mandal AK, Saklayen MG, Hillman NM, Markert RJ. Predictive factors for high mortality in hypernatremic patients. Am J Emerg Med 1997;15:130–2.
[250] Grunewald RW, Kinne RK. Osmoregulation in the mammalian kidney: the role of organic osmolytes. J Exp Zool 1999;283:708–24.
[251] Nakanishi T, Balaban RS, Burg MB. Survey of osmolytes in renal cell lines. Am J Physiol 1988;255:C181–191.
[252] Garcia-Perez A, Burg MB. Renal medullary organic osmolytes. Physiol Rev 1991;71:1081–115.
[253] Ho SN. Intracellular water homeostasis and the mammalian cellular osmotic stress response. J Cell Physiol 2006;206:9–15.
[254] Klawitter J, Rivard CJ, Capasso JM, Almeida NE, Berl T, Chan L. Metabonomic analysis of the effects of adaptation to hypertonicity in inner medullary collecting duct (IMCD3) cells. JASN 2004;15:90A.
[255] Burg MB. Molecular basis of osmotic regulation. Am J Physiol 1995;268:F983–996.

[256] Burg MB. Coordinate regulation of organic osmolytes in renal cells. Kidney Int 1996;49:1684–5.
[257] Yancey PH, Burg MB. Counteracting effects of urea and betaine in mammalian cells in culture. Am J Physiol 1990;258: R198–204.
[258] Grunewald JM, Grunewald RW, Kinne RK. Ion content and cell volume in isolated collecting duct cells: effect of hypotonicity. Kidney Int 1993;44:509–17.
[259] Grunewald JM, Grunewald RW, Kinne RK. Regulation of ion content and cell volume in isolated rat renal IMCD cells under hypertonic conditions. Am J Physiol 1994;267: F13–19.
[260] Dmitrieva NI, Cai Q, Burg MB. Cells adapted to high NaCl have many DNA breaks and impaired DNA repair both in cell culture and *in vivo*. Proc Natl Acad Sci USA 2004;101:2317–22.
[261] Dmitrieva NI, Michea LF, Rocha GM, Burg MB. Cell cycle delay and apoptosis in response to osmotic stress. Comp Biochem Physiol A Mol Integr Physiol 2001;130:411–20.
[262] Kultz D, Chakravarty D. Hyperosmolality in the form of elevated NaCl but not urea causes DNA damage in murine kidney cells. Proc Natl Acad Sci USA 2001;98:1999–2004.
[263] Alexander MR, Tyers M, Perret M, Craig BM, Fang KS, Gustin MC. Regulation of cell cycle progression by Swe1p and Hog1p following hypertonic stress. Mol Biol Cell 2001;12:53–62.
[264] Belli G, Gari E, Aldea M, Herrero E. Osmotic stress causes a G1 cell cycle delay and downregulation of Cln3/Cdc28 activity in *Saccharomyces cerevisiae*. Mol Microbiol 2001;39:1022–35.
[265] Copp J, Wiley S, Ward MW, van der Geer P. Hypertonic shock inhibits growth factor receptor signaling, induces caspase-3 activation, and causes reversible fragmentation of the mitochondrial network. Am J Physiol Cell Physiol 2005;288: C403–415.
[266] Desai BN, Myers BR, Schreiber SL. FKBP12-rapamycin-associated protein associates with mitochondria and senses osmotic stress via mitochondrial dysfunction. Proc Natl Acad Sci USA 2002;99:4319–24.
[267] Di Ciano C, Nie Z, Szaszi K, Lewis A, Uruno T, Zhan X, et al. Osmotic stress-induced remodeling of the cortical cytoskeleton. Am J Physiol Cell Physiol 2002;283:C850–865.
[268] Escote X, Zapater M, Clotet J, Posas F. Hog1 mediates cell-cycle arrest in G1 phase by the dual targeting of Sic1. Nat Cell Biol 2004;6:997–1002.
[269] Fumarola C, La Monica S, Guidotti GG. Amino acid signaling through the mammalian target of rapamycin (mTOR) pathway: role of glutamine and of cell shrinkage. J Cell Physiol 2005;204:155–65.
[270] Michea L, Ferguson DR, Peters EM, Andrews PM, Kirby MR, Burg MB. Cell cycle delay and apoptosis are induced by high salt and urea in renal medullary cells. Am J Physiol Renal Physiol 2000;278:F209–218.
[271] Morley SJ, Naegele S. Phosphorylation of eukaryotic initiation factor (eIF) 4E is not required for *de novo* protein synthesis following recovery from hypertonic stress in human kidney cells. J Biol Chem 2002;277:32855–9.
[272] Naegele S, Morley SJ. Molecular cross-talk between MEK1/2 and mTOR signaling during recovery of 293 cells from hypertonic stress. J Biol Chem 2004;279:46023–34.
[273] Zhang Z, Dmitrieva NI, Park JH, Levine RL, Burg MB. High urea and NaCl carbonylate proteins in renal cells in culture and *in vivo*, and high urea causes 8-oxoguanine lesions in their DNA. Proc Natl Acad Sci USA 2004;101:9491–6.
[274] Lockwood AH. Acute and chronic hyperosmolality. Effects on cerebral amino acids and energy metabolism. Arch Neurol 1975;32:62–4.
[275] Lohr JW, McReynolds J, Grimaldi T, Acara M. Effect of acute and chronic hypernatremia on myoinositol and sorbitol concentration in rat brain and kidney. Life Sci 1988;43: 271–6.
[276] Ko BC, Ruepp B, Bohren KM, Gabbay KH, Chung SS. Identification and characterization of multiple osmotic response sequences in the human aldose reductase gene. J Biol Chem 1997;272:16431–7.
[277] Rim JS, Atta MG, Dahl SC, Berry GT, Handler JS, Kwon HM. Transcription of the sodium/myo-inositol cotransporter gene is regulated by multiple tonicity-responsive enhancers spread over 50 kilobase pairs in the 5′-flanking region. J Biol Chem 1998;273:20615–21.
[278] Nakayama Y, Peng T, Sands JM, Bagnasco SM. The TonE/TonEBP pathway mediates tonicity-responsive regulation of UT-A urea transporter expression. J Biol Chem 2000;275: 38275–80.
[279] Ito T, Fujio Y, Hirata M, Takatani T, Matsuda T, Muraoka S, et al. Expression of taurine transporter is regulated through the TonE (tonicity-responsive element)/TonEBP (TonE-binding protein) pathway and contributes to cytoprotection in HepG2 cells. Biochem J 2004;382:177–82.
[280] Woo SK, Lee SD, Na KY, Park WK, Kwon HM. TonEBP/NFAT5 stimulates transcription of HSP70 in response to hypertonicity. Mol Cell Biol 2002;22:5753–60.
[281] Trama J, Go WY, Ho SN. The osmoprotective function of the NFAT5 transcription factor in T cell development and activation. J Immunol 2002;169:5477–88.
[282] Kojima R, Randall JD, Ito E, Manshio H, Suzuki Y, Gullans SR. Regulation of expression of the stress response gene, Osp94: identification of the tonicity response element and intracellular signalling pathways. Biochem J 2004;380:783–94.
[283] Kasono K, Saito T, Tamemoto H, Yanagidate C, Uchida S, Kawakami M, et al. Hypertonicity regulates the aquaporin-2 promoter independently of arginine vasopressin. Nephrol Dial Transplant 2005;20:509–15.

This page intentionally left blank

CHAPTER

46

Polyuria and Diabetes Insipidus

Daniel G. Bichet

Hôpital du Sacré-Coeur de Montréal, Departments of Medicine and Physiology, University of Montreal, Montréal, Québec, Canada

ARGININE VASOPRESSIN

Synthesis

Nonapeptides of the vasopressin family are the key regulators of water homeostasis in amphibia, reptiles, birds, and mammals. Since these peptides reduce urinary output, they are also referred to as antidiuretic hormones. Oxytocin and AVP (Figure 46.1) are synthesized in separate populations of magnocellular neurons of the supraoptic and paraventricular nuclei.[1] Oxytocin is most recognized for its key role in parturition and milk letdown in mammals.[2] The axonal projections of AVP- and oxytocin-producing neurons from supraoptic and paraventricular nuclei reflect the dual function of AVP and oxytocin as hormones and as neuropeptides, in that they project their axons to several brain areas, and to the neurohypophysis. The regulation of the release of AVP from the posterior pituitary is primarily dependent, under normal circumstances, on tonicity information relayed by central osmoreceptor neurons expressing TRPV1[3] (Figure 46.2) and peripheral osmoreceptor neurons expressing TRPV4.[4] AVP and its corresponding carrier, neurophysin II, are synthesized as a composite precursor by the magnocellular neurons of the supraoptic and paraventricular nuclei of the hypothalamus (for review see [5]). The precursor is packaged into neurosecretory granules and transported axonally in the stalk of the posterior pituitary. En route to the neurohypophysis, the precursor is processed into the active hormone. Pre-provasopressin has 164 amino acids, and is encoded by the 2.5 kb *AVP* gene located in chromosome region 20p13.[6,7] The *AVP* gene (coding for AVP and neurophysin II) and the *OXT* gene (coding for oxytocin and neurophysin I) are located in the same chromosome region, at a very short distance from each other (12 kb in humans) in head-to-head orientation. Data from transgenic mouse studies indicate that the intergenic region between the *OXT* and the *AVP* genes contains the critical enhancer sites for cell-specific expression in the magnocellular neurons.[5] It is phylogenetically interesting to note that *cis* and *trans* components of this specific cellular expression have been conserved between the *Fugu* isotocin (the homolog of mammalian oxytocin) and rat oxytocin genes.[8] Exon 1 of the *AVP* gene encodes the signal peptide, AVP, and the NH_2-terminal region of neurophysin II. Exon 2 encodes the central region of neurophysin II, and exon 3 encodes the COOH-terminal region of neurophysin II and the glycopeptide. Provasopressin is generated by the removal of the signal peptide from pre-provasopressin, and from the addition of a carbohydrate chain to the glycopeptide (Figure 46.3). Additional post-translational processing occurs within neurosecretory vesicles during transport of the precursor protein to axon terminals in the posterior pituitary, yielding AVP, neurophysin II, and the glycopeptide. The AVP–neurophysin II complex forms tetramers that can self-associate to form higher oligomers.[9] Neurophysins should be seen as chaperone-like molecules facilitating intracellular transport in magnocellular cells. In the posterior pituitary, AVP is stored in vesicles. Exocytotic release is stimulated by minute increases in serum osmolality (hypernatremia, osmotic regulation), and by more pronounced decreases in extracellular fluid (hypovolemia, non-osmotic regulation). Oxytocin and neurophysin I are released from the posterior pituitary by the suckling response in lactating females.

Immunocytochemical and radioimmunologic studies have demonstrated that oxytocin and vasopressin are synthesized in separate populations of the supraoptic nuclei and the paraventricular nuclei neurons,[10,11] the central and vascular projections of which have

Seldin and Giebisch's The Kidney, Fifth Edition.
DOI: http://dx.doi.org/10.1016/B978-0-12-381462-3.00046-X

© 2013 Elsevier Inc. All rights reserved.

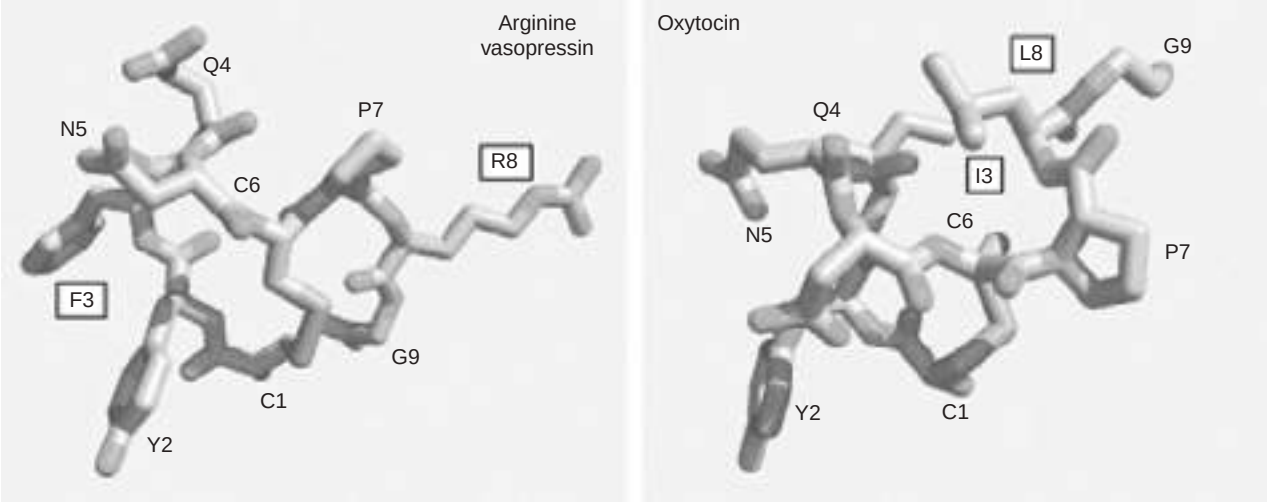

FIGURE 46.1 **Contrasting structures of arginine-vasopressin (AVP) and oxytocin (OT).** The peptides differ only by two amino acids (F3 → I3 and R8 → L8 in AVP and OT, respectively). *(The conformation of AVP was obtained from ref. [241]; and the conformation of OT was obtained from the Protein Data Bank (PDB Id 1XY1).)*

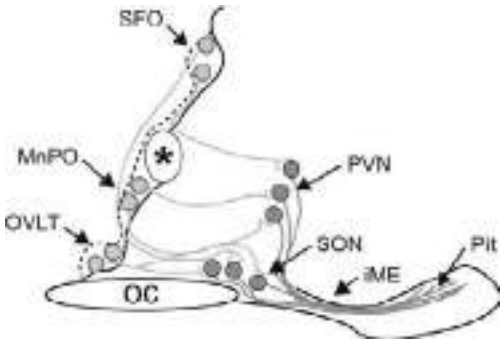

FIGURE 46.2 **Schematic representation of the osmoregulatory pathway of the hypothalamus (sagittal section of midline of ventral brain around the 3rd ventricle in mice).** Neurons (lightly filled circles) in the lamina terminalis (OVLT), median preoptic nucleus (MnPO) and subfornical organ (SFO) that are responsive to plasma hyptertonicity send efferent axonal projections (gray lines) to magnocellular neurons of the paraventricular (PVN) and supraoptic nuclei (SON). The OVLT is one of the brain circumventricular organs and is a key osmosensing site in the mammalian brain (*vide infra*). The processes (dark lines) of these magnocellular neurons form the hypothalamo–neurohypophysial pathway that courses in the median eminence to reach the posterior pituitary, where neurosecretion of vasopressin and oxytocin occurs. *(Modified from ref. [242].)*

been described in great detail.[12] Some cells express the *AVP* gene and other cells express the *OXT* gene. Immunohistochemical studies have revealed a second vasopressin neurosecretory pathway that transports high concentrations of the hormone to the anterior pituitary gland from parvocellular neurons to the hypophyseal portal system. In the portal system, the high concentration of AVP acts synergistically with corticotropin-releasing hormone (CRH) to stimulate adrenocorticotropic hormone (ACTH) release from the anterior pituitary. More than half of parvocellular neurons co-express both *CRH* and *AVP*. In addition, while passing through the median eminence and the hypophyseal stalk, magnocellular axons can also release AVP into the long portal system. Furthermore, a number of neuroanatomic studies have shown the existence of short portal vessels that allow communication between the posterior and anterior pituitary. Therefore, in addition to parvocellular vasopressin, magnocellular vasopressin is able to influence ACTH secretion.[13,14]

Mammals are Osmoregulators: the Cellular Perception of Tonicity to Stimulate Thirst and Vasopressin Release

Mammals are osmoregulators: they have evolved mechanisms that maintain extracellular fluid (ECF) osmolality near a stable value. Yet, although mammals strive to maintain a constant ECF osmolality, values measured in an individual can fluctuate around the set-point owing to intermittent changes in the rates of water intake and water loss (through evaporation or diuresis), and to variations in the rates of Na intake and excretion (natriuresis). In humans, for example, 40 minutes of strenuous exercise in the heat[15,16] or 24 hours of water deprivation[17] causes plasma osmolality to rise by more than 10 mosmol kg^{-1}. In a dehydrated individual, drinking the equivalent of two large glasses of water (~850 ml) lowers osmolality by approximately 6 mosmol kg^{-1} within 30minutes.[18] Similarly, ingestion of 13 g of salt increases plasma osmolality by approximately 5 mosmol kg^{-1} within 30 minutes.[19] Although osmotic perturbations larger than

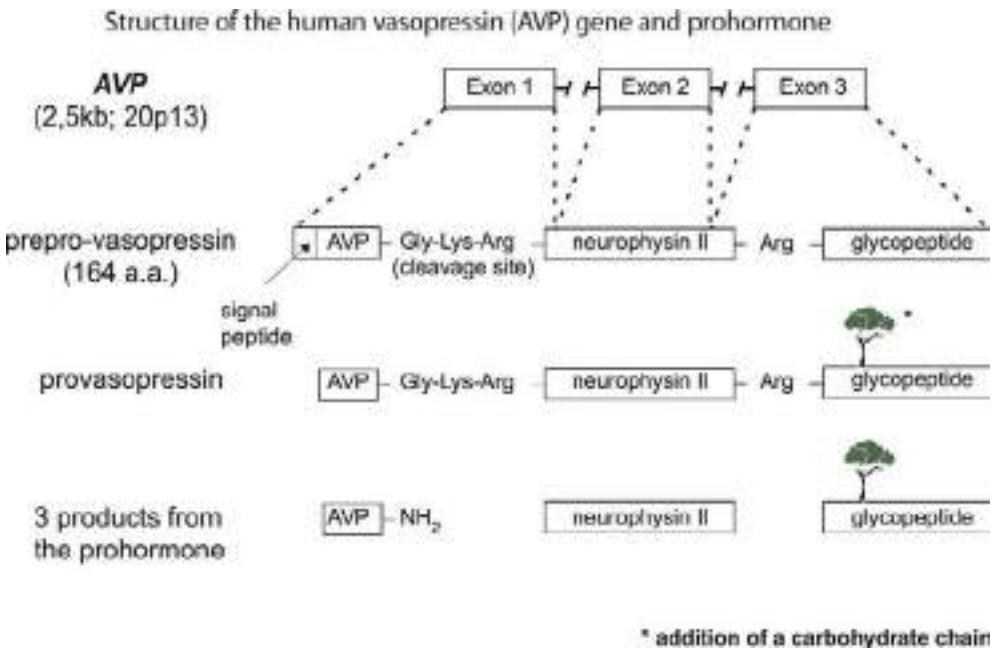

FIGURE 46.3 **Structure of the human vasopressin (AVP) gene and prohormone.** Cascade of vasopressin biosynthesis signal peptide; AVP, arginine-vasopressin; neurophysin; glycoprotein.

these can be deleterious to health, changes in the 1–3% range play an integral part in the control of body fluid homeostasis. Differences between the ECF osmolality and the desired set-point induce proportional homeostatic responses according to the principle of negative feedback.[3] ECF hyperosmolality stimulates the sensation of thirst to promote water intake, and the release of vasopressin to enhance water reabsorption in the kidney. By contrast, ECF hypoosmolality suppresses basal VP secretion in rats and humans.[20]

As summarized elegantly by Bourque,[3] early studies provided clear evidence that "cellular dehydration" (that is, cell shrinking) was required for thirst and vasopressin release to be stimulated during ECF hyperosmolality: these responses could be induced by infusions of concentrated solutions containing membrane-impermeable solutes, which extract water from cells, but not by infusions of solutes that readily equilibrate across the cell membrane (such as urea). Verney coined the term "osmoreceptor" to designate the specialized sensory elements. He further showed that these were present in the brain, and postulated that they might comprise "tiny osmometers" and "stretch receptors" that would allow osmotic stimuli to be "transmuted into electrical" signals.[21] Osmoreceptors are therefore defined functionally as neurons that are endowed with an intrinsic ability to detect changes in ECF osmolality, and it is now known that both cerebral and peripheral osmoreceptors contribute to the body fluid balance.

Although magnocellular neurons are themselves osmosensitive, they require input by glutamatergic afferents from the lamina terminalis to respond fully to osmotic challenges (Figure 46.2).

Hypertonicity is sensed by Organum Vasculosum Lamina Terminalis (OVLT) neurons expressing TRPV1 (Transient Receptor Potential Vanilloid-1, *vide infra*): OVLT serves as the brain's primary osmoreceptor area,[22] and neurons in this nucleus transduce hyperosmotic conditions into proportional increases in action-potential firing rate.[23] The information encoded by the electrical activity of these neurons is then relayed synaptically to diverse subsets of homeostatic effector neurons that induce appropriate osmoregulatory responses such as thirst, natriuresis, and antidiuretic hormone release.[3,24–27] The mechanical modulation of TRPV1 is well-demonstrated.[28]

Because the subfornical organ (SFO) and the organum vasculosum of the lamina terminalis (OVLT) lie outside the blood–brain barrier, they can integrate this information with endocrine signals borne by circulating hormones, such as angiotensin II (Ang-II), relaxin, and atrial natriuretic peptide (ANP). While circulating angiotensin II and relaxin excite both OT and vasopressin magnocellular neurons, ANP inhibits vasopressin neurons. The non-osmotic pathways are more physiologically described now as "osmoregulatory gain," since angiotensin II amplifies osmosensory transduction by enhancing the proportional relationship between osmolality, receptor potential, and action potential firing in rat supraoptic nucleus neurons[29] (Figure 46.4). Modifications in osmoregulatory gain induced by angiotensin explain why the changes in the

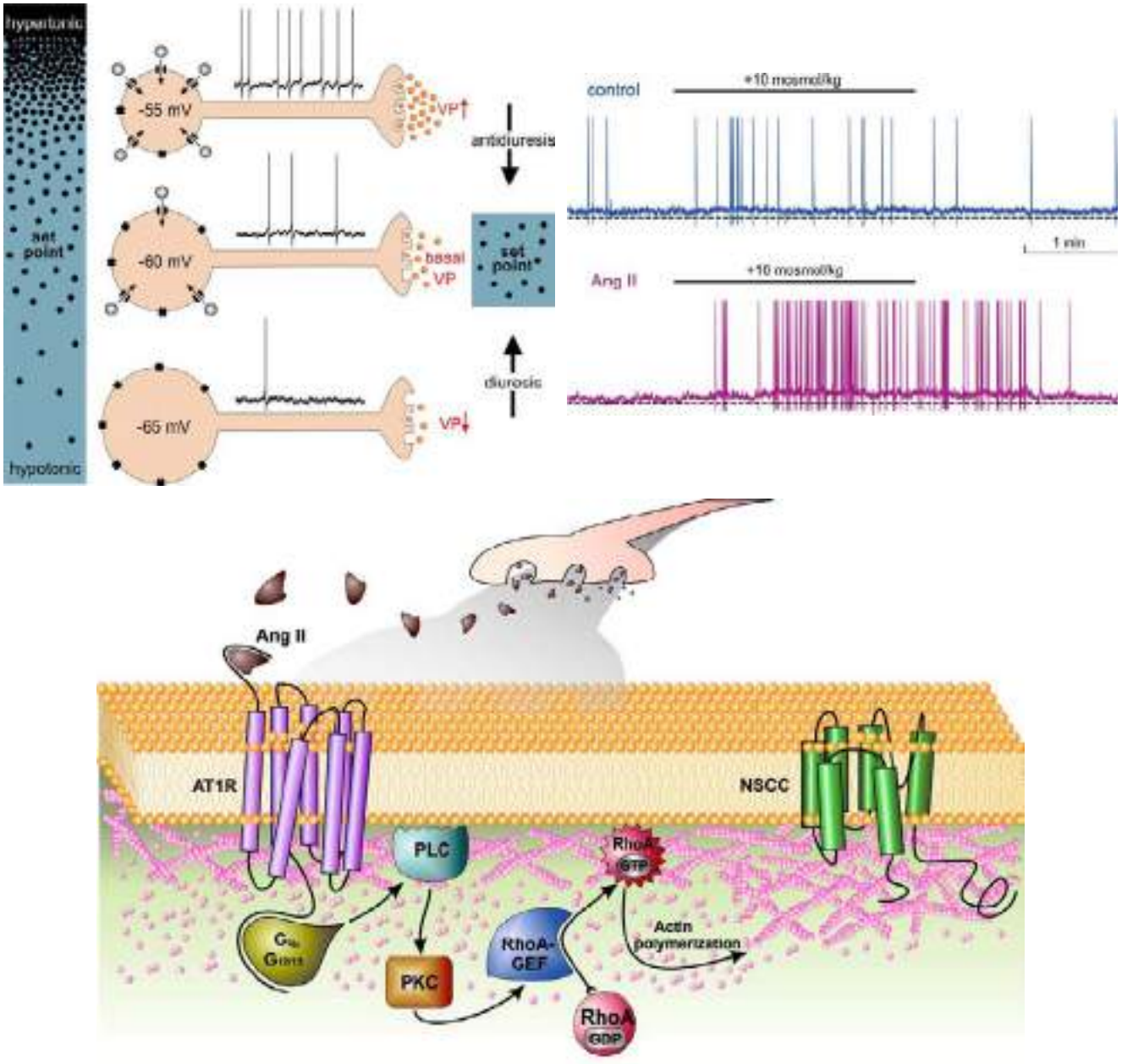

FIGURE 46.4 Upper left: Cell autonomous osmoreception in vasopressin neurons. Changes in osmolality cause inversely proportional changes in soma volume. Shrinkage activates nonselective cation channels (NSCCs) and the ensuing depolarization increases action potential firing rate and vasopressin (VP) release from axon terminals in the neurohypophysis. Increased VP levels in blood enhance water reabsorption by the kidney (antidiuresis) to restore extracellular fluid osmolality toward the set point. Hypotonic stimuli inhibit NSCCs. The resulting hyperpolarization and inhibition of firing reduces VP release and promotes diuresis. Upper right: Whole cell current clamp recordings from isolated MNCs (left) and averaged data from multiple cells show that the depolarizing and action potential firing responses induced by a hypertonic stimulus are significantly enhanced in the presence of 100 nM angiotensin II. Lower right: Hypothetical events mediating central angiotensin II enhancement of osmosensory gain. Angiotensin II released by afferent nerve terminals (e.g., during hypovolemia) binds to AT1 receptor (AT1R) coupled to G-proteins such as Gq or/and G12/13. Activated G-proteins signal through phospholipase C (PLC) and protein kinase C (PKC) to activate a RhoA-specific guanine nucleotide exchange factor (RhoA−GEF), such as p115RhoGEF or LARG (leukemia-associated Rho guanine−nucleotide exchange factor). Activation of RhoA−GEF converts inactive cytosolic RhoA (RhoA−GDP) into active, membrane-associated RhoA−GTP by promoting the exchange of GDP to GTP. ActivatedRhoA induces actin polymerization and increases submembrane F-actin density to enhance the mechanical gating of non-specific cation channels. *(With permission from ref. [243].)*

slope and threshold of the relationship between plasma osmolality and vasopressin secretion are potentiated by hypovolemia or hypotension, and are attenuated by hypervolemia or hypertension[30] (Figure 46.5).

The osmotic stimulation of AVP release by dehydration or hypertonic saline infusion, or both, is regularly used to test the AVP secretory capacity of the posterior pituitary. This secretory capacity can be assessed directly by comparing the plasma AVP concentration measured sequentially during a dehydration procedure with the normal values, and then correlating the plasma AVP with the urinary osmolality measurements obtained simultaneously[31] (Figure 46.6).

The AVP release can also be assessed indirectly by measuring plasma and urine osmolalities at regular intervals during the dehydration test.[32] The maximum urinary osmolality obtained during dehydration is compared with the maximum urinary osmolality obtained after the administration of vasopressin or 1-desamino-8-D-arginine vasopressin (dDAVP; Pitressin: 5 units subcutaneously (SQ) in adults; 1 unit SQ in children or dDAVP 1−4 mg intravenously over 5 to 10 minutes).

The nonosmotic stimulation of AVP release can be used to assess the vasopressin secretory capacity of the posterior pituitary in a rare group of patients with the essential hyponatremia and hypodipsia syndrome. Although some of these patients may have partial central diabetes insipidus, they respond normally to nonosmolar AVP release signals such as hypotension, emesis, and hypoglycemia.[33] In all other cases of suspected central diabetes insipidus, these nonosmotic stimulation tests will not give additional clinical information.[34]

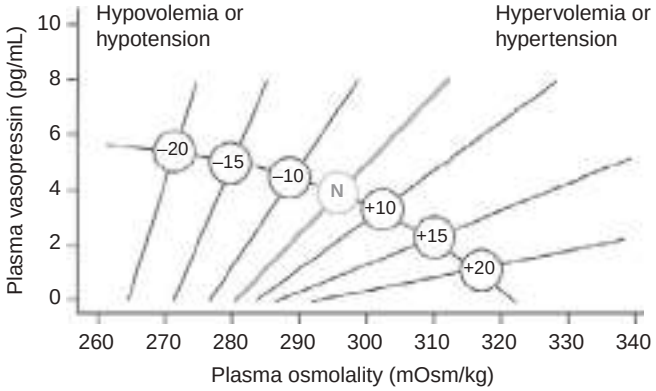

FIGURE 46.5 **Schematic representation of the relationship between plasma vasopressin and plasma osmolality in the presence of differing states of blood volume and/or pressure.** The line labeled N represents normovolemic normotensive conditions. Minus numbers to the left indicate percentage fall, and positive numbers to the right, percentage rise in blood volume or pressure. *(Data from Vokes, T. P., and Robertson, G. L. (1985) Physiology of secretion of vasopressin,* In *"Frontiers in Hormone Research: Diabetes Insipidus in Man," Vol. 13, 127−155, Czernichow, A. G. R. P., (ed.). S. Karger, Basel.*[244]*)*

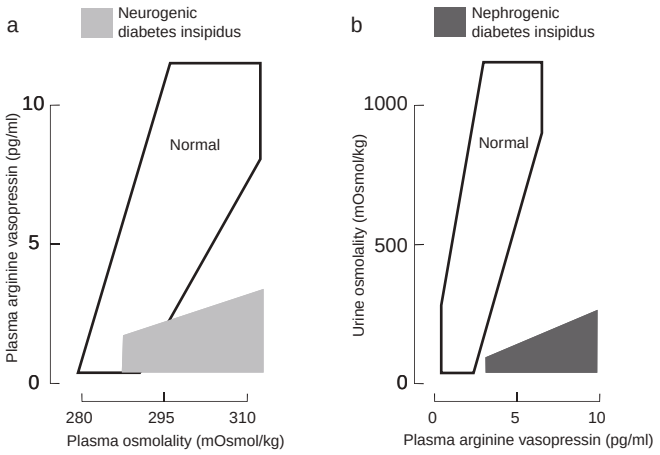

FIGURE 46.6 (a) Schematic diagram of the relationship between plasma arginine-vasopressin (AVP) and plasma osmolality during hypertonic saline infusion. In patients with neurogenic diabetes insipidus, plasma AVP is almost always subnormal relative to plasma osmolality. In contrast, patients with primary polydipsia or nephrogenic diabetes insipidus (NDI) have values within the normal range (light gray area). (b) Relationship between urine osmolality and plasma AVP during a dehydration test. Patients with NDI have hypotonic urine despite high plasma AVP. In contrast, patients with neurogenic diabetes insipidus or primary polydipsia have values within the normal range (dark gray area). *(from ref. [31].)*

Tonicity Information is Relayed by Central Osmoreceptor Neurons Expressing TRPV1 and Peripheral Osmoreceptor Neurons Expressing TRPV4

The osmotic regulation of the release of AVP from the posterior pituitary is primarily dependent, under normal circumstances, on tonicity information relayed by central osmoreceptor neurons expressing TRPV1,[3] and peripheral osmoreceptor neurons expressing TRPV4.[4]

The cellular basis for osmoreceptor potentials has been characterized using patch-clamp recordings and morphometric analysis in magnocellular cells isolated from the supraoptic nucleus of the adult rat. In these cells, stretch-inactivating cationic channels transduce osmotically evoked changes in cell volume into functionally relevant changes in membrane potential. In addition, magnocellular neurons also operate as intrinsic Na^+ detectors. The N-terminal variant of the transient receptor potential channel (TRPV1) is an osmoticaly activated channel expressed in the magnocellular cells producing vasopressin,[35] and in the circumventricular organs, the OVLT, and the SFO.[23] Since osmoregulation still operates in *Trpv1*$^{-/-}$ mice, other osmosensitive neurons or pathways must be able to compensate for loss of central osmoreceptor function.[23,35,36] Afferent neurons expressing the osmotically-activated ion channel, TRPV4, in the thoracic

dorsal root ganglia that innervate hepatic blood vessels and detect physiological hypoosmotic shifts in blood osmolality have recently been identified.[4] In mice lacking the osmotically-activated ion channel, TRPV4, hepatic sensory neurons no longer exhibit osmosensitive inward currents, and activation of peripheral osmoreceptors *in vivo* is abolished. In a large cohort of human liver transplantees, who presumably have denervated livers, plasma osmolality is significantly elevated compared to healthy controls, suggesting the presence of an inhibitory vasopressin effect of hyponatremia, perceived in the portal vein from hepatic afferents.[4] TRPV1 (expressed in central neurons) and TRPV4 (expressed in peripheral neurons) thus appear to play entirely complementary roles in osmoreception. Lechner et al. have thus identified the primary afferent neurons that constitute the afferent arc of a well-characterized reflex in man and more recently also in rodents.[37] This reflex engages the sympathetic nervous system to raise blood pressure and stimulate metabolism.[38,39] Of clinical interest, it has already been demonstrated that orthostatic hypotension and postprandial hypotension respond to water drinking.[40–42] Moreover, water drinking in man can prevent neutrally-mediated syncope during blood donation or after prolonged standing.[43] Finally, water drinking is also associated with weight loss in overweight individuals.[44] Other peripheral sensory neurons expressing other mechanosensitive proteins may also be involved in osmosensitivity.[45]

Cellular Actions of Vasopressin

The neurohypophyseal hormone AVP has multiple actions, including the inhibition of diuresis, contraction of smooth muscle, platelet aggregation, stimulation of liver glycogenolysis, modulation of adrenocorticotropic hormone release from the pituitary, and central regulation of somatic and higher functions (thermoregulation, blood pressure, autonomic expression of fear, neurobiology of attachment).[46–48] These multiple actions of AVP could be explained by the interaction of AVP with at least three types of G-protein-coupled receptors: the V1a (vascular hepatic) and V1b (anterior pituitary) receptors act through phosphatidylinositol hydrolysis to mobilize calcium[49]; and the V2 (kidney) receptor is coupled to adenylate cyclase.[48]

The transfer of water across the principal cells of the collecting ducts is now known at such a detailed level that billions of molecules of water traversing the membrane can be represented; see useful teaching tools at http://www.mpibpc.gwdg.de/abteilungen/073/gallery.html and http://www.ks.uiuc.edu/research/aquaporins. The 2003 Nobel Prize in chemistry was awarded to Peter Agre and Roderick MacKinnon, who solved two complementary problems presented by the cell membrane: how does a cell let one type of ion through the lipid membrane to the exclusion of other ions; and how does it permeate water without ions? This contributed to a momentum and renewed interest in basic discoveries related to the transport of water, and indirectly to diabetes insipidus.[50,51] The first step in the action of AVP (synthesized by du Vigneaud, Nobel Prize in Chemistry 1955)[52] on water excretion is its binding to arginine vasopressin type-2 receptors (hereafter referred to as V2 receptors) on the basolateral membrane of the collecting duct cells (Figure 46.7). The human *AVPR2* gene that codes for the V2 receptor is located in chromosome region Xq28, and has three exons and two small introns.[53,54] The sequence of the cDNA predicts a polypeptide of 371 amino acids with seven transmembrane, four extracellular, and four cytoplasmic domains. The activation of the V2 receptor on renal collecting tubules stimulates adenylyl cyclase via the stimulatory G-protein (Gs) (1994 Nobel Prize in Physiology and Medicine to Rodbell and Gilman for signal transduction and G-proteins), and promotes the cyclic adenosine monophosphate (cAMP)-mediated incorporation of water channels into the luminal surface of these cells.[55] E. Sutherland and T. Rall isolated cyclic adenosine monophosphate in 1956, and Sutherland was awarded the Nobel Prize in Physiology or Medicine in 1971.[56] There are two ubiquitously expressed intracellular cAMP receptors: (1) the classical protein kinase A (PKA) that is a cAMP-dependent protein kinase; and (2) the recently discovered exchange protein directly activated by cAMP that is a cAMP-regulated guanine nucleotide exchange factor. Both of these receptors contain an evolutionally-conserved cAMP-binding domain that acts as a molecular switch for sensing intracellular cAMP levels to control diverse biological functions.[57] Several proteins participating in the control of cAMP-dependent AQP2 trafficking have been identified; for example, A-kinase anchoring proteins tethering PKA to cellular compartments; phosphodiesterases regulating the local cAMP level; cytoskeletal components such as F-actin and microtubules; small GTPases of the Rho family controlling cytoskeletal dynamics; motor proteins transporting AQP2-bearing vesicles to and from the plasma membrane for exocytic insertion and endocytic retrieval; SNAREs inducing membrane fusions, hsc70, a chaperone important for endocytic retrieval. These processes are the molecular basis of the vasopressin-induced increase in the osmotic water permeability of the apical membrane of the collecting tubule.[58–60]

AVP also increases the water reabsorptive capacity of the kidney by regulating the urea transporter

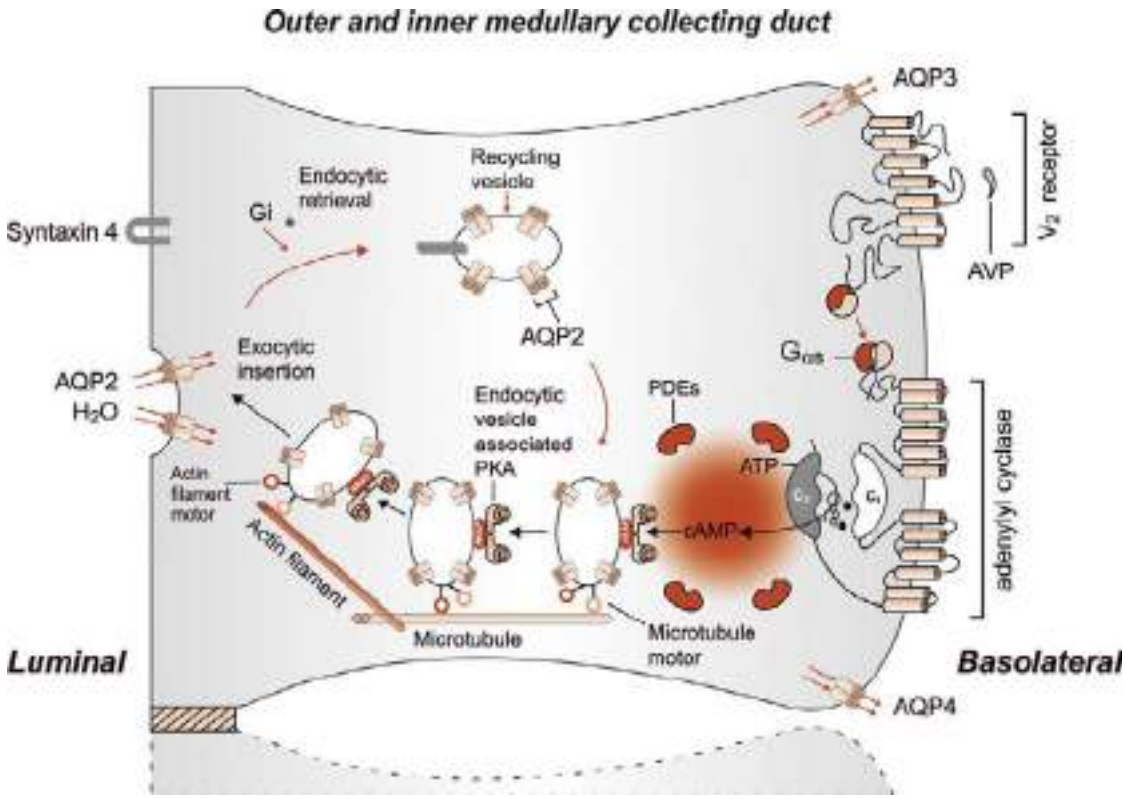

FIGURE 46.7 **Schematic representation of the effect of vasopressin (AVP) to increase water permeability in the principal cells of the collecting duct.** AVP is bound to the V2 receptor (a G-protein-linked receptor) on the basolateral membrane. The basic process of G-protein-coupled receptor signaling consists of three steps: a hepta-helical receptor that detects a ligand (in this case, AVP) in the extracellular milieu; a G-protein ($G_{\alpha s}$) that dissociates into a subunits bound to GTP and bg subunits after interaction with the ligand-bound receptor; and an effector (in this case, adenylyl cyclase) that interacts with dissociated G-protein subunits to generate small-molecule second messengers. AVP activates adenylyl cyclase, increasing the intracellular concentration of cAMP. The topology of adenylyl cyclase is characterized by two tandem repeats of six hydrophobic transmembrane domains separated by a large cytoplasmic loop, and terminates in a large intracellular tail. The dimeric structure (C_1 and C_2) of the catalytic domains is represented. Conversion of ATP to cAMP takes place at the dimer interface. Two aspartate residues (in C_1) coordinate two metal co-factors (Mg^{2+} or Mn^{2+}, represented here as two small black circles), which enable the catalytic function of the enzyme. Adenosine is shown as an open circle and the three phosphate groups (ATP) are shown as smaller open circles. Protein kinase A (PKA) is the target of the generated cAMP. The binding of cAMP to the regulatory subunits of PKA induces a conformational change, causing these subunits to dissociate from the catalytic subunits. These activated subunits (C) as shown here are anchored to an aquaporin-2 (AQP2)-containing endocytic vesicle via an A-kinase anchoring protein. The local concentration and distribution of the cAMP gradient is limited by phosphodiesterases (PDEs). Cytoplasmic vesicles carrying the water channels (represented as homotetrameric complexes) are fused to the luminal membrane in response to AVP, thereby increasing the water permeability of this membrane. The dissociation of the A-kinase anchoring protein from the endocytic vesicle is not represented. Microtubules and actin filaments are necessary for vesicle movement toward the membrane. When AVP is not available, AQP2 water channels are retrieved by an endocytic process, and water permeability returns to its original low rate. Aquaporin-3 (AQP3) and aquaporin-4 (AQP4) water channels are expressed constitutively at the basolateral membrane.

variants UT-A1/3, which are present in the inner medullary collecting duct, predominantly in its terminal part.[61] AVP also increases the permeability of principal collecting duct cells to sodium. In summary, as stated elegantly by Ward and colleagues,[62] in the absence of AVP stimulation, collecting duct epithelia exhibit very low permeabilities to sodium urea and water. These specialized permeability properties permit the excretion of large volumes of hypotonic urine formed during intervals of water diuresis. In contrast, AVP stimulation of the principal cells of the collecting ducts leads to selective increases in the permeability of the apical membrane to water (P_f), urea (P_{urea}), and Na (P_{Na}).

The actions of vasopressin in the distal nephron are possibly modulated by prostaglandin E2, nitric oxide,[63] and by luminal calcium concentration. PGE_2 is synthesized and released in the collecting duct, which expresses all four E-prostanoid receptors (EP1−4). Both EP2 and EP4 can signal via increased cAMP. Olesen et al. hypothesized that selective EP receptor stimulation could mimic the effects of vasopressin, and demonstrated that, at physiological levels, PGE_2 markedly increased apical membrane abundance and phosphorylation of AQP2 *in vitro* and *ex vivo*, leading to increased cell water permeability.[64] In their experiments, both EP2 and EP4 selective agonists were able to mimic

these effects. Furthermore, an EP2-agonist was able to positively regulate urinary-concentrating mechanisms in an animal model of nephrogenic diabetes insipidus where AVPR2 receptors were blocked by Tolvaptan, a non-peptide V2-antagonist. These results reveal an alternative mechanism for regulating water transport in the collecting duct that has major importance for understanding whole body water homeostasis, and provide a rationale for investigations into EP receptor-agonist use in X-linked nephrogenic diabetes insipidus treatment.

THE BRATTLEBORO RAT WITH AUTOSOMAL RECESSIVE NEUROGENIC DIABETES INSIPIDUS

The animal model of diabetes insipidus that has been most extensively studied is the Brattleboro rat. Discovered in 1961, the rat lacks vasopressin and its neurophysin, whereas the synthesis of the structurally-related hormone oxytocin is not affected by the mutation.[65] Its inability to synthesize vasopressin is inherited as an autosomal recessive trait. Schmale and Richter[66] isolated and sequenced the vasopressin gene from homozygous Brattleboro rats, and found that the defect is due to a single nucleotide deletion of a G residue within the second exon encoding the carrier protein neurophysin (Figure 46.8). The shift in the reading frame caused by this deletion predicts a precursor with an entirely different C-terminus. The messenger RNA (mRNA) produced by the mutated gene encodes a normal AVP, but an abnormal NPII moiety[66] which impairs transport and processing of the AVP-NPII precursor and its retention in the endoplasmic reticulum of the magnocellular neurons where it is produced.[67,68] Homozygous Brattleboro rats may still demonstrate some V2 (*vide infra*) antidiuretic effects, since the administration of a selective non-peptide V2-antagonist (SR 121463 A, 10 mg/kg i.p.) induced a further increase in urine flow rate (200 to 354 ± 42 mL/24 h) and a decline in urinary osmolality (170 to 92 ± 8 mmol/kg).[69] This decline in urine osmolality following the administration of a non-peptide V2 receptor antagonist could also be secondary to the "inverse agonist" properties of SR121463A: the intrinsic activity or "tone," of the V2R would be deactivated by the SR121463A compound (for the inverse agonist properties of SR121463A see [70]). There is also an alternative explanation to this relatively high urine osmolality of 170 since, in Brattleboro rats, low levels of hormonally-active AVP are produced from alternate forms of AVP preprohormone. Due to a process called molecular misreading, one transcript contains a 2 bp deletion downstream from the single nucleotide deletion that restores the reading frame, and produces a variant AVP preprohormone that is smaller in length by one amino acid and differs from the normal product by only 13 amino acids in the neurophysin II moiety.[71] Oxytocin, which is present at enhanced plasma concentrations in Brattleboro rats, may be responsible for the antidiuretic activity observed.[72,73] Oxytocin is not stimulated by increased plasma osmolality in humans.

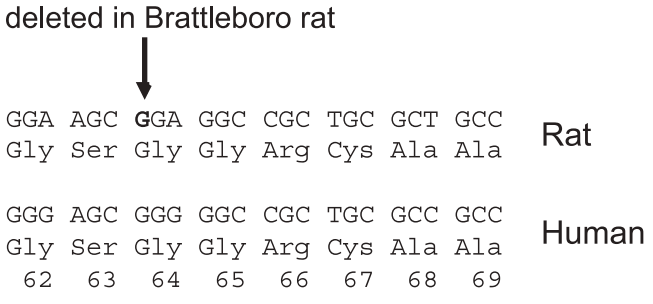
deleted in Brattleboro rat
GGA AGC GGA GGC CGC TGC GCT GCC
Gly Ser Gly Gly Arg Cys Ala Ala
Rat
GGG AGC GGG GGC CGC TGC GCC GCC
Gly Ser Gly Gly Arg Cys Ala Ala
62 63 64 65 66 67 68 69
Human

FIGURE 46.8 **Neurophysin II genomic and amino acid sequence showing the 1 bp (G) deleted in the Brattleboro rat.** The human sequence (GenBank entry M11166) is also shown. It is almost identical to the rat prepro sequence. In the Brattleboro rat, G1880 is deleted with a resultant frameshift after 63 amino acids (amino acid-1 is the first amino acid of neurophysin II).

KNOCKOUT MICE WITH URINARY CONCENTRATION DEFECTS

A useful strategy to establish the physiological function of a protein is to determine the phenotype produced by pharmacological inhibition of protein function or by gene disruption. Transgenic knockout mice deficient in AQP1, AQP2, AQP3, AQP4, and CLCNK1, NKCC2, NFAT5, AVPR2 or AGT have been engineered.[74–83] Angiotensinogen (AGT)-deficient mice are characterized by both concentrating and diluting defects secondary to a defective renal papillary architecture.[80] The *Aqp3*, *Aqp4*, *Clcnk1*, and *Agt* knockout mice have no identified human counterparts. Of interest, *AQP1*-null individuals have no obvious symptoms.[84] Yang et al.[85] have generated an AQP2-T126M "conditional knock-in" model of NDI, to recapitulate the clinical features of the naturally occurring human AQP2 mutation T126M.[86] The conditional knock-in adult mice showed polyuria, urinary hypoosmolality, and ER retention of AQP2-T126M in the collecting duct. Screening of candidate protein folding "correctors" in AQP2-T126M-transfected kidney cells showed increased AQP2-T126M plasma membrane expression with the Hsp90 inhibitor 17-allylamino-17-demethoxygeldanamycin (17-AAG), a compound currently in clinical trials for tumor therapy. 17-AAG increased

urine osmolality in the AQP2-T126M mice (without effect in AQP2 null mice), and partially rescued defective AQP2-T126M cellular processing. These proof-of-concept findings suggest the possibility of using existing drugs for therapy in some forms of NDI.

Mice lacking the AVPR2 receptor failed to thrive and died within the first week after birth due to hypernatremic dehydration.[83] Li et al.[87] generated mice in which the *Avpr2* gene could be conditionally deleted during adulthood by administration of 4-OH-tamoxifen. Adult mice displayed all characteristic symptoms of X-linked NDI, including polyuria, polydipsia, and resistance to the antidiuretic actions of vasopressin. Gene expression analysis suggested that activation of renal EP4 PGE_2 receptors might compensate for the lack of renal V2R activity in X-linked NDI mice, and both acute and chronic treatment of the mutant mice with a selective EP4 receptor agonist greatly reduced all major manifestations of XNDI. This beneficial effect is likely secondary to the intracellular generation of cAMP at the principal cell level by EP4 PGE_2 receptors.

As reviewed by Rao and Verkman,[88] extrapolation of data in mice to humans must be made with caution. For example, the maximum osmolality of mouse (< 3000 mOsm/kg H_2O) is much greater than that of human urine (1000 mOsmol/kg H_2O), and normal serum osmolality in mice is 330 to 345 mOsmol/kg H_2O, substantially greater than that in humans (280–290 mOsm/kg H_2O). Protein expression patterns, and thus the interpretation of phenotype studies, may also be species-dependent. For example, AQP4 is expressed in both proximal tubule and collecting duct in mouse, but only in collecting duct in rat and human.[88]

Ethylnitrosourea-mutagenized mice heterozygous for the F204V mutation in the *Aqp2* gene have been described,[89] and mice from the Jackson Laboratory with congenital progressive hydronephrosis bear the S256L mutation in *Aqp2* which affects its phosphorylation and apical membrane accumulation.[90,91]

QUANTITATING RENAL WATER EXCRETION

Diabetes insipidus is characterized by the excretion of abnormally large volumes of hypoosmotic urine (< 250 mmol/kg). This definition excludes osmotic diuresis, which occurs when excess solute is being excreted, as with glucose in the polyuria of diabetes mellitus. Other agents that produce osmotic diuresis are mannitol, urea, glycerol, contrast media, and loop diuretics. Osmotic diuresis should be considered when solute excretion exceeds 60 mmol/hour. The quantification of water excretion (free water clearance, osmolar clearance, free electrolyte water reabsorption, effective water clearance) is described elsewhere in this textbook.

CLINICAL CHARACTERISTICS OF DIABETES INSIPIDUS DISORDERS

Neurogenic Diabetes Insipidus

Common Forms

Failure to synthesize or secrete vasopressin normally limits maximal urinary concentration and, depending on the severity of the disease, causes varying degrees of polyuria and polydipsia. Experimental destruction of the vasopressin-synthesizing areas of the hypothalamus (supraoptic and paraventricular nuclei) causes a permanent form of the disease. Similar results are obtained by sectioning the hypophyseal hypothalamic tract above the median eminence. Sections below the median eminence, however, produce only transient diabetes insipidus. Lesions to the hypothalamic–pituitary tract are frequently associated with a three-stage response in experimental animals and in humans[92]: (1) an initial diuretic phase lasting from a few hours to 5 to 6 days; (2) a period of antidiuresis unresponsive to fluid administration (this antidiuresis is probably due to vasopressin release from injured axons and may last from a few hours to several days; because urinary dilution is impaired during this phase, continued water administration can cause severe hyponatremia); and (3) a final period of diabetes insipidus. The extent of the injury determines the completeness of the diabetes insipidus and, as already discussed, the site of the lesion determines whether the disease will be permanent.

Twenty-five percent of patients studied after transsphenoidal surgery developed spontaneous isolated hyponatremia, 20% developed diabetes insipidus, and 46% remained normonatremic. Normonatremia, hyponatremia, and diabetes insipidus were associated with increasing degrees of surgical manipulation of the posterior lobe and pituitary stalk during surgery.[93] Central diabetes insipidus observed after transphenoidal surgery is often transient, and only 2% of patients need long-term treatment with dDAVP.[94]

The causes of central diabetes insipidus in adults and in children are listed in Table 46.1.[95–98] Rare causes of central diabetes insipidus include leukemia, thrombotic thrombocytopenic purpura, pituitary apoplexy, sarcoidosis[99] and Wegener granulomatosis, xanthoma disseminatum,[100] septooptico dysplasia and agenesis of the corpus callosum,[101] metabolic anorexia nervosa, lymphocytic hypophysitis,[102] and necrotizing

TABLE 46.1 Etiology of Hypothalamic Diabetes Insipidus in Children and Adults

	Children (%)	Children and Young Adults (%)	Adults (%)
Primary brain tumor[a]	49.5	22.0	30.0
Before surgery	33.5		13.0
After surgery	16.0		17.0
Idiopathic (isolated or familial)	29.0	58.0	25.0
Histiocytosis	16.0	12.0	–
Metastatic cancer[b]	–		8.0
Trauma[c]	2.2	2.0	17.0
Postinfectious disease	2.2	6.0	–

Data from Czernichow, P., Pomarede, R., Brauner, R., Rappaport, R. (1985). Neurogenic diabetes insipidus in children. In "Frontiers of Hormone Research," 190–20, Czernichow, P., and Robinson, A. G. (eds.). S. Karger, Basel, Switzerland[95]*; Greger, N. G., Kirkland, R. T., Clayton, G. W., and Kirkland, J. L. (1986). Central diabetes insipidus. 22 years' experience. Am. J. Dis. Child* ***140****, 551–554*[96]*; Moses, A. M., Blumenthal, S. A., and Streeten, D. H. P. (1985). Acid–base and electrolyte disorders associated with endocrine disease: Pituitary and thyroid. In "Fluid, Electrolyte and Acid–Base Disorders," 851–892, Arieff, A. I., and de Fronzo, R. A., (eds.). Churchill Livingstone, New York*[98]*; Maghnie, M., Cosi, G., and Genovese, E., et al. (2000). Central diabetes insipidus in children and young adults. N. Engl. J. Med.* ***343****, 998–1007.*[97]

[a]*Primary malignancy: craniopharyngioma, dysgerminoma, meningioma, adenoma, glioma, astrocytoma.*

[b]*Secondary: metastatic from lung or breast, lymphoma, leukemia, dysplastic pancytopenia.*

[c]*Trauma could be severe or mild.*

infundibulo-hypophysitis.[103] Maghnie et al.[97] studied 79 patients with central diabetes insipidus: additional deficits in anterior pituitary hormones were documented in 61% of patients, a median of 0.6 years (range, 01–18.0 years) after the onset of diabetes insipidus. The most frequent abnormality was growth hormone deficiency (59%), followed by hypothyroidism (28%), hypogonadism (24%), and adrenal insufficiency (22%). Seventy-five percent of the patients with Langerhans cell histiocytosis had an anterior pituitary hormone deficiency that was first detected a median of 3.5 years after the onset of diabetes insipidus.[97] None of the patients with central diabetes insipidus secondary to *AVP* mutations developed anterior pituitary hormone deficiencies.

Rare Forms

AUTOSOMAL DOMINANT AND RECESSIVE NEUROGENIC DIABETES INSIPIDUS

Lacombe[104] and Weil[105] described a familial non-X-linked form of diabetes insipidus without any associated mental retardation. The descendants of the family described by Weil were later found to have autosomal dominant neurogenic diabetes insipidus.[106–108] Hereditary neurogenic diabetes insipidus (OMIM 125700)[109] is a well-characterized entity, secondary to mutations in *AVP* (OMIM 192340).[109] Patients with autosomal dominant neurogenic diabetes insipidus retain some limited capacity to secrete AVP during severe dehydration, and the polyuropolydipsic symptoms usually appear after the first year of life,[110] when the infant's demand for water is more likely to be understood by adults. In hereditary neurohypophyseal diabetes insipidus, termed familial neurohypophyseal diabetes insipidus (FNDI), levels of AVP are insufficient, and patients show a positive response to treatment with dAVP. Growth retardation might be observed in untreated children with autosomal dominant FNDI.[111]Over 60 mutations in the prepro-arginine-vasopressin-neurophysin II *AVP* gene located on chromosome 20p13 have been reported in dominant FNDI (adFNDI). Knock-in mice heterozygous for a nonsense mutation in the AVP carrier protein neurophysin II showed progressive loss of AVP-producing neurons over several months correlated with increased water intake, increased urine output, and decreased urine osmolality. The data suggest that vasopressin mutants accumulate as fibrillar aggregates in the endoplasmic reticulum and cause cumulative toxicity to magnocellular neurons, explaining the later age-of-onset.[112,113] To date, recessive FNDI, with early polyuric manifestations, has only been described in three studies.[114–116] Very early (first week of life) polyuric states are usually nephrogenic, but we and others have observed autosomal recessive central diabetes insipidus patients with early polyuria, dehydration episodes responding to dDAVP with specific mutations of the AVP gene.[114–117] A study by Christensen[118] examined the differences in cellular trafficking between dominant and recessive AVP mutants, and found that dominant forms were concentrated in the cytoplasm, whereas recessive forms were localized to the tips of neurites. The expression of regulated secretory proteins such as granins and prohormones, including pro-vasopressin, generates granule-like structures in a variety of neuroendocrine cell lines due to aggregation in the trans-Golgi.[119] Co-staining experiments unambiguously distinguished between these granule-like structures and the accumulations by pathogenic dominant mutants formed in the ER, since the latter, but not the trans-Golgi granules, co-localized with specific ER markers.[112] As studies concerning both dominant and recessive FNDI accumulate, it is becoming evident that FNDI exhibits a variable age-of-onset, and this may be related to the cellular handling of the mutant AVP. This progressive toxicity, sometimes called a toxic gain-of-function, shares mechanistic pathways with other neurodegenerative diseases, such as Huntington's and Parkinson's.

Of interest, errors in protein folding represent the underlying basis for many inherited diseases[120–122] and are also pathogenic mechanisms for *AVP*, *AVPR2*, and *AQP2* mutants. Why AVP-misfolded mutants are cytotoxic to AVP-producing neurons is an unresolved issue. Protein misfolding, an "unfolded protein response" in cells, and the accumulation of excess misfolded protein leading to apoptotic cell death are well-documented for autosomal dominant retinitis pigmentosa.[123]

WOLFRAM SYNDROME

Wolfram syndrome, also known as DIDMOAD, is an autosomal recessive neurodegenerative disorder accompanied by insulin-dependent diabetes mellitus and progressive optic atrophy. The acronym DIDMOAD describes the following clinical features of the syndrome: *d*iabetes *i*nsipidus, *d*iabetes *m*ellitus, *o*ptic *a*trophy, and sensorineural *d*eafness. An unusual incidence of psychiatric symptoms has also been described in patients with this syndrome. These included paranoid delusions, auditory or visual hallucinations, psychotic behavior, violent behavior, organic brain syndrome typically in the late or preterminal stages of their illness, progressive dementia, and severe learning disabilities or mental retardation or both. Patients with Wolfram syndrome develop diabetes mellitus and bilateral optical atrophy mainly in the first decade of life, the diabetes insipidus is usually partial and of gradual onset, and the polyuria can be wrongly attributed to poor glycemic control. Furthermore, a severe hyperosmolar state can occur if untreated diabetes mellitus is associated with an unrecognized posterior pituitary deficiency. The dilatation of the urinary tract observed in the DIDMOAD syndrome may be secondary to chronic high urine flow rates and, perhaps, to some degenerative aspects of the innervation of the urinary tract. The gene responsible for Wolfram syndrome, located in chromosome region 4p16.1, encodes a putative 890 amino acid transmembrane protein referred as *wolframin*. Wolframin is an endoglycosidase H-sensitive glycoprotein, which localizes primarily in the endoplasmic reticulum of a variety of neurons, including neurons in the supraoptic nucleus and neurons in the lateral magnocellular division of the paraventricular nucleus.[124,125] Disruption of the *Wfs1* gene in mice cause progressive β-cell loss and impaired stimulus-secretion coupling in insulin secretion, but central diabetes insipidus is not observed in $Wfs^{-/-}$ mice.[126] Miner1, another endoplasmic reticulum protein, is causative in Wolfram syndrome 2[127] and WFS1 negatively regulates a key transcription factor involved in ER stress signalling.[128]

SYNDROME OF HYPERNATREMIA AND HYPODIPSIA

Some patients with the hypernatremia and hypodipsia syndrome may have partial central diabetes insipidus. These patients also have persistent hypernatremia that is not due to any apparent extracellular volume loss, absence or attenuation of thirst, and a normal renal response to AVP. In almost all the patients studied, the hypodipsia has been associated with cerebral lesions in the vicinity of the hypothalamus. It has been proposed that in these patients there is a "resetting" of the osmoreceptor, because their urine tends to become concentrated or diluted at inappropriately high levels of plasma osmolality. However, using the regression analysis of plasma AVP concentration versus plasma osmolality, it has been shown that in some of these patients the tendency to concentrate and dilute urine at inappropriately high levels of plasma osmolality is due solely to a marked reduction in sensitivity or a gain in the osmoregulatory mechanism.[129] This finding is compatible with the diagnosis of partial central diabetes insipidus. In other patients, however, plasma AVP concentrations fluctuate in a random manner, bearing no apparent relationship to changes in plasma osmolality. Such patients frequently display large swings in serum sodium concentration, and frequently exhibit hypodipsia. It appears that most patients with "essential hypernatremia" fit one of these two patterns (Figure 46.9). Both of these groups of patients consistently respond normally to nonosmolar AVP release signals, such as hypotension, emesis, hypoglycemia or all three. These

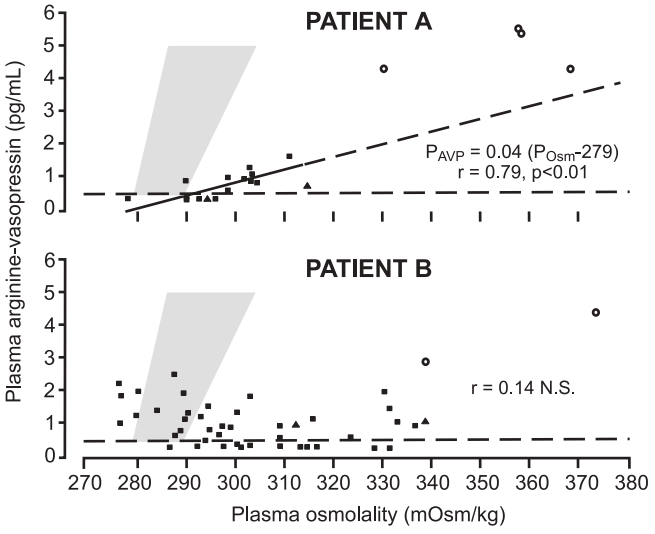

FIGURE 46.9 **Plasma arginine vasopressin (PAVP) as a function of "effective" plasma osmolality(P_{Osm}) in two patients with adipsic hypernatremia.** Open circles indicate values obtained on admission; filled squares indicate those obtained during forced hydration; filled triangles indicate those obtained after 1 to 2 weeks of ad libitum water intake; gray areas indicate range of normal values. *(From ref. [245].)*

observations suggest that: (1) the osmoreceptor may be anatomically, as well as functionally, separate from the nonosmotic efferent pathways and neurosecretory neurons for vasopressin, and a hypothalamic lesion may impair the osmotic release of AVP while the nonosmotic release of AVP remains intact; and (2) the osmoreceptor neurons that regulate vasopressin secretion are not synonymous with those that regulate thirst.

Hereditary Nephrogenic Diabetes Insipidus

In nephrogenic diabetes insipidus (NDI), the kidney is unable to concentrate urine despite normal or elevated concentrations of the antidiuretic hormone arginine vasopressin. In congenital NDI, the obvious clinical manifestations of the disease, that is polyuria and polydipsia, are present at birth and need to be immediately recognized to avoid severe episodes of dehydration. It is clinically useful to distinguish two types of hereditary NDI: a "pure" type characterized by loss of water only; and a complex type characterized by loss of water and ions. Patients who have congenital NDI and mutations in the *AVPR2* or *AQP2* genes have a pure NDI phenotype with loss of water but normal conservation of sodium, potassium, chloride, and calcium. Patients with inactivating mutations in genes (*SLC12A1*, *KCNJ1*, *CLCNKB*, *CLCNKA*, and *CLCNKB* in combination or *BSND*) that encode the membrane proteins of the thick ascending limb of the loop of Henle have a complex polyuropolydipsic syndrome with loss of water, sodium, chloride, calcium, magnesium, and potassium. Most (>90%) of pure congenital NDI patients have mutations in the *AVPR2* gene, the Xq28 gene coding for the vasopressin V2 (antidiuretic) receptor. In less than 10% of the families studied, congenital NDI has an autosomal recessive inheritance, and mutations have been identified in the *AQP2* gene located in chromosome region 12q13, that is, the vasopressin-sensitive water channel. When studied *in vitro*, most *AVPR2* mutations lead to receptors that are trapped intracellularly, and are unable to reach the plasma membrane. A minority of the mutant receptors reaches the cell surface, but is unable to bind AVP or to trigger an intracellular cAMP signal. Similarly, *AQP2* mutant proteins are trapped intracellularly and cannot be expressed at the luminal membrane. AVPR2 and AQP2-trafficking defects are correctable by chemical chaperones.

LOSS-OF-FUNCTION MUTATIONS OF *AVPR2*

X-linked NDI (OMIM 304800)[109] is secondary to *AVPR2* mutations, which result in a loss-of-function or dysregulation of the V2 receptor.[130] Males who have an *AVPR2* mutation have a phenotype characterized by early dehydration episodes, hypernatremia, and hyperthermia as early as the first week of life. Dehydration episodes can be so severe that they lower arterial blood pressure to a degree that is not sufficient to sustain adequate oxygenation to the brain, kidneys, and other organs. Mental and physical retardation and renal failure are the classical "historic" consequences of a late diagnosis and lack of treatment. Heterozygous females exhibit variable degrees of polyuria and polydipsia, because of skewed X-chromosome inactivation.[131,132]

Clinical Characteristics

The historic clinical characteristics include hypernatremia, hyperthermia, mental retardation, and repeated episodes of dehydration in early infancy.[133–136] Mental retardation, a consequence of repeated episodes of dehydration, was prevalent in the Crawford and Bode study,[133] in which only nine (11%) of 82 patients had normal intelligence. Early recognition and treatment of X-linked NDI with an abundant intake of water allows a normal lifespan with normal physical and mental development.[137] Two characteristics suggestive of X-linked NDI are the familial occurrence and the confinement of mental retardation to male patients. It is then tempting to assume that the family described in 1892 by McIlraith,[138] and discussed by Reeves and Andreoli[139] was an X-linked NDI family.

Crawford and Bode[133] clearly describe the early symptoms of the nephrogenic disorder and its severity in infancy. The first manifestations of the disease can be recognized during the first week of life. The infants are irritable, cry almost constantly and, although eager to suck, will vomit milk soon after ingestion unless prefed with water. The history given by the mothers often includes persistent constipation, erratic unexplained fever, and failure to gain weight. Although the patients characteristically show no visible evidence of perspiration, increased water loss during fever or in warm weather exaggerates the symptoms. Unless the condition is recognized early, children experience frequent bouts of hypertonic dehydration, sometimes complicated by convulsions or death; mental retardation is a frequent consequence of these episodes. The intake of large quantities of water, combined with the patient's voluntary restriction of dietary salt and protein intake, lead to hypocaloric dwarfism beginning in infancy. Frequently, lower urinary tract dilatation and obstruction, probably secondary to the large volume of urine produced,[140] develop in affected children. Dilatation of the lower urinary tract is also seen in primary polydipsic patients, and in patients with neurogenic diabetes insipidus.[141,142] Chronic renal insufficiency may occur

by the end of the first decade of life, and could be the result of episodes of dehydration with thrombosis of the glomerular tufts.[133]

History

In 1989, we observed that the administration of dDAVP, a V2-receptor agonist, increased plasma cAMP concentrations in healthy subjects, but had no effect in 14 male patients with X-linked NDI.[143] Intermediate responses were observed in obligate carriers of the disease, corresponding to half of the normal receptor response. On the basis of these results, we predicted that the defective gene in these patients with X-linked NDI was likely to code for a defective V2 receptor.[143] Since that time, a number of experimental results have confirmed our hypothesis: (1) the NDI locus was mapped to the distal region of the long arm of the X-chromosome[144–147]; (2) the V2 receptor was identified as a candidate gene for NDI[148]; (3) the human V2 receptor was cloned[53]; and (4) 214 putative disease-causing mutations have now been identified in the V2 receptor, and the list of mutations is still expanding[149,150] (Figure 46.10).

Population Genetics of *AVPR2* Mutations

X-linked NDI is generally a rare disease in which the affected male patients do not concentrate their urine after administration of AVP.[151] Because this form is a rare, recessive X-linked disease, female individuals are unlikely to be affected, but heterozygous female individuals can exhibit variable degrees of polyuria and polydipsia because of skewed X-chromosome inactivation. In Quebec, the incidence of this disease among male individuals was estimated to be approximately 8.8 in 1,000,000 male live births.[131] A founder effect of two particular *AVPR2* mutations,[152] one in Ulster Scot immigrants (the Hopewell mutation, W71X), and one

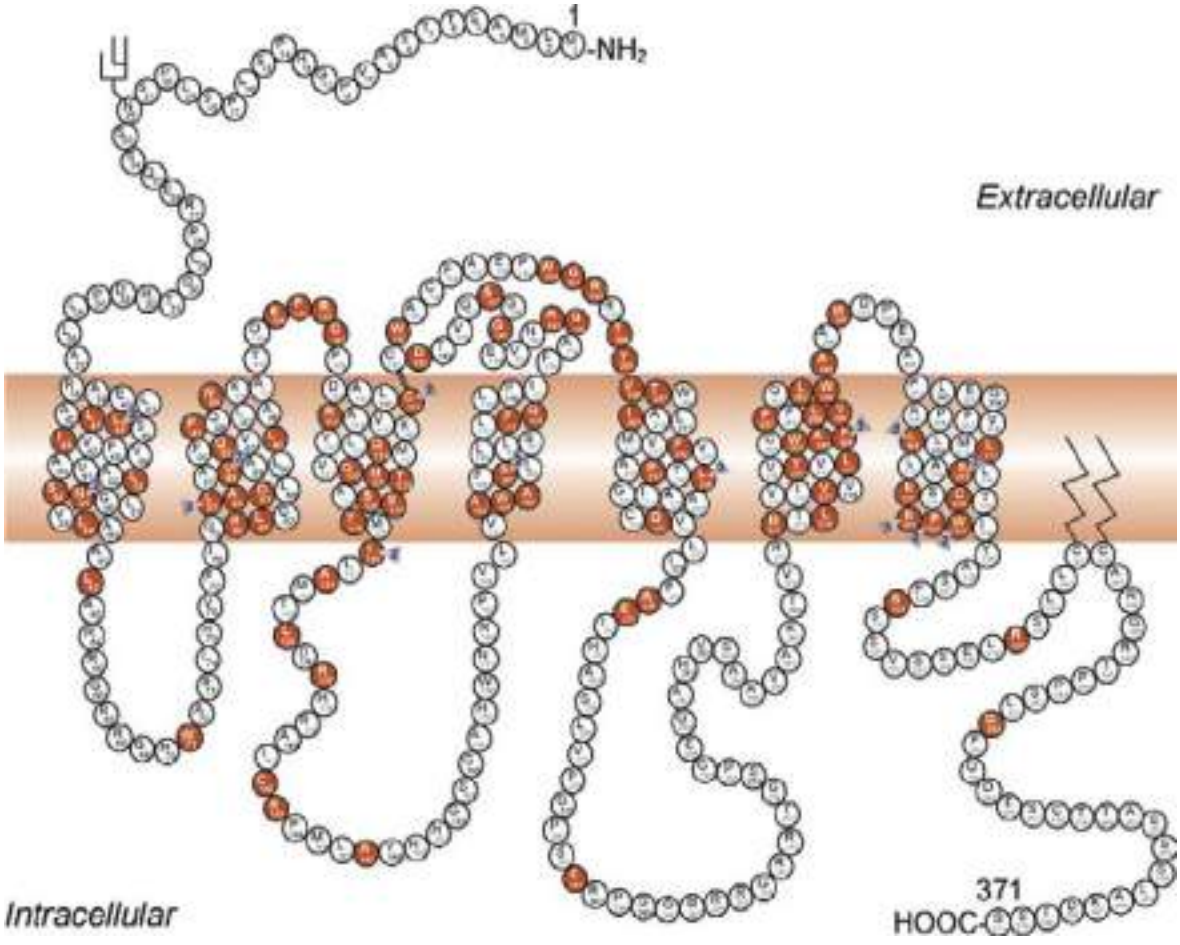

FIGURE 46.10 **Schematic representation of the V2 receptor and identification of 193 putative disease-causing AVPR2 mutations.** Predicted amino acids are shown as the one-letter amino acid code. A solid symbol indicates a codon with a missense or nonsense mutation; a number indicates more than one mutation in the same codon; other types of mutations are not indicated on the figure. There are 95 missense, 18 nonsense, 46 frameshift deletion or insertion, 7 inframe deletion or insertion, 4 splice-site, and 22 large deletion mutations, and one complex mutation.

in a large Utah kindred (the Cannon pedigree), result in an elevated prevalence of X-linked NDI in their descendants in certain communities in Nova Scotia, Canada, and Utah, United States.[117] These founder mutations have now spread all over the North American continent. We have identified the W71X mutation in 42 affected male individuals who reside predominantly in the Maritime Provinces of Nova Scotia and New Brunswick, and the L312X mutation in eight affected males who reside in the central United States. We know of 98 living affected male individuals of the Hopewell kindred, and 18 living affected male individuals of the Cannon pedigree.

We propose that all families with hereditary diabetes insipidus should have their molecular defect identified. The molecular identification underlying X-linked NDI is of immediate clinical significance, because early diagnosis and treatment of affected infants can avert the physical and mental retardation that results from repeated episodes of dehydration. Affected premature male infants may experience less severe polyuric symptoms, and may need only increased hydration during their first week without a need for hydrochlorothiazide treatment. Water should be offered every 2hours day and night, and temperature, appetite, and growth should be monitored. Admission to hospital may be necessary for continuous gastric feeding. The voluminous amounts of water kept in patients' stomachs will exacerbate physiological gastrointestinal reflux in infants and toddlers, and many affected boys frequently vomit. These young patients often improve with the absorption of an H_2 blocker, and with metoclopramide (which could induce extrapyramidal symptoms) or with domperidone, which seems to be better-tolerated and efficacious. As mentioned previously, all polyuric states (whether neurogenic, nephrogenic or psychogenic) can induce large dilatations of the urinary tract and bladder,[133,141,142] and bladder function impairment has been well-documented in patients who bear *AVPR2* or *AQP2* mutations.[153,154] Of interest, in mice with congenital progressive hydronephrosis (cph) homozygote for the S266L mutation (*Aqp2*) the congenital obstructive uropathy is likely a result of the polyuria.[90] Chronic renal failure secondary to bilateral hydronephrosis has been observed as a long-term complication in these patients. Renal and abdominal ultrasound should be done annually, and simple recommendations, including frequent urination and "double voiding" could be important to prevent these consequences.

Expression Studies

Classification of the defects of naturally occurring mutant human V2 receptors can be based on a similar scheme to that used for the LDL receptor. Mutations have been grouped according to the function and subcellular localization of the mutant protein whose cDNA has been transiently transfected in a heterologous expression system.[155] Using this classification, type 1 mutant V2 receptors reach the cell surface, but display impaired ligand binding and are consequently unable to induce normal cAMP production. The presence of mutant V2 receptors on the surface of transfected cells can be determined pharmacologically. By carrying out saturation-binding experiments using tritiated AVP, the number of cell surface mutant V2 receptors and their apparent binding affinity can be compared with that of the wild-type receptor. In addition, the presence of cell surface receptors can be assessed directly by using immunodetection strategies to visualize epitope-tagged receptors in whole-cell immunofluorescence assays.

Type 2 mutant receptors have defective intracellular transport. This phenotype is confirmed by carrying out, in parallel, immunofluorescence experiments on cells that are intact (to demonstrate the absence of cell surface receptors) or permeabilized (to confirm the presence of intracellular receptor pools). In addition, protein expression is confirmed by Western blot analysis of membrane preparations from transfected cells. It is likely that these mutant type 2 receptors accumulate in a pre-Golgi compartment, because they are initially glycosylated but fail to undergo glycosyl-trimming maturation.

Type 3 mutant receptors are ineffectively transcribed and lead to unstable mRNA, which are rapidly degraded. This subgroup seems to be rare, since Northern blot analysis of cells expressing mutant V2 receptors showed mRNA of normal quantity and molecular size.

Most of the *AVPR2* mutants that we and other investigators have tested are type 2 mutant receptors. They did not reach the cell membrane, and were trapped in the interior of the cell.[156–159] Other mutant G-protein-coupled receptors[160] and gene products that cause genetic disorders are also characterized by protein misfolding. Mutations that affect the folding of secretory proteins, integral plasma membrane proteins or enzymes destined to the endoplasmic reticulum, Golgi complex, and lysosomes result in loss-of-function phenotypes irrespective of their direct impact on protein function, because these mutant proteins are prevented from reaching their final destination.[161] Folding in the endoplasmic reticulum is the limiting step: mutant proteins which fail to correctly fold are retained initially in the endoplasmic reticulum and subsequently often degraded. Key proteins involved in the urine countercurrent mechanisms are good examples of this basic mechanism of misfolding. *AQP2* mutations responsible for autosomal recessive NDI are characterized by

misrouting of the misfolded mutant proteins, and are trapped in the endoplasmic reticulum.[162] Mutants that encode other renal membrane proteins that are responsible for Gitelman syndrome,[163] Bartter syndrome,[164,165] and cystinuria[166] are also retained in the endoplasmic reticulum.

The *AVPR2* missense mutations are likely to impair folding and to lead to rapid degradation of the misfolded polypeptide, and not to the accumulation of toxic aggregates (as is the case for AVP mutants), because the other important functions of the principle cells of the collecting duct (where *AVPR2* is expressed) are entirely normal. These cells express the epithelial sodium channel (ENaC). Decreased function of this channel results in a sodium-losing state.[167] This has not been observed in patients with *AVPR2* mutations. By contrast, another type of conformational disease is characterized by the toxic retention of the misfolded protein. The relatively common Z mutation in a_1-antitrypsin deficiency not only causes retention of the mutant protein in the endoplasmic reticulum, but also affects the secondary structure by insertion of the reactive center loop of one molecule into a destabilized b sheet of a second molecule.[168] These polymers clog up the endoplasmic reticulum of hepatocytes and lead to cell death and juvenile hepatitis, cirrhosis, and hepatocarcinomas in these patients.[169]

If the misfolded protein/traffic problem that is responsible for so many human genetic diseases can be overcome, and the mutant protein transported out of the endoplasmic reticulum to its final destination, these mutant proteins could be sufficiently functional.[120] Therefore, using pharmacological chaperones or pharmacoperones to promote escape from the endoplasmic reticulum is a possible therapeutic approach.[121,156,161] We used selective nonpeptide V2 and V1 receptor-antagonists to rescue the cell-surface expression and function of naturally occurring misfolded human V2 receptors.[158] Because the beneficial effect of nonpeptide V2 antagonists could be secondary to prevention and interference with endocytosis, we studied the R137H mutant previously reported to lead to constitutive endocytosis.[170] We found that the antagonist did not prevent the constitutive b-arresting-promoted endocytosis.[156] These results indicate that, as for other *AVPR2* mutants, the beneficial effects of the treatment result from the action of the pharmacological chaperones. These studies were confirmed *in vitro* with the use of non-peptide V2 agonists.[171] In clinical studies, we administered a nonpeptide vasopressin antagonist SR49059 to five adult patients who have NDI and bear the del62-64, R137H, and W164S mutations. SR49059 significantly decreased urine volume and water intake and increased urine osmolality whereas sodium, potassium, and creatinine excretions and plasma sodium levels were constant throughout the study.[156] This new therapeutic approach could be applied to the treatment of several hereditary diseases resulting from errors in protein folding and kinesis.[120,121]

Because most human gene-therapy experiments using viruses to deliver and integrate DNA into host cells are potentially dangerous,[172] other treatments are being actively pursued. Schöneberg and colleagues[173] used aminoglycoside antibiotics, because of their ability to suppress premature termination codons.[174] They demonstrated that geneticin, a potent aminoglycoside antibiotic, increased AVP-stimulated cAMP in cultured collecting duct cells prepared from E242X mutant mice. The urine concentrating ability of heterozygous mutant mice was also improved.

LOSS-OF-FUNCTION MUTATIONS OF AQP2 (OMIM 222000, 125800, 107777)

On the basis of desmopressin infusion studies and phenotypic characteristics of both male and female individuals who are affected with NDI, a non-X-linked form of NDI with a postreceptor (post-cAMP) defect was suggested.[109,175–177] A patient who presented shortly after birth with typical features of NDI, but who exhibited normal coagulation and normal fibrinolytic and vasodilatory responses to desmopressin, was shown to be a compound heterozygote for two missense mutations (R187C and S217P) in the *AQP2* gene.[178] To date, 46 putative disease-causing *AQP2* mutations have been identified in 52 NDI families (Figure 46.11). The oocytes of the African clawed frog (*Xenopus laevis*) have provided a most useful experimental system for studying the function of many channel proteins. This convenient expression system was key to the discovery of AQP1 by Agre,[179] because frog oocytes have very low permeability and survive even in freshwater ponds. Control oocytes are injected with water alone; test oocytes are injected with various quantities of synthetic transcripts from AQP1 or AQP2 DNA (cRNA). When subjected to a 20 mOsm osmotic shock, control oocytes have exceedingly low water permeability, but test oocytes become highly permeable to water. These osmotic water permeability assays demonstrated an absence or very low water transport for all of the cRNA with *AQP2* mutations. Immunofluorescence and immunoblot studies demonstrated that these recessive mutants were retained in the endoplasmic reticulum.

AQP2 mutations in autosomal recessive NDI, which are located throughout the gene, result in misfolded proteins that are retained in the endoplasmic reticulum. In contrast, the dominant mutations reported to date are located in the region that codes for the carboxyl-terminus of AQP2.[180–182] Dominant AQP2

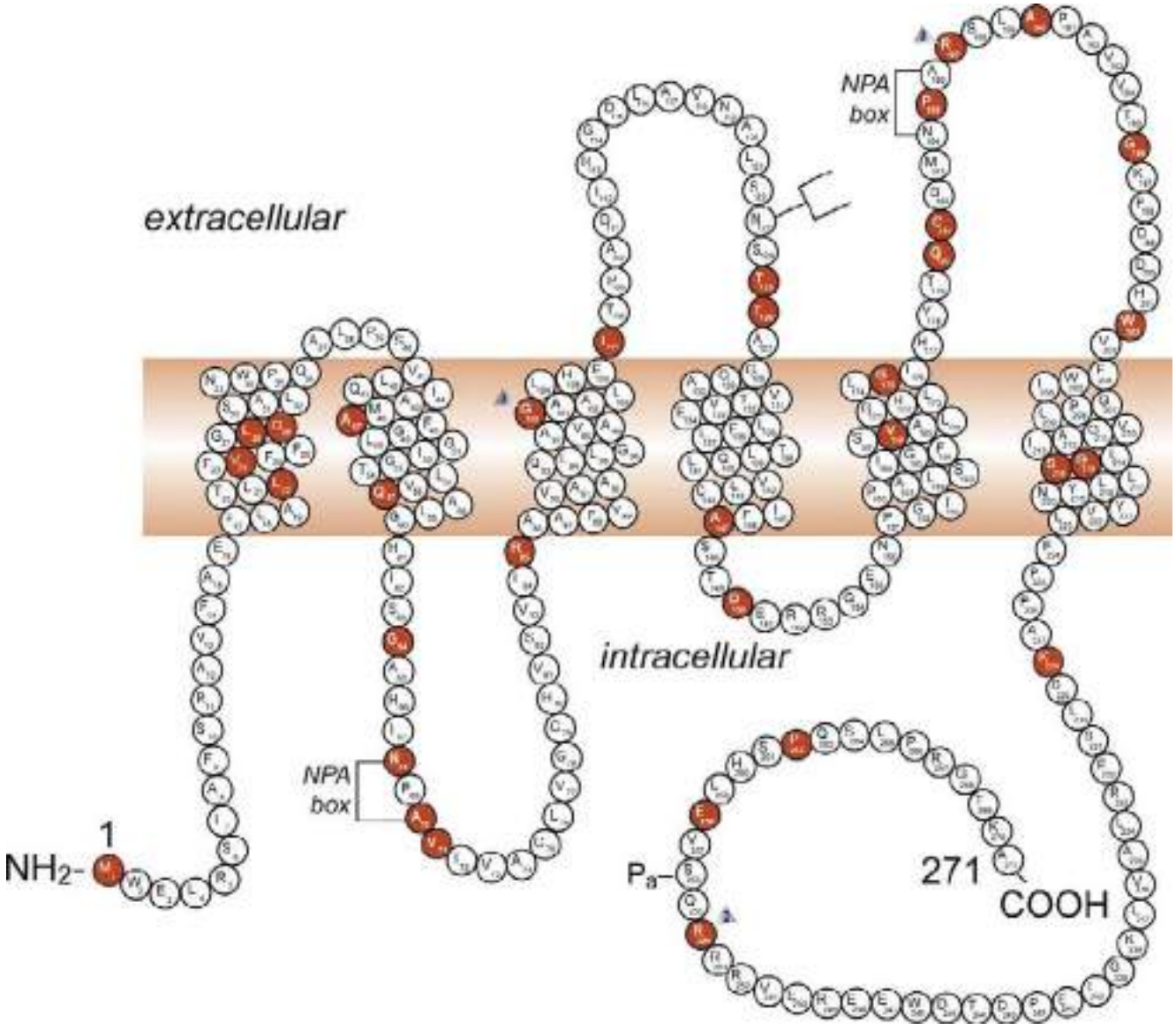

FIGURE 46.11 **A representation of the AQP2 protein and identification of 46 putative disease-causing AQP2 mutations.** A monomer is represented with six transmembrane helices. The location of the PKA phosphorylation site (Pa) is indicated. The extracellular, transmembrane, and cytoplasmic domains are defined according to *Deen, P. M., et al. (1994)*.[178] Solid symbols indicate the location of the mutations (for references, see Table 46.1): M1I; L22V; V24A; L28P; G29S; A47V; Q57P; G64R, N68S, A70D; V71M; R85X; G100X; G100V; G100R; I107D; 369delC; T125M; T126M; A147T; D150E; V168M; G175R; G180S; C181W; P185A; R187C; R187H; A190T; G196D; W202C; G215C; S216P; S216F; K228E; R254Q; R254L; E258K; and P262L. GenBank accession numbers—AQP2: AF147092, exon 1; AF147093, exons 2 through 4. NPA motifs and the N-glycosylation site are also indicated.

mutants form heterotetramers with wild-type AQP2 and are misrouted. Patients bearing these dominant mutations have a less severe phenotype compared to patients who are compound heterozygotes or homozygotes for recessive mutations: the patient and her daughter first described to bear the AQP2-E258K dominant mutation increased their urine osmolality to 350 mOsm/kg H_2O following dDAVP.[183] Also, the patient with a detailed phenotype described by Robertson and Kopp[184] increased her urine osmolality to 220 mOsm/kg H_2O during a mildly hypertonic dehydration, to 258 mOsm/kg H_2O after dDAVP, and to 305 mOsm/kg H_2O after hydrochlorothiazide and indomethacin. This patient was found to be heterozygous for the R254Q mutation, possibly interfering with the S256 phosphorylation site.[185] In the mutant AQP2 (763−772) knock-in mice, Sohara et al. demonstrated a slight increase in urine osmolality following dehydration, but a marked increase after the administration of Rolipram, a phosphodiesterase 4 inhibitor.[186]

COMPLEX POLYUROPOLYDIPSIC SYNDROME

In contrast to a pure NDI phenotype, with loss of water but normal conservation of sodium, potassium, chloride, and calcium, in Bartter syndrome, patients' renal-wasting starts prenatally, and polyhydramnios often leads to prematurity. Bartter syndrome (OMIM 601678, 241200, 607364, and 602522) refers to a group of autosomal recessive disorders caused by inactivating mutations in genes (*SLC12A1*, *KCNJ1*, *CLCNKB*, *CLCNKA*, and *CLCNKB* in combination or *BSND*) that encode membrane proteins of the thick ascending limb of the loop of Henle (for review see [187,188]). Although Bartter syndrome and Bartter mutations are commonly used as a diagnosis, it is likely, as explained by Jeck et al.,[189] that the two patients with a mild phenotype originally described by Dr. Bartter had Gitelman syndrome, a thiazide-like, salt-losing tubulopathy with a defect in the distal convoluted tubule.[189] As a consequence, salt-losing tubulopathy of the furosemide-type is a more physiologically appropriate definition.

Thirty percent of the filtered sodium chloride is reabsorbed in the thick ascending limb of the loop of Henle through the apically expressed sodium–potassium–chloride co-transporter NKCC2 (encoded by the *SLC12A1* gene), which uses the sodium gradient across the membrane to transport chloride and potassium into the cell. The potassium ions must be recycled through the apical membrane by the potassium channel ROMK (encoded by the *KCNJ1* gene). In the large experience of Seyberth and colleagues,[190] who studied 85 patients with a hypokalemic salt-losing tubulopathy, all 20 patients with *KCNJ1* mutations (except one) and all 12 patients with *SLC12A1* mutations were born as preterm infants after severe polyhydramnios. Of note, polyhydramnios is never seen during a pregnancy that leads to infants bearing *AVPR2* or *AQP2* mutations. The most common causes of increased amniotic fluid include maternal diabetes mellitus, fetal malformations and chromosomal aberrations, twin-to-twin transfusion syndrome, rhesus incompatibility, and congenital infections.[191] Postnatally, polyuria was the leading symptom in 19 of the 32 patients. Renal ultrasound revealed nephrocalcinosis in 31 of these patients. These patients with complex polyuropolydipsic disorders are often poorly-recognized, and may be confused with pure NDI. As a consequence, congenital polyuria does not suggest automatically *AVPR2* or *AQP2* mutations, and polyhydramnios, salt-wasting, hypokalemia, and nephrocalcinosis are important clinical and laboratory characteristics that should be assessed. In patients with Bartter syndrome (salt-losing tubulopathy/furosemide-type), the dDAVP test will only indicate a partial type of NDI. The algorithm proposed by Peters et al.[190] is useful, since most mutations in *SLC12A1* and *KCNJ1* are found in the carboxyl-terminus or in the last exon and, as a consequence, are amenable to rapid DNA sequencing.

Polyuria, polydipsia, electrolyte imbalance, and dehydration may also been seen in cystinosis, nephronophthisis, and apparent mineralocorticoid excess. Polyuria may be as mild as persistent enuresis and as severe as to contribute to death from dehydration and electrolyte abnormalities in infants with cystinosis who have acute gastroenteritis.[192] Nephronophthisis and apparent mineralocorticoid excess are also associated with low urine osmolality unresponsive to vasopressin.[193]

ACQUIRED NEPHROGENIC DIABETES INSIPIDUS

Acquired NDI is much more common than congenital NDI, but it is rarely as severe. The ability to produce hypertonic urine is usually preserved, even though there is inadequate concentrating ability of the nephron. Polyuria and polydipsia are therefore moderate (3–4 l/d).

The more common causes of acquired NDI are listed in Table 46.2. Lithium administration has become the most frequent cause; 54% of 1105 unselected patients on chronic lithium therapy developed NDI.[194] Nineteen percent of these patients had polyuria, as defined by a 24hour urine output exceeding 3 liters. The mechanism whereby lithium causes polyuria has been extensively studied. Lithium inhibits adenylyl cyclase in a number of cell types, including renal epithelia.[195,196] The dysregulation of aquaporin-2 expression is the result of cytotoxic accumulation of lithium which enters via the epithelial sodium channel (ENaC) on the apical membrane, and leads to the inhibition of signaling pathways that involve glycogen synthase kinase type 3 beta.[197] The concentration of lithium in urine of patients on well-controlled lithium therapy (i.e., 10 to 40 mOsmol/L) is sufficient to exert this effect. For patients on long-term lithium therapy, amiloride has been proposed to prevent the uptake of lithium in the collecting ducts, thus preventing the inhibitory effect of intracellular lithium on water transport.[198]

Primary Polydipsia

Primary polydipsia is a state of hypotonic polyuria secondary to excessive fluid intake. Primary polydipsia was extensively studied by Barlow and de Wardener in 1959[199]; however, the understanding of the

TABLE 46.2 Causes of Nephrogenic Diabetes Insipidus.

Narrow definition of NDI: water permeability of the collecting duct not increased by AVP
Congenital (idiopathic)
Hypercalcemia
Hypokalemia
Drugs:
Lithium
Nonpeptide vasopressin receptor (V2) antagonists
Demeclocycline
Amphotericin B
Methoxyflurane
Diphenylhydantoin
Nicotine
Alcohol
Broad definition of NDI: defective medullary countercurrent function
Renal failure, acute or chronic (especially interstitial nephritis or obstruction)
Medullary damage:
Sickle-cell anemia and trait
Amyloidosis
Sjögren syndrome
Sarcoidosis
Hypercalcemia
Hypokalemia
Protein malnutrition
Cystinosis

Modified from ref. [246]

pathophysiology of this disease has made little progress. Barlow and de Wardener[199] described seven women and two men who were compulsive water drinkers; their ages ranged from 48 to 59 years, except for one patient who was 24 years old. Eight of these patients had histories of previous psychological disorders, which ranged from delusions, depression, and agitation to frank hysterical behavior. The other patient appeared normal. The consumption of water fluctuated irregularly from hour to hour or from day to day; in some patients, there were remissions and relapses lasting several months or longer. In eight of the patients, the mean plasma osmolality was significantly lower than normal. Vasopressin tannate in oil made most of these patients feel ill; in one, it caused overhydration. In four patients, the fluid intake returned to normal after electroconvulsive therapy or a period of continuous narcosis; the improvement in three was transient, but in the fourth it lasted two years. Polyuric female subjects might be heterozygous for *de novo* or previously unrecognized *AVPR2* mutations, may bear *AQP2* mutations, and may be classified as compulsive water drinkers.[200] Therefore, the diagnosis of compulsive water drinking must be made with care, and may represent our ignorance of yet undescribed pathophysiological mechanisms. Robertson[200] has described under the name "dipsogenic diabetes insipidus" a selective defect in the osmoregulation of thirst. Three studied patients had, under basal conditions of *ad libitum* water intake, thirst, polydipsia, polyuria, and high-normal plasma osmolality. They had a normal secretion of AVP, but osmotic threshold for thirst was abnormally low. These dipsogenic diabetes insipidus cases might represent up to 10% of all patients with diabetes insipidus.[200]

Diabetes Insipidus and Pregnancy

Pregnancy in a Patient Known to Have Diabetes Insipidus

An isolated deficiency of vasopressin without a concomitant loss of hormones in the anterior pituitary does not result in altered fertility, and with the exception of polyuria and polydipsia, gestation, delivery, and lactation are uncomplicated.[201] Patients may require increasing dosages of dDAVP. The increased thirst may be due to a resetting of the thirst osmostat.[202]

Increased polyuria also occurs during pregnancy in patients with partial NDI.[203] These patients may be obligatory carriers of the NDI gene[204] or may be homozygotes, compound heterozygotes or may have dominant AQP2 mutations.

Syndromes of Diabetes Insipidus that Begin during Gestation and Remit after Delivery

Barron et al.[205] described three pregnant women in whom transient diabetes insipidus developed late in gestation and subsequently remitted postpartum. In one of these patients, dilute urine was present despite high plasma concentrations of AVP. Hyposthenuria in all three patients was resistant to administered aqueous vasopressin. Because excessive vasopressinase activity was not excluded as a cause of this disorder, Barron et al. labeled the disease vasopressin-resistant, rather than NDI.

A well-documented case of enhanced activity of vasopressinase has been described in a woman in the third trimester of a previously uncomplicated pregnancy.[206] She had massive polyuria and markedly

elevated plasma vasopressinase activity. The polyuria did not respond to large intravenous doses of AVP, but responded promptly to dDAVP, a vasopressinase-resistant analog of AVP. The polyuria disappeared with the disappearance of the vasopressinase. It is suggested that pregnancy may be associated with several different forms of diabetes insipidus, including central, nephrogenic, and vasopressinase mediated.[203,207,208]

Polyuria and Nocturia in Diabetes Insipidus, Nocturnal Polyuria in Enuretic Children

Polyuria could be constant during the day but also present at night: the urine is normally most concentrated in the morning due to lack of fluid ingestion overnight and increased vasopressin secretion during the late sleep period.[209] Neurons in the suprachiasmatic nucleus, the brain biological clock, send axonal projections toward the supraoptic nucleus, one of the hypothalamic nuclei producing vasopressin,[5] providing a possible anatomical substrate for the circadian modulation, an osmoregulatory gain during the late sleep period.[209] As a result, the first manifestation of a mild-to-moderate loss of concentrating ability is often nocturia. However, nocturia is not diagnostic of a defect in concentrating ability, since it can also be caused by other factors such as drinking before going to bed or, in men, by prostatic hypertrophy, which is characterized by urinary frequency rather than polyuria. Psychogenic polydipsic patients tend to ingest large amounts of fluid during the day but not at night, therefore nocturia is rarely seen in primary polydipsic patients.[199] The pattern of nocturnal polyuria in enuretic children is similar to that observed in acute sleep deprivation, and enuresis in children might be related to the failure of sleep to cause a reflex reduction in arterial pressure and urine production.[210,211]

INVESTIGATION OF A PATIENT WITH POLYURIA

Plasma sodium and osmolality are maintained within normal limits (136–143 mOsmol/l for plasma sodium; 275–290 mOsmol/kg for plasma osmolality) by a thirst–AVP–renal axis. Thirst and AVP release, both stimulated by increased osmolality, is a "double-negative" feedback system.[212] Even when the AVP component of this double-negative regulatory feedback system is lost, the thirst mechanism still preserves the plasma sodium and osmolality within the normal range, but at the expense of pronounced polydipsia and polyuria. Thus, the plasma sodium concentration or osmolality of an untreated patient with diabetes insipidus may be slightly greater than the mean normal value, but these small increases have no diagnostic significance. Polyuric patients should be asked about their thirst and their way to quench it: cold water will quench thirst more effectively in severely polyuric and dehydrated patients, irrespective of their etiology (central versus nephrogenic). Primary polydipsic patients may tend to absorb large quantities of water, ice-cold or not. Glucose-induced osmotic diuresis is more frequent than any cause of non-osmotic polyuria. High plasma glucose levels with polyuria could also be observed in brain-dead patients with diabetes insipidus receiving glucose infusions at a rate exceeding 500 ml/hour, which corresponds to the maximum (25 g/hour) possibility for glucose metabolism. The polyuria observed in post-obstructive diuresis is appropriate, representing an attempt to excrete the fluid retained during the period of obstruction.[213]

Excepting the context of brain trauma, brain surgery or long-term lithium administration, where the diagnosis of polyuria is obvious, a logical approach to the patient with polyuria is to search for arguments supporting known causes of polyuric states. Such arguments may be: (1) morphological (brain magnetic resonance imaging), including the presence of a hypothalamic tumour or mass related to a granulomatous or inflammatory process; (2) hormonal, suggesting that the posterior pituitary involvement is not isolated, but rather is associated with other signs of anterior pituitary deficits; (3) systemic, with the presence of a generalized inflammatory process or pituitary metastasis; (4) hereditary, with other members of the family affected with central or nephrogenic diabetes insipidus.

An abrupt onset of polyuria in an adult would suggest acquired central diabetes insipidus. Magnetic resonance imaging of the hypothalamic structures and of the posterior pituitary should be obtained to assess the posterior pituitary normal "bright spot," a possible surrogate of the posterior pituitary vasopressin content, and any accompanying lesions. Clinical and biochemical indices of associated anterior pituitary/hormone deficiency should also be obtained,[97] since additional deficits in anterior pituitary hormones were documented in 61% of patients, a median of 0.6 years after the onset of diabetes insipidus. The most frequent abnormality was growth hormone deficiency (59%), followed by hypothyroidism (28%), hypogonadism (24%), and adrenal insufficiency (22%). Seventy-five percent of the patients with Langerhans cell histiocytosis had an anterior pituitary hormone deficiency that was first detected a median of 3.5 years after the onset of diabetes insipidus.

In this context, the dehydration test is rarely necessary, and is only recommended for patients with isolated polyuria, a normal pituitary stalk and hypothalamic region on magnetic resonance imaging, and

with no familial history of polyuria. If plasma osmolality and/or sodium concentration under conditions of *ad libitum* fluid intake are above 295 mmol/kg and 143 mmol/L, the diagnosis of primary polydipsia is excluded.[214]

If severe polyuric symptoms and signs are documented, water should be restricted to only two to four hours during day time in infants, plasma sodium should be available every two hours during testing and should not exceed 145–148 in children and adults, since a maximal endogenous vasopressin stimulation (more than 3.5 pg/mL) should occur at this level with a maximal urine osmolality response (higher than 800 mOsm/kg H_2O). If delays of more than 60minutes are encountered to obtain plasma sodium or urine osmolalities during dehydration tests, these tests should be done in other institutions where almost immediate laboratory reports are obtained after blood samplings.

Theoretically, it should be relatively easy to differentiate between neurogenic diabetes insipidus, NDI, and primary polydipsia by comparing the osmolality of urine obtained during dehydration with that of urine obtained after the administration of dDAVP. Patients with neurogenic diabetes insipidus should reveal a rapid increase in urinary osmolality, whereas it should increase normally in response to moderate dehydration in patients with primary polydipsia. However, for several reasons, these distinctions may not be as clear as one might expect.[215] First, chronic polyuria resulting from any cause interferes with the maintenance of the medullary concentration gradient, and this "wash-out" effect diminishes the maximum concentrating ability of the nephron. The extent of the blunting varies in direct proportion to the severity of the polyuria. Hence, for any given basal urine output, the maximum urine osmolality achieved in the presence of saturating concentrations of AVP is depressed to the same extent in patients with primary polydipsia, neurogenic diabetes insipidus or NDI (Figure 46.12). Second, most patients with neurogenic diabetes insipidus maintain a small, but detectable, capacity to secrete AVP during severe dehydration, and urinary osmolality may then increase to greater than the plasma osmolality. Third, patients referred to as partial diabetes insipidus (either neurogenic or nephrogenic) and patients with acquired NDI have an incomplete response to AVP, and are able to concentrate their urine to varying degrees in a dehydration test. Finally, all polyuric states (whether neurogenic, nephrogenic or psychogenic) can induce large dilatations of the urinary tract and bladder.[141,142] As a consequence, the urinary bladder of these patients has an increased residual capacity, and changes in urinary osmolality induced by diagnostic maneuvers might be difficult to demonstrate.

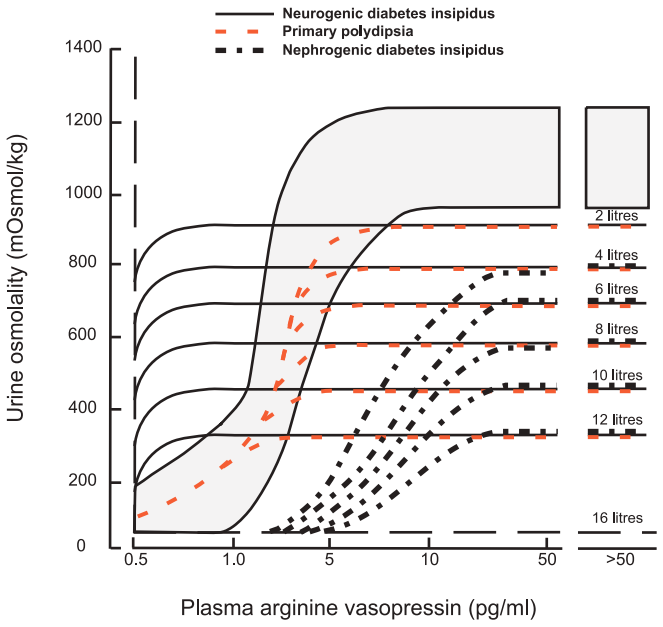

FIGURE 46.12 **Schematic diagram of the relationship between urine osmolality and plasma vasopressin in patients with polyuria of diverse cause and severity.** The shaded area represents the normal range. For each of the three categories of polyuria, the relationship is described by a family of sigmoid curves that differ in height. These differences in height reflect differences in maximum concentrating capacity due to "wash-out" of the medullary concentration gradient. They are proportional to the severity of the underlying polyuria (indicated in liters at the right-hand side of each plateau), and are largely independent of the cause. The three categories of diabetes insipidus differ principally in the submaximal or ascending portion of the dose–response curve. In patients with neurogenic diabetes insipidus, this part of the curve lies to the left of normal, reflecting increased sensitivity to the antidiuretic effects of very low concentrations of plasma vasopressin. In contrast, in patients with neurogenic diabetes insipidus, this part of the curve lies to the right of normal, reflecting decreased sensitivity to the antidiuretic effects of normal concentrations of plasma vasopressin. In primary polydipsia, this relationship is relatively normal. *(From ref. [215].)*

Indirect Tests for Diabetes Insipidus

The measurement of urinary osmolality after dehydration and dDAVP administration is usually referred to as "indirect testing," because AVP secretion is indirectly assessed through changes in urinary osmolalities.[32] The patient is maintained on a complete fluid-restriction regimen until urinary osmolality reaches a plateau, as indicated by an hourly increase of less than 30 mOsmol/kg for at least 3 successive hours. After measuring the plasma osmolality, 2 mg dDAVP are administered subcutaneously. Urinary osmolality is measured 30 and 60minutes later. The last urinary osmolality value obtained before the dDAVP injection, and the highest value obtained after the injection, are compared. In patients with severe neurogenic diabetes insipidus, urinary osmolality after dehydration is usually low (< 200 mOsmol/kg) and increases more than

50% after dDAVP administration. In patients with severe NDI, urinary osmolality after dehydration is also low (<200 mOsmol/kg), but does not increase after dDAVP administration (<20%). Urinary osmolality increases to variable degrees (10% to 50%) after dDAVP administration to patients with partial neurogenic or partial nephrogenic diabetes insipidus. In patients with primary polydipsia, maximum urinary osmolality will be obtained after dehydration (>295 mOsmol/kg) and does not increase after dDAVP administration (<10%).

Alternatively, plasma sodium and plasma and urinary osmolalities can be measured at the beginning of the dehydration procedure and at regular intervals (usually hourly) thereafter, depending on the severity of the polyuria.[216] For example, an 8-year-old patient (body weight 31 kg) with a clinical diagnosis of congenital NDI (later found to bear an *AVPR2* mutation) continued to excrete large volumes of urine (300 ml/h) during a short 4hour dehydration test. During this time, the patient suffered from severe thirst, his plasma sodium was 155 mOsmol/l, plasma osmolality was 310 mOsmol/kg, and urinary osmolality was 85 mOsmol/kg. The patient received 1 mg of dDAVP intravenously and was allowed to drink water. Repeated urinary osmolality measurements demonstrated a complete urinary resistance to dDAVP. It would have been dangerous and unnecessary to prolong the dehydration further in this young patient. Thus, the usual prescription of overnight dehydration should not be used in patients, and especially children, with severe polyuria and polydipsia (more than 30 ml/kg body weight per day). Great care should be taken to avoid any severe hypertonic state, arbitrarily defined as plasma sodium greater than 155 mOsmol/l.

Direct Tests of Diabetes Insipidus

The two approaches of Zerbe and Robertson are used,[217] although they are expensive, time-consuming, and difficult to do on young patients. In the first approach, during the dehydration test, plasma is collected hourly and assayed for AVP. The results are plotted on a nomogram depicting the normal relationship between plasma sodium or osmolality and plasma AVP in normal individuals (Figure 46.6a). If the relationship goes below the normal range, the disorder is diagnosed as neurogenic diabetes insipidus.

In the second approach, NDI can be differentiated from primary polydipsia by analyzing the relationship between plasma AVP and urinary osmolality at the end of the dehydration period (Figure 46.6b). However, definitive differentiation might be impossible, because a normal or even supranormal AVP response to increased plasma osmolality occurs in polydipsic patients. None of the patients with psychogenic or other forms of severe polydipsia studied by Robertson showed any evidence of pituitary suppression.[215]

In a comparison of diagnoses based on indirect versus direct tests of AVP function in 54 patients with polyuria of diverse cause, Robertson[215] found that the indirect test was reliable only for patients with severe defects. Three patients with severe NDI, and 16 of 17 patients with severe neurogenic diabetes insipidus were accurately diagnosed. However, the error rate of the indirect test was about 50% in diagnosing partial neurogenic diabetes insipidus, partial NDI or primary polydipsia in patients who were able to concentrate their urine to varying degrees when water-deprived. The benefits of combined direct and indirect testing of AVP function have been discussed by Stern and Valtin.[218] The diagnosis of primary polydipsia remains one of exclusion, and the cause could be psychogenic[199] or inappropriate thirst.[200,219] Psychiatric patients with polydipsia and hyponatremia have unexplained defects in urinary dilution, the osmoregulation of water intake or the secretion of vasopressin.[148]

Therapeutic Trial of dDAVP

In selected patients with an uncertain diagnosis, a closely monitored therapeutic trial of dDAVP (10 mg intranasally twice a day for 2 to 3 days) may be used to distinguish partial NDI from partial neurogenic diabetes insipidus or primary polydipsia. If dDAVP at this dosage causes a significant antidiuretic effect, NDI is effectively excluded. If polydipsia and polyuria are abolished and plasma sodium does not go below the normal range, the patient probably has neurogenic diabetes insipidus. Conversely, if dDAVP causes a reduction in urine output without reduction in water intake and hyponatremia appears, the patient probably has primary polydipsia. Since fatal water intoxication is a remote possibility, the dDAVP trial should be closely monitored. The methods of differential diagnosis of diabetes insipidus are described in Table 46.3.

Carrier Detection, Perinatal Testing, and Early Treatment

The identification of mutations in the genes that cause hereditary diabetes insipidus allows the early diagnosis and management of at-risk members of families with identified mutations. We encourage physicians who follow families with autosomal neurogenic, X-linked, and autosomal NDI to recommend mutation analysis before the birth of an infant, because early diagnosis and treatment can avert the physical and mental retardation associated with episodes of

TABLE 46.3 Differential Diagnosis of Diabetes Insipidus.

1. Measure plasma osmolality and/or sodium concentration under conditions of *ad libitum* fluid intake. If plasma osmolality is >295 mOsmol/kg and sodium is >143 mOsmol/l, the diagnosis of primary polydipsia is excluded and the work-up should proceed to step (5) and/or (6) to distinguish between NDI and neurogenic diabetes insipidus. *Otherwise*:
2. Perform a dehydration test. If urinary concentration does not occur before plasma osmolality reaches 295 mOsmol/kg and/or sodium reaches 143 mOsmol/l, the diagnosis of primary polydipsia is again excluded and the work-up should proceed to step (5) and/or (6). *Otherwise*:
3. Determine the ratio of urine to plasma osmolality at the end of the dehydration test. If it is <1.5, the diagnosis of primary polydipsia is again excluded and the work-up should proceed to step (5) and/or (6). *Otherwise*:
4. Perform a hypertonic saline infusion with measurement of plasma AVP and osmolality at intervals during the procedure. If the relationship between these two variables falls below the normal range, the diagnosis of neurogenic diabetes insipidus is established. *Otherwise*:
5. Perform a dDAVP infusion test. If urine osmolality increases by <150 mOsmol/kg above the value obtained at the end of the dehydration test, the diagnosis of NDI is established. *Alternatively*:
6. Measure urine osmolality and plasma AVP at the end of the dehydration test. If the relationship falls below the normal range, the diagnosis of NDI is established.

Data from ref. [219].

dehydration. Diagnosis of X-linked NDI was accomplished by mutation testing of cultured amniotic cells ($n = 7$), chorionic villus samples ($n = 10$) or cord blood obtained at birth ($n = 57$) in 74 of our patients. Thirty-five males were found to bear mutant sequences, 22 males were not affected, and nine females were not carriers. These affected patients were immediately given abundant water intake, a low-sodium diet, and hydrochlorothiazide. They never experienced episodes of dehydration, and their physical and mental development is normal. Gene analysis is also important for the identification of nonobligatory female carriers in families with X-linked NDI. Most females heterozygous for a mutation in the V2 receptor do not have clinical symptoms: few are severely affected.[131,220,221] Mutation detection in families with inherited neurogenic diabetes insipidus provides a powerful clinical tool for early diagnosis and management of subsequent cases, especially in early childhood, when diagnosis is difficult and the clinical risks are the greatest.[222]

Neurogenic diabetes insipidus (central or Wolfram) is easily treated with dDAVP.[223] All complications of congenital NDI are prevented by an adequate water intake. Thus, patients should be provided with unrestricted amounts of water from birth to ensure normal development. In addition to a low-sodium diet, the use of diuretics (thiazides) or indomethacin may reduce urinary output. This advantageous effect has to be weighed against the side-effects of these drugs (thiazides: electrolyte disturbances; indomethacin: reduction of the glomerular filtration rate and gastrointestinal symptoms).

RADIOIMMUNOASSAY OF AVP AND OTHER LABORATORY DETERMINATIONS

Radioimmunoassay of AVP

Three developments were basic to the elaboration of a clinically useful radioimmunoassay for plasma AVP[224,225]: (1) the extraction of AVP from plasma with petrol-ether and acetone and the subsequent elimination of nonspecific immunoreactivity; (2) the use of highly-specific and sensitive rabbit antiserum; and (3) the use of a tracer (^{125}I-AVP) with high specific activity. These same extraction procedures are still widely used,[161,198,213,216] and commercial tracers (^{125}I-AVP) and antibodies are available. AVP can also be extracted from plasma by using Sep-Pak C18 cartridges.[226–228]

Blood samples collected in chilled 7 ml lavender-stoppered tubes containing ethylenediaminetetraacetic acid are centrifuged at 4°C, 1000 g (3000 rpm in a usual laboratory centrifuge), for 20minutes. This 20minute centrifugation is mandatory for obtaining platelet-poor plasma samples, because a large fraction of the circulating vasopressin is associated with the platelets in humans.[229,230] The tubes may be kept for 2hours on slushed ice before centrifugation. Plasma is then separated, frozen at − 20°C and extracted within 6 weeks of sampling. Details for sample preparation (Table 46.4) and assay procedure (Table 46.5) can be found in writings by Bichet and colleagues.[229,231] An AVP radioimmunoassay should be validated by demonstrating: (1) a good correlation between plasma sodium or osmolality and plasma AVP during dehydration and infusion of hypertonic saline solution (Figure 46.6); and (2) the inability to obtain detectable values of AVP in patients with severe central diabetes insipidus. Plasma AVP immunoreactivity may be elevated in patients with diabetes insipidus following hypothamic surgery.[232]

In pregnant patients, the blood contains high concentrations of cystine aminopeptidase, which can (*in vitro*) inactivate enormous quantities (ng mL^{-1} min^{-1}) of AVP. However, phenanthrolene effectively inhibits these cystine aminopeptidases (Table 46.6).

Aquaporin-2 Measurements

Urinary AQP2 excretion could be measured by radioimmunoassay[233] or quantitative Western analysis,[234] and could provide an additional indication of the responsiveness of the collecting duct to AVP.

TABLE 46.4 Arginine Vasopressin Measurements: Sample Preparation.

4°C – Blood in EDTA tubes
Centrifugation 1000 g × 20 min.
Plasma frozen – 20°C
Extraction:
2 mL acetone + 1 mL plasma
1000 g × 30 min 4°C
Supernatant + 5 mL of petrol-ether
1000 g × 20 min 4°C
Freeze – 80°C
Throw nonfrozen upper phase
Evaporate lower phase to dryness
Store desiccated samples at – 20°C

TABLE 46.5 Arginine Vasopressin Measurements: Assay Procedure

Day 1	Assay set-up 400 μL/tube (200 μL sample or standard + 200 μL of antiserum or buffer). Incubation 80 hours, 4°C
Day 4	^{125}I-AVP 100 μL/tube 1000 cpm/tube. Incubation 72 hours, 4°C
Day 7	Separation dextran + charcoal

Data from ref. [247].

TABLE 46.6 Measurements of Arginine Vasopressin Levels in Pregnant Patients.

1,10-phenanthroline monohydrate (Sigma) solubilized with several drops of glacial acetic acid
0.1 mL/10 mL of blood

Plasma Sodium, Plasma, and Urine Osmolality

Measurements of plasma sodium, plasma, and urinary osmolality should be immediately available at various intervals during dehydration procedures. Plasma sodium is easily measured by flame photometry or with a sodium-specific electrode.[235] Plasma and urinary osmolalities are also reliably measured by freezing point depression instruments with a coefficient of variation at 290 mmol/kg of less than 1%.

At variance with published data,[229,217] we have found that plasma and serum osmolalities are equivalent (i.e., similar values are obtained). Blood taken in heparinized tubes is easier to handle, because the plasma can be more readily removed after centrifugation. The tube used (green-stoppered tube) contains a minuscule concentration of lithium and sodium, which does not interfere with plasma sodium or osmolality measurements. Frozen plasma or urinary samples can be kept for further analysis of their osmolalities, because the results obtained are similar to those obtained immediately after blood sampling, except in patients with severe renal failure. In the latter patients, plasma osmolality measurements are increased after freezing and thawing, but the plasma sodium values remain unchanged.

Plasma osmolality measurements can be used to demonstrate the absence of unusual osmotically active substances (e.g., glucose and urea in high concentrations, mannitol, ethanol).[236] With this information, plasma or serum sodium measurements are sufficient to assess the degree of dehydration and its relationship to plasma AVP. Nomograms describing the normal plasma sodium/plasma AVP relationship are equally as valuable as classic nomograms describing the relationship between plasma osmolality and effective osmolality (i.e., plasma osmolality minus the contribution of "ineffective" solutes: glucose and urea).

MAGNETIC RESONANCE IMAGING IN PATIENTS WITH DIABETES INSIPIDUS

Magnetic resonance imaging (MRI) permits visualization of the anterior and posterior pituitary glands and the pituitary stalk. The pituitary stalk is permeated by numerous capillary loops of the hypophyseal–portal blood system. This vascular structure also provides the principle blood supply to the anterior pituitary lobe, because there is no direct arterial supply to this organ. In contrast, the posterior pituitary lobe has a direct vascular supply. Therefore, the posterior lobe can be more rapidly visualized in a dynamic mode after administration of gadolinium (gadopentate dimeglumine) as contrast material during MRI. The posterior pituitary lobe is easily distinguished by a round, high-intensity signal (the posterior pituitary "bright spot") in the posterior part of the sella turcica on T1-weighted images. Loss of the pituitary hyperintense spot or bright spot on a T1-weighted MRI image reflects loss of functional integrity of the neurohypophysis, and is a non-specific indicator of neurohypophyseal diabetes insipidus regardless of the underlying cause.[97,237] It is now considered that the bright spot represents normal AVP storage in the posterior lobe of the pituitary, that the intensity is correlated with the amount of AVP, and that after 60 years of age the signal is often less intense, with irregularities in the normally smooth convex edge.[238,239] MRI is reported to be the best technique with which to evaluate the pituitary stalk and infundibulum in patients with idiopathic polyuria. A thickening or enlargement of the pituitary stalk may suggest an infiltrative process destroying the neurohypophyseal tract.[240]

TREATMENT

In most patients with complete hypothalamic diabetes insipidus, the thirst mechanism remains intact. Thus, hypernatremia does not develop in these patients, and they suffer only from the inconvenience associated with marked polyuria and polydipsia. If hypodipsia develops or access to water is limited, then severe hypernatremia can supervene. The treatment of choice for patients with severe hypothalamic diabetes insipidus is dDAVP, a synthetic, long-acting vasopressin analog with minimal vasopressor activity, but a large antidiuretic potency. The usual intranasal daily dose is between 5 and 20 mg. To avoid the potential complication of dilutional hyponatremia, which is exceptional in these patients as a result of an intact thirst mechanism, dDAVP can be withdrawn at regular intervals to allow the patients to become polyuric. Aqueous vasopressin (Pitressin) or dDAVP (4.0 mg/1 ml ampule) can be used intravenously in acute situations, such as after hypophysectomy or for the treatment of diabetes insipidus in the brain-dead organ donor. Pitressin tannate in oil and nonhormonal antidiuretic drugs are somewhat obsolete and now rarely used. For example, chlorpropamide (250–500 mg daily) appears to potentiate the antidiuretic action of circulating AVP, but troublesome side-effects of hypoglycemia and hyponatremia do occur.

The treatment of congenital NDI has been reviewed by Knoers and Monnens.[176] An abundant unrestricted water intake should always be provided, and affected patients should be carefully followed during their first years of life. Water should be offered every 2 hours day and night, and temperature, appetite, and growth should be monitored. The parents of these children easily accept setting their alarm clock every 2 hours during the night. Hospital admission may be necessary to allow continuous gastric feeding. A low-osmolar and low-sodium diet, hydrochlorothiazide (1–2 mg/kg/d) alone or with amiloride, and indomethacin (0.75–1.5 mg/kg) substantially reduce water excretion, and are helpful in the treatment of children. Many adult patients receive no treatment.

Acknowledgments

The author's work cited in this chapter was supported by the Canadian Institutes of Health Research, the Kidney Foundation of Canada, and the Fonds de la Recherche en Santé du Québec. We thank our co-workers, Marie-Françoise Arthus, Joyce Crumley, Mary Fujiwara, Michèle Lonergan, and Kenneth Morgan, and many colleagues who contributed families and ideas to our work.

References

[1] Richter D. Molecular events in the expression of vasopressin and oxytocin and their cognate receptors. Am J Physiol 1988;255:F207–19.

[2] Williams PD, Pettibone DJ. Recent advances in the development of oxytocin receptor antagonists. Curr Pharm Design 1996;2: 41–58.

[3] Bourque CW. Central mechanisms of osmosensation and systemic osmoregulation. Nat Rev Neurosci 2008;9:519–31.

[4] Lechner SG, Markworth S, Poole K, Smith ES, Lapatsina L, Frahm S, et al. The molecular and cellular identity of peripheral osmoreceptors. Neuron 2011;69:332–44.

[5] Burbach JP, Luckman SM, Murphy D, Gainer H. Gene regulation in the magnocellular hypothalamo–neurohypophysial system. Physiol Rev 2001;81:1197–267.

[6] Rao VV, Loffler C, Battey J, Hansmann I. The human gene for oxytocin-neurophysin I (OXT) is physically mapped to chromosome 20p13 by *in situ* hybridization. Cell Genet 1992;61:271–3.

[7] Sausville E, Carney D, Battey J. The human vasopressin gene is linked to the oxytocin gene and is selectively expressed in a cultured lung cancer cell line. J Biol Chem 1985;260:10236–41.

[8] Venkatesh B, Si-Hoe SL, Murphy D, Brenner S. Transgenic rats reveal functional conservation of regulatory controls between the Fugu isotocin and rat oxytocin genes. Proc Natl Acad Sci USA 1997;94:12462–6.

[9] Chen L, Rose JP, Breslow E, Yang D, Chang WR, Furey WFJ, et al. Crystal structure of a bovine neurophysin II dipeptide complex at 2.8 Angström determined from the single-wave length anomalous scattering signal of an incorporated iodine atom. Proc Natl Acad Sci USA 1991;88:4240–4.

[10] Swab D, Pool WC, Novelty F. Immunofluorescence of vasopressin and oxytocin in the rat hypothalamo–neurohypophyseal system. J Neural Transm 1975;36:195.

[11] Vandesande F, Dierickx K. Identification of the vasopressin producing and of the oxytocin producing neurons in the hypothalamic magnocellular neurosecretroy system of the rat. Cell Tissue Res 1975;164:153–62.

[12] Sofroniew M. Morphology of vasopressin and oxytocin neurones and their central and vascular projections, vol. 60. New York: Elsevier; 1983.

[13] Kalogeras KT, Nieman LN, Friedman TC, Doppman JL, Cutler GBJ, Chrousos GP, et al. Inferior petrosal sinus sampling in healthy human subjects reveals a unilateral corticotropin-releasing hormone-induced arginine vasopressin release associated with ipsilateral adrenocorticotropin secretion. J Clin Invest 1996;97:2045–50.

[14] Yanovski JA, Friedman TC, Nieman LK, Chrousos GP, Cutler Jr. GB, Doppman JL, et al. Inferior petrosal sinus AVP in patients with cushing's syndrome. Clin Endocrinol (Oxf) 1997;47:199–206.

[15] Edwards AM, Mann ME, Marfell-Jones MJ, Rankin DM, Noakes TD, Shillington DP. Influence of moderate dehydration on soccer performance: physiological responses to 45 min of outdoor match-play and the immediate subsequent performance of sport-specific and mental concentration tests. Br J Sports Med 2007;41:385–91.

[16] Saat M, Sirisinghe RG, Singh R, Tochihara Y. Effects of short-term exercise in the heat on thermoregulation, blood parameters, sweat secretion and sweat composition of tropic-dwelling subjects. J Physiol Anthropol Appl Human Sci 2005;24: 541–9.

[17] Shirreffs SM, Merson SJ, Fraser SM, Archer DT. The effects of fluid restriction on hydration status and subjective feelings in man. Br J Nutr 2004;91:951–8.

[18] Geelen G, Greenleaf JE, Keil LC. Drinking-induced plasma vasopressin and norepinephrine changes in dehydrated humans. J Clin Endocrinol Metab 1996;81:2131–5.

[19] Andersen LJ, Jensen TU, Bestle MH, Bie P. Gastrointestinal osmoreceptors and renal sodium excretion in humans. Am J Physiol Regul Integr Comp Physiol 2000;278:R287–94.

[20] Claybaugh JR, Sato AK, Crosswhite LK, Hassell LH. Effects of time of day, gender, and menstrual cycle phase on the human response to a water load. Am J Physiol Regul Integr Comp Physiol 2000;279:R966–73.
[21] Verney E. The antidiuretic hormone and the factors which determine its release. Proc R Soc London Ser B 1947;135:25–6.
[22] Ramsay DJ, Thrasher TN, Keil LC. The organum vasculosum laminae terminalis: a critical area for osmoreception. Prog Brain Res 1983;60:91–8.
[23] Ciura S, Bourque CW. Transient receptor potential vanilloid 1 is required for intrinsic osmoreception in organum vasculosum lamina terminalis neurons and for normal thirst responses to systemic hyperosmolality. J Neurosci 2006;26:9069–75.
[24] Denton DA, McKinley MJ, Weisinger RS. Hypothalamic integration of body fluid regulation. Proc Natl Acad Sci USA 1996;93:7397–404.
[25] Hollis JH, McKinley MJ, D'Souza M, Kampe J, Oldfield BJ. The trajectory of sensory pathways from the lamina terminalis to the insular and cingulate cortex: a neuroanatomical framework for the generation of thirst. Am J Physiol Regul Integr Comp Physiol 2008;294:R1390–401.
[26] Johnson AK. The sensory psychobiology of thirst and salt appetite. Med Sci Sports Exerc 2007;39:1388–400.
[27] McKinley MJ, Denton DA, Oldfield BJ, De Oliveira LB, Mathai ML. Water intake and the neural correlates of the consciousness of thirst. Semin Nephrol 2006;26:249–57.
[28] Ciura S, Liedtke W, Bourque CW. Hypertonicity sensing in organum vasculosum lamina terminalis neurons: a mechanical process involving TRPV1 but not TRPV4. J Neurosci 2011;31: 14669–76.
[29] Zhang Z, Bourque CW. Amplification of transducer gain by angiotensin II-mediated enhancement of cortical actin density in osmosensory neurons. J Neurosci 2008;28:9536–44.
[30] Robertson GL, Athar S. The interaction of blood osmolality and blood volume in regulating plasma vasopressin in man. J Clin Endocrinol Metab 1976;42:613–20.
[31] Zerbe RL, Robertson GL. Disorders of ADH. Med North Am 1984;13:1570.
[32] Miller M, Dalakos T, Moses AM, Fellerman H, Streeten DH. Recognition of partial defects in antidiuretic hormone secretion. Ann Intern Med 1970;73:721–9.
[33] Bichet DG, Kluge R, Howard RL, Schrier RW. Hyponatremic states. In: Seldin DW, Giebisch G, editors. The kidney: physiology and pathophysiology. 2nd ed. New York: Raven Press; 1992. p. 1727–51.
[34] Baylis PH, Gaskill MB, Robertson GL. Vasopressin secretion in primary polydipsia and cranial diabetes insipidus. Q J Med 1981;50:345–58.
[35] Sharif Naeini R, Witty MF, Seguela P, Bourque CW. An N-terminal variant of Trpv1 channel is required for osmosensory transduction. Nat Neurosci 2006;9:93–8.
[36] Taylor AC, McCarthy JJ, Stocker SD. Mice lacking the transient receptor vanilloid potential 1 channel display normal thirst responses and central Fos activation to hypernatremia. Am J Physiol Regul Integr Comp Physiol 2008;294:R1285–93.
[37] McHugh J, Keller NR, Appalsamy M, Thomas SA, Raj SR, Diedrich A, et al. Portal osmopressor mechanism linked to transient receptor potential vanilloid 4 and blood pressure control. Hypertension 2010;55:1438–43.
[38] Boschmann M, Steiniger J, Franke G, Birkenfeld AL, Luft FC, Jordan J. Water drinking induces thermogenesis through osmosensitive mechanisms. J Clin Endocrinol Metab 2007;92: 3334–7.
[39] Tank J, Schroeder C, Stoffels M, Diedrich A, Sharma AM, Luft FC, et al. Pressor effect of water drinking in tetraplegic patients may be a spinal reflex. Hypertension 2003;41:1234–9.
[40] Jordan J, Shannon JR, Black BK, Ali Y, Farley M, Costa F, et al. The pressor response to water drinking in humans: a sympathetic reflex? Circulation 2000;101:504–9.
[41] Schroeder C, Bush VE, Norcliffe LJ, Luft FC, Tank J, Jordan J, et al. Water drinking acutely improves orthostatic tolerance in healthy subjects. Circulation 2002;106:2806–11.
[42] Shannon JR, Diedrich A, Biaggioni I, Tank J, Robertson RM, Robertson D, et al. Water drinking as a treatment for orthostatic syndromes. Am J Med 2002;112:355–60.
[43] Claydon VE, Schroeder C, Norcliffe LJ, Jordan J, Hainsworth R. Water drinking improves orthostatic tolerance in patients with posturally related syncope. Clin Sci (Lond) 2006;110:343–52.
[44] Stookey JD, Constant F, Popkin BM, Gardner CD. Drinking water is associated with weight loss in overweight dieting women independent of diet and activity. Obesity (Silver Spring) 2008;16:2481–8.
[45] Coste B, Mathur J, Schmidt M, Earley TJ, Ranade S, Petrus MJ, et al. Piezo1 and Piezo2 are essential components of distinct mechanically activated cation channels. Science 2010;330: 55–60.
[46] Huber D, Veinante P, Stoop R. Vasopressin and oxytocin excite distinct neuronal populations in the central amygdala. Science 2005;308:245–8.
[47] Insel TR, Young LJ. The neurobiology of attachment. Nat Rev Neurosci 2001;2:129–36.
[48] Jard S. Mechanisms of action of vasopressin and vasopressin antagonists. Kidney Int Suppl 1988;26:S38–42.
[49] Nathanson MH, Moyer MS, Burgstahler AD, O'Carroll AM, Brownstein MJ, Lolait SJ. Mechanisms of subcellular cytosolic Ca^{2+} signaling evoked by stimulation of the vasopressin V1a receptor. J Biol Chem 1992;267:23282–9.
[50] Murata K, Mitsuoka K, Hirai T, Walz T, Agre P, Heymann JB, et al. Structural determinants of water permeation through aquaporin-1. Nature 2000;407:599–605.
[51] Tajkhorshid E, Nollert P, Jensen MO, Miercke LJ, O'Connell J, Stroud RM, et al. Control of the selectivity of the aquaporin water channel family by global orientational tuning. Science 2002;296:525–30.
[52] Ragnarsson U. The nobel trail of vincent du vigneaud. J Pept Sci 2007;13:431–3.
[53] Birnbaumer M, Seibold A, Gilbert S, Ishido M, Barberis C, Antaramian A, et al. Molecular cloning of the receptor for human antidiuretic hormone. Nature 1992;357:333–5.
[54] Seibold A, Brabet P, Rosenthal W, Birnbaumer M. Structure and chromosomal localization of the human antidiuretic hormone receptor gene. Am J Hum Genet 1992;51:1078–83.
[55] Raju TN. The Nobel chronicles. 1994: Alfred G Gilman (b 1941) and Martin Rodbell (1925–98). Lancet 2000;355:2259.
[56] Raju TN. The Nobel chronicles. 1971: Earl Wilbur Sutherland, Jr. (1915–74). Lancet 1999;354:961.
[57] Rehmann H, Wittinghofer A, Bos JL. Capturing cyclic nucleotides in action: snapshots from crystallographic studies. Nat Rev Mol Cell Biol 2007;8:63–73.
[58] Boone M, Deen PM. Physiology and pathophysiology of the vasopressin-regulated renal water reabsorption. Pflugers Arch 2008;456:1005–24.
[59] Nedvetsky PI, Tamma G, Beulshausen S, Valenti G, Rosenthal W, Klussmann E. Regulation of aquaporin-2 trafficking. Handb Exp Pharmacol 2009;:133–57.
[60] Nielsen S, Frokiaer J, Marples D, Kwon TH, Agre P, Knepper MA. Aquaporins in the kidney: from molecules to medicine. Physiol Rev 2002;82:205–44.
[61] Fenton RA, Shodeinde A, Knepper MA. UT-A urea transporter promoter, UT-A alpha, targets principal cells of the renal inner medullary collecting duct. Am J Physiol Renal Physiol 2006;290: F188–95.

[62] Ward DT, Hammond TG, Harris HW. Modulation of vasopressin-elicited water transport by trafficking of aquaporin2-containing vesicles. Annu Rev Physiol 1999;61:683–97.
[63] Morishita T, Tsutsui M, Shimokawa H, Sabanai K, Tasaki H, Suda O, et al. Nephrogenic diabetes insipidus in mice lacking all nitric oxide synthase isoforms. Proc Natl Acad Sci USA 2005;102:10616–21.
[64] Olesen ET, Rutzler MR, Moeller HB, Praetorius HA, Fenton RA. Vasopressin-independent targeting of aquaporin-2 by selective E-prostanoid receptor agonists alleviates nephrogenic diabetes insipidus. Proc Natl Acad Sci USA 2011;108:12949–54.
[65] Valtin H, North WG, Edwards BR, Gellai M. Animal models of diabetes insipidus. Front Horm Res 1985;13:105–26.
[66] Schmale H, Richter D. Single base deletion in the vasopressin gene is the cause of diabetes insipidus in Brattleboro rats. Nature 1984;308:705–9.
[67] Richter D. Reflections on central diabetes insipidus: retrospective and perspectives. In: Gross P, Richter D, Robertson GL, editors. Vasopressin. Paris: John Libbey Eurotext; 1993. p. 3–14.
[68] Schmale H, Bahnsen U, Fehr S, Nahke D, Richter D, editors. Hereditary diabetes insipidus in man and rat. Paris: John Libbey Eurotext; 1991.
[69] Serradeil-Le Gal C, Lacour C, Valette G, Garcia G, Foulon L, Galindo G, et al. Characterization of SR 121463A, a highly potent and selective, orally active vasopressin V2 receptor antagonist. J Clin Invest 1996;98:2729–38.
[70] Jean-Alphonse F, Perkovska S, Frantz MC, Durroux T, Mejean C, Morin D, et al. Biased agonist pharmacochaperones of the AVP V2 receptor may treat congenital nephrogenic diabetes insipidus. J Am Soc Nephrol 2009;20:2190–203.
[71] Evans DA, De Bree FM, Nijenhuis M, Van Der Kleij AA, Zalm R, Korteweg N, et al. Processing of frameshifted vasopressin precursors. J Neuroendocrinol 2000;12:685–93.
[72] Balment RJ, Brimble MJ, Forsling ML. Oxytocin release and renal actions in normal and Brattleboro rats. Ann NY Acad Sci US 1982;394:241–53.
[73] Chou CL, DiGiovanni SR, Luther A, Lolait SJ, Knepper MA. Oxytocin as an antidiuretic hormone II. Role of V2 vasopressin receptor. Am J Physiol 269 (Renal Fluid Electrolyte Physiol 1995;38:F78–85.
[74] Chou CL, Knepper MA, Hoek AN, Brown D, Yang B, Ma T, et al. Reduced water permeability and altered ultrastructure in thin descending limb of Henle in aquaporin-1 null mice. J Clin Invest 1999;103:491–6.
[75] Lopez-Rodriguez C, Antos CL, Shelton JM, Richardson JA, Lin F, Novobrantseva TI, et al. Loss of NFAT5 results in renal atrophy and lack of tonicity-responsive gene expression. Proc Natl Acad Sci USA 2004;101:2392–7.
[76] Ma T, Song Y, Yang B, Gillespie A, Carlson EJ, Epstein CJ, et al. Nephrogenic diabetes insipidus in mice lacking aquaporin-3 water channels. Proc Natl Acad Sci USA 2000;97:4386–91.
[77] Ma T, Yang B, Gillespie A, Carlson EJ, Epstein CJ, Verkman AS. Generation and phenotype of a transgenic knockout mouse lacking the mercurial-insensitive water channel aquaporin-4. J Clin Invest 1997;100:957–62.
[78] Ma T, Yang B, Gillespie A, Carlson EJ, Epstein CJ, Verkman AS. Severely impaired urinary concentrating ability in transgenic mice lacking aquaporin-1 water channels. J Biol Chem 1998;273:4296–9.
[79] Matsumura Y, Uchida S, Kondo Y, Miyazaki H, Ko SB, Hayama A, et al. Overt nephrogenic diabetes insipidus in mice lacking the CLC-K1 chloride channel. Nat Genet 1999;21:95–8.
[80] Okubo S, Niimura F, Matsusaka T, Fogo A, Hogan BL, Ichikawa I. Angiotensinogen gene null-mutant mice lack homeostatic regulation of glomerular filtration and tubular reabsorption. Kidney Int 1998;53:617–25.
[81] Takahashi N, Chernavvsky DR, Gomez RA, Igarashi P, Gitelman HJ, Smithies O. Uncompensated polyuria in a mouse model of Bartter's syndrome. Proc Natl Acad Sci USA 2000;97:5434–9.
[82] Yang B, Gillespie A, Carlson EJ, Epstein CJ, Verkman AS. Neonatal mortality in an aquaporin-2 knock-in mouse model of recessive nephrogenic diabetes insipidus. J Biol Chem 2001;276:2775–9.
[83] Yun J, Schoneberg T, Liu J, Schulz A, Ecelbarger CA, Promeneur D, et al. Generation and phenotype of mice harboring a nonsense mutation in the V2 vasopressin receptor gene. J Clin Invest 2000;106:1361–71.
[84] Preston GM, Smith BL, Zeidel ML, Moulds JJ, Agre P. Mutations in aquaporin-1 in phenotypically normal humans without functional CHIP water channels. Science 1994;265:1585–7.
[85] Yang B, Zhao D, Qian L, Verkman AS. Mouse model of inducible nephrogenic diabetes insipidus produced by floxed aquaporin-2 gene deletion. Am J Physiol Renal Physiol 2006;291:F465–72.
[86] Mulders SB, Knoers NVAM, van Lieburg AF, Monnens LAH, Leumann E, Wühl E, et al. New mutations in the AQP2 gene in nephrogenic diabetes insipidus resulting in functional but misrouted water channels. J Am Soc Nephrol 1997;8:242–8.
[87] Li JH, Chou CL, Li B, Gavrilova O, Eisner C, Schnermann J, et al. A selective EP4 PGE2 receptor agonist alleviates disease in a new mouse model of X-linked nephrogenic diabetes insipidus. J Clin Invest 2009;119:3115–26.
[88] Rao S, Verkman AS. Analysis of organ physiology in transgenic mice. Am J Physiol Cell Physiol 2000;279:C1–18.
[89] Lloyd DJ, Hall FW, Tarantino LM, Gekakis N. Diabetes insipidus in mice with a mutation in aquaporin-2. PLoS Genet 2005;1:e20.
[90] McDill BW, Li SZ, Kovach PA, Ding L, Chen F. Congenital progressive hydronephrosis (cph) is caused by an S256L mutation in aquaporin-2 that affects its phosphorylation and apical membrane accumulation. Proc Natl Acad Sci USA 2006;103:6952–7.
[91] Moeller HB, Olesen ET, Fenton RA. Regulation of the water channel aquaporin-2 by posttranslational modification. Am J Physiol Renal Physiol 2011;300:F1062–73.
[92] Verbalis JG, Robinson AG, Moses AM, editors. Postoperative and post-traumatic diabetes insipidus, vol. 13. Basel: S. Karger; 1985.
[93] Olson BR, Gumowski J, Rubino D, Oldfield EH. Pathophysiology of hyponatremia after transsphenoidal pituitary surgery. J Neurosurg 1997;87:499–507.
[94] Nemergut EC, Zuo Z, Jane Jr. JA, Laws Jr. ER. Predictors of diabetes insipidus after transsphenoidal surgery: a review of 881 patients. J Neurosurg 2005;103:448–54.
[95] Czernichow P, Pomarede R, Brauner R, editors. Neurogenic diabetes insipidus in children, vol. 13. Basel: S. Karger; 1985.
[96] Greger NG, Kirkland RT, Clayton GW, Kirkland JL. Central diabetes insipidus. 22 years' experience. Am J Dis Child 1986;140:551–4.
[97] Maghnie M, Cosi G, Genovese E, Manca-Bitti ML, Cohen A, Zecca S, et al. Central diabetes insipidus in children and young adults. N Engl J Med 2000;343:998–1007.
[98] Moses AM, Blumenthal SA, Streeten DH, editors. Acid–base and electrolyte disorders associated with endocrine disease: pituitary and thyroid. New York: Churchill Livingstone; 1985.

[99] Fery F, Plat L, van de Borne P, Cogan E, Mockel J. Impaired counterregulation of glucose in a patient with hypothalamic sarcoidosis. N Engl J Med 1999;340:852–6.
[100] Odell WD, Doggett RS. Xanthoma disseminatum, a rare cause of diabetes insipidus. J Clin Endocrinol Metab 1993;76:777–80.
[101] Masera N, Grant DB, Stanhope R, Preece MA. Diabetes insipidus with impaired osmotic regulation in septo-optic dysplasia and agenesis of the corpus callosum. Arch Dis Child 1994;70:51–3.
[102] Imura H, Nakao K, Shimatsu A, Ogawa Y, Sando T, Fujisawa I, et al. Lymphocytic infundibuloneurohypophysitis as a cause of central diabetes insipidus. N Engl J Med 1993;329:683–9.
[103] Ahmed SR, Aiello DP, Page R, Hopper K, Towfighi J, Santen RJ. Necrotizing infundibulo-hypophysitis: a unique syndrome of diabetes insipidus and hypopituitarism. J Clin Endocrinol Metab 1993;76:1499–504.
[104] Lacombe UL. De la polydipsie. Thesis of Medicine, no. 99. Imprimerie et Fonderie de Rignoux. Paris; 1841.
[105] Weil A. Ueber die hereditare form des diabetes insipidus. Archives fur Pathologische Anatomie und Physiologie and fur Klinische Medicine (Virchow's Archives) 1884;95:70–95.
[106] Camerer JW. Eine ergänzung des Weilschen diabetes-insipidus-stammbaumes. Archiv für Rassen-und Gesellschaftshygiene Biologie 1935;28:382–5.
[107] Dölle W. Eine weitere ergänzung des Weilschen diabetes-insipidus-stammbaumes. Zeitschrift für Menschliche Vererbungs- und Konstitutionslehre 1951;30:372–4.
[108] Weil A. Ueber die hereditare form des diabetes insipidus. Deutches Archiv fur Klinische Medizin 1908;93:180–290.
[109] McKusick VA. Mendelian inheritance in man and its online version, OMIM. Am J Hum Genet 2007;80:588–604.
[110] Rittig R, Robertson GL, Siggaard C, Kovacs L, Gregersen N, Nyborg J, et al. Identification of 13 new mutations in the vasopressin-neurophysin II gene in 17 kindreds with familial autosomal dominant neurohypophyseal diabetes insipidus. Am J Hum Genet 1996;58:107–17.
[111] Brachet C, Birk J, Christophe C, Tenoutasse S, Velkeniers B, Heinrichs C, et al. Growth retardation in untreated autosomal dominant familial neurohypophyseal diabetes insipidus caused by one recurring and two novel mutations in the vasopressin-neurophysin II gene. Eur J Endocrinol 2011;164: 179–87.
[112] Birk J, Friberg MA, Prescianotto-Baschong C, Spiess M, Rutishauser J. Dominant pro-vasopressin mutants that cause diabetes insipidus form disulfide-linked fibrillar aggregates in the endoplasmic reticulum. J Cell Sci 2009;122:3994–4002.
[113] Castino R, Davies J, Beaucourt S, Isidoro C, Murphy D. Autophagy is a prosurvival mechanism in cells expressing an autosomal dominant familial neurohypophyseal diabetes insipidus mutant vasopressin transgene. FASEB J 2005;19:1021–3.
[114] Abu Libdeh A, Levy-Khademi F, Abdulhadi-Atwan M, Bosin E, Korner M, White PC, et al. Autosomal recessive familial neurohypophyseal diabetes insipidus: onset in early infancy. Eur J Endocrinol 2009;162:221–6.
[115] Christensen JH, Kvistgaaard H, Knudsen J, Shaikh G, Tolmie J, Cooke S, et al. A novel deletion partly removing the avp gene causes autosomal recessive inheritance of early onset neurohypophyseal diabetes insipidus. Clin Genet 2011; epub ahead of print
[116] Willcutts MD, Felner E, White PC. Autosomal recessive familial neurohypophyseal diabetes insipidus with continued secretion of mutant weakly active vasopressin. Hum Mol Genet 1999;8:1303–7.
[117] Bichet DG, Arthus M-F, Lonergan M, Morgan K, Fujiwara TM. Hereditary central diabetes insipidus: Autosomal dominant and autosomal recessive phenotypes due to mutations in the *prepro-AVP-NPII* gene. J Am Soc Nephrol 1998;9:386A.
[118] Christensen JH, Siggaard C, Corydon TJ, Robertson GL, Gregersen N, Bolund L, et al. Differential cellular handling of defective arginine vasopressin (AVP) prohormones in cells expressing mutations of the AVP gene associated with autosomal dominant and recessive familial neurohypophyseal diabetes insipidus. J Clin Endocrinol Metab 2004;89:4521–31.
[119] Beuret N, Stettler H, Renold A, Rutishauser J, Spiess M. Expression of regulated secretory proteins is sufficient to generate granule-like structures in constitutively secreting cells. J Biol Chem 2004;279:20242–9.
[120] Cohen FE, Kelly JW. Therapeutic approaches to protein-misfolding diseases. Nature 2003;426:905–9.
[121] Ulloa-Aguirre A, Janovick JA, Brothers SP, Conn PM. Pharmacologic rescue of conformationally-defective proteins: implications for the treatment of human disease. Traffic 2004;5:821–37.
[122] Welch WJ, Howard M. Antagonists to the rescue. J Clin Invest 2000;105:853–4.
[123] Kennan A, Aherne A, Humphries P. Light in retinitis pigmentosa. Trends Genet 2005;21:103–10.
[124] Domenech E, Gomez-Zaera M, Nunes V. Study of the WFS1 gene and mitochondrial DNA in Spanish Wolfram syndrome families. Clin Genet 2004;65:463–9.
[125] Takeda K, Inoue H, Tanizawa Y, Matsuzaki Y, Oba J, Watanabe Y, et al. WFS1 (Wolfram syndrome 1) gene product: predominant subcellular localization to endoplasmic reticulum in cultured cells and neuronal expression in rat brain. Hum Mol Genet 2001;10:477–84.
[126] Ishihara H, Takeda S, Tamura A, Takahashi R, Yamaguchi S, Takei D, et al. Disruption of the WFS1 gene in mice causes progressive beta-cell loss and impaired stimulus-secretion coupling in insulin secretion. Hum Mol Genet 2004;13: 1159–70.
[127] Conlan AR, Axelrod HL, Cohen AE, Abresch EC, Zuris J, Yee D, et al. Crystal structure of Miner1: the redox-active 2Fe-2S protein causative in Wolfram Syndrome 2. J Mol Biol 2009;392:143–53.
[128] Fonseca SG, Ishigaki S, Oslowski CM, Lu S, Lipson KL, Ghosh R, et al. Wolfram syndrome 1 gene negatively regulates ER stress signaling in rodent and human cells. J Clin Invest 2010;120:744–55.
[129] Howard RL, Bichet DG, Schrier RW. Hypernatremic and polyuric states. In: Seldin DW, Giebisch G, editors. The kidney: physiology and pathophysiology. 2nd ed. New York: Raven Press, Ltd; 1992. p. 1753–78.
[130] Fujiwara TM, Bichet DG. Molecular biology of hereditary diabetes insipidus. J Am Soc Nephrol 2005;16:2836–46.
[131] Arthus M-F, Lonergan M, Crumley MJ, Naumova AK, Morin D, De Marco L, et al. Report of 33 novel *AVPR2* mutations and analysis of 117 families with X-linked nephrogenic diabetes insipidus. J Am Soc Nephrol 2000;11:1044–54.
[132] Nomura Y, Onigata K, Nagashima T, Yutani S, Mochizuki H, Nagashima K, et al. Detection of skewed X-inactivation in two female carriers of vasopressin type 2 receptor gene mutation. J Clin Endocrinol Metab 1997;82:3434–7.
[133] Crawford JD, Bode HH. Disorders of the posteriorpituitary in children. In: Gardner LI, editor. Endocrine and genetic diseases of childhood and adolescence. 2nd ed. Philadelphia: W.B. Saunders; 1975. p. 126–58.
[134] Forssman H. On the mode of hereditary transmission in diabetes insipidus. Nordisk Medicine 1942;16:3211–3.
[135] Waring AG, Kajdi L, Tappan V. Congenital defect of water metabolism. Am J Dis Child 1945;69:323–5.

[136] Williams RM, Henry C. Nephrogenic diabetes insipidus transmitted by females and appearing during infancy in males. Ann Int Med 1947;27:84–95.
[137] Niaudet P, Dechaux M, Trivin C, Loirat C, Broyer M. Nephrogenic diabetes insipidus: clinical and pathophysiological aspects. Adv Nephrol Necker Hosp 1984;13:247–60.
[138] McIlraith CH. Notes on some cases of diabetes insipidus with marked family and hereditary tendencies. Lancet 1892;2: 767–8.
[139] Reeves WB, Andreoli TE. Nephrogenic diabetes insipidus. In: Scriver CR, Beaudet AL, Sly WS, Valle D, editors. The metabolic basis of inherited disease. 7th ed. New York: McGraw-Hill; 1995. p. 3045–71.
[140] Streitz JMJ, Streitz JM. Polyuric urinary tract dilatation with renal damage. J Urol 1988;139:784–5.
[141] Boyd SD, Raz S, Ehrlich RM. Diabetes insipidus and nonobstructive dilatation of urinary tract. Urology 1980;16:266–9.
[142] Gautier B, Thieblot P, Steg A. Mégauretère, mégavessie et diabète insipide familial. Sem Hop 1981;57:60–1.
[143] Bichet DG, Razi M, Arthus M-F, Lonergan M, Tittley P, Smiley RK, et al. Epinephrine and dDAVP administration in patients with congenital nephrogenic diabetes insipidus. Evidence for a pre-cyclic AMP V2 receptor defective mechanism. Kidney Int 1989;36:859–66.
[144] Bichet DG, Hendy GN, Lonergan M, Arthus M-F, Ligier S, Pausova Z, et al. X-linked nephrogenic diabetes insipidus: from the ship hopewell to restriction fragment length polymorphism studies. Am J Hum Genet 1992;51:1089–102.
[145] Kambouris M, Dlouhy SR, Trofatter JA, Conneally PM, Hodes ME. Localization of the gene for X-linked nephrogenic diabetes insipidus to Xq28. Am J Med Genet 1988;29:239–46.
[146] Knoers N, van der Heyden H, van Oost BA, Monnens L, Willems J, Ropers HH. Three-point linkage analysis using multiple DNA polymorphic markers in families with X-linked nephrogenic diabetes insipidus. Genomics 1989;4:434–7.
[147] van den Ouweland AM, Knoop MT, Knoers VV, Markslag PW, Rocchi M, Warren ST, et al. Colocalization of the gene for nephrogenic diabetes insipidus (DIR) and the vasopressin type 2 receptor gene (AVPR2) in the Xq28 region. Genomics 1992;13:1350–2.
[148] Goldman MB, Luchins DJ, Robertson GL. Mechanisms of altered water metabolism in psychotic patients with polydipsia and hyponatremia. N Engl J Med 1988;318:397–403.
[149] Babey M, Kopp P, Robertson GL. Familial forms of diabetes insipidus: clinical and molecular characteristics. Nat Rev Endocrinol 2011;7:701–14.
[150] Spanakis E, Milord E, Gragnoli C. AVPR2 variants and mutations in nephrogenic diabetes insipidus: review and missense mutation significance. J Cell Physiol 2008;217:605–17.
[151] Bichet DG, Fujiwara TM. Nephrogenic diabetes insipidus. In: Scriver CR, Beaudet AL, Sly WS, editors. The metabolic and molecular basis of inherited disease. New York: McGraw Hill; 2001. p. 4181–204.
[152] Bichet DG, Arthus M-F, Lonergan M, Hendy GN, Paradis AJ, Fujiwara TM, et al. X-linked nephrogenic diabetes insipidus mutations in North America and the Hopewell hypothesis. J Clin Invest 1993;92:1262–8.
[153] Shalev H, Romanovsky I, Knoers NV, Lupa S, Landau D. Bladder function impairment in aquaporin-2 defective nephrogenic diabetes insipidus. Nephrol Dial Transplant 2004;19: 608–13.
[154] Ulinski T, Grapin C, Forin V, Vargas-Poussou R, Deschenes G, Bensman A. Severe bladder dysfunction in a family with ADH receptor gene mutation responsible for X-linked nephrogenic diabetes insipidus. Nephrol Dial Transplant 2004;19:2928–9.
[155] Hobbs HH, Russell DW, Brown MS, Goldstein JL. The LDL receptor locus in familial hypercholesterolemia: mutational analysis of a membrane protein. Annu Rev Genet 1990;24: 133–70.
[156] Bernier V, Lagace M, Lonergan M, Arthus MF, Bichet DG, Bouvier M. Functional rescue of the constitutively internalized V2 vasopressin receptor mutant R137H by the pharmacological chaperone action of SR49059. Mol Endocrinol 2004;18:2074–84.
[157] Hermosilla R, Oueslati M, Donalies U, Schonenberger E, Krause E, Oksche A, et al. Disease-causing V(2) vasopressin receptors are retained in different compartments of the early secretory pathway. Traffic 2004;5:993–1005.
[158] Morello JP, Salahpour A, Laperrière A, Bernier V, Arthus M-F, Lonergan M, et al. Pharmacological chaperones rescue cell-surface expression and function of misfolded V2 vasopressin receptor mutants. J Clin Invest 2000;105:887–95.
[159] Wuller S, Wiesner B, Loffler A, Furkert J, Krause G, Hermosilla R, et al. Pharmacochaperones post-translationally enhance cell surface expression by increasing conformational stability of wild-type and mutant vasopressin V2 receptors. J Biol Chem 2004;279:47254–63.
[160] Schoneberg T, Schulz A, Biebermann H, Hermsdorf T, Rompler H, Sangkuhl K. Mutant G-protein-coupled receptors as a cause of human diseases. Pharmacol Ther 2004;104: 173–206.
[161] Romisch K. A cure for traffic jams: small molecule chaperones in the endoplasmic reticulum. Traffic 2004;5:815–20.
[162] Tamarappoo BK, Verkman AS. Defective aquaporin-2 trafficking in nephrogenic diabetes insipidus and correction by chemical chaperones. J Clin Invest 1998;101:2257–67.
[163] Kunchaparty S, Palcso M, Berkman J, Velazquez H, Desir GV, Bernstein P, et al. Defective processing and expression of thiazide-sensitive Na-Cl co-transporter as a cause of Gitelman's syndrome. Am J Physiol 1999;277:F643–9.
[164] Hayama A, Rai T, Sasaki S, Uchida S. Molecular mechanisms of Bartter syndrome caused by mutations in the BSND gene. Histochem Cell Biol 2003;119:485–93.
[165] Peters M, Ermert S, Jeck N, Derst C, Pechmann U, Weber S, et al. Classification and rescue of ROMK mutations underlying hyperprostaglandin E syndrome/antenatal Bartter syndrome. Kidney Int 2003;64:923–32.
[166] Chillaron J, Estevez R, Samarzija I, Waldegger S, Testar X, Lang F, et al. An intracellular trafficking defect in type I cystinuria rBAT mutants M467T and M467K. J Biol Chem 1997;272: 9543–9.
[167] Bonnardeaux A, Bichet DG. Inherited disorders of the renal tubule. In: 9th ed. Taal MW, Marsden PA, Skorecki K, Yu ASL, Brenner BM, editors. Brenner & rector's the kidney, vol. 2. Philadelphia: Elsevier Saunders; 2012. p. 1584–625.
[168] Lomas DA, Evans DL, Finch JT, Carrell RW. The mechanism of Z alpha 1-antitrypsin accumulation in the liver. Nature 1992;357:605–7.
[169] Lawless MW, Greene CM, Mulgrew A, Taggart CC, O'Neill SJ, McElvaney NG. Activation of endoplasmic reticulum-specific stress responses associated with the conformational disease Z alpha 1-antitrypsin deficiency. J Immunol 2004;172:5722–6.
[170] Barak LS, Oakley RH, Laporte SA, Caron MG. Constitutive arrestin-mediated desensitization of a human vasopressin receptor mutant associated with nephrogenic diabetes insipidus. Proc Natl Acad Sci USA 2001;98:93–8.
[171] Robben JH, Kortenoeven ML, Sze M, Yae C, Milligan G, Oorschot VM, et al. Intracellular activation of vasopressin V2 receptor mutants in nephrogenic diabetes insipidus by nonpeptide agonists. Proc Natl Acad Sci USA 2009;106:12195–200.

[172] Glover DJ, Lipps HJ, Jans DA. Towards safe, non-viral therapeutic gene expression in humans. Nat Rev Genet 2005;6: 299–310.
[173] Sangkuhl K, Schulz A, Rompler H, Yun J, Wess J, Schoneberg T. Aminoglycoside-mediated rescue of a disease-causing nonsense mutation in the V2 vasopressin receptor gene *in vitro* and *in vivo*. Hum Mol Genet 2004;13:893–903.
[174] Mankin AS, Liebman SW. Baby, don't stop!. Nat Genet 1999;23:8–10.
[175] Brenner B, Seligsohn U, Hochberg Z. Normal response of factor VIII and von Willebrand factor to 1-deamino-8D-arginine vasopressin in nephrogenic diabetes insipidus. J Clin Endocrinol Metab 1988;67:191–3.
[176] Knoers N, Monnens LA. A variant of nephrogenic diabetes insipidus: V2 receptor abnormality restricted to the kidney. Eur J Pediatr 1991;150:370–3.
[177] Langley JM, Balfe JW, Selander T, Ray PN, Clarke JT. Autosomal recessive inheritance of vasopressin-resistant diabetes insipidus. Am J Med Genet 1991;38:90–4.
[178] Deen PM, Verdijk MA, Knoers NV, Wieringa B, Monnens LA, van Os CH, et al. Requirement of human renal water channel aquaporin-2 for vasopressin-dependent concentration of urine. Science 1994;264:92–5.
[179] Agre P. Aquaporin water channels (Nobel Lecture). Angew Chem Int Ed Engl 2004;43:4278–90.
[180] Kamsteeg EJ, Bichet DG, Konings IB, Nivet H, Lonergan M, Arthus MF, et al. Reversed polarized delivery of an aquaporin-2 mutant causes dominant nephrogenic diabetes insipidus. J Cell Biol 2003;163:1099–109.
[181] Kuwahara M, Iwai K, Ooeda T, Igarashi T, Ogawa E, Katsushima Y, et al. Three families with autosomal dominant nephrogenic diabetes insipidus caused by aquaporin-2 mutations in the C-terminus. Am J Hum Genet 2001;69:738–48.
[182] Marr N, Bichet DG, Lonergan M, Arthus MF, Jeck N, Seyberth HW, et al. Heteroligomerization of an Aquaporin-2 mutant with wild-type Aquaporin-2 and their misrouting to late endosomes/lysosomes explains dominant nephrogenic diabetes insipidus. Hum Mol Genet 2002;11:779–89.
[183] Mulders SM, Bichet DG, Rijss JPL, Kamsteeg E-J, Arthus M-F, Lonergan M, et al. An aquaporin-2 water channel mutant which causes autosomal dominant nephrogenic diabetes insipidus is retained in the Golgi complex. J Clin Invest 1998;102:57–66.
[184] Robertson GL, Kopp P. A novel dominant mutation of the aquaporin-2 gene resulting in partial nephrogenic diabetes insipidus. Global Conference Proceedings, NDI Foundation; April 26–28, 2002:7A.
[185] de Mattia F, Savelkoul PJ, Bichet DG, Kamsteeg EJ, Konings IB, Marr N, et al. A novel mechanism in recessive nephrogenic diabetes insipidus: wild-type aquaporin-2 rescues the apical membrane expression of intracellularly retained AQP2-P262L. Hum Mol Genet 2004;13:3045–56.
[186] Sohara E, Rai T, Yang SS, Uchida K, Nitta K, Horita S, et al. Pathogenesis and treatment of autosomal-dominant nephrogenic diabetes insipidus caused by an aquaporin 2 mutation. Proc Natl Acad Sci USA 2006;103:14217–22.
[187] Bichet DG. Nephrogenic diabetes insipidus: new developments. Nephrol Self-Assessment Progr 2004;3:187–91.
[188] Bichet DG, Fujiwara TM. Reabsorption of sodium chloride – lessons from the chloride channels. N Engl J Med 2004;350: 1281–3.
[189] Jeck N, Schlingmann KP, Reinalter SC, Komhoff M, Peters M, Waldegger S, et al. Salt handling in the distal nephron: lessons learned from inherited human disorders. Am J Physiol Regul Integr Comp Physiol 2005;288:R782–95.
[190] Peters M, Jeck N, Reinalter S, Leonhardt A, Tonshoff B, Klaus GG, et al. Clinical presentation of genetically defined patients with hypokalemic salt-losing tubulopathies. Am J Med 2002;112:183–90.
[191] Marek S, Tekesin I, Hellmeyer L, Komhoff M, Seyberth HW, Maier RF, et al. [Differential diagnosis of a polyhydramnion in hyperprostaglandin E syndrome: a case report]. Z Geburtshilfe Neonatol 2004;208:232–5.
[192] Gahl WA, Thoene JG, Schneider JA. Cystinosis. N Engl J Med 2002;347:111–21.
[193] Bockenhauer D, van't Hoff W, Dattani M, Lehnhardt A, Subtirelu M, Hildebrandt F, et al. Secondary nephrogenic diabetes insipidus as a complication of inherited renal diseases. Nephron Physiol 2010;116:p23–9.
[194] Boton R, Gaviria M, Batlle DC. Prevalence, pathogenesis, and treatment of renal dysfunction associated with chronic lithium therapy. Am J Kidney Dis 1987;10:329–45.
[195] Christensen S, Kusano E, Yusufi AN, Murayama N, Dousa TP. Pathogenesis of nephrogenic diabetes insipidus due to chronic administration of lithium in rats. J Clin Invest 1985;75:1869–79.
[196] Cogan E, Svoboda M, Abramow M. Mechanisms of lithium-vasopressin interaction in rabbit cortical collecting tubule. Am J Physiol 1987;252:F1080–7.
[197] Grunfeld JP, Rossier BC. Lithium nephrotoxicity revisited. Nat Rev Nephrol 2009;5:270–6.
[198] Christensen BM, Zuber AM, Loffing J, Stehle JC, Deen PM, Rossier BC, et al. alphaENaC-mediated lithium absorption promotes nephrogenic diabetes insipidus. J Am Soc Nephrol 2011;22:253–61.
[199] Barlow ED, de Wardener HE. Compulsive water drinking. Q J Med New Series 1959;28:235–58.
[200] Robertson GL. Dipsogenic diabetes insipidus: a newly recognized syndrome caused by a selective defect in the osmoregulation of thirst. Trans Assoc Am Physicians 1987;100:241–9.
[201] Amico JA. Diabetes insipidus and pregnancy. In: Czernichow AGRP, editor. Frontiers of hormone research. Basel: Karger; 1985. p. 266–77.
[202] Davison JM, Shiells EA, Philips PR, Lindheimer MD. Serial evaluation of vasopressin release and thirst in human pregnancy. Role of human chorionic gonadotrophin in the osmoregulatory changes of gestation. J Clin Invest 1988;81:798–806.
[203] Iwasaki Y, Oiso Y, Kondo K, Takagi S, Takatsuki K, Hasegawa H, et al. Aggravation of subclinical diabetes insipidus during pregnancy. N Engl J Med 1991;324:522–6.
[204] Forssman J. On hereditary diabetes insipidus, with special regard to a sex-linked form. Acta Med Scand 1945;159:1–196.
[205] Barron WM, Cohen LH, Ulland LA, Lassiter WE, Fulghum EM, Emmanouel D, et al. Transient vasopressin-resistant diabetes insipidus of pregnancy. N Engl J Med 1984;310:442–4.
[206] Durr JA, Hoggard JG, Hunt JM, Schrier RW. Diabetes insipidus in pregnancy associated with abnormally high circulating vasopressinase activity. N Engl J Med 1987;316:1070–4.
[207] Brewster UC, Hayslett JP. Diabetes insipidus in the third trimester of pregnancy. Obstet Gynecol 2005;105:1173–6.
[208] Hiett AK, Barton JR. Diabetes insipidus associated with craniopharyngioma in pregnancy. Obstet Gynecol 1990;76:982–4.
[209] Trudel E, Bourque CW. Central clock excites vasopressin neurons by waking osmosensory afferents during late sleep. Nat Neurosci 2010;13:467–74.
[210] Denton KM. In the arms of morpheus. Am J Physiol Renal Physiol 2012;302(2):F234–5.
[211] Mahler BT, Kamperis K, Schroeder M, Frokiaer J, Djurhuus JC, Rittig S. Sleep deprivation induces excess diuresis and natriuresis in healthy children. Am J Physiol Renal Physiol 2011;302 (2):F236–42.

[212] Leaf A. Nephrology forum: neurogenic diabetes insipidus. Kidney Int 1979;15:572–80.
[213] Bichet DG. Clinical manifestations and causes of nephrogenic diabetes insipidus. UpToDate, <www.uptodate.com>; 2011.
[214] Robertson GL. Diseases of the posterior pituitary. In: Felig D, Baxter JD, Broadus AE, editors. Endocrinology and metabolism. New York: McGraw-Hill; 1981. p. 251.
[215] Robertson GL. Diagnosis of diabetes insipidus. In: Czernichow AGRP, editor. Frontiers of hormone research, vol. 13. Basel: Karger; 1985. p. 176.
[216] Bichet D. Nephrogenic diabetes insipidus. In: Davison A, Cameron J, Grünfeld J, Kerr D, Ritz E, Winearls C, editors. Oxford textbook of clinical nephrology. New York: Oxford University Press; 2012, in press
[217] Zerbe RL, Robertson GL. A comparison of plasma vasopressin measurements with a standard indirect test in the differential diagnosis of polyuria. N Engl J Med 1981;305:1539–46.
[218] Stern P, Valtin H. Verney was right, but. N Engl J Med 1981;305:1581–2.
[219] Robertson GL. Differential diagnosis of polyuria. Annu Rev Med 1988;39:425–42.
[220] Oksche A, Dickson J, Schülein R, Seyberth HW, Müller M, Rascher W, et al. Two novel mutations in the vasopressin V2 receptor gene in patients with congenital nephrogenic diabetes insipidus. Biophys Biochem Res Com 1994;205:552–7.
[221] van Lieburg AF, Verdijk MAJ, Schoute F, Ligtenberg MJL, van Oost BA, Waldhauser F, et al. Clinical phenotype of nephrogenic diabetes insipidus in females heterozygous for a vasopressin type 2 receptor mutation. Hum Genet 1995; 96:70–8.
[222] Miller WL. Molecular genetics of familial central diabetes insipidus. J Clin Endocrinol Metab 1993;77:592–5.
[223] Bichet DG. Nephrogenic and central diabetes insipidus. In: Schrier RW, editor. Diseases of the kidney. 9th ed. New York: Lippincott Williams and Wilkins; 2012, in press.
[224] Robertson GL, Klein LA, Roth J, Gorden P. Immunoassay of plasma vasopressin in man. Proc Natl Acad Sci USA 1970;66: 1298–305.
[225] Robertson GL, Mahr EA, Athar S, Sinha T. Development and clinical application of a new method for the radioimmunoassay of arginine vasopressin in human plasma. J Clin Invest 1973;52:2340–52.
[226] Hartter E, Woloszczuk W. Radioimmunological determination of arginine vasopressin and human atrial natriuretic peptide after simultaneous extraction from plasma. J Clin Chem Clin Biochem 1986;24:559–63.
[227] LaRochelle Jr. FT, North WG, Stern P. A new extraction of arginine vasopressin from blood: the use of octadecasilyl-silica. Pflugers Arch 1980;387:79–81.
[228] Ysewijn-Van Brussel KA, De Leenheer AP. Development and evaluation of a radioimmunoassay for Arg8-vasopressin, after extraction with Sep-Pak C18. Clin Chem 1985; 31:861–3.
[229] Bichet DG, Arthus MF, Barjon JN, Lonergan M, Kortas C. Human platelet fraction arginine-vasopressin. Potential physiological role. J Clin Invest 1987;79:881–7.
[230] Preibisz JJ, Sealey JE, Laragh JH, Cody RJ, Weksler BB. Plasma and platelet vasopressin in essential hypertension and congestive heart failure. Hypertension 1983;5:I129–38.
[231] Bichet DG, Kortas C, Mettauer B, Manzini C, Marc-Aurele J, Rouleau JL, et al. Modulation of plasma and platelet vasopressin by cardiac function in patients with heart failure. Kidney Int 1986;29:1188–96.
[232] Seckl JR, Dunger DB, Bevan JS, Nakasu Y, Chowdrey C, Burke CW, et al. Vasopressin antagonist in early postoperative diabetes insipidus. Lancet 1990;335:1353–6.
[233] Kanno K, Sasaki S, Hirata Y, Ishikawa S, Fushimi K, Nakanishi S, et al. Urinary excretion of aquaporin-2 in patients with diabetes insipidus. N Engl J Med 1995;332:1540–5.
[234] Elliot S, Goldsmith P, Knepper M, Haughey M, Olson B. Urinary excretion of aquaporin-2 in humans: a potential marker of collecting duct responsiveness to vasopressin. J Am Soc Nephrol 1996;7:403–9.
[235] Maas AH, Siggaard-Andersen O, Weisberg HF, Zijlstra WG. Ion-selective electrodes for sodium and potassium: a new problem of what is measured and what should be reported. Clin Chem 1985;31:482–5.
[236] Gennari FJ. Current concepts. Serum osmolality. Uses and limitations. N Engl J Med 1984;310:102–5.
[237] De Buyst J, Massa G, Christophe C, Tenoutasse S, Heinrichs C. Clinical, hormonal and imaging findings in 27 children with central diabetes insipidus. Eur J Pediatr 2007;166:43–9.
[238] Cattin F, Bonneville F, Chayep C. Imagerie par resonance magnetique du diabete insipide. Feuillets de Radiologie 2005;45: 425–34.
[239] Fujisawa I. Magnetic resonance imaging of the hypothalamic-neurohypophyseal system. J Neuroendocrinol 2004;16: 297–302.
[240] Rappaport R. Magnetic resonance imaging in pituitary disease. Growth Genetics & Hormones 1995;11:1–5.
[241] Mouillac B, Chini B, Balestre M-N, Elands J, Trumpp-Kallmeyer S, Hoflack J, et al. The binding site of neuropeptide vasopressin V1a receptor. J Biol Chem 1995;270: 25771–7.
[242] Wilson Y, Nag N, Davern P, Oldfield BJ, McKinley MJ, Greferath U, et al. Visualization of functionally activated circuitry in the brain. Proc Natl Acad Sci USA 2002;99: 3252–7.
[243] Prager-Khoutorsky M, Bourque CW. Osmosensation in vasopressin neurons: changing actin density to optimize function. Trends Neurosci 2010;33:76–83.
[244] Vokes TP, Robertson GL. Physiology of secretion of vasopressin. In: Czernichow AGRP, editor. Frontiers in hormone research: diabetes insipidus in man, vol. 13. Basel: S. Karger; 1985. p. 127–55.
[245] Robertson G. The pathophysiology of ADH secretion. In: Tolis G, Labrie F, Martin JB, editors. Clinical neuroendocrinology: a pathophysiological approach. New York: Raven Press; 1979.
[246] Magner PO HM. Polyuria – a pathophysiological approach. Med North America 1987;15:2987–97.
[247] Davison JM, Gilmore EA, Durr J, Robertson GL, Lindheimer MD. Altered osmotic thresholds for vasopressin secretion and thirst in human pregnancy. Am J Physiol 1984;246: F105–9.

CHAPTER

47

The Molecular Biology of Renal K^+ Channels

WenHui Wang[1] *and Chou-Long Huang*[2]

[1]Department of Pharmacology, New York Medical College, Valhalla, NY, USA
[2]University of Texas, Southwestern Medical Center, Dallas, TX, USA

INTRODUCTION

Renal epithelial transport depends on the coordinated function of potassium channels with ion transporters (co-transporters, channels, and exchangers) and ion pumps in apical and basolateral membranes of distinct cell types along the nephron of the mammalian kidney. Potassium (K^+) channels are key members of this integrated transport system in renal epithelial cells. First, renal K^+ channels participate in generating cell membrane potential; since numerous transporters are electrogenic, changes in cell membrane potential could alter the transport rate of a given substance. Second, renal K^+ channels are involved in the volume regulation that is essential for preventing cell swelling or shrinking in the hypotonic or hypertonic environment. Third, renal K^+ channels play an important role in K^+ recycling which is essential for maintaining the function of several transport proteins, such as Na^+-K^+-ATPase. Finally, renal K^+ channels are extremely involved in K^+ secretion in the aldosterone-sensitive distal nephron (ASDN). Figure 47.1 is a scheme providing an overview regarding the role of K channels in different renal segments.

Since K^+ channels play such an important role in kidney function, understanding the structure and regulation of renal K^+ channels is essential to gaining insights into the molecular mechanisms of kidney potassium handling. In the past decades, the development of molecular biology and patch-clamp techniques has had a significant impact on the exploration of the molecular identity of some renal K^+ channels. This chapter summarizes our current understanding of the molecular identity of renal K^+ channels, and will specifically focus on the ROMK (Kir1; *KCNJ1*) channel. We will discuss similarities, as well as certain differences, in the properties of cloned K^+ channels compared to native K^+ channels expressed in the different nephron segments.

THE MOLECULAR BIOLOGY OF ROMK, A DISTAL K^+ SECRETORY CHANNEL

Structure of Inward Rectifying K^+ Channels and ROMK

The K^+ channel, *ROMK* (Kir1; *KCNJ1*[1]), belongs to a growing family of inwardly rectifying K^+ (Kir) channels[2] that are functionally characterized by high potassium selectivity and by either weak or strong inward rectification. To date, 16 Kir genes have been identified and classified into seven subfamilies (Kir1.x to Kir7.x). All Kir channels have a membrane topology consisting of two membrane-spanning domains (M1 and M2), an intervening H5 pore-forming region, and cytoplasmic amino (NH_2-) and carboxyl (COOH-)-terminal domains (Figure 47.2[3–5]). This membrane topology corresponds to the last two membrane spanning segments of the voltage-gated K^+ channels, suggesting a common ancestral origin.[6–8] The N- and C-terminal cytoplasmic regions of Kir channels provide regulatory domains (Figure 47.2) that can be phosphorylated by kinases,[9] and that interact with protons,[10–12] nucleotides,[13] and phosphoinositides.[14,15]

The three-dimensional structure of ROMK is not available, but it can be inferred from X-ray crystallographic structures of bacterial and eukaryotic K^+ channels. The first crystal structure of K^+ channel

Seldin and Giebisch's The Kidney, Fifth Edition.
DOI: http://dx.doi.org/10.1016/B978-0-12-381462-3.00047-1

© 2013 Elsevier Inc. All rights reserved.

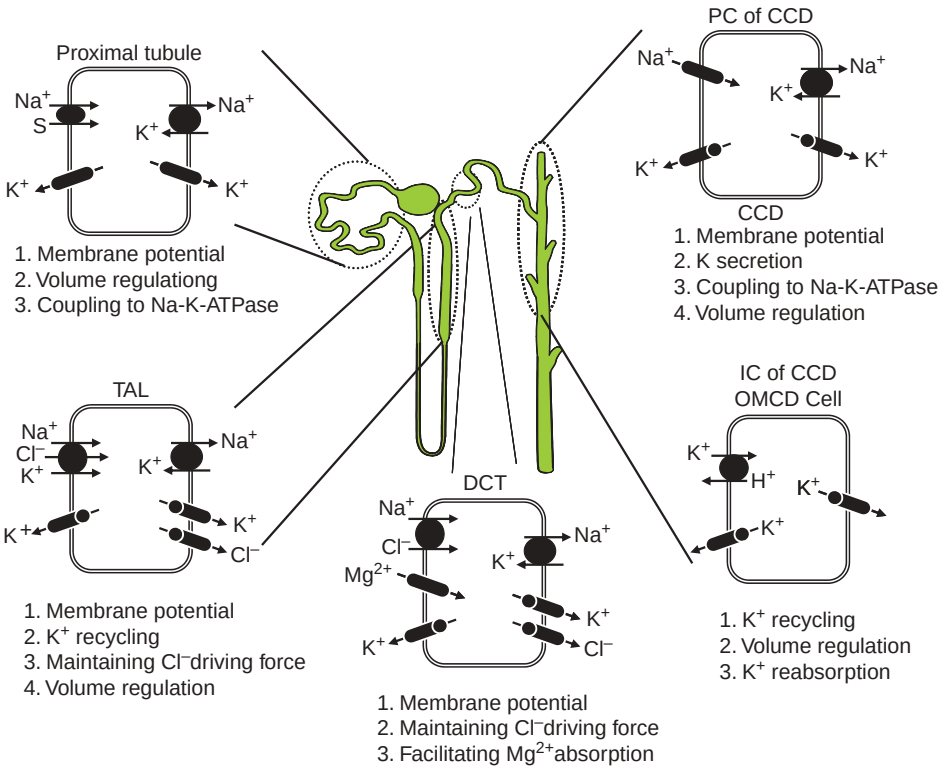

FIGURE 47.1 A cell model demonstrating the role of K channels in different renal segments.

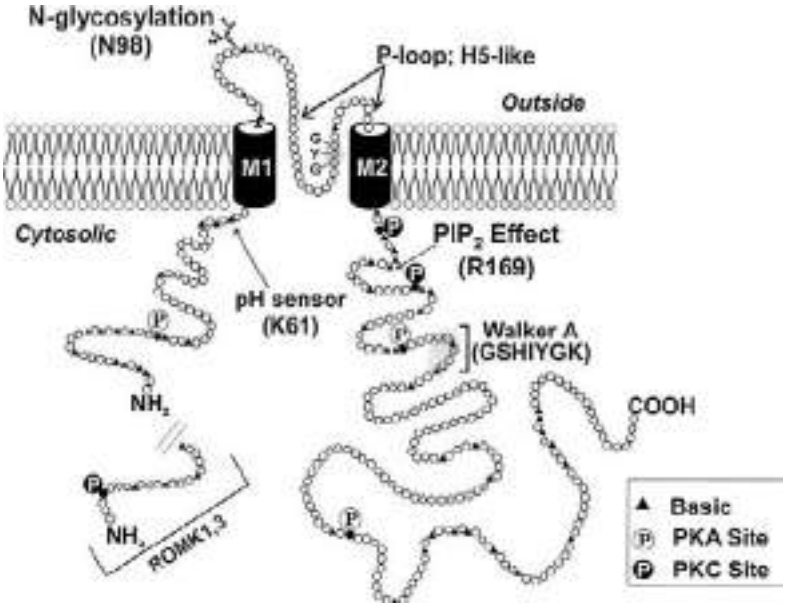

FIGURE 47.2 Topology of ROMK (Kir1.1) K^+ channel. M1 and M2 represent the two membrane-spanning domains characterizing the inward-rectifier family of potassium channel. Some important functional sites are indicated. A short amphipathic segment in the M1-M2 linking segment in ROMK forms the pore-forming (P-loop) or H5 region. The canonical T-X-G-Y-G amino acid sequence found in all K^+ channels is shown in the H5 segment. Numbering is based on amino acid sequence of ROMK2 (Kir1.1b).

determined is from *Streptomyces lividans* (KcsA).[16] Although not an inward rectifier K^+ channel, KcsA shares the same membrane topology with Kir channels with two membrane-spanning M1 and M2 segments, a H5 pore-forming region, and N- and C-terminal cytoplasmic domains. The amino acid sequence of KcsA is similar to the corresponding region of other K^+ channels, including vertebrate and invertebrate voltage-gated K^+ channel, inward rectifier, and calcium-activated K^+ channels. The crystal structure of KcsA reveals a tetramer with four identical subunits that encircle a central ion conduction pathway with four-fold symmetry (Figure 47.3). The M1 and M2 segments of each subunit form α-helices and are inserted into the

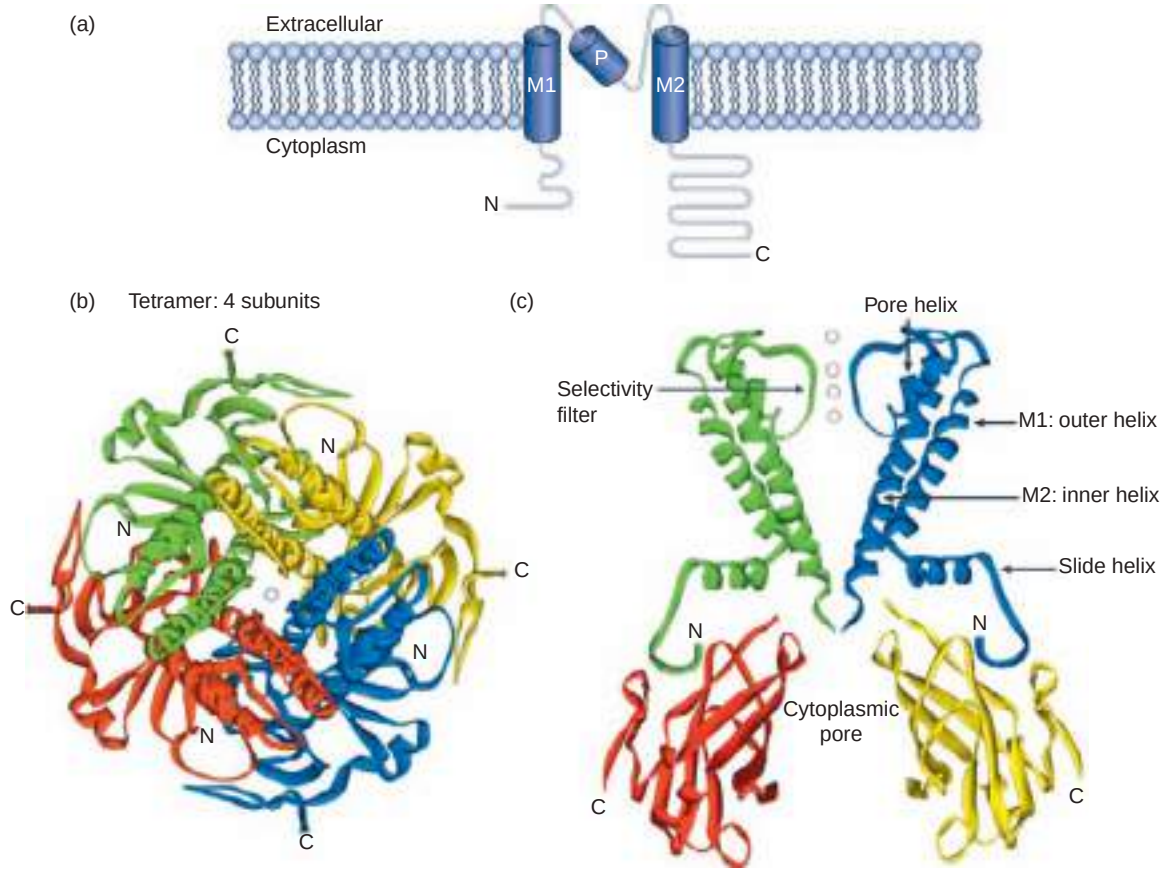

FIGURE 47.3 **Architecture of inwardly rectifying K (Kir) channels 276.** (a) A scheme of Kir channels: each subunit contains two transmembrane helices (M1 and M2), a channel pore (P), and both N- and C-termini. (b) The tetrameric structure of the KirBac1.1 channel4 (PDB ID:1P7B) viewed from the extracellular side. Each monomer is marked by red, green, yellow, and blue, respectively. The conduction pathway is indicated by a K ion (white). (c) Side view of two subunits of the KirBac1.1 illustrating the transmembrane domain (green and blue), the C-terminal domains of their neighbouring subunits (red and yellow) and K ions (white) in the selectivity filter. See color section at the back of the book.

tetramer such that M2 faces the central ion conduction pathway (termed inner helix), and M1 faces the lipid membrane (outer helix). Amino acids connecting M1 and M2 (from N to C) form the turret, a tilted pore helix that runs half-way through the membrane, and the selectivity filter bearing the Thr-X-Gly-Tyr-Gly (X is any amino acid) signature sequence of all K^+ channels. The inner helices are tilted with respect to the membrane, so that the subunits open like the petals of a flower facing the outside of the cell. Furthermore, the four inner helices pack against each other as a bundle near the intracellular aspect of the membrane, giving the appearance of an inverted teepee.

The ion conduction pathway (pore) of KcsA can be functionally divided into three parts that (from the outside of the cell) consist of the selectivity filter, a water-filled wide cavity near the middle of the membrane (the central cavity; ~10Å across), and the internal part of the pore made up of the anti-lipid facing amino acids of four inner helices. The selectivity filter (~12Å in length) is the narrowest part of the pore, and is lined by four evenly spaced layers of carbonyl oxygen atoms from amino acids X-Gly-Tyr-Gly, and a single layer of hydroxyl oxygen atoms from amino acid threonine. K^+ ions dehydrate and enter the selectivity filter in single file. The five layers of oxygen atoms form four consecutive K^+ ion-binding sites to stabilize dehydrated K^+ ions in the filter, which compensates for the energy required for dehydration. Due to repulsion between closely spaced ions, K^+ ions occupy only two of the four binding sites at a given time, in either 1,3 or 2,4 configuration. These unique structural and energetic features contribute to the extremely high selectivity (~1000 to 1 for K^+ over Na^+) yet fast conduction rate (up to ~10^8ions/sec) of K^+ channels for K^+ ions.

The crossing of four inner helices of KcsA as a bundle near the intracellular aspect of the membrane creates a point of structural constraint between the membrane pore and the cytoplasm, referred to as bundle crossing. Structural comparison of KcsA with

Mthk, a bacterial calcium-activated K^+ channel,[17] provides insights into how bundle crossing might function as an activation gate for K^+ channels. In KcsA, the inner helices are straight and the diameter of bundle crossing is about 3.5Å, suggesting that the crystal structure of KcsA is in closed conformation. In contrast, the crystal structure of Mthk, which is solved in the presence of high (Ca^{2+}), thus likely in the open conformation, reveals that inner helices are bent at a hinge point and splayed open so that the bundle crossing does not form a barrier to the flow K^+ ions between the central cavity and the cytoplasm. Thus, KcsA and Mthk structures likely represent closed and open pore conformations of many different K^+ channels, including ROMK. Conservation of a glycine residue at the inner helix hinge point in most K^+ channels supports this conclusion.

The structural studies of KcsA and Mthk do not include the cytoplasmic N- and C-terminal domains. The crystallographic structure of the bacterial inward rectifier K^+ channel KirBac1.1, including the transmembrane and cytoplasmic domains, provides the first insight into the intracellular domains of Kir channels.[18] The structures of the intracellular domains of eukaryotic Kir channels are determined in two ways. One uses only the N- and C-terminal cytoplasmic domains connected by an artificial kinker for crystallographic studies.[19] The other determines the structures of cytoplasmic domains, together with the transmembrane domains, using either a chimeric channel containing the outer three quarters of the membrane domains of KirBac3.1 and the inner one quarter of the membrane domain and the intracellular N- and C-terminal domains of Kir3.1[20] or the native form of inward rectifier K^+ channel from chicken (Kir2.2).[21] Overall, these studies reveal that the N-terminal cytoplasmic domain of one subunit interacts with the C-terminus of the adjacent subunit, and together form predominantly β-sheet structures. The four sets of associated N- and C-terminal domains assemble into a tetramer surrounding a water-filled cytoplasmic pore that extends coaxially from the transmembrane pore domain. Thus, the cytoplasmic pore extends the ion permeation pathway to ~60Å, nearly twice the length of the transmembrane pore. The apex of the cytoplasmic pore abutting the transmembrane domain is formed by a loop referred to as the "G-loop." In the crystal structures, the G-loops are in either a constricted or dilated conformation, likely representing closed and open states of the cytoplasmic pore, respectively.[19–21] Thus, Kir channels contain two regions along the length of ion conduction pathway that can adopt constricted or dilated conformation and function as the gates. One is the inner helix bundle crossing, and the other is the apex of the cytoplasmic pore formed by the G-loops.

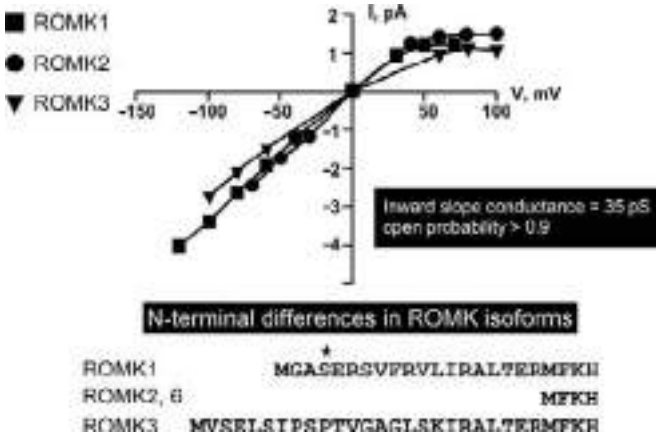

FIGURE 47.4 **The ROMK splice variants.** Current-voltage relationships for ROMK1, 2, and 3 are shown. Each of these variants has a similar I–V curve and calculated single channel conductance of ~35 pS. The open probability of these three channels is also similar and >0.9. ROMK1, 2, 3, and 6N-terminal amino acid sequences are shown using the single letter notation for residues. ROMK2 and 6 have an identical amino acid sequence. ROMK1 and ROMK3 have 19 and 26 additional N-terminal amino acids, respectively, compared to ROMK2 or 6. The asterisk in the ROMK1 sequence indicates a functional PKC phosphorylation site.

Interestingly, the plasma-membrane facing surface of the cytoplasmic pore contains many positively charged amino acids known to be important for binding to membrane phosphatidylinositol-4,5-bisphosphate (PIP_2)[4,22] (see section on "Regulation of ROMK by PIP_2" below). Interaction between these amino acids and membrane PIP_2 may alter the conformation of the G-loop and the inner helix bundle crossing to activate the channel.[19,20]

ROMK Channel Isoforms

Following the cloning of ROMK1 (Kir1.1a) from rat kidney,[3] three additional alternatively spliced forms of this channel were isolated (Figures 47.2 and 47.4), and named ROMK2 (Kir1.1b), ROMK3 (Kir1.1c)[23,24] and ROMK6 (Kir1.1d).[25] The encoded ROMK proteins differ at the beginning of the N-terminus – ROMK2 (also rat ROMK6, which has the same amino acid sequence as ROMK2; Figure 47.4[25]) has the shortest N-terminus, and splicing adds either 19 or 26 amino acids for ROMK1 or ROMK3, respectively (see Figures 47.2 and 47.4). Relative ROMK mRNA abundance measured by competitive PCR has shown that ROMK2 and ROMK3 are much more abundant than ROMK1 or ROMK6 in rat kidney.[26] In addition, a novel set of ROMK proteins, about one-third the size of native ROMK, has been suggested to be formed from alternative splicing of the ROMK core exon.[27] The significance of these putative

smaller channel proteins remains unclear. Six splice variants[28–30] have been identified in the human ROMK gene, *KCNJ1*, located on chromosome 11q24.[28] These six human transcripts apparently encode only three distinct polypeptides, two of which are similar to rat ROMK1 and ROMK2.[28] A rat homolog of the third human ROMK isoform has not been identified. Two ROMK homologs have also been cloned from human kidney, but their roles in renal function are unknown.[31]

ROMK Channel Localization

Rat ROMK1-3 are differentially expressed along the nephron from the thick ascending limb of Henle, TAL, to the outer medullary collecting duct, OMCD, (Figure 47.5[23,32]). The rat TAL and distal convoluted tubule, DCT, express ROMK2 and ROMK3 messenger RNA, while principal cells in the cortical collecting duct, CCD, express ROMK1 and ROMK2 transcripts (see Figure 47.5). The outer medullary collecting duct cells appear to express only ROMK1 transcripts. The general single channel properties of the ROMK1, 2, and 3 isoforms are similar, e.g., single channel conductance and open probability (Figure 47.4). Although the specific functional/regulatory consequences of the different isoforms have not been fully-elucidated, a serine at the fourth position in the extended N-terminus in ROMK1 has been shown to be required for sensitivity to arachidonic acid (Figures 47.2 and 47.4)[33] and protein kinase C[34] (see section on ROMK function below). Thus, ROMK1 may add distinct functional characteristics to ROMK channels. No specific role for the extended N-terminus of ROMK3 has yet been identified. Whether tetrameric ROMK channels are formed of different subunits (e.g., heterotetramers of ROMK2 and ROMK1 in the cortical collecting duct) or exist only as homotetramers is not known. Finally, ROMK transcripts are present in some other tissues,[3] including the early gravid uterus.[35] Roles for ROMK in these tissues have not been determined.

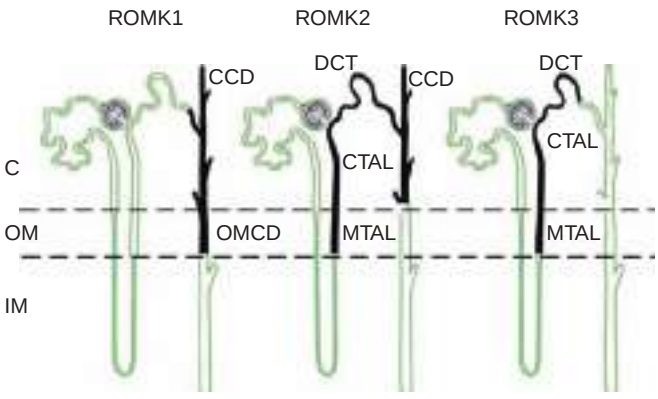

FIGURE 47.5 **The distribution of the ROMK 1, 2, and 3 isoforms along the rat nephron.** The shaded regions indicate the localization of ROMK transcripts and protein (CCD: cortical collecting duct; CTAL: cortical thick ascending limb; DCT: distal convoluted tubule; MTAL: medullary thick ascending limb; OMCD: outer medullary collecting duct). In the CCD and OMCD, ROMK is expressed only in principal cells.

Antibody generated to sequences of ROMK shared by all isoforms has demonstrated an apical pattern of channel protein expression in rat TAL (including macula densa cells), DCT, and early CNT cells, and principal cells of the CCD and OMCD.[36–39] This localization is consistent with the ROMK channel providing a K^+ secretory pathway in these renal epithelia.

ROMK Channel Properties are Similar to the Distal (SK) K^+ Secretory Channel

The single channel characteristics and regulatory properties of ROMK channels expressed in *X. laevis* frog oocytes are virtually identical to those of the native ATP-sensitive, small conductance (SK) channels in TAL cells[40,41] (Figure 47.6) and principal cells in the CCD[42–48](Figure 47.7). Similar kinetic characteristics of K^+, NH_4^+, and Tl^+ have been observed in the native secretory K^+ channel in the rat CCD and ROMK2 channels expressed in *X. laevis* oocytes,[49,50] leading Palmer and co-workers to conclude that the native SK and cloned ROMK channels were identical. A further characteristic of the low conductance secretory K^+ channel found in principal cells is a lack of sensitivity to external TEA^+.[42]

The general properties of ROMK channels expressed in *Xenopus* oocytes include: (1) weak inward rectification (Figure 47.4) that is dependent on the binding of cytosolic Mg^{2+} or other polyvalent cations to the channel pore[51–56]; (2) activation by protein kinase A-dependent phosphorylation processes[9,39,57,58]; (3) inhibition by high concentrations of MgATP[13]; (4) inhibition by slight reductions in cytosolic pH[59,60]; and (5) inhibition by arachidonic acid and protein kinase C.[33,34] When coupled with gene expression and protein localization studies, these functional similarities strongly suggest that ROMK makes up the pore-forming subunit of the renal distal SK potassium channel.[46,50]

Characteristics of the ROMK Channel Pore

CHANNEL KINETICS

ROMK channels are characterized by a high open probability (P_o) of greater than 0.9 for inward K^+ flux.[3,49,57,61] The high open probability results from one open state and two closed states. One closed state is very short (~1 ms; 99% frequency), and the other is longer (~40 ms) but very infrequent (~1%).[57,61] The infrequent closed state is due to blocking by divalent cations, as it can be abolished by EDTA.[61] Choe and

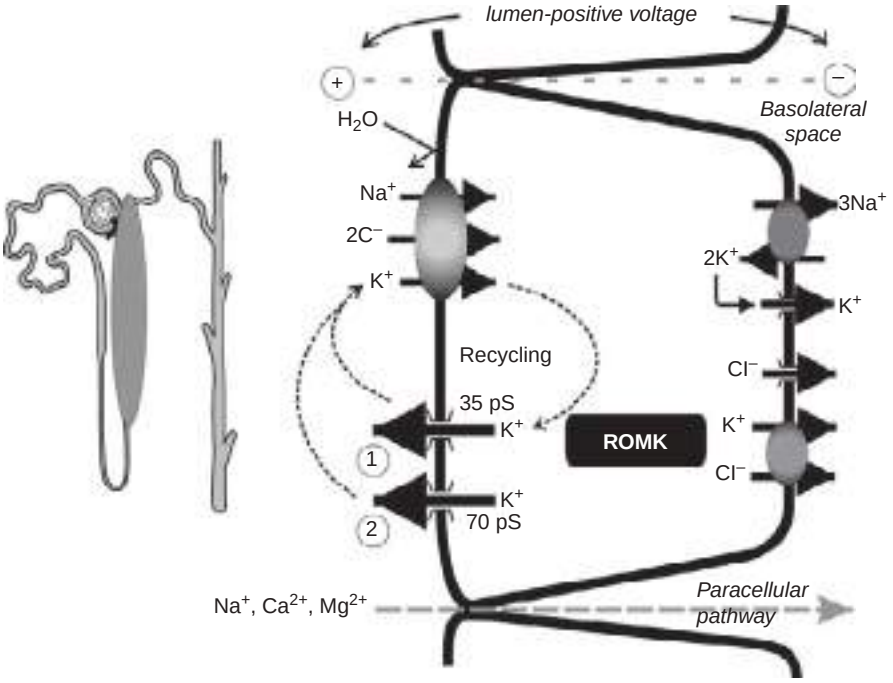

FIGURE 47.6 **Model for ion transport in the thick ascending limb.** The two types of apical K^+ channels are shown; 35 pS (also called the small K^+ or SK channel) and 70 pS channels. ROMK and SK functional and regulatory characteristics are essentially identical. It has been proposed that the 70 pS channel is also formed by ROMK in association with another channel subunit, but this remains to be demonstrated.

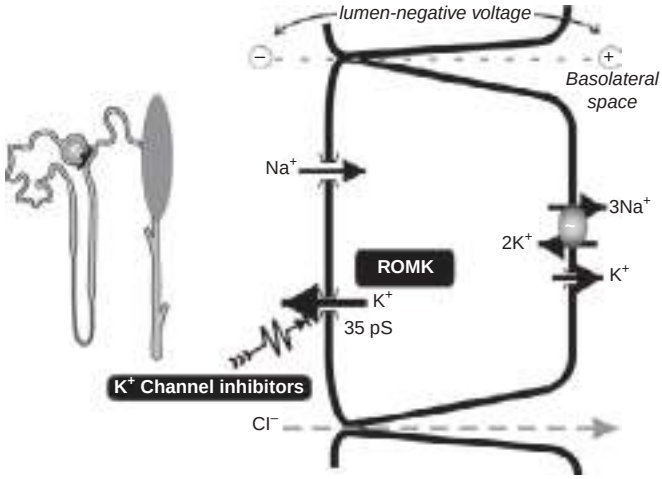

FIGURE 47.7 **Model for ion transport by the principal cell in the collecting duct.** The apical K^+ secretory channel in this cell is ROMK.

co-workers[61] have also suggested that the closed state of ROMK results from K^+ ions transiently blocking its own pathway. Such a model would not require large molecular motions, but rather small molecular oscillations.

CHANNEL RECTIFICATION

One of the fundamental characteristics of ROMK, as well as all Kir channels is inward rectification, the property of passing current more easily in the inward than in the outward direction (see Figure 47.4). Although this seems to be contrary to the role of ROMK in K^+ secretion, the inward rectification observed with ROMK, and with the kidney K^+ secretory channel, is "weak." The term "weak" rectification refers to the ability of ROMK to actually pass outward current, albeit to a lesser extent than inward current. Many of the other Kir channels are "strong" rectifiers, and characteristically pass little outward current. The very high open probability of the ROMK channel, usually >0.9, may help make up for the rectification effect on K^+ secretion. In other words, although the outward conductance (ease of passing K^+ secretory current) is less than the inward conductance, the channels are open most of the time, and thus are able to secrete large amounts of K^+. We now know that inward rectification of ROMK is due to blocking of the channel pore by Mg^{2+}[55] or polyamines like spermine or spermidine from the intracellular side.[52,53] Thus, it is possible that variations in the cytosolic concentrations of these inorganic and organic cations could provide an important mechanism regulating outward (i.e., K^+ secretory current. It was suggested that the inhibition of outward K^+ fluxes through ROMK by Mg^{2+} may contribute to K^+-wasting in the setting of Mg^{2+} deficiency.[62] A subsequent study by Yang et al.[63] examining the regulation of ROMK expressed in *Xenopus* oocytes and the native channel by intracellular and extracellular Mg^{2+} supports this idea.

Kinetic studies of inward rectification by Mg^{2+} and polyamines indicate that the effect is voltage-dependent and depends on the extracellular

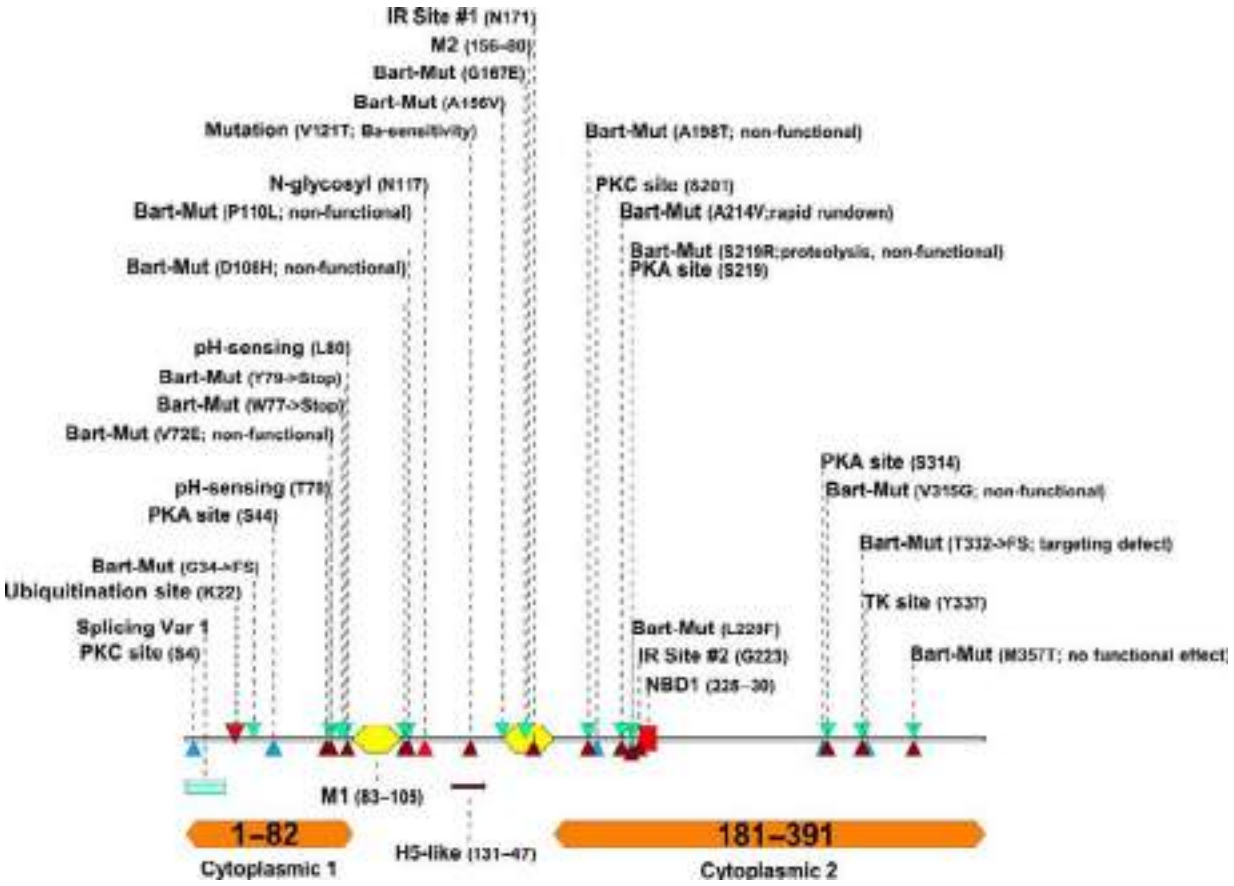

FIGURE 47.8 **The major functional and regulatory sites, and the Bartter's mutations are shown in this schematic representation of ROMK1, Kir1.1a** (see text for discussion).

concentration of K^+ (thus varies with the K^+ reversal potential in the constant intracellular (K^+)).[54,55,61,64,65] These findings suggest an interaction between permeant and blocking ions, and the presence of a variable energy well within the channel pore. The crystal structure of Kir revealing a long channel pore with multiple binding sites for K^+ and blocking ions is consistent with this idea.[19–21]

Electrophysiological studies have demonstrated the importance of the M2 segment and COOH-termini in determining the inward rectifying characteristics of inwardly rectifying K^+ channels.[54,56,66,67] Two residues are particularly important in determining whether the rectification is strong or weak. In strong inward rectifiers like IRK1 (Kir2.1),[5] a negatively charged residue, aspartic acid (D172 in IRK1), in the M2 membrane segment has been shown to be critical for strong inward rectification.[54,56] In ROMK the aspartate residue is replaced by asparagine (see Figure 47.8, IR Site #1, N171 in ROMK1), consistent with the weak rectification of this channel. A second residue located in the C-terminus has also been shown to be an important contributor to strong rectification in IRK1.[67] This glutamate residue (E224 in IRK1) is replaced by a glycine residue in ROMK (see Figure 47.8; IR Site #2). This C-terminal glycine residue in ROMK is a part of the Walker A site that contributes to the nucleotide-binding interactions (see Figure 47.1, and IR Site #2 in Figure 47.8) in the nucleotide-binding domain (NBD; Figure 47.8), and thus serves a different gating function in ROMK. As expected from this model, exchange of the ROMK C-terminus with that on IRK1 produces strong rectification in oocytes injected with the mutant ROMK channel.[66] Consistent with the electrophysiological results, the crystal structure of Kir2.2 reveals that the inner helices line the central cavity and the internal half of the membrane pore, and the side chain of D172 points to the center of the central cavity.[21] The binding sites for Mg^{2+} in the crystal structure of Kir2.2 were examined by soaking the crystal with 10 mM Sr^{2+}, an electron dense mimic of Mg^{2+}. Three density peaks due to Sr^{2+} are observed in the crystal of Kir2.2: one in the central cavity corresponding to the position of D172 and two in the cytoplasmic pore, referred to as the upper ring and lower ring of charges, respectively. The upper ring of charges consists of E224 of IRK1 and

an additional glutamate residue E229 from each of four subunits. The lower ring of charges consists of four D255, one from each subunit.[21]

Finally, two different extracts of venom have been suggested to specifically inhibit ROMK channels.[68,69] Both the snake toxin, δ-dendrotoxin,[68] the honey bee venom extract, tertiapin, and the modified compond, tertiapin-Q[69,70] appear to block ROMK activity by interacting with channel pore. Tertiapin-Q specifically blocks ROMK and Kir3.1, but not other Kir channels such as Kir4 and Kir5, and has been explored to estimate the density of ROMK channels in the CCD and CNT in response to dietary K^+ intake.[71] A study, however, indicates that tertiapin-Q can also block MaxiK (or BK, *hSlo1*) Ca^{2+}-activated K^+ channels.[72] Thus, caution should be exercised when utilizing tertiapin-Q to define ROMK activity under the condition in which MaxiK channels are activated by flow.

Regulation of the ROMK K^+ Channel

ROMK channel activity, like that of the native SK channel in TAL and principal cells, is regulated by a variety of factors that either activate or inhibit channel activity (Figure 47.9). The molecular mechanisms for these alterations in channel function are rapidly being identified.

PROTEIN KINASE A (PKA)

PKA-dependent phosphorylation processes activated by receptor-mediated events or alterations in cytosolic second messengers (e.g., cyclic AMP, cAMP) play important roles in regulating the native SK channel in principal cells of the CCD (Figure 47.10[45–48,73]). Phosphorylation-dephosphorylation processes also modulate the activity of the cloned ROMK K^+ channel.[9,33,34,57,58] K^+ channel activity in excised inside-out

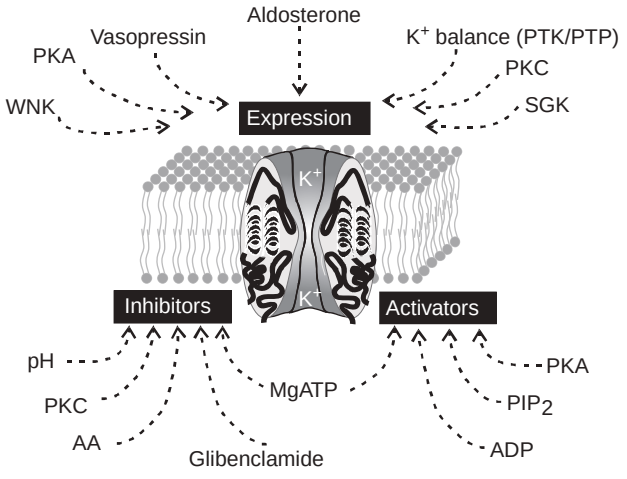

FIGURE 47.9 **The major identified regulators of ROMK channels.**

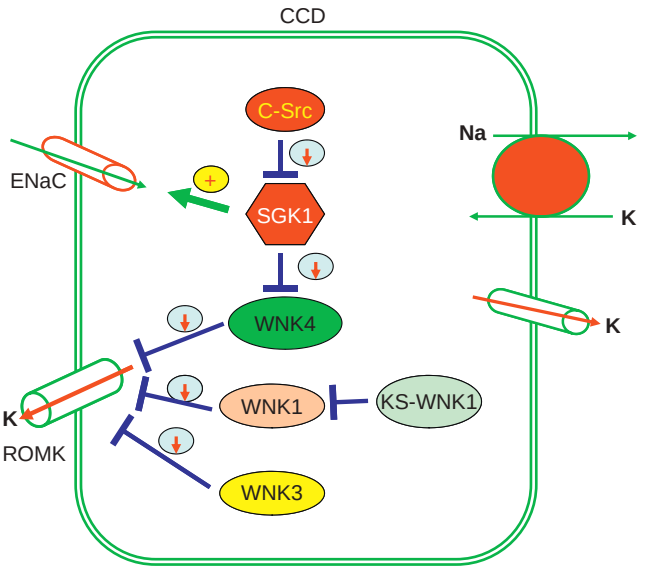

FIGURE 47.10 **A cell model illustrating the mechanism by which ROMK channel activity is regulated by the interaction among c-Src, SGK1, and WNKs in the CCD.**

patches of oocytes expressing ROMK requires activation by PKA-dependent phosphorylation processes.[58] Rundown or loss of ROMK channel activity in these patches occurs whenever phosphatase-mediated dephosphorylation activity is greater than phosphorylation (see also section on PIP_2 below for role of protein versus lipid kinases and phosphatases in the process of rundown and reactivation by MgATP).

The critical PKA phosphorylation sites are on the channel protein itself (see Figure 47.2). This has been demonstrated by several observations. First, ROMK protein expressed in HEK-293 cells can be phosphorylated by PKA.[9] Phosphopeptide analysis and mapping have shown three serine residues phosphorylated by PKA (one residue on the N-terminus (serine 25 in ROMK2) and two residues on the C-terminus (serine 200 and serine 294 in ROMK2)). Mutation of any single PKA phosphorylation site on ROMK2 reduces whole cell K^+ currents by 35–40% in oocytes; mutation of two or more of the three sites produces non-functional channels.[9] This is consistent with the critical role of PKA phosphorylation in channel activation. Second, at the single channel level the N-terminal and C-terminal PKA phosphorylation sites alter the channel activity, albeit differently.[57] None of the mutations with serine residues replaced by alanine alters the single channel conductance. Each of the C-terminal PKA phosphorylation site mutations, however, reduces open probability (P_o) by about 40%, due to the appearance of a new long closed state. This reduction in P_o is sufficient to account for the observed reduction in whole oocyte currents.[9] Replacing the N-terminal serine with alanine

does not change P_o, but does reduce the probability of finding functioning channels by about 60%. The mechanism for this reduction in active channels is not known at present. The mechanism by which PKA increases ROMK channel activity may include stimulation of surface expression and enhance the effect of PIP_2 on ROMK channels. It has been shown that stimulation of PKA increases the sensitivity of ROMK channels to PIP_2 in *Xenopus* oocytes.[74] Also, a recent study demonstrates that mutation of serine residue 44 to aspartate increases the surface delivery of ROMK1 channels.[75] One of the fundamental characteristics of SK channels in principal cells and in the TAL is their activation by Gs-coupled receptors or by the addition of cyclic AMP.[46] AKAPs are A-Kinase Anchoring Proteins that bind PKA holoenzyme (catalytic plus regulatory subunits), and maintain the enzyme at specific intracellular sites.[76,77] Wang and co-workers reported that ROMK1 channels expressed in *X. laevis* oocytes could not be activated by cyclic AMP unless expressed with an isoform of AKAP, AKAP79.[78] On the other hand, findings that ROMK channels carrying PKA site mutations exhibit reduced current in *Xenopus* oocytes in the absence of AKAP79 suggests that ROMK can be phosphorylated without AKAP79.[78] The role of AKAP in the native tissue is not determined. Some studies suggested that the Na/H exchange regulatory protein 2 (NHERF-2) might act as an AKAP, because NHERF-2 interacts with ROMK channels[79] and facilitates the stimulatory effect of SGK1 on ROMK channels.[80]

ARACHIDONIC ACID (AA)

Like the native SK channel in the CCD,[81] ROMK1 channels expressed in *Xenopus* oocytes are sensitive to arachidonic acid (AA[33,34]). The effect of AA is specific, since other fatty acids failed to mimic the effect of AA.[33] However, AA has little-to-no effect on the other two ROMK family members, ROMK2 and ROMK3.[34] Since the amino acid sequences of the ROMK channels are identical, with the exception of the N-terminus, the role of the N-terminus in mediating the effect of AA is strongly suggested. This is supported by the demonstration that deletion of the initial 37 aa of ROMK1 abolished the effect of AA. Moreover, a serine residue at the fourth position within the N-terminus of ROMK1 has been shown to play a crucial role in the AA-mediated inhibition of ROMK1, since mutation of this serine residue to alanine abolished the effect of AA (Figures 47.1 and 47.3[34]). Since this serine residue is a putative PKC phosphorylation site,[3] and AA has been shown to activate PKC, the effect of AA may depend on stimulation of a membrane-bound PKC.

PROTEIN KINASE C (PKC)

Activation of PKC phosphorylation processes inhibits the apical SK channel in the CCD.[48] ROMK1, which is exclusively expressed in collecting ducts, has three potential PKC phosphorylation sites involving serine residues: one on the N-terminus; and two on the C-terminal end. ROMK2 and ROMK3 only have the two C-terminal PKC phosphorylation sites (see Figures 47.2 and 47.4). Using an *in vitro* phosphorylation assay, it was observed that serine residue 4 in the N-terminus and serine residue 201 in the C-terminus are two major PKC-induced phosphorylation sites. The effect of PKC on ROMK channels is complex. It was demonstrated that phosphorylation of either serine residue 4 or 201 is essential for ROMK1 export to the plasma membrane.[18] On the other hand, stimulation of PKC *in vivo* has been shown to inhibit ROMK channel activity. The N-terminal serine residue at the fourth position appears to be most important to PKC-mediated K^+ channel inhibition of ROMK1. Interestingly, this is the same residue critical for the inhibitory effect of arachidonic acid (see Figure 47.4). However, it is possible that PKC-induced inhibition of ROMK channels may be indirect, resulting from a decrease in PIP_2 content. It was demonstrated that stimulation of PKC decreases the PIP_2 level in the plasma membrane.[82] Because PIP_2 is essential for maintaining ROMK channels in the open state, decreases in PIP_2 levels may contribute to the PKC-induced inhibition.

WNKS (WITH NO LYSINE KINASE)

WNKs are a family of four serine/threonine protein kinases named WNK1–4.[83,84] Among them, WNK1, 3, and 4 are expressed in the distal nephron.[85–87] The discovery that mutations in WNK1 and WNK4 cause the autosomal-dominant hypertension and hyperkalemia known as pseudohypoaldosteronism type 2 (PHA2) led to extensive characterization of their properties and function.[88] Evidence indicates that the WNK family plays an important role in the regulation of ROMK channels.[22,87,89–92] WNK1, 3, and 4 inhibits the ROMK channel activity (Figure 47.10), and the effect of WNKs on ROMK is mediated by stimulation of clathrin-dependent endocytosis.[22,89] Intersectin, a scaffold protein containing two Eps15 homology domains and four or five tandem SH3 domains, interacts with WNK1 and 4, which is required for the regulation of clathrin-mediated endocytosis of ROMK by WNKs.[93] In addition, a clathrin adaptor protein, Autosomal Recessive Hypercholesterolemia (ARH), has been shown to interact with ROMK, and the interaction may be involved in the stimulation of endocytosis of ROMK by WNK1.[16] Dysregulation of ROMK by

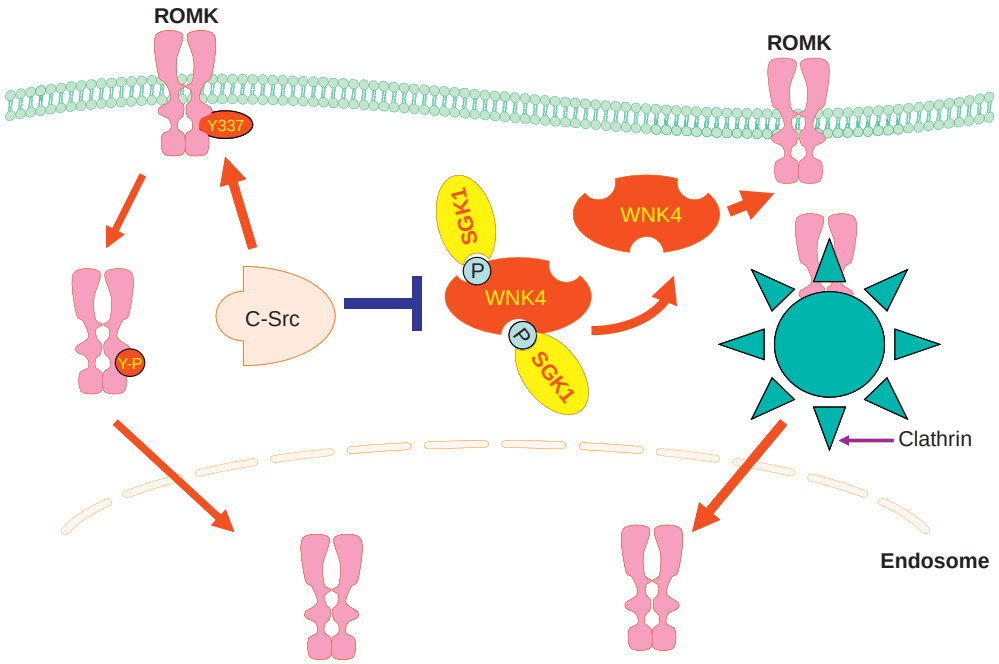

FIGURE 47.11 **A cell model demonstrating the regulation of ROMK1 channel in the CCD by Src-family PTK, SGK1, and WNK4.**

WNK1 and 4 may contribute to the hyperkalemia in PHA2.[94]

A kidney-specific splice form of WNK1 (KS-WNK1), in which an alternative 5′ exon replaces the first four exons of WNK1, is expressed in the distal nephron.[95] Unlike the long form of WNK1, KS-WNK1 lacks kinase activity and, by itself, does not regulate ROMK channels. However, KS-WNK1 antagonizes the inhibitory effect of WNK1 on ROMK.[90,92] It has been reported that high K^+ intake increases, whereas low K^+ intake decreases, the expression of KS-WNK1, and that increased KS-WNK1 expression attenuates the inhibitory effect of WNK1 on ROMK channels.[90,92] Thus, the alteration of the ratio between the long and short form of WNK1 may be an important mechanism by which a dietary K^+ intake regulates ROMK channel activity.

PROTEIN TYROSINE KINASE (PTK)

The ROMK channel is a substrate of PTK, and tyrosine residue 337 in the C-terminus of ROMK1 has been demonstrated to be a PTK phosphorylation site[95,97] (Figure 47.8). Tyrosine phosphorylation of ROMK is regulated by dietary K^+ intake: a low K^+ intake increases, whereas a high K^+ intake decreases, tyrosine phosphorylation.[98] The regulation of tyrosine phosphorylation of ROMK by K^+ diet is partially achieved by modulating the expression of Src family PTK in response to a dietary K^+ intake. Low K^+ increases, whereas a high K^+ suppresses, the expression of Src family PTK.[99] Immunostaining has also demonstrated that c-Src, the most ubiquitously distributed member of Src family PTK, is present in the thick ascending limb, connecting tubule, and cortical collecting duct.[96] Also, CD63, a tetra-spanning protein, increases c-Src activity by stimulating c-Src phosphorylation in tyrosine residue 416, thereby enhancing the c-Src-induced inhibition of ROMK channels.[100]

Although the fate of tyrosine phosphorylated ROMK is not completely understood, the stimulation of tyrosine phosphorylation of ROMK1 facilitates channel internalization (Figure 47.11[97]). Because ROMK1 is exclusively expressed in the connecting tubule and CCD, this mechanism should play an important role in K balance during K restriction. However, the upstream signaling which stimulates PTK is still not known. K restriction has been shown to stimulate renin and the angiotensin II system.[101–103] Moreover, micropuncture studies have revealed that luminal perfusion of angiotensin II inhibited K secretion in the distal nephron.[104] Patch-clamp experiments have further demonstrated that angiotensin II downregulates ROMK channels in the CCD, and that such inhibition could be demonstrated only in the CCD from K-restricted rats.[105] In addition, two lines of evidence indicate that superoxide is a mediator of the effect of K diet on the Src family PTK: (1) low K intake stimulates superoxide anion levels; and (2) incubation of M-1 cells, a cultured mouse CCD principal cell, with hydrogen peroxide increases the expression of c-Src.[106] The notion that superoxide anion could serve as a second messenger of low K intake on the Src family PTK is also supported by the finding that suppression of superoxide anion

attenuates the effect of low-K intake on c-Src expression, and diminishes the tyrosine phosphorylation of ROMK. Thus, superoxide and PTK pathway play important roles in maintaining K homeostasis.

ALDOSTERONE AND SERUM-GLUCOCORTICOID-INDUCED KINASE (SGK)

SGK1 has been reported to stimulate ROMK1 channels by facilitating the phosphorylation of ROMK channels at serine residue (Ser) 44, thereby enhancing the export of ROMK channels from the ER.[107,108] SGK1 also suppresses the effect of WNK4 on ROMK channels (Figure 47.10) through the phosphorylation of WNK4 at Ser 1169[91] and 1196.[109] Thus, the C-terminus containing Ser 1169 and 1196 was called the "switch-domain" for renal K secretion. Moreover, WNK1 has also been reported to stimulate SGK1 through PI3 kinase.[110] WNK1-induced activation of SGK1 could also play a role in mediating the effect of a high-K intake on K secretion. A large body of evidence suggests that SGK1 mediates, at least in part, the effect of aldosterone on renal K secretion.[91,111–113] For instance, the phenotype of SGK1 deletion is similar to MR knockout mice, and displays compromised renal K secretion in response to a high dietary K intake.[111] However, it is still not known whether the stimulatory effect of SGK on renal K secretion is the result of increased ENaC activity which in turn augments the electrochemical gradient for K secretion or due to a direct stimulation of ROMK channel insertion. It has shown that ROMK expression in the apical membrane of the TAL and CCD is actually increased rather than decreased in SGK null mice.[114] This suggests that the role of SGK in stimulating ROMK insertion may not be essential or can be replaced by other kinases, such as cAMP-dependent protein kinase A. A possible role of SGK in regulating renal K secretion by a daily dietary K intake has been suggested by the report that a high dietary K intake for 12hours stimulates SGK expression in the kidney.[115] Moreover, ROMK channel activity increased significantly in the CCD from rats on a high-K diet for only 6hours. Thus, SGK may regulate ROMK channel activity in the CT and CCD in response to a daily variation of dietary K intake.

INTERACTION OF PTK, SGK1, AND WNK4

As discussed above, WNK4 inhibits ROMK channels and K secretion in the CNT and the CCD. SGK1 reversed the inhibitory effect on ROMK channels by stimulation of WNK4 phosphorylation in serine residues 1169 and 1196. However, Wang and his associates have demonstrated that Src family PTK modulates the effect of SGK1 on WNK4, and abolishes the SGK1-induced phosphorylation of WNK4. Figure 47.11 is a model illustrating the role of the interaction among c-Src, SGK1, and WNK4 in regulating ROMK channels and K secretion. Activation of c-Src inhibits the SGK1-mediated phosphorylation of WNK4, thereby restoring the inhibitory effect of WNK4 on ROMK channels and K secretion.[116] The c-Src-dependent modulation of SGK1-WNK4 interaction may play a key role in preventing K loss during volume-depletion, and in stimulating K secretion during a high-K intake. Both volume-depletion and K secretion are expected to increase SGK1 expression. However, a high-K intake has been shown to suppress PTK activity, whereas volume-depletion does not inhibit PTK expression. Consequently, although a volume-depletion stimulates SGK1 activity, a high PTK activity blocks the effect of SGK1 and prevents K loss.

UBIQUITINATION

Ubiquitination plays an important role in the regulation of protein degradation and recycling by attaching ubiquitin molecules to lysine residues of substrate protein. Ubiquitination can further be classified into mono-ubiquitination by adding only one or two ubiquitin molecules to the substrate protein or polyubiquitination by attaching more than four ubiquitin molecules. The polyubiquitinated protein is subjected to degradation, whereas monoubiquitinated proteins are targeted to internalization and possibly recycling to the cell membrane. ROMK1 channel activity could be regulated by monoubiquitination, and the ubiquitin-binding site is on Lysine residue 22 on the N-terminus of ROMK1[117] (Figure 47.8). The physiological importance of monoubiquitination in the regulation of ROMK channel is still not clear. Because ROMK channel activity in the CCD decreases in response to stimulation of PTK, it would be interesting to determine whether monoubiquitination is required for the PTK-induced internalization of ROMK1 in the CCD. POSH (plenty of SH3) is an E3 ubiquitin ligase, and expression of POSH enhances the ubiquitination of ROMK, suggesting that POSH is involved in ubiquitination of ROMK channels.[118]

NUCLEOTIDES, THE CYSTIC FIBROSIS TRANSMEMBRANE CONDUCTANCE REGULATOR (CFTR), AND SULFONYLUREA RECEPTOR (SUR) PROTEINS

MgATP both activates and inhibits ROMK channels (Figure 47.9), with the net effect of nucleotide action being the integration of these opposite and complex events. Activation occurs by stimulation of PKA-mediated phosphorylation (see section on PKA, above) or by altering the generation of PIP_2 (,[15] and see section on regulation by PIP_2, below). These processes modulate channel-gating or plasma membrane channel density (e.g., by regulating trafficking of the channel to the

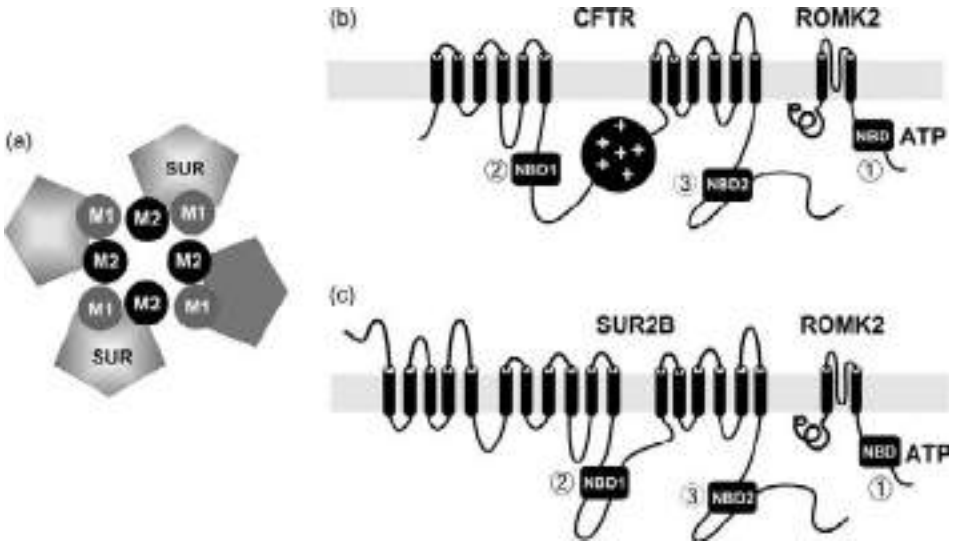

FIGURE 47.12 **Assembly of K_{ATP} and ROMK channels with ATP Binding Cassette (ABC) proteins.** (a) The proposed hetero-octameric complex forming ATP-sensitive (K_{ATP}) channels with four K_{IR} subunits and four sulfonylurea receptor (SUR) subunits. The M1 and M2 membrane segment arrangement is as shown in Figure 47.2a, with the M2 membrane segments lining the channel pore. (b) The topology of CFTR and ROMK channels proposed to form kidney K_{ATP} channels. A single nucleotide-binding domain (NBD, 1) is present on the C-terminus of ROMK, while two NBDs (numbered 2 and 3) are found on CFTR. (c) The topology of the sulfonylurea receptor, SUR2B, and ROMK proposed to form kidney K_{ATP} channels.

apical plasma membrane for the endoplasmic reticulum[75]). Inhibition of the SK secretory channel in CCD by MgATP[45] identifies this channel as belonging to a subgroup of Kir channels, referred to as ATP-sensitive or K_{ATP} channels (the classical K_{ATP} channels, Kir6.x; and Kir1.1 or ROMK channels[43,119]). The renal SK or K_{ATP} channel is somewhat less sensitive to ATP than the pancreatic β-cell or other K_{ATP} channels. As observed with other K_{ATP} channels,[119,120] addition of MgADP to MgATP-inhibited ROMK channels relieves the ATP block.[13] Thus, changes in the cytosolic MgATP concentration or in the MgATP/ADP ratio, as may occur with alterations in the activity of Na^+-K^+-ATPase, could modulate ROMK channel activity. This may provide one mechanism for coupling basolateral Na^+-pump activity with apical K^+ secretion in the principal cells of the CCD.

Channel inhibition by Mg-ATP is incompletely understood; however, the mechanism likely involves both direct binding of MgATP to the ROMK protein at an unconventional nucleotide-binding site (NBD; Figure 47.2b) and interaction with CFTR. The direct binding of ATP to K_{ATP} channels is supported by cross-linking of azido-ATP compounds to the channel proteins.[51,121,122] In addition, recent biochemical observations using fluorescent ATP analogs have shown that Mg-ATP can bind directly to K_{ATP} channels, including ROMK.[51,123,124] Both N- and C-terminal segments form the nucleotide-binding site which is situated at a region modeled to be involved in channel gating.[61,125,126] The crucial N-C-terminal interaction occurs between adjacent subunits; in other words, the nucleotide-binding site is intermolecular. As observed with other K_{ATP} channels,[119,120] addition of ADP to ATP-inhibited ROMK channels relieved the ATP block.[13]

Only a few studies have found that ATP can inhibit ROMK when expressed alone in *X. laevis* oocytes,[12,13,127] suggesting that direct binding of MgATP to ROMK is insufficient for channel inhibition. Several studies have demonstrated that ROMK channels may interact with CFTR or sulfonylurea receptor type 2B (SUR2B) (Figure 47.12a), and that such interaction is required for ATP sensitivity.[128–130] Moreover, a characteristic of K_{ATP} channels, including the renal SK channel, is their sensitivity to inhibition by sulfonylureas like glibenclamide.[119,131] The pancreatic β-cell K_{ATP} channel is formed by two subunits; a pore-forming polypeptide, Kir6.2; and the sulfonylurea-binding protein, SUR1 (an ABC (ATP-Binding Cassette) protein family member like CFTR[132–134]) in a 4:4 ratio (see Figure 47.12a[135–137]). Kir6.2 provides the K^+ channel permeation pathway and ATP binding-inhibition site, while SUR is required for sulfonylurea binding, and for certain aspects of regulation by nucleotides (e.g., ADP effects[133,138,139]). Two lines of evidence suggest that CFTR-ROMK interaction may play a key role for the sensitivity of ROMK to sulfonylurea agents: (1) CFTR is expressed in the same apical regions as ROMK channels in the CTAL and CCD,[140] and a functional

truncated hemi-CFTR is also expressed in the MTAL[141]; (2) glibenclamide- and Mg-ATP-sensitive whole cell K^+ currents in *X. laevis* oocytes are only observed when ROMK is co-expressed with CFTR.[127,142] In the kidney, glibenclamide induces natriuresis in rats,[143,144] and patch-clamp experiments have shown that 200 μM glibenclamide inhibits the apical SK channel in the rat TAL by about 60–70%.[40,145] The sensitivity of the SK channel in TAL to sulfonylureas is, however, much less than in other K_{ATP} channels.[43] Thus, the ability of glibenclamide to inhibit the K^+ secretory channels in renal distal tubule suggests that a SUR-like protein is associated with this channel, and is involved in the sulfonylurea effect (Figure 47.12C). However, the role of CFTR in regulating ATP-sensitivity of ROMK channels is still not completely understood.[146] Because the regulation of ROMK channels by ATP required PKA-dependent phosphorylation of CFTR, ATP-sensitivity of ROMK might be the result of the PKA-phosphorylation state of CFTR, rather than direct ATP regulation.[146]

INTRACELLULAR pH AND EXTRACELLULAR K

Small reductions in cytosolic pH reversibly inhibit ROMK channel activity expressed in *X. laevis oocytes*,[10–12,60,147] and the SK channel in TAL and CCD.[45,47,48,148] Lysine at position 80 on the N-terminus of ROMK1 (K61 on ROMK2; see Figures 47.2 and 47.8) is primarily responsible for conferring this pH-sensitivity, as mutation of this residue abolished pH-dependency[10,11,149]; although later studies have suggested an alternative role of lysine-80 in the pH regulation of ROMK1.[150,151] The pH-dependent gating of ROMK is rapidly reversible as long as the exposure to low pH (6.0–7.0) is short. Longer exposure to low pH results in "irreversibility." Schulte and co-workers have recently provided an explanation for the latter. The pH-dependent conformational change in ROMK apparently exposes N- and C-terminal cysteine residues forming disulfide bridges that lock the protein in a closed conformation. The disulfide bridges can be broken by DTT (dithiothreitol), resulting in channel reopening.

Cytosolic pH can also alter ROMK channel activity in another way. The $K_{1/2}$ for inhibition of ROMK channel activity is not fixed, but can be modulated by altering cytosolic side pH. McNicholas and co-workers[12] found that decreasing the pH from 7.4 to 7.2 on the cytosolic face of excised patches from oocytes expressing ROMK2 reduced the $K_{1/2}$ for MgATP inhibition from about 2.5 mM to $<$0.5 mM, almost a 10-fold increase in affinity with this small acidification. This effect appears to be independent of the lysine residue implicated in pH-dependent regulation of ROMK channel activity,[10,11] indicating that another pH sensor may be present on ROMK. This notion is supported by the report that the residues on the N-terminus of ROMK and the helix bundle crossing near the cytoplasmic end of the transmembrane pore have also been shown to modulate sensitivity to pH.[10,152] Relevant to the existence of multiple internal pH sensors is the finding that pH-dependent gating of ROMK1 is associated with conformational changes in both N- and C-termini.[147] The pH sensitivity of ROMK channels is controlled by extracellular K^+[153,154]. It has been shown that removal of extracellular K^+ inactivates ROMK channels which are closed by internal acidic pH. In the absence of extracellular K^+, intracellular alkalization fails to reactivate ROMK channels, and adding extracellular K^+ is required to reactivate ROMK channels. It has been suggested that internal pH-gating and external K^+-gating might act in the same amino acid (leucine residue 160 of ROMK2).[155] Acidification induces conformation changes, preventing K^+ access to the transmembrane pore from the cytoplasm.[152]

Not only affecting ATP sensitivity, change in pH also modulates the effect of polyamine block of ROMK channels. A negatively-charged glutamic acid residue in this C-terminal region (e.g., E224 in Kir2) has been shown to modulate block by Mg^{2+} or polyamines.[67] In addition, a histidine residue in Kir6.2 (H216, see Figure 47.2[156]) in a region corresponding to the Walker A site in ROMK, has been shown to mediate pH-dependent modulation of polyamine block of this K_{ATP} channel. Thus, this region of the C-terminus of Kir channels is involved in a variety of different gating functions (ATP, pH, polyamines).[157]

PHOSPHOINOSITIDES

Phospholipids, particularly PIP_2, have been shown to modulate Kir channels including ROMK1.[14,15,158] Exposure of inside-out patches from oocytes expressing Kir6.2 to PIP_2 reduces the ATP-sensitivity of this K_{ATP} channel, apparently by reducing the probability of ATP-binding to its receptor site.[158] Consequently, increasing concentrations of PIP_2 increase K_{ATP} channel activity. PIP_2 interacts with the pore-forming subunit rather than the SUR subunit of K_{ATP} channels, since PIP_2 modifies the ATP sensitivity of the C-terminal truncated Kir6.2 channel in the absence of SUR1.[158] ROMK, like many Kir channels, contains a high density of positively-charged amino acids just C-terminal to M2 (see Figure 47.2). Huang and co-workers[15] have shown that labeled phospholipid vesicles bind to a recombinant ROMK1 C-terminal fusion protein. These investigators implicated arginine 186 in the ROMK1 C-terminus (see Figure 47.2), as mutation of this residue to glutamine modified PIP_2 effects. Since PIP_2 is generated by ATP-dependent lipid kinases, Huang and co-workers have suggested that the stimulatory effect of MgATP may be due to the generation of PIP_2 by lipid

kinases.[15] Interaction with PIP_2 in the membrane is likely a general mechanism for activating Kir channels (see section on the structure of Kir and ROMK above).

REGULATION OF ROMK EXPRESSION IN KIDNEY (K^+ INTAKE, MINERALOCORTICOIDS, VASOPRESSIN, Klotho)

Since K^+ homeostasis is mainly controlled by aldosterone and the potassium-load, it is not surprising that ROMK mRNA expression in rat kidney is regulated by aldosterone, K^+ adaptation, and vasopressin (see Figure 47.9). It is well-established that rats fed a high-K^+ diet adapt by upregulating renal K^+ secretion and excretion.[159] This results, at least in part, from an increase in the SK channel density in CCD.[160] Wald and co-workers[161] found that K^+ deficiency reduces ROMK mRNA expression in both cortex and medulla, while K^+-loading increases ROMK transcript slightly only in medulla. Moreover, several studies have shown that K^+ deficiency decreased ROMK expression in the plasma membrane of the collecting duct,[162,163] presumably by stimulating internalization including clathrin and syntaxin-1A-dependent endocytosis.[164,165] The specific ROMK isoforms that changed with potassium were not assessed. Moreover, Frindt and co-workers[166] found that ROMK transcript abundance by *in situ* hybridization in the CCD was not affected by a high-K^+ diet. Thus, the high-K^+ diet-induced increase in density of active SK channels in principal cells in the CCD is not due to increased abundance of ROMK mRNA. Rather, changes in ROMK protein abundance, channel activation or ROMK channel translocation to the membrane are potential mechanisms to account for the high-K^+ adaptation effect on SK channels in the principal cells.

Mineralocorticoids also regulate ROMK abundance. Adrenalectomy decreased ROMK mRNA abundance in cortex, but increased transcript abundance in the medulla.[161] In this latter study, K^+ deficiency in adrenalectomized rats reduced ROMK mRNA to control levels, suggesting that the hyperkalemia associated with adrenalectomy was the cause for the increased ROMK message in medulla. In another study, White and colleagues[26] showed that aldosterone administration by minipump to adrenal intact rats increased ROMK transcripts in whole kidney. In the latter study, the ROMK2, 3, and 6 isoforms were increased by the mineralocorticoid. This latter study would be consistent with mineralocorticoid-mediated regulation of ROMK mRNA abundance in cortex. However, the glucocorticoid-responsive element responsible for transcriptional regulation of ROMK by mineralocorticoid has never been identified in the promoter region of the RMOK gene, *KCNJ1*.

Vasopressin, via cyclic AMP, stimulates K^+ secretion in principal cells,[47] and activates the apical K^+ channels in TAL cells[40,167] (see Figure 47.6). Although the activation of PKA by cAMP would phosphorylate ROMK (or the SK channel), it remains to be shown whether this is sufficient to account for the stimulation of K^+ channel activity or whether additional mechanisms, such as channel insertion into the membrane, are required. As discussed above, PKA-anchoring proteins appear to be required for cAMP activation of ROMK currents in oocytes[78] (see Figure 47.10).

Klotho is an aging-suppressing protein which is expressed in several organs, including the kidney. The application of the Klotho's extracellular domain increases the surface expression of ROMK1, and enhances urinary K^+ excretion.[168] The mechanism by which Klotho increases the expression of ROMK in the plasma membrane is by eliminating terminal sialic acids from N-glycan of ROMK. Consequently, underlying disaccharide galactose-N-acetylglucosamine is exposed and binds to galectin-1, a ubiquitous galactoside-binding lectin. Binding of ROMK to galectin-1 inhibits the clathrin-dependent endocytosis of ROMK. The physiological role of endogenous Klotho in K^+ homeostasis is unknown.

Lessons from Bartter's Syndrome

Bartter's syndrome[169] comprises a set of autosomal recessive renal tubulopathies characterized by hypokalemic metabolic alkalosis, salt-wasting, hyperreninemia, and hyperaldosteronsim.[170–173] Antenatal Bartter's syndrome is the most severe form of the inherited disorders, and is characterized by hyperprostaglandinemia (PGE_2). Antenatal Bartter's syndrome is genetically heterogeneous, resulting from mutations in one of five genes.[174] Three of the Bartter's genes encode the major Na^+, K^+, Cl^- transporters in the TAL: the *SLC12A1* gene encoding the apical Na-K-2Cl co-transporter[175,176]; the *CLCKB* basolateral Cl^- channel[177]; and the *KCNJ1* apical K^+ recycling channel, ROMK (see mutations in Figure 47.8[178–180]). Mutations in two other genes also produce the Bartter's phenotype – barttin and the extracellular calcium-sensing receptor (CaSR). Barttin is a membrane protein that is required for trafficking of the ClCKb channel to the basolateral membrane of TAL cells, and loss-of-function mutations in barttin result in the absence of basolateral Cl^- channel activity.[181] Gain-of function mutations in the CaSR result in inhibition of Na,K-ATPase, NKCC2, and apical 70 pS K channel activity.[174,182,183]

The effect of loss-of-function mutations in ROMK on TAL function can be understood, since apical K^+ recycling is crucial both to supplying K^+ to the Na-K-2Cl

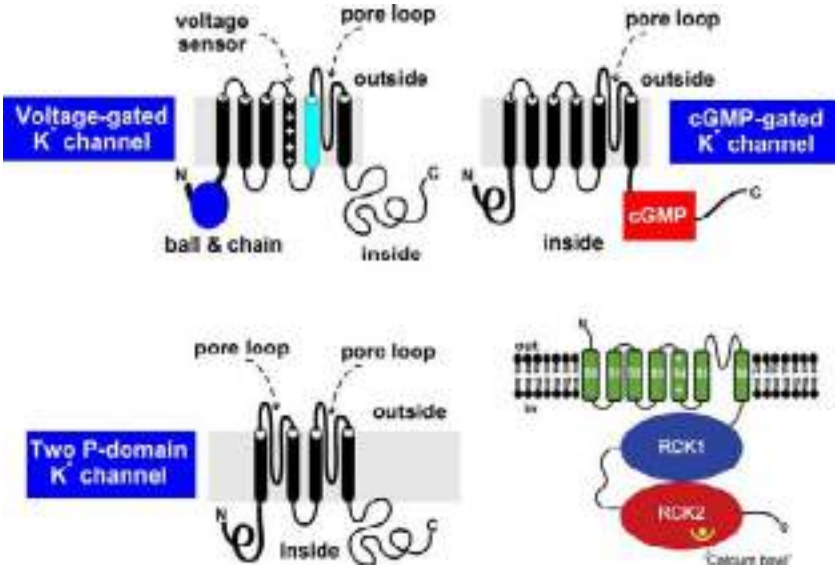

FIGURE 47.13 **Proposed topologies of the voltage-gated, cyclic nucleotide-gated, two-P-domain K^+ channel and Ca^{2+}-activated BK channels expressed in mammalian kidney.** The pore loops are indicated in each channel. Note the two pore loops for the two-P channel.

co-transporter, and to generation of the lumen-positive transepithelial voltage that drives 50% of the reabsorbed sodium through the paracellular pathway.[184,185] ROMK channels with some of the Bartter's mutations express either no or little function in *X. laevis* oocytes,[186–188] consistent with mutations in *KCNJ1* in Bartter's syndrome resulting in ROMK loss-of-function. Based on the location of the amino acid residue altered with certain KCNJ1 mutations (e.g., at or near phosphorylation sites or the nucleotide-binding site), the resultant ROMK channels would be expected to exhibit altered gating (see discussion above on "Regulation of the ROMK K^+ Channel"). A ROMK-deficient mouse has been developed and exhibits a Bartter's-like phenotype.[189,190]

While both human and mouse studies clearly demonstrate the importance of ROMK in TAL function, several questions regarding the resulting Bartter's phenotype remained. First, two types of apical K^+ channels have been observed in the rat TAL,[40] an SK channel with characteristics typical of ROMK and an intermediate conductance (~70 pS) channel that is similar only in some properties with ROMK. In rat TAL cells, however, the 70 pS channel predominates, so that mutations in the ROMK gene that generate inactive SK channels would only be expected to have minimal effect on the apical K^+ conductance of TAL cells. This has suggested that the intermediate conductance channel requires ROMK for function (e.g., either as a subunit or as a regulator). This possibility has been established by the absence of 70 pS K^+ channels in the TAL from ROMK null mice.[191] Second, ROMK comprises the apical K^+ secretory channel in principal cells of the CCD. Yet, Bartter's individuals with *KCNJ1* mutations are hypokalemic. This is due to the impairment of NaCl and fluid reabsorption in TAL which leads to increased NaCl and fluid delivery to the distal nephron, which stimulates K^+ secretion via the alternative flow-stimulated Maxi-K channel[94] (see section on "Maxi-K Channel" below).

OTHER RENAL POTASSIUM CHANNELS

Several other K^+ channels have been cloned from kidney-derived cell lines or are found in mammalian kidney (Figure 47.13). Physiological roles for these channels are less-defined than that for ROMK.

Ca^{2+}-Activated Big-Conductance K^+ Channels (BK, Maxi-K Channel)

The BK channel is composed of a pore-forming α-subunit (*Slo* 1), and an accessory β-subunit.[192,193] BK channel activity has been detected at the apical membrane of both principal cell (PC) and intercalated cell (IC), basolateral membrane of PC in the CNT and CCD[194,195] and in the podocytes where the BK channels may be involved in regulating glomerular filtration rate.[196]

BK IN THE APICAL MEMBRANE

Microperfusion experiments have demonstrated that BK channels are involved in mediated K^+ secretion during increased dietary K^+ intake.[197] However, the observation that the deletion of the BK channel α-subunit does not affect the net K^+ excretion in mice fed with a high-K^+ diet suggests that HK-induced stimulation of

ROMK channel expression and high plasma aldosterone level can compensate for deleting BK channels on K^+ secretion.[198] Although the role of BK channels in mediating flow-stimulated K^+ secretion has been firmly established,[198–201] it is still not completely-understood whether IC or PC is responsible for mediating the BK-dependent K^+ secretion. Patch-clamp experiments have demonstrated that apical BK channel activity is higher in IC than those in PC.[195] However, because IC has a low Na-K-ATPase activity, it is still arguable whether BK channels in IC significantly contribute to K^+ secretion in the collecting duct.[202] A recent study performed in *Kcnmb4*$^{-/-}$ mice in which the BK β4-subunit is deleted suggests the role of BK channels in IC in mediating flow-dependent K^+ secretion. Holtzclaw et al. have demonstrated that renal K^+ excretion was compromised in response to a HK intake in mice lacking the BK β4-subunit which is expressed in the apical membrane of IC in the CNT and CCD.[203] Furthermore, immunocytochemical staining shows that a high-K^+ intake decreased IC size in wild-type, but not in *Kcnmb4*$^{-/-}$, mice. Moreover, the flow rate speed was higher in knockout mice than those of wild-type mice. It is suggested that the BK channel in IC plays a role in K^+ secretion through decreasing IC size and increasing luminal volume of the CNT and the CCD, thereby creating conditions more favorable for K^+ secretion.

BK CHANNEL IN THE BASOLATERAL MEMBRANE

Immunocytochemical staining shows that BK α- and β1-subunits are expressed in the basolateral membrane of PC in the CNT and CCD, and their expression is stimulated by Na^+ restriction. The physiological function of basolateral BK channels in PC is possibly responsible for hyperpolarizing the basolateral membrane, thereby increasing the driving force for Na^+ absorption. The notion is supported by the observation that BK-β1($^{-/-}$) mice (*Kcnmb1*$^{-/-}$) have a higher Na^+ clearance than those of wild-type mice in response to low Na^+ intake.[204] The impaired function of basolateral BK channels in PC also affects the renal K^+ secretion in *Kcnmb1*$^{-/-}$ mice in response to a high-K^+ intake.[205] *Kcnmb1*$^{-/-}$ mice on a high-K^+ diet are hypertensive, volume-expanded, and have reduced urinary K^+ and Na^+ clearances, an effect which can be treated with mineralocorticoids receptor antagonist. This suggests that the impaired K^+ secretion results from high aldosterone levels which stimulate Na^+ transport in *Kcnmb1*$^{-/-}$ mice.

Regulation of BK Channels

DIETARY K^+ INTAKE

Real-time PCR analysis has demonstrated that a high K^+ intake stimulates the mRNA transcription of BK α-, β2-, and β4-subunits, but not β1, in the rabbit CCD.[206] Because a low-Na^+ intake, which increases aldosterone levels, fails to mimic the effect of a high-K^+ intake on the mRNA level of BK α- β2-, and β4-subunits, it excludes the role of aldosterone in regulating BK channel expression.[207] Also, the patch-clamp experiments demonstrated that a high-K^+ intake stimulates the BK channel activity in PC of the CCD.[194] Since inhibition of P38 and ERK activates BK channels in PC, and a high-K^+ intake suppresses both MAPK,[194] p38, and ERK, MAPK may be involved in mediating the effect of a high-K^+ intake on BK channels.

PKA AND PKC

Patch-clamp study has demonstrated that PKA and PKC inhibit BK channel activity in the PC of the CCD.[208] The role of PKA and PKC in regulating the flow-stimulated BK-dependent K^+ secretion in the CCD is also shown in the isolated perfused rabbit CCD. PKA induced a tonical inhibition of BK channels or an associated regulatory protein in PC. However, PKA has no inhibitory effect on BK channel in IC. It is possible that BK channels in PC and IC may be the results of different splice variants which respond to PKA in different ways.

CYTOCHROME P450 (CYP) EPOXYGENASE

BK channels in the PC are activated by CYP-epoxygenase-dependent metabolism of arachidonic acid, an effect which is also mimicked by 11,12-epoxyeicosatrienoic acid (11,12-EET), a main product of CYP-epoxygenase-dependent metabolism in the kidney.[209] Because a high-K^+ intake increased 11,12-EET levels in the CCD and stimulated the expression of CYP2C44 homolog, a main CYP-epoxygenase in the kidney, 11,12-EET may play a role in stimulating BK channel-dependent K^+ secretion during a high-K^+ intake. This notion is also supported by the finding that inhibition of CYP-epoxygenase abolished the flow-stimulated and BK-dependent K^+ excretion in the isolated rabbit CCD.[209]

Other 6-TM Renal K^+ Channels

The voltage-gated K^+ (Kv) channels are expressed in the kidney, and their function in regulating epithelial transport is well-documented.

KCNQ1 CHANNEL

KCNQ1 forms a small conductance (2–10 pS) Kv channel in kidney, existing as a heteromultimeric complex with KCNE1 (minK). MinK has a single transmembrane segment and is highly-expressed at the apical membrane. KCNQ1 and KCNE1 have been

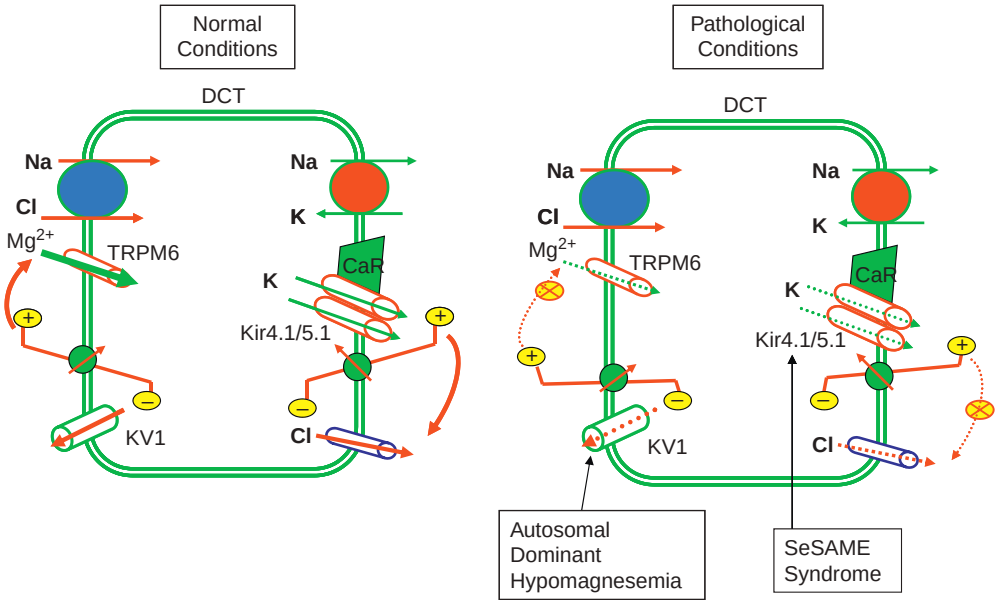

FIGURE 47.14 **A cell model illustrating the role of Kv1 and Kir4.1/5.1 in regulating Mg^{2+} transport and transepithelial Cl^- transport in the DCT.** SeSAME syndrome (for seizures, sensorineural deafness, ataxia, mental retardation and electrolyte imbalance).

extensively characterized in heart, where they play crucial roles in cardiac repolarization.[210–212] Mutations of these genes cause long QT syndrome. Immunostaining has demonstrated that voltage-gated K channels, such as ERG1 and KCNQ1, are expressed in the apical membrane of DCT and collecting duct.[213,214] The voltage-gated K^+ channels may prevent the membrane depolarization that occurs following stimulation of electrogenic Na^+-coupled transport of glucose or amino acids.[215] Accordingly, KCNE1 deficient mice exhibit a reduction in glucose and amino acid uptake, and defective volume regulation in the proximal tubule.[216] However, additional Kv channels and BK may also participate in stabilizing proximal tubule membrane potential during electrogenic Na^+ uptake.

KCNA1 FAMILY CHANNEL

A genetic study has revealed that voltage-gated K^+ channels (Kv1.1; KCNA1), which are expressed in the apical membrane of the DCT, play a role in regulating Mg^{2+} transport in the DCT.[217] A missense mutation in the Kv1.1 voltage-gated K channel caused human autosomal dominant hypomagnesemia. Figure 47.14 is a model illustrating the possible role of Kv1.1 in regulating Mg^{2+} transport in DCT. The activation of voltage-gated K channels is expected to hyperpolarize the apical membrane, thereby increasing the driving force for Mg^{2+} absorption through transient receptor potential cation channel 6 (TRPM6). Defective Kv1.1 channel function would impair the hyperpolarization of apical membrane potential, thereby decreasing the driving force for transepithelial Mg^{2+} transport through TRPM6.

KCNA10 is found at the apical membrane of the proximal tubule.[218] The *KCNA10* gene is located on 1p11–13, and transcripts are expressed in kidney, heart, and aorta. KCNA10 has 58% amino acid identity with Kv1.3, which also resides at 1p11–13.[219] The predicted secondary structure is identical to that of other Shaker-related K^+ channels, including intracellular N- and C-termini, 6 transmembrane segments, a voltage sensor (S4), and a pore (P) region. Unlike Shaker proteins, however, KCNA10 contains a putative cyclic nucleotide (CN)-binding domain at the C-terminus, suggesting that protein function is regulated by cyclic nucleotides (Figure 47.13).

2-TM Renal K^+ Channel (Non-ROMK)

Kir4.1 (KCNJ10), Kir4.2 (KCNJ15), AND Kir5.1 (KCNJ16) CHANNELS

Heteromeric Kir4.1/Kir5.1 and/or Kir4.1/Kir5.1 channels form the basolateral small conductance K^+ channel in distal nephron segments.[220] The inward rectifier K^+ channel, Kir4.1, was originally identified from rat brain, and exhibits 53% amino acid identity to ROMK1.[221,222] The kidney also expresses Kir4.1 mRNA, and the channel protein has been immunolocalized to the basolateral membrane of distal nephron segments, including DCT, CNT, and CCD.[223] Internal protons decrease Kir4.1 K^+ current by reducing open probability, however, internal protons also increase

channel conductance.[224] Mice with deletion of the Kir4.1 gene (KCN10) have been generated[225] but, due to early lethality in the neonatal stage, renal phenotype has not been examined.

Kir4.2 was originally cloned from human kidney and called Kir1.3.[31] While this study reported that Kir4.2 channels were not functional in *X. laevis* oocytes,[31] subsequent studies have shown that this protein forms inward rectifying K^+ channels that are inhibited by protein kinase C and internal protons.[220,226] Kir4.2 mRNA is found in human[31] and mouse[220] kidney, and in the latter species, specifically in the DCT.

The inward rectifier K^+ channel, Kir5.1, was also cloned from rat brain, but does not form functional K^+ channels by itself when expressed in *X. laevis* oocytes.[221] Kir5.1 mRNA is present in kidney,[221,227] and channel protein is abundantly expressed in PT, and in DCT and CCD segments,[228] where Kir4.1 is also expressed.[223] Recent studies have demonstrated that Kir4.1 or Kir4.2 can form heteromeric inward rectifying K^+ channels with Kir5.1 with distinct properties in the heterologous expression systems,[220,227,229] as well as in the native kidney.[227] The heteromeric interaction of Kir5.1 with other Kir K^+ channels is specific for Kir4.x channels, and requires a small region in the proximal COOH-terminus of Kir4.1.[229]

Patch-clamp experiments, immunocytochemical and molecular biological methods have confirmed the expression of several inwardly-rectifying K channels in the basolateral membrane.[204,230–233] Two lines of evidence suggest that Kir4.1/5.1 heterotetramers are the main type of K channels in the basolateral membrane in the ASDN: (1) the Kir4.1 protein is detected in the basolateral membrane of the DCT and the CCD[220,232]; and (2) the patch-clamp experiments have shown that Kir4.1/Kir5.1 channels form the major K channels in the basolateral membrane of principal cells (PC) in the CCD.[232] The most dramatic and specific effect of the Kir4.x-Kir5.1 assembly on K^+ channel function is the shift in the pKa for inhibition by internal protons from 6.0 to the physiologically relevant pKa of 7.4.[227,228,234,235] Internal pH sensitivity of Kir4.1-Kir5.1 is modulated by PIP_2,[236] similarly to Kir1.1 (ROMK).[237]

Kir4.1 has been shown to interact with Ca^{2+}-sensing receptor which inactivates the K channels.[238] Because Kir4.1 participates in generating the cell membrane potential, activation of Ca^{2+}-sensing receptor is expected to depolarize the membrane potential, thereby inhibiting transepithelial Na/Cl transport in the DCT. The importance of Kir4.1 in regulating membrane transport in the DCT is best demonstrated in patients with EAST (for epilepsy, ataxia, sensorineural deafness, and tubulopathy)[239] or SeSAME syndrome (for seizures, sensorineural deafness, ataxia, mental retardation and electrolyte imbalance).[240] The disease is caused by defective gene product encoding KCNJ10 (Kir4.1), which is expressed in a variety of tissues including in the basolateral membrane of the ASDN. The renal phenotypes of EAST/SeSAME syndrome are hypokalemia, metabolic alkalosis, and hypomagnesemia.[239,240] Figure 47.14 is a cell model illustrating the role of Kir4.1/5.1 in regulating NaCl transport in the DCT. Activation of Kir4.1/5.1 is expected to increase the negativity of basolateral membrane, thereby providing the driving force for Cl^- exit across the basolateral membrane. In contrast, defective Kir4.1 depolarizes the basolateral membrane, thereby diminishing the driving force for Cl^- exit across the basolateral membrane. Consequently, delivery of NaCl to the CNT and CCD is increased and leads to enhanced Na absorption in the CNT and CCD at the expense of K^+-wasting, resulting in hypokalemia and metabolic alkalosis. It was suggested that decreased basolateral membrane potential impairs Mg^{2+} absorption in the DCT, due to a compromised driving force for Mg^{2+}.[44]

Kir2.3 (KCNJ4) CHANNEL

In cortical collecting duct principal cells the maintenance of the negative membrane potential depends, at least in part, on the activity of an inwardly rectifying 18 pS K^+ channel. This basolateral K^+ channel has been suggested to be the inwardly rectifying K^+ channel, Kir2.3.[241] The kidney Kir2.3 was cloned from a mouse CCD cell line and its expression in kidney confirmed by Northern analysis.[241] When the MDCK cells were transfected with Kir2.3, the channel is expressed in the basolateral membrane,[242] and a basolateral sorting signal was identified at the COOH-terminal tail.[243,244] Kir 2.3 shares some biophysical properties with the native 18 pS K^+ channel, such as high open probability and channel conductance, 14.5 pS.[241]

Kir6.1 (KCNJ8) CHANNEL

Kir6.1 was originally cloned from a rat pancreatic islet cell cDNA library using Kir3.1 as a probe,[245] and belongs to the Kir6.x (ATP-sensitive; K_{ATP}) subfamily of inwardly rectifying K^+ channels.[2,246] Exogenous expression of Kir6.1 channels in *X. laevis* oocytes form ATP-sensitive channels only when co-expressed with a sulfonylurea receptor protein.[246,247] Although this inward rectifier is predominantly found in brain, heart, and vascular tissue, expression in kidney has been documented.[245,248] Kir6.1 has been localized to both mitochondria[249] and plasma membranes.[249,250] Upregulation of Kir6.1 mRNA has been observed following ischemic injury in rat kidney, consistent with the proposed role of K_{ATP} channel activation in protection from ischemic damage (e.g., in the heart[251]). Recently, Kir6.1 was cloned from rabbit proximal

tubule cDNA library, and expression of Kir6.1, SUR2A, and SUR2B in rabbit proximal tubule confirmed by PCR.[250] Functional studies in *X. laevis* oocytes suggested that Kir6.1 may form the basolateral ATP- and taurine-sensitive K^+ channel involved in the basolateral K^+ conductance of proximal tubules.[250] Adenylate kinase, which promotes phosphoryl transfer between ATP and ADP and associates with K_{ATP} channels,[252] has been cloned from the rabbit proximal tubule library,[253] and may associate with Kir6.1 in these cells to promote metabolic sensing.

Kir7.1 (KCNJ13) CHANNEL

The inward rectifier K^+ channel, Kir7.1, was originally cloned from human brain cDNA libraries after searching the GenBank expressed sequence Tag (EST) database using Kir1.1 and Kir6.2.[254,255] The Kir7.1 K^+ channel displays unusual K^+ permeation properties, with a low single channel conductance of 50 fS, low sensitivity to blocking by external Ba^{2+} or Cs^+, and very low dependence of conductance on external K^+.[254–256] PCR and Western blot analyses have identified Kir7.1 transcripts and protein, respectively, in rat, guinea pig, and human kidney.[254,255,257,258] Expression of Kir7.1 along the rat nephron was demonstrated by Western blots of microdissected nephron segments,[258] which showed K^+ channel protein in TAL, DCT, CNT, CCD, OMCD, and IMCD.[258] Immunostaining localized Kir7.1 to basolateral membranes of DCT and principal cells.[258] In the guinea pig, Kir7.1 protein is expressed in basolateral membranes of proximal tubule and TAL cells.[257] In the CCD, Kir7.1 is expressed in principal cells, but not intercalated cells. The unique pore properties of Kir7.1 and its localization close to Na-K-ATPase suggested that this K^+ channel may be functionally coupled to Na-K-ATPase, and involved in K^+ recycling across basolateral membranes.[258,259]

The Two-Pore K^+ Channels (K_t)

In CNT and CCD, a double-pore K channel (KCNK1) is expressed in the apical membrane.[38,260–262] However, the physiological function of the two-pore K channels in the CNT or CCD is still not clear. The most recently-discovered class of K^+ channels is characterized by a topology containing two pores or P-loops. These channels are also appropriately referred to as the "two pore domain" (or K_t, two-P, TWIK-related) K^+ channels (e.g., see [263]). K_t channels exhibit four membrane spanning domains consisting of two Kir-like domains that are linked in a single subunit (see Figure 47.13[263–269]). Structurally similar channels have been identified in the *C. elegans* genome project and represent the most abundant class of K^+ channels in this species.[270] The TWIK-related channels, including TWIK-1,[263,264,266–269,271] TWIK-2,[265] TREK-1,[263,272,273] TASK-1,[263,274] and TASK-2,[263] are all expressed in mammalian kidney.[263]

Both TWIK-1[267] and TWIK-2[265] express weakly inward-rectifying K^+ channels that are inhibited by intracellular acidification. Transcripts for TWIK-1 are expressed in rabbit cortical TAL and collecting duct,[269] and TWIK-1 protein has been localized to the brush border of proximal convoluted tubules, intracellular and apical border of intercalated cells in the CCD, and in cortical and medullary TAL cells.[266] TREK-1 gives rise to mechanosensitive outward-rectifying K^+ currents that are activated by arachidonic acid and are inhibited by protein kinases A and C.[272,275] TASK channels exhibit noninactivating outward-rectifying K^+ currents that are very sensitive to external pH.[263,274] While the properties of TWIK-related K^+ channels do not fit with any of the known native K^+ channels in kidney, their widespread expression in mammalian and other organisms (e.g., *C. elegans*) suggests either that they have been missed in patch-clamp recording or that they associate with other (unidentified to date) subunits to produce pores with native channel properties.

SUMMARY AND CONCLUSIONS

While we have gained significant insights into the structural diversity of K^+ channels expressed in the mammalian kidney, many new channels will likely be identified in the near future. Likewise, electrophysiological studies continue to expand our database of physiologically and pharmacologically distinct K^+ channels. The exciting challenge is to identify which channel genes encode which native channels. Given that many K^+ channels are probably comprised of more than one subunit (e.g., the K_{ATP} channels), this challenge is somewhat daunting, and will require many more years of investigation. Finally, we expect that new inherited disorders due to mutations in some of these channel genes (channelopathies) will be identified. These channelopathies will not only provide new insights into the physiological roles of K^+ channels, but will likely raise new questions as it has for ROMK mutations in Bartter's syndrome.

Acknowledgments

WHW is supported by DK54983 and CLH is supported by DK59530 from the National Institutes of Health.

References

[1] Hebert SC, Wang W-H. Structure and function of the low conductance K_{ATP} channel, ROMK. Wien Klin Wochenschr 1997;109:471–6.

[2] Nichols CG, Lopatin AN. Inward rectifier potassium channels. Ann Rev Physiol 1997;59:171–91.

[3] Ho K, Nichols CG, Lederer WJ, Lytton J, Vassilev PM, Kanazirska MV, et al. Cloning and expression of an inwardly rectifying ATP-regulated potassium channel. Nature 1993;362: 31–8.

[4] Jan LY, Jan YN. Cloned potassium channels from eukaryotes and prokaryotes. Ann Rev Neurosci 1997;20:91–123.

[5] Kubo Y, Baldwin TJ, Jan YN, Jan LY. Primary structure and functional expression of a mouse inward rectifier potassium channel. Nature 1993;362:127–33.

[6] Jan LY, Jan YN. Tracing the roots of ion channels. Cell 1992;715:715–8.

[7] Jan LY, Jan YN. Potassium channels and their evolving gates. Nature 1994;371:119–22.

[8] Jan LY, Jan YN. Voltage-gated and inwardly rectifying potassium channels. J Physiol 1997;505:267–82.

[9] Xu ZC, Yang Y, Hebert SC. Phosphorylation of the ATP-sensitive, inwardly rectifying K^+ channel, ROMK, by cyclic AMP-dependent protein kinase. J Biol Chem 1996;271: 9313–9.

[10] Choe H, Zhou H, Palmer LG, Sackin H. A conserved cytoplasmic region of ROMK modulates pH sensitivity, conductance, and gating. Am J Physiol (Renal Physiol) 1997;273: F516–29.

[11] Fakler B, Schultz JH, Yang J, Schulte U, Brändle U, Zenner HP, et al. Identification of a titratable lysine residue that determines sensitivity of kidney potassium channels (ROMK) to intracellular pH. EMBO J 1996;15:4093–9.

[12] McNicholas CM, MacGregor GG, Islas LD, Yang Y, Hebert SC, Giebisch G. pH-dependent modulation of the cloned renal K^+ channel, ROMK. Am J Physiol (Renal Physiol) 1998;275: F972–81.

[13] McNicholas CM, Yang Y, Giebisch G, Hebert SC. Molecular site for nucleotide binding on an ATP-sensitive renal K^+ channel (ROMK2). Am J Physiol (Renal Fluid Electrolyte Physiol) 1996;271:F275–85.

[14] Hilgemann DW, Ball R. Regulation of cardiac Na^+-Ca^{2+} exchange and K_{ATP} potassium channels by PIP_2. Science 1996;273:956–9.

[15] Huang C-L, Feng S, Hilgemann DW. Direct activation of inward rectifier potassium channels by PIP_2 and its stabilization by Gbg. Nature 1998;391:803–6.

[16] Fang L, Ganuti R, Kim BY, Wade JB, Welling PA. The ARH adaptor protein regulates endocytosis of the ROMK potassium secretory channel in mouse kidney. J Clin Invest 2009;119: 3278–89.

[17] Jiang Y, Lee A, Chen J, Cadene M, Chalt B, MacKinnon R. The open pore conformation of potassium channels. Nature 2002;417:523–6.

[18] Lin DH, Sterling H, Lerea KM, Giebisch G, Wang WH. Protein kinase C (PKC)-induced phosphorylation of ROMK1 is essential for the surface expression of ROMK1 channels. J Biol Chem 2002;277:44332–8.

[19] Pegan S, Arrabit C, Zhou W, Kwiatkowski W, Collins A, Slesinger PA, et al. Cytoplasmic domain structures of Kir2.1 and Kir3.1 show sites for modulating gating and rectification. Nat Neurosci 2005;8:279–87.

[20] Nishida M, Cadene M, Chait BT, MacKinnon R. Crystal structure of a Kir3.1-prokaryotic Kir channel chimera. EMBO J 2007;26:4005–15.

[21] Tao X, Avalos JL, Chen J, MacKinnon R. Crystal structure of the eukaryotic strong inward-rectifier K^+ Channel Kir2.2 at 3.1 + Å resolution. Science 2009;326:1668–74.

[22] Kahle KT, Wilson FH, Leng Q, Lalioti MD, O'Connell AD, Dong K, et al. WNK4 regulates the balance between renal NaCl reabsorption and K^+ secretion. Nat Genet 2003;35:372–6.

[23] Boim MA, Ho K, Shuck ME, Bienkowski MJ, Block JH, Slightom JL, et al. ROMK inwardly rectifying ATP-sensitive K^+ channel. II. Cloning and distribution of alternative forms. Am J Physiol 1995;268:F1132–40.

[24] Zhou H, Chepilko S, Schutt W, Choe H, Palmer LG, Sackin H. Mutations in the pore region of ROMK enhance Ba^{2+} block. Am J Physiol 1996;271:C1949–56.

[25] Kondo C, Isomoto S, Matsumoto S, Yamada M, Horio Y, Yamashita S, et al. Cloning and functional expression of a novel isoform of ROMK inwardly rectifying ATP-dependent K^+ channel, ROMK6 (Kir1.1f). FEBS Lett 1996;399:122–6.

[26] Hornby AH, White D. SJ. Regulation of distal nephron K^+ channels (ROMK) mRNA expression by aldosterone in rat kidney. J Physiol 1998;509:629–34.

[27] Beesley AH, Ortega B, White SJ. Splicing of a retained intron within ROMK K^+ channel RNA generates a novel set of isoforms in rat kidney. Am J Physiol (Cell Physiol) 1999;276: C585–92.

[28] Bock JH, Shuck ME, Benjamin CW, Chee M, Bienkowski MJ, Slightom JL. Nucleotide sequence analysis of the human KCNJ1 potassium channel locus. Gene 1997;188:9–16.

[29] Shuck ME, Block JH, Benjamin CW, Tsai T-D, Lee KS, Slightom JL, et al. Cloning and characterization of multiple forms of the human kidney ROM-K potassium channel. J Biol Chem 1994;269:24261–70.

[30] Yano H, Philipson LH, Kugler JL, Tokuyama Y, Davis EM, Le Beau MM, et al. Alternative splicing of human inwardly rectifying K^+ channel ROMK1 mRNA. Mol Pharmacol 1994;45: 854–60.

[31] Shuck ME, Piser TM, Block JH, Slightom JL, Lee KS, Bienkowski MJ. Cloning and characterization of two K^+ inward rectifier (K_{ir}) 1.1 potassium channel homologs from human kidney (K_{ir}1.2 and K_{ir}1.3). J Biol Chem 1997;272:586–93.

[32] Lee W-S, Hebert SC. The ROMK inwardly rectifying ATP-sensitive K^+ channel. I. Expression in rat distal nephron segments. Am J Physiol (Renal Fluid Electrolyte Physiol) 1995;268: F1124–31.

[33] Macica CM, Yang Y, Hebert SC, Wang W-H. Arachidonic acid inhibits the activity of the cloned renal K^+ channel, ROMK1. Am J Physiol (Renal Fluid Electrolyte Physiol) 1996;40:F588–94.

[34] Macica CM, Yang Y, Lerea K, Hebert SC, Wang W. Role of the NH_2 terminus of the cloned renal K^+ channel, ROMK1, in arachidonic acid-mediated inhibition. Am J Physiol (Renal Physiol) 1997;274:F175–81.

[35] Lundgren DW, Moore JJ, Chang SM, Collins PL, Chang AS. Gestational changes in the uterine expression of an inwardly rectifying K^+ channel, ROMK. Proc Soc Exp Biol Med 1997;216:57–64.

[36] Kohda Y, Ding W, Phan E, Housini I, Wang J, Star RA, et al. Localization of the ROMK potassium channel to the apical membrane of distal nephron in rat kidney. Kidney Internat 1998;54:1214–23.

[37] Mennitt PA, Wade JB, Ecelbarger CA, Palmer LG, Frindt G. Localization of ROMK channels in the rat kidney. J Am Soc Nephrol 1997;8:1823–30.

[38] Palmer LG. Potassium secretion and the regulation of distal nephron K channels. Am J Physiol 1999;277:F821–5.

[39] Xu JZ, Hall AE, Peterson LN, Bienkowski MJ, Eessalu TE, Hebert SC. Localization of the ROMK protein on apical

membranes of rat kidney nephron segments. Am J Physiol (Renal Physiol) 1997;273:F739–48.
[40] Wang W. Two types of K^+ channel in TAL of rat kidney. Am J Physiol (Renal Fluid Electrolyte Physiol) 1994;267-36: F599–605.
[41] Wang W, White S, Geibel J, Giebisch G. A potassium channel in the apical membrane of rabbit thick ascending limb of Henle's loop. Am J Physiol (Renal Fluid Electrolyte Physiol) 1990;258-27:F244–53.
[42] Frindt G, Palmer LG. Low-conductance K channels in apical membrane of rat cortical collecting tubule. Am J Physiol (Renal Fluid Electrolyte Physiol) 1989;256-25:F143–51.
[43] Misler S, Giebisch G. ATP-sensitive potassium channels in physiology, pathophysiology, and pharmacology. Curr Opin Nephrol Hypertens 1992;1:21–33.
[44] Schlatter E, Lohrmann E, Greger R. Properties of the potassium conductances of principal cells of rat cortical collecting ducts. Pflügers Arch 1992;420:39–45.
[45] Wang W, Giebisch G. Dual effect of adenosine triphosphate on the apical small conductance K^+ channel of the rat cortical collecting duct. J Gen Physiol 1991;98:35–61.
[46] Wang W, Hebert SC, Giebisch G. Renal K^+ channels: structure and function. Ann Rev Physiol 1997;59:413–36.
[47] Wang W, Sackin H, Giebisch G. Renal potassium channels and their regulation. Annu Rev Physiol 1992;54:81–96.
[48] Wang WH, Giebisch G. Dual modulation of renal ATP-sensitive K^+ channel by protein kinases A and C. Proc Natl Acad Sci USA 1991;88:9722–5.
[49] Chepilko S, Zhou H, Sackin H, Palmer LG. Permeation and gating properties of a cloned renal K^+ channel. Am J Physiol 1995;268:C389–401.
[50] Palmer LG, Choe H, Frindt G. Is the secretory K channel in the rat CCT ROMK? Am J Physiol (Renal Fluid Electrolyte Physiol) 1997;273:F404–10.
[51] Dong K, Tang L, MacGregor GG, Leng Q, Hebert SC. Novel nucleotide-binding sites in ATP-sensitive potassium channels formed at gating interfaces. EMBO J 2005;24:1318–29.
[52] Ficker E, Taglialatela M, Wible BA, Henley CM, Brown AM. Spermine and spermidine as gating molecules for inward rectifier K^+ channels. Science 1994;266:1068–72.
[53] Lopatin AN, Makhina EN, Nichols CG. Potassium channel block by cytoplasmic polyamines as the mechanism of intrinsic rectification. Nature 1994;372:366–9.
[54] Lu Z, MacKinnon R. Electrostatic tuning of Mg^{2+} affinity in an inward-rectifier K^+ channel. Nature 1994;371:243–6.
[55] Nichols CG, Ho K, Hebert SC. Mg^{2+}-dependent inward rectification of ROMK1 potassium channels expressed in *Xenopus* oocytes. J Physiol 1994;476:399–409.
[56] Wible BA, Taglialatela M, Ficker E, Brown AM. Gating of inwardly rectifying K^+ channels localized to a single negatively charged residue. Nature 1994;371:246–9.
[57] MacGregor GG, Xu J, McNicholas CM, Giebisch G, Hebert SC. Partially active channels produced by PKA site mutation of the cloned renal K^+ channel ROMK2. Am J Physiol (Renal Physiol) 1998;275:F415–22.
[58] McNicholas CM, Wang W, Ho K, Hebert SC, Giebisch G. Regulation of ROMK1 K^+ channel activity involves phosphorylation processes. Proc Natl Acad Sci USA 1994;91: 8077–81.
[59] Leipziger J, MacGregor GG, Cooper GJ, Xu J, Hebert SC, Giebisch G. PKA site mutations of ROMK2 channels shift the pH dependence to more alkaline values. Am J Physiol Renal Physiol 2000;279:F919–26.
[60] Tsai TD, Shuck ME, Thompson DP, Bienkowski MJ, Lee KS. Intracellular H^+ inhibits a cloned rat kidney outer medulla K^+ channel expressed in *Xenopus* oocytes. Am J Physiol 1995;268: C1173–8.
[61] Choe H, Sackin H, Palmer LG. Permeation and gating of an inwardly rectifying potassium channel. Evidence for a variable energy well. J Gen Physiol 1998;112:433–46.
[62] Huang CL, Kuo E. Mechanism of hypokalemia in magnesium deficiency. J Am Soc Nephrol 2007;18:2649–52.
[63] Yang L, Frindt G, Palmer LG. Magnesium modulates ROMK channel G comediated potassium secretion. J Am Soc Nephrol 2010;21:2109–16.
[64] Oliver D, Hahn H, Antz C, Ruppersberg JP, Fakler B. Interaction of permeant and blocking ions in cloned inward-rectifier K^+ channels. Biophys J 1998;74:2318–26.
[65] Spassova M, Lu Z. Coupled ion movement underlies rectification in an inward-rectifier K^+ channel. J Gen Physiol 1998;112: 211–21.
[66] Taglialatela M, Wible BA, Caporaso R, Brown AM. Specification of pore properties by the carboxyl terminus of inwardly rectifying K^+ channels. Science 1994;264:844–7.
[67] Yang J, Jan YN, Jan LY. Control of rectification and permeation by residues in two distinct domains in an inward rectifier K^+ channel. Neuron 1995;14:1047–54.
[68] Imredy JP, Chen C, MacKinnon R. A snake toxin inhibitor of inward rectifier potassium channel ROMK1. Biochemistry 1998;37:14867–74.
[69] Jin W, Lu Z. A novel high-affinity inhibitor for inward-rectifier K^+ channels. Biochemistry 1998;37:13291–9.
[70] Sackin H, Vasilyev A, Palmer LG, Krambis M. Permeant cations and blockers modulate pH gating of ROMK channels. Biophys J 2003;84:910–21.
[71] Frindt G, Palmer LG. Effects of dietary K on cell-surface expression of renal ion channels and transporters. Am J Physiol-Renal 2010;299:F890–7.
[72] Kanjhan R, Coulson EJ, Adams DJ, Bellingham MC. Tertiapin-Q blocks recombinant and native large conductance K channels in a use-dependent manner. J Pharmacol Exp Ther 2005;314: 1353–61.
[73] Wang WH, Giebisch G. The role of potassium and sodium channels in renal tubule electrolyte transport. Nippon Jinzo Gakkai Shi 1991;33:448–62.
[74] Liou HH, Zhou SS, Huang CL. Regulation of ROMK1 channel by protein kinase A via a phosphatidylinositol 4,5-bisphosphate-dependent mechanism. Proc Natl Acad Sci USA 1999;96: 5820–5.
[75] O'Connell AD, Leng Q, Dong K, MacGregor GG, Giebisch G, Hebert SC. Phosphorylation regulated ER retention signal in the ROMK potassium channel. Proc Natl Acad Sci USA 2005;102:9954–9.
[76] Faux MC, Scott JD. Molecular glue: kinase anchoring and scaffold proteins. Cell 1996;85:9–12.
[77] Pawson T, Scott JD. Signaling through scaffold, anchoring, and adaptor proteins. Science 1997;278:2075–80.
[78] Ali S, Chen X, Lu M, Xu J-C, Lerea KM, Hebert SC, et al. A kinase anchoring protein (AKAP) is required for mediating the effect of PKA on ROMK1. Proc Natl Acad Sci USA 1998;95: 10274–8.
[79] Yoo D, Flagg TP, Olsen O, Raghuram V, Foskett JK, Welling PA. Assembly and trafficking of a multiprotein ROMK (Kir1.1) channel complex by PDZ interactions. J Biol Chem 2004;279: 6863–73.
[80] Yun CC, Palmada M, Embark HM, Fedorenko O, Feng Y, Henke G, et al. The serum and glucocorticoid-inducible kinase SGK1 and the Na^+/H^+ exchange regulating factor NHERF2 synergize to stimulate the renal outer medullary K^+ channel ROMK1. J Am Soc Nephrol 2002;13:2823–30.

[81] Grantham JJ, Lowe CM, Dellasega M, Cole BR. Effect of hypotonic medium on K and Na content of proximal renal tubules. Am J Physiol (Renal Fluid Electrolyte Physiol) 1977;232:F42–9.
[82] Zeng WZ, Li XJ, Hilgemann DW, Huang CL. Protein kinase C inhibits ROMK1 channel activity via a phosphatidylinositol 4,5-bisphosphate-dependent mechanism. J Biol Chem 2003;278: 16852–6.
[83] Verissimo F, Jordan P. WNK kinases, a novel protein kinase subfamily in multi-cellular organisms. Oncogene 2001;20: 5562–9.
[84] Xu B, English JM, Wilsbacher JL, Stippec S, Goldsmith EJ, Cobb MH. WNK1, a novel mammalian serine/threonine protein kinase lacking the catalytic lysine in subdomain II. J Biol Chem 2000;275:16795–801.
[85] Kahle KT, Gimenez I, Hassan H, Wilson FH, Wong RD, Forbush B, et al. WNK4 regulates apical and basolateral Cl^- flux in extrarenal epithelia. P Natl Acad Sci 2004;101:2064–9.
[86] Kahle KT, Ring AM, Lifton RP. Molecular physiology of the WNK kinases. Ann Rev Physiol 2008;70:329–55.
[87] Leng Q, Kahle KT, Rinehart J, MacGregor GG, Wilson FH, Canessa CM, et al. WNK3, a kinase related to genes mutated in hereditary hypertension with hyperkaelemia, regulates the K^+ channel ROMK1 (Kir1.1). J Physiol 2006;571:275–86.
[88] Wilson FH, Disse-Nicodeme S, Choate KA, Ishikawa K, Nelson-Williams C, Desitter I, et al. Human hypertension caused by mutations in WNK kinases. Science 2001;293: 1107–12.
[89] Cope G, Murthy M, Golbang AP, Hamad A, Liu CH, Cuthbert AW, et al. WNK1 affects surface expression of the ROMK potassium channel independent of WNK4. J Am Soc Nephrol 2006;17:1867–74.
[90] Lazrak A, Liu Z, Huang CL. Antagonistic regulation of ROMK by long and kidney-specific WNK1 isoforms. Proc Natl Acad Sci 2006;103:1615–20.
[91] Ring AM, Leng Q, Rinehart J, Wilson FH, Kahle KT, Hebert SC, et al. An SGK1 site in WNK4 regulates Na^+ channel and K^+ channel activity and has implications for aldosterone signaling and K^+ homeostasis. Proc Natl Acad Sci 2007;104: 4025–9.
[92] Wade JB, Fang L, Liu J, Li D, Yang CL, Subramanya AR, et al. WNK1 kinase isoform switch regulates renal potassium excretion. Proc Nat Acad Sci 2006;103:8558–63.
[93] He G, Wang HR, Huang SK, Huang C-L. Intersectin links WNK kinase to endocytosis of ROMK1. J Clin Invest 2007;117:1078–87.
[94] Rodan AR, Huang CL. Distal potassium handling based on flow modulation of maxi-K channel activity. Curr Opin Nephrol Hypertens 2009;18(4):350–5.
[95] O'Reilly M, Marshall E, Speirs HJL, Brown RW. WNK1 a gene within a novel blood pressure control pathway, tissue-specifically generates radically different isoforms with and without a kinase domain. J Am Soc Nephrol 2003;14:2447–56.
[96] Lin DH, Sterling H, Yang B, Hebert SC, Giebisch G, Wang WH. Protein tyrosine kinase is expressed and regulates ROMK1 location in the cortical collecting duct. Am J Physiol Renal Physiol 2004;286:F881–92.
[97] Moral Z, Dong K, Wei Y, Sterling H, Deng H, Ali S, et al. Regulation of ROMK1 channels by protein-tyrosine kinase and -tyrosine phosphatase. J Biol Chem 2001;276:7156–63.
[98] Lin DH, Sterling H, Lerea KM, Welling P, Jin L, Giebisch G, et al. K depletion increases the protein tyrosine-mediated phosphorylation of ROMK. Am J Physiol Renal Physiol 2002;283:F671–7.
[99] Wei Y, Bloom P, Lin DH, Gu RM, Wang WH. Effect of dietary K intake on the apical small-conductance K channel in the CCD: role of protein tyrosine kinase. Am J Physiol Renal Physiol 2001;281:F206–12.
[100] Lin D, Kamsteeg EJ, Zhang Y, Jin Y, Sterling H, Yue P, et al. Expression of tetraspan protein CD63 activates protein-tyrosine kinase (PTK) and enhances the PTK-induced inhibition of ROMK channels. J Biol Chem 2008;283:7674–81.
[101] Ray PE, Suga SI, Liu XH, Huang X, Johnson RJ. Chronic potassium depletion induces renal injury, salt sensitivity, and hypertension in young rats. Kidney Int 2001;59:1850–8.
[102] Saikaley A, Bichet D, Kucharczyk J, Peterson LN. Neuroendocrine factors mediating polydipsia induced by dietary Na, Cl, and K depletion. Am J Physiol Regul Integr Comp Physiol 1986;251:R1071–7.
[103] Sealey JE, Clark I, Bull MB, Laragh JH. Potassium balance and the control of renin secretion. J. Clin. Invest 1970;49:2119–27.
[104] Wang T, Giebisch G. Effects of angiotensin II on electrolyte transport in the early and late distal tubule in rat kidney. Am J Physiol 1996;271:F143–9.
[105] Wei Y, Zavilowitz B, Satlin LM, Wang WH. Angiotensin II inhibits the ROMK-like small-conductance K channel in renal cortical collecting duct during dietary K restriction. J Biol Chem 2007;282:6455–62.
[106] Babilonia E, Wei Y, Sterling H, Kaminski P, Wolin MS, Wang WH. Superoxide anions are involved in mediating the effect of low K intake on c-Src expression and renal K secretion in the cortical collecting duct. J Biol Chem 2005;280:10790–6.
[107] O'Connell AD, Leng Q, Dong K, MacGregor GG, Giebisch G, Hebert SC. Phosphorylation-regulated endoplasmic reticulum retention signal in the renal outer-medullary K^+ channel (ROMK). Proc Nat Acad Sci 2005;102:9954–9.
[108] Yoo D, Kim BY, Campo C, Nance L, King A, Maouyo D, et al. Cell surface expression of the ROMK (Kir 1.1) channel is regulated by the aldosterone-induced kinase, SGK-1, and protein kinase A. J Biol Chem 2003;278:23066–75.
[109] Rozansky DJ, Cornwall T, Subramanya AR, Rogers S, Yong-Feng Y, David LL, et al. Aldosterone mediates activation of the thiazide-sensitive Na-Cl co-transporter through an SGK1 and WNK4 signaling pathway. J Clin Invest 2009;119: 2601–12.
[110] Xu B, Stippec S, Lazrak A, Huang CL, Cobb MH. WNK1 activates SGK1 by a phosphatidylinositol 3-kinase-dependent and non-catalytic mechanism. J Biol Chem 2005;280:34218–23.
[111] Huang DY, Wulff P, Volkl H, Loffing J, Richter K, Kuhl D, et al. Impaired regulation of renal K^+ elimination in the sgk1-knockout mouse. J Am Soc Nephrol 2004;15:885–91.
[112] Vallon V, Wulff P, Huang DY, Loffing J, Volkl H, Kuhl D, et al. Role of Sgk1 in salt and potassium homeostasis. Am J Physiol Regul Integr Comp Physiol 2005;288:R4–10.
[113] Verrey F, Summa V, Heitzmann D, Mordasini D, Vandewalle A, Feraille E, et al. Short-term aldosterone action on Na,K-ATPase surface expression: role of aldosterone-induced SGK1? Ann NY Acad Sci 2003;986:554–61.
[114] Huang DY, Wulff P, Volkl H, Loffing J, Richter K, Kuhl D, et al. Impaired regulation of renal K elimination in the sgk1-knockout mouse. JASN 2004;15:885–91.
[115] Palmer LG, Frindt G. Regulation of apical K channels in rat cortical collecting tubule during changes in dietary K intake. Am J Physiol 1999;277:F805–12.
[116] Yue P, Lin DH, Pan CY, Leng Q, Giebisch G, Lifton RP, et al. Src family protein tyrosine kinase (PTK) modulates the effect of SGK1 and WNK4 on ROMK channels. Proc Natl Acad Sci 2009;106:15061–6.
[117] Lin DH, Sterling H, Wang Z, Babilonia E, Yang B, Dong K, et al. ROMK1 channel activity is regulated by monoubiquitination. Proc Natl Acad Sci USA 2005;102:4306–11.

[118] Lin DH, Yue P, Pan CY, Sun P, Zhang X, Han Z, et al. POSH stimulates the ubiquitination and the clathrin-independent endocytosis of ROMK1 channels. J Biol Chem 2009;284: 29614–24.
[119] Ashcroft SJH, Ashcroft FM. Properties and functions of ATP-sensitive K-channels. Cell Signalling 1990;2:197–214.
[120] Kakei M, Kelly RP, Ashcroft SJH, Ashcroft FM. The ATP-sensitivity of K^+ channels in rat pancreatic B-cells is modulated by ADP. FEBS Lett 1986;208:63–6.
[121] Tanabe K, Tucker SJ, Ashcroft FM, Proks P, Kioka N, Amachi T, et al. Direct photoaffinity labeling of Kir6.2 by (g-^{32}P)ATP-(g)4- azidoanilide. Biochem Biophys Res Commun 2000;272: 316–9.
[122] Tanabe T, Tucker SJ, Matsuo M, Proks P, Ashcroft FM, Seino S, et al. Direct photoaffinity labeling of the Kir6.2 subunit of the ATP-sensitive K^+ channel by 8-azido-ATP. J Biol Chem 1999;274:3931–3.
[123] Dong K, Tang L, MacGregor GG, Hebert SC. Localization of the ATP/phosphatidylinositol 4,5 diphosphate-binding site to a 39-amino acid region of the carboxyl terminus of the ATP-regulated K^+ channel Kir1.1. J Biol Chem 2002;277: 49366–73.
[124] Vanoye CG, MacGregor GG, Dong K, Tang L, Buschmann AE, Hall AE, et al. The carboxyl termini of K_{ATP} channels bind nucleotides. J Biol Chem 2002;277:23260–70.
[125] Dabrowski M, Tarasov A, Ashcroft FM. Mapping the architecture of the ATP-binding site of the KATP channel subunit Kir6.2. J Physiol 2004;557:347–54.
[126] Doyle DA. Structural changes during ion channel gating. Trends Neurosci 2004;27:298–302.
[127] Ruknudin A, Schulze DH, Sullivan SK, Lederer WJ, Welling PA. Novel subunit composition of a renal epithelial K_{ATP} channel. J Biol Chem 1998;273:14165–71.
[128] Dong K, Xu J, Vanoye CG, Welch R, MacGregor GG, Giebisch G, et al. An amino acid triplet in the NH_2 terminus of rat ROMK1 determines interation with SUR2B. J Biol Chem 2001;276:44347–53.
[129] Lu M, Leng Q, Egan ME, Caplan MJ, Boulpaep E, Giebisch G, et al. CFTR is required for PKA-regulated ATP sensitivity of Kir1.1 potassium channels in mouse kidney. J Clin Invest 2006;116:797–807.
[130] McNicholas CM, Nason MW, Guggino WB, Schwiebert EM, Hebert S, Giebisch G, et al. The functional CFTR-NBF1 is required for ROMK2-CFTR interaction. Am J Physiol 1997;273: F843–8.
[131] Ashcroft SJH, Ashcroft FM. The sulfonylurea receptor. Biochim Biophys Acta 1992;1175:45–59.
[132] Aguilar-Bryan L, Nichols CG, Wechsler SW, Clement IV JP, Boyd III AE, González G, et al. Cloning of the b cell high-affinity sulfonylurea receptor: a regulator of insulin secretion. Science 1995;268:423–6.
[133] Babenko AP, Aguilar-Bryan L, Bryan J. A view of sur/KIR6.X, K_{ATP} channels. Ann Rev Physiol 1998;60:667–87.
[134] Bryan J, Aguilar-Bryan L. The ABCs of ATP-sensitive potassium channels: more pieces of the puzzle. COCB 1997;9:553–9.
[135] Clement JP, Kunjilwar K, Gonzalez G, Schwanstecher M, Panten U, Aguilar-Bryan L, et al. Association and stoichiometry of K_{ATP} channel subunits. Neuron 1997;18:827–38.
[136] Inagaki N, Gonoi T, Seino S. Subunit stoichiometry of the pancreatic b-cell ATP-sensitive K^+ channel. FEBS Letters 1997;409: 232–6.
[137] Lorenz E, Alekseev AE, Krapivinsky GB, Carrasco AJ, Clapham DE, Terzic A. Evidence for direct physical association between a K^+ channel (Kir6.2) and ATP-binding cassette protein (SUR1) which affects cellular distribution and kinetic behavior of an ATP-sensitive K^+ channel. Mol Cell Biol 1998;18:1652–9.
[138] Aguilar-Bryan L, Clement JP, Gonzalez G, Kunjilwar K, Babenko A, Bryan J. Toward understanding the assembly and structure of K_{ATP} channels. Physiol Rev 1998;78:227–45.
[139] Mikhailov MV, Proks P, Ashcroft FM, Ashcroft SJ. Expression of functionally active ATP-sensitive K-channels in insect cells using baculovirus. FEBS Lett 1998;429:390–4.
[140] Crawford I, Maloney PC, Zeitlin PL, Guggino WB, Hyde SC, Turley H, et al. Immunocytochemical localization of the cystic fibrosis gene product CFTR. Proc Natl Acad Sci USA 1991;88: 9262–6.
[141] Morales MM, Carroll TP, Morita T, Schwiebert EM, Devuyst O, Wilson PD, et al. Both the wild type and a functional isoform of CFTR are expressed in kidney. Am J Physiol (Renal Fluid Electrolyte Physiol) 1996;270:F1038–48.
[142] McNicholas CM, Guggino WB, Schwiebert EM, Hebert SC, Giebisch G, Egan ME. Sensitivity of a renal K^+ channel (ROMK2) to the inhibitory sulfonylurea compound, glibenclamide, is enhanced by co-expression with the ATP-binding cassette transporter cystic fibrosis transmembrane regulator. Proc Natl Acad Sci USA 1996;93:8083–8.
[143] Clark MA, Humphrey SJ, Smith MP, Ludens JH. Unique natriuretic properties of the ATP-sensitive K^+ channel blocker glyburide in concious rats. J Pharmacol Exp Ther 1993;165:933–7.
[144] Makita K, Takahashi K, Kerara A, Jacobson HR, Falck JR, Capdevila JH. Experimental and/or genetically controlled alterations of the renal microsomal cytochrome P450 epoxygenase induce hypertension in rats fed a high salt diet. J Clin Invest 1994;94:2414–20.
[145] Wang T, Wang W-H, Klein-Robbenhaar G, Giebisch G. Effects of glyburide on renal tubule transport and potassium-channel activity. Renal Physiol Biochem 1995;18:169–82.
[146] Lu M, Dong K, Egan ME, Giebisch GH, Boulpaep EL, Hebert SC. Mouse cystic fibrosis transmembrane conductance regulator forms cAMP-PKAG-regulated apical chloride channels in cortical collecting duct. Proc Natl Acad Sci 2010;107(13): 6082–7.
[147] Schulte U, Hahn H, Wiesinger H, Ruppersberg JP, Fakler B. pH-dependent gating of ROMK (K_{ir}1.1) channels involves conformational changes in both N and C termini. J Biol Chem 1998;273:34575–9.
[148] Schlatter E, Bleich M, Hirsch J, Greger R. pH-sensitive K^+ channels in the distal nephron. Nephrol Dial Trans 1993;8:488–90.
[149] Rapedius M, Haider S, Browner KF, Shang L, Sanson MSP, Baukroitz T, et al. Structural and functional analysis of the putative pH sensor in the Kir1.1 (ROMK) potassium channel. EMBO Rep 2006;7:611–6.
[150] Rapedius M, Fowler PW, Shang L, Sansom MSP, Tucker SJ, Baukrowitz T. H bonding at the helix-bundle crossing controls gating in Kir potassim channels. Neuron 2007;55(4):602–14.
[151] San Cristobal P, Pacheco-Alvarez D, Richardson C, Ring AM, Vazquez N, Rafiqi FH, et al. Angiotensin II signaling increases activity of the renal Na-Cl co-transporter through a WNK4-SPAK-dependent pathway. Proc Nat Acad Sci 2009;106: 4384–9.
[152] Zhang Y-Y, Sackin H, Palmer LG. Localization of the pH gate in Kir1.1 channels. Biophys J 2006;91:2901–9.
[153] Dahlmann A, Li M, Gao Z, McGarrigle D, Sackin H, Palmer LG. Regulation of Kir channels by intracellular pH and extracellular K^+: mechanisms of coupling. J Gen Physiol 2004;123: 441–54.
[154] Sackin H, Syn S, Palmer LG, Choe H, Walters DE. Regulation of ROMK by extracellular cations. Biophys J 2001;80:683–97.

[155] Sackin H, Nanazashvili M, Palmer LG, Krambis M, Walters DE. Structural locus of the pH gate in the Kir1.1 inward rectifier channel. Biophys J 2005;88:2597–606.
[156] Baukrowitz T, Tucker SJ, Schulte U, Benndorf K, Ruppersberg JP, Fakler B. Inward rectification in K_{ATP} channels: a pH switch in the pore. EMBO J 1999;18:847–53.
[157] Leng Q, MacGregor GG, Dong K, Giebisch G, Hebert SC. Subunit-subunit interactions are critical for proton sensitivity of ROMK: evidence in support of an intermolecular gating mechanism. Proc Nat Acad Sci USA 2006;103:1982–7.
[158] Baukrowitz T, Schulte U, Oliver D, Herlitze S, Krauter T, Tucker SJ, et al. PIP_2 and PIP as determinants for ATP inhibition of K_{ATP} channels. Science 1998;282:1141–4.
[159] Malnic G, Klose R, Giebisch G. Micropuncture study of renal potassium excretion in the rat. Am J Physiol 1964;206:674–86.
[160] Palmer LG, Antonian L, Frindt G. Regulation of apical K and Na channels and Na/K pumps in rat cortical collecting tubule by dietary K. J Gen Physiol 1994;104:693–710.
[161] Wald H, Garty H, Palmer LG, Popovtzer MM. Differential regulation of ROMK expression in kidney cortex and medulla by aldosterone and potassium. Am J Physiol 1998;275:F239–45.
[162] Chu PY, Quigley R, Babich V, Huang CL. Dietary potassium restriction stimulates endocytosis of ROMK channel in rat cortical collecting duct. Am J Physiol Renal Physiol 2003;285: F1179–87.
[163] Lin DH, Sterling H, Wang WH. The protein tyrosine kinase-dependent pathway mediates the effect of K intake on renal K secretion. Physiology (Bethesda) 2005;20:140–6.
[164] Sun TJ, Zeng WZ, Huang CL. Inhibition of ROMK potassium channel by syntaxin 1A. AJP - Renal Physiol 2005;288:F284–9.
[165] Zeng WZ, Babich V, Ortega B, Quigley R, White SJ, Welling PA, et al. Evidence for endocytosis of ROMK potassium channel via clathrin-coated vesicles. Am J Physiol Renal Physiol 2002;283:F630–9.
[166] Frindt G, Zhou H, Sackin H, Palmer LG. Dissociation of K channel density and ROMK mRNA in rat cortical collecting tubule during K adaptation. Am J Physiol 1998;274: F525–31.
[167] Reeves WB, McDonald GA, Mehta P, Andreoli TE. Activation of K^+ channels in renal medullary vesicles by cAMP-dependent protein kinase. J Membr Biol 1989;109:65–72.
[168] Cha SK, Hu MC, Kurosu H, Kuro-o M, Moe O, Huang CL. Regulation of renal outer medullary potassium channel and renal K^+ excretion by Klotho. Mol Pharmacol 2009;76:38–46.
[169] Bartter FC, Pronove P, Gill Jr JR, MacCardle RC, Diller E. Hyperplasia of the juxtaglomerular complex with hyperaldosteronoism and hypokalemic alkalosis. Am J Med 1962;33: 811–28.
[170] Asteria C. Molecular basis of Bartter's syndrome: new insights into correlation between genotype and phenotype. Eur J Endocrinol 1997;137:613–5.
[171] Guay-Woodford LM. Molecular insights into the pathogenesis of inherited renal tubular disorders. Curr Opin Nephrol Hypertens 1995;4:121–9.
[172] Karolyi L, Koch MC, Grzeschik KH, Seyberth HW. The molecular genetic approach to "Bartter's syndrome". J Mol Med 1998;76:317–25.
[173] Rodriguez-Soriano J. Bartter and related syndromes: the puzzle is almost solved. Pediatr Nephrol 1998;12:315–27.
[174] Hebert SC. Bartter syndrome. Curr Opin Nephrol Hypertens 2003;12:527–32.
[175] Simon DB, Karet FE, Hamdan JM, DiPietro A, Sanjad SA, Lifton RP. Bartter's syndrome, hypokalaemic alkalosis with hypercalciuria, is caused by mutations in the Na-K-2Cl cotransporter. NKCC2 Nat Genet 1996;13:183–8.
[176] Vargas-Poussou R, Feldmann D, Vollmer M, Konrad M, Kelly L, van den Heuvel LP, et al. Novel molecular variants of the Na-K-2Cl co-transporter gene are responsible for antenatal Bartter syndrome. Am J Hum Genet 1998;62:1332–40.
[177] Simon DB, Bindra RS, Mansfield TA, Nelson-Williams C, Mendonça E, Stone R, et al. Mutations in the chloride channel gene, *CLCNKB*, cause Bartter's syndrome type III. Nat Genet 1997;17:171–8.
[178] Karolyil L, Konrad M, Kockerling A, Ziegler A, Zimmermann DK, Roth B, et al. Mutations in the gene encoding the inwardly-rectifying renal potassium channel, ROMK, cause the antenatal variant of Bartter syndrome: evidence for genetic heterogeneity. Hum Mol Genet 1997;6:17–26.
[179] Simon DB, Karet FE, Rodriguez-Soriano J, Hamdan JH, DiPietro A, Trachtman H, et al. Genetic heterogeneity of Bartter's syndrome revealed by mutations in the K^+ channel, ROMK. Nat Geneti 1996;14:152–6.
[180] Vollmer M, Koehrer M, Topaloglu R, Strahm B, Omran H, Hildebrandt F. Two novel mutations of the gene for Kir 1.1 (ROMK) in neonatal Bartter syndrome. Pediatr Nephrol 1998;12:69–71.
[181] Estevez R, Boettger T, Stein V, Birkenhager R, Otto E, Hildebrandt F, et al. Barttin is a Cl^- channel b-subunit crucial for renal Cl^- reabsorption and inner ear K^+ secretion. Nature 2001;414:558–61.
[182] Vargas-Poussou R, Huang C, Hulin P, Houillier P, Jeunemaitre X, Paillard M, et al. Functional characterization of a calcium-sensing receptor mutation in severe autosomal dominant hypocalcemia with a Bartter-like syndrome. J Am Soc Nephrol 2002;13:2259–66.
[183] Watanabe S, Fukumoto S, Chang H, Takeuchi Y, Hasegawa Y, Okazaki R, et al. Association between activating mutations of calcium-sensing receptor and Bartter's syndrome. Lancet 2002;360:692–4.
[184] Bleich M, Schlatter E, Greger R. The luminal K^+ channel of the thick ascending limb of Henle's loop. Pflügers Arch 1990;415: 449–60.
[185] Greger R, Bleich M, Schlatter E. Ion channels in the thick ascending limb of Henle's loop. Renal Physiol Biochem 1990;13:37–50.
[186] Derst C, Konrad M, Köckerling A, Karschin A, Daut J, Seyberth HW. Mutations in the ROMK gene in antenatal Bartter syndrome are associated with impaired K^+ channel function. Biochem Biophys Res Comm 1997;230:641–5.
[187] Schwalbe RA, Bianchi L, Accili EA, Brown AM. Functional consequences of ROMK mutants linked to antenatal Bartter's syndrome and implications for treatment. Hum Mol Genet 1998;7:975–80.
[188] Schwalbe RA, Bianchi L, Accili EA, Brown AM. Functional consequences of ROMK mutants linked to antenatal Bartter's syndrome and implications for treatment. Hum Mol Genet 1998;7:975–80.
[189] Lorenz JN, Baird NR, Judd LM, Noonan WT, Andringa A, Doetschman T, et al. Impaired renal NaCl absorption in mice lacking the ROMK potassium channel, a model for type II Bartter's syndrome. J Biol Chem 2002;277:37871–80.
[190] Lu M, Wang T, Yan Q, Yang X, Dong K, Knepper MA, et al. Absence of small-conductance K^+ channel (SK) activity in apical membranes of thick ascending limb and cortical collecting duct in ROMK (Bartter's) knockout mice. J Biol Chem 2002;277:37881–7.
[191] Lu M, Wang T, Yan Q, Wang W, Giebisch G, Hebert SC. ROMK is required for expression of the 70 pS K channel in the thick ascending limb. Am J Physiol Renal Physiol 2004;286: F490–5.

[192] Lu R, Alioua A, Kumar Y, Eghbali M, Stefani E, Toro L. MaxiK channel partners: physiological impact. J Physiol 2006;570: 65–72.
[193] Salkoff L, Butler A, Ferreira G, Santi C, Wei A. High-conductance potassium channels of the SLO family. Nat Rev Neurosci 2006;7:921–31.
[194] Li DM, Wang ZJ, Sun P, Jin Y, Lin DH, Hebert SC, et al. Inhibition of mitogen-activated protein kinase stimulates the Ca^{2+}-dependent big conductance K channels (BK) in cortical collecting duct. Proc Natl Acad Sci USA 2006;103:19569–74.
[195] Palmer LG, Frindt G. High-conductance K channels in intercalated cells of the rat distal nephron. AJP - Renal Physiol 2007;292:F966–73.
[196] Morton MJ, Hutchinson K, Mathieson PW, Witherden IR, Saleem MA, Hunter M. Human podocytes possess a stretch-sensitive, Ca^{2+}-activated K^+ channel: potential implications for the control of glomerular filtration. J Am Soc Nephrol 2004;15:2981–7.
[197] Bailey MA, Cantone A, Yan QS, MacGregor GG, Leng Q, Amorim JB, et al. Maxi-K channels contribute to urinary potassium excretion in the ROMK-deficient mouse model of type II Bartter's syndrome and in adaptation to a high K diet. Kidney Int 2006;70:51–9.
[198] Rieg T, Vallon V, Sausbier M, Sausbier U, Kaissling B, Ruth P, et al. The role of the BK channel in potassium homeostasis and flow-induced renal potassium excretion. Kidney Int 2007;72:566–73.
[199] Liu W, Morimoto T, Woda C, Kleyman TR, Satlin LM. Ca^{2+} dependence of flow-stimulated K secretion in the mammalian cortical collecting duct. AJP - Renal Physiol 2007;293:F227–35.
[200] Taniguchi J, Imai M. Flow-dependent activation of maxi K^+ channels in apical membrane of rabbit connecting tubule. J Membr Biol 1998;164:35–45.
[201] Woda CB, Bragin A, Kleyman TR, Satlin LM. Flow-dependent K^+ secretion in the cortical collecting duct is mediated by a maxi-K channel. Am J Physiol Renal Physiol 2001;280: F786–93.
[202] Beck F-X, Dorge A, Giebisch G, Thurau K. Effect of diuretics on cell potassium transport: an electron microprobe study. Kidney Int 1990;37:1423–8.
[203] Holtzclaw JD, Grimm PR, Sansom SC. Intercalated cell BK-α/β4 channels modulate sodium and potassium handling during potassium adaptation. J Am Soc Nephrol 2010;21:634–45.
[204] Grimm PR, Irsik DL, Liu L, Holtzclaw JD, Sansom SC. Role of BK β1 in Na^+ reabsorption by cortical collecting ducts of Na^+-deprived mice. AJP - Renal Physiol 2009;297:F420–8.
[205] Grimm PR, Irsik DL, Settles DC, Holtzclaw JD, Sansom S. Hypertension of Kcnmb1$^{-/-}$ is linked to deficient K secretion and aldosteronism. Proc Nat Acad Sci 2009;106:11800–5.
[206] Najjar F, Zhou H, Morimoto T, Bruns JB, Li HS, Liu W, et al. Dietary K^+ regulates apical membrane expression of maxi-K channels in rabbit cortical collecting duct. Am J Physiol Renal Physiol 2005;289:F922–32.
[207] Estilo G, Liu W, Pastor-Soler N, Mitchell P, Carattino MD, Kleyman TR, et al. Effect of aldosterone on BK channel expression in mammalian cortical collecting duct. AJP - Renal Physiol 2008;295:F780–8.
[208] Liu W, Wei Y, Sun P, Wang WH, Kleyman TR, Satlin LM. Mechanoregulation of BK channel activity in the mammalian cortical collecting duct: role of protein kinases A and C. AJP - Renal Physiol 2009;297:F904–15.
[209] Sun P, Liu W, Lin DH, Yue P, Kemp R, Satlin LM, et al. Epoxyeicosatrienoic acid (EET) activates the Ca^{2+}-dependent bid conductance K channel in the cortical collecting duct. J Am Soc Nephrol 2009;20:513–23.
[210] Barhanin J, Lesage F, Guillemare E, Fink M, Lazdunski M, Romey G. KvLQT1 and IsK (minK) proteins associate to form the I_{ks} cardiac potassium current. Nature 1996;384:78–80.
[211] Sanguinetti MC, Curran ME, Zou A, Shen J, Spector PS, Atkinson DL, et al. Coassembly of K_vLQT1 and minK (IsK) proteins to form cardiac I_{Ks} potassium channel. Nature 1996;384:80–3.
[212] Wang Q, Curran ME, Splawski I, Burn TC, Millholland JM, VanRaay TJ, et al. Positional cloning of a novel potassium channel gene: KVLQT1 mutations cause cardiac arrhythmias. Nat Genet 1996;12:17–23.
[213] Carrisoza R, Salvador C, Bobadilla N, Trujillo J, Escobar L. Expression and immunolocalization of ERG1 potassium channels in the rat kidney. Histochem Cell Biol 2010;133:189–99.
[214] Zheng W, Verlander JW, Lynch IJ, Cash M, Shao J, Stow LR, et al. Cellular distribution of the potassium channel KCNQ1 in normal mouse kidney. AJP - Renal Physiol 2007;292:F456–66.
[215] Vallon V, Grahammer F, Richter K, Bleich M, Lang F, Barhanin J, et al. Role of KCNE1-dependent K^+ fluxes in mouse proximal tubule. J Am Soc Nephrol 2001;12:2003–11.
[216] Millar ID, Hartley JA, Haigh C, Grace AA, White SJ, Kibble JD, et al. Volume regulation is defective in renal proximal tubule cells isolated from KCNE1 knockout mice. Exp Physiol 2004;89:173–80.
[217] Glaudemans B, van der Wijst J, Scola RH, Lorenzoni PJ, Heister A, van der Kemp AW, et al. A missense mutation in the Kv1.1 voltage-gated potassium channel-encoding gene KCNA1 is linked to human autosomal dominant hypomagnesemia. J Clin Invest 2009;119:936–42.
[218] Yao X, Tian S, Chan H-Y, Biemesderfer D, Desir GV. Expression of KCNA10, a voltage-gated K channel, in glomerular endothelium and at the apical membrane of the renal proximal tubule. J Am Soc Nephrol 2002;13(12):2831–9.
[219] Orias M, Bray-Ward P, Curran ME, Keating MT, Desir GV. Genomic localization of the human gene for KCNA10, a cGMP-activated K channel. Genomics 1997;42:33–7.
[220] Lourdel S, Paulais M, Cluzeaud F, Bens M, Tanemoto M, Kurachi Y, et al. An inward rectifier K^+ channel at the basolateral membrane of the mouse distal convoluted tubule: similarities with Kir4-Kir5.1 heteromeric channels. J Physiol 2002;538: 391–404.
[221] Bond CT, Pessia M, Xia XM, Lagrutta A, Kavanaugh MP, Adelman JP. Cloning and expression of a family of inward rectifier potassium channels. Receptors Channels 1994;2:183–91.
[222] Takumi T, Ishii T, Horio Y, Morishige K, Takahashi N, Yamada M, et al. A novel ATP-dependent inward rectifier potassium channel expressed predominantly in glial cells. J Biol Chem 1995;270:16339–46.
[223] Ito M, Inanobe A, Horio Y, Hibino H, Isomoto S, Ito H, et al. Immunologicalization of an inwardly rectifying K^+ channel, K_{AB}-2 (Kir4.1), in the basolateral membrane of renal distal tubular epithelia. FEBS Lett 1996;388:11–5.
[224] Yang Z, Jiang C. Opposite effects of pH on open-state probability and single channel conductance of kir4.1 channels. J Physiol 1999;520(Pt 3):921–7.
[225] Kofuji P, Ceelen P, Zahs KR, Surbeck LW, Lester HA, Newman EA. Genetic inactivation of an inwardly rectifying potassium channel (Kir4.1 subunit) in mice: phenotypic impact in retina. J Neurosci 2000;20:5733–40.
[226] Pearson WL, Dourado M, Schreiber M, Salkoff L, Nichols CG. Expression of a functional Kir4 family inward rectifier K^+ channel from a gene cloned from mouse liver. J Physiol 1999;514(Pt 3):639–53.
[227] Tanemoto M, Kittaka N, Inanobe A, Kurachi Y. *In vivo* formation of a proton-sensitive K^+ channel by heteromeric

subunit assembly of Kir5.1 with Kir4.1. J Physiol 2000;525(Pt 3): 587–92.

[228] Tucker SJ, Imbrici P, Salvatore L, D'Adamo MC, Pessia M. pH dependence of the inwardly rectifying potassium channel, Kir5.1, and localization in renal tubular epithelia. J Biol Chem 2000;275:16404–7.

[229] Konstas AA, Korbmacher C, Tucker SJ. Identification of domains which control the heteromeric assembly of Kir5.1/Kir4.0 potassium channels. Am J Physiol Cell Physiol 2003;284: C910–7.

[230] Gray DA, Frindt G, Zhang YY, Palmer LG. Basolateral K^+ conductance in principal cells of rat CCD. AJP - Renal Physiol 2005;288:F493–504.

[231] Grimm PR, Foutz RM, Brenner R, Sansom SC. Identification and localization of BK-beta subunits in the distal nephron of the mouse kidney. AJP - Renal Physiol 2007;293:F350–9.

[232] Lachheb S, Cluzeaud F, Bens M, Genete M, Hibino H, Lourdel S, et al. Kir4.1/Kir5.1 channel forms the major K^+ channel in the basolateral membrane of mouse renal collecting duct principal cells. AJP - Renal Physiol 2008;294:F1398–407.

[233] Lourdel S, Paulais M, Cluzeaud F, Bens M, Tanemoto M, Kurachi Y, et al. An inward rectifier K^+ channel at the basolateral membrane of the mouse distal convoluted tubles: similarities with Kir4-Kir5.1 heteromeric channels. J Physiol 2002;538: 391–404.

[234] Pessia M, Imbrici P, D'Adamo MC, Salvatore L, Tucker SJ. Differential pH sensitivity of Kir4.1 and Kir4.2 potassium channels and their modulation by heteropolymerisation with Kir5.1. J Physiol 2001;532:359–67.

[235] Xu H, Cui N, Yang Z, Qu Z, Jiang C. Modulation of kir4.1 and kir5.1 by hypercapnia and intracellular acidosis. J Physiol 2000;524(Pt 3):725–35.

[236] Yang Z, Xu H, Cui N, Qu Z, Chanchevalap S, Shen W, et al. Biophysical and molecular mechanisms underlying the modulation of heteromeric Kir4.1-Kir5.1 channels by CO_2 and pH. J Gen Physiol 2000;116:33–45.

[237] Leung YM, Zeng WZ, Liou HH, Solaro CR, Huang CL. Phosphatidylinositol 4,5-bisphosphate and intracellular pH regulate the ROMK1 potassium channel via separate but interrelated mechanisms. J Biol Chem 2000;275:10182–9.

[238] Huang C, Sindic A, Hill CE, Hujer KM, Chan KW, Sassen M, et al. Interaction of the Ca^{2+}-sensing receptor with the inwardly rectifying potassium channels Kir4.1 and Kir4.2 results in inhibition of channel function. AJP - Renal Physiol 2007;292:F1073–81.

[239] Reichold M, Zdebik AA, Lieberer E, Rapedius M, Schmidt K, Bandulik S, et al. KCNJ10 gene mutations causing EAST syndrome (epilepsy, ataxia, sensorineural deafness, and tubulopathy) disrupt channel function. Proc Natl Acad Sci 2010;107:14490–5.

[240] Scholl UI, Choi M, Liu T, Ramaekers VT, Häusler MG, Grimmer J, et al. Seizures, sensorineural deafness, ataxia, mental retardation, and electrolyte imbalance (SeSAME syndrome) caused by mutations in KCNJ10. Proc Natl Acad Sci 2009;106:5842–7.

[241] Welling PA. Primary structure and functional expression of a cortical collecting duct K_{ir} channel. Am J Physiol 1997;273: F825–36.

[242] Le Maout S, Brejon M, Olsen O, Merot J, Welling PA. Basolateral membrane targeting of a renal-epithelial inwardly rectifying potassium channel from the cortical collecting duct, CCD- IRK3, in MDCK cells. Proc Natl Acad Sci USA 1997;94: 13329–34.

[243] Le Maout S, Welling PA, Brejon M, Olsen O, Merot J. Basolateral membrane expression of a K^+ channel, Kir 2.3, is directed by a cytoplasmic COOH-terminal domain. Proc Natl Acad Sci USA 2001;98:10475–80.

[244] Olsen O, Liu H, Wade JB, Merot J, Welling PA. Basolateral membrane expression of the Kir 2.3 channel is coordinated by PDZ interaction with Lin-7/CASK complex. Am J Physiol Cell Physiol 2002;282:C183–95.

[245] Inagaki N, Tsuura Y, Namba N, Masuda K, Gonoi T, Horie M, et al. Cloning and functional characterization of a novel ATP-sensitive potassium channel ubiquitously expressed in rat tissues, including pancreatic islets, pituitary, skeletal muscle, and heart. J Biol Chem 1995;270:5691–4.

[246] Seino S. ATP-sensitive potassium channels: a model of heteromultimeric potassium channel/receptor assemblies. Ann Rev Physiol 1999;61:337–62.

[247] Bryan J, Aguilar-Bryan L. Sulfonylurea receptors: ABC transporters that regulate ATP-sensitive K^+ channels. Biochim Biophys Acta 1999;1461:285–303.

[248] Erginel-Unaltuna N, Yang WP, Blanar MA. Genomic organization and expression of KCNJ8/Kir6.1, a gene encoding a subunit of an ATP-sensitive potassium channel. Gene 1998;211: 71–8.

[249] Suzuki M, Kotake K, Fujikura K, Inagaki N, Suzuki T, Gonoi T, et al. Kir6.1: a possible subunit of ATP-sensitive K^+ channels in mitochondria. Biochem Biophys Res Commun 1997;241: 693–7.

[250] Brochiero E, Wallendorf B, Gagnon D, Laprade R, Lapointe JY. Cloning of rabbit Kir6.1, SUR2A, and SUR2B: possible candidates for a renal K_{ATP} channel. Am J Physiol Renal Physiol 2002;282:F289–300.

[251] Akao M, Otani H, Horie M, Takano M, Kuniyasu A, Nakayama H, et al. Myocardial ischemia induces differential regulation of K_{ATP} channel gene expression in rat hearts. J Clin Invest 1997;100:3053–9.

[252] Carrasco AJ, Dzeja PP, Alekseev AE, Pucar D, Zingman LV, Abraham MR, et al. Adenylate kinase phosphotransfer communicates cellular energetic signals to ATP-sensitive potassium channels. Proc Natl Acad Sci USA 2001;98: 7623–8.

[253] Brochiero E, Coady MJ, Klein H, Laprade R, Lapointe JY. Activation of an ATP-dependent K^+ conductance in *Xenopus* oocytes by expression of adenylate kinase cloned from renal proximal tubules. Biochim Biophys Acta 2001;1510:29–42.

[254] Krapivinsky G, Medina I, Eng L, Krapivinsky L, Yang Y, Clapham DE. A novel inward rectifier K^+ channel with unique pore properties. Neuron 1998;20:995–1005.

[255] Partiseti M, Collura V, Agnel M, Culouscou JM, Graham D. Cloning and characterization of a novel human inwardly rectifying potassium channel predominantly expressed in small intestine. FEBS Lett 1998;434:171–6.

[256] Doring F, Derst C, Wischmeyer E, Karschin C, Schneggenburger R, Daut J, et al. The epithelial inward rectifier channel Kir7.1 displays unusual K^+ permeation properties. J Neurosci 1998;18:8625–36.

[257] Derst C, Hirsch JR, Preisig-Muller R, Wischmeyer E, Karschin A, Doring F, et al. Cellular localization of the potassium channel Kir7.1 in guinea pig and human kidney. Kidney Int 2001;59:2197–205.

[258] Ookata K, Tojo A, Suzuki Y, Nakamura N, Kimura K, Wilcox CS, et al. Localization of inward rectifier potassium channel Kir7.1 in the basolateral membrane of distal nephron and collecting duct. J Am Soc Nephrol 2000;11:1987–94.

[259] Nakamura N, Suzuki Y, Sakuta H, Ookata K, Kawahara K, Hirose S. Inwardly rectifying K^+ channel Kir7.1 is highly expressed in thyroid follicular cells, intestinal epithelial cells and choroid plexus epithelial cells: implication for a functional

coupling with Na^+,K^+-ATPase. Biochem J 1999;342(Pt 2): 329–36.

[260] Frindt G, Palmer LG. Apical potassium channels in the rat connecting tubule. Am J Physiol Renal Physiol 2004;287: F1030–7.

[261] Ho K. The ROMK-cystic fibrosis transmembrane conductance regulator connection: new insights into the relationship between ROMK and cystic fibrosis transmembrane conductance regulator channels. Curr Opin Nephrol Hypertens 1998;7:49–58.

[262] Satlin LM, Palmer LG. Apical K^+ conductance in maturing rabbit principal cell. Am J Physiol 1997;272:F397–404.

[263] Reyes R, Duprat F, Lesage F, Fink M, Salinas M, Farman N, et al. Cloning and expression of a novel pH-sensitive two pore domain K^+ channel from human kidney. J Biol Chem 1998;273:30863–9.

[264] Arrighi I, Lesage F, Scimeca J-C, Carle GF, Barhanin J. Structure, chromosome localization, and tissue distribution of the mouse *twik* K^+ channel gene. FEBS Lett 1998;425:310–6.

[265] Chavez RA, Gray AT, Zhao BB, Kindler CH, Mazurek MJ, Mehta Y, et al. TWIK-2, a new weak inward rectifing member of the tandem pore domain potassium channel family. J Biol Chem 1999;274:7887–92.

[266] Cluzeaud F, Reyes R, Escoubet B, Fay M, Lazdunski M, Bonvalet JP, et al. Expression of TWIK-1, a novel weakly inward rectifying potassium channel in rat kidney. Am J Physiol (Cell Physiol) 1998;275:C1602–9.

[267] Lesage F, Guillemare E, Fink M, Duprat F, Lazdunski M, Romey G, et al. TWIK-1 a ubiquitous human weakly inward rectifying K^+ channel with a novel structure. EMBO J 1996;15:1004–11.

[268] Lesage F, Guillemare E, Fink M, Duprat F, Lazdunski M, Romey G, et al. TWIK-1 a ubiquitous human weakly inward rectifying K^+ channel with novel structure. EMBO J 1996;15:1004–11.

[269] Orias M, Velazquez H, Tung F, Lee G, Desir GV. Cloning and localization of a double-pore K channel, KCNK1: exclusive expression in distal nephron segments. Am J Physiol 1997;273: F663–6.

[270] Wei A, Jegla T, Salkoff L. Eight potassium channel families revealed by the *C. elegans* genome project. Neuropharmacology 1996;35:805–29.

[271] Lesage F, Lauritzen I, Duprat F, Reyes R, Fink M, Heurteaux C, et al. The structure, function and distribution of the mouse TWIK-1K^+ channel. FEBS Lett 1997;402:28–32.

[272] Fink M, Duprat F, Lesage F, Reyes R, Romey G, Heurteaux C, et al. Cloning, functional expression and brain localization of a novel unconventional outward rectifier K^+ channel. EMBO J 1996;15:6854–62.

[273] Lesage F, Lazdunski M. Mapping of human potassium channel genes TREK-1 (*KCNK2*) and TASK (*KCNK3*) to chromosomes 1q41 and 2p23. Genomics 1998;51:478–9.

[274] Duprat F, Lesage F, Fink M, Reyes R, Heurteaux C, Lazdunski M. TASK a human background K^+ channel to sense external pH variations near physiological pH. EMBO J 1997;16: 5464–71.

[275] Patel AJ, Honore E, Maingret F, Lesage F, Fink M, Duprat F, et al. A mammalian two pore domain mechano-gated S-like K^+ channel. EMBO J 1998;17:4283–90.

This page intentionally left blank

CHAPTER

48

Extrarenal Potassium Metabolism

Vaibhav Sahni, Aleksandra Gmurczyk, Robert M. Rosa

The Feinberg School of Medicine, Northwestern University, Chicago, IL, USA

Internal potassium homeostasis is defined as the regulation of potassium distribution between the intracellular and extracellular fluid compartments, as distinct from the net gain or loss of potassium from the body. While the kidney plays the predominant role in maintaining external potassium balance, nonrenal tissues, especially muscle and liver, are quantitatively the most important organs involved in the regulation of internal potassium balance.

The ratio of potassium between intracellular and extracellular fluids is critically important, not only to the behavior of electrically excitable cells, such as muscle and nerve, but also to the vital processes of all living cells. The reason for this is that a major regulator of cell function is the transmembrane potential. The determinants of this membrane potential are described by the Goldman–Hodgkin–Katz equation, the most important term of which is the logarithm of the ratio of internal to external ionic activity of potassium.

Of the 3500 mEq of potassium found in the body of a 70 kg human, about 98% is confined to intracellular water (Figure 48.1). Of this, 80% is contained in muscle cells, at a concentration of about 150 mEq/liter. The remaining 2% of total body potassium (about 70 mEq) is located in the extracellular fluid (about 14 liters), where the normal concentration is 3.5–5.5 mEq/liter. The chief biological mechanism responsible for maintaining this 30-fold potassium gradient between cell water and extracellular fluid is the Na,K-ATPase pump, situated in the plasma membrane of all animal cells. A minor role is played by the inward transport of potassium coupled with sodium and chloride, via the Na–K–2Cl transporter in the plasma membrane of some cells. Transcellular distribution of potassium is also modulated by hormonal factors, such as insulin and catecholamines, by hydrogen ion balance, plasma osmolality, intracellular potassium content, and by factors that affect the passive movement of potassium through membrane channels, such as the level of intracellular calcium and pH (Table 48.1). Some of these factors, such as the activity of Na,K-ATPase and the distribution of hydrogen ions, may concurrently affect the potassium content of cells of the distal nephron, and thereby influence the external balance of potassium.

From a practical standpoint, a key determinant of transmembrane potential is the plasma potassium. Since the concentration of potassium inside cells far exceeds extracellular concentration, percentile changes in intracellular potassium are relatively small, even during extreme degrees of total body potassium surfeit, deficit or internal redistribution. The changes in extracellular potassium seen in diseased states are therefore much more likely to alter the membrane potential of cells than are concomitant changes in intracellular potassium. For this reason, a variety of mechanisms have evolved to preserve the extracellular concentration of potassium within the normal range.

If a moderate load of potassium (0.5 mEq/kg) is administered intravenously over 1 hour, about 40% of it is excreted into the urine at the end of that time. Within 3 hours, renal excretion is complete and the serum potassium, which initially increases by about 0.6 mEq/liter, returns to baseline.[1,2] The ability of the normal human kidney to excrete all of an oral load of potassium is more sluggish; while potassium excretion increases 6-10-fold within a few hours,[3–5] only about half of the load is excreted during the first 3–6 hours after it is ingested.[5–9] Of considerable interest, however, is recent evidence that is consistent with the existence of an unidentified "gut" and/or "hepatoportal factor" that senses potassium ingestion, and

Seldin and Giebisch's The Kidney, Fifth Edition.
DOI: http://dx.doi.org/10.1016/B978-0-12-381462-3.00048-3

© 2013 Elsevier Inc. All rights reserved.

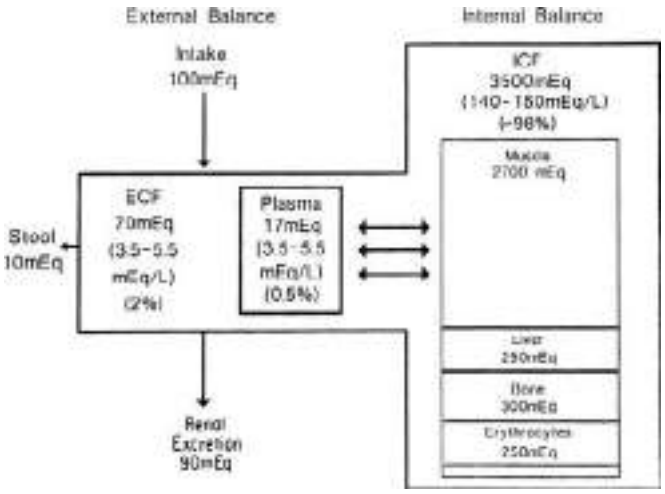

FIGURE 48.1 Internal potassium homeostasis in a 70 kg person. The potassium concentration in the extracellular fluid (ECF) depends on both the external balance (intake and output) and the internal balance (distribution between extracellular and intracellular fluid, ICF). Factors affecting internal balance are listed in Table 48.1. Note that the large ICF pool exists at a far greater K concentration than the small ECF pool; the ECF pool will therefore change more dramatically with changes in total body K or K distribution.

TABLE 48.1 Factors Affecting Internal Potassium Homeostasis

Factor	Effect on Potassium
Insulin	Enhanced cell uptake
β-Catecholamines	Enhanced cell uptake
α-Catecholamines	Impaired cell uptake
Acidosis	Impaired cell uptake and enhanced efflux[a]
Alkalosis	Enhanced cell uptake and reduced efflux[a]
External potassium balance	Loose correlation
Drugs	See text
Hyperosmolality	Enhance cell efflux

[a]*Degree varies with disturbance.*

rapidly initiates the process of renal potassium excretion in the absence of a significant change in plasma potassium concentration.[10,11]

Consumption of only 35 mEq of potassium by a 70 kg adult during an average meal (an amount equivalent to 1% of total body potassium) would, if confined exclusively to the extracellular space, raise the plasma potassium by 2.5 mEq/liter – enough to have pronounced effects on neuromuscular function. It is well-established, however, that a potassium load given to a normal human or dog has an apparent volume of distribution of 70–80% of body weight, somewhat greater than total body water,[6,12] instead of the 20% that represents extracellular fluid. In other words, only a small portion (about one quarter) of the 35 mEq of ingested potassium will normally remain in the extracellular compartment, raising the concentration of potassium in plasma by only about 0.6 mEq/liter. In contrast, a similar load of potassium administered to patients with deranged extrarenal potassium homeostasis may produce serious hyperkalemia.[13]

The cells also buffer plasma potassium during potassium depletion. In states of progressive potassium deficiency, as depletion worsens, a greater amount of potassium is lost from within cells to lessen the fall in external concentration, and to minimize the alteration in its intracellular to extracellular ratio.

These examples of potassium surfeit or deficit emphasize the critical role of internal potassium homeostasis in mitigating potentially dangerous changes in the plasma potassium. Disorders of the factors that mediate this adjustment thus may have substantial clinical importance and are the primary topic of this chapter.

POTASSIUM DEPLETION AND REPLETION

In many conditions, such as vomiting, diabetic ketoacidosis, and chronic renal failure, abnormalities of internal and external potassium homeostasis coexist. Just as internal potassium homeostasis can affect potassium uptake and excretion by the kidney, so changes in external potassium balance, by altering cellular potassium content, can independently influence internal potassium homeostasis.

Potassium Depletion

The idealized curvilinear relationship between total body potassium and the serum potassium concentration illustrated in Figure 48.2 is derived from several measurements in hypokalemic patients with positive potassium balance during replacement therapy,[14–16] and from unpublished data on hyperkalemic humans and animals.[17] In the early stages of depletion, extracellular potassium loss is proportionately greater than the loss of cellular potassium.[18] Nonetheless, since only a small fraction of total body potassium is extracellular, the quantity of potassium lost from the extracellular compartment is much smaller than that lost from inside cells.

In the early phases of hypokalemia (>2.5 mEq/liter), patients tend to display an almost linear relationship between total body potassium and the serum

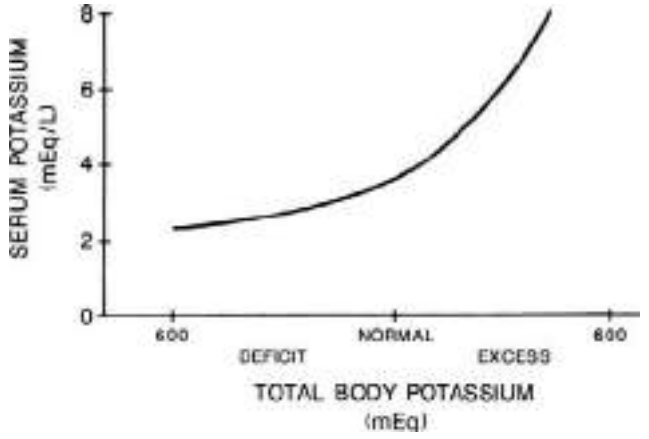

FIGURE 48.2 **Idealized relationship between the serum potassium concentration and the body potassium content.** *Reprinted with permission from ref. [17].*

potassium concentration. It has been observed that a change of 100–200 mEq in total body potassium (about 5%) is required to lower the serum potassium by 1.0 mEq/liter.[17] In such a situation, the extracellular potassium concentration would be expected to fall proportionately more (e.g., 4.0 to 3.0 mEq/liter) than the intracellular concentration (e.g., 140 to 133 mEq/liter). Because of the relationship of cell membrane potentials to the ratio of internal to external ionic activity of potassium, excessive extracellular potassium loss would be expected to hyperpolarize cells (resting membrane potential is increased). This expectation has been confirmed in studies of early potassium deficiency in both dogs[19] and humans.[20]

When potassium depletion becomes more severe, so that serum levels fall below about 2.5 mEq/liter, a further 1.0 mEq/liter fall will represent a much larger 200–400 mEq decrement in total body potassium (greater than 10%), reflecting a greater degree of potassium loss from within the cells[17,21] than occurred in the early phases of depletion. Decreased cell potassium content has, in fact, been observed in several tissues during severe hypokalemia.[15,22,23]

In severe potassium depletion cells tend to depolarize (resting membrane potential is decreased), at least in dogs[19] which, like humans, then develop weakness and muscle paralysis. Under conditions of chronic hypokalemia, however, there is also upregulation of the colonic form of H,K-ATPase (HKα2), which leads to enhanced potassium reabsorption from the gut.[24]

Potassium Repletion

During potassium repletion for severe hypokalemia, cellular potassium uptake is enhanced both in animals[25,26] and in humans[27]; that is, the administered potassium has an increased volume of distribution; as potassium is gained by the body and the stores become higher, the cellular uptake of potassium decreases. In anuric humans, for example, the cellular uptake of a potassium-load decreases as total body potassium increases.[27] Extracellular potassium then tends to rise and membrane potential decreases.[28] The important therapeutic caveat in the late phases of correction of potassium depletion is that less potassium administration is required than in earlier phases to increase serum potassium, which may rise suddenly to unexpected, dangerously hyperkalemic levels.[29]

As reviewed extensively by Sterns et al.,[27] the serum potassium alone is, at best, an extremely rough guide for estimating potassium replacement therapy, presumably because other factors, such as acid–base status, influence it. A low serum potassium value (e.g., 3.0 mEq/liter) may be associated with a range of total body deficits spanning a few hundred millequivalents (Figure 48.2).

The exact mechanisms that produce this curvilinear relationship are uncertain. They may stem in part from impairment of the electrogenic sodium pump.[19,30,31] During potassium depletion in rats, skeletal muscle potassium loss is associated with a reduced capacity for Na-K pumping and a reversible decrease in the number of [^{3}H] ouabain-binding sites.[32] A possible mechanism for suppression of the Na-K pump during potassium depletion is enhanced stimulation of alpha-adrenoreceptors[33] (see "Catecholamines"). In addition, even modest dietary potassium restriction provokes resistance to insulin-mediated cellular potassium uptake (see "Insulin").

INSULIN

The effect of insulin on potassium homeostasis was first demonstrated two years after its purification by Banting and Best. Harrop and Benedict,[34] and Briggs and Koechig[35] described the fall in serum potassium coincident with lowering of blood sugar when insulin was administered to diabetic patients, as well as in the non-diabetic human, dog, and rabbit. Later, there were reports of severe hypokalemia in insulin-treated patients with ketoacidosis who developed paralysis.[36]

Cellular Mechanism

The hypokalemic action of insulin derives from its capacity to cause net potassium uptake in skeletal muscle,[37–39] adipose tissue, and hepatic cells,[40–42] as well as other extrarenal sites.[43] This effect was formerly assumed to occur to preserve electrical neutrality when

insulin-mediated glucose uptake produced intracellular anionic sugars[44,45] and deposited potassium as an accompaniment of glycogen in the liver.[46]

This classical hypothesis did not explain the clinical observation that sudden lowering of serum potassium could precede the fall in blood sugar in insulin-treated diabetic coma. Zierler[47] first noted that insulin's effect on potassium movement in rat muscle occurred even in the absence of glucose; its known effect to increase sodium efflux *in vitro* also occurred without glucose.[48] Furthermore, enhancement of potassium disposal in the intact animal was separable temporally from glucose uptake[49,50] and occurred at plasma insulin concentrations having no measurable influence on uptake of glucose *in vivo*.[51] Different receptor mechanisms for potassium and glucose transport appear to exist.[45]

In vitro, insulin is known to stimulate both potassium uptake[52,53] and sodium efflux[37,54] in frog and rat muscle preparations. Similar effects have been reported in rat adipose tissue,[55] hepatocytes,[56] and other cells.[57] Considerable evidence[45] suggests that following binding to cell surface receptors,[58] insulin accelerates monovalent cation transport by stimulating Na,K-ATPase, the sodium-potassium pump. Most convincing is the fact that both insulin-stimulated net sodium efflux and potassium influx are blocked by ouabain.[37,52,54,59] *In vitro*, addition of insulin to purified plasma membrane of skeletal muscle increases the activity of the Na,K-ATPase.[60] Little evidence is currently available on whether insulin affects potassium permeability or potassium channels in skeletal muscle cells. Insulin activation of sodium−hydrogen exchange sensitive to amiloride[61] does not appear to be important to sodium-pump-mediated potassium uptake.[62] In adipocytes, insulin-stimulated uptake of K^+ and Rb^+ is inhibited by bumetanide and by removal of Cl^- from the extracellular fluid, suggesting a primary action of insulin on the Na−K−2Cl co-transporter.[63] On the other hand, in skeletal muscle, insulin does not appear to activate the co-transport of K^+ with Na^+ and Cl^-.[64] There is evidence, however, that the serum and glucocorticoid-inducible kinase SGK1 participates in the different signaling pathways that mediate the hypokalemic effect of insulin.[65]

Stimulation of active sodium−potassium transport by Na,K-ATPase could be due to a *de novo* increase in the number of sodium pump sites or to allosteric activation of existing sites. The latter theory is consistent with the rapid activation of transport that occurs,[66] as well as with the lack of new ouabain-binding sites[67,68] after exposure to insulin *in vitro*.

At least three molecular forms of the Na,K-ATPase catalytic subunit have been identified, designated alpha1, alpha2, and alpha3. In both rat and human skeletal muscles, insulin mediates the Na,K-ATPase alpha1- and alpha2-subunit translocation into the plasma membrane via a phosphatidylinositol 3-kinase-dependent mechanism.[69] In liver, the effect of insulin can be accounted for by increased intracellular sodium concentration.[56] Insulin also activates a KCl co-transporter uptake system in a cultured cell line resembling skeletal muscle.[70]

It should be noted that insulin is known to produce hyperpolarization of cellular membranes, not only in skeletal muscle,[71,72] but in a variety of other tissues.[73,74] This rapid effect appears to precede measurable increases in intracellular potassium.[39] Although stimulation of Na,K-ATPase could account for insulin's hyperpolarizing effect,[75] failure of ouabain to block it, at least in some studies, suggests that changes in ion permeability may be responsible. The role of hyperpolarization in mediating insulin effects on cation transport is uncertain. The effect of insulin to stimulate active sodium and potassium transport in skeletal muscle is mimicked by insulin-like growth factor I (IGF-I).[76]

In Vivo Effects

Abundant evidence therefore exists that insulin increases net uptake of potassium ions by several tissues *in vitro*. Since skeletal muscle is well-documented to respond to insulin and is the major body reservoir for potassium, it is most likely the dominant site for insulin-stimulated extrarenal potassium disposal *in vivo*. Human forearm muscle (and adipose tissue) increases potassium uptake during arterial infusion[51] of insulin.

Wilde[77] noted over half-a-century ago that injected potassium rapidly disappeared from the blood of cats, but was followed by a secondary rise in serum potassium. Recent investigation suggests that, at least during insulin infusion, hepatic disposal plays an important role in potassium homeostasis in the first hour of exposure to insulin in humans.[78] Splanchnic uptake accounted for two-thirds of the fall in plasma potassium during euglycemic hyperinsulinemia. In the second hour, net splanchnic uptake reversed, and peripheral tissues became the dominant site of potassium disposal.

That the effect of insulin on extrarenal potassium homeostasis is dose related is well-established[79,80] (Figure 48.3). In normal subjects, neither intramuscular nor subcutaneous administration of insulin, which achieved plasma insulin levels of about 50 μU/ml, decreased the plasma potassium.[81] Intravenous insulin injection, by comparison, produced 40-fold greater insulin levels, which were accompanied by a steady-state reduction in plasma potassium, with a maximal effect of about 30% occurring 50 minutes after insulin injection.

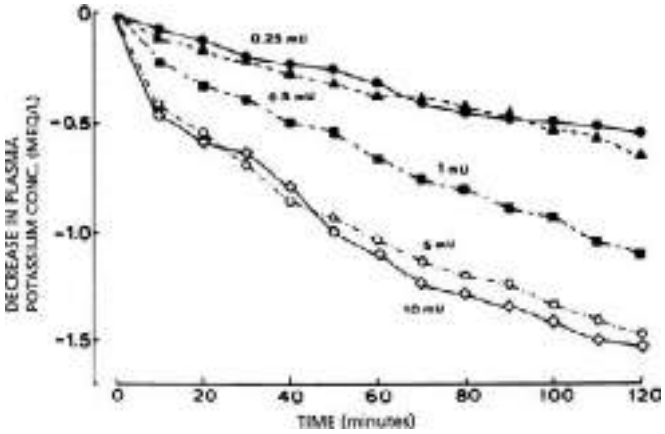

FIGURE 48.3 **Dose-related effect of euglycemic hyperinsulinemia on plasma potassium concentration.** Infusion of insulin at the doses shown produced plasma insulin levels of approximately 25, 50, 100, 500, and 1000 μU/ml above basal values. *Reprinted with permission from ref. [79].*

On the other hand, much smaller increments of insulin, about three-fold above basal values, either during constant venous[78,82] or intra-arterial infusion[49,51,83] also appear capable of augmenting potassium uptake *in vivo*.[27] Under conditions of prolonged potassium depletion, however, the expression of skeletal muscle Na,K-ATPase α2 isoform is decreased, which allows for enhanced efflux of potassium from muscle to the extracellular space.[84] Of particular interest is the observation that even modest dietary potassium restriction leads to a decrease in insulin-mediated cellular potassium uptake in rats in the absence of a fall in plasma potassium concentration.[85]

Clinical Implications

The relevance of these findings to a given clinical situation of exogenous potassium challenge will depend on the magnitude of potassium-load requiring disposal, and the elevation of insulin accompanying it. Following carbohydrate feeding, for example, increased liver uptake of potassium occurs.[46] Since peripheral venous insulin levels for 2 hours following oral glucose loading are elevated five-fold,[86] well within the range capable of augmenting potassium uptake, it seems likely that insulin contributes to the transient decrease in potassium that occurs after feeding.[87] Even basal circulating insulin levels may be essential to disposal of an acute potassium-load, since disposal is impaired when basal levels are decreased 50% by somatostatin.[88] The effect of carbohydrate meals to blunt or prevent hyperkalemia may be particularly important in anuric patients dependent on extracorporeal dialysis.[89]

During exogenous potassium challenge, the importance of insulin to potassium disposal by the intact organism deprived of endogenous insulin[90–93] or resistant to the actions of insulin[94] is well-established. As expected, supraphysiologic doses of exogenous insulin are capable of improving potassium tolerance.[92] Thus, for emergency treatment of hyperkalemia, the intravenous administration of insulin together with glucose is indicated, unless the patient is already hyperglycemic from diabetes in which case additional glucose is not warranted.

The ability of potassium-loading to stimulate the release of pancreatic insulin directly, in amounts sufficient to contribute to disposal of that potassium, is less clear. In pancreatic B-cells, ATP-sensitive K channels link cellular membrane potential to hormone secretion.[95] These channels control the transmembrane potential, and thereby the calcium channels that trigger glucose-induced insulin secretion.[96] Depolarization of the cell membrane (as expected with hyperkalemia) induces an increase in insulin secretion.[97] In humans[98] and intact dogs,[99–101] minor increments in blood potassium appear capable of triggering pancreatic insulin secretion. Since elevations in portal venous insulin far exceed those in the peripheral circulation when insulin release is stimulated,[100,102,103] it seems reasonable to conclude that, under conditions of significant hyperkalemia, induction of insulin release to promote potassium uptake does constitute a homeostatic feedback control system.

GLUCAGON

The effect of glucagon on extrarenal potassium disposal has been difficult to isolate, because the hormone also influences the secretion of insulin, epinephrine, and aldosterone. Administration of glucagon to cats does appear to mobilize potassium from the liver and produce a transient rise in arterial potassium levels.[104] In humans, the hyperkalemic response to the hormone appears to be only partly due to an epinephrine-like effect of glucagon to increase liver glycogenolysis.[105]

For example, aortic injection of glucagon in humans, which results in hepatic vein glucagon levels within the pathophysiologic range, causes a transient increment in hepatic vein potassium concentrations, but this precedes the slow rise in glucose in hepatic venous blood.[106] The specific source of the modest rise in hepatic venous potassium under these conditions has not been determined. Previous *in vitro* investigations using perfused rat liver suggest that glucagon releases potassium directly from the liver.[41,107] The effect would not appear to be due to diminished Na−K pump-mediated potassium uptake, since isolated rat hepatocytes

exposed to glucagon actually undergo stimulation of this cation pump.[108]

Systemic infusion of glucagon to physiologic levels tends to elevate plasma potassium slightly by an extrarenal mechanism, at least when glucagon-induced insulin secretion is suppressed by somatostatin, both in normal subjects[105] and in diabetic subjects.[109] It is unclear whether hyperglucagonemia, which occurs in decompensated diabetes mellitus,[110] uremia,[111] and exhausting exercise[112] affect potassium homeostasis. In the dog, potassium-stimulated insulin release appears to be accompanied by a modest rise in circulating glucagon.[92,112]

CATECHOLAMINES

The observation of D'Silva[113] in 1934 that epinephrine lowers the serum potassium in cats has since acquired important physiologic and clinical relevance.[114–116] Although D'Silva emphasized the rapid rise in the serum potassium that followed a bolus injection of epinephrine (now felt to be a consequence of transient hepatic discharge of potassium by alpha-adrenergic stimulation),[117–119] of greater significance was the sustained "after-fall" in serum potassium that he observed. This secondary decrease in potassium was found to persist throughout a 1 hour infusion of epinephrine.[120]

Since epinephrine inhibited the renal excretion of potassium,[121,122] its late hypokalemic action was attributed to net uptake of potassium by extrarenal tissues. Indeed, *in vivo* limb studies in dogs[123] and humans,[124,125] as well as tissue analysis and ion flux studies, supported accelerated uptake of potassium, primarily in skeletal muscle,[126] but also in liver[126] and heart,[127] in response to epinephrine. *In vitro*, epinephrine was demonstrated to stimulate potassium uptake, as well as sodium efflux, by isolated skeletal muscle in both rats[128,129] and humans.[128] A similar effect was present in rat diaphragm,[130] cat cardiac muscle,[131] and frog sartorius muscle.[132]

Because epinephrine may influence insulin secretion, it was necessary to show that its hypokalemic effect was independent of insulin.[133,134] Independence from renin-mediated aldosterone release was established by the lowering of potassium despite nephrectomy.[135,136] Since extrarenal potassium disposal was impaired when nephrectomized rats were subjected to adrenalectomy or to chemical sympathectomy,[93] both circulating adrenomedullary epinephrine, as well as peripheral sympathetic nervous activity, appeared to be important sources of sympathetic influence on potassium.

Beta-Adrenergic Effects

Epinephrine stimulates both alpha- and beta-adrenergic receptors.[137] The conclusion that its hypokalemic action was a result of beta-adrenergic stimulation derived from experiments many years later employing beta-agonists and beta-antagonists.[119,123] Isoproterenol, a nonspecific beta-agonist, reproduced the prolonged hypokalemia earlier observed by D'Silva, and this effect was reversed by the beta-adrenergic-antagonist propranolol; likewise, epinephrine's effects on cation flux were blocked by beta-antagonists.[1,114]

Beta-agonists and -antagonists have been used to establish that the stimulating effect of catecholamines on potassium uptake is mediated by the beta2-receptor subtype.[138,139] Epinephrine's effect on potassium is prevented by the presence of nonselective beta-antagonists such as propranolol[1,115,123,131,141–143] and timolol,[144] as well as by the nonspecific alpha-beta blocker labetalol.[145] Less reversal occurs with the partially beta1-selective-antagonists metoprolol[146] and atenolol.[144] No effect on potassium appears to be produced by the more specific beta1-antagonist practolol.[131,147] In addition, the selective beta2-antagonists butoxamine[138,148] and ICI-118551[149,150] are able to block the hypokalemic action of beta-agonists.

Numerous studies of beta-agonists have revealed that several beta2-agonists, including salbutamol,[151–155] terbutaline,[136,156–158] fenoterol,[159] and ritodrine[156] lower potassium levels, unlike the beta1-agonist ITP,[131] which has no effect. These pharmacologic studies therefore provide strong support for beta2 mediation of adrenergic effects to enhance potassium disposal.

Mechanism of Action

The specific cellular mechanism by which cell surface beta2-receptor stimulation augments transcellular potassium uptake in affected tissues has been evaluated in detail. Compelling evidence exists to support the proposal of Clausen[114] that beta2-stimulation initiates cyclic AMP formation,[160] which leads to activation of the sodium pump (Na,K-ATPase), and therefore electrogenic sodium efflux accompanied by potassium uptake.[161] Beta receptors are known to stimulate adenylate cyclase,[38,160,162] enhancing conversion of intracellular ATP to cyclic AMP.[163] Linkage of beta receptors and cyclic AMP is supported by the ability of theophylline to potentiate the effect of epinephrine on cation transport and membrane potential,[114] as well as by the increase in membrane potential that dibutyryl cyclic AMP and theophylline produce in rat diaphragm muscle.[164] Epinephrine, in stimulating cation transport, is well known to produce hyperpolarization of membranes in skeletal muscle.[114]

The sodium pump of muscle cells and lipocytes is activated by cyclic AMP. For example, Na,K-ATPase activity in smooth muscle membrane fragments is enhanced by exposure to cyclic AMP.[165] The most compelling evidence that catecholamine-mediated potassium influx involves the beta-adrenergic system through activation of the sodium pump, however, are the demonstrations in a series of experiments that potassium influx occurs as active movement of the cation against its electrochemical gradient[166]; ouabain blocks the ability of epinephrine to promote potassium influx in rat soleus muscle[129]; epinephrine markedly increases the ouabain-sensitive 22Na efflux by stimulating the Na−K pump in frog skeletal muscle, and this effect is blocked by propranolol[167]; epinephrine produces membrane hyperpolarization and transient decreases in extracellular potassium and intracellular sodium, which is blocked by ouabain, in isolated rat soleus muscle and human intercostal muscle[128]; and isoproterenol directly stimulates the Na−K pump in isolated rabbit myocytes.[168] While the specific sequence of events linking beta-adrenergic stimulation to sodium pump activity has not been delineated, phosphorylation of some portion of the sodium pump after beta2-receptor stimulation is presumably involved.[166] Beta-adrenergic agents also stimulate the cellular uptake of potassium via the Na−K−2Cl transporter in the skeletal muscle membrane of rats.[64]

There are numerous clinical examples showing that enhanced exogenous or endogenous beta-adrenergic stimulation augments extrarenal potassium uptake in humans. Whether high potassium levels can stimulate secretion of endogenous adrenomedullary epinephrine, and thereby form a homeostatic feedback loop, remains unresolved. Supraphysiologic levels of potassium *in vitro* can cause the release of catecholamines from isolated chromaffin cells[169] and perfused adrenal glands,[170] possibly related to the membrane depolarizing effect of a high potassium level. Induction of tyrosine hydroxylase, the rate-limiting enzyme in catecholamine biosynthesis,[171] by extremely high levels of potassium has also been observed. Reports that intra-arterial injections of KCl augment catecholamine release in cats[172] and in the dogfish shark[173] suggest a potential role for potassium as a catecholamine secretagogue *in vivo*.

Although specific stimulation of catecholamine release by potassium is not yet established, it is clear that physiologic elevations of endogenous catecholamines do enhance potassium uptake. Similar to the pharmacologic doses of epinephrine used in earlier animal reports of its protective effect during potassium-loading,[120,131,174] as well as its ability to lower basal potassium,[175] relatively small doses[1,140] have also been shown to enhance extrarenal disposal of an acute potassium-load. It has also been established that ambient potassium may be lowered when sustained epinephrine infusions[176] (Figure 48.4) elevate plasma concentrations of epinephrine to levels no higher than those observed in stressful conditions, such as myocardial infarction,[177] surgical stress,[178] and diabetic ketoacidosis.[179] By comparison, acute beta blockade does not appear to elevate fasting potassium levels,[176] suggesting that basal beta-adrenergic tone plays a limited role in potassium homeostasis in normal fasted individuals at rest.

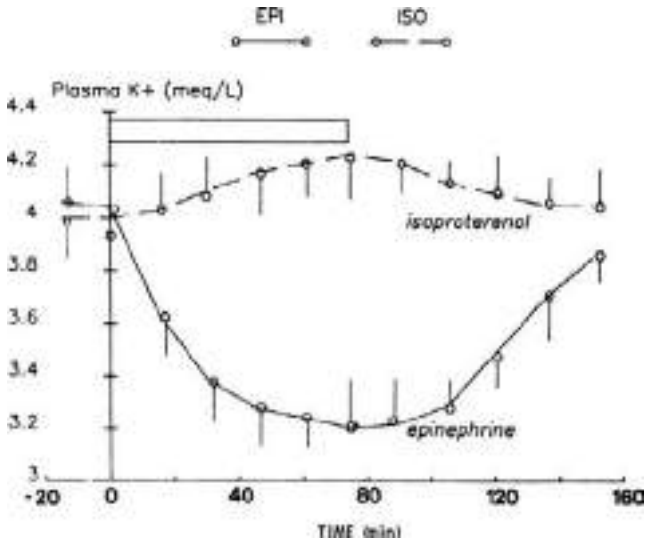

FIGURE 48.4 **Effect of epinephrine and isoproterenol infusions (long box) on the plasma potassium concentration.** The contrasting effects of the two beta-agonists probably are due to the relative beta2 selectivity of epinephrine at the dose given. Plasma epinephrine concentrations achieved by infusion were similar to those known to occur in myocardial infarction and other disorders. *Reprinted with permission from ref. [176].*

It has recently been appreciated, however, that there are two common physiologic circumstances in which endogenous catecholamines could act to defend against increments in extracellular potassium concentration. The first of these is postprandial disposal of dietary potassium. Feeding is now known to be associated with stimulation of the sympathetic nervous system.[180] Since only half of the potassium ingested in a meal is normally excreted within 6 hours,[7] enhanced beta-adrenergic-mediated extrarenal potassium disposal may help to limit elevations of serum potassium in the immediate postprandial period. In conjunction with enhanced potassium uptake due to insulin release, this mechanism would be particularly important in subjects at risk for hyperkalemia for any reason.

The second circumstance is the dramatic effect of catecholamine release during vigorous exertion to moderate the acute physiological hyperkalemia of

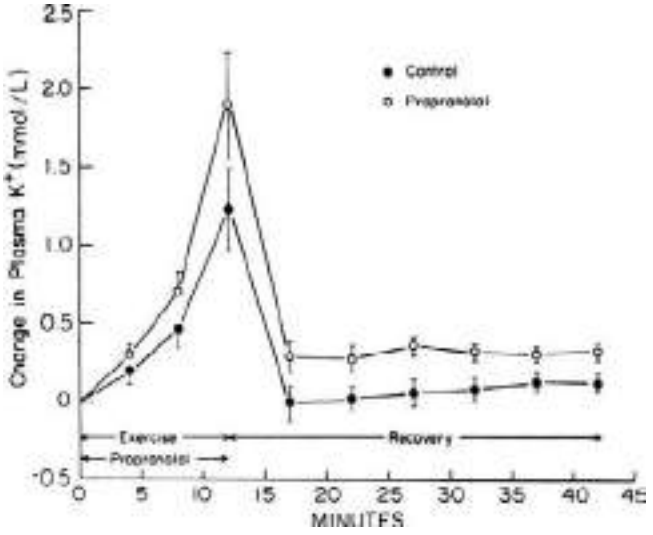

FIGURE 48.5 **Effect of adrenergic blockade on the plasma potassium concentration during vigorous exercise and recovery.** Beta-blockade with propranolol potentiated the rise of plasma potassium at peak exercise and prolonged its elevation during recovery. In the same subjects, alpha blockade with phentolamine was shown to lower the peak plasma potassium level, as well as the overall potassium curve. *Reprinted with permission from ref. [182].*

exercise. Catecholamines circulate at high levels during vigorous exercise, and the associated short-term elevation of potassium that is released into the circulation from working muscles is exaggerated by beta blockade[181,182] (Figure 48.5), suggesting that endogenous beta-adrenergic activity does protect against extreme hyperkalemia during exhaustive exercise. In this context, it is of particular interest that training leads to upregulation of the content of the Na,K-ATPase,[183] which serves to mitigate the rise in extracellular potassium concentration relative to the work performed.[184] Another mechanism that might mitigate the rise in extracellular potassium seen during exercise is AMP-activated protein kinase. This cellular enzyme, which is normally stimulated by exercise or ischemia, has been demonstrated to produce a decrease in plasma potassium when stimulated chemically in the rat.[185] This decrease does not appear, however, to be mediated by the Na,K-ATPase, and may instead be secondary to diminished efflux of potassium from the intracellular compartment.

Alpha-Adrenergic Effects

The fact that opposing alpha- and beta-adrenergic influences have in the past been reported on smooth muscle tone,[186] glucoregulatory hormones,[187] presynaptic membrane receptors,[188] and changes in intracellular second messengers[160,189] suggests the role of alpha-adrenergic agonists in potassium homeostasis. As noted previously, the early rise in extracellular potassium emphasized by D'Silva in 1934[113] was later attributed to alpha-mediated hepatic potassium release by the mixed alpha- and beta-agonist epinephrine.[119] This initial rise in potassium could be prevented by alpha blockade.[119] In addition, phenylephrine, a pure alpha-agonist, was observed to cause a sustained increase in potassium in dogs.[119,190]

When phenylephrine was infused into normal human subjects who were challenged with an intravenous potassium-load, the overall rise in plasma potassium was augmented by about 50%,[2] despite no change in insulin, renin, aldosterone or urinary potassium. In separate studies, addition of the alpha-antagonist phentolamine blocked the phenylephrine effect on potassium disposal. Neither alpha stimulation nor blockade appeared to affect the concentration of potassium in the absence of potassium-loading.

Other evidence suggests that the alpha effect might directly contribute to potassium homeostasis in certain circumstances. Alpha-receptor stimulation during vigorous exercise contributes to the acute rise in potassium that is maximal at peak exercise, and limits the dramatic fall due to potassium re-uptake during recovery.[182] Furthermore, during potassium depletion in rats, the sodium−potassium pump of skeletal muscle is suppressed by an increase in alpha-adrenergic activity mediated by nerves, an action that would mitigate the expected fall in plasma potassium concentration.[33] It is therefore speculated that enhanced alpha-agonist activity might act to preserve potassium similarly during a variety of acute illnesses, such as myocardial infarction[176] or delirium tremens,[191] where catecholamine stimulation of both beta- and alpha-receptors may coexist. Unopposed stimulation of alpha receptors may contribute to the impairment of potassium disposal caused by beta-receptor blockade.

Dopamine

The infusion of dopamine is known to augment glomerular filtration rate, renal plasma flow, osmolar clearance, sodium excretion,[192] and potassium excretion[193] in normal humans and animals. Levodopa, the metabolic precursor of dopamine, has also been reported to enhance renal potassium excretion,[194,195] and an increase in endogenous dopamine produced by protein feeding has been associated with augmented kaliuresis.[196] On the other hand, the dopamine antagonist metoclopramide also increases potassium excretion, an action ascribed to its blockade of tonic dopaminergic inhibition of aldosterone release.[197] Whether the dopaminergic system plays a role in extrarenal potassium homeostasis remains uncertain. Both dopamine and dobutamine lower plasma potassium

when infused into anesthetized dogs, but only by a few tenths of a mEq per liter.[198]While some studies demonstrate enhanced extrarenal potassium uptake into cells following administration of metoclopramide,[199–201] others demonstrate no such effect of either metoclopramide[202–204] or the dopamine agonist bromocriptine.[202,203,205] The discrepancy between these studies may well be attributed, at least in part, to the fact that metoclopramide is a nonspecific antagonist of dopamine.[206] The determination of the role, if any, of the dopaminergic system in extrarenal potassium homeostasis must await studies employing specific dopamine antagonists.

Clinical Implications

The clinical significance of epinephrine-induced hypokalemia is underscored by reports of hypokalemia occurring during acute illnesses, such as myocardial infarction, as well as during medical treatment with beta-agonists.[207] Struthers et al.[144] discovered that when epinephrine infusion produced circulating epinephrine levels similar to those found after myocardial infarction, the serum potassium fell from 4.06 to 3.22 mEq/liter in normal volunteers. This ability of small doses of epinephrine to diminish potassium levels was confirmed by Brown et al.[176] In this context, the frequency of hypokalemia during acute myocardial infarction has been observed to be 8 to 30%.[208–211] Concomitant therapy with diuretics may further increase the frequency of hypokalemia during myocardial infarction,[212,213] as it appears to do in normal subjects who are experimentally infused with epinephrine.[214]

Because several studies have suggested that hypokalemia is an independent risk factor for cardiac arrhythmias in patients with acute myocardial infarction, these observations may have clinical relevance. A higher incidence of atrial fibrillation[215] and ventricular arrhythmias are reported in hypokalemic compared with normokalemic patients during infarction.[209,216] In one report,[210] ventricular tachycardia or fibrillation increased three-fold (to 35%), and hospital mortality doubled in hypokalemic patients with myocardial infarction.

It must be appreciated, however, that the hypokalemia reported during earlier studies of epinephrine infusion occurred when high concentrations of plasma epinephrine were sustained by infusion. Whether elevations of plasma epinephrine during acute myocardial infarction are similarly sustained, rather than transient,[177] is uncertain. The contribution of circulating epinephrine to the hypokalemia that may occur during this form of acute illness therefore remains hypothetical. Nonetheless, pharmacologic data do suggest that such acutely ill patients may be protected from the hypokalemia that is sometimes associated with myocardial infarction by the use of beta blockers.[142,143,217] Whether the beneficial effect of beta blockade reported in this setting is due to diminution in hypokalemia-related arrhythmias is not known. That hypokalemia is not more prevalent in the setting of acute myocardial infarction may, in part, be a consequence of a simultaneous elevation in plasma norepinephrine, suggesting alpha-receptor stimulation that might antagonize the effect of epinephrine on potassium homeostasis.

Transient lowering of potassium levels has also been reported in other acute medical conditions[218–221] in which catecholamines might stimulate beta-adrenergic receptors capable of increasing cellular uptake of potassium. Pharmacologic therapy employing beta2-agonists such as terbutaline, ritodrine, and salbutamol to prevent premature labor[151,155,156,158,222] may produce a substantial degree of hypokalemia. Administration of salbutamol and albuterol in the treatment of bronchospasm[153,223] may also produce unwanted hypokalemia. In this context, it is important to appreciate that administration of inhaled beta2-agonists to healthy volunteers in doses similar to those used by asthmatic patients during an acute attack has produced decrements of plasma potassium by as much as 0.9 mEq/liter.[159] These observations raise the disturbing possibility that such usage of these agents may be the explanation for the high incidence of sudden death in adolescent asthmatics.[224] Hypokalemia in this setting might be further exaggerated by the concomitant use of theophylline[225] or other methylxanthines.[226,227] Theophylline not only increases the level of circulatory catecholamines, but also enhances catechol stimulation of adenylate cyclase by blocking inhibitory adenosine receptors. Hypokalemia associated with elevated levels of epinephrine has also been reported in patients admitted for trauma,[228] and in normal subjects who received endotoxin.[229] Sepsis induced in rats, moreover, increases the activity of Na,K-ATPase.[230]

The clinical significance of the adrenergic nervous system in potassium balance is also evident in the well-established effect of beta-antagonists to elevate extracellular potassium concentration. An example is the acute effect of propranolol to exaggerate the hyperkalemia of vigorous exercise.[182] Some,[231–233] but not all,[234,235] investigators have reported a 10–15% increase in ambient plasma potassium during chronic beta blockade with nonselective agents. In addition, one study suggests that the serum potassium may rise above 6 mEq/liter in patients on nonselective beta-blockers at the time of open heart surgery.[236] Transient hyperkalemia has been reported after cyclosporine

administration in patients on beta-blocking agents, but not when these are omitted.[237] Patients receiving succinylcholine anesthesia may also be at risk for the development of hyperkalemia.[238] Patients with end-stage renal failure on dialysis, moreover, regularly exhibit an increase in predialysis potassium of about 1 mEq/L when treated with propranolol.[239] Despite the clinical relevance of these studies describing an increase in extracellular potassium concentration in a variety of clinical conditions in patients receiving beta-blockers, it is important to realize that beta-blockers are unlikely to produce any significant increment in potassium concentration in subjects in whom the other mechanisms of potassium homeostasis are intact.

Since some studies do substantiate the anticipated absence of effect on potassium of cardioselective beta1-antagonists,[236,240,241] selected groups of patients at risk for hyperkalemia might be protected from significant elevations in potassium due to beta blockade by the use of such selective agents. Such patients include those with diabetes mellitus, hypoaldosteronism, and renal failure.

THYROID

Thyroid hormones enhance the activity of Na, K-ATPase in muscle cells,[242] accelerating the extrarenal disposal of potassium.[243] A portion of this effect can be ascribed to upregulation of beta-adrenergic receptors and an increase in beta-adrenergic responsiveness, but there appears to be a direct effect on cellular Na, K-ATPase as well.[243] Hypokalemic paralysis occasionally complicates thyrotoxicosis; in such cases urinary excretion of potassium is always low, reinforcing the hypothesis that the low serum potassium reflects a shift of potassium from the extracellular to the intracellular compartment rather than urinary losses of potassium. The hypokalemia and paralysis respond to the administration of beta-adrenergic-blocking agents.[244] This syndrome has been reported many times in Orientals, but is extremely rare in Caucasians and Blacks. It is not, moreover, associated with the inherited mutations in the calcium and sodium ion channels reported to cause familial hypokalemic periodic paralysis, but may in some cases be associated with a mutation in a channel mediating potassium efflux.[245] Hyperkalemia has been reported in hypothyroid dogs after exercise, but not in humans with hypothyroidism.[246]

ACID–BASE

Although acid–base balance affects potassium excretion by the kidney, shifts of potassium in and out of body cells are the initial way in which acid–base disturbances alter serum potassium. These movements are influenced by a variety of factors, including the changes in extracellular and intracellular pH, the degree of cellular buffering, the nature of the anion accompanying H^+, and the associated changes in hormonal and neural regulators of potassium uptake, including insulin and catecholamines.

The concentration of potassium in plasma tends to vary in the same direction as that of free hydrogen ions,[27,247–249] so that acidosis promotes hyperkalemia and alkalosis promotes hypokalemia. Since approximately 40% of the acid buffering capacity of the body is provided by intracellular proteins, largely in muscle cells,[250] and since potassium is the chief intracellular cation of muscle, the release of intracellular potassium is to be expected as a consequence of the intracellular buffering of hydrogen ions. Conversely, with repair of acidosis or during alkalosis, potassium will tend to move into cells. This exchange of K^+ for H^+ is not necessarily equimolar, and the routes across the plasma membrane that are responsible for such transfers have not been completely delineated. A simple reciprocal exchange of K^+ and H^+ via a single plasma membrane transporter has not been described in muscle cells.

Hydrogen Ion

The importance of pH in affecting internal potassium distribution during acidosis was demonstrated in early studies.[251–254] Fenn and Cobb[247] reported in 1934 that potassium exited from skeletal muscle *in vitro* when the bath pH was lowered, and moved into the tissue when blood at physiologic pH was substituted for acidic medium. They invoked the Donnan equilibrium to account for similarity in the intracellular to extracellular ratios of hydrogen and potassium ions, so that a decrease in that ratio produced by acidosis would be associated with a decrease in the ratio for potassium – that is, an increase in extracellular K^+. *In vivo* as well, an approximately linear relationship appears to exist between the potassium gradient and the pH gradient across muscle cell membranes, as predicted by the Donnan effect.[255,256] Nevertheless, the shifts in potassium observed in experimental situations are not always fully explained, either by the Donnan effect or by changes in membrane potential.[256,257]

Since the ratio Ki/Ke for skeletal muscle is approximately 30, the maintenance of a similar hydrogen ion ratio between intracellular and extracellular fluid would require an intracellular pH of approximately 5.92. However, intracellular pH is actually in the range of 6.9–7.0, so that the intracellular to extracellular proton ratio is only approximately 3 rather than 30. The

major reason for this is the operation of the amiloride-sensitive Na^+-H^+ antiporter, which transports H^+ out of cells by a secondary active mechanism that ultimately derives its energy from ATP via the Na,K-ATPase of plasma membranes.

Moreover, the direction of the movement of potassium during acute acid–base disorders is not uniform among various tissues.[257] During acute respiratory acidosis, potassium moves out of the cells in muscle and liver, but into cardiac muscle. Yet, in both skeletal and cardiac muscle, the ratio of intracellular to extracellular hydrogen ion concentration falls. As will be seen subsequently, powerful evidence has been adduced under both *in vitro* and *in vivo* conditions suggesting that, in some circumstances, the ionic ratios of hydrogen and potassium can be dissociated and transmembrane fluxes of potassium change in the face of a stable pH gradient.

Inhibition of the sodium–potassium pump of plasma membranes by an acid pH contributes importantly to the relationship between acidosis and plasma potassium. In every case in which it has been measured, an increase in plasma potassium associated with systemic acidosis is accompanied by a fall in intracellular potassium. The optimal pH for mammalian Na,K-ATPase is 7.5–7.6, whereas intracellular pH of muscle is 6.9–7.2.[258] The effect of pH on the activity of the sodium–potassium pump is exerted from the intracellular, rather than the extracellular, side of the membrane.[259,260] In bladder epithelial cells, for example, a reduction of intracellular pH by 0.3 units, from pH 7.2 to 6.9, reduced pump activity to about 70% of that at pH 7.2. On the other hand, alkalinizing the cell interior to pH 7.5 led to a 35% increase in sodium-pump activity.[260]

In addition to a direct effect of pH on the sodium–potassium transport enzyme, an indirect mechanism might involve the linked operation of the Na-H antiporter and the Na,K-ATPase. An attractive mechanism to explain the shift of potassium out of cells that occurs in acidosis involves the linked operation of these two transporters. Both of these transporters are present in the plasma membranes of most cells, including skeletal muscle. Acidification of the extracellular fluid would be expected to slow the rate at which hydrogen ions leave the cell and sodium ions enter, via the Na-H antiporter. The resultant decrease in intracellular sodium concentration would slow the Na-K pump, reduce active uptake of potassium by cells, and increase the concentration of potassium in extracellular fluid. A prediction of this hypothesis is that amiloride, which blocks the Na-H antiporter, would prevent the hyperkalemia produced by acidosis. It is not yet known whether this is the case, but amiloride does block the extracellular acidosis produced by KCl infusions.[261]

Finally, intracellular acidosis appears to open ATP-sensitive potassium channels in skeletal muscle by reducing the degree of channel inhibition by ATP, an action that might accelerate efflux of K^+ from muscle cells during anoxia or extreme acidosis.[262]

Mineral Acids

Acute mineral acidosis, produced by infusing HCl or NH_4Cl, elevated plasma potassium by an average of 0.7 mEq/liter per 0.1 unit decrease in blood pH, in 14 different studies summarized by Adrogue and Madias.[257] The results of these studies were extremely variable, however, ranging from 0.24 to 1.67 mEq/liter per 0.1 pH unit.

One reason for the variability in these reports is that the effect of mineral acid infusions on plasma potassium depends on the duration of the acidosis.[27,254,263,264] Immediately following an acute acid infusion there is a marked fall in extracellular pH and bicarbonate, followed by a gradual rise over the next 2 hours or so, as tissue buffering and respiratory compensation moderate the initial changes in blood pH.[249,250,254,264] Plasma potassium begins to rise early in the course of the infusion and increases progressively as buffering takes place, so that its concentration does not change in parallel with the change in pH. Late in the course of an acute acid-load, when cell buffers have been exhausted and intracellular pH drops sharply, plasma potassium rises more steeply.

It might be expected that the hyperkalemic response to an acid-load would be influenced by the state of muscle potassium. Experimental potassium depletion induced by DOCA (mean plasma K^+ 1.9 mEq/liter) did indeed attenuate the increase in plasma potassium produced by metabolic acidosis, but did not prevent it, and the percentage rise in plasma potassium from baseline induced by NH_4Cl acid-loading was not significantly different from that of controls.[265]

Clinical observations on the endogenous mineral acidosis of uremia, due to retention of sulfate and phosphate, suggest that the change in potassium that is observed when acidosis is corrected is of the magnitude expected in experimental mineral acidosis.[17,266]

Organic Acids

That changes in acidity are not the sole determinant of the kalemic response to acidosis is indicated by the disparate effects which mineral acidosis and nonmineral acidosis have on potassium. In humans and animals, infusion of organic acids such as acetic, lactic or beta-hydroxybutyric acid produce far smaller elevations of potassium than hydrochloric acid.[264,267–270]

The prevailing hypothesis is that the anions of organic acids, either by readily penetrating the intracellular compartment,[257] by entering cells as intact molecules[271] or by being formed endogenously within cells,[272] minimize the necessity for potassium cations to leave cells in exchange for hydrogen ions.[273] The addition of HCl to rat diaphragms *in vitro* results in a loss of potassium from the muscle,[253] whereas when extracellular pH is lowered by addition of acetic acid, beta-hydroxybutyric acid or lactic acid, no shift of potassium out of the cell is observed.[271]

For similar degrees of clinical severity, less elevation of serum potassium occurs with endogenous organic acidosis encountered in ill patients than with mineral acidosis, although the correlation of pH and serum potassium in clinical states of organic acidosis is further complicated by prior total body potassium depletion, oliguric renal failure, hypercatabolism, and other factors.[273] Ketone acids, for example, stimulate the secretion of insulin by the normal pancreas, while suppressing the secretion of glucagon. Infusions of hydrochloric acid, on the other hand, do not stimulate insulin secretion, but enhance plasma glucagon,[102] which in turn tends to elevate the serum potassium. The sympathoadrenal system, which is strongly activated in most clinical states accompanied by organic acidosis (e.g., diabetic or alcoholic ketoacidosis, and the lactic acidosis of circulatory shock), plays an important role in minimizing hyperkalemia, because of the hypokalemic action of beta-adrenergic stimulation. Moderately severe potassium depletion (as occurs in diabetic ketoacidosis) itself attenuates the increase in plasma potassium induced by metabolic acidosis.[265]

Untreated severe diabetic ketoacidosis is characterized by marked deficits (200−300 mEq) in total body potassium,[274] owing primarily to coincident potassium losses from the gastrointestinal tract or kidneys. Despite these losses, hypokalemia is uncommon, present in only 4% of episodes in one series,[275] probably because of concomitant acidosis. Serum potassium is usually normal or elevated at presentation,[276] but falls during successful treatment. Hypokalemia during recovery from diabetic ketoacidosis is most prominent in patients who initially received sodium bicarbonate.

Since insulin plays a significant role in cellular shifts of potassium, lack of insulin is presumably important in promoting hyperkalemia during diabetic ketoacidosis,[277] as it is in patients with hyperosmolar nonketotic coma, who may have severe hyperkalemia without acidosis.[278]

Similar to uncontrolled diabetes, several factors in lactic acidosis complicate the effect of acidemia *per se* on serum potassium. These include volume-depletion, prerenal azotemia, hypercatabolism, concomitant diabetes, catecholamine effects, and external potassium imbalance.[279] Although severe hyperkalemia is unusual in lactic acidosis, Perez et al.[273] have pointed out the absence of detailed studies on potassium in this varied disorder. In experimental lactic acid infusion in animals,[270] and in uncomplicated post-seizure lactic acidosis in humans,[272,280,281] potassium does not increase with the appearance of acidosis. However, in other forms of lactic acidosis, such as those earlier encountered due to phenformin therapy in diabetes,[276] and in other forms not associated with tissue hypoxia, mild elevation of potassium may occur.[272] Renal insufficiency may be a contributing factor in such patients. Most patients with alcoholic ketoacidosis have a normal extracellular potassium concentration,[282,283] although there is significant variability. The effects of rarer forms of organic acidosis on internal potassium homeostasis have been reviewed elsewhere in detail.[273]

Respiratory Acidosis

The effect of acute respiratory acidosis in elevating plasma potassium is, in general, smaller in magnitude than that of metabolic acidosis, though some effect can usually be detected.[248,255,284,285] A rise varying from 0.06 to 0.3 mEq K^+/liter per 0.1 pH unit was detected in 22 studies of mild to moderate respiratory acidosis.[257] More severe experimental acidosis, provoked by inhaled concentrations of CO_2 as high as 30%, induce more pronounced hyperkalemia.[257] In anephric dogs, the initial effect on potassium is small, but after 2 hours respiratory acidosis may increase to the range observed in metabolic acidosis.[27] On the other hand, in *in vitro* experiments, when the extracellular medium bathing isolated rat diaphragms was acidified by raising the ambient CO_2 from 2 to 10%, no shift in potassium was observed,[271] consistent with the ability of carbonic acid to permeate cells, as do other organic acids. Chronic respiratory acidosis produced in dogs was not attended by hyperkalemia.[285]

The increase in serum potassium induced by severe respiratory acidosis in intact rats could be roughly approximated from the decrease in $(H^+)_i/(H^+)_o$, and was attributed to the importance of the Donnan effect in producing these changes.[255] In addition, it is very likely that sympathoadrenal stimulation plays a major role in modulating serum potassium during respiratory acidosis *in vivo*, since it is well-established that acute hypercapnia results in an intense sympathetic discharge and an increase in the plasma concentration of epinephrine.[257,286] Glycogenolysis induced by epinephrine probably contributes to the initial release of glucose and potassium from the liver with hypercapnia, noted by Fenn and Asano,[287] and the hypokalemic effect of beta-adrenergic stimulation is likely to blunt the movement of potassium out of skeletal muscle that

would otherwise accompany acidosis. Probably for this reason, mild respiratory acidosis induced acutely in anesthetized patients was not found to elevate the plasma potassium,[288] although beta-adrenergic blockade produced marked hyperkalemia in hypercapneic animals.[289]

Bicarbonate

It has been suggested that the serum bicarbonate concentration, even at constant or "isohydric" pH, alters extrarenal potassium distribution and might account in part for the weak correlation between pH and serum potassium in many studies. Under conditions of constant blood pH, infusion of sodium bicarbonate appears to lower serum potassium,[257,290,291] and during acidosis in rats, potassium may correlate better with serum bicarbonate than with blood pH.[292] A similar correlation can be found in patients with hyperkalemia of diverse etiologies,[293] as well as in experimental acute ammonium chloride acidosis.[294] This has been taken to indicate that bicarbonate therapy, in addition to beneficially raising pH, corrects hyperkalemia directly, perhaps via intracellular transfer with the potassium cation.

Another explanation of the same data is that it is the quantity of acid buffered by cells, rather than the arterial pH, that governs the release of intracellular potassium. This would account for the fact that extracellular bicarbonate, rather than arterial pH, sometimes seems to exert an independent controlling influence on extracellular potassium. Effective buffering of an acid-load by intracellular and extracellular buffers, so as to produce a low serum bicarbonate and a normal arterial pH, involves the liberation of substantial amounts of potassium cations from intracellular proteins.[295] It can be inferred from the foregoing that alkali treatment of hyperkalemia should be most effective when the plasma bicarbonate is low and acidosis marked, and less so when plasma bicarbonate and pH are normal; this is indeed the case.[296] This result is also inherent in the finding that the changes in plasma potassium produced by metabolic alkalosis are smaller than those seen in metabolic acidosis.

Alkalosis

Metabolic and respiratory alkalosis are commonly associated with hypokalemia. In both, renal losses are important in initiating and perpetuating hypokalemia, but extrarenal adjustments are also involved. Acute alkalosis induced by infusions of sodium bicarbonate usually leads to a decrement in plasma potassium concentrations. The $\Delta(K)p/\Delta pH$ slope is usually smaller than that commonly observed in acute mineral acidosis, although the reported range is wide, from -0.09 to -0.42 mEq/liter per 0.1 pH unit.[257,297,298] The initial change is not attributable to kaliuresis. Acute respiratory alkalosis produces a comparable decrease in plasma potassium, although during voluntary overbreathing this fall may be counteracted by an increase in circulating norephinephrine which, as noted earlier, tends to increase plasma potassium.[299] It should be pointed out that most studies of extrarenal effects of metabolic alkalosis have involved the infusion of hypertonic solutions of sodium bicarbonate. Since hypertonicity itself promotes a rise in plasma potassium, this would tend to counteract any hypokalemic effect of alkalosis *per se*.

An intuitively appealing explanation for the extrarenal effect of alkalosis is replacement of H^+ associated with cellular buffers by potassium, in the reverse of the sequence discussed earlier by which acidosis releases intracellular potassium ions. Enhanced exchange of intracellular H^+ for extracellular Na^+ via the amiloride-sensitive Na^+-H^+ antiporter would accelerate cellular potassium accumulation by stimulating the Na, K-ATPase pump. In addition, intracellular alkalosis probably stimulates the sodium–potassium pump directly, as discussed earlier.

The combined effects of respiratory alkalosis on renal and extrarenal potassium handling commonly produce mild hypokalemia (around 3.0 mEq/liter) resistant to potassium replacement in hypocapneic patients who are artificially ventilated. Extreme hypocapneic alkalosis and hypokalemia, as seen in recently intubated patients who are overventilated, may produce serious cardiac arrhythmias.[300]

ALDOSTERONE

In addition to its action on the kidney to increase potassium excretion, aldosterone enhances potassium secretion into intestinal fluids and saliva. Aldosterone-induced colonic potassium secretion appears to occur through increased expression of luminal BK channels.[301] In chronic renal insufficiency, moreover, the colonic secretion of potassium is greatly enhanced.[302] In that sense, its effect on serum potassium can be said to have an extrarenal component. Aldosterone also has an independent action to accelerate renal acid excretion, and the consequent alkalosis itself has a secondary effect on cellular uptake of potassium. Apart from these mechanisms, there is no convincing evidence for a direct action of aldosterone to increase potassium uptake by muscle cells. For example, incubation of isolated rat diaphragms with

aldosterone results in a loss, rather than a gain, of intracellular potassium.[303,304]

An extrarenal action of aldosterone has been suggested in the past, because of several lines of evidence. First, in experimental animals, hyperkalemia after adrenalectomy seemed not to be entirely accounted for by a positive balance of potassium.[305] Furthermore, the fall in plasma potassium accompanying the administration of mineralocorticoids was not necessarily associated with an increase in potassium excretion.[306–308] Interpretation of such data is complicated, because of the effect of adrenal medullary hormones on extrarenal potassium uptake, and the renal action of mineralocorticoids to retain sodium and excrete acid, resulting in expansion of extracellular fluid volume and alkalosis, both of which might secondarily lower serum potassium.

Long-term treatment of dogs by Young and Jackson[308] with high doses of aldosterone altered the relationship between plasma potassium and total body exchangeable potassium, so that at any level of exchangeable potassium, plasma potassium was lower than in untreated animals. In these experiments, however, mean plasma bicarbonate was significantly higher in aldosterone-treated dogs than in controls, leaving open the possibility that aldosterone-induced alkalosis influenced potassium distribution.

Bia et al.[135] gave intravenous potassium loads to adrenalectomized and nephrectomized rats, and found that the acute administration of aldosterone prior to infusing potassium blunted the hyperkalemia. The differences they observed, however, were small, and could have been completely accounted for by a modest increase in the potassium concentration of gastrointestinal secretions (e.g., an increase of 20 mEq/liter in 1 ml of intestinal fluid) caused by the known action of aldosterone to increase intestinal potassium secretion.

The role of mineralocorticoids in the disposition of an oral potassium-load was studied in anephric humans by Sugarman and Brown.[309] Anephric patients were given 0.5 mEq/kg of KCl after 72 hours of either mineralocorticoid treatment (10 mg DOCA daily) or spironolactone (300 mg daily). The rise in serum potassium was delayed by DOCA, but the difference from control experiments with spironolactone was most marked at 1 hour, much less pronounced at 2 and 3 hours, and not present at 24 hours, suggesting that the mineralocorticoid had delayed absorption of potassium from the gastrointestinal tract. Chronic administration of high doses of mineralocorticoids is said to diminish serum potassium slightly in anuric patients, perhaps because of an increase in stool potassium.[310]

Finally, Alexander and Levinsky[311] reported that chronic potassium-loading improved extrarenal disposal of an acute potassium-load given after a night's fast, an effect abolished by adrenalectomy and restored by chronic (but not acute) high-dose mineralocorticoid replacement. They postulated that chronic hyperaldosteronism acts directly by enhancing cellular uptake of an acute potassium-load.[311] Another interpretation was offered by Spital and Sterns.[26] These investigators showed that, when dietary potassium is withdrawn from rats previously fed a high-potassium diet, high rates of potassium excretion persist and "overshoot," causing these animals to become progressively more depleted of potassium than controls. This "paradoxical potassium depletion" is responsible, at least in part, for extrarenal potassium adaptation, by creating a sink of potassium-hungry cells that avidly take up potassium, and thereby blunt the increment in plasma potassium after an acute potassium-load. Hyperaldosteronism magnifies urinary potassium losses during fasting, and thus promotes potassium depletion, which in turn facilitates the uptake into muscle of an acute potassium-load.[312]

In summary, aldosterone and other mineralocorticoid hormones do accelerate the disposal of potassium, but probably not by a direct effect on muscle. The changes observed can be accounted for by the known actions of aldosterone on the renal and gastrointestinal transport of sodium and potassium, and the separate action of aldosterone to produce systemic alkalosis by enhancing acid excretion.

RENAL FAILURE

In states of mild-to-moderate chronic renal failure, the ability to excrete potassium is well maintained by an adaptive increase in the rate of fractional potassium excretion to levels near the maximal for subjects with normal renal function.[313,314] As renal function declines further, however, so does the ability to excrete potassium in a timely manner.[315] With advanced renal failure, potassium is retained longer[5] and dependence on extrarenal disposal becomes more critical.

Whether extrarenal potassium disposal is enhanced, normal or impaired in the setting of uremia remains controversial.[316] Studies in which an oral potassium load was given found that patients with chronic renal failure excreted only one quarter[9] to one-half[7,8] the amount of potassium excreted by subjects with normal renal function over a comparable period of time. Nonetheless, an exaggerated rise in serum potassium did not always occur.[7,9] Reports of impaired extrarenal disposal of an oral potassium-load in patients with chronic renal failure might be criticized, either because the patients had higher basal serum potassium concentrations or might have

been more acidotic than the control subjects.[8,317,318] Another study that concluded that extrarenal potassium disposal was impaired in patients with chronic renal failure involved chronic rather than acute potassium-loading.[319] A more general criticism of studies administering oral potassium that might account for some of the discrepant conclusions, however, is the inherent difficulty of estimating the rate of gastrointestinal absorption of potassium in the setting of renal failure. With intravenous potassium-loading, however, most,[101,135,320] but not all[321] animal studies appear to show a discernible defect in extrarenal potassium disposal in the setting of renal failure. With rare exceptions,[320,322] however, these studies examined extrarenal potassium homeostasis immediately after acute nephrectomy, rather than in the uremic state.

If extrarenal potassium disposal is impaired in uremia, it cannot be a consequence of increased cellular potassium content or high total body potassium, since both are normal or low in this state.[323–328] Nor does there appear to be peripheral resistance to insulin-mediated potassium uptake,[329] despite the known resistance to the action of insulin on glucose metabolism in renal failure.[330] The chronic hyperinsulinemia of end-stage renal failure may afford some protection against hyperkalemia. Renin production, which might be expected to be suppressed in patients with end-stage renal disease, is normal or elevated in many patients. Furthermore, both hyperkalemia[27,331] and salt restriction[332] appear to stimulate aldosterone production adequately in the setting of chronic renal failure (in patients who do not have hyporeninemic hypoaldosteronism), and a lowering of the plasma potassium suppresses aldosterone secretion normally.[333]

Catecholamines circulate at increased levels in most,[334,335] but not all,[336] patients with renal failure. While it is likely that much, if not all, of this increase is a consequence of decreased renal excretion, the pressor and pulse responses to norepinephrine infusion have been reported to be impaired in renal failure.[334,336] Both intravenous[337] and inhaled[338] albuterol appear, however, to be effective and rapid therapeutic modalities to treat hyperkalemia in patients with advanced renal failure. If beta-adrenergic-mediated extrarenal potassium homeostasis is blunted in renal failure when compared with normal subjects,[339] it may well be in those whose endogenous plasma epinephrine levels are chronically elevated[340] or who are more acidemic. Contrarily, it should be appreciated that the administration of drugs that possess beta2-antagonist properties can produce significant hyperkalemia in patients with renal failure on dialysis.[239]

Impaired extrarenal disposal of potassium in uremia might conceivably be caused by high circulating levels of parathyroid hormone. Infusion of parathyroid hormone appears to impair extrarenal disposition of a potassium-load in nephrectomized rats,[341] an action ascribed to the enhancement of potassium efflux from cells produced by increasing intracellular calcium. Potassium tolerance in partially nephrectomized rats with chronic renal failure is improved by parathyroidectomy, and by administration of the calcium channel-blocker verapamil.[342]

Metabolic acidosis can impair cellular potassium uptake (see "Acid–Base"), and alkalinization has been demonstrated to reverse this effect in anuric patients.[318] Part of this effect of acidosis may be to diminish the activity of Na,K-ATPase, which has a pH optimum in the range of 7.5–7.6 in mammalian tissue.[258]

That the activity of the Na-K pump is impaired in the erythrocytes of some uremic subjects has been well-established.[343–349] The impairment is correlated with an increase in intracellular sodium of red blood cells. Also, the diminished pump activity is reversed when the red blood cells of uremic patients are incubated in normal plasma[344] or when the patients are dialyzed,[343,345,348,350] and the impairment is reproduced when normal erythrocytes are incubated in uremic plasma.[344,351] These studies suggest the presence of a circulating inhibitor of the Na-K pump in some uremics. Other investigators have reported a decrease in the number of pump sites, estimated by ouabain-binding, rather than in the activity of the pump (defined as the ion turnover rate per pump site) in the red blood cells of certain uremic patients.[352,353] Experimental uremia in rats decreases the Na,K-ATPase activity of skeletal muscle,[354] an effect reproduced by incubating normal muscle cells with uremic serum.[354] The excessive rise in plasma potassium exhibited by patients with chronic renal failure undergoing exercise is consistent, moreover, with an impairment in skeletal muscle Na,K-ATPase in humans with this condition,[355] although a higher baseline potassium concentration or a more acidotic state can be confounding variables in such studies.

MAGNESIUM

In a variety of clinical states, potassium-depletion accompanies magnesium-depletion. Among patients with hypokalemia, the coincidence of magnesium deficiency may range from less than 10%[356] to over 40%.[357,358] Clinical conditions with a high incidence of combined deficiencies in potassium and magnesium, such as diuretic administration, alcoholism, and diabetic ketoacidosis, generally involve a defect in renal conservation of potassium. Along with interest in the relationship between extrarenal magnesium and

potassium balances[359] has come information on the relationship of their movements in and out of cells.[360]

Because potassium and magnesium are the principal intracellular cations, it is not surprising that an important physiologic relationship might exist between them. For each, reduced intracellular concentrations may exist in certain states of depletion, out of proportion to the reduction in serum levels.[361,362] Furthermore, a high correlation is found between magnesium and potassium concentrations in extrarenal tissues, such as skeletal muscle.[363] A deficiency of magnesium evokes potassium-depletion in animals and humans. In rats, however, serum potassium remains normal,[364] whereas in human subjects, hypokalemia is often observed.[357,361]

A specific effect of magnesium-depletion on potassium homeostasis can be deduced from experimental magnesium deficiency states in which magnesium deficiency is associated with renal potassium-wasting.[365] One proposed mechanism is of importance to their internal homeostasis, insofar as it would involve a direct effect of magnesium depletion on the ability of both renal and extrarenal cells to preserve their potassium.[359,366] It is known that experimental dietary magnesium depletion in rats results in loss of cellular potassium in cardiac as well as skeletal muscle.[367] Furthermore, during magnesium depletion in both animals[368] and humans,[365] the intracellular deficiency of potassium cannot be restored by provision of potassium alone; correction of the magnesium deficiency is required. Clinical combined depletion may play a role in cardiac arrhythmias seen in patients with alcoholism or on diuretics,[357,369] underscoring the importance of magnesium replacement in the correction of refractory hypokalemia and cellular potassium-depletion.

Two extrarenal mechanisms have been suggested: reduced Na,K-ATPase activity; and increased cell membrane permeability to potassium. Cellular potassium-depletion due to diminished active potassium uptake mediated by Na,K-ATPase might occur because this cation pump requires cellular magnesium.[258] Animal studies have shown that magnesium-depletion is associated with a reduced concentration of Na−K pump units in rat skeletal muscle.[370] Reduced ouabain-binding, indicative of a decreased number of Na−K pumps, has also been found in humans treated with diuretics who developed low muscle potassium concentrations associated with hypomagnesemia.[371] Additional data suggest that magnesium-depletion may also exert its effect on intracellular potassium through an impairment of the activity of the sodium-potassium pump *per se*, rather than on the number of pump sites per cell.[372]

The second proposed mechanism of potassium loss would involve effects of magnesium on membrane potassium channels. In mammalian heart cells and in a cultured insulin-secreting cell line investigated by the patch-clamp technique, physiologic concentrations of intracellular magnesium block outward current by inhibiting the opening of ATP-sensitive potassium channels.[373,374] Magnesium may therefore play an important role in the low conductance of the outward potassium current through these channels[375] under normal conditions. Such a direct effect of magnesium on potassium channels might result in cellular potassium-depletion during magnesium deficiency.

DRUGS

Medications are the primary etiologic factor in as many as one-third of cases of clinically significant hyperkalemia,[376−379] and are contributing factors in more than 60% of hyperkalemic episodes in hospitalized adults.[380] Potassium supplements, angiotensin-converting enzyme inhibitors, angiotensin-II receptor-antagonists, potassium-sparing diuretics, trimethoprim, pentamidine, heparin, and prostaglandin-suppressing drugs that induce hyporeninemic hypoaldosteronism account for most of these cases; relative to those, hyperkalemia due to drugs that alter internal potassium distribution would appear to be uncommon.[377,381] As is true for drug-induced hyperkalemia in general, the risk of significant hyperkalemia is substantially increased in patients with diabetes mellitus, renal insufficiency, hypoaldosteronism, and in the elderly. In most other cases, the rise in potassium is mild.[377]

Impaired Extrarenal Disposal

Hyperkalemia due to beta-adrenergic-blockers, the most common class of medications that elevate potassium by extrarenal mechanisms, was discussed in an earlier section. A small, transient increase in serum potassium usually occurs in patients given depolarizing muscle relaxants, such as succinylcholine.[382−385] Exaggerated increments, however, may occur in patients with central nervous system diseases, spinal cord injury, increased intracranial pressure, and a variety of other ailments.[379] In such pathological states, the acetylcholine receptors may be increased beyond the junctional area.[386] Because potassium efflux from muscle end plates occurs during normal depolarization, massive efflux of the cation from such sensitized muscle can account for the hyperkalemia noted in patients with neurologic motor deficits, tetanus or muscle damage.[387] Succinylcholine-induced hyperkalemia may also be seen with neuroleptic malignant syndrome[388]

and skeletal muscle metastasis of a rhabdomyosarcoma.[389] Why burn patients and those with intracranial lesions not involving upper motor neurons[384] are also at risk is less apparent. In patients at risk, succinylcholine should be used with caution and in the smallest dose possible, and with pretreatment by nondepolarizing muscle relaxants.[387]

Muscle cell breakdown may also result in hyperkalemia in patients who develop myositis due to the HMG-CoA reductase inhibitor, lovastatin.[390] Such reactions are more likely when lovastatin is administered in combination with gemfibrozil, cyclosporine, and nicotinic acid.[391] HMG-CoA reductase inhibitors are commonly used in patients already predisposed to hyperkalemia due to diabetes mellitus or renal insufficiency.

Arginine HCl, in doses used for the correction of metabolic alkalosis, may increase serum potassium.[392] When this cationic amino acid is taken up by cells, potassium is displaced into the extracellular fluid. Hyperkalemia is more likely in patients with renal failure[393] who are unable to excrete this endogenous potassium-load, and in those with liver failure who are unable to metabolize the administered arginine normally.[394] The magnitude of potassium rise in normal subjects is under 1 mEq/liter[392]; it is not closely correlated with pH, and may occur in patients before correction of the alkalosis is accomplished.[394] Lysine HCl may also increase serum potassium levels. The antifibrinolytic agent epsilon aminocaproic acid (Amicar) has been reported to cause hyperkalemia as well,[395] although the mechanism underlying this effect is unclear.

Trivial increments in potassium may also occur at therapeutic or mildly toxic levels of cardiac glycosides.[396,397] Blockade of Na,K-ATPase-mediated potassium uptake with normal doses of digitalis has minimal effect on the serum potassium, since glycoside binding to skeletal muscle, the major body reservoir of potassium, is limited. At toxic concentrations of digitalis, however, such as following massive overdose, marked hyperkalemia is well-described and indicates a poor prognosis.[398,399] The toxic concentration of digitalis also prevents standard treatment of the hyperkalemia with calcium. Although no significant effect to retard potassium disposal in normal subjects with therapeutic digitalis levels has been published, it is likely that such an effect may exacerbate hyperkalemia in patients at risk. In patients with renal failure, for example, even modest digoxin toxicity resulting from therapeutic doses is reported to cause hyperkalemia.[400] In fact, of drugs known to induce hyperkalemia, digoxin was the most frequently encountered among patients with hyperkalemic episodes,[380] and nearly one quarter of these had toxic digoxin levels.

Nonsteroidal anti-inflammatory drugs produce hyperkalemia best attributed to their antikaliuretic effect, which results in positive potassium balance.[401,402] No impairment of extrarenal potassium homeostasis has been directly demonstrated.[380,403,404]

Lithium intoxication in animals is associated with a progressive elevation in serum potassium and electrocardiogram abnormalities characteristic of hyperkalemia. However, only at concentrations of plasma lithium (>10 mEq/liter) many times the therapeutic lithium levels (1 mEq/liter) attained in manic-depressive patients[405] do these changes occur. Increments in serum potassium of under 1 mEq/liter have been reported during chronic lithium therapy,[406] but frank hyperkalemia is rarely observed.[407] Lithium may displace intracellular potassium from human red blood cells and from skeletal muscle.[406] Amphotericin B (including the liposomal formulation) can cause severe hyperkalemia due to potassium released from the intracellular compartment when the dose is excessive, the rate of infusion is rapid or renal function is impaired.[408]

Enhanced Extrarenal Disposal

Drug-induced lowering of serum potassium by exogenous insulin and beta-adrenergic-agonists was described in detail earlier. Increased circulating catecholamine levels, as well as enhancement of catechol stimulation of adenylate cyclase, also appear to mediate in part the effect of methylxanthine derivatives such as theophylline. Hypokalemia due to beta-adrenergic stimulation may occur with severe theophylline toxicity[409] in humans. Propranolol is reported to block hypokalemia due to theophylline toxicity in the dog.[409] Whether therapeutic levels of aminophylline are important in acutely lowering serum potassium in humans is unclear.[410] Other methylxanthines, such as caffeine, might also be expected to decrease potassium concentrations,[227] not only by stimulating release of catecholamines, but also by their blockade of high-affinity (A1) adenosine receptors, which normally act to inhibit adenylate cyclase.

Several clinical studies have reported minor decreases in serum potassium levels in patients treated with calcium-antagonists, sometimes associated with increased urinary potassium losses.[411] Severe hypokalemia with heart block may complicate overdosage of verapamil.[412] Enhanced extrarenal potassium disposal has been demonstrated with the calcium channel-blockers verapamil, nifedipine, and nitrendipine.[413–415] In one study,[415] pretreatment with either verapamil or nifedipine reduced by about 40% the increment in plasma potassium produced over 1 hour by the

infusion of KCl in nephrectomized rats. The effect was not mediated by changes in pH, bicarbonate, insulin, aldosterone or the alpha- or beta-adrenergic systems. Diltiazem has been shown to reduce the interdialytic rate of increase in plasma potassium in patients with end-stage renal disease.[416] Diminished calcium-mediated potassium efflux from cells may be responsible, since increased intracellular calcium enhances potassium permeability *in vitro* (the Gardos effect)[417] in erythrocytes and other cells.[418] While this action would lower plasma potassium, the net effect of calcium channel-blockers in clinical practice is complicated by the fact that these agents also inhibit secretion of aldosterone,[419,420] which in turn would tend to produce potassium retention.

The increased use of thiopental infusions to achieve therapeutic barbiturate coma has been associated with extreme degrees of hypokalemia secondary to enhanced cellular uptake of potassium. Serious rebound hyperkalemia has ensued, moreover, following the administration of potassium to correct the hypokalemia and discontinuation of the thiopental.[421,422] The mechanism responsible for the hypokalemia is unknown, but could involve inhibition of voltage-dependent neuronal potassium currents. Overdosage of the antimalarial chloroquine has also been associated with hypokalemia, presumably from enhanced cellular uptake, but such cases are often confounded by concomitant administration of other medications.[423] High-dose intravenous methotrexate has been associated with the rapid development of tetraparesis and marked hypokalemia in one patient that appeared to be caused by enhanced extrarenal disposal of potassium.[424]

OTHER FACTORS

Two other factors that may clinically elevate serum potassium levels by affecting extrarenal potassium homeostasis are hyperosmolarity and cellular necrosis. Less well-described are the effects of barium, cesium, and body hypothermia to lower serum potassium levels by extrarenal shifts. A sudden increase in cell mass produced by rapid proliferation, moreover, may sequester potassium intracellularly and result in hypokalemia.

Hyperosmolarity

Hypertonic potassium-free solutions administered to normal human subjects fail to lower plasma potassium, despite expanding the extracellular fluid compartment.[425] This observation suggests that plasma potassium is maintained during the infusion by movement of potassium out of cells, impelled by an increase in its intracellular concentration, because of contraction of the intracellular volume. Potassium levels are maintained even when dilutional acidosis is prevented by incorporating bicarbonate into the hypertonic infusion.[426]

A modest rise in plasma potassium concentration (0.3−0.6 mEq/liter) can be produced in normal subjects by moderate increases in tonicity (10 mOsm/kg).[427] The effect is of clinical importance chiefly in diabetics, in whom plasma tonicity can be raised by 40−50 mOsm/kg during hyperglycemia, and who lack insulin-mediated potassium uptake. Glucose-induced hyperkalemia is more pronounced in diabetics deficient in aldosterone secretion[428] or during treatment with captopril,[429] but it may also be observed in diabetics with normal aldosterone responses. The standard 100 g oral glucose tolerance test produced an average increment of 1.3 mEq/liter in plasma potassium in four such patients.[430] The effect of hyperosmolarity on potassium homeostasis may also be present in patients with cerebral edema or with renal insufficiency when treated with large quantities of hypertonic mannitol.

Cellular Necrosis

When renal excretion and extrarenal disposal of potassium are exceeded, release of intracellular potassium into the extracellular compartment during cellular necrosis will result in hyperkalemia. The most common sources are muscle, tumor cells, and erythrocytes.

Traumatic muscle injury, due to motor vehicle accidents, alcoholism, cocaine abuse[431] or other etiologies, may produce life-threatening hyperkalemia, usually during rhabdomyolytic renal failure. Catabolic states, such as sepsis, compound fractures, burns, major surgery or overwhelming infections, result in protein breakdown to meet increased energy demands. Skeletal muscle, the source of protein loss, may release sufficient potassium to cause severe hyperkalemia, if renal excretory mechanisms are compromised.

Accelerated breakdown of a large leukemic tumor burden, especially during induction of chemotherapy, produces kaliuresis and may cause symptomatic hyperkalemia. Burkitt's lymphoma, a rapidly growing neoplasm, while not causing hyperkalemia even in azotemic patients prior to chemotherapy,[432] may result in hyperkalemia within hours of treatment, even in the absence of renal insufficiency. Fatal hyperkalemia has also been reported after initial tumor lysis therapy in acute lymphocytic leukemia, chronic lymphocytic

leukemia, and lymphosarcoma. The tumor lysis syndrome is only rarely reported after treatment of non-lymphomatous solid tumors.[433] Intensive supportive therapy probably accounts for the absence of hyperkalemia reported in some series.[434]

Transient hyperkalemia, in the absence of renal failure, occasionally occurs during hemolytic states such as congenital or acquired hemolytic anemia, hemoglobinopathy or transfusion reactions. Conversely, plasma potassium may fall during the rapid proliferation of erythrocytes and their precursors when severe pernicious anemia is successfully treated.[435–437]

Barium

Barium is a well-known inhibitor of potassium exit channels in muscle at concentrations of 1–5 mM.[438] *In vitro*, Ba^{2+}-treated muscle develops flaccid paralysis and depolarization secondary to this change in potassium permeability.[439] Hypokalemia is therefore a feature of barium poisoning, as are cardiac arrhythmias and skeletal muscle paralysis,[440] associated with depolarization of muscle fibers.[438] Barium poisoning is thought to be responsible for "Pa Ping paralysis" reported in Chinese patients who had eaten salt or drunk wine with a high content of barium salts.[441,442]

Cesium

Cesium chloride has been marketed as part of an alternative therapy for malignancy. Cesium appears in the periodic table below rubidium and potassium with a positive valence of 1; its salts are extremely toxic, causing hypokalemia, cardiac arrhythmias, prolonged Q-T interval, and torsade de pointes, probably like barium, by blocking potassium exit channels.[443]

Fluoride

Exposure to toxic levels of inorganic fluoride can produce hyperkalemia that is refractory to standard measures to increase cellular uptake of potassium such as glucose, insulin, and bicarbonate. The mechanisms appear to be decreased potassium influx due to impairment of Na,K-ATPase, further aggravated by a subsequent increase in intracellular calcium that enhances potassium efflux via the Gardos effect.[444]

Hypothermia

Acute transient hypokalemia has been described in patients with hypothermia associated with accidental trauma or following surgery.[445,446] When body temperature returns to normal, the hypokalemia disappears. Post-operative hypothermia (<36.5°C) was found in 40% of patients undergoing gastrointestinal and vascular surgery. Low serum potassium levels coincided with post-operative hypothermia in over half of these, whereas no patients with normothermia became hypokalemic. Urinary potassium losses did not account for the differences.[445] The hypokalemia of experimental hypothermia is not prevented by beta-adrenergic blockade.[447] It may be related to the alkalosis that regularly accompanies hypothermia because of the effect of lowered temperature to reduce the dissociation of carbonic acid.[448]

Race

The extrarenal disposal of an intravenous load of KCl is delayed in normal young African-Americans as compared with Caucasians, perhaps attributable to a racial tendency to lower Na,K-ATPase activity in the cells of African-Americans.[449]

References

[1] Rosa RM, Silva P, Young JB, Landsberg L, Brown RS, Rowe JW, et al. Adrenergic modulation of extrarenal potassium disposal. N Engl J Med 1980;302(8):431–4.

[2] Williams ME, Rosa RM, Silva P, Brown RS, Epstein FH. Impairment of extrarenal potassium disposal by alpha-adrenergic stimulation. N Engl J Med 1984;311(3):145–9.

[3] Keith NM, Osterberg AE, Burchell HB. Some effects of potassium salts in man. Ann Intern Med 1942;16:879–92.

[4] Keith NM, Osterberg AE, HE. King. The excretion of potassium by the normal and diseased kidney. Trans Assoc Am Physic 1940;55:219–22.

[5] Winkler AW, Hoff HE, Smith PK. The toxicity of orally administered potassium salts in renal insufficiency. J Clin Invest 1941;20:119–26.

[6] Bourdillon J. Distribution in body fluids and excretion of ingested ammonium chloride, potassium chloride, and sodium chloride. Am J Physiol 1937;120:411–9.

[7] Gonick HC, Kleeman CR, Rubini ME, Maxwell MH. Functional impairment in chronic renal disease. [3] Studies of potassium excretion. Am J Med Sci 1971;261(5):281–90.

[8] Keith NM, Osterberg AE. The tolerance for potassium in severe renal insufficiency. J Clin Invest 1947;26:773–83.

[9] Perez GO, Pelleya R, Oster JR, Kem DC, Vaamonde CA. Blunted kaliuresis after an acute potassium load in patients with chronic renal failure. Kidney Int 1983;24(5):656–62.

[10] Morita H, Fujiki N, Miyahara T, Lee K, Tanaka K. Hepatoportal bumetanide-sensitive $K(^{+})$-sensor mechanism controls urinary $K(^{+})$ excretion. Am J Physiol Regul Integr Comp Physiol 2000;278(5):R1134–9.

[11] Youn JH, McDonough AA. Recent advances in understanding integrative control of potassium homeostasis. Annu Rev Physiol 2009;71:381–401.

[12] Winkler AW, Smith PK. The apparent volume of distribution of potassium injected intravenously. J Biol Chem 1938;124:589–98.

[13] Perez GO, Oster JR, Pelleya R, Caralis PV, Kem DC. Hyperkalemia from single small oral doses of potassium chloride. Nephron 1984;36(4):270–1.

[14] Moore FD, Boling EA, Ditmore Jr. HB, Sicular A, Teterick JE, Ellison AE, et al. Body sodium and potassium. V. The relationship of alkalosis, potassium deficiency and surgical stress to acute hypokalemia in man; experiments and review of the literature. Metabolism 1955;4(5):379–402.
[15] Morgan DB, Cumberbatch M, Swaminathan R. The relation between plasma, erythrocyte and total body potassium in patients with hypokalemia. Miner Electrolyte Metab 1981;5: 233–9.
[16] Schwartz WB, Relman AS. Metabolic and renal studies in chronic potassium depletion resulting from overuse of laxatives. J Clin Invest 1953;32(3):258–71.
[17] Scribner BH, Burnell JM. Interpretation of the serum potassium concentration. Metabolism 1956;5(4):468–79.
[18] Knochel JP. Neuromuscular manifestations of electrolyte disorders. Am J Med 1982;72(3):521–35.
[19] Bilbrey GL, Herbin L, Carter NW, Knochel JP. Skeletal muscle resting membrane potential in potassium deficiency. J Clin Invest 1973;52(12):3011–8.
[20] Riecker G, Bolte HD, Rohl D. Hypokaliamie and membranpotential. Reanimation et Organes Artificiels 1954;1:41–50.
[21] Feig PU, Shook A, Sterns RH. Effect of potassium removal during hemodialysis on the plasma potassium concentration. Nephron 1981;27(1):25–30.
[22] Bergstrom J, Alvestrand A, Furst P, Hultman E, Sahlin K, Vinnars E, et al. Influence of severe potassium depletion and subsequent repletion with potassium on muscle electrolytes, metabolites and amino acids in man. Clin Sci Mol Med Suppl 1976;51(6):589–99.
[23] Patrick J, Bradford B. A comparison of leucocyte potassium content with other measurements in potassium-depleted rabbits. Clin Sci 1972;42(4):415–21.
[24] Giebisch G, Krapf R, Wagner C. Renal and extrarenal regulation of potassium. Kidney Int 2007;72(4):397–410.
[25] Miller H, Darrow D. Relation of muscle electrolyte to alteration in serum potassium and to the toxic effects of injected potassium chloride. Am J Physiol 1940;130:747–58.
[26] Spital A, Sterns RH. Paradoxical potassium depletion: a renal mechanism for extrarenal potassium adaptation. Kidney Int 1986;30(4):532–7.
[27] Sterns RH, Cox M, Feig PU, Singer I. Internal potassium balance and the control of the plasma potassium concentration. Medicine (Baltimore) 1981;60(5):339–54.
[28] Williams JA, Withrow CD, Woodbury DM. Effects of nephrectomy and KC1 on transmembrane potentials, intracellular electrolytes, and cell pH of rat muscle and liver *in vivo*. J Physiol 1971;212(1):117–28.
[29] Brown RS. Extrarenal potassium homeostasis. Kidney Int 1986;30(1):116–27.
[30] Cumberbatch M, Morgan DB. Erythrocyte sodium and potassium in patients with hypokalaemia. Clin Sci (Lond) 1983;64 (2):167–76.
[31] Levin ML, Rector Jr. FC, Seldin DW. Effects of potassium and ouabain on sodium transport in human red cells. Am J Physiol 1968;214(6):1328–32.
[32] Norgaard A, Kjeldsen K, Clausen T. Potassium depletion decreases the number of ^{3}H-ouabain binding sites and the active Na-K transport in skeletal muscle. Nature 1981;293(5835): 739–41.
[33] Akaike N. Sodium pump in skeletal muscle: central nervous system-induced suppression by alpha-adrenoreceptors. Science 1981;213(4513):1252–4.
[34] Harrop G, Benedict E. The role of phosphate and potassium in carbohydrate metabolism following insulin administration. Proc Soc Exp Biol Med 1923;20:430–1.
[35] Briggs A, Koechig I. Some changes in the composition of blood due to the injection of insulin. J Biol Chem 1924;58:721–30.
[36] Holler J. Potassium deficiency occurring during the treatment of diabetic acidosis. JAMA 1946;131:1186–9.
[37] Clausen T, Kohn PG. The effect of insulin on the transport of sodium and potassium in rat soleus muscle. J Physiol 1977;265 (1):19–42.
[38] Flatman JA, Clausen T. Combined effects of adrenaline and insulin on active electrogenic Na^+–K^+ transport in rat soleus muscle. Nature 1979;281(5732):580–1.
[39] Zierler KL. Effect of insulin on membrane potential and potassium content of rat muscle. Am J Physiol 1959;197:515–23.
[40] Berg T, Iversen JG. K^+ transport in isolated rat liver cells stimulated by glucagon and insulin *in vitro*. Acta Physiol Scand 1976;97(2):202–8.
[41] Burton SD, Mondon CE, Ishida T. Dissociation of potassium and glucose efflux in isolated perfused rat liver. Am J Physiol 1967;212(2):261–6.
[42] Lambotte L, Shoemaker W. Effect of insulin on hepatic K movements as influenced by hypothermia, barbiturate, and dibenzyline. Physiologist 1964;7: 184 A
[43] Gourley DR, Bethea MD. Insulin effect on adipose tissue sodium and potassium. Proc Soc Exp Biol Med 1964;115: 821–3.
[44] Groen J, Willebrands A, Kamminga E, Van Schothorst H, Godfried E. De invloed van toediening van glycose op het kaliumgehalte van het bloedserum bij normale personen en bijniet-diabetische patienten. Ned Milit Geneeskd Tijdschr 1950;94:2187–201.
[45] Moore RD. Effects of insulin upon ion transport. Biochim Biophys Acta 1983;737(1):1–49.
[46] Fenn WO. The deposition of potassium and phosphate with glycogen in rat livers. J Biol Chem 1939;128:297–307.
[47] Zierler KL. Effect of insulin on potassium efflux from rat muscle in the presence and absence of glucose. Am J Physiol 1960;198:1066–70.
[48] Creese R. Sodium fluxes in diaphragm muscle and the effects of insulin and serum proteins. J Physiol 1968;197(2):255–78.
[49] Andres R, Baltzan MA, Cader G, Zierler KL. Effect of insulin on carbohydrate metabolism and on potassium in the forearm of man. J Clin Invest 1962;41:108–15.
[50] Kestens PJ, Haxhe JJ, Lambotte L, Lambotte C. The effect of insulin on the uptake of potassium and phosphate by the isolated perfused canine liver. Metabolism 1963;12:941–50.
[51] Zierler KL, Rabinowitz D. Effect of very small concentrations of insulin on forearm metabolism. Persistence of its action on potassium and free fatty acids without its effect on glucose. J Clin Invest 1964;43:950–62.
[52] Gourley DR. Separation of insulin effects on K content and O_2 consumption of frog muscle with cardiac glycosides. Am J Physiol 1961;200:1320–6.
[53] Manery JF, Dryden EE, Still JS, Madapallimattam G. Enhancement (by ATP, insulin, and lack of divalent cations) of ouabain inhibition of cation transport and ouabain binding in frog skeletal muscle; effect of insulin and ouabain on sarcolemmal (Na + K)MgATPase. Can J Physiol Pharmacol 1977;55(1): 21–33.
[54] Moore RD. Effect of insulin upon the sodium pump in frog skeletal muscle. J Physiol 1973;232(1):23–45.
[55] Resh MD, Nemenoff RA, Guidotti G. Insulin stimulation of (Na^+,K^+)-adenosine triphosphatase-dependent 86Rb + uptake in rat adipocytes. J Biol Chem 1980;255(22):10938–45.
[56] Fehlmann M, Freychet P. Insulin and glucagon stimulation of (Na^+–K^+)-ATPase transport activity in isolated rat hepatocytes. J Biol Chem 1981;256(14):7449–53.

[57] De Luise MA, Harker M. Insulin stimulation of Na^+–K^+ pump in clonal rat osteosarcoma cells. Diabetes 1988;37(1):33–7.
[58] Czech MP. Molecular basis of insulin action. Annu Rev Biochem 1977;46:359–84.
[59] Grinstein S, Erlij D. Insulin unmasks latent sodium pump sites in frog muscle. Nature 1974;251(5470):57–8.
[60] Gavryck WA, Moore RD, Thompson RC. Effect of insulin upon membrane-bound ($Na^{++}K^+$)-ATPase extracted from frog skeletal muscle. J Physiol 1975;252(1):43–58.
[61] Moore RD. Stimulation of Na:H exchange by insulin. Biophys J 1981;33(2):203–10.
[62] Clausen T, Flatman JA. Effects of insulin and epinephrine on Na^+–K^+ and glucose transport in soleus muscle. Am J Physiol 1987;252(4 Pt 1):E492–9.
[63] Sargeant RJ, Liu Z, Klip A. Action of insulin on $Na(^+)$–$K(^+)$-ATPase and the $Na(^+)$–$K(^+)$–$2Cl^-$ co-transporter in 3T3-L1 adipocytes. Am J Physiol 1995;269(1 Pt 1):C217–25.
[64] Gosmanov AR, Thomason DB. Insulin and isoproterenol differentially regulate mitogen-activated protein kinase-dependent $Na(^+)$–$K(^+)$–$2Cl(^-)$ co-transporter activity in skeletal muscle. Diabetes 2002;51(3):615–23.
[65] Boini KM, Graf D, Kuhl D, Haussinger D, Lang F. SGK1 dependence of insulin induced hypokalemia. Pflugers Arch 2009;457(4):955–61.
[66] Resh MD. Insulin activation of (Na^+,K^+)-adenosinetriphosphatase exhibits a temperature-dependent lag time. Comparison to activation of the glucose transporter. Biochemistry 1983;22(12):2781–4.
[67] Clausen T, Hansen O. Active Na-K transport and the rate of ouabain binding. The effect of insulin and other stimuli on skeletal muscle and adipocytes. J Physiol 1977;270(2):415–30.
[68] Erlij D, Grinstein S. The number of sodium ion pumping sites in skeletal muscle and its modification by insulin. J Physiol 1976;259(1):13–31.
[69] Al-Khalili L, Yu M, Chibalin AV. Na^+,K^+-ATPase trafficking in skeletal muscle: insulin stimulates translocation of both alpha 1- and alpha 2-subunit isoforms. FEBS Lett 2003;536(1–3):198–202.
[70] Weil-Maslansky E, Gutman Y, Sasson S. Insulin activates furosemide-sensitive K^+ and Cl^- uptake system in BC3H1 cells. Am J Physiol 1994;267(4 Pt 1):C932–9.
[71] Zierler K, Rogus EM. Rapid hyperpolarization of rat skeletal muscle induced by insulin. Biochim Biophys Acta 1981;640(3):687–92.
[72] Zierler KL. Increase in resting membrane potential of skeletal muscle produced by insulin. Science 1957;126(3282):1067–8.
[73] Beigelman PM, Hollander PB. Effects of hormones upon adipose tissue membrane electrical potentials. Proc Soc Exp Biol Med 1964;116:31–5.
[74] LaManna VR, Ferrier GR. Electrophysiological effects of insulin on normal and depressed cardiac tissues. Am J Physiol 1981;240(4):H636–44.
[75] Moore RD, Rabovsky JL. Mechanism of insulin action on resting membrane potential of frog skeletal muscle. Am J Physiol 1979;236(5):C249–54.
[76] Dorup I, Clausen T. Insulin-like growth factor I stimulates active $Na(^+)$–K^+ transport in rat soleus muscle. Am J Physiol 1995;268(5 Pt 1):E849–57.
[77] Wilde W. The distribution of potassium in the cat after intravascular injection. J Biol Chem 1939;128:309–17.
[78] DeFronzo RA, Felig P, Ferrannini E, Wahren J. Effect of graded doses of insulin on splanchnic and peripheral potassium metabolism in man. Am J Physiol 1980;238(5):E421–7.
[79] Bia MJ, DeFronzo RA. Extrarenal potassium homeostasis. Am J Physiol 1981;240(4):F257–68.
[80] Cox M, Sterns RH, Singer I. The defense against hyperkalemia: the roles of insulin and aldosterone. N Engl J Med 1978;299(10):525–32.
[81] Guerra SM, Kitabchi AE. Comparison of the effectiveness of various routes of insulin injection: insulin levels and glucose response in normal subjects. J Clin Endocrinol Metab 1976;42(5):869–74.
[82] Minaker KL, Rowe JW. Potassium homeostasis during hyperinsulinemia: effect of insulin level, beta-blockade, and age. Am J Physiol 1982;242(6):E373–7.
[83] Fineberg SE, Merimee TJ. Effects of comparative perfusions of equimolar, single component insulin and proinsulin in the human forearm. Diabetes 1973;22(9):676–86.
[84] McDonough AA, Thompson CB, Youn JH. Skeletal muscle regulates extracellular potassium. Am J Physiol Renal Physiol 2002;282(6):F967–74.
[85] Chen P, Guzman JP, Leong PK, Yang LE, Perianayagam A, Babilonia E, et al. Modest dietary K^+ restriction provokes insulin resistance of cellular K^+ uptake and phosphorylation of renal outer medulla K^+ channel without fall in plasma K^+ concentration. Am J Physiol Cell Physiol 2006;290(5):C1355–63.
[86] Yalow RS, Berson SA. Immunoassay of endogenous plasma insulin in man. J Clin Invest 1960;39:1157–75.
[87] Young DB. Analysis of long-term potassium regulation. Endocr Rev 1985;6(1):24–44 [Winter]
[88] DeFronzo RA, Sherwin RS, Dillingham M, Hendler R, Tamborlane WV, Felig P. Influence of basal insulin and glucagon secretion on potassium and sodium metabolism. Studies with somatostatin in normal dogs and in normal and diabetic human beings. J Clin Invest 1978;61(2):472–9.
[89] Allon M, Dansby L, Shanklin N. Glucose modulation of the disposal of an acute potassium load in patients with end-stage renal disease. Am J Med 1993;94(5):475–82.
[90] Hiatt N, Yamakawa T, Davidson MB. Necessity for insulin in transfer of excess infused K to intracellular fluid. Metabolism 1974;23(1):43–9.
[91] Pettit GW, Vick RL. Contribution of pancreatic insulin to extrarenal potassium homeostasis: a two-compartment model. Am J Physiol 1974;226(2):319–24.
[92] Santeusanio F, Faloona GR, Knochel JP, Unger RH. Evidence for a role of endogenous insulin and glucagon in the regulation of potassium homeostasis. J Lab Clin Med 1973;81(6):809–17.
[93] Silva P, Spokes K. Sympathetic system in potassium homeostasis. Am J Physiol 1981;241(2):F151–5.
[94] DeFronzo RA. Obesity is associated with impaired insulin-mediated potassium uptake. Metabolism 1988;37(2):105–8.
[95] de Weille JR, Fosset M, Mourre C, Schmid-Antomarchi H, Bernardi H, Lazdunski M. Pharmacology and regulation of ATP-sensitive K^+ channels. Pflugers Arch 1989;414(Suppl. 1):S80–7.
[96] Petersen OH, Dunne MJ. Regulation of K^+ channels plays a crucial role in the control of insulin secretion. Pflugers Arch 1989;414(Suppl. 1):S115–20.
[97] Dawson CM, Lebrun P, Herchuelz A, Malaisse WJ, Goncalves AA, Atwater I. Effect of temperature upon potassium-stimulated insulin release and calcium entry in mouse and rat islets. Horm Metab Res 1986;18(4):221–4.
[98] Dluhy RG, Axelrod L, Williams GH. Serum immunoreactive insulin and growth hormone response to potassium infusion in normal man. J Appl Physiol 1972;33(1):22–6.
[99] Davidson MB, Hiatt N. Effect of KCl administration on insulin secretion in dogs. Isr J Med Sci 1972;8(6):752–4.
[100] Hiatt N, Davidson MB, Bonorris G. The effect of potassium chloride infusion on insulin secretion *in vivo*. Horm Metab Res 1972;4(2):64–8.

[101] Pettit GW, Vick RL, Swander AM. Plasma K plus and insulin: changes during KCl infusion in normal and nephrectomized dogs. Am J Physiol 1975;228(1):107–9.
[102] Adrogue HJ, Chap Z, Ishida T, Field JB. Role of the endocrine pancreas in the kalemic response to acute metabolic acidosis in conscious dogs. J Clin Invest 1985;75(3):798–808.
[103] Blackard WG, Nelson NC. Portal and peripheral vein immunoreactive insulin concentrations before and after glucose infusion. Diabetes 1970;19(5):302–6.
[104] Wolfson S, Ellis S. Effects of glucagon on plasma potassium. Proc Soc Exp Biol Med 1958;91:226–8.
[105] Massara F, Martelli S, Cagliero E, Camanni F, Molinatti GM. Influence of glucagon on plasma levels of potassium in man. Diabetologia 1980;19(5):414–7.
[106] Massara F, Cagliero E, Maccario M, Orzan F, Carini G. Pathophysiological doses of glucagon cause a transient increase of the hepatic vein potassium concentration in man. Miner Electrolyte Metab 1986;12(2):142–6.
[107] Finder AG, Boyme T, Shoemaker WC. Relationship of hepatic potassium efflux to phosphorylase activation induced by glucagon. Am J Physiol 1964;206:738–42.
[108] Lynch CJ, Bocckino SB, Blackmore PF, Exton JH. Calcium-mobilizing hormones and phorbol myristate acetate mediate heterologous desensitization of the hormone-sensitive hepatic Na^+/K^+ pump. Biochem J 1987;248(3):807–13.
[109] Cagliero E, Martina V, Massara F, Molinatti GM. Glucagon-induced increase in plasma potassium levels in type 1 (insulin-dependent) diabetic subjects. Diabetologia 1983;24 (2):85–7.
[110] Muller WA, Faloona GR, Unger RH. Hyperglucagonemia in diabetic ketoacidosis. Its prevalence and significance. Am J Med 1973;54(1):52–7.
[111] Bilbrey GL, Faloona GR, White MG, Knochel JP. Hyperglucagonemia of renal failure. J Clin Invest 1974;53(3): 841–7.
[112] Knochel JP. Role of glucoregulatory hormones in potassium homeostasis. Kidney Int 1977;11(6):443–52.
[113] D'Silva JL. The action of adrenaline on serum potassium. J Physiol 1934;82:393–8.
[114] Clausen T. Adrenergic control of Na^+–K^+-homoeostasis. Acta Med Scand Suppl 1983;672:111–5.
[115] Epstein FH, Rosa RM. Adrenergic control of serum potassium. N Engl J Med 1983;309(23):1450–1.
[116] Struthers AD, Reid JL. The role of adrenal medullary catecholamines in potassium homoeostasis. Clin Sci (Lond) 1984;66(4): 377–82.
[117] Coats RA. Effects of apamin on alpha-adrenoceptor-mediated changes in plasma potassium in guinea-pigs. Br J Pharmacol 1983;80(3):573–80.
[118] D'Silva JL. Action of adrenaline on the perfused liver. J Physiol 1936;87:181–8.
[119] Todd EP, Vick RL. Kalemotropic effect of epinephrine: analysis with adrenergic agonists and antagonists. Am J Physiol 1971;220(6):1964–9.
[120] Todd EP, Vick RL, Bonner FM, Leudke DW. The influence of the rate of infusion on the kalemotropic effect of epinephrine. Arch Int Physiol Biochim 1969;77(1):33–45.
[121] Katz LD, D'Avella J, DeFronzo RA. Effect of epinephrine on renal potassium excretion in the isolated perfused rat kidney. Am J Physiol 1984;247(2 Pt 2):F331–8.
[122] Smythe CM, Nickel JF, Bradley SE. The effect of epinephrine (USP), l-epinephrine, and l-norepinephrine on glomerular filtration rate, renal plasma flow, and the urinary excretion of sodium, potassium, and water in normal man. J Clin Invest 1952;31(5):499–506.
[123] Powell Jr. WJ, Skinner Jr. NS. Effect of the catecholamines on ionic balance and vascular resistance in skeletal muscle. Am J Cardiol 1966;18(1):73–82.
[124] De La Lande IS, Manson J, Parks VJ, Sandison AG, Skinner SL, Whelan RF. The local metabolic action of adrenaline on skeletal muscle in man. J Physiol 1961;157:177–84.
[125] Grob D, Liljestrand A, Johns RJ. Potassium movement in normal subjects: effect on muscle function. Am J Med 1957;23(3): 340–55.
[126] Vick RL, Todd EP, Luedke DW. Epinephrine-induced hypokalemia: relation to liver and skeletal muscle. J Pharmacol Exp Ther 1972;181(1):139–46.
[127] Glitsch HG, Haas HG, Trautwein W. The effect of adrenaline on the K and Na fluxes in the frog's atrium. Naunyn Schmiedebergs Arch Exp Pathol Pharmakol 1965;250:59–71.
[128] Ballanyi K, Grafe P. Changes in intracellular ion activities induced by adrenaline in human and rat skeletal muscle. Pflugers Arch 1988;411(3):283–8.
[129] Clausen T, Flatman JA. The effect of catecholamines on Na-K transport and membrane potential in rat soleus muscle. J Physiol 1977;270(2):383–414.
[130] Evans RH, Smith JW. Mode of action of catecholamines on skeletal muscle. J Physiol 1973;232(2):81P–2P.
[131] Lockwood RH, Lum BK. Effects of adrenergic agonists and antagonists on potassium metabolism. J Pharmacol Exp Ther 1974;189(1):119–29.
[132] Hays ET, Dwyer TM, Horowicz P, Swift JG. Epinephrine action on sodium fluxes in frog striated muscle. Am J Physiol 1974;227(6):1340–7.
[133] Deibert DC, DeFronzo RA. Epinephrine-induced insulin resistance in man. J Clin Invest 1980;65(3):717–21.
[134] Pettit GW, Vick RL. An analysis of the contribution of the endocrine pancreas to the kalemotropic actions of catecholamines. J Pharmacol Exp Ther 1974;190(2):234–42.
[135] Bia MJ, Tyler KA, DeFronzo RA. Regulation of extrarenal potassium homeostasis by adrenal hormones in rats. Am J Physiol 1982;242(6):F641–4.
[136] Olsson A, Persson S, Schroder R. Effects of terbutaline and isoproterenol on hyperkalemia in nephrectomized rabbits. Scand J Urol Nephrol 1977;12:35–8.
[137] Ahlquist RA. Study of the adrenotropic receptors. Am J Physiol 1948;153:586–600.
[138] Bia MJ, Lu D, Tyler K, De Fronzo RA. Beta adrenergic control of extrarenal potassium disposal. A beta-2 mediated phenomenon. Nephron 1986;43(2):117–22.
[139] Tannen RL. Potassium disorders. In: Kokko JP, Tannen RL, editors. Fluids and electrolytes. Philadelphia: Saunders; 1986. p. 150–228.
[140] DeFronzo RA, Bia M, Birkhead G. Epinephrine and potassium homeostasis. Kidney Int 1981;20(1):83–91.
[141] Ljunghall S, Joborn H, Rastad J, Akerstrom G. Plasma potassium and phosphate concentrations – influence by adrenaline infusion, beta-blockade and physical exercise. Acta Med Scand 1987;221(1):83–93.
[142] Vincent HH, Boomsma F, Man in't Veld AJ, Derkx FH, Wenting GJ, Schalekamp MA. Effects of selective and nonselective beta-agonists on plasma potassium and norepinephrine. J Cardiovasc Pharmacol 1984;6(1):107–14.
[143] Vincent HH, Man in't Veld AJ, Boomsma F, Schalekamp MA. Prevention of epinephrine-induced hypokalemia by nonselective beta blockers. Am J Cardiol 1985;56(6):10D–4D.
[144] Struthers AD, Reid JL, Whitesmith R, Rodger JC. The effects of cardioselective and non-selective beta-adrenoceptor blockade on the hypokalaemic and cardiovascular responses to adrenomedullary hormones in man. Clin Sci (Lond) 1983;65(2):143–7.

[145] Weidmann P, De Chatel R, Ziegler WH, Flammer J, Reubi F. Alpha and beta adrenergic blockade with orally administered labetalol in hypertension. Studies on blood volume, plasma renin and aldosterone and catecholamine excretion. Am J Cardiol 1978;41(3):570–6.
[146] Clausen T, Flatman JA. Beta 2-adrenoceptors mediate the stimulating effect of adrenaline on active electrogenic Na-K-transport in rat soleus muscle. Br J Pharmacol 1980;68(4):749–55.
[147] Lockwood RH, Lum BK. Effects of adrenalectomy and adrenergic antagonists on potassium metabolism. J Pharmacol Exp Ther 1977;203(1):103–11.
[148] Sugarman A, Kaji DM, Stein RM, Kahn T. Extrarenal potassium transport and the beta 2-adrenergic system. J Lab Clin Med 1984;103(6):912–21.
[149] Brown MJ. Hypokalemia from beta 2-receptor stimulation by circulating epinephrine. Am J Cardiol 1985;56(6):3D–9D.
[150] Struthers AD, Reid JL. Adrenaline causes hypokalaemia in man by beta 2 adrenoceptor stimulation. Clin Endocrinol (Oxf) 1984;20(4):409–14.
[151] Hastwell G, Lambert BE. The effect of oral salbutamol on serum potassium and blood sugar. Br J Obstet Gynaecol 1978;85(10):767–9.
[152] Leitch AG, Clancy LJ, Costello JF, Flenley DC. Effect of intravenous infusion of salbutamol on ventilatory response to carbon dioxide and hypoxia and on heart rate and plasma potassium in normal men. Br Med J 1976;1(6006):365–7.
[153] Smith SR, Kendall MJ. Inhaled bronchodilators and hypokalaemia. Lancet 1983;2(8343):218.
[154] Smith SR, Ryder C, Kendall MJ, Holder R. Cardiovascular and biochemical responses to nebulised salbutamol in normal subjects. Br J Clin Pharmacol 1984;18(4):641–4.
[155] Thomas DJ, Dove AF, Alberti KG. Metabolic effects of salbutamol infusion during premature labour. Br J Obstet Gynaecol 1977;84(7):497–9.
[156] Braden GL, von Oeyen PT, Germain MJ, Watson DJ, Haag BL. Ritodrine- and terbutaline-induced hypokalemia in preterm labor: mechanisms and consequences. Kidney Int 1997;51(6): 1867–75.
[157] Hurlbert BJ, Edelman JD, David K. Serum potassium levels during and after terbutaline. Anesth Analg 1981;60(10):723–5.
[158] Moravec MA, Hurlbert BJ. Hypokalemia associated with terbutaline administration in obstetrical patients. Anesth Analg 1980;59(12):917–20.
[159] Haalboom JR, Deenstra M, Struyvenberg A. Hypokalaemia induced by inhalation of fenoterol. Lancet 1985;1(8438): 1125–7.
[160] Insel PA. Identification and regulation of adrenergic receptors in target cells. Am J Physiol 1984;247(1 Pt 1):E53–8.
[161] Clausen T, Everts ME. Regulation of the Na,K-pump in skeletal muscle. Kidney Int 1989;35(1):1–13.
[162] Cheng LC, Rogus EM, Zierler K. Catechol a structural requirement for $(Na^+ + K^+)$-ATPase stimulation in rat skeletal muscle membrane. Biochim Biophys Acta 1977;464(2):338–46.
[163] Buur T, Clausen T, Holmberg E, Johansson U, Waldeck B. Desensitization by terbutaline of beta-adrenoceptors in the guinea-pig soleus muscle: biochemical alterations associated with functional changes. Br J Pharmacol 1982;76(2):313–7.
[164] Bray JJ, Hawken MJ, Hubbard JI, Pockett S, Wilson L. The membrane potential of rat diaphragm muscle fibres and the effect of denervation. J Physiol 1976;255(3):651–67.
[165] Scheid CR, Honeyman TW, Fay FS. Mechanism of beta-adrenergic relaxation of smooth muscle. Nature 1979;277(5691): 32–6.
[166] Scheid CR, Fay FS. Beta-adrenergic stimulation of 42K influx in isolated smooth muscle cells. Am J Physiol 1984;246(5 Pt 1): C415–21.
[167] Kaibara K, Akasu T, Tokimasa T, Koketsu K. Beta-adrenergic modulation of the Na^+–K^+ pump in frog skeletal muscles. Pflugers Arch 1985;405(1):24–8.
[168] Desilets M, Baumgarten CM. Isoproterenol directly stimulates the Na^+–K^+ pump in isolated cardiac myocytes. Am J Physiol 1986;251(1 Pt 2):H218–25.
[169] Douglas WW. Stimulus-secretion coupling: the concept and clues from chromaffin and other cells. Br J Pharmacol 1968;34 (3):453–74.
[170] Baker PF, Rink TJ. Catecholamine release from bovine adrenal medulla in response to maintained depolarization. J Physiol 1975;253(2):593–620.
[171] Silberstein SD, Lemberger L, Klein DC, Axelrod J, Kopin IJ. Induction of adrenal tyrosine hydroxylase in organ culture. Neuropharmacology 1972;11(5):721–6.
[172] Vogt M. The secretion of the denervated adrenal medulla of the cat. Br J Pharmacol 1952;7(2):325–30.
[173] Opdyke DF, Carroll RG, Keller NE. Systemic arterial pressor responses induced by potassium in dogfish, *Squalus acanthias*. Am J Physiol 1981;241(3):R228–32.
[174] Hiatt N, Chapman LW, Davidson MB. Influence of epinephrine and propranolol on transmembrane K transfer in anuric dogs with hyperkalemia. J Pharmacol Exp Ther 1979;209(2): 282–6.
[175] Massara F, Tripodina A, Rotunno M. Propranolol block of epinephrine-induced hypokaliaemia in man. Eur J Pharmacol 1970;10(3):404–7.
[176] Brown MJ, Brown DC, Murphy MB. Hypokalemia from beta2-receptor stimulation by circulating epinephrine. N Engl J Med 1983;309(23):1414–9.
[177] Karlsberg RP, Cryer PE, Roberts R. Serial plasma catecholamine response early in the course of clinical acute myocardial infarction: relationship to infarct extent and mortality. Am Heart J 1981;102(1):24–9.
[178] Halter JB, Pflug AE, Porte Jr. D. Mechanism of plasma catecholamine increases during surgical stress in man. J Clin Endocrinol Metab 1977;45(5):936–44.
[179] Christensen NJ. Plasma norepinephrine and epinephrine in untreated diabetics, during fasting and after insulin administration. Diabetes 1974;23(1):1–8.
[180] Landsberg L, Young JB. Fasting, feeding and regulation of the sympathetic nervous system. N Engl J Med 1978;298(23): 1295–301.
[181] Carlsson E, Fellenius E, Lundborg P, Svensson L. beta-Adrenoceptor blockers, plasma-potassium, and exercise. Lancet 1978;2(8086):424–5.
[182] Williams ME, Gervino EV, Rosa RM, Landsberg L, Young JB, Silva P, et al. Catecholamine modulation of rapid potassium shifts during exercise. N Engl J Med 1985;312(13):823–7.
[183] Clausen T. Hormonal and pharmacological modification of plasma potassium homeostasis. Fundam Clin Pharmacol 2010;24(5):595–605.
[184] McKenna MJ, Schmidt TA, Hargreaves M, Cameron L, Skinner SL, Kjeldsen K. Sprint training increases human skeletal muscle $Na(^+)$–$K(^+)$-ATPase concentration and improves K^+ regulation. J Appl Physiol 1993;75(1):173–80.
[185] Zheng D, Perianayagam A, Lee DH, Brannan MD, Yang LE, Tellalian D, et al. AMPK activation with AICAR provokes an acute fall in plasma $[K^+]$. Am J Physiol Cell Physiol 2008;294(1):C126–35.
[186] Lands AM, Arnold A, McAuliff JP, Luduena FP, Brown Jr. TG. Differentiation of receptor systems activated by sympathomimetic amines. Nature 1967;214(88):597–8.
[187] Imura H, Kato Y, Ikeda M, Morimoto M, Yawata M. Effect of adrenergic-blocking or -stimulating agents on plasma growth hormone, immunoreactive insulin, and blood free fatty acid levels in man. J Clin Invest 1971;50(5):1069–79.

[188] Westfall TC. Local regulation of adrenergic neurotransmission. Physiol Rev 1977;57(4):659–728.
[189] Jakobs KH, Saur W, Schultz G. Reduction of adenylate cyclase activity in lysates of human platelets by the alpha-adrenergic component of epinephrine. J Cyclic Nucleotide Res 1976;2(6): 381–92.
[190] Jauchem JR, Vick RL. Phenylephrine-induced hyperkalemia: role of the liver. Proc Soc Exp Biol Med 1980;163 (4):478–81.
[191] Wadstein J, Skude G. Does hypokalaemia precede delirium tremens? Lancet 1978;2(8089):549–50.
[192] McDonald Jr. RH, Goldberg LI, McNay JL, Tuttle Jr. EP. Effect of dopamine in man: augmentation of sodium excretion, glomerular filtration rate, and renal plasma flow. J Clin Invest 1964;43:1116–24.
[193] Meyer MB, McNay JL, Goldberg LI. Effects of dopamine on renal function and hemodynamics in the dog. J Pharmacol Exp Ther 1967;156(1):186–92.
[194] Finlay GD, Whitsett TL, Cucinell EA, Goldberg LI. Augmentation of sodium and potassium excretion, glomerular filtration rate and renal plasma flow by levodopa. N Engl J Med 1971;284(15):865–70.
[195] Granerus AK, Jagenburg R, Svanborg A. Kaliuretic effect of L-dopa treatment in parkinsonian patients. Acta Med Scand 1977;201(4):291–7.
[196] Williams M, Young JB, Rosa RM, Gunn S, Epstein FH, Landsberg L. Effect of protein ingestion on urinary dopamine excretion. Evidence for the functional importance of renal decarboxylation of circulating 3,4-dihydroxyphenylalanine in man. J Clin Invest 1986;78(6):1687–93.
[197] Carey RM, Thorner MO, Ortt EM. Effects of metoclopramide and bromocriptine on the renin–angiotensin–aldosterone system in man. Dopaminergic control of aldosterone. J Clin Invest 1979;63(4):727–35.
[198] Blevins RD, Whitty AJ, Rubenfire M, Maciejko JJ. Dopamine and dobutamine induce hypokalemia in anesthetized dogs. J Cardiovasc Pharmacol 1989;13(4):662–6.
[199] Bevilacqua M, Norbiato G, Raggi U, Micossi P, Baggio E, Prandelli M. Dopaminergic control of serum potassium. Metabolism 1980;29(4):306–10.
[200] Sager PT, DeFronzo RA. Dopaminergic regulation of extrarenal potassium metabolism. Miner Electrolyte Metab 1987;13(6): 385–92.
[201] Zanella MT, Bravo EL. *In vitro* and *in vivo* evidence for an indirect mechanism mediating enhanced aldosterone secretion by metoclopramide. Endocrinology 1982;111(5):1620–5.
[202] Carey RM, Thorner MO, Ortt EM. Dopaminergic inhibition of metoclopramide-induced aldosterone secretion in man. Dissociation of responses to dopamine and bromocriptine. J Clin Invest 1980;66(1):10–8.
[203] Pratt JH, Ganguly A, Parkinson CA, Weinberger MH. Stimulation of aldosterone secretion by metoclopramide in humans: apparent independence of renal and pituitary mediation. Metabolism 1981;30(2):129–34.
[204] Sowers JR, Brickman AS, Sowers DK, Berg G. Dopaminergic modulation of aldosterone secretion in man is unaffected by glucocorticoids and angiotensin blockade. J Clin Endocrinol Metab 1981;52(6):1078–84.
[205] Whitfield L, Sowers JR, Tuck ML, Golub MS. Dopaminergic control of plasma catecholamine and aldosterone responses to acute stimuli in normal man. J Clin Endocrinol Metab 1980;51(4):724–9.
[206] Taylor P. Cholinergic agonists. In: Goodman AG, Goodman LS, Rall TW, Murad F, editors. The pharmacological basis of therapeutics. 7th ed. New York: MacMillan; 1985. p. 108.
[207] Adrenaline and potassium: everything in flux. Lancet 1983;2 (8364):1401–1403.
[208] Donnelly T, Gray H, Simpson E, Rodger JC. Serum potassium in acute myocardial infarction. Scot Med J 1980;25:176.
[209] Madias JE, Shah B, Chintalapally G, Chalavarya G, Madias NE. Admission serum potassium in patients with acute myocardial infarction: its correlates and value as a determinant of in-hospital outcome. Chest 2000;118(4):904–13.
[210] Rolton H, Simpson E, Donnelly T, Rodger JC. Plasma potassium in acute myocardial infarction. Eur Heart J 1981;2 (Suppl. A):21 A.
[211] Thomas R, Hicks S. Myocardial infarction: ventricular arrhythmias associated with hypokalemia. Clin Sci 1981;61:32p.
[212] Johansson BW, Dziamski R. Malignant arrhythmias in acute myocardial infarction. Relationship to serum potassium and effect of selective and non-selective beta-blockade. Drugs 1984;28(Suppl. 1):77–85.
[213] Nordrehaug JE, Johannessen KA, von der Lippe G. Serum potassium concentration as a risk factor of ventricular arrhythmias early in acute myocardial infarction. Circulation 1985; 71(4):645–9.
[214] Struthers AD, Whitesmith R, Reid JL. Prior thiazide diuretic treatment increases adrenaline-induced hypokalaemia. Lancet 1983;1(8338):1358–61.
[215] Dyckner T, Helmers C, Lundman T, Wester PO. Initial serum potassium level in relation to early complications and prognosis in patients with acute myocardial infarction. Acta Med Scand 1975;197(3):207–10.
[216] Nordrehaug JE. Malignant arrhythmia in relation to serum potassium in acute myocardial infarction. Am J Cardiol 1985;56(6):20D–3D.
[217] Nordrehaug JE, Johannessen KA, von der Lippe G, Sederholm M, Grottum P, Kjekshus J. Effect of timolol on changes in serum potassium concentration during acute myocardial infarction. Br Heart J 1985;53(4):388–93.
[218] Amin DN, Henry JA. Propranolol administration in theophylline overdose. Lancet 1985;1(8427):520–1.
[219] Conci F, Procaccio F, Boselli L. Hypokalemia from beta2-receptor stimulation by epinephrine. N Engl J Med 1984;310:1329.
[220] Mikhailidis DP, Dandona P. Adrenaline and potassium. Lancet 1984;1(8369):170–1.
[221] Morgan DB, Young RM. Acute transient hypokalaemia: new interpretation of a common event. Lancet 1982;2(8301): 751–2.
[222] Smith SK, Thompson D. The effect of intravenous salbutamol upon plasma and urinary potassium during premature labour. Br J Obstet Gynaecol 1977;84(5):344–7.
[223] Rohr AS, Spector SL, Rachelefsky GS, Katz RM, Siegel SC. Efficacy of parenteral albuterol in the treatment of asthma. Comparison of its metabolic side effects with subcutaneous epinephrine. Chest 1986;89(3):348–51.
[224] Rubinstein S, Hindi RD, Moss RB, Blessing-Moore J, Lewiston NJ. Sudden death in adolescent asthma. Ann Allergy 1984;53(4):311–8.
[225] Wilson JD, Sutherland DC, Thomas AC. Has the change to beta-agonists combined with oral theophylline increased cases of fatal asthma? Lancet 1981;1(8232):1235–7.
[226] Flack JM, Ryder KW, Strickland D, Whang R. Metabolic correlates of theophylline therapy: a concentration-related phenomenon. Ann Pharmacother 1994;28(2):175–9.
[227] Lindinger MI, Graham TE, Spriet LL. Caffeine attenuates the exercise-induced increase in plasma [K^+] in humans. J Appl Physiol 1993;74(3):1149–55.
[228] Beal AL, Deuser WE, Beilman GJ. A role for epinephrine in post-traumatic hypokalemia. Shock 2007;27(4):358–63.

[229] Bundgaard H, Kjeldsen K, Suarez Krabbe K, van Hall G, Simonsen L, Qvist J, et al. Endotoxemia stimulates skeletal muscle Na^+-K^+-ATPase and raises blood lactate under aerobic conditions in humans. Am J Physiol Heart Circ Physiol 2003;284(3):H1028–34.
[230] O'Brien WJ, Lingrel JB, Fischer JE, Hasselgren PO. Sepsis increases skeletal muscle sodium, potassium-adenosinetriphosphatase activity without affecting messenger RNA or protein levels. J Am Coll Surg 1996;183(5):471–9.
[231] Pedersen EB, Kornerup HJ. Relationship between plasma aldosterone concentration and plasma potassium in patients with essential hypertension during alprenolol treatment. Acta Med Scand 1976;200(4):263–7.
[232] Pedersen G, Pedersen A, Pedersen EB. Effect of propranolol on total exchangeable body potassium and total exchangeable body sodium in essential hypertension. Scand J Clin Lab Invest 1979;39(2):167–70.
[233] Waal-Manning HJ. Metabolic effects of beta-adrenoreceptor blockers. Drugs 1976;11(Suppl. 1):121–6.
[234] Bauer JH. Effects of propranolol therapy on renal function and body fluid composition. Arch Intern Med 1983;143(5):927–31.
[235] Steiness E. Negative potassium balance during beta-blocker treatment of hypertension. Clin Pharmacol Ther 1982;31(6): 691–4.
[236] Petch MC, McKay R, Bethune DW. The effect of beta, adrenergic blockade on serum potassium and glucose levels during open heart surgery. Eur Heart J 1981;2(2):123–6.
[237] Pei Y, Richardson R, Greenwood C, Wong PY, Baines A. Extrarenal effect of cyclosporine a on potassium homeostasis in renal transplant recipients. Am J Kidney Dis 1993;22(2): 314–9.
[238] McCammon RL, Stoelting RK. Exaggerated increase in serum potassium following succinylcholine in dogs with beta blockade. Anesthesiology 1984;61(6):723–5.
[239] Arrizabalaga P, Montoliu J, Martinez Vea A, Andreu L, Lopez Pedret J, Revert L. Increase in serum potassium caused by beta-2 adrenergic blockade in terminal renal failure: absence of mediation by insulin or aldosterone. Proc Eur Dial Trans Assoc 1983;20:572–6.
[240] Arrizabalaga P, Montolio J, Martinez-Vea A, Andreu L, Lopez-Pedret J, Revert L. Increase in serum potassium caused by beta-2 adrenergic blockade in terminal renal failure: absence of mediation by insulin or aldosterone. Kidney Int 1983;24:427.
[241] Lundborg P. The effect of adrenergic blockade on potassium concentrations in different conditions. Acta Med Scand Suppl 1983;672:121–6.
[242] Ismail-Beigi F, Edelman IS. Effects of thyroid status on electrolyte distribution in rat tissues. Am J Physiol 1973;225(5): 1172–7.
[243] Kubota K, Ingbar SH. Influences of thyroid status and sympathoadrenal system on extrarenal potassium disposal. Am J Physiol 1990;258(3 Pt 1):E428–35.
[244] Lin SH, Lin YF. Propranolol rapidly reverses paralysis, hypokalemia, and hypophosphatemia in thyrotoxic periodic paralysis. Am J Kidney Dis 2001;37(3):620–3.
[245] Dias Da Silva MR, Cerutti JM, Arnaldi LA, Maciel RM. A mutation in the KCNE3 potassium channel gene is associated with susceptibility to thyrotoxic hypokalemic periodic paralysis. J Clin Endocrinol Metab 2002;87(11):4881–4.
[246] Schaafsma IA, van Ernst MG, Kouistra HS, Verkleij CB, Peeters ME, Boer P, et al. Exercise-induced hyperkalemia in hypothyroid dogs. Domest Anim Endocrinol 2002;22(2):113–25.
[247] Fenn WO, Cobb DM. The potassium equilibrium in muscle. J Gen Physiol 1934;17:629–56.
[248] Leibman J, Edelman IS. Interrelations of plasma potassium concentration, plasma sodium concentration, arterial pH and total exchangeable potassium. J Clin Invest 1959;38:2176–88.
[249] Swan RC, Pitts RF. Neutralization of infused acid by nephrectomized dogs. J Clin Invest 1955;34(2):205–12.
[250] Schwartz WB, Orning KJ, Porter R. The internal distribution of hydrogen ions with varying degrees of metabolic acidosis. J Clin Invest 1957;36(3):373–82.
[251] Burnell JM, Scribner BH, Uyeno BT, Villamil MF. The effect in humans of extracellular pH change on the relationship between serum potassium concentration and intracellular potassium. J Clin Invest 1956;35(9):935–9.
[252] Giebisch G, Berger L, Pitts RF. The extrarenal response to acute acid–base disturbances of respiratory origin. J Clin Invest 1955;34(2):231–45.
[253] Rogers TA. Tissue buffering in rat diaphragm. Am J Physiol 1957;191(2):363–6.
[254] Simmons DH, Avedon M. Acid–base alterations and plasma potassium concentration. Am J Physiol 1959;197:319–26.
[255] Brown Jr. EB, Goott B. Intracellular hydrogen ion changes and potassium movement. Am J Physiol 1963;204:765–70.
[256] Waddell WJ, Bates RG. Intracellular pH. Physiol Rev 1969; 49(2):285–329.
[257] Adrogue HJ, Madias NE. Changes in plasma potassium concentration during acute acid–base disturbances. Am J Med 1981;71(3):456–67.
[258] Skou JC. Enzymatic basis for active transport of Na^+ and K^+ across cell membrane. Physiol Rev 1965;45:596–617.
[259] Breitwieser GE, Altamirano AA, Russell JM. Effects of pH changes on sodium pump fluxes in squid giant axon. Am J Physiol 1987;253(4 Pt 1):C547–54.
[260] Eaton DC, Hamilton KL, Johnson KE. Intracellular acidosis blocks the basolateral Na-K pump in rabbit urinary bladder. Am J Physiol 1984;247(6 Pt 2):F946–54.
[261] Altenberg GA, Aristimuno PC, Amorena CE, Taquini AC. Amiloride prevents the metabolic acidosis of a KCl load in nephrectomized rats. Clin Sci (Lond) 1989;76(6):649–52.
[262] Davies NW, Standen NB, Stanfield PR. The effect of intracellular pH on ATP-dependent potassium channels of frog skeletal muscle. J Physiol 1992;445:549–68.
[263] Magner PO, Robinson L, Halperin RM, Zettle R, Halperin ML. The plasma potassium concentration in metabolic acidosis: a re-evaluation. Am J Kidney Dis 1988;11(3):220–4.
[264] Oster JR, Perez GO, Vaamonde CA. Relationship between blood pH and potassium and phosphorus during acute metabolic acidosis. Am J Physiol 1978;235(4):F345–51.
[265] Vaamonde CA, Oster JR, Alpert HC, Rodriguez GR. Effect of potassium depletion on acidosis-induced changes in plasma potassium concentration. Miner Electrolyte Metab 1985;11(6): 381–8.
[266] Schwarz KC, Cohen BD, Lubash GD, Rubin AL. Severe acidosis and hyperpotassemia treated with sodium bicarbonate infusion. Circulation 1959;19(2):215–20.
[267] Bettice JA, Gamble Jr. JL. Skeletal buffering of acute metabolic acidosis. Am J Physiol 1975;229(6):1618–24.
[268] Keating RE, Weichselbaum TE, Alanis M, Margraf HW, Elman R. The movement of potassium during experimental acidosis and alkalosis in the nephrectomized dog. Surg Gynecol Obstet 1953;96(3):323–30.
[269] Oster JR, Perez GO, Castro A, Vaamonde CA. Plasma potassium response to acute metabolic acidosis induced by mineral and nonmineral acids. Miner Electrolyte Metab 1980;4: 28–36.
[270] Tobin RB. Varying role of extracellular electrolytes in metabolic acidosis and alkalosis. Am J Physiol 1958;195(3):685–92.
[271] Rogers TA, Wachenfeld AE. Effect of physiologic acids on electrolytes in rat diaphragm. Am J Physiol 1958;193(3):623–6.
[272] Fulop M. Serum potassium in lactic acidosis and ketoacidosis. N Engl J Med 1979;300(19):1087–9.

[273] Perez GO, Oster JR, Vaamonde CA. Serum potassium concentration in acidemic states. Nephron 1981;27(4–5):233–43.
[274] Kreisberg RA. Diabetic ketoacidosis: new concepts and trends in pathogenesis and treatment. Ann Intern Med 1978;88(5): 681–95.
[275] Beigelman PM. Potassium in severe diabetic ketoacidosis. Am J Med 1973;54(4):419–20.
[276] Cohen AS, Vance VK, Runyan Jr. JW, Hurwitz D. Diabetic acidosis: an evaluation of the cause, course and therapy of 73 cases. Ann Intern Med 1960;52:55–86.
[277] Adrogue HJ, Lederer ED, Suki WN, Eknoyan G. Determinants of plasma potassium levels in diabetic ketoacidosis. Medicine (Baltimore) 1986;65(3):163–72.
[278] Arieff AI, Carroll HJ. Nonketotic hyperosmolar coma with hyperglycemia: clinical features, pathophysiology, renal function, acid–base balance, plasma-cerebrospinal fluid equilibria and the effects of therapy in 37 cases. Medicine (Baltimore) 1972;51(2):73–94.
[279] Madias NE. Lactic acidosis. Kidney Int 1986;29(3):752–74.
[280] Orringer CE, Eustace JC, Wunsch CD, Gardner LB. Natural history of lactic acidosis after grand-mal seizures. A model for the study of an anion-gap acidosis not associated with hyperkalemia. N Engl J Med 1977;297(15):796–9.
[281] Rodgrove HJ, Alabaster S. Lactic acidosis in seizures. N Engl J Med 1977;297(24):1352.
[282] Cooperman MT, Davidoff F, Spark R, Pallotta J. Clinical studies of alcoholic ketoacidosis. Diabetes 1974;23(5):433–9.
[283] Levy LJ, Duga J, Girgis M, Gordon EE. Ketoacidosis associated with alcoholism in nondiabetic subjects. Ann Intern Med 1973;78(2):213–9.
[284] Adler S, Fraley DS. Potassium and intracellular pH. Kidney Int 1977;11(6):433–42.
[285] Schwartz WB, Brackett Jr. NC, Cohen JJ. The response of extracellular hydrogen ion concentration to graded degrees of chronic hypercapnia: the physiologic limits of the defense of pH. J Clin Invest 1965;44:291–301.
[286] Nahas GG, Steinsland OS. Increased rate of catecholamine synthesis during respiratory acidosis. Respir Physiol 1968;5(1): 108–17.
[287] Fenn WO, Asano T. Effects of carbon dioxide inhalation on potassium liberation from the liver. Am J Physiol 1956;185(3): 567–76.
[288] Natalini G, Seramondi V, Fassini P, Foccoli P, Toninelli C, Caviliere S, et al. Acute respiratory acidosis does not increase plasma potassium in normokalaemic anaesthetized patients. A controlled randomized trial. Eur J Anaesthesiol 2001;18 (6):394–400.
[289] Takahashi T, Kato A, Miura Y, Karube T, Sakai M, Amagasa S. [The effect of beta-adrenergic blockade on the plasma potassium elevation induced by acute respiratory acidosis during halothane or fentanyl anesthesia]. Masui 1994;43(4):479–86.
[290] Abrams WB, Lewis DW, Bellet S. The effect of acidosis and alkalosis on the plasma potassium concentration and the electrocardiogram of normal and potassium depleted dogs. Am J Med Sci 1951;222(5):506–15.
[291] Kim WG, Brown Jr. EB. Potassium transfer with constant extracellular pH. J Lab Clin Med 1968;71(4):678–85.
[292] Farley DS, Adler S. Isohydric regulation of plasma potassium by bicarbonate in the rat. Kidney Int 1976;9(4):333–43.
[293] Fraley DS, Adler S. Correction of hyperkalemia by bicarbonate despite constant blood pH. Kidney Int 1977;12(5):354–60.
[294] Bushinsky DA, Coe FL. Hyperkalemia during acute ammonium chloride acidosis in man. Nephron 1985;40(1):38–40.
[295] Williams ME, Rosa RM, Epstein FH. Hyperkalemia. Adv Intern Med 1986;31:265–91.
[296] Blumberg A, Weidmann P, Shaw S, Gnadinger M. Effect of various therapeutic approaches on plasma potassium and major regulating factors in terminal renal failure. Am J Med 1988;85(4):507–12.
[297] Mostellar ME, Tuttle Jr. EP. Effects of alkalosis on plasma concentration and urinary excretion of inorganic phosphate in man. J Clin Invest 1964;43:138–49.
[298] Singer RB, Clark JK, Barker ES, Crosley Jr. AP, Elkinton JR. The acute effects in man of rapid intravenous infusion of hypertonic sodium bicarbonate solution. I. Changes in acid–base balance and distribution of the excess buffer base. Medicine (Baltimore) 1955;34(1):51–95.
[299] Krapf R, Caduff P, Wagdi P, Staubli M, Hulter HN. Plasma potassium response to acute respiratory alkalosis. Kidney Int 1995;47(1):217–24.
[300] Edwards R, Winnie AP, Ramamurthy S. Acute hypocapneic hypokalemia: an iatrogenic anesthetic complication. Anesth Analg 1977;56(6):786–92.
[301] Sorensen MV, Matos JE, Sausbier M, Sausbier U, Ruth P, Praetorious HA, et al. Aldosterone increases KCa1.1 (BK) channel-mediated colonic K^+ secretion. J Physiol 2008;586(Pt 17): 4251–64.
[302] Sorensen MV, Matos JE, Praetorius HA, Leipziger J. Colonic potassium handling. Pflugers Arch 2010;459(5): 645–56.
[303] Adler S. An extrarenal action of aldosterone on mammalian skeletal muscle. Am J Physiol 1970;218(3):616–21.
[304] Lim VS, Webster GD. The effect of aldosterone on water and electrolyte composition of incubated rat diaphragms. Clin Sci 1967;33(2):261–70.
[305] DeFronzo RA, Lee R, Jones A, Bia M. Effect of insulinopenia and adrenal hormone deficiency on acute potassium tolerance. Kidney Int 1980;17(5):586–94.
[306] Pan YJ, Young DB. Experimental aldosterone hypertension in the dog. Hypertension 1982;4(2):279–87.
[307] Young DB. Quantitative analysis of aldosterone's role in potassium regulation. Am J Physiol 1988;255(5 Pt 2):F811–22.
[308] Young DB, Jackson TE. Effects of aldosterone on potassium distribution. Am J Physiol 1982;243(5):R526–30.
[309] Sugarman A, Brown RS. The role of aldosterone in potassium tolerance: studies in anephric humans. Kidney Int 1988;34(3): 397–403.
[310] Singhal PC, Desroches L, Mattana J, Abramovici M, Wagner JD, Maesaka JK. Mineralocorticoid therapy lowers serum potassium in patients with end-stage renal disease. Am J Nephrol 1993;13(2):138–41.
[311] Alexander EA, Levinsky NG. An extrarenal mechanism of potassium adaptation. J Clin Invest 1968;47(4):740–8.
[312] Spital A, Sterns RH. Extrarenal potassium adaptation: the role of aldosterone. Clin Sci (Lond) 1989;76(2):213–9.
[313] Schwartz WB. Potassium and the kidney. N Engl J Med 1955;253(14):601–8.
[314] Seldin DW, Carter NW, Rector Jr. FC. Consequences of renal failure and their management. In: Strauss MB, Welt LG, editors. Diseases of the kidney. Boston: Little, Brown; 1963. p. 173–217.
[315] Elkinton JR, Tarail R, Peters JP. Transfers of potassium in renal insufficiency. J Clin Invest 1949;27:378–88.
[316] Salem MM, Rosa RM, Batlle DC. Extrarenal potassium tolerance in chronic renal failure: implications for the treatment of acute hyperkalemia. Am J Kidney Dis 1991;18(4):421–40.
[317] Fernandez J, Oster JR, Perez GO. Impaired extrarenal disposal of an acute oral potassium load in patients with endstage renal disease on chronic hemodialysis. Miner Electrolyte Metab 1986;12(2):125–9.

[318] Sterns RH, Feig PU, Pring M, Guzzo J, Singer I. Disposition of intravenous potassium in anuric man: a kinetic analysis. Kidney Int 1979;15(6):651–60.
[319] Kahn T, Kaji DM, Nicolis G, Krakoff LR, Stein RM. Factors related to potassium transport in chronic stable renal disease in man. Clin Sci Mol Med 1978;54(6):661–6.
[320] Bia M, DeFronzo R. The medullary collecting duct (MCD) does not play a primary role in potassium (K) adaptation following decreased GFR. Clin Res 1978;26: [457 A]
[321] Tuck ML, Davidson MB, Asp N, Schultze RG. Augmented aldosterone and insulin responses to potassium infusion in dogs with renal failure. Kidney Int 1986;30(6):883–90.
[322] Goecke IA, Bonilla S, Marusic ET, Alvo M. Enhanced insulin sensitivity in extrarenal potassium handling in uremic rats. Kidney Int 1991;39(1):39–43.
[323] Adesman J, Goldberg M, Castleman L, Friedman IS. Simultaneous measurement of body sodium and potassium using Na22 and K42. Metabolism 1960;9:561–9.
[324] Bergstrom J, Alvestrand A, Furst P, Hultman E, Widstam-Attorps U. Muscle intracellular electrolytes in patients with chronic uremia. Kidney Int Suppl 1983;16:S153–60.
[325] Bilbrey GL, Carter NW, White MG, Schilling JF, Knochel JP. Potassium deficiency in chronic renal failure. Kidney Int 1973;4(6):423–30.
[326] Mitch WE, Wilcox CS. Disorders of body fluids, sodium and potassium in chronic renal failure. Am J Med 1982;72(3): 536–50.
[327] Schultze G, Koeppe P, Molzahn M. Restoration of total body potassium in the course of long-term hemodialysis treatment. Miner Electrolyte Metab 1981;6:139–45.
[328] Spergel G, Bleicher SJ, Goldberg M, Adesman J, Goldner MG. The effect of potassium on the impaired glucose tolerance in chronic uremia. Metabolism 1967;16:581–5.
[329] Alvestrand A, Wahren J, Smith D, DeFronzo RA. Insulin-mediated potassium uptake is normal in uremic and healthy subjects. Am J Physiol 1984;246(2 Pt 1):E174–80.
[330] Westervelt Jr. FB. Uremia and insulin response. Arch Intern Med 1970;126(5):865–9.
[331] Cooke CR, Ruiz-Maza F, Kowarski A, Migeon CJ, Walker WG. Regulation of plasma aldosterone concentration in anephric man and renal transplant recipients. Kidney Int 1973;3(3): 160–6.
[332] Schrier RW, Regal EM. Influence of aldosterone on sodium, water and potassium metabolism in chronic renal disease. Kidney Int 1972;1(3):156–68.
[333] Cooke CR, Horvath JS, Moore MA, Bledsoe T, Walker WG. Modulation of plasma aldosterone concentration by plasma potassium in anephric man in the absence of a change in potassium balance. J Clin Invest 1973;52(12):3028–32.
[334] Campese VM, Romoff MS, Levitan D, Lane K, Massry SG. Mechanisms of autonomic nervous system dysfunction in uremia. Kidney Int 1981;20(2):246–53.
[335] Henrich WL, Katz FH, Molinoff PB, Schrier RW. Competitive effects of hypokalemia and volume depletion on plasma renin activity, aldosterone and catecholamine concentrations in hemodialysis patients. Kidney Int 1977;12(4): 279–84.
[336] Botey A, Gaya J, Montoliu J, Torras A, Rivera F, Lopez-Pedret J, et al. Postsynaptic adrenergic unresponsiveness in hypotensive haemodialysis patients. Proc Eur Dial Trans Assoc 1981;18:586–91.
[337] Montoliu J, Lens XM, Revert L. Potassium-lowering effect of albuterol for hyperkalemia in renal failure. Arch Intern Med 1987;147(4):713–7.
[338] Allon M, Dunlay R, Copkney C. Nebulized albuterol for acute hyperkalemia in patients on hemodialysis. Ann Intern Med 1989;110(6):426–9.
[339] Stemmer CL, Perez GO, Oster JR. Impairment of beta 2-adrenoceptor-stimulated potassium uptake in end-stage renal disease. J Clin Pharmacol 1987;27(8):628–31.
[340] Martinez Vea A, Montoliu J, Andreu L, Torras A, Gaya J, Lopez-Pedret J, et al. Beta adrenergic modulation of extrarenal potassium disposal in terminal uraemia. Proc Eur Dial Trans Assoc 1983;19:756–60.
[341] Sugarman A, Kahn T. Parathyroid hormone impairs extrarenal potassium tolerance in the rat. Am J Physiol 1988;254(3 Pt 2): F385–90.
[342] Soliman AR, Akmal M, Massry SG. Parathyroid hormone interferes with extrarenal disposition of potassium in chronic renal failure. Nephron 1989;52(3):262–7.
[343] Izumo H, Izumo S, DeLuise M, Flier JS. Erythrocyte Na,K pump in uremia. Acute correction of a transport defect by hemodialysis. J Clin Invest 1984;74(2):581–8.
[344] Kramer HJ, Gospodinov D, Kruck F. Functional and metabolic studies on red blood cell sodium transport in chronic uremia. Nephron 1976;16(5):344–58.
[345] Krzesinski JM, Rorive G. Sodium–lithium countertransport in red cells. N Engl J Med 1983;309:987–8.
[346] Walter U, Becht E. Red blood cell sodium transport and phosphate release in uremia. Nephron 1983;34(1):35–41.
[347] Welt LG, Sachs JR, McManus TJ. An ion transport defect in erythrocytes from uremic patients. Trans Assoc Am Physic 1964;77:169–81.
[348] Zannad F, Kessler M, Royer RJ, Robert J. Effect of hemodialysis on red blood cell Na^+–K^+-ATPase activity in terminal renal failure. Nephron 1985;40(1):127–8.
[349] Zannad F, Royer RJ, Kessler M, Huriet B, Robert J. Cation transport in erythrocytes of patients with renal failure. Nephron 1982;32(4):347–50.
[350] Quarello F, Boero R, Guarena C, Rosati C, Giraudo G, Giacchino F, et al. Acute effects of hemodialysis on erythrocyte sodium fluxes in uremic patients. Nephron 1985;41 (1):22–5.
[351] Cole CH, Balfe JW, Welt LG. Induction of a ouabain-sensitive ATPase defect by uremic plasma. Trans Assoc Am Physic 1968;81:213–20.
[352] Cheng JT, Kahn T, Kaji DM. Mechanism of alteration of sodium potassium pump of erythrocytes from patients with chronic renal failure. J Clin Invest 1984;74(5):1811–20.
[353] Kaji D, Thomas K. Na^+–K^+ pump in chronic renal failure. Am J Physiol 1987;252(5 Pt 2):F785–93.
[354] Druml W, Kelly RA, May RC, Mitch WE. Abnormal cation transport in uremia. Mechanisms in adipocytes and skeletal muscle from uremic rats. J Clin Invest 1988;81(4):1197–203.
[355] Sangkabutra T, Crankshaw DP, Schneider C, Fraser SF, Sostaric S, Mason K, et al. Impaired K^+ regulation contributes to exercise limitation in end-stage renal failure. Kidney Int 2003;63(1):283–90.
[356] Watson KR, O'Kell RT. Lack of relationship between Mg^{2+} and K^+ concentrations in serum. Clin Chem 1980;26(3):520–1.
[357] Whang R. Magnesium and potassium interrelationships in cardiac arrhythmias. Magnesium 1986;5(3–4):127–33.
[358] Whang R, Oei TO, Hamiter T. Frequency of hypomagnesmia associated with hypokalemia in hospitalized patients. Am J Clin Pathol 1979;71:610.
[359] Solomon R. The relationship between disorders of K^+ and Mg^+ homeostasis. Semin Nephrol 1987;7(3):253–62.
[360] Ryan MP. Interrelationships of magnesium and potassium homeostasis. Miner Electrolyte Metab 1993;19(4–5):290–5.
[361] Alfrey AC. Disorders of magnesium metabolism. In: Seldin DWaG G, editor. The kidney: physiology and pathophysiology. New York: Raven Press; 1985. p. 1281–95.

[362] Ladefoged K, Hagen K. Correlation between concentrations of magnesium, zinc, and potassium in plasma, erythrocytes and muscles. Clin Chim Acta 1988;177(2):157–66.
[363] Alfrey AC, Miller NL, Butkus D. Evaluation of body magnesium stores. J Lab Clin Med 1974;84(2):153–62.
[364] Manitius A, Epstein FH. Some observations on the influence of a magnesium-deficient diet on rats, with special reference to renal concentrating ability. J Clin Invest 1963;42(2):208–15.
[365] Shils ME. Experimental human magnesium depletion. Medicine (Baltimore) 1969;48(1):61–85.
[366] Whang R, Flink EB, Dyckner T, Wester PO, Aikawa JK, Ryan MP. Magnesium depletion as a cause of refractory potassium repletion. Arch Intern Med 1985;145(9):1686–9.
[367] Ryan MP, Whang R, Yamalis W, Aikawa JK. Effect of magnesium deficiency on cardiac and skeletal muscle potassium during dietary potassium restriction. Proc Soc Exp Biol Med 1973;143(4):1045–7.
[368] Whang R, Welt LG. Observations in experimental magnesium depletion. J Clin Invest 1963;42:305–13.
[369] Whang R, Oei TO, Aikawa JK, Ryan MP, Watanabe A, Chrysant SG, et al. Magnesium and potassium interrelationships, experimental and clinical. Acta Med Scand Suppl 1981;647:139–44.
[370] Kjeldsen K, Norgaard A. Effect of magnesium depletion on ^{3}H-ouabain binding site concentration in rat skeletal muscle. Magnesium 1987;6(1):55–60.
[371] Dorup I, Skajaa K, Clausen T, Kjeldsen K. Reduced concentrations of potassium, magnesium, and sodium-potassium pumps in human skeletal muscle during treatment with diuretics. Br Med J (Clin Res Ed) 1988;296(6620):455–8.
[372] Fischer PW, Giroux A. Effects of dietary magnesium on sodium-potassium pump action in the heart of rats. J Nutr 1987;117(12):2091–5.
[373] Findlay I. The effects of magnesium upon adenosine triphosphate-sensitive potassium channels in a rat insulin-secreting cell line. J Physiol 1987;391:611–29.
[374] Horie M, Irisawa H, Noma A. Voltage-dependent magnesium block of adenosine-triphosphate-sensitive potassium channel in guinea-pig ventricular cells. J Physiol 1987;387:251–72.
[375] Vandenberg CA. Inward rectification of a potassium channel in cardiac ventricular cells depends on internal magnesium ions. Proc Natl Acad Sci USA 1987;84(8):2560–4.
[376] Cannon-Babb ML, Schwartz AB. Drug-induced hyperkalemia. Hosp Pract (Off Ed) 1986;21(9A):99–107 111, 114-127
[377] Paice B, Gray JM, McBride D, Donnelly T, Lawson DH. Hyperkalaemia in patients in hospital. Br Med J (Clin Res Ed) 1983;286(6372):1189–92.
[378] Perazella MA. Drug-induced hyperkalemia: old culprits and new offenders. Am J Med 2000;109(4):307–14.
[379] Ponce SP, Jennings AE, Madias NE, Harrington JT. Drug-induced hyperkalemia. Medicine (Baltimore) 1985;64(6): 357–70.
[380] Rimmer JM, Horn JF, Gennari FJ. Hyperkalemia as a complication of drug therapy. Arch Intern Med 1987;147(5):867–9.
[381] Shemer J, Modan M, Ezra D, Cabili S. Incidence of hyperkalemia in hospitalized patients. Isr J Med Sci 1983;19(7):659–61.
[382] Brass EP, Thompson WL. Drug-induced electrolyte abnormalities. Drugs 1982;24(3):207–28.
[383] Gronert GA, Theye RA. Pathophysiology of hyperkalemia induced by succinylcholine. Anesthesiology 1975;43 (1):89–99.
[384] Iwatsuki N, Kuroda N, Amaha K, Iwatsuki K. Succinylcholine-induced hyperkalemia in patients with ruptured cerebral aneurysms. Anesthesiology 1980;53(1):64–7.
[385] Striker T, Morrow A. Effect of succinylcholine on the level of serum potassium in man. Anesthesiology 1968;29:214–5.
[386] Martyn JA, Richtsfeld M. Succinylcholine-induced hyperkalemia in acquired pathologic states: etiologic factors and molecular mechanisms. Anesthesiology 2006;104(1):158–69.
[387] Weintraub HD, Heisterkamp DV, Cooperman LH. Changes in plasma potassium concentration after depolarizing blockers in anaesthetized man. Br J Anaesth 1969;41(12):1048–52.
[388] George Jr. AL, Wood Jr. CA. Succinylcholine-induced hyperkalemia complicating the neuroleptic malignant syndrome. Ann Intern Med 1987;106(1):172.
[389] Krikken-Hogenberk LG, de Jong JR, Bovill JG. Succinylcholine-induced hyperkalemia in a patient with metastatic rhabdomyosarcoma. Anesthesiology 1989;70(3):553–5.
[390] Edelman S, Witztum JL. Hyperkalemia during treatment with HMG-CoA reductase inhibitor. N Engl J Med 1989;320(18): 1219–20.
[391] Grundy SM. HMG-CoA reductase inhibitors for treatment of hypercholesterolemia. N Engl J Med 1988;319(1):24–33.
[392] Alberti KG, Johnston H, Lauler D. The effect of arginine and its derivatives on potassium metabolism in the dog. Clin Res 1967;15:476.
[393] Hertz P, Richardson JA. Arginine-induced hyperkalemia in renal failure patients. Arch Intern Med 1972;130(5):778–80.
[394] Bushinsky DA, Gennari FJ. Life-threatening hyperkalemia induced by arginine. Ann Intern Med 1978;89(5 Pt 1): 632–4.
[395] Perazella MA, Biswas P. Acute hyperkalemia associated with intravenous epsilon-aminocaproic acid therapy. Am J Kidney Dis 1999;33(4):782–5.
[396] Edner M, Ponikowski P, Jogestrand T. The effect of digoxin on the serum potassium concentration. Scand J Clin Lab Invest 1993;53(2):187–9.
[397] Schmidt TA, Bundgaard H, Olesen HL, Secher NH, Kjeldsen K. Digoxin affects potassium homeostasis during exercise in patients with heart failure. Cardiovasc Res 1995;29(4):506–11.
[398] Bismuth C, Gaultier M, Conso F, Efthymiou ML. Hyperkalemia in acute digitalis poisoning: prognostic significance and therapeutic implications. Clin Toxicol 1973;6(2): 153–62.
[399] Smith TW, Willerson JT. Suicidal and accidental digoxin ingestion. Report of five cases with serum digoxin level correlations. Circulation 1971;44(1):29–36.
[400] Papadakis MA, Wexman MP, Fraser C, Sedlacek SM. Hyperkalemia complicating digoxin toxicity in a patient with renal failure. Am J Kidney Dis 1985;5(1):64–6.
[401] Clive DM, Stoff JS. Renal syndromes associated with nonsteroidal antiinflammatory drugs. N Engl J Med 1984;310 (9):563–72.
[402] Garella S, Matarese RA. Renal effects of prostaglandins and clinical adverse effects of nonsteroidal anti-inflammatory agents. Medicine (Baltimore) 1984;63(3):165–81.
[403] Clive D.M, Gurwitz J, Williams M, Rossetti R. Nonsteroidal antiinflammatory drugs (NSAID) do not impair potassium metabolism in normal humans. Paper presented at: 10th International Congress of Nephrology1990.
[404] Saris S, Lowenthal DT, Affrime MB, Rosenthal L, Swartz G. Lack of effect of nonsteroidsal anti-inflammatory drugs on exercise-induced hyperkalemia. N Engl J Med 1982;307(9): 559–60.
[405] Hariharasubramanian N, Devi D, Rao A. Serum potassium levels during lithium therapy of manic depressive psychosis. In: Johnson FN, Johnson S, editors. Lithium in medical practice. Baltimore: University Press; 1978. p. 205–8.
[406] McCusick V. The effect of lithium on the electrocardiogram of animals and relation of this effect to the ratio of the intracellular and extracellular concentrations of potassium. J Clin Invest 1954;33:598–610.

[407] Goggans FC. Acute hyperkalemia during lithium treatment of manic illness. Am J Psychiatry 1980;137(7):860–1.
[408] Groot OA, Trof RJ, Girbes AR, Swart NL, Beishuizen A. Acute refractory hyperkalaemia and fatal cardiac arrest related to administration of liposomal amphotericin B. Neth J Med 2008;66(10):433–7.
[409] Kearney TE, Manoguerra AS, Curtis GP, Ziegler MG. Theophylline toxicity and the beta-adrenergic system. Ann Intern Med 1985;102(6):766–9.
[410] Zantvoort FA, Derkx FH, Boomsma F, Roos PJ, Schalekamp MA. Theophylline and serum electrolytes. Ann Intern Med 1986;104(1):134–5.
[411] Trost BN, Weidmann P. Metabolic effects of calcium antagonists in humans, with emphasis on carbohydrate, lipid, potassium, and uric acid homeostases. J Cardiovasc Pharmacol 1988;12(Suppl. 6):S86–92.
[412] Minella RA, Schulman DS. Fatal verapamil toxicity and hypokalemia. Am Heart J 1991;121(6 Pt 1):1810–2.
[413] Davidovics Y, Peer G, Cabili S, Blum M, Serban I, Wollman Y, et al. Effect of verapamil on disposition of intravenous potassium in diabetic anephric uremic rats. Miner Electrolyte Metab 1993;19(2):99–102.
[414] Mimran A, Ribstein J, Sissmann J. Effects of calcium antagonists on adrenaline-induced hypokalaemia. Drugs 1993;46 (Suppl. 2):103–7.
[415] Sugarman A, Kahn T. Calcium channel blockers enhance extrarenal potassium disposal in the rat. Am J Physiol 1986;250 (4 Pt 2):F695–701.
[416] Solomon R, Dubey A. Diltiazem enhances potassium disposal in subjects with end-stage renal disease. Am J Kidney Dis 1992;19(5):420–6.
[417] Gardos G. The function of calcium in the potassium permeability of human erythrocytes. Biochim Biophys Acta 1958;30(3): 653–4.
[418] Burgess GM, Claret M, Jenkinson DH. Effects of quinine and apamin on the calcium-dependent potassium permeability of mammalian hepatocytes and red cells. J Physiol 1981;317:67–90.
[419] Capponi AM, Lew PD, Jornot L, Vallotton MB. Correlation between cytosolic free Ca^{2+} and aldosterone production in bovine adrenal glomerulosa cells. Evidence for a difference in the mode of action of angiotensin II and potassium. J Biol Chem 1984;259(14):8863–9.
[420] Nadler JL, Hsueh W, Horton R. Therapeutic effect of calcium channel blockade in primary aldosteronism. J Clin Endocrinol Metab 1985;60(5):896–9.
[421] Bouchard PM, Frenette AJ, Williamson DR, Perreault MM. Thiopental-associated dyskalemia in severe head trauma. J Trauma 2008;64(3):838–42.
[422] Jung JY, Lee C, Ro H, Kim HS, Joo KW, Kim Y, et al. Sequential occurrence of life-threatening hypokalemia and rebound hyperkalemia associated with barbiturate coma therapy. Clin Nephrol 2009;71(3):333–7.
[423] Clemessy JL, Favier C, Borron SW, Hantson PE, Vicaut E, Baud FJ. Hypokalaemia related to acute chloroquine ingestion. Lancet 1995;346(8979):877–80.
[424] Thuss-Patience PC, Peters U, Jurkat-Rott K, Pink D, Kretzschmar A, Dorken B, et al. Acute hypokalemic tetraparesis induced by intravenous methotrexate. J Clin Oncol 2003;21(9):1896–7.
[425] Seldin DW, Tarail R. Effect of hypertonic solutions on metabolism and excretion of electrolytes. Am J Physiol 1949;159(1): 160–74.
[426] Makoff DL, Da Silva JA, Rosenbaum BJ. On the mechanism of hyperkalaemia due to hyperosmotic expansion with saline or mannitol. Clin Sci 1971;41(5):383–93.
[427] Moreno M, Murphy C, Goldsmith C. Increase in serum potassium resulting from the administration of hypertonic mannitol and other solutions. J Lab Clin Med 1969;73 (2):291–8.
[428] Goldfarb S, Cox M, Singer I, Goldberg M. Acute hyperkalemia induced by hyperglycemia: hormonal mechanisms. Ann Intern Med 1976;84(4):426–32.
[429] Rado JP. Glucose-induced hyperkalemia during captopril treatment. Arch Intern Med 1983;143(2):389.
[430] Nicolis GL, Kahn T, Sanchez A, Gabrilove JL. Glucose-induced hyperkalemia in diabetic subjects. Arch Intern Med 1981;141(1):49–53.
[431] Singhal PC, Rubin RB, Peters A, Santiago A, Neugarten J. Rhabdomyolysis and acute renal failure associated with cocaine abuse. J Toxicol Clin Toxicol 1990;28(3):321–30.
[432] Cohen LF, Balow JE, Magrath IT, Poplack DG, Ziegler JL. Acute tumor lysis syndrome. A review of 37 patients with Burkitt's lymphoma. Am J Med 1980;68(4):486–91.
[433] Cech P, Block JB, Cone LA, Stone R. Tumor lysis syndrome after tamoxifen flare. N Engl J Med 1986;315(4):263–4.
[434] Tsokos GC, Balow JE, Spiegel RJ, Magrath IT. Renal and metabolic complications of undifferentiated and lymphoblastic lymphomas. Medicine (Baltimore) 1981;60(3):218–29.
[435] Hesp R, Chanarin I, Tait CE. Potassium changes in megaloblastic anaemia. Clin Sci Mol Med 1975;49(1):77–9.
[436] James GW, Abbott Jr. LD. Metabolic studies in pernicious anemia. I. Nitrogen and phosphorus metabolism during vitamin B12-induced remission. Metabolism 1952;1 (3):259–70.
[437] Lawson DH, Murray RM, Parker JL. Early mortality in the megaloblastic anaemias. Q J Med 1972;41(161):1–14.
[438] Sperelakis N, Schneider MF, Harris EJ. Decreased K^+ conductance produced by Ba^{++} in frog sartorius fibers. J Gen Physiol 1967;50(6):1565–83.
[439] Gallant EM. Barium-treated mammalian skeletal muscle: similarities to hypokalaemic periodic paralysis. J Physiol 1983;335: 577–90.
[440] Roza O, Berman LB. The pathophysiology of barium: hypokalemic and cardiovascular effects. J Pharmacol Exp Ther 1971; 177(2):433–9.
[441] Allen AS. Pa Ping, or Kiating paralysis. Chin Med J 1943;61:296–301.
[442] Huang K-W. Pa Ping (transient paralysis simulating family periodic paralysis). Chin Med J 1943;61:305–12.
[443] Dalal AK, Harding JD, Verdino RJ. Acquired long QT syndrome and monomorphic ventricular tachycardia after alternative treatment with cesium chloride for brain cancer. Mayo Clin Proc 2004;79(8):1065–9.
[444] McIvor ME. Acute fluoride toxicity. Pathophysiology and management. Drug Saf 1990;5(2):79–85.
[445] Bruining HA, Boelhouwer RU. Acute transient hypokalemia and body temperature. Lancet 1982;2(8310):1283–4.
[446] Koht A, Cane R, Cerullo LJ. Serum potassium levels during prolonged hypothermia. Intensive Care Med 1983;9(5): 275–7.
[447] Sprung J, Cheng EY, Gamulin S, Kampine JP, Bosnjak ZJ. Effects of acute hypothermia and beta-adrenergic receptor blockade on serum potassium concentration in rats. Crit Care Med 1991;19(12):1545–51.
[448] Ellis RJ, Hoover E, Gay WA, Ebert PA. Metabolic alterations with profound hypothermia. Arch Surg 1974;109 (5):659–63.
[449] Suh A, DeJesus E, Rosner K, Lerma E, Yu W, Young JB, et al. Racial differences in potassium disposal. Kidney Int 2004;66(3): 1076–81.

This page intentionally left blank

CHAPTER

49

Regulation of K^+ Excretion

Gerhard Malnic[1], *Gerhard Giebisch*[2], *Shigeaki Muto*[3], *Wenhui Wang*[4], *Matthew A. Bailey*[5] *and Lisa M. Satlin*[6]

[1]Universidade de Sao Paulo, Instituto de Ciencias Biomedicas, Departamento de Fisiologie e Biofisica, Sao Paulo, Brazil
[2]Department of Cellular & Molecular Physiology, Yale University School of Medicine, New Haven, CT, USA
[3]Department of Nephrology, Jichi Medical School, Shimotsuke, Tochigi, Japan
[4]Department of Pharmacology, New York Medical College, Valhalla, NY, USA
[5]British Heart Foundation Centre for Cardiovascular Science, The University of Edinburgh, Edinburgh, UK
[6]Department of Pediatrics, Mt. Sinai School of Medicine, New York, NY, USA

OVERVIEW OF K^+ DISTRIBUTION AND EXCRETION—INTERNAL AND EXTERNAL BALANCE

As the most abundant cation in intracellular fluid, K^+ plays an important role in a variety of cell functions. High K^+ concentration in cells and low K^+ concentration in extracellular fluid is essential for many cellular processes, including determining the electrical properties of cell membranes in both excitable (nerve, muscle) and nonexcitable (transporting epithelia) tissues.[514,515] Cell K^+ also contributes importantly to the effective osmolality of intracellular fluid, and thus to the regulation of cell volume.[316,514,515,568] Changes in cell K^+ modify intracellular acidity, and thereby indirectly influence a variety of metabolic processes.[4,274] These important functions depend on the coordinated action of a variety of regulatory mechanisms that serve to maintain total K^+ content (50–55 mmol/kg body weight) and distribution.[4,154,274]

INTERNAL K^+ BALANCE

Figure 49.1 schematically shows several features of the distribution of K^+ in the body. More than 98% of body K^+ resides within cells, principally in skeletal muscle, whereas only 2% of total body K^+ is located in the extracellular fluid space. Maintenance of K^+ homeostasis is challenging, because the daily dietary intake of K^+ in the adult (~70 mEq) typically approaches the total K^+ content normally present within the extracellular fluid space (~70 mEq in 17 L of extracellular fluid, with a K^+ concentration averaging ~4 mEq/l). To maintain zero balance in the adult, dietary intake of K^+ must be matched by its elimination, a task performed primarily by the kidney.

Ingested potassium enters the extracellular fluid by reabsorption from the small intestine, a process not subject to specific regulation.[264] K^+ that enters the extracellular fluid must temporarily and rapidly be translocated into cells to prevent dangerous increases in plasma K^+ levels. The buffering capacity of the combined cellular storage reservoirs, which includes muscle, liver, and red blood cells, is vast compared with the extracellular pool and is capable of sequestering large amounts of K^+. The biochemical and hormonal factors that influence the internal balance of K^+, typically by altering Na-K-ATPase activity, are listed in Figure 49.2.[7,259,479,480] Racial differences in K^+ distribution have also been reported.[495]

The steep K^+ concentration gradient across the cell membrane depends on the regulated interplay between active uptake by Na^+,K^+-ATPase and passive backleak through K^+ channels and carrier-mediated transport processes[514,515,568] (Figure 49.1b). When K^+ enters the extracellular fluid, active Na^+,K^+-ATPase-mediated K^+ uptake into cells occurs rapidly, and buffers against fluctuations of K^+ in the extracellular fluid. This process is efficient, and plasma K^+ concentration is kept

Seldin and Giebisch's The Kidney, Fifth Edition.
DOI: http://dx.doi.org/10.1016/B978-0-12-381462-3.00049-5

© 2013 Elsevier Inc. All rights reserved.

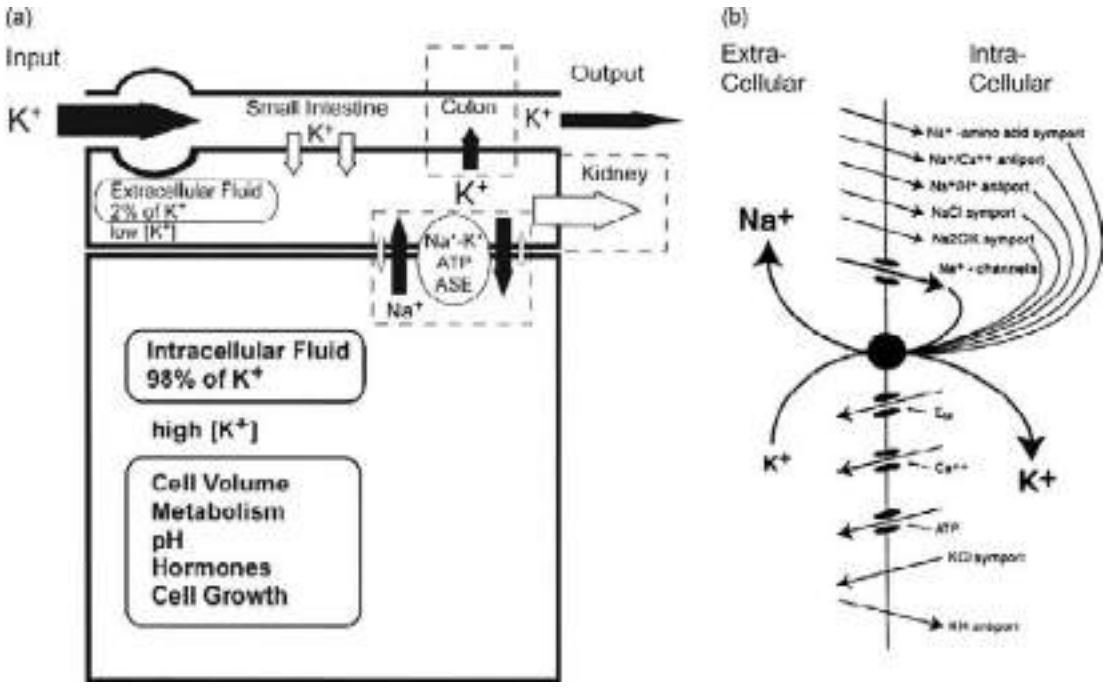

FIGURE 49.1 (a) Distribution of K^+ in the body and pathways of K^+ entry and exit. (b) Transporters involved in the distribution of K^+ and Na^+ across cell membranes. The activity of the Na^+,K^+-ATPase in cell membranes is opposed by several symporters, antiporters, and ion channels. *(From Giebisch, G. (2002). A trail of research on potassium. Kidney Int.* ***62****, 1498–1512, with permission.)*

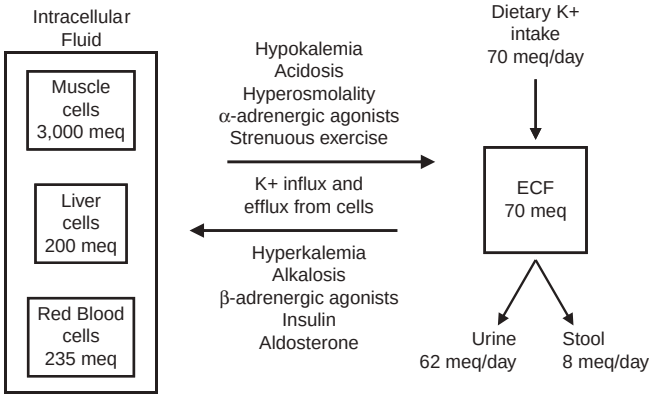

FIGURE 49.2 **Distribution of K^+ between the intracellular and extracellular (ECF) fluid compartments.** Only ≈2% of the total body K^+ is present in the ECF, with most of the remainder in intracellular fluid, here represented by three of the largest cellular compartments. The distribution of K^+ represents a balance between active uptake into cells by the Na^+,K^+-ATPase and the passive leak of K^+ out of cells. This balance is influenced by the K^+ concentration of the ECF, as well as by the factors listed above and below the two arrows. A typical daily K^+ intake of 70 meq/d is matched by the sum of a small excretion in the stool and the regulated excretion of K^+ by the kidneys. *(From Giebisch, G. (2002). A trail of research on potassium. Kidney Int.* ***62****, 1498–1512, with permission.)*

remarkably constant in the range from 3.5 to 5.0 mM.[53–55,97,98,102,478,479] Variations in K^+ intake are matched within hours by parallel adjustments in K^+ excretion, most of which is mediated by the kidney.[49,177–185,473,579–583] However, during exercise and ischemia, extracellular K^+ may quickly rise significantly. To minimize cell ATP decrease and loss of K^+ production of AMP-activated protein kinase (AMPK), under these conditions, is stimulated by an increase in intracellular AMP-to-ATP ratio favoring translocation of K^+ into cells in states of exercise and ischemia.[591,602] Although overshadowed by the kidney, the colon also excretes K^+ and responds to stimuli calling for a change in excretion rate.[29,30,151,216]

EXTERNAL K^+ BALANCE: THE ROLE OF THE KIDNEY

To accomplish excretion of the variable quantity of K^+ ingested daily, the kidney must first extract K^+ from blood in which K^+ circulates at a rather low concentration. Indeed, dietary K^+ may approximate that of sodium (80–120 mM/day), but the concentration of K^+ in plasma, and therefore the rate at which it is filtered by glomeruli, is only one-thirtieth of that of sodium. Nevertheless, the glomerular filtration rate (GFR) is normally high enough so that K^+ could be excreted by filtration alone. However, if the GFR is reduced to 10 to 15% of normal, as occurs with chronic renal failure, filtration alone would not be able to keep up with the normal dietary intake. Even if the GFR were reduced

TABLE 49.1 Main Features of Potassium Transport, Based on Clearance Experiments

1. K^+ secreted by renal tubules (excreted K^+ > filtered K^+)
2. K^+ excretion can be dissociated form the rate of glomerular filtration
3. Reabsorption of K^+ along the nephron precedes K^+ secretion
4. Secretion of K^+ occurs by exchange for Na^+
5. K^+ tolerance: Increased K excretion at relatively low K^+ in plasma
6. Reciprocal relation between urinary excretion of K^+ and H^+, carbonic anhydrase inhibitors induce kaliuresis
7. Adrenal steroids stimulate K^+ secretion

only by half, because not all filtered K^+ can escape reabsorption, it is likely that renal excretion would be inadequate and K^+ would be retained. Furthermore, even when GFR is normal, an excretion mechanism relying solely on filtration would have a limited capacity for adaptive increase, and could not achieve the 20-fold increase in K^+ excretion that has been observed in animals exposed to increased intake of K^+ by diets high in K^+ or parenteral infusions containing K^+. Indeed, net urinary K^+ excretion reflects not only glomerular filtration, but also tubular reabsorption and secretion. Clearance studies from as early as the 1940s revealed that the kidney is capable of secretion enabling the transfer of K^+ from plasma to tubule fluid.[48–52,177–186,187,292,330,345–347,379,473,474,583] Table 49.1 summarizes the main features of renal K^+ transport based on these studies.

A simplified but generally adequate view of renal K^+ handling is that proximal nephron segments between the glomerulus and the distal convoluted tubule (DCT) reabsorb a rather fixed fraction (80–90%) of the filtered K^+, whereas distal tubules and collecting ducts either secrete a variable quantity of K^+ into tubule fluid[49,177–187,221,320–324,379,485] or effectively reabsorb K^+.[119,179,325,371] By varying the rate and even the direction of K^+ transport, the distal nephron is able to respond homeostatically to changes in dietary K^+ intake or to changes in extracellular K^+ caused by other gains (parenteral administration, release from cellular pools) or losses (from the GI tract or skin). In people ingesting $\approx$70 mmol/day K^+, the usual rate of K^+ excretion in the postabsorptive period between meals is approximately 10–15% of the rate of K^+ filtration. In the hours following ingestion of K^+-rich meals, the rate of urinary excretion of K^+ can increase greatly to approach or even exceed the rate at which it is filtered. Such increments in K^+ excretion can be attributed to an increase in the quantity secreted by distal nephron segments. Increased secretion may not entirely account for increases in K^+ excretion in all cases, however, and variations in reabsorption by tubule segments, either proximal or distal to the main secretory sites, may become important in some circumstances.

If K^+ intake is reduced or eliminated (or if the body is depleted of K^+ by prior renal or nonrenal losses), urinary K^+ excretion declines rapidly as the deficit in total body K^+ increases. Within a few days K^+ excretion can be reduced to very low levels,[179,322–324] but K^+ conservation is less complete than that of sodium.[179]

General Aspects of K^+ Transport Along the Nephron

The generalization that filtered K^+ is largely reabsorbed by proximal nephron segments and that excreted K^+ is secreted by distal segments provides a useful framework for integrating information about renal handling of K^+, but a closer look at the cytologically distinct subdivisions of the nephron and the way each handles K^+ reveals a more complicated picture. K^+ is not continuously reabsorbed from all tubule segments proximal to the secretory sites in the distal tubules and collecting ducts. The rather constant fractional delivery of K^+ (10–20% of the filtered quantity) that has been found by collecting and analyzing samples of fluid from the earliest portion of the superficial DCT accessible to micropuncture is achieved by a sequence of reabsorption, secretion, and reabsorption as the glomerular filtrate travels through the proximal tubule and the loop of Henle.[179,322,323,324,325,466,470,471,473,579,583] Secretion of K^+ into loops of Henle has been documented only for the juxtamedullary nephron population[104,250,252,531]; however, it seems likely that the more superficial nephrons behave similarly.

Figures 49.3 and 49.4 represent schematic representations of the renal elements responsible for K^+ excretion. The location and naming of the subdivisions generally follow the scheme outlined by Kriz and Bankir.[281] Some features that distinguish superficial and deep nephrons are pictured. K^+ is filtered and reabsorbed from proximal convoluted tubules (PCT) of both superficial and deep nephrons. As the proximal straight tubule (PST) enters the outer medulla, the direction of K^+ transport reverses, and K^+ is secreted into the third proximal segment (S3) and the thin descending limb of the loop of Henle.[250–252] Higher K^+ concentrations are attained in loops of deeper nephrons that penetrate further into the inner medulla.

K^+ can be reabsorbed by thick ascending limbs (TALs), and net reabsorption probably occurs in both medullary and cortical TALs of both deep and superficial nephrons.[198,201,218] The portion of the distal tubule beyond the macula densa where each ascending limb contacts its parent glomerulus comprises several segments that are cytologically distinguishable. The DCT, extending beyond the

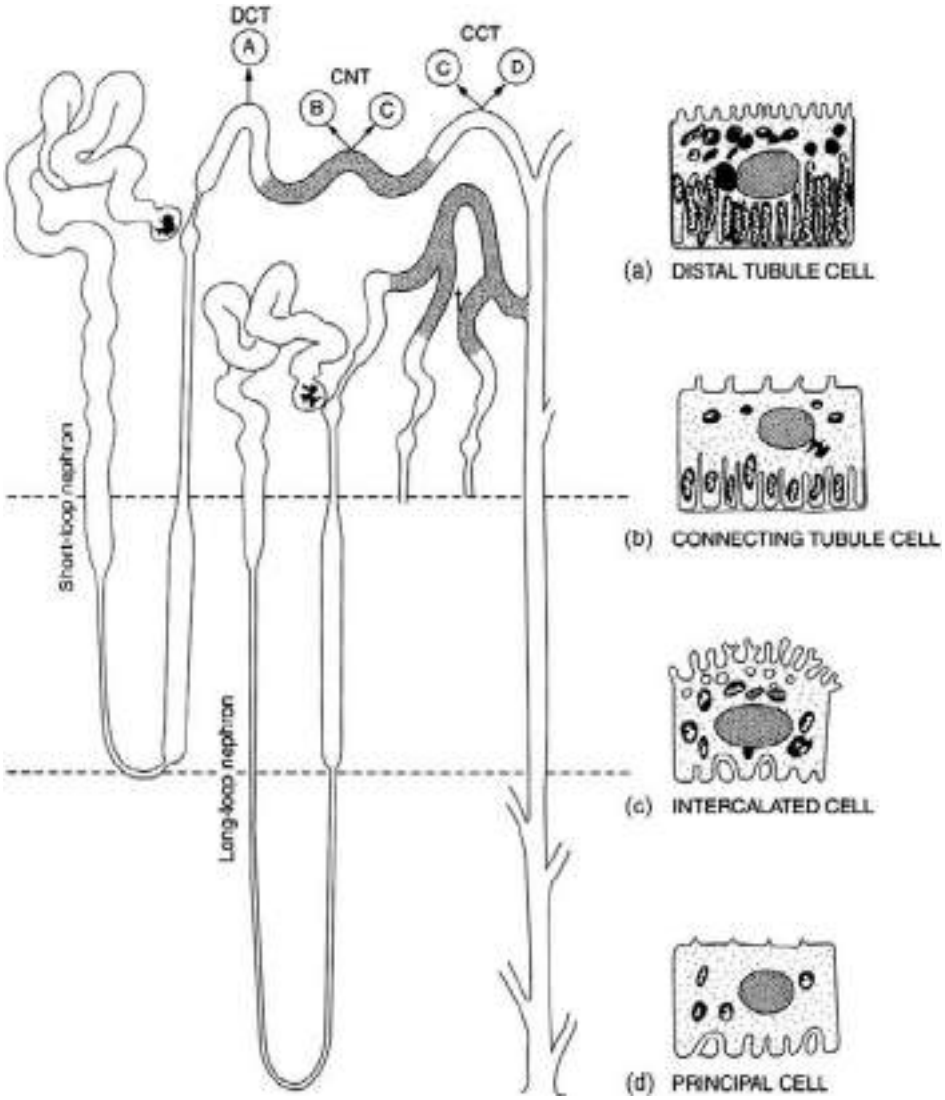

FIGURE 49.3 **Schematic illustration of the distal nephron segments** (CCT: cortical collecting tubule; CNT: connecting tubule; DCT: distal convoluted tubule). *(From ref. [244], with permission.)*

macula densa, is functionally distinct from the TAL segment, and probably contributes modestly to K^+ excretion.[451]

The next segment of the distal tubule – the connecting tubule (CNT), and the segment following it, the cortical collecting duct (CCD) – are major sites of K^+ secretion. In superficial nephrons, epithelium characteristic of the CCD appears some distance proximal to the first confluence of two distal tubules. This region has also been referred to as the late distal tubule or the initial collecting tubule (ICT).[28] In deeper nephrons, the CNTs frequently join to form arcades before flowing into the collecting duct. The separate segments of the distal tubule are discussed subsequently in more detail. K^+ is secreted into the collecting duct throughout the cortex, and probably in the outer stripe of the outer medulla as well.[485,486] However, in the inner stripe of the outer medulla, K^+ reabsorption appears once again and contributes to K^+ accumulation in the medullary interstitium. Both secretion and reabsorption of K^+ have been described along the terminal portions of the inner medullary collecting duct.[402,403,452,463,485–488]

K^+ Transport by Individual Nephron Segments

Glomerulus

K^+ ions that are free in plasma water pass across the glomerular capillary membrane with little hindrance. Nonfilterable proteins in plasma may bind a small fraction of K^+[294] and restrict filtration. The net negative charge on these plasma proteins tends to reduce K^+ concentration in glomerular filtrate relative to plasma water (Donnan equilibrium), but the concentration of

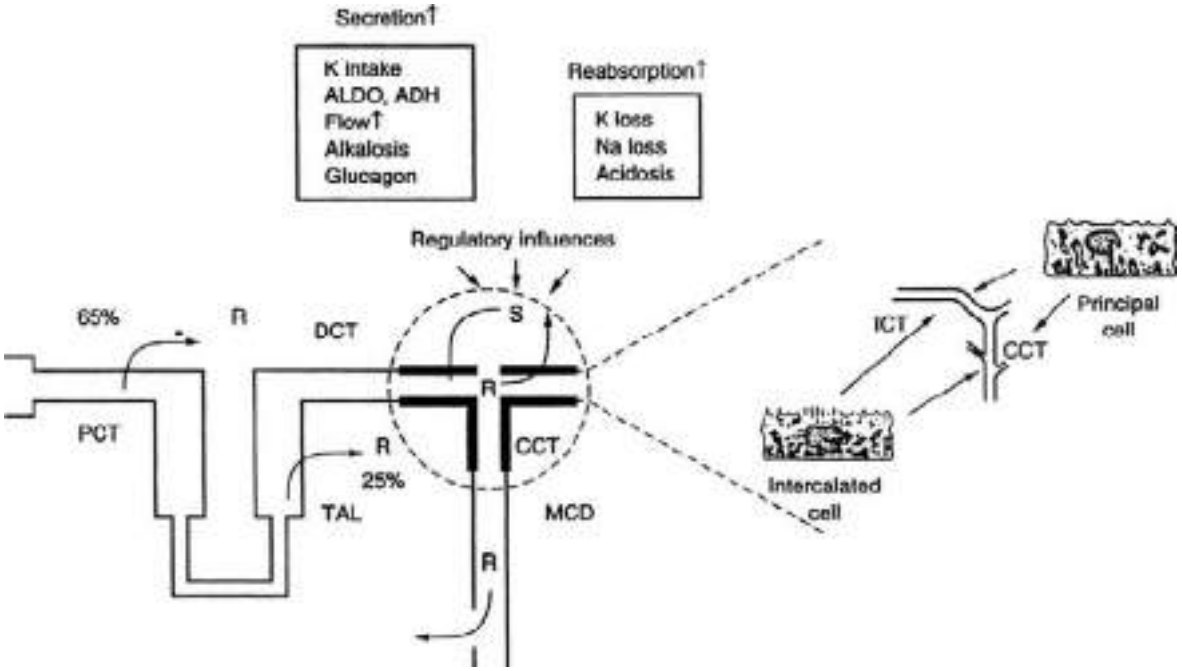

FIGURE 49.4 **Overview of K^+ transport along the nephron.** Secretion (S) largely determines the excretion of K^+ during normal and high K^+ intake; reabsorption (R) determines the excretion of K^+ in K^+ depletion. Note the cell heterogeneity in the distal nephron (see Figure 49.3) (ADH: antidiuretic hormone; ALDO: aldosterone; CCT: cortical collecting tubule; DCT: distal convoluted tubule; MCD: medullary collecting duct; PCT: proximal convoluted tubule; TAL: thick ascending limb of Henle). *(From Giebisch, G. (2002). A trail of research on potassium. Kidney Int. **62**, 1498–1512, with permission.)*

K^+ in plasma is approximately 6% lower than in plasma water. These factors tend to cancel each other out, and the concentrations of K^+ in glomerular filtrate and in plasma or serum, are approximately equal.

Although variations in GFR do cause proportional variations in the rate of K^+ filtration, they do not usually result in large changes in K^+ excretion, because mechanisms promoting glomerulotubular balance tend to stabilize the rate of K^+ delivery out of the proximal tubule and the loop of Henle. In the 1950s, when renal clearance methods were first applied systematically to the study of K^+ regulation by the kidney, it was observed that rates of glomerular filtration and final K^+ excretion could be varied independently of one another.[49,100,346,347] However, if GFR is reduced enough to decrease sodium and water excretion, the rate of K^+ excretion will also decrease.[49,100]

Proximal Convoluted Tubule: Direction, Magnitude, and Mechanism of Transport

Transepithelial K^+ Transport

Information about the direction and magnitude of K^+ transport processes along the nephron was obtained in the 1960s by *in vivo* micropuncture techniques.[193] The main features of K^+ transport in various nephron segments are summarized in Figure 49.4. Collections of tubular fluid samples showed that about 50% of filtered K^+ reaches the last accessible surface segment of the PCT.[322] Collections from sites close to the glomerulus showed that reabsorption of K^+, which occurs over most of the accessible proximal tubule,[59,179,322,325,399,553] may be preceded by a small K^+ leak into the lumen.[516] The downstream reabsorption of K^+ along the proximal tubule, like that of sodium, generally proceeds without developing a large concentration difference across the proximal tubule as a roughly similar fraction of water is also absorbed. Although K^+ concentration has been reported to increase slightly[40] or to remain unchanged[109] along the proximal tubule, a few studies have provided evidence that proximal reabsorption of K^+ can proceed against an electrochemical gradient, and that tubular fluid K^+ concentration may decline (by about 10%) between early and late proximal segments in rat kidneys.[61,268]

Three mechanisms participate in K^+ reabsorption by the proximal tubule: solvent drag; diffusion; and apparent active transport. First, the consistently observed association between K^+ transport and fluid transport suggests that a fraction of proximal K^+ absorption depends on the simultaneous rate of fluid

absorption.[61,62] This dependence of K^+ transport on net fluid transport, and the finding of low reflection coefficients of K^+,[550] support the notion of direct coupling of K^+ and fluid through the same transport pathway: a solvent drag mechanism.

Second, diffusion of K^+ from luminal to peritubular fluid may also occur because fluid absorption may raise the K^+ concentration in the proximal tubule, thus creating a concentration difference favoring K^+ absorption. *In vivo* microperfusion experiments show that proximal K^+ transport is very sensitive to changes in luminal K^+ concentration and transepithelial voltage.[61,62,550] The high K^+ permeability in the proximal tubule,[270] and the dependence of K^+ transport on the transepithelial electrochemical potential difference is consistent with diffusive movement through a paracellular pathway. However, barium, a potent K^+ channel-blocker, has been shown to block a significant fraction of K^+ reabsorption, implying possible participation of a transcellular route for reabsorption of K^+.[270,528] However, little is known about this pathway.

Third, the direction of the electrochemical driving force for K^+ in at least part of the proximal tubule, and the special microenvironment of the paracellular compartment between proximal tubule cells, provides theoretical support for apparent active K^+ absorption. Such movement of K^+ ions against an electrochemical potential gradient in the early proximal tubule is implied by experimental findings demonstrating both a concentration of K^+ in the tubule lumen below that in arterial plasma, and a lumen-negative transepithelial potential.[162,268,518] Moreover, dissociation between sodium-driven fluid movement and K^+ transport has also, albeit rarely, been observed. Micropuncture studies provide evidence that channel-dependent K^+ fluxes mediate a secretory component of K^+ movement into the early proximal tubule,[11,268,518] but K^+ reabsorption further downstream exceeds such secretory K^+ fluxes. Direct measurements of the electrochemical driving force for K^+ across the apical cell membrane in amphibian proximal tubules also support active K^+ reabsorption.[11,164] However, there is no evidence that K-H-ATPase activity identified in the apical membrane of mammalian proximal tubules[112,117] contributes to K^+ reabsorption.[538a,592]

A cell model summarizing the complex mechanisms involved in proximal tubular K^+ transport is pictured in Figure 49.5. It includes a sodium-K^+ exchange pump (Na^+,K^+-ATPase) in the basolateral membrane, a K^+ conductance in the apical membrane, and a pathway for K^+ transport between cells. Two pathways for K^+ exit across the basolateral membrane are shown: a conductive channel and a K-Cl co-transporter.[18,551] Note also that the transepithelial potential along the tubule changes from lumen-negative values in the early PCT to lumen-positive values in the late PCT.[162]

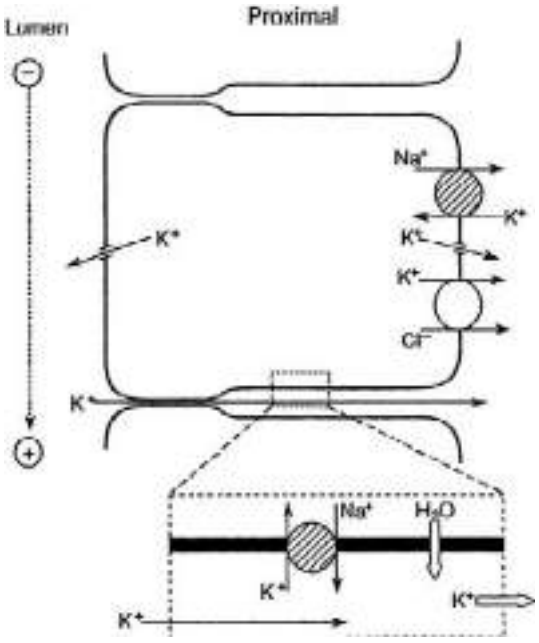

FIGURE 49.5 **Model of proximal tubule cell.** Transepithelial voltage is lumen-negative in S_1, and becomes lumen-positive in S_2. Enlargement of lateral membrane and the intercellular and extracellular spaces illustrates a postulated mechanism permitting absorption of potassium against a concentration gradient.

Weinstein has suggested that the apparent reabsorptive movement of K^+ against an electrochemical driving force does not require an active, directly energy-driven reabsorptive maechanism for K^+ in the apical cell membrane.[559] Given that Na^+,K^+-ATPase-driven uptake of K^+ does occur in the cell membranes lining the paracellular compartment between cells, such transport could deplete this compartment of K^+, particularly if the diffusion resistance to K^+ across the basolateral exit was low. A situation could then develop in which the luminal fluid equilibrates with the low-K^+ fluid in the interspace, effectively decreasing the K^+ concentration in the lumen below peritubular plasma levels. Exit of K^+ ions from the interspace into the peritubular fluid would be driven by bulk movement of fluid and K^+ along the hydrostatic pressure gradient that normally develops along the interspace from its luminal to basolateral end.

In the later part of the PCT, the transepithelial potential difference becomes lumen-positive, providing an additional driving force for net K^+ reabsorption.[162] It is likely that K^+ movement driven by the transepithelial voltage occurs through the paracellular shunt pathway. *In vivo* microperfusion experiments using mannitol to vary tubular fluid osmolarity reveal that the direction of net K^+ transport is

dependent on that of net fluid transport.[61,62] Previous observations had already shown that inhibition of proximal sodium and water transport would also block K^+ reabsorption,[59,181,234,579,581] an effect consistent with entrainment of K^+ ions by sodium-dependent fluid reabsorption.

Transepithelial electrochemical gradients of K^+ demonstrate the effect of changes in the electrical potential difference on tubule K^+ concentration.[456] Marked differences were observed between K^+-replete and K^+-depleted animals: whereas a lumen-positive potential was recorded in replete animals, the transepithelial potential difference was reversed in K^+-depleted animals, and the K^+ concentration ratio across the late proximal tubule was significantly elevated. These data support the view that diffusion along an electrochemical gradient can play a critical role in transport of K^+ across the proximal tubule.

Cell K^+ Transport

In proximal tubule cells, steady-state levels of cell K^+ depend on the balance between active uptake from interstitial fluid and passive leakage from the cytosol, either to the interstitium or to the tubule lumen. K^+ ions are actively taken up by the ATP-driven Na^+-K^+ exchange pump located in the basolateral membranes. Microelectrode measurements of basolateral membrane voltage and of K^+ activities show that the electrical potential difference across cell membranes of both amphibian and mammalian tubule cells is too small to account for the measured intracellular K^+ activity by passive distribution. Also, inhibitor studies indicate that ATPase-driven accumulation of K^+ is responsible for high cell K^+ concentrations. Inhibition of Na^+,K^+-ATPase activity reduces intracellular K^+ concentrations and content.[48,49,83,124,233,284,420,421,514,515]

The basolateral sodium-K^+ pump operates in an electrogenic mode: the rate at which sodium ions are pumped out of the cell exceeds the rate at which K^+ ions are taken in. The contribution of such an electrogenic cation exchange to the steady-state voltage across the basolateral membrane is probably small; however, sudden activation of the pump, either by raising cell sodium, by increasing extracellular K^+ from low levels or by warming tubules previously cooled, leads to rapid hyperpolarization of the basolateral cell membrane to levels that can exceed the equilibrium potential that could be generated by passive diffusion of K^+ ions.[48,49,83,124,148,150,233,390,420,421]

Figure 49.6 illustrates additional transporters in the basolateral membranes of proximal tubule cells. K^+ channels are present in both cell membranes, and serve several functions. They generate the cell-negative electrical potential which constitutes an important driving force for the entry of positively-charged solutes and the basolateral exit of negatively-charged solutes. Sodium-coupled electrogenic glucose and amino acid transport across the apical membrane of proximal tubule cells is facilitated by the cell-negative potential. Chloride diffusion, electrogenic Na^+-HCO_3 cotransport and Ca^{2+}/Na^+ exchange are also modulated by the magnitude of the K^+-dependent basolateral membrane potential.[513–515]

K^+ channels are also involved in volume regulation of proximal tubule cells.[237,419] Both apical and basolateral K^+ channels are activated by cell swelling, either directly by stretching of the membrane or indirectly, by volume-dependent Ca^{2+} entry through non-selective cation channels.[150,381,419] Apical K^+ channels are also sensitive to changes in membrane voltage, with depolarization leading to increased activity. Apical K^+ channels in the proximal tubule are critical in stabilizing the cell-negative potential, especially during depolarizing Na^+-coupled transport (i.e., with glucose or amino acids). The K^+ channel KCNQ1 and the accessory protein KCNE1 have been localized to the brush border of the mid-to-late proximal tubule.[516] They have been proposed to play a role in net K^+ secretion in the early proximal tubule, and in polarizing the brush border membrane to maintain the electrical driving force for Na^+-coupled transport. In support of this view, mice lacking KCNE1 exhibit increased renal excretion of Na^+ and glucose, and signs of volume-depletion.[516]

Basolateral K^+ channels are inhibited by an increase in cell ATP, by a fall in pH, by cyclic AMP and taurine,[217] and they have been implicated in renal cell damage by hypoxia.[400]

Coupling Between Sodium Transport and Basolateral K^+ Channels

The constancy of intracellular K^+ in the presence of large changes in transepithelial net sodium transport depends on appropriate modulations of the basolateral K^+ conductance.[453,454] Because a major pathway for sodium reabsorption is transcellular and involves the basolateral sodium-K^+ exchange pump, large changes in the rate of basolateral sodium extrusion necessarily cause large changes in K^+ uptake. However, by varying the magnitude of the basolateral-leak conductance in proportion to changes in pump rate, cells in renal[35–39,56,57,79,241,290,561,564] and other transporting epithelia[194] are able to maintain cytosolic K^+ activity, and cell volume, within narrow limits.

Pump-Leak Coupling

Transport-related changes in the coupling between active sodium extrusion across the basolateral membrane and apical and basolateral K^+ conductances are depicted in Figure 49.7a and 49.7b. Changes in cell

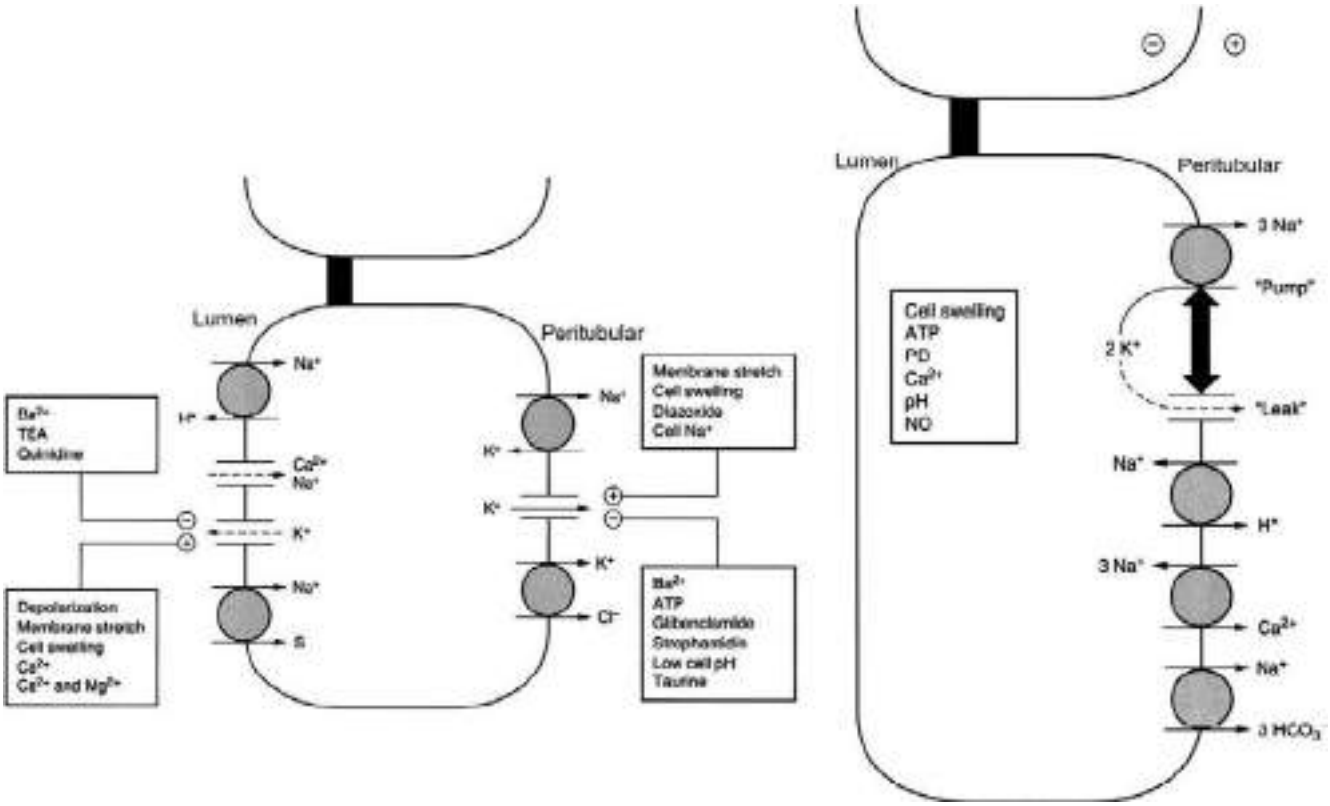

FIGURE 49.6 **Models of proximal tubule cells, including the main transport pathways and the apical and basolateral K^+ channels** (ATP: adenosine triphosphate; TEA: tetraethylammonium; NO: nitric oxide). Left: Model of a proximal tubule cell. Right: Relationship between the activity of basolateral Na,K-ATPase and the leak through K channels. The two-headed arrow indicates linkage between the pump and K channels; as K uptake increases, permeability to K increases, and *vice versa*. Factors that regulate transport pathways (left) and mediate the pump-leak coupling (right) are indicated in individual boxes. Basolateral transporters that may alter these variables are also shown (ATP: adenosine triphosphate). *(From Malnic, G., Bailey, M. A. and Giebisch, G. (2004). Control of renal potassium excretion. In "The Kidney," 7th ed., Vol. 1, 453–496, Brenner, B. (ed.). WB Saunders, Philadelphia, with permission.)*

volume and pH have a significant effect on K^+ channels, alkalosis increasing and acidosis decreasing the open probability.[35,210,282,286,362,446] During substrate-induced stimulation of proximal sodium transport, cell pH rises with a time-course that matches the observed increase in basolateral K^+ conductance.[38]

Changes in the concentration of Ca^{2+} in tubule cells, especially those correlated with fluctuations in cell volume and nitric oxide, may also couple basolateral Na^+, K^+-ATPase activity to K^+ permeability. Alterations in basolateral cell potential have also been implicated, since stimulation of electrogenic Na^+,K^+ pump activity hyperpolarizes tubule cells. Such membrane voltage changes are known to activate voltage-sensitive K^+ channels.[543]

Renal K^+ channel activity, including that of channels in the basolateral membrane of proximal tubule cells,[241,508] is also sensitive to alterations in cellular ATP.[35,36,508] Small amounts of ATP are required for the activity of some K^+ channels in the renal tubule, but millimolar concentrations inhibit K^+ channel activity. This effect is reversed by ADP,[217] and points to the involvement of the ATP/ADP ratio in the control of K^+ channel activity. It appears that transport-related changes in cell ATP levels modify cell K^+ conductance. Thus, stimulation of sodium transport in proximal tubules results in a significant fall in cell ATP, whereas inhibition of sodium transport increases cell ATP levels. This cross-talk mechanism, linking apical sodium transport to basolateral K^+ channel activity, is shown in Figure 49.7.[241,508,561] Thus, transport-related changes in the basolateral membrane potential of tubule cells may be involved in coupling the K^+ conductance to the pump activity. Measurements of the basolateral conductance of tubule cells,[233] as well as patch-clamp studies, in which the open probability of basolateral K^+ channels was examined as a function of the membrane potential,[343] show an increase in K^+ conductance with cell hyperpolarization. To the extent that stimulation of basolateral ATPase activity elevates the cell-negative potential, K^+ conductance would also be expected to increase interaction between basolateral and apical membrane transport.

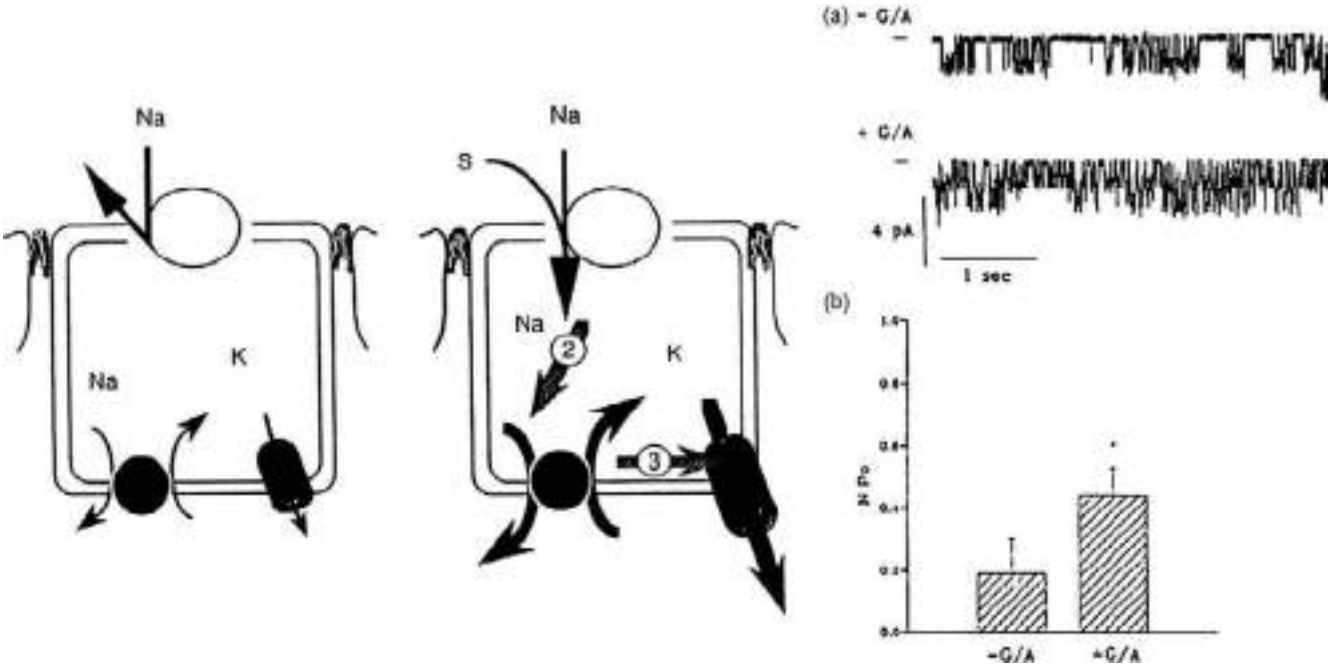

FIGURE 49.7 Left: Coupling between Na^+,K^+-ATPase activity and K^+ recycling in the basolateral membrane of proximal tubule cells.[36,37,198,512] Net rate of sodium transport was stimulated by addition of organic substrates (S; i.e., glucose or amino acid) to the lumen. Thus: (1) apical Na entry via Na-dependent substrate co-transporters is stimulated in the presence of substrates; (2) the Na^+, K^+-ATPase subsequently revs up so that active efflux of Na into the interstitium matches passive apical sodium entry; (3) ensuring that the increased active uptake of K^+ via the Na^+,K^+-ATPase will be efficiently recycled back across the basolateral membrane, K^+ channel activation ensues. *(Kidney Int. 1995; **48**, 1017–1023.)* Right: (A) Patch-clamp analysis of basolateral K^+ channel activity in isolated perfused proximal tubule. Data for experiments before (−) and during (+) perfusion of glucose and alanine (G/A). Horizontal bars indicate zero current. (B) Effect of luminal addition of glucose and alanine on single-K channel open probability (NP_o). $p < 0.02$. *(Am. J. Physiol. Renal 1993; **264**, F760–764.)*

Schultz has drawn attention to an additional relationship between transport events in the luminal and basolateral membrane of epithelial cells that involves changes in the pump-related K^+ conductance.[453,454] In leaky epithelia, such as the proximal tubule, stimulation of co-transport of sodium ions with organic solutes such as glucose or amino acids augments sodium entry across the apical membrane. Since the co-transporter carries positive current into the cell, the cell-negative electrical potential is reduced.[518] In tight epithelia, such as the CCD, mineralocorticoids increase apical sodium conductance, and thus bring about depolarization of the apical cell membrane.[64,65,275–277,356,358,361] The increase in K^+ conductance that occurs with stimulation of sodium pumping across the basolateral membrane also provides an important transport-sustaining feedback loop. The rise in potassium conductance hyperpolarizes the basolateral membrane and renders net transport more effective. An essential feature of these effects is that maneuvers that increase sodium transport tend to curtail further sodium entry, because the depolarization of the apical cell membrane reduces the electrochemical driving force for further sodium transport into the cell.

Loop of Henle: K^+ Recycling, Direction, Magnitude, and Mechanism of Transport

In vivo micropuncture and microperfusion studies show net reabsorption of K^+ between the last accessible segment of surface proximal tubules and the first accessible segment of surface distal tubules.[101,249,250,252,511–513] Thus, only a modest fraction, some 5–10% of the filtered K^+, reaches the early distal tubule (see Figure 49.4). As shown in Figure 49.3, this portion of the nephron comprises several morphologically and functionally distinct segments: the third segment of the proximal tubule (S3); the thin descending and thin ascending limbs; and the medullary and cortical thick ascending limbs of the loop of Henle.

The K^+ concentration in the loop of Henle fluid near the tip of the papilla can be as much as 10 times higher than the K^+ concentration in systemic plasma.[101,108,248–252] de Rouffignac and Morel[101] suggested that K^+ is added to tubule fluid along the descending limb of Henle's loop after being absorbed from the ascending limb and collecting duct. The phenomenon constitutes K^+ recycling (Figure 49.8). Jamison and coworkers further showed that K^+ delivery to the end of

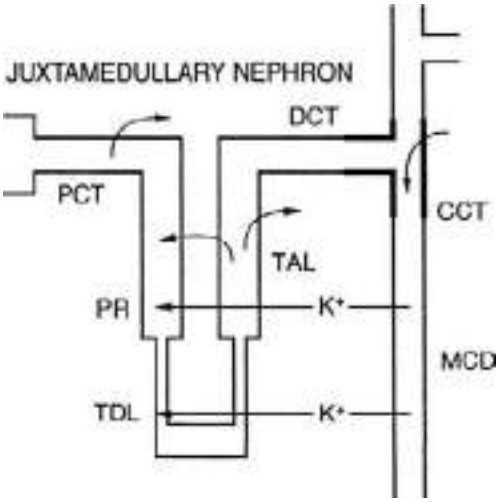

FIGURE 49.8 **Sites of K^+ movement into and out of the nephron.** The diagram emphasizes the movement of K^+ from the collecting ducts to the descending limbs of the loop of Henle via the medullary interstitium (CCT: cortical collecting tubule; DCT: distal convoluted tubule; MCD: medullary collecting duct; PCT: proximal convoluted tubule; PR: pars recta; TAL: thick ascending limb; TDL: thin descending limb). *(Field, M. J., and Giebisch, G. (1989). Mechanisms of segmental potassium reabsorption and secretion. In "The Regulation of Potassium Balance," 139–156, Seldin, D. W., and Giebisch, G. (eds.). Raven Press, New York, with permission.)*

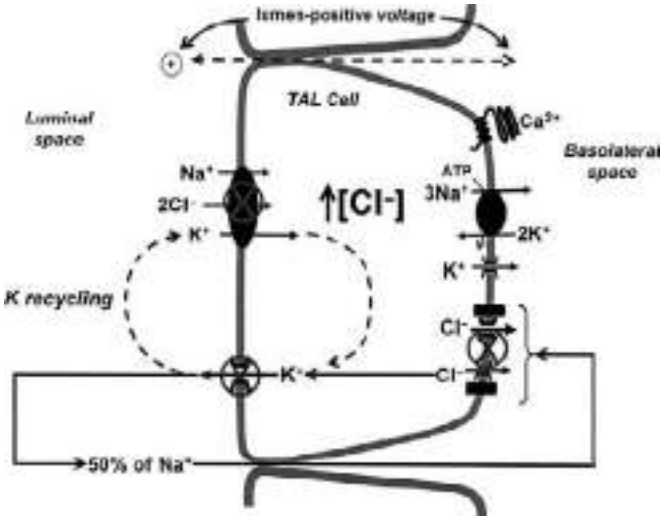

FIGURE 49.9 **Model of a thick ascending limb cell, including the main transport pathways and the apical and basolateral ion channels.** Potassium may also leave the cell across the basolaterall membrane by KCl co-transport (not shown). Note that the lumen-positive transepithelial potential difference drives cation reabsorption through the paracellular pathway (AA: arachidonic acid; ATP: adenosine triphosphate; CaR: extracellular calcium-sensing receptor; cGMP: cyclic guanonine monophosphate; 20-HETE: 20-hydroxyeicosatetraenoic acid; NO: nitric oxide; PKA: protein kinase A; PKC: protein kinase C; TALH: thick ascending limb of Henle; V_2: receptor for arginine vasopressin). *(From Malnic, G., Bailey, M. A. and Giebisch, G. (2004). Control of renal potassium excretion. In "The Kidney," 7th ed., Vol. 1, 453–496, Brenner, B. (ed.). WB Saunders, Philadelphia, with permission.)*

the descending limb of deep nephrons could equal the rate of K^+ filtration in normal rats,[252] and exceeded it in rats either fed a high-K^+ diet[32] or infused acutely with K^+.[15] The observation that isolated thin limbs of Henle lack a mechanism of active K^+ secretion[245,246] supports the view that K^+ enters the descending limb passively. If K^+ is also secreted into the proximal straight tubule of superficial nephrons,[552,578] and the delivery of K^+ to the DCT of deep nephrons is substantially less than the filtered quantity, then K^+ must be reabsorbed by ascending limbs in both populations of nephrons. Thus, K^+ is trapped in the medulla by countercurrent exchange between the ascending and descending limbs of the loop of Henle. Studies of isolated TAL perfused *in vitro* show that these segments are capable of absorbing K^+.[74]

As originally postulated by Jamison et al.[249] and shown in Figure 49.8, the main pathway by which K^+ can reach the renal medulla is absorption from the medullary collecting duct. Stokes[483–485] has shown that the outer medullary collecting duct is adequately permeable to both sodium and K^+, and therefore could permit K^+ reabsorption to occur passively. K^+ secretion by cells of the distal tubule and the cortical collecting duct into the tubular fluid provide the source of K^+ that accumulates in the renal medulla. Accordingly, more K^+ recycles with stimulation of secretion, whereas suppression of secretion attenuates the deposition of K^+ in the renal medulla. Thus, K^+ is secreted into tubule fluid in (at least) two sites along the nephron (see Figure 49.8), first into a proximal part of the nephron (the end-proximal tubule and descending limb), and second into a more distal region (the CT and CCD). When K^+ intake is suddenly increased after a period of K^+ deprivation, renal K^+ excretion, distal K^+ secretion, and K^+ recycling[110,129,130,214,223,249,494] all increase. Stokes also proposed that rising medullary K^+ concentrations inhibit NaCl and water absorption by the loop of Henle, and thus increase the flow rate and sodium concentration of fluid entering the distal tubule, providing optimum conditions for the distal segments to secrete K^+.[484] Medullary recycling is thus responsible for maintaining high concentrations of K^+ in the renal medulla. Such trapping of K^+ is also expected to limit reabsorptive loss of K^+ from the terminal collecting ducts.[579]

Thick Ascending Limb (TAL) Cell Transport Mechanisms

Studies of isolated mammalian TALs and amphibian (*Amphiuma*) early distal tubule have provided similar K^+ transport models (Figure 49.9). The primary driving

force for net K^+ reabsorption is again ATP-driven active Na^+-K^+ exchange across the basolateral membrane, which generates the steep sodium gradient for the entry of Na^+ across the apical cell membrane.

Apical Membrane

Entry of Na^+ is primarily mediated by an $Na^+ - 2Cl^- - K$ (or under certain conditions, Na,Cl) co-transport mechanism inhibited by the potent "loop" diuretics.[74–76,201–204,218,251,363,365–367,444] Also present in the apical membrane is a second pathway for sodium entry into cells, the Na-H exchanger (not shown in Figure 49.9). Conductive pathways for K^+ are found in both the apical and basolateral membranes.[201–204,218–220,363,365] The K^+ concentration gradient across the apical membrane favors K^+ secretion, which permits recycling of K^+ ions back to the tubule lumen. This back-diffusion provides a continuous luminal supply of K^+ for co-transport with sodium and chloride. The K^+ leak in the luminal membrane is also responsible for net K^+ secretion under those conditions in which the activity of the reabsorptive co-transport mechanism has been impaired.

Evidence supporting the operation of the $Na^+ - 2Cl^- - K^+$ co-transporter in the apical membrane includes the mutual dependence of these ions for transport. Net reabsorption of Na^+, K^+, and Cl^-, and the lumen-positive potential are abolished in the luminal absence of any of the three ions.[198,200–204] In addition, luminal application of furosemide also eliminates transport of all three ions, and collapses the transepithelial potential.[76,198,200,201,444] Interference with the co-transport system, either by appropriate luminal ion substitution or by administration of furosemide, lowers cell chloride and sodium activity, thereby supporting the view that the co-transport system is the main apical pathway for entry of these ions into the cell. Additional evidence for the requirement of a steady supply of luminal K^+ to safeguard $Na^+ - 2Cl^- - K^+$ co-transport in the cortical TAL is the observation that sodium reabsorption decreases sharply following the depletion of K^+ from the lumen or following the administration of K^+ channel-blockers.[537,538] These maneuvers also attenuate tubuloglomerular feedback.[519]

Morphological and electrophysiological criteria suggest the presence of at least two cell types in TALs, each with different permeability properties of the apical and basolateral cell membranes.[243,244,246] In the cortical TAL the K^+ permeability in the apical membrane exceeds that of the basolateral membrane, whereas the converse relationship was observed in the medullary TAL. These permeability differences may be associated with functional disparities, K^+ secretion being the prevalent transport mode in the cortical TAL, and reabsorption in the medullary TAL.[509]

Patch-clamp techniques have identified at least two K^+ channels in the apical membrane that mediate K^+ recycling.[58,217,540,544–547,548] The open probability of these apical K^+ channels is high, and they are inhibited by barium, low cell pH, millimolar concentration of ATP, and protein kinase C (PKC). Cell alkalinization and cyclic AMP, as well as NO and cyclic GMP, stimulate K^+ channels. Apical K^+ channels are also activated by furosemide, an effect mimicking the effects of aldosterone.[362,363,365,368] Aldosterone in amphibian early distal tubules, enhances apical Na-H exchange and alkalinizes cell pH. When furosemide is given, apical sodium entry is blocked and the intracellular sodium concentration decreases. As a consequence, the driving force for apical Na-H exchange increases and alkalinizes the cytoplasm. Because apical K^+ channels are stimulated by cell alkalinization, their activity increases.[362,363] This sequence of events explains why the full expression of the aldosterone effect on K^+ permeability depends on an intact Na-H exchange in the apical cell membrane.

A difference between the transport modes of cortical and medullary TAL segments has also been observed regarding the K^+ sensitivity of the apical co-transporter to K^+. Figure 49.10 shows two cell models in which vasopressin switches the apical sodium chloride transporter from a K^+-insensitive mode to one that depends critically on the presence of K^+ in the tubule lumen.[496a]

An interesting effect concerns the sequence of events following an increase in peritubular Ca^{2+}, which has been shown to inhibit both apical K^+ channels and $Na^+ - 2Cl^- - K^+$ co-transport.[217] Patch-clamp studies have demonstrated that the inhibitory effects of Ca^{2+} are mediated through activation of P450 and PKC.[539–542,546,547] It is likely that the extracellular Ca^{2+} ion-sensing receptor (CaSR) present on the basolateral membrane of the TAL[404,405] plays a role in this response. The CaSR is a G-protein-coupled surface receptor that is activated by increases in extracellular Ca^{2+} ion concentrations,[69] and has been shown to inhibit NaCl absorption and K^+ channels in the TAL by eicosanoids and P450 metabolites.[85,172]

Basolateral Membrane

As summarized in Figure 49.9, the basolateral membrane of TAL cells permits diffusion of both K^+ and chloride; however, the chloride conductance is dominant.[198,202,218,540] In addition to the K^+ conductance, $K^+ - Cl$ and the K^+-HCO_3^-[300] co-transport provide additional pathways for K^+ movement from cell to interstitium. Patch-clamp studies have defined a sodium-sensitive K^+ channel in the basolateral

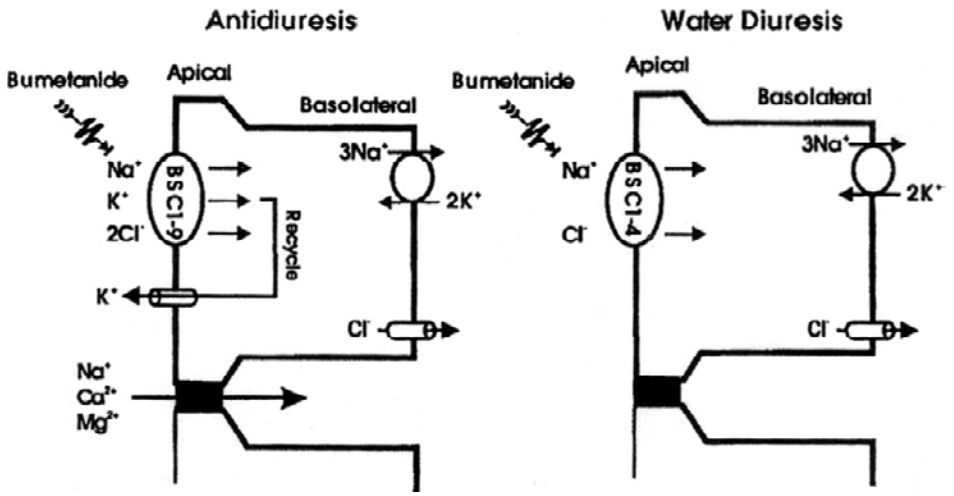

FIGURE 49.10 **Proposed model for thick ascending limb (TAL) function.** (a) Operation during water conservation. (b) Operation during maximal water diuresis. *(Am. J. Physiol. Renal 2001; **280**, F574–F582.)*

membrane.[383] These channels are stimulated by high cell sodium concentrations, providing coupling mechanisms between apical sodium uptake and basolateral ATP-dependent K^+ recycling. The Cl^- concentration gradient across the basolateral membrane favors diffusion of chloride from interstitium into the cell. Thus, both the luminal K^+ conductance and the basolateral Cl^- conductance tend to generate diffusion potentials oriented with the cell interior negative to the extracellular fluids. Because the K^+ concentration gradient across the apical membrane exceeds the Cl^- concentration gradient across the basolateral membrane, the voltage across the apical membrane exceeds the voltage across the basolateral membrane. These unequal electrical potential differences arranged in series generate a lumen-positive transepithelial voltage, which provides a driving force for reabsorption of K^+ and other cations by passive diffusion through the paracellular shunt pathway. The magnitude of passive paracellular K^+ reabsorption is difficult to assess because the transepithelial electrochemical gradient for passive K^+ reabsorption along the cortico–medullary axis is poorly defined.

Overall K^+ reabsorption along the loop of Henle is the result of two opposing events: secretion into the descending limb of Henle's loop as a consequence of K^+ recycling (see Figure 49.8); and K^+ reabsorption along the TAL of Henle's loop. Stimulation of K^+ secretion into the descending limb and enhanced delivery to the tip of Henle's loop have been demonstrated during K^+-loading by puncture of juxtamedullary nephrons.[249,250]

Several factors modulate K^+ reabsorption along the loop of Henle.[511,512] K^+ reabsorption is enhanced by restricting dietary K^+ intake, provided a constant load of fluid and K^+ is delivered into the loop of Henle; administration of a high-K^+ diet has the opposite effect.[511] Reabsorption of K^+ in perfused loops of Henle is stimulated by aldosterone R6TS.[107,465,468,473] However, no reduction in the rate of K^+ transport was observed in studies of perfused thick ascending limbs isolated from adrenalectomized animals.[577] Several factors modulate K^+ recycling and delivery into the distal tubule. Recycling of K^+ between the collecting duct and the descending limb of Henle's loop is enhanced following aldosterone administration in adrenalectomized animals.[223] Calcitonin reduced medullary recycling by inhibition of K^+ secretion into the distal tubule,[130] whereas vasopressin had the opposite effect.[129] Urea recycling increases delivery of fluid to principal cells and stimulates K^+ secretion.[214] Because ammonium ions may substitute for K^+ ions on the apical $Na^+ - 2Cl^- - K^+$ co-transport site, hyperkalemia may inhibit ammonium accumulation in the renal medulla and impede its translocation into the collecting tubule.[121,122]

The amphibian diluting segment normally reabsorbs K^+, but it may secrete K^+ following K^+-loading,[364] administration of loop diuretics,[363,365] alkalinization of the peritubular fluid[436] or administration of aldosterone.[545,567] Aldosterone stimulates both cell K^+ uptake and release into the lumen, an effect that is reversed by exposure to amiloride.[516] Acidosis inhibits the Na-K pump, as well as the K^+ channel.[196,199,209] In contrast, alkalosis stimulates both pump-mediated uptake of K^+ into cells, and passive K^+ efflux from the cells of the diluting segment.[210] Apical K^+ channel activity also increases with cell volume.[210]

Reversal of the direction of K^+ transport, from reabsorption to secretion, frequently follows administration

of loop diuretics. Free-flow micropuncture and loop perfusion studies[234,341] in the mammalian kidney, as well as perfusion of the amphibian diluting segment, show sharply reduced rates of K^+ reabsorption or reversal to net K^+ secretion following the inhibition of the apical $Na^+ - 2Cl^- - K^+$ co-transporter by furosemide,[74,76,511,512] torasemide,[512] ethacrinic acid,[75] and bumetanide.[512,523,524] The secretion of K^+ is the consequence of unopposed K^+ diffusion from the cell into the lumen.

Several experimental studies show that vasopressin enhances net sodium, chloride, and K^+ transport across the thick ascending limb of Henle.[218,220,319] Vasopressin action increases basolateral chloride permeability and accelerates chloride extrusion into the peritubular fluid. Vasopressin also enhances the affinity of the apical co-transporter for K^+ and augments the apical K^+ permeability. This increase in permeability speeds up apical membrane recycling of K^+ and stimulates $Na^+ - 2Cl^- - K^+$ co-transport. Loss-of-function mutations of the apical ROMK K^+ secretory channel can lead to Bartter's syndrome. Interference with recycling of K^+ ions in the apical membrane accounts for diminished sodium and K^+ reabsorption, and explains the urinary loss of sodium and K^+, hypokalemia, and high levels of aldosterone observed in this genetic disorder.[20,218]

Two mechanisms by which inhibition (or absence) of apical K^+ channels curtails sodium chloride and K^+ reabsorption in the TAL[20] are summarized in Figure 49.9. First, diminished K^+ recycling across the apical membrane lowers the turnover rate of $Na^+ - 2Cl^- - K^+$ co-transport. Second, the drastic reduction of the lumen-positive potential compromises the main driving force for passive movement of sodium through the paracellular pathway. Current flow across the basolateral membrane is largely carried by chloride ions which normally leave the cell along a favorable electrochemical gradient through chloride channels. Interference with such chloride exit from the cell is expected to increase its cell concentration and diminish apical activity of $Na^+ - 2Cl^- - K^+$ co-transport. This is illustrated in Bartter's Syndrome types 3, 4A, and 4B, in which either the basolateral chloride channels (CLCKA, CLCKB) or Barttin (BSDN) are mutated.[217]

DISTAL CONVOLUTED TUBULE CELL: DIRECTION, MAGNITUDE, AND MECHANISM OF TRANSPORT

The main pathways contributing to K^+ transport by DCT cells are shown in Figure 49.11. Two conductive pathways in the basolateral membrane allow for K^+ and Cl^- exit. K^+ is also able to exit the cell across the apical membrane, primarily through a K—Cl co-transporter, and, in some preparations, barium-sensitive K^+ channels.[590] The predominant path for sodium entry from the lumen is a Na—Cl co-transporter (slc12a3) that is blocked by thiazide diuretics, but not inhibited by bumetanide.[95,134,135,522–525] Amiloride-sensitive sodium channels may also be present in the apical membrane.[590] The junctional complexes between cells are cation-selective, and may permit diffusion of Na^+ and K^+ through the paracellular pathway from interstitium to lumen.

Evidence for the apical K-Cl co-transporter has come from microperfusion studies in rats.[134,135,522–525] K^+ secretion in this segment is increased when the luminal concentration of either K^+ or chloride is decreased. This increase in K^+ secretion occurs without a change in transepithelial voltage, and is not blocked by barium. Recirculation of chloride ions across the apical membrane is an important element of the mechanism of such K^+ secretion, particularly when luminal chloride concentrations are kept low by the administration of poorly-reabsorbable anions such as SO_4.[526] Under such conditions, thiazide diuretics, by blocking apical chloride entry via NaCl co-transport, inhibit K^+ secretion, consistent with K^+ ions entering the lumen by an electroneutral K-Cl co-transport mechanism.

Single channel analysis has demonstrated the presence of K^+ channels that modulate Na^+ and fluid reabsorption in this nephron segment (Figure 49.12). Of special interest is the function of KCNJ 10 Kir4.1 (KCNJ10), which provides an important pathway for basolateral K^+ recycling, especially by heteromerization with KCNJ 10 (Kir5.1).[287] This heteromeric complex is inhibited by low cell pH, and by activation of

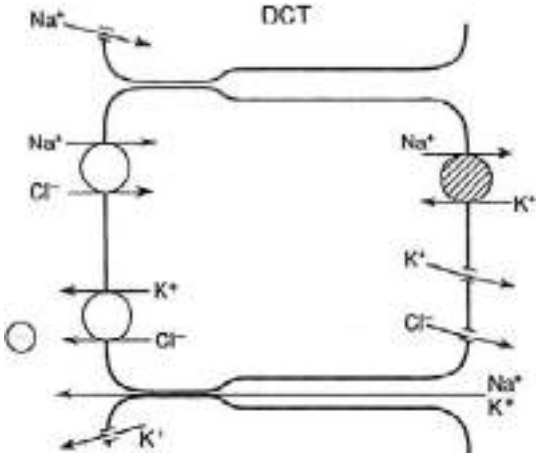

FIGURE 49.11 Model of distal convoluted tubule (DCT) cell. Some observations point to a lack of conductive pathways (channels) in the apical membrane; other studies have found evidence for Na and K conductances.

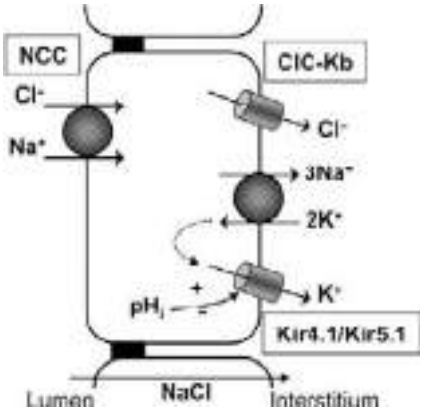

FIGURE 49.12 **Basolateral transport mechanisms in connecting tubule cells.** Note pH-sensitive K channels in the basolateral membrane. *(From ref. [24].)*

Ca^{2+} receptors.[24,287] Genetic dysfunction of this basolateral K^+ channel complex leads to salt-wasting due to diminished basolateral Na/K-ATPases activity, which results in high cell Na and a reduced driving force for passive Na entry across the apical membrane.[383a,401a]

Connecting Tubule and Cortical Collecting Duct Cells: Direction, Magnitude, and Mechanism of Transport

Two morphologically and functionally distinct cell types – principal cells and intercalated cells – determine K^+ transport in these segments, and play a major role in determining the magnitude of final urinary K^+ excretion (Figure 49.13). Principal cells, the most numerous cells in the initial collecting tubule (ICT), connecting tubule (CNT), and the cortical collecting duct (CCD) secrete K^+,[144–149,319–324,379–382,385,464,474] and are the cells subject to the most important regulatory influences. The less numerous intercalated cells also secrete K^+, but are capable of active K^+ reabsorption under certain conditions (dietary K^+ restriction) via an apical ATP-dependent electroneutral transport mechanism that mediates hydrogen ion secretion in exchange for K^+ reabsorption.[91,112,117,138,279,457–460,571,572]

K^+ Secretion

Figures 49.13–49.15 show the processes contributing to K^+ transport in the late DCT, CNT, and CCD. As pointed out above, the late distal convoluted tubule and collecting duct play a key role in K^+ homeostasis, but significant aldosterone-sensitive sodium reabsorption and K^+ secretion also occurs along the CNT. Collecting tubule K^+ secretion appears to become physiologically important whenever transport in the CNT is compromised or its transport capacity overwhelmed during ingestion of a high-K^+ diet.[416,560] Theoretical analysis, based on known morphology and transport parameters, has also supported the importance of CNT-mediated K^+ transport in maintaining K^+ homeostasis.[560]

Figure 49.13 summarizes the main transport processes mediating K^+ secretion in principal (and intercalated) cells. K^+ uptake across the basolateral membrane is again coupled to active sodium extrusion by the Na^+, K^+-ATPase, and provides for coupling between transepithelial sodium reabsorption and K^+ secretion. From the rapid depolarization of the basolateral membrane voltage caused by addition of ouabain to the peritubular bathing solution, it has been concluded that the Na–K^+ exchange pump operates in an electrogenic fashion, particularly following stimulation by desoxycorticosterone (DOC) treatment.[275,276,424,425,436] The basolateral pump responds to several stimuli known to modulate net K^+ transport, such as acid–base disturbances, changes in plasma K^+, and mineralocorticoid hormones.[175,176,184,185,187,276,312,314,356,360,424–427,465–469] Figure 49.13 also indicates the presence of a K^+ conductance in the basolateral membrane which, along with

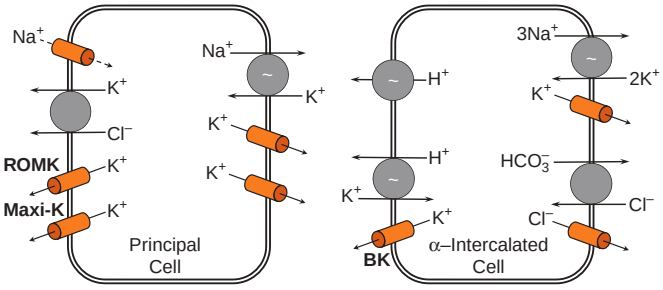

FIGURE 49.13 **Model of principal and intercalated cell, including apical and basolateral transport pathways.** Transcellular Na absorption proceeds through apical Na^+ channels and the basolateral Na^+-K^+ pump. K^+ secretion depends on K^+ uptake by Na^+-K^+ pump and movement through apical K^+ channels or K^+-Cl^- cotransporter. In intercalated cells, K is actively reabsorbed in the apical membrane by K/H-ATPase activity, and leaves cells in the basolateral membrane by K channels.

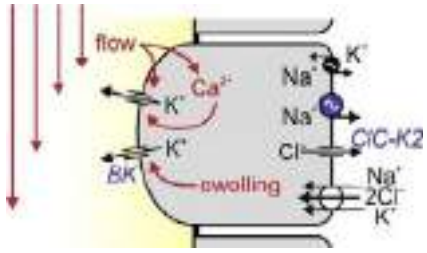

FIGURE 49.14 **Additional basolateral transport mechanisms (Na/2Cl/K transport) in principal and intercalated cells.** Note basolateral Na/2Cl/K transport. This model is consistent with passive paracellular Cl^--secretion.[575]

the high electrochemical gradient for K^+ efflux, is largely responsible for the cell negativity. Stimulation of the electrogenic Na^+-K^+-ATPase by aldosterone may drive the cell negativity to values exceeding the K^+ equilibrium potential, and reverse the direction of K^+ movement through basolateral K^+ channels (see section on adrenal steroids). Microperfusion studies in isolated CCDs have also identified a significant contribution of bumetanide-sensitive K^+ entry across the basolateral membrane of both principal and intercalated tubule cells (Figure 49.14).[310] Such K^+ transport, mediated by Na-K-2Cl co-transport (Slc12a2), is stimulated by high flow rate, and contributes to the well-established increase in K^+ secretion through BK (or maxi-K) channels.[574,575]

The apical membrane has both sodium and K^+ conductances. The sodium concentration gradient between lumen and cell favors diffusion of sodium ions into the cells, reducing the cell-negative voltage across the apical membrane relative to the voltage across the basolateral membrane. This asymmetrical electrical polarization of the apical and basolateral membranes favors diffusive movement of K^+ from cell to lumen, and is the source of the lumen-negative transepithelial potential difference which favors diffusive movement of K^+ from cell to lumen.

FIGURE 49.15 **Expression patterns of sodium and potassium transport systems and of their regulatory proteins along the distal convoluted tubule (DCT), connecting tubule (CNT), and cortical collecting duct (CCD).** In rat, mouse, and human, the sodium-chloride co-transporter (NCC) characterizes the DCT and co-localizes in the late DCT with the epithelial sodium channel (ENaC), which is also expressed in the CNT and CCD. The inwardly rectifying potassium channel (ROMK) and Na,K-ATPase are localized, respectively, in the apical and basolateral membrane along the aldosterone-sensitive distal nephron. Note that the expression of some regulatory proteins is restricted to the DCT and CNT, and does not extend to the CCD (MR: mineralocorticoid receptor; 11β-HSD2: 11β-hydroxysteroid dehydrogenase type 2; Sgk1: serum and glucocorticoid-inducible kinase; WNK4: with no lysine kinase 4; WNK1s: kidney-specific form with no lysine kinase 1; KLK1: tissue kallikrein). *(From Meneton, P., Loffing, J., and Warnock, D. G. (2004). Sodium and potassium handling by the aldosterone-sensitive distal nephron;the pivotal role of the distal and connecting tubule. Am. J. Physiol. Renal* ***287****, F593–F601; and Pluznick, J. L., Wei, P., Grimm, P. R., and Sansom, S. C. (2005). BK-ß1 subunit: Immunolocalization in the mammalian connecting tubule and its role in the kaliuretic response to volume expansion. Am. J. Physiol. Renal* ***288****, F846–F854, with permission.)*

Sodium entry across the apical epithelial sodium channel (ENaC; see Chapter 7 by Palmer and Sackin) and its electrogenic basolateral extrusion by the Na-K pump play a critical role in regulating apical K^+ transport by their depolarizing effect on the apical membrane potential. In animals fed a normal K^+ diet, K^+ secretion in the CCD is generally dependent on sodium absorption.[155,156,160,161,342,382,489] However, in rats fed a high-K^+ diet for as little as 18 hours, a significant fraction of K^+ excretion becomes amiloride-insensitive, and thus ENaC-independent, an observation consistent with the activation of a non-principal cell-mediated pathway in α-intercalated cells.[161] Diminished K^+ reabsorption in the proximal tubule may further compensate for compromised distal tubule K^+ secretion, as it has been shown that hyperkalemia suppresses proximal fluid and K^+ reabsorption.[67]

The apical membrane voltage of principal cells is depolarized following administration of mineralocorticoids.[179,350,356,359,360] In contrast, amiloride blocks ENaC and hyperpolarizes the apical membrane. The reduction in the driving force for K^+ excretion explains the K^+-sparing effect of this diuretic.[275,357,358,361] The K^+ conductance of the apical membrane is variable and increased by high-K^+ intake,[350,352,356,358,375,376,424–427,437,438,441,443] and vasopressin.[437,438,443] The apical K^+ conductance is reduced by intracellular acidification,[350,472,498] consistent with the K^+-sparing effect of acute acidosis.[470,475] Coupling between basolateral Na^+,K^+-ATPase activity and apical K^+ and sodium channels has also been observed, as evidenced by the coordinated changes of basolateral Na^+-K^+-ATPase activity and apical membrane Na^+ and K^+ conductances.[351]

K^+ Channels in the Aldosterone-Sensitive Distal Nephron (ASDN)

The apical sodium as well as apical and basolateral K^+ channels have been extensively studied by applying the patch-clamp technique to cultured amphibian kidney cells and to cells of isolated mammalian collecting ducts[81,157–161,179,183,187,217,379–382,407,540–548,563] (see also Chapter 47 by Wang and Huang).

Figures 49.15 to 49.17 summarize our present state of knowledge about apical and basolateral K^+ channels in principal and intercalated cells. The apical low-conductance secretory K^+ channel (SK) are highly K^+ selective, and have a high open probability. They are

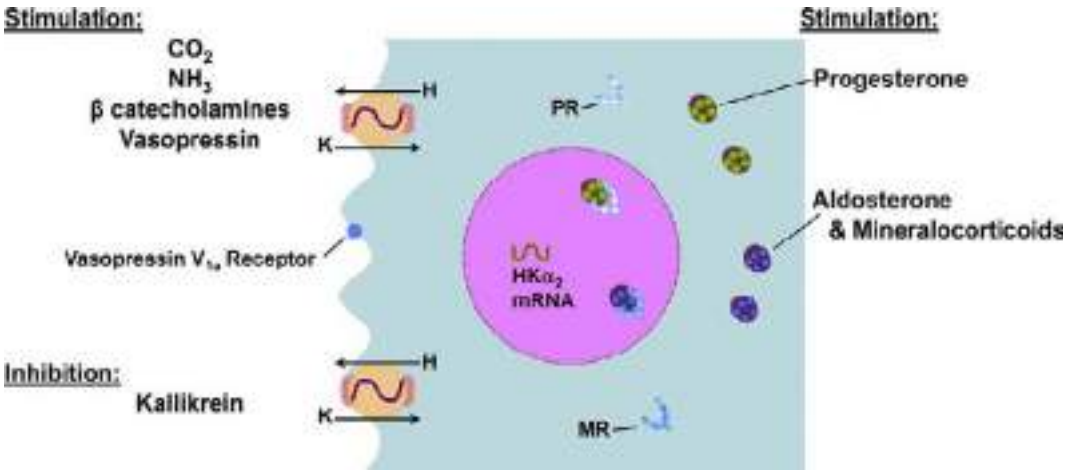

FIGURE 49.16 **Model of acid secreting (A-type) intercalated cells in the ICT and CCD.** These cells are the site of potassium absorption via an H,K-ATPase. Proton secretion is driven by an H-ATPase (not shown). *(Courtesy of Dr. Charles Wingo.)*

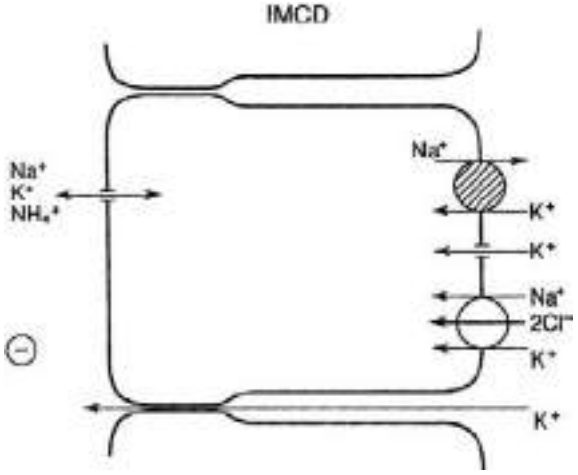

FIGURE 49.17 **Model of inner medullary collecting duct (IMCD) cell.** Apical cation channels are equally permeable to Na^+ and K^+.

stimulated by low concentrations of ATP and cyclic AMP-dependent protein kinase A, as well as by alkalinization of the cytoplasm. They are inhibited by barium, arachidonic acid, Ca^{2+}-calmodulin kinase II, millimolar concentrations of ATP, Ca^{2+}-dependent protein kinase C, and acidification of the intracellular fluid. The channel is sensitive to phosphorylation processes, so that protein phosphatase inhibitors are required to prevent channel "run-down," the decline in channel activity observed following excision of membrane patches. The open probability of the secretory K^+ channel is not markedly voltage-dependent, and Ca^{2+} ions do not directly affect channel activity in excised membrane patches. Increased channel activity is often reflected by recruitment of channels into the active apical membrane pool.[217] The K^+ channel is identical to ROMK (Kir1, KCNJ1), a cloned, inwardly rectifying, low-conductance, ATP-regulated K^+ channel.[157,158,217,227,603]

Whereas the SK/ROMK channel is present solely in connecting and principal cells, high conductance channels with characteristics associated with BK or (maxi-K) channels have been identified in both principal and intercalated cells both functionally,[158,160,195,240,303,385–387,430] and by immunolocalization.[205–208,354] The density of BK channels in intercalated cells exceeds that detected in principal cells in the distal nephron.

The open-probability of BK channels, as defined in split-open, isolated connecting tubules and cortical collecting tubules, is quite low at the resting membrane potential and basal intracellular Ca^{2+} concentration, although their single-channel conductance is about five times that of ROMK.[158,303,377,430,432,440–443] Apical BK channels are activated by membrane depolarization, elevation of $[Ca^{2+}]$, hypoosmotic stress, and/or membrane stretch,[120,160,224,239,377,490,491] and can be selectively blocked by iberiotoxin.[20,78,170] BK channels are generally comprised of pore-forming α-subunit, a member of the *slo* family of K^+ channels originally cloned from *Drosophila*, and a regulatory β-subunit.[17,131]

Cumulative evidence implicates the BK channel in mediating an important fraction of K^+ secretion in the CNT and CCD in response to high urinary flow rates[20,310,386,387,574,575] K^+-loading[20,354,385–387] and application of vasopressin to the lumen fluid,[10] and in the absence of ROMK in Bartter's syndrome.[20] BK channel-mediated K^+ secretion in the CCD is also dependent on a basolateral bumetanide sensitive chloride-dependent transport pathway, proposed to be NKCC1[310] (Figure 49.14). In support of this conclusion is the finding that mice with genetic disruption of NKCC1 exhibit higher serum potassium concentrations, with

inappropriately low urinary potassium excretion, compared to wild-type mice.[334,533]

The density of BK channels in intercalcalated cells exceeds that detected in principal cells in the distal nephron. It remains unsolved as to how intercalated cells maintain a high steady state K concentration for sustained luminal K^+ secretion as there is little immunodetectable[418] and functional[34,44,116,380,434] Na^+-K^+ pump activity in intercalated cells. A K-independent Na-ATPase identified biochemically in kidney[468] and present in CA MDCK may serve as an exit pathway for Na brought in by the apical NBCDE or BL NKCC.

Flow activation of BK channels is associated with an increase in delivery to and reabsorption of Na^+ by the distal nephron.[269,342,574,575] This in turn increases the driving force for passive K^+ efflux by depolarizing the apical membrane potential. High tubular fluid flow rates also lead to an increase in $[Ca^{2+}]_i$, via luminal Ca^{2+} entry and IP3-mediated store release to concentrations sufficient to stimulate Ca^{2+}-sensitive BK channels.[574] It has been suggested that high flow rates along connecting and collecting tubules activates apical Ca^{2+} channels, which in turn stimulate Ca-sensitive maxi-K channels.[574,575]

An unresolved problem concerns the contribution of Ca^{2+}-sensitive BK^+ channels to K^+ secretion under physiological flow conditions. Single channel analysis by patch-clamp techniques is limited to "split-open" tubules in the absence of membrane stretch. This renders evaluation of BK^+ channel activity difficult in conditions mimicking physiological flow rates of tubule fluid.

The basolateral K^+ channels, shown in Figure 49.13, are also K^+ selective. Some are activated by membrane hyperpolarization; all are inhibited by barium. Basolateral K^+ channels are characterized by several factors that distinguish them from their apical homologs.[225,226,315] First, a subpopulation responds to hyperpolarization by increased activity,[543] which contributes to the increase in basolateral membrane K^+ conductance following stimulation of electrogenic Na^+-K^+-ATPase activity. Second, basolateral K^+ channels are stimulated by NO and cGMP.[225,226,315] The evidence for the involvement of NO is the decline in basolateral K^+ channel activity by inhibiting nitric oxide synthase, whereas donors of exogenous NO stimulate these channels. Application of cGMP analogs also activate basolateral K^+ channels, and hyperpolarize the basolateral membrane. This induces an increase in the apical membrane potential through current flow via the paracellular pathway, and stimulates sodium entry across the apical membrane of principal cells.[315] Features shared by these channels are their lack of inhibition by ATP and a biphasic effect of changes in cell Ca^{2+}: whereas low concentrations stimulate basolateral K^+ channels (via activation of cGMP), high levels of Ca^{2+} inhibit K^+ channels.[225,226,315,445]

Apical Co-Transport of KCl

Microperfusion studies of superficial distal tubules in the rat and isolated rabbit CCDs provide evidence for an electroneutral K^+ and chloride co-transport mechanism in the apical membrane,[8,132–135,521–525] also shown in Figure 49.13. The key evidence for this mechanism is that K^+ secretion into the distal tubule is stimulated when the lumen is perfused with solutions with a low chloride concentration. This effect occurs without changes in the transepithelial voltage across the distal tubule wall, and persists in the presence of barium, a K^+ channel inhibitor. K-Cl co-transport may contribute to K^+ secretion when the concentration of chloride in the lumen declines. This may occur with the delivery of poorly reabsorbable anions, such as sulfate, phosphate, and especially bicarbonate into the distal tubule.[8,264] The molecular identity of this KCl co-transporter is not known.

K^+ REABSORPTION

In the distal nephron, intercalated cells mediate K^+ reabsorption (Figure 49.14). They are scattered among the principal cells of the cortical and outer medullary collecting duct, and also among the cells of the distal tubule (infrequently in the distal convoluted tubule, and more commonly in the connecting tubule and initial collecting tubule).[99,255,318] Several types of intercalated cells have been recognized: A-type cells secrete hydrogen ions; and B-type cells secrete bicarbonate ions. A third, "mixed" type, containing both Cl^-—HCO_3^- exchangers in the apical and basolateral membrane, has also been described.[558]

The A-type cells may also be responsible for K^+ reabsorption, as shown in Figures 49.14 and 49.16. Several important differences between intercalated cells and principal cells should be noted. Na^+, K^+-ATPase expression and activity in basolateral membranes of intercalated cells in tubules of the renal cortex is much lower than in principal cells.[258] However, it is possible but not yet proven that lack of this transport is compensated for by a K-independent, ouabain-insensitive Na^+-ATPase.[173,408] Moreover, intercalated cells also have low apical Na^+-conductances, but express large-conductance BK channels.[303,239,377,432]

Several isoforms of K^+-H^+-ATPase, distinguished by variable K^+/Na^+ sensitivities of the exchange processes, and by different sensitivities to inhibitors such as gastric K^+-H^+ blockers and ouabain, are responsible for active K^+ absorption in intercalated cells.[6,112,117,211,457–460,558,571,572] Two types of K^+-H^+-ATPase have been described in rat and mouse

cortical and outer medullary collecting tubules, and they are structurally identical to isoforms of K^+-H^+-ATPases cloned from gastric and colonic mucosa. Their importance is suggested by numerous functional studies.[70,112,117,122] However, a recent study, based on experiments in gastric and colonic K^+-H^+-ATPase knockout mice has provided strong evidence for an as yet unidentified additional transport mechanism for linked K^+ reabsorption and hydrogen ion secretion that is distinct from known K^+-H^+-ATPases.[384a] The importance of this transporter is underscored by its ability to compensate effectively for the loss-of-function of both gastric and colonic K^+-H^+-ATPase. Similar results have also been reported using the mouse cortical collecting tubule. Thus, the contribution of individual K^+-H^+-ATPases and other not-yet-identified transporters to the maintenance of K^+ and hydrogen ion balance is not fully-understood.

Two inhibitors of the gastric K^+-H^+-ATPase, omeprazole and SCH28080, decrease both K^+ absorption and hydrogen secretion in the distal tubule and the outer medullary collecting duct. K^+-H^+ exchange is increased during metabolic acidosis,[404,460] experimental K^+ depletion,[70,112,117,122,457–460,571,572,592] and during administration of a low-sodium diet.[457,458] Increased sensitivity to K^+ depletion was reported in mice lacking the colonic isoform of K^+-H^+-ATPase, although the ability of renal K^+ conservation was quite well-preserved, and most of the loss of K^+ occurred by fecal excretion.[333]

Several factors modulate the activity of apical K-H exchange, and are summarized in Figure 49.16. They include acid–base-related factors such as stimulation by ammonium and CO_2, catecholamines, kallikrein, vasopressin, and adrenal steroids.[571] Moreover, progesterone is also important for effective retention during K^+ deprivation.[125,126] Interference with K-H exchange also compromises effective Na retention.[571]

Morphological studies of the apical cell membrane of intercalated cells in K^+-depleted rats have shown changes in fine structure, such as an increase in the number of rod-shaped particles and amplification of the microplicae.[254–257,481] These alterations in membrane structure are specific for the luminal membrane of intercalated cells. Intercalated cells also undergo marked morphological amplification of their apical membranes following acidification.[110a] These changes suggest that K^+ reabsorption and hydrogen ion secretion are functionally linked.

Medullary Collecting Duct Cells

Several sections of the medullary collecting ducts have been distinguished on the basis of morphological and functional differences. The outer medulla can be grossly separated into outer and inner stripes, and the inner medulla can be subdivided into outer and inner halves. The inner medullary collecting duct is separated into initial and terminal segments. Most of these collecting duct segments participate in the regulation of K^+ excretion.

The medullary collecting duct in the outer stripe resembles the cortical collecting duct. K^+ secretion and sodium reabsorption continue,[485–487] and the cells lining this segment have morphological and functional properties similar to principal and intercalated cells.[255]

The collecting duct in the inner stripe is characterized by a different transport pattern. K^+ secretion is absent when isolated tubule segments are perfused with symmetrical solutions, and the apical cell membrane lacks significant K^+ conductance.[464] However, when transepithelial K^+ gradients are applied, significant K^+ movement occurs, presumably via the paracellular transport route.[459,464,570] K^+ depletion increases the passive K^+ permeability.[464] The generation of electrical potentials also activates passive K^+ movement. For instance, a lumen-positive potential, generated by electrogenic hydrogen ion secretion, induces signficant K^+ reabsorption. This coupling between K^+ and hydrogen movement may explain why augmented proton secretion is frequently associated with enhanced K^+ reabsorption.

An active K^+-hydrogen exchange mechanism has also been detected in collecting ducts isolated from the inner stripe of the outer medulla in K^+-depleted rabbits. Activation of this transporter also contributes to the stimulation of K^+ reabsorption and hydrogen ion secretion that is observed in K^+ depletion.[569]

Both reabsorption and secretion of K^+ have been observed in the inner medullary collecting duct. Figure 49.17 summarizes some of the known transport properties of inner medullary collecting duct cells.[410] An important feature of inner medullary collecting duct cells is a nonspecific cation channel in the apical membrane.[305] Depending on the apical transmembrane electrochemical driving forces, this channel may mediate both sodium reabsorption and K^+ secretion. At very high lumen K^+ concentrations, passive reabsorption of K^+ may also take place. The presence of a furosemide-sensitive Na^+-2Cl-K^+ co-transporter in the basolateral membrane of inner medullary collecting duct cells has also been reported.[90a,209,410]

CONTROL OF RENAL K^+ TRANSPORT

General Aspects of Regulation of Renal K^+ Transport

Figure 49.18 illustrates the difference between two distinct K^+ mechanisms involved in renal K^+

homeostasis. First, feedback control of K^+ excretion depends on changes in plasma K^+ concentration which, either directly or by modulating aldosterone release, alters renal K^+ secretion. A second mechanism, feed-forward control of K^+ excretion, depends on the local increase of K^+ concentration in the gastrointestinal tract, the liver, and possibly the cerebral circulation.[591] Such feed-forward control of extracellular K^+ homeostasis minimizes changes of plasma K^+ concentrations, and may account for the rapid response of the kidney to changes in gastrointestinal K^+ uptake.[89,369,591] The nature of the intestinal and cerebral K^+ receptor and the signaling mechanisms effecting changes in renal K^+ excretion are not known. Attention should also be drawn to evidence that the central nervous system participates in controlling renal K^+ excetion. Examples include the rapid increase in K^+ excretion following unilateral nephrectomy, diurnal fluctuations of K^+ excretion, and aldosterone-independent changes in K^+ balance in hypo- and hyperkalemic conditions.[392–397] Figure 49.19 summarizes known agents modulating K^+ secretion.

Proximal Tubule

The proximal tubule is the main site of K^+ reabsorption, but does not play an important role in the physiological regulation of K^+ excretion.[179] K^+ transport is largely dependent on sodium and fluid movement, and changes with variations of proximal tubule sodium and fluid reabsorption. Increased delivery of K^+ into the loop of Henle occurs during osmotic diuresis and inhibition of proximal tubule sodium and fluid transport.

Secretory potassium entry into the proximal straight tubule has been reported[250,252] (Figure 49.8). Such secretory transport has been demonstrated *in vitro*,[260,261] but it is likely that modest K^+ secretion also occurs *in vivo*. Given the increase in medullary K^+ concentration along the corticomedullary axis, K^+ ions may enter the tubule lumen by diffusion as part of the process of medullary recycling.[248,249]

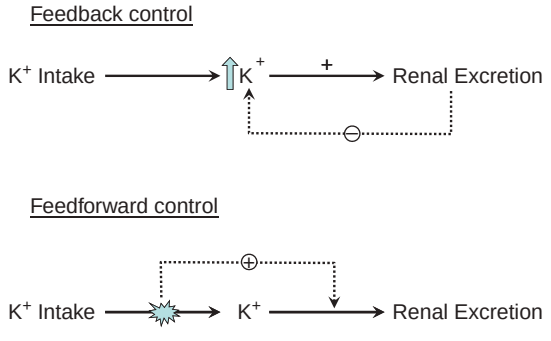

FIGURE 49.18 **The main control mechanisms safeguarding K homeostasis.[591]**

Thick Ascending Limb of Henle, Distal Convoluted Tubule, Connecting and Collecting Tubules

The TAL normally reabsorbs a significant fraction of filtered and recycled K^+. However, reabsorption may be significantly reduced or even replaced by net secretion, following inhibition of Na-2Cl-K co-transport or interference with apical K^+ recycling.[20,217,512] Diminished reabsorption of K^+ in the TAL may thus contribute to enhanced urinary excretion whenever TAL function is compromised.[20,234]

Modest rates of K^+ secretion have also been observed along the mammalian DCT, but changes in tubule flow rate and dietary K^+ intake do not affect K^+ secretion.[451] *In vivo* micropuncture and microperfusion experiments indicate that the DCT is the main site of action of thiazide diuretics.[94,95,522–525] An interesting relationship between sodium chloride and K^+ transport has been observed in microperfusion experiments. When apical sodium entry was stimulated by raising the Na concentration in the tubule lumen, K^+ secretion increased. It is likely that enhanced chloride entry increased cell chloride and stimulated K-Cl co-transport from cell to lumen.[521] Thus, recycling of chloride appears to play a significant role in K^+ secretion in DCT cells.

The CNT, ICT, and CCD are the main nephron sites that control K^+ excretion.[177–186,465,470,473,474,483–487,579–583,585] Information on the transport function of the ICT has been obtained by either free-flow or *in vivo* microperfusion studies. The CCD has also been investigated by *in vitro* microperfusion techniques. These tubule segments are distinguished by marked cell heterogeneity, and net transport of K^+ results from varying components of secretion and reabsorption of K^+. The most important systemic changes that affect these factors include K^+ intake, adrenal steroids, salt and water balance, and acid–base balance. Figure 49.19 summarized the main factors modulating K_r transport in DCT, CNT, and CCD.

Changes in K^+ Intake

Both increases and decreases in K^+ intake, as well as acute loading with K^+-containing fluids, initiate appropriate adjustments in renal K^+ excretion. Increases in K^+ intake tend to raise plasma K^+ concentration, which both affects the kidney directly and stimulates the adrenal glands to secrete aldosterone.[31,66,118] Decreases in K^+ intake or losses of K^+ that exceed intake tend to reduce total body K^+ content, plasma K^+ concentration, and aldosterone secretion.

K^+-Loading

Potassium secretion along the ICT rises sharply with parenteral administration of K^+-containing solutions.[179,182,185,473,474,491,579,583,585] The stimulation of K^+ secretion after acute K^+-loading has been demonstrated in both free-flow and microperfusion studies. Factors contributing to increased rates of secretion include increases in plasma K^+,[474,593] aldosterone levels,[66,118,145–147,166,482,487,585] and distal flow rate.[179,266,285,319,322] The independent and separate effects of these variables have been explored in microperfusion experiments in which flow rate, luminal ion concentrations, and the levels of both mineralocorticoids and glucocorticoids could be controlled.[121,123,154,155,416] Chronic K^+-loading increases the secretory capacity of the distal nephron so that at a given plasma K^+ level, renal K^+ excretion is significantly accelerated.[2,48,49,50,52,345–348,466] Figure 49.20 illustrates relationships between plasma K^+ concentration and either renal K^+ excretion or distal K^+ secretion in control animals, and in animals fed a high-K^+ diet, and Figure 49.21 provides an overview of the cell messengers involved. Pretreatment with the high-K^+ diet leads to powerful stimulation of K^+ secretion and a more rapid onset of kaliuresis.[228,352,585] This stimulation of K^+ secretion at normal or only slightly elevated plasma K^+ levels following chronic elevation of K^+ intake is a clear example of an adaptive change in renal function, and occurs even when plasma aldosterone is kept constant.[352] Full adaptation, though, does require an increase in mineralocorticoid levels.[140–147,381,382] Along with an enhanced rate of K^+ uptake by nonrenal cells,[7,53] the increased secretory capacity of distal tubule cells promotes K^+ tolerance – the ability of animals fed a high-K^+ diet to survive an acute K^+-load that would otherwise be fatal. As summarized in Figure 49.22, elevation of plasma K^+ also inhibits proximal fluid absorption, thereby increasing the delivery of fluid and Na into the distal nephron.[67]

A further example of K^+ adaptation is the ability of a reduced number of nephrons – such as in chronic renal failure – to sharply increase K^+ secretion and to maintain K^+ balance.[176] In addition to aldosterone, angiotensin II also increases ROMK activity, but only in animals fed a high-K diet.[556] A high-K diet increases not only the apical surface expression of ROMK, but also that of ENaC and of BK channels in both principal and intercalated cells in the CCD.[157] In contrast, NaCl co-transport expression in distal convoluted tubules was found to be decreased. Such redistribution of sodium reabsorption from NCC to nephron sites

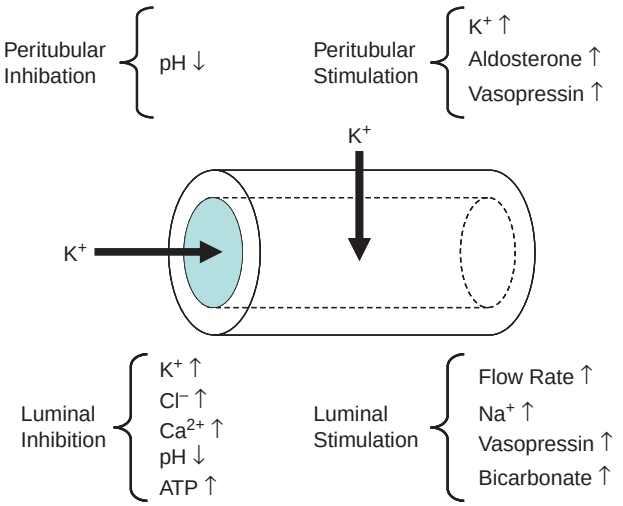

FIGURE 49.19 **Summary of luminal and basolateral factors modulating K transport in connecting and collecting tubule cells.**

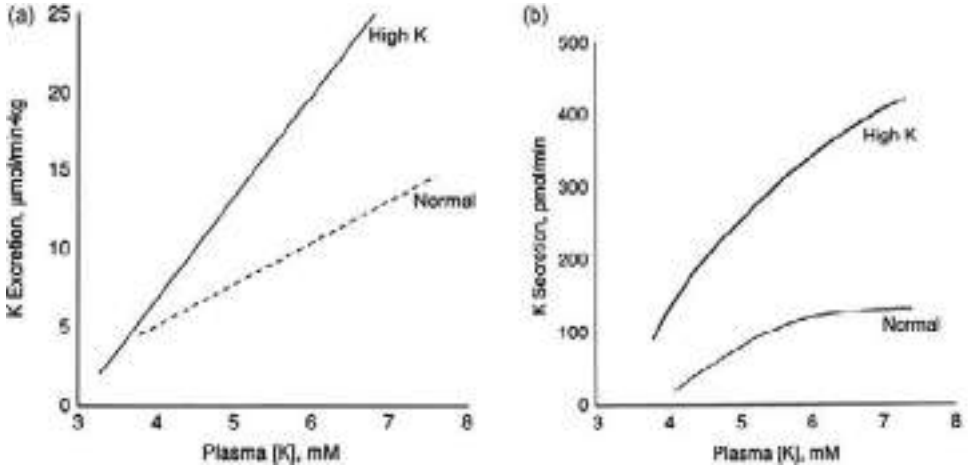

FIGURE 49.20 **(a) Relation between plasma K^+ concentration and renal K^+ excretion in rats on a control and high-K diet; and (b) distal tubule K^+ secretion.**

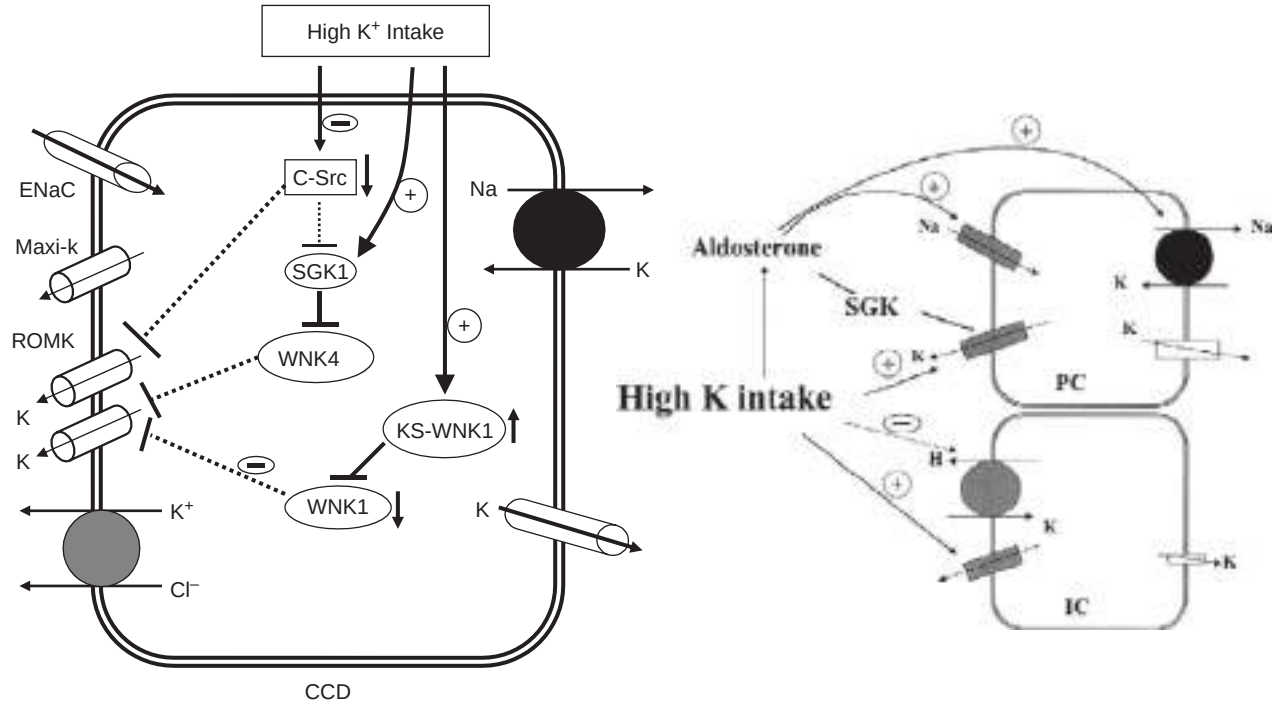

FIGURE 49.21 **Model of CCD cells illustrating the mechanisms by which high-K^+ diet increases K^+ secretion.** High-K^+ intake stimulates aldosterone secretion, which in turn activates ENaC and Na^+,K^+-ATPase in principle cells. Increased ENaC activity augments the driving force for K secretion, whereas stimulation of Na^+,K^+-ATPase can indirectly activate ROMK channel activity by a cross-talk mechanism. In addition, high K^+ intake can increase ROMK channel activity via modulation of the WNK pathway (see section on WNKs).

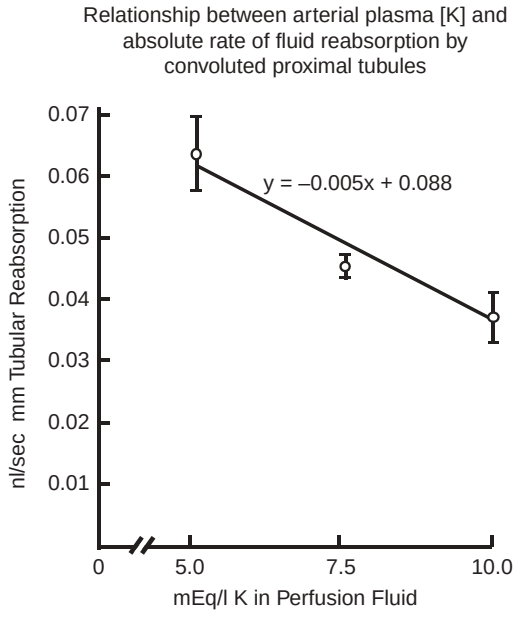

FIGURE 49.22 **Summary of the effects of changing peritubular K^+ concentration on proximal tubule fluid absorption.**[67]

with high ENaC expression provides an increase in the electrogenic driving force of K^+ secretion by the principal cell, and optimizes urinary K^+ excretion in hyperkalemic conditions.

Adaptive changes of K^+ transport have clear morphological and biochemical correlates in the distal tubule and CCD.[255–257,466,467,470] Proliferation of the basolateral cell membrane is highly significant in K^+-adapted animals, and is closely associated with a sharp increase in Na^+,K^+-ATPase.[113,114,156,163,254,296] Hyperkalemia and mineralocorticoids independently initiate the amplification of the basolateral membrane and the attendant increase in ATPase activity.[469] Thus, changes in basolateral membrane area, Na^+,K^+-ATPase content, and K^+ secretory rates are tightly coupled.[466,471,476] Morphological changes are apparent after 24 hours of increased K^+ intake and increase for about another week before a plateau is reached.[476] Increased K^+ excretion may continue beyond cessation of a high-K^+ intake.[348]

Principal cell basolateral membrane amplification also occurs with increased delivery of fluid and sodium ions to the ICT which occurs as a consequence of decreased proximal fluid absorption in hyperkalemic conditions[134,136,256,296,398] (Figure 49.22). The underlying mechanism appears to be stimulation of sodium reabsorption, which is linked to K^+ secretion. Another example is that chronic administration of furosemide to animals in which fluctuations of aldosterone and changes in electrolyte balance were prevented still leads to a sharp increase of K^+ secretion and sodium reabsorption.[469] Similar adaptation is observed in

unilaterally nephrectomized animals: K^+ balance is maintained by redistribution of Na^+ reabsorption from proximal to distal nephron sites and increased delivery of fluid into the distal nephron of the remaining nephron population.[109,467] Again, amplification of the basolateral membrane occurs predominantly in the principal cell population.

High-K^+ feeding also increases the pool of active ROMK in principal cells by diminishing apical removal of channels by endocytosis[157,161,539,544,546,548] and redistributing BK channels from an intracellular pool to the plasma membrane.[354] Figure 49.21 summarizes the change in cell messenger activity in response to increased K^+ intake. An important element responsible for stimulation of K^+ secretion is an increase in aldosterone release.[354] However, the effect of dietary potassium on stimulation of ROMK and BK channel activity is not due a direct hormonal effect, but reflects the mineralocorticoid-induced increase in apical ENaC and basolateral Na-K-ATPase activity, leading to enhancement of the electrochemical gradient favoring potassium secretion. The contribution of the BK channel towards excretion of a dietary potassium-load has been underscored by the finding that mice with genetic ablation of the β1-subunit of the BK channel exhibit, at baseline, low urinary potassium and sodium clearances, conditions that are exacerbated when the animals are fed a high-K^+ diet.[205–208]

In animals fed a normal K^+ diet, K^+ secretion in the CCD is completely dependent on sodium absorption.[342,483,489] However, distal potassium secretion may occur via a sodium-independent pathway in animals loaded with potassium for as little as 18 hours.[156,382] Moreover, basolateral sodium uptake via the Na/H exchanger has been proposed to be able to sustain basolateral pump activity in principal cells and potassium secretion in the CCD in the absence of significant sodium absorption.[353]

Dietary-induced stimulation of K^+ secretion is mediated not only by the aldosterone-dependent mechanisms described above, albeit indirectly, but also by aldosterone-independent mechanisms, a notion suggested by microperfusion studies that reveal that a high-K^+ diet stimulates potassium secretion in CCDs isolated from adrenalectomized rabbits.[352] A high-K^+ diet stimulates the expression of renal CYP2C23, a major CYP-epoxygenase, and increases the concentration of 11,12-epoxyeicosatrienoic acid (EET), a product of CYP-epoxygenase-dependent arachidonic acid metabolism in the CCD, which in turn stimulates BK channel activity,[497] CYP-epoxygenase-dependent arachidonic acid metabolism has been proposed to mediate regulation of renal K^+ secretion in response to dietary K^+ intake.[547]

A high-K^+ diet may not only diminish K^+ reabsorption by lowering H-K exchange,[569] but also by enhancing apical recycling of K^+ in intercalated cells by BK channels.[380]

K^+-Deprivation

Renal K^+ excretion drops sharply after withdrawal of K^+ from the diet and aldosterone secretion is suppressed. Concurrently, distal tubule K^+ secretion is markedly depressed or disappears altogether[142,175,177,371] to be replaced by net reabsorption.[119,322,371] K^+ reabsorption involves both active and passive transport mechanisms. Active K-H exchange is significantly increased in cortical and medullary collecting tubule segments.[70,112,117,571] An increase in passive K^+ permeability in the OMCD has been reported in states of K^+-depletion, and could favor accelerated K^+ reabsoprtion if the electrochemical gradient were favorable.

Figure 49.23 provides an overview of some of the transport changes that take place following administration of a low-K^+ diet.[539,540,546] Tyrosine phosphorylation of ROMK by Src initiates the endocytotic removal of apical K^+ channels. Specific tyrosine phosphorylation on the C-terminus of ROMK is critical, and superoxide production is closely associated with the low-K^+ response.[546] Notably, the reduction of apical K^+ channel density in response to K^+-depletion is independent of aldosterone, and consistent with previous findings of a direct effect of K^+ intake on K^+ excretion.[352]

Interestingly, upregulation of Na^+,K^+-ATPase activity has also been observed in tubules following K^+-depletion.[72,113] The original hypothesis that Na,K-ATPase was relocated to the apical membrane to facilitate K^+ reabsorption was not supported by immunological studies.[258] Thus, increased Na^+,K^+-ATPase-mediated K^+ uptake across the basolateral membrane requires increased backleak through basolateral K^+ channels.[113] It is well-established that K^+-depletion stimulates renal growth, a condition in which Na^+, K^+-ATPase might be expected to increase, but this relationship requires further exploration.[254]

K^+-depletion also involves changes in the distribution of H-K ATPases in cortical and outer medullary collecting ducts.[12,231,259] As shown in Figure 49.24, the ouabain-insensitive isoform of H-K-ATPase (type I) is downregulated in K^+-depletion and replaced by the type III isoform that is sensitive to inhibition by ouabain, and less selective for K^+ compared to sodium.[70,106a,117] Furthermore, remodeling of H-K-ATPases in K^+-depletion involves their targeting to principal cells,[117] instead of intercalated cells.

Since ammonium can substitute for K^+ on both Na-K-ATPase and Na-2Cl-K transporters, changes in extracellular K^+ exert a significant effect on acid excretion.[175,176,534] The interactions between K^+ and

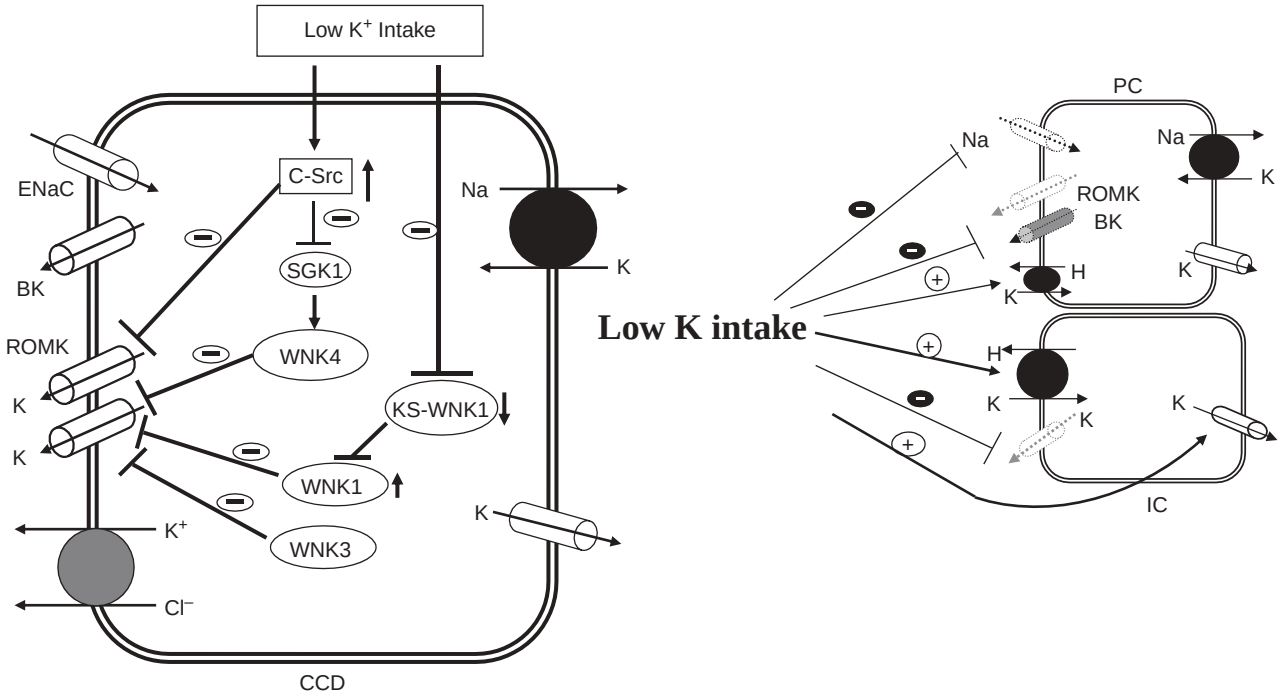

FIGURE 49.23 Model of CCD cells illustrating the mechanism by which low-K^+ diet decreases K^+ secretion. Low-K^+ intake reduces ROMK channel activity and thus K^+ secretion in principle cells via modulation of the WNK pathway and enhances apical H-K-ATPase activity in intercalated cells.

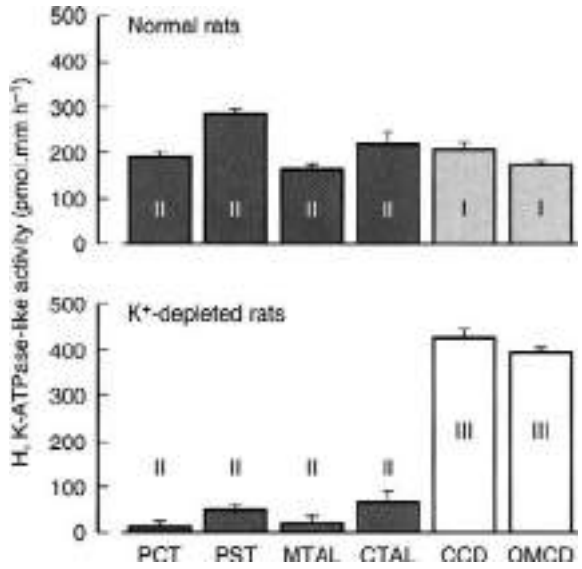

FIGURE 49.24 Distribution of three subtypes of H+,K+-ATPase-like activities, defined in the lower panel, along the nephron of normal rats and potassium-depleted rats.[117] All H-K-ATPase isoforms are sensitive to Sch28080. However, type I is insensitive to millimolar concentrations of ouabain whereas type III is sensitive to ouabain. Type II is inhibited by ouabain but is restricted in expression to the proximal tbule and thick ascending limb (TAL). Type III can be further distinguished from type II by its sensitivity to sodium and upregulation in response to K^+ depletion.[70,106a,117]

ammonium are summarized in Figure 49.25. Under conditions of K^+-depletion, the interstitial concentration of K^+ declines, and Na^+-K^+-ATPase-mediated uptake of ammonium in inner and outer MCD increases. Enhanced supply of cell hydrogen ion increases apical secretion, in part through the H-K exchange mechanism, thus stimulating K^+ reabsorption. Net K^+ secretion decreases further, since tubule trapping of ammonium blocks ROMK.[215] Hyperkalemia has the opposite effect. K^+ ions replace ammonium on Na^+,K^+-ATPase and the Na^+,K^+-2Cl co-transporter, which leads to diminished cell acidification and hydrogen ion availability for apical secretion. As a consequence, hyperkalemia may induce metabolic acidosis.[176]

Changes in aldosterone modulate, but are not fully responsible for, the renal response to K^+-deprivation. This mineralocorticoid modulates the urinary loss of K^+, but K^+ excretion continues to diminish when animals are put on a low-K^+ diet with clamped circulating aldosterone.[348–349]

In addition to aldosterone, progesterone has also been identified to be involved in the adaptive response to low-K intake.[126] Plasma concentrations of progesterone increase during K^+ restriction, and the efficiency of K^+ retention involves the stimulation of colonic H-K-ATPase in tubule cells.

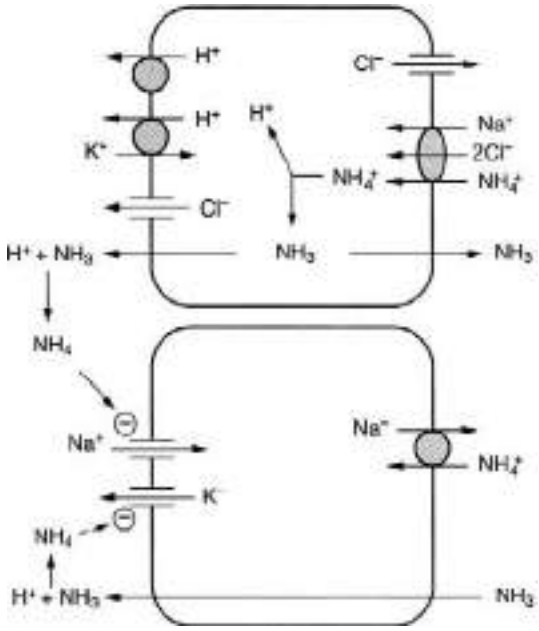

FIGURE 49.25 **Interaction between intercalated and principal cells.** Active K^+ reabsorption in the intercalated cell of the outer medullary collecting duct (OMCD) during K^+ depletion. Note that NH_4 can bind to the extracellular K^+ site of basolateral Na^+K^+-ATPase and the Na^+-Cl^--K^+ co-transporter and thereby stimulate H^+ secretion and K^+ reabsorption. Diffusion trapping of NH_4 in the tubule lumen directly inhibits K^+ secretion. *(From Malnic, G., Bailey, M. A., and Giebisch, G. (2004). Control of renal potassium excretion. In "The Kidney," 7th ed., Vol. 1, 453–496, Brenner, B. (ed.). WB Saunders, Philadelphia; and Wall, S. M. (2000). Impact of K^+ homeostasis on net acid secretion in rat terminal inner medullary collecting duct: Role of the Na-K-ATPase. Am. J. Kidney Dis. **36**, 1079–1088, with permission.)*

Finally, angiotensin II also plays a role in the tubule response to changes in K^+ intake. K-deprivation reduces apical ROMK activity, and patch-clamp experiments provide evidence for the involvement of AT1R receptor activation during inhibition of ROMK channels in rats given a low-K diet.[539,548]

Ultrastructural changes in medullary collecting ducts during K^+-depletion are largely confined to the intercalated cell population, and include a marked increase in the length of the apical cell membrane, an increase in the number of rod-shaped particles in the apical membrane, and a fall in the number of subapical cytoplasmic vesicles.[471] These morphological observations suggest an increase in the number of apical K^+ transporters, most likely the K,H-ATPase.

Interactions Between K^+ Channels and Magnesium

Changes in magnesium metabolism affect the kidney's ability to maintain normal K^+ balance. Magnesium deficiency tends to prevent restoration of K^+ balance following K^+ loss,[235] and recent evidence

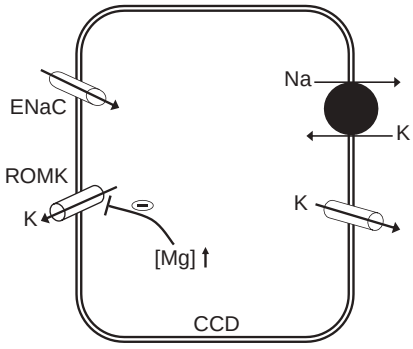

FIGURE 49.26 **Effect of changes in intracellular magnesium on ROMK channels in principal cells.**

has implicated involvement of apical ROMK channels in principal cells of the outer medulla[587]: a decrease in cell magnesium, during magnesium depletion, relieves K^+ channel inhibition and promotes enhanced K^+ secretion and kaliuresis whereas a rise in cell magnesium inhibits ROMK activity (Figure 49.26). Infusion of Mg decreases excretion of K^+ in the human kidney.

Adrenal Steroids

Mineralocorticoids have long been known to stimulate sodium reabsorption and, under appropriate conditions, enhance K^+ secretion. Figure 49.27 demonstrates the effects of aldosterone treatment on K^+ excretion.[594] Results from experiments in which mineralocorticoids were administered for prolonged periods of time until a steady-state was reached are shown. Aldosterone significantly enhances the efficiency of K^+ excretion, as evidenced by the fact that at each plasma K^+ concentration, more K^+ was excreted by animals with higher aldosterone levels. Expressed differently, as the aldosterone level rises, the same amount of K^+ can be excreted at progressively lower plasma K^+ levels. The direct stimulatory effect of mineralocorticoids on K^+ secretion by the distal tubule and CCD has been amply demonstrated.[55,93,145–148,222,356] Enhanced uptake of K^+ into extrarenal tissues has also been reported.[53,55,595]

The mechanism of aldosterone release from the adrenal glomerulosa involves two well-defined stimuli: cell depolarization by either an increase in extracellular K^+ or angiotensin II.[90] Both maneuvers enhance Ca^{2+} entry and aldosterone-synthase activation.[90] Recent evidence reveals that K^+ channel mutations characterized by diminished K^+ selectivity (increased Na permeability) result in cell depolarization and enhanced aldosterone production.[90]

The effects of mineralocorticoids on cell K^+ transport mechanisms of principal collecting duct cells are summarized in Figures 49.28a, 49.29 and 49.30. The effects of mineralocorticoids depend on the antecedent

hormonal condition, the duration of hormone treatment, and the modifying effects of sodium ions on K^+ transport.[96,146] Key aldosterone-sensitive transport mechanisms include the basolateral Na-K exchange pump, apical Na channels, and K^+ channels in both apical and basolateral membranes. Mineralocorticoid hormone action occurs in several steps summarized in Figure 49.29b. They include binding of aldosterone to cytoplasmic receptors to form the aldosterone–receptor complex, activation of the gene to initiate transcription, synthesis of new aldosterone-induced proteins, and actions on apical and basolateral transport operations. This process can be divided into early and late phases.

In the early phase, mineralocorticoids activate the apical sodium conductance, and thus stimulate sodium entry. With this increase in sodium entry and cell sodium activity, the basolateral pump turnover increases and K^+ secretion rises.[13,113,115,259,356,468,469] Enhanced sodium entry *per se* leads to rapid insertion of Na^+-K^+-ATPase units into the basolateral membrane from an enzyme pool whose magnitude depends on the antecedent aldosterone levels.[26,27,113,115,349] Thus, the acute effects of aldosterone include significant stimulation of Na^+,K^+-ATPase involving increased activity of individual pumps, and insertion of additional units.[115,259] Continued exposure to elevated mineralocorticoid levels results in late phase changes, including an additional increase in both K^+ and sodium transport rates, insertion of additional basolateral Na-K pump units, and further enhancement of the apical sodium and K^+ conductances.[153,276,356,424–427]

Also occurring in the late phase of mineralocorticoid administration are significant morphological changes in principal cells.[466–471,530,531] Mineralocorticoids have a direct effect on basolateral membrane amplification, independent of changes in K^+ balance and plasma K^+ levels.[469] However, sodium ions are required for full

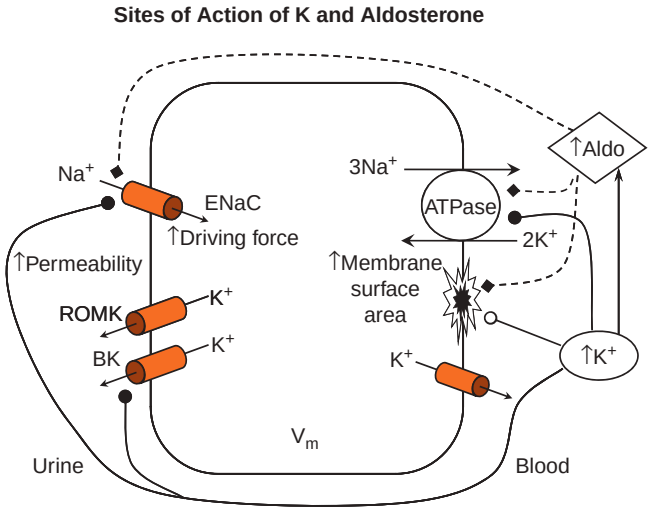

FIGURE 49.28 **Factors involved in the regulation of K^+ transport by aldosterone and peritubular K^+.** (1) Changes in peritubular K^+ increase apical K^+ and Na^+ channel activity, stimulate Na^+,K^+-ATPase activity, and augment the basolateral membrane area. High K^+ also activates the release of aldosterone. (2) Changes in aldosterone stimulate apical Na^+ channels but enhance K^+ channel activity only during chronic hyperkalemia. Similar to high K^+, aldosterone stimulates Na^+,K^+-ATPase activity and increases the basolateral membrane area and Na^+, K^+-ATPase activity. *(From ref. [150], courtesy of S. Hebert.)*

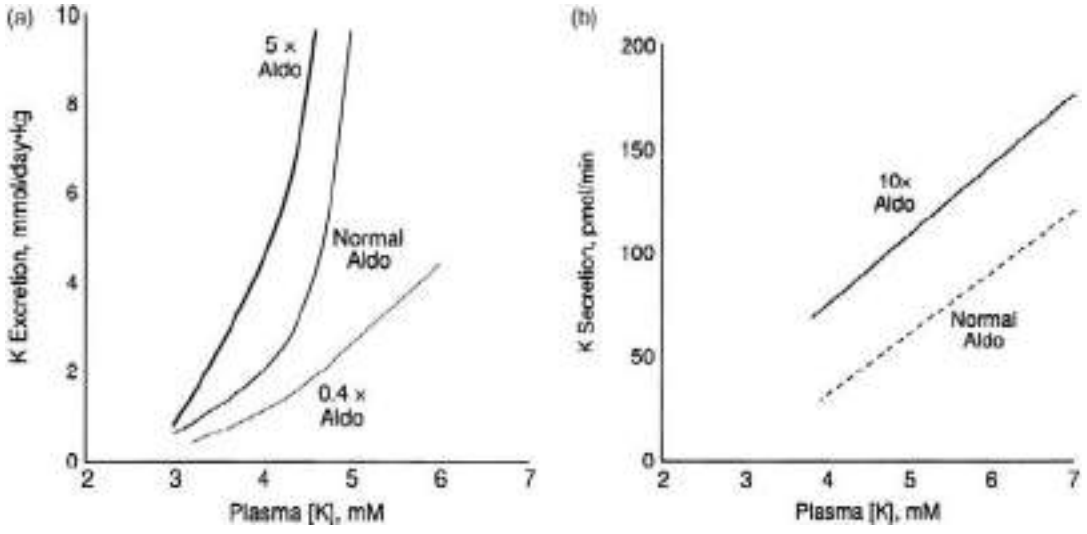

FIGURE 49.27 **Relation between K excretion and plasma K at different levels of aldosterone.** The relationship between plasma K^+ concentration and renal K^+ excretion (a) (*from ref. [415]*), and distal K^+ secretion (b) (*from ref. [416]*) is affected by circulating aldosterone. Effects of increased and decreased aldosterone are shown with respect to normal levels.

mineralocorticoid effects: morphological changes fail to develop fully during administration of a low-sodium diet.[476] In contrast to the changes observed in principal and connecting tubule cells, significant changes in basolateral membrane area fail to occur in intercalated cells during either diet- or hormone-induced stimulation of tubular K^+ secretion.[467,471]

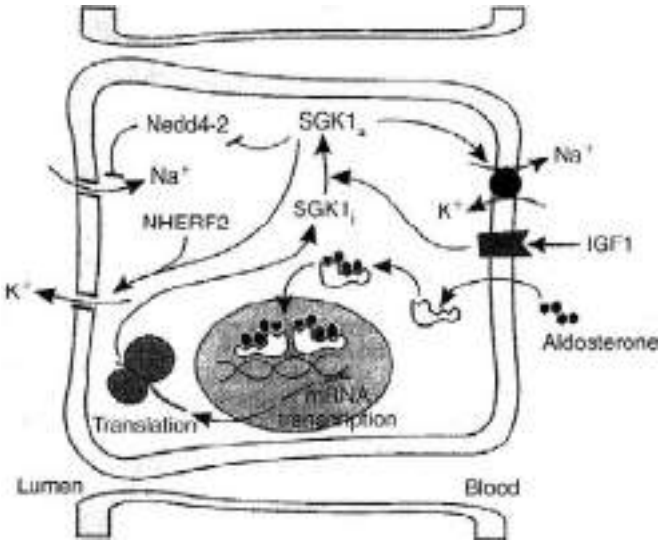

FIGURE 49.29 Effects of hormones on principle cell transport pathways. Aldo stimulate K^+ secretion via pathways shown in this cell model.

The electrophysiological consequences of high-K^+ and chronic mineralocorticoid administration are shown in Figure 49.30. The basolateral membrane voltage may hyperpolarize, and the direction of passive K^+ transport may reverse.[276,324] The mineralocorticoid-induced increase in the basolateral electrogenic Na-K exchange and basolateral K^+ conductance accounts for the rise in membrane potential above the K^+ equilibrium potential. The increase in membrane voltage provides a driving force for K^+ uptake into principal cells. This sequence of events suppresses the backflux of K^+ from cell to peritubular fluid, and increases the efficiency of K^+ secretion.

Measurements of proximal cell K^+ levels in tubules harvested from chronically mineralocorticoid-treated animals do not show an increase in cell K^+ content or activity.[375] This attests to the precise adjustments of basolateral pump activity to apical K^+ conductance. Possible mechanisms of this interaction between basolateral and apical transport mechanisms are mineralocorticoid-induced changes in cell ATP, Ca^{2+}, and pH levels. Were the stimulation of basolateral Na-K exchange to reduce cell ATP concentrations, apical K^+ channels would be released from inhibition. It is also possible that aldosterone activates basolateral Na-H exchange, alkalinizes the cytoplasm, and

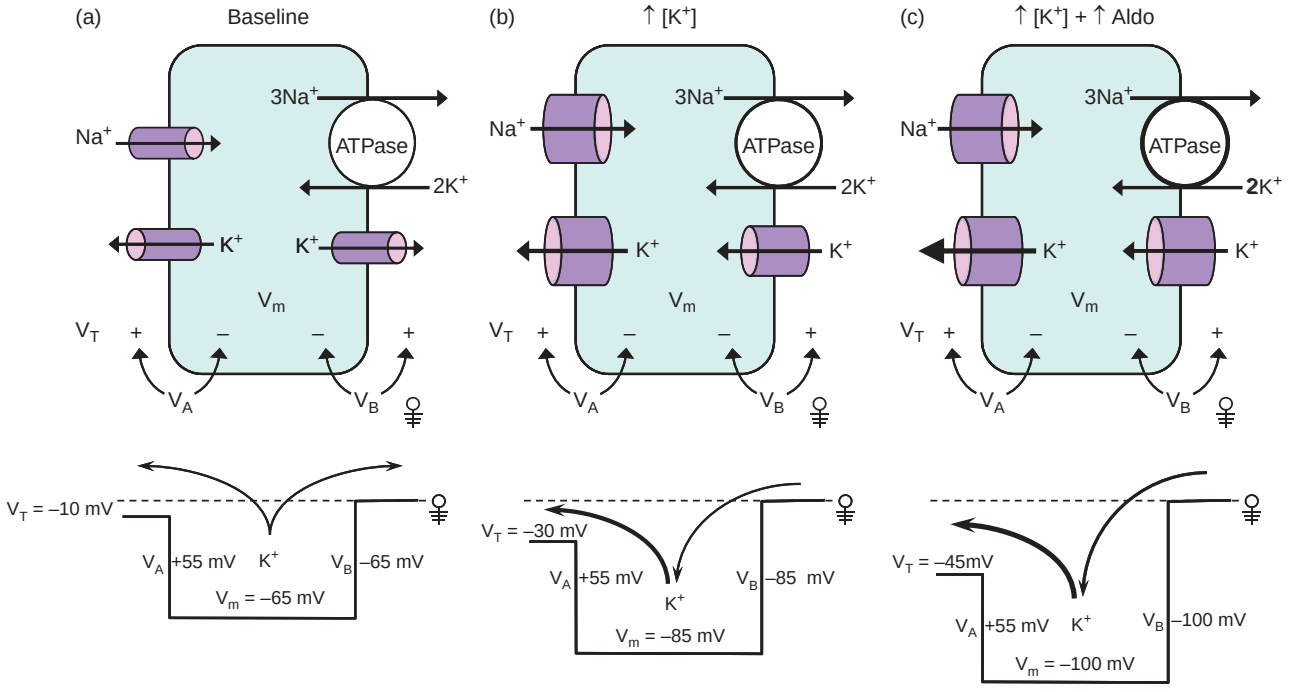

FIGURE 49.30 **Schema of cortical collecting tubule cell with key site of potassium transport.** Depending on the magnitude of the electrical potential difference across the basolateral cell membrane, potassium ions may either leave the cell (recycle) (a) or be taken up into the cell in parallel with pump-mediated potassium transport (b,c).

activates the apical secretory K^+ channels. Principal cells extrude hydrogen ions across the basolateral membrane by Na-H exchange,[86] and because aldosterone accelerates Na-H exchange in cells of the diluting segment,[362,368] this mechanism is an attractive possibility. Finally, cell Ca^{2+} changes could also be involved, owing to the effects of pump-induced alterations of cell sodium concentrations that affect Na^+/Ca^{2+} exchange.[445]

Sodium ions importantly modify the stimulating effect of mineralocorticoids on K^+ secretion. Thus, the kaliuretic effect of chronic desoxycorticosterone (DOC) treatment is effectively abolished by a low-sodium diet, and is amplified by a high-sodium intake.[455] Studies on single CCDs have confirmed the importance of an intact apical sodium entry mechanism, and an adequate lumen sodium supply, for the full stimulation of Na,K-ATPase activity that follows mineralocorticoid administration.[530,531] As pointed out above, switching from a low- to a high-cell-sodium environment induces a rapid increase of ATPase activity in proximal tubule cells.[113] Such prompt activation is consistent with a permissive role for Na in mineralocorticoid action mediated by the stimulating effect of sodium to insert pump units from a latent cytoplasmic pool into the basolateral membrane. Similarly, raising intracellular sodium concentrations enhances the cell surface expression of Na-K-ATPase α-subunit in mammalian cortical collecting duct principal cells. This process involves both c-AMP-dependent and cyclic-AMP-independent pathways.[113,188] Moreover, such activation of Na,K-ATPase is modulated by aldosterone, since cortical collecting ducts from aldosterone-depleted animals have a greatly diminished response to the change in ambient sodium, implying that the size of the cell sodium pool is strongly influenced by mineralocorticoids. In tubules from DOC-treated animals, amiloride significantly attenuates pump stimulation.[357] These results support the view that enhanced apical sodium entry into principal cells is necessary to allow full expression of mineralocorticoid stimulation of Na^+,K^+-ATPase activity. The efficacy of aldosterone-induced kaliuresis is also affected by urine flow rate.[145,147] Microperfusion experiments show that direct effects of aldosterone on K^+ transport are modified by simultaneous modulation of urine flow rate. Thus, although aldosterone enhances K^+ secretion in single distal tubules perfused at a constant rate, the antidiuretic effect of aldosterone may modulate the direct stimulation of aldosterone on K^+ excretion. On the other hand, dexamethasone does not stimulate potassium secretion in tubules perfused at a constant rate, but elicits K^+ transport stimulation through its enhancing effect on tubule flow rate.[147]

Aldosterone may act rapidly (<10 minutes) on renal distal nephron ion transport by a nongenomic mechanism. This is not affected by actinomycin D or spironolactone, and thus is independent of protein synthesis.[527] This nongenomic effect involves, primarily, stimulation of Na^+/H^+ exchange, and is thought to be mediated by specific membrane receptors for aldosterone. Membrane-binding sites of very low (0.1 nM) dissociation constant (Kd) for aldosterone which modulated Na^+/H^+ exchange were first described in human polymorphonuclear leucocytes. Such sites have no affinity for dexamethasone, corticosterone, ouabain, amiloride, and 18-hydroxyprogesterone.[140,505] Similar receptors for aldosterone were also found in pig kidney, but these had higher values of Kd for desoxycorticosterone acetate and corticosterone. These membrane receptors are different from the classical cytoplasmic mineralocorticoid receptors (MR), since MR knockout mice still display the nongenomic effect of aldosterone.[174] Activation of the nongenomic mechanism via membrane receptors includes a signaling path involving G-protein, inositol triphosphate, Ca^{2+}, and protein kinase C, as well as MAP-kinase.[527] ENaC-mediated current in isolated rabbit CCD is stimulated by nongenomic action of aldosterone.[527] Inasmuch as these nongenomic actions involve apical sodium channels, they could also have significant indirect effects on K^+ secretion.

Glucocorticoids

Abnormal function of the hypothalamic–pituitary–adrenal axis is often associated with deranged K^+ homeostasis.[63,123] In patients with low circulating levels of glucocorticoids, the excretory response to K^+-loading is blunted, even if aldosterone is normal. Glucocorticoid excess, in contrast, can be associated with kaliuresis and hypokalemia. The effect of glucocorticoids on urinary K^+ excretion largely reflects secondary stimulation of K^+ secretion in the distal nephron following glucocorticoid actions in proximal nephron segments. Glucocorticoids increase GFR, and also the delivery of sodium and fluid to the distal nephron[33]: these latter effects are strongly kaliuretic. Microperfusion experiments also support an indirect effect, since acute intravenous dexamethasone does not increase distal K^+ secretion when fluid and salt delivery are constant.

Nevertheless, studies suggest that chronically elevated glucocorticoids exert a direct mineralocorticoid-like effect on the distal nephron. Mineralocorticoid target genes are activated by glucocorticoid excess, even when aldosterone is normal, and patients with familial glucocorticoid receptor haploinsufficiency or apparent mineralococticoid excess are hypokalaemic despite low circulating aldosterone. These conditions

of corticosteroid cross-talk reflect the inherent affinity of the mineralocorticoid receptor for glucocorticoids.[16] As shown in Figure 49.31, the enzyme 11β-hydroxysteroid dehydrogenase type II (11βHSD2) converts active glucocorticoids to inactive metabolites. In the principal cell, 11βHSD2 brings mineralocorticoid receptor target proteins, such as ENaC, under the control of aldosterone.[16,22,280]

The 11βHSD2 barrier can be attenuated by mutations in the encoding gene or pharmacological inhibition of enzyme function: the hypokalemic hypertension of apparent mineralocorticoid excess or that following excess licorice consumption reflects glucocorticoid action in the distal nephron.[21,41] Micropuncture studies in rats confirm this,[23] and mice lacking 11βHSD2 maintain robust K^+ excretion despite severe hypokalemia.[22] Much of the K^+ excretion is amiloride-sensitive and is likely mediated by ROMK. However, kaliuresis is maintained after sodium handling is normalized and becomes resistant to amiloride. It is likely that such persistent K^+ excretion reflects BK-mediated K^+ secretion: 11βHSD2 null mice are severely polyuric and the increase in urine flow would activate BK channels.[20]

Some evidence suggests that glucocorticoids may also influence K^+ secretion by glucocorticoid receptor (GR) activation.[21,41] GR is expressed in the aldosterone-sensitive distal nephron of the rat, and it is this receptor, not MR, that translocates to the nucleus in response to physiological variations in aldosterone.[1,47] The physiological meaning of this is not resolved, but in mice with reduced levels of 11βHSD2 a high-salt diet causes hypokalemia and inappropriately high K^+ secretion in the distal nephron. The deranged K^+ homeostasis was prevented by GR blockade, and spironolactone was without effect.[41] In summary, there is strong evidence that chronic exposure to elevated glucocorticoids may directly influence K^+ secretion at this site, an effect above and beyond the kaliuresis triggered by rapid-onset events in more proximal segments.

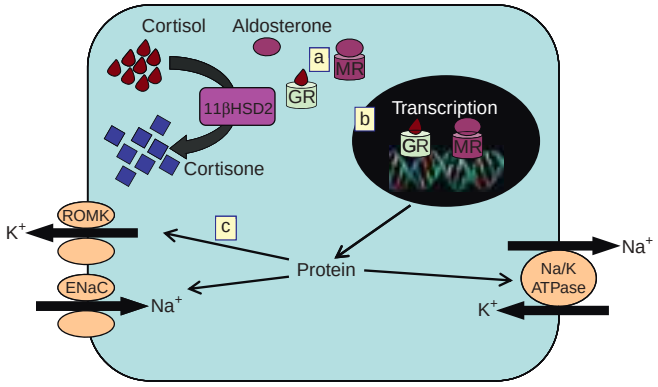

FIGURE 49.31 **The enzyme 11β hydroxysteroid dehydrogenase type 2 (11βHSD2) is co-expressed with the mineralocorticoid receptor (MR) in aldosterone target tissues, such as the principal cell of the collecting duct.** The enzyme converts cortisol, which is an agonist of the mineralocorticoid receptor (MR) to cortisone, which is not. This confers aldosterone-specificity on MR, placing transcription of aldosterone-induced proteins, such as ENaC, ROMK, and the basolateral Na/K-ATPase, under the control of the renin–angiotensin system. Recent data challenge the conventional view of corticosteroid action in the aldosterone-sensitive distal nephron, which expresses both the mineralocorticoid and glucocorticoid receptor (GR). As shown in (a), 11βHSD2 may also govern ligand access to GR, and GR translocation to the nucleus (b) is influenced by physiological changes in circulating aldosterone, and plays a permissive role in regulation of ENaC by aldosterone. Direct regulation of ROMK by GR is suggested (c) but the kaliuretic effects of glucocorticoids may also reflect activation of ENaC. *(Figure courtesy of Dr. Louise Evans.)*

WNKs (With No Lysine Kinase)

WNKs are serine/threonine protein kinases, and WNK1, 3, and 4 are expressed in the DCT and CCD.[127,229,253,331,562,598,604] A large body of evidence indicates that the WNK family plays an important role in the regulation of Na absorption and K^+ secretion. WNK4 suppresses the expression of the Na-Cl cotransporter (NCC) in the plasma membrane of the DCT, thereby inhibiting Na absorption.[253] In contrast, WNK1 stimulates NCC activity indirectly by antagonizing the inhibitory effect of WNK4. WNK1, 3, and 4 inhibit ROMK channel activity, and the effect of WNK on ROMK is mediated by stimulation of clathrin-dependent endocytosis. The inhibitory effect of WNK4 on ROMK1 does not require the kinase activity, because co-expression of the inactivated WNK4 inhibits expression of ROMK1 in *Xenopus* oocytes. The mutated gene products encoding inactivated WNK1 or WNK4 causes pseudohypoaldosteronism type II, a disease with characteristics of hypertension and low aldosterone levels. A kidney-specific splice form of WNK1 (KS-WNK1), in which an alternative 5′ exon replaces the first four exons of WNK1, is expressed in the DCT and CCD.[291] Unlike the long form of WNK1, KS-WNK1 lacks kinase activity and does not block ROMK channels. Moreover, KS-WNK1 can antagonize the inhibitory effect of WNK1. A high K^+ intake increases the expression of KS-WNK1, and accordingly attenuates the inhibitory effect of WNK1 on ROMK channels (Figure 49.32).[291,312] Thus, alteration of the ratio between the long and short forms of WNK1 may be an important mechanism by which a high-K intake stimulates ROMK channel activity. K^+ restriction has been reported to decrease the expression of KS-WNK1 and increase the long form WNK1. Consequently, the inhibitory effect of KS-WNK1 on WNK1 is diminished, and WNK1-mediated inhibition of ROMK channels is enhanced, in the CCD from animals fed a low-K diet.[236]

It should be noted that aldosterone is secreted both in the setting of intravascular volume depletion

(hypovolemia) and hyperkalemia. In the face of the hypovolemia, aldosterone promotes Na^+ retention and limits urinary K^+ loss. In hyperkalemia, aldosterone maximizes K^+ loss without Na^+ retention. This "aldosterone paradox" may be explained by changes in the relative expression and activities of WNK family members[127,229,236,253,331,493] (Figures 49.32 and 49.33).

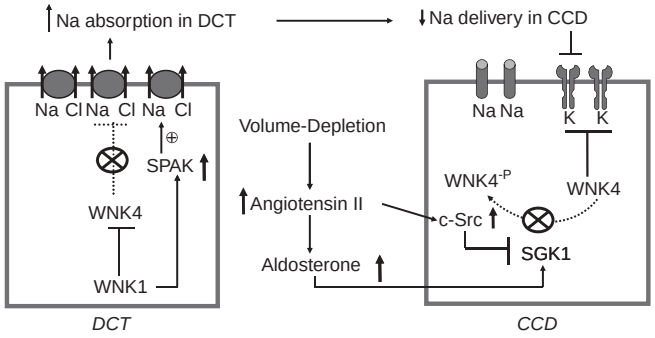

FIGURE 49.32 **A cell scheme illustrates the mechanism by which increasing dietary potassium intake facilitates K secretion.** A high-K intake increases KS-WNK4 expression which inhibits WNK1 function, thereby suppressing WNK1-mediated inhibition of WNK4. Thus, a high-K intake decreases NaCl co-transporter activity, and increases NaCl delivery to the connecting tubule and the CCD. A high-K intake also increases SGK1 activity which phosphorylates WNK4, thereby suppressing the WNK4-mediated inhibition of ROMK. Thus, a high-K intake stimulates K secretion in the connecting tubule and the CCD through increasing Na delivery and apical K^+ channel activity (CCD: cortical collecting duct; SGK1: serum-glucocorticoid-induced kinase 1; WNK: with-no-lysine kinase; KS-WNK1: kidney-specific WNK1).

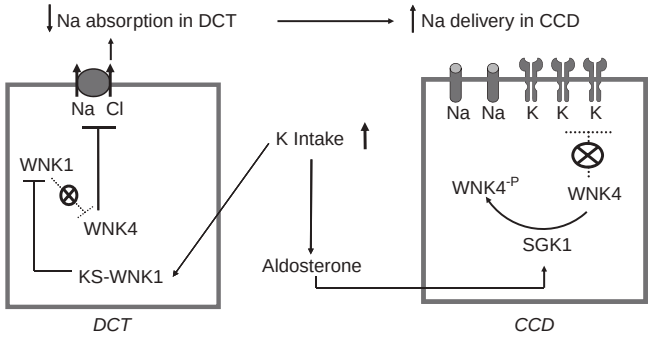

FIGURE 49.33 **A cell scheme illustrating the role of angiotensin II in regulating ROMK channels during volume-depletion.** Volume-depletion abolishes the inhibitory effect of WNK4 on the NaCl co-transporter through stimulation of SGK1-mediated WNK4, thereby increasing Na absorption in the distal nephron. Decreasing the Na delivery to the connecting tubule and the CCD diminishes the driving force for K secretion. In addition, the angiotensin II pathway inhibits SGK1-induced phosphorylation of WNK4 through activation of c-Src family protein tyrosine kinase, and leads to suppression of ROMK channel activity. A dotted line means a diminished effect (CCD: cortical collecting duct; DCT: distal convoluted tubule; SGK1: serum-glucocorticoid-induced kinase 1; WNK: with-no-lysine kinase).

Salt and Water Balance

K^+ excretion generally changes in association with modulation in sodium excretion. On the one hand, interventions that increase salt and water excretion – high-salt intake, extracellular volume expansion, saline infusion, administration of many diuretics acting upstream of the initial collecting tubule, and infusion of sodium salts of poorly-reabsorbable anions – all stimulate K^+ excretion.[59,180–186,234,267,326,399,470,582] On the other hand, maneuvers that diminish sodium excretion – rapid reduction of glomerular filtration rate, sodium-depletion, and volume-contraction – all decrease K^+ excretion. Thus, distal secretion of K^+ depends importantly on the delivery of sodium and tubule fluid to the sites of K^+ secretion.

Figure 49.34 illustrates the effect of different levels of sodium intake on the steady-state relationship between plasma K^+ and urinary K^+ excretion at clamped aldosterone levels.[596] K^+ excretion at a given plasma K^+ level is stimulated by augmenting sodium intake and a given rate of K^+ excretion occurs at lower plasma K^+ levels when sodium intake is elevated. This enhancement of K^+ excretion is thought to depend on increased delivery of fluid and sodium to the distal tubule and CCD.

Studies on single tubules, employing both micropuncture[260] and microperfusion[139,191,192,319] techniques, have fully confirmed that tubule fluid flow rate and luminal sodium concentration independently affect K^+ secretion. Figure 49.35 summarizes the effects of tubule flow rate and fluid sodium concentrations on K^+ secretion along the distal tubule. Increasing flow rate invariably stimulates K^+ secretion. For a given

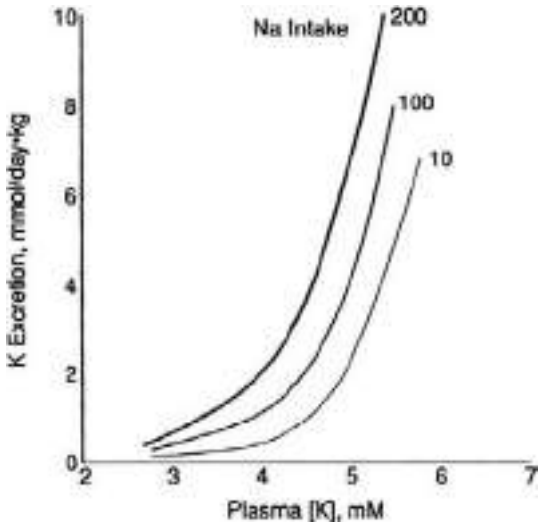

FIGURE 49.34 The relation between plasma K^+ concentration and renal K^+ excretion is affected by dietary Na intake. *(From ref. [596], with permission.)*

flow rate, K^+ secretion is augmented in animals with a high-K intake[266] or after mineralocorticoid administration[123,183]; it is decreased in animals on a low-K^+ diet.[266]

Three separate mechanisms underlie the increase of distal K^+ secretion with enhanced flow rate. The first involves electrophysiological linkage between sodium absorption and K^+ secretion. Increasing fluid delivery into the distal tubule increases the sodium concentration in the lumen, which in turn stimulates sodium absorption[267] and depolarizes the apical cell membrane, thus creating a more favorable electrochemical gradient for K^+ secretion. This effect is of greatest importance when luminal Na concentration shifts from low to high levels.[48,139,192,319,485]

An increase in tubular fluid flow rate also stimulates sodium absorption due to an increase in the open probability of ENaC.[342,433]

Enhanced sodium entry from the lumen into principal cells during augmented delivery of fluid stimulates the basolateral Na,K-ATPase and accelerates K^+ translocation into cells from the peritubular fluid. Thus, as long as basolateral pump activity responds to increased lumen delivery of sodium with increased Na-K exchange, K^+ secretion continues at a high enough rate to either prevent (in the lower range of lumen flow rates) or to curtail (in the higher range of lumen flow rates) a decline in the concentration of K^+ in the tubule lumen. If K^+ concentrations decline less than flow rate increases, K^+ secretion rates increase. Experimental conditions in which lumen K^+ concentrations remain constant during diuretic conditions,[232] and in which the concentration difference between cell interior and lumen remain unaltered despite marked stimulation of K^+ secretion (see Table 24 in [415]), underscore the importance of accelerated and coupled K^+ and sodium transport. By "clamping" the K^+ concentration in the lumen to fairly constant levels over the range of low physiological levels of tubule flow, the connecting and collecting tubule emerge as the major control site of K^+ excretion.[473]

A second mechanism that links increased delivery of fluid to the distal nephron to enhanced K^+ secretion may involve a flow-dependent fall of lumen K^+ concentration,[191,192] which increases the driving force for K^+ exit across the apical membrane. This mechanism permits K^+ secretion to increase under conditions in which increased sodium delivery into the distal tubule fails to stimulate basolateral Na-K-ATPase. Diminished apical sodium uptake and low lumen K^+ concentrations would hyperpolarize the apical membrane potential and tend to reduce the electrochemical driving force, favoring K^+ secretion. The functional state of the basolateral Na^+,K^+-ATPase transport system thus determines the extent to which increased fluid delivery stimulates K^+ secretion.

The third mechanism, illustrated in Figure 49.36, links changes in luminal flow to distal potassium secretion by activation of the BK channel. An increase in luminal flow rate transduces mechanical signals (circumferential stretch, shear stress, hydrodynamic bending moments on the cilium decorating the apical surface of virtually all renal epithelial cells) into increases in intracellular Ca^{2+} concentration, which in turn activate apical BK channels to secrete potassium, thereby enhancing urinary potassium excretion.[557,575]

Although apical sodium channels are a key pathway for entry of sodium into principal cells, K^+ excretion

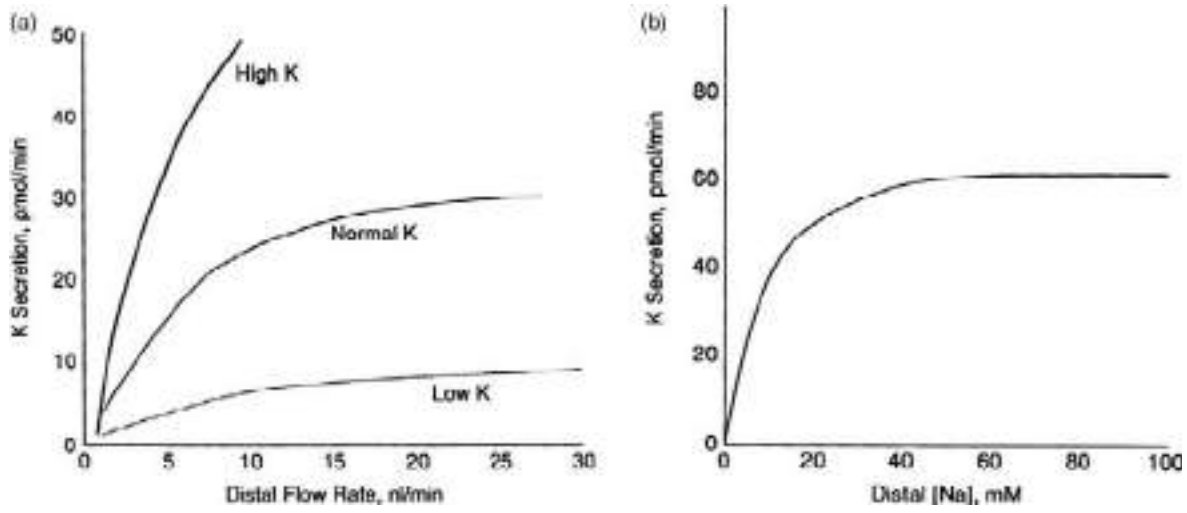

FIGURE 49.35 **(a) Relationship between distal flow rate and distal K secretion as affected by K intake. (b) Distal K secretion requires a luminal Na^+ concentration exceeding 25–35 mM.** The relation between flow rate of tubule fluid in distal tubule and distal K^+ secretion is affected by dietary intake: normal K^+ diet; low- K^+ diet; high- K^+ diet. *(From ref. [269], with permission.)*

appears not to be entirely dependent on apical sodium supply. Animals maintained on a low-sodium diet do respond with kaliuresis to acute K^+-loading,[384] as do animals given the ENaC inhibitior, amiloride.[589] Moreover, humans tolerate very well a diet high in K^+ and low in sodium.[374] An explanation for the apparent dissociation between apical sodium supply and maintained ability for K^+ secretion may be the presence of at least two additional sodium entry pathways in principal cells. These are located in the basolateral membrane, and include Na/H and Na/Ca^{2+} exchange.[86,295] Activity of these basolateral entry pathways may, at least in part, replace apical sodium supply and maintain K^+ secretion under conditions of low distal fluid and sodium delivery, especially under conditions of elevated levels of plasma K^+.[176] K^+ excretion independent of distal amiloride-sensitive Na transport has been confirmed in rats during high dietary K^+ intake.[156] Such Na-channel-independent K^+ excretion develops progressively during prolonged K-loading; it could be mediated, in part, by K^+ secretion in intercalated cells[206,354] and/or by reduced K^+ reabsorption along the proximal tubule and thick ascending limb of Henle's loop as a consequence of high plasma K^+ levels. The latter have been shown to lower proximal tubule Na and fluid reabsorption.[67,302]

Recent evidence, based on distal tubule perfusion studies, suggests a significant component of electroneutral sodium reabsorption (Figure 49.37), resistant to amiloride inhibition but sensitive to hydrochlorthiazide. Mechanistically, the transport process involves the parallel action of sodium-dependent Cl/bicarbonate exchange and sodium-independent chloride-bicarbonate exchange (pendrin). The presence of this transport in ß-intercalated cells is significant, because it would uncouple K^+ secretion from electrogenic sodium transport via Na channels in principal cells.[127,128]

The ability of the distal tubule and CCD to maintain a fairly constant K^+ concentration in the lumen over the physiological range of flow rates has two important consequences. First, the marked flow

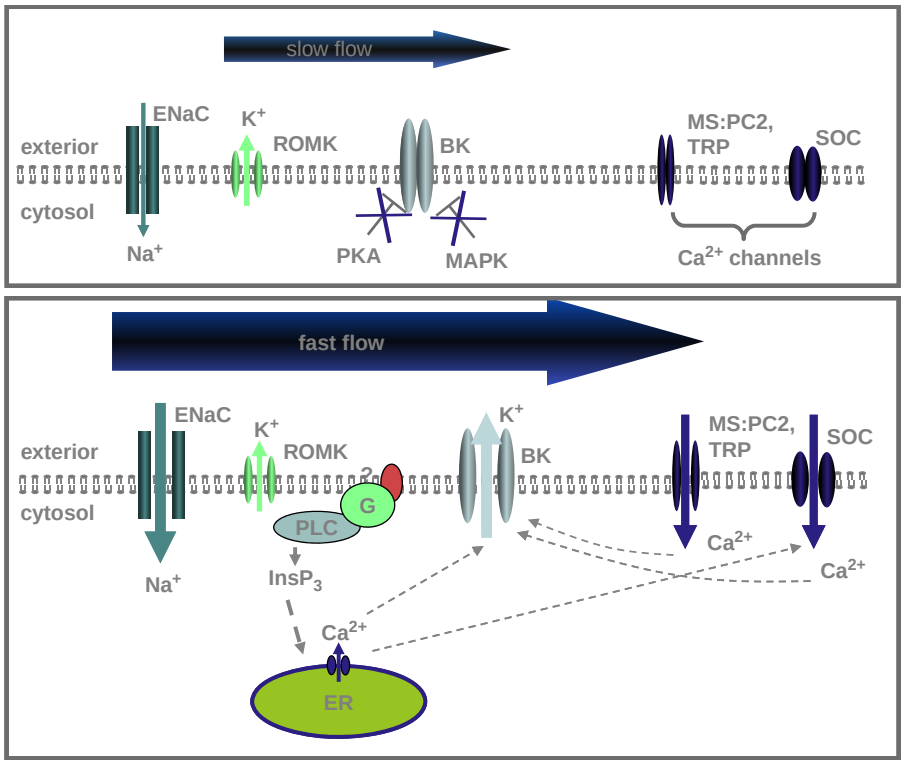

FIGURE 49.36 **Proposed model for the molecular physiology of flow-induced K^+ secretion (FIKS) in the distal nephron.** At slow "physiologic" flow rates, K^+ secretion requires electrogenic Na^+ absorption through ENaC, and is mediated by the SK/ROMK channel. The apical Ca^{2+}- and stretch-activated BK channel is tonically inhibited by PKA and MAPK. A rapid increase in tubular fluid flow rate associated with circumferential stretch of the CCD leads to shear or hydrodynamic impulses at the cilium or apical membrane and an increase in intracellular Ca^{2+} concentration ($[Ca^{2+}]_i$), due to luminal Ca^{2+} entry and internal store release. These hydrodynamic forces are associated with an increase in net Na^+ absorption and K^+ secretion, the latter mediated by Ca^{2+}-dependent activation of the BK channel. FIKS further requires microtubule integrity and possibly release of tonic channel inhibition. Mechanosensitive (MS) Ca^{2+} channels identified in the apical membrane of the distal nephron include polycystin 2, and the transient receptor vanilloid-4 (TRPV4) channels. Store-operated Ca^{2+} channels (SOC) also contribute to the flow-induced Ca^{2+} response.[574]

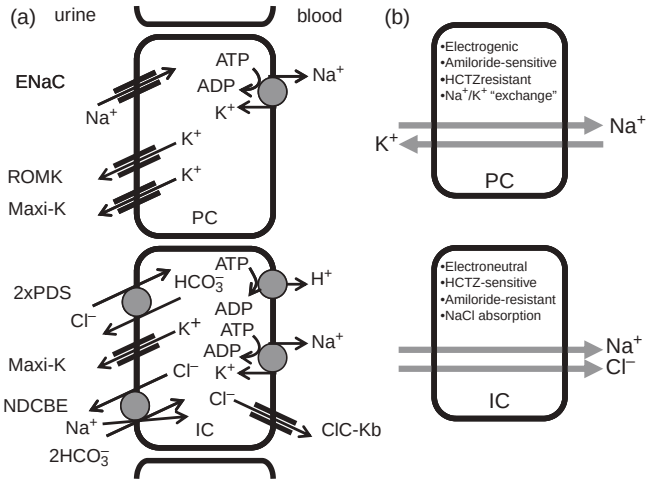

FIGURE 49.37 **Overview of the two major Na^+/* transport pathways in principal and intercalated cells, depicting electrogenic and electroneutral transport mechanisms.** *(From ref. [128].)*

dependence of K^+ secretion in the distal tubule and CCD endows the process of K^+ secretion with great sensitivity to changes in the delivery of sodium and fluid. This tubule segment is thus responsible for the enhanced rate of K^+ excretion that follows inhibition of sodium and fluid reabsorption upstream of the distal tubule and collecting duct ([234]; see "Diuretics" section below). Second, the ability of the distal nephron segments to "clamp" the K^+ concentration has implications for the physiological importance of those components of K^+ secretion that occur upstream during K^+ recycling. K^+ secreted upstream of the ICT determines the amount of K^+ secreted along the DCT and ICT as the tubule fluid approaches the "late" distal tubule. Hence, with stimulation of medullary K^+ recycling, the concentration of K^+ in the early distal tubule rises and approaches the "clamped" concentration across the initial collecting tubule. Thus, a smaller fraction of excreted K^+ is then contributed by distal secretion. Conversely, when medullary recycling of K^+ is minimal, and the concentration of K^+ in the fluid entering the distal tubule is low, a larger fraction of excreted K^+ has to be secreted by the distal tubule and the CCD.

A non-invasive method for evaluation of the transtubule gradient of K^+ (TTKG) in the CCD has been described.[565,566] Such estimates have been used to evaluate the effects of hormones, diuretics, and acid–base disturbances in patients. The method allows distinction between modulation of urine K^+ excretion by changes in flow rate and/or direct effects on K^+ secretion in principal cells. This approach has also shown that urea recycling, by enhancing flow rate in the cortical collecting tubule, provides a mechanism for aiding K^+ excretion.[214]

Chronic enhancement of sodium delivery into the distal nephron, for instance during treatment with loop diuretics, leads to both functional and morphological adjustments in the downstream tubule segments; these changes increase the capacity for sodium absorption and K^+ secretion in cells of the distal nephron.[136,257,296,344,466,467] Prolonged increased entry of sodium into cells of the distal tubule must be responsible for transport stimulation, because the functional and morphological changes persist when plasma aldosterone, vasopressin, and K^+ are held constant.[466,470] Increased transport in collecting duct segments following chronic treatment with diuretics that act on the loop of Henle or the distal convoluted tubule may curtail sodium excretion as well as promote K^+ secretion.[136] An increase in amiloride-sensitive K^+ secretion has been observed following uninephrectomy, and is linked to an initial increase in plasma K^+ concentration, and increased distal tubule fluid and sodium delivery.[25,46,109]

Renal sympathetic nerve activity affects renal K^+ excretion, most likely mediated by changes in glomerular filtration rate (GFR) and sodium excretion.[422] Renal denervation was shown to increase GFR, accompanied by enhanced sodium excretion, significant kaliuresis, and lowering of plasma K^+ concentration. Renal denervation lowers proximal sodium reabsorption, and the ensuing kaliuresis is best explained by enhanced sodium delivery to distal K-secreting nephron segments. An interesting observation concerns the relationship between distal tubule sodium reabsorption and K^+ secretion in a rat model of nephrotic syndrome. Although displaying high rates of sodium reabsorption in collecting ducts, K^+ secretion was not enhanced in tubules from such nephrotic rats. Inhibition of ROMK secretory K^+ channels was traced to the presence of high albumin in the tubule lumen. Moreover, nephrotic rats were shown to be less able to excrete K^+ when given a high-K^+ diet, an observation consistent with compromised apical K^+ channel activity.[149]

Non-chloride sodium salt also affects urinary K^+ excretion. Thus, the kaliuretic effects of sulfate, phosphate, and bicarbonate are well-established. Prolonged fasting and the enhanced excretion of short-chain fatty acids and organic acid radicals also promote K^+ loss.[306] Interestingly, infusion of sodium bicarbonate is more kaliuretic than similar amounts of sulfate.[80] It is generally assumed that the stimulating effect of poorly-reabsorbable anions on K^+ secretion is mediated by their effects on the lumen-negative potential.[321] Although there is evidence that the transepithelial potential difference effectively alters K^+ secretion,[179] it is unlikely that the effects of poorly-reabsorbable anions are solely mediated by changing the

transepithelial potential, because sulfate-induced enhancement has been shown to continue in the presence of effective blockade of sodium and K^+ channels. This suggests that stimulation of K^+ secretion in the presence of sulfate is mediated by low tubule chloride, which stimulates electroneutral K^+ chloride co-transport.[526] Perfusion studies also provide support for the notion that lumen alkalinization and bicarbonate directly stimulate K^+ secretion through augmenting electroneutral secretory K^+ chloride co-transport.[8]

Acid–Base Balance

Acid–base derangements have long been known to affect the excretion of K^+, and losses of K^+, particularly in states of alkalosis, are well-documented.[14,48–52,68,176,179,182,320,470,472] Figure 49.38 shows the striking dependence of renal K^+ excretion and distal K^+ secretion on blood pH. It is apparent that alkalosis stimulates, and acidosis depresses, K^+ excretion.

Clearance, stop-flow, micropuncture, and microperfusion studies indicate that the DCT and CCD are the main nephron sites where acid–base changes affect K^+ secretion. The right panel of Figure 49.38 shows results of a microperfusion study in which tubule flow rate and solute composition of luminal fluid were kept constant. Metabolic acidosis caused distal K^+ secretion to decrease, whereas metabolic alkalosis had the opposite effect. Direct effects of acid–base disorders on K^+ transport in these nephron segments can be distinguished from indirect effects that include changes of: (1) distal flow rate; (2) composition of fluid reaching the distal tubule; and (3) aldosterone levels.[472] Changes in plasma K^+ cannot be held responsible for acid–base related changes in K^+ excretion, because hyperkalemia is frequently associated with acidosis, whereas hypokalemia is commonly observed in alkalosis.[4,14,51,176,320]

The direct effects of acid–base disorders, summarized in Figure 49.39, involve modifications of both basolateral and apical transport functions in principal and intercalated cells. With regard to the basolateral membrane, alkalosis stimulates active K^+ uptake and increases the permeability to K^+ ions (Figure 49.40). The permeability increase in alkalosis shifts the membrane potential close towards the K^+ equilibrium potential, and minimizes K^+ loss from cells into the peritubular fluid. Acidosis has the opposite effect, including direct inhibition of basolateral Na^+,K^+-ATPase activity (Figure 49.41).[350] Acid–base related changes in the apical cell membrane are also observed and involve a striking sensitivity of both K^+ and sodium channel activity to cytosolic pH. Over a narrow and physiological pH range, acidosis (pH 7.0) suppresses and alkalosis (pH 7.4) stimulates sodium and K^+ channel activity.[158,159,217,544,546]

Additional stimuli modulating K^+ secretion in acid–base disturbances involve the delivery of tubule fluid with high Na^+ bicarbonate and low chloride concentrations to the distal nephron in metabolic alkalosis (Figure 49.42). Bicarbonate and other poorly-permeant anions act as osmotic diuretics and increase distal tubule flow rate and, as mentioned above, low lumen chloride concentration stimulates apical K-Cl secretion in distal convoluted and principal cells.[132,521,526] Bicarbonate also appears to activate K^+ excretion directly.[8,306] Figure 49.42 shows the results of *in vivo*

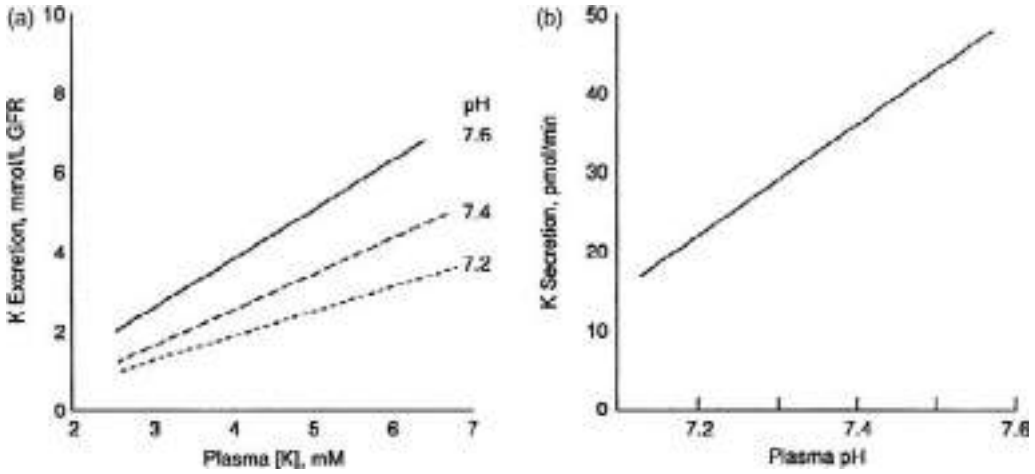

FIGURE 49.38 **(a) The relationship between plasma K^+ concentration and renal K^+ excretion is affected by plasma pH.** (*From Stanton, B. A., and Giebisch, G. (1991). Renal potassium transport. In "Handbook of Physiology: Renal Physiology," 813–874, Windhager, E. E. (ed.). Oxford University Press, New York, with permission.*) **(b) Distal K^+ secretion is affected by plasma pH.** (*From ref. [472], with permission.*)

microperfusion experiments in which luminal chloride was replaced with sulfate. Reducing luminal Cl concentration below 20 mM stimulates K^+ secretion into the distal tubule without changing the transepithelial voltage. Unidirectional flux measurements show that the increase in K^+ secretion occurs because the cell-to-lumen flux is enhanced. This enhanced secretory flux is not blocked by barium in the lumen.

Opposing effects of metabolic acidosis on K^+ excretion are summarized in Figure 49.41; metabolic acidosis may either inhibit or stimulate K^+ secretion. Direct actions of acidosis involve inhibition of K^+ secretion in distal nephron segments. In addition, indirect effects enhance K^+ secretion by elevating distal delivery of sodium-containing fluid following diminished proximal tubular bicarbonate transport. When flow rate along single distal tubules is kept constant, acidosis depresses K^+ secretion.[472] However, under free-flow conditions in intact tubules, K^+ secretion may rise as a consequence of increased fluid flow rate thought to result from inhibition of proximal transport during acidosis.[14] Such an increase in distal fluid and sodium delivery stimulates K^+ secretion during loading with ammonium chloride, in diabetic acidosis, and in proximal tubular acidosis. Taken together, it is clear that the effects of acid–base disturbances on K^+ excretion are mediated by two major components: direct effects related to pH, and secondary effects relating to the rate of delivery and composition of fluid entering the distal nephron. Increased aldosterone, possible related

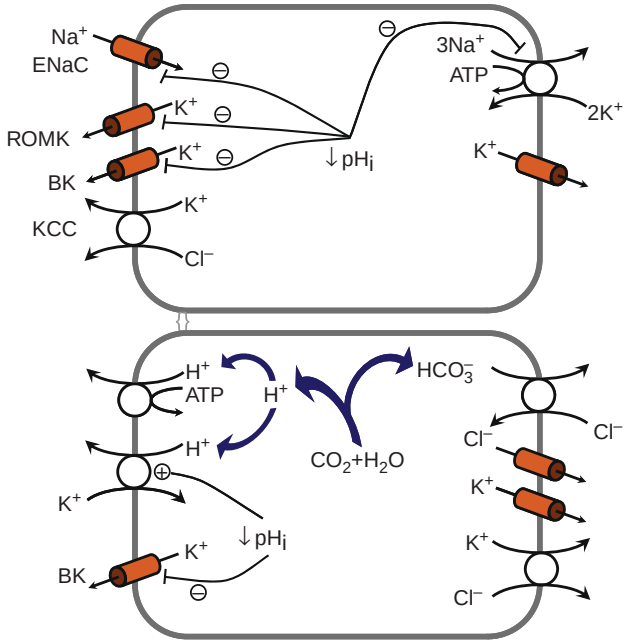

FIGURE 49.39 **Effects of pH changes on K^+ transport in principal (top) and intercalated (bottom) cells.** *(From ref. [14].)*

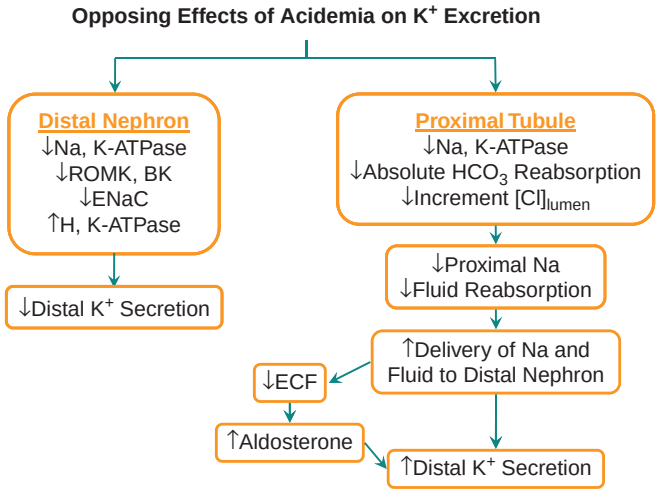

FIGURE 49.41 **Complex effects of acidemia on proximal and distal tubule potassium transport.**[14]

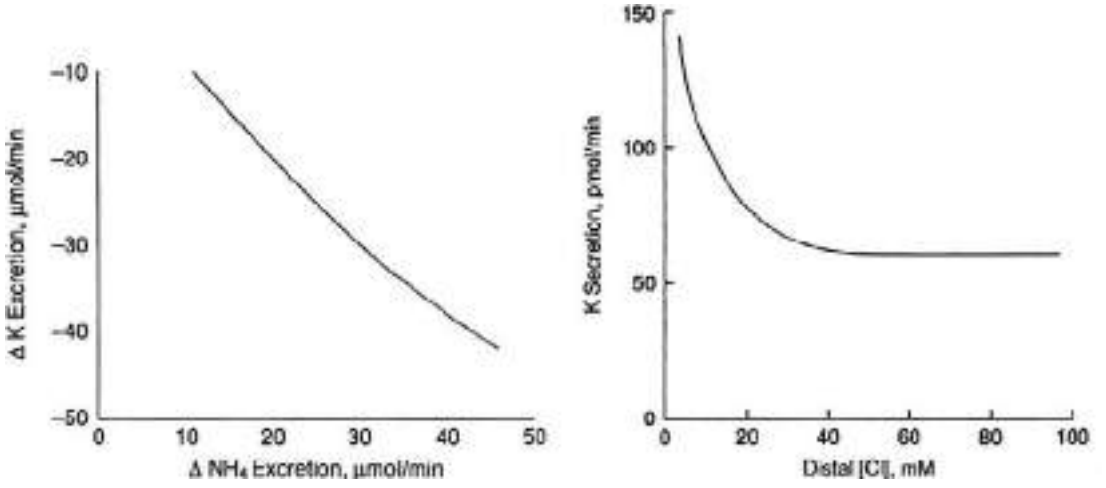

FIGURE 49.40 **Effects of acute alkalemia on K^+ excertion.**

to ECFV contraction, also contributes to kaliuresis during acidosis; K^+ excretion is reduced in acidosis when aldosterone levels are not allowed to increase.[473]

Metabolic alkalosis increases K^+ secretion by several mechanisms, both as a result of direct stimulation of K^+ secretion in principal cells and diminished K^+ reabsorption by K-H-ATPase in intercalated cells (Figure 49.40). Additionally, high delivery rates of bicarbonate-containing fluid into the distal tubule further promote K^+ secretion.[8,80,306]

It should be noted that the effects of respiratory acid–base disturbances on renal K^+ excretion are milder than those observed in metabolic acid–base disturbances.[14] In respiratory acidosis, the maintenance of significantly higher plasma bicarbonate concentrations sustains proximal tubule fluid reabsorption, and renal compensation of chronic respiratory acidosis restores plasma pH to normal more effectively than in metabolic acidosis.[14] Kaliuresis in respiratory alkalosis is also milder than that observed in metabolic alkalosis.

K^+ transport across the outer medullary collecting duct is also affected by changes in electrogenic hydrogen ion transport. Acidosis enhances electrogenic hydrogen secretion and tends to increase the lumen-positive potential, whereas alkalosis has the opposite effect. Passive K^+ reabsorption would thus be increased during acidosis and depressed in alkalosis. Independent of these indirect effects, metabolic acidosis has been shown to stimulate the activity of the apical K^+-H^+-ATPase in isolated rabbit CCDs.[458]

Renal production of ammonium is important not only to renal acid excretion, and therefore to maintenance of acid–base balance, but also to renal K^+ excretion. Tannen has drawn attention to the inverse relationship between urinary K^+ and ammonium excretion shown in Figure 49.42.[501,502] Studies in *in vivo* and isolated perfused kidneys have demonstrated that K^+ excretion is depressed when ammonium excretion is enhanced, an effect that has been localized in micropuncture studies to tubule sites beyond the ICT.[247] Studies of isolated perfused kidneys have systematically evaluated acid–base and endocrine factors modulating principal cell function.[445,446] The cell mechanism of the inhibitory effect of ammonium on K^+ excretion may involve competition between K^+ and ammonium at the K^+-binding site of the Na^+,K^+-ATPase in the basolateral membrane of principal tubule cells.[534]

Other Hormones

Vasopressin stimulates the secretion of K^+ ions across the distal tubule and CCD.[146,148,437,438,443,447] *In vivo* perfusion of the distal tubule and electrophysiological studies of K^+ transport in principal cells indicate that activation of K^+ secretion reflects an increase in apical sodium permeability.[443] Besides this effect on the driving force of K^+, patch-clamp studies have shown that vasopressin also increases the density of K^+ channels in the apical membrane of principal tubule cells.[82] The effects of vasopressin on K^+ secretion in cortical collecting ducts are sharply augmented by mineralocorticoid pretreatment.[438]

Luminal vasopressin also stimulates K^+ secretion via activation of V1 receptors.[10] This effect differs from the basolateral action, in that the V1 receptor is coupled to the phospholipase-IP3, Ca^{2+}-PKC signaling pathway, rather than cyclic AMP (Figure 49.43). A key role of Ca^{2+} was established by showing that chelators such as BAPTA abolished the luminal effects of vasopressin.

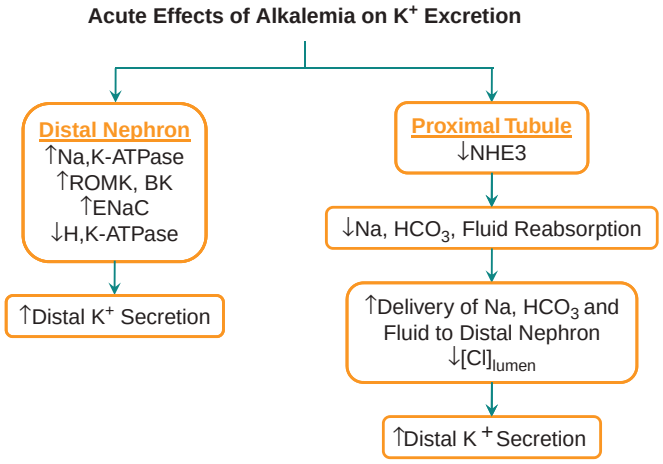

FIGURE 49.42 **Relation between luminal NH_4 (left) and Cl^- (right) concentration and K^+ secretion.** Distal K^+ secretion is inhibited by the presence of Cl^- in the tubule lumen and is stimulated when Cl^- concentration falls below 20 mM. *(From Velazquez, H., Ellison, D. H., and Wright, F. S. (1987). Chloride-dependent potassium secretion in early and late distal tubules. Am. J. Physiol. Renal* **253**, *F555–562, with permission.)* Changes in renal potassium excretion are negatively correlated with changes in ammonium excretion. *(From ref. [501,502], with permission.)*

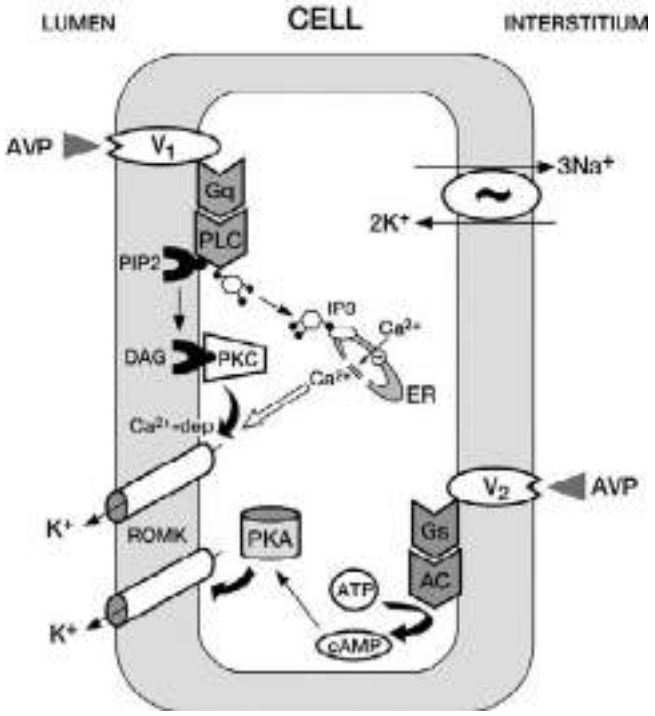

FIGURE 49.43 **Signaling mechanisms of luminal (V1 receptors) and basolateral (V2 receptors) action of AVP (arginine vasopressin) (PLC: phospholipase C; ER: endoplasmic reticulum).** *(From Amorim, J. B., Musa-Aziz, R., Mello-Aires, M., and Malnic, G. (2004). Signaling path of the action of AVP on distal K^+ secretion. Kidney Int.* ***66****, 696–704, with permission.)*

These observations strongly suggest that Ca^{2+}-sensitive B channels mediate the luminal effects of vasopressin. In contrast, the basolateral effects of vasopressin involve V2 receptors and the cAMP–PKA cascade which modulate ROMK channels.[82] The inhibitory effects on K^+ secretion of angiotensin and prostaglandins are similarly mediated by the phospholipase A-arachidonic acid pathway.[217]

Klotho, ATP, Catecholamines, Insulin, Glucagon, Kallikrein, and Guanilyn

Klotho, an age-suppressing agent, is expressed in distal tubule cells and regulates expression of ROMK channels in the kidney.[84] It not only increases ROMK abundance in HEK cells (human embryonic kidney cells), but also increases urinary K^+ excretion when given intravenously to rats. Diminished Klotho production associated with reduced renal mass and renal failure could contribute to impaired K^+ excretion. It is of interest that angiotensin II infusions curtail Klotho expression in the kidney. K^+ restriction activates the angiotensin II system, and its inhibitory effect on Klotho could account for diminished K^+ excretion during K-deprivation.[84]

Purinergic receptors and *ATP* affect K^+ transport in the kidney. Apical ATP reduces not only amiloride-sensitive Na transport,[128,297,298] but also decreases apical ROMK channel activity.[316] Consistent with inhibition of K^+ secretion by luminal ATP is the observation that mice lacking P2Y2 receptors display facilitated K^+ excretion accompanied by lower plasma K^+ concentrations.[406] A paracrine element of ATP-dependent regulation of tubule transport in collecting ducts has also been suggested: decreased Na reabsorption and diminished K^+ secretion as well as lowering of urinary ATP excretion result from ablation of renal purinergic receptors that are normally activated in intercalated tubule cells by enhanced tubule flow rate.[228a]

Both α- and β-adrenergic agonists affect K^+ transport by distal nephron segments. Care must be taken, however, to distinguish direct tubule effects from extrarenal effects, because epinephrine activates K^+ uptake in liver and muscle, and lowers plasma K^+ levels.[53,55] Nevertheless, when plasma K^+ levels are prevented from declining after epinephrine administration by infusion of K^+-containing fluids, renal K^+ excretion still falls. The epinephrine effect to suppress K^+ secretion or to enhance K^+ reabsorption has been localized to nephron sites beyond the initial collecting tubule.[104] Treatment with adrenergic agonists has been shown to reduce the lumen-negative voltage and chloride absorption in cortical collecting ducts.[242]

Insulin plays an important role in the regulation of extrarenal K^+ homeostasis,[53,103] but its renal effects are both modest and complex.[60,167,415] Insulin administration has been observed to reduce K^+ excretion,[104] but the role of changes of plasma K^+ and other hormones have proved difficult to resolve. In one clearance study, in which efforts were made to maintain constant K^+ levels in the blood, insulin modestly increased K^+ excretion.[415] In contrast, microperfusion of isolated CCDs with insulin *reduced* K^+ secretion.[167]

Glucagon has also been shown to have a significant effect on K^+ excretion. Its infusion induces a prompt increase in K^+ excretion, and it has been suggested that the effective excretion of K^+ following food intake may be related to glucagon release.[5]

Kallikrein is synthetized in distal connecting tubule cells,[87,128] and its release into the tubule fluid following a dietary K-load modulates downstream K^+ and Na transport.[137] Figure 49.44 illustrates its mode of action and that of other luminal agents. Following a dietary load of K, kallikrein is released into the tubule lumen and exerts its downstream action by inhibiting K^+ reabsorption by K/H exchange in intercalated cells. It also stimulates apical sodium channels in principal cells, depolarizing the apical membrane and enhancing the driving force for K^+ secretion. It is noteworthy that

the prompt kaliuresis following food intake was not associated with increased urinary aldosterone excretion.[87]

Guanylin and *uroguanylin* are peptides found in the gut and urine, and renal function studies demonstrate their ability to promote an increase in sodium and fluid excretion.[9] Perfusion studies in single rat distal tubules show that these peptides also inhibit K^+ secretion, most likely by modulating the activity of maxi-K channels. It is possible, but not certain, that guanilyn and uroguanylin are involved in the signaling between the gastrointestinal tract and the kidney with respect to changes in K^+ balance.

Diuretics

Diuretic drugs, used primarily to promote excretion of salt and water, also affect renal K^+ excretion.[73,134,135,171,181,186,201,234,345,524] Figure 49.45 illustrates the primary renal sites of action of compounds representative of three classes of diuretic drugs that act from the luminal side of tubule cells. Loop diuretics, such as furosemide, act mainly on the Na-K-2Cl co-transporter in the apical membrane of thick ascending limb cells.[74–76,198,201,234] Thiazide diuretics have their primary action on an Na-Cl co-transporter in cells of the distal convoluted tubule.[95,234,522–524] Loop and thiazide diuretics are both capable of increasing K^+ excretion. K^+-sparing diuretics, exemplified by amiloride and triamterene, block Na channels in principal cells of the ICT and CCD.[19,73,119,232,357] Renal K^+ excretion depends primarily on secretion by principal cells in the ICT and CCD. Amiloride targets these cells by a blocking ENaC, reducing the transepithelial potential difference and diminishing the driving focrce for K^+ secretion. Luminal Ca^{2+} also blocks ENaC, and has similar inhibitory effects on K^+ secretion.[372]

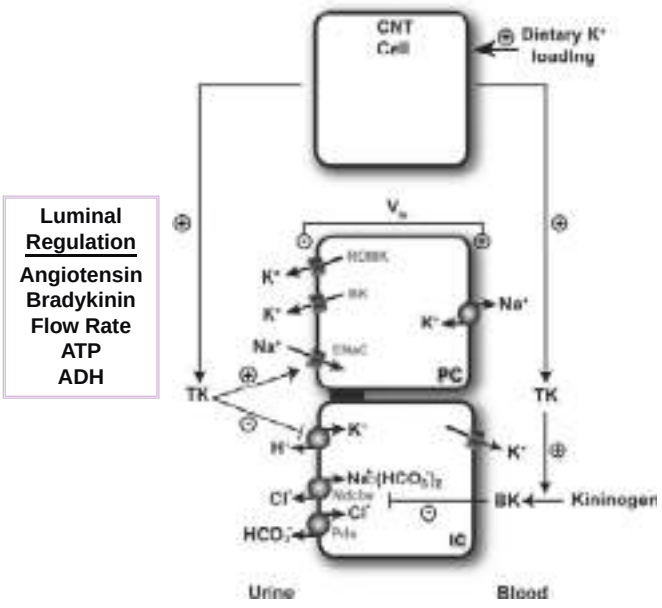

FIGURE 49.44 Regulation of distal tubule function by messengers. *(From ref. [128].)*

Loop diuretics increase renal K^+ excretion, in part by direct effects on TAL cells, and also by secondary effects on principal cells in the ICT and CCD. Thus, furosemide inhibition of the Na-K-2Cl co-transporter leaves the cell-to-lumen K^+ flux through apical membrane channels unopposed, resulting in either greatly reduced K^+ absorption or even reversal to produce net K^+ secretion, along the TAL.[201,511,512] The inhibition of Na and Cl absorption in the TAL also reduces medullary interstitial osmolality and results in decreased fluid absorption along the descending limb. Thus, loop diuretics not only decrease K^+ reabsorption in the thick ascending limb but, in addition, increase the rate of fluid delivery out of the loop of Henle and provide a flow rate stimulus to K^+ secretion along the distal tubule and collecting duct. Different degrees of kaliuresis have been observed in animal studies with furosemide and piretanide. The latter is less potent in promoting loss of K^+, owing to stimulation of bradykinin production which curtails sodium entry into collecting duct principal cells.[71]

Thiazide diuretics also promote renal K^+ excretion, largely via inhibition of the apical Na-Cl co-transporter in the DCT.[135,523–526] A likely explanation for the effect of thiazides to promote K^+ excretion is the increase in distal sodium and fluid delivery through inhibition of sodium chloride co-transport. By decreasing carbonic anhydrase-dependent sodium and bicarbonate reabsorption in the proximal tubule, thiazides also tend to increase the flow rate of fluid into the distal nephron.[234,522]

Osmotic diuretics exert their kaliuretic action largely by increasing fluid and sodium delivery into the distal tubule following proximal tubule transport inhibition. As described above, poorly permeant anions such as sulfate, phosphate bicarbonate, ferrocyanide, and hippurate not only augment distal fluid and sodium delivery, but also facilitate K^+ secretion by lowering lumen Cl^--concentration, thus stimulating K^+-chloride co-transport.[8,132] It should be noted, though, that with increased fluid loads delivered to the distal nephron, larger fractions of K^+ also enter the distal nephron. Additional mechanisms favoring K^+ loss during administration of diuretic agents also involve hormonal effects. As extracellular volume shrinks owing to urinary loss of sodium chloride, aldosterone and vasopressin release stimulate K^+ secretion.

Maturation of K^+ Transport

Somatic growth after birth is associated with a predictable increase in total body potassium content[77,152] and maintenance of a state of positive potassium balance.[106,111,496] Renal potassium clearance is low in newborns, even when corrected for the low glomerular filtration rate prevailing early in life.[106,430,496] Although infants, like adults, can excrete urinary potassium at a rate that exceeds its glomerular filtration, reflecting the capacity for net tubular secretion, they are unable to excrete an exogenously administered potassium load as efficiently as the adult.[313,330,510] Micropuncture studies in young (2-week-old) rats[299] and clearance studies in saline-expanded dogs[271] provide additional evidence for a limited secretory and enhanced reabsorptive capacity of the distal nephron to potassium early in life.

The physiologic processes contributing to net urinary potassium excretion in the neonate are similar to those already described in the fully-differentiated kidney, and include glomerular filtration, reabsorption (predominant) along the proximal tubule and loop of Henle, and bidirectional transport in the distal nephron. The fraction of the filtered load of potassium reabsorbed along the proximal tubule of suckling (2-week-old) rats is similar to that reabsorbed along the same segment in the adult.[299,462] In contrast, the TALH appears to undergo a significant developmental increase in its capacity for potassium reabsorption and diluting capacity, as evidenced by the findings in rats of significant increases in the: (1) fractional reabsorption of potassium along this segment, expressed as a percentage of delivered load, between the second and sixth weeks of postnatal life;[299] and (2) osmolarity of early distal fluid between the second and fourth weeks of life.[605] Molecular studies identify postnatal increases in abundance of mRNA encoding NKCC2 and Na-K-ATPase in rodent kidney, and in particular, in the medulla,[450,588] and Na-K-ATPase activity in rabbit TALH.[448]

Potassium secretion in the distal nephron, and specifically in the mammalian cortical collecting duct

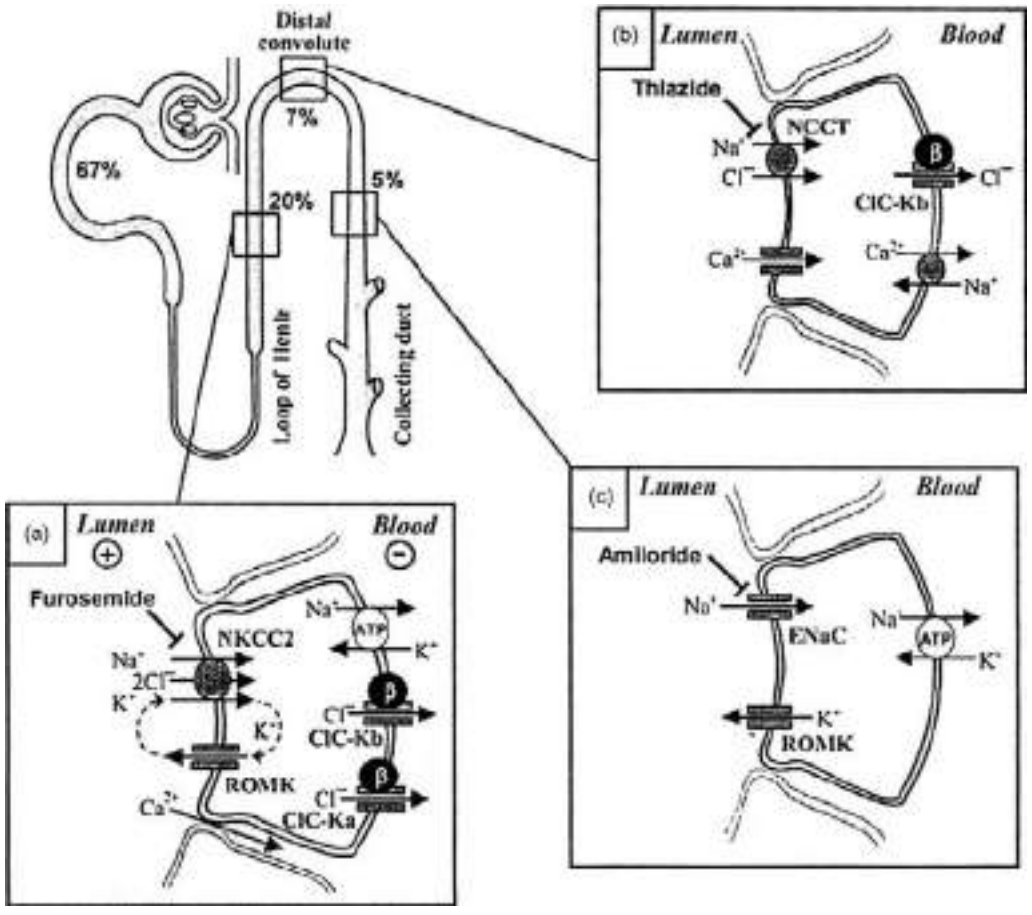

FIGURE 49.45 Distribution of NKCC2, ROMK, the CIC-ß-sub-unit Barttin, CIC-Kb, and NCCT along the nephron and site of action of the classic diuretic agents: (a) furosemide; (b) thiazide; and (c) amiloride. *(Acta Physiol. Scand. 2004, 181, 513–521.)*

(CCD) microperfused *in vitro*, is low early in life, and cannot be stimulated by high tubular (urinary) flow rates (Figure 49.46).[429,430] Indeed, basal potassium secretion cannot be detected in the rabbit CCD until after the third week of postnatal life, with potassium secretory rates increasing thereafter to reach adult levels by six weeks of age.[429] The limited capacity of the distal nephron for potassium secretion is due primarily to a paucity of apical conducting SK/ROMK channels in principal cells early in life.[431] The postnatal increase in apical channel activity reflects a developmental increase in number of channels, due to an increase in transcription and translation of channel proteins,[45,606] and not open probability which remained constant for all channels identified after the second week of life.[431] The electrochemical gradient favoring potassium secretion does not appear to be limiting early in life, as Na-K pump activity and the rate of net sodium absorption in the rabbit CCD at two weeks of age are 50–60% of that measured in the adult.[92,429,448] *In vivo* measurements of the sodium concentration in distal tubular fluid generally exceed 35 mEq/l both in healthy adult and suckling rats and thus should not restrict distal sodium secretion.[192,299,605]

Flow-induced potassium secretion, which is mediated by the Ca^{2+}- and stretch-activated BK channel, is a relatively late developmental event, first appearing in the rabbit CCD in the fifth week of postnatal life.[430,575] The detection of flow-induced potassium secretion coincides with the appearance of apical immunodetectable maxi-K channel α-subunit protein in this segment.[575] The absence of flow-induced potassium secretion early in life is not due to a limitation in the ability of the distal nephron to respond to an increase in luminal flow rate with an increase in net sodium absorption and/or intracellular Ca^{2+} concentration, responses required for flow-stimulated net potassium secretion; these flow-induced responses in CCDs from young animals are equivalent to those detected in the adult by the second week of postnatal life.[575]

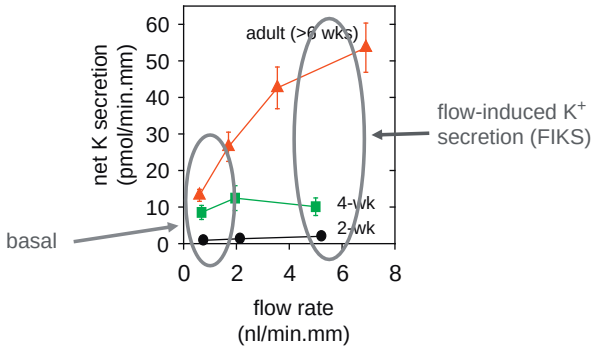

FIGURE 49.46 **Developmental changes in basal and flow-induced (FIKS) K^+ secretion in microperfused rabbit CCDs.** The maturing rabbit CCD is characterized by the relatively early appearance of basal K^+ secretion, mediated by SK/ROMK channels, at ~2 wks of age and, after the 4th week of postnatal life, BK channel-mediated FIKS. *Modified from ref. [429].*

The paucity of apical potassium secretory channels and relatively robust basolateral Na-K-ATPase activity prevailing in the CCD early in life requires that potassium translocated into the cell by the Na-K pump be recycled back into the interstitium via basolateral potassium channels to maintain a constant intracellular potassium concentration. Thus, the postnatal increase in transepithelial potassium secretion likely requires not only activation of apical potassium channels, but also modification of the magnitude of basolateral potassium recycling. Little is known about the developmental expression and regulation of renal basolateral potassium channels. Immunodetectable Kir7.1, which co-localizes with Na-K-ATPase at the basolateral membrane of distal nephron and principal cells of the fully differentiated CCD,[374a] is first observed in the cortical and medullary TAL by the end of the first postnatal week in rat, appearing in the DCT and CCD at three weeks of age.[497a] As the postnatal appearance of Kir7.1 coincides with that of ROMK in the CCD, Kir7.1 is not a likely candidate for basolateral potassium recycling in the early postnatal period. Kir7.1 has been proposed to contribute to urinary potassium excretion in response to potassium-loading by generating a transepithelial potential difference for sodium reabsorption which, in turn, provides the driving force for potassium secretion.[497a]

While the distal nephron is limited in its capacity for potassium secretion early in life, clearance studies suggest that newborn dogs absorb 25% more of the distal potassium load than their adult counterparts.[313] Functional assays of apical H-K-ATPase in rabbit collecting duct reveal that pump activity in neonatal intercalated cells is equivalent to that measured in mature cells.[91] Although these data alone do not predict transepithelial potassium absorption under physiologic conditions, the high distal tubular fluid potassium concentrations measured *in vivo* in the young rat may[299] facilitate H-K-ATPase-mediated potassium absorption in this part of the nephron.

Circadian Rhythm

Renal K^+ excretion varies during the 24-hour day.[337–339] Some of this variation occurs because of spacing between meals or other episodes of K^+ intake. However, even when K^+ ingestion is spread evenly throughout the day and night, a pattern of lower rates

of K^+ excretion at night and in the morning, and higher rates in the afternoon emerges.[337–339,397] Figure 49.47 shows the response of human subjects to an intravenous K^+ load, given either starting at midnight or midday. The relationship between plasma concentration and rate of renal K^+ excretion at different times of the day–night cycle is also summarized. It is apparent that the kaliuretic response was significantly diminished at night. Thus, higher concentrations of K^+ were required at night to effect K^+ excretion.

These daily fluctuations of K^+ excretion have not been fully explained. As with other circadian rhythms, the periodicity is entrained by the light–dark cycle, and depends on both central and peripheral pacemakers.[337–339] Notably, the DCT and CCD express several regulatory "Clock" genes, indicating operation of a local, intrarenal, pacemaker.[607] ENaC-, aquaporin 2-, and vasopressin-receptors have marked circadian rhythms which could indirectly influence the excretion of K^+. Also, it is likely that the changes in K^+ excretion are produced by changes in distal secretion. It has been reported that changes in aldosterone are not required,[393–397] but that the higher K^+ excretions during daytime may be related to enhanced bicarbonate loss in the urine.[477]

Integrated Regulation of K^+ Homeostasis

Renal K^+ excretion is regulated by multiple factors acting at several transport sites in response to influences originating outside the kidney. The final rate of excretion of K^+ is determined by the net effect of mechanisms that may be cooperating or competing. In some situations the individual regulatory factors may act together, while in other cases they may change in directions that tend to cancel one another. Reasonable predictions of the rate of K^+ excretion can be derived from knowledge of expected changes of individual factors.

Model calculations of tubule K^+ transport have provided interesting insights between water and K^+ transport. It was suggested that the increase in K^+ concentration along both the water-permeable connecting and collecting tubule was not only mediated by net secretion in principal cells, but also by vasopressin-dependent fluid equilibration.[560] Indeed, it becomes apparent that the initial K^+ concentration in both nephron segments may reach such high concentrations that they exceed the maximal transepithelial K^+ gradient that can be achieved by K^+ secretion in principal cells. As a consequence, both the CNT and CCD can become sites of modest, albeit significant, reabsorption of K^+. Calculations based on these cell models also allowed an assessment of the interactions between axial flow rate along the CNT and CCD, the sodium-load,

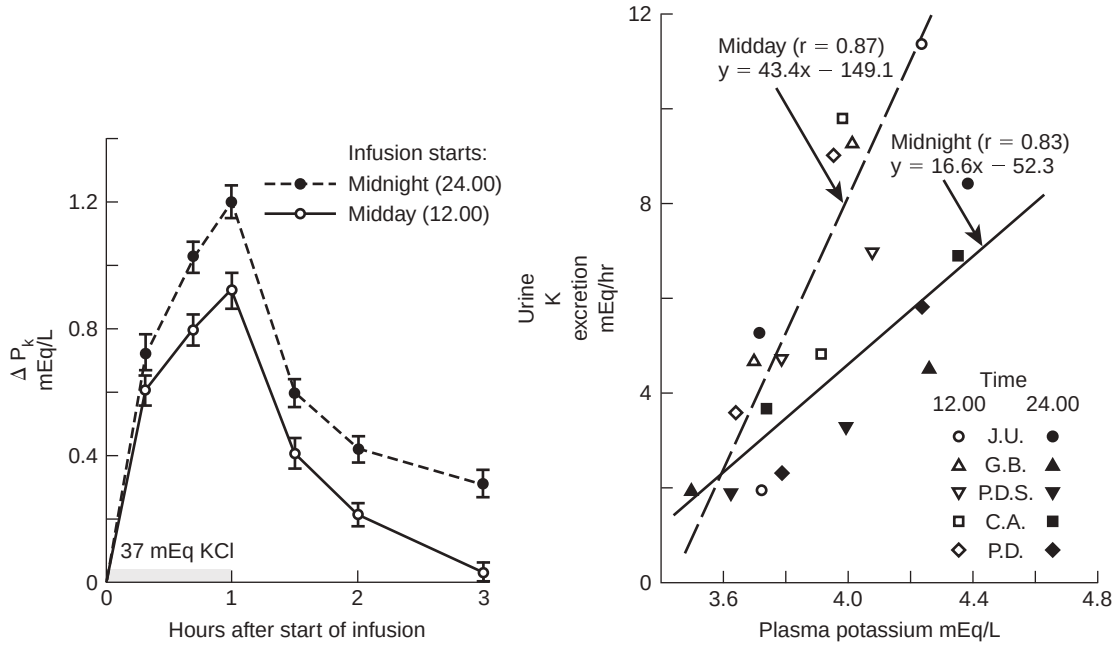

FIGURE 49.47 Left: Response of plasma potassium concentration (PK) in human subjects to intravenous infusion of 37 mEq of potassium chloride solution in 250 ml of water provided over 1 hour either starting at midnight (dashed line) or midday (solid line). Right: Relationship between plasma potassium concentration and rate of renal potassium excretion in human subject at midnight (dashed line) or midday (solid line). *(Am. J. Physiol. 1986, **250**, R735–R752.)*

transepithelial potential difference, and water permeability. It has also made possible an analysis of the factors leading to the typical kaliuresis produced by thiazides.[560]

An example of cooperative factors modulating K^+ transport is seen in the renal response to a high-K^+ intake. As noted previously, the increase in plasma K^+ concentration promotes K^+ uptake by K^+-secreting cells. It also stimulates the adrenal gland to secrete aldosterone, which in turn promotes K^+ secretion by cells of the distal nephron. Increased plasma K^+ concentration also inhibits sodium and fluid reabsorption by the proximal tubule, and thus increases flow rate into the distal nephron.

Evidence of the involvement of such factors in response to a change in K^+ intake was also obtained in a careful study employing human subjects.[391] Dietary K^+ was increased from 100 to 400 mmol/day. Renal K^+ excretion progressively increased so that external K^+ balance was restored within three days. During the first two hours after each meal, plasma K^+ rose by approximately 0.5 mM and then subsided, returning to the normal range before the next meal. Plasma aldosterone also increased after meals. The changes in plasma aldosterone (from 400 to 900 pM) were proportionately larger than the 10–20% increase in plasma K^+. Evidence that distal flow and sodium delivery increased after meals as well came from the observation that sodium excretion increased from 50 to 200 μmol/min. Thus, the concerted actions of multiple regulatory mechanisms improve the defense against the danger of hyperkalemia.

The effectiveness of aldosterone to stimulate K^+ secretion in principle cells is modulated by SGK1 (serum- and glucocorticoid-regulated kinase 1). This kinase affects several renal transport processes. Inspection of Figure 49.28 shows that the stimulation of apical sodium and K^+ channels, as well as of basolateral Na^+,K^+-ATPase through aldosterone, involves participation of SGK. Transcription and translation of SGK is upregulated by aldosterone,[89a,289,354a] and co-expression experiments in heterologous expression systems of SGK with Na^+ or K^+ channels, and with Na^+,K^+-ATPase, indicate increased activity of these transporters. It is significant that both the reabsorption of sodium, as well as the secretion of K^+, is impaired in SGK knockout mice. Compromised upregulation of urinary K^+ excretion during chronic K^+-loading was also demonstrated by maintenance of K^+ balance, but at elevated aldosterone levels.[520] SGK has been shown to enhance abundance of ROMK in the membrane of oocytes, a process that also involves the cooperative effect of NHERF (Na-H exchange regulating factor).[589a,589b] Increased activity of ROMK is also mediated by a significant shift in pH-sensitivity of the channel.[289]

Derangements in the regulation of aldosterone regulation can have important consequences for the maintenance of K^+ balance. The hypokalemia that appears in primary hyperaldosteronism has long been recognized.[175,176] Experimental administration of excess mineralocorticoid hormone (DOC) or aldosterone produces the effects seen in patients with adrenal overproduction of aldosterone. Sodium excretion falls initially, but within a few days it then increases until balance between intake and output is restored. Plasma sodium concentration does not change; however, arterial blood pressure is increased. The "escape" from the sodium-retaining effect of mineralocorticoid excess has been attributed to inhibition of Na reabsorption by factors related to extracellular fluid volume expansion,[213,273] and thiazide-sensitive Na-Cl co-transport has been defined as the key tubule transport that is downregulated during mineralocorticoid escape.[549] In contrast to sodium, K^+ excretion rises to levels exceeding K^+ intake, continues for a longer period, and results in hypokalemia. This continued stimulation of distal K^+ secretion appears to be related to the same volume-related inhibition of sodium reabsorption that limits the period of sodium retention. Inhibition of proximal sodium and fluid absorption leads to increased distal delivery of sodium and fluid, and therefore to a flow rate stimulus to K^+ secretion. Protective mechanisms, activated by the progressively increasing K^+ depletion, involve stimulation of K^+ reabsorption by H^+-K^+-ATPase which progressively restrains further K^+ loss.

It should be noted that some investigators are not satisfied that all stimuli acting to promote increased K^+ excretion have been identified. Rabinowitz and others have argued that increases in K^+ excretion after ingestion of K^+ are not fully-explained by changes in plasma K, circulating aldosterone or distal delivery of fluid and sodium.[105,168,393] These observations have recently been confirmed and extended, and it has been suggested that sensors in the gastrointestinal tract, the liver or the brain are involved in regulating K^+ homeostasis.[392–397] A gastrointestinal or hepatic K^+ sensor would explain the observation that a K^+-load given by infusion into the portal vein is more kaliuretic compared to the same amount of K^+ injected intravenously into the systemic circulation.[369] Moreover, by restricting the initial rise of K^+ to the hepatic circulation, kaliuresis could be induced without larger and potentially harmful fluctuations of K^+ in the general circulation.[89,343,369] Hepatic afferent nerve activity has been reported to increase with K^+ injection into the portal vein, but the mechanism modulating tubule transport of K^+ needs exploration.

When K^+ intake is restricted, reductions in plasma K^+ and circulating aldosterone withdraw the stimulus

to K^+ secretion, and renal K^+ excretion tends to fall. However, in some circumstances the integrated actions of all factors, because of competing priorities, fail to maintain K^+ balance. For example, if K^+ intake is being restricted along with other food because an individual has just undergone an abdominal operation, stress-related stimulation of aldosterone secretion may put high aldosterone levels in competition with low plasma K^+ levels, and cause the rate of K^+ excretion to exceed the rate of intake. Furthermore, if saline infusions are maintaining extracellular fluid volume and urine flow, a high flow rate of tubule fluid may further compromise the ability of the kidney to retain K^+.

In other circumstances, competition among the regulatory factors may actually serve the cause of K^+ homeostasis. Changes in sodium intake are a relevant example. Although changes in sodium intake lead to changes in circulating aldosterone and extracellular fluid volume, they do not result in important deviations from K^+ balance. Lack of sodium enhances proximal fluid reabsorption, and may decrease distal flow rate and diminish K^+ excretion. However, the simultaneous stimulation of the renin–angiotensin–aldosterone system acts to promote K^+ excretion. Similarly, with deprivation of water alone, competition among regulatory factors may also act to stabilize K^+ excretion. The K^+-retaining influence of low luminal flow rate is opposed by the stimulatory influence on K^+ secretion of increased circulating vasopressin.

Finally, in some acid–base disturbances, the net result of several influences on K^+ secretion may cause the kidney to excrete K^+ at rates exceeding K^+ intake, and thus to deplete body K^+. In metabolic alkalosis, plasma K^+ concentration tends to be low because cell uptake of K^+ is enhanced. Aldosterone levels are often elevated and also tend to promote K^+ secretion. Increased distal delivery of bicarbonate, associated with increased distal flow, and high luminal bicarbonate concentration permits the distal Cl concentration to fall to low levels, and thus further favor K^+ secretion of KCl co-transport.

In acute metabolic acidosis, decreased uptake of K^+ by distal cells tends to reduce K^+ secretion. However, as acidosis proceeds, proximal fluid absorption is increasingly inhibited and distal flow rate begins to increase. An additional factor favoring K^+ secretion is the elevation of aldosterone that has been observed in chronic metabolic acidosis. Taken together, it is important to recognize that renal K^+ excretion has multiple determinants, and that they may not always be responding only to changes in K^+ balance.

Acknowledgments

We are grateful to Dr. Fred Wright, who was a major contributor and co-author of previous chapters in the earlier issues. Ms. Leah Sanders and Mr. Duncan Wong have also contributed by careful editing of the manuscript and preparation of the figures.

We dedicate this chapter to Steve Hebert. He was an inspiration to all of us.

References

[1] Ackermann D, Gresko N, Carrel M, Loffing-Cueni D, Habermehl D, Gomez-Sanchez C, et al. *In vivo* nuclear translocation of mineralocorticoid and glucocorticoid receptors in rat kidney: differential effect of corticosteroids along the distal tubule. Am J Physiol 2010;299:F1473–1485.

[2] Adam WR, Dawborn JK. Potassium tolerance in rats. Aust J Exp Biol Med Sci 1972;50:757–86.

[3] Adams PR, Constanti A, Brown DA, Clark RB. Intracellular Ca^{2+} activates a fast voltage-sensitive K^+ current in vertebrate sympathetic neurones. Nature 1982;296:746–9.

[4] Adler S, Fraley DS. Potassium and intracellular pH. Kidney Int 1977;11:433–42.

[5] Ahloulay M, Dechaux M, Laborde K, Bankir L. Influence of glucagon on GFR and on urea and electrolyte excretion: direct and indirect effects. Am J Physiol 1995;269:F225–35.

[6] Ahn KY, Kone BE. Expression and cellular localization of mRNA encoding the "gastric"isoform of H^+-K^+-ATPase a-subunit in rat kidney. Am J Physiol 1995;268:F99–109.

[7] Alexander EA, Levinsky NG. An extrarenal mechanism for potassium adaptation. Clin Invest 1968;47:740–8.

[8] Amorin JB, Bailey MA, Musa-Aziz R, Giebisch G, Malnic G. Role of luminal anion and pH in distal tubule potassium secretion. Am J Physiol Renal 2003;284:F381–8.

[9] Amorim JBO, Musa-Aziz R, Lessa LMA, Malnic G, Fonteles MC. Effect of uroguanylin on potassium and bicarbonate transport in rat renal tubules. Can J Physiol Pharmacol 2006;84: 1003–10.

[10] Amorim JBO, Malnic G. VI receptors in luminal action of vasopressin (AVP) on distal K^+ secretion. Am J Physiol 2000;278: F809–16.

[11] Anagnostopoulos T, Planelles G. Cell and luminal activities of chloride, potassium, sodium and protons in the late distal tubule of *Necturus* kidney. J Physiol 1987;393:73–89.

[12] Antes LM, Kujubu DA, Fernandez PE. Hypokalemia and the pathology of ion transport molecules. Semin Nephrol 1998;18: 31–45.

[13] Aperia A, Holtback U, Syren ML, Svensson LB, Fryckstedt J, Greengard P. Activation/deactivation of renal Na^+,K^+-ATPase: a final common pathway for regulation of natriuresis. FASEB J 1994;8:436–9.

[14] Aronson PS, Giebisch G. Effects of pH on potassium: new explanations for old observations. J Am Soc Nephrol 2011;22:1981–9.

[15] Arrascue JF, Dobyan DC, Jamison RL. Potassium recycling in the renal medulla: effects of acute potassium chloride administration to rats fed a potassium-free diet. Kidney Int 1981;20: 348–52.

[16] Arriza JL, Weinberger C, Cerelli G, Glaser TM, Handelin BL, Housman DE, et al. Cloning of human mineralocorticoid receptor complementary DNA: structural and functional kinship with the glucocorticoid receptor. Science 1987;237:268–75.

[17] Atkinson NS, Robertson GA, Ganetzky B. A component of calcium-activated potassium channels encoded by the *Drosophila* slo locus. Science 1991;253:551–5.

[18] Avison MJ, Gullans SR, Ogino T, Giebisch T. Na^+ and K^+ fluxes stimulated by Na^+-coupled glucose transport: evidence for a Ba^{2+}-insensitive K^+ efflux pathway in rabbit proximal tubules. J Membr Biol 1988;105:197–205.

[19] Baer JE, Jones CB, Spitzer SA, Russo HF. The potassium sparing and natriuretic activity of N-amindino-3.4-diamino-6-chloropytazine-carboxyamide hydrochloride dihydrate (amiloride hydrochloride). J Pharmacol Exp Ther 1967;157:472–85.

[20] Bailey MA, Cantone A, Yan Q, MacGregor GG, Leng Q, Amorim JBO, et al. Maxi-K channels contribute to urinary potassium excretion in the ROMK-deficient mouse model of Type II Bartter's syndrome and in adaptation to a high-K diet. Kidney Int 2006;70:51–9.

[21] Bailey MA, Mullins JJ, Kenyon CJ. Mineralocorticoid and glucocorticoid receptors stimulate epithelial sodium channel activity in a mouse model of Cushing syndrome. Hypertension 2009;54: 890–6.

[22] Bailey MA, Paterson JM, Hodoke PW, Wrobel N, Bellamy CO, Brownstein DG, et al. A switch in the mechanism of hypertension in the syndrome of apparent mineralocorticoid excess. J Am Soc Nephrol 2008;19:47–58.

[23] Bailey MA, Unwin RJ, Shirley DG. *In vivo* inhibition of renal 11beta-hydroxysteroid dehydrogenase in the rat stimulates collecting duct sodium reabsorption. Clin Sci (Lond) 2001;101(2): 195–8.

[24] Bandulik S, Schmidt K, Bockenhauer D, Zdebik AA, Humberg E, Kleta R, et al. The salt-wasting phenotype of EAST syndrome, a disease with multifaceted symptoms linked to the KCNJ10 K^+ channel. Pflugers Arch 2011;461:423–35.

[25] Bank N, Aynedjian HS. A micropuncture study of potassium excretion by the remnant kidney. J Clin Invest 1973;52: 1480–90.

[26] Barlet-Bas C, Khadouri C, Marsy S, Doucet A. Enhanced intracellular sodium concentration in kidney cells recruits a latent pool of Na^+-K^+ATPase whose size is modulated by corticosteroids. J Biol Chem 1990;265:7799–803.

[27] Barlet-Bas C, Cheval L, Feraille E, et al. Regulation of tubular Na-KATPase. In: Hatano M, editor. Nephrology, Proceedings of the XIth International Congress of Nephrology. Berlin: Springer; 1991. p. 419–34.

[28] Barratt LJ, Rector Jr FC, Kokko JP, Tisher CC, Seldin DW. Transepithelial potential difference profile of the distal tubule of the rat kidney. Kidney Int 1975;8:368–75.

[29] Bastl C, Hayslett JP, Binder HJ. Increased large intestinal secretion of potassium in renal insufficiency. Kidney Int 1977;12: 9–16.

[30] Bastl C, Kliger AS, Binder HJ, Hayslett JP. Characteristics of potassium secretion in the mammalian colon. Am J Physiol 1978;234:F48–53.

[31] Bassett MH, White PC, Rainey WE. The regulation of aldosterone synthase expression. Molec and Cellular Endocrinol 2004;217:67–74.

[32] Battilana CA, Dobyan DC, Lacy FB, Bhattacharya J, Johnston PA, Jamison RL. Effect of chronic potassium loading on potassium secretion by the pars recta or descending limb of the juxtamedullary nephron in the rat. J Clin Invest 1978;62:1093–103.

[33] Baylis C, Handa RK, Sorkin M. Glucocorticoids and control of GFR. Semin Nephrol 1990;10:320–9.

[34] Beck FX, Dorge A, Blumner E, Giebisch G, Thurau K. Cell rubidium uptake: a method for studying functional heterogeneity in the nephron. Kidney Int 1988;33:642–51.

[35] Beck JS, Breton S, Mairbaurl H, Laprade R, Giebisch G. Relationship between sodium transport and intracellular ATP in isolated perfused rabbit proximal convoluted tubule. Am J Physiol 1991;261:F634–9.

[36] Beck JS, Hurst AM, Lapointe JV, Laprade R. Regulation of basolateral K^+ channels in proximal tubule studied during continuous microperfusion. Am J Physiol 1994;264:F496–501.

[37] Beck JS, Laprade R, Lapointe J-Y. Coupling between transepithelial Na^+ transport and basolateral K^+ conductance in renal proximal tubule. Am J Physiol 1994;266:F517–27.

[38] Beck JS, Breton S, Giebisch G, Laprade R. Potassium conductance regulation by pH in rabbit proximal convoluted tubules. Am J Physiol 1992;263:F453–8.

[39] Beck JS, Potts DJ. Cell swelling, co-transport activation and potassium conductance in isolated perfused rabbit kidney proximal tubules. J Physiol 1990;425:369–78.

[40] Beck LH, Senesky D, Goldberg M. Sodium-independent active potassium reabsorption in proximal tubule of the dog. Clin Invest 1973;52:2641–5.

[41] Bailey MA, Craigie E, Livingstone DE, Kotelevtsev YV, Al-Dujaili EA, Kenyon CJ, et al. Hsd1 lb2 haploinsufficiency in mice causes salt sensitivity of blood pressure. Hypertension 2011;57:515–20.

[42] Bailey MA, Mullins JJ, Kenyon CJ. Mineralocorticoid and glucocorticoid receptors stimulate epithelial sodium channel activity in a mouse model of Cushing syndrome. Hypertens 2009;54: 890–6.

[43] Bailey MA, Paterson JM, Hadoke PW, Wrobel N, Bellamy CO, Brownstein DG, et al. A switch in the mechanism of hypertension in the syndrome of apparent mineralocorticoid excess. J Am Soc Nephrol 2008;19:47–58.

[44] Beck FX, Dorge A, Blumner E, Giebisch G, Thurau K. Cell rubidium uptake: a method for studying functional heterogeneity in the nephron. Kidney Int 1988;33:642–51.

[45] Benchimol C, Zavilowitz B, Satlin LM. Developmental expression of ROMK mRNA in rabbit cortical collecting duct. Pediatr Res 2000;47:46–52.

[46] Bengele HR, Evan A, McNamara ER, Alexander EA. Tubular sites of potassium regulation in the normal and uninephrectomized rat. Am J Physiol 1978;234:F146–53.

[47] Bergann T, Fromm A, Borden SA, Fromm M, Schulzke JD. Glucocorticoid receptor is indispensable for physiological responses to aldosterone in epithelial Na^+ channel induction via the mineralocorticoid receptor in a human colonic cell line. Eur J Cell Biol 2011;90:432–9.

[48] Berliner RW. Renal secretion of potassium and hydrogen ions. Fed Proc 1952;11:695–700.

[49] Berliner RW. Renal mechanisms for potassium excretion. Harvey Lect 1961;55:141–71.

[50] Berliner RW, Kennedy TJ. Renal tubular secretion of potassium in the dog. Proc Soc Exp Biol Med 1948;67:542–5.

[51] Berliner RW, Kennedy TJ, Orloff J. Relationship between acidification of the urine and potassium metabolism. Am J Med 1951;11:274–82.

[52] Berliner RW, Kennedy Jr TJ, Hilton G. Renal mechanisms for excretion of potassium. Am J Physiol 1950;162:348–67.

[53] Bia MJ, DeFronzo RA. Extrarenal potassium homeostasis. Am J Physiol 1981;240:F257–68.

[54] Bia MJ, Tyler K, DeFronzo RA. The effect of dexamethasone on renal electrolyte excretion in the adrenalectomized rat. Endocrinology 1981;III:882–8.

[55] Bia MJ, Tyler KA, DeFronzo RA. Regulation of extrarenal potassium homeostasis by adrenal hormones in rats. Am J Physiol 1981;242:F461–8.

[56] Biagi B, Kubota T, Sohtell M, Giebisch G. Intracellular potentials in rabbit proximal tubules perfused in vitro. Am J Physiol 1981;240:F200–10.

[57] Biagi B, Sohtell M, Giebisch G. Intracellular potassium activity in the rabbit proximal straight tubule. Am J Physiol 1981;241: F677–86.

[58] Bleich M, Schlatter E, Greger R. K^+ channel of the thick ascending limb of Henle's loop. Pflugers Arch 1990;415:449–60.

[59] Bloomer HA, Rector Jr FC, Seldin DW. The mechanism of potassium reabsorption in the proximal tubule of the rat. J Clin Invest 1963;42:277–85.
[60] Boini KM, Graf D, Kuhl D, Haussinger K, Lang F. SGK1 dependence of insulin induced hypokalemia. Pflugers Arch 2009;457:955–61.
[61] Bomsztyk K, Wright FS. Effect of luminal potassium concentration and transepithelial voltage on potassium transport by the renal proximal tubule. Fed Proc 1983;42:304.
[62] Bomsztyk K, Wright FS. Dependence of ion fluxes on fluid transport by rat proximal tubule. Am J Physiol 1986;250: F680–9.
[63] Bouligand J, Delemer B, Hecart AC, Meduri G, Viengchareun S, Amazit L, et al. Familial glucocorticoid receptor haploinsufficiency by non-sense mediated mRNA decay, adrenal hyperplasia and apparent mineralocorticoid excess. PLoS One 2010;5: e13563.
[64] Boulpaep EL. Electrophysiology of the kidney [vol IVA] In: Giebisch G, Tosteson DC, Ussing HH, editors. Membrane transport in biology. Berlin: Springer-Verlag; 1979. p. 97–144.
[65] Boulpaep EL, Sackin H. Equivalent electrical circuit analysis and rheogenic pumps in epithelia. Fed Proc 1979;38:2030–6.
[66] Boyd JE, Mulrow PJ. Further studies of the influence of potassium upon aldosterone production in the rat. Endocrinology 1972;90:299–301.
[67] Brandis M, Keyes J, Windhager EE. Potassium-induced inhibition of proximal tubular fluid reabsorption in rats. Am J Physiol 1972;222:421–7.
[68] Brown EB, Goat B. Intracellular hydrogen ion changes and potassium movement. Am J Physiol 1963;204:765–70.
[69] Brown EM, Chattopadhyay N, Vassilev PM, Hebert SC. The calcium-sensing receptor (CaR) permits Ca^{2+} to function as a versatile extra-cellular first messenger. Recent Progr Horm Res 1998;53:257–80.
[70] Buffin-Meyer B, Younes-Ibrahim M, Barlet-Bas C, Cheval L, Marsy S, Doucet A. K depletion modifies the properties of Sch-28080-sensitive K-ATPase in rat collecting duct. Am J Physiol 1997;272:FI24.
[71] Buffin-Meyer B, Younes-Ibrahim M, El Mernissi G, Cheval L, Marsy S, Grima M, et al. Differential regulation of collecting duct Na^{+}-K^+-ATPase and K^+ excretion by furosemide and piretanide: role of bradykinin. J Am Soc Nephrol 2004;15:876–84.
[72] Buffin-Meyer B, Verbatz JM, Cheval L, Marsy S, Younes-Ibrahim M, Le Moal C, et al. Regulation of Na^+, K^+ATPase in the rat outer medullary collecting duct during potassium depletion. J Am Soc Nephrol 1998;9:538–50.
[73] Bull MB, Laragh JH. Amiloride. A potassium-sparing natriuretic agent. Circulation 1968;37:45–53.
[74] Burg MB. Thick ascending limb of Henle's loop. Kidney Int 1982;22:454–64.
[75] Burg MB, Green N. Effect of ethacrynic acid on the thick ascending limb of Henle's loop. Kidney Int 1973;4:301–8.
[76] Burg MB, Stoner L, Cardinal J, Green N. Furosemide effect on isolated perfused tubules. Am J Physiol 1973;225:119–24.
[77] Butte NF, Hopkinson JM, Wong WW, Smith EO, Ellis KJ. Body composition during the first 2 years of life: an updated reference. Pediatr Res 2000;47:578–85.
[78] Candia S, Garcia ML, Latorre R. Mode of action of iberiotoxin, a potent blocker of the large conductance $Ca^{(2+)}$-activated K^+ channel. Biophys J 1992;63:583–90.
[79] Cardinal J, Lapointe J-Y, Laprade R. Luminal and peritubular ionic substitutions and intracellular potential of the rabbit proximal convoluted tubule. Am J Physiol 1984;247:F352–64.
[80] Carlisle EJF, Donnelly SM, Ethier JH, Quaggin SE, Kaiser UB, Vasuvattakul S, et al. Modulation of the secretion of potassium by accompanying anions in humans. Kidney Int 1991;39: 1206–12.
[81] Carrisoza-Gaytan R, Salvador C, Satlin LM, Liu W, Zavilowitz B, Bobadilla NA, et al. Potassium secretion by voltage-gated potassium channel Kv1.3 in the rat kidney. Am J Physiol Renal Physiol 2010;299:F255–64.
[82] Cassola AC, Giebisch G, Wang W. Vasopressin increases density of apical low-conductance K^+ channels in rat CCD. Am J Physiol 1993;264:F502.
[83] Cemerikic D, Wilcox CS, Giebisch G. Intracellular potential and K^+ activity in rat kidney proximal tubular cells in acidosis and K^+ depletion. J Membr Biol 1982;69:159–65.
[84] Cha S-K, Hu M-C, Kurosu H, Kuro-o M, Moe O, Huang C-L. Regulation of renal outer medullary potassium channel and renal K^+ excretion by Klotho. Molec Pharmacol 2009;76:38–46.
[85] Cha S-K, Huang C, Ding Y, Qi X, Huang C-L, Miller RT. Calcium-sensing receptor decreases cell surface expression of the inwardly-rectifying K^+ channel, Kir4.1. J Biol Chem 2011;286:1828–35.
[86] Chaillet JR, Lopes AG, Boron WE. Basolateral Na-H exchange in the rabbit cortical collecting tubule. J Gen Physiol 1985;86: 785–812.
[87] Chambrey R, Picard N. Role of tissue kallikrein in regulation of tubule function. Curr Opin Nephrol Hypertens 2011;20: 523–8.
[88] Cheema-Dhadli S, Lin S-H, Keong-Chong C, Kamel KS, Halperin ML. Requirements for a high rate of potassium excretion in rats consuming a low electrolyte diet. J Physiol 2006;572:493–501.
[89] Chen P, Guzman JP, Leong PKK, Yang LE, Perianayagam A, Babilonia E, et al. McDonough. Modest dietary K^+ restriction provokes insulin resistance of cellular K^+ uptake and phosphorylation of renal outer medulla K^+ channel without fall in plasma K^+ concentration. Am J Physiol Cell Physiol 2006;290:C1355–63.
[89a] Chen SY, Bhargava A, Mastroberardino L, Meijer OC, Wang J, Buse P, et al. Epithelial sodium channel regulated by aldosterone-induced protein sgk. Proc Natl Acad Sci USA 1999;96(5):2514–9.
[90] Choi M, Scholl UI, Yue P, et al. K^+ channel mutations in adrenal aldosterone-producing adenomas and hereditary hypertension. Science 2011;331:768–71.
[90a] Chou CL, Yu MJ, Kassai EM, Morris RG, Hoffert JD, Wall SM, et al. Roles of basolateral solute uptake via NKCC1 and of myosin II in vasopressin-induced cell swelling in inner medullary collecting duct. Am J Physicol Renal Physiol 2008;295:F192–201.
[91] Constantinescu A, Silver RB, Satlin LM. H-K-ATPase activity in PNA-binding intercalated cells of newborn rabbit cortical collecting duct. Am J Physiol 1997;272:F167–77.
[92] Constantinescu AR, Lane JC, Mak J, Zavilowitz B, Satlin R. Na^+-K^+-ATPase-mediated basolateral rubidium uptake in the maturing rabbit cortical collecting duct. Am J Physiol Renal Physiol 2000;279:F1161–1168.
[93] Cortney MA. Renal tubular transfer of water and electrolytes in adrenalectomized rats. Am J Physiol 1969;216:589.
[94] Costanzo LS. Comparison of calcium and sodium transport in early and late rat distal tubules: effect of amiloride. Am J Physiol 1984;246:F937–45.
[95] Costanzo LS. Localization of diuretic action in microperfused rat distal tubules: Ca and Na transport. Am Physiol 1985;248: F197–211.
[96] Coutry N, Blot-Chabaud M, Mateo P, Bonvalet JP, Farman N. Time course of sodium induced Na^+-K^+-ATPase recruitment in rabbit cortical collecting tubule. Am J Physiol 1992;263:C61–8.

[97] Cox JR, Platts MM, Horn ME, Adams R, Miller HE. The effect of aldosterone on sodium and potassium distribution in man. J Endocrinol 1966;36:103–14.
[98] Cox M, Sterns RH, Singer I. The defense against hyperkalemia: the roles of insulin and aldosterone. N Engl J Med 1978;299: 525–32.
[99] Crayen M, Thoenes W. Architektur und cytologische Charakterisierung des distalen Tubulus der Rattenniere. Fortschr Zool 1975;23:279–88.
[100] Davidson DG, Levinsky NG, Berliner RW. Maintenance of potassium excretion despite reduction of glomerular filtration during sodium diuresis. J Clin Invest 1958; 37:548–55.
[101] De Rouffignac C, Morel E. Micropuncture study of water, electrolytes and urea movements along the loops of Henle in *Psammomys*. J Clin Invest 1969;48:474–86.
[102] DeFronzo RA, Bia M, Birkhead G., Epinephrine and potassium homeostasis. Kidney Int 198; 20: 83-91.
[103] DeFronzo RA, Goldberg M, Agus Z. The effects of glucose and insulin on renal electrolyte transport. J Clin Invest 1976;58:83–90.
[104] DeFronzo RA, Stanton B, Klein-Robbenhaar G, Giebisch G. Inhibitory effect of epinephrine on renal potassium sectetion: a micropuncture study. Am J Physiol 1983;245:F303–11.
[105] Dekel B, Nakhoul F, Abassii Z, Aviv R, Winaver J, Szylman P. Complete adaptation to chronic potassium loading after adrenalectomy: possible humoral mechanisms. J Lab Clin Med 1997;129:453–61.
[106] Delgado MM, Rohatgi R, Khan S, Holzman IR, Satlin LM. Sodium and potassium clearances by the maturing kidney: clinical-molecular correlates. Pediatr Nephrol 2003; 18:759–67.
[106a] Dherbecourt O, Cheval L, Bloch-Faure M, Meneton P, Doucet A. Molecular identification of Sch28080-sensitive K-ATPase activities in the mouse kidney. Pflugers Arch 2006;451(6):769–75.
[107] Dietl P, Good D, Stanton B. Adrenal corticosteroid action on the thick ascending limb. Semin Nephrol 1990;10: 350–64.
[108] Diezi J, Michaud P, Aceves J, Giebisch G. Micropuncture study of electrolyte transport across papillary collecting duct of the rat. Am J Physiol 1973;224:623–34.
[109] Diezi J, Michaud P, Grandchamp A, Giebisch G. Effects of nephrectomy on renal salt and water transport in the remaining kidney. Kidney Int 1976;10:450–62.
[110] Dobyan DC, Lacy FB, Jamison RL. Suppression of potassium-recycling in the renal medulla by short-term potassium deprivation. Kidney Int 1979;16:704–9.
[110a] Dorup J. Structural adaptation of intercalated cells in rat renal cortex to acute metabolic acidosis and alkalosis. J Ultrastruct Res 1985;92:119–31.
[111] Dorup I, Clausen T. Effects of potassium deficiency on growth and protein synthesis in skeletal muscle and the heart of rats. Br J Nutr 1989;62:269–84.
[112] Doucet A. H^+,K^+-ATPase in the kidney: localization and function in the nephron. Exp Nephrol 1997;5:271–6.
[113] Doucet A. Functional control of Na-K-ATPase in single nephron segments of the mammalian kidney. Kidney Int 1998;34:749–60.
[114] Doucet A, Katz AI. Renal potassium adaptation: Na-K-ATPase activity along the nephron after chronic potassium loading. Am J Physiol 1980;238:F380–6.
[115] Doucet A, Katz AI. Short-term effect of aldosterone on Na-K-ATPase in single nephron segments. Am J Physiol 1981;241: F273–8.
[116] Doucet A, Katz AI, Morel F. Determination of Na-K-ATPase activity in single segments of the mammalian nephron. Am J Physiol 1979;237:FI05–13.
[117] Doucet A, Marsy S. Characterization of K-ATPase activity in distal nephron: stimulation by potassium depletion. Am J Physiol 1987;253:F418–23.
[118] Douglas JG. Effects of high potassium diet on angiotensin II receptors and angiotensin-induced aldosterone production in rat adrenal glomerulosa cells. Endocrinology 1980;106:983–90.
[119] Duarte CG, Chomety F, Giebisch G. Effect of amiloride, ouabain, and furosemide on distal tubular function in the rat. Am J Physiol 1971;221:632–9.
[120] Dube L, Parent L, Sauve R. Hypotonic shock activates a maxi K^+ channel in primary cultured proximal tubule cells. Am J Physiol 1990;259:F348–56.
[121] DuBose Jr. TD. Hyperkalemic hyperchloremic metabolic acidosis: pathophysiologic insights. Kidney Int 1997;51:591–602.
[122] DuBose TD, Codina J, Burges A, Pressley TA. Regulation of H^+-K^+-ATPase expression in kidney. Am J Physiol 1995;269: F500–7.
[123] Dunbar DR, Khaled H, Evans LC, Al-Dujaili EA, Mullins LJ, Mullins JJ, et al. Transcriptional and physiological responses to chronic ACTH treatment by the mouse kidney. Physiological Genomics 2010;40:158–66.
[124] Edelman A, Curci S, Samarzija I, Frömter E. Determination of intracellular K^+ activity in rat kidney proximal tubular cells. Pflugers Arch 1978;378:37–45.
[125] Elabida B, Edwards A, Salhi A, Azroyan A, Fodstad H, Meneton P, et al. A physiological role for progesterone in male: involvement in the renal adaptation to dietary K^+ restriction. Kidney Int 2011; [in press]
[126] Elabida B, Edwards A, Salhi A, Azroyan A, Fodstad H, Meneton P, et al. Chronic potassium depletion increases adrenal progesterone production that is necessary for efficient renal retention of potassium. Kidney Int 2011;80:256–62.
[127] Eladari D, Chambrey R. WNKs: new concepts in the regulation of NaCl and K^+ balance. J Nephrol 2007;20:260–4.
[128] Eladari D, Chambrey R, Peti-Peterdi J. A new look at electrolyte transport in the distal tubule. Annu Rev Physiol 2012;74:325–49.
[129] Elalouf J-M, Roinel N, de Rouffignac C. Effects of dDAVP on rat juxtamedullary nephrons: stimulation of medullary K^+ recycling. Am J Physiol 1985;249:F291–8.
[130] Elalouf J-M, Roinel N, de Rouffignac C. Effects of human calcitonin on water and electrolyte movements in rat juxtamedullary nephrons: inhibition of medullary K^+ recycling. Pflugers Arch 1986;406:502–8.
[131] Elkins T, Ganetzky B, Wu CFA. *Drosophila* mutation that eliminates a calcium-dependent potassium current. Proc Natl Acad Sci USA 1986;83:8415–9.
[132] Ellison DH, Velazquez H, Wright FS. Stimulation of distal potassium sectetion by low lumen chloride in the presence of barium. Am J Physiol 1985;248:F638–49.
[133] Ellison DH, Velazquez H, Wright FS. Unidirectional potassium fluxes in the renal distal tubule: effects of chloride and barium. Am J Physiol 1986;250:F885–94.
[134] Ellison DH, Velazquez H, Wright FS. Mechanisms of sodium, potassium and chloride transport by the renal distal tubule. Miner Electrolyte Metab 1987;13:422–32.
[135] Ellison DH, Velazquez H, Wright FS. Thiazide-sensitive sodium chloride cotransport in early distal tubule. Am J Physiol 1987;253:F546–54.
[136] Ellison DH, Velazquez H, Wright FS. Adaptation of the distal convoluted tubule of the rat: structural and functional effects

of dietary salt intake and chronic diuretic infusion. J Clin Invest 1989;83:113–26.
[137] El Moghrabi S, Houillier P, Picard N, Sohet F, Wootla B, Bloch-Faure M, et al. Tissue kallikrein permits early renal adaptation to potassium load. Proc Natl Acad Sci USA 2010;107:13526–31.
[138] Emmons C, Kurtz I. Functional characterization of three intercalated cell subtypes in the rabbit outer cortical collecting duct. J Clin Invest 1994;93:417–23.
[139] Engbretson BG, Stoner LC. Flow-dependent potassium secretion by rabbit cortical collecting tubule *in vitro*. Am J Physiol 1987;253:F896–903.
[140] Engbretson BG, Beyenbach KW, Stoner LC. The everted renal tubule: a methodology for direct assessment of apical membrane function. Am J Physiol 1988;255:F1276–80.
[141] Estilo G, Liu W, Pastor-Soler N, Mitchell P, Carattino MD, Kleyman TR, et al. Effect of aldosterone on BK channel expression in mammalian cortical collecting duct. Am J Physiol Renal Physiol 2008;295:F780–8.
[142] Ethier JH, Kamel KS, Magner PO, Lemann Jr J, Halperin ML. The transtubular potassium concentration in patients with hypokalemia and hyperkalemia. Am J Kidney Dis 1990;15: 309–15.
[143] Evans LC, Mullins JJ, Kenyon C, et al. Progression of medullary atrophy and a urine concentrating defect in 11beta-hydroxysteroid dehydrogenase Type 2 knockout mice. Proc Physiol Soc 2010;19:PC248.
[144] Fang L, Garuti R, Kim B-Y, Wade JB, Welling PA. The ARH adaptor protein regulates endocytosis of the ROMK potassium secretory channel in mouse kidney. J Clin Invest 2009;119:3278–89.
[145] Field M, Giebisch G. Steroid effects on renal function. In: Laragh JH, Brenner BM, editors. Hypertension: pathophysiology, diagnosis and management. New York: Raven Press; 1990. p. 1273–85.
[146] Field MJ, Giebisch G. Hormonal control of renal potassium excretion. Kidney Int 1985;27:379–87.
[147] Field MJ, Stanton BA, Giebisch GH. Differential acute effects of aldosterone, dexamethasone and hyperkalemia on distal tubular potassium secretion in the rat kidney. J Clin Invest 1984;74:1792–802.
[148] Field MJ, Stanton BA, Giebisch GH. Influence of ADH on renal potassium handling: a micropuncture and microperfusion study in Brattleboro rats. Kidney Int 1984;25:502–11.
[149] Fila M, Brideau G, Morla L, Cheval L, Deschenes G, Doucet A. Inhibition of K^+ secretion in the distal nephron in nephrotic syndrome: possible role of albuminura. J Physiol 2011;14: 3611–21.
[150] Filipovic D, Sackin H. A calcium-permeable stretch-activated cation channel in renal proximal tubule. Am J Physiol 1991; 260:F119–29.
[151] Fisher KA, Binder HJ, Hayslett JP. Potassium secretion by colonic mucosal cells after potassium adaptation. Am J Physiol 1978;231:987–94.
[152] Flynn MA, Woodruff C, Clark J, Chase G. Total body potassium in normal children. Pediatr Res 1972;6:239–45.
[153] Fodstad H, Gonzalez-Rodriguez E, Bron S, Gaeggeler H, Guisan B, Rossier BC, et al. Effects of mineralocorticoid and K^+ concentration on K^+ secretion and ROMK channel expression in a mouse cortical collecting duct cell line. Am J Physiol Renal Physiol 2009;296:F966–75.
[154] Fraley DS, Adler S. Isohydric regulation of plasma potassium by bicarbonate in the rat. Kidney Int 1976;9:333–43.
[155] Frindt G, Houde V, Palmer LG. Conservation of Na^+ vs. K^+ by the rat cortical collecting duct. Am J Physiol Renal Physiol 2011;301:F14–20.
[156] Frindt G, Palmer LG. K^+ secretion in the rat kidney: Na^+ channel-dependent and -independent mechanisms. Am J Physiol Renal Physiol 2009;297:F389–96.
[157] Frindt G, Palmer LG. Effects of dietary K^+ on cell-surface expression of renal ion channels and transporters. Am J Physiol Renal Physiol 2010;299:F890–7.
[158] Frindt G, Palmer LG. Apical potassium channels in the rat collecting tubule. Am J Physiol Renal Physiol 2004;287:F1030–7.
[159] Frindt G, Palmer LG. Low-conductance K^+ channels in apical membrane of rat cortical collecting tubule. Am J Physiol 1989;256:F143–51.
[160] Frindt G, Palmer LG. Ca-activated K^+ channels in apical membrane of mammalian CCT, and their role in K^+ secretion. Am J Physiol 1987;252:F458–467.
[161] Frindt G, Shah A, Edvinsson J, Palmer LG. Dietary K^+ regulates ROMK channels in connecting tubule and cortical collecting duct of rat kidney. Am J Physiol Renal Physiol 2009;296: F347–54.
[162] Fromter E, Gessner K. Free flow potential profile along rat kidney proximal tubule. Pflugers Arch 1974;351:69–84.
[163] Fujii Y, Mujais SK, Katz AI. Renal potassium adaptation: role of the Na-K-ATP pump in rat cortical collecting tubules. Am J Physiol 1989;256:F79–284.
[164] Fujimoto M, Kubota I, Kotera K. Electrochemical profile of K^+ and CI ions across the proximal tubule of bullfrog kidneys. Contrib Nephrol 1977;6:114–23.
[165] Fujita T, Sato Y. Natriuretic and antihypertensive effects of potassium in DOCA-salt hypertensive rats. Kidney Int 1983;24:731–9.
[166] Funder JW, Blair-West JR, Coughlan JP, et al. Effect of plasma (K^+) on the secretion of aldosterone. Endocrinology 1969;85: 381–4.
[167] Furuya H, Tabei K, Muto S, Asano Y. Effect of insulin on potassium secretion in the rabbit cortical collecting tubule. Am J Physiol 1991;262:F30–5.
[168] Fuzman RI, Finkinshtein YA, Turner AY. Reflex mechanism of potassium homeostasis regulation. Nefrologia 1985;5:103–8.
[169] Gallazzini M, Attmane-Elakeb A, Mount DB, Hebert SC, Bichara M. Regulation by glucocorticoids and osmolality of expression of ROMK (Kir 1.1), the apical K^+ channel of thick ascending limb. Am J Physiol Renal Physiol 2003;284: F977–86.
[170] Galvez A, Gimenez-Gallego G, Reuben JP, Roy-Contancin L, Feigenbaum P, Kaczorowski GJ, et al. Purification and characterization of a unique, potent, peptidyl probe for the high conductance calcium-activated potassium channel from venom of the scorpion *Buthus tamulus*. J Biol Chem 1990;265:11083–90.
[171] Gamba G. The thiazide-sensitive Na^+-Cl^- cotransporter: molecular biology, functional properties, and regulation by WNKs. Am J Physiol Renal Physiol 2009;297:F838–48.
[172] Gamba G, Friedman PA. Thick ascending limb: the $Na(^+)$:K $(^+)$:2CL$(^-)$ co-transporter, NKCC2 and the calcium-sensing receptor, CaSR. Pflugers Arch 2009;458(1):61–74.
[173] Garg LC, Narang N. Ouabain-insensitive K-adenosine triphosphatase in distal nephron segments of the rabbit. J Clin Invest 1988;81:1204–8.
[174] Garg LC, Knepper MA, Burg MB. Mineralocorticoid effects on Na,K-ATPase in individual nephron segments. Am J Physiol 1991;240:F536–44.
[175] Gennari FJ. Hypokalemia. N Engl J Med 1998;339:451–9.
[176] Gennari FJ, Cohen JJ. Role of the kidney in potassium homeostasis: lessons from acid–base disturbances. Kidney Int 1975;8: 1–5.
[177] Giebisch G, Wang W. Potassium transport: from clearance to channels and pumps. Kidney Int 1995;49:1624–31.

[178] Giebisch G. Cell models of potassium transport in the renal tubule [Potassium transport: Physiology and pathophysiology] In: Giebisch G, editor. Current topics in membranes and transport, vo1. 28. Orlando, FL: Academic Press; 1987. p. 133
[179] Giebisch G. Renal potassium transport: mechanisms and regulation. Am J Physiol 1998;274:F817–33.
[180] Giebisch G. Some reflections on the mechanism of renal tubular potassium transport. Yale J Biol Med 1975;48:315–36.
[181] Giebisch G. Effects of diuretics on renal transport of potassium. Methods Pharmacol 1976;4A:121–64.
[182] Giebisch G. Renal potassium transport. In: Giebisch G, Tosteson DC, Ussing HH, editors. Membrane transport in biology, vol. IVA. Berlin: Springer-Verlag; 1978. p. 215–98.
[183] Giebisch G. Renal potassium channels: an overview. Kidney Int 1995;48:1004–9.
[184] Giebisch G. Recent advances in the field of renal potassium excretion: what can we learn from potassium channels? Yale J Biol Med 1998;70:311–22.
[185] Giebisch G, deMello-Aires M, Malnic G. Kinetics of potassium transport across single distal tubules of rat kidney. J Physiol 1973;232:47–70.
[186] Giebisch G, K1ein-Robbenhaar G, K1ein-Robbenhaar J, et al. Renal and extrarenal sites of actions of diuretics. Cardiovasc Drugs Ther 1993;7:11–21.
[187] Giebisch G, Wang W-H. Potassium transport – an update. J Nephrol 2010;23(S16):S97–104.
[188] Gonin S, Deschenes G, Roger F, Bens M, Martin PY, Carpentier JL, et al. Cyclic AMP increases cell surface expression of functional Na-K-ATPase units in mammalian cortical collecting duct principal cells. Mol Biol Cell 2001; 13:255–64.
[189] Good DW. Sodium-dependent bicarbonate absorption by cortical thick ascending limb of rat kidney. Am J Physiol 1985;248: F821–9.
[190] Good DW. Effects of potassium on ammonium transport by medullary thick ascending limb of the rat. Am J Physiol 1987;80:1358–65.
[191] Good DW, Velazquez H, Wright FS. Luminal influences on potassium secretion: low sodium concentration. Am J Physiol 1984;246:F609–19.
[192] Good DW, Wright FS. Luminal influences of potassium secretion: sodium concentration and fluid flow rate. Am J Physiol 1979;236:Fl92–205.
[193] Gottschalk CWO. Renal tubular function: lessons from micropuncture. Harvey Lect 1962-63;58:99–124.
[194] Grasset E, Gunter-Smith P, Schultz SG. Effects of Na-coupled alanine transport on intracellular K^+ activities and the K^+ conductance of the basolateral membranes of *Necturus* small intestine. J Membr Biol 1983;71:89–94.
[195] Gray DA, Frindt G, Zhang YY, Palmer LG. Basolateral K^+ conductance in principal cells of rat CCD. Am J Physiol Renal Physiol 2005;288:F493–504.
[196] Greenlee MM, Lynch IJ, Gumz ML, Cain BD, Wingo CS. Mineralocorticoids stimulate the activity and expression of renal H^+,K^+-ATPases. J Am Soc Nephrol 2011;22:49–58.
[197] Greenlee MM, Lynch IJ, Gumz ML, Cain BD, Wingo CS. The renal H,K-ATPases. Curr Opin Nephrol Hypertens 2010;19: 478–82.
[198] Greger R. Ion transport mechanisms in thick ascending limb of Henle's loop of mammalian nephrons. Physiol Rev 1985;65: 760–97.
[199] Greger R, Oberleithner H, Schlatter E, Cassola AC, Weidtke C. Chloride activity in cells of isolated perfused cortical thick ascending limbs of rabbit kidney. Pflugers Arch 1983;399:29–41.
[200] Greger R, Schlatter E. Presence of luminal K, a prerequisite for active NaCl transport in the cortical thick ascending limb of Henle's loop of rabbit kidney. Pflugers Arch 1981;392: 92–4.
[201] Greger R, Schlatter E. Cellular mechanism of the action of loop diuretics on the thick ascending limb of Henle's loop. Klin Woehensehr 1983;61:1019–27.
[202] Greger R, Schlatter E. Properties of the basolateral membrane of the cortical thick ascending limb of Henle's loop of rabbit kidney. A model for secondary active chloride transport. Pflugers Arch 1983;396:325–34.
[203] Greger R, Gogelein H. Role of K^+ conductive pathways in the nephron. Kidney Int 1987;31:1055–64.
[204] Greger R, Schlatter E. Properties of the lumen membrane of the cortical thick ascending limb of Henle's loop of rabbit kidney. Pflugers Arch 1983;396:315–24.
[205] Grimm PR, Foutz RM, Brenner R, Sansom SC. Identification and localization of BK-beta subunits in the distal nephron of the mouse kidney. Am J Physiol Renal Physiol 2007;293: F35–359.
[206] Grimm PR, Irsik DL, Liu L, Holtzclaw JD, Sansom SC. Role of BKbeta1 in Na^+ reabsorption by cortical collecting ducts of Na^+-deprived mice. Am J Physiol Renal Physiol 2009;297: F420–8.
[207] Grimm PR, Irsik DL, Settles DC, Holtzclaw JD, Sansom SC. Hypertension of $Kcnmb1^{-/-}$ is linked to deficient K^+ secretion and aldosteronism. Proc Natl Acad Sci USA 2009;106: 11800–5.
[208] Grimm PR, Sanson SC. BK channels and a new form of hypertension. Kidney Int 2010;78:956–62.
[209] Grupp C, Pavenstadt-Grupp R, Grunewald W, Bevan C, Stokes III JB, Kinne RK. A Na-K-CI cotransporter in isolated rat papillary collecting duct cells. Kidney Int 1989;36:201–9.
[210] Guggino WE, Oberleithner H, Giebisch G. The amphibian diluting segment. Am J Physiol 1988;254:F615–27.
[211] Gumz ML, Lynch IJ, Greenlee MM, Cain BD, Wingo CS. The renal H^+-K^+-ATPases: physiology, regulation, and structure. Am J Physiol Renal Physiol 2010;298:F12–21.
[212] Gunter-Smith PJ, Grasset E, Schultz SG. Sodium-coupled amino acid and sugar transport by *Necturus* small intestine. An equivalent circuit analysis of a rheogenic cotransport system. J Membr Biol 1982;66:25–39.
[213] Hall JE, Granger JP, Smith MJ, Premen AJ. Role of renal hemodynamics and 58: regulation of potassium excretion arterial pressure in aldosterone "escape.". Hypertension 1984;6(Suppl. 1):183–92.
[214] Halperin ML, Gowrishankar M, Mallie JP, Sonnenberg H, Oh M. Urea recycling: an aid to the excretion of potassium during antidiuresis. Nephron 1996;72:507–11.
[215] Hamm LL, Gillespie C, Klahr S. Ammonium chloride inhibits Na^+ and K^+ transport in the cortical collecting tubule. Contrib Nephrol 1985;47:125.
[216] Hayslett JP, Halevy J, Pace PE, Binder HJ. Demonstration of net potassium absorption in mammalian colon. Am J Physiol 1982;242:G209–14.
[217] Hebert SC, Desir G, Giebisch G, Wang WH. Molecular diversity and regulation of renal potassium channels. Physiol Rev 2005;85:319–71.
[218] Hebert SC, Andreoli TE. Control of NaCl transport in the thick ascending limb. Am J Physiol 1984;246:F745–56.
[219] Hebert SC, Friedman PA, Andreoli TE. Effects of antidiuretic hormone on cellular conductive pathways in mouse medullary thick ascending limbs of Henle: 1. ADH increases transcellular conductance pathways. Membr Biol 1984;80:201–9.

[220] Hebert SC, Andreoli TE. Effects of antidiuretic hormone on cellular conductive pathways in mouse medullary thick ascending limbs of Henle: II. Determinants of the ADH-mediated increases in transepithelial voltage and in net Cl^- absorption. J Membr Biol 1984;80:221–33.

[220a] Heller BI, Hammarsten JF, Stutzman FL. Concerning the effects of magnesium sulfate on renal function, electrolyte excretion, and clearance of magnesium. J Clin Invest 1953;32:858–61.

[221] Hierholzer K. Secretion of potassium and acidification in collecting ducts of mammalian kidney. Am J Physiol 1961;201: 318–24.

[222] Hierholzer K, Wiederholt M, Holzgreve H, et al. Micropuncture study of renal transtubular concentration gradients of sodium and potassium in adrenalectomized rats. Pflugers Arch 1965;285:193–210.

[223] Higashihara E, Kokko JP. Effects of aldosterone on potassium recycling in the kidney of adrenalectomized rats. Am J Physiol 1985;248:F219–27.

[224] Hirsch J, Leipziger J, Frobe U, Schlatter E. Regulation and possible physiological role of the Ca^{2+}-dependent K^+ channel of cortical collecting ducts of the rat. Pflugers Arch 1993;422: 492–8.

[225] Hirsch J, Schlatter E. K channels in the basolateral membrane of rat cortical collecting duct are regulated by a cGMP-dependent protein kinase. Pflugers Arch 1995;429:338–44.

[226] Hirsch J, Schlatter E. K channels in the basolateral membrane of rat cortical collecting duct. Kidney Int 1995;48:1036–46.

[227] Ho K, Nichols CG, Lederer WL, Lytton J, Vassilev PM, Kanazirska MV, et al. Cloning and expression of an inwardly rectifying ATP-regulated potassium channel. Nature 1993;362:31–8.

[228] Holtzclaw JD, Grimm PR, Sansom SC. Intercalated cell BK-alpha/beta4 channels modulate sodium and potassium handling during potassium adaptation. J Am Soc Nephrol 2010;21:634–45.

[228a] Holtzclaw JD, Cornelius RJ, Hatcher LI, Sansom SC. Coupled ATP and potassium efflux from intercalated cells. Am J Physicol Renal Physicol 2011;300:F1319–26.

[229] Hoorn EJ, Nelson JH, McCoprmick JA, Ellison DH. The WNK kinase network regulating sodium, potassium, and blood pressure. J Am Soc Nephrol 2011;22:605–14.

[230] Hoover RS, Angiotensin II. A candidate for an aldosterone-independent mediator of potassium preservation during volume depletion. Kidney Int 2011;79:377–9.

[231] Horisberger J-D, Doucet A. Renal ion translocating ATPases: the P type family 139. In: Seldin DW, Giebisch G, editors. The kidney: physiology and pathophysiology. 3rd ed. Philadelphia: Lippincott Williams & Wilkins; 2002. p. 139–70.

[232] Horisberger J-D, Giebisch G. Potassium-sparing diuretics. Renal Physiol 1987;10:198–200.

[233] Horisberger J-D, Giebisch G. Voltage dependence of the basolateral membrane conductance in the *Amphiuma* collecting tubule. J Membr Biol 1988;105:257–63.

[234] Hropot M, Fowler N, Karlmark B, Giebisch G. Tubular action of diuretics: distal effects on electrolyte transport and acidification. Kidney Int 1985;28:477–89.

[235] Huang C-L, Kuo E. Mechanism of hypokalemia in magnesium deficiency. J Am Soc Nephrol 2007;18:2649–52.

[236] Huang C-L, Yang S-S, Lin S-H. Mechanism of regulation of renal ion transport by WNK kinases. Curr Opin Nephrol Hypertens 2008;17:519–25.

[237] Hunter M. Stretch-activated channels in the basolateral membrane of single proximal cells of frog kidney. Pflugers Arch 1990;416:448–53.

[238] Hunter M, Cohen BJ, Forrest JA, et al. Patch-clamp recordings from cultured amphibian kidney cell (A6). Kidney Int 1984;25: 303.

[239] Hunter M, Lopes A, Boulpaep E, Giebisch G. Regulation of single K-channels from apical membrane of rabbit collecting tubule. Am J Physiol 1986;251:F725–33.

[240] Hunter M, Lopes AG, Boulpaep EL, Giebisch GH. Single channel recordings of calcium-activated potassium channels in the apical membrane of rabbit cortical collecting tubules. Proc Natl Acad Sci USA 1984;81:4237–9.

[241] Hurst AM, Beck JS, Laprade R, Lapointe JY. Na^+ pump inhibition down regulates an ATP-sensitive K^+ channel in rabbit proximal convoluted tubule. Am J Physiol 1993;264: F760–4.

[242] Iino Y, Troy JL, Brenner BM. Effects of catecholamines on electrolyte transport in cortical collecting tubules. J Membr Biol 1981;61:67–73.

[243] Imai M. The connecting tubule: a functional subdivision of the rabbit distal nephron segments. Kidney Int 1979; 15:346–56.

[244] Imai M, Nakamura R. Function of distal convoluted and connecting tubules studied by isolated nephron fragments. Kidney Int 1982;22:465–72.

[245] Imai M, Taniguchi J, Tabei K. Function of thin loops of Henle. Kidney Int 1987;31:565–79.

[246] Imai M, Taniguchi J, Yoshitomi K. Transition of permeability properties along the descending limb of long-loop nephron. Am J Physiol 1988;254:F323–8.

[247] Jaeger P, Karlmark B, Giebisch G. Ammonium transport in rat cortical tubule: relationship to potassium metabolism. Am J Physiol 1983;245:F593–600.

[248] Jamison R, Muller-Suur R. Potassium recycling. In: Giebisch G, editor. Current topics in membranes and transport, vol. 28. Orlando: Academic Press; 1987. p. 115–31.

[249] Jamison RL. Potassium recycling. Kidney Int 1987;31:695–703.

[250] Jamison RL, Lacy FB, Pennell JP, Sanjana VM. Potassium secretion by the descending limb of pars recta of the juxtamedullary nephron *in vivo*. Kidney Int 1976;9:323–32.

[251] Jamison RL, Sonnenberg H, Stein JH. Questions and replies: role of the collecting tubule in fluid, sodium, and potassium balance. Am J Physiol 1979;237:F247–61.

[252] Jamison RL, Work J, Schafer JA. New pathways for potassium transport in the kidney. Am J Physiol 1982;242:F297–312.

[253] Kahle KT, Ring AM, Lifton RP. Molecular physiology of the WNK kinases. Annu Rev Physiol 2008;70:329–55.

[254] Kaissling B. Structural aspects of adaptive changes in renal electrolyte excretion. Am J Physiol 1982;243:F211–26.

[255] Kaissling B, Kriz W. Structural analysis of rabbit kidney. Berlin: Springer; 1979.

[256] Kaissling B, LeHir M. Distal tubular segments of the rabbit kidney after adaptation to altered Na- and K-intake. 1. Structural changes. Cell Tissue Res 1982;224:469–92.

[257] Kaissling B, Stanton BA. Adaptation of distal tubule and collecting duct to increased sodium delivery. 1. Ultrastructure. Am J Physiol 1988;255:F1256–68.

[258] Kashgarian M, Biemesderfer D, Caplan M, Forbush III B. Monoclonal antibody to Na, K-ATPase: immunocytochemical localization along nephron segments. Kidney Int 1985;28:899–913.

[259] Katz AI. Renal Na-K-ATPase: its role in tubular sodium and potassium transport. Am J Physiol 1982;242:F207–19.

[260] Kaufman JS, Hamburger RJ. Potassium transport in the isolated proximal convoluted tubule. Am J Physiol 1982;244: F297–313.

[261] Kaufman JS, Hamburger RJ. Passive potassium transport in the isolated proximal convoluted tubule. J Physiol 1985;248: F228–32.
[262] Kawahara K. A stretch-activated K^+ channel in the basolateral membrane of *Xenopus* kidney proximal tubule cells. Pflugers Arch 1990;415:624–9.
[263] Kawahara K, Hunter M, Giebisch G. Calcium-activated potassium channels in the luminal membrane of *Amphiuma* diluting segment: voltage-dependent block by intracellular Na^+ upon depolarisation. Pflügers Archiv 1990;416:422–7.
[264] Kaunitz JD, Barrett KE, McRoberts JA. Electrolyte secretion and absorption: small intestine and colon. In: 2nd ed. Yamada T, editor. Textbook of Gastroenterology, vol. 1. Philadelphia JB: Lippincott; 1995. p. 316–61.
[265] Keith NM, King HE, Osterberg AE. Serum concentration and renal clearance of potassium in severe renal insufficiency in man. Arch Intern Med 1943;71:675–701.
[266] Khuri RN, Strieder WN, Giebisch G. Effects of flow rate and potassium intake on distal tubular potassium transfer. Am J Physiol 1975;228:1249–61.
[267] Khuri R, Wiederholt M, Strieder N, Giebisch G. Effects of graded solute diuresis on renal tubular sodium transport in the rat. Am J Physiol 1975;228:1261–8.
[268] Khuri RN, Agulian SK, Bogharian K. Electrochemical potentials of potassium in proximal renal tubule of rat. Pflugers Arch 1974;346:319–26.
[269] Khuri RN, Strieder N, Giebisch G. Effects of flow rate and potassium intake on distal tubular potassium transfer. Am J Physiol 1975;228:1249–61.
[270] Kibble JD, Wareing M, Wilson RW, Green R. Effect of barium on potassium diffusion across the proximal convoluted tubule of the anesthetized rat. Am J Physiol 1995;268:F778–83.
[271] Kleinman LI, Banks RO. Segmental nephron sodium and potassium reabsorption in newborn and adult dogs during saline expansion. Proc Soc Exp Biol Med 1983;173:231–7.
[272] Knauf H, Mutschler E, Velazquez H, Giebisch G. Torasemide significantly reduces thiazide-induced potassium- and magnesium-loss despite supra-additive natriuresis. Eur J Clin Pharmacol 2009;65:465.
[273] Knox FG, Romero JE. Mechanism for escape from the sodium retaining effects of mineralocorticoids. In: Kaufman XI, Wambach G, Helber A, Meuer KA, editors. Mineralocorticoids and hypertension. Berlin: Springer-Verlag; 1983. p. 81–100.
[274] Koefoed-Johnsen V, Ussing HH. The nature of the frog skin potential. Acta Physiol Scand 1985;42:298–308.
[275] Koeppen BM, Biagi BA, Giebisch GH. Intracellular microelectrode characterization of the rabbit cortical collecting duct. Am J Physiol 1983;244:F35–47.
[276] Koeppen BM, Giebisch G. Mineralocorticoid regulation of sodium and potassium transport by the cortical collecting duct. In: Graves S, editor. Regulation and development of membrane transport processes. New York: Wiley; 1983. p. 89–104.
[277] Koeppen BM. Conductive properties of the rabbit outer medullary collecting duct: inner stripe. Am J Physiol 1985;248: F500–6.
[278] Kokko JP. Variations in the permeability and transport along the distal tubule. Proceedings of the VIIth international congress on nephrology. Basel: Karger; 1978 [225–233]
[279] Kone BE, Renal H-K-ATPase: structure, function, and regulation. Miner Electrolyte Metab 1996;22:349–65.
[280] Kotelevtsev Y, Brown RW, Fleming S, Kenyon C, Edwards CR, Seckl JR, et al. Hypertension in mice lacking 11beta-hydroxysteroid dehydrogenase type 2. J Clin Invest 1999;103: 683–9.
[281] Kriz XI, Bankir L. A standard nomenclature for structures of the kidney. Am J Physiol 1988;254:FI–8.
[282] Kubokawa M, Mori Y, Fujimoto K, Kubota T. Basolateral pH-sensitive K^+ channels mediate membrane potential of proximal tubule cells in bullfrog kidney. Jpn Physiol 1998; 48:1–8.
[283] Kubokawa M, Wang XI, McNicholas CM, Giebisch G. Role of Ca^{2+}/CaMK II in Ca^{2+}-induced K^+ channel inhibition in rat CCD principal cell. Am J Physiol 1995;268:F211–9.
[284] Kubota T, Biagi BA, Giebisch G. Intracellular potassium activity measurements in single proximal tubules of *Necturus* kidney. J Membr Biol 1983;73:51–60.
[285] Kunau RT, Webb ML, Botman SE. Characteristics of the relationship between the flow rate of tubular fluid and potassium transport in the distal tubule of the rat. J Clin Invest 1974;54:1488–95.
[286] Kuwahara M, Ishibashi K, Krapf R. Rector FC Jr, Berry CA. Effect of lumen pH on cell pH and cell potential in rabbit proximal tubules. Am J Physiol 1989;256:F1075–83.
[287] Lachheb S, Cluzeaud F, Bens M, Genete M, Hibino H, Lourdel S, et al. Kir4.1/Kir5.1 channel forms the major K^+ channel in the basolateral membrane of mouse renal collecting duct principal cells. Am J Physiol Renal Physiol 2008;294: F1398–407.
[288] Lalioti MD, Zhang J, Vollkman HM, Kahle KT, Hoffman KE, Toka HR, et al. Wnk4 controls blood pressure and potassium homeostasis via regulation of mass and activity of the distal convoluted tubule. Nature 2006;38:1124–32.
[289] Lang F, Shumilina E. Regulation of ion channels by the serum- and glucocorticoid-inducible kinase SGK1. FASEB J 2012; [Epub ahead of print].
[290] Lapointe JY, Garneau L, Bell PD, Cardinal J. Membrane cross-talk in the mammalian proximal tubule during alterations in transepithelial sodium transport. Am J Physiol 1990;258: F339–45.
[291] Lazrak A, Liu Z, Huang C-L. Antagonistic regulation of ROMK by long and kidney-specific WNK1 isoforms. Proc Natl Acad Sci 2006;103:1615–20.
[292] Leaf A, Camara AA. Renal tubular secretion of potassium in man. J Clin Invest 1949;28:1526–33.
[293] LeGrimellec E. Micropuncture study along the proximal convoluted tubule. Pflugers Arch 1975;354:133–50.
[294] LeGrimellec C, Poujeol P, de Rouffignac E. ^{3}H-inulin and electrolyte concentrations in Bowman's capsule in rat kidney. Pflugers Arch 1975;354:117–31.
[295] LeGrimellec C, Roinel N, Morel F. Simultaneous Mg, Ca, P K, Na and Cl analysis in rat tubular fluid. III. During acute Ca plasma loading. Pflugers Arch 1974;346:171–88.
[296] LeHir M, Kaissling B, Dubach UE. Distal tubular segments of the rabbit kidney after adaptation to altered Na- and K-intake. II. Changes in Na-K-ATPase activity. Cell Tissue Res 1982;224:493–504.
[297] Lehrmann H, Thomas J, Kim SJ, Jacobi C, Leipziger J. Luminal P2Y2 receptor-mediated inhibition of Na^+ absorption in isolated perfused mouse CCD. J Am Soc Nephrol 2002;13:10–8.
[298] Leipziger J. Control of epithelial transport via luminal P2 receptors. Am J Physiol Renal Physiol 2003;284:F419–32.
[299] Lelievre-Pegorier M, Merlet-Benicho C, Roinel N, de Rouffignac C. Developmental pattern of water and electrolyte transport in rat superficial nephrons. Am J Physiol 1983;245: F15–21.
[300] Leviel F, Borensztein B, Houillier P, Paillard M, Bichara M. Electroneutral K^+/HCO_3^- cotransport in cells of medullary thick ascending limb of rat kidney. J Clin Invest 1992;90: 869–78.

[301] Leviel F, Hubner CA, Houillier P, Morla L, El Moghrabi S, Brideau G, et al. The Na^+-dependent chloride-bicarbonate exchanger SLC4A8 mediates an electroneutral Na^+ reabsorption process in the renal cortical collecting ducts of mice. J Clin Invest 2010;120(5):1627–35.

[302] Levine DZ, Walker T, Nash LA, Raman S. Effects of KCl infusions on proximal tubular function in normal and potassium-depleted rats. Kidney Int 1973;4:318–25.

[303] Li D, Wang Z, Sun P, Jin Y, Lin DH, Hebert SC, et al. Inhibition of MAPK stimulates the Ca^{2+}-dependent big-conductance K^+ channels in cortical collecting duct. Proc Natl Acad Sci USA 2006;103:19569–74.

[304] Li Z, Cai T, Tian J, Xie JX, Zhao X, Liu L, et al. NaKtide, a Na/K-ATPase-derived peptide Src inhibitor, antagonizes ouabain-activated signal transduction in cultured cells. J Biol Chem 2009;284:21066–76.

[305] Light DB, McCann FV, Keller TM, Stanton BA. Amiloride-sensitive cation channel in apical membrane of inner medullary collecting duct. Am J Physiol 1988;255:F278–85.

[306] Lin S-H, Cheema-Dhadli S, Gowrishankar M, Marliss EB, Kamel KS, Halperin ML. Control of excretion of potassium: lessons from studies during prolonged total fasting in human subjects. Am J Physiol 1997;273:F796–800.

[307] Linas SL, Peterson LN, Anderson RJ, Aisenbrey GA, Simon FR, Berl T. Mechanism of renal potassium conservation in the rat. Kidney Int 1979;15:601–11.

[308] Lindinger MI, Franklin TW, Lands LC, Pedersen PK, Welsh DG, Heigenhauser GJ. $NaHCO_3$ and $KHCO_3$ ingestion rapidly increases renal electrolyte excretion in humans. J Appl Physiol 2000;88:540–50.

[309] Liu W, Pastor-Soler NM, Schreck C, Zavilowitz B, Kleyman TR, Satlin LM. Luminal flow modulates H^{+-}ATPase activity in the cortical collecting duct (CCD). Am J Physiol Renal Physiol 2011;302:F205–15.

[310] Liu W, Schreck C, Coleman RA, Wade JB, Hernandez Y, Zavilowitz B, et al. Role of NKCC in BK channel-mediated net K^+ secretion in the CCD. Am J Physiol Renal Physiol 2011;301: F1088–91.

[311] Liu W, Xu S, Woda C, Kim P, Weinbaum S, Satlin LM. Effect of flow and stretch on the $[Ca^{2+}]_i$ response of principal and intercalated cells in cortical collecting duct. Am J Physiol Renal Physiol 2003;285:F998–1012.

[312] Liu Z, Wang H-R, Huang C-L. Regulation of ROMK channel and K^+ homeostasis by kidney-specific WNK1 kinase. J Biol Chem 2009;284:12198–206.

[313] Lorenz JM, Kleinman LI, Disney TA. Renal response of newborn dog to potassium loading. Am J Physiol 1986;251: F513–9.

[314] Lourdel S, Paulais M, Cluzeaud F, Bens M, Tanemoto M, Kurachi Y, et al. An inward rectifier K^+ channel at the basolateral membrane of the mouse distal convoluted tubule: similarities with Kir4-Kir5.1 heteromereic channels. J Physiol 2002;538 (2):391–404.

[315] Lu M, Wang WH. Nitric oxide regulates the low-conductance K^+ channel in the basolateral membrane of the cortical collecting duct. Am J Physiol 1996;270:C1336–42.

[316] Lu M, Hebert SC, Giebisch G. Hydrolyzable ATP and PIP_2 modulate the small-conductance K^+ channel in apical membranes of rat cortical collecting duct. J Gen Physiol 2002;120: 603–15.

[317] Lynch IJ, Greenlee MM, Gumz ML, Rudin A, Xin S-L, Wingo CS. Heterogeneity of H-K-ATPase-mediated acid secretion along the mouse collecting duct. Am J Physiol Renal Physiol 2000;298:F408–15.

[318] Madsen KM, Tisher CE. Structural–functional relationships along the distal nephron. Am J Physiol 1986;250:F1–15.

[319] Malnic G. Berliner RW; Giebisch G. Flow dependence of K^+ secretion in cortical distal tubules of the rat. Am J Physiol 1989;256:F932–41.

[320] Malnic G, De Mello-Aires M, Giebisch G. Potassium transport across renal distal tubules during acid–base disturbances. Am J Physiol 1971;221:1192–208.

[321] Malnic G, Giebisch G. Some electrical properties of distal tubular epithelium in the rat. Am J Physiol 1972;223:797–808.

[322] Malnic G, Klose RM, Giebisch G. Micropuncture study of renal potassium excretion in the rat. Am J Physiol 1964;206: 674–86.

[323] Malnic G, Klose RM, Giebisch G. Microperfusion study of distal tubular potassium and sodium transfer in rat kidney. Am J Physiol 1966;211:548–99.

[324] Malnic G, Klose RM, Giebisch G. Micropuncture study of distal tubular potassium and sodium transport in rat nephron. Am J Physiol 1966;211:529–47.

[325] Marsh DJ, Ullrich KJ, Rumrich G. Micropuncture analysis of the behavior of potassium ions in rat renal cortical tubules. Pflugers Arch 1963;277:107–19.

[326] Matsumura Y, Cohen B, Guggino WE, Giebisch G. Regulation of the basolateral potassium conductance of the Necturus proximal tubule. J Membr Biol 1984;79:153–61.

[327] Mauerer UR, Boulpaep EL, Segal AS. Properties of an inwardly rectifying ATP-sensitive K^+ channel on the basolateral membrane of renal proximal tubule. J Gen Physiol 1998;111:139–60.

[328] Mauerer UR, Boulpaep EL, Segal AS. Regulation of an inwardly rectifying ATP-sensitive K^+ channel on the basolateral membrane of renal proximal tubule. J Gen Physiol 1998;111:161–80.

[329] McCance RA, Widdowson EM. Alkalosis with disordered kidney function. Lancet 1937;2:247–9.

[330] McCance R, Widdowson EM. The response of the new-born piglet to an excess of potassium. J Physiol 1958;141:88–96.

[331] McCormick JA, Yang C-L, Ellison DH. WNK kinases and renal sodium transport in health and disease. Hypertension 2008;51:588–96.

[332] Mello-Aires M, Malnic G. Renal handling of sodium and potassium during hypochloremic alkalosis in the rat. Pflugers Arch 1972;331:215–25.

[333] Meneton P, Schultheis PJ, Greeb J, Nieman ML, Liu LH, Clarke LL, et al. Increased sensitivity to K^+ deprivation in colonic H, K-ATPase-deficient mice. J Clin Invest 1998;101:536–42.

[334] Meyer JW, Flagella M, Sutliff RL, Lorenz JN, Nieman ML, Weber CS, et al. Decreased blood pressure and vascular smooth muscle tone in mice lacking basolateral Na^+-K^+-$2Cl^-$ cotransporter. Am J Physiol Heart Circ Physiol 2002;283: H1846–1855.

[335] Michell AR, Debnam ES, Unwin RJ. Regulation of renal function by the gastrointestinal tract: potential role of gut-derived peptides and hormones. Annu Rev Physiol 2008; 70:379–403.

[336] Molony DA, Reeves WB, Hebert SC, Andreoli TE. ADH increases apical NaK-2CI entry in mouse medullary thick ascending limbs of Henle. Am J Physiol 1987;252:F177–87.

[337] Moore-Ede MD, Meguid MM, Fitzpatrick GF, Boyden CM, Ball MR. Circadian variation in response to potassium infusion. Clin Pharmacol Ther 1978;23:218–27.

[338] Moore-Ede MD. Physiology of the circadian timing system: predictive versus reactive homeostasis. Am J Physiol 1986;250: R735–52.

[339] Moore-Ede MC, Herd JA. Renal electrolyte circadian rhythms: independence from feeding and activity patterns. Am J Physiol 1977;232:FI28–35.

[340] Morel F. Sites of hormone action in the mammalian nephron. Am J Physiol 1981;240:FI59–64.

[341] Morgan TO, Tadokoro M, Martin D, Berliner RW. Effect of furosemide on Na^+ and K^+ transport studied by microperfusion of the rat nephron. Am J Physiol 1970;218:292–7.

[342] Morimoto T, Liu W, Woda C, Carattino MS, Wei Y, Hughey RP, et al. Mechanism underlying flow-stimulation of Na absorption in the mammalian collecting duct. Am J Physiol 2006;291:F663–9.

[343] Morita H, Fujiki N, Miyahara T, Lee K, Tanaka K. Heptoportal bumetanide-sensitive K^+-sensor mechanism controls urinary K^+ excretion. Am J Physiol 2000;278:R1134–9.

[344] Morsing P, Velazquez H, Wright FS, Ellison DH. Adaptation of the distal convoluted tubule of the rat. II. Effects of chronic thiazide infusion. Am J Physiol 1991;261:FI37–43.

[345] Mudge GH, Ames 3rd A, Foulks J, Gilman A. Effects of drugs on renal secretion of potassium in the dog. Am J Physiol 1950;161:151–8.

[346] Mudge GH, Foulks J, Gilman A. The renal excretion of potassium. Proc Soc Exp Biol Med 1948;67:545–7.

[347] Mudge GH, Foulks J, Gilman A. Renal secretion of potassium in the dog during cellular dehydration. Am J Physiol 1950;161:159–66.

[348] Mujais WK. Renal memory after potassium adaptation: role of Na^+-K + -ATPase. Am J Physiol Renal 1988;254:F845.

[349] Mujais SK, Chekal MA, Jones WJ, Hayslett JP, Katz AI. Regulation of renal Na-K ATPase in the rat: role of the natural mineralo- and glucocorticoid hormones. J Clin Invest 1984;73:13–9.

[350] Muto S. Potassium transport in the mammalian collecting duct. Physiol Rev 2001;81:85–116.

[351] Muto S, Asano Y, Seldin D, Giebisch G. Basolateral Na^+ pump modulates apical Na^+ and K^+ conductances in rabbit cortical collecting ducts. Am J Physiol 1999;276:FI43–58.

[352] Muto S, Sansom SC, Giebisch G. Effects of high K^+ diet on the electrical properties of cortical collecting ducts from adrenalectomized rabbits. J Clin Invest 1988;81:376–80.

[353] Muto S, Tsuruoka S, Miyata Y, Fujimura A, Kusano E, Wang W, et al. Basolateral Na^+/H^+ exchange maintains potassium secretion during diminished sodium transport in the rabbit cortical collecting duct. Kidney Int 2009;75:25–30.

[354] Najjar F, Zhou H, Morimoto T, Bruns JB, Li HS, Liu W, et al. Dietary K^+ regulates apical membrane expression of maxi-K channels in rabbit cortical collecting duct. Am J Physiol Renal Physiol 2005;289:922–32.

[354a] Náray-Fejes-Tóth A, Canessa C, Cleaveland ES, Aldrich G, Fejes-Tóth G. sgk is an aldosterone-induced kinase in the renal collecting duct. Effects on epithelial Na^+ channels. J Biol Chem 1999;274(24):16973–8.

[355] Nichols CG, Ho K, Hebert SC. M^+-dependent inward rectification of ROMKl potassium channels expressed in *Xenopus* oocytes. J Physiol 1994;476:399–409.

[356] O'Neil RG. Aldosterone regulation of sodium and potassium transport in the cortical collecting tubule. Semin Nephrol 1990; l0:365–74.

[357] O'Neil RG, Boulpaep EL. Effect of amiloride on the apical cell membrane cation channels of a sodium-absorbing, potassium-secreting renal epithelium. J Membr Biol 1979;50:365–87.

[358] O'Neil RG, Boulpaep EL. Ionic conductive properties and electrophysiology of the rabbit cortical collecting tubule. Am J Physiol 1982;243:F81–95.

[359] O'Neil RG, Hayhurst RA. Sodium-dependent modulation of the renal Na-K-ATPase: influence of mineralocorticoids on the cortical collecting duct. J Membr Biol 1985;85:169–79.

[360] O'Neil RG, Helman SI. Transport characteristics of renal collecting tubules: influences of DOCA and diet. Am J Physiol 1977;233:F544–58.

[361] O'Neil RG, Sansom SE. Characterization of apical cell membrane Na^+ and K^+ conductances of cortical collecting duct using microelectrode techniques. Am J Physiol 1984;247: FI4–24.

[362] Oberleithner H, Dietl P, Munich G, Weigt M, Schwab A. Relationship between luminal Na^+H^+ exchange and luminal K^+ conductance in diluting segment of frog kidney. Pflugers Arch 1985;405:5110–4.

[363] Oberleithner H, Giebisch G, Lang F, Wang W. Cellular mechanism of the furosemide sensitive transport system in the kidney. Klin Wochenschr 1982;60:1173–9.

[364] Oberleithner H, Guggino W, Giebisch G. Potassium transport in the distal tubule of *Amphiuma* kidney: effects of potassium adaptation. Pflugers Arch 1983;396:185–91.

[365] Oberleithner H, Guggino W, Giebisch G. The effect of furosemide on luminal sodium, chloride and potassium transport in the early distal tubule of *Amphiuma* kidney: effects of potassium adaptation. Pflugers Arch 1983;396:27–33.

[366] Oberleithner H, Lang F, Greger R, Wang W, Giebisch G. Effect of luminal potassium transport on cellular sodium activity in the early distal tubule of *Amphiuma* kidney. Pflugers Arch 1983;396:34–40.

[367] Oberleithner H, Lang F, Wang W, Giebisch G. Effects of inhibition of chloride transport on intracellular sodium activity in distal amphibian nephron. Pflugers Arch 1982;394:55–60.

[368] Oberleithner H, Weight M, Westphale HD, Wang W. Aldosterone activates Na/H exchange and raises cytoplasmic pH in target cells of the amphibian kidney. Proc Natl Acad Sci USA 1987;84:1464–88.

[369] Oh K-S, Oh YT, Kim S-W, Kita T, Kang I, Youn JH. Gut sensing of dietary K^+ intake increases renal K^+ secretion. Am J Physiol Integr Comp Physiol 2011;301:R421–9.

[370] Ohno-Shosaku T, Kubota T, Yamaguchi J, Fujimoto M. Regulation of inwardly rectifying K^+ channels by intracellular pH in opossum kidney cells. Pflugers Arch 1990; 416:138–43.

[371] Okusa MD, Unwin RJ, Velazquez H, Giebisch G, Wright FS. Active potassium absorption by the renal distal tubule. Am J Physiol 1992;31:F488.

[372] Okusa MD, Velazquez H, Ellison DH, Wright FS. Luminal calcium regulates potassium transport by the renal distal tubule. Am J Physiol 1990;258:F423–8.

[373] Okusa MD, Velazquez H, Wright FS. Effect of Na-channel blockers and lumen Ca on K^+ secretion by rat renal distal tubule. Am J Physiol 1991;260:F459–65.

[374] Oliver WJ, Cohen EL, Neel JV. Blood pressure, sodium intake, and sodium related hormones in the Yanomamo Indians, a "no-salt" culture. Circulation 1975;52:146.

[374a] Ookata K, Tojo A, Suzuki Y, Nakamura N, Kimura K, Wilcox CS, Hirose S. Localization of inward rectifier potassium channel Kir7.1 in the basolateral membrane of distal nephron and collecting duct. J Am Soc Nephrol 2000;11:1987–94.

[375] Ornt DB, Radke KJ, Scandling JD. Effect of aldosterone on renal potassium conservation in the rat. Am J Physiol 1996;270: EI003–l008.

[376] Ornt DB, Tannen RL. Demonstration of an intrinsic renal adaptation for K^+ conservation in short-term K^+ depletion. Am J Physiol 1983;245:F329–38.

[377] Pacha J, Frindt G, Sackin H, Palmer LG. Apical maxi K^+ channels in intercalated cells of cortical collecting tubule. Am J Physiol 1991;261:F696–705.

[378] Pallone TL, Cao C, Zhang Z. Inhibition of K^+ conductance in descending vasa recta pericytes by ANG II. Am J Physiol Renal Physiol 2004;287:F1213–22.

[379] Palmer LG, Choe H, Frindt G. Is the secretory K^+ channel in the rat CCT ROMK?. Am J Physiol 1997;273:F404–10.
[380] Palmer LG, Frindt G. High-conductance K^+ channels in intercalated cells of the rat distal nephron. Am J Physiol Renal Physiol 2007;292:F966–73.
[381] Palmer LG, Sackin H. Regulation of renal ion channels. FASEB J 1988;2:3061–5.
[382] Palmer L. Potassium secretion and the regulation of distal nephron K^+ channels. Am J Physiol 1999;277:F821–5.
[383] Paulais M, Lachheb S, Teulon J. A Na^+- and Cl^--activated K^+ channel in the thick ascending limb of mouse kidney. J Gen Physiol 2006;127:205–15.
[383a] Paulais M, Bloch-Faure M, Picard N, Jacques T, Ramakrishnan SK, Keck M, et al. Renal phenotype in mice lacking the Kir5.1 (Kcnj16) K^+ channel subunit contrasts with that observed in SeSAME/EAST syndrome. Proc Natl Acad Sci USA 2011;108(25):10361–6.
[384] Peterson LN, Wright FS. Effect of sodium intake on renal potassium excretion. Am J Physiol 1977;233:F225–34.
[384a] Petrovic S, Spicer Z, Greeley T, Shull GE, Soleimani M. Novel Schering and ouabain-insensitive potassium-dependent proton secretion in the mouse cortical collecting duct. Am J Physiol Renal Physiol 2002;282(1):F133–43.
[385] Pluznick JL, Sansom SC. BK channels in the kidney: role in K^+ secretion and localization of molecular components. Am J Physiol Renal Physiol 2006;291:F517–29.
[386] Pluznick JL, Wei P, Carmines PK, Sansom SC. Renal fluid and electrolyte handling in BKCa-beta1$^{-/-}$ mice. Am J Physiol Renal Physiol 2003;284:F1274–1279.
[387] Pluznick JL, Wei P, Grimm PR, Sansom SC. BK-β1 subunit: immunolocalization in the mammalian connecting tubule and its role in the kaliuretic response to volume expansion. Am J Physiol Renal Physiol 2005;288:F846–54.
[388] Praetorius HA, Leipziger J. ATP release from non-excitable cells. Purinergic Signalling 2009;5:433–46.
[389] Praetoriuis HA, Leipziger J. Intrarenal purineregic signaling in the control of renal tubular transport. Annu Rev Physiol 2010;72:377–93.
[390] Proverbio F, Whittembury G. Cell electrical potential during enhanced Na extrusion in guinea-pig cortex slices. J Physiol 1975;250:559–78.
[391] Rabelink TJ, Koomans HA, Hene J, Dorhout-Mees EJ. Early and late adjustment to potassium loading in humans. Kidney Int 1990;38:942–7.
[392] Rabinowitz L. Aldosterone and renal potassium excretion. Renal Physiol (Basel) 1979-80;2:229–43.
[393] Rabinowitz L. Homeostatic regulation of potassium excretion. J Hypertens 1989;7:433–42.
[394] Rabinowitz L, Aizman RI. The central nervous system in potassium homeostasis. Frontiers in Neuroendocrinol 1993; 14:1–26.
[395] Rabinowitz L, Berlin R, Yamauchi H. Plasma potassium and diurnal cyclic potassium excretion in the rat. Am J Physiol 1987;253:F1178–81.
[396] Rabinowitz L, Gunther RA. Renal potassium excretion in sheep during sodium sulfate, phosphate, and chloride infusion. Am J Physiol 1978;234:F371–5.
[397] Rabinowitz L, Wydner CJ, Smith KM, Yamauchi H. Diurnal potassium excretory cycles in the rat. Am J Physiol 1986;250: F930–41.
[398] Rastegar A, Biemesderfer D, Kashgarian M, Hayslett JP. Changes in membrane surfaces of collecting duct cells in potassium adaptation. Kidney Int 1980;18:293–301.
[399] Rector Jr FC, Bloomer HA, Seldin DW. Proximal tubular reabsorption of potassium during mannitol diuresis in rats. J Lab Clin Med 1964;63:100–5.
[400] Reeves WE, Shah SV. Activation of potassium channels contributes to hypoxic injury in proximal tubules. J Clin Invest 1994;94:2289–94.
[401] Reeves WE, Winters Q, Zimniak L, Andreoli TE. Medullary thick limbs: renal concentrating segments. Kidney Int 1996;50: S154–64.
[401a] Reichold M, Zdebik AA, Lieberer E, Rapedius M, Schmidt K, Bandulik S, et al. KCNJ10 gene mutations causing EAST syndrome (epilepsy, ataxia, sensorineural deafness, and tubulopathy) disrupt channel function. Proc Natl Acad Sci USA 2010;107(32):14490–5.
[402] Reineck HJ, Osgood RW, Ferris TF, Stein JH. Potassium transport in the distal tubule and collecting duct of the rat. Am J Physiol 1975;219:1403–9.
[403] Reineck HJ, Osgood RW, Stein JH. Net potassium addition beyond the superficial distal tubule of the rat. Am J Physiol 1978;235:F104–10.
[404] Riccardi D, Hall AE, Chattopadhyay N, Xu JZ, Brown EM, Hebert SC. Localization of the extracellular Ca^{2+}-(polyvalent) cation-sensing receptor in kidney. Am J Physiol Renal Physiol 1998;274:F611–22.
[405] Riccardi D, Lee WS, Lee K, Segre GV, Brown EM, Hebert SC. Localization of the extracellular Ca^{2+}-sensing receptor and PTH/PTHrP receptor in rat kidney. Am J Physiol 1996;271: F951–6.
[406] Rieg T, Bundey RA, Chen Y, Deschenes G, Junger W, Insel PA, et al. Mice lacking P2Y2 receptors have salt-resistant hypertension and facilitated renal Na^+ and water reabsorption. FASEB J 2007;21:3717–26.
[407] Rieg T, Vallon V, Sausbier M, Sausbier U, Kaissling B, Ruth P, et al. The role of the BK channel in potassium homeostasis and flow-induced renal potassium excretion. Kidney Int 2007;72: 566–73.
[408] Rocafull MA, Romero FJ, Thomas LE, del Castillo JR. Isolation and cloning of the K^+-independent, ouabain-insensitive Na^+-ATPase. Biochim Biophys Acta 2011;1808:1684–700.
[409] Rocha AS, Kokko JP. Sodium chloride and water transport in the medullary thick ascending limb of Henle: evidence for active chloride transport. J Clin Invest 1973;52:612–23.
[410] Rocha AS, Kudo LH. Water, urea, sodium, chloride, and potassium transport in the *in vitro* isolated perfused papillary collecting duct. Kidney Int 1982;22:485–91.
[411] Rodan AR, Cheng C-J, Huang C-L. Recent advances in distal tubular potassium handling. Am J Physiol Renal Physiol 2011;300:F821–7.
[412] Rodan AR, Huang C-L. Distal potassium handling based on flow modulation of maxi-K channel activity. Curr Opin Nephrol Hypertens 2009;18:350–6.
[413] Rodriguez HJ, Hogan WE, Hellman RN, Klahr S. Mechanism of activation of renal Na^+-K^+-ATPase in the rat: effects of potassium loading. Am J Physiol 1980;238:F315–23.
[414] Rodriguez HJ, Sinha SK, Starling J, Klahr S. Regulation of renal Na^+-K^+ATPase in the rat by adrenal steroids. Am J Physiol 1981;241:F186–95.
[415] Rosetti L, Robbenhaar GK, Giebisch G, Smith D, DeFronzo R. Effect of insulin on renal potassium metabolism. Am J Physiol 1987;252:F60–4.
[416] Rubera I, Loffing J, Palmer LG, Frindt G, Fowler-Jaeger N, Sauter D, et al. Collecting duct-specific gene inactivation of αENaC in the mouse kidney does not impair sodium and potassium balance. J Clin Invest 2003;112:554–65.
[417] Rutledge JC, Rabinowitz L. Kaliuretic regulatory factors in the rat. Am J Physiol Renal Physiol 1987;253:F1182–96.
[418] Sabolic I, Herak-Kramberger CM, Breton S, Brown D. Na/K-ATPase in intercalated cells along the rat nephron

revealed by antigen retrieval. J Am Soc Nephrol 1999;10: 913–22.
[419] Sackin H. Stretch-activated potassium channels in renal proximal tubule. Am J Physiol 1987;241:F540–55.
[420] Sackin H, Boulpaep EL. Isolated perfused salamander proximal tubule. II. Monovalent ion replacement and rheogenic transport. Am J Physiol 1981;241:F540–55.
[421] Sackin H, Boulpaep EL. Rheogenic transport in rhe renal proximal tubule. J Gen Physiol 1983;82:819–51.
[422] Salman IM, Sattar MA, Abdullah NA, Ameer OZ, Basri F, Hussain NM, et al. Role of renal sympathetic nervous system in the control of renal potassium handling. J Nephrol 2010;23:291–6.
[423] Sampio MS, Bezerra IP, Pecanha FL, Fonseca PH, Capella MA, Lopes AG. Lack of Na^+,K^+-ATPase expression in intercalated cells may be compensated by Na^+-ATPase: a study on MDCK-C11 cells. Cell Mol Life Sci 2008;65:3093–9.
[424] Sansom SE, Agulian S, Muto S, Illig V, Giebisch G. K activity of CCD principal cells from normal and DOCA-treated rabbits. Am J Physiol 1989;256:F136–42.
[425] Sansom SE, Muto S, Giebisch G. Na-dependent effects of DOCA on cellular transport properties of CCDs from ADX rabbits. Am J Physiol 1987;253:F753–9.
[426] Sansom SC, O'Neil RG. Mineralocorticoid regulation of apical cell membrane Na^+ and K^+ transport of rhe cortical collecring duct. *Am J*. Am J Physiol 1985;248:F858–68.
[427] Sansom SE, O'Neil RG. Effects of mineralocorticoids on transport properties of cortical collecting duct basolateral membrane. Am J Physiol 1986;241:F743–57.
[428] Sastrasinh S, Tannen RL. Effect of potassium on renal NH3 production. Am J Physiol 1983;244:F383–91.
[429] Satlin LM. Postnatal maturation of potassium transport in rabbit cortical collecting duct. Am J Physiol 1994;266:F57–65.
[430] Satlin LM. Regulation of potassium transport in the maturing kidney. Semin Nephrol 1999;19(2):155–65.
[431] Satlin LM, Palmer LG. Apical K^+ conductance in maturing rabbit principal cell. Am J Physiol 1997;272:F397–404.
[432] Satlin LM, Palmer LP. The apical Na^+ conductance in the maturing rabbit principal cell. Am J Physiol 1996;279:F391–7.
[433] Satlin LM, Sheng S, Woda CB, Kleyman TR. Epithelial sodium channels are regulated by flow. Am J Physiol 2001;280:F1010–8.
[434] Sauer M, Flemmer A, Thurau K, Beck FX. Sodium entry routes in principal and intercalated cells of the isolated perfused cortical collecting duct. Pflugers Arch 1990;416:88–93.
[435] Scandling JD, Ornt DB. Mechanism of potassium depletion during chronic metabolic acidosis in the rat. Am J Physiol 1987;252:Fl22–130.
[436] Schafer C, Westphale HJ, Oberleithner H. Contrasting action of H^+ and Ca^{2+} on K^+-transport in diluting segment of frog kidney. Cell Physiol Biochem 1991;1:286–93.
[437] Schafer JA, Troutman SL. Effect of ADH on rubidium transport in isolated perfused rat cortical collecting tubule. Am J Physiol 1986;250:F1063–72.
[438] Schafer JA, Troutman SL, Schlatter E. Vasopressin and mineralocorticoid increase apical membrane driving force for K^+ secretion in rat CCD. Am J Physiol 1990;258:F199–210.
[439] Schafer JA, Work J. Transport properties of the pars recta. Nephrology 1985;1:186–95.
[440] Schlatter E, Bleich M, Hirsch J, Markstahler U, Fröbe U, Greger R. Cation specificity and pharmacological properties of the Ca^{2+}-dependent K^+ channel of rat cortical collecting ducts. Pflugers Arch 1993;422:481–91.
[441] Schlatter E, Lohrmann E, Greger R. Properties of the potassium conductances of principal cells of rat cortical collecting ducts. Pflugers Arch 1992;420:39–45.
[442] Schlatter E. Regulation of ion channels in the cortical collecting duct. Renal Physiol Biochem 1993;16:21–36.
[443] Schlatter E. Antidiuretic hormone regulation of electrolyte transport in the distal nephron. Renal Physiol Biochem 1989;12:65–84.
[444] Schlatter E, Greger R, Widtke C. Effect of "high ceiling" diuretics on active salt transport in the cortical thick ascending limb of Henle's loop of rabbit kidney. Correlation of chemical structure and inhibitory potency. Pflugers Arch 1983;396:210–7.
[445] Schlatter E, Haxelmans S, Ankorina I. Correlation between intracellular activities of Ca^{2+} and Na^+ in rat cortical collecting duct: a possible coupling mechanism between Na^+-K^+-ATPase and basolateral K^+ conductance. Kidney Blood Press Res 1996;19:24–31.
[446] Schlatter E, Haxelmans S, Hirsch J, Leipziger J. pH dependence of K^+ conductances of rat cortical collecting duct principal cells. Pflugers Arch 1994;428:631–40.
[447] Schlatter E, Schafer JA. Electrophysiological studies in principal cells of rat cortical collecting tubules. ADH increases the apical membrane Na^+-conductance. Pflugers Arch 1987;409: 81–92.
[448] Schmidt U, Horster M. Na-K-activated ATPase: activity maturation in rabbit nephron segments dissected *in vitro*. Am J Physiol 1977;233:F55–60.
[449] Schmidt U, Schmid J, Schmid H, Dubach UC. Sodium- and potassium-activated ATPase. A possible target of aldosterone. J Clin Invest 1975;55:655–60.
[450] Schmitt R, Ellison DH, Farman N, Rossier BC, Reilly RF, Reeves WB, et al. Developmental expression of sodium entry pathways in rat nephron. Am J Physiol 1999;276:F367–381.
[451] Schnermann J, Steipe B, Briggs JP. *In situ* studies of distal convoluted tubule in rat. II. K^+ secretion. Am J Physiol 1987;252: F970–6.
[452] Schon DA, Backman KA, Hayslett JP. Role of the medullary collecting duct in potassium excretion in potassium-adapted animals. Kidney Int 1981;20:655–62.
[453] Schultz SG. Homocellular regulatory mechanisms in sodium-transporting epithelia: avoidance of extinction by "flush-through". Am J Physiol 1981;21:F579–90.
[454] Schultz SG. Homocellular regulatory mechanisms in sodium-transporting epithelia: an extension of the Koefoed-Johnsen-Ussing model. Semin Nephrol 1982;2:343–7.
[455] Seldin DW, Welt LG, Cart JH. The role of sodium salts and adrenal steroids in the production of hypokalemic alkalosis. Yale J Biol Med 1956;29:229–47.
[456] Shirley DG, Walter SJ, Folkerd EJ, Unwin RJ, Bailey MA. Transepithelial electrochemical gradient in the proximal convoluted tubule during potassium depletion in the rat. J Physiol (Lond) 1998;513:551–7.
[457] Silver RB, Choe H, Frindt G. Low-NaCI diet increases H-K-ATPase in intercalated cells from rat cortical collecting duct. Am J Physiol 1998;275:F94–102.
[458] Silver RB, Frindt G, Mennitt P, Satlin LM. Characterization and regulation of H-K-ATPase in intercalated cells of rabbit cortical collecting duct. J Exp Zool 1997;279:443–55.
[459] Silver RB, Frindt G. Functional identification of H^+/K^+-ATPase in intercalated cells of cortical collecting tubule. Am J Physiol 1993;264:F259–66.
[460] Silver RB, Mennitt PA, Satlin LM. Stimulation of apical H-K-ATPase in intercalated cells of cortical collecting duct with chronic metabolic acidosis. Am J Physiol 1996;270: F539.
[461] Simon BB, Karel FE, Rodriguez-Soriano J, Hamdan JH, DiPietro A, Trachtman H, et al. Genetic heterogeneity of

Bartter's syndrome revealed by mutations in the K^+ channel, ROMK. Nature Gen 1996;14:152–6.

[462] Solomon S. Absolute rates of sodium and potassium reabsorption by proximal tubule of immature rats. Biol Neonate 1974;25:340–51.

[463] Sonnenberg H. Medullary collecting duct function in antidiuretic and in salt- or water-diuretic rats. Am J Physiol 1974;226:501–6.

[464] Stanton BA. Characterization of apical and basolateral membrane conductances of rat inner medullary collecting duct. Am J Physiol 1989;256:F862–8.

[465] Stanton B. Regulation by adrenal corticosteroids of sodium and potassium transport in loop of Henle and distal tubule of rat kidney. J Clin Invest 1986;78:1612–20.

[466] Stanton B. Renal potassium adaptation: cellular mechanisms and morphology. In: Giebisch G, editor. Current topics in membranes and transport, vol. 28. Orlando: Academic Press; 1987. p. 225–67.

[467] Stanton B, Kaissling B. Adaptation of distal tubule and collecting duct to increased sodium delivery. II. Na^+ and K^+ transport. Am J Physiol 1988;255:FI269–1275.

[468] Stanton B, Giebisch G, Klein-Robbenhaar G, Wade J, DeFronzo RA. Effects of adrenalectomy and chronic adrenal corticosteroid replacement on potassium transport in rat kidney. J Clin Invest 1985;75:1317–26.

[469] Stanton B, Pan L, Deetjen P, Guckian V, Giebisch G. Independent effects of aldosterone and potassium on induction of potassium adaptation in rat kidney. Clin Invest 1987;79: 198–206.

[470] Stanton BA. Renal potassium transport: morphological and functional adaptations. Am J Physiol 1989;257:R989–97.

[471] Stanton BA, Biemesderfer D, Wade JB, Giebisch G. Structural and functional study of the rat distal nephron: effects of potassium adaptation and potassium depletion. Kidney Int 1981;19:36–48.

[472] Stanton BA, Giebisch G. Effects of pH on potassium transport by renal distal tubule. Am J Physiol 1982;242:F544–51.

[473] Stanton BA, Giebisch G. Renal potassium transport Renal physiology In: Windhager EE, editor. Handbook of physiology. New York: Oxford University Press; 1991. p. 813–74

[474] Stanton BA, Giebisch GH. Potassium transport by the renal distal tubule: effects of potassium loading. Am J Physiol 1982;243:F487–93.

[475] Stanton BA, Guggino WB, Giebisch G. Acidification of the basolateral solution reduces potassium conductance of the apical membrane. Ped Proc 1982;41:1006.

[476] Stanton BA, Janzen A, Klein-Robbenhaar G, DeFronzo RA, Wade J, Giebisch G. Ultrastructure of rat initial collecting tubule: effect of adrenal corticosteroid treatment. J Clin Invest 1985;75:1327–34.

[477] Sterns RH. Oscillations of plasma K^+ and insulin during K^+ infusion in awake anephric dogs. Am J Physiol 1982;243: F44–52.

[478] Sterns RH, Cox M, Feig PU, Singer I. Internal potassium balance and the control of the plasma potassium concentration. Medicine 1981;60:339–54.

[479] Sterns RH, Cox M, Feig PU, Singer I. Internal potassium balance and the control of the plasma potassium concentration. Medicine (Baltimore) 1981;60:339–54.

[480] Sterns RH, Feig PU, Pring M, Guzzo J, Singer I. Disposition of intravenous potassium in anuric man: a kinetic analysis. Kidney Int 1979;15:651–60.

[481] Stetson DL, Wade JB, Giebisch G. Morphologic alterations in the rat medullary collecting duct following potassium depletion. Kidney Int 1980;17:45–56.

[482] Stokes JB. Potassium intoxication: pathogenesis and treatment. In: Seldin DW, Giebisch G, editors. The regulation of potassium balance. New York: Raven Press; 1989. p. 269–302.

[483] Stokes JB. Potassium secretion by cortical collecting tubule: relation to sodium absorption, luminal sodium concentration, and transepithelial voltage. Am J Physiol 1981;241: F395–402.

[484] Stokes JB. Consequences of potassium recycling in the renal medulla. Effects on ion transport by the medullary thick ascending limb of Henle's loop. J Clin Invest 1982;70:219–29.

[485] Stokes JB. Ion transport by the cortical and outer medullary collecting tubule. Kidney Int 1982;22:473–84.

[486] Stokes JB. Na and K^+ transport across the cortical and outer medullary collecting tubule of the rabbit: evidence for diffusion across the outer medullary portion. Am J Physiol 1982;242:F514–20.

[487] Stokes JB. Ion transport by the collecting duct. Semin Nephrol 1993;13:202–12.

[488] Stokes JB, Ingram MJ, Williams AD, Ingram D. Heterogeneity of the rabbit collecting tubule: localization of mineralocorticoid hormone action to the cortical portion. Kidney Int 1981;20:340–7.

[489] Stoner LC, Burg MB, Orloff J. Ion transport in cortical collecting tubule: effect of amiloride. Am J Physiol 1974;227(2): 453–9.

[490] Stoner LC, Viggiano SC. Environmental KCl causes an upregulation of apical membrane maxi K^+ and ENaC channels in everted *Ambystoma* collecting tubule. J Membr Biol 1998;162: 107–16.

[491] Stoner LC, Viggiano SC. Elevation of basolateral K^+ induces K^+ secretion by apical maxi K^+ channels in *Abystoma* collecting tubule. Am J Physiol 1999;276:R616–621.

[492] Stow LR, Gumz ML, Lynch IJ, Greenlee MM, Rudin A, Cain BD, et al. Aldosterone modulates steroid receptor binding to the endothelin-1 gene (edn1). J Biol Chem 2009;284: 30087–96.

[493] Subramanya AR, Yang C-L, McCormick JA, Ellison DH. WNK kinases regulate sodium chloride and potassium transport by the aldosterone-sensitive distal nephron. Kidney Int 2006;70: 630–4.

[494] Sufit CR, Jamison RL. Effect of acute potassium load on reabsorption in Henle's loop in the rat. Am J Physiol 1983;245: F569–76.

[495] Suh A, DeJesus E, Rosner K, Lerma E, Yu W, Young JB, et al. Racial differences in potassium disposal. Kidney Int 2004;66: 1076–81.

[496] Sulyok E, Nemeth M, Tenyi I, Csaba IF, Varga F, Gyory E, et al. Relationship between maturity, electrolyte balance and the function of the renin–angiotensin–aldosterone system in newborn infants. Biol Neonate 1979;35:60–5.

[496a] Sun A, Grossman EB, Lombardi M, Hebert SC. Vasopressin alters the mechanism of apical CI^- entry from Na^+:CI^- to Na^+:K^+:2CI^- cotransport in mouse medulltary thick ascending limb. J Membr Biol 1991;120:83–94.

[497] Sun P, Liu W, Lin DH, Yue P, Kemp R, Satlin LM, et al. Epoxyeicosatrienoic acid activates BK channels in the cortical collecting duct. J Am Soc Nephrol 2009;20:513–23.

[497a] Suzuki Y, Yasuoka Y, Shimohama T, Nishikitani M, Nakamura N, Hirose S, Kawahara K. Expression of the K^+ channel Kir7.1 in the developing rat kidney: role in K^+ excretion. Kidney Int 2003;63:969–75.

[498] Tabei K, Muto S, Furuya H, Sakairi Y, Ando Y, Asano Y. Potassium secretion is inhibited by metabolic acidosis in rabbit cortical collecting ducts *in vitro*. Am J Physiol Renal 1995;268: F490–5.

[499] Taniguchi J, Imai M. Flow-dependent activation of maxi K^+ channels in apical membrane of rabbit connecting tubule. J Membr Biol 1998;164:35–45.
[500] Taniguchi J, Tsuruoka S, Mizuno A, Sato J, Fujimura A, Suzuki M. TRPV4 as a flow sensor in flow-dependent K^+ secretion from the cortical collecting duct. Am J Physiol Renal Physiol 2007;292:F667–73.
[501] Tannen RL. Effect of potassium on renal acidification and acid–base homeostasis. Semin Nephrol 1987; 7:263–72.
[502] Tannen RL. Potassium and acid–base balance. In: Giebisch G, editor. Current topics in membranes and transport, vol. 28. Orlando: Academic Press; 1987. p. 207–23.
[503] Teulon J, Anagnostopoulos T. Proximal cell K^+ activity: technical problems and dependence on plasma K^+ concentration. Am J Physiol 1982;243:FI2–8.
[504] Tian J, Xie Z-J. The Na-K-ATPase and calcium-signaling microdomains. Physiol 2008;23:205–11.
[505] Tomita K, Pisano J, Knepper MA. Control of sodium and potassium transport in the cortical collecting duct of the rat. Effects of bradykinin, vasopressin, and deoxycorticosterone. J Clin Invest 1985;76:132–6.
[506] Toussaint C, Vereerstraeten P. Effects of blood pH changes on potassium excretion in the dog. Am J Physiol 1962;202: 768–72.
[507] Tsai TD, Shuck ME, Thompson DP, Bienkowski MJ, Lee Ks. Intracellular H^+ inhibits a cloned rat outer medullary K^+ channel expressed in *Xenopus* oocytes. Am J Physiol 1995;268: C1173–8.
[508] Tsuchiya K, Wang W, Giebisch G, Welling PA. ATP is a coupling modulator of parallel Na^+/K^+ ATPase-K^+ channel activity in the renal proximal tubule. Proc Natl Acad Sci USA 1992;89:6418–22.
[509] Tsuruoka S, Koseki C, Muto S, Tabei K, Imai M. Axial heterogeneity of potassium transport across hamster thick ascending limb of Henle's loop. Am J Physiol Renal 1994;267:F121.
[510] Tudvad F, McNamara H, Barnett HL. Renal response of premature infants to administration of bicarbonate and potassium. Pediatrics 1954;13:4–16.
[511] Unwin R, Capasso G, Giebisch G. Potassium and sodium transport along the loop of Henle: effects of altered dietary potassium intake. Kidney Int 1994;46:1092–9.
[512] Unwin RJ, Capasso G, Giebisch G, et al. Loop of Henle (LOH) potassium transport and the urinary concentrating mechanism. In: DeSanto NG, Capasso G, editors. Acid–base and electrolyte balance. Naples: Institute Italy Pere Gli Studi Filosofici; 1995. p. 243–56.
[513] Unwin R, Capasso G, Giebisch G Water and electrolyte transport along the rat loop of Henle: effect of chronic dietary potassium adaptation and restriction. In: Proceedings of the 11th International Congress of Nephrology. Tokyo: 1990;493a.
[514] Ussing HH. The alkali metal ions in isolated systems and tissues. Handbuch der experimentellen Pharmakologie. Heidelberg: SpringerVerlag; 1960 [1–195]
[515] Ussing HH, Leaf A. Transport across multimembrane systems. In: Giebisch G, Tosteson DC, Ussing HH, editors. Membrane transport in biology, vol. 3. New York: Springer-Verlag; 1978. p. 1.
[516] Vallon V, Grahammer F, Richter K, Bleich M, Lang F, Barhanin J, et al. Role of KCNE1-dependent K^+ fluxes in mouse proximal tubule. J Am Soc Nephrol 2001;12:2003–11.
[517] Vallon V. P2 receptors in the regulation of renal transport mechanisms. Am J Physiol Renal Physiol 2008;294:F10–27.
[518] Vallon V, Grahammer F, Volkl H, Sandu CD, Richter K, Rexhepaj R, et al. KCNQ1-dependent transport in renal and gastrointestinal epithelia. Proc Natl Acad Sci 2005;102(49): 17864–9.
[519] Vallon V, Osswald H, Blantz RC, Thomson S. Potential role of luminal potassium in tubuloglomerular feedback. J Am Soc Nephrol 1997;8:1831–7.
[520] Vallon V, Wulff P, Huang DY, Loffing J, Völkl H, Kuhl D, et al. Role of Sgk1 in salt and potassium homeostasis. Am J Physiol Regul Integr Comp Physiol 2005;288:R4–10.
[521] Velazquez H, Ellison DH, Wright FS. Chloride-dependent potassium secretion in early and late distal tubules. Am J Physiol 1987;253:F555–562.
[522] Velazquez H. Thiazide diuretics. Renal Physiol 1987;10: 184–97.
[523] Velazquez H, Giebisch G. Effects of diuretics on specific transport systems. Semin Nephrol 1988;8:295–304.
[524] Velazquez H, Wright FS. Control by drugs of renal potassium handling. Annu Rev Pharmacol Toxicol 1986;26:293–309.
[525] Velazquez H, Wright FS. Effects of diuretic drugs on Na, Cl, and K^+ transport by rat renal distal tubule. Am J Physiol 1986;250:FI013–l023.
[526] Velazquez H, Wright FS, Good DW. Luminal influences on potassium secretion: chloride replacement with sulfate. Am J Physiol 1982;242:F46–55.
[527] Verrey F. Early aldosterone effects. Exp Nephrol 1998;6:294–301.
[528] Vestri S, Malnic G. Mechanism of potassium transport across proximal tubule epithelium in the rat. Braz J Med Biol Res 1990;23:1195–9.
[529] Wade JB, Fang L, Coleman RA, Liu J, Grimm PR, Wang T, et al. Differential regulation of ROMK (Kir1.1) in distal nephron segments by dietary potassium. Am J Physiol Renal Physiol 2011;300:F1385–93.
[530] Wade JB, O'Neil RG, Pryor JL, Boulpaep EL. Modulation of cell membrane area in renal collecting tubules by corticosteroid hormones. J Cell Biol 1979;81:439–45.
[531] Wade JB, Stanton BA, Field MJ, Kashgarian M, Giebisch G. Morphological and physiological responses to aldosterone: time course and sodium dependence. Am J Physiol 1990;259: F88–94.
[532] Wagner CA. New roles for renal potassium channels. J Nephrol 2010;23(1):5–8.
[533] Wall SM, Knepper MA, Hassell KA, Fischer MP, Shodeinde A, Shin W, et al. Hypotension in NKCC1 null mice: role of the kidneys. Am J Physiol Renal Physiol 2006;290:F409–416.
[534] Wall SM, Koger LM. NH_4 transport mediated by Na^+K^+-ATPase in rat inner medullary collecting duct. Am J Physiol 1994;167:F660–70.
[535] Wang T. Renal outer medullary potassium channel knockout models reveal thick ascending limb function and dysfunction. Clin Exp Nephrol 2012;16:49–54.
[536] Wang T, Malnic G, Giebisch G, Chan YL. Renal bicarbonate absorption in the rat: 4. Bicarbonate transport mechanisms in the early and late distal tubule. J Clin Invest 1993;91:2776–84.
[537] Wang T, Wang W, Klein-Robbenhaar G, Giebisch G. Effects of a novel KATP channel blocker on renal tubule function and.K channel activity. J Pharmacol Exp Ther 1995;273:1382–9.
[538] Wang T, Wang W, Klein-Robbenhaar G, Giebisch G. Effects of glyburide on renal tubule transport and potassium-channel activity. Renal Physiol Biochem 1995;18:169–82.
[538a] Wang T, Yang CL, Abbiati T, Schultheis PJ, Shull GE, Giebisch G, et al. Mechanism of proximal tubule bicarbonate absorption in NHE3 null mice. Am J Physiol 1999;277(2 Pt 2): F298–302.
[539] Wang W, Giebisch G. Regulation of potassium (K) handling in the renal collecting duct. Pflugers Arch 2009;458:157–68.

[540] Wang W, Hebert SC, Giebisch G. Renal K^+ channels: structure and function. Annu Rev Physiol 1997;59:413–6.
[541] Wang W. Two types of potassium channels in thick ascending limb of rat kidney. Am J Physiol 1994;267:F599–605.
[542] Wang WH, Geibel J, Giebisch G. Mechanism of apical K^+ channel modulation in principal renal tubule cells. J Gen Physiol 1993;101:673–94.
[543] Wang WH. Regulation of the hyperpolarization-activated K^+ channel in the lateral membrane of the cortical collecting duct. J Gen Physiol 1995;106:25–43.
[544] Wang W, Geibel J, Giebisch G. Regulation of the small conductance K^+ channels in the apical membrane of rat cortical collecting tubule. Am J Physiol 1990;259:F494–502.
[545] Wang W, Henderson RM, Geibel J, White S, Giebisch G. Mechanism of aldosterone-induced increase of K^+ conductance in early distal renal tubule cells of the frog. J Membr Biol 1989;111:277–89.
[546] Wang WH. View of K^+ secretion through the apical K^+ channel of cortical collecting duct. Kidney Int 1995;48:1024–30.
[547] Wang WH, Lu M, Hebert SC. P450 metabolites mediate extracellular Ca^{2+}-induced inhibition of apical K^+ channels in the thick ascending limb of the rat kidney. Am J Physiol 1996;266: F813–22.
[548] Wang W-H, Yue P, Sun P, Lin D-H. Regulation and function of potassium channels in aldosterone-sensitive distal nephron. Curr Opin Nephrol Hypertens 2010;19:463–70.
[549] Wang XY, Masilamani S, Nielsen J, Kwon TH, Brooks HL, Nielsen S, Knepper MA. The renal thiazide-sensitive Na-Cl cotransporter as a mediator of the aldosterone-escape phenomenon. J Clin Invest 2001;108:215–22.
[550] Wareing M, Wilson RW. Kibble JD, Green R. Estimated potassium reflection coefficient in perfused proximal convoluted tubules of the anaesthetized rat *in vivo*. J Physiol 1995;488.1: 153–61.
[551] Warnock DG, Eveloff J. K-Cl cotransport systems. Kidney Int 1989;36:412–7.
[552] Wasserman AG, Agus ZS. Potassium secretion in the rabbit proximal straight tubule. Am J Physiol 1983;245:FI67–74.
[553] Watson JF, Clapp IR, Berliner RW. Micropuncture study of potassium concentration in proximal tubule of dog, rat, and *Necturus*. J Clin Invest 1964;43:595–605.
[554] Wei Y, Babilonia E, Sterling H, Jin Y, Wang W-H. Mineralocorticoids decrease the activity of the apical small-conductance K^+ channel in the cortical collecting duct. Am J Physiol Renal Physiol 2005;289:F1065–71.
[555] Wei Y, Zavilowitz B, Satlin LM, Wang W-H. Angiotensin II inhibits the ROMK-like small conductance K^+ channel in renal cortical collecting duct during dietary potassium restriction. J Biol Chem 2007;282:6455–62.
[556] Wei Y, Zavilowitz B, Ren J, Liui W, Chan P, Estilio G, et al., Angiotensin type 2 (AT2) receptor regulates renal potassium secretory channel activity during high dietary potassium adaptation. (personal communication)
[557] Weinbaum S, Duan Y, Satlin LM, Wang T, Weinstein AM. Mechanotransduction in the renal tubule. Am J Physiol Renal Physiol 2010;299:F1220–1236.
[558] Weiner ID, Milton AE. H^+-K^+-ATPase in rabbit cortical collecting duct B-type intercalated cell. Am J Physiol 1996;270: F518–30.
[559] Weinstein AM. Modeling the proximal tubule: complications of the paracellular pathway. Am J Physiol 1988;254:F297–305.
[560] Weinstein AM. A mathematical model of rat distal convoluted tubule. II. Potassium secretion along the connecting segment. Am J Physiol Renal Physiol 2005;289:721–41.
[561] Welling PA. "Cross-talk" and the role of KATP channels in the proximal tubule. Kidney Int 1995;48:1017–23.
[562] Welling PA, Chang Y-PC, Delpire E, Wade JB. Multigene kinase network, kidney transport, and salt in essential hypertension. Kidney Int 2010;77:1063–9.
[563] Welling PA, Ho K. A comprehensive guide to the ROMK potassium channel: form and function in health and disease. Am J Physiol Renal Physiol 2009;297:F849–63.
[564] Welling PA, O'Neil RG. Cell swelling increases basolateral membrane Cl and K^+ conductances of the rabbit proximal straight tubule. Kidney Int 1987;31:452.
[565] West ML, Bendz O, Chen CB, Singer GG, Richardson RM, Sonnenberg H, et al. Development of a test to evaluate the transtubular potassium concentration gradient in the cortical collecting duct *in vivo*. Miner Electrolyte Metab 1986;12: 226–33.
[566] West ML, Marsden PA, Richardson RM, Zettle RM, Halperin ML. New clinical approach to evaluate disorders of potassium excretion. Miner Electrolyte Metab 1986;12:234–8.
[567] Westphale HI, Schafer C, Oberleithner H. Aldosterone stimulates cellular K^+ uptake and K^+ release in the diluting segment of the frog kidney. Cell Physiol Biochem 1991;1: 89–97.
[568] Whittembury G, Grantham RR. Cellular aspects of renal sodium transport and cell volume regulation. Kidney Int 1976;9:103–20.
[569] Wingo CS. Potassium transport by the medullary collecting tubule of the rabbit: effects of variation in K^+ intake. Am J Physiol 1987;253:Fl136–1141.
[570] Wingo CS. Potassium secretion by the cortical collecting tubule: effect of CI gradients and ouabain. Am J Physiol 1989;256:F306–13.
[571] Wingo CS, Cain BD. The renal H-K-ATPase: physiological significance and role in potassium homeostasis. Annu Rev Physiol 1993;55:323–47.
[572] Wingo CS, Straub SS. Active proton secretion and potassium absorption in the rabbit outer medullary collecting duct. Functional evidence for proton potassium-activated adenosine triphosphatase. J Clin Invest 1989;84:361–5.
[573] Wirz H. Untersuchungen ueber die Nierenfinktion in adrenalektomierten Katzen. Relv Physiol Pharmacol Acta 1945; 3:589.
[574] Woda CB, Bragin A, Kleyman TR, Satlin LM. Flow-dependent K^+ secretion in the cortical collecting duct is mediated by a maxi-K channel. Am J Physiol 2001;280:F786–93.
[575] Woda CB, Miyawaki N, Ramalakshmi S, Ramkumar M, Rojas R, Zavilowitz B, et al. Ontogeny of flow-stimulated potassium secretion in rabbit cortical collecting duct: functional and molecular aspects. Am J Physiol Renal Physiol 2003;285: F629–639.
[576] Woodhall PB, Tisher CC. Response of the distal tubule and cortical collecting duct to vasopressin in the rat. J Clin Invest 1973;52:3095–108.
[577] Work I, Jamison RL. Effect of adrenalectomy on transport in the rat medullary thick ascending limb. J Clin Invest 1987;80:1160–4.
[578] Work I, Troutman SL, Schafer JA. Transport of potassium in the rabbit pars recta. Am J Physiol 1982;242:F226–37.
[579] Wright FS. Renal potassium handling. Semin Nephrol 1987;7:174–84.
[580] Wright FS. Increasing magnitude of electrical potential along the renal distal tubule. Am J Physiol 1971;220:624–38.
[581] Wright FS. Sites and mechanisms of potassium transport along the renal tubule. Kidney Int 1977;11:415–32.

[582] Wright FS. Flow dependent transport processes: filtration, absorption, secretion. Am J Physiol 1982;243:FI–l1.
[583] Wright FS, Giebisch G. Renal potassium transport: contributions of individual nephron segments and populations. Am J Physiol 1978;235:F515–27.
[584] Wright FS, Schnermann J. Interference with feedback control of glomerular filtration rate by furosemide, triflocin and cyanide. J Clin Invest 1974;53:1695–708.
[585] Wright FS, Strieder N, Fowler NB, Giebisch G. Potassium secretion by distal tubule after potassium adaptation. Am J Physiol 1971;221:437–48.
[586] Xu Z-C, Yang Y, Hebert SC. Phosphorylation of the ATP-sensitive, inwardly-rectifying K^+ channel, ROMK, by cyclic AMP-dependent protein kinase. J Biol Chem 1996;271:9313–9.
[587] Yang L, Frindt G, Palmer LG. Magnesium modulates ROMK channel-mediated potassium secretion. J Am Soc Nephrol 2010;21:2109–16.
[588] Yasui M, Marples D, Belusa R, Eklof AC, Celsi G, Nielsen S, et al. Development of urinary concentrating capacity: role of aquaporin-2. Am J Physiol 1996;271:F461–468.
[589] Yeyati NL, Etcheverry JC, Adrogue HJ. Kaliretic response to potassium loading in amiloride-treated dogs. Ren Physiol Biochem 1990;13:190–9.
[589a] Yoo D, Kim BY, Campo C, Nance L, King A, Maouyo D, Welling PA. Cell surface expression of the ROMK channel is regulated by the aldostrerone-induced kinase, SGK-1, and protein kinase A. J Biol Chem 2003;278:23066–75.
[589b] Yoo D, Flagg TP, Olsen O, Raghuram V, Foskett JK, Welling PA. Assembly and trafficking of a multiprotein ROMK channel complex by PDZ interactions. J Biol Chem 2004;279:6863–73.
[590] Yoshitomi K, Shimizu T, Taniguchi I, Imai M. Electrophysiological characterization of rabbit distal convoluted tubule cell. Pflugers Arch 1989;414:457–63.
[591] Youn JH, McDonough AA. Recent advances in understanding integrative control of potassium homeostasis. Annu Rev Physiol 2009;71:381–401.
[592] Younes-Ibrahim M, Barlet-Bas C, Buffin-Meyer B, Cheval L, Rajerison R, Doucet A. Ouabain-sensitive and -insensitive K-ATPases in rat nephron: effect of K^+ depletion. Am J Physiol 1995;268:F1141–7.
[593] Young DB. Relationship between plasma potassium concentration and renal potassium excretion. Am J Physiol 1982;242: F599–603.
[594] Young DB. Quantitative analysis of aldosterone role in potassium regulation. Am J Physiol 1988;255:FI269–I275.
[595] Young DB, Jackson TE. Effects of aldosterone on potassium distribution. Am J Physiol 1982;243:R526–30.
[596] Young DB, Jackson TE, Tipayamontri U, Scott RC. Effects of sodium intake on steady-state potassium excretion. Am J Physiol 1984;246:F772–8.
[597] Young DB, Paulsen AW. Interrelated effects of aldosterone and plasma potassium on potassium excretion. Am J Physiol 1983;244:F28–34.
[598] Yue P, Lin D-H, Pan C-Y, Leng Q, Giebisch G, Lifton RP, et al. Src family protein tyrosine kinase (PTK) modulates the effect of SGK1 and WNK4 on ROMK channels. Proc Natl Acad Sci USA 2009;106:15061–6.
[599] Yue P, Sun P, Lin D-H, Pan C, Xing W, Wang W-H. Angiotensin II diminishes the effect of SGK1 on the WNK4-mediated inhibition of ROMK1 channels. Kidney Int 2010;79 (4):423–31.
[600] Zalups RK, Stanton BA, Wade JB, Giebisch G. Structural adaptation in initial collecting tubule following reduction in renal mass. Kidney Int 1985;27:636–42.
[601] Zeidel ML, Seifter JL, Lear S, Brenner BM, Silva P. Atrial peptides inhibit oxygen consumption in kidney medullary collecting duct cells. Am J Physiol 1986;251:F379–83.
[602] Zheng D, Perianayagam A, Lee DH, Brannan MD, Yang LE, Tellalian D, et al. AMPK activation with AICAR provokes an acute fall in plasma [K^+]. Am J Physiol Cell Physiol 2008;294: C126–35.
[603] Zhou HS, Tate S, Palmer LG. Primary structure and functional properties of an epithelia K^+ channel. Am J Physiol 1994;166: C809–24.
[604] Zhuang J, Zhang X, Wang D, Li J, Zhou B, Shi Z, et al. WNK4 kinase inhibits Maxi K^+ channel activity by a kinase-dependent mechanism. Am J Physiol Renal Physiol 2011;301:F410–9.
[605] Zink H, Horster M. Maturation of diluting capacity in loop of Henle of rat superficial nephrons. Am J Physiol 1977;33: F519–24.
[606] Zolonitskaya A, Satlin LM. Developmental expression of ROMK in rat kidney. Am J Physiol 1999;276:F825–36.
[607] Zuber AM, Centeno G, Pradervand S, Nikolaeva S, Maquelin L, Cardinaux L, et al. Molecular clock is involved in predictive circadian adjustment of renal function. Proc Natl Acad Sci USA 2009;106(38):16523–8.

This page intentionally left blank

CHAPTER

50

Physiopathology of Potassium Deficiency

Francesco Trepiccione, Miriam Zacchia and Giovambattista Capasso

Chair of Nephrology, Department of Internal Medicine, Faculty of Medicine, Second University of Naples, Italy

INTRODUCTION

Hypokalemia is a common clinical disorder that can be the end-result of: (1) potassium (K^+) redistribution between plasma and intracellular fluid (ICF); (2) insufficient K^+ intake; (3) disproportionate K^+ excretion. It is commonly defined as a plasma K^+ concentration less than 3.5 mmol/L, but this level infrequently causes trouble unless it has fallen rapidly: patients are usually symptomatic when plasma K^+ is lower than 2.5 mmol/L. Major muscle weakness have a tendency to occur at plasma K^+ less than 2 mmol/L.

The average K^+ intake in a typical western diet is roughly 70 mmol.[1] The intestine absorbs almost all of the ingested K^+; only negligible quantities of K^+ are excreted in the feces. The kidney plays an important role in K^+ balance, which is the result of glomerular filtration, extensive proximal tubule reabsorption, and highly regulated secretory/reabsorbtive processes located along the distal tubule and the collecting duct (CD).[2] Total body K^+ is roughly 55 mmol/kg of body weight, with 98% distributed to the intracellular fluid (primarily in muscle, liver, and erythrocytes) and 2% in the extracellular fluid. Na/K-ATPase actively pumps K^+ into the cell and preserves the electrochemical gradient between the intra- and extracellular pool.

NEW CONCEPTS ON THE INTEGRATIVE CONTROL OF K^+ HOMEOSTASIS

Feedback Control of K^+ Homeostasis

A large increase in plasma K^+ concentration triggers aldosterone release from the adrenal glands. Aldosterone, in turn, stimulates the activity and synthesis of both Na/K-ATPase and luminal K^+ channels in CD principal cells, thus promoting K^+ excretion.[3] In addition, aldosterone enhances K^+ secretion in the distal colon, which can exert an essential role when renal function is reduced.[4]

On the other hand, if plasma K^+ concentration decreases as a consequence of reduced K^+ intake or increased K^+ excretion, then feedback regulation redistributes K^+ from ICF to plasma. At the same extent, skeletal muscle becomes insulin-resistant to K^+ (but not glucose) uptake, blocks the entry of K^+ from plasma into the cell. Hypokalemia also causes a decreased expression of skeletal muscle Na/K-ATPase 2 isoform, thus allowing a leak of K^+ from ICF to the plasma.[5] The low plasma K^+ concentration suppresses adrenal aldosterone release so that the kidney reduces urinary K^+ excretion.

Feedforward Control of K^+ Homeostasis

However, besides the classic feedback control, some findings suggest a feedforward control.[6] It is clear that plasma K^+ stimulates aldosterone secretion only at supra-physiological levels, with little effect within the physiological range.[7] Indeed, it has been shown that, in sheep, a meal intake produced a substantial kaliuresis in the absence of changes in plasma aldosterone concentration.[8] From these experiments it was concluded that the increased renal K^+ excretion following a meal cannot be explained by changes in aldosterone concentration, but it may be dependent on the existence of a kaliuretic reflex arising from *sensors* in the splanchnic bed (i.e., gut, portal circulation, and/or liver) (Figure 50.1).

One of the potential effectors of the feedforward control of serum K^+ is glucagon. Glucagon secretion is definitely stimulated after a protein-rich meal, and intraportal glucagon infusion produces significant increases in renal blood flow and glomerular filtration

Seldin and Giebisch's The Kidney, Fifth Edition.
DOI: http://dx.doi.org/10.1016/B978-0-12-381462-3.00050-1

© 2013 Elsevier Inc. All rights reserved.

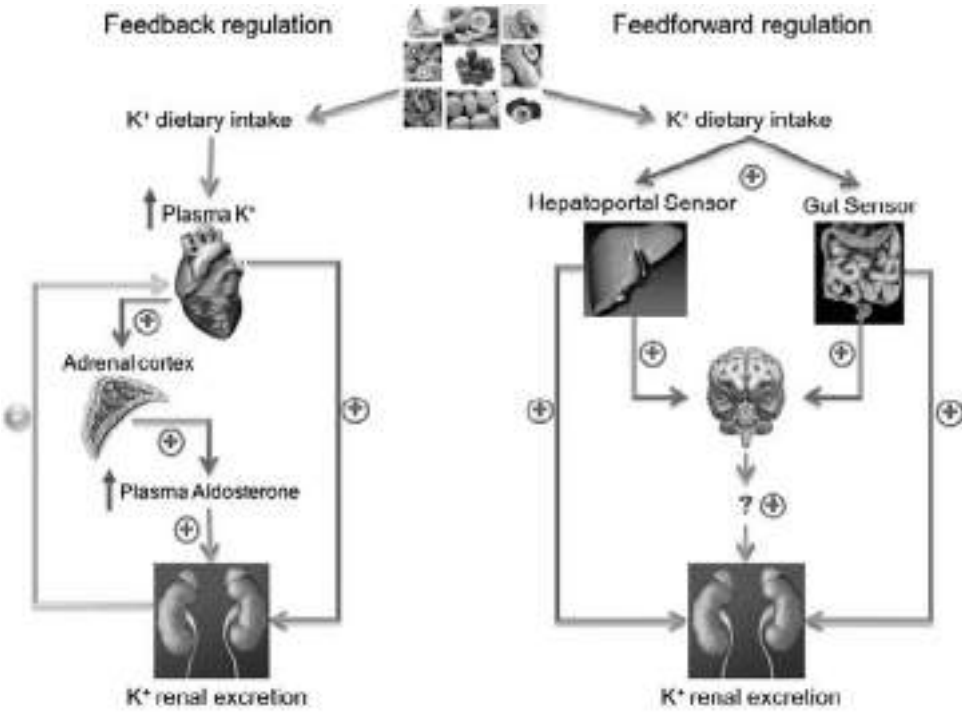

FIGURE 50.1 **Schematic diagram illustrating feedback versus feedforward control of K^+ homeostasis.** Left: In feedback control, an increase in ECF [K^+] is the signal that stimulates urinary K^+ excretion. Right: In feedforward control, an increase in [K^+] in the gut is sensed during K^+ intake and stimulates urinary K^+ excretion independently from a rise in ECF [K^+].

rate (GFR), suggesting the existence of a hepatorenal axis.[9]

The feedforward regulation may act through three different mechanisms: (1) insulin release rapidly stimulates cellular K^+ uptake into insulin-responsive tissues; (2) glucagon, through cAMP released from the liver, quickly increases renal K^+ excretion after a protein-rich meal; (3) a yet-unidentified gut factor senses K^+ ingestion and enhances renal K^+ excretion. When plasma K^+ level increases despite these layers of control, feedback regulation is activated. Aldosterone acts only after a certain time, it is not involved in rapid control of K^+ homeostasis, but it can chronically increase K^+ secretion until plasma K^+ is normalized.[6]

Assessment of Urinary K^+ Excretion

Several urine parameters are used to identify whether hypokalemia is dependent on renal loss. Renal K^+ excretion can be assessed with a 24 hour urine collection or a spot urine test determining the K^+: creatinine ratio. A 24-hour urinary K^+ excretion lower than 15 mEq or a K^+ (mmol)/creatinine (mmol) ratio <1 suggests an extrarenal cause of hypokalemia.

In the clinical practise, as an initial test to address the origin of K^+ losses, a random urine K^+ is used. However, this approach is hampered by the effect of renal water handling on urine K^+ concentration. Determining the transtubular K^+ gradient (TTKG) is still an accepted way to assess renal K^+ handling:

$$TTKG = [uk/(uOsmolality/sOsmolality)]/sk$$

Tubular fluid K^+ concentration in the last part of the CD is mainly dependent on aldosterone, because most K^+ secretion takes place in the CD. Thereafter, urinary K^+ concentration increases as a consequence of water reabsorption. The TTKG reflects the tubular fluid K^+ concentration at the end of the cortical CD, by accounting for water reabsorption that takes place distal of where K^+ secretion has ended.

However, there are few limitations to the clinical use of this formula.[10] First, the calculation assumes that there is no significant solute transport and only water reabsorption along the medullary CD. Any Na^+ or urea reabsorption in this segment would tend to lower urine osmolality and cause the TTKG to overestimate the gradient for K^+ secretion in the upstream CD. Second, there must be optimal conditions for K^+ secretion at the time that the TTKG is measured. In this regard, urinary Na^+ should be no less than 25 mEq/L, to guarantee that Na^+ delivery to the CD is not rate-limiting in K^+ secretion. In addition, urine osmolality should be equal to or higher than the plasma. A higher urine osmolality indicates increased vasopressin

release, which is known to stimulate K^+ secretion in the CD.

Hypokalemia Associated With Intracellular Shift

The regulation of K^+ distribution between the intracellular and extracellular space is known as internal K^+ balance. Even though the kidney is in charge of the preservation of total body K^+, factors that adjust internal balance are central to the removal of acute K^+-loads. A large K^+ intake could potentially double extracellular K^+ concentration in the absence of a rapid shift into the cells. This process is mainly regulated by insulin and catecholamines, with a minor role of metabolic and respiratory alkalosis.

Hypokalemic periodic paralysis is a rare disorder characterized by muscle weakness or paralysis as a result of the sudden movement of K^+ into cells. Measurement of the TTKG at the time of the attacks typically shows values of <1. The attacks may be triggered by exercise, stress, intake of large quantities of carbohydrates, and increased release of catecholamines or insulin.[11]

This disorder is classified as primary, due to a genetic defect or acquired, due to drugs or glandular diseases. The genetic forms are associated with mutations in genes encoding for subunits of muscular sodium, calcium, and potassium channels. Mutations in the α-subunit of the calcium channel [dihydropyridine (DHP)-receptor] (CACNA1S) gene and the α-subunit of the sodium channel (SCN4A) have been described. Loss of function mutations of CACNA1S reduce current density. A mutation in the KCNJ2 gene encoding for the inward-rectifying potassium channel Kir2.1 causes Andersen-Tawil syndrome, characterized by the triad of periodic muscle weakness, cardiac arrhythmias, and multiple dysmorphic features (short stature, hypertelorism, micrognathia).[12] Whether hypokalemia determines the attack is not well-established. The onset of attacks occurs generally between 15 and 35 years of age; the severity of the clinical manifestations range from rare episodes in a lifetime to daily and severe attacks. The attacks can be triggered by all conditions which favor hypokalemia, such as physical exercise, a carbohydrate-rich meal, alcohol, and cold. Myalgia after the attack is a frequent complaint. The acquired form is mainly associated with thyrotoxicosis. Excess thyroid hormone may predispose to paralytic episodes by increasing Na/K-ATPase activity. The activity of this pump is further induced by catecholamines, which are typically increased in this setting. The underlying cause of thyrotoxicosis is most commonly Graves disease, but it can also be a solitary thyroid adenoma (Plummer disease).[13] The acute attacks of hypokalemic periodic paralysis are best treated with intravenous KCl and propranolol.

It is important to administer KCl in non-dextrose-containing solutions, because glucose will stimulate insulin release, potentially exacerbating K^+ shift into the cells. Propranolol (a nonspecific adrenergic β-blocker) blocks the effects of catecholamines, and inhibits the peripheral conversion of T4 to T3.

Extrarenal K^+ Loss from the Body

Diarrhea is a common cause of hypokalemia due to gastrointestinal loss. Secretory diarrhea may be the consequence of two processes that can occur either alone or together. First, it may be related to inhibition of active intestinal NaCl and $NaHCO_3$ reabsorption and, second, it may be dependent on increased active secretion of Cl^- coupled to passive secretion of an identical quantity of Na^+ in order to maintain the electrochemical balance. Under both circumstances, the stool electrolyte composition is analogous to plasma with a high concentration of NaCl and a much lower K^+ concentration. Despite the low K^+ concentration in the stool, large K^+ losses can take place in the setting of large fecal fluid volume.

Hypokalemia may also be associated with infectious diarrhea. In particular, malaria and leptospirosis may cause alterations in fluid and electrolyte balance. Hypokalemia is particularly frequent in children with severe malaria, and may arise within several hours of initiation of therapy. Hypokalemia develops in about one-third of patients with leptospirosis. Such patients are at risk of both gastrointestinal and renal losses. In the outer membrane of the organism there is a substance that has an inhibitory effect on the Na/K-ATPase within the nephron. It has been hypothesized that this inhibitory effect reduces Na^+ reabsorption along the proximal tubule, thus increasing distal Na^+ delivery, resulting in kaliuresis.[14] Hypokalemia may also be associated with watery diarrhea and achlorhydria, a condition secondary to hypersecretion of vasoactive intestinal polypeptide (VIP). In adults, this syndrome is most commonly a complication of pancreatic islet cell tumors, and sometimes of bronchogenic carcinoma, medullary thyroid carcinoma or retroperitoneal histiocytoma. There are now few reports describing chronic watery diarrhea and hypokalemia due to adrenal pheochromocytoma containing immunoreactive VIP.[15]

A recent report describes five consecutive patients with acute or subacute colonic pseudo-obstruction suffering a typical secretory diarrhea characterized by very high fecal K^+ concentrations (over 100 mEq/kg)

and low Na^+ concentration (Ogilvie syndrome). These elevated fecal concentrations of K^+ in large volume diarrhea induced important outputs of K^+ salts responsible for profound hypokalemia and decreased urinary excretion of K^+.[16]

RENAL K^+-LOSING SYNDROMES

Bartter Syndrome (BS)

BS results from a defect in any of the major components of NaCl reabsorbtive machinery along the TAL. So far, mutations of five genes have been described. The defect determines renal loss of water and electrolytes resulting in hypovolemia, with a compensatory increase in renin and aldosterone levels.

Genetic and Molecular Biology

BS type I is sustained by mutations of the SLC12A1 gene, encoding the kidney-specific furosemide-sensitive NKCC2.[17] A number of point mutations have been described in homozygosis or compound heterozygosis, mostly frameshift and non-conservative missense mutations. To date, over 30 mutations in the SLC12A1 gene have been reported[18]; phenotypic variability among patients with SLC12A1 mutations may be due to the effect of genetic mutations on protein function, and milder phenotypes may correlate with residual NKCC2 function.[19]

BS type II depends on inactivating mutations of the KCNJ1 gene, encoding the K^+ channel ROMK.[20] These channels are the main renal K^+ secretory channels. Along the TAL, ROMK mediates K^+ efflux to the lumen, which is critical for supporting Na/K-2Cl absorption via NKCC2. At this level of the nephron, ROMK channels contribute to the generation of the lumen-positive transepithelial voltage which allows paracellular calcium and magnesium absorption. An inactivating mutation of ROMK is thought to inhibit salt reabsorption along the TAL. Over 35 genetic mutations have been described, such as missense mutations, frameshift mutations, and stop codons which result in a truncated protein.[21] The majority of these mutations reduces or eliminates ROMK surface expression, as a consequence of misfolding and/or mistrafficking; others compromise K^+ permeation and channel regulation. Besides the TAL, ROMK channels are also expressed along the apical membrane of principal cells in the cortical CD, where they mediate K^+ secretion into the lumen. A defect in ROMK results in the classical BS phenotype, including the presence of hypokalemia. This finding brought attention to its role in K^+ secretion. Subsequent studies have demonstrated that, in the absence of functional ROMK channels, K^+ secretion is guaranteed by the upregulation of flux-sensitive Maxi-K channels along the CD in mice.[22]

BS type III depends on the mutation of the kidney-specific Cl^- channel, CLC-K. Two genes belonging to the CLC family are involved in Cl^- efflux across the basolateral membrane, CLCNKA and CLCNKB. Their products are nearly identical at protein level, and both channels are associated with the Barttin subunit, essential for their insertion on plasma membrane and their activity. These channels differ only in their distribution along the nephron, with CLC-Ka expressed predominantly along the TAL, while CLC-Kb is expressed along the DT.[23] CLCKNB defects are associated with a Bartter phenotype in humans; a high rate of deletions encompassing the entire gene has been described,[24] together with frameshift and splice-site mutations. These mutations are supposed to disrupt the protein, altering its function. The predominant location of CLCKb along the DT explains why this variant of BS is less commonly associated with a defect in concentrating mechanism, and with hypercalciuria. There is no evidence CLCKNA mutations may generate a Bartter like syndrome. ClCk1 (the ortholog of CLC-Ka)-deficient mice show a phenotype of nephrogenic diabetes insipidus.[25] However a combination of defects in both CLCNKA and CLCNKB genes result in a phenotype of antenatal BS.[23]

BS type IV refers to the mutations in the BSND gene product. In contrast to other BS variants, the gene does not encode for an ion channel or transporter, but for an accessory subunit of CLC-Ka and CLC-Kb, defined as Barttin. CLC-K/Barttin Cl^- channels also localize in the cochlea, along the basolateral membrane of marginal cells of the stria.[26] Barttin has been found mutated in patients suffering from BS; different mutations generate phenotypes of varying severity. In heterologous expression, CLC-K channels do not yield currents in the absence of a functional Barttin subunit, suggesting that Barttin is essential for their function. As in the TAL, CLC-K channels participate in Cl^- reabsorption in the inner ear. Recent studies have shown that the Barttin subunit is essential for the generation of endocochlear potential; in the absence of Barttin, the degeneration of cochlear outer cells and the collapse of endolymphatic space may contribute to the pathogenesis of deafness in this BS subtype.[27]

BS type V depends on the activating mutation of the calcium-sensing receptor (CaSR). The protein is expressed in the parathyroid and in the kidney, and it is mainly involved in calcium and magnesium homeostasis. Along the TAL the CaSR is expressed on the basolateral membrane and it can inhibit salt absorption. A case report showed that activating mutations of the CaSR gene associated with a BS phenotype inhibit ROMK, explaining the inhibition of salt absorption at

this site.[28] A number of gain-of-function mutations of the CaSR gene have been identified as causing an inherited form of hypocalcemia/hypoparathyroidism (autosomal-dominant hypoparathyroidism). Whether those disarrangements lead to a different phenotype is still unknown.

Mutations in these five genes do not explain all cases of BS, and many patients do not get a genetic diagnosis. It is presumable that other genes are involved in the pathogenesis of this syndrome. Recently a role has been proposed for claudins, a family of transmembrane proteins expressed within the tight junction. Mutation in claudin-16 is associated with familiar hypomagnesemia with hypercalciuria and nephrocalcinosis. A single nucleotide substitution has been found in the extracellular domain of claudin-8 in four African-American BS patients.[29] The effect of the mutation on protein function has not yet been addressed.

Pathophysiology

The defective NaCl absorption along the TAL caused by mutations in any of these five genes leads to an increased salt delivery to the distal nephron. The subsequent volume-depletion leads to a compensatory hyper-reninemia. Mice models of BS type I and II show early onset of polyuria, metabolic alkalosis, increased calcium and magnesium urinary excretion, and hyperprostaglandinemia, a phenotype which resembles the abuse of loop diuretics. The activation of RAAS leads to a compensatory increase in Na^+ absorption along the PT and the aldosterone-sensitive segments of the nephron. The latter favors K^+ secretion along the CD, enhancing the kaliuretic effect of the increased Na^+ delivery. Clinical differences among BS subtypes depend on the specific physiological role of the causative gene in the kidney and in other organs.

Type II BS is characterized by relatively mild hypokalemia compared with type I, and by the dual role of ROMK in the kidney in controlling NaCl absorption along the TAL (through K^+ recycling) and K^+ secretion along the CD. The presence of hypokalemia is ensured by the activation of the flux-sensitive Maxi-K channels which mediate urinary K^+ secretion along the distal nephron. However, newborn infants suffering from type II BS show transient hyperkalemia before developing normohypokalemia later in the infancy. This effect may be due to the delay in BK-dependent K^+ secretion, which later is responsible for urinary K^+ excretion.[30]

The widespread distribution of CLC-K channels along the distal nephron and the compensatory activation of Cl^- absorption through other channels explains why CLCKNB mutations may result in a pure BS phenotype, GS phenotype or a combination of these.[23] Hypercalciuria and nephrocalcinosis are typical signs of type I and II BS, but are rare in type III[24]; however, a broad spectrum of phenotypes has been associated with mutations of the CLCNKB gene, ranging from antenatal BS to classic BS and Gitelman-like syndrome, without any correlation with the type of genetic mutation. Additional studies are needed for a better understanding of the phenotypic variability.

The presence of deafness is a hallmark of type IV BS. Barttin, as pointed out above, is necessary for CLC-K channels trafficking to the membrane. ClCK-barttin complex is expressed in the kidney and in the inner ear. Mice lacking a functional CLC-Ka have a phenotype resembling nephrogenic diabetes insipidus, with high vasopressin plasma levels, and low osmolality of renal papilla even after water restriction, suggesting a role in the urinary concentrating mechanism. CLCKB-null mice show the classic form of BS, whereas only a defect of Barttin determines deafness. In the inner ear CLC-K/Barttin channels participate in Cl^- transcellular extrusion across the basolateral membrane. It is possible that the absence of CLC-Kb could be compensated by the CLC-Ka-Barttin in the inner ear, while the absence of Barttin equals a double defect in CLC-k a and b, leading to deafness.[23] Hypercalciuria and nephrocalcinosis are the main features of type V BS. Activating mutation of the CaSR leads to autosomal dominant hypoparathyroidism, characterized by hypocalcaemia and hyperphosphoremia, with low-normal PTH levels.[31]

Clinical Presentation

Clinically, BS is divided into antenatal and classic BS with or without deafness.

Antenatal BS, or *hyper-prostaglandin E BS*, is the most severe form, characterized by polyhydramnios for excessive urinary output and premature birth. It is sustained by type I and II, and sometimes type III. After birth, patients have a life-threatening clinical course, with fever, vomiting, and lethargy. Biochemical analysis shows the presence of metabolic alkalosis, hypokalemia, isohypostenuria, and hypercalciuria. Nephrocalcinosis is frequent. High urinary prostaglandin excretion of E2 or its metabolites is typical of the antenatal form, and high levels of renin and aldosterone are secondary to volume-depletion. The reason for the high urinary and plasma prostaglandin levels is still unknown, but it seems to be secondary to the defect of NaCl absorption along the TAL.

Classic BS is sustained more often by type III BS. Clinical appearance occurs during infancy or childhood, in the absence of polyhydramnios and prematurity. The clinical course is milder than the antenatal subtype; patients manifest polyuria, polydipsia, vomiting, and dehydration. Nephrocalcinosis is an

infrequent sign, and a less severe defect in urinary concentrating mechanism is present.

BS with sensorineural deafness. The presentation of patients with type IV BS shows remarkable variation, ranging from prenatal diagnosis with severe polyhydramnios and prematurity to late diagnosis.[32]

Gitelman Syndrome

Gitelman syndrome (GS) differs from BS because of the presence of hypocalciuria and hypomagnesaemia. It is often diagnosed in adulthood.

Genetics and Molecular Biology

The syndrome correlates with mutations of the SLC12A3 gene located on chromosome 16q, encoding the thiazide-sensitive sodium-chloride co-transporter (NCC). The transporter is expressed on the apical membrane of distal tubule, and represents the major NaCl transport pathway in this segment. More than 140 mutations have been described; the majority of mutations are missense substitutions, but frameshift and splice-site mutations have also been described.[33] Heterozygous subjects show a tendency for low blood pressure, while the complete GS phenotype occurs only in homozygosis. De Jong et al. have performed, in *xenopus laevis* oocytes, functional and immunohistochemical analysis of mutant human NCC of GS subjects.[34] This study has found class I mutants, characterized by the absence of significant metazolone-sensitive Na^+ uptake with undetectable protein distribution on the membrane, and class II mutants, which exhibited significant, albeit low, metazolone-sensitive Na^+ uptake, while NCC staining was equally present in plasma membrane and cytoplasm. These findings suggest that some mutations compromise NCC abundance in plasma membrane (class I), leading to a defect in protein activity; other mutations only partly impair NCC routing to the membrane, as suggested by the presence of mutant NCC both on plasma membrane and cytoplasm. However, different mechanisms are involved in the impaired trafficking for the two classes of mutations, and the precise mechanism has still to be established. Previous studies suggest the role of defective post-translational changes, such as protein glycosylation, which seems to be required for proper folding and trafficking to plasma membrane.[35] A minority of patients with GS phenotype show mutations in the CLCNKB gene, which is also responsible for BS type III.

Pathophysiology

Both NCC and CLC-Kb dysfunction result in decreased Na^+ and Cl^- absorption along the DT. The volume-contraction resulting from defective NaCl absorption determines a compensatory activation of RAAS, which promotes electrogenic Na^+ absorption along the CD through ENaC. The latter enhances K^+ and H^+ secretion along the CD, favoring hypokalemia and metabolic alkalosis. The pathogenesis of hypocalciuria and hypomagnesemia refers to a not yet completely-elucidated mechanism. Micropuncture experiments have demonstrated an increased Ca^{2+} absorption along the proximal tubule (PT) after chronic administration of thiazides, whereas DT calcium absorption was unaffected.[36] This hypothesis is supported by the presence of thiazide-induced hypocalciuria in a mouse model lacking the calcium channel (TRPV5) along the DT. These findings demonstrate that increased calcium absorption parallels a compensatory increased Na^+ absorption along the PT secondary to volume-contraction. Other studies suggest that enhanced calcium absorption along the DT participates in the generation of hypocalciuria. In a mouse model of GS, the expression of TRPV5 and TRPV6 were increased, and TRPV5 is also overexpressed in renal tissue from patients with GS.[37]

Hypomagnesemia, another hallmark which distinguishes GS from BS, has a controversial origin. Magnesium is freely filtered by the glomerulus, and it is reabsorbed in a small fraction along the PT. The majority of Mg^{2+} is reabsorbed along the TAL, via paracellular pathway, and DT, via transcellular pathway. In the latter, Mg^{2+} reabsorption is mediated by the transient receptor potential cation channel, TRPM6. In NCC knockout mice a downregulation of TRPM6 in DT has been shown.[36] This effect could explain the defective Mg^{2+} absorption, and the subsequent hypomagnesemia.

The clinical phenotype in CLCNKB mutations is extremely variable; several reports have described subjects with phenotypic features of GS without any defect in SLC12A3 gene, carrying homozygous mutations of CLCNKB gene[38] or mixed BS-GS phenotype.[39]

Clinical Presentation

GS is characterized by an extreme inter- and intrafamilial phenotype variability, varying from mild or undiagnosed forms to severe conditions complicated by growth retardation, ventricular arrhythmias, and neuromuscular symptoms. In most cases the diagnosis occurs in adulthood. The patients suffer from tetany, especially during conditions which determine further Mg^{2+} loss, like vomiting or diarrhea. Some patients experience fatigue which compromises daily activities, in relation to the degree of hypokalemia. In contrast with BS, those patients do not manifest polyuria and growth retardation. Chronic K^+ and Mg^{2+} deficiency may predispose to a higher risk for ventricular

arrhythmias. However, lethal arrhythmias have been reported rarely in GS patients, and may be related to underlying triggering mechanisms besides hypokalemia. Riviera et al. have described a subgroup of GS patients with severe phenotype, characterized by early onset, and severe neuromuscular and cardiac symptoms.[40] Almost all patients of the subgroup were male, and showed a higher incidence of splicing mutation leading to a truncated transcript compared with mild and classic GS. This study suggests that male gender and splicing mutations, resulting in a severe protein dysfunction, may account for the clinical severity of GS. Biochemical analysis shows hypocalciuria, hypokalemia, and hypomagnesemia. Although hypocalciuria and hypomagnesemia have been considered necessary for the diagnosis of GS, recently a report of a GS patient with a proven mutation in the GS gene did not manifest those signs. Plasma renin and aldosterone levels are only slightly increased compared with BS.

Liddle Syndrome

Liddle syndrome (LS) is an autosomal dominant disease leading to hypertension. Besides the early onset of hypertension, it is characterized by hypokalemic metabolic alkalosis, with downregulation of RAAS. In the last 10 years the Lifton group has identified several mutations mapping in β- and γ-ENaC subunits, resulting in the expression of a higher number of channels in the plasma membrane.

Genetic and Molecular Biology

ENaC is comprised of three subunits, α, β, and γ, which are assembled at stoichiometry α2βγ. Several studies have suggested that also αβ and αγ are functional channels. The first description of Liddle syndrome (LS) in literature was correlated with the mutation in the gene encoding the β-ENaC subunit, resulting in a premature stop codon which leads to the loss of the last amino acids of the C-terminus.[41] Genetic screening of subjects suffering from LS has showed that the syndrome also segregates with mutations of the gene encoding for the γ-subunit. The expression of either truncated γ- or β-ENaC subunit increases amiloride-sensitive Na^+ uptake in oocytes.[42] These findings suggest that the C-terminus of β- and γ-subunits is a crucial region for the activity of the channel. Different investigations have found that most mutations resulting in LS phenotype are mapped on a highly-conserved PPPXY sequence (PPY motif) of the C-terminus in β and γ; disruption of the motif preserves the channel from inhibitory stimuli.

Pathophysiology

The amiloride-sensitive ENaC is an ion channel which mediates Na^+ absorption along the distal segment of CNT and CD. ENaC channels are positively regulated by aldosterone and vasopressin. In mice, aldosterone has been shown to activate ENaC via the ser/thr kinase Sgk1. This kinase induces ENaC activation partly through the inhibition of ENaC downregulation by the E3 ubiquitine ligase, Nedd4-2, which targets ENaC to degradation in cultured cells.[43] Sgk1 phosphorylates Nedd4-2 to an inhibitory site, thus preventing ENaC removal from the plasma membrane.[44] Mutations in β- and γ-subunits of ENaC in LS result in a constitutive activation of ENaC activity.[45] These mutations impair the PY motif in the C-terminus, which is required for Nedd4-2-mediated ENaC ubiquitination. In the absence of the binding site, Nedd4-2 fails to target the channel for degradation. However, these mutations increase the overall ENaC expression at the apical membrane, contributing to increased Na^+ absorption. The resulting volume-expansion explains the suppression of RAAS. Interestingly, mice bearing a LS deletion revealed normal aldosterone response.[46] Consistently, in cultured cell, aldosterone, vasopressin, and Sgk1 are still able to increase ENaC surface abundance in the presence of LS causative mutations,[47] suggesting that Nedd4-2 is not necessary for aldosterone-dependent increased ENaC activity. However, in LS patients, constitutive increased ENaC activity leads to volume-expansion, high blood pressure, and suppressed RAAS.[48] As a consequence of increased channel activity along the CD, patients do manifest hypokalemia and metabolic alkalosis. Mice bearing LS become hypertensive only when fed a high-salt diet.[49]

Clinical Presentation

LS was first described in 1963 as a condition resembling hyperaldosteronism, because of the coexistence of hypertension, hypokalemia, and metabolic alkalosis. However, due to the low/normal levels of plasma aldosterone this condition is described as pseudohyperaldosteronism of the second type. Hypertension usually develops at an early age in affected individuals, and worsens throughout the lifetime. Recently, Tapolyia *et al*. have proposed the presence of serum bicarbonate over 25 mmol/L, K^+ levels lower than 4 mEq/L, plasma renin activity lower than 0.35 μU/ml/h, and plasma aldosterone levels lower than 15 ng/dl as screening criteria for LS. Based on these criteria, this group found a prevalence of 6.7% patients that satisfied the criteria for likely LS in a cross-sectional investigation of 149 hypertensive patients with hypokalemia and metabolic alkalosis.[50] Hypertension is usually refractory to common antihypertensive drugs, while it is responsive to the use of the ENaC inhibitor, amiloride.

RENAL CHANGES IN K^+ DEFICIENCY

Morphology

Experimental Studies

Hypokalemic states are associated with several renal morphological alterations. The severity and exposure time to hypokalemia are fundamental to the development of renal injuries. Mild hypokalemia ranging among 3.6±0.2 is not associated with significant glomerular or tubular abnormalities in Sprague-Dawley rats.[51] Renal hypertrophy is a universal finding in studies of K^+-depletion (KD) since the early report by Schraeder et al. in 1937. This renal growth has distinct morphologic characteristics. The increase in kidney mass is not uniform, being more prominent in the outer medulla, as reflected in the relative contribution of the different zones to total kidney weight in K^+ deficient rats.[52]

The growth process consists of both hyperplasic and hypertrophic components. Despite the fact that hypokalemic mice present a different metabolic behavior (metabolic acidosis), they develop morphological abnormalities of CD similar to rats and humans. K^+ deficient mice show morphological alterations in outer medulla CD (OMCD) after three days of a low-K^+ diet. CD epithelial cells from K^+ deficient mice have a higher proliferation rate than control mice. Intercalated cells show PCNA positive staining (proliferation marker) more than principal cells. No signs of cellular hypertrophy are detected at this time point in CD epithelial cells, despite IC already display an enlargement of the apical membrane domain. After 14 days of a low-K^+ diet both principal and IC cells appear hypertrophic as evaluated at EM level. In hypokalemia-induced morphologic alteration of OMCD, hyperplasia precedes the development of cellular hypertrophy. Transcriptome analysis of OMCD suggests Gdf15 (growth differentiation factor 15) increases significantly from day 3 to day 14 of the low-K^+ diet. It could be a potential candidate in driving the switch from hyperplasia to hypertrophy. Gdf15 belongs to the TGFβ superfamily, and it could be a growth-stop signal in OMCD.[53]

The growth-promoting effect of K^+ deficiency is not limited by the state of the organ. It occurs in intact, as well as in previously damaged, kidneys. Peterson *et al*.[54] have shown that institution of K^+ deficiency in a model of remnant kidney (5/6 nephrectomy) led to an increase in renal mass and RNA content beyond that expected of the surgical ablation alone.

CD is the main nephron site where morphologic alterations occur in K^+ deficiency. Glomerular and vascular lesions have rarely been observed in pure K^+ deficiency, and changes in proximal convoluted tubules have been limited to vacuolar degeneration. While several studies demonstrate the occurrence of morphologic changes in individual CD cells, conflicting statements have been made regarding the proportion of cell types and number. Hansen *et al*.[55] observed extensive swelling of the epithelium of the CD involving both principal and intercalated cells along the OMCD (Figure 50.2). No changes were observed in either principal or intercalated cells of the initial CD.[56] Intercalated cells in the MCD segment develop extensive microplicae over the entire luminal surface with increased luminal surface boundary length,[55] whereas no change was observed in basolateral membrane length or in the luminal or basolateral aspects of principal cells[57] (Figure 50.3). This increased luminal surface could be due to the fusion of the cytoplasmic vesicles with the apical membrane domain. A large number of rod-shaped structures are opened in the lumen in this way. This event is thought to be useful for H^+ secretion and K^+ reabsorption through H^+-ATPase or H^+-K^+-ATPase activity, respectively. There are conflicting findings about the proportion of intercalated and principal cells in any part of the CD in K^+ deficiency. Evidences indicate the development of morphologic changes in individual cells as well as an increase in cell number.

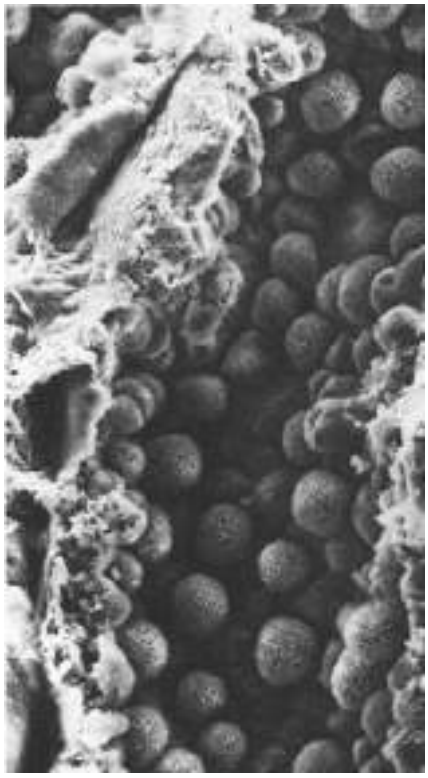

FIGURE 50.2 **Electron microscopy of rat collecting duct in ISOM.** This is a representative picture of hypertrophy of A-type-intercalated cells. *(With permission from Hansen, G. P. et al. [55])*

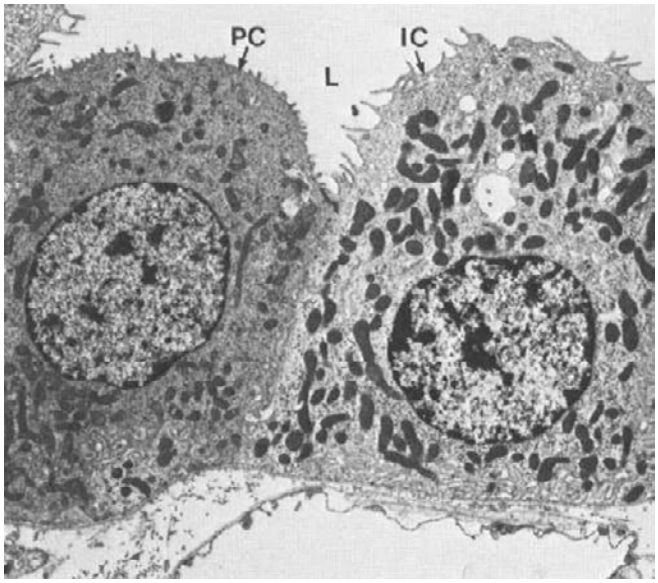

FIGURE 50.3 **Electron microscopy of rat medullary collecting duct, showing a representative picture of hypokalemia-induced morphological changes in both principal and intercalated cells.** *(With permission from Stetson, D. L. et al. [57])*

Recently, progressive capillary loss has been identified in hypokalemic nephropathy. This injury was first observed in the ISOM after 2 weeks of a K-restriction diet, expanded to the OSOM at 4 weeks, and then to the cortex by week 12. Capillary loss significantly correlated with local macrophage infiltration and low endothelial cell proliferation rate, an effect probably secondary to a decrease of VEGF and eNOS expression.[58]

The most remarkable ultrastructural change is the accumulation of cytoplasmic droplets in tubular cells of the medulla. The appearance of droplets starts from the CD at the tip of the papilla, and then extends upward into the outer medulla until the corticomedullary junction. The extension depends on the duration of K^+ deficiency. Besides epithelial cells, interstitial and other cells in the medulla also show cytoplasmic droplets, with considerable enlargement of cell volume. With K^+ repletion, the droplets reversed progressively.[59] The droplets are believed to be the consequence of phospholipids dysregulation,[60] and their lysosomal origin is suggested by the presence of hydrolytic enzymes. It has been suggested that increased ammonia production secondary to hypokalemia may contribute to vacuolation of nucleated cells in KD.[61] In fact, ammonia has been shown to induce vacuolization of lysosomes, inhibition of endocytosis, and lysosomial protein degradation. Another hypothesis is that the cytoplasmic droplets could be related to a cellular autophagy phenomenon. Lipid droplets share common protein with the autophagosome in hepatocytes and cardiac myocytes,[62] and those organelles may be an expression of autophagy. Ureteral ligation in K^+ deficient rats is followed by resolution of droplets, presumably because of increased renal medullary K^+ content.[63] The severity of droplet formation depends on the method of induction of K^+ deficiency, with minimal droplet formation developing with DOCA-induced compared with dietary deficiency.[64]

Tubular and interstitial apoptosis is observed during K^+ deficiency. Apoptotic cells are located mainly in the outer medulla. Bcl-2 protein distributed in the tubules of the outer medulla is significantly decreased in KD rats, while immunoreactivity for Bax protein tends to increase above control levels. These results suggest that apoptosis is associated with progression of cellular proliferation in hypokalemic nephropathy, and a decrease in bcl2 may be involved in promoting this apoptotic process.[65]

Human Studies

Unlike experimental studies where K^+ deficiency can be induced selectively, clinical observations are frequently based on complex conditions where K^+ deficiency is complicated by numerous other alterations, including Na^+ and acid–base homeostasis. The issue is even more complex if we consider additional factors like duration of disease, and therapeutic interventions that may substantially alter histopathologic manifestations in humans. Finally, clinical data are usually limited to cortical biopsies, and sampling of medullary and papillary structures may be lacking. An important observation comes from autopsy studies in healthy Thai adults who died of vehicular accidents. K^+ deficiency prevails among the healthy population of northeast Thailand. In this study, none of the patients had renal histopathological change compatible with a diagnosis of focal or diffuse interstitial nephritis, and there were minimal renal tubulo-interstitial changes.[66]

Glomerular changes consisted mostly of a reduction in capillary surface and Bowman capsule areas, and an increase in the mesangial space. The glomerular shrinkage was not associated with any alterations in cellular constitution of the tuft.[67] Of note is the increase in juxtaglomerular complex size in many of the patients to levels comparable to, or even exceeding, those observed in BS. Such findings underscore the non-specificity of this change, which is likely secondary to defective Cl^- absorption in the thick ascending limb, rather than a characteristic feature of BS. Tubular vacuolization was not a frequent or pathognomic observation, although it was considered characteristic by Conn and Johnson, who coined the term kaliopenic nephropathy in 1956. More important for the prognosis of these patients is the occurrence of degenerative changes such as tubular atrophy, dilatation, epithelial

flattening, and thickening of the basement membrane.[68] Again, these alterations are non-specific, and reflect evidence of chronic injury. Increased interstitial surface area and lymphocytic cellular infiltration were frequent. PAS-positive granules have been observed in some of these patients in all medullary cells when available in the specimen.

Taken together, these observations suggest that many of the renal changes seen in K^+ deficient animals have their counterparts in clinical cases. Some of these changes (glomerular shrinkage, tubular atrophy, interstitial fibrosis) indicate irreversible renal damage, and the occurrence of renal insufficiency in this group of patients has been convincingly demonstrated.[69] Indeed, in some young women the condition has led to end-stage renal disease.[70] Elements of the kaliopenic nephropathy mixed to morphological changes secondary to hypertension are also found in patients with primary aldosteronism. The apparently additive insults of hypertension and K^+ deficiency are illustrated in the study of 18 patients with primary aldosteronism by Danforth *et al*.[71] Moderate to severe hypertensive changes (fibrous thickening of small vessels and glomerular hyalinization) and kaliopenic lesions (vacuolization and degeneration of tubular epithelia) were observed in 14 (78%) and 16 (89%) patients, respectively. The hypertensive changes appeared to be more severe in this group than in subjects with primary hypertension of similar severity, suggesting a possible synergistic effect of K^+ deficiency.

Tubular Function

A heterogeneous pattern of structural and functional changes occurs along the nephron, with a progressive increase from proximal to distal segments.

Proximal Convoluted Tubule

SODIUM CHLORIDE

Transport along the proximal tubule has been extensively studied in both acute and chronic K^+ deficiency models with micropuncture and isolated tubule techniques. An acute change in K^+ concentration in the perfusion bath below 2.5 mM inhibits NaCl transport in isolated and perfused PT from rabbit.[72] Decrements in NaCl reabsorption, as evidenced by decreased net fluid absorption in this segment, have also been observed during capillary microperfusion with hypokalemic solutions in rats.[73] Studies in K^+ deficient animals show a different pattern of alterations in transport. Walter *et al*.[74] performed micropuncture studies on anesthetized rats which had been kept on a K deficient diet for 2 weeks. In these animals total glomerular filtration rate (GFR) and single-nephron filtration rate were significantly lower than controls. Fractional reabsorption by the proximal convoluted tubule was enhanced, and end proximal fluid delivery was markedly reduced. These observations are in line with other studies showing reduced fractional excretion of lithium in K^+ deficiency,[75] presumably a surrogate measurement for enhanced proximal Na^+ reabsorption.

Chronic K^+ deficiency, but not an acute luminal exposure, leads to increased NaCl reabsorption. K^+ deficiency increased the expression of both the adrenergic receptor $alfa_{2B}$,[76] and AT1 (angiotensin II receptors)[77] in rat PT. These changes are coupled with an increase in renin and angiotensin II level, as demonstrated in many species. The higher Na^+ reabsorption could be in part transcellular, mainly driven by several Na^+ transporters upregulated in hypokalemia (*vide infra*).

Hypokalemic rats have an increased expression of Na-H exchanger 3 (NHE3) in membrane fractions of renal cortex and outer stripe of the outer medulla (OSOM). Immunohistochemistry confirms that NHE3 labeling is increased in the luminal membrane domain of the PT of hypokalemic rats.[78] However, Wang *et al*.[79] found no change in the expression of NHE3 mRNA and its cognate protein after 6 and 14 days in rats on a low-K^+ diet. The mRNA levels for NHE1, NHE2, and NHE4 also remained unchanged at 6 and 14 days of the low-K^+ diet. These apparent inconsistencies between protein expression and mRNA levels could be due to a posttranslational level of regulation of NHE3, as recently found in hypertensive models.[80] In parallel with Na^+ reabsorption, NHE3 promotes proton extrusion. This mechanism is functional for net bicarbonate reabsorption through the PT.

BICARBONATE

Chronic K^+ deficiency is associated with metabolic alkalosis and an increase in bicarbonate reabsorption, as demonstrated by free-flow micropuncture and microperfusion studies in rats.[81] In contrast, acute exposure of proximal tubules to ow (K^+ 2 mM) in capillary microperfusion experiments had no effect on bicarbonate reabsorption.[73] The mechanism of enhanced bicarbonate reabsorption is mediated by stimulation of NHE3 and the basolateral $Na/3HCO_3$-co-transporter.[75] In OKP cells, low-K medium causes a decrease in intracellular pH, which leads to increased NHE3 activity.[82] Accordingly, NHE3 total protein abundance and immunostaining along the apical membrane of PT and TAL were dramatically increased in hypokalemic rats.

The bicarbonate basolateral exit pathway from the PT cells is mediated by the sodium bicarbonate

co-transporter (NBC1). During K^+ deficiency states both the activity and mRNA expression of NBC1 are increased.[83] It is not clear if the upregulation of NBC1 causes the lowering intracellular pH or whether it is a consequence of the higher bicarbonate reabsorption.

Angiotensin II could promote bicarbonate reabsorption in the PT. In fact, angiotensin II is found to increase NBC1 expression in rat PT, while it is debated whether it also regulates NHE3 function.[84]

AMMONIUM

Metabolic alkalosis developing during K^+ deficiency is also sustained by increased bicarbonate generation from the ammoniagenesis pathway in the PT. Chronic hypokalemia is associated with increased ammonium excretion in humans as well.[85] K^+ deficiency leads to a three-fold increase in ammonia production in the S1, and to a two-fold increase in S2 segments of PT.[86] No changes in ammonia production were observed in the S3 segment (pars recta) or in the thick ascending limb or distal convoluted tubule. The increased ammonia production in S1 occurred in both superficial and juxtamedullary nephrons, with a greater extent in the former. The primary mechanism by which K^+ deficiency stimulates renal ammonia production is not precisely known. Increased renal ammonia production and excretion, despite the simultaneous presence of metabolic alkalosis, suggest that intracellular factors, rather than extracellular pH, modulate renal ammonia metabolism. Intracellular acidosis that occurs in K^+ deficiency may initiate the adaptive response in ammoniagenesis. Both mitochondrial (glutamine transaminase activity) and cytosolic (phosphoenolypyruvate carboxykinase, PEPCK) enzymes involved in glutamine catabolism and gluconeogenesis are increased in the hypokalemic state.[87] This pathway induces a net gain of new bicarbonate production. K^+ repletion leads to prompt decreases in ammonia production.[88] Although mice present a species-different acid–base adaptation to hypokalemia, namely metabolic acidosis, they share a high urinary ammonium excretion with rats. Hypokalemic mice show an increase of glutamine transporter SNAT3. SNAT3, normally located in the S3 segment of the PT, spreads to S1 and S2 segments during K^+ deficiency, supporting the increase ammoniagenesis in the PT[89] (Figure 50.4).

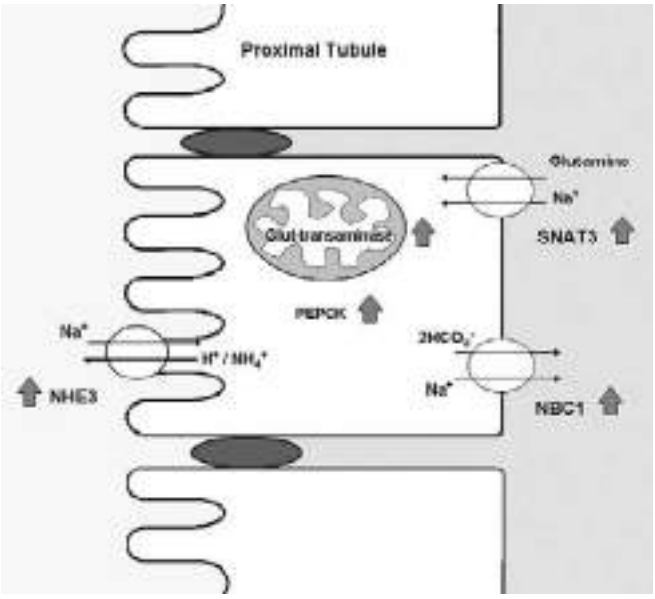

FIGURE 50.4 **Hypokalemia increases ammoniagenesis in proximal tubule cells.** Hypokalemia-induced ammoniagenesis is proved by an increased expression of PEPCK and glutamine transaminase.[87] Therefore, hypokalemic mice present an upregulation of SNAT-3, the sodium-coupled glutamine importer along the whole proximal tubule.[89] These effects are coupled to upregulation of NHE3[78] and NBC-1[145] transporters involved in proximal tubule bicarbonate reabsorption.

PHOSPHATE

Chronic K^+ deficiency is associated with low serum phosphate (Pi) and an increase urinary Pi excretion in rats and mice. Key regulators of renal Pi excretion are the Na dependent co-transporter NaPi IIa and NaPi IIc, expressed almost exclusively in the kidney. Another group of Pi transporters, Pit-1 and Pit-2, have been described.[90] In hypokalemia, a phosphaturic phenotype is associated with a differential regulation of the different NaPi transporters. NaPi IIa protein abundance in brush border membranes (BBM) and protein targeting to the apical membrane are increased, while NaPi IIc and PiT2 are decreased in animals fed with a low-K diet. In addition, NaPi IIc relocates from the apical membrane domain to cytoplasmic vesicles.[91] The downregulation of NaPi IIc seems to sustain the hypokalemia-induced urinary phosphate loss.

OTHER PROXIMAL TUBULE DYSFUNCTION

Chronic K^+ deficiency causes hypocitraturia. Urinary citrate excretion is mainly a function of citrate absorption along the proximal tubule, a process mediated by the Na-dicarboxilate co-transporter NaDC1, and citrate metabolism. Levi *et al.*[92] have shown an increased NaDC1 activity on renal cortical BBM from K^+ deficient rats. Hypokalemia may also participate in proximal tubular dysfunctions observed in children with primary distal renal tubular acidosis. Indeed, in these patients, correction of hypokalemia ameliorates low molecular weight proteinuria, phosphaturia, and generalized aminoaciduria.

Loop of Henle

SODIUM CHLORIDE

Eknoyan *et al*.[93] were the first to suggest that a defect in Na^+ transport by the thick ascending limb (TAL) could explain the concentrating defect of K^+ deficiency. Micropuncture and microperfusion studies showed diminished net Cl^- reabsorption between the latest proximal and earliest distal segment, as well as increased luminal Cl^- concentration at the latter site. These findings were consistent with impaired TAL absorption, and the defect was only partially corrected with indomethacin. Gutsche *et al*.,[94] using the micro stop-flow technique, have provided evidence for defective Na^+ transport in the TAL of K^+ deficient rats. The severity of the defect correlated with the decrease in plasma K^+ concentration, and was rapidly reversed with acute K^+ administration. In addition, net NaCl transport is inhibited by reduction in bath K^+ concentration in isolated perfused TAL.[95]

A more recent study has uncovered the molecular basis of the observed defects in electrolyte reabsorption in the TAL. In rats, NKCC2 mRNA expression in medulla is decreased about 56 and 51% after 6 and 14 days of K^+ restriction diet respectively. Functional studies in tubular suspensions of medullary TAL from K^+ deficient rats demonstrated a 45 and 37% decreased NKCC2 activity at 6 and 14 days, respectively. NKCC2 protein abundance of membrane fraction from renal ISOM is downregulated in rats fed for 4 days on a K^+ restricted diet. Immunohistochemical localization confirms a lower expression of NKCC2 in mTAL.[78] Na/K-ATPase plays a key role in the Na^+-dependent transport in this nephron segment. Despite the increase in the number of Na/K-ATPase units, the transport capacity of the Na/K pump, determined by ouabain-sensitive Rb uptake, was reduced in mTAL from K^+ deficient rats. Inhibition of the Na/K pump was the consequence of a reduced affinity for Na.[96]

BICARBONATE AND AMMONIUM

Basolateral and apical Na-H exchangers (NHEs) in TAL are involved in NH_4^+ and HCO_3^- absorption, respectively. The NH_4^+ absorption rate in Henle's loop is increased in K^+ deficiency, which may be secondary to the increased NH_4^+ concentration in luminal fluid and/or to an increased NH_4^+ absorptive capacity of TAL. HCO_3^- absorptive capacity in Henle's loop is unchanged in K^+ deficiency, despite the presence of metabolic alkalosis. The effects of K^+ deficiency on the expression of basolateral NHE-1 and the expression of apical NHE3 in TAL have been examined by Laghmani *et al*.[97] NHE1 protein abundance was similarly increased (approximately 90%) at 2 and 5 weeks of K^+ deficiency, while NHE1 mRNA amount in TAL cells was increased at 2 weeks, and returned to normal values by 5 weeks. NHE3 protein abundance and mRNA remained unchanged after 2 weeks of K^+ deficiency. NHE3 mRNA was reduced by approximately 50% at 5 weeks. In K^+ deficiency, the increased NHE1 expression may support an increased TAL NH_4^+ absorptive capacity. The lack of change in NHE3 expression, despite the presence of metabolic alkalosis, is in agreement with the unchanged HCO_3^- absorptive capacity of Henle's loop. Recently, an electro-neutral, Na-dependent HCO_3^--co-transporter (NBCn1) has been cloned and localized at the basolateral side of the mTAL. Several results show NBCn1 is fundamental for NH_4^+ reabsorption in the TAL. NH_4^+ entering the mTAL cell via the furosemide-sensitive NKCC2 transporter dissociates into H^+ and NH_3. The NH_3 leaves the cell via non-ionic diffusion preferentially through the basolateral membrane. The remaining proton may either be transported directly via a basolateral NHE1 and/or could be buffered by basolateral import of HCO_3^- through NBCn1. During hypokalemia, NBCn1 protein abundance is strongly upregulated in ISOM. In addition, *in vitro* perfusion of isolated mTAL shows hypokalaemia induced a three-fold upregulation of Na-coupled HCO_3^- influx[98] (Figure 50.5).

Distal Tubule

SODIUM CHLORIDE

Along the DT downregulation of the main Na^+ transporter has been reported. Rats fed a low-K^+ diet for 4 days present a downregulation of sodium chloride co-transporter (NCC) in the membrane fraction of cortex and OSOM. Immunoistochemistry confirms the reduced expression of NCC in the convolute distal tubule cells.[78]

BICARBONATE

In DT, the rate of bicarbonate absorption is not altered in K^+ deficiency, despite a lower delivery rate and the presence of a greater lumen-to-plasma bicarbonate concentration difference due to the higher plasma and lower luminal levels.[99] Micropuncture experiments have demonstrated that bicarbonate reabsorption along the distal tubule of K^+ deficient rats was increased when delivery rates of bicarbonate reached levels similar to those in controls. In the DT, bicarbonate reabsorption is relatively insensitive to peritubular alkalinization, and the systemic alkalosis does not affect acid secretion.[100] The mechanism, therefore, is not self-limiting, and no "braking" of the enhanced bicarbonate reabsorption occurs. This is due to enhanced electrogenic proton secretion (H^+-ATPase) as demonstrated by *in vivo* microperfusion of the superficial distal tubule in K^+ deficient animals.[101]

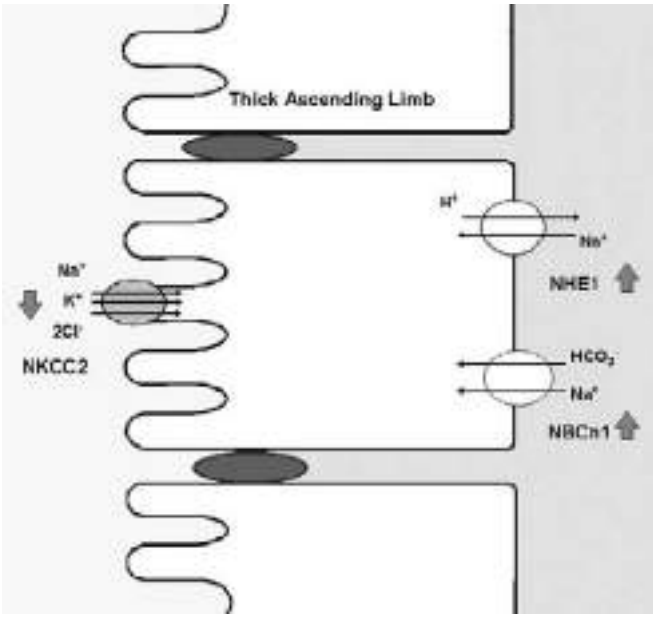

FIGURE 50.5 **Hypokalemia impairs sodium chloride absorption in the TAL, mainly inhibiting both the activity and expression of the NKCC2.**[78] The reduction of sodium chloride absorption in the TAL contributes to the urinary concentrating defect. Ammonium absorption is increased along the TAL, sustained by the upregulation of basolateral NHE1[97] and NBCn1.[98]

POTASSIUM

K^+ secretion in the segments of the distal nephron accessible to micropuncture (the early distal convoluted tubule, the connecting tubule, and the initial collecting tubule), is reduced to near zero in K^+ deficiency.[56]

Collecting Duct

This segment is the site of major structural changes in K^+ deficiency, and the alterations in its transport functions are primarily responsible for metabolic alkalosis and defective urinary concentrating ability.

SODIUM

Along the connecting tubule, as well as the cortical, outer, and inner medullary CD, Na^+ uptake occurs through the luminal amiloride-sensitive epithelial Na^+ channel (ENaC), and it is driven by the electrogenic potential induced by the basolateral Na/K-ATPase. During hypokalemic states, all ENaC subunits (α, β and γ) are downregulated in renal samples from cortex-OSOM, and in whole kidneys as well. This has been ascribed to the hypokalemia-induced inhibition of aldosterone secretion.[78] Despite this finding, K^+ deficiency produces a striking, time-dependent increase in Na/K-ATPase activity, mainly in the CD in ISOM. After 3 weeks of a K-free diet, Na/K-ATPase activity was over four-fold higher than control animals.[102] The increased protein activity was larger than the extent of tubular volume or protein content, indicating that it is not merely a reflection of the concomitant hypertrophy observed in this region of the nephron. Na/K-ATPase activity returned to baseline after 7 days of K^+ repletion.[102] In association with the increased activity, it has been described that two weeks of K^+ deficiency induced a marked increase in the α1- and β1-subunits of Na/K-ATPase in medullary, but not in the cortical portion of the CD.[103] These observations are interesting, because enhanced activity of Na/K-ATPase would likely promote K^+ secretion and urinary loss, thus exacerbating the hypokalemia. Because the ISOM segment of the CD plays an important role in K^+ homeostasis, the upregulation of the Na/K-ATPase has been associated with a potential kaliferic function. To reconcile these observations, Hayashi and Katz[102] proposed that the induced Na^+ pumps were localized to the luminal domain, thus facilitating active K^+ reabsorption instead of secretion. Further evidence is needed to support this hypothesis. During a hypokalemic state, in the medullary interstitium a lower K^+ and an increased NH_4^+ concentration develop (see below). NH_4^+ and K^+ compete for the same transport site of the Na/K-ATPase. Upregulation of the Na/K-ATPase in the IMCD promotes ammonium uptake, primarily from the reduced interstitial K^+ concentration.[104] This phenomenon could be another explanation for the paradox of the Na/K-ATPase upregulation.

Proton Secretion

The development of metabolic alkalosis in sustained by the increased bicarbonate absorption and generation along the PT, as well as the enhanced proton secretion along the CD. Physiologically, the proteins responsible for proton secretion are mainly the H-ATPase and H/K-ATPase.

The effects of K^+ deficiency on the activity and distribution of the H-ATPase in the Sprague-Dawley rat were assessed by Bailey *et al.*[101] K^+ deficiency increased electrogenic H-ATPase activity in rat distal tubule, with an increased insertion of pumps into the apical membrane.[105] These findings were confirmed and expanded by Silver *et al.*[106] The rate of pH(i) recovery in intercalated cells (ICs) in response to an acute acid-load (a measure of plasma membrane H-ATPase activity) was three times larger after K^+ deficiency as compared to controls. This was associated with a change in the distribution of membrane-bound proton pumps in the IC population of cortical CD from K^+ deficient rats. Immunocytochemical analysis of rats CDs showed that K^+ deficiency increased the number of ICs with tight apical H-ATPase staining, and

decreased the number of cells with diffuse basolateral H-ATPase staining. Taken together, these data indicate that chronic K^+ deficiency induces a marked increase in plasma membrane H-ATPase activity in individual ICs.

The ability of A-ICs to secrete protons into the lumen is strictly coupled to bicarbonate extrusion on the basolateral side, and it is blocked when an impairment of bicarbonate extrusion occurs. The latter is mainly mediated by the anion exchanger-1 (AE-1) and other members of this family. During K^+ deficiency, protein abundance of AE-1 increases in cortex and OSOM, and this is coupled with a strong upregulation of another anion exchanger, SLC26A7.[107] In MDCK cells, SLC26A7 was found to translocate from the endosomal compartment to the basolateral membrane in response to a low-K^+ media.[108]

H/K-ATPase promotes luminal acidification and K^+ reabsorption. Two isoforms, H/Kα1 (gastric) and H/Kα2 (colonic), are expressed along the entire length of the CD from the early connecting tubule to the inner medullary CD. This localization is consistent among species. In rat CD, H/K-ATPase is expressed mainly in intercalated cells.[109] Chronic K^+ deficiency (3 weeks) led to a generalized increase in H/K-ATPases activity along the CD segments, with the greater increments occurring in CNT > CCD > MCD. This is in contrast to the morphologic changes that occur in the CD in K^+ deficiency, which display a hypertrophic response with the hierarchy: MCD > CCD > CNT.[102] Studies from single H/Kα1 and H/Kα2 knockout mice show an impairment in acid secretion during normal diet, confirming the crucial role of this transporter in renal acid–base balance. Data from H/Kα2 null mice demonstrated increased fecal K^+ loss, without significant differences in K^+ urinary excretion. A compensatory activation of the H/Kα1 subunits might be responsible for K^+ secretion in the absence of functional H/Kα2-subunits. Investigation of double H/Kα1 and H/Kα1,2-null mice on a K^+ deficient diet will provide insight into the functional importance of H/K-ATPases in K^+ deficient conditions.[109]

Pendrin belongs to a superfamily of Cl/anion exchangers, and has been localized in the apical side of non-type-A IC of the cortical CD. Reduced bicarbonate secretion was demonstrated in a pendrin knockout mouse model. In chronic K^+ deficiency, known to elicit a metabolic alkalosis, pendrin protein levels are decreased and pendrin expression is shifted to an intracellular pool with the relative number of pendrin positive cells reduced. These results are in agreement with a potential role of pendrin in bicarbonate secretion and regulation of acid–base transport in the cortical CD.[110] These adaptations occurring during K^+ deficiency are similar to those observed in chronic metabolic acidosis. Considering that metabolic alkalosis suppresses distal acidification, the stimulation by K^+ deficiency overcomes the effect of the alkalemic state. K^+ deficiency thus exerts a primary, aldosterone and Na^+-independent, stimulatory effect on hydrogen ion secretion in the CD, most likely at the level of the putative proton pump (Figure 50.6).

POTASSIUM

K^+ deficiency results in a decrease in urinary K^+ excretion of variable magnitude, depending on the species. In all species, however, the decline in K^+ excretion does not match the reduced intake, and a persistently negative K^+ balance is observed. In humans, short-term dietary K^+ deprivation (intake of less than 1 mEq/day) induces a decline in urinary K^+ excretion which is still higher than intake, with a gradual adaptation reaching a maximum within 5 to 7 days. In rats fed a low-K diet, urinary K^+ excretion falls promptly and parallels intake by 72 to 96 hours after the institution of a K^+ deficient diet.[111] The conservation of K^+ can be conceived as being due to attenuation of kaliuretic mechanisms, in part by resistance to normally kaliuretic influences, and in part by activation of kaliferic ones. Both phenomena have to be examined in the context of renal and systemic adaptations to K^+ deficiency, with differences in short-term and

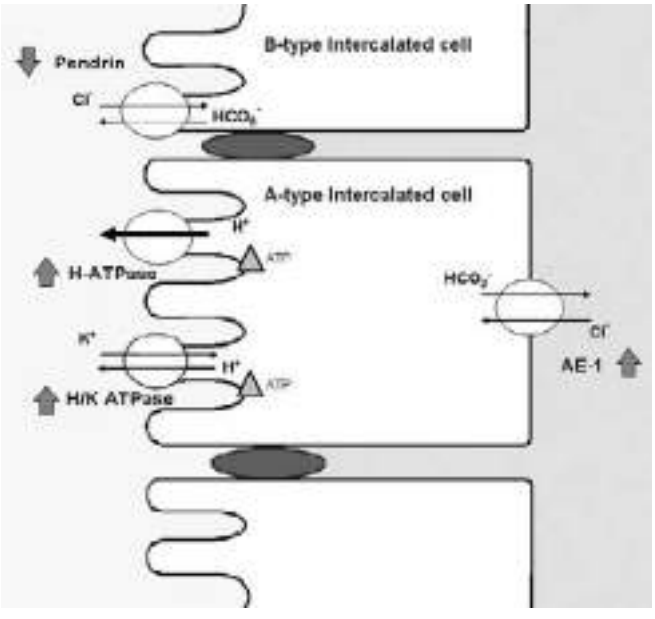

FIGURE 50.6 **Hypokalemia led to a metabolic alkalosis in rats and humans.** In addition to a proximal tubule effect, an increased acid secretion has been described in type-A-intercalated cells. Both H^+-ATPase[106] and H^+/K^+-ATPase[146] showed increased expression, along with an upregulation of AE-1.[107] B-type-intercalated cells showed a reduced expression of the bicarbonate secreting transporter, pendrin.[110] This latter finding supports K^+ depletion also impairing urinary bicarbonate secretion.

long-term K^+ deficiency. K^+ secretion in the CCD is markedly attenuated, but may not cease even with profound degrees of K^+ deficiency.[112] The reduced level of K^+ secretion is coupled with a decreased response to kaliuretic factors. Malnic *et al*.[112] have shown that K^+ deficient rats maintain their ability to increase K^+ secretion in response to increments in tubular flow, albeit at a much lower level. Finally, K^+ deficient humans are resistant to the kaliuretic influence of high urine flux, osmotic diuresis, and metabolic alkalosis. It has been suggested that an "escape" from kaliuretic influences may occur in K^+ deficient conditions, a concept which resembles the escape from the Na^+-retaining effects of chronic mineralocorticoid administration. Thus, no kaliuretic response is observed in rats when DOCA is administered 72 hours after initiation of K^+ deficiency.[111] In contrast, resistance to the kaliuretic effects of mineralocorticoids does not appear in short-term (7–10 days) K^+ deficient humans, in whom administration of DOCA is associated with a kaliuresis, despite the presence of hypokalemia and a large negative K^+ balance.

K restriction suppresses renal K^+ secretion and enhances its absorption.[113] This is achieved by both inhibiting apical K^+ channels in principal cells and stimulating K^+ absorption in intercalated cells. In CCD a molecular mechanism has been proposed to explain the inhibition of ROMK channels during severe and moderate hypokalemia. Low-K^+ intake increases renal superoxide anion generation, which stimulates PTK (protein tyrosine kinase) activity and MAPK (mitogen-activated protein kinase) phosphorylation. PTK inhibits ROMK activity through a tyrosine-mediated phosphorylation. MAPK can inhibit the activity of the ROMK-like SK and BK channels. Moreover, MAPK and PTK may have a positive feedback on each other. Since activation of PTK and MAPK inhibits the apical K-secretory channels, renal K^+secretion is suppressed during K^+ restriction states[114] (Figure 50.7).

The decline in aldosterone levels and the increase of angiotensin II that accompany K^+ deficiency contribute to renal K^+ conservation. It has been proven that angiotensin II has an inhibitory effect on ROMK channels and, on the other hand, antagonists of the AT-1 receptor abolish the renal ability of K^+ conservation during K-restricted diet by preventing the tyrosine phosphorylation of the ROMK channels.[115] In K^+ deficiency states, the ratio of long versus kidney-specific Wnk1 isoforms represents a novel K-saving mechanism along the aldosterone-sensitive segments of the nephron (*vide infra*).

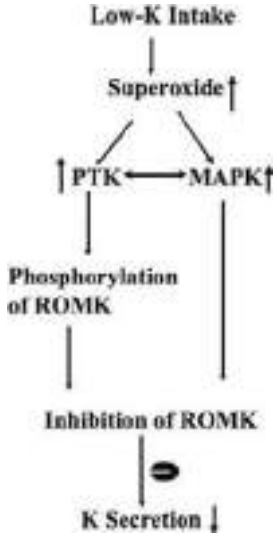

FIGURE 50.7 **Cascade of events leading to the K^+-sparing effect in the CD during K^+ depletion states.** Low extracellular K^+ stimulates an inactivating phosphorylation of ROMK channels through PTK and MAPK kinases.[114]

UREA

The concentrating defect of K^+ deficiency occurs in association with a reduced osmolality of the medullary interstitium. Urea uptake in the kidney is mediated by a family of transporter proteins that include the renal urea transporter UT-A, and the erythrocyte urea transporter UT-B. UT-A1 and UT-A3 are localized in the distal part of the IMCD, and UT-A2 is localized in the descending thin limb of Henle's loop, while UT-B is localized in vasa recta. K^+ deficiency is associated with reduced expression of UT-A1, UT-A3, and UT-B, but with increased expression of UT-A2. These data suggest that the impairment of urea absorption in the terminal IMCD (UT-A1 and -A3), and the impairment of the vasa recta urea recycling, could play a key role in lowering the medullary osmolality of K^+ deficient mice.[116]

WATER

The concentrating defect of K^+ deficiency is manifest primarily as a limitation of maximal urinary concentrating ability, rather than persistent hyposthenuria. K^+ deficiency also results in polydypsia, thus accentuating polyuria independent of the urinary concentrating defect. In humans, thirst is a prominent symptom of experimental K^+ deficiency.[117] In rats, the increased water intake precedes the development of the urinary concentrating defect, and restriction of fluid intake in the initial phase attenuates the polyuria; however, it does not prevent the development of the urinary concentrating defect.[118]

In humans, the concentrating defect has been observed in pathologic and experimental K^+ deficiency. The degree of K^+ deficiency also relates to the severity of the urinary concentrating defect in the rat. The rat,

however, is still capable of generating a maximally-concentrated urine for the first week,[118] while by 2 weeks the concentrating defect is fully established.[119]

Hypokalemic rats keep the basal water permeability at control level, whereas the response to vasopressin is significantly diminished.[120] These results are coupled with *in vitro* experiments where extracellular K^+ has been explored in rat renal papillary CD cells in culture.[121] Exposure of these cells to a K^+-free medium for more than 24 hours was associated with an attenuated cellular cAMP response to both vasopressin and forskolin. Hypokalemia results in decreased aquaporin-2 (AQP2) expression in principal cells of rat CD (cortical and medullary), in parallel with the development of polyuria. K^+ repletion is associated with normalization of AQP2 expression and urine output.[122]

Whether prostaglandin (PG) synthesis interferes with the action of vasopressin and the AQP2 system is not univocal among species. In rats, neither PGE_2 excretion nor papillary tissue content[118,123] is affected by K^+ deficiency. On the same line, indomethacin failed to reverse the concentrating defect, despite effective inhibition of medullary tissue prostaglandin synthesis.[118] The concentrating defect in K^+ deficiency is likely multifactorial; reduction in vasopressin response and in medullary interstitial osmolality are contributing mechanisms acting in a complementary fashion. Impaired NaCl reabsorption in the TAL and alteration in urea recycling limits the establishment of a hypertonic interstitium. The latter is a prerequisite for urine concentration, and it may be amplified by polydypsia and the consequent medullary washout. In addition, an impaired response of the CD to vasopressin contributes to the concentrating defect. Recently a tonicity-responsive enhancer-binding protein (TonEBP) has been identified as a transcriptional factor activated by hypertonicity. TonEBP, among other functions, plays a critical role in protecting renal medullary cells from the deleterious effects of hypertonicity. It is a key regulator of urinary concentration through the regulation of AQP2 and UT-A transcription, in a vasopressin-independent manner. K^+ deficiency conditions are associated with a downregulation of TonEBP in both inner and outer medullary CD and TAL. In the descending thin limb, TonEBP translocates from the nucleus to the cytoplasmic compartment where it is inactive. Lower interstitial osmolality occurring during K^+ deficiency could reduce TonEBP expression, and so contribute to the downregulation of AQP2 and UT-A[124] (Figure 50.8).

There is also evidence in K^+ deficiency for a decrease in inner medullary organic osmolytes which might precede the renal concentrating defect. Aldose-reductase (an osmoregulatory protein) mRNA abundance was reduced in K^+ deficiency.[125]

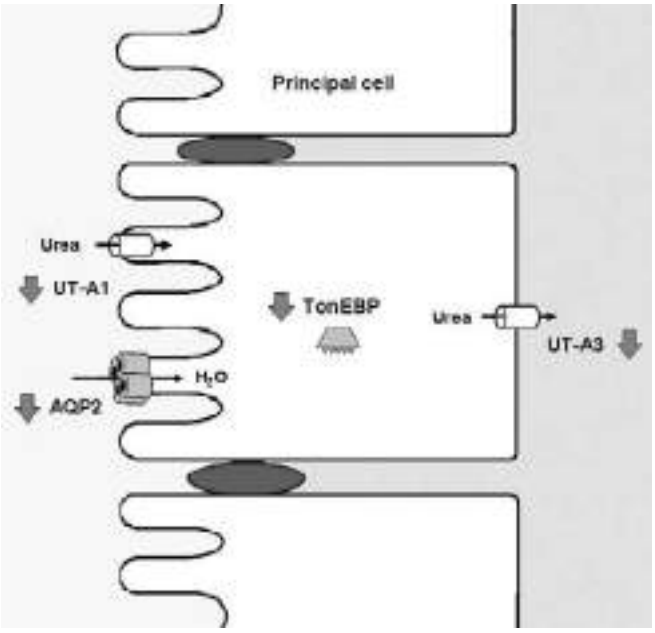

FIGURE 50.8 **A model of the urinary concentration impairment during K^+ deficiency.** In addition to a TAL-dependent low interstitial tonicity generation, principal cells along the CD play a key role. It has been described that K^+ deficiency downregulates AQP2 expression, mainly in cortical and OSOM CD.[122] In a mice model of K^+ deficiency, UT-A1 and UT-A3 are dowregulated.[116] TonEBP could promote the downregulation of urea transporters and AQP2.[124]

System Biology Approach to Hypokalemia

Since the discoding of the human genome, a novel scientific approach has been widely diffuse in health science: so-called systems biology. Systems biology aims to observe any biological system in an holistic way. It examines multiple components of a biological system *simultaneously* through high-throughput techniques (transcriptomics, metabolomics, and proteomics), and integrates the data with mathematical models. Systems biology methods produce a vast amount of data to generate hypotheses on how the observed system works. It offers new opportunities to understand complex systems.

The OMCD transcriptome of hypokalemic mice has been compared with one from mice treated with an NH_4Cl-load. Data were determined by using the serial analysis for gene expression (SAGE) microassay; a cluster analysis of changed tags has been reported in this study. Hypokalemic mice showed overexpression of tags belonging to the cluster of proliferation and apoptosis, while tags of the transport cluster were predominant in NH_4Cl-induced acidotic mice. Several transcripts have been identified in these clusters, and they are listed in the study from Cheval *et al.*[126]

The proteome of kidneys from mild and severe hypokalemic mice has been examined by Thongboonkerd

et al.[127] Chronic (8 weeks K^+ deficient diet) hypokalemic mice were compared with normokalemic mice. Two-dimensional gel-based MALDI-MS and/or Q-TOF MS/MS techniques were carried out on whole kidney samples. Thirty-three proteins induced by K^+ deficiency were identified. They are mainly metabolic enzymes and cytoskeletal proteins. Some of them are involved in the osmoregulatory process of the papillary interstitium, such as aldose reductase. A complete list of the altered proteins is also available.

SYSTEMIC EFFECTS OF K^+ DEPLETION

Healthy individuals may well tolerate short periods of mild K^+ deficiency; however, high K^+ deficiency may induce severe renal, cardiac, and neurologic injuries, and glucose intolerance. Indeed, reduced K^+ intake correlates directly with higher blood pressure in both normotensive and hypertensive individuals.

K^+ and Hypertension

Hypertension is a major health problem in developed countries. It has been extensively demonstrated that the occurrence of hypertension is associated with salt (NaCl) intake. There is evidence that dietary K^+ intake may participate in determining sensitivity to salt-induced hypertension.

Compared with our Paleolithic ancestors, the common Western diet contains a larger amount of Na^+ (150 versus 20 mmol per day), the majority (approximately 75%) is added to food products by manufacturers. While salt intake has been growing dramatically since the Paleolithic period, K^+ intake has been lessening (50 versus 320 mmol per day). This drop in K^+ intake is a consequence of reduced intake of fruits and vegetables in the diet. Epidemiologic studies have demonstrated that dietary K^+ is inversely related to the occurrence of hypertension, independently of salt intake.[128] An international study of electrolyte excretion and blood pressure performed on a large cohort of subjects, distributed in various countries, demonstrated that K^+ excretion is negatively and independently correlated with blood pressure.[129] Furthermore, K^+ supplementation (60 mmol KCl per day) decreased blood pressure in hypertensive patients with diuretic-induced hypokalemia.[130]

The role of dietary K^+ in controlling blood pressure has been assessed by the Dietary Approaches to Stop Hypertension (DASH) trial.[131] Slightly hypertensive individuals were arbitrarily assigned to either a control diet or to the DASH diet (a diet rich in vegetables, fruits, and low-fat dairy products); subgroups of participants on each diet were divided to ingest either low, intermediate or high amounts of Na^+ (approximately 50, 100, and 150 mmol, respectively, per day). The DASH diet markedly reduced blood pressure, independent of Na^+ intake (Figure 50.9). According to a Scientific Statement issued by the American Heart Association, the beneficial blood pressure-lowering effect of the DASH diet is largely a function of its high K^+ content (about 120 mmol/day in the 2100 Kcal DASH diet versus approximately 60 mmol/day in the control diet).[132] The effect of K^+ supplementation on blood pressure was further confirmed in a meta-analysis of 33 clinical trials.[133]

The mechanisms by which low dietary K^+ intake increases blood pressure have been investigated.[134] It has been shown that the hypertensive effect of K^+ deficiency is prevented by lowering daily Na^+ intake. K^+ deficiency seems, at least partially, to enhance renal Na^+ reabsorption. This mechanism could be sustained by WNK1.[135]

New Physiologic Concepts in Aldosterone-Dependent Sodium and K^+ Handling

Aldosterone is an important regulator of the final composition of urine through its effects on the distal

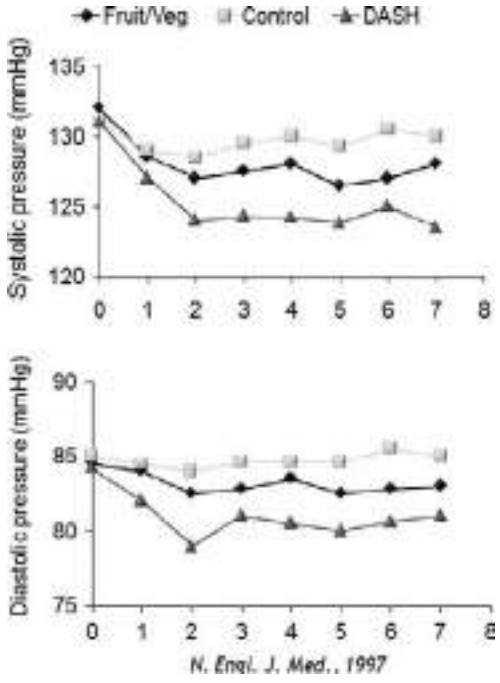

FIGURE 50.9 **Progression of weekly blood pressure measurements during control diet, fruit- and vegetable-enriched diet and DASH diet.** Control diet was typical of the diets of a substantial number of Americans with a K^+ content about 25th percentile of US consumption. The fruits- and vegetables-diet provided potassium and magnesium at levels close to the 75th percentile of consumption. The DASH diet had a K^+ content about 75th percentile of US consumption, and a reduced amount of saturated fat, total fat, and cholesterol. *(Adapted from Appel et al. [131])*

nephron. ENaC are activated by aldosterone, thus creating a lumen-negative potential. The luminal electronegativity supplies the driving force for Cl^- reabsorption through the paracellular pathway and K^+ and H^+ secretion. In such a way, Na^+ and K^+ homeostasis are finely tuned together. Aldosterone secretion is extremely sensitive to extracellular fluid volume depletion and hyperkalemia. In volume-depletion conditions, aldosterone increases salt reabsorption restoring extracellular fluid volume without generating hypokalemia. During hyperkalemia, aldosterone increases renal K^+ excretion, without concomitant renal salt retention.

The ability of the kidney to respond to increased aldosterone with two different physiologic adaptations (salt retention without K^+ secretion during volume-depletion states, and K^+ secretion without salt retention during hyperkalemia) is still a subject of debate. Recent data suggest a potential implication of the WNK kinase.[136] WNK (with no lysine) kinases are a novel family of large serine/threonine protein kinases that are conserved in multicellular organisms.[137] At present, there are four known mammalian WNK family members: WNK1, WNK2, WNK3, and WNK4. WNK4 is widely-expressed in epithelial tissues. Full-length WNK1 is ubiquitous, and is also known as long WNK1 (L-WNK1); an alternatively spliced WNK1 isoform is specifically expressed in the kidney and is, therefore, known as kidney-specific WNK1 (KS-WNK1). KS-WNK1 is an antagonist of L-WNK1.[138] L-WNK1 has been demonstrated to enhance the activity of both ENaC[139] and NCC; the latter occurs through the inhibition of WNK4, which in turn is capable of inhibiting NCC. Both L-WNK1 and WNK4 inhibit ROMK. Interestingly, KS-WNK1 antagonizes L-WNK1 with respect to its effects on ROMK, NCC, and ENaC. Therefore, a positive ratio of L-WNK1 to KS-WNK1 increases the rate of Na^+ reabsorption via ENaC and NCC, and decreases the rate of K^+ secretion by inhibiting ROMK. However, these effects uncouple Na^+ reabsorption from K^+ secretion. These mechanisms may be central to enlighten the hypotensive effect of K^+ supplementation in salt-sensitive hypertension. Indeed, high K^+ stimulates aldosterone secretion, which would be predicted to stimulate a hypertensive, rather than a hypotensive, effect. The abundance of ROMK in the apical membrane of distal nephron is regulated by dietary K^+ intake.[140] It has been reported that high- and low-K^+ intake increases and decreases KS-WNK1 expression, respectively. Low-K^+ intake also increases the expression of L-WNK1 in the kidney. The ratio of L-WNK1 to KS-WNK1 in the kidney is, therefore, increased when K^+ intake is low, and reduced when intake is high. So, by increasing the ratio of L-WNK1 to KS-WNK1, the kidney simultaneously conserves K^+ and Na^+ during K^+ deficiency (Figure 50.10). This effect could be implicated in the pathogenesis of salt-sensitive hypertension, and explain the positive action of high-K^+ intake on blood pressure.

K^+ Depletion and Glucose Intolerance

Insulin controls both K^+ and glucose homeostasis. It is possible that there is a common pathway between the two systems. Insulin-resistance is usually correlated with hyperinsulinemia, because pancreatic β-cells raise insulin secretion to balance insulin resistance.[141] The resulting hyperinsulinemia may induce hypokalemia from excessive cellular K^+ uptake, if the effect of insulin on K^+ uptake is not similarly reduced. In fact, a weakened insulin effect on K^+ fluxes in obesity and diabetes has been demonstrated,[142] which are both correlated with insulin resistance with respect to glucose metabolism.

There are data indicating that there are two distinct varieties of insulin resistance: resistance to cellular glucose uptake observed in type 2 diabetes; and resistance to cellular K^+ uptake observed during K^+ deficiency or fasting.

The molecular mechanisms involved in the differential regulation of glucose versus K^+ cellular uptake by insulin are not known. It is highly probable that these pathways are related to post-binding actions of insulin to its receptor, which is a common step in the regulation of K^+ and glucose uptake. The resistance of

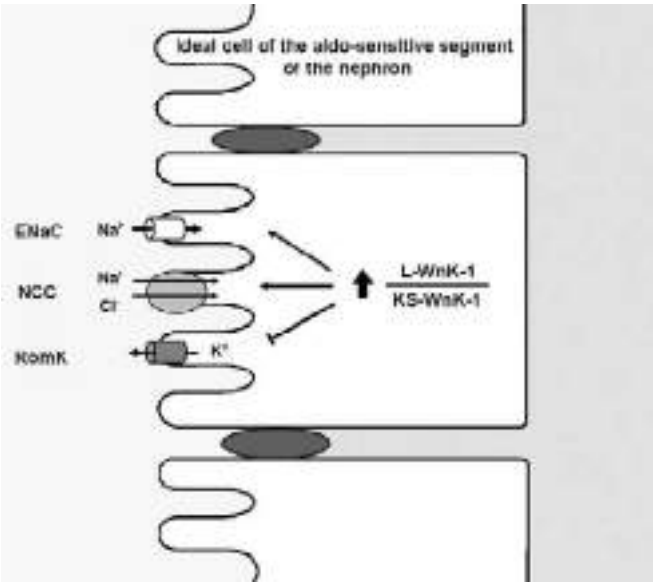

FIGURE 50.10 **The role of WNK in Na^+ and K^+ handling along the aldosterone-sensitive segments.** Hypokalemia induces an increase in the ratio of L-WNK1 to KS-WNK1 in the kidney, which decreases renal K^+ secretion in order to conserve K^+; however, this also causes reabsorption of Na^+ via ENaC and NCC.[140]

muscle cell glucose uptake during insulin resistance is attributed to an impairment of insulin signaling at the level of PI3-kinase, which involves GLUT4 trafficking.[143] Insulin has been suggested to trigger cellular K^+ uptake by activating the Na^+ pump.[144] It has also been anticipated that activation in the kidney, during K^+ deprivation, of NADPH oxidase, superoxide anion production, and PTK activities may affect insulin stimulation of K^+ cellular uptake.

Hypokalemia may play a role in the well-known association between the use of thiazide diuretics and the development of diabetes. It has been estimated that a decrease of 1 mEq/L K^+ may cause an approximately 10 mg/dl increase in glucose. These data are confirmed by the observation that glucose levels can be normalized after K^+ repletion in patients who have hypokalemia. The mechanism of thiazide-induced hyperglycemia is thought to be the consequence of decreased insulin released from the pancreatic beta cell. ATP-sensitive K^+ channels link cell metabolism to electrical activity, thereby playing an important role in the control of insulin secretion.

References

[1] Greenlee M, Wingo CS, McDonough AA, Youn JH, Kone BC. Narrative review: evolving concepts in potassium homeostasis and hypokalemia. Ann Intern Med 2009;150(9):619–25.

[2] Giebisch GH, Wang WH. Potassium transport – an update. J Nephrol 2010;23(Suppl 16):S97–104.

[3] Wang W. Regulation of renal K transport by dietary K intake. Annu Rev Physiol 2004;66:547–69.

[4] Giebisch G, Krapf R, Wagner C. Renal and extrarenal regulation of potassium. Kidney Int 2007;72(4):397–410.

[5] McDonough AA, Thompson CB, Youn JH. Skeletal muscle regulates extracellular potassium. Am J Physiol Renal Physiol 2002;282(6):F967–74.

[6] Youn JH, McDonough AA. Recent advances in understanding integrative control of potassium homeostasis. Annu Rev Physiol 2009;71:381–401.

[7] Rabinowitz L. Aldosterone and potassium homeostasis. Kidney Int 1996;49(6):1738–42.

[8] Rabinowitz L. Model of homeostatic regulation of potassium excretion in sheep. Am J Physiol 1988;254(2 Pt 2):R381–8.

[9] Bankir L, Martin H, Dechaux M, Ahloulay M. Plasma cAMP: a hepatorenal link influencing proximal reabsorption and renal hemodynamics? Kidney Int Suppl 1997;59:S50–6.

[10] Choi MJ, Ziyadeh FN. The utility of the transtubular potassium gradient in the evaluation of hyperkalemia. J Am Soc Nephrol 2008;19(3):424–6.

[11] El-Hennawy AS, Nesa M, Mahmood AK. Thyrotoxic hypokalemic periodic paralysis triggered by high carbohydrate diet. Am J Ther 2007;14(5):499–501.

[12] Finsterer J. Primary periodic paralyses. Acta Neurol Scand 2008;117(3):145–58.

[13] Tagami T, Usui T, Shimatsu A, Naruse M. Toxic thyroid adenoma presenting as hypokalemic periodic paralysis. Endocr J 2007;54(5):797–803.

[14] Sitprija V. Altered fluid, electrolyte and mineral status in tropical disease, with an emphasis on malaria and leptospirosis. Nat Clin Pract Nephrol 2008;4(2):91–101.

[15] Ikuta S, Yasui C, Kawanaka M, Aihara T, Yoshie H, Yanagi H, et al. Watery diarrhea, hypokalemia and achlorhydria syndrome due to an adrenal pheochromocytoma. World J Gastroenterol 2007;13(34):4649–52.

[16] Blondon H, Bechade D, Desrame J, Algayres JP. Secretory diarrhoea with high faecal potassium concentrations: a new mechanism of diarrhoea associated with colonic pseudo-obstruction? Report of five patients. Gastroenterol Clin Biol 2008;32(4):401–4.

[17] Simon DB, Karet FE, Rodriguez-Soriano J, Hamdan JH, DiPietro A, Trachtman H, et al. Genetic heterogeneity of Bartter's syndrome revealed by mutations in the K^+ channel, ROMK. Nat Genet 1996;14(2):152–6.

[18] Adachi M, Asakura Y, Sato Y, Tajima T, Nakajima T, Yamamoto T, et al. Novel SLC12A1 (NKCC2) mutations in two families with Bartter syndrome type 1. Endocr J 2007;54(6):1003–7.

[19] Pressler CA, Heinzinger J, Jeck N, Waldegger P, Pechmann U, Reinalter S, et al. Late-onset manifestation of antenatal Bartter syndrome as a result of residual function of the mutated renal Na^+-K^+-$2Cl^-$ co-transporter. J Am Soc Nephrol 2006;17(8):2136–42.

[20] Simon DB, Karet FE, Rodriguez-Soriano J, Hamdan JH, DiPietro A, Trachtman H, et al. Genetic heterogeneity of Bartter's syndrome revealed by mutations in the K^+ channel, ROMK. Nat Genet 1996;14(2):152–6.

[21] International Collaborative Study Group for Bartter-like Syndromes. Mutations in the gene encoding the inwardly-rectifying renal potassium channel, ROMK, cause the antenatal variant of Bartter syndrome: evidence for genetic heterogeneity. Hum Mol Genet 1997;6(1):17–26.

[22] Bailey MA, Cantone A, Yan Q, MacGregor GG, Leng Q, Amorim JB, et al. Maxi-K channels contribute to urinary potassium excretion in the ROMK-deficient mouse model of Type II Bartter's syndrome and in adaptation to a high-K diet. Kidney Int 2006;70(1):51–9.

[23] Kramer BK, Bergler T, Stoelcker B, Waldegger S. Mechanisms of disease: the kidney-specific chloride channels ClCKA and ClCKB, the Barttin subunit, and their clinical relevance. Nat Clin Pract Nephrol 2008;4(1):38–46.

[24] Konrad M, Vollmer M, Lemmink HH, van den Heuvel LP, Jeck N, Vargas-Poussou R, et al. Mutations in the chloride channel gene CLCNKB as a cause of classic Bartter syndrome. J Am Soc Nephrol 2000;11(8):1449–59.

[25] Matsumura Y, Uchida S, Kondo Y, Miyazaki H, Ko SB, Hayama A, et al. Overt nephrogenic diabetes insipidus in mice lacking the CLC-K1 chloride channel. Nat Genet 1999;21(1):95–8.

[26] Estevez R, Boettger T, Stein V, Birkenhager R, Otto E, Hildebrandt F, et al. Barttin is a Cl^- channel beta-subunit crucial for renal Cl^- reabsorption and inner ear K^+ secretion. Nature 2001;414(6863):558–61.

[27] Rickheit G, Maier H, Strenzke N, Andreescu CE, De Zeeuw CL, Muenscher A, et al. Endocochlear potential depends on Cl^- channels: mechanism underlying deafness in Bartter syndrome IV. EMBO J 2008;27(21):2907–17.

[28] Watanabe S, Fukumoto S, Chang H, Takeuchi Y, Hasegawa Y, Okazaki R, et al. Association between activating mutations of calcium-sensing receptor and Bartter's syndrome. Lancet 2002;360(9334):692–4.

[29] Chen YH, Lin JJ, Jeansonne BG, Tatum R, Lu Q. Analysis of claudin genes in pediatric patients with Bartter's syndrome. Ann N Y Acad Sci 2009;1165:126–34.

[30] Welling PA, Ho K. A comprehensive guide to the ROMK potassium channel: form and function in health and disease. Am J Physiol Renal Physiol 2009;297(4):F849–63.
[31] Geibel JP. The calcium-sensing receptor. J Nephrol 2010;23 (Suppl 16):S130–5.
[32] Miyamura N, Matsumoto K, Taguchi T, Tokunaga H, Nishikawa T, Nishida K, et al. Atypical Bartter syndrome with sensorineural deafness with G47R mutation of the beta-subunit for ClC-Ka and ClC-Kb chloride channels, barttin. J Clin Endocrinol Metab 2003;88(2):781–6.
[33] Knoers NV, Levtchenko EN. Gitelman syndrome. Orphanet J Rare Dis 2008;3:22.
[34] de Jong JC, Van DV, van den Heuvel LP, Willems PH, Knoers NV, Bindels RJ. Functional expression of mutations in the human NaCl co-transporter: evidence for impaired routing mechanisms in Gitelman's syndrome. J Am Soc Nephrol 2002;13(6):1442–8.
[35] Kunchaparty S, Palcso M, Berkman J, Velasquez H, Desir GV, Bernstein P, et al. Defective processing and expression of thiazide-sensitive Na–Cl co-transporter as a cause of Gitelman's syndrome. Am J Physiol 1999;277(4 Pt 2):F643–9.
[36] Nijenhuis T, Vallon V, van der Kemp AW, Loffing J, Hoenderop JG, Bindels RJ. Enhanced passive Ca^{2+} reabsorption and reduced Mg^{2+} channel abundance explains thiazide-induced hypocalciuria and hypomagnesemia. J Clin Invest 2005;115 (6):1651–8.
[37] Yang SS, Lo YF, Yu IS, Lin SW, Chang TH, Hsu YJ, et al. Generation and analysis of the thiazide-sensitive Na^+–Cl^- co-transporter (Ncc/Slc12a3) Ser707X knockin mouse as a model of Gitelman syndrome. Hum Mutat 2010;31(12):1304–15.
[38] Enriquez R, Adam V, Sirvent AE, Garcia-Garcia AB, Millan I, Amoros F. Gitelman syndrome due to p.A204T mutation in CLCNKB gene. Int Urol Nephrol 2010;42(4):1099–102.
[39] Jeck N, Konrad M, Peters M, Weber S, Bonzel KE, Seyberth HW. Mutations in the chloride channel gene, CLCNKB, leading to a mixed Bartter–Gitelman phenotype. Pediatr Res 2000;48 (6):754–8.
[40] Riveira-Munoz E, Chang Q, Godefroid N, Hoenderop JG, Bindels RJ, Dahan K, et al. Transcriptional and functional analyses of SLC12A3 mutations: new clues for the pathogenesis of Gitelman syndrome. J Am Soc Nephrol 2007;18 (4):1271–83.
[41] Shimkets RA, Warnock DG, Bositis CM, Nelson-Williams C, Hansson JH, Schambelan M, et al. Liddle's syndrome: heritable human hypertension caused by mutations in the beta subunit of the epithelial sodium channel. Cell 1994;79 (3):407–14.
[42] Schild L, Canessa CM, Shimkets RA, Gautschi I, Lifton RP, Rossier BC. A mutation in the epithelial sodium channel causing Liddle disease increases channel activity in the *Xenopus laevis* oocyte expression system. Proc Natl Acad Sci USA 1995;92 (12):5699–703.
[43] Abriel H, Loffing J, Rebhun JF, Pratt JH, Schild L, Horisberger JD, et al. Defective regulation of the epithelial Na^+ channel by Nedd4 in Liddle's syndrome. J Clin Invest 1999;103(5):667–73.
[44] Henry PC, Kanelis V, O'Brien MC, Kim B, Gautschi I, Forman-Kay J, et al. Affinity and specificity of interactions between Nedd4 isoforms and the epithelial Na^+ channel. J Biol Chem 2003;278(22):20019–28.
[45] Lifton RP. Molecular genetics of human blood pressure variation. Science 1996;272(5262):676–80.
[46] Dahlmann A, Pradervand S, Hummler E, Rossier BC, Frindt G, Palmer LG. Mineralocorticoid regulation of epithelial Na^+ channels is maintained in a mouse model of Liddle's syndrome. Am J Physiol Renal Physiol 2003;285(2):F310–8.
[47] Auberson M, Hoffmann-Pochon N, Vandewalle A, Kellenberger S, Schild L. Epithelial Na^+ channel mutants causing Liddle's syndrome retain ability to respond to aldosterone and vasopressin. Am J Physiol Renal Physiol 2003;285(3):F459–71.
[48] Warnock DG. Liddle syndrome: an autosomal dominant form of human hypertension. Kidney Int 1998;53(1):18–24.
[49] Pradervand S, Wang Q, Burnier M, Beermann F, Horisberger JD, Hummler E, et al. A mouse model for Liddle's syndrome. J Am Soc Nephrol 1999;10(12):2527–33.
[50] Tapolyai M, Uysal A, Dossabhoy NR, Zsom L, Szarvas T, Lengvarsky Z, et al. High prevalence of Liddle syndrome phenotype among hypertensive US Veterans in Northwest Louisiana. J Clin Hypertens (*Greenwich*) 2010;12(11):856–60.
[51] Reungjui S, Hu H, Mu W, Roncal CA, Croker BP, Patel JM, et al. Thiazide-induced subtle renal injury not observed in states of equivalent hypokalemia. Kidney Int 2007;72(12):1483–92.
[52] Ordonez NG, Toback FG, Aithal HN, Spargo BJ. Zonal changes in renal structure and phospholipid metabolism during reversal of potassium depletion nephropathy. Lab Invest 1977;36(1):33–47.
[53] Cheval L, Duong Van Huyen JP, Bruneval P, Verbavatz JM, Elalouf JM, Doucet A. Plasticity of mouse renal collecting duct in response to potassium depletion. Physiol Genomics 2004;19 (1):61–73.
[54] Peterson LN, Carpenter B, Guttierrez GA, Fajardo C, Levine DZ. Potassium depletion enhances renal compensatory hypertrophy in the nephrectomized rat. Miner Electrolyte Metab 1987;13(1):57–62.
[55] Hansen GP, Tisher CC, Robinson RR. Response of the collecting duct to disturbances of acid–base and potassium balance. Kidney Int 1980;17(3):326–37.
[56] Stanton BA, Biemesderfer D, Wade JB, Giebisch G. Structural and functional study of the rat distal nephron: effects of potassium adaptation and depletion. Kidney Int 1981;19(1):36–48.
[57] Stetson DL, Wade JB, Giebisch G. Morphologic alterations in the rat medullary collecting duct following potassium depletion. Kidney Int 1980;17(1):45–56.
[58] Reungjui S, Roncal CA, Sato W, Glushakova OY, Croker BP, Suga S, et al. Hypokalemic nephropathy is associated with impaired angiogenesis. J Am Soc Nephrol 2008;19(1):125–34.
[59] Sarkar K, Levine DZ. Ultrastructural changes in the renal papillary cells of rats during maintenance and repair of profound potassium depletion. Br J Exp Pathol 1979;60(2):120–9.
[60] Toback FG, Ordonez NG, Bortz SL, Spargo BH. Zonal changes in renal structure and phospholipid metabolism in potassium-deficient rats. Lab Invest 1976;34(2):115–24.
[61] O'Reilly DS. Increased ammoniagenesis and the renal tubular effects of potassium depletion. J Clin Pathol 1984;37 (12):1358–62.
[62] Shibata M, Yoshimura K, Furuya N, Koike M, Ueno T, Komatsu M, et al. The MAP1-LC3 conjugation system is involved in lipid droplet formation. Biochem Biophys Res Commun 2009;382 (2):419–23.
[63] Sarkar K, Nash LA, Levine DZ. Effects of ureteral ligation on renal medullary lesions of potassium depletion. Br J Exp Pathol 1983;64(6):677–83.
[64] Sarkar K, Levine DZ. Minimal medullary droplets in DOCA-induced potassium depletion of rats. Invest Urol 1978;15 (4):280–3.
[65] Kimura T, Nishino T, Maruyama N, Hamano K, Kubo A, Iwano M, et al. Expression of Bcl-2 and Bax in hypokalemic nephropathy in rats. Pathobiology 2001;69(5):237–48.
[66] Lelamali K, Khunkitti W, Yenrudi S, Panichaphongse V, Huiprasert L, Sitprija V, et al. Potassium depletion in a healthy north-eastern Thai population: no association with tubulointerstitial injury. Nephrology (Carlton) 2003;8(1):28–32.

[67] Riemenschneider T, Bohle A. Morphologic aspects of low-potassium and low-sodium nephropathy. Clin Nephrol 1983;19(6):271–9.
[68] Aithal HN, Toback FG, Dube S, Getz GS, Spargo BH. Formation of renal medullary lysosomes during potassium depletion nephropathy. Lab Invest 1977;36(2):107–13.
[69] Cremer W, Bock KD. Symptoms and course of chronic hypokalemic nephropathy in man. Clin Nephrol 1977;7(3):112–9.
[70] bdel-Rahman EM, Moorthy AV. End-stage renal disease (ESRD) in patients with eating disorders. Clin Nephrol 1997;47 (2):106–11.
[71] Danforth Jr DN, Orlando MM, Bartter FC, Javadpour N. Renal changes in primary aldosteronism. J Urol 1977;117(2):140–4.
[72] Cardinal J, Duchesneau D. Effect of potassium on proximal tubular function. Am J Physiol 1978;234(5):F381–5.
[73] Chan YL, Biagi B, Giebisch G. Control mechanisms of bicarbonate transport across the rat proximal convoluted tubule. Am J Physiol 1982;242(5):F532–43.
[74] Walter SJ, Shore AC, Shirley DG. Effect of potassium depletion on renal tubular function in the rat. Clin Sci (Lond) 1988;75 (6):621–8.
[75] Shirley DG, Walter SJ, Folkerd EJ, Unwin RJ, Bailey MA. Transepithelial electrochemical gradients in the proximal convoluted tubule during potassium depletion in the rat. J Physiol 1998;513(Pt 2):551–7.
[76] Huang L, Wei YY, Momose-Hotokezaka A, Dickey J, Okusa MD. Alpha 2B-adrenergic receptors: immunolocalization and regulation by potassium depletion in rat kidney. Am J Physiol 1996;270(6 Pt 2):F1015–26.
[77] Fryer JN, Burns KD, Ghorbani M, Levine DZ. Effect of potassium depletion on proximal tubule AT1 receptor localization in normal and remnant rat kidney. Kidney Int 2001;60 (5):1792–9.
[78] Elkjaer ML, Kwon TH, Wang W, Nielsen J, Knepper MA, Frøkiaer J, et al. Altered expression of renal NHE3, TSC, BSC-1, and ENaC subunits in potassium-depleted rats. Am J Physiol Renal Physiol 2002;283(6):F1376–88.
[79] Wang Z, Baird N, Shumaker H, Soleimani M. Potassium depletion and acid–base transporters in rat kidney: differential effect of hypophysectomy. Am J Physiol 1997;272(6 Pt 2): F736–43.
[80] Riquier AD, Lee DH, McDonough AA. Renal NHE3 and NaPi2 partition into distinct membrane domains. Am J Physiol Cell Physiol 2009;296(4):C900–10.
[81] Capasso G, Kinne R, Malnic G, Giebisch G. Renal bicarbonate reabsorption in the rat. I. Effects of hypokalemia and carbonic anhydrase. J Clin Invest 1986;78(6):1558–67.
[82] Yang X, Amemiya M, Peng Y, Moe OW, Preisig PA, Alpern RJ. Acid incubation causes exocytic insertion of NHE3 in OKP cells. Am J Physiol Cell Physiol 2000;279(2):C410–9.
[83] Soleimani M, Burnham CE. Physiologic and molecular aspects of the Na^+:HCO_3^- cotransporter in health and disease processes. Kidney Int 2000;57(2):371–84.
[84] Turban S, Beutler KT, Morris RG, Masilamani S, Fenton RA, Knepper MA, et al. Long-term regulation of proximal tubule acid–base transporter abundance by angiotensin II. Kidney Int 2006;70(4):660–8.
[85] Tizianello A, Garibotto G, Robaudo C, Saffioti S, Pontremoli R, Bruzzone M, et al. Renal ammoniagenesis in humans with chronic potassium depletion. Kidney Int 1991;40(4):772–8.
[86] Nonoguchi H, Takehara Y, Endou H. Intra- and inter-nephron heterogeneity of ammoniagenesis in rats: effects of chronic metabolic acidosis and potassium depletion. Pflugers Arch 1986;407(3):245–51.
[87] Fraley DS, Adler S, Rankin B, Curthoys N, Zett B. Relationship of phosphate-dependent glutaminase activity to ammonia excretion in potassium deficiency and acidosis. Miner Electrolyte Metab 1985;11(3):140–9.
[88] Sastrasinh S, Sastrasinh M. Renal mitochondrial glutamine metabolism during K^+ depletion. Am J Physiol 1986;250(4 Pt 2):F667–73.
[89] Busque SM, Wagner CA. Potassium restriction, high protein intake, and metabolic acidosis increase expression of the glutamine transporter SNAT3 (Slc38a3) in mouse kidney. Am J Physiol Renal Physiol 2009;297(2):F440–50.
[90] Murer H, Biber J. Phosphate transport in the kidney. J Nephrol 2010;23(Suppl 16):S145–51.
[91] Breusegem SY, Takahashi H, Giral-Arnal H, Wang X, Jiang T, Verlander JW, et al. Differential regulation of the renal sodium-phosphate co-transporters NaPi-IIa, NaPi-IIc, and PiT-2 in dietary potassium deficiency. Am J Physiol Renal Physiol 2009;297(2):F350–61.
[92] Levi M, McDonald LA, Preisig PA, Alpern RJ. Chronic K depletion stimulates rat renal brush-border membrane Na-citrate co-transporter. Am J Physiol 1991;261(5 Pt 2):F767–73.
[93] Eknoyan G, Martinez-Maldonado M, Suki WN, Richie Y. Renal diluting capacity in the hypokalemic rat. Am J Physiol 1970;219(4):933–7.
[94] Gutsche HU, Peterson LN, Levine DZ. *In vivo* evidence of impaired solute transport by the thick ascending limb in potassium-depleted rats. J Clin Invest 1984;73(4):908–16.
[95] Greger R. Cation selectivity of the isolated perfused cortical thick ascending limb of Henle's loop of rabbit kidney. Pflugers Arch 1981;390(1):30–7.
[96] Buffin-Meyer B, Marsy S, Barlet-Bas C, Cheval L, Younes-Ibrahim M, Rajerison R, et al. Regulation of renal Na^+,K (+)-ATPase in rat thick ascending limb during K^+ depletion: evidence for modulation of Na^+ affinity. J Physiol 1996;490(Pt 3):623–32.
[97] Laghmani K, Richer C, Borensztein P, Paillard M, Froissart M. Expression of rat thick limb Na/H exchangers in potassium depletion and chronic metabolic acidosis. Kidney Int 2001;60 (4):1386–96.
[98] Jakobsen JK, Odgaard E, Wang W, Elkjaer ML, Nielsen S, Aalkjaer C, et al. Functional up-regulation of basolateral Na^+-dependent HCO_3^- transporter NBCn1 in medullary thick ascending limb of K^+-depleted rats. Pflugers Arch 2004;448 (6):571–8.
[99] Capasso G, Kinne R, Malnic G, Giebisch G. Renal bicarbonate reabsorption in the rat. I. Effects of hypokalemia and carbonic anhydrase. J Clin Invest 1986;78(6):1558–67.
[100] Capasso G, Jaeger P, Giebisch G, Guckian V, Malnic G. Renal bicarbonate reabsorption in the rat. II. Distal tubule load dependence and effect of hypokalemia. J Clin Invest 1987;80 (2):409–14.
[101] Bailey M, Capasso G, Agulian S, Giebisch G, Unwin R. The relationship between distal tubular proton secretion and dietary potassium depletion: evidence for up-regulation of H^+-ATPase. Nephrol Dial Transplant 1999;14(6):1435–40.
[102] Hayashi M, Katz AI. The kidney in potassium depletion. I. Na^+-K^+-ATPase activity and [^{3}H]ouabain binding in MCT. Am J Physiol 1987;252(3 Pt 2):F437–46.
[103] McDonough AA, Magyar CE, Komatsu Y. Expression of Na (+)-K(+)-ATPase alpha- and beta-subunits along rat nephron: isoform specificity and response to hypokalemia. Am J Physiol 1994;267(4 Pt 1):C901–8.
[104] Wall SM, Fischer MP, Kim GH, Nguyen BM, Hassell KA. In rat inner medullary collecting duct, NH uptake by the Na,K-

ATPase is increased during hypokalemia. Am J Physiol Renal Physiol 2002;282(1):F91–102.
[105] Bailey MA, Fletcher RM, Woodrow DF, Unwin RJ, Walter SJ. Upregulation of H^+-ATPase in the distal nephron during potassium depletion: structural and functional evidence. Am J Physiol 1998;275(6 Pt 2):F878–84.
[106] Silver RB, Breton S, Brown D. Potassium depletion increases proton pump ($H^{(+)}$-ATPase) activity in intercalated cells of cortical collecting duct. Am J Physiol Renal Physiol 2000;279 (1):F195–202.
[107] Barone S, Amlal H, Kujala M, Xu J, Karet F, Blanchard A, et al. Regulation of the basolateral chloride/base exchangers AE1 and SLC26A7 in the kidney collecting duct in potassium depletion. Nephrol Dial Transplant 2007;22(12): 3462–70.
[108] Xu J, Worrell RT, Li HC, Barone SL, Petrovic S, Amlal H, et al. Chloride/bicarbonate exchanger SLC26A7 is localized in endosomes in medullary collecting duct cells, and is targeted to the basolateral membrane in hypertonicity and potassium depletion. J Am Soc Nephrol 2006;17(4):956–67.
[109] Gumz ML, Lynch IJ, Greenlee MM, Cain BD, Wingo CS. The renal H^+-K^+-ATPases: physiology, regulation, and structure. Am J Physiol Renal Physiol 2010;298(1):F12–21.
[110] Wagner CA, Finberg KE, Stehberger PA, Lifton RP, Geibisch GH, Aronson PS, et al. Regulation of the expression of the Cl^-/anion exchanger pendrin in mouse kidney by acid–base status. Kidney Int 2002;62(6):2109–17.
[111] Linas SL, Peterson LN, Anderson RJ, Aisenbrey GA, Simon FR, Berl T. Mechanism of renal potassium conservation in the rat. Kidney Int 1979;15(6):601–11.
[112] Malnic G, Berliner RW, Giebisch G. Flow dependence of K^+ secretion in cortical distal tubules of the rat. Am J Physiol 1989;256(5 Pt 2):F932–41.
[113] Wang W. Regulation of renal K transport by dietary K intake. Annu Rev Physiol 2004;66:547–69.
[114] Wang ZJ, Sun P, Xing W, Pan C, Lin DH, Wang WH. Decrease in dietary K intake stimulates the generation of superoxide anions in the kidney and inhibits K secretory channels in the CCD. Am J Physiol Renal Physiol 2010;298(6): F1515–22.
[115] Jin Y, Wang Y, Wang ZJ, Lin DH, Wang WH. Inhibition of angiotensin type 1 receptor impairs renal ability of K conservation in response to K restriction. Am J Physiol Renal Physiol 2009;296(5):F1179–84.
[116] Jung JY, Madsen KM, Han KH, Yang CW, Knepper MA, Sands JMJ, et al. Expression of urea transporters in potassium-depleted mouse kidney. Am J Physiol Renal Physiol 2003;285 (6):F1210–24.
[117] Garella S, Chang B, Kahn SI. Alterations of hydrogen ion homeostasis in pure potassium depletion: studies in rats and dogs during the recovery phase. J Lab Clin Med 1979;93 (2):321–31.
[118] Berl T, Aisenbrey GA, Linas SL. Renal concentrating defect in the hypokalemic rat is prostaglandin independent. Am J Physiol 1980;238(1):F37–41.
[119] Peterson LN. Time-dependent changes in inner medullary plasma flow rate during potassium-depletion. Kidney Int 1984;25(6):899–905.
[120] Carney S, Rayson B, Morgan T. A study *in vitro* of the concentrating defect associated with hypokalaemia and hypercalcaemia. Pflugers Arch 1976;366(1):11–7.
[121] Ishikawa S, Saito T, Kuzuya T. Role of potassium in vasopressin-induced production of cyclic AMP in rat renal papillary collecting tubule cells in culture. J Endocrinol 1987;113(2):199–204.
[122] Marples D, Frokiaer J, Dorup J, Knepper MA, Nielsen S. Hypokalemia-induced downregulation of aquaporin-2 water channel expression in rat kidney medulla and cortex. J Clin Invest 1996;97(8):1960–8.
[123] Beck N, Shaw JO. Thromboxane B2 and prostaglandin E2 in the K^+-depleted rat kidney. Am J Physiol 1981;240(2): F151–7.
[124] Jeon US, Han KH, Park SH, Lee SD, Sheen MR, Jung JY, et al. Downregulation of renal TonEBP in hypokalemic rats. Am J Physiol Renal Physiol 2007;293(1):F408–15.
[125] Nakanishi T, Yamauchi A, Yamamoto S, Sugita M, Takamitsu Y. Potassium depletion modulates aldose reductase mRNA in rat renal inner medulla. Kidney Int 1996;50(3):828–34.
[126] Cheval L, Morla L, Elalouf JM, Doucet A. Kidney collecting duct acid–base "regulon.". Physiol Genomics 2006;27 (3):271–81.
[127] Thongboonkerd V, Chutipongtanate S, Kanlaya R, Songtawee N, Sinchaikul S, Parichatikanond P, et al. Proteomic identification of alterations in metabolic enzymes and signaling proteins in hypokalemic nephropathy. Proteomics 2006;6(7): 2273–85.
[128] Langford HG. Dietary potassium and hypertension: epidemiologic data. Ann Intern Med 1983;98(5 Pt 2):770–2.
[129] Intersalt Cooperative Research Group 14. Intersalt: an international study of electrolyte excretion and blood pressure. Results for 24 hour urinary sodium and potassium excretion. BMJ 1988;297(6644):319–28.
[130] Kaplan NM, Carnegie A, Raskin P, Heller JA, Simmons M. Potassium supplementation in hypertensive patients with diuretic-induced hypokalemia. N Engl J Med 1985;312 (12):746–9.
[131] Appel LJ, Moore TJ, Obarzanek E, Vollmer WM, Svetkey LP, Sacks FM, et al. A clinical trial of the effects of dietary patterns on blood pressure. DASH Collaborative Research Group. N Engl J Med 1997;336(16):1117–24.
[132] Appel LJ, Brands MW, Daniels SR, Karanja N, Elmer PJ, Sacks FM. Dietary approaches to prevent and treat hypertension: a scientific statement from the American Heart Association. Hypertension 2006;47(2):296–308.
[133] Whelton PK, He J, Cutler JA, Brancati FL, Appel LJ, Follmann D, et al. Effects of oral potassium on blood pressure. Meta-analysis of randomized controlled clinical trials. JAMA 1997;277(20):1624–32.
[134] Grimm Jr RH, Neaton JD, Elmer PJ, Svendsen KH, Levin J, Segal M, et al. The influence of oral potassium chloride on blood pressure in hypertensive men on a low-sodium diet. N Engl J Med 1990;322(9):569–74.
[135] Huang CL, Kuo E. Mechanisms of disease: WNK-ing at the mechanism of salt-sensitive hypertension. Nat Clin Pract Nephrol 2007;3(11):623–30.
[136] Kahle KT, Wilson FH, Leng Q, Lalioti MD, O'Connell AD, Dong K, et al. WNK4 regulates the balance between renal NaCl reabsorption and K^+ secretion. Nat Genet 2003;35 (4):372–6.
[137] Xu B, English JM, Wilsbacher JL, Stippec S, Goldsmith EJ, Cobb MH. WNK1, a novel mammalian serine/threonine protein kinase lacking the catalytic lysine in subdomain II. J Biol Chem 2000;275(22):16795–801.
[138] Subramanya AR, Yang CL, Zhu X, Ellison DH. Dominant-negative regulation of WNK1 by its kidney-specific kinase-defective isoform. Am J Physiol Renal Physiol 2006;290(3): F619–24.
[139] Xu BE, Stippec S, Chu PY, Lazrak A, Li XJ, Lee BH, et al. WNK1 activates SGK1 to regulate the epithelial sodium channel. Proc Natl Acad Sci USA 2005;102(29):10315–20.

[140] Chu PY, Quigley R, Babich V, Huang CL. Dietary potassium restriction stimulates endocytosis of ROMK channel in rat cortical collecting duct. Am J Physiol Renal Physiol 2003;285(6):F1179–87.
[141] Bergman RN, Ader M, Huecking K, Van CG. Accurate assessment of beta-cell function: the hyperbolic correction. Diabetes 2002;51(Suppl 1):S212–20.
[142] Arslanian S, Austin A. Impaired insulin mediated potassium uptake in adolescents with IDDM. Biochem Med Metab Biol 1991;46(3):364–72.
[143] Graham TE, Kahn BB. Tissue-specific alterations of glucose transport and molecular mechanisms of intertissue communication in obesity and type 2 diabetes. Horm Metab Res 2007;39(10):717–21.
[144] Benziane B, Chibalin AV. Frontiers: skeletal muscle sodium pump regulation: a translocation paradigm. Am J Physiol Endocrinol Metab 2008;295(3):E553–8.
[145] Soleimani M, Burnham CE. Physiologic and molecular aspects of the Na^+:HCO_3^- co-transporter in health and disease processes. Kidney Int 2000;57(2):371–84.
[146] Mujais SK, Chen Y, Nora NA. Discordant aspects of aldosterone resistance in potassium depletion. Am J Physiol 1992;262(6 Pt 2):F972–9.

This page intentionally left blank

CHAPTER

51

Clinical Disorders of Hyperkalemia

Kamel S. Kamel[1], *Shih-Hua Lin*[2], *Sung-Sen Yang*[2] *and Mitchell Halperin*[1]

[1]Renal Division, St. Michael's Hospital, University of Toronto, Toronto, Canada
[2]Division of Nephrology, Department of Medicine, Tri-Service General Hospital, National Defense Medical Center, Taipei, Taiwan, Republic of China

INTRODUCTION

Hyperkalemia is a common electrolyte disorder that may have detrimental effects, the most serious of which is a cardiac arrhythmia.[1] There is large variability among patients in the absolute concentration of potassium (K^+) ions in plasma (P_K), which leads to electrocardiographic changes and cardiac toxicity of hyperkalemia. From a diagnosis of the cause of hyperkalemia perspective, the basis of hyperkalemia will be a shift of K^+ out of cells if the time course for its development is short and/or if there is little K^+ intake. On the other hand, chronic hyperkalemia implies that there is a defect in the regulation of the excretion of K^+ by the kidney.

Basic Concept for the Movement of K^+ Ions Across Cell Membranes

K^+ is the principal cation in cells. The movement of K^+ ions across cell membranes has two requirements; first, there must be a driving force; second there must be an open K^+ channel in a cell membrane.

Driving Force

K^+ are kept inside the cell by an electrical force; the cell interior has a negative voltage. It follows that a more negative cell voltage is required to shift K^+ into cells. The negative voltage in cells is generated by the activity of the electrogenic cation pump, the Na^+, K^+ ATPase (Na-K-ATPase). This pump exports three sodium (Na^+) ions while importing only two K^+ ions; hence there is a net export of {1/3} of a positive charge per Na^+ that exits from cells via the Na-K-ATPase (Figure 51.1). Because, intracellular anions are largely macromolecular phosphates such as RNA, DNA, and phospholipids, which remain inside the cell, a negative intracellular voltage is generated when Na^+ exits the cell via the electrogenic Na-K-ATPase.

There are three ways to acutely increase ion pumping by the Na-K-ATPase: First, a rise in the concentration of its rate-limiting substrate—intracellular Na^+; second, an increase in the affinity for Na^+ or in the V_{max} of the existing Na-K-ATPase units in cell membranes; third, an increase in the number of active Na-K-ATPase pump units in the cell membrane by recruitment of new units. A chronic increase in Na-K-ATPase pump activity requires the synthesis of new pump units as occurs with exercise training.[2]

The driving force for the secretion of K^+ by principal cells in the late distal convoluted tubule, the connecting segments and the cortical collecting duct (the abbreviation CCD is used in this Chapter to indicate all these nephron segments) is a lumen-negative voltage. This lumen-negative voltage is generated by the electrogenic reabsorption of Na^+ (reabsorption of more Na^+ ions than of their accompanying anion, chloride (Cl^-) ions).

Ion Channels for K^+

There are several different types of channels that permit the diffusion of K^+ through cell membranes.[3,4] Some of these channels are regulated by voltage, others by ligands such as calcium ions (Ca^{2+}), and yet others by metabolites such as adenosine di-phosphate

Seldin and Giebisch's The Kidney, Fifth Edition.
DOI: http://dx.doi.org/10.1016/B978-0-12-381462-3.00051-3

© 2013 Elsevier Inc. All rights reserved.

(ADP)—the latter are called K_{ATP} channels. Because K^+ ions do not reach diffusion equilibrium, control is exerted not only by modulating the number but also the conductance and gating of these channels.

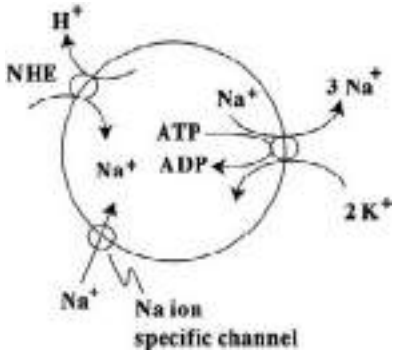

FIGURE 51.1 Na-K-ATPase activity and the export of positive voltage. The Na-K-ATPase generates the electrical driving force for K^+ entry into cells providing that the source of Na^+ pumped out is either Na^+ that existed in cells or Na^+ that entered cells in an electroneutral fashion via NHE. If the source of Na^+ pumped were Na^+ that entered cells via a Na^+ ion channel, the voltage in cells would become less negative. While K^+ channel conductance does limit the rate of K^+ exit, a higher concentration of K^+ in the ICF compartment that resulted from ion pumping by the Na-K-ATPase can still cause the electrogenic exit of K^+. *Reproduced with permission (224).*

The major K^+ channel that adjusts the intracellular voltage is the K^+_{ATP} channel.[5] It is a misnomer to call these channels K^+_{ATP} as the concentration of ATP in cells does not change sufficiently to provide a signal for regulating these channels. The signal that regulates these channels may be the result of a change in the concentration of a related nucleotide, ADP. When the concentration of ADP rises, K^+_{ATP} channels will open; conversely, when the concentration of ADP falls, K^+_{ATP} channels will close. This regulation of K^+_{ATP} channels adjusts the negative voltage in cells, which in turn regulates other ion channels. The best example is the voltage-gated Ca^{2+} channel, which is opened by a less negative voltage in cells. Ionized Ca^{2+} is a major signal for regulation of a number of intracellular processes.

Example: Regulation of the K^+_{ATP} channel by ADP plays a critical role in the release of insulin.[6] When the concentration of glucose in plasma ($P_{Glucose}$) is high, a metabolic signal is generated in ß-cells of the pancreas to cause the release of insulin (Figure 51.2). When the rate of oxidation of glucose rises in ß-cells, the concentration of ADP in these cells falls. This lower concentration of ADP causes the K^+_{ATP} channels to close and thus the ICF compartment becomes less negative because fewer K^+ ions (positive charges) exit ß-cells. This less negative voltage in ß-cells increases the conductance of voltage-gated Ca^{2+} channels and hence the

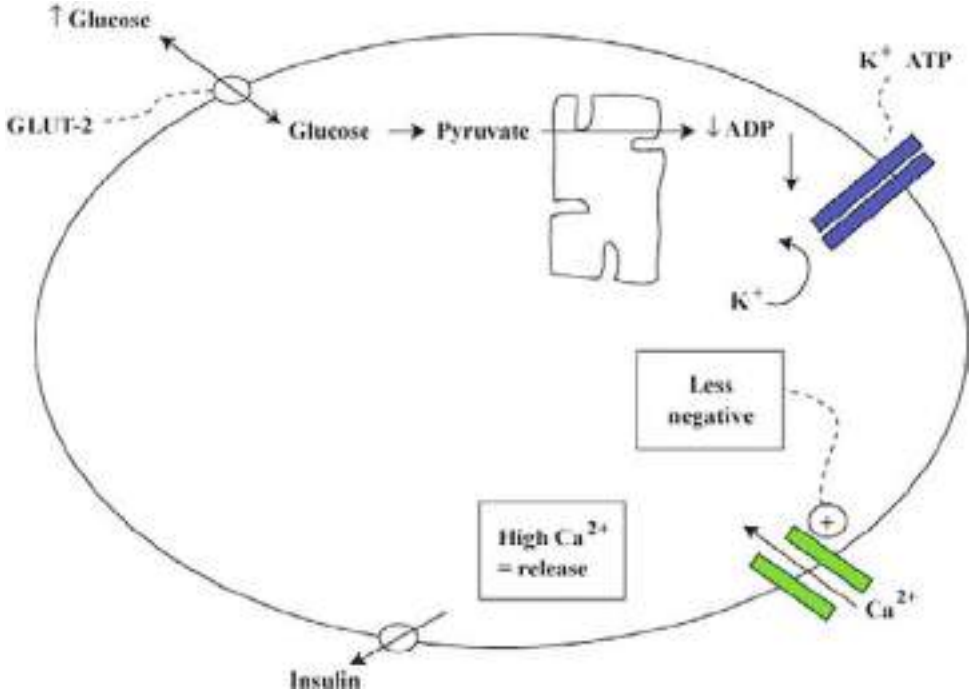

FIGURE 51.2 Signal system to release insulin from ß-cells of the pancreas. The large oval represents a ß-cell of the pancreas. When the $P_{Glucose}$ rises, the $ICF_{Glucose}$ rises to the same extent because of the type of glucose transporter (GLUT-2) in these cells. When glucose is oxidized, the concentration of ADP falls, and this permits K_{ATP} channels to be closed. As a result, less K^+ and positive voltage exits, which causes the ICF compartment to become less negative. This opens voltage-gated Ca^{2+} channels and hence the ionized Ca^{2+} concentration in their cytosol increases. A higher ionized Ca^{2+} in these cells causes the release of insulin.

intracellular concentration of ionized Ca^{2+} rises—this provides the signal to release insulin from ß-cells (Figure 51.2).

A similar logic can be used to deduce how the blood flow to exercising muscle may be controlled using intracellular Ca^{2+} as the signal[7] (Figure 51.3). During a sprint, L-lactic acid is released from skeletal muscle cells. When lactic acid enters vascular smooth muscle cells, H^+ and/or lactate anions lead to the opening of the K^+_{ATP} channels. As a result, K^+ exit and the voltage in these cells become more negative. This causes closure of voltage-gated Ca^{2+} channels and less entry of Ca^{2+} into cells and hence vasodilatation.

Several types of K^+ channels including renal outer medullary K^+ channels, ROMK ($K_{ir}1.1$) (which have similar biophysical prosperities and regulatory mechanism as that of the small conductance K^+ channels identified in mouse and rat CCD), a Ca^{2+} activated big-conductance K^+ channel (BK) and the double-pore K^+ channel, are expressed in the apical membrane of principal cells in CCD.[8,9] ROMK are the K^+ channels most important for the secretion of K^+ in CCD.[9,10] Big K^+ conductance "BK" or maxi-K^+ channels are activated by a rise in intracellular Ca^{2+} and are thought to play an important role in flow dependent K^+ secretion.[11,12] Although these channels likely mediate K^+ secretion in patients with Bartter's syndrome that is due to a loss of function mutation in ROMK,[13] their role in physiological regulation of renal excretion of K^+ is not clear. BK channel activity has been detected in both principal cells and intercalated cells in CCD. It is difficult to explain the contribution of BK located in intercalated cells to K^+ secretion as these cells have low Na-K-ATPase pump content. BK channel activity is increased in the CCD from rats on a high K^+ diet.[14] Furthermore, in BK-α subunit knocked mice, increase in flow failed to stimulate K^+ secretion in distal nephron.[15] Notwithstanding, deletion of BK-α subunit does not affect net K^+ excretion in mice fed a high K^+ diet. It is important to recall that the role of these channels was examined in laboratory rodents which consume 10-fold more K^+ per kg body weight and close to three-fold more Na^+ per kg body weight compared to human subjects consuming a typical Western diet. Therefore, it is possible that the BK channel may provide a way for a "speedy" K^+ excretion if there is a large intake of K^+ and if flow through CCD were augmented. Although, the same limitations imposed by the magnitude of the lumen negative voltage on the rate of secretion of K^+ by these channels will apply, it is possible that "conductance" through ROMK may be rate limiting when there is a need for a high rate of excretion of K^+ over a short period of time.

REGULATION OF K^+ HOMEOSTASIS

Regulation of K^+ homeostasis has two important aspects:

1. Control of the trans-cellular distribution of K^+, which is vital for survival because it limits acute changes in the P_K.

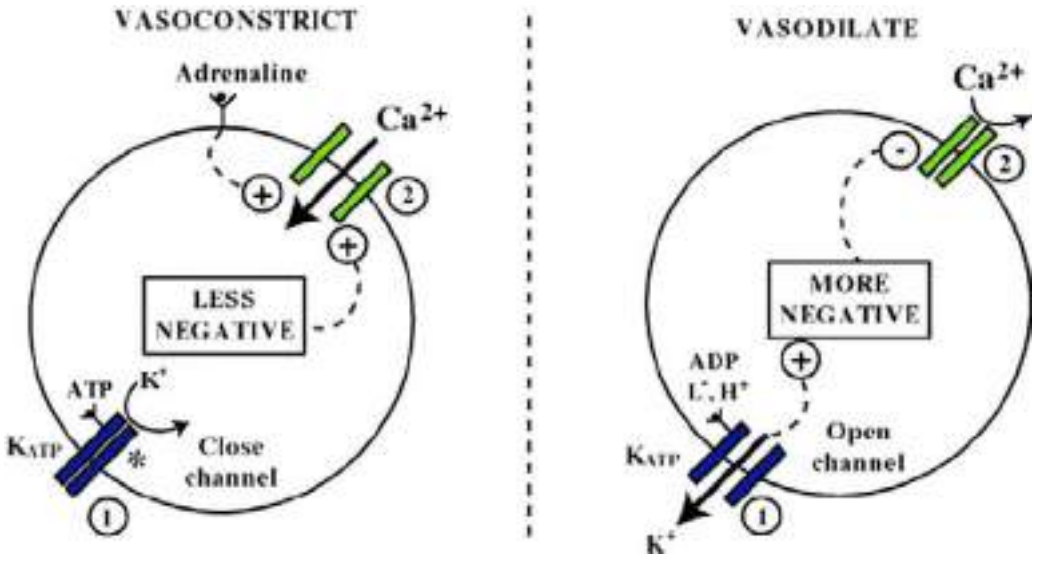

FIGURE 51.3 Vasoconstrictor tone in vascular smooth muscle cells. The circles represent vascular smooth muscle cells. When the ICF has a less negative voltage because its K^+_{ATP} channels (shown in blue) are closed, the voltage-gated Ca^{2+} channels (shown in green) can be maintained in an open configuration permitting a rise in the ICF [Ca^{2+}]. Hence there will be an increase in vasoconstriction (shown to the left of the dashed line). In contrast, during a sprint, K^+_{ATP} channels will open because of a high concentration of L-lactate anions (L^-) and H^+. This will lead to a more negative ICF voltage and closure of their voltage-gated Ca^{2+} channels and thereby vasodilatation and increase in blood flow to muscles.

2. The regulation of K^+ excretion by the kidney, which maintains overall K^+ balance; nevertheless, this is a much slower process.

Acute Control of the Plasma K^+

Distribution of K^+ between the ECF and ICF Compartments

THE Na-K-ATPase

The activity of the Na-K-ATPase is higher when the concentration of its substrate, Na^+ in cells rises. The impact of this increase in the net exit of Na^+ on the trans-membrane voltage, however, depends on whether the Na^+ entry step into cells is electroneutral or electrogenic.

Electroneutral Entry of Na^+ into Cells: This occurs when Na^+ ions enter cells in exchange for hydrogen ions (H^+) via the Na^+/H^+ exchanger-1 (NHE-1) (Figure 51.4, left side).[16] The NHE-1 is normally inactive in cell membranes, as can be deduced from the fact that the concentrations of its substrates (Na^+ in the extracellular fluid (ECF) and H^+ in the intracellular fluid (ICF) compartment) are considerably higher than that of its products (Na^+ in the ICF compartment and H^+ in the ECF compartment) in steady state. The two major activators of NHE-1 are a higher concentration of H^+ in the ICF compartment near NHE -1[17] and insulin.[18] Monocarboxylic acids (e.g., L-lactic acid) enter cells on the monocarboxylic acid cotransporter (M-CT)[19,20] (Figure 51.4). If the M-CT is located in close proximity to NHE in a cell membrane, the release of H^+ from these acids may cause a high concentration of H^+ in the local area of NHE-1, which activates NHE-1 and hence increases the electroneutral entry of Na^+ into cells (Figure 51.4, left side).[21]

Electrogenic entry of Na^+ into Cells: The Na^+ channel in cell membranes is normally gated by voltage. When open, one cationic charge enters the cell per Na^+ transported. Since only 1/3 of a charge exits per Na^+ ion that is exported out of the cell via the Na-K-ATPase (Figure 51.1); the net effect would be to diminish the degree of intracellular negative voltage and this leads to net exit of K^+ out of cells. This explains a rise in the P_K during intense exercise.[22,23] It could explain the development of hyperkalemia in patients with hyperkalemic periodic paralysis.[24,25]

Hormones that Affect the Distribution of K^+

Catecholamines: FXYD1 (phospholemman) interacts with the catalytic α subunit of the Na-K-ATPase and modulates its activity. Un-phosphorylated FXYD1 binds to the α subunit and this inhibits the pump activity by decreasing its affinity for Na^+ and/or its V_{max}. ß-$_2$ adrenergic agonists activate adenalyate cyclase and this leads to stimulation of the conversion of ATP to cAMP. This second messenger, in turn, activates protein kinase-A, which induces phosphorylation of the FXYD1; this disrupts its interaction with α subunit of the Na-K-ATPase and results in an increase in the affinity of the Na-K-ATPase for intracellular Na^+.[26,27] The increase in export of pre-existing intracellular Na^+ (Figure 51.1) increases the negative voltage in cells and causes a shift of K^+ into cells.

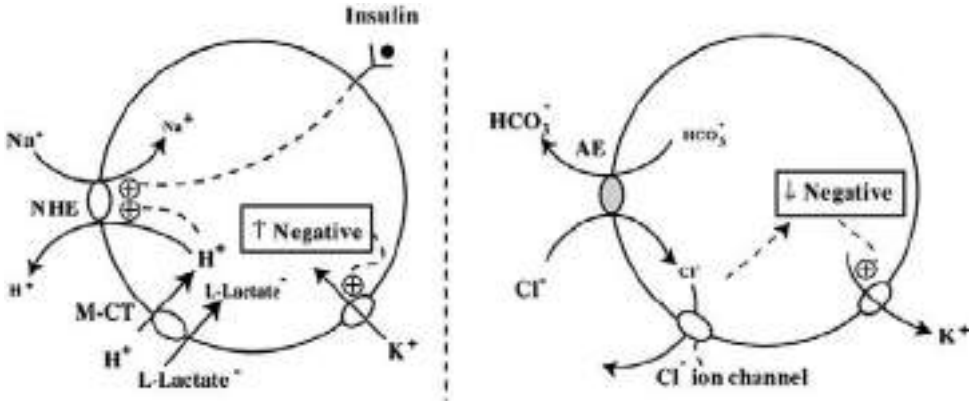

FIGURE 51.4 **Role of NHE-1 and AE in the shift of K^+ across cell membranes.** The circle represents a cell membrane. NHE and the AE are normally *inactive* in cell membranes. As shown to the left of the dashed vertical line, there are two major activators of NHE, insulin and a higher concentration of H^+ in the ICF compartment. Monocarboxylic acids (e.g., L-lactic acid) enter cells on the monocarboxylic acid cotransporter (M-CT). If the M-CT is located in close proximity to NHE-1 in cell membrane, the release of H^+ from these acids may cause a high concentration of H^+ in the local area of NHE-1, which activates NHE-1. Activation of NHE-1 increases the electroneutral entry of Na^+ into cells. As Na^+ exit via the electrogenic Na-K-ATPase, the net effect is a more negative intracellular voltage and the entry of K^+ into cells. As shown on the right, when the AE is activated and there are favorable concentration differences, HCO_3^- will be exported and Cl^- enter cells. The intracellular negative voltage will drive the exit of Cl^-; from cells through their specific ion channel. This latter step will lead to the export of negative voltage from cells and the subsequent exit of K^+.

An acute shift of K^+ into cells and hypokalemia is observed in conditions associated with a surge of catecholamines (e.g., patients with a subarachnoid hemorrhage, myocardial ischemia, and/or an extreme degree of anxiety).[28] ß$_2$-agonists may be used to induce a shift of K^+ into cells in patients with hyperkalemia in an emergency setting. Non-specific ß-blockers are being used for therapy of the subtype of hypokalemic periodic paralysis associated with hyperthyroidism.[29,30]

Insulin: Insulin increases the activity of the Na-K-ATPase and its expression in the plasma membrane through a phosphoinositide 3-kinase, atypical protein kinase C (aPKC), and extracellular signal regulated kinases 1 and 2 (ERK1/2). ERK1/2 kinase phosphorylation of the Na-K-ATPase α subunit promotes translocation of Na-K-ATPase from an intracellular pool to the cell membrane.[31,32] aPKC phosphorylation of FXYD1 leads to an increase in the V_{max} of the Na-K ATPase.[27] Insulin may also have an effect in augmenting the electroneutral entry of Na^+ into cells via NHE-1.[18] This, in conjunction with increasing the number and activity of the Na-K-ATPase on the cell surface, causes the voltage in cells to become more negative (Figure 51.4, left side). Notwithstanding the glucose transporter, GLUT4 and Na-K-ATPase do not co-localize to the same skeletal muscle intracellular vesicles and hence, the effect of insulin to shift K^+ into cells is separate from its effect on glucose entry into these cells.[33]

Insulin has been utilized clinically in the treatment of patients with an emergency due to the adverse cardiac effects of hyperkalemia. In contrast, in patients with diabetic ketoacidosis, a lack of action of insulin results in a shift of K^+ out of cells and the development of hyperkalemia despite a total body deficit of K^+.

Acid–Base Influences

When an acid is added to the body, most of the H^+ are buffered in the ICF compartment.[34] Monocarboxylic acids (e.g., L-lactic acid) enter cells on the M-CT,[19,20] and, as mentioned above, release of their H^+ near NHE-1 may activate NHE-1 and increase the electroneutral entry of Na^+ into cells and hence, in the presence of insulin, may cause a shift of K^+ into cells.[21]

A shift K^+ out of cells may occur in patients with metabolic acidosis due to acids that are not transported on MC-T (e.g., metabolic acidosis due to a gain of HCl acid owing to loss of $NaHCO_3$ in a patient with diarrhea, ingestion of citric acid[35]). A possible mechanism to explain how this may occur is illustrated in (Figure 51.4, right side**)**. Activation of the Cl^-/bicarbonate (HCO_3^-) anion exchanger (AE) will cause HCO_3^- to exit and Cl^- to enter cells.[36] Since cells have Cl^- channels in their membrane,[37] the rise in the concentration of Cl^- in the ICF in conjunction with the usual negative voltage forces Cl^- to exit. As this exit of Cl^- is electrogenic, it causes a less negative voltage in cells and K^+ will exit from cells.

Several clinical implications follow from this analysis:

1. If hyperkalemia is present in a patient with metabolic acidosis due to accumulation of monocarboxylic organic acid, other causes for hyperkalemia than the acidemia should be sought (e.g., lack of insulin in patients with diabetic ketoacidosis, tissue injury, and a lack of ATP to drive the Na-K-ATPase in patients with L-lactic acidosis due to hypoxia[38–40]).
2. Metabolic acidosis due to inorganic acids (addition of HCl) causes a shift of K^+ out of cells. Patients with chronic hyperchloremic metabolic acidosis (e.g., patients with chronic diarrhea or those with renal tubular acidosis (RTA)) however, usually have a low P_K because of excessive loss of K^+ in the diarrhea fluid in the former[41] or the urine in the later.[42]

Respiratory acid–base disorders, on the other hand, cause only small changes in the P_K as there is little movement of Na^+ or Cl^- across cell membranes in these disorders.[43,44]

Tissue Catabolism

Hyperkalemia may be seen in patients with crush injury or those with tumor-lysis syndrome.[45] In these patients, factors that compromise the ability of the kidney to excrete K^+ are usually present as well. Patients with diabetic ketoacidosis, have a total body K^+ depletion but hyperkalemia is commonly present due to a shift of K^+ from cells secondary to a lack of insulin. The corollary is that during therapy, complete replacement of the deficit of K^+ must await the provision of cellular constituents (phosphate, amino acids, Mg^{2+}, etc.) and the presence of anabolic signals.

LONG-TERM REGULATION OF K^+ HOMEOSTASIS

Control of the renal excretion of K^+ maintains overall daily K^+ balance. Although the usual intake of K^+ in adults eating a typical western diet is close to 1 mmol of K^+/kg body weight, the rate of excretion of K^+ can match an intake of more than 200 mmol/day with only a minor rise in the P_K.[46]

Control of K^+ secretion occurs primarily in the CCD.[47,48] Two factors influence the rate of excretion of K^+ in CCD; the flow rate in the terminal CCD, and the net secretion of K^+ by principal cells in the CCD which raises the luminal concentration of K^+ ($[K^+]_{CCD}$).

K^+ Secretion

The secretory process for K^+ by principal cells in the CCD, has two elements. First, a trans-epithelial lumen negative voltage must be generated by electrogenic reabsorption of Na^+ via epithelial Na^+ channels (ENaC) (Figure 51.5). Second, open ROMK channels must be present in the luminal membrane of principal cells.[49]

Aldosterone actions lead to an increase in the number of open ENaC units in the luminal membrane of principal cells in CCD[50] (Figure 51.5). The steps involved include binding of aldosterone to its receptor in the cytoplasm of principal cells, entry of this hormone-receptor complex into the nucleus, and then the synthesis of new proteins including the serum and glucocorticoid regulated kinase-1 (SGK-1).[51,52] SGK-1 increases the expression of ENaC in the apical membrane of principal cells. The mechanism seems to be related to the effect of SGK-1 to phosphorylate and inactivate the ubiquitin ligase Nedd-4-2.[53] Nedd-4-2 ubiquinates ENaC subunits, leading to their removal from the cell membrane and degradation in proteasomes. Therefore, inhibition of the Nedd-4-2 induced endocytosis of ENaC leads to increased expression of ENaC in the luminal membrane, which increases the transport of Na^+.[54,55] Another mechanism by which aldosterone activates ENaC involves proteolytic cleavage of the channel by serine proteases. Aldosterone induces production of "channel activating proteases" (CAP 1–3).[56] These proteases activate ENaC by increasing their open-probability, rather than by increasing their expression in the luminal membrane.

The driving force for Na^+ reabsorption in the CCD is a higher concentration of Na^+ in the lumen of CCD than that in principal cells (~10–15 mmol/L) and a negative voltage inside cells, owing to the actions of the Na-K-ATPase at the basolateral membrane of these cells. The concentration of Na^+ in luminal fluid is limited by the presence of urea osmoles and that the osmolality of luminal fluid in CCD will be equal to plasma osmolality in the presence of vasopressin. The rate of electrogenic Na^+ reabsorption is limited by constraints on the magnitude of luminal negative voltage that can be generated in CCD because of limitations on transport of Cl^-. At a trans-epithelial lumen negative voltage of −61 mV and a plasma Cl^- of 100 mmol/L, the minimum luminal Cl^- concentration would be 10 mmol/L. Therefore, under most circumstances, the concentration of Na^+ in luminal fluid is sufficient for the activity of ENaC. Variations in the luminal concentration of Na^+ in the CCD do not regulate the net secretion of K^+.[57]

The reabsorption of Na^+ in the CCD can be electroneutral, if the rate of reabsorption of its major accompanying anion Cl^- matches its rate of reabsorption, or electrogenic, if more Na^+ than Cl^- are reabsorbed in CCD (Figure 51.5). The pathway(s) for the reabsorption of Cl^- in the CCD is (are) not well defined, but it is thought that paracellular pathways play an important role.[58,59] Recently an electroneutral, thiazide-sensitive and amiloride-resistant Na^+-Cl^- transport was identified in the intercalated cells of the cortical collecting duct in mice.[60,61] This seems to be mediated by the parallel activity of the Na^+-dependent Cl^-/HCO_3^- exchanger (NDCBE), which promotes the electroneutral exchange of one intracellular Cl^- with one Na^+, two HCO_3^- and the Na^+ independent Cl^-/HCO_3^- exchanger (pendrin). This transport mechanism is apparently responsible for as much as 50% of Na^+-Cl^- transport in CCD of the mouse while mineralocorticoids act. To play a role in modulating the rate of K^+ secretion, this mechanism of electroneutral NaCl reabsorption needs to be expressed in the late DCT and the connecting tubule.

An increase in the concentration of HCO_3^- and/or an alkaline luminal fluid pH seem to increase the amount of K^+ secreted in the CCD. It was suggested that this

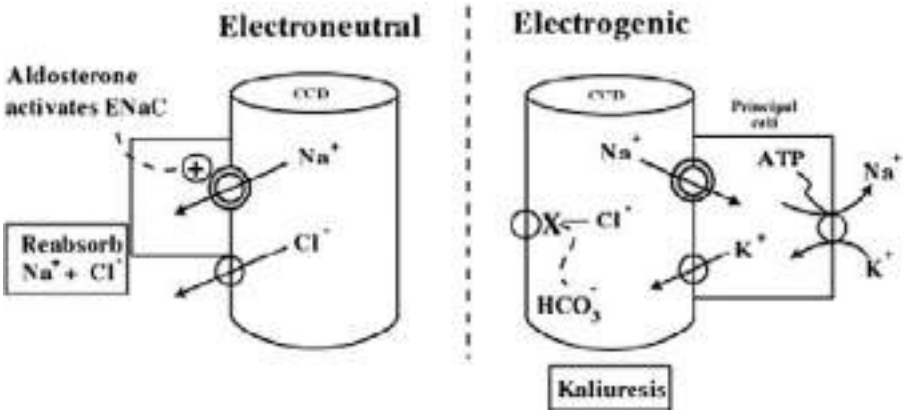

FIGURE 51.5 Electrogenic and electroneutral reabsorption of Na^+ in the CCD. The barrel-shaped structures represent the CCD and the rectangles represent principal cells. Na^+ is reabsorbed via ENaC; this reabsorption is increased by aldosterone (the shaded enlarged circle). Net secretion of K^+ occurs through its specific ion channel (ROMK). Electroneutral reabsorption of Na^+ is shown on the left and an example of electrogenic reabsorption of Na^+ (the presence of HCO_3^- or an alkaline luminal pH) is shown to the right of the dashed vertical line. *Reproduced with permission (224).*

may be due to a decrease in the apparent permeability of Cl^-[62] and/or an increase in ROMK open probability in this nephron segment. It is also possible that the increase in luminal HCO_3^- concentration in CCD, inhibits the Cl^-/HCO_3^- exchanger (pendrin), and hence the NDCBE and the electroneutral NaCl reabsorption,[60] perhaps leading to a higher rate of electrogenic reabsorption of Na^+.

If the rate of reabsorption of Na^+ in CCD is not appreciably higher than the rate of reabsorption of Cl^-, a large lumen-negative voltage cannot develop. The hyperkalemia in patients with the syndrome of "Familial Hyperkalemia with Hypertension" (also known as type II pseudohypoaldosteronism or Gordon's syndrome) may be an example for this pathophysiology.[58,63] Two factors are important to achieve this near-equal rate of ion transport in the CCD. First, low delivery of Na^+ and Cl^- to the CCD occurs because the reabsorption of Na^+ and Cl^- is augmented in the distal convoluted tubule because of increased activity of Na^+-Cl^-cotransporter (NCC). Second, effective arterial blood volume expansion suppresses the release of aldosterone; this leads to fewer numbers of open ENaC in the luminal membrane of principal cells in CCD. Hence the rate of reabsorption of Cl^- in the CCD may match that of Na^+.

ROMK channels are abundant and have a high open-probability on a K^+-rich diet.[9,64] Therefore ROMK channels do not seem to be rate-limiting for net secretion of K^+ unless the P_K falls to the mid-3 mmol/L range in rats.[65] Dietary K^+ intake is an important regulator of ROMK channels. Low K^+ intake decreases, whereas a high K^+ intake increases the number of ROMK channels in the luminal membrane of principal cells.[66] The membrane trafficking of ROMK is modulated by phosphorylation of tyrosine in the channel protein, such that phosphorylation of tyrosine stimulates endocytosis and de-phosphorylation of tyrosine induces exocytosis. K^+ depletion increases the expression and activity of the protein tyrosine kinase and tyrosine phosphorylation of ROMK channels results in their endocytosis.[67] Angiotensin II (ANG_{II}) inhibits ROMK activity in K^+-restricted rats, but not in rats on a usual K^+ diet.[68] The effect of ANG_{II} may be mediated via activating NADPH oxidase II and the production of superoxide anions, which increases the expression of protein tyrosine kinase.[69–71] The WNK (*With No Lysine*) kinases seem to play a role in modulating K^+ secretion. There are two isoforms of WNK1; a ubiquitous full-length WNK1 (WNK1-L) and a kidney-specific, short WNK1 lacking the kinase domain (WNK1-S).[72] WNK1-L induces endocytosis of ROMK[73] whereas WNK1-S inhibits this effect of WNK1-L. The ratio of WNK1-S to WNK1-L transcripts is reduced by K^+ restriction (more endocytosis of ROMK) and is increased by K^+ loading (less endocytosis of ROMK).[74,75]

Flow Rate in the CCD

When vasopressin acts and aquaporin-2 water channels (AQP2) have been inserted in the luminal membrane of principal cells, the late distal nephron is permeable to water, the osmolality of fluid in the terminal CCD is equal to the plasma osmolality and hence is relatively fixed. Therefore, the flow rate in terminal CCD is determined by the number of osmoles in the luminal fluid.

The osmoles that are present in the lumen of the terminal portion of CCD are largely urea, NaCl, and K^+ with an accompanying anion. While there is little reabsorption or secretion of electrolytes in the nephron segments distal to terminal CCD, and hence the number of electrolyte osmoles in terminal CCD is close to their rate of excretion in the urine, this is not the case for urea. A quantitative analysis of the process of intra-renal urea recycling reveals that the amount of urea delivered to the early DCT is about two-fold larger than the quantity of urea that is excreted in the urine. In the following paragraphs, we shall illustrate that urea recycling aids the excretion of K^+; this process is especially important in subjects with disorders or those who are taking drugs that lead to a less lumen-negative voltage in the CCD.[76]

Urea Recycling, Process and Quantitative Analysis

For simplicity, we shall begin with the absorption of urea in the inner medullary collecting duct (MCD) (Figure 51.6). This absorption requires the presence of urea transporters in the luminal membrane of cells of the inner MCD (vasopressin phosphorylates and causes the insertion of urea transporters UT-A1 in the luminal membrane of cells in this nephron segment[77]), and a higher concentration of urea in the luminal fluid in the inner MCD than that in the interstitial fluid in the inner medulla. This later requirement is achieved because all the segments of the distal nephron that are upstream to the inner MCD, are likely to be impermeable to urea, but most of the water delivered to the early DCT is reabsorbed in the CCD and MCD owing to the insertion of AQP2 into the luminal membranes of principal cells. The concentration of urea rises to higher than 600 mmol/L in the luminal fluid that is delivered to the inner MCD (Figure 51.6).

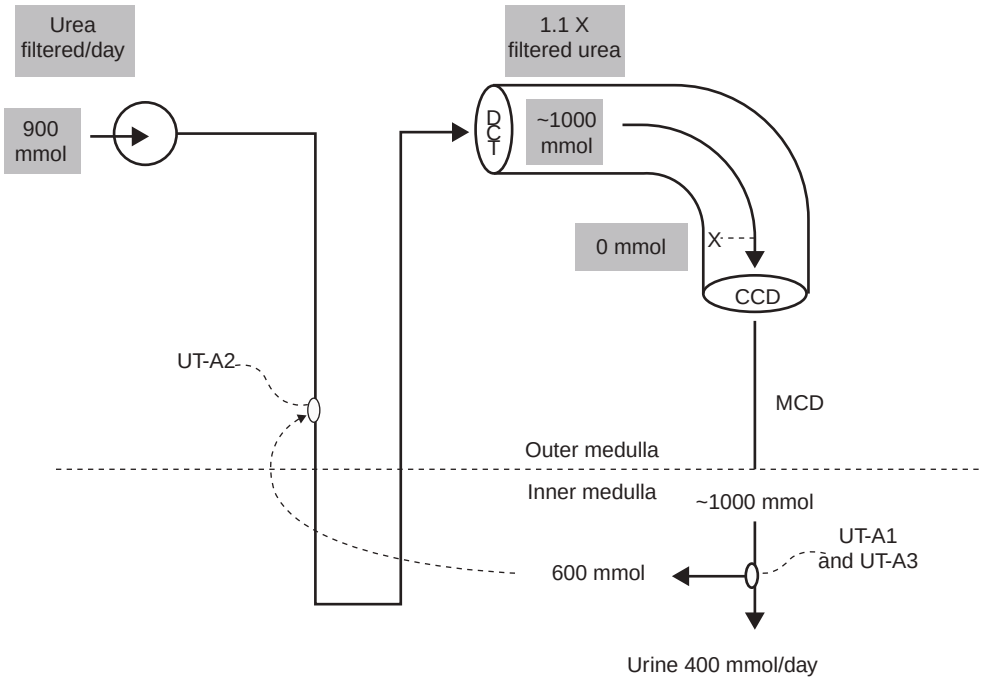

FIGURE 51.6 An overview of intra-renal urea recycling. In micropuncture studies in rats, the amount of urea in luminal fluid in early distal tubule was 1.1 times the amount that was filtered. Extrapolated to adult human with a GFR of 180 L/day and a plasma urea of 5 mmol/L, 1000 mmol of urea would be delivered to early CCD per day. Since ~400 mmol of urea are excreted daily in an adult human subjects who consumes a typical Western diet, then ~600 mmol of urea are reabsorbed down stream from the DCT and recycled back to DCT. Based on the presence of urea transporters, it is likely that the urea is reabsorbed in the inner MCD and added into the luminal fluid in the descending thin limbs of the loop of Henle of superficial nephrons that have their bends deeper in the medulla via UT-A2.

The bulk of the urea that is reabsorbed in the inner MCD leaves the inner medulla via the ascending vasa recta, because it has UT-A2 and, as a result, is permeable to urea. Once in the deep outer medulla, most urea will enter the luminal fluid of the descending thin limbs (DtL) of the loop of Henle of superficial nephrons that have their bends deep in the outer medulla, as they possess the UT-A2 and the concentration of urea is higher in the interstitial compartment than in the luminal fluid of the DtL, which allows for a high rate of delivery of urea to the early DCT.[78,79]

To obtain a quantitative estimate of the amount of urea that is recycled, one needs an estimate of the amount of urea that is delivered to the early DCT and the amount of urea that is excreted in the urine over a given period of time. Since the amount of urea delivered to the early DCT cannot be measured in human subjects, it is essential to use data from experiments using the micropuncture technique in the early DCT in fed rats. In these studies,[80] the amount of urea in the early DCT was 1.1 times the amount of urea that was filtered. Extrapolated to a human adult with a GFR of 180 L/day, and a plasma urea concentration of 5 mmol/L, a reasonable estimate of the daily delivery of urea to the early DCT is approximately 1000 mmol/day. Since subjects eating a typical Western diet excrete close to 400 mmol of urea per day, the amount of urea that recycles would be approximately 600 mmol per day.

Importance of Urea Recycling for the Excretion of K^+

This process of urea recycling adds an extra 2 L to the flow rate in terminal CCD (600 mosmol divided by a luminal fluid osmolality that is equal to that in plasma or ~300 mOsm/L). A reasonable estimate of the number of liters of fluid that exit the terminal CCD per day is close to 5 L (1500 mosmol/day in the terminal CCD (1000 mosmol of urea/day and 500 mosmol/day of electrolytes) divided by 300 mosmol/L). This means, in quantitative terms that 40% of the flow rate in terminal CCD is the result of this process of recycling of urea.

Implications for the Patient with Hyperkalemia

Patients who develop chronic hyperkalemia have a renal defect that is characterized by an inability to

generate a sufficiently large trans-epitheleal (TE) lumen-negative voltage in the CCD to secrete all their daily intake of K^+ while maintaining a normal P_K. These patients, however, will achieve a steady state in which they will excrete all the K^+ they ingest and absorb that is not lost via non-renal routes. To understand how this steady state is achieved, we shall consider how a K^+ load of 70 mmol/day is handled in normal subjects and a patient with an electrical defect that leads to a diminished ability to raise the concentration of K^+ in the lumen of terminal CCD ($[K^+]_{CCD}$) (Figure 51.7).

Normal subjects have a much larger capacity to secrete K^+ in their CCD compared to the usual daily intake of K^+; they excrete most of their daily intake over a relatively short period of time close to noon. This likely reflects an increase in the lumen negative voltage in CCD owing to a larger delivery of $NaHCO_3$ to the CCD at the time of the alkaline tide in urine pH. If a normal subject has a P_K of 4 mmol/L and a TE voltage in the CCD of -61 mvolts, the $[K^+]$ in luminal fluid in CCD would be 10 times the P_K or 40 mmol/L. If this voltage could be maintained while 1-L of fluid exits the CCD, 40 mmol of the 70 mmol of K^+ would be excreted in this time period (approximately five hours). For the next 19-hours, if 4-L of fluid would exit the terminal CCD with a concentration of K^+ of only close to 8 mmol/L, the remaining 30 mmol of K^+ can be excreted to achieve K^+ balance.

Let us now consider a patient who has a large defect that leads to a lumen negative TE voltage in the CCD of only −29.1 mvolts (Table 51.1 and Figure 51.7). At this TE voltage, the K_{CCD}/P_K can rise to a value of only three. At a P_K of 4.7 mmol/L, the $[K^+]_{CCD}$ will be close to 14 mmol/L; hence at the usual flow rate in terminal CCD of 5-L/day, this patient could excrete 70 mmol of K^+ daily and maintain a normal P_K. The point to emphasize is that this precise balance is dependant on intra-renal urea recycling and thereby maintaining the daily flow rate in the terminal CCD of 5-L. Therefore, if this patient were to be put on a protein restricted diet (decrease the number of osmoles of urea in the terminal CCD), a smaller number of liters of fluid will exit the CCD per day and hyperkalemia may develop. To put this in a quantitative perspective, if the number of liters exiting the CCD per day were 4-L instead of 5-L, and if the K_{CCD}/P_K were three, while this patient continued to consume 70 mmol of K^+/day, in steady state, the P_K will need to rise to 5.8 mmol/L to maintain K^+ balance and only if this maximum rate of K^+ secretion is maintained throughout the 24 hours period. To further emphasize this point, consider a patient who may

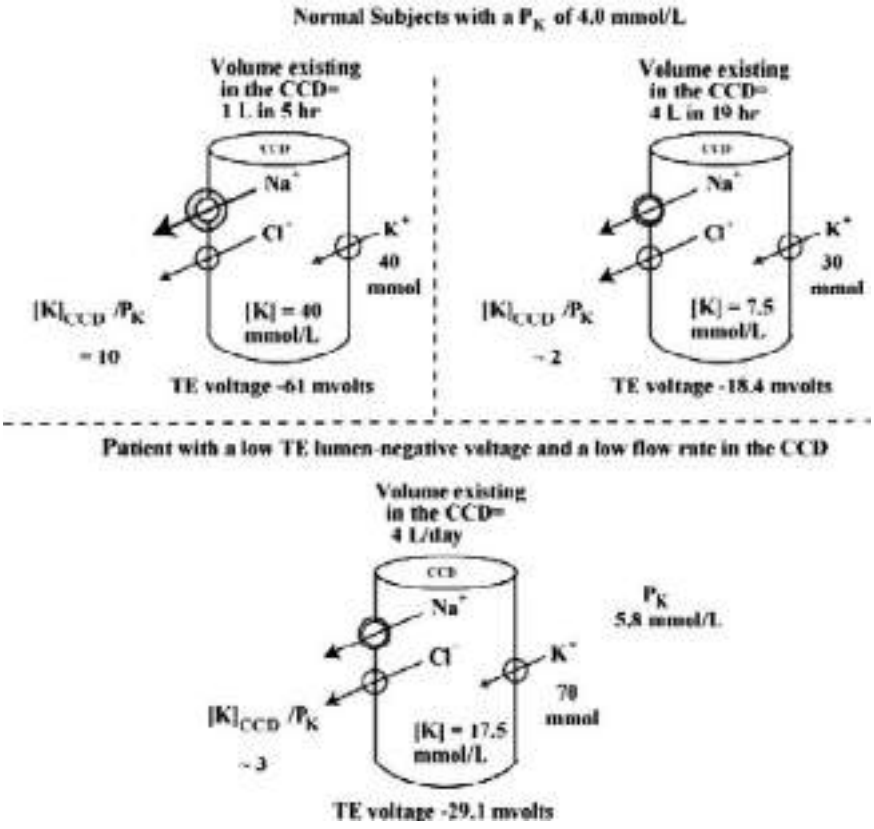
Normal Subjects with a P_K of 4.0 mmol/L
Volume existing in the CCD= 1 L in 5 hr
Volume existing in the CCD= 4 L in 19 hr
CCD
Na^+
Cl^-
K^+
40 mmol
30 mmol
$[K]_{CCD}/P_K$ = 10
$[K]_{CCD}/P_K$ ~ 2
[K] = 40 mmol/L
[K] = 7.5 mmol/L
TE voltage -61 mvolts
TE voltage -18.4 mvolts
Patient with a low TE lumen-negative voltage and a low flow rate in the CCD
Volume existing in the CCD= 4 L/day
P_K 5.8 mmol/L
70 mmol
$[K]_{CCD}/P_K$ ~ 3
[K] = 17.5 mmol/L
TE voltage -29.1 mvolts

FIGURE 51.7 Excretion of K^+ in normal subjects and in patients with chronic hyperkalemia. The barrel-shaped structures represent the CCD. Over the 24-hour period, both the normal subject and the patient with a low TE voltage reabsorb 70 mmol more Na^+ than Cl^-; and hence excrete 70 mmol of K^+, as they are in balance for K^+. The top portion of the figure describes normal subjects (P_K 4.0 mmol/L). The left section of the top portion illustrates the excretion of K^+ when it is at its usual maximum rate (close to noon) whereas its right portion illustrates this secretory process when K^+ excretion usually declines. In the bottom portion is a patient with a disorder that leads to a lower TE lumen negative voltage in CCD. At TE voltage of −29.1 mvolts, $K^+_{CCD}/P_K = 3$. If the flow rate in terminal CCD declines to 4 L/day, K^+ balance can be maintained but his P_K will rise to 5.8 mmol/L.

TABLE 51.1 Interaction Between the Transepithelial (TE) Voltage, the P_K and Rate of Flow, on the Rate of Secretion in the CCD

TE Voltage (mvolts)	$[K]_{CCD}/P_K$	P_K (mmol/L)	$[K]_{CCD}$ (mmol/L)	Flow Rate$_{CCD}$ (L/day)	$K_{Excretion}$ (mmol/day)
−29.1	3	4.7	14.4	5	70
−29.1	3	5.8	18	4	70
−29.1	3	7.8	24	3	70
−18.4	2	7.2	10	5	70

The $[K^+]_{CCD}/P_K$ is calculated from the TE voltage using the Nernst equation. The numbers are the P_K and the flow rate in terminal CCD per day that are required to achieve a rate of K^+ excretion of approximately 70 mmol/day at a reduced voltage in CCD. Note that even with a large decrease in TE voltage in CCD to −29.1 mvolts, K^+ balance is achieved without a large rise in P_K if the flow rate in terminal CCD is at its usual value of 5 L per day. If the flow rate in terminal CCD were to decrease to 4 L per day, the P_K must rise to 5.8 mmol/L to excrete the daily intake of 70 mmol of K^+ and remain in K^+ balance.

have markedly impaired urea recycling due to a disease that involves the inner medulla (perhaps an example may be a patient with sickle cell disease). This patient may have a flow rate in the terminal CCD that is only 3-L/day rather than 5-L/day. If such a patient has a disease that leads to a reduced ability to generate a high lumen negative TE voltage in the CCD, a more severe degree of hyperkalemia will develop unless K^+ intake is markedly reduced. In quantitative terms, if the TE voltage in the CCD is −29.1 mvolts, the $[K]_{CCD}$ will be three-fold higher than P_K. Therefore, if the volume of filtrate that exits the terminal CCD is only 3-L/day, the P_K would have to be close to 8 mmol/L to excrete 70 mmol of K^+/day.

Integration of the Response to Dietary K^+ Intake: A Paleolithic Perspective

Virtually all our major control mechanisms developed in Paleolithic times; the important ones provided an advantage for survival. There have been no pressures in modern times that have enough control strength to over-ride these control mechanisms. The diet of our most ancient ancestors consisted mainly of fruit and berries; a diet that provides sugar, K^+ and organic anions, but little NaCl. In addition, this intake of K^+ was episodic, but large at times. Therefore, there was a need to have a mechanism in place to rapidly shift K^+ into the liver before it reaches the heart to avoid the risk of cardiac arrhythmia. Furthermore, the renal response needed to be orchestrated to switch from a NaCl conservation mode to a K^+ excretion mode. It is important in this regard to note that aldosterone can be a NaCl retaining or a kaliuretic hormone, in what has been dubbed as the "aldosterone paradox". In more detail, when aldosterone acts, it causes the insertion of a larger number of open ENaC units in the luminal membrane of principal cells in CCD, which permits both NaCl retention or K^+ secretion. Thus, there must be another signal to select one of these possible effects. Of note, the secretagogue for aldosterone is ANG_{II} when its release is in response to a low effective arterial blood volume. On the other hand, a higher P_K directly stimulates the release of aldosterone, however, ANG_{II} in this setting, will be suppressed.

Shift of K^+ into Hepatocytes

While it is well known that there is a rise in the $P_{L\text{-lactate}}$ in portal venous blood after absorption of dietary glucose,[81] the physiological importance of this high $P_{L\text{-lactate}}$ was not evident when viewed solely in metabolic terms. We suggested that a possible function of this high portal $P_{L\text{-lactate}}$ is to prevent hyperkalaemia in hepatic venous blood following the absorption of K^+ from the diet.[21] The process begins by increasing the rate of aerobic glycolysis in enterocytes; as a result of performing more work by intestinal cells and thereby the generation of more ADP, the other substrate (beside glucose) for glycolysis. This extra metabolic work occurs because the sodium linked glucose transporter (SLGT) in this location is SLGT-1. Hence, when 1 mmol of glucose is absorbed, 2 mmol of Na^+ must be absorbed; therefore more ATP will be converted to ADP to absorb a given quantity of glucose.[82] Should glycolysis occur at a faster rate than that of pyruvate oxidation, L-lactate will released into the portal vein. In the liver, the uptake of L-lactic acid on the M-CT could lead to a rise the concentration of H^+ in the sub-membrane region of hepatocytes and hence activation of NHE-1. This electroneutral entry of Na^+ into hepatocytes and its subsequent exit via Na^+/K^+-ATPase in an electrogenic fashion, will lead to a higher negative intracellular voltage and hence the retention of K^+ in hepatocytes. This mechanism requires the presence of insulin,[21] which is released in response to the dietary sugar load with the

ingestion of fruit and berries. Perhaps, because of its effect, to cause the translocation of more Na^+/K^+-ATPase units to the cell surface of hepatocytes, insulin is required for this effect of L-lactic acid to cause a shift of K^+ into hepatocytes.

Integration of the Renal Response to Dietary K^+ Intake

WNK Kinases

Available evidence indicates that this complex network of with-no-lysine kinases (WNKs); WNK4 and WNK1, via effects on NCC and ROMK normally function as a switch to change the aldosterone response of the kidney to either conserve Na^+ or excrete K^+, depending on whether the release of aldosterone is induced by a change in dietary Na^+ or dietary K^+ intake.[83,84]

WNK4 is thought to inhibit NCC activity by reducing its plasma membrane abundance, by diverting post-Golgi NCC to the lysosome for degradation.[85] The expected kaliuresis owing to increased delivery of NaCl to CCD is prevented because WNK4 inhibits ROMK, an effect that involves clathrin-mediated endocytosis.[86,87] SGK-1, when ANG_{II} is suppressed as in conditions of high K^+ intake, phosphorylates WNK4 and reverses its inhibition of ROMK.[88] ANG_{II} has been shown to inhibit ROMK activity in K^+-restricted rats, but not in rats on their usual dietary K^+ intake.[68] The effect of ANG_{II} may be mediated via activating NADPH oxidase II and the production of superoxide anions, which increases the expression of protein tyrosine kinase such as c-Src.[69–71] Src family protein tyrosine kinase phosphorylates ROMK and results in their endocytosis.[89,90] Therefore, ANG_{II} release due to low Na^+ intake or a K^+ restricted diet inhibits ROMK directly via protein tyrosine kinase or indirectly via blocking SGK-1 mediated WNK4 phosphorylation, which restores WNK4 inhibition of ROMK.

ANG_{II} signaling through the ANG_{II} receptor phosphorylates and converts WNK4 from an inhibiting mode to an NCC-activating kinase form. The activating form of WNK4 induces a phosphorylation cascade, whereby WNK4 phosphorylates the intermediary kinases, STE 20/SPS 1-related proline, alanine-rich kinase (SPAK) and perhaps also the oxidative stress responsive protein type 1 (ORS1). Phosphorylated-SPAK/ORS1 in turn phosphorylates and activates NCC.[91] Since the release of aldosterone in states of hypovolemia (or low salt intake) is mediated by ANG_{II}, but not when the stimulus of the release of aldosterone is due to hyperkalemia, this may provide a mechanism to signal the need of actions of aldosterone as a NaCl retaining hormone. In this setting, the effect of ANG_{II} to inhibit ROMK prevents kaliuresis in response to the release of aldosterone and SGK-1. Although SGK-1 phosphorylates WNK4, this does not mimic the stimulatory effects of ANG_{II}.[92] The dual requirement for both SGK-1 and ANG_{II} signaling to switch WNK4 from being an inhibitor to an activator of NCC would provide a mechanism to integrate the effects of high aldosterone and ANG_{II} for appropriate activation of NCC in hypovolemia. It would also explain why high aldosterone and SGK-1 activation induced by a high-K diet does not stimulate NCC transport, in which case ANG_{II} is not elevated.

In response to a large intake of K^+, in the absence of ANG_{II}, WNK4 will be in its NCC inhibiting mode and hence more NaCl will be delivered downstream. Aldosterone, acting via SGK-1, increases the number of open ENaC subunits in the luminal membrane of principal cells in CCD and hence the electrogenic reabsorption of Na^+. Nevertheless, for this result in kaliuresis, ROMK channels in an open configuration must be present in the luminal membrane of principal cells. When ANG_{II} is suppressed, SGK-1 mediated phosphorylation of WNK4 reverses WNK4 effect to inhibit ROMK.

As mentioned above, alternative promoter usage of the WNK1 gene produces a kidney-specific short form of WNK1, called WNK1-S, and a more ubiquitous long form, called WNK1-L.[72] WNK1-L inhibits ROMK by inducing endocytosis of the channel protein; WNK1-S isoform inhibits this effect of WNK1-L. The relative abundance of the WNK1 isoforms is regulated by dietary K^+. The ratio of WNK1-S to WNK1-L transcripts is reduced by K^+ restriction (greater endocytosis of ROMK) and increased by K^+ loading (reduced endocytosis of ROMK).[74,75] WNK1-L up-regulates NCC by blocking the inhibitory form of WNK4 or directly via phosphorylation of SPAK/ORS1.[93] WNK1-L has also been reported to activate SGK-1 through PI3 kinase.[94] WNK1-S, on the other hand, antagonizes the effects of WNK1-L and therefore indirectly inhibits NCC.

Modulation by the Delivery of HCO_3^- to the CCD

An increased delivery of HCO_3^- and/or a rise in the pH of luminal fluid in CCD may provide a signal to augment the secretion of K^+.[62,95] The effect may be due to a decrease in the electroneutral component of Na^+ reabsorption in the CCD, which would increase the magnitude of the luminal negative voltage, if accompanied by an increase in electrogenic Na^+ reabsorption. Alternatively, or in addition, luminal alkalinization may increase the number of open ROMK in the luminal membrane of principal cells in the CCD.

In Paleolithic times, the major source of dietary K^+ was from fruit and berries. The anions ingested along with this K^+ were a family of organic anions that can be metabolized to neutral end products plus HCO_3^-. In addition, a higher P_K is associated with alkalinization in the cells of the proximal convoluted tubule (PCT), which leads to inhibition of the reabsorption of HCO_3^-.[96] The end result is the delivery of more HCO_3^- to the CCD, which promotes aldosterone to exert its kaliuretic effect.[97] On the other hand, ANG_{II}, which mediates the release of aldosterone in response to decreased effective circulating volume, is a potent activator of Na^+/H^+ exchanger-3 (NHE-3) and the reabsorption of HCO_3^- in the cells of the PCT.[98] Therefore, there will be diminished delivery of HCO_3^- to the CCD, which will allow for more electroneutral rather than electrogenic reabsorption of Na^+ in this nephron segment and hence more NaCl retention and less kaliuresis.[97]

Medullary Recycling of K^+

The Paleolithic diet provided little NaCl. Nevertheless, there is a need to deliver one mmol of Na^+ to the CCD to secrete one mmol of K^+. Therefore, there must be a mechanism to increase the delivery of Na^+ to the CCD when there is a need to excrete a large K^+ load. Notwithstanding, it is also essential to minimize the excretion of Na^+ and Cl^- to stay in salt balance.

To increase distal delivery of Na^+, the kidney must make an investment.[99] By this we mean that, the kidney must reabsorb some of the $KHCO_3$ delivered to the MCD to increase the medullary interstitial concentration of K^+.[100,101] While it may seem counter-productive to have active reabsorption of K^+, when a high rate of excretion is needed, this process in fact increases the rate of excretion of K^+ by increasing the distal delivery of Na^+. In more detail, a rise in the medullary interstitial concentration of K^+ will lead to depolarization of cells of the medullary thick ascending limb of the loop of Henle. This will diminish the exit of Cl^- from these cells, as this is an electrogenic process, which carries a negative charge out of the cell. The subsequent increase in intracellular Cl^- concentration inhibits the reabsorption on Na and Cl in the medullary thick ascending limb of the loop of Henle and hence increases their delivery to the distal nephron.[102] This reabsorption of $KHCO_3$ could be achieved via the K^+/H^+-ATPase, which is likely to be present in the luminal membrane of cells in the MCD because of a prior state of depletion of K^+ before the large intake of K^+ occurred.[103] As the rise in P_K is sustained, there will be less K^+/H^+-ATPase units in the luminal membrane of MCD cells. Hence, the medullary interstitial concentration of K^+ will fall and a large natriuresis is avoided.

Intra-Renal Urea Recycling

The second source of dietary K^+ is from ingestion of animal organs (e.g., muscle and liver, which are rich in RNA). The principal anions that accompany this K^+ load are organic phosphates (which are ultimately metabolized to inorganic monovalent phosphate ($H_2PO_4^-$)) or sulfate anions. The key point here, is that unlike HCO_3^-, $H_2PO_4^-$ and sulfate anions do not augment the secretion of K^+ unless the concentration of Cl^- in luminal fluid in the CCD is very low.[57] There is, however, a symbiotic relationship with another constituent in the diet, protein, because when its constituent amino acids are oxidized, urea is produced.[104] The process of urea recycling aids the excretion of K^+ because it increases the number of liters of fluid that exit the terminal CCD.[76] Owing to the process of urea recycling, as calculated above, the flow rate in terminal CCD is increased by about 2-L per day.

CLINICAL TOOLS TO ASSESS THE CONTROL OF THE RENAL EXCRETION OF K^+

Examine the Rate of Excretion of K^+: There is no normal rate of K^+ excretion. Normal subjects in steady state excrete all the K^+ they eat and absorb from the GI tract. Therefore to assess the renal response in a patient with hyperkalemia, we use the expected rate of K^+ excretion in normal subjects who were given a K^+ load; these subjects could augment their rate of excretion of K^+ to greater than 200 mmol/day—this was achieved with only a minor increase in P_K.[46,105] Notwithstanding, to develop chronic hyperkalemia, there must be a defect in the renal excretion of K^+. Nevertheless, in the steady state, these patients will excrete all the K^+ they ingest and absorb that is not lost via non-renal routes. Therefore, a patient with chronic hyperkalemia and a rate of excretion of K^+ that is higher than the 'usual', has a defect in renal K^+ excretion; in addition, a large K^+ intake contributes to the degree of hyperkalemia in this patient.

To assess the rate of excretion of K^+, a 24-hr urine collection is not necessary. One can use the ratio of the concentrations of K^+ and creatinine in a spot urine sample ($U_K/U_{Creatinine}$) despite the diurnal variation in K^+ excretion.[95] This analysis is predicated on the fact that creatinine is excreted at a near-constant rate throughout the day.[106] Moreover, a $U_K/U_{Creatinine}$ in spot urines provides more relevant information because the stimulus to drive K^+ excretion (e.g., P_K) can be known at that time. The expected value in a patient with hyperkalemia is >20 mmol K^+/mmol creatinine (>200 mmol K^+/g creatinine).

The Transtubular K^+ Concentration Gradient (TTKG)

The TTKG was developed to provide a semi-quantitative reflection of the driving force to secrete K^+ in the CCD.[107,108] The lynch pin in this calculation was to adjust the concentration of K^+ in the urine (U_K) for the amount of water that is reabsorbed in downstream nephron segments (i.e., the MCD) to estimate the concentration of K^+ in the luminal fluid in the terminal CCD ($[K_{CCD}]$). To calculate the $[K_{CCD}]$, one divides the U_K by the ratio of urine osmolality (U_{Osm}) to the plasma osmolality (P_{Osm}) (i.e., U_{Osm}/P_{Osm}), as the P_{Osm} should be equal to the osmolality in the luminal fluid in the terminal CCD when vasopressin acts and AQP2 are present in the luminal membranes of the CCD.

The assumption made when using the U_{Osm}/P_{Osm} ratio to adjust for the amount of water that was reabsorbed in the MCD is that the majority of the osmoles delivered to the MCD were not reabsorbed in this nephron segment.[95] While, in the absence of a marked degree of contraction of the effective circulating volume, the amount of electrolytes reabsorbed in the MCD should not pose a problem, this is, however, not true for urea because of intra-renal urea recycling.[76] As estimated above, $\approx$600 mmol of urea are reabsorbed downstream from CCD per day. Therefore, the calculated $[K^+]_{CCD}$ obtained from $U_K/(U_{Osm}/P_{Osm})$ is likely to be appreciably higher than the actual value *in vivo* (same amount of K^+ but a larger volume of water in the terminal CCD). While adjustments in the calculation of the TTKG can be made to account for this error in subjects in whom the rate of excretion of urea is close to the usual (400 mmol/day), if the rate of excretion of urea deviates appreciably from its usual rate of excretion, one does not know the amount of urea that is recycled relative to the amount that is excreted, and hence an adjustment in the calculation to estimate $[K^+]_{CCD}$ is not possible. Furthermore, other factors may affect this process of urea recycling (e.g., vasopressin, ANG_{II}) which further complicates the interpretation of the TTKG. Therefore, we do not use the TTKG in the clinical assessment of patients with a dyskalemia, we think the $U_K/U_{Creatinine}$ provides the clinician with the information needed to assess the renal response in these patients.

CLINICAL APPROACH TO THE PATIENT WITH HYPERKALEMIA

A list of causes of hyperkalemia is provided in Table 51.2. The steps in the clinical approach to the patient with hyperkalemia are illustrated in Flow Charts 51.1–51.3.

Address Emergencies

It is imperative to recognize when hyperkalemia represents a medical emergency because therapy must take precedence over diagnosis. One must also anticipate the dangers associated with each mode of therapy and take steps to prevent them from occurring.

Hyperkalemia constitutes a medical emergency, primarily due to its effect on the heart.[109–111] To understand the effects of hyperkalemia on cardiac myocytes, we start from phase 4 of the action potential, the resting phase (associated with diastole). Since the cell membrane is most permeable to K^+ and relatively impermeable to other ions during this phase of action potential, the resting membrane potential (RMP) is determined by the K^+ equilibrium potential across the

TABLE 51.2 Causes of Hyperkalemia

- High intake of K^+
  - Only if combined with low excretion of K^+
- Shift of K^+ out of cells
  - Tissue breakdown (e.g., rhabdomyolsis), exhaustive exercise
  - Na/K-ATPase problem
    - Tissue hypoxia
    - Lack of a stimulus (e.g., inhibition of insulin release by α–adrenergic surge, use of non selective ß-blockers (small effect if only factor))
    - Inhibition of Na/K-ATPase (e.g., by drugs e.g., digoxin)
  - α-adrenergic surge
  - Hyperosmolality (e.g., administration of mannitol)
  - Metabolic acidosis due to acids that can not be transported on the nonocarboxylic acid cotransprter (e.g., HCl , citric acid)
  - Increase K^+ efflux from cells (administration of succinylcholine, floride intoxication)
  - Rare causes (e.g., hyperkalemic periodic paralysis)
- Diminished K^+ loss in the urine
  - Advanced chronic renal insufficiency
  - Low $[K^+]_{CCD}$ (diminished electrogenic reabsorption of Na^+ in the CCD)
    - Primary decrease in flux of Na^+ through ENaC
      - Very low delivery of Na^+ to the CCD
      - Low levels of aldosterone (e.g., Addison's disease,
      - Blockade of the aldosterone receptor (e.g., spironolactone)
      - Low ENaC activity (Type I pesudohypoaldosteronism)
      - Blockade of ENaC (e.g., amiloride, triamterene, trimethoprim-like drugs)
    - Cl^- reabsorbed at a similar rate as Na^+
      - Increased reabsorption of Na^+ and Cl^- in the distal convoluted tubule (e.g., Familial Hypertension with Hyperkalemia (WNK 4 or WNK1 mutations), drugs (e.g., calcineurin inhibitors), some patients with diabetic nephropathy and hyporeninemic hypoaldosteronism).
      - Increased electroneutral reabsorption of Na^+ and Cl^- in CCD due to Cl^- shunt in the CCD or parallel activity of the Cl/HCO_3 exchanger (pendrin) and the Na dependent Cl/HCO_3 exchanger (NDCBE) (e.g., some of the causes of hyporeninemic hypoaldosteronism)

FLOW CHART 51.1

INITIAL STEPS IN THE PATIENT WITH HYPERKALEMIA

The initial step in the clinical approach to the patient with hyperkalemia is to determine if there is an emergency that demands urgent therapy.
Source: Reproduced with permission (224).

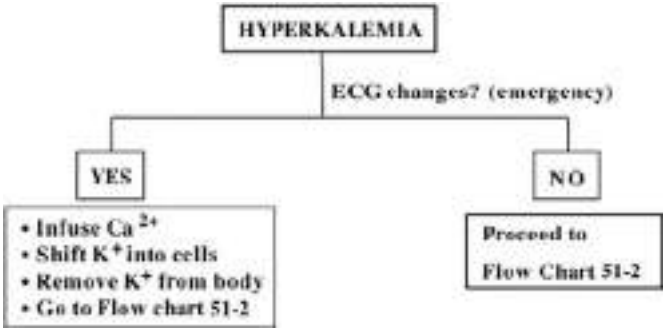

FLOW CHART 51.2

DETERMINE IF THERE IS A SHIFT OF K^+ OUT OF CELLS

Determine if a shift of K^+ out of cells is likely by assessing the time course for the rise in the P_K and whether there was little intake of K^+. If there is no reason to suspect a shift of K^+ out of cells, pseudohyperkalemia should be ruled out.
Source: Reproduced with permission (224).

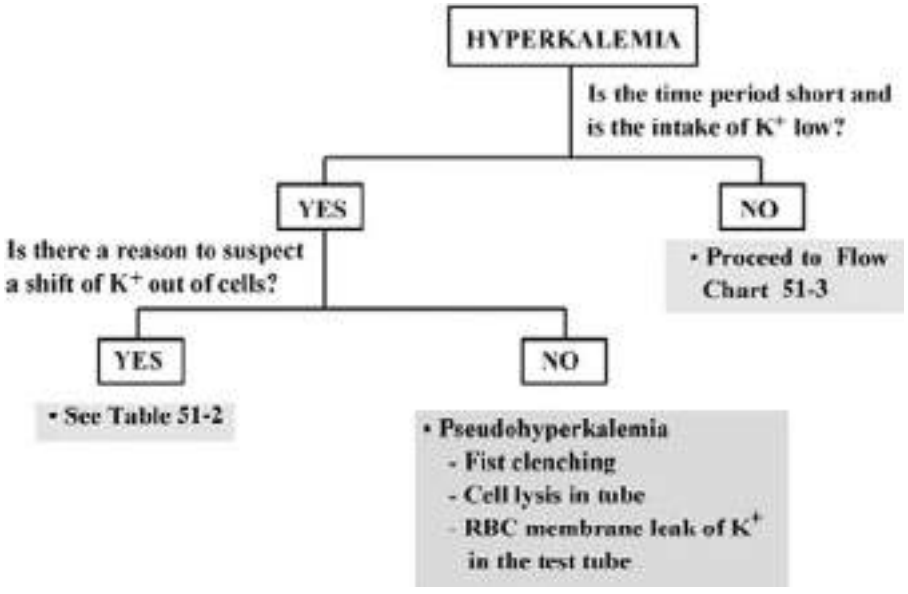

cell membrane. During hyperkalemia, the ratio of K_{in} to K_{out} will be reduced, the RMP will become less negative (i.e., the cell membrane will become depolarized). Stage 0 of action potential is the rapid depolarization phase. This phase is due to opening of the fast Na^+ channels causing a rapid increase in membrane conductance to Na^+ and thus a rapid influx of Na^+ ions into cells. The magnitude of Na^+ inward current

FLOW CHART 51.3

BASIS FOR THE LOW RATE OF EXCRETION OF K^+

Patients with chronic hyperkalemia can be divided into two groups based on their effective arterial blood volume. In this analysis, we assumed that there is an adequate distal delivery of Na^+.

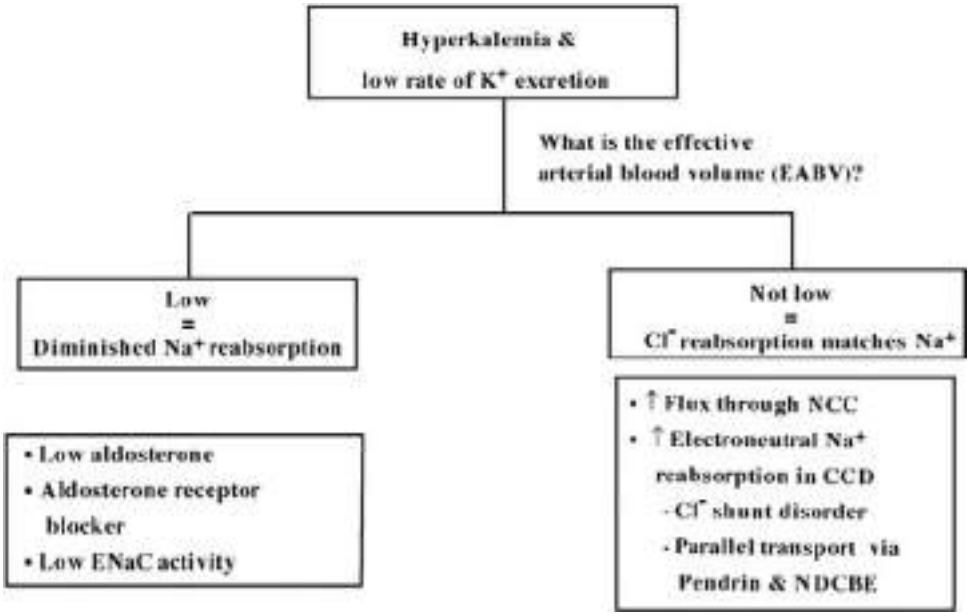

determines the rate of rise of action potential upstroke (Vmax), which determines the speed of impulse propagation. The ability of the cell to open the fast Na^+ channels during phase 0 is related to the membrane potential at the onset of depolarization. If RMP is less negative, fewer Na^+ channels become activated during depolarization, thus the magnitude of the inward Na^+ current and the V_{max} of the action potential diminishes. The decrease in V_{max} results in a reduction in myocardial conduction, with progressive prolongation of the P wave, PR interval, and QRS complex. V_{max} is greatest when RMP is about -75 mV, RMP that is associated with 50% reduction in V_{max} is -65 mV (a rise in plasma K from 4–5 mmol/L to 8–10 mmol/L).

The rapid delayed rectifier K channel (I_{Kr}) is mostly responsible for the efflux of K^+ seen during phase 3 of the cardiac action potential; the rapid repolarization phase. For reasons that are not well understood, the I_{Kr} current is sensitive to extracellular K^+ levels; as extracellular K^+ rises, K^+ conductance through these channels increases, so that more K^+ leave the myocytes in a given time period. This leads to shortening of the repolarization time, which is thought to be responsible for some of the electrocardiographic manifestations observed with a modest degree of hyperkalemia such as ST-T segment depression, peaked T waves and QT shortening.

The earliest ECG manifestations of hyperkalemia include the appearance of narrow based, peaked "tent shaped" symmetrical T waves. These T waves are of relatively short duration, which help distinguish them from the broad T waves typically seen in patients with myocardial infarction or intra-cerebral accidents.[112] Peaked T waves are usually seen at K^+ concentration of >5.5 mM.

As serum K^+ increases to >6.5 mM, the manifestations of slow cardiac conduction become apparent: broad flat P wave (delayed sino-atrial conduction), prolonged PR interval (delayed atrioventricular conduction), wide QRS complex (delayed intra-ventricular conduction). The QRS complex may take the appearance of right or left bundle branch block. A clue that these electrocardiographic changes are due to hyperkalemia and not bundle branch disease is that in hyperkalemia the conduction delay persists throughout the QRS complex and not just in the initial portion (as in left bundle branch block) or in the terminal portion (as in right bundle branch block). Also, the width of T wave is close to that of QRS complex. In intraventricular conduction abnormalities due to other

causes or in ventricular ectopic rhythm, the T wave is much wider than the QRS complex.

As K^+ levels reach 8–9 mmol/L, there are absent P waves indicating atrial arrest. The QRS complex continues to widen and eventually blends with the T wave producing the classical sine wave. The SA node may continue to stimulate the ventricle without evidence of atrial electrical activity producing a sino-ventricular rhythm. As hyperkalemia worsens and the K^+ level reaches 10 mEq/L, sino-ventricular conduction no longer occurs, ventricular fibrillation and asystole are imminent.

It is important to note that this correlation between the absolute level of P_K and the ECG changes is based largely on experiments with the acute infusion of K^+ in animals. There is large variability among patients in the absolute P_K leading to ECG changes and cardiac toxicity of hyperkalemia.[113] Variables include the rapidity of the onset of hyperkalemia,[111,114] underlying cardiac disease, and the presence or absence of hypocalcemia, acidemia, and/or hyponatremia. In a retrospective review of the frequency of ECG changes in patients with hyperkalemia,[115] the ECG had poor sensitivity for diagnosing hyperkalemia, with only 55% of patients with plasma K^+ >6.8 mmol/L manifested peaked T waves. Notwithstanding, 14 out of 90 patients in this case series developed cardiac arrhythmia or cardiac arrest, a number of them did not have any ECG changes on their initial presentation. Therefore, it is our view that severe hyperkalemia, i.e., P_K >7.0 mmol/L should be treated as an emergency with maneuvers to induce a shift of K^+ into cells; even in the absence of ECG changes, and perhaps at even lower P_K (e.g., >6.5 mmol/L) in the presence of hypocalcemia, acidemia and/or hyponatremia.

Determine if the Cause of the Hyperkalemia is a Shift of K^+ out of Cells *In Vivo* or *In Vitro*

Is the time period short and/or has the intake of K^+ been low?

If the answer is yes, there are three options to consider:

There Is Destruction of Cells in the Body

In this case, the diagnosis is usually obvious (e.g., crush injury).

There Is a Shift of K^+ out of Cells in the Body

This may occur in conditions in which there is a less negative voltage in cells. This may be due to tissue hypoxia affecting the Na-K-ATPase (conditions causing hypoxic lactic acidosis), lack of a stimulus for Na-K-ATPase (e.g., lack of insulin in patients with diabetic ketoacidosis, α-adrenergic surge causing inhibition of the release of insulin or directly causing a shift of K^+ out of cells, β_2-adrenergic blockade especially under conditions of α-adrenergic surge). A shift of K^+ may also occur in conditions of metabolic acidosis due to non- monocarboxylic acids, i.e., acids that can not be transported on M-CT (e.g., metabolic acidosis due to a gain of HCl acid owing to loss of $NaHCO_3$ in a patient with diarrhea, ingestion of citric acid[35]). Digoxin inhibits Na-K-ATPase, digoxin overdose can result in hyperkalemia.[116] Bufadienolide, a structurally similar glycoside, is present in high concentration in the skin and venom gland of the toad *Bufo marinus*. The ingestion of such toads or their extracts can result in fatal hyperkalemia.[117] Several cases of hyperkalemia have been reported after the ingestion of certain herbal aphrodisiac pills containing large amounts of toad venom. The stems, leaves, flowers and roots of yellow oleander contain high concentration of cardiac glycosides, ingestion of yellow oleando for deliberate self-harm has been reported especially in South Asia.[118] Acute hyperkalemia may occur during exhaustive exercise or status epilepticus.[119] Severe hyperkalemia has been described as a complication of the administration of mannitol for the treatment or prevention of cerebral edema.[120,121] Succinylcholine depolarizes muscle cells, resulting in the efflux of K^+ through acetylcholine receptors in conditions that may lead to up-regulation of acetylcholine receptors.[122] Floride can open the Ca^{2+} sensitive K^+ channel,[123] floride intoxication can lead to fatal hyperkalemia.[124] A positive family history for acute hyperkalemia suggests that there may be a molecular basis for this disorder (e.g., hyperkalemic periodic paralysis).

Pseudohyperkalemia May Be Present

Pseudohyperkalemia is caused by the release of K^+ during or after venipuncture.[125] Excessive fist clenching during blood sampling may increase K^+ release from local muscle and thus raise the measured P_K.[126,127] Pseudohyperkalemia can be present in cachectic patients because the normal T-tubule architecture in skeletal muscle may be disturbed. This permits more K^+ to be released into venous blood, even without excessive fist clenching during blood sampling. Thrombocytosis (especially megakaryocytosis),[128] leukocytosis (especially due fragile leukemia cells)[129,130] and/or erythrocytosis may cause pseudohyperkalemia due to release of K^+ from cells.[131,132] Cooling of blood prior to the separation of cells from plasma is a recognized cause of pseudohyperkalemia.[133] There are several hereditary subtypes of pseudohyperkalemia, caused by an increase in the passive K^+ permeability of erythrocytes. The P_K increases in blood samples from these patients that have been left at room temperature. Interestingly, eleven pedigrees of

patients with autosomal dominant hemolysis and pseudohyperkalemia were found to have single point mutations in the anion exchanger, AE1.[134] These mutations reduce anion transport in red cells and convert AE1 to a non-selective cation channel.

Is the Rate of Excretion of K^+ High Enough in a Patient with Hyperkalemia?

In a patient with chronic hyperkalemia, pseudohyperkalemia should be first ruled out. To assess the renal response in a patient with hyperkalemia, we use the expected rate of K^+ excretion in normal subjects who were given a K^+ load; these subjects could augment their rate of excretion of K^+ to greater than 200 mmol/day—this was achieved with only a minor increase in P_K.[46,105] Patients with chronic hyperkalemia have a defect in K^+ excretion (i.e., they excrete much less than 200 mmol K^+/g creatinine or 20 mmol K^+/mmol creatinine in their urine).

In a Patient with Chronic Hyperkalemia, Determine the Basis for the Low $U_K/U_{Creatinine}$

There are two possible mechanisms for a lower than expected U_K/U_{Cr} in a patient with hyperkalemia. First, the most common mechanism is a less negative voltage in the lumen of the CCD due to a lower rate of electrogenic reabsorption of Na^+ in the CCD (Figure 51.5). Second, even if a lumen-negative voltage could be generated, the secretion of K^+ might still be low if there were too few ROMK channels with a high open-probability in the luminal membrane of the CCD. While no diseases have been directly attributed to this pathophysiology, we must still include it in the differential diagnosis.

There are two major categories of disorders that lead to a low lumen-negative voltage in CCD: Disorders that lead to a diminished rate of reabsorption of Na^+ via ENaC, and disorders that lead to reabsorption of Na^+ and of Cl^- in CCD occurring at near equal rates.

Diminished Reabsorption of Na^+ via ENaC in the CCD

The first subgroup with this pathophysiology consists of patients who have a marked decrease in the effective arterial blood volume; these patients may have a sufficiently very low delivery of Na^+ to the CCD to limit the rate of secretion of K^+. The hallmark for this diagnosis is the excretion of urine with a very low concentration of Na^+. The second subgroup consists of patients who have lesions that lead to a diminished number of open ENaC units in the luminal membrane of principal cells in the CCD. Accordingly, the reabsorption of Na^+ cannot occur at high enough rate to generate a large lumen-negative voltage in the CCD. The basis of this lower rate of reabsorption of Na^+ includes low $P_{Aldosterone}$ levels (e.g., adrenal insufficiency), blockade of the aldosterone receptor in principal cells, molecular defects that diminish the number of ENaC units in the luminal membrane of the CCD, the presence of cationic compounds in the lumen of the CCD that block ENaC (e.g., the use of the potassium-sparing diuretics amiloride or triamterene or cationic antimicrobial agents such as trimethoprim). These patients have a low effective arterial blood volume and a higher than expected rate of excretion of Na^+ and Cl^- in the presence of a low effective arterial blood volume, and a high $P_{Renin\ mass}$ (with the exception of the patients with hyporenenimic hypoaldosteronism due to decreased production of renin). The $P_{Aldosterone}$ is helpful to determine the reason for the diminished Na^+ reabsorption via ENaC in the CCD.

Reabsorption of Na^+ and Cl^- at Near-Equal Rates in the CCD

In one subgroup of patients with this pathophysiology, the site of the lesion might be in the early DCT where there is enhanced electroneutral reabsorption of Na^+ and Cl^- via NCC. Accordingly, the delivery of Na^+ and Cl^- to the CCD is not sufficiently large to permit the rate of reabsorption of Na^+ to exceed the rate of reabsorption of Cl^- in the CCD by an appreciable amount. In addition, there is a diminished number of open ENaC units in the luminal membranes of principal cells in CCD because of the suppression of release of aldosterone by an expanded effective arterial blood volume. These patients are expected to have a rise in K^+ excretion with the administration of a thiazide type diuretic.

In another subgroup of patients, the defect might be due to enhanced electroneutral reabsorption of NaCl in CCD. The term "chloride shunt disorder" has been coined to describe this pathophysiology, implying that perhaps there is increased permeability for Cl^- through the paracellular pathway.[135] Given the large concentration difference for Cl^- and the relatively small transepithelial voltage difference, if there were increased paracellular permeability for Cl^-, perhaps the movement of Cl^- would be into instead of out of the lumen of the CCD. The defect could also be one of increased electroneutral reabsorption of NaCl by the parallel activity of the Na^+-dependent Cl^-/HCO_3^- exchanger (NDCBE) and the Na^+ independent Cl^-/HCO_3^- exchanger; pendrin.[60] Nevertheless, this transport mechanism has been detected in the cortical collecting duct; to play a role in modulation of K^+ secretion it needs to be expressed in the late

distal tubule and/or the connecting segment. Patients with this pathophysiology of enhanced electroneutral reabsorption of NaCl in the CCD, are expected to have a rise in K^+ excretion with increasing the delivery of HCO_3^- to CCD, e.g., induced with administration of acetazolamide.

SPECIFIC CAUSES OF HYPERKALEMIA

A list of the causes of hyperkalemia based on their possible underlying pathophysiology is provided in Table 51.2 and a list of drugs that may cause hyperkalemia is shown in Table 51.3.

Chronic Renal Insufficiency

Hyperkalemia occurs frequently in patients with advanced, chronic kidney disease and it is due to a diminished ability to excrete K^+. There are two major reasons that lead to a diminished rate of excretion of K^+. First, decreased flow rate in the terminal CCD. In more detail, flow rate in terminal CCD is directly related to the number of luminal osmoles in the lumen of terminal CCD when vasopressin acts.[95] The major osmoles in terminal CCD are urea and $Na^+ + Cl^-$. The number of osmoles of $Na^+ + Cl^-$ in the terminal CCD may be diminished because of dietary salt restriction and/or the use of diuretics that may induce decreased effective arterial blood volume. The number of urea osmoles in the terminal CCD may be decreased because of dietary protein restriction and also diminished intra-renal urea recycling owing to medullary interstitial disease involving the inner MCD. The second reason for diminished rate of excretion of K^+, is a low $[K^+]_{CCD}$. Two factors may contribute to this low $[K^+]_{CCD}$. Although the flow rate in the CCD may be decreased, as there is a very large reduction in the number of residual functioning nephrons in these patients, the flow rate through each remaining CCD segment may be very high. When the flow rate per CCD is high, the ability to reabsorb more Na^+ than Cl^- in the CCD is diminished and the lumen-negative voltage may not be high enough to raise the $[K^+]_{CCD}$ sufficiently. In addition, these patients may be taking drugs that compromise the ability to excrete K^+. Prominent on the list are drugs that diminish the secretion of aldosterone (ACE-inhibitors or angiotensin II receptor blockers) and aldosterone receptor blockers (e.g., spironolactone). The degree of hyperkalemia will obviously be more severe when the intake of K^+ is particularly high, due for example to the intake of salt substitutes that contain KCl or the ingestion of a large volume of fruit juice.[136]

TABLE 51.3 Drugs that can Cause Hyperkalemia

- **Drugs containing K** (only increase P_K if K^+ excretion is compromised)
  - KCl tablets, salt substitutes
- **Drugs causing a K shift from ICF to ECF**
  - Cell depolarizers such as succinylcholine
  - Drugs that inhibit Na/K ATPase e.g., digitalis overdose
  - Chemotherapy causing tumor lysis
  - Drugs impairing insulin release from β-cells such as α-adrenergic agonists, octreiode
  - β_2-adrenergic receptor blockers
- **Drugs which interfere with K excretion in the urine:**
  - Drugs that cause acute renal failure or interstitial nephritis
  - Drugs that inhibit the release of renin e.g., NSAIDs
  - Drugs that inhibit the release of aldosterone (e.g., heparin)
  - Drugs that interfere with the renin- ANG_{II} axis (e.g., direct renin blockers, converting enzyme inhibitors and ANG_{II} receptor blockers)
  - Aldosterone receptor blockers (e.g., spironolactone)
  - Drugs that block ENaC in the CCD (e.g., amiloride, trimethoprim)
  - Drugs the interfere with activation of ENaC via proteolytic cleavage (e.g., nafamostat mesylate)

Addison's Disease[137]

The most common cause of this disorder used to be bilateral adrenal destruction due to tuberculosis, but now autoimmune disease either as an isolated disorder or as part of polyglandular endocrinopathy accounts for the majority of cases.[138] HIV is now the most important infectious cause of adrenal insufficiency,[139] with CMV the most likely cause in this setting. Nevertheless, the list includes other infectious diseases including disseminated fungal infections. Additional causes of Addison's disease include adrenal infiltration by amyloidosis, metastatic carcinoma or lymphoma, adrenal hemorrhage or infarction, as may occur in patients with the anti-phospholipid antibody syndrome,[140] and drugs that impair the synthesis of aldosterone (e.g. heparin, ketoconazole[141] and possibly fluconazole).

Patients with chronic primary adrenal insufficiency may present with chronic malaise, fatigue, anorexia, generalized weakness, and weight loss. Salt craving is a distinctive feature in some patients. Hyperpigmentation is evident in nearly all patients. In most patients, the blood pressure is low and postural symptoms of dizziness and syncope are common. The P_K is usually close to 5.5 mmol/L, unless a significant degree of intravascular volume depletion diminishes the flow rate in CCD, leading to a more severe degree of hyperkalemia. Nevertheless, hyperkalemia is not seen on presentation in approximately one third of the cases.[142] The absence of hyperkalemia in such a large percentage of patients is probably due to a low dietary K^+ intake. Other possible abnormal laboratory findings

include hyponatremia, hyperchloremic metabolic acidosis, hypoglycemia, and eosinophilia. Some patients may present with acute adrenal crisis and shock.

The diagnosis can be established by finding a low $P_{Aldosterone}$ and $P_{Cortisol}$, high $P_{Renin\ mass}$, and a blunted cortisol response to the administration of ACTH.

Adrenal crisis is an emergency that requires immediate restoration of the intravascular volume with administration of intravenous saline and correction of the cortisol deficiency with the administration of dexamethasone or hydrocortisone. Beware of raising the P_{Na} too rapidly if hyponatremia is present because of the risk of osmotic demyelination in a catabolic patient.[143] The administration of cortisol can lead, indirectly, to a fall in the circulating level of vasopressin.[144] We prefer to give dDAVP at the outset of therapy to avoid a large water diuresis that could result in a sudden and excessive rise in the P_{Na}.

Patients with chronic adrenal insufficiency should receive replacement therapy with both a glucocorticoid and a mineralocorticoid. For the former, 25 mg of hydrocortisone (15 mg in the morning and 10 mg in the afternoon) is usually given. For mineralocorticoid replacement, fludrocortisone in a single dose of 50 to 200 μg is usually used. Dose adjustments are made based on patients' symptoms, ECF volume status, the blood pressure and the P_K.

Hyperkalemia Due to Inherited Disorders of Aldosterone Biosynthesis

The inherited enzymes deficiency involved in aldosterone biosynthesis include 21-hydroxylase, 3-hydroxysteroid dehydrogenase, cholesterol desmolase and aldosterone-synthetase deficiency. Except for aldosterone-synthetase deficiency, the other three disorders (also called congenital adrenal hyperplasia) are combined with glucocorticoid deficiency because the cortisol biosynthesis is also affected in these three disorders.[145] Salt wasting, hyponatremia, hyperkalemia and hypotension are common features. Among them, 21-hydrolyase deficiency is the most common, and more easily recognized in affected females who usually have masculine-type genitalia at birth due to excess secretion of fetal adrenal androgen. The diagnosis is confirmed by the findings of elevated serum 17-hydroxyprogesterone, the substrate for the absent enzyme. Patients with 3-hydroxysteroid dehydrogenase and cholesterol desmolase deficiency usually have the signs of sex steroid deficiency, which distinguishes them from patients with 21-hydrolyase deficiency who have manifestations of androgen excess. In patients with aldosterone-synthetase defects, aldosterone synthesis is decreased but corticosterone secretion is enhanced and its concentration in serum is elevated. Aldosterone-synthetase defects can be divided into two types: Type I corticosterone methyl oxidase (COMI) defect and type II corticosterone methyl oxidase (COMII) defect.[146] Serum 18-hydroxycorticosterone is deficient in patients with COMI defect, but increased in patients with COMII defect.

Pseudohypoaldosteronism Type I

The underlying pathophysiology in patients with pseudohypoaldosteronism type 1 (PHA-1) resembles "closed" ENaC in the luminal membrane of principal cells in the CCD. There are two different forms of this disorder with two different modes of inheritance.

Autosomal Dominant Disorder: This is due to loss of function mutations involving the mineralocorticoid receptor.[147] The clinical disorder is usually mild and often remits with time.

Autosomal Recessive Form: This results from various mutations involving all the three subunits of ENaC.[148] Unlike the autosomal dominant form of PHA-1, the disease is permanent, and does not improve in adulthood. Patients usually present in the neonatal period with renal salt wasting, hyperkalemia, metabolic acidosis, failure to thrive, and weight loss. ENaC activity is also impaired in the lung and this leads to excessive airway fluid and recurrent lower respiratory tract infections.

Patients fail to respond to exogenous mineralocorticoids and their $P_{Aldosterone}$ and $P_{Renin\ activity}$ are markedly elevated. Treatment includes supplementation with NaCl and inducing the loss of K^+ through the GI tract. Dialysis may be required for treatment of life-threatening hyperkalemia.

Syndrome of Hyporeninemic Hypoaldosteronism

Patients with this syndrome represent a heterogeneous group with regard to the pathophysiology of their disorder.

A Group with Low Capability of Producing Rennin: The basis of this group of disorders may be destruction of, or a biosynthetic defect in the juxtaglomerular apparatus, that leads to a low $P_{Renin\ mass}$ and thereby to a low $P_{Aldosterone}$.[149,150] Accordingly, there is a less negative luminal voltage in CCD due to less ENaC activity and hence a lower rate of reabsorption of Na^+ in CCD. These patients will tend to have low effective arterial blood volume. Patients with this disorder are expected to have a significant rise in their U_K/U_{Cr} with the administration of exogenous mineralocorticoids.

A Group with Low Stimulus to Produce Rennin: A subset of these patients are those with "Familial

Hyperkalemia with Hypertension" (also known as Pseudohypoaldosteronism type II (PHA-II) or Gordon's syndrome). Patients with this disorder behave like a gain-of-function in the thiazide-sensitive NCC with enhanced reabsorption of Na^+ and Cl^- in DCT;[58] the molecular defects leading to this disorder are discussed below.

This enhanced upstream reabsorption of Na^+ and Cl^- results in a low delivery of Na^+ and Cl^- to the CCD, which compromises the ability of this nephron segment to reabsorb more Na^+ than Cl^-, and thereby leads to a diminished excretory capacity for K^+. ECF volume expansion is a hallmark of the pathophysiology and it results in a low $P_{Renin\ mass}$, and thereby a lower than expected $P_{Aldosterone}$ given the hyperkalemia. Accordingly, these patients are not expected to have an appreciable rise in their U_K/U_{Cr} with exogenous mineralocorticoids, but their hyperkalemia should resolve with the administration of thiazide diuretics (higher Na^+ and Cl^- delivery to the CCD, and more reabsorption of Na^+ than Cl^- in CCD if more ENaC are open due to release of renin and aldosterone as the intravascular volume becomes less expanded).

A similar set of clinical findings to those described above but without a known molecular lesion may occur in other patients, most commonly patients with diabetic nephropathy.[149] Support is given to the hypothesis that suppression of renin release in these patients is the result of volume expansion by the findings that circulating atrial natriuretic peptide blood levels are elevated in these patients,[151] and many will respond to either $NaCl^-$ restriction or to furosemide with an increased P_{Renin} activity.[151,152] A similar pathophysiology (i.e., that suppression of renin release is due to intravascular volume expansion) has been suggested in patients with chronic renal failure[153] and patients with lupus nephritis with hyperkalemia and hyporeninemic hypoaldosteronism.[154] The basis of the disorder remains to be established. It is possible that the reabsorption of Na^+ and Cl^- may be augmented in the DCT akin to patients with "Familial Hyperkalemia with Hypertension". Interesting in this regard with respect to patients with type II DM, who may have hyperinsulinemia and the metabolic syndrome, is that chronic insulin infusion in rats is associated with the retention of NaCl due to its enhanced reabsorption in different nephron segments including the DCT and with less WNK4 expression in the renal cortex.[155] Furthermore, Obese Zuker rats were shown to be more sensitive to thiazides than their lean counterparts with a greater natriuresis , kaliuresis and drop in BP on thiazides.[156] Reduced renal cortical expression of WNK4 was also observed in this model. It is also interesting to note that work in cell culture indicates the involvement of PI3-kinase in activating WNK-1.[89] As mentioned above, WNK1 up-regulates NCC by blocking the inhibitory form of WNK4 or via phosphorylation of SPAK/ORS1.

It is also possible that ECF volume expansion and hyperkalemia in these patients may reflect an increased electroneutral NaCl reabsorption in CCD, perhaps a "Cl shunt" disorder[135]or possibly increased electroneutral reabsorption of NaCl by the parallel activity of the Na^+-dependent Cl^-/HCO_3^- exchanger (NDCBE) and the Na^+ independent Cl^-/HCO_3^- exchanger; pendrin[60] Patients with this pathophysiology of enhanced electroneutral reabsorption of $Na^+ + Cl^-$ in the CCD, are expected to have a rise in K^+ excretion with induction of bicarbonaturia (e.g., administration of acetazolamide).

Differentiation between these two groups of patients with hyporeninemic hypoaldosteronism has implications for therapy. The use of exogenous mineralocorticoids (9 α-fludrocortisone) is of benefit for the first group of patients as it results in both a kaliuresis and re-expansion of the intravascular volume due to retention of Na^+. Diuretic therapy would pose a threat to these patients because it would cause a more severe degree of decreased effective arterial blood volume. In contrast, mineralocorticoids may aggravate the hypertension in those who have excessive reabsorption of Na^+ and Cl^- in the DCT. In this group of patients, the administration of a thiazide diuretic to inhibit NCC should enhance the kaliuresis and lower the blood pressure. The administration of diuretics to patients with enhanced electroneutral Na^+ and Cl^- reabsorption in the CCD may increase their rate of excretion of K^+ by increasing the flow rate in the CCD. The activity of K^+ secretion may be increased by inducing bicarbonaturia; loss of HCO_3^- may have to be replaced to avoid the development of metabolic acidosis.

Familial Hyperkalemia with Hypertension

The term pseudohypoaldosteronism type II (PHAII) is misleading from a physiologic perspective because patients with this syndrome have salt retention and hypertension, findings associated with more rather than with less aldosterone effect.

The cause for increased reabsorption of Na^+ and Cl^- in the DCT in this disorder has been clarified recently.[58] Major deletions in the gene encoding for WNK kinase-1 and missense mutations in WNK4 were reported in these patients. When activated by ANG_{II}, WNK4 normally causes an increased luminal NCC phosphorylation and thus activity through SPAK/OSR1 (Figure 51.8).[157] PHAII-WNK4 mutants activate NCC *in vivo* by enhancing the SPAK/OSR1-NCC phosphorylation signaling,[158] an effect which is not further augmented by ANG_{II}, consistent with gain-of-function

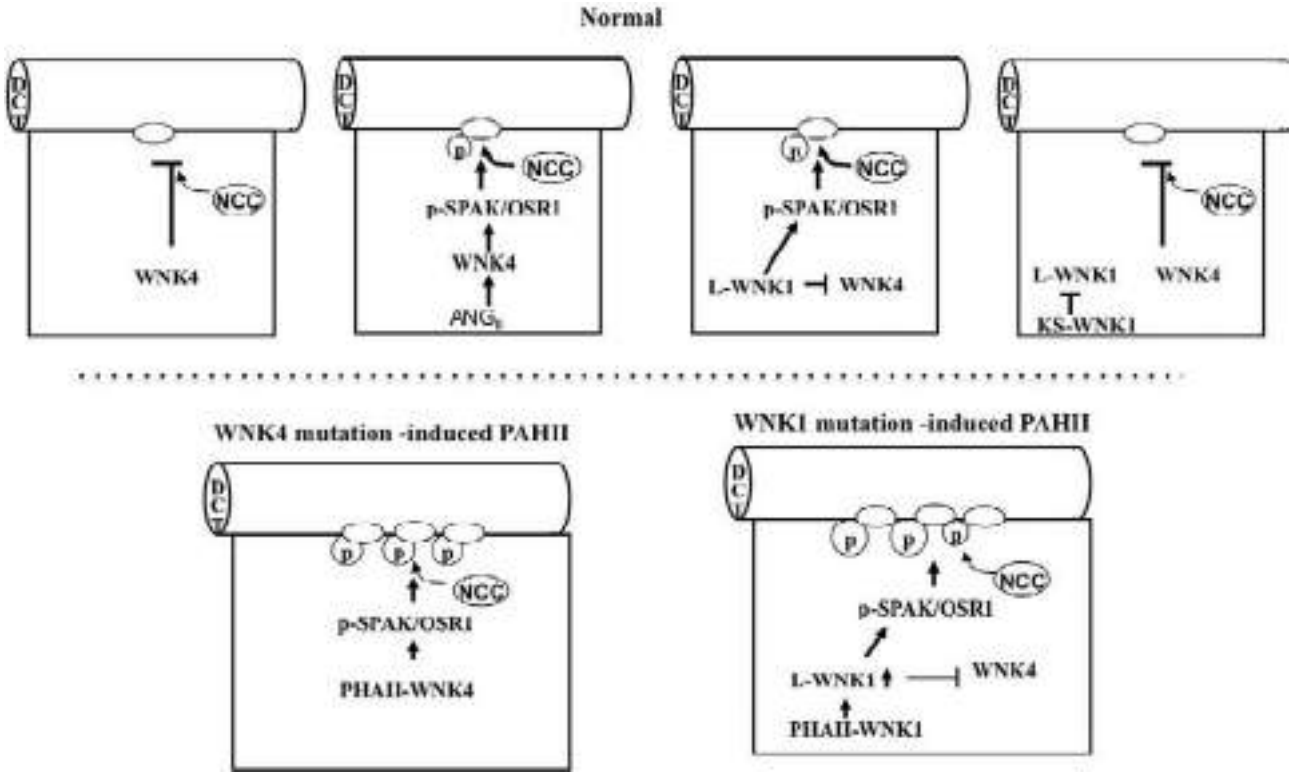

FIGURE 51.8 **Mutations in WNK kinases causing "Familial Hyperkalemia with Hypertension".** WNK4 is thought to inhibit NCC activity by reducing its plasma membrane abundance, by diverting post-Golgi NCC to the lysosome for degradation. When activated by ANG_{II}, WNK4 normally causes an increased luminal NCC phosphorylation and thus activity through SPAK/OSR1. WNK1-L up-regulates NCC by blocking the inhibitory form of WNK4 or by phosphorylation of SPAK/ORSI. WNK1-S has a dominant-negative effect on WNK1-L. PHAII-WNK4 mutants activate NCC *in vivo* by enhancing the SPAK/OSR1- NCC phosphorylation signaling, an effect which is not further augmented by ANG_{II}, consistent with gain-of-function mutations resulting in constitutive activation of the signaling pathway. When the intron1 of WNK1 gene is deleted, both WNK1-L and WNK1-S are increased in DCT and the imbalance of the WNK1-L/WNK1-S ratio leads to an activation of the NCC.

mutations resulting in constitutive activation of the signaling pathway. Thus, reabsorption of Na^+ and Cl^- by NCC in the DCT will be augmented.

The molecular defect in WNK1 is a removal of intron bases that leads to NCC activation (gain of function). There are two isoforms of WNK1; a ubiquitous full-length (WNK1-L) and a kidney-specific, WNK1 lacking the kinase domain (WNK1-S).[159] WNK1-L has an antagonistic effect on the inhibitory form of WNK4, and can also activate SPAK/OSR1-NCC signaling pathway.[93] WNK1-S has a dominant-negative effect on WNK1-L. When the intron 1 of WNK1 gene is deleted, both WNK1-L and WNK1-S are increased in DCT and the imbalance of the WNK1-L/WNK1-S ratio leads to an activation of the NCC.

The higher activity of the thiazide-sensitive NCC could explain the hypertension, hyperkalemia, and the suppressed $P_{Renin\ mass}$ that are common features in this disorder. Because of the enhanced reabsorption of Na^+ and Cl^- via NCC in the DCT, the delivery of Na^+ and Cl^- to the CCD is not sufficiently large to permit the rate of reabsorption of Na^+ to exceed the rate of reabsorption of Cl^- in the CCD by an appreciable amount. In addition, there is a diminished number of open ENaC units in the luminal membranes of principal cells because of the suppression of release of aldosterone by an expanded effective arterial blood volume. The overall result is to cause low luminal negative voltage in the CCD and the development of hyperkalemia. The increased NCC activity in these patients accounts for the marked fall in blood pressure in some patients who are treated with thiazide diuretics.[160]

Hyperkalemic Periodic Paralysis

The defect in this disorder seems to be in the regulation of a specific population of Na^+ channels (the tetrodotoxin sensitive Na^+ channels) in the cell membrane. This syndrome has an autosomal dominant inheritance

and is the result of a mutation in the α-subunit of the skeletal muscle Na^+ channel gene ($Na_v1.4$ encoded by *SCN4A gene*).[24] When the muscle is stimulated to contract, Na^+ influx depolarizes the cell. As the resting membrane potential approaches -50 mV, normal Na^+ channels close. In patients with hyperkalemic periodic paralysis, these defective Na^+ channels fail to close, the persistent Na^+ influx leads to membrane depolarization and drives an outward efflux of K^+ into the ECF compartment, causing hyperkalemia. Depending on the absolute voltage, lesser changes may result in myotonia, while larger changes can cause paralysis. Weakness is triggered by a variety of circumstances including rest after exercise, K^+-rich food, cold environment, emotional stress and fasting. Acute attacks of hyperkalemic periodic paralysis can be treated by inducing a shift of K^+ into cells with $ß_2$-adrenergics.[161] Inducing a large K^+ loss should be avoided. Acetozolamide seems to be effective in prevention of recurrence of attacks, though its mechanism of action is not clear.

Drugs Associated with Hyperkalemia

In general, drugs that cause hyperkalemia can be classified into those that affect the shift of K^+ into cells and those that impair the renal excretion of K^+.

Drugs that Affect Cellular Redistribution of K^+

Non-selective ß-adrenergic blockers may diminish the $ß_2$-adrenergic mediated shift of K^+ into cells.[162] In general, only a minor rise in the P_K is observed. Nevertheless, more significant degrees of hyperkalemia may develop after vigorous exercise[163] or the intake of drugs that may impair the excretion of K^+ by the kidney.

Digitalis overdose may be accompanied by hyperkalemia as a result of the inhibition of the Na-K-ATPase pump.[164,165]

The use of depolarizing agents such as succinylcholine during anesthesia may cause a shift of K^+ from cells and cause hyperkalemia.[122] The hyperkalemic effect of succinylcholine is more pronounced in patients with conditions that may lead to up-regulation of acetylcholine receptors in skeletal muscles such as neuromuscular injury (upper or lower motor neuron lesion), immobilization, muscle inflammation, muscle trauma or burn injury.[166]

Arginine hydrochloride used in the treatment of hepatic coma and severe metabolic alkalosis[167,168] and epsilon-aminocaproic acid,[169] a synthetic amino acid structurally similar to lysine and arginine used to treat severe hemorrhage also causes an efflux of K^+ from cells, resulting in life-threatening hyperkalemia, especially in patients with impaired renal function.

Hyperkalemia may also result from inhibition of insulin secretion by the somatostatin agonist octreotide.[170]

Impaired K^+ redistribution via the activation of the K^+ channel by fluoride poisoning[171,172] leads to life-threatening hyperkalemia and may be ameliorated by the administration of quinidine and amiodarone.[173]

Drugs that Interfere with Renal K^+ Excretion

Drugs that Inhibit the Release of Renin; Non-Steroidal Anti-Inflammatory Drugs (NSAIDS): Secretion of renin by cells in the afferent glomerular arterioles and by cells of the macula densa in the early DCT appears to be mediated in part by locally produced prostaglandins via COX-2.[174] As a result, prostaglandin synthesis inhibition can lead to low $P_{Renin\ mass}$ and low $P_{Aldosterone}$.[175,176] NSAIDs also blunt the adrenal response to hyperkalemia, which is at least partially dependent on prostaglandins. It is not surprising that COX-2 inhibitors produce identical effects to those of non-selective NSAIDS.[177,178] The rise in the P_K is small in normal subjects, but a significant degree of hyperkalemia may develop in the presence of certain diseases or with the intake of drugs that may impair the renal excretion of K^+.

Drugs that Interfere with the Renin-Angiotensin-Aldosterone Axis

Direct Renin Blockers, Angiotensin Converting Enzyme (ACE) Inhibitors and Angiotensin II Receptor Blockers: The two major stimuli for the release of aldosterone are ANG_{II} and an increase in the P_K. The effect of hyperkalemia to stimulate the release of aldosterone acts in concert with ANG_{II} that is generated locally within the adrenal glomerulosa.[179] Blocking both of these actions is expected to reduce aldosterone secretion and thereby impair the renal excretion of K^+. Of note, however, aldosterone levels are not fully suppressed in patients on chronic therapy with ACE inhibitors.[180] Furthermore, there are no reported studies that examined the effect of exogenous mineralocorticoids on the renal excretion of K^+ in patients who develop hyperkalemia while on drugs that block the renin-angiotensin-aldosterone system (RAAS).

Notwithstanding, as show in Table 51.1, hyperkalemia will likely not occur, even if there is a large reduction in TE voltage in the CCD unless there is decreased flow rate in the terminal CCD. A deficiency of actions of ANG_{II} may diminish intra-renal urea recycling by reducing urea reabsorption in the inner MCD as A_{II} stimulates the transport of urea in the inner MCD in the presence of vasopressin,[181] or

possibly by decreasing vasoconstrictor tone to blood vessels that descend into the renal medulla, and thereby wash urea out of the deeper region of the outer medulla as a result of diminishing the driving force for urea entry into the descending thin limbs of superficial nephrons. Hence, the hyperkalemia seen in some patients on ACE inhibitors or ARBs may be due to a combination of diminished electrical driving force for the net secretion of K^+ in the CCD and a diminished rate of flow in the terminal CCD due to a decrease in urea recycling.

In patients with hypertension without risk factors for hyperkalemia, the incidence of hyperkalemia with RAAS inhibitor mono-therapy is low (<2%), whereas rates are higher with dual RAAS blockade (5%).[182] The incidence of hyperkalemia is also increased in patients with congestive heart failure or chronic kidney disease (5% to 10%). However, these estimates are based on data from patients in a study setting and hence may not reflect the incidence of hyperkalemia in an outpatient setting. The rise in the P_K is less than 0.5 mmol/L in patients with relatively normal renal function. In contrast, more severe hyperkalemia may be seen in patients with chronic kidney disease, concurrent use of a drug that impairs renal K^+ excretion such as a potassium-sparing diuretic or a non-steroidal anti-inflammatory drug, and in the elderly patients.

Drugs that Inhibit Aldosterone Synthesis; Heparin: Aldosterone synthesis is selectively reduced in patients who are treated with heparin.[183–185] This seems to be due to an effect of heparin that leads to a reduction in the number and affinity of adrenal ANG_{II} receptors. It has been estimated that hyperkalemia occurs in about 7% of patients receiving heparin. Both unfractionated and low-molecular weight heparin can cause hyperkalemia. Hyperkalemia due to prophylactic subcutaneous unfractionated heparin (5000 units twice daily) has also been reported. Nevertheless, the degree of decrease in the $P_{Aldosterone}$ may not be of sufficient magnitude to affect the renal excretion of K^+ in many patients who receive this drug. Severe hyperkalemia occurs only if some other disorder that leads to impairment in K^+ excretion is present such as renal insufficiency or if the patient is taking an ACE inhibitor, or a potassium-sparing diuretic.

Aldosterone Receptor Antagonists; Spironolactone and Eplerenone: Hyperkalemia is of particular concern in patients on the non-specific mineralocorticoid receptor antagonist, spironolactone,[186] or the selective mineralocorticoid receptor antagonist eplerenone, especially given the increasing indications to combine spironolactone or eplerenone with ACE-inhibitors and/or ARBs in patients with renal and cardiac disease. Heart failure, diabetes, and chronic kidney disease increase the risk of hyperkalemia from these agents. The prevalence of hyperkalemia associated with the combined use of mineralocorticoid receptor antagonists and ACE-inhibitors/ARBs appears to be much higher in clinical practice (~10%) than what has been reported in large clinical trials, perhaps in part due to the use of higher than recommended doses. The incidence of hyperkalemia is dose dependent with detectable effects even at doses of 25 mg spironolactone per day, at higher doses, the risk of severe hyperkalemia increases. Juurlink et al.,[186] in a population-based study of computerized drug prescription records and hospitalizations in Ontario, Canada, studied the correlation between the rate of spironolactone prescription for patients with heart failure on ACE-inhibitors, following the publication of "The Randomized Aldactone Evaluation Study" with hyperkalemia and associated morbidity. The frequency with which spironolactone was prescribed to patients with heart failure who were taking an ACE inhibitor rose significantly after the publication of RALES (from 30 prescriptions per 1000 patients in early 1999 to 149 prescriptions per 1000 patients by late 2001). Over the same interval, there were significant increases among these patients in the rates of hospital admissions for hyperkalemia (from 4.0 to 11.0 per 1000) and of in-hospital death from hyperkalemia (from 0.7 to 2.0 per 1000). Notwithstanding, a study from the United Kingdom found a similar increase in spironolactone use after the publication of RALES, but without an increase in hyperkalemia or admissions to hospital for hyperkalemia.[187]

Drugs that Block ENaC; Trimethoprim and Pentamidine: The cationic form of trimethoprim and pentamidine causes hyperkalemia and salt wasting by blocking ENaC in the lumen of the CCD.[188] Patients with HIV and pneumocystis carinii pneumonia treated with trimethoprim not infrequently develop hyperkalemia.[189–191] Although this was attributed to the use of high doses of trimethoprim in these patients, trimethoprim may cause a rise in P_K when used in conventional doses. In a study of hospitalized patients treated with standard doses of trimethoprim,[192] significant hyperkalemia occurred in greater than 50%, with severe hyperkalemia (>5.5 mmol/L) in 21% of these patients. Risk factors for hyperkalemia due to usual-dose of trimethoprim include renal insufficiency, hyporeninemic hypoaldosteronism, and concomitant use of ACE-inhibitors and ARBs.[192]

Another factor that may explain the observed high incidence of hyperkalemia in patients with HIV and pneumocystis carinii pneumonia treated with trimethoprim is the low flow rate in the terminal CCD. Because the dietary intake in this group of patients is likely very poor, the number of osmoles (urea and NaCl) in terminal CCD will be low and hence a lower number of liters of fluid will exit CCD. If protein intake is low

delivery of urea to the inner MCD will be diminished and hence intra-renal urea recycling will be decreased. In addition to its effect to diminish the rate of excretion of K^+, a low flow rate in terminal CCD also increases the concentration of trimethoprim in the lumen of the CCD for a given amount of this drug (same quantity of trimethoprim is now in a smaller volume). Hence the ability of trimethoprim to block ENaC in principal cells in the CCD will be enhanced.[193] This also may be a contributing factor to the development of hyperkalemia in patients receiving conventional doses of trimethoprim.

If hyperkalemia develops over a short period of time or in the absence of a large intake of K^+, its most likely cause is a shift of K^+ out of cells. For example, a shift of K^+ from cells may occur due to suppression of the release of insulin by α-adrenergics released in response to contracted effective arterial blood volume owing to the effect of trimethoprim to block ENaC and cause renal salt wasting.[194]

With regard to therapy, loop diuretics may help by lowering the concentration of trimethoprim in the luminal fluid in the CCD. Enough NaCl must be given to re-expand the effective arterial blood volume. Because only the protonated form of trimethoprim blocks ENaC,[188] increasing the delivery of HCO_3 to the CCD should cause less trimethoprim to be in its cationic form and hence minimize its ENaC blocking effect. Inducing bicarbonaturia with acetazolamide is a rationale therapeutic option when continuation of trimethoprim is necessary and blockade of ENaC is likely. Enough alkali would need to be given to avoid the development of metabolic acidosis.

Calcineurine Inhibitors (Cyclosporin, Tacrolimus): Hyperkalemia develops in some patients receiving cyclosporin or tacrolimus following organ transplantation. The pathophysiology of hyperkalemia and the clinical signs in these patients resembles that of "Familial Hyperkalemia with Hypertension".[195] In a recent study, Hoorn et al.[196] demonstrated that in wild-type mice tacrolimus caused salt-sensitive hypertension and increased the abundance of phosphorylated NCC and the NCC-regulatory kinases WNK3, WNK4 and SPAK. Hydrochlorothiazide reversed tacrolimus-induced hypertension. Tacrolimus treated mice developed hyperkalemia when they consumed a high K^+ chow. Kidney transplant recipients treated with tacrolimus had a greater fractional excretion of Cl^- in response to bendroflumethiazide, a drug that blocks NCC, than individuals not treated with tacrolimus; renal NCC abundance was also greater in these patients.

Nafamostat Mesylate Interferes With Activation of ENaC Via Proteolytic Cleavage: Activation of ENaC by aldosterone involves proteolytic cleavage of the channel by serine proteases such as CAP1. These proteases activate ENaC by increasing the open probability of the channel rather than by increasing its expression at the cell surface. Nafamostat mesylate is a potent serine protease inhibitor that has been widely used in Japan for the treatment of acute pancreatitis, disseminated intravascular coagulation and as an anticoagulant in hemodialysis.[197] It can cause hyperkalemia primarily by decreasing urinary K^+ excretion.[198] The mechanism is related to the metabolites of nafamostat that inhibits these aldosterone-inducible, membrane-associated, channel activating proteases.[199]

THERAPY OF HYPERKALEMIA

Medical Emergencies

The major danger of a severe degree of hyperkalemia is a cardiac arrhythmia. Because mild ECG changes may progress rapidly to a dangerous arrhythmia, any patient with an ECG abnormality related to hyperkalemia should be considered as a medical emergency. Because some patients may develop cardiac arrhythmia or even cardiac arrest in the absence of changes associated with hyperkalemia in the initial ECG, it is our view that severe hyperkalemia, i.e., P_K >7.0 mmol/L, should be treated as an emergency with maneuvers to induce a shift of K^+ into cells even in absence of ECG changes, and perhaps at even lower P_K, e.g., >6.5 mmol/L, in the presence of hypocalcemia, acidemia and or hyponatremia. Notwithstanding, those who develop hyperkalemia after extreme exercise (the super-marathon[200]), most patients on chronic hemodialysis, and infants seem to tolerate even severe hyperkalemia without adverse effects.

Antagonize the Cardiac Effects of Hyperkalemia

In cells in which the rate of rise of action potential upstroke (V_{max}) is dependant on the inward Na^+ current, administration of calcium alters the relation between the V_{max} and the RMP at the onset of depolarization such that V_{max} is greater at less negative RMP, and hence conduction velocity is increased.[109]

A 10 ml of a 10% solution of calcium chloride contains about three times the amount of elemental calcium compared to calcium gluconate. Calcium gluconate, however, is preferred because of less risk of tissue necrosis if it extravasates. The usual dose of Ca gluconate is 1000 mg (10 ml of a 10% solution) infused over 2–3 minutes. The effect of IV calcium occurs in one to three minutes but lasts for only 30–60 minutes. This dose can be repeated in five minutes if ECG changes persist, or if they recur. Extreme caution

should be exerted in patients on digitalis because hypercalcemia may aggravate digitalis toxicity. It is recommended that Ca be given in hyperkalemic patients on digitalis only if there is loss of P wave, or a wide QRS complex. In this case calcium gluconate should be diluted in 100 ml of D5W and infused over 20–30 minutes to avoid acute hypercalcemia. The administration of digoxin-specific antibody fragments is the preferred therapy in these patients.

Induce a Shift of K^+ into the ICF

Insulin: A number of studies support the use of insulin to treat acute hyperkalemia.[201–205] The effect of insulin on plasma K^+ levels is independent of its hypoglycemic effect, which may be impaired in patients with end stage renal disease. The usual recommended dose of insulin is 10 units of regular insulin given as intravenous bolus. The insulin regimen, however, that was shown in studies to achieve close to a 1 mmol/L fall in P_K at 60 minutes, was the infusion of about 20 units of regular insulin over that period of time. This seems to achieve and maintain the supra-physiological levels of insulin in plasma that are required for a maximal shift of K^+ into cells. Hypoglycemia is definitely a risk. In the study by Blumberg et al.,[201] giving this dose of insulin and 20 g of glucose, 50% of their patients developed hypoglycemia. Hypoglycemia was avoided when the same dose of insulin was used but 60 g of glucose were infused over the one hour period.

ß$_2$-Adrenergic Agonists: ß$_2$-adrenergic stimulation lowers the P_K in patients with renal failure.[202–204,206–211] Albuterol (Salbutamol), a selective β_2-agonist, as inhaled/nebulized or IV is the most widely studied and used; only the inhaled form however, is available in the United States and Canada. Allon et al.[209] observed a decline in the P_K 1.0 mmol/L that lasted for two hours with 20 mg of albuterol given by nebulizer. There was a minimal increase in heart rate and a notable absence of cardiovascular side effects. However, since 20 to 40% of patients with ESRD are resistant to this therapy and it is not possible to predict non-responders, we do not recommend β_2-agonist as a sole emergency therapy. Moreover, we are concerned about the safety of these drugs in the doses used for the treatment of hyperkalemia, which are four to eight times that prescribed for the treatment of acute asthma. It is to be noted that in many of the studies using these agents, patients were selected for the study and patients on β-blockers (who are likely to have cardiac disease) were excluded. In some studies, patients with angina, myocardial infarction within six months, and patients with unstable heart rhythm were excluded.

The combination of nebulized ß$_2$-agonists and insulin was reported to produce a greater fall in P_K (1.2 mmol/L) compared with either drug alone (~0.65 mmol/L).[202] One should note however that only 10 units of regular insulin as an intravenous bolus was given in this study and the magnitude of the fall in P_K was lower than that observed in other studies using higher doses of insulin as an infusion.[201,203] Thus, it remains uncertain whether ß$_2$-agonists would have a P_K lowering effect additive to that of higher doses of insulin.

$NaHCO_3$: A number of studies have found $NaHCO_3$ therapy to be ineffective as the sole treatment of hyperkalemia.[201,212,213] It is noteworthy that these studies were performed in stable hemodialysis patients who did not have significant acidemia (i.e., NHE-1 was presumably inactive). Studies that examined the combined use of $NaHCO_3$ with insulin also have conflicting results.[203,205] Thus the question remains, "Would $NaHCO_3$ be effective in patients with a more significant degree of acidemia?" There are no data in the literature to answer this question definitively.[214] Given this uncertainty, we only use $NaHCO_3$ in addition to other therapies to treat emergency hyperkalemia in patients with a significant degree of acidemia. Caution is warranted because an excessive administration of $NaHCO_3$ has the risk of inducing hypernatremia, ECF volume expansion, carbon dioxide retention, and hypocalcemia.

Non-Medical Emergency

Removal of K^+ From the Body

It is important to appreciate that a very much less K^+ loss is needed to lower the P_K from 7.0 to 6.0 mM than to lower it from 6.0 to 5.0 mM.[215] Hence creating a modest K^+ loss can be very important when there is a severe degree of hyperkalemia.

Enhancing the Excretion Of K^+ in the Urine

While a number of maneuvers may be suggested to increase the excretion of K^+ in the urine, there are no data to support their efficacy, particularly in the acute setting. The administration of a loop diuretic may induce kaliuresis by increasing the flow rate in the terminal CCD. One should avoid intravascular volume depletion as this may lead to the opposite effect of decreasing flow in the terminal CCD. Kaliuresis may be also enhanced by giving a mineralocorticoid (e.g., 100–300 μg florinef) and possibly by inducing bicarbonaturia with a carbonic anhydrase inhibitor. $NaHCO_3$ may need to be given to replace the HCO_3^- lost in the urine.

Cation Exchange Resins

Sodium polysterene sulfonate (SPS) is a cross linked polymer to which reactive sulfonic groups are attached, and preloaded with a the cation, Na^+. When SPS is placed in a solution, its reactive sulfonate group exchange their bound Na^+ for another cation in the solution. SPS has been long used by clinicians for the treatment of hyperkalemia with the assumption that it exchanges its bound Na^+ with K^+ in the lumen of GI tract and hence causes the loss of K^+ in stool.

SPS contains 4 mEq of Na^+ per gram, which could be available for exchange for K^+ in the lumen of the GI tract. Based on the affinity of SPS to Na^+ and K^+,[216] and if one considers the measured concentrations of Na^+ and K^+ at different sites in the lumen of the gastrointestinal tract, it seems that the only favorable site for this exchange to take place is in the lumen of the rectum (or perhaps the entire colon). Notwithstanding, other cations such as NH_4^+, Ca^{2+} and Mg^{2+} will compete with K^+ for this exchange with Na^+. But even if the exchange of Na^+ for K^+ were to occur in the colon, there is only a small amount of K^+ in the lumen of the colon to bind the resin. The amount of K^+ excreted via the GI tract in normal subjects is about, 9 mmol/day. It has been suggested that patients with ESRD have an enhanced colonic excretion of K^+. Balance data are conflicting and the bulk of evidence would suggest that uremic patients may excrete a few extra mmol of K^+ than normal subjects in their stool.[217]

One possible theoretical benefit to the use of cation exchange resins is if they were to bind K^+ and lower its concentration in luminal water, this may enhance the net secretion of K^+ by the recto-sigmoid colon. While the administration of several doses of SPS over a number of days may increase the loss of K^+ via the GI tract, the question is how to achieve a large loss of K^+ from the GI tract over a short period of time if this to be used to achieve the loss of K^+ in a patient with moderately severe hyperkalemia? The limiting factor for a large K^+ loss via the GI tract is stool volume. As shown by Emmett et al.,[216] the administration of 60 g of sorbitol, an osmotic cathartic, to normal subjects, the mean stool weight was 788 g over 12 hours and the total K^+ output was 26 ± 2 mmol over that time period. The addition of resin did not add much in terms of K^+ loss, as the total K^+ output was 30 ± 6, mmol over 12-hour period.

Two studies are commonly quoted to support the use of SPS in the treatment of hyperkalemia. In the study by Flinn et al.[218] SPS was given four times per day and the results for the P_K were reported on day five. Importantly, patients were given sufficient amount of sorbitol to produce a "satisfactory" diarrhea. Although the number of patients was rather small, one group of patients was treated with sorbitol alone, and had an average reduction by day five of treatment in P_K that was larger than patients treated with both resin and sorbitol.

Scherr et al.[219] treated 30 patients with hyperkalemia and oliguria with SPS, most patients did not require laxatives as constipation occurred only occasionally. The mean fall in the P_K in the group that received SPS orally was 0.9 ± 0.1 mmol/L in the first 24 hours. K^+ excretion in stool was not measured, so there is no evidence that the administration of resin caused a fecal loss of K^+ sufficient to account for the fall in P_K. In fact, some patients had quite impressive falls in P_K in the first 24 hours. For instance, one patient had a fall of 2.8 mmol/L, after oral resin 40 grams. The results are difficult to explain if SPS has a K^+ binding capacity *in vivo* of about 1 mmol per gram.

An increasing concern with the use of SPS in sorbitol is the development of intestinal necrosis, which usually involves the ileum and the colon. While the incidence of this complication is not exactly known and is likely to be rather low considering the frequency with which it is used, it is however, frequently fatal. Most cases were reported initially in patients in the post-operative period (e.g., post renal transplant) or in critically ill patients given resin enema.[220,221] Recently however, McGowan et al.[222] reported 11 cases of intestinal necrosis over a period of nine years that were temporally related to the use of SPS in sorbitol, four of which were fatal. All patients received oral SPS, only two of them were postoperative (both of them had orthopedic surgery) and only four had ESRD that required dialysis. The harm has generally been attributed to the use of 70% sorbitol.[223] There does seem to be some concern however that the resin itself may be involved.[222] In September of 2009, the FDA recommended against the "concomitant use of sorbitol" with Kayexalate® powder because of concerns about the risk of colonic necrosis and other gastrointestinal side effects. This warning however did not apply to premixed sodium polystyrene sulfonate in 33% sorbitol. There is concern however, that at least some of the more recent reports of colonic necrosis followed use of premixed preparation containing 33% sorbitol.[220]

In patients with life-threatening hyperkalemia, there is no role for the use of resins or attempting to induce K^+ loss via the intestinal tract. In a patient with moderately severe hyperkalemia in whom the decision is made not to start dialysis, to induce K^+ loss in stool, the goal of therapy should be to induce diarrhea. The addition of resin adds little in terms of K^+ loss to the induction of diarrhea alone. If the patient does not develop diarrhea, this treatment is not likely to be effective. Since there is concern about the use of

sorbitol 33%, the role of other cathartics need to be explored. Since, it seems that the most K^+ loss is achieved with the use of cathartics that induce secretory diarrhea, drugs like bisacodyl may be considered.

Dialysis

Hemodialysis is more effective than peritoneal dialysis for removing K^+. Removal rates of K^+ can approximate 35 mmol/hr with a dialysate bath K^+ concentration of 1−2 mM. A glucose-free dialysate is preferable to avoid the glucose-induced release of insulin and the subsequent shift of K^+ into cells, lessening the removal of K^+. For the same reason, one should consider discontinuing the insulin/glucose infusion once hemodialysis is initiated.

References

[1] Halperin ML, Kamel KS. Potassium. Lancet 1998;352:135−42.

[2] Clausen T. Na^+-K^+ pump regulation and skeletal muscle contractility. Physiol Rev 2003;83:1269−324.

[3] Desir GV. The structure, regulation and pathophysiology of potassium channels. Curr Opin Nephrol Hypertens 1995;4: 402−5.

[4] Clapp LH, Tinker A. Potassium channels in the vasculature. Curr Opin Nephrol Hypertens 1998;7:91−8.

[5] Misler S, Giebisch G. ATP-sensitive potassium channels in physiology, pathophysiology, and pharmacology. Curr Opin Nephrol Hypertens 1992;1:21−33.

[6] Ashcroft FM. K(ATP) channels and insulin secretion: a key role in health and disease. Bioch Soc Transact 2006;34:243−6.

[7] Landry DW, Oliver JA. The pathogenesis of vasodilatory shock. New Engl J Med 2001;345:588−95.

[8] Wang WH, Yue P, Sun P, Lin DH. Regulation and function of potassium channels in aldosterone-sensitive distal nephron. Curr Opin Nephrol Hypertens 2010;19:463−70.

[9] Welling PA, Ho K. A comprehensive guide to the ROMK potassium channel: form and function in health and disease. Am J Physiol 2009;297:F849−863.

[10] Hebert SC, Wang WH. Structure and function of the low conductance KATP channel, ROMK. Wien Klin Wochenschr 1997;109:471−6.

[11] Woda CB, Bragin A, Kleyman TR, Satlin LM. Flow-dependent K+ secretion in the cortical collecting duct is mediated by a maxi-K channel. Am J Physiol 2001;280:F786−793.

[12] Sansom SC, Welling PA. Two channels for one job. Kidney Int 2007;72:529−30.

[13] Bailey MA, Cantone A, Yan Q, MacGregor GG, Leng Q, Amorim JB, et al. Maxi-K channels contribute to urinary potassium excretion in the ROMK-deficient mouse model of Type II Bartter's syndrome and in adaptation to a high-K diet. Kidney Int 2006;70:51−9.

[14] Najjar F, Zhou H, Morimoto T, Bruns JB, Li HS, Liu W, et al. Dietary K+ regulates apical membrane expression of maxi-K channels in rabbit cortical collecting duct. Am J Physiol 2005;289:F922−932.

[15] Rieg T, Vallon V, Sausbier M, Sausbier U, Kaissling B, Ruth P, et al. The role of the BK channel in potassium homeostasis and flow-induced renal potassium excretion. Kidney Int 2007;72: 566−73.

[16] Counillon LL, Pouyssegur RJ. The members of the Na+/H+ exchanger gene family: their structure, function, expression, and regulation. In: Seldin DW, Giebisch G, editors. The kidney: physiology & pathophysiology. Philadelphia PA: Lippincott Williams & Wilkins; 2000. p. 223−34.

[17] Juel C. Regulation of pH in human skeletal muscle: adaptations to physical activity. Acta Physiol (Oxf) 2008;19:17−24.

[18] Moore RD. Stimulation of Na:H exchange by insulin. Biophys J 1981;33:203−10.

[19] Juel C, Bangsbo J, Graham T, Saltin B. Lactate and potassium fluxes from human skeletal muscle during and after intense, dynamic, knee extensor exercise. Acta Physiol Scand 1990;140: 147−59.

[20] Juel C, Halestrap AP. Lactate transport in skeletal muscle-role and regulation of the monocarboxylate transporter. J Physiol 1999;517:633−42.

[21] Cheema-Dhadli S, Chong CK, Kamel KS, Halperin ML. An acute infusion of lactic acid lowers the concentration of potassium in arterial plasma by inducing a shift of potassiun into cells of the liver in fed rats. Neph Physiol 2012; 120:7−15

[22] Medbo JI, Sejersted OM. Plasma potassium changes with high intensity exercise. J Physiol 1990;421:105−22.

[23] Clausen T. Hormonal and pharmacological modification of plasma potassium homeostasis. Fundam Clin Pharmacol 2010; 24:595−605.

[24] Fontaine B, Khurana TS, Hoffman EP, et al. Hyperkalemic periodic paralysis and the adult muscle sodium channel alpha-subunit gene. Science 1990;250:1000−2.

[25] Hayward LJ, Kim JS, Lee MY, Zhou H, Kim JW, Misra K, et al. Targeted mutation of mouse skeletal muscle sodium channel produces myotonia and potassium-sensitive weakness. J Clin Invest 2008;118:1437−49.

[26] Clausen T. Regulation of active Na^+-K^+ transport in skeletal muscle. Physiol Rev 1986;66:542−80.

[27] Bibert S, Roy S, Schaer D, Horisberger JD, Geering K. Phosphorylation of phospholemman (FXYD1) by protein kinases A and C modulates distinct Na,K-ATPase isozymes. J Biol Chem 2008;283:476−86.

[28] Rosa RM, Silva P, Young JB, Landsberg L, Brown RS, Rowe JW, et al. Adrenergic modulation of extrarenal potassium disposal. New Engl J Med 1980;302:431−4.

[29] Lin SH, Lin YF. Propranolol rapidly reverses paralysis, hypokalemia and hypophosphatemia in thyrotoxic periodic paralysis. Am J Kidney Dis 2001;37:620−4.

[30] Conway MJ, Seibel JA, Eaton RP. Thyrotoxicosis and hypokalemic periodic paralysis: improvement with beta blockade. Ann Intern Med 1974;81:332−6.

[31] Al-Khalili L, Yu M, Chibalin AV. Na^+,K^+-ATPase trafficking in skeletal muscle: insulin stimulates translocation of both alpha 1- and alpha 2-subunit isoforms. FEBS Lett 2003;536: 198−202.

[32] Benziane B, Chibalin AV. Frontiers: skeletal muscle sodium pump regulation: a translocation paradigm. Am J Physiol Endocrinol Metab 2008;295:E553−558.

[33] Nguyen TQ, Maalouf NM, Sakhaee K, Moe OW. Comparison of insulin action on glucose versus potassium uptake in humans. Clin J Am Soc Nephrol 2011;6:1533−9.

[34] Swan RC, Pitts RF. Neutralization of infused acid by nephrectomized dogs. J Clin Invest 1995;34:205−12.

[35] DeMars C, Hollister K, Tomassoni A, Himmelfarb J, Halperin ML. Citric acidosis: a life-threatening cause of metabolic acidosis. Ann Emerg Med 2001;38:588−91.

[36] Alper S. The band 3-related anion exchanger (AE) gene family. Ann Rev Physiol 1991;53:549−64.

[37] Waldegger S, Jentsch TJ. From tonus to tonicity: physiology of CIC chloride channels. J Am Soc Nephrol 2000;11:1331–9.
[38] Orringer CE, Eustace JC, Wunsch CD, Gardner LB. Natural history of lactic acidosis after grand-mal seizures. New Eng J Med 1977;297:796–9.
[39] Fulop M. Serum potassium in lactic acidosis and ketoacidosis. N Engl J Med 1979;300:1087–9.
[40] Magner PO, Robinson L, Halperin RM, Zettle R, Halperin ML. The plasma potassium concentration in metabolic acidosis: a reevaluation. Am J Kidney Dis 1988;11:220–4.
[41] Field M. Intestinal transport and the pathophysiology of diarrhea. J Clin Invest 2003;111:931–43.
[42] Sebastian A, McSherry E, Morris Jr RC. Renal potassium wasting in renal tubular acidosis (RTA): its occurrence in types 1 and 2 RTA despite sustained correction of systemic acidosis. J Clin Invest 1971;50:667–78.
[43] Adrogue HJ, Madias NE. Changes in plasma potassium concentration during acute acid–base disturbances. Am J Med 1982;71:456–67.
[44] Bercovici M, Chen C, Goldstein M, Stinebaugh B, Halperin M. Effect of acute changes in the $PaCO_2$ on acid–base parameters in normal dogs and dogs with metabolic acidosis or alkalosis. Can J Physiol Pharmacol 1983;61:166–73.
[45] Arrambide K, Toto RD. Tumor lysis syndrome. Semin Nephrol 1993;13:273–80.
[46] van Buren M, Rabelink TJ, van Rijn HJM, Koomans HA. Effects of acute NaCl, KCl and $KHCO_3$ loads on renal electrolyte excretion in humans. Clin Sci 1992;83:567–74.
[47] Giebisch G. Renal potassium transport: mechanisms and regulation. Am J Physiol 1998;274:F817–833.
[48] Wang WH, Giebisch G. Regulation of potassium (K) handling in the renal collecting duct. Pflugers Arch: Eur J Physiol 2009;458:157–68.
[49] Wang WH, Hebert SC. The molecular biology of renal K^+ channels. In: Seldin DW, Giebisch G, editors. The kidney: physiology & pathophysiology. Philadelphia PA: Lippincott Williams & Wilkins; 2000. p. 235–49.
[50] Garty H. Regulation of the epithelial Na^+ channel by aldosterone: open questions and emerging answers. Kidney Int 2000;57:1270–6.
[51] Farman N, Boulkroun S, Courtois-Coutry N. Sgk: an old enzyme revisited. J Clin Invest 2002;110:1233–4.
[52] Flores SY, Debonneville C, Staub O. The role of Nedd4/Nedd4-like dependant ubiquitylation in epithelial transport processes. Pflugers Arch–Eur J Physiol 2003;446:334–8.
[53] Kamynina E, Tauxe C, Staub O. Distinct characteristics of two human Nedd4 proteins with respect to epithelial Na(+) channel regulation. Am J Physiol 2001;281:F469–477.
[54] Vallon V, Lang F. New insights into the role of serum- and glucocorticoid-inducible kinase SGK1 in the regulation of renal function and blood pressure. J Am Soc Nephrol 2005;14: 59–66.
[55] Debonneville C, Flores SY, Kamynina E, Plant PJ, Tauxe C, Thomas MA. et al. Phosphorylation of Nedd4-2 by Sgk1 regulates epithelial Na(+) channel cell surface expression. EMBO J 20:7052-7059.
[56] Vuagniaux G, Vallet V, Jaeger NF, Hummler E, Rossier BC. Synergistic activation of ENaC by three membrane-bound channel-activating serine proteases (mCAP1, mCAP2, and mCAP3) and serum- and glucocorticoid-regulated kinase (Sgk1) in Xenopus. Oocytes. J Gen Physiol 2002;120:191–201.
[57] Velazquez H, Wright FS, Good DW. Luminal influences on potassium secretion: chloride replacement with sulfate. Am J Physiol 1982;242:F46–55.
[58] Wilson FH, Disse-Nocodeme S, Choate KA, Ishikawa K, Nelson-Williams C, Desitter I, et al. Human hypertension caused by mutations in WNK kinases. Science 2001;293: 1107–12.
[59] Stokes JB. Ion transport by the collecting duct. Sem Nephrol 1993;13:202–12.
[60] Leviel F, Hubner CA, Houillier P, Morla L, El Moghrabi S, Brideau G, et al. The $Na+$-dependent chloride-bicarbonate exchanger SLC4A8 mediates an electroneutral $Na+$ reabsorption process in the renal cortical collecting ducts of mice. J Clin Invest 2010;120:1627–35.
[61] Eladari D, Hubner CA. Novel mechanisms for NaCl reabsorption in the collecting duct. Curr Opin Nephrol Hypertens 2011; 20:506–11.
[62] Carlisle EJF, Donnelly SM, Ethier J, Quaggin SE, Kaiser U, Vasuvattakul S, et al. Modulation of the secretion of potassium by accompanying anions in humans. Kidney Int 1991;39: 1206–12.
[63] Yang C-L, Angell J, Mitchell R, Ellison DH. WNK kinases regulate thiazide-sensitive Na-Cl cotransport. J Clin Invest 2003;111:1039–45.
[64] Palmer LG, Frindt G. Regulation of apical K channels in rat cortical collecting tubule during changes in dietary K intake. Am J Physiol 1999;277:F805–812.
[65] Cheema-Dhadli S, Lin SH, Keong-Chong C, Kamel KS, Halperin ML. Requirements for a high rate of potassium excretion in rats consuming a low electrolyte diet. J Physiol (London) 2006;572:493–501.
[66] Wang WH. Regulation of renal K transport by dietary K intake. Ann Rev Physiol 2004;66:547–69.
[67] Lin DH, Sterling H, Yang B, Hebert SC, Giebisch G, Wang WH. Protein tyrosine kinase is expressed and regulates ROMK1 location in the cortical collecting duct. Am J Physiol 2003;286: F881–892.
[68] Wei Y, Zavilowitz B, Satlin LM, Wang WH. Angiotensin II inhibits the ROMK-like small conductance K channel in renal cortical collecting duct during dietary potassium restriction. J Biol Chem 2007;282:6455–62.
[69] Babilonia E, Wei Y, Sterling H, Kaminski P, Wolin M, Wang WH. Superoxide anions are involved in mediating the effect of low K intake on c-Src expression and renal K secretion in the cortical collecting duct. J Biol Chem 2005;280: 10790–6.
[70] Babilonia E, Lin D, Zhang Y, Wei Y, Yue P, Wang WH. Role of gp91phox -containing NADPH oxidase in mediating the effect of K restriction on ROMK channels and renal K excretion. J Am Soc Nephrol 2007;18:2037–45.
[71] Youn JH, McDonough AA. Recent advances in understanding integrative control of potassium homeostasis. Ann Rev Physiol 2009;71:381–401.
[72] Delaloy C, Lu J, Houot AM, Disse-Nicodeme S, Gasc JM, Corvol P, et al. Multiple promoters in the WNK1 gene: one controls expression of a kidney-specific kinase-defective isoform. Mol Cell Biol 2003;23:9208–21.
[73] Cope G, Murthy M, Golbang AP, Hamad A, Liu CH, Cuthbert AW, et al. WNK1 affects surface expression of the ROMK potassium channel independent of WNK4. J Am Soc Nephrol 2006;17:1867–74.
[74] Lazrak A, Liu Z, Huang CL. Antagonistic regulation of ROMK by long and kidney-specific WNK1 isoforms. Proc Natl Acas Sci USA 2006;103(5):1615–20.
[75] Wade JB, Fang L, Liu J, Li D, Yang CL, Subramanya AR, et al. WNK1 kinase isoform switch regulates renal potassium excretion. Proc Natl Acas Sci USA 2006;103:8558–63.
[76] Kamel KS, Halperin ML. Intrarenal urea recycling leads to a higher rate of renal excretion of potassium: an hypothesis with clinical implications. Curr Opin Nephrol Hypertens 2011;20: 547–54.

[77] Zhang C, Sands JM, Klein JD. Vasopressin rapidly increases phosphorylation of UT-A1 urea transporter in rat IMCDs through PKA. J Am Soc Nephrol 2002;282:F85–90.
[78] Fenton RA, Chou CL, Stewart GS, Smith CP, Knepper MA. Urinary concentrating defect in mice with selective deletion of phloretin-sensitive urea transporters in the renal collecting duct. Proc Natl Acas Sci USA 2004;101:7469–74.
[79] Fenton RA. Urea transporters and renal function: lessons from knockout mice. Curr Opin Nephrol Hypertens 2008;17: 513–8.
[80] Lassiter WE, Gottschalk CW, Mylle M. Micropuncture study of net transtubular movement of water and urea in non-diuretic mammalian kidney. Am J Physiol 1961;200:1139–46.
[81] McGarry JD, Kuwajima M, Newgard CB, Foster DW, Katz J. From dietary glucose to liver glycogen: the full circle round. Ann Rev Nutr 1987;7:51–73.
[82] Halperin ML, Rolleston FS. In: Harmon A, editor. Clinical detective stories: a problem-based approach to clinical cases in energy and acid–base metabolism. 1st ed. London, England: Portland Press; 1993.
[83] Welling PA, Chang YP, Delpire E, Wade JB. Multigene kinase network, kidney transport, and salt in essential hypertension. Kidney Int 2010;77:1063–9.
[84] Hoorn EJ, Nelson JH, McCormick JA, Ellison DH. The WNK kinase network regulating sodium, potassium, and blood pressure. J Am Soc Nephrol 2011;22:605–14.
[85] Subramanya AR, Ellison DH. Sorting out lysosomal trafficking of the thiazide-sensitive Na-Cl Co-transporter. J Am Soc Nephrol 2010;21:7–9.
[86] Huang CL, Yang SS, Lin S-H. Mechanism of regulation of renal ion transport by WNK kinases. Curr Opin Nephrol Hypertens 2008;17:519–25.
[87] He G, Wang HR, Huang SK, Huang CL. Intersectin links WNK kinases to endocytosis of ROMK1. J Clin Invest 2007;117: 1078–87.
[88] Ring AM, Leng Q, Rinehart J, Wilson FH, Kahle KT, Hebert SC, et al. An SGK1 site in WNK4 regulates Na^+ channel and K^+ channel activity and has implications for aldosterone signaling and K^+ homeostasis. Proc Natl Acas Sci USA 2007;104: 4025–9.
[89] Lin DH, Sterling H, Yang B, Hebert SC, Giebisch G, Wang WH. Protein tyrosine kinase is expressed and regulates ROMK1 location in the cortical collecting duct. Am J Physiol 2004;286:F881–892.
[90] Wei Y, Bloom P, Lin D, Gu R, Wang WH. Effect of dietary K intake on apical small-conductance K channel in CCD: role of protein tyrosine kinase. Am J Physiol 2001;281:F206–212.
[91] San-Cristobal P, Pacheco-Alvarez D, Richardson C, Ring AM, Vazquez N, Rafiqi FH, et al. Angiotensin II signaling increases activity of the renal Na-Cl cotransporter through a WNK4-SPAK-dependent pathway. Proc Natl Acas Sci USA 2009;106: 4384–9.
[92] Vallon V, Schroth J, Lang F, Kuhl D, Uchida S. Expression and phosphorylation of the Na^+-Cl^- cotransporter NCC in vivo is regulated by dietary salt, potassium, and SGK1. Am J Physiol 2009;297:F704–712.
[93] Moriguchi T, Urushiyama S, Hisamoto N, Iemura S, Uchida S, Natsume T, et al. WNK1 regulates phosphorylation of cation-chloride-coupled cotransporters via the STE20-related kinases, SPAK and OSR1. J Biol Chem 2005;280:42685–93.
[94] Xu BE, Stippec S, Lazrak A, Huang CL, Cobb MH. WNK1 activates SGK1 by a phosphatidylinositol 3-kinase-dependent and non-catalytic mechanism. J Biol Chem 2005;280: 34218–23.
[95] Steele A, deVeber H, Quaggin SE, Scheich A, Ethier J, Halperin ML. What is responsible for the diurnal variation in potassium excretion? Am J Physiol 1994;36:R554–560.
[96] Kurtzman NA, White MG, Rogers PW. The effect of potassium and extracellular volume on renal bicarbonate reabsorption. Metab 1973;22:483–92.
[97] Halperin ML, Kamel KS. Dynamic interactions between integrative physiology and molecular medicine: the key to understand the mechanism of action of aldosterone in the kidney. Can J Physiol Pharm 2000;78:587–94.
[98] Cogan MG. Angiotensin II: a powerful controller of sodium transport in the early proximal tubule. Hypertension 1990;15:451–8.
[99] Cheema-Dhadli S, Chong C-K, Lin S-H, Kamel KS, Halperin ML. Control of potassium excretion, a Paleolithic approach. Curr Opin Nephrol Hypertens 2006;15:430–6.
[100] Jamison RL. Potassium recycling. Kidney Int 1987;31:695–703.
[101] Cheema-Dhadli S, Lin S-H, Chong CK, Kamel KS, Halperin ML. Requirements for a high rate of potassium excretion in rats consuming a low electrolyte diet. J Physiol (London) 2006;572:493–501.
[102] Stokes JB. Consequences of potassium recycling in the renal medulla. Effects of ion transport by the medullary thick ascending limb. J Clin Invest 1982;70:219–29.
[103] Gumz ML, Lynch IJ, Greenlee MM, Cain BD, Wingo CS. The renal H + -K + -ATPases: physiology, regulation, and structure. Am J Physiol 2010;298:F12–21.
[104] Jungas RL, Halperin ML, Brosnan JT. Lessons learnt from a quantitative analysis of amino acid oxidation and related gluconeogenesis in man. Physiol Rev 1992;72:419–48.
[105] Talbott JH, Schwab RS. Recent advances in the biochemistry and therapeutics of potassium salts. New Engl J Med 1940;222:585–90.
[106] Cockcroft DW, Gault MH. Prediction of creatinine clearance from serum creatinine. Nephron 1979;16:31–41.
[107] West ML, Bendz O, Chen CB, Singer G, Richardson RMA, Sonnenberg H, et al. Development of a test to evaluate the transtubular potassium concentration gradient in the cortical collecting duct in vivo. Min Electrolyte Metab 1986;12: 226–33.
[108] Ethier JH, Kamel KS, Magner PO, Lemann JJ, Halperin ML. The transtubular potassium concentration in patients with hypokalemia and hyperkalemia. Am J Kidney Dis 1990;15: 309–15.
[109] Parham WA, Mehdirad AA, Biermann KM, Fredman CS. Hyperkalemia revisited. Tex Heart Inst J 2006;33:40–7.
[110] Cohen HC, Rosen KM, Pick A. Disorders of impulse conduction and impulse formation caused by hyperkalemia in man. Am Heart J 1975;89:501–9.
[111] Surawicz B. Relationship between electrocardiogram and electrolytes. Am Heart J 1967;73:814–34.
[112] Somers MP, Brady WJ, Perron AD, Mattu A. The prominent T wave: electrocardiographic differential diagnosis. Am J Emerg Med 2002;20:243–51.
[113] Szerlip HM, Weiss J, Singer I. Profound hyperkalemia without electrocardiographic manifestations. Am J Kidney Dis 1986;7:461–5.
[114] Paice B, Gray JM, McBride D, Donnelly T, Lawson DH. Hyperkalaemia in patients in hospital. Br Med J 1983;286: 1189–92.
[115] Montague BT, Ouellette JR, Buller GK. Retrospective review of the frequency of ECG changes in hyperkalemia. Clin J Am Soc Nephrol 2008;3:324–30.

[116] Bismuth C, Gaultier M, Conso F, Efthymiou ML. Hyperkalemia in acute digitalis poisoning: prognostic significance and therapeutic implications. Clin Toxicol 1973;6:153–62.
[117] Gowda RM, Cohen RA, Khan IA. Toad venom poisoning: resemblance to digoxin toxicity and therapeutic implications. Heart 2003;89:e14.
[118] Bandara V, Weinstein SA, White J, Eddleston M. A review of the natural history, toxinology, diagnosis and clinical management of Nerium oleander (common oleander) and the vetia peruviana (yellow oleander) poisoning. Toxicon 2010;56: 273–81.
[119] Warden JC. Fatal hyperkalaemia in status epilepticus. Med J Aust 1966;1:22–5.
[120] Flynn BC. Hyperkalemic cardiac arrest with hypertonic mannitol infusion: the strong ion difference revisited. Anesth Analg 2007;104:225–6.
[121] Hassan ZU, Kruer JJ, Fuhrman TM. Electrolyte changes during craniotomy caused by administration of hypertonic mannitol. J Clin Anesth 2007;19:307–9.
[122] Gronert GA, Theye RA. Pathophysiology of hyperkalemia induced by succinylcholine. Anesthesiology 1975;43:89–99.
[123] Cummings CC, McIvor ME. Fluoride-induced hyperkalemia: the role of Ca2 + -dependent K + channels. Am J Emerg Med 1988;6:1–3.
[124] Baltazar RF, Mower MM, Reider R, Funk M, Salomon J. Acute fluoride poisoning leading to fatal hyperkalemia. Chest 1980;78:660–3.
[125] Wiederkehr MR, Moe OW. Factitious hyperkalemia. Am J Kidney Dis 2000;36:1049–53.
[126] Bailey IR, Thurlow VR. Is suboptimal phlebotomy technique impacting on potassium results for primary care? Ann Clin Biochem 2008;45:266–9.
[127] Seimiya M, Yoshida T, Sawabe Y, Sogawa K, Umemura H, Matsushita K, et al. Reducing the incidence of pseudohyperkalemia by avoiding making a fist during phlebotomy: a quality improvement report. Am J Kidney Dis 2010;56: 686–92.
[128] Graber M, Subramani K, Corish D, Schwab A. Thrombocytosis elevates serum potassium. Am J Kidney Dis 1988;12:116–20.
[129] Kim A, Biteman B, Malik UF, Siddique S, Martin MR, Ali SA, et al. A case of pseudohyperkalemia in a patient presenting with leucocytosis and high potassium level: a case report. Cases J 2010;3:73.
[130] Ruddy KJ, Wu D, Brown JR. Pseudohyperkalemia in chronic lymphocytic leukemia. J Clin Oncol 2008;26:2781–2.
[131] Sevastos N, Theodossiades G, Archimandritis AJ. Pseudohyperkalemia in serum: a new insight into an old phenomenon. Clin Med Res 2008;6:30–2.
[132] Sevastos N, Theodossiades G, Savvas SP, Tsilidis K, Efstathiou S, Archimandritis AJ. Pseudohyperkalemia in patients with increased cellular components of blood. Am J Med Sci 2006;331: 17–21.
[133] Sodi R, Davison AS, Holmes E, Hine TJ, Roberts NB. The phenomenon of seasonal pseudohypokalemia: effects of ambient temperature, plasma glucose and role for sodium-potassium-exchanging-ATPase. Clin Biochem 2009;42: 813–8.
[134] Bruce LJ, Robinson HC, Guizouarn H, Borgese F, Harrison P, King MJ, et al. Monovalent cation leaks in human red cells caused by single amino-acid substitutions in the transport domain of the band 3 chloride-bicarbonate exchanger, AE1. Nat Genet 2005;37:1258–63.
[135] Schambelan M, Sebastian A, Rector Jr FC. Mineralocorticoid-resistant renal hyperkalemia without salt wasting (type II pseudohypoaldosteronism): role of increased renal chloride reabsorption. Kidney Int 1981;19:716–27.
[136] Mueller BA, Scott MK, Sowinski KM, Prag KA. Noni juice (morinda citrifolia): hidden potential for hyperkalemia? Am J Kidney Dis 2000;35:310–2.
[137] Chakera AJ, Vaidya B. Addison disease in adults: diagnosis and management. Am J Med 2010;123:409–13.
[138] Orth DN, Kovacs WJ. The adrenal cortex. In: 9th ed. Wilson JD, Foster DW, Kronenberg HM, Larsen PR, editors. Williams textbook of endocrinology, 1998. Philadelpha, PA: WB Saunders Company; 1998. p. 550.
[139] Mayo J, Collazos J, Martinez E, Ibarra S. Adrenal function in the human immunodeficiency virus-infected patient. Arch Intern Med 2002;162:1095–8.
[140] Espinosa G, Santos E, Cervera R, Piette JC, de la Red G, Gil V, et al. Adrenal involvement in the antiphospholipid syndrome: clinical and immunologic characteristics of 86 patients. Medicine 2003;82:106–18.
[141] Tucker WSJ, Snell BB, Island DP, Gregg CR. Reversible adrenal insufficiency induced by ketoconazole. JAMA 1985;253: 2413–4.
[142] Gagnon RF, Halperin ML. Possible mechanisms to explain the absence of hyperkalemia in a patient with addison's disease. Nephrol Dial Transpl 2001;16:1280–4.
[143] Lin SH, Hsu Y-J, Chiu J-S, Chu S-J, Davids MR, Halperin ML. Osmotic demyelination syndrome: a potentially avoidable disaster. Quart J Med 2003;96:935–47.
[144] Raff H. Glucocorticoid inhibition of neurohypophysial vasopressin secretion. Am J Physiol 1987;252:R635–644.
[145] White PC, Speiser PW. Congenital adrenal hyperplasia. Endocr Rev 2000;21:245–91.
[146] White PC. Disorders of aldosterone biosynthesis and action. Mol Cell Endocrinol 2004;217:81–7.
[147] Bonny O, Rossier BC. Disturbances of Na/K balance: pseudohypoaldosteronism revisted. J Am Soc Nephrol 2002;13: 2399–414.
[148] Schild L. The ENaC channel as the primary determinant of two human diseases: liddle's syndrome and pseudohypoaldosteronism. Neprhologie 1996;17:395–400.
[149] DuBose Jr TD. Hyperkalemic hyperchloremic metabolic acidosis: pathophysiologic insights. Kidney Int 1997;51: 591–602.
[150] Lush DJ, King JA, Fray JC. Pathophysiology of low renin syndromes: sites of renal renin secretory impairment and prorenin overexpression. Kidney Int 1993;43:983–99.
[151] Chan R, Sealey JE, Michelis MF, Swan A, Pfaffle AE, Devita MV, et al. Renin-aldosterone system can respond to furosemide in patients with hyperkalemic hyporeninism. J Lab Clin Med 1998;132:229–35.
[152] Klemm SA, Gordon RD, Tunny TJ, Finn WL. Biochemical correction in the syndrome of hypertension and hyperkalaemia by severe dietary salt restriction suggests renin-aldosterone suppression critical in pathophysiology. Clin Exp Pharm Physiol 1990;17:191–5.
[153] Oh MS, Carroll HJ, Clemmens JE. A mechanism for hyporeninemic hypoaldosteronism in chronic renal disease. Metabolism 1974;23:1157–66.
[154] Lee FO, Quismorio Jr FP, Troum OM, Anderson PW, Do YS, Hsueh WA. Mechanisms of hyperkalemia in systemic lupus erythematosus. Arch Intern Med 1988;148:397–401.
[155] Song J, Hu X, Riazi S, Tiwari S, Wade JB, Ecelbarger CA. Regulation of blood pressure, the epithelial sodium channel (ENaC), and other key renal sodium transporters by chronic insulin infusion in rats. Am J Physiol 2006;290: F1055–1064.

[156] Bickel CA, Verbalis JG, Knepper MA, Ecelbarger CA. Increased renal Na-K-ATPase, NCC, and beta-ENaC abundance in obese Zucker rats. Am J Physiol 2001;281:F639–648.
[157] Ohta A, Rai T, Yui N, Chiga M, Yang SS, Lin SH, et al. Targeted disruption of the Wnk4 gene decreases phosphorylation of Na-Cl cotransporter, increases Na excretion and lowers blood pressure. Hum Mol Genet 2009;18: 3978–86.
[158] Yang SS, Morimoto T, Rai T, Chiga M, Sohara E, Ohno M, et al. Molecular pathogenesis of pseudohypoaldosteronism type II: generation and analysis of a Wnk4(D561A/ +) knockin mouse model. Cell Metab 2007;5:331–44.
[159] Yang CL, Zhu X, Ellison DH. The thiazide-sensitive Na-Cl cotransporter is regulated by a WNK kinase signaling complex. J Clin Invest 2007;117:3403–11.
[160] Mayan H, Vered I, Mouallem M, Tzadok-Witkon M, Pauzner R, Farfel Z. Pseudohypoaldosteronism type II: marked sensitivity to thiazides, hypercalciuria, normomagnesemia, and low bone mineral density. J Clin Endo Metab 2002;87:3248–54.
[161] Wang P, Clausen T. Treatment of attacks in hyperkalaemic familial periodic paralysis by inhalation of salbutamol. Lancet 1976;1:221–3.
[162] DeFronzo RA, Bia M, Birkhead G. Epinephrine and potassiun homeostasis. Kidney Int 1981;20:83.
[163] Williams ME, Gervino EV, Rosa RM, Landsberg L, Young JB, Silva P, et al. Catecholamine modulation of rapid potassium shifts during exercise. N Eng J Med 1985;312:823–7.
[164] Woolf AD, Wenger T, Smith TW, Lovejoy FHJ. The use of digoxin-specific fab fragments for severe digitalis intoxication in children. N Eng J Med 1992;326:1739–44.
[165] Smith TW, Willerson JT. Suicidal and accidental digoxin ingestion. Report of five cases with serum digoxin level correlations. Circulation 1971;44:29–36.
[166] Martyn JA, Richtsfeld M. Succinylcholine-induced hyperkalemia in acquired pathologic states: etiologic factors and molecular mechanisms. Anesthesiology 2006;104:158–69.
[167] Bushinsky DA, Gennari FJ. Life-threatening hyperkalemia induced by arginine. Ann Int Med 1978;89:632–4.
[168] Dickerman HW, Walker WG. Effect of cationic amino acid infusion on potassium metabolism in vivo. Am J Physiol 1964;206:403–8.
[169] Perazella MA, Biswas P. Acute hyperkalemia associated with intravenous epsilon-aminocaproic acid therapy. Am J Kidney Dis 1999;33:782–5.
[170] Adabala M, Jhaveri KD, Gitman M. Severe hyperkalaemia resulting from octreotide use in a haemodialysis patient. Nephrol Dial Transpl 2010;25:3439–42.
[171] McIvor ME, Cummings CE, Mower MM, Wenk RE, Lustgarten JA, Baltazar RF, et al. Sudden cardiac death from acute fluoride intoxication: the role of potassium. Ann Emerg Med 1987;16:777–81.
[172] Baltazar RF, Mower MM, Reider RMF, Salomon J. Acute fluoride poisoning leading to fatal hyperkalemia. Chest 1980;78: 660–3.
[173] Su M, Chu J, Howland MA, Nelson LS, Hoffman RS. Amiodarone attenuates fluoride-induced hyperkalemia in vitro. Acad Emerg Med 2003;10:105–9.
[174] Peti-Peterdi J, Harris RC. Macula densa sensing and signaling mechanisms of renin release. J Am Soc Nephrol 2010;21:1093–6 [Epub 2010/04/03].
[175] Tan SY, Shapiro R, Franco R, Stockard H, Mulrow PJ. Indomethacin-induced prostaglandin inhibition with hyperkalemia. A reversible cause of hyporeninemic hypoaldosteronism. Ann Int Med 1979;90:783–5.
[176] Mactier RA, Khanna R. Hyperkalemia induced by indomethacin and naproxen and reversed by fludrocortisone. South Med J 1988;81:799–801.
[177] Harris RC. Jr Cyclooxygenase-2 inhibition and renal physiology. Am J Cardiol 89:10D-7D.
[178] Lam Q, Schneider HG. Hyperkalaemia with cyclooxygenase-2 inhibition and hypoaldosteronism. Int Med J 2005;35: 572–3.
[179] Kifor I, et al. Potassium stimulated angiotensin release from adrenal capsules and enzymatically digested cells of the zona gloerulosa. Endocrinol 1991;129:823–31.
[180] Textor SC, Bravo EL, Fouad FM, Tarazi RC. Hyperkalemia in azotemic patients during angiotensin-converting enzyme inhibition and aldosterone reduction with captopril. Am J Med 1982;158:26–32.
[181] Kato A, Klein JD, Zhang C, Sands JM. Angiotensin II increases vasopressin-stimulated facilitated urea permeability in rat terminal IMCDs. Am J Physiol 2000;279:F835–840.
[182] Weir MR, Rolfe M. Potassium homeostasis and renin-angiotensin-aldosterone system inhibitors. Clin J Am Soc Nephrol 2010;5:531–48.
[183] Sherman RA, et al. Suppression of aldosterone production by low-dose heparin. Am J Nephrol 1985;6:165–8.
[184] Siebels M, Andrassy K, Vecsei P, Seelig HP, Back T, Nawroth P, et al. Dose dependent suppression of mineralocorticoid metabolism by different heparin fractions. Thromb Res 1992;66:467–73.
[185] Oster JR, Singer I, Fishman LM. Heparin-induced aldosterone suppression and hyperkalemia. Am J Med 1995;98: 575–86.
[186] Juurlink DN, Mamdani MM, Lee DS, Kopp A, Austin PC, Laupacis A, et al. Rates of hyperkalemia after publication of the randomized aldactone evaluation study. N Eng J Med 2004;351:543–51.
[187] Wei L, Struthers AD, Fahey T, Watson AD, Macdonald TM. Spironolactone use and renal toxicity: population based longitudinal analysis. Brit M J 2010;340:c1768.
[188] Schreiber MS, Chen C-B, Lessan-Pezeshki M, Halperin ML, Schlanger LE, Patnaik A, et al. Antikaliuretic action of trimethoprim is minimized by raising urine pH. Kidney Int 1996;49: 82–7.
[189] Choi MJ, Fernandez PC, Patnaik A, Coupaye-Gerard B, D'Andrea D, Zerlip H, et al. Trimethoprim induced hyperkalemia in a patient with AIDS. N Eng J Med 1993;328: 703–6.
[190] Greenberg S, Reiser IW, Chou S-Y, Porush JG. Trimethoprim-sulfamethoxazole induces reversible hyperkalemia. Ann Int Med 1993;119:291–5.
[191] Velazquez H, Perazella MA, Wright FS, Ellison DH. Renal mechanism of trimethoprim-induced hyperkalemia. Ann Int Med 1993;119:295–301.
[192] Antoniou T, Gomes T, Juurlink DN, Loutfy MR, Glazier RH, Mamdani MM. Trimethoprim-sulfamethoxazole-induced hyperkalemia in patients receiving inhibitors of the renin-angiotensin system: a population-based study. Arch Intern Med 2010;170:1045–9.
[193] Schreiber M, Halperin ML. Urea excretion rate as a contributor to trimethoprim-induced hyperkalemia. Ann Intern Med 1994;120:166–7.
[194] Porte DJ. Sympathetic regulation of insulin secretion. Arch Intern Med 1969;123:252–60.
[195] Kamel K, Ethier JH, Quaggin S, Levin A, Albert S, Carlisle EJF, et al. Studies to determine the basis for hyperkalemia in recipients of a renal transplant who are treated with cyclosporin. J Am Soc Nephrol 1992;2:1279–84.

[196] Hoorn EJ, Walsh SB, McCormick JA, Furstenberg A, Yang CL, Roeschel T, et al. The calcineurin inhibitor tacrolimus activates the renal sodium chloride cotransporter to cause hypertension. Nat Med 2011;17:1304–9.
[197] Iwashita K, Kitamura K, Narikiyo T, Adachi M, Shiraishi N, Miyoshi T, et al. Inhibition of prostasin secretion by serine protease inhibitors in the kidney. J Am Soc Nephrol 2003;14: 11–6.
[198] Kitagawa H, Chang H, Fujita T. Hyperkalemia due to nafamostat mesylate. N Eng J Med 1995;332:687.
[199] Muto S, Imai M, Asano Y. Mechanisms of the hyperkalemia caused by nafamostat mesilate: effects of its two metabolites on Na^+ and K^+ transport properties in the rabbit cortical collecting duct. Br J Pharmacol 1994;111:173–8.
[200] McKechnie JK, Leary WP, Joubert SM. Some electrocardiographic and biochemical changes recorded in marathon runners. South Afr Med J 1967;41:722–5.
[201] Blumberg A, Weidmann P, Shaw S, Gnadinger M. Effect of various therapeutic approaches on plasma potassium and major regulating factors in terminal renal failure. Am J Med 1988;85:507–12.
[202] Allon M, Copkney C. Albuterol and insulin for treatment of hyperkalemia in hemodialysis patients. Kidney Int 1990;38:869–72.
[203] Allon M, Shanklin N. Effect of bicarbonate administration on plasma potassium in dialysis patients: interactions with insulin and albuterol. Am J of Kidney Dis 1996;28:508–14.
[204] Lens XM, Montoliu J, Cases A, Campistol JM, Revert L. Treatment of hyperkalemia in renal failure: salbutamol v. Insulin. Nephrol Dial 1989;4:228–32.
[205] Kim HJ. Combined effect of bicarbonate and insulin with glucose in acute therapy of hyperkalemia in end-stage renal disease patients. Nephron 1996;72:476–82.
[206] Montoliu J, Lens XM, Revert L. Potassium-lowering effect of albuterol for hyperkalemia in renal failure. Arch Intern Med 1987;147:713–7.
[207] Liou HH, Chiang SS, Wu SC, et al. Hypokalemic effects of intravenous infusion or nebulization of salbutamol in patients with chronic renal failure. Am J Kidney Dis 1994;23:266–70.
[208] Kemper MJ, Harps E, Muller-Wiefel DE. Hyperkalemia: therapeutic options in acute and chronic renal failure. Clin Nephrol 1995;46:67–9.
[209] Allon M, Dunlay R, Copkney C. Nebulized albuterol for acute hyperkalemia in patients on hemodialysis. Ann Intern Med 1989;110:426–9.
[210] Montoliu J, Almirall J, Ponz E, Campistol JM, Revert L. Treatment of hyperkalemia in renal failure with salbutamol inhalation. J Int Med 1990;228:35–7.
[211] Mandelberg A, Krupnik Z, Houri S. Salbutamol metered-dose inhaler with spacer for hyperkalemia: how fast? how safe?. Chest 1999;115:617–22.
[212] Guttierez R, Schlessinger F, Oster JR, Rietberg B, Perez GO. Effect of hypertonic versus isotonic sodium bicarbonate on plasma potassium concentration in patients with end-stage renal disease. Miner Electrolyte Metab 1991;17:297–302.
[213] Blumberg A, Weidmann P, Ferrari P. Effect of prolonged bicarbonate administration on plasma potassium in terminal renal failure. Kidney Int 1992;41:369–74.
[214] Kamel KS, Wei C. Controversial issues in treatment of hyperkalemia. Nephrol Dialysis Transpl 2003;18:2215–8.
[215] Sterns RH, Guzzo J, Feig PU, Singer I. Internal potassium balance and the control of the plasma potassium concentration. Medicine 1981;60:339–54.
[216] Emmett M, Hootkins RE, Fine KD. Effect of three laxatives and a cation exchange resin on fecal sodium and potassium excretion. Gastroenterology 1995;108:752–60.
[217] Agarwal R, Afzalpurkar R, Fordtran J. Pathophysiology of potassium absorption and secretion by the human intestine. Gastroenterology 1994;107:548–71.
[218] Flinn RB, Merrill JP, Welzant WR. Treatment of the oliguric patient with a new sodium-exchange resin and sorbitol. N Eng J Med 1961;264:111–5.
[219] Scherr L, Ogden DA, Mead AW. Management of hyperkalemia with a cation-exchange resin. N Eng J Med 1961;264:115–9.
[220] Sterns RH, Rojas M, Bernstein P, Chennupati S. Ion-exchange resins for the treatment of hyperkalemia: are they safe and effective? J Am Soc Nephrol 2010;21:733–5.
[221] Gerstman BB, Kirkman R, Platt R. Intestinal necrosis associated with postoperative orally administered sodium polystyrene sulfonate in sorbitol. Am J Kidney Dis 1992;20:159–61.
[222] McGowan CE, Saha S, Chu G, Resnick MB, Moss SF. Intestinal necrosis due to sodium polystyrene sulfonate (Kayexalate) in sorbitol. South Med J 2009;102:493–7.
[223] Lillemoe KD, Romolo JL, Hamilton SR, Pennington LR, Burdick JF, Williams GM. Intestinal necrosis due to sodium polystyrene (Kayexalate) in sorbitol enemas: clinical and experimental support for the hypothesis. Surgery 1987;101:267–72.
[224] Halperin ML. The ACID truth and BASIC facts–with a Sweet Touch, an enLYTEnment, 5th ed. Toronto: RossMark Medical Publishers; 2004.

CHAPTER

52

Control of Intracellular pH

Mark O. Bevensee[1] *and Walter F. Boron*[2]

[1]Departments of Cell, Developmental and Integrative Biology, University of Alabama at Birmingham, 1918 University Boulevard, Birmingham, AL 35294

[2]Physiology and Biophysics, Case Western Reserve University School of Medicine, 10900 Euclid Avenue, Cleveland, OH 44106

Because virtually every biological process is sensitive to changes in pH (for reviews, see refs.[1,2,3]), acid–base homeostasis is of critical importance to cells and organisms, and has attracted considerable attention. Until relatively recently, acid–base homeostasis, for both clinicians and basic scientists, has been synonymous with pH regulation in the two most easily accessed compartments, blood and cerebrospinal fluid (CSF). The pH in these extracellular compartments (pH_o) is certainly important for organisms. For example, alterations in pH_o may affect various extracellular biochemical reactions (e.g., hemostasis, complement fixation) and influence binding of various substances (e.g., hormones, metals, therapeutic agents) to plasma proteins or cell surface receptors. Moreover, certain ion channels[4,5] as well as transporters that move solutes across cell membranes are sensitive to pH_o changes. Nevertheless, the number of processes sensitive to changes of extracellular pH pales in comparison with the myriad processes sensitive to alterations in intracellular pH (pH_i). Thus, pH_i homeostasis should be a matter of central importance not only for individual cells, but also for the organism composed of these cells.

Although cellular metabolism can modulate pH_i, the regulation of pH_i is the province of membrane proteins that transfer acid–base equivalents across the plasma membrane. In addition, transporters that carry acid–base equivalents across organellar membranes can transiently modify pH_i or can participate in the buffering of cytoplasmic H^+.

Since the last edition of this book, the field of pH_i regulation has continued to advance in the following broad areas: (1) the multiplicity of transport pathways responsible for pH_i regulation, and (2) molecular mechanisms by which these pathways operate.

Elucidating the multiplicity of transport pathways in pH_i regulation: A common theme is that patterns of pH_i regulation in particular cell types is characteristic of the cell and complex. As a result, without previous knowledge of a cell's physiology, it may be impossible to predict its response to a particular maneuver. For example, switching the extracellular buffer from a non-CO_2/HCO_3^- buffer to CO_2/HCO_3^- usually causes an abrupt fall in pH_i, due to influx of the highly permeant CO_2. On the other hand, some cell membranes show no evidence whatsoever of being permeable to gases such as CO_2[6] or NH_3.[7,8,6] In fact, some of the CO_2 permeability of membranes may require "gas" channels.[9,10,11,12] For cells with CO_2-permeable membranes, the response to the initial CO_2-induced acidification may—depending on the cell type and initial pH_i —be a pH_i recovery that is totally absent,[13] partial,[14] complete,[15] or even excessive.[16–23]

Underlying the diversity of pH_i regulation is its complexity. Thus, a particular cell type may possess numerous plasma-membrane transporters that regulate pH_i, each with its own unique properties. For example, five genes encode Na^+-coupled HCO_3^- transporters, and these generally have multiple variants, each of which has a characteristic expression profile that depends on cell type and developmental stage, and susceptibility to regulatory mechanisms. Since the last edition of this book, investigators have described many new variants of transporters and have clarified the roles that they play in pH_i regulation.

pH_i regulation is also complex in that Na^+–H^+ exchangers, Na^+-coupled HCO_3^- transporters, and other

Seldin and Giebisch's The Kidney, Fifth Edition.
DOI: http://dx.doi.org/10.1016/B978-0-12-381462-3.00052-5

© 2013 Elsevier Inc. All rights reserved.

acid–base transporters may be under the concerted control of humoral agents[20,24–28] or other environmental influences, such as acidosis[29] or hypertonicity (see ref. [30]). In the case of pH_o changes, certain G-protein-coupled receptors can detect extracellular H^+.[31] In addition, charges in the basolateral concentration of $[CO_2]$ and $[HCO_3^-]$ per se—independent of basolateral pH—are powerful regulators of acid–base transport in the proximal tubule.[32]

Given the complexity and diversity of patterns of pH_i regulation, one must examine pH_i physiology anew for each previously unexplored cell type.

Understanding the molecular mechanisms of pH_i regulation: Since the last edition of this book, the field has seen further major advances in the molecular physiology of acid–base transporters. Many of these carriers are discussed in greater detail in Chapter 53 on Na^+-coupled HCO_3^- transporters, Chapter 54 on anion exchangers, and refs. [167,713,714] on Na^+-H^+ exchangers. The reader may also consult a review on Na^+-coupled HCO_3^- transporters.[33]

Scope of this chapter: In this chapter, we shall first consider the methodologies available for making pH_i measurements. We shall then examine the factors that contribute to changes in pH_i: the thermodynamic forces acting on hydrogen ions (H^+) and other charged acids/bases; the permeation of the cell membrane by electrically neutral acids and bases; the buffering power of the intracellular fluid; and transporters that regulate pH_i by moving H^+, bicarbonate ions (HCO_3^-) and/or other weak acid/bases across the plasma membrane. Because space does not permit us to summarize the vast array of acid–base transporters, we will focus on transporters that play a major role in pH_i regulation. Emerging from this discussion will be a model of pH_i regulation. Finally, in light of this model, we will consider several factors that fundamentally alter pH_i regulation: alterations in pH_o; temperature changes; metabolic inhibitors and hypoxia; cell shrinkage; hormones, growth factors, and oncogenes.

METHODS FOR MEASURING pH_i

Of the techniques available for measuring pH_i, we shall consider the four that are currently of greatest utility. These techniques differ from one another in terms of their theoretical foundations, the precise cellular properties that they measure, as well as in their accuracy and sensitivity.

pH-Sensitive Microelectrodes

In the mid 1990s, it was beginning to look like the use of pH microelectrodes might become a dying art, except for their restricted use for measuring pH_i in large invertebrate cells. However, the emergence of the *Xenopus* oocyte expression system and the cloning of numerous acid–base transporters over the past couple of decades have breathed new life into an old technology.

When a pH electrode and an indifferent reference electrode are placed in a solution, the voltage difference between the electrodes (E_X) is linearly related to the solution pH (pH_X):

$$pH_X = pH_S + (E_X - E_S)\frac{F}{RT \ln 10} \qquad (52.1)$$

pH_S is the pH of a standard solution, E_S is the voltage difference in this standard, and F/(RT ln 10) is the theoretical slope (~58 mV per pH-unit change at 22°C) of the line relating pH to voltage. The actual slope is determined empirically.

Although the pH sensor can be any of several materials (e.g., platinum-hydrogen, antimony, tungsten, or a liquid membrane), the most reliable remains pH-sensitive glass. Glass has the advantages of long lifetime, long-term stability, as well as insensitivity to cations other than H^+ (at physiological pH), redox reactions, and various gases. Several styles of glass pH-sensitive microelectrodes are available, including Hinke's exposed-tip design,[34] Roger Thomas' recessed-tip design,[35] and Roger Thomas' eccentric design.[36,37] Glass electrodes are particularly well suited to measure pH_i of relatively large cells (e.g., squid axons), or to measure pH_o. However, because it is difficult to fabricate glass microelectrodes that are small enough to be used with small cells, glass electrodes generally have been abandoned in favor of electrodes with liquid-membrane sensors, which are easier to make, but have a much shorter lifetime, are less stable, and are sometimes sensitive to drugs and other parameters.

Ideally, the pH and reference microelectrodes must impale a single cell. An acceptable alternative may be to place them in two identical cells, or in cells that are electrically coupled. Another solution is to employ a double-barreled electrode.[38,39] Unfortunately, for each barrel, there is a trade-off between tip size and electrode performance. The larger the two barrels of a double-barreled electrode, the better the electrode performance, but the greater the cell damage caused by impalement. The performance of liquid-membrane electrodes can be improved by using a concentric design in which a saline-filled pipette is threaded into the column of a liquid-membrane sensor, thereby reducing the overall longitudinal resistance between the sensor at the electrode's tip and the electrical contact in the electrode's barrel.[40–43] Fedirko et al.[40] have described a simplified approach for implementing this concentric design for H^+- and Ca^{2+}-selective microelectrodes, permitting rapid measurements of extracellular pH and Ca^{2+} transients in rat hippocampal brain slices.

pH-sensitive electrodes, particularly those with glass sensors, remain the method of choice for monitoring pH_i in relatively large cells. Not only are these electrodes highly sensitive (< 0.01 pH units), they are probably more precise and accurate than dyes. Moreover, the microelectrodes report pH and cell voltage simultaneously, and in real time. The "pH_i" that they report is almost certainly that of the bulk cytoplasm (i.e., the fluid in direct contact with the plasma membrane), uncontaminated by the pH of organelles. Disadvantages of using microelectrodes for measuring pH_i include the time and skill required for making and using them. In addition, one can only use conventional microelectrodes on cells large enough to sustain the impalement.

Although small mammalian cells generally do not easily tolerate impalement, pH-sensitive microelectrodes placed near the extracellular side of the plasma membrane of a mammalian cell can be used to measure H^+ fluxes due to acid–base transporter activity. Using an elegant "self-referencing" pH microelectrode technique with Chinese hamster ovary (CHO) fibroblasts, Fuster et al.[44] measured the continual extracellular H^+ gradient when a cell-attached patch pipette was repetitively positioned close to and away from an extracellular pH electrode. H^+ fluxes due to altered Na^+–H^+ exchanger activity were quantitated from changes in the extracellular H^+ gradient elicited by altering the cytoplasm via pipette perfusion. Electrodes with relatively large tips (15–20 μm) have been used to monitor surface pH transients in oocytes and glean important information about the permeability to CO_2 and NH_3 in the study of gas channels.[45–48]

Distribution of Weak Acids and Bases

Cell membranes are generally far more permeable to neutral molecules than to charged ones of similar shape and size. Thus, if a cell is exposed to a monoprotic weak acid HA ($HA \rightleftarrows H^+A^-$), the neutral molecule rapidly enters the cell (Figure 52.1). Assuming for the moment that A^- cannot penetrate the membrane, the entry of HA continues until HA is in equilibrium across the cell membrane, that is, when the concentration of HA inside the cell ($[HA]_i$) is the same as that outside ($[HA]_o$). Because entering HA dissociates to H^+ and A^-, the equilibration of HA across the membrane is necessarily accompanied by a fall in pH_i. This principle underlies the pH_i changes caused by neutral weak acids and bases that we will discuss below in the Section on "Effects of Weak Acids and Bases on pH_i". Provided that the dissociation constant ($K = [H^+] \times [A^-]/[HA]$) is the same both inside and outside the cell, then, at equilibrium,

$$\frac{[H^+]_i}{[H^+]_o} = \frac{[A^-]_o}{[A^-]_i} \tag{52.2}$$

Because the transmembrane distribution ratios of A^- and H^+ are inversely related, we can use Equation 52.2 to compute pH_i.

The weak acid most commonly used to calculate pH_i is 5,5-dimethyl-2,4-oxazolidinedione (DMO), employed as ^{14}C-DMO; benzoic acid has also been used.[49,50] Regardless of the weak acid used, the amount of radioactivity in the intra- or extracellular fluid is proportional to the total concentration of the probe ($[A^-] + [HA]$). pH_i is computed from the following equation, which must include the concentrations of the total probe because it is impossible to measure $[A^-]$ directly:

$$pH_i = pK + \log\left[\frac{([A^-]_i + [HA]_i)}{([A^-]_o + [HA]_o)}(10^{pH_i - pK} + 1)\right] \tag{52.3}$$

One can use a similar approach to compute pH_i from the distribution of a permeant weak base, such as methylamine.[51] Reviews by Waddell and Butler[52] and by Roos and Boron[3] contain more detailed descriptions and discuss potential difficulties of the weak-acid/base method.

The major advantages of the weak-acid/base method include its technical simplicity and applicability to even very small cells. The parameter actually measured is not the pH of the cytoplasm, but rather a volume–weighted mean pH of all intracellular compartments in which the weak acid or base is distributed. The practical sensitivity of this approach is 0.03–0.05 pH units—considerably less than the microelectrode technique. The major disadvantage of the weak-acid/base approach is that continuous pH_i measurements are not possible.

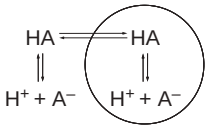

FIGURE 52.1 The distribution of a monoprotic weak acid across the cell membrane. When placed in the external solution, HA passively enters the cell, where it dissociates to form H^+ and A^-. Once $[HA]_i = [HA]_o$, the equilibrium $HA \rightarrow H^+ + A^-$ holds in both the intracellular and extracellular fluids.

pH-Sensitive Dyes

Absorbance

Molecules with an absorbance, fluorescence excitation, and/or fluorescence emission spectrum sensitive to pH may be convenient probes for measuring pH_i. When exposed to light, pH-sensitive dye molecules may absorb some of the light as electrons make the

transition to a higher-energy state. From the intensities of incident light (I_o) and the light transmitted through the solution (I), we can compute the absorbance (A):

$$A = \log \frac{I_o}{I} \tag{52.4}$$

According to the Beer-Lambert law, A at a particular wavelength (A_λ) is proportional to both the length of the light's path through the solution (l) and the concentration of the dye (C):

$$A_\lambda = \varepsilon_{\lambda,pH}\, lC \tag{52.5}$$

where the proportionality constant $\varepsilon_{\lambda,pH}$ is the dye's extinction coefficient at a particular wavelength and pH. The wavelength dependence of $\varepsilon_{\lambda,pH}$ defines the shape of the absorbance spectrum, and the pH dependence of $\varepsilon_{\lambda,pH}$ defines how this shape is affected by changes in pH. However, A_λ depends not only upon pH, but also upon l and C. Although l and C are extremely difficult to ascertain in a live cell, we can obtain the absorbance data at two wavelengths (λ_1 and λ_2), and compute the absorbance ratio ($A_{\lambda 1}/A_{\lambda 2}$):

$$\frac{A_{\lambda 1}}{A_{\lambda 2}} = \frac{\varepsilon_{\lambda 1,pH}\, lC}{\varepsilon_{\lambda 2,pH}\, lC} = \frac{\varepsilon_{\lambda 1,pH}}{\varepsilon_{\lambda 2,pH}} \tag{52.6}$$

Thus, because the l and C terms cancel out, the absorbance ratio in Equation 52.6, depends only on pH. By choosing two wavelengths such that $\varepsilon_{\lambda 1,pH}/\varepsilon_{\lambda 2,pH}$ varies considerably with pH, one can obtain sensitive pH measurements. Experimenters using fluorescein derivatives typically use the peak absorbance wavelength (~510 nm), and the isosbestic wavelength (~440 nm), where ε is insensitive to pH changes. Monitoring dye absorbance at the isosbestic wavelength is attractive because one can determine the extent of dye loss during the experiment, assuming l is constant.

An advantage of absorbance for measuring pH_i is that it tends to be extremely stable and sensitive. On the other hand, because absorbance is proportional to l and C, a relatively high intracellular dye concentration is required, even for thick preparations (e.g., renal tubules).

Fluorescence

After absorbing a photon, most molecules return to the ground state by gradually losing energy through a series of random collisions with other molecules (see ref.[53]). Some dyes, however, can lose a quantum of energy from an excited singlet state by emitting a photon (i.e., fluorescing). The intensity of emitted fluorescent light (I_{emit}) can be measured with a photomultiplier tube (e.g., see ref.[19]) or an intensified [CCD] television camera, which provides imaging data (e.g., see ref.[54]). At most wavelengths, I_{emit} is sensitive to pH, but at all wavelengths, I_{emit} is sensitive to dye concentration as well as other parameters (e.g., position of cell in the incident light beam). Therefore, one usually employs a ratio technique to generate a parameter more uniquely related to pH. With the *fluorescence-excitation ratio* approach, commonly used with fluorescein dyes such as BCECF, one alternately excites at two wavelengths while monitoring I_{emit} at one wavelength. With the *fluorescence-emission ratio* approach, commonly used with some rhodamine dyes such as SNARF-1, one excites at one wavelength, while monitoring I_{emit} simultaneously at two wavelengths. By analogy with the absorbance ratio approach, one chooses three wavelengths to optimize the pH sensitivity of the ratio. A strength of the fluorescence-emission ratio approach is that the simultaneous capture of I_{emit} at two wavelengths improves temporal resolution (see below).

Fluorescence measurements offer the advantage of being extremely sensitive. Thus, it is possible to quantitate the fluorescence from small amounts of dye, even in a microdomain within a single cell. In addition, one can use fluorescence with two-dimensional imaging, confocal microscopy, and multi-photon microscopy. Because fluorescence is more sensitive than absorbance to the environment of the dye molecule, fluorescence measurements are in principle more prone to artifact.

Bleaching and Photodynamic Damage

Excessive illumination can photolyse (i.e., bleach) dye molecules, causing a progressive decrease in the concentration of native dye. Among the photolysis products may be free radicals that react with cellular components and injure the cell ("photodynamic damage"). Excessive illumination can also cause a time-dependent shift in the apparent intracellular calibration curve of the dye,[19] presumably due to bleaching-induced generation of dye-related products with spectral characteristics slightly different than those of the parent compound.

Bleaching can be particularly problematic during experiments on single cells, where the number of dye molecules and thus the number of emitted photons is low. The problem is that the limiting signal-to-noise ratio (S/N) is proportional to the square root of the number of photons measured. One can increase the number of emitted photons by increasing the intensity of the excitation light source, but at the expense of exacerbating the bleaching and photodynamic damage. The damage can be minimized either by illuminating continuously with low-intensity light for longer, or by limiting the duty cycle of high-intensity exciting light.[19] Thus, one must sometimes trade off pH_i resolution (i.e., S/N) against time resolution. In imaging experiments, where a cell may be represented by thousands of picture elements (pixels), the photon emission rate per pixel is exceedingly low. Here, one must trade off pH_i resolution, time resolution, and

spatial resolution (i.e., the number of pixels that must be grouped to compute pH_i values).

More recent advances in fluorescence microscopy have helped to minimize the predicament of good pH_i vs. spatial/temporal resolution. For example, two-photon excitation laser scanning microscopy is a relatively new imaging technique that has allowed investigators to reduce photobleaching of ion-sensitive fluorescent dyes, even while acquiring high spatial and temporal resolution recordings.[55,56] Multiphoton imaging technology is based on the general quantum principle that a molecule can exhibit fluorescence after absorbing two photons simultaneously when excited by high-intensity light of twice the wavelength necessary for single-photon absorption. Excitation at the higher wavelengths (and thus lower energies) reduces overall photobleaching of the dye. Two-photon microscopy has been particularly useful in measuring intracellular Ca^{2+} transients with excellent spatial resolution in tissues and cellular microdomains (see[57–60]). The technique has also been used with pH-sensitive dyes.[61] For example, intracellular pH has been measured with BCECF in microdomains of the epidermis,[62] and with SNARF-4 in villous enterocytes *in vivo*.[63]

Calibration

SIMULTANEOUS MICROELECTRODE MEASUREMENTS

Because dyes interact with cytoplasmic components, the spectroscopic properties of an intracellular dye differ, sometimes markedly, from those of the same dye examined in a cuvette. Therefore, intracellular dye calibration is essential. One calibration approach is to use a second, independent method for measuring pH_i in either the same cell, or another cell under similar conditions. For example, simultaneous measurements with a pH-sensitive microelectrode have confirmed that the absorbance indicator dimethylcarboxyfluorescein in salamander proximal-tubule cells,[64] and the fluorescence indicator BCECF in leech glial astrocytes[65] yield reasonable values.

NIGERICIN APPROACH

The most popular approach has been to monitor intracellular absorbance or fluorescence while using the high-$[K^+]_o$/nigericin technique[66] to clamp pH_i to predetermined values. Nigericin is a carboxylic ionophore that exchanges K^+ (and to a lesser extent Na^+) for H^+ across cell membranes. If one is successful in choosing $[K^+]_o$ to match $[K^+]_i$, then pH_i should equal pH_o. Thus, by altering pH_o, one can measure the dye's spectral properties over a range of pH_i values. A detailed calibration spanning a wide pH_i range can be obtained for each experiment. Alternately, one can perform the detailed calibration on one set of cells, and routinely perform only a single-point calibration.[19] Potential problems with the high-$[K^+]_o$/nigericin technique have been discussed in some detail.[67]

In using nigericin-containing solutions for dye calibration, one must be careful to cleanse the perfusion system completely after each calibration procedure. Even trace amounts of nigericin can interfere with the assessment of pH_i-regulating mechanisms, by mimicking a K^+-H^+ exchanger and by increasing "background acid loading[a]" through nigericin-mediated exchange of internal K^+ for external H^+.[17,68]

NULL-POINT APPROACH

A novel calibration technique, originally proposed for microelectrodes by Szatkowski and Thomas,[69] but applied to dyes by Eisner et al.,[70] involves sequentially exposing the cell to a permeant weak acid and weak base. As discussed below, the size of a pH_i change elicited by a weak acid/base depends on the initial pH_i. It is thus possible to compute the initial pH_i from the magnitude of the change of the pH_i indicator. Eisner et al.[70] have extended this approach by introducing an elegant null-point technique, in which one experimentally determines a combination of weak-acid and weak-base concentrations that produces no change in the measured fluorescence. The null-point approach can be particularly useful in assessing the validity of other dye-calibration procedures, particularly the high-$[K^+]_o$/nigericin technique.[71–73]

Choice of Dyes

BCECF

The most popular dye for fluorescence measurements of pH_i is the fluorescein derivative BCECF,[74] which has four negatively-charged carboxylate groups and a phenolic -OH moiety that is titrated by pH changes. The dye can be directly loaded into large cells (e.g., *Xenopus* oocytes) with an injection pipette, or into small mammalian cells by diffusion from a patch pipette during whole-cell recordings.[75,76] However, BCECF is usually loaded into cells as an uncharged acetoxymethylester (AM) precursor that easily permeates most plasma membranes. Intracellular esterases hydrolyze BCECF-AM to yield four or five formaldehyde molecules for each charged BCECF molecule trapped inside the cell. The time required for dye loading can vary greatly among cell types, from 1 minute to tens of minutes. Less conventional methods for dye loading—including scrape loading, osmotic lysis, and electroporation—are examined in more detail in

[a]We define "acid loading" as any process that causes pH_i to fall. Examples include the uptake of H^+, the loss of HCO_3^-, or the metabolic production of H^+.

Giuliano and Taylor.[77] BCPCF, with carboxypropyl groups, is a derivative of BCECF that can be used as a dual-emission pH indicator.[78]

OTHER DYES

Both pyranine-based[79] and rhodamine-based dyes[80,81] have also been used for monitoring pH_i. Rhodamine dyes such as the seminaphthorhodafluor (SNARF) dyes are excited and emit at longer wavelengths than the fluorescein derivatives. An advantage of SNARF is that its fluorescence-emission spectrum is pH sensitive, in addition to its absorbance and fluorescence-excitation spectra. Thus, the dye can be used in the dual-emission mode, and is therefore more useful than fluorescein derivatives for confocal microscopy, in which one typically excites at only one wavelength. Dual-emission dyes also enable the user to sample more frequently, and to avoid the delay in alternating between two excitation wavelengths. SNARF-1 can be used simultaneously with Fura-2 for monitoring both pH_i and $[Ca^{2+}]_i$.[82] In general however, one should be cautious in using multiple ion-sensitive dyes simultaneously to avoid quenching artifacts.[83]

MEASUREMENT OF pH IN ORGANELLES

pH-sensitive fluorescent dyes with lower pK values are available (e.g., from Life Technologies™/Molecular Probes®) for pH measurements in acidic organelles such as lysosomes. Some of these dyes include the weak-base LysoSensor probes,[84,85] the aminorhodamine dye pHrodo,[86] and the fluorinated fluorescein dye Oregon Green.[87,88] These probes can be targeted to appropriate organelles by a cell's own endocytic pathway.

Investigators have also developed ingenious methods for targeting pH-sensitive probes to organelles. As reviewed by Maxfield and Yamashiro,[89] pH-sensitive indicators can be targeted to the endocytic pathway following pinocytosis or receptor-mediated endocytosis. Kim et al.[90] have measured Golgi pH with either a rhodamine- or fluorescein-labeled β subunit of verotoxin, which accumulates in the Golgi complex after receptor-mediated endocytosis and retrograde transport. Grinstein's group has also measured pH in the endoplasmic reticulum[91] and the *trans*-Golgi network[92] by creating chimeric proteins with organelle-specific retrieval signals, and subsequently tagging them with pH-sensitive fluorophores before internalization. A similar approach has been used to measure the pH of recycling endosomes.[93,94] The Machen group has examined pH regulation in the secretory pathway by targeting biotin-labelled pH probes to organelles expressing avidin-chimera proteins.[95–97] Seksek et al.[98] have used a different technique to measure the *trans*-Golgi pH of fibroblasts. They injected the cells with 70-nm liposomes containing membrane-impermeable pH-sensitive fluorophores; the liposomes then fused with the *trans*-Golgi. As described in the next section, investigators have also measured the pH of organelles by fusing pH-sensitive green fluorescent protein (GFP) variants or associated biosensors to organellar localization signals.

GREEN-FLUORESCENT PROTEIN (GFP)

Another fluorophore that has become useful in the pH field is GFP, which is a natural product of the jellyfish *Aequorea victoria*, and typically used to label proteins expressed in cells.[99,100] Several researchers have engineered GFP mutants such as pHluorins[101] that are sensitive to pH changes in the physiological range, and can be targeted to the cytosol or organelles.[102–108] Wild-type or mutant fluorescent proteins such as GFP and YFP can also be fused together to create ratiometric pH biosensors, and subsequently target the biosensors to organelles such as the mitochondria.[109] Tantama et al.[110] have recently engineered—from the red fluorescent protein mKeima—a pH-sensitive, dual-excitation/ratiometric variant called pHRed. This variant would be particularly useful during simultaneous measurements requiring the use of other more blue-shifted fluorescent probes. Moreover, upon two-photon, single-wavelength excitation, pHRed exhibits modest pH-sensitive changes in fluorescence lifetime that could be used to obtain rough estimates of pH_i.

Compared to more traditional pH indicators, pH-sensitive GFP mutants are advantageous in displaying a low rate of photobleaching while remaining trapped inside of cells. pHluorins linked to markers of synaptic vesicles (synaptopHluorins) undergo marked changes in fluorescence upon exocytosis at synaptic terminals and have therefore been used to characterize synaptic vesicle cycling associated with presynaptic activity.[101–112] Such vesicular cycling has been examined in transgenic mice expressing synaptopHluorin.[113] It is intriguing to speculate on the potential applicability of pH-sensitive GFPs to examine cellular pH physiology. Indeed, pHluorin constructs have been used to measure pH_i of fungi, plants, and yeast,[114–116] as well as transiently transfected HEK293 cells and astrocytes (Liu and Bevensee, unpublished). One could perform *in vivo* pH_i measurements on targeted cells that are induced by a specific promoter to express a pH-sensitive GFP. Metzger et al.[117] successfully measured pH_i in cerebellar slices from a generated transgenic mouse expressing a pH- and chloride-sensitive yellow-green variant of GFP (EYFP) under the control of a neuronal potassium channel promoter.

Differential Dye Loading

One can exploit differential dye loading in preparations to target dyes to specific cells or locations. For

example, intercalated cells in the cortical collecting tubule of the kidney incorporate BCECF-AM much more rapidly than the neighboring principal cells.[118] In a somewhat different application, Chu et al.[119] found that mouse colonic crypt cells exclude SNARF, which can then be used to measure extracellular pH changes in the intact epithelium. Also, a probenecid-sensitive organic-anion transporter can extrude BCECF from some cells including thyroid cells,[120] and epithelial kidney and intestinal cells.[121,122] In an elegant study, Harris et al.[123] used BCECF to measure the pH of the lateral intracellular space (LIS) of MDCK cell monolayers by first loading the cells with BCECF, and subsequently allowing organic transporters to move the dye into the LIS.

BCECF generally stains the cytoplasm rather uniformly, although in some cells the nuclear region is more intense than peripheral areas.[124] Working on Ehrlich ascites tumor cells, Thomas et al.[66] found that 6-carboxyfluorescein is confined to the cytoplasm, but fluorescein is distributed in both the mitochondria and cytoplasm. Furthermore, Slayman et al.[125] found that BCECF can accumulate in vacuoles of the fungus *Neurospora* when the cells are exposed to BCECF-AM.

One can evaluate a dye's intracellular compartmentalization by monitoring the fluorescence loss elicited by selectively permeabilizing different compartments with detergents. For example, most of the BCECF loaded into rat hippocampal CA1 neurons appears to be in the cytoplasm because 0.01% saponin reduces the fluorescence signal by ~96%.[126] Both absorbance- and fluorescence-derived estimates of pH_i can be influenced by dye in compartments other than the cytoplasm, depending upon each compartment's volume, dye concentration and pK, and pH.

Nuclear Magnetic Resonance

Certain atomic nuclei, among them ^{31}P and ^{19}F, possess a quantum mechanical property termed "spin," and behave as tiny bar magnets with magnetic moments. When an atomic nucleus of this type is placed in an external magnetic field, the magnetic moment precesses with a characteristic frequency about the axis of the applied field. The nucleus can be excited to a high-energy state by irradiating it with an oscillating magnetic field of the same frequency (i.e., resonance frequency) as the precession frequency. The resonance frequency depends not only on the identity of the atomic nucleus (e.g., ^{31}P), but also on its chemical environment, which influences the strength of the magnetic field at the nucleus. Thus, the resonance frequencies for ^{31}P in $HPO_4^{=}$ and HPO_4^{-} are slightly different because of the different chemical environments of the ^{31}P. Because the exchange rate of ^{31}P between individual $HPO_4^{=}$ and HPO_4^{-} ions is very rapid, nuclear magnetic resonance (NMR) detects only a single inorganic phosphate peak, the location of which depends on $[HPO_4^{-}]/[HPO_4^{=}]$. Because the dependence of this ratio on pH is described by a modified pH-titration curve ($H_2PO_4^{-} \rightleftarrows HPO_4^{=} + H^+$; $pK_a' = \sim 6.8$), the position of the inorganic phosphate peak is a good index of pH_i.

A major advantage of ^{31}P-NMR is that, in addition to providing nearly continuous measurements of pH_i, it can also be used to monitor levels of a variety of phosphorus-containing compounds, such as ATP. The pH_i value derived from NMR measurements is predominantly the pH of the cytoplasm. However, the inorganic phosphate peak for the cytosol may overlap with the inorganic-phosphate peaks from other intracellular compartments, as well as the extracellular space. The mitochondrial inorganic phosphate peak can in some cases[127] be resolved from that of the cytoplasmic peak. NMR measurements have been made on whole organs, whole small animals, and human limbs.[128]

pH_i can also be measured by NMR with ^{19}F-labeled probes having pK values in the physiological range.[129] As discussed by Deutsch,[130] ^{19}F-labeled probes are advantageous over ^{31}P in that background signals are low, and the fluorinated probes are highly visible and sensitive to the environment. Commonly used probes such as fluoroanilines, derivatives of fluoroisobutyric acid, and fluorinated pyridoxins are generally introduced into cells as methyl esters, similar to the approach used for pH-sensitive dyes. Aside from cost and the need for technical expertise, the major disadvantage of NMR is its relatively low sensitivity. Thus, a considerable mass of ^{31}P or ^{19}F is required for detection, precluding the use of the technique with single cells. For reviews, see refs[128,131,132].

As reviewed by Gallagher et al.,[133] related approaches for estimating pH_i include a comparison of ^{13}C signals for CO_2 and HCO_3^{-}, the use of ^{89}Y-labeled compounds, and pH-sensitive exchange of ^1H_2O between bulk water and water bound to a gadolinium complex.

FORCES AFFECTING THE PASSIVE MOVEMENT OF H^+ AND OTHER CHARGED ACIDS AND BASES

Forces Affecting H^+

Until the 1930s, it was generally assumed that hydrogen ions were in electrochemical equilibrium across the cell membrane, as defined by the Nernst equation:

$$V_m = \frac{RT}{F} \ln \frac{[H^+]_o}{[H^+]_i} \qquad (52.7)$$

Here, V_m is the voltage difference across the plasma membrane (the unit is the volt), R is the universal gas content (8.31 joules • $^{\circ}K^{-1}$ • equivalent^{-1}), T is absolute temperature, F is Faraday's constant (96,486 coulombs • equivalent^{-1}), and the subscripts *o* and *i* refer to extracellular and intracellular, respectively. In terms of pH, the foregoing equation becomes

$$V_m = (0.0585\ V) \times (pH_i - pH_o) \qquad (52.8)$$

assuming a temperature of 22°C. Thus, if H^+ were in equilibrium, then pH_i would be one unit lower than pH_o for each −58.5 mV of membrane potential. However, such a situation would present severe problems for the cell, inasmuch as V_m changes would shift the equilibrium distribution of H^+, and thus alter pH_i and pH_i-sensitive processes. It was not until the mid-1930s that Fenn and colleagues,[134,135] in experiments on frog skeletal muscle, demonstrated that pH_i is higher than expected for H^+ to be in electrochemical equilibrium. The authors, in effect, estimated V_m from the ratio $[K^+]_o/[K^+]_i$, and measured pH_i using the weak-acid method.

Nowadays, both V_m and pH_i can be measured directly, and for nearly all cells studied, pH_i is well above the equilibrium pH_i. In vertebrate skeletal muscle, for example, V_m is ~ -90 mV and pH_i is ~ 7.1[3]. Given a pH_o of 7.4, Equation 52.8 predicts an equilibrium pH_i of ~5.9, far lower than the actual pH_i. Rather than calculating equilibrium pH, one could equally well compute equilibrium potential for H^+, that is, the membrane voltage required for H^+ to be in equilibrium across the membrane (E_H). In skeletal-muscle example introduced above ($pH_i = 7.1$, $pH_o = 7.4$), the E_H computed from Equation 52.7 or Equation 52.8 is ~ -18 mV. Because the actual V_m (−90 mV) is more negative than E_H, H^+ is drawn into the relatively negative cell, driven by an electrochemical gradient of 90−18 or 72 mV. Thus, there is a substantial electrochemical gradient (1.2 pH units or 72 mV) favoring the passive influx of H^+. If the cell membrane were permeable to H^+, then the resultant H^+ influx would represent a *chronic intracellular acid load* (i.e., an acid load imposed on the cell for an indefinite period) that would tend to lower pH_i.

In the above discussion, we made no assumptions about the mechanism of the hypothetical influx of H^+. It had generally been thought that H^+ flux across the plasma membrane occurs via nonspecific pathways. However, as extensively reviewed by DeCoursey,[136,137] voltage-activated, Zn^{2+}-inhibited H^+ currents were first described in snail neurons,[138] and have subsequently been characterized in numerous other cell types, including epithelial cells (e.g., kidney cells), connective tissue, skeletal muscle, lymphocytes, macrophages, granulocytes, and microglia. Ramsey et al.[139] and Sasaki et al.[140] independently identified the first cDNA encoding a Zn^{2+}-sensitive, voltage-gated proton channel, termed H_v1 (also known as VSOP). As first shown by Meech and Thomas, the channel is closed at normal V_m levels, when the H^+ electrochemical gradient favors the passive influx of H^+. However, strong depolarization not only reverses the H^+ gradient—now favoring the passive efflux of H^+—but also opens the channels. Thus, as reviewed by Capasso et al.,[141] as long as the cell is highly depolarized, this channel functions as an H^+-efflux pathway that can contribute to acid extrusion, defined below in our discussion of pH_i regulation. Murphy et al.,[142] used the NH_4^+-prepulse technique to acid load rat alveolar epithelial cells, and computed the acid-extrusion rate from the subsequent pH_i recovery. They observed similar Zn^{2+}-sensitive acid extrusion, regardless of whether the cells were depolarized with high-K^+ solutions, and concluded that H_v1 channels must have been contributing to the pH_i recovery. However, it is not clear whether—under conditions of 'normal' membrane voltage—the H^+ electrochemical gradient would be outward and the H_v1 channels would be open. In the absence of data showing that the Zn^{2+} effects are reduce/eliminated by the knockdown/knockout of H_v1, one must entertain the hypothesis that Zn^{2+} had nonspecific effects and that H_v1 did not contribute to pH_i regulation.

The depolarization threshold for channel activation is lowered by increasing the pH_o-to-pH_i gradient. Although the single-channel conductance is low for H_v1, high protein expression in cells account for macroscopic H^+ currents that can exceed K^+ currents.

It has become clear that H_v1 is functionally coupled to NADPH oxidases (NOX), and plays a critical role in removing the protons formed as byproducts during the generation of O_2^-[143–145]; for reviews, see refs[137,146]. This H_v1 activity is important during neutrophil phagocytosis,[147] signaling in immune cells, as well as in spermatozoa activation (see ref. [141]).

Forces Affecting Charged Weak Acids/Bases

In general, the passive fluxes of ionic weak acids (e.g., NH_4^+) and bases (e.g., HCO_3^-) also impose a chronic intracellular acid load. As noted earlier (see Equation 52.2), whenever a neutral weak acid (HA) is equilibrated across the cell membrane ($[HA]_i = [HA]_o$), the transmembrane distribution ratio for H^+ is the reciprocal of the distribution ratio for the anionic conjugate weak base (A^-). Consider, for example, the CO_2/HCO_3^- buffer system. If (1) $[CO_2]_i$ equals $[CO_2]_o$, (2) CO_2 is in equilibrium with H^+ and HCO_3^- both

inside and outside the cell, and (3) the equilibrium constant is the same inside and outside the cell, then:

$$\frac{[H^+]_i}{[H^+]_o} = \frac{[HCO_3^-]_o}{[HCO_3^-]_i} \quad (52.9)$$

That is, the electrochemical gradient for HCO_3^- (and that for any other monovalent anion that can be described by a similar equation) is equal to but opposite to the gradient for H^+. Inasmuch as H^+ normally leaks into cells, HCO_3^- and other anionic weak bases tend to leak out, also decreasing pH_i. In crayfish muscle, the transmitter GABA opens Cl^- channels that are also permeable to HCO_3^-.[148] The resultant HCO_3^- efflux can reduce pH_i by as much as 0.4. A similar $GABA_A$-activated HCO_3^- conductance is present in cells from turtle cerebellum[149] and rat hippocampus.[150,151] This $GABA_A$-activated HCO_3^- conductance can be inhibited by antagonists of $GABA_A$ receptors such as picrotoxin. In a similar fashion, HCO_3^- movement through glycine-activated Cl^- channels alters pH_i.[75] Other anionic weak bases that seem to penetrate at least some cell membranes include the DMO anion,[152] formate,[153] propionate,[154] and salicylate.[153]

We can make a similar analysis for cationic weak acids ($HB^+ \rightleftarrows H^+ + B$). If the electrically neutral conjugate weak base (B) is equilibrated across the cell membrane (i.e., $[B]_i = [B]_o$), if the equilibrium $HB^+ \rightleftarrows H^+ + B$ holds on both sides of the membrane, and if the equilibrium constant is the same on both sides of the membrane, then:

$$\frac{[H^+]_i}{[H^+]_o} = \frac{[HB^+]_i}{[HB^+]_o} \quad (52.10)$$

That is, the electrochemical gradient for HB^+ is in the same direction as that for H^+. Thus, similar to H^+, cationic weak acids such as NH_4^+ tend to enter the cell and produce a chronic intracellular acid load.

Energetics of pH_i Regulation

The preceding analysis shows that, under the conditions that normally prevail in most cells (e.g., $pH_i \cong 7.1$, $V_m \cong -60$), the electrochemical gradients affecting H^+ and charged monovalent weak acids/bases (provided the neutral species equilibrates across the membrane) generally favor fluxes that would lower pH_i. Note that the above thermodynamic analysis addresses only the net *direction* of these passive fluxes, and does not address the *rate* of intracellular acid loading. These passive fluxes are depicted for a model cell in Figure 52.2. Additional acid-loading mechanisms include carrier-mediated transport of H^+ into or HCO_3^- out of cells, as well as metabolism that generates acidic byproducts. Acid-loading mechanisms such as passive fluxes, carrier-mediated transport, and metabolism are "chronic" because they act continuously to lower pH_i. Maintaining a normal pH_i requires that acid loading be matched by a comparable—and continuous—extrusion of acid. By definition, this acid extrusion[b] must be an active (i.e., energy-requiring) process. Acid extrusion can be accomplished either by the active uptake of alkali (e.g., OH^- or HCO_3^-) and/or the active removal of acid (e.g., H^+).

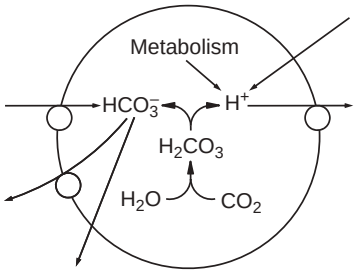

FIGURE 52.2 Factors affecting cellular H^+ balance. In a typical mammalian cell, membrane potential (V_m) might be −60 mV (inside negative) and extracellular pH (pH_o) approximately 7.4. In order for H^+ to be in electrochemical equilibrium, pH_i would have to be approximately 6.4. This is far lower than typical values, which range from 6.8 to 7.6, depending upon the cell type. Thus, H^+ tends to enter the cell passively (*inward arrow*). The same gradient that drives H^+ into the cell would also tend to drive HCO_3^- out (*outward arrow*), thereby lowering pH_i. The cell would also be acidified by any transporters that mediate the efflux of HCO_3^- (*curved arrow*), and perhaps by the metabolic generation of acid (*arrow*). In order for pH_i to be kept at its normal, relatively alkaline value, transporter(s) must actively remove acid from the cell, or accumulate an alkali such as HCO_3^-. Together, such active processes are referred to as "acid extrusion."

EFFECTS OF WEAK ACIDS AND BASES ON pH_i

Effects of CO_2 and Other Neutral Weak Acids

In the section above on "Distribution of Weak Acids and Bases" for measuring pH_i, we discussed the flux of neutral weak acids and bases across the cell membrane. In general, solutions containing the weak acid HA always contain the conjugate weak base A^-. However, because membranes are usually far more permeable to HA than to A^-, HA fluxes generally have a greater effect on pH_i.

Flux of the Neutral Weak Acid

When a cell is exposed to a neutral weak acid, HA enters and dissociates into A^- and H^+, thereby causing pH_i to fall:

[b]We define "acid extrusion" as any process that causes pH_i to rise. Examples include the efflux of H^+ and the uptake of HCO_3^-.

$$HA \rightarrow A^- + H^+ \quad (52.11)$$

This movement of the neutral weak acid (or a neutral weak base such as NH_3, discussed below) has been termed non-ionic diffusion. This process continues until $[HA]_i$ equals $[HA]_o$. Subsequently, there should be no further change in pH_i, provided there is no flux of A^- and no change in the rates of acid–base transporter activity. Although CO_2 is often regarded as a weak acid, it is not an acid at all. Only after reacting with H_2O does CO_2 yield the true weak acid, H_2CO_3, which then dissociates (as described above for the idealized weak acid HA):

$$CO_2 + H_2O \rightarrow H_2CO_3 \rightarrow HCO_3^- + H^+ \quad (52.12)$$

These two reactions can be combined into a single one with an overall apparent equilibrium constant ($K_a' = [HCO_3^-][H^+]/[CO_2]$). The enzyme carbonic anhydrase (CA) greatly accelerates the formation of HCO_3^- from CO_2 by catalyzing the reaction:

$$CO_2 + OH^- \xrightarrow{CA} HCO_3^- \quad (52.13)$$

which generates H^+ by virtue of consuming OH^-. The mechanism by which CA catalyzes this reaction is examined in more detail by Liljas et al.[155] In the absence of CA, the reaction can also occur, particularly under alkaline conditions (i.e., pH >8).

In the example of Figure 52.3, a cell is successively exposed to solutions equilibrated with 1, 2 and 5% CO_2 (constant $[HCO_3^-]_o = 10$ mM). Each time, CO_2 produces a rapid and sustained fall of pH_i. The period during the CO_2 exposure in which pH_i is relatively stable is termed the *plateau phase*. The magnitude of the CO_2-induced acidification is inversely related to the intracellular buffering power (β; see below). The magnitude of the pH_i decrease also increases with $[CO_2]_o$. The degree of dissociation is governed by the relationship between pH_i and pK_a', which, in logarithmic form, is the familiar Henderson-Hasselbalch equation:

$$pH_i = pK_a' + \log \frac{[HCO_3^-]_i}{[CO_2]_i} \quad (52.14)$$

where pK_a' is ~6.1 at 37°C. Therefore, if pH_i is 7.1, 10 molecules of incoming CO_2 dissociate into H^+ plus HCO_3^- for each molecule of CO_2 that remains CO_2. If the initial pH_i is only 6.1, then this ratio falls to 1:1, and fewer incoming CO_2 molecules dissociate. There are two practical consequences of this rule. First, the lower the initial pH_i, the smaller the magnitude of acidification elicited by the subsequent exposure to the CO_2. Second, as one raises $[CO_2]_o$ by fixed increments, the magnitude of the acidification is not proportional to the successive $[CO_2]_o$ increment. Thus, in Figure 52.3, the ΔpH_i produced by 2% CO_2 is less than twice as large as that produced by 1% CO_2, and that produced by 5% CO_2 is substantially less than five times that produced by 1% CO_2.

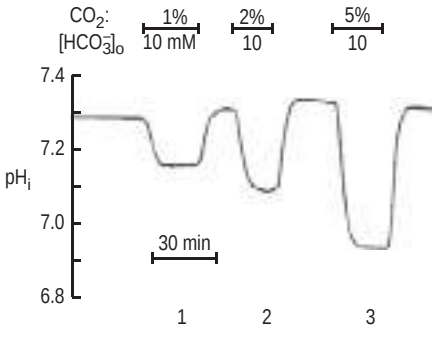

FIGURE 52.3 Effect of CO_2 on pH_i. A giant barnacle muscle fiber was exposed to CO_2 at three different levels: 1% ($pH_o = 7.5$), 2% ($pH_o = 7.2$), and 5% ($pH_o = 6.8$). After its entry into the cell, CO_2 is rapidly hydrated to H_2CO_3, which in turn dissociates into H^+ and HCO_3^-, causing pH_i to fall. Removing CO_2 reverses these processes. pH_i was measured with an exposed-tip pH-sensitive microelectrode, of the design of Hinke.[621] *(Reproduced from ref. [165].)*

Although investigators have long believed that all gases penetrate all membranes simply by dissolving in the membrane lipid, Waisbren et al.[6] demonstrated the first membrane with negligible permeability to a dissolved gas (i.e., CO_2 and NH_3). Moreover, Nakhoul et al.[11] and Cooper and Boron[9] identified the first gas channel—AQP1, which is permeable to CO_2. Later work showed that AQP1 is also permeable to NH_3[48] and that rhesus (Rh) proteins can be permeable to both CO_2[156] and NH_3.[157–159] In human erythrocytes, AQP1 and the Rh complex, together, are responsible for ~90% of the CO_2 permeability.[160,46] Thus, at least two families of proteins can function as gas channels. Furthermore, just as ion channels display ion selectivity, the AQPs and Rh proteins display gas selectivity. Based on CO_2- or NH_3-mediated changes in the surface pH of oocytes expressing AQP or Rh-family members, the sequence of CO_2/NH_3 selectivity is AQP4 ≅ AQP5 > AQP1 > AmtB > RhAG.[47]

Weak acids such as acetic acid,[161] lactic acid,[162] and DMO[152] can also elicit intracellular acidifications, which have $[HA]_o$ and pH_i dependencies similar to those described for CO_2. Aside from the dissolved gases discussed in the previous paragraph, many nonvolatile neutral weak acids and bases may move through plasma membranes—at least in part—via protein pathways (e.g., channels, transporters) in addition to any traffic through the lipid phase of the membrane. In a general sense, all such fluxes can be thought of as non-ionic diffusion, regardless of the mechanism. CO_2

is unusual, however, in that $[CO_2]_o$ is easily controlled, independent of $[HCO_3^-]_o$, either by the experimenter (who can equilibrate solutions with a known CO_2 mixture) or by the intact organism (which can alter its external respiration). Of course, the price one pays for varying $[CO_2]$ at constant $[HCO_3^-]$ is that—at equilibrium—pH must vary as well, as predicted by Equation 52.14. In the laboratory, it is possible to overcome this limitation by using out-of-equilibrium CO_2/HCO_3^- solutions (see below) to change only one of the three parameters (pH, CO_2, or HCO_3^-) at a time. For nonvolatile weak acids, the experimenter can only manipulate the total concentration of extracellular buffer ($[TA]_o = [HA]_o + [A^-]_o$) and pH. When $[TA]_o$ is fixed, changes in pH_o produce reciprocal alterations in $[HA]_o$ and $[A^-]_o$, so that the magnitude of the HA-induced pH_i decrease is very pH_o sensitive.

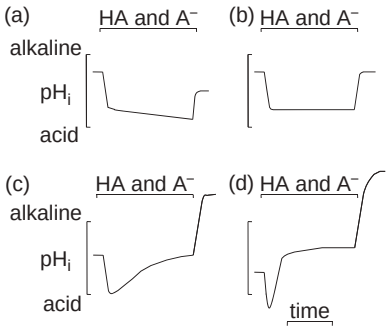

FIGURE 52.4 Hypothetical responses of a cell to the application of a neutral weak acid (HA) and its conjugate weak base (A^-). In all cases, the initial effect is a rapid fall in pH_i, due to the influx and partial dissociation of HA. The decrease in pH_i halts once $[HA]_i = [HA]_o$. The subsequent course of pH_i depends on the balance among (1) the passive efflux of A^- (which will lower pH_i), (2) transporters (e.g., $Cl^- - HCO_3^-$ exchanger) that lower pH_i, and (3) transporters (e.g., $Na^+ - H^+$ exchanger) that raise pH_i. a: Acid loading exceeds acid extrusion, and pH_i falls during the plateau phase. When external HA/A^- is removed, the recovery of pH_i falls short of the initial value. b: Acid loading exactly balances acid extrusion, and pH_i is stable during the plateau phase. When external HA/A^- is removed, pH_i returns to its initial value. c: Introducing HA/A^- does not fundamentally alter either acid loading or acid extrusion. pH_i returns to exactly its initial level by the end of the plateau phase. When external HA/A^- is removed, pH_i overshoots its initial value. d: Introducing HA/A^- promotes acid extrusion more than acid loading. During the plateau phase, pH_i recovers to a value that is higher than the initial pH_i. When external HA/A^- is removed, pH_i overshoots its initial value by even more than in case C.

Flux of the Anionic, Conjugate Weak Base

In the preceding discussion, we assumed that the movement of the uncharged weak acid HA was the only factor affecting pH_i. In other words, we excluded the possibilities that: (1) the charged species A^- can traverse the cell membrane and significantly affect pH_i, and (2) acid–base transporters as well as metabolic processes that generate acid–base equivalents can alter the overall balance between acid extrusion/loading. In the absence of these complicating effects, applying and withdrawing HA/A^- would produce the pH_i changes illustrated in Figure 52.4b.

What would happen if A^-, as well as HA, were able to cross the membrane passively? At the instant a cell is exposed to a solution containing HA and A^-, the electrochemical gradient for A^- would be inward (assuming that the initial $[A^-]_i$ were sufficiently low). Initially then, both HA and A^- would enter, the HA tending to lower pH_i, and the A^- tending to raise pH_i. A significant permeability of the membrane to A^- would reduce the initial rate of the HA-induced acidification. Eventually, however, the generation of A^- from incoming HA, as well as the influx of A^-, would raise $[A^-]_i$ to such a level that A^- would tend to exit the cell passively, as described earlier. In addition, a transporter might move A^- out of the cell; for example, a $Cl^- - HCO_3^-$ exchanger normally moves HCO_3^- out of the cell. Subsequently, the efflux of A^- would lower pH_i, both during the initial HA-induced acidification and during the later plateau phase, as illustrated in Figure 52.4a. This A^- efflux represents what might be termed a "semi-chronic" acid load, inasmuch as the pH_i decrease would continue until $[A^-]_i$ was so low that A^- was equilibrated across the membrane. Removing external HA/A^- would elicit a rapid rise in pH_i due to the efflux of HA from the cell. Note, however, that pH_i would rise to a value less than the initial pH_i. The magnitude of the shortfall would be directly related to the net acid loading due to A^- efflux. The pH_i changes illustrated in Figure 52.4a, presumably due to permeability of the membrane to the A^- form of a weak acid, have been observed in snail neurons exposed to salicylic acid.[153]

Acid-extrusion mechanisms can also influence the pH_i changes of a cell exposed to HA/A^-. In practice, the effects described below are due to one or more acid-extruders that outstrip acid loaders. These transporters are described in more detail later, as are their effects on the dynamics of pH_i regulation. We introduce these transporters here only to complete our consideration of pH_i transients elicited by HA/A^-. Consider a cell that is permeable to HA, but not to A^-, and that has an acid-extrusion mechanism that is unaffected by A^- (e.g., $Na^+ - H^+$ exchange). Applying HA/A^- would acutely acid load the cell, due to the influx of HA, and subsequent formation of A^- and H^+. However, an acid-extruder stimulated by the pH_i decrease would remove this acute acid load and return pH_i to exactly its starting value (Figure 52.4C). Note that removing HA/A^- causes pH_i to overshoot its

initial value by a substantial amount. The magnitude of the overshoot is directly related to the net amount of acid extruded during the HA/A^- exposure. This pattern of pH_i changes, including a complete recovery of pH_i during the plateau phase, is observed in snail neurons acid loaded by exposure to CO_2/HCO_3^-.[15] Other examples have been reported in which the plateau-phase pH_i recovery is incomplete.

As illustrated in Figure 52.4d, exposing a cell to HA/A^- may cause the pH_i during the plateau phase to rise to a value even greater than the initial pH_i. For example, if the cell had an acid extruder that is stimulated either by HA or A^-, then the influx of HA would initially acidify the cell. However, the stimulated acid extruder would not merely return pH_i to its initial value, as in Figure 52.4c, but increase pH_i beyond the initial value, as in Figure 52.4d. We can provide two such examples in which A^- stimulates acid extrusion and thereby elicits pH_i changes similar to those in Figure 52.4d: (1) exposing renal mesangial cells to CO_2/HCO_3^- stimulates a Na^+-driven HCO_3^- uptake mechanism,[19,163] and (2) adding acetic acid/acetate to the lumen of a rabbit S3 proximal tubule stimulates a Na^+/acetate cotransporter.[161,164] HA can also stimulate acid extrusion. In the rabbit proximal tubule, CO_2 per se appears to stimulate Na^+-H^+ exchange and H^+ pumping.[22]

Effects of NH_3 and Other Neutral Weak Bases

Solutions containing the neutral weak base B also contain its conjugate weak acid HB^+. Because membranes are usually far more permeable to B than to HB^+, B fluxes tend to have a greater effect on pH_i.

Flux of the Neutral Weak Base

When a cell is exposed to a neutral weak base, B enters and associates with H^+ to form HB^+, causing pH_i to rise:

$$B + H^+ \rightarrow HB^+ \qquad (52.15)$$

This process continues until $[B]_i$ equals $[B]_o$. Subsequently, there should be no further change in pH_i, provided there is no flux of HB^+ and no change in the rates of acid–base transporter activity. Removing external B reverses the reaction as written in Equation 52.15, and B passively diffuses out of the cell. pH_i should then return to exactly its initial level. An example of the effect of the weak base NH_3 is shown in Figure 52.5. Applying 20 mM total ammonium (i.e., $[NH_3]_o + [NH_4^+]_o$) causes pH_i first to rise, and then stabilize (segment ab, pulse 1). Removing the NH_3/NH_4^+ elicits a fall in pH_i to a value somewhat lower than the initial one (compare points a and c). The reason for this

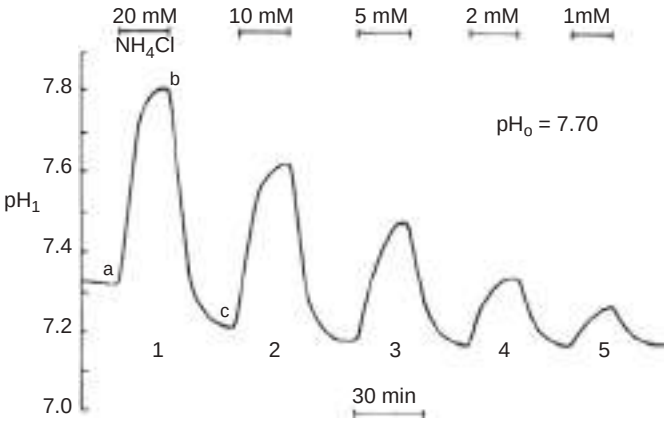

FIGURE 52.5 Effects of brief exposures to NH_3 on pH_i. A giant barnacle muscle fiber was exposed to NH_3 at five different levels of $[NH_3] + [NH_4^+]$: 20, 10, 5, 2, and 1 mM. Because pH_o was 7.70 throughout, $[NH_3]_o$ was approximately 312, 156, 78, 31, and 16 μM, respectively, in the five pulses. After its entry into the cell, NH_3 rapidly combines with H^+ to form NH_4^+. The resulting rise in pH_i continues until $[NH_3]_i = [NH_3]_o$. Removing external NH_3/NH_4^+ reverses these processes. Between NH_3/NH_4^+ pulses, the external solution was buffered with 5-mM HEPES to pH 7.5. pH_i was measured with an exposed-tip pH-sensitive microelectrode, of the design of Hinke.[621] *(Reproduced from ref. [165].)*

small pH_i undershoot will become clear below. As discussed above for HA-induced acidifications, the magnitude of the NH_3-induced alkalinization depends upon intracellular buffering power, $[NH_3]_o$, and the degree to which entering NH_3 is protonated. The last is governed by the relation:

$$pH_i = pK_a' + \log \frac{[NH_3]_i}{[NH_4^+]_i} \qquad (52.16)$$

where pK_a' (~9.2 at 22°C) is the acid dissociation constant. Thus, at the initial pH_i of 7.3 (point a), approximately 99.4% of entering NH_3 is protonated to form NH_4^+, whereas at a pH_i of 7.8 (point b), only approximately 98% is protonated. The dependence of the protonation of NH_3 on the difference $(pK_a' - pH_i)$ has two consequences, analogous to the two discussed earlier for CO_2. First, the higher the initial pH_i, the smaller the magnitude of the alkalinization elicited by the subsequent exposure to the NH_4^+. Second, as one raises $[NH_3]_o$ by fixed increments, the magnitude of the alkalinization with each successive $[NH_3]_o$ increment does not increase in proportion. Thus, in Figure 52.5, the alkalinization produced by 10 mM total NH_4^+ is less than twice as great as that produced by 5 mM total NH_4^+.

In Figure 52.5, the magnitude of the NH_4^+-induced alkalinization actually depends more on $[NH_3]_o$ than on $[\text{total } NH_4^+]_o$. Thus, the NH_4^+-induced alkalinizations will be identical for solutions in which $[\text{total } NH_4^+]$ and pH_o are varied reciprocally so as to keep

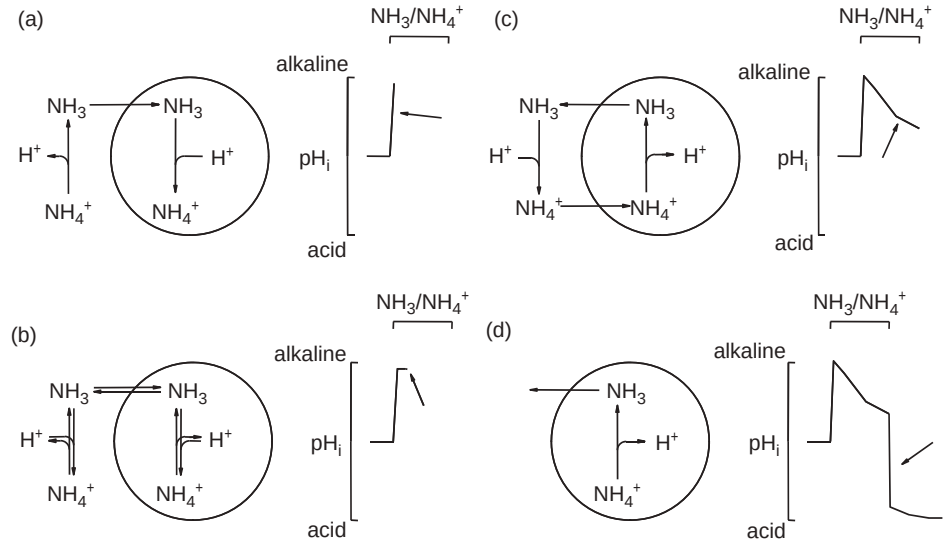

FIGURE 52.6 The NH_4^+ prepulse technique. a: When a cell is first exposed to a solution containing NH_4^+ and NH_3, there is a rapid increase in pH_i, due to the influx of NH_3. This rise in pH_i is blunted if NH_4^+ can also enter the cell. b: Eventually, $[NH_3]_i$ rises to the point where $[NH_3]_i$ transiently equals $[NH_3]_o$. Here, NH_4^+ is in equilibrium with NH_3 and H^+, both inside and outside the cell. pH_i is transiently stable. c: During the plateau phase, the entry of NH_4^+ leads to the formation of intracellular NH_3, which then exits the cell. This sets up a shuttling system for carrying H^+ into the cell. The NH_4^+ may enter via a simple conductive pathway, or be transported by a carrier such as the Na^+–K^+ pump or $Na^+/K^+/Cl^-$ cotransporter. Other acid loading processes (e.g., Cl^-–HCO_3^- exchange or metabolism) could also contribute to the plateau-phase acidification. d: Upon removing external NH_3/NH_4^+, most of the intracellular NH_4^+ gives up its H^+ and exits the cell as NH_3. Because NH_4^+ had accumulated in the cell during the plateau (either because of NH_4^+ uptake per se or other acid-loading processes), pH_i undershoots its initial value and the cell is acid loaded.

$[NH_3]_o$ constant.[165] Neutral weak bases such as lidocaine,[166] procaine,[166] and methylamine[51] also elicit intracellular alkalinizations that have $[B]_o$ and pH_i dependencies similar to those described for NH_3.

As noted above, the bacterial protein AmtB, an Rh homolog, functions as a gas channel permeable to NH_3.[47,48,157–159] In addition, aquaporins 1, 4, 5,[47] and AQP8[168] are permeable to NH_3.

It is possible to target the weak base NH_3 and selectively raise the pH of a specific intracellular compartment. For example, Carraro-Lacroix et al.[169] raised the pH of lysosomes by first endocytotically targeting urease to the lysosome compartment, and then exposing the cells to urea. The urease—now in the lysosomes—catalyzed the hydrolysis of the urea to produce one molecule of CO_2 but two of the weak base NH_3. Both because of the 2:1 stoichiometry of generated NH_3:CO_2 and the low initial lysosomal pH, the NH_3 dominates and the net effect is the NH_3-driven consumption of H^+ to form NH_4^+, thereby selectively alkalinizing the lysosome.

Flux of the Cationic, Conjugate Weak Acid

When one exposes a cell to a weak base, the dominant effect on pH_i generally reflects the influx of the highly permeant neutral weak base (e.g., NH_3). However, the flux of the conjugate weak acid (e.g., NH_4^+) may produce pH_i decreases that are substantial or even dominant. The effects on pH_i of applying and withdrawing NH_3/NH_4^+ can be separated into four steps. When a cell is exposed to NH_3/NH_4^+, the rapid influx of NH_3 leads to an initial rise in pH_i (Figure 52.6a). However, this alkalinization is actually blunted by the simultaneous, although smaller, influx of NH_4^+. The most general mechanism of NH_4^+ influx is the passive diffusion of NH_4^+,[170] although the carrier-mediated transport of NH_4^+ into cells can be substantial. For example, NH_4^+ can enter cells by substituting for K^+ on the Na^+–K^+ pump[171] and/or the $Na^+/K^+/Cl^-$ cotransporter.[7] Although most of the entering NH_4^+ remains NH_4^+, a small fraction (governed by the differences between pK_a' and pH_i) dissociates to form NH_3 and H^+. When external NH_3/NH_4^+ is removed, the NH_4^+ that previously entered, but failed to dissociate, now dissociates into NH_3 (which rapidly leaves the cell) and H^+ (which is trapped within the cell). As a consequence, the final pH_i (point c in Figure 52.5) is slightly lower than the initial value (point a).

The acidifying effect of NH_4^+ is much more evident when the NH_3/NH_4^+ exposure lasts beyond the initial influx (Figure 52.6a) and equilibration of NH_3 (Figure 52.6b). During an extended plateau phase, the continuing net influx of NH_4^+ produces a plateau-phase acidification, as illustrated in Figure 52.6c. In cells with a Cl^-–HCO_3^- exchanger (e.g., sheep cardiac

Purkinje fibers), this plateau-phase acidification may be augmented by efflux of HCO_3^- in exchange for Cl^-.[172] When the external NH_3/NH_4^+ is eventually withdrawn, the pH_i undershoot is greatly exaggerated (Figure 52.6d). The magnitude of the undershoot reflects the previous influx of NH_4^+. The longer the exposure to NH_3/NH_4^+, the more extensive the plateau-phase acidification, and the larger the undershoot. This undershoot represents an acute intracellular acid load. Indeed, the NH_4^+-prepulse technique is widely used for acid loading cells in studies of pH_i regulation.[170]

If the NH_4^+ electrochemical gradient is reversed during the plateau phase, in a cell for which the dominant mechanism of NH_4^+ entry is a passive flux, then pH_i rises during the plateau phase and the pH_i undershoot is converted to a shortfall.[165]

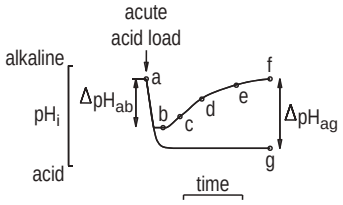

FIGURE 52.7 Determination of intracellular buffering power (β_i) in an intact cell from the pH_i change produced by an acute acid load. β_i is defined as the amount of strong acid injected (mmole/liter of cytoplasm) divided by the negative of the resultant fall in pH_i. Injecting acid, however, causes a biphasic change in pH_i: a rapid fall (segment ab), followed by a slower recovery (*bcdef*). The latter is due to extrusion of acid from the cell by one or more active transport processes. The true β_i must be computed from the pH_i change (ΔpH_{ag}) that would have occurred had all acid extrusion been blocked (segment ag). If the ΔpH_i instead is computed from the pH_i at points b, c, d, e or f, the computed β_i will be, at best, artifactually high (in the case of ΔpH_{ab}) and, at worst, will approach infinity (in the case of $\Delta pH_{af} = 0$). If the acid load is applied by exposing the cell to CO_2, then the active transport of HCO_3^- into the cell can sometimes cause the pH_i at point f to be greater than the pH_i at point a. In this case, ΔpH_{af} is <0, and the computed β_i will be negative.

INTRACELLULAR BUFFERING

Role of Buffering in pH_i Regulation

In the broadest sense, a pH buffer is any system that moderates the effects of an acid load by reversibly consuming H^+, or of an alkali load by reversibly releasing H^+. As we shall see, buffering in the intracellular fluid (e.g., the cytosol) is considerably more complex than in the blood and extracellular fluids. One can determine the buffering power (β) of either the extra- or intracellular fluid by applying an acute acid or alkali load, and measuring the resultant change in pH. β is defined as the amount of strong base (or strong acid) required to raise (or lower) pH by a given amount. Strictly speaking, the definition is given in differential notation. However, if the amount of base added (ΔB, given in mM) and the resultant pH increase (ΔpH) are sufficiently small, then β is approximated by:

$$\beta = \frac{\Delta B}{\Delta pH} \qquad (52.17)$$

This definition was originally proposed in slightly different form by Koppel and Spiro in 1914[173,174] and later modified to its present state independently by Michaelis[175] and Van Slyke.[176] Note that β is always a positive number; for a strong acid, ΔB and ΔpH are both negative. β is usually reported in mM per pH unit.

Among the several methods available for applying acid and alkali loads to the cytoplasm, the most direct is by injection of acid[151,77] or alkali into the cell with a micropipette. Such an acute acid load produces an abrupt fall in pH_i (see Figure 52.7, segment ab), the extent of which is determined by the amount of acid injected, the intracellular buffering power, and the ability of pH_i-regulatory mechanisms to blunt the pH_i decrease. As discussed in later sections, these pH_i-regulatory mechanisms can actively extrude acid from the cell and thereby return pH_i to its initial value (segment b–f). If we were to calculate β blindly, then we would see that the apparent β depends critically on the time of the ΔpH_i measurement following the acid load. For example, the apparent β is relatively low at point b and rises to infinity at point f, where ΔpH_i is zero.

An approach for avoiding the above ambiguity is to define intracellular buffering power (β_i) under conditions in which we completely block pH_i regulation. In this case, pH_i would follow the trajectory indicated by ag in Figure 52.7, the observed ΔpH_i at "infinite" time would be relatively large, and the computed β would be smaller than any of the possibilities described above. There are three justifications for excluding acid–base transport processes from the definition of β_i: *(a)* As we have just seen, excluding cellular transport processes makes the calculated β_i time independent (provided we allow enough time for pH_i to fall). *(b)* As we shall see later, transport of acid and/or base can generally be distinguished from buffering mechanisms by applying transport inhibitors or performing ion substitutions in the extracellular fluid. *(c)* Generally, these transport processes are not fully reversible. The buffering mechanisms included in our definition of β_i fall into three categories: *(a)* weak acids and bases (i.e., chemical buffers), *(b)* biochemical reactions consuming or releasing H^+, and *(c)* transport of acids or bases across organellar membranes. These mechanisms, which will be discussed in more detail later, can be justifiably grouped because there is presently no practical basis for distinguishing among them

when examining cytosolic pH regulation. Furthermore, they proceed very rapidly compared to the time currently required to measure pH_i.

Buffering mechanisms abate pH_i changes produced by acute acid and alkali loads that otherwise could damage the cell. However, these mechanisms cannot prevent a change in pH_i, only reduce its magnitude. Furthermore, buffering mechanisms cannot restore pH_i to its initial value following an acid or alkali load. Such recoveries are brought about by transport of acid and/or base across the cell membrane. As an illustration, consider the response of the cell to an acute intracellular acid load, as in Figure 52.7. Cellular buffers respond very rapidly, typically consuming more than 99.99% of the applied acid and limiting the initial fall in pH_i (*ag*). Active transport mechanisms respond more slowly, extruding acid from the cell and returning pH_i toward normal (b–f). During the transport-mediated pH_i recovery, H^+ previously taken up by the buffering mechanisms is now released and extruded from the cell. By the time pH_i returns to its initial level (f), the entire acid load has been extruded from the cell, and cellular buffering mechanisms have been returned to their pre-acid-loading state (a). Buffering mechanisms play no role in the steady state; in this case, acid loading exactly balances acid extrusion, and the state of cellular buffers is unchanged.

Mechanisms of Intracellular Buffering

The total intracellular buffering power (β^T) is the sum of chemical (i.e., weak-acid/base equilibria), biochemical, and organellar buffering powers.

Chemical Buffering

A weak base (B) of valence *n* reacts with H^+ to produce its conjugate weak acid (HB) of valence n + 1:

$$B^n + H^+ \rightarrow HB^{n+1} \tag{52.18}$$

This equilibrium is described by the relation:

$$K_a' = \frac{[B^n][H^+]}{HB^{n+1}} \tag{52.19}$$

where K_a' is the apparent acid dissociation constant. This relation can also be expressed in logarithmic form, whereupon it takes the form of Equation 52.16. Starting with the definition of β (Equation 52.17) and the statement of chemical equilibrium (Equation 52.19), one can express β as a function of $[H^+]$, K_a', and total buffer concentration.[173,175]

$$\beta = \frac{2.3K_a'[H^+]}{(K_a' + [H^+])^2}[TB] \tag{52.20}$$

where 2.3 approximates ln(10), and [TB] is the concentration of total buffer (i.e., $[TB] = [B^n] + [HB^{n+1}]$). By obtaining the derivative of β with respect to $[H^+]$ (i.e., $d\beta/d[H^+]$) and setting this equal to zero, one can show that β is maximal when $[H^+]$ equals K_a'.[173] This maximal buffering power (β^{max}) is simply:

$$\beta^{max} \cong 0.58\,[TB] \tag{52.21}$$

Although the pH of maximal buffering power is in general unique to the buffer, all buffers have the same molar buffering power ($\beta^{max}/[TB]$), and the same dependence of β on the difference $pH - pK_a'$. If more than one buffer is present, then β^T is simply the sum of the individual buffering powers, each computed from Equation 52.20.

The foregoing equation describing β was derived by taking the partial derivative of $[B^n]$ with respect to pH at a fixed [TB]. That is, the analysis applies only to buffers in a closed system, in which [TB] is constant. Closed-system buffers include a solution of a nonvolatile buffer (e.g., inorganic phosphate) in a beaker, a solution of a volatile buffer (e.g., CO_2/HCO_3^-) in a capped syringe, and an impermeant buffer (e.g., a protein) in the cytoplasm of a cell. In such a closed system, β for CO_2/HCO_3^- would be rather low at normal pH_i values, because pH_i (~7.0) is far higher than the pK_a' of 6.1. However, cells are generally not a closed system with respect to CO_2/HCO_3^-. Rather, CO_2 usually freely exchanges with the extracellular fluid (ECF) so that the total intracellular CO_2 (i.e., $[CO_2]_i + [HCO_3^-]_i$) can change appreciably during intracellular acid–base disturbances. For example, when H^+ is added to cytoplasm containing CO_2/HCO_3^-, H^+ combines with HCO_3^- according to the reactions:

$$H^+ + HCO_3^- \rightarrow H_2CO_3 \rightarrow H_2O + CO_2 \tag{52.22}$$

The cytoplasmic CO_2 so formed is lost to the ECF. Thus, it is $[CO_2]_i$ that remains constant, while $[HCO_3^-]_i$ and [total CO_2]$_i$ both fall. Because there is no buildup of CO_2 within the cell, the extent of the reaction in Equation 52.22 is limited only by the availability of HCO_3^-. The amount of H^+ absorbed (i.e., buffered) by the CO_2/HCO_3^- system exactly equals the amount of HCO_3^- that disappears. That is:

$$\beta^{CO_2} = \frac{\Delta[HCO_3^-]}{\Delta pH} \tag{52.23}$$

where β^{CO_2} is the CO_2 buffering power. When this equation, in differential form, is combined with the Henderson-Hasselbalch equation, it can be shown that:

$$\beta^{CO_2} = 2.3\,[HCO_3^-] \tag{52.24}$$

when $[CO_2]$ is held constant. At very high pH values, when the equilibrium $H^+ + CO_3^{2-} \rightleftarrows HCO_3^-$ cannot be

ignored, the term 4.6 $[CO_3^{2-}]$ must be added to the right-hand side of Equation 24. This equation describes the buffering power of CO_2/HCO_3^- in an open system, such as a solution in a beaker equilibrated with gaseous CO_2. Because most cell membranes are highly permeable to CO_2, this gas rapidly equilibrates across membranes and stabilizes $[CO_2]_i$, provided the ECF behaves as an infinite reservoir for CO_2. Thus, an isolated cell *in vitro* behaves as an open system for CO_2/HCO_3^-. Because the intact organism has mechanisms (e.g., alveolar ventilation in higher vertebrates) for stabilizing $[CO_2]$ in the ECF, CO_2/HCO_3^- behaves as an open-system buffer *in vivo*, both in the extra- and intracellular spaces.

In an open system, the CO_2/HCO_3^- buffer pair generally makes a substantial contribution to β^T. For example, at a pH_i of 7.1, the buffering power of all non-CO_2 buffers in rat renal mesangial cells is only about 10 mM,[19] whereas the computed β^{CO_2} is nearly 29 mM when the cell is equilibrated with 5% CO_2. Thus, β^{CO_2} accounts for nearly 75% of the β^T of 39 mM/pH unit.

It is essential to distinguish clearly between open- and closed-system buffers of a cell. The cell is a closed system for intracellular buffers that do not readily cross the cell membrane (e.g., inorganic phosphate and the imidazole groups of proteins). Thus, these buffers are influenced by the attributes of the cell (e.g., volume, temperature, and metabolic state), and not those of the extracellular fluid. These are termed *intrinsic buffers*.[165] Biochemical and organellar buffering mechanisms (*vide infra*) are also intrinsic, and the total intrinsic buffering power (β^I) is the sum of biochemical, organellar, and intrinsic chemical buffering powers.

The cell is an open system when one member of the buffer pair readily crosses the cell membrane. The buffering power of such a buffer pair is very sensitive to extracellular conditions. As noted earlier, β^{CO_2} is proportional to $[HCO_3^-]_i$, which in turn is completely determined by pH_i and the extracellular P_{CO_2} (assuming that CO_2 equilibrates across the cell membrane). The cell also behaves as an open system for buffers other than CO_2/HCO_3^-. These are generally conjugate pairs of which one member is a small, neutral molecule. Examples include NH_3/NH_4^+ and acetic acid/acetate. Regardless of whether the charged species is a cation or an anion, the intracellular buffering power of an open-system buffer pair is always $2.3 \times [\text{charged species}]_i$, provided the neutral species is equilibrated across the cell membrane. Thus, the intracellular buffering power of such a buffer pair is sensitive not only to the total amount of the buffer in the ECF (i.e., $[TB]_o$), but also to pH_o. As with CO_2/HCO_3^-, these other open-system buffers can sometimes be the dominant component of β^T. For example, β^I in squid axons is $\sim$9 mM.[170] When these axons are exposed to a pH_o–7.7 NH_3/NH_4^+ solution containing only 10 mM total ammonium, $[NH_4^+]_i$ rises to 10 mM. The computed β^{NH_3} is 23 mM, nearly 70% of β^T. Because the buffering power of such open-system buffers is so sensitive to factors external to the cell (e.g., pH_o), these buffers are termed *extrinsic*.[165] The total chemical buffering power of a cell is the sum of the buffering powers of the individual conjugate acid/base buffer pairs, be they intrinsic (closed system) or extrinsic (open system).

Biochemical Buffering

Because certain biochemical reactions consume or release H^+ and are pH_i sensitive, they can act as H^+ buffers.[3] Examples include hydrolysis of ATP (which releases H^+) and hydrolysis of phosphocreatine (which consumes H^+). During the Cori cycle, the liver converts lactic acid into glucose, whereas skeletal muscle breaks down the glucose to produce ATP and more lactic acid. Also, H^+ buffering can arise when reactions induce a change in the pK_a' of an ionizable group. A classic example is the buffering reactions of oxygenated versus deoxygenated hemoglobin.

A well studied example of biochemical buffering are reactions involving intermediary metabolites in rat brain.[179] Cells that are acutely acid loaded with an increase of P_{CO_2} in the ECF respond by reducing intracellular levels of several acid metabolic intermediates (i.e., the acids of lactate, pyruvate, citrate, α-ketoglutarate, malate, glutamate, and aspartate), while raising those of glucose and glucose-6-phosphate. These observations are consistent with the hypothesis that reducing pH_i inhibits a step in the glycolytic pathway, possibly the phosphofructokinase reaction. Indeed, mouse muscle phosphofructokinase is markedly sensitive to pH changes[180]; reducing *in-vitro* pH from 7.2 to 7.1 produces more than a 90% inhibition. Rat-brain cells respond in the opposite fashion to acute intracellular alkali loads. Increases in pH_i induced by lowering the P_{CO_2} in the ECF lead to increased levels of lactate and pyruvate.[181] Thus, the biochemical machinery of these cells seems to respond appropriately to pH_i changes, consuming H^+ in response to intracellular acid loads and releasing H^+ in response to alkali loads. The extent to which such biochemical reactions contribute to overall buffering power can be computed from changes in steady-state metabolite levels, provided that such changes are reciprocally linked to the production or consumption of neutral and/or readily diffusible molecules. For example, the consumption of one citrate molecule removes three H^+, whereas malate removes two, and pyruvate, one. From data on rat brain,[182] the buffering power of biochemical reactions amounts to about half that provided by all non-CO_2 physicochemical buffers. Biochemical buffering power can be defined and quantitated in a manner analogous to

chemical (*vide supra*) and organellar (*vide infra*) buffering powers [see Equation 52.17]. The biochemical buffering reaction can be written as:

$$R^n + q\ H^+ \rightleftarrows P^{n+q} \qquad (52.25)$$

where R is the reactant, P is the product, n is the valence, and q is the H^+ stoichiometry ($q > 0$). The biochemical buffering power is thus:

$$\beta = \frac{\Delta[R^n] \cdot q}{\Delta pH} \qquad (52.26)$$

As noted above, biochemical and organellar (*vide infra*) buffering mechanisms, in addition to closed-system chemical buffers, comprise the intrinsic buffers.

Organellar Buffering

H^+-transport systems have been identified or implicated in many intracellular organelles,[3,183] including mitochodria,[184–191] lysosomes,[192] sarcoplasmic reticulum,[193] Golgi network,[92,90] endosomes,[194–198] chromaffin granules,[199,192] and zymogen granules.[200] In addition, three of the cloned Na-H exchangers (NHE6, 7, and 9) are found in organellar membranes where they may contribute to organellar pH regulation.[167,713] For reviews of vesicular H^+ pumps, see refs.[201,202] It would be reasonable to expect decreases in cytoplasmic pH to stimulate H^+ uptake and/or inhibit H^+ extrusion by at least some organelles, and increases in pH_i to produce the opposite effects. Such buffering would lead to a net transfer of H^+ into these organelles following intracellular acid loads, and a net movement of H^+ into the cytoplasm following alkali loads. A transfer of acid or base across organellar membranes would constitute a *de facto* buffer mechanism for the bulk intracellular fluid. Although the extent to which such hypothetical organellar buffering mechanisms contribute to β^T is not established, it can be inferred from published data that changes in extraorganellar pH can produce at least small changes in the intraorganellar pH of mitochondria,[127] lysosomes,[192] and sarcoplasmic reticulum vesicles.[193] Organellar buffering power can be defined and quantitated in a manner analogous to that for physicochemical and biochemical buffering [see Equation 52.17]. The organellar buffering reaction is written:

$$\text{organelle}() + H^+ \rightleftarrows \text{organelle}(H^+) \qquad (52.27)$$

where the parentheses refer to organellar contents. Organellar buffering power is thus:

$$\beta = \frac{\Delta[\text{organelle}()]}{\Delta pH_i} \qquad (52.28)$$

Organellar buffers, along with the biochemical and closed-system chemical buffers, comprise β^I.

Measurement of Intracellular Buffering Power

Titration of Cell Homogenates

The easiest method for estimating β_i is to homogenize a tissue sample and titrate the homogenate. The slope of the pH titration curve is the buffering power of the homogenate. However, some disadvantages limit the accuracy of this technique. First, homogenization may disrupt cellular organelles and thus obscure the organellar buffering contribution. Second, homogenization-induced changes in metabolism must be prevented, for example by quick-freezing the sample before homogenization,[203] and then performing the titration either at low temperature[203] or in the presence of an inhibitor such as fluoride.[182] Blocking metabolism will reduce biochemical buffering, and reducing temperature generally increases pK_a' values, thereby altering chemical buffering.

Microinjection

The most straightforward approach for estimating β_i in an intact cell is to microinject a known amount of acid or base into a cell and monitor the resultant change in pH_i. The microinjection can be achieved either by iontophoresis[15] or by pressure injection.[177] This technique enables one to compute the total β_i (i.e., sum of physicochemical, biochemical, and organellar buffering) of the cell. For small neurons incubated in a CO_2-free solution, the iontophoresis and pressure-injection methods give β_i values of 10.8 mM/pH unit[15] and 10.3 mM/pH unit,[177] respectively. Disadvantages of this direct *in-vitro* titration approach include the necessity of using cells that (1) are large enough to withstand the microelectrode impalements, and (2) have a sufficiently compact geometry to permit rapid equilibration of the injected acid or base throughout the cell.

Weak-Acid and Base Methods

An approach that, at least in principle, is applicable to cells of all shapes and sizes, is measurement of the pH_i change produced by exposing the cell to a neutral weak acid HA ($HA \rightleftarrows H^+ + A^-$), or weak base B ($HB \rightleftarrows H^+ + B$). As discussed earlier, exposing a cell to a neutral weak acid leads to a decrease in pH_i as HA enters the cell and partially dissociates into H^+ and A^-. The entry and dissociation halt once $[HA]_i = [HA]_o$. The extent of the dissociation depends on the weak acid's pK_a', as well as the initial pH_i. Virtually all of the released H^+ is consumed by intracellular buffers (Figure 52.8A and B); the remaining fraction is responsible for the accompanying pH_i decrease. Although HA/A^- is a buffer, it does not participate in buffering the acid load imposed by the intracellular dissociation of HA. Similarly, a B/BH^+ buffer

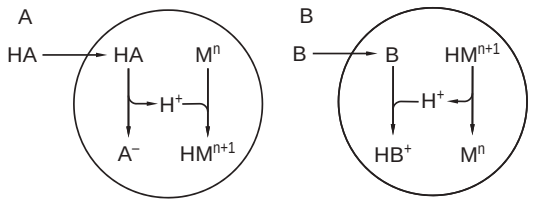

FIGURE 52.8 Measurement of intracellular buffering power by exposure to a neutral weak acid or base. A: When a cell is exposed to a neutral weak acid (HA), HA enters the cell, where some of it dissociates into H^+ and A^-. Virtually all of this H^+ is taken up by buffers (M; valence = n) that are titrated to their conjugate weak acids (HM; valence = n + 1). Thus, for each A^- formed, almost exactly one H^+ is consumed by non-HA/A^- buffers. $\beta = -\Delta[A^-]_i/\Delta pH_i$. B: When a cell is exposed to a weak base, B, the base enters the cell, where some of it combines with H^+ to form HB^+. Virtually all of this H^+ is derived from buffers (HM; valence = n + 1) that are titrated to their conjugate weak bases (HM; valence = n). Thus, for each HB^+ formed, almost exactly one H^+ is released by non-B/HB^+ buffers. $\beta = -\Delta\,[HB^+]_i/\Delta pH_i$.

system can not buffer changes in pH_i caused by the entry (or exit) of B. Because the dissociation of HA leads to the formation of one A^- for each H^+, the magnitude of the intracellular acid load is $\Delta[A^-]_i$. This amount of added acid is the additive inverse of the amount of base added (ΔB) in the preceding definition of β:

$$\beta_i = \frac{\Delta B}{\Delta pH_i} = \frac{-\Delta[A^-]_i}{\Delta pH_i} \qquad (52.29)$$

Note that β_i is the non-HA/A^- buffering power of the cell. It is the sum of chemical, biochemical, and organellar buffering. ΔpH_i is directly measured, and $\Delta[A^-]_i$ is calculated from final and initial values of pH_i and $[HA]_o$. In the simplest case, the initial $[A^-]_i$ is zero, and final $[A^-]_i$ is given by:

$$[A^-]_i = [HA]\cdot 10^{pH_i - pK_a'} \qquad (52.30)$$

assuming $[HA] = [HA]_i = [HA]_o$. A commonly used weak acid for measuring β_i is CO_2, for which:

$$\beta_i = \frac{\Delta B}{\Delta pH_i} = \frac{-\Delta[HCO_3^-]_i}{\Delta pH_i} \qquad (52.31)$$

β_i is the non-CO_2/HCO_3^- or intrinsic buffering power, β_i^I. Once β_i^I is known, the total intracellular buffering power (β_i^T) can be obtained by computing the open-system CO_2 buffering power:

$$\beta_i^T = \beta_i^I + \beta_i^{CO_2} \qquad (52.32)$$

where $\beta_i^{CO_2}$, the CO_2 buffering power, is given by $2.3 \times [HCO_3^-]_i$, as outlined above.

There are as many as three major drawbacks of using the weak-acid method to measure β. First, $[HA]_i$ may not exactly equal $[HA]_o$. In rapidly metabolizing cells for instance, $[CO_2]_i$ may exceed $[CO_2]_o$. Second, the pH_i decrease elicited by the entry of HA may stimulate acid-extrusion mechanisms (i.e., pH_i-regulating systems described below). Thus, the actual ΔpH_i may be smaller than if all acid–base transport had been blocked (Figure 52.7). By underestimating ΔpH_i, one will overestimate β_i. This error should in principle be eliminated by blocking the pH_i-regulating systems.[165] One can also minimize the error by extrapolating the pH_i-versus-time curve back to a point at which acid extrusion is judged to have had no effect on pH_i.[17,204–206] For example, in the hypothetical experiment of Figure 52.7, one could extrapolate the pH_i recovery (i.e., bcdef) back to the time of the acid load. A third potential drawback of the weak-acid method is that the weak acid could indirectly alter pH_i by modifying cellular metabolism. Thus, it is critical that the weak acid affect pH_i only by entering and dissociating into H^+ and A^-. Otherwise, any other effect on pH_i will lead to an error in the calculation of β_i.

The intrinsic intracellular buffering power can also be determined by exposing a cell to a neutral weak base, B (Figure 52.8B). As described in the preceding section, exposing a cell to B leads to a pH_i increase as most of the entering B combines with H^+ to form HB^+. The entry of B and the alkali loading of the cell continues until $[B]_i = [B]_o$. Almost all of the entering H^+ that is converted to HB^+ is derived from cellular buffers. The minute amount that comes from the pool of free H^+ is responsible for the rise in pH_i. Thus, the change in $[HB^+]_i$ is equivalent to the amount of strong base added to the intracellular fluid:

$$\beta_i = \frac{\Delta B}{\Delta pH_i} = \frac{\Delta[HB^+]_i}{\Delta pH_i} \qquad (52.33)$$

In the simplest case, the initial $[HB^+]_i$ is zero, and the final $[HB^+]_i$ is calculated from the statement of chemical equilibrium:

$$[HB^+]_i = [B]\cdot 10^{pK_a' - pH_i} \qquad (52.34)$$

assuming that $[B] = [B]_i = [B]_o$. The most commonly used weak base is NH_3:

$$\beta_i = \frac{\Delta B}{\Delta pH_i} = \frac{\Delta[NH_4^+]_i}{\Delta pH_i} \qquad (52.35)$$

$[NH_4^+]_i$ is determined in a manner analogous to that outlined earlier for $[HCO_3^-]_i$. Note that β_i in this case is the non-NH_3/NH_4^+ buffering power (i.e., the buffering power of all buffers other than NH_3/NH_4^+). If the NH_3 titration is performed in the absence of CO_2/HCO_3^-, then the measured β_i is β_i^I. If CO_2/HCO_3^- is present, then the measured β_i is $\beta_i^I + \beta_i^{CO_2} = \beta_i^T$. An approach commonly used with NH_4^+ is to compute β from the pH_i decrease caused by decreasing or withdrawing

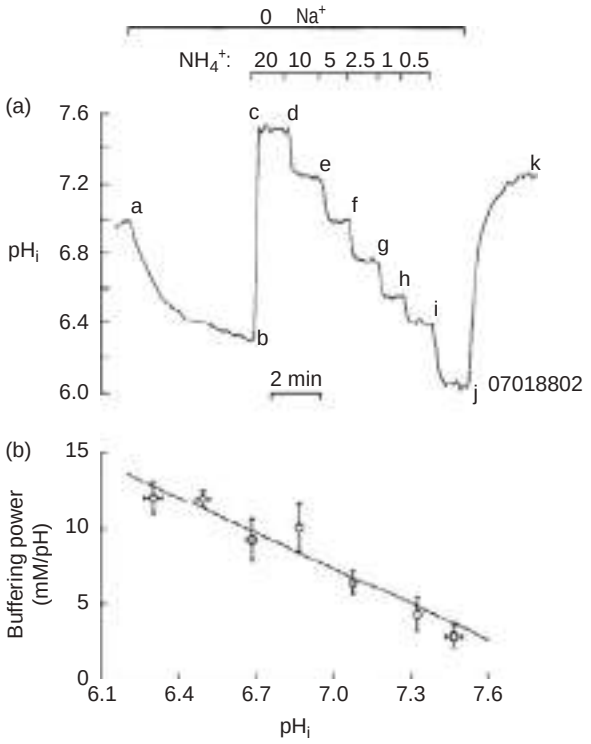

FIGURE 52.9 The dependence of intrinsic intracellular buffering power on pH_i. a: The effect on pH_i of stepwise reductions in $[NH_4^+]_o$ in the absence of CO_2/HCO_3^-. Na^+ was removed to block acid-extruding mechanisms. The subsequent reduction in $[NH_4^+]_o$ from 20 to 10 to 5 to 2.5 to 1 to 0.5 to 0 mM produced discrete acid loads. This experiment was performed on a single renal mesangial cell, the pH_i of which was measured using BCECF and a microscope-based fluorometry system. b: Computation of β_i. The acid load imposed by each stepwise reduction in $[NH_4^+]_o$ was computed from the change in $[NH_4^+]_i$. The latter was calculated from $[NH_4^+]_o$, pH_o and pH_i. The mean buffering power in the pH_i range covered by the stepwise fall in pH_i was computed as $\beta_i = \Delta[NH_4^+]_i/\Delta pH_i$. *(Reproduced from ref. [19].)*

external NH_4^+. During such experiments, one usually blocks acid-extrusion mechanisms (e.g., by removing external Na^+) that would likely counteract the acidification. By reducing $[NH_4^+]_o$ in a stepwise fashion (Figure 52.9a), one can compute β_i as a function of pH_i (Figure 52.9b), as has been done in mesangial cells[19] and gastric parietal cells.[207] An alternate approach one can use with NH_4^+ is to compute β_i from the pH_i increase that accompanies stepwise increases of external NH_4^+.[17]

ACID–BASE TRANSPORT SYSTEMS

Acid–base transporters can be divided into two groups: acid loaders and acid extruders. Acid loaders move H^+ into, or base equivalents (e.g., OH^- or HCO_3^-) out of, cells and generally contribute to the recovery of pH_i from acute intracellular alkali loads. In contrast, acid extruders move H^+ out of, or base equivalents into, cells and generally contribute to the recovery of pH_i from acute intracellular acid loads. In the remainder of this section, we discuss major acid–base transporters in each of these two categories. For each transporter, we will examine at least the following three issues: (1) general function and molecular identity, (2) energetics and role in pH_i regulation, and (3) effects of pharmacological agents. Please consult the following relevant chapters in this book on the molecular biology of Na^+-coupled HCO_3^- transporters (Chapter 53) and anion exchangers (Chapter 54), as well as refs.[167,713,714] on Na^+–H^+ exchangers.

Acid-Loading Mechanisms

Introduction

As noted above, passive fluxes of H^+, monovalent cationic acids (e.g., NH_4^+), and monovalent anionic bases (e.g., HCO_3^-) are governed by the electrochemical gradient for the ion in question, and normally tend to acidify the cell. In principle, such passive transport processes could be exploited for protecting the cell against alkaline loads. Nevertheless, such passive processes generally do not appear to have a substantial impact on pH_i. A notable exception discussed above is the $GABA_A$-activated Cl^- channel at the crayfish neuromuscular junction[148] and in cells from turtle cerebellum[149] and rat hippocampus.[150,151] This Cl^- channel can conduct HCO_3^- and thus mediate a substantial HCO_3^- efflux that lowers pH_i. For the most part, however, major acid-loading transport pathways are HCO_3^- transporters—the most common ones being Cl^-–HCO_3^- exchange and Na^+/HCO_3^- cotransport.

Cl^-–HCO_3^- and Cl^-–OH^- Exchangers

GENERAL FUNCTION AND MOLECULAR IDENTITY

Found in a wide variety of animal-cell membranes, Cl^-–HCO_3^- exchangers normally couple the influx of Cl^- to the efflux of HCO_3^- (Figure 52.10a–h). Na^+-independent Cl^-–HCO_3^- exchangers (to distinguish them from the Na^+-dependent Cl^-–HCO_3^- exchangers discussed later) are thought to serve two major functions in non-epithelial cells: regulation of intracellular pH (pH_i), and regulation of intracellular $[Cl^-]$. The erythrocyte exchanger is known as the "band 3 protein" because of its position on SDS-polyacrylamide gels (for review, see ref.[208]) Band 3 has also been termed AE1 because it was the first "anion exchanger" to be cloned and sequenced[209]). As described in greater detail in Chapter 54, the AE gene subfamily comprises at least three related genes AE1, AE2, and AE3. The AE gene

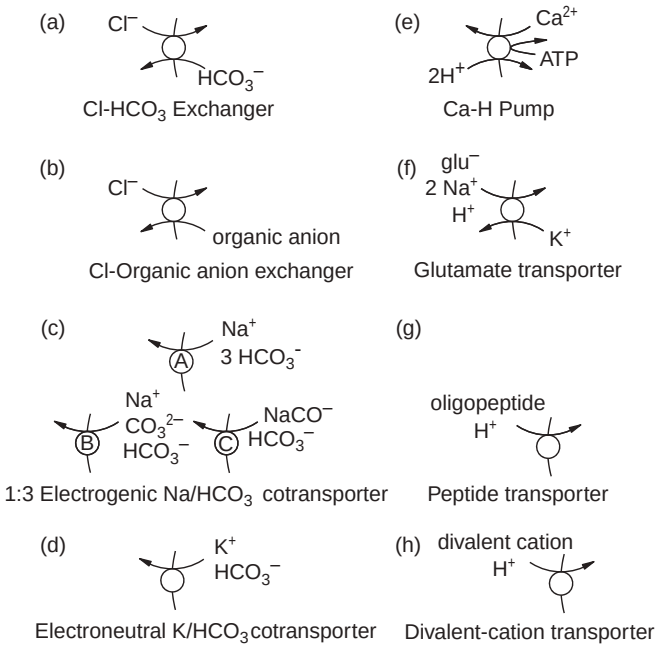

FIGURE 52.10 Acid-loading mechanisms. A: Cl^-—HCO_3^- exchanger. B: Cl^--organic anion exchanger. C: 1:3 Electrogenic N^+/HCO_3^- cotransporter. The electrogenic Na^+/HCO_3^- cotransporter present in the basolateral membranes of epithelial cells has a stoichiometry of 3 HCO_3^- equivalents for each Na^+. Three alternative models are shown. D: Electroneutral K^+/HCO_3^- cotransporter. E: Ca^{2+}—H^+ pump. F: Glutamate transporter. G: Peptide transporter. H: Divalent-cation transporter.

subfamily is a branch of the bicarbonate-transporter (SLC4) family that includes the Na^+-coupled HCO_3^- transporter subfamily (see Chapter 53). Several members of the SLC26 family can also mediate Cl^-—HCO_3^- exchange.[210,211] However, unlike the AE family, which virtually always exhibits a Cl^-: HCO_3^- stoichiometry of 1:1, the SLC26 family can exhibit stoichiometries of 1:2, 1:1, or 2:1[212–214]; for review, see ref.[211].

INVOLVEMENT OF Cl^- AND HCO_3^-/OH^-; ENERGETICS

Red cell AE1 mediates electroneutral homo- or hetero-exchange of monovalent anions with a 1:1 stoichiometry, exhibiting a substrate preference of $Cl^- \sim HCO_3^- \sim NO_3^- > Br^- > F^- > I^-$ > divalent oxyanions.[215,216] Sulfate is cotransported with H^+.[217] Monovalent anion exchange can be reasonably well modeled by a ping-pong kinetic scheme, thought to reflect the alternation of an anion binding site between one side and the other of the membrane.[218–221] Because the Cl^-:HCO_3^- stoichiometry is 1:1, the transporter is electroneutral. Thus, the direction of net transport is determined by the sum of the chemical gradients for Cl^- (i.e., $[Cl^-]_i/[Cl^-]_o$) and HCO_3^- (i.e., $[HCO_3^-]_i/[HCO_3^-]_o$). Because the inward Cl^- gradient is generally greater than the inward HCO_3^- gradient in cells other than erythrocytes, the former dominates, driving HCO_3^- out of the cell. The transporter is easily reversed, however, by inverting the sum of the Cl^- and HCO_3^- gradients. Indeed, a classic pH_i assay for Cl^-—HCO_3^- exchange activity involves removing external Cl^- that evokes a rapid pH_i increase.[222,223] In some cell types, the transporter can also be reversed by lowering $[HCO_3^-]_i$, as would occur during severe intracellular acid loads. The exchanger operating in reverse then becomes an acid extruder, moving HCO_3^- into the cell and contributing to the pH_i recovery from the acid load.

Some Cl^-—HCO_3^- exchangers have a very high affinity for HCO_3^- and transport can take place with low levels of HCO_3^- ($\sim$100 μM) in a nominally HCO_3^--free solution. For example, removing external Cl^- from the solution bathing rat osteoclasts can elicit a dramatic DIDS-sensitive pH_i increase, even in the nominal absence of CO_2/HCO_3^-.[224] However, vigorously bubbling the solutions with 100% N_2 gas greatly reduces the pH_i increase.

Sun et al.[225] reported the presence of a Cl^-—OH^- exchanger (or H^+/Cl^- cotransporter), which operates in parallel with a "conventional" Cl^-—HCO_3^- exchanger, in guinea-pig ventricular myocytes. The putative Cl^-—OH^- exchanger is Cl^- dependent; it is activated by low pH_o[225] and also by high pH_i.[226] The evidence that it is a Cl^-—OH^- exchanger—rather than a Cl^-—HCO_3^- exchanger—is that it functions as an acid loader in the presence or absence of CO_2/HCO_3^-, and is insensitive to DIDS.[225] The activation of the exchanger by lowering pH_o is unaffected by a CO_2-free, 100% N_2 atmosphere.[227] As attractive as it is to conclude that the transporter is a Cl^-—OH^- exchanger, it is difficult to rule out the possibilities that: (1) ambient and metabolically produced CO_2/HCO_3^- have not been totally eliminated, and (2) the transporter has an exceedingly high affinity for HCO_3^-. Putative Cl^-—OH^- exchange activity also contributes to NaCl reabsorption in intestinal epithelial cells.[228]

Based on experiments on rat-brain synaptosomes, Martínez-Zaguilán et al.[229] have concluded that a H^+/Cl^- cotransporter is responsible for (1) the pH_i increase elicited by removing extracellular Cl^-, and (2) the faster pH_i recovery from an acid load in the absence of extracellular Cl^-. However, it is generally difficult to distinguish H^+ transport in one direction from OH^- and/or HCO_3^- transport in the opposite direction.

The CLC gene family encodes proteins that are either Cl^- channels or Cl^-—H^+ exchangers.[230] While ClC1, ClC2, ClC-Ka, and ClC-Kb are plasma-membrane Cl^- channels, ClC3 through ClC7 are thought to be vesicular Cl^-—H^+ exchangers. Although these ClCs are primarily expressed intracellularly, low levels of ClC4, ClC5, and ClC6 expression are observed

at the plasma membrane, leading to Cl^-–H^+ exchanger activity at this location.[231,230] The other ClCs in this group (i.e., ClC3 and ClC7) are also likely to be exchangers because each member of the group possesses a key glutamate residue that is necessary for such exchange.

DEPENDENCE ON pH_i

By analogy to acid extruders, which are often stimulated by decreases in pH_i, one might expect acid loaders such as Cl^-–HCO_3^- exchange to be stimulated by increases in pH_i. Indeed, Cl^-–HCO_3^- exchange activity in many cells including Vero and L-cells,[232] mesangial cells,[163] and lymphocytes[233] is low but measurable at pH_i values as low as 6.5, increases to somewhat higher levels in the physiological pH_i range, and then rises very steeply as pH_i increases above ~7.6.

In more recent expression studies, the widely distributed AE2 also appears to exhibit greater activity at more alkaline pH_i values.[234–236] The pH sensor is located somewhere within the C-terminal transmembrane domain,[237,238] and its apparent pK_a is modulated by residues within the N-terminal cytoplasmic domain.[237,239,240] Multiple histidines within the transmembrane domain contribute to AE2 activity, as well as pH_i and pH_o sensitivies.[241] Furthermore, residues within the first putative re-entrant loop of AE2 also contribute to pH_i and/or pH_o sensitivities.[242]

EFFECTS OF PHARMACOLOGICAL AGENTS

The non-erythroid Cl^-–HCO_3^- exchanger is blocked by stilbene derivatives such as DIDS and SITS,[113,243] as well as the noncompetitive inhibitor niflumic acid.[244,245] Some of the more potent AE inhibitors include oxonol dyes at the nanomolar level.[246–249]

Electrogenic Na^+/HCO_3^- Cotransporters

GENERAL FUNCTION AND MOLECULAR IDENTITY

Present in the basolateral membrane of several epithelia, including the renal proximal tubule, is an electrogenic Na^+/HCO_3^- cotransporter[13] that mediates the isodirectional flux of one Na^+ and—in the simplest model—three HCO_3^- ions.[250] In epithelia, the cotransporter normally mediates a net efflux of Na^+ and HCO_3^- (see below), and therefore functions as an acid loader (Figure 52.10C). In the early proximal tubule, Na^+/HCO_3^- cotransport appears to be the major route of HCO_3^- efflux across the basolateral membrane. The transporter thus plays a key role in HCO_3^- reabsorption, and probably makes an important contribution to Na^+ reabsorption as well.

Our understanding of Na/Bicarbonate Cotransporters (or NBCs), as well as other bicarbonate transporters has expanded immensely over the past 16 years with the molecular identification of these proteins. As described in Chapter 53, ten *SLC4* genes encode members of the family of bicarbonate transporters including electrogenic and electroneutral NBCs, the Na-driven Cl^-–HCO_3^- exchanger (NDCBE), and the Na^+-independent anion exchangers (AEs). At the amino-acid level, the transporters share considerable homology to one another, and are therefore predicted to have similar membrane topologies.

INVOLVEMENT OF Na^+ AND HCO_3^-; ENERGETICS

In the salamander proximal tubule, the cotransporter has an absolute requirement for both Na^+ and HCO_3^-.[13] The cotransporter in rabbit proximal convoluted tubules can still function even in the absence of added HCO_3^-,[251] probably due to intracellular formation of HCO_3^- from metabolically-derived CO_2. Removing external HCO_3^- elicits a rapid fall in pH_i and $[Na^+]_i$, and a near-instantaneous depolarization of the basolateral membrane. A similar pattern of changes is caused by removing external Na^+. All effects are fully reversible. The DIDS-sensitive depolarization elicited by removing Na^+, which makes it appear as though Na^+ is moving as an anion, is practically diagnostic of electrogenic Na^+/HCO_3^- cotransport.

A 1:3 stoichiometry is accounted for by any of the schemes outlined in Figure 52.10C.[252] The model in which Na^+ exits together with one CO_3^{2-} and one HCO_3^- (Figure 52.10C, model B) is supported by the observation that SO_3^{2-} stimulates Na^+ uptake by basolateral membrane vesicles,[253] presumably by interacting at a CO_3^{2-} site. However, more recent studies indicate that NBCe1-A—at least as expressed in *Xenopus* oocytes—does not interact with either SO_3^- or HCO_3^-.[254,255] In preliminary work, Grichtchenko and Boron[256] as well as Lee et al.[257] performed a more direct assessment of CO_3^{2-} transport by using extracellular pH electodes to measure NBCe1-induced changes in surface pH (pH_s) of *Xenopus* oocytes expressing both the transporter and extracellular-facing carbonic anhydrase (CAIV). Depolarization-induced activation of the NBC elicited an expected decrease in pH_s as base equivalents were transported into the cell. However, applying a CA inhibitor caused the magnitude of the pH_s decrease to increase rather than to diminish. The larger response is consistent with the hypothesis that NBCe1 mediates CO_3^{2-} transport and that the role of CAIV is to consume H^+ generated as the reaction $HCO_3^- \rightarrow CO_3^{2-} + H^+$ replenishes CO_3^{2-} near the cell surface.

The direction of net cotransport is determined by the combined transmembrane gradients for Na^+, HCO_3^- and voltage. If one focuses on Na^+, then the epithelial cotransporter acts as an auxiliary Na^+ pump. As far as its classification as a primary, secondary or

tertiary active Na^+ transporter is concerned, the cotransporter occupies an unusual niche. The Na^+–K^+ pump directly or indirectly establishes the membrane voltage. This pump also indirectly establishes the Na^+ gradient that energizes the Na^+–H^+ exchanger, which raises pH_i and thereby establishes the HCO_3^- gradient. These voltage and HCO_3^- gradients, directly or indirectly established by the Na^+–K^+ pump, drive the epithelial Na^+/HCO_3^- cotransporter in the direction of the net Na^+ efflux. Thus, this Na^+ extrusion can be viewed as a secondary/tertiary active transport process.

EFFECTS OF PHARMACOLOGICAL AGENTS

Similar to Cl^-–HCO_3^- exchangers, Na^+/HCO_3^- cotransporters are inhibited by stilbene derivatives such as DIDS[13]; for review, see ref.[258]. Cloned NBCe1 expressed in oocytes can also be inhibited by benzamil,[259] the non-steroidal anti-inflammatory drug tenidap,[259,260] niflumic acid,[261] and diBAC oxonol dyes.[261] Recently, the *N*-cyanosulphonamide S0858 has been identified as an NBC inhibitor in renal epithelial cells[262] and ventricular myocytes.[263,264]

Electroneutral K^+/HCO_3^- Cotransporter

GENERAL FUNCTION AND MOLECULAR IDENTITY

A K^+/HCO_3^- cotransporter (Figure 52.10D), presumably electroneutral, has been documented in squid giant axons, where it normally mediates the efflux of one K^+ and one HCO_3^- ion.[265] Because the transporter moves HCO_3^- out of the axon, it functions as an acid loader. A similar transporter has been reported in cells of the medullary thick ascending limb of rat kidney,[266,267] and may exist in cultured cortical astrocytes of rat (Bevensee and Boron, unpublished). In mammalian glia, K^+/HCO_3^- cotransport may contribute to the pH_i decrease following an acute intracellular alkali load.

INVOLVEMENT OF K^+ AND HCO_3^-; ENERGETICS

In the squid giant axon dialyzed with a fluid containing K^+, but lacking Na^+ and Cl^-, the cotransporter moves K^+ and HCO_3^- out of the axon, eliciting a pH_i decrease.[265] Under the appropriate conditions, the K^+/HCO_3^- cotransporter can also operate in the forward direction, moving HCO_3^- into the squid giant axon.[268,269] Exposing axons dialyzed with a fluid devoid of K^+, Na^+, and Cl^- to an artificial seawater containing K^+ and CO_2/HCO_3^- elicits a pH_i decrease (due to CO_2 entry), followed by a pH_i increase (due to K^+/HCO_3^- influx). The HCO_3^- fluxes mediated by K^+/HCO_3^- cotransporter can be enhanced by using out-of-equilibrium CO_2/HCO_3^- solutions to introduce HCO_3^- exclusively to either the inside or outside of the axon.[268,270]

As mentioned above, two independent groups have also reported DIDS-sensitive, K^+-coupled HCO_3^- transport in the medullary thick ascending limb (mTAL), either from tubule suspensions[266] or perfused tubules.[267] In the perfused-tubule study,[267] luminal DIDS increased transepithelial HCO_3^- reabsorption—a finding consistent with DIDS-sensitive K^+-coupled HCO_3^- transport opposing HCO_3^- reabsorption.

EFFECTS OF PHARMACOLOGICAL AGENTS

While the transporter in the mTAL is sensitive to stilbene derivatives such as DIDS, the K^+/HCO_3^- cotransporter in the squid giant axon is not. However, quaternary ammonium ions introduced into the cell inhibit inwardly directed cotransport.[268] The potency of inhibition increases with increasing alkyl chain length of the quaternary ammonium ion. For example, the apparent K_i for phenylpropyltetraethylammonium or PPTEA (~91 μM) is ~850-fold less than the apparent K_i for tetraethylammonium or TEA (~78 mM).

Ca^{2+}-$2H^+$ Exchange Pump

GENERAL FUNCTION AND MOLECULAR IDENTITY

The P-type ATPase family includes not only the Na^+-K^+ and H^+-K^+ pumps, but also the Ca^{2+} pumps, of which there are two types—the sarcoplasmic (endoplasmic) reticulum Ca^{2+}-ATPase (SERCA) and the plasma membrane Ca^{2+}-ATPase (PMCA). These Ca^{2+} pumps, along with Na^+/Ca^{2+} exchangers, contribute to Ca_i^{2+} regulation by pumping Ca^{2+} either out of the cells across the plasma membrane (PMCAs) or back into intracellular stores (SERCAs). In both cases, the pumps exchange Ca^{2+} for H^+. Thus, from the standpoint of pH_i, the PMCAs, which take up H^+ as they extrude Ca^{2+} across the plasma membrane, function as acid loaders (Figure 52.10E).

Four PMCAs (PMCA1-4) have been cloned and characterized (for reviews, see refs. [271–274]). The cDNAs encode proteins with ~1200 amino acids. Based on hydropathy analysis, the PMCAs have ten transmembrane α-helices (TM 1-10) with both the N- and C-termini being cytoplasmic. The ATPase catalytic domain lies between TM 4 and TM 5. According to molecular modeling data, PMCAs have a predicted structure similar to the crystallized SERCAs, with the following cytosolic domains: actuator (A), nucleotide-binding (N), and phosphorylation (P).[271] Based on localization studies (for review, see ref. [275]). PMCA1 and PMCA4 are expressed ubiquitously. In contrast, PMCA2 and PMCA3 are found predominantly in the nervous system. mRNA encoding all four isoforms have been found in kidney.[276,277] However, PMCA levels of mRNA and protein are highest in the distal

tubule, particularly in the distal convoluted tubule.[278,279]

INVOLVEMENT OF Ca^{2+}; ENERGETICS

It has been known for some time that the plasma-membrane Ca^{2+} pump in erythrocytes exchanges Ca^{2+} for H^+.[280,281] Schwiening et al.[282] have used Ca^{2+}- and pH-sensitive microelectrodes to demonstrate that the plasma membrane Ca^{2+} pump in snail neurons also exchanges extracellular H^+ for intracellular Ca^{2+}. In this preparation, activation of the Ca^{2+} pump (generated by increasing intracellular Ca^{2+} with depolarization or iontophoretic Ca^{2+} injection) elicits an increase in extracellular Ca^{2+}, and a simultaneous increase in extracellular pH. Both the increase in extracellular Ca^{2+} and pH can be inhibited by the Ca^{2+}-pump inhibitor vanadate. A similar Ca^{2+} pump, present in hippocampal neurons,[283] appears responsible for causing an increase in the extracellular pH of the hippocampal slice elicited by stimuli-induced neuronal activity.[284–286]

Glutamate Transporters

GENERAL FUNCTION AND MOLECULAR IDENTITY

In the mammalian CNS, the predominant excitatory amino acids glutamate and aspartate are transported from the extracellular space back into neurons and glial cells by ion-coupled glutamate transporters in the SLC1 family.[287] Since 1992, cDNAs encoding several of these electrogenic glutamate transporters have been cloned and characterized.[288–296] As reviewed in refs.[290,297,298], these transporters are predominantly expressed in the nervous system, but also in certain epithelial cells. The L-glutamate/L-aspartate transporters EAAT1 (or GLAST1) and EAAT2 (or GLT1) are mainly found in glia, whereas EAAT3 (or EAAC1) and EAAT4 are found predominantly in neurons. EAAT3 is also expressed in liver, as well as the small intestine and kidney where it mediates the uptake of glutamate and aspartate across the apical membrane.[299] EAAT4 is expressed in cerebellum, whereas EAAT5 is predominantly expressed in retina.

INVOLVEMENT OF GLUTAMATE/ASPARTATE, Na^+, AND K^+; ENERGETICS

Using the results from $^{22}Na^+$ and [^{14}C]glutamate uptake studies, as well as pH_i measurements, on *Xenopus* oocytes expressing EAAT3, Kanai et al.[300] concluded that the protein transports 1 glutamate, 2 Na^+ and 1 H^+ into the cell, in exchange for 1 K^+, which moves out of the cell (Figure 52.10F). This stoichiometry, which predicts a net movement of one positive charge into the cell, agrees with that proposed for the glutamate transporter in salamander retinal glia based on kinetic analysis.[301] Adding either glutamate or aspartate to the extracellular fluid causes a steep fall in pH_i,[300] consistent with the influx of H^+ or the efflux of alkali. H^+ appears to be the transported acid–base species because the EAAT3-induced change in pH (but not the transporter current) is inhibited by amino acids with a higher pK (e.g., cysteine) than glutamate—a finding consistent with transport of the amino acid coupled to H^+ as an ion pair, followed by H^+ dissociation and a subsequent drop in pH.[302]

Peptide and Divalent-Cation Transporters

Although most solute exchangers and cotransporters in animal cells are Na^+ driven, some are H^+ coupled (Figure 52.10g and h). The absorption of oligopeptides and peptide-based antibiotics by intestinal and proximal-tubule epithelial cells is mediated by two members of the SLC15 family, H^+/oligopeptide transporters PepT1 (SLC15A1) and PepT2 (SLC15A2; for reviews, see refs. [303,304]). PepT1 and PepT2 transport the same di- and tri-peptides, but with different affinities/capacities.[303] PepT1 exhibits low-affinity, high-capacity transport, whereas PepT2 exhibits the opposite: high-affinity, low-capacity transport. Both transporters are expressed in kidney (among other tissues), with PepT1 found in the S1 segment of the proximal tubule and PepT2 found in the S3 segment.[305,306] Other members of the peptide transporter family include PTH1 (SLC15A4) and PTH2 (SLC15A3), both of which can transport histidine as well as di- and tripeptides in a H^+-coupled manner (for review, see ref.[303]).

The cDNA encoding PepT1 has 707 amino acids with 12 putative membrane-spanning segments.[307] Based on the recent crystal structure of a prokaryotic homologue, PepT proteins possess a large central hydrophilic cavity where peptide binds, and a smaller extracellular one where H^+ binds.[308] In oocytes expressing PepT1, the net transport of dipeptides occurs with a proton:dipeptide stoichiometry of 1:1[309] and causes a steep fall in pH_i.[300,309] For negatively charged dipeptides, one H^+ binds to the cation site of the transporter, whereas another H^+ neutralizes the dipeptide on the peptide site. The net transport stoichiometry of negatively charged dipeptides is therefore 1 proton for 1 neutralized dipeptide.

15 years ago, Gunshin et al.[310] cloned the cDNA encoding a mammalian divalent-cation transporter (DCT1)—now called the divalent metal transporter (DMT)—which mediates intestinal non-heme Fe^{2+} absorption. DMT contains 561 amino acids with 12 putative membrane-spanning domains (see review by Mackenzie and Hediger[311]). By Northern blotting, DMT is ubiquitously expressed; heavily so in the duodenum. In kidney, DMT is expressed at the apical membrane of the thick ascending limb of the loop of Henle, the distal nephron, and collecting ducts, as well

as intracellularly throughout the nephron.[312] DMT is electrogenic, and cotransports any one of a group of metals (e.g., Fe^{2+}, Zn^{2+}, Mn^{2+}, Co^{2+}, Cd^{2+}, Cu^{2+}, Ni^{2+}, Pb^{2+}) together with one H^+. By analogy with the EAATs and PepT1, adding Fe^{2+} to the extracellular fluid of an oocyte expressing DMT leads to a rapid fall in pH_i, consistent with the influx of H^+.

Other Transporters that Carry Strong or Weak Acids or Bases

We have discussed several major categories of transporters that act as acid loaders. Two of these—the Cl^--HCO_3^- exchangers and Na^+/HCO_3^- cotransporters—specifically play a role in regulating pH. However, any transporter that carries a proton or a weak acid or base could affect pH. A quick perusal of the 40^+ families of SLC proteins[313] reveals that about half of these families include members that transport either H^+ or weak acids or weak bases. In addition, several other families of transport proteins (e.g., vacuolar H^+ pump, gastric H^+-K^+ pump) can carry acids or bases. Although most of these transporters do not regulate pH, they can impact pH. The extent of this impact depends on the rate of transport and—for transported substances other than H^+ or OH^-—the pK of the substance, and the pH of the compartments on either side of the membrane across which the transport occurs.

Acid-Extrusion Mechanisms

Introduction

As discussed earlier, acid extrusion, that is, the movement of H^+ (or protonated monovalent weak acids) out of cells, or the movement of OH^- or HCO_3^- (or monovalent weak bases) into cells, generally occurs against a steep energy gradient. Based on their source of energy, acid-extrusion mechanisms can be divided into three groups: primary, secondary and tertiary active transporters (see ref. [314]). Primary active transport mechanisms, also called pumps, derive their energy from electron transport (e.g., the electron transport chain that drives H^+ out of mitochondria) or, as with the transporters such as the H^+ pump considered below, from the hydrolysis of ATP. Secondary active transport systems (e.g., Na^+—H^+ exchange) derive their energy from the electrochemical gradient of an ion (e.g., Na^+)—a gradient that is in turn established by a primary active transporter (e.g., Na^+—K^+ pump). Finally, tertiary active transporters (e.g., the monocarboxylate system) are driven by an ion gradient established by a secondary active transporter.

From the point of view of feedback control, the effectiveness of an acid extruder would be enhanced greatly if decreases in pH_i increased transport. The most productive approach for studying the pH_i dependence of acid extruders in intact cells has been to load cells with acid acutely, as schematized in Figure 52.11A–D. The acid load can be applied by prepulsing with NH_4^+,[170] microinjecting H^+,[177] dialyzing with a low-pH solution,[315] or reducing pH_o in the temporary presence of nigericin.[316] In the model experiment of Figure 52.11A, the pH_i decrease produced by the acid load (segment ab) is followed by a rapid recovery to the initial pH_i (bcd). In the most general case, this pH_i recovery is mediated by one or more acid extruders, but may be opposed by one or more acid loaders. Identifying the component of pH_i recovery that is mediated by a particular transporter requires that the transporter be specifically, instantaneously, and completely inhibited. Such inhibitors exist for two of the acid extruders that we will discuss below, the Na^+-driven Cl^-—HCO_3^- exchanger and the Na^+—H^+ exchanger. Figure 52.11A illustrates three possible outcomes (indicated by broken curves following the

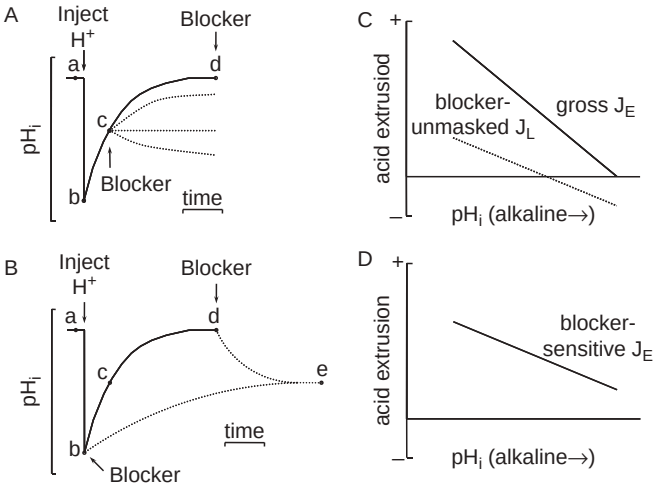

FIGURE 52.11 Determining the pH_i dependence of an acid–base transporter. The pH_i dependence of the Na^+-driven Cl^-—HCO_3^- exchanger. A: Hypothetical experiment illustrating how an inhibitor (e.g., DIDS) can be used to ascertain the component of a pH_i recovery from an acid load that is mediated by an acid extruder such as the Na^+-driven Cl^-—HCO_3^- exchanger. The blocker is applied at the arrow (point c). The broken curves illustrate three possible effects of the blocker on the pH_i recovery. B: Another hypothetical experiment illustrating a different approach for determining the pH_i-dependence of an acid extruder during the pH_i recovery from an acid load. The blocker is applied either at the time of the acid load, or after the pH_i recovery (broken curves). C: The pH_i dependence of "gross" acid extrusion (gross J_E) is calculated from the pH_i recovery in the absence of blocker (bcd) in panel B. The pH_i dependence of "blocker-unmasked" acid loading (blocker-unmasked J_L) is calculated from the pH_i recovery in the presence of blocker (be), or the pH_i decrease elicited by applying the blocker after the pH_i recovery (de) in panel B. D: The pH_i dependence of "blocker-sensitive" acid extrusion (blocker-sensitive J_E) is calculated by subtracting the plot of blocker-unmasked J_L from the plot of gross J_E in panel C.

arrow) of applying such an agent during a pH_i recovery due at least in part to a mechanism sensitive to the blocker. First, applying the blocker may slow but not halt the pH_i recovery. This result indicates that a second, blocker-insensitive acid-extruder also contributes to the pH_i recovery. Second, the blocker may completely eliminate the pH_i recovery, indicating that the entire recovery is due to a blocker-sensitive mechanism(s). However, complete blockade by the blocker does not rule out the possibility that the blocker-sensitive, acid-extrusion process is opposed by a less potent blocker-sensitive, acid-loading process. Third, applying the blocker may not only halt the pH_i recovery, but may also unmask a slow pH_i decline. This result implies that the blocker-sensitive, acid-extrusion process is opposed by at least one blocker-insensitive acid loader.

In any of the above three eventualities, the difference in rates of pH_i change (dpH_i/dt) immediately before and immediately after applying the blocker at point c in Figure 52.11A is the component of the pH_i recovery—at the pH_i value prevailing at point c—that is due to blocker-sensitive transporters. In order to convert this blocker-sensitive dpH_i/dt to a net acid-extrusion rate (J_E), we must multiply this dpH_i/dt by the total intracellular buffering power (β^T) prevailing at the pH_i of the blocker application, as well as the inverse of the surface-to-volume ratio (ρ):

$$J_E = (\beta^T/\rho) \times (dpH_i/dt)_{\text{blocker-sensitive}} \qquad (52.36)$$

Because acid–base transporters are generally sensitive to changes in pH_i, this analysis must be repeated over a range of pH_i values to produce a plot of the pH_i dependence of the blocker-sensitive flux(es).

Rather than repeating the experiment in Figure 52.11A many times, each with a different pH_i at the instant we apply the blocker (i.e., point *c*), we could employ a more practical approach, which requires only three types of experiments. First, we monitor the pH_i recovery—in the absence of blocker—over the entire pH_i range indicated by bcd in Figure 52.11B. At regular pH_i intervals during this recovery, we compute the "gross" dpH_i/dt, from which we compute the gross J_E (Figure 52.11C).

Second, we monitor the pH_i recovery in an experiment in which the blocker is present during the entire pH_i recovery. If the blocker-sensitive transporter is the only acid extruder present in the cell, then pH_i will not recover at all, or may even decline. On the other hand, if other acid extruders are present (as is more often the case), then pH_i will recover slowly and incompletely, as in be in Figure 52.11C. At regular pH_i intervals during this abbreviated recovery, we compute the "blocker-insensitive" dpH_i/dt, from which we compute the blocker-insensitive J_E (Figure 52.11C).

Third, we allow pH_i to recover fully (bcd), and then add the blocker. If, during the steady state indicated by point d, one or more acid loaders oppose the blocker-sensitive acid extruder, as is typically the case, then applying the blocker will cause pH_i to drift downward (de). The initial rate of pH_i decline at point d reflects the rate of acid loading (J_L) at the pH_i at d. At regular pH_i intervals during this pH_i decline, we compute the "blocker-unmasked" dpH_i/dt, from which we compute the blocker-unmasked J_L (Figure 52.11C).

Finally, at each pH_i value, we subtract the blocker-unmasked J_L from the blocker-insensitive J_E in Figure 52.11D. The result is the pH_i dependence of the "blocker-sensitive" J_E (i.e., the flux mediated by the transporter of interest). This approach was first used by Boron et al.[317] to determine the pH_i dependence of the Na^+-driven Cl^-–HCO_3^- exchanger of barnacle muscle, and then by Boyarsky et al.[318] to determine the pH_i dependence of the Na^+–H^+ exchanger of renal mesangial cells. Others extended this approach to study the pH_i dependence of Na^+–H^+ exchange in IEC-6 colonic cells,[319] UMR-106 osteoblastic cells ,[320] osteoclasts,[124] rabbit S3 proximal tubules,[206] ventricular myocytes,[321] rat hippocampal astrocytes,[17] and shrunken mesangial cells.[322] Finally, the approach outlined in Figure 52.11B–D also has been used to determine the pH_i dependence of the Na^+-driven Cl^-–HCO_3^- exchanger in NIH 3T3 cells transformed with the c-H-*ras* oncogene,[323] and the pH_i dependence of the H^+ pump in rabbit S3 proximal tubules[206] and osteoclasts.[124]

H^+ Pumps

GENERAL FUNCTION AND MOLECULAR IDENTITY

An electrogenic vacuolar-type H^+ pump (Figure 52.12A, left) is present in the proximal tubule and distal nephron of the kidney (for reviews, see refs. [201,324,325] and Chapter 56), as well as in macrophages and neutrophils ,[326,327] osteoclasts,[328] tumor cells,[329] and goblet cells of the insect midgut.[330] Similar H^+ pumps are present in clathrin-coated vesicles and other organellar membranes (for reviews, see refs. [201,331,324,325]).

The V-type H^+ pump is composed of two domains, V_0 and V_1. The V_0 domain, which is comprised of at least five different subunits, is involved in translocating H^+ across the membrane. The V_1 domain, which is comprised of at least eight different subunits, is involved in ATP hydrolysis and contains the catalytic nucleotide binding sites. A more complete review of the structure and function of the V_0 and V_1 subunits of the pump are presented in refs. [324,325,332,333]. Similar vacuolar H^+ pumps have been examined in *Neurospora* and plant cells.[334–336]

Immunohistological studies with antibodies raised against various subunits of the H^+ pump have revealed expression of the pump throughout the

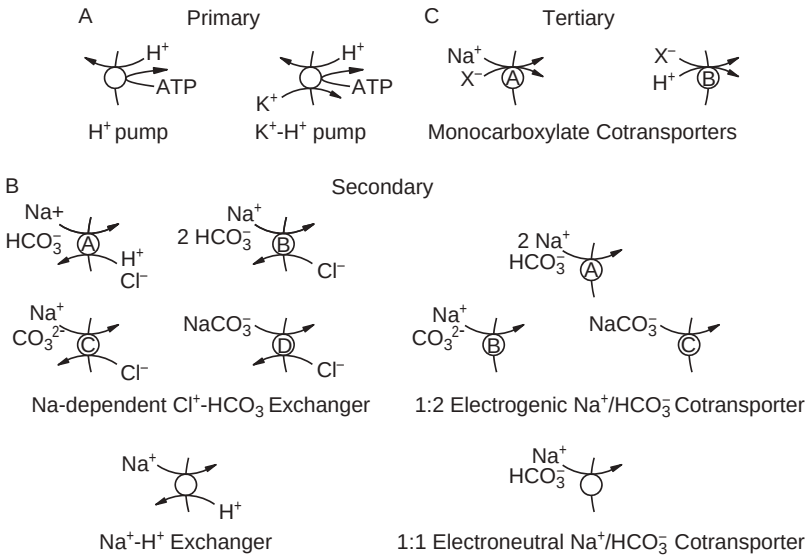

FIGURE 52.12 Acid-extrusion mechanisms. **A**: Primary active transport mechanisms include the electrogenic H^+ pump and the electroneutral K^+—H^+ pump. **B**: Secondary active transporters include the Na^+-driven Cl^-—HCO_3^- exchanger (four models of which are shown), the Na^+—H^+ exchanger, the 1:2 electrogenic Na^+/HCO_3^- cotransporter, and the 1:1 electroneutral Na^+/HCO_3^- cotransporter. **C**: The tertiary active transport system consists of a Na^+/monocarboxylate cotransporter that brings the monocarboxylate (X^-) into the cell, and an H^+/monocarboxylate cotransporter that uses the energy stored in the X^- gradient to drive H^+ out of the cell. In renal proximal tubules, the Na^+/monocarboxylate cotransporter is confined to the luminal membrane.

nephron on both apical and basolateral membranes.[337] In the cortical collecting tubule, the H^+ pump is localized to the apical membrane of α intercalated cells (which secrete acid) and the basolateral membranes of β intercalated cells (which secrete alkali).[338–340] Vacuolar H^+ pumps are also present at the apical membrane of the proximal tubule.[338–340]

ENERGETICS

The extrusion of H^+ by this primary active transporter is not coupled directly to the movement of other ions that might balance electrical charge. Rather, this pump is electrogenic. Because the H^+ pump is driven by the hydrolysis of ATP, which provides a substantial amount of energy, it is capable of generating a large H^+ gradient across the cell membrane. For example, if the voltage across the membrane were zero, then the H^+ pump could establish a pH difference of about three pH units. On the other hand, when compared to other H^+ transporters, H^+ pumps have a relatively low transport rate. Thus, the H^+ pump is expressed in epithelia needing a high-gradient/low-capacity H^+ transporter. An H^+ pump contributes to pH_i regulation in a number of cells, including macrophages and neutrophils,[327] osteoclasts,[124] renal cells,[341,342] glial cells,[343,344] and corneal epithelial cells.[345]

K^+—H^+ Exchange Pumps

GENERAL FUNCTION AND MOLECULAR IDENTITY

As discussed earlier, K^+—H^+ exchange pumps (Figure 52.12A, right) are members of the P-type ATPase family. Both the gastric and non-gastric H^+—K^+ pumps are ATP-driven transporters that exchange intracellular H^+ for extracellular K^+. However, the gastric and non-gastric pumps differ in their molecular biology, localization, functional properties, and pharmacological sensitivities (for reviews, see refs.[346–349] and Chapter 3).

Both the gastric and non-gastric forms of the H^+—K^+ pump are present in the collecting duct of the kidney, where their major role may be in K^+ preservation (for reviews, see refs[346–349]). For example, during K^+ depletion, mRNA and protein levels of the non-gastric form are raised in multiple nephron segments.

INVOLVEMENT OF K^+; ENERGETICS

In using the energy from ATP hydrolysis, H^+—K^+ pumps can establish extremely large pH gradients. For instance, gastric parietal cells (see ref.[350] can produce gastric secretions containing as much as 140 mM HCl (i.e., pH $\sim$0.7). In parietal cells of rabbit gastric glands, applying omeprazole (which blocks H^+—K^+ pumps) reduces pH_i by nearly 0.1 in glands stimulated with histamine and IBMX, though not in resting glands. This result implies that the H^+—K^+ pump contributes to the maintenance of pH_i in stimulated parietal cells.

Functional studies of non-gastric H^+—K^+ pumps have been performed *in vitro* using expression systems such as the *Xenopus* oocyte and HEK-293 cells. In such expression systems, the non-gastric pumps exchange extracellular K^+ for intracellular H^+. However, the pumps may also possess the ability to transport Na^+ (for reviews, see refs.[347,351]).

Na^+-Driven Cl^-—HCO_3^- Exchanger

GENERAL FUNCTION AND MOLECULAR IDENTITY

A secondary active transport system that exchanges external Na^+ and HCO_3^- for internal Cl^- and H^+ (or its equivalent, *vide infra*) was first identified in invertebrate cells such as squid axons[352,353] and snail

neurons.[354] Indeed, the work on the squid axon was the first evidence for the dynamic regulation of pH_i.[170] This transport mechanism makes an important contribution to pH_i regulation in mammalian neurons.[355] Not certain is the precise identity of the transported acid–base equivalents, inasmuch as pH_i measurements cannot clearly distinguish inward movements of HCO_3^-, CO_3^{2-} or $NaCO_3^-$ from one another, or from outward movements of H^+. All four schemes outlined in Figure 52.12B (top left) can account for the data. For simplicity, we shall refer to the transporter as the Na^+-driven Cl^-–HCO_3^- exchanger.

As mentioned earlier and described in greater detail in Chapter 54, investigators have cloned the cDNA encoding the Na^+-driven Cl^-–HCO_3^- exchanger (NDCBE or SLC4A8) and have also examined the transport properties of the protein.[356] When expressed in *Xenopus* oocytes, human NDCBE exhibits all the functional hallmarks of the endogenously expressed transporter. For instance, stimulation of NDCBE activity in oocytes causes an increase in pH_i that (1) requires external Na^+ and HCO_3^-, (2) can be inhibited by stilbenes, and (3) correlates with a decrease in intracellular Cl^-.[356] Using the surface-pH measurement technique described above for examining CO_3^{2-} transport by NBCe1, Grichtchenko and Boron[357] as well as Lee et al.[257] have provided preliminary evidence that NDCBE can also transport CO_3^{2-}.

DEPENDENCE ON pH_i AND CALCULATION OF ACID EXTRUSION RATES

Using the approach outlined above in Figures 52.11B–D, Boron et al.[317] separately determined the pH_i dependence of the Na^+-driven Cl^-–HCO_3^- exchanger of barnacle muscle at pH_o values of 6.8, 7.4, 8.0, and 8.6 (at a fixed $[CO_2]$ of 0.4%). As shown in Figure 52.13, the flux is highest at low pH_i values, and gradually falls toward zero at a pH_i of ~7.4—the threshold for activating the exchanger. This work was the first to demonstrate threshold behavior for an acid extruder; similar work followed on the Na^+–H^+ exchanger (see below). The pH_i sensitivity of acid extrusion in Figure 52.13 is probably not a Michaelis-Menten type of dependence on intracellular H^+, which would translate into a sigmoid (rather than a linear) acid-extrusion-rate-versus-pH_i relationship. The pH_i sensitivity may reflect an allosteric site for intracellular H^+ (*vide infra*).

It is important to recognize that, for two reasons, an analysis of the type shown in Figure 52.13 is far more valuable than a simple plot of the pH_i recovery rate (dpH_i/dt) versus pH_i. First, because the above analysis includes buffering power, the result is a flux rather than merely a rate of change in pH_i. This consideration is important when buffering power changes appreciably

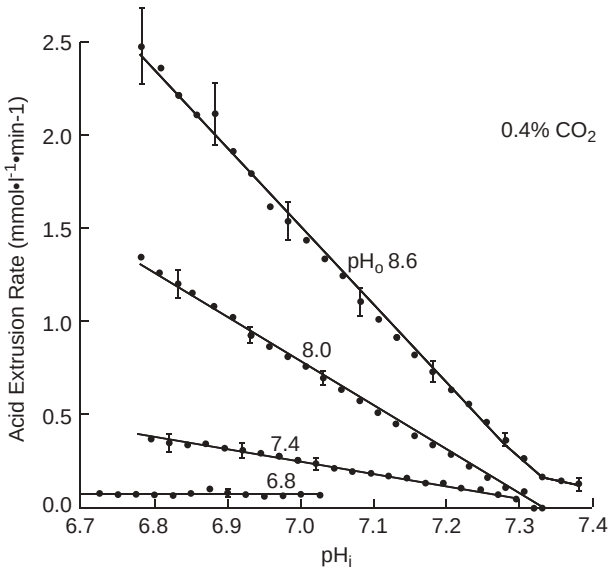

FIGURE 52.13 **The pH_i dependence of the Na^+-driven Cl^-–HCO_3^- exchanger from giant barnacle muscle fibers.** The rate of pH_i recovery from an acid load (NH_4^+ prepulse) was determined over a range of pH_i values, multiplied by the sum of intrinsic and HCO_3^- buffering powers (both of which vary with pH_i), and corrected for an acidification unmasked by applying SITS. *(Reproduced from ref. [317].)*

over the pH_i range in question, or if a transporter is to be compared under conditions when buffering power is expected to vary. Second, the above analysis takes into account processes other than the transporter in question; these other processes may contribute to the pH_i recovery (or lack thereof!). Failing to make this correction can lead to a serious over- or underestimation of the flux due to the transporter of interest.

DEPENDENCE ON pH_O

Although the Na^+-driven Cl^-–HCO_3^- exchange rate is stimulated at low values of pH_i, it is apparently inhibited at low values of pH_o. For example, both in barnacle muscle and squid giant axons, decreases in pH_o—produced by lowering $[HCO_3^-]_o$ at a fixed P_{CO_2}—cause J_E to decrease.[358,359] However, at least for the squid axon, this apparent inhibition at low pH_o may be only illusory: when pH_o is decreased at a fixed $[NaCO_3^-]_o$, the inhibition disappears.[358] Thus, at least in squid axons, the transporter per se may be relatively pH_o insensitive. Most methods of producing acidosis may inhibit Na^+-driven HCO_3^- transport because they simultaneously lower $[NaCO_3^-]_o$.

INVOLVEMENT OF Na^+, Cl^-, AND HCO_3^-

The Na^+-driven Cl^-–HCO_3^- exchanger has an absolute requirement for external Na^+,[15] external HCO_3^-[360] or a related species, and internal Cl^-.[315] Removing any one of these three ions from the appropriate side of the

membrane completely blocks acid extrusion. Moreover, Na^+ and Cl^- are actually transported along with acid equivalents.[15,315] The observed stoichiometry is one Na^+ entering the cell, one Cl^- exiting, and two acid equivalents neutralized intracellularly. This stoichiometry is consistent with all four models presented in Figure 52.12B (top left). The prediction that Na^+-driven Cl^-—HCO_3^- exchange should be electroneutral is supported by the observations that transport neither alters[165,361] nor is altered by V_m.[352]

ENERGETICS

The models of Figure 52.12B (top left) make equivalent energetic predictions, based upon which physiological gradients for Na^+, Cl^-, and HCO_3^- should support Na^+-driven Cl^-—HCO_3^- exchange with no external source of energy.[3] The major predicted energy source is the steep Na^+ gradient, established by the Na^+—K^+ pump. This model of a secondary active transporter, driven only by ion gradients, is supported by the observation that transport can be reversed by reversing gradients for Na^+ and/or HCO_3^-.[317,362,363] Curiously, however, the transporter in squid axons requires ATP; not as an energy source, but probably for an essential phosphorylation event or as an essential cofactor.[364]

THE pH_i THRESHOLD

In barnacle muscle, the activity of the Na^+-driven Cl^-—HCO_3^- exchanger falls toward zero as pH_i approaches a pH_i threshold of ~7.4 (see Figure 52.13). This reduction in transport does not reflect the inavailability of energy, however, which is sufficient to drive pH_i to ~8.0. Threshold behavior is thus probably due to an allosteric effect of H^+ on the transporter or an essential activator. This hypothesis is supported by the observation that the barnacle-muscle Na^+-driven Cl^-—HCO_3^- exchanger, in addition to mediating net acid extrusion, also mediates what appears to be Na^+—Na^+[362] and Cl^-—Cl^-[365] exchange. Like acid extrusion, these ancillary transporter activities are also stimulated by reducing pH_i below the threshold.

SENSITIVITY TO PHARMACOLOGICAL AGENTS

The Na^+-driven Cl^-—HCO_3^- exchanger is blocked by the stilbene derivatives 4-isothiocyano-4′-acetamido-2,2′-stilbene disulfonate (SITS) and 4,4′-diisothiocyano-2,2′-stilbene disulfonate (DIDS). The site of permanent action is apparently a free amino group on the transporter that reacts with the isothiocyano moiety of the stilbene to form an *N,N*-disubstituted thiourea (Edman reaction). However, even stilbene derivatives lacking an isothiocyano group can inhibit the transporter, although the inhibition is often less than complete and is reversible. Thus, 4,4′-dinitro-2,2′-stilbene disulfonate (DNDS), at a concentration of 1 mM, reversibly inhibits the squid-axon transporter by approximately 80%.[366] By analogy to the erythrocyte Cl^-—HCO_3^- exchanger, the Na^+-driven Cl^-—HCO_3^- exchanger probably forms a reversible, ionic complex with each of the aforementioned stilbenes. This interaction presumably involves the negatively charged sulfonate groups on the stilbene and cationic moieties on the transporter. The stilbenes with amino-reactive groups (i.e., SITS and DIDS) subsequently form a covalent bond that eventually blocks transport irreversibly. Interesting, the inhibition of squid-axon Na^+-driven Cl^-—HCO_3^- exchanger by DNDS is apparently competitive with Na^+ as well as with HCO_3^-—a finding that is quantitatively consistent with the hypothesis that DNDS actually competes with the $NaCO_3^-$ ion pair for binding.[366]

Two non-stilbene amino-reactive agents also inhibit Na^+-driven Cl^-—HCO_3^- exchange.[165] The inhibition by *p*-isothiocyanatobenzenesulfonate is irreversible, as is its reaction with free amino groups. The inhibition by pyridoxal phosphate is reversible, as is its reaction with free amines. Na^+-driven Cl^-—HCO_3^- exchange is also reversibly inhibited by relatively high levels (~0.5 mM) of furosemide.[352,365]

Na^+—H^+ Exchangers

GENERAL FUNCTION AND MOLECULAR IDENTITY

Na^+—H^+ exchangers (Figure 52.12B, bottom left) have been identified in the plasma membranes of a wide variety of vertebrate cells (for reviews, see refs.[167,714]). At least two functional classes of Na^+—H^+ exchangers have been identified. The first, which is apparently the most widespread version, are the Na^+—H^+ exchangers of nonepithelial cells[171,316,373–378] as well as the basolateral membranes of many epithelial cells.[64,379] This distribution is characteristic of what have been regarded as "housekeeping" transporters (e.g., Na^+—K^+ pump and Na^+—Ca^{2+} exchanger), which are inhibited by relatively low concentrations of 5-amino-substituted amiloride analogs, (e.g., EIPA). The second class of exchangers is the one characteristically located at the apical membrane of epithelia such as the renal proximal tubule.[164,380–385] It is inhibited by only relatively high concentrations of the aforementioned amiloride analogs. These two pharmacologically distinct Na^+—H^+ exchangers have been identified on the apical and basolateral membranes of LLC-PK1 cells.[386] A third pharmacological class of Na^+—H^+ exchanger is found in rat astrocytes[387] and hippocampal neurons.[205,355,388,389] These cells have a Na^+-driven acid extruder that functions in the nominal absence of HCO_3^-, and is not inhibited even by high levels of amiloride and/or amiloride analogs.

A cDNA encoding a Na^+—H^+ exchanger (NHE1) was first cloned by Sardet et al.,[390] using an expression

strategy. At present, eight additional NHE isoforms (NHE1 to NHE9) have been identified, all members of the SLC9 family.[167,713,714] The sequence comparisons, tissue distributions, and functions of the various NHE isoforms are examined in Chapter 53. In the remainder of this section, we will examine the role of Na^+-H^+ exchange in pH_i regulation.

DEPENDENCE ON pH_i

The first convincing evidence that decreases in pH_i stimulate Na^+-H^+ exchange came from experiments on membrane vesicles, in which low pH_i stimulates amiloride-sensitive Na^+ efflux.[391] This result, analogous to the Cl^--influx and Na^+-efflux data on the Na^+-driven $Cl^--HCO_3^-$-exchanger, extends the allosteric-H^+-site hypothesis to the Na^+-H^+ exchanger.

One can also determine the pH_i dependence of the Na^+-H^+ exchanger in experiments on intact cells. However, an examination of the literature describing the pH_i dependence of Na^+-H^+ exchangers reveals that many investigators assume that the Na^+-H^+ exchanger is the only factor contributing to the recovery of pH_i from an acute acid load. In support of this conclusion, they point out that the recovery occurs in the nominal absence of HCO_3^- and is inhibited by blockers of the Na^+-H^+ exchanger. However, there is a serious flaw in this line of reasoning. It is true that, after a cell containing a Na^+-H^+ exchanger is acutely acid loaded, there is a more-or-less exponential pH_i recovery (e.g., see bcd in Figure 52.11A) that may be prevented by pretreating with amiloride analogs. However, this result only proves that an intact Na^+-H^+ exchanger is required for the pH_i recovery. Such experiments do not address the issue of how background acid-loading processes influence the rate of the pH_i recovery, and thus can not—by themselves—provide the pH_i sensitivity of the Na^+-H^+ exchanger.

An analysis of the pH_i sensitivity of Na^+-H^+ exchange in intact cells requires that one rule out, or at least account for, background acid-loading processes that oppose the action of the exchanger, as discussed above in connection with Figure 52.11. In experiments on isolated hepatocytes in the nominal absence of HCO_3^-,[392,393] applying amiloride has no effect the steady-state pH_i. This implies that both Na^+-H^+ exchange and background acid loading are inactive at this pH of ~7. During the recovery from an acid load, amiloride analogs block the pH_i recovery, but do not unmask a background acid-loading process. Thus, in these cells, the product of (β^T/ρ) and the gross pH_i recovery rate is the true net Na^+-H^+ exchange rate, which varies with pH_i in a nearly linear fashion (Figure 52.14A and B).

In many other cells, however, applying an amiloride analog causes a sizeable fall in steady-state

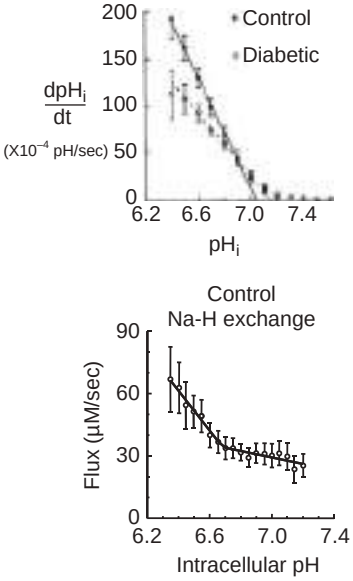

FIGURE 52.14 Two patterns of pH_i dependence of the Na^+-H^+ exchanger. A: The Na^+-H^+ exchanger of rat hepatocytes exhibits true pH_i threshold behavior. Although applying EIPA completely blocks the recovery of pH_i from an acid load, EIPA has no effect on pH_i after the pH_i recovery is completed. Thus, the exchanger is inactive in the normal steady state. The experiments were performed on single freshly disaggregated hepatocytes in the nominal absence of CO_2/HCO_3^-. pH_i was measured using BCECF and a microscope-based fluorometry system. *(Reproduced from ref. [392].)* B: The Na^+-H^+ exchanger in rat mesangial cells is active in the steady state. Applying EIPA in the steady state unmasks a sizeable acidification, indicating that the exchanger is normally active. The experiments were performed on single cells (passage 2–5) in the nominal absence of CO_2/HCO_3^-. *(Reproduced with permission from ref. [318].)*

pH_i,[376,394,395] as indicated by de in Figure 52.11B, implying that both acid loading and Na^+-H^+ exchange were active at the original steady-state pH_i. A similar EIPA-induced pH_i decrease occurs in renal mesangial cells. The pH_i dependence of the true Na^+-H^+ exchange rate thus can be computed only after correcting the gross pH_i recovery rate for EIPA-insensitive acid extrusion and EIPA-unmasked acid loading, as discussed in connection with Figure 52.11B–D. The result for the mesangial cell is the curve shown in Figure 52.14B that indicates that the Na^+-H^+ exchanger is substantially less pH_i sensitive in the physiological range than under conditions of severe acid loading.[318]

DEPENDENCE ON pH_o

The Na^+-H^+ exchanger is inhibited by decreases in pH_o. In intact cells, lowering pH_o decreases the rate at which pH_i recovers from an acid load.[396,397] In crayfish neurons, the pH_i recovery halts completely at the pH_o at which the energy required to move one H^+ out of the cell equals that released by moving one Na^+ in.[397] In brush border membrane vesicles from the renal

cortex, the pH_o dependence of Na^+-H^+ exchange is described by a simple pH titration curve with a pK_a of 7.45.[398] Based on kinetic analyses, external H^+, Na^+, Li^+, and amiloride all compete for a common site on the exchanger (for review, see ref. [367]).

INVOLVEMENT OF Na^+

Acid extrusion by the Na^+-H^+ exchanger in intact cells is blocked by removing extracellular Na^+.[171,396,397] Furthermore, in the presence of extracellular Na^+, acid extrusion is accompanied by a rise in intracellular Na^+ activity[171,396,397] that is blocked when acid extrusion is blocked by lowering pH_o.[396] Reported values of the apparent K_m for external Na^+ vary over a fairly wide range, between ~5 mM and ~40 mM at a pH_o of 7.4.[64,399–403] Accordingly, external Na^+ nearly saturates the transporter at a normal pH_o. The K_m values tend to be inversely related to pH_o, consistent with competition between external Na^+ and H^+ (for review, see ref. [367]). In membrane-vesicle studies, the exchanger can transport Li^+ in place of Na^+.[382] Indeed, Li^+ transport by the exchanger is a key element of the "proton-suicide" technique used to kill cells with a functional Na^+-H^+ exchanger.[404]

EFFECTS OF PHARMACOLOGICAL AGENTS

Amiloride is a K^+-sparing diuretic that inhibits apical ENaC Na^+ channels in tight epithelia; K_i values are in the range 0.1 to 1 μM.[405,406] However, at substantially higher concentrations, amiloride also inhibits certain Na^+-H^+ exchangers (K_i: 3 to 1000 μM; see refs.[407,408]) and Na^+-Ca^{2+} exchange (K_i: 300 to 1100 μM; see refs.[409,410]). The inhibition of Na^+-H^+ exchange by amiloride has generally been found to be purely competitive with respect to external Na^+,[377,400,411,412] although both mixed-type[413] and noncompetitive inhibition[414] have been reported. Because of the competition with Na^+, millimolar levels of amiloride generally are necessary to inhibit Na^+-H^+ exchange at physiological Na^+ concentrations.[171,396,397,411] Structure-function relationships, which have been reviewed in some detail,[406,407,415] indicate that different regions of the amiloride molecule alter the molecule's affinity for the apical Na^+ channel, the Na^+-Ca^{2+} exchanger, or the Na^+-H^+ exchanger. HOE compounds such as HOE694 and HOE642 (cariporide) are relatively new Na^+-H^+ exchange inhibitors that have different affinities for several NHE isoforms, with NHE1 being the most sensitive. Similar to amiloride, the base structure of HOE compounds is guanidinium. However, unlike amiloride and its sister compounds, HOE compounds have an attached benzene ring.

Electroneutral and Electrogenic Na^+/HCO_3^- Cotransporters

As discussed earlier, an electrogenic Na^+/HCO_3^- cotransporter with a Na^+:HCO_3^- stoichiometry of 1:3 is present on the basolateral membrane of proximal tubule cells of the kidney, where it mediates Na^+ and HCO_3^- reabsorption, and therefore functions as an acid loader. A member of the SLC4 family, NBCe1 (SLC4A4) is responsible for HCO_3^- transport in the proximal tubule. A second transporter, NBCe2 (SLC4A5), which is expressed at high levels in hepatocytes, can also mediate electrogenic Na^+/HCO_3^- cotransport with an apparent Na^+:HCO_3^- stoichiometry of 1:3.[416] In mouse choroid epithelial cells, NBCe2 has a Na^+:HCO_3^- stoichiometry of 1:3.[417] However, both NBCe1[418,419] and NBCe2[420] can also operate with a stoichiometry of 1:2, in which case they move Na^+ and HCO_3^- into cells, and therefore function as acid extruders. An electrogenic Na^+/HCO_3^- cotransporter with a Na^+:HCO_3^- stoichiometry of 1:2 (Figure 52.12B, top right) has been documented in both invertebrate and mammalian glial cells (for reviews, see refs.[421–424]).

An electroneutral Na^+/HCO_3^- cotransporter with a Na^+:HCO_3^- stoichiometry of 1:1 (Figure 52.12B, bottom right) has been described in sheep Purkinje fibers,[425] guinea pig myocytes,[426] and vascular smooth-muscle cells.[427] As described in more detail in Chapter 53, two SLC4 members, NBCn1[428,429] and NBCn2 (aka, NCBE)[430] mediate electroneutral Na^+/HCO_3^- cotransport.

Monocarboxylate Transporters

GENERAL FUNCTION AND MOLECULAR IDENTITY OF MCTS

Na^+-independent transport of monocarboxylates such as lactate occurs by a process of cotransport with H^+ (or exchange with OH^-) across the plasma membranes of most cell types (for review, see ref. [431]). The responsible transporters are members of the SLC16 family, which includes 14 members.[432,433] The two best characterized monocarboxylate transporters are MCT1 (SLC16A1)[434] and MCT2 (SLC16A7).[435] However, only MCT1-MCT4 exhibit H^+-coupled monocarboxylate transport. In fact, most of the other family members have yet to be functionally characterized. The sequences of the encoded proteins are predicted to have 12 transmembrane (TM) segments, with a large intracellular loop between TM 6 and 7 and greatest conservation in the predicted transmembrane regions. Although both MCT1 and MCT2 have broad tissue distributions, in the kidney, MCT1 is expressed on the basolateral membrane of proximal tubule cells, and MCT2 is expressed on the basolateral membrane of medullary collecting duct cells.[435]

SUBSTRATE SPECIFICITY AND ENERGETICS OF THE MCTS

MCT isoforms appear to have different affinities for the same substrates. For example, both MCT1 and MCT2 transport lactate and pyruvate,[435] but MCT2 has a much higher apparent affinity for pyruvate.[436]

In all cells examined, H^+/X^- cotransport appears to be electroneutral[162,437] (see ref.[431]). Because MCT-mediated transport of monocarboxylates involves cotransport with H^+, the net driving force depends on the gradients of both monocarboxylate and H^+ across the plasma membrane. Depending on the direction of the net driving force, MCTs can mediate either the influx or efflux of monocarboxylates. As described below, MCT1 on the basolateral membrane of renal proximal-tubule cells acts in conjunction with an apical Na^+/monocarboxylate (Na^+/X^-) cotransporter to facilitate transepithelial lactate reabsorption.

EFFECTS OF PHARMACOLOGICAL AGENTS ON MCTS

MCT1 and MCT2, but not MCT3 and MCT4, are inhibited substantially by α-cyano-4-hydroxycinnamate (CHC).[432,435,438] However, because CHC has yet to be widely tested on other classes of transporters, it is not clear whether this compound is specific for MCTs.

THE Na^+/MONOCARBOXYLATE COTRANSPORTER

The Na^+/X^- cotransporter is rather nonspecific, capable of transporting D- and L-lactate, pyruvate, acetate, and other monocarboxylates. The cotransporter is found in apical membranes of both the proximal tubule and small intestine.[162,439] The Na^+/X^- cotransporter appears to be electrogenic (moving more Na^+ than X^-) in mammals,[198,440–442] but electroneutral in amphibians.[162] Investigators have found that one member of the SLC5 family of "Na^+/glucose cotransporters", namely SLC5A8, encodes an electrogenic sodium-coupled monocarboxylate transporter (SMCT; see refs.[443–446]). In addition, zebrafish SLC5A12 encodes an electroneutral SMCT.[446] As expected, the transporters are relatively nonselective for monocarboxylates, although substrate affinities can vary among the transporters.

INTERACTION OF Na^+/X^- AND H^+/X^- COTRANSPORTERS

Some proximal-tubule cells possess both a Na^+/X^- cotransporter at the apical membrane and an MCT at the basolateral membrane (Figure 52.12C). Acting in concert, these two monocarboxylate transporters can extrude substantial amounts of acid while reabsorbing monocarboxylates.[161,162]

The first step of the acid-extruding process is the coupled entry of Na^+ and X^- across the apical membrane, an example of secondary active transport. Because the pK_a' governing the dissociation of monocarboxylic acids ($HX \rightleftarrows H^+ + X^-$) is generally far below pH_i, very little of the entering X^- can combine with H^+ to form HX, and thus Na^+/X^- cotransport by itself is "pH_i silent". In the second step, X^- entering via luminal Na^+/X^- cotransport rapidly exits across the basolateral membrane via MCT—along with H^+. In this system, basolateral H^+/X^- cotransport is an example of tertiary active transport because the extrusion of H^+ is driven by an X^- gradient that is, in turn, established by the luminal Na^+/X^- cotransporter, a secondary active transporter. The net effect is the transepithelial reabsorption of monocarboxylate from lumen to blood.

Following the coupled uptake of Na^+ and X^- across the apical membrane, the extrusion of Na^+ across the basolateral membrane by the Na^+–K^+ pump contributes to transepithelial Na^+ reabsorption. Indeed, acetate promotes volume reabsorption.[447]

The Regulation of pH_i

INTRODUCTION

In the preceding sections, we have discussed a wide range of factors that influence pH_i. In this and the following section, we will examine how these factors interact to produce transient changes in pH_i and, finally, to establish a steady-state pH_i.

FUNDAMENTAL LAW OF pH_i REGULATION

What determines the stability of pH_i? It is intuitively obvious that pH_i will remain constant as long as the rate of acid extrusion out of the cytoplasm (J_E) is equal to the rate of acid loading into the cytoplasm (J_L)[c]. pH_i will rise if J_E exceeds J_L, and pH_i will fall if J_L exceeds J_E. The rate of pH_i change is proportional to the difference between J_E and J_L, proportional to the surface-to-volume ratio (ρ), but inversely proportional to buffering power:

[c]We define acid-extrusion and acid-loading rates as fluxes (J), with the units of moles per unit area of cell surface, per unit time. In practice, such a definition is practical for calculating values from experiments only if the cell has a very simple geometry (e.g., cylinder in the case of an axon). For most mammalian cells, which have complicated geometries, investigators express acid-loading and acid-extrusion rates in what we would term "pseudofluxes" (φ),[448] with the units of moles per unit volume of cytoplasm, per unit time. In the case of a pseudoflux, the surface-to-volume ratio is folded into the φ value. One must use caution in dealing with φ values, which can change with cell swelling or shrinkage, even without a change in the true underlying acid–base "flux".

$$\frac{d\mathrm{pH}_i}{dt} = \frac{\rho}{\beta}(J_E - J_L) \qquad (52.37)$$

Equation 52.37 makes good intuitive sense. If $J_E = J_L$, then $d\mathrm{pH}_i/d\mathrm{t} = 0$, and the cell is in a steady state with respect to pH_i. Should J_E exceed J_L, pH_i must increase because $d\mathrm{pH}_i/d\mathrm{t}$ will be greater than zero. Furthermore, the rate of this alkalinization is expected to increase as the difference between J_E and J_L increases. If J_E and J_L are unequal, then the rate of pH_i change must be proportional to the surface-to-volume ratio (ρ). Thus, pH_i transients tend to be faster in smaller cells. Finally, the rate of pH_i change must be strongly influenced by β. If β were infinite, then pH_i would be fixed, regardless of J_E and J_L. Conversely, if β approached zero, then even a small difference between J_E and J_L would cause pH_i to change very rapidly.

Factors that Influence the Steady-State pH_i

A Graphical Representation of Equation 52.37

Figure 52.15 is a plot of J_E and J_L as a function of pH_i for a hypothetical cell. The shape of the J_E curve is modeled after that reported for the Na^+–H^+ exchanger of cultured mesangial cells,[318] whereas the shape of the J_L curve is modeled after that reported for Cl^-–HCO_3^- exchange in several cells.[163,232] It is clear from Equation 52.37 that pH_i can be in a steady state (i.e., $d\mathrm{pH}_i/d\mathrm{t} = 0$) only if J_E and J_L are equal. Thus, in Figure 52.15, the steady-state pH_i is determined by the intersection of the J_E and J_L curves. By using the graphical model in Figure 52.15, one can evaluate how steady-state pH_i is altered by either acid–base disturbances, which we will discuss below, or by other factors such as hormones, mitogens, and oncogenes. Some examples will be presented below, from which the following three key concepts will emerge.

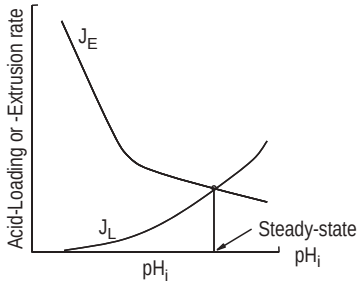

FIGURE 52.15 Dependence of acid-extrusion rate (J_E) and acid-loading rate (J_L) on pH_i for a hypothetical cell. The shapes of the curves are similar to those describing the Na^+–H^+ exchanger and background acid-loading process in renal mesangial cells.

Buffering Power Does Not Influence Steady-State pH_i

Buffering is important for cells because it reduces the magnitude of the pH_i excursions that result from acute (i.e., one-time-only) acid and alkali loads. However, buffering does not prevent pH_i changes; it only minimizes them. Moreover, after an acute acid or alkali load, buffering cannot return pH_i to normal. As we will see in the next paragraph, it is the acid-extruding mechanisms that are responsible for returning pH_i toward normal. According to Equation 52.37, β only influences the rate of pH_i recovery from such an acid load.

Acute Acid or Alkali Loads Do Not Affect Steady-State pH_i

Consider the consequences of an acute acid load (e.g., an injection of H^+ or an influx of a weak acid that leads to the intracellular generation of H^+). The vast majority of H^+ introduced into the cell is neutralized by buffers (the small amount of unbuffered H^+ is responsible for the pH_i decrease). pH_i can return to normal only when the entire acid load—both the additional free H^+ and the added H^+ that is reversibly neutralized by buffers—is extruded from the cell. During such a pH_i recovery, acid extruders remove free H^+ from the cytoplasm, and buffers then partially replenish these extruded protons. Thus, during the pH_i recovery, the added protons move from the buffers to the cytoplasm, from where the acid extruders translocate them to the outside of the cell. If there has been no fundamental change in the properties of the acid loaders and acid extruders, then pH_i will return precisely to its initial value. Thus, by themselves, acute acid and alkali loads produce only transient changes in pH_i.

Only Fundamental Changes in Acid-Extruding and Acid-Loading Processes Can Affect Steady-State pH_i

Consider the consequences of modifying the pH_i dependence of an acid-extruding process in such a way that the intersection of the J_E and J_L curves in Figure 52.15 is altered. Such a change in transporter kinetics would produce a shift in steady-state pH_i. Note that, whereas a change in the J_E and/or J_L curves is required for a shift in steady-state pH_i, the J_E and J_L curves can shift without a change in steady-state pH_i. For example, if there were appropriate offsetting changes in both curves, then it would be possible for the steady-state pH_i to remain unaltered, even though J_E and J_L were modified.

Examples of Intracellular Acid–Base Disturbances

Acute Intracellular Acid Load

Figure 52.16A–F illustrates the time course of pH_i in a hypothetical experiment in which we acutely acid load a cell (segment *ab*) and monitor the subsequent pH_i recovery (*bcd*). Figure 52.16B is reproduced Figure 52.15 and shows the pH_i dependencies of J_E and J_L, as well as J_E and J_L values at different times during segment *abcd* in Figure 52.16A. As described above, the intersection of the J_E and J_L curves at point *a* in Figure 52.16B determines the initial steady-state pH_i, where $dpH_i/dt = 0$.

We could regard the acute acid load as a square-wave increase in J_L. The product of the width (i.e., duration) of the square wave, the height of the square wave, and the surface-to-volume ratio is the amount of acid we are loading into the cell. Dividing this amount by β yields the magnitude of the pH_i decrease, which is represented in Figure 52.16A as an instantaneous fall in pH_i (*ab*). This imposed decrease in pH_i causes J_E to rise (*b* on the J_E curve) and J_L to fall (*b* on the J_L curve). According to Equation 52.37, because J_E now exceeds J_L, pH_i must increase. However, as the pH_i recovery proceeds (*bcd*), J_E gradually falls and J_L rises. Eventually, J_E and J_L come into balance at point *d*, which is identical to point *a*. Thus, as long as an acute intracellular acid load does not produce fundamental changes in the kinetics of either acid extrusion or acid loading, the effect on pH_i is only transitory. Stated differently, if the pH_i dependencies of J_E and J_L in Figure 52.16B are unchanged, then steady-state pH_i also is unchanged. In principle, the precise shape of the pH_i recovery (*bcd*) could be obtained by integrating Equation 52.37. An acute alkaline load will have the opposite effects on pH_i, and can be analyzed in an analogous way.

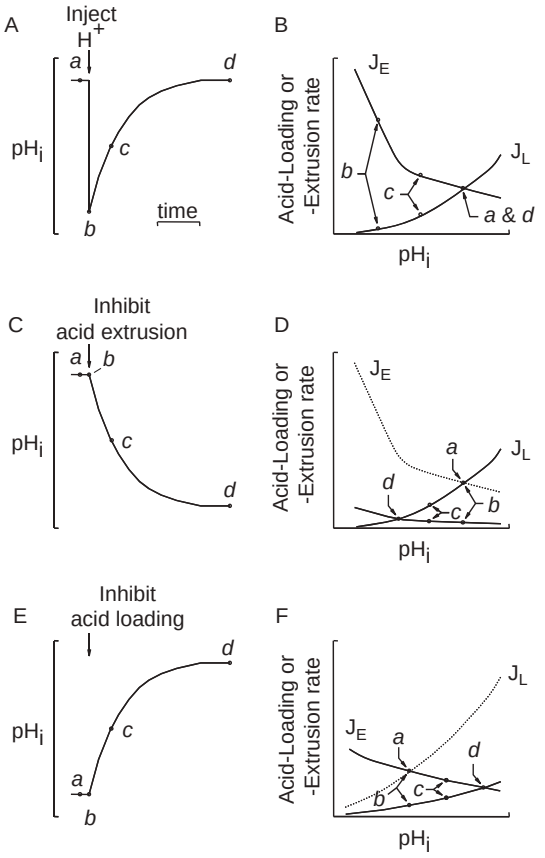

FIGURE 52.16 Response of a hypothetical cell to three insults to intracellular acid–base homeostasis. A and B: An acute intracellular acid load produces no fundamental change in the kinetics of acid extrusion and acid loading. Initially, pH_i is described by point *a* in panel A, and J_E and J_L balance each other, as described by point *a* in panel B. The acid load, which causes pH_i to fall to point b (panel A), also causes J_E to rise and J_L to fall, as described by the *b* points (panel B). Because J_E now exceeds J_L, pH_i recovers (segment *bcd* in panel A). During this recovery, J_E gradually decreases and J_L gradually increases until they reach their original values at point *d* (panel B). C and D: Inhibiting acid extrusion is assumed to reduce J_E by 75% over the entire pH_i range. The original J_E-pH_i relationship is given by the broken curve. Because J_L exceeds J_E immediately after the insult (points *b* in panel D), pH_i declines (panel C). As pH_i declines (*bcd* in panel C), however, J_E slowly increases and J_L decreases until they once again come into balance at point *d* (panel D), which describes the new steady state. E and F: Inhibiting acid loading is assumed to reduce J_L by 75% over the entire pH_i range. The original J_L-pH_i relationship is given by the broken curve. Because J_E exceeds J_L immediately after the insult (points *b* in panel F), pH_i rises (panel E). As pH_i rises (*bcd* in panel E), J_L slowly increases and J_E decreases until they once again come into balance at point *d* (panel F), which describes the new steady state.

Chronic Inhibition of Acid Extrusion

Imagine that our hypothetical cell, initially in a steady state described by point *a* in Figure 52.16C and Figure 52.16D, is treated with sufficient HOE694 (an inhibitor of Na^+–H^+ exchange) to reduce J_E to approximately one eighth of its original level at all pH_i values in Figure 52.16D. Thus, immediately after this reduction in Na^+–H^+ exchange rate, J_L is unchanged (point *b* on the J_L curve), but J_E is greatly reduced (point *b* on the J_E curve). According to Equation 52.37, because J_L now exceeds J_E, pH_i must slowly fall (*bcd* in Figure 52.16C). However, as pH_i declines, J_E rises and J_L falls (e.g., point *c* in Figure 52.16D). Eventually, J_E and J_L come into balance at point *d*, where pH_i now stabilizes. If β does not depend steeply on pH_i, then the rate of pH_i decline during *bcd* will be greatest at point *b*, where the difference (J_L–J_E) is greatest. Thus, a chronic inhibition of acid extrusion causes steady-state pH_i to fall.

Chronic Inhibition of Acid Loading

Imagine that our hypothetical cell, initially in a steady state described by point *a* in Figure 52.16E and Figure 52.16F, is treated with sufficient DIDS (an inhibitor of $Cl^--HCO_3^-$ exchange) to reduce J_L to approximately one fourth of its original value over the entire pH_i range indicated in Figure 52.16F. In Figure 52.16F, the reduced acid loading is represented by shifting the J_L-pH_i curve downward. Thus, immediately after this inhibition of $Cl^--HCO_3^-$ exchange, J_E is unchanged (point *b* on the J_E curve), but J_L is substantially reduced (point *b* on the J_L curve). According to Equation 52.37, because J_L is now much less than the unchanged J_E, pH_i must slowly rise (*bcd* in Figure 52.16E). However, this gradual increase of pH_i causes J_E to fall and J_L to rise (e.g., point *c* in Figure 52.16F). Eventually, J_E and J_L come into balance at point *d*, where pH_i stabilizes. Thus, a chronic inhibition of acid loading causes steady-state pH_i to rise.

FACTORS INFLUENCING pH_i

Interaction of pH_i and pH_o

Introduction

It is well established that changes in pH_o can affect pH_i, and also that changes in pH_i can be accompanied by changes in pH_o.[449,450] Such interactions between intra- and extra-cellular acid–base metabolism are almost certainly mediated by changes in acid–base transport across the cell membrane. We have already discussed several such transport processes, including (1) non-ionic diffusion of weak acids and bases (including metabolites), regardless of whether the transport occurs through the lipid phase of the membrane or via membrane proteins; (2) passive flux of charged weak acids and bases through channels; and (3) acid–base movement via a variety of transporters. In the remainder of this section, we will examine how an alteration on one side of the cell membrane can alter transport and thus produce a pH change on the other side.

Effects of the "Classical" Changes in Extracellular Acid–Base Status on pH_i

One can define at least six simple disturbances of extracellular acid–base status, each of which has a unique effect on pH_i. Four of these are the "classic" extracellular disturbances: metabolic acidosis and alkalosis, as well as respiratory acidosis and alkalosis. The other two extracellular acid–base disturbances, isohydric hyper- and hypocapnia, are unusual in that they produce alterations in pH_i with no change in pH_o.

METABOLIC ACIDOSIS

A sudden extracellular acidification produced by a reduction of $[HCO_3^-]_o$ at a fixed P_{CO_2} is expected to alter pH_i only by mechanisms that we shall describe as "chronic." The reductions in pH_o and/or $[HCO_3^-]_o$ are expected to inhibit acid-extrusion processes, but stimulate acid-loading processes. Such kinetic changes could be produced by alterations in any rate-determining parameter, such as pH_o, $[Na^+]_o$, $[Na^+]_i$, binding constants, or the density of transporters. The net effect is expected to be a gradual but sustained decline in pH_i, similar to that schematized in Figure 52.16C. The modeling of this problem is similar to that described above in Figure 52.16D, except that not only would J_E decrease, but J_L would increase as well. The time course of the pH_i decline depends on β and on the pH_i dependencies of J_E and J_L. The actual value of the new steady-state pH_i would, of course, be independent of β.

The predictions of the foregoing analysis have been confirmed experimentally. Measurements of steady-state pH_i with DMO indicate that metabolic acidosis lowers pH_i in mammalian skeletal and cardiac muscle.[3,451] The time course of this intracellular acidification has also been monitored with pH-sensitive microelectrodes in several vertebrate cells.[13,204,452,453]

METABOLIC ALKALOSIS

A sudden extracellular alkalinization produced by raising $[HCO_3^-]_o$ at a fixed P_{CO_2} is expected to have chronic effects on acid extrusion, acid loading, and pH_i that are opposite to those described above for metabolic acidosis. Metabolic alkalosis generally produces a gradual but sustained pH_i increase, similar to that schematized in Figure 52.16E. The modeling of this problem would be similar to that of Figure 52.16F, except that, not only would J_E increase, but J_L would decrease as well. Steady-state pH_i measurements with DMO in mammalian muscle[451,454] have confirmed the foregoing prediction that pH_i should rise during metabolic acidosis.

RESPIRATORY ACIDOSIS

A sudden extracellular acidification produced by an increase in P_{CO_2} is expected to alter pH_i by both acute and chronic mechanisms. In the laboratory, it is possible to produce a respiratory acidosis in which $[HCO_3^-]_o$ is constant. However, *in vivo*, respiratory acidosis is always accompanied by a rise in $[HCO_3^-]_o$. Regardless of the effect on $[HCO_3^-]_o$, the "acute" effect of respiratory acidosis is produced by the influx of CO_2, which elicits a rapid fall in pH_i. This represents an acute intracellular acid load from which the cell would fully recover if the kinetics of acid-extruding and acid-loading mechanisms were not fundamentally altered

by the accompanying fall in pH_o. The expected "chronic" effects of respiratory acidosis are qualitatively the same as for metabolic acidosis: an inhibition of J_E and a stimulation of J_L. These chronic effects will tend to lower steady-state pH_i, as in metabolic acidosis. Indeed, pH_i determinations by the DMO technique[3,451] show that respiratory acidosis does reduce steady-state pH_i. In principle, the time course of the pH_i decrease could be predicted from our discussion of CO_2-induced acidifications (the acute effect) and from Equation 52.37 (the chronic effect). Thus, β, initial pH_i, initial and final P_{CO_2}, and the kinetics of acid extrusion and acid loading would all influence the time course of acidification. All these parameters except β would also influence the final steady-state pH_i. After the acute effect (i.e., the rapid CO_2-induced pH_i fall), respiratory acidosis could then produce: (1) A slower but sustained pH_i decline (chronic effect), (2) no further pH_i change (i.e., immediate stabilization), or (3) a pH_i recovery that is either partial, complete or—at least in principle—even exaggerated. Which of the three steady-state outcomes we observe depends upon the relationship between J_E and J_L.

RESPIRATORY ALKALOSIS

The pH_i changes produced by respiratory alkalosis, and the mechanisms effecting these changes, are opposite those produced by respiratory acidosis. The effect on acid extrusion is noteworthy because the imposed rise in pH_o is expected to stimulate acid extrusion, whereas the resultant increase in pH_i (caused by the efflux of CO_2) is expected to inhibit or even totally block acid extrusion. Thus, the expected time course of pH_i after its rapid initial rise could be: (1) A further, slower increase to a new steady state, (2) no change, or (3) a decline. Studies with pH-sensitive microelectrodes have demonstrated the first pattern in mouse skeletal muscle,[204] and steady-state pH_i measurements have confirmed that respiratory alkalosis causes a sustained elevation of pH_i.[3,451]

ISOHYDRIC HYPERCAPNIA

Raising P_{CO_2} at constant pH_o (i.e., raising P_{CO_2} and $[HCO_3^-]_o$ proportionally) produces a rapid fall in pH_i,[170,35] due to the influx of CO_2, just as does respiratory acidosis (*vide supra*). However, for at least two reasons, the long-term influences on pH_i can be very different from those produced by respiratory acidosis. First, because pH_o is fixed, one expects no immediate inhibition of acid extrusion or stimulation of acid loading. Thus, the cell should be better able to resist the acute acid load caused by the influx of CO_2. Second, because $[HCO_3^-]_o$ is higher in isohydric hypercapnia than respiratory acidosis, acid loading due to the passive and carrier-mediated efflux of HCO_3^- should be lower than during respiratory acidosis. Third, the aforementioned increase in $[HCO_3^-]_o$ could also stimulate HCO_3^--dependent acid extrusion (e.g., Na^+-driven $Cl^- - HCO_3^-$ exchange). According to recent data, raising $[CO_2]$ per se (i.e., in the nominal absence of HCO_3^-) can stimulate H^+ extrusion from proximal-tubule cells.[32] Thus, although isohydric hypercapnia is expected to elicit the same initial, CO_2-induced fall in pH_i as respiratory acidosis, the final steady-state pH_i should be higher, as has been confirmed in mammalian skeletal muscle.[451]

The time course of pH_i during isohydric hypercapnia depends on the four previously mentioned factors (i.e., β, initial pH_i, initial and final P_{CO_2}, and the kinetics of acid extrusion and acid loading). In salamander proximal-tubule cells, pH_i does not recover from the initial fall, due to the very high HCO_3^- efflux across the basolateral membrane, via NBC.[13] In cells with lesser degrees of HCO_3^--dependent acid loading, pH_i makes a partial or even complete recovery.[455,3,14] Finally, in cells with dominant HCO_3^--dependent acid-extrusion mechanisms, such as smooth muscle[16] and renal mesangial cells,[19] isohydric hypercapnia increases steady-state pH_i. In both dissociated CA1 neurons[355,456] and cultured astrocytes[17] from the rat hippocampus, the degree of this pH_i increase becomes less and less at progressively higher initial values of pH_i. The pH_i increase produced by isohydric hypercapnia in the rabbit proximal tubule[457] may reflect stimulation of apical $Na^+ - H^+$ exchange and H^+ pumping,[206,458] likely involving sensors for basolateral CO_2 and HCO_3^-.[32]

ISOHYDRIC HYPOCAPNIA

Lowering P_{CO_2} at constant pH_o (i.e., lowering P_{CO_2} and $[HCO_3^-]_o$ proportionally) produces an initial rise in pH_i due to CO_2 efflux, as in respiratory alkalosis. The long-term influences on pH_i are the opposite of those described above for isohydric hypercapnia. Thus, the final steady-state pH_i is expected to be somewhat lower in isohydric hypocapnia than in respiratory alkalosis, as confirmed for mammalian skeletal muscle.[459] The time course of changes in pH_i during isohydric hypocapnia has been monitored in several cells, especially during the transition between normal $P_{CO_2}/[HCO_3^-]$ to nominally CO_2/HCO_3^--free conditions. As expected, the reduction in P_{CO_2} at constant pH_o causes an abrupt increase in pH_i (due to CO_2 efflux), followed by a partial return of pH_i toward normal (probably due to inhibition of acid extrusion and stimulation of acid loading at high pH_i). In mesangial cells, the switch from 10% CO_2/50 mM HCO_3^- ($pH_o = 7.4$) to 5% CO_2/25 mM HCO_3^- ($pH_o = 7.4$) causes an abrupt increase in pH_i that represents an acute intracellular alkali load. The subsequent recovery

of pH_i, due primarily to Cl^-–HCO_3^- exchange, can then be examined at physiological levels of extracellular CO_2 and HCO_3^-.[25] A similar approach has been used by Ou-yang et al.[460] to examine Cl^-–HCO_3^- exchanger activity in neurons cultured from the rat cortex.

Use of Out-of-Equilibrium CO_2/HCO_3^- to make Isolated Changes in Extracellular $[CO_2]$, $[HCO_3^-]$, and pH—One at a Time

In 1995, Zhao et al.[270] introduced a rapid-mixing technique that allows one to create out-of-equilibrium (OOE) CO_2/HCO_3^- solutions with virtually any combination of $[CO_2]$, $[HCO_3^-]$, and pH in the pathophysiological pH range. The approach is to mix the outputs of two syringes—each containing a different combination of equilibrated $[CO_2]$, $[HCO_3^-]$, and pH—and then rapidly (<200 ms) deliver the newly mixed solution to the cells, while continuously sweeping away the solution after it has contacted the cells.

Sensors for Extracellular $[CO_2]$, $[HCO_3^-]$, and pH

Zhou et al.[32] used the powerful OOE approach to alter, systematically, the basolateral (BL) $[CO_2]$, $[HCO_3^-]$, and pH—one at a time—in experiments on isolated, perfused rabbit proximal tubules. They found that increasing $[CO_2]_{BL}$—while holding $[HCO_3^-]_{BL}$ and pH_{BL} fixed—caused an increase in the rate of HCO_3^- reabsorption (measured during a period of $\sim$20 min). This is the appropriate response to the "respiratory" part of acute respiratory acidosis. Conversely, increasing $[HCO_3^-]_{BL}$—while holding $[CO_2]_{BL}$ and pH_{BL} fixed—caused the rate of HCO_3^- reabsorption to decrease. This is the appropriate response to the "metabolic" part of acute metabolic acidosis. Finally, they found that increasing pH_{BL} (which also increased pH_i)—while holding $[CO_2]_{BL}$ and $[HCO_3^-]_{BL}$ fixed—had no effect on the rate of HCO_3^- reabsorption. In other words—at least during acute stresses—the proximal tubule is incapable of responding to changes in pH_{BL} (or pH_i) per se. Rather, the tubule responds to changes in the basolateral concentrations of the two major buffers, CO_2 and HCO_3^-. These data are consistent with the hypothesis that the proximal tubule has some sort of sensor or sensors that detect extracellular levels of CO_2 and extracellular HCO_3^-. The response to increased $[CO_2]_{BL}$ is blocked by nanomolar levels of compounds believed to be specific for the ErbB family of receptor tyrosine kinases, but not by an inhibitor of Src kinases.[461]

Although proximal-tubule cells apparently do not respond to pH_{BL} changes per se, Ludwig et al.[31] identified two G-protein–coupled receptors (GPCRs) that do respond to changes in extracellular pH. The first is the ovarian cancer GPCR (OGR1). Lowering pH_o from 7.8 to 6.8 converts OGR1 from its fully inactivated to its fully activated state, which causes an increase in inositol phosphate formation. According to additional work by Tomura et al.,[462] OGR1 can lead to an increase in $[cAMP]_i$ via phospholipase C and the cyclooxygenase pathway. OGR1 is highly expressed in osteoblasts, lung, intestine, and kidney. The second pH-sensitive GPCR identified by Ludwig et al.[31] is GPR4, which also appears to signal through cAMP. Shortly thereafter, other investigators identified additional pH-sensitive GPCRs with homology to OGR1 and GPR4, including G2A (from G2 accumulation)[463] and T Cell Death-Associated Gene 8 (TDAG8).[464,465] Acid-induced activation of these additional receptors signals through inositol phosphate accumulation for G2A and cAMP accumulation and RhoA activation for TDAG8 (for a review by Tomura et al., see ref. [466]).

In addition to the above GPCRs, several ion channels are pH sensitive. Thus, it is possible that changes in pH_o could signal via changes in membrane potential. The first such channel to be identified was the Na^+-permeable channel ASIC.[467] This channel is activated by large ($\sim$1 pH unit) and rapid pH_o decreases.[468] pH also modulates 2P-domain K^+ channels (TASK, TALK, TREK, & TWIK). TASKs are acidosis inhibited, whereas TALKs are alkalosis activated.[469] TASK-1 (pK $\sim$7.3) is very sensitive to pH_o variations [470] and TASK-3 has a pK of $\sim$6.6.[471,472] For a thoughtful discussion of mechanisms by which kidney cells may sense intra- or extracellular acid–base disturbances, see the review by Brown and Wagner.[473]

Effects of Intracellular pH Changes on pH_o

The pH of the bulk extracellular fluid (pH_{ECF}) is closely regulated by the respiratory and renal systems. Nevertheless, the movement of acids and bases across cell membranes can modify pH_{ECF}. For example, in the central nervous system, where the neurons and glial cells are in close apposition to one another, acid–base transport across the cell membranes can profoundly alter pH_o (for reviews, see refs. [2,474–476]). Acid–base movement across cell membranes can result in either parallel or reciprocal changes in pH_i and pH_o. Parallel decreases in pH_i and pH_o can occur when an increased rate of lactic acid production (which lowers pH_i) leads to the subsequent efflux of lactic acid via H^+/Lac^- cotransport (which lowers pH_o). The efflux of lactic acid minimizes the fall in pH_i. Reciprocal increases in pH_i and decreases in pH_o occur in gall-bladder epithelial cells due to Na^+–H^+ exchange,[449] and in depolarized snail neurons due to a voltage-activated conductance pathway.[450] In both of the above examples, stabilization of pH_i occurs at the expense of pH_o homeostasis.

Role of the Extracellular Fluid in pH_i Regulation

It is well established that changes in pH_o will elicit reciprocal changes in pH_i. A general rule of thumb: the magnitude of a pH_i change will be ~1/3 the magnitude of the pH_o change. However, $\Delta pH_i/\Delta pH_o$ can vary considerably among cells, being as high as 0.7 in mesenteric vascular smooth muscle,[477] carotid-body glomus cell,[478] and CNS neurons.[479] As noted above, extracellular metabolic acidosis causes a sustained fall in pH_i. The overall effect of this acidosis on acid–base transport is therefore a net transfer of acid from the ECF to the ICF of all accessible cells, causing pH_o to increase somewhat toward normal, but at the expense of causing pH_i to decrease throughout the organism. One interpretation of these reciprocal changes in pH_i and pH_o is that cells act as a pH buffer for the ECF, preventing large fluctuations in pH_o. For example, "healthy" cells taking up H^+ minimize the fall in pH_o due to the release of lactic acid by a subpopulation of hypoxic cells. The partial uptake of this acid from the ECF by the healthy cells may thus be viewed as a mechanism for distributing the acid insult among all cells accessible to the ECF, until such time that the renal and respiratory systems can correct the acid–base disturbance.

In the steady state in most animals, there is a net transfer of metabolically generated acid from cells to the ECF, and from the ECF to the urine, as depicted in Figure 52.17. In the kidney, tubules from both the proximal nephron[13,383,380,396] and distal nephron[341,480] are comprised of cells that regulate pH_i much as would nonepithelial cells; they respond to intracellular acid loads by extruding acid. However, these cells are unique in that HCO_3^- efflux, which provides the major intracellular acid load, is limited to the cells' basolateral (or blood-side) membrane.[13,178,481–484] On the other hand, acid extruders (e.g., the Na^+–H^+ exchanger and H^+ pump) are generally most active at the luminal membrane.[164,380,485] Thus, the acid extruded into the ECF from non-renal cells enters renal-tubule cells via basolateral HCO_3^- efflux, lowering renal-tubule pH_i. Presumably stimulated by this pH_i decrease, luminal acid extruders move the acid into the tubule lumen. Thus, the regulation of pH_i by certain renal-tubule cells ultimately leads to acid excretion by the kidney. The renal-tubule cells therefore provide the following final link between pH_i and pH_o: pH_i regulation by renal-tubule cells is responsible for pH_o regulation, which in turn makes possible pH_i regulation by the body's other cells.

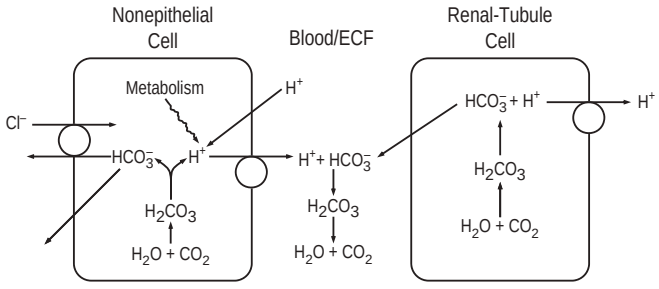

FIGURE 52.17 Schematic representation of factors affecting H^+ balance in the single cell and whole organism. A nonepithelial cell is acid-loaded by metabolic production of acid, by HCO_3^- efflux, and by H^+ influx. pH_i is maintained by a mechanism that extrudes acid from the cell into the ECF and blood. This acid effectively gains entry into certain renal tubule cells by the efflux of HCO_3^- across the renal tubule basolateral membrane. This HCO_3^- efflux, in turn, acid-loads the renal tubule cell and stimulates extrusion of acid across the luminal membrane and into the urine. Thus, the necessity of pH_i regulation by these renal tubule cells brings about pH_i regulation of the blood, which in turn keeps the extracellular pH high enough for nonepithelial cells to regulate their pH_i.

Temperature Changes

Decreasing the temperature generally produces a pH increase in both the blood and intracellular fluid. For reviews, see refs. [3,486]. In principle, a temperature change could alter pH_i in at least three ways: (1) By modifying the pK_a' of pH buffers, (2) by modifying the pK_a' of enzymes or transporters involved in acid–base homeostasis, or (3) by changing the activation energy for an enzymatic reaction or transport process.

Effect of Temperature Changes on the pK_a' of Buffers

The intergrated form of the van't Hoff equation predicts that, in a closed system (i.e., for a fixed total amount of buffer), a buffer's pK should vary inversely with temperature:

$$pK_1 - pK_2 = \frac{\Delta H}{R \ln 10}\left[\frac{1}{T_1} - \frac{1}{T_2}\right] \qquad (52.38)$$

where ΔH is the heat of ionization, R is the universal gas constant, T_1 and T_2 are two absolute temperatures, and the subscripts 1 and 2 refer to pK_a' values at the corresponding two temperatures. If a solution contains only one buffer, then a temperature change will produce parallel shifts in pK_a' and pH. In the case of a solution containing several buffers (e.g., intracellular fluid), the temperature-induced pH shift depends on the sum of the individual pK shifts, each weighted by the buffer's relative contribution to total buffering.[487]

Reeves and Malan[488] have analyzed the pH_i changes produced by temperature shifts in frog muscle *in vivo*. Over the same temperature range, the *in-vivo* pH_i values in these experiments are approximated by the *in-vitro* pH values of a mixture of imidazole, phosphate, and CO_2/HCO_3^-, all at physiological levels.

These frog-muscle data seem consistent with the idea that temperature changes can shift steady-state pH_i by shifting pK_a' of buffers, and thus releasing or consuming H^+. However, this interpretation is inconsistent with the general principle that only alterations in the properties of acid–base transporters can change steady-state pH_i. Consider the example of raising temperature, which would lower the pK_a' values of intracellular buffers, thereby releasing H^+. This represents an acute intracellular acid load, no different in principle from the acid load produced by the injection of H^+. If the only effect of the temperature increase were to lower pK_a' values of buffers, then pH_i would abruptly decrease and subsequently recover to its initial value over the course of a few minutes. The only lasting effect would be subtle changes in the pH_i profile of β. Thus, although there can be little doubt that temperature changes elicit a rapid release or consumption of H^+, we must look to other mechanisms to account for changes in steady-state pH_i.

Effect of Temperature Changes on Enzymes and Transporters

The effects of temperature changes on acid–base transporters and other enzymes affecting pH_i are not well documented. The effects are most likely of two sorts: (1) A temperature-induced shift in the pK_a' of an ionizable group on an enzyme or transport protein could affect the kinetics of the reaction or transport process. (2) Raising the temperature speeds reactions by increasing the energy of the reactants. As far as pK_a' shifts are concerned, a change in temperature would be expected to alter the ionization state of titratable groups on proteins, with effects being greatest for groups with pK_a' values similar to the prevailing pH. For instance, a rise in temperature would lower the pK_a' of an amino group of a protein, thereby reducing the fraction of molecules with a positive charge at that position. Conversely, the fraction of molecules with a negatively charged carboxyl group would rise. Such alterations in ionization could lead to conformational changes that could have major effects on protein function.

As far as direct effects of temperature changes on reaction rates are concerned, enzymatic reaction rates as well as passive and active fluxes of ions all are expected to fall with decreasing temperature, although to varying degrees. In mouse soleus muscle, reducing the temperature from 37°C to 28°C causes the acid-extrusion rate to fall by 65%.[171] Similarly, in cultured astrocytes from rat hippocampus, reducing the temperature from 37°C to room temperature causes the acid-extrusion rate elicited by exposing the cells to CO_2/HCO_3^- to fall by ~40% (unpublished data). In a study on cultured fetal rat hippocampal neurons, Baxter and Church[388] have presented evidence that the Na^+-driven $Cl^- - HCO_3^-$ exchanger contributes to the maintenance of steady-state pH_i at 18°C–22°C, but not at 37°C. In these neurons, increasing temperature may activate the $Na^+ - H^+$ exchanger more than the Na^+-driven $Cl^- - HCO_3^-$ exchanger. In addition to cellular changes brought about by temperature shifts, whole-body physiological changes (e.g., hormone levels, P_{CO_2}, plasma $[HCO_3^-]$) may also influence pH_i.

Metabolic Inhibitors and Anoxia/Hypoxia

Metabolic inhibitors, anoxia/hypoxia and ischemia generally produce slow decreases in pH_i. Metabolic inhibitors have been examined most closely in isolated nerve and muscle preparations using pH-sensitive microelectrodes. Both azide and 2,4-dinitrophenol (DNP) produce two-stage decreases in pH_i:[35,170] an abrupt fall followed by a slower one. The abrupt pH_i decrease is probably due to the influx and dissociation of the protonated weak-acid form of the inhibitor, whereas the slower pH_i decrease may be caused by a net increase in the production of acidic metabolites, confounded perhaps by a decrease in the rate of acid extrusion. Squid axons that are exposed to hydrocyanic acid ($HCN \rightleftarrows H^+ + CN^-$; $pK_a' = \sim 10$) display only a slow decrease in pH_i,[170] the origin of which is likely the same as those of the slow phase of the azide and DNP-induced acidifications. The failure of HCN to produce a rapid pH_i decrease in squid axons is due to its high pK_a'; at physiological pH_i, only a small fraction of incoming HCN dissociates into CN^- and H^+.

Ischemia and anoxia/hypoxia can also elicit decreases in pH_i due to the lactic acid production that results from increased glycolysis in the absence of oxidative phosphorylation (see refs. [489,490]). For example, using ^{31}P-NMR to measure the pH_i of beating rat hearts, Gadian et al.[128] observed that ischemia produced a gradual fall in pH_i from 7.05 to 6.2 in 13 min. However, in hearts previously depleted of glycogen, the pH_i fall triggered by a subsequent episode of ischemia is reduced by ~50%.[491] Similarly, preincubating the hearts in 2-deoxyglucose, which inhibits phosphorylase b and thus glycogen breakdown, reduces the ischemia-induced pH_i decrease by ~25%. Although anoxia/hypoxia might be expected to decrease pH_i by interfering with active-transport processes that extrude acid, the effects of anoxia/hypoxia appear to be more complex and are likely to depend on several factors including the cell type, the experimental preparation (e.g., cells *in situ* vs. cells in culture), duration of anoxia/hypoxia, and the presence vs. the absence of CO_2/HCO_3^-, as well as other parameters that influence the relative activity of various acid–base transporters.

For example, in the isolated turtle heart, anoxia inhibits a DIDS-sensitive, Na^+- and HCO_3^--dependent mechanism by ~50%.[492] In contrast, acute anoxia appears to stimulate a stilbene-sensitive, electrogenic Na^+-coupled HCO_3^- transporter in rat hippocampal neurons.[493] Anoxia/ischemia or subsequent reoxygenation has also been shown to stimulate Na^+–H^+ exchange activity in mammalian neurons and astrocytes,[493–498] and such stimulation can involve kinases such as ERK1/2 and protein kinases A and C.[497,499,500]

Hypoxia-induced changes in acid–base transporter expression are also complex. For example, exposing mice to chronic hypoxia (11% O_2) for two or four weeks decreases the expression of NBCn1 and NBCn2 in cerebral cortex, subcortex, cerebellum, and hippocampus in both neonatal and adult mice.[501] Similar hypoxic results were obtained for NDCBE expression in adult mice, although neonatal animals displayed delayed or absent responses in some of these brain regions.[502] Specific acid–base transporters appear to play important roles in regulating pH_i, ion homeostasis, and perhaps signaling pathways associated with hypoxia-induced cell death.[503] For example, exposing cultured neurons or hippocampal slices to 1% hypoxia for five to seven days causes neuronal damage that is inhibited by the bicarbonate-transport inhibitor DIDS, but exacerbated by NHE inhibitors.[504]

Effects of Cell Shrinkage on pH_i

Effect of Hypertonic Solutions on Na^+–H^+ and Cl^-–HCO_3^- Exchange

In several cell types, including erythrocytes,[505–511] lymphocytes,[374] mesangial cells,[322] glioma cells,[399,512] and barnacle muscle,[513,514] shrinking a cell in a hypertonic medium stimulates the exchange of external Na^+ for internal H^+. In at least *Amphiuma* red blood cells (RBCs), shrinkage in hypertonic solutions also stimulates the exchange of external Cl^- for internal HCO_3^-. Because the H^+ extruded from the cells is derived almost exclusively from buffers, and because the HCO_3^- is derived from the freely diffusible CO_2 and H_2O, these movements of H^+ and HCO_3^- are "osmotically silent." Thus, the net effect of Na^+–H^+ and Cl^-–HCO_3^- exchange is an uptake of NaCl—along with osmotically obligated H_2O—and a recovery of cell volume termed a *volume-regulatory increase* (VRI). As discussed below, shrinkage appears to activate the Na^+–H^+ exchanger directly. However, the stimulation of the Cl^-–HCO_3^- exchanger appears to be indirect, reflecting by the rise in pH_i caused by the activated Na^+–H^+ exchanger.[515]

Interestingly, in lymphocytes, the shrinkage-induced activation of the Na^+–H^+ exchanger is observed only after volume-regulatory decrease that follows a previous cell swelling.[374] Regulation of cell volume per se is discussed in Chapter 5. For other reviews of cell-volume regulation, see refs.[370,371,516–522].

Mechanism by which Shrinkage/Hypertonicity Affects Na^+–H^+ Exchange

Just how cells sense shrinkage is unknown. However, we are beginning to understand more about the signal-transduction processes involved in the acute and chronic responses to shrinkage. Hypertonicity can trigger the rapid dephosphorylation of phosphatidylinositol-5-kinase type I β (PIP5KIβ) that activates the enzyme and increases the rate of PIP_2 synthesis.[523] On a longer time scale, kinases in the Ste20 family, with the subsequent activation of the MAPK pathway, are critical for the chronic response to hypertonic shock in yeast (for reviews, see refs. [524,525]) and mammalian cells (for a review, see ref. [526]).

How does acute cell shrinkage affect one of the key endpoints of the signal-transduction cascade, namely, the Na^+–H^+ exchanger? Most investigators have not observed a hyperosmotic-induced phosphorylation of NHE1,[527] although Rigor et al.[528] have recently reported that the shrinkage of red blood cells from *Amphiuma tridactylum* does activate NHE1 through direct phosphorylation of the C terminus. There is more evidence that the phosphorylation of other proteins is likely to be involved. For example, in work on primary rat astrocytes[529] and confluent C6 glioma cells,[512] Shrode et al. have discovered that shrinkage appears to stimulate Na^+–H^+ exchange through phosphorylation of myosin light chain. Kinases such as tyrosine kinases, MAPKs, and Janus kinase 2 (Jak2) also appear to be involved;[530–533] for a review, see ref. [519]. For example, the general tyrosine kinase inhibitor genistein inhibits both tyrosine kinase-mediated protein phosphorylation and hypertonic-induced stimulation of NHE1 in polymorphonuclear leukocytes.[533]

According to results from an intriguing structure-function study involving chimeras of NHE1 (stimulated by shrinkage) and NHE2 (not stimulated by shrinkage), the extracellular loop between TM domains 1 and 2 of NHE2 is sufficient to inhibit shrinkage-induced activation of the exchanger.[534]

How does acute shrinkage mechanistically alter the Na^+–H^+ exchanger? Shrinkage is thought to increase the transporter's affinity for intracellular H^+.[535] However, Dunham and colleagues[536,537] have reported that cell shrinkage stimulates Na^+–H^+ exchange activity in dog RBCs by reducing the transporter's affinity for external Na^+ at an extracellular inhibitory site.

Other insights into the events linking shrinkage to the acute stimulation of Na^+–H^+ exchange come from work on dog RBCs, lymphocytes, and/or giant-barnacle muscle fibers. First, although Na^+–H^+

exchange appears inactive in these cells under physiological conditions, it can be stimulated by either a decrease in pH_i,[374,538] a decrease in cell volume,[374,508,514] or an increase in $[Li^+]_i$.[538,539] Second, the shrinkage-induced activation of Na^+-H^+ exchange requires Cl^-,[540,508] specifically intracellular Cl^-.[514,541] In rat mesangial cells as well, the shrinkage-induced increase in pH_i is inhibited by preincubating the cells in a Cl^--free solution for a minimum of ~15 min (and presumably decreasing $[Cl^-]_i$ considerably). Third, in barnacle muscle fibers, the shrinkage-induced activation of Na^+-H^+ exchange is inhibited by GDPβS,[513] suggesting involvement of a G protein in the signal transduction system. Consistent with this last observation, Na^+-H^+ exchange is stimulated by either GTPγS, AlF_3, or cholera toxin (CTX).[541] However, the CTX effect is not via a classic G_s pathway, inasmuch as neither cAMP nor cAMP analogs stimulate Na^+-H^+ exchange. It should be emphasized that the data do not prove that CTX stimulates the Na^+-H^+ exchanger by the same signal transduction pathway as does shrinkage. Finally, in barnacle muscle fibers, the Cl^- requirement in the shrinkage-induced activation of the exchanger is at or before activation of the heterotrimeric G protein.[541]

K^+-H^+ Exchange

Cala has observed that an exchange of internal K^+ for external H^+ contributes to the *volume-regulatory decrease* (VRD) that occurs after swelling *Amphiuma* RBCs.[506] This exchange is inhibited in the nominal absence of Ca^{2+}, and is stimulated by applying the Ca^{2+} ionophore A23187, suggesting that increases in $[Ca^{2+}]_i$ may activate K^+-H^+ exchange. Two observations are of special interest. First, increased $[Ca^{2+}]_i$ failed to stimulate K^+-H^+ exchange when Na^+-H^+ exchange was stimulated by shrinkage. Second, if the cells were shrunken (so that Na^+-H^+ exchange should have been stimulated) and then pretreated with amiloride (to block Na^+-H^+ exchange), then swelling failed to activate K^+-H^+ exchange. However, amiloride did not inhibit swelling-activated K^+-H^+ exchange when the drug was applied for the first time to swollen cells. These data led Cala to suggest that Na^+-H^+ and K^+-H^+ exchange may be mediated by the same entity.[542] K^+-H^+ exchange can also be activated by millimolar concentrations of *N*-ethylmaleimide (NEM).[543]

Hormones, Chronic Stress, Growth Factors and Oncogenes

Hormones

A number of hormones modulate transepithelial acid−base transport in various nephron segments (for examples, see refs. [544−547]). In addition, hormones modulate specific acid−base transporters in a variety of cells, including those from the kidney. The Na^+-H^+ exchanger is the transporter that has most often been the subject of these hormone studies—probably reflecting the transporter's popularity rather than its unique sensitivity to hormonal control. Below, we will review some of the hormones that can alter the activity of acid−base transporters, particularly those in the kidney.

GLUCOCORTICOIDS

Elevations in plasma levels of glucocorticoids in response to metabolic acidosis increases acid excretion in the kidney by stimulating Na^+-H^+ exchange, thereby increasing H^+ secretion and HCO_3^- reabsorption. In studies on brush-border membrane vesicles, Na^+-H^+ exchange rates are higher in vesicles obtained from adrenalectomized (adx) animals treated with the glucocorticoid dexamethazone than in adx animals treated with the mineralocorticoid aldosterone, or in adx animals receiving no supplementation.[548,549,550] In proximal-tubule cells isolated from the kidney, Bidet et al.[551] have shown that even a 1-hr treatment with dexamethazone can enhance Na^+-H^+ exchange. The dexamethazone increases the V_{max} of the transporter, and stimulates new protein synthesis. Glucocorticoids exert their effect predominantly on the Na^+-H^+ exchange isoform NHE3. For example, in ileal brush-border membranes from animals injected with methylprednisolone, the glucocorticoid stimulates both the activity and mRNA levels of NHE3, but not of NHE2 or NHE1.[552] In opossum kidney (OKP) cells, glucocorticoids increases both Na^+-H^+ exchange activity[553] and NHE3 mRNA levels.[554] Hydrocortisone raises both the activity and protein level of NHE-3 in OKP cells subjected to acidosis.[555] Data are consistent with a non-genomic component to glucocorticoid-induced activation of NHE3 that involves both the stimulation of protein kinase SGK1 and the presence of the Na^+-H^+ exchanger regulatory factor NHERF2.[556,557] Glucocorticoids can also enhance the stimulatory effect of insulin on NHE3 activity and expression in OKP cells.[558,559]

Glucocorticoids appear to stimulate Na^+/HCO_3^- cotransport as well. For example, removing hydrocortisone from the medium of cultured proximal tubule cells causes a decrease in Na^+/HCO_3^- activity, whereas returning the hydrocortisone or adding dexamethasone increases the activity of the transporter.[560] In addition, both NBCe1 activity and mRNA levels are increased 80−90% in proximal tubules from rats four days after subcutaneous injection with glucocorticoids.[561]

Aldosterone can have both non-genomic (short term) and genomic effects (long term) on Na^+-H^+ exchange. For example, in both renal and non-renal

cells, applying aldosterone elicits a stimulation of the Na^+-H^+ exchanger after a maximum delay of 20 min[562–565] (see ref. [566]), probably due to an alkali shift in the set point of the transporter.[567] However, a 30-min exposure of aldosterone to the frog early distal tubule also stimulates Na^+-H^+ exchange activity, but due to increased expression of the transporter. In this frog-tubule preparation, the stimulation can be inhibited by transcription or translation inhibitors.[568] In a nongenomic fashion, aldosterone also stimulates NHE3 activity in the medullary thick ascending limb of the kidney[569,570] through an ERK-dependent pathway.[571] In immortalized proximal-tubule epithelial cells from the spontaneously hypertensive rat (SHR), aldosterone also stimulates NHE activity through a process requiring H_2O_2 production.[572] As presented in greater detail in Chapter 35, aldosterone also stimulates the V-type H^+ pump in the distal tubule.

CATECHOLAMINES

The catecholamines norepinephrine and dopamine both influence acid–base transporter activity in the kidney. Norepinephrine has been proposed to stimulate Na^+-H^+ exchanger activity in the proximal tubule,[573,574] probably through activation of α_{1A}- and/or α_{1B}-adrenergic receptors.[575] However, in working on the *Ambystoma* proximal tubule, Abdulnour-Nakhoul et al.[576] found that norepinephrine has no effect on Na^+-H^+ exchanger activity, but rather, elicits an increase in pH_i by inhibiting NBC-mediated HCO_3^- efflux. Norepinephrine also increases $Cl^--HCO_3^-$ exchange activity to a greater extent in immortalized proximal-tubule epithelial cells from SHR than normotensive rats, perhaps due to elevated H_2O_2 production.[577] Catecholamines also can influence expression of acid–base transporters. For example, a 15-day whole-animal infusion of norepinephrine increases the expression of both NHE3 and NBCe1 in rat kidney cortex.[578]

Regarding dopamine, it is well established that this catecholamine inhibits Na^+-H^+ exchanger activity in the brush-border membrane of the proximal tubule.[579–584] Such inhibition is mediated through both cAMP/PKA-dependent and -independent events,[579,580,584] and can involve endocytotic removal of NHE3 transporters from the apical membrane.[585] Working on isolated proximal tubules from rabbit, Kunimi et al.[586] have demonstrated that dopamine also inhibits Na^+/HCO_3^- cotransporter activity, although such inhibition was not observed in tubules from hypertensive rats. Dopamine has also been shown to inhibit $Cl^--HCO_3^-$ exchanger activity in immortalized proximal-tubule cells from normotensive, but not hypertensive rats.[587]

Other agents that can influence acid–base activity in the kidney include adenosine, which stimulates Na^+/HCO_3^- cotransporter activity in the proximal tubule,[588] as well as cholinergic agonists that stimulate the cotransporter in proximal-tubule cells.[589,590]

THYROID HORMONES

The effect of thyroid hormone levels on Na^+-H^+ exchange activity has been examined in brush-border vesicles obtained from the renal cortex of hypo-, eu-, and hyperthyroid rats.[550,591–593] Compared to vesicles derived from euthyroid animals, those derived from hypothyroid animals had only half the normal Na^+-H^+ exchange activity, whereas those derived from hyperthyroid animals had twice the normal exchanger activity. In both cases, the altered Na^+-H^+ exchange activity is due to an increase in the V_{max} of the transporter, rather than a decrease in the apparent K_m for Na^+. The effect of thyroid hormones triiodo-L-thyronine (T_3) and L-thyroxine (T_4) on Na^+-H^+ exchange has also been examined in cultured cells. In opossum kidney cells, both T_3 and T_4 stimulate amiloride-sensitive $^{22}Na^+$ uptake,[594] probably by increase the transcription of NHE3.[595]

Thyroid hormone levels also can influence the expression of acid–base transporters. For example, inducing mild hypothyroidism in rats reduces expression of NHE3 and NBCe1 in proximal-tubule brush-border membranes (BBM), but increases expression of AE1 in the distal nephron.[596] Following metabolic acidosis, expression of both NBCe1 in the proximal-tubule BBM and AE1 in the distal nephron are elevated in the hypothyroid vs. control animals. Thyroid hormone also appears to contribute to the developmental switch in expression of NHE8 to NHE3 in the proximal tubule.[597]

PARATHYROID HORMONE, ANGIOTENSIN II, AND CYCLIC AMP

In the renal proximal tubule, HCO_3^- reabsorption is inhibited by PTH,[545,598,599] which increases intracellular levels of cAMP. At the level of brush-border membrane vesicles, PTH and cAMP analogs both reduce Na^+-H^+ exchange activity,[600] whereas parathyroidectomy of the donor animal increases Na^+-H^+ exchange activity.[601] At the cellular level, PTH and cAMP both inhibit Na^+-H^+ exchange in renal epithelial cell lines[602,603] and in rat medullary thick ascending limb (MTAL) tubule suspensions.[604] Based on work by Weinman and colleagues (see ref. [605]), the inhibitory effect of cAMP in the proximal tubule requires the presence of the Na^+-H^+ exchange regulatory factory NHERF-1, which is a PDZ adaptor protein that can bind to the carboxy terminus of NHE3.[606,607] The outcome of PTH stimulation is probably a shift in the pH_i

sensitivity of Na^+-H^+ exchange,[608] likely associated with PTH-induced phosphorylation of NHE3.[609,610] PTH can also have a delayed secondary effect of stimulating internalization of NHE3 from apical membranes.[609,610,611] Long-term PTH exposure also reduces NHE3 expression in OKP cells through a PKA-dependent reduction in NHE3 promoter activity.[612]

PTH and cAMP can also inhibit HCO_3^- transporters. Treatments that raise $[cAMP]_i$ inhibit apical $Cl^-{-}HCO_3^-$ exchange in the *Necturus* gallbladder epithelium,[613] as well as in renal epithelial cells.[614] Similarly PTH appears to inhibit Na^+/HCO_3^- cotransport activity in rabbit renal basolateral membranes via G proteins and a calmodulin-dependent protein kinase.[615] Increases in cAMP and activated Ca^{2+}-dependent protein kinases also inhibit Na^+/HCO_3^- cotransport in these basolateral membranes.[616] As described above for cAMP-mediated inhibition of NHE3, NHERF-1 is also involved in cAMP-mediated inhibiton of NBCe1, although there is no direct association between the two proteins.[617,618]

Low doses of Ang II (e.g., 10^{-11} M in an isolated rabbit proximal tubule, or 10^{-9} M in an anesthetized rat) stimulate Na^+-H^+ exchange and/or Na^+/HCO_3^- cotransport in the proximal tubule,[546,619–627] distal tubule,[628–630] and cortical collecting duct.[631] On the other hand, higher doses of Ang II (e.g., 10^{-9} M or 10^{-6} M in the above preparations) inhibit these transporters.[619,624,627,632,633] Long-term effects of Ang II include regulation of NBCe1 expression in the proximal tubule. For example, expression levels of NBCe1—but not NHE3—in the kidney increase when rats are infused with Ang II, but decrease when infused with the AT1-receptor blocker candesartan.[634] Regarding the signal-transduction pathway, in renal cortical basolateral membrane vesicles[635] and OKP cells,[636] Ang II stimulation of the exchanger involves G-protein activation. Ang II stimulation of Na^+/HCO_3^- cotransporter activity in OKP cells involves activation of Src family tyrosine kinases (SFKs) and the classic MAPK pathway.[637]

In isolated perfused superficial S1 segments of the rabbit proximal tubule, Ang II stimulates both Na^+-H^+ exchange and Na^+/HCO_3^- cotransport,[621] as judged from rates of pH_i change measured at relatively low pH_i values. Interestingly, Ang II has very little effect on steady-state pH_i. Thus, if Ang II indeed stimulates both transporters in the physiological pH_i range, then the combined increase in activities of the acid extruder and acid loader serves to increase transepithelial HCO_3^- reabsorption without altering pH_i. Ang II can also stimulate the Na^+-H^+ exchangers on the apical[638] and basolateral[632] sides of macula densa cells. Recently, Queiroz-Leite et al. have reported that chronic exposure of OKP cells to low levels of Ang II increases NHE mRNA and protein levels through transcriptional activation involving the Sp1/Egr-1 binding site and P450, PI3K, PKA, and MAPK signaling pathways.[639]

Ang II can be internalized by AT_1 receptor–mediated endocytosis through a microtubule-dependent pathway, and subsequently increase NHE3 mRNA levels through direct stimulation of MAP kinases ERK1/2 and increased transcription.[640–642]

Ang II can also stimulate other acid–base transporters. For example, in cat papillary muscles of the ventricular myocardium, Ang II stimulates $Cl^-{-}HCO_3^-$ exchange via activation of a PKC-dependent pathway.[643] However, in cat ventricular myocytes, Ang II stimulates total NBC activity through reactive oxygen species (ROS)-stimulation of ERK,[644] but inhibits electrogenic NBC through p38 kinase.[645] In the kidney, Ang II has been shown to stimulate the H^+ pump in isolated proximal-tubule cells by colchicine-sensitive apical membrane insertion.[342]

Chronic Stresses

CHRONIC METABOLIC ACIDOSIS AND ALKALOSIS

Chronic metabolic acidosis typically increases Na^+-H^+ exchange activity in the kidney, whereas chronic metabolic alkalosis has the opposite effect. For example, brush-border membrane vesicles derived from animals with chronic metabolic acidosis have increased Na^+-H^+ exchange activity,[601] due to an increase in the apparent V_{max}, rather than to a decrease in the K_m for Na^+.[646,550] Increases in the activity of Na^+-H^+ exchange have been observed in other preparations, such as membrane vesicles of rabbit kidney proximal tubules previously incubated in a low-pH solution,[647] and cells from the medullary thick ascending limb (mTAL) of rats subjected to metabolic acidosis.[648] In the mTAL, such activation is paralleled by increases in NHE3 mRNA and protein levels,[648] but not NHE1 mRNA levels.[649] Working with cultured proximal-tubule cells, Alpern et al.[650] found that *chronic* metabolic and respiratory acidosis increases Na^+-H^+ exchange activity via new protein synthesis. This effect, as well as increased expression of NHE3 mRNA, is blocked by overexpressing Csk,[651] a natural inhibitor of Src kinases. Recall that in acute experiments (see above) on isolated perfused proximal tubules, CO_2 appears to signal through a receptor tyrosine kinase, not Src.

Chronic metabolic acidosis/alkalosis can also elicit changes in the activity of other acid–base transporters. For example, the increase in apical Na^+-H^+ exchange activity with metabolic acidosis is paralleled by an increase in basolateral Na^+/HCO_3^- cotransporter activity.[29,647,652] Kwon et al.[653] used semiquantitative immunoblotting and immunohistochemistry to

examine the effect of chronic metabolic acidosis on the expression of three Na^+-coupled HCO_3^- transporters in rat kidney. The acidosis increased NBCn1 abundance in the medullary thick ascending limb and another NBCn1 variant in intercalated cells, but had no effect on NBCe1 abundance in the proximal tubule.

Metabolic acidosis also causes an increase in the activity of apical H^+ pumps in the kidney,[654,655,656] presumably contributing to the increase in HCO_3^- reabsorption. In fact, chronic acidosis stimulates the redistribution of H^+ pumps to the apical surface of collecting-duct intercalated cells, whereas chronic alkalosis stimulates the redistribution to the basolateral surface.[657] *In vitro* chronic acidosis also increases the expression of the H^+-K^+ pump in HEK-293 cells.[658] Finally, Sabolic et al.[657] observed that expression levels of $Cl^-{-}HCO_3^-$ exchange increase in the cortical collecting duct (CCD) of rats subjected to chronic metabolic acidosis (consistent with increased HCO_3^- reabsorption by α intercalated cells), but decrease in animals subjected to chronic metabolic alkalosis. Consistent with this observation is work by the Schwartz group on the rabbit CCD. They found that chronic metabolic acidosis decreases apical Cl^-–base exchange (and pendrin mRNA and protein expression) of the β-intercalated cells, but increases basolateral Cl^-–base exchange (and AE1 expression) of the α-intercalated cells.[659,655] Such expression changes are rapidly reversed with alkali loading for only 6–20 h.[659] In ref.[660], Schwartz and Alexander review the adaptive changes to the pH physiology of CCD intercalated cells subjected to acid–base disturbances.

CHRONIC HYPERCAPNIA

Na^+-H^+ exchange activity is increased in renal brush-border vesicles derived from animals that were chronically hypercapnic.[661] Chronic respiratory acidosis also increases levels of band 3 mRNA in the kidney.[662] Working on either opossum kidney cells or cultures of proximal-tubule cells, Arruda and colleagues have found that 10% CO_2 (i.e., respiratory acidosis) has a biphasic stimulatory effect on NBCe1 activity that initially (within 5 min) involves activation of Src family kinases and phosphatidylinositol 3-kinase and increased membrane insertion of NBCe1.[663–666] Later (24 h), these authors observe increases in mRNA and protein levels. Chronic hypercapnia can also alter the expression of acid–base transporters with dependence on tissue and stage of development. For example, exposing mice to 8 or 12% CO_2 for two weeks increases the expression of: (1) NHE1 and NBCn1 in the brain, heart, and kidney, and (2) NBCe1 in the heart and kidney of neonatal vs. adult mice.[667] Exposing rats to an atmosphere of 8% CO_2 + 13% O_2 for 10 days increases the expression of NBCe1 in the proximal tubule, but decreases the expression of pendrin in connecting tubules and cortical collecting ducts.[668]

RENAL HYPERTROPHY, HIGH PROTEIN DIET AND CHRONIC K^+ DEPLETION

Renal hypertrophy can increase the activity of several acid–base transporters (for review, see ref. [669]). Brush-border membrane vesicles derived from the remnant kidney following a uninephrectomy exhibit increased Na^+-H^+ exchange activity.[326,670] Interestingly, the denervation associated with the uninephrectomy may be the predominant stimulus. Indeed, the hypertrophy-induced activation of Na^+-H^+ exchange elicited by the uninephrectomy can be mimicked by contralateral denervation.[671] Nevertheless, hypertrophy of renal proximal-tubule cells *in vitro* does lead to an increase of Na^+-H^+ exchange activity.[672] In microperfusion studies of rat proximal tubule, Preisig and Alpern[673] demonstrated that the hyperfiltration preceding a decrease in renal mass increases the activities of both Na^+-H^+ exchange and Na^+/HCO_3^- cotransport.

Rats fed a 40% protein diet, rather than a 6% protein diet, also yield cortical brush-border membrane vesicles with enhanced Na^+-H^+ exchange activity, and these effects of uninephrectomy and high-protein diet are additive.[326,670] A high-protein diet in rats promotes distal HCO_3^- reabsorption through endothelin-stimulated activities of the Na^+-H^+ exchanger and H^+ pump.[674] In the case of the H^+ pump, endothelin acts through an increase in aldosterone levels.[675]

Finally, K^+ depletion also can increase the expression and function of renal acid–base transporters, enhancing overall HCO_3^- reabsorption. For example, vesicles derived from K^+-depleted rats exhibit enhanced Na^+-H^+ exchange and Na^+/HCO_3^- cotransport activity due to increases in apparent V_{max} values, with no changes in the apparent K_m values for Na^+.[676] K^+ depletion appears to increase NBCe1 mRNA expression and activity in the proximal tubule, and induce them in the mTAL and inner medullary collecting duct.[677] K^+ depletion also increases expression and activity of K^+-H^+ pumps[346,349] and H^+ pumps in the distal nephron.[678] In the case of the H^+ pumps, Barone et al.[679] present evidence that K^+ depletion increases expression of the H^+ pump on the apical membrane of α-intercalated cells in the collecting ducts and, in these same cells, upregulates SLC26A7 and AE1 on the basolateral membranes.

Growth Factors

CLASSICAL MODEL OF GROWTH-FACTOR EFFECTS ON pH_i

A potential role for pH_i in mitogenesis is suggested by the observation that growth-factor-induced

proliferation of both fibroblasts[680] and mesangial cells[27] is blocked at relatively low pH_i values, and rises sharply as pH_i enters the physiological range. Indeed, there are numerous examples in which adding a mitogen to quiescent cells, in the nominal absence of CO_2/HCO_3^-, causes a sustained increase in pH_i.[24,378,395,681–686] Because the mitogen-induced pH_i increase is prevented either by removing Na^+[681,395] or by pretreating with amiloride or an amiloride analog,[394,395,681] many investigators had deduced that the increase in pH_i is due to stimulation of $Na^+–H^+$ exchange (for more examples, see ref. [351]). Furthermore, in fibroblast mutants lacking $Na^+–H^+$ exchange, mitogens fail to elicit proliferation, or to alkalinize the cells.[404,680] Wang et al.[687] have reported that a P19 embryonal carcinoma cell line lacking $Na^+–H^+$ exchange has a reduced ability to grow and differentiate. The ability to differentiate can be resurrected by reintroducing the exchanger into the cells. These data led to an attractive hypothesis: (1) In quiescent cells, pH_i is too low to sustain proliferation. (2) Mitogens, it addition to affecting other cellular functions, stimulate $Na^+–H^+$ exchange. (3) This stimulation of $Na^+–H^+$ exchange elevates pH_i to a range that is permissive for proliferation. Thus, according to this model, pH_i would play a central role in proliferation.

EFFECT OF MITOGENS ON pH_i IN THE PRESENCE OF CO_2/HCO_3^-

One of the first hints that the mitogen-pH_i model described above might be incomplete was the observation that A431 cells incubated in the presence of CO_2/HCO_3^- do not alkalinize in response to FCS plus EGF.[20] Mesangial cells,[24] fibroblasts,[18] and NIH 3T3 cells[685] also fail to alkalinize. In fact, in mesangial cells, all 13 mitogens or other agents that increased steady-state pH_i in the nominal absence of CO_2/HCO_3^- caused pH_i to decrease in the presence of this physiological buffer.[27] In all four of the aforementioned cell types, the steady-state pH_i in the presence of CO_2/HCO_3^- is substantially higher than observed in the absence of CO_2/HCO_3^-, with or without mitogen. Thus, it seems that, at least for some cells, the pH_i prevailing in the presence of CO_2/HCO_3^- is high enough to put pH_i in a range permissive for proliferation, and that pH_i remains in this permissive range even after a mitogen-induced acidification. Although the pH_i increase elicited by mitogens in the absence of CO_2/HCO_3^- is real, it appears that a change in pH_i is not an intrinsic part of the mitogenic response.

TRANSPORTERS AFFECTED BY MITOGENS IN THE PRESENCE OF CO_2/HCO_3^-

The effect of growth factors on the activity of acid–base transporters of cells incubated in the presence of CO_2/HCO_3^- has been examined in some preparations. In renal mesangial cells, application of arginine vasopressin (AVP)[688,25] or epidermal growth factor (EGF)[688] "activates" all three of the following acid–base transporters known to be present: the $Na^+–H^+$ exchanger, the Na^+-driven $Cl^–HCO_3^-$ exchanger, and the $Cl^–HCO_3^-$ exchanger. The two acid-extrusion mechanisms, assayed at the single pH_i of 6.6, were stimulated by ~100%. The acid loader, assayed at the single pH_i of 7.7, was stimulated to an even greater extent, ~140%. AVP also stimulates both $Na^+–H^+$ and $Cl^–HCO_3^-$ exchange in the A10 vascular-smooth-muscle cell line.[689] It should be emphasized that none of the data discussed thus far address the issue of whether in fact the growth factors stimulated the transporters in the physiological pH_i range (i.e., approximately 7.1–7.3 for these cells).

Growth factors can also have time-dependent effects on pH_i and acid–base transporters. For example, in working on mesangial cells, Ganz et al.[688] observed that both AVP and EGF, which are thought to act through different signal transduction pathways, have similar effects on the time courses of the three aforementioned transporters. Both growth factors elicit an immediate (i.e., within ten min) increase in the activities of all three transporters (assayed at the single pH_i values indicated above). The immediate response is followed within an hour by a fall in the activities of all three transporters, even though the activities remain substantially above control levels. Finally, there is a transient dip in the activities of all three transporters at times corresponding to the period of the maximal rate of increase in cell number (~35–~45 h for AVP and ~12–~20 h for EGF). Growth factors can have "early" and "late" effects on $Na^+–H^+$ exchange in vascular smooth muscle cells (for review, see ref. [690]). The "late" effect can include increased expression of the exchanger.

EFFECT OF GROWTH FACTORS ON THE pH_i DEPENDENCE OF THE $Na^+–H^+$ EXCHANGER

In the past, many investigators believed that the pH_i dependence of the $Na^+–H^+$ exchanger is linear, and that the exchanger is inactive at the physiological (i.e., "threshold") pH_i. Investigators also believed that the mitogen-induced increase in pH_i that is observed in the absence of CO_2/HCO_3^- exclusively reflects stimulation of $Na^+–H^+$ exchange in the physiological pH_i range. According to this view, mitogens cause an alkaline shift and/or an increase in the steepness of the $Na^+–H^+$ exchange activity vs. pH_i relationship, without having other effects on acid extrusion and/or acid loading. Indeed, careful analyses of the pH_i dependence of $Na^+–H^+$ exchanger activity in intact

hepatocytes indicates that Na^+-H^+ exchange activity can vary linearly with pH_i,[392,393] and that a mitogen can shift this line in the alkaline direction.[393] However, as discussed above (pH_i dependence of Na^+-H^+ exchange), it is now clear that the approach often used to reach similar conclusions in other cells (i.e., comparison of pH_i recovery rates with and without amiloride at a single low pH_i) is seriously flawed.

Applying the approach used to generate the pH_i dependence of Na^+-H^+ exchange activity in Figure 52.11A or Figure 52.11B leads to the conclusion that AVP has a complex pH_i- and time-dependent effect on Na^+-H^+ exchange in mesangial cells. At short times (~8 min) after applying AVP, the pH_i dependence of Na^+-H^+ exchange activity (similar to that shown in Figure 52.14A) becomes linear in such a way that the transporter is unaffected at pH_i values below 6.7, but inhibited at higher pH_i values. At longer times (~14 min), the new linearized plot is shifted to more alkaline values. In the new "stimulated" steady state, the Na^+-H^+ exchanger is more active at pH_i values below ~6.9, but less active at higher pH_i values. How can AVP therefore raise pH_i in the absence of CO_2/HCO_3^-, if the Na^+-H^+ exchanger is inhibited in the physiological pH_i range? The answer seems to be that AVP has an even greater inhibitory effect on background acid-loading processes. Thus, AVP causes pH_i to rise in mesangial cells in the absence of CO_2/HCO_3^- not because the growth factor stimulates Na^+-H^+ exchange, but because it inhibits Na^+-H^+ exchange to a lesser extent than it inhibits background acid loading.

Oncogenes

Hagag et al.[691] found that microinjecting the v-H-*ras* p21 gene product into mouse NIH 3T3 cells causes a rapid and sustained pH_i increase that is inhibited by amiloride or low $[Na^+]_o$. Thus, a functional Na^+-H^+ exchanger is required for the *ras*-induced pH_i increase, though these data do not prove that *ras* actually stimulates the exchanger. Doppler et al.[49] took a different approach, transfecting NIH 3T3 cells with the v-*mos* or Ha-*ras* oncogene under the control of the MMTV-LTR promoter. They found that expression of either oncogene, upon addition of a glucocorticoid, elicited an increase in pH_i as well as progression into the S phase of the cell cycle. Expression of the proto-oncogene of Ha-*ras* (i.e., the normal cell product) had no effect on pH_i and was only weakly mitogenic. The pH_i increase associated with expression of the Ha-*ras* oncogene was blocked by dimethylamiloride,[692] demonstrating a requirement for a functional Na^+-H^+ exchanger. In NIH 3T3 cells transformed with the c-H-*ras* oncogene, Kaplan and Boron[323] found that a higher steady-state pH_i—compared to that of the non-transformed cells—was due to an alkali shift of ~0.7 pH unit in the pH_i dependencies of both the Na^+-H^+ exchanger and a Na^+-coupled HCO_3^- transporter.

It is now well established that cancer cells often exist in an acidic environment and that acid extruders help maintain the pH_i of many cancer cells at a relatively alkaline level (for reviews, see refs. [693–695]). Moreover, many cancers exhibit an upregulation of Na^+-coupled HCO_3^- transporters.[696–699] Curiously, cancer cells seem to go out of their way to create the acidic environment in which they exist—a strategy that appears to confer a selective advantage. A key element in creating a low pH_o in solid tumors is the overexpression of hypoxia-inducible extracellular carbonic anhydrases, particularly CAIX and CAXII[700–706] (for review, see ref.[707]). It appears that these enzymes convert the copious amounts of CO_2 exiting from the cells into HCO_3^- and H^+, thereby lowering pH_o but helping the cells maintain a relatively high pH_i.[708–710] Not surprisingly, CAIX has become a therapeutic target.[711,712]

References

[1] Busa WB, Nuccitelli R. Metabolic regulation via intracellular pH. Am J Physiol 1984;246:R409–38.

[2] Chesler M. The regulation and modulation of pH in the nervous system. Prog Neurobiol 1990;34:401–27.

[3] Roos A, Boron WF. Intracellular pH. Physiol Rev 1981;61:296–434.

[4] Somjen GG, Tombaugh GC. pH modulation of neuronal excitability and central nervous system functions. In: Kaila K, Ransom BR, editors. pH and brain function. New York: Wiley-Liss, Inc.; 1998. p. 373–93.

[5] Traynelis SF. pH modulation of ligand-gated ion channels. In: Kaila K, Ransom BR, editors. pH and brain function. New York: Wiley-Liss, Inc.; 1998. p. 417–46.

[6] Waisbren SJ, Geibel JP, Modlin IM, Boron WF. Unusual permeability properties of gastric gland cells. Nature 1994;368:332–5.

[7] Kikeri D, Sun A, Zeidel ML, Hebert SC. Cell membranes impermeable to NH_3. Nature 1989;339:478–80.

[8] Singh SK, Binder HJ, Geibel JP, Boron WF. An apical permeability barrier to NH_3/NH_4^+ in isolated, perfused colonic crypts. Proc Natl Acad Sci USA 1995;92:11573–7.

[9] Cooper GJ, Boron WF. Effect of PCMBS on CO_2 permeability of *Xenopus* oocytes expressing aquaporin 1 or its C189S mutant. Am J Physiol 1998;275:C1481–6.

[10] Forster RE, Gros G, Lin L, Ono Y, Wunder M. The effect of 4,4′-diisothiocyanato-stilbene-2,2′-disulfonate on CO_2 permeability of the red blood cell membrane. Proc Natl Acad Sci USA 1998;95:15815–20.

[11] Nakhoul NL, Davis BA, Romero MF, Boron WF. Effect of expressing the water channel aquaporin-1 on the CO_2 permeability of *Xenopus* oocytes. Am J Physiol 1998;274:C543–8.

[12] Prasad GV, Coury LA, Fin F, Zeidel ML. Reconstituted aquaporin 1 water channels transport CO_2 across membranes. J Biol Chem 1998;273:33123–6.

[13] Boron WF, Boulpaep EL. Intracellular pH regulation in the renal proximal tubule of the salamander: basolateral HCO_3^- transport. J Gen Physiol 1983;81:53–94.

[14] Wenzl E, Sjaastad MD, Weintraub WH, Machen TE. Intracellular pH regulation in IEC-6 cells, a cryptlike intestinal cell line. Am J Physiol 1989;G732–40.

[15] Thomas RC. The effect of carbon dioxide on the intracellular pH and buffering power of snail neurones. J Physiol (Lond) 1976;255:715–35.
[16] Aickin CC. Direct measurement of intracellular pH and buffering power in smooth muscle cells of guinea-pig vas deferens. J Physiol (Lond) 1984;349:571–85.
[17] Bevensee MO, Weed RA, Boron WF. Intracellular pH regulation in cultured astrocytes from rat hippocampus. I. Role of HCO_3^-. J Gen Physiol 1997;110:453–65.
[18] Bierman AJ, Cragoe Jr EJ, de Laat SW, Moolenaar WH. Bicarbonate determines cytoplasmic pH and suppresses mitogen-induced alkalinization in fibroblastic cells. J Biol Chem 1988;263:15253–6.
[19] Boyarsky G, Ganz MB, Sterzel B, Boron WF. pH regulation in single glomerular mesangial cells. I. Acid extrusion in absence and presence of HCO_3^-. Am J Physiol 1988;255: C844–56.
[20] Cassel D, Whiteley B, Zhuang YX, Glaser L. Mitogen-independent activation of Na^+/H^+ exchange in human epidermoid carcinoma A431 cells: regulation by medium osmolarity. J Cell Physiol 1985;122:178–86.
[21] Deitmer JW, Schlue W-R. The regulation of intracellular pH by identified glial cells and neurones in the central nervous system of the leech. J Physiol (Lond) 1987;388:261–83.
[22] Nakhoul NL, Chen LK, Boron WF. Effect of basolateral CO_2/HCO_3^- on intracellular pH regulation in the rabbit S3 proximal tubule. J Gen Physiol 1993;102:1171–205.
[23] Putnam RW. pH regulatory transport systems in a smooth muscle-like cell line. Am J Physiol 1990;258:C470–9.
[24] Ganz MB, Boyarsky G, Boron WF, Sterzel RB. Effects of angiotensin II and vasopressin on intracellular pH of glomerular mesangial cells. Am J Physiol 1988;254:F787–94.
[25] Ganz MB, Boyarsky G, Sterzel RB, Boron WF. Arginine vasopressin enhances pH_i regulation in the presence of HCO_3^- by stimulating three acid–base transport systems. Nature 1989;337:648–51.
[26] Ganz MB, Pekar SK, Perfetto MC, Sterzel RB. Arginine vasopressin promotes growth of rat glomerular mesangial cells in culture. Am J Physiol 1988;255:F898–906.
[27] Ganz MB, Perfetto MC, Boron WF. Effects of mitogens and other agents on rat mesangial cell proliferation, pH, and Ca^{2+}. Am J Physiol 1990;259:F269–78.
[28] Moolenaar WH, Yarden Y, de Laat SW, Schlessinger J. Epidermal growth factor induces electrically silent Na^+ influx in human fibroblasts. J Biol Chem 1982;257:8502–6.
[29] Preisig PA, Alpern RJ. Chronic metabolic acidosis causes an adaptation in the apical membrane Na/H antiporter and basolateral membrane $Na(HCO_3)_3$ symporter in the rat proximal convoluted tubule. J Clin Invest 1988;82:1445–53.
[30] Noel J, Pouysségur J. Hormonal regulation, pharmacology, and membrane sorting of vertebrate Na^+/H^+ exchanger isoforms. Am J Physiol 1995;268:C283–96.
[31] Ludwig MG, Vanek M, Guerini D, Gasser JA, Jones CE, Junker U, et al. Proton-sensing G-protein-coupled receptors. Nature 2003;425:93–8.
[32] Zhou Y, Zhao J, Bouyer P, Boron WF. Evidence from renal proximal tubules that HCO_3^- and solute reabsorption are acutely regulated not by pH but by basolateral HCO_3^- and CO_2. Proc Natl Acad Sci USA 2005;102:3875–80.
[33] Parker MD, Boron WF. The divergence, actions, roles, and relatives of sodium-coupled bicarbonate transporters. Physiol Rev in press.
[34] Hinke JAM. Cation-selective microelectrodes for intracellular use. In: Eisenman G, editor. Glass electrodes for hydrogen and other cations. Principle and practice. New York: Dekker; 1967. p. 464–77.
[35] Thomas RC. Intracellular pH of snail neurones measured with a new pH-sensitive glass micro-electrode. J Physiol (Lond) 1974;238:159–80.
[36] Schwiening CJ, Thomas RC. A vacuum silanization technique for eccentric double-barrelled ion-sensitive microelectrodes made with aluminosilicate glass. J Physiol (Lond) 1990;425:8P.
[37] Thomas RC. Eccentric double micropipette suitable both for pH_i micro-electrodes and for intracellular iontophoresis. J Physiol (Lond) 1986;371:24P.
[38] De Hemptinne A. A double-barrel pH micro-electrode for intracellular use [proceedings]. J Physiol 1979;295:5P–6P.
[39] Matsumura Y, Aoisi S, Kajino K, Fujimoto M. The double-barreled microelectrode for the measurement of intracellular pH, using liquid ion-exchanger, and its biological application. Proc 28th Int Congr Physiol Sci 1980;14:572.
[40] Fedirko N, Svichar N, Chesler M. Fabrication and use of high-speed, concentric H^+- and Ca^{2+}-selective microelectrodes suitable for in vitro extracellular recording. J Neurophysiol 2006;96:919–24.
[41] Orme F. Liquid ion-exchanger microelectrodes. In: Lavellee M, Schanne OF, Hebert NC, editors. Glass microelectrodes. New York: Wiley; 1969. p. 376–95.
[42] Ujec E, Keller O, Kriz N, Pavlik V, Machek J. Double-barrel ion selective [K^+, Ca^{2+}, Cl^-] coaxial microelectrodes (ISCM) for measurements of small and rapid changes in ion activities. In: Sykova E, Pavel H, Vyklicky L, editors. Ion-selective microelectrodes and their use in excitable tissues. New York: Plenum Press; 1981. p. 41–5.
[43] Ujec E, Keller O, Machek J, Pavlik V. Low impedance coaxial K^+ selective microelectrodes. Pflügers Arch 1979;382:189–92.
[44] Fuster D, Moe OW, Hilgemann DW. Lipid- and mechanosensitivities of sodium/hydrogen exchangers analyzed by electrical methods. Proc Natl Acad Sci USA 2004;101:10482–7.
[45] Chen LM, Zhao J, Musa-Aziz R, Pelletier MF, Drummond IA, Boron WF. Cloning and characterization of a zebrafish homologue of human AQP1: a bifunctional water and gas channel. Am J Physiol Regul Integr Comp Physiol 2010;299:R1163–74.
[46] Endeward V, Musa-Aziz R, Cooper GJ, Chen L, Pelletier MF, Virkki LV, et al. Evidence that Aquaporin 1 is a major pathway for CO_2 transport across the human erythrocyte membrane. FASEB J 2006;20:1974–81.
[47] Musa-Aziz R, Chen LM, Pelletier MF, Boron WF. Relative CO_2/NH_3 selectivities of AQP1, AQP4, AQP5, AmtB, and RhAG. Proc Natl Acad Sci USA 2009;106:5406–11.
[48] Musa-Aziz R, Jiang L, Chen LM, Behar KL, Boron WF. Concentration-dependent effects on intracellular and surface pH of exposing *Xenopus* oocytes to solutions containing NH_3/NH_4^+. J Membr Biol 2009;228:15–31.
[49] Doppler W, Jaggi R, Groner B. Induction of v-*mos* and activated Ha-*ras* oncogene expression in quiescent NIH 3T3 cells causes intracellular alkalinisation and cell-cycle progression. Gene 1987;54:147–53.
[50] L'Allemain G, Paris S, Pouysségur J. Growth factor action and intracellular pH regulation in fibroblasts. Evidence for a major role of the Na^+/H^+ antiport. J Biol Chem 1984;259:5809–15.
[51] Boron WF, Roos A. Comparison of microelectrode DMO and methylamine methods for measuring intracellular pH. Am J Physiol 1976;231:799–809.
[52] Waddell WJ, Butler TC. Calculation of intracellular pH from the distribution of 5,5-dimethyl-2,4-oxazolidenedione (DMO). Application to skeletal muscle of the dog. J Clin Invest 1959;38:720–9.
[53] Bevensee MO, Boron WF. Fluorescence indicators. In: Kaila K, Ransom BR, editors. pH and brain function. New York: Wiley-Liss, Inc; 1998. p. 129–51.

[54] Paradiso AM, Tsien RY, Machen TE. Digital image processing of intracellular pH in gastric oxyntic and chief cells. Nature 1987;325:447–50.
[55] Denk W, Svoboda K. Photon upmanship: why multiphoton imaging is more than a gimmick. Neuron 1997;18:351–7.
[56] Svoboda K, Denk W, Kleinfeld D, Tank DW. *In vivo* dendritic calcium dynamics in neocortical pyramidal neurons. Nature 1997;385:161–5.
[57] Dunn KW, Young PA. Principles of multiphoton microscopy. Nephron Exp Nephrol 2006;103:e33–40.
[58] Göbel W, Helmchen F. In vivo calcium imaging of neural network function. Physiology (Bethesda) 2007;22:358–65.
[59] Rubart M. Two-photon microscopy of cells and tissue. Circ Res 2004;95:1154–66.
[60] Zipfel WR, Williams RM, Webb WW. Nonlinear magic: multiphoton microscopy in the biosciences. Nat Biotechnol 2003;21:1369–77.
[61] Hille C, Berg M, Bressel L, Munzke D, Primus P, Lohmannsröben HG, et al. Time-domain fluorescence lifetime imaging for intracellular pH sensing in living tissues. Anal Bioanal Chem 2008;391:1871–9.
[62] Hanson KM, Behne MJ, Barry NP, Mauro TM, Gratton E, Clegg RM. Two-photon fluorescence lifetime imaging of the skin stratum corneum pH gradient. Biophys J 2002;83:1682–90.
[63] Chen M, Singh A, Xiao F, Dringenberg U, Wang J, Engelhardt R, et al. Gene ablation for PEPT1 in mice abolishes the effects of dipeptides on small intestinal fluid absorption, short-circuit current, and intracellular pH. Am J Physiol Gastrointest Liver Physiol 2010;299:G265–74.
[64] Chaillet JR, Lopes AG, Boron WF. Basolateral Na-H exchange in the rabbit cortical collecting tubule. J Gen Physiol 1985;86:795–812.
[65] Nett W, Deitmer JW. Simultaneous measurements of intracellular pH in the leech giant glial cell using 2′,7′-bis-(2-carboxyethyl)-5,6-carboxyfluorescein and ion-sensitive microelectrodes. Biophys J 1996;71:394–402.
[66] Thomas JA, Buchsbaum RN, Zimniak A, Racker E. Intracellular pH measurements in Ehrlich ascites tumor cells utilizing spectroscopic probes generated in situ. Biochemistry 1979;18:2210–8.
[67] Chaillet JR, Boron WF. Intracellular calibration of a pH-sensitive dye in isolated perfused salamander proximal tubules. J Gen Physiol 1985;86:765–94.
[68] Richmond PH, Vaughan-Jones RD. Assessment of evidence for K^+–H^+ exchange in isolated type-1 cells of neonatal rat carotid body. Pflügers Arch 1997;434:429–37.
[69] Szatkowski MS, Thomas RC. New method for calculating pH_i from accurately measured changes in pH_i induced by a weak acid and base. Pflügers Arch 1986;407:59–63.
[70] Eisner DA. Kenning NA, O'Neill SC, Pocock G, Richards CD, Valdeolmillos M. A novel method for absolute calibration of intracellular pH indicators. Pflügers Arch 1989;413:553–8.
[71] Boyarsky G, Hanssen C, Clyne LA. Inadequacy of high K^+/nigericin for calibrating BCECF. I. Estimating steady-state intracellular pH. Am J Physiol 1996;271:C1131–45.
[72] Boyarsky G, Hanssen C, Clyne LA. Inadequacy of high K^+/nigericin for calibrating BCECF. II. Intracellular pH dependence of the correction. Am J Physiol 1996;271:C1146–56.
[73] Boyarsky G, Hanssen C, Clyne LA. Superiority of *in vitro* over *in vivo* calibrations of BCECF in vascular smooth muscle cells. FASEB J 1996;10:1205–12.
[74] Rink TJ, Tsien RY, Pozzan T. Cytoplasmic pH and free Mg^{2+} in lymphocytes. J Cell Biol 1982;95:189–96.
[75] Lückermann M, Trapp S, Ballanyi K. GABA-and glycine-mediated fall of intracellular pH in rat medullary neurons in situ. J Neurophysiol 1997;77:1844–52.
[76] Trapp S, Lückermann M, Brooks PA, Ballanyi K. Acidosis of rat dorsal vagal neurons *in situ* during spontaneous and evoked activity. J Physiol (Lond) 1996;496:695–710.
[77] Giuliano KA, Taylor DL. Light-optical-based reagents for the measurement and manipulation of ions, metabolites, and macromolecules in living cells. In: Kraicer J, Dixon SJ, editors. Methods in neurosciences, Vol. 27. San Diego, CA: Academic Press; 1995.
[78] Liu J, Diwu Z, Klaubert DH. Fluorescent molecular probes III. 2′7′-bis-(3-carboxypropyl)-5-(and 6)-carboxyfluorescein (BCPCF): a new polar dual-excitation and dual emission pH indicator with a PKA of 7.0. Bioorg Med Chem 1997;7:3069–72.
[79] Giuliano K, Gillies RJ. Determination of intracellular pH of BALB/c-3T3 cells using the fluorescence of pyranine. Anal Biochem 1987;167:362–71.
[80] Tsien RY. Fluorescent indicators of ion concentration. Methods Cell Biol 1989;30:127–56.
[81] Whitaker JE, Haugland RP, Ryan D, Hewitt PC, Haugland RP, Prendergast FG. Fluorescent rhodol derivatives: versatile, photostable labels and tracers. Anal Biochem 1992;207:267–79.
[82] Martínez-Zaguilán R, Martínez GM, Lattanzio F, Gillies RJ. Simultaneous measurement of intracellular pH and Ca^{2+} using the fluorescence of SNARF-1 and fura-2. Am J Physiol 1991;260:C297–307.
[83] Martínez-Zaguilán R, Parnami G, Lynch RM. Selection of fluorescent ion indicators for simultaneous measurements of pH and Ca^2. Cell Calcium 1996;19:337–49.
[84] Carrithers MD, Dib-Hajj S, Carrithers LM, Tokmoulina G, Pypaert M, Jonas EA, et al. Expression of the voltage-gated sodium channel NaV1.5 in the macrophage late endosome regulates endosomal acidification. J Immunol 2007;178:7822–32.
[85] Lewis CJ, Cobb BA. Carbohydrate oxidation acidifies endosomes, regulating antigen processing and TLR9 signaling. J Immunol 2010;184:3789–800.
[86] Strunnikova NV, Barb J, Sergeev YV, Thiagarajasubramanian A, Silvin C, Munson PJ, et al. Loss-of-function mutations in Rab escort protein 1 (REP-1) affect intracellular transport in fibroblasts and monocytes of choroideremia patients. PLoS One 2009;4:e8402.
[87] Haggie PM, Verkman AS. Unimpaired lysosomal acidification in respiratory epithelial cells in cystic fibrosis. J Biol Chem 2009;284:7681–6.
[88] Soyombo AA, Tjon-Kon-Sang S, Rbaibi Y, Bashllari E, Bisceglia J, Muallem S, et al. TRP-ML1 regulates lysosomal pH and acidic lysosomal lipid hydrolytic activity. J Biol Chem 2006;281:7294–301.
[89] Maxfield FR, Yamashiro DJ. In: Steer CJ, Hanover JA, editors. Intracellular trafficking of proteins. Cambridge, UK: Cambridge University Press; 1991. p. 157–82.
[90] Kim JH, Lingwood CA, Williams DB, Furuya W, Manolson MF, Grinstein S. Dynamic measurement of the pH of the Golgi complex in living cells using retrograde transport of the verotoxin receptor. J Cell Biol 1996;134:1387–99.
[91] Kim JH, Johannes L, Goud B, Antony C, Lingwood CA, Daneman R, et al. Noninvasive measurement of the pH of the endoplasmic reticulum at rest and during calcium release. Proc Natl Acad Sci USA 1998;95:2997–3002.
[92] Demaurex N, Furuya W, D'Souza S, Bonifacino JS, Grinstein S. Mechanism of acidification of the *trans*-Golgi network (TGN). *In situ* measurements of pH using retrieval of TGN38 and furin from the cell surface. J Biol Chem 1998;273:2044–51.

[93] D'Souza S, Garcia-Cabado A, Yu F, Teter K, Lukacs G, Skorecki K, et al. The epithelial sodium-hydrogen antiporter Na^+/H^+ exchanger 3 accumulates and is functional in recycling endosomes. J Biol Chem 1998;273:2035–43.

[94] Teter K, Chandy G, Quinones B, Pereyra K, Machen T, Moore HP. Cellubrevin-targeted fluorescence uncovers heterogeneity in the recycling endosomes. J Biol Chem 1998;273:19625–33.

[95] Wu MM, Grabe M, Adams S, Tsien RY, Moore HP, Machen TE. Mechanisms of pH regulation in the regulated secretory pathway. J Biol Chem 2001;276:33027–35.

[96] Wu MM, Llopis J, Adams S, McCaffery JM, Kulomaa MS, Machen TE, et al. Organelle pH studies using targeted avidin and fluorescein-biotin. Chem Biol 2000;7:197–209.

[97] Wu MM, Llopis J, Adams SR, McCaffery JM, Teter K, Kulomaa MS, et al. Studying organelle physiology with fusion protein-targeted avidin and fluorescent biotin conjugates. Methods Enzymol 2000;327:546–64.

[98] Seksek O, Biwersi J, Verkman AS. Direct measurement of *trans*-Golgi pH in living cells and regulation by second messangers. J Biol Chem 1995;270:4967–70.

[99] Chalfie M, Tu Y, Euskirchen G, Ward WW, Prasher DC. Green fluorescent protein as a marker for gene expression. Science 1994;263:802–5.

[100] Marshall J, Molloy R, Moss GWJ, Howe JR, Hughes TE. The jellyfish green fluorescent protein: a new tool for studing ion channel expression and function. Neuron 1995;14:211–5.

[101] Miesenbock G, De Angelis DA, Rothman JE. Visualizing secretion and synaptic transmission with pH-sensitive green fluorescent proteins. Nature 1998;394:192–5.

[102] Disbrow GL, Aanover JA, Schlegel R. Endoplasmic reticulum-localized human papillomavirus type 16 E5 protein alters endosomal pH but not *trans*-Golgi pH. J Virol 2005;79:5839–46.

[103] Jankowski A, Kim JH, Collins RF, Daneman R, Walton P, Grinstein S. *In situ* measurements of the pH of mammalian peroxisomes using the fluorescent protein pHluorin. J Biol Chem 2001;276:48748–53.

[104] Kneen M, Farinas J, Li Y, Verkman AS. Green fluorescent protein as a noninvasive intracellular pH indicator. Biophys J 1998;74:1591–9.

[105] Llopis J, McCaffery JM, Miyawaki A, Farquhar MG, Tsien RY. Measurement of cytosolic, mitochondrial, and Golgi pH in single living cells with green fluorescent proteins. Proc Natl Acad Sci USA 1998;95:6803–8.

[106] Machen TE, Chandy G, Wu M, Grabe M, Moore HP. Cystic fibrosis transmembrane conductance regulator and H^+ permeability in regulation of Golgi pH. JOP 2001;2:229–36.

[107] Nakamura N, Tanaka S, Teko Y, Mitsui K, Kanazawa H. Four Na^+/H^+ exchanger isoforms are distributed to Golgi and post-Golgi compartments and are involved in organelle pH regulation. J Biol Chem 2005;280:1561–72.

[108] Robey RB, Ruiz O, Santos AV, Ma J, Kear F, Wang LJ, et al. pH-dependent fluorescence of a heterologously expressed *Aequorea* green fluorescent protein mutant: in situ spectral characteristics and applicability to intracellular pH estimation. Biochemistry 1998;37:9894–901.

[109] Ogata M, Awaji T, Iwasaki N, Fujimaki R, Takizawa M, Maruyama K, et al. A new mitochondrial pH biosensor for quantitative assessment of pancreatic β-cell function. Biochem Biophys Res Commun 2012;421:20–6.

[110] Tantama M, Hung YP, Yellen G. Imaging intracellular pH in live cells with a genetically encoded red fluorescent protein sensor. J Am Chem Soc 2011;133:10034–7.

[111] Sankaranarayanan S, De Angelis D, Rothman JE, Ryan TA. The use of pHluorins for optical measurements of presynaptic activity. Biophys J 2000;79:2199–208.

[112] Yuste R, Miller RB, Holthoff K, Zhang S, Miesenbock G. Synapto-pHluorins: chimeras between pH-sensitive mutants of green fluorescent protein and synaptic vesicle membrane proteins as reporters of neurotransmitter release. Methods Enzymol 2000;327:522–46.

[113] Li Z, Burrone J, Tyler WJ, Hartman KN, Albeanu DF, Murthy VN. Synaptic vesicle recycling studied in transgenic mice expressing synaptopHluorin. Proc Natl Acad Sci USA 2005;102:6131–6.

[114] Bagar T, Altenbach K, Read ND, Bencina M. Live-cell imaging and measurement of intracellular pH in filamentous fungi using a genetically encoded ratiometric probe. Eukaryot Cell 2009;8:703–12.

[115] Karagiannis J, Young PG. Intracellular pH homeostasis during cell-cycle progression and growth state transition in *Schizosaccharomyces pombe*. J Cell Sci 2001;114:2929–41.

[116] Schulte A, Lorenzen I, Böttcher M, Plieth C. A novel fluorescent pH probe for expression in plants. Plant Methods 2006;2:7.

[117] Metzger F, Repunte-Canonigo V, Matsushita S, Akemann W, ez-Garcia J, Ho CS, et al. Transgenic mice expressing a pH and Cl^- sensing yellow-fluorescent protein under the control of a potassium channel promoter. Eur J Neurosci 2002;15:40–50.

[118] Schwartz GJ, Barasch J, Al Awqati Q. Plasticity of functional epithelial polarity. Nature 1985;318:368–71.

[119] Chu S, Brownell WE, Montrose MH. Quantative confocal imaging along the crypt-to-surface axis of colonic crypts. Am J Physiol 1995;269:C1557–64.

[120] Gerard C, Boudier JA, Mauchamp J, Verrier B. Evidence for probenecid-sensitive organic anion transporters on polarized thyroid cells in culture. J Cell Physiol 1990;144:354–64.

[121] Allen CN, Harpur ES, Gray TJ, Simmons NL, Hirst BH. Efflux of bis-carboxyethyl-carboxyfluorescein (BCECF) by a novel ATP-dependent transport mechanism in epithelial cells. Biochem Biophys Res Commun 1990;172:262–7.

[122] Collington GK, Hunter J, Allen CN, Simmons NL, Hirst BH. Polarized efflux of 2′,7′-bis(2-carboxyethyl)-5(6)-carboxyfluorescein from cultured epithelial cell monolayers. Biochem Pharmacol 1992;44:417–24.

[123] Harris PJ, Chatton JY, Tran PH, Bungay PM, Spring KR. pH, morphology, and diffusion in lateral intercellular spaces of epithelial cell monolayers. Am J Physiol 1994;266:C73–80.

[124] Ravesloot JH, Eisen T, Baron R, Boron WF. Role of Na-H exchangers and vacuolar H^+ pumps in intracellular pH regulation in neonatal rat osteoclasts. J Gen Physiol 1995;105:177–208.

[125] Slayman CL, Moussatos VV, Webb WW. Endosomal accumulation of pH indicator dyes delivered as acetoxymethyl esters. J Exp Biol 1994;196:419–38.

[126] Bevensee MO, Schwiening CJ, Boron WF. Use of BCECF and propidium iodide to assess membrane integrity of acutely isolated CA1 neurons from rat hippocampus. J Neurosci Methods 1995;58:61–75.

[127] Shullman RG, Brown TR, Ugurbil K, Ogawa S, Cohen SM, den Hollander JA. Cellular applications of ^{31}P and ^{13}C nuclear magnetic resonance. Science 1979;205:160–6.

[128] Gadian DG, Radda GK, Dawson MJ, Wilkie DR. pH_i measurements of cardiac and skeletal muscle using ^{31}P-NMR. In: Nuccitelli R, Deamer DW, editors. Intracellular pH. Its measurement, regulation, and utilization in cellular functions. New York: Liss, Inc.; 1982. p. 61–77.

[129] Deutsch CJ, Taylor JS. Intracellular pH as measured by ^{19}F NMR. Ann NY Acad Sci 1987;508:33–47.

[130] Deutsch CJ, Taylor JS. NMR spectroscopy of cells and organisms, Vol. 2. Boca Raton, FL: CRC Press; 1987.

[131] Gillies RJ, Alger JR, den Hollander JA, Shulman RG. Intracellular pH measured by NMR: methods and results. In: Nuccitelli R, Deamer DW, editors. Intracellular pH: Its measurment, regulation, and utilization in cellular functions. New York: Liss, Inc.; 1982. p. 79–104.
[132] Okerlund LS, Gillies RJ. Measurement of pH and Na^+ by nuclear magnetic resonance. In: Grinstein S, editor. Na^+/H^+ Exchange. Boca Raton, FL: CRC Press, Inc; 1987. p. 21–43.
[133] Gallagher FA, Kettunen MI, Brindle KM. Imaging pH with hyperpolarized ^{13}C. NMR Biomed 2011;24:1006–15.
[134] Fenn WO, Cobb DM. The potassium equilibrium in muscle. J Gen Physiol 1934;17:629–56.
[135] Fenn WO, Maurer FW. The pH of muscle. Protoplasma 1935;24:337–45.
[136] DeCoursey TE. Voltage-gated proton channels and other proton transfer pathways. Physiol Rev 2003;83:475–579.
[137] DeCoursey TE. Voltage-gated proton channels find their dream job managing the respiratory burst in phagocytes. Physiology (Bethesda) 2010;25:27–40.
[138] Thomas RC, Meech RW. Hydrogen ion currents and intracellular pH in depolarized voltage-clamped snail neurones. Nature 1982;299:826–8.
[139] Ramsey IS, Moran MM, Chong JA, Clapham DE. A voltage-gated proton-selective channel lacking the pore domain. Nature 2006;440:1213–6.
[140] Sasaki M, Takagi M, Okamura Y. A voltage sensor-domain protein is a voltage-gated proton channel. Science 2006;312: 589–92.
[141] Capasso M, DeCoursey TE, Dyer MJ. pH regulation and beyond: unanticipated functions for the voltage-gated proton channel, HVCN1. Trends Cell Biol 2011;21:20–8.
[142] Murphy R, Cherny VV, Morgan D, DeCoursey TE. Voltage-gated proton channels help regulate pH_i in rat alveolar epithelium. Am J Physiol Lung Cell Mol Physiol 2005;288:L398–408.
[143] Henderson LM, Chappell JB, Jones OT. Superoxide generation by the electrogenic NADPH oxidase of human neutrophils is limited by the movement of a compensating charge. Biochem J 1988;255:285–90.
[144] Henderson LM, Chappell JB, Jones OTG. The superoxide-generating NADPH oxidase of human neutrophils is electrogenic and associated with an H^+ channel. Biochem J 1987;246:325–9.
[145] Henderson M, Chappell JB, Jones WTG. Internal pH changes associated with the activity of NADPH oxidase of human neutrophils. Biochem J 1988;251:563–7.
[146] Musset B, Cherny VV, Morgan D, DeCoursey TE. The intimate and mysterious relationship between proton channels and NADPH oxidase. FEBS Lett 2009;583:7–12.
[147] Morgan D, Capasso M, Musset B, Cherny VV, Rios E, Dyer MJ, et al. Voltage-gated proton channels maintain pH in human neutrophils during phagocytosis. Proc Natl Acad Sci USA 2009;106:18022–7.
[148] Kaila K, Voipio J. Postsynaptic fall in intracellular pH induced by GABA-activated bicarbonate conductance. Nature 1987;330: 163–5.
[149] Chen JC, Chesler M. A bicarbonate-dependent increase in extracellular pH mediated by $GABA_A$ receptors in turtle cerebellum. Neurosci Lett 1990;116:130–5.
[150] Chen JC, Chesler M. Extracellular alkaline shifts in rat hippocampal slice are mediated by NMDA and non-NMDA receptors. J Neurophysiol 1992;68:342–4.
[151] Kaila K, Paalasmaa P, Taira T, Voipio J. pH transients due to monosynaptic activation of $GABA_A$ receptors in rat hippocampal slices. Neuro Report 1992;3:105–8.
[152] Keifer DW, Roos A. Membrane permeability to the molecular and ionic forms of DMO in barnacle muscle. Am J Physiol 1981;240:C73–9.
[153] Sharp AP, Thomas RC. The effects of chloride substitution on intracellular pH in crab muscle. J Physiol (Lond) 1981;312: 71–80.
[154] Keifer DW. Effect of weak acids on pH regulation and anion transport in barnacle muscle fibers. Am J Physiol 1981;241: C193–9.
[155] Liljas A, Hakansson K, Jonsson BH, Xue Y. Inhibition and catalysis of carbonic anhydrase. Eur J Biochem 1994;219:1–10.
[156] Ripoche P, Goossens D, Devuyst O, Gane P, Colin Y, Verkman AS, et al. Role of RhAG and AQP1 in NH_3 and CO_2 gas transport in red cell ghosts: a stopped-flow analysis. Transfus Clin Biol 2006;13:117–22.
[157] Khademi S, O'Connell 3rd J, Remis J, Robles-Colmenares Y, Miericke LJW, Stroud RM. Mechanism of ammonia transport by Amt/MEP/Rh: Structure of AmtB at 1.35 angstrom. Science 2004;305:1587–94.
[158] Nakhoul NL, Hering-Smith KS, Abdulnour-Nakhoul SM, Hamm LL. Transport of NH_3/NH_4^+ in oocytes expressing aquaporin-1. Am J Physiol Renal Physiol 2001;281:F255–63.
[159] Zheng L, Kostrewa D, Berneche S, Winkler FK, Li XD. The mechanism of ammonia transport based on the crystal structure of AmtB of *Escherichia coli*. Proc Natl Acad Sci USA 2004;101:17090–5.
[160] Endeward V, Cartron JP, Ripoche P, Gros G. RhAG protein of the Rhesus complex is a CO_2 channel in the human red cell membrane. FASEB J 2008;22:64–73.
[161] Nakhoul NL, Boron WF. Acetate transport in the S3 segment of the rabbit proximal tubule and its effect on intracellular pH. J Gen Physiol 1988;92:395–412.
[162] Siebens AW, Boron WF. Effect of electroneutral luminal and basolateral lactate transport on intracellular pH in salamander proximal tubules. J Gen Physiol 1987;90:799–831.
[163] Boyarsky G, Ganz MB, Sterzel B, Boron WF. pH regulation in single glomerular mesangial cells. II. Na^+-dependent and -independent $Cl^- - HCO_3^-$ exchangers. Am J Physiol 1988;255: C857–69.
[164] Nakhoul NL, Lopes AG, Chaillet JR, Boron WF. Intracellular pH regulation in the S3 segment of the rabbit proximal tubule in HCO_3^--free solutions. J Gen Physiol 1988;92:369–93.
[165] Boron WF. Intracellular pH transients in giant barnacle muscle fibers. Am J Physiol 1977;233:C61–73.
[166] Bianchi CP, Bolton TC. Action of load anesthetics on coupling systems in muscle. J Pharmacol Exp Ther 1967;157:388–405.
[167] Casey JR, Grinstein S, Orlowski J. Sensors and regulators of intracellular pH. Nat Rev Mol Cell Biol 2010;11:50–61.
[168] Saparov SM, Liu K, Agre P, Pohl P. Fast and selective ammonia transport by aquaporin-8. J Biol Chem 2007;282:5296–301.
[169] Carraro-Lacroix LR, Jaumouillé V, Fairn GD, Grinstein S. A weak base-generating system suitable for selective manipulation of lysosomal pH. Traffic 2011;12:1490–500.
[170] Boron WF, De Weer P. Intracellular pH transients in squid giant axons caused by CO_2, NH_3 and metabolic inhibitors. J Gen Physiol 1976;67:91–112.
[171] Aickin CC, Thomas RC. An investigation of the ionic mechanism of intracellular pH regulation in mouse soleus muscle fibres. J Physiol (Lond) 1977;273:295–316.
[172] Vaughan-Jones RD. Chloride-bicarbonate exchange in the sheep cardiac Purkinje fibre. In: Nuccitelli R, Deamer DW, editors. Intracellular pH: Its measurement, regulation and utilization in cellular functions. New York: Liss, Inc.; 1982. p. 239–52.

[173] Koppel M, Spiro K. Uber die Wirkung von Moderatoren (Puffern) bei der Verschiebung des Saure-Basengleichgewichtes in biologischen Flussigkeiten. Biochem Z 1914;65:409–39.
[174] Roos A, Boron WF. The buffer value of weak acids and bases: origin of the concept, and first mathematical derivation and application of physico-chemical systems. The work of M. Koppel and K. Spiro (1914). Respir Physiol 1980;40:1–32.
[175] Michaelis L. Die Wasserstoffionenkonzentration. Berlin: Springer; 1922.
[176] Van Slyke DD. On the measurement of buffer values and on the relationship of buffer value to the dissociation constant of the buffer and the concentration and the reaction of the buffer solution. J Biol Chem 1922;52:525–70.
[177] Meech RW, Thomas RC. Effect of measured calcium chloride injections on the membrane potential and internal pH of snail neurones. J Physiol (Lond) 1980;298:111–29.
[178] Akiba T, Alpern RJ, Eveloff J, Calamina J, Warnock DG. Electrogenic sodium/bicarbonate cotransport in rabbit renal cortical basolateral membrane vesicles. J Clin Invest 1986;78:1472–8.
[179] Folbergrova J, MacMillan V, Siesjö BK. The effect of hypercapnic acidosis upon some glycolytic and Krebs cycle-associated intermediates in the rat brain. J Neurochem 1972;19:2507–17.
[180] Trivedi B, Danforth WH. Effect of pH on the kinetics of frog muscle phosphofructokinase. J Biol Chem 1966;241:4110–2.
[181] MacMillan V, Siesjö BK. The influence of hypocapnea upon intracellular pH and upon some carbohydrate substrates, amino acids and organic phosphates in the brain. J Neurochem 1973;21:1283–99.
[182] Siesjö BK, Messeter K. Factors determining intracellular pH. In: Siesjö BK, Sorensen SC, editors. Ion homeostasis of the brain. Copenhagen: Munksgaard; 1971. p. 244–62.
[183] Rudnick G. ATP-driven H^+ pumping into intracellular organelles. Annu Rev Physiol 1986;48:403–13.
[184] Boyer PD, Chance B, Ernster L, Mitchell P, Racker E, Slater EC. Oxidative phosphorylation and photophosphorylation. Annu Rev Biochem 1977;46:955–1025.
[185] Fillingame RH. The proton translocating pumps of oxidative phosphorylation. Annu Rev Biochem 1980;49:1079–113.
[186] Mitchell P. Coupling of phosphorylation to electron and hydrogen ion transfer by a chemi-osmotic type of mechanism. Nature 1961;191:144–8.
[187] Mitchell P. Chemiosmotic coupling in oxidative and photosynthetic phosphorylation. Biol Rev 1966;41:445–502.
[188] Mitchell P. Vertorial chemistry and the molecular mechanics of chemiosmotic coupling: power transmission by proticity. Biochem Soc Trans 1976;4:399–430.
[189] Mitchell P. The Ninth Sir Hans Krebs Lecture. Compartmentaion and communication in living systems. Ligand conduction: a general catalytic principle in chemical, osmotic and chemiosmotic reaction systems. Eur J Biochem 1979;95:1–20.
[190] Skulachev VP. Energy coupling in biological membranes. In: Racker E, editor. MTP international reviews of science: biochemistry, Vol. 3. London: Butterworth; 1975.
[191] Skulachev VP. Transmembrane electrochemical H^+ potential as a convertible energy source for the living cell. FEBS Lett 1977;74:1–9.
[192] Ohkuma S, Poole B. Fluorescence probe measurement of the intralysosomal pH in living cells and the perturbation of pH by various agents. Proc Natl Acad Sci USA 1978;75:3327–31.
[193] Nomura K, Nakamura Y. Determination of the intravesicular pH of fragmented sarcoplasmic reticulum with 5,5-dimethyl-2,4 oxazolidinedione. J Biochem 1976;80:1393–9.
[194] D'Souza S, Garcia-Cabado A, Yu F, Teter K, Lukacs G, Skorecki K, et al. The epithelial sodium-hydrogen antiporter Na^+/H^+ exchanger 3 accumulates and is functional in recycling membranes. J Biol Chem 1998;273:2035–43.
[195] Gurich RW, Warnock DG. Electrically neutral Na^+–H^+ exchange in endosomes obtained from rabbit renal cortex. Am J Physiol 1986;251:F702–9.
[196] Hilden SA, Bose Ghoshroy K, Madias NE. Na^+–H^+ exchange, but not Na^+–K^+-ATPase, is present in endosome-enriched microsomes from rabbit renal cortex. Am J Physiol 1990;258: F1311–9.
[197] Nass R, Rao R. Novel localization of a Na^+/H^+ exchanger in a late endosomal compartment of yeast. Implications for vacuole biogenesis. J Biol Chem 1998;273:21054–60.
[198] Van Dyke RW. Na^+/H^+ exchange modulates acidification of early rat liver endocytic vesicles. Am J Physiol 1995;269: C943–54.
[199] Haigh JR, Phillips JH. A sodium/proton antiporter in chromaffin-granule membranes. Biochem J 1989;257: 499–507.
[200] Anderie I, Thévenod F. Evidence for involvement of a zymogen granule Na^+/H^+ exchanger in enzyme secretion from rat pancreatic acinar cells. J Membrane Biol 1996;152:195–205.
[201] Forgac M. Structure and function of vacuolar class of ATP-driven proton pumps. Physiol Rev 1989;69:765–96.
[202] Gluck S. V-ATPases of the plasma membrane. J Exp Biol 1992;172:29–37.
[203] Furusawa K, Kerridge MT. The hydrogen ion concentration of the muscles of the cat. J Physiol (Lond) 1927;63:33–41.
[204] Aickin CC, Thomas RC. Microelectrode measurement of the intracellular pH and buffering power of mouse soleus muscle fibres. J Physiol (Lond) 1977;267:791–810.
[205] Bevensee MO, Cummins TR, Haddad GG, Boron WF, Boyarsky G. pH regulation in single CA1 neurons acutely isolated from the hippocampi of immature and mature rats. J Physiol (Lond) 1996;494:315–28.
[206] Chen LK, Boron WF. Acid extrusion in S3 segment of rabbit proximal tubule: I. Effect of bilateral CO_2/HCO_3^-. Am J Physiol 1995;268:F179–92.
[207] Wenzl E, Machen TE. Intracellular pH dependence of buffer capacity and anion exchange in the parietal cell. Am J Physiol 1989;257:G741–7.
[208] Cabantchik ZI, Knauf PA, Rothstein A. The anion transport system of the red blood cell: the role of membrane protein evaluated by the use of 'probes'. Biochim Biophys Acta 1978;515:239–302.
[209] Kopito RR, Lodish HF. Primary structure and transmembrane orientation of the murine anion exchange protein. Nature 1985;316:234–8.
[210] Mount DB, Romero MF. The SLC26 gene family of multifunctional anion exchangers. Pflügers Arch 2004;447:710–21.
[211] Ohana E, Yang D, Shcheynikov N, Muallem S. Diverse transport modes by the solute carrier 26 family of anion transporters. J Physiol 2009;587:2179–85.
[212] Ko SB, Shcheynikov N, Choi JY, Luo X, Ishibashi K, Thomas PJ, et al. A molecular mechanism for aberrant CFTR-dependent HCO_3^- transport in cystic fibrosis. EMBO J 2002;21:5662–72.
[213] Shcheynikov N, Wang Y, Park M, Ko SB, Dorwart M, Naruse S, et al. Coupling modes and stoichiometry of Cl^-/HCO_3^- exchange by slc26a3 and slc26a6. J Gen Physiol 2006;127:511–24.
[214] Shcheynikov N, Yang D, Wang Y, Zeng W, Karniski LP, So I, et al. The Slc26a4 transporter functions as an electroneutral $Cl^-/I^-/HCO_3^-$ exchanger: role of Slc26a4 and Slc26a6 in I^- and

HCO_3^- secretion and in regulation of CFTR in the parotid duct. J Physiol 2008;586:3813–24.
[215] Bamberg E, Passow H. The band 3 proteins: anion transporters, binding proteins, and senescent antigens. Progress in cell research. 2nd ed. Amsterdam: Elsevier; 1992.
[216] Jennings ML. Structure and function of the red blood cell anion transport protein. Annu Rev Biophys Biophys Chem 1989;18:397–430.
[217] Milanick MA, Gunn RB. Proton-sulfate co-transport: mechanism of H^+ and sulfate addition to the chloride transporter of human red blood cells. J Gen Physiol 1982;79:87–113.
[218] Cabantchik ZI, Greger R. Chemical probes for anion transporters of mammalian cell membranes. Am J Physiol 1992;262: C803–27.
[219] Fröhlich O, Gunn RB. Erythrocyte anion transport: the kinetics of a single-site obligatory system. Biochim Biophys Acta 1986;864:169–94.
[220] Knauf PA, Law FY, Leung TW, Gehret AU, Perez ML. Substrate-dependent reversal of anion transport site orientation in the human red blood cell anion-exchange protein, AE1. Proc Natl Acad Sci USA 2002;99:10861–4.
[221] Restrepo D, Cronise BL, Snyder RB, Knauf PA. A novel method to differentiate between ping-pong and simultaneous kinetics and its application to the anion exchanger of the HL60 cell. J Gen Physiol 1992;100:825–46.
[222] Chaillet JR, Amsler K, Boron WF. Optical measurement of intracellular pH in single LLC-PK1 cells: demonstration of Cl-HCO_3 exchange. Proc Natl Acad Sci USA 1986;83:522–6.
[223] Vaughan-Jones RD. Regulation of chloride in quiescent sheep-heart Purkinje fibres studied using intracellular chloride and pH-sensitive micro-electrodes. J Physiol (Lond) 1979;295: 111–37.
[224] Siegel WK, Ravesloot JH, Baron R, Boron WF. The anion exchanger of neonatal rat osteoclasts. FASEB J 1993;7:A13.
[225] Sun B, Leem CH, Vaughan-Jones RD. Novel chloride-dependent acid loader in the guinea-pig ventricular myocyte: part of a dual acid-loading mechanism. J Physiol (Lond) 1996;495:65–82.
[226] Leem CH, Vaughan-Jones RD. Sarcolemmal mechanisms for pH_i recovery from alkalosis in the guinea-pig ventricular myocyte. J Physiol (Lond) 1998;509:487–96.
[227] Leem CH, Vaughan-Jones RD. Choride-hydroxyl exchange in the guinea-pig ventricular myocyte: no role for bicarbonate. J Mol Cell Cardiol 1997;29:2483–9.
[228] Gill RK, Ramaswamy K, Dudeja PK. Mechanisms and regulation of NaCl absorption in the human intestine. Research signpost. Recent research developments in physiology. Trivandrum (India): Research Signpost; 2003. p. 643–77.
[229] Martínez-Zaguilán R, Gillies RJ, Sanchez-Armass S. Regulation of pH in rat brain synaptosomes. II. Role of Cl^-. J Neurophysiol 1994;71:2249–57.
[230] Plans V, Rickheit G, Jentsch TJ. Physiological roles of CLC Cl^-/H^+ exchangers in renal proximal tubules. Pflügers Arch 2009;458:23–7.
[231] Neagoe I, Stauber T, Fidzinski P, Bergsdorf EY, Jentsch TJ. The late endosomal ClC-6 mediates proton/chloride countertransport in heterologous plasma membrane expression. J Biol Chem 2010;285:21689–97.
[232] Olsnes S, Tonnessen TI, Sandvig K. pH-regulated anion antiport in nucleated mammalian cells. J Cell Biol 1986;102: 967–71.
[233] Mason MJ, Smith JD, Garcia-Soto JD, Grinstein S. Internal pH-sensitive site couples Cl^-–HCO_3^- exchange to Na^+–H^+ antiport in lymphocytes. Am J Physiol 1989;256: C428–33.
[234] Humphreys BD, Jiang L, Chernova MN, Alper SL. Functional characterization and regulation by pH of murine AE2 anion exchanger expressed in *Xenopus* oocytes. Am J Physiol 1994;267:C1295–307.
[235] Jiang L, Stuart-Tilley A, Parkash J, Alper SL. pH_i and serum regulate AE2-mediated Cl^-/HCO_3^- exchange in CHOP cells of defined transient transfection status.. Am J Physiol 1994;267::C845–56.
[236] Lee BS, Gunn RB, Kopito RR. Functional differences among nonerythroid anion exchangers expressed in a transfected human cell line. J Biol Chem 1991;266:11448–54.
[237] Stewart AK, Chernova MN, Kunes YZ, Alper SL. Regulation of AE2 anion exchanger by intracellular pH: critical regions of the NH_2-terminal cytoplasmic domain. Am J Physiol Cell Physiol 2001;281:C1344–54.
[238] Zhang Y, Chernova MN, Stuart-Tilley AK, Jiang L, Alper SL. The cytoplasmic and transmembrane domains of AE2 both contribute to regulation of anion exchange by pH. J Biol Chem 1996;271:5741–9.
[239] Kurschat CE, Shmukler BE, Jiang L, Wilhelm S, Kim EH, Chernova MN, et al. Alkaline-shifted pH_o sensitivity of AE2c1-mediated anion exchange reveals novel regulatory determinants in the AE2 N-terminal cytoplasmic domain. J Biol Chem 2006;281:1885–96.
[240] Stewart AK, Kerr N, Chernova MN, Alper SL, Vaughan-Jones RD. Acute pH-dependent regulation of AE2-mediated anion exchange involves discrete local surfaces of the NH_2-terminal cytoplasmic domain. J Biol Chem 2004;279:52664–76.
[241] Stewart AK, Kurschat CE, Burns D. Banger N, Vaughan-Jones RD, Alper SL. Transmembrane domain histidines contribute to regulation of AE2-mediated anion exchange by pH. Am J Physiol Cell Physiol 2007;292:C909–18.
[242] Stewart AK, Kurschat CE, Vaughan-Jones RD, Alper SL. Putative re-entrant loop 1 of AE2 transmembrane domain has a major role in acute regulation of anion exchange by pH. J Biol Chem 2009;284:6126–39.
[243] Olsnes S, Ludt J, Tonnessen TI, Sandvig K. Bicarbonate/chloride antiport in Vero cells: II. Mechanisms for bicarbonate-dependent regulation of intracellular pH. J Cell Physiol 1987;132:192–202.
[244] Cousin JL, Motais R. Inhibition of anion permeability by amphiphilic compounds in human red cell: evidence for an interaction of niflumic acid with the band 3 protein. J Membr Biol 1979;46:125–53.
[245] Knauf PA, Mann NA. Use of niflumic acid to determine the nature of the asymmetry of the human erythrocyte anion exchange system. J Gen Physiol 1984;83:703–25.
[246] Alper SL, Chernova MN, Williams J, Zasloff M, Law FY, Knauf PA. Differential inhibition of AE1 and AE2 anion exchangers by oxonol dyes and by novel polyaminosterol analogs of the shark antibiotic, squalamine. Biochem Cell Biol 1988;76: 799–806.
[247] Knauf PA, Law FY, Hahn K. An oxonol dye is the most potent known inhibitor of band 3-mediated anion exchange. Am J Physiol 1995;269:C1073–7.
[248] Knauf PA, Raha NM, Spinelli LJ. The noncompetitive inhibitor WW781 senses changes in erythrocyte anion exchanger (AE1) transport site conformation and substrate binding. J Gen Physiol 2000;115:159–73.
[249] Raha NM, Spinelli LJ, Knauf PA. WW-781, a potent reversible inhibitor of red cell Cl^- flux, binds to band 3 by a two-step mechanism. Am J Physiol 1993;265:C521–32.
[250] Soleimani M, Grassl SM, Aronson PS. Stoichiometry of Na^+–HCO_3^- cotransport in basolateral membrane vesicles isolated from rabbit renal cortex. J Clin Invest 1987;79:1276–80.

[251] Krapf R, Alpern RJ, Rector Jr. FC, Berry CA. Basolateral membrane Na/base cotransport is dependent on CO_2/HCO_3 in the proximal convoluted tubule. J Gen Physiol 1987;90:833–53.
[252] Lopes AG, Siebens AW, Giebisch G, Boron WF. Electrogenic Na/HCO_3 cotransport across the basolateral membrane of the isolated perfused *Necturus* proximal tubule. Am J Physiol 1987;253:F340–50.
[253] Soleimani M, Aronson PS. Ionic mechanism of sodium bicarbonate cotransport in rabbit renal basolateral membrane vesicles. J Biol Chem 1989;264(31):18302–8.
[254] Grichtchenko II, Hogan EM, Boron WF. Extracellular HCO_3^- directly inhibits HCO_3^- efflux in *Xenopus* oocytes expressing the electrogenic rat kidney Na/HCO_3 cotransporter (rkNBC). FASEB J 1999;13:A65.
[255] Grichtchenko II, Romero MF, Boron WF. Extracellular HCO_3^- dependence of electrogenic Na/HCO_3 cotransporters cloned from salamander and rat kidney. J Gen Physiol 2000;115: 533–45.
[256] Grichtchenko II, Boron WF. Surface-pH measurements in voltage-clamped *Xenopus* oocytes co-expressing NBCe1 and CAIV: evidence for $CO_3^=$ transport. FASEB J 2002;16:A795.
[257] Lee S-K, Grichtchenko II, Boron WF. Distinguishing HCO_3^- from CO_3^{2-} transport by NBCe1-A. FASEB J 2011;25:656–9.
[258] Romero MF, Boron WF. Electrogenic Na^+/HCO_3^- cotransporters: cloning and physiology. Annu Rev Physiol 1999;61: 699–723.
[259] Ducoudret O, Diakov A, Müller-Berger S, Romero MF, Frömter E. The renal Na-HCO_3^- cotransporter expressed in *Xenopus laevis* oocytes: inhibition by tenidap and benzamil and effect of temperature on transport rate and stoichiometry. Pflügers Arch 2001;442:709–17.
[260] Lu J, Boron WF. Reversible and irreversible interactions of DIDS with the human electrogenic Na/HCO_3 cotransporter (hNBCe1-A): role of lysines in the KKMIK motif of TM5. Am J Physiol Cell Physiol 2007;292:C1787–98.
[261] Liu X, Williams JB, Sumpter BR, Bevensee MO. Inhibition of the Na/bicarbonate cotransporter NBCe1-A by diBAC oxonol dyes relative to niflumic acid and stilbenes. J Membr Biol 2007;215:195–204.
[262] Schwab A, Rossmann H, Klein M, Dieterich P, Gassner B, Neff C, et al. Functional role of Na^+–HCO_3^- cotransport in migration of transformed renal epithelial cells. J Physiol 2005;568:445–58.
[263] Ch'en FF, Villafuerte FC, Swietach P, Cobden PM, Vaughan-Jones RD. S0859, an *N*-cyanosulphonamide inhibitor of sodium-bicarbonate cotransport in the heart. Br J Pharmacol 2008;153:972–82.
[264] Yamamoto T, Swietach P, Rossini A, Loh SH, Vaughan-Jones RD, Spitzer KW. Functional diversity of electrogenic Na^+–HCO_3^- cotransport in ventricular myocytes from rat, rabbit and guinea pig. J Physiol 2005;562:455–75.
[265] Hogan EM, Cohen MA, Boron WF. K^+ and HCO_3^--dependent acid–base transport in squid giant axons: I. Base efflux. J Gen Physiol 1995;106:821–44.
[266] Leviel F, Borensztein P, Houillier P, Paillard M, Bichara M. Electroneutral K^+/HCO_3^- cotransport in cells of medullary thick ascending limb of rat kidney. J Clin Invest 1992;90:869–78.
[267] Watts III BA, Good DW. An apical K^+-dependent HCO_3^- transport pathway opposes transepithelial HCO_3^- absorption in rat medullary thick ascending limb. Am J Physiol Renal Physiol 2004;287:F57–63.
[268] Davis BA, Hogan EM, Cooper GJ, Bashi E, Zhao J, Boron WF. Inhibition of K/HCO_3 cotransport in squid axons by quaternary ammonium ions. J Membrane Biol 2001;183:25–32.
[269] Hogan EM, Cohen MA, Boron WF. K^+-and HCO_3^--dependent acid–base transport in squid giant axons: II. Base influx. J Gen Physiol 1995;106:845–62.
[270] Zhao J, Hogan EM, Bevensee MO, Boron WF. Out-of-equilibrium CO_2/HCO_3^- solutions and their use in characterizing a new K/HCO_3 cotransporter. Nature 1995;374:636–9.
[271] Brini M, Carafoli E. Calcium pumps in health and disease. Physiol Rev 2009;89:1341–78.
[272] Carafoli E. Biogenesis: plasma membrane calcium ATPase: 15 years of work on the purified enzyme. FASEB J 1994;8: 993–1002.
[273] Guerini D, Coletto L, Carafoli E. Exporting calcium from cells. Cell Calcium 2005;38:281–9.
[274] Monteith GR, Roufogalis BD. The plasma membrane calcium pump—a physiological perspective on its regulation. Cell Calcium 1995;18:459–70.
[275] Guerini D. The significance of the isoforms of plasma membrane calcium ATPase. Cell Tissue Res 1998;292:191–7.
[276] Caride AJ, Chini EN, Homma S, Penniston JT, Dousa TP. mRNA encoding four isoforms of the plasma membrane calcium pump and their variants in rat kidney and nephron segments. J Lab Clin Med 1998;132:149–56.
[277] Magosci M, Yamaki M, Penniston JT, Dousa TP. Localization of mRNAs coding for isozymes of plasma membrane Ca^{2+}-ATPase pump in rat kidney. Am J Physiol 1992;263:F7–14.
[278] Borke JL, Caride A, Verma AK, Penniston JT, Kumar R. Plasma membrane calcium pump and 28-kDa calcium binding protein in cells of rat kidney distal tubules. Am J Physiol 1989;257:F842–9.
[279] Magyar CE, White KE, Rojas R, Apodaca G, Friedman PA. Plasma membrane Ca^{2+}-ATPase and NCX1 Na^+/Ca^{2+} exchanger expression in distal convoluted tubule cells. Am J Physiol Renal Physiol 2002;283:F29–40.
[280] Carafoli E, Zurini M. The Ca^{2+}-pumping ATPase of plasma membranes. Biochim Biophys Acta 1982;683:279–301.
[281] Niggli V, Sigel E, Carafoli E. The purified Ca^{2+} pump of human-erythrocyte membranes catalyzes an electroneutral Ca^{2+}–H^+ exchange in reconstituted liposomal systems. J Biol Chem 1982;257:2350–6.
[282] Schwiening CJ, Kennedy HJ, Thomas RC. Calcium-hydrogen exchange by the plasma membrane Ca-ATPase of voltage-clamped snail neurons. Proc R Soc Lond 1993;253:285–9.
[283] Trapp S, Lückermann M, Kaila K, Ballanyi K. Acidosis of hippocampal neurones mediated by a plasmalemmal Ca^{2+}/H^+ pump. Neuro Report 1996;7:2000–4.
[284] Paalasmaa P, Kaila K. Role of voltage-gated calcium channels in the generation of activity-induced extracellular pH transients in the rat hippocampal slice. J Neurophysiol 1996;75:2354–60.
[285] Paalasmaa P, Taira T, Voipio J, Kaila K. Extracellular alkaline transients mediated by glutamate receptors in the rat hippocampal slice are not due to a proton conductance. J Neurophysiol 1994;72:2031–3.
[286] Smith SE, Gottfried JA, Chen JCT, Chesler M. Calcium dependence of glutamate receptor-evoked alkaline shifts in hippocampus. Neuro Report 1994;5:2441–5.
[287] Kanai Y, Hediger MA. The glutamate/neutral amino acid transporter family SLC1: molecular, physiological and pharmacological aspects. Pflügers Arch 2004;447:469–79.
[288] Arriza JL, Eliasof S, Kavanaugh MP, Amara SG. Excitatory amino acid transporter 5, a retinal glutamate transporter coupled to a chloride conductance. Proc Natl Acad Sci USA 1997;94:4155–60.
[289] Arriza JL, Fairman WA, Wadiche JI, Murdoch GH, Kavanaugh MP, Amara SG. Functional comparisons of three glutamate

transporter subtypes cloned from human motor cortex. J Neurosci 1994;14:5559–69.
[290] Danbolt NC. Glutamate uptake. Prog Neurobiol 2001;65:1–105.
[291] Danbolt NC, Storm-Mathisen J, Kanner BI. An [$Na^+ + K^+$] coupled L-glutamate transporter purified from rat brain is located in glial cell processes. Neuroscience 1992;51:295–310.
[292] Fairman WA, Vandenberg RJ, Arriza JL, Kavanaugh MP, Amara SG. An excitatory amino-acid transporter with properties of a ligand-gated chloride channel. Nature 1995;375:599–603.
[293] Kanai Y, Hediger MA. Primary structure and functional characterization of a high-affinity glutamate transporter. Nature 1992;360:467–71.
[294] Kanai Y, Stelzner M, Nussberger S, Khawaja S, Hebert SC, Smith CP, et al. The neuronal and epithelial human high affinity glutamate transporter. J Biol Chem 1994;269:20599–606.
[295] Pines G, Danbolt NC, Bjoras M, Zhang Y, Bendahan A, Eide L, et al. Cloning and expression of a rat brain L-glutamate transporter. Nature 1992;360:464–7.
[296] Storck T, Schulte S, Hofmann K, Stoffel W. Structure, expression, and functional analysis of a Na^+-dependent glutamate/aspartate transporter from rat brain. Proc Natl Acad Sci USA 1992;89:10955–9.
[297] Robinson MB. The family of sodium-dependent glutamate transporters: a focus on the GLT-1/EAAT2 subtypes. Neurochem Int 1999;33:479–91.
[298] Seal RP, Amara SG. Excitatory amino acid transporters: a family in flux. Annu Rev Pharmacol Toxicol 1999;39:431–56.
[299] Hediger MA. Glutamate transporters in kidney and brain. Am J Physiol 1999;277:F487–92.
[300] Kanai Y, Nussberger S, Romero MF, Boron WF, Hebert SC, Hediger MA. Electrogenic properties of the epithelial and neuronal high affinity glutamate transporter. J Biol Chem 1995;270:16561–8.
[301] Bouvier M, Szatkowski M, Amato A, Attwell D. The glial cell glutamate uptake carrier countertransports pH-changing anions. Nature 1992;360:471–4.
[302] Zerangue N, Kavanaugh MP. Flux coupling in a neuronal glutamate transporter. Nature 1996;383:634–7.
[303] Daniel H, Kottra G. The proton oligopeptide cotransporter family SLC15 in physiology and pharmacology. Pflügers Arch 2004;447:610–8.
[304] Ganapathy V, Brandsch M, Leibach FH. Intestinal transport of amino acids and peptides. In: Johnson LR, editor. Physiology of the Gastrointestinal Tract. New York: Raven Press; 1994. p. 1773–94.
[305] Shen H, Smith DE, Yang T, Huang YG, Schnermann JB, Brosius III FC. Localization of PEPT1 and PEPT2 proton-coupled oligopeptide transporter mRNA and protein in rat kidney. Am J Physiol 1999;276:F658–65.
[306] Smith DE, Pavlova A, Berger UV, Hediger MA, Yang T, Huang YG, et al. Tubular localization and tissue distribution of peptide transporters in rat kidney. Pharm Res 1998;15:1244–9.
[307] Fei YJ, Kanai Y, Nussberger S, Ganapathy V, Leibach FH, Romero MF, et al. Expression cloning of a mammalian proton-coupled oligopeptide transporter. Nature 1994;368:563–6.
[308] Newstead S, Drew D, Cameron AD, Postis VL, Xia X, Fowler PW, et al. Crystal structure of a prokaryotic homologue of the mammalian oligopeptide-proton symporters, PepT1 and PepT2. EMBO J 2011;30:417–26.
[309] Steel A, Nussberger S, Romero MF, Boron WF, Boyd CAR, Hediger MA. Stoichiometry and pH-dependence of the mammalian proton-dependent oligopeptide transporter PepT1. J Physiol (Lond) 1997;498:563–9.
[310] Gunshin H, Mackenzie B, Berger UV, Gunshin Y, Romero MF, Boron WF, et al. Cloning and characterization of a mammalian proton-coupled metal-ion transporter. Nature 1997;388:482–8.
[311] Mackenzie B, Hediger MA. SLC11 family of H^+-coupled metal-ion transporters NRAMP1 and DMT1. Pflügers Arch 2004;447:571–9.
[312] Ferguson CJ, Wareing M, Ward DT, Green R, Smith CP, Riccardi D. Cellular localization of divalent metal transporter DMT-1 in rat kidney. Am J Physiol Renal Physiol 2001;280:F803–14.
[313] Hediger MA, Romero MF, Peng JB, Rolfs A, Takanaga H, Bruford EA. The ABCs of solute carriers: physiological, pathological and therapeutic implications of human membrane transport proteins. Introduction. Pflügers Arch 2004;447:465–8.
[314] Aronson PS. Identifying secondary active transport in epithelia. Am J Physiol 1981;240:F1–11.
[315] Russell JM, Boron WF. Role of chloride transport in regulation of intracellular pH. Nature 1976;264:73–4.
[316] Grinstein S, Cohen S, Rothstein A. Cytoplasmic pH regulation in thymic lymphocytes by an amiloride-sensitive Na^+/H^+ antiport. J Gen Physiol 1984;83:341–69.
[317] Boron WF, McCormick WC, Roos A. pH regulation in barnacle muscle fibers: dependence on intracellular and extracellular pH. Am J Physiol 1979;237:C185–93.
[318] Boyarsky G, Ganz MB, Cragoe Jr EJ, Boron WF. Intracellular-pH dependence of Na-H exchange and acid loading in quiescent and arginine vasopressin-activated mesangial cells. Proc Natl Acad Sci USA 1990;87:5921–4.
[319] Sjaastad MD, Wenzl E, Machen TE. pH_i dependence of Na-H exchange and H delivery in IEC-6 cells. Am J Physiol 1992;262:C164–70.
[320] Gupta A, Schwiening CJ, Boron WF. Effects of CGRP, forskolin, PMA, and ionomycin on pH_i dependence of Na-H exchange in UMR-106 cells. Am J Physiol 1994;266:C1083–92.
[321] Leem CH, Lagadic-Gossmann D, Vaughan-Jones RD. Characterization of intracellular pH regulation in the guinea-pig ventricular myocyte. J Physiol (Lond) 1999;517:159–80.
[322] Bevensee MO, Bashi E, Schlue W-R, Boyarsky G, Boron WF. Shrinkage-induced activation of Na^+/H^+ exchange in rat renal mesangial cells. Am J Physiol 1999;276:C674–83.
[323] Kaplan D, Boron WF. Long-term expression of c-H-*ras* stimulates Na-H and Na^+-dependent Cl-HCO_3 exchange in NIH-3T3 fibroblasts. J Biol Chem 1994;269:4116–24.
[324] Jefferies KC, Cipriano DJ, Forgac M. Function, structure and regulation of the vacuolar (H^+)-ATPases. Arch Biochem Biophys 2008;476:33–42.
[325] Toei M, Saum R, Forgac M. Regulation and isoform function of the V-ATPases. Biochemistry 2010;49:4715–23.
[326] Seifter JL, Harris RC. Adaptation of Na^+–H^+ exchange in the proximal tubule: Studies in microvillus membrane vesicles. In: Aronson PS, Boron WF, editors. Current topics in membranes and transport, Vol. 26. Na-H exchange, intracellular pH and Cell function. Orlando, Fla: Academic Press; 1986. p. 245–61.
[327] Swallow CJ, Grinstein S, Rotstein OD. A vacuolar type H^+-ATPase regulates cytoplasmic pH in murine macrophages. J Biol Chem 1990;265:7645–54.
[328] Chatterjee D, Chakraborty M, Leit M, Neff L, Jamsa-Kellokumpu S, Fuchs R, et al. Sensitivity to vanadate and isoforms of subunits A and B distinguish the osteoclast proton pump from other vacuolar H^+ ATPases. Proc Natl Acad Sci USA 1992;89:6257–61.
[329] Martínez-Zaguilán R, Lynch RM, Martínez GM, Gillies RJ. Vacuolar-type H^+-ATPases are functionally expressed in plasma membranes of human tumor cells. Am J Physiol 1993;265:C1015–29.

[330] Wieczorek H, Putzenlechner M, Zeiske W, Klein U. A vacuolar-type proton pump energizes K^+/H^+ antiport in an animal plasma membrane. J Biol Chem 1991;266:15340–7.
[331] Forgac M. Structure, function and regulation of the vacuolar (H^+)-ATPases. FEBS Lett 1998;440:258–63.
[332] Forgac M. Structure and properties of the vacuolar (H^+)-ATPases. J Biol Chem 1999;274:12951–4.
[333] Stevens TH, Forgac M. Structure, function and regulation of the vacuolar (H^+)-ATPase. Annu Rev Cell Dev Biol 1997;13: 779–808.
[334] Bowman BJ, Allen R, Wechser MA, Bowman EJ. Isolation of genes encoding the *Neurospora* vacuolar ATPase. Analysis of *vma-2* encoding the 57-kDa polypeptide and comparison to *vma-1*. J Biol Chem 1988;263:14002–7.
[335] Bowman EJ, Tenney K, Bowman BJ. Isolation of genes encoding the *Neurospora* vacuolar ATPase. Analysis of *vma-1* encoding the 67-kDa subunit reveals homology to other ATPases. J Biol Chem 1988;263:13994–4001.
[336] Zimniak L, Dittrich P, Gogarten JP, Kibak H, Taiz L. The cDNA sequence of the 69-kDa subunit of the carrot vacuolar H^+-ATPase. J Biol Chem 1988;263:9102–12.
[337] Wagner CA, Finberg KE, Breton S, Marshansky V, Brown D, Geibel JP. Renal vacuolar H^+-ATPase. Physiol Rev 2004;84: 1263–314.
[338] Brown D, Hirsch S, Gluck S. An H^+-ATPase in opposite plasma membrane domains in kidney epithelial cell subpopulations. Nature 1988;331:622–4.
[339] Brown D, Hirsch S, Gluck S. Localization of a proton-pumping ATPase in rat kidney. J Clin Invest 1988;82:2114–26.
[340] Silva F, Schulz W, Davis L, Xie XS, Stone DK. Immunocytochemical localization of the clathrin-coated vesicle proton pump (ccv-pp). Kidney Int 1987;31:416.
[341] Selvaggio AM, Schwartz JH, Bengele HH, Gordon FD, Alexander EA. Mechanisms of H^+ secretion by inner medullary collecting duct cells. Am J Physiol 1988;254:F391–400.
[342] Wagner CA, Giebisch S, Lang F, Geibel JP. Angiotensin II stimulates vesicular H^+-ATPase in rat proximal tubular cells. Proc Natl Acad Sci USA 1998;95:9665–8.
[343] Pappas CA, Ransom BR. A depolarization-stimulated, bafilomycin-inhibitable H^+ pump in hippocampal astrocytes. Glia 1993;9:280–91.
[344] Philippe JM, Dubois JM, Rouzaire-Dubois B, Cartron PF, Vallette F, Morel N. Functional expression of V-ATPases in the plasma membrane of glial cells. Glia 2002;37:365–73.
[345] Wu X, Torres-zamorano V, Yang H, Reinach PS. ETA receptor mediated inhibition of intracellular pH regulation in cultured bovine corneal epithelial cells. Exp Eye Res 1998;66:699–708.
[346] Greenlee MM, Lynch IJ, Gumz ML, Cain BD, Wingo CS. The renal H,K-ATPases. Curr Opin Nephrol Hypertens 2010;19: 478–82.
[347] Gumz ML, Lynch IJ, Greenlee MM, Cain BD, Wingo CS. The renal H^+–K^+-ATPases: physiology, regulation, and structure. Am J Physiol Renal Physiol 2010;298:F12–21.
[348] Jaisser F, Beggah AT. The nongastric H^+–K^+-ATPases: molecular and functional properties. Am J Physiol 1999;276: F812–24.
[349] Silver RB, Soleimani M. H^+-K^+-ATPases: regulation and role in pathophysiological states. Am J Physiol 1999;276:F799–811.
[350] Rabon EC, Reuben MA. The mechanism and structure of the gastric H,K-ATPase. Annu Rev Physiol 1990;52:321–44.
[351] Moolenaar WH. Effects of growth factors on intracellular pH regulation. Annu Rev Physiol 1986;48:363–76.
[352] Boron WF, Russell JM. Stoichiometry and ion dependencies of the intracellular-pH-regulating mechanism in squid giant axons. J Gen Physiol 1983;81:373–99.
[353] Russell JM, Boron WF. Intracellular pH regulation in squid giant axons. In: Nuccitelli R, Deamer DW, editors. Intracellular pH. Its measurement, regulation, and utilization in cellular functions. New York: Liss, Inc.; 1982. p. 221–37.
[354] Thomas RC. Snail neuron intracellular pH regulation. In: Nuccitelli R, Deamer DW, editors. Intracellular pH. Its Measurement, Regulation, and Utilization in Cellular Function. New York: Liss, Inc.; 1982. p. 189–204.
[355] Schwiening CJ, Boron WF. Regulation of intracellular pH in pyramidal neurons from the rat hippocampus by Na^+-dependent Cl^-–HCO_3^- exchange. J Physiol (Lond) 1994;475:59–67.
[356] Grichtchenko II, Choi I, Zhong X, Bray-Ward P, Russell JM, Boron WF. Cloning, characterization, and chromosomal mapping of a human electroneutral Na^+-driven Cl-HCO_3 exchanger. J Biol Chem 2001;276:8358–63.
[357] Grichtchenko II, Boron WF. Surface-pH gradient measurements in *Xenopus* oocytes co-expressing the Na^+-driven Cl-HCO_3 exchanger (NDCBE1) and CAIV: evidence for $CO_3^=$ transport. FASEB J 2002;16:A797.
[358] Boron WF, Knakal RC. Na^+-dependent Cl–HCO_3 exchange in the squid axon. Dependence on extracellular pH. J Gen Physiol 1992;99:817–37.
[359] Boron WF, McCormick WC, Roos A. pH regulation in barnacle muscle fibers: dependence on extracellular sodium and bicarbonate. Am J Physiol 1981;240:C80–9.
[360] Boron WF, De Weer P. Active proton transport stimulated by CO_2/HCO_3^- blocked by cyanide. Nature 1976;259:240–1.
[361] Thomas RC. Ionic mechanism of the H^+ pump in a snail neurone. Nature 1976;262:54–5.
[362] Russell JM, Boron WF, Brodwick MS. Intracellular pH and Na fluxes in barnacle muscle with evidence for reversal of the ionic mechanism of intracellular pH regulation. J Gen Physiol 1983;82:47–78.
[363] Thomas RC. Reversal of the pH_i-regulating system in a snail neuron. In: Boulpaep EL, editor. Current topics in membranes and transport. Cellular mechanisms of renal tubular ion transport. New York: Academic Press; 1980. p. 23–9.
[364] Boron WF, Hogan E, Russell JM. pH-sensitive activation of the intracellular-pH regulation system in squid axons by ATP-γ-S. Nature 1988;332:262–5.
[365] Boron WF, Russell JM, Brodwick MS, Keifer DW, Roos A. Influence of cyclic AMP on intracellular pH regulation and chloride fluxes in barnacle muscle fibres. Nature 1978;276: 511–3.
[366] Boron WF, Knakal RC. Intracellular pH-regulating mechanism of the squid axon. Interaction between DNDS and extracellular Na^+ and HCO_3^-. J Gen Physiol 1989;93:123–50.
[367] Aronson PS. Kinetic properties of the plasma membrane Na^+–H^+ exchanger. Annu Rev Physiol 1985;47:545–60.
[368] Counillon L, Pouysségur J. The members of the Na^+/H^+ exchanger gene family: their structure, function, expression and regulation. In: Seldin DW, Giebisch G, editors. The kidney: physiology and pathophysiology, Vol. 3. Philadelphia: Lippincott Williams and Wilkins; 2000.
[369] Frelin C, Vigne P, Ladoux A, Lazdunski M. The regulation of the intracellular pH in cells from vertebrates. Eur J Biochem 1988;173:3–14.
[370] Grinstein S, Rotin D, Mason MJ. Na^+/H^+ exchange and growth factor-induced cytosolic pH changes. Role in cellular proliferation. Biochim Biophys Acta 1989;988:73–97.
[371] Hoffman EK, Simonsen LO. Membrane mechanisms in volume and pH regulation in vertebrate cells. Physiol Rev 1989;69:315–82.
[372] Wakabayashi S, Shigekawa M, Pouysségur J. Molecular physiology of vertebrate Na^+/H^+ exchangers. Physiol Rev 1997;77: 51–74.

[373] Cassel D, Rothenberg P, Zhuang YX, Deuel TF, Glaser L. Platelet-derived growth factor stimulates Na^+/H^+ exchange and induces cytoplasmic alkalinization in NR6 cells. Proc Natl Acad Sci USA 1983;80:6224–8.

[374] Grinstein S, Clarke CA, Rothstein A. Activation of Na^+/H^+ exchange in lymphocytes by osmotically induced volume changes and by cytoplasmic acidification. J Gen Physiol 1983;82:619–38.

[375] Moolenaar WH, Boonstra J, van der Saag PT, de Laat SW. Sodium/proton exchange in mouse neuroblastoma cells. J Biol Chem 1981;256:12883–7.

[376] Moolenaar WH, Tertoolen LGJ, de Laat SW. The regulation of cytoplasmic pH in human fibroblasts. J Biol Chem 1984;259:7563–9.

[377] Paris S, Pouysségur J. Biochemical characterization of the amiloride-sensitive Na^+/H^+ antiport in chinese hamster lung fibroblasts. J Biol Chem 1983;258:3503–8.

[378] Rothenberg P, Glaser L, Schlesinger P, Cassel D. Activation of Na^+/H^+ exchange by epidermal growth factor elevates intracellular pH in A431 cells. J Biol Chem 1983;258:12644–53.

[379] Biemesderfer D, Reilly RF, Exner M, Igarashi P, Aronson PS. Immunocytochemical characterization of Na^+–H^+ exchanger isoform NHE-1 in rabbit kidney. Am J Physiol 1992;263: F833–40.

[380] Alpern RJ, Chambers M. Cell pH in the rat proximal convoluted tubule: Regulation by luminal and peritubular pH and sodium concentration. J Clin Invest 1986;78:502–10.

[381] Ives HE, Yee JV, Warnock DG. Asymmetric distribution of the Na^+/H^+ antiporter in the renal proximal tubule epithelial cell. J Biol Chem 1983;258:13513–6.

[382] Kinsella JL, Aronson PS. Properties of the Na^+–H^+ exchanger in renal microvillus membrane vesicles. Am J Physiol 1980;238: F461–9.

[383] Kurtz I. Apical Na^+/H^+ antiporter and glycolysis-dependent H^+-ATPase regulate intracellular pH in the rabbit S3 proximal tubule. J Clin Invest 1987;80:928–35.

[384] Sasaki S, Shiigai T, Takeuchi J. Intracellular pH in the isolated perfused rabbit proximal tubule. Am J Physiol 1985;249: F417–23.

[385] Schwartz GJ, Weinstein AM, Steele RE, Stephenson JL, Burg MB. Carbon dioxide permeability of rabbit proximal convoluted tubules. Am J Physiol 1981;240:F231–44.

[386] Haggerty JG, Agarwal N, Reilly RF, Adelberg EA, Slayman CW. Pharmacologically different Na/H antiporters on the apical and basolateral surfaces of cultured porcine kidney cells (LLC-PK1). Proc Natl Acad Sci USA 1988;85:6797–801.

[387] Boyarsky G, Ransom B, Schlue W-R, Davis MBE, Boron WF. Intracellular pH regulation in single cultured astrocytes from rat forebrain. Glia 1993;8:241–8.

[388] Baxter KA, Church J. Characterization of acid extrusion mechanisms in cultured fetal rat hippocampal neurones. J Physiol (Lond) 1996;493:457–70.

[389] Raley-Susman KM, Cragoe Jr EJ, Sapolsky RM, Kopito RR. Regulation of intracellular pH in cultured hippocampal neurons by an amiloride-insensitive Na^+/H^+ exchanger. J Biol Chem 1991;266:2739–45.

[390] Sardet C, Franchi A, Pouysségur J. Molecular cloning, primary structure, and expression of the human growth factor-activatable Na^+/H^+ antiporter. Cell 1989;56:271–80.

[391] Aronson PS, Nee J, Suhm MA. Modifier role of internal H^+ in activating the Na^+–H^+ exchanger in renal microvillus membrane vesicles. Nature 1982;299:161–3.

[392] Boyarsky G, Rosenthal N, Barrett E, Boron WF. Effect of diabetes on Na^+–H^+ exchange by single isolated hepatocytes. Am J Physiol 1991;260:C167–75.

[393] Stewart DJ. Sodium-proton exchanger in isolated hepatocytes exhibits a set point. Am J Physiol 1988;255:G346–51.

[394] Ladoux A, Krawice I, Damais C, Frelin C. Phorbol esters and chemotactic factor induce distinct changes in cytoplasmic Ca^{2+} and pH in granulocytic like HL60 cells. Biochim Biophys Acta 1989;1013:55–9.

[395] Moolenaar WH, Tsien RY, van der Saag PT, de Laat SW. Na^+/H^+ exchange and cytoplasmic pH in the action of growth factors in human fibroblasts. Nature 1983;304:645–8.

[396] Boron WF, Boulpaep EL. Intracellular pH regulation in the renal proximal tubule of the salamander. Na-H exchange. J Gen Physiol 1983;81:29–52.

[397] Moody Jr WJ. The ionic mechanism of intracellular pH regulation in crayfish neurones. J Physiol (Lond) 1981;316: 293–308.

[398] Aronson PS, Suhm MA, Nee J. Interaction of external H^+ with the Na^+–H^+ exchanger in renal microvillus membrane vesicles. J Biol Chem 1983;258:6767–71.

[399] Jean T, Frelin C, Vigne P, Lazdunski M. The Na^+/H^+ exchange system in glial cell lines. Properties and activation by an hyperosmotic shock. Eur J Biochem 1986;160:211–9.

[400] Kinsella JL, Aronson PS. Amiloride inhibition of the Na^+–H^+ exchanger in renal microvillus. Am J Physiol 1981;241:F374–9.

[401] Kinsella JL, Aronson PS. Interaction of NH_4^+ and Li^+ with the renal microvillus membrane Na^+–H^+ exchanger. Am J Physiol 1981;241:C220–6.

[402] Rindler MJ, Saier MH. Evidence for Na^+/H^+ antiport in cultured dog kidney cells (MDCK). J Biol Chem 1981;256: 10820–5.

[403] Warnock DG, Reenstra WW, Yee VJ. Na^+/H^+ antiporter of brush border vesicles: studies with acridine orange uptake. Am J Physiol 1982;242:F733–9.

[404] Pouysségur J, Sardet C, Franchi A, L'Allemain G, Paris S. A specific mutation abolishing Na^+/H^+ antiport activity in hamster fibroblasts precludes growth at neutral and acidic pH. Proc Natl Acad Sci USA 1984;81:4833–7.

[405] Alvarez de la Rosa D, Canessa CM, Fyfe GK, Zhang P. Structure and regulation of amiloride-sensitive sodium channels. Annu Rev Physiol 2000;62:573–94.

[406] Benos DJ. Amiloride: a molecular probe of sodium transport in tissues and cells. Am J Physiol 1982;242:C131–45.

[407] Benos DJ. Amiloride: chemistry, kinetics, and structure-activity relationships Na^+/H^+ exchange. Boca Raton, FL: CRC Press; 1988. p. 121–36.

[408] Mahnensmith RL, Aronson PS. The plasma membrane sodium-hydrogen exchanger and its role in physiological processes. Circ Res 1985;56:773–88.

[409] Kaczorowski GJ, Barros F, Dethmers JK, Trumble MJ. Inhibition of Na^+/Ca^{2+} exchange in pituitary plasma membrane vesicles by analogues of amiloride. Biochemistry 1985;24:1394–403.

[410] Schellenberg GD, Anderson L, Cragoe Jr EJ, Swanson PD. Inhibition of synaptosomal membrane Na^+–Ca^{2+} exchange transport by amiloride and its analogues. Mol Pharmacol 1985;27:537–43.

[411] Rindler MJ, Taub M, Saier Jr MH. Uptake of $^{22}Na^+$ by cultured dog kidney cells (MDCK). J Biol Chem 1979;254:11431–9.

[412] Vigne P, Frelin C, Lazdunski M. The amiloride-sensitive Na^+/H^+ exchange system in skeletal muscle cells in culture. J Biol Chem 1982;257:9394–400.

[413] Ives HE, Yee VJ, Warnock DG. Mixed type inhibition of the renal Na^+/H^+ antiporter by Li^+ and amiloride. J Biol Chem 1983;258:9710–6.

[414] Moran A. Sodium-hydrogen exchange system in LLC-PK1 epithelium. Am J Physiol 1987;252:C63–7.

[415] Frelin C, Vigne P, Barbry P, Lazdunski M. Molecular properties of amiloride action and of its Na^+ transporting targets. Kidney Int 1987;32:785–93.
[416] Sassani P, Pushkin A, Gross E, Gomer A, Abuladze N, Dukkipati R, et al. Functional characterization of NBC4: a new electrogenic sodium-bicarbonate cotransporter. Am J Physiol Cell Physiol 2002;282:C408–16.
[417] Millar ID, Brown PD. NBCe2 exhibits a 3 HCO_3^- :1 Na^+ stoichiometry in mouse choroid plexus epithelial cells. Biochem Biophys Res Commun 2008;373:550–4.
[418] McAlear SD, Liu X, Williams JB, McNicholas-Bevensee CM, Bevensee MO. Electrogenic Na/HCO_3 cotransporter (NBCe1) variants expressed in *Xenopus* oocytes: functional comparison and roles of the amino and carboxy termini. J Gen Physiol 2006;127:639–58.
[419] Sciortino CM, Romero MF. Cation and voltage dependence of rat kidney electrogenic Na^+–HCO_3^- cotransporter, rkNBC, expressed in oocytes. Am J Physiol 1999;277:F611–23.
[420] Virkki LV, Wilson DA, Vaughan-Jones RD, Boron WF. Functional characterization of human NBC4 as an electrogenic Na^+–HCO_3^- cotransporter (NBCe2). Am J Physiol Cell Physiol 2002;282:C1278–89.
[421] Deitmer JW. pH regulation in invertebrate glia. In: Kaila K, Ransom BR, editors. pH and brain function. New York: Wiley-Liss; 1998. p. 233–52.
[422] Deitmer JW, Rose CR. pH regulation and proton signalling by glial cells. Prog Neurobiol 1996;48:73–103.
[423] McAlear SD, Bevensee MO. pH regulation in non-neuronal brain cells and interstitial fluid. In: Hertz L, editor. Non-neuronal cells of the nervous system: Function and dysfunction. Amsterdam: Elsevier; 2003. p. 707–45.
[424] Rose CR, Ransom BR. pH regulation in mammalian glia. In: Kaila K, Ransom BR, editors. pH and brain function. New York: Wiley-Liss; 1998. p. 253–75.
[425] Dart C, Vaughan-Jones RD. Na^+–HCO_3^- symport in the sheep cardiac Purkinje fibre. J Physiol (Lond) 1992;451:365–85.
[426] Fonteriz RI, Vaughan-Jones RD, Lagadic-Gossmann D. Hypoxia inhibits acid extrusion from the guinea-pig isolated ventricular myocyte. J Physiol (Lond) 1993;467:332P.
[427] Aalkjær C, Hughes A. Chloride and bicarbonate transport in rat resistance arteries. J Physiol (Lond) 1991;436:57–73.
[428] Choi I, Aalkjær C, Boulpaep EL, Boron WF. An electroneutral sodium/bicarbonate cotransporter NBCn1 and associated sodium channel. Nature 2000;405:571–5.
[429] Pushkin A, Abuladze N, Lee I, Newman D, Hwang J, Kurtz I. Cloning, tissue distribution, genomic organization, and functional characterization of NBC3, a new member of the sodium bicarbonate cotransporter family. J Biol Chem 1999;274:16569–75.
[430] Parker MD, Musa-Aziz R, Rojas JD, Choi I, Daly CM, Boron WF. Characterization of human SLC4A10 as an electroneutral Na/HCO_3 cotransporter (NBCn2) with Cl^- self-exchange activity. J Biol Chem 2008;283:12777–88.
[431] Poole RC, Halestrap AP. Transport of lactate and other monocarboxylates across mammalian plasma membranes. Am J Physiol 1993;264:C761–82.
[432] Halestrap AP, Meredith D. The *SLC16* gene family-from monocarboxylate transporters (MCTs) to aromatic amino acid transporters and beyond. Pflügers Arch 2004;447:619–28.
[433] Meredith D., Christian H.C. The SLC16 monocaboxylate transporter family. Xenobiotica
[434] Garcia CK, Goldstein JL, Pathak RK, Anderson RG, Brown MS. Molecular characterization of a membrane transporter for lactate, pyruvate, and other monocarboxylates: implications for the Cori cycle. Cell 1994;76:865–73.
[435] Garcia CK, Brown MS, Pathak RK, Goldstein JL. cDNA cloning of MCT2, a second monocarboxylate transporter expressed in different cells than MCT1. J Biol Chem 1995;270:1843–9.
[436] Lin RY, Vera JC, Chaganti RS, Golde DW. Human monocarboxylate transporter 2 (MCT2) is a high affinity pyruvate transporter. J Biol Chem 1998;273:28959–65.
[437] Deuticke B. Monocarboxylate transport in erythocytes. J Membr Biol 1982;70:89–103.
[438] Yoon H, Fanelli A, Grollman EF, Philp NJ. Identification of a unique monocarboxylate transporter (MCT3) in retinal pigment epithelium. Biochem Biophys Res Commun 1997;234: 90–4.
[439] Wright EM. Transport of carboxylic acids by renal mamebrane vesicles. Annu Rev Physiol 1985;47:127–41.
[440] Barac-Nieto M, Murer H, Kinne R. Lactate-sodium cotransport in rat renal brush border membranes. Am J Physiol 1980;239:F496–506.
[441] Mengual R, Leblanc G, Sudaka P. The mechanism of Na^+-L-lactate cotransport by brush-border membrane vesicles from horse kidney. Analysis by isotopic exchange kinetics of a sequential model and stoichiometry. J Biol Chem 1983;258:15071–8.
[442] Samarzija I, Molnar V, Frömter E. The stoichiometry of Na^+ coupled anion absorption across the brushborder membrane of rat renal proximal tubule. Adv Physiol Sci 1981;11:419–23.
[443] Coady MJ, Chang MH, Charron FM, Plata C, Wallendorff B, Sah JF, et al. The human tumour suppressor gene *SLC5A8* expresses a Na^+-monocarboxylate cotransporter. J Physiol 2004;557:719–31.
[444] Gopal E, Fei Y-J, Miyauchi S, Zhuang L, Prasad PD, Ganapathy V. Sodium-coupled and electrogenic transport of B-complex vitamin nicotinic acid by slc5a8, a member of the Na/glucose co-transporter gene family. Biochem J 2005;388:309–16.
[445] Miyauchi S, Gopal E, Fei YJ, Ganapathy V. Functional identification of SLC5A8, a tumor suppressor down-regulated in colon cancer, as a Na^+-coupled transporter for short-chain fatty acids. J Biol Chem 2004;279:13293–6.
[446] Plata C, Sussman CR, Sindić A, Liang JO, Mount DB, Josephs ZM, et al. Zebrafish Slc5a12 encodes an electroneutral sodium monocarboxylate transporter (SMCTn): A comparison to the electrogenic SMCT (SMCTe/Slc5a8). J Biol Chem 2007.
[447] Schafer JA, Andreoli TE. Anion transport processes in the mammalian superficial proximal straight tubule. J Clin Invest 1976;58:500–13.
[448] Bevensee MO, Boron WF. Manipulation and regulation of cytosolic pH. In: Kraicer J, Dixon SJ, editors. Measurement and manipulation of intracellular ions. San Diego: Academic Press; 1995.
[449] Reuss L, Costantin JL. Cl^-/HCO_3^- exchange at the apical membrane of *Necturus* gallbladder. J Gen Physiol 1984;83:801–18.
[450] Thomas RC. Changes in the surface pH of voltage-clamped snail neurones apparently caused by H^+ fluxes through a channel. J Physiol (Lond) 1988;398:313–27.
[451] Adler S, Roy A, Relman AS. Intracellular acid–base regulation. I. The response of muscle cells to changes in CO_2 tension or extracellular bicarbonate concentration. J Clin Invest 1965;44:8–20.
[452] Deitmer JW, Ellis D. Interactions between the regulation of the intracellular pH and sodium activity of sheep cardiac Purkinje fibres. J Physiol (Lond) 1980;304:471–88.
[453] Ellis D, Thomas RC. Direct measurement of the intracellular pH of mammalian cardiac muscle. J Physiol (Lond) 1976;262:755–71.
[454] Heisler N. Intracellular pH of isolated rat diaphragm muscle with metabolic and respiratory changes of extracellular pH. Respir Physiol 1975;23:243–55.

[455] Boron WF. Transport of H^+ and of ionic weak acids and bases. J Membrane Biol 1983;72:1–16.
[456] Smith GA, Brett C, Church J. Effects of noradrenaline on intracellular pH in acutely dissociated adult rat hippocampal CA1 neurones. J Physiol (Lond) 1998;512:487–505.
[457] Nakhoul NL, Chen LK, Boron WF. Intracellular pH regulation in rabbit S3 proximal tubule: basolateral $Cl–HCO_3$ exchange and $Na\text{-}HCO_3$ cotransport. Am J Physiol 1990;258:F371–81.
[458] Chen LK, Boron WF. Acid extrusion in S3 segment of rabbit proximal tubule: II. Effect of basolateral CO_2/HCO_3^-. Am J Physiol 1995;268:F193–203.
[459] Adler S, Roy A, Relman AS. Intracellular acid–base regulation. II. The interaction between CO_2 tension and extracellular bicarbonate in the determination of muscle cell pH. J Clin Invest 1965;44:21–30.
[460] Ou-yang Y, Mellergard P, Siesjö BK. Regulation of intracellular pH in single rat cortical neurons in vitro: a microspectrofluorometric study. J Cereb Blood Flow Metab 1993;13:827–40.
[461] Zhou Y, Bouyer P, Boron WF. Role of a tyrosine kinase in the CO_2-induced stimulation of HCO_3^- reabsorption by rabbit S2 proximal tubules. Am J Physiol Renal Physiol 2006;291: F358–67.
[462] Tomura H, Wang JQ, Komachi M, Damirin A, Mogi C, Tobo M, et al. Prostaglandin I_2 production and cAMP accumulation in response to acidic extracellular pH through OGR1 in human aortic smooth muscle cells. J Biol Chem 2005;280:34458–64.
[463] Murakami N, Yokomizo T, Okuno T, Shimizu T. G2A is a proton-sensing G-protein-coupled receptor antagonized by lysophosphatidylcholine. J Biol Chem 2004;279:42484–91.
[464] Ishii S, Kihara Y, Shimizu T. Identification of T cell death-associated gene 8 (TDAG8) as a novel acid sensing G-protein-coupled receptor. J Biol Chem 2005;280:9083–7.
[465] Wang JQ, Kon J, Mogi C, Tobo M, Damirin A, Sato K, et al. TDAG8 is a proton-sensing and psychosine-sensitive G-protein-coupled receptor. J Biol Chem 2004;279:45626–33.
[466] Tomura H, Mogi C, Sato K, Okajima F. Proton-sensing and lysolipid-sensitive G-protein-coupled receptors: a novel type of multi-functional receptors. Cell Signal 2005;17:1466–76.
[467] Waldmann R, Champigny G, Bassilana F, Heurteaux C, Lazdunski M. A proton-gated cation channel involved in acid-sensing. Nature 1997;386:173–7.
[468] Alvarez de la Rosa D, Krueger SR, Kolar A, Shao D, Fitzsimonds RM, Canessa CM. Distribution, subcellular localization and ontogeny of ASIC1 in the mammalian central nervous system. J Physiol 2003;546:77–87.
[469] Lesage F. Pharmacology of neuronal background potassium channels. Neuropharmacology 2003;44:1–7.
[470] Duprat F, Lesage F, Fink M, Reyes R, Heurteaux C, Lazdunski M. TASK, a human background K^+ channel to sense external pH variations near physiological pH. EMBO J 1997;16: 5464–71.
[471] Chapman CG, Meadows HJ, Godden RJ, Campbell DA, Duckworth M, Kelsell RE, et al. Cloning, localisation and functional expression of a novel human, cerebellum specific, two pore domain potassium channel. Brain Res Mol Brain Res 2000;82:74–83.
[472] Rajan S, Wischmeyer E, Xin LG, Preisig-Müller R, Daut J, Karschin A, et al. TASK-3, a novel tandem pore domain acid-sensitive K^+ channel: an extracellular histidine as pH sensor. J Biol Chem 2000;275:16650–7.
[473] Brown D, Wagner CA. Molecular mechanisms of acid–base sensing by the kidney. J Am Soc Nephrol 2012;10.1681/ASN.2012010029.
[474] Chesler M. Regulation and modulation of pH in the brain. Physiol Rev 2003;83:1183–221.
[475] Chesler M, Kaila K. Modulation of pH by neuronal activity. Trends Neurosci 1992;15:396–402.
[476] Ransom BR. Glial modulation of neural excitability mediated by extracellular pH: a hypothesis. Prog Brain Res 1992;94: 37–46.
[477] Austin C, Wray S. Extracellular pH signals affect rat vascular tone by rapid transduction into intracellular pH changes. J Physiol (Lond) 1993;466:1–8.
[478] Buckler KJ, Vaughan-Jones RD, Peers C, Lagadic-Gossmann D, Nye PCG. Effects of extracellular pH, Pco_2 and HCO_3^- on intracellular pH in isolated type-1 cells of the neonatal rat carotid body. J Physiol (Lond) 1991;444:703–21.
[479] Bouyer P, Bradley SR, Zhao J, Wang W, Richerson GB, Boron WF. Effect of extracellular acid–base disturbances on the intracellular pH of neurones cultured from rat medullary raphe or hippocampus. J Physiol (Lond) 2004;559:85–101.
[480] Weiner ID, Hamm LL. Regulation of intracellular pH in the rabbit cortical collecting tubule. J Clin Invest 1990;85:274–81.
[481] Alpern RJ. Mechanism of basolateral membrane $H^+/OH^-/HCO_3^-$ transport in the rat proximal convoluted tubule. A sodium-coupled electrogenic process. J Gen Physiol 1985;86: 613–36.
[482] Alpern RJ, Chambers M. Basolateral membrane Cl/HCO_3 exchange in the rat proximal convoluted tubule. Na-dependent and independent modes. J Gen Physiol 1987;89:581–98.
[483] Kurtz I. Basolateral membrane Na^+/H^+ antiport, Na^+/base cotransport, and Na^+- independent Cl^-/base exchange in the rabbit S_3 proximal tubule. J Clin Invest 1989;83:616–22.
[484] Yoshitomi K, Burckhardt BC, Frömter E. Rheogenic sodium-bicarbonate cotransport in the peritubular cell membrane of rat renal proximal tubule. Pflügers Arch 1985;405:360–6.
[485] Ives HE, Yee VJ, Warnock DG. The Na^+/H^+ antiporter of the rabbit proximal tubules is confined to the luminal membrane. Kidney Int 1983;23:233.
[486] Reeves RB. The interaction of body temperature and acid–base balance in ectothermic vertebrates. Annu Rev Physiol 1977;39: 559–86.
[487] Burton RF. The role of buffers in body fluids. Mathematical analysis. Respir Physiol 1973;18:34–42.
[488] Reeves RB, Malan A. Model studies of intracellular acid–base temperature responses in ectotherms. Respir Physiol 1976;28:49–63.
[489] Herman B, Gores GJ, Nieminen AL, Kawanishi T, Harman A, Lemasters JJ. Calcium and pH in anoxic and toxic injury. Toxicol 1990;21:127–48.
[490] Yao H, Haddad GG. Calcium and pH homeostasis in neurons during hypoxia and ischemia. Cell Calcium 2004;36:247–55.
[491] Garlick PP, Radda GK, Seeley PJ. Studies of acidosis in the ischaemic heart of phosphorus nuclear magnetic resonance. Biochem J 1979;184:547–54.
[492] Shi H, Hamm PH, Meyers RS, Lawler RG, Jackson DC. Mechanisms of pH_i recovery from NH_4Cl-induced acidosis in anoxic isolated turtle heart: a ^{31}P-NMR study. Am J Physiol 1997;272:R6–15.
[493] Yao H, Gu XQ, Haddad GG. The role of HCO_3^--dependent mechanisms in pH_i regulation during O_2 deprivation. Neuroscience 2003;117:29–35.
[494] Bevensee MO, Boron WF. Effects of acute hypoxia on intracellular-pH regulation in astrocytes cultured from rat hippocampus. Brain Res 2008;1193:143–52.
[495] Diarra A, Sheldon C, Brett CL, Baimbridge KG, Church J. Anoxia-evoked intracellular pH and Ca^{2+} concentration changes in cultured postnatal rat hippocampal neurons. Neuroscience 1999;93:1003–16.

[496] Jørgensen NK, Petersen SF, Damgaard I, Schousboe A, Hoffmann EK. Increases in $[Ca^{2+}]_i$ and changes in intracellular pH during chemical anoxia in mouse neocortical neurons in primary culture. J Neurosci Res 1999;56:358–70.

[497] Kintner DB, Su G, Lenart B, Ballard AJ, Meyer JW, Ng LL, et al. Increased tolerance to oxygen and glucose deprivation in astrocytes from Na^+/H^+ exchanger isoform 1 null mice. Am J Physiol Cell Physiol 2004;287:C12–21.

[498] Sheldon C, Church J. Reduced contribution from Na^+/H^+ exchange to acid extrusion during anoxia in adult rat hippocampal CA1 neurons. J Neurochem 2004;88:594–603.

[499] Sheldon C, Church J. Intracellular pH response to anoxia in acutely dissociated adult rat hippocampal CA1 neurons. J Neurophysiol 2002;87:2209–24.

[500] Yao H, Gu XQ, Douglas RM, Haddad GG. Role of Na^+/H^+ exchanger during O_2 deprivation in mouse CA1 neurons. Am J Physiol Cell Physiol 2001;281:C1205–10.

[501] Chen LM, Choi I, Haddad GG, Boron WF. Chronic continuous hypoxia decreases the expression of SLC4A7 (NBCn1) and SLC4A10 (NCBE) in mouse brain. Am J Physiol Regul Integr Comp Physiol 2007;293:R2412–20.

[502] Chen LM, Haddad GG, Boron WF. Effects of chronic continuous hypoxia on the expression of SLC4A8 (NDCBE) in neonatal versus adult mouse brain. Brain Res 2008;1238:85–92.

[503] Prentice HM. Key contributions of the Na^+/H^+ exchanger subunit 1 and HCO_3^- transporters in regulating neuronal cell fate in prolonged hypoxia. Am J Physiol Regul Integr Comp Physiol 2008;294:R448–50.

[504] Xue J, Zhou D, Yao H, Haddad GG. Role of transporters and ion channels in neuronal injury under hypoxia. Am J Physiol Regul Integr Comp Physiol 2008;294:R451–7.

[505] Cala PM. Volume regulation by *Amphiuma* red blood cells: The membrane potential and its implications regarding the nature of the ion flux pathways. J Gen Physiol 1980;76:683–708.

[506] Cala PM. Cell volume regulation by *Amphiuma* red blood cells: The role of Ca^{2+} as a modulator of alkali metal/H^+ exchange. J Gen Physiol 1983;82:761–84.

[507] Kregenow FM, Caryk T, Siebens AW. Further studies of the volume-regulatory response of *Amphiuma* erythrocytes in hypertonic media. Evidence for amiloride-sensitive Na/H exchange. J Gen Physiol 1985;86:565–84.

[508] Parker JC, Castranova V. Volume-responsive sodium and proton movements in dog red blood cells. J Gen Physiol 1984;84:379–401.

[509] Parker JC, Glosson PS. Interactions of sodium-proton exchange mechanism in dog reg blood cells with *N*-phenylmaleimide. Am J Physiol 1987;253:C60–5.

[510] Siebens AW, Kregenow FM. Analysis of amiloride-sensitive volume regulation in *Amphiuma* red cells. Fed Proc 1980;39:379.

[511] Siebens AW, Kregenow FM. Volume-regulatory responses of *Amphiuma* red cells in anisotonic media: the effect of amiloride. J Gen Physiol 1985;86:527–64.

[512] Shrode LD, Klein JD, Douglas PB, O'Neill WC, Putnam RW. Shrinkage-induced activation of Na^+/H^+ exchange: role of cell density and myosin light chain phosphorylation. Am J Physiol 1997;272:C1968–79.

[513] Davis BA, Hogan EM, Boron WF. Role of G proteins in stimulation of Na-H exchange by cell shrinkage. Am J Physiol 1992;262:C533–6.

[514] Davis BA, Hogan EM, Boron WF. Shrinkage-induced activation of Na^+–H^+ exchange in barnacle muscle fibers. Am J Physiol 1994;266:C1744–53.

[515] Humphreys BD, Jiang L, Chernova MN, Alper SL. Hypertonic activation of AE2 anion exchanger in *Xenopus* oocytes via NHE-mediated intracellular alkalinization. Am J Physiol 1995;268:C201–9.

[516] Cala PM. Volume-sensitive alkali metal-H transport in *Amphiuma* red blood cells. In: Aronson PS, Boron WF, editors. Current topics in membranes and transport, Vol. 26. Na-H exchange, intracellular pH and cell function. Orlando, Fla: Academic Press; 1986. p. 79–99.

[517] Grinstein S, Rothstein A. Mechanisms of regulation of the Na^+/H^+ exchanger. J Membrane Biol 1986;90:1–12.

[518] Hallows KR, Knauf PA. Principles of cell volume regulation. In: Strange K, editor. Cellular and molecular physiology of cell volume regulation. Boca Raton, FL: CRC Press; 1994. p. 3–29.

[519] Hoffmann EK, Lambert IH, Pedersen SF. Physiology of cell volume regulation in vertebrates. Physiol Rev 2009;89:193–277.

[520] Kregenow FM. Osmoregulatory salt transporting mechanisms: control of cell volume in anisotonic media. Annu Rev Physiol 1981;43:493–505.

[521] Lang F, Busch GL, Ritter M, Völkl H, Waldegger S, Gulbins E, et al. Functional significance of cell volume regulatory mechanisms. Physiol Rev 1998;78:247–306.

[522] Lang F, Busch GL, Völkl H, Häussinger D. Cell volume: a second message in regulation of cell function. News Physiol Sci 1995;10:18–22.

[523] Yamamoto M, Chen MZ, Wang YJ, Sun HQ, Wei Y, Martinez M, et al. Hypertonic stress increases phosphatidylinositol 4,5-bisphosphate levels by activating PIP5KIβ. J Biol Chem 2006;281:32630–8.

[524] Hohmann S. Osmotic stress signaling and osmoadaptation in yeasts. Microbiol Mol Biol Rev 2002;66:300–72.

[525] Klipp E, Nordlander B, Kruger R, Gennemark P, Hohmann S. Integrative model of the response of yeast to osmotic shock. Nature Biotechnology 2005;23:975–82.

[526] Sheikh-Hamad D, Gustin MC. MAP kinases and the adaptive response to hypertonicity: functional preservation from yeast to mammals. Am J Physiol Renal Physiol 2004;287:F1102–10.

[527] Grinstein S, Woodside M, Sardet C, Pouysségur J, Rotin D. Activation of the Na^+/H^+ antiporter during cell volume regulation. J Biol Chem 1992;267:23823–8.

[528] Rigor RR, Damoc C, Phinney BS, Cala PM. Phosphorylation and activation of the plasma membrane Na^+/H^+ exchanger (NHE1) during osmotic cell shrinkage. PLoS One 2011;6:e29210.

[529] Shrode LD, Klein JD, O'Neill WC, Putnam RW. Shrinkage-induced activation of Na^+/H^+ exchange in primary rat astrocytes: role of myosin light-chain kinase. Am J Physiol 1995;269:C257–66.

[530] Alexander RT, Grinstein S. Na/H exchangers and the regulation of volume. Acta Physiol (Oxf) 2006;187:159–67.

[531] Garnovskaya MN, Mukhin YV, Vlasova TM, Raymond JR. Hypertonicity activates Na^+/H^+ exchange through Janus kinase 2 and calmodulin. J Biol Chem 2003;278:16908–15.

[532] Gillis D, Shrode LD, Krump E, Howard CM, Rubie EA, Tibbles LA, et al. Osmotic stimulation of the Na^+/H^+ exchanger NHE1: relationship to the activation of three MAPK pathways. J Membr Biol 2001;181:205–14.

[533] Krump E, Nikitas K, Grinstein S. Induction of tyrosine phosphorylation and Na^+/H^+ exchanger activation during shrinkage of human neutrophils. J Biol Chem 1997;272:17303–11.

[534] Su X, Pang T, Wakabayashi S, Shigekawa M. Evidence for involvement of the putative first extracellular loop in differential volume sensitivity of the Na^+/H^+ exchangers NHE1 and NHE2. Biochemistry 2003;42:1086–94.

[535] Grinstein S, Rothstein A, Cohen S. Mechanism of osmotic activation of Na^+/H^+ exchange in rat thymic lymphocytes. J Gen Physiol 1985;85:765–87.

[536] Dunham PB. Cell shrinkage activates Na^+/H^+ exchange in dog red cells by relieving inhibition of exchange by Na^+ in isotonic medium. Blood Cells Mol Dis 2004;32:389–93.
[537] Dunham PB, Kelley SJ, Logue PJ. Extracellular Na^+ inhibits Na^+/H^+ exchange: cell shrinkage reduces the inhibition. Am J Physiol Cell Physiol 2004;287:C336–44.
[538] Davis BA, Hogan EM, Boron WF. Activation of Na-H exchange by intracellular lithium in barnacle muscle fibers. Am J Physiol 1992;263:C246–56.
[539] Parker JC. Na-proton exchange in dog red blood cells. In: Aronson PS, Boron WF, editors. Current topics in membranes and transport, Vol. 26. Na-H exchange, intracellular pH, and cell function. Orlando, FL: Academic Press; 1986. p. 101–14.
[540] Parker JC. Glutaraldehyde fixation of sodium transport in dog red blood cells. J Gen Physiol 1984;84:789–803.
[541] Hogan EM, Davis BA, Boron WF. Intracellular Cl^- dependence of Na-H exchange in barnacle muscle fibers under normotonic and hypertonic conditions. J Gen Physiol 1997;110:629–39.
[542] Cala PM. Volume regulation by *Amphiuma* red blood cells: characteristics of volume sensitive K/H and Na/H exchange. Mol Physiol 1985;8:199–214.
[543] Adorante JS, Cala PM. Activation of electroneutral K flux in *Amphiuma* red blood cells by *N*-ethylmaleimide. Distinction between K^+/H^+ exchange and KCl cotransport. J Gen Physiol 1987;90:209–27.
[544] Garcia-Austt J, Good DW, Burg MB, Knepper MA. Deoxycorticosterone-stimulated bicarbonate secretion in rabbit cortical collecting ducts: effects of luminal chloride removal and in vivo acid loading. Am J Physiol 1985;249:F205–12.
[545] Iino Y, Burg MB. Effect of parathyroid hormone on bicarbonate absorption by proximal tubules in vitro. Am J Physiol 1979;236:F387–91.
[546] Liu FY, Cogan MG. Angiotensin II: a potent regulator of acidification in the rat early proximal convoluted tubule. J Clin Invest 1987;80:272–5.
[547] Paillard M, Bichara M. Peptide hormone effects on urinary acidification and acid–base balance: PTH, ADH, and glucagon. Am J Physiol 1989;256:F973–85.
[548] Freiberg JM, Kinsella J, Sacktor B. Glucocorticoids increase the Na^+–H^+ exchange and decrease the Na^+ gradient-dependent phosphate-uptake systems in renal brush border membrane vesicles. Proc Natl Acad Sci USA 1982;79:4932–6.
[549] Kinsella JL, Freiberg JM, Sacktor B. Glucocorticoid activation of Na^+/H^+ exchange in renal brush border vesicles: kinetic effects. Am J Physiol 1985;248:F233–9.
[550] Sacktor B, Kinsella JL. Hormonal regulation of renal Na^+–H^+ exchange activity. In: Aronson PS, Boron WF, editors. Current topics in membranes and transport, Vol. 26. Na-H exchange, intracellular pH, and cell function. Orlando, FL: Academic Press; 1986. p. 223–43.
[551] Bidet M, Merot J, Tauc M, Poujeol P. Na^+–H^+ exchange in proximal cells isolated from kidney. II. Short-term regulation by glucocorticoids. Am J Physiol 1987;253:F945–51.
[552] Yun CH, Gurubhagavatula S, Levine SA, Montgomery LT, Brant SR, Cohen ME, et al. Glucocorticoid stimulation of ileal Na^+ absorptive cell brush border Na^+/H^+ exchange and association with an increase in message for NHE3, an epithelial Na^+/H^+ isoform. J Biol Chem 1993;268:206–11.
[553] Baum M, Cano A, Alpern RJ. Glucocorticoids stimulate Na^+/H^+ antiporter in OKP cells. Am J Physiol 1993;264: F1027–31.
[554] Baum M, Amemiya M, Dwarakanath V, Alpern RJ, Moe OW. Glucocorticoids regulate NHE-3 transcription in OKP cells. Am J Physiol 1996;270:F164–9.
[555] Ambuhl PM, Yang X, Peng Y, Preisig PA, Moe OW, Alpern RJ. Glucocorticoids enhance acid activation of the Na^+/H^+ exchanger 3 (NHE3). J Clin Invest 1999;103:429–35.
[556] He P, Lee SJ, Lin S, Seidler U, Lang F, Fejes-Toth G, et al. Serum- and glucocorticoid-induced kinase 3 in recycling endosomes mediates acute activation of Na^+/H^+ exchanger NHE3 by glucocorticoids. Mol Biol Cell 2011;22:3812–25.
[557] Yun CC, Chen Y, Lang F. Glucocorticoid activation of Na^+/H^+ exchanger isoform 3 revisited. The roles of SGK1 and NHERF2. J Biol Chem 2002;277:7676–83.
[558] Fuster DG, Bobulescu IA, Zhang J, Wade J, Moe OW. Characterization of the regulation of renal Na^+/H^+ exchanger NHE3 by insulin. Am J Physiol Renal Physiol 2007;292: F577–85.
[559] Klisic J, Hu MC, Nief V, Reyes L, Fuster D, Moe OW, et al. Insulin activates Na^+/H^+ exchanger 3: biphasic response and glucocorticoid dependence. Am J Physiol Renal Physiol 2002;283:F532–9.
[560] Ruiz OS, Wang LJ, Pahlavan P, Arruda JA. Regulation of renal $Na–HCO_3$ cotransporter: III. Presence and modulation by glucocorticoids in primary cultures of the proximal tubule. Kidney Int 1995;47:1669–76.
[561] Ali R, Amlal H, Burnham CE, Soleimani M. Glucocorticoids enhance the expression of the basolateral Na^+:HCO_3^- cotransporter in renal proximal tubules. Kidney Int 2000;57: 1063–71.
[562] Oberleithner H, Weigt M, Westphale HJ, Wang W. Aldosterone activates Na^+–H^+ exchange and raises cytoplasmic pH in target cells of the amphibian kidney. Proc Natl Acad Sci USA 1987;84:1464–8.
[563] Wehling M, Kasmayr J, Theisen K. Fast effects of aldosterone on electrolytes in human lymphocytes are mediated by the sodium-proton exchanger of the cell membrane. Biochem Biophys Res Commun 1989;164:961–7.
[564] Wehling M, Kasmayr J, Theisen K. Rapid effects of mineralocorticoids on sodium-proton exchanger: genomic or nongenomic pathway?. Am J Physiol 1991;260:E719–26.
[565] Weigt M, Dietl P, Silbernagl S, Oberleithner H. Activation of luminal Na^+/H^+ exchange in distal nephron of frog: an early response to aldosterone. Pflügers Arch 1987;408:609–14.
[566] Wehling M. Nongenomic aldosterone effects: the cell membrane as a specific target of mineralocorticoid action. Steroids 1995;60:153–6.
[567] Cooper GJ, Hunter M. Na^+–H^+ exchange in frog early distal tubule: effect of aldosterone on the set-point. J Physiol (Lond) 1994;479:423–32.
[568] Cooper GJ, Hunter M. Role of *de novo* protein synthesis and calmodulin in rapid activation of Na^+–H^+ exchange by aldosterone in frog diluting segment. J Physiol (Lond) 1996;491: 219–23.
[569] Good DW, George T, Watts III BA. Aldosterone inhibits HCO_3^- absorption via a nongenomic pathway in medullary thick ascending limb. Am J Physiol Renal Physiol 2002;283: F699–706.
[570] Good DW, George T, Watts III BA. Nongenomic regulation by aldosterone of the epithelial NHE3 Na^+/H^+ exchanger. Am J Physiol Cell Physiol 2006;290:C757–63.
[571] Watts III BA, George T, Good DW. Aldosterone inhibits apical NHE3 and HCO_3^- absorption via a nongenomic ERK-dependent pathway in medullary thick ascending limb. Am J Physiol Renal Physiol 2006;291:F1005–13.
[572] Pinto V, Pinho MJ, Hopfer U, Jose PA, Soares-da-Silva P. Oxidative stress and the genomic regulation of aldosterone-stimulated NHE1 activity in SHR renal proximal tubular cells. Mol Cell Biochem 2008;310:191–201.

[573] Gesek FA, Schoolwerth AC. Effects of alpha-adrenergic agonists on intracellular and intramitochondrial pH in rat proximal nephrons. Am J Physiol 1989;257:F623–30.

[574] Nord EP, Howard MJ, Hafezi A, Moradeshagi P, Vaystub S, Insel PA. Alpha$_2$ adrenergic agonists stimulate $Na^+–H^+$ antiport activity in the rabbit renal proximal tubule. J Clin Invest 1987;80:1755–62.

[575] Liu F, Nesbitt T, Drezner MK, Friedman PA, Gesek FA. Proximal nephron Na^+/H^+ exchange is regulated by α_{1A}- and α_{1B}-adrenergic receptor subtypes. Mol Pharmacol 1997;52: 1010–8.

[576] Abdulnour-Nakhoul S, Khuri RN, Nakhoul NL. Effect of norepinephrine on intracellular pH in kidney proximal tubule: role of Na^+-$(HCO_3^-)_n$ cotransport. Am J Physiol 1998;275: F33–45.

[577] Simão S, Fraga S, Jose PA, Soares-Da-Silva P. Oxidative stress and α1-adrenoceptor-mediated stimulation of the Cl^-/HCO_3^- exchanger in immortalized SHR proximal tubular epithelial cells.. Br J Pharmacol 2008;153:1445–55.

[578] Sonalker PA, Tofovic SP, Bastacky SI, Jackson EK. Chronic noradrenaline increases renal expression of NHE-3, NBC-1, BSC-1 and aquaporin-2. Clin Exp Pharmacol Physiol 2008;35: 594–600.

[579] Felder CC, Albrecht FE, Campbell T, Eisner GM, cAMP-independent Jose PA. cAMP-independent G protein-linked inhibition of Na^+/H^+ exchange in renal brush border by D_1 dopamine agonists. Am J Physiol 1993;264:F1032–7.

[580] Felder CC, Campbell T, Albrecht F, Jose PA. Dopamine inhibits $Na^+–H^+$ exchanger activity in renal BBMV by stimulation of adenylate cyclase. Am J Physiol 1990;259:F297–303.

[581] Gesek FA, Schoolwerth AC. Hormonal interactions with the proximal $Na^+–H^+$ exchanger. Am J Physiol 1990;258: F514–21.

[582] Jadhav AL, Liu Q. DA1 receptor mediated regulation of $Na^+–H^+$ antiport activity in rat renal cortical brush border membrane vesicles. Clin Exp Hypertens A 1992;14:653–66.

[583] Sheikh-Hamad D, Wang YP, Jo OD, Yanagawa N. Dopamine antagonizes the actions of angiotensin II in renal brush-border membrane. Am J Physiol 1993;264:F737–43.

[584] Wiederkehr MR, Di Sole F, Collazo R, Quinones H, Fan L, Murer H, et al. Characterization of acute inhibition of Na/H exchanger NHE-3 by dopamine in opossum kidney cells. Kidney Int 2001;59:197–209.

[585] Hu MC, Fan L, Crowder LA, Karim-Jimenez Z, Murer H, Moe OW. Dopamine acutely stimulates Na^+/H^+ exchanger (NHE3) endocytosis via clathrin-coated vesicles. Dependence on protein kinase A-mediated NHE3 phosphorylation. J Biol Chem 2001;276:26906–15.

[586] Kunimi M, Seki G, Hara C, Taniguchi S, Uwatoko S, Goto A, et al. Dopamine inhibits renal Na^+:HCO_3^- cotransporter in rabbits and normotensive rats but not in spontaneously hypertensive rats. Kidney Int 2000;57:534–43.

[587] Pedrosa R, Jose PA, Soares-da-Silva P. Defective D_1-like receptor-mediated inhibition of the Cl^-/HCO_3^- exchanger in immortalized SHR proximal tubular epithelial cells. Am J Physiol Renal Physiol 2004;286:F1120–6.

[588] Takeda M, Yoshitomi K, Imai M. Regulation of $Na^+–3HCO_3^-$ cotransport in rabbit proximal tubule convoluted tubule via adenosine A_1 receptor. Am J Physiol 1993; 265:F511–9.

[589] Robey RB, Ruiz OS, Baniqued J, Mahmud D, Espiritu DJ, Bernardo AA, et al. SFKs, Ras, and the classic MAPK pathway couple muscarinic receptor activation to increased $Na–HCO_3$ cotransport activity in renal epithelial cells. Am J Physiol Renal Physiol 2001;280:F844–50.

[590] Ruiz OS, Qiu YY, Cardoso LR, Arruda JA. Regulation of the renal $Na–HCO_3$ cotransporter: VII. Mechanism of the cholinergic stimulation. Kidney Int 1997;51:1069–77.

[591] Kinsella JL, Cujdik T, Sacktor B. Further studies of the effect of thyroid hormones on $Na^+–H^+$ exchange in renal brush-border membrane vesicles (BBMV). Ann NY Acad Sci 1985;456:445–7.

[592] Kinsella JL, Cujdik T, Sacktor B. Kinetic studies on the stimulation of $Na^+–H^+$ exchange activity in renal brush border membranes isolated from thyroid hormone-treated rats. J Membr Biol 1986;91:183–91.

[593] Kinsella JL, Sacktor B. Thyroid hormones increase $Na^+–H^+$ exchange activity in renal brush border membranes. Proc Natl Acad Sci USA 1985;82:3606–10.

[594] Yonemura K, Cheng L, Sacktor B, Kinsella JL. Stimulation by thyroid hormone of $Na^+–H^+$ exchange activity in cultured opossum kidney cells. Am J Physiol 1990;258:F333–8.

[595] Cano A, Baum M, Moe OW. Thyroid hormone stimulates the renal Na/H exchanger NHE3 by transcriptional activation. Am J Physiol 1999;276:C102–8.

[596] Mohebbi N, Kovacikova J, Nowik M, Wagner CA. Thyroid hormone deficiency alters expression of acid–base transporters in rat kidney. Am J Physiol Renal Physiol 2007;293: F416–27.

[597] Gattineni J, Sas D, Dagan A, Dwarakanath V, Baum M. Effect of thyroid hormone on the postnatal renal expression of NHE8. Am J Physiol Renal Physiol 2008;294:F198–204.

[598] Dennis V, Brazy PC. Sodium, phosphate, glucose, bicarbonate and lamanine interactions in the isolated proximal convoluted tubule of the rabbit kidney. J Clin Invest 1979;237:387–97.

[599] Gullans SR, Brazy PC, Dennis VW, Mandel LJ. Interactions between gluconeogenesis and sodium transport in rabbit proximal tubule. Am J Physiol 1984;246:F859–69.

[600] Kahn AM, Dolson GM, Hise MK, Bennett SC, Weinman EJ. Parathyroid hormone and dibutyryl cAMP inhibit Na^+/H^+ exchange in renal brush border vesicles. Am J Physiol 1985;248:F212–8.

[601] Cohn DE, Klahr S, Hammerman MR. Metabolic acidosis and parathyroidectomy increase $Na^+–H^+$ exchange in brush border vesicles. Am J Physiol 1983;:F217–22.

[602] Moran A, Montrose MH, Murer H. Regulation of $Na^+–H^+$ exchange in cultured opossum kidney cells by parathyroid hormone, atrial natriuretic peptide and cyclic nucleotides. Biochim Biophys Acta 1988;969:48–56.

[603] Pollock AS, Warnock DG, Strewler GJ. Parathyroid hormone inhibition of $Na^+–H^+$ antiporter activity in a cultured renal cell line. Am J Physiol 1986;250:F217–25.

[604] Borensztein P, Juvin P, Vernimmen C, Poggioli J, Paillard M, Bichara M. cAMP-dependent control of Na^+/H^+ antiport by AVP, PTH, and PGE2 in rat medullary thick ascending limb cells. Am J Physiol 1993;264:F354–64.

[605] Weinman EJ, Cunningham R, Wade JB, Shenolikar S. The role of NHERF-1 in the regulation of renal proximal tubule sodium-hydrogen exchanger 3 and sodium-dependent phosphate cotransporter 2a. J Physiol 2005;567:27–32.

[606] Weinman EJ, Steplock D, Shenolikar S. CAMP-mediated inhibition of the renal brush border membrane $Na^+–H^+$ exchanger requires a dissociable phosphoprotein cofactor. J Clin Invest 1993;92:1781–6.

[607] Weinman EJ, Steplock D, Wang Y, Shenolikar S. Characterization of a protein cofactor that mediates protein kinase A regulation of the renal bruch border membrane $Na^+–H^+$ exchanger. J Clin Invest 1995;95:2143–9.

[608] Miller RT, Pollock AS. Modification of the internal pH sensitivity of the Na^+/H^+ antiporter by parathyroid hormone in a cultured renal cell line. J Biol Chem 1987;262:9115–20.

[609] Collazo R, Fan L, Hu MC, Zhao H, Wiederkehr MR, Moe OW. Acute regulation of Na^+/H^+ exchanger NHE3 by parathyroid hormone via NHE3 phosphorylation and dynamin-dependent endocytosis. J Biol Chem 2000;275:31601–8.

[610] Fan L, Wiederkehr MR, Collazo R, Wang H, Crowder LA, Moe OW. Dual mechanisms of regulation of Na/H exchanger NHE-3 by parathyroid hormone in rat kidney. J Biol Chem 1999;274:11289–95.

[611] Zhang Y, Norian JM, Magyar CE, Holstein-Rathlou N-H, Mircheff AK, McDonough AA. In vivo PTH provokes apical NHE3 and NaPi2 redistribution and Na-K-ATPase inhibition. Am J Physiol 1999;276:F711–9.

[612] Bezerra CN, Girardi AC, Carraro-Lacroix LR, Rebouças NA. Mechanisms underlying the long-term regulation of NHE3 by parathyroid hormone. Am J Physiol Renal Physiol 2008;294: F1232–7.

[613] Reuss L, Petersen KU. Cyclic AMP inhibits Na^+/H^+ exchange at the apical membrane of *Necturus* gallbladder epithelium. J Gen Physiol 1985;85:409–29.

[614] Harada H, Kanai Y, Anzai M, Suketa Y. cAMP activates Cl^-/HCO_3^- exchange for regulation of intracellular pH in renal epithelial cells. Biochim Biophys Acta 1991;1092: 404–7.

[615] Ruiz OS, Qiu YY, Wang LJ, Arruda JA. Regulation of the renal Na-HCO_3 cotransporter: V. Mechanism of the inhibitory effect of parathyroid hormone. Kidney Int 1996;49:396–402.

[616] Ruiz OS, Arruda JA. Regulation of the renal Na-HCO_3 cotransporter by cAMP and Ca-dependent protein kinases. Am J Physiol 1992;262:F560–5.

[617] Bernardo AA, Kear FT, Santos AVP, Ma J, Steplock D, Robey RB, et al. Basolateral Na^+/HCO_3^- cotransport activity is regulated by the dissociable Na^+/H^+ exchanger regulatory factor. J Clin Invest 1999;104:195–201.

[618] Weinman EJ, Evangelista CM, Steplock D, Liu MZ, Shenolikar S, Bernardo A. Essential role for NHERF in cAMP-mediated inhibition of the Na^+-HCO_3^- co-transporter in BSC-1 cells. J Biol Chem 2001;276:42339–46.

[619] Coppola S, Frömter E. An electrophysiological study of angiotensin II regulation of Na-HCO_3 cotransport and K conductance in renal proximal tubules. I. Effect of picomolar concentrations. Pflügers Arch 1994;427:143–50.

[620] Eiam-Ong S, Hilden SA, Johns CA, Madias NE. Stimulation of basolateral Na^+–HCO_3^- cotransporter by angiotensin II in rabbit renal cortex. Am J Physiol 1993;265:F195–203.

[621] Geibel JP, Giebisch G, Boron WF. Angiotensin II stimulates both Na^+–H^+ exchange and Na^+/HCO_3^- cotransport in the rabbit proximal tubule. Proc Natl Acad Sci USA 1990;87: 7917–20.

[622] Harris PJ. Regulation of proximal tubule function by angiotensin. Clin Exp Pharmacol Physiol 1992;19:213–22.

[623] Harris PJ, Hiranyachattada S, Antoine AM, Walker L, Reilly AM, Eitle E. Regulation of renal tubular sodium transport by angiotensin II and atrial natriuretic factor. Clin Exp Pharmacol Physiol 1996;3:S112–8.

[624] Horita S, Zheng Y, Hara C, Yamada H, Kunimi M, Taniguchi S, et al. Biphasic regulation of Na^+–HCO_3^- cotransporter by angiotensin II type 1A receptor. Hypertension 2002;40:707–12.

[625] Reilly AM, Harris PJ, Williams DA. Biphasic effect of angiotensin II on intracellular sodium concentration in rat proximal tubule. Am J Physiol 1995;269:F374–80.

[626] Saccomani MP, Bonadonna RC, Caveggion E, DeFronzo RA, Cobelli C. Bicarbonate kinetics in humans: identification and validation of a three-compartment model. Am J Physiol 1995;269:E183–92.

[627] Zhou Y, Bouyer P, Boron WF. Effects of angiotensin II on the CO_2 dependence of HCO_3^- reabsorption by the rabbit S2 renal proximal tubule. Am J Physiol Renal Physiol 2006;290: F666–73.

[628] Barreto-Chaves MLM, Mello-Aires M. Effect of luminal angiotensin II and ANP on early and late cortical distal tubule HCO_3^- reabsorption. Am J Physiol 1996;271:F977–84.

[629] Levine DZ, Iacovitti M, Buckman S, Burns KD. Role of angiotensin II in dietary modulation of rat late distal tubule bicarbonate flux in vivo. J Clin Invest 1996;97:120–5.

[630] Wang T, Egbert ALJ, Abbiati T, Aronson PS, Giebisch G. Mechanisms of stimulation of proximal tubule chloride transport by formate and oxalate. Am J Physiol 1996;271: F446–50.

[631] Schlatter E, Haxelmans S, Ankorina I, Kleta R. Regulation of Na^+/H^+ exchange by diadenosine polyphosphates, angiotensin II, and vasopressin in rat cortical collecting duct. J Am Soc Nephrol 1995;6:1223–9.

[632] Bell PD, Peti-Peterdi J. Angiotensin II stimulates macula densa basolateral sodium/hydrogen exchange via type 1 angiotensin II receptors. J Am Soc Nephrol 1999;10:S225–9.

[633] Coppola S, Frömter E. An electrophysiological study of angiotensin II regulation of Na–HCO_3 cotransport and K conductance in renal proximal tubules. II. Effect of micromolar concentrations. Pflügers Arch 1994;427:151–6.

[634] Turban S, Beutler KT, Morris RG, Masilamani S, Fenton RA, Knepper MA, et al. Long-term regulation of proximal tubule acid–base transporter abundance by angiotensin II. Kidney Int 2006;70:660–8.

[635] Ruiz OS, Qiu YY, Wang LL, Arruda JA. Regulation of the renal Na-HCO_3 cotransporter: IV. Mechanisms of the stimulatory effect of angiotensin II. J Am Soc Nephrol 1995;6: 1202–8.

[636] Cano A, Miller RT, Alpern RJ, Preisig PA. Angiotensin II stimulation of Na-H antiporter activity is cAMP independent in OKP cells. Am J Physiol 1994;266:C1603–8.

[637] Robey RB, Ruiz OS, Espiritu DJ, Ibanez VC, Kear FT, Noboa OA, et al. Angiotensin II stimulation of renal epithelial cell Na/HCO_3 cotransport activity: a central role for Src family kinase/classic MAPK pathway coupling. J Membrane Biol 2002;187:135–45.

[638] Peti-Peterdi J, Bell PD. Regulation of macula densa Na:H exchange by angiotensin II. Kidney Int 1998;54:2021–8.

[639] Queiroz-Leite GD, Peruzzetto MC, Neri EA, Rebouças NA. Transcriptional regulation of the Na^+/H^+ exchanger NHE3 by chronic exposure to angiotensin II in renal epithelial cells. Biochem Biophys Res Commun 2011;409:470–6.

[640] Li XC, Hopfer U, Zhuo JL. AT_1 receptor-mediated uptake of angiotensin II and NHE-3 expression in proximal tubule cells through a microtubule-dependent endocytic pathway. Am J Physiol Renal Physiol 2009;297:F1342–52.

[641] Li XC, Zhuo JL. Selective knockdown of AT_1 receptors by RNA interference inhibits Val5-ANG II endocytosis and NHE-3 expression in immortalized rabbit proximal tubule cells. Am J Physiol Cell Physiol 2007;293:C367–78.

[642] Li XC, Zhuo JL. Intracellular ANG II directly induces in vitro transcription of TGF-β1, MCP-1, and NHE-3 mRNAs in isolated rat renal cortical nuclei via activation of nuclear AT_{1a} receptors. Am J Physiol Cell Physiol 2008;294:C1034–45.

[643] Camilión de Hurtado MC, Alvarez BV, Pérez NG, Ennis IL, Cingolani HE. Angiotensin II activates Na^+-independent Cl^-–HCO_3 exchange in ventricular myocardium. Circ Res 1998;82:473–81.

[644] De Giusti VC, Garciarena CD, Aiello EA. Role of reactive oxygen species (ROS) in angiotensin II-induced stimulation of the

cardiac Na^+/HCO_3^- cotransport. J Mol Cell Cardiol 2009;47:716–22.
[645] De GV, Orlowski A, Aiello EA. Angiotensin II inhibits the electrogenic Na^+/HCO_3^- cotransport of cat cardiac myocytes. J Mol Cell Cardiol 2010;49:812–8.
[646] Kinsella J, Cujdik T, Sacktor B. Na^+–H^+ exchange activity in renal brush border membrane vesicles in response to metabolic acidosis: the role of glucocorticoids. Proc Natl Acad Sci USA 1984;81:630–4.
[647] Soleimani M, Bizal GL, McKinney TD, Hattabaugh YJ. Effect of in vitro metabolic acidosis on luminal Na^+/H^+ exchange and basolateral Na^+:HCO_3^- cotransport in rabbit kidney proximal tubules. J Clin Invest 1992;90:211–8.
[648] Laghmani K, Borensztein P, Ambuhl P, Froissart M, Bichara M, Moe OW, et al. Chronic metabolic acidosis enhances NHE-3 protein abundance and transport activity in the rat thick ascending limb by increasing NHE-3 mRNA. J Clin Invest 1997;99:24–30.
[649] Laghmani K, Richer C, Borensztein P, Paillard M, Froissart M. Expression of rat thick limb Na/H exchangers in potassium depletion and chronic metabolic acidosis. Kidney Int 2001;60:1386–96.
[650] Horie S, Moe O, Tejedor A, Alpern RJ. Preincubation in acid medium increases Na/H antiporter activity in cultured renal proximal tubule cells. Proc Natl Acad Sci U S A 1990;87:4742–5.
[651] Yamaji Y, Amemiya M, Cano A, Preisig PA, Miller RT, Moe OW, et al. Overexpression of csk inhibits acid-induced activation of NHE-3. Proc Natl Acad Sci USA 1995;92:6274–8.
[652] Akiba T, Rocco VK, Warnock DG. Parallel adaptation of the rabbit renal cortical sodium/proton antiporter and sodium/bicarbonate cotransporter in metabolic acidosis and alkalosis. J Clin Invest 1987;80:308–15.
[653] Kwon TH, Fulton C, Wang W, Kurtz I, Frokiær J, Aalkjær C, et al. Chronic metabolic acidosis upregulates rat kidney Na-HCO_3^- cotransporters NBCn1 and NBC3 but not NBC1. Am J Physiol Renal Physiol 2002;282:F341–51.
[654] Soleimani M, Bookstein C, Singh G, Rao MC, Chang EB, Bastani B. Differential regulation of Na^+/H^+ exchange and H^+-ATPase by pH and HCO_3^- in kidney proximal tubules. J Membr Biol 1995;144:209–16.
[655] Tsuruoka S, Schwartz GJ. Adaptation of rabbit cortical collecting duct HCO_3^- transport to metabolic acidosis in vitro. J Clin Invest 1996;97:1076–84.
[656] Tsuruoka S, Schwartz GJ. Metabolic acidosis stimulates H^+ secretion in the rabbit outer medullary collecting duct (inner stripe) of the kidney. J Clin Invest 1997;99:1420–31.
[657] Sabolić I, Brown D, Gluck SL, Alper SL. Regulation of AE1 anion exchanger and H^+-ATPase in rat cortex by acute metabolic acidosis and alkalosis. Kidney Int 1997;51:125–37.
[658] Codina J, Opyd TS, Powell ZB, Furdui CM, Petrovic S, Penn RB, et al. pH-dependent regulation of the α-subunit of H^+–K^+-ATPase (HKα2). Am J Physiol Renal Physiol 2011;301:F536–43.
[659] Purkerson JM, Tsuruoka S, Suter DZ, Nakamori A, Schwartz GJ. Adaptation to metabolic acidosis and its recovery are associated with changes in anion exchanger distribution and expression in the cortical collecting duct. Kidney Int 2010;78:993–1005.
[660] Schwartz JH, Alexander EA. Adaptation of intercalated cells along the collecting duct to systemic acid/base changes. Kidney Int 2010;78:949–51.
[661] Zeidel ML, Seifter JL. Regulation of Na/H exchange in renal microvillus vesicles in chronic hypercapnia. Kidney Int 1988;34:60–6.
[662] Teixeira Da Silva Jr. JC, Perrone RD, Johns CA, Madias NE. Rat kidney band 3 mRNA modulation in chronic respiratory acidosis. J Am Physiol 1991;260:F204–9.
[663] Bernardo AA, Espiritu DJ, Ruiz OS, Robey RB, Arruda JA. The role of phosphatidylinositol 3-kinase (PI3K) in CO_2 stimulation of the Na^+/HCO_3^- cotransporter (NBC). J Membr Biol 2003;191:141–8.
[664] Espiritu DJ, Yang VL, Bernardo AA, Arruda JA. Regulation of renal Na^+/HCO_3^- cotransporter stimulation by CO_2: role of phosphorylation, exocytosis and protein synthesis. J Membr Biol 2004;199:39–49.
[665] Ruiz OS, Qiu YY, Wang LJ, Cardoso LR, Arruda JAL. Regulation of renal Na–HCO_3 cotransporter: VIII. Mechanism Of stimulatory effect of respiratory acidosis. J Membr Biol 1998;162:201–8.
[666] Ruiz OS, Robey RB, Qiu YY, Wang LJ, Li CJ, Ma J, et al. Regulation of the renal Na–HCO_3 cotransporter. XI. Signal transduction underlying CO_2 stimulation. Am J Physiol 1999;277:F580–6.
[667] Kanaan A, Douglas RM, Alper SL, Boron WF, Haddad GG. Effect of chronic elevated carbon dioxide on the expression of acid–base transporters in the neonatal and adult mouse. Am J Physiol Regul Integr Comp Physiol 2007;293:R1294–302.
[668] De Seigneux S, Malte H, Dimke H, Frøkiaer J, Nielsen S, Frische S. Renal compensation to chronic hypoxic hypercapnia: downregulation of pendrin and adaptation of the proximal tubule. Am J Physiol Renal Physiol 2007;292:F1256–66.
[669] Capasso G, Mollica F, Saviano C, De Santo NG. Tubule effects of glomerular hyperfilteration: an integrated view. Semin Nephrol 1995;15:419–25.
[670] Harris RC, Seifter JL, Brenner BM. Adaptation of Na^+–H^+ exchange in renal microvillus membrane vesicles. Role of dietary protein and uninephrectomy. J Clin Invest 1984;74:1979–87.
[671] Mackovic-Basic M, Fan R, Kurtz I. Denervation inhibits early increase in Na^+–H^+ exchange after uninephrectomy but does not suppress hypertrophy. Am J Physiol 1992;263:F328–34.
[672] Fine LG, Badie-Dezfooly B, Lowe AG, Hamzeh A, Wells J, Salehmoghaddam S. Stimulation of Na^+/H^+ antiport is an early event in hypertrophy of renal proximal tubular cells. Proc Natl Acad Sci USA 1985;82:1736–40.
[673] Preisig PA, Alpern RJ. Increased Na/H antiporter and Na/$3HCO_3$ symporter activities in chronic hyperfiltration. A model of cell hypertrophy. J Gen Physiol 1991;97:195–217.
[674] Khanna A, Simoni J, Hacker C, Duran MJ, Wesson DE. Increased endothelin activity mediates augmented distal nephron acidification induced by dietary protein. J Am Soc Nephrol 2004;15:2266–75.
[675] Khanna A, Simoni J, Wesson DE. Endothelin-induced increased aldosterone activity mediates augmented distal nephron acidification as a result of dietary protein. J Am Soc Nephrol 2005;16:1929–35.
[676] Soleimani M, Bergman JA, Hosford MA, McKinney TD. Potassium depletion increases luminal Na^+/H^+ exchange and basolateral Na^+:CO_3^{2-}:HCO_3^- cotransport in rat renal cortex. J Clin Invest 1990;86:1076–83.
[677] Amlal H, Habo K, Soleimani M. Potassium deprivation upregulates expression of renal basolateral Na^+–HCO_3^- cotransporter (NBC-1). Am J Physiol 2000;279:F532–43.
[678] Bailey MA, Fletcher RM, Woodrow DF, Unwin RJ, Walter SJ. Upregulation of H^+-ATPase in the distal nephron during potassium depletion: structural and functional evidence. Am J Physiol 1998;275:F878–84.

[679] Barone S, Amlal H, Kujala M, Xu J, Karet F, Blanchard A, et al. Regulation of the basolateral chloride/base exchangers AE1 and SLC26A7 in the kidney collecting duct in potassium depletion. Nephrol Dial Transplant 2007;22:3462–70.

[680] Pouysségur J, Franchi A, L'Allemain G, Paris S. Cytoplasmic pH, a key determinant of growth factor-induced DNA synthesis in quiescent fibroblasts. FEBS Lett 1985;190:115–9.

[681] Grinstein S, Cohen S, Goetz JD, Rothstein A, Gelfand EW. Characterization of the activation of Na^+/H^+ exchange in lymphocytes by phorbol esters. Change in the cytoplasmic pH-dependence of the antiport. Proc Natl Acad Sci USA 1985;82:1429–33.

[682] Quinn DA, Dahlberg CG, Bonventre JP, Scheid CR, Honeyman T, Joseph PM, et al. The role of Na^+/H^+ exchange and growth factors in pulmonary artery smooth muscle cell proliferation. Am J Resp Cell Mol Biol 1996;14:139–45.

[683] Schuldiner S, Rozengurt E. Na^+/H^+ antiport in Swiss 3T3 cells: mitogenic stimulation leads to cytoplasmic alkalinization. Proc Natl Acad Sci USA 1982;79:7778–82.

[684] Strazzabosco M, Poci C, Spirli C, Zsembery A, Granato A, Massimino ML, et al. Intracellular pH regulation in Hsp G2 cells: effects of epidermal growth factor, transforming growth factor-alpha, and insulinlike growth factor-II on Na^+/H^+ exchange activity. Hepatology 1995;22:588–97.

[685] Szwergold BS, Brown TR, Freed JJ. Bicarbonate abolishes intracellular alkalinization in mitogen- stimulated 3T3 cells. J Cell Physiol 1989;138:227–35.

[686] Vicintini M, Villereal ML. Activation of Na^+/H^+ exchange in cultured fibroblasts: synergism and antagonism between phorbol ester, Ca^{2+} ionophore, and growth factors. Proc Natl Acad Sci USA 1985;82:8053–6.

[687] Wang H, Singh D, Fliegel L. The Na^+/H^+ antiporter potentiates growth and retinoic acid-induced differentiation of P19 embryonal carcinoma cells. J Biol Chem 1997;272:26545–9.

[688] Ganz MB, Boron WF. Long-term effects of growth factors on pH and acid–base transport in rat glomerular mesangial cells. Am J Physiol 1994;266:F576–85.

[689] Kikeri D, Zeidel ML, Ballermann BJ, Brenner BM, Hebert SC. pH regulation and response to AVP in A10 cells differ markedly in the presence vs. absence of CO_2–HCO_3^-. Am J Physiol 1990;259:C471–83.

[690] Lucchesi PA, Berk BC. Regulation of sodium-hydrogen exchange in vascular smooth muscle. Cardiovasc Res 1995;29: 172–7.

[691] Hagag N, Lacal JC, Graber M, Aaronson S, Viola MV. Microinjection of *ras* p21 induces a rapid rise in intracellular pH. Mol Cell Biol 1987;7:1984–8.

[692] Maly K, Oberhuber H, Woppler W, Hoflacher J, Jaggi R, Groner B, et al. Effect of Ha-ras on phosphatidylinositol metabolism, Na^+/H^+-antiporter and mobilization of intracellular calcium. Adv Enzyme Reg 1988;27:121–31.

[693] Chiche J, Brahimi-Horn MC, Pouysségur J. Tumour hypoxia induces a metabolic shift causing acidosis: a common feature in cancer. J Cell Mol Med 2010;14:771–94.

[694] Parks SK, Chiche J, Pouysségur J. pH control mechanisms of tumor survival and growth. J Cell Physiol 2011;226:299–308.

[695] Swietach P, Hulikova A, Vaughan-Jones RD, Harris AL. New insights into the physiological role of carbonic anhydrase IX in tumour pH regulation. Oncogene 2010;29:6509–21.

[696] Ahmed S, Thomas G, Ghoussaini M, Healey CS, Humphreys MK, Platte R, et al. Newly discovered breast cancer susceptibility loci on 3p24 and 17q23.2. Nat Genet 2009;41:585–90.

[697] Chen Y, Choong LY, Lin Q, Philp R, Wong CH, Ang BK, et al. Differential expression of novel tyrosine kinase substrates during breast cancer development. Mol Cell Proteomics 2007;6: 2072–87.

[698] Izumi H, Torigoe T, Ishiguchi H, Uramoto H, Yoshida Y, Tanabe M, et al. Cellular pH regulators: potentially promising molecular targets for cancer chemotherapy. Cancer Treat Rev 2003;29:541–9.

[699] Long J, Shu XO, Cai Q, Gao YT, Zheng Y, Li G, et al. Evaluation of breast cancer susceptibility loci in Chinese women. Cancer Epidemiol Biomarkers Prev 2010;19:2357–65.

[700] Beasley NJ, Wykoff CC, Watson PH, Leek R, Turley H, Gatter K, et al. Carbonic anhydrase IX, an endogenous hypoxia marker, expression in head and neck squamous cell carcinoma and its relationship to hypoxia, necrosis, and microvessel density. Cancer Res 2001;61:5262–7.

[701] Chiche J, Ilc K, Laferrière J, Trottier E, Dayan F, Mazure NM, et al. Hypoxia-inducible carbonic anhydrase IX and XII promote tumor cell growth by counteracting acidosis through the regulation of the intracellular pH. Cancer Res 2009;69:358–68.

[702] Ivanov S, Liao S-Y, Ivanova A, Danilkovitch-Miagkova A, Tarasova N, Weirich G, et al. Expression of hypoxia-inducible cell-surface transmembrane carbonic anhydrases in human cancer. Am J Pathol 2001;158:905–19.

[703] Li Y, Wang H, Oosterwijk E, Selman Y, Mira JC, Medrano T, et al. Antibody-specific detection of CAIX in breast and prostate cancers. Biochem Biophys Res Commun 2009;386:488–92.

[704] Morimoto K, Nishimori I, Takeuchi T, Kohsaki T, Okamoto N, Taguchi T, et al. Overexpression of carbonic anhydrase-related protein XI promotes proliferation and invasion of gastrointestinal stromal tumors. Virchows Arch 2005;447:66–73.

[705] Span PN, Bussink J, Manders P, Beex LV, Sweep CG. Carbonic anhydrase-9 expression levels and prognosis in human breast cancer: association with treatment outcome. Br J Cancer 2003;89:271–6.

[706] Svastova E, Witarski W, Csaderova L, Kosik I, Skvarkova L, Hulikova A, et al. Carbonic anhydrase IX interacts with bicarbonate transporters in lamellipodia and increases cell migration via its catalytic domain. J Biol Chem 2012;287:3392–402.

[707] Swietach P, Vaughan-Jones RD, Harris AL. Regulation of tumor pH and the role of carbonic anhydrase 9. Cancer Metastasis Rev 2007;26:299–310.

[708] Švastová E, Hulíková A, Rafajová M, Zat'ovičová M, Gibadulinová A, Casini A, et al. Hypoxia activates the capacity of tumor-associated carbonic anhydrase IX to acidify extracellular pH. FEBS Lett 2004;577:439–45.

[709] Swietach P, Patiar S, Supuran CT, Harris AL, Vaughan-Jones RD. The role of carbonic anhydrase 9 in regulating extracellular and intracellular pH in three-dimensional tumor cell growths. J Biol Chem 2009;284:20299–310.

[710] Swietach P, Wigfield S, Cobden P, Supuran CT, Harris AL, Vaughan-Jones RD. Tumor-associated carbonic anhydrase 9 spatially coordinates intracellular pH in three-dimensional multicellular growths. J Biol Chem 2008;283:20473–83.

[711] Supuran CT. Development of small molecule carbonic anhydrase IX inhibitors. BJU Int 2008;101(Suppl. 4):39–40.

[712] Vitale RM, Alterio V, Innocenti A, Winum JY, Monti SM, De SG, et al. Carbonic anhydrase inhibitors. Comparison of aliphatic sulfamate/bis-sulfamate adducts with isozymes II and IX as a platform for designing tight-binding, more isoform-selective inhibitors. J Med Chem 2009;52:5990–8.

[713] Ohgaki R, van IJzendoorn SCD, Matsushita M, Hoekstra D, Kanazawa H. Organellar Na^+/H^+ exchangers: Novel players in organellar pH regulation and their emerging functions. Biochem 2011;50:443–50.

[714] Orlowski J, Grinstein S. Diversity of the mammalian sodium/proton exchanger SLC9 gene family. Pflügers Arch 2004;447:549–65.

This page intentionally left blank

CHAPTER

53

SLC4 Sodium-Driven Bicarbonate Transporters

Ira Kurtz

Department of Medicine, Brain Research Institute, David Geffen School of Medicine at UCLA, Los Angeles, California, USA

The SLC4 (*sol*ute *c*arrier 4) family is a group of a membrane proteins that share sequence homology and in general mediate the transport of bicarbonate. It should be noted that bicarbonate transport is not unique to the SLC4 family. The structurally unrelated SLC26 family has at least three proteins that mediate $Cl^- - HCO_3^-$ exchange. In this chapter, the biology of SLC4 Na^+-dependent bicarbonate transporters will be highlighted. The outlier in the SLC4 family is the SLC4A11 gene product (NaBC1) that lacks the ability to transport bicarbonate and is currently characterized as an electrogenic sodium-borate transporter. Whether SLC4 transporters mediate bicarbonate and/or carbonate transport is unclear and therefore when the word bicarbonate or the chemical symbol HCO_3^- is used throughout the chapter with reference to SLC4 mediated ion transport, it refers to both HCO_3^- and/or CO_3^{2-}.

In this chapter, while extra-renal studies will be highlighted, an emphasis will be placed on the biology of specific sodium-coupled SLC4 proteins in the kidney.

FUNCTIONAL CATEGORIZATION OF THE SLC4 FAMILY

A dendrogram of the SLC4 family of proteins is shown in Fig. 53.1. The 10 different SLC4 gene products can be logically subdivided functionally and structurally into four groups that differ primarily in their Na^+- and Cl^--dependence and electrogenic properties. Although various categorizations have been proposed, the following is a convenient scheme:

Na^+-independent $Cl^- - HCO_3^-$ exchangers: 3 homologous transporters, AE1, AE2, and AE3 (*SLC4A1, -2,-3* respectively) that mediate $Cl^- - HCO_3^-$ exchange have been well characterized. A fourth member, AE4, has also been reported to function as a $Cl^- - HCO_3^-$ exchanger. However, as will be discussed, the amino acid sequence of AE4 is more homologous to sodium-coupled SLC4 transporters.

$Na^+ - HCO_3^-$ cotransporters: There are 3 well-characterized members of the SLC4 family that transport Na^+ and HCO_3^- without concomitant net Cl^-transport. NBCe1 (*SLC4A4* gene) and NBCe2 (*SLC4A5* gene) are sodium bicarbonate cotransporters that are chloride-independent and electrogenic in that their HCO_3^- to Na^+ transport coupling is >1 (2:1, or 3:1). NBCn1 (*SLC4A7* gene) is an electroneutral $Na^+ - HCO_3^-$ cotransporter with a coupling ratio of 1:1.

Na^+-driven $Cl^- - HCO_3^-$ exchangers: Two SLC4 transporters have been reported to mediate $Na^+ - HCO_3^-$ cotransport in exchange for chloride. The literature regarding the functional properties of the first reported mammalian transporter, NCBE (SLC4A10), is somewhat confusing. Although this transporter is reported by several groups to mediate Na^+-dependent $Cl^- - HCO_3^-$ exchange, a separate study in oocytes has shown that chloride is not transported under physiologic conditions, and accordingly the protein was renamed NBCn2 ($Na^+ - HCO_3^-$ cotransporter electroneutral 2). The details of the discrepant findings in this area are discussed below. The second reported transporter in this group, NDCBE (*SLC4A8* gene), is a well-characterized Na^+-driven $Cl^- - HCO_3^-$ exchanger.

Electrogenic Na-borate cotransporter: NaBC1 has been reported to mediate the electrogenic transport of

Seldin and Giebisch's The Kidney, Fifth Edition.
DOI: http://dx.doi.org/10.1016/B978-0-12-381462-3.00053-7

© 2013 Elsevier Inc. All rights reserved.

$Na^+ - BO_4^-$ in the presence of borate, or $Na^+ - OH^-$ cotransport with coupling ratio of Na^+:anion of at least 2 (electrogenic) in the absence of borate. The lack of a clear role for borate transport in various tissues where this transporter is expressed raises questions regarding the actual function of NaBC1 physiologically.

Several SLC4 transporters expressed in the kidney have been localized at the transcript/or protein level in various nephron segments and cell types (Tables 53.1–53.3; Fig. 53.2). Studies involving the expression of SLC4 transcripts in the kidney have been done in several mammalian species including mouse, rat, rabbit and human. In addition to documented known species differences, SLC4 proteins typically have a number of specific variants (due to splicing and/or alternate promoter usage) whose localization in the kidney and functional properties have not been thus far thoroughly investigated. This fact increases significantly the complexity of addressing the actual protein expression pattern and functional characteristics of each SLC4 transporter in various renal cell types.

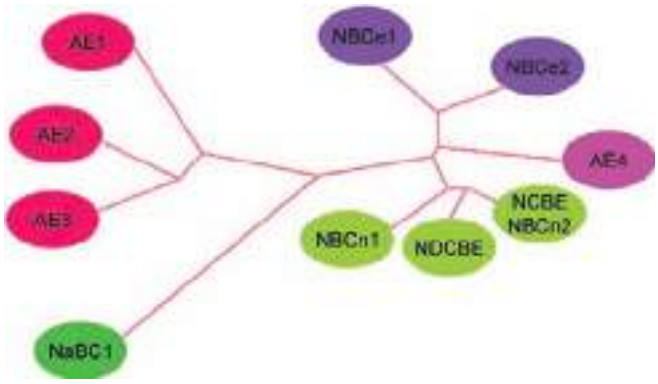

FIGURE 53.1 Dendrogram of SLC4 transporters.

The kidney and brain share the property of having various cell types that express different bicarbonate transporter proteins. Although most SLC4 transporters have in common the property of transporting bicarbonate, cells in the kidney and brain are likely taking advantage of the unique and specific properties of each transporter. The uniqueness of SLC4 proteins stems from the fact that these transporters differ significantly in their ion (Na^+, Cl^-) dependence, coupling ratios, membrane targeting, substrate affinities, developmental expression, regulation by factors pH/phosphorylation, and protein-protein interaction. These differences also account for the fact that functionally, SLC4

TABLE 53.1 Immunolocalization of Na^+-driven SLC4 Transporters in Kidney

Transporter	Location	Apical	Basolateral	Human	Rat	Mouse
NBCe1	PT		+	+	+	+
NBCe2	OMCD	N/A	N/A	+		
	P(U)	+		+		
NBCn1	mTAL		+	+	+	
	OMCD–αIC		+			
	IMCD 2 & 3		+			
	P(U)*				+	
NaBC1**	Podocytes			+	+	
	PT	+	+	+	+	
	tDL		+		+	+****
	CCD – IC***	+		+		
	OMCD – IC***	+		+		
	IMCD		+	+		

*LacZ staining.
**NaBC1 does not transport Na bicarbonate.
***IC type not specified.
****immunolocalization and LacZ staining only in the tDL in mouse.
PT – proximal tubule.
OMCD – outer medullary collecting duct.
P(U) – pelvis (uroepithelium).
tDL – thin descending limb.
mTAL – medullary thin descending limb.
IMCD – inner medullary collecting duct.

TABLE 53.2 SLC4 Na^+-driven Transporters that Have Not Been Immunolocalized in Kidney

Transporters	Technique	Location	Human	Rat	Mouse
NCBE/ NBCn2	Northern: weak		+		
NDCBE	Northern: weak		+		
	RT-PCR	cortex (weak), medulla	+		
	RT-PCR	inner medulla		+	
	Western	cortex/CCD			+

TABLE 53.3 AE4 Immunolocalization in the Kidney

Location	Apical	Basolateral	Rat	Mouse	Rabbit	Reference
CCD: βIC	+				+	194, 208
CCD: αIC	+	+			+	96
CCD: αIC, βIC		+	+			96
CCD: βIC		+		+		21, 72

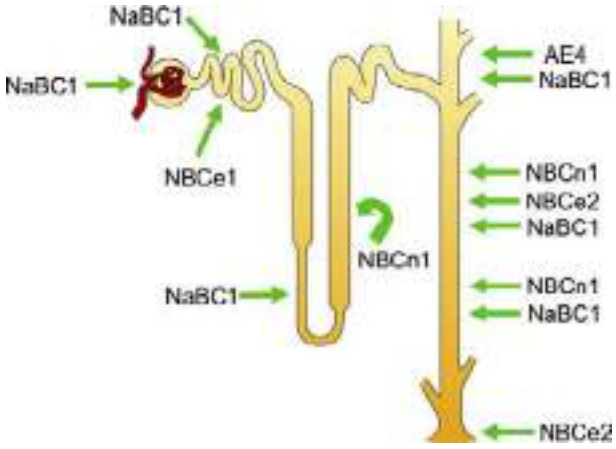

FIGURE 53.2 Immunlocolization of Na^+-driven SLC4 transporters in the kidney. The data is derived from studies in human, rat, mouse and rabbit. Species differences exist as shown in Tables 53.1 and 53.3.

transporters have various direct and indirect physiological roles in the kidney including transepithelial bicarbonate transport, intracellular pH regulation, and transport of Cl^-, Na^+ and possibly NH_4^+.

Because SLC4 transporters are expressed not only in the kidney but also in various extrarenal organs and cell types, diseases associated with mutations in these transporters or targeted disruption in mice result in both a renal and extrarenal phenotype (Table 53.4).

SODIUM BICARBONATE COTRANSPORTERS (ELECTROGENIC)

NBCe1 (SLC4A4 Gene)

Structural Variants

Our knowledge regarding the structure of sodium-dependant SLC4 transporters has until recently been extrapolated from the large body of data obtained from studies on the AE1 anion exchanger.[1] More recent studies of NBCe1 reveal very interesting structural and functional differences from AE1.[2] Three variants of the SLC4A5 gene have been well characterized.[3,4] All three NBCe1 variants mediate electrogenic $Na^+ - HCO_3^-$ cotransport, but differ in their N- and C-terminal extremities, regulation, and intrinsic activity. In kidney, NBCe1-A (or kNBC1) is predominantly expressed in S1 and S2 proximal tubule cells where it mediates the basolateral efflux of HCO_3^-, thereby contributing to the reabsorption of ~80% of the filtered bicarbonate load.[5–9] In addition to the proximal tubule, NBCe1-A is also expressed in the eye[10,11] and salivary gland.[12] NBCe1-A transcripts have also been detected in nasal submucosal glands in turbinate mucosa and nasal polyps.[13]

The second NBCe1 variant, NBCe1-B (or pNBC1), which is identical to NBCe1-A except for its unique N-terminus (85 aa replacing the 41 aa in NBCe1-A) was originally cloned from pancreas and is expressed in pancreatic duct epithelial cells where it contributes to basolateral bicarbonate flux from blood to cell, during the process of secretin-evoked pancreatic fluid secretion.[14,15] NBCe1-B is also widely expressed in various other tissues including, colon, skeletal muscle, eye, airway submucosal glands, heart, gall bladder, and nasal mucosa.[10,11,14,16–19] The third variant, NBCe1-C, has a unique C terminus (61 aa replaces 46 in NBCe1-A or B) that ends in a type I PDZ-binding motif.[4] The N-termini of NBCe1-B and NBCe1-C are identical and unlike the N-terminus of NBCe1-A, interact with the IP3 receptor binding protein IRBIT resulting in a stimulation of transport activity.[20,21] More recently additional transcript have been reported.[21A]

Topological and Structural Properties

Of the NBCe1 variants, the structural topology of NBCe1-A has been most thoroughly studied and provides a topologic framework for other Na^+-driven SLC4 bicarbonate transporters (Fig. 53.3). NBCe1-A is an oligomer wherein the predominant oligomeric state of the cotransporter is dimeric.[22] The NBCe1-A monomer is a ~140-kDa glycoprotein containing 1035 amino

TABLE 53.4 Phenotype with Altered SLC4 Function

Transporter	Human	Mouse
NBCe1	pRTA	pRTA
	band keratopathy	intestine obstruction
	glaucoma, cataracts	spleen abnormalities
	intracerebral calcification	enamel defect
	enamel defect	
	↑ amylase, ↑ lipase	
NBCe2	hypertension	hyperchloremic metabolic acidosis
		hyporeninemic hypoaldosteronism
		hypertension
NBCn1		Usher 2B- like syndrome
NDCBE		↓ CCD electroneutral NaCl transport
NCBE/ NBCn2	↑ seizure propensity	↓ cerebral ventricle size
		↓seizure threshold
NaBC1	CHED2; Harboyan Syndrome; FECD	CHED2 – like
		↓ urine osmolarity
		↑urine volume
		↑excretion of Na^+, K^+, Cl^-, Mg^{2+}
		↓ urinary [Ca^{2+}]
AE4		no phenotype

acids and is composed of 14 transmembrane regions (TMs).[2,22] The N-terminal transmembrane region has 8 TMs homologous to the SLC4 transporter AE1.[2] Both the extreme N- and C-termini of NBCe1-A are located in cytoplasm, with a large extracellular loop between transmembrane segment (TM) 5 and 6 containing two glycosylation sites.[2,23] Importantly, although NBCe1-A forms a structural oligomer, each monomeric subunit maintains its own independent transport activity.[22]

Previous topological models of NBCe1 were based on the assumption that the cotransporter resembles AE1 which has been extensively studied structurally.[24] The C-terminal transmembrane region of the two transporters share 40% sequence homology but differ structurally. NBCe1-A lacks the two AE1 reentrant loops and extensive substituted cysteine scanning mutagenesis analysis showed that the C-terminal transmembrane region of NBCe1-A is tightly folded unlike AE1 resembling in various aspects the bacterial Na^+-leucine cotransporter, LeuT.[2]

An extensive mutatgenesis study of NBCe1-A has demonstrated several key residues that are critical for its function.[25] Domain swapping studies of the cotransporter have also shed light on its functional properties and have suggested the electrogenicity of NBCe1-A is determined by the interaction of TMs in the lipid bilayer.[24] Arg^{298} in the N-terminus may be involved in constructing a "HCO_3^- tunnel".[26] Residue Thr^{442} in TM 1 is thought to form an external gate for the transported ions.[27] Proposed TM8 has several residues found to be involved in forming the ion translocation pore.[28] Interestingly, substitution of Asp^{555} to glutamic acid in the proposed TM 5 of NBCe1-A induced an outward rectifying Cl^- current and altered the transport substrate selectivity, indicating it plays an important role in HCO_3^- selectivity.[29]

Inhibitors

Asp^{555} is in close proximity of the proposed 4,4′-diisothiocyanatostilbene-2,2′-disulfonate DIDS (a functional inhibitor) binding site of NBCe1-A (Lys^{559}).[29] From the extracellular side, DIDS blocks NBCe1 reversibly by binding to a KKMIK motif at the putative extracellular end of TM5.[30] The apparent affinity of the interaction decreases at more negative voltages possibly due to alterations in the conformation of the cotransporter as the membrane voltage changes.[30,31] DIDS is also capable of blocking the cotransporter from the intracellular side at an unknown site.[32] In addition to DIDS, NBCe1-A is also blocked by the nonsteroidal inflammatory agent Tenidap from the extracellular or intracellular side.[32] NBCe1-B is sensitive to the anion channel inhibitors phloretin, niflumic acid, NPPB, and glybenclamide.[31] NBCe1 is inhibited by the N-cyanosulphonamide compound S0859 however the inhibition is not specific.[33] Benzamil has also been reported to inhibit NBCe1-A.[32]

Familial Proximal Renal Tubular Acidosis: Molecular Mechanisms Involving NBCe1

Patients with autosomal recessive mutations in NBCe1 have an unique phenotype that can be diagnosed clinically that includes severe hyperchloremic acidosis, with extra-renal manifestations including growth and mental retardation, basal ganglia calcification, cataracts, corneal opacities (band keratopathy), glaucoma, elevated serum amylase and lipase, and defects in the enamel consistent with amelogenesis imperfecta.[2,34–43] Regarding the renal phenotype, this "experiment of nature" demonstrates the importance of NBCe1-A in mediating proximal tubule bicarbonate reclamation; the extrarenal manifestations demonstrate the importance of NBCe1- variants in eye (NBCe1-A, NBCe1-B;[10,11]), brain (NBCe1-B, NBCe1-C;[44]), and tooth ameloblasts (NBCe1-B;[45,46]). Thus far,

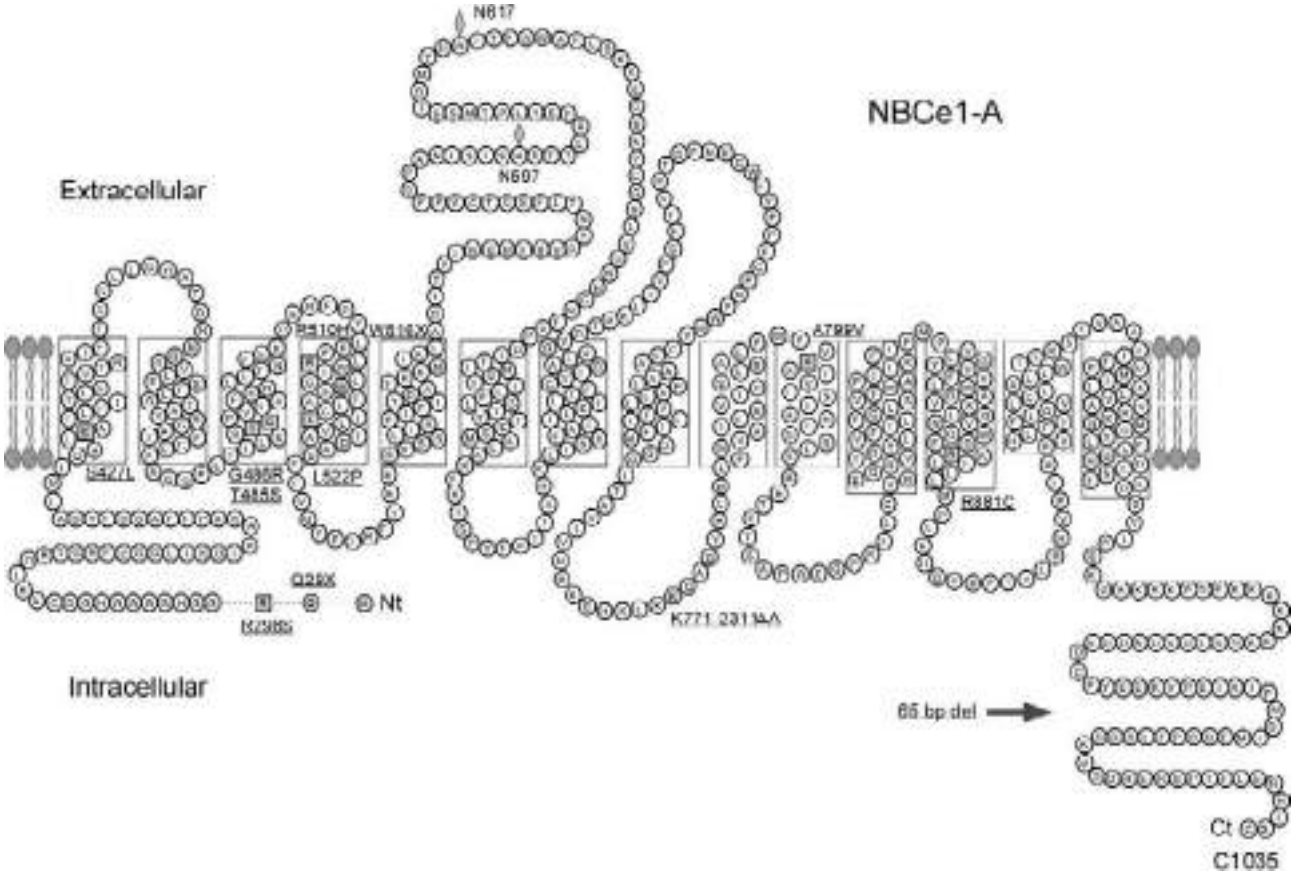

FIGURE 53.3 Topology of NBCe1-A. The transporter has 14 TMs with cytoplasmic N- and C-termini. The location of the known pRTA mutations is depicted. A large extracellular loop between TM5 and 6 typifies the Na^+-driven SLC4 bicarbonate transporters. Note that NBCe1-A lacks the two AE1 (SLC4A1) re-entrant loops.

the following mutants have been described: eight missense mutations (R298S, S427L, T485S, G486R, R510H, L522P, A799V, and R881C), 2 nonsense mutations (Q29X, W516X), a frameshift deletion at nucleotide 2311A, and a C-terminal 65 base-pair deletion from exon 23 to intron 23 predicted to truncate the intracytoplasmic C-terminus (Fig. 53.3, Table 53.5). Other than the NBCe1-A-Q29X mutation which only affects NBCe1-A, the NBCe1-B and -C variants are also mutated resulting in the extrarenal manifestations in this disorder.

The disease causing mechanism of the nonsense/frameshift mutations is due to absence of the full-length NBCe1 protein, whereas the missense mutations result from either reduced transport function and/or impaired plasma membrane processing (R510H, L522P, and R881C; (53, 114, 122)). The functional and targeting defects caused by NBCe1-A pRTA missense mutations have been analyzed in Xenopus oocyte, ECV304 cells, Madin-Darby canine kidney cells, and HEK293 cells with sometimes differing results. In general, mutant membrane transporter proteins are thought to have reduced function as a result of three possible mechanisms that are not mutually exclusive: (1) misfolding of the transporter protein resulting in ER retention; (2) alteration of the ion translocation (permeation) pathway; and (3) impairment of the transporter conformation (static/dynamic) required for substrate translocation.[2]

Missense Mutations

Recent studies have focused on the topologic/structural/functional implications of the residues in NBCe1 that are mutated in pRTA[2]; (Table 53.5). Arg^{298} is located in the cytoplasmic N-terminus of NBCe1-A and resides in a tightly folded aqueous inaccessible conformation based on: (1) homology modeling to the crystallized cytoplasmic domain structure of AE1 and (2) biotin maleimide labeling assays. It has been suggested that Arg^{298} may be involved in constructing a "HCO_3^- tunnel" in NBCe1-A and that mutation R298S disrupts the local structure of the ion permeation pathway thereby impairing the HCO_3^- entry.[2,26] The remaining missence pRTA residues

TABLE 53.5 SLC4A4 Mutations: Molecular Mechanisms

Mutation	Location	Effect	Mechanism
Q29X*	N-terminus	truncation	—
R298S	N-terminus	↓ function	ion permeation pathway
S427L	TM1	↓ function	voltage sensing
T485S	TM3	↓ function	protein conformation
G486R	TM3	↓ function	protein conformation
R510H	TM4	misfolding	ER retention
W516X	TM4	truncation	—
L522P	TM4	misfolding	ER retention
2311delA	IL4	truncation	—
A799V	TM10	↓ function	protein conformation
R881C	TM12	misfolding	ER retention
65bp-del	C-terminus	truncation	—

NBCe1-A only
TM Transmembrane
IL Intracellular Loop

have recently been localized in the transporter (Fig. 53.3): Ser^{427} to TM 1, Thr^{485}, Gly^{486} to TM 3, Arg^{510} and Leu^{522} to TM 4, Ala^{799} to TM 10, and Arg^{881} to TM 12.[2]

All pRTA residues do not appear to line an ion translocation pore and are likely located in the protein/lipid bilayer complex. Considering the structural change or charge alteration for most of the missense mutations involved in pRTA, it is conceivable that these TM residing mutations would affect protein folding/helix packing in the lipid bilayer, which could lead to significant loss of mutant protein transport function. However, other than R510H, L522P, and R881C, which cause protein intracellular retention, the remaining pRTA causing mutations (S427L, T485S, G486R, and A799V) process to the plasma membrane and retain 10–50% transport function. These findings essentially rule out the possibility that the reduced transport function of the membrane-processed pRTA causing mutations is caused by dramatic protein misfolding.

Mutation of Ser^{427} to leucine induces a failure of the transporter to reverse its direction even at very negative membrane potentials.[35] In addition, the transport is 10% of wild-type NBCe1-A.[35] Ser^{427} has been proposed to be involved in helix interaction and leucine mutation may disrupt NBCe1-A "voltage sensing," affect a Na^+ coordination site, or alter the local conformation required for normal function. Ser^{427} is located in TM 1 adjacent to Ala^{428}, a residue that lines the substrate translocation pore.[27] The bulky side chain of leucine may alter the geometry of the ion translocation pore and impair transport.

The T485S mutation[36] is of interest because of the following considerations: (1) Serine and threonine both belong to the same amino acid category (nucleophilic) and have the same pK_a; (2) structurally, serine closely resembles threonine, but lacks a $-CH_3$ group; (3) mutation of Thr^{485} to serine/cysteine impairs NBCe1-A function by 50%. These observations suggest that the $-CH_3$ group of threonine at position 485 may have a unique role in maintaining the structure of NBCe1-A for normal ion translocation. Valine substitution restored NBCe1-A transport activity to 75% that of the wild-type, despite the fact that it is a hydrophobic amino acid. Moreover isoleucine substitution impaired transport function by 50% also highlighting the potential importance of the $-OH$ group at the 485 position.[2] Based on these findings, it has been proposed that Thr^{485} may reside in a space confined position involving both $-CH_3$ and $-OH$ chemistry that is critical for maintaining NBCe1-A in a conformation required for normal transport function. Indeed, when both $-CH_3$ and $-OH$ groups are removed at this particular amino acid position (alanine substitution), the transport function is decreased to 30% of the wild type.[2] This mechanism may also be applicable to the G486R mutation, which resides adjacent to $Thr.^{485}$

The L522P mutation causing pRTA is not processed to the plasma membrane in *Xenopus* oocytes, ECV 304, and Madin-Darby canine kidney cells, whereas an L522C mutant does not impair membrane processing.[2,34,43] This suggests that it is the proline residue rather than the loss of leucine that causes intracellular retention of NBCe1-A. Arg^{510} and Leu^{522} both reside in TM 4, a helix that carries signal anchor and stop transfer sequences,[23] and has several residues whose mutation cause protein intracellular retention. TM 4 in NBCe1-A may act as a scaffolding helix that is important for the second stage folding of the transporter. Therefore, it is predictable that a helix disruption mutation (L522P) would significantly misfold the transporter.

The R510H and R881C mutants are also misfolded causing ER retention.[38,47,48] Although R881C was partially expressed on the plasma membrane in the *Xenopus* oocytes and had significant transport activity it was fully retained intracellularly in Madin-Darby canine kidney cells and HEK cells.[2,36,48] Arg^{510} and Arg^{881} are localized to TM 4 and 12, respectively, and do not reside in surface or re-entrant loops as was previously thought.[49] Misfolding of NBCe1-A caused by these two mutations suggests that the arginine at positions 510 and 881 is involved in forming ionic interactions within the TMs to maintain the overall folding of the protein.

Potential Mutant–Specific Therapy in Proximal Renal Tubular Acidosis

In one of the nonsense mutations of NBCe1-A causing proximal RTA, a wt-CAG sequence encoding glutamine has been replaced by a UAG stop codon sequence resulting in premature truncation.[39] Deciphering the rules dictating read-through efficiency is of primary importance for pharmacological treatment of renal tubular acidosis resulting from mutations causing premature stop codons (PSC). Aminoglycosides offer a potential therapeutic approach to treat PSC mutations by inducing ribosomal read-through.[50,51] Aminoglycosides bind to the internal loop of helix 44 of the 16S ribosomal RNA, a region termed the decoding site.[52] In both prokaryotes and eukaryotes, aminoglycosides induce miscoding by mimicking the conformation change in 16S rRNA that would be induced by a correct codon–anticodon pair, thereby compromising the integrity of codon–anticodon proofreading during translation. As a general rule, glutamine is inserted at nonsense UAG or UAA read-through sites, whereas UGA sites miscode to tryptophan.[52]

Recent studies have shown that the NBCe1-A-Q29X mutation can be rescued *in vitro* by treatment with aminoglycoside antibiotics.[53] These findings represent the first evidence that in the presence of the NBCe1-A-Q29X mutation that causes proximal renal tubular acidosis, full-length functional NBCe1-A protein can be produced. In particular these studies offer the opportunity to treat the eye phenotype locally without systemic toxicity. Recently the aminoglycoside derivative NB54 was designed which has significantly less toxicity, with stop-codon read-through potency that is significantly greater than gentamicin likely due to the presence of the flexible N-1-AHB group (*S*)-2-hydroxy-4-aminobutyl group at the N-1 position).[54] In addition non-aminoglycoside compounds such PTC124 may prove efficacious.[55]

Additional Lessons Learned from Mice with Targeted Disruption of SLC4A4

Mice with disruption of the Slc4a4 gene (NBCe1$^{-/-}$ mice) have a more severe (and fatal) phenotype than patients.[56] In addition to severe hyperchloremic metabolic acidosis, they have severe volume depletion, hyponatremia, splenomegaly, intestinal obstructions, and die before weaning. In addition, NBCe1$^{-/-}$ mice also have abnormal dentition as do patients. Paine et al. showed that enamel producing ameloblast cells express AE2a apically and NBCe1-B basolaterally.[45,46] Based on this data, they hypothesized that ameloblasts mediate regulated transcellular bicarbonate secretion during the various phases of enamel formation. Results in NBCe1$^{-/-}$ mice demonstrated that normal enamel development in mammals requires the NBCe1-B variant.[57]

The physiologic importance of NBCe1 in mediating intestinal bicarbonate secretion is exemplified by the intestinal obstruction phenotype in NBCe1$^{-/-}$ mice.[56] NBCe1-B is widely expressed throughout the gastrointestinal tract.[14,58] In the possum ileum, the transporter is predominantly expressed in the mid region of the villi, with lower levels of expression in the crypts,[59] whereas in the murine colon its expression is higher in crypts than in surface cells.[60,61] Although NBCn1 (SLC4A7) is also thought to function as a basolateral bicarbonate uptake mechanism in the intestine,[60–63] NBCe1 is expressed at significantly higher levels than NBCn1,[19] and in addition mice with targeted disruption of SLC4A7 don't have an obvious intestinal phenotype.[64]

Gain of Function

No gain of function mutations have been thus far described.

SYSTEMIC FACTORS AFFECTING NBCe-1 FUNCTION IN THE KIDNEY

Mechanism of enhanced bicarbonate excretion in Na^+ loading. In rats NaCl and $NaHCO_3$ loading reduces the expression of NHE3 and NBCe1 in the proximal tubule potentially contributing to prevention of volume overload and metabolic alkalosis (during bicarbonate loads).[65]

Metabolic alkalosis-potassium depletion: enhanced bicarbonate reclamation: Potassium depletion results in an increase in renal bicarbonate reabsorption proximally and distally.[66–68] Amlal et al. suggested that the upregulation of NBCe1 in the proximal tubule could contribute to the maintenance of metabolic alkalosis.[69] Of note although NBCe1 is normally not expressed in the mTAL and IMCD, the authors reported an increase in the expression of NBCe1 in these nephron segments.

Sympathetic nervous system: norepinephrine: Sonalker reported that long-term (15 days) infusions of noradrenaline (600 ng/min) in rats led to an ~2.5 fold increase in the expression of NBCe1 on Western blotting of rat cortex.[70] The underlying mechanism was not characterized but may have relevance to proximal tubule handling of sodium during alterations in sympathetic outflow to the kidney.

Dopamine: Dopamine decreased the activity of NBCe1 in rabbit and rat proximal tubules but not in spontaneously hypertensive SHR rats.[71] Interestingly, dopamine inhibited the activity of NBCe1 when the cotransporter operated with the 3 HCO_3^-:1 Na^+

stoichiometry.[71] In SHR a defect of DA1 receptor signaling could contribute to the development of hypertension.

PTH: Functional activity of NBCe1 is decreased by PTH in rat tubules *in vivo*.[72] In rabbit tubules perfused *in vivo* under normal conditions, PTH has no effect.[73] In rat tubules pre-incubated in DMEM (Delbecco's modified Eagles medium) + norepinephrine, PTH inhibits the cotransporter possibly via a cAMP dependent mechanism.[71]

Hypertension: In the SHR rat with spontaneous hypertension, Sonalker reported that NBCe1 protein expression was increased ~2 fold in comparison to control WKY rats.[74] However in a separate study, in immortalized proximal tubule SHR cells, NBCe1 activity was reported to be less than normal.[75]

Renal transplant rejection: In a rat model of acute renal transplant rejection, Velic reported down-regulation of NHE-3 but up-regulation of NBCe1-A.[76] These findings may account for changes in proximal tubule bicarbonate transport following renal transplantation.

FK506: The calcineurin inhibitor FK506 has been reported to cause pRTA.[77] Chronic metabolic acidosis per se has no effect on NBCe1-A expression in the kidney.[78] In rats FK506 administration was found to decrease the protein abundance of NBCe1-A in the cortex without a change in acid−base status.

Lithium Toxicity: Chronic lithium toxicity is associated with histologic changes in the kidney and distal renal tubular acidosis.[79] In rats, lithium administration leads to an increase in NBCe1 expression perhaps as a compensatory mechanism.[80]

Ureteral Obstruction: Chronic ureteral obstruction is associated with chronic renal failure and a hyperkalemic distal renal tubular acidosis.[81] In neonatal rats chronic ureteral obstruction resulted in a significant decrease in NBCe1-A expression in the proximal tubule.[82]

Extrarenal Tissues: Role of NBCe-1-B/C in Various Organs and Selective Disease States

Cardiac physiology, ischemia, and reperfusion injury: Several studies have discussed the importance of electrogenic NBC transport in ventricular electrophysiology and function. The data in the literature is sometimes difficult to interpret because NBCe1, NBCe2, and NBCn1 are expressed in the heart and the molecular basis for a given functional effect is not often clearly established. Villa-Abrille showed electrogenic $Na^+ - HCO_3^-$ cotransport modulates resting membrane potential and action potential duration in cat ventricular myocytes.[83] Yamamoto et al. emphasized the functional diversity of electrogenic NBC activity in various species.[84] Schafer et al. demonstrated that following reoxygenation of rat myocytes initially exposed to anoxia, sodium bicarbonate cotransport is responsible for ~50% of the pH_i recovery.[85] DIDS (an NBCe1 and NBCe2 inhibitor) blocked calcium oscillations that cause hypercontracture of the cells.[85] Khandouri et al. have reported an increase in NBCe1-B in myocardium from humans with heart failure.[86] In addition, NBCe1 mRNA and protein was reported to be increased in the rat heart following myocardial infarction.[87] An antibody against NBCe1 significantly improved the post-ischaemic cardiac function.[86] Verdonck hypothesized that the NBCe1-B transporter might contribute to the incidence of arrhythmias in heart failure.[88]

Cystic Fibrosis: NBCe1-B is expressed on the basolateral membrane of pancreatic duct cells in humans.[89,90] In cystic fibrosis pancreatic bicarbonate secretion is decreased and it has been hypothesized that an alteration in basolateral membrane voltage (resulting from defective CFTR transport), impairs NBCe1-B basolateral bicarbonate uptake.[91] IRBIT has been recently shown to be a key coordinator of epithelial fluid and HCO_3^- secretion in murine intralobular pancreatic ducts via independent activation of NBCe1-B and CFTR.[20,21] Interestingly, NBCe1 knockout mice and patients with NBCe1 loss of function mutations do not have a cystic fibrosis phenotype although evidence for pancreatic involvement (elevated amylase or lipase) has been reported in patients.[38,42,56]

Duodenal ulcers: NBCe1-B is expressed in the duodenum, and contributes to transepithelial HCO_3 secretion and potential duodenal cell pHi regulation.[63] Duodenal bicarbonate secretion is thought to protect the duodenal mucosa from acid-related injury.[92] However patients with cystic fibrosis, who have impaired duodenal bicarbonate secretion, paradoxically don't develop duodenal ulcers.[93] Studies in rats support the role of intracellular bicarbonate in the protection of duodenal epithelial cells from ulcer formation.[94]

CNS. Upregulation of NBCe1 (NBCe1-B/C) mediated HCO_3 transport in specific neurons of the brain may prevent excessive extracellular acidosis and inhibit neuronal activity as part of a negative feedback mechanism.[95,96] In seizure-prone gerbils, at 30 minutes postictally, NBCe1 immunoreactivity is substantially elevated in the hippocampus (CA1-, -2, and -3 regions).[97] By three hours, elevated NBCe1 staining is also detectable in the dentate gyrus (and the granule layer).[97]

Molecular Regulation of NBCe1 Function and Membrane Expression

Cytosolic N- and C-terminus: Truncation mutant studies of heterologously expressed NBCe1 variants in

oocytes have shown that unique amino terminus of NBCe1-A stimulates transporter activity (autostimulatory domain (ASD)), whereas the unique amino terminus of the B and C variants inhibits activity.[98] The N-terminus in NBCe1-B and NBCe1-C has accordingly been termed an autoinhibitory domain (AID). The mechanism involved is currently unknown but likely involves interaction(s) between the specific amino terminus and the transport pathway and/or binding to cytosolic factors. In contrast, the carboxy termini affect the plasma membrane expression without affecting cotransporter function.[36,47,98]

In mammalian cells however, Espiru et al. reported that truncation of the N- or C- termini failed to prevent targeting to the plasma membrane (HEK293 cells) or to the basolateral membrane of OK cells.[99] These results differ from Li et al. who showed mistargeting of the C-terminal mutant to the apical membrane with residual basolateral expression in MDCK cells[100] and identified a QQPFLS carboxyl-terminal motif as a basolateral targeting sequence. Horita et al. reported that C-terminal truncation resulted in intracellular NBCe1 localization.[36] Length of truncation, duration of heterologous expression, and cell type may account for these differences. Moreover single point mutation analysis may provide a more informative approach to deciphering the residues that are required for proper folding of the transporter and escape from the ER.[25]

PKA-dependent phosphorylation: Given the prevailing Na^+, HCO_3^- and basolateral membrance voltage in proximal tubule cells, the Nerst equation predicts that for NBCe1-A to mediate the flux of sodium bicarbonate from cell to blood, the ion transport stoichiometry of NBCe1-A is 1 Na^+:3 HCO_3^-.[101–103] Interestingly, the ratio is 1:2 in certain heterologous expression systems such as HEK293 cells and oocytes.[32,104–106] Studies in a mouse proximal and distal tubule cells lines have reported that the stoichiometry of both NBCe1-A and NBCe1-B is cell-type dependent and variable suggesting that unknown cytosolic factors in the proximal tubule interact with NBCe1-A (and NBCe1-B) and modulate the stoichiometry.[107,108] In a proximal tubule cell line, the shift in NBCe1-A stoichiometry from 1:3 to 1:2 is mediated by protein kinase A-dependent phosphorylation of Ser^{982}.[108] Thr^{49} in the unique amino-terminus of NBCe1-B was found to play an important role in modulating the cAMP-induced increase in cotransporter current without altering its stoichiometry.[109] Accordingly, cAMP has also been found to increase intestinal NBCe1-B mediated transport in part via a change in membrane expression.[19,61]

PKC-dependent phosphorylation: ANG II has a biphasic effect on NBCe1 transport in both oocytes and renal proximal tubule cells.[110–114] Studies in oocytes have reported that the ANG II-induced inhibition of NBCe1-A is mediated by the Ca^{2+}-insensitive PKCε isoform that increases its association with NBCe1-A in the membrane, and AII-induced Ca^{2+} mobilization may trigger decreased NBCe1-A surface expression via the AT_{1B} receptor.[113,115] In addition to affecting cell membrane expression, intracellular calcium modulates the stoichiometry of the cotransporter. Specifically, in oocytes expressing NBCe1-A it has been reported that an increase in cytosolic Ca^{2+} shifts the transport stoichiometry from 1:2 to 1:3, possibly via a phosphorylation (PKC) event.[32] Data in a rat parotid cell line suggest that NBCe1-A and NBCe1-B participate in constitutive and stimulated (carbachol) endocytosis regulated by conventional PKCs (PKCαβγ) and by a novel PKCδ.[116] This data may only have relevance in secretory epithelia involving NBCe1-B transport such as salivary duct, ileum, and colon.[19,59,116]

Phosphatidylinositol 4,5-bisphosphate (PIP_2): PIP_2 is noteworthy because in addition to its role as a precursor of the Ca^{2+}-mobilizing inositol triphosphate (IP_3) and the kinase-activating diacylglycerol (DAG), PIP_2 can regulate solute movement.[117] NBCe1 and other members of the SLC4 family have a stretch of C-terminal lysines that may interact electrostically with PIP_2. In voltage-clamped oocytes heterologously expressing NBCe1 (-A, -B, and -C) variants, PIP_2 increased both the B and C variant currents.[118] It has been hypothesized that the NBCe1-A may not respond to exogenous PIP_2 because it may have a higher affinity for endogenous PIP_2 compared to the B and C variants or that a putative autoinhibitory domain in the B and C variants might be masked by PIP_2.[118]

Intracellular Mg^{2+}: When heterologously expressed in oocytes, a phenomenon of NBCe1-A-rundown occurs.[118] The majority of NBCe1-A rundown is likely due to Mg^{2+}-dependent phosphatase (5′-lipid phosphatase) activity because the rundown is largely inhibited by removing bath Mg^{2+}, both in the presence or absence of vanadate and F^-.[118] It has been suggested that the 5′-lipid phosphatase dephosphorylates PIP_2 to PIP.[118] While removing bath Mg^{2+} inhibits NBCe1-A rundown, raising bath Mg^{2+} appears to inhibit NBCe1-A directly.[118] Yamaguchi and Ishikawa reported that intracellular Mg^{2+} inhibits NBCe1-B expressed in mammalian HEK 293 and NIH3T3 cells.[31,119] An N-terminal deletion mutant was less sensitive to Mg^{2+} compared to wild-type NBCe1-B, consistent with the view that the inhibition may be associated, directly or indirectly, with the N-terminal region. Inhibition of NBCe1-mediated transport via an increase in cytosolic Mg^{2+} during ischemia may reduce post-ischemic dysfunction in kidney (NBCe1-A) and heart (NBCe1-B) possibly by keeping the intracellular Na^+

concentration lower and thereby preventing Ca^{2+} overload.

IRBIT: The NBC1-B variant is activated by IRBIT whereas the NBCe1-A is not.[20] IRBIT binds to the N-terminal 1−42 residues of NBCe1-B that are not present in NBCe1-A. Phosphorylation of the PEST (Pro-Glu-Ser-Thr) domain is required for IRBIT binding and activation.[20,120,121] Regulation of NBCe1-B by IRBIT suggests that IRBIT may regulate fluid and HCO_3^- secretion in secretory tissues such as the pancreatic duct.[21]

ATP: In oocytes expressing NBCe1-A, when ATP is applied to the intracellular surface of oocyte membrane patches with low transport activity, the cotransporter current increased.[32] This activation is not due to active ATP-driven transport. The non-hydrolysable ATP analog AMP-PNP does not mimic the effect of ATP.[32] It has been hypothesized that ATP may phosphorylate NBCe1-A by means of an unidentified protein kinase.

Carbonic anhydrase II (CAII): It has been proposed the CAII interacts with an NBCe1 C-terminal a $D^{986}NDD^{989}$ motif forming a transport metabolon that transfers bicarbonate intra-molecularly between the two proteins.[122−124] This hypothesis is of interest given the known expression of CAII in the cytosol of proximal tubule cells.[125] In addition, direct interaction between NBCe1 and membrane bound CAIV has been reported.[126] The data in the literature is both in favor and against the existence of a "transport metabolon;" in part due to difference in techniques employed and the sensitivity/specificity of the measurements utilized.[122,124,127−129] Recently, the question was readdressed using the substituted cysteine accessibility method which showed that the C-terminal tails of the NBCe1-A dimer are highly structured and may sterically prevent CA II binding.[130] Against the quantitative importance of a transport metabolon with CAII is an experiment of nature wherein patients and mice with loss of proximal tubule CAII function do not have as severe proximal renal tubular acidosis as might be predicted; or in comparison to patients with NBCe1 mutations.[131,132] Moreover, neither an alteration in either renal bicarbonate handling or hypobicarbonatemia has thus far been reported in patients or mice with loss of CA IV function.[133−135]

NBCe2: (SLC4A5 Gene)

Structural Variants and Tissue Distribution

NBCe2 (or NBC4) is an electrogenic sodium bicarbonate cotransporter encoded by SLC4A5.[136−139] Interestingly, NBCe2 and $p150^{Glued}$ were originally reported to be encoded by the same locus, DCTN1-SLC4A5, that spans ~230 kilobases on chromosome 2p13 and contains 66 exons.[140] $p150^{Glued}$ is a component of the dynactin heteromultimeric complex of proteins which is required for dynein-mediated vesicle and organelle transport by microtubules.[141] In eukaryotes, it is rare for a single gene to encode two functionally unrelated proteins. More recent studies suggest that SLC4A5 has its own promoter.[142] Six variants have been reported; 4 that are valid splice variants from full-length transcripts (NBCe2-A, -B, -C, and -D;[136,137]) and 2 additional variants[143] that are invalid given they are not found in the SLC4A5 genomic sequence. The most widely expressed variant is NBCe2-C (also called NBC4-C) consists of 1121 aa and is ~145 kDa.[144]

NBCe2 transcripts are expressed in several tissues including brain (human cerebellum, cerebrum, hippocampus, and choroid plexus), heart, kidney, testis, pancreas, muscle, and peripheral blood leukocytes.[58,136,137] At the protein level, NBCe2 has been immunolocalized to the apical membrane of uroepithelial cells and unspecified collecting duct cells in rats.[58,144] In humans, NBCe2 is expressed on the apical membrane of a subset of collecting duct cells in the renal outer medulla.[58] In extra-renal tissues the transporter is expressed in the basolateral membrane of hepatocytes,[144] the apical membranes of cholangiocytes,[143] apical membrane of rat choroid plexus epithelial cells[145] (not detectable in human choroid plexus[58,146]), skeletal muscle,[17] and the basolateral membrane of polarized Calu-cells[16] (suggesting the transporter might be expressed in airway submucosal glands).

Functional Properties

When expressed in mammalian cells NBCe2-C elicits, a Na^+-driven, DIDS-sensitive- bicarbonate flux in the absence of chloride.[138] Similar findings were subsequently reported in oocytes expressing the transporter.[139] NBCe2-C is electrogenic and mediates a hyperpolarization when cells are exposed to bicarbonate and a depolarization when Na^+ is removed. These responses are analogous to those induced by NBCe1. Like NBCe1, NBCe2 appears to function with a Na^+:HCO_3^- stoichiometry of 1:2[139] or 1:3.[138] In mouse choroid plexus epithelial cells, Millar et al. measured a small DIDS-sensitive, Na^+-dependent, HCO_3^--induced outward current.[147] Based on the reversal potential obtained from I-V plots, and the known localization of NBCe2 to the apical membrane of choroid epithelial cells, it was concluded the measured function was mediated by NBCe2 functioning with a 1:3 Na^+:HCO_3^- stoichiometry. Given that the membrane potential of the choroid plexus epithelial cells is −35 mV to −60 mV, NBCe2 would mediate bicarbonate secretion. In a study addressing the potential importance in apical choroid plexus bicarbonate transport, in a mouse model where basolateral bicarbonate influx mediated

by NCBE/NBCn2 (see below) was disrupted, apical NHE activity but not NBCe2 was up-regulated.[148] Moreover, DIDS-sensitive HCO_3^- recovery (presumably assaying NBCe2) in these mice did not function in an inward transport mode. Thus far in native kidney tubules, there are no studies which have addressed the functional contribution of NBCe2 to either transcellular bicarbonate transport and/or intracellular pH regulation.

Hypertension

The Family Blood Pressure Program in 2002 found an association between the *SLC4A5* gene and hypertension.[149] In African Americans 5 SNPs in the *SLC4A5* gene showed significant association with pulse pressure. In Utah pedigrees, at baseline and after a 10-year follow-up period, the association of *SLC4A5* polymorphisms and hypertension was subsequently reported.[150] A meta-analysis of three studies (HyperGEN, HERITAGE, and Family Study and Genetics of Hypertension in Blacks) was done to determine LOD scores for systolic and diastolic blood pressure in African-American and Nigerian families, and linkage evidence showed an association with 2p14–p13.1 where *SLC4A5* is located.[151] In another meta-analysis, the region flanking the *SLC4A5* locus (2p12–q22) was also suggested to be important in whites for blood pressure variation. Finally, *SLC4A5* has been proposed as a promising candidate gene for variations in the blood pressure response to drugs that inhibit the renin-angiotensin system.[152] In a recent analysis, the observed association with resting and submaximal-exercise cardiovascular and metabolic traits in the HERITAGE Family Study were not found to be due variation in the promoter or coding SNPs of the *SLC4A5* gene.[142] Further studies are therefore required to clarify the role of NBCe2 in human hypertension.

Targeted Disruption in the Mouse

Targeted disruption of the Slc4a5 gene results in significant abnormalities in intracerebral ventricle volume, intracranial pressure, and CSF electrolyte levels.[153] In the retina, there is loss of photoreceptors, ganglion cells, and retinal detachment. In a separate study, mice with loss of NBCe2 were shown to have increased blood pressure, a compensated metabolic acidosis and hyporeninemic hypoaldosteronism, elevated fluid intake and urine excretion and an increased glomerular filtration rate.[154] It was suggested that the loss of sodium bicarbonate reabsorption by SLC4A5 initiates compensatory bicarbonate reabsorption via other sodium-bicarbonate transporters.

SODIUM BICARBONATE COTRANSPORTERS (ELECTRONEUTRAL)

NBCn1 (SLC4A7 Gene)

Structural Variants

Pushkin et al. characterized NBC3 (encoded by the SLC4A7 gene), the first electroneutral stilbene-insensitive sodium bicarbonate cotransporter,[155,156] which was subsequently renamed NBCn1.[157] Eight different protein variants (rat and/or human) generated by the SLC4A7 gene have been documented from as many as 16 protein variants that are predicted based on alternative promoter usage and/or splicing.[155,158–159] The documented variants are named NBCn1-(A-H).[158] The first variant characterized from human skeletal muscle cDNA, NBCn1-A (originally NBC3), has 1214 aa and is ~180–200 kDa.[155,160,161] NBCn1 variants have been sub-categorized based on motifs or "cassettes" that they contain. For example, NBCn1-A has an N-terminus that begins with the peptide sequence MERF and contains cassettes I (13 aa) and II (124 aa in human; 123 aa in rat) but lacks a C-terminal cassette III (36 aa). Certain cassettes are homologous to sequences in other Na^+-driven bicarbonate transporters (cassettes I and III), whereas cassette II is unique to NBCn1. Differences in stilbene sensitivity have not been systematically addressed in each of the variants.

Recently, Yang et al. demonstrated the effect of a specific NBCn1 cassette on its function and expression.[162] In NBCn1-A, B, C, and D, cassette II (derived from exon 7 in the SLC4A7 gene) contains multiple putative phosphorylation sites and comprises 20% of the cytoplasmic amino terminus. This cassette has been a focus of attention because it is unique among the SLC4 family in being present only in NBCn1. Transcripts from skeletal muscle,[155] cardiac (apex, atrium and atrioventricular nodes) tissues[163] and embryonic hippocampus neurons[159] express this cassette. Cassette II has been shown to regulate the function and expression of the cotransporter, and may have auto-inhibitory functional activity analogous to the N-terminus of NBCe1-B, -C.[162]

Expression Pattern

Several facts should be considered regarding the expression of NBCn1 variants: (1) Although NBCn1 is expressed in various tissues (transcript and/or protein level) including choroid plexus epithelia, hippocampus, vascular smooth muscle, heart, duodenum, colon, aorta, liver, pancreas, skeletal muscle, spleen, oteoclasts, salivary gland and kidney, the localization of each protein variant in these tissues and in the kidney,[58,62,155,157,161,163–168] has not been

systematically addressed because variant specific antibodies are unavailable. (2) Published findings of the expression of NBCn1 in the kidney are not in uniform agreement potentially due to technical issues, epitope differences being detected, protein-protein interactions *in vivo*, species heterogeneity, and the presence of multiple NBCn1 variants.[78,160–162,167–169] Similarly, differences in NBCn1 choroid plexus expression between species and among mouse strains has been documented.[170]

Despite these complexities, it is currently agreed that the cotransporter is localized to the basolateral membrane of the mTAL in humans and rats.[58,78,161,167,168] In rats but not humans, NBCn1 is expressed on the basolateral membrane of α intercalated cells in the outer medulla.[168] In the rat, inner medullary collecting duct IMCD2 and IMCD3 cells express the cotransporter on the basolateral membrane.[168] Expression of NBCn1 transcripts have also been found by β-galactosidase staining of transgenic mice with a LacZ insertion into the *SLC4A7* gene.[62] This study showed that the cotransporter is located in additional cells types in the mouse kidney including afferent arterioles, glomeruli, arcuate arteries, uroepithelial cells, and urinary bladder.[58,62]

Interaction with PDZ Binding Proteins

Pushkin et al. first showed C-terminal PDZ interacting domain of NBCn1-A (NBC3) can bind to the PDZ-binding protein NHERF-1.[171] Similarly in the eye and inner ear, NBCn1 is organized via PDZ interactions into a supermolecular network of proteins that are mutated in patients with various forms of USHER syndrome;[171A] the most common cause of combined blindness and deafness in humans. NBCn1 per se has not thus far been found to be mutated in this syndrome.

Systemic Factors Affecting NBCn1 Expression in Kidney and Extrarenal Organs

Chronic metabolic acidosis: It has been suggested that countercurrent transfer of NH_4^+ from the medullary thick ascending limb (mTAL) to the outer medullary collecting duct may be modulated by basolateral NBCn1 transport in the mTAL.[167] In keeping with this hypothesis, mTAL NBCn1 expression is upregulated in chronic metabolic acidosis when transepithelial NH_4^+ transport is increased.[167] In cultured mTAL cells, ^{14}C-MA uptake is increased suggesting that acidic conditions increase NBCn1 mediated transport.[172] The upregulation may provide a constant supply of HCO_3^- to the cell and enhance NH_4^+/NH_3 uptake by buffering intracellular H^+ loads. Upregulation of NBCn1 during acidosis is not unique to the kidney and has been demonstrated in neurons where it is associated with glutamate excitotoxicity.[173]

Chronic respiratory acidosis: Studies in mice have shown a developmental and tissue specific effect of chronic respiratory acidosis on NBCn1 expression.[174] The effect of hypercapnia on kidney NBCn1 expression was detected in P2 mice but not neonates or adults. Which cell type in the kidney was involved in the increased expression of NBCn1 was not studied.

K^+depletion: In rats with K^+ depletion, outer medullary collecting duct NBCn1 expression is increased.[175] As in chronic metabolic acidosis, upregulation of the cotansporter may play a role in enhancing countercurrent transfer of NH_4^+ from the mTAL to the outer medullary collecting duct.

Lithium toxicity: Chronic lithium administration induces histologic changes in the kidney associated with dRTA and nephrogenic diabetes insipidus.[79] In rats, lithium administration increased the protein expression of NBCn1 in the inner stripe of the outer medulla ~250%. Presumably, this was due to increased expression on the basolateral membrane of α intercalated cells in the inner stripe of the outer medulla.[168] The relevance to human disease is unclear given that NBCn1 has not been immunolocalized to these cells.[58]

Ureteral Obstruction: Congenital ureteral obstruction is associated with chronic renal failure and a urinary acidification defect.[81] In a neonatal rat model of ureteral obstruction, down-regulation of NBCn1 in medullary thick ascending limbs and outer medullary collecting duct α intercalated cells was detected.[82]

FK506: The calcineurin inhibitor has been shown to decrease the protein abundance of NBCn1 in the rat medulla.[176]

PTH induced hypercalcemia and metabolic alkalosis: Chronic hyperparathyroidism is accompanied by hypercalcemia and mild metabolic alkalosis.[177] Chronic PTH administration in rats led to a decreased expression of NBCn1 in medullary thick ascending limbs and IMCD2 cells in the inner medullary collecting duct.

Hypoxia: In the brain, chronic hypoxia leads to a decreased expression of NBCn1 that is out of proportion to the decrease in brain protein levels.[178] It has been suggested that this effect may reduce energy consumption. Whether this effect is more widespread and a similar decrease in expression of the cotransporter occurs in renal ischemia remains to be determined.

CSF-1-mediated osteoclast survival: NBCn1 is expressed (transcripts and protein) in osteclasts and is thought to play a role in cell survival. The ability of CSF-1 to prolong osteoclast survival requires functional NBCn1.[4]

Functional Properties, Na^+ Current, and Unique Inhibitor Profile

All NBCn1 variants that have been studied thus far have a 1:1 Na^+:HCO_3^- transport stoichiometry and are electroneutral.[155,157,159] In contrast to other members of the SLC4 family, bicarbonate flux mediated by NBCn1 variants are essentially stilbene-insensitive.[155,157,179] Pushkin et al.[155] first suggested that this is due to the replacement of the highly conserved lysine in the conserved putative stilbene-binding motif (K(M/L)XK) by aspartic acid; corresponding to Lys^{542} in human AE1. This may block negatively charged stilbene disulfonates from binding to the transporter. Currently there are no known specific inhibitors of the cotransporter.

NBCn1 produces a steady state ionic current[157,159] that is in part mediated by Na^+, thermodynamically uncoupled to HCO_3^-, and stimulated by stilbenes. The current is not inhibited by amiloride, tetrodotoxin, ouabain, furosemide, or niflumic acid[159] and is possibly generated from the C-terminal transmembrane region of the cotransporter.[24] Using the current to assess the function of the NBCn1-B and D (without casette II) variants, it has been suggested that cassette II may act as an autoinhibitory domain.[162] NBCn1 is inhibited by the N-cyanosulphonamide compound S0859 nonspecifically.[33,180] Whether Tenidap also nonspecifically inhibits the transporter is unknown.

Function in the Kidney

mTAL Transport

Isolated perfused medullary thick ascending limbs have a stilbene-insensitive basolateral sodium driven bicarbonate transport process (electrogenicity has not been studied) thought to be mediated by NBCn1.[167] The expression of NBCn1 and basolateral sodium-driven bicarbonate transport are both increased in chronic metabolic acidosis.[167,172] It has been suggested that NBCn1 mediates basolateral bicarbonate influx to prevent intracellular acidification resulting from apical NH_4^+ influx via NKCC2 coupled to basolateral NH_3 efflux. This hypothesis assumes however that H^+ equivalents released intracellularly from NH_4^+ are not independently transported across the basolateral membrane. Interestingly, mTALs from the NBCn1 KO mouse with normal acid–base status show no difference in transepithelial NH_4^+ transport (Kurtz and Good unpublished observation). Basolateral HCO_3^- uptake mediated by NBCn1 may also function as a regulator of mTAL pHi rather than affecting transepithelial transport.

IMCD Transport

There is little information on the role of NBCn1 in the IMCD. In non-perfused rat IMCD segments adhering to coverslips, a stilbene-insensitive basolateral sodium driven bicarbonate transport process has been reported.[168] Unlike the mTAL, chronic metabolic acidosis has no effect on the expression of NBCn1 in the IMCD. The function of the basolateral transport process has not been examined during chronic metabolic acidosis.

SLC4A7 Gene Disruption in the Mouse

Currently there is no known renal phenotype reported with loss or gain of NBCn1 function. In mice with targeted disruption of NBCn1, a sensorineural phenotype has been described.[64] These mice have visual impairment due to gradual loss of photoreceptors. In addition they have hearing abnormalities due to gradual loss of hair cells, spiral ganglia neurons, and spiral ligament type II and IV fibrocytes.[181] The symptoms are similar to those associated with Usher Syndrome 2B, which maps to chromosome 3p22 (genetic locus of the SLC4A7 gene).[182,183] Given the expression of the transporter in heart and blood vessels, it remains a possibility that subtle change in hemodynamics exist in mammals with loss of NBCn1 function.

Na^+-DRIVEN $Cl^- - HCO_3^-$ EXCHANGER

NDCBE (SLC4A8 Gene)

Structural Variants

The first NDCBE clone was identified (but not functionally characterized) in a screen of 100 cDNA clones from human brain.[184] NDCBE (original name kNBC-3) was then cloned and partially characterized from a human NT-2 cell line,[185] and mouse IMCD cells.[186] The transporter was first shown to function as an electroneutral Na^+-driven Cl^--bicarbonate exchanger by Grichtchenko et al.[187] Human NDCBE (encoded by the *SLC4A8* gene) has been detected by Northern analysis in brain (predominant), testis, kidney, and ovary,[187] and by RT-PCR in human kidney medulla, duodenum, ileum, choroid plexus, hippocampus, and cerebrum.[58] In mouse, transcript expression has been reported to be either highest in testes with less expression in brain;[188] or conversely expressed at high levels in brain.[186] In rat, by RT-PCR, NDCBE transcripts were found in testis, cerebrum, cerebellum, eye, kidney inner medulla, and submandibular gland.[58] Currently, four human NDCBE variants have been characterized functionally and named NDCBE-

A,-B,-C,-D.[187,189] These variants differ in their cytoplasmic N- and C- termini. The longest variant is NDCBE-A composed of 1093 aa and is ~135 kDa.[188,190] In NDCBE-B, the C-terminal 66 aa are replaced by 17 aa that are specific for this variant. NDCBE-C is identical to NDCBE-A except that it is truncated by 53 aa in its N-terminus. Similarly, NDCBE-D is identical to NDCBE-B except that it also is also shortened by 53 aa in its N-terminus. A transcript whose amino acid sequence is identical to NDCBE-D has also been isolated from human heart that differs in its 5′-UTR.[189]

There are no studies with variant specific antibodies that have addressed the localization of the known NDCBE variants in the kidney. In mouse kidney, NDCBE transcripts were reported to be highest in the inner medulla.[186] In a study using an N-terminal antibody (against rat) that would be predicted to detect the NDCBE-A and -B variants, no clear staining of human kidney was detected although transcripts (by PCR) were detected in the medulla (no distinction was made between outer or inner segment) and less so in the cortex.[58] Despite its absence in the kidney, anti-NDCBE immunoreactivity was detected using the same antibody in human hippocampus pyramidal cells.[58] In the rat brain N-terminal antibodies predicted to detect both NDCBE-A and -B variants have localized the transporter to cerebellar Purkinje cells.[58,190] In rat, neurons in the cerebral cortex, CA1-3 and hipoocampal dentate gyrus, substantia nigra, medulla, and cerebellar granular cells express the transporter.[190]

Functional Properties

NDCBE transports $Na^+ - HCO_3^-$ in exchange for Cl^- in an electroneutral fashion. Thermodynamically, 2 HCO_3^-- (or 1 CO_3^{2-}) with 1 Na^+ are exchanged for 1 Cl^- in each transport cycle.[187] This transport stoichiometry is required for the transporter to function electroneutrally. Interestingly, based on ^{36}Cl studies in NDCBE heterologously expressed in xenopus oocyes, the estimated unidirectional Cl^- flux is sevenfold higher than expected and does not occur in the absence of bicarbonate.[187] Therefore, it appears that the majority of Cl^- flux is not being utilized thermodynamically in exchange for $Na^+ - HCO_3^-$ but rather in exchange for Cl^- (i.e. Cl^- self exchange). Removal of extracellular Cl^- impairs ^{36}Cl efflux suggesting that either NDCBE requires that Cl^- bind to an extracellular Cl^- modifier site following removal of Cl^-, or that under these conditions NDCBE mediates electroneutral $Na^+ - HCO_3^-$ cotransport. Regarding the differences in function among the characterized human variants, the unique 17-aa C-terminus of NDCBE-B/D appears to be autoinhibitory in an oocyte expression system.[189]

Hypoxia

In the neonatal mouse brain, chronic hypoxia decreased NDCBE expression in hippocampus and subcortex.[191] In adult mice, expression was also decreased in cerebral cortex and cerebellum. It was hypothesized that changes in expression may adaptively reduce energy expenditure or modulate neuronal pHi.

Function in the Kidney

IMCD Cultured Cells

In a mouse immortalized IMCD cell line acid stress upregulates NDCBE message and a DIDS-sensitive Na^+- and HCO_3^--dependent dependent pH_i recovery.[185] How faithfully these cells mirror the native inner medullary collecting duct is unclear since they also express NBCe1 which is not found in the IMCD *in vivo*.

Targeted Disruption in the Mouse

The role of NDCBE in intercalated cells in the CCD has recently been reported.[188] Approximately 50% of Na^+ absorption in the rat collecting duct is thiazide sensitive and amiloride insensitive.[192] The transporter(s) responsible for this effect in the CCD has been unclear because the known target for thiazides, NCC, is restricted to the distal convoluted tubule.[193] In a recent study, Leviel suggested that NDCBE coupled with pendrin play a role in mediating thiazide-sensitive electroneutral uptake of NaCl in the mouse CCD.[188] Specifically, a Na^+-driven bicarbonate transport process was detected in mouse CCDs that was: (1) absent in mice with targeted disruption of the *SLC4A8* gene, and (2) inhibited by luminal thiazides. Importantly, whether NDCBE is immunolocalized to the apical membrane of CCD intercalated cells has not been determined. Interestingly, thiazides are not able to inhibit NDCBE in an oocyte expression system.[188]

SLC4 TRANSPORTERS WHOSE FUNCTION IS CONTROVERSIAL

NCBE/NBCn2 (SLC4A10 Gene)

Functional Properties

The terminology regarding the name of the SLC4A10 gene product has undergone several revisions in part because of the discrepant functional properties reported in the literature. Wang et al. first cloned the transporter from a mouse insulinoma cell line and named it NCBE (Na^+-driven $Cl^- - HCO_3^-$ exchanger).[194] NCBE was reported by several different

groups to be a Na^+-driven $Cl^- - HCO_3^-$ exchanger.[145,194,195] Subsequently, in the presence of physiologic chloride concentrations, Parker et al. reported that the transporter mediates electroneutral $Na^+ - HCO_3^-$ cotransport similar to NBCn1 and was renamed NBCn2.[196] Interestingly, the transporter simultaneously performed Cl^--self exchange and therefore there was no *net* chloride transport (equal Cl^- flux in both directions) detected under physiological conditions. In the absence of extracellular Cl^- (non-physiologic conditions), the transporter mediated sodium-driven chloride-bicarbonate exchange at a low rate.[196]

Recently, the function of the *SLC4A10* gene product has again been revisited. Damkier et al. reported that *SLC4A10* expressed in stably transected NIH-3T3 cells mediated $Na^+ - HCO_3^-$-cotransport in exchange for Cl^- in an electroneutral fashion (Na^+-driven $Cl^- - / HCO_3^-$ exchange) as Wang et al. originally reported.[197] The authors proposed that the protein be re-named NCBE. Moreover these authors reported that E890, E892, H976, and H980 played an important role in the functional properties of the transporter.

Structural Variants

NCBE/NBCn2-A is composed of 1088 aa and is ~140–150 kDa.[194] The original clone is referred to here as NCBE/NBCn2-A because additional variants have been reported. In general, the mammalian *SLC4A10* gene contains two inserts (cassettes) that account for the known transcripts. Full length cDNAs have been found in mammals for four variants NCBE/NBCn2-A (1088 aa), NCBE/NBCn2-B (originally named rb1NCBE; 1118 aa), NCBE/NBCn2-C (originally named rb2NCBE; 1106 aa) and a partial clone from rat that is possibly NCBE/NBCn2-D (1136 aa).[195,198] At the protein level, evidence for NCBE/NBCn2-D has recently been reported.[198] The transcripts for NCBE/NBCn2-A and NCBE/NBCn2-B contain the 39-bp cassette B that encodes 3 aa and an early stop codon, whereas NCBE/NBCn2-C and NCBE/NBCn2-D contain cassette A (90-bp) in the N-terminus.

Regulation

Although little is known about the regulation of the transporter, Yong-Sun Lee et al. have reported that NCBE/NBCn2-C (originally named rb2NCBE) is inhibited by PKA activation, and that it interacts with EBP50/actin cytoskeleton via a PDZ motif.[199]

Expression in Extrarenal Tissues

NCBE/NBCn2 transcripts are highly expressed in the brain and weakly in rat kidney, testes, ileum, pancreas and pituitary.[194] In mouse, Hubner et al. reported the developmental expression pattern in mouse brain, and that NCBE/NBCn2 is also expressed in stomach, and duodenum.[200] At the protein level the transporter is expressed in the basolateral membrane of choroid plexus cells,[144,190,198,201,202] cerebral cortex,[195,198,201] hippocampus,[195,198,203] cerebellum,[203,195,198] brainstem[198] and lateral superior olive.[198] The most abundant variant is NCBE/NBCn2-A.[198] In the kidney, NCBE/NBCn2 has not been detected at the protein level, however, weak expression has been reported on Northern blotting of human kidney. Although epithelial cells in the kidney do not appear to express the transporter, it is possible that renal nerves in the parenchyma account for the Northern data.

Human Phenotype and Targeted Disruption in the Mouse

As might be predicted from the known expression pattern, loss of NCBE/NBCn2 results in a brain phenotype. Sebat et al. reported a pair of identical twins from a large cohort of patients with autism with chromosomal deletion involving exon 1 of *SLC4A10*.[204] Gurnett et al. described a 13-year-old girl with moderate mental retardation, delayed speech and partial complex epilepsy with a translocation breakpoint of *SLC4A10* on chromosome 2q24.[205] In contrast, mice with targeted disruption of *SLC4A10* have an increased seizure threshold and small ventricles.[201] The latter finding is of interest given the potential importance of NCBE/NBCn2 to transepithelial choroid plexus bicarbonate transport.[144,170] No renal phenotype has thus far been reported.

Electrogenic Na^+–Borate Cotransporter

NaBC1 (SLC4A11 Gene)

The protein encoded by *SLC4A11* was initially called BTR1 (Bicarbonate Transporter Related protein-1) based on sequence homology with other members of the SLC4 family.[206] Motivated by homology with the borate transporter BOR1 in Arabidopsis,[207] Park et al. reported that the transporter was an electrogenic sodium-borate cotransporter and was renamed NaBC1.[208,209] In the absence of borate, the transporter functioned as an electrogenic $Na^+ - OH^-$ cotransporter.[208,209] Questions regarding its functional properties and therefore the appropriate name for the transporter remain, given the lack of documented physiological requirements for borate transport in the tissues expressing NaBC1 in health and disease states.

Expression in the Kidney and Extrarenal Tissues

Studies in human and rat tissues have demonstrated the widespread expression pattern of NaBC1. The

transporter can be localized apically or basolaterally. NaBC1 was originally identified at the protein level in rat kidney, parotid gland, submandibular gland (SMG), pancreas, liver, and spleen.[209] In cornea, NaBC1 is expressed mainly in sensory tissues including endothelial cells with less expression in the epithelial cell layer.[58,210,211] In the inner ear, fibrocytes in the striae vascularis express the transporter.[210,211] In the pancreas NaBC1 is localized to the apical membrane of intercalated ducts.[58] Both the apical membrane of choroid plexus epithelial cells and choroid plexus endothelial cells express NaBC1.[58] In addition, peripheral nerves express the transporter.[58] In kidney, NaBC1 is more widely expressed than any of the SLC4 proteins. These regions include the glomerulus (podocytes), proximal tubule (brush border), nerves near afferent arterioles, basolateral membrane of thin descending limbs in the outer medulla, and basolateral membrane of IMCD cells in the inner medulla.[58] *SLC4A11* transcripts (RT-PCR) have been detected in human stomach and duodenum.

NaBC1 Cell Biology

In knockdown experiments, NaBC1, functioning as a cellular borate influx pathway was reported to be required for cell proliferation.[208,209] In a large scale examination of various intestinal SLC transporter families (including SLC4), administration of various bacteria to mice significantly decreased the expression of intestinal *SLC4A11* (by RT-PCR).[212] The significance of this finding is unknown.

CHED2 Disease and Harboyan Syndrome

Corneal hereditary dystrophy type 2 (CHED2) is caused by mutations in the SLC4A11 gene.[213] Some patients with mutations in the transporter also develop Harboyan syndrome in which perceptive hearing loss and nystagmus are also present.[214] No patients with SLC4A11 mutations have been described with isolated hearing abnormalities. No renal phenotype has been reported in humans despite the widespread localization of NaBC1 in the human kidney.[58]

Targeted Disruption of SLC4A11 in the Mouse

In the first report of targeted disruption of *SLC4A11* in the mouse, sensory tissues were examined.[211] NaBC1 was highly expressed in the corneal endothelial cell layer with less staining in epithelial cells. However unlike humans with mutations in NaBC1, the corneal phenotype was not as severe. Both auditory brain responses and vestibular evoked potential waveforms were abnormal demonstrating the importance of NaBC1 in the visual-auditory-vestibular system. NaBC1 appears be required for generating the inner ear endocochlear potential.[210]

In a second study in mice lacking NaBC1, a renal phenotype was uncovered.[210] LacZ expression and an NaBC1 antibody were used to determine the localization of the transporter in wild-type mice. Unlike the human and rat data, NaBC1 was confined to the thin descending limb at the cortical/outer medullary border. No expression was found in the glomerulus, proximal tubule, nerves or the collecting duct. The urine of the KO mice had a reduced osmolarity, an increased urine volume, increased excretion of sodium, potassium, chloride, and magnesium and a decreased urinary concentration of calcium. It was suggested that NaBC1 in the thin descending limb of Henle is essential for urinary concentration, and that the transporter plays a role in the countercurrent multiplication system. The molecular basis for these findings is still unclear. Further studies are needed to determine its exact transport function.

AE4 (SLC4A9 Gene)

Functional Properties and Expression Pattern in Kidney and Extrarenal Tissues

The function of AE4 is also controversial and there appears to be significant species differences in its kidney expression pattern. AE4 was first cloned from rabbit renal β-intercalated cells and characterized by Tsuganezawa et al.[215] The rabbit transporter is 995 aa and ~110 kDa. Northern analysis of rabbit kidney showed greatest expression in the cortex and the transporter was localized to the apical membrane of rabbit beta intercalated cells. When expressed in oocytes and COS-7 cells AE4 was reported to function as a DIDS-insensitive Na^+-independent $Cl^- - HCO_3^-$ exchanger. Parker et al.[206] and Lipovitch et al.[216] subsequently reported the sequence of the human orthologue. Subsequently, Ko et al. reported that rat AE4 functions as a DIDS-sensitive Na^+-independent $Cl^- - HCO_3^-$ Cl exchanger.[217] In addition, human AE4 expressed in oocytes functioned as a $Cl^- - HCO_3^-$ exchanger. Although AE4 had been reported to function as a Na^+ + -independent $Cl^- - HCO_3^-$ exchanger,[215,217,218] its structure closely resembled SLC4 Na^+-dependent transporters (Fig. 53.1). Indeed in a preliminary report, Parker et al. reported that AE4 is an electroneutral $Na^+ - HCO_3^-$ cotransporter.[219]

Although the transporter was initially localized to the apical membrane of rabbit collecting duct β-intercalated cells, subsequent studies have not verified this finding uniformly (Table 53.3). After the initial report, AE4 has been immunolocalized to the apical and lateral membranes of rabbit CCD α-intercalated cells.[217]

A subsequent study showed apical co-localization in rabbit with peanut lectin (a β-intercalated cell marker).[218] In the rat, the transporter was localized to the basal and lateral membrane of CCD α- and β-intercalated cells.[217] In the mouse it is expressed predominantly on the basolateral membrane of cortical collecting duct β-intercalated cells.[220,221]

While northern analysis has shown that AE4 expression predominates in rabbit, human and mouse kidney,[215,216,221] transcripts were also detected in rat stomach and caecum.[217] At the protein level, localization of AE4 was reported in mouse and rabbit gastric surface mucous and duodenal villus cells, and mouse submandibular gland[217] where AE4 is reported to function as an apical $Cl^- - HCO_3^-$ exchanger.[218] However, in a LacZ transgenic mouse, no expression was found in stomach, intestine or colon yet expression in β-intercalated cells was confirmed.[221]

Structural Variants

Multiple splice variants of AE4 have been reported in humans because of selective inclusion/exclusion of part of exons 8, 10, 11, 19 and 20, whereas the use of exons 4–7, 9 and 12–17 appeared constant.[216] It has been suggested that these multiple splice variants may result from inefficient spliceosomal processing.[216] Hentschke et al. in mouse reported 4 different variants resulting potentially from alternative promoter useage.[221] The finding that there are potentially multiple AE4 variants expressed in the kidney cortical collecting duct may account in part for the discrepant immunocytochemistry findings in the literature.

Regulation

In a rat cortical collecting duct cell line (RCCD1 cells), 48 hours of extracellular metabolic alkalosis had no effect on AE4 expression.[222]

Absence of AE4 Expression in the Foxi1$^{-/-}$ Mouse

Mice with targeted disruption of forkhead transcription factor Foxi1$^{-/-}$ develop distal renal tubular acidosis.[220] The cortical collecting ducts of these mice have one cell type that has characteristics of intercalated and principal cells (expression of both AQP2 and CAII). These cells fail to express various acid/base transport proteins including the B_1 subunit of the apical H^+-ATPase, pendrin, and AE4.

Mice with Targeted Disruption of AE4

AE4$^{-/-}$ mice do not have an overt phenotype and have no significant decrease in duodenal upper villous epithelial $Cl^- - HCO_3^-$ exchange activity.[223] Studies of CCD β-intercalated function were not reported.

References

[1] Alper SL. Molecular physiology and genetics of Na^+-independent SLC4 anion exchangers. J Exp Biol 2009;212:1672–83.

[2] Zhu Q, Kao L, Azimov R, Newman D, Liu W, Pushkin A, et al. Topological location and structural importance of the NBCe1-A residues mutated in proximal renal tubular acidosis. J Biol Chem 2010;285: 13416–26.

[3] Abuladze N, Song M, Pushkin A, Newman D, Lee I, Nicholas S, et al. Structural organization of the human NBC1 gene: kNBC1 is transcribed from an alternative promoter in intron 3. Gene 2000;251:109–22.

[4] Bevensee MO, Schmitt BM, Choi I, Romero MF, Boron WF. An electrogenic Na^+–HCO_3^- cotransporter (NBC) with a novel COOH-terminus, cloned from rat brain. Am J Physiol Cell Physiol 2000;278:C1200–11.

[5] Abuladze N, Lee I, Newman D, Hwang J, Pushkin A, Kurtz I. Axial heterogeneity of sodium-bicarbonate cotransporter expression in the rabbit proximal tubule. Am J Physiol 1998;274: F628–3.

[6] Burnham CE, Amlal H, Wang Z, Shull GE, Soleimani M. Cloning and functional expression of a human kidney Na^+: HCO_3^- cotransporter. J Biol Chem 1997;272:19111–4.

[7] Maunsbach AB, Vorum H, Kwon TH, Nielsen S, Simonsen B, Choi I, et al. Immunoelectron microscopic localization of the electrogenic Na/HCO_3 cotransporter in rat and ambystoma kidney. J Am Soc Nephrol 2000;11:2179–89.

[8] Romero MF, Hediger MA, Boulpaep EL, Boron WF. Expression cloning and characterization of a renal electrogenic Na^+/HCO_3^- cotransporter. Nature 1997;387:409–13.

[9] Schmitt BM, Biemesderfer D, Romero MF, Boulpaep EL, Boron WF. Immunolocalization of the electrogenic Na^+–HCO_3^- cotransporter in mammalian and amphibian kidney. Am J Physiol 1999;276:F27–38.

[10] Bok D, Schibler MJ, Pushkin A, Sassani P, Abuladze N, Naser Z, et al. Immunolocalization of electrogenic sodium-bicarbonate cotransporters pNBC1 and kNBC1 in the rat eye. Am J Physiol Renal Physiol 2001;281:F920–5.

[11] Usui T, Hara M, Satoh H, Moriyama N, Kagaya H, Amano S, et al. Molecular basis of ocular abnormalities associated with proximal renal tubular acidosis. J Clin Invest 2001;108:107–15.

[12] Brandes A, Oehlke O, Schumann A, Heidrich S, Thevenod F, Roussa E. Adaptive redistribution of NBCe1-A and NBCe1-B in rat kidney proximal tubule and striated ducts of salivary glands during acid–base disturbances. Am J Physiol Regul Integr Comp Physiol 2007;293:R2400–11.

[13] Lee SH, Park JH, Jung HH, Oh JW, Lee HM, Jun HS, et al. Expression and distribution of ion transport mRNAs in human nasal mucosa and nasal polyps. Acta Otolaryngol 2005;125:745–52.

[14] Abuladze N, Lee I, Newman D, Hwang J, Boorer K, Pushkin A, et al. Molecular cloning, chromosomal localization, tissue distribution, and functional expression of the human pancreatic sodium bicarbonate cotransporter. J Biol Chem 1998;273: 17689–95.

[15] Gross E, Abuladze N, Pushkin A, Kurtz I, Cotton CU. The stoichiometry of the electrogenic sodium bicarbonate cotransporter pNBC1 in mouse pancreatic duct cells is 2 HCO_3^-:1 Na^+. J Physiol 2001;531:375–82.

[16] Kreindler JL, Peters KW, Frizzell RA, Bridges RJ. Identification and membrane localization of electrogenic sodium bicarbonate cotransporters in Calu-3 cells. Biochim Biophys Acta 2006;1762:704–10.

[17] Kristensen JM, Kristensen M, Juel C. Expression of Na^+/HCO_3^- co-transporter proteins (NBCs) in rat and human skeletal muscle. Acta Physiol Scand 2004;182:69–76.

[18] Moser AJ, Gangopadhyay A, Bradbury NA, Peters KW, Frizzell RA, Bridges RJ. Electrogenic bicarbonate secretion by prairie dog gallbladder. Am J Physiol Gastrointest Liver Physiol 2007;292:G1683–94.

[19] Yu H, Riederer B, Stieger N, Boron WF, Shull GE, Manns MP, et al. Secretagogue stimulation enhances NBCe1 (electrogenic Na^+/HCO_3^- cotransporter) surface expression in murine colonic crypts. Am J Physiol Gastrointest Liver Physiol 2009;297:G1223–31.

[20] Shirakabe K, Priori G, Yamada H, Ando H, Horita S, Fujita T, et al. IRBIT, an inositol 1,4,5-trisphosphate receptor-binding protein, specifically binds to and activates pancreas-type Na^+/HCO_3^- cotransporter 1 (pNBC1). Proc Natl Acad Sci U S A 2006;103:9542–7.

[21] Yang D, Shcheynikov N, Zeng W, Ohana E, So I, Ando H, et al. IRBIT coordinates epithelial fluid and HCO_3^- secretion by stimulating the transporters pNBC1 and CFTR in the murine pancreatic duct. J Clin Invest 2009;119:193–202.

[21A] Liu Y, Xu JY, Wang DK, Wang L, Chen LM. Cloning and identification of two novel NBCe1 splice variants from mouse reproductive tract tissues: a comparative study of NCBT genes. Genomics 2011;98:112–9.

[22] Kao L, Sassani P, Azimov R, Pushkin A, Abuladze N, Peti-Peterdi J, et al. Oligomeric structure and minimal functional unit of the electrogenic sodium bicarbonate cotransporter NBCe1-A. J Biol Chem 2008;283:26782–94.

[23] Tatishchev S, Abuladze N, Pushkin A, Newman D, Liu W, Weeks D, et al. Identification of membrane topography of the electrogenic sodium bicarbonate cotransporter pNBC1 by *in vitro* transcription/translation. Biochemistry 2003;42:755–65.

[24] Choi I, Soo Yang H, Boron WF. The electrogenicity of the rat sodium-bicarbonate cotransporter NBCe1 requires interactions among transmembrane segments of the transporter. J Physiol 2007;578:131–42.

[25] Abuladze N, Azimov R, Newman D, Sassani P, Liu W, Tatishchev S, et al. Critical amino acid residues involved in the electrogenic sodium-bicarbonate cotransporter kNBC1-mediated transport. J Physiol 2005;565:717–30.

[26] Chang MH, DiPiero J, Sonnichsen FD, Romero MF. Entry to "formula tunnel" revealed by SLC4A4 human mutation and structural model. J Biol Chem 2008;283:18402–10.

[27] Zhu Q, Azimov R, Kao L, Newman D, Liu W, Abuladze N, et al. NBCe1-A transmembrane segment 1 lines the ion translocation pathway. J Biol Chem 2009;284:8918–29.

[28] McAlear SD, Bevensee MO. A cysteine-scanning mutagenesis study of transmembrane domain 8 of the electrogenic sodium/bicarbonate cotransporter NBCe1. J Biol Chem 2006;281:32417–27.

[29] Yang HS, Kim E, Lee S, Park HJ, Cooper DS, Rajbhandari I, et al. Mutation of aspartate 555 of the sodium/bicarbonate transporter SLC4A4/NBCe1 induces chloride transport. J Biol Chem 2009;284:15970–9.

[30] Lu J, Boron WF. Reversible and irreversible interactions of DIDS with the human electrogenic Na/HCO_3 cotransporter NBCe1-A: role of lysines in the KKMIK motif of TM5. Am J Physiol Cell Physiol 2007;292:C1787–98.

[31] Yamaguchi S, Ishikawa T. Electrophysiological characterization of native $Na^+–HCO_3^-$ cotransporter current in bovine parotid acinar cells. J Physiol 2005;568:181–97.

[32] Muller-Berger S, Ducoudret O, Diakov A, Fromter E. The renal $Na\text{-}HCO_3$-cotransporter expressed in Xenopus laevis oocytes: change in stoichiometry in response to elevation of cytosolic Ca2 + concentration. Pflugers Arch 2001;442:718–28.

[33] Ch'en FF, Villafuerte FC, Swietach P, Cobden PM, Vaughan-Jones RD. S0859, an N-cyanosulphonamide inhibitor of sodium-bicarbonate cotransport in the heart. Br J Pharmacol 2008;153:972–82.

[34] Demirci FY, Chang MH, Mah TS, Romero MF, Gorin MB. Proximal renal tubular acidosis and ocular pathology: a novel missense mutation in the gene (SLC4A4) for sodium bicarbonate cotransporter protein (NBCe1). Mol Vis 2006;12:324–30.

[35] Dinour D, Chang MH, Satoh J, Smith BL, Angle N, Knecht A, et al. A novel missense mutation in the sodium bicarbonate cotransporter (NBCe1/SLC4A4) causes proximal tubular acidosis and glaucoma through ion transport defects. J Biol Chem 2004;279:52238–46.

[36] Horita S, Yamada H, Inatomi J, Moriyama N, Sekine T, Igarashi T, et al. Functional analysis of NBC1 mutants associated with proximal renal tubular acidosis and ocular abnormalities. J Am Soc Nephrol 2005;16:2270–8.

[37] Horita S, Yamada H, Inatomi J, Sekine T, Igarashi T, Seki G, et al. Mechanism of NBC1 inactivation by mutations identified in patients with proximal renal tubular acidosis and ocular abnormalities. J Am Soc Nephrol 2003;14:302A.

[38] Igarashi T, Inatomi J, Sekine T, Cha SH, Kanai Y, Kunimi M, et al. Mutations in SLC4A4 cause permanent isolated proximal renal tubular acidosis with ocular abnormalities. Nat Genet 1999;23:264–6.

[39] Igarashi T, Inatomi J, Sekine T, Seki G, Shimadzu M, Tozawa F, et al. Novel nonsense mutation in the Na^+/HCO_3^- cotransporter gene (SLC4A4) in a patient with permanent isolated proximal renal tubular acidosis and bilateral glaucoma. J Am Soc Nephrol 2001;12:713–8.

[40] Igarashi T, Inatomi J, Sekine T, Seki G, Yamada H, Horita S, et al. Mutational and functional analysis of the Na^+/HCO_3 cotransporter gene (SLC4A4) in patients with permanent isolated proximal renal tubular acidosis and ocular abnormalities. J Am Soc Nephrol 2003;14:302A.

[41] Igarashi T, Sekine T, Inatomi J, Seki G. Unraveling the molecular pathogenesis of isolated proximal renal tubular acidosis. J Am Soc Nephrol 2002;13:2171–7.

[42] Inatomi J, Horita S, Braverman N, Sekine T, Yamada H, Suzuki Y, et al. Mutational and functional analysis of SLC4A4 in a patient with proximal renal tubular acidosis. Pflugers Arch 2004;448:438–44.

[43] Suzuki M, Vaisbich MH, Yamada H, Horita S, Li Y, Sekine T, et al. Functional analysis of a novel missense NBC1 mutation and of other mutations causing proximal renal tubular acidosis. Pflugers Arch 2008;455:583–93.

[44] Majumdar D, Maunsbach AB, Shacka JJ, Williams JB, Berger UV, Schultz KP, et al. Localization of electrogenic Na/bicarbonate cotransporter NBCe1 variants in rat brain. Neuroscience 2008;155:818–32.

[45] Lacruz RS, Nanci A, Kurtz I, Wright JT, Paine ML. Regulation of pH During Amelogenesis. Calcif Tissue Int 86: 91–103.

[46] Paine ML, Snead ML, Wang HJ, Abuladze N, Pushkin A, Liu W, et al. Role of NBCe1 and AE2 in secretory ameloblasts. J Dent Res 2008;87:391–5.

[47] Li HC, Szigligeti P, Worrell RT, Matthews JB, Conforti L, Soleimani M. Missense mutations in $Na^+:HCO_3^-$ cotransporter NBC1 show abnormal trafficking in polarized kidney cells: a basis of proximal renal tubular acidosis. Am J Physiol Renal Physiol 2005;289:F61–71.

[48] Toye AM, Parker MD, Daly CM, Lu J, Virkki LV, Pelletier MF, et al. The human NBCe1-A mutant R881C, associated with proximal renal tubular acidosis, retains function but is mistargeted in polarized renal epithelia. Am J Physiol Cell Physiol 2006;291:C788–801.

[49] Boron WF. Acid–base transport by the renal proximal tubule. J Am Soc Nephrol 2006;17:2368–82.
[50] Burke JF, Mogg AE. Suppression of a nonsense mutation in mammalian cells *in vivo* by the aminoglycoside antibiotics G-418 and paromomycin. Nucleic Acids Res 1985;13:6265–72.
[51] Karimi R, Pavlov MY, Buckingham RH, Ehrenberg M. Novel roles for classical factors at the interface between translation termination and initiation. Mol Cell 1999;3:601–9.
[52] Nilsson M, Ryden-Aulin M. Glutamine is incorporated at the nonsense codons UAG and UAA in a suppressor-free Escherichia coli strain. Biochim Biophys Acta 2003;1627:1–6.
[53] Azimov R, Abuladze N, Sassani P, Newman D, Kao L, Liu W, et al. G418-mediated ribosomal read-through of a nonsense mutation causing autosomal recessive proximal renal tubular acidosis. Am J Physiol Renal Physiol 2008;295:F633–41.
[54] Nudelman I, Rebibo-Sabbah A, Cherniavsky M, Belakhov V, Hainrichson M, Chen F, et al. Development of novel aminoglycoside (NB54) with reduced toxicity and enhanced suppression of disease-causing premature stop mutations. J Med Chem 2009;52:2836–45.
[55] Welch EM, Barton ER, Zhuo J, Tomizawa Y, Friesen WJ, Trifillis P, et al. PTC124 targets genetic disorders caused by nonsense mutations. Nature 2007;447:87–91.
[56] Gawenis LR, Bradford EM, Prasad V, Lorenz JN, Simpson JE, Clarke LL, et al. Colonic anion secretory defects and metabolic acidosis in mice lacking the NBC1 Na^+/HCO_3^- cotransporter. J Biol Chem 2007;282:9042–52.
[57] Lacruz RS, Nanci A, White SN, Wen X, Wang H, Zalzal SF, et al. The sodium bicarbonate cotransporter (NBCe1) is essential for normal development of mouse dentition. *J Biol Chem* 285: 24432–38.
[58] Damkier HH, Nielsen S, Praetorius J. Molecular expression of SLC4-derived Na^+-dependent anion transporters in selected human tissues. Am J Physiol Regul Integr Comp Physiol 2007;293:R2136–46.
[59] Bartolo RC, Harfoot N, Gill M, McLeod BJ, Butt AG. Secretagogues stimulate electrogenic HCO_3^- secretion in the ileum of the brushtail possum, Trichosurus vulpecula: evidence for the role of a Na^+/HCO_3^- cotransporter. J Exp Biol 2009;212:2645–55.
[60] Bachmann O, Juric M, Seidler U, Manns MP, Yu H. Basolateral ion transporters involved in colonic epithelial electrolyte absorption, anion secretion, and cellular homeostasis. *Acta Physiol (Oxf)*.
[61] Bachmann O, Rossmann H, Berger UV, Colledge WH, Ratcliff R, Evans MJ, et al. cAMP-mediated regulation of murine intestinal/pancreatic Na^+/HCO_3^- cotransporter subtype pNBC1. Am J Physiol Gastrointest Liver Physiol 2003;284: G37–45.
[62] Boedtkjer E, Praetorius J, Fuchtbauer EM, Aalkjaer C. Antibody-independent localization of the electroneutral Na^+–HCO_3^- cotransporter NBCn1 (slc4a7) in mice. Am J Physiol Cell Physiol 2008;294:C591–603.
[63] Praetorius J, Hager H, Nielsen S, Aalkjaer C, Friis UG, Ainsworth MA, et al. Molecular and functional evidence for electrogenic and electroneutral Na^+–HCO_3^- cotransporters in murine duodenum. Am J Physiol Gastrointest Liver Physiol 2001;280:G332–43.
[64] Bok D, Galbraith G, Lopez I, Woodruff M, Nusinowitz S, BeltrandelRio H, et al. Blindness and auditory impairment caused by loss of the sodium bicarbonate cotransporter NBC3. Nat Genet 2003;34:313–9.
[65] Amlal H, Chen Q, Greeley T, Pavelic L, Soleimani M. Coordinated down-regulation of NBC-1 and NHE-3 in sodium and bicarbonate loading. Kidney Int 2001;60:1824–36.
[66] Capasso G, Jaeger P, Giebisch G, Guckian V, Malnic G. Renal bicarbonate reabsorption in the rat. II. Distal tubule load dependence and effect of hypokalemia. J Clin Invest 1987;80:409–14.
[67] Rector Jr FC, Bloomer HA, Seldin DW. Effect of potassium deficiency on the reabsorption of bicarbonate in the proximal tubule of the rat kidney. J Clin Invest 1964;43:1976–82.
[68] Roberts KE, Randall HT, Sanders HL, Hood M. Effects of potassium on renal tubular reabsorption of bicarbonate. J Clin Invest 1955;34:666–72.
[69] Amlal H, Habo K, Soleimani M. Potassium deprivation upregulates expression of renal basolateral Na^+–HCO_3^- cotransporter (NBC-1). Am J Physiol Renal Physiol 2000;279:F532–43.
[70] Sonalker PA, Tofovic SP, Bastacky SI, Jackson EK. Chronic noradrenaline increases renal expression of NHE-3, NBC-1, BSC-1 and aquaporin-2. Clin Exp Pharmacol Physiol 2008;35: 594–600.
[71] Kunimi M, Seki G, Hara C, Taniguchi S, Uwatoko S, Goto A, et al. Dopamine inhibits renal Na^+:HCO_3^- cotransporter in rabbits and normotensive rats but not in spontaneously hypertensive rats. Kidney Int 2000;57:534–43.
[72] Pastoriza-Munoz E, Harrington RM, Graber ML. Parathyroid hormone decreases HCO_3 reabsorption in the rat proximal tubule by stimulating phosphatidylinositol metabolism and inhibiting base exit. J Clin Invest 1992;89:1485–95.
[73] Sasaki S, Marumo F. Mechanisms of inhibition of proximal acidification by PTH. Am J Physiol 1991;260:F833–38.
[74] Sonalker PA, Tofovic SP, Jackson EK. Increased expression of the sodium transporter BSC-1 in spontaneously hypertensive rats. J Pharmacol Exp Ther 2004;311:1052–61.
[75] Pedrosa R, Goncalves N, Hopfer U, Jose PA, Soares-da-Silva P. Activity and regulation of Na^+–HCO_3^- cotransporter in immortalized spontaneously hypertensive rat and Wistar-Kyoto rat proximal tubular epithelial cells. Hypertension 2007;49:1186–93.
[76] Velic A, Hirsch JR, Bartel J, Thomas R, Schroter R, Stegemann H, et al. Renal transplantation modulates expression and function of receptors and transporters of rat proximal tubules. J Am Soc Nephrol 2004;15:967–77.
[77] O'Gorman MA, Fivush B, Wise B, Colombani P, Burdick J, Schwarz KB. Proximal renal tubular acidosis secondary to FK506 in pediatric liver transplant patients. Clin Transplant 1995;9:312–6.
[78] Kwon TH, Fulton C, Wang W, Kurtz I, Frokiaer J, Aalkjaer C, et al. Chronic metabolic acidosis upregulates rat kidney Na–HCO_3 cotransporters NBCn1 and NBC3 but not NBC1. Am J Physiol Renal Physiol 2002;282:F341–51.
[79] Alexander MP, Farag YM, Mittal BV, Rennke HG, Singh AK. Lithium toxicity: a double-edged sword. Kidney Int 2008;73:233–7.
[80] Kim YH, Kwon TH, Christensen BM, Nielsen J, Wall SM, Madsen KM, et al. Altered expression of renal acid–base transporters in rats with lithium-induced NDI. Am J Physiol Renal Physiol 2003;285:F1244–57.
[81] Batlle DC, Arruda JA, Kurtzman NA. Hyperkalemic distal renal tubular acidosis associated with obstructive uropathy. N Engl J Med 1981;304:373–80.
[82] Wang G, Li C, Kim SW, Ring T, Wen J, Djurhuus JC, et al. Ureter obstruction alters expression of renal acid–base transport proteins in rat kidney. Am J Physiol Renal Physiol 2008;295:F497–506.
[83] Villa-Abrille MC, Petroff MG, Aiello EA. The electrogenic Na^+/HCO_3^- cotransport modulates resting membrane potential and action potential duration in cat ventricular myocytes. J Physiol 2007;578:819–29.

[84] Yamamoto T, Swietach P, Rossini A, Loh SH, Vaughan-Jones RD, Spitzer KW. Functional diversity of electrogenic Na^+—HCO_3^- cotransport in ventricular myocytes from rat, rabbit and guinea pig. J Physiol 2005;562:455–75.

[85] Schafer C, Ladilov YV, Siegmund B, Piper HM. Importance of bicarbonate transport for protection of cardiomyocytes against reoxygenation injury. Am J Physiol Heart Circ Physiol 2000;278:H1457–63.

[86] Khandoudi N, Albadine J, Robert P, Krief S, Berrebi-Bertrand I, Martin X, et al. Inhibition of the cardiac electrogenic sodium bicarbonate cotransporter reduces ischemic injury. Cardiovasc Res 2001;52:387–96.

[87] Sandmann S, Yu M, Kaschina E, Blume A, Bouzinova E, Aalkjaer C, et al. Differential effects of angiotensin AT1 and AT2 receptors on the expression, translation and function of the Na^+—H^+ exchanger and Na^+—HCO_3^- symporter in the rat heart after myocardial infarction. J Am Coll Cardiol 2001;37:2154–65.

[88] Verdonck F, Volders PG, Vos MA, Sipido KR. Intracellular Na^+ and altered Na^+ transport mechanisms in cardiac hypertrophy and failure. J Mol Cell Cardiol 2003;35:5–25.

[89] Marino CR, Jeanes V, Boron WF, Schmitt BM. Expression and distribution of the Na^+—HCO_3^- cotransporter in human pancreas. Am J Physiol 1999;277:G487–94.

[90] Satoh H, Moriyama N, Hara C, Yamada H, Horita S, Kunimi M, et al. Localization of Na^+—HCO_3^- cotransporter (NBC-1) variants in rat and human pancreas. Am J Physiol Cell Physiol 2003;284:C729–37.

[91] Shumaker H, Amlal H, Frizzell R, Ulrich II CD, Soleimani M. CFTR drives Na^+—$nHCO_3^-$ cotransport in pancreatic duct cells: a basis for defective HCO_3^- secretion in CF. Am J Physiol 1999;276:C16–25.

[92] Tuo BG, Sellers ZM, Smith AJ, Barrett KE, Isenberg JI, Dong H. A role for CagA/VacA in Helicobacter pylori inhibition of murine duodenal mucosal bicarbonate secretion. Dig Dis Sci 2004;49:1845–52.

[93] Lepore MJ. Cystic fibrosis of the pancreas in the adult. Gastroenterology 1963;44:696–7.

[94] Akiba Y, Furukawa O, Guth PH, Engel E, Nastaskin I, Sassani P, et al. Cellular bicarbonate protects rat duodenal mucosa from acid-induced injury. J Clin Invest 2001;108: 1807–16.

[95] Chesler M. The regulation and modulation of pH in the nervous system. Prog Neurobiol 1990;34:401–27.

[96] Ransom BR. Glial modulation of neural excitability mediated by extracellular pH: a hypothesis. Prog Brain Res 1992;94:37–46.

[97] Kang TC, An SJ, Park SK, Hwang IK, Suh JG, Oh YS, et al. Alterations in Na^+/H^+ exchanger and Na^+/HCO_3^- cotransporter immunoreactivities within the gerbil hippocampus following seizure. Brain Res Mol Brain Res 2002;109:226–32.

[98] McAlear SD, Liu X, Williams JB, McNicholas-Bevensee CM, Bevensee MO. Electrogenic Na/HCO_3 cotransporter (NBCe1) variants expressed in Xenopus oocytes: functional comparison and roles of the amino and carboxy termini. J Gen Physiol 2006;127:639–58.

[99] Espiritu DJ, Bernardo AA, Arruda JA. Role of NH_2 and COOH termini in targeting, stability, and activity of sodium bicarbonate cotransporter 1. Am J Physiol Renal Physiol 2006;291: F588–96.

[100] Li HC, Worrell RT, Matthews JB, Husseinzadeh H, Neumeier L, Petrovic S, et al. Identification of a carboxyl-terminal motif essential for the targeting of Na^+—HCO_3^- cotransporter NBC1 to the basolateral membrane. J Biol Chem 2004;279:43190–7.

[101] Kurtz I, Petrasek D, Tatishchev S. Molecular mechanisms of electrogenic sodium bicarbonate cotransport: structural and equilibrium thermodynamic considerations. J Membr Biol 2004;197:77–90.

[102] Pushkin A, Kurtz I. SLC4 base (HCO_3^-, CO_3^{2-}) transporters: classification, function, structure, genetic diseases, and knockout models. Am J Physiol Renal Physiol 2006;290: F580–99.

[103] Soleimani M, Grassi SM, Aronson PS. Stoichiometry of Na^+—HCO_3^- cotransport in basolateral membrane vesicles isolated from rabbit renal cortex. J Clin Invest 1987;79:1276–80.

[104] Ducoudret O, Diakov A, Muller-Berger S, Romero MF, Fromter E. The renal Na—HCO_3^- cotransporter expressed in Xenopus laevis oocytes: inhibition by tenidap and benzamil and effect of temperature on transport rate and stoichiometry. Pflugers Arch 2001;442:709–17.

[105] Heyer M, Muller-Berger S, Romero MF, Boron WF, Fromter E. Stoichiometry of the rat kidney Na^+—HCO_3^- cotransporter expressed in Xenopus laevis oocytes. Pflugers Arch 1999;438:322–9.

[106] Shao XMKL, Kurtz I. A new delta current method for estimating the transport stoichiometry of electrogenic transporters. FASEB J 2010;815:815.

[107] Gross E, Hawkins K, Abuladze N, Pushkin A, Cotton CU, Hopfer U, et al. The stoichiometry of the electrogenic sodium bicarbonate cotransporter NBC1 is cell-type dependent. J Physiol 2001;531:597–603.

[108] Gross E, Hawkins K, Pushkin A, Sassani P, Dukkipati R, Abuladze N, et al. Phosphorylation of Ser982 in the sodium bicarbonate cotransporter kNBC1 shifts the HCO_3^- : Na^+ stoichiometry from 3: 1 to 2: 1 in murine proximal tubule cells. J Physiol 2001;537:659–65.

[109] Gross E, Fedotoff O, Pushkin A, Abuladze N, Newman D, Kurtz I. Phosphorylation-induced modulation of pNBC1 function: distinct roles for the amino- and carboxy-termini. J Physiol 2003;549:673–82.

[110] Coppola S, Fromter E. An electrophysiological study of angiotensin II regulation of $Na—HCO_3$ cotransport and K conductance in renal proximal tubules. I. Effect of picomolar concentrations. Pflugers Arch 1994;427:143–50.

[111] Coppola S, Fromter E. An electrophysiological study of angiotensin II regulation of $Na—HCO_3$ cotransport and K conductance in renal proximal tubules. II. Effect of micromolar concentrations. Pflugers Arch 1994;427:151–6.

[112] Horita S, Zheng Y, Hara C, Yamada H, Kunimi M, Taniguchi S, et al. Biphasic regulation of Na^+—HCO_3^- cotransporter by angiotensin II type 1A receptor. Hypertension 2002;40:707–12.

[113] Perry C, Blaine J, Le H, Grichtchenko II. PMA- and ANG II-induced PKC regulation of the renal Na^+—HCO_3^- cotransporter (hkNBCe1). Am J Physiol Renal Physiol 2006;290:F417–27.

[114] Zheng Y, Horita S, Hara C, Kunimi M, Yamada H, Sugaya T, et al. Biphasic regulation of renal proximal bicarbonate absorption by luminal AT(1A) receptor. J Am Soc Nephrol 2003;14:1116–22.

[115] Perry C, Le H, Grichtchenko II. ANG II and calmodulin/CaMKII regulate surface expression and functional activity of NBCe1 via separate means. Am J Physiol Renal Physiol 2007;293:F68–77.

[116] Perry C, Baker OJ, Reyland ME, Grichtchenko II. PKC {alpha}{beta}{gamma}- and PKC{delta}-dependent endocytosis of NBCe1-A and NBCe1-B in salivary parotid acinar cells. Am J Physiol Cell Physiol 2009;297:C1409–23.

[117] Hilgemann DW, Feng S, Nasuhoglu C. The complex and intriguing lives of PIP2 with ion channels and transporters. Sci STKE 2001;2001:re19.

[118] Wu J, McNicholas CM, Bevensee MO. Phosphatidylinositol 4,5-bisphosphate (PIP2) stimulates the electrogenic Na/HCO_3 cotransporter NBCe1-A expressed in Xenopus oocytes. Proc Natl Acad Sci U S A 2009;106:14150–5.

[119] Yamaguchi S, Ishikawa T. The electrogenic Na^+–HCO_3^- cotransporter NBCe1-B is regulated by intracellular Mg^{2+}. Biochem Biophys Res Commun 2008;376:100–4.

[120] Devogelaere B, Nadif Kasri N, Derua R, Waelkens E, Callewaert G, Missiaen L, et al. Binding of IRBIT to the IP3 receptor: determinants and functional effects. Biochem Biophys Res Commun 2006;343:49–56.

[121] Devogelaere B, Verbert L, Parys JB, Missiaen L, De Smedt H. The complex regulatory function of the ligand-binding domain of the inositol 1,4,5-trisphosphate receptor. Cell Calcium 2008;43:17–27.

[122] Gross E, Pushkin A, Abuladze N, Fedotoff O, Kurtz I. Regulation of the sodium bicarbonate cotransporter kNBC1 function: role of Asp986, Asp988 and kNBC1-carbonic anhydrase II binding. J Physiol 2002;544:679–85.

[123] Morgan PE, Pastorekova S, Stuart-Tilley AK, Alper SL, Casey JR. Interactions of transmembrane carbonic anhydrase, CAIX, with bicarbonate transporters. Am J Physiol Cell Physiol 2007;293:C738–48.

[124] Pushkin A, Abuladze N, Gross E, Newman D, Tatishchev S, Lee I, et al. Molecular mechanism of kNBC1-carbonic anhydrase II interaction in proximal tubule cells. J Physiol 2004;559:55–65.

[125] Lonnerholm G, Wistrand P. Carbonic anhydrase in the human fetal gastrointestinal tract. Biol Neonate 1983;44:166–76.

[126] Alvarez BV, Loiselle FB, Supuran CT, Schwartz GJ, Casey JR. Direct extracellular interaction between carbonic anhydrase IV and the human NBC1 sodium/bicarbonate co-transporter. Biochemistry 2003;42:12321–9.

[127] Becker HM, Deitmer JW. Carbonic anhydrase II increases the activity of the human electrogenic Na^+/HCO_3^- cotransporter. J Biol Chem 2007;282:13508–21.

[128] Lu J, Daly CM, Parker MD, Gill HS, Piermarini PM, Pelletier MF, et al. Effect of human carbonic anhydrase II on the activity of the human electrogenic Na/HCO_3 cotransporter NBCe1-A in Xenopus oocytes. J Biol Chem 2006;281:19241–50.

[129] Piermarini PM, Kim EY, Boron WF. Evidence against a direct interaction between intracellular carbonic anhydrase II and pure C-terminal domains of SLC4 bicarbonate transporters. J Biol Chem 2007;282:1409–21.

[130] Zhu Q, Kao L, Newman D, Kurtz I. The C-terminal tails of the NBCe1-A dimer are structured: relevance to CAII binding. JASN 2010.

[131] Bourke E, Delaney VB, Mosawi M, Reavey P, Weston M. Renal tubular acidosis and osteopetrosis in siblings. Nephron 1981;28:268–72.

[132] Brechue WF, Kinne-Saffran E, Kinne RK, Maren TH. Localization and activity of renal carbonic anhydrase (CA) in CA-II deficient mice. Biochim Biophys Acta 1991;1066:201–7.

[133] Rebello G, Ramesar R, Vorster A, Roberts L, Ehrenreich L, Oppon E, et al. Apoptosis-inducing signal sequence mutation in carbonic anhydrase IV identified in patients with the RP17 form of retinitis pigmentosa. Proc Natl Acad Sci U S A 2004;101:6617–22.

[134] Shah GN, Ulmasov B, Waheed A, Becker T, Makani S, Svichar N, et al. Carbonic anhydrase IV and XIV knockout mice: roles of the respective carbonic anhydrases in buffering the extracellular space in brain. Proc Natl Acad Sci U S A 2005;102:16771–6.

[135] Yang Z, Alvarez BV, Chakarova C, Jiang L, Karan G, Frederick JM, et al. Mutant carbonic anhydrase 4 impairs pH regulation and causes retinal photoreceptor degeneration. Hum Mol Genet 2005;14:255–65.

[136] Pushkin A, Abuladze N, Newman D, Lee I, Xu G, Kurtz I. Cloning, characterization and chromosomal assignment of NBC4, a new member of the sodium bicarbonate cotransporter family. Biochim Biophys Acta 2000;1493:215–8.

[137] Pushkin A, Abuladze N, Newman D, Lee I, Xu G, Kurtz I. Two C-terminal variants of NBC4, a new member of the sodium bicarbonate cotransporter family: cloning, characterization, and localization. IUBMB Life 2000;50:13–9.

[138] Sassani P, Pushkin A, Gross E, Gomer A, Abuladze N, Dukkipati R, et al. Functional characterization of NBC4: a new electrogenic sodium-bicarbonate cotransporter. Am J Physiol Cell Physiol 2002;282:C408–16.

[139] Virkki LV, Wilson DA, Vaughan-Jones RD, Boron WF. Functional characterization of human NBC4 as an electrogenic Na^+–HCO_3^- cotransporter (NBCe2). Am J Physiol Cell Physiol 2002;282:C1278–89.

[140] Pushkin A, Abuladze N, Newman D, Tatishchev S, Kurtz I. Genomic organization of the DCTN1-SLC4A5 locus encoding both NBC4 and p150(Glued). Cytogenet Cell Genet 2001;95:163–8.

[141] Gill SR, Schroer TA, Szilak I, Steuer ER, Sheetz MP, Cleveland DW. Dynactin, a conserved, ubiquitously expressed component of an activator of vesicle motility mediated by cytoplasmic dynein. J Cell Biol 1991;115:1639–50.

[142] Stutz AM, Teran-Garcia M, Rao DC, Rice T, Bouchard C, Rankinen T. Functional identification of the promoter of SLC4A5, a gene associated with cardiovascular and metabolic phenotypes in the HERITAGE Family Study. Eur J Hum Genet 2009;17:1481–9.

[143] Xu J, Wang Z, Barone S, Petrovic M, Amlal H, Conforti L, et al. Expression of the Na^+–HCO_3^- cotransporter NBC4 in rat kidney and characterization of a novel NBC4 variant. Am J Physiol Renal Physiol 2003;284:F41–50.

[144] Abuladze N, Pushkin A, Tatishchev S, Newman D, Sassani P, Kurtz I. Expression and localization of rat NBC4c in liver and renal uroepithelium. Am J Physiol Cell Physiol 2004;287:C781–9.

[145] Bouzinova EV, Praetorius J, Virkki LV, Nielsen S, Boron WF, Aalkjaer C. Na^+-dependent HCO_3^-- uptake into the rat choroid plexus epithelium is partially DIDS sensitive. Am J Physiol Cell Physiol 2005;289:C1448–56.

[146] Praetorius J, Nielsen S. Distribution of sodium transporters and aquaporin-1 in the human choroid plexus. Am J Physiol Cell Physiol 2006;291:C59–67.

[147] Millar ID, Brown PD. NBCe2 exhibits a 3 HCO_3^-:1 Na^+ stoichiometry in mouse choroid plexus epithelial cells. Biochem Biophys Res Commun 2008;373:550–4.

[148] Damkier HH, Prasad V, Hubner CA, Praetorius J. Nhe1 is a luminal Na^+/H^+ exchanger in mouse choroid plexus and is targeted to the basolateral membrane in Ncbe/Nbcn2-null mice. Am J Physiol Cell Physiol 2009;296:C1291–1300.

[149] Barkley RA, Chakravarti A, Cooper RS, Ellison RC, Hunt SC, Province MA, et al. Positional identification of hypertension susceptibility genes on chromosome 2. Hypertension 2004;43:477–82.

[150] Hunt SC, Xin Y, Wu LL, Cawthon RM, Coon H, Hasstedt SJ, et al. Sodium bicarbonate cotransporter polymorphisms are associated with baseline and 10-year follow-up blood pressures. Hypertension 2006;47:532–6.

[151] Rice T, Cooper RS, Wu X, Bouchard C, Rankinen T, Rao DC, et al. Meta-analysis of genome-wide scans for blood pressure in African American and Nigerian samples. The national heart,

lung, and blood institute genelink project. Am J Hypertens 2006;19:270–4.
[152] Padmanabhan S, Wallace C, Munroe PB, Dobson R, Brown M, Samani N, et al. Chromosome 2p shows significant linkage to antihypertensive response in the British Genetics of Hypertension Study. Hypertension 2006;47:603–8.
[153] Kao L, Kurtz LM, Shao X, Papadopoulos MC, Liu L, Bok D, et al. Severe neurologic impairment in mice with targeted disruption of the electrogenic sodium bicarbonate cotransporter NBCe2 (Slc4a5 gene). *J Biol Chem* 286: 32563–74.
[154] Groger N, Vitzthum H, Frohlich H, Kruger M, Ehmke H, Braun T, et al. Targeted mutation of SLC4A5 induces arterial hypertension and renal metabolic acidosis. *Hum Mol Genet* 21: 1025–36.
[155] Pushkin A, Abuladze N, Lee I, Newman D, Hwang J, Kurtz I. Cloning, tissue distribution, genomic organization, and functional characterization of NBC3, a new member of the sodium bicarbonate cotransporter family. J Biol Chem 1999;274: 16569–75.
[156] Pushkin A, Abuladze N, Lee I, Newman D, Hwang J, Kurtz I. Mapping of the human NBC3 (SLC4A7) gene to chromosome 3p22. Genomics 1999;57:321–2.
[157] Choi I, Aalkjaer C, Boulpaep EL, Boron WF. An electroneutral sodium/bicarbonate cotransporter NBCn1 and associated sodium channel. Nature 2000;405:571–5.
[158] Boron WF, Chen L, Parker MD. Modular structure of sodium-coupled bicarbonate transporters. J Exp Biol 2009;212: 1697–706.
[159] Cooper DS, Saxena NC, Yang HS, Lee HJ, Moring AG, Lee A, et al. Molecular and functional characterization of the electroneutral Na/HCO_3 cotransporter NBCn1 in rat hippocampal neurons. J Biol Chem 2005;280:17823–30.
[160] Pushkin A, Yip KP, Clark I, Abuladze N, Kwon TH, Tsuruoka S, et al. NBC3 expression in rabbit collecting duct: colocalization with vacuolar H^+-ATPase. Am J Physiol 1999;277: F974–81.
[161] Vorum H, Kwon TH, Fulton C, Simonsen B, Choi I, Boron W, et al. Immunolocalization of electroneutral $Na–HCO_3^-$ cotransporter in rat kidney. Am J Physiol Renal Physiol 2000;279: F901–9.
[162] Yang HS, Cooper DS, Rajbhandari I, Park HJ, Lee S, Choi I. Inhibition of rat $Na^+–HCO_3^-$- cotransporter (NBCn1) function and expression by the alternative splice domain. Exp Physiol 2009;94:1114–23.
[163] Cooper DS, Lee HJ, Yang HS, Kippen J, Yun CC, Choi I. The electroneutral sodium/bicarbonate cotransporter containing an amino terminal 123-amino-acid cassette is expressed predominantly in the heart. J Biomed Sci 2006;13:593–5.
[164] Bouyer P, Sakai H, Itokawa T, Kawano T, Fulton CM, Boron WF, et al. Colony-stimulating factor-1 increases osteoclast intracellular pH and promotes survival via the electroneutral Na/HCO_3 cotransporter NBCn1. Endocrinology 2007;148:831–40.
[165] Damkier HH, Nielsen S, Praetorius J. An anti-NH2-terminal antibody localizes NBCn1 to heart endothelia and skeletal and vascular smooth muscle cells. Am J Physiol Heart Circ Physiol 2006;290:H172–80.
[166] Gresz V, Kwon TH, Vorum H, Zelles T, Kurtz I, Steward MC, et al. Immunolocalization of electroneutral $Na^+–HCO_3^-$ cotransporters in human and rat salivary glands. Am J Physiol Gastrointest Liver Physiol 2002;283:G473–80.
[167] Odgaard E, Jakobsen JK, Frische S, Praetorius J, Nielsen S, Aalkjaer C, et al. Basolateral Na^+-dependent HCO_3^- transporter NBCn1-mediated HCO_3^- influx in rat medullary thick ascending limb. J Physiol 2004;555:205–18.
[168] Praetorius J, Kim YH, Bouzinova EV, Frische S, Rojek A, Aalkjaer C, et al. NBCn1 is a basolateral $Na^+–HCO_3^-$ cotransporter in rat kidney inner medullary collecting ducts. Am J Physiol Renal Physiol 2004;286:F903–12.
[169] Kwon TH, Pushkin A, Abuladze N, Nielsen S, Kurtz I. Immunoelectron microscopic localization of NBC3 sodium-bicarbonate cotransporter in rat kidney. Am J Physiol Renal Physiol 2000;278:F327–336.
[170] Damkier HH, Brown PD, and Praetorius J. Epithelial pathways in choroid plexus electrolyte transport. Physiology (Bethesda) 25: 239–249.
[171] Pushkin A, Abuladze N, Newman D, Muronets V, Sassani P, Tatishchev S, et al. The COOH termini of NBC3 and the 56-kDa H^+-ATPase subunit are PDZ motifs involved in their interaction. Am J Physiol Cell Physiol 2003;284:C667–73.
[171A] Reiners J, Nagel-Wolfrum K, Jurgens K, Marker T, Wolfrum U. Molecular basis of human Usher syndrome: deciphering the meshers of the Usher protein network provider insight into the pathomechanisma of the Usher disease. Exp Eye Res 2066;83:97–119.
[172] Lee S, Lee HJ, Yang HS, Thornell IM, Bevensee MO, and Choi I. Sodium-bicarbonate cotransporter NBCn1 in the kidney medullary thick ascending limb cell line is upregulated under acidic conditions and enhances ammonium transport. Exp Physiol 95: 926–37.
[173] Park HJ, Rajbhandari I., Yang HS, Lee S, Cucoranu D, Cooper DS, et al. Neuronal expression of sodium/bicarbonate cotransporter NBCn1 (SLC4A7) and its response to chronic metabolic acidosis. Am J Physiol Cell Physiol 298: C1018–28.
[174] Kanaan A, Douglas RM, Alper SL, Boron WF, Haddad GG. Effect of chronic elevated carbon dioxide on the expression of acid–base transporters in the neonatal and adult mouse. Am J Physiol Regul Integr Comp Physiol 2007;293:R1294–302.
[175] Jakobsen JK, Odgaard E, Wang W, Elkjaer ML, Nielsen S, Aalkjaer C, et al. Functional up-regulation of basolateral Na^+-dependent HCO_3^- transporter NBCn1 in medullary thick ascending limb of K^+-depleted rats. Pflugers Arch 2004;448: 571–8.
[176] Mohebbi N, Mihailova M, Wagner CA. The calcineurin inhibitor FK506 (tacrolimus) is associated with transient metabolic acidosis and altered expression of renal acid–base transport proteins. Am J Physiol Renal Physiol 2009;297: F499–509.
[177] Hulter HN, Peterson JC. Acid–base homeostasis during chronic PTH excess in humans. Kidney Int 1985;28:187–92.
[178] Chen LM, Choi I, Haddad GG, Boron WF. Chronic continuous hypoxia decreases the expression of SLC4A7 (NBCn1) and SLC4A10 (NCBE) in mouse brain. Am J Physiol Regul Integr Comp Physiol 2007;293:R2412–20.
[179] Park M, Ko SB, Choi JY, Muallem G, Thomas PJ, Pushkin A, et al. The cystic fibrosis transmembrane conductance regulator interacts with and regulates the activity of the HCO_3- salvage transporter human $Na^+–HCO_3^-$ cotransport isoform 3. J Biol Chem 2002;277:50503–9.
[180] Lauritzen G, Jensen MB, Boedtkjer E, Dybboe R, Aalkjaer C, Nylandsted J, et al. NBCn1 and NHE1 expression and activity in DeltaNErbB2 receptor-expressing MCF-7 breast cancer cells: contributions to pHi regulation and chemotherapy resistance. *Exp Cell Res* 316: 2538–53.
[181] Lopez IA, Acuna D, Galbraith G, Bok D, Ishiyama A, Liu W, et al. Time course of auditory impairment in mice lacking the electroneutral sodium bicarbonate cotransporter NBC3 (slc4a7). Brain Res Dev Brain Res 2005;160:63–77.
[182] Hmani-Aifa M, Ben Arab S, Kharrat K, Orten DJ, Boulila-Elgaied A, Drira M, et al. Distinctive audiometric features

between USH2A and USH2B subtypes of Usher syndrome. J Med Genet 2002;39:281–3.
[183] Hmani M, Ghorbel A, Boulila-Elgaied A, Ben Zina Z, Kammoun W, Drira M, et al. A novel locus for Usher syndrome type II, USH2B, maps to chromosome 3 at p23-24.2. Eur J Hum Genet 1999;7:363–7.
[184] Nagase T, Ishikawa K, Suyama M, Kikuno R, Miyajima N, Tanaka A, et al. Prediction of the coding sequences of unidentified human genes. XI. The complete sequences of 100 new cDNA clones from brain which code for large proteins *in vitro*. DNA Res 1998;5:277–86.
[185] Amlal H, Burnham CE, Soleimani M. Characterization of Na^+/HCO_3^- cotransporter isoform NBC-3. Am J Physiol 1999;276: F903–13.
[186] Wang Z, Conforti L, Petrovic S, Amlal H, Burnham CE, Soleimani M. Mouse Na^+: HCO_3^- cotransporter isoform NBC-3 (kNBC-3): cloning, expression, and renal distribution. Kidney Int 2001;59:1405–14.
[187] Grichtchenko II, Choi I, Zhong X, Bray-Ward P, Russell JM, Boron WF. Cloning, characterization, and chromosomal mapping of a human electroneutral Na^+-driven $Cl–HCO_3$ exchanger. J Biol Chem 2001;276:8358–63.
[188] Leviel F, Hubner CA, Houillier P, Morla L, El Moghrabi S, Brideau G, et al. The Na^+-dependent chloride-bicarbonate exchanger SLC4A8 mediates an electroneutral Na^+ reabsorption process in the renal cortical collecting ducts of mice. *J Clin Invest* 120: 1627–1635.
[189] Parker MD, Bouyer P, Daly CM, Boron WF. Cloning and characterization of novel human SLC4A8 gene products encoding Na^+-driven Cl^-/HCO_3^- exchanger variants NDCBE-A, -C, and -D. Physiol Genomics 2008;34:265–76.
[190] Chen LM, Kelly ML, Parker MD, Bouyer P, Gill HS, Felie JM, et al. Expression and localization of Na-driven Cl-HCO_3-exchanger (SLC4A8) in rodent CNS. Neuroscience 2008;153:162–74.
[191] Chen LM, Haddad GG, Boron WF. Effects of chronic continuous hypoxia on the expression of SLC4A8 (NDCBE) in neonatal versus adult mouse brain. Brain Res 2008;1238: 85–92.
[192] Terada Y, Knepper MA. Thiazide-sensitive NaCl absorption in rat cortical collecting duct. Am J Physiol 1990;259: F519–28.
[193] Schmitt R, Ellison DH, Farman N, Rossier BC, Reilly RF, Reeves WB, et al. Developmental expression of sodium entry pathways in rat nephron. Am J Physiol 1999;276: F367–81.
[194] Wang CZ, Yano H, Nagashima K, Seino S. The Na^+-driven Cl^-/HCO_3^- exchanger. Cloning, tissue distribution, and functional characterization. J Biol Chem 2000;275:35486–90.
[195] Giffard RG, Lee YS, Ouyang YB, Murphy SL, Monyer H. Two variants of the rat brain sodium-driven chloride bicarbonate exchanger (NCBE): developmental expression and addition of a PDZ motif. Eur J Neurosci 2003;18:2935–45.
[196] Parker MD, Musa-Aziz R, Rojas JD, Choi I, Daly CM, Boron WF. Characterization of human SLC4A10 as an electroneutral Na/HCO_3 cotransporter (NBCn2) with Cl- self-exchange activity. J Biol Chem 2008;283:12777–88.
[197] Damkier HH, Aalkjaer C, Praetorius J. Na^+-dependent HCO_3^- import by the slc4a10 gene product involves Cl^- export. *J Biol Chem*.
[198] Liu Y, Xu K, Chen LM, Sun X, Parker MD, Kelly ML, et al.. Distribution of NBCn2 (SLC4A10) splice variants in mouse brain. *Neuroscience* 169: 951–64.
[199] Lee YS, Ouyang YB, Giffard RG. Regulation of the rat brain Na^+-driven Cl^-/HCO_3^--exchanger involves protein kinase a and a multiprotein signaling complex. FEBS Lett 2006;580: 4865–71.
[200] Hubner CA, Hentschke M, Jacobs S, Hermans-Borgmeyer I. Expression of the sodium-driven chloride bicarbonate exchanger NCBE during prenatal mouse development. Gene Expr Patterns 2004;5:219–23.
[201] Jacobs S, Ruusuvuori E, Sipila ST, Haapanen A, Damkier HH, Kurth I, et al. Mice with targeted Slc4a10 gene disruption have small brain ventricles and show reduced neuronal excitability. Proc Natl Acad Sci U S A 2008;105:311–6.
[202] Praetorius J, Nejsum LN, Nielsen SA. SCL4A10 gene product maps selectively to the basolateral plasma membrane of choroid plexus epithelial cells. Am J Physiol Cell Physiol 2004;286: C601–10.
[203] Chen LM, Kelly ML, Rojas JD, Parker MD, Gill HS, Davis BA, et al. Use of a new polyclonal antibody to study the distribution and glycosylation of the sodium-coupled bicarbonate transporter NCBE in rodent brain. Neuroscience 2008;151: 374–85.
[204] Sebat J, Lakshmi B, Malhotra D, Troge J, Lese-Martin C, Walsh T, et al. Strong association of de novo copy number mutations with autism. Science 2007;316:445–9.
[205] Gurnett CA, Veile R, Zempel J, Blackburn L, Lovett M, Bowcock A. Disruption of sodium bicarbonate transporter SLC4A10 in a patient with complex partial epilepsy and mental retardation. Arch Neurol 2008;65:550–3.
[206] Parker MD, Ourmozdi EP, Tanner MJ. Human BTR1, a new bicarbonate transporter superfamily member and human AE4 from kidney. Biochem Biophys Res Commun 2001;282:1103–9.
[207] Takano J, Noguchi K, Yasumori M, Kobayashi M, Gajdos Z, Miwa K, et al. Arabidopsis boron transporter for xylem loading. Nature 2002;420:337–40.
[208] Park M, Li Q, Shcheynikov N, Muallem S, Zeng W. Borate transport and cell growth and proliferation. Not only in plants. Cell Cycle 2005;4:24–6.
[209] Park M, Li Q, Shcheynikov N, Zeng W, Muallem S. NaBC1 is a ubiquitous electrogenic Na^+-coupled borate transporter essential for cellular boron homeostasis and cell growth and proliferation. Mol Cell 2004;16:331–41.
[210] Groger N, Frohlich H, Maier H, Olbrich A, Kostin S, Braun T, et al. SLC4A11 prevents osmotic imbalance leading to corneal endothelial dystrophy, deafness, and polyuria. *J Biol Chem* 285: 14467–74.
[211] Lopez IA, Rosenblatt MI, Kim C, Galbraith GC, Jones SM, Kao L, et al. Slc4a11 gene disruption in mice: cellular targets of sensorineuronal abnormalities. J Biol Chem 2009;284: 26882–96.
[212] Kotka M, Lieden A, Pettersson S, Trinchieri V, Masci A, D'Amato M, et al. Solute carriers (SLC) in inflammatory bowel disease: a potential target of probiotics? J Clin Gastroenterol 2008;(42 Suppl 3 Pt 1):S133–5.
[213] Vithana EN, Morgan P, Sundaresan P, Ebenezer ND, Tan DT, Mohamed MD, et al. Mutations in sodium-borate cotransporter SLC4A11 cause recessive congenital hereditary endothelial dystrophy (CHED2). Nat Genet 2006;38:755–7.
[214] Desir J, Moya G, Reish O, Van Regemorter N, Deconinck H, David KL, et al. Borate transporter SLC4A11 mutations cause both Harboyan syndrome and non-syndromic corneal endothelial dystrophy. J Med Genet 2007;44:322–6.
[215] Tsuganezawa H, Kobayashi K, Iyori M, Araki T, Koizumi A, Watanabe S, et al. A new member of the HCO_3^- transporter superfamily is an apical anion exchanger of beta-intercalated cells in the kidney. J Biol Chem 2001;276:8180–9.
[216] Lipovich L, Lynch ED, Lee MK, King MC. A novel sodium bicarbonate cotransporter-like gene in an ancient duplicated

region: SLC4A9 at 5q31. Genome Biol 2001;2: [RESEARCH0011]

[217] Ko SB, Luo X, Hager H, Rojek A, Choi JY, Licht C, et al. AE4 is a DIDS-sensitive Cl^-/HCO_3^- exchanger in the basolateral membrane of the renal CCD and the SMG duct. Am J Physiol Cell Physiol 2002;283:C1206–18.

[218] Xu J, Barone S, Petrovic S, Wang Z, Seidler U, Riederer B, et al. Identification of an apical Cl^-/HCO_3^- exchanger in gastric surface mucous and duodenal villus cells. Am J Physiol Gastrointest Liver Physiol 2003;285:G1225–34.

[219] Parker MD, Boron WF, Tanner MJ. Characterization of human "AE4" as an electroneutral sodium bicarbonate cotransporter. FASEB J 2002;16:A796.

[220] Blomqvist SR, Vidarsson H, Fitzgerald S, Johansson BR, Ollerstam A, Brown R, et al. Distal renal tubular acidosis in mice that lack the forkhead transcription factor Foxi1. J Clin Invest 2004;113:1560–70.

[221] Hentschke M, Hentschke S, Borgmeyer U, Hubner CA, Kurth I. The murine AE4 promoter predominantly drives type B intercalated cell specific transcription. Histochem Cell Biol 2009;132:405–12.

[222] Rivarola V, Ford P, Chara O, Parisi M, Capurro C. Functional and molecular adaptation of Cl/HCO_3^- exchanger to chronic alkaline media in renal cells. Cell Physiol Biochem 2005;16:271–80.

[223] Simpson JE, Schweinfest CW, Shull GE, Gawenis LR, Walker NM, Boyle KT, et al. PAT-1 (Slc26a6) is the predominant apical membrane Cl^-/HCO_3^- exchanger in the upper villous epithelium of the murine duodenum. Am J Physiol Gastrointest Liver Physiol 2007;292:G1079–88.

CHAPTER

54

The SLC4 Anion Exchanger Gene Family

Andrew K. Stewart[1] *and Seth L. Alper*[2]

[1]Renal Division and Molecular and Vascular Medicine Division, Beth Israel Deaconess Medical Center, Department of Medicine, Harvard Medical School, Boston, MA, USA

[2]Renal Division, Beth Israel Deaconess Medical Center, Department of Medicine, Harvard Medical School, Boston, MA, USA

INTRODUCTION

Optimal function of mammalian cells requires tight control of the acid–base status of intracellular and extracellular compartments. The pH of arterial blood is approximately 7.35–7.45, whereas intracellular pH is normally 7.1–7.3.[1] The CO_2/bicarbonate (HCO_3^-) buffer pair is the body's major pH buffer system for maintenance of pH homeostasis. CO_2 and HCO_3^- also serve as substrates and products in numerous metabolic pathways. Up to fifteen carbonic anhydrase gene products accelerate the slow aqueous equilibration of CO_2 and HCO_3^- inside and outside cells by up to five orders of magnitude. Rapid plasmalemmal HCO_3^- transport across cell plasma membranes by Na^+-dependent and Na^+-independent HCO_3^- transporters is critical for intracellular and extracellular carbonic anhydrases to maintain this equilibrium in the face of changing metabolic demands. At least two gene superfamilies encode Na^+-independent Cl^-/HCO_3^- exchange polypeptides: the SLC4 "bicarbonate transporter superfamily" and the SLC26 "sulfate permease" multi-anion transporter superfamily. Under normal physiological conditions, the Cl^-/HCO_3^- exchangers among the polypeptides encoded by both gene superfamilies are bicarbonate extruders (acid loaders) and Cl^- loaders. Thus, both sets of Cl^-/HCO_3^- exchangers contribute to regulation of intracellular pH (pH_i), cell volume, tonicity, and intracellular [Cl^-].[2–4]

This chapter will focus on the Na^+-independent Cl^-/HCO_3^- exchangers of the SLC4 gene family: AE1/SLC4A1, AE2/SLC4A2, and AE3/SLC4A3. Other members of the SLC4 gene family will also be briefly introduced. The SLC4[2–19] and the SLC26 gene families.[20–26] have been reviewed previously.

The AE Anion Exchangers Among the SLC4 And SLC26 Superfamilies.

The SLC4 bicarbonate transporter superfamily (Fig. 54.1) includes autosomal genes encoding at least three electroneutral Na^+-independent anion exchangers (SLC4A1–3/AE1–3), three Na^+-bicarbonate cotransporters (the electrogenic SLC4A4/NBCe1 and SLC4A5/NBCe2 and the electroneutral SLC4A7/NBCn1), and Na^+-dependent anion exchangers (SLC4A8/NBCDE and SLC4A10/NCBE). The transport mechanisms of three SLC4 proteins remain controversial. SLC4A10, originally described as a Na^+-dependent Cl^-/HCO_3^- exchanger[27,28] has also been described as an electroneutral Na^+-bicarbonate cotransporter NBCn2.[29] SLC4A9 was originally described as a Na^+-independent Cl^-/HCO_3^- exchanger,[30,31] despite the strong phylogenetic prediction of Na^+-dependent transport. The most divergent mammalian member of the family, SLC4A11/BTR1/NaBC1[32] was first reported as an electrogenic Na^+-borate cotransporter important for cell proliferation,[33] but the result has remained unconfirmed despite SLC4A11's phylogenetic proximity to the SLC4 homologs AtBor1 of *A. thaliana* and YNL275w/Bor1 of *S. cerevisiae*, both responsible for maintenance of nontoxic cellular borate levels in the face of elevated environmental borate.[34,35] SLC4 genes are represented in all metazoans, including the fruitfly *D. melanogaster*,[36] the

Seldin and Giebisch's The Kidney, Fifth Edition.
DOI: http://dx.doi.org/10.1016/B978-0-12-381462-3.00054-9

© 2013 Elsevier Inc. All rights reserved.

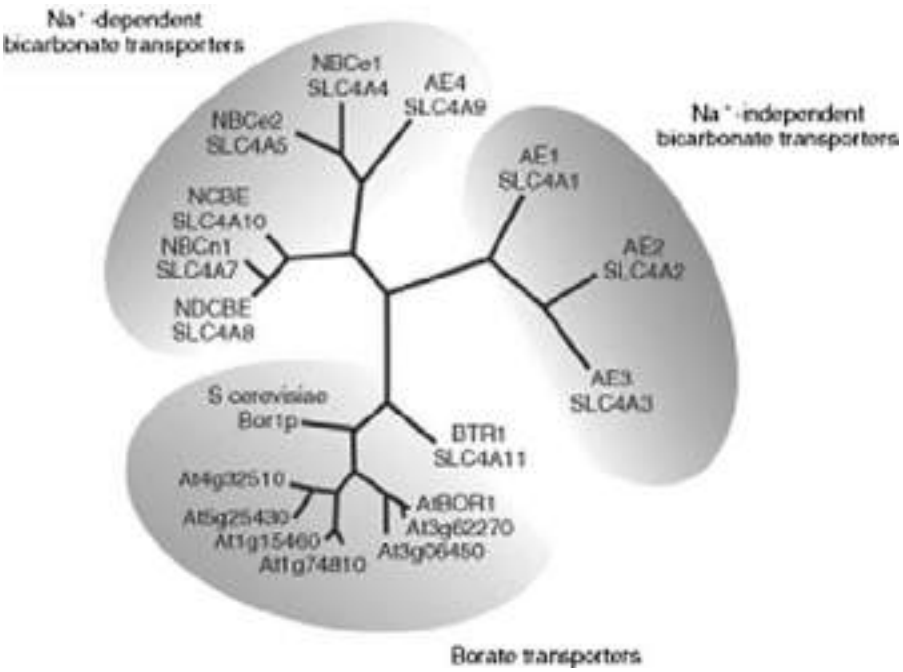

FIGURE 54.1 Phylodendrogram of human SLC4 gene family polypeptides grouped into the three clades of Na^+-independent bicarbonate transporters (red), all Cl^-/HCO_3^- exchangers; Na^+-dependent bicarbonate transporters (blue), including electrogenic and electroneutral Na^+/HCO_3^- cotransporters and Na^+-dependent Cl^-/HCO_3^- exchangers; and borate transporters (green). BTR/SLC4A11 is an electrogenic Na^+-borate cotransporter. The borate transporter clade includes proteins from *S. cerevisiae* (yeast) and *A. thaliana* (plant) of yet undefined transport mechanism. *(Modified from,[579] with permission).*

mosquito *A. aedes*,[37,38] the roundworm *C. elegans*,[39–41] the zebrafish *D. rerio*[42,43] and the pufferfish *T. nigroviridis*,[44] as well as in unicellular eukaryotes.[34,45–47] An SLC4-related gene was also recently reported in a marine prokaryotic genome.[48]

The most extensively studied member of the SLC4 gene family is SLC4A1/AE1 (also known as "band 3"), a Cl^-/HCO_3^- exchanger abundant in erythrocytes of vertebrates and elasmobranchs, but apparently absent from erythrocytes of the jawless fishes.[49] AE1 is also expressed in the Type A intercalated cells of kidney collecting duct in mammals and birds, and at much lower levels in heart and distal colon. Mutations in the SLC4A1/AE1 gene (Table 54.3) are associated with dominant hereditary spherocytic anemia, dominant Southeast Asian ovalocytosis and stomatocytic cation leak syndromes, and dominant and recessive forms of distal renal tubular acidosis.[2–4,13] AE2 is expressed widely among epithelial and other cell types, with highest expression in subsets of epithelial cells including gastric parietal cells, choroid plexus, proximal colonic enterocytes, and thick ascending limb cells. AE3 is expressed at highest levels in brain, heart, and retina, and at lower levels in smooth muscle and epithelial cells. Mutations in the genes encoding SLC4A2/AE2 and SLC4A3/AE3 have not been directly linked to Mendelian human disease, but mutations in the SLC4A4/NBCe1 electrogenic Na^+-bicarbonate cotransporter gene cause the recessive syndrome of proximal renal tubular acidosis, ocular abnormalities, and elevated pancreatic amylase,[50,51] sometimes accompanied by migraine.[52,53] Mutations in the SLC4A11 (nominal Na^+-borate cotransporter) gene are associated with congenital hereditary endothelial dystrophy of the cornea type 2[54,55] associated with vision loss, and with Harboyan syndrome (with added hearing loss). Mouse Slc4 knockout disease models for Na^+-dependent HCO_3^- transporters for which corresponding human genetic diseases remain unidentified are *slc4a5*$^{-/-}$[56] and *slc4a10*$^{-/-}$ mice[57] exhibiting altered choroid plexus function with decreased cerebral ventricular volume; *slc4a7*$^{-/-}$ mice with retinal and cochlear degeneration[58] and mild hypertension resistant to exacerbation by angiotensin II;[59] *slc4a8*$^{-/-}$ mice with coincident absence of Slc26a4/pendrin lack electroneural NaCl reabsorption by cortical collecting duct Type B intercalated cells;[60] and *slc4a11*$^{-/-}$ mice that exhibit, in addition to corneal and auditory abnormalities shared with the corresponding human diseases, polyuria likely related to renal medullary thin limb dysfunction in the countercurrent multiplier mechanism.[61,62]

Cl^-/HCO_3^- exchange and other anion exchange functions are also mediated by SLC26 polypeptides. The SLC26 gene family was identified first among Neurospora sulfate transporters, and subsequently in vertebrates[63,64] and throughout the evolutionary tree,[20] including prokaryotes.[65,66] Polypeptide products of the 11 SLC26 genes transport a wide range of monovalent and divalent anions including sulfate (SO_4^{2-}), chloride (Cl^-), bicarbonate (HCO_3^-), hydroxyl anion (OH^-), oxalate, and formate. Although unrelated in sequence to the SLC4 gene family, at least three of the SLC26 anion exchangers can mediate Cl^-/HCO_3^-

exchange: the congenital chloride-losing diarrhea gene SLC26A3/DRA,[67–69] the Pendred syndrome gene SLC26A4/Pendrin,[70,71] and SLC26A6/Pat-1/CFEX.[72,73] SLC26A7,[74] SLC26A9,[75] and SLC26A11[76,77] also mediate Cl^-/HCO_3^- exchange, but SLC26A7[78] and SLC26A9[79] also appear to function as anion channels. SLC26A2 mediates sulfate/Cl^- exchange[80,81] in chondrocytes, hepatocytes and enterocytes. SLC26A6 and SLC26A1 mediate enterocyte and proximal tubule oxalate/Cl^- exchange.[82,83]

AE DOMAIN STRUCTURE AND ALTERNATIVE TRANSCRIPTS

The AE polypeptide products of the SLC4A1–3 and SLC4A9 genes share a tripartite domain structure as predicted by hydropathy analysis and confirmed by chemical and antibody reactivity studies (Fig. 54.2). A long N-terminal cytoplasmic domain extends for 400–700 amino acids (aa) before the polypeptide chain enters the lipid bilayer. Overall % aa identity of this region among the AE polypeptides is only ~35%, but short stretches within the region are highly conserved (Fig. 54.3). The N-terminal domain of AE1 binds to cytoskeletal proteins, but binding partners of the N-terminal domains of AE2 and AE3 remain less well investigated. The transmembrane domains of ~500 aa in length (Fig. 54.2) are modeled to traverse the bilayer approximately 12–14 times, with at least one large extracellular loop carrying 1,2, or 3 N-glycans. The AE transmembrane domains share a higher overall aa identity of ~65%, with yet greater sequence identity among the putative transmembrane spans (Fig. 54.3). When expressed in *Xenopus* oocytes and in HEK 293 human embryonic kidney cells, the transmembrane domain of AE1 mediates anion transport in the absence of all but the membrane-proximal ~30 aa of the N-terminal cytoplasmic domain.[84–86] The transmembrane domain is followed by a short C-terminal cytoplasmic tail of ~35–40 aa, and harbors a putative binding site for carbonic anhydrase II[87] (but see[14]).

The majority of AE polypeptide variants described to date vary in their N-terminal amino acid sequences (Fig. 54.2). This variation derives from alternative promoter usage resulting in distinct 5′ mRNA exons expressed in tissue-specific and cell type-specific patterns.[88–91] The AE1 and AE3 genes encode two such 5′-variant transcripts encoding proteins with distinct N-terminal aa sequences. The AE2 genes of rat and human express four 5′-variant transcripts, and the mouse gene expresses five such transcripts.[91,92] Two additional transcripts of the AE3 gene encode alternate 3′-transcripts encoding predicted soluble proteins[93] devoid of intrinsic anion transport function. The AE4 gene encodes at least four (Fig. 54.2)[31] and possibly many more variant transcripts.[94] Unusual among the AE genes in its greater sequence similarity with Na^+-dependent than with Na^+-independent SLC4 polypeptides (Fig. 54.1), AE4 may nonetheless function as a Na^+-independent anion exchanger[30,31,95] (but see[7]).

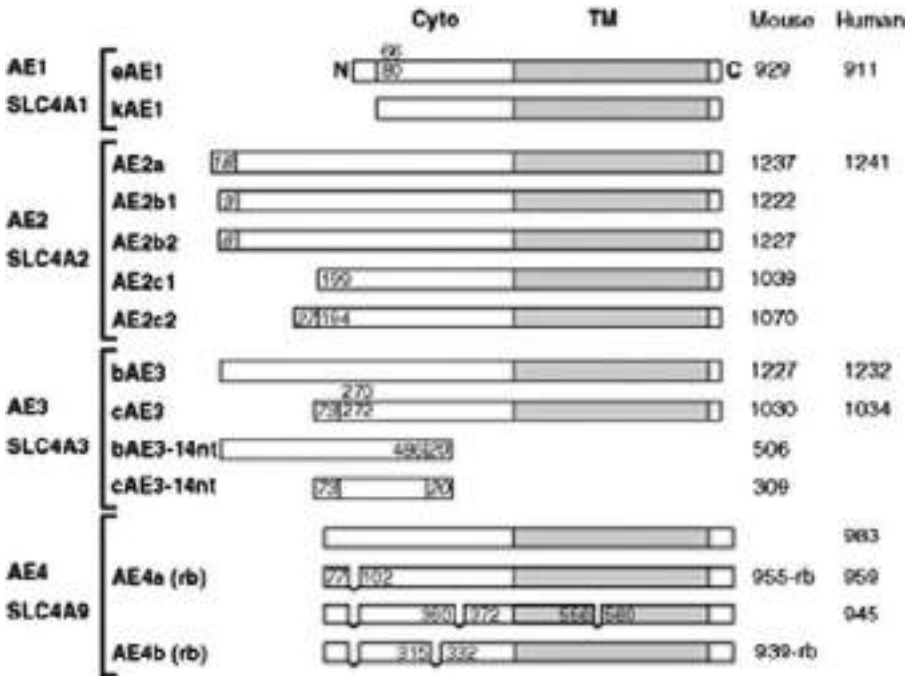

FIGURE 54.2 Schematic of polypeptide variants expressed from the SLC4 Na^+-independent transporters AE1, AE2, and AE3. Also shown are four of the many predicted polypeptide products of the AE4/SLC4A9 gene, found by some but not all to encode Na^+-independent Cl^-/HCO_3^- exchange function, despite their inclusion in the Na^+-dependent clade (Fig. 54.1). Blue indicates predicted transmembrane domains. Total polypeptide lengths (aa) at right. Length (aa) of variant N-terminal domains is indicated within leftmost boxes, and of variant C-terminal domains within rightmost boxes (for the AE3–14nt variants). Aa of junctions indicated in middle boxes. rb, rabbit.

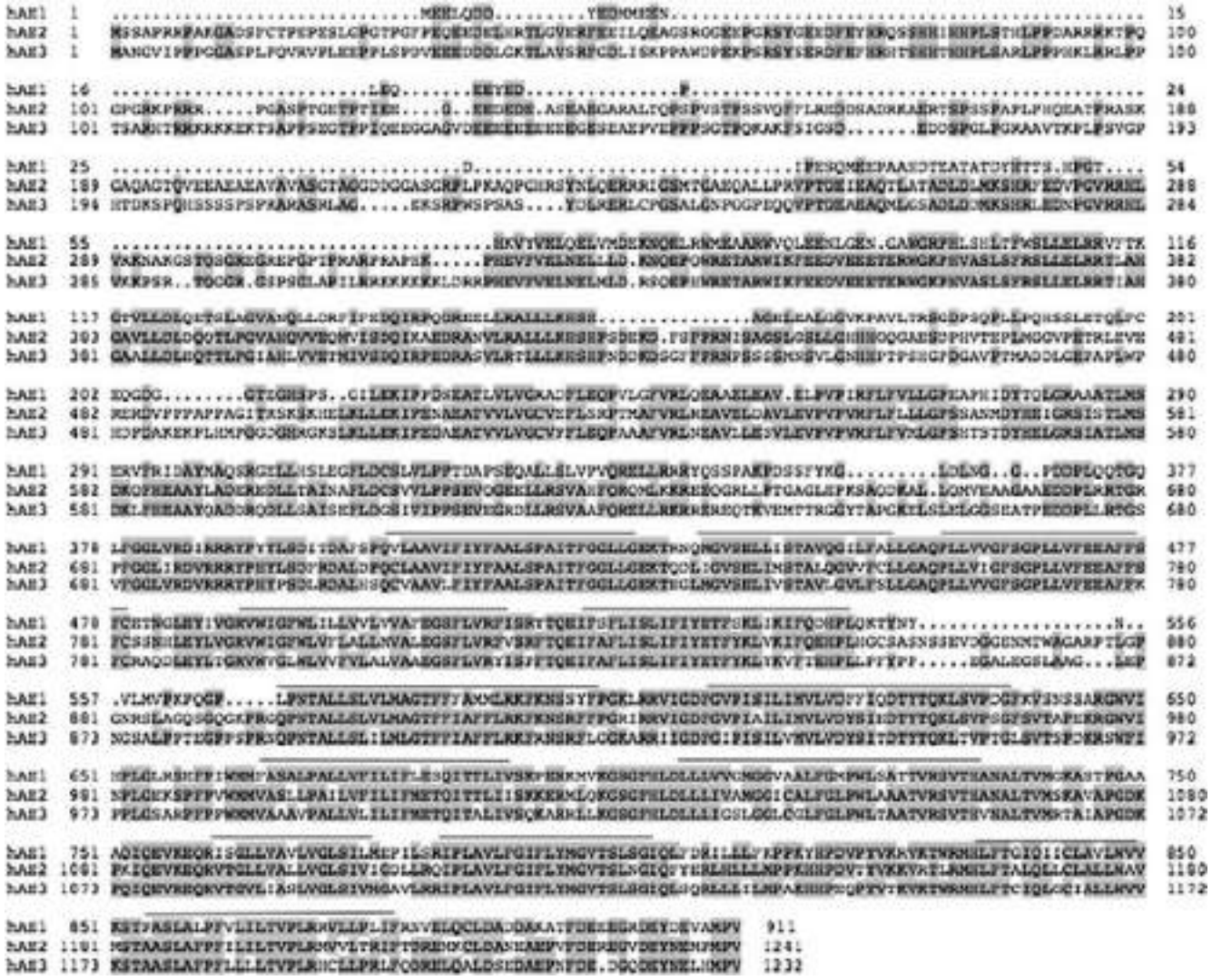

FIGURE 54.3 Amino acid sequence alignment of the Na^+-independent bicarbonate transporter clade of the human SLC4 family, including the Cl^-/HCO_3^- exchanger polypeptides AE1/SLC4A1 (eAE1, NP_000333), AE2/SLC4A2 (AE2a, NP_003031), and AE3/SLC4A3 (bAE3, NP_005061). Alignment was performed with DNAStar software, with manual revision. Conserved residues are highlighted in gray. Putative transmembrane spans are overlined, guided by models of[233] and.[237]

The AE anion exchangers mediate electroneutral, bidirectional exchange of monovalent anions, capable of hetero-exchange and homo-exchange (Fig. 54.4A). They can also mediate cotransport of divalent anions (sulfate and oxalate are the best studied) with a proton in homoexchange or in heteroexchange for monovalent chloride (Fig. 54.4B). Exchange is believed to be via a "ping-pong" mechanism, also known as a "sequential" or an "alternating sites" mechanism (Fig. 54.4C), on the basis of biochemical, kinetic, and spectroscopic changes measured during studies of anion substitution and ligand inhibition.[9,96,97] Extensive functional investigation of AE1 in intact red cells has been accompanied by study of recombinant AE polypeptides in the major expression systems of *Xenopus* oocytes[98] and HEK 293 cells,[85] as well as in CHO,[99] K562,[100] MDCK,[101–103] and Sf9 insect cells,[104] *S. cerevisia*,[105] and *E. coli*.[106]

LOCALIZATION AND FUNCTION OF ANION EXCHANGERS IN TISSUES

AE1 is essential for postnatal survival in humans[107] zebrafish,[43] mice[108,109] and cattle.[110] AE1 is expressed at highest levels in erythrocytes as the eAE1 polypeptide, constituting 25% of total membrane protein and 50% of intrinsic membrane protein. This high density in the red cell membrane is needed for rapid HCO_3^- transport during the sub-second traversal of

pulmonary capillaries (and most other non-sinusoidal capillary beds). Sparingly soluble CO_2 generated by cellular metabolism diffuses across capillary endothelial cells into red cells. There it is converted by erythroid cytoplasmic carbonic anhydrases into highly soluble HCO_3^- and promptly exported by eAE1 in exchange for extracellular Cl^-. The H^+ liberated by the OH^--consuming carbonic anhydrase reaction is buffered by hemoglobin to enhance oxygen release to hypoxic tissues.[111]

In the pulmonary capillaries this process operates in reverse, with entry of extracellular HCO_3^- into the red cell in exchange for cytoplasmic Cl^-. The newly transported intracellular HCO_3^- is used by red cell carbonic anhydrase to generate CO_2, which diffuses down its concentration gradient into the alveolar lumen for exhalation. At the same time, hemoglobin's surrender of H^+ to the OH^- newly generated by carbonic anhydrase enhances hemoglobin binding of O_2 diffusing into the red cell from the alveolus. This reversible Cl^-/HCO_3^- exchange cycle of the red cell, shuttling between hypoxic, hypercarbic peripheral capillaries and hyperoxic, hypocarbic pulmonary capillaries, increases by five- to eight-fold the total CO_2 carrying capacity of the blood[112] (~90% HCO_3^-, 5% free CO_2, and 5% carbamino-hemoglobin and other carbamino-CO_2).[113]

The role of oxygen tension in controlling the rate of mammalian eAE1-mediated anion exchange remains controversial, with reports of both hypoxic stimulation[114] and hypoxic inhibition.[115] eAE1 also mediates H^+-cotransport of sulfate[116] and oxalate[117] in exchange for Cl^-. Elevated erythroid oxalate transport has been correlated with hyperoxaluria and oxalate nephrolithiasis,[117,118] but AE1 polymorphisms have not correlated with oxalate lithiasis. eAE1 has been proposed to contribute to erythroid transport of nitric oxide (NO) or its metabolites as part of red-cell facilitated vasodilation,[119,120] by a nitrite transport-independent mechanism[121] possibly involving AE1 S-nitrosothiolation.[119] However, the stilbene disulfonate-insensitivity of erythroid NO transport, and its undiminished transport by hagfish and lamprey red cells that lack AE1, suggest a dominant AE1-independent NO transport mechanism.[122]

The kidney isoform of AE1 is a truncated form of erythroid AE1, lacking the initial 65 (human) N-terminal amino acids due to transcriptional initiation of kAE1 mRNA from an alternative promoter in exon 3 of the AE gene. kAE1 is expressed in the basolateral membrane of Type A intercalated cells of the mammalian renal collecting duct,[123–125] where it is essential for normal distal urinary acidification.[13,109] AE1 is also expressed at lower levels in glomerular podocytes,[126] heart[127,128] (whether as a tissue-specific transcript variant remains controversial), and in distal colon of rat[129] but not human.[130] Recently, AE1 was localized in the sensory cilia of olfactory neurons.[131]

The AE2/SLC4A2 Cl^-/HCO_3^- exchanger is the most widely expressed of the Na^+-independent SLC4 anion exchangers, and in the mouse is essential for post-weaning survival.[132] In the basolateral membrane of gastric parietal cells,[133] AE2 is required for normal gastric acid secretion.[132] AE2 is required for normal osteoclast activity,[134,135] and for normal male fertility.[136] AE2 is also expressed (Fig. 54.14) in conjunctival epithelium,[137] in odontoblasts and ameloblasts[138,139] in choroid plexus epithelial cells,[140] intestinal enterocytes,[141] respiratory epithelium,[142,143] and in biliary ductular epithelium.[144–146] AE2 is expressed along the length of the nephron (Fig. 54.13), at highest levels in basolateral membranes of medullary thick ascending limb and inner medullary collecting duct.[147–149] AE2 has also been noted in basolateral membrane of macula densa in mouse,[149] rat,[148] and rabbit,[150] where it may possibly contribute to glomerulotubular feedback. The near-ubiquitous distribution of AE2 suggests that AE2 also serves a homeostatic, housekeeping function in the regulation of intracellular pH (pH_i), intracellular chloride concentration and cell volume regulation in renal epithelial cells as well as in other tissues. In some circumstances, as in IMCD cells, AE2 may contribute to transepithelial anion secretion.

AE3 expression is prominent in heart,[151,152] brain,[85,153] retina,[154] adrenal gland,[155] as well as at lower levels in smooth muscle[156] and in epithelial cells of kidney and gut.[153] AE3 can modulate seizure threshold in mice,[155] but its role in renal and cardiac function remains little understood, slowed in part by questionable histochemical specificity of some antibodies as judged by absence of immunostaining in knockout tissue (unpublished results). AE4/SLC4A9 appears apical in gastric surface mucous and duodenal villus cells,[95] but shows species-dependent cell polarity and cell type-specificity in immunostained intercalated cells.[30,31,157] The antibodies may prove unreliable or species-specific, since the AE4 promoter exhibits Type B-intercalated cell specificity.[158] The physiological function of AE4 remains unclear.[159]

AE1 N-TERMINAL CYTOPLASMIC DOMAIN STRUCTURE AND BINDING PROTEINS

Much structural information available for AE anion exchangers derives from study of the abundant erythroid AE1 (eAE1) polypeptide. The N-terminal cytoplasmic domain is attached to and may anchor cytoskeletal protein complexes at the inner face of the erythroid plasma membrane, as shown in Fig. 54.5.

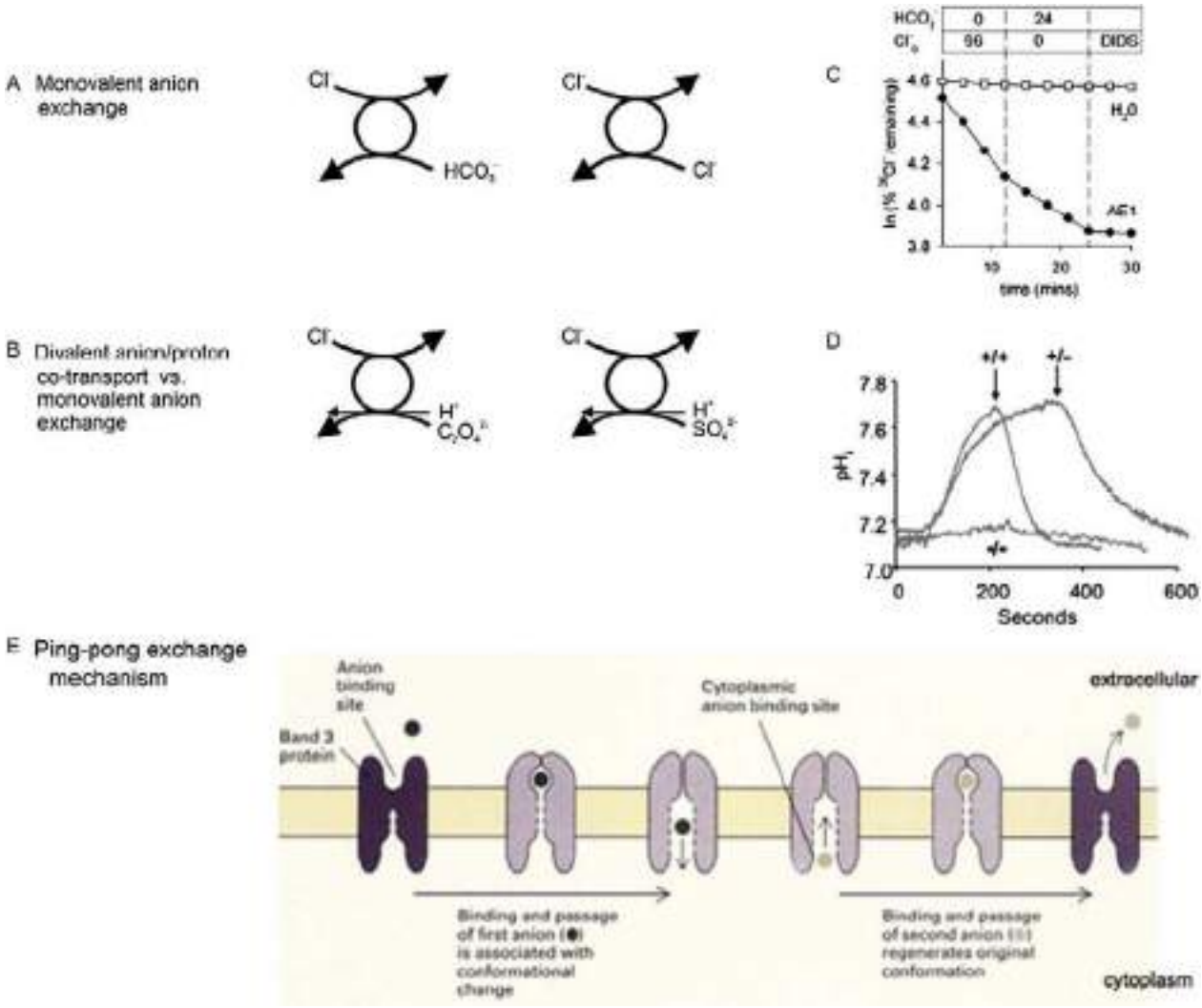

FIGURE 54.4 Anion exchange modes of electroneutral Na^+-independent SLC4 polypeptides. A. Schematic of monovalent anion exchange. B. Schematic of monovalent anion exchange with a divalent anion/proton pair. The spectrum of transported anion substrates is more extensive than portrayed in A and B (see.[229] C. Example of $^{36}Cl^-$ efflux from an AE1-expressing oocyte in exchange for extracellular Cl^- or HCO_3^-, then inhibited by extracellular DIDS. D. Reversible Cl^-/HCO_3^- exchange by BCECF-AM-loaded osteoclasts from wildtype ($^{+/+}$), heterozygous ($^{+/-}$) and homozygous ($^{-/-}$) Ae2(a,b) knockout mice (from[580] with permission). E. The ping-pong (sequential) exchange mechanism is believed applicable to the transport modes portrayed in A and B *(C modified from[581] with permission).*

eAE1 is linked to the spectrin-actin cytoskeleton through its binding of the linker protein ankyrin. Ankryin copy number is ~20% that of eAE1 monomers. eAE1 in the red cell membrane appears to be homodimeric[160,161] or homotetrameric as bound to ankyrin.[162,163] eAE1 also binds tightly to protein 4.2 and glycophorin A, and with lower apparent affinity to protein 4.1, an actin-binding component of the cytoskeletal junctional complex (Fig. 54.5). Less direct interactions have been detected with NH_3 channel RhAG[164] and with water/CO_2 channel AQP1,[165] but see.[166,167] AE1 participates in an erythroid membrane macromolecular complex[164,168] established early during erythropoiesis.[169]

The X-ray structure of the recombinant dimeric N-terminal cytoplasmic domain of eAE1 overexpressed in *E. coli* and crystallized at pH 4.8 has been solved at 2.6 A resolution[106] (Fig. 54.6). The eAE1 monomers are intertwined through "domain swapping" of individual dimerization domains via leucine zipper interactions. The monomers show near two-fold symmetry around an axis at the dimer interface, and the dimers are packed in the crystal as tetramers. The N-terminal 54 amino acids (aa) and the membrane-proximate C-terminal-most 19 aa of eAE1 were disordered in the crystal, and so not visualized. The 20–25 aa immediately preceding entry of the polypeptide chain into the lipid bilayer[170] were omitted from the crystallized

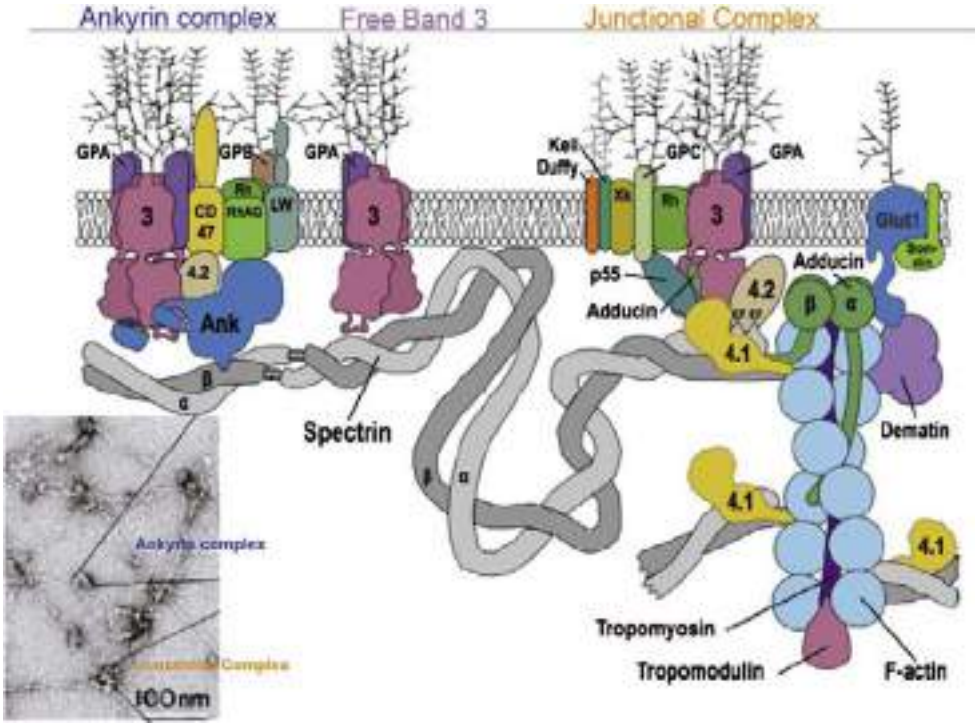

FIGURE 54.5 Three populations of AE1/SLC4A1 (Band 3) envisioned in the the erythrocyte membrane and underlying cytoskeleton: 1) free, unbound AE1 dimers; 2) AE1 tetramers in complex with the ankyrin/spectrin complex (blue in transmission electron micrograph at lower left), associated with AE1-binding proteins glycophorin A (GPA), protein 4.2, and with the RhCDE/RhAG/GPB/CD47/LW complex; 3) AE1 dimers of the spectrin/actin/Protein 4.1 junctional complex (orange in micrograph at lower left) with AE1-binding proteins GPA, adducin and protein 4.2, with associated protein 4.1/p55, GPC, Kell/XK, Duffy, and Glut1/stomatin, all linked to the spectrin/actin/tropomyosin/tropomodulin complex(*Adapted with permission from*[582,583]).

recombinant polypeptide, guided by earlier protease accessibility studies. The absence of this junctional structure renders uncertain the orientation of the AE1 N-terminal cytoplasmic domain with respect to its adjacent transmembrane domain. This eAE1 crystal structure has been used to model the corresponding region of SLC4A2/AE2,[171] and will provide the template for structural analysis of the recently crystallized recombinant N-terminal cytoplasmic domain of the homologous electrogenic sodium bicarbonate cotransporter SLC4A4/NBCe1A.[172]

The soluble eAE1 N-terminal cytoplasmic domain undergoes several structural changes upon pH shift from 6.0 to 10.0, including elongation of the Stokes radius and the axial ratio, increased intrinsic fluorescence, decreased thermal stability, and increased protein segmental motion.[162,173] The crystal structure of the eAE1 N-terminal cytoplasmic domain is more compact than predicted by the domain's solution properties, possibly reflecting the acidic crystallization pH. The crystal structure can be modeled to undergo an alkaline pH-induced elongation in the region of the dimerization domain (Fig. 54.6), leading to separation of the peripheral protein binding domain from the dimerization domain,[173] supported by intradimer luminescence resonance energy transfer (LRET) measurements between Cys201 residues in adjacent monomers.[174] Single particle fluorescence resonance energy transfer (FRET) measurements document two populations of conformers at neutral pH, with inter-Cys201 distances similar to those measured by LRET at extreme pH values. However, this distance is larger when estimated "in situ" in endogenous AE1 present in KI-stripped inside-out red cell vesicles. Moreover, the pH-dependence of that distance differs from that of pure recombinant N-terminal cytoplasmic domain prepared from inside-out vesicles, further suggesting distinct conformations in the two experimental systems,[174] and the potential for considerable plasticity of conformation dependent on local environment and binding partners.

Many functions have been assigned to the N-terminal cytoplasmic domain of eAE1 (Table 54.1). Glycolytic enzymes translocated from cytosol to membrane binding sites[175] where they may form macromolecular complexes to regulate ATP production in concert with metabolic demand. Aldolase binding to AE1 requires two sites within aa 1–23, including aa

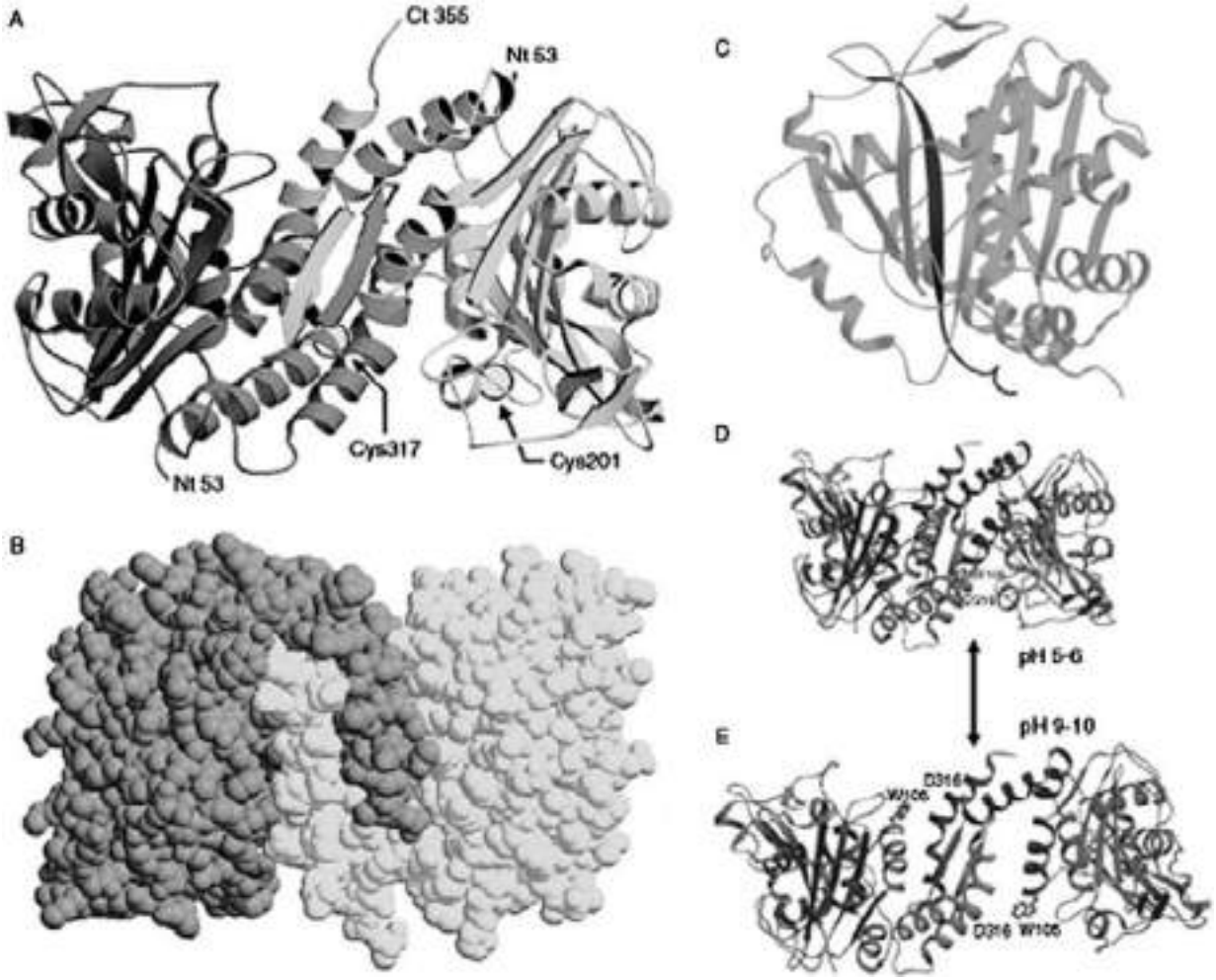

FIGURE 54.6 X-ray crystal structure of the dimeric N-terminal cytoplasmic domain of human AE1/SLC4A1, showing the structured portion (aa 55–356) from the 379 aa domain. A. Ribbon diagram. B. Space-filling model of dimer showing interlocking arms of monomeric units. C. Ribbon diagram viewed from a different angle, showing aa 55–65 (dark strand) present in eAE1, but missing in kAE1. D. and E. Reversible conformations of dimeric cytoplasmic domain predicted for pH 6 (D) and pH 10 (E), perhaps explaining the alkalinization-induced Stokes radius increase of 11 A and the doubling of intrinsic fluorescence. *(A–C reproduced with permmission from[106]; D and E reproduced with permission from[173]).*

6–10 and aa 19–23. Glyceraldehyde-3-phosphate dehydrogenase binds to either of two sites located within aa 1–11 or within 12–23. Phosphofructokinase binds to aa 12–23, but AE1 does not contribute the membrane binding sites for lactate dehydrogenase and pyruvate kinase.[176] Thus, organization of the entire glycolytic complex at the red cell membrane requires not only AE1 but additional membrane proteins. Oxygen tension[175] and hemoglobin binding to the eAE1 N-terminal region also contribute to membrane association of glycolytic enzymes. Glycolytic enzymes are largely membrane-localized in inactive form in oxygenated erythrocytes through binding to N-terminal residues of eAE1. Deoxygenation leads to enzyme release and translocation to the cytosol, thus derepressing erythroid glycolytic flux.[177] Glycolytic enzymes of *Ae1*$^{-/-}$ mouse red cells exhibit oxygenation-independent, constitutively cytosolic localization.[178] The eAE1 peptide aa 1–10 bound with low affinity to tetrameric hemoglobin, and decreased hemoglobin cooperativity to the same degree as did the entire N-terminal cytoplasmic domain, or as 2,3-diphosphoglycerate.[179] AE1 N-terminal cytosolic domain mutants with enhanced hemoglobin binding accelerated polymerization of sickle hemoglobin in solution,[180] suggesting a possible point of therapeutic intervention in sickle disease. Conversely, hemoglobin also induced conformational change in AE1.[181–183]

The major human AE1 binding site for erythroid ankyrin is a surface loop comprising aa 175–185.[184] The AE1-ankyrin interaction, although critical for membrane stability, was insensitive to shear stress in

TABLE 54.1 AE1 Residues of Defined Function

Location	eAE1 Residue	Importance/Function	Reference
N-term cytoplasmic	1–11, 12–23	GAPDH binding site	176,446
	12–23	Deoxy-hemoglobin/hemichrome binding site	513,514
	Y8, Y21	p72syk phosphorylation sites, Y8 inhibits binding of glycolytic enzymes	175,515–517
	6–10, 19–23	Aldolase binding site	176
	12–23	Phosphofructokinase binding site	176
	T42	Major casein kinase 1 phosphorylation site	360
	1–54	Disordered in crystal	106
	55–65, 175–185	Required for Ankyrin-1 binding site	184
	Y105, D316	Postulated to contribute inter-monomeric H bond related to pH-sensitive elongation, Trp fluorescence, thermal stability	106
	C201, C317	Able to form inter-monomeric disulfide link	220
	202–211, 357–9	Disordered in crystal	106
	208–225	Contributes to dimer: dimer interface of tetramer	106
	252–261	Contributes to dimer: dimer interface of tetramer	106
	S303	Minor casein kinase 1 phosphorylation site	360
	314–344	Dimerization arm	106
	343–347	Required for Protein 4.1 binding site	189
	K360	Cytoplasmic domain trypsin cleavage site	518
	G381	Deletion abolishes function but maintains surface expression	170
	357–399	Flexible link between N-term cyto and transmembrane domains	106
	Y359	Cytoplasmic domain chymotrypsin cleavage site.	
		Secondary p53/56lyn phosphorylation site, requires prior syk phosphorylation of Y8/Y21; SHP-2 binding to phospho-Y359 allows dephosphorylation of Y8, Y21, Y904.	
		Required for basolateral targeting in polarized MDCK cells	209,479,519
C-term transmembrane	K430	EC1 site of extracellular eosin-maleimide binding, reductive methylation; inhibits function	520
	C479	TM3 site reacts with PCMBS, unreactive with maleimides	235
	K539	EC3 covalent binding site for DIDS/H_2-DIDS, SITS and DNFB; inhibits function	521,522
	K542	EC3 alternate covalent binding site for DIDS (not H_2(DIDS) when K542 mutated	523
	K551, K562	EC3 sites of inter-monomeric crosslinking with BSSS within dimer	218
	M559	Oxidized by Chloramine T (N-chloro-p-toluenesulfoamide)	230
	K590	Inner TM6 covalent binding site for phenyl isothiocyanate and DNFB; inhibits function	521,524,525
	Q630	EC4 extracellular papain cleavage site; inhibits function	526–528
	N642	EC4 N-glycosylation site; glycan not required for trafficking or function	470
	E681	Inner TM8 binding site for extracellular Woodward's Reagent K; inhibits function	

(*Continued*)

TABLE 54.1 (*Continued*)

Location	eAE1 Residue	Importance/Function	Reference
		Reduction by borohydride leads to H + -independent sulfate self-exchange.	254,265
	H734	Intracellular DEPC labeling site, as assigned based on mutagenesis and function in oocytes.	300
	M741	Oxidized by Chloramine T, partially blocked by DNDS and by DEPC.	230
	K743	Intracellular trypsin cleavage site (at low ionic strength)	529,530
	H834	Intracellular DEPC labeling site; modification decreases sulfate affinity, but not substrate-induced conforational change	303,531
	C843	Inner TM13 palmitoylation site	532,533
	K851	Outer TM13 PLP binding site and H_2DIDS intramonomeric crosslinking site; inhibitory	522
	C885	C-term cyto tail NEM labeling site	237
	886–890	Carbonic anhydrase 2 binding site; stimulatory	322
	886–911	Alanine scan mutagenesis reduces V_{max} for sulfate transport in S. cerevisiae.	326
	R901	C-terminal cyto tail site of hydroxyphenylglyoxal binding, reduced in H_2-DIDS-locked outward conformation of AE1. Modification or mutations reduces V_{max} for sulfate transport.	296
	D902EY	Involved in binding GAPDH to kAE1	350
	Y904	Secondary p53/56lyn phosphorylation site, requires prior syk phosphorylation of Y8/Y21	
		Required for basolateral targeting in polarized MDCK cells.	209,479
	M909	Oxidized by Chloramine T	230
	878–911	Binds cytoplasmic N-terminal tail of glycophorin A in vitro and in yeast two hybrid.	347
	893–911	Encodes or activates red cell ghosts glycophorin A protease.	347

resealed red cells.[185] Mouse red cells lacking the corresponding critical Ae1 aa 188–199, despite loss of ability to bind ankyrin *in vitro*, were found to retain 60% of AE1 cytoskeletal binding in red cells that were less destabilized than predicted.[186] The sustained cytoskeletal binding was later attributed in part to interaction with adducin[187] and to the junctional complex. Increased cytoskeletal attachment of AE1 gradually reduces AE1 mobility in the plane of the plasma membrane during erythroid development.[188] Binding of the N-terminal 30 kDa membrane-association domain of protein 4.1R was localized to the LRRRY motif at AE1 aa 343–347 by ligand blot,[189] whereas solution binding methods indicated a predominant role for sites near the far N-terminus of the cytoplasmic domain.[190] ~20% of erythroid protein 4.1 binds to AE1, with larger proportions bound to glycophorin C and to p55/dematin.[191] Phosphatidylinositol-4,5-bisphosphate (PIP2) decreased protein 4.1 binding to AE1 while increasing binding to glycophorin C.[192] Single particle tracking experiments in wildtype and mutant mouse red cells suggest that ~40% of eAe1 is bound to ankyrin, ~33% is bound to adducin, and 27% is unattached to cytoskeletal proteins (Fig. 54.5).[193]

The ribbon diagram of Fig. 54.6C shows as a dark β strand the eAE1 aa 55–65 that are absent from kidney AE1 (kAE1, Fig. 54.2) of renal collecting duct Type A intercalated cells. Absence from kAE1 of this β-strand and the preceeding erythroid-specific residues predicts a structure quite different from that of eAE1, consistent with the inability of kAE1 to bind erythroid ankyrin[194] protein 4.1R, and aldolase.[195] The lack of ankyrin binding by kAE1 corresponds to apparent absence of erythroid ankyrin in Type A intercalated cells.[196] The influence of eAE1-specific aa 1–65 (absent from kAE1) on the conformation of the N-terminal cytoplasmic domain is further suggested by the ability of the common, clinically benign polymorphism K56E (band 3 Memphis, Table 54.3) to retard the SDS-polyacrylamide gel mobility of the N-terminal 60 kDa chymotryptic fragment of erythroid AE1. An additional influence on the structure of the transmembrane domain is suggested by the decreased erythroid transport rate for the (slowly transported putative) substrate, phosphoenolpyruvate.[197]

The erythroid-specific protein 4.2 closely associated with eAE1 during fractionation, and interacted when coexpressed in *Xenopus* oocytes.[198] Genetic deficiency

of AE1 in human hereditary spherocytosis or in knockout animals can be associated with decreased protein 4.2.[199] Conversely, the hereditary elliptocytosis or spherocytosis of protein 4.2 deficiency is associated with partial reduction in abundance of erythroid AE.[200] Incorporation of protein 4.2 into band 3 proteoliposomes slightly reduced anion transport.[201] In contrast, coexpression of protein 4.2 in *Xenopus* oocytes increased AE1-mediated anion transport,[198] whereas some protein 4.2 spherocytosis mutants lacked this phenotype. Protein 4.2 may also link AE1 to the Rh complex via red cell CD47.[202]

Undefined AE1 residues bind to aa 200−211 of protein 4.2, immediately adjacent protein 4.2's ankryin-binding site at aa 187−200.[203] AE1 cleavage at aa 45 and aa 205 by erythroid caspase 3 decreased binding of protein 4.2.[204] Since activated red cell caspase 3 also promotes externalization of phosphatidylserine,[205] a marker and agent of terminal red cell aging[206] and a signal for erythrophagocytosis,[207] the band 3-protein 4.2 interaction may signal erythrocyte removal from the circulation. In HEK-293 cells, AE1 hereditary spherocytosis mutant polypeptides E40K, G130R, and P327R exhibited diminished binding to co-expressed protein 4.2, with decreased protein 4.2. The AE1 transmembrane domain did not interact with protein 4.2.[208]

The tyrosine kinases Syk and Lyn bind to human eAE1 and phosphorylate its N-terminal cytoplasmic domain at Y8, Y21, and Y359. The phosphorylation state of these Tyr residues regulates glycolytic enzyme binding,[175] but likely not anion transport.[117,209] eAE1 tyrosine phosphorylation is increased by malaria parasite invasion, the oxidative stress of sickle disease, thalassemia, G6PD deficiency, and normal cell aging, as well as by hypertonic cell shrinkage. Tyrosine phosphorylation also promotes AE1 dissociation from the cytoskeleton and promotes mobility in the membrane,[210] perhaps adaptive responses to the above stresses.

A calponin homology domain of human kAE1 (aa 27−189, corresponding to aa 92−254 of eAE1) was shown to bind to the C-terminal catalytic domain of integrin-linked kinase in the endoplasmic reticulum, traffic together to the basolateral membrane leading to increased surface expression with proportionately increased transport activity, although without the expected increase in actin cytoskeletal association.[211] The AE1 N-terminal cytoplasmic domain has also been shown to interact with the C-terminal tail of GLUT1.[212] Although the N-terminal cytoplasmic domain of AE2 may bind erythroid ankyrin,[213] others detected no ankyrin binding to N-terminal cytoplasmic domains of kAE1, AE2, or cAE3.[194,214] AE2 binding to the distinct Golgi ankyrin Ank_{195}[215] may contribute to membrane anchoring of the Golgi cytoskeleton.[216] AE3 N-terminal cytoplasmic domain binding proteins have not been reported.

AE1 C-TERMINAL TRANSMEMBRANE DOMAIN STRUCTURE AND BINDING PROTEINS

The C-terminal transmembrane domains of AE1, AE2,[86,217] and AE3[85] suffice to mediate anion exchange in the absence of their corresponding N-terminal cytoplasmic domains. The native or detergent-solubilized transmembrane domains of AE1,[160,218−220] AE2,[221] and AE3[222] are dimers or higher-order oligomers. Figs 54.7A−F shows 18A resolution cryo-electron microscopy images of the dimeric, H_2-DIDS-crosslinked transmembrane domain of solubilized eAE1 in tubular crystals,[223] supporting earlier electron microscopic images of negatively stained two-dimensional crystals.[224,225] Higher resolution (Fig. 54.7A) electron microscopic images of 2D crystals (Fig. 54.7G) revealed outlines of several transmembrane helices,[226] allowing identification of an overall fold with similarities to the Clc Cl^-/H^+ exchanger gene superfamily.[226] This similarity has prompted consideration of an AE1 transmembrane domain model incorporating anti-parallel V-shaped motifs[227] differing from that previously derived from topographically directed mutagenesis and labeling studies (as in Fig. 54.8).

Growth of three-dimensional crystals suitable for high resolution X-ray diffraction has proven difficult for the transmembrane domain of eAE1[228] and for the *S. cerevisiae* SLC4 putative borate transporter polypeptide YNL275w/Bor1p (Fig. 54.1).[34,35,47] This difficulty may reflect in part the conformational flexibility of AE1 required to accommodate a wide range of anion substrate dimensions,[229] and the possibly increased susceptibility of AE1 Met residues to oxidation by peroxides accumulating in polyoxyethylene detergents such as C12E8.[230] Polytopic transmembrane domains of prokaryotic membrane proteins overexpressed in *E. coli* have proven more amenable to crystallization and have provided insight into SLC26-related anion transporter structure.[65,66,231] The recent description of a marine prokaryotic SLC4 anion transporter[48] suggests that this or another route to crystallization and structure determination[46,232] will soon bear fruit for a prototype SLC4 anion transporter transmembrane domain.

In the absence of a high resolution crystal structure, indirect studies of SLC4 transmembrane domain structure have relied upon chemical modification of native or detergent-solubilized erythroid eAE1, and site-directed mutagenesis studies of recombinant AE1 (Table 54.1) and AE2 (Table 54. 2). Fig. 54.8 presents a

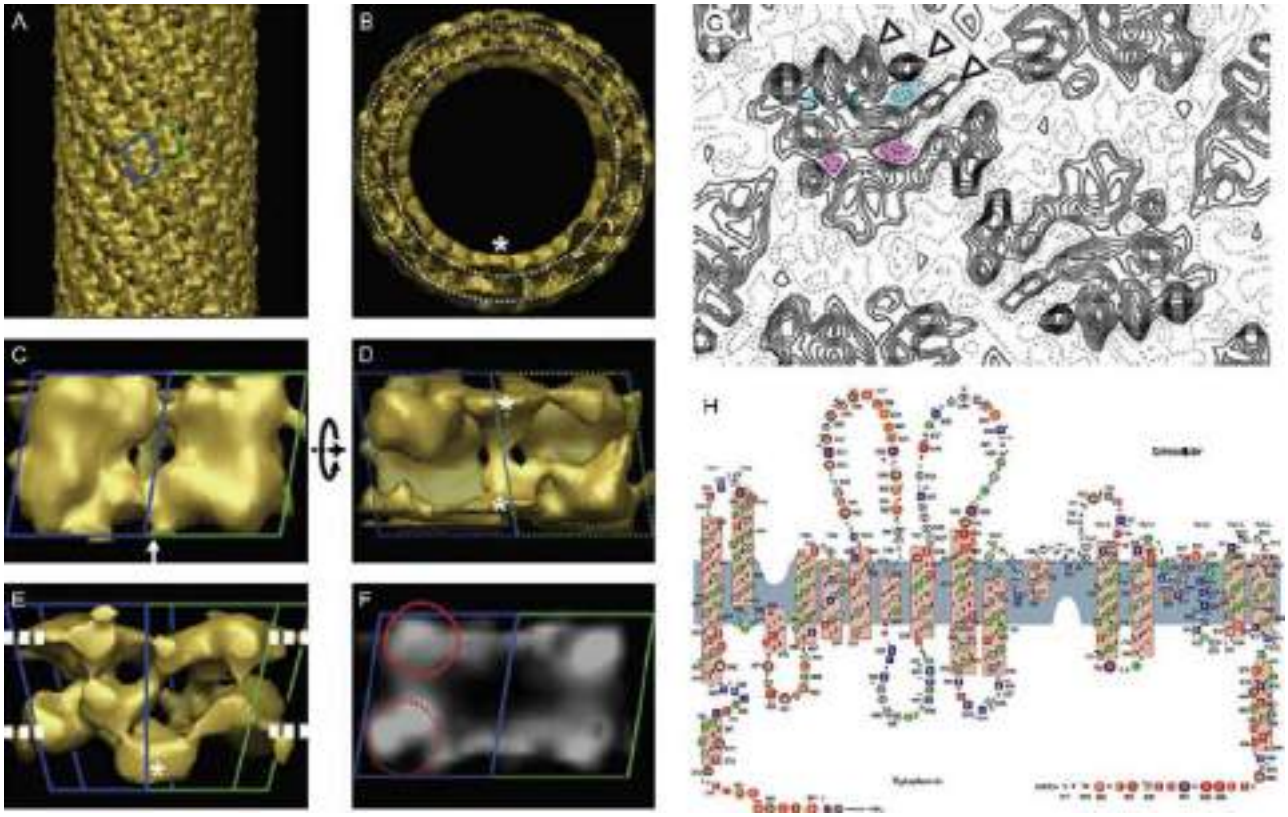

FIGURE 54.7 A. Three-dimensional image reconstruction (18 A resolution) of a tubular crystal of H_2-DIDS-crosslinked human AE1 transmembrane domain (TMD) in outward conforation (side view with boxes demarcating two protomers of a dimer). B. End-on view, with white dotted lines estimating boundaries of lipid bilayer. Asterisk in B, D, and E marks 20A protrusions on extracellular surface. The intracellular (C) and extracellular (D) surfaces of the AE1 TMD dimer unit cell boxed in (A). E. AE1 TMD dimer viewed along the tube axis (through the membrane plane, with membrane boundaries estimated by white dotted lines. Projection image of AE1 TMD dimer from cytoplasmic side, with circles suggesting subdomains of one protomer. (*A–F reproduced with permission from*[223]). G. Two-dimensional crystal projection map (7.5 A resolution) of H_2-DIDS-crosslinked AE1 TMD dimer in outward conformation (*reproduced with permission from*[226]). H. Topology of AE1 TMD modeled on the anti-parallel V-shaped repeat structure of the *E. coli* Clc Cl Figure Legends See color plate section at the back of the book.

topographical model of the secondary structure of eAE1, based on hydropathy analysis[233] updated by scanning cysteine accessibility mutagenesis data[234–238] (but without considering the 2D crystal EM data shown in Fig. 54.7). The model is also informed by proteolytic, glycolytic, and chemical labeling studies (Table 54.1), identification of polymorphic blood group antigen sites recognized by extracellular antibodies (Fig. 54.8 and Table 54.3), and scanning N-glycosylation insertional mutagenesis studies.[239–241] These latter studies suggest that folding of the transmembrane domain in the endoplasmic reticulum (as measured by *in vitro* translation) differs from that in the plasma membrane, and likely undergoes further maturation during transit to the cell surface.[240] The proposal of two flexible re-entrant loop regions suggested by accessibility of introduced Cys residues to impermeant reagents from either side of the cell membrane[237] deviates considerably from earlier models based solely on hydropathy analysis.[233] A model of AE1 transmembrane helix packing was proposed based on groups of two or more complementary subfragments of the AE1 transmembrane domain capable of partial reconstitution of wildtype chloride transport activity.[242–244] Intra- and intersubunit distance constraints have been proposed based upon fluorescence resonance energy transfer (FRET) and luminescence resonance energy transfer experiments (LRET) between inhibitor binding sites or between inhibitor probes and targeted cysteine probes.[174,245,246] FRET experiments have been extended to single dimeric AE1 subdomains on coverslip,[247] allowing measurement of the kinetics of single molecule conformational changes. Intermolecular FRET has also been used to estimate the local pH_i gradient change produced by AE1-mediated Cl^-/HCO_3^- exchange in the immediate intracellular vicinity of the AE1 polypeptide expressed in HEK-293 cells.[248]

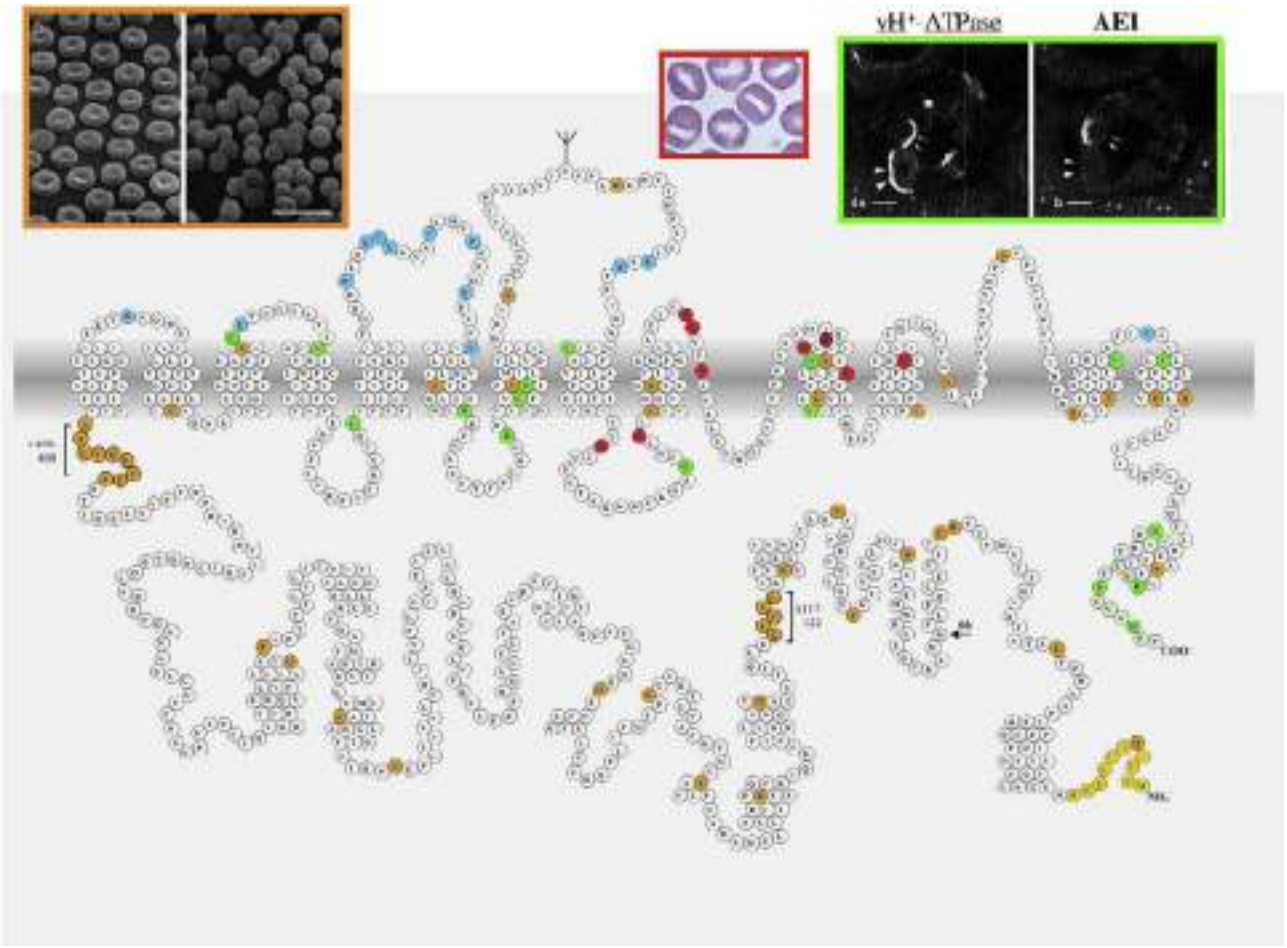

FIGURE 54.8 Proposed topographical model for human AE1/SLC4A1, with natural amino acid variants. Met 66 (arrow) marks start of kidney AE1. Polymorphisms encoding blood group antigens are in blue. Mutations associated with hereditary spherocytic anemia and ovalocytosis are in orange, and include missense, nonsense, splicing, and deletion mutations. Missense mutations associated with hereditary cation-leak stomatocytosis are in red. Mutations associated with dominant and recessive distal renal tubular acidosis are in green. Terminal deletions are in lighter orange and green. Upper left: scanning electron micrographs of bovine wild-type erythrocytes and AE1(−/−) spherocytes (HS, modified with permission from[110]). Upper center, Wright-Giemsa-stained human stomatocytes. Upper right: consecutive semithin sections of rat kidney cortex immunostained for vH^+-ATPase (left) and AE1 (right). Note that only Type A intercalated cell with apical vH^+-ATPase expresses basolateral kAE1 (Modified from[3] with permission). See color plate section at the back of the book.

MECHANISMS OF SLC4/AE ANION TRANSPORT

The anion exchangers AE1, AE2 and AE3 transport monovalent anions (i.e. Cl^- for HCO_3^-) by a mechanism of obligatory one-for-one electroneutral exchange (Fig. 54.4). Each AE1 transport unit in the intact human red cell exchanges Cl^- for HCO_3^- or another Cl^- ~50,000/sec at 37°C.[249] AE1-mediated exchange in the red cell is tightly coupled such that net Cl^- movement driven by the transmembrane electrical potential is at least 10,000 times slower than unidirectional[36] Cl^- flux in the context of homo- or hetero-exchange.[9,250] The tight coupling is reflected in the obligatory trans-anion dependence of unidirectional anion movement. Electroneutral one-for-one monovalent exchange has been rigorously demonstrated for eAE1 expressed in *Xenopus* oocytes.[251] The tight coupling of anion exchange may allow higher anion:cation selectivity than permitted by the pore of an ion channel, with consequent reduction in the metabolic cost of volume regulation.[9] Transport of divalent anions such as sulfate and oxalate requires cotransport with a proton,[116,117] by a mechanism in which divalent anion binding facilitates cis-binding of protons, and proton binding facilitates subsequent binding of divalent anion.[252,253]

Kinetic and other studies generally support a ping-pong mechanism for AE1-mediated anion exchange, in which the substrate binding site faces either the cytosolic compartment (inward conformation) or the

TABLE 54.2 AE2 Residues of Defined Function

Location	AE2a Residue	Importance/Function	Reference
N-term cytoplasmic	127–134, 145–149	Deletion or Ala substitution alkaline-shifts $pH_{o(50)}$	375
	150–175	Progressive deletion acid-shifts $pH_{o(50)}$	375
	H313/H317	Ala substitution acid-shifts $pH_{o(50)}$	171
	E318/E322	Ala Substitution acid-shifts $pH_{o(50)}$, reduces pH_i sensitivity	171
	F320	Ala, Tyr substitution acid-shifts $pH_{o(50)}$, reduces pH_i sensitivity	171
	L323	Ala substitution acid-shifts $pH_{o(50)}$, reduces pH_i sensitivity	171
	W336	Ala substitution acid-shifts $pH_{o(50)}$, reduces pH_i sensitivity	373
	E338	Ala substitution reduces pH_i sensitivity	373
	R341	Ala substitution acid-shifts $pH_{o(50)}$, reduces pH_i sensitivity	373
	W342	Ala substitution reduces pH_i sensitivity	373
	I343	Ala substitution reduces pH_i sensitivity	373
	F345	Ala substitution reduces pH_i sensitivity	373
	E346	Ala or Asp substitution acid-shifts $pH_{o(50)}$, reduces pH_i sensitivity	373
	E347	Ala or Asp substitution acid-shifts $pH_{o(50)}$, reduces pH_i sensitivity	373
	W356	Ala substitution reduces pH_i sensitivity	171
	H360	Glu substitution acid-shifts $pH_{o(50)}$, reduces pH_i sensitivity	171
	403–408	Ala substitution acid-shifts $pH_{o(50)}$	171
C-term transmembrane	R789	Glu and Ser substitution reduces AE-mediated Cl^- transport but with wild-type surface expression	298
	E888 (EC3)	Ala substitution acid-shifts $pH_{o(50)}$	298
	K889 (EC3)	Ala substitution acid-shifts $pH_{o(50)}$	298
	R921 (IC3)	Thr substitution reduces pH_i sensitivity	298
	F922 (IC3)	Tyr substitution reduces pH_i sensitivity	298
	D970/K971 (EC4)	Ala/Ser substitution increases pH_i sensitivity	298
	E981 (EC4)	Leu substitution acid-shifts $pH_{o(50)}$	298
	K982 (EC4)	Tyr substitution acid-shifts $pH_{o(50)}$	298
	E1007 (inner TM8)	His, Gly, Lys substitution abolishes Cl^- transport; Q substitution makes sulfate transport H^+-independent	302
	H1029 (TM9)	Ala substitution inhibits Cl^- transport; wild-type surface expression	302
	A1051	Ser substitution alkaline-shifts $pH_{o(50)}$	377
	A1053	Thr substitution alkaline-shifts $pH_{o(50)}$	377
	R1056	Ala substitution inhibits Cl^- transport; wild-type surface expression	298
	S1068	Gly substitution acid-shifts $pH_{o(50)}$, reduces pH_i sensitivity	377
	V1071	Ser substitution acid-shifts $pH_{o(50)}$, reduces pH_i sensitivity	377
	A1072	Gly substitution acid-shifts $pH_{o(50)}$, reduces pH_i sensitivity	377
	D1075	Ala substitution acid-shifts $pH_{o(50)}$	298
	P1077	Ala substitution reduces pH_i sensitivity	298

(*Continued*)

TABLE 54.2 (*Continued*)

Location	AE2a Residue	Importance/Function	Reference
	I1079	Asp/Glu/Lys/Phe/Thr/Tyr substitution reduces pH_i sensitivity, Glu or Lys substitution acid-shifts $pH_{o(50)}$.	
		Cys substitution increases pH_i sensitivity and alkaline-shifts $pH_{o(50)}$	377
	R1107	Ser substitution reduces pH_i sensitivity	298
	R1134	Cys substitution inhibits Cl^- transport; apparent lack of surface expression	298
	H1144	Tyr substitution alkaline-shifts $pH_{o(50)}$	302
	H1145	Ala substitution alkaline-shifts $pH_{o(50)}$, increases pH_i sensitivity	302
	R1155	Lys substitution increases pH_i sensitivity	298
	R1202	Leu substitution increases pH_i sensitivity	298

extracellular compartment (outward conformation) (Fig. 54.4). Anions may bind and unbind, likely at rates near the diffusion limit, before unbinding is prevented by an initial conformational change sometimes envisioned as closure of an "external gate". This gate closure is coincident with or induces formation of the oppositely directed conformational state sometimes envisioned as opening of an "internal gate". In this state the translocated anion can be released to the other compartment, and the next half-cycle of transport can proceed in the opposite direction. Thus, binding of substrate to one conformational state induces a conformational transition to the other state, accompanied by anion translocation and transport. The conformational transition occurs only upon protein binding of anion on one side.[254,255] The characteristic rank order of anion transport rates by AE1[229] and AE2[256] reflects not binding affinity but rather the extent to which binding of each anion lowers the transition state free energy for the conformational transition. Such a mechanism may allow coexistence of high substrate specificity with the low binding affinities required for anions present at concentrations of 5–150 mM, often with low transmembrane concentration gradients.[257] A postulated short-lived "occluded state" of anion binding hypothesized to accompany the AE1 transition state between inward and outward conformations has not been experimentally detected.

The ping-pong model of completely separate steps for anion exit and entry is supported by several lines of evidence. The strongest evidence is from the "half-turnover" experiments of Jennings,[258] which created conditions to detect the number of $^{36}Cl^-$ anions which rapidly effluxed from resealed red cell ghost membranes into an extracellular medium without permeant trans-anion. This number nearly equaled the number of AE1 polypeptides per red cell, and suggested that each polypeptide had undergone the transition from inward to outward conformation, completing only a half cycle of transport before encountering the absence of rapidly transportable anion in the extracellular medium. Further evidence includes findings that alteration of transmembrane Cl^- gradients controlled the proportion of AE1 polypeptides in the outward conformation (as detected by binding of inhibitors favoring the outward-facing state), that reaction of an outward-binding inhibitors such as DIDS prevented binding of the inward-state inhibitor, NAP-taurine,[259] and that binding of inhibitor to the external side of AE1 blocked Cl^- binding on both sides of the protein, as measured by ^{35}Cl-NMR.[260] In addition, red cell exposure to the external inhibitor H_2DIDS promoted uphill Cl^- efflux,[261] consistent with recruitment of inward-facing AE1-Cl^- complex to the outward facing state where, immediately after Cl^- release, the transporter conformation is frozen by inhibitor binding.

The anion binding sites on the cytoplasmic and extracellular faces of the polypeptide are non-equivalent, with yet undefined binding pockets comprising distinct sets of aa residues on inner and outer faces of AE1 (Fig. 54.8). Thus, whereas symmetrical Cl^- concentrations favor a 6-fold preponderance of the inward conformation of AE1 (reflecting a 6-fold higher relative Cl^- binding affinity vs HCO_3^-), symmetrical HCO_3^- concentrations in the absence of Cl^- favor a 10-fold preponderance of the outward conformation (with its 10-fold higher relative affinity for HCO_3^-.[262] This substrate-specific asymmetry of AE1 affects apparent affinities for substrates and inhibitors. When the carrier is unloaded, the inward facing form (the lower free energy state in Cl^-) is favored over the outward facing form (higher energy state) such that the apparent substrate affinity is higher for external than for internal substrate.[263]

Although the above data support an alternating sites model for AE1-mediated anion transport, evidence for

TABLE 54.3 AE1 Mutations

Band 3	Mutation		Ref
A. SLC4A1 (AE1) MTATIONS ASSOCIATED WITH RED CELL SHAPE CHANGE			
Southeast Asian ovalocytosis	Δ400−408	ovalocytosis (MIM:109270,130600,166900)	453,534,535
High transport (HT)	P868L	acanthocytosis, increased sulfate transport.	293
B. SLC4A1 (AE1) MUTATIONS ASSOCIATED WITH HEREDITARY SPHEROCYTOSIS (MIM:109270)			
Genas	nt 89 (G→A) from cap site in 5′ untranslated region; 33% decrease in mRNA		536
Neapolis	Splice donor mutation retains intron 2 in primary transcript to yield two variant mRNAs: variant 1: intron 2 retention; polypeptide terminates after 19 neocodons.		
	variant 2: Δ1−11; exon 2 skipping leads to deletion of first 11 aa to encode near full-length polypeptide with initiator codon at Met 12.		
	Severe HS in homozygotes 12% eAE1 protein; mild HS in heterozyotes, 82% of eAE1 protein.		446
Montefiore	E40K	recessive hemolytic anemia with protein 4.2 deficiency	444
Foggia	H55T-fs	1-nt deletion	537
Kagoshima	E56fs	1-nt deletion (A)	538
Hodonin	W81X	mutant mRNA undetected	442
Capetown	E90K	compound heterozygote with Prague III, both mRNAs present	539,540
Napoli I	S100F-fs-term; nt 447insT; mutant mRNA undetected		537
Fukuyama I	R112−113 fs, 2-nt del (AC) aa		200
Nachod	Δ117−12 intron-5 splice acceptor mutation, maybe near ankyrin binding site		442
Fukuoka	G130R	asymptomatic alone, recessive, exacerbated HS when in trans with G714R Okinawa	541
Mondego	P147S	in cis with E40K Montefiore; in trans with V488M Coimbra.	542
	Enhances severity of heterozygous HS V488M Coimbra		
Lyon, Osnabruck	R150X		536,543
Worcester	L170−172 fs 1-nt insertion; mutant mRNA undetected	442	
Fukuyama II	D183 fs	1-nt insertion	541
Campinas	Q203 fs	followed by 13-aa neosequence, 1-nt insertion.	448
	incomplete dRTA by furosemide test, resiting bicarbonaturia		
Bohain	V241 fs	1-nt deletion	544
Princeton	A273−275 fs	1-nt insertion; mutant mRNA undetected	442
Boston	A285D		442
Tuscaloosa	P327R		545
Noirterre	Q330X		546
Bruggen	P419 fs	1-nt deletion	543
Benesov	G455E	in TM2	442
Bicetre II	A456 fs	1-nt deletion	544

(*Continued*)

TABLE 54.3 (*Continued*)

Band 3	Mutation		Ref
Pribram	S477 fs	1-nt deletion in splice acceptor, intron-12 retention, terminates after 7 neocodons	442
		small amount mutant mRNA detected, mutant protein not detected	
		also incomplete RTA by $CaCl_2$ load test, bicarbonaturia following HCO_3^- load	447
Coimbra	V488M	exacerbated by in trans−double-mutant E40K/P147S	542
Bicetre I	R490C		544
Evry	W492 fs	1-nt deletion	544
Milano	I500G followed by duplicated aa 478−499; mutant protein undetected		547
Dresden	R518C		543
(Mexico)	G580fs63X	frameshift, 4 nt duplication, frameshift	548
Smichov	I616 fs	1-nt deletion, mutant mRNA undetected	442
Trutnov	Y628X	mutant mRNA undetected	442
Hobart	R646−647 fs 1-nt deletion, mutant mRNA undetected		442
Osnabruck II	M663−664 fs		543
Tambau	M663K	de novo mutation	549
Most	L707P		442
Okinawa	G714R	HS more severe when in trans with band 3 Fukuoka	200
Prague II	R760Q	mutant polypeptide not detected	540
Hradec Kralove	R760W		540
Chur	G771D	mutant mRNA present at normal level	550
Napoli II	I783N	mutant mRNA present, mutant protein undetected	537
Jablonec	R808C		540
Nara	R808H		538
Prague I	V822 fs	10-nt duplication	540
Birmingham	H834P		442
Philadelphia	T837M		442
Tokyo	T837A	mutant mRNA present at normal level	551
Prague III	R870W	in compound heterozygote with Capetown E90K, both mRNAs present	539,540
Vesuvio	T894 fs	1-nt deletion replaces C-terminal 18 aa with 133 aa neoseq.	
		silent polymorphism 904 TAC-to-TAT in trans.	
		mutant mRNA present, mutant protein undetected	552
C. SLC4A1 (AE1) MUTATIONS ASSOCIATED WITH RED CELL CATION LEAK SYNDROMES			
Southeast Asian ovalocytosis	Δ400−408		318
Blackburn	L687P		318
Horam	D705Y		318

(*Continued*)

TABLE 54.3 (*Continued*)

Band 3	Mutation		Ref
Hemel	S731P		318
Hurstpierpoint	H734R		318
	R730C		553
New Haven	E758K		554
Prague II	R760Q		318
	S762R		456
Ceinge	G796R		555
D. SLC4A1 (AE1) MUTATIONS ASSOCIATED WITH DISTAL RENAL TUBULAR ACIDOSIS (MIM:179800,602272,109270)			
Capetown	E90K	compound heterozygous recessive dRTA	556
Sotheast Asian Ovalocytosis	Δ400−408	compound heterozygous recessive dRTA	see below
Edmonton	C479W	compound heterozygous recessive dRTA	557
Coimbra	V488M	homozygote shows complete absence of erythroid AE1, with hydrops fetalis, hemolytic anemia, accompanying recessive	107
		dRTA heterozygote exhibits dominant dRTA with HS	see below
Kaohsiung	E522K	compound heterozygous recessive dRTA	558
dRTA	R589H	dominant dRTA	468,469,559
dRTA	R589C	dominant dRTA	469
dRTA	R589S	dominant dRTA	469
dRTA	R602H	dominant dRTA as compound heterozygote with SAO	560
dRTA	G609R	dominant dRTA	477
dRTA	S613F	dominant dRTA	469
Courcouronnes	S667P	compound heterozygous recessive dRTA	561
Bangkok I	G701D	homozygous recessive dRTA	483
Unimas	Q759H	recessive dRTA as compound heterozygote with SAO	562
dRTA	S773P	recessive dRTA as compound heterozygote with G701D	488
dRTA	ΔV850	homozygous recessive dRTA, and as compound heterozygote with SAO	485
dRTA	A858D	homozygous recessive dRTA, and as compound heterozygote with SAO	485,563
dRTA	A888L/889X dominant dRTA		564
Walton	R901X	dominant dRTA, frameshift from 13-bp duplication	559
Qingdao	D905Gfs15	dominant dRTA	565
dRTA	M909T	dominant	
E. SLC4A1 (AE1) POLYMORPHISMS ASSOCIATED WITH BLOOD GROUP ANTIGENS			
NFLD	E429D	plus P561A	566
ELO	R432W		567
Fra	E480K		568
Rb(a)	P548L		569

(*Continued*)

TABLE 54.3 (*Continued*)

Band 3	Mutation		Ref
Tr(a)	K551N		569
WARR	T552I		570
Vga	Y555H	plus silent L441L	567
Wd(a)	V557M		569
BOW	P561S		568
Wu	G565A		567,571
Jna	P566S		572
KREP	P566A		572
Moa	R656H		567
Bpa	N569K		567
Swa	R646Q		573
Sw!	R646W		
Hga	R656C		567
Wright b +	E658	common allele	349
Wright a +	E658K	rare allele (a + /b + ⊕1:1000 in general population)	349
Dia, Memphis II	P854L	Diego a + antigen, rare allele	574
Dib	P854	common variant	574
F. SLC4A1 (AE1) ASYMPTOMATIC POLYMORPHIC VARIANTS			
Bangkok II	M31T	in cis with Memphis I and the dRTA mutation G701D	483
Napoli II	D38A		537,575
Memphis I	K56E	80% decreased phosphoenolpyruvate transport	575,576
Intron-3 polymorphisms		c87t, c242t*, g259a*, a580g (numbered from 5′ end of intron-3)	485
		(kAE1 promoter region); *, linked with Memphis I polymorphism	
Variant	E72D	found in HS assoc with other mutation	
Variant	R112S		575
Variant	I442F		575
Variant	M586L		575
Variant	I688V		575
Variant	S690G		575
Variant	R832H		575
variant	A858S		577
Variant	V862I		575
G. ANIMAL MODELS			
B. taurus	Bovine equivalent of human R646X. Erythroid AE1 absent, also reductions in spectrin, ankyrin, actin, 4.2		110
	Systemic acidosis with urine of less than maximally acidic pH		493
D. rerio	Zebrafish retsina ret(b245) 1.5- to 2-cM deletion encompassing AE1 gene		43

(*Continued*)

TABLE 54.3 (*Continued*)

Band 3	Mutation	Ref
	ret(tr265) E456G (aligns with human E472)	43
	Slightly reduced mRNA in early embryo, nonfunctional protein	
	ret(tr217) frameshift 13 nt insertion at nt 503 (creates new splice acceptor in intron 5), greatly reduced mRNA, severely truncated protein	43
	All genotypes show phenotype of dyserythropoietic anemia type II (binuclearity with failure of cytokinesis)	
M. musculus	Mouse AE1(− / −). Insertion/disruption of exons 9–11	108,164
M. musculus	Mouse AE1(− / −). Insertion/disruption of exon 3	489,490
M. musculus	Band 3 wan. mAE1 Q85X missense terminator. Severe recessive HS	492
	Heterozygotes nonanemic	
	Wan/wan on C3H background, no post-weaning survival, better on mixed background	578

a second anion binding site on AE1 detectable at non-physiological conditions shows that a simple ping-pong model cannot suffice to explain the AE1 transport mechanism (summarized by[257]). This alternate Cl^- binding site in human eAE1 appears to interact with E681, believed to constitute part of the main anion translocation pathway.[264,265] Thus, alternating site models of other types have not been ruled out.[266,267] Cysteine scanning and other mutagenesis studies have implicated many residues as potentially contributing primarily or secondarily to the AE1 anion translocation pathway.[235,237,238,268,269] Additional clues have been provided by similar structure-function experiments performed on Na^+-dependent SLC4 anion transporters.

PHARMACOLOGY OF SLC4/AE ANION EXCHANGERS

Anion exchange inhibitors are often of low specificity and low or modest potency, with apparent affinities sensitive to substrate concentration. Use of the inhibitors at effective concentrations may exert "off-target effects" which, though not monitored, may influence the measurement.[270] Thus small molecule inhibitors have proven only moderately helpful in assignment of anion transport in cells or tissues to the action of specific polypeptides. eAE1 in the intact red cell is an exception, due to the combination of its high abundance in the red cell membrane and the absence of other erythroid anion exchangers. Although these small molecule inhibitors are useful in the study of recombinant AE anion exchanger function, Cl^-/HCO_3^- exchange function in intact cells and tissues can be more specifically studied with RNA interference techniques or with comparison of cells from knockout and wildtype mice.

All the SLC4 anion exchangers are inhibited by the stilbene derivatives, SITS, DIDS (4,4′-diisothiocyanostilbene-2,2′-disulfonate) and H_2DIDS.[271] These inhibitors each have two negatively charged sulfonate groups, at least one of which is believed to interact with the anion translocation pathway. The two isothiocyanate groups of DIDS and H_2DIDS and the single group of SITS can slowly react covalently with free amino groups. Inhibition of AE1 by SITS and DIDS occurs initially via rapid, reversible electrostatic ionic interaction, followed by a slower, irreversible covalent reaction. In human AE1 the lysine residue that interacts with the isothiocyanate moiety of stilbene disulfonates is K539, located at the junction of TM5 and the third extracellular loop. A DIDS-reaction motif encompassing this lysine (KLXK, X = hydrophobic residue, e.g., I or Y) is conserved in AE2 and AE3, and in many other SLC4 polypeptides. DIDS inhibits in the rank order of AE1 > AE3 > AE2, with apparently competitive kinetics of non-covalent inhibition.[256,272] Whereas rat AE4 is DIDS-sensitive,[30] rabbit AE4a may be DIDS-insensitive.[31] DIDS sensitivity may be modulated by membrane lipid composition or other factors.[273,274]

Conformation-sensitive reversible inhibitors of AE1 include eosin-maleimide, niflumic and flufenamic acids and other nonsteroidal anti-inflammatory drugs, NAP-taurine, and the oxonol dyes (WW781 and diBA(5)C4), which prefer the outward conformation and are variably sensitive to [Cl^-]. DiBA(5)C4 is among the most potent AE1 inhibitors, with sub-nanomolar potency.[272] Experiments with these AE1 inhibitors have provided additional support for the ping-pong model and for asymmetric disposition of inward and outward conformations.[9] eAE1 anion exchange was also potently inhibited by the non-stilbene blockers NS1652[275] and NS3623.[276] The polyaminosterol MSI-1361 exhibited greater potency against AE2 than AE1 expressed in *Xenopus* oocytes.[277] S20787 inhibited cardiomyocyte

Cl^-/HCO_3^- exchange,[278,279] but tests against the recombinant cardiac anion exchangers AE3 and SLC26A6 remain to be reported. Many additional drugs inhibit AE1 and uncharacterized cellular anion exchange activities at low or moderate potency, including dipyridamole, tenidap, pyridoxal phosphate,[280] topiramate and other carbonic anhydrase inhibitors,[281,282] and others.[270] Cl^-/HCO_3^- exchange activities of intestinal SLC26A3/DRA and renal SLC26A4/pendrin exhibit little or no DIDS sensitivity, in contrast to the DIDS-sensitive SLC26A6 and moderately DIDS-sensitive SLC26A7.[20,23]

THE ANION TRANSLOCATION PATHWAY OF AE1

The anion substrate translocation pathway of AE1 remains undefined. The anion translocation pathway might in principle traverse either a single subunit of the oligomer or the subunit interface. However, a single functional subunit within a dimer appears sufficient to mediate Cl^-/HCO_3^- exchange in red cells[219] and in *Xenopus* oocytes for AE1[283] and for AE2 (Stewart and Alper, unpublished). Moreover, the noncooperative kinetics of monovalent anion transport by the solubilized dimeric polypeptide as well as in intact cells support independent anion translocation pathways within subunits of each oligomer. Nonetheless, numerous studies with fluorescent AE1 ligands such as DBDS[96,264,266] and with mutant-wildtype AE1 heterooligomers[103,284,285] suggest that perturbation of one promoter can alter the conformation of the partner protomer within the dimer/oligomer.

Several regions of the transmembrane domain have drawn particular attention as likely components of or contributors to the anion translocation pathway within the AE1 monomer. Most prominent among these is human AE1 E681 (mouse E699) near the membrane cytoplasmic face, whose modification with the glutamate-reactive Woodward's Reagent K inhibits transport.[286,287] Subsequent borohydride reduction cleaves the adduct and converts the glutamate carboxyl group to an alcohol, creating a norleucine substitution. hAE1 so modified severely inhibits red cell Cl^- exchange, increases Cl^- conductance, and greatly accelerates newly proton-independent sulfate transport[254] as obligatory electrogenic sulfate/Cl^- exchange,[288] demonstrating that tight coupling of anion exchange by AE1 need not be electroneutral. Similar properties were exhibited by the corresponding mouse AE1 mutant E699Q,[268] whereas other substitutions at E699 led to complete loss-of-function. Thus hAE1 E681 appears to be a proton binding site for proton/sulfate cotransport, and likely constitutes part of the gated permeability barrier for the anion translocation pathway. Biophysical modeling predicts the the Cl^- influx half-cycle of electrogenic $sulfate_i/Cl_o$ exchange is accompanied by movement of nearly one positive charge through most of the membrane electric field, with a small negative charge accompanying sulfate on the return cycle.[288] E681 of hAE1 is highly conserved in the SLC4 family, and the corresponding residue of AE2 likely plays a similar role.[289]

Since the anion translocation pathway through the AE1 polypeptide likely includes an external vestibule, the electric field within the translocation pathway may traverse a distance shorter than the thickness of the membrane bilayer. FRET[290] and NMR experiments[291] showing that bound Woodward's Reagent K prevents binding of neither Cl^- nor DIDS to AE1 suggest that the site of DIDS interaction with the AE1 transport pathway resides within the outer half of the electric field. An external vestibule was also consistent with results of scanning Cys accessibility studies of residues surrounding E681 in the Cys-less AE1 transmembrane domain.[234] Some Cys insertion mutants in TM8 external to E681 were nonfunctional at the cell surface. Among the functional Cys insertions preceding and extending beyond E681, those accessible to maleimide reagent labeling defined a surface of the TM8 helix plausibly contributing to the anion translocation pathway.[235] However the functional inhibition produced by the maleimide adducts of these introduced Cys residues was usually modest, unlike the more dramatic inhibition of NBCe1/SLC4A4 by modification of a Cys insertion at L750 (corresponding to hAE1 K677, one putative helical turn above the critical E681).[292] Similar Cys scan experiments in the C-terminal portion of the AE1 transmembrane domain identified hAE1 aa S852-L857 in the putative last extracellular loop as likely contributors to a "charge filter"[238] proposed to impede access of cations to the anion-preferring vestibule. The adjacent acanthocytosis-associated recessive AE1 mutation P868L near the final transmembrane span increased DIDS-sensitive sulfate uptake in intact patient red cells with normal polypeptide abundance.[293] Single Cys substitutions into wildtype AE1 have also contributed to the repetoire of residues that directly or indirectly contribute to the anion translocation pathway.[294]

Covalent modification and mutagenesis studies have highlighted additional C-terminal transmembrane domain amino acid residues important for anion transport. Although some mutations prevented surface delivery of AE polypeptides in heterologous expression systems, others reduced or abolished activity of protein in the plasma membrane. Chemical modification and mutagenesis studies of eAE1 transport suggest that among the Arg residue(s) essential for anion

translocation[295] is R901,[296] mutagenesis or modification of which reduces V_{max} for sulfate transport in *S. cerevisiae*. However, the AE1 distal renal tubular acidosis mutant R901X exhibits apparently normal transport in both human erythrocytes[297] and *Xenopus* oocytes, in which truncation of even 10 additional C-terminal aa retained Cl^-/Cl^- exchange activity.[283] Charge-modifying mutations of R789, R1056, and R1134 attenuated or abolished transport in mouse AE2.[298] Charge-modifying mutations of the Lys residues that bind to and are crosslinked by the isothiocyanate groups of H_2DIDS altered not only reversible antagonist binding, but also apparent sulfate affinity.[299]

His residues have also been implicated in AE-mediated Cl^- transport by the reduced anion transport of mouse AE1 His mutants H721Q, H752S, H837Q, and H852Q.[300] Introduction into these His-to-Gln substitution mutants of the additional mutation K558N (the DIDS isothiocyanate-binding Lys) partially or completely rescued Cl^- transport in *Xenopus* oocytes.[301] In contrast for AE2, only H1029 (corresponding to mAE1 H721) proved critical for AE2-mediated Cl^- transport.[302] Mouse AE1 H752, which alters pH dependence of anion exchange,[301] and human AE1 H834[303] (corresponding to mAE1 H852) have both been proposed as chief targets of inhibitory covalent modification by diethyl pyrocarbonate (DEPC).

ANION CONDUCTANCE ASSOCIATED WITH AE1

The relationship between AE1-mediated anion exchange and the dominant (though small) anion conductance of the human erythrocyte has been a question of long standing. Erythroid anion conductance is considerably larger in nucleated erythrocytes, and often sensitive to activation by hypotonic swelling. AE1 of the nucleated, hormone-regulated trout erythrocyte is unique among AE1 polypeptides in conferring on Xenopus oocytes not only Cl^-/anion exchange function, but also a large anion conductance accompanied by increased taurine transport[274,304] and increased cation conductance.[305] Although expression of so many distinct properties suggests coincident activation of endogenous *Xenopus* permeabilities by heterologous protein overexpression, mutagenesis studies to date[306,307] remain consistent with the hypothesis that trout AE1 can mediate both anion exchange and anion conductance. Thus, defined mutations in TM7 of trout AE1 modified anion conductance magnitude and selectivity without apparent change in the tested anion exchange properties, whereas mutations in more C-terminal regions altered both anion conductance and exchange.[307,308] In contrast oocyte expression of AE1 from skate and from zebrafish[309] and zebrafish AE2[42] was unaccompanied by increased anion conductance.

The parallel inhibition in the human red cell of anion exchange and of ~65% of anion conductance by stilbene disulfonates and other inhibitors suggests this fraction of red cell anion conductance might be mediated by AE1. The conductance mode could represent an infrequent AE1 "malfunction" in which unliganded carrier undergoes the conformational transition between inward and outward states or could represent anion "tunneling" directly through or adjacent to AE1 in the absence of conformational change.[250] AE1-mediated Cl^- conductance is supported indirectly by at least two observations. First, the red cell of the *ae1*$^{-/-}$ mouse[108] lacks both DIDS-sensitive sulfate uptake and DIDS-sensitive anion conductance.[310] The specificity of this observation is tempered by the destabilization of the fragile *ae1*$^{-/-}$ red cell membrane, which is deficient in additional membrane proteins[164,310] among which may be a DIDS-sensitive AE1-independent anion channel, one of several endogenous anion channel activities detectable in human red cells.[311–314] Second, expression in *Xenopus* oocytes of a human eAE1 construct from which the two transmembrane spans 6 and 7 are deleted induced DIDS-sensitive anion conductance, while partially retaining electroneutral anion exchange function. Importantly, the K539A mutation reduced DIDS sensitivity of both exchange and conductance transport modes in this mutant construct.[315]

Expression in *Xenopus* oocytes of AE1 from the nucleated red cell of the skate, *Raja erinaceae* also induced regulated osmolyte permeability and cation conductance properties[316,317] (but see[309]). Interestingly, small cation and osmolyte permeabilities were also associated with deletion of two transmembrane spans in hAE1,[315] reminiscent of the genetic association between reduced Cl^- transport function and low-level cation permeability in stomatocytosis mutants of human AE1.[318] Additional mutations in human AE1 have been reported to produce in oocytes divergent changes in anion exchange and anion conductance.[294,319] Thus, the tightly coupled anion exchange mechanism of AE1 (and of other SLC4 AEs) can apparently be altered in selectivity and in mechanism by single missense mutations.

THE AE1 C-TERMINAL CYTOPLASMIC TAIL: CARBONIC ANHYDRASE BINDING, ANION SELECTIVITY, AND OTHER FUNCTIONS

The final transmembrane span of AE1 terminates in a C-terminal cytoplasmic tail approximately 33–36 aa in length, the N-terminal half of which is required for

AE1 trafficking to the cell surface.[283,320] The moderately well conserved LDADD motif at aa 896−890 of the hAE1 C-terminal cytoplasmic tail binds in some assays to the positively charged N-terminus of carbonic anhydrase II (CAII),[87,321,322] and has been proposed to constitute a bicarbonate transport metabolon.[323,324] CAII co-immunoprecipitated with AE1, and soluble multimeric glutathione-S-transferase (GST) fusion constructs of the AE1 C-terminal tail exhibited saturable binding to immobilized CAII. The carbonic anhydrase inhibitor acetazolamide partially inhibited AE1-mediated Cl^-/HCO_3^- exchange[283,323] without inhibiting Cl^-/Cl^- exchange in *Xenopus* oocytes.[283] Mutation of the LDADD CAII-binding motif of AE1 abolished Cl^-/HCO_3^- exchange in both HEK-293 cells[323] and in oocytes, but failed to reduce Cl^-/Cl^- exchange.[283] Heterologous CAII overexpression failed to stimulate Cl^-/HCO_3^- exchange activity of coexpressed AE1, AE2, or AE3 in HEK-293 cells, but overexpression of catalytically inactive CAII inhibited AE activity. This inhibition was prevented by either missense mutations in the AE1 LDADD motif or by deletion of the 17 N-terminal aa of CAI,[323] both of which prevented CAII binding to the GST-AE1 fusion protein in the solid-phase binding assay without reduction of AE1 surface expression in cells. An AE1-CA2 C-terminal fusion protein did not transport HCO_3^- faster than wildtype AE1 in HEK-293 cells, but was insensitive to inhibition by excess catalytically inactive CA2.[325] In *Xenopus* oocytes, overexpression of heterologous wt but not mutant CAII mildly stimulated AE1-mediated Cl^-/HCO_3^- exchange, but not Cl^-/Cl^- exchange. An intact LDADD CAII-binding motif within a nonfunctional, surface-expressed mutant AE1 polypeptide rescued (within an AE1 heterodimer) Cl^-/HCO_3^- exchange activity in a coexpressed AE1 mutant itself unable to transport HCO_3^- but competent for Cl^-/Cl^- exchange.[283] These data show that residues of the AE1 C-terminal cytoplasmic tail are required for trafficking to the cell surface, can discriminate between transport of Cl^- and HCO_3^-, and can convey that discrimination between subunits within the AE1 dimer. The data are also consistent with the modified sulfate transport caused by mutation of these C-terminal residues.[296,326]

The CAII-binding motif is moderately conserved across the SLC4 gene family. AE2 and AE3 overexpressed in HEK293 cells were each inhibited by coexpressed mutant CA2. Recombinant CAII also interacted with fusion proteins encoding C-terminal tails of recombinant $Na^+-HCO_3^-$ cotransporters SLC4A4 and SLC4A7,[327] Cl^-/HCO_3^- exchanger SLC26A6,[328] and Na^+/H^+ exchanger NHE1.[329,330] SLC4A4 was also activated by CAI and CAII.[331] Acetazolamide treatment or co-expression of catalytically inactive CAII also partially inhibited apparent activity of these transporters.

The ecto-carbonic anhydrase activities of glycosylphosphatidyl-inositol-linked CAIV[332] and transmembrane carbonic anhydrases CAIX[333] interacted with extracellular loops of AE polypeptides, and have been proposed to constitute extracellular components of a bicarbonate transport metabolon assembled on both sides of the plasma membrane.[324] Recombinant CAIV also bound to recombinant fusion protein containing an ecto-loop from NBCe1/SLC4A4,[334] an interaction disrupted by the CAIV missense mutations associated with human autosomal dominant rod-cone dystrophy.[335] CAXIV together with CAIV enhanced AE3-mediated Cl^-/HCO_3^- exchange in hippocampal neurons.[336] CA−AE physical interaction has in some cases been conferred by overexpression pulldown experiments. Carbonic anhydrase coexpression has also been shown to enhance SLC16/MCT-mediated H^+/lactate cotransport,[337] although in part through poorly understood, non-enzymatic effects.[338,339]

Additional data, however, question the bicarbonate transport metabolon hypothesis.[14] Thus, CAII did not bind to free AE1 C-terminal cytoplasmic tail peptide, nor to immobilized GST-AE1 C-terminal peptide fusion protein.[340] Injection of supplemental CAII into oocytes expressing electrogenic SLC4A4/NBCe1 failed to activate $Na^+-HCO_3^-$ cotransport currents in *Xenopus* oocytes even while accelerating intracellular CO_2 hydration in an ethoxazolamide-sensitive[341] or acetazolamide-sensitive manner.[342] $Na^+-HCO_3^-$ cotransport current mediated by a GFP-NBCe1-CAII tripartite fusion protein was no greater in magnitude than that of GFP-NBCe1 without the appended CAII, although the tripartite fusion protein again accelerated ethoxazolamide-sensitive CO_2 hydration.[341] Similarly, CAIV coexpression with NBCe1 increased the extracellular juxtamembrane pH gradient with minimal effect on NBCe1-mediated current.[343] Moreover, a pRTA/migraine mutant of NBCe1 lacking the putative CA2 binding sites expressed normal activity in *Xenopus* oocytes.[342] Thus, in these experimental settings, neither intracellular nor extracellular carbonic anhydrase increased NBCe1 turnover.

Acceleration of HCO_3^- transport by cytoplasmic and ecto-carbonic anhydrases bound closely to the internal and external vestibules of SLC4 HCO_3^- transporters, as proposed by the metabolon hypothesis, suggests that dissociation of translocated HCO_3^-, rather than anion translocation itself, is rate-limiting for anion exchange. Although a rate-limiting anion dissociation step could be consistent with the kinetics of (Woodward's Reagent K-modified) AE1 E681-OH,[265] this condition has not been reported for wild-type AE1. Since bulk intracellular diffusion coefficients of CO_2 and HCO_3^- differ only slightly and are both fast relative to transmembrane anion exchange, and since the oocyte

plasma membrane is not freely permeable to CO_2, then maximizing proximity of carbonic anhydrase activity with HCO_3^- transporters may not enhance rates of SLC4 polypeptide-mediated transmembrane HCO_3^- transport,[341] except perhaps in physiological settings of enhanced intracellular or regional pH gradients.[344,345] Thus, the relationship between HCO_3^- transporters and carbonic anhydrases remains debated.

The short AE1 cytoplasmic C-terminal tail binds additional proteins. The intracellular N-terminal tail of glycophorin A, which facilitates hAE1 trafficking to the surface membrane,[346] binds to the AE1-C-terminal tail.[347] Stabilizing this interaction, the C-terminal ecto-domain of glycophorin A which modulates AE1 anion transport rates[346] interacts via aa R61 with the hAE1 fourth ecto-loop variant E658K to form Wright (a/b) blood group antigens.[348,349] GAPDH binds to the kAE1 C-terminal tail without altered GAPDH activity and in an AE1 phosphorylation-insensitive manner. siRNA knockdown of GAPDH in AE1-expressing MDCK cells increases intracellular retention of AE1, with reduced AE1 at the surface membrane.[350] Several additional candidate binding proteins detected by yeast two hybrid studies using AE C-terminal cytoplasmic tails or larger fragments as bait include the PDZ proteins syntenin and Pick-1[351] (never validated), α-cardiac actin[352] (not validated in native tissue) and the cell-cycle protein p16.[353] The proposed kAE1-specific binding protein kanadaptin[354] was later shown to be a protein of the nucleus and mitochondrion[355,356] unable to bind kAE1.[357] AE2, like AE1, can interact with p16.[358] The C-terminal tail of AE2 also binds GAPDH.[350] AE3-binding proteins have not been described.

ACUTE REGULATION OF ANION EXCHANGERS

Phosphorylation of Anion Exchangers

Human eAE1 is a substrate for serine/threonine kinases and for tyrosine kinases, AE1 phosphorylation does not regulate anion transport rate[265] in the absence of oxidative stress or coincident glucose-6-phosphatase deficiency.[359] Casein kinase I phosphorylated recombinant hAE1 N-terminal cytoplasmic domain at T42 and less completely at S303.[360] Tyrosine kinases p72(syk) and p56/53(lyn) phosphorylated human eAE1 in cells exposed to oxidative[359,361] or hypertonic stress, or subjected to elevated intracellular $[Ca^{2+}]$.[362] Diamide crosslinking and clustering of red cell AE1 was associated with its enhanced tyrosine phosphorylation in the setting of increased phosphorylation and membrane recruitment of p72(syk). These phenomena are irreversible in G6PD-deficient red cells,[363] and lead to release of hemichrome-containing vesicles.[364] In acanthocytic red cells of patients with choreo-acanthocytosis, AE1 was heavily phosphorylated at the Y904, a functional target of p53/56(lyn), but not at Y8, a target of syk.[365] Phosphorylation of eAE1 Y8 and Y21 facilitated secondary phosphorylation of Y359 and Y904 in human red cells,[209] and these residues were susceptible to dephosphorylation by erythroid tyrosine phosphatases PTP1B and SHP-2. Phosphorylation of hAE1 Y8 and possibly also Y21 inhibited binding of glycolytic enzymes to the red cell membrane,[175] associated with hypoxic activation of glycolysis in parallel with glycolytic enzyme dissociation from the membrane,[210] events that may occur during passage through the hypoxic renal medulla. Downregulation of hAE1 tyrosine phosphorylation may regulate red cell vesiculation during the red cell senescence process.[362]

In the skate red cell, hypotonic swelling activated AE1 Tyr phosphorylation in parallel with increased osmolyte permeability, but swelling-activated AE1 tetramerization, altered AE1 binding to ankyrin and protein 4.1, and AE1 trafficking from intracellular lipid raft-containing vesicular fraction to the plasma membrane were all independent of AE1 tyrosine phosphorylation.[366] In human kidney AE1 lacking Y8 and Y21, phosphorylation of Y904 and Y359 is crucial to normal basolateral targeting of kAE1 expressed in polarized MDCK cell monolayers.[367] Tyrosine phosphorylation also contributes to basolateral targeting of chicken kidney AE1,[101] and hAE1 Y904 is conserved in AE2 and AE3.

Rabbit AE2a may be activated by PKC in gastric parietal cell.[90] MEK/MAPK pathway activity during first metaphase leads to Ae2 removal from the mouse oocyte plasma membrane in parallel with reduction in oocyte Cl^-/HCO_3^- activity.[368] Angiotensin II-induced PKC-dependent phosphorylation of rat bAE3 Ser 67 in HEK-293 cells increased Cl^-/HCO_3^- exchange activity without changing surface expression.[369] This phosphorylation event may contribute to hypertrophy of rat cardiomyocytes but not in those of mouse, which express only cAE3 and in which SLC26A6 may be the major Cl^-/HCO_3^- exchanger.[370]

Acute Regulation By pH

The acute regulation of AE2 (and other pH-sensitive SLC4 bicarbonate transporters) requires a "pH sensor(s)" (likely delocalized rather than a unique amino acid residue), is postulated to promote a protein conformational change leading to altered anion transport activity. This regulation is proposed to occur through concerted pH-sensing actions of both N-terminal cytoplasmic and C-terminal transmembrane domains of the protein. The AE anion exchanger gene products differ considerably

in their acute regulation by pH. Native erythrocyte AE1-mediated Cl^-/HCO_3^- exchange[371] and AE1-mediated Cl^-/Cl^- exchange in *Xenopus* oocytes[217,256] both display broad pH versus activity profiles, consistent with the eAE1's role in facilitating CO_2 mobilization from the respiring tissues to the lungs for exhalation.[372] In contrast, the widely expressed, non-erythroid anion exchangers AE2 and AE3 are acutely regulated by changes in pH_i,[373] with activation by alkaline pH consistent with their roles in pH_i recovery from alkaline loads, and inhibition by acid pH appropriate for downregulation of their acid-loading function. Whereas mouse AE1 expressed in *Xenopus* oocytes is relatively insensitive to changes in bath pH between five and nine, mouse AE2 expressed in oocytes[86,217,256] is acutely and independently regulated by pH_o and pH_i, and is also highly sensitive to pH_i when expressed in cultured cells.[99,374] AE3 is also regulated by pH_i when transiently transfected in HEK293 cells[374] or expressed in *Xenopus* oocytes.[373]

In *Xenopus* oocytes, AE2-mediated Cl^-/Cl^- exchange is regulated by intracellular pH_i at constant pH_o and by extracellular pH_o at constant pH_i.[86,373] AE2a-mediated Cl^-/Cl^- exchange is regulated by extracellular pH_o with a pH value at which activity is half-maximal ($pH_{o(50)}$) of 6.9. Structure-function experiments have indicated that regulation of AE2 by changes in pH_o is via a pH sensor(s) that resides within the C-terminal transmembrane domain of AE2[217] and can be regulated/modified by critical amino acid residues in the cytoplasmic N-terminal domain.[86,171,217,373] Removal of the cytoplasmic N-terminal domain acid shifts the $pH_{o(50)}$ of AE2-mediated Cl^- transport and abolishes pH_i regulation of AE2.[86] These findings suggest the presence of a "pH sensor" motif within the AE2 TMD that interacts directly/indirectly with sensor components in the cytoplasmic N-terminal domain to modulate anion exchange activity in responses to changes in pH_i and pH_o. All AE2 N-terminal polypeptide variants displayed similar sensitivity to inhibition by acid pH_i. AE2b1 and AE2b2 resembled AE2a in regulation by pH_o, whereas the gastric parietal cell-specific AE2c1 displayed a significantly alkaline shifted $pH_{o(50)}$ value due to the absence in AE2c1 of AE2a aa 127–134 and aa 145–149.[375]

Additional stretches of non-contiguous residues of the AE2 N-terminal domain present in all five N-terminal variant AE2 polypeptides[92,149] are important for pH regulation of AE2,[171,373] and are predicted by structural modeling to contribute to surface features of the folded cytoplasmic domain.[171] For example, aa 336–347 critical for regulation of AE2 by pH are highly conserved across the entire SLC4 bicarbonate transporter superfamily. Thus, the AE3 Glu residues corresponding to the functionally important E346 and E347 of AE2 are also important for pH_i regulation of cAE3.[373]

The mechanism by which AE2 integrates acute regulation of transport activity by pH_i and pH_o involves both cytoplasmic and transmembrane domains. Attempts to localize the AE2 TMD pH sensor have identified as candidate contributing residues nonconserved histidines,[302] nonconserved charge residues, and other amino acid residues of the TMD.[298] More recently AE1–AE2 chimera studies identified subdomains of AE2 that contribute to different regulatory phenotypes, including regulation by pH.[376] These studies indicated that the Ae2 pH sensor probably did not comprise a single amino acid but rather multiple TMD regions or amino acids interacting to confer on AE2-mediate anion exchange regulation by pH.

Biochemical and cysteine scanning mutagensis studies of AE1 have identified a structure comprising 12–14 TMD including two putative re-entrant loops. The second re-entrant loop and the last two TMD have been proposed to contribute to the AE1 anion selectivity filter. The first re-entrant loop is comprised of ~38 aa, nine of which are not conserved between AE1 and AE2. Mutagenesis studies of these 9 nonconserved amino acids identified single amino acids and regions of charged amino acids including the ^{1075}DKPK^{1078} motif within the AE2 RL1 as crucial components of the pH sensor.[377] Replacement of the AE1 RL1 with the AE2 RL1 or introduction of regions of AE2 RL1 amino acids into the AE1 RL1 failed to confer AE2-like pH sensitivity on AE1. In contrast, introduction of the same AE2 RL1 residues into the RL1 of the pH-insensitive chimera $AE2_{(1-920)}/AE1_{(613-929)}$ conferred AE2-like pH sensitivity to pH_i but not to pH_o.

These data show that H^+ sensing by the pH-sensitive regulatory domain of AE2 likely involves broad conformational change that includes a localized, charged, surface of the cytoplasmic domain and a region of re-entrant loop 1 within the TMD. A role for rapid trafficking events in acute AE2 regulation by pH is likely, but remains inadequately explored.

Acute Regulation by Ammonium and Hypertonicity

All N-terminal AE2 variant polypeptides expressed in *Xenopus* oocytes are activated by hypertonicity[375,378] and by exposure to NH_4Cl.[375,379] AE1 does not share these regulatory properties. Hypertonicity alkalinizes oocyte pH_i through cJNK-dependent stimulation of an unusual Cl^--dependent Na^+/H^+ exchange activity.[380] Thus, activation of AE2 by hypertonicity is consistent, at least in part, with AE2 activation by alkalinization. NH_4Cl activates AE2 despite acidifying the *Xenopus*

oocyte, and so overrides AE2 inhibition by acidic pH_i. Renal medullary and colonic [Na_4^+] are maximal with respect to AE2 stimulation, and so might render endogenous AE2 locally insensitive to inhibition by acidic pH_i.

AE2 stimulation by Na_4^+ and by hypertonicity requires similar regions of both N-terminal cytoplasmic and C-terminal transmembrane domains,[381] but the individual amino acids required differ. Alanine scan of the N-terminal region 336–347 identified single mutations that abolish or attenuate one or both types of stimulation. Chelation of intracellular Ca^{2+} attenuated AE2 stimulation by both Na_4^+ and hypertonicity. Calmidazolium inhibited both basal and stimulated AE2-mediated anion exchange in an apparently CaM kinase-independent manner, via residues in the C-terminal transmembrane domain and independent of the N-terminal cytoplasmic domain.[381]

DEVELOPMENTAL AND CHRONIC REGULATION OF ANION EXCHANGERS

The proximal erythroid promoter regions of AE1 genes have been studied in mouse,[382,383] human,[100] and chicken.[384,385] pH-sensitive repression of chicken AE1 transcription by the vErbA erythroleukemia oncogene contributed to oncogenic block of erythroid differentiation.[386] Newly biosynthesized eAE1 assembled into preformed cytoskeleton during *in vitro* differentiation of chicken erythroid precursors,[387] but appeared to contribute at least temporally to cytoskeletal assembly in murine erythroid precursors.[388]

kAE1 expression in kidney is restricted to collecting duct Type A acid-secreting intercalated cells, but is absent from Type B cells and from non-A non-B cells. Although rabbit primary and immortalized (lectin-defined) Type B intercalated cells in culture can give rise to cells expressing markers of principal cells and of Type A intercalated cells,[389] the developmental relationships among intercalated and principal cells *in vivo* remain unknown. However, mice lacking the transcription factor Foxi1 developed a collecting duct populated by a uniform cell type expressing both the principal cell marker AQP2 and the intercalated cell marker CAII, but lacking expression of immunodetectable vH^+-ATPase, AE1, and AE4.[157] Rescue experiments with Foxi-1 *in vivo* and *in vitro* promise a major advance in understanding of collecting duct and intercalated cell development. The promoter for AE4, preferentially active in Type B intercalated cells,[158] was directly regulated by Foxi1.[390] Foxi1 also regulates development and ion transporter expression in intercalated cell-like dermal ionocytes of *Xenopus*[391] and zebrafish.[392] Zebrafish ionocytes express (kAE1-like) basolateral Ae1b,[393] product of a gene distinct from erythroid Ae1a.[43]

The kAE1 promoter includes intron 3, but the 5′-extent of sequence required for optimal kAE1 transcription remains unknown, as the kAE1 promoter has not yet been tested *in vivo* or in very short-lived primary cultures of GFP-marked murine intercalated cells.[394] AE1 accumulates in increasing numbers of mouse cortical collecting duct intercalated cells between postnatal days three to 18, coordinated with development of HCO_3^- reabsorption and with expression of other acid–base transporters. During the same period pendrin-expressing intercalated cells disappear from the medullary collecting duct.[395] In rabbit collecting duct the balance between Type A intercalated cells and non-A intercalated cells appeared to be regulated by apoptosis.[396] Intercalated cells of rat inner medullary collecting duct proliferated during chronic systemic lithium treatment, but not all new cells expressed AE1.[397]

AE1 mRNA in Type A intercalated cells of adult rat kidney cortex is upregulated in acute[398] or chronic metabolic acidosis[125] and in chronic respiratory acidosis,[399] but down-regulated in acute metabolic alkalosis.[398,400] AE1 upregulation in chronic metabolic acidosis is part of a collecting duct acid–base "regulon" of >25 co-regulated transcripts in mouse kidney.[401] Chronic acidosis-induced increase in AE1 was associated with Type A intercalated cell (and principal cell) proliferation in mouse,[402] but not in rabbit.[400] Chronic lithium treatment led to increased AE1 and intercalated cell proliferation in IMCD, as part of a generalized IMCD remodeling response.[397] Water deprivation of normal rats decreased AE1 mRNA and protein in outer medulla while increasing both mRNA and protein encoding SLC26A7.[403] Similarly, ddAVP administration to Brattleboro rats suppressed collecting duct kAE1 abundance in parallel with increased corticosterone and decreased serum [HCO_3^-],[404] but dramatically upregulated SLC26A7 in outer medullary collecting duct intercalated cells without change in vH^+-ATPase abundance.[405] AE1 mRNA in rat distal colon was upregulated by aldosterone[129] but the aldosterone-increased acidification of the rabbit outer medullary collecting duct[406,407] has not yet been correlated with mineralocorticoid regulation of collecting duct AE1 expression. Rat distal colon AE1 mRNA levels exhibit circadian regulation in tandem with electrolyte absorption and mRNAs of SLC26A3, NHE3, KCC1, and NKCC1, in a feeding-sensitive manner.[408]

AE2 regulation in kidney has been studied in thick limb and in collecting duct. In the rabbit cortical collecting duct principal cell, AE2 mRNA decreased in metabolic acidosis and increased in metabolic alkalosis.[409] AE2 expression in rat thick ascending limb was

regulated by chronic acid−base and NaCl loading.[410] In both cortical (cTAL) and medullary thick ascending limb (mTAL) chronic oral NaCl loading increased basolateral membrane AE2 abundance, whereas NH_4Cl loading increased AE2 expression only in cTAL. Cortical AE2 abundance was unchanged by loading with $NaHCO_3^-$ or KCl, and decreased with $KHCO_3^-$ loading. $NaHCO_3^-$ loading increased AE2 only in outer medulla. AE2b but not AE2a was selectively upregulated in rat cTAL basolateral membrane in response to chronic NH_4Cl loading.[147]

The five 5′-variant transcripts of mouse AE2 (Fig. 54.2) are transcribed from four promoters in the AE2 gene expressed in tissue-specific patterns.[149,375,411] AE2c1 is expressed almost uniquely in stomach, with minor expression in uterus in the mouse.[375] In rabbit stomach, parietal and mucous cells expressed unique proportional distributions of AE2 variant transcripts.[90] The four AE2 promoters of the rat and human genes transcribe only four AE2 mRNAs.[91,92,148,412] The AE2a transcript is expressed at higher abundance than other AE2 isoforms in kidney.[148,149] The mechanisms of differential regulation of AE2 variant polypeptide levels have been little studied, but the human AE2b promoter was selectively regulated by the transcription factor HNF1α expressed in kidney.[413] The human AE2 b1 promoter exhibits a polymorphism of yet unknown significance to transcriptional regulation.[414]

Hormonal regulation of AE2 is developmentally and tissue-specific, but remains little understood. In neonatal rat small intestine, AE2 was downregulated by thyroxine, but was unchanged by dexamethasone.[415] Dexamethasone increased HCO_3^- secretion in bile duct units and intrahepatic cholangiocytes of rat, in parallel with upregulated AE2 protein but unchanged AE2 mRNA.[416] Hepatic AE2 levels were decreased in liver and biliary epithelial cells of primary biliary cirrhosis patients,[417−419] in part likely due to upregulation of miR-506.[420] The combination of ursodeoxycholic acid and glucocorticoids, effective for a subset of patients with primary biliary cirrhosis, selectively activated transcription of AE2b1 and AE2b2 transcripts through enhanced p300-related interactions between HNF1 and the glucocorticoid receptor.[421] Some,[422,423] but not other, association studies[424,425,426] have linked AE2 polymorphisms to either risk, autoimmune phenotype, or ursodeoxycholate responsiveness of primary biliary cirrhosis.

AE2 was decreased in salivary glands of Sjogren's Syndrome patients.[427] Chronic exposure to oxidative stress upregulated AE2 mRNA and protein in human bronchial epithelial cells and in intact rat lung, in parallel with activation of transcription factor AP-1.[428] AE2 expression was regulated by the Von Hippel Lindau gene product, with several-fold increase in AE2 mRNA and protein in non-tumorigenic 786-O-VHL renal cell carcinoma cells despite reduction in Cl^-/HCO_3^- exchange activity, as compared to tumorigenic, VHL-deficient 786-O cells. NHE3 mRNA was similarly elevated, and NHE-mediated recovery from acid load was similarly reduced.[429] Hepatocellular carcinoma samples also exhibited several-fold increased AE2 mRNA levels compared to adjacent normal liver,[430] and anti-sense reduction in AE2 expression induced apoptosis in several hepatocarcinoma cell lines.[431] AE2 overexpression in colon carcinoma cells was transcriptionally regulated by EGR1, and led to extranuclear sequestration of p16 and enhanced ERK phosphorylation. AE2 abundance in clinical colon carcinoma specimens correlated with expression of proliferation markers and with poor prognosis.[358] In contrast, siRNA knockdown of AE2 attenuated high glucose-induced apoptosis in endothelial cells.[432] Ae2 mRNA was greatly decreased in enamel organs of mice deficient in matrix metalloproteinase 20.[433]

The study of regulated AE2 trafficking in polarized epithelial cells remains in early stages. AE2 is exclusively basolateral in most epithelial cells. However, AE2 in human hepatocytes has been localized near or in the apical canalicular membrane in liver,[146] gall bladder and bile duct,[434] and in cultured bile duct epithelial cells.[144] Several AE2 isoforms expressed as C-terminal GFP fusion proteins trafficked basolaterally in polarized MDCK monolayers and apically in primary hepatocyte biliary ductule units,[435] with sorting to either cell pole microtubule-dependent. However, fusion with C-terminal GFP altered trafficking of AE1 in MDCK cells and regulation of AE2 in *Xenopus* oocytes (Stewart, Prabakaran, Alper, unpublished). In addition, AE2 was retained in intracellular vesicular structures in polarized WIF-B cells.[436] The putative AE2-binding, trafficking, and anchoring/scaffolding proteins that might govern the distinct steady-state localizations of AE2 polypeptides in renal and hepatic epithelial cells remain unidentified.

Regulation of renal expression of AE3 or AE4 has not yet been reported. In the developing mouse heart, however, brain AE3 (bAE3) and cardiac AE3 (cAE3) mRNAs are equally abundant, but bAE3 levels decrease dramatically during postnatal cardiac development.[89] In contrast, adult rat and human heart continue to express both bAE3 and cAE3. Stable AE3 expression in adult heart might reflect functional dominance of SLC26A6-mediated Cl^-/HCO_3^- exchange in the adult mouse heart.[370] However, the 2−4-fold higher Cl^-/HCO_3^- exchange activity of SHR rat cardiomyocytes compared with those from WKY rats corresponded to higher levels of bAE3 mRNA and lower cAE3 mRNA levels, suggesting a possible role for bAE3 in this model of hypertensive cardiac

hypertrophy.[437] AE3 is widely expressed in brain, with reduced hippocampal AE3 expression in the *Nhe1*$^{-/-}$ mouse.[438] AE3 is differentially regulated in mouse heart and brain, with chronic hypercapnia decreasing AE3 expression in both neonatal and adult brain, but increasing AE3 expression in neonatal hearts.[439]

AE1 DEFICIENCY DISEASES OF ERYTHROCYTES

Loss-of-function mutations in the human AE1 gene on chromosome 17q22 cause hereditary erythroid and kidney diseases (Table 54.3). Mutations in the human AE2 and AE3 genes have not been directly linked to disease with Mendelian inheritance. The AE1-related erythroid dyscrasias include hemolytic anemias characterized by spherocytosis, ovalocytosis, or stomatocytosis, nearly all caused by dominant heterozygous mutations. AE1-associated distal renal tubular acidosis (dRTA) in the Americas and Europe is caused most often by dominant heterozygous mutations, and in Southeast Asia by recessive homozygous or compound heterozygous mutations. With rare exceptions among the dominant human mutations, and very few among the recessive mutations, the red cell disorders and the kidney diseases are caused by discrete sets of mutations (Fig. 54.8). Homozygosity for the dominant disease mutations is encountered only rarely, and is assumed in most cases to be embryonic-lethal. It is marked by life-threatening hemolytic anemia and severe acidosis, and phenocopied by engineered AE1 knockouts in mouse and zebrafish, and by spontaneous bovine AE1 deficiency.

Hereditary Spherocytosis

Hereditary spherocytic anemia (HS) is characterized by increased osmotic fragility, and reflects a reduced erythroid surface area-to-volume ratio arising from exo- and endo-vesiculation from the unstable membrane of mechanically fragile red cells. Most cases result from dominantly inherited heterozygous deficiency of extrinsic proteins of the erythroid cytoskeleton (β spectrin, ankyrin-1, protein 4.2) but up to 65% of cases exhibit eAE1 deficiency.[440,441] In addition to splenomegaly and jaundice, the more severe hemolytic anemias are accompanied by leg ulcers, hemochromatosis, cholelithiasis, and other problems. The clinical presentation is generally milder in HS associated with AE1 mutations than from other causes,[199,442] and is remarkable for the absence of detectable renal acidification defect.

HS mutations include nonsense, frameshift, and missense mutations (Table 54.3) and are distributed across the entire AE1 coding region (Fig. 54.8). Mutant transcripts are usually absent or of reduced abundance, with moderate compensatory upregulation of the wild-type polypeptide representing increased transcription or post-transcriptional stabilization. Most HS mutant AE1 polypeptides expressed in *Xenopus* oocytes or HEK 293 cells fail to reach the plasma membrane with retention in endoplasmic reticulum or proximal Golgi, and some are misfolded as judged by altered stilbene disulfonate binding.[443] The severe recessive HS caused by the AE1 mutation E40K[444] is accompanied by 90% reduction in erythroid abundance of the AE1-binding protein 4.2. Conversely, the recessive protein 4.2 Nippon mutation is accompanied by 50% reduction in eAE1 abundance.[445] Most HS-associated AE1 mutations are not accompanied by defective distal urinary acidification. The rare exceptions include the severe recessive HS mutation V488M[107] and possibly also Band 3 Neapolis,[446] as well as the unexplained bicarbonaturia reported in HS patients with the heterozygous AE1 mutants S477fs[447] and Q203fs.[448]

BENIGN ERYTHROID PHENOTYPES OF AE1 POLYPEPTIDE VARIANTS

Human AE1 polymorphisms in extracellular loops of the C-terminal transmembrane domain encode minor blood group antigens classified as the Diego blood group system, generally considered of minimal clinical consequence for transfusion compatibility. Recently, however, an acute hemolytic transfusion reaction was associated with AE1-borne Wr(a) incompatibility.[449] Definition of these extracellular polymorphisms (Fig. 54.8) has provided important constraints on evolving models of AE1 topography within the membrane.[10] Anti-AE1 auto-antibodies directed against extracellular epitopes of human AE1 have been proposed either to mediate or to accelerate the complement-assisted removal of aged red cells by reticuloendothelial macrophages.[207] The antigens involved are hypothesized to arise from oxidative modification of AE1, and can target N-glycan carbohydrate antigens.[450] The benign erythroid phenotype of acanthocytosis can be associated with familial central nervous system disease. In one such family the dominant AE1 mutation P868L was associated with elevated erythroid sulfate transport rate and selectively altered red cell binding of H_2-DIDS,[293] consistent with altered conformation at the "second" isothiocyanate binding site at AE1 K851. However, the relationship of this mutation to altered red cell shape and to the neurological disease remains unclear.

Southeast Asian Ovalocytosis (SAO) is an asymptomatic, heterozygous condition associated with several indices of increased red cell rigidity including resistance to plasmodial invasion,[451] and is associated with reduced mortality from cerebral malaria.[452] The AE1 SAO mutant allele encodes a polypeptide with the inframe deletion Δ400−408 that is present in the red cell membrane at normal abundance, but neither transports anions nor binds stilbene disulfonates.[283,453] AE1 SAO is not dominant negative with respect to anion transport,[219] but nonetheless alters the conformation of bound wildtype protein.[170,284]

Cold-stored SAO red cells exhibit a cation leak,[454] and SAO has recently been recognized as a variant of the "hereditary stomatocytosis with cation leak syndromes",[455,456] sometimes presenting clinically as pseudohyperkalemia. In addition to SAO, nine dominant mutations in AE1 have been found to be associated with the red cell cation leak syndromes of cryohydrocytosis, spherocytosis with low temperature cation leak, and shallow slope hereditary stomatocytosis.[318] All stomatocytosis mutations are located in the proximate portion of the second half of the transmembrane domain. These AE1 mutants expressed in *Xenopus* oocytes exhibited moderately-to-severely reduced anion transport accompanied by low magnitude cation fluxes variably sensitive to some inhibitors of wildtype AE1-mediated anion transport. Mutagenesis experiments have supported the hypothesis that the mutations create cation leak pathways through the AE1 polypeptide,[294] but pharmacological results are less supportive. No renal acidification or salt-wasting phenotype has yet been noted in hereditary stomatospherocytosis with cation leak. However, AE1 mutations associated with cation permeability have promoted speculation that oxidatively modified AE1 may contribute to the still unidentified, deoxygenation-activated cation conductance specific to sickle erythrocytes.[457]

AE1 AND DISTAL RENAL TUBULAR ACIDOSIS (dRTA)

Heritable dRTA is caused by mutations in genes encoding components of the Type A intercalated cell acidification mechanism. dRTA is characterized by hyperchloremic metabolic acidosis in the presence of submaximal urinary acidification, usually defined as inability to acidify urine below pH 5.5. Normal proximal tubular function is marked by the absence of bicarbonaturia. The disease is associated with any combination of hypokalemia (severe enough on occasion to provoke weakness and arrhythmia), nephrocalcinosis, nephrolithiasis, growth retardation, rickets, polyuria, nausea and vomiting, and systemic dehydration. "Incomplete dRTA" marked by lack of spontaneous acidosis can be revealed by failure to acidify urine pH below 5.5 in response to standardized acid loading. In humans, dRTA genes of this class identified to date (Fig. 54.9) include the *AE1/SLC4A1* gene encoding the basolateral Cl^-/HCO_3^- exchanger kAE1, the *ATP6V1B1* and *ATP6V1A4* genes encoding B1 and A4 subunits of the apical membrane vH^+-ATPase, and the *CA2* gene encoding the cytosolic carbonic anhydrase CAII (causing mixed proximal-distal RTA).[2,285] dRTA genes described in knockout mice but not yet found in humans include K-Cl cotransporter KCC4/SLC12A7,[458] Cl^-/HCO_3^- exchanger/anion channel SLC26A7,[459] vasopressin-1a receptor,[460] apical ammonia channel RhCG,[461] H,K-ATPase subunits α1 and α2[462] and the matrix protein hensin/muclin/DMBT1[463−465] (but see [466,467]). As some identified familial dRTA cohorts remain without genetic diagnosis, additional dRTA genes will likely be defined as exome and whole genome sequencing becomes more widely available.

AE1-Associated Dominant dRTA

The nine AE1 mutations reported to date in patients with dominantly inherited dRTA are noted in Table 54.3. None of these dominant mutations have been found in the homozygous state, suggesting embryonic lethality. Unlike AE1 HS mutations, all dominant and recessive dRTA mutations of AE1 are missense mutations located in the AE1 transmembrane domain (Fig. 54.8). Dominant dRTA associated with mutant AE1 has been reported with few exceptions in Caucasians, and is unaccompanied by an erythroid phenotype. Erythroid AE1 abundance is normal in patients with heterozygous dRTA-associated AE1 mutations. Thus, whereas presumed AE1 haploinsufficiency in the Type A intercalated cells of HS patients suffices for normal urinary acidification, haploinsufficiency in the setting of dRTA mutations is pathological for the Type A intercalated cell, but inconsequential for the erythrocyte. This suggests a tissue-specific dominant- negative mechanism of disease for AE1-associated dRTA mutations. Two major mechanisms have been described to date (Fig. 54.10): hetero-oligomerization with dominant intracellular retention, and mutant mistargeting to the apical membrane.

In the absence of a robust cultured cell model of differentiated Type A intercalated cells, dRTA-associated AE1 mutant polypeptide function has been studied in *Xenopus* oocytes, HEK-293 cells, and MDCK cells grown on plastic, glass or permeable filter supports. In patient erythrocytes dRTA mutant AE1 polypeptides exhibited wildtype anion transport activity, while in

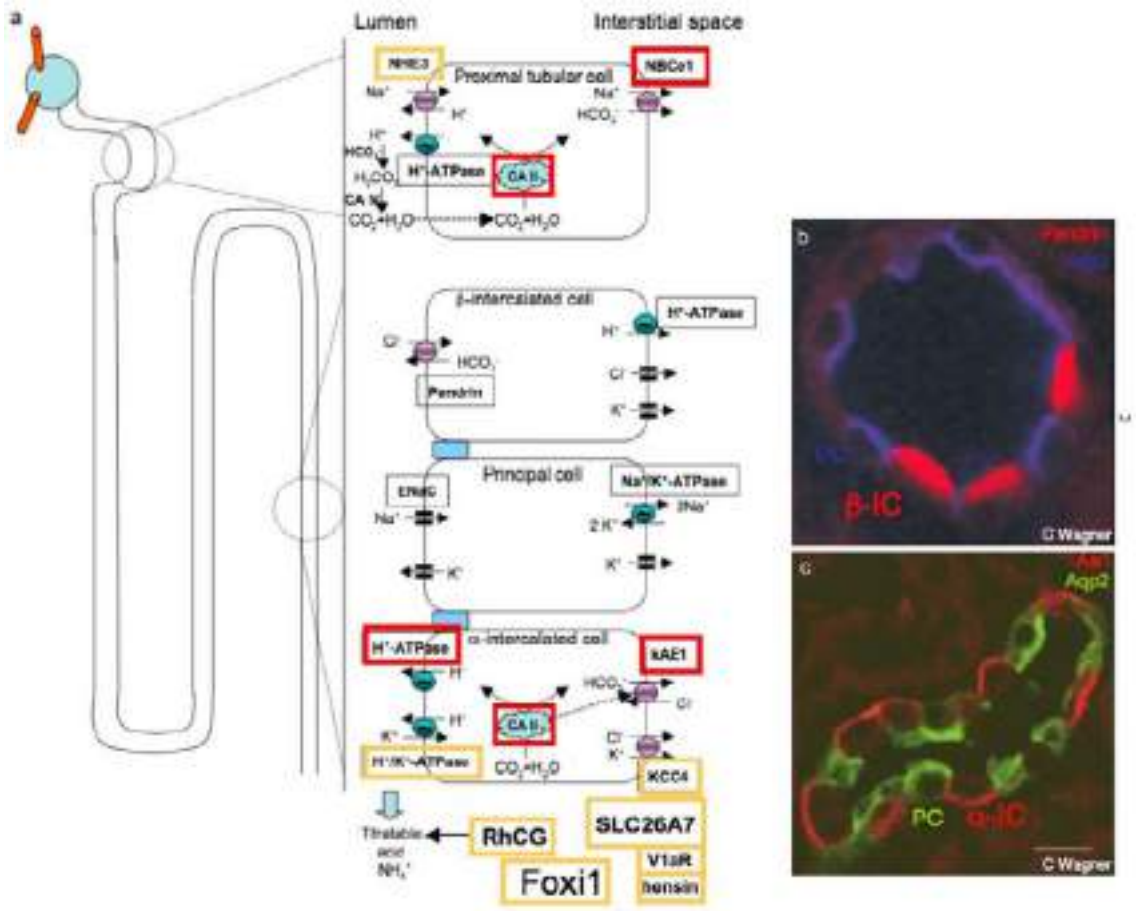

FIGURE 54.9 A. Schematic model of renal acidifying mechanisms: Bicarbonate reabsorption in proximal tubular cells and H^+ secretion in α-intercalated cells of the collecting duct. In the proximal tubule, H^+ is secreted at the apical membrane by the NHE3 Na^+/H^+ exchanger and by the vacuolar H^+-ATPase. Membrane-bound carbonic anhydrase CA IV (not shown) accelerates formation of CO_2 from H_2CO_3 generated by protonation of filtered HCO_3^-. CO_2 enters the tubular cell by diffusion and likely also via AQP1. H_2CO_3 is formed in the presence of cytosolic CA II, and HCO_3^- is transported out of the cell at the basolateral surface by Na^+/HCO_3^- cotransporter NBCe1. In Type A (α)-intercalated cells of the cortical collecting duct, H^+ is transported out of the cell into the lumen by vacuolar H^+-ATPase and, in K^+-depleted conditions, perhaps also by H^+/K^+-ATPase. HCO_3^- generated inside the cells leaves via anion exchanger 1 (kAE1) in exchange for Cl^- entry across the basolateral membrane. Basolateral Cl^- recycling is depicted with KCC4 K^+/Cl^- cotransporter, but may require Cl^- channel(s) in humans. Type B (β)-intercalated cells secrete HCO_3^- in exchange for Cl^- via their apical anion exchanger pendrin. In contrast to α-intercalated cells they can express a basolateral vH^+-ATPase. The principal cells are involved in Na^+ reabsorption and K^+ secretion. (Modified with permission from[285]). Red boxes indicate human dRTA genes. Orange boxes indicate dRTA genes identified in knockout mice, but as yet unassociated with human dRTA. B. Immunofluorescence micrograph of mouse cortical collecting duct showing β-intercalated cells expressing apical pendrin (red) in relation to principal cells expressing apical AQP2 (purple) (Reproduced with permission from[584]). C. Immunofluorescence micrograph of mouse cortical collecting duct showing α-intercalated cells expressing basolateral ae1/slc4a1 (red) in relation to (green) AQP2-expressing principal cells *(Reproduced with permission from[585]).*

Xenopus oocytes they exhibited 50−100% of wildtype anion transport activity[468,469] without a dominant negative phenotype.[468] An explanation for the dominant inheritance of the dRTA was sought in altered AE1 trafficking to the surface of renal epithelial cells. A technical advance enhancing these studies in HEK-293 cells replaced the high-mannose, Endo H-resistant wildtype N-glycan assembled at hAE1 N643 in the fourth exofacial loop with a novel N-glycosylation site in the third exofacial loop in the triple mutant N642D/Y555N/V557T.[470] Additional dRTA mutations could be introduced into this more easily tracked construct without alteration of trafficking attributable to the engineered glycan. Another important approach utilized an ecto-reactive anti-AE1 monoclonal antibody.

Expression of erythroid and of kidney forms of the AE1 dRTA mutant R589H in nonpolarized HEK-293 cells revealed intracellular retention of most kAE1 R589H, in contrast to normal surface expression of eAE1 R589H likely reflecting the different structures

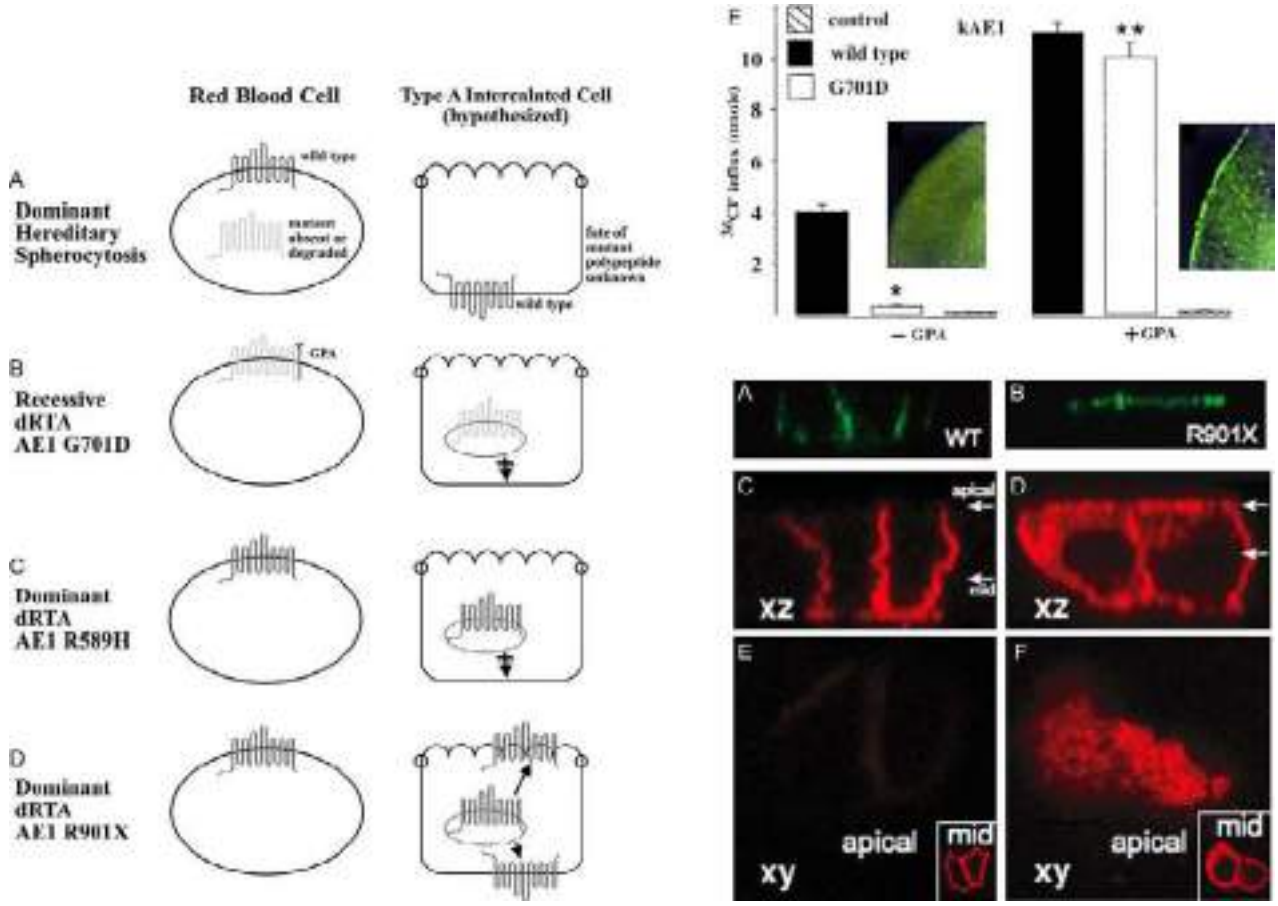

FIGURE 54.10 Pathophysiology of mutant AE1 trafficking in recessive and dominant forms of distal renal tubular acidosis (dRTA). A. Dominant hereditary spherocytosis. In red cells, the mutant erythroid AE1 (eAE1) polypeptide is usually absent or degraded. The wildtype eAE1 polypeptide is at the cell surface at 50−80% of normal level. In Type A intercalated cells, the wt kidney AE1 (kAE1) polypeptide is believed to be at the basolateral surface, but surface abundance and fate of the mutant polypeptide are unknown. B. Recessive dRTA is exemplified by AE1 G701D. In red cells, eAE1 G701D is believed to associate normally with the AE1-binding transmembrane protein, glycophorin A. This association allows normal accumulation and function in the red cell membrane. G701D and other recessive mutants fail to traffic to the surface of the *Xenopus* oocyte and (it is thought) to the surface of the intercalated cell. The coexpression of glycophorin A rescues surface expression and function of kAE1 G701D in the oocyte. The intercalated cell lacks glycophorin A. C. Dominant dRTA is exemplified by AE1 R589H. In the red cell, eAE1 is of normal abundance, surface localization, and function. In *Xenopus* oocytes, AE1 R589H exhibits only mildly diminished function. In the intercalated cell, kAE1 R589H acts as a dominant negative mutant, binding to and preventing surface accumulation of the WT AE1 polypeptide. D. A different mechanism of dominant dRTA is exemplified by AE1 R901X. AE1 901X is of normal abundance and function in red cells, and exhibits near normal function in oocytes. In transiently transfected MDCK cells, kAE1 R901X is present not only in the basolateral membrane, but also at or near the apical surface. In stably transfected cells, the mutant is present only in the apical membrane. The resultant functional short-circuiting of acid secretion could explain the dominant negative clinical phenotype. (Modified with permission from[199]). E. The recessive dRTA mutant AE1 G701D is rescued by coexpression glycophorin A in *Xenopus* oocytes. Bar graphs show $^{36}Cl^-$ influx into oocytes expressing wildtype kAE1 (black) or kAE1 G701D (white) compared with control (water-injected) oocytes (cross-hatched) in the absence (left graph) or presence of co-expressed glycophorin A (right bars). AE1 immunoflorescence shows AE1 G701D expression is absent from the oocyte surface (left inset) whereas coexpression with glycophorin A (right inset) rescues surface expression of kAE1 G701D (modified with permission from[483]). Lower right: AE1 immunoflorescence shows localization of dominant dRTA mutant AE1 901X. Unlike basolateral expression of wildtype kAE1 in stably (A) or transiently transfected, confluent MDCK cells (C, E), the dominant dRTA mutant AE1 R901X accumulates either at the apical membrane in stable transfectants (B) or at both apical and basolateral membranes in transiently transfected cells (D, F). *Modified with permission from*[473]*(A, B) and from*[102]*(C−F).*

and interactions of the N-terminal cytoplasmic domains of eAE1 and kAE1. Wildtype kAE1 surface expression was reduced by transiently coexpressed kAE1 R589H.[471]

MDCK cells offered the advantages of complex processing of the native N-glycan of heterologous AE1 and the possibility of trafficking in a polarized cell system. Low transient transfection efficiency[472] and variable rates of transgene extinction in stable transfectants[473] initially encountered in polarized MDCK cells were overcome by development of recombinant replication-deficient pseudotyped retrovirus,[474]

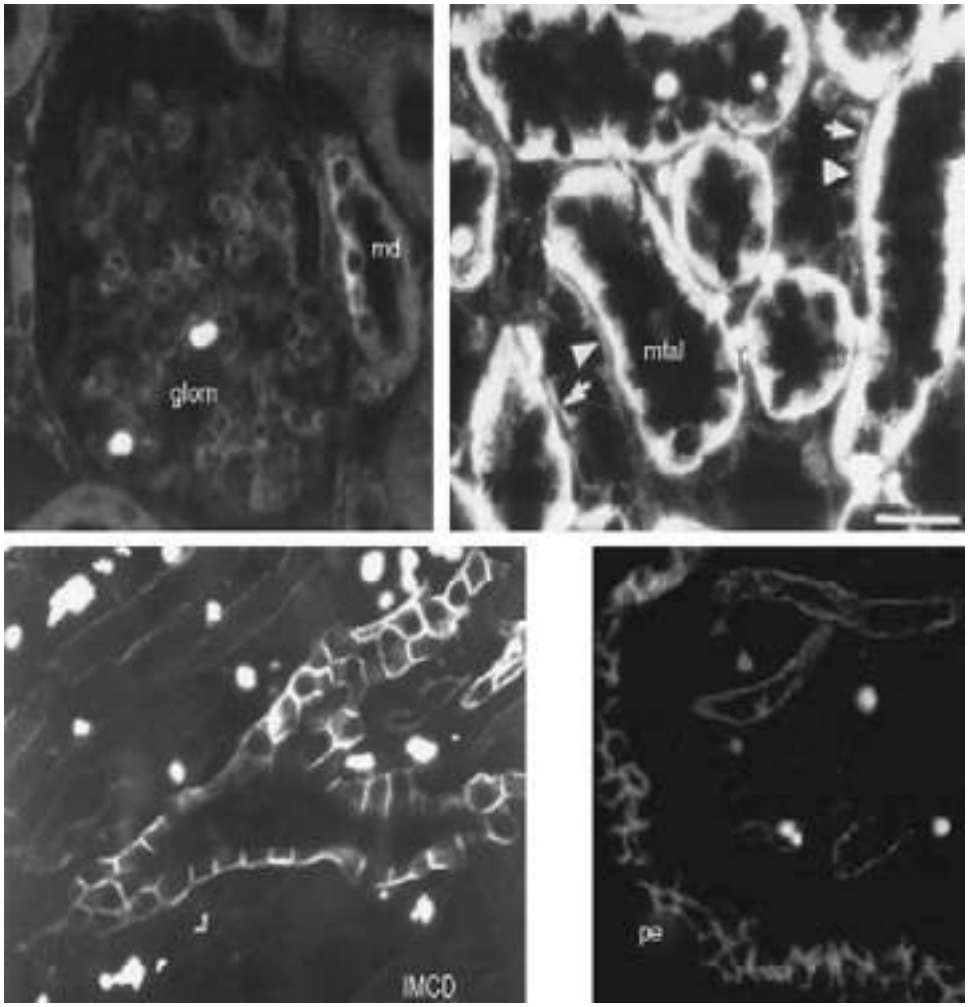

FIGURE 54.11 Basolateral expression of Ae2 in rat kidney. A. Ae2 in the basolateral membrane of rat macula densa cells (md), adjacent to the glomerulus (glom). B. Ae2 in the basolateral membrane of rat medullary thick ascending limb cells (mtal), adjacent to collecting ducts expressing low levels of Ae2 in the basolateral membrane of principal cells (arrowheads) and cross-reactive ae1 in the basolateral membrane of α-intercalated cells. C. Ae2 in the basolateral membrane of rat inner medullary collecting duct cells (IMCD) and adjacent thin limbs. (*A–C from,*[148] with permission). D. Ae2 in the basolateral membrane of mouse kidney papillary epithelial cells (pe), and papillary collecting duct cells. In all panels, bright round structures are red cells with cross-reactive Ae1. *(From,*[586] *with permission).*

adenovirus,[103] and lentivirus vectors to boost infection efficiency, modulate toxic overexpression, and increase sensitivity of AE1 transgene immunodetection. Both nonpolarized and polarized MDCK cells overexpressing dominant dRTA kAE1 mutants R589H and S613F retained the mutant polypeptides in endoplasmic reticulum, with some protein also in lysosomes and other structures, and contrasted with basolateral localization of wildtype kAE1. Coexpression of epitope-tagged wildtype kAE1 with kAE1 dominant mutant R589H inhibited surface delivery and accumulation of wildtype protein, and accelerated its degradation.[103] Sections from a heavily scarred kidney resected from a heterozygous AE1 R589H dRTA patient revealed decreased frequency of Type A intercalated cells with reduced apical vH^+-ATPase staining, but AE1 staining was uninformative.[475] However, the well-preserved morphology of a clinically indicated renal biopsy from a dRTA patient heterozygous for AE1 S613F[469] revealed diffuse, decreased AE1 immunostaining with loss of basolateral localization, accompanied by reduced and vH^+-ATPase staining with loss of apical localization in Type A intercalated cells smaller in both number and size than in control kidney.[476] These human data are consistent with the dominant negative trafficking behavior of dominant negative dRTA kAE1 mutations polarized MDCK cells. The dominant dRTA phenotype contrasted with that of a Sjogren's

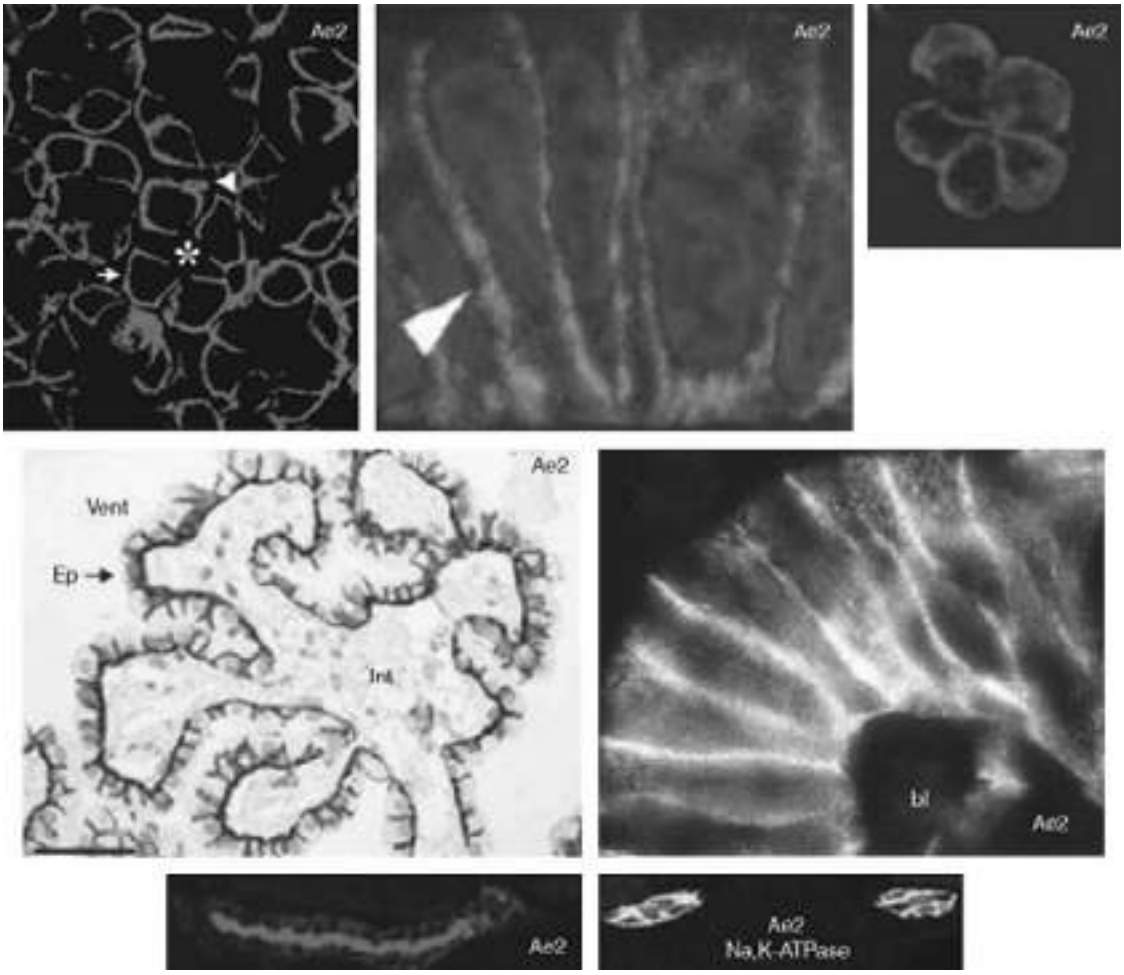

FIGURE 54.12 A–D. Basolateral expression of Ae2 in extrarenal tissues. A. Basolateral Ae2 in parietal cells of mouse gastric mucosa (from ,[132] with permission). Basolateral Ae2 in human Calu-3 cell monolayer (from,[143] with permission). C. Basolateral Ae2 in mouse submandibular gland acinar cell cluster (from,[587] with permission). D. Basolateral Ae2 in mouse choroid plexus epithelial cells (from,[588] with permission). E. Basolateral Ae2 in mouse colonic surface mucosa (from,[141] with permission). F, G. Apical Ae2 in pronephric duct of zebrafish in longitudinal section (F) and in transverse section costained with basolateral Na,K-ATPase α subunit *(from,[42] with permission).*

syndrome patient with dRTA, in which collecting duct immunoreactivity of both vH^+-ATPase and kAE1 was completely absent.[476]

The second trafficking mechanism by which heterozygous AE1 mutations give rise to dominant dRTA is mistargeting to the apical membrane, leading to a postulated apical HCO_3^- secretion that can short-circuit the normal vH^+-ATPase-mediated apical H^+ secretion (Fig. 54.10). AE1 dominant dRTA mutant 901X was expressed normally at the surface of red cells[297] and *Xenopus* oocytes,[283] but was retained in the endoplasmic reticulum of HEK-293 cells, where the mutant also trapped cotransfected wildtype kAE1.[297] kAE1 901X was similarly retained in MDCK cells grown on glass, but in transiently transfected filter-grown MDCK or rat IMCD cells kAE1 was present in both basolateral and apical membranes, in addition to intracellular membranes.[102] However, in stably transfected MDCK cells, AE1 901X accumulated exclusively in the apical membrane with apparent wildtype stability[473] (Fig. 54.12). AE1 dominant dRTA mutant G609R similarly localized in polarized MDCK cells more in the apical than basolateral membrane, in contrast to its normal surface expression in erythrocytes and *Xenopus* oocytes.[477]

Basolateral sorting of kAE1 does not require the sorting protein adaptin AP-1B.[102] A yeast two-hybrid screen recently identified adaptin AP-1A as interacting with the AE1 C-terminal Y904DEV907 sequence. The interaction was validated in HEK-293 cells, and knockdown of endogenous AP-1A reduced surface expression of kAE1.[478] Confirmation of the functional interaction of AP-1A with kAE1 in polarized epithelial cells is awaited. Another potential explanation for

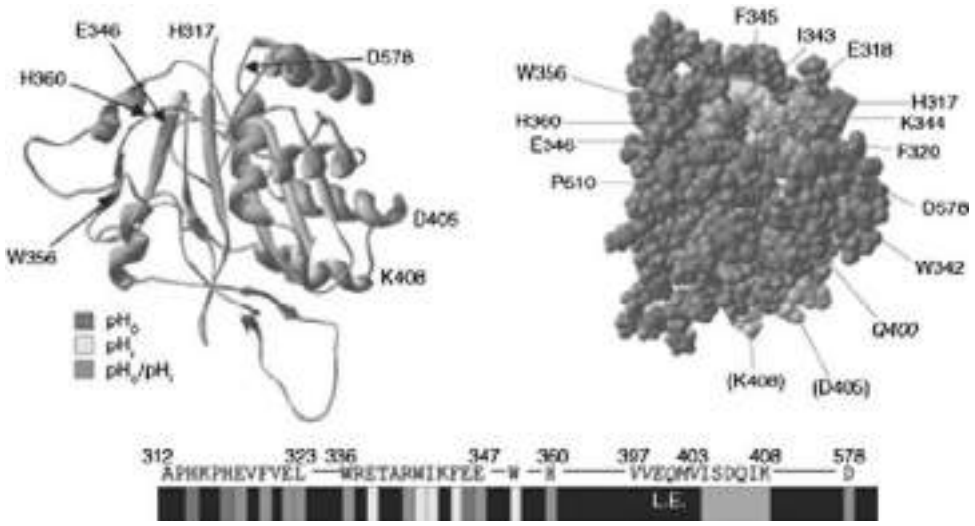

FIGURE 54.13 Amino acid residues of mouse Ae2 N-terminal cytoplasmic domain that contribute to anion transport regulation by extracellular (pH_o) and intracellular pH (pH_i). A. Ribbon diagram of Ae2 aa 317–623 modeled on the crystal structure of human AE1. B. Space-filling structure of the same region of Ae2. C. Linear sequence of portions of the Ae2 N-terminal cytoplasmic domain. In each panel, red marks residues in which mutations alter regulation by pH_o only, yellow marks residues in which mutations alter regulation by pH_i only, and orange marks residues in which mutation alters regulation by both pH_i and pH_o *(from,*[171] *with permission).*

apical accumulation of dRTA AE1 mutant R901X is loss of the tyrosine phosphorylation site Y904, required along with Y359 for basolateral accumulation in polarized MDCK cells.[479] Identification of the responsible tyrosine kinase(s) and PTyr-dependent trafficking/scaffolding proteins of the Type A intercalated cell is awaited, and promises to provide more detailed understanding of the altered targeting of dominant dRTA mutant AE1 polypeptides. Whereas Y904 is conserved among AE1 orthologs, and in AE2 and AE3, Y359 is not conserved in AE2 and AE3. A parallel to the N-terminal YVEL motif important in the basolateral trafficking of chicken kidney AE1 variant AE1−4[480] has not been detected in human or mouse kAE1.

Both wildtype kAE1 and dominant negative mutants R589H and R901X are ubiquitinated, then deglycosylated (likely in the cytosol) prior to undergoing proteosomal degradation. The half-life of the mutant polypeptides is shorter than the 15−17 hour half-life of wildtype protein in polarized MDCK cells.[481] The mutant proteins can be partially rescued from ER retention (in the case of mutant R589H or from the apical surface and some ER retention (in the case of R901X) to the basolateral surface of polarized MDCK cells in the context of a mutation that prevents N-glycosylation. Partial basolateral surface rescue was achieved by inhibition of the ER-localized interaction between mutant polypeptides and the ER folding lectin chaperonin, calnexin by castanospermine inhibition of AE1 N-glycan trimming in the ER. Polarized cell exposure to the small molecule chemical chaperones MAL (an Hsc70 modulator) or to C3 or C4 (developed as CFTR ΔF508 correctors) also led to partial rescue of basolateral expression of dominant mutant polypeptides,[481] suggesting possible therapeutic approaches to dominant dRTA caused by AE1 mutations.

AE1-Associated Recessive dRTA

Recessive dRTA has been associated with twelve AE1 mutations found in homozygous or compound heterozygous patients (Table 54.3). Most cases have been reported from Thailand, Malaysia, and Papua-New Guinea, and were frequently accompanied by hematological dyscrasia and (in Thailand) a co-inherited hemoglobinopathy.[482,483] All mutants described to date appear to share a mechanism of intercalated cell-specific intracellular retention[103,483–485] (Fig. 54.10). The first described was AE1 G701D in homozygous patients with normal erythroid eAE1 abundance and anion transport activity.[483] However, both eAE1 and kAE1 forms of the G701D mutant were non-functional in *Xenopus* oocytes due to failure of surface expression. Coexpression in oocytes of the erythroid AE1-binding protein glycophorin A completely rescued functional surface expression of both erythroid and kidney forms of AE1 G701D[483] (Fig. 54.10). As glycophorin A is not expressed in kidney, recessive dRTA mutant AE1 G701D has a conditional recessive

phenotype: normal in the presence of glycophorin A but incapable of normal trafficking in its absence. In contrast, wildtype AE1 surface trafficking does not require glycophorin A, but is potentiated by it.[486]

Expression of kAE1 G701D in HEK-293 cells[487] and in polarized MDCK cells led to its intracellular retention in the Golgi compartment.[103] Consistent with the clinical phenotype of heterozygous family members, coexpressed wildtype kAE1 rescued kAE1 G701D to the basolateral surface of polarized MDCK cells.[103] Additional recessive dRTA AE1 mutants subsequently described[485] (Table 54.3) exhibited similar conditional recessive phenotypes. The anion transport activities of the recessive loss-of-function mutant ΔV850 and the clinically less severe loss-of-function dominant mutant A858D were each potentiated by coexpressed glycophorin A in *Xenopus* oocytes.

Multiple instances of AE1-linked dRTA arise from compound heterozygosity with one rare recessive dRTA allele and one common SAO allele. An example is the AE1 A858D/SAO compound heterozygote with very low erythroid anion transport activity despite half-normal eAE1 polypeptide content. Correspondingly, coexpression in *Xenopus* oocytes of AE1 SAO prevented glycophorin A rescue of AE1 A858D to the surface.[485] kAE1 SAO itself is retained inside polarized MDCK cells.[481] dRTA also results from AE1 compound heterozygosity for two rare dRTA alleles, as in AE1 A858D/ΔV850. AE1 A858D expressed alone in polarized MDCK cells was retarded in exit from endoplasmic reticulum but reached the basolateral membrane, whereas AE1 ΔV850 expressed alone was retained in the endoplasmic reticulum. The coexpressed mutants hetero-oligomerized and, although AE1 A858D slightly enhanced surface delivery of coexpressed *nonfunctional* AE1 ΔV850, ΔV850 decreased surface expression of the coexpressed partially *functional* AE1 A858D.[484]

Glycophorin A rescue experiments for recessive dRTA-associated AE1 mutants R602H, Q759H, and S773P have not been reported. AE1 S773P was discovered in a compound heterozygote dRTA patient with a G701D allele. Although the folding-defective mutant kAE1 S773P was retained and degraded in endoplasmic reticulum in HEK-293 cells,[488] the mutant trafficked at near wild-type levels to the basolateral membrane of polarized MDCK cells. Consistent with clinical phenotype, however, coexpression in MDCK cells of AE1 G701D with the S773P mutant impaired AE1 S773P expression at the basolateral membrane.[103] Neither inhibition of N-glycan processing, genetically engineered prevention of N-glycosylation, nor exposure to small molecule chemical chaperones MAL, C3, or C4 led to detectable rescue of basolateral surface expression for kAE1 SAO or recessive kAE1 mutant G701D.[481]

dRTA With Complete Absence of AE1 and AE1 Knockout Models

Heterozygosity for putative loss-of-function mutation AE1 V488M was diagnosed in a newborn child of two parents, each with mild hereditary spherocytosis due to heterozygosity for the same mutation.[107] The homozygous child was born with life-threatening hydrops fetalis and hemolytic anemia with poikilocytotic red cells devoid of AE1. Renal tubular acidosis was noted at age 3 months, and nephrocalcinosis shortly thereafter. Intensive support with frequent blood transfusion and bicarbonate supplementation allowed survival.

Mouse models of complete AE1 deficiency phenocopy the hydrops fetalis of complete AE1 deficiency in the human. Two engineered *ae1*$^{-/-}$ mouse models showed severe growth retardation, severe hemolytic anemia with spherocytosis and poikilocytosis, severe hypercoagulation syndrome, and death of most mice before weaning.[108,489,490] In red cells from both mouse models, the ultrastructure of the red cell cytoskeleton unexpectedly remained intact in the absence of Ae1, leading to the proposal that the associated membrane fragility arose from destabilization of bilayer lipid in the absence of the membrane's major intrinsic protein.[108,489] The hypercoagulable state was attributed to propensity of the increased fraction of Ae1$^{-/-}$ red cells with externalized annexin V, those likely undergoing premature cell death (eryptosis),[491] to activate the prothrombinase complex,[490] a mechanism apparently not applicable to human red cells.[491] The spontaneous mouse hemolytic anemia mutant *wan* is caused by homozygosity for the AE1 mutation Q85X, and is marked by no survival post-weaning. Decreased clinical severity on mixed strain backgrounds led to the demonstration of modifier genes for the severity of hemolytic anemia,[492] one of which maps near the β-spectrin locus.

The small surviving fraction of *ae1* −/− mice[108] included fertile males. This facilitated subsequent generation of sufficient numbers of weanlings to document at age 12 wks a syndrome of complete dRTA, with spontaneous metabolic acidosis disproportionately exacerbated by an acid load well tolerated by wildtype and heterozygous mice.[109] The acidosis was accompanied by inappropriately alkaline urine pH and by reduced Cl^-/HCO_3^- exchange activity in isolated medullary collecting ducts, with compensatory upregulation of a pharmacologically distinct Cl^-/HCO_3^- exchange activity of unknown identity. Intercalated cells devoid of Ae1 remained present and exhibited reduced abundance of both vH^+-ATPase and of pendrin, but mRNA levels of candidate basolateral Cl^-/HCO_3^- exchangers Ae4 and Slc26a7 were

unchanged. *ae1* −/− mice also exhibited nephrocalcinosis accompanied by hypercalciuria, hyperphosphaturia, and hypocitraturia. An unexpectedly severe urinary concentrating defect with mildly decreased renal function (possibly prerenal) was accompanied by increased inner medullary AQP2 largely retained intracellularly. Possible hypokalemia was masked by hemolysis, and severe renal hemosiderosis may have contributed to the mild renal insufficiency and concentrating defect.[109] Nonetheless, the *ae1*$^{-/-}$ mouse was the first mouse model of complete dRTA with genetic deficiency of a human dRTA gene product. Ongoing attempts to analyze mice with normal eAE1 expression together with selective kAE1 deficiency or kAE1 missense mutations will accelerate future studies of the development, course, and treatment of AE1 mutation-associated dRTA.

Dominantly inherited perinatal hemolytic anemia and apparent renal tubular acidosis in a bovine cohort was associated with the heterozygous mutation AE1 646X.[110] Red cells completely lacked AE1, and coexpressed AE1 R664X suppressed wildtype anion transport in *Xenopus* oocytes. Recombinant bovine AE1 R664X polypeptide and the wildtype/R664X hetero-oligomer in HEK-293 or K562 erythroleukemia cells exhibited endoplasmic reticulum-associated proteosomal degradation, independent of ubiquitination or N-glycosylation and without aggresome formation.[493] Metabolic acidosis in the heterozygous AE1 646X cattle was notably unaccompanied by compensatory respiratory acidosis,[110] consistent with the incomplete respiratory compensation noted in mice with renal tubular acidosis lacking either carbonic anhydrase 2[494] or AE1,[109] and consistent with the coordinate roles of both eAE1 and CA2 in the respiratory disposal of metabolic CO_2. Bovine AE1 R664X represents the most severe dominant negative spherocytosis mutation yet reported, thus far unique in its phenotypic expression in both red cells and kidney.

Ae1 mutations were isolated among chemically mutagenized zebrafish screened for anemia phenotypes. Three recessive loss-of-function alleles of AE1 deficiency in zebrafish with severely reduced erythropoiesis were partially rescued by either zebrafish or mouse *Ae1* cRNAs. The observation of a dyserythropoietic phenotype in Ae1a mutants led to discovery of an Ae1a requirement for normal cytokinesis late zebrafish erythroblasts, with a similar but less prominent effect detectable in bone marrow of the *ae1*$^{-/-}$ mouse.[43] However, dyserythropoietic changes have not been reported in human AE1-associated dominant hereditary spherocytosis, and the clinically distinct human congential dyserythropoietic anemias are unlinked to *AE1*. Neither AE1a nor AE2b[495] are expressed in zebrafish pronephric duct. The systemic physiological functions of zebrafish pronephric duct Ae[42] (Fig. 54.14) remain unexplored.

KNOCKOUT MOUSE MODELS OF DEFICIENCY OF AE2/SLC4A2 AND AE3/SLC4A3

Complete knockout of the *ae2* gene in the mouse allows live births, but severe growth retardation and failure to thrive leads to death before weaning.[132] Gastric mucosal hypoplasia and achlorhydria was associated with reduced numbers of H^+,K^+-ATPase-positive parietal cells with underdeveloped secretory canaliculi lacking AE2. Knockout mice were also deaf (consistent with AE localization in cochlea), ataxic, edentulous,[132] and osteopetrotic[135] consistent with an essential role for AE2 in osteoclast function. A similar, recessive osteopetrotic phenotype is shown by Red Angus cattle with a homozygous large deletion of the AE2 gene region encoding exons 2 and 3.[496] However, genome-wide association studies have not yet implicated human AE2 as a risk modifier for low bone density.

An independently generated AE2 knockout mouse was devoid of AE2a, AE2b1, and AE2b2,[136] but appears to have retained expression of AE2c isoforms and possibly others expressed as a compensatory response ($ae2_{a,b}^{-/-}$ mice). This otherwise grossly healthy mouse model exhibited male infertility, consistent with AE2 localization in epididymis,[497] and osteopetrosis in long bones but not in calvariae.[134] Although basal gastric acid secretion was unimpaired in four month old mice, carbachol/histamine-stimulated secretion was reduced 70%, and was accompanied by increased parietal cell turnover without apoptosis.[498] Thus, the gastric-specific AE2c1 isoform is not sufficient for normal murine gastric acid secretion.

Although modest shRNA suppression of AE2 abundance in normal rat cholangiocytes reduced both unstimulated and secretin-stimulated Cl^-/HCO_3^- exchange,[499] biliary flow and secretion of both HCO_3^- and bile acids were increased rather than decreased in $ae2_{a,b}^{-/-}$ mice compared to wildtype littermates.[500] This observation, parallels the increased pancreatic HCO_3^- secretion observed in mice lacking the apical pancreatic ductal Cl^-/HCO_3^- exchanger slc26a6[501,502] and is consistent with the elevated cAMP levels in $ae2_{a,b}^{-/-}$ murine embronic fibroblasts, which reflect activation of bicarbonate-sensitive soluble adenylyl cyclase by the pH_i elevation secondary to loss of physiological AE2-mediated acid loading.[503] $ae2_{a,b}^{-/-}$ mice exhibit splenomegaly and immune dysregulation, and most develop

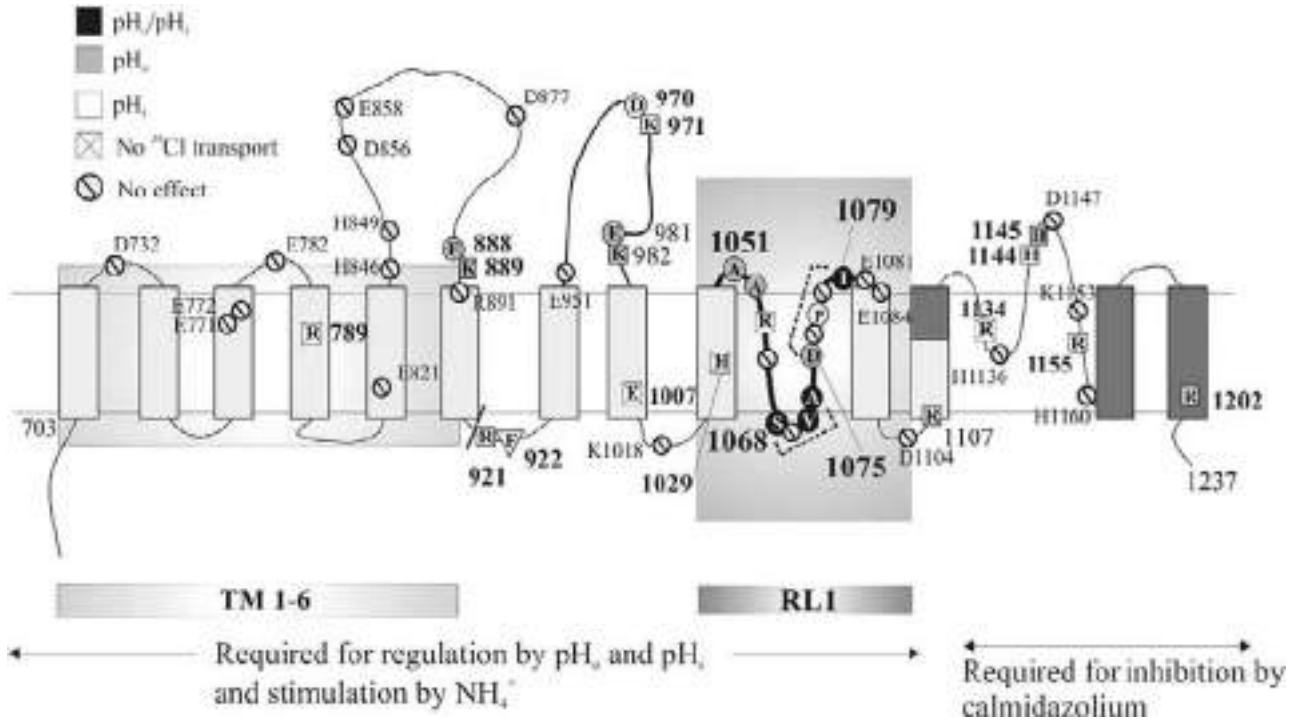

FIGURE 54.14 Mouse Ae2 transmembrane domain (TMD) residues involved in regulation of anion exchange. Re-entrant loop (RL1) in the Ae2 transmembrane domain is important for acute regulation of anion exchange by pH. Shaded areas indicate transmembrane (TMD) subdomains and individual amino acids identified from mutagenesis studies that contribute in a critical way to acute regulation of AE2 by pH, simulation by Na_4^+ and required for inhibition by calmidazolium. The indicated critical amino acids in the RL1 likely interact with as yet unidentified residues in TMD 1−6 or/and in the cytoplasmic N-terminal domain and contribute to the AE2 "pH sensor" function that regulates anion exchange. TMD residues involved in regulation by pH_o are gray, those involved in regulation by pH_i are in white and residues involved in regulation by both pH_o and pH_i are in black. Bisected open circles indicate residues for which mutation did not alter regulation of AE2 by pH. Boxes with X indicate residues for which mutation reduced transport activity below levels required for study of inhibitory regulation *(modified from,[377] with permission).*

anti-mitochondrial antibodies and other auto-immune abnormalities reminiscent of those in human patients. About one third of *ae2*$_{a,b}^{-/-}$ mice develop portal inflamation.[504,505] Proximal colonic epithelium of *ae2*$^{-/-}$ mice shows reduced cAMP-stimulated Cl^- secretion by proximal colonic epithelium,[506] and AE2 knockdown also reduces cAMP-stimulated Cl^- secretion by Calu3 cells.[507] Thus, in some secretory epithelial tissues, Ae2 is the predominant basolateral Cl^- loader. No renal phenotype has yet been reported in either *ae2* knockout mouse strain.

The *ae3*$^{-/-}$ mouse was grossly normal despite wildtype AE3 expression by or before gestational day 11. However, the *ae3*$^{-/-}$ mouse exhibited increased susceptibility to pharmacologically-induced generalized seizures, with increased seizure-associated mortality. The lowered seizure threshold was associated with complete absence of wildtype DIDS-sensitive Cl^-/HCO_3^- exchange activity in CA3 neuronal cell bodies monitored in hippocampal slices,[155] and unaccompanied by compensatory changes in brain mRNA levels of other Slc4 genes, or of Slc26a11, Slc12 Cl^- cotransporters, or Slc9 Na^+/H^+ exchangers. This murine seizure phenotype reinforces the previously documented association of human AE3 polymorphism A867D with seizure history among multiplex families with idiopathic generalized epilepsy.[508] In HEK-293 cells, AE3 A867D exhibited reduced function that was not explained by decreased cell surface abundance.[509]

Ae3-/- mice develop retinal degeneration after four to six months of age,[510] suggesting important homeostatic roles for Ae3 in retinal pigment epithelial cells, muller, and horizontal cells. Late-onset, recessive progressive retinal atrophy in Golden Retriever dogs was recently shown to cosegregate with a frameshift terminator mutation at transmembrane domain residue E868 (661 in cAE3).[511] Although *ae3*$^{-/-}$ mice have not revealed a cardiac phenotype, loss of AE3 expression in the hypertrophic cardiomyopathy transgenic mouse model expressing cardiac α-tropomyosin E180G greatly accelerated cardiac decompensation.[512] No renal phenotype has been reported in the *ae3*$^{-/-}$ mouse.

CONCLUSION

Transmembrane, transepithelial, and systemic transport of HCO_3^- and CO_2 is central to body pH and volume homeostasis. The Na^+-independent, electroneutral Cl^-/HCO_3^- exchangers AE1/band 3 and the related AE2 and AE3 polypeptides of the SLC4 gene family play central roles in these processes, along with Na^+-dependent SLC4 HCO_3^- transporters, and with anion transporters of the SLC26 gene family. The SLC4/AE anion exchangers regulate intracellular pH and, through their polarized localization in renal and other epithelial cells, regulate compartmental and systemic pH. SLC4/AE anion exchangers also regulate cell volume and modulate the cellular equilibrium potential for Cl^-, thus contributing to determination of driving forces for multiple ion transporter pathways. In polarized epithelial cells of kidney and other tissues, anion exchange in concert with cation transport can mediate transepithelial solute secretion or reabsorption.

These physiological functions come to the fore in tissues in which deletion or deficiency of an AE anion exchanger unmasks a lack of functional redundancy. Such is the case with AE1 in the human diseases hereditary spherocytosis, and heritable distal renal tubular acidosis. Hereditary stomatocytosis is an example of mutations that combine loss-of-fnction with gain of novel function (cation permeability). Genetic manipulation of AE2 and AE3 in mice, along with *in vitro* experiments, have suggested human AE2 as a candidate risk modifier gene determining bone density, gastric acidification and differentiation, male fertility, and epithelial secretion, and human AE3 as a candidate risk modifier for seizure disorder, late-onset blindness, and heart failure.

Recent advances in recombinant DNA technology, genome sequencing, model system genetic engineering to modulate gene expression in cultured cells and intact animals, structure determination, and single molecule spectroscopy have each contributed to rapidly accelerating progress in our understanding of the structure and function of SLC4/AE anion exchangers. The coming years should provide atomic-level insight into the structure of an SLC4 transmembrane domain, allowing visualization of the anion translocation pathway(s). Such structure will encourage reevaluation of existing kinetic data, revising mechanistic models that reconcile the requirements of the highest known rates of non-channel ion transport with very high anion:cation selectivity, broad anion specificity, and low substrate anion affinity. Ongoing discovery and characterization of AE-binding proteins will increase understanding of AE regulation. Together, the resulting insights will enhance our growing understanding of the way in which AE anion exchanger function at the cell and organ levels fits into the "systems biology" of cell and organismic pH, Cl^- and volume regulation.

References

[1] Vaughan-Jones RD, Spitzer KW. Role of bicarbonate in the regulation of intracellular pH in the mammalian ventricular myocyte. Biochem Cell Biol = Biochimie et Biologie Cellulaire 2002;80(5):579–96.

[2] Alper SL. Genetic diseases of acid–base transporters. Annu Rev Physiol 2002;64:899–923.

[3] Alper SL. Molecular physiology of SLC4 anion exchangers. Exp Physiol 2006;91(1):153–61.

[4] Alper SL. Molecular physiology and genetics of Na^+-independent SLC4 anion exchangers. J Exp Biol 2009;212(Pt 11): 1672–83.

[5] Pushkin A, Kurtz I. SLC4 base (HCO_3^-, CO_3 2-) transporters: classification, function, structure, genetic diseases, and knockout models. Am J Physiol Renal Physiol 2006;290(3):F580–99.

[6] Toye AM. Defective kidney anion-exchanger 1 (AE1, band 3) trafficking in dominant distal renal tubular acidosis (dRTA). Biochem Soc Symp 2005;72:47–63.

[7] Romero MF, Fulton CM, Boron WF. The SLC4 family of HCO_3 transporters. Pflugers Arch 2004;447(5):495–509.

[8] Shayakul C, Alper SL. Defects in processing and trafficking of the AE1 Cl^-/HCO_3^- exchanger associated with inherited distal renal tubular acidosis. Clin Exp Nephrol 2004;8(1):1–11.

[9] Knauf PA, Pal P. Band 3 Mediated Transport. In: Bernhardt I, Ellory JC, editors. Red cell membrane transport in health and disease. Berlin: Springer; 2003. p. 253–301.

[10] Jarolim P. Disorders of Band 3. In: Bernhardt I, Ellory JC, editors. Red cell membrane transport in health and disease. New York: Springer; 2003.

[11] Sterling D, Casey JR. Bicarbonate transport proteins. Biochem Cell Biol = Biochimie et Biologie Cellulaire 2002;80(5):483–97.

[12] Wrong O, Bruce LJ, Unwin RJ, Toye AM, Tanner MJ. Band 3 mutations, distal renal tubular acidosis, and Southeast Asian ovalocytosis. Kidney Int 2002;62(1):10–9.

[13] Alper SL. Familial renal tubular acidosis. J Nephrol 2010;23 (Suppl. 16):S57–76.

[14] Boron WF. Evaluating the role of carbonic anhydrases in the transport of HCO_3^- related species. Biochim Biophys Acta 2010;1804(2):410–21.

[15] Boron WF, Chen L, Parker MD. Modular structure of sodium-coupled bicarbonate transporters. J Exp Biol 2009;212(Pt 11): 1697–706.

[16] Majumdar D, Bevensee MO. Na-coupled bicarbonate transporters of the solute carrier 4 family in the nervous system: function, localization, and relevance to neurologic function. Neuroscience 2010;171(4):951–72.

[17] Casey JR, Grinstein S, Orlowski J. Sensors and regulators of intracellular pH. Nat Rev 2010;11(1):50–61.

[18] Cordat E, Casey JR. Bicarbonate transport in cell physiology and disease. Biochem J 2009;417(2):423–39.

[19] Almomani EY, Chu CY, Cordat E. Mis-trafficking of bicarbonate transporters: implications to human diseases. Biochem Cell Biol = Biochimie et Biologie Cellulaire 2011;89(2):157–77.

[20] Mount DB, Romero MF. The SLC26 gene family of multifunctional anion exchangers. Pflugers Arch 2004;447(5):710–21.

[21] Dawson PA, Markovich D. Pathogenetics of the human SLC26 transporters. Curr Med Chem 2005;12(4):385–96.

[22] Soleimani M, Xu J. SLC26 chloride/base exchangers in the kidney in health and disease. Semin Nephrol 2006;26(5):375–85.
[23] Alper SL, Stewart AK, Chernova MN, Zolotarev AS, Clark JS, Vandrope DH. Anion exchangers in flux: functional differences between human SLC26A6 and mouse slc26a6 polypeptides. In: Chadwick DJ, Goode J, editors. Epithelial Anion Transport in Health and Disease: the role of the SLC26 Transporters Family. Novartis Foundation Symposium vol. 273. London: John Wiley; 2006. p. 107–19; discussion 119–125, 261–264.
[24] Sharma AK, Rigby AC, Alper SL. STAS domain structure and function. Cell Physiol Biochem 2011;28(3):407–22.
[25] Ohana E, Yang D, Shcheynikov N, Muallem S. Diverse transport modes by the solute carrier 26 family of anion transporters. J Physiol 2009;587(Pt 10):2179–85.
[26] Dorwart MR, Shcheynikov N, Yang D, Muallem S. The solute carrier 26 family of proteins in epithelial ion transport. Physiol (Bethesda, Md) 2008;23:104–14.
[27] Wang CZ, Yano H, Nagashima K, Seino S. The Na^+-driven Cl^-/HCO_3^- exchanger. Cloning, tissue distribution, and functional characterization. J Biol Chem 2000;275(45):35486–90.
[28] Damkier HH, Aalkjaer C, Praetorius J. Na^+-dependent HCO_3^- import by the slc4a10 gene product involves Cl^- export. J Biol Chem 2010;285(35):26998–7007.
[29] Parker MD, Musa-Aziz R, Rojas JD, Choi I, Daly CM, Boron WF. Characterization of human SLC4A10 as an electroneutral Na/HCO_3 cotransporter (NBCn2) with Cl^- self-exchange activity. J Biol Chem 2008;283(19):12777–88.
[30] Ko SB, Luo X, Hager H, Rojek A, Choi JY, Licht C, et al. AE4 is a DIDS-sensitive Cl^-/HCO_3^- exchanger in the basolateral membrane of the renal CCD and the SMG duct. Am J Physiol Cell Physiol 2002;283(4):C1206–18.
[31] Tsuganezawa H, Kobayashi K, Iyori M, Araki T, Koizumi A, Watanabe S, et al. A new member of the HCO_3^- transporter superfamily is an apical anion exchanger of beta-intercalated cells in the kidney. J Biol Chem 2001;276(11):8180–9.
[32] Parker MD, Ourmozdi EP, Tanner MJ. Human BTR1, a new bicarbonate transporter superfamily member and human AE4 from kidney. Biochem Biophys Res Commun 2001;282(5):1103–9.
[33] Park M, Li Q, Shcheynikov N, Zeng W, Muallem S. NaBC1 is a ubiquitous electrogenic Na + -coupled borate transporter essential for cellular boron homeostasis and cell growth and proliferation. Mol Cell 2004;16(3):331–41.
[34] Takano J, Noguchi K, Yasumori M, Kobayashi M, Gajdos Z, Miwa K, et al. Arabidopsis boron transporter for xylem loading. Nature 2002;420(6913):337–40.
[35] Zhao R, Reithmeier RA. Expression and characterization of the anion transporter homologue YNL275w in Saccharomyces cerevisiae. Am J Physiol Cell Physiol 2001;281(1):C33–45.
[36] Sciortino CM, Shrode LD, Fletcher BR, Harte PJ, Romero MF. Localization of endogenous and recombinant Na^+-driven anion exchanger protein NDAE1 from Drosophila melanogaster. Am J Physiol Cell Physiol 2001;281(2):C449–63.
[37] Piermarini PM, Grogan LF, Lau K, Wang L, Beyenbach KWA. SLC4-like anion exchanger from renal tubules of the mosquito (Aedes aegypti): evidence for a novel role of stellate cells in diuretic fluid secretion. Am J Physiol 2010;298(3):R642–60.
[38] Linser PJ, Neira Oviedo M, Hirata T, Seron TJ, Smith KE, Piermarini PM, et al. Slc4-like anion transporters of the larval mosquito alimentary canal. J Insect Physiol 2012;58(4):551–62.
[39] Bellemer A, Hirata T, Romero MF, Koelle MR. Two types of chloride transporters are required for GABA(A) receptor-mediated inhibition in C. Elegans. EMBO J 2011;30(9):1852–63.
[40] Liao VH, Liu JT, Li WH, Yu CW, Hsieh YC. Caenorhabditis elegans bicarbonate transporter ABTS-1 is involved in arsenite toxicity and cholinergic signaling. Chem Res Toxicol 2010;23(5):926–32.
[41] Sherman T, Chernova MN, Clark JS, Jiang L, Alper SL, Nehrke K. The abts and sulp families of anion transporters from Caenorhabditis elegans. Am J Physiol Cell Physiol 2005;289(2):C341–51.
[42] Shmukler BE, Kurschat CE, Ackermann GE, Jiang L, Zhou Y, Barut B, et al. Zebrafish slc4a2/ae2 anion exchanger: cDNA cloning, mapping, functional characterization, and localization. Am J Physiol Renal Physiol 2005;289(4):F835–49.
[43] Paw BH, Davidson AJ, Zhou Y, Li R, Pratt SJ, Lee C, et al. Cell-specific mitotic defect and dyserythropoiesis associated with erythroid band 3 deficiency. Nat Genet 2003;34(1):59–64.
[44] Tang CH, Lee TH. The novel correlation of carbonic anhydrase II and anion exchanger 1 in gills of the spotted green pufferfish, Tetraodon nigroviridis. J Exp Zool A Ecol Genet Physiol 2007;307(7):411–8.
[45] Terbach N, Shah R, Kelemen R, Klein PS, Gordienko D, Brown NA, et al. Identifying an uptake mechanism for the antiepileptic and bipolar disorder treatment valproic acid using the simple biomedical model Dictyostelium. J Cell Sci 2011;124(Pt 13):2267–76.
[46] Tokuda N, Igarashi K, Shimamura T, Yurugi-Kobayashi T, Shiroishi M, Ito K, et al. Cloning, expression and purification of the anion exchanger 1 homologue from the basidiomycete Phanerochaete chrysosporium. Protein Expr Purif 2011;79(1):81–7.
[47] Takano J, Kobayashi M, Noda Y, Fujiwara T. Saccharomyces cerevisiae Bor1p is a boron exporter and a key determinant of boron tolerance. FEMS Microbiol Lett 2007;267(2):230–5.
[48] Parker MD, Boron WF. Expression and characterization of a prokaryotic SLC4-like anion transporter from nitrococcus mobilis. J Am Soc Nephrol 2007;:592A.
[49] Hagerstrand H, Danieluk M, Bobrowska-Hagerstrand M, Holmstrom T, Kralj-Iglic V, Lindqvist C, et al. The lamprey (Lampetra fluviatilis) erythrocyte; morphology, ultrastructure, major plasma membrane proteins and phospholipids, and cytoskeletal organization. Mol Membr Biol 1999;16(2):195–204.
[50] Igarashi T, Inatomi J, Sekine T, Cha SH, Kanai Y, Kunimi M, et al. Mutations in SLC4A4 cause permanent isolated proximal renal tubular acidosis with ocular abnormalities. Nat Genet 1999;23(3):264–6.
[51] Usui T, Hara M, Satoh H, Moriyama N, Kagaya H, Amano S, et al. Molecular basis of ocular abnormalities associated with proximal renal tubular acidosis. J Clin Invest 2001;108(1):107–15.
[52] Demirci FY, Chang MH, Mah TS, Romero MF, Gorin MB. Proximal renal tubular acidosis and ocular pathology: a novel missense mutation in the gene (SLC4A4) for sodium bicarbonate cotransporter protein (NBCe1). Mol Vis 2006;12:324–30.
[53] Suzuki M, Van Paesschen W, Stalmans I, Horita S, Yamada H, Bergmans BA, et al. Defective membrane expression of the Na^+-HCO_3^- cotransporter NBCe1 is associated with familial migraine. Proc Nat Acad Sci USA 2010;107(36):15963–8.
[54] Vithana EN, Morgan P, Sundaresan P, Ebenezer ND, Tan DT, Mohamed MD, et al. Mutations in sodium-borate cotransporter SLC4A11 cause recessive congenital hereditary endothelial dystrophy (CHED2). Nat Genet 2006;38(7):755–7.
[55] Vilas GL, Morgan PE, Loganathan SK, Quon A, Casey JR. A biochemical framework for SLC4A11, the plasma membrane protein defective in corneal dystrophies. Biochemistry 2011;50(12):2157–69.

[56] Kao L, Kurtz LM, Shao X, Papadopoulos MC, Liu L, Bok D, et al. Severe neurologic impairment in mice with targeted disruption of the electrogenic sodium bicarbonate cotransporter NBCe2 (Slc4a5 gene). J Biol Chem 2011;286(37):32563–74.

[57] Jacobs S, Ruusuvuori E, Sipila ST, Haapanen A, Damkier HH, Kurth I, et al. Mice with targeted Slc4a10 gene disruption have small brain ventricles and show reduced neuronal excitability. Proc Nat Acad Sci USA 2008;105(1):311–6.

[58] Bok D, Galbraith G, Lopez I, Woodruff M, Nusinowitz S, BeltrandelRio H, et al. Blindness and auditory impairment caused by loss of the sodium bicarbonate cotransporter NBC3. Nat Genet 2003;34(3):313–9.

[59] Boedtkjer E, Praetorius J, Matchkov VV, Stankevicius E, Mogensen S, Fuchtbauer AC, et al. Disruption of Na^+, HCO cotransporter NBCn1 (slc4a7) inhibits NO-mediated vasorelaxation, smooth muscle Ca_2 sensitivity, and hypertension development in mice. Circulation 2011;124(17):1819–29.

[60] Leviel F, Hubner CA, Houillier P, Morla L, El Moghrabi S, Brideau G, et al. The Na + -dependent chloride-bicarbonate exchanger SLC4A8 mediates an electroneutral Na + reabsorption process in the renal cortical collecting ducts of mice. J Clin Invest 2010;120(5):1627–35.

[61] Groger N, Frohlich H, Maier H, Olbrich A, Kostin S, Braun T, et al. SLC4A11 prevents osmotic imbalance leading to corneal endothelial dystrophy, deafness, and polyuria. J Biol Chem 2011;285(19):14467–74.

[62] Lopez IA, Rosenblatt MI, Kim C, Galbraith GC, Jones SM, Kao L, et al. Slc4a11 gene disruption in mice: cellular targets of sensorineuronal abnormalities. J Biol Chem 2009;284(39):26882–96.

[63] Bissig M, Hagenbuch B, Stieger B, Koller T, Meier PJ. Functional expression cloning of the canalicular sulfate transport system of rat hepatocytes. J Biol Chem 1994;269(4):3017–21.

[64] Markovich D, Bissig M, Sorribas V, Hagenbuch B, Meier PJ, Murer H. Expression of rat renal sulfate transport systems in Xenopus laevis oocytes. Functional characterization and molecular identification. J Biol Chem 1994;269(4):3022–6.

[65] Price GD, Woodger FJ, Badger MR, Howitt SM, Tucker L. Identification of a SulP-type bicarbonate transporter in marine cyanobacteria. Proc Nat Acad Sci USA 2004;101(52):18228–33.

[66] Felce J, Saier Jr MH. Carbonic anhydrases fused to anion transporters of the SulP family: evidence for a novel type of bicarbonate transporter. J Mol Microbiol Biotechnol 2004;8(3): 169–76.

[67] Schweinfest CW, Henderson KW, Suster S, Kondoh N, Papas TS. Identification of a colon mucosa gene that is down-regulated in colon adenomas and adenocarcinomas. Proc Nat Acad Sci USA 1993;90(9):4166–70.

[68] Hoglund P, Haila S, Socha J, Tomaszewski L, Saarialho-Kere U, Karjalainen-Lindsberg ML, et al. Mutations of the Down-regulated in adenoma (DRA) gene cause congenital chloride diarrhoea. Nat Genet 1996;14(3):316–9.

[69] Melvin JE, Park K, Richardson L, Schultheis PJ, Shull GE. Mouse down-regulated in adenoma (DRA) is an intestinal Cl^-/HCO_3^- exchanger and is up-regulated in colon of mice lacking the NHE3 Na^+/H^+ exchanger. J Biol Chem 1999;274(32): 22855–61.

[70] Everett LA, Glaser B, Beck JC, Idol JR, Buchs A, Heyman M, et al. Pendred syndrome is caused by mutations in a putative sulphate transporter gene (PDS). Nat Genet 1997;17(4):411–22.

[71] Soleimani M, Greeley T, Petrovic S, Wang Z, Amlal H, Kopp P, et al. Pendrin: an apical $Cl^-/OH^-/HCO_3^-$ exchanger in the kidney cortex. Am J Physiol Renal Physiol 2001;280(2):F356–64.

[72] Knauf F, Yang CL, Thomson RB, Mentone SA, Giebisch G, Aronson PS. Identification of a chloride-formate exchanger expressed on the brush border membrane of renal proximal tubule cells. Proc Nat Acad Sci Usa 2001;98(16):9425–30.

[73] Chernova MN, Jiang L, Friedman DJ, Darman RB, Lohi H, Kere J, et al. Functional comparison of mouse slc26a6 anion exchanger with human SLC26A6 polypeptide variants: differences in anion selectivity, regulation, and electrogenicity. J Biol Chem 2005;280(9):8564–80.

[74] Petrovic S, Barone S, Xu J, Conforti L, Ma L, Kujala M, et al. SLC26A7: a basolateral Cl^-/HCO_3^- exchanger specific to intercalated cells of the outer medullary collecting duct. Am J Physiol Renal Physiol 2004;286(1):F161–9.

[75] Xu J, Henriksnas J, Barone S, Witte D, Shull GE, Forte JG, et al. SLC26A9 is expressed in gastric surface epithelial cells, mediates Cl^-/HCO_3^- exchange, and is inhibited by $NH4^+$. Am J Physiol Cell Physiol 2005;289(2):C493–505.

[76] Xu J, Barone S, Li H, Holiday S, Zahedi K, Soleimani M. Slc26a11, a chloride transporter, localizes with the vacuolar H^+-ATPase of A-intercalated cells of the kidney. Kidney Int 2011;80 (9):926–37.

[77] Stewart AK, Shmukler BE, Vandorpe DH, Reimold F, Heneghan JF, Nakakuki M, et al. SLC26 anion exchangers of guinea pig pancreatic duct: molecular cloning and functional characterization. Am J Physiol Cell Physiol 2011;301(2):C289–303.

[78] Kim KH, Shcheynikov N, Wang Y, Muallem S. SLC26A7 is a Cl^- channel regulated by intracellular pH. J Biol Chem 2005;280 (8):6463–70.

[79] Dorwart MR, Shcheynikov N, Wang Y, Stippec S, Muallem S. SLC26A9 is a Cl^- channel regulated by the WNK kinases. J Physiol 2007;584(Pt 1):333–45.

[80] Heneghan JF, Akhavein A, Salas MJ, Shmukler BE, Karniski LP, Vandorpe DH, et al. Regulated transport of sulfate and oxalate by SLC26A2/DTDST. Am J Physiol Cell Physiol 2010;298(6): C1363–75.

[81] Ohana E, Shcheynikov N, Park M, Muallem S. Solute carrier family 26 member a2 (Slc26a2) protein functions as an electroneutral SOFormula/OH-/Cl^- exchanger regulated by extracellular Cl. J Biol Chem 2012;287(7):5122–32.

[82] Aronson PS. Essential roles of CFEX-mediated Cl^--oxalate exchange in proximal tubule NaCl transport and prevention of urolithiasis. Kidney Int 2006;70(7):1207–13.

[83] Dawson PA, Russell CS, Lee S, McLeay SC, van Dongen JM, Cowley DM, et al. Urolithiasis and hepatotoxicity are linked to the anion transporter Sat1 in mice. J Clin Invest 2010;120 (3):706–12.

[84] Grinstein S, Ship S, Rothstein A. Anion transport in relation to proteolytic dissection of band 3 protein. Biochim Biophys Acta 1978;507(2):294–304.

[85] Kopito RR, Lee BS, Simmons DM, Lindsey AE, Morgans CW, Schneider K. Regulation of intracellular pH by a neuronal homolog of the erythrocyte anion exchanger. Cell 1989;59(5): 927–37.

[86] Stewart AK, Chernova MN, Kunes YZ, Alper SL. Regulation of AE2 anion exchanger by intracellular pH: critical regions of the NH_2-terminal cytoplasmic domain. Am J Physiol Cell Physiol 2001;281(4):C1344–54.

[87] Vince JW, Reithmeier RA. Carbonic anhydrase II binds to the carboxyl terminus of human band 3, the erythrocyte C1-/HCO_3- exchanger. J Biol Chem 1998;273(43):28430–7.

[88] Alper SL. The band 3-related anion exchanger (AE) gene family. Annu Rev Physiol 1991;53:549–64.

[89] Linn SC, Askew GR, Menon AG, Shull GE. Conservation of an AE3 Cl^-/HCO_3^-exchanger cardiac-specific exon and promoter region and AE3 mRNA expression patterns in murine and human hearts. Circ Res 1995;76(4):584–91.

[90] Rossmann H, Bachmann O, Wang Z, Shull GE, Obermaier B, Stuart-Tilley A, et al. Differential expression and regulation of AE2 anion exchanger subtypes in rabbit parietal and mucous cells. J Physiol 2001;534(Pt 3):837–48.

[91] Wang Z, Schultheis PJ, Shull GE. Three N-terminal variants of the AE2 Cl^-/HCO_3^-exchanger are encoded by mRNAs transcribed from alternative promoters. J Biol Chem 1996;271(13): 7835–43.

[92] Medina JF, Lecanda J, Acin A, Ciesielczyk P, Prieto J. Tissue-specific N-terminal isoforms from overlapping alternate promoters of the human AE2 anion exchanger gene. Biochem Biophys Res Commun 2000;267(1):228–35.

[93] Morgans CW, Kopito RR. Generation of truncated brain AE3 isoforms by alternate mRNA processing. J Cell Sci 1993;106(Pt 4):1275–82.

[94] Lipovich L, Lynch ED, Lee MK, King MC. A novel sodium bicarbonate cotransporter-like gene in an ancient duplicated region: SLC4A9 at 5q31. Genome Biol 2001;2(4): RESEARCH0011

[95] Xu J, Barone S, Petrovic S, Wang Z, Seidler U, Riederer B, et al. Identification of an apical Cl^-/HCO_3^- exchanger in gastric surface mucous and duodenal villus cells. Am J Physiol Gastrointest Liver Physiol 2003;285(6):G1225–34.

[96] Salhany JM. Erythrocyte band 3 protein. Boca Raton, FL: CRC Press; 1990. pp..1–213

[97] Jennings ML. Structure and function of the red blood cell anion transport protein. Annu Rev Biophys Biophys Chem 1989;18:397–430.

[98] Hanke-Baier P, Raida M, Passow H. Comparison of murine band 3 protein-mediated Cl- transport as measured in mouse red blood cells and in oocytes of Xenopus laevis. Biochim Biophys Acta 1988;940(1):136–40.

[99] Jiang L, Stuart-Tilley A, Parkash J, Alper SL. pHi and serum regulate AE2-mediated Cl^-/HCO_3^- exchange in CHOP cells of defined transient transfection status. Am J Physiol 1994;267 (3 Pt 1):C845–56.

[100] Philipp S, Kneussel M, Konig J, Appelhans H. Molecular analysis of regulation of gene expression of the human erythroid anion exchanger (AE) 1. FEBS Lett 1998;438(3):315–20.

[101] Adair-Kirk TL, Cox KH, Cox JV. Intracellular trafficking of variant chicken kidney AE1 anion exchangers: role Of alternative NH_2 termini in polarized sorting and Golgi recycling. J Cell Biol 1999;147(6):1237–48.

[102] Devonald MA, Smith AN, Poon JP, Ihrke G, Karet FE. Non-polarized targeting of AE1 causes autosomal dominant distal renal tubular acidosis. Nat Genet 2003;33(2):125–7.

[103] Cordat E, Kittanakom S, Yenchitsomanus PT, Li J, Du K, Lukacs GL, et al. Dominant and recessive distal renal tubular acidosis mutations of kidney anion exchanger 1 induce distinct trafficking defects in MDCK cells. Traffic 2006;7(2):117–28.

[104] Dale WE, Textor JA, Mercer RW, Simchowitz L. Expression and characterization of the human erythrocyte anion exchanger in a baculovirus/Sf-9 cell system. Protein Expr Purif 1996;7(1):1–11.

[105] Groves JD, Falson P, le Maire M, Tanner MJ. Functional cell surface expression of the anion transport domain of human red cell band 3 (AE1) in the yeast Saccharomyces cerevisiae. Proc Nat Acad Sci USA 1996;93(22):12245–50.

[106] Zhang D, Kiyatkin A, Bolin JT, Low PS. Crystallographic structure and functional interpretation of the cytoplasmic domain of erythrocyte membrane band 3. Blood 2000;96 (9):2925–33.

[107] Ribeiro ML, Alloisio N, Almeida H, Gomes C, Texier P, Lemos C, et al. Severe hereditary spherocytosis and distal renal tubular acidosis associated with the total absence of band 3. Blood 2000;96(4):1602–4.

[108] Peters LL, Shivdasani RA, Liu SC, Hanspal M, John KM, Gonzalez JM, et al. Anion exchanger 1 (band 3) is required to prevent erythrocyte membrane surface loss but not to form the membrane skeleton. Cell 1996;86(6):917–27.

[109] Stehberger PA, Shmukler BE, Stuart-Tilley AK, Peters LL, Alper SL, Wagner CA. Distal renal tubular acidosis in mice lacking the AE1 (band 3) Cl^-/HCO_3^- exchanger (slc4a1). J Am Soc Nephrol 2007;:18 in press

[110] Inaba M, Yawata A, Koshino I, Sato K, Takeuchi M, Takakuwa Y, et al. Defective anion transport and marked spherocytosis with membrane instability caused by hereditary total deficiency of red cell band 3 in cattle due to a nonsense mutation. J Clin Invest 1996;97(8):1804–17.

[111] Swietach P, Tiffert T, Mauritz JM, Seear R, Esposito A, Kaminski CF, et al. Hydrogen ion dynamics in human red blood cells. J Physiol 2010;588(Pt 24):4995–5014.

[112] Wieth JO, Andersen OS, Brahm J, Bjerrum PJ, Borders Jr CL. Chloride–bicarbonate exchange in red blood cells: physiology of transport and chemical modification of binding sites. Philos Trans R Soc Lond B Biol Sci 1982;299(1097):383–99.

[113] Boron WF. Transport of oxygen and carbon dioxide in the blood. In: Boron WF, Boulpaep EL, editors. Medical physiology: a cellular and molecular approach. Philadelphia: Saunders; 2003. p. 654–68.

[114] Drew C, Ball V, Robinson H, Clive Ellory J, Gibson JS. Oxygen sensitivity of red cell membrane transporters revisited. Bioelectrochem (Amsterdam, Netherlands) 2004;62(2): 153–8.

[115] Galtieri A, Tellone E, Romano L, Misiti F, Bellocco E, Ficarra S, et al. Band-3 protein function in human erythrocytes: effect of oxygenation-deoxygenation. Biochim Biophys Acta 2002;1564 (1):214–8.

[116] Jennings ML. Proton fluxes associated with erythrocyte membrane anion exchange. J Membr Biol 1976;28(2-3):187–205.

[117] Jennings ML, Adame MF. Characterization of oxalate transport by the human erythrocyte band 3 protein. J Gen Physiol 1996;107(1):145–59.

[118] Baggio B, Gambaro G, Borsatti A, Clari G, Moret V. Relation between band 3 red blood cell protein and transmembrane oxalate flux in stone formers. Lancet 1984;2 (8396):223–4.

[119] Pawloski JR, Hess DT, Stamler JS. Export by red blood cells of nitric oxide bioactivity. Nature 2001;409(6820):622–6.

[120] Gladwin MT. Role of the red blood cell in nitric oxide homeostasis and hypoxic vasodilation. Adv Exp Med Biol 2006;588:189–205.

[121] Jensen FB. Nitrite transport into pig erythrocytes and its potential biological role. Acta Physiol Scand 2005;184(3):243–51.

[122] Jensen FB, Rohde S. Comparative analysis of nitrite uptake and hemoglobin-nitrite reactions in erythrocytes: sorting out uptake mechanisms and oxygenation dependencies. Am J Physiol 2010;298(4):R972–82.

[123] Alper SL, Darman RB, Chernova MN, Dahl NK. The AE gene family of Cl/HCO_3^- exchangers. J Nephrol 2002;15(Suppl. 5): S41–53.

[124] Alper SL, Kopito RR, Libresco SM, Lodish HF. Cloning and characterization of a murine band 3-related cDNA from kidney and from a lymphoid cell line. J Biol Chem 1988;263(32): 17092–9.

[125] Huber S, Asan E, Jons T, Kerscher C, Puschel B, Drenckhahn D. Expression of rat kidney anion exchanger 1 in type A intercalated cells in metabolic acidosis and alkalosis. Am J Physiol 1999;277(6 Pt 2):F841–9.

[126] Wu F, Saleem MA, Kampik NB, Satchwell TJ, Williamson RC, Blattner SM, et al. Anion exchanger 1 interacts with nephrin in podocytes. J Am Soc Nephrol 2010;21(9):1456–67.

[127] Papageorgiou P, Shmukler BE, Stuart-Tilley AK, Jiang L, Alper SL. AE anion exchangers in atrial tumor cells. Am J Physiol Heart Circ Physiol 2001;280(3):H937–45.

[128] Richards SM, Jaconi ME, Vassort G, Puceat M. A spliced variant of AE1 gene encodes a truncated form of Band 3 in heart: the predominant anion exchanger in ventricular myocytes. J Cell Sci 1999;112(Pt 10):1519–28.
[129] Rajendran VM, Black J, Ardito TA, Sangan P, Alper SL, Schweinfest C, et al. Regulation of DRA and AE1 in rat colon by dietary Na depletion. Am J Physiol Gastrointest Liver Physiol 2000;279(5):G931–42.
[130] Alrefai WA, Tyagi S, Nazir TM, Barakat J, Anwar SS, Hadjiagapiou C, et al. Human intestinal anion exchanger isoforms: expression, distribution, and membrane localization. Biochim Biophys Acta 2001;1511(1):17–27.
[131] Hengl T, Kaneko H, Dauner K, Vocke K, Frings S, Mohrlen F. Molecular components of signal amplification in olfactory sensory cilia. Proc Nat Acad Sci USA 2010;107(13):6052–7.
[132] Gawenis LR, Ledoussal C, Judd LM, Prasad V, Alper SL, Stuart-Tilley A, et al. Mice with a targeted disruption of the AE2 Cl^-/HCO_3^- exchanger are achlorhydric. J Biol Chem 2004;279(29):30531–9.
[133] Stuart-Tilley A, Sardet C, Pouyssegur J, Schwartz MA, Brown D, Alper SL. Immunolocalization of anion exchanger AE2 and cation exchanger NHE-1 in distinct adjacent cells of gastric mucosa. Am J Physiol 1994;266(2 Pt 1):C559–68.
[134] Josephsen K, Praetorius J, Frische S, Gawenis LR, Kwon TH, Agre P, et al. Targeted disruption of the Cl^-/HCO_3^- exchanger Ae2 results in osteopetrosis in mice. Proc Nat Acad Sci USA 2009;106(5):1638–41.
[135] Wu J, Glimcher LH, Aliprantis AO. HCO_3^-/Cl^- anion exchanger SLC4A2 is required for proper osteoclast differentiation and function. Proc Nat Acad Sci USA 2008;105(44): 16934–9.
[136] Medina JF, Recalde S, Prieto J, Lecanda J, Saez E, Funk CD, et al. Anion exchanger 2 is essential for spermiogenesis in mice. Proc Nat Acad Sci USA 2003;100(26):15847–52.
[137] Turner HC, Alvarez LJ, Candia OA. Identification and localization of acid–base transporters in the conjunctival epithelium. Exp Eye Res 2001;72(5):519–31.
[138] Bronckers AL, Lyaruu DM, Jansen ID, Medina JF, Kellokumpu S, Hoeben KA, et al. Localization and function of the anion exchanger Ae2 in developing teeth and orofacial bone in rodents. J Exp Zool B Mol Dev Evol 2009;312B(4):375–87.
[139] Josephsen K, Takano Y, Frische S, Praetorius J, Nielsen S, Aoba T, et al. Ion transporters in secretory and cyclically modulating ameloblasts: a new hypothesis for cellular control of preeruptive enamel maturation. Am J Physiol Cell Physiol 2010;299(6): C1299–307.
[140] Alper SL, Stuart-Tilley A, Simmons CF, Brown D, Drenckhahn D. The fodrin-ankyrin cytoskeleton of choroid plexus preferentially colocalizes with apical Na^+K^+-ATPase rather than with basolateral anion exchanger AE2. J Clin Invest 1994;93(4): 1430–8.
[141] Alper SL, Rossmann H, Wilhelm S, Stuart-Tilley AK, Shmukler BE, Seidler U. Expression of AE2 anion exchanger in mouse intestine. Am J Physiol 1999;277(2 Pt 1):G321–32.
[142] Lubman RL, Danto SI, Chao DC, Fricks CE, Crandall ED. Cl (-)-HCO_3^- exchanger isoform AE2 is restricted to the basolateral surface of alveolar epithelial cell monolayers. Am J Respir Cell Mol Biol 1995;12(2):211–9.
[143] Loffing J, Moyer BD, Reynolds D, Shmukler BE, Alper SL, Stanton BA. Functional and molecular characterization of an anion exchanger in airway serous epithelial cells. Am J Physiol Cell Physiol 2000;279(4):C1016–23.
[144] Tietz PS, Marinelli RA, Chen XM, Huang B, Cohn J, Kole J, et al. Agonist-induced coordinated trafficking of functionally related transport proteins for water and ions in cholangiocytes. J Biol Chem 2003;278(22):20413–9.
[145] Garcia C, Montuenga LM, Medina JF, Prieto J. In situ detection of AE2 anion-exchanger mRNA in the human liver. Cell Tissue Res 1998;291(3):481–8.
[146] Martinez-Anso E, Castillo JE, Diez J, Medina JF, Prieto J. Immunohistochemical detection of chloride/bicarbonate anion exchangers in human liver. Hepatol (Baltimore, Md. 1994;19 (6):1400–6.
[147] Frische S, Zolotarev AS, Kim YH, Praetorius J, Alper S, Nielsen S, et al. AE2 isoforms in rat kidney: immunohistochemical localization and regulation in response to chronic NH4Cl loading. Am J Physiol Renal Physiol 2004;286(6):F1163–70.
[148] Alper SL, Stuart-Tilley AK, Biemesderfer D, Shmukler BE, Brown D. Immunolocalization of AE2 anion exchanger in rat kidney. Am J Physiol 1997;273(4 Pt 2):F601–14.
[149] Stuart Tilley AK, Shmukler BE, Brown D, Alper SL. Immunolocalization and tissue-specific splicing of AE2 anion exchanger in mouse kidney. J-Am-Soc-Nephrol 1998;9(6): 946–59.
[150] Komlosi P, Frische S, Fuson AL, Fintha A, Zsembery A, Peti-Peterdi J, et al. Characterization of basolateral chloride/bicarbonate exchange in macula densa cells. Am J Physiol Renal Physiol 2005;288(2):F380–6.
[151] Linn SC, Kudrycki KE, Shull GE. The predicted translation product of a cardiac AE3 mRNA contains an N terminus distinct from that of the brain AE3 Cl^-/HCO_3^- exchanger. Cloning of a cardiac AE3 cDNA, organization of the AE3 gene, and identification of an alternative transcription initiation site. J Biol Chem 1992;267(11):7927–35.
[152] Yannoukakos D, Stuart-Tilley A, Fernandez HA, Fey P, Duyk G, Alper SL. Molecular cloning, expression, and chromosomal localization of two isoforms of the AE3 anion exchanger from human heart. Circ Res 1994;75(4):603–14.
[153] Kudrycki KE, Newman PR, Shull GE. cDNA cloning and tissue distribution of mRNAs for two proteins that are related to the band 3 Cl^-/HCO_3^- exchanger. J Biol Chem 1990;265(1): 462–71.
[154] Kobayashi S, Morgans CW, Casey JR, Kopito RR. AE3 anion exchanger isoforms in the vertebrate retina: developmental regulation and differential expression in neurons and glia. J Neurosci 1994;14(10):6266–79.
[155] Hentschke M, Wiemann M, Hentschke S, Kurth I, Hermans-Borgmeyer I, Seidenbecher T, et al. Mice with a targeted disruption of the Cl^-/HCO_3^- exchanger AE3 display a reduced seizure threshold. Mol Cell Biol 2006;26(1):182–91.
[156] Brosius III FC, Pisoni RL, Cao X, Deshmukh G, Yannoukakos D, Stuart Tilley AK, et al. AE anion exchanger mRNA and protein expression in vascular smooth muscle cells, aorta, and renal microvessels. Am-J-Physiol 1997;273(6 Pt 2): F1039–47.
[157] Blomqvist SR, Vidarsson H, Fitzgerald S, Johansson BR, Ollerstam A, Brown R, et al. Distal renal tubular acidosis in mice that lack the forkhead transcription factor Foxi1. J Clin Invest 2004;113(11):1560–70.
[158] Hentschke M, Hentschke S, Borgmeyer U, Hubner CA, Kurth I. The murine AE4 promoter predominantly drives type B intercalated cell specific transcription. Histochem Cell Biol 2009;132(4):405–12.
[159] Simpson JE, Schweinfest C, Shull GE, Gawenis L, Walker NM, Boyle KT, et al. PAT-1 (Slc26a6) is the predominant apical membrane Cl^-/HCO_3^- exchanger in the upper villous epithelium of murine duodenum. Am J Physiol Gastrointest Liver Physiol 2007;292(4):G1079–88.

[160] Casey JR, Reithmeier RA. Analysis of the oligomeric state of band 3, the anion transport protein of the human erythrocyte membrane, by size exclusion high performance liquid chromatography. Oligomeric stability and origin of heterogeneity. J Biol Chem 1991;266(24):15726–37.
[161] Vince JW, Sarabia VE, Reithmeier RA. Self-association of band 3, the human erythrocyte anion exchanger, in detergent solution. Biochim Biophys Acta 1997;1326(2):295–306.
[162] Thevenin BJ, Low PS. Kinetics and regulation of the ankyrin-band 3 interaction of the human red blood cell membrane. J Biol Chem 1990;265(27):16166–72.
[163] Van Dort HM, Knowles DW, Chasis JA, Lee G, Mohandas N, Low PS. Analysis of integral membrane protein contributions to the deformability and stability of the human erythrocyte membrane. J Biol Chem 2001;276(50):46968–74.
[164] Bruce LJ, Beckmann R, Ribeiro ML, Peters LL, Chasis JA, Delaunay J, et al. A band 3-based macrocomplex of integral and peripheral proteins in the RBC membrane. Blood 2003;101 (10):4180–8.
[165] Endeward V, Musa-Aziz R, Cooper GJ, Chen LM, Pelletier MF, Virkki LV, et al. Evidence that aquaporin 1 is a major pathway for CO_2 transport across the human erythrocyte membrane. Faseb J 2006;20(12):1974–81.
[166] Hub JS, de Groot BL. Does CO2 permeate through aquaporin-1? Biophys J 2006;91(3):842–8.
[167] Ripoche P, Goossens D, Devuyst O, Gane P, Colin Y, Verkman AS, et al. Role of RhAG and AQP1 in NH3 and CO2 gas transport in red cell ghosts: a stopped-flow analysis. Transfus Clin Biol 2006;13(1-2):117–22.
[168] Burton NM, Bruce LJ. Modelling the structure of the red cell membrane. Biochem Cell Biol = Biochimie et Biologie Cellulaire 2011;89(2):200–15.
[169] Satchwell TJ, Bell AJ, Pellegrin S, Kupzig S, Ridgwell K, Daniels G, et al. Critical band 3 multiprotein complex interactions establish early during human erythropoiesis. Blood 2011;118(1):182–91.
[170] Kanki T, Young MT, Sakaguchi M, Hamasaki N, Tanner MJ. The N-terminal region of the transmembrane domain of human erythrocyte band 3. Residues critical for membrane insertion and transport activity. J Biol Chem 2003;278 (8):5564–73.
[171] Stewart AK, Kerr N, Chernova MN, Alper SL, Vaughan-Jones RD. Acute pH-dependent regulation of AE2-mediated anion exchange involves discrete local surfaces of the NH2-terminal cytoplasmic domain. J Biol Chem 2004;279(50):52664–76.
[172] Gill HS, Boron WF. Expression and purification of the cytoplasmic N-terminal domain of the Na/HCO_3 cotransporter NBCe1-A: structural insights from a generalized approach. Protein Expr Purif 2006;49(2):228–34.
[173] Zhou J, Low PS. Characterization of the reversible conformational equilibrium in the cytoplasmic domain of human erythrocyte membrane band 3. J Biol Chem 2001;276(41): 38147–51.
[174] Pal P, Holmberg BE, Knauf PA. Conformational changes in the cytoplasmic domain of human anion exchanger 1 revealed by luminescence resonance energy transfer. Biochemistry 2005;44 (42):13638–49.
[175] Campanella ME, Chu H, Low PS. Assembly and regulation of a glycolytic enzyme complex on the human erythrocyte membrane. Proc Nat Acad Sci USA 2005;102(7):2402–7.
[176] Chu H, Low PS. Mapping of glycolytic enzyme binding sites on human erythrocyte band 3. Biochem J 2006;:.
[177] Lewis IA, Campanella ME, Markley JL, Low PS. Role of band 3 in regulating metabolic flux of red blood cells. Proc Nat Acad Sci USA 2009;106(44):18515–20.
[178] Campanella ME, Chu H, Wandersee NJ, Peters LL, Mohandas N, Gilligan DM, et al. Characterization of glycolytic enzyme interactions with murine erythrocyte membranes in wild-type and membrane protein knockout mice. Blood 2008;112(9): 3900–6.
[179] Zhang Y, Manning LR, Falcone J, Platt O, Manning JM. Human erythrocyte membrane band 3 protein influences hemoglobin cooperativity. Possible effect on oxygen transport. J Biol Chem 2003;278(41):39565–71.
[180] Rotter MA, Chu H, Low PS, Ferrone FA. Band 3 catalyzes sickle hemoglobin polymerization. Biophys Chem 2010;146(2-3):55–9.
[181] Demehin AA, Abugo OO, Jayakumar R, Lakowicz JR, Rifkind JM. Binding of hemoglobin to red cell membranes with eosin-5-maleimide-labeled band 3: analysis of centrifugation and fluorescence data. Biochemistry 2002;41(27):8630–7.
[182] Salhany JM, Cordes KA, Gaines ED. Light-scattering measurements of hemoglobin binding to the erythrocyte membrane. Evidence for transmembrane effects related to a disulfonic stilbene binding to band 3. Biochemistry 1980;19(7):1447–54.
[183] Shaklai N, Yguerabide J, Ranney HM. Interaction of hemoglobin with red blood cell membranes as shown by a fluorescent chromophore. Biochemistry 1977;16(25):5585–92.
[184] Chang SH, Low PS. Identification of a critical ankyrin-binding loop on the cytoplasmic domain of erythrocyte membrane band 3 by crystal structure analysis and site-directed mutagenesis. J Biol Chem 2003;278(9):6879–84.
[185] Anong WA, Weis TL, Low PS. Rate of rupture and reattachment of the band 3-ankyrin bridge on the human erythrocyte membrane. J Biol Chem 2006;281(31):22360–6.
[186] Stefanovic M, Markham NO, Parry EM, Garrett-Beal LJ, Cline AP, Gallagher PG, et al. An 11-amino acid beta-hairpin loop in the cytoplasmic domain of band 3 is responsible for ankyrin binding in mouse erythrocytes. Proc Nat Acad Sci USA 2007;104(35):13972–7.
[187] Anong WA, Franco T, Chu H, Weis TL, Devlin EE, Bodine DM, et al. Adducin forms a bridge between the erythrocyte membrane and its cytoskeleton and regulates membrane cohesion. Blood 2009;114(9):1904–12.
[188] Kodippili GC, Spector J, Kang GE, Liu H, Wickrema A, Ritchie K, et al. Analysis of the kinetics of band 3 diffusion in human erythroblasts during assembly of the erythrocyte membrane skeleton. Br J Haematol 2010;150(5):592–600.
[189] Jons T, Drenckhahn D. Identification of the binding interface involved in linkage of cytoskeletal protein 4.1 to the erythrocyte anion exchanger. EMBO J 1992;11(8):2863–7.
[190] Lombardo CR, Willardson BM, Low PS. Localization of the protein 4.1-binding site on the cytoplasmic domain of erythrocyte membrane band 3. J Biol Chem 1992;267(14):9540–6.
[191] Hemming NJ, Anstee DJ, Staricoff MA, Tanner MJ, Mohandas N. Identification of the membrane attachment sites for protein 4.1 in the human erythrocyte. J Biol Chem 1995;270(10):5360–6.
[192] An X, Zhang X, Debnath G, Baines AJ, Mohandas N. Phosphatidylinositol-4,5-biphosphate (PIP2) differentially regulates the interaction of human erythrocyte protein 4.1 (4.1R) with membrane proteins. Biochemistry 2006;45(18):5725–32.
[193] Kodippili GC, Spector J, Hale J, Giger K, Hughes MR, McNagny KM, et al. Analysis of the mobilities of band 3 populations associated with ankyrin protein and junctional complexes in intact murine erythrocytes. J Biol Chem 2012;287 (6):4129–38.
[194] Ding Y, Casey JR, Kopito RR. The major kidney AE1 isoform does not bind ankyrin (Ank1) in vitro. An essential role for the 79 NH2-terminal amino acid residues of band 3. J Biol Chem 1994;269(51):32201–8.

[195] Wang CC, Moriyama R, Lombardo CR, Low PS. Partial characterization of the cytoplasmic domain of human kidney band 3. J Biol Chem 1995;270(30):17892–7.
[196] Piepenhagen PA, Peters LL, Lux SE, Nelson WJ. Differential expression of Na^+-K^+-ATPase, ankyrin, fodrin, and E-cadherin along the kidney nephron. Am J Physiol 1995;269(6 Pt 1): C1417–32.
[197] Ideguchi H, Okubo K, Ishikawa A, Futata Y, Hamasaki N. Band 3-Memphis is associated with a lower transport rate of phosphoenolpyruvate. Br J Haematol 1992;82(1):122–5.
[198] Toye AM, Ghosh S, Young MT, Jones GK, Sessions RB, Ramauge M, et al. Protein-4.2 association with band 3 (AE1, SLCA4) in Xenopus oocytes: effects of three natural protein-4.2 mutations associated with hemolytic anemia. Blood 2005;105 (10):4088–95.
[199] Alper SL. Diseases of mutations in the SLC4A1/AE1 polypeptide. In: Broer S, Wagner CA, editors. Membrane transport diseases. New York: Kluwer Academic/Plenum; 2003. p. 39–63.
[200] Kanzaki A, Hayette S, Morle L, Inoue F, Matsuyama R, Inoue T, et al. Total absence of protein 4.2 and partial deficiency of band 3 in hereditary spherocytosis. Br J Haematol 1997;99(3): 522–30.
[201] Malik S, Sami M, Watts A. A role for band 4.2 in human erythrocyte band 3 mediated anion transport. Biochemistry 1993;32 (38):10078–84.
[202] Bruce LJ, Ghosh S, King MJ, Layton DM, Mawby WJ, Stewart GW, et al. Absence of CD47 in protein 4.2-deficient hereditary spherocytosis in man: an interaction between the Rh complex and the band 3 complex. Blood 2002;100(5):1878–85.
[203] Su Y, Ding Y, Jiang M, Jiang W, Hu X, Zhang Z. Associations of protein 4.2 with band 3 and ankyrin. Mol Cell Biochem 2006;289(1–2):159–66.
[204] Mandal D, Baudin-Creuza V, Bhattacharyya A, Pathak S, Delaunay J, Kundu M, et al. Caspase 3-mediated proteolysis of the N-terminal cytoplasmic domain of the human erythroid anion exchanger 1 (band 3). J Biol Chem 2003;278(52):52551–8.
[205] Mandal D, Mazumder A, Das P, Kundu M, Basu J. Fas-, caspase 8-, and caspase 3-dependent signaling regulates the activity of the aminophospholipid translocase and phosphatidylserine externalization in human erythrocytes. J Biol Chem 2005;280 (47):39460–7.
[206] Lang KS, Lang PA, Bauer C, Duranton C, Wieder T, Huber SM, et al. Mechanisms of suicidal erythrocyte death. Cell Physiol Biochem 2005;15(5):195–202.
[207] Arese P, Turrini F, Schwarzer E. Band 3/complement-mediated recognition and removal of normally senescent and pathological human erythrocytes. Cell Physiol Biochem 2005;16 (4–6):133–46.
[208] Bustos SP, Reithmeier RA. Protein 4.2 interaction with hereditary spherocytosis mutants of the cytoplasmic domain of human anion exchanger 1. Biochem J 2011;433(2):313–22.
[209] Brunati AM, Bordin L, Clari G, James P, Quadroni M, Baritono E, et al. Sequential phosphorylation of protein band 3 by Syk and Lyn tyrosine kinases in intact human erythrocytes: identification of primary and secondary phosphorylation sites. Blood 2000;96(4):1550–7.
[210] Ferru E, Giger K, Pantaleo A, Campanella E, Grey J, Ritchie K, et al. Regulation of membrane-cytoskeletal interactions by tyrosine phosphorylation of erythrocyte band 3. Blood 2011;117(22):5998–6006.
[211] Keskanokwong T, Shandro HJ, Johnson DE, Kittanakom S, Vilas GL, Thorner P, et al. Interaction of integrin-linked kinase with the kidney chloride/bicarbonate exchanger, kAE1. J Biol Chem 2007;282(32):23205–18.
[212] Jiang W, Ding Y, Su Y, Jiang M, Hu X, Zhang Z. Interaction of glucose transporter 1 with anion exchanger 1 in vitro. Biochem Biophys Res Commun 2006;339(4):1255–61.
[213] Jons T, Drenckhahn D. Anion exchanger 2 (AE2) binds to erythrocyte ankyrin and is colocalized with ankyrin along the basolateral plasma membrane of human gastric parietal cells. Eur J Cell Biol 1998;75(3):232–6.
[214] Ding Y, Kobayashi S, Kopito R. Mapping of ankyrin binding determinants on the erythroid anion exchanger, AE1. J Biol Chem 1996;271(37):22494–8.
[215] Holappa K, Kellokumpu S. Targeting of the AE2 anion exchanger to the Golgi apparatus is cell type-dependent and correlates with the expression of Ank(195), a Golgi membrane skeletal protein. FEBS Lett 2003;546(2–3):257–64.
[216] Holappa K, Munoz MT, Egea G, Kellokumpu S. The AE2 anion exchanger is necessary for the structural integrity of the Golgi apparatus in mammalian cells. FEBS Lett 2004;564(1–2): 97–103.
[217] Zhang Y, Chernova MN, Stuart-Tilley AK, Jiang L, Alper SL. The cytoplasmic and transmembrane domains of AE2 both contribute to regulation of anion exchange by pH. J Biol Chem 1996;271(10):5741–9.
[218] Jennings ML, Nicknish JS. Localization of a site of intermolecular cross-linking in human red blood cell band 3 protein. J Biol Chem 1985;260(9):5472–9.
[219] Jennings ML, Gosselink PG. Anion exchange protein in Southeast Asian ovalocytes: heterodimer formation between normal and variant subunits. Biochemistry 1995;34(11): 3588–95.
[220] Taylor AM, Zhu Q, Casey JR. Cysteine-directed cross-linking localizes regions of the human erythrocyte anion-exchange protein (AE1) relative to the dimeric interface. Biochem J 2001;359(Pt 3):661–8.
[221] Zolotarev AS, Shmukler BE, Alper SL. AE2 anion exchanger polypeptide is a homooligomer in pig gastric membranes: a chemical cross-linking study. Biochemistry 1999;38(26): 8521–31.
[222] Pushkin AV, Tsuprun VL, Abuladze NK, Newman D, Kurtz I. Oligomeric structure of bAE3 protein. IUBMB Life 2000;50 (6):397–401.
[223] Yamaguchi T, Fujii T, Abe Y, Hirai T, Kang D, Namba K, et al. Helical image reconstruction of the outward-open human erythrocyte band 3 membrane domain in tubular crystals. J Struct Biol 2010;169(3):406–12.
[224] Wang DN, Sarabia VE, Reithmeier RA, Kuhlbrandt W. Three-dimensional map of the dimeric membrane domain of the human erythrocyte anion exchanger, band 3. EMBO J 1994;13 (14):3230–5.
[225] Wang DN, Kuhlbrandt W, Sarabia VE, Reithmeier RA. Two-dimensional structure of the membrane domain of human band 3, the anion transport protein of the erythrocyte membrane. EMBO J 1993;12(6):2233–9.
[226] Yamaguchi T, Ikeda Y, Abe Y, Kuma H, Kang D, Hamasaki N, et al. Structure of the membrane domain of human erythrocyte anion exchanger 1 revealed by electron crystallography. J Mol Biol 2010;397(1):179–89.
[227] Hirai T, Hamasaki N, Yamaguchi T, Ikeda Y. Topology models of anion exchanger 1 that incorporate the anti-parallel V-shaped motifs found in the EM structure. Biochem Cell Biology = Biochimie et Biologie Cellulaire 2011;89(2):148–56.
[228] Lemieux MJ, Reithmeier RA, Wang DN. Importance of detergent and phospholipid in the crystallization of the human erythrocyte anion-exchanger membrane domain. J Struct Biol 2002;137(3):322–32.

[229] Cabantchik ZI, Greger R. Chemical probes for anion transporters of mammalian cell membranes. Am J Physiol 1992;262(4 Pt 1):C803–27.

[230] Li C, Takazaki S, Jin X, Kang D, Abe Y, Hamasaki N. Identification of oxidized methionine sites in erythrocyte membrane protein by liquid chromatography/electrospray ionization mass spectrometry peptide mapping. Biochemistry 2006;45(39):12117–24.

[231] Babu M, Greenblatt JF, Emili A, Strynadka NC, Reithmeier RA, Moraes TF. Structure of a SLC26 anion transporter STAS domain in complex with acyl carrier protein: implications for E. coli YchM in fatty acid metabolism. Structure 2010;18(11): 1450–62.

[232] Bonar P, Casey JR. Purification of functional human Cl^-/HCO_3^- exchanger, AE1, over-expressed in Saccharomyces cerevisiae. Protein Expr Purif 2010;74(1):106–15.

[233] Wood P. The anion exchange proteins: homology and secondary structure. ProgCellRes 1992;2:325–52.

[234] Tang XB, Fujinaga J, Kopito R, Casey JR. Topology of the region surrounding Glu681 of human AE1 protein, the erythrocyte anion exchanger. J Biol Chem 1998;273(35):22545–53.

[235] Tang XB, Kovacs M, Sterling D, Casey JR. Identification of residues lining the translocation pore of human AE1, plasma membrane anion exchange protein. J Biol Chem 1999;274 (6):3557–64.

[236] Fujinaga J, Tang XB, Casey JR. Topology of the membrane domain of human erythrocyte anion exchange protein, AE1. J Biol Chem 1999;274(10):6626–33.

[237] Zhu Q, Lee DW, Casey JR. Novel topology in C-terminal region of the human plasma membrane anion exchanger, AE1. J Biol Chem 2003;278(5):3112–20.

[238] Zhu Q, Casey JR. The substrate anion selectivity filter in the human erythrocyte Cl^-/HCO_3^- exchange protein, AE1. J Biol Chem 2004;279(22):23565–73.

[239] Popov M, Tam LY, Li J, Reithmeier RA. Mapping the ends of transmembrane segments in a polytopic membrane protein. Scanning N-glycosylation mutagenesis of extracytosolic loops in the anion exchanger, band 3. J Biol Chem 1997;272 (29):18325–32.

[240] Popov M, Li J, Reithmeier RA. Transmembrane folding of the human erythrocyte anion exchanger (AE1, band 3) determined by scanning and insertional N-glycosylation mutagenesis. Biochem J 1999;339(Pt 2):269–79.

[241] Cheung JC, Li J, Reithmeier RA. Topology of transmembrane segments 1–4 in the human chloride/bicarbonate anion exchanger 1 (AE1) by scanning N-glycosylation mutagenesis. Biochem J 2005;390(Pt 1):137–44.

[242] Groves JD, Tanner MJ. Structural model for the organization of the transmembrane spans of the human red-cell anion exchanger (band 3; AE1). Biochem J 1999;344(Pt 3):699–711.

[243] Groves JD, Tanner MJ. Topology studies with biosynthetic fragments identify interacting transmembrane regions of the human red-cell anion exchanger (band 3; AE1). Biochem J 1999;344(Pt 3):687–97.

[244] Groves JD, Wang L, Tanner MJ. Functional reassembly of the anion transport domain of human red cell band 3 (AE1) from multiple and non-complementary fragments. FEBS Lett 1998;433(3):223–7.

[245] Pal P, Lebedev D, Salim S, Knauf PA. Substrates induce conformational changes in human anion exchanger 1 (hAE1) as observed by fluorescence resonance energy transfer. Biochemistry 2006;45(20):6279–95.

[246] Basu A, Mazor S, Casey JR. Distance measurements within a concatamer of the plasma membrane Cl/HCO exchanger, AE1. Biochemistry 2010;49(43):9226–40.

[247] Pal P, Lesoine JF, Lieb MA, Novotny L, Knauf PA. A novel immobilization method for single protein spFRET studies. Biophys J 2005;89(2):L11–3.

[248] Johnson DE, Casey JR. Cytosolic H + microdomain developed around AE1 during AE1-mediated Cl^-/HCO_3^- exchange. J Physiol 2011;589(Pt 7):1551–69.

[249] Brahm J. Temperature-dependent changes of chloride transport kinetics in human red cells. J Gen Physiol 1977;70(3): 283–306.

[250] Frohlich O. The "tunneling" mode of biological carrier-mediated transport. J Membr Biol 1988;101(3):189–98.

[251] Shcheynikov N, Wang Y, Park M, Ko SB, Dorwart M, Naruse S, et al. Coupling modes and stoichiometry of Cl^-/HCO_3^- exchange by slc26a3 and slc26a6. J Gen Physiol 2006; 127(5):511–24.

[252] Milanick MA, Gunn RB. Proton-sulfate co-transport: mechanism of H + and sulfate addition to the chloride transporter of human red blood cells. J Gen Physiol 1982;79(1): 87–113.

[253] Milanick MA, Gunn RB. Proton-sulfate cotransport: external proton activation of sulfate influx into human red blood cells. Am J Physiol 1984;247(3 Pt 1):C247–59.

[254] Jennings ML, Smith JS. Anion-proton cotransport through the human red blood cell band 3 protein. Role of glutamate 681. J Biol Chem 1992;267(20):13964–71.

[255] Knauf P. Kinetics of Anion Transport. Red Cell Memb 1989;171–200.

[256] Humphreys BD, Jiang L, Chernova MN, Alper SL. Functional characterization and regulation by pH of murine AE2 anion exchanger expressed in Xenopus oocytes. Am J Physiol 1994;267(5 Pt 1):C1295–307.

[257] Knauf PA, Pal P. Band 3 mediated transport. In: Bernhardt I, Ellory JC, editors. Red cell membrane transport in health and disease. New York: Springer; 2003. p. 253–301.

[258] Jennings ML. Stoichiometry of a half-turnover of band 3, the chloride transport protein of human erythrocytes. J Gen Physiol 1982;79(2):169–85.

[259] Grinstein S, McCulloch L, Rothstein A. Transmembrane effects of irreversible inhibitors of anion transport in red blood cells. Evidence for mobile transport sites. J Gen Physiol 1979;73 (4):493–514.

[260] Falke JJ, Pace RJ, Chan SI. Direct observation of the transmembrane recruitment of band 3 transport sites by competitive inhibitors. A 35Cl NMR study. J Biol Chem 1984;259 (10):6481–91.

[261] Jennings ML, Whitlock J, Shinde A. Pre-steady state transport by erythrocyte band 3 protein: uphill countertransport induced by the impermeant inhibitor H2DIDS. Biochem Cell Biol = Biochimie et biologie cellulaire 1998;76(5):807–13.

[262] Knauf PA, Law FY, Leung TW, Gehret AU, Perez ML. Substrate-dependent reversal of anion transport site orientation in the human red blood cell anion-exchange protein, AE1. Proc Nat Acad Sci USA 2002;99(16):10861–4.

[263] Gunn RB, Frohlich O. Asymmetry in the mechanism for anion exchange in human red blood cell membranes. Evidence for reciprocating sites that react with one transported anion at a time. J Gen Physiol 1979;74(3):351–74.

[264] Salhany JM, Sloan RL, Cordes KS. The carboxyl side chain of glutamate 681 interacts with a chloride binding modifier site that allosterically modulates the dimeric conformational state of band 3 (AE1). Implications for the mechanism of anion/proton cotransport. Biochemistry 2003;42(6): 1589–602.

[265] Jennings ML. Evidence for a second binding/transport site for chloride in erythrocyte anion transporter AE1 modified at glutamate 681. Biophys J 2005;88(4):2681–91.

[266] Salhany JM, Cordes KS, Sloan RL. Band 3 (AE1, SLC4A1)-mediated transport of stilbenedisulfonates. II: evidence for transmembrane allosteric interactions between the "primary" stilbenedisulfonate binding site and the stilbenedisulfonate efflux site. Blood Cells Mol Dis 2006;37(3):149–54.

[267] Salhany JM. Allosteric effects in stilbenedisulfonate binding to band 3 protein (AE1). Cell Mol Biol (Noisy-le-Grand, France) 1996;42(7):1065–96.

[268] Chernova MN, Jiang L, Crest M, Hand M, Vandorpe DH, Strange K, et al. Electrogenic sulfate/chloride exchange in Xenopus oocytes mediated by murine AE1 E699Q. J Gen Physiol 1997;109(3):345–60.

[269] Chernova MN, Stewart AK, Barry PN, Jennings ML, Alper SL. Mouse Ae1 E699Q mediates SO42-i/anion-o exchange with [SO42-]i-dependent reversal of wild-type pHo sensitivity. Am J Physiol Cell Physiol 2008;295(2):C302–12.

[270] Culliford S, Ellory C, Lang HJ, Englert H, Staines H, Wilkins R. Specificity of classical and putative Cl(-) transport inhibitors on membrane transport pathways in human erythrocytes. Cell Physiol Biochem 2003;13(4):181–8.

[271] Barzilay M, Cabantchik ZI. Anion transport in red blood cells. II. Kinetics of reversible inhibition by nitroaromatic sulfonic acids. Membr Biochem 1979;2(2):255–81.

[272] Knauf PA, Law FY, Hahn K. An oxonol dye is the most potent known inhibitor of band 3-mediated anion exchange. Am J Physiol 1995;269(4 Pt 1):C1073–7.

[273] van't Hof W, Malik A, Vijayakumar S, Qiao J, van Adelsberg J, Al-Awqati Q. The effect of apical and basolateral lipids on the function of the band 3 anion exchange protein. J Cell Biol 1997;139(4):941–9.

[274] Fievet B, Gabillat N, Borgese F, Motais R. Expression of band 3 anion exchanger induces chloride current and taurine transport: structure-function analysis. EMBO J 1995;14(21):5158–69.

[275] Bennekou P, Pedersen O, Moller A, Christophersen P. Volume control in sickle cells is facilitated by the novel anion conductance inhibitor NS1652. Blood 2000;195(5):1842–8.

[276] Bennekou P, de Franceschi L, Pedersen O, Lian L, Asakura T, Evans G, et al. Treatment with NS3623, a novel Cl-conductance blocker, ameliorates erythrocyte dehydration in transgenic SAD mice: a possible new therapeutic approach for sickle cell disease. Blood 2001;97(5):1451–7.

[277] Alper SL, Chernova MN, Williams J, Zasloff M, Law FY, Knauf PA. Differential inhibition of AE1 and AE2 anion exchangers by oxonol dyes and by novel polyaminosterol analogs of the shark antibiotic squalamine. Biochem Cell Biol = Biochimie et biologie cellulaire 1998;76(5):799–806.

[278] Lagadic-Gossmann D, Le Prigent K, Baut GL, Caignard DH, Renard P, Scalbert E, et al. Effects of S20787 on pHi-regulating mechanisms in isolated rat ventricular myocytes. J Cardiovasc Pharmacol 1996;28(4):547–52.

[279] Loh SH, Tsai CS, Lin CI, Jin JS, Vaughan-Jones RD. Effect of S20787, a novel Cl–HCO_3- exchange inhibitor, on intracellular pH regulation in guinea pig ventricular myocytes. J Biomed Sci 2001;8(5):395–405.

[280] Kawano Y, Okubo K, Tokunaga F, Miyata T, Iwanaga S, Hamasaki N. Localization of the pyridoxal phosphate binding site at the COOH-terminal region of erythrocyte band 3 protein. J Biol Chem 1988;263(17):8232–8.

[281] Morgan PE, Supuran CT, Casey JR. Carbonic anhydrase inhibitors that directly inhibit anion transport by the human Cl^-/HCO_3^- exchanger, AE1. Mol Membr Biol 2004;21(6):423–33.

[282] Leniger T, Thone J, Wiemann M. Topiramate modulates pH of hippocampal CA3 neurons by combined effects on carbonic anhydrase and Cl^-/HCO_3^- exchange. Br J Pharmacol 2004;142 (5):831–42.

[283] Dahl NK, Jiang L, Chernova MN, Stuart-Tilley AK, Shmukler BE, Alper SL. Deficient HCO_3^- transport in an AE1 mutant with normal Cl− transport can be rescued by carbonic anhydrase II presented on an adjacent AE1 protomer. J Biol Chem 2003;278(45):44949–58.

[284] Kuma H, Abe Y, Askin D, Bruce LJ, Hamasaki T, Tanner MJ, et al. Molecular basis and functional consequences of the dominant effects of the mutant band 3 on the structure of normal band 3 in Southeast Asian ovalocytosis. Biochemistry 2002;41(10):3311–20.

[285] Kurschat CE, Alper SL. Hereditary renal tubular acidosis. In: Mount DB, Pollak MR, editors. Molecular and genetic basis of renal disease: a companion to brenner and rector's the kidney. Philadephia: Elsevier; 2007in press

[286] Jennings ML, Anderson MP. Chemical modification and labeling of glutamate residues at the stilbenedisulfonate site of human red blood cell band 3 protein. J Biol Chem 1987;5262 (4):1691–7.

[287] Jennings ML, Al-Rhaiyel S. Modification of a carboxyl group that appears to cross the permeability barrier in the red blood cell anion transporter. J Gen Physiol 1988;92(2):161–78.

[288] Jennings ML. Rapid electrogenic sulfate-chloride exchange mediated by chemically modified band 3 in human erythrocytes. J Gen Physiol 1995;105(1):21–47.

[289] Sekler I, Lo RS, Kopito RR. A conserved glutamate is responsible for ion selectivity and pH dependence of the mammalian anion exchangers AE1 and AE2. J Biol Chem 1995;270 (48):28751–8.

[290] Knauf PA, Law FY, Leung TW, Atherton SJ. Relocation of the disulfonic stilbene sites of AE1 (band 3) on the basis of fluorescence energy transfer measurements. Biochemistry 2004;43 (38):11917–31.

[291] Bahar S, Gunter CT, Wu C, Kennedy SD, Knauf PA. Persistence of external chloride and DIDS binding after chemical modification of Glu-681 in human band 3. Am J Physiol 1999;277(4 Pt 1):C791–9.

[292] McAlear SD, Bevensee MO. A cysteine-scanning mutagenesis study of transmembrane domain 8 of the electrogenic sodium/bicarbonate cotransporter NBCe1. J Biol Chem 2006;281 (43):32417–27.

[293] Bruce LJ, Kay MM, Lawrence C, Tanner MJ. Band 3 HT, a human red-cell variant associated with acanthocytosis and increased anion transport, carries the mutation Pro-868− > Leu in the membrane domain of band 3. Biochem J 1993;293(Pt 2): 317–20.

[294] Barneaud-Rocca D, Borgese F, Guizouarn H. Dual transport properties of anion exchanger 1: the same transmembrane segment is involved in anion exchange and in a cation leak. J Biol Chem 2011;286(11):8909–16.

[295] Wieth JO, Bjerrum PJ, Borders Jr CL. Irreversible inactivation of red cell chloride exchange with phenylglyoxal, and arginine-specific reagent. J Gen Physiol 1982;79(2):283–312.

[296] Takazaki S, Abe Y, Kang D, Li C, Jin X, Ueda T, et al. The functional role of arginine 901 at the C-terminus of the human anion transporter band 3 protein. J Biochem (Tokyo) 2006;139 (5):903–12.

[297] Toye AM, Bruce LJ, Unwin RJ, Wrong O, Tanner MJ. Band 3 Walton, a C-terminal deletion associated with distal renal tubular acidosis, is expressed in the red cell membrane but retained internally in kidney cells. Blood 2002;99 (1):342–7.

[298] Stewart AK, Kurschat CE, Alper SL. Role of nonconserved charged residues of the AE2 transmembrane domain in regulation of anion exchange by pH. Pflugers Arch 2007;454(3): 373–84.

[299] Wood PG, Muller H, Sovak M, Passow H. Role of Lys 558 and Lys 869 in substrate and inhibitor binding to the murine band 3 protein: a study of the effects of site-directed mutagenesis of the band 3 protein expressed in the oocytes of Xenopus laevis. J Membr Biol 1992;127(2):139–48.

[300] Muller-Berger S, Karbach D, Konig J, Lepke S, Wood PG, Appelhans H, et al. Inhibition of mouse erythroid band 3-mediated chloride transport by site-directed mutagenesis of histidine residues and its reversal by second site mutation of Lys 558, the locus of covalent H2DIDS binding. Biochemistry 1995;34(29):9315–24.

[301] Muller-Berger S, Karbach D, Kang D, Aranibar N, Wood PG, Ruterjans H, et al. Roles of histidine 752 and glutamate 699 in the pH dependence of mouse band 3 protein-mediated anion transport. Biochemistry 1995;34(29):9325–32.

[302] Stewart AK, Kurschat CE, Burns D, Banger N, Vaughan-Jones RD, Alper SL. Transmembrane domain histidines contribute to regulation of AE2-mediated anion exchange by pH. Am J Physiol Cell Physiol 2007;292(2):C909–18.

[303] Jin XR, Abe Y, Li CY, Hamasaki N. Histidine-834 of human erythrocyte band 3 has an essential role in the conformational changes that occur during the band 3-mediated anion exchange. Biochemistry 2003;42(44):12927–32.

[304] Fievet B, Perset F, Gabillat N, Guizouarn H, Borgese F, Ripoche P, et al. Transport of uncharged organic solutes in Xenopus oocytes expressing red cell anion exchangers (AE1s). Proc Nat Acad Sci USA 1998;95(18):10996–1001.

[305] Guizouarn H, Gabillat N, Motais R, Borgese F. Multiple transport functions of a red blood cell anion exchanger, tAE1: its role in cell volume regulation. J Physiol 2001;535(Pt 2): 497–506.

[306] Borgese F, Renard C, Gabillat N, Pellissier B, Guizouarn H. Molecular mapping of the conductance activity linked to tAE1 expressed in Xenopus oocyte. Biochim Biophys Acta 2004;1664 (1):80–7.

[307] Martial S, Guizouarn H, Gabillat N, Pellissier B, Borgese F. Consequences of point mutations in trout anion exchanger 1 (tAE1) transmembrane domains: evidence that tAE1 can behave as a chloride channel. J Cell Physiol 2006;207(3): 829–35.

[308] Martial S, Guizouarn H, Gabillat N, Pellissier B, Borgese F. Importance of several cysteine residues for the chloride conductance of trout anion exchanger 1 (tAE1). J Cell Physiol 2007;213(1):70–8.

[309] Guizouarn H, Christen R, Borgese F. Phylogeny of anion exchangers: could trout AE1 conductive properties be shared by other members of the gene family? Biochim Biophys Acta 2005;1726(3):244–50.

[310] Alper SL, Vandorpe DH, Stuart Tilley A, Rotter M, Lux SE, et al. Absence of DIDS-sensitive Cl conductance in red cells of AE1 (band 3) -/- mice. J Am Soc Nephrol 1998;9: 151A.

[311] Thomas SL, Bouyer G, Cueff A, Egee S, Glogowska E, Ollivaux C. Ion channels in human red blood cell membrane: actors or relics? Blood Cells Mol Dis 2011;46(4):261–5.

[312] Decherf G, Bouyer G, Egee S, Thomas SL. Chloride channels in normal and cystic fibrosis human erythrocyte membrane. Blood Cells Mol Dis 2007;39(1):24–34.

[313] Bouyer G, Cueff A, Egee S, Kmiecik J, Maksimova Y, Glogowska E, et al. Erythrocyte peripheral type benzodiazepine receptor/voltage-dependent anion channels are upregulated by Plasmodium falciparum. Blood 2011;118(8): 2305–12.

[314] Skals M, Jensen UB, Ousingsawat J, Kunzelmann K, Leipziger J, Praetorius HA. Escherichia coli alpha-hemolysin triggers shrinkage of erythrocytes via K(Ca)3.1 and TMEM16A channels with subsequent phosphatidylserine exposure. J Biol Chem 2010;285(20):15557–65.

[315] Parker MD, Young MT, Daly CM, Meech RW, Boron WF, Tanner MJA. Conductive pathway generated from fragments of the human red cell anion exchanger, AE1. J Physiol 2007;581 (Pt 1):33–50.

[316] Koomoa DL, Musch MW, Myers DE, Goldstein L. Expression of the skate (Raja erinacea) AE1 osmolyte channel in Xenopus laevis oocytes: monovalent cation permeability. J Membr Biol 2004;198(1):23–9.

[317] Koomoa DL, Musch MW, Goldstein L. The activation pathway of the volume-sensitive organic osmolyte channel in Xenopus laevis oocytes expressing skate anion exchanger 1 (AE1). J Membr Biol 2005;208(3):241–50.

[318] Bruce LJ, Robinson HC, Guizouarn H, Borgese F, Harrison P, King MJ, et al. Monovalent cation leaks in human red cells caused by single amino-acid substitutions in the transport domain of the band 3 chloride-bicarbonate exchanger, AE1. Nat Genet 2005;37(11):1258–63.

[319] Guizouarn H, Martial S, Gabillat N, Borgese F. Point mutations involved in red cell stomatocytosis convert the electroneutral anion exchanger 1 to a nonselective cation conductance. Blood 2007;110(6):2158–65.

[320] Cordat E, Li J, Reithmeier RA. Carboxyl-terminal truncations of human anion exchanger impair its trafficking to the plasma membrane. Traffic 2003;4(9):642–51.

[321] Vince JW, Carlsson U, Reithmeier RA. Localization of the Cl^-/HCO_3^-anion exchanger binding site to the amino-terminal region of carbonic anhydrase II. Biochemistry 2000;39(44): 13344–9.

[322] Vince JW, Reithmeier RA. Identification of the carbonic anhydrase II binding site in the Cl(-)/HCO(3)(-) anion exchanger AE1. Biochemistry 2000;39(18):5527–33.

[323] Sterling D, Reithmeier RA, Casey JR. A transport metabolon. Functional interaction of carbonic anhydrase II and chloride/bicarbonate exchangers. J Biol Chem 2001;276 (51):47886–94.

[324] Purkerson JM, Schwartz GJ. The role of carbonic anhydrases in renal physiology. Kidney Int 2007;71(2):103–15.

[325] Sowah D, Casey JR. An intramolecular transport metabolon: fusion of carbonic anhydrase II to the COOH terminus of the Cl^-/HCO_3^- exchanger, AE1. Am J Physiol Cell Physiol 2011;301(2):C336–46.

[326] Takazaki S, Abe Y, Yamaguchi T, Yagi M, Ueda T, Kang D, et al. Arg 901 in the AE1 C-terminal tail is involved in conformational change but not in substrate binding. Biochim Biophys Acta 2012;1818(3):658–65.

[327] Loiselle FB, Morgan PE, Alvarez BV, Casey JR. Regulation of the human NBC3 Na^+/HCO_3^- cotransporter by carbonic anhydrase II and PKA. Am J Physiol Cell Physiol 2004;286(6): C1423–33.

[328] Alvarez BV, Vilas GL, Casey JR. Metabolon disruption: a mechanism that regulates bicarbonate transport. EMBO J 2005;24(14):2499–511.

[329] Li X, Alvarez B, Casey JR, Reithmeier RA, Fliegel L. Carbonic anhydrase II binds to and enhances activity of the Na^+/H^+ exchanger. J Biol Chem 2002;277(39):36085–91.

[330] Li X, Liu Y, Alvarez BV, Casey JR, Fliegel L. A novel carbonic anhydrase II binding site regulates NHE1 activity. Biochemistry 2006;45(7):2414–24.

[331] Schueler C, Becker HM, McKenna R, Deitmer JW. Transport activity of the sodium bicarbonate cotransporter NBCe1 is enhanced by different isoforms of carbonic anhydrase. PloS One 2011;6(11):e27167.

[332] Sterling D, Alvarez BV, Casey JR. The extracellular component of a transport metabolon. Extracellular loop 4 of the human AE1 Cl^-/HCO_3^- exchanger binds carbonic anhydrase IV. J Biol Chem 2002;277(28):25239–46.

[333] Morgan PE, Pastorekova S, Stuart-Tilley AK, Alper SL, Casey JR. Interactions of transmembrane carbonic anhydrase, CAIX, with bicarbonate transporters. Am J Physiol Cell Physiol 2007;293(2):C738–48.

[334] Alvarez BV, Loiselle FB, Supuran CT, Schwartz GJ, Casey JR. Direct extracellular interaction between carbonic anhydrase IV and the human NBC1 sodium/bicarbonate co-transporter. Biochemistry 2003;42(42):12321–9.

[335] Yang Z, Alvarez BV, Chakarova C, Jiang L, Karan G, Frederick JM, et al. Mutant carbonic anhydrase 4 impairs pH regulation and causes retinal photoreceptor degeneration. Hum Mol Genet 2005;14(2):255–65.

[336] Svichar N, Waheed A, Sly WS, Hennings JC, Hubner CA, Chesler M. Carbonic anhydrases CA4 and CA14 both enhance AE3-mediated Cl^--HCO_3^- exchange in hippocampal neurons. J Neurosci 2009;29(10):3252–8.

[337] Becker HM, Klier M, Schuler C, McKenna R, Deitmer JW. Intramolecular proton shuttle supports not only catalytic but also noncatalytic function of carbonic anhydrase II. Proc Nat Acad Sci USA 2011;108(7):3071–6.

[338] Becker HM, Deitmer JW. Nonenzymatic proton handling by carbonic anhydrase II during H^+-lactate cotransport via monocarboxylate transporter 1. J Biol Chem 2008;283(31):21655–67.

[339] Becker HM, Klier M, Deitmer JW. Nonenzymatic augmentation of lactate transport via monocarboxylate transporter isoform 4 by carbonic anhydrase II. J Membr Biol 2010;234 (2):125–35.

[340] Piermarini PM, Kim EY, Boron WF. Evidence against a direct interaction between intracellular carbonic anhydrase II and pure C-terminal domains of SLC4 bicarbonate transporters. J Biol Chem 2007;282(2):1409–21.

[341] Lu J, Daly CM, Parker MD, Gill HS, Piermarini PM, Pelletier MF, et al. Effect of human carbonic anhydrase II on the activity of the human electrogenic Na/HCO_3 cotransporter NBCe1-A in Xenopus oocytes. J Biol Chem 2006;281(28):19241–50.

[342] Yamada H, Horita S, Suzuki M, Fujita T, Seki G. Functional role of a putative carbonic anhydrase II-binding domain in the electrogenic Na^+-HCO-cotransporter NBCe1 expressed in Xenopus oocytes. Channels (Austin, Tex. 2011;5(2):106–9.

[343] Grichtchenko II, Boron WF. Surface pH measurements in voltage-clamped Xenopus oocytes co-expressing NBCe1 and CAIV: evidence for carbonate transport. FASEB J 2002;:A795.

[344] Swietach P, Patiar S, Supuran CT, Harris AL, Vaughan-Jones RD. The role of carbonic anhydrase 9 in regulating extracellular and intracellular ph in three-dimensional tumor cell growths. J Biol Chem 2009;284(30):20299–310.

[345] Hulikova A, Vaughan-Jones RD, Swietach P. Dual role of CO_2/HCO_3^- formula buffer in the regulation of intracellular pH of three-dimensional tumor growths. The Journal of biological chemistry. Apr 22;286(16):13815–26.

[346] Young MT, Tanner MJ. Distinct regions of human glycophorin A enhance human red cell anion exchanger (band 3; AE1) transport function and surface trafficking. J Biol Chem 2003;278(35):32954–61.

[347] Fu G, Wang T, Yang B, Lv F, Shi C, Jiang X, et al. Purification and characterization of the human erythrocyte band 3 protein C-terminal domain. Biochemistry 2004;43(6):1633–8.

[348] Telen MJ, Chasis JA. Relationship of the human erythrocyte Wrb antigen to an interaction between glycophorin A and band 3. Blood 1990;76(4):842–8.

[349] Bruce LJ, Ring SM, Anstee DJ, Reid ME, Wilkinson S, Tanner MJ. Changes in the blood group Wright antigens are associated with a mutation at amino acid 658 in human erythrocyte band 3: a site of interaction between band 3 and glycophorin a under certain conditions. Blood 1995;85(2):541–7.

[350] Su Y, Blake-Palmer KG, Fry AC, Best A, Brown AC, Hiemstra TF, et al. Glyceraldehyde 3-phosphate dehydrogenase is required for band 3 (anion exchanger 1) membrane residency in the mammalian kidney. Am J Physiol Renal Physiol 2011; 300(1):F157–66.

[351] Cowan CA, Yokoyama N, Bianchi LM, Henkemeyer M, Fritzsch B. EphB2 guides axons at the midline and is necessary for normal vestibular function. Neuron 2000;26(2): 417–30.

[352] Moura Lima PR, Salles TS, Costa FF, Saad ST. alpha-cardiac actin (ACTC) binds to the band 3 (AE1) cardiac isoform. J Cell Biochem 2003;89(6):1215–21.

[353] Fu GH, Wang Y, Xi YH, Shen WW, Pan XY, Shen WZ, et al. Direct interaction and cooperative role of tumor suppressor p16 with band 3 (AE1). FEBS Lett 2005;579(10):2105–10.

[354] Chen J, Vijayakumar S, Li X, Al-Awqati Q. Kanadaptin is a protein that interacts with the kidney but not the erythroid form of band 3. J Biol Chem 1998;273(2):1038–43.

[355] Hubner S, Bahr C, Gossmann H, Efthymiadis A, Drenckhahn D. Mitochondrial and nuclear localization of kanadaptin. Eur J Cell Biol 2003;82(5):240–52.

[356] Hubner S, Jans DA, Xiao CY, John AP, Drenckhahn D. Signal- and importin-dependent nuclear targeting of the kidney anion exchanger 1-binding protein kanadaptin. Biochem J 2002;361 (Pt 2):287–96.

[357] Kittanakom S, Keskanokwong T, Akkarapatumwong V, Yenchitsomanus PT, Reithmeier RA. Human kanadaptin and kidney anion exchanger 1 (kAE1) do not interact in transfected HEK 293 cells. Mol Membr Biol 2004;21(6):395–402.

[358] Song LJ, Liu RJ, Zeng Z, Alper SL, Cui HJ, Lu Y, et al. Gastrin inhibits a novel, pathological colon cancer signaling pathway involving EGR1, AE2, and P-ERK. J Mol Med (Berlin, Germany) 2012;: [Epub ahead of print]

[359] Teti D, Crupi M, Busa M, Valenti A, Loddo S, Mondello M, et al. Chemical and pathological oxidative influences on band 3 protein anion-exchanger. Cell Physiol Biochem 2005;16(1–3): 77–86.

[360] Wang CC, Tao M, Wei T, Low PS. Identification of the major casein kinase I phosphorylation sites on erythrocyte band 3. Blood 1997;89(8):3019–24.

[361] Bordin L, Zen F, Ion-Popa F, Barbetta M, Baggio B, Clari G. Band 3 tyr-phosphorylation in normal and glucose-6-phospate dehydrogenase-deficient human erythrocytes. Mol Membr Biol 2005;22(5):411–20.

[362] Minetti G, Ciana A, Balduini C. Differential sorting of tyrosine kinases and phosphotyrosine phosphatases acting on band 3 during vesiculation of human erythrocytes. Biochem J 2004;377 (Pt 2):489–97.

[363] Pantaleo A, Ferru E, Giribaldi G, Mannu F, Carta F, Matte A, et al. Oxidized and poorly glycosylated band 3 is selectively phosphorylated by Syk kinase to form large membrane clusters in normal and G6PD-deficient red blood cells. Biochem J 2009;418(2):359–67.

[364] Pantaleo A, Ferru E, Carta F, Mannu F, Simula LF, Khadjavi A, et al. Irreversible AE1 tyrosine phosphorylation leads to membrane vesiculation in G6PD deficient red cells. PloS one 2011;6 (1):e15847.

[365] De Franceschi L, Tomelleri C, Matte A, Brunati AM, Bovee-Geurts PH, Bertoldi M, et al. Erythrocyte membrane changes

of chorea-acanthocytosis are the result of altered Lyn kinase activity. Blood 2011;118(20):5652–63.

[366] Perlman DF, Musch MW, Goldstein L. Cell membrane surface expression and tyrosine kinase regulate the osmolyte channel (skAE1) in skate erythrocytes. Acta Physiol (Oxford, England) 2006;187(1-2):87–91.

[367] Williamson RC, Brown AC, Mawby WJ, Toye AM. Human kidney anion exchanger 1 localisation in MDCK cells is controlled by the phosphorylation status of two critical tyrosines. J Cell Sci 2008;121(Pt 20):3422–32.

[368] Zhou C, Tiberi M, Liang B, Alper SL, Baltz JM. HCO_3^-/Cl^- exchange inactivation and reactivation during mouse oocyte meiosis correlates with MEK/MAPK-regulated Ae2 plasma membrane localization. PloS One 2009;4(10):e7417.

[369] Alvarez BV, Fujinaga J, Casey JR. Molecular basis for angiotensin II-induced increase of chloride/bicarbonate exchange in the myocardium. Circ Res 2001;89(12):1246–53.

[370] Alvarez BV, Kieller DM, Quon AL, Markovich D, Casey JR. Slc26a6: a cardiac chloride-hydroxyl exchanger and predominant chloride-bicarbonate exchanger of the mouse heart. J Physiol 2004;561(Pt 3):721–34.

[371] Funder J, Wieth JO. Chloride transport in human erythrocytes and ghosts: a quantitative comparison. J Physiol 1976;262(3): 679–98.

[372] Jennings M. Cellular anion transport. Kidney: Physiol Pathophysiol 1992;:113–45.

[373] Stewart AK, Chernova MN, Shmukler BE, Wilhelm S, Alper SL. Regulation of AE2-mediated Cl- transport by intracellular or by extracellular pH requires highly conserved amino acid residues of the AE2 NH2-terminal cytoplasmic domain. J Gen Physiol 2002;120(5):707–22.

[374] Lee BS, Gunn RB, Kopito RR. Functional differences among nonerythroid anion exchangers expressed in a transfected human cell line. J Biol Chem 1991;266(18):11448–54.

[375] Kurschat CE, Shmukler BE, Jiang L, Wilhelm S, Kim EH, Chernova MN, et al. Alkaline-shifted pHo sensitivity of AE2c1-mediated anion exchange reveals novel regulatory determinants in the AE2 N-terminal cytoplasmic domain. J Biol Chem 2006;281(4):1885–96.

[376] Stewart AK, Kurschat CE, Vaughan-Jones RD, Shmukler BE, Alper SL. Acute regulation of mouse AE2 anion exchanger requires isoform-specific amino acid residues from most of the transmembrane domain. J Physiol 2007;584(Pt 1):59–73.

[377] Stewart AK, Kurschat CE, Vaughan-Jones RD, Alper SL. Putative re-entrant loop 1 of AE2 transmembrane domain has a major role in acute regulation of anion exchange by pH. J Biol Chem 2009;284(10):6126–39.

[378] Humphreys BD, Jiang L, Chernova MN, Alper SL. Hypertonic activation of AE2 anion exchanger in Xenopus oocytes via NHE-mediated intracellular alkalinization. Am J Physiol 1995;268(1 Pt 1):C201–9.

[379] Humphreys BD, Chernova MN, Jiang L, Zhang Y, Alper SL. NH4Cl activates AE2 anion exchanger in Xenopus oocytes at acidic pHi. Am J Physiol 1997;272(4 Pt 1):C1232–40.

[380] Goss GG, Jiang L, Vandorpe DH, Kieller D, Chernova MN, Robertson M, et al. Role of JNK in hypertonic activation of Cl^--dependent Na^+/H^+ exchange in Xenopus oocytes. Am J Physiol Cell Physiol 2001;281(6):C1978–90.

[381] Chernova MN, Stewart AK, Jiang L, Friedman DJ, Kunes YZ, Alper SL. Structure-function relationships of AE2 regulation by Ca_i2^+-sensitive stimulators Na_4^+ and hypertonicity. Am J Physiol Cell Physiol 2003;284(5):C1235–46.

[382] Frazar TF, Weisbein JL, Anderson SM, Cline AP, Garrett LJ, Felsenfeld G, et al. Variegated expression from the murine band 3 (AE1) promoter in transgenic mice is associated with mRNA transcript initiation at upstream start sites and can be suppressed by the addition of the chicken beta-globin 5′ HS4 insulator element. Mol Cell Biol 2003;23(14):4753–63.

[383] Sahr KE, Daniels BP, Hanspal M. Identification of the proximal erythroid promoter region of the mouse anion exchanger gene. Blood 1996;88(12):4500–9.

[384] Kim HR, Kennedy BS, Engel JD. Two chicken erythrocyte band 3 mRNAs are generated by alternative transcriptional initiation and differential RNA splicing. Mol Cell Biol 1989;9(11): 5198–206.

[385] Cox KH, Adair-Kirk TL, Cox JV. Four variant chicken erythroid AE1 anion exchangers. Role of the alternative N-terminal sequences in intracellular targeting in transfected human erythroleukemia cells. J Biol Chem 1995;270(34): 19752–60.

[386] Zenke M, Kahn P, Disela C, Vennstrom B, Leutz A, Keegan K, et al. v-erbA specifically suppresses transcription of the avian erythrocyte anion transporter (band 3) gene. Cell 1988;52(1): 107–19.

[387] Cox JV, Stack JH, Lazarides E. Erythroid anion transporter assembly is mediated by a developmentally regulated recruitment onto a preassembled membrane cytoskeleton. J Cell Biol 1987;105(3):1405–16.

[388] Lehnert ME, Lodish HF. Unequal synthesis and differential degradation of alpha and beta spectrin during murine erythroid differentiation. J Cell Biol 1988;107(2):413–26.

[389] Fejes-Toth G, Naray-Fejes-Toth A. Differentiation of renal beta-intercalated cells to alpha-intercalated and principal cells in culture. Proc Nat Acad Sci USA 1992;89(12):5487–91.

[390] Kurth I, Hentschke M, Hentschke S, Borgmeyer U, Gal A, Hubner CA. The forkhead transcription factor Foxi1 directly activates the AE4 promoter. Biochem J 2006;393(Pt 1):277–83.

[391] Quigley IK, Stubbs JL, Kintner C. Specification of ion transport cells in the Xenopus larval skin. Deve (Cambridge, England) 2011;138(4):705–14.

[392] Esaki M, Hoshijima K, Nakamura N, Munakata K, Tanaka M, Ookata K, et al. Mechanism of development of ionocytes rich in vacuolar-type H(+)-ATPase in the skin of zebrafish larvae. Dev Biol 2009;329(1):116–29.

[393] Lee YC, Yan JJ, Cruz SA, Horng JL, Hwang PP. Anion exchanger 1b, but not sodium-bicarbonate cotransporter 1b, plays a role in transport functions of zebrafish H + -ATPase-rich cells. Am J Physiol Cell Physiol 2011;300(2):C295–307.

[394] Miller RL, Zhang P, Smith M, Beaulieu V, Paunescu TG, Brown D, et al. V-ATPase B1-subunit promoter drives expression of EGFP in intercalated cells of kidney, clear cells of epididymis and airway cells of lung in transgenic mice. Am J Physiol Cell Physiol 2005;288(5):C1134–44.

[395] Bonnici B, Wagner CA. Postnatal expression of transport proteins involved in acid–base transport in mouse kidney. Pflugers Arch 2004;448(1):16–28.

[396] Kim J, Cha JH, Tisher CC, Madsen KM. Role of apoptotic and nonapoptotic cell death in removal of intercalated cells from developing rat kidney. Am J Physiol 1996;270(4 Pt 2): F575–92.

[397] Christensen BM, Kim YH, Kwon TH, Nielsen S. Lithium treatment induces a marked proliferation of primarily principal cells in rat kidney inner medullary collecting duct. Am J Physiol Renal Physiol 2006;291(1):F39–48.

[398] Sabolic I, Brown D, Gluck SL, Alper SL. Regulation of AE1 anion exchanger and H(+)-ATPase in rat cortex by acute metabolic acidosis and alkalosis. Kidney Int 1997;51(1):125–37.

[399] Da Silva Junior JC, Perrone RD, Johns CA, Madias NE. Rat kidney band 3 mRNA modulation in chronic respiratory acidosis. Am J Physiol 1991;260(2 Pt 2):F204–9.

[400] Purkerson JM, Tsuruoka S, Suter DZ, Nakamori A, Schwartz GJ. Adaptation to metabolic acidosis and its recovery are associated with changes in anion exchanger distribution and expression in the cortical collecting duct. Kidney Int 2010;78 (10):993–1005.
[401] Cheval L, Morla L, Elalouf JM, Doucet A. The kidney collecting duct acid–base "regulon". Physiol Genomics 2006;27(3): 271–81.
[402] Welsh-Bacic D, Nowik M, Kaissling B, Wagner CA. Proliferation of acid-secretory cells in the kidney during adaptive remodelling of the collecting duct. PloS one 2011;6(10): e25240.
[403] Barone S, Amlal H, Xu J, Kujala M, Kere J, Petrovic S, et al. Differential regulation of basolateral Cl^-/HCO_3^- exchangers SLC26A7 and AE1 in kidney outer medullary collecting duct. J Am Soc Nephrol 2004;15(8):2002–11.
[404] Amlal H, Sheriff S, Faroqui S, Ma L, Barone S, Petrovic S, et al. Regulation of acid–base transporters by vasopressin in the kidney collecting duct of Brattleboro rat. Am J Nephrol 2006;26 (2):194–205.
[405] Petrovic S, Amlal H, Sun X, Karet F, Barone S, Soleimani M. Vasopressin induces expression of the Cl^-/HCO_3^- exchanger SLC26A7 in kidney medullary collecting ducts of Brattleboro rats. Am J Physiol Renal Physiol 2006;290(5):F1194–201.
[406] Stone DK, Seldin DW, Kokko JP, Jacobson HR. Mineralocorticoid modulation of rabbit medullary collecting duct acidification. A sodium-independent effect. J Clin Invest 1983;72(1):77–83.
[407] Stone DK, Seldin DW, Kokko JP, Jacobson HR. Anion dependence of rabbit medullary collecting duct acidification. J Clin Invest 1983;71(5):1505–8.
[408] Sotak M, Polidarova L, Musilkova J, Hock M, Sumova A, Pacha J. Circadian regulation of electrolyte absorption in the rat colon. Am J Physiol Gastrointest Liver Physiol 2011;301(6): G1066–74.
[409] Fejes-Toth G, Rusvai E, Cleaveland ES, Naray-Fejes-Toth A. Regulation of AE2 mRNA expression in the cortical collecting duct by acid/base balance. Am J Physiol 1998;274(3 Pt 2): F596–601.
[410] Quentin F, Eladari D, Frische S, Cambillau M, Nielsen S, Alper SL, et al. Regulation of the Cl^--HCO_3^- exchanger AE2 in rat thick ascending limb of Henle's loop in response to changes in acid–base and sodium balance. J Am Soc Nephrol 2004;15 (12):2988–97.
[411] Lecanda J, Urtasun R, Medina JF. Molecular cloning and genomic organization of the mouse AE2 anion exchanger gene. Biochem Biophys Res Commun 2000;276(1):117–24.
[412] Medina JF, Acin A, Prieto J. Molecular cloning and characterization of the human AE2 anion exchanger (SLC4A2) gene. Genomics 1997;39(1):74–85.
[413] Malumbres R, Lecanda J, Melero S, Ciesielczyk P, Prieto J, Medina JF. HNF1alpha upregulates the human AE2 anion exchanger gene (SLC4A2) from an alternate promoter. Biochem Biophys Res Commun 2003;311(1):233–40.
[414] Lecanda J, Urtasun R, Recalde S, Prieto J, Medina JF. A novel polymorphism IVS2 + 843C > T in the alternate promoter b1 of the human AE2 anion exchanger gene. Hum Mutat 2001;17(1): 82.
[415] Chow A, Zhou W, Jacobson R. Regulation of AE2 Cl^-/HCO_3^- exchanger during intestinal development. Am J Physiol 1996;271(2 Pt 1):G330–7.
[416] Alvaro D, Gigliozzi A, Marucci L, Alpini G, Barbaro B, Monterubbianesi R, et al. Corticosteroids modulate the secretory processes of the rat intrahepatic biliary epithelium. Gastroenterology 2002;122(4):1058–69.
[417] Prieto J, Qian C, Garcia N, Diez J, Medina JF. Abnormal expression of anion exchanger genes in primary biliary cirrhosis. Gastroenterology 1993;105(2):572–8.
[418] Medina JF, Martinez A, Vazquez JJ, Prieto J. Decreased anion exchanger 2 immunoreactivity in the liver of patients with primary biliary cirrhosis. Hepatology (Baltimore, Md. 1997;25(1): 12–7.
[419] Medina JF. Role of the anion exchanger 2 in the pathogenesis and treatment of primary biliary cirrhosis. Dig Dis (Basel, Switzerland) 2011;29(1):103–12.
[420] Banales JM, Saez E, Uriz M, Sarvide S, Urribarri AD, Splinter P, et al. Upregulation of mir-506 leads to decreased AE2 expression in biliary epithelium of patients with primary biliary cirrhosis. Hepatol (Baltimore, Md.) 2012;: doi: 101002/hep.25691. [Epub ahead of print]
[421] Arenas F, Hervias I, Uriz M, Joplin R, Prieto J, Medina JF. Combination of ursodeoxycholic acid and glucocorticoids upregulates the AE2 alternate promoter in human liver cells. J Clin Invest 2008;118(2):695–709.
[422] Aiba Y, Nakamura M, Joshita S, Inamine T, Komori A, Yoshizawa K, et al. Genetic polymorphisms in CTLA4 and SLC4A2 are differentially associated with the pathogenesis of primary biliary cirrhosis in Japanese patients. J Gastroenterol 2011;46(10):1203–12.
[423] Poupon R, Ping C, Chretien Y, Corpechot C, Chazouilleres O, Simon T, et al. Genetic factors of susceptibility and of severity in primary biliary cirrhosis. J Hepatol 2008;49 (6):1038–45.
[424] Hirschfield GM, Liu X, Han Y, Gorlov IP, Lu Y, Xu C, et al. Variants at IRF5-TNPO3, 17q12-21 and MMEL1 are associated with primary biliary cirrhosis. Nat Genet 2010;42(8):655–7.
[425] Liu X, Invernizzi P, Lu Y, Kosoy R, Lu Y, Bianchi I, et al. Genome-wide meta-analyses identify three loci associated with primary biliary cirrhosis. Nat Genet 2010;42(8):658–60.
[426] Juran BD, Atkinson EJ, Larson JJ, Schlicht EM, Lazaridis KN. Common genetic variation and haplotypes of the anion exchanger SLC4A2 in primary biliary cirrhosis. Am J Gastroenterol 2009;104(6):1406–11.
[427] Vazquez JJ, Vazquez M, Idoate MA, Montuenga L, Martinez Anso E, Castillo JE, et al. Anion exchanger immunoreactivity in human salivary glands in health and Sjogren's syndrome. Am-J-Pathol 1995;146(6):1422–32.
[428] Turi JL, Jaspers I, Dailey LA, Madden MC, Brighton LE, Carter JD, et al. Oxidative stress activates anion exchange protein 2 and AP-1 in airway epithelial cells. Am J Physiol Lung Cell Mol Physiol 2002;283(4):L791–8.
[429] Karumanchi SA, Jiang L, Knebelmann B, Stuart-Tilley AK, Alper SL, Sukhatme VP. VHL tumor suppressor regulates Cl^-/HCO_3^-exchange and Na^+/H^+ exchange activities in renal carcinoma cells. Physiol Genomics 2001;5(3):119–28.
[430] Wu TT, Hsieh YH, Wu CC, Tsai JH, Hsieh YS, Huang CY, et al. Overexpression of anion exchanger 2 in human hepatocellular carcinoma. Chin J Physiol 2006;49(4):192–8.
[431] Hwang JM, Kao SH, Hsieh YH, Li KL, Wang PH, Hsu LS, et al. Reduction of anion exchanger 2 expression induces apoptosis of human hepatocellular carcinoma cells. Mol Cell Biochem 2009;327(1–2):135–44.
[432] Huang QR, Li Q, Chen YH, Li L, Liu LL, Lei SH, et al. Involvement of anion exchanger-2 in apoptosis of endothelial cells induced by high glucose through an mPTP-ROS-Caspase-3 dependent pathway. Apoptosis 2010;15(6):693–704.
[433] Tye CE, Sharma R, Smith CE, Bartlett JD. Altered ion-responsive gene expression in Mmp20 null mice. J Dent Res 2010;89(12):1421–6.

[434] Schwabe K, Cetin Y. Guanylin and functional coupling proteins in the hepatobiliary system of rat and guinea pig. Histochem Cell Biol 2012;137(5):580–97.
[435] Aranda V, Martinez I, Melero S, Lecanda J, Banales JM, Prieto J, et al. Shared apical sorting of anion exchanger isoforms AE2a, AE2b1, and AE2b2 in primary hepatocytes. Biochem Biophys Res Commun 2004;319(3):1040–6.
[436] Gradilone SA, Tietz PS, Splinter PL, Marinelli RA, LaRusso NF. Expression and subcellular localization of aquaporin water channels in the polarized hepatocyte cell line, WIF-B. BMC physiology. 2005; 5:13.
[437] Chiappe de Cingolani G, Morgan P, Mundina-Weilenmann C, Casey J, Fujinaga J, Camilion de Hurtado M, et al. Hyperactivity and altered mRNA isoform expression of the Cl^-/HCO_3^- anion-exchanger in the hypertrophied myocardium. Cardiovasc Res 2001;51(1):71–9.
[438] Xue J, Douglas RM, Zhou D, Lim JY, Boron WF, Haddad GG. Expression of Na^+/H^+ and HCO_3^--dependent transporters in Na^+/H^+ exchanger isoform 1 null mutant mouse brain. Neuroscience 2003;122(1):37–46.
[439] Kanaan A, Douglas RM, Alper SL, Boron WF, Haddad GG. Effect of chronic elevated carbon dioxide on the expression of acid–base transporters in the neonatal and adult mouse. Am J Physiol 2007;293(3):R1294–302.
[440] Rocha S, Costa E, Rocha-Pereira P, Ferreira F, Cleto E, Barbot J, et al. Erythrocyte membrane protein destabilization versus clinical outcome in 160 Portuguese Hereditary Spherocytosis patients. Br J Haematol 2010;149(5):785–94.
[441] Mariani M, Barcellini W, Vercellati C, Marcello AP, Fermo E, Pedotti P, et al. Clinical and hematologic features of 300 patients affected by hereditary spherocytosis grouped according to the type of the membrane protein defect. Haematologica 2008;93(9):1310–7.
[442] Jarolim P, Murray JL, Rubin HL, Taylor WM, Prchal JT, Ballas SK, et al. Characterization of 13 novel band 3 gene defects in hereditary spherocytosis with band 3 deficiency. Blood 1996;88 (11):4366–74.
[443] Quilty JA, Reithmeier RA. Trafficking and folding defects in hereditary spherocytosis mutants of the human red cell anion exchanger. Traffic 2000;1(12):987–98.
[444] Rybicki AC, Qiu JJ, Musto S, Rosen NL, Nagel RL, Schwartz RS. Human erythrocyte protein 4.2 deficiency associated with hemolytic anemia and a homozygous 40glutamic acid- > lysine substitution in the cytoplasmic domain of band 3 (band 3Montefiore). Blood 1993;81(8):2155–65.
[445] Yawata Y, Kanzaki A, Yawata A, Doerfler W, Ozcan R, Eber SW. Characteristic features of the genotype and phenotype of hereditary spherocytosis in the Japanese population. Int J Hematol 2000;71(2):118–35.
[446] Perrotta S, Borriello A, Scaloni A, De Franceschi L, Brunati AM, Turrini F, et al. The N-terminal 11 amino acids of human erythrocyte band 3 are critical for aldolase binding and protein phosphorylation: implications for band 3 function. Blood 2005;106(13):4359–66.
[447] Rysava R, Tesar V, Jirsa Jr M, Brabec V, Jarolim P. Incomplete distal renal tubular acidosis coinherited with a mutation in the band 3 (AE1) gene. Nephrol Dial Transplant 1997;12(9): 1869–73.
[448] Lima PR, Gontijo JA, Lopes de Faria JB, Costa FF, Saad ST. Band 3 Campinas: a novel splicing mutation in the band 3 gene (AE1) associated with hereditary spherocytosis, hyperactivity of Na^+/Li^+ countertransport and an abnormal renal bicarbonate handling. Blood 1997;90 (7):2810–8.
[449] Boctor FN. Overt immediate hemolytic transfusion reaction attributable to anti-Wr(a). Immunohematology/American Red Cross 2008;24(3):113–5.
[450] Janvier D, Lam Y, Galicier L, Bierling P. A new cold autoagglutinin specificity: the third external loop of band 3. Transfusion. Jan;50(1):47–52.
[451] Cortes A, Benet A, Cooke BM, Barnwell JW, Reeder JC. Ability of Plasmodium falciparum to invade Southeast Asian ovalocytes varies between parasite lines. Blood 2004;104(9):2961–6.
[452] Allen SJ, O'Donnell A, Alexander ND, Mgone CS, Peto TE, Clegg JB, et al. Prevention of cerebral malaria in children in Papua New Guinea by southeast Asian ovalocytosis band 3. Am J Trop Med Hyg 1999;60(6):1056–60.
[453] Schofield AE, Reardon DM, Tanner MJ. Defective anion transport activity of the abnormal band 3 in hereditary ovalocytic red blood cells. Nature 1992;355(6363):836–8.
[454] Bruce LJ, Ring SM, Ridgwell K, Reardon DM, Seymour CA, Van Dort HM, et al. South-east asian ovalocytic (SAO) erythrocytes have a cold sensitive cation leak: implications for in vitro studies on stored SAO red cells. Biochim Biophys Acta 1999;1416(1–2):258–70.
[455] Stewart GW. Hemolytic disease due to membrane ion channel disorders. Curr Opin Hematol 2004;11(4):244–50.
[456] Guizouarn H, Borgese F, Gabillat N, Harrison P, Goede JS, McMahon C, et al. South-east Asian ovalocytosis and the cryohydrocytosis form of hereditary stomatocytosis show virtually indistinguishable cation permeability defects. Br J Haematol 2011;152(5):655–64.
[457] Browning JA, Staines HM, Robinson HC, Powell T, Ellory JC, Gibson JS. The effect of deoxygenation on whole-cell conductance of red blood cells from normal individuals and sickle cell patients. Blood 2007;109(6):2622–9.
[458] Boettger T, Hubner CA, Maier H, Rust MB, Beck FX, Jentsch TJ. Deafness and renal tubular acidosis in mice lacking the K-Cl co-transporter Kcc4. Nature 2002;416(6883):874–8.
[459] Xu J, Song P, Nakamura S, Miller M, Barone S, Alper SL, et al. Deletion of the chloride transporter slc26a7 causes distal renal tubular acidosis and impairs gastric acid secretion. J Biol Chem 2009;284(43):29470–9.
[460] Izumi Y, Hori K, Nakayama Y, Kimura M, Hasuike Y, Nanami M, et al. Aldosterone requires vasopressin V1a receptors on intercalated cells to mediate acid–base homeostasis. J Am Soc Nephrol 2011;22(4):673–80.
[461] Biver S, Belge H, Bourgeois S, Van Vooren P, Nowik M, Scohy S, et al. A role for Rhesus factor Rhcg in renal ammonium excretion and male fertility. Nature 2008;456(7220):339–43.
[462] Lynch IJ, Rudin A, Xia SL, Stow LR, Shull GE, Weiner ID, et al. Impaired acid secretion in cortical collecting duct intercalated cells from H-K-ATPase-deficient mice: role of HKalpha isoforms. Am J Physiol Renal Physiol 2008;294(3):F621–7.
[463] Takito J, Al-Awqati Q. Conversion of ES cells to columnar epithelia by hensin and to squamous epithelia by laminin. J Cell Biol 2004;166(7):1093–102.
[464] Gao X, Eladari D, Leviel F, Tew BY, Miro-Julia C, Cheema F, et al. Deletion of hensin/DMBT1 blocks conversion of beta- to alpha-intercalated cells and induces distal renal tubular acidosis. Proc Nat Acad Sci USA 2010;107(50):21872–7.
[465] Al-Awqati Q. Terminal differentiation in epithelia: the role of integrins in hensin polymerization. Annu Rev Physiol 2011;73:401–12.
[466] Renner M, Bergmann G, Krebs I, End C, Lyer S, Hilberg F, et al. DMBT1 confers mucosal protection in vivo and a deletion variant is associated with Crohn's disease. Gastroenterology 2007;133(5):1499–509.

[467] De Lisle RC, Xu W, Roe BA, Ziemer D. Effects of Muclin (Dmbt1) deficiency on the gastrointestinal system. Am J Physiol Gastrointest Liver Physiol 2008;294(3):G717–27.
[468] Jarolim P, Shayakul C, Prabakaran D, Jiang L, Stuart-Tilley A, Rubin HL, et al. Autosomal dominant distal renal tubular acidosis is associated in three families with heterozygosity for the R589H mutation in the AE1 (band 3) Cl^-/HCO_3^-exchanger. J Biol Chem 1998;273(11):6380–8.
[469] Bruce LJ, Cope DL, Jones GK, Schofield AE, Burley M, Povey S, et al. Familial distal renal tubular acidosis is associated with mutations in the red cell anion exchanger (band 3, AE1) gene. J Clin Invest 1997;100(7):1693–707.
[470] Li J, Quilty J, Popov M, Reithmeier RA. Processing of N-linked oligosaccharide depends on its location in the anion exchanger, AE1, membrane glycoprotein. Biochem J 2000;349(Pt 1):51–7.
[471] Quilty JA, Li J, Reithmeier RA. Impaired trafficking of distal renal tubular acidosis mutants of the human kidney anion exchanger kAE1. Am J Physiol Renal Physiol 2002;282(5): F810–20.
[472] Karet FE. Inherited distal renal tubular acidosis. J Am Soc Nephrol 2002;13(8):2178–84.
[473] Toye AM, Banting G, Tanner MJ. Regions of human kidney anion exchanger 1 (kAE1) required for basolateral targeting of kAE1 in polarised kidney cells: mis-targeting explains dominant renal tubular acidosis (dRTA). J Cell Sci 2004;117(Pt 8):1399–410.
[474] Cheung JC, Cordat E, Reithmeier RA. Trafficking defects of the Southeast Asian ovalocytosis deletion mutant of anion exchanger 1 membrane proteins. Biochem J 2005;392(Pt 3): 425–34.
[475] Shayakul C, Jarolim P, Zachlederova M, Prabakaran D, Cortez-Campeao D, Kalabova D, et al. Characterization of a highly polymorphic marker adjacent to the SLC4A1 gene and of kidney immunostaining in a family with distal renal tubular acidosis. Nephrol Dial Transplant 2004;19(2):371–9.
[476] Walsh S, Turner CM, Toye A, Wagner C, Jaeger P, Laing C, et al. Immunohistochemical comparison of a case of inherited distal renal tubular acidosis (with a unique AE1 mutation) with an acquired case secondary to autoimmune disease. Nephrol Dial Transplant 2007;22(3):807–12.
[477] Rungroj N, Devonald MA, Cuthbert AW, Reimann F, Akkarapatumwong V, Yenchitsomanus PT, et al. A novel missense mutation in AE1 causing autosomal dominant distal renal tubular acidosis retains normal transport function but is mistargeted in polarized epithelial cells. J Biol Chem 2004;279 (14):13833–8.
[478] Sawasdee N, Junking M, Ngaojanlar P, Sukomon N, Ungsupravate D, Limjindaporn T, et al. Human kidney anion exchanger 1 interacts with adaptor-related protein complex 1 mu1A (AP-1 mu1A). Biochem Biophys Res Commun 2010;401 (1):85–91.
[479] Toye AM, Williamson RC, Brown A, Mawby W, Banting G. Kidney anion exchanger 1 is phosphorylated on N and C-terminal tyrosines Y359 and Y904 that are essential for basolateral localization. J Am Soc Nephrol 2006;17:3A.
[480] Dorsey FC, Muthusamy T, Whitt MA, Cox JV. A novel role for a YXXPhi motif in directing the caveolin-dependent sorting of membrane-spanning proteins. J Cell Sci 2007;120(Pt 15): 2544–54.
[481] Patterson ST, Reithmeier RA. Cell surface rescue of kidney anion exchanger 1 mutants by disruption of chaperone interactions. J Biol Chem 2010;285(43):33423–34.
[482] Khositseth S, Sirikanaerat A, Khoprasert S, Opastirakul S, Kingwatanakul P, Thongnoppakhun W, et al. Hematological abnormalities in patients with distal renal tubular acidosis and hemoglobinopathies. Am J Hematol 2008;83(6):465–71.
[483] Tanphaichitr VS, Sumboonnanonda A, Ideguchi H, Shayakul C, Brugnara C, Takao M, et al. Novel AE1 mutations in recessive distal renal tubular acidosis. Loss-of-function is rescued by glycophorin A. J Clin Invest 1998;102(12):2173–9.
[484] Cordat E, Reithmeier RA. Expression and interaction of two compound heterozygous distal renal tubular acidosis mutants of kidney anion exchanger 1 in epithelial cells. Am J Physiol Renal Physiol 2006;291(6):F1354–61.
[485] Bruce LJ, Wrong O, Toye AM, Young MT, Ogle G, Ismail Z, et al. Band 3 mutations, renal tubular acidosis and South-East Asian ovalocytosis in Malaysia and Papua New Guinea: loss of up to 95% band 3 transport in red cells. Biochem J 2000;350(Pt 1):41–51.
[486] Groves JD, Tanner MJ. The effects of glycophorin A on the expression of the human red cell anion transporter (band 3) in Xenopus oocytes. J Membr Biol 1994;140(1):81–8.
[487] Sawasdee N, Udomchaiprasertkul W, Noisakran S, Rungroj N, Akkarapatumwong V, Yenchitsomanus PT. Trafficking defect of mutant kidney anion exchanger 1 (kAE1) proteins associated with distal renal tubular acidosis and Southeast Asian ovalocytosis. Biochem Biophys Res Commun 2006;350(3): 723–30.
[488] Kittanakom S, Cordat E, Akkarapatumwong V, Yenchitsomanus PT, Reithmeier RA. Trafficking defects of a novel autosomal recessive distal renal tubular acidosis mutant (S773P) of the human kidney anion exchanger (kAE1). J Biol Chem 2004;279(39):40960–71.
[489] Southgate CD, Chishti AH, Mitchell B, Yi SJ, Palek J. Targeted disruption of the murine erythroid band 3 gene results in spherocytosis and severe haemolytic anaemia despite a normal membrane skeleton. Nat Genet 1996;14(2):227–30.
[490] Hassoun H, Wang Y, Vassiliadis J, Lutchman M, Palek J, Aish L, et al. Targeted inactivation of murine band 3 (AE1) gene produces a hypercoagulable state causing widespread thrombosis in vivo. Blood 1998;92(5):1785–92.
[491] Akel A, Wagner CA, Kovacikova J, Kasinathan RS, Kiedaisch V, Koka S, et al. Enhanced suicidal death of erythrocytes from gene-targeted mice lacking the Cl^-/HCO_3^- exchanger AE1. Am J Physiol Cell Physiol 2007;292(5):C1759–67.
[492] Peters LL, Swearingen RA, Andersen SG, Gwynn B, Lambert AJ, Li R, et al. Identification of quantitative trait loci that modify the severity of hereditary spherocytosis in wan, a new mouse model of band-3 deficiency. Blood 2004;103(8):3233–40.
[493] Ito D, Koshino I, Arashiki N, Adachi H, Tomihari M, Tamahara S, et al. Ubiquitylation-independent ER-associated degradation of an AE1 mutant associated with dominant hereditary spherocytosis in cattle. J Cell Sci 2006;119(Pt 17):3602–12.
[494] Lien YH, Lai LW. Respiratory acidosis in carbonic anhydrase II-deficient mice. Am J Physiol 1998;274(2 Pt 1):L301–4.
[495] Shmukler BE, Clark JS, Hsu A, Vandorpe DH, Stewart AK, Kurschat CE, et al. Zebrafish ae2.2 encodes a second slc4a2 anion exchanger. Am J Physiol 2008;294(3):R1081–91.
[496] Meyers SN, McDaneld TG, Swist SL, Marron BM, Steffen DJ, O'Toole D, et al. A deletion mutation in bovine SLC4A2 is associated with osteopetrosis in Red Angus cattle. BMC genomics 2010;11:337.
[497] Jensen LJ, Stuart-Tilley AK, Peters LL, Lux SE, Alper SL, Breton S. Immunolocalization of AE2 anion exchanger in rat and mouse epididymis. Biol Reprod 1999;61(4):973–80.
[498] Recalde S, Muruzabal F, Looije N, Kunne C, Burrell MA, Saez E, et al. Inefficient chronic activation of parietal cells in Ae2a, $b^{-/-}$ mice. Am J Pathol 2006;169(1):165–76.
[499] Banales JM, Arenas F, Rodriguez-Ortigosa CM, Saez E, Uriarte I, Doctor RB, et al. Bicarbonate-rich choleresis induced by

secretin in normal rat is taurocholate-dependent and involves AE2 anion exchanger. Hepatol (Baltimore, Md. 2006;43(2): 266–75.

[500] Mardones Hiche P, Medina J, Prieto J, Oude Elferink R. The role of anion exchanger 2 in bile secretion. Eur J Gastroenterol 2006;:A50.

[501] Ishiguro H, Namkung W, Yamamoto A, Wang Z, Worrell RT, Xu J, et al. Effect of Slc26a6 deletion on apical Cl^-/HCO_3^-exchanger activity and cAMP-stimulated bicarbonate secretion in pancreatic duct. Am J Physiol Gastrointest Liver Physiol 2007;292(1):G447–55.

[502] Wang Y, Soyombo AA, Shcheynikov N, Zeng W, Dorwart M, Marino CR, et al. Slc26a6 regulates CFTR activity in vivo to determine pancreatic duct HCO(3)(-) secretion: relevance to cystic fibrosis. EMBO J 2006;1925(21):5049–57.

[503] Mardones P, Medina JF, Elferink RP. Activation of cyclic AMP Signaling in Ae2-deficient mouse fibroblasts. J Biol Chem 2008;283(18):12146–53.

[504] Salas JT, Banales JM, Sarvide S, Recalde S, Ferrer A, Uriarte I, et al. Ae2a,b-deficient mice develop antimitochondrial antibodies and other features resembling primary biliary cirrhosis. Gastroenterology 2008;134(5):1482–93.

[505] Fickert P, Trauner M. When lightning strikes twice: the plot thickens for a dual role of the anion exchanger 2 (AE2/SLC4A2) in the pathogenesis and treatment of primary biliary cirrhosis. J Hepatol 2009;50(3):633–5.

[506] Gawenis LR, Bradford EM, Alper SL, Prasad V, Shull GE. AE2 Cl^-/HCO_3^- exchanger is required for normal cAMP-stimulated anion secretion in murine proximal colon. Am J Physiol Gastrointest Liver Physiol 2010;298(4):G493–503.

[507] Shan J, Huang J, Liao J, Robert R, Hanrahan JW. Anion secretion by a model epithelium: more lessons from Calu-3. Acta Physiol (Oxford, England) 2011;202(3):523–31.

[508] Sander T, Toliat MR, Heils A, Leschik G, Becker C, Ruschendorf F, et al. Association of the 867Asp variant of the human anion exchanger 3 gene with common subtypes of idiopathic generalized epilepsy. Epilepsy Res 2002;51(3):249–55.

[509] Vilas GL, Johnson DE, Freund P, Casey JR. Characterization of an epilepsy-associated variant of the human Cl^-/HCO_3^- exchanger AE3. Am J Physiol Cell Physiol 2009;297(3): C526–36.

[510] Alvarez BV, Gilmour GS, Mema SC, Martin BT, Shull GE, Casey JR, et al. Blindness caused by deficiency in AE3 chloride/bicarbonate exchanger. PloS one 2007;2(9):e839.

[511] Downs LM, Wallin-Hakansson B, Boursnell M, Marklund S, Hedhammar A, Truve K, et al. A frameshift mutation in golden retriever dogs with progressive retinal atrophy endorses SLC4A3 as a candidate gene for human retinal degenerations. PloS one 2011;6(6):e21452.

[512] Al Moamen NJ, Prasad V, Bodi I, Miller ML, Neiman ML, Lasko VM, et al. Loss of the AE3 anion exchanger in a hypertrophic cardiomyopathy model causes rapid decompensation and heart failure. J Mol Cell Cardiol 2011;50(1):137–46.

[513] Walder JA, Chatterjee R, Steck TL, Low PS, Musso GF, Kaiser ET, et al. The interaction of hemoglobin with the cytoplasmic domain of band 3 of the human erythrocyte membrane. J Biol Chem 1984;259(16):10238–46.

[514] Chu H, Breite A, Ciraolo P, Franco RS, Low PS. Characterization of the deoxyhemoglobin binding site on human erythrocyte band 3: implications for O2 regulation of erythrocyte properties. Blood 2008;111(2):932–8.

[515] Low PS, Allen DP, Zioncheck TF, Chari P, Willardson BM, Geahlen RL, et al. Tyrosine phosphorylation of band 3 inhibits peripheral protein binding. J Biol Chem 1987;262(10): 4592–6.

[516] Yannoukakos D, Meyer HE, Vasseur C, Driancourt C, Wajcman H, Bursaux E. Three regions of erythrocyte band 3 protein are phosphorylated on tyrosines: characterization of the phosphorylation sites by solid phase sequencing combined with capillary electrophoresis. Biochim Biophys Acta 1991;1066 (1):70–6.

[517] Yannoukakos D, Vasseur C, Piau JP, Wajcman H, Bursaux E. Phosphorylation sites in human erythrocyte band 3 protein. Biochim Biophys Acta 1991;1061(2):253–66.

[518] Groves JD, Tanner MJ. Co-expressed complementary fragments of the human red cell anion exchanger (band 3, AE1) generate stilbene disulfonate-sensitive anion transport. J Biol Chem 1995;270(16):9097–105.

[519] Bordin L, Brunati AM, Donella-Deana A, Baggio B, Toninello A, Clari G. Band 3 is an anchor protein and a target for SHP-2 tyrosine phosphatase in human erythrocytes. Blood 2002;100 (1):276–82.

[520] Cobb CE, Beth AH. Identification of the eosinyl-5-maleimide reaction site on the human erythrocyte anion-exchange protein: overlap with the reaction sites of other chemical probes. Biochemistry 1990;29(36):8283–90.

[521] Abe Y, Chaen T, Jin XR, Hamasaki T, Hamasaki N. Massspectrometric analyses of transmembrane proteins in human erythrocyte membrane. J Biochem (Tokyo) 2004;136(1): 97–106.

[522] Okubo K, Kang D, Hamasaki N, Jennings ML. Red blood cell band 3. Lysine 539 and lysine 851 react with the same H2DIDS (4,4′-diisothiocyanodihydrostilbene-2,2′-disulfonic acid) molecule. J Biol Chem 1994;269(3):1918–26.

[523] Garcia AM, Lodish HF. Lysine 539 of human band 3 is not essential for ion transport or inhibition by stilbene disulfonates. J Biol Chem 1989;264(33):19607–13.

[524] Sigrist H, Kempf C, Zahler P. Interaction of phenylisothiocyanate with human erythrocyte band 3 protein. I. Covalent modification and inhibition of phosphate transport. Biochim Biophys Acta 1980;597(1):137–44.

[525] Brock CJ, Tanner MJ, Kempf C. The human erythrocyte anion-transport protein. Partial amino acid sequence, conformation and a possible molecular mechanism for anion exchange. Biochem J 1983;213(3):577–86.

[526] Jennings ML, Adams-Lackey M, Denney GH. Peptides of human erythrocyte band 3 protein produced by extracellular papain cleavage. J Biol Chem 1984;259(7):4652–60.

[527] Matsuyama H, Kawano Y, Hamasaki N. Anion transport activity in the human erythrocyte membrane modulated by proteolytic digestion of the 38,000-dalton fragment in Band 3. J Biol Chem 1983;258(24):15376–81.

[528] St V, Haest CW, Deuticke B. Complex effects of papain on function and inhibitor sensitivity of the red cell anion exchanger AE1 suggest the presence of different transport subsites. J Membr Biol 2001;179(3):205–21.

[529] Jennings ML, Anderson MP, Monaghan R. Monoclonal antibodies against human erythrocyte band 3 protein. Localization of proteolytic cleavage sites and stilbenedisulfonate-binding lysine residues. J Biol Chem 1986;261(19):9002–10.

[530] Kuma H, Shinde AA, Howren TR, Jennings ML. Topology of the anion exchange protein AE1: the controversial sidedness of lysine 743. Biochemistry 2002;41(10):3380–8.

[531] Takazaki S, Abe Y, Yamaguchi T, Yagi M, Ueda T, Kang D, et al. Mutation of His 834 in human anion exchanger 1 affects substrate binding. Biochim Biophys Acta 2010;1798 (5):903–8.

[532] Okubo K, Hamasaki N, Hara K, Kageura M. Palmitoylation of cysteine 69 from the COOH-terminal of band 3 protein in the human erythrocyte membrane. Acylation occurs in the middle

of the consensus sequence of F–I-IICLAVL found in band 3 protein and G2 protein of Rift Valley fever virus. J Biol Chem 1991;266(25):16420–4.

[533] Kang D, Karbach D, Passow H. Anion transport function of mouse erythroid band 3 protein (AE1) does not require acylation of cysteine residue 861. Biochim Biophys Acta 1994;1194 (2):341–4.

[534] Jarolim P, Palek J, Amato D, Hassan K, Sapak P, Nurse GT, et al. Deletion in erythrocyte band 3 gene in malaria-resistant Southeast Asian ovalocytosis. Proc Nat Acad Sci USA 1991;88(24):11022–6.

[535] Mohandas N, Winardi R, Knowles D, Leung A, Parra M, George E, et al. Molecular basis for membrane rigidity of hereditary ovalocytosis. A novel mechanism involving the cytoplasmic domain of band 3. J Clin Invest 1992;89(2):686–92.

[536] Alloisio N, Maillet P, Carre G, Texier P, Vallier A, Baklouti F, et al. Hereditary spherocytosis with band 3 deficiency. Association with a nonsense mutation of the band 3 gene (allele Lyon), and aggravation by a low-expression allele occurring in trans (allele Genas). Blood 1996;88(3):1062–9.

[537] Miraglia del Giudice E, Vallier A, Maillet P, Perrotta S, Cutillo S, Iolascon A, et al. Novel band 3 variants (bands 3 Foggia, Napoli I and Napoli II) associated with hereditary spherocytosis and band 3 deficiency: status of the D38A polymorphism within the EPB3 locus. Br J Haematol 1997;96(1):70–6.

[538] Kanzaki A, Hayette S, Morle L, Inoue F, Matsuyama R, Inoue T, et al. Molecular and genetic characteristics in Japanese patients with hereditary spherocytosis: frequent Band 3 mutations and rarer ankyrin mutations. Blood 1997;90(suppl. 1):6b.

[539] Bracher NA, Lyons CA, Wessels G, Mansvelt E, Coetzer TL. Band 3 Cape Town (E90K) causes severe hereditary spherocytosis in combination with band 3 Prague III. Br J Haematol 2001;113(3):689–93.

[540] Jarolim P, Rubin HL, Brabec V, Chrobak L, Zolotarev AS, Alper SL, et al. Mutations of conserved arginines in the membrane domain of erythroid band 3 lead to a decrease in membrane-associated band 3 and to the phenotype of hereditary spherocytosis. Blood 1995;85(3):634–40.

[541] Inoue T, Kanzaki A, Kaku M, Yawata A, Takezono M, Okamoto N, et al. Homozygous missense mutation (band 3 Fukuoka: G130R): a mild form of hereditary spherocytosis with near-normal band 3 content and minimal changes of membrane ultrastructure despite moderate protein 4.2 deficiency. Br J Haematol 1998;102(4):932–9.

[542] Alloisio N, Texier P, Vallier A, Ribeiro ML, Morle L, Bozon M, et al. Modulation of clinical expression and band 3 deficiency in hereditary spherocytosis. Blood 1997;90(1):414–20.

[543] Eber SW, Gonzalez JM, Lux ML, Scarpa AL, Tse WT, Dornwell M, et al. Ankyrin-1 mutations are a major cause of dominant and recessive hereditary spherocytosis. Nat Genet 1996;13 (2):214–8.

[544] Dhermy D, Galand C, Bournier O, Boulanger L, Cynober T, Schismanoff PO, et al. Heterogenous band 3 deficiency in hereditary spherocytosis related to different band 3 gene defects. Br J Haematol 1997;98(1):32–40.

[545] Jarolim P, Palek J, Rubin HL, Prchal JT, Korsgren C, Cohen CM. Band 3 Tuscaloosa: Pro327–Arg327 substitution in the cytoplasmic domain of erythrocyte band 3 protein associated with spherocytic hemolytic anemia and partial deficiency of protein 4.2. Blood 1992;80(2):523–9.

[546] Jenkins PB, Abou-Alfa GK, Dhermy D, Bursaux E, Feo C, Scarpa AL, et al. A nonsense mutation in the erythrocyte band 3 gene associated with decreased mRNA accumulation in a kindred with dominant hereditary spherocytosis. J Clin Invest 1996;97(2):373–80.

[547] Bianchi P, Zanella A, Alloisio N, Barosi G, Bredi E, Pelissero G, et al. A variant of the EPB3 gene of the anti-Lepore type in hereditary spherocytosis. Br J Haematol 1997;98(2):283–8.

[548] Sanchez-Lopez JY, Camacho-Torres AL, Ibarra B, Tintos JA, Perea FJ. Analysis of the SLC4A1 gene in three Mexican patients with hereditary spherocytosis: report of a novel mutation. Genet Mol Biol 2010;33(1):9–11.

[549] Lima PR, Baratti MO, Chiattone ML, Costa FF, Saad ST. Band 3Tambau: a de novo mutation in the AE1 gene associated with hereditary spherocytosis. Implications for anion exchange and insertion into the red blood cell membrane. Eur J Haematol 2005;74(5):396–401.

[550] Maillet P, Vallier A, Reinhart WH, Wyss EJ, Ott P, Texier P, et al. Band 3 Chur: a variant associated with band 3-deficient hereditary spherocytosis and substitution in a highly conserved position of transmembrane segment 11. Br J Haematol 1995;91(4):804–10.

[551] Iwase S, Ideguchi H, Takao M, Horiguchi-Yamada J, Iwasaki M, Takahara S, et al. Band 3 Tokyo: Thr837– >Ala837 substitution in erythrocyte band 3 protein associated with spherocytic hemolysis. Acta Haematol 1998;100(4):200–3.

[552] Perrotta S, Polito F, Cone ML, Nobili B, Cutillo S, Nigro V, et al. Hereditary spherocytosis due to a novel frameshift mutation in AE1 cytoplasmic COOH terminal tail: band 3 Vesuvio. Blood 1999;93(6):2131–2.

[553] Stewart AK, Kedar PS, Shmukler BE, Vandorpe DH, Hsu A, Glader B, et al. Functional characterization and modified rescue of novel AE1 mutation R730C associated with overhydrated cation leak stomatocytosis. Am J Physiol Cell Physiol 2011;300(5):C1034–46.

[554] Stewart AK, Vandorpe DH, Heneghan JF, Chebib F, Stolpe K, Akhavein A, et al. The GPA-dependent, spherostomatocytosis mutant AE1 E758K induces GPA-independent, endogenous cation transport in amphibian oocytes. Am J Physiol Cell Physiol 2010;298(2):C283–97.

[555] Iolascon A, De Falco L, Borgese F, Esposito MR, Avvisati RA, Izzo P, et al. A novel erythroid anion exchange variant (Gly796Arg) of hereditary stomatocytosis associated with dyserythropoiesis. Haematologica 2009;94(8):1049–59.

[556] Jamard B, Allard J, Caron P, Corberand JX, Blanchard A, Vargas-Poussou R, et al. Distal renal tubular acidosis and ovalocytosis: a case report. Osteoporos Int 2008;19(1):119–22.

[557] Chu C, Woods N, Sawasdee N, Guizouarn H, Pellissier B, Borgese F, et al. Band 3 Edmonton I, a novel mutant of the anion exchanger 1 causing spherocytosis and distal renal tubular acidosis. Biochem J 2010;426(3):379–88.

[558] Chang YH, Shaw CF, Jian SH, Hsieh KH, Chiou YH, Lu PJ. Compound mutations in human anion exchanger 1 are associated with complete distal renal tubular acidosis and hereditary spherocytosis. Kidney Int 2009;76(7):774–83.

[559] Karet FE, Gainza FJ, Gyory AZ, Unwin RJ, Wrong O, Tanner MJ, et al. Mutations in the chloride-bicarbonate exchanger gene AE1 cause autosomal dominant but not autosomal recessive distal renal tubular acidosis. Proc Nat Acad Sci USA 1998;95(11):6337–42.

[560] Vasuvattakul S, Yenchitsomanus PT, Thuwajit P, Kaitwatcharachai C, Vachuanichsanong P, Laosombat V, et al. Compound heterozygosity of AE1 genes cause recessive distal renal tubular acidosis in Southeast Asian Ovalcytosis. J Am Soc Nephrol 1999;10:444A.

[561] Toye AM, Williamson RC, Khanfar M, Bader-Meunier B, Cynober T, Thibault M, et al. Band 3 Courcouronnes (Ser667Phe): a trafficking mutant differentially rescued by wild-type band 3 and glycophorin A. Blood 2008;111(11): 5380–9.

[562] Choo KE, Nicoli TK, Bruce LJ, Tanner MJ, Ruiz-Linares A, Wrong OM. Recessive distal renal tubular acidosis in Sarawak caused by AE1 mutations. Pediatr Nephrol 2006;21 (2):212–7.
[563] Shmukler BE, Kedar PS, Warang P, Desai M, Madkaikar M, Ghosh K, et al. Hemolytic anemia and distal renal tubular acidosis in two Indian patients homozygous for SLC4A1/AE1 mutation A858D. Am J Hematol 2010;85(10):824–8.
[564] Cheidde L, Vieira TC, Lima PR, Saad ST, Heilberg IP. A novel mutation in the anion exchanger 1 gene is associated with familial distal renal tubular acidosis and nephrocalcinosis. Pediatrics 2003;112(6 Pt 1):1361–7.
[565] Shao L, Xu Y, Dong Q, Lang Y, Yue S, Miao Z. A novel SLC4A1 variant in an autosomal dominant distal renal tubular acidosis family with a severe phenotype. Endocrine 2010;37 (3):473–8.
[566] McManus K, Pongoski J, Coghlan G, Zelinski T. Amino acid substitutions in human erythroid protein band 3 account for the low-incidence antigens NFLD and BOW. Transfusion 2000;40(3):325–9.
[567] Jarolim P, Rubin HL, Zakova D, Storry J, Reid ME. Characterization of seven low incidence blood group antigens carried by erythrocyte band 3 protein. Blood 1998;92 (12):4836–43.
[568] McManus K, Lupe K, Coghlan G, Zelinski T. An amino acid substitution in the putative second extracellular loop of RBC band 3 accounts for the Froese blood group polymorphism. Transfusion 2000;40(10):1246–9.
[569] Jarolim P, Murray JL, Rubin HL, Smart E, Moulds JM. Blood group antigens Rb_a, Tr_a, and Wd_a are located in the third ectoplasmic loop of erythroid band 3. Transfusion 1997;37 (6):607–15.
[570] Jarolim P, Murray JL, Rubin HL, Coghlan G, Zelinski TA. Thr552– >Ile substitution in erythroid band 3 gives rise to the Warrior blood group antigen. Transfusion 1997;37(4): 398–405.
[571] Zelinski T, McManus K, Punter F, Moulds M, Coghlan G. A Gly565– >Ala substitution in human erythroid band 3 accounts for the Wu blood group polymorphism. Transfusion 1998;38(8):745–8.
[572] Poole J, Hallewell H, Bruce L, Tanner MJ, Zupanska B, Kusnierz-Alejska G. Identification of two new Jn^{a+} individuals and assignment of Jn^a to erythrocyte band 3. Transfusion 1997;37(Suppl.):90S.
[573] Zelinski T, Rusnak A, McManus K, Coghlan G. Distinctive Swann blood group genotypes: molecular investigations. Vox Sang 2000;79(4):215–8.
[574] Bruce LJ, Anstee DJ, Spring FA, Tanner MJ. Band 3 Memphis variant II. Altered stilbene disulfonate binding and the Diego (Dia) blood group antigen are associated with the human erythrocyte band 3 mutation Pro854– >Leu. J Biol Chem 1994;269(23):16155–8.
[575] NCBI. NCBI Genbank P02730 (gi: 114787) citations of LocusLink SLC4A1 dbSNP, (<http://www.ncbi.nlm.nih.gov./SNP/snp_ref.cgi?locusId = 6521/>). [cited; Available from: (<http://www.ncbi.nlm.nih.gov./SNP/snp_ref.cgi?locusId = 6521/>).
[576] Yannoukakos D, Vasseur C, Driancourt C, Blouquit Y, Delaunay J, Wajcman H, et al. Human erythrocyte band 3 polymorphism (band 3 Memphis): characterization of the structural modification (Lys 56–Glu) by protein chemistry methods. Blood 1991;78(4):1117–20.
[577] Xu XG, He J, He YM, Tao SD, Ying YL, Zhu FM, et al. Distribution of Diego blood group alleles and identification of four novel mutations on exon 19 of SLC4A1 gene in the Chinese Han population by polymerase chain reaction sequence-based typing. Vox Sang 2011;100(3):317–21.
[578] Boles MK, Wilkinson BM, Wilming LG, Liu B, Probst FJ, Harrow J, et al. Discovery of candidate disease genes in ENU-induced mouse mutants by large-scale sequencing, including a splice-site mutation in nucleoredoxin. PloS Genet 2009;5(12): e1000759.
[579] Frommer WB, von Wiren N. Plant biology: ping-pong with boron. Nature 2002;420(6913):282–3.
[580] Jansen ID, Mardones P, Lecanda F, de Vries TJ, Recalde S, Hoeben KA, et al. Ae2(a,b)-deficient mice exhibit osteopetrosis of long bones but not of calvaria. Faseb J 2009;23 (10):3470–81.
[581] Darnell J, Lodish H, Baltimore D. Molecular cell biology. 2nd ed. New York: W. H. Freeman; 1990. p. 531–582
[582] Korsgren C, Peters LL, Lux SE Protein 4.2 binds to the carboxyl-terminal EF-hands of erythroid alpha-spectrin in a calcium- and calmodulin-dependent manner. J Biol Chem. Feb;285(7):4757–4770.
[583] Bennett V, Baines AJ. Spectrin and ankyrin-based pathways: metazoan inventions for integrating cells into tissues. Physiol Rev 2001;81(3):1353–92.
[584] Wagner CA, Finberg KE, Stehberger PA, Lifton RP, Giebisch GH, Aronson PS, et al. Regulation of the expression of the Cl^-/anion exchanger pendrin in mouse kidney by acid–base status. Kidney Int 2002;62(6):2109–17.
[585] Finberg KE, Wagner CA, Bailey MA, Paunescu TG, Breton S, Brown D, et al. The B1-subunit of the H^+ ATPase is required for maximal urinary acidification. Proc Nat Acad Sci USA 2005;102(38):13616–21.
[586] Stuart-Tilley AK, Shmukler BE, Brown D, Alper SL. Immunolocalization and tissue-specific splicing of AE2 anion exchanger in mouse kidney. J Am Soc Nephrol 1998;9(6): 946–59.
[587] Nguyen HV, Stuart-Tilley A, Alper SL, Melvin JE. Cl^-/HCO_3^- exchange is acetazolamide sensitive and activated by a muscarinic receptor-induced $Ca^{2+}{}_i$ increase in salivary acinar cells. Am J Physiol Gastrointest Liver Physiol 2004;286 (2):G312–20.
[588] Praetorius J, Kim YH, Bouzinova EV, Frische S, Rojek A, Aalkjaer C, et al. NBCn1 is a basolateral Na^+-HCO_3^- cotransporter in rat kidney inner medullary collecting ducts. Am J Physiol Renal Physiol 2004;286(5):F903–12.

This page intentionally left blank

CHAPTER

55

Cellular Mechanisms of Renal Tubular Acidification

L.Lee Hamm[1], *Robert J. Alpern*[2] *and Patricia A. Preisig*[2,3]

[1]Department of Internal Medicine, Tulane University, New Orleans, LA

[2]Department of Internal Medicine, Yale University, New Haven CT

[3]Department of Cellular and Molecular Physiology, Yale University, New Haven, CT

To maintain acid–base balance, the renal tubules secrete hydrogen ions into the lumen at a rate equal to the sum of extrarenal acid generation and bicarbonate filtration. In this chapter we review the cellular mechanisms responsible for transepithelial hydrogen secretion along the nephron and describe the regulators of these processes.

PROXIMAL TUBULE

The fluid entering the proximal tubule is the glomerular ultrafiltrate, which is in Donnan equilibrium with plasma and has a bicarbonate concentration of approximately 25 mEq/L. The proximal convoluted tubule secretes H ions that acidify the luminal fluid leading to the reabsorption of approximately 14 apart from 75% of filtered bicarbonate and decreasing luminal bicarbonate concentration to 5–10 mEq/L and luminal pH from 7.4 to ~6.8. The proximal straight tubule has a smaller capacity for H secretion, but also contributes to bicarbonate reabsorption. With an acidic luminal fluid (relative to the peritubular space) and a relatively small transepithelial voltage [−2 (early proximal tubule) to +2 (late proximal tubule) mV], transepithelial H secretion requires active transport.

The proximal tubule cell voltage is between −50 and −70 mV relative to the peritubular fluid and cell pH of between 7.15 and 7.30.[1–5] Using these values, it can be calculated that protons (hydrogen ions) can enter the cell across the basolateral membrane passively (or equivalently base can passively exit the cell across the basolateral membrane), while H ion secretion across the apical membrane from the cell to the luminal fluid is against the electrochemical gradient, and thus, requires active transport.

Apical Membrane H/HCO_3 Transport Mechanisms

Proton Secretion vs *HCO_3 Absorption*

Net acidification of the tubular fluid may be mediated by apical membrane H secretion or HCO_3 absorption. These two processes, shown in Figure 55.1, have been distinguished using the disequilibrium pH. The mechanisms shown in Figure 55.1 involve two reactions in series. The association/dissociation of H_2CO_3 (carbonic acid) to or from H and HCO_3 (reaction 1) occurs instantaneously, while the association/dissociation of H_2CO_3 to or from CO_2 and H_2O (reaction 2) is very slow. Carbonic anhydrase catalyzes the latter reaction such that in its presence all constituents are at equilibrium. In the absence of luminal carbonic anhydrase, the second reaction will not be at equilibrium and the relative concentrations of the substrates can be used to determine the direction in which the reactions are occurring, and, thus, whether there is direct H secretion or direct HCO_3 absorption.

If carbonic anhydrase is present in the lumen, H_2CO_3 will be in equilibrium with CO_2 and H_2O, and H_2CO_3 concentration will be that calculated from the concentration of CO_2 and the equilibrium constant for the second reaction. Equivalently, using the equilibrium constants for the above reactions, the

Seldin and Giebisch's The Kidney, Fifth Edition.
DOI: http://dx.doi.org/10.1016/B978-0-12-381462-3.00055-0

© 2013 Elsevier Inc. All rights reserved.

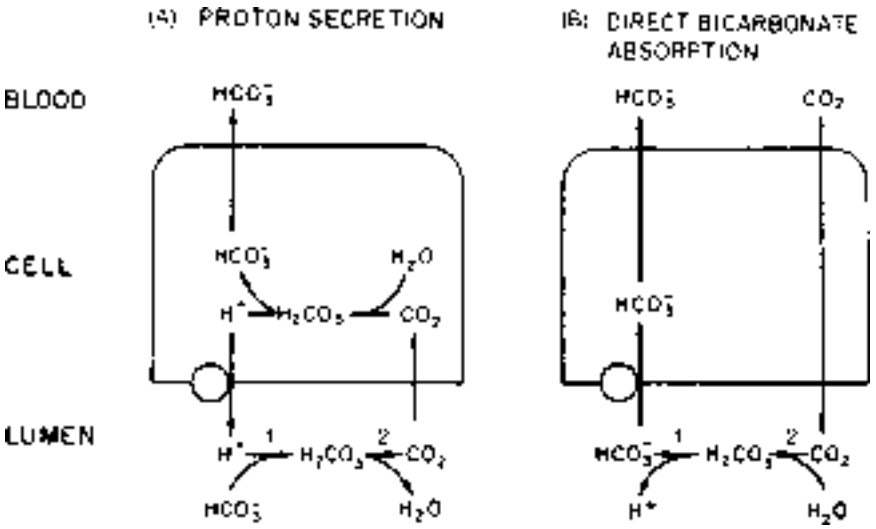

FIGURE 55.1 Mechanisms of luminal acidification: A, proton secretion, or B, direct HCO_3 absorption. *(In: Brenner BM, Seldin DW, eds, The Kidney. Philadelphia: W.B. Saunders, 1994:408–471, with permission.)*

concentrations of H, HCO_3 and CO_2 will be those predicted for equilibrium. But, if carbonic anhydrase is absent from the luminal fluid and H secretion is the mechanism by which the tubular fluid is acidified (Figure 55.1a), reactions 1 and 2 will move to the right, but the H_2CO_3 concentration will be greater than that predicted for equilibrium with CO_2, and H and HCO_3 concentrations, while in equilibrium with H_2CO_3, will also be greater than that predicted for equilibrium with CO_2. Conversely, if luminal carbonic anhydrase is absent and HCO_3 absorption is the mechanism by which the tubular fluid is acidified (Figure 55.1b), luminal H_2CO_3, H, and HCO_3 concentrations will all be lower than that predicted for equilibrium with CO_2.

Using slightly different approaches, three groups of investigators have examined this issue.[6–8] All found that under baseline conditions the system is in equilibrium and measured *in situ* pH (H ion concentration) is equal to the predicted equilibrium pH. However, after systemic infusion of a carbonic anhydrase inhibitor luminal pH drops below that predicted for equilibrium (an acid disequilibrium pH), demonstrating secretion of H (Figure 55.1a).

These results provide two extremely important conclusions. First, they demonstrate that the mechanism(s) responsible for luminal fluid acidification involve H secretion rather than HCO_3 absorption across the proximal tubule apical membrane. This conclusion has been confirmed by numerous studies (see below) that have directly identified H rather than HCO_3 transport mechanisms on the apical membrane. The second conclusion of equal importance is that the luminal fluid is normally exposed to carbonic anhydrase. This luminal carbonic anhydrase allows secreted H ions to be buffered quickly, preventing an acid disequilibrium pH that would oppose continued H secretion. This latter point is discussed further below.

Mechanisms of Apical Membrane H/HCO_3 Transport

The discussion below first describes the mechanisms that mediate apical membrane H secretion and then discusses possible backleak mechanisms. The description of the H secretory mechanisms is oriented along lines of coupling to metabolism. The term *primary active transport* describes transport mechanisms directly coupled to the consumption of metabolic energy (ATP), such as the H-ATPase. *Secondary active transport* refers to a transporter that couples the transport of H to that of a second ion, for which a favorable driving force is established by another transporter that is directly coupled to energy consumption. An example of secondary active transport is Na/H exchange. *Tertiary active transport* refers to the presence of three transporters functioning in series, where the first transporter is directly coupled to energy utilization and establishes a favorable electrochemical gradient for molecular species *A*. A second transporter is a coupled transporter that uses the electrochemical gradient for species *A* to establish a favorable electrochemical gradient for species *B*, and the third transporter then uses the electrochemical gradient for species *B* to transport acid or base (species *C*) against its electrochemical gradient. There is now good evidence that all of these mechanisms are present in the proximal tubule. The primary and secondary transport mechanisms play key roles in net acid secretion, while the tertiary transport mechanisms most likely contribute significantly to NaCl reabsorption, and play a minimal role in net acid secretion.

Primary Active Transport: H-ATPase

Five lines of evidence suggest the presence of an apical membrane H translocating ATPase. These include the demonstration of: (1) an H translocating ATPase in apical membrane vesicle preparations, (2) a role of an H-ATPase in the defense of cell pH against an acid load, (3) electrogenic H secretion in the microperfused proximal tubule, (4) apical membrane immunohistochemical labeling with antibodies against purified vacuolar H-ATPase subunits, and (5) a component of HCO_3 absorption that cannot be attributed to secondary or tertiary active H secretion.

Kinne-Saffrin and Kinne were the first to demonstrate the presence of HCO_3-stimulated H-ATPase activity and ATP-dependent H translocation in brush border membrane vesicles.[9–11] This H translocating ATPase is not of mitochondrial origin as it was insensitive to oligomycin.

In the rat proximal tubule microperfused *in vivo* symmetrically with Na-free solutions, Yoshitomi et al. found that cell pH decreases and then returns to control levels.[12] Similarly, Alpern found that rat proximal tubules perfused symmetrically with Na-free solutions develop an alkaline cell pH in the steady state.[1] Both of these observations are best explained by the presence of a Na-independent alkalinizing mechanism in these cells. Kurtz more specifically examined this phenomenon in the S3 proximal tubule perfused *in vitro* utilizing the fluorescent measurement of cell pH.[13] Following an acute intracellular acid load (NH_3/NH_4^+ prepulse), cell pH is rapidly defended in the complete absence of Na. This cell alkalinization is inhibited by luminal dicyclohexylcarbodiimide (DCCD) and N-ethylmaleimide (NEM), two inhibitors of vacuolar H-ATPases. Nakhoul et al. demonstrated that S3 proximal tubules, acidified by removal of luminal and peritubular Na, returned their cell pH to values more alkaline than control cell pH.[14] In these studies, the cell alkalinization was not inhibited by DCCD. All of these studies demonstrate the ability of the proximal tubule cell to transport protons out in response to cell acidification in the complete absence of extracellular Na. Based on our current knowledge of transporters capable of active H efflux from cells, the only Na-independent mechanism that has been identified is the H-ATPase. However, the lack of specificity of the inhibitors, DCCD and NEM, precludes a definitive interpretation from the above studies.

A third line of evidence suggesting the presence of an apical membrane H-ATPase is the demonstration of electrogenic H secretion. Fromter and Gessner first reported that when luminal and peritubular capillaries of rat proximal convoluted tubules are perfused at fast rates with bicarbonate Ringer's solutions (containing no organic components), transepithelial voltage is +1 mV in the early proximal tubule and +0.2 mV in the late proximal tubule.[15] This lumen positive voltage is not affected by ouabain but is inhibited by acetazolamide, a carbonic anhydrase inhibitor.[16] These results demonstrate electrogenic H secretion. While they are consistent with an apical membrane electrogenic H transporting mechanism, they are also consistent with a basolateral membrane electrogenic H/HCO_3 transport mechanism in series with any apical membrane conductance that need not mediate H transport.

Perhaps the best evidence for an apical membrane H-ATPase is the demonstration of the labeling of the apical membrane with antibodies against the purified vacuolar H-ATPase.[17,18] High resolution immunogold labeling demonstrated that the H-ATPase is located at the neck of the apical invaginations between the clathrin-coated domains and the microvilli.[17,19]

Lastly, as will be discussed below (see "Role of Apical Membrane H/HCO_3 Transport Mechanisms in Transepithelial H Secretion"), there is good evidence that a component of proximal tubule HCO_3 absorption exists that is not attributable to secondary or tertiary active transport mechanisms.[20–22]

Based on all of the above, there is strong evidence for the existence of a proximal tubule apical membrane H translocating ATPase of the vacuolar type that contributes to luminal acidification. Its molecular composition was reviewed, this will be described in greater detail later in this Chapter under the "Distal Nephron," and its role in proximal tubule function will be discussed below.[19,23–25]

Secondary Active Transport: Na/H Exchange

The apical membrane Na/H antiporter mediates most of $NaHCO_3$ absorption and all of transcellular NaCl absorption in the proximal tubule.[22,26] Na/H antiporters represent a form of secondary active transport in that they are not directly coupled to metabolism, but rather use the low cell Na concentration established by the ouabain-sensitive basolateral membrane Na,K-ATPase to drive the 'uphill' extrusion of protons. Na/H antiporters are inhibited by amiloride and more potently by amiloride analogs with hydrophobic substitutions at the 5-amino nitrogen atom.[27] Three pieces of evidence are consistent with a Na/H antiporter on the proximal tubule apical membrane.

Murer, Hopfer and Kinne were the first to demonstrate that apical membrane vesicles prepared from rat renal cortex possess Na/H antiporter activity.[28] The antiporter acidifies the external medium in response to an inwardly directed Na gradient, and an outwardly

directed H gradient drives ^{22}Na uptake. The Na/H antiporter is coupled in a 1:1 manner such that transport is electroneutral. Similar results were reported by Warnock et al. and by Kinsella and Aronson.[29,30]

Subsequent studies in vesicles demonstrated that the apical membrane Na/H antiporter displays saturation kinetics with respect to external Na with a K_{Na} of approximately 5–15 mEq/l at pH 7.5.[29,30] External protons compete with external Na for a single site such that increases in external H concentration decrease the apparent affinity for Na, the K_H is 35 nM.[31] The Na/H antiporter is inhibited by amiloride and lithium. Kinsella and Aronson showed that lithium and amiloride compete with Na at the external site and Ives et al. showed that the inhibition by lithium and amiloride involves both competitive and noncompetitive interactions.[32,33,34] As will be discussed below, the Na/H antiporter is exquisitely sensitive to the H concentration on the inside (cytoplasmic side) of the vesicle.[35]

An apical membrane Na/H antiporter has also been demonstrated in the intact tubule by measuring the effect of luminal Na on cell pH. Boron and Boulpaep measured cell pH using a pH-sensitive microelectrode in the *in vitro* perfused salamander proximal tubule and found that following an acid load cell pH recovery is accelerated in the presence of luminal Na, an effect that is blocked by luminal amiloride.[36] Sasaki et al. measured cell pH in the *in vitro* perfused rabbit proximal straight tubule using a pH sensitive microelectrode and showed that luminal Na removal and readdition causes cells to acidify and realkalinize, respectively.[4] Alpern and Chambers measured cell pH in the *in vivo* perfused rat proximal convoluted tubule microfluorimetrically and found similarly that luminal Na removal causes cell acidification and Na readdition causes cell alkalinization.[37] In the studies of Sasaki et al. and Alpern and Chambers, the cell pH change was blocked by amiloride and by amiloride analogs.[37,4]

The last line of evidence supporting the existence of an apical membrane Na/H antiporter is the demonstration of the dependence of HCO_3 absorption on Na transport. In the *in vivo* microperfused rat proximal convoluted tubule and the *in vitro* microperfused rabbit proximal convoluted tubule and proximal straight tubule, HCO_3 absorption is almost entirely inhibited by removal of Na from luminal and peritubular fluids or inhibition of the Na,K-ATPase.[20,38–41] As will be discussed below, these results suggest a role for the Na/H antiporter in HCO_3 absorption, but are complicated by other possible interpretations. A more convincing result is inhibition of HCO_3 absorption by addition of amiloride to the luminal fluid.[20–22]

In summary, the above studies provide strong evidence for an apical membrane amiloride-sensitive, electroneutral Na/H antiporter in the proximal tubule.

Sardet et al. was the first to clone a complementary DNA (cDNA) for a human amiloride-sensitive Na/H antiporter.[42] Based on the sequence, the Na/H antiporter is predicted to be a 99 kDa protein with an amino terminal domain, 10–12 transmembrane spanning regions, and a carboxy terminal hydrophilic region representing a large cytoplasmic tail. Three putative N-linked glycosylation sites (aa 75, 370, and 410) have been identified and the C-terminus possesses several potential phosphorylation sites. The isoform encoded by this cDNA is now referred to as NHE1.

Subsequent studies from multiple labs have identified at least 8 other isoforms, with 3 isoforms (NHEs 1, 3, and 8) expressed in the proximal tubule.[43–46] NHE1 is ubiquitously expressed with few exceptions, and is probably the most important isoform for cell pH and volume defense, cell growth, migration, adhesion, and other 'housekeeping' functions. In the proximal tubule cell, NHE1 is expressed on the basolateral membrane. Haggarty et al. demonstrated that the apical membrane Na/H antiporter of LLC-PK_1 cells (proximal tubule cell line) has an IC_{50} of 13 μM for EIPA (ethylisopropylamiloride) (classified as amiloride-resistant), whereas the basolateral membrane Na/H antiporter has an IC_{50} of 44 nM (amiloride sensitive).[47] The inhibitor sensitivity of the LLC-PK_1 apical membrane transporter is similar to that found in apical membrane vesicles prepared from renal cortex, while the inhibitor sensitivity of the basolateral membrane Na/H antiporter is similar to that of the "housekeeping" isoform.[48–50]

Substantial evidence suggests that NHE3 is the apical membrane Na/H antiporter of the proximal tubule. (1) Immunohistochemical studies have localized NHE3 to the apical membrane of the proximal tubule and thick ascending limb (Figure 55.2).[51,52] (2) NHE3 mRNA is highly expressed in kidney cortex.[53,54] (3) NHE3 is inhibited by amiloride, amiloride analogs, and HOE694, with sensitivities similar to that of the apical membrane Na/H antiporter.[48,49,55](4) In cultured cells and in intact animals, regulation of NHE3 protein and mRNA abundances by glucocorticoids, thyroid hormone, and acidosis parallels regulation of the proximal tubule Na/H antiporter.[56–61] (5) In cultured cells regulation of NHE3 activity (defined as EIPA resistant activity) parallels regulation of the proximal tubule apical membrane Na/H antiporter in that both are stimulated by angiotensin II and endothelin,[62,63] and both are inhibited by parathyroid hormone and protein kinase A.[64] (6) Lastly, mice in which the NHE3 gene has been knocked out develop a mild metabolic

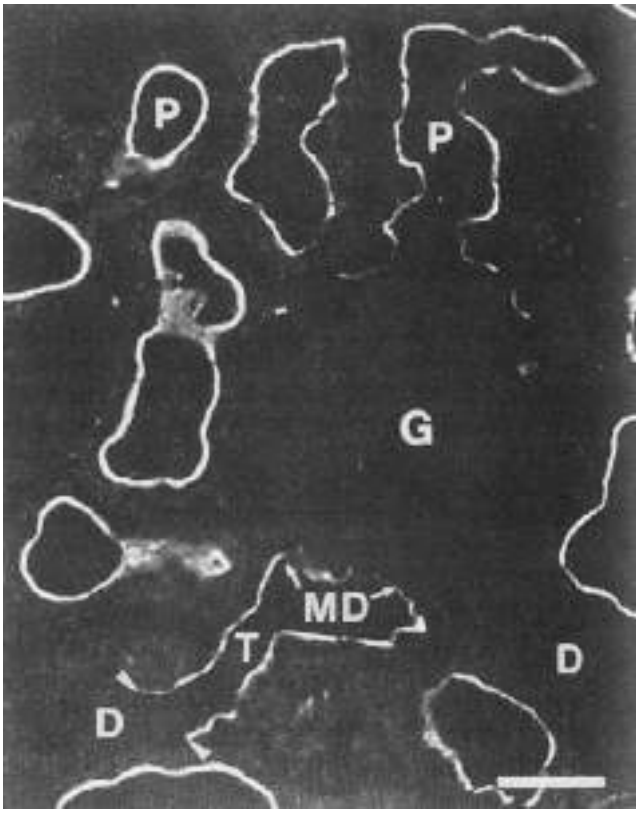

FIGURE 55.2 Immunohistochemical localization of NHE3 in rat kidney cortex. NHE3 is expressed on the apical membrane of the proximal tubule (*P*) and thick ascending limb (*T*), but is not expressed in the distal convoluted tubule (*D*) or glomerulus (*G*). *(From Amemiya M, Loffing J, Lotscher M, Kaissling B, Alpern RJ, Moe OW. Expression of NHE-3 in the apical membrane of rat renal proximal tubule and thick ascending limb. Kidney Int 1995,48:1206-1215, with permission.)*

acidosis and proximal tubule HCO_3 absorption is inhibited by 61%.[65,66]

In NHE3 null mice, about 60% of the remaining HCO_3 absorption is inhibited by bafilomycin, a vacuolar H-ATPase inhibitor, demonstrating a significant role for the H pump in mediating NHE3-independent HCO_3 absorption.[66] The mechanism of H secretion mediation of the remaining 40% of HCO_3 absorption remains controversial. A small EIPA-sensitive component of HCO_3 absorption was observed by some, but not all labs, in mice null for both NHE2 and NHE3, suggesting expression of another Na/H antiporter isoform.[67,66] In support of expression of another NHE isoform, Aronson's group demonstrated expression of an invertebrate NHE isoform (NHE8) in the proximal tubule and localized expression to the apical membrane by *in situ* hybridization, immunoblotting, and immunofluorescence microscopy.[68,69] Apical membrane NHE8 is highly expressed in neonates, likely accounting for much of the NHE activity when apical membrane NHE3 protein expression is scant at this age.[70,71] In both neonatal mice and rats, acid feeding-induced increases in NHE activity are prevented by a dose of EIPA that inhibits NHE8, but not NHE3 activity, and both NHE3 and NHE8 apical membrane protein abundances are increased.[72] With maturation apical membrane expression switches from predominately NHE8 to NHE3 expression, but total cortical NHE8 expression is higher than in the neonatal proximal tubule, suggesting that NHE8 may serve predominantly as an intracellular organelle exchanger in adults.[71] Regulation of this maturational switch appears to be under endocrine control, with both thyroid hormone and glucorticoids being responsible.[71,73,74] However, studies in senile rats provide support for NHE8 contributing to apical membrane Na/H exchange even in the adult by the finding that age-related decreases in proximal acidification occur without changes in NHE3 or H-ATPase expression, but with decreased abundance of both NHE8 mRNA and protein.[75]

Molecular biological studies have provided some characterization of NHE3. The protein has 12 transmembrane domains and a large cytoplasmic C-terminal domain. Transmembrane domain IV is implicated in ion transport, with amiloride inhibition mediated by transmembrane domain IX, and regulation of transporter activity mediated by the C-terminal tail.[76] In the C-terminal tail are binding domains or phosphorylation sites for NHERF [required for cAMP inhibition of NHE3 through EPAC (exchange protein directly activated by cAMP)-dependent and PKA-dependent mechanisms), CHP [(calcineurin homologous protein) involved in ezrin-dependent increases in NHE3 abundance and constitutive function], casein kinase 2 (involved in exocytic and delivery of newly synthesized protein to the membrane surface), PKA phosphorylation sites (which when phosphorylated by PKA do not alter NHE3 activity).[77–81] In addition there is evidence for novel phosphorylation sites that when dephosphorylated by a calyculin A-sensitive phosphatase (likely PP1) stimulate NHE3 activity. It is likely that these sites are functionally significant, but their effect masked by the net contribution of other known phosphorylation sites.

Tertiary Active H Transport

Aronson was the first to propose that active H extrusion could be mediated by tertiary active transport.[82] Siebens and Boron first demonstrated such a process in the Ambystoma proximal tubule perfused *in vitro*.[83] This segment, which contains a basolateral membrane Na,K-ATPase, possesses an apical membrane Na/lactate cotransporter and a basolateral membrane lactate/hydroxyl exchanger (or equivalently an H/lactate

cotransporter). These transporters working in series could effect the active extrusion of protons, but the proton extrusion would be across the basolateral membrane.

Nakhoul and Boron found evidence for such a system in the S3 segment of the rabbit proximal tubule.[14,84] This segment, which contains a basolateral membrane Na,K-ATPase, possesses an apical membrane Na/acetate cotransporter, and pathways for acetic acid movement (equivalent to H/acetate cotransport or acetate/OH countertransport) on the apical and basolateral membranes. The acetic acid pathways may merely represent nonionic diffusion across the lipid bilayer rather than a specific transporter. With this model, the Na,K-ATPase establishes a low cell Na concentration that provides a driving force for the Na/acetate cotransporter, mediating acetate uptake across the apical membrane. The high cell acetate concentration can then drive protons (equivalently as acetic acid nonionic diffusion, H/acetate cotransport, or acetate/OH countertransport) out across the apical or basolateral membrane.

Nakhoul et al. showed that this system participates in the defense of cell pH against an acid load. The role of this system on transepithelial H secretion or transepithelial acetate transport depends on whether the "acetic acid" exits across the apical or basolateral membrane. The contribution of tertiary active transport systems to transepithelial H secretion was addressed by Geibel et al. who demonstrated that in tubules incubated in the absence of CO_2/HCO_3, acetate stimulates transepithelial H secretion, but in tubules perfused in the presence of CO_2/HCO_3, acetate addition inhibits rates of transepithelial H secretion.[85] These data suggest that the acetate tertiary active system does not contribute significantly to transepithelial H secretion under physiologic conditions.

Chloride/Base Exchange

The previous sections have discussed mechanisms responsible for active H extrusion. The proximal tubule also possesses a number of pathways that lead to the net backleak of acid from the lumen into the cell across the apical membrane. These transporters are chloride-dependent and exchange chloride (moving from lumen to cell) for another anion, such as OH, HCO_3, formate, or oxalate (moving from cell to lumen, equivalent to a backleak of acid).[43] Evidence for such transport on the apical membrane has come from several studies.

Lucci and Warnock were the first to suggest the presence of apical membrane anion exchange.[86] In *in vivo* microperfused rat proximal tubule, NaCl absorption is inhibited by luminal addition of disulfonic stilbenes or high doses of furosemide (10^{-3} M), agents that inhibit the red cell Cl/HCO_3 exchanger. Baum also found in the *in vitro* perfused rabbit proximal convoluted tubule that luminal addition of disulfonic stilbenes inhibits Cl absorption.[87]

Using apical membrane vesicles isolated from rabbit renal cortex, Warnock and Yee demonstrated that a pH gradient (inside pH greater than outside pH) drives ^{36}Cl uptake into vesicles.[88] Shiuan and Weinstein found similar results.[89] Both groups found that pH gradients drive Cl uptake even in the presence of a voltage clamp, suggesting direct chemical coupling of Cl and base transport. Burnham et al. found similar results measuring the effect of Cl gradients on proton transport measured by acridine orange.[90] Chen et al. demonstrated Cl/OH exchange using a Cl-sensitive fluorescent dye to measure Cl transport.[91] On the other hand, Seifter et al. showed that when apical membrane vesicles are voltage clamped, pH gradients do not drive Cl uptake.[92] Other investigators have also been unable to demonstrate Cl driven H transport using acridine orange.[93,94] The reason for this discrepancy is not clear, but is most likely due to the low level of Cl/OH exchanger activity. Even those investigators who demonstrated Cl/OH exchanger activity found that it is far less than Na/H antiporter activity. Cl/OH exchange in vesicles is inhibited by disulfonic stilbenes.[89,91]

Karnisky and Aronson showed that formate gradients are able to drive the countertransport of Cl, and Cl gradients are able to drive the countertransport of formate in rabbit renal apical membrane vesicles.[95,96] The rate of this transporter is far greater than that found by other investigators for Cl/OH exchange. Similar evidence was found for a Cl/oxalate exchanger.[95] Based on this they proposed that the physiologically relevant Cl/base exchangers were Cl/formate and Cl/oxalate exchangers.

Measuring cell pH microfluorimetrically in the *in vivo* perfused rat proximal convoluted tubule, Alpern showed that if basolateral cell pH defense mechanisms are inhibited, changes in luminal Cl concentration affect cell pH in a manner consistent with Cl/base exchange.[97] If 1 mM formate is added to luminal and peritubular solutions, the effect of Cl removal and addition increases 3-fold and all effects of luminal Cl substitution are blocked by addition of DIDS to the luminal fluid. Similar results were found by Baum in the *in vitro* perfused rabbit proximal convoluted tubule.[98] Thus, these studies demonstrate Cl/base exchange, and confirm the vesicle results, namely Cl/OH and Cl/formate exchange with Cl/formate exchange activity being greater than Cl/OH exchange activity.

Further support for these anion exchangers is derived from volume flux measurements. The addition of formate or Cl to the luminal fluid increases the

proximal tubule volume and Cl absorption.[99,100] This increase is inhibited by DIDS, an anion exchange inhibitor, suggesting that NaCl absorption is mediated by parallel Na/H and Cl/base exchangers with the H and base recycling. Support for this model comes from the observation that amiloride inhibits Cl absorption in the absence of added formate or oxalate, and that EIPA inhibits the formate-induced stimulation of Cl absorption.[26,87,99] The demonstration that oxalate-dependent Cl transport is not EIPA-sensitive, but is sulfate-dependent, while formate-dependent Cl transport is sulfate-independent, but EIPA-sensitive has lead to a proximal tubule model in which formate-stimulated NaCl absorption is dependent on Na/H exchange, while oxylate-stimulated NaCl absorption is dependent on Na-sulfate cotransport in parallel with sulfate-oxalate exchange.[99,101,102] In the case of formate and OH, stimulation of anion exchange not only increases the rate of NaCl absorption, but inhibits the rate of luminal acidification.

The quantitative role of Cl/base exchangers in proximal tubule/base exchangers in proximal tubule luminal acidification is unclear, but likely to be small. Three studies have been unable to demonstrate an effect of luminal and peritubular Cl removal on net HCO_3 absorption, while one lab found that luminal DIDS stimulates net HCO_3 absorption.[38,40,87,103] Thus, in summary, the Cl/formate, Cl/OH, and Cl/oxalate exchangers appear to function in parallel with Na-dependent transport mechanism to mediate net NaCl absorption from the lumen to cell.[26,87,99,101,102] In circumstances where Na/H exchange is coupled to "base" secretion, net H secretion is reduced. The role of the Cl/base exchangers in proximal tubule function is discussed in more detail in Chapter 33: "Sodium and Chloride Transport: Proximal Nephron."

H Leak

An H leak pathway in the apical membrane, especially in the late proximal tubule, would provide an additional backleak pathway for secreted acid. Reenstra et al. showed that brush border membranes possess a significant H/OH permeability.[104] Ives measured internal buffer capacity of vesicles and was able to calculate an H permeability that is not inhibited by amiloride or DCCD and, thus, is not due to proton movement across the Na/H antiporter or the H-ATPase.[105]

Preisig and Alpern measured apical membrane proton permeability by examining the rate of change of cell pH in response to a rapid luminal pH change.[106] Apical membrane Na- and Cl-coupled transporters were inhibited by perfusing tubules in the absence of luminal and peritubular Na and Cl and rates of change in cell pH were converted to fluxes by measuring buffer capacity. These studies demonstrated an apical membrane proton permeability of 0.52 cm/sec, a value that is in close agreement with that calculated by Ives from vesicle studies when corrected for the surface area of the brush border membrane.[105]

Role of Apical Membrane H/HCO_3 Transport Mechanisms in Transepithelial H Secretion

As shown in Figure 55.3, the proximal tubule apical membrane possesses an H-ATPase, a Na/H antiporter and tertiary active transport mechanisms all capable of effecting active acid extrusion. In addition, possible apical membrane net proton backleak pathways include the Cl/HCO_3, Cl/OH, and Cl/formate exchangers as well as proton diffusion across the membrane. As discussed above, the Cl/base exchangers and tertiary active transport mechanisms probably play a very small, if any, role in proximal tubule acidification, and thus, won't be discussed further.

Using the apical membrane H permeability (see above), Preisig and Alpern calculated that a passive H leak from lumen to cell would be of minor quantitative importance in the early proximal tubule where the luminal pH is close to 7.4 (and cell pH ~7.3). However, in the late proximal tubule with a luminal pH of ~6.8, 1/3 of secreted protons could leak back across the apical membrane.[106]

The role of the Na/H antiporter in mediating transepithelial HCO_3 absorption has been studied in a number of ways. In *in vivo* and *in vitro* perfused proximal

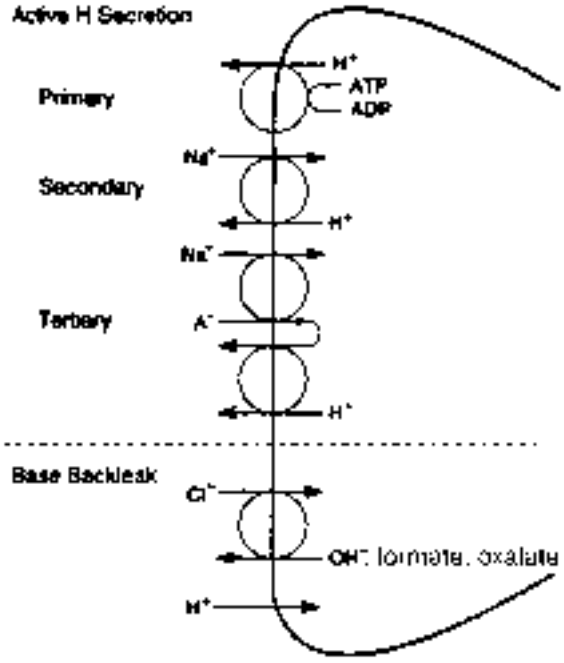

FIGURE 55.3 Apical membrane H transport mechanisms. *(From Alpern RJ. Cell mechanisms of proximal tubule acidification. Physiol Rev 1990,70:79-114, with permission.)*

tubules, either complete Na removal from luminal and peritubular fluids or inhibition of the Na,K-ATPase by peritubular ouabain or peritubular K removal inhibits most of HCO_3 absorption.[20,38–41] While these studies were initially interpreted as demonstrating that all apical membrane H secretion is Na-coupled and utilizes the lumen-to-cell Na gradient established by the Na,K-ATPase, they are equally consistent with a Na-coupled, electrogenic mechanism mediating HCO_3 efflux on the basolateral membrane working in series with a Na-independent H secretory mechanism on the apical membrane, which was demonstrated to be the situation (see below). However, inhibition of the Na,K-ATPase leads to cell depolarization, which inhibits the electrogenic Na/HCO_3 cotransporter on the basolateral membrane, as shown in studies in which inhibition of the Na,K-ATPase in the bullfrog proximal tubule causes a cell alkalinization.[107] This observation is consistent with inhibition of base exit, and not consistent with inhibition of apical membrane Na-independent H secretion, as that would have resulted in cell acidification. Thus, while the effect of both Na removal and Na,K-ATPase inhibition on HCO_3 absorption are consistent with an important role of the Na/H antiporter in HCO_3 absorption, neither can quantify the magnitude of this contribution.

The best approach toward quantifying the contribution of the Na/H antiporter has been to examine the effect of inhibiting the apical membrane Na/H antiporter on HCO_3 absorption. Howlin et al. and Chan and Giebisch demonstrated that luminal amiloride significantly inhibits the rate of HCO_3 absorption in the *in vivo* microperfused rat proximal convoluted tubule.[20,21] However, neither group found the magnitude of inhibition to be as large as expected if the Na/H antiporter mediates all of the H secretion involved in HCO_3 absorption.

To further examine this issue, Preisig et al. looked at the effect of high concentrations of luminal amiloride and t-butyl amiloride (a more potent analog) on transepithelial HCO_3 absorption.[22] In the *in vivo* microperfused tubule, these investigators found that both agents inhibit only 45% of HCO_3 absorption. While one interpretation of this observation is that the Na/H antiporter mediates only a fraction of transepithelial HCO_3 absorption, other interpretations are that the rat Na/H antiporter is insensitive to these agents or that the inhibitor concentration is not consistent along the perfused segment. Preisig et al. then showed that when corrections are made for the measured luminal inhibitor concentration profile (amiloride and its analogs are highly lipophic and diffuse out of the lumen along the length of the perfused segment), and for the luminal [HCO_3] profile, Na/H antiporter activity, assayed as the rate of change in cell pH in response to luminal Na removal or addition, is inhibited by amiloride and t-butyl amiloride as predicted by vesicle studies. Thus, these studies concluded that an amiloride-sensitive Na/H antiporter mediates approximately 65% of transepithelial HCO_3 absorption, with the remaining 35% mediated by an amiloride-insensitive, Na-independent mechanism. This conclusion is supported by the observation that in NHE3 null mice, proximal tubule HCO_3 absorption is inhibited by 61%.[65]

The studies by Preisig et al. were performed in the absence of organic anions in the perfused lumen making it very unlikely that tertiary active transport mechanisms are responsible for the remaining 39% of HCO_3 absorption. Thus, the most likely explanation is that the H-ATPase mediates the remaining 35% of transepithelial HCO_3 absorption. Bank et al. have more directly demonstrated a role of the H-ATPase in HCO_3 absorption by showing that luminal DCCD, an inhibitor of vacuolar H-ATPases, inhibits 21% of proximal tubule HCO_3 absorption.[108]

Basolateral Membrane H/HCO_3 Transport Mechanisms

Because cell pH is above electrochemical equilibrium, basolateral membrane base efflux can occur passively.

Electrogenic $Na/3HCO_3$ Cotransport

Studies have uniformly demonstrated that the key basolateral membrane base efflux mechanism is an electrogenic $Na/3HCO_3$ cotransporter. Evidence for this rests on results that have demonstrated: (1) effects of this transporter on cell pH and cell voltage, (2) the presence of this transporter in basolateral membrane vesicles, and (3) the importance of this transporter in transepithelial HCO_3 absorption.

In intact tubules, initial studies examined the electrogenicity of basolateral membrane H/HCO_3 movement. It was reasoned that if cell pH and HCO_3 concentration are above electrochemical equilibrium, a simple basolateral membrane $H/OH/HCO_3$ conductance could mediate base efflux and transepithelial H secretion. Burckhardt et al. provided evidence for a large basolateral membrane H/HCO_3 conductance in the *in vivo* perfused rat proximal convoluted tubule.[109] When HCO_3 concentration is rapidly decreased from 30 to 3 mEq/L, cells rapidly depolarize and then slowly repolarize. A subsequent increase in peritubular HCO_3 concentration leads to a rapid hyperpolarization followed by a slow depolarization. This basolateral membrane conductance is inhibited by acetazolamide and peritubular SITS. While initial studies had

difficulty demonstrating such a HCO_3 conductance in the *in vitro* perfused rabbit proximal convoluted and straight tubules, improvements in the perfusion technique that permit sufficiently rapid fluid changes, led to confirmation of Burckhardt et al.'s finding.[110]

Further evidence for the electrogenicity of basolateral membrane HCO_3 transport in the intact tubule is the voltage sensitivity of bicarbonate movement. Alpern measured cell pH microfluorimetrically in the *in vivo* perfused rat proximal convoluted tubule and showed that increasing peritubular K concentration from 5 to 50 mEq/L (a maneuver that causes cell depolarization) causes a rapid cell alkalinization that is reversible when peritubular K concentration is reduced back to 5 mEq/L.[1] While these studies suggest the presence of a voltage-sensitive $H/OH/HCO_3$ transport mechanism on this membrane, they were also consistent with a K/HCO_3 cotransporter. To examine this possibility, the studies were repeated in the presence of 2 mM peritubular barium. Barium inhibits the basolateral membrane K conductance, preventing changes in peritubular K concentration from affecting cell voltage.[2,111] In addition, by inhibiting the K conductance, barium itself leads to a cell depolarization.[2,111] Barium addition causes cell alkalinization, and prevents any subsequent effect of changing peritubular K concentration on cell pH.[1] These results are consistent with the presence of a voltage-sensitive $H/OH/HCO_3$ transport mechanism in the proximal tubule cell. While these studies did not specifically address which membrane the transport mechanism is on, the studies by Burckhardt et al. demonstrated a HCO_3 conductance on the basolateral, but not on the apical membrane.

While initially it was felt that Burckhardt et al.'s studies represent a simple HCO_3 conductance on the basolateral membrane, Boron and Boulpaep suggested a more complex transport mechanism.[112] These investigators used ion selective microelectrodes in the *in vitro* perfused salamander proximal tubule and found that lowering the peritubular HCO_3 concentration causes a rapid cell depolarization, indicative of a HCO_3 conductance. However, peritubular acidification also led to cell acidification and a decrease in intracellular Na activity, and lowering peritubular Na concentration causes cell depolarization, cell acidification, and a decrease in cell Na activity. The cell depolarization in response to lowering peritubular Na concentration is in the wrong direction for a Na conductance and is more suggestive of a Na-coupled anion current. In further studies these investigators found that all of the above changes occur in the absence of Cl and are blocked by SITS. Considered together these studies provided the evidence suggesting a directly coupled Na/HCO_3 cotransport mechanism that transports more HCO_3 than Na ions and, thus, is electrogenic.

The first suggestion that such a transport mechanism exists in the mammalian nephron was made by Biagi and Sohtell, who measured cell voltage in the *in vitro* perfused proximal convoluted tubule and proximal straight tubule.[110,113] These investigators found that lowering peritubular HCO_3 or Na concentration leads to a spike depolarization that is blocked by SITS. Once again, the cell depolarization occurring in response to lowering peritubular Na concentration is in the wrong direction for a simple Na conductance.

Subsequent studies performed by Alpern and Yoshitomi et al. measured cell pH in the *in vivo* perfused rat proximal tubule and confirmed the existence of an electrogenic Na/HCO_3 cotransporter.[1,12] Alpern found that decreasing peritubular pH causes cell acidification. Additionally, lowering peritubular Na concentration from 147 to 25 mEq/L (replacing Na with either choline or tetramethylammonium) causes cell pH to decrease by 0.2 pH units, an effect that persists in the complete absence of Cl.[114]

The above studies are consistent with three possible mechanisms of coupling between Na and HCO_3: parallel Na and HCO_3 conductances, amiloride-sensitive Na/H antiport, or SITS-sensitive Na/HCO_3 cotransport. To determine if the results are attributable to parallel Na and HCO_3 conductances, Alpern examined the Na-dependence of basolateral membrane H/HCO_3 permeability.[1] If the HCO_3 conductance were Na-independent, complete Na removal should have no effect on basolateral membrane H/HCO_3 permeability. The results showed that complete removal of Na from luminal and peritubular fluid inhibits basolateral membrane H/HCO_3 permeability by greater than 90%, demonstrating direct coupling between Na and HCO_3. In subsequent studies, SITS, but not amiloride blocked the effect of peritubular Na on cell pH. Lastly, Alpern demonstrated that the effect of cell depolarization (raising peritubular K concentrations) on cell pH was prevented if lumen and peritubular capillaries were perfused with Na-free solutions. Taken together these studies suggest a directly coupled, electrogenic Na/HCO_3 cotransport mechanism similar to that found in the salamander.

Yoshitomi et al. found similar results, measuring cell voltage, pH and Na activity using ion sensitive microelectrodes.[12] Lowering peritubular HCO_3 concentration causes a rapid cell depolarization, a decrease in cell pH, and a decrease in cell Na activity. Decreasing peritubular Na concentration also causes a rapid cell depolarization and a decrease in cell pH. SITS inhibits the effects of both lowering peritubular pH and peritubular Na concentration. Lastly, luminal and peritubular Na removal inhibits the effect of changing peritubular HCO_3 concentration on cell voltage and cell pH. In subsequent studies, Sasaki et al., and

Lopes et al. found similar results in the rabbit proximal straight tubule and the Necturus proximal tubule, respectively.[115,116] Thus, all of these studies consistently demonstrate an electrogenic, SITS-sensitive Na/HCO_3 cotransport mechanism on the proximal tubule basolateral membrane.

This question has also been addressed in basolateral membrane vesicles.[117,118] Akiba et al. found that addition of HCO_3 to the extravesicular fluid increases the rate of ^{22}Na uptake.[117] SITS has no effect on ^{22}Na uptake in the absence of HCO_3, but inhibits the HCO_3-dependent increment. Addition of valinomycin (a K ionophore) in the presence of an inwardly directed K gradient causes an internal positive voltage. This maneuver has no effect on ^{22}Na uptake in the absence of HCO_3, but accelerates the uptake in the presence of HCO_3, an effect that is in the wrong direction for a Na conductance.

Grassl and Aronson demonstrated in rabbit cortical basolateral membrane vesicles that pH gradients drive ^{22}Na uptake.[118] Whereas the effect is small in the absence of exogenous CO_2/HCO_3, it is large in its presence. In addition, a valinomycin-generated positive interior voltage drives ^{22}Na uptake, but only in the presence of HCO_3. Lastly, using acridine orange to measure H transport, Grassl and Aronson found that Na gradients ($[Na]_{in} > [Na]_{out}$) drives HCO_3 out of vesicles leading to acidification of the intravesicular space. ^{22}Na uptake is blocked in a dose-dependent fashion by DIDS and is unaffected by amiloride. In the studies of Akiba et al. and Grassl and Aronson, Cl was absent from all fluids.[117,118] Thus, these studies demonstrate the presence of an electrogenic, stilbene sensitive, Na-coupled HCO_3 transport mechanism. Grassl et al. found similar results in rat cortical basolateral membranes.[119]

Stoichiometry: Based on the electrogenicity demonstrated above, it was concluded that the basolateral membrane Na-dependent HCO_3 transporter carries a greater number of HCO_3 than Na ions. If the free energy for HCO_3 efflux is calculated, it can be predicted that a $Na/2HCO_3$ co-transporter will not be able to function in the HCO_3 efflux mode, unless directly coupled to energy.[120,121] Thus, it was predicted that the stoichiometry is a minimum of 3 HCO_3:1 Na. Yoshitomi et al. directly examined this question by comparing the SITS-sensitive voltage response to a 10-fold reduction in peritubular HCO_3 concentration with the response to a 10-fold reduction in peritubular Na concentration, and found the former to be 2.95-fold greater.[12] They also demonstrated that a reduction in peritubular HCO_3 concentration causes a 3.1-fold greater HCO_3 than Na flux out of the cell. Thus, both studies suggest a stoichiometry of 3 HCO_3:1 Na.

A 3:1 stoichiometry was confirmed by Soleimani et al. in basolateral membrane vesicles by demonstrating that in the presence of valinomycin (to increase K permeability) the HCO_3 and K concentration gradients required for no net Na movement yield a stoichiometry of 1 Na:3 HCO_3:2 negative charges.[122]

Base species transported: Thus far in the discussion this basolateral membrane transporter has been described as a Na/HCO_3 cotransport mechanism, based on a strong transporter dependence on the presence of HCO_3.[117,118] Krapf et al. examined the dependence of the transporter on exogenous CO_2/HCO_3 in the *in vitro* perfused rabbit proximal convoluted tubule utilizing the fluorescent measurement of cell pH.[123] These investigators found that in the absence of exogenous CO_2/HCO_3, the transporter functions at 1/3 of its control rate. While these results could be interpreted as suggesting that the transporter is able to run in the absence of CO_2/HCO_3, it is also possible that metabolism was producing sufficient CO_2 and HCO_3 to run the transporter at a slow rate. In agreement with this latter interpretation, the transporter flux measured in the absence of exogenous CO_2/HCO_3 is completely inhibited by acetazolamide, a carbonic anhydrase inhibitor, or by cyanide, a metabolic inhibitor. There should be no requirement for carbonic anhydrase if the transporter carries H or OH. In addition, the transporter is unaffected by cyanide when studied in the presence of exogenous CO_2/HCO_3. Thus, these results agree with the vesicle studies and suggest that the transporter has an absolute dependence on HCO_3.

Soleimani and Aronson performed further studies that suggest that carbonate (CO_3^{2-}) is also a substrate.[122] They found that with a constant extravesicular HCO_3 concentration, increasing carbonate concentration increases ^{22}Na uptake into basolateral membrane vesicles. Sulfite, a structural analog of carbonate, also stimulates ^{22}Na uptake in the presence of CO_2/HCO_3, but not in the absence of CO_2/HCO_3, an effect that is blocked by the disulfonic stilbene, DNDS. Lastly, using an equilibrium approach similar to that described above, a stoichiometry of 1 Na:1 sulfite:1 HCO_3 was derived, with carbonate and sulfite competing for a similar site. The last issue addressed in these studies was whether three separate binding sites exist or whether Na and carbonate formed a $NaCO_3^-$ ion pair that then interacts with a single site, while HCO_3 interacts at another site. Multiple pieces of evidence are against the ion pair model. First, lithium, which is more likely to form an ion pair with carbonate than is Na, is a less effective substrate for the transporter. Secondly, oxalate and phosphate, anions that participate in ion pair formation with Na, do not interact with the transporter. Lastly, harmaline, an inhibitor of Na transporters, competes with Na on the $Na/3HCO_3$

transporter. Such an interaction would be unlikely if the transporter possessed only two transport sites with both binding negatively charged substrates. Thus, it appears that the transporter is actually a $Na/HCO_3/CO_3$ cotransporter rather than a $Na/3HCO_3$ cotransporter.

Romero et al. cloned the cDNA for the electrogenic $Na/3HCO_3$ transporter from *Ambystoma tigrium*.[124] This cDNA, referred to as NBC1 (*N*a *B*icarbonate *C*otransporter *e*lectrogenic *1*) encodes a 1035 amino acid protein, the same size as and ~80% identical to the human and rat sequence.[125,126] The human and rat mRNAs are larger than the amphibian kidney mRNA, with the human and rat mRNA ~7.5 kb in length and the amphibian mRNA 4.2 kb.[125,126] The difference is due to an extensive 3-prime non-coding region in the human and rat transcript.[126]

Human NBCe1 is highly expressed in both the kidney and pancreas, the two differing only in their N-terminal sequence. The kidney transcript is expressed predominantly in the kidney, while the pancreas transcript is expressed in multiple tissues.[126] In kidney the protein localizes to the basolateral membranes of the proximal tubule.[127] More detailed reviews of HCO_3-coupled transporters have been published and the transporters are discussed in Chapter 54.[128,129]

Na/H Antiporter

Many segments along the nephron possess basolateral membrane Na/H antiporters that likely participate in housekeeping functions. Boron and Boulpaep found that the salamander proximal tubule possesses Na/H antiporters on apical and basolateral membranes.[36] Ives et al. and Sabolic and Burckhardt did not find any Na/H antiporter activity in basolateral membrane fractions from rabbit renal cortex.[130,131] While Grassl and Aronson found some pH-dependent ^{22}Na uptake in the absence of HCO_3, it is not inhibited by amiloride.[118] In the *in vivo* perfused rat proximal convoluted tubule Alpern found that the effect of basolateral Na changes on cell pH is not inhibited by amiloride and in the *in vitro* perfused rabbit proximal convoluted tubule Krapf et al. found similar results.[1,123] Kurtz found an amiloride-sensitive basolateral membrane Na/H antiporter in the S3 proximal tubule and Geibel et al. reported a basolateral membrane Na/H antiporter in S1 and S2 proximal tubule segments dissected from the most juxtamedullary portions of the nephron.[13,132] By immunohistochemistry, Biemesderfer et al. found inhomogeneous labeling of the proximal tubule basolateral membrane with anti-NHE1 antibodies.[133] Taken together these studies suggest that a Na/H antiporter may be expressed on the basolateral membrane of juxtamedullary proximal tubule, but not likely in cortical proximal tubules. More recently evidence for regulation of a basolateral membrane Na/H antiporter in the S3 segment was demonstrated by examining the effect of aldosterone on intracellular pH recovery rate. The basolateral membrane NHE1 appears to be regulated by both genomic (1h via a mineralocorticoid receptor) and non-genomic (2–15 min, likely via a glucocorticoid receptor) mechanisms. At lower concentration ranges (10^{-12} M aldosterone) intracellular [Ca] is increased and NHE1 activity is stimulated, while at higher concentrations (10^{-6} M) intracellular [Ca] decreases and NHE1 activity is inhibited.[134]

Cl/Base Exchange: Na-Dependent and Na-Independent Modes

Edelman et al. first demonstrated the presence of basolateral membrane Cl/HCO_3 exchange in Necturus proximal tubule using Cl-sensitive microelectrodes.[135] Guggino et al. confirmed these results and, in addition, found that the transporter is coupled to Na.[136] Lowering basolateral Cl concentration causes intracellular Cl activity to decrease. Removal of peritubular HCO_3 leads to an increase in cell Cl activity, while changes in peritubular pH in the absence of exogenous HCO_3 have no effect on intracellular Cl activity. When cell pH is modulated by NH_3/NH_4^+ addition and removal, cell Cl activity changes in a manner consistent with Cl/HCO_3 exchange, repeating these maneuvers in the absence of exogenous CO_2/HCO_3 causes a marked decrease in the response of intracellular Cl activity. Lowering peritubular Na concentration leads to an increase in intracellular Cl activity. In addition, cell acidification by NH_3/NH_4^+ addition and removal causes a decrease in Cl activity that is blocked if Na is simultaneously removed from the peritubular fluid. Taken together these findings suggest a $NaHCO_3/Cl$ exchange mechanism. On the basis of other studies that fail to find basolateral membrane electrogenic Cl movement, it was concluded that the transporter is a $Na(HCO_3)_2/Cl$ exchanger.[137,138] A similar transporter has been found in many invertebrate and vertebrate cells and, in these cells, is felt to be an important mechanism responsible for cell pH defense against an acid load.

Alpern and Chambers examined whether such a transport mechanism is present on the basolateral membrane of the rat proximal tubule by studying the effect of peritubular Cl on cell pH.[114] In tubules perfused in the absence of luminal and peritubular Cl, peritubular Cl addition causes cells to acidify by 0.14 pH units, an effect that is blocked by peritubular SITS. In addition, if Cl is added to the peritubular perfusate in the complete absence of luminal and

peritubular Na, cells acidify by only 0.02 pH units. These studies suggest the presence of a small amount of Na-independent and a much larger amount of Na-dependent Cl/HCO_3 exchange activity.

However, the above results are also consistent with a basolateral membrane Cl conductance functioning in parallel with the electrogenic $Na/3HCO_3$ cotransporter. Preisig and Alpern addressed this issue by examining the Cl-dependence of the basolateral membrane H/HCO_3 permeability.[139] If changes in peritubular Cl only affect cell pH by changing voltage and secondarily modifying $Na/3HCO_3$ cotransporter activity, Cl removal should not affect basolateral membrane H/HCO_3 permeability. However, complete removal of Cl from luminal and peritubular solutions leads to a 35% decrease in basolateral membrane H/HCO_3 permeability. Because complete removal of Na from luminal and peritubular fluids leads to a greater than 90% inhibition of basolateral membrane H/HCO_3 permeability, taken together these results suggest that at least 25% of H/HCO_3 permeability is mediated by a Na and Cl-coupled H/HCO_3 transporter.[1,12] The remaining fraction of H/HCO_3 permeability, which is not inhibited by Na removal, may represent a Cl/HCO_3 exchanger. Sasaki and Yoshiyama found similar results using microelectrodes to measure intracellular Cl and pH in the rabbit proximal straight tubule perfused *in vitro*.[140] Decreases in peritubular Cl concentration cause a cell alkalinization and decreases in peritubular pH lead to an increase in cell Cl activity, with both effects inhibited by peritubular SITS. Total Na removal from luminal and peritubular fluids prevents most of the effect of bath pH on cell Cl activity. And, lastly, removal of luminal and peritubular Cl slows the cell pH response to peritubular acidification by 26% and slows the cell pH response to lowering peritubular Na concentration by 19%. These results demonstrate a Na-dependent Cl/HCO_3 exchanger. Kurtz and Nakhoul et al. have reported basolateral membrane Na-independent Cl/HCO_3 exchange in the S3 segment of the rabbit proximal tubule perfused *in vitro*.[141,142]

While studies in the intact tubule seem to consistently demonstrate the presence of a Na-dependent Cl/HCO_3 exchanger, studies in basolateral membranes have been much less consistent. Grassl et al. found that a pH gradient ($pH_{in} > pH_{out}$) can drive ^{36}Cl uptake in rabbit cortical basolateral membrane vesicles.[143] In the presence of CO_2/HCO_3, a similar pH gradient leads to a 6-fold greater accumulation of ^{36}Cl. This effect is not inhibited by voltage clamping the vesicles, but is inhibited by DIDS. Grassl et al. did not find Na-dependence of HCO_3-driven ^{36}Cl uptake. In subsequent studies examining the effect of Cl and Cl gradients on HCO_3-stimulated ^{22}Na uptake, results were not consistent with a $Na(HCO_3)_2/Cl$ exchanger.[118]

In rat basolateral membrane vesicles, Grassl et al. demonstrated that symmetrical Cl addition to the inside and outside of vesicles stimulates HCO_3-dependent ^{22}Na uptake and that a Cl gradient ($Cl_{in} > Cl_{out}$) further stimulates uptake.[119] Chen and Verkman used a Cl-sensitive fluorescent dye to examine the effect of pH gradients on Cl uptake into rabbit cortical basolateral membrane vesicles.[144] These authors demonstrated that pH gradients ($pH_{in} > pH_{out}$) stimulate Cl uptake, an effect that is enhanced by the presence of CO_2/HCO_3 and inhibited by H_2DIDS. Na gradients ($Na_{in} > Na_{out}$) also stimulate Cl uptake, but only in the presence of CO_2/HCO_3.

Based on all of the above data, it appears that the basolateral membrane contains a Cl/HCO_3 exchanger that demonstrates less transporter activity in intact S1 and S2 proximal tubules compared to the S3 proximal tubule. While vesicle studies are clearly consistent with this observation, there is controversy as to the existence of Na-dependent Cl/HCO_3 exchange.

H Leak

Preisig and Alpern measured basolateral membrane H permeability, using an approach similar to that described for apical membrane H permeability.[106] The permeability, 0.67 cm/sec, was similar to that found in the apical membrane.

Role of Basolateral Membrane Transporters

Three types of experiments taken together strongly suggest that the majority of base efflux mediating transepithelial HCO_3 absorption involves the electrogenic, Cl-independent, Na/HCO_3 cotransporter on the basolateral membrane. As mentioned above, such a transporter has a stoichiometry allowing it to run passively in the base efflux direction.[12,122] First, proximal tubule HCO_3 absorption is almost entirely inhibited by removal of luminal and peritubular Na, but is unaffected by removal of luminal and peritubular Cl.[20,38–40,103] Second, and consistent with the above, most of the basolateral membrane H/HCO_3 permeability is Na-dependent and Cl-independent.[1,12,139,140] Third, in studies in which the cell is depolarized by addition of barium to the peritubular fluid, transepithelial HCO_3 absorption is inhibited, implying conductive base efflux.[103] In addition, SITS, an inhibitor of anion exchangers, including the $Na/3HCO_3$ cotransporter, inhibits transepithelial HCO_3 absorption when applied to the peritubular fluid.[145]

The effect of SITS could also implicate involvement of the Na-independent and -dependent Cl/HCO_3 exchangers, however, the observation that peritubular Cl removal does not affect HCO_3 absorption suggests

that these transporters are relatively unimportant in mediating HCO_3 reabsorption.[38,40,103] In addition, the activity of the Na-independent Cl/HCO_3 transporter is very low. And the Na-dependent Cl/HCO_3 exchanger would tend to run Na and HCO_3 into the cell and Cl out of the cell, and thus, would not contribute to transepithelial HCO_3 absorption. This transport could, however, function as a Cl efflux mechanism mediating transepithelial NaCl absorption. It could also function in the defense of cell pH, but Krapf et al. found no effect of Cl removal on cell pH defense in the proximal tubule.[146]

Lastly, while a basolateral H leak could contribute to net basolateral base efflux, Preisig and Alpern calculated that this pathway would be expected to mediate only 2% of base efflux.[106] Figure 55.4 summarizes the basolateral membrane H/HCO_3 transport pathways discussed above.

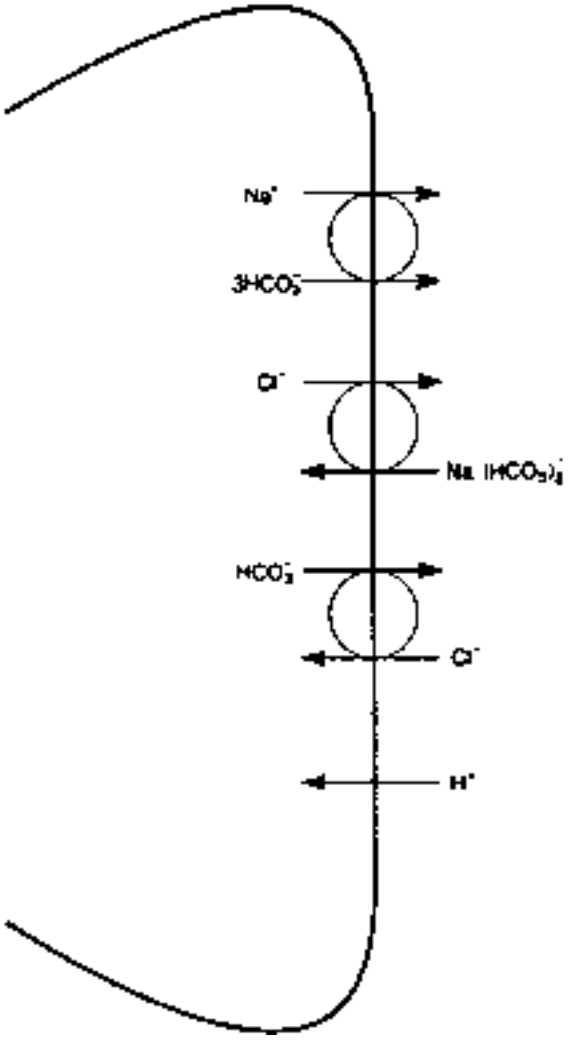

FIGURE 55.4 Basolateral membrane H/HCO_3 transport mechanisms. *(From Alpern RJ. Cell mechanisms of proximal tubule acidification. Physiol Rev 1990,70:79-114, with permission.)*

Leak Pathways

Proton secretion across the apical membrane of the proximal tubule decreases luminal pH and HCO_3 concentration to values below those found in plasma. This sets up gradients for passive back diffusion of base into the lumen. Possible diffusing species include H, OH, HCO_3, and non-HCO_3 buffers. In rabbit proximal convoluted tubules perfused with acidic solutions in the absence of CO_2/HCO_3, in either the absence or presence of luminal organic solutes, the measured transepithelial H permeability is ~ 0.31 cm/sec at 30°C.[147,148] This value agrees well with the transcellular H permeability of 0.3 cm/sec, calculated from individually measured apical and basolateral membrane H permeabilities, suggesting that the majority of transepithelial H diffusion is transcellular.[106] This conclusion is consistent with studies showing that the activation energy for H diffusion is not consistent with diffusion in aqueous solutions.[149]

HCO_3 permeability of the proximal tubule has been measured using two approaches. One approach, using diffusion potentials to measure the ratio of the HCO_3 to Cl permeability combined with a measured tracer Cl permeability, determined a HCO_3 permeability of 1.3×10^{-5} cm/sec in rabbit proximal convoluted tubules.[150] Using a similar approach in the *in vivo* microperfused rat proximal convoluted tubule a slightly higher HCO_3 permeability of 9.8×10^{-5} cm/sec was determined.[151]

A second approach was to measure the rate of net HCO_3 diffusion in response to an imposed HCO_3 gradient in the presence of acetazolamide to inhibit active H secretion and slow the rate of conversion of CO_2 to HCO_3. Although it is impossible to remove H and OH ions and, thus, to prevent their diffusion, the above reported H permeability suggests that transepithelial H/OH diffusion is minimal compared to the HCO_3 flux. Using this approach, measured HCO_3 permeabilities vary between 1.7 and 3.5×10^{-5} cm/sec in the rat proximal convoluted tubule and between 1.4 and 2.0×10^{-5} cm/sec in the rabbit proximal convoluted tubule.[152–155] Measured permeabilities are similar when measured in the lumen to peritubular or peritubular to lumen direction.

Both Schwartz and Hamm et al. found that removal of luminal organic buffers decreases the rate of passive acid efflux from an acidic luminal fluid.[147,148] These results suggest that organic acid efflux could also participate as a passive leak. However, such a flux is unlikely to be of major physiologic importance, as most

organic acids are removed from the luminal fluid early in the proximal tubule before the luminal fluid has been extensively acidified.

Using the above measured permeabilities, passive fluxes can be calculated. In the early proximal tubule these will be insignificant because luminal pH changes little. However, in the late proximal tubule, where the luminal fluid is acidified, passive leaks become more important. Alpern et al. measured a net transepithelial HCO_3 absorption rate in the presence of a late proximal tubule-like fluid of 12 pEq/mm·min.[152] Using the measured HCO_3 permeability, the calculated rate of paracellular HCO_3 backleak is 30 pEq/mm·min, leading to a calculated net transcellular H secretory flux of 42 pEq/mm·min. As discussed earlier under "Apical Membrane Mechanisms," in the late proximal tubule there is a sufficient electrochemical driving force to drive 17 pEq/mm·min of protons from lumen to cell (H "absorption"). Thus, the apical membrane must secrete 59 pEq/mm·min of H in order to effect a net transepithelial H secretory flux (equivalently a transepithelial HCO_3 reabsorptive flux) of 12 pEq/mm·min.

Role of Carbonic Anhydrase

In the proximal tubule carbonic anhydrase is localized to the apical membrane, basolateral membrane, and cytoplasm. The cytoplasmic carbonic anhydrase is type II carbonic anhydrase, while apical and basolateral membrane carbonic anhydrases are type IV. The interested reader is referred elsewhere for an in depth discussion of carbonic anhydrase localization in the proximal tubule.[156–158] In the present chapter we will review evidence establishing a role for carbonic anhydrase in transepithelial H secretion.

A number of investigators demonstrated that carbonic anhydrase plays a role in HCO_3 absorption in the proximal tubule.[159–163] As described at the beginning of the Chapter, luminal carbonic anhydrase facilitates transepithelial H secretion (and HCO_3 reabsorption) by catalyzing the dissociation of HCO_3 to CO_2 and OH, with OH neutralizing secreted H. This prevents the generation of an acid disequilibrium pH (see discussion above), which would secondarily slow the rate of apical membrane H secretory transporters.[6–8] The importance of luminal carbonic anhydrase has been best demonstrated by studying the effect of cell-impermeant luminal carbonic anhydrase inhibitors on HCO_3 absorption. In the presence of these inhibitors HCO_3 reabsorption is inhibited by 80–100%, confirming a key role for luminal carbonic anhydrase in this process.[161,162]

H secretion across the apical membrane generates OH ions within the cell that must exit across the basolateral membrane to have net transepithelial H secretion. While carbonic anhydrase inhibitors confined to the luminal fluid are able to inhibit most of HCO_3 absorption, the effect on luminal pH is different than that observed with inhibitors that can enter the cell. Inhibitors confined to the luminal fluid cause a more profound acid disequilibrium pH compared to cell permeant inhibitors.[161,162] This observation suggests that cell permeant carbonic anhydrase inhibitors block acidification at an additional step. This possible second location could be base diffusion across the cell or base efflux across the basolateral membrane.

Diffusion of H/OH across aqueous solutions is generally a limiting process because of the low H and OH concentrations. Thus, although the diffusion coefficients for H and OH are large, the fact that these entities exist in nanomolar concentrations limits the amount of diffusion. Acid and base diffusion is best accomplished when H/OH combines with buffers existing in millimolar concentrations, and allowing these buffers to then diffuse across the cell.[164,165] Thus, OH generated at the apical membrane can diffuse to the basolateral membrane by combining with CO_2 forming millimolar concentrations of HCO_3 or by combining with non-HCO_3 buffers forming the basic buffer species. The former reaction requires carbonic anhydrase, while the latter process requires mobile buffers within the cell. Measurements of intracellular non-HCO_3 buffer capacity demonstrate significant concentrations of intracellular buffers. Krapf et al. demonstrated that these non-HCO_3 buffers are, in fact, mobile, and thus, that carbonic anhydrase-dependent conversion of OH to HCO_3 is not required for OH diffusion to the basolateral membrane.[123]

Therefore, it appears that the second requirement for carbonic anhydrase is related to base efflux across the basolateral membrane. As described previously in this Chapter, the basolateral membrane base efflux mechanism carries a HCO_3 and a carbonate (CO_3) ion, rather than either OH or H ions. Therefore, OH formed when an H ion is secreted across the apical membrane must be converted to HCO_3 and CO_3 either within the cell or at the basolateral membrane prior to efflux. A number of studies demonstrated that the effect of a peritubular pH change on cell voltage or cell pH is blocked by carbonic anhydrase inhibitors.[109,110,123] This implies that carbonic anhydrase is required to supply HCO_3 and CO_3 to the transporter and/or to allow the HCO_3 and/or CO_3 ions, once they have been transported across the membrane, to react with interstitial buffers on the extracellular side of the basolateral membrane. Alternatively, the carbonic anhydrase inhibitors could have a direct inhibitory effect on the transporter protein. In support of the former, Soleimani and Aronson demonstrated in basolateral membrane

vesicles that the effect of acetazolamide (carbonic anhydrase inhibitor) on $Na/3HCO_3$ cotransporter activity is due to effects on substrate concentration rather than direct inhibition of the transport protein itself.[166]

In summary, carbonic anhydrase has two roles in proximal tubule transepithelial H secretion. The first is to minimize decreases in luminal pH when H ions are secreted into the lumen by rapidly converting the secreted H to CO_2 and H_2O thereby allowing H secretion to continue at a faster rate. The second role is to facilitate conversion of the cytoplasic OH, formed by the generation of the H that was secreted, to HCO_3 and CO_3 that can then exit across the basolateral membrane. This latter step could be mediated by either cytoplasmic or basolateral membrane carbonic anhydrase. In addition, it is possible, but unproven, that basolateral membrane carbonic anhydrase could further enhance acidification by facilitating conversion of HCO_3 and CO_3 that exit across the basolateral membrane to OH and H, which then can titrate non-HCO_3 buffers in the peritubular interstitium.

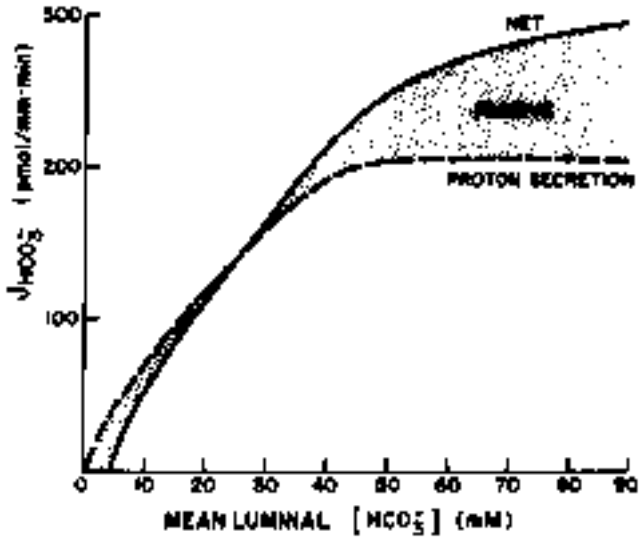

FIGURE 55.5 Dependence of HCO_3 absorption on mean luminal HCO_3 concentration. Solid line indicates net HCO_3 absorption, shaded area indicates passive paracellular HCO_3 flux, and dashed line indicates rate of active transcellular H secretion. *(From Alpern RJ, Cogan MG, Rector FC Jr. Effect of luminal bicarbonate concentration on proximal acidifi cation in the rat. Am J Physiol 1982,243:F53–F59, with permission.)*

Regulation of Acidification

Proximal tubule acidification involves transcellular H secretion in parallel with paracellular HCO_3 backleak. Other leak pathways are relatively minor. Net HCO_3 absorption can be regulated by modification of the transcellular or the paracellular flux, but regulation of the transcellular flux is more frequently observed. Below a number of the important proximal nephron acidification regulatory determinants are discussed.

Luminal HCO_3 Concentration

Malnic and de Mello Aires examined the effect of luminal HCO_3 concentration and pH on the rate of HCO_3 absorption using the split droplet technique.[167] In these classic studies, the pH of a luminal split drop was measured with an antimony electrode and the HCO_3 concentration calculated. It was noted that HCO_3 concentration decreases by first order kinetics, implying that the rate of H secretion is linearly related to luminal HCO_3 concentration. This dependence of H secretion on luminal HCO_3 concentration was confirmed in other split droplet studies and in *in vivo* microperfusion studies.[152,168]

Alpern et al., varying luminal perfusate HCO_3 concentration in the *in vivo* microperfusion setting, showed that the measured rate of HCO_3 absorption increases as a function of mean luminal HCO_3 concentrations below 45 mEq/L [Figure 55.5, solid line (net)].[152] At concentrations greater than 45 mEq/L the rate of HCO_3 absorption tends toward a plateau.

Increases in luminal HCO_3 concentration also increase the rate of passive HCO_3 absorption. Using their measured HCO_3 permeability, Alpern et al. calculated the contribution of passive HCO_3 diffusion to net HCO_3 flux (Figure 55.5, shaded area).[152] When net HCO_3 flux is corrected for the passive HCO_3 flux, the rate of transcellular H secretion can be determined (Figure 55.5, dashed line). As shown, at luminal HCO_3 concentrations above 45 mEq/L, the rate of transcellular H secretion plateaus. At HCO_3 concentrations in the physiologic range (20–25 mM), the major effect of luminal HCO_3 concentration on net HCO_3 absorption is on the rate of proton secretion.

While it is tempting to ascribe the results of Figure 55.5 to a saturable H secretory process, it is important to remember that HCO_3 is not a substrate for the apical membrane transport mechanisms. As discussed above, HCO_3 reabsorption is mediated by H transport mechanisms, and thus, the process is most likely sensitive to luminal H concentration (pH). At high luminal HCO_3 concentrations, large changes in HCO_3 concentration lead to small changes in luminal pH and even smaller changes in luminal H concentration, whereas at low luminal HCO_3 concentrations small changes in HCO_3 concentration can lead to significant changes in luminal pH and even larger changes in luminal H concentration. This would give the appearance that the H secretory process is saturable. This thesis is supported by the direct observations of Aronson et al. who demonstrated that Na/H

antiporter rate is sensitive to external H concentration, with H competing with Na at a single site.[31]

Increases in luminal HCO_3 concentration directly stimulate the apical membrane Na/H antiporter and H-ATPase. In the steady state, the rate of the basolateral membrane $Na/3HCO_3$ transporter must increase to a similar extent as apical membrane H secretion. The most likely signal that increases the rate of the basolateral membrane transporter is an increase in cell pH, resulting from the increased rate of apical membrane H secretion. Alpern et al. demonstrated that increasing luminal pH from 6.6 to 7.3 increases cell pH by only 0.1 pH unit, while a similar increase in luminal pH stimulates transepithelial H secretion three-fold.[37,152] Thus, the basolateral membrane $Na/3HCO_3$ transporter must be exquisitely sensitive to cell pH, such that increases of 0.1 pH unit can increase the rate of the transporter threefold. Apical membrane transporters undergo a similar stimulation in this setting, but in response to a 0.7 pH unit increase in driving force (pH 7.3−6.6). One possible mechanism for the apparent exquisite sensitivity of the basolateral membrane cotransporter is that each turnover of the transporter carries three base equivalents. Thus, kinetically the transporter may be driven by the cube of the OH or HCO_3 concentration. In a proximal tubule mathematical kinetic model based on the ($[HCO_3]$),[3] Verkman and Alpern demonstrated that the $Na/3HCO_3$ cotransporter is sufficient sensitivity to cell pH to explain the experimentally observed changes in transporter rate.[169]

Luminal Flow Rate

When glomerular filtration rate increases, it is important that proximal tubule rates of H secretion increase in proportion. This maintains glomerulotubular balance and prevents increases in GFR from leading to marked bicarbonaturia and development of a metabolic acidosis. Both *in vivo* and *in vitro* microperfusion studies have demonstrated a marked flow dependence of HCO_3 absorption.[145,170,171]

One mechanism by which increases in luminal flow rate can stimulate HCO_3 absorption is by altering the luminal HCO_3 concentration profile.[172,173] Normally, as glomerular ultrafiltrate proceeds down the tubule lumen, HCO_3 concentration progressively decreases because the rate of HCO_3 absorption is proportionally greater than the rate of volume absorption. At faster luminal flow rates (higher GFR), the same rate of HCO_3 absorption would lead to a lesser fall in luminal HCO_3 concentration, which would then stimulate H secretion. Chan et al. and Alpern et al. examined the flow dependence of HCO_3 absorption as a function of mean luminal HCO_3 concentration.[145,170] Both investigators found that while increases in luminal flow rate cause increases in mean luminal HCO_3 concentration, this can account for only a small fraction of the stimulation of HCO_3 absorption. Chan et al. and Wang et al. also showed that changes in luminal flow rate do not affect paracellular HCO_3 permeability, and thus, the effect of flow is on transcellular H secretion.[153,171,174]

To more directly demonstrate this effect of flow rate on transcellular proton secretion, Preisig examined the effect of luminal flow rate on rat proximal tubule cell pH when the basolateral membrane $Na/3HCO_3$ transporter is inhibited.[175] Because cell pH was measured at the site of the perfusion pipette, results are not complicated by changes in the axial luminal HCO_3 concentration profile. Increases in luminal flow rate cause an immediate increase in cell pH that is reversible on decreasing luminal flow rate. This observation proves that increases in luminal flow rate lead to increases in the rate of H secretion. Preisig also showed that the apical membrane H secretory transporter that is stimulated by flow is the Na/H antiporter.[175] Du et al. found a similar flow-dependence of apical membrane proton secretion in the mouse proximal tubule, but concluded that both the Na/H antiporter and H-ATPase were similarly stimulated.[171,174] Consistent with NHE3 being involved in flow-dependent stimulation of H secretion are studies in NHE3-deficient mice, where it was shown that glomerular-tubular balance is significantly reduced.[176]

One possible mechanism for the effect of luminal flow rate on H secretion is a flow-dependent luminal diffusion barrier. According to this theory, a luminal diffusion barrier exists among the brush border microvilli, which impedes diffusion of secreted protons out into the center of the lumen and of HCO_3 from the lumen to the apical membrane. The acid pH in the vicinity of the H transporters in the microvilli then slows the rate of H secretion. Increases in luminal flow rate would decrease the magnitude of the diffusion barrier such that the local pH in the vicinity of the H transporters would increase, and, thus, the driving force for H secretion would increase. In this model, however, one would not expect increases in flow rate to stimulate H secretion if luminal HCO_3 concentration is already in the range where rates of H secretion are insensitive to it (see Figure 55.5, luminal HCO_3 concentration >45 mEq/L). These are the kinetics observed by Alpern et al. when H secretion was examined as a function of mean luminal HCO_3 concentration.[170] Increases in luminal flow rate stimulate H secretion at low luminal HCO_3 concentrations but have no effect on the apparent maximal rate. Similarly, Preisig found no effect of luminal flow rate on cell pH when luminal perfusate pH ($[HCO_3]$) is high.[175]

Wang et al. have proposed another mechanism mediating the flow dependence of H secretion and HCO_3 absorption.[171,174] By modeling the force (torque)

put on the apical membrane microvilli by increases in luminal flow rate, they demonstrated a linear relationship between luminal flow rate and the change in torque and between the change in torque and the change in the rate of HCO_3 absorption. This effect of flow is dependent on an intact actin cytoskeleton. Thus, they concluded that the microvilli serve as sensors of luminal flow rate, and then, in an actin-dependent manner, regulate Na/H antiporter and H-ATPase activity in a proportional manner.

All of the above studies examined the effect of acute changes in luminal flow rate on HCO_3 absorption. Preisig and Alpern created a model of chronic nephron hyperfiltration by combining uninephrectomy with high dietary protein intake.[177] Microperfused rat proximal tubules exposed to chronic hyperfiltration of 12–18 days duration absorbed HCO_3 at faster rates than tubules in control animals (sham operation and normal protein diet). This occurred in spite of the fact that both groups of tubules were microperfused at similar perfusion rates. Thus, there is a chronic adaptation in the capacity for HCO_3 absorption with chronic exposure to higher luminal flow rates.

Harris et al. demonstrated that the flow-induced stimulation of Na/H antiporter activity that occurs secondary to either an increase in dietary protein intake or uninephrectomy appears kinetically as an increase in the V_{max} of Na/H antiporter activity with no change in the Na affinity.[178] Addition of $NaHCO_3$ to the diet (to neutralize the acid load from the high protein diet) did not prevent the stimulation of Na/H antiporter activity. Similar results were found in the remnant kidney model where the stimulation of Na/H antiporter activity is most likely secondary to chronic increases in single nephron glomerular filtration rate.[179,180]

Measuring cell pH fluorescently in the *in vivo* microperfused proximal tubule, Preisig and Alpern demonstrated that both apical membrane Na/H antiporter and basolateral membrane $Na/3HCO_3$ cotransporter activities are increased in parallel by approximately 30 and 100% after 24 hrs and 12–18 days, respectively, of hyperfiltration.[177] Harris et al. found a similar percent stimulation of Na/H antiporter activity after 24 hrs of hyperfiltration.[178]

Peritubular (Extracellular) HCO_3 Concentration, pCO_2, and pH

Acute regulation: Acutely increasing peritubular [HCO_3] inhibits proximal tubule HCO_3 absorption, while decreasing peritubular [HCO_3] stimulates HCO_3 absorption.[145,155,168,181–185] Similarly, acute decreases in pCO_2 inhibit and acute increases in pCO_2 stimulate HCO_3 absorption.[155,182,183,185–188]

Alpern showed that changes in peritubular [HCO_3] do not affect HCO_3 permeability, and have minimal effect on paracellular HCO_3 diffusion.[181] Thus, the major effect of peritubular [HCO_3] is on the rate of transcellular proton secretion. This effect is mediated by a direct effect on basolateral membrane $Na/3HCO_3$ cotransporter activity, and, likely, secondarily affects the rate of apical membrane H transporters through resulting changes in cell pH. Alpern and Chambers demonstrated that a 0.7 pH unit change in peritubular pH causes a 0.3 pH unit change in cell pH.[37] This rather large change in cell pH indicates that cell pH is more responsive to changes in systemic or blood pH than to changes in luminal pH, as decreases in luminal pH of 0.7 pH units result in a 0.1 pH unit change in cell pH. Teleologically, such a system seems reasonable in view of the large variations in luminal pH along the length of the proximal tubule, and the generally small changes in blood pH under physiologic conditions.

In the steady state, net changes in apical and basolateral membrane H transport must be equal, so the change in cell pH reflects the change in driving force required for equal changes in apical and basolateral transport. If cell pH changes by 0.3 pH units in response to a 0.7 pH unit change in peritubular pH, the change in driving force across the basolateral membrane transporter is 0.4 pH units and that across the apical membrane is 0.3 pH units. Thus, in this setting, the transporters seem to be of relatively equal sensitivity. As discussed above, the $Na/3HCO_3$ transporter is exquisitely sensitive to changes in cell pH and may also be very sensitive to changes in peritubular pH. In contrast, the apical membrane Na/H antiporter is relatively insensitive to changes in luminal pH, but most likely more sensitive to changes in cell pH (see below).

The response to changes in pCO_2 is complex. As noted above, increases in pCO_2 stimulate HCO_3 absorption and decreases in pCO_2 inhibit HCO_3 absorption. Because of the high proximal tubule CO_2 permeability, any changes in pCO_2 will have immediate and similar effects on luminal, cell, and peritubular pH. The resulting final pHs will be those required to generate equal changes in apical and basolateral membrane fluxes in the new steady state. Krapf et al. found that changes in extracellular fluid pCO_2 lead a cell pH change that is $^2/_3$rds the magnitude of the change in extracellular fluid pH.[146] Thus, respiratory acidosis (an increase in pCO_2) is associated with equal acidification of luminal and peritubular fluids and a cell acidification that is $^2/_3$rds the magnitude of the extracellular pH change. In the steady state, the larger decrease in peritubular pH compared to cell pH will increase the driving force across the $Na/3HCO_3$ co-transporter in favor of increased transporter activity, and can explain the

increased rate of HCO_3 transport across on the basolateral membrane.

On the apical membrane side, the larger decrease in luminal pH compared to cell pH would decrease the driving force for H secretion. However, respiratory acidosis is associated with an increase in apical membrane H transport, which implies that the apical membrane H secretory mechanisms are more sensitive to changes in cell pH than to changes in luminal pH.

Two possible mechanisms exist for increased sensitivity of Na/H antiporter activity to cell pH compared to its sensitivity to luminal pH. First, when Na/H antiporter activity is examined as a function of internal H concentration, transporter activity is greater at acidic pHs than would be expected for simple substrate interaction, suggesting allosteric regulation.[35] In more convincing studies, these investigators measured the rate of amiloride-sensitive Na efflux when internal pH was lowered. Lowering internal pH would be expected to inhibit Na efflux from vesicles by competition between H and Na for the same site. However, lowering intravesicular pH actually accelerated amiloride-sensitive ^{22}Na efflux, providing definitive demonstration for allosteric up-regulation of Na/H antiporter activity by more acidic internal pHs.

This allosteric activation has been demonstrated for most of the NHE isoforms, and the domains responsible identified by detailed studies of NHE1. Wakabayashi et al. showed that deletion of the C-terminus (amino acids 636-815) of NHE1 has no affect on cell pH regulation of antiporter activity, however, deletion of amino acids 567–635 (also in the C-terminal cytoplasmic domain of NHE1) decreases antiporter sensitivity to cell pH.[189]

A second mechanism that could impart sensitivity to cell pH is regulation of apical membrane NHE3 abundance via trafficking. Proximal tubule endosomes contain both H-ATPases and an amiloride-insensitive Na/H antiporter.[190,191] Schwartz and Al-Awqati demonstrated that rapid cell acidification leads to exocytosis of previously endocytosed fluorescein-labeled dextran, raising the possibility that insertion of endosomal transporters into the apical membrane is another mechanism by which transport capacity increases in acidosis.[192]

In the above discussion, the effects of acute changes in pH, $[HCO_3]$, and pCO_2 on HCO_3 absorption were described. In detailed studies varying pH, $[HCO_3]$, and pCO_2 independently, Boron et al. found that acute regulation of proximal tubule acidification processes is mediated by changes in peritubular $[HCO_3]$ and pCO_2, and not pH per se, and have proposed the existence of HCO_3 and pCO_2 sensors on the basolateral side of the cell.[182,185]

While all of the above described acute effects are large, the changes required to elicit them were also large and frequently non-physiologic. If proximal tubular H/HCO_3 transport processes are to participate in the kidney's defense against physiologic changes in the daily metabolic acid load (primarily determined by the composition of the diet), mechanisms that sense and respond to minimal changes in acid–base parameters are required. These more sensitive mechanisms most likely mediate the chronic adaptations in transporter activity.

Chronic regulation: Using the *in vivo* microperfused rat proximal tubule preparation, Kunau et al. demonstrated that chronic acid feeding causes a marked stimulation in HCO_3 absorption that is greater than was seen by Alpern et al. in an acute metabolic acidosis model, in spite of the fact that the decrease in plasma $[HCO_3]$ in the chronic studies was far less than in the acute studies.[181,193] Similarly, Cogan found that chronic hypercapnea stimulated proximal tubule HCO_3 absorption to a far greater degree than did acute hypercapnea.[194]

Cohn et al. demonstrated that Na/H antiporter activity is increased in apical membrane vesicles prepared from dogs with chronic metabolic acidosis compared to control dogs.[195] In that the increased Na/H antiporter activity persisted *in vitro* when studied under control conditions (pH 7.4), this observation demonstrates a memory effect and not an effect secondary to a change in driving force across the transporter. Tsai et al. and Kinsella et al. found similar results in apical membrane vesicles prepared from rabbit and rat kidney cortex, respectively, and Tsai et al. demonstrated that the effect of acidosis is on the Vmax with no effect on transporter affinity for Na.[196,197]

Similar acid-induced stimulation of the basolateral membrane $Na/3HCO_3$ cotransporter has been found. When compared under the same conditions (pH 7.4), Akiba et al. (using rabbit apical and basolateral membrane vesicles) and Preisig and Alpern (using the *in vivo* microperfused rat proximal tubule) demonstrated parallel increases in apical membrane Na/H antiporter activity and basolateral membrane $Na/3HCO_3$ cotransporter activity when preparations from animals with a chronic metabolic acidosis are compared to preparations from control animals.[139,198] Both studies demonstrated that the increase in activities is due to a memory effect and not merely a change in transporter driving force. Akiba et al. also demonstrated a decrease in $Na/3HCO_3$ cotransporter activity in basolateral membrane vesicles prepared from animals with chronic metabolic alkalosis, and a trend for inhibition of Na/H antiporter activity in apical membrane vesicles prepared from the same animals.

Similar studies have been performed in chronic respiratory acidosis, but with mixed results. Some investigators have found increases in apical membrane Na/H antiporter and/or basolateral membrane Na/3HCO_3 activities, while other investigators have found that a chronic respiratory acidosis has no effect on the activity of either transporter.[199–204] The reason for these discrepancies is not clear, it is possible that hemodynamic changes leading to decreases in GFR in some models are obscuring a stimulatory effect.

Further examination of acid regulation of Na/H antiporter activity demonstrated that NHE3 is the NHE isoform regulated by acidosis, and that the increased activity is associated with an increase in brush border NHE3 protein abundance, with no measurable change in renal cortical NHE3 mRNA abundance.[55,56] While it is not clear *in vivo* whether the increase in apical membrane NHE3 protein abundance is due to trafficking of existing transporters from the cytoplasm to the membrane or requires a simultaneous increase in total cell NHE3 protein, cell culture studies suggest it is the former (see below).

Acid activated signaling pathway: To elucidate the signaling pathway that mediates NHE3-stimulation by extracellular acidity, Amemiya et al. established an opossum kidney (OKP) cell culture model in which cells incubated in control (pH 7.4) or acid media (pH 6.6 to 7.2) demonstrate increased activity of an EIPA-resistant Na/H antiporter (kinetics consistent with NHE3).[57] While the stimulatory effect of media acidification on NHE3 activity is evident within 6 hrs and remains elevated at 24 hrs, NHE3 mRNA and protein abundances are only significantly increased at 12 and 24 hrs, respectively, suggesting that, at least the initial increase in NHE3 activity, is not dependent on increases in whole cell protein abundance (Figure 55.6).[57,205] In support of this conclusion, media acidification increases NHE3 activity in the absence of protein synthesis (cycloheximide).[57] Acid stimulation of NHE3 activity correlates with significant increases in apical membrane NHE3 abundance, which also significantly increases by 6 hrs and persists at 24 hrs, suggesting that the increase in NHE3 activity is mediated by trafficking of protein to the apical membrane (Figure 55.6).[205] Exocytic movement of NHE3 to the apical membrane requires an intact cytoskeleton and the increase in apical membrane abundance is required for acid-induced stimulation of NHE3 activity.[205]

A typical western diet that contains animal protein generates about 0.5–1.0 mEq/kg/day of non-volatile acid through metabolism, which must be excreted mEq-for-mEq by the kidneys to maintain acid–base homeostasis. Through buffering mechanisms, this daily acid addition does not significantly change extracellular pH. Thus, a key biological question is how the body

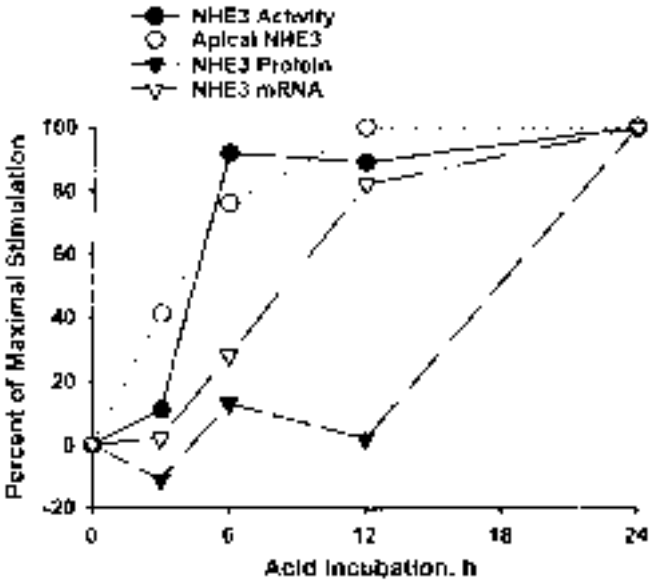

FIGURE 55.6 Time course for the effect of acid on NHE3. NHE3 activity, apical NHE3 protein abundance, total cellular NHE3 protein abundance, and NHE3 mRNA abundance are plotted as the percentage of maximal stimulation *vs* time. *(From Yang X, Amemiya M, Peng Y, Moe OW, Preisig PA, Alpern RJ. Acid incubation causes exocytic insertion of NHE3 in OKP cells. Am J Physiol 2000,279:C410–C419, with permission.)*

responds to the need and senses the precise amount of acid that must be excreted daily. The most likely explanation is that cells respond to "unmeasurable" changes in extracellular pH. If this is the case, sensing mechanisms must be exquisitely sensitive. Ambühl et al. showed that acid feeding increases apical membrane NHE3 protein abundance with changes in extracellular pH of less than 0.1 pH unit.[56] In fact, after seven days of acid feeding plasma pH and HCO_3 concentration are not significantly different from control, while apical membrane NHE3 protein abundance continues to rise (Figure 55.7).[56] Strong evidence suggests that changes in intracellular pH are the signal that initiates the physiological response in that K depletion [extracellular alkalosis and intracellular acidosis (see below)] elicits the same proximal tubule responses as a metabolic acidosis (extracellular and intracellular acidosis).

Endocrine and autocrine pathways have been shown to be involved in mediating the proximal tubule response to an acid load (also see below). In rats, metabolic acidosis is associated with an increase in plasma cortisol levels, and adrenalectomy prevents the acidosis-induced stimulation of Na/H antiporter activity.[197,206,207] In OKP cells, addition of low concentrations of hydrocortisone to the media (that alone do not stimulate NHE3 activity) increase the magnitude of the effect of media acidification on NHE3 activity and whole cell protein abundance, with no effect on

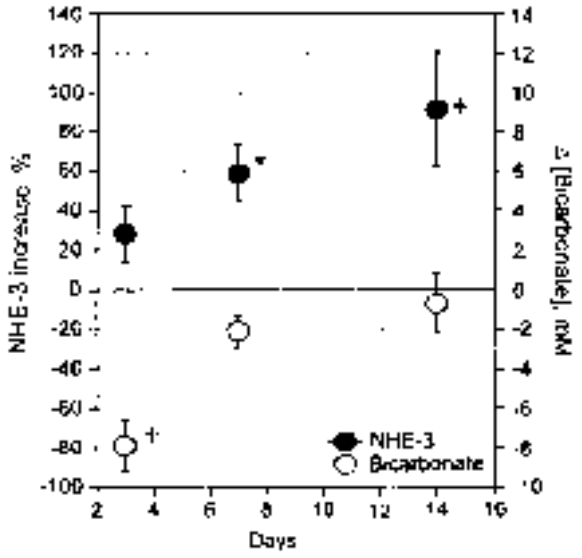

FIGURE 55.7 Acid-induced increase in NHE3 protein abundance (*solid circles*) and decrease in plasma bicarbonate concentration (Δ[bicarbonate], *open circles*) are plotted as a function of duration of treatment. *(From Ambühl PM, Amemiya M, Danczkay M, Lotscher M, Kaissling B, Moe OW, Preisig PA, Alpern RJ. Chronic metabolic acidosis increases NHE3 protein abundance in rat kidney. Am J Physiol 1996,271: F917–F925, with permission.)*

acid-induced increases in NHE3 mRNA abundance.[208] Additional studies demonstrate that the enhanced effect seen in the presence of low dose hydrocortisone is not dependent on protein synthesis, but rather mediated by increased trafficking of NHE3 to the apical membrane.[208] Aldosterone is without effect on NHE3 activity. Taken together, these studies suggest that in the presence of an acid load, low dose glucocorticoids interact synergistically with the acid load to stimulate NHE3 translation and trafficking. Glucocorticoids can also directly increase NHE3 activity, and protein and mRNA abundance, and thus, contribute to the response to an acidosis (see below).

Endothelin also plays a role in acid regulation of NHE3 activitiy. Metabolic acidosis increases renal cortical endothelin levels and endothelin-1 stimulates NHE3 activity (see below).[209,210] In mice in which the ET_B receptor has been knocked out in the kidney, acid feeding does not increase NHE3 activity in renal cortical brush border membrane vesicles, whereas NHE3 activity is significantly increased in vesicles prepared from wild-type mice, demonstrating acid regulation of NHE3 through the ET_B receptor.[211]

Studies elucidating the acid-activated signaling pathway have been performed in OKP cells. In this model, as with *in vivo* models, an intracellular acidification appears to be the key to the adaptation as NHE3 activity is stimulated by both media acidification and exposing cells to weak acids or an NH_4Cl prepulse, maneuvers that acidify the cell but have no effect on extracellular pH.[212] Incubation of OKP cells in acid media activates the non-receptor tyrosine kinases Pyk2 and c-Src and the MAP kinases ERK (extracellular regulated kinase) 1 and 2. Inhibition of Pyk2 kinase [with expression of $pyk2^{K457A}$ (a dominant negative Pyk2) or an siRNA against Pyk2], c-Src kinase [with overexpression of *csk* (*c-Src k*inase, an endogenous inhibitor of Src family kinases), expression of $c\text{-}src^{K295M}$ (a dominant negative c-Src), or expression of $pyk2^{Y402F}$ (a mutant Pyk2 that prevents c-Src binding to Pyk2 and subsequent c-Src activation)], or the ERK 1,2 kinases with PD98059 blocks acid stimulation of NHE3 activity.[212–215] Media acidification also increases transcriptional expression of *c-fos*, *c-Jun*, *junB*, and *egr-1*.[216]

More recent studies have explored the relationship between these acid-activated signaling intermediates and found that downstream of a cell acidification are two parallel pathways.[217,218] One pathway involves Pyk2 and c-Src and the other pathway ERK1 and 2 and the immediate early genes *c-fos* and *c-jun* and their associated increase in activity of the transcription factor AP-1. Following exposure to acid media, Pyk2 is activated within 30 sec, and its activation is required for activation of c-Src kinase, which occurs 90 sec following exposure to acidic media, placing Pyk2 "upstream" of c-Src in the signaling pathway.[213] Studies demonstrating that Pyk2 can be activated by acid in a cell free system over a physiologically relevant pH range (maximal autophosphorylation achieved with a 0.2 pH unit decrease and maximal kinase activity achieved with a 0.4 pH unit decrease) established Pyk2 as the likely proximal tubule cell pH sensor responsible for initiating activation of the acid-activated signaling pathway that mediates the increase in NHE3 activity.[213] Inhibiting acid activation of Pyk2 kinase with the dominant negative $pyk2^{K457A}$ or $siRNA_{Pyk2}$ or inhibiting c-Src kinase with the dominant negative $c\text{-}Src^{K295M}$, while preventing NHE3 activation, do not prevent acid activation of ERK 1 and 2 kinase or the increase in *c-fos* mRNA abundance.[218] These data establish that two parallel pathways are activated by cell acidification and that both are required for acid stimulation of NHE3 activity.

In both cultured OKP cells and *in vivo*, media acidification or acid feeding, respectively, increases endothelin-1 (ET-1) expression.[209,219] The human ET-1 promoter contains an AP-1 binding site between nt -104 and -109. As mentioned above, media acidification increases *c-fos* and *c-Jun* expression and AP-1 activity.[220] Using a luciferase assay, Laghmani et al. showed that acid stimulation of ET-1 transcription is mediated by the above mentioned AP-1 binding site in the ET-1 promoter.[221] Preliminary data from our laboratory suggests that both Pyk2 and c-Src activation are also

required for acid-induced increases in ET-1 transcription, suggesting convergence of the two parallel acid-activated signaling pathways (Figure 55.8).[217] ET-1 stimulation of NHE3 activity is mediated by the ET_B (and not the ET_A) receptor and mediates acid regulation of NHE3 activity.[63,211]

Failure to excrete the daily acid load generated on a typical Western style diet leads to bone demineralization and muscle protein breakdown.[222–224] Described above is the effect of this acid load on NHE3 activity and the acid-activated signaling pathways that likely mediated this effect. However, the renal proximal tubule role in excreting this daily acid load involves more than just stimulation of NHE3 activity. In addition, the apical membrane Na-dependent citrate co-transporter (NaDC-1) and basolateral membrane Na-HCO_3^- (NBC1) activities, NH_3 synthesis, and citrate metabolism are all stimulated. Stimulation of NHE3 activity serves to enhance both proton (H^+) and NH_4^+ secretion, the latter by NHE3 functioning in the Na^+/NH_4^+ exchange mode.[225] Increased NH_3 synthesis involves stimulation of mitochondrial glutaminase (GA) and glutamate dehydrogenase (GDH) activities.[226] Increased citrate metabolism involves stimulation of mitochondrial aconitase (mAcon) (mitochondrial metabolism) and cytoplasmic ATP citrate lyase (ACL) (cytoplasmic metabolism) activities.[227,228] Enhanced citrate reabsorption and metabolism serves to decrease base loss (citrate metabolism generates 3 HCO_3^-/citrate). In addition, the products of citrate metabolism, oxaloacetate (OAA) and acetyl CoA, provide substrates for gluconeogenesis and fatty acid synthesis, respectively, and OAA is also a product of the ammoniagenic process.[226] Thus, the combined effect of stimulating these transport and metabolic processes are enhanced net acid excretion, gluconeogenesis, and possibly fat synthesis.

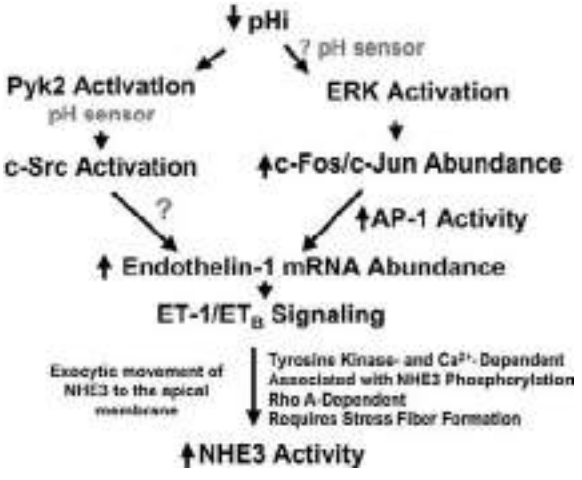

FIGURE 55. 8 Proposed acid-activated signaling pathways that mediates acid stimulation of NHE3 activity.

Preisig and Alpern used both *in vitro* (OKP cell line) and *in vivo* (C57Bl6 and various WT and KO transgenic mouse lines) models to identify the pathways that coordinately regulate the proximal tubule response to an acid load and determined that two apparently parallel pathways are involved. One pathway, involves Pyk2, the endothelin B receptor and calcineurin and the other Nocturnin, a deadenylase member of the circadian gene family (unpublished observations). As described above, Pyk2 serves as a pH sensor for activation of the proximal tubule response. Pyk2, the endothelin B receptor, and the Ca^{2+}/calmodulin/calcineurin pathway, but not the Nocturnin pathway is required for acid stimulation of both NHE3 and NaDC-1 activities. Pyk2 is required for acid stimulation of the three above mentioned mitochondrial enzymes (GA, GDH, and mAcon), while the endothelin B receptor is required for acid stimulation of only GA and GDH and Nocturnin is not required for stimulation of the mitochondrial enzymes, but is required for acid stimulation of the citrate metabolic enzymes (mAcon and ACL) (unpublished observations). Taken together, it appears that the Pyk2/endothelin B receptor/calcineurin pathway mediates acid regulation of apical membrane transport and ammoniagenesis, while citrate metabolism is regulated by the parallel pathway that requires nocturnin.

Perhaps consistent with the absence of an effect of apical membrane transport or ammoniagenic enzymes, Nocturnin knockout mice do not demonstrate a more severe metabolis acidosis when fed an acid diet (unpublished observation). In contrast, Pyk2 and endothelin B receptor knockout mice develop a more severe metabolic acidosis within the first week, but the difference progressively disappears, as has been shown by many investigators in chronic metabolic acidosis studies (unpublished observation).

Potassium Depletion

Using *in vivo* microperfusion Chan et al. compared rates of HCO_3 absorption in control and K depleted animals, demonstrating a 23% stimulation associated with K depletion, while acute changes in peritubular K concentration were without effect.[145] Soleimani and McKinney demonstrated parallel increases in Na/H antiporter and Na/3HCO_3 cotransporter activities in apical and basolateral membrane vesicles, respectively, prepared from K depleted animals and Amemiya et al. demonstrated increased NHE3 activity in OKP cells incubated in low K media.[229,230] The stimulation in transporter activities is an effect on the V_{max} with no effect on Na affinity. These increases in transporter activities, which mimic the adaptation to an acid load,

are likely mediated by an intracellular acidification as Adam and coworkers showed with ^{31}P NMR spectroscopy that the average renal intracellular pH is lower in K depleted animals and incubation of OKP cells in low K media leads to intracellular acidification.[229,231]

Extracellular Fluid Volume

Free flow micropuncture studies have found varying results regarding the effects of extracellular fluid volume on HCO_3 reabsorption. Cogan demonstrated that volume expansion has only a slight inhibitory effect on $NaHCO_3$ absorption, while Bichara et al. found a much larger effect on $NaHCO_3$ absorption.[232,233] Mercier et al. observed that prior parathyroidectomy prevents the large effect of volume expansion on $NaHCO_3$ absorption and proposed that the difference between the results of Cogan and Bichara et al. may be due to effects on PTH secretion.[234]

In vivo microperfusion studies identified two possible mechanisms by which expansion of extracellular fluid volume can inhibit proximal tubule $NaHCO_3$ absorption. First, Alpern et al. found that extracellular fluid volume expansion increases the paracellular HCO_3 permeability by 50%, which agrees with studies showing that transepithelial electrical resistance also decreases.[181,235,236] Second, Alpern demonstrated that changes in proximal tubule volume absorption modify the rate of $NaHCO_3$ absorption, an effect that is not due to changes in solvent drag, but, rather, represents a modification of transcellular H secretion, possibly mediated by changes in interstitial pH and HCO_3 concentration with secondary changes in transcellular H secretion as discussed above.[159] Consistent with this hypothesis, apical membrane NHE3 activity is regulated by hormones known to be involved in the regulation of extracellular volume (see below) and NHE3 knock out mice are hypotensive, hypovolemic, and have a mild metabolic acidosis.[44,237]

Moe et al. examined the effects of chronic changes in dietary Na intake on Na/H antiporter activity assayed in brush border membrane vesicles, comparing rats that had been placed on either a low or high NaCl intake for four days.[238] The 20% increase in Na/H antiporter activity observed in vesicles made from kidney cortex harvested from the rats on the low salt diet was associated with an effect on the Vmax and no effect on Na affinity. An increase in Na/H antiporter activity would increase both proximal tubular $NaHCO_3$ absorption and proximal tubular NaCl absorption.

A possible mechanism for dietary salt regulation of NHE3 was suggested by studies by Yang et al. that showed that following three weeks of a high salt diet, NHE3 phosphorylation on Ser^{552} doubled and was associated with the phosphorylated NHE3, dipeptidyl peptidase IV (DPPIV), myosin VI and the angiotensin II type 2 receptor being redistributed from the low-density plasma membrane-enriched fractions to higher-density intracellular membrane-enriched fractions and the phosphorylated NHE3, myosin VI and the angiotensin II type 2 receptor relocalized to the base of the microvilli (observed by confocal microscopy).[239] These observations are consistent with studies showing that DPPIV catalytic activity is required for NHE3-mediated $NaHCO_3$ reabsorption.[240]

Hormonal Regulation

Parathyroid Hormone: Free flow micropuncture studies demonstrated that parathyroid hormone (PTH) inhibits proximal tubular HCO_3 absorption in dogs and rats.[241,242] *In vitro* microperfusion studies in rabbit proximal tubules also demonstrated that addition of PTH to the peritubular fluid inhibits HCO_3 absorption.[243–245] This effect is mediated by inhibition of transcellular HCO_3 absorption, and is not associated with a change in HCO_3 permeability.[244,245] Using apical membrane vesicles prepared from proximal tubule suspensions or OK cells exposed to PTH, it was shown that PTH decreases Na/H antiporter activity, and that this effect is mediated by a PTH-induced modification of the internal pH sensitivity of NHE3.[64,246,247] Consistent with PTH having an inhibitory effect on NHE3 activity, Cohn et al. showed that *in vivo* thyroparathyroidectomy increases Na/H antiporter activity, assayed in apical membrane vesicles.[195]

The effects of PTH on Na/H antiporter activity are similar to those of dibutyryl or 8-bromo cyclic AMP.[244–246] In brush border membrane vesicles, OK cells, and Na/H antiporters reconstituted into liposomes, cyclic AMP-dependent protein kinase (protein kinase A) directly inhibits Na/H antiporter activity.[248–252] An important role for protein kinase A is confirmed by the observation that expression of a dominant negative protein kinase A catalytic subunit blocks inhibition of NHE3 by cAMP.[253] Moe et al. found that purified protein kinase A phosphorylates the cytoplasmic domain of NHE3 *in vitro*, and that 8-bromo cAMP phosphorylates NHE3 in cultured cells.[253,254] In *Xenopus* oocytes, 8-bromo cAMP inhibits wild type NHE3 activity, but not $NHE3_{\Delta cyto}$, in which the cytoplasmic domain is deleted.[254] It remains controversial as to which site in the cytoplasmic tail is phosphorylated by PKA/cAMP and mediates the inhibitory effect. Kurashima et al. found that both Ser^{605} and Ser^{634} (both in the cytoplasmic domain) are required for PKA regulation of NHE3, but only Ser^{605} is phosphorylated.[255] Zhao et al. found that cAMP phosphorylates multiple serines on the NHE3 cytoplasmic tail, and that phosphorylation of both Ser^{552} and Ser^{605} are required for PKA-mediated inhibition of

NHE3 activity.[253] The reason for this discrepancy is not clear. Kocinsky et al. generated Ser^{552}- and Ser^{605}-specific antibodies and demonstrated that in rat kidney cortex Ser^{552} is phosphorylated to a much greater extent than Ser^{605} in control animals, and that the Ser^{552}-phosphorylated NHE3 is localized to the coated pit region of the brush border membrane, where NHE3 is inactive. Consistent with this, Kocinsky et al. demonstrated that although phosphorylation of NHE3 at Ser^{552} and Ser^{605} is regulated by PKA both *in vivo* and *in vitro*, phosphorylation of these sites does not directly alter NHE3 activity.[78,79]

An alternative mechanism of PKA-mediated inhibition of NHE3 activity was proposed by Bezerra et al. who demonstrated that following exposure to PTH, decreased NHE3 activity was associated with diminished NHE3 surface expression and total cellular NHE3 protein and mRNA abundances, and a decrease in mRNA stability. Additional studies demonstrated that PTH exposure results in a PKA-dependent inhibitory effect on the NHE3 promoter that was responsible for the reduced mRNA half-life stablility.[256]

NHE3 regulation by protein kinase A also involves reorganization of the cytoskeleton and involvement of a second factor, NHERF-1 (Na/H exchange regulator factor, also known as ezrin binding protein 50).[257–262] NHERF-1 was identified by Weinman et al., when a brush border membrane protein fraction that did not contain Na/H antiporter activity was found to bestow regulation of the antiporter by protein kinase A.[263,264] *In vitro* studies demonstrated that NHERF-1 inhibits NHE3 activity, and that in NHERF-1 null cells or in the NHERF-1 knock-out mouse, PTH is without effect on NHE3 activity, a response that can be reinstated by expression of NHERF-1 in NHERF-1 null cells.[257,265,266]

NHERF-1 is one of four members of the NHERF family, the other three members being NHERF-2 [also called E3KARP (NHE3 kinase A regulatory protein)], NHERF-3 (also known as PDZK1), and NHERF-4 (also known as IKEPP). These proteins range in size from 337 to 519 amino acids. NHERF-1 and -2 contain ERM (ezrin, radixin, moesin) binding domains, while NHERF-3 and -4 do not.[267] NHERF-1 and -2 have two PDZ protein binding domains, while NHERF-3 and -4 have four PDZ domains. Weinman et al. have shown that the C-terminal PDZ domain (aa 150-241) in NHERF-1 is primarily responsible for NHE3 inhibition by cAMP.[266] Ezrin, an actin binding protein of the ERM family, links membrane proteins to the actin cytoskeleton.[259] Ezrin is also a protein kinase A binding protein, and studies have shown that interactions between NHE3, NHERF-1, and ezrin are required for protein kinase A-mediated phosphorylation and inhibition of NHE3 activity.[268] Thus, NHERF-1 appears to function as a scaffolding protein within the NHE3 regulatory signaling complex.

Rat proximal tubule and OK cells express only NHERF-1, while human, mouse, and possibly rabbit proximal tubules express both NHERF-1 and -2.[261] In mice, NHERF-1 distributes to the microvillus and co-localizes with NHE3, while NHERF-2 is localized predominantly in a submicrovillar region.[261,262] Although there is controversy regarding whether only NHERF-1 or both NHERF-1 and -2 play a role in cAMP-mediated inhibition of NHE3 activity, the studies mentioned above showing no cAMP regulation of NHE3 activity in the NHERF-1 knock-out mouse, which does express NHERF-2, suggests that only NHERF-1 mediates this effect.[258,265,269] Consistent with a link between NHE3, NHERF-1, ezrin, and the actin cytoskeleton, *in vivo* studies demonstrate that following PTH infusion, NHE3 retracts from the tips to the base of proximal tubule microvilli.[270]

Hruska et al. have found that PTH can also activate phospholipase C in proximal tubule cells leading to increased levels of inositol trisphosphate and diacylglycerol.[271] The increase in inositol trisphosphate leads to an increase in cell Ca^{2+} that may directly modify Na/H antiporter activity or activate other cell kinases. Increases in diacylglycerol activate protein kinase C, which may modify Na/H antiporter activity either directly or indirectly. Weinman et al. and Mellas et al. have found that protein kinase C directly increases Na/H antiporter activity in apical membrane vesicles and proximal tubule cell suspensions, respectively.[272,273] Inconsistent with these findings, Baum and Hays found that protein kinase C activation inhibits HCO_3 absorption in the *in vitro* perfused rabbit proximal tubule.[274] However, Wang and Chan showed in the *in vivo* perfused rat proximal tubule that this inhibition may be due to prolonged activation of protein kinase C, and that the acute effect is a stimulation of transcellular HCO_3 absorption.[275] Studies in cell culture have also yielded conflicting results with both stimulation and inhibition of NHE3 by protein kinase C reported.[49,276–279]

It has also been difficult to define the effect of increases in intracellular Ca^{2+} on Na/H antiporter activity. Both stimulation and inhibition of proximal tubular HCO_3 absorption have been observed with calcium ionophores.[280–282] Bertrand et al. found that NHE1 is stimulated by increases in cell Ca^{2+}, an effect mediated by Ca^{2+}-dependent binding of calmodulin to amino acids 636-656 in the cytoplasmic domain.[283] This cytoplasmic region was shown to inhibit the pH activation of NHE1, an effect blocked by binding of calmodulin.[284] NHE3, on-the-other-hand, is not regulated by cell Ca^{2+}, but a chimera containing the N-terminal half

of NHE3 and the Ca^{2+}-sensitive C-terminal half of NHE1 reinstated Ca^{2+}-induced regulation.[285]

Angiotensin II and Aldosterone: Liu and Cogan demonstrated that angiotensin II (Ang II) is a potent stimulator of proximal tubular HCO_3 absorption.[286,287] This effect occurs predominantly in the early proximal tubule but is also present in the late proximal tubule. The effect on HCO_3 absorption is independent of renal nerve activity. Geibel et al. reported that Ang II added to *in vitro* perfused proximal tubules increases both Na/H antiporter and $Na/3HCO_3$ cotransporter activities, consistent with other conditions that regulate transepithelial HCO_3 absorption.[288] Saccomani et al. showed that the effect of Ang II is on the V_{max} of Na/H antiporter activity, and is without effect on Na affinity.[289]

Cano et al. found that Ang II concentrations of 10^{-9}–10^{-12} M stimulate NHE3 activity, 10^{-8} M has no effect, and higher concentrations (10^{-6} M) inhibit the antiporter in cultured OKP cells.[62] This biphasic concentration response is similar to that previously reported for the effect of Ang II on transepithelial Na transport.[290,291] It is not presently clear whether the effects of high concentrations are physiologically relevant, however, Seikely et al. reported that luminal and peritubular capillary Ang II concentrations are in the range of 10^{-9}–10^{-8} M, suggesting that high concentrations may not be physiologically relevant.[292]

Liu and Cogan demonstrated that the Ang II effect on HCO_3 absorption is associated with a decrease in luminal cAMP concentration and that pertussis toxin pretreatment of the whole animal blocks the effects of Ang II on HCO_3 absorption and luminal cAMP concentration.[287] These results agree with other studies that show that Ang II inhibits adenylyl cyclase in renal cortical homogenates and in primary cultures of renal proximal tubules.[293,294] However, other pathways must also be important, as Cano et al. found in OKP cells that low concentrations of Ang II increase NHE3 activity without altering cAMP production.[62]

High concentrations of Ang II increase intracellular Ca^{2+} concentration.[295,296] However, these Ang II concentrations are associated with inhibition of solute flux in *in vivo* and *in vitro* studies.[290,291] Ang II also signals through protein kinase C, CaM kinase, phospholipase A_2, and the non-receptor tyrosine kinase c-Src.[297] The physiological effects of Ang II signaling through these pathways vary from preparation to preparation, and thus, the key physiological pathways are not yet clear.[297]

The effects of chronic exposure to Ang II (16 hrs to 7 days) has revealed conflicting results. In OKP cells 16 hr exposure to 10^{-7} M Ang II increases NHE3 activity and mRNA abundance, both effects inhibited by actinomycin D (inhibitor of transcription).[298] In tissues harvested from rodents infused with Ang II, 7 days exposure to a pressor dose increases NHE3 activity in brush border membrane vesicles and increases both mRNA and protein abundance in renal cortex and brush border membrane vesicles, respectively.[299] In contrast, another study found that 3 days exposure to a non-pressor dose of either Ang II or Ang II Type 1 (AT1) receptor blocker has no effect on NHE3 protein abundance in cortical or whole kidney homogenates, respectively, but Ang II increases and the AT1 receptor blocker decreases abundance of the basolateral membrane $NaHCO_3$ cotransporter in the same tissue preparation.[300] The cause of the difference between the two studies with respect to the Ang II effect on NHE3 is not known, but may be due to the use of an Ang II dose that raises blood pressure in the former study and one that has no effect on blood pressure in the latter study.

Angiotensin II at a concentration that stimulates NHE3 activity (10−7 M) also stimulates H-ATPase activity in a SV40-transformed rat proximal tubule cell line. This effect does not involve changes in mRNA or protein abundances of the B2 subunit, but is associated with increased cell surface expression of the V-ATPase. Tyrosine kinases, PI3K and p38 all were required for the effect of Angiotensin II on H-ATPase activity.[301]

In adrenalectomized rats, aldosterone stimulates NHE3-dependent proximal tubule volume absorption, an effect that is associated with an increase in brush border NHE3 protein abundance without a change in cortical NHE3 protein abundance.[302] Studies by Drumm et al. suggest that this effect is mediated through the EGF receptor, with aldosterone increasing EGF receptor expression in primary cultures of human renal proximal tubule epithelial cells.[303] More recently, tubule perfusion studies have suggested that luminal or peritubular aldosterone has a non-genomic stimulatory effect on HCO3 reabsorption in the proximal tubule, an effect that appears dependent on glucocorticoid receptors.[304]

Endothelin: The endothelins are important regulators of proximal tubule transport, mediating changes in volume absorption and regulation of the acidification process.[211,217,305–308] Endothelin-1 (ET-1) stimulates apical membrane Na/H antiporter activity in rat and rabbit proximal tubule.[309,310] In wild type OKP cells ET-1 does not regulate NHE3, however, ET-1 stimulation of NHE3 activity can be induced in OKP cells transfected with the endothelin B (ET_B), but not the endothelin A (ET_A), receptor.[63] This effect of ET-1 is mediated 50% by increases in cell Ca^{2+} and CaM (Ca^{2+}-calmodulin) kinase, and 50% by tyrosine kinase pathways.[63,311] In addition, stimulation of NHE3 activity is associated with phosphorylation and trafficking of NHE3 to the apical membrane.[312,313]

As a family, the endothelins are locally acting autocrine/paracrine factors. As mentioned above, in both cultured OKP cells and *in vivo*, media acidification or acid feeding, respectively, increases ET-1 expression, an effect that is mediated through an AP1 site in the ET-1 promoter.[209,219,221] Also as mentioned above, in mice in which the ET_B receptor has been knocked out in the kidney, acid feeding does not increase NHE3 activity in renal cortical brush border membrane vesicles, whereas NHE3 activity is significantly increased in vesicles prepared from wild-type mice, demonstrating that the effect of acid on proximal tubule NHE3 activity is indirect, and mediated by ET-1 signaling through the ET_B receptor.[211]

Given that the effect of acid on NHE3 activity is indirect and mediated by the ET-1/ET_B signaling pathway, recent studies have sought to determine which signaling intermediates in the acid-activated signaling pathway are "up-stream" and which ones are "down-stream" of ET-1/ET_B. Results have demonstrated that two non-receptor tyrosine kinases Pyk2 and c-Src and the MAP kinases ERK 1 and 2 are required for acid, but not ET-1 stimulation of NHE3 activity, placing them "up-stream" of ET-1/ET_B,.[213–215,217,314]

Catecholamines: Chan demonstrated that addition of catecholamines to the peritubular capillary fluid increases HCO_3 absorption in the microperfused proximal tubule and Nord et al. showed that catecholamines increase Na/H antiporter activity in proximal tubule cell suspensions.[315,316] These studies demonstrated that the catecholamine effect is mediated by α_2 agonists. Non-specific α agonists inhibit adenylyl cyclase in renal cortical tubules and α_2 agonists inhibit adenylyl cyclase in renal cortical homogenates.[317,318] Thus, the possibility exists that both α_2 agonists and Ang II stimulate NHE3 activity by inhibiting adenylyl cyclase through a $G\alpha_i$ protein. Recent studies have shown that α_1 adrenergic receptor stimulation also increases NHE3 activity, but this effect is mediated by MAPK.[319] Lastly, β_2 adrenergic agonists can activate NHE3 by inducing β_2 adrenergic receptor binding to NHERF through binding of a NHERF PDZ domain with the last few residues of the C-terminal cytoplasmic domain of the receptor.[320]

Glucocorticoids: Glucocorticoids administered *in vivo* increase Na/H antiporter activity in apical membrane vesicles from renal cortex.[321] Glucocorticoids added to the media of primary cultures of proximal tubule or OKP cells stimulate NHE3 activity, demonstrating a direct effect of glucocorticoids on the Na/H antiporter.[322,323] In both OKP cells and proximal tubules harvested from rabbits given glucocorticoids, the increase in NHE3 activity is mediated by stimulation of NHE3 transcription leading to increases in NHE3 mRNA abundance, effects that are blocked by preventing transcription or protein synthesis with actinomycin D or cycloheximide, respectively, or by blocking the glucocorticoid receptor with RU486.[58,59,324]

The above studies address the chronic mechanism by which glucocorticoids stimulate NHE3 activity. Studies have shown that glucocorticoid-induced stimulation of NHE3 activity preceeds the increase in NHE3 protein abundance, suggesting that the acute effects on NHE3 activity are mediated by another mechanism.[324] Consistent with this, the acute effects are blocked by the glucocorticoid receptor blocker RU486, but are insensitive to actinomycin D or cycloheximide.[324] Moe et al. demonstrated that acute regulation of NHE3 activity is mediated by dexamethasone-induced exocytic trafficking of NHE3 protein to the apical membrane.[325] Additional studies demonstrated that dexamthasone-induced phosphorylation of Ser[663] by serum- and glucocorticoid-inducible kinase (SGK1) preceeds this and is required for the dexamethasone-induced stimulation of NHE3 activity and the increase in apical membrane protein expression.[326]

As discussed above, in addition to directly stimulating NHE3 activity, glucocorticoids synergistically increase the effect of acidosis on NHE3 protein abundance.[208]

Insulin: In the proximal tubule insulin stimulates volume absorption, ammonia synthesis and excretion, and Na/H antiporter activity.[327–329] In OK cells the signaling mechanism mediating insulin stimulation of NHE3 activity is time-dependent.[330] Chronic exposure (24 hrs) stimulates NHE3 activity through the PI3K-SGK1 signaling pathway, while the pathway that mediates acute regulation (1-2 hrs) is not known, but has been shown not to involve the PI3K-SGK1 or cbl/CAP/TC10 (complex that assembles caveolae, which NHE3 may associate with) pathways, increases in apical membrane NHE3 expression, NHE3 phosphorylation, or association with megalin.[330]

LOOP OF HENLE AND THICK ASCENDING LIMB

The loop of Henle reabsorbs 10-20% of filtered HCO_3^-.[331] At least two important phenomena contribute to bicarbonate reabsorption in the loop of Henle. First, reabsorption of water in the descending limb concentrates the luminal fluid and elevates the HCO_3 concentration to ~10-25 mM, raising luminal pH.[332,333] The second phenomena is the reabsorption of HCO_3 by the thick ascending limb (TAL).[334,335] The initial elevation of luminal HCO_3 concentration facilitates reabsorption in the TAL, where reabsorption of bicarbonate is dependent on luminal HCO_3^- concentration and is

gradient limited as in the proximal tubule. In other words, the TAL cannot lower luminal HCO_3 concentration below ~5 mM,[334] if the fluid delivered to the TAL had a low HCO_3 concentration, as present at the end of the proximal tubule, HCO_3 could not be reabsorbed in the TAL. The alkalinization of luminal fluid is also important in raising luminal ammonia concentrations and hence the transport of ammonium from the loop to the collecting tubules.[336]

Earlier micropuncture studies demonstrated that ~50–70% of the HCO_3 remaining at the end of the accessible superficial proximal tubule is reabsorbed prior to the superficial distal tubule.[332,337] The site of this HCO_3 reabsorption was established when Good and colleagues found that rat cortical and medullary TAL perfused *in vitro* reabsorb HCO_3 at a rate of up to ~20 pmole/mm·min, comparable to that in collecting tubule segments.[334,335] (The late proximal tubule *in vivo* probably reabsorbs only a small amount of the filtered HCO_3.) Subsequent studies indicated that the general features of acid–base transport in the rat TAL are those depicted in Figure 55.9.[338] The apical H extrusion process is predominantly sodium-dependent and amiloride-sensitive, i.e., Na-H exchange.[334,339,340] The predominant apical membrane Na-H exchanger in the TAL is the NHE3 isoform.[341,342] However, NHE2 is also present on the apical membrane of the TAL.[343,344] A luminal vacuolar type of H-ATPase is also present

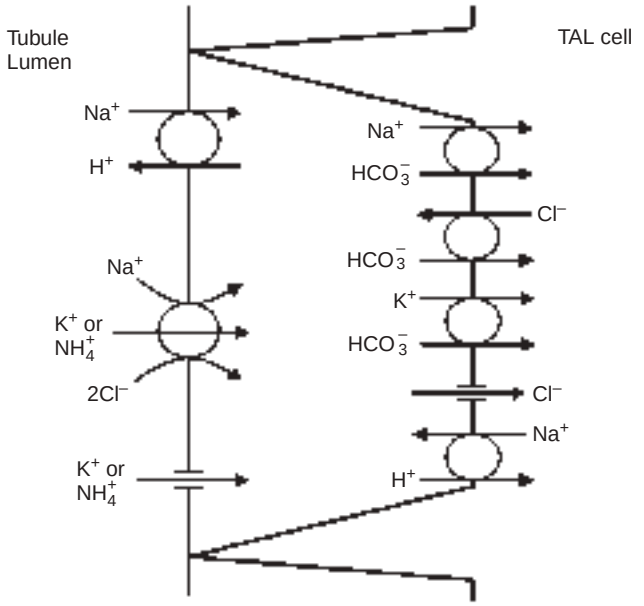

FIGURE 55.9 Model of acid–base transport in the thick ascending limb (TAL). Not shown is carbonic anhydrase, which is important in facilitating acid–base transport in this segment. Also not shown is apical H^+-ATPase, which may have a role in H^+ secretion. See text for additional details.

but its role in transepithelial HCO_3 transport in the TAL is not established.[17,338,340,345,346] Similarly, K-ATPase activity and a K^+-dependent HCO_3 transport pathway (possibly a K^+–HCO_3^- cotransporter) have been found in TAL but their roles are not clear either.[347,348]

The basolateral extrusion of HCO_3 probably occurs via a Na/HCO_3 cotransporter as in the proximal tubule. Krapf identified a sodium-dependent, chloride-independent, SITS-sensitive HCO_3 transport system on the basolateral membrane of the rat cortical TAL.[349] Similar findings were reported for the mouse medullary TAL.[340] Electroneutral NBC 2 (also known as NBCn1, *Na-Bi*carbonate *Co*-transporter) is thought to be the predominate mechanism, at least in the medullary portion of the TAL.[350,351] In addition, basolateral Cl/HCO_3 exchange (AE2, anion exchanger 2) and K-HCO_3 transport are present and may be involved in transepithelial HCO_3 transport.[352–358] AE2 may mediate some of the adaptive changes that occur in acid–base transport in the TAL.[359,360]

Other acid–base transporters are present in the TAL as well. Basolateral Na-H exchange (NHE-1 and NHE-4) probably functions in pH_i and cell volume regulation, in regulation of apical Na-H exchange, and in absorption of NH_4^+.[133,357,361–363] The apical and basolateral Na-H exchangers appear to be functionally linked, increasing in activity of the basolateral Na-H exchanger are accompanied by increases in the apical rates as well.[364,365] NHE1 is proposed to control activity of NHE3, and consequently HCO_3^- reabsorption, by a mechanism involving a change in cellular polymerized actin.[366]

Basolateral chloride channels are present in the TAL but the role in acid–base transport has not been well defined. ClC-Kb/barttin (ClC-K2/barttin in rodents, barttin—a small necessary accessory protein) is present in the TAL,[367] distal convoluted tubule, and intercalated cells of the collecting duct. Mutations in either ClC-Kb or barttin leads to Bartter's syndrome, discussed elsewhere.[368]

The TAL also reabsorbs ammonium, probably via NH_4^+ movement on the apical Na-K-2Cl cotransporter, and possibly via apical K channels.[335,369–373] The lumen positive voltage may also drive some paracellular movement of NH_4^+.[369,370] Of particular note, the apical membrane of the TAL has been recognized to have an extremely low permeability to NH_3, compared to most other biological membranes.[340,372,373] Transport of ammonium across the basolateral membrane is likely via NHE4 and possibly NH_3 diffusion.[371] NHE4 adapts to metabolic acidosis to increase TAL absorption and ultimate excretion of ammonium.[374] Ammonia transport is discussed further in another chapter.

As in most nephron segments involved in acid–base transport, bicarbonate reabsorption in the TAL is dependent on carbonic anhydrase.[334] The rat TAL has both cytosolic and apical and basolateral membrane carbonic anhydrase,[157] the rabbit TAL, which does not have carbonic anhydrase, does not reabsorb HCO_3.[375,376] Human and mouse TAL also have carbonic anhydrase and therefore may reabsorb HCO_3.[375,377]

Regulation of HCO_3 reabsorption in the TAL has been examined both *in vivo* and *in vitro*. Acute and chronic metabolic acidosis stimulate, and chronic chloride depletion metabolic alkalosis inhibits, HCO_3 reabsorption in the TAL.[378,379] Acidosis increases NHE-3 and basolateral Na-HCO_3^- co-transport.[350,341] NHE-3 decreases with metabolic alkalosis.[380] However the effects of metabolic alkalosis on HCO_3 reabsorption i*n vivo* appear to vary with some experimental models perhaps due to opposing influences of the acid–base status and sodium and HCO_3 delivery. HCO_3^- reabsorption increases as luminal HCO_3^- concentration increases.[334,381]

Sodium chloride or sodium bicarbonate loading *in vivo* increase HCO_3 reabsorption in the TAL via mechanisms involving both NHE3 and NHE1,[382] and sodium depletion reduces HCO_3 reabsorption.[379] These effects of sodium balance have been thought to result from changes in sodium delivery rather than from changes in mineralocorticoids.[379] However, recently aldosterone has been shown to inhibit TAL HCO_3^- reabsorption by a non-genomic inhibition of NHE3.[383,384] Glucocorticoids and aldosterone at high doses have been reported to stimulate HCO_3 reabsorption *in vivo*.[345,378,385] Angiotensin II inhibits TAL HCO_3^- reabsorption via a P-450 dependent mechanism.[386] A variety of other peptide hormones have also been found to alter HCO_3 reabsorption in the TAL both *in vivo* and *in vitro*. Arginine vasopressin (AVP) and glucagon acting via cAMP inhibit HCO_3 reabsorption.[387–389] Nerve growth factor can either inhibit or stimulate TAL HCO_3 reabsorption, depending upon the presence or absence of other regulatory factors,[390] inhibiting HCO_3 reabsorption via ERK.[391] The effect of PTH is complex. *In vitro*, PTH modestly inhibits HCO_3 reabsorption,[388] however, *in vivo* PTH infusion enhances loop HCO_3 reabsorption in thyroparathyroidectomized rats, perhaps in part from an increased load of bicarbonate.[392] Toll-like receptor 4 (TLR4) and TLR2 activation inhibit NHE3 and TAL bicarbonate reabsorption.[393–395]

Osmolality and furosemide also alter HCO_3 reabsorption in this segment. Increases in osmolality, signaling via tyrosine kinase pathways, decrease apical Na/H exchange and HCO_3 reabsorption,[363,396] *in vivo*, this may be an additive factor with AVP during states of antidiuresis. Hyposmolality stimulates HCO_3 reabsorption via a PI-3 kinase mechanism.[397,398] However, PGE_2 reverses inhibition of HCO_3 absorption by AVP (but not hyperosmolality), this reversal occurs via PKC and pertussis toxin sensitive G protein pathways.[399,400] Furosemide stimulates TAL HCO_3 reabsorption, possibly due to decreased cell Na (and hence increased Na-H exchange) or cell hyperpolarization.[334,388] This effect may contribute to the enhanced urine acidification observed with furosemide.

An interesting effect is that basolateral NHE1 appears to regulate activity of apical NHE3, and consequently HCO_3^- reabsorption, by a mechanism involving a change in cellular polymerized actin.[366]

DISTAL NEPHRON

Luminal fluid delivered to the distal nephron is normally low in [HCO_3] and pH, usually 5-7 mEq/L and 6.5–6.7, respectively.[332,337] The distal tubule reabsorbs this remaining HCO_3 via H secretion, as in the proximal tubule. In contrast to the proximal tubule, however, net H secretion continues after reabsorption of virtually all of luminal HCO_3, lowering luminal and urine pH to less than 5.5 under appropriate conditions. This process requires active H secretion and an epithelium able to maintain large concentration gradients for H and HCO_3. H secretion or HCO_3 reabsorption in the distal tubule is generally considered to result from primary H secretion. Supporting primary H secretion are studies demonstrating an acid luminal disequilibrium pH under certain circumstances in the superficial distal tubule, in the cortical and outer medullary collecting tubules, and in papillary collecting tubules.[6,401–406]

The distal nephron, beyond the thick ascending limb, is composed of several distinct segments and a diversity of cell types, several of which are involved in acid–base transport, primarily H secretion. Some segments of the distal tubule can secrete HCO_3, at least under some circumstances. Despite this diversity, the general mechanisms of luminal H secretion (HCO_3 reabsorption) are likely similar along the distal nephron. A general model of an H secreting cell is depicted in Figure 55.10. This model originated from studies of the turtle urinary bladder and has been best confirmed in studies of intercalated cells of the rabbit cortical collecting tubule and outer medullary collecting tubule.[407–409] (The turtle bladder, an ancestral and embryologic relative of the collecting tubule, had been extensively used in the past as an *in vitro* model of distal nephron acid–base transport but will not be reviewed here.) The general features of H secreting cells in the distal nephron are the apical H pump, a basolateral Cl/HCO_3 exchanger, and a basolateral Cl channel. In addition, an apical H,K-ATPase is present in many of these cells.[410–412] In most, if not all, H

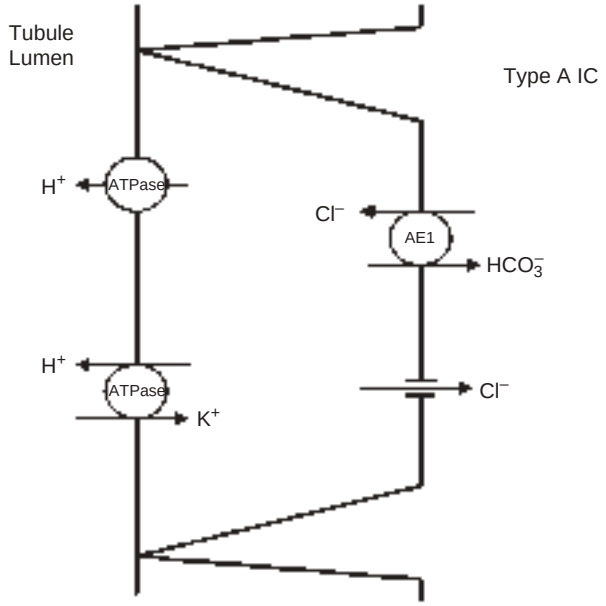

FIGURE 55.10 Model of H^+ secreting type A intercalated cell. Other transporters (such as Na^+-H^+ exchanger) may be present, but are probably not involved in transepithelial acid–base transport.

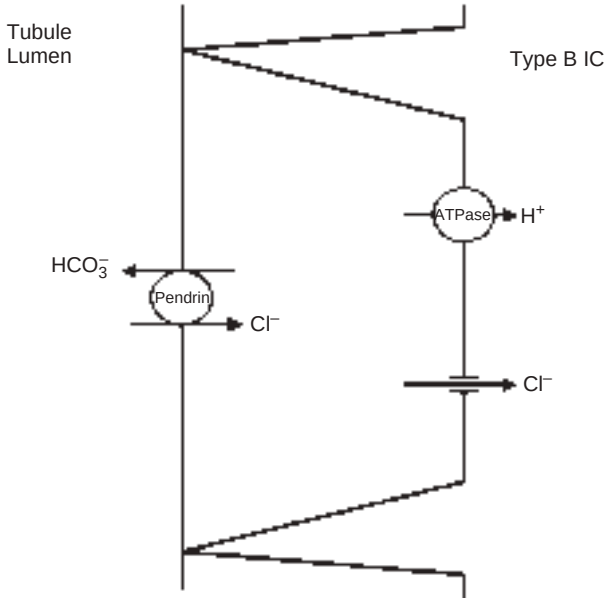

FIGURE 55.11 Model of HCO_3^- secreting type B intercalated cell of the cortical collecting duct. Other transporters (such as Na^+-H^+ exchanger) may be present, but are probably not involved in transepithelial acid–base transport.

secreting cells, the process is accelerated by cytosolic and/or membrane associated carbonic anhydrase. The primary apical H pump is a vacuolar type H-ATPase, at least in most of these cells.[413,414] The basolateral Cl/HCO_3 exchanger is related to the red cell Cl/HCO_3 exchanger, band 3 protein, which has been extensively studied.[415,416] Each of these features of the H secreting cell will be discussed in depth subsequently.

The opposite process, HCO_3 secretion, is modeled in Figure 55.11. The general features are apical Cl/HCO_3 exchange, basolateral H extrusion, and a basolateral Cl channel.[408,409] An apical H,K-ATPase may be present in some HCO_3 secreting cells but is not depicted in Figure 55.11 since the role in transepithelial transport is not clear.[417,418] HCO_3 secretion occurs in cells with carbonic anhydrase. HCO_3 secretion has been reported in the rat superficial distal tubule, the rat and rabbit cortical collecting tubule, and the turtle urinary bladder.[419–423] The models in Figures 55.10 and 55.11 will be used as starting points for the discussion of specifics segments and specific cellular mechanisms.

Some methodological considerations limit complete integration of the available studies of acid–base transport in the distal nephron. The evidence for the models depicted in Figures 55.10 and 55.11 derives mostly from studies of the turtle bladder and rabbit, rat, and mouse collecting tubules perfused *in vitro*. However, almost all of the *in vivo* physiology of distal acidification is derived from studies of rats. In addition, most of the biochemical and immunocytochemical studies (e.g., of H-ATPase) have been performed in the rat and mouse. Although most of the information on rats and rabbits is complementary, some differences are apparent, as discussed below, these differences limit direct extrapolation of data between species. In contrast to the rat and human, the rabbit usually excretes an alkaline urine with little ammonium present. Studies of cultured mammalian cells have complemented the studies of intact nephron segments.

Distal Tubule

Micropuncture studies of rats have usually defined the distal tubule as beginning just after the macula densa and extending to the first junction with another renal tubule. The distal tubule includes as many as four distinct morphologic segments or regions in sequence: a short portion of the thick ascending limb, the distal convoluted tubule, the connecting segment, and the initial collecting tubule.[424] In the rat and human, there is a gradual transition from the distal convoluted tubule to the collecting duct, so that the connecting segment has four cell types: distal convoluted tubule cells, connecting tubule cells, intercalated cells, and principal cells (the latter two described in detail for the collecting duct in the section below).[424] Also the intercalated cells are divided into at least two configurations, type A and type B, as described below.[425] The type A cells are presumed to secrete H,

based on the presence of apical H-ATPase and basolateral Cl/HCO_3 exchange, and morphologic changes with respiratory acidosis. By analogy with the cortical collecting tubule, the type B intercalated cells may be involved in HCO_3 secretion. As discussed below, there are other intercalated cells now classified as non-A, non-B cells.

Numerous micropuncture studies have demonstrated net H secretion (or HCO_3 reabsorption) in the superficial distal tubule of the rat.[426–432] The early distal tubule appears to reabsorb HCO_3 via both Na-H exchange and H-ATPase whereas the late distal tubule has H-ATPase and H,K-ATPase, the latter particularly during potassium depletion.[433–436] The Na-H exchanger is probably NHE2.[342,437,438] Colonic H,K-ATPase is clearly present in some cells of the connecting segment and early CCD.[433,434] Free flow micropuncture and *in vivo* and *in vitro* microperfusion studies have also demonstrated net HCO_3 secretion in this segment.[387,422,439,440] Net HCO_3 transport varies markedly with diet, acid-loading, and other conditioning of the animals and with tubule flow rate.[441] Studies using variations in luminal Cl concentration have suggested that separate processes of HCO_3 reabsorption and HCO_3 secretion are present in the late distal tubule just as in the cortical collecting tubule.[442,435] Since the cellular and molecular mechanisms of these processes have been elucidated better using *in vitro* microperfusion of rabbit cortical collecting tubules, the discussion of these mechanisms will be described in the next section.

Cortical Collecting Duct (CCD)

In a pivotal group of studies, McKinney et al. demonstrated that the rabbit CCD perfused *in vitro* can either reabsorb or secrete HCO_3, depending on the acid–base conditioning of the animals.[442–444] Subsequent studies extended these findings to rat and mouse CCD.[419,445–447] Considerable evidence suggests that bicarbonate reabsorption and bicarbonate secretion are separate processes mediated by distinct cell types as in Figures 55.10 and 55.11.[408]

The CCD consists of principal cells (PC) and more than two types of intercalated cells (IC). The principal cells represent ⅔ of CCD cells and mediate sodium, water, and probably most, if not all, of potassium transport under normal conditions.[448] Most evidence suggests that the principal cells are not involved in transepithelial acid–base transport. The PCs do possess several acid–base transporters on the basolateral membrane: Na-H exchanger, Na-independent Cl/HCO_3 exchanger, and Na/HCO_3 cotransporter.[449–451] These processes probably function to regulate pH_i. Direct studies of pH_i in PC have not identified any apical membrane acid–base transporters.[450,451] Also, immunocytochemical studies have failed to find immunoreactivity for H-ATPase, band 3 type protein (Cl/HCO_3 exchanger), and H,K-ATPase.[17,416,452] PCs do have a few intramembranous rod-shaped particles, which are associated with H-ATPase.[453] Hence, the weight of evidence for the PC suggests no involvement in transepithelial acid–base transport.

Two types of intercalated cells, A and B cells, are responsible for bicarbonate reabsorption and secretion, respectively, in the CCD. (Types A and B are sometimes used to only indicate rat cells, whereas α and β are used for rabbit cells, here A and B refer to any experimental species.) The model of separate intercalated cells (IC) is derived from several lines of evidence and is analogous to transport in the turtle urinary bladder.[454] Morphologically, the rat CCD has two distinct types of IC, both of which stain for carbonic anhydrase.[424,425,455,456] The type A cell has a mixture of apical microplicae and microvilli by scanning electron microscopy, immunoreactivity for H-ATPase on the apical membrane and for band 3 protein on the basolateral membrane, and apical intramembranous rod-shaped particles (which are associated with H-ATPase as described below).[17,415,425,457] The type B cell has a few apical microvilli and no immunoreactivity for band 3 protein, immunoreactivity for H-ATPase and rod-shaped particles are present on the basolateral membrane[415,425,457–459] (Figure 55.12). Pendrin is also located on the apical membranes of rat (and mouse) type B IC.[460,461] All of these characteristics agree with the models in Figures 55.10 and 55.11. These features are best resolved in rat CCD, in the rabbit CCD, IC do not clearly separate into types based on morphology.[453] In fact, rod-shaped particles are present in all rabbit CCD IC on both the apical and basolateral membranes, although to varying extent.[453] However, rabbit CCD IC do demonstrate heterogeneity with respect to other characteristics. Most rabbit CCD IC, especially in the outer cortex, have apical peanut lectin binding, and these cells exhibit characteristics of type B or HCO_3 secreting IC: predictable changes in cell pH with changes in luminal Cl or HCO_3, and cell acidification on removal of peritubular Cl.[416,451,462,463] In the rabbit, the type B IC (peanut lectin positive) usually exhibit diffuse staining for H-ATPase, rather than basolateral staining as in the rat type B IC.[464] Some rabbit CCD IC do have immunoreactivity for apical H-ATPase and basolateral band 3 protein (type A IC).[416,464] The type A IC in the rabbit CCD can also be identified by the endocytosis of fluorescent macromolecules, this presumably occurs in the recycling of apical membrane H-ATPase as discussed below.[462,192,465] These cells exhibit cell alkalinization on removal of basolateral Cl.[462,465]

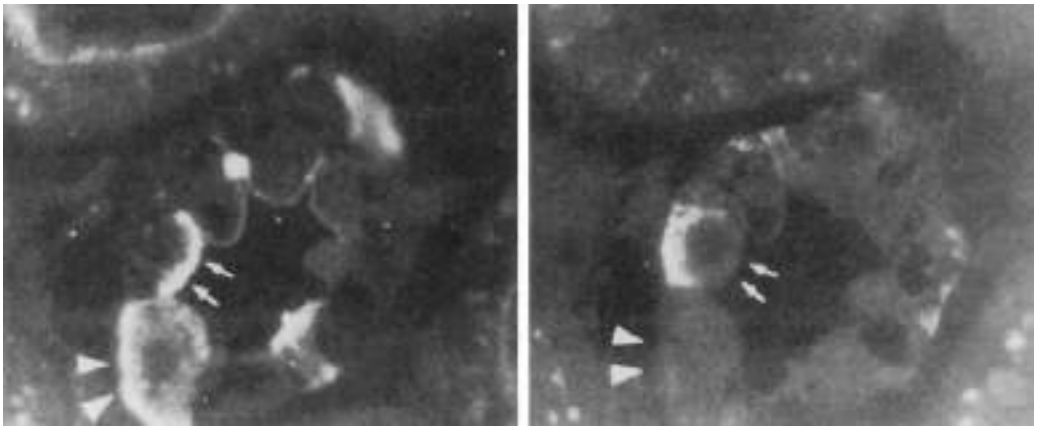

FIGURE 55.12 Left panel shows section of rat kidney cortex immunolabelled with antibodies against the H^+-ATPase (31-kD subunit). One cell (*arrows*) has apical staining (type A IC), while another has basolateral staining (*arrowheads*, type B IC). Right panel shows adjacent section stained with anti-band 3 antibody. The type A cell has basolateral staining. *(From Alper S, Natale S, Gluck S, Lodish HF, Brown D. Subtypes of intercalated cells in rat kidney collecting duct defined by antibodies against erythroid band 3 and renal vacuolar H^+-ATPase. Proc Natl Acad Sci USA 1989,86:5429–5433, with permission.)*

Type A IC become more abundant as the CCD approaches the junction with the medulla in the rabbit.[466,467] Although the morphologic differences between species are complex, both experimental species, rat and rabbit, exhibit IC cells resembling the models in Figures 55.10 and 55.11.

Importantly, IC have recently been found to be involved in regulation of NaCl reabsorption.[468,469] Cl can obviously be directly transported by pendrin on the apical membrane of type B IC but luminal pH/HCO_3 and voltage are also altered by H^+ secretion by type A IC, thereby modulating Na^+ transport.

Other types of IC exist based on a variety of experimental techniques and findings.[467,470,471] These are currently referred to as "non-A, non-B IC." These cells have both H-ATPase and pendrin on the apical membrane and neither H-ATPase or AE1 on the basolateral membrane. Some earlier investigators had called one group of such intercalated cells γ and G cells in rabbit and rat CCD respectively, defined functionally by both apical and basolateral Cl/HCO_3 in studies of intracellular pH.[470,471] These cells are only clearly identified so far by intracellular pH studies demonstrating both apical and basolateral Cl/HCO_3 exchange. The normal function and adaptive response of these non A, non B cells have not been clearly established. These cells may represent a versatile cell type able to respond to acid or base loads or other stimuli.There has been clear *in vitro* evidence that some CCD cells undergo significant functional changes with acid loads.[472,473] In contrast to the distinct classifications of subtypes, studies of cellular distribution of H-ATPase in rat CCD and OMCD demonstrate a spectrum of distribution ranging from predominantly apical location, to predominantly cytoplasmic, to predominantly basolateral, depending upon the acid–base status of the animal.[474] This regulation is discussed further below.

Both A and B IC probably have basolateral Cl channels as in Figures 55.10 and 55.11, and basolateral Na-H exchange to regulate intracellular pH.[451,475,476] (Actually, much of the data for type A IC in the CCD derives from studies on the IC of the outer medullary collecting duct, in which all of the IC are type A.) Rabbit IC also exhibit immunoreactivity for H, K-ATPase as discussed below.[452] Regulation of CCD HCO_3 transport, including the possibility of modulation of cell type, will be discussed in a subsequent section.

CCD from most untreated normal rabbits exhibit spontaneous HCO_3 secretion,[379,423,477–479] CCD from most untreated rats exhibit spontaneous HCO_3 absorption.[419,445] However, in both species, simultaneous secretion and reabsorption are probably occurring in separate cell types. Separate processes can be inferred from transepithelial flux studies which selectively abolish HCO_3 reabsorption (with removal of luminal HCO_3 or peritubular Cl) or alternatively abolish HCO_3 secretion (with removal of luminal Cl or basolateral HCO_3).[480,445,481] HCO_3 reabsorption can also be inhibited by basolateral disulfonic stilbenes.[404,478] Simultaneous HCO_3 secretion and H secretion can also be inferred from studies demonstrating an acid disequilibrium pH in rabbit CCD which have net HCO_3 secretion.[406]

The separate process of H secretion (or HCO_3 reabsorption) in the CCD appears to be analogous to the same process in the outer medullary collecting duct, where no HCO_3 secretion occurs.[406] The process is electrogenic (generating a lumen positive

transepithelial voltage in the absence of Na transport), sodium-independent, and sensitive to inhibition by acetazolamide.[404,444] Some data suggest that CCD H secretion is increased by mineralocorticoids independent of the increased lumen negative transepithelial voltage,[404] however, HCO_3 secretion in the CCD is also increased by mineralocorticoids administered *in vivo*.[480] As discussed below, *in vivo* and *in vitro* acid loads increase net HCO_3 reabsorption in the CCD. However, unidirectional HCO_3 reabsorption is stimulated less than unidirectional HCO_3 secretion is inhibited.[480–484]

Bicarbonate secretion in the CCD is electroneutral, sodium-independent, coupled to Cl absorption, and sensitive to acetazolamide.[443,478,479,485] The distinction between the apical Cl/HCO_3 exchanger in type B cells and the basolateral Cl/HCO_3 exchanger in type A cells will be discussed below. As discussed in detail below, the HCO_3 secretory process is decreased by *in vivo* or *in vitro* acid loads and is increased by *in vivo* mineralocorticoids (at least in alkalotic animals).[478,480,481,486]

In sum, the CCD has at least two different types of intercalated cells mediating separate processes of HCO_3 reabsorption and HCO_3 secretion. Net HCO_3 transport depends upon the sum of these processes which are determined by the conditioning of the animal. The transport proteins responsible for these processes will be discussed below.

Outer Medullary Collecting Duct (OMCD)

The OMCD is distinct from both the CCD and the inner medullary collecting duct. Both the rat and rabbit OMCD reabsorb HCO_3, no HCO_3 secretion has been reported.[419,477,487] In the rat, IC constitute 1/3 of the cells in the OMCD in both the outer and inner stripe ($OMCD_{os}$ and $OMCD_{is}$, respectively).[424,456] However, in the rabbit $OMCD_{is}$, only the outer portion has IC, the cells of the inner $OMCD_{is}$ differ from both PC and IC and have been termed "inner stripe cells".[407,453] The IC of the OMCD resemble type A IC of the CCD, these cells have apical or diffuse staining for H-ATPase, basolateral staining for band 3 protein, and cytoplasmic staining for H,K-ATPase.[416,464,452] The rabbit OMCD IC do not bind peanut lectin,[416] and in contrast to the type A IC of the CCD, only −2 of the OMCD IC endocytose macromolecules.[467] Studies of pH_i in OMCD IC demonstrate characteristics of the prototypical type A cell in Figure 55.10: Na-independent acid extrusion and basolateral Cl/HCO_3 exchange.[488] Electrophysiologic studies clearly distinguish PC and IC, the IC have a lower basolateral membrane voltage, a predominantly Cl selective basolateral membrane, and virtually no measurable ionic conductance across the apical membrane.[489,490] All of these findings are consistent with IC mediating the HCO_3 reabsorption observed in the $OMCD_{os}$ of the rabbit. As was the case for HCO_3 reabsorption in the CCD, HCO_3 reabsorption in the $OMCD_{os}$ is sodium-independent and coupled to basolateral Cl/HCO_3 exchange.[487] In contrast to the CCD, HCO_3 reabsorption is relatively insensitive to inhibition by carbonic anhydrase.[487]

As indicated by the morphologic differences with the $OMCD_{os}$, the $OMCD_{is}$ is functionally distinct. In contrast to the $OMCD_{os}$ and CCD which contain PC, the $OMCD_{is}$ has not been reported to reabsorb Na. All inner stripe cells ($OMCD_{is}$) in the rabbit have apical intramembranous rod shaped particles (associated with H-ATPase), although in varying density.[453] However, only some cells stain for H-ATPase (apical location) and basolateral band 3 protein.[17,416,464] The cells also exhibit heterogeneity for the uptake of the pH sensitive dyes 6-carboxyfluorescein and BCECF (from the lumen).[467,491] However, these differences among cells do appear to represent quantitative differences of functional activity, but may not indicate qualitative differences of cell type as in the CCD.[492] As expected for type A cells, the cells of the $OMCD_{is}$ do not bind peanut lectin and do not endocytose macromolecules.[416,467] Studies of pH_i demonstrate basolateral Cl/HCO_3 exchange and Na-independent H extrusion which is sensitive to NEM.[475,493,494] In addition, these cells demonstrate basolateral Na-H exchange in the recovery of pH_i from acid loads.[475] OMCDis IC also express an apical $Na\text{-}HCO_3^-$ cotransporter (NBC3) that functions predominantly in intracellular pH homeostasis.[495] Functionally, HCO_3 reabsorption in the $OMCD_{is}$ is electrogenic (lumen positive transepithelial voltage), sodium-independent, and coupled to basolateral Cl/HCO_3 exchange.[496,497] In contrast to the CCD, the rabbit $OMCD_{is}$ does not have a luminal disequilibrium pH, this finding indicates the functional presence of luminal carbonic anhydrase.[405] (An acid disequilibrium pH can be demonstrated with addition of carbonic anhydrase inhibitors to the luminal solution.) As discussed below, some functional evidence suggests that HCO_3 reabsorption in the $OMCD_{is}$, particularly from potassium depleted rabbits, is mediated at least in part by H,K-ATPase.[412,498]

In sum, both segments of the OMCD only reabsorb HCO_3, in contrast to the more complex situation in the CCD. However, the process of HCO_3 reabsorption is basically the same as in the type A cell of the CCD: apical vacuolar type H-ATPase and H,K-ATPase, and basolateral Cl/HCO_3 exchange by a band 3 protein.

Inner Medullary Collecting Duct (IMCD)

The IMCD is divided into the initial and terminal segments, $IMCD_i$ and $IMCD_t$ respectively, based on

distinct morphology and function, the transition between these segments occurs after the initial 1/3 to 1/2 of the IMCD.[424,499,500] The $IMCD_i$ corresponds to the $IMCD_1$ in other terminology, and the $IMCD_t$ corresponds to the $IMCD_2$ plus the $IMCD_3$. The rat $IMCD_i$ contains −10% IC, in the rabbit, the $IMCD_i$ resembles the inner stripe cells of the $OMCD_{is}$.[121,500] The cells of the $IMCD_i$ have apical rod shaped particles and membrane associated carbonic anhydrase, the $IMCD_t$ lacks these features.[453,500] The $IMCD_t$ cells are homogeneous without IC and are referred to as IMCD cells.[453,500] Immunoreactivity for H-ATPase, band 3 protein, and H,K-ATPase have not been found or reported in the IMCD, except in the IC of the $IMCD_i$. Although NEM-sensitive ATPase activity (ascribed to H-ATPase) has been reported in some studies of the $IMCD_i$, the cellular location of this activity is not known.[453,501,502] H,K-ATPase activity has been found in the IMCD, as discussed below.

The IMCD has been studied with micropuncture, microcatheterization, and microperfusion techniques in the rat.[503,504] These studies indicate luminal acidification, sodium-independent bicarbonate reabsorption, and an acid disequilibrium pH (at least during systemic bicarbonate infusion).[401,403,505–511] A few *in vitro* microperfusion studies of acid–base transport in the IMCD have been reported. Ishibashi et al. found no luminal acidification in the rabbit IMCD.[512] Wall et al. found some H secretion and HCO_3 reabsorption in the rat IMCD (both $IMCD_i$ and $IMCD_t$) perfused *in vitro*, but the rate appeared to be less than reported *in vivo*.[504,513]

Because of the limited studies of intact IMCD *in vitro*, cell culture and suspension studies of IMCD cells assume additional importance. Cell cultures and suspensions of rat and rabbit IMCD demonstrate both Na-dependent and Na-independent H extrusion.[514–523] The Na dependent process (Na-H exchange) has now been localized to the basolateral membrane, indicative of a role in pH_i regulation and not in urine acidification.[515,524] The exact nature and cellular origin of the Na-independent H extrusion have been problematic, particularly for the $IMCD_t$ where no IC and conflicting evidence for vacuolar-type H-ATPase are found. However, as discussed below, significant evidence for H,K-ATPase in the IMCD is now available.[410,504] Other studies find evidence for H-ATPase.[520,525] Basolateral acid–base transport processes in IMCD cells have been studied also. Studies of pH_i in perfused and cultured rat IMCD have demonstrated basolateral Cl/HCO_3 exchange that may represent AE1 and AE2 (discussed below).[526–528] Cultured IMCD cells have also been reported to possess basolateral Na-coupled HCO_3 transport.[529]

Cellular Mechanisms of H Secretion in the Distal Nephron

H-ATPase

Much evidence exists for a H-ATPase mediating H secretion in the mammalian distal nephron and in particular the cortical and outer medullary collecting ducts.[530,531] In addition, as previously discussed, H-ATPase mediates some component of H secretion/HCO_3 reabsorption in the proximal tubule. Although the initial evidence for H-ATPase mediating urine acidification derived from turtle bladder, most of the subsequent biochemical data has been from bovine and rat kidney.[413,409,532] The initial evidence supportive of a H-ATPase was a report by Dixon and Al-Awqati demonstrating a DCCD-sensitive increase in intracellular ATP in turtle bladders with an imposed electrical or H gradient, a result consistent with a reversible, H-ATPase.[532]

The H-ATPase involved in urine acidification is a member of a novel class of proton-translocating ATPases, the vacuolar H-ATPases.[19,530] These proton pumps acidify the interior of a variety of intracellular organelles: endosomes, Golgi-derived vesicles, lysosomes, endoplasmic reticulum, and chromaffin granules.[533] Plasma membrane localization, associated with cellular H extrusion, has been reported in kidney tubule cells, osteoclasts, macrophages, epididymis, vas deferens, and interdental cells in the inner ear. This class of H-ATPase has ancestral relationships to the F_1F_0 H-ATPases, the class containing the mitochondrial ATP synthetase, this relationship is indicated by some sequence homology and by structural similarities.[414,533,534] The vacuolar H-ATPases contain 8–10 protein subunits, ranging in molecular weight from 12,000 to 116,000. A distinguishing feature of this class of H-ATPase is the pattern of inhibitor sensitivity: sensitivity to N-ethylmaleimide (NEM), 7-chloro-4-nitrobenz-2-oxa-1,3-diazole (NBD-C1), dicyclohexylcarbodiimide (DCCD), omeprazole, and bafilomycin, resistance to vanadate, azide, and oligomycin.[414,533] H-ATPase is also inhibited by cadmium.[530] The holoenzyme has a molecular weight of 500-700 kDa. The H-ATPase from kidney has been purified, reconstitution restores both ATP hydrolysis and ATP-dependent H transport.[535–537] By analogy with the F_1F_0 H-ATPases, the vacuolar H-ATPases have been modeled to have: (1) several globular, cytoplasmic subunits involved in ATP hydrolysis, (2) multiple copies of small intramembranous subunits forming the H channel, and (3) other subunits possibly involved in membrane anchoring or in coupling between ATP hydrolysis and H transport.[413,414,533,534] These subunits are located in two distinct domains or sectors, a predominantly

transmembrane V_0 sector responsible for proton translocation and a cytosolic V_1 sector involved in ATP hydrolysis and regulation (Figure 55.13).[530] Several subunits have more than one isoform which are selectively expressed in various tissues. There are 4 isoforms of the α subunit suggesting distinct roles, but all 4 are expressed in IC.[538] Intercalated cells selectively express a unique isoform of the B or 56 KD subunit, B1.[539] However, the B2 subunit is also expressed in IC.[540] Mutations in the B1 subunit and the a4 subunit (genes Atp6v1b1 and Atp6v0a4 respectively) have been characterized as causing distal reanl tubular acidosis.[541,542]

The evidence that an H-ATPase of the vacuolar class mediates urine acidification derives from several lines of evidence. First, the physiology of distal tubule H secretion correlates well with the biochemical information: electrogenic, sodium-independent ATP-requiring process.[404,496,543] Second, antibodies directed against H-ATPase stain the apical plasma membranes of rat intercalated cells.[17,18,415,458] Third, rabbit outer medullary collecting ducts from the inner stripe have H secretion which is sensitive to luminal NEM.[493] Also, affinity purified H-ATPase form arrays of stud-like structures in liposomes which are identical to structures observed in apical membranes of H secreting cells.[544] And finally mutations in H-ATPases subunits cause distal renal tubular acidosis.[19]

Because of the unique inhibitor sensitivity of vacuolar H-ATPase (i.e., NEM sensitivity, and resistance to many other inhibitors), NEM-sensitive ATPase activity has been used to localize and quantitate activity in various nephron segments.[346,501,502,545,546] Although the segmental localization and chronic adaptation (e.g., to acid loads and mineralocorticoids) often correspond to expectations based on other data, the interpretation of NEM-sensitive ATPase activity must be cautious because of the non-specific nature of NEM and because of the presence of intracellular vacuolar H-ATPase associated with cellular organelles. In other words, NEM sensitive ATPase activity may not accurately reflect plasma membrane H pump.

Regulation of renal H-ATPase probably occurs via several mechanisms.[19,530] Since the pump is electrogenic, the rate of H secretion will vary depending on the transmembrane voltage which is influenced predominantly by the rate of Na transport in the distal nephron. Cl may directly activate the pump.[414,547] And Cl dissipates the transmembrane voltage in intracellular organelles allowing acidification,[414,533] however, in the apical membranes of the IC of the collecting ducts, such a Cl channel has not been found functionally[489,488,548] except in cultured cells.[549] The chloride channel ClC-5 colocalizes with H-ATPase in type A ICs, but the functional activity is unknown.[550] Also Slc26a11 has also been localized in IC and could serve this function.[551]

The best characterized and probably most important mode of regulation of H-ATPase is targeting and recycling of pumps into and out of the apical membrane discussed in the section on "regulation of distal nephron acidification" below. Regulated assembly and disassembly of the subunits is also a well characterized mechanism of regulation in some systems,[530,552,553] regulated assembly of the V_0 and V_1 domains leading to membrane insertion is coupled to glucose metabolizing enzymes and the phosphatidylinositol-3-kinase pathway.[530,554–556] The latter signaling mechanism

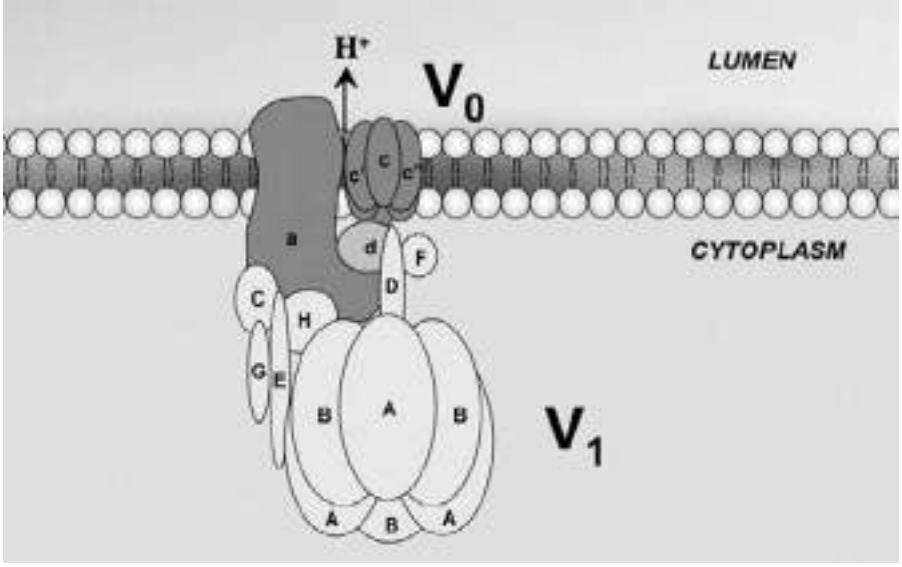

FIGURE 55.13 Model of H-ATPase. *(From Breton S, Brown D. New insights into the regulation of V-ATPase-dependent proton secretion. Am J Physiol Renal Physiol 2006,172:1107–1119, with permission.)*

may regulate H-ATPase via interaction with actin.[555] Other mechanisms of modulation of pump activity may include the lipid environment, cytosolic regulatory factors, and possibly activator and inhibitory proteins.[414,531,557–559] Transcriptional and translational regulation of H-ATPases do not appear to be important mechanisms, although the 31 kD subunit increases in IC with acidosis.[560]

H,K-ATPase

H,K-ATPases are also present in various distal nephron segments and contribute to acid secretion and HCO_3 reabsorption particularly in certain states such as potassium deficiency.[412,561–564] H,K-ATPases secrete H^+ and absorb K in an electroneutral manner. K-ATPase activity, insensitive to sodium and ouabain but sensitive to inhibitors of the gastric H,K-ATPase, was initially identified in distal nephron segments.[565,566] The impact of these findings was then amplified by a series of studies demonstrating the effect of these same inhibitors on HCO_3 transport.[410–412] Several approaches have demonstrated the presence and function of at least two isoforms of H,K-ATPase, HKα1 and HKα2, defined below.[410–412] Functionally, H secretion via H,K-ATPase has been identified by loss of function on K removal or by use of inhibitors such as omeprazole or SCH28080 (Schering-Plough).[412,567] K-ATPase activity, distinct from Na,K-ATPase, has also been used.[565,566]

H,K-ATPases are K- dependent ATPases of the E1,E2 class (P-type ATPase) and consist of two subunits, the α catalytic subunit and the β subunit. Four isoforms of the α subunit of H,K-ATPase have been isolated, cloned, and sequenced,[410] these are designated as HKα1, HKα2, HKα3, and HKα4 cloned from rat stomach,[568] rat distal colon,[569] toad bladder,[570] and human skin,[571] respectively. The HKα1, 2, and 4 isoforms have been referred to as gastric, colonic isoforms and ATPlAL1, respectively, ATP1AL1, also known as α4, is probably the human ortholog of the α2 gene.[572] The colonic α2 subunit has at least two molecular variants.[434,573,574] The four known α isoforms have different, but still incompletely defined, inhibitor sensitivity (reviewed in[410,412]). The HKα1 or gastric isoform is sensitive to omeprazole and SCH28080 but not to ouabain. The HKα2 or colonic isoform is sensitive to ouabain but not SCH28080. Both SCH28080 and ouabain inhibit HKα3 and HKα4, note, however, that no mammalian form of HKα3 has been identified yet. Other isoforms or variants have been suggested based on various discrepancies (between enzymatic activities and molecular events, and between model systems),[562,575–577] but recent work in knock-out mice suggest that gastric and colonic isoforms do account for K-ATPase enzymatic activities (an area of discrepancy and controversy particularly in rats).[578] Two β subunits have been shown to interact with H,K-ATPases, a gastric 2 isoform which is also expressed in kidney and the β1 subunit of Na,K-ATPase.[561,562,579–584]

The relative role of H,K-ATPase (versus H-ATPase), distribution of isoforms, and regulation have been examined. Both HKα1 and HKα2 mRNA have been found all along the collecting duct.[410] Mice with knockouts for either gastric or colonic H,K-ATPase have normal acid–base status,[585,586] but this may result from compensatory adaptations. In the CCD, H,K-ATPase functions in H^+ secretion at least after potassium depletion.[412,587] In the $OMCD_{is}$ under normal conditions, 35–70% of HCO_3 reabsorption appears to be mediated via H,K-ATPase.[588,589] Increased HCO_3 reabsorption in response to metabolic acidosis is secondary to increased H-ATPase[482,589,590] but the acute response to respiratory acidosis may be H,K-ATPase, at least in CCD.[591] But metabolic acidosis does stimulate H,K-ATPase activity.[417,592] Calcitonin and isoproterenol both stimulate H-K-ATPase activity, presumably in distinct IC populations, but the physiologic roles are not clear.[593,594]

Some data suggests a role for H,K-ATPase in HCO_3 secretion.[587,595] However, an apical H,K-ATPase (not basolateral as expected for HCO_3^- secretion) appears to be present in type β IC.[417,418,433,434,596] HKα2 is increased in CCD with metabolic alkalosis.[595]

With potassium depletion, increased HCO_3 reabsorption appears to be predominantly SCH28080 sensitive H,K-ATPase.[498,588,590] However, most information suggests that HKα2 (not usually SCH28080 sensitive) is the predominant isoform induced by potassium depletion particularly in medullary collecting ducts.[597–601] However, HKα1 may be also induced in CCD in potassium depletion.[598] Several studies of IMCD also demonstrate that SCH28080 inhibitable H secretion is present under basal conditions and stimulated by potassium depletion.[504,518] Other studies of cultured IMCD cells, however, have found predominantly H-ATPase.[520,525] As alluded to above, the isoforms of H,K-ATPase responsible for various functional findings are not entirely clarified. Some evidence suggests that an unidentified, H,K-ATPase isoform may be induced by hypokalemia or that the properties of known isoforms may be altered in potassium depletion.[562,577]

H,K-ATPase may play a role in sodium transport since sodium can substitute for potassium to accomplish sodium absorption and low Na diets up-regulate H,K-ATPase activity.[602–604] NH_4 may also substitute for H and thereby H,K-ATPase function in NH_4 secretion.[605–607] Isoproterenol and calcitonin stimulate collecting duct H,K-ATPase activity via a cAMP and ERK dependent manner.[593,594]

Basolateral Cl/HCO_3 Exchange

Early studies of H secretion in the turtle bladder and collecting tubule suggested basolateral Cl/HCO_3 exchange which was sensitive to disulfonic stilbenes (SITS and DIDS).[497,511,608] Inhibition of basolateral Cl/HCO_3 exchange inhibits luminal H secretion.[487,497,511] Studies of pH_i in IC of rabbit are also consistent with basolateral Na-independent Cl/HCO_3 exchange.[462,467,475,494] Studies using antibodies directed against the red cell Cl/HCO_3 exchanger (band 3 protein or anion exchanger AE1, SLC4A1) demonstrated immunoreactivity with mitochondria rich cells of the turtle bladder and with type A IC of rat, rabbit and human collecting ducts.[415,416,457,609,665,711] The molecular details of AE1 and the related kidney protein were subsequently elucidated.[612–616] A single gene encodes both the red cell and the kidney AE1 protein, however, an alternate start site leads to an mRNA in the kidney which has exons 1–3 deleted.[352,613,616] The major kidney AE1 protein therefore has a truncated N-terminus, this region of the protein is part of the cytoplasmic domain not directly involved in Cl/HCO_3 exchange.[611,617] SLC26A7 may also contribute to basolateral Cl^-/HCO_3^- exchange in the medullary CD and be regulated by distinct stimuli such as hypertonicity.[618–620]

The driving force for basolateral Cl/HCO_3 exchange would appear to be a concentration gradient of Cl from basolateral solution to cell, since most studies of pH_i in the collecting tubule suggest that the intracellular [HCO_3] in H secreting cells is close to or below extracellular [HCO_3].[475,462,467,488,494] Primary active H secretion across the apical membrane potentially produces cell alkalinization and elevation of intracellular [HCO_3], HCO_3 then is extruded across the basolateral membrane. Evidence does not support conductive pathways or significant sodium-coupled pathways for this HCO_3 exit in most distal nephron H secreting cells.[475,494,527] Cell Cl is undoubtedly lowered by a basolateral Cl channel as in Figure 55.10, the cell negative transmembrane voltage will drive Cl exit from the cell. Studies of IC in the CCD and $OMCD_{os}$ and of inner stripe cells have demonstrated that the basolateral membranes are predominantly Cl conductive.[548,489,621,622]

Few studies have directly addressed the regulation of either the basolateral Cl/HCO_3 exchanger or the basolateral Cl channels. However, two studies have examined the kinetics of the basolateral Cl/HCO_3 exchanger in intact $OMCD_{is}$. Breyer et al. reported a K_m for extracellular Cl of −10 mM, while Hays and Alpern reported a K_m of −114 mM.[475,494] The higher value of Hays and Alpern was measured in the presence of competing HCO_3 and thus represents an apparent K_m under physiologic conditions. This value would indicate that changes in extracellular [Cl] in the physiologic range could have important effects on $OMCD_{is}$ H secretion. In either case, the K_m for Cl is much higher than for H secretion in the turtle bladder (K_m <1 mM measured in the absence of HCO_3 which competes with Cl). Basolateral AE1 in the collecting duct does adapt to acid–base conditions.[623,624]

Although principal cells in the CCD also have basolateral Cl/HCO_3 exchange, the identity of the protein responsible is not clear.[450,451] Antibodies to AE1 protein do not label PC basolateral membrane, although this could be a result of low density of the transporter in these cells.[415,416] The PC Cl/HCO_3 exchanger is not active under normal conditions, but is activated by elevations in pH_i.[451,625] Similarly, all inner stripe cells and inner medullary collecting tubule cells apparently exhibit Cl/HCO_3 exchange,[475,494,514,527] but only some of the inner stripe cells and no $IMCD_t$ cells label with antibodies against AE1.[416,457] Basolateral Cl/HCO_3 in the collecting duct which is not accounted for by AE1 may be AE2. AE2 is on the basolateral membrane of some collecting duct cells, particularly in the inner medulla.[353,526,626,627] AE4 may also mediate some of basolateral HCO_3 transport.[628] SLC26A7 may also mediate basolateral Cl/HCO_3 exchange in the OMCD.[618,620] As noted above, cultured IMCD cells do exhibit basolateral Na-HCO_3 symport.[524]

In sum, cellular HCO_3 is extruded in most H secreting cells of the distal nephron by a truncated form of band 3 or AE1 protein. Cl/HCO_3 exchange also occurs in other cells, but the molecular identity of the other exchangers is not resolved. Basolateral chloride channels are discussed below.

Cellular Mechanisms of HCO_3 Secretion

Apical Cl/HCO_3 Exchange

The apical process in HCO_3 secreting IC is the Cl/HCO_3 exchanger pendrin, SLC26A4. The functional properties were established by transepithelial flux studies and directly demonstrated by studies of pH_i in rabbit IC.[443,451,462,478,479] Transepithelial flux studies of HCO_3 and Cl first demonstrated Cl/HCO_3 exchange in CCD.[476,478,479] Studies of cell pH have subsequently clearly shown apical Cl/HCO_3 exchange in CCD IC. For instance, changes in luminal Cl or HCO_3 alter cell pH in a predictable fashion.[451,467] These cells also show cellular acidification with removal of basolateral Cl, indicative of apical Cl/HCO_3 exchange, presumably as basolateral Cl is removed, cell Cl is depleted, and Cl will enter the cell across the apical membrane in exchange for extrusion of cellular HCO_3.[451,462] Prior

removal of luminal Cl, before removal of basolateral Cl, blocks the cell acidification.[451] Physiologic studies demonstrate that the apical exchanger differs from the basolateral exchanger present in type A IC.[478,629] Also, the apical membranes of type B IC (or most IC of the rabbit CCD) do not stain with antibodies to AE1 protein, in contrast to the basolateral membranes of type A IC.[415,416,457,610,611] The apical Cl/HCO_3 exchanger in B IC is likely not the same protein as the basolateral Cl/HCO_3 exchanger in type A IC. The exchanger appears to function in transepithelial anion transport but does not appear to be involved in acute regulation of intracellular pH.[625] The exchanger has little if any role in cell pH recovery from acid loads and also may not be activated by cell alkalinization.[625] The exchanger actually exchanges Cl for Cl (Cl self exchange) at a rate greater than Cl/HCO_3 exchange.[476,629,630] The exchanger appears to be activated by cAMP as discussed below.[478,631,632] The K_m for luminal Cl is 10 mM in the rabbit CCD,[632] with the apparent halide affinity $Cl^- \sim Br^- > I^- > F^-$.[633]

Pendrin has now been established as the apical Cl/HCO_3 exchanger in B IC. Pendrin (SLC26a4) is the gene product, originally identified as an iodine transporter defective in Pendred's Syndrome, an autosomal recessive deafness and goiter. It localizes to the apical membrane of HCO_3 secreting type B IC and non- A, non-B IC. CCD from pendrin knock-out mice does not secrete HCO_3.[460,447,634] Pendrin expression and apical localization increase with alkali loads and mineralocorticoids and decrease with acid loads.[460,635–638] Pendrin likely has both cytosolic and extracellular pH regulatory sites.[639] Pendrin expression also responds to chloride balance and appears to be involved in blood pressure regulation.[640,637,641,642]

In contrast to studies implicating pendrin, some earlier evidence suggested that the apical Cl/HCO_3 exchanger in Type B IC is a form of AE1.[643–646] These investigators suggest that the kidney form of AE1 is not detected by usual immunocytochemical methods because the antigen is Alatent@ or hidden in the apical domain of B cells.[643] Another anion exchanger AE4 has also been proposed to account for apical Cl/HCO_3 exchange, at least in the rabbit.[647] However, other studies find properties of AE4 (such as a lack of change with acid–base perturbations) that differ from CCD HCO_3 secretion.[628]

Basolateral H Extrusion

HCO_3 secretion in the turtle bladder and mammalian CCD is active and acetazolamide sensitive.[409,443] The basolateral H extrusion mechanism in bicarbonate secreting cells is the active driving force for HCO_3 secretion. The molecular mechanism of H extrusion in these cells is undoubtedly a vacuolar H-ATPase, at least in large part.[408] In the rat, antibodies against vacuolar ATPase stain the basolateral membrane of a portion of IC in the CCD,[17,415,458,474] H-ATPase may be be stabilized there by association wih NHERF1.[530] In the rabbit CCD, most lectin positive cells (B IC) have diffuse cytoplasmic, rather than basolateral, immunoreactivity for H-ATPase.[464] However, all the physiologic data in rabbit CCD are consistent with basolateral H-ATPase.[416,443,479] Although Na-H exchange is present on the basolateral membranes of type B IC (to regulate pH_i),[451] HCO_3 secretion in the rabbit CCD is insensitive to ouabain, peritubular amiloride, and removal of sodium.[416,443,479,648] [One study did show a decrease in HCO_3 secretion with removal of sodium.[443]] Na-H exchange appears to mediate all of the pHi recovery from intracellular acid loads in type B IC.[451] Rod shaped particles are present in both membranes of rabbit CCD IC and in the basolateral membrane of some rat IC, as discussed alone.[453,459] The possible role of H, K-ATPase in HCO_3 secretion has not been tested in the CCD. In sum, most evidence is consistent with basolateral H-ATPase mediating HCO_3 secretion.

BASOLATERAL CHLORIDE CHANNELS AND OTHER TRANSPORTERS

Basolateral Cl channels are present in both type A and type B IC. A predominant basolateral Cl conductance has been clearly demonstrated by electrophysiologic techniques in type A IC of CCD and $OMCD_{os}$ and in inner stripe cells of $OMCD_{is}$.[489,490,548,622] The possible role of these channels in regulation or modulation of HCO_3 reabsorption is unknown. Cl channels presumably recycle Cl across the basolateral membrane, extruding Cl which enters the cells on the basolateral Cl/HCO_3 exchanger. The exact nature of Cl channels in IC (e.g., selectivity, unit conductance, molecular identity, etc.) has not been clearly determined. Although chloride channels have been isolated from the kidney, the exact function of these is still unsettled.[649] In addition, two potential regulators of chloride channels, P-glycoprotein and CFTR, have been found in collecting ducts among other sites in the kidney.[649,650] In the rat $IMCD_i$, a basolateral HCO_3 conductance is found, without a basolateral Cl channel.[651]

The apical membranes of H secreting cells do *not* appear to possess functional Cl channels despite the usual association of vacuolar H-ATPase with Cl channels, this conclusion is based on electrophysiologic studies which show the fractional resistance of the apical membranes of these cells to be approximately 1.[489,490,548] Since Cl secretion is stoichiometrically equal to H secretion (or HCO_3 reabsorption) in the $OMCD_{is}$ which has no other active transport, Cl flux presumably occurs via the paracellular pathway, driven by the lumen positive voltage.[497] In cultured CCD cells which

resemble IC cells, an apical Cl channel has been observed in excised patches, however, these channels were not usually open in cell-attached patches.[549] The chloride channel ClC-5 has been found to colocalize with H-ATPase in Type A IC but its function there is unknown.[550] ClC-5 which also is located in the proximal tubule may function in endocytosis rather than in transepithelial transport,[550] ClC-5 is mutated in Dent's disease, which is characterized by hypercalciuria and kidney stones.

Cl channels in the basolateral membranes of type B IC have been studied little via electrophysiologic techniques.[622] However, tracer flux experiments in rabbit CCD have indirectly shown several important features of these channels.[476] In the CCD, Cl reabsorption occurs via two pathways.[476] First, Cl is reabsorbed via the paracellular pathway as sodium is absorbed, Cl moving down an electrochemical gradient, predominantly due to the lumen negative transepithelial voltage. Second, Cl is reabsorbed via the type B IC. With sodium reabsorption blocked, Cl moves predominantly via the latter pathway which involves the series of the apical Cl/HCO_3 exchanger (or Cl/Cl self exchanger) and the basolateral Cl channel.[476] Inhibition of transepithelial Cl self exchange by peritubular chloride channel blockers is evidence for the presence of basolateral Cl channels in type B IC. cAMP appears to activate these channels in conjunction with acceleration of apical Cl/HCO_3 exchange (or Cl/Cl self exchange).[629,632] Also low concentrations of intracellular HCO_3 activate these channels.[40,630,652] These channels are inhibited by typical Cl channel blockers such as DPC (diphenylamine-2-carboxylic acid) and anthracene-9-carboxylate.[629,652] The chloride channel ClC-3 has been localized to type B IC.[653]

Electroneutral NBC-3 (or NBCn1) is in the apical membrane of Type A IC and OMCD cells, and in the basolateral membranes of Type B IC and IMCD cells,[654–656] but the exact role and function in transepithelial acid–base transport is unknown.[495,657] The KCl co-transporter KCC4 is in the basolateral membrane of type A IC and may have a role in acid secretion.[658]

Role of Carbonic Anhydrase

Carbonic anhydrase (CA) facilitates acid–base transport in the distal nephron, just as in the proximal tubule and the thick ascending limb discussed previously.[157,158,659] Both histochemical methods (e.g. Hanson's technique) and immunocytochemical methods, and more recently molecular techniques, have been used to localize CA along the distal nephron. Principal cells either do not stain for CA or stain weakly. In contrast, intercalated cells along the distal nephron have intense cytoplasmic CA staining,[375,377,660,661] probably representing Type II CA.[377,662–665] CA II may be important in the development of the IC phenotype.[530] In addition to cytosolic CA, mouse and rabbit IC have membrane associated CA staining, particularly on the apical membrane.[375,453] In the rat, IC do not have membrane associated CA staining[660] or immunoreactivity for CA type IV, the predominant renal membrane associated with CA.[666] In the human kidney, in contrast to other species, all distal convoluted tubule cells are reportedly positive for CA,[377,664,667] in the rat, distal convoluted tubule cells have basolateral membrane staining.[661] In the rabbit $OMCD_{is}$, staining for CA is predominantly in the apical membrane but there is variability along the length of the segment, the number of positive cells increasing from outer to inner zone of $OMCD_{is}$,[453] rabbit $OMCD_{is}$ and $IMCD_i$ have CA type IV by RT-PCR.[668] Although the $IMCD_i$ has predominantly membrane staining as in the $OMCD_{is}$, the $IMCD_t$ does not have CA staining at least in the rabbit,[453] mouse,[375] and probably the rat.[661] Cells in the human kidney IMCD do stain for both CA II and IV.[664,669] Studies of rat IMCD also demonstrate CA activity.[514,670] Another isozyme of membrane associated CA, CA XII, has been shown in the basolateral membranes of the TAL, the distal tubule, and principal cells of the collecting duct.[671–673] Obviously, variations in species, cell types, and techniques prevent a cohesive understanding of the role of CA along the distal nephron. However, CA is present in most, if not all, distal nephron cells involved in acid–base transport. Despite the membrane staining in some cells, functional studies discussed below demonstrate no luminal CA in most distal nephron segments.

Acid–base transport, both HCO_3 reabsorption and secretion, in each segment of the distal nephron is sensitive to inhibition of CA.[443,444,477,481,487,510,511] Bicarbonate reabsorption in the papillary collecting duct (or $IMCD_t$) is also sensitive to CA inhibition,[510,511] despite the apparent lack of staining for CA by either histochemical or immunocytochemical methods,[661,662,666] this may indicate a lack of sensitivity of the localization methods. Both CA II and CA IV are induced by metabolic acidosis in those nephron segments expressing basal activity.[668,674]

Several segments of the distal nephron have been found to have a spontaneous acid disequilibrium pH, this not only indicates H secretion, as opposed to base absorption, but also implies the functional absence of luminal CA. A spontaneous acid disequilibrium pH has been found in the superficial distal tubule, the CCD, $OMCD_{os}$, and papillary collecting duct.[6,401,403,405,406] The acid disequilibrium pH, but not

H secretion or HCO_3 reabsorption, can be eliminated by perfusion of tubules with exogenous carbonic anhydrase.

The acid luminal disequilibrium pH in the distal nephron is important in at least two regards. First, a low luminal pH maintains luminal NH_3 concentrations low, favoring NH_3 diffusion into the collecting duct. Second, the lack of luminal CA is important in the elevation of urinary pCO_2 above plasma pCO_2, infusion of CA lowers urinary pCO_2 to blood levels.[401,675] In the presence of luminal HCO_3, H secretion in the distal nephron acidifies the luminal fluid, but in the absence of CA, the formation of CO_2 from HCO_3 and carbonic acid is slow. CO_2 formed in the inner medullary collecting duct does not diffuse into the adjacent vasa recta because of a high pCO_2 in these structures, a result of trapping of CO_2 in the medullary countercurrent system.[401] CO_2 formed in the renal pelvis or below does not rapidly diffuse out, presumably because of a low surface-to-volume ratio in these structures.

Functional evidence for luminal CA has been found in two distal nephron segments, the $OMCD_{is}$ of the rabbit and the $IMCD_i$ of the rat.[405,668,676] In the $OMCD_{is}$ this was initially shown by a disequilibrium pH which was apparent only during perfusion with a carbonic anhydrase inhibitor.[405] Later studies demonstrated inhibition of bicarbonate reabsorption by membrane impermanent CA inhibitors.[677] To demonstrate luminal CA in the rat $IMCD_i$ *in vitro*, H were generated in the lumen by creating a lumen-to-peritubular NH_3 gradient, pulling the reaction $NH_4^+ \rightarrow NH_3 + H$ to the right, with this protocol, no disequilibrium pH was present in $IMCD_i$ whereas an acid disequilibrium pH was produced in the $IMCD_t$.[676] Luminal CA in these segments of the distal nephron may facilitate reabsorption of any remaining HCO_3 presented to the distal nephron.[676]

Thus, cellular CA facilitates acid–base transport in the distal nephron. However, in most distal nephron segments, the functional absence of luminal CA results in an acid luminal disequilibrium pH, facilitating trapping of NH_3/NH_4^+.

Regulation of Distal Nephron Acidification

Peritubular and Luminal pH

Both *in vivo* and *in vitro* studies have demonstrated that systemic or peritubular pH modify distal nephron acid–base transport.[441,485,678] This regulation has both acute and chronic components. Acutely systemic pH alters U-B pCO_2 (urine pCO_2–blood pCO_2), an index of distal nephron H secretion.[401,679,680] Also acute metabolic acidosis has been found to stimulate inner medullary H secretion.[509] Although some studies have demonstrated systemic pH effects in the distal tubule,[436,483,484] some prior studies have not found changes in superficial distal tubule acid–base transport in acute metabolic acidosis.[430,431] Several studies have addressed acute changes in acid–base transport in isolated perfused rabbit collecting ducts. This decreases in peritubular $[HCO_3]$ and pH increase net HCO_3 reabsorption in both cortical and outer medullary collecting ducts.[512,681,682] Also increasing peritubular pCO_2 increases HCO_3 reabsorption in the $OMCD_{os}$ and $OMCD_{is}$.[683] Results of studies examining the effect of pCO_2 on CCD have differed. Breyer and colleagues reported no change in net HCO_3 transport with elevation of pCO_2,[681] however, similar studies by McKinney and Davidson reported increased net HCO_3 reabsorption.[683] This discrepancy may result from different rates of bicarbonate secretion or bicarbonate reabsorption in the control condition, no studies have addressed the effects of elevations of pCO_2 on unidirectional HCO_3 secretion.

Acutely increased H secretion or HCO_3 reabsorption with decreased peritubular pH may result from several mechanisms. Decreased peritubular $[HCO_3]$ will directly accelerate basolateral Cl/HCO_3 exchange in H secreting cells.[494] This will secondarily lower pH_i. Decreases in cell pH (independent of pCO_2 or $[HCO_3]$) have been shown to accelerate apical H secretion, at least in the turtle bladder.[684] The effect of cell pH on H secretion is likely to result, at least in part, by direct effects on the H pump, via both kinetic and thermodynamic effects.[409,684–687] However, the direct effects of pHi on the kinetics of H-ATPase may be small.[413] Increased pCO_2 will also lower cell pH since CO_2 is extremely permeable across cell membranes. Increased H secretion may then result from effects of lowered cell pH. The increased H secretion with increased CO_2 can not result from thermodynamic effects since luminal pH will be decreased just as cell pH. Recent studies of mechanisms of pH regulation of acid–base transport have focused on potential pH and/or HCO_3^- "sensors." GPR4, a G protein coupled receptor, appears to be such a pH sensitive receptor located in the collecting duct that may serve to regulate acid–base homeostasis.[688] H-ATPase itself and soluble adenylyl cyclase (discussed below) are potential pH/HCO_3 sensing mechanisms.[689]

The best characterized mechanism of acute (and perhaps chronic) regulation of H-ATPase is insertion and removal from tubulovesicular structures and the plasma membrane. The process of membrane recycling resembles the insertion and retrieval of clathrin coated vesicles but is not associated with clathrin or calveolin in the collecting tubule.[530,690,691] Exocytic insertion of H pumps is also microtubule/

microfilament dependent and similar to mechanisms of neurosecretory exocytosis, involving SNARE and SNAP proteins.[692,693] A variety of intracellular proteins may be involved in the trafficking machinery: syntaxin 1A, SNAP23, cellubrevin, ARNO, and Arf6.[530,693–695] H-ATPase subunits may also interact interact with the actin cytoskeleton for localization and trafficking.[530] Changes in cell calcium (discussed below) may be involved in the interaction of H-ATPases and the actin cytoskeleton.

The exocytic insertion of H pumps into the apical membrane from subapical endocytic vesicles was historically demonstrated early for increased pCO_2 but may be applicable for decreased cell pH in general and a variety of other stimulators of acidification.[465,690,696] The exocytic insertion of H pumps was first demonstrated in the turtle bladder, but has since been extended to both the proximal tubule and the collecting tubule.[192,697,698] Studies using fluorescent probes attached to macromolecules (dextran or albumin usually) demonstrate luminal endocytosis into acidic subapical vesicles with lowering pCO_2. On stimulation of H secretion with increased pCO_2 or with application of weak acids, these vesicles fuse with the apical membrane, releasing their contents and presumably inserting more H pumps into the plasma membrane.[192,462,465,697] In the turtle bladder, there is simultaneous increased apical H secretion, an increase in apical surface area of H secreting cells, and increased electrical capacitance,[696,698–700] in rabbit $OMCD_{is}$ there is no apparent acute change in surface area.[683] However, morphologic studies of rat type A intercalated cells after several hours of increased pCO_2 do demonstrate this fusion and apparent recycling of rod shaped intramembranous particles (associated with H-ATPase) between subapical tubulovesicular structures and plasma membrane, apical surface area is increased and subapical vesicles are decreased.[425,455,701] Similar changes occur with metabolic acidosis *in vivo*.[702,703]

One component of the relationship between decreased intracellular pH and exocytosis is an increase in cell calcium, buffering of cell calcium prevents the exocytosis and the increase in H secretion.[692,704] The exocytic process and increased H secretion are also sensitive to colchicine and other inhibitors of microtubule and microfilament function.[683,697,698,705] The increase in H secretion with increased pCO_2 may return cell pH back towards normal, yet transepithelial transport remains stimulated.[704] Other conditions, previously thought to alter H secretion directly by changes in pH_i, may also have other mechanisms of action. For instance, acetazolamide increases cell pH but additional mechanisms of inhibition of H secretion seem likely, acetazolamide appears to induce apical endocytosis which could be responsible in part for reduced H secretion.[699,706] In sum, acute changes in peritubular and cell pH alter H transport by at least two mechanisms: (1) direct effects on the H pump and on the basolateral Cl/HCO_3 exchange process, and (2) exocytic insertion of additional H pumps with stimulation. Recycling of H-ATPase between apical membrane and subapical tubulovesicular structures appears to be an important mechanism of the regulation of H secretion in the collecting duct.[465,690,696]

Chronic changes in systemic pH or peritubular pH induce additional changes in distal nephron acid–base transport. This is best illustrated by *in vitro* studies of collecting tubules which have been obtained from animals which have been loaded with acid or base. McKinney and colleagues first reported that rabbit CCD could either reabsorb or secrete HCO_3 *in vitro*, depending on the prior *in vivo* conditioning of the animals.[405,423,443] Similar results have since been obtained in rat cortical collecting ducts perfused *in vitro* and rat superficial distal tubules perfused *in vivo*.[419,422,439] Inner medullary collecting ducts also adapt to metabolic acidosis or alkalosis.[507,508,511,513] In contrast to these results, rabbit outer medullary collecting ducts (both $OMCD_{is}$ and $OMCD_{os}$) perfused *in vitro* have not consistently shown adaptation to either acid loads or respiratory acidosis *in vivo*.[477,487,589,707] The adaptations of the CCD occur rapidly after *in vivo* signals, one hour after an acid load in rabbits and one hour after chloride depletion alkalosis in rats, but the changes persist *in vitro* for relatively long times (greater than an hour) despite incubation in solutions of normal pH.[445,708] Speculatively, the signals for these changes in acid–base transport may not require changes in extracellular pH per se since feeding or high protein diets which cause little or no change in plasma pH alter transport,[429,422,709] the signals for any pH-independent changes associated with acid or protein loads are not known. However, at least for pendrin expression, changes in chloride excretion in addition to acid–base status are important.[710]

The cellular mechanisms of the changes in the cortical collecting duct have been examined by Schwartz, Al-Awqati, and colleagues. Early studies suggested that type A and type B cells could interconvert or reverse polarity.[462] In these studies, type A and B intercalated cells were defined by endocytosis of macromolecules and peanut lectin binding, respectively.[462] With acid loading of rabbits, an increased number of type A cells and a decreased number of type B cells were found. Since cellular proliferation was excluded and the total number of intercalated cells remained constant, reversal of cell polarity was proposed. Subsequent studies by Satlin et al. examined lectin

positive cells during continuous exposure to an acid peritubular media *in vitro*, after 3–5 hours, cells lost peanut lectin binding, developed endocytosis, and exhibited decreased apical Cl/HCO_3 exchange.[486] Subsequent studies of acidosis *in vitro* have shown both decreased HCO_3 secretion and increased HCO_3 reabsorption via H-ATPase.[482] Further studies demonstrated that with acid incubation, some type B IC not only lose apical Cl/HCO_3 exchange, but acquire basolateral Cl/HCO_3 exchange, an effect mediated in part by the extracellular protein hensin.[473,472,711] Purkerson et al. using immunofluorescence for AE1 and pendrin have confirmed this model of variation in these anion exchangers with acidosis and recovery.[712] Although these results do not confirm strictly defined reversal of polarity, they do demonstrate remarkable cellular remodeling. Even though reversal of polarity in the strictest sense has been controversial based on the differences in the apical and basolateral Cl/HCO_3 exchangers discussed previously, Al-Awqati and collaborators demonstrated reversal of polarity in an immortalized β IC cell line *in vitro*, in addition to the findings in perfused tubules sited above.[643,644,713] In this cell line reversal of polarity is dependent on seeding density, subsequent studies demonstrated that the mediator of this reversal of polarity was the extracellular matrix protein, hensin/DMBT1, interacting with integrins and two secreted proteins, galectin-3 and cypA (a cis-trans prolyl isomerase).[472,643,644,711,713,714] Blocking antibodies against hensin prevent the polarity reversal, and deletion of hensin blocks conversion of B to A IC.[473,715] Galectin-3 facilitates hensin's role in the adaptation to acidosis.[716] Other studies demonstrated that the response to acidosis involving hensin requires cyclophilins, evidenced by inhibition by cyclosporine A.[717]

Bastani et al.,[474] examining cellular H-ATPase distribution in rat CCD using immunocytochemistry, found a spectrum of patterns ranging between prototypical B cells to prototypical A cells, with H-ATPase on the basolateral and apical membranes, respectively. The distribution of H-ATPase polarity in this spectrum varies with acid or base loads.[474] Besides distribution in apical and/or basolateral membranes, H-ATPase in IC resides in submembrane vesicles in the cytoplasm. Other morphologic studies of the rat CCD have shown that respiratory acidosis induces distinct changes in type A cells but no clear evidence of interconversion of cell types.[425] Another study of rat CCD found a constant percentage of intercalated cells with apical H-ATPase, suggesting no reversal of polarity, the remaining IC cells had an inverse proportion of cells with basolateral staining and with diffuse cytoplasmic H-ATPase immunoreactivity, suggesting alterations between these two forms only.[458] The presence of significant numbers of intercalated cells with diffuse cytoplasmic staining for H-ATPase (rather than apical or basolateral membrane staining) has led to an alternative hypothesis that some cells are "hybrid cells" able to change function depending on conditions.[464,474,690] Two functional studies using rabbit CCD suggest that acid loading *in vivo* results in tubules with dramatically reduced unidirectional HCO_3 secretion, but with minimal increases in unidirectional HCO_3 reabsorption.[413,480] This would be consistent with altered function of type B intercalated cells in rabbits, but with little effect of acid loads on type A cells, the latter would correspond with the lack of effect of acid loads on outer medullary collecting duct HCO_3 reabsorption.[477,487] In contrast, studies of CCD from rats with chloride depletion metabolic alkalosis suggest that both HCO_3 reabsorption and HCO_3 secretion are altered.[445] Also, studies of both rabbit CCD and $OMCD_{is}$ demonstrate adaptation of HCO_3 reabsorption, in addition to changes in HCO_3 secretion in CCD.[482,589] Recent studies in rats suggest that type A IC in the cortical and outer medullary CD proliferate in response to systemic acidosis and that growth differentiation factor 15 is involved early in this process.[718,719] In sum, dramatic changes occur in the structure and function of intercalated cells of the CCD with acid loads, however, the exact nature and mediators of these changes remain under study. Clearly, intercalated cells exhibit considerable variation in phenotype and remarkable plasticity.

Besides these "remodeling" changes in CCD, additional mechanisms of adaptation of transport may also occur with chronic acid loading. The adaptations in the IMCD during acidosis are unlikely to result from any changes in intercalated cells since these are not present in the inner medulla. Metabolic acidosis has been reported to increase NEM-sensitive ATPase at least in the CCD.[346,502] However, there are varying results regarding whether mRNAs for H-ATPase subunits increase with acidosis.[474,560]

Luminal pH may also alter distal nephron acid–base transport based on findings in turtle bladder studies.[720] In these studies, H secretion decreased linearly with decreases in mucosal pH, a result of a decreased H pump rather than an H leak.[720] Assuming that a low luminal pH does inhibit collecting duct H secretion, increased delivery of luminal buffers will enhance H secretion by decreasing changes in luminal pH as H secretion occurs. Some *in vivo* microperfusion studies of the rat superficial distal tubule have demonstrated increased HCO_3 reabsorption with increased loads.[426,428]

Although the effect of luminal pH or buffer delivery has not been well studied in distal nephron segments, microperfusion studies have confirmed that the rabbit CCD and $OMCD_{is}$ and the rat superficial distal tubule

have low H and HCO_3 permeabilities.[428,681] Also studies of pH_i in $OMCD_{is}$ and IMCD have shown minimal changes with luminal pH.[494,527] Similar findings have been reported in the principal cells of the CCD.[625] Therefore, pH_i of distal nephron cells appears to be predominantly affected by peritubular pH rather than by luminal pH. However, luminal HCO_3 does influence pH_i of type B intercalated cells, as expected with an apical Cl/HCO_3 exchanger.[625]

In sum, systemic and luminal pH alter distal nephron H secretion and HCO_3 reabsorption. The mechanisms are multiple: acute kinetic and thermodynamic effects on membrane transporters, acute insertion of additional transporters into the plasma membrane, and chronic alterations in cellular structure and function. As discussed below, endogenous hormones such as prostacyclins and endothelin may mediate some of these changes.

Sodium and Chloride Delivery and Transepithelial Voltage

Clearance studies have clearly shown that the delivery of sodium and the nature of the accompanying anion have marked influences on distal nephron acidification.[721–723] Increasing sodium delivery, especially in the presence of nonreabsorbable anions, increases H secretion, this effect is most evident in animals with volume depletion or increased mineralocorticoids.[722] However, as reviewed above, luminal H secretion is independent of Na in all of the distal nephron segments past the TAL.[404,430,444,496,511] The effect of sodium delivery and the accompanying anion can be explained by the electrogenic nature of distal H secretion.[543,685,724] H secretion in the CCD and $OMCD_{is}$ has been shown to be both electrogenic and sensitive to the transepithelial voltage.[404,496,725] In the CCD, sodium reabsorption results in a lumen negative transepithelial voltage which will stimulate H secretion, with increased mineralocorticoids or a nonreabsorbable anion the magnitude of the lumen negative voltage will be increased, resulting in more H secretion. In the $OMCD_{is}$, sodium reabsorption does not occur, and H secretion results in a lumen positive transepithelial voltage.[477,496,725] H secretion in the IMCD also appears to be electrogenic, at least in part,[516] however, the influence of transepithelial voltage is unknown in this segment. In the rat superficial distal tubule, luminal flow rate and HCO_3 delivery are also important determinants of HCO_3 transport.[426,428,439]

Chloride concentrations are also an important determinant of distal nephron acid–base transport. Several studies have clearly shown that chloride concentrations in the luminal and peritubular solutions alter net HCO_3 transport in the CCD.[442,479,726] Based on the models in Figures 55.10 and 55.11, HCO_3 reabsorption depends on the presence of peritubular Cl, and HCO_3 secretion depends on the presence of luminal Cl, this has been experimentally verified.[442,479,480] Changes in Cl delivery *in vivo* may be important since the K_m for luminal Cl/HCO_3 exchange in HCO_3 secretion is 5–10 mM,[632] this range of concentrations is relevant for considerations of the maintenance and repair of chloride depletion metabolic alkalosis. The plasma concentrations of Cl may also be physiologically important since some studies have suggested that the K_m for $OMCD_{is}$ Cl/HCO_3 exchange is 115 mM, i.e., in the physiologic range.[494] Chloride concentration gradients may also alter H secretion by altering transepithelial voltage.[725,726]

Mineralocorticoids

Mineralocorticoids are an important determinant of net acid excretion by the kidneys[727,728] and may mediate the effects of extracellular fluid volume on distal nephron acidification.[729] Several mechanisms explain the stimulation of H secretion in the distal nephron. First, mineralocorticoids are well known to stimulate Na reabsorption and the lumen negative transepithelial voltage in the CCD, H secretion will increase secondary to the altered voltage. Second, mineralocorticoids directly stimulate H secretion in the CCD and $OMCD_{is}$, independent of Na transport.[404,496] Some of this response occurs after only a few hours and can be observed *in vitro*. Recently, a rapid nongenomic stimulation of H-ATPase activity by aldosterone was reported in OMCD,[730] a transient rise in intracellular calcium and a requirement for PKC were found in this response. Chronic mineralocorticoids also increase NEM sensitive ATPase.[501,546] Therefore mineralocorticoid stimulation of H secretion may have both early and late mechanisms of action, as has been shown for stimulation of Na transport. Mineralocorticoids also stimulate inner medullary collecting duct H secretion, probably independent of Na reabsorption.[731] Mineralocorticoids also have effects on H,K-ATPases and ammonia transporters. The effects on H,K-ATPase include increased mRNA of H,K-ATPase $\alpha 2$.[732] These effects interact with luminal V1a AVP receptors in IC.[733] Another potential mechanism of mineralocorticoid stimulation of H secretion is via potassium depletion, discussed below.

Mineralocorticoids also stimulate HCO_3 secretion in the CCD.[446,734] Acid-loading of mineralocorticoid-treated animals eliminates this HCO_3 secretion.[480] Therefore, the increased HCO_3 secretion may be secondary to the systemic alkalosis produced by mineralocorticoids. However, the effect of mineralocorticoids to

increase HCO_3 secretion could be direct, but still inhibitable by acid loading.

Potassium

Clinically potassium depletion is usually associated with metabolic alkalosis and inappropriate urine acidification. However, the direct effects of K depletion on distal nephron acidification are complicated by changes in aldosterone secretion.[735] Potassium depletion *per se* decreases aldosterone levels, clinically however, K depletion often occurs in conditions associated with increased mineralocorticoids. Potassium depletion appears to potentiate the effects of mineralocorticoids to increase H excretion.[736]

Hypokalemia significantly increases HCO_3 reabsorption in the superficial distal tubule.[426,427] The effect of *in vivo* potassium depletion on distal acidification has been addressed in several studies. Initially McKinney and Davidson studied K depleted rabbits and found increased HCO_3 reabsorption in the CCD and decreased HCO_3 reabsorption in OMCD, mineralocorticoids administered to the K depleted animals increased both CCD and $OMCD_{is}$ HCO_3 absorption.[737] The K depleted animals had decreased aldosterone levels and metabolic acidosis, which complicates the interpretation. Hays et al. also studied K depleted rabbits, but their animals were alkalotic, despite the alkalosis, no HCO_3 secretion was found in CCD and HCO_3 reabsorption in $OMCD_{is}$ was unchanged from control values.[737] These studies suggest that K depletion is associated with increased or inappropriate collecting duct H secretion or HCO_3 reabsorption, especially considering the suppression of aldosterone in the experimental models.

As discussed previously (see section on H,K-ATPase), Wingo found that HCO_3 reabsorption in $OMCD_{is}$ from K depleted animals is sensitive to luminal omeprazole, an inhibitor of gastric H,K-ATPase.[498] Other studies also suggest increased H,K-ATPase activity in collecting ducts from K depleted animals.[565] Since these early studies, a variety of studies (discussed previously) have found increased H,K-ATPase along the collecting duct in potassium depletion.[410,412] Increased membrane insertion of H-ATPase in K depletion is another probable mechanism of increased collecting duct H secretion since an increased number of rod-shaped particles is found in IC, as in acidosis.[738] Other studies demonstrate enhanced apical H^+ATPase, and basolateral AE1 and Slc26a7 during K depletion.[739]

Endothelin: Endothelin has been shown to mediate some of the effects of systemic acid loads on distal tubule acid−base transport.[210] Acid loading of rats increases renal cortical interstitial endothelin-1 (ET-1), and inhibition of Type B endothelin receptors blunts the HCO_3 secretory and reabsorptive changes induced by acid loading.[210] Infusion of ET-1 *in vivo* increases H^+ secretion via Na-H exchange and decreases HCO_3 secretion in rat superficial distal tubules.[436,740] Acidosis directly increases ET-1 secretion by renal microvascular endothelial cells.[741] Further *in vitro* studies indicate that the ET_B receptor and signaling via NO-guanylate cyclase is involved in the down-regulation of HCO_3^- secretion in the CCD in response to acidosis.[742] Thus, intra-renal endothelin may play an important role in regulating distal nephron acid−base transport.[743]

A variety of other hormones have also been implicated as having effects on acid−base transport in the distal nephron.[744,745] However, the exact role and physiology of all of these is not as well characterized as that of mineralocorticoids, and the physiologic role is expected to be less important.

Parathyroid hormone (PTH) and Calcium: PTH has been implicated in stimulating distal nephron acidification.[392,506,746,747] PTH is released in response to HCl induced acidosis.[746] PTH increases H secretion in the toad bladder.[748] However, the effect of PTH to increase distal acidification in the rat may be predominantly secondary to an increased distal delivery of phosphate,[747] phosphate could stimulate distal acidification both as a buffer and as a poorly reabsorbable anion as discussed previously. Of note in regard to the possibility of a direct effect of PTH on the distal nephron, PTH stimulates adenylate cyclase in the distal convoluted tubule and connecting segment, but not in the collecting tubule of either rat or rabbit.[749] Calcium may also stimulate distal acidification.[750]

Arginine vasopressin (AVP or antidiuretic hormone): ADH has been reported to increase rat distal nephron acidification.[387,744] Net bicarbonate secretion is converted to net bicarbonate reabsorption both in superficial distal tubules *in vivo* and in the rat CCD *in vitro*.[387,751] The mechanism and responsible cell type have not been established. Glucagon has been shown to stimulate net HCO_3 secretion in the rat superficial distal tubule *in vivo*.[389] The mechanism has not been delineated but glucagon is known to stimulate cAMP in both cortical and medullary collecting ducts of the rat.[749] Bicarbonate reabsorption is stimulated by cAMP in the rabbit $OMCD_{is}$ *in vitro*,[752] however, the primary hormones which stimulate this action are not known. Prostaglandin E_2 inhibits, and indomethacin stimulates, HCO_3 reabsorption in the $OMCD_{is}$ to a modest extent.[752]

Isoproterenol and cAMP: Isoproterenol increases HCO_3 secretion in the cortical collecting tubule via a cyclic AMP dependent action.[478] The mechanism probably involves activation of both the apical Cl/HCO_3

exchanger and the basolateral Cl channel in type B intercalated cells.[631,632,478,629] The evidence for these separate actions are a decreased intracellular pH and an increase in the apparent chloride conductance of the CCD.[631,632] Bicarbonate secretion in the turtle bladder is also sensitive to cAMP, but in this case the stimulated secretion may be via an electrogenic mechanism.[753,754,755,756] Of note, turtle bladder HCO_3 secretion also responds to activation of protein kinase C, whereas CCD HCO_3 transport is not altered by this mechanism.[757,758] In contrast, isoproterenol (or VIP) may increase HCO_3 reabsorption in the rat distal tubule.[744]

Recent studies have directly implicated cAMP and PKA in regulating the expression and distribution of H-ATPase.[759] The metabolic sensor AMPK (AMP-activated kinase) can override the effects of cAMP/PKA. The upstream activators and physiologic integration of these findings are not clear but the bicarbonate stimulated soluble adenylyl cyclase (sAC) has been suggested.[760]

Prostacyclin (PGI_2): PGI_2 increases rat distal tubule HCO_3 secretion, probably via a cAMP dependent process.[761] And importantly, alkali loads increase urinary metabolites of PGI_2.[761] Therefore, PGI_2 may mediate some of the transport changes induced by alkali loads *in vivo*.

Angiotensin II: Angiotensin II has a variety of effects on distal nephron acid−base transport.[762] Angiotensin II was found to stimulate HCO_3 secretion in rabbit CCD[763] but to increase HCO_3 reabsorption is rat distal tubule.[744,764] Recently AII has been found to increase H secretion via H-ATPase insertion into the apical membrane of type A IC in mice, this effect may be important not only in acid−base transport but also in facilitating NaCl reabsorption in the CCD.[765] Increased H-ATPase activity may also occur in type B IC.[766] In the OMCD, angiotensin II reduced HCO_3 reabsorption.[461]

References

[1] Alpern RJ. Mechanism of basolateral membrane H/OH/HCO_3 transport in the rat proximal convoluted tubule. J Gen Physiol 1985;86:613−36.

[2] Biagi B, Kubota T, Sohtell M, Giebisch G. Intracellular potentials in rabbit proximal tubules perfused *in vitro*. Amer J Physiol 1981;240:F200−10.

[3] Fromter E. Viewing the kidney through microlectrodes. Amer J Physiol 1984;247:F695−705.

[4] Sasaki S, Shiigai T, Takeuchi J. Intracellular pH in the isolated perfused rabbit proximal tubule. Amer J Physiol 1985;249:F417−23.

[5] Yoshitomi K, Fromter E. Cell pH of rat renal proximal tubule in vivo and the conductive nature of peritubular $HCO_3(OH^-)$ exit. Pflugers Arch 1984;402:300−5.

[6] DuBose Jr. TD, Pucacco LR, Carter NW. Determination of disequilibrium pH in the rat kidney in vivo: evidence for hydrogen secretion. Amer J Physiol 1981;240:F138−46.

[7] Rector Jr. FC, Carter NW, Seldin DW. The mechanism of bicarbonate reabsorption in the proximal and distal tubules of the kidney. J Clin Invest 1965;44:278−90.

[8] Vieira FL, Malnic B. Hydrogen ion secretion by rat renal cortical tubules as studied by an antimony microelectrode. Amer J Physiol 1968;214:710−8.

[9] Kinne-Saffran E, Beauwens R, Kinne R. An ATP-driven proton pump in brush-border membranes from rat renal cortex. J Membr Biol 1982;64:67−76.

[10] Kinne-Saffran E, Kinne R. Presence of a bicarbonate stimulated ATPase in the brush border microvillus membranes of the proximal tubule. Proc Soc Exp Biol Med 1974;146:751.

[11] Kinne-Saffran E, Kinne R. Further evidence for the existence of an intrinsic bicarbonate-stimulated Mg^{+231}-ATPase in brush border membranes isolated from rat kidney cortex. J Membr Biol 1979;49:235−51.

[12] Yoshitomi K, Burckhardt BCh, Fromter E. Rheogenic sodium-bicarbonate cotransport in the peritubular cell membrane of rat renal proximal tubule. Pflugers Arch 1985;405:360−6.

[13] Kurtz I. Apical Na/H antiporter and glycolysis-dependent H-ATPase regulate intracellular pH in the rabbit S_3 proximal tubule. J Clin Invest 1987;80:928−35.

[14] Nakhoul NL, Lopes AG, Chaillet JR, Boron WF. Intracellular pH regulation in the S3 segment of the rabbit proximal tubule in HCO3-free solutions. J Gen Physiol 1988; 92:369−93.

[15] Fromter E, Gessner K. Active transport potentials, membrane diffusion potentials, and streaming potentials across rat kidney proximal tubule. Pflugers Arch 1974;351:85−98.

[16] Fromter E, Gessner K. Effect of inhibitors and diuretics on electrical potential differences in rat kidney proximal tubule. Pflugers Arch 1978;357:209−24.

[17] Brown D, Hirsch S, Gluck S. Localization of a proton-pumping ATPase in rat kidney. J Clin Invest 1988;82:2114−26.

[18] Silva F, Schultz W, Davis L, Xie XS, Stone DK. Immunocytochemical localization of the clathrin-coated vesicle proton pump (CCV-PP). Kidney Int 1987;31:416 [Ref Type: Abstract].

[19] Wagner CA, Finberg KE, Breton S, Marshansky V, Brown D, Geibel JP. Renal vacuolar H^+-ATPase. Physiol Rev 2004;84:1263−314.

[20] Chan YL, Giebisch G. Relationship between sodium and bicarbonate transport in the rat proximal convoluted tubule. Amer J Physiol 1981;240:F222−30.

[21] Howlin KJ, Alpern RJ, Rector Jr. FC. Amiloride inhibition of proximal tubular acidification. Amer J Physiol 1985;248:F773−8.

[22] Preisig PA, Ives HE, Cragoe EJ, Alpern RJ, Rector Jr. FC. Role of the Na/H antiporter in rat proximal tubule bicarbonate absorption. J Clin Invest 1987;80:970−8.

[23] Harvey WR. Voltage coupling of primary H^+ V-ATPasees to secondary Na^+- or K^+-dependent transporters. J Exp Biol 2009;212:1620−9.

[24] Saroussi S, Nelson N. The little we know on the structure and machinery of V-ATPase. J Exp Biol 2009;212:160−1610.

[25] Valles P, Lapointe MSWJ, Batlle D. Kidney vacuolar H+-ATPase: physiology and regulation. Sem Nephrol 2006;26: 361−74.

[26] Preisig PA, Rector Jr. FC. Role of Na-H antiport in rat proximal tubule NaCl absorption. Amer J Physiol 1988;255:F461−5.

[27] Kleyman TR, Cragoe Jr. EJ. Amiloride and its analogs as tools in the study of ion transport. J Membr Biol 1988;105:1−21.

[28] Murer H, Hopfer U, Kinne R. Sodium/proton antiport in brush-border membrane vesicles isolated from rat small intestine and kidney. Biochem J 1976;154:597–604.
[29] Kinsella JL, Aronson PS. Properties of the Na-H exchanger in renal microvillus membrane vesicles. Amer J Physiol 1980;238: F467–9.
[30] Warnock DG, Reenstra WW, Yee VJ. Na/H antiporter of brush border vesicles: studies with acridine orange uptake. Amer J Physiol 1982;242:F733–9.
[31] Aronson PS, Suhm MA, Nee J. Interaction of external H with the Na-H exchanger in renal microvillus membrane vesicles. J Biol Chem 1983;258:6767–71.
[32] Ives HE, Yee VJ, Warnock DG. Mixed-type inhibition of the renal Na/H antiporter by Li and amiloride: evidence for a modifier site. J Biol Chem 1983;258:9710–6.
[33] Kinsella JL, Aronson PS. Amiloride inhibition of the Na-H exchanger in renal microfillus membrane vesicles. Amer J Physiol 1981;241:F374–9.
[34] Kinsella JL, Aronson PS. Interaction of NH_4 and Li with the renal microvillus membrane Na-H exchanger. Amer J Physiol 1981;241:C220–6.
[35] Aronson PS, Nee J, Suhm MA. Modifier role of internal H in activating the Na-H exchanger in renal microvillus membrane vesicles. Nature 1982;299:161–3.
[36] Boron WF, Boulpaep EL. Intracellular pH regulation in the renal proximal tubule of the salamander: Na-H exchange. J Gen Physiol 1983;81:29–52.
[37] Alpern RJ, Chambers M. Cell pH in the rat proximal convoluted tubule: regulation by luminal and peritubular pH and sodium concentration. J Clin Invest 1986;78:502–10.
[38] Burg MB, Green N. Bicarbonate transport by isolated perfused rabbit proximal convoluted tubules. Amer J Physiol 1977;233: F307–14.
[39] Chantrell[e B, Cogan MG, Rector Jr. FC. Evidence for coupled sodium/hydrogen exchange in the rat superficial proximal convoluted tubule. Pflugers Arch 1982;395:186–9.
[40] McKinney TD, Burg MB. Bicarbonate and fluid absorption by renal proximal straight tubules. Kidney Int 1977;21:1–8.
[41] Sasaki S, Berry CA, Rector Jr. FC. Effect of potassium concentration on bicarbonate reabsorption in the rabbit proximal convoluted tubule. Amer J Physiol 1983;224:F122–8.
[42] Sardet C, Franchi A, Pouyssegur J. Molecular cloning, primary structure, and expression of the human growth factor-activatable Na/H antiporter. Cell 1989;56:271–80.
[43] Aronson PS. Ion exchangers mediating Na^+, HCO_3^-, and Cl^- transport in the renal proximal tubule. J Nephrol 2006;19 (**Suppl.**):S3–10.
[44] Bobulescu IA, DiSole F, Moe OW. Na^+/H^+ exchangers: physiology and link to hypertension and organ ischemia. Curr Opin Nephrol Hypertens 2005;14:485–94.
[45] Bobulescu IA, Moe OW. Na^+/H^+ exchanger in renal regulation of acid–base balance. Sem Nephrol 2006;26:334–44.
[46] Tse CM, Levine SA, Yun CHC, Montrose MH, Little PJ, Pouyssegur J, et al. Cloning and expression of a rabbit cDNA encoding a serum-activated ethylisopropylamiloride-resistant epithelial Na/H exchanger isoform (NHE-2). J Biol Chem 1993;268:11917–24.
[47] Haggerty JG, Agarwal N, Reilly RF, Adelberg EA, Slayman CW. Pharmacologically different Na/H antiporters on the apical and basolateral surfaces of cultured porcine kidney cells (LLC-PK_1). Proc Natl Acad Sci USA 1988;85:6797–801.
[48] Orlowski J. Heterologous expression and functional properties of amiloride high affinity (NHE-1) and low affinity (NHE-3) isoforms of the rat Na/H exchanger. J Biol Chem 1993;268: 16369–77.
[49] Tse CM, Levine SA, Yun CHC, Brant SR, Pouyssegur J, Montrose MH, et al. Functional characteristics of a cloned epithelial Na/H exchanger (NHE3): Resistance to amiloride and inhibition by protein kinase C. Proc Natl Acad Sci USA 1993;90:9110–4.
[50] Yu FH, Shull GE, Orlowski J. Functional properties of the rat Na/H exchanger NHE-2 isoform expressed in Na/H exchanger-deficient Chinese hamster ovary cells. J Biol Chem 1993;268:11925–8.
[51] Amemiya M, Loffing J, Lotscher M, Kaissling B, Alpern RJ, Moe OW. Expression of NHE-3 in the apical membrane of rat renal proximal tubule and thick ascending limb. Kidney Int 1995;48:1206–15.
[52] Biemesderfer D, Pizzonia J, Abu-Alfa A, Exner M, Reilly R, Igarashi P, et al. NHE3: a Na/H exchanger isoform of renal brush border. Amer J Physiol 1993;265:F736–42.
[53] Orlowski J, Kandasamy RA, Shull GE. Molecular cloning of putative members of the Na/H exchanger gene family. J Biol Chem 1992;267:9331–9.
[54] Tse CM, Brant SR, Walker MS, Pouyssegur J, Donowitz M. Cloning and sequencing of a rabbit cDNA encoding an intestinal and kidney-specific Na/H exchanger isoform (NHE-3). J Biol Chem 1992;267:9340–6.
[55] Wu MS, Biemesderfer D, Giebisch G, Aronson P. Role of NHE3 in mediating renal brush border Na^+-H^+ exchange. Adaptation to metabolic acidosis. J Biol Chem 1996;271: 32749–52.
[56] Ambühl PM, Amemiya M, Danczkay M, Lotscher M, Kaissling B, Moe OW, et al. Chronic metabolic acidosis increases NHE3 protein abundance in rat kidney. Amer J Physiol 1996;271: F917–25.
[57] Amemiya M, Yamaji Y, Cano A, Moe OW, Alpern RJ. Acid incubation increases NHE-3 mRNA abundance in OKP cells. Amer J Physiol 1995;269:C126–33.
[58] Baum M, Amemiya M, Dwarakanath V, Alpern RJ, Moe OW. Glucocorticoids regulate NHE-3 transcription in OKP cells. Amer J Physiol 1996;270:F164–9.
[59] Baum M, Moe OW, Gentry DL, Alpern RJ. Effect of glucocorticoids on renal cortical NHE-3 and NHE-1 mRNA. Amer J Physiol 1994;267:F437–42.
[60] Cano A, Baum M, Moe OW. Thyroid hormone stimulates the renal Na/H exchanger NHE3 by transcriptional activation. Amer J Physiol 1999;276:C102–8.
[61] Yun CHC, Gurubhagavatula S, Levine SA, Montgomery JLM, Brant SR, Cohen ME, et al. Glucocorticoid stimulation of ileal Na absorptive cell brush border Na/H exchange and association with an increase in message for NHE-3, an epithelial Na/H exchanger isoform. J Biol Chem 1993;268: 206–11.
[62] Cano A, Miller RT, Alpern RJ, Preisig P. Angiotensin II stimulation of Na/H antiporter activity is cAMP-independent in OKP cells. Amer J Physiol 1994;266:C1603–8.
[63] Chu TS, Peng Y, Cano A, Yanagisawa M, Alpern RJ. $Endothelin_B$ receptor activates NHE-3 by a Ca^{2+}-dependent pathway in OKP cells. J Clin Invest 1996;97:1454–62.
[64] Pollock AS, Warnock DG, Strewler GJ. Parathyroid hormone inhibition of Na-H antiporter activity in a cultured renal cell line. Amer J Physiol 1986;250:F217–25.
[65] Schultheis PJ, Clarke LL, Meneton P, Miller ML, Soleimani M, Gawenis LR, et al. Renal and intestinal absorptive defects in mice lacking the NHE3 Na^+/H^+ exchanger. Nature Genet 1998;19:282–5.
[66] Wang T, Yang CL, Abbiati T, Schultheis PJ, Shull GE, Giebisch G, et al. Mechanism of proximal tubule bicarbonate absorption in NHE3 null mice. Am J Physiol 1999;277: F298–302.

[67] Choi JY, Shah M, Lee MG, Schultheis PJ, Shull GE, Muallem S, et al. Novel amiloride-sensitive sodium-dependent proton secretion in the mouse proximal convoluted tubule. J Clin Invest 2000;105:1141–6.
[68] Goyal S, Mentone SA, Aronson PS. Immunolocalization of NHE8 in rat kidney. Amer J Physiol 2005;288:F530–8.
[69] Goyal S, Vanden Heuvel G, Aronson PS. Renal expression of novel Na^+/H^+ exchanger isoform NHE8. Amer J Physiol 2003;284:F467–73.
[70] Becker AM, Zhang J, Goyal S, Dwarakanath V, Aronson PS, Moe OW, et al. Ontogeny of NHE8 in the rat proximal tubule. Amer J Physiol 2007;293:F255–61.
[71] Bobulescu IA, Moe OW. Luminal Na + /H + exchange in the proximal tubule. Pflugers Arch 2009;458:5–21.
[72] Twombley K, Gattineni J, Bobulescu IA, Dwarakanath V, Baum M. Effect of metabolic acidosis on neonatal proximal tubule acidification. Amer J Physiol 2010;299:R1360–8.
[73] Baum M, Biemesderfer D, Gentry D, Aronson PS. Ontogeny of rabbit renal cortical NHE3 and NHE1: effect of glucocorticoids. Amer J Physiol 1995;268:F815–20.
[74] Gattineni J, Sas D, Dagan A, Dwarakanath V, Baum M. Effect of thyroid hormone on the postnatal renal expression of NHE8. Amer J Physiol 2008;294:F198–204.
[75] Fiori M, Gras EG, Amorena C. Decreased NHE8 isoform expression and defective acidification in proximal convoluted tubules of senile rats. Age (Omaha) 2009;31:77–84.
[76] Alexander RT, Grinstein S. Tethering, recycling and activation of the epithelian sodium-proton exchanger, NHE3. J Exp Biol 2009;212:1630–7.
[77] DiSole F, Babich V, Moe OW. The calcineurin homologous protein-1 increases Na^+/H^+-exchanger 3 trafficking via ezrin phosphorylation. J Amer Soc Nephrol 2009;20:1776–86.
[78] Kocinsky HS, Dynia DW, Wang T, Aronson PS. NHE3 phosphorylation at serines 552 and 605 does not directly affect NHE3 activity. Amer J Physiol 2007;293:F212–8.
[79] Kocinsky HS, Girardi ACC, Biemesderfer D, Nguyen T, Mentone SA, Orlowski J, et al. Use of phospho-specific antibodies to determine the phosphorylation of endogenous Na^+/H^+ exchanger NHE3 at PKA consensus sites. Amer J Physiol 2005;289:F249–58.
[80] Murtazina R, Kovbasnjuk O, Zachos NC, Li X, Chen Y, Hubbard A, et al. Tissue-specific regulation of sodium/proton exchanger isoform 3 activity in Na + /H + exchanger regulatory factor 1 (NHERF1) null mice. J Biol Chem 2007;282: 25141–51.
[81] Sarker R, Grønborg M, Cha B, Mohan S, Chen Y, Pandey A, et al. Casein kinase 2 binds to the C terminus of Na + /H + exchanger 3 (NHE3) and stimulates NHE3 basal activity by phosphorylating a separate site in NHE3. Mol Biol Cell 2008;19:3859–70.
[82] Aronson P. Mechanisms of active H^+ secretion in the proximal tubule. Amer J Physiol 1983;243:F647–59.
[83] Siebens AW, Boron WF. Effect of electroneutral luminal and basolateral lactate transport on intracellular pH in salamander proximal tubules. J Gen Physiol 1987;90:799–831.
[84] Nakhoul NL, Boron WF. Acetate transport in the S3 segment of the rabbit proximal tubule and its effect on intracellular pH. J Gen Physiol 1988;92:395–412.
[85] Geibel J, Giebisch G, Boron WF. Effects of acetate on luminal acidification processes in the S3 segment of the rabbit proximal tubule. Amer J Physiol 1989;257:F586–94.
[86] Lucci MS, Warnock DG. Effects of anion-transport inhibitors on NaCl reabsorption in the rat superficial proximal convoluted tubule. J Clin Invest 1979;64:570–9.
[87] Baum M. Evidence that parallel Na-H and Cl-HCO_3(OH) antiporters transport NaCl in the proximal tubule. Amer J Physiol 1987;252:F338–45.
[88] Warnock DG, Yee VJ. Chloride uptake by brush border membrane vesicles isolated from rabbit renal cortex: coupling to proton gradients and K diffusion potentials. J Clin Invest 1981;67:103–15.
[89] Shiuan D, Weinstein SW. Evidence for electroneutral chloride transport in rabbit renal cortical brush border membrane vesicles. Amer J Physiol 1984;247:F837–47.
[90] Burnham C, Munzesheimer C, Rabon E, Sachs G. Ion pathways in renal brush border membranes. Biochim Biophys Acta 1982;685:260–72.
[91] Chen PY, Illsley NP, Verkman AS. Renal brush-border chloride transport mechanisms characterized using a fluorescent indicator. Amer J Physiol 1988;254:F114–20.
[92] Seifter JL, Knickelbein R, Aronson PS. Absence of Cl-OH exchange and NaCl cotransport in rabbit renal microvillus membrane vesicles. Amer J Physiol 1984;247:F753–9.
[93] Cassano G, Stieger B, Murer H. Na/H- and Cl/OH-exchange in rat jejunal and rat proximal tubular brush border membrane vesicles. Pflugers Arch 1984;400:309–17.
[94] Ives HE, Chen PY, Verkman AS. Mechanism of coupling between Cl^- and OH^- transport in renal brush-border membranes. Biochim Biophys Acta 1986;863:91–100.
[95] Karniski LP, Aronson PS. Anion exchange pathways for Cl transport in rabbit renal microvillus membranes. Amer J Physiol 1987;253:F513–21.
[96] Karniski LP, Aronson PS. Chloride/formate exchange with formic acid recycling: a mechanism of active chloride transport across epithelial membranes. Proc Natl Acad Sci USA 1985;82:6362–5.
[97] Alpern RJ. Apical membrane chloride/base exchange in the rat proximal convoluted tubule. J Clin Invest 1987;79:1026–30.
[98] Baum M. Effect of luminal chloride on cell pH in rabbit proximal tubule. Amer J Physiol 1988;254:F677–83.
[99] Wang T, Egbert Jr. AL, Abbiati T, Aronson PS, Giebisch G. Mechanisms of stimulation of proximal tubule chloride transport by formate and oxalate. Amer J Physiol 1996;271:F446–50.
[100] Wang T, Giebisch G, Aronson PS. Effects of formate and oxalate on volume absorption in rat proximal tubule. Amer J Physiol 1992;263:F37–42.
[101] Aronson PS. Role of SLC26A6-mediated Cl^--oxalate exchange in renal physiology and pathophysiology. J Nephrology 2010;23:S158–64.
[102] Aronson PS, Giebisch G. Mechanisms of chloride transport in the proximal tubule. Amer J Physiol 1997;273:F179–92.
[103] Sasaki S, Berry CA. Mechanism of bicarbonate exit across basolateral membrane of the rabbit proximal convoluted tubule. Amer J Physiol 1984;246:F889–96.
[104] Reenstra WW, Warnock DG, Yee VJ, Forte JG. Proton gradients in renal cortex brush-border membrane vesicles: demonstration of a rheogenic proton flux with acridine orange. J Biol Chem 1981;256:11663–6.
[105] Ives HE. Proton/hydroxyl permeability of proximal tubule brush border vesicles. Amer J Physiol 1985;248:F78–86.
[106] Preisig PA, Alpern RJ. Contributions of cellular leak pathways to net $NaHCO_3$ and NaCl absorption. J Clin Invest 1989;83:1859–67.
[107] Wang W, Messner G, Oberleithner H, Lang F, Deetjen P. The effect of ouabain on intracellular activities of K, Na, Cl, H and Ca^{2+} in proximal tubules of frog kidneys. Pflugers Arch 1984;401:6–13.

[108] Bank N, Aynedjian HS, Mutz BF. Evidence for a DCCD-sensitive component of proximal bicarbonate reabsorption. Amer J Physiol 1985;249:F636–44.
[109] Burckhardt B-C, Sato K, Fromter E. Electrophysiological analysis of bicarbonate permeation across the peritubular cell membrane of rat kidney proximal tubule. I. Basic observations. Pflugers Arch 1984;401:43–51.
[110] Biagi BA, Sohtell M. Electrophysiology of basolateral bicarbonate transport in the rabbit proximal tubule. Amer J Physiol 1986;250:F267–72.
[111] Burckhardt B-C, Cassola AC, Fromter E. Electrophysiological analysis of bicarbonate permeation across the peritubular cell membrane of rat kidney proximal tubule. II. Exclusion of HCO_3-effects on other ion permeabilities and of coupled electroneutral HCO_3-transport. Pflugers Arch 1984;401:43–51.
[112] Boron WF, Boulpaep EL. Intracellular pH regulation in the renal proximal tubule of the salamander: basolateral HCO_3 transport. J Gen Physiol 1983;81:53–94.
[113] Biagi BA. Effects of the anion transport inhbitor, SITS, on the proximal straight tubule of the rabbit perfused in vitro. J Membr Biol 1985;88:25–31.
[114] Alpern RJ, Chambers M. Basolateral membrane Cl/HCO_3 exchange in the rat proximal convoluted tubule: Na-dependent and -independent mechanisms. J Gen Physiol 1987;89:581–98.
[115] Lopes AG, Siebens AW, Giebisch G, Boron WF. Electrogenic Na/HCO_3 cotransport across basolateral membrane of isolated perfused Necturus proximal tubule. Amer J Physiol 1987;253: F340–50.
[116] Sasaki S, Shiigai T, Yoshiyama N, Takeuchi J. Mechanism of bicarbonate exit across basolateral membrane of rabbit proximal straight tubule. Amer J Physiol 1987;252:F11–8.
[117] Akiba T, Alpern RJ, Eveloff J, Calamine J, Warnock DG. Electrogenic sodium/bicarbonate cotransport in rabbit renal cortical basolateral membrane vesicles. J Clin Invest 1986;78: 1472–8.
[118] Grassl SM, Aronson PS. Na/HCO_3 co-transport in basolateral membrane vesicles isolated from rabbit renal cortex. J Biol Chem 1986;261:8778–83.
[119] Grassl SM, Holohan PD, Ross CR. HCO_3 transport in basolateral membrane vesicles isolated from rat renal cortex. J Biol Chem 1987;262:2682–7.
[120] Alpern RJ. Cell mechanisms of proximal tubule acidification. Physiol Rev 1990;70:79–114.
[121] Preisig PA, Alpern RJ. Basolateral membrane $H/OH/HCO_3$ transport in the proximal tubule. Amer J Physiol 1989;256: F751–65.
[122] Soleimani M, Aronson PS. Ionic mechanism of $Na{:}HCO_3$ cotransport in renal basolateral membrane vesicles (BLMV). J Biol Chem 1989;264:18302–8.
[123] Krapf R, Alpern RJ, Rector Jr. FC, Berry CA. Basolateral membrane Na/base cotransport is dependent on CO_2/HCO_3 in the proximal convoluted tubule. J Gen Physiol 1987;90:833–53.
[124] Romero MF, Hediger MA, Boulpaep EL, Boron WF. Expression cloning and characterization of a renal electrogenic Na^+/HCO_3^- cotransporter. Nature 1997;387:409–13.
[125] Romero MF, Fong P, Berger UV, Hediger MA, Boron WF. Cloning and functional expression of rNBC, an electrogenic $Na^+–HCO_3^-$ cotransporter from rat kidney. Amer J Physiol 1998;274:F425–32.
[126] Soleimani M. Functional and molecular properties of Na^+: HCO_3-cotransporters (NBC). Minerva Urol Nefrol 2003;55: 131–40.
[127] Aalkjær C, Frische S, Leipziger J, Nielson S, Praetoruis J. Sodium coupled bicarbonate transporters in the kidney, an update. Acta Physiol Scand 2004;181:505–12.
[128] Bernardo AA, Bernardo CM, Espiritu DJ, Arruda JAL. The sodium bicarbonate cotransporter: structure, function, and regulation. Sem Nephrol 2006;26:352–60.
[129] Boron WF, Chen L, Parker MD. Modular structure of sodium-coupled bicarbonate transporters. J Exp Biol 2009;212: 1697–706.
[130] Ives HE, Yee VJ, Warnock DG. Asymmetric distribution of the Na/H antiporter in the renal proximal tubule epithelial cell. J Biol Chem 1983;258:13513–6.
[131] Sabolic I, Burckhardt G. Proton pathways in rat renal brush border and basolateral membranes. Biochim Biophys Acta 1983;734:210–20.
[132] Geibel J, Giebisch G, Boron WF. Basolateral sodium-coupled acid–base transport mechanisms of the rabbit proximal tubule. Amer J Physiol 1989;257:F790–7.
[133] Biemesderfer D, Reilly RF, Exner M, Igarashi P, Aronson PS. Immunocytochemical characterization of Na-H exchanger isoform NHE-1 in rabbit kidney. Amer J Physiol 1992;263: F833–40.
[134] Leite-Dellova DCA, Oliveira-Souza M, Malnic G, Mello-Aires M. Genomic and nongenomic dose-dependent biphasic effect of aldosterone on Na^+/H^+ exchanger in proximal S3 segment: role of cytosolic calcium. Amer J Physiol 2008;295:F1342–52.
[135] Edelman I, Bouthier M, Anagnostopoulos T. Chloride distribution in the proximal convoluted tubule of *Necturus* kidney. J Membr Biol 1981;62:7–17.
[136] Guggino WB, London R, Boulpaep EL, Giebisch G. Chloride transport across the basolateral cell membrane of the *Necturus* proximal tubule: dependence on bicarbonate and sodium. J Membr Biol 1983;71:227–40.
[137] Guggino WB, Boulpaep EL, Giebisch G. Electrical properties of chloride transport across the *Necturus* proximal tubule. J Membr Biol 1982;65:185–96.
[138] Shindo T, Spring KR. Chloride movement across the basolateral membrane of proximal tubule cells. J Membr Biol 1981;58:35–42.
[139] Preisig PA, Alpern RJ. Chronic metabolic acidosis causes an adaptation in the apical membrane Na/H antiporter and basolateral membrane $Na(HCO_3)_3$ symporter in the rat proximal convoluted tubule. J Clin Invest 1988;82:1445–53.
[140] Sasaki S, Yoshiyama N. Interaction of chloride and bicarbonate transport across the basolateral membrane of rabbit proximal straight tubule. J Clin Invest 1988;81:1004–11.
[141] Kurtz I. Basolateral membrane Na/H antiport, Na/base cotransport, and Na-independent Cl/base exchange in the rabbit S_3 proximal tubule. J Clin Invest 1989;83:616–22.
[142] Nakhoul NL, Chen LK, Boron WF. Intracellular pH regulation in the rabbit S3 proximal tubule. Basolateral $Cl{-}HCO_3$ exchange and $Na{-}HCO_3$ cotransport. Amer J Physiol 1990;258:F371–81.
[143] Grassl SM, Karniski LP, Aronson PS. $Cl–HCO_3$ exchange in rabbit renal cortical basolateral membrane vesicles (BLMV). Kidney Int 1985;27:282 [Ref Type: Abstract].
[144] Chen PY, Verkman AS. Sodium-dependent chloride transport in basolateral membrane vesicles isolated from rabbit proximal tubule. Biochemistry 1988;27:655–60.
[145] Chan YL, Biagi B, Giebisch G. Control mechanisms of bicarbonate transport across the rat proximal convoluted tubule. Amer J Physiol 1982;242:F532–43.
[146] Krapf R, Berry CA, Alpern RJ, Rector Jr. FC. Regulation of cell pH by ambient bicarbonate, carbon dioxide tension, and pH in the rabbit proximal convoluted tubule. J Clin Invest 1988;81: 381–9.
[147] Hamm LL, Pucacco LR, Kokko JP, Jacobson HR. Hydrogen ion permeability of the rabbit proximal convoluted tubule. Amer J Physiol 1984;246:F3–11.

[148] Schwartz GJ. Na-dependent H efflux from proximal tubule: evidence for reversible Na-H exchange. Amer J Physiol 1981;241:F380–5.
[149] Rubio CR, Mangili OC, deMello GB, Malnic G. Effect of temperature on proximal tubular acidification. Pflugers Arch 1982;393:71–6.
[150] Warnock DG, Yee VJ. Anion permeabilities of the isolated perfused rabbit proximal tubule. AmerJ Physiol 1982;242:F395–405.
[151] Fromter E, Muller CW, Wick T. Permeability properties of the proximal tubular epithelium of the rat kidney studied with electrophysiological methods. In: Giebisch G, editor. Electrophysiology of epithelial cells. Stuttgart: Schattauer; 1971. p. 119–46.
[152] Alpern RJ, Cogan MG, Rector Jr FC. Effect of luminal bicarbonate concentration on proximal acidification in the rat. Amer J Physiol 1982;243:F53–9.
[153] Chan YL, Malnic G, Giebisch G. Passive driving forces of proximal tubular fluid and bicarbonate transport: gradient-dependence of H secretion. Amer J Physiol 1983;245:F622–33.
[154] Holmberg C, Kokko JP, Jacobson HR. Determination of chloride and bicarbonate permeabilities in proximal convoluted tubules. Amer J Physiol 1981;241:F386–94.
[155] Sasaki S, Berry CA, Rector Jr. FC. Effect of luminal and peritubular HCO_3 concentrations and PCO_2 on HCO_3 reabsorption in rabbit proximal convoluted tubules perfused in vitro. J Clin Invest 1982;70:639–49.
[156] Alpern RJ, Warnock DG, Rector Jr FC. Renal acidification mechanisms. In: Brenner BM, Rector Jr FC, editors. The kidney. Philadelphia: W.B. Saunders; 1986. p. 206–49.
[157] Dobyan DC, Bulger RE. Renal carbonic anhydrase. Amer J Physiol 1982;243:F311–24.
[158] Preisig PA, Toto RD, Alpern RJ. Carbonic anhydrase inhibitors. Renal Physiol 1987;10:136–59.
[159] Alpern RJ. Bicarbonate-water interactions in the rat proximal convoluted tubule: an effect of volume flux on active proton secretion. J Gen Physiol 1984;84:753–70.
[160] Cogan MG, Maddox DA, Warnock DG, Lin ET, Rector Jr FC. Effect of acetazolamide on bicarbonate reabsorption in the proximal tubule of the rat. Amer J Physiol 1979;237:F447–54.
[161] Lucci MS, Pucacco LR, DuBose Jr. TD, Kokko JP, Carter NW. Direct evaluation of acidification by rat proximal tubule: role of carbonic anhydrase. Amer J Physiol 1980;238:F372–9.
[162] Lucci MS, Tinker JP, Weiner IM, DuBose Jr. TD. Function of proximal tubule carbonic anhydrase defined by selective inhibition. Amer J Physiol 1983;245:F443–9.
[163] Lucci MS, Warnock DG, Rector Jr. FC. Carbonic anhydrase-dependent bicarbonate reabsorption in the rat proximal tubule. Amer J Physiol 1979;236:F58–65.
[164] Gros G, Moll W. Facilitated diffusion of CO_2 across albumin solutions. J Gen Physiol 1974;64:356–71.
[165] Gros G, Moll W, Hoppe H, Gros H. Proton transport by phosphate diffusion–a mechanism of facilitated CO_2 transfer. J Gen Physiol 1976;67:773–90.
[166] Soleimani M, Aronson PS. Effects of acetazolamide on Na-HCO_3 cotransport in basolateral membrane vesicles isolated from rabbit renal cortex. J Clin Invest 1989;83:945–51.
[167] Malnic G, deMello-Aires M. Kinetic study of bicarbonate reabsorption in proximal tubule of the rat. Amer J Physiol 1971;220:1759–67.
[168] Ullrich KJ, Rumrich G, Baumann K. Renal proximal tubular buffer-(glycodiazine) transport. Pflugers Arch 1975;357: 149–63.
[169] Verkman AS, Alpern RJ. Kinetic transport model for cellular regulation of pH and solute concentration in the renal proximal tubule. Biophys J 1987;51:533–46.
[170] Alpern RJ, Cogan MG, Rector Jr FC. Flow dependence of proximal tubular bicarbonate absorption. Amer J Physiol 1983;245: F478–84.
[171] Du Z, Yan Q, Duan Y, Weinbaum S, Weinstein AM, Wang T. Axial flow modulates proximal tubule NHE3 and H-ATPase activities by changing microvillus bending moments. Amer J Physiol 2006;290:F289–96.
[172] Barfuss DW, Schafer JA. Flow dependence of nonelectrolyte absorption in the nephron. Amer J Physiol 1979;236: F163–74.
[173] Wright FS. Flow-dependent transport processes: filtration, absorption, secretion. Amer J Physiol 1982;243:F1–11.
[174] Wang T. Flow-activated transport events along the nephron. Curr Opin Nephrol Hypertens 2006;15:530–6.
[175] Preisig PA. Luminal flow rate regulates proximal tubule H-HCO_3 transporters. Amer J Physiol 1992;262:F47–54.
[176] Cantone A, Wang T, Pica A, Simeon M, Capasso G. Use of transgenic mice in acid–base balance studies. J Nephrol 2006;19:S121–7.
[177] Preisig PA, Alpern RJ. Increased Na/H antiporter and Na/$3HCO_3$ symporter activities in chronic hyperfiltration. J Gen Physiol 1991;97:195–217.
[178] Harris RC, Seifter JL, Brenner BM. Adaptation of Na-H exchange in renal microvillus membrane vesicles. J Clin Invest 1984;74:1979–87.
[179] Cohn DE, Hruska KA, Klahr S, Hammerman MR. Increased Na-H exchange in brush border vesicles from dogs with renal failure. Amer J Physiol 1982;243:F293–9.
[180] Nord EP, Hafezi A, Kaunitz JD, Trizna W, Fine LG. pH gradient-dependent increased Na-H antiport capacity of the rabbit remnant kidney. Amer J Physiol 1985;249:F90–8.
[181] Alpern RJ, Cogan MG, Rector Jr FC. Effects of extracellular fluid volume and plasma bicarbonate concentration on proximal acidification in the rat. J Clin Invest 1983;71:736–46.
[182] Boron WF. Acid–base transport by the renal proximal tubule. J Amer Soc Nephrol 2006;17:2368–82.
[183] deMello-Aires M, Malnic G. Peritubular pH and PCO_2 in renal tubular acidification. Amer J Physiol 1975;228:1766–74.
[184] Giebisch G, Malnic G, deMello GB, deMello-Aires M. Kinetics of luminal acidification in cortical tubules of the rat kidney. J Physiol 1977;167:571–99.
[185] Zhou Y, Zhao J, Bouyer P, Boron WF. Evidence from renal proximal tubules that HCO_3^- and solute reabsorption are acutely regulated not by pH but by basolateral HCO_3^- and CO_2. Proc Natl Acad Sci USA 2005;102:3875–80.
[186] Cogan MG. Effects of acute alterations in PCO_2 on proximal HCO_3, Cl, and H_2O reabsorption. Amer J Physiol 1984;246: F21–6.
[187] Jacobson HR. Effects of CO_2 and acetazolamide on bicarbonate and fluid transport in rabbit proximal tubules. Amer J Physiol 1981;240:F54–62.
[188] Levine DZ. Effect of acute hypercapnia on proximal tubular water and bicarbonate absorption. Amer J Physiol 1971;221:1164–70.
[189] Wakabayashi S, Bertrand B, Shigekawa M, Fafournoux P, Pouyssegur J. Growth factor activation and "H^+-sensing" of the Na^+/H^+ exchanger isoform 1 (NHE1). J Biol Chem 1994;269:5583–8.
[190] Gurich RW, Warnock DG. Electrically neutral Na-H exchange in endosomes obtained from rabbit renal cortex. Amer J Physiol 1986;251:F702–9.
[191] Sabolic I, Haase W, Burckhardt G. ATP-dependent H^+ pump in membrane vesicles from rat kidney cortex. Amer J Physiol 1985;248:F835–44.

[192] Schwartz GJ, Al-Awqati Q. Carbon dioxide causes exocytosis of vesicles containing H pumps in isolated perfused proximal and collecting tubules. J Clin Invest 1985;75:1638–44.
[193] Kunau Jr. RT, Hart JI, Walker KA. Effect of metabolic acidosis on proximal tubular total CO_2 absorption. Amer J Physiol 1985;249:F62–8.
[194] Cogan MG. Chronic hypercapnia stimulates proximal bicarbonate reabsorption in the rat. J Clin Invest 1984;74:1942–7.
[195] Cohn DE, Klahr S, Hammerman MR. Metabolic acidosis and parathyroidectomy increase Na/H exchange in brush border vesicles. Amer J Physiol 1983;245:F217–22.
[196] Tsai CJ, Ives HE, Alpern RJ, Yee VJ, Warnock DG, Rector Jr FC. Increased V_{max} for Na/H antiporter activity in proximal tubule brush border vesicles from rabbits with metabolic acidosis. Amer J Physiol 1984;147:F339–43.
[197] Kinsella JL, Cujkit T, Sactor B. Na-H exchange activity in renal brush border membrane vesicles in response to metabolic acidosis: the role of glucocorticoids. Proc Natl Acad Sci USA 1984;81:630–4.
[198] Akiba T, Rocco VK, Warnock DG. Parallel adaptation of the rabbit renal cortical sodium/proton antiporter and sodium/bicarbonate cotransporter in metabolic acidosis and alkalosis. J Clin Invest 1987;80:308–15.
[199] Talor Z, Yang WC, Shuffield J, Sack E, Arruda JAL. Chronic hypercapnia enhances V_{max} of Na-H antiporter of renal brush-border membranes. Amer J Physiol 1987;253:F394–400.
[200] Yang WC, Arruda JAL, Talor Z. Na-H antiporter in posthypercapnic state. Amer J Physiol 1987;253:F833–40.
[201] Krapf R. Mechanisms of adaptation to chronic respiratory acidosis in the rabbit proximal tubule. J Clin Invest 1989;83: 890–6.
[202] Ruiz OS, Arruda JAL, Talor Z. Na-HCO_3 cotransport and Na-H antiporter in chronic respiratory acidosis and alkalosis. Amer J Physiol 1989;256:F414–20.
[203] Zeidel ML, Seifter JL. Regulation of Na/H exchange in renal microvillus vesicles in chronic hypercapnia. Kidney Int 1988;34:60–6.
[204] Northrup TE, Garella S, Pertucucci E, Cohen JJ. Acidemia alone does not stimulate rat renal Na-H antiporter activity. Amer J Physiol 1988;255:F237–43.
[205] Yang X, Amemiya M, Peng Y, Moe OW, Preisig PA, Alpern RJ. Acid incubation causes exocytic insertion of NHE3 in OKP cells. Am J Physiol 2000;279:C410–9.
[206] May RC, Kelly RA, Mitch WE. Metabolic acidosis stimulates protein degradation in rat muscle by a glucocorticoid-dependent mechanism. J Clin Invest 1986;77:614–21.
[207] Welbourne TC. Acidosis activation of the pituitary-adrenal-renal glutaminase I axis. Endocrinology 1976;99:1071–9.
[208] Ambühl PM, Yang X, Peng Y, Preisig PA, Moe OW, Alpern RJ. Glucocorticoids enhance acid activation of Na^+/H^+ exchanger 3 (NHE3). J Clin Invest 1999;103:429–35.
[209] Licht C, Laghmani K, Yanagisawa M, Preisig PA, Alpern RJ. An autocrine role for endothelin-1 in the regulation of proximal tubule NHE3. Kidney Int 2004;65:1320–6.
[210] Wesson DE. Endogenous endothelins mediate increased distal tubule acidification induced by dietary acid in rats. J Clin Invest 1997;99:2203–11.
[211] Laghmani K, Preisig PA, Moe OW, Yanagisawa M, Alpern RJ. Endothelin-1/endothelin-B receptor-mediated increases in NHE3 activity in chronic metabolic acidosis. J Clin Invest 2001;107:1563–9.
[212] Yamaji Y, Tsuganezawa H, Moe OW, Alpern RJ. Intracellular acidosis activates c-Src. Amer J Physiol 1997;272:C886–93.
[213] Li S, Sato S, Yang X, Preisig PA, Alpern RJ. Pyk2 activation is integral to acid stimulation of sodium/hydrogen exchanger 3. J Clin Invest 2004;114:1782–9.
[214] Tsuganezawa H, Sato S, Yamaji Y, Preisig PA, Moe OW, Alpern RJ. Role of *c-Src* and ERK in acid-induced activation of NHE3. Kidney Int 2002;62:41–50.
[215] Yamaji Y, Amemiya M, Cano A, Preisig PA, Miller RT, Moe OW, et al. Overexpression of *csk* inhibits acid-induced activation of NHE-3. Proc Natl Acad Sci USA 1995;92:6274–8.
[216] Yamaji Y, Moe OW, Miller RT, Alpern RJ. Acid activation of immediate early genes in renal epithelial cells. J Clin Invest 1994;94:1297–303.
[217] Preisig PA. The acid-activated signaling pathway: starting with Pyk2 and ending with increased NHE3 activity. Kidney Int 2007;72:1324–9.
[218] Li S, Preisig PA, Alpern RJ. Pyk2 is necessary for acid regulation of NHE3 activity, but not for regulation of *c-fos* mRNA expression. J Am Soc Nephrol 2003;14:15A [Ref Type: Abstract]
[219] Yang X, Gariepy CE, Yanagisawa M, Preisig PA, Alpern RJ. Media acidification stimulates endothelin-1 (ET-1) synthesis and receptor binding in OKP cells. J Am Soc Nephrol 2001;12:12A [Ref Type: Abstract]
[220] Horie S, Moe O, Yamaji Y, Cano A, Miller RT, Alpern RJ. Role of protein kinase C and transcription factor AP-1 in the acid-induced increase in Na/H antiporter activity. Proc Natl Acad Sci USA 1992;89:5236–40.
[221] Laghmani K, Preisig PA, Yanagisawa M, Alpern RJ. Transcriptional regulation of the endothelin-1 (ET-1) gene by metabolic acidosis: role of AP-1. J Am Soc Nephrol 2000;6A: [Ref Type: Abstract]
[222] Alpern RJ, Sakhaee K. The clinical spectrum of chronic metabolic acidosis: homeostatic mechanisms produce significant morbidity. Am J Kid Dis 1997;29:291–302.
[223] Ince BA, Anderson EJ, Neer RM. Lowering dietary protein to U.S. recommended dietary allowance levels reduces urinary calcium excretion and bone resorption in young women. J Clin Endocrinol Metab 2004;89:3801–7.
[224] Jehle S, Anetti A, Muser J, Hulter HN, Krapf R. Partial neutralization of the acidogenic western diet with potassium citrate increases bone mass in postmenopausal women with osteoporosis. J Amer Soc Nephrol 2006;17:3213–22.
[225] Preisig PA. The acid-activated signaling pathway:starting with Pyk2 and ending with increased NHE3 activity. Kidney Int 2007;72:1324–9.
[226] Curthoys NP. In: Alpern RJ, Hebert SC, editors. Renal Ammonium Ion Production and Excretion. In The Kidney – Physiology and Pathophysiology. New York: Elsevier; 2008. p. 1601–20.
[227] Melnick JZ, Preisig PA, Moe OW, Srere PA, Alpern RJ. Renal cortical mitochondrial aconitase is regulated in hypo- and hypercitraturia. Kidney Int 1998;54:160–5.
[228] Melnick JZ, Srere PA, Elshourbagy NA, Moe OW, Preisig PA, Alpern RJ. Adenosine triphosphate citrate lyase mediates hypocitraturia in rats. J Clin Invest 1996;98:2381–7.
[229] Amemiya M, Tabei K, Kusano E, Asano Y, Alpern RJ. Incubation of OKP cells in low-K^+ media increases NHE3 activity after early decrease in intracellular pH. Am J Physiol 1999;276:C711–6.
[230] Soleimani M, McKinney TD. Potassium depletion increases Na/H exchange and Na:CO_3:HCO_3 cotransport in rat renal cortex. Clin Res 1989;37:585A.
[231] Adam WR, Koretsky AP, Weiner MW. ^{31}P NMR in vivo measurement of renal intracellular pH: effects of acidosis and K depletion in rats. Amer J Physiol 1986;251:F904–10.
[232] Bichara M, Paillard M, Corman B, de Rouffignac C, Leviel F. Extracellular volume expansion and peritubular protein modulate $NaHCO_3$ and NaCl transport in the rat proximal tubule and Henle's loop. Amer J Physiol 1984;247:F140–50.

[233] Cogan MG, Maddox DA, Lucci MS, Rector Jr FC. Control of proximal bicarbonate reabsorption in normal and acidotic rats. J Clin Invest 1979;64:1168–80.
[234] Mercier O, Bichara M, Paillard M, Gardin JP, Leviel F. Parathyroid hormone contributes to volume expansion-induced inhibition of proximal reabsorption. Amer J Physiol 1985;248:F100–3.
[235] Boulpaep EL. Permeability changes of the proximal tubule of Necturus during saline loading. Amer J Physiol 1972;222: 517–31.
[236] Seely JF. Effects of peritubular oncotic pressure on rat proximal tubule electrical resistance. Kidney Int 1973;4:28–35.
[237] Alexander RT, Grinstein S. Na^+/H^+ exchangers and the regulation of volume. Acta Physiol Scand 2006;187:159–67.
[238] Moe OW, Tejedor A, Levi M, Seldin DW, Preisig PA, Alpern RJ. Dietary NaCl modulates Na-H antiporter activity in renal cortical apical membrane vesicles. Amer J Physiol 1991;260: F130–7.
[239] Yang LE, Sandberg MB, Can AD, Pihakaski-Maunsbach K, McDonough. AA. Effects of dietary salt on renal Na + transporter subcellular distribution, abundance, and phosphorylation status. Amer J Physiol 2008;295:F1003–16.
[240] Girardi ACC, Fukuda LE, Rossoni LV, Malnic G, Rebouças NA. Dipeptidyl peptidase IV inhibition downregulates Na + - H + exchanger NHE3 in rat renal proximal tubule. Amer J Physiol 2008;294:F414–22.
[241] Bank N, Aynedjian HS. A micropuncture study of the effect of parathyroid hormone on renal bicarbonate reabsorption. J Clin Invest 1976;58:336–44.
[242] Puschett JB, Zurbach P. Acute effects of parathyroid hormone on proximal bicarbonate transport in the dog. Kidney Int 1976;9:501–10.
[243] Iino Y, Burg MB. Effect of parathyroid hormone on bicarbonate absorption by proximal tubules in vitro. Amer J Physiol 1979;236:F387–91.
[244] McKinney TD, Myers P. Bicarbonate transport by proximal tubules: effect of parathyroid hormone and dibutyryl cyclic AMP. Amer J Physiol 1980;238:F166–74.
[245] McKinney TD, Myers P. PTH inhibition of bicarbonate transport by proximal convoluted tubules. Amer J Physiol 1980;239: F127–34.
[246] Kahn AM, Dolson GM, Hise MK, Bennett SC, Weinman EJ. Parathyroid hormone and dibutyryl cAMP inhibit Na/H exchange in renal brush border vesicles. Amer J Physiol 1985;248:F212–8.
[247] Miller RT, Pollock AS. Modification of the internal pH sensitivity of the Na/H antiporter by parathyroid hormone in a cultured renal cell line. J Biol Chem 1987;262: 9115–20.
[248] Collazo R, Fan L, Hu MC, Zhao H, Wiederkehr MR, Moe OW. Acute regulation of Na^+/H^+ exchanger NHE3 by parathyroid hormone via NHE3 phosphorylation and dynamin-dependent endocytosis. J Biol Chem 2000;275:31601–8.
[249] Fan L, Wiederkehr MR, Collazo R, Wang H, Crowder LA, Moe OW. Dual mechanisms of regulation of Na/H exchanger NHE-3 by parathyroid hormone in rat kidney. J Biol Chem 1999;274:11289–95.
[250] Honegger KJ, Capuano P, Winter C, Bacic D, Strange G, Wagner CA, et al. Regulation of sodium-proton exchanger isoform 3 (NHE3) by PKA and exchange protein directly activated by cAMP (EPAC). Proc Natl Acad Sci U S A 2006;103:803–8.
[251] Weinman EJ, Dubinsky WP, Shenolikar S. Reconstitution of cAMP-dependent protein kinase regulated renal Na-H exchanger. J Membr Biol 1988;101:11–8.
[252] Weinman EJ, Shenolikar S, Kahn AM. cAMP-associated inhibition of Na-H exchanger in rabbit kidney brush-border membranes. Amer J Physiol 1987;252:F19–25.
[253] Zhao H, Wiederkehr MR, Fan L, Collazo RL, Crowder LA, Moe OW. Acute inhibtion of Na/H exchanger NHE-3 by cAMP. J Biol Chem 1999;274:3978–87.
[254] Moe OW, Amemiya M, Yamaji Y. Activation of protein kinase A acutely inhibits and phosphorylates Na/H exchanger NHE-3. J Clin Invest 1995;96:2187–94.
[255] Kurashima K, Yu FH, Cabado AG, Szabo EZ, Grinstein S, Orlowski J. Identification of sites required for down-regulation of Na^+/H^+ exchanger NHE3 activity by cAMP-dependent protein kinase. J Biol Chem 1997;272:28672–9.
[256] Bezerra CNA, Girardi ACC, Carraro-Lacroix LR, Rebouças NA. Mechanisms underlying the long-term regulation of NHE3 by parathyroid hormone. Amer J Physiol 2008;294:F1232–7.
[257] Cunningham R, Steplock D, Wang F, Huang H, Xiaofei E, Shenolikar S, Weinman EJ. Defective parathyroid hormone regulation of NHE3 activity and phosphate adaptation in cultured NHERF-$1^{-/-}$ renal proximal tubule cells. J Biol Chem 2004;279: 37815–21.
[258] Shenolikar S, Voltz JW, Cunningham R, Weinman EJ. Regulation of ion transport by the NHERF family of PDZ proteins. Physiology 2004;19:362–9.
[259] Szászi K, Grinstein S, Orlowski J, Kapus A. Regulation of the epithelial Na^+/H^+ exchanger isoform by the cytoskeleton. Cell Physiol Biochem 2000;10:265–72.
[260] Szászi K, Kurashima K, Kaibuchi K, Grinstein S, Orlowski J. Role of the cytoskeleton in mediating cAMP-dependent protein kinase inhibition of the epithelial Na^+/H^+ exchanger NHE3. J Biol Chem 2001;276:40761–8.
[261] Weinman EJ, Cunningham R, Shenolikar S. NHERF and regulation of the renal sodium-hydrogen exchanger NHE3. Pflugers Arch 2005;450:137–44.
[262] Weinman EJ, Cunningham R, Wade JB, Shenolikar S. The role of NHERF-1 in the regulation of renal proximal tubule sodium-hydrogen exchanger 3 and sodium-dependent phosphate cotransporter 2a. J Physiol 2005;567:27–32.
[263] Weinman EJ, Steplock D, Schenolikar S. cAMP-mediated inhibition of the renal brush border membrane Na-H exchanger requires a dissociable phosphoprotein cofactor. J Clin Invest 1993;92:1781–6.
[264] Weinman EJ, Steplock D, Wang Y, Shenolikar S. Characterization of a protein cofactor that mediates protein kinase A regulation of the renal brush border membrane Na^+-H^+ exchanger. J Clin Invest 1995;95:2143–9.
[265] Weinman EJ, Steplock D, Shenolikar S. NHERF-1 uniquely transduces the cAMP signals that inhibit sodium-hydrogen exchange in mouse renal apical membranes. Febs Lett 2003;536:141–4.
[266] Weinman EJ, Steplock D, Tate K, Hall RA, Spurney RF, Shenolikar S. Structure -function of Recombinant Na/H Exchange Regulatory Factor (NHE-RF). J Clin Invest 1998;101: 2199–206.
[267] Donowitz M, Cha B, Zachos NC, Brett CL, Sharma A, Tse C-M, et al. NHERF family and NHE3 regulation. J Physiol 2005;567: 3–11.
[268] Weinman EJ, Steplock D, Donowitz M, Shenolikar S. NHERF associations with sodium-hydrogen exchanger isoform 3 (NHE3) and ezrin are essential for cAMP-mediated phosphorylation and inhibition of NHE3. Biochemistry 2000;39:6123–9.
[269] Yun CHC, Oh S, Zizak M, Steplock D, Tsao S, Tse C-M, et al. cAMP-mediated inhibition of the epithelial brush border Na^+/H^+ exchanger, NHE3, requires an associated regulatory protein. Proc Natl Acad Sci USA 1997;94:3010–5.

[270] Yang LE, Maunsbach AB, Leong PKK, McDonough AA. Differential traffic of proximal tubule Na^+ transporters during hypertension or PTH: NHE3 to base of microvilli vs. NaPi2 to endosomes. Amer J Physiol 2004;287:F896–906.

[271] Hruska KA, Moskowitz D, Esbrit P, Civitelli R, Westbrook S, Huskey M. Stimulation of inositol trisphosphate and diacylglycerol production in renal tubular cells by parathyroid hormone. J Clin Invest 1987;79:230–9.

[272] Mellas J, Hammerman MR. Phorbol ester-induced alkalinization of canine renal proximal tubular cells. Amer J Physiol 1986;250:F451–9.

[273] Weinman EJ, Shenolikar S. Protein kinase C activates the renal apical membrane Na/H exchanger. J Membr Biol 1986;93: 133–9.

[274] Baum M, Hays SR. Phorbol myristate acetate and dioctanoylglycerol inhibit transport in rabbit proximal convoluted tubule. Amer J Physiol 1988;254:F9–14.

[275] Wang T, Chan YL. Time- and dose-dependent effects of protein kinase C on proximal bicarbonate transport. J Membr Biol 1990;117:131–9.

[276] Kandasamy RA, Yu FH, Harris R, Boucher A, Hanrahan JW, Orlowski J. Plasma membrane Na^+/H^+ exchanger isoforms (NHE-1, -2, and -3) are differentially responsive to second messenger agonists of the protein kinase A and C pathways. J Biol Chem 1995;270:29209–16.

[277] Levine SA, Montrose MH, Tse CM, Donowitz M. Kinetics and regulation of three cloned mammalian Na^+/H^+ exchangers stably expressed in a fibroblast cell line. J Biol Chem 1994;368: 25527–35.

[278] Wiederkehr MR, Zhao H, Moe OW. Acute regulation of Na/H exchanger NHE-3 activity by protein kinase C: role of NHE3 phosphorylation. Amer J Physiol 1999;276:C1205–17.

[279] Yip J, Ko WH, Viberti G, Huganir RL, Donowitz M, Tse C-M. Regulation of the epithelial brush border Na^+/H^+ exchanger isoform 3 stably expressed in fibroblasts by fibroblast growth factor and phorbol esters is not through changes in phosphorylation of the exchanger. J Biol Chem 1997;272:18473–80.

[280] Chatsudthipong V, Chan YL. Calcium ion and proximal tubular transport of fluid and bicarbonate in the rat kidney. Proc. Ninth Intl.Congr.Nephrol 1984;380A: [Ref Type: Conference Proceeding]

[281] Friedman PA, Figueiredo JF, Maack T, Windhager EE. Sodium-calcium intractions in the renal proximal convoluted tubule of the rabbit. Amer J Physiol 1981;240:F558–68.

[282] Liu F-Y, Cogan MG. Effects of intracellular calcium on proximal bicarbonate absorption. Amer J Physiol 1990;259:F451–7.

[283] Bertrand B, Wakabayashi S, Ikeda T, Pouyssegur J, Shigekawa M. The Na^+/H^+ exchanger isoform 1 (NHE1) is a novel member of the calmodulin-binding proteins. J Biol Chem 1994;269: 13703–9.

[284] Wakabayashi S, Bertrand B, Ikeda T, Pouyssegur J, Shigekawa M. Mutation of calmodulin-binding site renders the Na^+/H^+ exchanger (NHE1) highly H^+-sensitive and Ca^{2+} regulation-defective. J Biol Chem 1994;269:13710–5.

[285] Wakabayashi S, Ikeda T, Noel J, Schmitt B, Orlowski J, Pouyssegur J, et al. Cytoplasmic domain of the ubiquitous Na^+/H^+ exchanger NHE1 can confer Ca^{2+} responsiveness to the apical isoform NHE3. J Biol Chem 1995;270:26460–5.

[286] Liu FY, Cogan MG. Angiotensin II: a potent regulator of acidification in the rat early proximal convoluted tubule. J Clin Invest 1987;80:272–5.

[287] Liu FY, Cogan MG. Angiotensin II(AII) stimulates early proximal bicarbonate absorption in the rat by decreasing cyclic adenosine monophosphate. J Clin Invest 1989;84:83–91.

[288] Geibel J, Giebisch G, Boron WF. Angiotensin II stimulates both Na-H exchange and Na/HCO_3 cotransport in the rabbit proximal tubule. Proc Natl Acad Sci USA 1990;87:7917–20.

[289] Saccomani G, Mitchell KD, Navar LG. Angiotensin II stimulation of Na/H exchange in proximal tubule cells. Amer J Physiol 1990;258:F1188–95.

[290] Harris PJ, Young JA. Dose-dependent stimulation and inhibition of proximal tubular sodium reabsorption by angiotensin II in the rat kidney. Pflugers Arch 1977;367:295–7.

[291] Schuster VL, Kokko JP, Jacobson HR. Angiotensin II directly stimulates sodium transport in rabbit proximal convoluted tubules. J Clin Invest 1984;73:507–15.

[292] Seikaly MG, Arant Jr. BS, Seney Jr. FD. Endogenous angiotensin concentrations in specific intrarenal fluid compartments of the rat. J Clin Invest 1990;86:1352–7.

[293] Douglas JG. Angiotensin receptor subtypes of the kidney cortex. Amer J Physiol 1987;253:F1–7.

[294] Woodcock EA, Johnston CI. Inhibition of adenylate cyclase by angiotensin II in rat renal cortex. Endocrinology 1982;111: 1687–91.

[295] Dominguez JH, Snowdowne KW, Freudenrich CC, Brown T, Borle AB. Intracellular messenger for action of angiotensin II on fluid transport in rabbit proximal tubule. Amer J Physiol 1987;252:F423–8.

[296] Welsh C, Dubyak G, Douglas JG. Relationship between phospholipase C activation and prostaglandin E_2 and cyclic adenosine monophosphate production in rabbit tubular epithelial cells. J Clin Invest 1988;81:710–9.

[297] Alpern RJ. Endocrine control of acid–base balance. In: Fray J, editor. Handbook of physiology: section 7: endocrinology: hormonal regulation of water and electrolyte balance. New York: American Physiological Society, Oxford University Press; 2000. p. 570–606.

[298] Xu L, Dixit MP, Nullmeyer KD, Xu H, Kiela PR, Lynch RM, et al. Regulation of Na^+/H^+ exchanger-NHE3 by angiotensin-II in OKP cells. Biochemica et Biophysica Acta 2006;1758:519–26.

[299] Dixit MP, Xu L, Xu H, Bai L, Collins JF, Ghishan FK. Effect of angiotensin-II on renal Na^+/H^+ exchanger-NHE3 and NHE2. Biochemica et Biophysica Acta 1664;38-44:2004.

[300] Turban S, Beutler KT, Morris RG, Masilamani S, Fenton RA, Knepper MA, et al. Long-term regulation of proximal tubule acid–base transporter abundance by angiotensin II. Kidney Int 2006;70:660–8.

[301] Carraro-Lacroix LR, Girardi ACC, Malnic G. Long-term regulation of vacuolar H + -ATPase by angiotensin II in proximal tubule cells. Pflugers Arch 2009;458:969–79.

[302] Krug AW, Papavassiliou F, Hopfer U, Ullrich KJ, Gekle M. Aldosterone stimulates surface expression of NHE3 in renal proximal brush borders. Pflugers Arch 2003;446:492–6.

[303] Drumm K, Kress TR, Gassner B, Krug AW, Gekle M. Aldosterone stimulates activity and surface expression of NHE3 in human primary renal proximal tubule epithelial cells (RTEC). Cell Physiol Biochem 2006;17:021–8.

[304] Pergher PS, Leite-Dellova D, deMello-Aires M. Direct action of aldosterone on bicarbonate reabsorption in in vivo cortical proximal tubule. Amer J Physiol 2009;296:F1185–93.

[305] Garcia NH, Garvin JL. Endothelin's biphasic effect on fluid absorption in the proximal straight tubule and its inhibitory cascade. J Clin Invest 1994;93:2572–7.

[306] Laghmani K, Preisig PA, Alpern RJ. The role of endothelin in proximal tubule proton secretion and the adaptation to a chronic metabolic acidosis. J Nephrol 2002;15(Suppl. 5): S75–87.

[307] Wesson DE. Endothelin role in kidney acidification. Sem Nephrol 2006;26:393–8.
[308] Wesson DE. Regulation of kidney acid excretion by endothelins. Kidney Int 2006;70:2066–73.
[309] Eiam-Ong S, Hilden SA, King AJ, Johns CA, Madias NE. Endothelin-1 stimulates the Na^+/H^+ and Na^+/HCO_3^- transporters in rabbit renal cortex. Kidney Int 1992;42:18–24.
[310] Guntupalli J, DuBose TD. Effects of endothelin on rat renal proximal tubule Na^+-P_i cotransport and Na^+/H^+ exchange. Amer J Physiol 1994;266:F658–66.
[311] Chu TS, Tsuganezawa H, Peng Y, Cano A, Yanagisawa M, Alpern RJ. Role of tyrosine kinase pathways in ET_B receptor activation of NHE3. Amer J Physiol 1996;271:C763–71.
[312] Peng Y, Amemiya M, Yang X, Fan L, Moe OW, Yin HL, et al. ET_B receptor activation causes exocytic insertion of NHE3 in OKP cells. Amer J Physiol 2001;280:F34–42.
[313] Peng Y, Moe OW, Chu T-S, Preisig PA, Yanagisawa M, Alpern RJ. ET_B receptor activation leads to activation and phosphorylation of NHE3. Amer J Physiol 1999;276:C938–45.
[314] Li S, Alpern RJ, Preisig PA. Rho A kinase, but not Pyk2, c-Src, or ERK1,2 function downstream of ET-1/ET_B in acid-induced NHE3 stimulation. J Am Soc Nephrol 2005;16:122A [Ref Type: Abstract]
[315] Chan YL. Adrenergic control of bicarbonate absorption in the proximal convoluted tubule of the rat kidney. Pflugers Arch 1980;388:159–64.
[316] Nord EP, Howard MJ, Hafezi A, Moradeshagi P, Vaystub S, Insel PA. $Alpha_2$ adrenergic agonists stimulate Na-H antiport activity in the rabbit renal proximal tubule. J Clin Invest 1987;80:1755–62.
[317] Guder WG, Rupprecht A. Antagonism between parathyroid hormone and norepinephrine on cyclic adenosine-3′:5′-monophosphate (cAMP) levels in isolated tubules from rat kidney cortex. Pflugers Arch 1975;254:177–86.
[318] Woodcock EA, Johnston CI. Selective inhibition by epinephrine of parathyroid hormone-stimulated adenylate cyclase in rat renal cortex. Amer J Physiol 1982;242:F721–6.
[319] Liu F, Gesek FA. a1-adrenergic receptors activate NHE1 and NHE3 through distict signaling pathways in epithelial cells. Amer J Physiol 2001;280:F415–25.
[320] Hall RA, Premont RT, Chow C-W, Blitzer JT, Pitcher JA, Claing A, et al. The B_2-adrenergic receptor interacts with the Na^+/H^+-exchanger regulatory factor to control Na^+/H^+ exchange. Nature 1998;392:626–30.
[321] Kinsella JL, Freiberg JM, Sacktor B. Glucocorticoid activation of Na/H exchange in renal brush border vesicles: kinetic effects. Amer J Physiol 1985;248:F233–9.
[322] Baum M, Cano A, Alpern RJ. Glucocorticoids stimulate Na/H antiporter in OKP cells. Amer J Physiol 1993;264:F1027–31.
[323] Bidet M, Merot J, Tauc M, Poujeol P. Na-H exchanger in proximal cells isolated from kidney. II. Short-term regulation by glucocorticoids. Amer J Physiol 1987;253:F945–51.
[324] Wang D, Zhang H, Lang F, Yun CC. Acute activation of NHE3 by dexamethasone correlates with activation of SGK1 and requires a functional glucocorticoid receptor. Amer J Physiol 2007;292:C396–404.
[325] Bobulescu IA, Dwarakanath V, Zou L, Zhang J, Baum M, Moe OW. Glucocorticoids acutely increase cell surface Na^+/H^+ exchanger-3 (NHE3) by activation of NHE3 exocytosis. Amer J Physiol 2005;289:F685–91.
[326] Wang D, Sun H, Lang F, Yun CC. Activation of NHE3 by dexamethasone requires phosphorylation of NHE3 at Ser663 by SGK1. Amer J Physiol 2005;289:C802–10.
[327] Baum M. Insulin stimulates volume absorption in the rabbit proximal convoluted tubule. J Clin Invest 1987;79:1104–9.
[328] Chobanian MC, Hammerman MR. Insulin stimulates ammoniagenesis in canine renal proximal tubular segments. Amer J Physiol 1987;253:F1171–7.
[329] Krivosikova Z, Spustova V, Dzurik R. Participation of P-dependent and P-independent glutaminases in rat kidney ammoniagenesis and their modulation by metabolic acidosis. Physiol Res 1998;47:177–83.
[330] Fuster DG, Bobulescu IA, Zhang J, Wade J, Moe OW. Characterization of the regulation of renal Na^+/H^+ exchanger NHE3 by insulin. Amer J Physiol 2007;292:F577–85.
[331] Capasso G, Unwin R, Rizzo M, Pica A, Giebisch G. Bicarbonate transport along the loop of Henle: molecular mechanisms and regulation. J Nephrol 2002;15(Suppl 5):S88–96.
[332] Buerkert J, Martin D, Trigg D. Segmental analysis of the renal tubule in buffer production and net acid formation. Amer J Physiol 1983;244:F442–54.
[333] DuBose Jr. TD, Lucci MS, Hogg RW, Pucacco LR, Kokko JP, Carter NW. Comparison of acidification parameters in superficial and deep nephrons of the rat. Amer J Physiol 1983;244: F497–503.
[334] Good DW. Sodium-dependent bicarbonate absorption by cortical thick ascending limb of rat kidney. Amer J Physiol 1985;248:F821–9.
[335] Good DW, Knepper MA, Burg MB. Ammonia and bicarbonate transport by thick ascending limb of rat kidney. Amer J Physiol 1984;247:F35–44.
[336] Good DW, Caflisch CR, DuBose Jr. TD. Transepithelial ammonia concentration gradients in inner medulla of the rat. Amer J Physiol 1987;252:F491–500.
[337] DuBose Jr. TD, Pucacco LR, Lucci MS, Carter NW. Micropuncture determination of pH, PCO_2, and total CO_2 concentration in accessible structures of the rat renal cortex. J Clin Invest 1979;64:476–82.
[338] Good DW. Bicarbonate absorption by the thick ascending limb of Henle's loop. Sem Nephrol 1990;10:132–8.
[339] Good DW, Watts III BA. Functional roles of apical membrane Na^+/H^+ exchange in rat medullary thick ascending limb. Amer J Physiol 1996;270:F691–9.
[340] Kikeri D, Azar S, Sun A, Zeidel ML, Hebert SC. Na-H antiporter and Na-$(HCO_3)_n$ symporter regulate intracellular pH in mouse medullary thick limbs of Henle. Amer J Physiol 1990;258:F445–56.
[341] Laghmani K, Borensztein P, Ambühl P, Froissart M, Bichara M, Moe OW, et al. Chronic metabolic acidosis enhances NHE-3 protein abundance and transport activity in the rat thick ascending limb by increasing NHE-3 mRNA. J Clin Invest 1997;99:24–30.
[342] Wang T, Hropot M, Aronson PS, Giebisch G. Role of NHE isoforms in mediating bicarbonate reabsorption along the nephron. Amer J Physiol 2001;281:F1117–22.
[343] Sun AM, Liu Y, Dworkin LD, Tse C-M, Donowitz M, Yip KP. Na^+/H^+ exchanger isoform 2 (NHE2) is expressed in the apical membrane of the medullary thick ascending limb. J Membr Biol 1997;160:85–90.
[344] Vallon V, Schwark JR, Richter K, Hropot M. Role of Na^+/H^+ exchanger NHE3 in nephron function: micropuncture studies with S3226, an inhibitor of NHE3. Amer J Physiol 2000;278: F375–9.
[345] Good DW, Kurtz I. Effects of chronic metabolic acidosis (CMA) and mineralocorticoid on H/HCO_3 transport in rat medullary thick ascending limb (MAL). Kidney Int 1989;35:454.
[346] Sabatini S, Laski ME, Kurtzman NA. NEM-sensitive ATPase activity in rat nephron: effect of metabolic acidosis and alkalosis. Amer J Physiol 1990;258:F297–304.

[347] Watts III BA, Good DW. An apical K^+-dependent HCO_3^- transport pathway opposes transepithelial HCO_3^- absorption in rat medullary thick ascending limb. Am J Physiol Renal Physiol 2004;287:F57–63.

[348] Younes-Ibrahim M, Barlet-Bas C, Buffin-Meyer B, Cheval L, Rajerison R, Doucet A. Ouabain-sensitive and -insensitive K-ATPases in rat nephron: effect of K depletion. Am J Physiol 1995;268:F1141–7.

[349] Krapf R. Basolateral membrane H/OH/HCO_3 transport in the rat cortical thick ascending limb. J Clin Invest 1988;82:234–41.

[350] Kwon TH, Fulton C, Wang W, Kurtz I, Frokiaer J, Aalkjaer C, et al. Chronic metabolic acidosis upregulates rat kidney Na-HCO cotransporters NBCn1 and NBC3 but not NBC1. Am J Physiol Renal Physiol 2002;282:F341–51.

[351] Vorum H, Kwon TH, Fulton C, Simonsen B, Choi I, Boron W, et al. Immunolocalization of electroneutral Na-HCO_3^- cotransporter in rat kidney. Am J Physiol Renal Physiol 2000;279: F901–9.

[352] Alper SL, Darman RB, Chernova MN, Dahl NK. The AE gene family of Cl/HCO_3^- exchangers. J Nephrol 2002;15:S41–53.

[353] Alper SL, Stuart-Tilley A, Biemesderfer D, Shmukler BE, Brown D. Immunolocalization of AE2 anion exchanger in rat kidney. Amer J Physiol 1997;273:F601–14.

[354] Blanchard A, Leviel F, Bichara M, Podevin RA, Paillard M. Interactions of external and internal K^+ with K^+-HCO_3^- cotransporter of rat medullary thick ascending limb. Am J Physiol 1996;271:C218–25.

[355] Bourgeois S, Masse S, Paillard M, Houillier P. Basolateral membrane Cl^--, Na^+-, and K^+-coupled base transport mechanisms in rat MTALH. Am J Physiol Renal Physiol 2002;282: F655–68.

[356] Eladari D, Blanchard A, Leviel F, Paillard M, Stuart-Tilley A, Alper SL, et al. Functional and molecular characterization of luminal and basolateral Cl^-/HCO_3^- exchangers of rat thick ascending limbs. Amer J Physiol 1998;275:F334–42.

[357] Hebert SC. Hypertonic cell volume regulation in mouse thick limbs. II. Na-H and Cl–HCO_3 exchange in basolateral membranes. Amer J Physiol 1986;250:C920–31.

[358] Leviel F, Eladari D, Blanchard A, Poumarat JS, Paillard M, Podevin RA. Pathways for HCO-3 exit across the basolateral membrane in rat thick limbs. Am J Physiol 1999;276:F847–56.

[359] Frische S, Zolotarev AS, Kim YH, Praetorius J, Alper S, Nielsen S, et al. AE2 isoforms in rat kidney: immunohistochemical localization and regulation in response to chronic NH_4Cl loading. Am J Physiol Renal Physiol 2004;286:F1163–70.

[360] Quentin F, Eladari D, Frische S, Cambillau M, Nielsen S, Alper SL, et al. Regulation of the Cl^-/HCO_3^- exchanger AE2 in rat thick ascending limb of Henle's loop in response to changes in acid–base and sodium balance. J Am Soc Nephrol 2004;15:2988–97.

[361] Bourgeois S, Meer LV, Wootla B, Block-Faure M, Chambrey R, Shull GE, et al. NHE4 is critical for the renal handling of ammonia in rodents. J Clin Invest 2010;120:1895–904.

[362] Chambrey St R, John PL, Eladari D, Quentin F, Warnock DG, Abrahamson DR, et al. Localization and functional characterization of Na^+/H^+ exchanger isoform NHE4 in rat thick ascending limbs. Am J Physiol—Ren Fluid Electrolyte Physiol 2001;281:F707–17.

[363] Good DW. Hyperosmolality inhibits bicarbonate absorption in rat medullary thick ascending limb via a protein-tyrosine kinase-dependent pathway. J Biol Chem 1995;270:9883–9.

[364] Good DW, George T, Watts III BA. Basolateral membrane Na^+/H^+ exchange enhances HCO_3 absorption in rat medullary thick ascending limb: evidence for functional coupling between basolateral and apical membrane Na^+/H^+ exchangers. Proc Natl Acad Sci USA 1995;92:12525–9.

[365] Watts III BA, George T, Good DW. Nerve growth factor inhibits HCO_3^- absorption in renal thick ascending limb through inhibition of basolateral membrane Na^+/H^+ exchange. J Biol Chem 1999;274:7841–7.

[366] Watts III BA, George T, Good DW. The basolateral NHE1 Na^+/H^+ exchanger regulates transepithelial HCO_3^- absorption through actin cytoskeleton remodeling in renal thick ascending limb. J Biol Chem 2005;280:11439–47.

[367] Uchida S, Sasaki S, Nitta K, Uchida K, Horita S, Nihei H, et al. Localization and Functional Characterization of Rat Kidney-specific Chloride Channel, C1C-K1. J Clin Invest 1995;95: 104–13.

[368] Simon DB, Bindra RS, Mansfield TA, Nelson-Williams C, Mendonca E, Stone R, et al. Mutations in the chloride channel gene, *CLCNKB*, cause Bartter's syndrome type III. Nature Genet 1997;17:171–8.

[369] Garvin JL, Burg MB, Knepper MA. Active NH_4 absorption by the thick ascending limb. Amer J Physiol 1988;255:F57–65.

[370] Good DW. Active absorption of NH_4 by rat medullary thick ascending limb: inhibition by potassium. Amer J Physiol 1988;255:F78–87.

[371] Kikeri D, Sun A, Zeidel ML, Hebert SC. Cell membranes impermeable to NH_3. Nature 1989;339:478–80.

[372] Kikeri D, Sun A, Zeidel ML, Herbert SC. Cellular NH_4^+/K^+ transport pathways in mouse medullary thick limb of Henle. J Gen Physiol 1992;99:435–61.

[373] Watts III BA, Good DW. Effects of Ammonium on Intracellular pH in Rat Medullary Thick Ascending Limb: Mechanisms of Apical Membrane NH_4^+ Transport. J Gen Physiol 1994;103: 917–36.

[374] Houillier P, Bourgeois S. More actors in ammonia absorption by the thick ascending limb. Amer J Physiol 2012;302:F293–7.

[375] Dobyan DC, Magill LS, Friedman PA, Hebert SC, Bulger RE. Carbonic anhydrase histochemistry in rabbit and mouse kidneys. Anat Rec 1982;204:185–97.

[376] Lino Y, Burg MB. Effect of acid–base status *in vivo* on bicarbonate transport by rabbit renal tubules *in vitro*. Jpn J Physiol 1981;31:99–107.

[377] Lonnerholm G, Wistrand PJ. Carbonic anhydrase in the human kidney: a histochemical and immunocytochemical study. Kidney Int 1984;25:886–98.

[378] Capasso G, Unwin R, Ciani F, DeSanto NG, DeTommaso G, Russo F, et al. Bicarbonate transport along the loop of Henle II. Effects of acid–base, dietary, and neurohormonal determinants. J Clin Invest 1994;94:830–8.

[379] Good DW. Adaptation of HCO_3 and NH_4 transport in rat MTAL: effects of chronic metabolic acidosis and Na intake. Amer J Physiol 1990;258:F1345–53.

[380] Laghmani K, Chambrey R, Froissart M, Bichara M, Paillard M, Borensztein P. Adaptation of NHE-3 in the rat thick ascending limb: effects of high sodium intake and metabolic alkalosis. Amer J Physiol 1999;276:F18–26.

[381] Capasso G, Unwin R, Agulian S, Giebisch G. Bicarbonate transport along the loop of Henle I. Microperfusion studies of load and inhibitor sensitivity. J Clin Invest 1991;88:430–7.

[382] Good DW, George T, Watts III BA. High sodium intake increases HCO_3^- absorption in medullary thick ascending limb through adaptations in basolateral and aplical Na^+/H^+ exchangers. Amer J Physiol 2011;301:F334–43.

[383] Good DW, George T, Watts III BA. Aldosterone inhibits HCO absorption via a nongenomic pathway in medullary thick ascending limb. Am J Physiol Renal Physiol 2002;283: F699–706.

[384] Good DW, George T, Watts III BA. Nongenomic regulation by aldosterone of the epithelial NHE3 Na^+/H^+ exchanger. Am J Physiol Cell Physiol 2006;290:C757–63.

[385] Unwin R, Capasso G, Giebisch G. Bicarbonate transport along the loop of Henle effects of adrenal steroids. Amer J Physiol 1995;268:F234–9.
[386] Good DW, George T, Wang DH. Angiotensin II inhibits HCO-3 absorption via a cytochrome P-450-dependent pathway in MTAL. Am J Physiol 1999;276:F726–36.
[387] Bichara M, Mercier O, Houillier P, Paillard M, Leviel F. Effects of antidiuretic hormone on urinary acidification and on tubular handling of bicarbonate in the rat. J Clin Invest 1987;80:621–30.
[388] Good DW. Inhibition of bicarbonate absorption by peptide hormones and cyclic adenosine monophosphate in rat medullary thick ascending limb. J Clin Invest 1990;85:1006–13.
[389] Mercier O, Bichara M, Delahousse M, Prigent A, Leviel F, Paillard M. Effects of glucagon on H/HCO_3 transport in Henle's loop, distal tubule, and collecting ducts in the rat. Amer J Physiol 1989;257:F1003–14.
[390] Good DW. Nerve growth factor regulates HCO3-absorption in thick ascending limb: modifying effects of vasopressin. Amer J Physiol 1998;274:C931–9.
[391] Watts III BA, Good DW. ERK mediates inhibition of Na^+/H^+ exchange and HCO_3^- absorption by nerve growth factor in MTAL. Am J Physiol Renal Physiol 2002;282:F1056–63.
[392] Bichara M, Mercier O, Paillard M, Leviel F. Effects of parathyroid hormone on urinary acidification. Amer J Physiol 1986;251:F444–53.
[393] Good DW, George T, Watts III BA. Lipopolysaccharide directly alters renal tubule transport through distinct TLR4-dependent pathways in basolateral and apical membranes. Amer J Physiol 2009;297:F866–74.
[394] Good DW, George T, Watts III BA. Toll-like receptor 2 mediates inhibition of HCO_3^- absorption by bacterial lipoprotein in medullary thick ascending limb. Amer J Physiol 2010;299:F536–44.
[395] Watts III BA, George T, Sherwood ER, Good DW. Basolateral LPS inhibits NHE3 and HCO_3^- absorption through TLR4/MyD88-dependent ERK activation in medullary thick ascending limb. Amer J Physiol 2011;301:C1296–306.
[396] Good DW, Molina JJ. Effects of osmolality on bicarbonate absorption by medullary thick ascending limb. Kidney Int 1990;37:537.
[397] Good DW, Di Mari JF, Watts III BA. Hyposmolality stimulates Na^+/H^+ exchange and HCO_3^- absorption in thick ascending limb via PI 3-kinase. Am J Physiol Cell Physiol 2000;279:C1443–54.
[398] Watts III BA, Good DW. Hyposmolality stimulates apical membrane Na^+/H^+ exchange and HCO_3^- absorption in renal thick ascending limb 2955. J Clin Invest 1999;104:1593–602.
[399] Good DW. PGE_2 reverses AVP inhibition of HCO_3 absorption in rat MTAL by activation of protein kinase C. Amer J Physiol 1996;270:F978–85.
[400] Good DW, George T. Regulation of HCO_3 absorption by prostaglandin E_2 and G proteins in rat medullary thick ascending limb. Amer J Physiol 1996;270:F711–7.
[401] DuBose Jr. TD. Hydrogen ion secretion by the collecting duct as a determinant of the urine to blood PCO_2 gradient in alkaline urine. J Clin Invest 1982;69:145–56.
[402] DuBose Jr. TD. Application of the disequilibrium pH method to investigate the mechanism of urinary acidification. Amer J Physiol 1983;245:F535–44.
[403] Graber ML, Bengele HH, Schwartz JH, Alexander EA. pH and pCO_2 profiles of the rat inner medullary collecting duct. Amer J Physiol 1981;241:F659–68.
[404] Koeppen BM, Helman SI. Acidification of luminal fluid by the rabbit cortical collecting tubule perfused in vitro. Amer J Physiol 1982;242:F521–31.
[405] Star RA, Burg MB, Knepper MA. Luminal disequilibrium pH and ammonia transport in outer medullary collecting duct. Amer J Physiol 1987;252:F1148–57.
[406] Star RA, Kurtz I, Mejia R, Burg MB, Knepper MA. Disequilibrium pH and ammonia transport in isolated perfused cortical collecting ducts. Amer J Physiol 1987;253:F1232–42.
[407] Hamm LL, Hering-Smith KS. Acid–base transport in the collecting duct. Sem Nephrol 1993;13:246–55.
[408] Schuster VL. Bicarbonate reabsorption and secretion in the cortical and outer medullary collecting tubule. Sem Nephrol 1990;10:139–47.
[409] Steinmetz PR. Cellular organization of urinary acidification. Amer J Physiol 1986;251:F173–87.
[410] DuBose Jr. TD, Codina J. H,K-ATPase. Curr Opin Nephrol Hypertens 1996;5:411–6.
[411] Wingo CS, Cain BD. The renal H-K-ATPase: physiological significance and role in potassium homeostasis. Annu Rev Physiol 1993;55:323–47.
[412] Wingo CS, Smolka AJ. Function and structure of H-K-ATPase in the kidney. Amer J Physiol 1995;269:F1–16.
[413] Gluck S, Kelly S, Al-Awqati Q. The proton translocating ATPase responsible for urinary acidification. J Biol Chem 1982;257:9230–3.
[414] Stone DK, Xie XS. Proton translocating ATPases: issues in structure and function. Kidney Int 1988;33:767–74.
[415] Alper S, Natale S, Gluck S, Lodish HF, Brown D. Subtypes of intercalated cells in rat kidney collecting duct defined by antibodies against erythroid band 3 and renal vacuolar H^+-ATPase. Proc Natl Acad Sci USA 1989;86:5429–33.
[416] Schuster VL, Bonsib SM, Jennings ML. Two types of collecting duct mitochondria-rich (intercalated) cells: lectin and band 3 cytochemistry. Amer J Physiol 1986;251:C347–55.
[417] Silver RB, Mennitt PA, Satlin LM. Stimulation of apical H-K-ATPase in intercalated cells of cortical collecting duct with chronic metabolic acidosis. Am J Physiol 1996;270:F539–47.
[418] Weiner ID, Milton AE. H^+ -K^+ -ATPase in rabbit cortical collecting duct B-type intercalated cell. Amer J Physiol 1996;270:F518–30.
[419] Atkins JL, Burg MB. Bicarbonate transport by isolated perfused rat collecting ducts. Amer J Physiol 1985;249:F485–9.
[420] Cohen L. HCO_3-Cl exchange transport in the adaptive response to alkalosis by turtle bladder. Amer J Physiol 1980;239:F167–74.
[421] Leslie BR, Schwartz JH, Steinmetz PR. Coupling between Cl absorption and HCO_3 secretion in turtle urinary bladder. Amer J Physiol 1973;225:610–7.
[422] Levine DZ, Iacovitti M, Nash L, Vandorpe D. Secretion of bicarbonate by rat distal tubules in vivo. J Clin Invest 1988;81:1873–8.
[423] McKinney TD, Burg MB. Bicarbonate transport by rabbit cortical collecting tubules: effect of acid and alkali loads in vivo on transport in vitro. J Clin Invest 1977;60:766–8.
[424] Tisher CC, Madsen KM. Anatomy of the kidney. In: Brenner BM, editor. The kidney. Philadelphia: W.B. Saunders Co.; 1996. p. 3–71.
[425] Verlander JW, Madsen KM, Tisher CC. Effect of acute respiratory acidosis on two populatons of intercalated cells in rat cortical collecting duct. Amer J Physiol 1987;253:F1142–56.
[426] Capasso G, Jaeger P, Giebisch G, Guckian V, Malnic G. Renal bicarbonate reabsorption in the rat. II. Distal tubule load dependence and effect of hypokalemia. J Clin Invest 1987;80:409–14.

[427] Capasso G, Kinne R, Malnic G, Giebisch G. Renal bicarbonate reabsorption in the rat. I. Effects of hypokalemia and carbonic anhydrase. J Clin Invest 1986;78:1558–67.
[428] Chan YL, Malnic G, Giebisch G. Renal bicarbonate reabsorption in the rat: III. Distal tubule perfusion study of load dependence and bicarbonate permeability. J Clin Invest 1989;84:931–8.
[429] Kunau RT, Walker KA. Total CO absorption in the distal tubule of the rat. Amer J Physiol 1987;252:F468–73.
[430] Levine DZ. An in vivo microperfusion study of distal tubule bicarbonate reabsorption in normal and ammonium chloride rats. J Clin Invest 1985;75:588–95.
[431] Malnic GM, deMello-Aires M, Giebisch G. Micropuncture study of renal tubular hydrogen iion transport in the rat. Amer J Physiol 1972;222:147–58.
[432] Lucci MS, Pucacco LR, Carter NW, DuBose Jr. TD. Evaluation of bicarbonate transport in the rat distal tubule: effects of acid–base status. Amer J Physiol 1982;243:F335–41.
[433] Fejes-Toth G, Naray-Fejes-Toth A. Immunohistochemical localization of colonic H-K-ATPase to the apical membrane of connecting tubule cells. Am J Physiol Renal Physiol 2001;281: F318–25.
[434] Verlander JW, Moudy RM, Campbell WG, Cain BD, Wingo CS. Immunohistochemical localization of H-K-ATPase alpha (2c)-subunit in rabbit kidney. Am J Physiol Renal Physiol 2001;281:F357–65.
[435] Wang T, Malnic G, Giebisch G, Chan YL. Renal bicarbonate reabsorption in the rat. IV. Bicarbonate transport mechanisms in the early and late distal tubule. J Clin Invest 1993;91: 2776–84.
[436] Wesson DE. Na/H exchange and H-K ATPase increase distal tubule acidification in chronic alkalosis. Kidney Int 1998;53:945–51.
[437] Bailey MA, Giebisch G, Abbiati T, Aronson PS, Gawenis LR, Shull GE, et al. NHE2-mediated bicarbonate reabsorption in the distal tubule of NHE3 null mice. J Physiol 2004;561: 765–75.
[438] Chambrey R, Warnock DG, Podevin R-A, Bruneval P, Mandet C, Belair M-F, et al. Immunolocalization of the Na^+/H^+ exchanger isoform NHE2 in rat kidney. Am J Physiol 1998;275: F379–86.
[439] Iacovitti M, Nash L, Peterson LN, Rochon J, Levine DZ. Distal tubule bicarbonate accumulation in vivo. J Clin Invest 1986;78:1658–65.
[440] Tsuruoka S, Schwartz GJ. Mechanisms of HCO_3^- secretion in the rabbit connecting segment. Amer J Physiol 1999;277: [t-74]
[441] Levine DZ. Single nephron studies: implications for acid–base regulation. Kidney Int 1990;38:744–61.
[442] Levine DZ, Bandorpe D, Iacovitti M. Luminal chloride modulates rat distal tubule bidirectional bicarbonate flux in vivo. J Clin Invest 1990;85:1793–8.
[443] McKinney TD, Burg MB. Bicarbonate secretion by rabbit cortical collecting tubules in vitro. J Clin Invest 1978;61: 1421–7.
[444] McKinney TD, Burg MB. Bicarbonate absorption by rabbit cortical collecting tubules in vitro. Amer J Physiol 1978;234: F141–5.
[445] Gifford JD, Sharkins K, Work J, Luke RG, Galla JH. Total CO_2 transport in rat cortical collecting duct in chloride-depletion alkalosis. Amer J Physiol 1990;258:F848–53.
[446] Knepper MA, Good DW, Burg MB. Ammonia and bicarbonate transport by rat cortical collecting ducts perfused in vitro. Amer J Physiol 1985;249:F870–7.
[447] Royaux IE, Wall SM, Karniski LP, Everett LA, Suzuki K, Knepper MA, et al. Pendrin, encoded by the Pendred syndrome gene, resides in the apical region of renal intercalated cells and mediates bicarbonate secretion. Proc Natl Acad Sci U S A 2001;98:4221–6.
[448] O'Neil RG, Hayhurst RA. Functional differentiation of cell types of cortical collecting duct. Amer J Physiol 1985;248: F449–53.
[449] Chaillet JR, Lopes AG, Boron WF. Basolateral Na-H exchange in the rabbit cortical collecting tubule. J Gen Physiol 1985;86: 795–812.
[450] Wang X, Kurtz I. H^+/Base transport in principal cells characterized by confocal fluorescence imaging. Amer J Physiol 1990;259:C365–73.
[451] Weiner ID, Hamm LL. Regulation of intracellular pH in the rabbit cortical collecting tubule. J Clin Invest 1990;85: 274–81.
[452] Wingo CS, Madsen KM, Smolka A, Tisher CC. H-K-ATPase immunoreactivity in cortical and outer medullary collecting duct. Kidney Int 1990;38:985–90.
[453] Ridderstrale Y, Kashgarian M, Koeppen B, Giebisch G, Stetson D, Ardito T, et al. Morphological heterogeneity of the rabbit collecting duct. Kidney Int 1988;34:655–70.
[454] Steinmetz PR. Characteristics of hydrogen ion transport in urinary bladder of water turtle. J Am Soc Nephrol 2000;11: 1160–9.
[455] Madsen KM, Tisher CC. Structural-functional relationships along the distal nephron. Amer J Physiol 1986;250: F1–15.
[456] Verlander JW, Madsen KM, Tisher CC. Structural and functional features of proton and bicarbonate transport in the rat collecting duct. Sem Nephrol 1991;11:465–77.
[457] Verlander JW, Madsen KM, Low PS, Allen DP, Tisher CC. Immunocytochemical localization of band 3 protein in the rat collecting duct. Amer J Physiol 1988;255:F115–25.
[458] Brown D, Hirsch S, Gluck S. An H-ATPase in opposite plasma membrane domains in kidney epithelial cell subpopulations. Nature 1988;331:622–4.
[459] Brown D, Orci L. Junctional complexes and cell polarity in the urinary tubule. J Electr Micro Tech 1988;9:145.
[460] Kim YH, Kwon TH, Frische S, Kim J, Tisher CC, Madsen KM, et al. Immunocytochemical localization of pendrin in intercalated cell subtypes in rat and mouse kidney. Am J Physiol Renal Physiol 2002;283:F744–54.
[461] Wall SM. Mechanisms of NH_4^+ and NH_3 transport during hypokalemia. Acta Physiol Scand 2003;179:325–30.
[462] Schwartz GJ, Barasch J, Al-Awqati Q. Plasticity of functional epithelial polarity. Nature 1985;318:368–71.
[463] Weiner ID, Hamm LL. Use of fluorescent dye BCECF to measure intracellular pH in cortical collecting tubule. Amer J Physiol 1989;256:F957–64.
[464] Schuster VL, Gluck S. Co-existence of H^+-ATPase and band 3 $Cl–HCO_3$ exchanger in rabbit collecting duct intercalated cells. Kidney Int 1989;35:463.
[465] Schwartz GJ, Al-Awqati Q. Regulation of transepithelial H^+ transport by exocytosis and endocytosis. Ann Rev Physiol 1986;48:153–61.
[466] Emmons C, Matsuzaki K, Stokes JB, et al. Axial heterogeneity of cortical collecting duct cell types. Kidney Int 1989;35:453.
[467] Schwartz GJ, Satlin LM, Bergmann JE. Fluorescent characterization of collecting duct cells: a second H^+-secreting type. Amer J Physiol 1988;255:F1003–14.
[468] Eladari D, Chambrey R, Peti-Peterdi J. A new look at electrolyte transport in the distal tubule. Annu Rev Physiol 2012;74:325–49.
[469] Wall SM, Pech V. Pendrin and sodium channels: relevance to hypertension. J Nephrology 2010;23:S118–23.

[470] Emmons C, Kurtz I. Functional characterization of three intercalated cell subtypes in the rabbit outer cortical collecting duct. J Clin Invest 1994;93:417–23.
[471] Weiner ID, Weill AE, New AR. Distribution of Cl^-/HCO_3^- exchange and intercalated cells in rabbit cortical collecting duct. Amer J Physiol 1994;267:F952–64.
[472] Al Awqati Q. Terminal differentiation of intercalated cells: the role of hensin. Annu Rev Physiol 2003;65:567–83.
[473] Schwartz GJ, Tsuruoka S, Vijayakumar S, Petrovic S, Mian A, Al-Awqati Q. Acid incubation reverses the polarity of intercalated cell transporters, an effect mediated by hensin. J Clin Invest 2002;109:89–99.
[474] Bastani B, Purcell H, Hemken P, Trigg D, Gluck S. Expression and distribution of renal vacuolar proton-translocating adenosine triphosphatase in response to chronic acid and alkali loads in the rat. J Clin Invest 1991;88:126–36.
[475] Breyer MD, Jacobson HR. Regulation of rabbit medullary collecting duct cell pH by basolateral Na/H and Cl/base exchange. J Clin Invest 1989;84:996–1004.
[476] Schuster VL, Stokes JB. Chloride transport by the cortical and outer medullary collecting duct. Amer J Physiol 1987;253: F203–12.
[477] Lombard WE, Kokko JP, Jacobson HR. Bicarbonate transport in cortical and outer medullary collecting tubules. Amer J Physiol 1983;244:F289–96.
[478] Schuster VL. Cyclic adenosine monophosphate-stimulated bicarbonate secretion in rabbit cortical collecting tubules. J Clin Invest 1985;75:2056–64.
[479] Star RA, Burg MB, Knepper MA. Bicarbonate secretion and chloride absorption by rabbit cortical collecting ducts. J Clin Invest 1985;76:1123–30.
[480] Garcia-Austt J, Good DW, Burg MB, Knepper MA. Deoxycorticosterone-stimulated bicarbonate secretion in rabbit cortical collecting ducts: effects of luminal chloride removal and in vivo acid loading. Amer J Physiol 1985;249: F205–12.
[481] Hamm LL, Hering-Smith K, Vehaskari VM. Control of bicarbonate transport in collecting tubules from normal and remnant kidneys. Amer J Physiol 1989;256:F680–7.
[482] Tsuruoka S, Schwartz GJ. Adaptation of rabbit cortical collecting duct HCO_3^- transport to metabolic acidosis in vitro. J Clin Invest 1996;97:1076–84.
[483] Wesson DE. Reduced bicarbonate secretion mediates increased distal tubule acidification induced by dietary acid. Amer J Physiol 1996;271:F670–8.
[484] Wesson DE. Dietary HCO_3 reduces distal tubule acidification by increasing cellular HCO_3 secretion. Amer J Physiol 1996;271:F132–42.
[485] Levine DZ, Jacobson HR. The regulation of renal acid secretion: new observations from studies of distal nephron segments. Kidney Int 1986;29:1099–109.
[486] Satlin LM, Schwartz GJ. Cellular remodeling of HCO_3-secreting cells in rabbit renal collecting duct in response to an acidic environment. J Cell Biol 1989;109:1279–88.
[487] McKinney TD, Davidson KK. Bicarbonate transport in collecting tubules from outer stripe of outer medulla of rabbit kidneys. Amer J Physiol 1987;253:F816–22.
[488] Kuwahara M, Sasaki S, Marumo F. Cell pH regulation in rabbit outer medullary collecting duct cells: mechanisms of HCO_3^--independent processes. Amer J Physiol 1990;259: F902–9.
[489] Koeppen BM. Conductive properties of the rabbit outer medullary collecting duct: outer stripe. Amer J Physiol 1986;250: F70–6.
[490] Koeppen BM. Electrophysiological identification of principal and intercalated cells in the rabbit outer medullary collecting duct. Pflugers Arch 1987;409:138–41.
[491] Hamm LL, Weiner ID. Differential loading of luminal BCECF in the inner stripe of the outer medullary collecting duct (OMCD(is). J Amer Soc Nephrol 1990;1:649A.
[492] Weiner ID, Wingo CS, Hamm LL. Regulation of intracellular pH in two cell populations of inner stripe of rabbit outer medullary collecting duct. Amer J Physiol 1993;265: F406–15.
[493] Hays S, Alpern RJ. Mechanism and regulation of apical membrane Na-independent H^+ efflux in the inner stripe of the outer medullary collecting tubule (OMiCT). Kidney Int 1990;37:538A.
[494] Hays SR, Alpern RJ. Basolateral membrane Na-independent Cl/HCO_3 exchange in the inner stripe of the rabbit outer medullary collecting tubule. J Gen Physiol 1992;95:347–67.
[495] Yip KP, Tsuruoka S, Schwartz GJ, Kurtz I. Apical H^+/base transporters mediating bicarbonate absorption and pH(i) regulation in the OMCD. Am J Physiol Renal Physiol 2002;283: F1098–104.
[496] Stone DK, Seldin DW, Kokko JP, Jacobson HR. Mineralocorticoid modulation of rabbit medullary collecting duct acidification: a sodium independent effect. J Clin Invest 1983;72:77–83.
[497] Stone DK, Seldin DW, Kokko JP, Jacobson HR. Anion dependence of rabbit medullary collecting duct acidification. J Clin Invest 1983;71:1505–8.
[498] Wingo CS. Active proton secretion and potassium absorption in the rabbit outer medullary collecting duct: functional evidence for H/K-ATPase. J Clin Invest 1989;84:361–5.
[499] Clapp WL, Madsen KM, Verlander JW, Tisher CC. Morphologic heterogeneity along the rat inner medullary collecting duct. Lab Invest 1989;60:219.
[500] Madsen KM, Clapp WL, Verlander JW. Structure and function of the inner medullary collecting duct. Kidney Int 1988;34: 441–54.
[501] Garg LC, Narang N. Effects of aldosterone on NEM-sensitive ATPase in rabbit nephron segments. Kidney Int 1988;34: 13–7.
[502] Garg LC, Narang N. Stimulation of N-ethylmaleimide ATPase in the collecting duct segments of rat by metabolic acidosis. Can J Physiol Pharmacol 1985;63:1291–6.
[503] Wall SM, Knepper MA. Acid–base transport in the inner medullary collecting duct. Sem Nephrol 1990;10:148–58.
[504] Wall SM, Truong AV, DuBose TD. H^+-K^+-ATPase mediates net acid secretion in rat terminal inner medullary collecting duct. Am J Physiol 1996;271:F1037–44.
[505] Bengele HH, Graber ML, Alexander EA. Effect of respiratory acidosis on acidification by the medullary collecting duct. Amer J Physiol 1983;244:F89–94.
[506] Bengele HH, McNamara ER, Alexander EA. Effect of acute thyroparathyroidectomy on nephron acidificatoin. Amer J Physiol 1984;246:F569–74.
[507] Bengele HH, McNamara ER, Schwartz JH, Alexander EA. Acidification adaptation along the inner medullary collecting duct. Amer J Physiol 1988;255:F1155–9.
[508] Bengele HH, Schwartz JH, McNamara ER, Alexander EA. Chronic metabolic acidosis augments acidification along the inner medullary collecting duct. Amer J Physiol 1986;250: F690–4.
[509] Graber ML, Bengele HH, Mroz E, Lechene C, Alexander EA. Acute metabolic acidosis augments collecting duct acidification rate in the rat. Amer J Physiol 1981;241:F669–76.

[510] Richardson RMA, Kunau Jr. RT. Bicarbonate reabsorption in the papillary collecting duct: effect of acetazolamide. Amer J Physiol 1982;243:F74–80.
[511] Ullrich KJ, Papavassiliou F. Bicarbonate reabsorption in the papillary collecting duct of rats. Pflugers Arch 1981;289:271–5.
[512] Ishibashi M, Sasaki S, Yoshiyama N, et al. Generation of pH gradient across the rabbit collecting duct segments perfused in vitro. Kidney Int 1987;31:930–96.
[513] Wall SM, Sands JM, Flessner MF, Nonoguchi H, Spring KR, Knepper MA. Net acid transport by isolated perfused inner medullary collecting ducts. Amer J Physiol 1990;258: F75–84.
[514] Brion LP, Schwartz JH, Lachman HM, Zavilowitz BJ, Schwartz GJ. Development of H^+ secretion by cultured renal inner medullary collecting duct cells. Amer J Physiol 1989;257:F486–501.
[515] Hering-Smith K, Cragoe Jr. E, Weiner EJ, Hamm LL. Inner medullary collecting duct Na^+–H^+ exchanger. Amer J Physiol 1991;260:C1300–7.
[516] Kikeri D, Zeidel ML. Intracellular pH regulation in freshly isolated suspensions of rabbit inner medullary collecting duct cells: role of Na^+:H^+ antiporter and H^+-ATPase. J Amer Soc Nephrol 1990;1:890–901.
[517] Kleinman JG, Blumenthal S, Wiessner JH, Reetz KL, Lewand DL, Mandel NS, et al. Regulation of pH in rat papillary tubule cells in primary culture. J Clin Invest 1987;80:1660–9.
[518] Ono S, Guntupalli J, DuBose Jr. TD. Role of H^+-K^+-ATPase in pHi regulation in inner medullary collecting duct cells in culture. Amer J Physiol 1996;270:F852–61.
[519] Prigent A, Bichara M, Paillard M. Hydrogen transport in papillary collecting duct of rabbit kidney. Amer J Physiol 1985;248: C241–6.
[520] Schwartz JH. Renal acid–base transport: the regulatory role of the inner medullary collecting duct. Kidney Int 1995;47: 333–41.
[521] Selvaggio AM, Schwartz JH, Bengele HH, Gordon FD, Alexander EA. Mechanisms of H^+ secretion by inner medullary collecting duct cells. Amer J Physiol 1988;254:F391–400.
[522] Wall SM, Kraut JA, Muallem S. Modulation of Na^+-H^+ exchange activity by intracellular Na^+, H^+, and Li^+ in IMCD cells. Amer J Physiol 1988;255:F331–9.
[523] Wall SM, Muallem S, Kraut JA. Detection of a Na^+-H^+ antiporter in cultured rat renal papillary collecting duct cells. Amer J Physiol 1987;253:F889–95.
[524] Hart D, Nord EP. Polarized distribution of Na^+/H^+ antiport and Na^+/HCO_3^- cotransport in primary cultures of renal inner medullary collecting duct cells. J Biol Chem 1991;66: 2374–82.
[525] Schwartz JH, Masion SA, Nichols RD, Alexander EA. Intracellular modulation of acid secretion in rat inner medullary collecting duct cells. Amer J Physiol 1994;266:F94–101.
[526] Obrador G, Yuan H, Shih TM, Wang YH, Shia MA, Alexander EA, et al. Characterization of anion exchangers in an inner medullary collecting duct cell line. J Amer Soc Nephrol 1998;9:746–54.
[527] Star RA. Basolateral membarne sodium-independent Cl^-/HCO_3^- exchanger in rat inner medullary collecting duct cell. J Clin Invest 1990;85:1959–66.
[528] Weill AE, Tisher CC, Conde MF, Weiner ID. Mechanisms of bicarbonate transport by cultured rabbit inner medullary collecting duct cells. Amer J Physiol 1994;266:F466–76.
[529] Kim C, Nord EP, Kraut JA. Cl^-/HCO_3^- exchange of inner medullary collecting duct (IMCD) cells is predominantly a Na^+-independent process. Kidney Int 1989;35:456A.
[530] Breton S, Brown D. New insights into the regulation of V-ATPase-Dependent proton secretion. AmJPhysiol Renal Physiol 2006.
[531] Gluck S, Bastani B, Nelson R, et al. Properties and function of the kidney vacuolar H^+ ATPase: a versatile proton pump responsible for urinary acidification. Springer-Verlag; 1991 [Ref Type: Conference Proceeding]
[532] Dixon TE, Al-Awqati Q. Urinary acidification in turtle bladder is due to a reversible proton translocating ATPase. Proc Natl Acad Sci USA 1979;76:3135–8.
[533] Forgac M. Structure and function of vacuolar class of ATP-driven proton pumps. Physiol Rev 1989;69:765–96.
[534] Stone DK, Crider B, Xie XS. Structural properties of vacuolar proton pumps. Kidney Int 1990;38:649–53.
[535] Gluck S, Caldwell J. Proton translocating ATPase from bovine kidney medulla partial purification and reconstitution. Amer J Physiol 1988;254:F71–9.
[536] Gluck S, Caldwell J. Immunoaffinity purification and characterization of vacuolar H ATPase from bovine kidney. J Bio Chem 1987;262:15780–9.
[537] Stone DK, Xie XS, Wu LT, Racker E. Proton translocating ATPases of clathrin-coated vesicles, renal medulla and Ehrlich ascites tumor cells. In: Forte J, Warnock D, Rector Jr FC, editors. Hydrogen ion transport in epithelia. New York: Wiley Press; 1984. p. 219–30.
[538] Schulz N, Dave MH, Stehberger PA, Chau T, Wagner CA. Differential localization of vacuolar H + -ATPases containing a1, a2, a3 or a4 (ATP6V0A1-4) subunit isoforms along the nephron. Cell Physiol Biochem 2007;20:109–20.
[539] Nelson RD, Guo XL, Masood K, Brown D, Kalkbrenner M, Gluck S. Selectively amplified expression of an isoform of the vacuolar H-ATPase 56-kilodalton subunit in renal intercalated cells. Proc Natl Acad Sci USA 1992;89:3541–5.
[540] Paunescu TG, Da SN, Marshansky V, McKee M, Breton S, Brown D. Expression of the 56-kDa B2 subunit isoform of the vacuolar H^+-ATPase in proton-secreting cells of the kidney and epididymis. Am J Physiol Cell Physiol 2004;287: C149–62.
[541] Alper SL. Genetic diseases of acid–base transporters. Annu Rev Physiol 2002;64:899–923.
[542] Borthwick KJ, Karet FE. Inherited disorders of the H^+-ATPase. Curr Opin Nephrol Hypertens 2002;11:563–8.
[543] Al-Awqati Q. H transport in urinary epithelia. Amer J Physiol 1978;235:F77–88.
[544] Brown D, Gluck S, Hartwig JH. Structure of the novel membrane coating material in proton-secreting epithelial cells and identification as an H ATPase. J Clin Biol 1987;105:1637–48.
[545] Ait-Mohamed AK, Marsy S, Barlet C, Khadouri G, Doucet A. Characterization of N-ethylmaleimide-sensitive proton pump in the kidney. J Biol Chem 1986;261:12526–33.
[546] Mujais SK. Effects of aldosterone on rat collecting tubule N-ethylmaleimide-sensitive adenosine triphosphatase. J Lab Clin Med 1989;109:34–9.
[547] Stone DK, Tsai SJ, Xie XS. Chloride directly stimulates the bovine brain clathrin-coated vesicle and renal medulla proton pumps. Kidney Int 1987;31:417.
[548] Koeppen BM. Conductive properties of the rabbit outer medullary collecting duct: inner stripe. Amer J Physiol 1985;248: F500–6.
[549] Light DB, Schwiebert EM, Fejes-Toth G, Naray-Fejes-Toth A, Karlson KH, McCann FV, et al. Chloride channels in the apical membrane of cortical collecting duct cells. Amer J Physiol 1990;258:F273–80.

[550] Gunther W, Luchow A, Cluzeaud F, Vandewalle A, Jentsch TJ. CIC-5, the chloride channel mutated in Dent's disease, colocalizes with the proton pump in endocytotically active kidney cells. Proc Natl Acad Sci USA 1998;95:8075–80.

[551] Xu J, Barone S, Li H, Holiday S, Zahedi K, Soleimani M. Slc26a11, a chloride transporter, localizes with the vacuolar H^+-ATPase of A-intercalated cells in the kidney. Kidney Int 2011;80:926–37.

[552] Gluck SL, Iyori M, Holliday LS, Kostrominova T, Lee BS. Distal urinary acidification from homer smith to the present. Kidney Int 1996;49:1660–4.

[553] Gluck SL, Underhill D, Iyori M, Holliday LS, Kostrominova T, Lee BS. Physiology and biochemistry of the kidney vacuolar H^+ATPase. Annu Rev Physiol 1996;58:427–45.

[554] Lu M, Holliday LS, Zhang L, Dunn Jr. WA, Gluck SL. Interaction between aldolase and vacuolar H^+-ATPase: evidence for direct coupling of glycolysis to the ATP-hydrolyzing proton pump. J Biol Chem 2001;276:30407–13.

[555] Sautin YY, Lu M, Gaugler A, Zhang L, Gluck SL. Phosphatidylinositol 3-kinase-mediated effects of glucose on vacuolar H + -ATPase assembly, translocation, and acidification of intracellular compartments in renal epithelial cells. Mol Cell Biol 2005;25:575–89.

[556] Su Y, Zhou A, Al-Lamki RS, Karet FE. The a-subunit of the V-type H^+-ATPase interacts with phosphofructokinase-1 in humans. J Biol Chem 2003;278:20013–8.

[557] Xie XS, Crider BP, Stone DK. Isolation of a protein activator of the clathrin-coated vesicle proton pump. J Biol Chem 1993;268: 25063–7.

[558] Zhang K, Wang ZQ, Gluck S. A cytosolic inhibitor of vacuolar H-ATPases from mammalian kidney. J Biol Chem 1992;267: 14539–42.

[559] Zhang K, Wang ZQ, Gluck S. Identification and partial purification of a cytosolic activator of vacuolar H-ATPases from mammalian kidney. J Biol Chem 1992;267:9701–5.

[560] Fejes-Toth G, Naray-Fejes-Toth A. Effect of acid/base balance on H-ATPase 31 kD subunit mRNA levels in collecting duct cells. Kidney Int 1995;48:1420–6.

[561] Caviston TL, Campbell WG, Wingo CS, Cain BD. Molecular identification of the renal H^+,K^+-ATPases. Semin Nephrol 1999;19:431–7.

[562] Doucet A, Horisberger J. Renal Ion-Translocating ATPases: the P-Type family. In: Seldin D, Giebisch G, editors. The kidney: physiology and pathophysiology. Philadelphia: Lippincott Williams & Wilkins; 2000. p. 140–70.

[563] Gumz ML, Lynch IJ, Greenlee MM, Cain BD, Wingo CS. The renal H^+-K^+-ATPases: physiology, regulation and structure. Amer J Physiol 2010;298:F12–21.

[564] Silver RB, Soleimani M. H^+-K^+-ATPases: regulation and role in pathophysiological states. Am J Physiol 1999;276:F799–811.

[565] Doucet A, Marsy S. Characterization of K-ATPase activity in distal nephron: stimulation by potassium depletion. Amer J Physiol 1987;253:F418–23.

[566] Garg LC, Narang N. Ouabain-insensitive K ATPase activity in distal nephron segments of the rabbit. J Clin Invest 1988;81: 1204–8.

[567] Sachs G, Munson K, Balaji VN, Aures-Fischer D, Hershey SJ, Hall K. Functional domains of the gastric H-K-ATPase. J Bioenerg Biomembr 1989;21:573–88.

[568] Shull GE, Lingrel JB. Molecular cloning of the rat stomach (H + K)-ATPase. J Biol Chem 1986;261:16788–91.

[569] Crowson MS, Shull GE. Isolation and characterization of a cDNA encoding the putative distal colon H,K-ATPase. J Biol Chem 1992;267:13740–8.

[570] Jaisser F, Horisberger J-D, Geering K, Rossier BC. Mechanisms of urinary K and H excretion: primary structure and functional expression of a novel H,K-ATPase. J Cell Biol 1993;123:1421–9.

[571] Grishin AV, Sverdlov VE, Kostina MB, Modyanov NN. Cloning and characterization of the entire cDNA encoded by ATPIAL1 a member of the human Na,K/H,K-ATPase gene family. Febs Lett 1994;349:144–50.

[572] Kraut JA, Helander KG, Helander HF, Iroezi ND, Marcus EA, Sachs G. Detection and localization of H^+-K^+-ATPase isoforms in human kidney. Am J Physiol Renal Physiol 2001;281: F763–8.

[573] Kone BC, Higham SC. A novel N-terminal splice variant of the rat H^+-K^+-ATPase alpha2 subunit. Cloning, functional expression, and renal adaptive response to chronic hypokalemia. J Biol Chem 1998;273:2543–52.

[574] Zies DL, Wingo CS, Cain BD. Molecular regulation of the HKalpha2 subunit of the H^+,K^+-ATPases. J Nephrol 2002;15 (Suppl. 5):S54–60.

[575] Jaisser F, Beggah AT. The nongastric H^+-K^+-ATPases: molecular and functional properties. Am J Physiol 1999;276:F812–24.

[576] Laroche-Joubert N, Marsy S, Doucet A. Cellular origin and hormonal regulation of $K(^+)$-ATPase activities sensitive to Sch-28080 in rat collecting duct. Am J Physiol Renal Physiol 2000;279:F1053–9.

[577] Petrovic S, Spicer Z, Greeley T, Shull GE, Soleimani M. Novel Schering and ouabain-insensitive potassium-dependent proton secretion in the mouse cortical collecting duct. Am J Physiol - *Ren Fluid Electrolyte Physiol* 2002;282:F133–43.

[578] Dherbecourt O, Cheval L, Bloch-Faure M, Meneton P, Doucet A. Molecular identification of Sch28080-sensitive K-ATPase activities in the mouse kidney. Pflugers Arch 2006;451:769–75.

[579] Callaghan JM, Tan SS, Khan MA, Curran KA, Campbell WG, Smolka. AJ, et al. Renal expression of the gene encoding the gastric H^+-K^+-ATPase beta-subunit. Amer J Physiol 1995;268: F363–74.

[580] Campbell-Thompson ML, Verlander JW, Curran KA, Campbell WG, Cain BD, Wingo CS, et al. In situ hybridization of H-K-ATPase B-subunit mRNA in rat and rabbit kidney. Am J Physiol 1995;269:F345–54.

[581] Codina J, Delmas-Mata JT, DuBose Jr TD. The alpha-subunit of the colonic H^+,K^+-ATPase assembles with beta1-Na^+,K^+-ATPase in kidney and distal colon. J Biol Chem 1998;273: 7894–9.

[582] Codina J, Kone BC, Delmas-Mata J, DuBose Jr TD. Functional expression of the colonic H^+,K^+-ATPase alpha-subunit. Pharmacologic properties and assembly with X^+,K^+-ATPase beta-subunits. J Biol Chem 1996;271:29759–63.

[583] Kraut JA, Hiura J, Shin JM, Smolka A, Sachs G, Scott D. The $Na(^+)$-$K(^+)$-ATPase beta 1 subunit is associated with the HK alpha 2 protein in the rat kidney. Kidney Int 1998;53:958–62.

[584] Sangan P, Kolla SS, Rajendran VM, Kashgarian M, Binder HJ. Colonic H-K-ATPase beta-subunit: identification in apical membranes and regulation by dietary K depletion. Am J Physiol 1999;276:C350–60.

[585] Meneton P, Schultheis PJ, Greeb J, Nieman ML, Liu LH, Clarke LL, et al. Increased sensitivity to K^+ deprivation in colonic H, K-ATPase-deficient mice. J Clin Invest 1998;101:536–42.

[586] Spicer Z, Miller ML, Andringa A, Riddle TM, Duffy JJ, Doetschman T, et al. Stomachs of mice lacking the gastric H,K-ATPase alpha -subunit have achlorhydria, abnormal parietal cells, and ciliated metaplasia. J Biol Chem 2000;275:21555–65.

[587] Gifford JD, Rome L, Galla JH. H-K-ATPase activity in rat collecting duct segments. Amer J Physiol 1992;262:F692–5.

[588] Armitage FE, Wingo CS. Luminal acidification in K-replete OMCDi: contributions of H-K-ATPase and bafilomycin-Al-sensitive H-ATPase. Amer J Physiol 1994;267:F450–8.

[589] Tsuruoka S, Schwartz GJ. Metabolic acidosis stimulates H^+ secretion in the rabbit outer medullary collecting duct (Inner Stripe) of the kidney. J Clin Invest 1997;99:1420–31.

[590] Guntupalli J, Onuigbo M, Walls S, Alpern RJ, DuBose Jr. TD. Adaptation to low-K^+ media increases H^+-K^+-ATPase but not H + -ATPase-mediated pHi recovery in OMCD1 cells. Amer J Physiol 1997;273:C558–71.

[591] Zhou X, Wingo CS. Stimulation of total CO2 flux by 10% CO2 in rabbit CCD: role of an apical Sch-28080- and Ba-sensitive mechanism. Amer J Physiol 1994;267:F114–20.

[592] Silver RB, Frindt G, Mennitt P, Satlin LM. Characterization and regulation of H-K-ATPase in intercalated cells of rabbit cortical collecting duct. J Exp Zool 1997;279:443–55.

[593] Laroche-Joubert N, Marsy S, Luriau S, Imbert-Teboul M, Doucet A. Mechanism of activation of ERK and H-K-ATPase by isoproterenol in rat cortical collecting duct. Am J Physiol Renal Physiol 2003;284:F948–54.

[594] Laroche-Joubert N, Marsy S, Michelet S, Imbert-Teboul M, Doucet A. Protein kinase A-independent activation of ERK and H,K-ATPase by cAMP in native kidney cells: role of Epac I. J Biol Chem 2002;277:18598–604.

[595] Fejes-Toth G, Rusvai E, Longo KA, Naray-Fejes-Toth A. Expression of colonic H-K-ATPase mRNA in cortical collecting duct: regulation by acid/base balance. Amer J Physiol 1995;269:F551–7.

[596] Silver RB, Frindt G. Functional identification of H-K-ATPase in intercalated cells of cortical collecting tubule. Amer J Physiol 1993;264:F259–66.

[597] Ahn KY, Park KY, Kim KK, Kone B. Chronic hypokalemia enhances exprssion of the H^+-K^+-ATPase a_2-subunit gene in renal medulla. Am J Physiol 1996;271:F314–21.

[598] Ahn KY, Turner PB, Madsen KM, Kone BC. Effects of chronic hypokalemia on renal expression of the "gastric" H^+-K^+-ATPase alpha-subunit gene. Amer J Physiol 1996;270:F557–66.

[599] DuBose Jr. TD, Codina J, Burges A, Pressley TA. Regulation of H^+-K^+-ATPase expression in kidney. Amer J Physiol 1995;269: F500–7.

[600] Kraut JA, Hiura J, Besancon M, Smolka A, Sachs G, Scott D. Effect of hypokalemia on the abundance of HKa_1 HKa_2 protein in the rat kidney. Am J Physiol 1997;272:F744–50.

[601] Nakamura S, Wang Z, Galla JH, Soleimani M. K^+ depletion increases HCO_3^- reabsorption in OMCD by activation of colonic H^+-K^+-ATPase. Am J Physiol 1998;274:F687–92.

[602] Cougnon M, Bouyer P, Planelles G, Jaisser F. Does the colonic H,K-ATPase also act as an Na,K-ATPase? Proc Natl Acad Sci USA 1998;96:6516–20.

[603] Silver RB, Choe H, Frindt G. Low-NaCl diet increases H-K-ATPase in intercalated cells from rat cortical collecting duct. Am J Physiol 1998;275:F94–102.

[604] Zhou X, Wingo CS. H-K-ATPase enhancement of Rb efflux by cortical collecting duct. Am J Physiol 1992;263:F43–8.

[605] Codina J, Pressley TA, DuBose Jr TD. The colonic H^+,K^+-ATPase functions as a Na^+-dependent $K^+(NH_4^+)$-ATPase in apical membranes from rat distal colon. J Biol Chem 1999;274:19693–8.

[606] Cougnon M, Bouyer P, Jaisser F, Edelman A, Planelles G. Ammonium transport by the colonic $H(^+)$-$K(^+)$-ATPase expressed in Xenopus oocytes. Am J Physiol 1999;277: C280–7.

[607] Nakamura S, Amlal H, Galla JH, Soleimani M. NH_4^+ secretion in inner medullary collecting duct in potassium deprivation: role of colonic H^+-K^+-ATPase. Kidney Int 1999;56:2160–7.

[608] Fischer JL, Husted RF, Steinmetz PR. Chloride dependence of the HCO_3 exit step in urinary acidification by the turtle bladder. Amer J Physiol 1983;245:F564–8.

[609] Drenckhahn D, Oelmann M, Schaaf P, Wagner M, Wagner S. Band 3 is the basolateral anion exchanger of dark epithelial cells of turtle urinary bladder. Amer J Physiol 1987;252: C570–4.

[610] Drenckhahn D, Schluter K, Allen DP, Bennett V. Colocalization of band 3 with ankyrin and spectrin at the basal membrane of intercalated cells in the rat kidney. Science 1985;230:1287–9.

[611] Wagner S, Vogen R, Lietzke R, Koob R, Drenckhahn D. Immunochemical characterization of a band 3-like anion exchanger in collecting duct of human kidney. Amer J Physiol 1987;253:F213–21.

[612] Alper S, Kopito RR, Lodish HF. A molecular biological approach to the study of anion transport. Kidney Int 1987;32: S117–8.

[613] Brosius III FC, Alper SL, Garcia AM, Lodish HF. The major kidney band 3 gene transcript predicts an aminoterminal truncated band 3 polypeptide. J Biol Chem 1989;264:7784–7.

[614] Kopito RR, Andersson M, Lodish HF. Structure and organization of the murine band 3 gene. J Biol Chem 1987;262:8035–40.

[615] Kopito RR, Lodish HF. Primary structure and transmembrane orientation of the murine anion exchange protein. Nature 1985;316:234–8.

[616] Kudrycki KE, Shull GE. Primary structure of the rat kidney band 3 anion exchange protein deduced from a cDNA. J Biol Chem 1989;264:8185–92.

[617] Janoshazi A, Ojcius DM, Kone B, Seifter JL, Solomon AK. Relation between the anion exchange protein in kidney medullary collecting duct cells and red cell band 3. J Membr Biol 1988;103:181–9.

[618] Petrovic S, Barone S, Xu J, Conforti L, Ma L, Kujala M, et al. SLC26A7: a basolateral Cl^-/HCO_3^- exchanger specific to intercalated cells of the outer medullary collecting duct. Am J Physiol Renal Physiol 2004;286:F161–9.

[619] Sun X, Petrovic S. Increased acid load and deletion of AE1 increases Slc26a7 expression. Nephron Physiol 2008;109: 29–35.

[620] Xu J, Worrell RT, Li HC, Barone SL, Petrovic S, Amlal H, et al. Chloride/bicarbonate exchanger SLC26A7 is localized in endosomes in medullary collecting duct cells and is targeted to the basolateral membrane in hypertonicity and potassium depletion. J Am Soc Nephrol 2006;17:956–67.

[621] Koeppen BM. Electrophysiology of collecting duct H secretion: effect of inhibitors. Amer J Physiol 1989;256:F79–84.

[622] Muto S, Yasoshima K, Yoshitomi K, et al. Electrophysiological identification of a- and b-intercalated cells and their distribution along the rabbit distal nephron segments. J Clin Invest 1990;86:1829–39.

[623] Sabolic I, Brown D, Gluck S, Alper S. Regulation of AE1 anion exchanger and H^+ -ATPase in rat cortex by acute metabolic acidosis and alkalosis. Kidney Int 1997;51:125–37.

[624] Verlander JW, Madsen KM, Cannon JK, Tisher CC. Activation of acid-secreting intercalated cells in rabbit collecting duct with ammonium chloride loading. Amer J Physiol 1994;266: F633–45.

[625] Weiner ID, Hamm LL. Regulation of Cl^-/HCO_3^- exchange in the rabbit cortical collecting tubule. J Clin Invest 1991;87: 1553–8.

[626] Fejes-Toth G, Rusvai E, Cleaveland ES, Naray-Fejes-Toth A. Regulation of AE2 mRNA expression in the cortical collecting duct by acid/base balance. Am J Physiol 1998;274:F596–601.

[627] Stuart-Tilley AK, Shmukler BE, Brown D, Alper SL. Immunolocalization and tissue-specific splicing of AE2 anion

exchanger in mouse kidney. J Am Soc Nephrol 1998;9: 946–59.
[628] Ko SB, Luo X, Hager H, Rojek A, Choi JY, Licht C, et al. AE4 is a DIDS-sensitive Cl^-/HCO_3^- exchanger in the basolateral membrane of the renal CCD and the SMG duct. Am J Physiol Cell Physiol 2002;283:C1206–18.
[629] Tago K, Schuster VL, Stokes JB. Regulation of Cl^- self-exchange by cAMP in cortical collecting tubule. Amer J Physiol 1986;251: F40–8.
[630] Tago K, Schuster VL, Stokes JB. Stimulation of chloride transport by HCO_3^--CO_2 in rabbit cortical collecting tubule. Amer J Physiol 1986;251:F49–56.
[631] Hayashi M, Yamaji Y, Iyori M, Kitajima W, Saruta T. Effect of isoproterenol on intracellular pH of the intercalated cells in the rabbit cortical collecting ducts. J Clin Invest 1991;87:1153–7.
[632] Schuster VL. Cyclic adenosine monophosphate-stimulated anion transport in rabbit cortical collecting duct: kinetics, stoichiometry, and conductive pathways. J Clin Invest 1986;78: 1621–30.
[633] Emmons C. Halide transport patterns of apical anion exchange in rabbit cortical collecting duct intercalated cells. Amer J Physiol 1996;271:F799–805.
[634] Soleimani M, Greeley T, Petrovic S, Wang Z, Amlal H, Kopp P, et al. Pendrin: an apical $Cl^-/OH^-/HCO_3^-$ exchanger in the kidney cortex. Am J Physiol Renal Physiol 2001;280: F356–64.
[635] Frische S, Kwon TH, Frokiaer J, Madsen KM, Nielsen S. Regulated expression of pendrin in rat kidney in response to chronic NH_4Cl or $NaHCO_3$ loading. Am J Physiol Renal Physiol 2003;284:F584–93.
[636] Petrovic S, Wang Z, Ma L, Soleimani M. Regulation of the apical Cl^-/HCO_3^- exchanger pendrin in rat cortical collecting duct in metabolic acidosis. Am J Physiol Renal Physiol 2003;284: F103–12.
[637] Verlander JW, Hassell KA, Royaux IE, Glapion DM, Wang ME, Everett LA, et al. Deoxycorticosterone upregulates PDS (Slc26a4) in mouse kidney: role of pendrin in mineralocorticoid-induced hypertension. Hypertension 2003; 42:356–62.
[638] Wagner CA, Finberg KE, Stehberger PA, Lifton RP, Giebisch GH, Aronson PS, et al. Regulation of the expression of the Cl^-/ anion exchanger pendrin in mouse kidney by acid–base status. Kidney Int 2002;62:2109–17.
[639] Azroyan A, Laghmani K, Crambert G, Mordasini D, Doucet A, Edwards A. Regulation of pendrin by pH, dependence on glycosylation. Biochem J 2011;434:61–72.
[640] Quentin F, Chambrey R, Trinh-Trang-Tan MM, Fysekidis M, Cambillau M, Paillard M, et al. The Cl^-/HCO_3^- exchanger pendrin in the rat kidney is regulated in response to chronic alterations in chloride balance. Am J Physiol Renal Physiol 2004;287:F1179–88.
[641] Verlander JW, Kim YH, Shin W, Pham TD, Hassell KA, Beierwaltes WH, et al. Dietary Cl^- restriction upregulates pendrin expression within the apical plasma membrane of type B intercalated cells. Am J Physiol Renal Physiol 2006.
[642] Wall SM, Kim YH, Stanley L, Glapion DM, Everett LA, Green ED, et al. NaCl restriction upregulates renal Slc26a4 through subcellular redistribution: role in Cl^- conservation. Hypertension 2004;44:982–7.
[643] Al-Awqati Q, Vijayakumar S, Hikita C, Chen J, Takito J. Phenotypic plasticity in the intercalated cell: the hensin pathway. Amer J Physiol 1998;275:F183–90.
[644] van Adelsberg J, Edwards JC, Takito J, Kiss B, Al-Awqati Q. An induced extracellular matrix protein reverses the polarity of band 3 in intercalated epithelial cells. Cell 1994;76:1053–61.
[645] van Adelsberg JS, Edwards JC, Al-Awqati Q. The apical Cl/ HCO_3 exchanger of b intercalated cells. J Biol Chem 1993;268:11283–9.
[646] van't Hof W, Malik A, Vijayakumar S, Qiao J, van Adelsberg J, Al-Awqati Q. The effect of apical and basolateral lipids on the function of the band 3 anion exchange protein. J Cell Biol 1997;139:941–9.
[647] Tsuganezawa H, Kobayashi K, Iyori M, Araki T, Koizumi A, Watanabe S, et al. A new member of the HCO_3^- transporter superfamily is an apical anion exchanger of beta-intercalated cells in the kidney. J Biol Chem 2001;276:8180–9.
[648] Husted RF, Eyman E. Chloride-bicarbonate exchange in the urinary bladder of the turtle: independence from sodium ion. Biochim Biophys Acta 1980;595:305–8.
[649] Reeves WB, Andreoli TE. Chloride channels in renal epithelial cells. Curr Opin Nephrol Hypertens 1996;5:406–10.
[650] Ernest S, Bello-Reuss E. P-glycoprotein functions and substrates: possible roles of MDR1 gene in the kidney. Kidney Int Suppl 1998;65:S11–7.
[651] Stanton BA. Characterization of apical and basolateral membrane conductances of rat inner medullary collecting duct. Amer J Physiol 1989;256:F862–8.
[652] Matsuzaki K, Schuster VL, Stokes JB. Reduction in sensitivity to Cl^- channel blockers by HCO_3^-/CO_2 in rabbit cortical collecting duct. Amer J Physiol 1989;257:C102–9.
[653] Obermuller N, Gretz N, Kriz W, Reilly RF, Witzgall R. The swelling-activated chloride channel CIC-2, the chloride channel CIC-3, and CIC-5, a chloride channel mutated in kidney stone disease, are expressed in distinct subpopulations of renal epithelial cells. J Clin Invest 1998;101:635–42.
[654] Kwon TH, Pushkin A, Abuladze N, Nielsen S, Kurtz I. Immunoelectron microscopic localization of NBC3 sodium-bicarbonate cotransporter in rat kidney. American Journal of Physiology. Renal Fluid & Electrolyte Physiology.|American. Journal of Physiology. Renal Physiology 2000;278:F327–36.
[655] Praetorius J, Kim YH, Bouzinova EV, Frische S, Rojek A, Aalkjaer C, et al. NBCn1 is a basolateral Na^+–HCO_3^- cotransporter in rat kidney inner medullary collecting ducts. Am J Physiol Renal Physiol 2004;286:F903–12.
[656] Pushkin A, Abuladze N, Lee I, Newman D, Hwang J, Kurtz I. Cloning, tissue distribution, genomic organization, and functional characterization of NBC3, a new member of the sodium bicarbonate cotransporter family. J Biol Chem 1999;274: 16569–75.
[657] Gross E, Kurtz I. Structural determinants and significance of regulation of electrogenic Na^+-HCO_3^- cotransporter stoichiometry. Am J Physiol Renal Physiol 2002;283:F876–87.
[658] Boettger T, Hubner CA, Maier H, Rust MB, Beck FX, Jentsch TJ. Deafness and renal tubular acidosis ini mice lacking the K-Cl co-transporter Kcc4. Nature 2002;416:874–8.
[659] Schwartz GJ. Physiology and molecular biology of renal carbonic anhydrase. J Nephrol 2002;15(Suppl. 5):S61–74.
[660] Lonnerholm G. Histochemical demonstration of carbonic anhydrase activity in the rat kidney. Acta Physiol Scand 1971;81: 433–9.
[661] Lonnerholm G, Ridderstrale Y. Intracellular distribution of carbonic anhydrase in the rat kidney. Kidney Int 1980;17:162–74.
[662] Brown D, Kumpulainen T, Roth J, Orci L. Immunohistochemical localization of carbonic anhydrase in postnatal and adult rat kidney. Amer J Physiol 1983;245: F110–8.

[663] Brown D, Roth J, Kumpulainen T, Orci L. Ultrastructural immunochtochemical localization of carbonic anhydrase: presence in intercalated cells of the rat collecting tubule. Histochemistry 1982;75:209–13.
[664] Spicer SS, Sens MA, Tashian RE. Immunocytochemical demonstration of carbonic anhydrase in human epithelial cells. J Histochem Cytochem 1982;30:864–73.
[665] Spicer SS, Stoward PJ, Tashian RE. The immunohistolocalization of carbonic anhydrase in rodent tissues. J Histochem Cytochem 1979;27:820–31.
[666] Brown D, Zhu XL, Sly WS. Localization of membrane-associated carbonic anhydrase type IV in kidney epithelial cells. Proc Natl Acad Sci USA 1990;87:7457–61.
[667] Lonnerholm G. Histochemical demonstration of carbonic anhydrase in the human kidney. Acta Physiol Scand 1973;88: 455–68.
[668] Tsuruoka S, Kittelberger A, Schwartz GJ. Carbonic anhydrase II and IV mRNA in rabbit nephron segments: stimulation during metabolic acidosis. Amer J Physiol 1998;274:F259–67.
[669] Lonnerholm G, Wistrand PJ. Membrane-bound carbonic anhydrase IV in the human kidney. Acta Physiol Scand 1991;141: 231–4.
[670] Kleinman J, Bain J, Riley D, Pscheidt R. Intercalated (IC) and principal (PC) cells of inner medullary collecting duct (IMCD). Kidney Int 1990;37:540A.
[671] Kyllonen MS, Parkkila S, Rajaniemi H, Waheed A, Grubb JH, Shah GN, et al. Localization of carbonic anhydrase XII to the basolateral membrane of H^+-secreting cells of mouse and rat kidney. J Histochem Cytochem 2003;51:1217–24.
[672] Parkkila S, Parkkila AK, Saarnio J, Kivela J, Karttunen TJ, Kaunisto K, et al. Expression of the membrane-associated carbonic anhydrase isozyme XII in the human kidney and renal tumors. J Histochem Cytochem 2000;48:1601–8.
[673] Schwartz GJ, Kittelberger AM, Watkins RH, O'Reilly MA. Carbonic anhydrase XII mRNA encodes a hydratase that is differentially expressed along the rabbit nephron. Am J Physiol Renal Physiol 2003;284:F399–410.
[674] Winkler CA, Kittelberger A, Schwartz GJ. Expression of carbonic anhydrase IV mRNA in rabbit kidney stimulation by metabolic acidosis. Amer J Physiol 1997;272:F551–60.
[675] Ochwadt BK, Pitts RF. Effects of intravenous infusion of carbonic anhydrase on carbon dioxide tension of alkaline urine. Amer J Physiol 1956;185:426–9.
[676] Wall SM, Flessner MF, Knepper MA. Distribution of luminal carbonic anhydrase activity along rat inner medullary collecting duct. Amer J Physiol 1991;260:F738–48.
[677] Tsuruoka S, Schwartz. GJ. HCO_3^- absorption in rabbit outer medullary collecting duct: role of luminal carbonic anhydrase. Amer J Physiol 1998;274:F139–47.
[678] Breyer MD, Jacobson HR. Mechanisms and regulation of renal H^+ and HCO_3^- transport. Am J Nephrol 1987;7:150–61.
[679] Gougoux A, Vinay P, Lemieux G, Duran MA, Chen CB, Goldstein MB, et al. Studies on the mechanism whereby acidemia stimulates collecting duct hydrogen ion secretion in vivo. Kidney Int 1981;20:643–8.
[680] Gougoux A, Vinay P, Lemieux G, Richardson RMA, Tam SC, Goldstein MB, et al. Effect of blood pH on distal nephron hydrogen ion secretion. Kidney Int 1980;17:615–21.
[681] Breyer MD, Kokko JP, Jacobson HR. Regulation of net bicarbonate transport in rabbit cortical collecting tubule by peritubular pH, carbon dioxide tension, and bicarbonate concentration. J Clin Invest 1986;77:1650–60.
[682] Jacobson HR. Medullary collecting duct acidification: effects of potassium, HCO_3^- concentration, and pCO_2. J Clin Invest 1984;74:2107–14.
[683] McKinney TD, Davidson KK. Effects of respiratory acidosis on HCO_3 transport by rabbit collecting tubules. Amer J Physiol 1988;255:F656–65.
[684] Cohen LH, Steinmetz PR. Control of active proton transport in turtle urinary bladder by cell pH. J Gen Physiol 1980;76: 381–93.
[685] Al-Awqati Q, Muller A, Steinmetz PR. Transport of H against electrochemical gradients in turtle urinary bladder. Amer J Physiol 1977;233:F502–8.
[686] Schwartz JH, Steinmetz PR. CO_2 requirements for H secretion by the isolated turtle bladder. Amer J Physiol 1971;220: 2051–7.
[687] Steinmetz PR. Cellular mechanisms of urinary acidification. Physiol Rev 1974;54:890–956.
[688] Sun X, Yang LV, Tiegs BC, Arend LJ, McGraw DW, Penn RB, et al. Deletion of the pH sensor GPR4 decreases renal acid excretion. J Amer Soc Nephrol 2010;21:1745–55.
[689] Brown D, Paunescu TG, Breton S, Marshansky V. Regulation of the V-ATPase in kidney epithelial cells: dual role in acid–base homeostasis and vesicle trafficking. Journal of Exp Biology 2009;212:1762–72.
[690] Brown D. Membrane recycling and epithelial cell function. Amer J Physiol 1989;256:F1–12.
[691] Brown D, Orci L. The "coat" of kidney intercalated cell tubulovesicles does not contain clathrin. Amer J Physiol 1986;250: C605–8.
[692] Alexander EA, Brown D, Shih T, McKee M, Schwartz JH. Effect of acidification on the location of H^+-ATPase in cultured inner medullary collecting duct cells. Amer J Physiol 1999;276: [t-63]
[693] Banerjee A, Li G, Alexander EA, Schwartz JH. Role of SNAP-23 in trafficking of H^+-ATPase in cultured inner medullary collecting duct cells. Am J Physiol—Cell Physiol 2001;280: C775–81.
[694] Li G, Yang Q, Alexander EA, Schwartz JH. Syntaxin 1A has a specific binding site in the H3 domain that is critical for targeting of H^+-ATPase to apical membrane of renal epithelial cells. Am J Physiol Cell Physiol 2005;289:C665–72.
[695] Nicoletta JA, Ross JJ, Li G, Cheng Q, Schwartz J, Alexander EA, et al. Munc-18-2 regulates exocytosis of H^+-ATPase in rat inner medullary collecting duct cells. Am J Physiol Cell Physiol 2004;287:C1366–74.
[696] Stetson DL. Turtle urinary bladder: regulation of ion transport by dynamic changes in plasma membrane area. AmerJ Physiol 1989;257:R973–81.
[697] Gluck S, Cannon C, Al-Awqati Q. Exocytosis regulates urinary acidification in turtle bladder by rapid insertion of H pumps into the luminal membrane. Proc Natl Acad Sci USA 1982;79:4327–31.
[698] Stetson DL, Steinmetz PR. Role of membrane fusion in CO_2 stimulation of proton secretion by turtle bladder. Amer J Physiol 1983;245:C113–20.
[699] Dixon TE, Clausen C, Coachman D. Constitutive and transport-related endocytic pathways in turtle bladder epithelium. J Membr Biol 1988;102:49–58.
[700] Husted RF, Mueller AL, Kessel RG, Steinmetz PR. Surface characteristics of carbonic-anhydrase-rich cells in turtle urinary bladder. Kidney Int 1981;19:491–502.
[701] Madsen KM, Tisher CC. Cellular response to acute respiratory acidosis in rat medullary collecting duct. Amer J Physiol 1983;245:F670–9.
[702] Dorup J. Structural adaptation of intercalated cells in rat renal cortex to acute metabolic acidosis and alkalosis. J Ultrastructure Res 1985;92:119–31.
[703] Madsen KM, Tisher CC. Response of intercalated cells of rat outer medullary collecting duct to chronic metabolic acidosis. Lab Invest 1984;51:268–76.

[704] van Adelsberg J, Al-Awqati Q. Regulation of cell pH by Ca-mediated exocytotic insertion of H-ATPase. J Cell Biol 1986;102:1638–45.
[705] Arruda JAL, Sabatini S, Mola R, Dytko G. Inhibition of H secretion in the turtle bladder by colchicine and vinblastine. J Lab Clin Med 1980;96:450–9.
[706] Graber ML, Dixon T, Coachman D, Devine P. Acetazolamide inhibits acidification by the turtle bladder independent of cell pH. Amer J Physiol 1989;256:F923–31.
[707] Laski ME, Kurtzman NA. Collecting tubule adaptation to respiratory acidosis induced in vivo. Amer J Physiol 1990;258: F15–20.
[708] Laski ME, Jackley TL. The adaptation of cortical collecting tubules to acidosis is a rapid event. Clin Res 1989;37:494A.
[709] McKinney TD, Davidson KK. Effect of potassium depletion and protein intake in vivo on renal tubular bicarbonate transport in vitro. Amer J Physiol 1987;252:F509–16.
[710] Hafner P, Grimaldi R, Capuano P, Capasso G, Wagner CA. Pendrin in the mouse kidney is primarily regulated by Cl^- excretion, but also by systemic metabolic acidosis. Amer J Physiol 2008;295:C1658–67.
[711] Schwartz GJ, Al-Awqati Q. Role of hensin in mediating the adaptation of the cortical collecting duct to metabolic acidosis. Curr Opin Nephrol Hypertens 2005;14:383–8.
[712] Purkerson JM, Tsuruoka S, Suter DZ, Nakamori A, Schwartz GJ. Adaptation to metabolic acidosis and its recovery are associated with changes in anion exchanger distribution and expression in the cortical collecting duct. Kidney Int 2010;78:993–1005.
[713] Takito J, Hikata C, Al-Awqati Q. Hensin, a new collecting duct protein involved in the in vitro plasticity of intercalated cell polarity. J Clin Invest 1996;98:2324–31.
[714] Al-Awqati Q, Gao XB. Differentiation of intercalated cells in the kidney. Physiology 2012;26:266–72.
[715] Gao X, Eladari D, Leviel F, Tew BY, Miro-Julia C, Cheema F, et al. Deletion of hensin/DMBT1 blocks conversion of beta-to-alpha intercalated cells and induces distal renal tubular acidosis. Proc Natl Acad Sci U S A 2010;107:21872–7.
[716] Schwaderer AL, Vijayakumar S, Al-Awqati Q, Schwartz GJ. Galectin-3 expression is induced in renal beta-intercalated cells during metabolic acidosis. Am J Physiol Renal Physiol 2006;290:F148–58.
[717] Watanabe S, Tsuruoka S, Vijayakumar S, Fischer G, Zhang Y, Fujimura A, et al. Cyclosporin A produces distal renal tubular acidosis by blocking peptidyl prolyl cis-trans isomerase activity of cyclophilin. Am J Physiol Renal Physiol 2005;288:F40–7.
[718] Duong Van Huyen JP, Cheval L, Bloch-Faure M, Belair MF, Heudes D, Bruneval P, et al. GDF15 triggers homeostatic proliferation of acid-secreting collecting duct cells. J Amer Soc Nephrol 2008;19:1965–74.
[719] Welsh-Bacic D, Nowik M, Kaissling B, Wagner CA. Proliferation of acid-secretory cells in the kidney during adaptive remodelling of the collecting duct. PLoS ONE 2011;6: e25240.
[720] Steinmetz PR, Lawson LR. Effect of luminal pH of ion permeability and flows of Na and H in turtle bladder. Amer J Physiol 1971;220:1573–80.
[721] Bank N, Schwartz WB. The influence of anion penetrating ability on urinary acidification and the excretion of titratable acid. J Clin Invest 1960;39:1516–25.
[722] Schwartz WB, Jenson RL, Relman AS. Acidification of the urine and increased ammonium excretion without change in acid–base equilibrium: sodium reabsorption as a stimulus to the acidifying process. J Clin Invest 1955;34:673–80.
[723] Tam SC, Goldstein MB, Stinebaugh BJ, Chen CB, Gougoux A, Halperin ML. Studies on the regulation of hydrogen ion secretion in the collecting duct in vivo: Evaluation of factors that influence the urine minus blood PCO_2 difference. Kidney Int 1981;20:636–42.
[724] Ziegler TW, Fanestil DD, Ludens JH. Influence of transepithelial potential difference on acidification in the toad urinary bladder. Kidney Int 1976;10:279–86.
[725] Laski ME, Kurtzman NA. Characterization of acidification in the cortical and medullary collecting tubule of the rabbit. J Clin Invest 1983;72:2050–9.
[726] Laski ME, Warnock DG, Rector Jr. FC. Effects of chloride gradients on total CO_2 flux in the rabbit CCT. Amer J Physiol 1983;244:F112–21.
[727] Hulter HN, Ilnicki LP, Harbottle JA, Sebastian A. Impaired renal H secretion and NH_3 production in mineralocorticoid-deficient glucocorticoid-replete dogs. Amer J Physiol 1977;232: F136–46.
[728] Hulter HN, Licht JH, Glynn RD, Sebastian A. Renal acidosis in mineralocorticoid deficiency is not dependent on NaCl depletion or hyperkalemia. Amer J Physiol 1979;236:F283–94.
[729] Tam SC, Goldstein MB, Richardson RMA, Robson WLM, Stinebaugh BJ, Halperin ML. Effect of extracellular fluid volume contraction on distal-nephron hydrogen ion secretoin in vivo. J Lab Clin Med 1980;96:442–9.
[730] Winter C, Schulz N, Giebisch G, Geibel JP, Wagner CA. Nongenomic stimulation of vacuolar H^+-ATPases in intercalated renal tubule cells by aldosterone. Proc Natl Acad Sci USA 2004;101:2636–41.
[731] DuBose Jr. TD, Caflisch CR. Effect of selective aldosterone deficiency on acidification in nephron segments of the rat inner medulla. J Clin Invest 1988;82:1624–32.
[732] Greenlee MM, Lynch IJ, Gumz ML, Cain BD, Wingo CS. Mineralocorticoids stimulate the activity and expression of renal H^+,K^+-ATPase. J Amer Soc Nephrol 2011;22:49–58.
[733] Izumi Y, Hori K, Nakayama Y, Kimura M, Hasuike Y, Nanami M, et al. Aldosterone requires vasopressin V1a receptors on intercalated cells to mediate acid–base homeostasis. J Amer Soc Nephrol 2011;22:673–80.
[734] Knepper MA, Good DW, Burg MB. Mechanism of ammonia secretion by cortical collecting ducts of rabbits. Amer J Physiol 1984;247:F729–38.
[735] Jones JW, Sebastian A, Hulter HN. Systemic and renal acid–base effects of chronic dietary potassium depletion in humans. Kidney Int 1982;21:402–10.
[736] Hulter HN, Licht JH, Sebastian A. K deprivation potentiates the renal acid excretory effect of mineralocorticoid: obliteration by amiloride. Amer J Physiol 1978;235:F298–309.
[737] Hays SR, Seldin DW, Kokko JP, Jacobson HR. Effect of K depletion on HCO_3 transport across rabbit collecting duct segments. Kidney Int 1986;29:368A.
[738] Stetson DL, Wade JB, Giebisch G. Morphologic alterations in the rat medullary collecting duct following potassium depletion. Kidney Int 1980;17:45–56.
[739] Barone S, Amlal H, Kujala M, Xu J, Karet F, Blanchard A, et al. Regulation of the basolateral chloride/base exchangers AE1 and SLC26A7 in the kidney collecting duct in potassium depletion. Nephrol Dialysis Transplant 2007;22:3462–70.
[740] Wesson DE, Dolson GM. Endothelin-1 increases rat distal tubule acidification in vivo. Amer J Physiol 1997;273:F586–94.
[741] Wesson DE, Simoni J, Green. DF. Reduced extracellular pH increases endothelin-1 secretion by human renal microvascular endothelial cells. J Clin Invest 1998;101:578–83.
[742] Tsuruoka S, Watanabe S, Purkerson JM, Fujimura A, Schwartz GJ. Endothelin and nitric oxide mediate adaptation of the

cortical collecting duct to metabolic acidosis. Am J Physiol Renal Physiol 2006;291:F866–73.
[743] Wesson DE. Physiologic and pathophysiologic renal consequences of H^+-stimulated endothelin secretion. Am J Kidney Dis 2000;35:LII–.
[744] Levine DZ, Lacovitti M, Buckman S, Harrison V. In vivo modulation of rat distal tubule net HCO_3 flux by VIP, isoproterenol, angiotensin II, and ADH. Amer J Physiol 1994;266: F878–83.
[745] Paillard M, Bichara M. Peptide hormone effects on urinary acidification and acid–base balance: PTH, ADH, and glucagon. Amer J Physiol 1989;256:F973–85.
[746] Bichara M, Mercier O, Borensztein P, Paillard M. Acute metabolic acidosis enhances circulating parathyroid hormone, which contributes to the renal response against acidosis in the rat. J Clin Invest 1990;86:430–43.
[747] Mercier O, Bichara M, Paillard M, Prigent A. Effects of parathyroid hormone and urinary phosphate on collecting duct hydrogen secretion. Amer J Physiol 1986;251:F802–9.
[748] Frazier LW. Effects of parathyroid hormone on H and NH_3/NH_4 excretion in toad urinary bladder. J Membr Biol 1976;30:187–96.
[749] Morel F. Sites of hormone action in the mammalian nephron. Amer J Physiol 1981;240:F159–64.
[750] Wagner CA, Devuyst O, Bourgeois S, Mohebbi N. Regulated acid–base transport in the collecting duct. Pflugers Arch 2009;458:137–56.
[751] Tomita K, Pisano JJ, Burg MB, Knepper MA. Effects of vasopressin and bradykinin on anion transport by the rat cortical collecting duct. J Clin Invest 1986;77:136–41.
[752] Hays S, Kokko JP, Jacobson HR. Hormonal regulation of proton secretion in rabbit medullary collecting duct. J Clin Invest 1986;78:1279–86.
[753] Durham JH, Matons C. Cl^- induced increment in short circuiting current of the turtle bladder: effects of in vivo acid base state. Biochim Biophys Acta 1984;769:297–310.
[754] Durham JH, Matons C, Brodsky WA. Vasoactive intestinal peptide stimulates alkali excretion in turtle urinary bladder. Amer J Physiol 1987;252:C428–35.
[755] Satake N, Durham JH, Ehrenspeck G, Brodsky WA. Active electrogenic mechanisms for alkali and acid transport in turtle bladders. Amer J Physiol 1983;244:C259–69.
[756] Stetson DL, Beauwens R, Palmisano J, Mitchell PP, Steinmetz PR. A double-membrane model for urinary bicarbonate secretion. Amer J Physiol 1985;249:F546–52.
[757] Durham JH, Schneider E, Matons C, Brodsky WA. Two independent neurohormonally induced reaction cascade for up retulation of alkali secretion. Kidney Int 1988;33:339.
[758] Hays SR, Baum M, Kokko JP. Effects of protein kinase C activation on sodium, potassium, chloride, and total CO_2 transport in the rabbit cortical collecting tubule. J Clin Invest 1987;80: 1561–70.
[759] Gong F, Alzamora R, Smolak C, Li H, Naveed S, Neumann D, et al. Vacuolar H^+-ATPase apical accumulation in kidney intercalated cells is regulated by PKA and AMP-activated protein kinase. Amer J Physiol 2010;298:F1162–9.
[760] Paunescu TG, Ljubojevic M, Russo LM, Winter C, McLaughlin MM, Wagner CA, et al. cAMP stimulates apical V-ATPase accumulation, microvillar elongation, and proton extrusion in kidney collecting duct A-intercalated cells. Amer J Physiol 2010;298:F643–54.
[761] Wesson DE. Prostacyclin increases distal tubule HCO_3 secretion in the rat. Amer J Physiol 1996;271:F1183–92.
[762] Geibel JP. Distal tubule acidification. J Nephrol 2006;19(Suppl. 9):S18–26.
[763] Weiner ID, New AR, Milton AE, Tisher CC. Regulation of luminal alkalinization and acidification in the cortical collecting duct by angiotensin II. Amer J Physiol 1995;269:F730–8.
[764] Wang T, Giebisch G. Effects of angiotensin II on electrolyte transport in the early and late distal tubule in rat kidney. Amer J Physiol 1996;271:F143–9.
[765] Pech V, Zheng W, Pham TD, Verlander JW, Wall SM. Angiotensin II activates H^+-ATPase in type A intercalated cells. J Amer Soc Nephrol 2008;19:84–91.
[766] Wagner CA, Mohebbi N, Uhlig U, Giebisch GH, Breton S, Brown D, et al. Angiotensin II stimulates H-ATPase activity in intercalated cells from isolated mouse connecting tubules and cortical collecting ducts. Cell Physiol Biochem 2011;28:513–20.

CHAPTER

56

Chemoreceptors, Breathing and pH

Eugene Nattie

The Geisel School of Medicine at Dartmouth, Lebanon, New Hampshire, USA

INTRODUCTION

Our thinking on mammalian acid–base regulation focuses on pH. Intracellular pH, which is of great importance in the maintenance of normal protein function, is regulated by membrane ion transporters, intracellular buffers, and by changes in cell metabolism.[94,111] The success of intracellular pH regulation is dependent on the extracellular pH being constrained in its variation.[107] Renal processes can alter extracellular proton and bicarbonate balance by changes in ion excretion. In this chapter we focus on how breathing can affect the partial pressure of carbon dioxide in extracellular fluid, here the partial pressure of carbon dioxide in arterial blood, $PaCO_2$. The traditional approach utilizes the straightforward relationships shown in Eqs 1 and 2.

$$CO_2 + H_2O = H_2CO_3^- = H^+ + HCO_3^- \quad (59.1)$$

$$pH = pK^- + \log([HCO_3^-]/[S \times PCO_2]) \quad (59.2)$$

where S = the solubility of CO_2 in blood and pK^- is a combined dissociation constant.

Note that pH can be affected by primary changes in either bicarbonate or PCO_2. Arterial bicarbonate changes by a small amount as CO_2 is changed due to the presence of blood buffers. But by far the most important changes in arterial bicarbonate occur either as the result of a primary metabolic disturbance, which changes the ionic composition of blood thereby affecting bicarbonate, or as the result of the kidney, which can also change the ionic composition of blood thereby affecting bicarbonate.

CO_2

Ventilation and CO_2

Arterial blood pH is the clinically relevant extracellular variable because changes in breathing alter the $PaCO_2$ directly. The $PaCO_2$ is determined by the ratio of CO_2 production and alveolar ventilation. For a constant metabolic rate (and CO_2 production), an increase in alveolar ventilation will lower the $PaCO_2$ and, conversely, a decrease in alveolar ventilation will elevate the $PaCO_2$. Both events have acid–base consequences. Hyperventilation eliminates CO_2 faster than it is being produced and, as a result, pH increases; hypoventilation eliminates CO_2 more slowly than it is being produced and, as a result, pH decreases. The changes are quantitatively speaking not small. If alveolar ventilation doubles, the normal $PaCO_2$ of 40 mm Hg will quickly attain a new value of 20 mm Hg. Arterial pH will quickly change from the normal value of 7.40 to 7.70. Conversely, if alveolar ventilation is reduced by half, arterial PCO_2 will quickly attain a new value of 80 mm Hg. Arterial pH will change from the normal value of 7.4 to 7.10. Changes in alveolar ventilation quickly and dramatically affect $PaCO_2$ and pH. A 10% increase in alveolar ventilation will decrease $PaCO_2$ by 4 mm Hg and increase arterial pH from 7.40 to 7.45 all within seconds. This change in arterial pH is determined by the decrease in PCO_2 and by the effectiveness of blood buffers, which include most importantly the red blood cell hemoglobin concentration. In the absence of any protein buffers, the pH change would be much greater. If the hyperventilation and

Seldin and Giebisch's The Kidney, Fifth Edition.
DOI: http://dx.doi.org/10.1016/B978-0-12-381462-3.00056-2

© 2013 Elsevier Inc. All rights reserved.

hypocapnia are sustained, there are secondary renal adjustments that act to excrete more bicarbonate and to lessen the initial alkalosis. These events take minutes to hours and are governed by the lowered PCO_2. Changes in PCO_2, whether decrease or increase, are quickly reflected in all blood and tissue compartments due to the diffusability of CO_2.

Tissue CO_2

Tissue PCO_2 levels are determined by the arterial value, the tissue rate of CO_2 production, and the amount of tissue blood flow. Changes in blood flow and cell metabolism can affect cell PCO_2 and pH for any given arterial PCO_2. For example, the brain has blood vessels that determine blood flow resistance and are very sensitive to changes in CO_2. An increase in $PaCO_2$ would tend to directly cause an increase in tissue and cell PCO_2 and a decrease in their pH. The strong vasodilatory action of high CO_2 on cerebral vessels would decrease resistance and allow blood flow to increase, which would clear more CO_2 and indirectly minimize the increase in tissue and cell PCO_2. Tissue and cell PCO_2 and pH are determined by blood flow for any $PaCO_2$ value and by metabolic rate.

CO_2 and Ventilation

A change in pH is detected by a physiological process called chemoreception. The pH sensors are present in the peripheral blood at the bifurcation of the carotid artery, the carotid body,[26,38,43,54,67] and within the brainstem at multiple locations.[5,56,69–72,105,106] Both the carotid body and the brainstem respond to a fall in pH, for example, by increased stimulation of breathing, which lowers $PaCO_2$ and tends to minimize the initial acidosis. This feedback control of the alveolar ventilation level, and hence the $PaCO_2$, by chemoreceptor-detected changes in pH is the essence of this chapter. The body can detect small pH changes at many sites and quickly bring about a change in breathing that acts to correct the initial perturbation. It is an appropriate response to correct pH. This system detects arterial pH at the carotid body and at the central chemoreceptors; it likely detects a pH value somewhere between the arterial and brain interstitial fluid pH.

PERIPHERAL CHEMORECEPTORS

Location of Carotid Body

The carotid body is well located to detect changes in arterial pH and PCO_2. In fact, this location at the bifurcation of the carotid body rapidly detects small changes in $PaCO_2$ that reflect minor variations in the normal level of alveolar ventilation, and thus serves admirably as a feedback control detector site for the maintenance of a normal level of alveolar ventilation. This site is also a useful one for the detection of pH changes that reflect abnormal physiology, but for this purpose it is difficult to construct an argument that makes this anatomical location of special utility. In fact, a chemoreceptor site closer to the tissue location of altered metabolism in a metabolic acid–base disorder might theoretically be of greater use. For example, mixed venous CO_2 receptors have long been sought for in order to explain the tight link between increased metabolism in muscular exercise and alveolar ventilation. Here venous CO_2 levels rise; but arterial PCO_2 remains normal or decreases slightly as alveolar ventilation changes to match the increase in metabolic rate. Sporadically, the discovery of mixed venous chemoreceptors has been reported, but none of these have stood the test of time. Specific central chemoreceptor locations in the brain might well reflect tissue and cell PCO_2 and pH, that is, tissue chemoreceptors may be present.

Carotid Body Function

The carotid body is a fascinating tissue. It is quite small, and is difficult to find by gross anatomical dissection, but has a large metabolic rate and a high perfusion. This tissue is arguably the only and certainly the major detector of low O_2 levels. Hypoxia strongly excites the carotid body with powerful stimulatory effects on breathing and arousal.[38,43,54] It is the detector for the hypoxia emergency warning system, and also detects changes in PCO_2, including values that may drop below normal. In non-rapid eye movement sleep, apneas that occur within seconds of a transient hyperventilation have been attributed to hypocapnia sensed at the carotid body. Thus, in sleep there is a tonic nervous activity from the carotid body to the brain that maintains a normal level of ventilation. Transient diminution of this activity by brief hypocapnia can lead to apnea, the cessation of breathing.[26,108] There is evidence as well for tonic carotid afferent activity that is important in the maintenance of appropriate levels of ventilation in wakefulness.[17,38] Surgical removal of the carotid bodies in experimental animals and in humans results in a stable new steady state of hypoventilation. The animal then maintains a "normal" $PaCO_2$ that is a few mmHg higher than in animals with intact peripheral chemoreceptors. This state is maintained despite the presence of central chemoreceptors.[31,38,67,100] It seems that normal ventilation

requires the tonic afferent input from peripheral chemoreceptors. In 1938, Heymans received the Nobel Prize for the discovery of the carotid body. He proposed that the carotid body was the major detector of CO_2, as well as for hypoxia.[43]

CENTRAL CHEMORECEPTORS

There is clear evidence for receptors within the brain that detect changes in PCO_2 or pH and bring about a change in ventilation. The ventilatory response to changes in pH as mediated by central chemoreceptors is very sensitive. Figure 56.1 shows data obtained from unanesthetized goats in a series of classic experiments.[34,89] Alveolar ventilation, VA, is plotted against the pH in cerebrospinal fluid. The shaded area presents data obtained during chronic metabolic acidosis and alkalosis maintained for days in the goats as they breathed air or inhaled CO_2 from 0 to 10%. Note that in these steady-state conditions of chronic metabolic acid–base disorders, the response of alveolar ventilation to changes in cerebral pH is very sensitive—it doubles for a cerebrospinal fluid (CSF) pH change from 7.33 to 7.28. The X symbols in Fig. 56.1 will be discussed below.

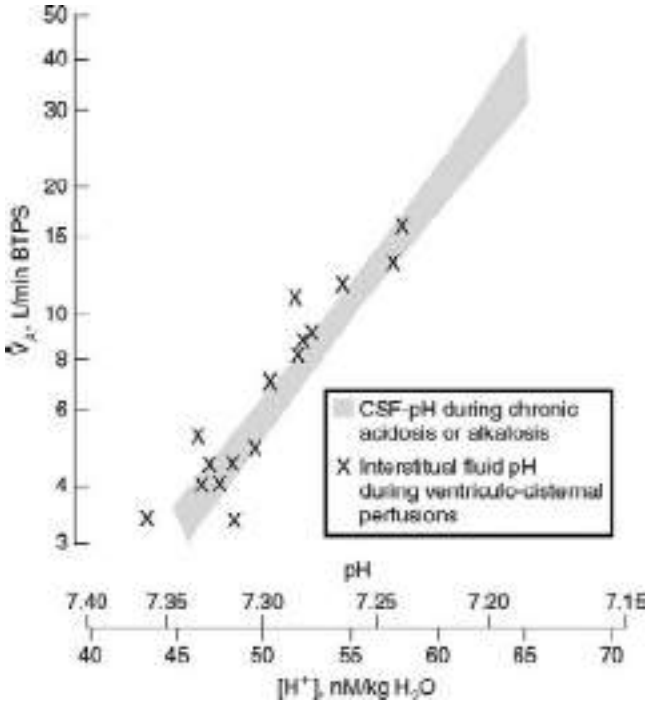

FIGURE 56.1 The alveolar ventilation response to chronic acid–base disorders and to inhaled CO_2 is shown versus the pH measured in cerebrospinal fluid in the shaded area, which presents ±SEM (standard error of measurement) of 81 separate measurements obtained in five goats. The crosses derive from experiments in which the goats had ventriculo-cisternal perfusion of cerebrospinal fluid with differing bicarbonate concentrations. Alveolar ventilation in these cases is plotted versus the pH calculated for a site that lies three-quarters of the distance along the concentration gradient between ventricular cerebrospinal fluid and blood. *(With permission of the American Physiological Society, from Figure 12, from ref. [34].)*

History: Ventrolateral Medulla

The presence of central chemoreceptors was first suggested by the continued presence of a ventilatory response to an increase in $PaCO_2$ after surgical removal of the peripheral chemoreceptors[31,38,42,67] and solidified by the presence of a ventilatory response to an acid load applied directly into the cerebral ventricles.[55] Direct application of small pieces of cotton, soaked in an acidic solution, to various brainstem surfaces further localized the site of central chemoreception to the surface of the ventral lateral medulla,[56,60,105,117] a site that still captures the imagination of investigators.[62] All of these studies were performed under surgical anesthesia, which has a powerful depressant effect on the sensitivity of the ventilatory response to CO_2, and required very acidic stimuli. Further, the blood supply to the medulla arises from vessels on the ventral surface, which could have easily carried the stimulus to deeper structures.[13,58] Cooling or coagulation of this area decreased ventilatory output dramatically in anesthetized animals.[14,106]

The effects of anesthesia on chemosensitivity cannot be overemphasized. For example, Akilesh et al.[4] found that in rats, the change in ventilation breathing 7% CO_2 compared to breathing air is decreased by about 70% with the introduction of anesthesia. There are many similar examples of how much anesthesia affects the chemoreceptor response sensitivity.[37,87] Nevertheless, these early studies demonstrated that chemoreception is present in the medulla, and it is accessible from the ventral medullary surface.

Widespread Central Chemoreception

More recently, a series of studies have led to the proposal that central chemoreception is a phenomenon that is widely present in the hindbrain.[16,32,69–72] Before proceeding, a few clarifying definitions are warranted. A functional definition for chemoreception refers to a ventilatory response to a change in CO_2/pH. Chemosensitivity or chemodetection refers to the response of a described unit, say a particular type of neuron, to changes in CO_2/pH. Chemosensitivity and chemodetection do not necessarily translate to chemoreception, that is, the presence of a type of neuron with

a known sensitivity *in vitro* to changes in CO_2/pH does not necessarily mean that the neuron is important in a chemoreceptor response, one that involves a change in ventilation *in vivo*.

A number of experimental approaches support the concept that central chemoreception is a widely distributed function within the hindbrain. Experiments using expression of the early gene, c-fos, following exposure to elevated CO_2, described the presence of activated neurons at locations near the ventral lateral medullary surface, as proposed in early studies, but also deeper in the brainstem at other locations including the locus ceruleus, nucleus tractus solitarius, medullary raphe, rostral aspect of the ventral respiratory group, and fastigial nucleus of the cerebellum.[28,88,90,95,102,116] Studies of neurons in slice preparations of the medulla that included the deeper nucleus tractus solitarious, locus ceruleus, and medullary raphe have all described neurons that were excited by CO_2.[24,53,91,96,98,99] These experimental approaches did not demonstrate chemoreception, however. The neurons expressing c-fos could have been "downstream" to the actual chemodetector cells, and the neurons in the slice preparations were not connected to a ventilatory output.

A series of experiments have utilized the approach of examining the ventilatory response to a small region of focal acidosis produced at various sites within the brainstem. While studying the role of carbonic anhydrase in cerebral pH regulation, Coates et al.[15] noted that focal application of acetazolamide, an inhibitor of carbonic anhydrase, resulted in focal acidosis. They then used tiny 1-nl injections of acetazolamide to produce very focal acidosis in the brainstem of anesthetized cats and rats.[6,16] The presence of a ventilatory response following such injections indicated the presence of chemoreception at that site. Central chemoreception was present at many locations, including the retrotrapezoid nucleus (RTN) just below the ventral medullary surface (a possible site for the older surface chemoreceptors), nucleus tractus solitarious, locus ceruleus, midline medullary raphe, rostral aspect of the ventral respiratory group, and fastigial nucleus in the core of the cerebellum (the same sites as described by the c-fos studies). Focal acidosis produced by the 1-nl injections of acetazolamide resulted in an increase in fictive ventilatory output in these anesthetized animals, which provided functional evidence for multiple central chemoreceptor locations. Brain pH measurements showed the tissue pH change to be similar to that observed with a 20-mm Hg increase in arterial PCO_2 in anesthetized animals. A second approach to induce a focal acidosis in various regions of the brainstem utilizes reverse microdialysis with a CO_2 laden artificial cerebrospinal fluid (aCSF)[60–62], which reduced brain tissue pH by an amount like that observed with an increase in arterial PCO_2 of 5-6 mm Hg, a small stimulus intensity[63]. This approach demonstrated ventilatory responses in the sites shown in Fig. 56.2.

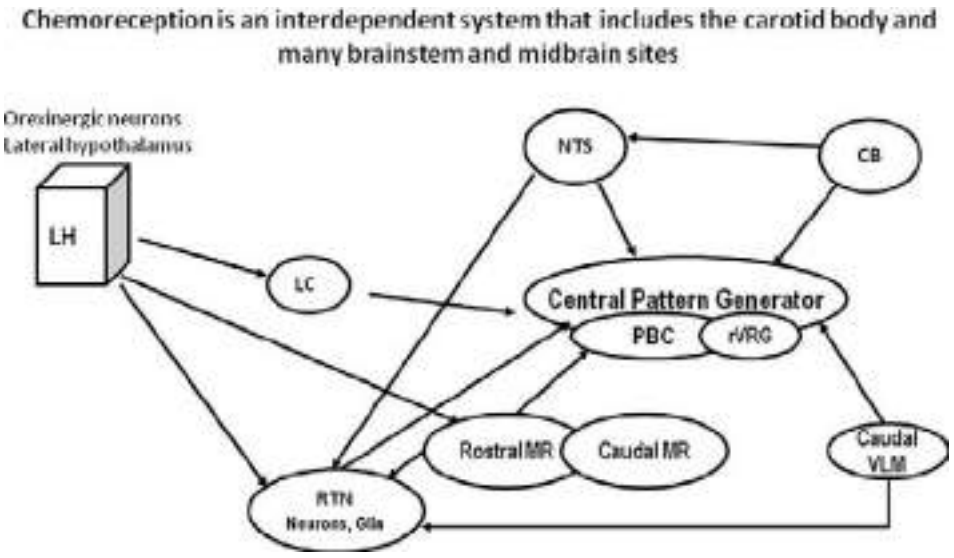

FIGURE 56.2 A simplified, schematic view of chemoreceptor sites that, when stimulated, can increase ventilation in wakefulness. Solid lines identify connections known to be present in wakefulness. LH, lateral hypothalamus; LC, locus ceruleus; NTS, nucleus tractus solitarius; CB, carotid body; PBC, pre-Bötzinger complex; rVRG, rostral ventral respiratory group; MR, medullary raphe; VLM, ventrolateral medulla. (Modified from Figure 1 in: Nattie, E. Julius H. Comroe, Jr. distinguished lecture: central chemoreception: then. . .and now. Apply Physiol 110:1–8, 2011.)

Putative Chemoreceptor Cell Type

What cell type is responsible for the detection of CO_2 or pH within the brainstem chemoreceptor sites? This seemingly simple question has proven difficult to answer because there are numerous possibilities. While it is difficult to study the response of a given cell type to acidic stimulation in a brainstem slice preparation or in cultured neurons, it is even more difficult to interpret *in vivo* findings of chemoreception. Nonetheless, there is *in vitro* and *in vivo* complementary evidence for involvement of serotonergic, noradrenergic, and glutamatergic neurons. This evidence is discussed below.

Serotonergic Neurons

Serotonergic neurons are chemosensitive when studied in slices taken from young rats or in neurons taken from newborn rats and grown in culture for several days.[96–99,119–121] These neurons are in the midline medullary raphe in close proximity to large penetrating blood vessels. The blood supply of the medulla arises from vessels on the ventral surface that penetrate deep into the tissue supplying neurons through to the dorsal aspect of the medulla.[13] A serotonergic neuron in culture will increase its firing rate with a mild CO_2 stimulus, e.g., from 1 to 3 Hz. If expressed as the percent change in firing rate, these neurons are quite sensitive in this reduced preparation. This sensitivity *in vitro*, response to mild stimulus intensities, and anatomical proximity to large vessels has been interpreted to indicate that serotonergic neurons are major central chemoreceptors. *In vivo* data support this hypothesis. Serotonergic neurons can be specifically destroyed by injection of a cell toxin, saporin, which has been conjugated to an antibody to the serotonin transport protein (anti-SERT-SAP).[84] The antibody recognizes the serotonergic cell, the conjugate is internalized, the saporin is released, and, over a period of days, the cell is killed. Such injections reduce the number of serotonergic neurons in the medullary raphe region of the rat by 28%, and also reduce the ventilatory response to CO_2 by 15 and 18%, respectively, in wakefulness and in NREM sleep. Serotonergic neurons are clearly involved in chemoreception. These data do not prove that they are chemodetector neurons *in vivo*.

One can inhibit serotonergic neurons reversibly by stimulation of serotonin 1A receptors, which are primarily inhibitory autoreceptors, by direct application via reverse microdialysis of 8-OH-DPAT ((R)-(+)-8-hydroxy-2(di-n-propylamino)tetralin). When this is done in the medullary raphe region of the unanesthetized rat, the CO_2 response is reduced. Dialysis of 10 mM 8-OH-DPAT reduces the CO_2 response by ~20%, while dialysis of 30 mM 8-OH-DPAT reduces it by 40% (Taylor et al., unpublished observations). When DPAT is dialyzed in the medullary raphe region of the unanesthetized newborn piglet, the CO_2 response is again reduced, but only in piglets older than seven days. In younger piglets, dialysis of DPAT increases the CO_2 response.[59] Serotonergic neurons are clearly involved in chemoreception but not in the early postnatal period. Again, these data do not prove that they are chemodetector neurons *in vivo*.

Finally, daily focal administration of the SERT inhibitor, fluoxetine, over 21 days in the unanesthetized rat, which should make more serotonin available in the medullary raphe region, results in an enhanced ventilatory response to CO_2.[114]

Serotonergic neurons cell bodies are located in specific sites within the brainstem and have very widespread connections within the higher brain and spinal cord. They are most active in terms of firing rate in wakefulness and less so in NREM sleep, and are almost quiescent in REM sleep. Their main function remains incompletely understood; the concept that they may be chemodetectors important in ventilatory chemoreception is somewhat paradoxical.

In sum, these *in vitro* data showing the sensitivity of serotonergic neurons to CO_2 but not proving their involvement in chemoreception, and these *in vivo* data showing that serotonergic neurons are involved in chemoreception but not demonstrating that they are directly chemosensitive, present a constellation of findings most easily interpreted as involving serotonergic neurons as chemodetectors. It is likely that these serotonergic neurons also modulate other aspects in regulating breathing and, in respect to chemoreception, they may act as modulators as well as detectors.

Glutamatergic Neurons

Glutamatergic neurons in the region of the retrotrapezoid nucleus (RTN) have also been proposed as the central chemosensitive neurons. The RTN, at first glance, is a rather unimpressive group of small, difficult-to-find neurons that lie in a small sliver of space between the ventral border of the facial nucleus and the ventral surface of the medulla. This group of neurons was discovered at about the same time by two quite different experimental approaches. In one, viral retrograde tracers injected into the phrenic motor nucleus demonstrated the presence of second-order neurons at this site;[27,109] in the other, very small injections in the RTN of an excitatory amino acid toxin, kainic acid, stopped breathing and substantially reduced the ventilatory response to CO_2 in anesthetized cats

and rats.[76,77] A series of studies then showed in unanesthetized rats that:

1. Focal stimulation of the RTN by reverse microdialysis of a CO_2-rich artificial cerebrospinal fluid stimulated breathing, which indicated the presence of chemoreception in the RTN.[57]
2. Dialysis of the GABA-A receptor agonist muscimol decreased the ventilatory response to CO_2, supporting the presence of chemoreception in the RTN.[78]
3. Dialysis of the GABA-A receptor antagonist, bicuculline, stimulated breathing, which indicated the presence of a tonic GABAergic inhibition in the RTN.[83]
4. Stimulation of neuronal activity in the RTN by CO_2, which supported the presence of chemoreception in the RTN.[18,82]
5. Unilateral excitatory amino acid toxin-induced lesions reduced the ventilatory response to CO_2, but had no effect on baseline breathing or on the response to hypoxia supporting the presence of chemoreception in the RTN.[4]
6. Bilateral lesions of RTN neurons that express the neurokinin-1 receptor by injection of a cell-specific toxin, substance P (the ligand for the neurokinin-1 receptor) conjugated to the cell toxin saporin, decreased the ventilatory response to CO_2 and induced hypoventilation, which supported the presence of chemoreception in the RTN.[81]

Recent studies have identified the putative chemoreceptor neuron within the RTN as glutamatergic.[62] In anesthetized rats, RTN neuronal activity was shown to be sensitive to CO_2 delivered to the whole rat, even when other aspects of the respiratory control network were inhibited by systemic administration of a broad-spectrum glutamate receptor antagonist or by an opioid receptor antagonist. Further, the excitable neurons were shown by juxtacellular labeling to express the RNA message for the glutamate transport protein, VGLUT2, thereby identifying the neurons as glutamatergic. These authors also found that nearby serotonergic neurons were not responsive to CO_2, but they did not test serotonergic neurons at other sites where they are plentiful. Studies in brainstem slices also showed these glutamatergic neurons to be CO_2 sensitive. The RTN is a central chemoreceptor site, and glutamatergic neurons in the RTN certainly seem to be involved in chemoreception and may be chemodetector neurons at this site.

Noradrenergic Neurons

Like serotonergic neurons, the noradrenergic neurons have cell body localization within the brainstem with widespread projections into the higher brain and spinal cord, fire in a state-dependent manner with firing greatest during wakefulness, followed by NREM sleep, which in turn is followed by REM sleep, and seem to play a role in both basic physiological control as well as in the modulation of higher nervous system behaviors. When studied in brainstem slices, the noradrenergic neurons of the locus ceruleus are chemosensitive, which suggests that they could be involved in chemoreception. In brain slices, the locus ceruleus cell firing rate is increased by ~56% as bathing medium CO_2 is increased from 5 to 10% CO_2,[91] and by 93% as the bathing medium CO_2 is increased to 15%.[35] In anesthetized rats, hypercapnia increases the locus ceruleus neuron firing rate together with splanchnic nerve activity even after denervation of the carotid bodies.[29] The baseline firing rate of one neuron was ~3 Hz; on average, the firing rate increased by 20% at 5% CO_2 and 47% at 10% CO_2.[29] The expression of the early gene, c-fos, is also increased in TH-ir neurons of the locus ceruleus region in response to increased CO_2 (15% CO_2 for 60 minutes), which suggests a role for these cells in central chemoreception.[41] Focal acidification of the locus ceruleus region by microinjection of acetazolamide increases fictive ventilatory output (phrenic nerve activity) in anesthetized cats and rats, indicating that this location contains chemoreceptors that can affect breathing.[16] Cell-specific killing of noradrenergic neurons in locus ceruleus and in other brainstem regions, that is, the A5, C1, and C3 regions, decreases the ventilatory response to CO_2 in rats during sleep and wakefulness (Li and Nattie, unpublished observations). Injections of the cell-specific toxin, anti-DBH-SAP, into the fourth ventricle, reduced the number of TH-ir cell profiles counted in the A6 region by 84% and in the A5 region by 78%. These injections had little effect on TH-ir cells in more rostral sites as demonstrated by the lack of effect on TH-ir cell profile counts in a portion of the A9 region. This was associated with a 25–28% reduction in the ventilatory response to systemic hypercapnia in both sleep and wakefulness.

Cholinergic Receptors

There is *in vivo* evidence suggesting that muscarinic cholinergic receptors in the region of the retrotrapezoid nucleus are also involved in central chemoreception.[63] In anesthetized cats, focal inhibition of muscarinic receptors by application of antagonists to the ventral medullary surface and by their microinjection into the ventral medullary tissue decreased the ventilatory response to CO_2. Use of relatively specific muscarinic-receptor subtype antagonists produced effects suggesting that the M3 subtype was most potently involved; a greater fraction of M3 receptor antagonist injections inhibited the CO_2 response than did M1 or M2 receptor antagonist injections.[75]

Small Ventral Surface Cells

A number of investigators have noted the presence of small cells along the ventral medulla surface that express the early gene c-fos after CO_2 stimulation. These cells have been proposed as chemodetectors.[8,39,117] The size and character of these cells differ from the glutamatergic neurons that have been recently proposed in this region as chemodetectors.[62] In fact, they resemble glial cells. Could glia be central chemodetectors? There is evidence to support the idea that glia can, at the least, modulate central chemoreception. Focal inhibition of glial function in the RTN by microdialysis of fluorocitrate, which preferentially inhibits metabolism in glia, results in the development of focal acidosis and stimulation of breathing in anesthetized rats.[30] In unanesthetized rats, fluorocitrate application focally into the RTN region stimulates breathing both in air and in various CO_2 levels.[46] If glia can be depolarized, and thus "excited," by changes in pH, their release of substances like ATP or glutamate could act like "neurotransmitters," which can then stimulate nearby neurons (see Putnam et al.[94]). Glia seems to regulate local interstitial fluid (ISF) pH, and thus they likely modulate central chemoreceptor function.

ATP and P2X Receptors

There is quite a bit of evidence from experiments in anesthetized animals that supports a role of some type for ATP and P2X receptors in central chemoreception. P2X receptors are present in the ventral lateral medulla; application of P2 receptor antagonists decreases the ventilatory response to CO_2, ATP is released from cells in the ventrolateral medulla during CO_2 stimulation, and application of ATP to this region stimulates breathing.[112] These observations suggest that ATP release with subsequent stimulation of cells with purogenic receptors is involved in central chemoreception.

Why so Many Central Chemoreceptor Sites?

Which sites are the most important? There is no evidence as yet to show that one central chemoreceptor site, or that one central chemodetector cell type, is of primary importance in the unanesthetized mammal. Much evidence obtained both *in vitro* and *in vivo* supports a role for medullary raphe serotonergic neurons, RTN glutamatergic neurons, and medullary noradrenergic neurons in central chemoreception. The quantitative nature of responses to focal acidic stimulation is basically similar in anesthetized or unanesthetized animals at all sites tested, which include the RTN, medullary raphe, locus ceruleus, nucleus tractus solitarius, rostral aspect of the ventral respiratory group, and fastigial nucleus of the cerebellum. Similarly, lesions of the RTN, medullary raphe, and medullary noradrenergic cells, and focal inhibition of the RTN or the medullary raphe all decreased the ventilatory response to CO_2 but none abolished it. In fact, the largest proportional inhibition that has been observed in conscious animals has been a ~40% decrease in the ventilatory response to CO_2: (1). following destruction of RTN neurons by an excitatory neurotoxin,[4] and (2). following reversible inhibition of medullary raphe serotonergic neurons by reverse microdialysis of 8-OH-DPAT, an inhibitor of serotonergic neurons (Taylor et al., unpublished observations). In the first case, this effect was measured 18 days following induction of the lesion; in the second case, the effect was measured immediately. No one has as yet produced a total lesion or total inhibition of all neurons located at a single anatomical location or of all neurons identified by a single chemical phenotype. One possible exception is an experiment in which neonatal rats were treated with a serotonergic toxin, 5,7-dyhydroxytryptamine.[61] When studied as adults, these rats showed a decrease of about 50% in ventilatory response to CO_2. Because no histology was performed, the extent of the serotonergic lesion is unknown, although tissue levels of serotonin were dramatically reduced.

Given the presence of multiple cell types that are chemosensitive *in vitro* together with *in vivo* observations that indicate chemoreception occurs at sites containing these neurons and that lesions or neuronal inhibition at these sites interfere with the ventilatory response to CO_2, it seems unlikely that there is a predominant chemodetector neuron or chemosensitive site. The sum of all the evidence supports the concept of multiple central chemoreceptor sites and multiple chemodetector cells.

Why is Central Chemoreception Such a Distributed Property?

A number of hypotheses, briefly described in the following, have been proposed to answer this question:[32,70–72]

Geographic Specificity

Various brain regions, in a geographic or anatomical sense, each have their own set and type of chemoreceptors. These could be organized among physiological functions, such as control of blood pressure versus breathing, or within a single function, such as the various brainstem sites involved in the control of breathing.

Stimulus Intensity

Sites may vary according to stimulus threshold and stimulus intensity required to bring about a response. To obtain the very high overall sensitivity of the system, many or all sites must be stimulated at the same time.

Stimulus Specificity

CO_2 may stimulate some sites, and pH may stimulate others. Some may detect intracellular pH, and others extracellular pH.

Temporal Specificity

Some sites may be oriented to detect blood pH, others to detect brain interstitial fluid pH or to detect cell pH. These various sites may detect pH changes at different times during an acid–base event.

Syncytium

Chemodetector cells at certain sites could be part of a network connected by low-resistance junctions.[25] This could be a way to enhance the system response to a small focal response at the cellular level.

Arousal State

Some sites could respond in sleep, others in wakefulness, and still others in both states. Evidence from focal stimulation studies supports this to some extent.

The role of various central chemoreceptor sites has been evaluated in unanesthetized animals by employing the technique of reverse microdialysis to deliver CO_2 into restricted brainstem regions. By equilibration of artificial cerebrospinal fluid with high CO_2 concentrations, and by rapid flow through the dialysis system, a focal and moderate level of tissue acidosis can be produced. In the rat, such focal acidosis in the region of the retrotrapezoid nucleus increases ventilation in wakefulness,[57] whereas in the midline medullary raphe region it does so in sleep (Fig. 56.3).[79] These two sites are within a millimeter or so of each other anatomically. The fact that focal CO_2 administration at the medullary raphe increases ventilation by affecting breathing frequency only in sleep, while focal CO_2 administration in the RTN increases ventilation via an effect on tidal volume only in wakefulness, provides functional evidence that this technique does produce a focal stimulus. These data also suggest that various chemoreceptor sites may have different roles. Focal CO_2 administration in the nucleus tractus solitarius increases ventilation in both sleep and wakefulness via an effect on both breathing frequency and tidal volume.[80] In the unanesthetized goat, focal acidification in the medullary raphe increases ventilation in wakefulness,[44] and focal acidification at two medullary raphe sites produces twice the effect on breathing.[45] The stimulus intensity observed with focal CO_2 dialysis in rats, as measured by tissue pH electrodes, is similar to that observed with a 6-mm Hg increase in $PaCO_2$. The goat studies used a similar stimulus intensity.

Evolutionary Considerations

Satinoff[101] published the idea of a hierarchical control system for mammalian temperature regulation, with levels in the hierarchy determined by physiological processes added during steps in evolution.

New demands cause new mechanisms and new sites of regulation. It is possible that the presence of multiple central chemoreceptor sites is the result of a similar evolution. As organisms progressed during evolutionary time, major events occurred, each of which could have resulted in the development of a new chemoreceptor site with new functional emphasis. For example, the transition from water-to-air breathing, development of homeothermy, requirement for sleep, and further differentiation of sleep into NREM and REM components, could have been associated with the need for the development of a new chemoreceptor site and mechanism.

What is the Role of Peripheral versus Central Chemoreceptors?

If we group the central chemoreceptors together, the issue remains of the importance and function of the central chemoreceptors versus that of the peripheral chemoreceptors. Heymans and Bouckaert,[43] among others, have argued that the peripheral chemoreceptors can explain most of the chemical control of breathing while others, most notably Pappenheimer and colleagues,[34,89] have suggested that the opposite is more likely. Experiments with clearly interpretable results have not been forthcoming. There have been many attempts to surgically remove the carotid bodies and then compare the sensitivity of the ventilatory response to CO_2 to that observed prior to peripheral chemodenervation. Generally, these studies in both anesthetized and in unanesthetized animals have suggested that the peripheral chemoreceptor can account for 20–40% of the total CO_2 response.[38,42,67] The problem that makes the interpretation of these data difficult is that the carotid bodies provide a tonic afferent excitatory input to the respiratory control system. Thus, peripheral chemodenervation removes both a tonic source of system excitation as well as the CO_2-dependent increase in excitation. Consequently, a subsequent reduced sensitivity to CO_2 cannot be interpreted as the outcome of losing CO_2 detection alone. In fact, this loss of a tonic excitation may be the explanation for the common observation in chemodenervated animals and humans

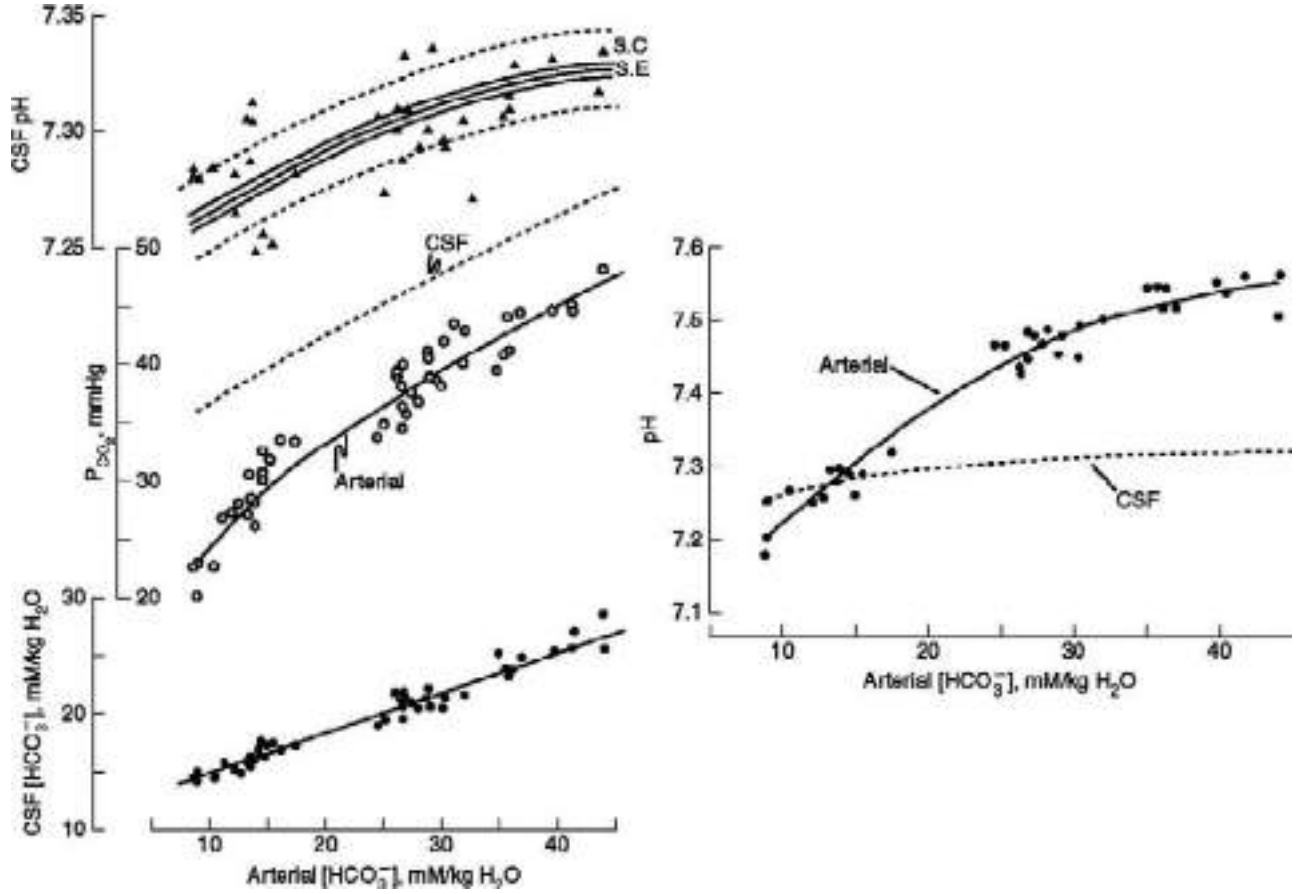

FIGURE 56.3 The three panels at the left show pH and bicarbonate in cerebrospinal fluid, and both CSF and $PaCO_2$ versus arterial bicarbonate in five goats with chronic acid–base disturbances. The panel at the right shows both arterial and CSF pH versus arterial bicarbonate. These data are very representative of such data obtained in humans with chronic acid–base disorders. Note that CSH pH changes very little in comparison to arterial pH, and that this results from both a smaller change in CSF bicarbonate than in blood and from the changes in $PaCO_2$ that reflect chemoreceptor-induced changes in alveolar ventilation. (*With permission, from Figures 2 and 3, in.* [34])

that hypoventilation ensues following peripheral chemodenervation. The remaining chemoreceptor sites do not make up for the loss of peripheral excitatory input from the carotid bodies. This absence of recovery following chemodenervation also occurs after removal of at least one central chemoreceptor site, the RTN.[81] Here, with bilateral destruction of RTN neurons, the unanesthetized rat also hypoventilates while breathing air at rest. The rat behaves just like it does following loss of the carotid bodies. Following RTN destruction, the remaining chemoreceptors, including the carotid body, do not make up for the presumed loss of tonic excitatory input from neurons within the RTN region. The RTN can be viewed as containing glutamatergic chemodetector neurons as well as providing tonic excitation to the respiratory control system.

Smith and Dempsey have used an elegant preparation that has the potential to unravel how peripheral and central chemoreceptor sites interact.[25,108] In the dog, these authors denervated the peripheral chemoreceptor on one side and created an investigator-controlled perfusion system for the other side. They controlled the PO_2 and PCO_2 of peripheral and central chemoreceptors independently. The major finding from these studies to date is the importance of the peripheral chemoreceptors in detecting rapid changes in $PaCO_2$ either as hypocapnia or hypercapnia. In various experiments, responses to changes in $PaCO_2$ at the carotid body are on average twice as fast as when the change in $PaCO_2$ is isolated to the central chemoreceptors. Remarkably, these data are in agreement with deductions made from analysis of time constants of the ventilatory response to single breath changes in CO_2 in humans with and without peripheral chemoreceptors.[31] They also agree with older data in decerebrate cats.[9] The possible role of peripheral chemoreceptors as a rapid-response detector is intriguing and important, as Dempsey and colleagues[26] have shown that in some

cases, apneas in sleep may be potentiated by sudden, rapid decreases in PCO_2 brought about by transient increases in ventilation that involve only a few breaths.

PARADOX: CENTRAL CHEMORECEPTORS LOCATED IN AN ENVIRONMENT WITH TIGHT pH REGULATION

Acid–Base Regulation in Brain Fluids

The central nervous system has two extracellular compartments; the ventricles containing CSF, and tissue interstitial fluid (ISF). CSF and ISF have different volumes, 10 and 20% of brain weight, respectively, and communicate without diffusional restriction. The ionic composition of both is regulated and this provides a stable chemical environment for neuronal function.[22,23,33,34,36,51,68] As a first approximation, we can estimate brain ISF pH by measurement of CSF pH. CSF pH is regulated by a combination of ion secretory and exchange processes at the choroid plexus and blood–brain barrier (BBB), which determine the ionic composition of CSF and ISF, respectively, and cerebral blood flow and alveolar ventilation, which determine ISF PCO_2.[68] CSF pH changes very little in acid–base disturbances.[22,33,34] Figure 56.4 shows the small change in CSF pH that accompanies chronic experimental acid–base disturbances produced in goats that vary arterial bicarbonate from less than 10 to more than 40 mmol/liter. The figure also shows that CSF pH changes much less than arterial pH under these conditions. Also in Fencl et al.,[34] a summary of data obtained from nine separate studies of humans with chronic acid–base disorders showed the very same relationships. These goat data are fully representative of the changes in these variables observed in human subjects. ISF pH homeostasis provides a stable environment for cell pH regulation and allows normal neuronal function at the membrane and synaptic levels. Disorders of pH caused by ionic or CO_2 imbalance initiate both types of brain responses—ionic and blood flow/ventilatory. The brain can regulate its own ionic environment—as the kidney does systemically—and alter brain and body PCO_2. This regulatory system for brain ISF pH contributes to body pH homeostasis as well.

Choroid Plexus

Specialized cells in choroid plexus secrete the CSF, a clear colorless liquid with low protein content (~25 mg/100 ml) in comparison to plasma (~6.5 gm/100 ml). It circulates through the ventricles and exits to the venous system via the arachnoid villi. CSF secretion involves a number of ion exchange proteins in choroid plexus epithelium.[48] Facing CSF, a sodium/potassium ATPase extrudes sodium, decreasing cell sodium concentration and maintaining the sodium concentration gradient from plasma to cell. At the plasma membrane, sodium/proton and chloride/bicarbonate antiporters operate to enhance sodium and chloride entry. Cell carbonic anhydrase catalyzes the rapid production of bicarbonate and protons used for these ion exchanges. Sodium chloride cotransport appears at both membranes as well.[48] The secreted CSF has a higher sodium and chloride concentration and lower potassium concentration and pH than does plasma.

Blood–Brain Barrier

Not all CSF originates in the choroid plexus. Pollay and Curl[92] perfused a portion of the rabbit fourth ventricle after removing the plexus. Dilution of their perfusate indicated the presence of a fluid added from the brain. This fluid, which accumulated at one third the rate of total CSF, was thought to originate at the capillary endothelial cells that form the BBB. Brain capillaries, because of endothelial tight junctions, have no Starling-type bulk-flow fluid exchange with ISF, and this barrier has low ion permeabilities, low hydraulic conductivity, and high electrical resistance.[11,103,104] Thus, ion movement that accounts for the observed fluid flow must occur by a secretory process.

Ion transport proteins are present at the BBB.[8,11] As reviewed by Schielke and Betz,[103] an amiloride-sensitive nonselective cation channel,[7,8,118] a sodium/chloride cotransport protein, and sodium/proton[64] and chloride/bicarbonate antiporters[110] are found at the barrier. At the ISF-facing membrane, there is a sodium/potassium ATPase.[12,88] The sodium/proton antiporter has been demonstrated in isolated cerebral capillaries,[7] and potassium and chloride channels have been suggested based on observations made in analogous systems. This model can account for an actively secreted ISF originating at brain capillary endothelium and provides possible sites for ISF pH regulation.

Bulk Flow of Interstitial Fluid

Brain ISF can move by a pressure-dependent bulk flow through ISF spaces into ventricular CSF.[19,20,48] The clearance of 900-, 4000-, and 69,000-Da tracer molecules injected into brain parenchyma was found to be similar, results explicable by bulk flow but not diffusion.[19] Part of this clearance occurs via ventricular CSF, and part by other pathways, such as cervical lymphatics.[113] Thus, a CSF-like fluid formed by secretory

processes at the endothelial cells moves by bulk flow through ISF to the ventricles or to cervical lymphatics.[48,113] This flow pathway for brain ISF raises the following questions: What is the role of ventricular CSF in the regulation of ISF? Is CSF merely an effluent drainage system or does it modify brain ISF? Tracer molecules perfused via the cerebral ventricular system do enter the parenchyma (e.g.,[10]) by diffusion or bulk flow if the normal flow-determining pressure gradients are disturbed. It seems reasonable to suggest that ISF, especially near the ventricles, is exposed to the ionic constituents of CSF. This would help to maintain ISF ion concentrations within the narrow range required for normal neuronal function.

Potassium

As an example, we consider the role of choroid plexus and BBB in the tight regulation of ISF and CSF potassium.[11,52] Potassium measurements by ion-selective electrodes in rats of different ages show that ISF potassium regulation is present, developmentally, before that of ventricular CSF.[49] Sodium/potassium ATPases, described at the brain-facing surface of both choroid plexus and BBB cells, have a K_m of 3 mM, the normal ISF and CSF concentration.[104] Cotransport of potassium with chloride is present at the choroid plexus and, perhaps, at the BBB, and many potassium channels have been identified in capillary endothelial cells.[52] Mechanisms exist at both choroid plexus and the BBB for potassium regulation in brain ISF and CSF. Such a model should also apply to pH regulation in brain ISF and CSF.

PCO_2 at Choroid Plexus

The bicarbonate concentration of freshly secreted CSF depends on the PCO_2. At choroid plexus, an increase in PCO_2 increases the bicarbonate, and decreases the chloride, concentrations of secreted CSF.[51,65,66] The sodium concentration is also increased in the immediate response.[50,65,66] These ionic responses are involved in CSF pH regulation—as the bicarbonate concentration increases, the pH of the secreted fluid is less acidic. With a decrease in PCO_2, the reverse occurs—bicarbonate decreases and chloride increases. The mechanisms for these changes in the ionic character of secreted CSF involve sodium/proton and chloride/bicarbonate antiporters as: (1) Antagonists of these proteins inhibit the CSF bicarbonate response to hypercapnia;[73,74] (2) the full CSF bicarbonate response to hypercapnia requires the presence of carbonic anhydrase;[122] (3) changes in pH affect choroid plexus cell ion concentrations and sodium entry from blood to CSF via an amiloride-sensitive process.[64]

PCO_2 at Blood–Brain Barrier

At the BBB, CO_2 sensitive ionic processes help to regulate ISF pH, and may affect the composition of ventricular CSF. In anesthetized cats, hypercapnia quickly increased cortical-surface ISF bicarbonate concentrations and decreased chloride concentrations.[2,3] The responses were thought to reflect glia–ISF exchange of chloride and bicarbonate, a rapid cell response to regulate ISF pH. However, such an exchange would acidify the glia. An alternative explanation places the bicarbonate/chloride exchange at capillary endothelial cells. Katsura et al.[50] measured ISF and brain tissue ions of rat cortex in response to hypercapnia. ISF bicarbonate and sodium increased, and chloride decreased, within minutes. Tissue bicarbonate also increased within minutes, as found by others.[65,122] A chloride for bicarbonate and sodium for proton exchange between cell and ISF was proposed; that is, cells lost bicarbonate, or gained H^+, and ISF pH was regulated at the expense of cell pH. The major observation to support this interpretation was the absence of any measurable change in tissue (cell) sodium and chloride content. But, due to the small size of the ISF space and the greater sodium and chloride concentration in ISF than in the cells, it is difficult to detect changes in cell sodium or chloride by whole-tissue measurements. The CO_2-stimulated changes in ISF sodium, chloride, and bicarbonate could arise from BBB processes.

The view that brain cells lose bicarbonate during hypercapnia in order to regulate ISF pH requires greater acidification of the cells involved. Simultaneous measurements of brain cell and ISF pH using 31P-NMR show that cell pH decreases: (1) Less than ISF pH after 10 minutes of hypercapnia;[93] (2) less than blood pH following 50 minutes of hypercapnia.[86] That cell pH changes minimally in acute hypercapnia does not support the idea of cell acidification for regulating ISF pH. The rapid changes in brain ISF sodium, bicarbonate, and chloride during hypercapnia appear to represent events that occur between ISF and blood, rather than cell and ISF. Thus, rapid ion movements at the BBB likely play an important role in ISF pH regulation in hypercapnia. Such ISF pH regulation would optimize cell pH regulation at neuronal and glial membranes.

Bicarbonate Entry from Blood

ISF pH changes rapidly following changes in blood pH produced by infusion of acid or base with arterial

PCO_2 maintained at a constant value. In the steady state, the ISF pH changes are approximately one-third of those in blood.[21,47,115] Measurements on the cortical surface in anesthetized cats given a bolus infusion of sodium bicarbonate with constant arterial PCO_2 showed a rapid increase in ISF bicarbonate accompanied by a decrease in ISF chloride.[3] In contrast, no change in CSF pH[21,47] or cell pH[1] is observed in these types of acute experiments. In chronic systemic acid–base disorders, CSF pH does change in the direction of the change in blood pH but by a very small amount, much less than in blood and, presumably, ISF.[33,34,89]

SUMMARY

Brain ISF is produced by capillary endothelial cells and moves through the interstitium via clearance of bulk flow by ventricular CSF and cervical lymphatics. ISF pH is, in part, regulated by ionic processes at the choroid plexus and BBB. Both CO_2 and blood bicarbonate (ions) have independent effects.[40,85] Some of these processes respond to changes in PCO_2, although the means by which they are controlled is unknown. It is likely that cell pH affects ion transport proteins.

BREATHING AND pH REGULATION

Effectiveness of Breathing in pH Regulation

Chemoreceptors provide a very sensitive means by which ventilation can be stimulated by a small decrease in pH; conversely, they are inhibited by a small increase in pH (see Fig. 56.1). The peripheral chemoreceptors can be viewed as a detector with rapid-response dynamics, and the central chemoreceptors as having slower dynamics. We can demonstrate, by means of simple calculations, the effectiveness of this very sensitive central chemoreceptor system to small changes in cerebral pH in regulating peripheral arterial pH as well as brain pH. Under normal baseline conditions in humans, arterial pH is 7.40, $PaCO_2$ is 40 mm Hg, arterial bicarbonate is 24 mmol/liter, and CSF pH is 7.3. In metabolic acidosis with arterial bicarbonate decreasing from the normal value of 24 mmol/liter to, say, 20 mmol/liter, without any ventilatory response such that $PaCO_2$ remains at 40 mm Hg, and arterial pressure will decrease from 7.40 to 7.32. With this mild acidosis in the presence of a ventilatory response, in humans the $PaCO_2$ will decrease by about 5 mm Hg to a value of ~35 mm Hg (see data for humans, Figure 13 in Feldman et al.[32]). The corresponding pH will be 7.38. The increase in alveolar ventilation, which will decrease $PaCO_2$ from 40 to 35 mm Hg, has a substantial effect on pH regulation. The fall in $PaCO_2$ reduces the decrease in pH from 7.40 to 7.38 instead of 7.32 or a change in pH of 0.2 pH units instead of 0.8 pH units. The ventilatory response to the acidosis reduces the arterial pH change in this example by 75%.

Where Do Chemoreceptors Detect the pH Change?

Examination of Fig. 56.4 shows that in these chronic acid–base disturbances, the ventilatory response (as inferred from the observed changes in $PaCO_2$, or as observed directly from the measured alveolar ventilation in Fig. 56.1) could be related either to the large changes in arterial pH shown in the right panel or to the smaller changes in CSF pH shown also in the right panel. In an elegant set of experiments and deductions, Pappenheimer, Fencl, and colleagues[34,89] performed a perfusion of the entire brain ventricular system in goats with chronic acid–base disturbances using fluids of varying bicarbonate concentration. They then related alveolar ventilation in all conditions, chronic acid–base disorders, CO_2 inhalation, and ventriculo-cisternal perfusion of differing HCO_3 concentrations, to pH at one site only, a virtual site that lies three-quarters of the distance between the large ventricle CSF and arterial blood. All of the ventilatory responses fit one stimulus location only with pH calculated for this site. The pH at this site is represented by the X symbols in Fig. 56.1. Referring to Fig. 56.4, we can imagine that the pH detected by central chemoreceptors lies between arterial and CSF pH, but closer to arterial pH.

SUMMARY

In a metabolic acid–base disturbance, CSF bicarbonate changes less than blood bicarbonate due to the presence of ionic secretory processes at choroid plexus and the BBB that regulate CSF bicarbonate. In addition, central chemoreceptors detect the acidosis, most likely at a site lying between arterial blood and CSF. The central chemoreceptors increase alveolar ventilation, which decreases $PaCO_2$ as well as the PCO_2 in tissue and in CSF. This CO_2 change further minimizes the degree of acidosis in CSF and it acts importantly to diminish the pH change in arterial blood. Peripheral chemoreceptors also contribute to the increase in alveolar ventilation. This complex system has a set of ionic regulatory processes to control brain fluid ions, and a superimposed ventilatory system response to control brain CO_2 that mirrors, in the body, the set of ionic regulatory processes in the kidney that control body fluid

ions, which also has superimposed a ventilatory system response to control $PaCO_2$.

Acknowledgments

Dr. Aihua Li is an essential contributor to the author's work. The lab has been generously supported by the National Institutes of Health (grant HL 28066).

References

[1] Adler S, Simplaceanu V, Ho C. Brain pH in acute isocapnic metabolic acidosis and hypoxia: a 31P- nuclear magnetic resonance study. Am J Physiol 1990;258:F34–40.

[2] Ahmad HR, Loeschcke HH. Fast bicarbonate-chloride exchange between brain cells and brain extracellular fluid in respiratory acidosis. Pflügers Arch 1982;395:293–9.

[3] Ahmad HR, Loeschcke HH. Fast bicarbonate-chloride exchange between plasma and brain extracellular fluid at maintained PCO_2. Pflügers Arch 1982;395:300–5.

[4] Akilesh MR, Kamper M, Li A, Nattie EE. Effects of unilateral lesions of the retrotrapezoid nucleus on breathing in awake rats. J Appl Physiol 1997;82:469–79.

[5] Ballantyne D, Scheid P. Central chemosensitivity of respiration: a brief overview. Respir Physiol 2001;129:5–12.

[6] Bernard DG, Li A, Nattie EE. Evidence for central chemoreception in the medullary raphé. J Appl Physiol 1996;80:108–15.

[7] Betz AL. Sodium transport in capillaries isolated from rat brain. J Neurochem 1983;41:1150–7.

[8] Betz AL, Goldstein GW. The basis for active transport at the blood–brain barrier. In: Eisenberg HM, Suddith RL, editors. Advances in experimental medicine biology. New York: Plenum; 1981. p. 5–15.

[9] Borison HL, Gonsalves SF, Montgomery SP, McCarthy LE. Dynamics of respiratory VT response to isocapnic pHa forcing in chemodenervated cats. J Appl Physiol 1978;45:502–11.

[10] Borison HL, Borison R, McCarthy LE. Brain stem penetration by horseradish peroxidase from cerebrospinal fluid spaces in the cat. Exp Neurol 1980;69:271–89.

[11] Bradbury MWB. The blood–brain barrier. Transport across the cerebral endothelium. Circ Res 1985;57:213–22.

[12] Bradbury MWB, Stulcová B. Efflux mechanism contributing to the stability of the potassium concentration in cerebrospinal fluid. J Physiol (Lond) 1970;208:415–30.

[13] Bradley SR, Pieribone VA, Wang W, Severson CA, Jacobs RA, Richerson GB. Chemosensitive serotonergic neurons are closely associated with large medullary arteries. Nat Neurosci 2003;5:401–2.

[14] Budzinska K, von Euler C, Kao FF, Panteleo T, Yamamoto Y. Effects of graded focal cold block in the rostral areas of the medulla. Acta Physiol Scand 1985;124:329–40.

[15] Coates EL, Li A, Nattie EE. Acetazolamide on the ventral medulla of the cat increases phrenic output and delays the ventilatory response to CO_2. J Physiol (Lond) 1991;441:433–51.

[16] Coates EL, Li A, Nattie EE. Widespread sites of brainstem ventilatory chemoreceptors. J Appl Physiol 1993;75:5–14.

[17] Cohen MI. Tonic chemoreceptor input as the background for respiratory rhythm. In: Trouth CO, Millis RM, Kiwull-Schöne HF, Schläfke ME, editors. Ventral brainstem mechanisms and control of respiration and blood pressure. New York: Marcel Dekker; 1995. p. 797–9.

[18] Connelly CA, Ellenberger HH, Feldman JL. Respiratory activity in retrotrapezoid nucleus in cat. Am J Physiol 1990;258:L33–44.

[19] Cserr HF, Cooper DN, Suri PK, Patlak CS. Efflux of radiolabeled polyethylene glycols and albumin from rat brain. Am J Physiol 1981;240:F319–28.

[20] Cserr HF, Patlak CS. Secretion and bulk flow of interstitial fluid. In: Bradbury MWB, editor. Physiology and pharmacology of the blood–brain barrier. New York: Springer-Verlag; 1992. p. 245–61.

[21] Davies DG, Nolan WF. Cerebral interstitial fluid acid–base status follows arterial acid–base perturbations. J Appl Physiol 1982;53:1551–5.

[22] Davson H, Segal MB. Acid-base relations in the central nervous system. In: Davson H, Segal MB, editors. Physiology of the CSF and blood–brain barriers. Boca Raton, FL: CRC Press; 1996. p. 459–88.

[23] Davson H, Welch K. The relations of blood, brain and cerebrospinal fluid. In: Siesjö BK, Sorenson SC, editors. Ion homeostasis of the brain, 10. New York: Academic Press; 1971. p. 9–28.

[24] Dean JB, Lawing WL, Millhorn DE. CO_2 decreases membrane conductance and depolarizes neurons in the nucleus tractus solitarius. Exp Brain Res 1989;76:656–61.

[25] Dean JB, Ballantyne D, Cardone DL, Erlichman JS, Solomon IC. Role of gap junctions in CO_2 chemoreception and respiratory control. Am J Physiol Lung Cell Mol Physiol 2002;283:L665–70.

[26] Dempsey JA. Crossing the apnoeic threshold: causes and consequences. Exp Physiol 2004;90:13–24.

[27] Dobbins EG, Feldman JL. Brainstem network controlling descending drive to phrenic motoneurons in rat. J Comp Neurol 1994;347:64–86.

[28] Dreshaj IA, Haxhiu MA, Martin RJ. Role of the medullary raphe nuclei in the respiratory response to CO_2. Respir Physiol 1998;111:15–23.

[29] Elam M, Yao T, Thorén P, Svensson TH. Hypercapnia and hypoxia: chemoreceptor-mediated control of locus ceruleus neurons and splanchnic, sympathetic nerves. Brain Res 1981;222:373–81.

[30] Erlichman JS, Li A, Nattie EE. Ventilatory effects of glial dysfunction in a rat brain stem chemoreceptor region. J Appl Physiol 1998;85:1599–604.

[31] Fatemian M, Nieuwenhuijs DJ, Teppema LJ, Meinesz S, van der Mey AG, Dahan A, Robbins PA. The respiratory response to carbon dioxide in humans with unilateral and bilateral resections of the carotid bodies. J Physiol (Lond) 2003;549:965–73.

[32] Feldman JL, Mitchell GS, Nattie EE. Breathing: rhythmicity, plasticity, chemosensitivity. Ann Rev Neurosci 2003;26:239–66.

[33] Fencl V. Acid–base balance in cerebral fluids. In: Fishman AP, editor. Handbook of physiology. Vol. II. Control of breathing, Part 1. Bethesda, MD: American Physiological Society; 1986. p. 115–40.

[34] Fencl V, Miller TB, Pappenheimer JR. Studies on the respiratory response to disturbances of acid–base balance, with deductions concerning the ionic composition of cerebral fluids. Am J Physiol 1966;210:459–72.

[35] Filosa JA, Dean JB, Putnam RW. Role of intracellular and extracellular pH in the chemosensitive response of rat locus coeruleus neurones. J Physiol (Lond) 2002;541:493–509.

[36] Fishman R. Cerebrospinal fluid in diseases of the nervous system. Philadelphia: WB Saunders; 1992.

[37] Forster HV, Ohtake PJ, Pan LG, Lowry TF. Effects on breathing of ventrolateral medulla cooling in awake goats. J Appl Physiol 1995;78:258–65.

[38] Forster HV, Pan LG, Lowry TF, Serra A, Wenninger J, Martino P. Important role of carotid chemoreceptor afferents in control of breathing of adult and neonatal mammals. Respir Physiol 2000;119:199–208.

[39] Fukuda Y, Honda Y. pH sensitivity of cells located at the ventrolateral surface of the cat medulla oblongata in vitro. Pflügers Arch 1976;364:243–7.
[40] Hasan FM, Kazemi H. The dual contribution theory of regulation of CSF HCO3 in respiratory acidosis. J Appl Physiol 1976;40:559–67.
[41] Haxhui MA, Tolentino-Silva F, Pete G, Kc P, Mack SO. Monoaminergic neurons, chemosensation and arousal. Respir Physiol 2001;129:191–210.
[42] Heeringa J, Berkenbosch A, DeGoede J, Olievier CN. Relative contribution of central and peripheral chemoreceptors to the ventilatory response of CO_2 during hyperoxia. Respir Physiol 1979;37:365–79.
[43] Heymans C, Bouckaert C. Les chémo-récepteurs du sinus carotidien. Ergebn Physiol 1939;41:28–55.
[44] Hodges MR, Klum L, Leekley T, Brozoski DT, Bastasic J, Davis J, Davis S, Wenninger JM, Feroah TR, Pan LG, Forster HV. Effects on breathing in awake and sleeping goats of focal acidosis in the medullary raphe. J Appl Physiol 2004;96:1815–24.
[45] Hodges MR, Martino P, Davis S, Opansky C, Pan LG, Forster HV. Effects on breathing of focal acidosis at multiple medullary raphe sites in awake goats. J Appl Physiol 2004;97:2303–9.
[46] Holleran J, Babbie M, Erlichman JS. Ventilatory effects of impaired glial function in a brain stem chemoreceptor region in the conscious rat. J Appl Physiol 2001;90:1539–47.
[47] Javaheri S, De Hemptine A, Vanheel B, Leusen I. Changes in brain ECF pH during metabolic acidosis and alkalosis: a microelectrode study. J Appl Physiol 1983;55:1849–53.
[48] Johanson CE. Ventricles and cerebrospinal fluid. In: Conn PM, editor. Neuroscience in medicine. Philadelphia: JB Lippincott; 1995. p. 171–96.
[49] Jones HC, Keep RF. The control of potassium concentration in the cerebrospinal fluid and brain interstitial fluid of developing rats. J Physiol (Lond) 1987;383:441–53.
[50] Katsura K, Kristián T, Nair R, Siesjö BK. Regulation of intra- and extracellular pH in the rat brain in acute hypercapnia: a reappraisal. Brain Res 1994;651:47–56.
[51] Kazemi H, Johnson DC. Regulation of cerebrospinal fluid acid–base balance. Physiol Rev 1986;66:953–1037.
[52] Keep RF, Xiang J, Betz AL. Potassium transport at the blood–brain and blood–CSF barriers. In: Drewes LR, Betz AL, editors. Frontiers in cerebral vascular biology: transport and its regulation. New York: Plenum Press; 1993. p. 43–54.
[53] Kogo N, Arita H. In vivo study on medullary H^+-sensitive neurons. J Appl Physiol 1990;69:1408–12.
[54] Lahiri S, Mokashi A, Huang W, Sherpa AK, Di Giulio C. Stimulus interaction between CO_2 and almitrine in the cat carotid chemoreceptors. J Appl Physiol 1989;76:232–8.
[55] Leuson IR. Chemosensitivity of the respiratory center. Influence of CO_2 in the cerebral ventricles on respiration. Am J Physiol 1954;176:39–44.
[56] Loeschcke HH. Central chemosensitivity and the reaction theory. J Physiol (Lond) 1982;332:1–24.
[57] Li A, Randall M, Nattie EE. CO_2 microdialysis in the retrotrapezoid nucleus of the rat increases breathing in wakefulness but not in sleep. J Appl Physiol 1999;87:910–9.
[58] Lipscomb WT, Boyarski LL. Neurophysiological investigations of medullary chemosensitive areas of respiration. Respir Physiol 1972;16:362–76.
[59] Messier ML, Li A, Nattie EE. Inhibition of medullary raphe serotonergic neurons has age-dependent effects on the CO_2 response in newborn piglets. J Appl Physiol 2004;96:1909–19.
[60] Mitchell RA, Loeschcke HH, Massion WH, Severinghaus JW. Respiratory responses mediated through superficial chemosensitive areas on the medulla. J Appl Physiol 1963;18:523–33.
[61] Mueller RA, Towle AC, Breese GR. Supersensitivity to the respiratory stimulatory effect of TRH in 5,7-dihydroxytryptamine-treated rats. Brain Res 1984;298:370–3.
[62] Mulkey DK, Stornetta RL, Weston MC, Simmons JR, Parker A, Bayliss DA, Guyenet PG. Respiratory control by ventral surface chemoreceptor neurons in rats. Nat Neurosci 2004;7:1360–9.
[63] Monteau R, Morin D, Hilaire G. Acetylcholine and central chemosensitivity: in vitro study in the newborn rat. Respir Physiol 1990;81:241–54.
[64] Murphy VA, Johanson CE. Na^{+}-H^{+} exchange in choroid plexus and CSF in acute metabolic acidosis or alkalosis. Am J Physiol 1990;258:F1528–37.
[65] Nattie EE. Brain and cerebrospinal fluid ionic composition and ventilation in acute hypercapnia. Respir Physiol 1980;40: 309–22.
[66] Nattie EE. Ionic mechanisms of cerebrospinal fluid acid–base regulation (brief review). J Appl Physiol 1983;54:3–12.
[67] Nattie EE. Ventilation during acute HCl infusion in intact and chemodenervated conscious rabbits. Respir Physiol 1983;54: 97–107.
[68] Nattie EE. Control and disturbances of cerebrospinal fluid pH. In: Ransom B, Kaila K, editors. pH and brain function. New York: John Wiley and Sons; 1998. p. 629–50.
[69] Nattie EE. Central chemoreceptors, pH, and respiratory control. In: Ransom B, Kaila K, editors. pH and brain function. New York: John Wiley and Sons; 1998. p. 535–60.
[70] Nattie E. CO_2, brainstem chemoreceptors and breathing. Prog Neurobiol 1999;59:299–331.
[71] Nattie E. Multiple sites for central chemoreception: their roles in response sensitivity and in sleep and wakefulness. Respir Physiol 2000;122:223–35.
[72] Nattie EE. Central chemosensitivity, sleep, and wakefulness. Respir Physiol 2001;129:257–68.
[73] Nattie EE, Adams JM. DIDS decreases CSF HCO_3 and increases breathing in response to CO_2 in awake rabbits. J Appl Physiol 1988;64:397–403.
[74] Nattie EE, Giddings B. Effects of amiloride and diethylpyrocarbonate on CSF HCO_3 and ventilation in hypercapnia. J Appl Physiol 1988;65:242–8.
[75] Nattie EE, Li A. Ventral medulla sites of muscarinic receptor subtypes involved in cardiorespiratory control. J Appl Physiol 1990;69:33–41.
[76] Nattie EE, Li A. Lesions in the retrotrapezoid nucleus decrease ventilatory output in anesthetized or decerebrate cats. J Appl Physiol 1991;71:1363–75.
[77] Nattie EE, Li A. Retrotrapezoid nucleus lesions decrease phrenic activity and CO_2 sensitivity in rats. Respir Physiol 1994;97:63–77.
[78] Nattie EE, Li A. Muscimol dialysis in the retrotrapezoid nucleus region inhibits breathing in the awake rat. J Appl Physiol 2000;89:153–62.
[79] Nattie EE, Li A. CO_2 dialysis in the medullary raphe of the rat increases ventilation in sleep. J Appl Physiol 2001;90:1247–57.
[80] Nattie EE, Li A. CO_2 dialysis in the nucleus tractus solitarius region of rat increases ventilation in sleep and wakefulness. J Appl Physiol 2002;92:2119–30.
[81] Nattie EE, Li A. Substance P-saporin lesion of neurons with NK1 receptors in one chemoreceptor site in rats decreases ventilation and chemosensitivity. J Physiol (Lond) 2002;544: 603–16.
[82] Nattie E, Fung ML, Li St A, John WM. Responses of respiratory modulated and tonic units in the retrotrapezoid nucleus to CO_2. Respir Physiol 1993;94:35–50.
[83] Nattie E, Shi J, Li A. Bicuculline dialysis in the retrotrapezoid nucleus (RTN) region stimulates breathing in the awake rat. Respir Physiol 2001;124:179–93.

[84] Nattie EE, Li A, Richerson GB, Lappi DA. Medullary serotonergic neurons and adjacent neurons that express neurokinin-1 receptors are both involved in chemoreception in vivo. J Physiol (Lond) 2004;556:235–53.
[85] Nattie EE, Romer LCSF. HCO_3 regulation in isosmotic conditions: the role of brain PCO_2 and plasma HCO_3. Respir Physiol 1978;33:177–98.
[86] Nishimura M, Johnson DC, Hitzig BM, Okunieff P, Kazemi H. Effects of hypercapnia on brain pHi and phosphate metabolite regulation by 31P-NMR. J Appl Physiol 1989;66:2181–8.
[87] Ohtake PJ, Forster HV, Pan LG, Lowry TF, Korducki MJ, Aaron EA, Weiss EM. Ventilatory responses to cooling the ventrolateral medullary surface of awake and anesthetized goats. J Appl Physiol 1995;78:247–57.
[88] Okada Y, Chen Z, Jiang W, Kuwana S, Eldridge FL. Anatomical arrangement of hypercapnia-activated cells in the superficial ventral medulla of rats. J Appl Physiol 2002;93: 427–39.
[89] Pappenheimer JR, Fencl V, Heisey SR, Held D. Role of cerebral fluids in control of respiration as studied in unanesthetized goats. Am J Physiol 1965;208:436–50.
[90] Pete G, Mack SO, Haxhiu MA, Walbaum S, Gauda EB. CO_2-induced c-Fos expression in brainstem preprotachykinin mRNA containing neurons. Respir Physiol Neurobiol 2002;130: 265–374.
[91] Pineda J, Aghajanian GK. Carbon dioxide regulates the tonic activity of locus ceruleus neurons by modulating a proton- and polyamine-sensitive inward rectifier potassium current. Neuroscience 1997;77:723–43.
[92] Pollay M, Curl F. Secretion of cerebrospinal fluid by the ventricular ependyma of the rabbit. Am J Physiol 1967;213: 1031–8.
[93] Portman MA, Lassen NA, Cooper TG, Sills AM, Potchen EJ. Intra- and extracellular pH of the brain in vivo studies by 31P-NMR during hyper- and hypocapnia. J Appl Physiol 1991;71: 2168–72.
[94] Putnam RW, Filosa JA, Ritucci NA. Cellular mechanisms involved in CO_2 and acid signaling in chemosensitive neurons. Am J Physiol Cell Physiol 2004;287:C1493–526.
[95] Ribas-Salgueiro JL, Gaytán SP, Crego R, Pásaro R, Ribas J. Highly H^+-sensitive neurons in the caudal ventrolateral medulla of the rat. J Physiol (Lond) 2003;549:181–94.
[96] Richerson GB. Response to CO_2 of neurons in the rostral ventral medulla in vitro. J Neurophysiol 1995;36:207–16.
[97] Richerson GB. Cellular mechanisms of sensitivity to pH in the mammalian respiratory system. In: Kaila K, Ransom BR, editors. pH and brain function. New York: Wiley-Liss; 1998. p. 509–33.
[98] Richerson GB, Wang W, Tiwari J, Bradley SR. Chemosensitivity of serotonergic neurons in the rostral ventral medulla. Respir Physiol 2001;129:175–90.
[99] Richerson GB. Serotonin neurons as CO_2 sensors that maintain pH homeostasis. Nat Rev Neurosci 2004;5:449–61.
[100] Rodman JR, Curran AK, Henderson KS, Dempsey JA, Smith CA. Carotid body denervation in dogs: eupnea and the ventilatory response to hyperoxic hypercapnia. J Appl Physiol 2001;91:328–35.
[101] Satinoff E. Neural organization and evolution of thermal regulation in mammals. Science 1978;201:16–22.
[102] Sato M, Severinghaus JW, Basbaum AI. Medullary CO_2 chemoreceptor neuron identification by c-fos immunohistochemistry. J Appl Physiol 1992;73:96–100.
[103] Schielke GP, Betz AL. Electrolyte transport. In: Bradbury MWB, editor. Physiology and pharmacology of the blood–brain barrier. New York: Springer-Verlag; 1992. p. 221–43.
[104] Schielke GP, Moises HC, Betz AL. Potassium activation of the Na,K-pump in isolated brain microvessels and synaptosomes. Brain Res 1990;524:291–6.
[105] Schläfke ME. Central chemosensitivity: a respiratory drive. Rev Physiol Biochem Pharm 1981;90:171–2.
[106] Schläfke ME, Kille JF, Loeschcke HH. Elimination of central chemosensitivity by coagulation of a bilateral area on the ventral medullary surface in awake cats. Pflügers Arch 1979;378: 231–41.
[107] Siesjö BK. The regulation of cerebrospinal fluid pH. Kidney Int 1972;1:360–74.
[108] Smith CA, Saupe KW, Henderson KS, Dempsey JA. Ventilatory effects of specific carotid body hypocapnia in dogs during wakefulness and sleep. J Appl Physiol 1995;79: 689–99.
[109] Smith JC, Morrison DE, Ellenberger HH, Otto MR, Feldman JL. Brainstem projections to the major respiratory neuron populations in the medulla of the cat. J Comp Neurol 1989; 281:69–96.
[110] Smith QR, Rapoport SI. Carrier-mediated transport of chloride across the blood–brain barrier. J Neurochem 1984;42:754–63.
[111] Somero G. Protons, osmolytes, and fitness of internal milieu for protein function. Am J Physiol 1986;251:R197–213.
[112] Spyer KM, Dale N, Gourine AV. ATP is a key mediator of central and peripheral chemosensory transduction. Exp Physiol 2004;89:53–9.
[113] Szentistványi I, Patlak CS, Ellis RA, Cserr HF. Drainage of interstitial fluid from different regions of rat brain. Am J Physiol 1984;246:F835–844.
[114] Taylor NC, Li A, Green A, Kinney HC, Nattie EE. Chronic fluoxetine microdialysis into the medullary raphe nuclei of the rat, but not systemic administration, increases the ventilatory response to CO_2. J Appl Physiol 2004;97:1763–73.
[115] Teppema LJ, Barts PWJA, Folgering HTH, Evers JAM. Effects of respiratory and (isocapnic) metabolic arterial acid–base disturbances on medullary extracellular fluid pH and ventilation in cats. Respir Physiol 1983;53:379–95.
[116] Teppema LJ, Veening JG, Kranenburg A, Dahan A, Berkenbosch AAD, Olievier C. Expression of c-fos in the rat brainstem after exposure to hypoxia and to normoxic and hyperoxic hypercapnia. J Comp Neurol 1997;388:169–90.
[117] Trouth CO, Loeschcke HH, Berndt J. A superficial substrate on the ventral surface of the medulla oblongata influencing respiration. Pflügers Arch 1979;339:135–52.
[118] Vigne P, Champigny G, Marsault R, Barbry P, Frelin C, Lazdunski M. A new type of amiloride-sensitive cationic channel in endothelial cells of brain microvessels. J Biol Chem 1989;264:7663–8.
[119] Wang W, Richerson GB. Development of chemosensitivity of rat medullary raphe neurons. Neuroscience 1999;90: 1001–11.
[120] Wang W, Pizzonia JH, Richerson GB. Chemosensitivity of rat medullary raphe neurones in primary tissue culture. J Physiol (Lond) 1998;511:433–50.
[121] Wang W, Tiwari JK, Bradley SR, Zaykin AV, Richerson GB. Acidosis-stimulated neurons of the medullary raphé are serotonergic. J Neurophysiol 2001;85:2224–35.
[122] Wichser J, Kazemi H. CSF bicarbonate regulation in respiratory acidosis and alkalosis. J Appl Physiol 1975;38:504–11.

This page intentionally left blank

CHAPTER

57

Renal Ammonium Ion Production and Excretion

Norman P. Curthoys

Department of Biochemistry and Molecular Biology, Colorado State University, Fort Collins, Colorado, USA

INTRODUCTION

The maintenance of systemic acid–base balance is essential for survival. Increased renal ammoniagenesis and gluconeogenesis from plasma glutamine constitute an essential physiological response to metabolic acidosis that partially restores acid–base balance.[1–3] Onset of acidosis triggers a rapid and pronounced increase in extraction and catabolism of plasma glutamine within the renal proximal convoluted tubule. The mitochondrial phosphate-activated glutaminase (GA) catalyzes the initial reaction in the primary pathway for the renal catabolism of glutamine and is a key regulator of the increased renal ammoniagenesis and gluconeogenesis.[4] Glutamine extracted by the kidney is both deamidated and deaminated to yield two ammonium ions. The increased renal ammoniagenesis provides an expendable cation that facilitates the excretion of titratable acid while conserving sodium and potassium ions. In rats and humans, the resulting α-ketoglutarate is primarily converted to glucose.[5] This pathway generates HCO_3^- ions that partially compensate the systemic acidosis. During chronic acidosis, this adaptive response is sustained, in part, by cell-specific increases in expression of various enzymes and transport proteins. The adaptive increases in GA and the cytosolic phospho*enol*pyruvate carboxykinase (PEPCK) are paradigms for characterization of the mechanisms that mediate the pH-responsive regulation of renal gene expression. The pronounced increase in GA results from stabilization of the GA mRNA, while the more rapid increase in PEPCK is initiated by activating transcription of the *PCK1* gene[6] and sustained, in part, by a gradual stabilization of the PEPCK mRNA. A decrease in intracellular pH activates multiple signal transduction pathways within proximal tubule cells that mediate the increased expression of PEPCK[7] and the exocytosis[8] and increased expression[9] of NHE3, the apical Na^+/H^+ exchanger. The latter protein contributes to the active translocation of H^+ and NH_4^+ ions into the urine.[10,11] A significant portion of the ammonium ions, generated in the proximal tubule, is subsequently reabsorbed within the medullary thick ascending limb to produce a high interstitial concentration of ammonium ions within the renal medulla.[12] This gradient provides the driving force for the final transport of ammonium ions into the urine that occurs via specific ammonia channels[13] located within the basolateral and apical membranes of the collecting ducts.[14] All of these steps are subject to fine regulation to ensure that the level of renal ammonium ion production and excretion are appropriate to sustain normal acid–base balance. As a result, excess production of acid or insufficient adaptations lead to various pathophysiologies.[15]

ROLE OF RENAL AMMONIUM ION PRODUCTION AND EXCRETION IN THE MAINTENANCE OF ACID–BASE BALANCE

All higher eukaryotes maintain the pH of the extracellular fluid and of various intracellular compartments within narrow limits. For example, in humans, normal arterial plasma pH is set at 7.40 ± 0.04. Blood pH values outside this narrow range define an acidosis ($pH<7.36$) or an alkalosis ($pH>7.44$). The relative concentrations of HCO_3^- and CO_2 are the primary

Seldin and Giebisch's The Kidney, Fifth Edition.
DOI: http://dx.doi.org/10.1016/B978-0-12-381462-3.00057-4

© 2013 Elsevier Inc. All rights reserved.

determinants of plasma pH. The reaction of H^+ with HCO_3^- to form H_2CO_3 has a pK of 6.1 and thus would appear to be a relatively ineffective buffer at pH 7.4. However, the resulting carbonic acid is rapidly equilibrated with CO_2 and H_2O by multiple carbonic anhydrases. The combined reactions provide an effective buffer system due to the ability of the lungs to maintain a constant CO_2 concentration through changes in the rate of respiration. A constant blood pH of 7.40 is produced by maintaining a pCO_2 of 40 mmHg and a blood HCO_3^- concentration of 24 mM. The kidney contributes to the maintenance of a constant blood HCO_3^- concentration by recovering nearly all of the HCO_3^- that is filtered by the glomeruli. In humans, the daily filtered load of HCO_3^- is approximately 4000 mmol.

About 70–80 percent of the filtered HCO_3^- is reabsorbed in the proximal tubule.[16] This process requires the pumping of H^+ ions into the tubular lumen via NHE3, the apical Na^+/H^+ exchanger, and various H^+-ATPases (Figure 57.1). A luminal carbonic anhydrase uses the H^+ ions to protonate the filtered HCO_3^- to form CO_2 and H_2O. After diffusing into the epithelial cells of the proximal tubule, a cytosolic carbonic anhydrase hydrates the CO_2 to reform HCO_3^- and regenerate the excreted H^+ ions. The HCO_3^- ions are then transported across the basolateral membrane by NBC1, a $Na^+/3HCO_3^-$ cotransporter. The overall process of HCO_3^- absorption is inhibited by alkalosis and hypocalcemia and is increased by acidosis, hypercalcemia and by increased levels of angiotensin II.[17] Additional regulation occurs in the distal nephron segments that are responsible for the recovery of the HCO_3^- that remains in the fluid leaving the proximal tubule.[18,19] The type A intercalated cells within the cortical and outer medullary collecting ducts secrete H^+ ions via the apical H^+-ATPase and an electroneutral H^+/K^+-ATPase. The reabsorbed HCO_3^- is subsequently transported across the basolateral membrane by AE1, a HCO_3^-/Cl^- antiporter.

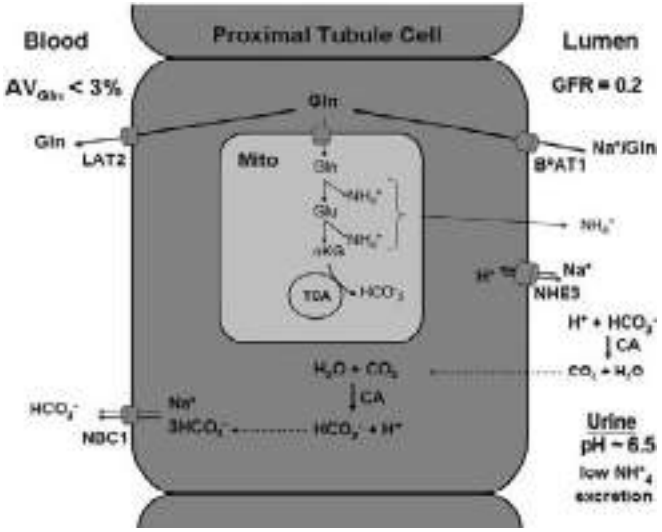

FIGURE 57.1 Pathways of bicarbonate reabsorption and glutamine catabolism within the renal proximal tubule during normal acid–base balance. The glomerular filtrate is slightly acidified by the apical Na^+/H^+ exchanger (NHE3). The translocated H^+ ions titrate most of the filtered HCO_3^- ions producing carbonic acid which is converted to CO_2 and H_2O by the apical carbonic anhydrase (CA). The CO_2 diffuses into the proximal tubule and is hydrated by the cellular carbonic anhydrase (CA) to reform HCO_3^- ions that are then translocated across the basolateral membrane by the $Na^+/3HCO_3^-$ cotransporter (NBC1). The glutamine (Gln) filtered by the glomeruli is transported across the apical membrane by a Na^+-dependent neutral amino acid transporter (B^oAT1). Most of the recovered glutamine is then transported across the basolateral membrane by a Na^+-independent neutral amino acid transporter (LAT2). A small proportion of the recovered glutamine is transported into the mitochondria where it is catabolized to generate the basal level of ammonium ions that are excreted in the slightly acidified urine.

Catabolic pathways result in a net production of volatile and non-volatile acids. The major acid generated as a product of carbohydrate and fat catabolism is CO_2 which is reversibly hydrated to form carbonic acid. A normal individual generates approximately 20 moles of CO_2 per day. However, this acid is volatile and is effectively expelled by the lungs. In contrast, the catabolism of protein also produces non-volatile acids including H_2SO_4 and H_3PO_4. These are strong acids that rapidly dissociate to generate H^+ ions and the corresponding anions. The H^+ ions combine with HCO_3^- to form CO_2 and H_2O. However, this process causes a decrease in blood HCO_3^- concentration and a corresponding decrease in blood pH. The average person eating a western diet generates about 70 mmol per day of nonvolatile acids from the catabolism of proteins and amino acids. To maintain normal acid–base balance, the kidneys of this individual must accomplish the net synthesis of an equivalent amount of HCO_3^- ions.

The renal production of HCO_3^- is primarily accomplished by the extraction and catabolism of plasma glutamine.[2] This process occurs largely within the proximal convoluted tubule and is primarily initiated by the mitochondrial glutaminase (GA) and glutamate dehydrogenase (GDH). The combined reactions accomplish the deamidation and oxidative deamination of glutamine and generate two ammonium ions and α-ketoglutarate:

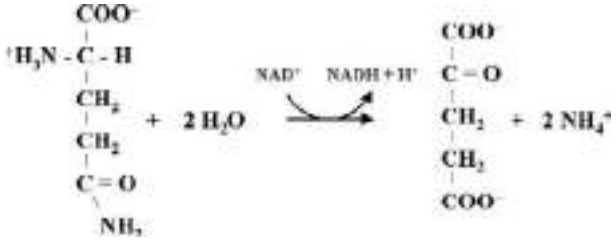

The subsequent conversion of α-ketoglutarate to phospho*enol*pyruvate is accomplished by reactions of the tricarboxylic acid cycle and the phospho*enol*pyruvate carboxykinase (PEPCK). This process also generates two HCO_3^- and two H^+ ions:

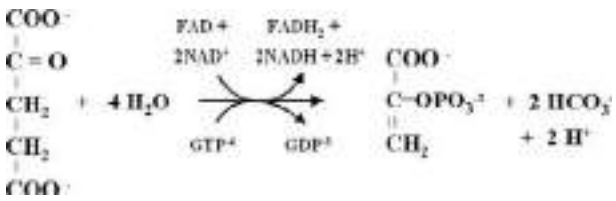

The two H^+ ions that are produced in these reactions are consumed when the phospho*enol*pyruvate is either converted to glucose, a neutral molecule, or is oxidized to CO_2 and H_2O. The net effect of the combined reactions is the catabolism of glutamine to yield two NH_4^+, two HCO_3^- ions, and one-half molecule of glucose. For this process to result in the net production of HCO_3^- ions, the resulting NH_4^+ ions must be excreted in the urine. Ammonium ions that are added to the renal venous blood are utilized in the liver to form urea, a process that consumes HCO_3^- ions.[20] Therefore, the amount of ammonium ions excreted in the urine is equivalent to the net production of HCO_3^- ions by the kidney.

PATHWAYS OF RENAL AMMONIAGENESIS

During normal acid–base balance, the kidneys extract and metabolize very little of the plasma glutamine.[21] The measured rat renal arterial-venous difference is less than three percent of the arterial concentration of glutamine, whereas only seven percent of the plasma glutamine is extracted by the human kidneys even after an overnight fast.[22] Therefore, renal uptake is significantly less than the fraction of plasma glutamine that is filtered by the glomeruli and enters the lumen of the nephron (Figure 57.1). Most of the filtered glutamine is reabsorbed within the proximal convoluted tubule.[23] This uptake is probably mediated by B^oAT1, a Na^+-dependent neutral amino acid transporter that is localized to the apical membrane of the small intestine and the renal proximal tubule.[24] Mutations in the *SLC6A19* gene that encodes this transporter are associated with Hartnup's disorder.[24,25] Most of the recovered glutamine is subsequently transported across the basolateral membrane via the LAT2 isoform (SLC7A8) of the Na^+-independent system L family of amino acid transporters.[26,27] Transporters of this family have a preference for leucine, but also recognize a broad range of neutral amino acids including glutamine. The LAT2 isoform is expressed predominantly in the basolateral membrane of intestinal epithelial cells and the renal proximal tubule.[28] Thus, it functions in the cellular release of glutamine that was absorbed from the intestinal lumen or the glomerular filtrate. However, it also catalyzes an exchange of extracellular and intracellular amino acids[29] that may contribute to basolateral glutamine uptake by intestinal epithelial cells in a post-absorptive state and by the proximal tubule during metabolic acidosis.

Utilization of the small fraction of extracted plasma glutamine requires its transport into the mitochondrial matrix where glutamine is deamidated by a phosphate-activated GA and then oxidatively deaminated by GDH (Fig. 57.1). Glutamine uptake occurs via a mersalyl-sensitive electroneutral uniporter.[30] The mitochondrial glutamine transporter has been purified from rat kidney and was shown by reconstitution in lipid vesicles to be specific for glutamine and asparagine and inhibited by various thiol reagents.[31] Kinetic measurements using isolated rat renal mitochondria indicated that the rate of glutamine transport is not rate limiting for glutamine catabolism.[32,33] However, the basal level of GA is much greater than what is required to accomplish the basal catabolism of glutamine. Therefore, either the activity of the mitochondrial glutamine transporter or the GA must be largely inhibited or inactivated *in vivo* during normal acid–base balance to account for the effective reabsorption of glutamine. Finally, during normal acid–base balance, the urine is only slightly acidified. Thus, only two-thirds of the ammonium ions produced from glutamine are trapped in the tubular lumen and are excreted.[34] The remainder is added to the renal venous blood.

ACUTE REGULATION OF RENAL AMMONIAGENESIS

Acute onset of a metabolic acidosis produces acute alterations in the interorgan metabolism of glutamine[35] which support the rapid and pronounced changes in glutamine catabolism that occur in the kidney (Figure 57.2). Typically, acute acidosis has been induced by stomach loading rats with 2.0 mmol NH_4Cl/100 g body weight.[36] Within 1 to 3 h, the arterial plasma glutamine concentration is increased twofold, primarily due to an increased release of glutamine from muscle tissue.[37] Significant renal extraction of glutamine becomes evident as the arterial plasma concentration is increased.[36] After 3 h, net extraction reaches 25% of the plasma glutamine, a level that slightly exceeds the percent filtered by the glomeruli. Thus, the direction of the basolateral glutamine

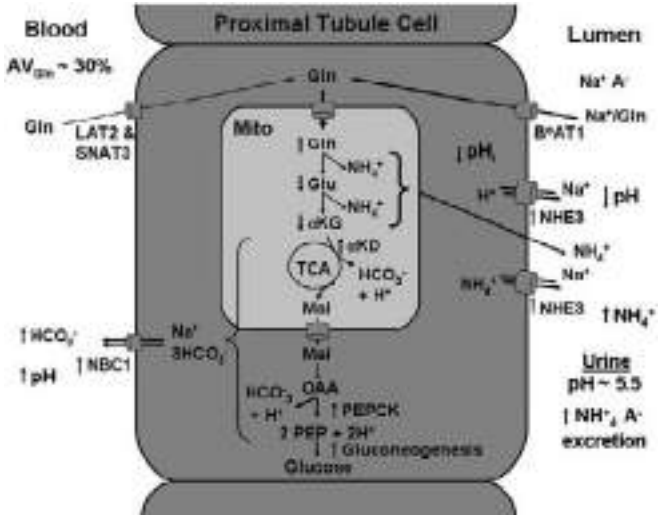

FIGURE 57.2 Pathway of glutamine catabolism within the renal proximal tubule during acute acidosis. The onset of an acute acidosis leads to a rapid reversal of glutamine (Gln) flux across the basolateral membrane that may be due to the exchange activity of LAT2 or the increased expression of SNAT3. Acute acidosis also produces a decrease in intracellular pH (pH_i) that activates flux through the mitochondrial glutamine transporter and α-ketoglutarate dehydrogenase (αKD). The combined effects produce an increase in mitochondrial glutamine and a decrease in glutamate (Glu) and α-ketoglutarate (αKG) levels that increase flux through glutaminase and glutamate dehydrogenase, respectively. The rapid transcriptional activation of the phospho*enol*pyruvate carboxykinase (PEPCK) gene may also contribute to the decrease in cellular glutamate and α-ketoglutarate levels. The acute translocation and activation of NHE3 causes a prompt acidification of the urine and facilitates the apical transport of ammonium ions. The combined increases in renal ammonium ion excretion and gluconeogenesis produce a net synthesis of HCO_3^- ions that are transported across the basolateral membrane by the Na^+-dependent bicarbonate transporter (NBC1).

transport must be reversed in order for the proximal convoluted tubule cells to extract glutamine from both the glomerular filtrate and the venous blood. Adrenalectomized rats exhibit an impaired ability to increase plasma glutamine and to extract glutamine during onset of acute acidosis, suggesting that this response may be mediated, at least in part, by an adrenal hormone.[36] Within 4 h, plasma HCO_3^- decreased from 28 mM to 17 mM, urine pH decreased from 7.2 to 5.8, and renal ammonium ion excretion increased 6-fold.[34] The prompt acidification of the urine may result from the rapid translocation[38] and acute activation[39] of NHE3, the apical Na^+/H^+ exchanger. This process facilitates the rapid removal of cellular ammonium ions[40] and ensures that the bulk of the ammonium ions generated from the amide and amine nitrogens of glutamine are excreted in the urine.

The acute increase in renal ammoniagenesis from plasma glutamine is initiated more rapidly than the adaptive increases in the levels of GA and GDH.[34,41] The rapid increase in ammoniagenesis may result from an acute activation of the mitochondrial glutamine transporter.[42] In addition, the cellular concentrations of glutamate and α-ketoglutarate within the renal cortex are decreased significantly in acute acidosis.[43] The latter compounds are products and potent inhibitors of the GA and GDH reactions, respectively. The decrease in concentrations of the two regulatory metabolites may result from a pH-induced activation of α-ketoglutarate dehydrogenase[43] and the rapid induction of PEPCK.[44,45] The increased level of the latter enzyme would facilitate the cataplerotic removal of intermediates of the tricarboxylic acid cycle. Thus, increased renal catabolism of glutamine initially results from a rapid activation of key transport processes, an increased availability of glutamine, and a decrease in product inhibition of the GA and GDH activities. The net effect is a rapid and pronounced increase in the excretion of ammonium ions and titratable acid in the urine.[34]

Various indirect studies also support the hypothesis that changes in product inhibition may contribute to the acute regulation of renal catabolism of glutamine. For example, inhibition of glutamate uptake both *in vivo*[46] and in renal cell culture[47] reduces the cellular glutamate concentration and stimulates flux through GA leading to increased ammoniagenesis. In addition, a mutation in GDH, that increases *in vivo* activity by reducing GTP inhibition, is responsible for the hyperinsulinism/hyperammonium syndrome.[48] Similarly, systemic activation of GDH can be produced by feeding rats a non-metabolizable analog of leucine that functions as an allosteric activator of GDH. The latter protocol produced a mild hyperammonemia that resulted from a renal specific increase in ammoniagenesis.[49] All of these observations support the concept that acute activation of flux through GA and GDH may contribute to the acute regulation of renal ammoniagenesis.

Only a few studies have characterized the changes in renal glutamine extraction and ammoniagenesis that occur in humans during acute[50] and chronic acidosis.[51] Both studies enrolled hypertensive patients who were undergoing renal vein catheterization to assess plasma renin activity. In the acute study, half of the patients were fed 3 doses of NH_4Cl during the 24 h before catheterization.

This protocol produced a significant decrease in arterial pH (7.41 to 7.33), arterial HCO_3^- (23 mM to 15 mM), and urine pH (5.6 to 4.7), but increased total renal ammonium ion production by only 60%. The acidotic patients exhibited no significant changes in arterial glutamine or renal extraction of glutamine (~6%), but did exhibit an increased extraction of plasma glycine, proline and ornithine.[50] During chronic acidosis, glutamine extraction by the human kidney was

increased even though blood glutamine levels were decreased.[51] The combined data indicate that the mechanism to increase renal catabolism of plasma glutamine is not acutely activated in humans and that amino acids in addition to glutamine may contribute to total renal ammoniagenesis.

CHRONIC ADAPTATIONS TO METABOLIC ACIDOSIS

Role of Increased Gene Expression

During chronic metabolic acidosis, the acute decreases in the renal concentrations of glutamate and α-ketoglutarate are partially compensated and the arterial plasma glutamine concentration is decreased to 70% of normal.[1] However, the kidneys now extract nearly 40% of the total plasma glutamine[21,34] in a single pass through this organ (Figure 57.3). Renal catabolism of glutamine is now sustained by increased expression of the genes that encode various ion transporters and key enzymes of glutamine metabolism.[6] Following onset of acidosis, a rapid induction of PEPCK gene expression occurs only within the S1 and S2 segments of the proximal tubule.[52] The more gradual increase in the levels of the mitochondrial GA[53,54] and GDH[55] also occur solely within the proximal convoluted tubule. Previous micropuncture studies[56] and assays using microdissected nephron segments[57] established that the preponderance of renal ammoniagenesis in normal or acidotic rats occurs within the convoluted portion of the proximal tubule. The decreases in plasma pH and HCO_3^- concentration during metabolic acidosis produce a comparable and sustained decrease in the intracellular pH (pH_i) of the proximal convoluted tubule.[58,59] Thus, the adaptive increases in gene expression may be initiated by a decrease in pH_i. This hypothesis is supported by the findings that similar changes in gene expression occur in response to feeding a high protein diet or chronic hypokalemia, conditions that decrease intracellular pH but produce either no change in extracellular pH or a pronounced alkalosis, respectively.[6,60] The adaptations in GA and PEPCK levels result from increased rates of synthesis of the proteins[61,62] that correlate with comparable increases in the levels of their respective mRNAs.[45,63] However, the increase in GA results from the selective stabilization of the GA mRNA,[64–66] whereas the more rapid increase in PEPCK activity is initiated by enhanced transcription of the *PCK1* gene.[67] The activities of the apical Na^+/dicarboxylate co-transporter, NaDC-1,[68] the mitochondrial glutamine transporter,[42] the basolateral SNAT3 glutamine transporter (SLC38A3),[69] the apical Na^+/H^+ exchanger, NHE3,[9] the basolateral Na^+-$3HCO_3^-$ co-transporter, NBC1,[9] the medullary Na^+K^+-$2Cl^-$ co-transporter,[70] and the ammonia channel, RhCG[71] are also increased during chronic acidosis.

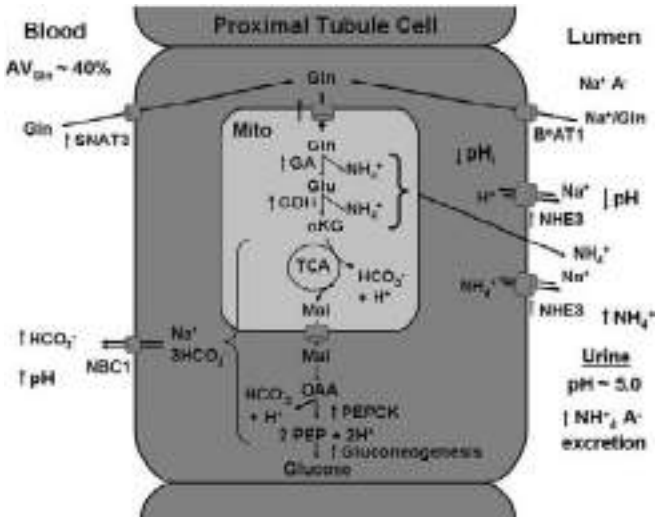

FIGURE 57.3 Pathway of glutamine catabolism within the renal proximal tubule during chronic acidosis. Increased renal catabolism of glutamine is sustained during chronic acidosis by increased expression of the genes that encode glutaminase (GA), glutamate dehydrogenase (GDH), phospho*enol*pyruvate carboxykinase (PEPCK), the mitochondrial glutamine transporter, the apical Na^+/H^+ exchanger (NHE3), and the basolateral glutamine transporter (SNAT3). The increased protein expression is indicated by the arrows. Increased expression of NHE3 contributes to the transport and trapping of ammonium ions in the luminal fluid. The combined increases in renal ammonium ion excretion and gluconeogenesis result in a net synthesis of HCO_3^- ions that are transported across the basolateral membrane by the $Na^+/3HCO_3^-$ co-transporter (NBC1).

The adaptation in the NaDC-1 transporter contributes to an increased reabsorption and metabolism of citrate within the proximal tubule. This reduces the excretion of a weak acid in the urine. Following cellular uptake, citrate is metabolized through one of two pathways, a cytoplasmic pathway involving citrate lyase or a mitochondrial pathway involving the citric acid cycle.[72] During acidosis, the activities of cytoplasmic citrate lyase and mitochondrial aconitase are also increased.[68] Since both pathways generate HCO_3^-, the increased reabsorption of citrate is equivalent to a decrease in base excretion.[60] Enhanced catabolism of citrate also produces substrates that support the increased gluconeogenesis. By contrast, the onset of acidosis produced a decreased transcription of the apical sodium-dependent phosphate transporter, NaPi-II, in rat kidney and in OK cells.[73,74] This adaptation may contribute to an increased excretion of phosphate, a titratable acid. However, the onset of acidosis in mice decreased the expression of NaPi-IIa and NaPi-IIb mRNAs, but increased levels of both isoforms in isolated brush border membranes.[75] Thus, the transient

increase in phosphaturia may be caused by a direct effect of H^+ ion concentration on the activity of the phosphate transporter.

Chronic acidosis also leads to a pronounced increase in the levels of the SNAT3 glutamine transporter (SLC38A3) in rat kidney.[76] Adaptive increases in this transporter also occur in response to chronic dietary potassium restriction and a high protein intake, conditions that also cause an increase in renal ammonia synthesis and excretion.[77] A comprehensive survey of the adaptive response of known amino acid transporters in mouse kidney, demonstrated that only the basolateral SNAT3 transporter exhibits a rapid and pronounced increase in both mRNA and protein levels during onset of acidosis.[78] Surprisingly, expression of the y^+-LAT1 (SLC7A7), a basolateral cationic/neutral amino acid exchanger subunit, was decreased significantly during acidosis. The SNAT3 transporter has a high affinity for glutamine.[79] It was initially cloned by its homology to the vesicular GABA transporter.[80] It catalyzes a Na^+-dependent uptake of glutamine that is coupled to the efflux of H^+ ions.[26,81] However, under physiological conditions, this reaction is reversible. Thus, it can also catalyze H^+ ion uptake coupled to glutamine efflux. In brain, the SNAT3 transporter is expressed primarily in glial cells,[80] while in liver, it is found solely in the perivenous hepatocytes.[82] Under normal acid–base conditions, it is localized solely to the basolateral membrane of the proximal straight tubules within the outer stripe of the outer medulla in rat kidney.[69] All of these cell types express high levels of glutamine synthetase.[83] Thus, the SNAT3 transporter may function primarily to catalyze a pH-dependent release of glutamine. However, during chronic acidosis, increased expression of the SNAT3 transporter occurs primarily in the basolateral membranes of the S1 and S2 segments of proximal tubule, the site of increased glutamine catabolism.[76] Given the sustained increase in H^+ ion concentration within these cells, the increased expression of the SNAT3 transporter is likely to contribute to the basolateral uptake of glutamine. Therefore, the adaptive increase in the SNAT3 transporter may contribute to both the rapid reversal of glutamine transport across the basolateral membrane that occurs during acute acidosis and the elevated and sustained extraction of plasma glutamine during chronic acidosis.

The increase in apical Na^+/H^+ exchanger activity sustains the acidification of the fluid in the tubular lumen and contributes to the active transport of ammonium ions.[8,84] Thus, the increased renal ammoniagenesis continues to provide an expendable cation that facilitates the excretion of titratable acids while conserving sodium and potassium ions. The increased Na^+/H^+ exchanger activity also promotes the tubular reabsorption of HCO_3^- ions. In humans, the α-ketoglutarate generated from glutamine is primarily converted to glucose and to a lesser extent oxidized to CO_2[5]. Either process requires the cataplerotic activity of PEPCK to convert intermediates of the tricarboxylic acid cycle to phospho*enol*pyruvate. This product is either utilized to initiate gluconeogenesis or converted to pyruvate that re-enters the mitochondria and is oxidized to CO_2. However, both pathways generate 2 HCO_3^- ions per mole of α-ketoglutarate. Activation of NBC1, the basolateral $Na^+/3HCO_3^-$ co-transporter, facilitates the translocation of reabsorbed and of *de novo*-synthesized HCO_3^- ions into the renal venous blood. However, this process occurs without an increase in the level of the NBC1 protein.[85] Thus, the combined adaptations also create a net renal release of HCO_3^- ions that contribute to the ability of the kidney to partially restore acid–base balance. In addition to these adaptations, the renal proximal tubule undergoes an extensive hypertrophy during chronic acidosis.[86]

Difference gel electrophoresis along with proteomic and bioinformatic techniques were used to identify proteins that are differentially expressed in the rat renal proximal convoluted tubule during metabolic acidosis.[44] Tubules were prepared by incubation of minced rat renal cortex with collagenase and purified by Percoll density gradient centrifugation.[87] The purity of the isolated proximal convoluted tubules was confirmed by western blot analyses using antibodies to proteins that are expressed only within a single cortical segment of the nephron. This analysis indicated that the purified tubules retained proteins that are expressed only in this segment, but essentially lacked proteins specific for the thick ascending limb, distal tubule, and cortical collecting duct. Nearly 2000 protein spots were resolved when the proximal tubule lysates were fractionated by two-dimensional gel electrophoresis. The protein spots that were differentially expressed were picked and analyzed by mass spectrometry. This analysis identified 21 proteins which are increased between 1.5- and 8.4-fold, including GA (8.4-fold), PEPCK (7.0-fold) and GDH (3.0-fold), and 16 proteins that are decreased between .67- and .03-fold.[44] The observed changes indicate that amino acid catabolism, an ER-stress response, and Ca^{++}-signaling are activated, while conversion of glycine to creatine, oxidation of pyruvate, and fatty acid catabolism are decreased in the proximal convoluted tubule during chronic metabolic acidosis. Many of the observed changes, including activation of an ER-stress response, were confirmed by western blot analysis.

A recent microarray analysis[88] characterized the mRNA isolated from whole kidneys of control mice and of mice that were made acidotic by providing 0.28 M NH_4Cl as the drinking water. After 2 d, this protocol produced a significant acidosis (arterial blood

pH of 7.10 and 12 mM HCO_3^-) that was partially compensated by seven days. Microarray analysis detected 13,000 mRNAs or ~40% of the genes on the mouse genomic array. The levels of 333 mRNAs were up-regulated and another 342 were down-regulated during both acute and chronic acidosis. Cluster analysis indicated that a large proportion of the regulated genes encode solute transporters and proteins involved in cell growth, proliferation, apoptosis, ammoniagenesis, water homeostasis, and energy metabolism. As expected, the mRNAs that encode GA, GDH, PEPCK and the SNAT3 transporter were among those that exhibited the most pronounced increases. The changes in five mRNAs were confirmed by RT-PCR of mRNA isolated from dissected S1 and S2 segments. It remains uncertain which of the other changes occur within the proximal convoluted tubule, within other cell types, or within multiple segments of the nephron. However, this analysis clearly established that expression of a very large number of genes is altered in the kidney in response to acidosis.

Properties of Mitochondrial Glutaminase

The human *GLS1* gene that encodes the kidney-type GA[89] spans 82 kb on chromosome 2, contains 19 exons and uses alternative splicing and different polyadenylation sites to form multiple mRNAs. The human, rat and mouse kidney-type GA genes have identical exon and intron lengths. The primary GA mRNA expressed in rat kidney, termed KGA mRNA, lacks the sequence encoded by exon 15 and utilizes alternative polyadenylation signals to produce a more abundant 5.0-kb and a less abundant 3.6-kb mRNA that encode the same protein sequence.[90] The two mRNAs are coordinately increased and decreased in response to changes in acid–base balance.[45,91] Thus, it is unlikely that differential selection of the polyadenylation site contributes to altered expression of the KGA mRNA. The first sixteen amino acids of this sequence form an amphipathic α-helix that functions as a mitochondrial targeting sequence.[90]

A variant of the human KGA cDNA, termed GAC, was initially cloned from a human carcinoma cDNA library.[92] The human GAC mRNA is formed by splicing together the sequences contained in exons 1 through 15 of the *GLS1* gene, but lacks sequence encoded by exons 16 through 19. As a result, the GAC mRNA contains a unique C-terminal coding sequence and 3′-untranslated region. Both the KGA and GAC mRNAs are highly expressed in human kidney.[92] However, the cell specific expression of the two GA mRNAs in human kidney has not been characterized. The rat and pig orthologs of the human KGA and GAC cDNAs have also been cloned and sequenced.[89] From the cloned sequences, it appears that the KGA and GAC mRNAs contain an identical 5′-sequence and thus may be produced from the same promoter. The unique C-terminal sequences of the two kidney-type GA proteins are highly conserved in the three species, suggesting that they may form distinct functional domains.

Eukaryotic GA has been purified from pig[93] and rat[94] kidney, from pig,[95] rat[96] and cow brain,[97] and from Erlich ascites-tumor cells.[98] All of these protocols were reported before it was realized that multiple isoforms are produced from the KGA gene. Based upon subsequent analysis, it is likely that the purified rat and pig enzymes are predominately the KGA isoform. The enzymes were solubilized from mitochondria by treatment with Triton X-100, freeze-thaw fractionation, or lyophilization in the presence of a borate and phosphate buffer. The solubilized GA undergoes extensive polymerization in the presence of borate and phosphate (MW>10,000,000), whereas dialysis into a Tris-phosphate buffer produces an active tetrameric enzyme with an apparent mass of 250,000 Da. This reversible association-dissociation was used to purify the GA either by repeated precipitation and solubilization or by repeated chromatography on a gel filtration column. Truncated forms of the recombinant GA protein containing an N-terminal His_6-tag have been expressed in bacteria and purified by Ni^+-affinity chromatography.[99] More recently, a highly conserved core fragment of GA (amino acids 221 to 533) has been co-crystallized with bound glutamate. The 3-dimensional structure of this complex is available from the Protein Data Bank (http://www.rcsb.org/pdb/explore/explore.do?structureId=3CZD).

The kinetic properties of the kidney-type GA have been characterized using permeabilized mitochondrial extracts[100,101] or the highly purified enzyme.[93] The GA activity is greatly enhanced by the addition of a broad range of polyvalent anions. The most commonly used activator is phosphate, which produces half-maximal activation at concentrations of 20–30 mM. However, the physiological activator of the GA is unknown. The kidney-type GA exhibits a relatively low K_M for glutamine and is strongly inhibited by glutamate.[101] The K_M for glutamine decreases from 36 to 4 mM as the phosphate concentration is increased from 5 to 100 mM. Glutamate was found to be a competitive inhibitor with respect to glutamine at both high and low concentrations of phosphate. However, the K_I for glutamate increased from 5 to 52 mM with increasing phosphate. These results indicate that glutamine and glutamate interact with the same site, but the conformation and specificity of this site is determined by the concentration of the activator.

The kinetic properties of the GAC variant of the mitochondrial GA have not been characterized. However, a truncated form of recombinant GA that lacks either C-terminal domain retains full activity and similar kinetic properties.[99] Thus, the distinct C-terminal domains of the kidney-type GA may function as protein binding domains that lead to association with an anchoring protein of the inner mitochondrial membrane or with different enzymes of glutamate metabolism. This hypothesis is supported by the finding that the C-terminal domain of the human liver-type GA binds to a unique GA-interacting protein.[102]

The biosynthesis and submitochondrial localization of the rat kidney KGA has been studied extensively. Pulse-chase experiments performed both *in vitro*[103] and in cultured cells[104] established that the rat kidney KGA is translated as a 74-kDa cytosolic precursor that is rapidly translocated into the mitochondrial matrix where it undergoes two sequential processing reactions that are catalyzed by the matrix processing peptidase.[105] The initial reaction removes the N-terminal mitochondrial targeting signal to form a 72-kDa intermediate. This product is subsequently cleaved at either of two sites to form either a minor 68-kDa or the predominant 66-kDa subunit. The deduced sequence of the 66-kDa subunit indicates that mitochondrial KGA lacks a membrane spanning domain or a targeting sequence that would initiate the translocation of the mature subunit to the intermembrane space.[89,90] Submitochondrial fractionation and biophysical studies indicate that the mature GA is either localized in the matrix compartment or loosely associated with the inner surface of the inner mitochondrial membrane.[4] Digitonin and Lubrol fractionation and swell-shrink sonication techniques were used to demonstrate that the rat renal GA is associated with the inner surface of the inner mitochondrial membrane.[106] Similar studies suggested that the rat renal GA is contained primarily within the mitochondrial matrix.[107] Either localization is consistent with the relative concentration of detergent required to release the mitochondrial GA and the inability to inhibit enzyme activity with membrane impermeable sulfhydral reagents and Fab antibodies that rapidly inactivate the solubilized GA.[108]

As a result of the submitochondrial localization of the GA, the catabolism of glutamine requires its initial translocation across the inner mitochondrial membrane. Glutamine uptake in mitochondria isolated from normal rats is mediated through glutamine/glutamate and glutamine/malate antiporters.[109] However, transport of glutamine into mitochondria prepared from acidotic rats occurs through a uniport mechanism[110] that uses a unique carrier.[32,111] Characterization of this process is made difficult by the rapid rate of mitochondrial transport, the high level of GA activity, and the lack of a specific and effective GA inhibitor. Thus, it has not been possible to measure initial rates of glutamine transport in intact mitochondria in the absence of metabolism.[112] However, experiments performed with isolated inner membrane vesicles that lack GA activity also indicate that the activity of the glutamine transporter is increased during both acute and chronic acidosis.[42,30] The rat renal mitochondrial glutamine uniporter has been purified and partially characterized by reconstitution into lipid vesicles.[31] However, neither a cDNA nor the gene that encodes the transporter has been cloned or identified, respectively. Thus, this important step in glutamine metabolism remains poorly characterized.

Stabilization of GA mRNA

The level of GA activity is increased in rat kidney during progressive development of chronic acidosis.[4] In normal rat kidney, the mitochondrial GA is greatest in the distal tubule and collecting duct, intermediate in the proximal convoluted tubule, and very low in glomeruli and the proximal straight tubule.[53,54] Within 1 d following the onset of acidosis, the GA activity is increased 2-fold, but only within the proximal convoluted tubule. Due to the cell specificity of the increase and the greater level of activity associated with distal tubules, 2 to 3 d are required to observe a significant increase in the GA activity measured in a crude homogenate of whole kidney. The total GA activity increases gradually and eventually plateaus after 7 d of acidosis at a value that is 3-fold greater than normal. However, this increase is due to a 7- to 8-fold increase in GA activity[53,54] and protein[44] within the proximal convoluted tubule. This adaptation correlates with the increased renal NH_4^+ ion synthesis that occurs in the proximal convoluted tubule. The physiological function of the non-responsive, but significant levels of GA in the distal segments of the nephron is unknown.

Immunological and pulse labeling experiments established that the increase in renal GA activity is due to the presence of an increased amount of protein[113] that results from a corresponding increase in the relative rate of GA synthesis.[62] However, the increase in GA occurs without an increase in the rate of transcription of the GA mRNA,[45] suggesting that this adaptation is due to a selective stabilization of the GA mRNA. Eukaryotic mRNAs contain a 5′-^{7Me}GpppG cap and a 3′-poly(A) tail that bind initiation factors and poly(A) binding proteins, respectively. Protein-protein interactions between eIF4E and the poly(A) binding protein form a circular structure that stabilizes the mRNA and enhances translation. Rapid degradation of a mammalian mRNA is initiated by the binding of specific

proteins to AU-rich elements within the 3′-UTR.[114–116] The RNA binding proteins recruit a poly(A)-specific deadenylase[117] and the exosome, a complex of 3′→5′ exonucleases,[118] to remove the poly(A) tail and accomplish the rapid 3′→5′ degradation of the deadenylated mRNA. Alternatively, the deadenylated mRNA may undergo decapping and 5′→3′ exonucleolytic degradation. Recent studies have identified cytoplasmic loci termed processing bodies, which contain the decapping enzyme, Dcp1/Dcp2, and a 5′→3′ exonuclease, Xrn1.[119] Thus, processing bodies are thought to constitute the site of 5′→3′ degradation. A third mechanism of mRNA turnover is initiated by sequence-specific endonucleolytic cleavage that generates sites for rapid exonucleolytic degradation by the exosome and the processing bodies.[120]

The presence of a sequence element that regulates the turnover of the GA mRNA was initially demonstrated by stable expression of various β-globin (βG) reporter mRNAs[64] in LLC-PK_1-F^+ cells, a pH-responsive line of porcine proximal tubule-like cells.[121] Expression of the parent βG construct produced a high level of a very stable mRNA ($t_{\{1/2\}}$>30 h). The turnover of the βG mRNA was not affected by transfer of the cells to acidic medium. A second construct, pβG-GA, includes the 956-bp segment that encodes the 3′-nontranslated sequence that is common to the two rat KGA mRNAs that are produced by use of alternative polyadenylation sites. The βG-GA mRNA exhibits a decreased expression that results from its more rapid turnover ($t_{\{1/2\}}$ = 4.6 h). Transfer of the cells expressing this construct to acidic medium resulted in a pronounced stabilization and a gradual induction of the βG-GA mRNA. These studies indicated that the 3′-nontranslated segment contains a pH-responsive instability element (pH-RE).

RNA gel-shift assays established that a direct repeat of 8-base AU sequences within the 3′-UTR of the GA mRNA functions as a specific protein binding site.[66] Site-directed mutation of both 8-base AU-sequences completely abolished protein binding and the pH-responsive stabilization of the βG-GA mRNA.[65] In addition, insertion of a 29-bp segment containing either the direct repeat or a single 8-base AU-sequence was sufficient to impart a 5-fold pH-responsive stabilization to a chimeric βG mRNA. Thus, the 8-base AU-sequence is both necessary and sufficient to function as a pH-RE. Extracts prepared from the renal cortex of rats that were made acutely acidotic exhibit an increased protein binding to the pH-RE.[122] The time course of the increase in binding activity correlated with the temporal increase in GA mRNA.

A tetracycline-responsive promoter system was developed to perform a pulse-chase analysis of the degradation of various chimeric βG mRNAs in LLC-PK_1-F^+ cells.[123] This approach accomplishes the rapid shut-off of the synthesis of a single mRNA and avoids potential indirect effects that may be caused by the use of a general transcription inhibitor.[124] With this approach, the measured half-life of the βG-GA mRNA is 2.9 h in cells maintained in normal medium and is increased >5-fold when the cells are transferred to acidic medium. RNase H cleavage and Northern analysis of the 3′-ends established that rapid deadenylation occurred concomitant with the rapid decay of the βG-GA mRNA in cells grown in normal medium. Stabilization of the βG-GA mRNA in acidic medium is associated with a pronounced decrease in the rate and extent of deadenylation. Mutation of the pH-RE within the βG-GA mRNA blocked the pH-responsive stabilization but not the rapid degradation, whereas insertion of only a 29-bp segment containing the pH-RE was sufficient to produce both rapid degradation and pH-responsive stabilization.

A biotinylated oligoribonucleotide containing the pH-RE was used as an affinity ligand to purify the pH-RE binding protein from a cytosolic extract of rat renal cortex.[125] The purified protein retained the same specific binding properties as observed with crude extracts. Mass spectroscopic analysis of the purified protein identified 11 peptides (~50% sequence coverage) that are identical to tryptic peptides derived from rat ζ-crystallin/NADPH:quinone reductase (ζ-cryst). This identification was confirmed by western blot analysis. In addition, specific antibodies to ζ-cryst blocked the formation of the complex between the pH-RE and either a crude cytosolic extract or the purified protein. Purified recombinant ζ-cryst also binds with high affinity and specificity to the two AU-sequences in the GDH mRNA.[126] Thus, ζ-cryst is the primary protein in extracts of rat kidney cortex that binds to the pH-RE. A second protein purified by the affinity protocol was identified as the T-cell restricted intracellular antigen-related protein (TIAR). This protein functions as the matrix for formation of stress granules[127] that constitute a site for the triage and remodeling of mRNA/proteins complexes in response to multiple stress conditions.[128,129] However, the affinity purified TIAR did not bind to the pH-RE and antibodies to TIAR did not block the binding interaction between the pH-RE and a protein in a cytosolic extract.[125]

To test the function of ζ-cryst binding, adenoviruses were produced that over express mouse ζ-cryst or a shRNA that is specific for the porcine ζ-cryst. Neither a pronounced over expression (50-fold) nor a significant knockdown (85%) of ζ-cryst in LLC-PK_1-F^+ cells had an effect on the normal turnover or the pH-responsive stabilization of the βG-GA mRNA.[130] Thus, ζ-cryst binding is not likely to be the rate limiting or sole factor that accounts for the rapid degradation or the

pH-responsive stabilization of GA mRNA. The process of mRNA stabilization in the proximal tubules may involve additional proteins or redundant pathways, such that the knockdown of ζ-cryst has very little effect on the overall process. Alternatively, the endogenous ζ-cryst may be present in such large excess that a small fraction of the normal level is sufficient to mediate the turnover of the GA mRNA.

RNA gel shift assays demonstrated that the recombinant p40 AUF1 also binds to the pH-RE of the GA mRNA with high affinity and specificity.[123] AUF1 is a known RNA binding protein that interacts with the 3′-UTRs of various unstable mRNAs including c-myc,[131] TNFα,[132] GM-CSF,[133] and COX-2.[134] AUF1 was also identified as hnRNPD,[135] a protein that shuttles between the nucleus and the cytoplasm.[136] Four isoforms of AUF1 (p37, p40, p42 and p45) are produced by alternative splicing of the initial AUF1 transcript.[135] Western blot analysis demonstrated that rat kidney cortex and various kidney cell lines express multiple isoforms of AUF1.[123] Additional experiments have established that recombinant HuR also binds to the pH-RE (unpublished data of Y. J. Lee and N. P. Curthoys). HuR is normally sequestered in the nucleus. However, in response to various stress conditions, HuR is translocated to the cytosol where it binds to AU-rich elements and promotes mRNA stabilization.[137] Recent studies indicate that the nuclear/ctyoplasmic distribution of HuR is determined by its level of phosphorylation.[138] Therefore, AUF1 and HuR may augment or counteract the effect of ζ-cryst and contribute to the regulation of the turnover of the GA mRNA.

Proteomic analysis of rat renal proximal tubules isolated from control and from 1 d, 3 d and 7 d acidotic rats identified two proteins including PEPCK that are fully induced within 1 d and eight proteins that exhibit more gradual induction profiles similar to GA and GDH.[44] All of the mRNAs that encode the latter proteins and the PEPCK mRNA contain an AU-sequence that is highly homologous to the pH-RE found in the GA mRNA. More recent studies have established that a pH-responsive stabilization contributes to the sustained increase in PEPCK mRNA in LLC-PK_1-F^+ cells treated with acidic medium. Thus, selective mRNA stabilization may be the predominant mechanism by which protein expression is increased or sustained in response to acidosis.

Enhanced Expression of PEPCK mRNA

The cytosolic isoform of PEPCK is a primary site of regulation of both hepatic and renal gluconeogenesis.[67] However, this activity is not regulated by allosteric mechanisms or by covalent modifications. Instead, it is regulated solely by mechanisms that determine the level of the PEPCK mRNA and thereby control the level of the PEPCK protein. This is accomplished through changes in either the rate of synthesis or the rate of degradation of the PEPCK mRNA. The *PCK1* gene that encodes the cytosolic PEPCK is composed of 10 exons and 9 introns and is approximately 6 kb in length.[139] It encodes a single 2.6-kb mRNA that is translated into a 69 kDa protein. The level of PEPCK mRNA in rat kidney is increased rapidly following acute onset of acidosis.[45] The increase is initiated within 1 h and reaches a maximum within 7 h at a level that is 6-fold greater than normal. Transcription run off experiments[45] indicated that changes in the relative rate of transcription of the *PCK1* gene account for the initial induction of PEPCK mRNA. Furthermore, the observed changes in PEPCK mRNA levels closely correlated with earlier data that measured changes in the relative rates of PEPCK protein synthesis in normal and acidotic rats.[61] However, the 6-fold induced level of PEPCK mRNA is sustained in rats that are made chronically acidotic even though the relative rate of transcription gradually decreases and plateaus at a level that is only 2-fold greater than observed in normal rats.[91]

Various segments of the PEPCK promoter, as well as the core promoter (-460 to +73 bp) containing specific block mutations in regulatory elements, have been extensively analyzed in transgenic animals to determine their role in controlling *PCK1* gene expression.[140] The wild type core promoter fused to the bovine growth hormone (bGH) gene contains all of the information necessary to insure appropriate expression and hormonal regulation in liver. A larger 2.3-kb segment of the PEPCK promoter was required to drive expression of the transgene in adipose tissue. However, both of these constructs were expressed at low levels in the kidney. In contrast, a CRC362 transgene that contains only 362 bp of the promoter but all of the downstream exons and introns of the rat *PCK1* gene was expressed at normal levels in the kidney.[141] This transgene differed from the endogenous gene only by the substitution of a segment of the chicken *PCK1* gene into the portion of the final exon that encodes the 3′-UTR of the PEPCK mRNA. The latter construct also exhibits a significant renal-specific induction when the transgenic mice were made acidotic.[142] These observations suggest that only 362 bp of the promoter along with an element in a downstream exon or intron is sufficient to recapitulate the pH-responsive induction of the *PCK1* gene.[142]

LLC-PK_1-F^+ cells exhibit a pH-responsive induction of PEPCK mRNA.[143] Previous attempts to identify a pH-responsive element by transient expression of

various PEPCK-chloramphenicol acetyltransferase reporter constructs in LLC-PK_1-F^+ cells produced contradictory results.[144–146] However, these studies clearly established that binding of HNF-1 to the P2 element is essential for basal expression of the renal PEPCK and that this protein:DNA interaction may contribute to increased expression during acidosis. Other experiments have established that in kidney, C/EBP_β[147] and ATF-2[7] bind to the CRE-1 element within the *PCK1* promoter.

Previous studies have also demonstrated that the half-life of the PEPCK mRNA is increased in liver in response to cAMP[148] and glucocorticoids.[149] Increased stability may also contribute to the sustained induction of renal PEPCK mRNA during chronic acidosis.[91] The tetracycline-responsive promoter system was used to quantify the half-life of various chimeric β-globin-PEPCK (βG-PCK) mRNAs in LLC-PK_1-F^+ cells.[150] The βG-PCK-1 mRNA, which contains the entire 3′-UTR of the PEPCK mRNA, was degraded with a half-life of 1.2 h. RNase H treatment indicated that rapid deadenylation occurred concomitant with degradation of the βG-PCK-1 mRNA. Previous studies[151] indicated that PCK-7, a 50-nt segment at the 3′-end of the 3′-UTR, binds an unidentified protein that may contribute to the rapid decay of the PEPCK mRNA. However, the chimeric βG-PCK-7 mRNA has a half-life of 17 h. Inclusion of the adjacent PCK-6 segment, a 23-bp AU-rich region, produced the βG-PCK-6/7 mRNA that has a half-life of 3.6 h. The βG-PCK-3 mRNA that contains the 3′-half of the 3′-UTR was degraded with the same half-life. Surprisingly, the βG-PCK-2 mRNA, containing the 5′-end of the 3′-UTR, was also degraded rapidly ($t_{\{1/2\}} = 5.4$ h). RNA gel-shift analyses established that AUF1 binds to the PCK-7, PCK-6 and PCK-2 segments with high affinity and specificity. Mutational analysis indicated that AUF1 binds to a UUAUUUUAU sequence within PCK-6 and an AU-rich element and adjacent CU-region within a stem-loop structure in PCK-7. The two AU-rich elements are highly conserved in all of the mammalian *PCK1* genes that have been sequenced. Thus, AUF1 binds to multiple destabilizing elements within the 3′-UTR that participate in the rapid turnover of the PEPCK mRNA.

RNA gel-shift assays established that purified recombinant HuR also binds with high affinity and specificity to same AU-rich elements and CU-sequence that bind recombinant p40-AUF1[250]. siRNA knockdown of HuR decreased basal expression and significantly inhibited the pH-responsive increase in PEPCK protein. Therefore, the pH-responsive stabilization of PEPCK mRNA in LLC-PK_1-F^+ cells, and possibly in the renal proximal tubule, may be mediated by a remodeling of the competitive interaction of HuR and AUF1 with the elements that mediate the rapid turnover of the mRNA. Thus, the same mechanism that accounts for the more gradual induction of the GA mRNA may also contribute to the sustained increase in PEPCK mRNA levels during chronic acidosis.

SIGNAL TRANDSDUCTION PATHWAYS THAT MEDIATE THE ADAPTIVE RESPONSES TO ACIDOSIS

Increased Expression of PEPCK

Analysis of the signal transduction pathways that mediate the pH-responsive induction of PEPCK gene expression[6] and the translocation and activation of NHE3[60] provide excellent paradigms to characterize the molecular mechanisms by which proximal tubule cells sense a slight decrease in intracellular pH and rapidly activate renal ammoniagenesis. The transfer of LLC-PK_1-F^+ cells to an acidic medium produced a rapid and pronounced increase in phosphorylation and activation of ERK1/2 and p38 MAPKs.[7] The potential involvement of the MAPK pathways was examined by determining the effects of specific inhibitors on basal and acid-induced PEPCK mRNA levels. SB203580, a specific p38 MAPK inhibitor, produced a dose-dependent inhibition of the pH-responsive induction of PEPCK mRNA and blocked phosphorylation of the downstream transcription factor, ATF-2. By contrast, the ERK1/2 inhibitors, PD098059 and U0126, and the JNK specific inhibitor, curcumin, had no effect on basal or acid-induced PEPCK mRNA levels. The octanucleotide sequence of the CRE-1 site in the PEPCK promoter (TTACGTCA) is a perfect match to the consensus element for binding ATF-2.[152] Gel-shift analysis using a labeled oligonucleotide containing the CRE-1 element produced a band that was partially supershifted with antibodies specific for ATF-2. Subsequent experiments[153] using dominant negative and constitutively active constructs of MKK3 and MKK6, the kinases that are immediately upstream of p38 MAPK, confirmed the role of p38 MAPK in mediating the pH-responsive induction of PEPCK. Thus, the SB-sensitive p38 MAPK/ATF-2 pathway may function as the pH-responsive signaling network for induction of PEPCK mRNA during acidosis.[154] However, the signaling mechanism that functions upstream of p38 MAPK to sense changes in intracellular pH in LLC-PK_1-F^+ cells is unknown. In addition, the pH-responsive increase in GA mRNA levels in LLC-PK_1-F^+ cells is not blocked by SB203580, suggesting that either a kinase upstream of the p38 MAPK or an alternative signaling pathway may mediate this response.[7]

Transforming growth factor-β (TGF-β) is a primary mediator of renal hypertrophy and was hypothesized

to enhance the catabolism of glutamine by activating GA and NHE3 gene expression.[155] Western blot analyses established that TGF-β activated the ERK1/2, p38 MAPK and Smad1/5/8 pathways in LLC-PK$_1$-F$^+$ cells, but not the JNK and Smad2/3 pathways.[156] However, TGF-β caused only a transient increase in PEPCK mRNA levels, but produced a gradual and stable increase in GA mRNA. In addition, the effects of acidic medium and TGF-β were additive. Therefore, TGF-β is not likely to mediate the altered gene expression that occurs following onset of metabolic acidosis.

Translocation and Activation of NHE3

The majority of the apical H^+ ion secretion in the proximal tubule is mediated by NHE3.[157] The development of chronic acidosis produces a gradual increase in total NHE3 protein in the S1 and S2 segments of the proximal tubule and in the medullary thick ascending limb of the rat kidney.[158] The NHE3 abundance is increased 60% by 7 d and nearly 2-fold by 14 d. In the medullary thick ascending limb, NHE3 activity, mRNA levels and protein abundance are increased about 70% during chronic metabolic acidosis.[159] A more rapid response occurs in OKP cells, a clonal line of opossum proximal tubule-like cells. Transfer of OKP cells to an acidic medium produced an increase in NHE3 mRNA levels that was initially detectable at 12 h and that reached a 2-fold increase after 24 h.[160] Interestingly, the abundance of the NHE3 protein within the apical membrane, as measured by surface biotinylation, is increased 2-fold within 6 h of transferring OKP cells to acidic medium.[38] Thus, the increase in apical Na^+/H^+ antiporter abundance precedes the increase in mRNA levels. The associated increase in apical activity is inhibited by ethylisopropylamiloride, an NHE3-specific inhibitor. The acute activation of NHE3 is caused by an increase in the rate of exocytosis and is inhibited by latrunculin B, an inhibitor of microfiliment formation. This process is mediated by a Rho kinase-dependent formation of stress fibers.[161] Therefore, the prompt acidification of the urine during acute onset of acidosis[40] may result from a rapid increase in translocation of the NHE3 protein to the apical membrane.

Treatment of OKP cells with endothelin-1 (ET-1), which binds to ET(B) receptors, also causes a 2- to 3-fold increase in apical abundance of NHE3.[162] This response occurs within 15 min and with no change in the level of total NHE3. Activation of the ET-1 signaling stimulates exocytosis of NHE3 and increases phosphorylation of multiple serine and threonine residues within NHE3.[163] The increase in phosphorylation exhibits a time course, an ET(B) receptor specificity, and a concentration dependence similar to the ET-1 activation of NHE3 translocation, suggesting that the two processes are linked. The potential *in vivo* role of the ET-1/ET(B) receptor signaling pathway in the response to metabolic acidosis was examined using ET (B) receptor deficient mice.[164] Acid ingestion for 7 d increased renal cortical ET-1 mRNA expression 2.4-fold in both wild type and ET(B) receptor deficient mice, but caused a greater acidosis in the homozygous deficient animals. Chronic acidosis also increased apical membrane NHE^3 in wild type, but not in ET(B) deficient mice. The combined studies indicate that increased synthesis of ET-1 and activation of the ET(B) receptor may mediate the increased apical expression of NHE3. Similar studies indicate that the pH-responsive increase in NaDC-1, the apical citrate transporter, is also mediated by the ET-1/ET(B) signaling pathway.[165]

Incubation of MCT cells, an SV40 transformed mouse proximal tubule cell line, in acidic medium for 30−45 sec produced a 2-fold increase in activity of c-Src,[166] a soluble tyrosine kinase. The pH-responsive increase in apical NHE3 activity in OKP cells was selectively inhibited by herbimycin A, a tyrosine kinase inhibitor, and by overexpression of carboxyl-terminal src kinase (csk), a physiological inhibitor of c-Src.[167] Additional studies demonstrated that expression of a dominant negative c-Src construct prevented the increase in NHE3 activity.[168] These observations indicate that a decrease in pH_i leads to rapid activation of c-Src and that the family of soluble protein tyrosine kinases plays a key role in the pH-responsive translocation of NHE3. More recent studies have identified Pyk2, a member of the focal adhesion kinase family of tyrosine kinases, as the upstream activator of c-Src.[169] Incubation of OKP cells in acidic medium caused a rapid, but transient increase in phosphorylation of Pyk2. Expression of a dominant negative form of Pyk2 or a Pyk2-specific siRNA blocked activation of c-Src and the downstream increase in NHE3.

Isolated Pyk2 is phosphorylated and activated *in vitro* by treatment with a slightly acidic medium.[169] The data suggest that autoactivation of Pyk2 may function as the sensor of a slight decreases in pH_i and initiate the downstream events that lead to increased expression of NHE3.[170] However, the principle effect of the *in vitro* activation is to decrease the K_M of Pyk2 for ATP from 129 μM to 51 μM. As a result, the pH-responsive activation of Pyk2 was only observed using 10 μM ATP as the substrate. Therefore, to function as an *in vivo* pH-sensor, Pyk2 must be localized to a region of the cell that maintains a lower than normal level of ATP.[60] The Pyk2 pathway is also involved in activation of basolateral HCO_3^- secretion.[171]

The combined studies suggest that activation of Pyk2 and c-Src function upstream of the increased synthesis and release of ET-1 that in turn binds to the ET(B) receptor and activates the translocation of NHE3.[60]

Treatment of MCT cells with acidic medium also causes a rapid activation of the ERK1/2 MAPK pathway that may activate transcription of multiple immediate early response genes, including *c-fos*, and *c-jun*.[172] This response is not blocked by inhibitors of Pyk2/c-Src/ET-1 pathway. However, the ERK1/2 inhibitor, PD98059, does inhibit the pH-responsive activation of NHE3.[168] Therefore, cross-talk between the two independently activated pathways may be required to activate the transcription and release of ET-1 that initiates the translocation and increased apical expression of the NHE3.[60]

The pH-responsive induction of PEPCK is not blocked by tyrosine kinase inhibitors.[7] Thus, it is unlikely that the Pyk-2/c-Src/ET-1 pathway contributes to increased expression of PEPCK. Therefore, multiple signaling pathways may be activated in response to a decrease in pH_i. Alternatively, the two pathways were characterized primarily in porcine and opossum kidney cells, respectively. Thus, different species may utilize different signaling pathways to mediate the adaptive response to acidosis. The physiological response of the kidney to metabolic acidosis has not been characterized in either the pig or the opossum. Therefore, further analysis of the signaling pathways should utilize a more physiologically relevant model system.

COUNTERCURRENT TRANSPORT OF AMMONIUM IONS

Secretion of Ammonium Ions within the Proximal Tubule

Initial micropuncture studies established a strong correlation between the level of ammonium ions in the luminal fluid of the late proximal convoluted tubule and the level of renal ammonium ion excretion.[173,174] Subsequent studies using dissected tubular segments indicated that the bulk of the ammonium ions produced by the kidney are synthesized in the proximal convoluted tubule.[57] Therefore, secretion into the luminal fluid of the proximal tubule is the initial step in renal excretion of ammonium ions. It was initially hypothesized that this process occurred by diffusion trapping.[175] This model assumes that the concentrations of ammonium ions (NH_4^+) and ammonia (NH_3) are maintained in equilibrium and that biological membranes allow the rapid diffusion of ammonia, but exhibit low permeability to ammonium ions. As a result, ammonia would rapidly equilibrate across the membrane and ammonium ions would accumulate in a compartment that exhibits a decreased pH. Thus, acidification of the luminal fluid would provide a sufficient driving force to account for tubular secretion and excretion of ammonium ions. While diffusion trapping clearly contributes to renal excretion, the transport of both ammonia and ammonium ions are now known to be mediated by specific proteins.

In the early portion of the proximal tubule, the preferential secretion of ammonium ions into the luminal fluid occurs before the development of a significant pH gradient.[176] The pH gradient in this portion of the nephron, as measured by *in vitro* microperfusion, is not sufficient to account for the observed ammonium ion secretion.[177] A significant portion of the measured ammonium ion secretion was inhibited by amiloride and this effect was only partially reversed by lowering the pH of the luminal perfusate.[11] These observations suggest that luminal secretion of ammonium ions is mediated, in part, by NHE3, the apical Na^+/H^+ exchanger. Experiments performed with isolated brush border membrane vesicles also indicated that ammonium ion transport can occur via the apical Na^+/H^+ exchanger.[10] However, both the basolateral and the apical membranes of the proximal tubule exhibit a high permeability to ammonia.[178] Additional studies demonstrated that ammonia entry into the lumen of the proximal tubule is affected by luminal pH and by the flow rate.[179] Thus, transport via NHE3 may be the dominant mechanism of ammonium ion secretion within the S1 segment, the initial portion of the proximal convoluted tubule, whereas diffusion and trapping of ammonia may be the primary mechanism within the S2 segment where significant acidification of the luminal fluid has occurred.

The rat S3 segment, the terminal straight portion of the proximal tubule, has a very low level of mitochondrial GA activity[53] and thus is unlikely to be a major site of ammoniagenesis. However, this segment, which extends into the outer stripe of the outer medulla, may participate in transepithelial transport of ammonium ions. Countercurrent transport of ammonium ions produces a high interstitial concentration within the medulla. As a result, basolateral uptake may result from the binding of NH_4^+, in place of K^+, to the basolateral Na^+/K^+-ATPase.[180] Subsequent apical secretion may occur via diffusion and trapping of ammonia within the acidified luminal fluid. Recycling at this site may contribute to the maintenance of the zonal gradient of ammonium ions.

Renal ammonium ion production and excretion are inversely affected by the concentration of K^+ ions.[181,182] Hypokalemia is associated with an increase in ammonium ion production that leads to an

increased excretion in spite of an increase in urinary pH. In contrast, hyperkalemia suppresses renal ammonium ion excretion. Microperfusion studies performed with isolated mouse S2 segments indicate that altered K^+ ion concentration has opposing effects on ammonium ion production by the proximal tubule.[183] Reduced K^+ ion concentrations enhanced ammonium ion production, whereas elevated K^+ concentrations inhibited production. These results are consistent with the observed effects of hypo- and hyperkalemia. However, reduced K^+ ion concentrations reduced proximal tubular ammonium ion secretion, whereas net secretion was unchanged with elevated K^+ ion concentrations. Thus, altered K^+ ion concentration must also affect the transport of ammonium ions that occurs within the loop of Henle and the collecting ducts.

Microperfusion studies also indicate that production and secretion of ammonium ions within the proximal tubule is regulated, in part, by angiotensin II.[184] Addition of physiological concentrations of angiotensin II to the basolateral surface of mouse S2 segments produced an increase in intracellular Ca^{++}, stimulated ammonium ion production, and enhanced luminal acidification.[185] However, unexpectedly, luminal secretion of ammonium ions was inhibited slightly. In contrast, the addition of angiotensin II to the luminal perfusate produced a similar increase in ammonium production, but stimulated an amiloride-sensitive increase in ammonium ion secretion in parallel with the increase in luminal acidification.[186] The effects of luminal angiotensin II were blocked by saralasin, an angiotensin II receptor inhibitor, and by nifedipine, a calcium channel blocker.

Additional studies were performed to compare the effects of luminal angiotensin II on ammonium ion secretion in perfused S2 tubules that were isolated from normal and acutely acidotic mice.[187] Tubules isolated from acutely acidotic mice exhibit an adaptive increase in ammonium ion secretion that was blocked when losartan was co-administered during the induction of acidosis. The addition of angiotensin II to the luminal fluid enhanced ammonium ion production and secretion to a greater extent in tubules isolated from the acidotic mice compared to normal mice. The stimulatory effects of angiotensin II were also blocked by losartan. Similar results were obtained using microperfused S2 segments obtained from mice feed NH_4Cl for 7 d.[188] In the latter studies, losartan also blocked the acid-induced apical expression of NHE3, but had no effect on the increased expression of GA or PEPCK. Recent studies also demonstrated that acute feeding (18 h) of NH_4Cl produced a 2-fold increase in total and apical surface expression of AT(1), the type 1 angiotensin II receptor.[189] The acute increase in cell surface expression of AT(1) was reproduced by treatment of cultured mouse S1 proximal tubules cells with an acidic medium for two hours and was blocked by colchicine. The combined data suggest that angiotensin II may play an important role in the adaptive increase in proximal tubular ammonium ion production and secretion by stimulating NHE3 translocation during the acute onset of acidosis. However, the effect of angiotensin II is not specific for NHE3. Infusion of angiotensin II in rats caused an acute (20 min) increase in the translocation of multiple proteins from subapical cytoplasmic vesicles to the apical brush border membrane.[190]

Reabsorption of Ammonium Ions in the Medullary Thick Ascending Limb

Microperfusion studies demonstrated that ammonium ions are reabsorbed from the luminal fluid between the proximal tubule and the accessible portion of the distal convoluted tubule.[74,96] However, the descending and ascending thin limbs of the loop of Henle exhibit high permeabilities for both ammonia and ammonium ions.[191,192] Therefore, this segment probably functions to equilibrate the ammonium ions within the interstitial space and the luminal fluid. Such a process could contribute to the countercurrent multiplication by recycling ammonium ions that have accumulated within the medulla. The primary site of ammonium ion reabsorption is the thick ascending limb of the loop of Henle.[193] Between 40 and 80% of the ammonium ions contained within the terminal portion of the proximal convoluted tubule are reabsorbed within this segment.[56] This process generates the corticomedullary concentration gradient that facilitates the final transport of ammonium ions into the collecting duct and their excretion in the urine.

The medullary thick ascending limb is a further site of luminal fluid acidification and HCO_3^- reabsorption. The developing pH gradient would favor the further translocation of ammonium ions into the luminal fluid. Therefore, reabsorption within this segment is not mediated by diffusion and trapping of ammonia. The addition of NH_4Cl to most cells causes a rapid alkalinization of the cytosol due to the more rapid entry of ammonia that is subsequently protonated and thereby reduces the intracellular concentration of H^+ ions. In contrast, the addition of NH_4Cl to the luminal surface of the medullary thick ascending limb causes a rapid acidification of the cytosol1.[195] This observation suggests that the apical membrane of the thick ascending limb is relatively impermeable to ammonia, while ammonium ions are rapidly and selectively transported into the cell. Some of the entering ammonium ions undergo rapid deprotonation to increase the

concentration of H^+ ions. Numerous studies have demonstrated that ammonium ion reabsorption by the thick ascending limb is sensitive to furosemide and is inhibited by K^+ ions.[196] Studies with apical membrane vesicles prepared from medullary thick ascending limbs also demonstrated that ammonium ions stimulated a bumentanide-sensitive Na^+ uptake and inhibited a bumentanide-sensitive rubidium ion flux.[197] These observations are consistent with ammonium ion transport via the apical Na^+-K^+-$2Cl^-$ cotransporter, BSC1/$NKCC_2$. Inhibitor studies suggest that in normal acid–base balance approximately two-thirds of the ammonium ion reabsorption within the thick ascending limb balance is mediated by BSC1/$NKCC_2$. Hyperkalemia also causes a reduction in ammonium ion reabsorption within the thick ascending limb and a reduced medullary interstitial concentration of ammonium ions.[198] Competition between NH_4^+ and K^+ ions for binding to the BSC1/$NKCC_2$ transporter could account for the reduction in ammonium ion excretion that is associated with hyperkalemia.[199] The remainder of the ammonium ion uptake within the thick ascending limb may occur via a barium- and verapamil-sensitive electroneutral K^+/NH_4^+ antiporter[200] that is localized within the apical membrane.[201]

The medullary thick ascending limbs express both an apical (NHE3) and basolateral (NHE1) Na^+/H^+ exchanger. NHE3 may contribute to the acidification of the luminal fluid and reduce the intracellular acidifying effect of the rapid entry of ammonium ions.[202] In isolated perfused tubules, the transepithelial transport of HCO_3^- ions is inhibited by addition of amiloride to the basolateral, but not the luminal surface of the thick ascending limb.[203] Thus, the NHE1 may contribute to the reabsorption of HCO_3^- ions.

During metabolic acidosis, the medullary thick ascending limb exhibits an increased rate of ammonium ion reabsorption.[204] This increase results from increased delivery from the proximal tubule and an adaptive increase in the level of the BSC1/NKCC2 transporter.[205] Incubation of isolated rat medullary thick ascending limb segments in an acidic medium produced a nearly 2-fold increase in BSC1/$NKCC_2$ transport activity and a corresponding increase in BSC1/NKCC2 mRNA and protein levels. Similar adaptations were observed in medullary thick ascending limb segments that were isolated from chronically acidotic rats. This adaptive increase is not mediated by increased transcription, but is due to selective stabilization of the BSC1/$NKCC_2$ mRNA.[70] This response requires the 3′-UTR of the BSC1/$NKCC_2$ mRNA, which contains four AU-rich sequences in which 7 of the 8 nucleotides are identical to the pH-REs that mediate the adaptive increases in GA and GDH mRNAs.[6] More recent experiments[206] have demonstrated that deletion of a single AU-rich sequence (ARE3) was sufficient to block the pH-responsive increase in BSC1/NKCC2 mRNA. Mouse TAL cells exhibit a two-fold increase in ζ-cryst when the cells are treated with an acidic medium. Over expression of mouse ζ-cryst also resulted in an increased level of wild type BSC1/$NKCC_2$ mRNA, but not the construct lacking ARE3. In addition, cells that over express ζ-cryst failed to exhibit a further increase in BSC1/NKCC2 mRNA when treated with acidic medium. Finally, siRNA knockdown of ζ-cryst (by 60%) reduced the basal level and completely abolished the pH-responsive increase in BSC1/$NKCC_2$ mRNA. Thus, this study provides convincing evidence that ζ-cryst plays an essential role in determining the level of BSC1/$NKCC_2$ mRNA in TAL cells.

Chronic metabolic acidosis also causes an adaptive increase in NHE3 mRNA and protein levels in the rat medullary thick ascending limb.[159] The mechanism and significance of this adaptation is uncertain, since selective inhibition of the apical Na^+/H^+ exchanger has no effect on ammonium ion reabsorption.[202] However, this adaptation may contribute to the increased HCO_3^- reabsorption that occurs within the thick ascending limb during acidosis.[194]

EXCRETION OF AMMONIUM IONS

Approximately 80% of the excreted ammonium ions are translocated across the cells of the collecting duct. The various segments of the collecting duct exhibit a very low permeability to ammonium ions, but are highly permeable to ammonia.[207] A portion of this secretion occurs within the cortical collecting duct[56] even though the interstitial concentration of ammonium ions within the cortex is relatively low. The mechanism for uptake of ammonium ions into the epithelial cells of this segment is not well defined. The observation that ammonium secretion by the cortical collecting duct is not inhibited by ouabain suggests that this transport is not mediated by the basolateral Na^+/K^+-ATPase.[194] However, this protein may contribute to ammonium ion uptake within the inner medulla where the interstitial concentration of ammonium ions is sufficient to effectively compete with K^+ ions for binding to the Na^+/K^+-ATPase.[208] A basolateral K^+/NH_4^+ antiporter has been defined in cultured mouse inner medullary collecting duct cells, but not in isolated segments.[209] Finally, a Na^+-K^+-$2Cl^-$ cotransporter, BSC2/NKCC1, has been immunolocalized to the basolateral membranes of the α-intercalated cells of the outer and initial inner medullary collecting ducts of the rat[210] and the terminal portion of the inner medullary collecting ducts of the mouse.[211] The observation that expression of BSC2/NKCC1 is increased in the rat

collecting duct during chronic acidosis suggests that this transporter may contribute to the basolateral uptake of ammonium ions.[212]

The process of apical secretion of ammonia is tightly coupled to the process of luminal acidification.[213] Within the rat, the cortical and outer medullary segments of the collecting duct lack a luminal carbonic anhydrase.[214,215] Thus, the combination of the secreted H^+ and luminal HCO_3^- ions results in the formation of carbonic acid that slowly dissociates to form CO_2 and H_2O. The resulting disequilibrium in carbonic acid produces a greater luminal acidification that contributes to the trapping of ammonia. Evidence for this hypothesis was obtained by the observation that infusion of carbonic anhydrase markedly reduces ammonium ion secretion in the cortical collecting duct.[213] During chronic acidosis, there is a marked increase in ammonium ion secretion along the entire length of the collecting duct.[56] This increase is paralleled by a corresponding increase in acid secretion. Within the inner medullary collecting duct, the increased luminal acidification is primarily mediated by an H^+/K^+-ATPase.[216] Consistent with this conclusion, intercalated cells from mice deficient in the alpha(1) and alpha(2) subunits of the H^+/K^+-ATPase exhibit a reduced acid excretion.[217]

The mammalian genome encodes a family of ammonia transport proteins, two of which participate in renal ammonium ion excretion.[218,219] Initially, the erythroid Rh antigen, Rh associated glycoprotein (RhAG), was shown to have structural homology to the family of yeast and plant ammonia transport proteins.[220] Subsequent cloning led to the identification of two additional mammalian homologs, RhBG and RhCG, that are selectively expressed in tissues that transport ammonia.[221] In the rat kidney, RhBG is expressed in the basolateral membrane of the distal convoluted tubule, the connecting segment and the cortical collecting duct.[222] Within the outer and inner medullary collecting ducts, RhGB expression appears to be limited to the α-intercalated cells that are involved in acid secretion. In the mouse, the pendrin-positive β-intercalated cells, which mediate HCO_3^- secretion during alkalosis, do not express basolateral RhBG immunoreactivity.[223] RhCG has an identical distribution along the rat nephron except that it was initially localized to the apical membrane.[224] However, more recent studies indicate that RhCG is expressed in both the basolateral and apical membranes.[225] Within the collecting duct, expression of both RhBG and RhCG is greater in the α-intercalated cells than in the principal cells.[223,224] Because the former cells are the primary site of H^+ ion secretion within the collecting duct, the disequilibrium decrease in luminal pH would be greatest in the region adjacent to the apical membrane of the α-intercalated cells. The high levels of the two ammonia transporters in these cells would facilitate the rapid transport and subsequent luminal trapping of ammonia.[14]

The X-ray crystallographic structure of an ammonia channel, the AmtB protein from *E. coli*, was recently solved at a 1.35 Å resolution.[226] The integral protein has 11 membrane-spanning α-helices. It also contains a vestibule that recruits ammonium ions, a binding site for an NH_4^+ ion, and a 20 Å long hydrophobic channel that lowers the pK_a for ammonium ions from 9 to less than 6. The channel conducts ammonia by forming favorable hydrogen bonding interactions with specific histidine residues that are conserved in all members of the family of ammonia transporters including the mammalian RhBG and RhCG proteins.[226] Thus, the latter proteins are also likely to function as specific channels to facilitate the rapid diffusion of ammonia.[13] While most membranes exhibit moderate permeability to ammonia, the expression of an ammonia channel would accelerate ammonia transport at sites where diffusion through the bilayer is slow relative to the physiological need. The cell specific expression of RhBG and RhCG within the kidney and in various non-renal tissues is consistent with this hypothesis.

Initial studies indicated that the cellular content and localization of RhBG are unaltered by development of chronic acidosis.[227] Furthermore, the total knockout of the *RhBG* gene had no apparent effect on systemic ammonium ion metabolism or ammonia permeability in isolated perfused collecting ducts.[228] In addition, the knockout mice responded to a chronic acid challenge with an appropriate increase in ammonium ion excretion. Thus, it was concluded that RhBG is not essential for the physiologic transport of ammonia, but may instead function as an ammonia sensor.[229] However, a more recent study demonstrates that the level of RhBG is increased in both the cortex and outer medulla in response to a metabolic acidosis that is induced by HCl administration.[230] In addition, mice which lack RhBG only in intercalated cells exhibit normal acid–base parameters and normal levels of ammonium ion excretion when fed a standard diet. However, mice with the cell-specific knockout exhibit a decreased response in ammonium ion excretion during early onset of metabolic acidosis, but not after 5 d of acid feeding. Therefore, the RhBG expressed in the intercalated cells may contribute to increased ammonium ion excretion during onset of acidosis. Previous studies established that mice exhibit a decrease in glutamine synthetase levels during metabolic acidosis.[231] Surprisingly, the intercalated cell specific knockout of RhBG resulted in a decreased expression of glutamine synthetase during normal acid–base balance and a greater than normal decrease following 5 d of metabolic acidosis.[230] Thus, the greater decrease in glutamine synthetase may

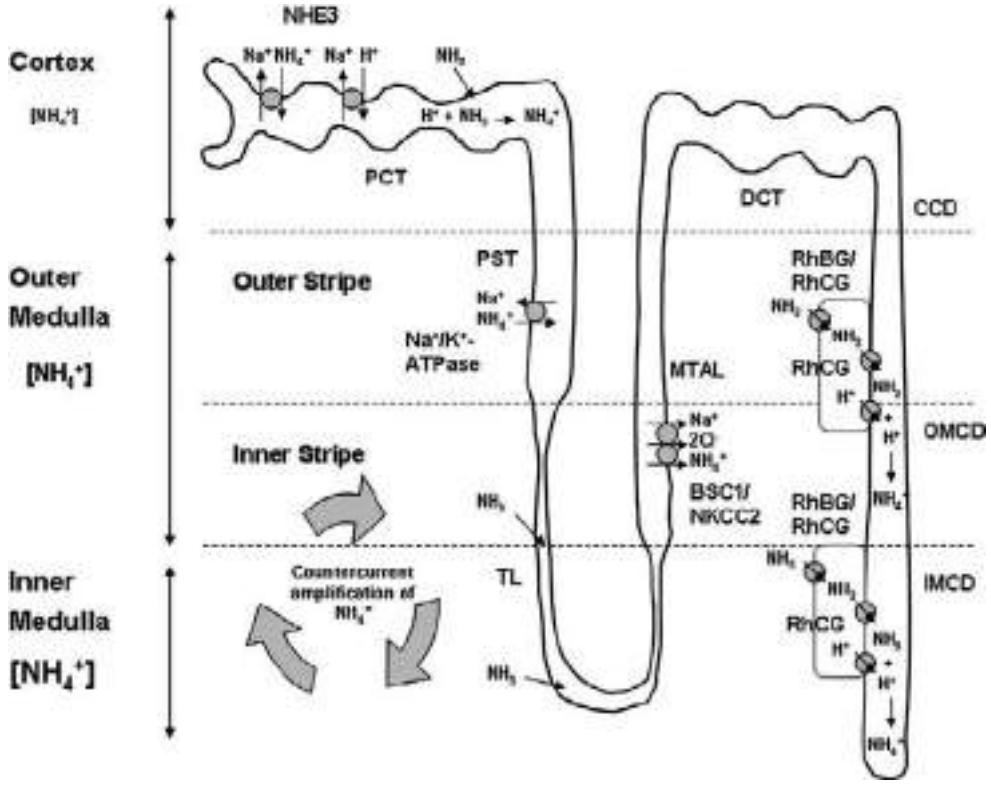

FIGURE 57.4 Primary sites and mechanisms of ammonium ion transport within the kidney. Ammonium ion transport in the proximal tubule is primarily mediated by NHE3, the apical Na^+/H^+ exchanger, by ammonia diffusion and trapping, and by the basolateral Na^+/K^+-ATPase. The formation of a corticomedullary gradient of ammonium ions is accomplished primarily by the secondary active transport of ammonium ions out of the medullary thick ascending limb by the apical Na^+-K^+-$2Cl^-$ cotransporter, BSC1/NKCC2, and by the reentry of ammonia within the thin limb of the loop of Henle. The transport of ammonia within the collecting duct is mediated primarily by the basolateral (RhBG & RhCG) and apical (RhCG) ammonia channels and by the trapping of ammonium ions in the acidified luminal fluid. The various segments of the nephron are abbreviated as: PCT, proximal convoluted tubule; PST, proximal straight tubule, TL, thin limb of the loop of Henle; MTAL, medullary thick ascending limb; DCT, distal convoluted tubule; CCD, cortical collecting duct; OMCD, outer medullary collecting duct; and IMCD, inner medullary collecting duct.

contribute to the appropriate level of ammonium ion excretion observed in the knockout mice when fed a normal diet or when fully adapted to a chronic acidosis.

Immunostaining[71] and immunogold-labeling[227] experiments indicate that the levels of RhCG are selectively increased in the apical membrane during chronic acidosis. The observed increases occur without a corresponding increase in RhCG mRNA and may result from increased apical targeting or the selective expansion of the apical membrane in the intercalated cells of the medullary collecting duct. Mice lacking RhCG exhibit abnormal urinary acidification and reduced ammonium ion excretion during NH_4Cl-induced metabolic acidosis.[232] Microperfused collecting ducts isolated from acidotic *RhCG*$^{(-/-)}$ mice exhibit reduced ammonia permeability and transepithelial transport. Similar defects were observed when RhCG was knocked out only the collecting duct[233] or the intercalated cells.[234] The combined data indicate that RhCG expression in both types of cells is necessary to produce the appropriate increase in renal ammonium ion excretion during metabolic acidosis.

The overall process of proximal tubular secretion of ammonium ions, reabsorption with the medullary thick ascending limb, and re-entry of ammonia in the collecting duct is summarized in Figure 57.4.

PATHOPHYSIOLOGY

The overall process of renal ammonium ion synthesis and excretion is both complex and finely regulated. It is exquisitely designed to generate an amount of HCO_3^- ions that is equivalent to the daily production of non-volatile acids. The primary pathway of HCO_3^- and ammonium ion synthesis within the proximal tubule is well delineated. In addition, considerable progress has been made in understanding how the expression of genes that encode key enzymes and

transporters is regulated during chronic acidosis. However, knowledge of the acute mechanisms that rapidly sense relatively minor changes in intercellular pH and activate specific signaling pathways to produce appropriate changes in ammonium ion production and transport and achieve the correct level of ammonium excretion is less satisfying. A major deficiency is the lack of knowledge of the molecular mechanism of mitochondrial glutamine transport and the regulation of this key step in ammoniagenesis.

In humans, the level of ammonium ion excretion is increased at least 5-fold in response to chronic acidosis.[235] However, pronounced renal insufficiencies in humans result in a proportionate reduction in ammonium ion production and excretion.[236] Various investigators demonstrated that in rats a 65–80% ablation of the kidneys is necessary to produce a reduction in total ammonium ion excretion and a reduced response to a high protein diet[237] or acid load.[238] However, even with this level of ablation, the ammonium ion production per remaining nephron is increased to partially compensate for the loss of renal tissue.[238,239] Thus, the processes of renal ammoniagenesis and excretion exhibit a high capacity and broad adaptive range.

The ability of the kidneys to contribute to acid–base balance by excreting the appropriate level of ammonium ions is also significantly influenced by various hormones including glucocorticoids,[240] endothelin[60] and the aldosterone/angiotensin system.[241] Glucocorticoids are essential to produce the appropriate increases in PEPCK[61] and SNAT3, the basolateral glutamine transporter.[242] In addition, glucocorticoids,[243] endothelin[60] and angiotensin II[188] enhance the translocation of NHE3 to the apical membrane. Furthermore, K^+ ion homeostasis1[82] also affects acid–base balance, in part, from the fact that NH_4^+ and K^+ ions compete for binding to a number of transport proteins and, in part, from the effect of extracellular K^+ ion concentration on intercellular pH. As a result, various conditions that result in adrenal insufficiency,[240] altered angitensin II levels,[241,244] hyperkalemia[245,246] and hypokalemia[247] can adversely affect renal ammonium ion excretion and acid–base balance. An impaired ability to acidify the luminal fluid, due to defects in H^+ transporters or a back leak of H^+, results in an inappropriate level of ammonium ion secretion and causes a distal renal tubular acidosis. In contrast, proximal renal tubular acidosis is produced by a defect in HCO_3^- reabsorption within the proximal tubule. This condition also causes a decrease in ammonium ion production due to an increase in intercellular pH[248] and in ammonium ion excretion due to the production of a more alkaline urine.[249] The pathophysiologies associated with each of these conditions are described in detail in other chapters of this monograph.

FUTURE DIRECTIONS

Our current knowledge of the adaptations in the renal production and excretion of ammonium ions that occur in response to changes in acid–base balance has been derived largely from hypothesis-driven experiments. Through this approach, a number of genes that are differentially expressed in the various segments of the nephron have been identified. Characterization of the increased expression of the mitochondrial GA has defined a novel mechanism of pH-responsive mRNA stabilization. The characterization of the cytosolic PEPCK gene has served as a paradigm to characterize the mechanism of pH-responsive changes in transcription. Activation of NHE3 has served as the paradigm for characterization of acid-induced translocation of key transporters to the plasma membrane. Limited progress has also been made in identifying the signal transduction pathways that mediate this adaptive response. However, given the complexity of this process and the number of participating cell types, the expression of a large number of additional genes are likely to also respond to changes in acid–base balance. Further understanding of the complexity and the regulation of this important physiological process may be derived from the application of genomic and proteomic techniques to identify the broad set of genes that are differentially expressed in individual nephron segments in response to changes in acid–base balance. The resulting data will identify the full spectra of genes that are activated or repressed by metabolic acidosis or alkalosis and classify those which are regulated through transcriptional or post-transcriptional mechanisms. It may also identify sets of genes, and their associated regulatory elements, that are temporally affected by mechanisms that have not, as yet, been characterized. Such techniques can also be used to more fully characterize the signal transduction pathways that mediate and coordinate the overall response.

References

[1] Brosnan JT, Lowry M, Vinay P, Gougoux A, Halperin ML. Renal ammonium production–une vue canadienne. Can J Physiol Pharmacol 1987;65:489–98.
[2] Halperin ML. Metabolic aspects of metabolic acidosis. Clin Invest Med 1993;16:294–305.
[3] Tannen RL, Sahai A. Biochemical pathways and modulators of renal ammoniagenesis. Miner Electrolyte Metab 1990;16:249–58.
[4] Curthoys NP, Watford M. Regulation of glutaminase activity and glutamine metabolism. Annu Rev Nutr 1995;15:133–59.
[5] Gerich JE, Meyer C, Woerle HJ, Stumvoll M. Renal gluconeogenesis: its importance in human glucose homeostasis. Diabetes Care 2001;24:382–91.
[6] Curthoys NP, Gstraunthaler G. Mechanism of increased renal gene expression during metabolic acidosis. Am J Physiol Renal Physiol 2001;281:F381–90.

[7] Feifel E, Obexer P, Andratsch M, Euler S, Taylor L, Tang A, et al. p38 MAPK mediates acid-induced transcription of PEPCK in LLC-PK(1)-FBPase(+) cells. Am J Physiol Renal Physiol 2002;283:F678–88.
[8] Bobulescu IA, Moe OW. Na^+/H^+ exchangers in renal regulation of acid–base balance. Semin Nephrol 2006;26:334–44.
[9] Preisig PA, Alpern RJ. Chronic metabolic acidosis causes an adaptation in the apical membrane Na/H antiporter and basolateral membrane $Na(HCO_3)_3$ symporter in the rat proximal convoluted tubule. J Clin Invest 1988;82:1445–53.
[10] Kinsella JL, Aronson PS. Interaction of NH_4^+ and Li^+ with the renal microvillus membrane Na^+-H^+ exchanger. Am J Physiol 1981;241:C220–6.
[11] Nagami GT. Luminal secretion of ammonia in the mouse proximal tubule perfused in vitro. J Clin Invest 1988;81:159–64.
[12] Karim Z, Attmane-Elakeb A, Bichara M. Renal handling of NH_4^+ in relation to the control of acid–base balance by the kidney. J Nephrol 2002;15:S128–34.
[13] Knepper MA, Agre P. Structural biology. The atomic architecture of a gas channel. Science 2004;305:1573–4.
[14] Weiner ID. The Rh gene family and renal ammonium transport. Curr Opin Nephrol Hypertens 2004;13:533–40.
[15] Alpern RJ. Trade-offs in the adaptation to acidosis. Kidney Int 1995;47:1205–15.
[16] Aalkjaer C, Frische S, Leipziger J, Nielsen S, Praetorius J. Sodium coupled bicarbonate transporters in the kidney, an update. Acta Physiol Scand 2004;181:505–12.
[17] Stern R. Fluid, Electrolytes and Acid–Base Disturbances. NephSAPTM 2004;3:192–231.
[18] Capasso G, Unwin R, Rizzo M, Pica A, Giebisch G. Bicarbonate transport along the loop of Henle: molecular mechanisms and regulation. J Nephrol 2002;15:S88–96.
[19] de Mello-Aires M, Malnic G. Distal tubule bicarbonate transport. J Nephrol 2002;15:S97–111.
[20] Haussinger D. Liver regulation of acid–base balance. Miner Electrolyte Metab 1997;23:249–52.
[21] Squires EJ, Hall DE, Brosnan JT. Arteriovenous differences for amino acids and lactate across kidneys of normal and acidotic rats. Biochem J 1976;160:125–8.
[22] Meyer C, Stumvoll M, Dostou J, Welle S, Haymond M, Gerich J. Renal substrate exchange and gluconeogenesis in normal postabsorptive humans. Am J Physiol Endocrinol Metab 2002;282: E428–34.
[23] Silbernagl S. Tubular reabsorption of L-glutamine studied by free-flow micropuncture and microperfusion of rat kidney. Int J Biochem 1980;12:9–16.
[24] Kleta R, Romeo E, Ristic Z, Ohura T, Stuart C, Arcos-Burgos M, et al. Mutations in SLC6A19, encoding B0AT1, cause Hartnup disorder. Nat Genet 2004;36:999–1002.
[25] Seow HF, Broer S, Broer A, Bailey CG, Potter SJ, Cavanaugh JA, et al. Hartnup disorder is caused by mutations in the gene encoding the neutral amino acid transporter SLC6A19. Nat Genet 2004;36:1003–7.
[26] Bode BP. Recent molecular advances in mammalian glutamine transport. J Nutr 2001;131:2475S–85S.
[27] Park SY, Kim JK, Kim IJ, Choi BK, Jung KY, Lee S, et al. Reabsorption of neutral amino acids mediated by amino acid transporter LAT2 and TAT1 in the basolateral membrane of proximal tubule. Arch Pharm Res 2005;28:421–32.
[28] Rossier G, Meier C, Bauch C, Summa V, Sordat B, Verrey F, et al. LAT2, a new basolateral 4F2hc/CD98-associated amino acid transporter of kidney and intestine. J Biol Chem 1999; 274:34948–54.
[29] Pineda M, Fernandez E, Torrents D, Estevez R, Lopez C, Camps M, et al. Identification of a membrane protein, LAT-2, that Co-expresses with 4F2 heavy chain, an L-type amino acid transport activity with broad specificity for small and large zwitterionic amino acids. J Biol Chem 1999;274:19738–44.
[30] Sastrasinh S, Sastrasinh M. Glutamine transport in submitochondrial particles. Am J Physiol 1989;257:F1050–8.
[31] Indiveri C, Abruzzo G, Stipani I, Palmieri F. Identification and purification of the reconstitutively active glutamine carrier from rat kidney mitochondria. Biochem J 1998;333:285–90.
[32] Goldstein L, Boylan JM. Renal mitochondrial glutamine transport and metabolism: studies with a rapid-mixing, rapid-filtration technique. Am J Physiol 1978;234:F514–21.
[33] Kovacevic Z, Bajin K. Kinetics of glutamine-efflux from liver mitochondria loaded with the ^{14}C-Labeled substrate. Biochim Biophys Acta 1982;687:291–5.
[34] Sleeper RS, Vertuno LL, Strauss F, Preuss HG. Effects of acid challenge on in vivo and in vitro rat renal ammoniagenesis. Life Sci 1978;22:1561–71.
[35] Tamarappoo BK, Joshi S, Welbourne TC. Interorgan glutamine flow regulation in metabolic acidosis. Miner Electrolyte Metab 1990;16:322–30.
[36] Hughey RP, Rankin BB, Curthoys NP. Acute acidosis and renal arteriovenous differences of glutamine in normal and adrenalectomized rats. Am J Physiol 1980;238:F199–204.
[37] Schrock H, Cha CJ, Goldstein L. Glutamine release from hindlimb and uptake by kidney in the acutely acidotic rat. Biochem J 1980;188:557–60.
[38] Yang X, Amemiya M, Peng Y, Moe OW, Preisig PA, Alpern RJ. Acid incubation causes exocytic insertion of NHE3 in OKP cells. Am J Physiol Cell Physiol 2000;279:C410–9.
[39] Horie S, Moe O, Tejedor A, Alpern RJ. Preincubation in acid medium increases Na/H antiporter activity in cultured renal proximal tubule cells. Proc Natl Acad Sci U S A 1990;87:4742–5.
[40] Tannen RL, Ross BD. Ammoniagenesis by the isolated perfused rat kidney: the critical role of urinary acidification. Clin Sci (Lond) 1979;56:353–64.
[41] Wright PA, Packer RK, Garcia-Perez A, Knepper MA. Time course of renal glutamate dehydrogenase induction during NH_4Cl loading in rats. Am J Physiol 1992;262:F999–1006.
[42] Sastrasinh M, Sastrasinh S. Effect of acute pH change on mitochondrial glutamine transport. Am J Physiol 1990;259:F863–6.
[43] Lowry M, Ross BD. Activation of oxoglutarate dehydrogenase in the kidney in response to acute acidosis. Biochem J 1980;190: 771–80.
[44] Curthoys NP, Taylor L, Hoffert JD, Knepper MA. Proteomic analysis of the adaptive response of rat renal proximal tubules to metabolic acidosis. Am J Physiol Renal Physiol 2007;292: F140–7.
[45] Hwang JJ, Curthoys NP. Effect of acute alterations in acid–base balance on rat renal glutaminase and phosphoenolpyruvate carboxykinase gene expression. J Biol Chem 1991;266:9392–6.
[46] Carter P, Welbourne T. Glutamate transport regulation of renal glutaminase flux in vivo. Am J Physiol 1997;273:E521–7.
[47] Welbourne T, Nissim I. Regulation of mitochondrial glutamine/glutamate metabolism by glutamate transport: studies with (^{15}) N. Am J Physiol Cell Physiol 2001;280:C1151–9.
[48] MacMullen C, Fang J, Hsu BY, Kelly A, de Lonlay-Debeney P, Saudubray JM, et al. Hyperinsulinism/hyperammonemia syndrome in children with regulatory mutations in the inhibitory guanosine triphosphate-binding domain of glutamate dehydrogenase. J Clin Endocrinol Metab 2001;86:1782–7.
[49] Treberg JR, Clow KA, Greene KA, Brosnan ME, Brosnan JT. Systemic activation of glutamate dehydrogenase increases renal ammoniagenesis: implications for the hyperinsulinism/hyperammonemia syndrome. Am J Physiol Endocrinol Metab 2010;298:E1219–25.

[50] Tizianello A, Deferrari G, Garibotto G, Robaudo C, Acquarone N, Ghiggeri GM. Renal ammoniagenesis in an early stage of metabolic acidosis in man. J Clin Invest 1982;69:240–50.
[51] Deferrari G, Garibotto G, Robaudo C, Saffioti S, Russo R, Sala MR, et al. Renal ammoniagenesis and interorgan flow of glutamine in chronic metabolic acidosis. Contrib Nephrol 1994;110: 144–9.
[52] Schoolwerth AC, deBoer PA, Moorman AF, Lamers WH. Changes in mRNAs for enzymes of glutamine metabolism in kidney and liver during ammonium chloride acidosis. Am J Physiol 1994;267:F400–6.
[53] Curthoys NP, Lowry OH. The distribution of glutaminase isoenzymes in the various structures of the nephron in normal, acidotic, and alkalotic rat kidney. J Biol Chem 1973;248:162–8.
[54] Wright PA, Knepper MA. Phosphate-dependent glutaminase activity in rat renal cortical and medullary tubule segments. Am J Physiol 1990;259:F961–70.
[55] Wright PA, Knepper MA. Glutamate dehydrogenase activities in microdissected rat nephron segments: effects of acid–base loading. Am J Physiol 1990;259:F53–9.
[56] Sajo IM, Goldstein MB, Sonnenberg H, Stinebaugh BJ, Wilson DR, Halperin ML. Sites of ammonia addition to tubular fluid in rats with chronic metabolic acidosis. Kidney Int 1981;20:353–8.
[57] Good DW, Burg MB. Ammonia production by individual segments of the rat nephron. J Clin Invest 1984;73:602–10.
[58] Ackerman JJ, Lowry M, Radda GK, Ross BD, Wong GG. The role of intrarenal pH in regulation of ammoniagenesis: [^{31}P] NMR studies of the isolated perfused rat kidney. J Physiol 1981;319:65–79.
[59] Sahai A, Laughrey E, Tannen RL. Relationship between intracellular pH and ammonia metabolism in LLC-PK$_1$ cells. Am J Physiol 1990;258:F103–8.
[60] Preisig PA. The acid-activated signaling pathway: starting with Pyk2 and ending with increased NHE3 activity. Kidney Int 2007;72:1324–9.
[61] Iynedjian PB, Ballard FJ, Hanson RW. The regulation of phosphoenolpyruvate carboxykinase (GTP) synthesis in rat kidney cortex. The role of acid–base balance and glucocorticoids. J Biol Chem 1975;250:5596–603.
[62] Tong J, Harrison G, Curthoys NP. The effect of metabolic acidosis on the synthesis and turnover of rat renal phosphate-dependent glutaminase. Biochem J 1986;233:139–44.
[63] Cimbala MA, Lamers WH, Nelson K, Monahan JE, Yoo-Warren H, Hanson RW. Rapid changes in the concentration of phosphoenolpyruvate carboxykinase mRNA in rat liver and kidney. Effects of insulin and cyclic AMP. J Biol Chem 1982;257: 7629–36.
[64] Hansen WR, Barsic-Tress N, Taylor L, Curthoys NP. The 3′-nontranslated region of rat renal glutaminase mRNA contains a pH-responsive stability element. Am J Physiol 1996;271: F126–31.
[65] Laterza OF, Curthoys NP. Specificity and functional analysis of the pH-responsive element within renal glutaminase mRNA. Am J Physiol Renal Physiol 2000;278:F970–7.
[66] Laterza OF, Hansen WR, Taylor L, Curthoys NP. Identification of an mRNA-binding protein and the specific elements that may mediate the pH-responsive induction of renal glutaminase mRNA. J Biol Chem 1997;272:22481–8.
[67] Hanson R, Reshef L. Regulation of phosphoenolpyruvate carboxykinase (GTP) gene expression. Annu Rev Biochem 1997;66: 581–611.
[68] Aruga S, Wehrli S, Kaissling B, Moe OW, Preisig PA, Pajor AM, et al. Chronic metabolic acidosis increases NaDC-1 mRNA and protein abundance in rat kidney. Kidney Int 2000;58:206–15.
[69] Karinch AM, Lin CM, Wolfgang CL, Pan M, Souba WW. Regulation of expression of the SN1 transporter during renal adaptation to chronic metabolic acidosis in rats. Am J Physiol Renal Physiol 2002;283:F1011–9.
[70] Karim Z, Attmane-Elakeb A, Sibella V, Bichara M. Acid pH increases the stability of BSC1/NKCC2 mRNA in the medullary thick ascending limb. J Am Soc Nephrol 2003;14: 2229–36.
[71] Seshadri RM, Klein JD, Kozlowski S, Sands JM, Kim YH, Han KH, et al. Renal expression of the ammonia transporters, Rhbg and Rhcg, in response to chronic metabolic acidosis. Am J Physiol Renal Physiol 2006;290:F397–408.
[72] Simpson DP. Citrate excretion: a window on renal metabolism. Am J Physiol 1983;244:F223–34.
[73] Ambuhl PM, Zajicek HK, Wang H, Puttaparthi K, Levi M. Regulation of renal phosphate transport by acute and chronic metabolic acidosis in the rat. Kidney Int 1998;53:1288–98.
[74] Jehle AW, Hilfiker H, Pfister MF, Biber J, Lederer E, Krapf R, et al. Type II Na-Pi cotransport is regulated transcriptionally by ambient bicarbonate/carbon dioxide tension in OK cells. Am J Physiol 1999;276:F46–53.
[75] Nowik M, Picard N, Stange G, Capuano P, Tenenhouse HS, Biber J, et al. Renal phosphaturia during metabolic acidosis revisited: molecular mechanisms for decreased renal phosphate reabsorption. Pflugers Arch 2008;457:539–49.
[76] Solbu TT, Boulland JL, Zahid W, Lyamouri Bredahl MK, Amiry-Moghaddam M, Storm-Mathisen J, et al. Induction and targeting of the glutamine transporter SN1 to the basolateral membranes of cortical kidney tubule cells during chronic metabolic acidosis suggest a role in pH regulation. J Am Soc Nephrol 2005;16:869–77.
[77] Busque SM, Wagner CA. Potassium restriction, high protein intake, and metabolic acidosis increase expression of the glutamine transporter SNAT3 (Slc38a3) in mouse kidney. Am J Physiol Renal Physiol 2009;297:F440–50.
[78] Moret C, Dave MH, Schulz N, Jiang JX, Verrey F, Wagner CA. Regulation of renal amino acid transporters during metabolic acidosis. Am J Physiol Renal Physiol 2007;292: F555–66.
[79] Christensen HN. Role of amino acid transport and countertransport in nutrition and metabolism. Physiol Rev 1990;70:43–77.
[80] Chaudhry FA, Reimer RJ, Krizaj D, Barber D, Storm-Mathisen J, Copenhagen DR, et al. Molecular analysis of system N suggests novel physiological roles in nitrogen metabolism and synaptic transmission. Cell 1999;99:769–80.
[81] Chaudhry FA, Reimer RJ, Edwards RH. The glutamine commute: take the N line and transfer to the A. J Cell Biol 2002;157:349–55.
[82] Gu S, Roderick HL, Camacho P, Jiang JX. Identification and characterization of an amino acid transporter expressed differentially in liver. Proc Natl Acad Sci U S A 2000;97:3230–5.
[83] Taylor L, Curthoys NP. Glutamine Metabolism: role in acid–base balance. Biochem Molec Biol Ed 2004;32:291–304.
[84] Bobulescu IA, Moe OW. Luminal Na($^+$)/H ($^+$) exchange in the proximal tubule. Pflugers Arch 2009;458:5–21.
[85] Kwon TH, Fulton C, Wang W, Kurtz I, Frokiaer J, Aalkjaer C, et al. Chronic metabolic acidosis upregulates rat kidney Na-HCO cotransporters NBCn1 and NBC3 but not NBC1. Am J Physiol Renal Physiol 2002;282:F341–51.
[86] Liu B, Preisig PA. Compensatory renal hypertrophy is mediated by a cell cycle-dependent mechanism. Kidney Int 2002;62: 1650–8.
[87] Doctor RB, Chen J, Peters LL, Lux SE, Mandel LJ. Distribution of epithelial ankyrin (Ank3) spliceoforms in renal proximal and distal tubules. Am J Physiol 1998;274:F129–38.

[88] Nowik M, Lecca MR, Velic A, Rehrauer H, Brandli AW, Wagner CA. Genome-wide gene expression profiling reveals renal genes regulated during metabolic acidosis. Physiol Genomics 2008;32:322–34.
[89] Porter LD, Ibrahim H, Taylor L, Curthoys NP. Complexity and species variation of the kidney-type glutaminase gene. Physiol Genomics 2002;9:157–66.
[90] Shapiro RA, Farrell L, Srinivasan M, Curthoys NP. Isolation, characterization, and in vitro expression of a cDNA that encodes the kidney isoenzyme of the mitochondrial glutaminase. J Biol Chem 1991;266:18792–6.
[91] Hwang JJ, Perera S, Shapiro RA, Curthoys NP. Mechanism of altered renal glutaminase gene expression in response to chronic acidosis. Biochemistry 1991;30:7522–6.
[92] Elgadi KM, Meguid RA, Qian M, Souba WW, Abcouwer SF. Cloning and analysis of unique human glutaminase isoforms generated by tissue-specific alternative splicing. Physiol Genomics 1999;1:51–62.
[93] Kvamme E, Tveit B, Svenneby G. Glutaminase from pig renal cortex. I. Purification and general properties. J Biol Chem 1970;245:1871–7.
[94] Curthoys NP, Kuhlenschmidt T, Godfrey SS. Regulation of renal ammoniagenesis. Purification of phosphate-dependent glutaminase from rat kidney. Arch Biochem Biophys 1976;174:82–9.
[95] Svenneby G, Torgner IA, Kvamme E. Purification of phosphate-dependent pig brain glutaminase. J Neurochem 1973;20:1217–24.
[96] Haser WG, Shapiro RA, Curthoys NP. Comparison of the phosphate-dependent glutaminase obtained from rat brain and kidney. Biochem J 1985;229:399–408.
[97] Chiu JF, Boeker EA. Cow brain glutaminase: partial purification and mechanism of action. Arch Biochem Biophys 1979;196:493–500.
[98] Quesada AR, Sanchez-Jimenez F, Perez-Rodriguez J, Marquez J, Medina MA, Nunez de Castro I. Purification of phosphate-dependent glutaminase from isolated mitochondria of Ehrlich ascites-tumour cells. Biochem J 1988;255: 1031–5.
[99] Kenny J, Bao Y, Hamm B, Taylor L, Toth A, Wagers B, et al. Bacterial expression, purification, and characterization of rat kidney-type mitochondrial glutaminase. Protein Expr Purif 2003;31:140–8.
[100] Roberg B, Torgner IA, Laake J, Takumi Y, Ottersen OP, Kvamme E. Properties and submitochondrial localization of pig and rat renal phosphate-activated glutaminase. Am J Physiol Cell Physiol 2000;279:C648–57.
[101] Shapiro RA, Morehouse RF, Curthoys NP. Inhibition by glutamate of phosphate-dependent glutaminase of rat kidney. Biochem J 1982;207:561–6.
[102] Olalla L, Aledo JC, Bannenberg G, Marquez J. The C-terminus of human glutaminase L mediates association with PDZ domain-containing proteins. FEBS Lett 2001;488:116–22.
[103] Perera SY, Chen TC, Curthoys NP. Biosynthesis and processing of renal mitochondrial glutaminase in cultured proximal tubular epithelial cells and in isolated mitochondria. J Biol Chem 1990;265:17764–70.
[104] Perera SY, Voith DM, Curthoys NP. Biosynthesis and processing of mitochondrial glutaminase in HTC hepatoma cells. Biochem J 1991;273:265–70.
[105] Srinivasan M, Kalousek F, Curthoys NP. In vitro characterization of the mitochondrial processing and the potential function of the 68-kDa subunit of renal glutaminase. J Biol Chem 1995;270:1185–90.
[106] Curthoys NP, Weiss RF. Regulation of renal ammoniagenesis. Subcellular localization of rat kidney glutaminase isoenzymes. J Biol Chem 1974;249:3261–6.
[107] Kalra J, Brosnan JT. The subcellular localization of glutaminase isoenzymes in rat kidney cortex. J Biol Chem 1974;249: 3255–60.
[108] Shapiro RA, Haser WG, Curthoys NP. The orientation of phosphate-dependent glutaminase on the inner membrane of rat renal mitochondria. Arch Biochem Biophys 1985;243:1–7.
[109] Atlante A, Passarella S, Minervini GM, Quagliariello E. Glutamine transport in normal and acidotic rat kidney mitochondria. Arch Biochem Biophys 1994;315:369–81.
[110] Brosnan JT, Hall B. The transport and metabolism of glutamine by kidney-cortex mitochondria from normal and acidotic rats. Biochem J 1977;164:331–7.
[111] Adam W, Simpson DP. Glutamine transport in rat kidney mitochondria in metabolic acidosis. J Clin Invest 1974;54: 165–74.
[112] Shapiro RA, Curthoys NP. Characterization of the apparent rates of glutamine transport in rat renal mitochondria. FEBS Lett 1978;91:49–52.
[113] Curthoys NP, Kuhlenschmidt T, Godfrey SS, Weiss RF. Phosphate-dependent glutaminase from rat kidney. Cause of increased activity in response to acidosis and identity with glutaminase from other tissues. Arch Biochem Biophys 1976;172:162–7.
[114] Chen CY, Shyu AB. AU-rich elements: characterization and importance in mRNA degradation. Trends Biochem Sci 1995;20:465–70.
[115] Garneau NL, Wilusz J, Wilusz CJ. The highways and byways of mRNA decay. Nat Rev Mol Cell Biol 2007;8:113–26.
[116] Parker R, Song H. The enzymes and control of eukaryotic mRNA turnover. Nat Struct Mol Biol 2004;11:121–7.
[117] Gao M, Fritz DT, Ford LP, Wilusz J. Interaction between a poly (A)-specific ribonuclease and the 5′ cap influences mRNA deadenylation rates in vitro. Mol Cell 2000;5:479–88.
[118] van Hoof A, Parker R. The exosome: a proteasome for RNA? Cell 1999;99:347–50.
[119] Anderson P, Kedersha N. RNA granules: post-transcriptional and epigenetic modulators of gene expression. Nat Rev Mol Cell Biol 2009;10:430–6.
[120] Wang Z, Kiledjian M. Identification of an erythroid-enriched endoribonuclease activity involved in specific mRNA cleavage. Embo J 2000;19:295–305.
[121] Gstraunthaler G, Handler JS. Isolation, growth, and characterization of a gluconeogenic strain of renal cells. Am J Physiol 1987;252:C232–8.
[122] Laterza OF, Curthoys NP. Effect of acidosis on the properties of the glutaminase mRNA pH-response element binding protein. J Am Soc Nephrol 2000;11:1583–8.
[123] Schroeder JM, Ibrahim H, Taylor L, Curthoys NP. Role of deadenylation and AUF1 binding in the pH-responsive stabilization of glutaminase mRNA. Am J Physiol Renal Physiol 2006;290:F733–40.
[124] Loflin PT, Chen CY, Xu N, Shyu AB. Transcriptional pulsing approaches for analysis of mRNA turnover in mammalian cells. Methods 1999;17:11–20.
[125] Tang A, Curthoys NP. Identification of zeta-crystallin/ NADPH:quinone reductase as a renal glutaminase mRNA pH response element-binding protein. J Biol Chem 2001;276: 21375–80.
[126] Schroeder JM, Liu W, Curthoys NP. pH-responsive stabilization of glutamate dehydrogenase mRNA in LLC-PK_1-F^+ cells. Am J Physiol Renal Physiol 2003;285:F258–65.

[127] Kedersha NL, Gupta M, Li W, Miller I, Anderson P. RNA-binding proteins TIA-1 and TIAR link the phosphorylation of eIF-2 alpha to the assembly of mammalian stress granules. J Cell Biol 1999;147:1431–42.
[128] Anderson P, Kedersha N. Stress granules. Curr Biol 2009;19: R397–8.
[129] Kedersha N, Stoecklin G, Ayodele M, Yacono P, Lykke-Andersen J, Fritzler MJ, et al. Stress granules and processing bodies are dynamically linked sites of mRNP remodeling. J Cell Biol 2005;169:871–84.
[130] Ibrahim H, Lee YJ, Curthoys NP. Renal response to metabolic acidosis: role of mRNA stabilization. Kidney Int 2008;73:11–8.
[131] Wilson GM, Lu J, Sutphen K, Suarez Y, Brewer B, Villaneuva-Feliciano EC, Ysla RM, Charles S, Brewer G. Phosphorylation of p40AUF1 regulated binding to A + U-rich mRNA destabilizing elemants and protein-induced changes in ribonucleoprotein structure. J Biol Chem 2003;278:33039–48.
[132] Wilson GM, Lu J, Sutphen K, Sun Y, Huynh Y, Brewer G. Regulation of A + U-rich element-directed mRNA turnover involving reversible phosphorylation of AUF1. J Biol Chem 2003;278:33029–38.
[133] Shaw G, Kamen R. A conserved AU sequence from the 3′ untranslated region of GM-CSF mRNA mediates selective mRNA degradation. Cell 1986;46:659–67.
[134] Lasa M, Mahtani KR, Finch A, Brewer G, Saklatvala J, Clark AR. Regulation of cyclooxygenase 2 mRNA stability by the mitogen-activated protein kinase p38 signaling cascade. Mol Cell Biol 2000;20:4265–74.
[135] Wagner BJ, DeMaria CT, Sun Y, Wilson GM, Brewer G. Structure and genomic organization of the human AUF1 gene: alternative pre-mRNA splicing generates four protein isoforms. Genomics 1998;48:195–202.
[136] Dreyfuss G, Matunis MJ, Pinol-Roma S, Burd CG. hnRNP proteins and the biogenesis of mRNA. Annu Rev Biochem 1993;62:289–321.
[137] Fan XC, Steitz JA. Overexpression of HuR, a nuclear-cytoplasmic shuttling protein, increases the in vivo stability of ARE-containing mRNAs. Embo J 1998;17:3448–60.
[138] Kim HH, Gorospe M. Phosphorylated HuR shuttles in cycles. Cell Cycle 2008;7:3124–6.
[139] Beale EG, Chrapkiewicz NB, Scoble HA, Metz RJ, Quick DP, Noble RL, et al. Rat hepatic cytosolic phosphoenolpyruvate carboxykinase (GTP). Structures of the protein, messenger RNA, and gene. J Biol Chem 1985;260:10748–60.
[140] Hanson RW, Patel YM. Phosphoenolpyruvate carboxykinase (GTP): the gene and the enzyme. Adv Enzymol Relat Areas Mol Biol 1994;69:203–81.
[141] Eisenberger CL, Nechushtan H, Cohen H, Shani M, Reshef L. Differential regulation of the rat phosphoenolpyruvate carboxykinase gene expression in several tissues of transgenic mice. Mol Cell Biol 1992;12:1396–403.
[142] Cassuto H, Olswang Y, Heinemann S, Sabbagh K, Hanson RW, Reshef L. The transcriptional regulation of phosphoenolpyruvate carboxykinase gene in the kidney requires the HNF-1 binding site of the gene. Gene 2003;318:177–84.
[143] Gstraunthaler G, Holcomb T, Feifel E, Liu W, Spitaler N, Curthoys NP. Differential expression and acid–base regulation of glutaminase mRNAs in gluconeogenic LLC-PK$_{(1)}$-FBPase$^{(+)}$ cells. Am J Physiol Renal Physiol 2000;278:F227–37.
[144] Cassuto H, Olswang Y, Livoff AF, Nechushtan H, Hanson RW, Reshef L. Involvement of HNF-1 in the regulation of phosphoenolpyruvate carboxykinase gene expression in the kidney. FEBS Lett 1997;412:597–602.
[145] Drenowska K, Craig M, Digiovanni S, McCarty J, Moorman A, Lamars W, et al. PEPCK mRNA localization in proximal tubule and gene regulation during metabolic acidosis. J Physiol Phram 2002;53:3–20.
[146] Holcomb T, Liu W, Snyder R, Shapiro R, Curthoys NP. Promoter elements that mediate the pH response of PCK mRNA in LLC-PK$_1^-$F$^+$ cells. Am J Physiol 1996;271:F340–6.
[147] Liu X, Wall QT, Taylor L, Curthoys NP. C/EBPbeta contributes to cAMP-activated transcription of phosphoenolpyruvate carboxykinase in LLC-PK$_{(1)}^-$F$^+$ cells. Am J Physiol Renal Physiol 2001;281:F649–57.
[148] Hod Y, Hanson RW. Cyclic AMP stabilizes the mRNA for phosphoenolpyruvate carboxykinase (GTP) against degradation. J Biol Chem 1988;263:7747–52.
[149] Petersen DD, Magnuson MA, Granner DK. Location and characterization of two widely separated glucocorticoid response elements in the phosphoenolpyruvate carboxykinase gene. Mol Cell Biol 1988;8:96–104.
[150] Hajarnis S, Schroeder JM, Curthoys NP. 3′-Untranslated region of phosphoenolpyruvate carboxykinase mRNA contains multiple instability elements that bind AUF1. J Biol Chem 2005;280:28272–80.
[151] Laterza OF, Taylor L, Unnithan S, Nguyen L, Curthoys NP. Mapping and functional analysis of an instability element in phosphoenolpyruvate carboxykinase mRNA. Am J Physiol Renal Physiol 2000;279:F866–73.
[152] Cheong J, Coligan JE, Shuman JD. Activating transcription factor-2 regulates phosphoenolpyruvate carboxykinase transcription through a stress-inducible mitogen-activated protein kinase pathway. J Biol Chem 1998;273:22714–8.
[153] O'Hayre M, Taylor L, Andratsch M, Feifel E, Gstraunthaler G, Curthoys NP. Effects of constitutively active and dominant negative MAPK kinase (MKK) 3 and MKK6 on the pH-responsive increase in phosphoenolpyruvate carboxykinase mRNA. J Biol Chem 2006;281:2982–8.
[154] Yang J, Reshef L, Cassuto H, Aleman G, Hanson RW. Aspects of the control of phosphoenolpyruvate carboxykinase gene transcription. J Biol Chem 2009;284:27031–5.
[155] Welbourne T, Routh R, Yudkoff M, Nissim I. The glutamine/glutamate couplet and cellular function. News Physiol Sci 2001;16:157–60.
[156] Andratsch M, Feifel E, Taylor L, O'Hayre M, Schramek H, Curthoys NP, et al. TGF-beta signaling and its effect on glutaminase expression in LLC-PK$_1$-FBPase$^+$ cells. Am J Physiol Renal Physiol 2007;293:F846–53.
[157] Laghmani K, Preisig PA, Alpern RJ. The role of endothelin in proximal tubule proton secretion and the adaptation to a chronic metabolic acidosis. J Nephrol 2002;15:S75–87.
[158] Ambuhl PM, Amemiya M, Danczkay M, Lotscher M, Kaissling B, Moe OW, et al. Chronic metabolic acidosis increases NHE3 protein abundance in rat kidney. Am J Physiol 1996;271:F917–25.
[159] Laghmani K, Borensztein P, Ambuhl P, Froissart M, Bichara M, Moe OW, et al. Chronic metabolic acidosis enhances NHE-3 protein abundance and transport activity in the rat thick ascending limb by increasing NHE-3 mRNA. J Clin Invest 1997;99:24–30.
[160] Amemiya M, Yamaji Y, Cano A, Moe OW, Alpern RJ. Acid incubation increases NHE-3 mRNA abundance in OKP cells. Am J Physiol 1995;269:C126–33.
[161] Yang X, Huang HC, Yin H, Alpern RJ, Preisig PA. RhoA required for acid-induced stress fiber formation and trafficking and activation of NHE3. Am J Physiol Renal Physiol 2007;293: F1054–64.
[162] Peng Y, Amemiya M, Yang X, Fan L, Moe OW, Yin H, et al. ET (B) receptor activation causes exocytic insertion of NHE3 in OKP cells. Am J Physiol Renal Physiol 2001;280:F34–42.

[163] Peng Y, Moe OW, Chu T, Preisig PA, Yanagisawa M, Alpern RJ. ETB receptor activation leads to activation and phosphorylation of NHE3. Am J Physiol 1999;276:C938–45.
[164] Laghmani K, Preisig PA, Moe OW, Yanagisawa M, Alpern RJ. Endothelin-1/endothelin-B receptor-mediated increases in NHE3 activity in chronic metabolic acidosis. J Clin Invest 2001;107:1563–9.
[165] Liu L, Zacchia M, Tian X, Wan L, Sakamoto A, Yanagisawa M, et al. Acid regulation of NaDC-1 requires a functional endothelin B receptor. Kidney Int 2010. [Epub:Aug11].
[166] Yamaji Y, Tsuganezawa H, Moe OW, Alpern RJ. Intracellular acidosis activates c-Src. Am J Physiol 1997;272:C886–93.
[167] Yamaji Y, Amemiya M, Cano A, Preisig PA, Miller RT, Moe OW, et al. Overexpression of csk inhibits acid-induced activation of NHE-3. Proc Natl Acad Sci U S A 1995;92:6274–8.
[168] Tsuganezawa H, Sato S, Yamaji Y, Preisig PA, Moe OW, Alpern RJ. Role of c-SRC and ERK in acid-induced activation of NHE3. Kidney Int 2002;62:41–50.
[169] Li S, Sato S, Yang X, Preisig PA, Alpern RJ. Pyk2 activation is integral to acid stimulation of sodium/hydrogen exchanger 3. J Clin Invest 2004;114:1782–9.
[170] Gluck SL. Acid sensing in renal epithelial cells. J Clin Invest 2004;114:1696–9.
[171] Espiritu DJ, Bernardo AA, Robey RB, Arruda JA. A central role for Pyk2-Src interaction in coupling diverse stimuli to increased epithelial NBC activity. Am J Physiol Renal Physiol 2002;283:F663–70.
[172] Yamaji Y, Moe OW, Miller RT, Alpern RJ. Acid activation of immediate early genes in renal epithelial cells. J Clin Invest 1994;94:1297–303.
[173] Glabman S, Kose RM, Giebisch G. Micropuncture study of ammonia excretion in the rat. Am J Physiol 1963;205:127–32.
[174] Hayes Jr. CP, Mayson JS, Owen EE, Robinson RR. A Micropuncture Evaluation of Renal Ammonia Excretion in the Rat. Am J Physiol 1964;207:77–83.
[175] Pitts R. Production and excretion of ammonia in relation to acid–base regulation. In: Orloff J, Berliner R, editors. Handbook of physiology, section 8: renal physiology. Washington, DC: American Physiology Society; 1973. p. 455–97.
[176] Good DW, DuBose Jr. TD. Ammonia transport by early and late proximal convoluted tubule of the rat. J Clin Invest 1987;79:684–91.
[177] Nagami GT, Kurokawa K. Regulation of ammonia production by mouse proximal tubules perfused in vitro. Effect of luminal perfusion. J Clin Invest 1985;75:844–9.
[178] Preisig PA, Alpern RJ. Pathways for apical and basolateral membrane NH3 and NH_4^+ movement in rat proximal tubule. Am J Physiol 1990;259:F587–93.
[179] Simon EE, Hamm LL. Ammonia entry along rat proximal tubule in vivo: effects of luminal pH and flow rate. Am J Physiol 1987;253:F760–6.
[180] Garvin JL, Burg MB, Knepper MA. Ammonium replaces potassium in supporting sodium transport by the Na-K-ATPase of renal proximal straight tubules. Am J Physiol 1985;249:F785–8.
[181] Sastrasinh S, Tannen RL. Effect of potassium on renal NH_3 production. Am J Physiol 1983;244:F383–91.
[182] Tannen RL. Relationship of renal ammonia production and potassium homeostasis. Kidney Int 1977;11:453–65.
[183] Nagami GT. Effect of bath and luminal potassium concentration on ammonia production and secretion by mouse proximal tubules perfused in vitro. J Clin Invest 1990;86:32–9.
[184] Nagami GT, Kraut JA. Acid–base regulation of angiotensin receptors in the kidney. Curr Opin Nephrol Hypertens 2010;19:91–7.
[185] Nagami GT. Effect of angiotensin II on ammonia production and secretion by mouse proximal tubules perfused in vitro. J Clin Invest 1992;89:925–31.
[186] Nagami GT. Effect of luminal angiotensin II on ammonia production and secretion by mouse proximal tubules. Am J Physiol 1995;269:F86–92.
[187] Nagami GT. Enhanced ammonia secretion by proximal tubules from mice receiving NH(4)Cl: role of angiotensin II. Am J Physiol Renal Physiol 2002;282:F472–7.
[188] Nagami GT. Role of angiotensin II in the enhancement of ammonia production and secretion by the proximal tubule in metabolic acidosis. Am J Physiol Renal Physiol 2008;294: F874–80.
[189] Nagami GT, Chang JA, Plato ME, Santamaria R. Acid loading in vivo and low pH in culture increase angiotensin receptor expression: enhanced ammoniagenic response to angiotensin II. Am J Physiol Renal Physiol 2008;295:F1864–70.
[190] Riquier-Brison AD, Leong PK, Pihakaski-Maunsbach K, McDonough AA. Angiotensin II stimulates trafficking of NHE3, NaPi2, and associated proteins into the proximal tubule microvilli. Am J Physiol Renal Physiol 2010;298: F177–86.
[191] Flessner MF, Knepper MA. Ammonium and bicarbonate transport in isolated perfused rodent ascending limbs of the loop of Henle. Am J Physiol 1993;264:F837–44.
[192] Flessner MF, Mejia R, Knepper MA. Ammonium and bicarbonate transport in isolated perfused rodent long-loop thin descending limbs. Am J Physiol 1993;264:F388–96.
[193] Attmane-Elakeb A, Amlal H, Bichara M. Ammonium carriers in medullary thick ascending limb. Am J Physiol Renal Physiol 2001;280:F1–9.
[194] Knepper MA, Good DW, Burg MB. Ammonia and bicarbonate transport by rat cortical collecting ducts perfused in vitro. Am J Physiol 1985;249:F870–7.
[195] Kikeri D, Sun A, Zeidel ML, Hebert SC. Cell membranes impermeable to NH_3. Nature 1989;339:478–80.
[196] Good DW. Ammonium transport by the thick ascending limb of Henle's loop. Annu Rev Physiol 1994;56:623–47.
[197] Kinne R, Kinne-Saffran E, Schutz H, Scholermann B. Ammonium transport in medullary thick ascending limb of rabbit kidney: involvement of the Na^+,K^+,$Cl^{(-)}$-cotransporter. J Membr Biol 1986;94:279–84.
[198] DuBose Jr. TD, Good DW. Chronic hyperkalemia impairs ammonium transport and accumulation in the inner medulla of the rat. J Clin Invest 1992;90:1443–9.
[199] Good DW. Effects of potassium on ammonia transport by medullary thick ascending limb of the rat. J Clin Invest 1987;80:1358–65.
[200] Amlal H, Paillard M, Bichara M. NH_4^+ transport pathways in cells of medullary thick ascending limb of rat kidney. NH_4^+ conductance and $K^+/NH_4^+(H^+)$ antiport. J Biol Chem 1994;269:21962–71.
[201] Attmane-Elakeb A, Boulanger H, Vernimmen C, Bichara M. Apical location and inhibition by arginine vasopressin of K^+/H^+ antiport of the medullary thick ascending limb of rat kidney. J Biol Chem 1997;272:25668–77.
[202] Good DW, Watts 3rd BA. Functional roles of apical membrane Na^+/H^+ exchange in rat medullary thick ascending limb. Am J Physiol 1996;270:F691–9.
[203] Good DW, George T, Watts 3rd BA. Basolateral membrane Na^+/H^+ exchange enhances $HCO3^-$ absorption in rat medullary thick ascending limb: evidence for functional coupling between basolateral and apical membrane Na^+/H^+ exchangers. Proc Natl Acad Sci U S A 1995;92:12525–9.

[204] Good DW. Adaptation of HCO_3^- and NH_4^+ transport in rat MTAL: effects of chronic metabolic acidosis and Na^+ intake. Am J Physiol 1990;258:F1345–53.

[205] Attmane-Elakeb A, Mount DB, Sibella V, Vernimmen C, Hebert SC, Bichara M. Stimulation by in vivo and in vitro metabolic acidosis of expression of rBSC-1, the Na^+-K^+(NH_4^+)-$2Cl^-$ cotransporter of the rat medullary thick ascending limb. J Biol Chem 1998;273:33681–91.

[206] Szutkowska M, Vernimmen C, Debaix H, Devuyst O, Friedlander G, Karim Z. z-crystallin/NADPH quinone reductase mediates the acid-pH-induced increase in the stability of BSC1 cotransporter mRNA. Kidney Int 2009;76:730–8.

[207] Flessner MF, Wall SM, Knepper MA. Permeabilities of rat collecting duct segments to NH_3 and NH_4^+. Am J Physiol 1991;260:F264–72.

[208] Wall SM, Koger LM. NH_4^+ transport mediated by Na(+)-K(+)-ATPase in rat inner medullary collecting duct. Am J Physiol 1994;267:F660–70.

[209] Amlal H, Soleimani M. K^+/NH_4^+ antiporter: a unique ammonium carrying transporter in the kidney inner medulla. Biochim Biophys Acta 1997;1323:319–33.

[210] Ginns SM, Knepper MA, Ecelbarger CA, Terris J, He X, Coleman RA, et al. Immunolocalization of the secretory isoform of Na-K-Cl cotransporter in rat renal intercalated cells. J Am Soc Nephrol 1996;7:2533–42.

[211] Kaplan MR, Plotkin MD, Brown D, Hebert SC, Delpire E. Expression of the mouse Na-K-2Cl cotransporter, mBSC2, in the terminal inner medullary collecting duct, the glomerular and extraglomerular mesangium, and the glomerular afferent arteriole. J Clin Invest 1996;98:723–30.

[212] Ikebe M, Nonoguchi H, Nakayama Y, Tashima Y, Tomita K. Upregulation of the secretory-type Na(+)/K(+)/2Cl(-)-cotransporter in the kidney by metabolic acidosis and dehydration in rats. J Am Soc Nephrol 2001;12:423–30.

[213] Star RA, Kurtz I, Mejia R, Burg MB, Knepper MA. Disequilibrium pH and ammonia transport in isolated perfused cortical collecting ducts. Am J Physiol 1987;253: F1232–42.

[214] Flessner MF, Wall SM, Knepper MA. Ammonium and bicarbonate transport in rat outer medullary collecting ducts. Am J Physiol 1992;262:F1–7.

[215] Wall SM, Flessner MF, Knepper MA. Distribution of luminal carbonic anhydrase activity along rat inner medullary collecting duct. Am J Physiol 1991;260:F738–48.

[216] Wall SM, Truong AV, DuBose Jr. TD. H(+)-K(+)-ATPase mediates net acid secretion in rat terminal inner medullary collecting duct. Am J Physiol 1996;271:F1037–44.

[217] Lynch IJ, Rudin A, Xia SL, Stow LR, Shull GE, Weiner ID, et al. Impaired acid secretion in cortical collecting duct intercalated cells from H-K-ATPase-deficient mice: role of HKalpha isoforms. Am J Physiol Renal Physiol 2008;294:F621–7.

[218] Weiner ID, Hamm LL. Molecular mechanisms of renal ammonia transport. Annu Rev Physiol 2007;69:317–40.

[219] Weiner ID, Verlander JW. Molecular physiology of the Rh ammonia transport proteins. Curr Opin Nephrol Hypertens 2010;19:471–7.

[220] Marini AM, Urrestarazu A, Beauwens R, Andre B. The Rh (rhesus) blood group polypeptides are related to NH_4^+ transporters. Trends Biochem Sci 1997;22:460–1.

[221] Liu Z, Chen Y, Mo R, Hui C, Cheng JF, Mohandas N, et al. Characterization of human RhCG and mouse Rhcg as novel nonerythroid Rh glycoprotein homologues predominantly expressed in kidney and testis. J Biol Chem 2000;275:25641–51.

[222] Quentin F, Eladari D, Cheval L, Lopez C, Goossens D, Colin Y, et al. RhBG and RhCG, the putative ammonia transporters, are expressed in the same cells in the distal nephron. J Am Soc Nephrol 2003;14:545–54.

[223] Verlander JW, Miller RT, Frank AE, Royaux IE, Kim YH, Weiner ID. Localization of the ammonium transporter proteins RhBG and RhCG in mouse kidney. Am J Physiol Renal Physiol 2003;284:F323–37.

[224] Eladari D, Cheval L, Quentin F, Bertrand O, Mouro I, Cherif-Zahar B, et al. Expression of RhCG, a new putative NH(3)/NH(4)(+) transporter, along the rat nephron. J Am Soc Nephrol 2002;13:1999–2008.

[225] Kim HY, Verlander JW, Bishop JM, Cain BD, Han KH, Igarashi P, et al. Basolateral expression of the ammonia transporter family member Rh C glycoprotein in the mouse kidney. Am J Physiol Renal Physiol 2009;296:F543–55.

[226] Khademi S, O'Connell III J, Remis J, Robles-Colmenares Y, Miercke LJ, Stroud RM. Mechanism of ammonia transport by Amt/MEP/Rh: structure of AmtB at 1.35 A. Science 2004;305:1587–94.

[227] Seshadri RM, Klein JD, Smith T, Sands JM, Handlogten ME, Verlander JW, et al. Changes in subcellular distribution of the ammonia transporter, Rhcg, in response to chronic metabolic acidosis. Am J Physiol Renal Physiol 2006;290:F1443–52.

[228] Chambrey R, Goossens D, Bourgeois S, Picard N, Bloch-Faure M, Leviel F, et al. Genetic ablation of Rhbg in the mouse does not impair renal ammonium excretion. Am J Physiol Renal Physiol 2005;289:F1281–90.

[229] Chambrey R, Goossens D, Quentin F, Eladari D. Rh glycoproteins in epithelial cells: lessons from rat and mice studies. Transfus Clin Biol 2006;13:154–8.

[230] Bishop JM, Verlander JW, Lee HW, Nelson RD, Weiner AJ, Handlogten ME, et al. Role of the Rhesus Glycoprotein, Rh B Glycoprotein, in renal ammonia excretion. Am J Physiol Renal Physiol 2010. [Epub:Aug18].

[231] Conjard A, Komaty O, Delage H, Boghossian M, Martin M, Ferrier B, et al. Inhibition of glutamine synthetase in the mouse kidney: a novel mechanism of adaptation to metabolic acidosis. J Biol Chem 2003;278:38159–66.

[232] Biver S, Belge H, Bourgeois S, Van Vooren P, Nowik M, Scohy S, et al. A role for Rhesus factor Rhcg in renal ammonium excretion and male fertility. Nature 2008;456:339–43.

[233] Lee HW, Verlander JW, Bishop JM, Igarashi P, Handlogten ME, Weiner ID. Collecting duct-specific Rh C glycoprotein deletion alters basal and acidosis-stimulated renal ammonia excretion. Am J Physiol Renal Physiol 2009;296:F1364–75.

[234] Lee HW, Verlander JW, Bishop JM, Nelson RD, Handlogten ME, Weiner ID. Effect of intercalated cell-specific Rh C glycoprotein deletion on basal and metabolic acidosis-stimulated renal ammonia excretion. Am J Physiol Renal Physiol 2010;299: F369–79.

[235] Tizianello A, Deferrari G, Garibotto G, Robaudo C, Bruzzone M, Passerone GC. Renal ammoniagenesis during the adaptation to metabolic acidosis in man. Contrib Nephrol 1982;31:40–6.

[236] Tizianello A, De Ferrari G, Garibotto G, Gurreri G, Robaudo C. Renal metabolism of amino acids and ammonia in subjects with normal renal function and in patients with chronic renal insufficiency. J Clin Invest 1980;65:1162–73.

[237] Schoolwerth AC, Sandler RS, Hoffman PM, Klahr S. Effects of nephron reduction and dietary protein content on renal ammoniagenesis in the rat. Kidney Int 1975;7:397–404.

[238] MacClean AJ, Hayslett JP. Adaptive change in ammonia excretion in renal insufficiency. Kidney Int 1980;17:595–606.

[239] Buerkert J, Martin D, Trigg D, Simon E. Effect of reduced renal mass on ammonium handling and net acid formation by the superficial and juxtamedullary nephron of the rat. Evidence

for impaired reentrapment rather than decreased production of ammonium in the acidosis of uremia. J Clin Invest 1983;71:1661–75.

[240] Hamm LL, Ambuhl PM, Alpern RJ. Role of glucocorticoids in acidosis. Am J Kidney Dis 1999;34:960–5.

[241] Wagner CA, Kovacikova J, Stehberger PA, Winter C, Benabbas C, Mohebbi N. Renal acid–base transport: old and new players. Nephron Physiol 2006;103:1–6.

[242] Karinch AM, Lin CM, Meng Q, Pan M, Souba WW. Glucocorticoids have a role in renal cortical expression of the SNAT3 glutamine transporter during chronic metabolic acidosis. Am J Physiol Renal Physiol 2007;292:F448–55.

[243] Bobulescu IA, Dwarakanath V, Zou L, Zhang J, Baum M, Moe OW. Glucocorticoids acutely increase cell surface Na^+/H^+ exchanger-3 (NHE3) by activation of NHE3 exocytosis. Am J Physiol Renal Physiol 2005;289:F685–91.

[244] Wagner CA. Metabolic acidosis: new insights from mouse models. Curr Opin Nephrol Hypertens 2007;16:471–6.

[245] DeFronzo RA. Hyperkalemia and hyporeninemic hypoaldosteronism. Kidney Int 1980;17:118–34.

[246] Szylman P, Better OS, Chaimowitz C, Rosler A. Role of hyperkalemia in the metabolic acidosis of isolated hypoaldosteronism. N Engl J Med 1976;294:361–5.

[247] Tizianello A, Garibotto G, Robaudo C, Saffioti S, Pontremoli R, Bruzzone M, et al. Renal ammoniagenesis in humans with chronic potassium depletion. Kidney Int 1991;40:772–8.

[248] Halperin ML, Kamel KS, Ethier JH, Magner PO. What is the underlying defect in patients with isolated, proximal renal tubular acidosis? Am J Nephrol 1989;9:265–8.

[249] Brenes LG, Sanchez MI. Impaired urinary ammonium excretion in patients with isolated proximal renal tubular acidosis. J Am Soc Nephrol 1993;4:1073–8.

[250] Mufti J, Hajarnis S, Shepardson K, Gummadi L, Taylor L, Curthoys NP. Role of AUF1 and HuR in the pH-responsive stabilization of phosphoenolpyruvate carboxykinase mRNA in LLC-PK1-F cells. Am J Physiol Renal Physiol 2011;301:F1066–77.

This page intentionally left blank

CHAPTER

58

Clinical Syndromes of Metabolic Alkalosis

Orson W. Moe, Robert J. Alpern and Donald W. Seldin

Department of Internal Medicine, University of Texas Southwestern Medical Center, Dallas, TX, USA
Office of the Dean Yale University School of Medicine, New Haven, CT, USA

INTRODUCTION

Homeostatic control of acid–base parameters within discreet limits is vital to all living organisms. Acid–base disturbances are conditions that reflect underlying pathophysiology, which can stem from a broad range of etiologies. In humans with a filtration-reabsorption nephron, >4,000 mEq of HCO_3^- is filtered daily at the glomerulus and virtually all of it is reabsorbed by the tubules (Figure 58.1).

HCO_3^- absorption is an energy-requiring process. Under normal circumstances with a more or less fixed capacity to reabsorb elevated filtered [HCO_3^-], the renal tubule does not commensurately increase energy consumption or bicarbonate reabsorption therefore bicarbonaturia invariably ensues. Given this background, one wonders why metabolic alkalosis should supervene. In contrast to metabolic acidosis where the pathophysiology reflects increased acid production, reduced acid excretion, or both, the maintenance of metabolic alkalosis is a quintessential disease of altered renal HCO_3^- handling. Even though extrarenal factors contribute, the final effectors of maintaining a high plasma [HCO_3^-] reside in the kidney. Metabolic alkalosis is a tubulopathy.

A few definitions are necessary. *Alkalosis* denotes an excess of base in total body fluids. *Alkalemia* refers to a state of decreased H^+ activity in the plasma (increased plasma pH). Alkalosis can exist with little alkalemia due to respiratory compensation and without alkalemia because alkalosis might be part of a mixed acid–base disturbance. Conversely, alkalemia can be present without total body alkalosis. The adjective *metabolic* denotes that the disturbance is caused by a primary gain of base (e.g., HCO_3^-) or loss of H^+ from the body; as opposed to primary disturbances in carbon dioxide excretion.

The only compartment that is accessible to clinical testing is the ECF; hence ECF composition has defined most clinical acid–base disorders. Note that the direction of alterations in intracellular fluid (ICF) H^+ activity might differ from ECF.[1,2] The pathogenesis of metabolic alkalosis involves two distinct derangements—*generation* and *maintenance*. The increased ECF [HCO_3^-] that characterizes metabolic alkalosis is usually due to excessive ECF HCO_3^- content with noted exceptions such as massive contraction of ECFV around a constant amount of HCO_3^-, or shift of H^+ into cells with intracellular K^+ depletion. ECF HCO_3^- addition might occur through oral or intravenous routes. Of equal importance is H^+ removal from ECF which is tantamount to HCO_3^- addition.

H^+ can leave the body (external H^+ loss) through the gastrointestinal tract by vomiting or the kidney through stimulated urinary H^+ excretion. In either case, H^+ loss is synonymous with formation of HCO_3^- from the gastric or renal cell, respectively, which then enters the ECF. Alternatively, H^+ can move from the ECF into the ICF (internal H^+ loss) as seen in K^+ depletion. The phase of metabolic alkalosis in which addition to the ECF exceeds HCO_3^- exit from ECF thus raising ECF [HCO_3^-], is called the *generation phase*.[3] Normally, excess ECF HCO_3^- is readily and rapidly excreted by the kidneys. Persistent excess ECF HCO_3^-

Seldin and Giebisch's The Kidney, Fifth Edition.
DOI: http://dx.doi.org/10.1016/B978-0-12-381462-3.00058-6

© 2013 Elsevier Inc. All rights reserved.

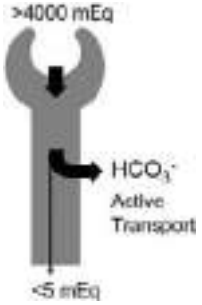

FIGURE 58.1 Filtration-absorption mechanism of bicarbonate handling by the nephron.

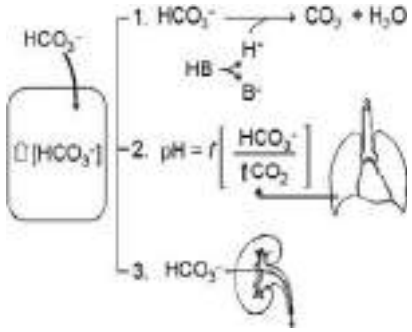

FIGURE 58.2 Three lines of defense against a HCO_3^- load: 1. Redistribution and buffer. 2. Hypoventilation to increase pCO_2. 3. Renal excretion of HCO_3^-.

content and concentration is usually due to inhibition of the ability of the kidney to excrete HCO_3^-. This is referred to as the *maintenance phase*.

Metabolic alkalosis is the most common acid–base disorder in hospitalized patients.[4] The magnitude of metabolic alkalosis correlates with morbidity,[5] mostly as a marker of severe underlying conditions but also a direct contributor to adverse events. A careful approach guided by the known pathophysiology of this order can direct diagnosis and management of the underlying disorders.

In this chapter, we will cover how one normal copes with the defense against high extracellular fluid HCO_3^- concentration, the systemic factors that act on the kidney to "reset" the plasma HCO_3 concentration, the proximal and distal tubular mechanisms responsible for this feat and finally, the clinical syndromes of metabolic alkalosis.

DEFENSE AGAINST EXCESS EXTRACELLULAR FLUID (ECF) HCO_3

As with any acid–base disturbance, one can envision three fronts of defense (Figure 58.2). First, the excess base confronts constituents of the fluid compartments, which harbors chemical components of defense. Second, the ventilatory system adjusts one determinant of ECFV pH, namely the CO_2 tension, to minimize the pH deviation. Third and the most important of all is the definite correction by the kidney with external elimination of the excessive base.

Systemic Response to ECF HCO_3^- Addition

Distribution of HCO_3^- Added to ECFV

Unlike a non-decomposable anion such as sulfate, HCO_3^- is partially dissipated by body buffers,[6] so its distribution does not fit into a single body compartment. The apparent distribution space of added HCO_3^-

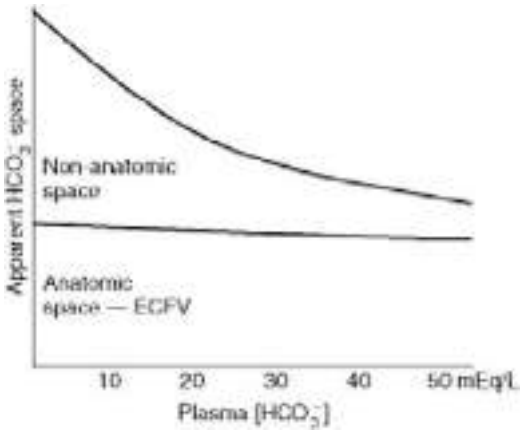

FIGURE 58.3 Apparent HCO_3^- space. This entity is theoretically partitioned into anatomic ECF volume and a non-anatomic space whose size is dependent on existing plasma $[HCO_3^-]$.

has been partitioned into anatomic and non-anatomic divisions (Figure 58.3).

The "anatomic" division refers to mainly the ECF compartment where added HCO_3^- is freely distributed. The "non-anatomic" division refers to the theoretical volume that accommodates the added HCO_3^- which cannot be accounted for by the anatomic space (ECF). This presumably represents some HCO_3^- that has entered cells and some that has been titrated by H^+ released from non-HCO_3^- buffers (such as hemoglobin and phosphate) thus constituting a virtual "space." At normal pH, these two divisions are approximately equal and together yield a total apparent HCO_3^- space of about 40 to 50% of total body weight.[6,7] Apparent HCO_3^- space is inversely related to preexisting ECF $[HCO_3^-]$, with the non-anatomic fraction decreasing in size as the ECF $[HCO_3^-]$ increases.[8] Decreasing size of the non-anatomic division with increasing ECF $[HCO_3^-]$ is due to progressive narrowing of the titration range for non-HCO_3^- buffers at higher ECF $[HCO_3^-]$.[8] Thus, a higher preexisting ECF $[HCO_3^-]$ indicates

greater titration of non-HCO_3^- buffers, causing a greater rise in ECF [HCO_3^-] in response to a given quantity of added HCO_3^-. As with H^+, HCO_3^- added to ECF is buffered by cellular and extracellular processes.[7] Compared to acid, a smaller fraction of added base is buffered in the cell,[9] so a greater fraction of added HCO_3^- is retained in the ECF. In addition, there is less stabilization of intracellular pH in the alkaline range compared to the acid range.[10] This highlights the importance of rapid renal HCO_3^- removal in the systemic defense against excess ECF HCO_3^-.

Respiratory Response to a Primary Increase in ECF [HCO_3^-]

Respiratory mechanisms alleviate but do not fully correct the elevated plasma pH (Figure 58.2). The pH increase from added ECF HCO_3^- is attenuated by a concomitant rise in pCO_2. The acute component begins within seconds of HCO_3^- addition due to neutralization of added HCO_3^- by H^+ derived from titrated non-HCO_3^- buffers as follows:

$$NaHCO_3 + H\ Buffer \rightarrow NaBuffer + H_2CO_3 \rightarrow CO_2 + H_2O$$

The CO_2 generated by this reaction stimulates ventilation, returning pCO_2 toward but not precisely to normal. This acute response is followed by a more chronic one commencing at about 1 hour in which the alkalemia suppresses ventilation, leading to a sustained increase in pCO_2.[11,12] This effect on the central ventilatory centers is probably mediated through alkalinization of cerebral interstitial fluid.[13] The hypercapneic response to metabolic alkalosis takes several hours to complete and attenuates the rise in body fluid pH (but does not return pH to normal). In general, the pCO_2 increase in metabolic alkalosis is about 0.74 mm Hg for every 1 mEq/L increase in ECF [HCO_3^-].[14,15] The compensatory fall in alveolar ventilation is limited by hypoventilatory hypoxemia which can override the pH effect.

Renal Excretion of HCO_3^-

Despite the importance of buffering and respiratory responses which provides transient amelioration, the kidney has the ultimate responsibility for disposal of excess ECF HCO_3^-. Although its usual task is to completely recover filtered HCO_3^- and excrete a nearly HCO_3^--free urine, the normal kidney has an extraordinary capacity to excrete HCO_3^-. The normal kidney excretes ingested HCO_3^- more rapidly than it excretes ingested H^+.[16]

The classic experiment of Pitts and Lotspeich (Figure 58.4) demonstrated that renal HCO_3^- reabsorption does not increase after plasma [HCO_3^-] is beyond about 24 mM- a "threshold" at the whole organism

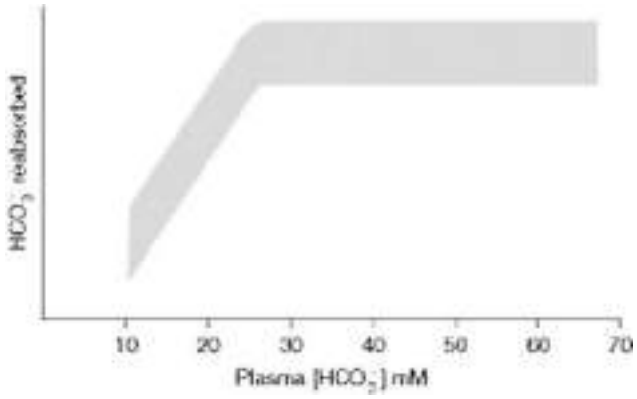

FIGURE 58.4 Whole kidney HCO_3^- absorption as a function of plasma [HCO_3^-]. HCO_3^- reabsorption increases as plasma [HCO_3^-] increases (assuming constant glomerular filtration rate) up to a point which is the plasma [HCO_3^-] threshold beyond which bicarbonaturia ensues. The inflection point is not sharp in the sense that there is a slight splay. Above the threshold the maximal capacity of renal HCO_3^- reabsorption is reached.

level.[17] Bicarbonaturia commence beyond the threshold which is when the tubular reabsorptive capacity is reach (Figure 58.4). The inflection point does not have a sharp angle but rather has a splay (Figure 58.4). Chronic oral $NaHCO_3^-$ loads as large as 24 mEq/kg/day are readily excreted in humans with minimal changes in ECF [HCO_3^-],[18] and acute intravenous loads are excreted entirely within 24 hours.[7] The kidney also increases excretion of organic anions (e.g. citrate) which are HCO_3^- equivalents (metabolism of which produces HCO_3^-) in response to ingested HCO_3^-,[19] contributing to the defense against metabolic alkalosis. Urine HCO_3^- excretion in response to administered HCO_3^- might theoretically be mediated by increased glomerular filtration rate (GFR), reduced tubule HCO_3^- reabsorption, or a combination of both. Intravenous isotonic $NaHCO_3^-$ induces massive urinary HCO_3^- excretion with minimal or no change in GFR[20] highlighting the importance of the renal tubule in mediating bicarbonaturia. Acute HCO_3^- infusion reduces fractional HCO_3^- reabsorption in the proximal[21] and distal nephron.[22] In addition, juxtamedullary nephrons excrete proportionally more HCO_3^- than do superficial ones in response to an acute intravenous HCO_3^- load.[23] Thus, the fixed or even suppressed capacity of HCO_3^- reabsorption is the predominant mechanism that mediates bicarbonaturia in response to an acute HCO_3^- load.

Acute HCO_3^- infusion tests the nephron's response to extreme HCO_3^- loads and massive bicarbonaturia is the usual response. However, mammals are rarely exposed to such massive alkali insults in their natural habitats and more subtle means of base excretion are utilized such as reduced net acid excretion and

citraturia.[24] More physiologic alkali challenges have been modeled using dietary $NaHCO_3$. Chronic oral $NaHCO_3^-$ reduces urine net acid excretion (urine ammonium + titratable acid − urine base) by decreasing excretion of ammonium and titratable acid as well as by increasing organic anion (primarily citrate) and HCO_3^- excretion.[25] Decreased ammonium and titratable acid excretion with maintained GFR is caused by decreased distal nephron acidification.

The inference from clearance studies was confirmed by direct measurements showing reduced acidification in distal[26] and collecting[27] tubules in animals ingesting $NaHCO_3$. Because HCO_3^- is both reabsorbed (mediated largely through H^+ secretion) and secreted in the distal[28,29] and collecting[27] tubule, decreased acidification in these distal segments can actually be mediated by increased HCO_3^- secretion and/or decreased H^+ secretion. Animals chronically ingesting $NaHCO_3$ have increased HCO_3^- secretion in the distal[30,31] and collecting[27] tubule while distal tubule H^+ secretion is less affected.[32] H^+ ingestion increases H^+-ATPase staining activity in collecting ducts.[33,34] Thus, stimulated HCO_3^- secretion is more prominent than reduced H^+ secretion as the predominant mechanism by which dietary HCO_3^- decreases distal nephron acidification.

Renal Disposal of Excess ECF HCO_3^-

Peritubular and Luminal Acid–Base Composition

Because increased ECF [HCO_3^-] is accompanied by simultaneous increase in [HCO_3^-] in the proximal tubule luminal fluid *in vivo*, it is difficult to separate the effects of peritubular from luminal acid − base changes on tubular HCO_3^- reabsorption in response to ECF [HCO_3^-] addition. This is best studied by measuring renal tubule HCO_3^- reabsorption in response to unilateral changes of acid–base composition in a renal tubule or its adjacent peritubular capillary *in vivo*.

In the proximal tubule, increased peritubular [HCO_3^-] and pH decrease net HCO_3^- reabsorption and increased luminal [HCO_3^-] increases it (Figures 58.5 and 58.6).[26,35] When H^+ secretion (transcellular active transport) is measured with varying luminal [HCO_3^-] at two levels of constant plasma [HCO_3^-],[36] two features are evident. First, the proximal HCO_3^- threshold is not 25 mM but rather 40-50 mM.[36] The threshold depicted in Figure 58.4 of 24 mM is a whole animal phenomenon. Second, increase in peritubular [HCO_3^-] reduces the HCO_3^- transport capacity of the proximal tubule (Figure 58.6). Acute increases in plasma [HCO_3^-] and pH (peritubular) also decrease distal tubule HCO_3^- reabsorption *in vivo*.[37] On the other hand, increases in luminal [HCO_3^-] increases HCO_3^- reabsorption in both proximal[35] and distal[37] tubules. Acute HCO_3^- addition

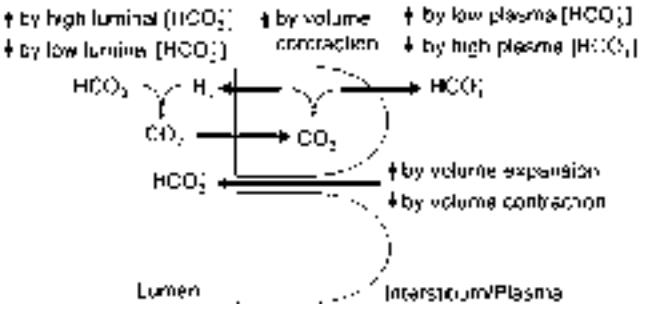

FIGURE 58.5 Regulation of proximal tubule transcellular HCO_3^- absorption (H^+ secretion). Transcellular bicarbonate reabsorption is regulated by both luminal and plasma [HCO_3^-] and pH, and ECF volume while paracellular HCO_3^- back-leak is regulated by extracellular fluid volume.

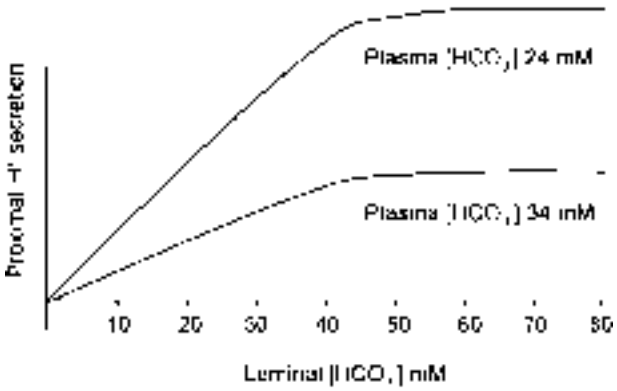

FIGURE 58.6 Interaction of luminal and plasma [HCO_3^-] on rate of transcellular H^+ secretion in rat proximal tubule. At each level of luminal [HCO_3^-], plasma [HCO_3^-] influences proximal acidification.

to ECF will inhibit both proximal and distal HCO_3^- reabsorption by increasing peritubular [HCO_3^-] but the concurrent increase in luminal [HCO_3^-] will stimulate proximal absorption and depending on whether the increased luminal [HCO_3^-] is translated axially down the nephron, it may offset the distal effect of increased peritubular [HCO_3^-].

ECF Volume and Dietary NaCl

Classic clearance studies showed increasing bicarbonaturia as ECF [HCO_3^-] (and HCO_3^- filtered load) rises above baseline in response to isotonic $NaHCO_3^-$ infusion[17] suggesting that the kidney ordinarily operates near its maximal capacity for HCO_3^- reabsorption. Renal HCO_3^- reabsorption can be dramatically enhanced above control levels when ECF [HCO_3^-] and filtered HCO_3^- load are increased with hypertonic $NaHCO_3^-$ infusion with minimal concomitant volume expansion.[38,39] In the absence of volume expansion, proximal tubule HCO_3^- reabsorption increases robustly in response to increasing luminal [HCO_3];[36] showing

partial saturation at a luminal [HCO_3] that is nearly twice that of plasma.[36] These studies highlight the kidneys' large intrinsic capacity for HCO_3^- reabsorption—an ability that is important in maintaining metabolic alkalosis.

Renal HCO_3^- reabsorption is inversely related to the state of effective ECF volume (Figure 58.5).[40] Volume expansion decreases fractional HCO_3^- reabsorption in the proximal convoluted tubule whether it is achieved with isotonic Ringers solution or with salt-poor hyperoncotic albumin.[41] Decreased proximal tubule HCO_3^- reabsorption induced by volume expansion is due to increased HCO_3^- permeability from peritubular blood to the tubule lumen, which likely increase "back-leak" of HCO_3^- into the tubule lumen and reducing net HCO_3^- reabsorption;[36] volume expansion induced no changes in proximal tubule H^+ secretion.[36] Thus, adequate ECF volume is an important permissive factor for renal excretion of excess ECF HCO_3^-. Dietary restriction or excess of NaCl yields subtle changes in ECF volume and influence steady-state ECF [HCO_3^-] via modulation of renal HCO_3^- excretion. Animals ingesting a NaCl-restricted diet have higher plasma [HCO_3^-] and lower urinary HCO_3^- excretion.[32] Furthermore, humans given $NaHCO_3$ increase their ECF [HCO_3^-] when they concomitantly ingest an NaCl-restricted diet.[42] Dietary NaCl restriction also increases ECF [HCO_3^-] in animals[43] and humans[44] with uremic acidosis. Dietary NaCl also induce distal HCO_3^- secretion.[32] Thus, supplemental dietary NaCl facilitates excretion of HCO_3^- added to ECF.

Potassium Status

K^+ deficiency is associated with intracellular acidosis independent of the extracellular pH.[45] To a renal epithelial cell, this likely provides a signal that calls for augmentation of HCO_3^- absorption. K^+ depletion causes metabolic alkalosis in rats[46] and humans[14] by multiple mechanisms, some of which are not fully clarified. Because K^+ depletion causes renal Cl^- wasting,[47] the effects of K^+ depletion with respect to renal HCO_3^- handling might be due in part to KCl depletion. Renal HCO_3^- reabsorption is greater in K^+-deplete compared to K^+-replete animals, and K^+ loading augments urinary HCO_3^- excretion in response to HCO_3^- infusion at all levels of ECF volume.[48] Acute $NaHCO_3$ infusion induces less renal HCO_3^- excretion and higher ECF [HCO_3^-] in KCl-deplete animals compared to K^+-replete ones.[22,49] Thus, KCl depletion reduces renal ability to excrete excess ECF HCO_3^- and helps to maintain metabolic alkalosis. There is a very modest increase in the mRNAs for the subunits of H,K-ATPases in the outer medulla;[50–52] the physiologic significance of this finding is not known.

Hormones Affecting Renal HCO_3^- Excretion

Addition of HCO_3^- to the ECF may modulate renal HCO_3^- excretion. ECF volume expansion due to $NaHCO_3$ administration decreases angiotensin II and aldosterone levels,[2] both being stimulatory hormones for renal tubule HCO_3^- reabsorption.[53,54] More importantly, euvolemic increases in ECF [HCO_3^-] and pH generated by dialysis decrease plasma aldosterone concentration.[45] Vasoactive intestinal peptide which increases after meals,[55] increases distal tubule HCO_3^- secretion,[30] possibly facilitating postprandial urinary HCO_3^- excretion. Dietary $NaHCO_3$ increases urinary prostacyclin, which also augments distal tubule HCO_3^- secretion.[31] Altered actions of these and other agonists induced by ECF HCO_3^- addition might contribute to urinary HCO_3^- excretion. In contrast, disturbances in such responses might contribute to the persistence of excess ECF HCO_3^- and maintenance of metabolic alkalosis.

MECHANISMS OF METABOLIC ALKALOSIS

When the rate of HCO_3^- generation or administration exceeds the capacity of regulatory mechanisms to immediately correct it, transient disequilibrium metabolic alkalosis can occur. Most commonly, the generation of excess ECF HCO_3^- is not sustained and ECF acid–base composition is returned to normal. Sustained metabolic alkalosis is hard to achieve with normal renal HCO_3^- excretory ability[18] and invariably involves compromised renal ability to excrete HCO_3^- and/or failure to reduce net acid excretion.

Generation of Excess ECF HCO_3^-

Figure 58.7 summarizes the factors that generate the elevation of plasma [HCO_3^-] which is broadly segregated into alkali (HCO_3^-) gain and H^+ loss. It is important to indicate that generation alone cannot beget the clinical syndrome without augmenting maintenance factors.

Exogenous Alkali (HCO_3^-) Gain

Administration of HCO_3^- or its precursors adds HCO_3^- to ECF and causes sustained metabolic alkalosis if renal HCO_3^- excretion is compromised. Some patients ingest $NaHCO_3$ to relieve indigestion, whereas others receive intravenous $NaHCO_3$ for various reasons. Large amounts of HCO_3^- precursors such as citrate might be administered during massive blood transfusions or plasmapheresis, which when metabolized, adds HCO_3^- to ECF. Metabolizable organic

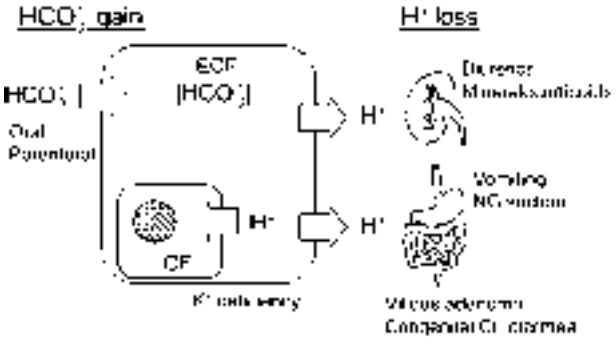

FIGURE 58.7 Generation of high plasma [HCO_3^-]. Elevation of [HCO_3^-] in the ECF can result from gain of HCO_3^- equivalent or loss of H^+ into the ICF, or out of the body via the kidney or gastrointestinal tract. Decrease of a massively expanded ECFV from isotonic NaCl and water loss (e.g., aggressive natriuretic therapy) around a fixed amount of HCO_3^- can raise the plasma [HCO_3^-] (not shown in figure). Note this requires a large fall in ECFV. For instance, if a grossly expanded ECFV of 28 L with a ECF [HCO_3^-] of 24 mM is reduced to 22 L by a 6 L NaCl-water loss, the resultant ECFV [HCO_3^-] will rise to 30 mM.

anions such as ketoacids and lactate are also HCO_3^- precursors. Treatment of organic acidosis with HCO_3^- might generate excess ECF HCO_3^- when the inciting metabolic disturbance is corrected and retained organic anions are metabolized. Metabolic alkalosis can be encountered transiently in these settings but is eventually corrected if renal HCO_3^- excretory mechanisms are intact. Dialysis against a dialysate with high [HCO_3^-] in an anephric patient can also generate metabolic alkalosis until the HCO_3^- is neutralized by endogenous acid production.

External H^+ Loss

Extrarenal H^+ loss primarily is due to gastric fluid loss from vomiting or nasogastric suction is the most common extrarenal H^+ loss that generates metabolic alkalosis. Gastric parietal cells add H^+ to the lumen and HCO_3^- to adjacent perigastric blood.[56] Gastric fluid entering the duodenum is neutralized by HCO_3^--containing pancreatic and biliary secretions,[57] so that acid−base balance is maintained under normal circumstances. External gastric fluid loss perturbs this balance as well as increases gastric pH, stimulating further luminal H^+ addition and perigastric HCO_3^- addition.[56] The generated excess ECF HCO_3^- initially causes bicarbonaturia with urine Na^+ and K^+ losses;[58] both of these contribute to the subsequent maintenance of metabolic alkalosis. Less commonly, extrarenal external H^+ loss generates metabolic alkalosis through lower GI fluid losses in some unusual diarrheal states. Diarrheal fluids are commonly alkali but H^+-rich diarrheal fluids occur with some villous adenomata[59] and with congenital chloridorrhea.[60]

Renal H^+ loss is another important source. For each mEq of renal net acid excretion, a mEq of HCO_3^- is added to ECF.[16] When renal acid excretion (HCO_3^- generation) exceeds H^+ addition (HCO_3^- consumption) to the body, excess ECF HCO_3^- accumulation occurs. Loop diuretics increase renal acid excretion,[61] and increase ECF [HCO_3^-],[62] and chronic administration of these agents can induce metabolic alkalosis, particularly when combined with a low intake of dietary Na and K.[63] Mineralocorticoids increase urine net acid excretion and ECF [HCO_3^-][64] by increasing distal nephron H^+-ATPase and H^+ secretion.[52] Ingestion of a NaCl-restricted diet blunts the ability of mineralocorticoid to induce volume expansion and metabolic alkalosis.[65] The combination of increased mineralocorticoid activity with inappropriately high distal Na^+ delivery greatly enhances distal nephron acidification[66] and K^+ loss, which further augments distal acidification[67] by increasing ammonium production[68] and activating distal nephron H^+,K^+-ATPase.[52]

Internal H^+ Shift

Potassium depletion induces metabolic alkalosis by multiple mechanisms.[66] Severe K^+ depletion induces movement of ECF H^+ into ICF in partial cationic replacement of lost intracellular K^+,[69] generating ECF HCO_3 by mechanisms discussed earlier. Conversely, K^+ repletion of K^+-depleted animals with metabolic alkalosis decreases ECF [HCO_3] in part by titration of ECF HCO_3^- by H^+ exiting from ICF in cationic exchange for administered K^+.[70] In severe K^+ depletion, there may be an enormous amount of H^+ accumulation in the cell such that there may be a total body H^+ excess hence warranting the designation of "metabolic acidosis" even though the ECF [HCO_3^-] may be high.[71] This is a potentially confusing but important concept to grasp.

No Net loss or Gain of H^+/HCO_3^-

Not shown in Figure 58.7 is what is referred to as "contraction alkalosis." ECF [HCO_3^-] can theoretically be increased by decreasing ECF volume around a constant HCO_3^- content through reductions in ECF NaCl and H_2O. In the purest form of contraction alkalosis, there is no true generation of HCO_3^-. In clinical settings, this mechanism of increased ECF [HCO_3^-] rarely occurs in isolation but more often exists in concert with other mechanisms that generate HCO_3^- such as GI and renal H^+ loss. Experimental models that explore this mechanism of generating metabolic alkalosis have been created in animals subjected to acute urinary losses induced by furosemide.[72] The rise in ECF [HCO_3^-] in this setting cannot be attributed exclusively to reduced ECF volume because furosemide also increases excretion of K^+ and H^+,[61] each of which generates metabolic

alkalosis. The rise in ECF [HCO_3^-] in these animals is proportionately less than the decrease in ECF volume, due in part to HCO_3^- entry into ICF, titration by non-HCO_3^- buffers, and urinary HCO_3^- excretion.[60,73]

Maintenance of Excess ECF HCO_3^-

While metabolic acidosis can result from acid production overwhelming maximal renal acid excretion, alkalosis is maintained primarily by compromising renal HCO_3^- excretion. In settings where metabolic alkalosis is due exclusively to excess HCO_3^- ingestion or generation, the disorder is self-limited and is associated with alkaline urine, reflecting an appropriate renal response. In sustained metabolic alkalosis, the urine is not alkaline, reflecting little to no urine HCO_3^- excretion in the presence of elevated plasma [HCO_3^-].

As shown in Figure 58.8, high plasma [HCO_3^-] can be maintained by low GFR or increased renal tubule HCO_3^- reabsorption. The following section describes factors that play a role in the chronic maintenance of excess ECF HCO_3^-: (1) Decreased GFR. (2) K^+ depletion. (3) ECFV depletion or Cl^- depletion. (4) Mineralocorticoid excess. The latter three are the most important.

Decreased GFR

Reduction in GFR can theoretically normalize the amount of HCO_3^- filtered despite a high plasma [HCO_3^-]. Indeed, the level of GFR reduction in some experimental models of chronic metabolic alkalosis yields a filtered HCO_3^- load (GFR x plasma [HCO_3^-]) and absolute renal HCO_3^- reabsorption that is not different from control.[74] This will be a mechanism of maintenance where low GFR is the sole culprit and there is no tubulopathy. Administration of crystalloid to this model increases GFR and reduces the ECF [HCO_3^-].[74] Infusion of atrial natriuretic peptide increases GFR and reduces excess ECF HCO_3^-.[75] However, establishing reduction of GFR as a major maintenance factor for metabolic alkalosis has been problematic. In some models of chronic metabolic alkalosis, GFR is comparable to control[49] or even higher.[76] Exogenous HCO_3^- administration to animals with reduced GFR still induces appropriate urinary HCO_3^- excretion[77] indicating that tubular responses return acid–base status towards normal despite low GFR. In humans, the slight GFR reduction in subjects with chronic metabolic alkalosis contributes minimally to maintenance compared to enhanced renal tubular HCO_3^- reabsorption. Most published studies show that GFR is normal[78] to slightly reduced[79] in humans with chronic metabolic alkalosis. In human studies that did show reduced GFR, the level of GFR reduction is not sufficient to account for the rise in ECF HCO_3^-, indicating a concomitant enhancement of renal HCO_3^- reabsorption must exist.[80,79] Kunau and coworkers convincing showed that isohydric expansion of ECFV in the presence of renal arterial restriction to keep GFR low successfully resulted in bicarbonaturioa and correction of alkalosis.[81] In summary, GFR reduction may contribute but does not play a major role in maintaining chronic metabolic alkalosis in humans. A tubulopathy has to come to play.

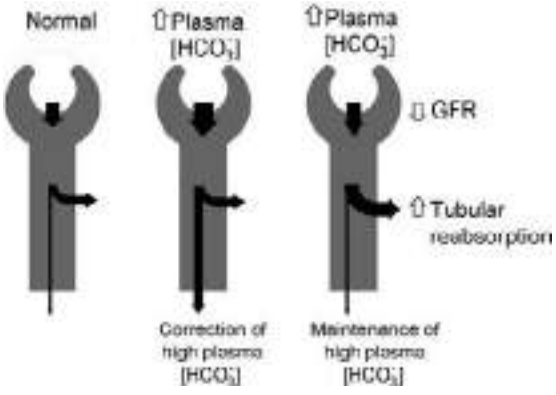

FIGURE 58.8 Renal maintenance of high plasma [HCO_3^-]. Normally there is little or no HCO_3^- in the urine (left panel). With elevation of plasma [HCO_3^-], the increased filtered load leads to obligatory bicarbonaturia and correction of the alkalosis (middle panel). High plasma [HCO_3^-] can be maintained by either reduced GFR or increased tubular reabsorption (right panel); the latter being much more important.

K^+ Depletion

Depletion of total body K^+ maintains metabolic alkalosis by multiple complex mechanisms (Table 58.1). K^+ depletion reduces urine HCO_3^- excretion in response to administered HCO_3^-.[22,48] Thus, K^+ depletion limits renal HCO_3^- excretion after generation of metabolic alkalosis. Decreased renal HCO_3^- excretion has been shown to be mediated by increased HCO_3^- reabsorption in both the proximal[81,82] and distal[67,82] nephron in animals with K^+ depletion.

TABLE 58.1 Mechanisms by which K^+ Depletion Contributes to Metabolic Alkalosis

Reduction of GFR
Increased ammonia production
Hypocitraturia
Increased proximal tubule acidification
Increased distal tubule acidification
Increased renal Cl^- wasting

Increased renal tubule HCO_3^- reabsorption might be due to reduced intracellular pH in renal tubule cells of K^+-depleted animals.[83] This electrolyte abnormality also increases renal ammonia production,[68] which would facilitate augmented net H^+ excretion,[84] the latter generating and maintaining metabolic alkalosis by the mechanisms discussed earlier. Potassium depletion causes renal Cl^- wasting[47] and thereby volume depletion, which can maintain metabolic alkalosis. Severe K^+ depletion can also decrease GFR,[85] which might contribute somewhat to maintain metabolic alkalosis. As noted earlier, K^+ depletion enhances metabolic alkalosis induced by exogenous mineralocorticoids.[64] However, K^+-depletion *per se* reduces mineralocorticoid production.[86] which is expected to reduce renal acidification.[52] Nevertheless, K^+-depleted animals with metabolic alkalosis and reduced serum aldosterone levels[87] still have increased proximal[49] and distal[49,87] tubule acidification, suggesting that other factors can increase renal acid excretion in this setting. K^+ depletion clearly is an important maintenance factor for metabolic alkalosis and should be searched for and treated if found in patients with metabolic alkalosis as part of the management of patients with this acid–base disorder.

ECF Volume Depletion

Reduced ECF volume is probably the single most important maintenance factor for metabolic alkalosis in the clinical setting in humans[78] and is a feature of many experimental models of this acid–base disorder.[3] In a gastric acid loss model of metabolic alkalosis in humans, volume repletion reduces excess ECF HCO_3^- leading to correction of the alkalosis.[58] In support of the pivotal importance of ECF volume depletion rather than hypochloremia is the demonstration that in diuretic-induced hypochloremic alkalosis, expansion of ECF volume with hypochloric solutions corrected the metabolic alkalosis without raising the serum chloride concentration.[88] Still unsettled is whether total body Cl^- depletion independent of ECF volume depletion can maintain metabolic alkalosis. Nevertheless even in purported volume-replete experimental models of metabolic alkalosis in which the removed NaCl is replaced with equimolar $NaHCO_3$, ECF volume depletion can occur due to a shift of ECF $NaHCO_3$ into ICF as HCO_3^- space is larger than ECF.[1] Volume-deplete subjects clearly excrete less of an administered HCO_3^- load compared to volume-replete or volume-expanded ones.[48,89] Dietary NaCl restriction increases activity of the proximal tubule Na^+/H^+ exchanger.[90] In addition, dietary NaCl restriction reduces luminal Cl^- delivery in the distal tubule,[32] limiting the Cl^- available to promote luminal HCO_3^- secretion.[91,92] Depending on the degree, volume depletion can also decrease GFR[93] and stimulate the renin-angiotensin system[94] and increase angiotensin II, which increases HCO_3^- reabsorption in both the proximal[95] and distal[30] nephron.

Cl^- Depletion

A longstanding controversy has been whether Cl^- depletion *per se* contributes to metabolic alkalosis independent of ECF volume contraction. In support of this view is the fact that Cl^- administration to some Cl^--deplete experimental models of metabolic alkalosis decreases ECF [HCO_3^-] independent of changes in both ECF volume[96,97] and body K^+ stores.[58,96,97]

Although suggestive, interpretive issues still cloud unequivocal proof that Cl^- depletion independent of ECF volume depletion maintains metabolic alkalosis. The intimate relationship of total body Cl^- to ECF volume renders separating the two, even experimentally, exceedingly difficult. Models in which NaCl removal is replaced with equimolar $NaHCO_3$ can induce ECF volume depletion due to shifts of Na^+ out of the ECF as HCO_3^- is distributed in the non-anatomic space as indicated earlier.[1] Experimental models where reduction of total body Cl^- is not accompanied by detectable ECF volume contraction[49,98] are difficult to reconcile with clinical practice where Cl^- depletion is almost invariably associated with ECF volume depletion. Cl^- depletion and repletion both carry changes in the accompanying cation which is either Na^+ or K^+; both of which can affect HCO_3^- homeostasis per se. The one mechanism that Cl^- can affect distal HCO_3^- secretion independent of Na^+ and K^+ is by activiting distal Cl^-/HCO_3^- exchange. Thus far, data supporting Cl^- depletion per se as an independent factor independent of ECF volume and K^+ depletion are not conclusive.

Excess Mineralocorticoid Activity

Hypermineralocorticoid states have long been associated with metabolic alkalosis[3,99] and correction of the excess mineralocorticoid state in humans effectively reduces excess ECF HCO_3^-.[65] Two points are noteworthy. First, one is referring to a primary increase in mineralocorticoid activity rather than the elevation in response to volume contraction or hyperkalemia.[94] High aldosterone activity in subjects with volume depletion contributes to maintenance of excess HCO_3^- where distal Na^+ delivery is high such as in gastric alkalosis with bicarbonaturia and in diuretic therapy. Second, excess mineralocorticoid activity denotes a heightened state of biologic activity rather than just levels of mineralocorticoids. One action of mineralocorticoids is to increase distal nephron and net acid excretion acidification,[54,100] which can generate and maintain excess ECF HCO_3^-.

The ability of mineralocorticoids to generate and maintain metabolic alkalosis depends on the Na^+

and K^+ status of the subject. It is very important to note that humans on a low-salt diet given mineralocorticoid do not develop metabolic alkalosis or hypokalemia.[65,101,102] Exogenous mineralocorticoids lead to minor changes in net acid excretion in K^+-replete dogs in contrast to a large increase in acid excretion in K^+-deplete animals.[64] Patients with primary hyperaldosteronism with the most severe K^+ depletion have the worst metabolic alkalosis.[103] This illustrates the importance of multiple factors in the maintenance of metabolic alkalosis.

Derangements in Renal Acidification in Metabolic Alkalosis

How do the above factors act to maintain the abnormal tubular function? There is a prevailing but yet unproven dogma that the renal tubule is completely normal but simply misdirected by the incoming signals to maintain a high rate of acid excretion and low rate of HCO_3^- secretion in the face of a high plasma [HCO_3^-]; somewhat of a mendicant organ just blindly taking orders so to speak. Unflattering as it may sound, this is widely believed to be true mainly due to the rapid reversal when the principal defects of ECFV contraction, K^+ depletion, and high mineralocorticoid activity are corrected.

Different experimental models of metabolic alkalosis may use diverse generation and maintenance mechanisms.[49] In several models, it is maintained by increased whole-kidney HCO_3^- reabsorption, which stems from both proximal and distal mechanisms. One difficulty in interpretation of the current body of animal data is the heterogeneity of the models and to a lesser extent species variation. Table 58.2 summarizes the documented or predicted changes in the three pivotal pathophysiologic factors affecting renal acidification in various models of metabolic alkalosis. ECF volume contraction and K^+ depletion increases proximal acidification. All three factors affect distal acidification.

TABLE 58.2 Mechanisms of Metabolic Alkalosis in Selected Models

Model	ECFV↓	K^+↓	MC↑
$NaHCO_3$ load	−	±	−
Replace NaCl with $NaHCO_3$	+/−	+	+/−
Diuretic	−	−	+
K^+ depletion	+/−	+	−
Exogenous MC	−	+	+

ECFV, extracellular fluid volume; MC, mineralocorticoid.

Proximal Tubule and Thick Ascending Limb

This is best exemplified by the classic experiment of Maddox and Gennari.[104] Absolute proximal tubule HCO_3^- absorption increases with increasing filtered HCO_3^- (Figure 58.9). When metabolic alkalosis is induced with acute infusion of $NaHCO_3$, filtered load is increased but reabsorption is not, resulting in massive bicarbonaturia. During the maintenance phase of chronic metabolic alkalosis, even when both the plasma [HCO_3^-] and filtered load are as high as in the acute situation, proximal HCO_3^- continues to increase (Figure 58.9) instead of the expected inhibition by high plasma [HCO_3^-] (Figures 58.5 and 58.9). This finding indicates there are intrinsic changes in the proximal tubule epithelium.

Proximal tubule HCO_3^- reabsorption is increased in K^+- and Cl^--deplete model of diuretic-induced metabolic alkalosis.[49,76] The increase is related in part to the augmented filtered HCO_3^- load delivered to the proximal tubule.[49,76] The effect of increased luminal [HCO_3^-] on HCO_3^- reabsorption in the proximal tubule is offset by the increased ECF [HCO_3].[35] ECF volume contraction also increases proximal tubule Na^+/H^+ exchange activity[40] and the proximal tubule autocrine/paracrine renin angiotensin system.[105] Thus, proximal tubule HCO_3^- reabsorption is not decreased, as would be expected to be homeostatically appropriate in the setting of excess ECF HCO_3.

The stimulation of proximal tubule HCO_3^- reabsorption by K^+ depletion[81] is possibly mediated by intracellular acidification.[83] Chronic hypokalemia increases the proximal tubule ensemble of Na^+/H^+ exchanger (NHE3),[106,107] ammoniagenic enzymes.[68,108,109] Na^+-dicarboxylate (citrate) cotransporter (NaDC-1)[110] and citrate metabolism[111] and Na-bicarbonate cotransporter[106] and expression of angiotensin II receptor, AT1;[112]

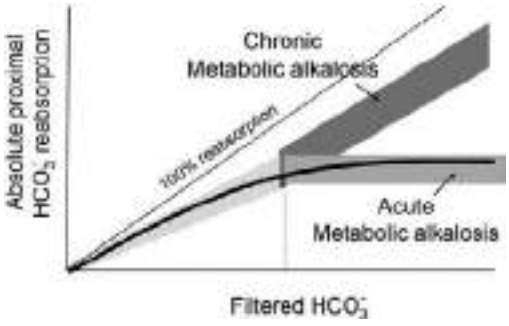

FIGURE 58.9 The relationship of absolute proximal tubule HCO_3^- absorption as a function of filtered load of HCO_3^- under free flow condition. The dotted line denotes the normal filtered load. The heavy solid line represents the normal relationship between filtered and absorbed HCO_3^-. In the acute setting, this is only a very small deviation from normal. In chronic metabolic alkalosis, tubular reabsorption is increased so the increased filtered load is reclaimed.

probably all mediated by intracellular acidification. Inhibition of the proximal Na-sulfate cotransporter NaSi-1[113] does not affect proximal acidification *per se* but the increased distal sulfate delivery of a non-absorbable anion can increase distal H^+ secretion. Note that simple $NaHCO_3$ loading without persistent metabolic alkalosis led to a decrease of NHE3[114] and NBC-1[115] suggesting the conglomerate changes listed above are involved with the maintenance of metabolic alkalosis. Other possible explanations of the increased proximal tubule HCO_3^- reabsorption in metabolic alkalosis is volume depletion,[116] with its attendant changes in proximal tubule HCO_3^- permeability[35] and its resulting hormonal changes, including stimulation of the renin-angiotensin system.[94,105] In addition, diuretic-induced metabolic alkalosis is associated with increased renal endothelin-1 secretion,[87] which can increase Na^+/H^+ exchange.[117] These changes are summarized in Figure 58.10.

Derangements in the thick ascending limb are less consistent in metabolic alkalosis. Absorption of HCO_3^- is increased by either $NaHCO_3$ or NaCl administration but reduced by NaCl restriction.[118] The effect of ECF volume may dominate over the effects of high plasma pH and $[HCO_3^-]$. K^+ depletion may facilitate delivery of ammonium to the collecting thus contributing to increase net acid excretion.[84] The role of the thick limb in the maintenance of metabolic alkalosis is unclear.

Distal Convoluted and Collecting Tubule

In distal renal tubular acidosis or overproduction acidosis, distal H^+ secretion is insufficient to effect the net acid excretion so as to maintain net acid balance,[89] but the distal nephron nevertheless contributes to overall acid excretion to correct the acidosis. In contrast, metabolic alkalosis is maintained by distal acidification that is inappropriately increased which makes it the guilty party resulting in maintenance of the alkalosis.

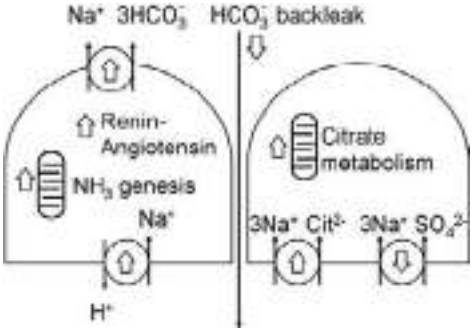

FIGURE 58.10 Proximal tubule pathophysiology in metabolic alkalosis. Changes are caused predominantly by effective ECF volume contraction and K^+ deficiency. A host of metabolic and transport changes that culminate in increased proximal H^+ secretion and HCO_3^- absorption.

In a KCl-deplete model of diuretic-induced metabolic alkalosis, HCO_3^- reabsorption measured *in situ* in the surface distal tubule is increased.[49] Both fractional and absolute HCO_3^- reabsorption in the distal tubule are higher[49] so this is not just due to increased filtered load but rather to augmented distal tubule H^+ secretion.[29,119] Although distal tubule HCO_3^- secretion is also increased, likely driven by increased plasma $[HCO_3^-]$,[29] the increased HCO_3^- secretion is smaller in magnitude compared to the increased H^+ secretion so that net distal tubule acidification is increased.[49] This can be mediated by ECF volume contraction, K^+ deficiency or high aldosterone.

K^+ depletion increases distal acidification[120] mediated in part by stimulated distal nephron colonic isoform of H^+,K^+-ATPase activity.[37,87,121,122] Animals with diuretic-induced K^+-depletion and chronic metabolic alkalosis also have increased distal tubule Na^+/H^+ activity mediated in part by endogenous endothelins.[87] On the other hand, K^+ depletion decreases aldosterone secretion,[86] that is expected to decrease distal nephron H^+-ATPase activity[52] and decrease distal nephron acidification. In a diuretic-induced K^+-depletion model of metabolic alkalosis, neither aldosterone levels nor H^+-ATPase activity are increased, yet distal acidification is stimulated.[87] In addition, K^+ depletion increases proximal ammonia production by inducing ammoniagenic enzymes,[123,124] which in the presence of increased distal acidification, increases urine net acid excretion.[84] Therefore, K^+ depletion increases distal nephron acidification mediated by increased activity of at least two distal nephron H^+ transporters. This augmented distal nephron acidification hampers excretion of excess ECF HCO_3^-. Potassium depletion can both generate and maintain metabolic alkalosis.

Mineralocorticoids can increase distal nephron acidification by a number of mechanisms. Mineralocorticoids increase collecting tubule Na^+ reabsorption and luminal electronegativity,[125] which increases electrogenic acidification.[125] Aldosterone also increases activity of collecting tubule Na^+/K^+-ATPase,[125] lowering intracellular Na^+ and thereby stimulating luminal Na^+/H^+ exchanger.[37] Finally, aldosterone directly stimulates activity of H^+-ATPase, a major H^+ transporter in the cortical and medullary collecting tubule.[52] The ECF $[HCO_3^-]$ of animals with metabolic alkalosis is higher when activities of both H^+-ATPase (stimulated by high mineralocorticoid levels) and H^+,K^+-ATPase (stimulated by K^+ depletion) are increased, compared to isolated increased activity of either transporter.[52]

In acute alkali loading, the anion-exchanger-1 (AE1) on the basolateral membrane of acid-secreting β-intercalated cells is much reduced consistent with an appropriate compensation to lower H^+ secretion.[126] It is unclear what is causing the impairment of this

compensation in chronic metabolic alkalosis. One possibility is the limited luminal Cl^- in ECF volume contraction due to increased proximal Cl^- absorption. Regardless of whether there are more Cl^-/HCO_3^- exchangers, paucity of luminal Cl^- can impair the apical Cl^-/HCO_3^- exchange and HCO_3^- secretion in this segment.[91,127,128]

An apical membrane Cl^-/base exchanger in the distal nephron, Pendrin (gene product of *Slc26A4*), should be the main player in base secretion in the collecting duct and theoretically assume a central pathogenic role in the maintenance of metabolic alkalosis. $NaHCO_3$ loading *per se* increases pendrin expression suggesting it does defend against alkalosis.[129,130] In a model of hypermineralocorticoid activity, pendrin is upregulated presumably to augment apical HCO_3^- secretion [131] but in a K^+ depletion model, Pendrin is down regulated suggesting that it is actually the culprit.[132] Pendrin-/- animals at baseline do not have high plasma [HCO_3^-] but when subjected to induction of metabolic alkalosis have higher plasma [HCO_3^-] than Pendrin + / + animals.[131] Interestingly, K^+ depletion did not elicit increased Pendrin expression[130] despite the fact that the ECF [HCO_3^-] is high. This discrepancy may be attributable to the presence of intracellular acidosis in K^+ depletion. At present, although one expected Pendrin to assume a central role in maintaining metabolic alkalosis, the experimental data are inconclusive.

One player that has recently been implicated in the maintenance of metabolic alkalosis is the epithelial Na^+ channel ENaC. While ENaC is considered to be mainly important for Na^+ absorption and K^+ secretion, it does provide the luminal negative voltage that is important for H^+. As discussed below, dominant gain-of-function mutations of ENaC subunits can lead to metabolic alkalosis. The presence of alkalemia per se appears to stimulate ENaC independent of aldosterone activity which can contribute to the heightened acidification.[133]

The delivery of Na^+ salts of poorly reabsorbable anions increases distal nephron acidification in association with increased mineralocorticoid activity.[93] Na^+ absorption without an accompanying anion greatly increases luminal electronegativity[134] and promotes distal H^+ secretion.[93] Non-reabsorbable anions that can induce this phenomenon include sulfate,[135] nitrate,[93] and the penicillin class of antibiotics.[136,137] The pathophysiology of distal acidification is summarized in Figure 58.11.

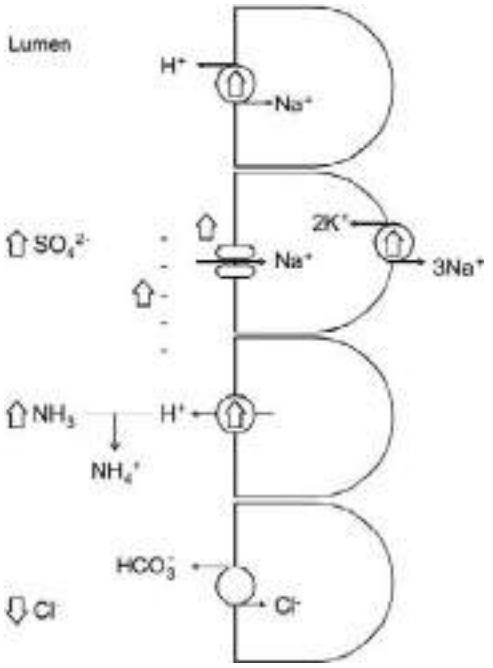

FIGURE 58.11 Distal tubule pathophysiology in metabolic alkalosis. The changes can be caused by K^+ depletion, hypermineralocorticoid activity and effective ECF volume contraction. The changes include increased H^+ secretion, reduced HCO_3^- absorption, increased luminal negativity and buffer capacity.

Consideration of an Intrinsic Tubular Defect

Although there is no doubt that metabolic alkalosis can only be sustained by changes in the renal tubules. Thus far, one is working with the assumption that the kidney is merely being misdirected by the incoming signals described above. There are some highly fundamental questions that need to be considered. Is the kidney capable of independently sensing and setting plasma pH and [HCO_3^-]? The sensing of pH and [HCO_3^-] are fundamentally different biologic processes that utilize different molecular mechanisms. If such sensing ability exists, why is the kidney not responding to the higher plasma [HCO_3^-] but remaining obedient to the erroneous signals. Does metabolic alkalosis represent a state where there is a resetting of the sensors in the kidney? There is strong *in vitro* evidence that renal epithelial cells can sense and respond to changes in ambient pH and [HCO_3^-].[138] A host of proteins with pH and [HCO_3^-] sensing capabilities have been identified and a subset of them is expressed in the kidney.[139] Direct sensing of intracellular [HCO_3^-] is performed by the soluble adenylyl cyclase (sAC) which is also expressed in the rodent and human kidney.[140,141] Recently, a tyrosine kinase, the insulin-related receptor (IRR) was shown to be an extracellular pH sensor that reacts to alkaline pH changes.[142] Despite the fact that the pH required for activation is way higher than the typical clinical range (>7.9), genetic disruption of IRR resulted in blunted bicarbonaturia and higher plasma [HCO_3^-] in response to HCO_3^- loading in situations where ECF volume contraction K^+ deficiency or

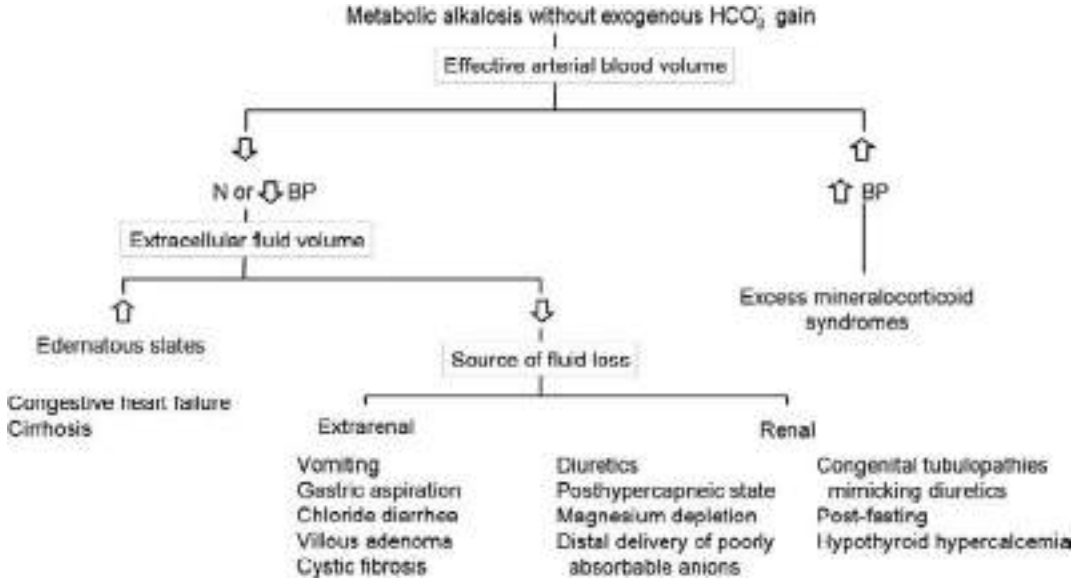

FIGURE 58.12 Summary of pathophysiology of maintenance of metabolic alkalosis. In one model, the three principal signals extrinsic to the kidney govern renal acidification to render the urine HCO_3^- and maintains a high ECFV [HCO_3^-]. The renal tubules are not defective but simply misguided. In the bottom situation, an alternative concept is presented. H^+ or HCO_3^- sensors in the kidney are reset to a new set-point to regulate renal acidification to maintain ECFV [HCO_3^-] at a higher level independent of incoming signals. These two mechanisms are not necessarily mutually exclusive.

heightened mineralocorticoid activity is are unlikely to be present.[142] This is the first demonstration that a primary renal defect in HCO_3^- sensing can "reset" the plasma [HCO_3^-] at least transiently without invoking the triple cardinal systemic factors that maintain metabolic alkalosis which is conceptually completely different from the classic view of the renal tubules responding to the three cardinal incoming signals. It will be extremely informative to explore whether renal "resetting" actually occurs in the common syndromes of metabolic alkalosis.

CLINICAL SYNDROMES OF METABOLIC ALKALOSIS

Approach to Patients with Metabolic Alkalosis

The first presentation to a clinician is almost always a chemical one often with the serendipitous discovery of an elevated ECF [HCO_3^-] or total CO_2 on the panel of serum electrolytes. The level of ECF pH elevation combined with associated life-threatening conditions that are caused or exacerbated by the alkalosis will determine whether therapeutic interventions are required to acutely lower ECF pH. Rapid intervention lowers pH either chemically by adding acid (usually HCl),[143] or diffusively with dialysis,[144] independent of the pathophysiology and/or etiology of the metabolic alkalosis. These interventions treat the chemistry but not necessarily the underlying disorder. Thus correction of the chemistry by whatever means does not negate the search for and treatment of the underlying cause. If acute intervention is not necessary, then the principal duty for the clinician is to identify the underlying conditions causing the disorder and address them. As one peruses through the individual clinical syndromes in the following section, always keep in mind that one is dealing with a disorder of renal HCO_3^- absorption and the three salient factors that lead to maintenance of this state are decreased circulating volume as sensed by the kidneys, K^+ deficiency, and hypermineralocorticoid activity on the renal tubule.

History and Physical Examination

A careful history frequently reveals the etiology of metabolic alkalosis. The clinician should probe for factors that might generate excess ECF HCO_3^-, such as intake of HCO_3^- and/or its metabolic precursors, or H^+ loss as might occur from the GI tract (i.e., vomiting) or the kidney (i.e., diuretics). One should also assess the patient's ability to excrete excess ECF HCO_3^- by determining whether the patient has renal failure, loss of body fluids, and/or poor dietary NaCl intake. Furthermore, the clinician must inquire about factors that maintain metabolic alkalosis, such as conditions that cause volume depletion and intake of medications that might induce renal excretion of H^+ and/or K^+ (e.g., diuretics, mineralocorticoids).

By far, the two most important elements of the physical exam in determining the etiology of metabolic alkalosis are the blood pressure and indicators of the ECF volume. One of the major mediators through which decreased ECF volume maintains metabolic alkalosis is reduced effective arterial volume. Some pathologic conditions such as heart failure, liver failure, and nephrotic syndrome alter systemic hemodynamics in such a way as to reduce renal perfusion pressure even when ECF volume is increased. These conditions are often referred to as states of decreased *effective* arterial blood volume (EABV).

Laboratory Investigation

Because respiratory acidosis can also increase ECF [HCO_3^-] due to the physiologic response to elevated pCO_2,[13] arterial blood gases should be done to rule out this respiratory disorder. The distinction is often but not invariable achieved by history and physical examination alone. Metabolic alkalosis is confirmed by demonstrating a primary increase in ECF [HCO_3^-], with any rise in pCO_2 being secondary. The laboratory values most pertinent in determining the etiology are those that assess EABV such as urine [Cl^-] and [Na^+], and those that determine the degree of activation of the renin-angiotensin-aldosterone system, including serum levels of renin and aldosterone. Not all these laboratory studies are needed in every patient with metabolic alkalosis. Selected use of laboratory determinations with the history and physical exam can permit the clinician to arrive at the diagnosis.

Consequences of Metabolic Alkalosis

Metabolic alkalosis in the outpatient setting is most commonly mild, and its clinical importance often relates to identifying the underlying metabolic disorder such as hypermineralocorticoid states, K^+ deficiency, or natriuretic overuse. In the inpatient setting, it can be a severe metabolic disturbance with marked elevations of ECF pH and associated life-threatening consequences. Combined metabolic and respiratory alkalosis is the most common acid–base disturbance in critically ill patients.[145] Studies of this patient population show a direct correlation between ECF pH $>$ 7.48 and mortality.[146] This relationship represents not only a marker of the catastrophic underlying conditions but also direct consequences of alkalemia as well. The direct adverse effects of metabolic alkalosis are summarized in Table 58.3. While we repeatedly emphasize the need to search and treat the underlying disorder, the direct adverse effects of a high [HCO_3^-] and pH justify chemical correction even if one cannot rectify the root of the problem.

TABLE 58.3 Adverse Effects of Metabolic Alkalosis

1. Ventilatory depression
2. Vasoconstriction
3. Decreased O_2 delivery by hemoglobin
4. Cardiac arrhythmias

Metabolic alkalosis decreases ventilation causing hypercapnea and hypoxemia[11–13,99,147,148] and it can do so with some severity, particularly in patients with underlying lung disease, causing severe hypoxia.[148] This effect is mediated via both central and peripheral chemoreceptors.[149,150] Metabolic alkalosis has many other untoward cardiovascular effects, such as vasoconstriction of various systemic vascular beds.[151] Vasoconstriction has been documented in isolated coronary strips, saphenous, and mesenteric veins *in vitro* by alkaline pH produced either by raising [HCO_3^-] or lowering pCO_2.[152–154] In intact organisms, a high plasma [HCO_3^-] and/or pH reduces blood flow to coronary arteries leading to myocardial ischemia[152] and cerebral vasculature leading to compromised CNS function.[155,156] The adverse consequences of hypoxia are compounded by the alkalosis-induced leftward shift of the hemoglobin-O_2 dissociation curve, which increases O_2 affinity decrease release to tissues.[151,157] In combination with vasoconstriction and hypoxia, this further reduces tissue O_2 delivery, resulting in anaerobic metabolism, possibly contributing to the anion gap frequently described in patients with severe metabolic alkalosis.[158]

Alkalosis lowers the threshold for cardiac arrhythmias, especially those associated with digitalis.[159–161] Arrhythmias concomitant with metabolic alkalosis are reported to be refractory to treatment until the alkalosis is corrected.[161] However, the number of subjects in these reports is relatively small and it is difficult to establish the correct incidence. Critically ill patients frequently have lots of reason to have cardiac dysrhythmias.

Metabolic Alkalosis with Exogenous HCO_3 Gain

Distinct clinical syndromes will be discussed. It is important to state that these conditions may involve exogenous HCO_3^- gain but are usually associated with impaired renal HCO_3^- excretion in order for sustained metabolic alkalosis to be present. Subjects with normal ability to excrete HCO_3^- can ingest large and chronic oral loads of HCO_3^- and its metabolic precursors (e.g., citrate, lactate) without developing sustained elevations of plasma [HCO_3^-]. Acute infusion of up to 1500 mEq of $NaHCO_3$ only transiently elevated plasma

[HCO_3^-].[7] Even chronic administration of this magnitude only raised plasma [HCO_3^-] slightly.[18] Treatment includes limiting or discontinuing alkali intake and increasing renal excretory ability. Other sources of exogenous HCO_3^- include those given during cardiopulmonary arrest, metabolism of citrate in stored blood given during massive transfusions or plasmapheresis, and metabolism of organic acids (e.g., ketoacids) in combination with HCO_3^- therapy for metabolic acidosis.[123]

Non-absorbable antacids (aluminum and magnesium carbonate) can cause metabolic alkalosis when intake is combined with cation exchange resins.[162] The metal carbonate salts usually form metal Cl^- salts when they contact gastric HCl, consuming gastric H^+. When the metal salts reach the HCO_3^--rich upper small bowel, they form insoluble metal carbonate salts which are excreted. Under usual circumstances, ingestion of these metal carbonate salts results in equimolar H^+ and HCO_3^- excretion without changing acid-base balance. However, concomitant ingestion of exchange resin binds the aluminum or magnesium of the antacid, precluding these metals from forming insoluble carbonate salts in the HCO_3^--rich fluid of the upper small intestine. The cation liberated by the exchange resin, usually Na^+, combines with HCO_3^- to form easily absorbable $NaHCO_3$ Consequently, ingestion of the metal carbonate salts with exchange resins leads to consumption of secreted gastric H^+, but subsequent reabsorption of $NaHCO_3$ causing a net HCO_3^- gain. Metabolic alkalosis is sustained when base excretion from the ECF is limited. This is one syndrome where continued exogenous base ingestion does contribute to the metabolic alkalosis.

Milk-Alkali syndrome. Metabolic alkalosis occurs in patients with peptic ulcer disease who ingest large quantities of milk and antacids or more recently in patients on calcium alkali salts for osteoporosis or habitual chewing of betel nuts in Asia.[163–165] Each Alka-Seltzer tablet for instance contained 1.9 g of $NaHCO_3$. Important components of the milk alkali syndrome include high alkali intake, reduced glomerular filtration, and increased tubular reabsorption of HCO_3^-. Hypercalcemia impairs, but the suppressed parathyroid hormone can stimulate proximal HCO_3^- reabsorption. Hypercalcemia also has loop diuretic-like effect that produces Na^+, Cl^- and K^+ wasting via the basolateral calcium sensing receptor.[166] The main mechanism of metabolic alkalosis in the milk alkali syndrome is likely ECF volume contraction. The combination of high urinary calcium and alkaline urine can also lead to nephrocalcinosis.[167] Treatment consists of discontinuation of alkali and calcium.

Metabolic Alkalosis without Exogenous HCO_3 Gain

When history excludes exogenous HCO_3^- gain, the presence or absence of hypertension can be used to categorize patients for subsequent workup. Figure 58.12 provides a general outline. It is important to state that this type of algorithm serves as a guide and to streamline the approach and under no circumstance should it replace the critical thinking that is required to identify the underlying pathophysiology of a patient with metabolic alkalosis. Two critical points in this diagnostic algorithm are the determination of whether there is hypertension and whether effective arterial blood volume is decreased. The latter is not always obvious on clinical grounds alone. Thereafter, whether or not EABV is decreased will further sort the diagnostic possibilities and guide the clinician as to the necessary laboratory tests. Although physical exam findings indicative of ECF volume depletion can be rapidly and cheaply obtained, bear in mind that they may have questionable value in extrapolating to the assessment of effective renal perfusion.[168] Urine indices including fractional excretion of Na^+ and Cl^- have a better predictive value for renal perfusion in such patients.[168]

Metabolic Alkalosis with Decreased Effective Arterial Blood Volume

Decreased EABV with expanded ECFV (edema). This encompasses all the patients with edematous states who despite the expanded ECF volume, have reduced renal perfusion which provides the main contribution to maintenance of metabolic alkalosis. Congestive heart failure is the most relevant condition for discussion in this instance.[169] Metabolic alkalosis occurs in patients with cirrhosis but is often buried in a host of metabolic and respiratory acid–base disturbances.[170,171] The generating and maintenance mechanisms of metabolic alkalosis are not completely understood although multiple hypotheses abound.[172] In addition to the impaired renal perfusion from the primary disease, edematous patients are almost invariably treated with diuretics, most of which will increase H^+ excretion, providing a mechanism for generation of metabolic alkalosis. Further reduction in EABV as well as diuretic-induced K^+ depletion maintains the disorder. Treatment of metabolic alkalosis in these patients is a formidable challenge because they need diuretic therapy. One can improve renal perfusion by reducing diuretic dose, and/or including agents that do not increase renal H^+ and K^+ excretion (e.g., K^+-sparing diuretics amiloride, triamterene, and spironolactone). The most effective treatment is correction or improvement of the underlying disease.

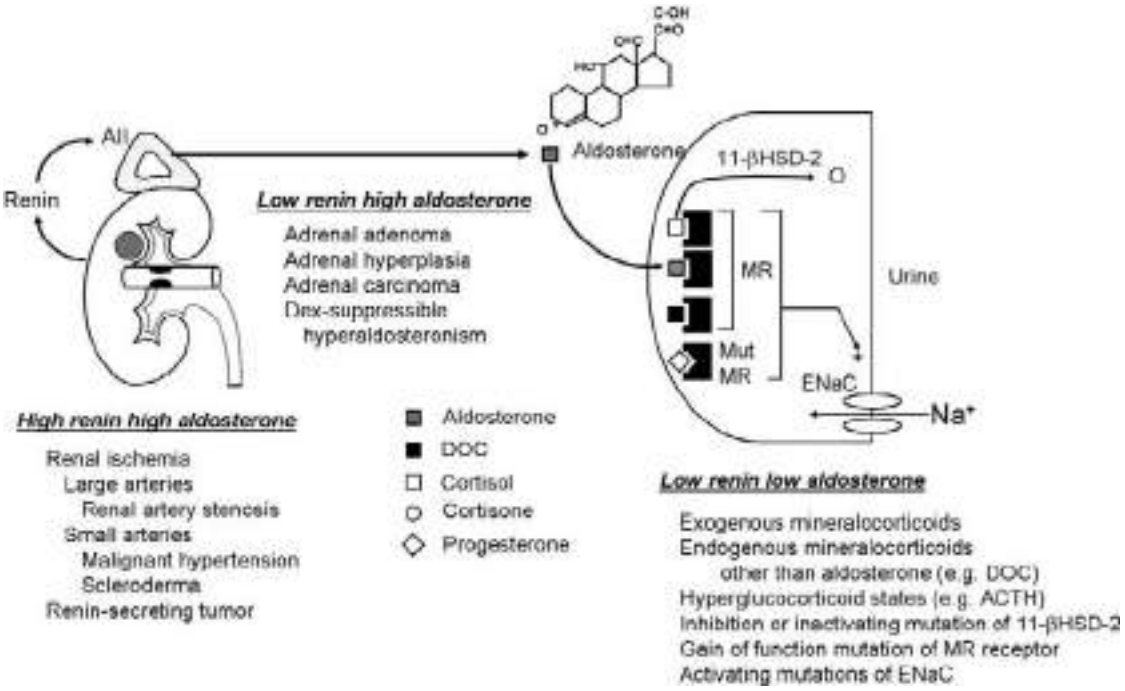

FIGURE 58.13 Hypermineralocorticoid states with hypertension and metabolic alkalosis. Three categories based on renin and aldosterone levels are shown. Left panel- Renal-originated renin disorders. Middle panel-Adrenal disorders. Right panel- Systemic and end organ disorders. DOC: Desoxycorticosterone. 11-βHSD-2: 11-beta-hydroxysteroid dehydrogenase type 2. ENaC: Epithelial Na^+ channel. MR: Mineralocorticoid receptor. Mut MR: Mutant mineralocorticoid receptor.

Decreased EABV without expanded ECF volume (edema). This is the largest group of patients with metabolic alkalosis without hypertension. Decreased ECF and EABV are expected to induce renal conservation of Na^+ and Cl^-, the major cation and anion of ECF. This is indeed true in patients with extrarenal fluid and solute losses; the most important of which derive from the gastrointestinal tract (Fig. 58.13). The gastrointestinal fluid loss can generate and maintain metabolic alkalosis. The second and equally important subgroup is renal fluid loss (Fig. 58.13). This broad group of diseases elegantly illustrates some of the most fascinating mechanisms of generation and maintenance of metabolic alkalosis. Specific syndromes will be discussed below.

Gastric alkalosis. Gastric fluid contains about 80-100 mEq/L of HCl and varying amounts of Na^+ and K^+. Removal of gastric HCl in humans raises ECF HCO_3^-. The estimated reduction in ECF volume can account for only minor part of the rise in ECF [HCO_3^-][78] so HCO_3^- must be added to the ECF.[73] This is initially associated with an alkaline urine and decreased urine net acid excretion, with about half of the latter mediated by bicarbonaturia.[78] In this dysequilibrium state, bicarbonaturia is accompanied by renal Na^+ and K^+ loss.[78] This is one instance where low urinary [Cl^-] is accompanied paradoxically by high urinary [Na^+] because of the obligatory natriuresis in bicarbonaturia.

Although the cation that accompanies HCO_3^- at the glomerular filtrate is primarily Na^+, the high aldosterone activity at the distal tubule causes exchange of luminal Na^+ for K^+ which results in significant K^+ wasting. Alkalosis may itself increase renal K^+ excretion.[173] This sets the stage for the maintenance phase which is mediated by both ECF volume and K^+ depletion. A few days following cessation of gastric HCl removal, urine pH and net acid excretion return to acid values with little or no Na^+, K^+, or HCO_3^- in the urine despite persistent metabolic alkalosis and the subject is in acid–base balance.[78] These data are consistent with an inappropriate renal tubule response to the persistent excess ECF HCO_3^-. Direct measurements of GFR show this parameter to be no different from control, consistent with an overall increase in renal tubular HCO_3^- reabsorption.[78] KCl or NaCl administration increases urine pH and decreases net acid excretion with subsequent normalization of ECF [HCO_3^-].[78] Treatment involve cessation of gastric loss. If nasogastric suction cannot be discontinued, gastric HCl production might be reduced with H_2-blockers or H^+/K^+ ATPase inhibitors.[174] The cornerstone of therapy is disruption of maintenance by NaCl and KCl replacement.

Congenital chloride diarrhea and villous adenoma. In contrast to gastric fluid, lower intestinal content tends to be alkaline so its loss should not generate metabolic alkalosis. This disorder was discovered in the 1940s where infants present with profuse watery diarrhea, high stool Cl^- and the cardinal feature of metabolic alkalosis.[175,176] Two decades elapsed before the pathophysiology guided the proper nomenclature of congenital chloridorrhea or congenital chloride diarrhea.[177] This is an autosomal recessive disease that seems to cluster in Finland[178] and the Middle East[179] and is due to mutation of the Cl^-/HCO_3^- exchanger DRA (*down-regulated in colonic adenoma*; gene product of *SLC26A3*) in the ileal and colonic luminal membrane. Of the list of congenital diarrheal syndromes,[180] this is the only one that causes metabolic alkalosis. The functional lesion has been identified physiologically,[60,181] and subsequently confirmed by the molecular identity[182,183] of the defect. Stool $[Cl^-]$ far exceeds stool $[Na^+ + K^+]$ giving rise to a "cation gap" which is primarily NH_4^+. Parallel activities of Na^+/H^+ exchange and Cl^-/HCO_3^- exchange results in net NaCl absorption. When Cl^-/HCO_3^- exchange exceeds Na^+/H^+ exchange as it does in the colon, it normally creates an alkaline lumen normally. With inactivating mutations of the DRA Cl^-/HCO_3^- exchanger, Na^+/H^+ exchange runs in isolation and converts the intestine into an acid-secreting epithelium. Luminal free H^+ is buffered by NH_3 from the blood or NH_3 generated by the bacterial flora. The end result is copious amounts of Cl^- in the stool accompanied mainly by NH_4^+ and to a lesser extent Na^+ and K^+. Metabolic alkalosis is generated by H^+ loss and maintained by continued H^+ loss, ECF volume, and K^+ depletion from both diarrheal and renal origins. Kaliuresis is a result of intermittent bicarbonaturia, distal Na^+ delivery, and volume-stimulated high aldosterone activity. The only treatment is lifetime replacement of NaCl, KCl, and water.

Rarely, metabolic alkalosis develops in patients with villous adenomata of the colon as first described by Bartter and colleagues in 1965.[184] The secretory nature of these tumors elaborate up to 3 L/day of a clear fluid with high concentration of Cl^-, Na^+, K^+ and variable amount of NH_4^+.[59,185,186] When the concentration of NH_4^+ is high enough, it generates and maintains metabolic alkalosis with mechanisms similar to that described fro congenital chloride diarrhea. Not all villous adenomata cause metabolic alkalosis.

Recent reports suggest another often overlooked cause of extrarenal ECF loss is cystic fibrosis which can present with metabolic alkalosis due to volume contraction and K^+ deficiency.[187–189] The next group of disorders involves primarily renal loss of H^+ as a generating mechanism.

Diuretic-induced metabolic alkalosis. Diuretics are the most common cause of metabolic alkalosis. Loop and thiazide diuretics induce a hypotonic urine with low $[HCO_3^-]$ and comparatively high $[Cl^-]$, reducing ECF volume while preserving ECF HCO_3^- content.[190] Diuretics generate metabolic alkalosis by several mechanisms. They induce a small degree of contraction alkalosis which is quantitatively of minor importance.[191] Since both loop and thiazide diuretics are kaliuretics, the loss of K^+ cause some H^+ shift into cell.[69] the most important generating factor is loss of H^+ into the urine. Furosemide and thiazides are the prime examples where distal Na^+ delivery is uncoupled to aldosterone levels; both are high. This results in excessive distal H^+ secretion and high net acid generation,[61] and metabolic alkalosis ensues. Once generated, the alkalosis is maintained by volume contraction, K^+ deficiency and high aldosterone. Patients with persistent diuretic-induced metabolic alkalosis have acidic urine, indicative of a failure of the renal tubules to respond appropriately to the excess ECF HCO_3^-. Finally, loop diuretics may have direct stimulatory effects on distal H^+ secretion as there is experimental data showing the H^+ secretion can remain higher than control levels even when NaCl and KCl are replaced intravenously.[62,192] However, this increment in H^+ secretion is probably not sufficient to maintain high plasma $[HCO_3^-]$ as diuretic-induced metabolic alkalosis is decreased with NaCl and KC1 repletion.[190] One needs to exercise caution in the interpretation of urinary electrolytes in diuretic users. Urinary $[Na^+]$ and $[Cl^-]$ may be extremely high or low depending how the measurement is timed with the administration of the drug.

Post-hypercapneic state. Chronic respiratory acidosis is associated with the physiologic compensatory increase in ECF HCO_3^- which is mediated by cellular buffering (primarily erythrocytes) in minutes and within a few hours by a renal response of increased net acid excretion resulting in a resetting of plasma $[HCO_3^-]$ to about 0.3 mEq/L for every 1 mm Hg rise in pCO_2. When the chronically elevated pCO_2 is suddenly decreased (e.g., intubation and mechanical ventilation) ECF $[HCO_3^-]$ often fails to decrease leading to a metabolic alkalosis.[193] The immediate bicarbonaturia obligates urinary Na^+ and K^+ losses. Along with the volume-stimulated aldosterone activity, the bicarbonaturia ceases before ECF $[HCO_3^-]$ completely returns to normal and the patient settles on a new steady state of maintenance of metabolic alkalosis. Urinary $[Cl^-]$ is generally very low but urinary $[Na^+]$ may not be low during the bicarbonaturic phase. Patients with chronic respiratory acidosis who experience this reduction in pCO_2 require adequate NaCl and KCl supplement to effect the necessary

urinary excretion of HCO_3^- to reduce ECF [HCO_3^-] to normal.

Magnesium depletion. Severe magnesium (Mg^{2+}) depletion causes hypokalemia and metabolic alkalosis. Humans with experimentally-induced Mg^{2+} depletion waste K^+ in the urine possibly through an aldosterone-related mechanism and the kaliuresis can be blocked by spironolactone.[194,195] The absence of hypertension suggests that the excess mineralocorticoid activity is not primary and may be secondary to defective renal Na^+ conservation. Mg^{2+} deficiency can result from a variety of acquired causes such as cisplatin[196] or aminoglycoside toxicity,[197] or from congenital defects in ion channels or paracellular proteins.[198] These conditions are reviewed in detail in another chapter. The mechanism of generation and maintenance is not entirely clear but K^+ deficiency is likely the culprit. Mg^{2+} and K^+ repletion is the definitive treatment.

Distal delivery of poorly absorbable anions. The administration of poorly absorbable anions that end up in the distal nephron in conjunction with high mineralocorticoid activity results in hypokalemic metabolic alkalosis.[93,134] This is another example where urinary [Cl^-] is not accompanied by low urinary [Na^+]. All anions are comparatively less absorbable than Cl^-. Of intermediate permeability is HCO_3^- as encountered in patients with gastric alkalosis with ongoing vomiting and bicarbonaturia.[78] Other common clinical examples include non-reabsorbable anionic antibiotics such as penicillin, ampicillin, and carbenicillin.[122,136] These patients are particularly susceptible when they have concomitant volume depletion.[93] These patients respond to removal of the offending agent and/or restoration of depleted ECF volume. Excessive urinary sulfate and nitrate can also cause dissociation of urinary Na^+ and Cl^- experimentally but clinical scenarios of significant "sulphaturia" and "nitraturia" are not encountered.

Congenital tubulopathies mimicking diuretics. This is a group of rare Mendelian genetic diseases that has seen enormous progress in the last decade. A brief account will be delivered here. More detailed discussions of these diseases are found elsewhere in this textbook.

In 1962, Bartter and associates reported patients with hypokalemic metabolic alkalosis, normal to low blood pressure and increased plasma renin and angiotensin.[199] In addition, these patients have hypercalciuria, impaired vasopressor effect to exogenous angiotensin II, hyperprostaglandinuria, and histologically, they have hyperplasia of the juxtaglomerular cell. The original cluster of findings that have become cardinal features of Bartter's syndrome are all accurate but it was difficult to discern primary vs. secondary findings. Over the years these features have stimulated a variety of conjectures that experienced everything from popularity to notoriety. Almost 20 years after the original description, Bartter himself proposed that this is a disorder of primary renal NaCl wasting and all other features are secondary.[200] Now this genetic thick ascending limb tubulopathy is known to be caused by a heterogeneous group of inactivating mutations of the Na-K-2Cl cotransporter, the ROMK K^+ channel, Cl^- channels ClC-Ka and ClC-Kb, Cl^- channel subunit Barttin, and activating mutations of the calcium sensing receptor.[201] The final common pathway is disruption of the transcellular NaCl resorptive ensemble in the thick ascending limb with a phenotype identical to a perpetual state of loop diuretic administration. The mechanisms of maintenance include volume contraction, K^+ depletion, excess aldosterone with increased distal Na^+ delivery, and Mg^{2+} depletion.

A similar but distinct parallel cause of genetic hypokalemic metabolic alkalosis, Gitelman's syndrome, was described in 1966.[202] Gitelman's can be distinguished from Bartter's clinically by older age of onset, less severe phenotype and hypo instead of hypercalciuria.[203] Gitelman's syndrome is homogeneously due to inactivating mutations of the Na-Cl cotransporter.[204] Akin to Bartter's patients, Gitelman's patients live with a phenotype resembling lifelong thiazide therapy. The mechanism of metabolic alkalosis is similar to that of Bartter's syndrome.

Post-fasting metabolic alkalosis. Early in starvation ketoacidosis, ketoanions are excreted as Na^+ and K^+ salts, and a minority as undissociated ketoacids. With the activation of renal ammoniagenesis, most ketoanions are excreted with NH_4^+ which creates a new steady where ketoacid production is matched by heightened renal NAE.[205–207] Patients develop metabolic alkalosis upon glucose refeeding following a prolonged fast.[208] Generation of excess ECF HCO_3^- and its maintenance persists for about a week after glucose refeeding and then ECF [HCO_3^-] returns to its pre-fast level.[208] Metabolic alkalosis and its short-term maintenance in this setting might be due to the increased net acid excretion caused by augmented ammoniagenesis in response to fasting-induced ketosis.[123] Glucose refeeding stops ketoacid production quickly and converts plasma ketoanions to base equivalents, but the increased net acid excretion normalizes more slowly to match the new and lower metabolic acid production.[37] Thus, net acid excretion is temporarily greater than intrinsic H^+ production, leading to excess ECF HCO_3^- generation. When net acid excretion eventually decreases to match intrinsic H^+ production after a few days, the physiologic renal HCO_3^- excretory mechanisms would normalize ECF HCO_3^-. Although physiologically plausible, this explanation is not

entirely supported by the data.[208] Intracellular H^+ movement generating ECF HCO_3^- has also been proposed as a contributing factor.[123] Both glucose and insulin can stimulate proximal tubule $NaHCO_3$ absorption.[208–210] During early refeeding, the kidney is extremely antinatriuretic to the point that the patients becomes edematous—a condition called refeeding edema. The mechanism of the maintenance phase is equally obscure. In short, the etiology for this uncommon form of metabolic alkalosis remains unresolved.

Hypoparathyroid hypercalcemia. Interestingly, the hypercalcemia due to hyperparathyroidism can be associated with a very mild metabolic alkalosis, hyperchloremic metabolic acidosis, or no acid–base disturbance.[211,212] In contrast, hypercalcemia from accelerated bone release such as in malignancy, metabolic alkalosis is frequently seen.[213,214] This is likely due to increased alkali release from dissolution of calcium carbonate combined with impaired renal HCO_3^- excretion. Suppressed parathyroid hormone may increase proximal HCO_3^- absorption[215,46,216,217] by inhibition of the Na^+/H^+ exchanger.[218,219] Hypercalcemia *per se* can directly stimulate H^+ secretion.[220] Through the calcium sensing receptor, hypercalcemia also has a loop diuretic effect on the thick ascending limb via inhibition of the apical K^+ channel.[221]

Metabolic Alkalosis with Hypertension

Most patients in this group have increased renal mineralocorticoid effects that generate and maintain metabolic alkalosis by the mechanisms discussed earlier. Patients can be categorized according to EABV although the clinical evaluation of this parameter can be challenging. Urine [Cl^-] and [Na^+] are less helpful diagnostically in these patients with metabolic alkalosis because few of them have decreased EABV and thus few will have decreased urine Cl^- or Na^+ excretion. The most important challenge facing the clinician is diagnosing the cause. Measurement of serum renin and aldosterone levels is the most helpful laboratory test to categorize patients for more detailed investigation. This constitutes one of the most fascinating assemblage of etiologies for metabolic alkalosis and hypertension. The best approach to organize these disorders is by the renin and aldosterone levels (Figure 58.13).

High renin and high aldosterone. These are primarily renal disorders (Figure 58.13). These patients have primary increases in renin secretion uncoupled from feedback mechanisms that normally turn off renin production, leading to increased aldosterone secretion and metabolic alkalosis by the mechanisms discussed earlier. Rare renin-producing tumors and juxtaglomerular hyperplasia cause metabolic alkalosis, although the most prominent feature is severe hypertension.[222,223] Metabolic alkalosis and hyperaldosteronism is unusual but has been described in patients with renal artery stenosis.[224,225] A prevalence of 10% has been suggested but the true prevalence is probably unknown as many cases may be due to diuretic-induced metabolic alkalosis. Another confounder is simultaneous renal artery stenosis and unrelated primary hyperaldosteronism.[226,227] A classic state of hyperreninemic hyperaldosteronism is found in patients with small vessel disease such as malignant hypertension, vasculitis, or scleroderma where renal ischemia stimulates renin secretion, secondary hyperaldosteronism, and hypokalemic metabolic alkalosis.[228,229] Renin-secreting tumors are rare but have been described with numerous histologic types- hemangiopericytoma, hamartomas, Wilm's tumor, and even pulmonary malignancies.[222,223,230–232]

Low Renin and High Aldosterone. These are primarily adrenal diseases (Figure 58.14) where aldosterone has achieved autonomy escaping the control by renin-angiotensin and renin secretion is suppressed. A common cause is an adrenal adenoma.[233] Surgical resection of the adenoma usually corrects both the hypertension and metabolic alkalosis. Patients in this group can also have bilateral adrenal hyperplasia. Although bilateral adrenal resection corrects both the hypertension and metabolic alkalosis,[233] the resulting adrenal insufficiency favors pharmacologic suppression of mineralocorticoid secretion or inhibition of its action. A biochemical adjunct to discern adrenal adenoma from hyperplasia is postural changes in aldosterone levels. Serum aldosterone levels tend to decrease with upright posture in patients with adenomas, whereas they increase in patients with hyperplasia.[233] Because of the less than perfect predictive value of this test and the improved resolution of computerized tomography, this postural test is seldom done. Non-functional anatomic lesions are quite common so radiographic adrenal adenomas require biochemical validation of hyperaldosteronism and adrenal venous samples to confirm the source of aldosterone before commitment to surgery.

In a rare variant of bilateral adrenal hyperplasia described by Biglieri and associates known as indeterminate hyperaldosteronism, exogenous mineralocorticoids seem to normalize aldosterone levels.[234] Very little is known about this exceeding rare condition. In 1966, Laidlaw and associates described patients whose aldosterone levels decreased with administration of the pure glucocorticoid dexamethasone. This group of disorders have been termed glucocorticoid suppressible aldosteronism.[82] Lifton and associates described the molecular defect in this condition when two tandem genes CYP11B1 and CYP11B2 encoding for 11-β-hydroxylase and aldosterone synthase respectively

undergoes unequal cross-over so the ACTH-responsive 5′-flanking promoter region of 11-β-hydroxylase is driving the transcription of aldosterone synthase. The end result is control of aldosterone synthase by ACTH[235,236] leading to hypersecretion of aldosterone uncoupled from its feedback inhibition but suppressible by dexamethasone. A similar autosomal dominant syndrome has been described with the exception that the hyerpaldosteronism is not suppressible and they do not harbor the hybrid CYP11B1/CYP11B2 gene described above.[237,238] A number of candidates were excluded and a locus has recently been mapped.[239,240]

Rarely, metabolic alkalosis can be due to pure aldosterone secretion by an adrenal cortical carcinoma.[241] Adrenal carcinomas more commonly secrete desoxycorticosterone and corticosterone, which has mineralocorticoid activity and suppress both renin and aldosterone.[242]

Low renin and low aldosterone. This group of diseases is represented on the right panel of Figure 58.14 and can be subdivided into three categories: (1) A hormone other than aldosterone is activating a normal mineralocorticoid receptor. (2) A gain-of-function mutation of the receptor resulting in its activation. (3) Activation of transport mechanisms downstream to the receptor.

Patients with Cushing's syndrome can secrete mineralocorticoids other than aldosterone such as desoxycorticosterone causing most clinical features of aldosteronism including hypokalemic metabolic alkalosis and hypertension.[242] Although aldosterone levels are usually not increased in Cushing's syndrome,[243] 30 to 40% of these patients do develop hypokalemic metabolic alkalosis due to secretion of non-aldosterone mineralocorticoids[244] and to mineralocorticoid effects of corticosterone.[245] Hypokalemic metabolic alkalosis is very common when Cushing's syndrome is caused by ectopic adrenocorticotropic hormone (ACTH) secretion because these patients frequently secrete high levels of corticosterone, desoxycorticosterone, and cortisol.[246] The principal treatment strategy for these syndromes is identification and correction of the underlying disorder.

Exogenous mineralocorticoids, both synthetic and natural, can produce the entire syndrome of aldosterone excess including hypokalemic metabolic alkalosis.[234] Excessive intake of the synthetic mineralocorticoid fludrocortisone acetate, causes hypokalemic metabolic alkalosis with physiology not unlike that of endogenous compounds.

Glucocorticoids such as cortisol can activate the mineralocorticoid receptor with similar in vitro affinity as aldosterone due to the much higher (2-3 log orders) plasma levels compared to aldosterone.[247] However, the mineralocorticoid receptor is usually protected from glucocorticoids by the co-expression of the type 2 11-β-hydroxysteroiddehydrogenase enzyme (11-β-HSD-2).[247] In the absence of adequate 11-β-HSD-2 activity in mineralocorticoid target tissues, a hypermineralocorticoid state will emerge. This can occur when cortisol levels are so high that 11-β-HSD-2 is overwhelmed as in ACTH-secreting tumors. In addition, glycyrrhizic acid or its hydrolytic product glycyrrhetinic acid, compounds found in natural but not synthetic licorice and in some chewing tobaccos, is an inhibitor of 11-β-HSD-2, and can cause the syndrome.[248–250] In addition to acquired inhibitors of 11-β-HSD-2, a genetic syndrome of apparent mineralocorticoid excess was described in the 1970s[251,252] Inactivating mutations of the 11-β-HSD-2 enzyme can cause its inactivation which leaves the mineralocorticoid receptor unprotected from the physiologic levels of cortisol.[253,254]

A number of adrenogenital syndromes can cause hypokalemic metabolic alkalosis due to production of various steroids with mineralocorticoid activity. Defective 11-hydroxylation blocks conversion of desoxycortisol to cortisol and desoxycorticosterone to corticosterone. Although aldosterone synthesis is intact, the relative glucocorticoid deficiency associated with this syndrome drives adrenal steroid synthesis, accumulating high levels of desoxycortisol and desoxycorticosterone upstream from the block. These compounds have less mineralocorticoid activity than aldosterone, but their high levels can exert marked mineralocorticoid effects.[234]

A less common syndrome involves defective 17-hydroxylation, which blocks conversion of pregnanediol to 17-pregnanediol and progesterone to 17-hydroxyprogesterone. These are steroid precursors to cortisol, androgens, and estrogens. The reduced cortisol levels lead to increased ACTH secretion with stimulates both desoxycorticosterone and aldosterone synthesis. Exogenous glucocorticoids reduce mineralocorticoid production and metabolic alkalosis in both syndromes.

The above syndromes involves the engagement of the mineralocorticoid receptor by steroid ligands with natural affinity and for various reasons indicated above, these steroids achieve levels far above the physiologic state. The next syndrome involves a different mechanism where the mineralocorticoid receptor acquires affinity for a novel ligand which results in it activation.

Geller, Lifton and colleagues reported a gain-of-function mutation of the mineralocorticoid receptor that causes constitutive receptor activation and alters receptor specificity so progesterone and other steroids lacking 21-hydroxyl groups, even antagonists become potent agonists. This mutations explains the progesterone-induced hypertension in pregnancy but

these patients tend not to develop K^+ wasting or metabolic alkalosis.[255]

A final cause of hypermineralocorticoid state is a constitutive activation of an aldosterone effector (Figure 58.13). A channelopathy that has received a lot of attention is one described by Liddle and associates back in 1963.[256] Liddle's syndrome is a rare autosomal dominant disorder exhibiting all the clinical features of mineralocorticoid excess but without increased secretion of any identifiable mineralocorticoid nor could it be reversed by inhibition of steroid synthesis or mineralocorticoid receptor blockers.[256–258] However, inhibitors of electrogenic distal tubule Na^+ reabsorption reversed the electrolyte abnormalities and normalized the elevated blood pressure,[258] consistent with an intrinsic tubule defect. The genetic lesion is now known to be due to mutations of the epithelial Na^+ channel which lead to reduced channel degradation and excessive apical Na^+ absorption.[259–261] The molecular mechanisms of how these mutant channels lead to a dominant trait of excessive Na^+ current is discussed elsewhere in the textbook. The mechanism of generation and maintenance of metabolic alkalosis is the same as with the other hypermineralocorticoid states. These patients can be treated with diuretics with direct effects on the renal tubule to inhibit the electrogenic Na^+ channel, such as amiloride and triamterene, and with K^+ supplements.

CONCLUDING REMARKS

Metabolic alkalosis is a common clinical acid–base disorder in both inpatients and outpatients. It is generally mild but it can have significant adverse effects particularly in the critically ill patient. In the ambulatory setting, the alkalosis *per se* is likely of no dire effect. Its predominant clinical importance resides in its role as a sentinel for the underlying conditions causing it, which might have grave consequences if remain unrecognized. Clinicians must pursue an expeditious and scientifically-based diagnostic tactic. While the use of diagnostic algorithms assists thought organization and streamlines the process, it is not intended to and under no circumstances should it replace the rigorous analysis based on pathophysiology.

Of all the acid–base disturbances encountered clinically or experimentally, metabolic alkalosis exemplifies the quintessential renal disorder of HCO_3^- transport. It is virtually impossible to induce sustained elevations of plasma [HCO_3^-] in normal individuals with even massive HCO_3^- infusion or ingestion. Given the vast capacity of the filtration-reabsorption nephron to excrete excess ECF HCO_3^-, the renal derangements in metabolic alkalosis are indeed remarkable and involve complex mechanisms. The overall scheme of generation and maintenance is summarized in Figure 58.13. If this is the prototypical tubulopathy that resets the plasma [HCO_3^-], the general consensus still favors the paradigm that there is no intrinsic defect in the renal tubule. It is simply a state of misguidance by incoming signals which presides over the kidney; a state akin to the salt retention and edema in renal hypoperfusion. It is important to note that it is still not proven that there is absolutely no intrinsic defect in the kidney; it is simply based on absence of proof.

The quest to uncover pathophysiology is of utmost importance and priority in clinical medicine which may be slowly, but dangerously and steadily eroding. Instead of resorting to rote memory of diagnostic algorithms and lists, the superb clinician is compelled to pose three kinds of questions regarding this state of inappropriately augmented renal HCO_3^- absorption. First is *what*. Almost all metabolic alkalotic syndromes work through a combination of the three pivotal pathophysiologic mechanisms: Contraction of effective arterial blood volume, K^+ deficiency, and excessively high mineralocorticoid activity. Decades of investigation furnished this foundation. Second is *how*. The mechanisms by which renal HCO_3^- is altered by each of these three pathophysiologic factors are complex and incompletely understood but what is known is summarized in this chapter. The third and most difficult but interesting and important question to ponder is *why*. Here one can merely speculate. Since HCO_3^- is a major ECF anion and the defense of the integrity of the circulation and organ perfusion is of such paramount importance, the kidney will recruit all mechanisms to maintain ECF volume, even at the expense of sacrificing on the chemical milieu of body fluids. Circulatory volume is preserved at the expense of plasma pH. This situation is akin to the hyponatremia seen in compromised effective arterial blood volume where the kidney foregoes osmoregulation to defend circulatory volume, or the massive sodium retention in edematous states. One can view this as a trade-off for a greater good. In the case of K^+ deficiency, the proximal nephron may be attempting to reclaim all HCO_3^- to prevent further K^+ wastage which will occur downstream in the distal nephron if significant luminal HCO_3^- is present. In addition to K^+ conservation, the intracellular acidosis in K^+ deficiency is signaling both the proximal and distal renal epithelial to defend against an apparent "acid excess state" even though the H^+ have simply migrated from the extracellular to intracellular space. Primary escalation of mineralocorticoid activity is elegantly manifested in the host of disorders of the renin-angiotensin-aldosterone axis from elevation of renin to inappropriate activation of mineralocorticoid

effector targets. This is a manifestation *par excellence* of the multiple roles of mineralocorticoids in regulating Na^+, K^+ and H^+ handling by the kidney. The uncoupled situation of the excessive luminal Na^+ with high mineralocorticoid activity leads to excessive H^+ secretion in a fashion quite inappropriate and oblivious to the high plasma [HCO_3^-]. Finally, a most fundamental question remains as to whether the kidney can sense and set plasma [HCO_3^-] and whether metabolic alkalosis represents an intrinsic disorder in the tubule rather than simply a state of obedient but misguided behavior in response to erroneous commands.

Although much has been learned about the pathophysiology of metabolic alkalosis, much more remains to be uncovered using a synergistic combination of bedside physiology and bench research. Efforts devoted to this cause can only result in improved care of patients and heightened interests for practitioners.

References

[1] Garella S, Cohen JJ, Northrup TE. Chloride-depletion metabolic alkalosis induces ECF volume depletion via internal fluid shifts in nephrectomized dogs. Eur J Clin Invest 1991;21:273–9.

[2] Rubin SI, Sonnenberg B, Zettle R, Halperin ML. Metabolic alkalosis mimicking the acute sequestration of HCl in rats: bucking the alkaline tide. Clin Invest Med 1994;17:515–21.

[3] Seldin DW, Rector Jr FC. Symposium on acid–base homeostasis. The generation and maintenance of metabolic alkalosis. Kidney Intern 1972;1:321.

[4] Hodgkin JE, Soeprono FF, Chan DM. Incidence of metabolic alkalemia in hospitalized patients. Crit Care Med 1980;8:725–8.

[5] Grace WJ, Barr DP. Complications of alkalosis. Am J Med 1948;4:331–7.

[6] Swan RC, Axelrod DR, Pitts RF. Distribution of sodium bicarbonate infused into nephrectomized dogs. J Clin Invest 1955;34:1795–801.

[7] Singer RB, Clark JK, Barker ES, Crosley Jr. AP, Elkinton JR. The acute effects in man of rapid intravenous infusion of hypertonic sodium bicarbonate solution. I. Changes in acid–base balance and distribution of the excess buffer base. Medicine 1955;34: 51–95.

[8] Adrogue HJ, Brensilver J, Cohen JJ, Madias NE. Influence of steady- state alterations in acid–base equilibrium on the fate of administered bicarbonate in the dog. J Clin Invest 1983;71: 867–83.

[9] Swan RC, Pitts RF. Neutralization of infused acid by nephrectomized dogs. J Clin Invest 1955;34:205–12.

[10] Adler S, Roy A, Relman AS. Intracellular acid–base regulation. II. The interaction between CO-2 tension and extracellular bicarbonate in the determination of muscle cell pH. J Clin Invest 1965;44:21–30.

[11] Heinemann HO, Goldring RM. Bicarbonate and the regulation of ventilation. Am J Med 1974;57:361–70.

[12] Stone DJ. Respiration in man during metabolic alkalosis. J Appl Physiol 1962;17:33–7.

[13] Fencl V, Miller TB, Pappenheimer JR. Studies on the respiratory response to disturbances of acid–base balance, with deductions concerning the ionic composition of cerebral interstitial fluid. Am J Physiol 1966;210:459–72.

[14] Jones JW, Sebastian A, Hulter HN, Schambelan M, Sutton JM, Biglieri EG. Systemic and renal acid–base effects of chronic dietary potassium depletion in humans. Kidney Intern 1982;21:402–10.

[15] Madias NE, Bossert WH, Androgue HJ. Ventilatory response to chronic metabolic acidosis and alkalosis in the dog. J Appl Physiol 1984;56:1640–6.

[16] Dubose TDJ, Cogan MG, Rector FCJ. acid–base disorders. In: Brenner BM, editor. The kidney. 5th ed. Philadelphia: W.B. Saunders; 1996. p. 932.

[17] Pitts RF, Lotspeich WD. Bicarbonate and the renal regulation of acid–base balance. Am J Physiol 1946;147:138–54.

[18] van Goidsenhoven GM, Gray OV, Price AV, Sanderson PH. The effect of prolonged administration of large doses of sodium bicarbonate in man. Clin Sci (Lond) 1954;13:383–401.

[19] Packer RK, Curry CA, Brown KM. Urinary organic anion excretion in response to dietary acid and base loading. J Am Soc Nephrol 1995;5:1624–9.

[20] Wesson DE. Glomerular filtration effects of acute volume expansion: importance of chloride. Kidney Intern 1987;32: 238–45.

[21] Cogan MG, Maddox DA, Rector FCJ. Determinants of bicarbonate reabsorption in the rat proximal tubule. Kidney Intern 1978;14:753–61.

[22] Wesson DE. Depressed distal tubule acidification corrects chloride-deplete in rats. Am J Physiol 1990;259:F636–44.

[23] Frommer JP, Wesson DE, Laski ME, Kurtzman NA. Juxtamedullary nephrons during actute metabolic alkalosis in the rat. Am J Physiol 1985;249:F107–16.

[24] Cheema-Dhadli S, Lin SH, Halperin ML. Mechanisms used to dispose of progressively increasing alkali load in rats. Am J Physiol Renal Physiol 2002;282:F1049–55.

[25] Lemann Jr. J, Lennon EJ, Goodman AD, Litzow JR, Relman AS. The net balance of acid in subjects given large loads of acid or alkali. J Clin Invest 1965;44:507–17.

[26] Chan YL, Malnic G, Giebisch G. Renal bicarbonate reabsorption in the rat. III. Distal tubule perfusion study of load dependence and bicarbonate permeability. Clin Invest 1989; 84:931–8.

[27] Atkins JL, Burg MB. Bicarbonate transport by isolated perfused rat collecting ducts. Am J Physiol (Renal Fluid Electrolyte Physiol) 1985;249:F485–9.

[28] Levine DZ, Iacovitti M, Harrison V. Bicarbonate secretion *in vivo* by rat distal tubules during alkalosis induced by dietary chloride restriction and alkali loading. J Clin Invest 1991;87: 1513–8.

[29] Wesson DE, Dolson GM. Augmented bidirectional HCO_3 transport by rat distal tubules in chronic alkalosis. Am J Physiol 1991;261:F308–17.

[30] Levine DZ, Iacovitti M, Buckman S, Harrison V. In vivo modulation of rat distal tubule net HCO3 flux by VIP, isoproterenol, angiotensin II, and ADH. Am J Physiol 1994;266:F878–83.

[31] Wesson DE. Prostacyclin increases distal tubule HCO3 secretion in the rat. Am J Physiol 1996;271:F1183–92.

[32] Wesson DE. Dietary HCO3 reduces distal tubule acidification by increasing cellular HCO3 secretion. Am J Physiol 1996;271: F132–42.

[33] Bastani B, Purcell H, Hemken P, Trigg D, Gluck S. Expression and distribution of renal vacuolar proton-traslocating adenosine triphosphatase in response to chronic acid and alkali loads in the rat. J Clin Invest 1991;88:126–36.

[34] Sabatini S, Laski ME, Kurtzman NA. NEM-sensitive ATPase activity in rat nephron: effect of metabolic acidosis and alkalosis. Am J Physiol 1990;258:F297–304.
[35] Alpern RJ, Cogan MG, Rector FCJ. Effects of extracellular fluid volume and plasma bicarbonate concentration on proximal acidification in the rat. J Clin Invest 1983;71:736–46.
[36] Alpern RJ, Cogan MG, Rector FCJ. Effect of luminal bicarbonate concentration on proximal acidification in the rat. Am J Physiol 1982;243:F53–9.
[37] Giebisch G, Malnic G, De Mello GB, De Mello AM. Kinetics of luminal acidification in cortical tubules of the rat kidney. J Physiol 1977;267:571–99.
[38] Purkerson ML, Lubowitz H, White RW, Bricker NS. On the influence of extracellular fluid volume expansion on bicarbonate reabsorption in the rat. J Clin Invest 1969;48:1754–60.
[39] Slatopolsky E, Hoffsten P, Purkerson M, Bricker NS. On the influence of extraceller fluid volume expansion and of uremia on bicarbonate reabsorption in man. J Clin Invest 1970;49: 988–98.
[40] Kurtzman NA. Regulation of renal bicarbonate reabsorption by extracellular volume. J Clin Invest 1970;49:586–95.
[41] Levine DZ, Nash LA, Chan T, Dubrovskis AH. Proximal bicarbonate reabsorption during ringer and albumin infusions in the rat. J Clin Invest 1976;57:1490–7.
[42] Cogan MG, Carniero AV, Tatsuno J, et al. Normal diet NaCl variation can affect the renal set-point for plasma pH-(HCO3-) maintenance. J Am Soc Nephrol 1990;1:193–9.
[43] Espinel GH. The influence of salt intake on the metabolic acidosis of chronic renal failure. J Clin Invest 1975;56:286–91.
[44] Lameire N, Matthys E. Influence of progressive salt restriction on urinary bicarbonate wasting in uremic acidosis. Am J Kid Dis 1986;8:151–8.
[45] Jones GV, Wall BM, Williams HH, Presley DN, Sapir DG, Cooke CR. Modulation of plasma aldosterone by physiological changes in hydrogen ion concentration. Am J Physiol 1992;262: R269–75.
[46] Bank N, Aynedjian HS. A micropuncture study of renal bicarbonate and chloride reabsorption in hypokalaemic alkalosis. Clin Sci 1965;29:159–70.
[47] Luke RG, Levitin H. Impaired renal conservation of chloride and the acid–base changes associated with potassium depletion in the rat. Clin Sci 1967;32:511–26.
[48] Kurtzman NA, White MG, Rogers PW. The effect of potassium and extracellular volume on renal bicarbonate reabsorption. Metabolism 1973;22:481–92.
[49] Wesson DE. Augmented bicarbonate reabsorption by bothe the proximal and distal nephron maintains chloride-deplete metabolic alkalosis in rats. J Clin Invest 1989;84:1460–9.
[50] Cheval L, Duong Van Huyen JP, Bruneval P, Verbavatz JM, Elalouf JM, Doucet A. Plasticity of mouse renal collecting duct in response to potassium depletion. Physiological genomics 2004;19:61–73.
[51] Cheval L, Morla L, Elalouf JM, Doucet A. Kidney collecting duct acid–base "regulon". Physiological genomics 2006;27: 271–81.
[52] Eiam-Ong S, Kurtzman NA, Sabatini S. Regulating of collecting tubule adenosine triphosphatases by aldosterone and potassium. J Clin Invest 1993;91:2385–92.
[53] Liu FY, Cogan MG. Angiotensin II: a potent regulator of acidification in the rat early proximal convoluted tubule. J Clin Invest 1987;80:272–5.
[54] Stone DK, Seldin DW, Kokko JP, Jacobson HR. Mineralocorticoid modulation of rabbit medullary collecting duct acidification. A sodium-independent effect. J Clin Invest 1983;72:77–83.
[55] Ebeid EM, Escourrou J, Murray P. Pathophysiology of VIP. In: Bloom SR, editor. Gut hormones. Edinburgh: Churchill Livingstone; 1978. p. 479–83.
[56] Wolfe MM, Soll AH. The physiology of gastric acid secretion. NEJM 1988;319:1707–15.
[57] Argent BE, Case RM. Pancreatic ducts: cellular mechanism and control of bicarbonate secretion. In: Johnson LR, editor. Physiology of the gastrointestinal tract. 3rd ed. New York: Raven Press; 1994.
[58] Kassirer JP, Schwartz WB. Correction of metabolic alkalosis in man without repair of potassium deficiency. A re-evaluation of the role of potassium. Am J Med 1966;40:19–26.
[59] Deysine M. Villous adenomas of the colon complicated by electrolyte imbalance. Dis Colon Rectum 1968;11:289–91.
[60] Holmberg C, Perheentupa J, Launiala K. Colonic electrolyte transport in health and in congenital chloride diarrhea. J Clin Invest 1975;56:302–10.
[61] Rastogi SP, Crawford C, Wheeler R, Flanigan W, Arruda JA. Effect of furosemide on urinary acidification in distal renal tubular acidosis. J Lab Clin Med 1984;104:271–82.
[62] Bosch JP, Goldstein MH, Levitt MF, Kahn T. Effect of chronic furosemide administration on hydrogen ion and sodium excretion in the dog. Am J Physiol 1977;232:F397–404.
[63] Kahn T, Kaufman AM, Mac-Moune FL. Response to repeated frusemide administration on low chloride and low sodium intake in the rat. Clin Sci (Lond) 1983;64:565–72.
[64] Hulter HN, Sigala JF, Sebastian A. K + deprivation potentiates the renal alkalosis-producing effect of mineralocorticoid. Am J Physiol 1978;235:F298–309.
[65] Seldin DW, Welt LG, Cort JH. The role of sodium salts and adrenal steroids in the production of hypokalemic alkalosis. Yale J Biol Med 1956;29:229–47.
[66] Alpern RJ, Emmett M, Seldin DW. Metabolic alkalosis. In: Seldin DW, Giebisch G, editors. The kidney: physiology and pathophysiology. 2nd ed. New York: Raven Press; 1992. p. 2733–59.
[67] Capasso G, Kinne R, Malnic G, Giebisch G. Renal bicarbonate reabsorption in the rat. I. Effects of hypokalemia and carbonic anhydrase. J Clin Invest 1986;78:1558–67.
[68] Tannen RL, McGill J. Influence of potassium on renal ammonia production. Am J Physiol 1976;231:1178–84.
[69] Cooke RE, Segar WE, Cheek DB, Coville FE, Darrow DC. The extrarenal correction of alkalosis associated with potassium deficiency. J Clin Invest 1952;31:798–805.
[70] Scheich A, Donnelly S, Cheema-Dhadli S, Schweigert M, Vasuvattakul S, Halperin ML. Does saline "correct" the abnormal mass balance in metabolic alkalosis associated with chloride depletion in the rat? Clin Invest Med 1994;17:448–60.
[71] Scheich A, Donnelly S, Cheema-Dhadli S, Schweigert M, Vasuvattakul S, Halperin ML. Does saline correct the abnormal mass balance in metabolic alkalosis associated with chloride depletion in the rat? Clin Invest Med 1994;17: 448–60.
[72] Lecompte F, Brun M, Paillard M. contraction alkalosis in the awake rat: study of its generation and 24-hour follow-up. Kidney Intern 1978;14:557–66.
[73] Garella S, Chang BS, Kahn SI. Dilution acidosis and contraction alkalosis: review of a concept. Kidney Intern 1975;8:279–83.
[74] Cogan MG, Liu FY. Metabolic alkalosis in the rat. Evidence that reduced glomerular filtration rather than enhanced tubular bicarbonate reabsorption is responsible for maintaining the alkalotic state. J Clin Invest 1983;71:1141–60.
[75] Cogan MG. Atrial natriuretic factor ameliorates chronic metabolic alkalosis by increasing glomerular filtration. Science 1985;229:1405–7.

[76] Maddox DA, Horn JF, Famiano FC, Gennari FJ. Load dependence of proximal tubular fluid and bicarbonate reabsorption in the remnant kidney of the Munich-Wistar rat. J Clin Invest 1986;77:1639–49.
[77] Arrud JA, Carrasquillo T, Cubria A, Rademacher DR, Kurtzman NA. Bicarbonate reabsorption in chronic renal failure. Kidney Intern 1976;9:481–8.
[78] Kassirer JP, Schwartz WB. The response of normal man to selective depletion of hydrochloric acid. Factors in the genesis of persistent gastric alkalosis. Am J Med 1966;40:10–8.
[79] Schwartz WB, Relman AS. Metabolic and renal studies in chronic potassium depletion resulting from overuse of laxatives. J Clin Invest 1953;32:258–71.
[80] Berger BE, Cogan MG, Sebastian A. Reduced glomerular filtration and enhanced bicarbonate reabsorption maintain metabolic alkalosis in humans. Kidney Intern 1984;26:205–8.
[81] Kunau Jr. RT, Frick A, Rector Jr FC, Seldin DW. Micropuncture study of the proximal tubular factors responsible for the maintenance of alkalosis during potassium deficiency in the rat. Clin Sci 1968;34:223–31.
[82] Sutherland DJ, Ruse JL, Laidlaw JC. Hypertension, increased aldosterone secretion and low plasma renin activity relieved by dexamethasone. Can Med Assoc J 1966;95:1109–19.
[83] Adam WR, Koretsky AP, Weiner MW. 31P-NMR in vivo measurement of renal intracellular pH: effects of acidosis and K + depletion in rats. Am J Physiol 1986;251:F904–10.
[84] Knepper MA, Packer R, Good DW. Ammonium transport in the kidney. Physiol Rev 1989;69:179–249.
[85] Abbrecht PH. Effects of potassium deficiency on renal function in the dog. J Clin Invest 1969;48:432–42.
[86] Boyd JE, Palmore WP, Mulrow PJ. Role of potassium in the control of aldosterone secretion in the rat. Endocrinology 1971;88: 556–65.
[87] Wesson DE. Na/H exchange and HK ATPase increase distal tubule acidification in chronic alkalosis. Kidney Intern 1998;53:945–51.
[88] Cohen JJ. Correction of metabolic alkalosis by the kidney after isomertric expansion of extracellular fluid. J Clin Invest 1968;47:1181–92.
[89] Kurtzman NA. Disorders of distal acidification. Kidney Intern 1990;38:720–7.
[90] Moe OW, Tejedor A, Levi M, Seldin DW, Preisig PA, Alpern RJ. Dietary NaCl modulates Na(+)-H + antiporter activity in renal apical membrane vesicles. Am J Physiol 1991;260: F130–7.
[91] Levine DZ, Vandorpe D, Iacovitti M. Luminal chloride modulates rat distal tubule bidirectional bicarbonate flux in vivo. J Clin Invest 1990;85:1793–8.
[92] Wesson DE, Dolson GM. Enhanced HCO3 secretion by distal tubule contributes to NaCl-induced correction of chronic alkalosis. Am J Physiol 1993;264:F899–906.
[93] Stinebaugh B, Miller RB, Relman AS. The influence of nonreabsorbable anions on acid excretion. Clin Sci 1969;36: 53–65.
[94] Romero JC, Staneloni RJ, Dufau ML, et al. Changes in fluid compartments, renal hemodynamics, plasma renin and aldosterone secretion induced by low sodium intake. Metabolism 1968;17:10–9.
[95] Liu FY, Cogan MG. Angiotensin II stimulates early proximal bicarbonate absorption in the rat by decreasing cyclic adenosine monophosphate. J Clin Invest 1989;84:83–91.
[96] Galla JH, Bonduris DN, Luke RG. Correction of acute chloride-depletion alkalosis in the rat without volume expansion. Am J Physiol 1983;244:F217–21.
[97] Wall BM, Byrum GV, Galla JH, Luke RG. Importance of chloride for the correction of chronic metabolic alkalosis in the rat. Am J Physiol 1987;253:F1031–9.
[98] Luke RG, Galla JH. Chloride-depletion alkalosis with a normal extracellular fluid volume. Am J Physiol 1983;245: F419–24.
[99] Javaheri S, Kazemi H. Metabolic alkalosis and hypoventilation in humans. Am Rev Respir Dis 1987;136:1011–6.
[100] Wesson DE. Dietary acid increases blood and renal coritcal acid content in rats. Am J Physiol 1998;274:F97–103.
[101] Relman AS, Schwartz WB. The effect of DOCA on electrolyte balance in normal man and its relation to sodium chloride intake. Yale J Biol Med 1952;24:540–58.
[102] Harrington JT, Hulter HN, Cohen JJ, Madias NE. Mineralocorticoid-stimulated renal acidification: the critical rose of dietary sodium. Kidney Intern 1986;30:43–8.
[103] Kassirer JP, London AM, Goldman DM, Schwartz WB. On the pathogenesis of metabolic alkalosis in hyperaldosteronism. Am J Med 1970;49:306–15.
[104] Maddox DA, Gennari FJ. Load dependence of proximal tubular bicarbonate reabsorption in chronic metabolic alkalosis in the rat. J Clin Invest 1986;77:709–16.
[105] Tank JE, Henrich WL, Moe OW. Regulation of glomerular and proximal tubule renin mRNA by chronic changes in dietary NaCl. Am J Physiol 1997;273:F892–8.
[106] Soleimani M, Bergman JA, Hosford MA, McKinney TD. Potassium depletion increases luminal Na + /H + exchange and basolateral Na + :CO3 = :HCO3$^-$ cotransport in rat renal cortex. J Clin Invest 1990;86:1076–83.
[107] Amemiya M, Tabei K, Kusano E, Asano Y, Alpern RJ. Incubation of OKP cells in low-K + media increases NHE3 activity after early decrease in intracellular pH. Am J Physiol 1999;276:C711–6.
[108] Nonoguchi H, Takehara Y, Endou H. Intra- and inter-nephron heterogeneity of ammoniagenesis in rats: effects of chronic metabolic acidosis and potassium depletion. Pflugers Arch 1986;407:245–51.
[109] Sastrasinh S, Sastrasinh M. Renal mitochondrial glutamine metabolism during K + depletion. Am J Physiol 1986;250: F667–73.
[110] Levi M, McDonald LA, Preisig PA, Alpern RJ. Chronic K depletion stimulates rat renal brush-border membrane Na-citrate cotransporter. Am J Physiol 1991;261:F767–73.
[111] Melnick JZ, Preisig PA, Moe OW, Srere P, Alpern RJ. Renal cortical mitochondrial aconitase is regulated in hypo- and hypercitraturia. Kidney Intern 1998;54:160–5.
[112] Burns KD, Smith IB. Potassium depletion stimulates mRNA expression of proximal tubule AT1 angiotensin II receptors. Nephron 1998;78:73–81.
[113] Markovich D, Wang H, Puttaparthi K, et al. Chronic K depletion inhibits renal brush border membrane Na/sulfate cotransport. Kidney Intern 1999;55:244–51.
[114] Akiba T, Rocco VK, Warnock DG. Parallel adaptation of the rabbit renal cortical sodium/proton antiporter and sodium/bicarbonate cotransporter in metabolic acidosis and alkalosis. J Clin Invest 1987;80:308–15.
[115] Amlal H, Chen Q, Greeley T, Pavelic L, Soleimani M. Coordinated down-regulation of NBC-1 and NHE-3 in sodium and bicarbonate loading. Kidney Int 2001;60:1824–36.
[116] Sabatini S. The cellular basis of metabolic alkalosis. Kidney Intern 1996;49:906–17.
[117] Chu TS, Peng Y, Cano A, Yanagisawa M, Alpern RJ. Endothelin (B) receptor activates NHE-3 by a Ca2^{+-}dependent pathway in OKP cells. J Clin Invest 1996;97:1454–62.

[118] Good DW. Adaptation of HCO3 and NH + 4 transport in rat MTAL: effects of chronic acidosis and Na + intake. Am J Physiol 1990;258:F1345–53.
[119] Wesson DE, Dolson GM. Maximal proton secretory rate of rat distal tubules is higher during chronic metabolic alkalosis. Am J Physiol 1991;261:F753–9.
[120] Chan YL, Biagi B, Giebisch G. Control mechanisms of bicarbonate transport across the rat proximal convoluted tubule. Am J Physiol 1982;242:F532–43.
[121] Wingo CS. Active proton secretion and potassium absorption in the rabbit outer medullary collecting duct. Functional evidence for proton-potassium-activated adenosine triphosphatase. J Clin Invest 1989;84:361–5.
[122] Buffin-Meyer B, Younes-Ibrahim M, Barlet-Bas C, Cheval L, Marsy S, Doucet A. K depletion modifies the properties of Sch-28080-sensitive K-ATPase in rat collecting duct. Am J Physiol 1997;272:F124–31.
[123] Garella S. Clinical acid–base disorders. In: Cameron S, Davidson AM, Grunfeld JP, Kerr D, Ritz E, editors. Oxford textbook of clinical nephrology. Oxford: Oxford University Press; 1992. p. 944–5.
[124] Madison LL, Seldin DW. Ammonia excretion and renal enzymatic adaptation in human subjects, as disclosed by administration of precursor amino acids. J Clin Invest 1958; 37:1615–27.
[125] O'Neil RG. Aldosterone regulation of sodium and potassium transport in the cortical collecting duct. Semin Nephrol 1990;10:365–74.
[126] Sabolic I, Brown D, Gluck SL, Alper SL. Regulation of AE1 anion exchanger and H(+)-ATPase in rat cortex by acute metabolic acidosis and alkalosis. Kidney Intern 1997;51: 125–37.
[127] Gifford JD, Sharkins K, Work J, Luke RG, Galla JH. Total CO2 transport in rat cortical collecting duct in chloride-depletion alkalosis. Am J Physiol 1990;258:F848–53.
[128] Star RA, Burg MB, Knepper MA. Bicarbonate secretion and chloride absorption by rabbit cortical collecting ducts. Role of chloride/bicarbonate exchange. J Clin Invest 1985;76:1123–30.
[129] Frische S, Kwon TH, Frokiaer J, Madsen KM, Nielsen S. Regulated expression of pendrin in rat kidney in response to chronic NH4Cl or NaHCO3 loading. Am J Physiol 2003;284: F584–93.
[130] Wagner CA, Finberg KE, Stehberger PA, et al. Regulation of the expression of the Cl^-/anion exchanger pendrin in mouse kidney by acid–base status. Kidney Intern 2002;62:2109–17.
[131] Verlander JW, Hassell KA, Royaux IE, et al. Deoxycorticosterone upregulates PDS (Slc26a4) in mouse kidney: role of pendrin in mineralocorticoid-induced hypertension. Hypertension 2003;42:356–62.
[132] Wagner CA, Finberg KE, Stehberger PA, et al. Regulation of the expression of the Cl^-/anion exchanger pendrin in mouse kidney by acid–base status. Kidney Int 2002;62:2109–17.
[133] Pech V, Pham TD, Hong S, et al. Pendrin modulates ENaC function by changing luminal HCO3. J Am Soc Nephrol 2010;21:1928–41.
[134] Clapp JR, Rector FCJ, Seldin DW. Effect of unreabsorbed anions on proximal and distal transtubular potentials in rats. Am J Physiol 1962;202:781–6.
[135] Morris RC, Piel CF, Audioun E. Effects of sodium phosphate and sulfate on renal acidification in two patients with renal tubular acidosis. Pediatrics 1965;36:899–904.
[136] Stapleton FB, Nelson B, Vats TS, Linshaw MA. Hypokalemia associated with antibiotic treatment. Evidence in children with malignant neoplasms. Am J Dis Child 1976;130:1104–8.
[137] Cabizuca SV, Dresser KB. Carbenicillin-associated with hypokalemic alkalosis. JAMA 1976;236:956–7.
[138] Preisig PA. The acid-activated signaling pathway: starting with Pyk2 and ending with increased NHE3 activity. Kidney Int 2007;72:1324–9.
[139] Seuwen K, Ludwig MG, Wolf RM. Receptors for protons or lipid messengers or both? Journal of receptor and signal transduction research 2006;26:599–610.
[140] Buck J, Levin LR. Physiological sensing of carbon dioxide/bicarbonate/pH via cyclic nucleotide signaling. Sensors Basel Sensors 2011;11:2112–28.
[141] Geng W, Wang Z, Zhang J, Reed BY, Pak CY, Moe OW. Cloning and characterization of the human soluble adenylyl cyclase. Am J Physiol Cell Physiol 2005;288:C1305–16.
[142] Deyev IE, Sohet F, Vassilenko KP, et al. Insulin receptor-related receptor as an extracellular alkali sensor. Cell Metab 2011;13:679–89.
[143] Worthley LI. The rational use of i.v. hydrochloric acid in the treatment of metabolic alkalosis. Br J Anaesth 1977;49:811–7.
[144] Ayus JC, Olivero JJ, Adrogue HJ. Alkalemia associated with renal failure. Correction by hemodialysis with low-bicarbonate dialysate. Arch Intern Med 1980;140:513–5.
[145] Wilson RF, Gibson D, Percinel AK, et al. Severe alkalosis in critically ill surgical patients. Arch Surg 1972;105:197–203.
[146] Anderson LE, Henrich WL. Alkalemia-associated morbidity and mortality in medical and surgical patients. South Med J 1987;80:729–33.
[147] Bear R, Goldstein M, Phillipson E, et al. Effect of metabolic alkalosis on respiratory function in patients with chronic obstructive lung disease. Can Med Assoc J 1977;117:900–3.
[148] Shear L, Brandman IS. Hypoxia and hypercapnia caused by respiratory compensation for metabolic alkalosis. Am Rev Respir Dis 1973;107:836–41.
[149] Pokorski M, Lahiri S. Relative peripheral and central chemosensory responses to metabolic alkalosis. Am J Physiol 1983;245:R873–80.
[150] Schuitmaker JJ, Berkenbosch A, DeGoede J, Olievier CN. Ventilatory responses to respiratory and metabolic acid–base disturbances in cats. Respir Physiol 1987;67:69–83.
[151] Mitchell JH, Wildenthal K, Johnson Jr. JR. The effects of acid–base disturbances on cardiovascular and pulmonary function. Kidney Intern 1972;1:375–89.
[152] Yasue H, Omote S, Takizawa A, Nagao M, Nosaka K, Nakajima H. Alkalosis-induced coronary vasoconstriction: effects of calcium, diltiazem, nitroglycerin, and propranolol. Am Heart J 1981;102:206–10.
[153] Rinaldi GJ, Amado CE, Cingolani HE. Interaction between calcium and hydrogen ions in canine coronary arteries. J Mol Cell Cardiol 1987;19:773–84.
[154] Vanhoutte P, Clement D. Effect of pH and PCO2 changes on the reactivity of isolated venous smooth muscle. Arch Int Physiol Biochim 1968;76:144–6.
[155] Betz E, Heuser D. Cerebral cortical blood flow during changes of acid–base equilibrium of the brain. J Appl Physiol 1967;23:726–33.
[156] Lubash GD, Cohen BD, Young CW, Silverman GM, Rubin AL. Severe metabolic alkalosis with neurologic abnormalities; report of a case. NEJM 1958;258:1050–2.
[157] Hsia CC. Respiratory function of hemoglobin. N Eng J Med 1998;338:239–47.
[158] Adrogue HJ, Brensilver J, Madias NE. Changes in the plasma anion gap during chronic metabolic acid–base disturbances. Am J Physiol 1978;235:F291–7.
[159] Brater DC, Morrelli HF. Systemic alkalosis and digitalis related arrhythmias. Acta Med Scand 1981;647:79–85.
[160] Ayres SM, Grace WJ. Inappropriate ventilation and hypoxemia as causes of cardiac arrhythmias. The control of

arrhythmias without antiarrhythmic drugs. Am J Med 1969; 46:495–505.
[161] Lawson NW, Butler III GH, Ray CT. Alkalosis and cardiac arrhythmias. Anesth Analg 1973;52:951–64.
[162] Madias NE, Levey AS. Metabolic alkalosis due to absorption of "nonabsorbable" antacids. Am J Med 1983;74:155–8.
[163] Hardt LL, Rivers AB. Toxic manifestations following the alkaline treatment of peptic ulcer. Arch Intern Med 1923;31: 171–80.
[164] Lin SH, Lin YF, Cheema-Dhadli S, Davids MR, Halperin ML. Hypercalcaemia and metabolic alkalosis with betel nut chewing: emphasis on its integrative pathophysiology. Nephrol Dial Transplant 2002;17:708–14.
[165] Lin SH, Lin YF, Shieh SD. Milk-alkali syndrome in an aged patient with osteoporosis and fractures. Nephron 1996;73:496–7.
[166] Hebert SC, Brown EM, Harris HW. Role of the Ca(2 +)-sensing receptor in divalent mineral ion homeostasis. J Exp Biol 1997;200:295–302.
[167] Orwoll ES. The milk-alkali syndrome: current concepts. Arch Intern Med 1982;97:242–8.
[168] Chung HM, Kluge R, Schrier RW, Anderson RJ. Clinical assessment of extracellular fluid volume in hyponatremia. Am J Med 1987;83:905–8.
[169] Oster JR, Preston RA, Materson BJ. Fluid and electrolyte disorders in congestive heart failure. Semin Nephrol 1994;14:485–505.
[170] Funk GC, Doberer D, Osterreicher C, Peck-Radosavljevic M, Schmid M, Schneeweiss B. Equilibrium of acidifying and alkalinizing metabolic acid–base disorders in cirrhosis. Liver Int 2005;25:505–12.
[171] Bernardi M, Predieri S. Disturbances of acid–base balance in cirrhosis: a neglected issue warranting further insights. Liver Int 2005;25:463–6.
[172] Haussinger D, Steeb R, Gerok W. Ammonium and bicarbonate homeostasis in chronic liver disease. Klin Wochenschr 1990;68:175–82.
[173] Stanton BA, Giebisch G. Effects of pH on potassium transport by renal distal tubule. Am J Physiol 1982;242:F544–51.
[174] Barton CH, Vaziri ND, RLea Ness, Saiki JK, Mirahmadi KS. Cimetidine in the management of metabolic alkalosis induced by nasogastric drainage. Arch Surg 1979;114:70–4.
[175] Darrow DC. Congenital alkalosis with diarrhea. J Pediat 1945;26:519–32.
[176] Gamble JL, Fahey KR, Appleton J, McLachlan E. Chronic alkalosis with diarrhea. J Pediat 1945;26:509–18.
[177] Perheentupa J, Eklund J, Kojo N. Familial chloride diarrhea (congenital alkalosis with diarrhea). Acta Paediatr Scand Suppl 1965;159:119–20.
[178] Höglund P, Haila S, Gustavson KH, et al. Clustering of private mutations in the congenital chloride diarrhea/down-regulated in adenoma gene. Hum Mutat 1998;11:321–7.
[179] Kagalwalla AF. Congenital chloride diarrhea. J Clin Gastroenterol 1994;19:36–40.
[180] Makela S, Kere J, Holmberg C, Hoglund P. SLC26A3 mutations in congenital chloride diarrhea. Hum Mutat 2002;20:425–38.
[181] Bieberdorf FA, Gorden P, Fordtran JS. Pathogenesis of congenital alkalosis with diarrhea. Implications for the physiology of normal ileal electrolyte absorption and secretion. J Clin Invest 1972;51:1958–68.
[182] Schweinfest CW, Henderson KW, Suster S, Kondoh N, Papas TS. Indentification of a colon mucosa gene that is down-regulated in colon adenomas and adenocarcinomas. Proc Natl Acad Sci USA 1993;90:4166–70.
[183] Höglund P, Haila S, Socha J, et al. Mutations in the down-regulated in adenoma (DRA) gene cause congenital chloride diarrhea. Nat Genet 1996;14:316–9.
[184] Pilch YH, Kiser WS, Bartter FC. A case of villous adenoma of the rectum with hyperaldosteronism and unusual renal manifestations. Am J Med 1965;39:483–91.
[185] Bondo B, Pedersen SA. Villous adenoma of the rectum associated with severe electrolyte imbalance. Report of a case. Acta Chir Scand 1968;:.
[186] Birzgalis AR, Tweedle DE. Large villous adenoma of the stomach causing severe electrolyte disturbance. J R Coll Surg Edinb 1993;38:170–1.
[187] Sweetser LJ, Douglas JA, Riha RL, Bell SC. Clinical presentation of metabolic alkalosis in an adult patient with cystic fibrosis. Respirology 2005;10:254–6.
[188] Yalcin E, Kiper N, Dogru D, Ozcelik U, Aslan AT. Clinical features and treatment approaches in cystin fibrosis with pseudo Bartter syndrome. Ann Trop Paediatr 2005;25:119–24.
[189] Dave S, Honney S, Raymond J, Flume PA. An unusual presentation of cystic fibrosis in an adult. Am J Kid Dis 2005;45: e41–4.
[190] Wilcox CS. Diuretics. In: Brenner BM, editor. The kidney. 5th ed. Philadelphia: W.B. Saunders; 1996. p. 2315.
[191] Cannon PJ, Heinemann HO, Albert MS, Laragh JH, Winters RW. "Contraction" alkalosis after diuresis of edematous patients with ethacrynic acid. Ann Intern Med 1965;62: 979–90.
[192] Gyory AZ, Lissner D. Independence of ethacrynic acid-induced renal hydrogen ion excretion of sodium-volume depletion in man. Clin Sci Mol Med 1977;53:125–32.
[193] Schwartz WB, Cohen JJ. The nature of renal response to chronic disorders of acid–base equilibrium. Am J Med 1978;64:417–28.
[194] Shils ME. Experimental human magnesium depletion. Medicine 1969;48:61–85.
[195] Francisco LL, Sawin LL, Dibona GF. Mechanism of negative potassium balance in the magnesium-deficient rat. Proc Soc Exp Biol Med 1981;168:382–8.
[196] Schilsky RL, Anderson T. Hypomagnesemia and renal magnesium wasting in patients receiving cisplatin. Arch Intern Med 1979;90:929–31.
[197] Bar RS, Wilson HE, Mazzaferri EL. Hypomagnesemic hypocalcemia secondary to renal magnesium wasting. Arch Intern Med 1975;82:646–9.
[198] Conrad M, Weber S. Recent advances in molecular genetics of hereditary magnesium-losing disorders. J Am Soc Nephrol 2003;147:249–60.
[199] Bartter FC, Pronove P, Gill JRJ, Maccardle RC. Hyperplasia of the juxtaglomerular complex with hyperaldosteronism and hypokalemic alkalosis. A new syndrome. Am J Med 1962;33: 811–28.
[200] Bartter FC. On the pathogenesis of Bartter's syndrome. Miner Electrolyte Metab 1980;3:61–5.
[201] Hebert SC. Bartter syndrome. Curr Opin Nephrol Hypertens 2003;12:527–32.
[202] Gitelman HJ, Graham JB, Welt LG. A new familial disorder characterized by hypokalemia and hypomagnesemia. Trans Am Assoc Phys 1966;79:221–35.
[203] Bettinelli A, Bianchetti MG, Girardin E, et al. Use of calcium excretion values to distinguish two forms of primary renal tubular hypokalemic alkalosis: Bartter and Gitelman syndromes. Journal of Pediatrics 1992;120:38–43.
[204] Simon DB, Nelson-Williams C, Bia MJ, et al. Gitelman's variant of Bartter's syndrome, inherited hypokalaemic alkalosis, is

caused by mutations in the thiazide-sensitive Na-Cl transporter. Nat Genet 1996;12:24–30.
[205] Rapoport A, From GL, Husdan H. Metabolic studies in prolonged fasting. I. Organic metabolism and kidney function. Metabolism 1965;14:31–46.
[206] Rapoport A, From GL, Husdan H. Metabolic studies in prolonged fasting. II. Organic metabolism. Metabolism 1965;14: 47–58.
[207] Veverbrants E, Arky RA. Effects of fasting and refeeding. I. Studies on sodium, potassium and water excretion on a constant electrolyte and fluid intake. J Clin Endocrin Metab 1969;29:55–62.
[208] Stinebaugh BJ, Schloeder FX. Glucose-induced alkalosis in fasting subjects. Relationship to renal bicarbonate reabsorption during fasting and refeeding. J Clin Invest 1972;51:1326–36.
[209] Baum M. Insulin stimulates volume absorption in the rabbit proximal convoluted tubule. J Clin Invest 1987;79:1104–19.
[210] Suki WN, Herbert CS, Stinebaugh BJ, Martinez-Maldonado M, Eknoyan G. Effects of glucose on bicarbonate reabsorption in the dog kidney. J Clin Invest 1974;54:1–8.
[211] Massry SG, Kurokawa K, Arieff AI, Ben-Issac C. Metabolic acidosis of hyperparathyroidism. Arch Intern Med 1974;134: 385–7.
[212] Hulter HN. Effects and interrelationships of PTH, Ca2 + , vitamin D, and Pi in acid–base homeostasis. Am J Physiol 1985;248:F739–52.
[213] Heinemann HO. Metabolic alkalosis in patients with hypercalcemia. Metabolism 1965;14:1137–52.
[214] Barzel US. Systemic alkalosis in hypoparathyroidism. J Clin Endocrin Metab 1969;29:917–8.
[215] Nordin BEC. The effects of intravenous parathyroid extract on urinary pH, bicarbonate and electrolyte excretion. Clin Sci 1960;19:311–9.
[216] Diaz-Buxo JA, Ott CE, Cuche JL, Marchand GR, Wilson DM, Knox FG. Effects of extracellular fluid volume contraction and expansion on the bicarbonaturia of parathyroid hormone. Kidney Intern 1975;8:105–9.
[217] Puschett JB, Zurbach O. Acute effects of parathyroid hormone on proximal tubule bicarbonate transport in the dog. Kidney Intern 1976;9:501–10.
[218] Fan L, Wiederkehr MR, Collazo R, Huang H, Crowder LA, Moe OW. Dual mechanisms of regulation on Na/H exchanger NHE-3 by parathyroid hormone in rat kidney. J Biol Chem 1999;274:11289–95.
[219] Collazo R, Fan L, Zhao H, Wiederkehr M, Moe OW. Acute regulation of Na + /H + exchanger NHE3 by parathyroid hormone via NHE3 phosphorylation and dynamin-dependent endocytosis. J Biol Chem 2000;275:31601–8.
[220] Crumb CK, Martinez-Maldonado M, Eknoyan G, Suki WN. Effects of volume expansion, purified parathyroid extract, and calcium on renal bicarbonate absorption in the dog. J Clin Invest 1974;54:1287–94.
[221] Wang WH, Lu M, Hebert SC. Cytochrome P-450 metabolites mediate extracellular Ca(2 +)-induced inhibition of apical K + channels in the TAL. Am J Physiol 1996;271:C103–11.
[222] Conn JW, Cohen EL, Lucas CP, et al. Primary reninism. Hypertension, hyperreninemia, and secondary aldoseronism due to renin-producting juxtaglomerular cell tumors. Arch Intern Med 1972;130:682–96.
[223] Eddy RL, Sanchez SA. Renin-secreting renal neoplasm and hypertension with hypokalemia. Arch Intern Med 1971;75: 725–9.
[224] Bunchman TE, Sinaiko AR. Renovascular hypertension presenting with hypokalemic metabolic alkalosis. Pediatr Nephrol 1990;4:169–70.
[225] Ruby ST, Burch A, White WB. Unilateral renal artery stenosis seen initially as severe and symptomatic hypokalemia. Arch Surg 1993;128:346–8.
[226] Mansoor GA, Tendler BE, Anwar YA, Uwaifo G, White WB. Coexistence of atherosclerotic renal artery stenosis with primary hyperaldosteronism. J Hum Hypertens 2000;14: 151–3.
[227] Stokes GS, Monaghan JC, Roche J, Grunstein H, Gordon RD. Concurrence of primary aldosteronism and renal atery stenosis. Clin Exp Pharmacol Physiol 1992;19:300–3.
[228] Hollenberg NK, Epstein M, Basch RI, Couch NP, Hickler RB, Merrill JP. Renin secretion in essential and accelerated hypertension. Am J Med 1969;47:855–9.
[229] Laragh JH, Ulick S, Januszewicz V, Deming QB, Kelly WG, Lieberman S. Aldosterone secretion and primary and malignant hypertension. J Clin Invest 1960;39:1091–106.
[230] Mitchell JD, Baxter TJ, Blair-West JR, McCredie DA. Renin levels in nephroblastoma (Wilms' tumour). Report of a renin secreting tumour. Arch Dis Child 1970;45:376–84.
[231] Hirose M, Arakawa K, Kikuchi M, et al. Primary reninism with renal hamartomaous alteration. JAMA 1974;230:1288–92.
[232] Genest J, Rojo-Ortega JM, Kuchel O, et al. Malignant hypertension with hypokalemia in a patient with renin-producing pulmonary carcinoma. Trans Assoc Am Physicians 1975;88: 192–201.
[233] Weinberger MH. Primary aldosteronism: diagnosis and differentiation of subtypes. Arch Intern Med 1984;100:300–2.
[234] Biglieri EG, Stockigt JR, Schambelan M. Adrenal mineralocorticoids causing hypertension. Am J Med 1972;52:623–32.
[235] Lifton RP, Dluhy RG, Powers M, et al. A chimaeric 11 beta-hydroxylase/aldosterone synthase gene causes glucocorticoid-remediable aldosteronism and human hypertension. Nature 1992;355:262–5.
[236] Pascoe L, Curnow KM, Slutsker L, et al. Glucocorticoid-suppressible hyperaldosteronism results from hybrid genes created by unequal crossovers between CYP11B1 and CYP11B2. Proc Natl Acad Sci USA 1992;89:8327–31.
[237] Greco RG, Carroll JE, Morris DJ, Grekin RJ, Melby JC. Familial hyperaldosteronism, not suppressed by dexamethasone. J Clin Endocrin Metab 1982;55:1013–6.
[238] Torpy DJ, Gordon RD, Lin JP, et al. Familial hyperaldosteronism type-II: description of a large kindred and exclusion of the aldosterone synthase (CYP11B2) gene. J Clin Endocrin Metab 1998;83:3214–8.
[239] Jackson RV, Lafferty A, Torpy DJ, Stratakis C. New genetic insights in familial hyperaldosteronism. Ann NY Acad Sci 2002;970:77–88.
[240] Lafferty AR, Torpy DJ, Stowasser M, et al. A novel genetic locus for low renin hypertension: familial hyperaldosteronism type II maps to chromosome 7 (7p22). J Med Genet 2000;37:831–5.
[241] Greathouse DJ, McDermott MT, Kidd GS, Hofeldt FD. Pure primary hyperaldosteronism due to adrenal cortical carcinoma. Am J Med 1984;76:1132–6.
[242] Alterman SL, Dominguez C, Lopez-Gomez A, Lieber AL. Primary adrenocortical cancer causing aldosteronism. Cancer 1969;24:602–9.
[243] Cost WS. A mineralocorticoid excess syndrome presumably due to excessive secretions of corticosterone. Lancet 1963;16:362–3.
[244] Christy NP, Laragh JH. Pathogenesis of hypokalemic alkalosis in Cushing's syndrome. Nord Hyg Tidskr 1961;265:1083–8.
[245] Gwinup G, Gantt CL, Hamwi GJ. The production of hypokalemic alkalosis with hydrocortisone in subjects with adrenal insufficiency. Metabolism 1964;13:836.

[246] Schambelam M, Slaton Jr. PE, Biglieri EG. Mineralocorticoid production in hyperadrenocorticism. Role in pathogenesis of hypokalemic alkalosis. Am J Med 1971;51:299–303.
[247] Mantero F, Palermo M, Petrelli MD, Tedde R, Stewart PM, Shackleton CH. Apparent mineralocorticoid excess: type I and type II. Steroids 1996;61:193–6.
[248] Blachley JD, Knochel JP. Tobacco chewer's hypokalemia: licorice revisited. NEJM 1980;302:784–5.
[249] Louis LH, Conn JW. Preparation of glycyrrhizinic acid, the electrolyte-active principle of licorice: its effects upon metabolism and upon pituitary-adrenal function of man. J Lab Clin Med 1956;47:20–8.
[250] Stewart PM, Wallace AM, Valentino R, Burt D, Shackleton CH, Edwards CR. Mineralocorticoid activity of liquorice: 11-beta-hydroxysteroid dehydrogenase deficiency comes of age. Lancet 1987;2:821–4.
[251] New MI, Levine LS, Biglieri EG, Pariera J, Ulick S. Evidence for an unidentified steroid in a child with apparent mineralocorticoid hypertension. J Clin Endocrin Metab 1977;44:924–33.
[252] Ulick S, Levine LS, Gunczler P, et al. A syndrome of apparent mineralocorticoid excess associated with defects in the peripheral metabolism of cortisol. J Clin Endocrin Metab 1979;49:757–64.
[253] Wilson RC, Krozowski ZS, Li K, et al. A mutation in the HSD11B2 gene in a family with apparent mineralocorticoid excess. J Clin Endocrin Metab 1995;80:2263–6.
[254] Mune T, Rogerson FM, Nikkila H, Agarwal AK, White PC. Human hypertension caused by mutations in the kidney isozyme of 11 beta-hydroxysteroid dehydrogenase. Nat Genet 1995;10:394–9.
[255] Geller DS, Farhi A, Pinkerton N, et al. Activating mineralocorticoid receptor mutation in hypertention exacerbated by pregnancy. Science 2000;289:119–23.
[256] Liddle GW, Bledso T, Coppage Jr. WS. A familial renal disorder simulating primary aldosteroism but with negligible aldosterone secretion. Trans Assoc Am Physicians 1963;76: 199–213.
[257] Rodriguez JA, Biglieri EG, Schambelan M. Pseudohyperaldosteronism with renal tubular resistance to mineralocorticoid hormones. Trans Assoc Am Physicians 1981;94:172–82.
[258] Wang C, Chan TK, Yeung RT, Coghlan JP, Scoggins BA, Stockigt JR. The effect of triamterene and sodium intake on renin, aldosterone, and erythrocyte sodium transport in Liddle's syndrome. J Clin Endocrin Metab 1981;52:1027–32.
[259] Hansson JH, Nelson-Williams C, Suzuki H, et al. Hypertension caused by a truncated epithelial sodium channel gamma subunit: genetic heterogeneity of Liddle syndrome. Nat Genet 1995;11:76–82.
[260] Shimkets RA, Warnock DG, Bositis CM, et al. Liddle's syndrome: heritable human hypertension caused by mutations in the beta subunit of the epithelial sodium channel. Cell 1994;79:407–14.
[261] Snyder PM, Price MP, McDonald FJ, et al. Mechanism by which Liddle's syndrome mutations increase activity of a human epithelial Na + channel. Cell 1995;83:969–78.

This page intentionally left blank

CHAPTER

59

Clinical Syndromes of Metabolic Acidosis

Reto Krapf, Donald W. Seldin and Robert J. Alpern

Kantonsspital Bruderholz, University of Basel, Bruderholz/Basel, Switzerland
University of Texas Southwestern Medical Center, Dallas, Texas, USA
Yale University School of Medicine, New Haven, Connecticut, USA

INTRODUCTION

The maintenance of normal systemic acid–base regulation requires the subtle integration of a number of organ functions and physiologic mechanisms such as extracellular and cellular buffering processes and integrated responses of the kidney, lung, liver, gastrointestinal tract, and skeleton. Disturbances of acid–base homeostasis are the predictable consequences of many pathophysiological processes. Their recognition may lead the clinician to the diagnosis of specific diseases and/or complications thereof. In addition, it has become increasingly clear that adaptation to acid–base disturbances is characterized by a number of important metabolic and endocrine derangements. Thus, whereas there is no evidence that there is any defense of extracellular pH to any homeostatic value or "set-point," there is evidence for homeostatic regulation of intracellular pH. Such regulation of intracellular pH affords unimpaired function of a multitude of cellular, enzymatic, and molecular processes. However, many adverse and clinically important effects of systemic acid–base disturbances *in vivo* have been recognized that might be viewed as maladaptive or constituting a "trade-off" for the maintenance of acid–base homeostasis.

In this chapter, we review the renal and systemic response to acidosis or acid load. Next, special emphasis is placed on the clinical consequences of acidosis such as on protein, divalent ion, and bone metabolism, and sodium and potassium balance as well as secondary endocrine disturbances. Finally, the various clinical entities of metabolic acidosis and their diagnostic recognition are described. The number of cited references had to be reduced for this edition. Therefore, not all important work of all authors that have contributed to the knowledge of the field could be cited. The reader will find additional references in the second to fourth editions of this book.

DEFINITION OF METABOLIC ACIDOSIS

Metabolic acidosis is the acid–base disturbance initiated by a primary decrease in plasma bicarbonate concentration. The resultant acidification of neural chemoreceptors stimulates ventilation and leads to a predictable secondary hypocapnia. The primary hypobicarbonatemia causing metabolic acidosis can occur due to: (1) loss of bicarbonate salts from the gastrointestinal tract or kidney, (2) excess of noncarbonic acid presented to body buffers from endogenous or exogenous sources, and/or (3) a decrease in the kidney's set-point for regulation of plasma bicarbonate concentration. The latter circumstance might or might not be associated with a decrease in the kidney's ability to excrete acid.

Metabolic acidosis is defined as acute on the basis of the characterization of an early steady-state period in which stable acid–base and electrolyte composition is observed during at least the initial six hours after an acid load.[319,376] Within 120 minutes after an acid load and following a large net retention of administered acid, renal net acid excretion is significantly increased[376] and is fully augmented within 72 hours. Net acid excretion is increased to values whereby the rate of acid excretion approaches the rate of endogenous acid production. Daily acid balance is again essentially achieved and the steady state of chronic metabolic acidosis has occurred.[98,207] In chronic

Seldin and Giebisch's The Kidney, Fifth Edition.
DOI: http://dx.doi.org/10.1016/B978-0-12-381462-3.00059-8

© 2013 Elsevier Inc. All rights reserved.

metabolic acidosis, the occurrence of an approach to daily acid balance permits the maintenance of stable but depressed plasma bicarbonate concentrations. The resulting decrease in plasma bicarbonate concentration in such conditions of extrarenal metabolic acidosis reflects the magnitude and anionic character of the acid load/production as well as the potency of the acid excretory response. Large variations in naturally occurring diet-induced acid production from 0 to 150 mmol protons/day correlate inversely and significantly with ambient plasma bicarbonate concentration,[214] and lower bicarbonate concentrations are associated with higher blood acidity. Thus, normal subjects ingesting higher acid loads occupy the lower domains of the normal range of plasma bicarbonate concentration, whereas those that self-select smaller acid loads exhibit bicarbonate values within the upper domain of the normal range of values. The observation that higher acid-generating diets produce relatively small decrements in plasma bicarbonate and small increments in blood acidity reflects the potency of renal acid excretory mechanisms to adjust to changes in acid load as well as other factors such as primary or secondary changes in $PaCO_2$ as discussed in subsequent sections. Thus, plasma bicarbonate concentrations within the clinically normal range do not signify the rigorous absence of an acidotic process.

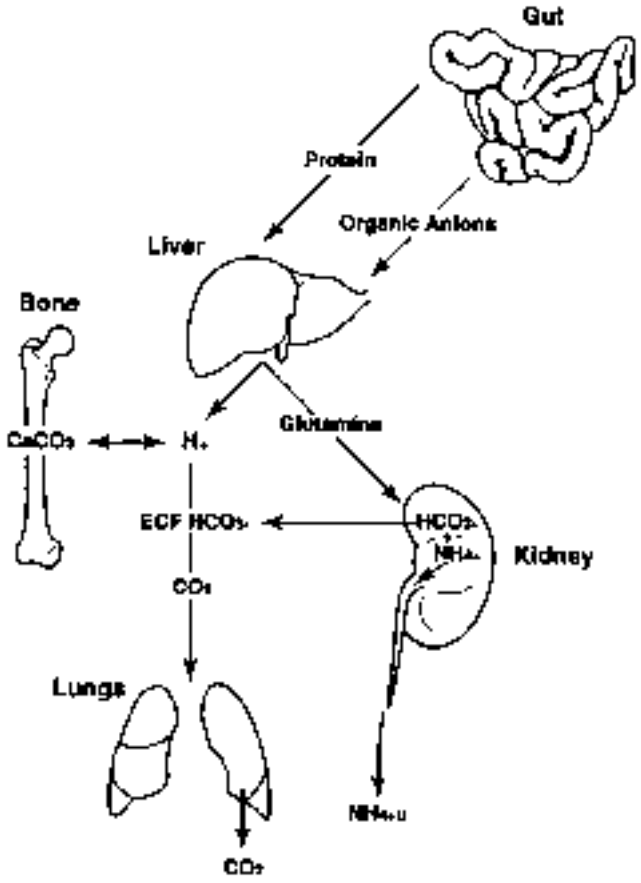

FIGURE 59.1 Integration of liver, lung, kidney, bone, and gut in regulation of acid–base homeostasis. Endogenous acid (H^+) production occurs primarily during metabolism of dietary protein in the liver. Protons produced titrate HCO_3^- in the extracellular fluid with generation of CO_2, which is eliminated by the lungs. Glutamine supply from the liver to the kidney is the prerequisite for renal production of HCO_3^- (added to the extracellular fluid) and NH_4^+ (excreted with urine) and thus allows regeneration of HCO_3^-. Bone-derived base (CO_3^{2-}) is recruited to buffer H^+ during normal variations of acid production. Depending on diet composition, up to 50% of H^+ produced during protein metabolism is titrated by base (organic anions) resorbed through the gastrointestinal tract.

SYSTEMIC AND RENAL ACID–BASE HOMEOSTASIS

Systemic acid–base homeostasis requires the coordinated and integrated action of the lung, kidney, liver, skeleton, and gastrointestinal tract (Fig. 59.1). Cellular metabolism produces about 15,000 mmol of CO_2 daily that, if received as a nonvolatile acid or a volatile acid in a closed system would constitute a major acid load according to the following relationship:

$$CO_2 + H_2O \rightarrow H_2CO_3 \rightarrow HCO_3^- + H^+$$

Although equimolar quantities of acid and base are produced by the dissociation of carbonic acid, the produced protons would be expected to have a much greater influence on acid–base equilibrium due to the basal concentration of H^+ being six orders of magnitude lower than the corresponding value for bicarbonate (40 nmol/liter vs 25mmol/liter).

However, under steady-state circumstances the HCO_3^-/H_2CO_3 buffer system behaves as an "open" buffer system, whereby CO_2/H_2CO_3 is eliminated at a rate necessary to maintain $PaCO_2$ at the level dictated by alveolar ventilation, the rate of that is, in turn, controlled by neural chemoreceptors. Accordingly, when regulation of alveolar ventilation is undisturbed, only noncarbonic acids normally contribute to net acid production or to appreciable acid retention.

In the healthy individual, the primary source and magnitude of an acid load results from hepatic metabolism of dietary protein. Neutral amino acids are metabolized without net proton consumption or production, and metabolism of dicarboxylic amino acids consumes protons, while sulfur-containing as well as cationic amino acid catabolism results in net hepatic proton production. Due to the prevalence of sulfur-containing amino acids in the animal protein-rich nutrients typical of the "Western diet," endogenous acid production is around 1 mmol per kilogram of body weight per day.[161]

Endogenous acid production is also influenced by organic acid production from neutral precursors and alkali lost through stool.[225] Many of the clinical syndromes of metabolic acidosis are characterized by an increase in organic acid production and/or organic acid metabolism (such as ketoacidosis, lactic acidosis) and will be discussed in subsequent sections.

Hepatorenal Interactions

As illustrated in Fig. 59.1, the proton load produced by hepatic amino acid metabolism will titrate extracellular bicarbonate resulting in production of CO_2 that is eliminated by the lungs. To maintain plasma bicarbonate constant, the kidney has two pivotal tasks. First, it must reclaim the bicarbonate present in the glomerular ultrafiltrate (filtered load of bicarbonate) and, second, it must regenerate bicarbonate to replete the bicarbonate consumed during endogenous acid production. The first task is accomplished by virtually complete tubular reabsorption or reclamation of the filtered bicarbonate along the nephron (predominantly in the proximal tubule). The kidney regenerates bicarbonate (bicarbonate neogenesis) by excretion of protons either as ammonium (NH_4^+) or as titratable acid (TA) in amounts sufficient to offset those protons produced daily by oxidation of dietary foodstuffs. The amount of renal proton excretion or, equivalently, bicarbonate neogenesis/regeneration is measured as net acid excretion (NAE), which reflects the sum of NH_4^+ and titratable acid excretion minus any urinary bicarbonate excreted (that which escapes tubular reabsorption):

$$\text{Net acid excretion} = NH_4^+U + TAU - HCO_3^-U$$

The rate of renal hydrogen ion secretion is thus expressed as the sum of excreted hydrogen ions (NAE) and filtered bicarbonate reabsorbed:

$$\text{Renal } H^+ \text{ secretion} = HCO_3^- \text{ reabsorption} + NH_4 + U + TAU$$

where

$$HCO_3^- \text{ reabsorption} = (GFR \times [HCO_3^-]\text{plasma}) - HCO_3^-U$$

Excretion of NH_4^+ requires the interaction of hepatic and renal glutamine metabolism and intact renal ammoniagenesis. Urea synthesis in peripheral hepatocytes consumes equal amounts of bicarbonate and NH_4^+ and thus is without impact on acid–base balance. However, a small fraction of NH_4^+ is diverted to glutamine synthesis in hepatocytes located in the center of the hepatic lobule and such hepatic production of glutamine has been argued to be an important homeostatic substrate for renal NH_4^+/net acid excretion.[155,156] Acidemia stimulates and alkalemia inhibits glutamine synthesis.[155,156] Under certain conditions, acidemia has been demonstrated to be associated with decreased urea synthesis thereby increasing the supply of NH_4^+ for glutamine synthesis, raising the question that the liver might control the renal acid excretory response to metabolic acidosis.[278] Nevertheless, a significant role for acute metabolic acidosis in altering urea production rate *in vivo* has not been found when tested robustly in rats.[158] In addition, in humans, a negative correlation between ureagenesis and plasma HCO_3^- concentration was observed over a wide range of HCO_3^- concentrations that were altered both chronically and acutely (Fig. 59.2).[173] Thus, the ureageneic process per se may even be maladaptive for acid–base regulation in

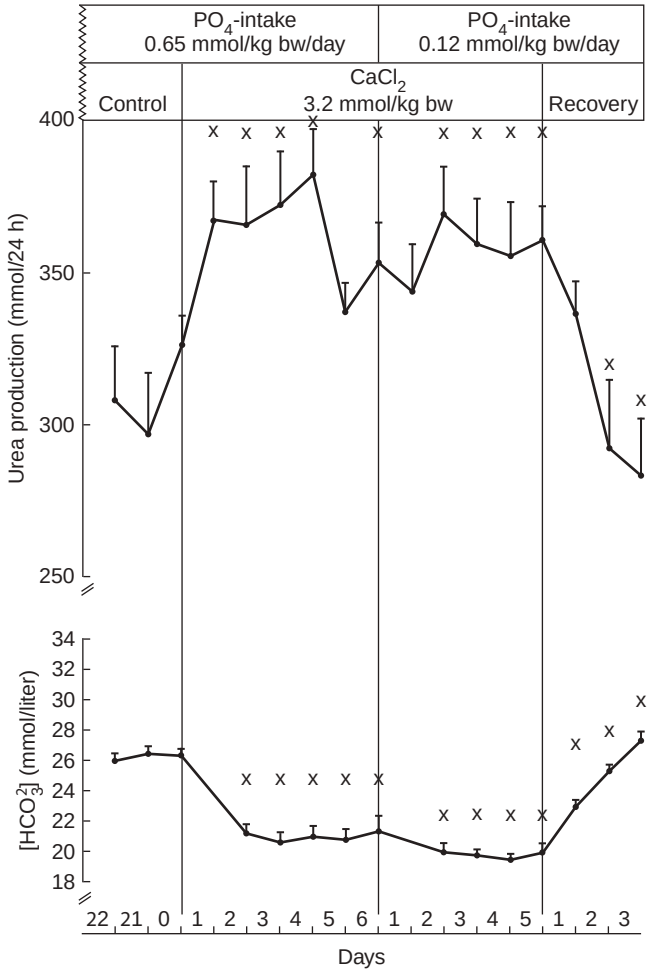

FIGURE 59.2 Effect of $CaCl_2$-induced chronic metabolic acidosis on 24 urea production rates in normal human subjects. Acidosis increases urea production rate significantly and independently of variations in the oral intake of phosphate. *(With permission, from Hosch M, Muser J, Hulter HN, Krapf R. Ureagenesis: evidence for lack of hepatic regulation of acid–base equilibrium in humans. Am J Renal Physiol 2003;286:F94–F99.)*

humans and does not appear to have a discernible homeostatic effect on acid–base equilibrium. It is likely that other metabolic pathways operate in metabolic acidosis to offset the accelerated HCO_3^- consumption of ureagenesis (e.g., oxidation of glutamate or other alkali generating reactions), but this issue has not been addressed experimentally either in animals or humans.

Glutamine supply to the kidneys is also increased by enhanced release of glutamine from skeletal muscle[317] and increased intestinal glutamine absorption, thus providing higher levels of glutamine in the splanchnic circulation.[4] In aggregate, acidemia increases glutamine synthesis or release and delivery of glutamine to the kidney.

In the proximal tubule, two deamidation/deamination steps, both positively regulated by low pH (glutamine deaminase, glutamate dehydrogenase) yield two NH_4^+ and two HCO_3^- molecules. NH_4^+ and HCO_3^- are then separated, NH_4^+ is excreted in the urine and HCO_3^- is added to the extracellular fluid. Therefore, glutamine catabolism in the kidney leads to excretion of protons (as NH_4^+) and reabsorption of equal amounts of HCO_3^-. Excess glutamine, not taken up by the kidney, is returned to the liver and deamidated/deaminated, a process that stimulates ureagenesis, inhibits further glutamine synthesis and thus constitutes a feed-back loop regulating glutamine (and thus potential NH_4^+ and bicarbonate) supply to the kidney. In contrast to the kidney, HCO_3^- and NH_4^+ are not physically partitioned or differentially excreted in the liver, but metabolized with a stoichiometry of 1:1 during ureagenesis. It is thus renal control of NH_4^+ excretion, not hepatic control of glutamine vs. urea synthesis that relates changes in plasma acid–base composition to changes in NH_4^+ metabolism and thus to possible effects on acid–base balance.

Role of the Gut

The gut affects acid–base homeostasis not only by absorbing sulfur-containing amino acids, but also by absorbing potential base. Organic anions in the gut are intrinsic to a whole food diet and are also derived in situ from dietary carbohydrates, protein and fat. They are absorbed (constituting potential base), or excreted in feces (around 10 to 60 mmol/day) or intestinally metabolized to organic acids by bacteria with subsequent reaction with HCO_3^- in ileum and colon. The amount of enterally absorbed base from a human whole food diet has been estimated to be about 50% of the magnitude of endogenous acid production.[222]

The amount of base absorbed can be estimated as the difference between diet and stool anion gaps. In both diet and feces, alkali content is estimated as the sum of noncombustible cations ($Na^+ + K^+ + Ca^{2+} + Mg^{2+}$) minus the sum of noncombustible anions ($Cl^- + 1.8$ P), where 1.8 represents the average valence of phosphate at pH 7.4.[224]

The same arithmetic version of the urinary anion gap ($[Na^+ + K^+ + Ca^{2+} + Mg^{2+}] - [Cl^- + 1.8$ P]) has also been shown to be correlated directly and positively with the diet-stool anion gap in metabolically controlled human subjects.[276] This would allow an estimate of gastrointestinal alkali absorption without measuring stool composition. However, the urinary anion gap cannot reliably estimate gut base absorption under conditions in which net systemic organic acid production is altered or in which net bone accretion or dissolution prevails (i.e., typical clinically encountered conditions) as this construct of the urinary anion gap reflects the combined effects of cellular and bone buffering, endogenous organic acid production as well as gastrointestinal base absorption.

There is only weak evidence that intestinal absorption might adapt to acidosis. An insignificant decrement in the stool anion gap of 7 mEq/day was noted during the first six days of acid loading (potential secondary systemic gain of alkali) in human subjects, but this decrement subsequently decreased to only 2.5 mEq/day during prolonged acidosis.[225] The measured 2.5 mEq/day increment in gut base absorption in metabolic acidosis is a very small response in comparison to the simultaneous increment in renal net acid excretion (from 44 to 247 mEq/day).[225] Thus, quantitative considerations and the fact that the estimation of the stool anion gap rests completely on an unknown valence for phosphate, and that only 5% of the fecal phosphate is dialyzable (suggesting that most of stool phosphate is either intracellular or sequestered in calcium/magnesium salts) are the most important arguments against an adaptive role of the gut in acidosis.

Role of Bone

Bone is a large reservoir of exchangeable base as calcium carbonate and dibasic phosphate. Exogenous and endogenous metabolic acid loads, both acute and chronic, liberate calcium and base (carbonate) from bone.[57,58] Calcium is subsequently lost in the urine.[222]

There is evidence from human studies (reviewed in Lemann et al.[224]) that when acid production is increased experimentally, renal net acid excretion does not increase as much as acid production. The difference in acid neutralization (i.e., the positive acid balance) is attributed to bone buffering of retained protons (or liberation of bone base) (Fig. 59.3). Similarly, renal net acid excretion does not decrease as much as acid production when base ($KHCO_3$) is administered. Under

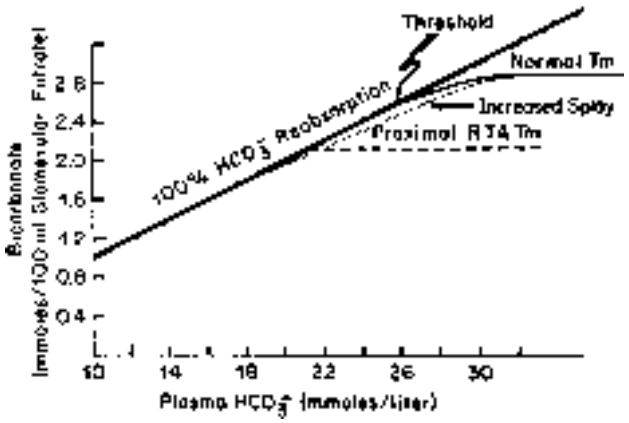

FIGURE 59.3 The relationship between plasma bicarbonate concentration and renal tubular reabsorption of bicarbonate is demonstrated for both normal individuals and patients with proximal renal tubular acidosis (RTA). The renal bicarbonate threshold represents the plasma bicarbonate concentration at which bicarbonate first appears in the urine. The bicarbonate T_{max} (or Tm) represents the bicarbonate concentration at which maximal renal tubular bicarbonate reabsorption occurs. The portion of the curve between the threshold and the T_{max} is called the splay.

these experimental conditions, subjects are likely in small negative acid or positive base balance, with incorporation of base into bone. Positive acid balance is accompanied by equivalent cation loss (loss of Ca^{++} and possibly K and/or Na from bone), negative acid balance by equivalently positive cation balance (incorporation of Ca^{++} and K and/or Na). Scanning ion microprobe analysis indicates that bone buffer content (i.e., HCO_3^- and phosphate) is decreased significantly in mouse calvariae in *in vitro* models of both acute and chronic metabolic acidosis. This consumption of proton buffers may attenuate the severity of both acute and chronic metabolic acidosis, but does so at the expense of a decrease in bone mineral content.[60]

Based on these and other observations that acidotic normal subjects and patients with renal failure that were shown to be in positive acid balance and yet were able to maintain stable plasma bicarbonate concentrations,[147,223] it is assumed that bone contributes in a quantitative important way to proton buffering in response to acid loads. However, in the chronic acidosis of renal failure, quantitative considerations of the required large magnitude of bone alkali have raised the possibility that available bone alkali content is insufficient to offset a possible underexcretion of acid relative to that needed for daily acid balance. While it has been argued that increased gut organic anion absorption may account for this needed base,[361] such a conclusion is not a compelling one when based on a computation of acid balance that depends on a constant and assumed phosphate valence for whole food diets and stool (see Role of Gut section).

Renal Regulation of Acid–Base Equilibrium

As discussed, the kidney maintains a stable $[HCO_3^-]p$ through two processes: (1) HCO_3^- reclamation, the reabsorption of filtered HCO_3^-, and (2) HCO_3^- regeneration, the neogenesis of HCO_3^- that has been decomposed by the invasion of fixed acids into the extracellular fluid or HCO_3^- lost from the body through extrarenal or renal routes.

The relationship between the $[HCO_3^-]p$ and renal HCO_3^- reclamation is shown in Fig. 59.4. When the $[HCO_3^-]p$ is reduced below the normal range, about 25 mEq/liter, the kidney reclaims all filtered HCO_3^-. As the $[HCO_3^-]p$ increases toward normal, complete HCO_3^- reclamation continues until a critical HCO_3^- concentration is reached. This concentration is about 25 mmol/liter in normal humans' "bicarbonate threshold," and thus explains that normal subjects excrete only trivial quantities of bicarbonate in their urine (usually less than 5 mmol/day). Above the bicarbonate threshold, some filtered bicarbonate escapes reclamation and is excreted in the urine. As the $[HCO_3^-]p$ increases further, HCO_3^- reclamation also increases, but not in proportion to the increment in the filtered HCO_3^- load. Therefore, despite greater reclamation, increasing quantities of HCO_3^- enter the urine. Finally,

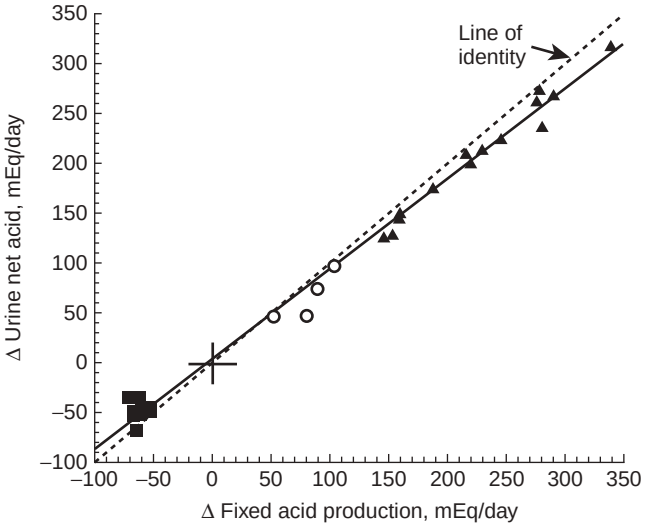

FIGURE 59.4 Changes from control in daily urinary net acid excretion in relation to changes from control in daily endogenous fixed acid production among healthy adults given different acid and base loads. If all endogenous acid produced were eliminated by the kidney, the values should fall on the line of identity. The figure illustrates, however, that acid balances become positive when acid production is increased markedly reflecting buffering by bone. Similarly, acid balances become negative when large amount of base is given reflecting buffering of base by bone. *(With permission, from Lemann J Jr, Bushinsky DA, Hamm LL. Bone buffering of acid and base in humans. Am J Physiol Renal Physiol 2003;54:F811–F832.)*

a $[HCO_3^-]p$ is reached beyond which further increases elicit no greater HCO_3^- reclamation. At this $[HCO_3^-]p$ (about 28 mEq/liter in normal humans), an apparent maximal reabsorptive rate, or apparent T_{max} for HCO_3^-, has been achieved. When the $[HCO_3^-]p$ increases above the apparent T_{max}, the resultant increment in the filtered HCO_3^- load is entirely excreted into the urine.

In addition to HCO_3^- reclamation (reabsorption), the kidney must also regenerate the HCO_3^-, that has been decomposed by the entry of fixed acids into the extracellular fluid (ECF) or lost in urine or stool. The kidney regenerates HCO_3^- by excreting acid. The vast majority of protons are excreted in the form of NH_4^+ or titratable acid as the free proton concentration at the minimal urinary pH of 4.5 is less than 0.1 mmol/liter. The net effect of renal acidification can be measured as net acid excretion.

$$\text{Net Acid excretion} = NH_4^+ + \text{Titratable Acid} - HCO_3^-$$

Quantitatively, changes in renal NH_4^+ excretion account for most of the changes in renal acid excretion both in response to changes in endogenous acid production and in the adaptation to acid–base disturbances. In adaptation to changes in acid load, NH_4^+ excretion is regulated at multiple levels including glutamine supply to the kidney, production of NH_3 in the proximal tubule (ammoniagenesis), secretion of NH_3 into the tubular lumen and various transport processes of NH_3/NH_4^+ along the nephron. (For a discussion of these mechanisms, see Chapters 54 and 56)

Phosphate and organic anions such as citrate, acetate, beta-hydroxybutyrate and creatinine contribute as filtered buffers to titratable acid excretion. Amongst these substances, the buffer pair di- and mono-basic phosphate $(HPO_4^-/H_2PO_4^-)_2$ is the most important buffer due to its pKa of 6.8 and urinary excretion values on the order of 20 to 50 mmol/day. Titration of the other potentially titratable species is severely limited due to their pKa values residing below 5.0. The importance of phosphate as a urinary proton buffer is illustrated by the effects of both neutral phosphate loading and depletion. Increases in neutral phosphate load significantly enhance net acid excretion[315] and are able to generate as well as maintain metabolic alkalosis even without a concomitant increase in renal cation resorption or sodium avidity.[174,206] Although phosphate delivery to distal acidification sites has been demonstrated to be rate limiting for renal acid secretion in acidotic dogs,[180] under phosphate loading conditions, the generation of phosphate-induced secondary hyperparathyroidism appears to provide the major stimulus to enhanced renal acid excretion.[177] Phosphate depletion reduces both phosphate and titratable acid excretion and induces positive hydrogen balance.[140] It is unclear whether these changes are best explained by a rate-limiting role of luminal phosphate for renal acid excretion or by the observed renal HCO_3^- wasting.[140]

Determination of Net Acid Excretion

Although enzymatic ammonium assays in serum are widely performed in clinical medicine and this assay method is valid in urine, ammonium values are seldom requested in urine for reasons that have not been reported. As an alternative to requesting an ammonium value in urine, a simplified version of the urinary anion gap is frequently used as an indirect index of ammonium excretion:[142]

$$\text{Urinary anion gap} = Na^+u - K^+u - Cl^-u$$

The rationale is that in chronic metabolic acidosis, ammonium excretion is elevated, is a cation, and balances part of the negative charge of the major urinary cation, chloride. Thus, the urinary anion gap should become progressively negative as the rate of ammonium excretion increases in response to acidosis or to acid loads. However, the urinary anion gap is not a quantitative index of ammonium excretion.[381] Its potential role in the clinical differential diagnosis of hyperchloremic metabolic acidosis will be discussed in subsequent sections.

Calculation of titratable acid requires determination of urinary pH (UpH), blood pH (BbpH), urine phosphate, estimation of the pKa (near 6.8) and an arithmetic computation:

$$\begin{aligned}\text{TAexc} = &[[\text{Pexc}/\text{antilog}\,(\text{UpH} - \text{pK}')] + 1]] \\ &- [[\text{Pexc}/\text{antilog}\,(\text{BpH} - \text{pK}')] + 1]]\end{aligned}$$

Although use of a pKa phosphate value of 6.8 is sufficient for most clinical purposes, the pK′ of phosphate can be corrected for ionic strength and pH for improved accuracy.[319]

CLINICAL CONSEQUENCES

Ventilatory Response to Acidosis: Homeostatic and/or Maladaptive?

The most characteristic clinical manifestation of metabolic acidosis is hyperventilation. Because the depth of ventilation increases to a much greater degree than the respiratory rate, hyperventilation may not be clinically apparent until acidemia becomes severe. Then,

patients may experience labored breathing and their chief complaint is dyspnea.

Metabolic acidosis rapidly causes secondary hyperventilation, which reduces the $PaCO_2$ and tends to increase the blood pH toward normal. This secondary respiratory response is usually fully developed in 12–24 hours. Peripheral chemoreceptors in the carotid and aortic bodies and central chemoreceptors on the ventral surface of the medulla trigger the respiratory response to metabolic acidosis. Some controversy still exists as to which chemoreceptors are more important.

During acute metabolic acidosis (initial six hours after an acid load) $PaCO_2$ falls by 0.85 mm Hg for every millimole-per-liter decrease in $[HCO_3^-]p$ (Fig. 59.5). In response to sustained acidosis, the respiratory response is further stimulated and is maximal by 24 hours. Then, $PaCO_2$ is decreased by about 1.1 mm Hg for each millimole-per-liter fall in $[HCO_3^-]p$ in acidotic human subjects.[208] Several other helpful guides can be used at the bed side to determine whether respiratory compensation is appropriate: (1) metabolic acidosis should reduce the $PaCO_2$ so that it approximates the decimal digits of the pH. For example, when metabolic acidosis reduces the pH to 7.30, the pCO_2 should be about 30 mm Hg. Maximal hyperventilation in patients with extreme acidemia will reduce the $PaCO_2$ to about 10 mm Hg. (2) Another useful rule is that the $PaCO_2$ should approximate the $[HCO_3^-]p + 15$. 9. (3) In uncomplicated metabolic acidosis the decrease in $PaCO_2$ after full adaptation may also be calculated as follows:

$$PaCO_2 = 1.5[HCO_3^-] + 8 \pm 2$$

The respiratory response to metabolic acidosis may be slightly different in patients with different forms of metabolic acidosis. For example, it has been suggested that lactic acidosis generates greater hyperventilation and a lower $PaCO_2$ than equally severe ketoacidosis. This could be the result of a lower intracellular pH in the patients with lactic acidosis. However, others find that secondary hyperventilation in lactic acidosis is not different from other metabolic acidoses.[107,128]

A chronically low $PaCO_2$ (hypocapnia) lowers the $[HCO_3^-]p$ as a result of transient bicarbonaturia or decreased renal net acid excretion. In dogs, experimental hypocapnia caused the kidney to decrease $[HCO_3^-]p$ (transient renal acid retention) even in the context of metabolic acidosis with preexisting hypobicarbonatemia.[76,235] The decrease in $[HCO_3^-]$ was strictly proportional to the induced hypocapnia over a wide range of $PaCO_2$ values and $[HCO_3^-]p$ (fall in $[HCO_3^-]p$ of 0.54 mmol/liter per 1-mm Hg fall in $PaCO_2$). The hypocapnia-induced decrement in $[HCO_3^-]p$ was sufficient to increase blood acidity. These findings

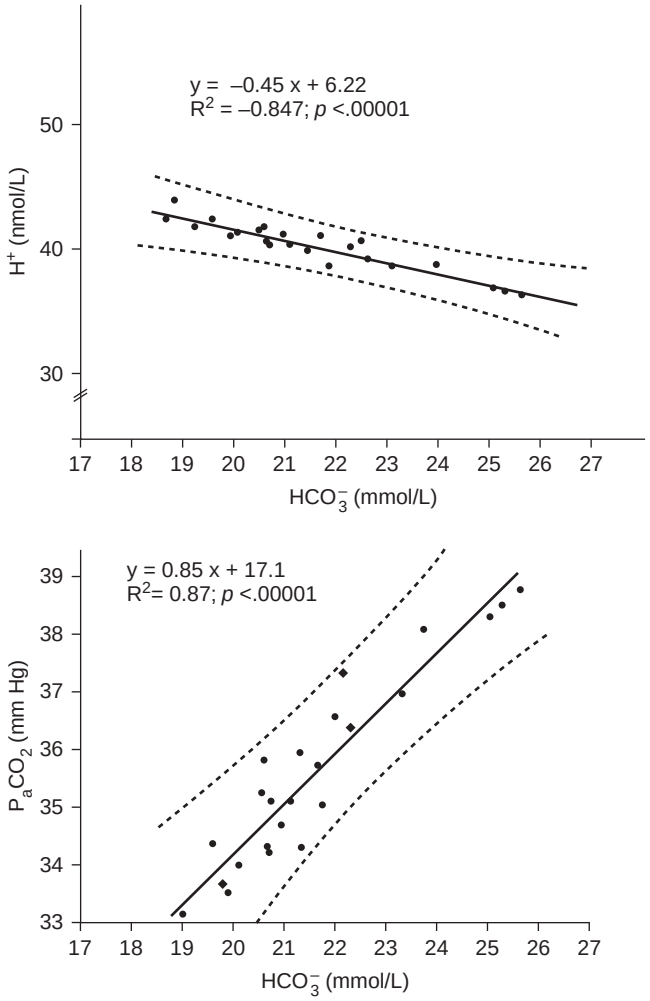

FIGURE 59.5 Relations of $PaCO_2$ to plasma bicarbonate and blood hydrogen ion concentrations in acidotic subjects. The shaded area represents the 95% confidence limits for uncomplicated, acute metabolic acidosis. *(With permission, from Wiederseiner JM, Muser J, Lutz T, Hulter HN, Krapf R. Acute metabolic acidosis: characterization and diagnosis of the disorder and the plasma potassium response. J Am Soc Nephrol 2004;15:1589–1596.)*

demonstrated that the renal response to metabolic acidosis is not primarily geared at the defense of pH[76] and that secondary hypocapnia elicits a maladaptive renal response.[235] In contrast to dogs, however, humans exhibit an alkalemic response to hypocapnia (increase in blood pH) (Fig. 59.6) irrespective of the presence or absence of preexisting metabolic acidosis ($[HCO_3^-]p$ between 25 and 10 mmol/liter),[209] despite the finding that hypocapnia also caused transient renal acid retention. The reason for this species difference is that the inhibitory effect of hypocapnia on renal acid excretion (decrease of $[HCO_3^-]p$ by 0.41 mmol/liter per 1-mm Hg fall in $PaCO_2$) is too small in humans to offset the direct alkalemic effect of the decrease in $PaCO_2$ as dictated by the HCO_3^- Henderson-Hasselbalch

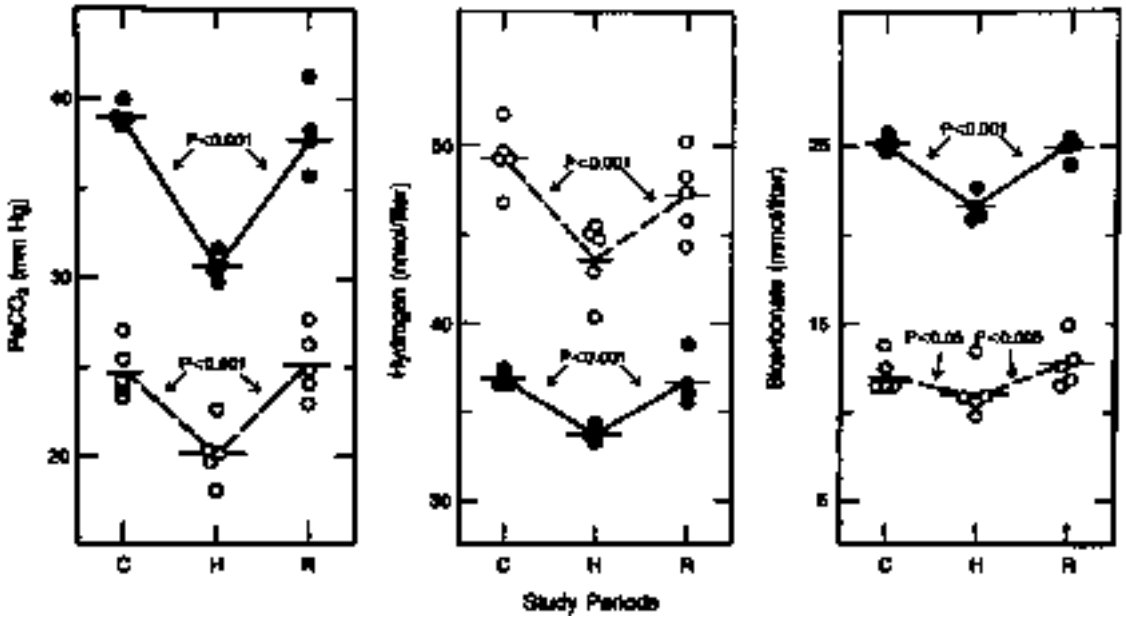

FIGURE 59.6 Steady-state plasma acid–base indexes during control (C), hypocapnia (H), and recovery (R) in normal subjects with and without experimentally induced (NH4CL feeding) acidosis. Solid lines and circles represent subjects with preexisting acidosis. Hypocapnia elicits an alkalemic response irrespective of the control steady-state plasma bicarbonate concentration. *(With permission, from Krapf R, Beeler I, Hertner D, Hulter HN. Chronic respiratory alkalosis. The effect of sustained hyperventilation on renal regulation of acid–base equilibrium. N Engl J Med 1991;324:1394–1401.)*

equation. However, if the slope of line for the relation of the $[HCO_3^-]p$ on $PaCO_2$ extends to $[HCO_3^-]p$ below 10 mmol/liter, it can be predicted that at the lowest end of the range of values for $[HCO_3^-]p$, hypocapnia might worsen acidemia in humans as well as dogs.[208] Figure 59.7 illustrates these differences in the prediction of blood $[H^+]$ when chronic hypocapnia is superimposed on chronic metabolic acidosis when a $[HCO_3^-]/PaCO_2$ slope of 0.54 is used (as reported for dogs; dashed lines) or when a $[HCO_3^-]/PaCO_2$ slope of 0.41 is used as reported for normal human subjects.[209]

Metabolic and Endocrine Consequences of Metabolic Acidosis

Effects of Acidosis on Nitrogen Balance and Protein Metabolism

Metabolic acidosis results in reversible growth failure in children with tubular acidosis and in rats.[248] It affects protein metabolism both by accelerating proteolysis (resulting in negative nitrogen balance) and amino acid oxidation and by decreasing protein synthesis.[244,293] Quantitatively, metabolic acidosis may be the most important factor[18] in the wasting syndrome associated with many illnesses—that is, uremia,[284] sepsis, trauma, and chronic diarrhea—and thus may affect adversely the prognosis of these conditions.[203]

Among the different proteolytic pathways, metabolic acidosis activates the ATP-dependent ubiquitin-26S proteasome pathway, which mediates muscle proteolysis.[16,255] The balance between glucocorticoids and insulin regulates mRNA expression of ubiquitin-proteasome genes and thus muscle proteolysis. Glucocorticoid activity is stimulated in acidosis[327] and, both *in vitro* and *in vivo*, the acidosis-induced stimulation of skeletal muscle proteolysis as well as the induction of ubiquitin-26S proteasome gene expression was shown to be glucocorticoid-dependent.[188] Insulin is the chief counterregulatory factor opposing the catabolic effects of glucocorticoids via the ubiquitin-proteasome pathway.[26] Since there is evidence for insulin resistance in metabolic acidosis,[3,94,325,326] and acidosis was shown to impair insulin signaling via insulin-receptor substrate-1, associated phosphoinositide 3-kinase (PI3K) in muscle cells,[123] both increased glucocorticoid activity and impaired insulin signaling might mediate increased rates of proteolysis in response to acidosis. In addition, decreased concentrations of free IGF-1, an inhibitor of ubiquitin gene expression, and altered thyroid function (mild primary hypothyroidism) have been reported in metabolic acidosis[53,54] and constitute additional potential mechanisms for increased proteolysis.

Protein synthesis is also affected by metabolic acidosis. Muscle protein synthesis and albumin synthesis

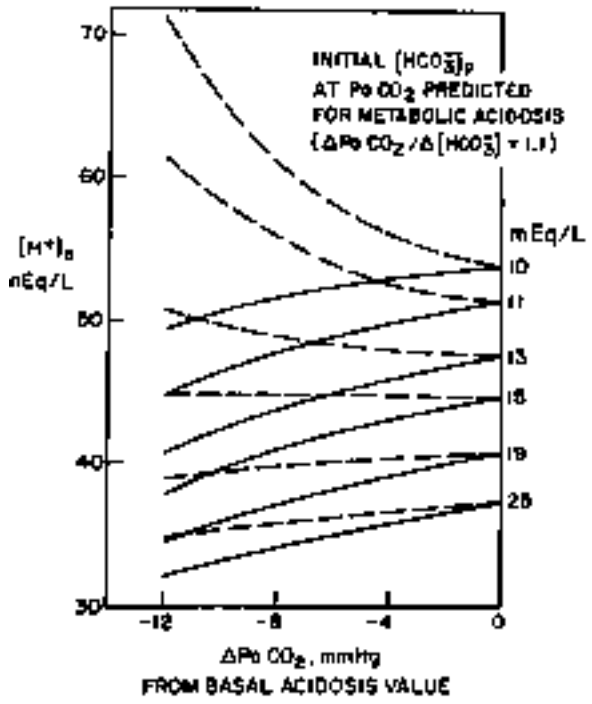

FIGURE 59.7 Nomogram for predicting blood $[H^+]$ when chronic hypocapnia is superimposed on chronic metabolic acidosis over a range of values of initial $[HCO_3^-]$. Solid lines represent the blood $[H^+]$ responses (nmol/liter) to hypocapnia in humans with initial plasma $[HCO_3^-]$ from 10 to 25 mmol/liter, based on the slope of $[HCO_3^-]/PaCO_2 = 0.41$. (*From Gonick HC. Trace metals and the kidney. Miner Electrolyte Metab 1978;1:107–120.*) The dashed lines show the blood $[H^+]$ responses when a $[HCO_3^-]/PaCO_2$ slope of 0.54 (reported for dogs and used in most textbooks) is applied. $\Delta PaCO_2$ values represent changes in $PaCO_2$ from the intial $PaCO_2$ using a relationship of $PaCO_2/HCO_3^- = 1.1$, which is characteristic of uncomplicated metabolic acidosis. Hypocapnia results in a uniform alkalemic response when the human slope is employed, while a deflection point for acidemic versus alkalemic response is apparent at initial $[HCO_3^-]p$ <16 mmol/liter when the canine slope is used. If the slope of 0.41 extends to inital $[HCO_3^-]p$ <10 mmol/liter, it can be calculated that a deflection point would exist between very low $[HCO_3^-]p$ between 6 and 8 mmol/liter. *(With permission, from Krapf R, Hulter HN. Renal response to chronic hypocapnia: qualitative differences between dogs and humans? Clin Chem 1992;38:444–445.)*

(the latter only after several days of metabolic acidosis) are inhibited in humans,[18,200] but not in rats.[242] Correction of acidosis has been effective in both increasing free IGF-1 and albumin serum concentrations[375] as well as in conserving muscle mass and protein homeostasis in patients with chronic renal failure and metabolic acidosis (cited in Kleger et al.[200]).

Effects of Metabolic Acidosis on Sodium Homeostasis

It is well known that both acute and chronic metabolic acidosis are associated with natriuresis.[97,156] Both proximal and distal tubular sodium reabsorption appear to be inhibited.[72,98,226,240,366] The proximal effect is the result of downregulated organic-anion stimulated NaCl absorption,[366] while HCO_3^- reabsorption is enhanced as a consequence of increased expression and activity of Na^+/H^+ exchange (sodium–hydrogen exchanger isoform 3, NHE-3).[11,37] The natriuresis of acidosis induces extracellular volume depletion and increased renin-angiotensin-aldosterone activity, which significantly counteracts and limits the acidosis-induced negative sodium balance and weight loss.[169] Inhibition of angiotensin II action by the AT-1 receptor antagonist losartan resulted in decreased renal net acid excretion in pre-existing metabolic acidosis.[169] Therefore, distal nephron angiotensin II activity is a coregulator of the renal-tubular response to metabolic acidosis and, thereby, is important in determining the severity of acidosis. Increased aldosterone is also expected to limit the severity of metabolic acidosis by stimulation of distal nephron acidification. However, inhibition of aldosterone action by spironolactone exacerbated human metabolic acidosis by an extrarenal mechanism (increased endogenous acid production[169] precluding an analysis of its effect on renal acidification. Thus, the quantitative role of acidosis-induced hyperaldosteronism in the tubular response to metabolic acidosis and the resultant severity of metabolic acidosis remain to be determined.

Effects of Metabolic Acidosis on Potassium Homeostasis

Both extrarenal cellular potassium shifts and the renal regulation of potassium transport have been examined in metabolic acidosis. Contrary to a widely expressed opinion, there is no compelling evidence—either in acute mineral or acute organic acidosis—for a demonstrable increase in plasma potassium in response to acidosis.[2,376] Under carefully controlled conditions, arterialized venous plasma potassium increased nonsignificantly by only +0.02 mmol/liter per mmol/liter decrease in plasma $[HCO_3^-]$ in acute, NH_4Cl-induced metabolic acidosis in normal human subjects.[376] Previous studies in dogs and humans (cited in Wiederseiner et al.[376]) had described both unchanged and increased plasma potassium concentrations albeit with unusually large variances. Failure to detect hyperkalemia in the most recent and some of the previous reports[376] does not preclude, however, the existence of acidosis-induced net K^+/H^+ exchange across cell membranes with efflux of K^+ from cells. The finding of a hyperinsulinemic response (with concomitant decrease in glucagon concentration and unchanged catecholamine levels) in response to

acidosis suggests that an insulin response counterregulates any acidemia-induced cellular potassium efflux, resulting in stable plasma potassium concentrations.[376] This occurred despite an increase in the insulin/glucose ratio, suggesting the insulin resistance in acute acidosis may not involve transcellular potassium balance. A similar mechanism may operate in acute organic acidosis.[3] In the case of organic acidosis, organic anions may enter cells along with protons thus obviating exit of potassium.[280] In conclusion, acidosis-induced hyperinsulinemia seems to prevent acidosis-induced hyperkalemia. The plasma potassium response in acutely acidotic subjects with insulin deficiency or preexisting insulin resistance needs further investigation. In the clinical setting, therefore, the plasma potassium response must always be interpreted with a diligent analysis of the presence of factors in addition to acidemia that are known to influence potassium distribution between intra- and extracellular spaces such as changes in osmolality, sympathoadrenergic activity, aldosterone, and the activity of glucoregulatory hormones (insulin and glucagon).

Acute metabolic acidosis (less than two hours) initially reduces renal potassium excretion, based in large part on effects in the CCT. Experimental reduction of luminal pH in the isolated perfused CCT results in diminished K secretion.[40] The effect of acute acidification of CCT principal cells is believed to be mediated by the effect of cellular acidity to decrease the open probability of potassium channels in the apical membrane.[367] Metabolic acidosis of longer duration is a potent stimulus of renal K excretion and may lead chronically to significant hypokalemia and substantial potassium depletion.[209,307,327] This increase in potassium excretion is probably the consequence of increased volume/sodium delivery to the distal tubule and collecting duct[338] and hyperaldosteronism.[309,313,327]

Effect of Metabolic Acidosis on Divalent Ion, PTH, and 1,25 $(OH)_2D$ Metabolism

Metabolic acidosis profoundly affects calcium and phosphate metabolism resulting in calcium loss from bone[57] in association with hypercalciuria.[222,223] Hypercalciuria is the result of an increase in filtered load and decreased tubular reabsorption of calcium, the cellular mechanisms of which are poorly understood although calcium reabsorption is correlated with luminal $[HCO_3^-]$ in the distal tubule. Important clinical sequelae of the resultant negative calcium balance are a metabolic bone disease with poorly characterized features of osteomalacia/low formation rate/high resorption rate[7,290,298] and calcium nephrolithiasis. Metabolic acidosis induces hypophosphatemia in association with increased renal phosphate clearance and increased fractional excretion of phosphate; in brief, metabolic acidosis induces renal phosphate depletion.[207,222,223] The mechanism of decreased tubular phosphate reabsorption in the proximal tubule is likely to be complex. High ambient proton concentration was shown to stimulate phosphate transport by a glucocorticoid-dependent, posttranslational mechanism.[190] Isohydric decreases in $[HCO_3^-]/PaCO_2$, on the other hand, stimulated phosphate transport in OK-cells via a transcriptional effect.[190] In addition, metabolic acidosis has been shown to decrease [IGF-1]s in humans, providing a plausible mechanism for decreased renal phosphate reabsorption. Thus, metabolic acidosis seems to affect renal regulation of phosphate reabsorption both directly (via effects of acid−base changes on phosphate transport) and indirectly via endocrine changes (increased glucocorticoid activity, decreased IGF-1 levels).[50,326] The relative importance of these mechanisms remains to be elucidated.

Acute and chronic metabolic acidosis was demonstrated to induce renal magnesium wasting and hypomagnesemia.[239,286] The cellular mechanisms of acidosis-induced renal magnesium wasting are largely unknown, although extracellular acidity has been shown to decrease magnesium uptake in mouse distal tubular cells.[85]

In animals, metabolic acidosis was found to decrease $[1,25(OH)_2D]$s,[217] an effect generally attributed to decreased activity of renal 1-alpha-hydroxylase.[218] However, chronic metabolic acidosis was demonstrated repeatedly to increase $[1,25(OH)_2D]$s (by stimulation of its production rate) and to concomitantly decrease [PTH]s in humans.[207,239] The effects of metabolic acidosis on ionized calcium concentration (hypercalcemia not observed or very mild in humans, but prevalent in rats) and on the severity of phosphate depletion/hypophosphatemia seem to differ among species. Thus, it is likely that the changes in $[1,25(OH)_2D]$s and [PTH]s observed are primarily determined by the occurrence or the severity of acidosis-induced hypercalcemia, which has been shown to override other potent stimuli of $1,25(OH)_2D$ production including phosphate depletion unless the latter is quite severe.[59,176]

It is interesting to speculate that the elevated $[1,25(OH)_2D]$s in response to metabolic acidosis could serve a homeostatic role, or, that elevated $[1,25(OH)_2D]$s could contribute to the normal acid excretory response to an acid load/acidosis. This question merits investigation in as much as vitamin D deficiency was shown to result in metabolic acidosis in chicks[37] and chronic $1,25(OH)_2D$ administration results in metabolic alkalosis (in part of renal origin) in thyroparathyroidectomized dogs.[178]

In summary, metabolic acidosis in humans induces (1) hypercalciuria due to release of calcium from bone and decreased renal tubular calcium reabsorption, (2) renal phosphate depletion and hypophosphatemia, (3) renal magnesium wasting, and (4) increases [1,25(OH) 2D]s and decreases in intact [PTH]s.

Effect of Metabolic Acidosis on Bone

The effects of metabolic acidosis on bone mineral content—that is, reduced levels of mineral sodium, potassium, carbonate, calcium, and phosphate—are consistent with the role of bone as a proton buffer. In mouse calvariae *in vitro*, exposure to acid media (low HCO_3^-) induces initial physicochemical mineral dissolution. Cell-mediated bone resorption follows and is characterized by both increased osteoclastic and inhibited osteoblastic activities paralleled by alterations in the expression of a number of osteoclastic and osteoblastic genes.[62] In particular, increased osteoblastic RNA expression of the osteoclast activator RANK-ligand with unchanged expression of its soluble decoy receptor, osteoprotegerin, may provide a central mechanism by which metabolic acidosis enhances osteoclastogenesis and osteoclast activity. The effect is mediated—at least in part—by acidosis-induced enhancement of osteoblastic prostaglandin E2 (PGE2) secretion. Both RANK-L expression and cell-mediated calcium efflux from bone are inhibited by cyclooxygenase inhibition, confirming the central role of acidosis-induced PGE2 stimulation.[61]

Since glucocorticoid activity is increased in metabolic acidosis[326] and glucocorticoids are known to dramatically decrease bone mineral content, it is possible that acidosis-induced hyperglucocorticoidism might contribute to calcium efflux from bone. Surprisingly, however, *in vitro* cortisol inhibited rather than stimulated acid-induced, cell-mediated osteoclastic bone resorption through a decrease in osteoblastic PGE2 production.[212]

Other Endocrine Effects of Metabolic Acidosis

Endothelin

Metabolic acidosis induces renal endothelial cells to release endothelin-1, which was demonstrated to play a key role in the renal defense to an acid load. Both proximal acidification (by activation of the proximal tubule Na/H antiporter, NHE-3) and collecting duct acidification are stimulated involving signaling via the endothelin receptor B (ETB). In the distal tubule, both direct (endothelin-induced activation of Na^+/H^+ exchange) and indirect (stimulation of H^+-ATPase via endothelin-induced increases in aldosterone) effects may be operative to stimulate proton secretion.[197] When ETB is inhibited by the unselective ET-receptor antagonist bosentan (Tracleer) in rats or ETB is knocked out in mice, the metabolic acidosis resulting from a given acid load is more severe.[215,371] The mechanisms of acid-induced increased endothelin expression and endothelin-1/ETB signaling are complex, but quite well characterized and involve activation of a putative acid-sensor, a proline rich tyrosine kinase 2, Pyk2.[227] Interpretation of the effects of bosentan in rats to decrease distal H^+ secretion has been difficult since bosentan has also induced a decrease in chronic net acid excretion/endogenous acid production, which in itself, dictates lower tubular acidification rates along the nephron. In summary, renal endothelin-1 acting via ETB receptor is quantitatively important in the renal defense against an acid load in mice and rats. The importance of the acid-induced renal endothelin response has not yet been investigated in humans.

Growth Hormone (GH)/IGF-1 Axis

Important effects of metabolic acidosis on the GH/IGF-1 endocrine axis were suggested by the observation[250] that growth retardation in children with renal-tubular acidosis was reversible upon administration of alkali. In humans, IGF-1 serum concentrations are decreased in response to metabolic acidosis. The primary abnormality in humans and rats is most likely due to peripheral insensitivity to GH action with GH secretion rates presumably elevated based on the demonstration of an exaggerated increase in GH in response to stimulation by GH releasing hormone.[53,279] The recent observations that administration of GH both partially corrected metabolic acidosis by a renal mechanism (primarily by an increase in ammonium excretion)[327] and corrected acidosis-induced negative nitrogen balance, corrected renal phosphate depletion as well as hypophosphatemia and attenuated renal magnesium wasting[239] is evidence for the notion that acidosis-induced changes in the GH/IGF1 endocrine axis may be important in the mediation of some important metabolic effects of metabolic acidosis.

Thyroid Hormones

Chronic metabolic acidosis in humans mildly decreases freeT3 and freeT4 and significantly increases TSH serum concentrations with no change in reverse T3,[54] findings consistent with a primary thyroidal decrease in thyroid hormone secretion, that is, mild primary hypothyroidism. The quantitative importance of these changes in thyroid function with respect to acidosis-induced negative nitrogen balance and to renal acidification is presently unknown.

Catecholamines

Acidosis induces release of catecholamines, which attenuate both the negative inotropic effect of acidosis on cardiac contractility and the peripheral vasodilatory effect of acidemia.[256] With severe acidosis, catecholamine responsiveness decreases and cardiac collapse may result. Acidosis can also decrease the ventricular fibrillation threshold.[139] Peripheral arterial vasodilatation is a direct effect of acidosis but is also offset by catecholamine release, so that peripheral vascular resistance remains relatively constant. However, in the venous system, the direct effect of acidosis is vasoconstriction, which is further enhanced by catecholamine release.[323] Peripheral venoconstriction can shift blood from the peripheral vascular system to the pulmonary vascular bed. In patients with severe acidosis, this may contribute to pulmonary edema. Therapeutic administration of $NaHCO_3$ constitutes an important additional risk factor.

It is not known whether the catecholamine response affects the renal response to acidosis in humans, although alpha-adrenergic stimulation has been shown to enhance proximal tubule bicarbonate reabsorption in rats.[67]

In moderately severe acute metabolic acidosis in humans (decrease of $[HCO_3^-]p$ from 25 to about 19 mmol/liter), there was no significant effect on catecholamine levels.[376] Thus, the effects described previously may be more applicable to severe forms of metabolic acidosis or to a pattern of sympathetic stimulation that does not result in overt systemic catecholamine spillover.

Glucocorticoids

Observations carried out in rats suggest that increased glucocorticoid activity in response to metabolic acidosis might modulate acidosis-induced increase in protein degradation, at least in part.[245] It is also possible that increased glucocorticoid activity could co-determine the systemic and renal response to an acid load, given the effects of glucocorticoids on renal acidification[181] and renal tubular acid–base transport mechanisms.[27,198] Chronic metabolic acidosis in humans significantly increases glucocorticoid activity based on determination of the daily urinary excretion rates of cortisone and cortisol.[327] In addition, neutralization of dietary acid production (decrease in renal acid excretion from ~80 to 10 mEq/day) significantly decreased urinary free-cortisol and THF excretion over 24 hours in normal humans.[244] However, reports from another group indicated that chronic metabolic acidosis did not affect cortisol homeostasis in humans[313] as analyzed by serum profile and urinary 17-OH-corticosteroid excretion rates. The reasons for this discrepancy are not clear.

Effects of Metabolic Acidosis on Renal Citrate Metabolism

The effects of metabolic acidosis on renal citrate metabolism have important clinical consequences and are, therefore, briefly discussed here. Citrate is derived from carbohydrate metabolism and contains three negatively charged carboxyl groups. Complete oxidation of citrate thus generates three HCO_3^- ions per mole and thus increased renal reabsorption and metabolism of citrate would be expected to serve a homeostatic role in the adaptation to metabolic acidosis. Citrate is freely filtered at the glomerulus and reabsorbed and metabolized almost exclusively in the proximal tubules (Fig. 59.8), with these processes determining the amount of urinary citrate excretion.[44] In metabolic acidosis, tubular reabsorption is increased and urinary excretion decreased due to both increased protonation of trivalent to divalent citrate, the substrate for the sodium/citrate cotransporter in the proximal tubule and increased expression and activity of Na^+/citrate cotransporter NaDC1.[15,191] In addition, cellular (i.e., cytoplasmic) metabolism of citrate (Fig. 59.8) is increased in the proximal tubule. Enhanced cytoplasmic metabolism in response to metabolic acidosis is mediated by a specific increase in renal ATP citrate lyase activity and expression.[251] Mitochondrial citrate metabolism is also stimulated in metabolic acidosis as shown by the increased activity of mitochondrial aconitase, the first step in mitochondrial citrate metabolism.[252] These findings are clinically important

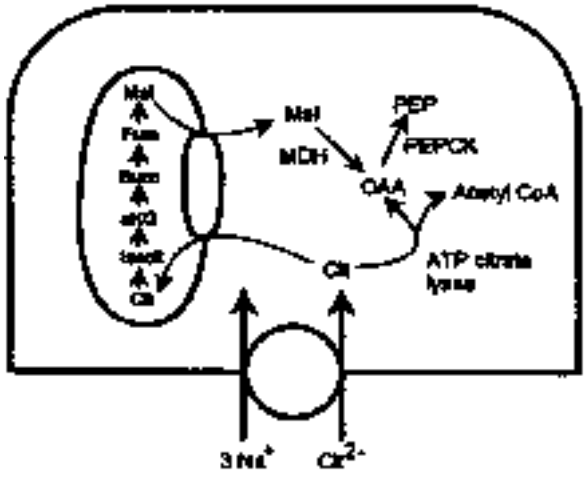

FIGURE 59.8 Citrate metabolism in the proximal tubule. *(With permission, from Alper S. Genetic diseases of acid–base transporters. Annu Rev Physiol 2002;64:899–923.)*

because of citrate's role in calcium complexation, inhibition of stone formation and prevention of nephrocalcinosis. Indeed, a high proportion of patients with nephrolithiasis have low urinary citrate levels.[269] A high-protein intake (which increases endogenous acid production) decreases urinary citrate excretion in rats by renal mechanisms described previously.[10]

Miscellaneous Clinical Effects of Metabolic Acidosis

Renal Growth

In contrast to the growth inhibitory effect in nonrenal tissue, metabolic acidosis leads to hyperplasia and hypertrophy in renal tissue with an apparent predilection for the renal tubules.[230] Interestingly, acidosis induces metabolic effects in the kidney that also contrast with its systemic consequences: renal IGF1 levels are increased and renal protein degradation is decreased.[112,136] Decreased protein degradation is a cell-cycle independent mechanism for renal hypertrophy. Whether cell-cycle dependent mechanisms (via cyclin kinases) are important in metabolic acidosis as they are in diabetic nephropathy or compensatory renal hypertrophy remains to be investigated.

Based on the hypothesis that renal hypertrophy is associated with progression of renal disease, it is possible that acidosis might accelerate the rate of decline of renal function in renal insufficiency. The following evidence from animal studies suggests that such an effect of acidosis may be present: (1) ammonia has been proposed to be responsible for tissue injury, possibly by acting as a convertase for the alternate pathway of complement activation.[266] (2) The remnant kidney model in the rat is associated with increased ammoniagenesis by residual nephrons.[233] (3) Systemic alkalinization has been shown to reduce ammoniagenesis and to mitigate proteinuria and the histological damage typically seen in this model.[267]

Acidosis-induced promotion of growth may be most relevant in polycystic kidney disease. Patients with hyperaldosteronism and potassium depletion (which leads to intracellular acidosis and stimulation of ammoniagenesis) were shown to have a greatly increased incidence of renal cysts.[353] Furthermore, in Han:SPRD rats, a rat model for polycystic kidney disease, induction of acidosis by NH_4Cl enhances, while systemic alkalinization by HCO_3^- slows the rate of cyst formation.[356] Thus, correction of acidosis may be most important in patients with polycystic kidney diseases. However, no human studies have yet been performed to evaluate the effect of complete correction of acidosis on the progressive decline in renal function both in cystic and non-cystic kidney diseases.

O_2 and CO_2 Dissociation Curves

Metabolic acidosis, as mediated by an increase in hydrogen ion concentration, shifts the hemoglobin saturation curve to the right, that is, less oxygen is bound to hemoglobin for a given PO_2. This circumstance provides for acute acidosis-enhanced oxygen release in tissues. Quantitatively, this effect is quite small; however, at least for the pH changes observed *in vivo* and can be estimated using the Bohr factor (BF):

$$BF = \Delta \log P50/\Delta pH$$

where P50 is the half-saturation PO_2, normally around 27 mm Hg (3.6 kPa). Since the Bohr factor in human blood is about 0.5, it can be calculated that a change in blood pH of 0.1 U will shift the half-saturation of hemoglobin by about 1 mm Hg. When metabolic acidosis persists beyond 6–8 hours, the dissociation curve is shifted back toward its normal position (leftward) due to the more prolonged effect of acidosis to decrease erythrocyte 2,3-diphosphoglycerate. It is not known with certainty which of these effects is predominant during sustained metabolic acidosis *in vivo*.

Hemoglobin displays a higher affinity for hydrogen ion in the reduced form (Haldane effect) and roughly half of acute buffering of an acid load is due to nonbicarbonate buffers including Hb. The decrease in oxygen saturation (or increase in reduced hemoglobin) for a given PO_2 associated with acute acidosis could therefore increase the hemoglobin buffering capacity of an acute systemic acid load and thus limit the fall in $[HCO_3^-]p$. At the same time, the Haldane effect increases the CO_2 transport capacity of blood at the low pCO_2 values of metabolic acidosis. The quantitative *in vivo* contribution of the Haldane effect to the early plasma bicarbonate response to acid loads remains to be determined.

The Trade-Off Hypothesis

As was described earlier and shown in Fig. 59.9A, normal acid–base balance is achieved and maintained when renal net acid excretion equals endogenous acid production at normal $[HCO_3^-]p$. As illustrated in Fig. 59.9B, an increase in endogenous acid production leads to renal and extrarenal cellular adaptations, ultimately increasing net acid excretion to again balance endogenous acid production. While it was demonstrated that increases in dietary-induced acid production correlate inversely and significantly with $HCO_3^-]p$ during metabolic balance studies,[214] $[HCO_3^-]p$ generally does not fall out of the wide normal range when determined in clinical practice. Thus, an ongoing acidotic process may be present albeit not recognized due to the efficient adaptation of acid excretory

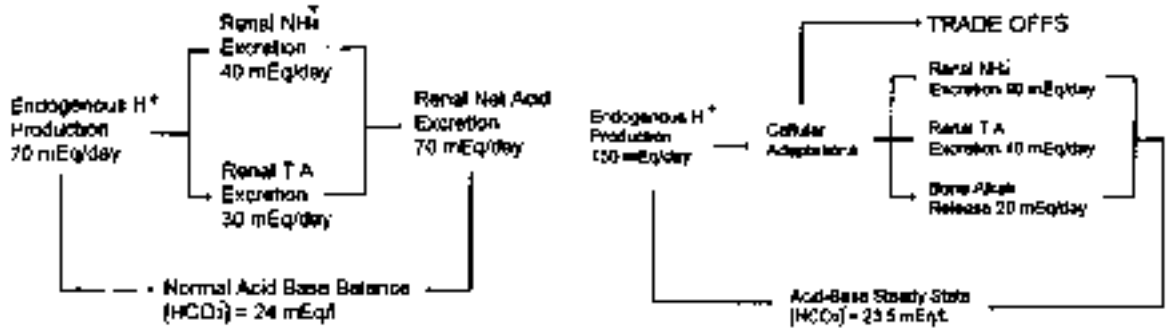

FIGURE 59.9 (A) Shows concept of acid–base balance. (B) Depicts trade-offs, that is, cellular adaptations due to increased acid production. *(With permission, from Alpern RJ, Sakhaee K. The clinical spectrum of chronic metabolic acidosis: homeostatic mechanisms produce significant morbidity. Am J Kidney Dis 1997;29:291–302.)*

mechanisms and the imperfections of routine laboratory analysis. The term eubicarbonatemic[9] metabolic acidosis (Table 59.1) circumscribes this entity. It is instructive to review, therefore, to which extent some of the metabolic and endocrine effects of metabolic acidosis discussed previously also occur during normal dietary variation of acid production and/or during physiologic declines in acid excretion such as during the aging process.[125]

Habitual ingestion of protein-rich diets has repeatedly been linked to clinical disorders, in particular nephrolithiasis, osteoporosis, and fracture incidence.[1,48,228] The potential clinical and epidemiological relevance of the trade-offs of the adaptation to increases in endogenous acid production or decreases in acid excretion (minimal metabolic acidosis) was demonstrated recently by the finding—both in postmenopausal women and young adults—that neutralizing endogenous acid-production by oral administration of $KHCO_3$ significantly decreased urinary nitrogen losses, induced positive calcium and phosphate balances by decreasing renal excretion of these ions and decreased markers of bone resorption.[124,244,321] Thus, eubicarbonatemic metabolic acidosis may be an important cause of osteoporosis, nephrolithiasis and loss of lean body mass. Therefore, although the degree of diet-dependent (and other etiologies of) eubicarbonatemic metabolic acidosis (Table 59.1) is mild as judged by the degree of perturbation of blood acid–base equilibrium, it cannot be considered mild as judged by its adverse biological consequences and may be of great epidemiological and economic impact when considered under the aspects of dietary habits and increased longevity.

TABLE 59.1 Causes of Eubicarbonatemic Metabolic Acidosis

Western diet
Age
Chronic diarrhea
Incomplete distal tubular acidosis
Mild renal insufficiency

There is a large literature on positive epidemiological associations between diets assumed to be acid-generating (prototype: Western diet rich in animal, dairy, and wheat-flour proteins) and osteoporosis, bone loss, and/or fracture rates.[165] However, an equally large literature supports beneficial effects of animal protein (acid generating) on bone, which is probably explained by the protein-induced stimulation of GH/IGF1 axis and/or stimulatory effects on intestinal calcium absorption.[166,205] Thus, evaluation of the role of diet-induced endogenous acid production on bone mineral content (osteoporosis) and fracture rates will need to be performed in a prospective, long-term clinical trial where endogenous acid production is effectively neutralized.

CLINICAL DISORDERS

Daily metabolic reactions generate and consume several thousand milliequivalents of organic acids, including lactic, pyruvic, citric, and acetoacetic acids. The metabolic conversion of organic acids to neutral products, such as glucose, consumes both the organic anion and the H^+ ion. Metabolic conversion of organic acids to H_2O and CO_2, which is exhaled, also removes both the organic anion and H^+ from body fluids. Normally, organic acid generation and consumption rates are balanced, so that acid accumulation does not occur. However, if organic acids are generated more rapidly than they are consumed, their accumulation results in metabolic acidosis. To the extent that this occurs, the accumulating H^+ decomposes HCO_3^-, while the concentration of organic anions increases. For

example, when lactic acid accumulates, the products are:

$$\text{H lactate} + HCO_3^-$$
$$\text{lactate}^- + H_2CO_3$$
$$H_2O + CO_2$$

The increase in [lactate$^-$] and decrease in [HCO_3^-] are reciprocal. One may assume that ECF lactate$^-$ replaces HCO_3^-. The accumulated lactate represents decomposed HCO_3^-. In addition, because lactate can be metabolized and thereby regenerate HCO_3^-, the accumulated lactate also represents potential HCO_3^-. When lactate$^-$ is converted to glucose or oxidized to H_2O and CO_2, lactic acid is removed from the ECF and HCO_3^- is regenerated, as follows:

The generation of HCO_3^- from such organic anions does not require renal intervention. Contrast these events with the accumulation of an inorganic acid such as HCl:

In this case, Cl^- replaces HCO_3^- in the ECF and also represents decomposed HCO_3^-—. However, unlike lactate$^-$, Cl^- cannot be metabolized. Regeneration of HCO_3^- must be accomplished by the kidney, which filters NaCl, reabsorbs the Na^+, and excretes H^+. This results in increased net acid excretion and HCO_3^- regeneration.

Infused sodium salts of organic acids such as Na lactate are converted to $NaHCO_3$ when the anion is metabolized to neutral products or oxidized to H_2O and CO_2. Metabolism of the organic anion, such as lactate, is accompanied by H^+, which is derived from plasma water, as illustrated here:

Therefore, metabolism of the sodium salts of lactate, citrate, acetate, and other organic anions generates 1 mole of $NaHCO_3$ for each mole of carboxylate.

Anion Gap Acidosis

The ionic profile of normal serum is depicted in Fig. 59.10. The law of electroneutrality states that the quantity of positive charges in any solution must equal the quantity of negative charges. If every ion present in serum is measured in charge units such as metabolic equivalents per liter, then electroneutrality is found. However, if only the quantitatively most important electrolytes—Na^+, Cl^-, and HCO_3^- are considered, then [Na^+]p normally exceeds the sum of [Cl^-]p + [HCO_3^-]p. This difference, [Na^+] − ([Cl^-] + [HCO_3^-]), is the anion gap. The anion gap calculated in this manner is normally 12 + 4 mEq/liter (+ 2 standard deviations). Note that [K^+]p is not included in the calculation due to its relatively minor quantitative contribution.

The anion gap does not measure any specific ionic constituent. It includes the net unmeasured negative protein charge (primarily from albumin), inorganic phosphate, sulfate, organic anions, and other ions less unmeasured cations such as potassium, calcium, and magnesium. The anion gap is used to classify the metabolic acidoses and is also a clue to the presence of various mixed acid−base disorders. These aspects of anion gap interpretation are reviewed in the following sections.

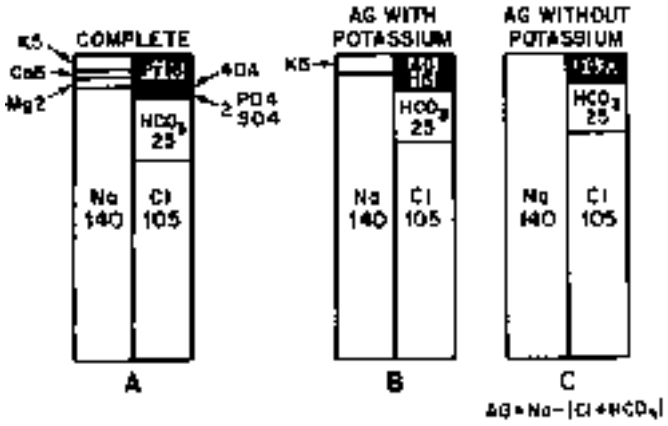

FIGURE 59.10 Ionic anatomy of serum. Normal serum electrolyte pattern and the calculation of the anion gap (AG). Numbers refer to serum concentration in mEq/liter. OA, organic acids, Pr, proteins. *(Adapted from Field M, Block MB, Levin R, Rall DP. Significance of blood lactate elevations among patients with acute leukemia and other nephroplastic proliferative disorders. Am J Med 1966;40:528–547.)*

Occasionally, the anion gap is abnormally small, or even negative. This may be due to random measurement errors. If a low anion gap exists, each electrolyte measurement should be reconfirmed. Systematic errors that depress the [Na^+]p (e.g., pseudohyponatremia due to hyperlipidemia or hyperproteinemia) or increase the [Cl^-]p (e.g., pseudohyperchloremia due to bromism) produce reproducible reductions in the anion gap. Increased concentrations of cations other than Na^+ (e.g., abnormal cationic myeloma proteins, extreme hypermagnesemia, lithium poisoning) also depress the anion gap because [Cl^-]p increases without a proportionate change in [Na^+]. Table 59.2 lists the causes of a reduced or negative anion gap.

H^+, which accumulates in the ECF, is primarily buffered by the following reaction:

$$H^+ + HCO_3^- \rightarrow H_2CO_3 \rightarrow CO_2 + H_2O$$

To the extent that H^+ accumulates, a nearly equimolar decrease in [HCO_3^-]p occurs. If HA, a strong acid, accumulates in the ECF, then the reduction in [HCO_3^-]p is accompanied by a similar increase in [A^-]. The net effect of HA addition to the ECF is the replacement of HCO_3^- by A^-. If HA represents HCl, then the decrease

TABLE 59.2 Causes of Low Anion Gap

Reduced concentration of unmeasured anions
Dilution
Hypoalbuminemia
Hyperchloremic metabolic acidosis
Systemic underestimate of $[Na^+]p$
Extreme hypernatremia
Hyperviscosity
Displacement of water by hyperlipidemia or hyperproteinemia
Systemic overestimate of $[Cl^-]p$
Other halides—bromide, iodide
Increased concentration of nonsodium cations
Multiple myeloma—paraproteinemias
Extreme hypercalcemia, hypermagnesemia, lithium intoxication

in $[HCO_3^-]p$ is counterbalanced by a similar increase in $[Cl^-]p$, while the anion gap remains relatively stable. (The anion gap actually decreases slightly, because a decrease in pH increases H^+ binding by proteins. This reduces the net negative charge on proteins, principally albumin.) Alternatively, if HA is any non-HCl acid (i.e., lactic, acetoacetic, phosphoric, sulfuric), then HA accumulation in the ECF decreases the $[HCO_3^-]p$ and reciprocally increases the anion gap. Figures 59.11 and 59.12 illustrate the development of hyperchloremic and anion gap metabolic acidoses. The causes of hyperchloremic and anion gap metabolic acidoses are listed in Table 59.3.

Occasional patients develop mixed anion gap and hyperchloremic acidosis. Such hybrid metabolic acidoses may occur when early renal failure progresses toward overt uremia.[372] Hyperchloremic metabolic acidosis occurs commonly with early renal disease as a result of inadequate ammonia synthesis and excretion. At this time, the GFR is still adequate to excrete the normal exogenous and endogenous anion load (phosphate, sulfate, etc.). The hyperchloremic acidosis that develops in this setting is a form of type IV renal tubular acidosis. Later, when renal function deteriorates, anion retention develops and typical uremic–anion gap acidosis evolves. In the intervening period, mixed hyperchloremic–anion gap acidosis may exist as shown in Fig. 59.13.[374]

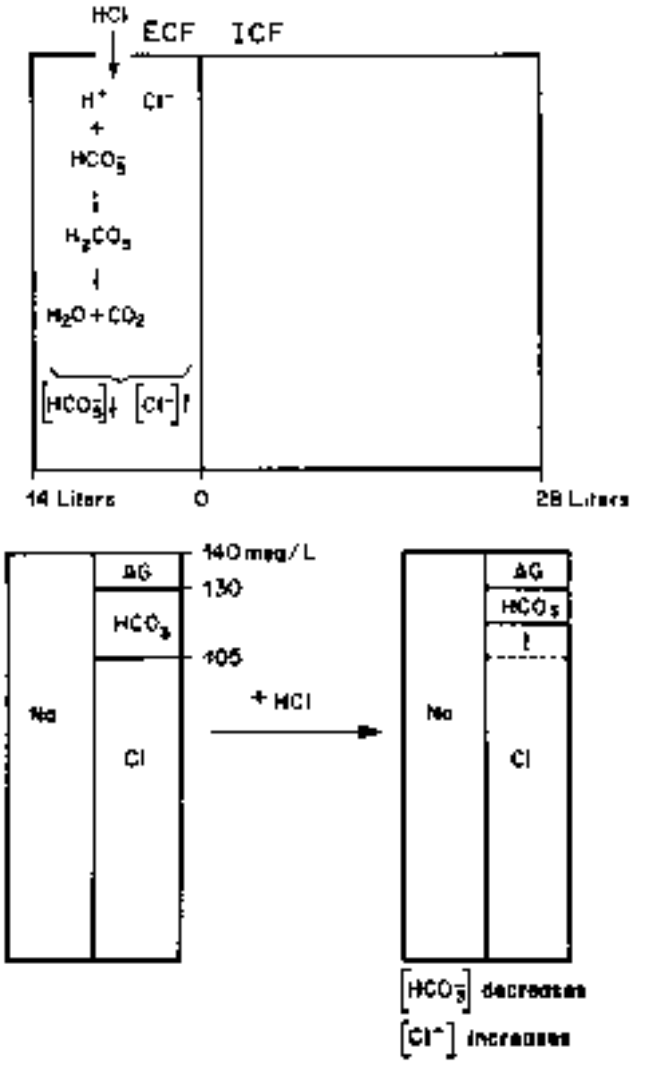

FIGURE 59.11 The addition of 10 mmol/liter of HCl to ECF results in a proportionate reduction in $[HCO_3^-]s$ and increase in $[Cl^-]$. Hyperchloremic acidosis develops while the anion gap remains unchanged.

Ketoacidosis

Ketoacidosis is usually due to an accumulation of acetoacetic acid and beta-OH butyric acid in the ECF. Mild ketoacidosis develops in normal individuals during starvation. More severe fasting ketoacidosis may develop in chronic alcoholics, pregnant women, and young children. The most common cause of severe ketoacidosis is untreated, or inadequately treated, insulin-dependent diabetes mellitus. Several inherited enzyme disorders also generate severe ketoacidosis and lactic acidosis during a fast. They include glucose-6-phosphatase deficiency (von Gierke disease), and fructose-1,6-bisphosphatase deficiency. Ketoacids other than acetoacetic acid and beta-butyric acid can accumulate in children with enzyme defects that produce branched chain organic acidurias and disorders of propionate metabolism.

Ketogenesis

Figures 59.14 and 59.15 illustrate the endocrine regulation of fatty acid release from adipose triglyceride stores and fatty acid metabolism within hepatic cells.

Hormone-sensitive lipase in adipose tissue is normally inhibited by relatively low levels of insulin.

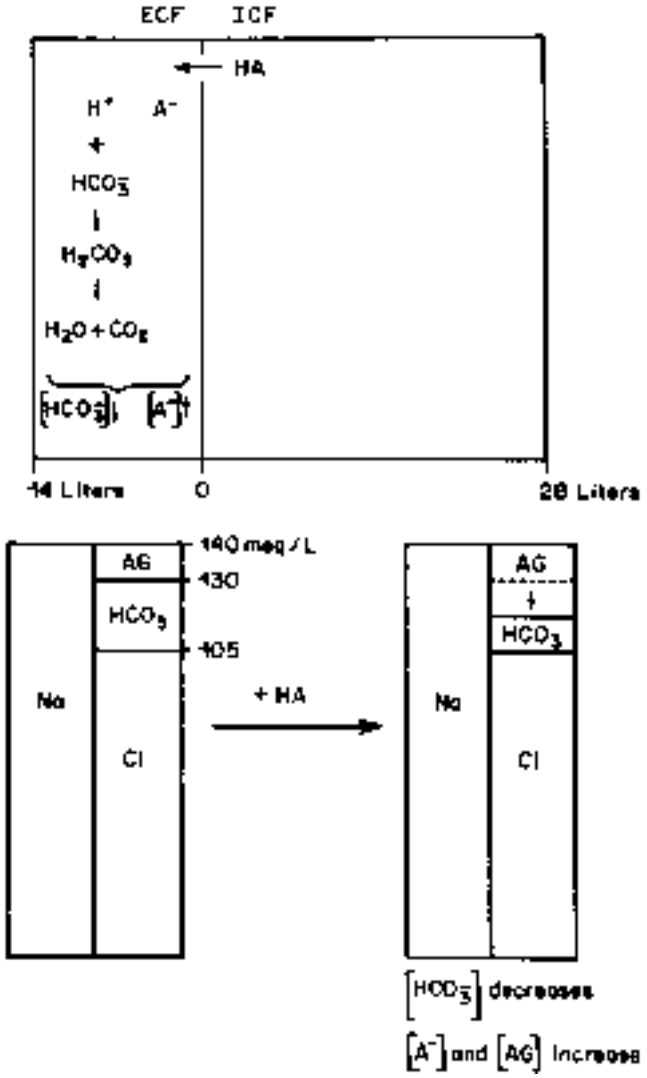

FIGURE 59.12 The addition of 10 mmol/liter of a strong non-HCl acid (HA) (i.e., lactic acid, ketoacids) reduces the [HCO_3^-] and proportionately increases [A^-]. This increases the anion gap while the [Cl^-]s concentration remains relatively stable.

TABLE 59.3 Causes of Hyperchloremic and Anion Gap Metabolic Acidosis

Elevated anion gap acidosis
Ketoacidosis
Lactic acidosis
Methanol poisoning
Ethylene glycol poisoning
Paraldehyde poisoning
Salicylate poisoning
Uremia
Congenital organic acidosis
D-lactic acidosis
Hyperchloremic (normal anion gap) acidoses
Renal
Hypokalemia: proximal tubular acidosis (RTA II), classic, distal tubular acidosis (RTA I), mixed type RTA (RTA III)
Hyperkalemia: generalized distal tubular acidosis (RTA IV)—mineralocorticoid deficiency, mineralocorticoid resistance, tubular voltage defects
Recovery from high anion gap acidosis (renal loss of "potential" HCO_3^-)
Gastrointestinal
Diarrhea
Pancreatic fistula (pancreas transplantation)
Ingestion of HCO_3^--binding salts or resins (CaCl2, cholestyramine)
Mixed gastrointestinal-renal
Uretorosigmoidostomy
Rectal baldder
Ileal loop bladder
Ureterointestinal segments
Other
Posthypocapnia
HCl or HCl precursor infusion or ingestion
Dilution acidosis

Catecholamine, cortisol, growth hormone, and glucagon activate this enzyme (Fig. 59.14). Fasting progressively reduces insulin and elevates the abovementioned counter-regulatory hormones. This triggers lipolysis. Fatty acids released from the triglycerides in adipose tissue flow to the liver where they may potentially enter several metabolic pathways (Fig. 59.15). One involves their combination with glycerol phosphate to reform triglycerides and other lipids. Alternatively, they can enter mitochondria and undergo beta-oxidation to provide energy. This mitochondrial entry step is not passive, but rather is a tightly regulated, carrier-mediated process. Within hepatocyte cytoplasm, long chain fatty acids must first be activated by enzymatic conversion to their acyl-CoA derivatives. Then carnitine palmitoyl transferase I (CPT I), an enzyme associated with the mitochondrial outer membrane, links the acyl-CoA derivatives to carnitine. Now the carnitine–fatty acid complex can cross the inner mitochondrial membrane via a specific acyl-carnitine translocase. At the inner surface of the inner membrane, carnitine is removed by CPT II, reforming the acyl-CoA activated form of the fatty acid. The released carnitine shuttles back through the membrane to be used again as a fatty acid carrier. Within mitochondria, the fatty acyl-CoA undergoes beta-oxidation, which sequentially splits two carbon acetyl-CoA fragments from the long fatty acid molecule.

Two major catabolic pathways generate acetyl-CoA in mitochondria: (1) pyruvate oxidation via the pyruvate dehydrogenase reaction (see Lactic Acidosis section) (Fig. 59.17), and (2) fatty acid oxidation via beta-oxidation. Acetyl-CoA can be further oxidized by the Krebs cycle to yield CO_2 and energy. Acetyl-CoA can also exit from the mitochondria to be used in synthetic reactions (Fig. 59.15).

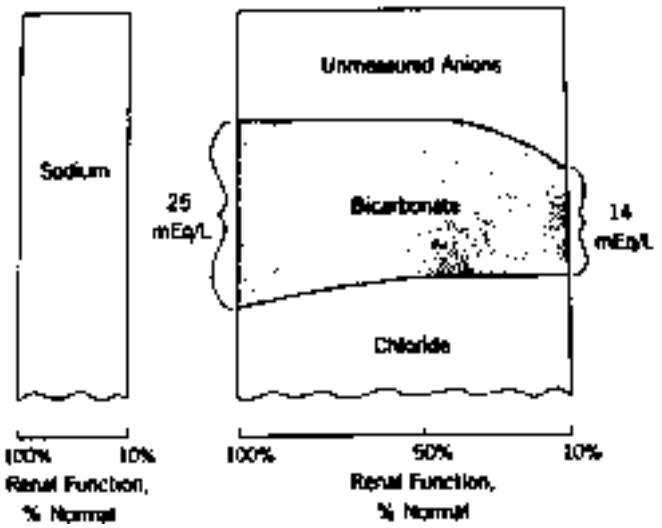

FIGURE 59.13 Early renal failure impairs NH_4^+ excretion before anion retention develops. This results in hyperchloremic metabolic acidosis. As renal failure progresses and the GFR falls, anion retention eventuates. Uremic-anion gap metabolic acidosis will develop. Between these extremes, combined hyperchloremic and anion gap metabolic acidosis is a common finding. *(From Weinstein B, Irreverre I, Watkin DM. Lung carcinoma, hypouricemia and aminoaciduria. Am J Med 1965;39:520–526, with permission.)*

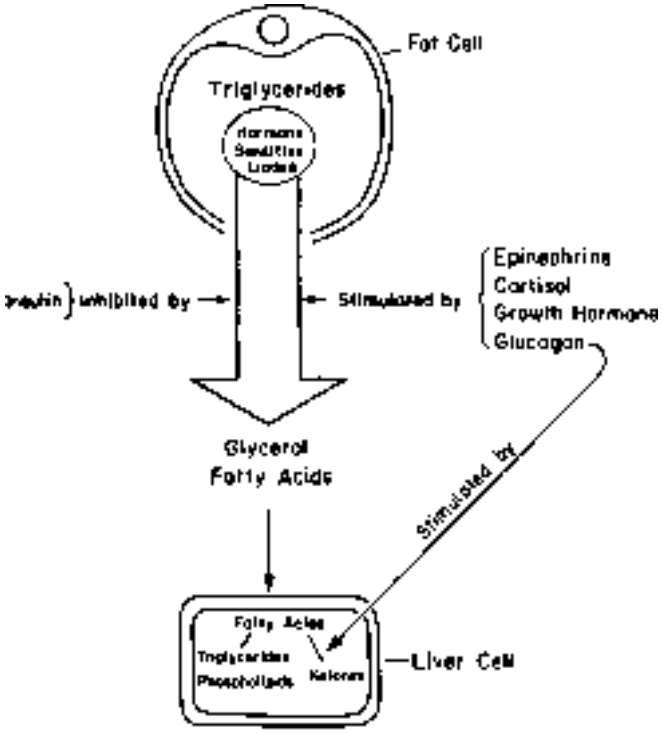

FIGURE 59.14 The release of fatty acids from adipose triglyceride stores under the control of hormone-sensitive lipase.

When the concentration of acetyl-CoA within mitochondria increases markedly, the oxidative capacity of the Krebs cycle is exceeded and ketoacids are generated. Two molecules of acetyl-CoA first condense to form acetoacetyl-CoA. This is then converted into acetoacetic acid via the 3-hydroxy 3-methylglutaryl-CoA pathway.

The low insulin and high glucagon levels produced by a fast create the conditions required for ketogenesis. Adipose tissue hormone-sensitive lipase is activated, releasing fatty acids that are delivered to the liver (Fig. 59.14). Within hepatocytes, the fatty acids are converted to acyl-CoA derivatives and then flow into the mitochondria via the CPT and translocase systems. CPT I is deinhibited by the low cytoplasmic malonyl-CoA levels. Consequently, transport of fatty acyl CoA across the mitochondrial membranes is greatly enhanced with subsequent generation of large quantities of acetyl-CoA via beta-oxidation. Malonyl-CoA levels are low, because acetyl-CoA carboxylase, the enzyme responsible for its production, is inhibited when insulin levels are reduced and glucagon levels are increased.

Acetyl-CoA oxidation by the Krebs cycle may not keep pace with the production rate, so acetyl-CoA accumulates. Relatively low Krebs cycle oxidation is in part due to low oxaloacetate levels. Acetyl-CoA must combine with oxaloacetate to form citrate in order to enter the Krebs cycle. Fasting stimulates oxaloacetate transport out of mitochondria to be converted into glucose. Low mitochondrial oxaloacetate levels limit acetyl-CoA oxidation by the Krebs cycle and acetyl-CoA levels to increase. As its concentration increases, it is converted to acetoacetic acid.

A feed-back mechanism for the regulation of ketoacid production by hydrogen ion concentration is suggested by the observation that in circumstances were ketoacid production is stimulated (fasting obese subjects), acid feeding inhibits, while alkali feeding stimulates ketoacid production. Decreased availability of free fatty acids is an important factor in mediating the inhibition of ketoacid production in response to a decrease in pH.[170] The clinical importance of this apparent feedback mechanism remains to be demonstrated.

The acetoacetic acid that is produced during ketogenesis can be converted to beta-OH butyric acid or to acetone (Fig. 59.16). Acetoacetic acid decomposes to acetone nonenzymatically. Acetoacetic acid and beta-OH butyric acid are interconverted by beta-OH butyrate dehydrogenase, which requires the NAD^+/NADH couple as cosubstrates. At equilibrium, the beta-OH butyrate/acetoacetate ratio is normally about 2:1. However, this ratio varies with the mitochondrial $NADH/NAD^+$ ratio. Both acetoacetic acid and beta-OH butyric acid are almost completely dissociated at

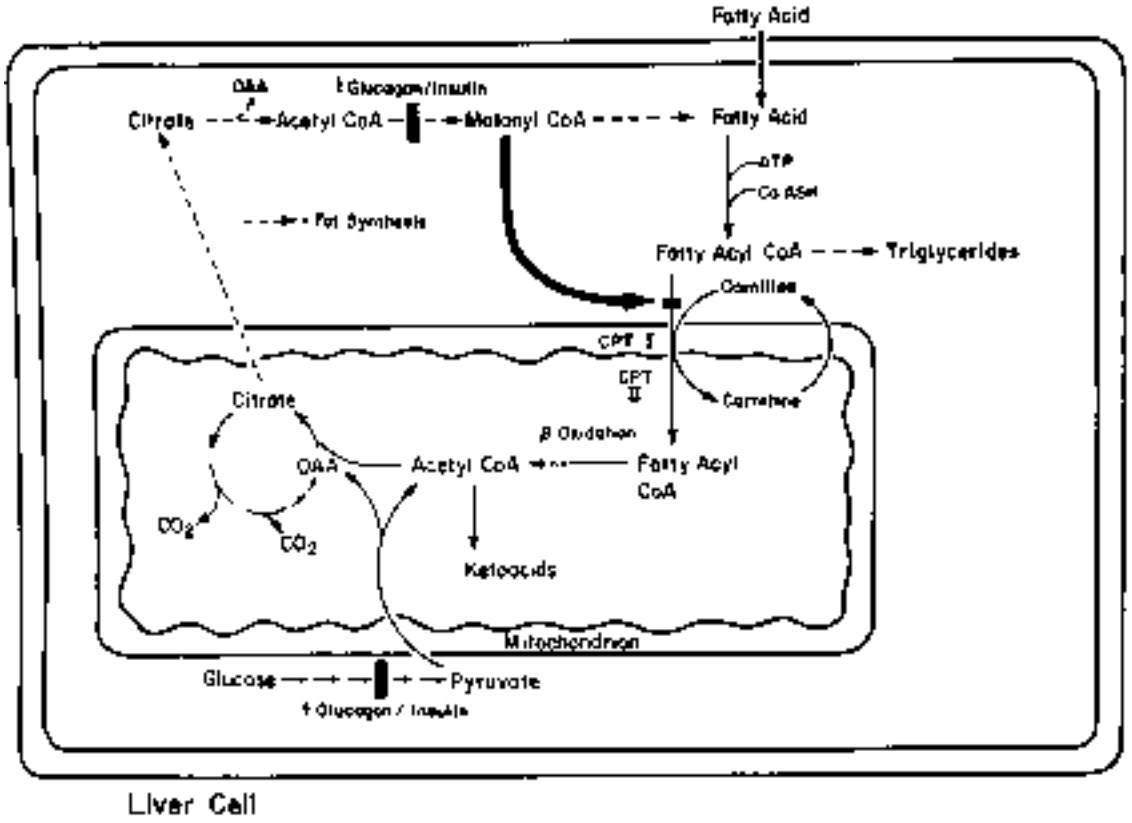

FIGURE 59.15 Fat metabolism in hepatic parenchymal cells. The oxidation of long-chain fatty acids requires that they first be activated in cytoplasm (converted to acyl-CoA derivatives) and then transported into mitochondria. Mitochondria entry is controlled at the level of carnitine palmitoyl transferase I (CPT I). This enzyme is inhibited by malonyl-CoA. When appropriately stimulated, liver cells can also synthesize fatty acids from acetyl-CoA. The fat synthetic pathway is indicated by dashed arrows. These synthetic and oxidative pathways are under the control of insulin and glucagon. OAA, oxaloacetate.

physiologic pH (pK = 3.6 and 4.4, respectively). To the extent that these acids accumulate in ECF, the $[HCO_3^-]$p falls and the anion gap increases. The anion gap increase represents the sum of the beta-OH butyrate and acetoacetate concentrations. Although beta-OH butyrate usually predominates (2:1), the severity of the acidosis is independent of the specific accumulating acid. However, these two acids have different chemical characteristics that affect diagnostic studies. The nitroprusside test for ketones and ketoacids detects acetoacetate (usually about 30% of the plasma ketoacids) but not beta-OH butyrate. If the $NADH/NAD^+$ ratio increases, acetoacetate is shifted to beta-OH butyrate (Fig. 59.16). Under these conditions the nitroprusside reaction decreases, or even becomes negative, despite significant ketoacidosis. Clinically, the nitroprusside reaction can be negative in severe diabetic ketoacidosis probably due to coexisting lactic acidosis (which increases the $NADH/NAD^+$ redox ratio) due to volume depletion, vomiting, and poor hemodynamics. Upon institution of treatment (correction of volume depletion, insulin administration), $NADH/NAD^+$ ratio decreases and the nitroprusside reaction becomes positive. This scenario is the predictable consequence of successful treatment and does not reflect worsening ketoacidosis. Alcoholic ketoacidosis may also produce a high $NADH/NAD^+$ ratio, frequently resulting in a weak nitroprusside reaction.[159] Thus, while the nitroprusside test is a very useful diagnostic tool in patients with ketoacidosis, redox state alterations reduce its value as an index of therapeutic response. Other parameters, such as the clinical status of the patient, the arterial pH, the plasma $[HCO_3^-]$, and changes in the anion gap, should be used to monitor therapy.

Acetone, nonenzymatically derived from acetoacetic acid, is a ketone but not an acid and, therefore, does not reduce the $[HCO_3^-]$p or increase the anion gap. Contrary to current beliefs in most textbooks, acetone does not react with nitroprusside. Acetone is volatile and primarily excreted by the lungs. Small quantities of acetone are also excreted by the kidneys and converted into glucose. Serum acetone levels may increase markedly when severe ketoacidosis develops and then

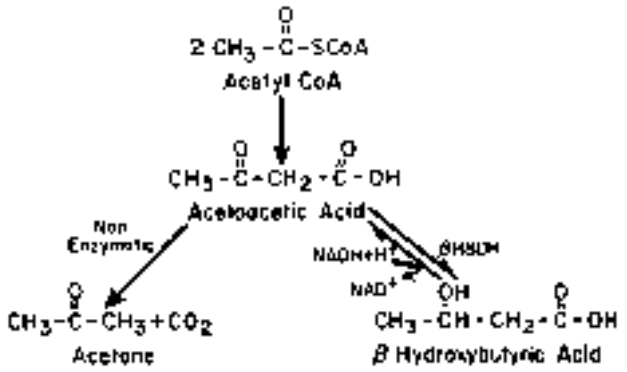

FIGURE 59.16 Ketone body metabolism. The interrelationship among acetoacetic acid, alpha-hydroxybutyric acid (not a true ketoacid), and acetone is shown. The arrow from acetyl-CoA to acetoacetic acid encompasses the intermediate formation of acetoacetic-CoA, and beta-OH alpha-methyl-glutaryl-CoA. β HBDH, beta-hydroxybutyrate dehydrogenase.

persist for several days after resolution of the ketoacidosis.

Isopropyl, or rubbing alcohol, is rapidly metabolized to acetone. Therefore isopropyl alcohol poisoning generates an acetone breath odor, but not ketoacidosis and no positive nitroprusside reaction.[17] The $[HCO_3^-]p$ and anion gap remain normal unless other complications ensue. High acetone levels will raise the plasma osmolality and lead to an osmolar gap.

Clinical Syndromes of Ketoacidosis

Starvation Ketosis

Starvation will generate modest ketoacidosis in normal individuals.[282] During the initial 10–14 hours of fasting, glucose levels are maintained primarily by glycogenolysis. After glycogen stores are depleted, gluconeogenesis becomes the major source of glucose. Hepatic energy requirements are maintained by the oxidation of fatty acids. Accelerated lipolysis and hepatic fatty acid oxidation lead to ketoacidosis, as discussed previously. After 1–2 weeks, the blood ketoacid concentration stabilizes at about 5–6 mEq/liter and the $[HCO_3^-]p$ falls to 18–20 mEq/liter. More fulminant ketoacidosis is aborted as a result of ketoacid-induced release of insulin from pancreatic islet cells.[237] Despite continued starvation, the resultant increase in insulin levels blunts lipolysis. With continued starvation, glucagon and catecholamine levels also decrease toward the normal range and this also slows ketoacid generation. However, pregnant women and young children are particularly vulnerable to more severe ketoacidosis during starvation. In such patients, oral refeeding is frequently impossible due to anorexia, vomiting, and abdominal pain.

Diabetic Ketoacidosis

Diabetic ketoacidosis is usually the result of absolute, or relative, insulin deficiency combined with high glucagon levels. It may be the presenting clinical manifestation of a previously undiagnosed diabetic patient. More often, ketoacidosis occurs in treated diabetic patients because the established insulin program is discontinued or because a superimposed illness, or stress, increases their insulin requirements. Infection, trauma, surgery, and emotional stress activate counter-regulatory hormones that oppose the action of insulin and increase insulin requirements.

Reduced insulin activity, combined with elevated glucagon levels, stimulates glycogenolysis, gluconeogenesis, lipolysis, and fatty acid oxidation. Simultaneously, peripheral glucose utilization falls. Accelerated glucose generation combines with decreased utilization to raise glucose levels. Hepatic ketoacid production exceeds CNS and peripheral ketoacid utilization so that ketoacidosis ensues. Renal Na^+, K^+, and water losses occur as a result of glucose-driven solute diuresis as well as the excretion of large quantities of ketosalts. This leads to volume contraction and renal insufficiency. Nausea, anorexia, and vomiting contribute to the volume deficit and complicate the acid–base abnormalities.

Alcoholic Ketoacidosis

Alcoholic ketoacidosis develops in susceptible individuals who chronically abuse alcohol.[253] Typically, a period of heavy alcohol ingestion is followed by a period of nausea, vomiting, and starvation and then the development of ketoacidosis. Alcoholic ketoacidosis may represent an extreme form of starvation ketosis. However, in these subjects, starvation combines with alcohol withdrawal and volume depletion to elevate markedly counter-regulatory hormones, especially catecholamines. This further accelerates lipolysis and markedly increases fatty acid levels. The fatty acids are oxidized by the liver, which is metabolically primed by low insulin and high glucagon levels.

This form of ketoacidosis is often associated with lactic acidosis and, sometimes, hypoglycemia. Lactic acidosis is in part due to volume depletion resulting from vomiting and decreased oral intake. In addition, ethanol oxidation increases the $NADH/NAD^+$ ratio, which exacerbates lactic acidosis. The high $NADH/NAD^+$ ratio also drives the acetoacetate toward beta-OH butyrate and reduces the nitroprusside reaction.

Hypoglycemia may be the result of glycogen depletion, starvation, and impaired gluconeogenesis. Since the enzymatic steps governing the conversion of non-carbohydrate precursors (e.g., amino acids) to glucose are NAD^+ dependent, the increase in the NADH/

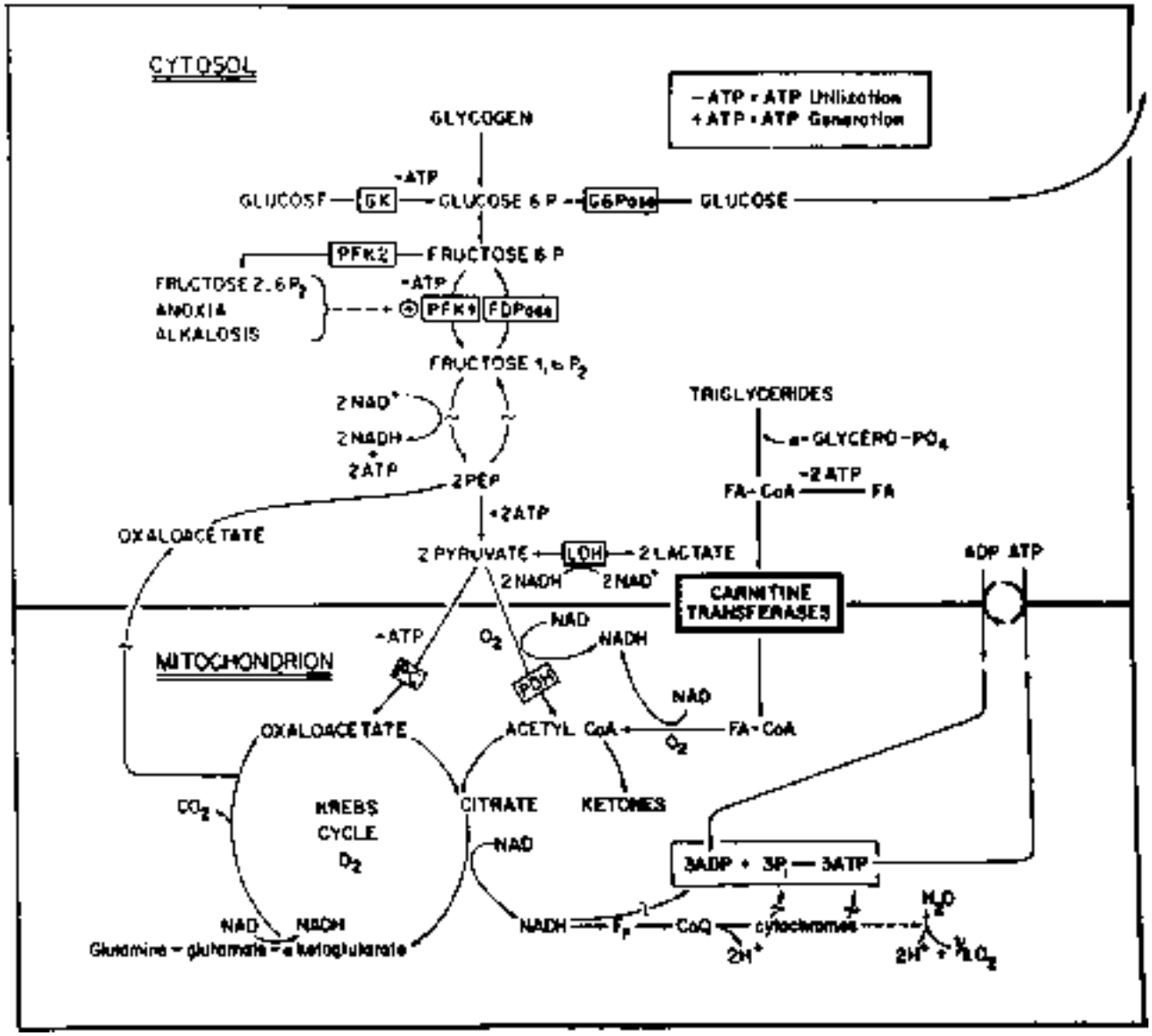

FIGURE 59.17 The metabolic pathways that generate pyruvate and lactate and the pathways that consume pyruvate are summarized. FBPase, fructose bisphosphatase; G6Pase, glucose-6-phosphatase; GK, glucokinase; LDH, lactate dehydrogenase; PC, pyruvate carboxylase; PDH, pyruvate dehydrogenase; PFK, phosphofructokinase.

NAD^+ ratio sharply reduces gluconeogenesis.[236] When this occurs in a setting of hepatic glycogen depletion owing to starvation, hypoglycemia may result.

Alcoholic ketolactic acidosis can generally be rapidly reversed by the intravenous infusion of glucose and saline. Volume expansion improves the circulatory status and reduces catecholamine levels, reversing two factors contributing to lactic acidosis. The glucose infusion corrects hypoglycemia (if present) and increases the insulin/glucagon ratio, thereby suppressing ketoacid production and permitting resolution of the ketoacidosis. Exogenous insulin is rarely necessary unless patients have coexistent diabetes mellitus.

Inborn Errors of Metabolism

Glucose-6-phosphatase and fructose-1,6-bisphosphatase deficiency predispose to both lactic and ketoacidosis. The pathogenesis of these mixed organic acidoses is explained in the next section.

Other rare enzyme disorders also result in ketoacidosis. In some, the accumulating ketoacids are acetoacetic acid and beta-OH butyric acid. However, a variety of other unusual ketoacids can also accumulate.

Lactic Acidosis

Pyruvate, Lactate, and Energy Metabolism Pyruvic and lactic acid metabolism are shown in Fig. 59.17. The

oxidation of glucose and, to a much smaller degree, the deamination of alanine, generates pyruvate, which has four metabolic fates: (1) enter mitochondria and be oxidized to acetyl-CoA via pyruvate dehydrogenase. (2) Enter mitochondria and be carboxylated to form oxaloacetate via pyruvate carboxylase. (3) Remain in cytosol and be aminated to alanine. (4) Remain in cytosol and be reduced to lactic acid.

In most cells, the major metabolic pathway for pyruvate is mitochondrial oxidation to acetyl-CoA. Generally, the rate of mitochondrial pyruvate uptake and oxidation matches the pyruvate generation rate and the cytosol pyruvate concentration is stabilized. Should mitochondrial uptake fail to increase in response to accelerated generation, the pyruvate concentration increases. Decreased mitochondrial uptake, during periods of rapid generation, will increase the pyruvate concentration sharply.

The metabolic–hormonal set of the cell determines how pyruvate, acetyl-CoA, and oxaloacetate are used. In the fed state, energy-yielding substrate is abundant. Exogenous carbohydrates are partially oxidized and partially used to synthesize glycogen and fat. In the fasted state, adipose tissue releases fatty acids, which are oxidized; oxaloacetate and other protein-derived substrates are used to synthesize glucose.

Krebs cycle oxidation of acetyl-CoA transfers electrons and protons, representing chemical potential energy, from this compound to NAD^+, forming $NADH + H^+$. The energy is subsequently released in small steps as the electrons flow down the mitochondrial respiratory (electron transport) chain from the $NADH + H^+$, eventually reduce to oxygen, and form H_2O (Fig. 59.17, bottom at right).

Lactate–Pyruvate Relationship

Lactate dehydrogenase (LDH) catalyzes the interconversion of pyruvic and lactic acids. This reaction requires the cosubstrate $NADH/NAD^+$ couple (Fig. 59.17). A dynamic equilibrium exists between these compounds. Under normal conditions, this reaction is poised toward the left, producing a lactate/pyruvate ratio of about 10:1. At equilibrium,

$$\frac{(\text{pyruvate})(\text{NADH})(H^+)}{\text{lactate}} = \frac{(\text{lactate})(NAD^+)}{[\text{pyruvate}][\text{NADH}][H^+]/[NAD^+]}$$

or

$$\text{lactate} = K\,[\text{pyruvate}][\text{NADH}][H^+]/[NAD^+]$$

where K is the equilibrium constant for the LDH reaction.

The cytosolic lactate concentration is determined by the cytosolic pyruvate concentration, the $NADH/NAD^+$ (redox) ratio, and the cell pH. It is evident that lactate concentrations can increase for three reasons: (1) lactate may increase as a consequence of an increased pyruvate concentration. The lactate/pyruvate ratio would remain about 10:1. (2) Lactate may increase due to a high $NADH/NAD^+$ ratio; the lactate/pyruvate ratio will increase and can exceed 40:1. (3) Lactate may increase as a result of a combined increase of pyruvate concentration and the $NADH/NAD^+$ ratio. This is the usual finding in patients with severe lactic acidosis.

When the $NADH/NAD^+$ or redox ratio and the pyruvate concentration increase together, then lactate levels rise markedly. Huckabee[175] suggested the separation of clinical lactic acidoses into those with normal and those with elevated $NADH/NAD^+$ ratios (as reflected by the lactate/pyruvate ratio) and proposed the concept of "excess lactate." This represents the component of elevated lactate not directly attributed to increased pyruvate. Excess lactate is due to a $NADH/NAD^+$, or redox, shift. Clinically significant lactic acidosis is always associated with a redox shift and excess lactate. Pyruvate concentrations are not routinely measured; however, a redox shift (increased $NADH/NAD^+$ ratio and a lactate/pyruvate ratio greater than 10:1) almost always exists when the blood lactate concentration exceeds 5 mEq/liter. Therefore, this concept of "excess lactate" has been of little clinical use, but it might be useful in conditions like respiratory alkalosis where lactate may be increased separating this entity from incipient lactic acidosis.

Normal Lactate Metabolism

Under steady-state conditions, lactic acid generation and utilization rates are perfectly matched. Tissues that normally release relevant amounts of lactic acid are the skin, brain, exercising muscle, renal medulla, intestine, and red blood cells. Lactic acid is normally taken up and metabolized by the liver.[78] The kidneys also metabolize small amounts of lactic acid.[386] Lactic acid produced in peripheral tissues can be converted back to glucose up by the liver (Cori-cycle). The normal rate of lactic acid generation and utilization is about 15–20 mEq/kg/day (1000–1400 mEq/day). However, these rates can increase markedly. A change in lactate production is usually matched by a parallel change in utilization. The normal steady-state plasma lactate concentration is 1–2 mEq/liter.

When lactate uptake falls behind production, lactate levels increase. Strenuous exercise accelerates muscle lactate production and simultaneously decreases hepatic perfusion. Hepatic lactate uptake lags behind production and lactate levels increase as much as 10–15 mEq/liter. The concentration of serum HCO_3^- falls reciprocally. During postexercise recovery, lactate levels gradually decline as a result of slower production and improved hepatic uptake.[52]

An apparent negative feedback of systemic proton concentration similar to the one described for ketoacid

production has also been demonstrated for lactic acid production.[171] The quantitative importance of this effect in clinical acid–base disturbances is unknown, however.

Ischemia and Lactic Acidosis

Ischemia simultaneously accelerates lactate production and decreases lactate utilization. The final physiologic proton acceptor is oxygen and oxygen deficits impair the oxidation of NADH to NAD^+. NADH accumulates and the $NADH/NAD^+$ ratio increases. A second consequence of tissue oxygen deficits is the failure of oxidative phosphorylation. The energy required to drive the reaction $ADP + P_i - ATP$ is derived from the transfer of electrons and protons from NADH down the electron transport chain to oxygen. If this process is blocked, ATP falls and ADP increases. Therefore oxygen deficiency will generate high $NADH/NAD^+$ and high ADP/ATP ratios.

Oxygen deficiency will also increase the pyruvate concentration. This is due to reduced pyruvate uptake combined with accelerated pyruvate production. Mitochondrial pyruvate utilization requires intact oxidative metabolism. Pyruvate oxidation to acetyl-CoA (via pyruvate dehydrogenase [PDH]) requires NAD^+. Pyruvate carboxylation to oxaloacetate (via pyruvate carboxylase [PC]) requires ATP. Therefore mitochondrial hypoxia decreases pyruvate flux through both reactions and mitochondrial pyruvate uptake decreases. Energy (ATP)-depleted cells compensate by accelerating anaerobic glycolysis. The conversion of glucose into pyruvic and lactic acids is primarily controlled by the rate-limiting enzyme phosphofructokinase-1 (PFK-1). The activity of this allosteric enzyme is increased by hypoxia and energy depletion. ATP inhibits the enzyme while the ATP breakdown products ADP, AMP, and inorganic phosphate activate it. This enzyme also is activated by an alkaline pH and by the regulatory intermediate, fructose-2,6-bisphosphate. Phosphofructokinase-1 [PFK-1] irreversibly phosphorylates fructose-6-phosphate to fructose-1,6-bisphosphate. The enzyme is activated by AMP, ADP, and phosphate, and inhibited by ATP. The glucose regulatory hormones, insulin and glucagon, also regulate the activity of this enzyme. They act through the metabolic intermediate, fructose-2,6-bisphosphate, which is also derived from fructose-6-phosphate. The enzyme phosphofructokinase-2 [PFK-2] converts fructose-6-phosphate into fructose-2,6-bisphosphate. Fructose-2,6-bisphosphate exerts a strong positive effect on PFK-1. Fructose-2,6-bisphosphate levels are increased by insulin, stimulating glycolysis, and decreased by glucagon, inhibiting glycolysis. (Hypoxia and ischemia probably do not directly affect fructose-2,6-bisphosphate levels.) Acceleration of anaerobic glycolysis by ischemia is termed the Pasteur effect.

Thus, ischemia simultaneously accelerates glycolysis, increasing the rate of pyruvate generation, and slows mitochondrial pyruvate uptake. The elevated $NADH/NAD^+$ ratio produced by ischemia drives pyruvate to lactate. Therefore lactate levels increase sharply because high pyruvate levels are combined with a high $NADH/NAD^+$ ratio.

Clinical Syndromes of Lactic Acidosis

Table 59.4 lists the major clinical syndromes associated with lactic acidosis. Most commonly, lactic acidosis results when inadequate oxygen is supplied to a large mass of tissue. Circulatory failure characteristically produces lactic acidosis. Generalized underperfusion triggers the metabolic cascade described previously. Major sources of lactate are skeletal muscle and the intestinal tract. In acute lung injury such as shock lung or the adult respiratory distress syndrome, the lung can also become a major source of lactate. Circulatory failure also reduces hepatic perfusion, superimposing diminished lactate uptake on accelerated production. Plasma lactate concentrations reflect the severity of the process and may be a useful prognostic indicator.[72]

Severe acute arterial hypoxemia, in the absence of decreased perfusion, can generate lactic acidosis.[175] However, this rarely occurs with chronic hypoxemia because multiple compensatory mechanisms generally maintain tissue oxygenation. Increased cardiac output, polycythemia, and a decreased hemoglobin–oxygen affinity, owing to high red cell 2,3-diphosphoglyceric acid levels, maintain tissue oxygen delivery. Therefore, patients with uncomplicated chronic obstructive lung disease rarely develop lactic acidosis despite severe hypoxemia. When lactic acidosis develops in such patients it is usually the result of a superimposed process such as hypotension, sepsis, or superimposed acute hypoxia.

Carbon monoxide poisoning frequently produces lactic acidosis.[56] Carbon monoxide binds to hemoglobin more avidly than oxygen, reducing hemoglobin's oxygen-carrying capacity. In addition, the carbon monoxide–hemoglobin complex shifts the oxygen–hemoglobin dissociation relationship so that hemoglobin's affinity for oxygen increases. This reduces oxygen release to tissues. Hence less oxygen is transported to tissues and less is released. Furthermore, cardiac output, which is usually increased by acute hypoxia, does not generally increase in patients with

carbon monoxide poisoning.[56] Oxygen chemoreceptors, responsible for the afferent limb of this response, respond primarily to arterial PO_2, and the PO_2 does not fall with carbon monoxide poisoning. The displaced oxygen-carrying capacity, left shift of the oxygen–hemoglobin dissociation curve, and deficient cardiovascular response sharply reduce tissue oxygenation. Finally, carbon monoxide binds directly to the electron transport molecule cytochrome a3 and depresses oxidative phosphorylation and mitochondrial respiration. The net result is accelerated lactic acid production and lactic acidosis.

Severe anemia, especially when due to iron deficiency or methemoglobinemia, may trigger lactic acidosis.[328] Anemia directly reduces the oxygen-carrying capacity. In addition, iron is a critical constituent of several electron carriers in the respiratory chain and severe deficiency can depress oxidative metabolism.[117]

Poisons can block oxygen uptake by mitochondria despite normal oxygen delivery. Cyanide is a compound that binds to cytochromes a and a3, blocking the flow of electrons to oxygen. ATP generation falls and the oxidation of NADH to NAD^+ decreases, resulting in lactic acidosis.[155] The arterial–venous O_2 gradient across vascular beds decreases as a result of depressed oxygen uptake. Iatrogenic cyanide poisoning can occur when patients are exposed to nitroprusside for prolonged periods of time. Nitroprusside is metabolized to cyanide, which is then converted to thiocyanate, a less toxic molecule that is excreted by the kidneys. However, impaired renal and hepatic function can result in cyanide poisoning.[184]

2,4-Dinitrophenol (used in manufacturing of dyes, as wood preservative, insecticide or as a reagent) is a compound that poisons mitochondria via another mechanism.[254] This agent uncouples oxidative phosphorylation. Uncouplers do not block the oxidation of NADH to NAD^+, nor do they prevent the flow of protons and electrons to oxygen. However, they separate these energy-releasing reactions from the phosphorylation of ADP to ATP. NADH oxidation, uncoupled from ATP generation, becomes unregulated and rapid. Chemical energy is converted into heat and calories are burned. Similar mitochondrial uncouplers have been used as weight-reducing agents but they can produce life-threatening lactic acidosis.

Many congenital mitochondrial enzyme abnormalities can affect lactate metabolism. Various components of complex enzyme systems such as pyruvate carboxylase, pyruvate dehydrogenase, and the cytochrome electron transport system can be affected. Severe inherited disorders of this type are rapidly fatal. More subtle defects, compatible with life, result in chronic lactic acidosis. Affected individuals typically develop worse acidosis during exercise, when the metabolic load delivered to these enzyme systems is increased. Many also develop severe muscle dysfunction and progressive neurologic abnormalities.

Acquired defects of critical enzyme systems can also generate lactic acidosis. One such example is beriberi, a nutritional disorder due to thiamine deficiency. Thiamine is a required cofactor for several enzyme complexes, including pyruvate dehydrogenase. Severe thiamine deficiency reduces pyruvate dehydrogenase activity and depresses mitochondrial pyruvate oxidation (Fig. 59.17). In addition, high output heart failure occurs frequently and contributes to the development of lactic acidosis. Beriberi lactic acidosis is promptly reversed by the administration of thiamine.[363]

The biguanide metformin is used to treat type II diabetes mellitus, particularly in obese patients. It is not appreciably metabolized and excreted primarily by the kidneys. Metformin can accumulate in patients whose kidney function is impaired, especially in the elderly. High concentrations of biguanides reduce the activity of several mitochondrial enzymes, especially pyruvate dehydrogenase.[86] Although lactic acidosis is 10 to 20 times less frequent with metformin than with phenformin (withdrawn from the market), many cases have been reported generally, but not exclusively, when one of the contraindications for the drug (renal impairment, liver disease, cardiac and respiratory insufficiency, etc.) was overlooked. Estimated mortality remains high at 50%. Metformin can be removed from the body by hemodialysis.

The activity of pyruvate dehydrogenase is increased by insulin[351] and may be decreased in diabetic patients. This may predispose diabetic patients to development of lactic acidosis. However, when lactic acidosis occurs in diabetic patients, it is usually due to a superimposed disorder such as volume contraction or sepsis. Acute inorganic phosphate depletion lowers ATP levels and can produce lactic acidosis. Such a sequence can develop due to severe intracellular phosphate depletion (as in the hyperalimentation-induced phosphate depletion syndrome) or when phosphate is trapped within the cytoplasm. Such phosphate trapping can occur after intravenous infusion of organic substances (such as fructose, xylitol) or when phosphorylated intracellular organic anions can not be efficiently metabolized due to enzymatic deficiencies (i.e., fructose-1-phosphate aldolase in fructose intolerance). Acute reductions in the intracellular inorganic phosphate concentration slow the generation of ATP from ADP. Simultaneously, the Pasteur effect accelerates anaerobic glycolysis. Decreased oxidative phosphorylation combines with accelerated anaerobic glycolysis to generate lactic acidosis.

ADP and AMP accumulate due to decreased rates of ATP synthesis and are metabolized to inosine-5-

monophosphate, which is then converted into ADP, AMP, and uric acid (ATP breakdown products). Therefore, hyperuricemia and hyperuricosuria are observed typically in the phosphate depletion syndrome. Hypermagnesemia is also observed and is the consequence of magnesium release from adenine nucleotide complexes, and impaired renal function. ATP depletion also causes hepatic and renal cortical dysfunction. Hepatic necrosis elevates serum transaminase levels. Proximal renal tubule dysfunction produces a Fanconi syndrome.[260] In addition to the energy depletion, some phosphorylated sugars, such as the fructose-1-phosphate, accumulate in the liver and kidneys and may also have direct toxic effects.

Similar pathophysiological sequences (i.e., trapping of phosphate to organic anions) occur in hereditary glucose-6-phosphate deficiency (von Gierke disease) where glucose release from glucose-6-phosphate is blocked and in hereditary fructose-1,6-bisphosphate deficiency, where generation of glucose during gluconeogenesis is blocked.

The mitochondrial encephalomyopathies—Kearns–Sayre syndrome (KSS), myoclonic epilepsy with ragged fibers (MERRF), mitochondrial encephalopathy, lactic acidosis, and stroke-like episodes (MELAS)—are all causes of lactic acidosis. In these disorders, pyruvate or acetyl CoA utilization in the mitochondrion is impaired due to defects in proteins of the electron transfer chain.

Nucleoside analogs, widely used in HIV-treatment disrupt the mitochondrial DNA that encodes for the respiratory chain proteins and, thereby, inhibits the transport of pyruvate into the mitochondria and have been reported to cause lactic acidosis in HIV positive patients when used as single agents or, more frequently in combination. Hyperlactatemia developed in about 8% or 73 out of 880 patients of a large cohort of HIV-positive, with only one patient developing severe lactic acidosis (anion gap >16).[38]

Lactic acidosis can develop when lactate production accelerates within local compartments. Hepatic lactate uptake in these conditions may be normal, high, or low. Lactic acidosis associated with strenuous exercise is due to rapid generation of lactic acid in muscle, which is released into the systemic circulation and temporarily exceeds hepatic uptake. Hepatic lactate uptake often falls because strenuous exercise reduces hepatic blood flow. Exhaustive exercise may increase lactate levels above 12 mEq/liter with rapid normalization within one hour.[52] Similar mechanisms may generate lactic acidosis following seizures[280] and after exertion-related heat stroke[164] or strychnine intoxication.[41]

Malignancies, including leukemia, lymphoma, and oat cell lung cancer, may produce chronic lactic acidosis.[115] Afflicted patients often have a large tumor mass. Multiple factors may contribute to this form of lactic acidosis: (1) malignant cells often have a rapid metabolic rate,[35,303] (2) rapidly growing bulky tumors may outstrip their blood supply and develop hypoxic foci, (3) enzymatic defects, which accelerate lactate production, may occur(,[35,303] and (4) extensive metastatic liver disease may decrease hepatic lactate uptake. Cancer-associated lactic acidosis may persist for weeks to months. It is usually refractory to treatment unless the tumor burden can be reduced. Exogenous $NaHCO_3$ infusions are usually not helpful and can actually accelerate lactic acid production.[122] A low systemic pH may break the lactic acid synthetic rate[171] and efforts to increase the pH can stimulate lactate production. The chronic loss of lactate into the urine represents caloric wastage and contributes to weight loss and development of cachexia.[116] Lactic acidosis can be associated with the tumor lysis syndrome.

Severe hepatic dysfunction will depress lactate uptake. However, lactic acidosis is uncommon in patients with uncomplicated liver disease.[294] When such patients develop lactic acidosis, an associated disorder that accelerates lactate generation (such as hypotension or sepsis) usually exists.[239] In some cases, arteriovenous shunting results in a large mass of underperfused tissue.[33] Some malnourished patients with combined liver and renal failure (frequently requiring dialysis) may develop a form of chronic lactic acidosis.[251] This is not due to clinically apparent hypotension, diminished tissue perfusion, or hypoxia. It frequently occurs during a fast and is often accompanied by hypoglycemia. Antecedent starvation often depletes glycogen stores so these patients become dependent on gluconeogenesis to maintain blood glucose levels. Low insulin levels combine with high levels of glucagon, growth hormone, glucocorticoid, and catecholamines to drive gluconeogenesis, lipolysis, and protein catabolism. However, hepatic uptake of glucose precursors, especially alanine and lactate, is reduced, in part as a result of poor hepatic function. The inadequate gluconeogenic response leads to hypoglycemia. Lactic acid increases as decreased hepatic lactate uptake combines with accelerated peripheral generation (due, in general, to hypotension or sepsis). The lactic acidosis further depresses hepatic alanine uptake, which exacerbates the hypoglycemia. Most of these biochemical abnormalities are rapidly reversed by the infusion of glucose. The complex interrelationships among liver failure, renal disease, malnutrition, lactic acidosis, and hypoglycemia are not fully understood. Glucose must play a central role because its infusion rapidly reverses the syndrome.

Increased catecholamine levels, of either endogenous or exogenous origin, raise lactic acid levels slightly.[175] Epinephrine accelerates glycogenolysis and glycolysis while inhibiting mitochondrial pyruvate

uptake. This increases both pyruvate and lactate levels. As long as the $NADH/NAD^+$ ratio remains normal, the increase in lactate remains relatively small (< 5 mEq/liter). However, if catecholamine levels increase markedly, then tissue perfusion is compromised, owing to intense peripheral vasoconstriction and cardiac dysfunction. This elevates the $NADH/NAD^+$ ratio and clinically significant lactic acidosis will then occur.[150] Severe lactic acidosis may also occur in patients with pheochromocytomas[195] or cocaine intoxication as a result of similar metabolic pathology.[192]

Sodium valproate and germanium poisoning can both cause lactic acidosis, the pathogenesis of which is unclear.[106,210] Propofol, an anesthetic drug, can rarely cause lactic acidosis and rhabdomyolysis when applied over extended periods of time and in high doses. Lactic acidosis probably is due to propofol's uncoupling of beta-oxidation at complex II of the respiratory chain.[362]

Therapy for Lactic Acidosis

The treatment of lactic acidosis must be directed at the underlying pathophysiology. When lactic acid is overproduced, the root cause of overproduction should be identified and, if possible, eliminated. The therapeutic approach in patients with lactic acidosis due to shock, sepsis, asphyxia, and poisons is generally self-evident. Despite this, mortality of lactic acidosis remains high and treatment strategies directed at later steps in the metabolic cascade have been evaluated.

Dichloroacetate,[34] which stimulates pyruvate dehydrogenase, accelerates mitochondrial pyruvate oxidation (Fig. 59.17). Improved mitochondrial pyruvate uptake should decrease cytosol concentrations of pyruvate and lactate. Unfortunately, despite these theoretical promises, dichloroacetate had no effect on the course of lactic acidosis when evaluated in a prospective multicenter trial[335] and cannot be recommended as a treatment option for lactic acidosis.

Treatment of lactic acidosis with $NaHCO_3$ infusions and other alkalinizing salts is generally ineffective. Even if the pH and $[HCO_3^-]$ are transiently increased, acidemia promptly recurs unless the basic pathology is reversed. Some animal models of lactic acidosis are even accompanied by poorer survival after $NaHCO_3$ therapy.[13,334] $NaHCO_3$ infusions acutely increase CO_2 generation when H^+ combines with HCO_3^- to form CO_2. If ventilation does not accelerate appropriately, the arterial pCO_2 will increase. Even when the arterial pCO_2 remains normal, capillary, venous, and tissue CO_2 tensions may increase after $NaHCO_3$ infusions. This reduces intracellular pH as CO_2 rapidly diffuses into cells.[300] Recently, a new alkalinizing salt called carbicarb (a combination of Na_2CO_3 and $NaHCO_3$), which should generate less CO_2, has been introduced. However, preliminary studies suggesting this salt may be advantageous compared with $NaHCO_3$[31] were not confirmed in animal models[17] or appropriately designed clinical studies. Thus, the reason why these drugs are of no proven benefit may be explained by the possibility that mortality is not determined by lactic acidosis per se, but rather by its underlying cause such as shock and sepsis.

The infusion of large quantities of hypertonic $NaHCO_3$ can produce hypernatremia and intracellular dehydration. Hypernatremia may be forestalled by appropriate hydration; however, the resultant volume expansion may produce pulmonary edema. If the lactic acidosis is reversed and large quantities of $NaHCO_3$ have been infused, then rebound metabolic alkalosis often develops.[372] The exogenous HCO_3^- combines with HCO_3^- regenerated from circulating lactate to elevate the blood $[HCO_3^-]p$.

Hemodialysis/hemofiltration and peritoneal dialysis can simultaneously deliver HCO_3^-, remove lactate, normalize electrolytes, and stabilize the extracellular fluid (ECF) volume. However, plasma lactate clearance rates achieved by these methods are so low (less than 3% of total lactate clearance) that they cannot be recommended as treatment options.[231]

POISON-ASSOCIATED ANION GAP ACIDOSIS

Alcohols

Alcohols and Osmolal Gap

Under most conditions sodium salts, urea, and glucose generate the osmotic pressure of blood plasma. The plasma osmolality can be calculated using the following equation:

$$\text{osmolality} = 2[Na^+]\text{mmol/liter} + \text{BUN mmol/liter} + \text{glucose mmol/liter}$$

If concentrations of BUN and glucose are expressed as percent milligrams, the values need to be divided by 2.8 (BUN) and 18 (glucose). When the calculated osmolality is compared with the measured osmolality, they should agree to within 10–15 mOsm/liter. When the measured osmolality is greater than the calculated osmolality by 15 mOsm or more, the osmolal gap is increased and one of two possibilities usually obtains. The first possibility is that the serum $[Na^+]$ measurement is spuriously low, resulting in a reduced calculated osmolality. For example, pseudohyponatremia due to hyperlipidemia or hyperproteinemia can reduce the calculated osmolality while the measured

osmolality reflects the true plasma water [Na^+]. When this occurs the measured osmolality is usually normal, while the calculated osmolality is abnormally low. The second possibility is that solutes other than sodium salts, urea, or glucose are present in plasma and elevate its osmolality. Low molecular weight solutes such as mannitol, alcohols, ethylene glycol, and acetone can achieve high plasma concentrations, and thereby elevate measured osmolality. In such cases, the difference between the measured and calculated osmolality is proportional to the concentration of that solute. Methanol's molecular weight is 32 mg/mmol. Therefore a methanol concentration of 32 mg/100 ml = 320 mg/liter = 10 mOsm/liter. Table 59.5 shows the contribution of various clinically pertinent solutes to measured osmolality.

The foregoing discussion is based on plasma osmolality measurements made with freezing point depression osmometers. Some osmometers in clinical practice use deviations in vapor pressure to measure osmolality. Although this methodology is appropriate for measuring the osmotic contributions of most solutes, it will not detect volatile solutes such as small alcohols. Therefore freezing point depression osmometers must be used if the difference between measured and calculated osmolality is to be a helpful screening test for such intoxications. However, this calculation is a screening test and both false negative and false positive results may occur.[314,339]

Ethanol Intoxication

Ethanol intoxication is an important cause of both ketoacidosis and lactic acidosis,[211] both of which were discussed in previous sections.

Methanol Poisoning

Methanol, or wood alcohol, is used as an industrial solvent, antifreeze ingredient (especially in windshield washing solutions), and canned solid fuel component. The ingestion of 60–250 ml is potentially lethal in adults. Chronic alcoholics may knowingly, or accidentally, use methanol as an inexpensive ethanol substitute.[30] Methanol poisoning produces initial inebriation similar to ethanol intoxication. Methanol oxidation, primarily by the liver, generates several toxic products, including formaldehyde and formic acid. They begin to accumulate 6–24 hours after ingestion and produce vomiting, abdominal pain, visual disturbances, confusion, and coma. High formic acid levels generate an anion gap metabolic acidosis.[249] Hypoxia, hypotension, and cardiac dysfunction may also produce lactic acidosis. Methanol metabolites that interfere with normal mitochondrial function can potentiate the lactic acidosis.

Both formic acid and formaldehyde are toxic to retinal cells and the optic nerve.[249] Ocular toxicity includes blurred vision, optic disc swelling, pupillary dilation, and blindness. Fundoscopy may be diagnostic of methanol intoxication. Nausea, vomiting, and abdominal pain occur and may be due to pancreatitis. CNS toxicity results in confusion, seizures, coma, and death.

Methanol poisoning must be treated aggressively. An aqueous slurry of activated charcoal, 1–2 g per kilogram of body weight, is administered by mouth or nasogastric tube. This may be followed by a purgative, such as sorbitol (30–50 ml of 70% solution) to hasten transit of unabsorbed alcohol and charcoal through the gastrointestinal tract. Forced vomiting (ipecac syrup) should be reserved for only the most recent intoxications (minutes) as it will severely limit the ability to ingest and retain activated charcoal.

The next phase of therapy is directed at inhibition of alcohol dehydrogenase, the major methanol-oxidizing enzyme system. The relatively specific and potent inhibitor of alcohol dehydrogenase, fomepizole (4-methylpyrazole) blocks development of the anion gap metabolic acidosis as well as other toxic consequences of methanol poisoning and was safe and effective in series of both adult and pediatric intoxications.[46,87] The drug is given at a dose of 15 mg/kg of body weight over 30 minutes intravenously, followed by 10 mg/kg of body weight over the next 12 hours for four consecutive doses.

If fomepizole is not available, metabolism of methanol by alcohol dehydrogenase can be competitively inhibited by ethanol.[247] Alcohol dehydrogenase has a greater affinity for ethanol than for methanol (or ethylene glycol) and ethanol competitively inhibits the oxidation of other alcohols. A therapeutically effective blood ethanol level is 100–150 mg/dl. The ethanol can be administered by mouth, nasogastric tube, intravenously, or via dialysis. An initial loading dose of approximately 600 mg/kg produces the requisite level. In a 70-kg adult, this represents about 42 g of ethanol. The alert patient may ingest 4 oz of 80-proof whiskey. Alternatively, 500 ml of a 10% ethanol solution may be infused intravenously. Subsequent dosing will depend on the rate of ethanol metabolism. Nonalcoholic subjects require about 5 g/hr of ethanol to maintain an adequate level (about 60 ml/hr of a 10% solution, specific weight of ethanol = 0.79). Chronic alcoholics more rapidly metabolize ethanol because of chronic activation of alcohol dehydrogenase. They will require about 10 g/hr (120 ml/hr of a 10% solution).[247] If dialysis is initiated, the ethanol infusion rate must be doubled. Alternatively, ethanol may be added to the dialysate at a concentration of about 100 mg/dl. Folic acid should be given because it may increase formic acid metabolism to CO_2.

Reversal of metabolic acidosis may ameliorate methanol toxicity. Therefore aggressive alkalinization has been recommended. This may be accomplished by parenteral $NaHCO_3$ infusion. However, volume expansion and hypernatremia complicate hypertonic $NaHCO_3$ infusions. Alkalinization can be achieved more rapidly and effectively with hemodialysis. Hemodialysis also rapidly removes methanol and its toxic metabolic products (see subsequent recommendations). Peritoneal dialysis is much less effective than hemodialysis.[196] Forced diuresis is relatively ineffective because renal methanol clearance is very low.

Ethylene Glycol Poisoning

Ethylene glycol is the principal constituent of most automotive engine antifreeze, brake fluid and power steering fluid products and is a widely used organic solvent. It is rarely used as a pharmaceutical solvent (i.e., for lorazepam vials). This colorless and slightly sweet alcohol is sometimes illegally used to enhance the flavor of low quality wine.

Chronic alcoholics may knowingly ingest ethylene glycol as an inexpensive ethanol substitute. However, accidental or suicidal poisoning is more common. Although the lethal adult dose is about 100 ml, occasional individuals survive ingestion of much larger quantities. Similar to methanol, ethylene glycol itself is slightly toxic but is rapidly oxidized to multiple more toxic products, including glycolates and oxalates. Several of these metabolites are relatively strong acids that accumulate and generate an anion gap metabolic acidosis.[130] In addition, cardiovascular collapse occurs commonly and may precipitate lactic acidosis.

Ethylene glycol poisoning usually produces inebriation, nausea, and vomiting soon after ingestion. The ingestion of large quantities may rapidly result in coma, seizures, and death. More commonly, initial mild symptoms persist for about 12 hours and are followed by a second wave of more severe clinical and biochemical alterations.[126] During the latent period, toxic metabolic products accumulate and generate a progressive anion gap metabolic acidosis.[130] Calcium deposition and chelation reduce the ionized $[Ca^{2+}]$, resulting in tetany and seizures. Calcium oxalate precipitates in the lungs, heart, kidneys, and brain.[126]

Patients who survive these initial phases often develop oliguric renal failure, associated with severe flank pain. This may become the dominant clinical problem.[126] Renal failure is partially due to calcium oxalate deposition and may be irreversible. A variety of persistent neurologic deficits, possibly due to neural calcium oxalate deposits, may develop in long-term survivors.

Ethylene glycol intoxication should be considered in patients presenting with confusion, obtundation, or coma and an unexplained anion gap metabolic acidosis. Suspicion increases if the patient has a psychiatric, suicidal, or chronic alcohol abuse history. Other laboratory findings include a large osmolal gap, anion gap metabolic acidosis, and calcium oxalate crystals in the urine. Qualitative analysis of ethylene glycol in blood, urine, or gastric fluid is necessary for definitive diagnosis.

The initial management of ethylene glycol poisoning parallels that described for methanol poisoning. A charcoal slurry is then administered to bind residual ethylene glycol and prevent further absorption. Purgatives that speed gastrointestinal transit may be useful.

Ethylene glycol is also oxidized by alcohol dehydrogenase in the cytoplasm of hepatic cells. Blocking this enzymatic reaction markedly reduces ethylene glycol's toxicity.[365] As with methanol intoxication, ethanol can be used as a competitive substrate for alcohol dehydrogenase. A therapeutic blood ethanol concentration is 100−150 mg/100 ml (see Methanol Poisoning section). However, fomepizole (4-methylpyrazole) has an affinity to alcohol dehydrogenase that is at least three orders of magnitude greater than ethanol and is the treatment of choice in ethylene glycol intoxication.[47]

Severe metabolic acidosis may be treated with parenteral $NaHCO_3$. However, large quantities of $NaHCO_3$ produce volume expansion and may precipitate pulmonary edema. Cardiac and pulmonary toxicity secondary to calcium oxalate deposition increases the likelihood of pulmonary edema in response to a volume challenge.

Pyridoxine and thiamine (100 mg each intravenously per day) are cofactors for the metabolism of ethylene glycol metabolites and should be administered.

Unlike methanol, renal excretion of ethylene glycol and its metabolites is significant. When renal function is adequate, forced diuresis with furosemide and mannitol can be effective.[339] Precautions must be taken to forestall sodium and other electrolyte deficits that can be induced by the diuresis. The effectiveness of such diuresis is greatly amplified if metabolism of ethylene glycol is simultaneously reduced by inhibition of the alcohol dehydrogenase enzyme system. Severe poisoning should be treated with hemodialysis.[127] Ethylene glycol and toxic metabolic products are removed, metabolic acidosis and electrolyte abnormalities are reversed, and volume status normalized.

Ionized calcium levels fall as a result of calcium oxalate precipitates and chelates. To some extent, metabolic acidosis ameliorates the low ionized calcium levels by reducing calcium binding to proteins. Therefore alkalinization may exacerbate hypocalcemic symptomatology and produce tetany and seizures. Dialysis simultaneously corrects the acidosis and

hypocalcemia because oxalate is removed while calcium and alkali are infused.

Indications for Dialysis in Ethylene Glycol and Methanol Poisoning

Firm indications for recommending dialysis are not available. The following indications are, however, generally accepted:

- Methanol or ethylene glycol plasma concentrations in excess of 25 mg/100 ml in asymptomatic patients.
- Ingestion of more than 175 mg/kg body weight of either poison.
- Sustained metabolic acidosis and visual disturbances (methanol).
- Unexplained metabolic acidosis with a high anion gap and a high osmolal gap in a setting where assays for methanol or ethylene glycol plasma concentrations are not readily available.

Paraldehyde Poisoning

Chronic paraldehyde poisoning used to be a rare cause of anion gap metabolic acidosis but paraldehyde (used as a sedative for delirium tremens) is no longer manufactured (see third edition of this book).

Salicylate Poisoning

Salicylate poisoning is a relatively common disorder that produces a characteristic spectrum of clinical, acid–base, and electrolyte abnormalities.[69] Salicylate preparations include salicylic acid, acetylsalicylic acid (aspirin), sodium salicylate, and methylsalicylate. Acetylsalicylic acid is rapidly hydrolyzed by the liver to salicylic acid.

At toxic concentrations, salicylate uncouples oxidative phosphorylation, which accelerates oxygen utilization, heat generation, and CO_2 production;[254] in consequence, hyperthermia and hypoglycemia may result. Multiple other oxidative enzyme systems are inhibited by high salicylate levels. Salicylate also directly stimulates the central respiratory center, increasing minute ventilation.[299] The hyperventilatory response usually more than compensates forthe accelerated CO_2 production, resulting in a respiratory alkalosis (especially in adults).

The metabolic acidosis produced by salicylate poisoning is multifactorial. As mentioned previously, a variety of enzymatic reactions are inhibited and oxidative phosphorylation is uncoupled. Simultaneously, the low pCO_2 increases intracellular pH, which accelerates glycolysis as a result of phosphofructokinase-1 activation. This contributes to the development of lactic acidosis. Vomiting and decreased oral intake produce Na^+ and K^+ depletion. Hypokalemia can generate cardiac arrhythmias. Volume depletion also contributes to the lactic acidosis. Ketoacidosis may develop, especially in young children and pregnant women. In consequence, the anion gap metabolic acidosis is due to an accumulation of lactate, ketoacids, salicylate, and other organic acids.[129] The molecular weight of salicylate is 138 mg/mmol. Therefore, a salicylate level of 100 mg/100 ml will contribute about 7 mEq/liter to the anion gap.

Usually, salicylate poisoning results in a mixed acid–base disturbance, that is metabolic acidosis and coexisting respiratory alkalosis. The age of the patient has an important impact on whether acidemia or alkalemia dominates. Metabolic acidosis is generally more severe in infants and young children, while adults typically manifest a normal or alkaline blood pH.[129,380] The systemic pH will affect the degree of neurotoxicity and the patient survival rate. The low pKa of salicylic acid indicates that more than 99% will be ionized in the physiologic pH range. However, it is the minute unionized fraction of salicylic acid that readily penetrates lipid cell membranes, while the ionized fraction penetrates poorly. The concentration of un-ionized salicylate increases when blood pH falls. For example, its concentration doubles when the blood pH falls from 7.4 to 7.1. Thus, acidemia increases the concentration of un-ionized salicylate, which readily enters parenchymal and brain cells. This nonionic diffusion accounts for the increased mortality rate associated with acidemia in this disorder.[129]

A number of biochemical abnormalities can occur in salicylate-poisoned individuals. Hypoglycemia often develops[80] probably due to interactions with the sulfonylurea receptor. Even when the blood glucose level is normal, brain glucose concentrations may be reduced.[354] Extreme hypouricemia is due to inhibition of renal tubule urate reabsorption by high salicylate levels.[385] Hypokalemia develops as a result of urinary potassium losses, which are exacerbated by alkalinization of distal renal tubule cells (owing to respiratory alkalosis) in a setting of increased distal delivery of sodium salts (nonreabsorbed salicylate) and enhanced Na^+ reabsorption (due to volume depletion). In addition, starvation and vomiting may contribute to the potassium deficits. In alkalotic patients, potassium may also be redistributed from the extracellular fluid into cells.

Clinical manifestations of salicylate poisoning include hyperventilation, confusion, coma, and seizures.[69,129] Noncardiogenic pulmonary edema may occur, especially with chronic salicylate intoxication.[167] Tinnitus, deafness, and vertigo are common complaints. Hyperthermia, in the absence of infection, may occur and reflects increased heat production.

Hemorrhagic manifestations are rare, but severe intoxication can lead to ecchymoses, petechia, and prolonged bleeding related to platelet dysfunction and hypoprothrombinemia (secondary to factor VII synthesis inhibition). Impaired renal function results from salt depletion and salicylate inhibition of renal production of vasodilatory prostaglandins.

The urinary excretion of salicylate metabolites can generate a false positive reaction for ketones (nitroprusside test) and for glucose (reducing substances). Renal glycosuria can, however, develop as a result of proximal tubule dysfunction. A positive glucose oxidase test identifies the presence of true glycosuria. Fanconi's syndrome rarely develops.

Blood salicylate measurements must be interpreted with respect to the time elapsed from ingestion. The decrease in salicylate levels follows first-order kinetics. Toxicity is common with peak levels above 30 mg/100 ml, while severe toxicity and fatalities occur when peak levels exceed 100 mg/100 ml.

Guidelines for the treatment of salicylate intoxication are listed in Table 59.6. The use of gastric lavage is controversial due to side effects (aspiration), limited efficacy and the possibility to enhance propagation of salicylates to the small bowel. However, aggregation of salicylates and gastroparesis are arguments to perform gastric lavage. Gastric lavage may be indicated early after ingestion and the indication is probably best made after endoscopic evaluation. Activated charcoal should be administered (see Methanol Poisoning section). Hypokalemia, hypoglycemia, and metabolic acidosis must be treated aggressively. Hypoprothrombinemia can be corrected with parenteral vitamin K or fresh frozen plasma infusions.

Renal salicylate excretion is accelerated by induction of a large diuresis and alkaline urine. Salicylate filtered by the glomerulus is both reabsorbed and secreted by the renal tubules. In part, it is reabsorbed as undissociated salicylic acid via the process of nonionic diffusion. This occurs when the urine pH is lower than the blood pH. Conversely, if the urine pH exceeds the blood pH, then ionized salicylate is trapped in the urine. If urine pH above 7.5 can be achieved, salicylate clearance may increase several-fold above the glomerular filtration rate. Increased urine flow will also augment salicylate excretion by reducing its concentration in tubular fluid. An alkaline diuresis, with urine flow of about 2 ml/min, should be induced. This can be accomplished with $NaHCO_3$ infusions. However, if the patient is already alkalemic, such infusions must be used cautiously. Further elevation of blood pH can cause severe tetany and seizures.

Inducing bicarbonate diuresis with acetazolamide is discouraged because of its potential to create or aggravate systemic acidosis, which is not always preventable by exogenous $NaHCO_3$ in clinical practice. Acetazolamide's efficacy to remove salicylate is also in doubt since a controlled comparison of bicarbonate administration vs bicarbonate plus acetazolamide in salicylate-toxic dogs resulted in no significant increase in salicylate excretion. Whereas acetazolamide administration does alkalinize the final urine, it results in a disequilibrium pH in the proximal tubule lumen (lower value than the equilibrium value due to its ability to delay the dehydration of luminal carbonic acid) and thus may not provide luminal alkalinity at the nephron site critical for salicylate dissociation.

Hepatic salicylate metabolism is dependent on availability of glycine. Administration of glycine was shown to increase excretion of conjugated salicylic acid and, therefore, elimination of salicylates.[274]

Intravenous fluids to replace volume, induce diuresis, provide $NaHCO_3$, and replace K^+ must be administered cautiously. Increased capillary permeability predisposes these patients to noncardiogenic pulmonary edema, as well as cerebral edema.[167]

If salicylate intoxication is severe and associated with progressive metabolic and/or neurologic derangements, hemodialysis should be used and can be life-saving.[69] Dialysis is also required in those patients who develop acute renal failure or have preexisting renal disease. Hemodialysis very efficiently removes salicylate and corrects metabolic acidosis, electrolyte abnormalities, and volume status. Charcoal hemoperfusion is equally effective as hemodialysis.[134] Peritoneal dialysis, however, is only about one-fourth as effective as hemodialysis[344] and is not recommended as a treatment option.

Uremic Acidosis

As renal mass decreases, several interrelated abnormalities account for the development of metabolic acidosis. Net renal acid excretion (NH_4^+ + titratable acid $- HCO_3^-$) must equal net systemic acid generation to maintain acid balance. Renal insufficiency affects each component of net acid excretion. First, renal ammonia production decreases progressively as nephron mass is reduced.[102] In addition to decreased renal ammonia synthesis, the countercurrent medullary NH_4^+ gradient, which is critical for normal NH_4^+ excretion, becomes deranged. Low ammonia concentrations in the deep medulla decrease ammonia entry into the collecting ducts. The development of hyperkalemia also contributes to the reduction in NH_4^+ synthesis and excretion. Although the ammonia excretory rate—factored for GFR—increases, the absolute ammonia excretory rate falls markedly[102] because of the reduced nephron mass.

Decreased NH_4^+ excretion forces the kidney to become dependent on titratable acid to maintain acid balance. Titratable acid formation is a function of urine pH and the urine concentration of titratable buffers, especially phosphate. As the GFR declines, phosphate excretion may remain relatively constant as a result of increased parathyroid hormone and phosphorus levels. However, when the GFR falls below 25–30 ml/min, phosphorus clearance is generally reduced. Low phosphorus intake, the use of phosphorus binders, and calcium phosphate depositional disease will further depress renal phosphorus excretion.

Despite chronic renal insufficiency, renal tubules usually maintain the ability to acidify the urine maximally.[147,282,295,318,330] For varying periods of time, increased titratable acid excretion can offset the reduction in NH_4^+ excretion. Later, as titratable acid falls, in part due to decreased phosphate excretion, net acid excretion falls below net acid generation and metabolic acidosis ensues.

The third element of net acid excretion is excretion of HCO_3^-. Proximal tubule HCO_3^- reabsorption has been reported to be high, normal, and low with chronic renal failure.[14,216] Chronic renal failure may increase proximal tubule Na^+/H^+ antiporter activity, contributing to enhanced HCO_3^- reabsorption.[77] On the other extreme, proximal tubule HCO_3^- reabsorption may fall for several reasons in these patients. Volume expansion, hyperparathyroidism, solute diuresis, and overperfused residual nephrons may all reduce proximal HCO_3^- eabsorption. However, when patients with overt volume expansion are excluded or Na^+ is restricted from the diet, the HCO_3^- reabsorptive capacity of most patients with renal insufficiency is relatively normal.[14,216] Nevertheless, the aforementioned factors probably increase the fraction of filtered HCO_3^- delivered to the distal tubule, where it is reabsorbed. To the extent that this occurs, limited distal H^+ secretory capacity is utilized for HCO_3^- reabsorption rather than generation of titratable acid and NH_4^+. The consequence of this abnormal physiology can be demonstrated when metabolic acidosis in uremic patients is reversed with exogenous HCO_3^- that is then stopped.[316] The subsequent decline in serum [HCO_3^-] is more rapid than expected from the accrual of endogenous fixed acids. In these subjects, the urine pH often becomes alkaline and remains so until the serum [HCO_3^-] is reduced.[318] A relatively high urine pH combined with severely restricted NH_4^+ excretion results in a very low or negative net acid excretion. As the plasma [HCO_3^-] falls, distal HCO_3^- delivery decreases sufficiently to permit a reduction in luminal pH: titratable acid is again generated and urine pH may be maximally lowered. Occasional patients with chronic renal failure develop true HCO_3^- reabsorptive defects and spill a large fraction of filtered HCO_3^- when the plasma [HCO_3^-] is normal or slightly reduced.

Most patients with severe chronic renal failure generate normal amounts of endogenous acid unless dietary intake is markedly altered. However, their acid excretory rate is 10–20 mEq/day lower than their acid generation rate. Despite continued positive accrual of acid, the serum [HCO_3^-] usually stabilizes. This occurs because the excess acid is buffered by bone-derived alkali. It is likely however, that bone alkali is insufficient to compensate for the decrease in renal acid excretion at least in the long term. Whether increased gut organic anion absorption accounts for the needed base[360] remains to be established.

Most patients with uremic acidosis develop an anion gap elevation that approximates the reduction in [HCO_3^-]p. The excess anion gap is due to retention of phosphate, sulfate, and a variety of organic acids. These acids are generated by normal metabolic processes and the accumulated anions represent decomposed HCO_3^-. Anion retention largely reflects a reduction in the GFR. Thus, the metabolic acidosis is due to tubular malfunction, while the elevated anion gap is due to the GFR reduction. In many patients with renal failure, these two abnormalities progress in parallel, producing a 1:1 correlation between the increase in anion gap and decrease in HCO_3^-. However, with early renal failure (creatinine 2–4 mg/100 ml), a hyperchloremic pattern may develop. When the GFR falls below 20 ml/min, hyperchloremia usually recedes and is replaced by an increased anion gap.[374] Occasionally, hyperchloremic acidosis remains the dominant pattern until much later in the course. In these patients, hyperchloremic acidosis is usually due to a reduction in renal acid excretion that exceeds the fall in glomerular filtration. Sodium salts of fixed acids, representing decomposed sodium bicarbonate, are filtered and excreted. Normally, they would be excreted as NH_4^+ salts or with titratable acid; instead, they are excreted as Na^+ or K^+ salts. Hemodialysis can also generate a hyperchloremic component as organic and inorganic acid anions may be removed more rapidly than HCO_3^- is replaced. Combined anion gap and hyperchloremic acidosis in patients with renal failure is discussed in the section on plasma acid–base profile.

Congenital Organic Acidoses

Inborn errors of metabolism can result in organic acidosis due to the accumulation of lactic acid, the classic ketoacids (acetoacetic acid and beta-OH butyric acid), and a variety of other organic acid intermediates, including several long chain ketoacids. Tables 59.4 and 59.7 list the different causes of congenital organic

TABLE 59.4 Causes of Lactic Acidosis

Decreased ATP production
Circulatory failure
Volume depletion
Severe heart failure
Massive pulmonary emboli
Shock: sepsis, anaphylaxis, drugs (nitroprusside)
Tissue hypoxia
Acute respiratory failure
Carbon monoxide poisoning
Severe anemia
Methhemoglobinemia
Mitochondrial defects
Electron transport defects: carbon monoxide, cyanide, severe iron deficiency
Decreased oxidative phosphorylation: salicylate and 2,4-dinitrophenol intoxication
Mitochondrial enzyme defects: pyruvate carboxylase, pyruvate dehdrogenase, cytochrome oxidase defects, MELAS syndrome
Decreased pyruvate utilization: metformin, acute thiamin deficiency (beriberi)
Phosphate trapping: fructose, xylitol, sorbitol, glucose-6-phosphatase deficiency (von Gierke disease)
Other: nucleoside analogs (zidovudine, fialuridine), propofol
Lactate overproduction (with relative ATP deficiency)
Muscle hyperactivity
Severe exertion
Seizure
Exertional heat stroke
Strychnine poisoning
Hypothermia
Disseminated malignant neoplasia (leukemia, lymphoma)
Tumor lysis syndrome
Shock lung, ARDS
Gluconeogenetic enzyme defects
Glucose-6-phosphatase defect (von Gierke disease)
Fructose-1,6-diphosphatase defect
Catecholamine excess (iatrogenic, pheochromocytoma, cocaine poisoning)
Methanol
Ethylene glycol
Ethanol
Zinc phosphide
Decreased lactate utilization
Advanced liver disease
Sodium valproate
Germanium

TABLE 59.5 Contributions of Clinically Pertinent Solutes to Osmolality

Substance	Molecular Weight	Amount (mOsm/liter) Generated by Concentration of 100 mg/dl
Acetone	58	17
Ethanol	46	22
Ethyl ether	26	38
Isopropanol	60	17
Mannitol	182	5.5
Methanol	32	31
Ethylene glycol	62	16

acidosis. For more information, the reader is referred to textbooks dedicated to detailed discussions of inborn errors of metabolism or to the OMIM (Online Mendelian Inheritance in Man) database (www.ncbi.nlm.nih.gov/entrez).

D-Lactic Acidosis

Lactic acid exists in L- and D-optical stereo isomer forms. The L-optical isomer is generated and used in the cells of higher animals, whereas D-lactate is primarily a product of bacterial metabolism. D-Lactic acid is generated by bacteria in the gastrointestinal tract and is excreted into the stool. However, certain pathologic conditions may lead to systemic absorption of bacterial derived D-lactic acid. D-Lactate will then accumulate in the ECF because this compound is slowly metabolized.[157] This unique form of lactic acidosis can occur in short-bowel syndrome and after ileal–jejunal bypass operations. The disorder may be precipitated by the ingestion of carbohydrates, a systemic illness, or therapy that alters the enteric bacterial flora (i.e., broad-spectrum antibiotics, ingestion of yogurt or D-Lactobacillus tablets to treat diarrhea, and possibly the use of lactulose).

D-Lactic acidosis is commonly associated with CNS abnormalities, such as obtundation, confusion, and ataxia. These symptoms may represent a direct neurotoxic effect of D-lactate or may be a manifestation of some other organic acids or unidentified toxins.

The diagnosis of D-lactic acidosis should be considered in patients with gastrointestinal pathology who develop otherwise unexplained anion gap metabolic acidosis. The enzymatic assay for lactic acid uses stereospecific L-lactate dehydrogenase (L-LDH). Therefore, it will not detect D-lactic acid. The diagnosis of D-lactic acidosis can be established with an analogous assay using the enzyme D-LDH. D-Lactate can also be measured with lactic acid analytic techniques that are not stereospecific, such as gas–liquid chromatology.

Immediate treatment should include elimination of all oral intake of food and parenteral nutrition. Poorly absorbed antibiotics (vancomycin, neomycin, and kanamycin) or metronidazol are used to suppress intestinal flora in both the short term and long term. Low-carbohydrate diets or use of fructose or starch instead of glucose are also worth trying.[359]

TABLE 59.6 Treatment of Salicylate Poisoning

General support
Correction of electrolyte disturbances (potassium)
Glucose infusion (neuroglycopenia)
Elimination of toxin
Noninvasive methods
Activated charcoal (1–2 g/kg body weight initially, then 0.5–1 g/kg body weight every 2–4 hours (3–4 times)
Sodium bicarbonate: blood pH should be around 7.5, urine pH >8.0
Glycine, 8 g taken orally initially, 4 g every 2 hours for 16 hours
Invasive methods
(Gastroscopic) lavage in combination with activated charcoal before and after lavage
Hemoperfusion/hemodialysis

TABLE 59.7 Causes of Congenital Organic Acidosis (MIM Number)

Lactic acidosis
Glucose-6-phosphatase deficiency (glycogen storage disease 1, 322200)
Fructose-1,6-bisphosphatase deficiency (229700)
Phosphoenolpyruvate carboxykinase deficiency (261650)
Pyruvate carboxylase deficiency (312170)
Pyruvate dehydrogenase deficiency (608769)
Cytochrome oxidase defects (516030–516050)
Mitochondrial encephalopathy, lactic acidosis and stroke-like epilepsy (MELAS syndrome 540000)
Kearns-Sayer syndrome (KSS, 530000)
Myoclonic epilepsy with ragged fibers (MERRF, 545000)
Ketoacidosis
Hypervalinemia (277100)
Hyperleucin-isoleucinemia (238340)
Maple syrup urine disease (branched chain ketoaciduria, 238340)
Isovaleric acidemia (243500)
Mixed or other organic acidosis
Glutaric aciduria II (231680)
Ethyl-malonic-adipic aciduria (602473)
Propionicacidemia (606054)
Beta-methylcrotonyl-CoA-carboxylase deficienca (601557)
Methylmalonyl-CoA-mutase deficiency (277400)
Pyroglutamic acidemia (alpha oxoprolinuria, 260130)
Tyrosinemia I, III (276700, 276710)

MIM, Mendelian Inheritance in Man.

Hyperchloremic Metabolic Acidosis

Hyperchloremic acidosis develops when $NaHCO_3$ or other forms of alkali (i.e., Na ketone salts) is lost from the ECF, or HCl or other chloride salts that generate HCl are added to the ECF. Hyperchloremia occurs because the ECF contracts about a fixed quantity of chloride or because exogenous chloride (from NaCl, HCl, or other chloride salts) is added to the ECF. In many circumstances, both mechanisms are responsible. These mechanisms are further characterized in Anion Gap Acidosis and Hyperchloremic Acidosis. The differential diagnosis of hyperchloremic metabolic acidosis is listed in Table 59.3.

Hypokalemic Renal Tubular Acidosis

Proximal Renal Tubular Acidosis

The proximal tubule assumes a pivotal role in reclamation of filtered HCO_3^- and thus preservation of HCO_3^- stores. Around 80% of filtered bicarbonate (around 4 moles/day in a subject with normal GFR) is reabsorbed in this segment via processes that involve apical proton secretion (Na^+/H^+ exchange and ATP driven proton secretion) and basolateral HCO_3^- exit via sodium-coupled HCO_3^- transporters.

The low intracellular [Na^+] also energizes the reabsorption of other filtered solutes including glucose, phosphate, uric acid, amino acids, and organic anions. These compounds and anions are reabsorbed by specific Na^+-linked symporters.

Generalized dysfunction of proximal tubule transport results in $NaHCO_3$ excretion combined with glycosuria, phosphaturia, aminoaciduria, and so on. This combination of multiple proximal tubule defects defines the renal Fanconi syndrome (Lignac–de Toni–Debre–Fanconi syndrome). Less commonly, HCO_3^- wasting occurs as an isolated proximal tubule defect.

As illustrated in Fig. 59.18, a reduction in proximal tubule HCO_3^- reclamation will deliver a larger HCO_3^- load to distal tubule segments that have limited HCO_3^- reclamation capacity. The resulting $NaHCO_3$ diuresis reduces the [HCO_3^-]p and generates ECF volume depletion. Activation of the renin-angiotensin-aldosterone system stimulates distal tubule Na^+ reabsorption and K^+ secretion. Ingested NaCl is retained, partially reversing the ECF contraction. The net effect of these alterations is the development of a hypokalemic, hyperchloremic metabolic acidosis. Several factors combine to produce a steady-state and reestablish relatively normal fractional HCO_3^- reabsorption: (1) the low [HCO_3^-]p reduces the filtered HCO_3^- load. (2) The lower [HCO_3^-]p increases transcellular H^+ secretion and should decrease HCO_3^- back leak in the late proximal tubule. (3) Volume contraction increases HCO_3^- reabsorption. (4) Hypokalemia increases HCO_3^- reabsorption.

As fractional HCO_3^- reabsorption by the proximal tubule increases toward normal, a smaller quantity of $NaHCO_3$ is delivered to distal segments and is normally reabsorbed. Now, normal distal tubule acidification can proceed so that titratable acid and ammonia excretion return to normal. HCO_3^- decomposed by metabolic and dietary acids and HCO_3^- lost in stool can

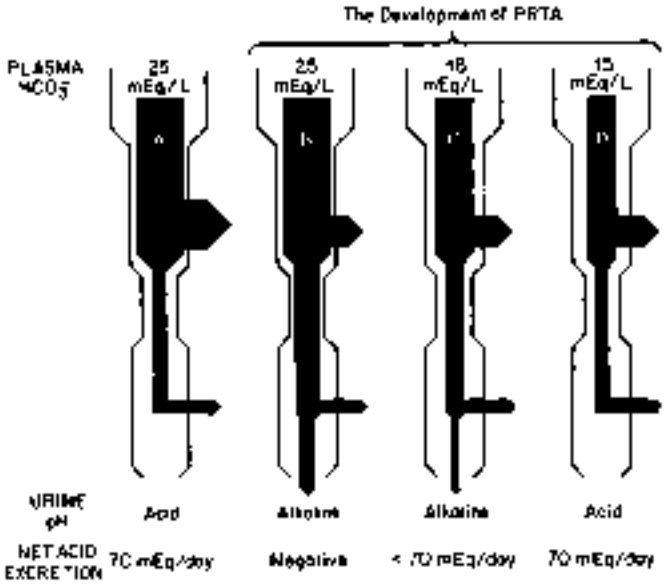

FIGURE 59.18 Schematic representation of the development of the proximal renal tubular acidification (PRTA) defect. (A) Normally, approximately 85% of the bicarbonate load is reabsorbed in the proximal tubule and the remaining 15% is reabsorbed in distal segments. As the urine is further acidified, net urine is generated. (B) The development of a proximal tubule acidification defect decreases the fraction of filtered bicarbonate reabsorbed in the proximal tubule (e.g., in this case, to 60%). Increased delivery of bicarbonate to the distal tubule overwhelms its bicarbonate reabsorptive capacity and leads to severe bicarbonaturia. An alkaline urine and negative net acid excretion result. (C) As the serum bicarbonate concentration declines, less bicarbonate is filtered and less is delivered to the distal tubule. The severity of the bicarbonaturia is decreased. (D) When the plasma bicarbonate is sufficiently reduced, proximal bicarbonate reabsorption is sufficient to reabsorb most of the filtered bicarbonate and thereby reduce distal tubule bicarbonate delivery. Under these conditions, the distal tubule can reabsorb the delivered bicarbonate and normally acidify the urine. In this new steady state, net acid excretion will again be equivalent to net acid production, albeit at the expense of a reduced serum bicarbonate concentration. *(Adapted from Ochwadt BK, Pitts RF. Effect of intravenous infusion of carbonic anhydrase on carbon dioxide tension of alkaline urine. Am J Physiol 1956;185:426–429.)*

now be regenerated by the kidney and acid balance is restored.

Potassium balance may also be restored when these patients achieve acid–base steady-state conditions. As the acidosis evolves, distal $NaHCO_3$ delivery combines with volume contraction and hyperaldosteronism to accelerate distal tubule K^+ secretion. In the steady state, dietary NaCl replaces $NaHCO_3$, restoring ECF volume. Aldosterone levels fall, distal $NaHCO_3$ delivery decreases toward normal, and K^+ secretion is reduced. Mild hypokalemia may persist, reflecting a total body deficit, but K^+ balance is restored and hypokalemia is rarely severe.[322] In the steady state, acid balance is reestablished, albeit at the expense of a lower plasma [HCO_3^-]. This is not true in patients with distal real tubular acidosis (RTA) or uremic acidosis. In those disorders, acid balance is persistently positive. This distinction may account, in part, for the differing skeletal manifestations that develop with these disorders. The skeleton plays a major buffering role in disorders associated with chronic positive acid balance. Thus, with distal RTA, skeletal dissolution helps stabilize the [HCO_3^-]p but also releases Ca^{2+} and Mg^{2+}, which are excreted into the urine. Acidemia (low luminal pH) also reduces renal tubular Ca^{2+} reabsorption.[206] Consequently, overt hypercalciuria develops in about one third of patients with distal RTA.[45] This is in part the reason these patients develop nephrocalcinosis and nephrolithiasis (other contributing factors include hypocitraturia and an alkaline urine pH—discussed later). These patients also develop osteomalacia and children have impaired skeletal growth. Skeletal mobilization of alkaline calcium salts also develops in other chronic metabolic acidoses associated with positive acid balance, such as uremic acidosis. In contrast, isolated proximal RTA does not mobilize skeletal buffers, perhaps because acid balance is reestablished. Hypercalciuria does not develop in these patients; first, because skeletal mobilization does not occur. Second, the increased delivery of HCO_3^- to the distal tubule will stimulate distal Ca^{2+} reabsorption despite systemic acidemia.[285] Furthermore, the two other factors that contribute to nephrocalcinosis and nephrolithiasis in patients with distal RTA also do not occur in those with proximal RTA. Patients with proximal RTA are able to acidify their urine when they are in a steady state and have relatively high urine citrate excretion. The importance of citrate to urine calcium solubility was discussed earlier (Effects of Metabolic Acidosis on Renal Citrate Metabolism section) and subsequently in relationship to distal RTA. Although systemic acidosis and K^+ depletion usually decrease urine citrate excretion, proximal RTA is an exception to this rule. A generalized defect in proximal tubule organic anion reabsorption apparently offsets any tendency to reduce urine citrate excretion (see Hypokalemic Distal Renal Tubular Acidosis section). Thus, nephrocalcinosis and nephrolithiasis are distinctly uncommon in patients with proximal RTA.[221] When phosphate wasting and vitamin D abnormalities complicate proximal RTA, skeletal pathology including rickets and osteomalacia may develop.

Recently, a few patients with isolated proximal tubular acidosis were found to have impaired ammonium excretion when confronted with acid load.[42] These patients could theoretically be in chronic positive acid balance. It remains to be seen whether the defect in this patient segment is decreased ammoniagenesis in the proximal tubule and/or additional more distal

effects such as the one caused by carbonic anhydrase II deficiency in type 3 RTA. Table 59.8 lists the many causes of proximal RTA.

Primary Proximal Renal Tubular Acidosis

Primary proximal RTA is defined as the occurrence of the tubule defect or defects in the absence of any other underlying process or etiology. Primary proximal RTA occurs in children and much less commonly in adults. Idiopathic proximal RTA of children often improves with time.[265,301] Proximal HCO_3^- wasting may be isolated or occur together with full-blown Fanconi's syndrome. Autosomal dominant, autosomal recessive, and sex-linked inheritance patterns have been reported.[43,125]

In autosomal dominant proximal RTA no genetic defect has been reported. The gene encoding NHE-3 (SLC9A3) is considered a candidate as SLC9A3 knock-out mice have combined renal and intestinal defects in HCO_3^- (re)absorption.

In autosomal recessive proximal RTA with ocular abnormalities several mutations in the gene SLC4A4, encoding for the kidney Na/HCO_3 cotransporter (kNBC1) have been described. kNBC1 is localized on the basolateral membrane of the proximal tubule and is—acting in series with the luminal Na/H antiporter (NHE-3)—part of the major pathway of HCO_3^- reabsorption in the proximal nephron. This type of RTA presents with growth failure, and ocular abnormalities (band keratopathy, cataracts, glaucoma) and mental retardation. The ocular and brain abnormalities are consistent with the finding that kidney isoform kNBC1 is also expressed in various ocular tissues and the brain.[186]

No genetic defect has been reported for proximal RTA with sex-linked inheritance.

Inherited Mixed Renal Tubular Acidosis

Various genetic defects of the carbonic anhydrase II gene (CA II) have been described. Patients with this deficiency exhibit a mixed form of tubular acidosis with proximal and distal components, retarded growth, osteopetrosis and cerebral calcifications. Bone marrow or stem cell transplantation corrected only the extrarenal manifestations of this disorder.[8] CA II is known to be expressed by osteoclasts and in proximal and distal nephron segments explaining the increased bone mass and the mixed acidosis with features of both HCO_3^- wasting and defective H^+ secretion. Heterogeneity exists among different defects and the severity of the osteopetrotic phenotype. The metabolic acidosis in these patients is assumed to counteract—albeit incompletely—excessive bone thickening generated by the CA II-dependent inhibition of osteoclast activity.[373]

TABLE 59.8 Causes of Proximal Tubular Acidosis (RTA II)

- Primary
  - Hereditary
    - Autosomal-dominant
    - Autosomal-recessive with ocular abnormalities (SLC4A4, kNBC1 deficiency)
    - Sporadic
  - Transient in infancy
    - Mixed-type RTA (type III, with additional distal RTA)
    - Autosomal recessive with osteopetrosis (carbonic anhydrase II, CA II deficiency)
- Secondary
  - Genetic—familial
    - Disorders of amino acid metabolism: cystinosis, tyrosinemia
    - Disorders of carbohydrate metabolism: galactosemia, hereditary fructose intolerance, glycogen storage disease with Fanconi syndrome
    - Wilson's disease (copper accumulation)
    - Lowe syndrome (oculo-cerebral-renal syndrome)
    - Metachromatic leukodystrophy
  - Dysproteinemic states
    - Multiple myeloma
    - Light-chain disease
    - Monoclonal gammopathy
    - Amyloidosis
  - Excess parathyroid hormone
    - Primary hyperparathyroidism
    - Secondary hyperparathyroidism: renal failure, vitamin D deficiency, abnormal vitamin D metabolism
  - Drugs−chemicals
    - Carbonic anhydrase inhibitors: acetazolamide, mafenide (Sulfamylon)
    - Ifosfamide
    - Tacrolimus (FK 506)
    - Lithium
    - Streptozotocin
    - Methyl-3-chromonew
    - Maleic acid
    - D-Serine
    - Toluene (glue sniffing)
    - Cadmium
    - Lead
    - Mercury
    - Outdated tetracycline
  - Interstitial renal disease
    - Sjögren syndrome
    - Medullary cystic disease
    - Post-transplant (rejection)
    - Chronic renal vein thrombosis
    - Balkan nephropathy
  - Miscellaneous
    - Malignancy
    - Nephrotic syndrome
    - Paroxysmal nocturnal hemoglobinuria (iron deposition)
    - Congenital heart disease
    - Bone fibroma

Secondary Proximal Renal Tubular Acidosis

The secondary varieties of proximal RTA with and without Fanconi's syndrome occur more commonly than the primary forms. Many secondary forms are

associated with hereditary abnormalities of amino acid or carbohydrate metabolism.

Cystinosis is an autosomal recessive lysosomal storage disease caused by mutations in the lysosomal cystine transporter CTNS. Defects in the transporter lead to intracellular cystine accumulation, widespread cellular destruction, Fanconi's syndrome, renal glomerular failure later in childhood. This disorder remains the most common childhood cause of Fanconi's syndrome[379] (see: www.ncbi.nlm.nih.gov/entrez/dispomim.cgi?id = 219800). Treatment with oral cysteamine (beta-mercaptoethylamine), a free thiol that reduces lysosomal cysteine levels and can prevent or delay the complications of cystinosis. A FISH-based method for early molecular diagnosis of the most common 57 kb CTNS deletion mutation is available.[28]

Other organs, including the liver, spleen, and pancreas, muscles, and CNS also accumulate cystine and may develop abnormalities. Occasional patients have a very benign clinical course with minimal renal involvement. Such patients who are asymptomatic may be diagnosed during routine ophthalmologic evaluation when ocular cystine deposits are noted.

Other inherited disorders of amino acid or carbohydrate metabolism such as type I tyrosinemia, galactosemia, and fructose intolerance are listed in Table 59.8. Patients with the X-linked hereditary nephrolithiasis syndrome (Dent's disease) have features of a generalized proximal tubule disorder such as low molecular weight proteinuria, aminoaciduria, and phosphaturia. Interestingly, however, acidosis is not observed in this disease caused by a defect in one of the chloride channel genes (CLCN5).[229]

Lowe's syndrome (oculocerebral syndrome) also exhibits features of Fanconi's syndrome and is caused by mutations in OCRL1, encoding a phosphatidylinositol 4,5-bisphosphate (PIP2) 5-phosphatase (www.ncbi.nlm.nih.gov/entrez/dispomim.cgi?id = 309000). Some mutations in OCRL1 do not cause classical Lowe's syndrome but rather develop a Dent's phenotype without acidosis.[172] The reason and mechanism of this phenotypic heterogeneity remain to be elucidated.

Multiple myeloma is the most common cause of acquired adult Fanconi's syndrome. Some Bence Jones proteins, which are reabsorbed and catabolized by proximal tubule cells, are toxic to these cells.[306,333] Patients with isolated light chain disease,[118,163] benign monoclonal gammopathy,[163] and Bence Jones–protein associated amyloidosis[118,163] have developed Fanconi's syndrome. Fanconi's syndrome occurs more commonly in disorders with monoclonal κ light chains than those with λ light chains. In adult patients with apparent "idiopathic" Fanconi's syndrome the diagnosis of multiple myeloma should always be considered because occult forms of myeloma may become overt years after development of the renal dysfunction.

Primary hyperparathyroidism has been associated clinically with hyperchloremic metabolic acidosis[25,243,261] and large doses of PTH have been shown to suppress proximal tubule HCO_3^- reabsorption at least in part by inhibiting Na^+/H^+ exchange.[284,306] However, experimentally induced chronic PTH excess in humans induces only a transient metabolic acidosis followed by a mild metabolic alkalosis, both generated and maintained by a renal mechanism.[177] Thus, the clinically observed acid–base disturbances in primary and secondary hyperparathyroidism are not the result of isolated proximal PTH action, but rather constitute the final consequence of many, in part opposing mechanisms such as more distal effects of PTH, alkali recruitment from bone, hypercalcemia (which stimulates renal H^+ secretion), phosphaturia, underlying or associated renal disease and secondary changes in 1,25 $(OH)_2D$ levels.[179]

Fanconi's syndrome may develop in individuals with vitamin D deficiency and other disorders of vitamin D metabolism.[154] Secondary hyperparathyroidism often complicates these disorders and may contribute to the tubule dysfunction. Hypocalcemia and hypophosphatemia may also alter proximal tubule function. Administration of appropriate vitamin D metabolites can ameliorate or correct Fanconi's syndrome.

Pharmacologic inhibition of membrane-bound carbonic anhydrase IV in the proximal tubule lumen will generate proximal RTA and have a diuretic effect.[74] Such diuretics are especially useful in patients with metabolic alkalosis. They are also used to reduce intraocular pressure in patients with glaucoma.

Drugs and toxins can damage proximal tubule cells. Outdated tetracycline was responsible for several Fanconi's syndrome epidemics.[127,153] Ifosfamide and tacrolimus (FK506) were reported to cause proximal tubular acidosis in children.[275,330] Fanconi's syndrome was also described in HIV^+ patients, but the pathogenesis (i.e., side effects of drugs therapy, etc.) was not investigated. Aristolochic acid, an ingredient in Chinese herbs, is also believed to be a causal agent in Fanconi's syndrome.[383] Chronic exposure to heavy metals, such as cadmium, lead, and mercury, damages the proximal tubule and can lead to proximal RTA.[70,71,145,219] Damage due to copper deposition with Wilson's disease has already been noted.[375] Other toxins such as D-serine, toluene (glue sniffing), maleic acid, and methyl-3-chromone may also damage proximal tubule cells.[133,162,283]

A variety of interstitial renal diseases, including Sjögren's syndrome, medullary cystic disease, kidney transplant rejection,[377] Balkan nephropathy, and

chronic renal vein thrombosis,[63] have been associated with Fanconi's syndrome.

Some patients with nephrotic syndrome develop proximal tubule abnormalities.[39] Tubule function may be adversely affected by a large reabsorbed protein load. However, uncomplicated nephrotic syndrome does not usually produce proximal tubule defects. When nephrotic syndrome is complicated by renal vein thrombosis, proximal tubule defects become more common.[63] The added vascular insult may increase interstitial damage and lead to the proximal tubule dysfunction. Immunologic tubule injury may also contribute to tubule dysfunction in these patients.

Malignancy may be associated with proximal tubular dysfunction. Fanconi's syndrome has been identified in patients with monocytic and myelomonocytic leukemia as well as lymphoma.[143] Isolated renal tubule uric acid and amino acid wasting can occur with Hodgkin's disease and lung cancer.[29,371]

Hypokalemic ("Classic") Distal Renal Tubular Acidosis

Patients with hypokalemic distal RTA cannot generate a maximally acid urine (<5.5) despite spontaneous or induced metabolic acidosis. This reduces titratable acid and ammonium excretion and results in positive acid balance. Hyperchloremic acidosis, usually associated with hypokalemia and hypercalciuria, ensues. Proximal reabsorption of HCO_3^- and other solutes is preserved. Generalized distal tubule dysfunction is not present, as affected patients tend to be hypokalemic.

In inherited or primary forms of distal RTA, the transport defects in the alpha intercalated cells of the medullary collecting duct are responsible pathogenetically. In these cells, mutations of the genes encoding for the vacuolar H^+-ATPase and basolateral Cl^-/HCO_3^- exchanger (kAE1) have been identified. An additional candidate is the gene for the H^+/K^+-ATPase expressed in cortical and outer medullary collecting duct cells.

The precise localization of the defect(s) in the distal segments and the cellular basis for acquired, classic distal renal tubular acidosis are not well defined and probably heterogeneous. Phenomenologically, the distal acidification defect can be due to abnormal proton secretory pumps that decrease distal H^+ secretion, increase distal tubule permeability to H^+ (which leaks back), or increase HCO_3^- permeability (which leaks into the lumen). Absence of H^+-ATPase in the collecting duct has been found in some, but not all examined patients with Sjögren's syndrome and distal RTA.[89] Candidate transporter defects are H^+-ATPase and basolateral Cl/HCO_3^- in type A intercalated cells and H^+/K^+-ATPase in cortical and outer medullary collecting duct cells (see Primary Distal Renal Tubular Acidosis section). Absence of H^+-ATPase in the collecting duct has been found in some, but not all examined patients with Sjögren's syndrome and distal RTA.[89]

Sodium and potassium wasting are prominent features of distal RTA and result from complex mechanisms. Normally, 50–100 mEq of net acid are produced daily from dietary precursors, metabolic generation, and stool alkali losses. The acid anions, such as PO_42^-, SO_42^-, and Cl^-, transiently replace decomposed HCO_3^- in the ECF. Normally, the kidney filters these anions as Na^+ salts and then reabsorbs the Na^+ in exchange for H^+, which generates NH_4^+ or titratable acid. Thus, regenerated HCO_3^- is returned to the ECF together with Na^+, while the acid anion is excreted into the urine together with a proton. Decomposed bicarbonate is regenerated when the proton and anion are excreted. Excretion of NH_4^+ and the anion or titratable acid and the anion is equivalent, from the acid–base perspective, to excretion of the original acid itself.

Impaired distal H^+ secretion decreases the excretion of these anions as acids and increases their excretion as Na^+ or K^+ salts. ECF contraction and metabolic acidosis result. Acidosis further decreases proximal sodium reabsorption aggravating activation of the renin–angiotensin–aldosterone axis and thus augmenting distal tubule Na^+ reabsorption and K^+ secretion. Histological damage to the medullary collecting duct might also contribute to potassium losses. Dietary NaCl is retained and partially ameliorates the ECF contraction. The net effect is hyperchloremic acidosis and hypokalemia.

Chronic metabolic acidosis and chronic positive acid balance activate skeletal buffering mechanisms. As bone is mobilized, alkali, calcium, magnesium, and phosphate are added to the ECF. This accounts, in part, for the hypercalciuria that develops in many patients with distal RTA. In addition, systemic acidemia may reduce renal tubule calcium absorption in the distal convoluted tubules. Stone formation and renal calcification are commonly observed in untreated distal RTA patients.

The acidosis-induced negative calcium balance observed in distal RTA and, in addition, direct effects of acidosis on bone (inhibition of osteoblasts and stimulation of osteoclasts) (see Role of Bone section), have been shown to effectively decrease bone mass (which can then be improved by alkali treatment).[101] The prevalence of distal RTA in otherwise unexplained "primary" osteoporosis is unknown. However, incomplete distal RTA was found in 9 out of 48 patients with osteoporosis, where other secondary causes had been excluded.[369]

Another important factor that contributes to renal calcification and stone formation is renal citrate

excretion. For the reasons discussed earlier, citrate excretion is greatly diminished in metabolic acidosis. As discussed previously, one exception to this general response to acidosis and acidemia is proximal RTA. The diffuse tubule dysfunction, which commonly occurs together with proximal RTA in Fanconi's syndrome, reduces citrate absorption and thereby increases its renal excretion. This may not be true of pure proximal RTA without any element of Fanconi's syndrome. The proximal RTA produced by acetazolamide decreases urine citrate excretion and is associated with renal calcification.[329]

Citrate is an important calcium chelator that solubilizes urinary calcium.[88,262,273] Low urine citrate levels, a high urine pH (which increases calcium phosphate precipitation), and hypercalciuria combine to produce nephrolithiasis and nephrocalcinosis in patients with distal RTA (see Effects of Metabolic Acidosis on Renal Citrate Metabolism section).

Additional clinical features of distal RTA include secondary erythrocytosis (due to increased erythropoietin concentrations[6]) and renal cyst formation.[187] The pathogenesis of both increased erythropoietin secretion and cyst formation is unknown. Table 59.9 lists disorders associated with distal renal tubular acidosis.

TABLE 59.9 Causes of Distal Renal Tubular Acidosis

Primary
Autosomal-dominant distal RTA (type Ia): defect of AE1 (SLC4A1)
Autosomal-recessive distal RTA with sensorineural deafness (type Ib): defect of B1 subunit of H + ATPase, ATP6V1B1
Autosomal-recessive distal RTA without sensorineural deafness (type Ic): Defect of a4 subunit of H + ATPase, ATP6V0A4
Autosomal-recessive, unclassified: rare AE1, SLC4A1, mutations
Mixed RTA (type III) with osteopetrosis: defect in carbonic anhydrase II (CA II)
H^+/K^+-ATPase defect
Secondary to genetically transmitted diseases
Ehlers–Danlos syndrome
Hereditary elliptocystosis
Sickle cell disease
Carbonic anhydrase deficiency
Medullary cystic disease
Wilson's disease
Fabry's disease
Hereditary hypercalciuria
Hereditary fructose intolerance
Familial hypergammaglobulinemia
Secondary to autoimmune disorders
Polyconal hypergammaglobulinemia
Hyperglobulinemic purpura
Cryoglobulinemia
Sjögren syndrome
Thyreoiditis
Pulmonary fibrosis
Chronic active hepatitis
Primary biliary cirrhosis
Systemic lupus erythematosus
Arteritis
Hypercalciuria
Primary hyperparathyroidism
Vitamin D intoxication
Hyperthyroidism
Idiopathic hypercalciuria
Medullary sponge kidney
Drugs and toxins
Amphotericin B
Lithium
Vanadate
Toluene (glue sniffing)
Analgesics
Cyclamate
Tubulointerstitial disease
Balkan nephropathy
Chronic pyelonephritis
Obstructive uropathy
Renal transplantation
Leprosy
Jejuno–ileal bypass with oxaluria
Miscellaneous
Hepatic cirrhosis
Empty sella syndrome
Osteopetrosis

Primary or Inherited Distal Renal Tubular Acidosis

Both autosomal-dominant and autosomal-recessive inheritance patterns exist in primary distal RTA. The phenotypic spectrum is large and ranges from asymptomatic, mild acidosis, incidental renal stones or renal calcifications to severe metabolic acidosis, stunted growth, rickets or osteomalacia and early nephrocalcinosis with renal failure. In general, dominant forms are associated with a milder phenotype.[193]

Autosomal dominant distal RTA (type Ia, [O]MIM 179800) occurs in patients who are heterozygous for mutations in the SLC4A1 gene encoding for the kidney anion exchanger AE1 (kAE1).[194] kAE1 is expressed on the basolateral surface of type-A intercalated cells in the collecting duct and mediates HCO_3^- reabsorption via Cl^-/HCO_3^- exchange. Several mutants have been identified, which, surprisingly, retain near normal transport function, but seem to be mistargeted away from their proper basolateral destination.[199,305] Thus, the mutations described thus far identify autosomal-dominant distal RTA as a protein trafficking disorder.

The erythroid Cl^-/HCO_3^- exchanger (band 3, eAE1) is the product of the same gene. Defects in this gene lead to spherocytosis. However, erythroid disorders associated with AE1 mutations exhibit no concurrent renal dysfunction, while patients with autosomal-dominant distal RTA lack erythroid abnormalities. The only human exception is one single case with complete deficiency of the eAE1 polypeptide (band 3 Coimbra) exhibiting clinically both phenotypes (i.e., severe hemolytic anemia and distal RTA).[297] The mechanisms

by which a particular mutation in the AE1 gene leads to the clinical phenotype of either spherocytosis or distal RTA remain to be elucidated.[324]

Recessive distal RTA is genetically heterogeneous and occurs with and without sensorineural deafness. Both affected genes encode for subunits of the apical proton pump (H^+-ATPase) in type A intercalated cells. In distal RTA, type Ib (MIM 267300), with sensorineural deafness, B1 subunit gene of the H^+-ATPase is affected by various mutations (ATP6V1B1).

A similar phenotype with milder sensorineural deafness manifested in adulthood, occurs as the result of several mutations in the a4 subunit of the proton pump (ATP6V0A4).[343] Deafness is thought to result from hair cell damage due to changes in the acid−base and electrolyte milieu of the endolymph. Epithelial cells surrounding the endolymphatic space express the H^+-ATPase. The high potassium concentration in endolymph (around 140 mmol/liter) creates a positive endolymph potential that results in passive proton efflux. To maintain pH at around 7.40 active proton transport into the endolymph is necessary. Accordingly, systemic alkali treatment corrects acidosis in these patients but apparently cannot prevent progressive loss of hearing.[50]

Autosomal-recessive distal RTA with normal hearing (distal RTA, type Ic, MIM 602722) is caused by mutations in the ATP6N1B gene, which encodes for an 840−amino acid, kidney-specific isoform of ATP6N1A. The encoded protein constitutes a noncatalytic, accessory subunit of the proton pump.[331]

One reported case of a child with renal and probably intestinal K^+ wasting, distal RTA, renal magnesium wasting may represent the first example of an inherited deficiency in the colonic H^+/K^+-ATPase.[328] However, no genetic analysis is currently available. Acquired forms of classical distal RTA lend further support to the identification of H^+/K_+-ATPase as a candidate gene: vanadate, an inhibitor of H,K-ATPase, but not vacuolar H^+-ATPase, causes hypokalemic distal RTA and decreased H^+/K^+-ATPase activity in rats.[83] Also, vanadate contamination of drinking water has been linked to endemic hypokalemic distal RTA in Thailand.[271] Rat models of distal tubular acidosis induced by urinary tract obstruction or lithium were recently associated with decreased H^+/K^+-ATPase activity in the medullary collecting duct, with enhanced or unchanged activities in the cortical collecting duct.[108] Thus, acquired or congenital defects in H^+/K^+-ATPase may cause classical distal RTA.

Mice lacking the K-Cl cotransporter Kcc4 exhibit deafness and renal tubular acidosis. Apart from the inner ear, Kcc4 is expressed—as are H^+-ATPase and kAE1—in type A intercalated cells of the medullary collecting duct and may be necessary for basolateral chloride extrusion (permitting continued basolateral CL^-/HCO_3^- exchange). A human disorder has not been described, but this finding supports the central role of the alpha-intercalated cells in the pathogenesis of distal RTA and establishes the K-Cl cotransporter Kcc4 as an additional candidate gene for primary, distal RTA.[36]

Secondary Distal Renal Tubular Acidosis

As described previously, distal RTA can lead to hypercalciuria and nephrocalcinosis. However, distal RTA can also result from tubular damage caused by hypercalciuria and nephrocalcinosis of any cause. Reported causes include hyperparathyroidism,[296] hypervitaminosis D,[114] and hyperthyroidism.[185]

Distal RTA occurs frequently in patients with autoimmune diseases. Kidney biopsies often reveal lymphocytic interstitial nephritis,[151] which may be responsible for the acidification defect. This form of RTA occurs in patients with Sjögren syndrome,[111,348] chronic active hepatitis, and primary biliary cirrhosis.[141,285] Lymphocytic cytotoxicity specific to renal tissue and autoantibodies directed to renal collecting duct cells have been identified in several such patients.

Several drugs and toxins can produce distal RTA. Amphotericin B, a cation-selective ionophore and may increase H^+ back leak. Unlike most other forms of distal RTA, the capacity to generate a normal U-B pCO_2 gradient is maintained[103,105,248,340] (see Diagnosis of Proximal and Hypokalemic Distal Renal Tubular Acidosis section). Other drugs and toxins, including toluene,[23,263] analgesics,[338] and cyclamates[384] can produce distal RTA. They probably act through a variety of different mechanisms. Toluene thus causes both distal and proximal tubular acidosis, but organic acidosis by overproduction of hippuric acid resulting from the metabolism of toluene is an additional factor in the genesis of metabolic acidosis.[65]

A variety of tubulointerstitial diseases may produce distal RT. Transplanted kidneys can develop both proximal and distal RTA.[24,32,259,377] Transient proximal RTA occurs frequently in the immediate posttransplant period. Distal acidification defects may occur months to years after the transplant. The distal defect may be secondary to chronic cellular rejection.[259] Batlle et al.[24] studied renal acidification defects in transplant patients and identified a number of pathogenic mechanisms. Multiple defects were also found when distal RTA developed in patients with chronic obstructive uropathy.[20] The abnormalities included intrinsic acidification defects, decreased renin (and aldosterone) production, and renal resistance to aldosterone.

As indicated previously, a form of endemic distal RTA was identified in Thailand[270] that has been linked

to vanadate contamination of drinking water. Affected subjects are at high risk for sudden (nocturnal) death probably caused by cardiac arrhythmias due to potassium depletion. The relatively high prevalence of hypokalemic periodic paralysis in the same population may increase the frequency of severe hypokalemic side effects.[271]

Patients with early or incomplete distal RTA may not manifest the full-blown syndrome. These patients cannot normally acidify their urine and therefore excrete reduced quantities of titratable acid. However, they maintain apparently normal acid–base balance by increasing renal ammonia excretion, decreasing citrate excretion and increasing bone buffering.[55,350] Patients with incomplete distal RTA are often discovered during a family screening when a relative with classic distal RTA is diagnosed. They may also be identified during nephrolithiasis evaluation. These patients are not acidemic, but they are hypercalciuric and have low urine citrate levels. Therefore they develop renal stones and nephrocalcinosis. Oral alkali therapy will increase urine citrate, reduce urine calcium, and decrease stone formation and nephrocalcinosis.

Diagnosis of Proximal and Hypokalemic Distal Renal Tubular Acidosis

A hypokalemic, hyperchloremic, low bicarbonate pattern is consistent with a diagnosis of proximal or hypokalemic distal renal tubular acidosis. Chronic respiratory alkalosis can produce an identical plasma electrolyte pattern as metabolic acidosis and must be ruled out by the history, physical examination, and arterial blood gas analysis. The anion gap provides a differential clue. It tends to be slightly reduced with hyperchloremic acidosis (as a result of proton buffering by albumin, which decreases its negative charge) and slightly increased by respiratory alkalosis (as a result of increased organic acid levels and decreased proton buffering by albumin increasing its negative charge).

If acidosis is confirmed, other forms of hyperchloremic metabolic acidoses, especially acidosis secondary to diarrhea, must be excluded usually by the history. Before embarking on an extensive and expensive evaluation of renal acidification defects and their underlying disease states, it is necessary to determine if the acidosis is of renal or extrarenal origin. In the typical clinical circumstance, there is usually some doubt regarding this classification when the patient is evaluated initially. This major differential diagnostic hurdle can be easily surmounted with a measurement of net acid excretion (NAE): elevated NAE correlates with extrarenal acidosis, and normal or reduced NAE with renal acidosis. In brief, the normal kidney responds to systemic acidosis by increasing NAE.

When RTA is the most likely possibility, the proximal and hypokalemic distal types must be differentiated. Patients with proximal RTA are able to normally acidify the urine once the $[HCO_3^-]p$ is reduced acutely to values below the renal threshold. In contrast, patients with hypokalemic distal RTA cannot normally acidify the urine whether the $[HCO_3^-]s$ is normal or markedly reduced. Therefore, while a UpH of less than 5.5 effectively rules out classic distal RTA, it is still compatible with a diagnosis of proximal RTA.

Diagnostic Tests for Distal RenalTubular Acidosis

Patients with distal RTA have low urine NH_4^+ excretion rates, which is a major reason they develop metabolic acidosis and positive acid balance. Reduced urine NH_4^+ excretion is partly due to decreased collecting duct trapping because of the high urine pH. In addition, the medullary countercurrent NH_4^+ concentration gradient is probably disrupted in many of these patients as a result of tubulointerstitial disease. The urine NH_4^+ excretion rate helps differentiate distal RTA from other forms of chronic hyperchloremic metabolic acidosis. Occasional patients with metabolic acidosis whose renal acidification mechanism is normal have a urine pH above 5.5 despite severe acidemia. Markedly increased renal ammoniagenesis and ammonia excretion in these patients raise the urine pH by virtue of NH_3's property as a diffusible base (Fig. 59.19B). Hypokalemia is an important stimulus to renal ammonia synthesis and excretion.[349] Therefore patients with chronic diarrhea and hypokalemic hyperchloremic metabolic acidosis may develop a high urine pH despite maximal renal acidification.[21] Although the high urine pH suggests a diagnosis of RTA, the high ammonia excretion rate rules out that possibility. The urine anion gap, defined as $UNa + UK - UCl$, estimates the urine $[NH_4^+]$.[142] Patients with metabolic acidosis whose $UCl > UNa + UK$ (i.e., negative urine anion gap) generally excrete more than 80 mEq/liter NH_4^+ in the urine, ruling out a diagnosis of distal RTA. When the $UCl < UNa + UK$ (i.e., positive urine anion gap), then urine NH_4^+ excretion is relatively low and a diagnosis of distal RTA is possible.[21,142] However, the interpretation of urine electrolytes and the urine anion gap will be confounded if large quantities of HCO_3^-, or organic anions, such as ketoacid salts, are present in the urine. Bicarbonate should be excluded by measuring urine pH, while ketosalts are excluded by the clinical circumstances and urine dipstick. It must be recalled that the urinary anion gap,

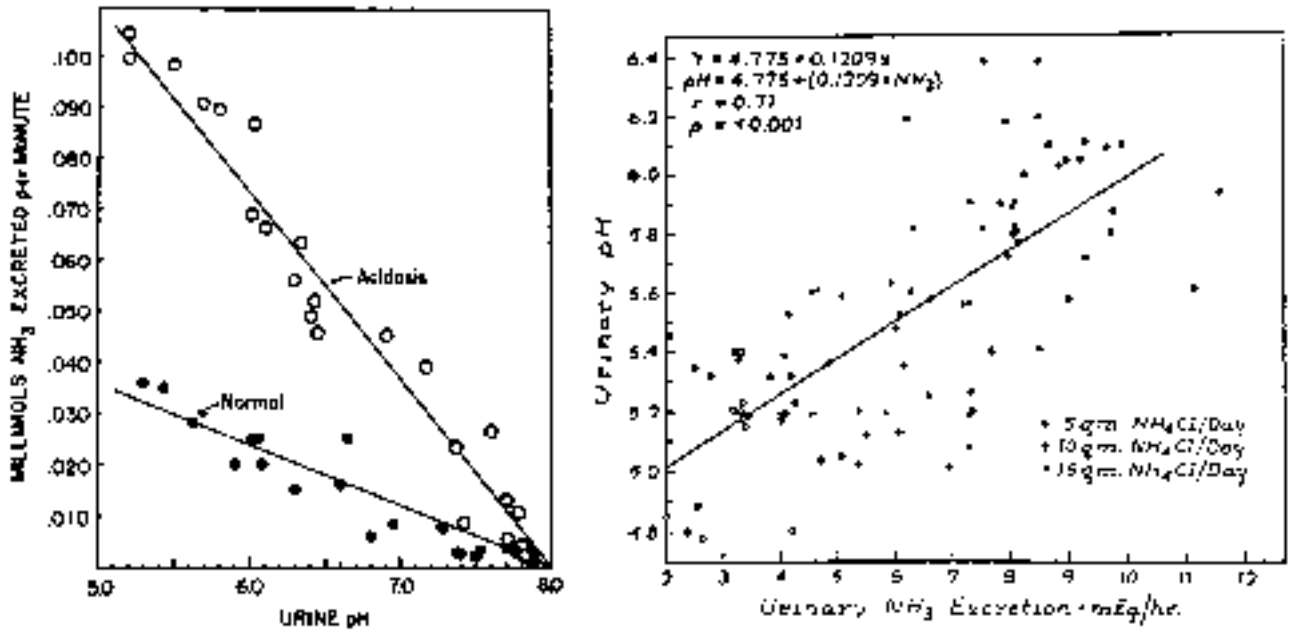

FIGURE 59.19 (A) The relation between urine pH and ammonia excretion in a single animal under conditions of normal acid–base balance in chronic acidosis. Urine pH was varied by the intravenous infusion of sodium bicarbonate. Note that the animal excretes a greater quantity of ammonia at any given urine pH under conditions of chronic acidosis. (*With permission, from Pitts RF. The renal excretion of acid. Fed Proc 1948;7:418.*) (B) The relationship between ammonia excretion and urinary pH during chronic NH_4Cl loads. As the chronic acid load was increased in stepwise fashion, mean urinary ammonia excretion increased. Note that the urine pH also increased progressively as the NH_4Cl load increased from 5 to 10 or 10 to 15 g/day. Thus, more severe chronic metabolic acidosis was associated with a higher urine pH, as well as higher ammonia excretion rates. *(With permission, from Madison LL, Mebane D, Unger RH, Lochner A. The hypoglycemic action of ketones. II. Evidence for a stimulatory feedback of ketones on the pancreatic beta cells. J Clin Invest 1964;43:408–415.)*

although often helpful for clinical diagnostic purposes, gives only crude estimates of renal NH_4^+ excretion.

Patients with incomplete distal RTA always require an acidification test to establish this diagnosis. By definition, these patients are not spontaneously acidemic under basal conditions.[55,110] The acid load should reduce the plasma $[HCO_3^-]$ by 4–5 mEq/liter. The most commonly used, standardized acidification test is ingestion of a single dose of NH_4Cl, 100 mg/kg body weight over 30–40 min. The NH_4Cl may first be dissolved in water to improve its absorption. Following ingestion of the NH_4Cl, sequential urine specimens are collected over six hours. The $[HCO_3^-]p$ is measured prior to and three hours after the oral NH_4Cl load and should decrease by 4–5 mEq/liter to document adequate NH_4Cl absorption and systemic acidification. The normal response to this acidosis is urine acidification with the pH falling below 5.5.

An alternative acidification test may be used when patients cannot tolerate ammonia loads (i.e., patients with hepatic insufficiency who may develop encephalopathy). The ingestion of $CaCl_2$ 2 mEq/kg will generate a metabolic acidosis.[281] Ingested $CaCl_2$ ionizes and within the intestine the Ca^{2+} binds CO_3^{2-} (principally from pancreatic secretions) to form relatively insoluble $CaCO_3$. Ingested Cl^- is absorbed in exchange for secreted HCO_3^-. The net effect of these reactions is the excretion of $CaCO_3$ into the stool and systemic acidification, equivalent to a NH_4Cl or HCl load.

Urinary tract infections and bacteriuria can confound the interpretation of urine pH measurements. Urease from bacteria split urea into CO_2 and NH_3. The NH_3 combines with H^+, which increases the urine pH. A diagnostic work-up for RTA, undertaken in the presence of a persistent urinary tract infection, mandates precautions to mitigate urine stasis by ensuring a rapid urine flow rate. Urine must be promptly collected and analyzed and potent bactericidal agents should be placed in the collection container. The (U-B) pCO_2 gradient can also be a helpful diagnostic tool under such circumstances.[104,105,160]

The gradient between urinary and blood pCO_2 [(U-B) pCO_2] after an intravenous $NaHCO_3$ load is probably proportional to distal tubule proton secretion and can be used as a diagnostic test for distal RTA. Pitts and Lotspeich[291] provided the experimental basis for this test: Bicarbonate loading delivers large quantities of $NaHCO_3$ to the distal tubule and stimulates proton

secretion. Owing to the absence of carbonic anhydrase, the H_2CO_3 that is generated does not rapidly dehydrate and instead is delivered to more distal tubule segments, the ureters and bladder. The H_2CO_3 relatively slowly dehydrates to form H_2O and CO_2 in these structures, where the medullary countercurrent system and surface-to-volume relationship are not favorable to rapid CO_2 dissipation. In consequence, the urine pCO_2 increases. Thus, a high urine−blood (U-B) pCO_2 gradient is accepted as evidence for distal tubule proton secretion.

Since the (U-B) pCO_2 gradient is influenced importantly by urinary pH, nonbicarbonate buffers, and HCO_3 concentration, it is best measured under standardized conditions, that is, during an intravenous $NaHCO_3$ load. $NaHCO_3$, at a concentration of 500 mEq/liter, is infused at 3 ml/min. The pH and pCO_2 of sequential urine specimens are determined. Steady-state urine values are usually achieved 2−4 hours after the infusion is initiated when the urine pH exceeds 7.5. At this time, the (U-B) pCO_2 gradient should be greater than 20−30 mm Hg.[23] Most patients with distal RTA cannot generate a normal gradient, which is consistent with the notion that most cases of distal RTA are caused by defective distal proton secretion. One exception is amphotericin-induced RTA, which likely is due to a H^+ back leak; such patients can generate a normal (U-B) pCO_2 gradient.[105]

Increased distal delivery of Cl^- (by administering furosemide) or SO_4^{2-} (by Na_2SO_4 infusion) can also be used to estimate distal H^+ secretion. Due to the low permeability of these anions in the collecting ducts, a more lumen negative transepithelial potential and thus a stimulus for H^+ (and K^+) secretion are created.[19,24]

In summary, distal RTA is generally confirmed by systemic acidemia, a relatively high urine pH, and a low ammonium excretion rate or—indirectly—a positive urinary anion. Other common features include nephrocalcinosis, nephrolithiasis, hypercalciuria and hypocitraturia.

Diagnostic Tests for Proximal Renal Tubular Acidosis

Patients with proximal RTA are able to normally acidify their urine if their $[HCO_3^-]p$ is adequately reduced. However, as the $[HCO_3^-]p$ is increased, for example, by administering exogenous $NaHCO_3$, urinary pH increases and bicarbonaturia develops while the $[HCO_3^-]p$ is still below the normal range. Intravenous HCO_3^- titration experiments are required to identify accurately proximal RTA. However, a diagnosis can usually be established with oral $NaHCO_3$ administration. Simultaneous measurement of urine and serum bicarbonate and creatinine concentrations permits the fractional bicarbonate excretion rate to becalculated:

$$[HCO_3^-]u \times [Cr]s/[HCO_3^-]s \times [Cr]u \times 100\% = \text{fractional excretion } HCO_3^-$$

Patients with proximal RTA excrete greater than 10−15% of the filtered HCO_3^- load as the $[HCO_3^-]p$ approaches normal.

Although isolated bicarbonate wasting can occur, most patients with proximal RTA have other proximal tubule reabsorptive defects. Glucose, amino acids, uric acid, lysozyme, beta-2-microglobulin, light chains, and other small proteins are abnormally excreted. Decreased phosphate reabsorption results in renal phosphate wasting and hypophosphatemia, which can lead to growth retardation, rickets, and osteomalacia. Detection of increased urinary excretion of these proximally reabsorbed molecules is, therefore, an important clue to the identification of proximal RTA in an acidotic patient. Hypercalciuria and hypocitraturia are uncommon with proximal RTA. In consequence, nephrolithiasis and nephrocalcinosis do not occur with increased frequency.

Treatment of Hypokalemic Distal Renal Tubular Acidosis

The therapy of hypokalemic distal RTA begins with an effort to establish, and if possible remove, an underlying process. Thus, RTA secondary to a drug or toxin is most appropriately treated by its elimination. When an underlying process cannot be eliminated or treated, therapy directed at the chemical abnormalities may be initiated.

Patients with distal RTA cannot completely regenerate that HCO_3^- decomposed by normal acid loads. This leads to hypokalemic hyperchloremic acidosis, ECF volume depletion, secondary hyperaldosteronism, hypercalciuria, and hypocitraturia. The administration of an adequate quantity of oral bicarbonate will reverse most of these abnormalities. Adults generally require between 50 and 100 mEq of HCO_3^- or HCO_3^- precursors.

Larger quantities, up to 15 mEq/kg/day of $NaHCO_3^-$ may be required in children with distal RTA.[250] In these children, an element of proximal HCO_3^- wasting exists in addition to the distal tubule defect. Although it is possible that volume expansion, produced by the administered $NaHCO_3$, has reduced the proximal HCO_3^- reabsorptive rate, careful studies in several patients exclude this possibility. Direct measurement of ECF and renin levels suggests volume contraction.[250] High doses of $NaHCO_3$ therapy are necessary for these children to achieve normal growth

rates. This form of combined distal and proximal RTA has been called type III RTA in the past. However, as these children mature, the HCO_3^- wasting component decreases and classic distal RTA evolves.[250]

The ingestion of adequate quantities of HCO_3^- normalizes the acid–base status of these patients. Furthermore, ECF volume is expanded, reducing renin, angiotensin, and aldosterone levels. This ameliorates the renal K^+ wasting. Early in the course of therapy, HCO_3^- administration may produce profound hypokalemia unless K^+ is aggressively replaced. Once the initial K^+ deficit is corrected, additional potassium supplements are often not required.

Bicarbonate therapy can restore normal growth in children and stop skeletal mobilization in adults.[101,250] Hypercalciuria decreases, urine citrate increases, and renal stone formation and nephrocalcinosis decrease.[149,262]

Some of the available HCO_3^- salts and HCO_3^- salt precursors are listed in Table 59.10. Sodium bicarbonate tablets and baking soda are inexpensive and readily available. One teaspoon (about 4.5 grams) of baking soda contains 50–60 mEq of sodium bicarbonate, and is an adequate daily dose for many adults with distal RTA. The gas generated by oral HCO_3^- may be unpleasant and occasionally diarrhea results from the osmotic load. These side effects are diminished by dividing the doses and limiting each dose to one-half teaspoon (2 to 2.5 grams). An alternative alkali source is Shohl's solution, which contains sodium citrate and citric acid constituted to provide 1 mEq/ml of potential sodium bicarbonate. Shohl's solution does not generate CO_2 gas. Compared with $NaHCO_3$, sodium citrate delivers a smaller osmotic load due to citrate's trivalent charge. One millimole of Na citrate provides 3 mEq of potential HCO_3^- and represents 4 mOsm; an equivalent dose of $NaHCO_3$ delivers 6 mOsm. Shohl's solution is commercially available as Bicitra. However, all citrate compounds markedly enhance the GI absorption of aluminum.[258] Therefore, caution must be exercised when these drugs are prescribed and they should never be used together with aluminum-containing compounds.

Most patients with distal RTA do not require supplemental potassium following initial potassium repletion. However, for the occasional patient who does need additional potassium, potassium-containing alkali salts listed in Table 59.10 may be used. If $NaHCO_3$ salts produce sodium retention and edema, dietary NaCl should be restricted and diuretics may be administered cautiously.

TABLE 59.10 Oral $NaHCO_3$ and Bicarbonate Precursors

$NaHCO_3$ tablets	3.9 mEq/325-mg tablet
Baking soda ($NaHCO_3$)	60 mEq/teaspoon
Shohl's solution: bicitra	
Na citrate	1 mEq/mL
Citric acid	1 mEq/mL
Polycitra	
Na citrate	1 mEq/mL
K citrate	1 mEq/mL
Citric acid	1 mEq/mL
Kaon (K gluconate)	1.33 mEq/mL
	5 mEq/tablet
K-lyte ($KHCO_3$ and K citrate)	25 or 50 mEq/tablet

Treatment of Proximal Renal Tubular Acidosis

The treatment of proximal RTA is most effective when an underlying process can be reversed or eliminated. When this is not possible, treatment may be directed at the biochemical abnormalities. However, proximal RTA is a more difficult disorder to treat than distal RTA. Although exogenous $NaHCO_3$ can increase the $[HCO_3^-]p$, the proximal HCO_3^- reabsorptive capacity is exceeded and bicarbonaturia results. To the extent that administered $NaHCO_3$ expands volume, HCO_3^- wasting will also be worsened. Increased distal $NaHCO_3$ delivery also accelerates renal potassium wasting. Figure 59.20 shows that patients with proximal RTA develop bicarbonaturia and K^+ wasting when exogenous $NaHCO_3$ is administered. By contrast, patients with distal RTA respond to $NaHCO_3$ treatment by reducing renal K^+ excretion.[322]

If alkali salts are administered to patients with proximal RTA, large doses (10–30 mEq/kg/day) will be required. Bicarbonate retention can be improved by modest volume depletion. Thiazide diuretics may be used to contract the ECF volume and increase proximal HCO_3^- reabsorption.[43,292] However, thiazide diuretics may exacerbate renal K^+ wasting. In such cases, potassium-sparing diuretics may be useful. Dietary NaCl restriction is also used to reduce volume. Patients with proximal RTA are in a tenuous state of potassium balance and frequent determinations of serum $[K^+]$ are required to avoid both hypokalemia and hyperkalemia.

When generalized proximal defects result in Fanconi's syndrome, oral phosphate salts and vitamin D metabolites are required to treat the resulting skeletal abnormalities.[4] Modest volume depletion also promotes phosphate retention. Normal growth may be restored with such therapy.

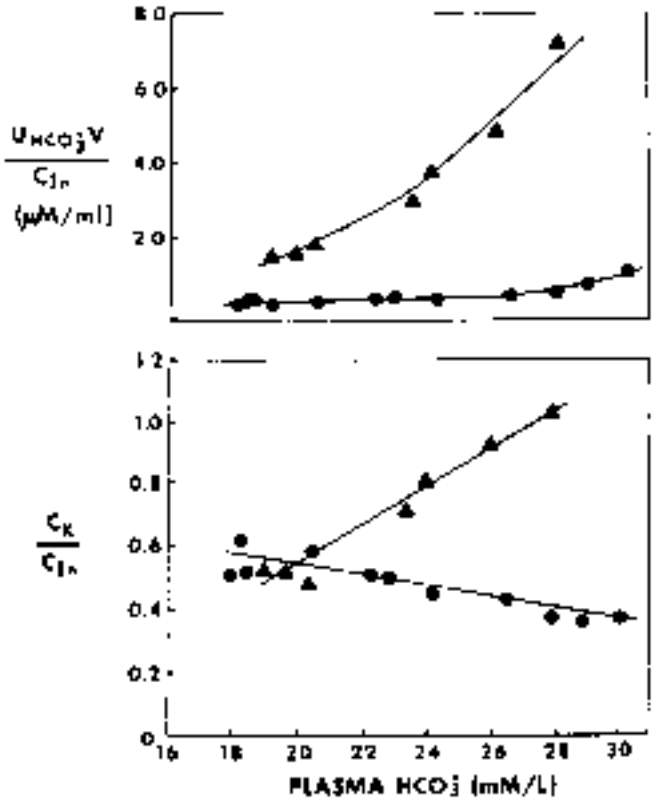

FIGURE 59.20 Fractional excretion of bicarbonate and potassium as a function of the plasma bicarbonate concentration in patients with proximal (triangle) and distal (circle) renal tubular acidosis.

Generalized Distal Tubular Acidosis (Hyperkalemic Renal Tubular Acidosis)

Aldosterone-sensitive tissues include the sweat glands, salivary glands, colon, and distal renal tubule. Aldosterone stimulates sodium reabsorption in the cortical collecting tubule, which usually increases the negative potential difference at this site. This electric potential enhances the secretion of protons and potassium.[241] Potassium deficiency will increase distal tubule H^+ secretion. Aldosterone also stimulates active H^+ secretion via the proton ATPase independent of Na^+ reabsorption.[341]

Decreased aldosterone activity in the distal renal tubule reduces Na^+ reabsorption, K^+ secretion, and H^+ secretion. Salts of decomposed HCO_3^-, which would normally be excreted with NH_4^+ or titratable acid, are instead excreted as sodium salts. This results in a hyperchloremic metabolic acidosis and ECF contraction. In addition to the direct decrease of H^+ secretion secondary to reduced aldosterone activity, the development of hyperkalemia inhibits renal ammoniagenesis and decreases renal NH_4^+ excretion. Decreased NH_4^+ excretion is the major reason these patients develop metabolic acidosis.[347,350]

Animal models show that mineralocorticoid deficiency does not block the capacity to generate a normal pH gradient across an epithelial membrane but does reduce the rate of H^+ secretion. A normally acid urine pH can be achieved despite a rate defect, if urine buffer levels are very low. However, urine pH rises rapidly when buffer is made available. This phenomenon has been documented in mineralocorticoid-deficient animals and in humans.[347]

Szylman and associates[347] suggested the critical role played by hyperkalemia in this form of metabolic acidosis. Reducing the serum potassium concentration with the administration of kayexalate resulted in increased renal ammonia excretion, which correlated with correction of acidosis.[347,349] That study did not establish a role for renal mechanisms in correcting the acidosis, however, because renal net acid excretion was not reported and kayexalate is known to bind to gut NH_4^+ and to increase plasma bicarbonate by that mechanism.[361] Moreover, increased urine ammonia represents additional urine buffer. The rate defect imposed by the low aldosterone activity will increase the urine pH and correspondingly reduce titratable acidity.[183] This sequence is illustrated in Fig. 59.21. Dietary correction of hyperkalemia in hyperkalemic distal RTA with renal insufficiency produced a greater increase in ammonia excretion than the reduction in titratable acid so that metabolic acidosis improved.[238] However, there was a large extrarenal component to the increase in plasma bicarbonate. In adrenalectomized mineralocorticoid deficient dogs with normal kidneys studied following withdrawal of aldosterone, but continuing on physiologic glucocorticoid replacement, the degree of acidosis and magnitude of reduction in NAE was similar whether or not hyperkalemia was prevented by a low potassium intake.[183] When hyperkalemia was permitted, the decrement in NAE was due to reduced NH_4 excretion, whereas with maintained normokalemia, the decrement in NAE was due to reduced titratable acid excretion, suggesting that, without structural renal damage, the aldosterone deficiency-induced H^+ secretory rate defect is sufficient to explain the acidosis and is independent of potassium-induced alterations in buffer (NH_3) availability. Thus, while hyperkalemia is not the critical factor in the pathogenesis in this form of metabolic acidosis, hyperkalemia has the potential to aggravate acidosis by limiting buffer (NH_3) availability in circumstances where alternative urinary buffers (i.e., phosphate) are severely limited.[180]

The various syndromes that reduce aldosterone activity or action are listed in Table 59.11. They are divided into three major categories: (1) defective adrenal gland aldosterone synthesis due to generalized destruction, damage localized to the zona glomerulosa, or enzymatic defects that reduce mineralocorticoid

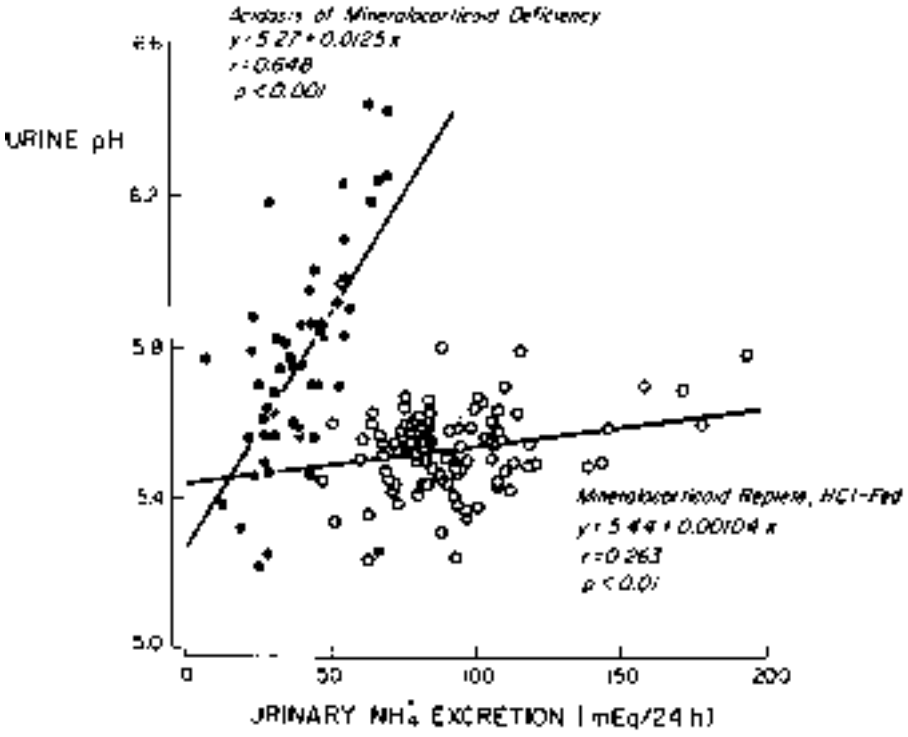

FIGURE 59.21 Urine pH as a function of urine ammonia excretion in two groups of dogs during steady-state metabolic acidosis-fed HCl: mineralocorticoid-deficient dogs (closed circle) and mineralocorticoid-replete dogs (open circle). *(With permission, from Hulter HN, Ilnicki LP, Harbottle JA, Sebastian A. Impaired renal H^+ secretion and NH3 production in mineralocorticoid-deficient glucocorticoid-replete dogs. Am J Physiol 1977;326: F136–F146.)*

synthesis; (2) decreased aldosterone synthesis by a normal adrenal gland as a result of reduced angiotensin II stimulation (hyporeninemic hypoaldosteronism); and (3) genetic or acquired forms of generalized dysfunction of the collecting duct with features of resistance to mineralocorticoid action. These disturbances comprise inherited disorders of aldosterone sensitivity due to either mineralocorticoid receptor defects or disturbances in aldosterone-sensitive Na^+ or Cl^- reabsorption, and acquired forms, that is, generalized destruction of aldosterone-sensitive nephron segments, notably the collecting duct, and pharmacologic interference with mineralocorticoids.

Primary Adrenocortical Deficiency

Destruction of the adrenal cortex by infection, tumor, hemorrhage, or an autoimmune process produces Addison's disease. Severe damage results in combined glucocorticoid and mineralocorticoid deficiencies. The glucocorticoid deficiency produces anorexia, weight loss, GI distress, hypoglycemia, weakness, and inability to mount a normal "stress" reaction. Mineralocorticoid deficiency produces renal salt wasting, hyperkalemia, and metabolic acidosis. Most patients with Addison's disease can be treated adequately without mineralocorticoid replacement despite combined deficiencies. Glucocorticoid replacement and generous quantities of NaCl will maintain acid and K^+ balance. Delivery of large amounts of Na^+ to the distal tubule will stimulate K^+ and H^+ secretion, even in the absence of mineralocorticoid activity. However, electrolyte balance in these patients is precarious. If salt ingestion is limited, or Na^+-rich fluids are lost (i.e., diarrhea), then negative Na^+ balance rapidly develops, ECF volume shrinks, and renal distal tubule Na^+ delivery falls. In the absence of aldosterone, K^+ excretion and H^+ excretion are sharply reduced, leading to hyperkalemia and metabolic acidosis. Therefore, if salt intake is restricted or ECF deficits develop, mineralocorticoid replacement becomes mandatory for maintenance of normal electrolyte balance.

Adrenal Enzyme Defects

Figure 59.22 shows the scheme for adrenal steroid synthesis. Severe proximal enzyme defects block the conversion of cholesterol to progesterone and produce profound neonatal adrenal insufficiency. This disorder is usually rapidly fatal. Patients with partial proximal defects can survive. Defects of more distal enzymes in this metabolic pathway are also compatible with life.

The most common congenital adrenal enzyme defect is 21-hydroxylase deficiency.[266] This disorder is usually inherited with an autosomal recessive pattern. The block can affect both glucocorticoid and mineralocorticoid synthesis or only the glucocorticoid pathway. Although complete 21-hydroxylase deficiency may be fatal unless promptly diagnosed and treated, children

TABLE 59.11 Causes of Mineralocorticoid Deficiency and Resistance

Primary mineralocorticoid deficiency
Combined glucocorticoid and mineralocorticoid deficiencies
Addison's disease
Bilateral adrenalectomy
Bilateral adrenal destruction
Congenital adrenal enzyme defects: 21-hydroxylase deficiency,3-b-OH dehydrogenase deficiency, desmolase deficiency
Isolated mineralocorticoid deficiency
Familial methyloxidase deficiency
Transient mineralocorticoid deficiency of infancy
Chronic idiopathic hypoaldosteronism
Chronic heparin therapy
Hyporeninemic hypoaldosteronism
Diabetic nephropathy
Tubulointerstitial disease
Volume expansion
Prostaglandin inhibitors
Acquired mineralocorticoid resistance
Renal insufficiency: renal disease with disproportionate medullary destruction
Drugs: spironolactone, amiloride, triamterene
Congenital mineralocorticoid resistance
With salt wasting and hypotension: pseudohypoaldosteronism type I
Autosomal-dominant renal form: defect in mineralocorticoidreceptor expression (MLR)
Autosomal-recessive multiorgan form: defects in alpha (SNCC1A), beta (SNCC1B), and gamma (SNCC1G) subunits of ENaC
With salt retention and hypertension: pseudohypoaldosteronism type II (Gordon's syndrome)
Defects in WNK1 and WNK4 kinases

with mild 21-hydroxylase deficiency survive without specific therapy. However, ACTH levels increase markedly in response to relative glucocorticoid deficiency and drive steroid synthesis. The 21-hydroxylase block shifts steroid precursors toward androgen synthesis (Fig. 59.22). This results in the adrenogenital syndrome. The children grow rapidly, and males prematurely virilize while females develop ambiguous genitalia. Exogenous glucocorticoid administration will decrease ACTH production, slow androgen synthesis, and reverse virilization. However, supraphysiologic quantities of glucocorticoids may be necessary to completely normalize androgen levels. These higher doses will produce iatrogenic Cushing's syndrome. Recent work indicates that androgen antagonists should be combined with glucocorticoids to prevent Cushing's syndrome yet reverse virilization.[82]

The 21-hydroxylase step is required for mineralocorticoid synthesis. Different isoenzymes may catalyze this reaction in the zona fasciculata (glucocorticoids) and zona glomerulosa (mineralocorticoids).[332] In some children, the 21-hydroxylase defect principally affects glucocorticoid synthesis in the zona fasciculata while mineralocorticoid synthesis is normal. In others, both the glucocorticoid and mineralocorticoid pathways are affected. When mineralocorticoid synthesis is reduced, variable degrees of salt wasting, hyperkalemia, and hyperchloremic acidosis result. Exogenous mineralocorticoid is usually required to normalize the electrolyte pattern. Generally, these exogenous mineralocorticoid requirements will decrease with time.

21-Hydroxylase deficiency accounts for about 90% of all cases of adrenogenital syndrome. Much less common are 11-hydroxylase deficiency and 17-hydroxylase enzyme deficiency, which also produce adrenogenital syndrome. These enzymes are not required to synthesize mineralocorticoids. Instead, affected children overproduce mineralocorticoids and therefore develop hypertension and metabolic alkalosis.

Final conversion of corticosterone to aldosterone requires sequential oxidations of the 18-methyl group. These oxidations are catalyzed by two methyl oxidase enzymes. Hereditary defects of these oxidases produce aldosterone deficiency, renal salt wasting, hyperkalemia, and hyperchloremic acidosis.[95] These enzymes are also inhibited by chronic heparin administration.[79,220,379] Hyperkalemia and metabolic acidosis may develop with chronic heparin therapy, especially in patients with renal insufficiency.

The salt wasting and volume depletion that occur in these patients will stimulate renin synthesis. However, potassium retention and hyperkalemia will suppress renin synthesis.[320] Therefore, renin levels may be high, normal, or low, depending on the net effect of several offsetting stimuli.

Hyporeninemic Hypoaldosteronism

Most patients with adrenal enzyme defects that lead to mineralocorticoid deficiency have high plasma renin levels as a result of volume contraction. In contrast, patients with hyporeninemic hypoaldosteronism have low renin activity. Presumably, aldosterone deficiency in these patients results from decreased renin secretion and angiotensin generation. The low renin and angiotensin levels may reflect specific juxtaglomerular apparatus damage, generalized renal damage, volume expansion, or pharmacologic inhibition of renin or angiotensin II.

Hyporeninemic hypoaldosteronism most often occurs in elderly individuals with mild renal insufficiency.[310,312] Many also have diabetes mellitus. The single most common biochemical abnormality they develop is asymptomatic hyperkalemia. Hyperchloremic acidosis occurs in about 50%.[90]

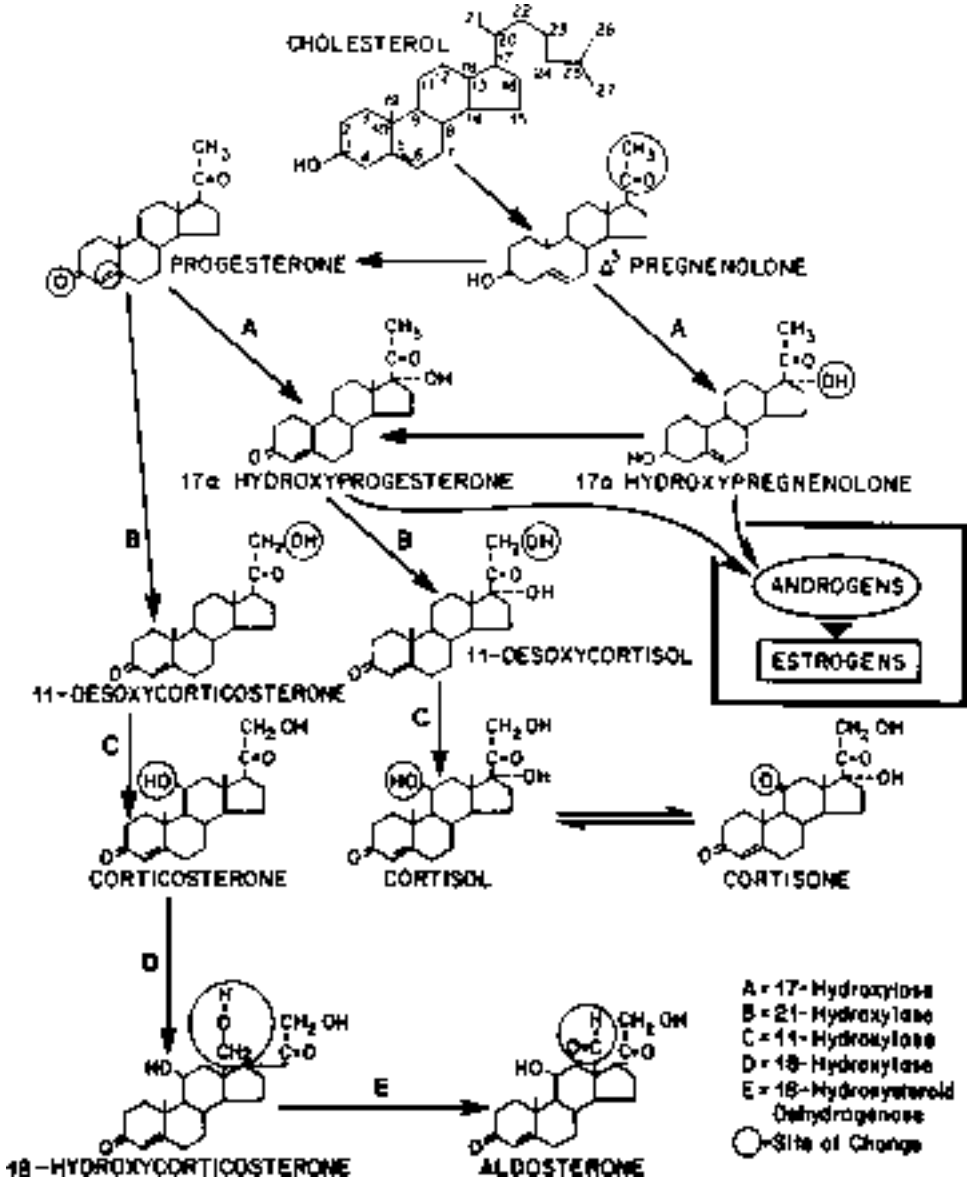

FIGURE 59.22 Adrenal metabolic reactions leading from cholesterol to mineralocorticoids,glucocorticoids, and sex hormones.

Several hypotheses have been advanced to explain the syndrome of hyporeninemic hypoaldosteronism. Multiple defects may exist in different patients or within a single patient. The most widely accepted explanation attributes the syndrome to juxtaglomerular injury resulting from an inflammatory, vascular, or immunologic insult. For example, autonomic neuropathy can suppress renin release. Pharmacologic suppression and physiologic suppression by volume expansion may also occur. Decreased renin secretion reduces angiotensin activation, which in turn decreases aldosterone release. The low aldosterone levels are ultimately responsible for the biochemical and clinical features of the syndrome.

The role of volume expansion in this syndrome remains unsettled. Clinical probes of volume status may be inadequate in these patients. Orthostatic hypotension may signal autonomic insufficiency rather than volume contraction. Edema may develop as a result of hypoalbuminemia rather than volume expansion. If volume expansion is primary, then diuresis should reverse the disorder. Indeed, diuretics are occasionally successful,[277] but more often this approach fails. However, in these patients ECF volume may not have been adequately reduced. Furthermore, chronic suppression of renin and aldosterone synthesis may require a prolonged period of stimulation before an appropriate response can be elicited.

An alternative hypothesis locates the primary lesion in the adrenal gland. Reduced renin levels could then be secondary to hyperkalemic suppression.[320] Several adrenal aldosterone synthetic defects have been described in diabetic patients.[96] Insulin may be necessary for a normal zona glomerulosa response to various stimuli, especially hyperkalemia.[81,90,287] Although aldosterone usually increases in response to angiotensin II infusions in these patients, the magnitude of this response may not be appropriate.[90] However, most patients with well-defined adrenal aldosterone secretory defects (i.e., 21-hydroxylase deficiency) develop high renin levels despite hyperkalemia.

Theoretically, a syndrome of inappropriate ANP secretion would be predicted to produce hyporeninemic hypoaldosteronism, but no such syndrome has been observed yet.

The increased proclivity of diabetics for development of this syndrome has several possible explanations.[364] First, diabetic vascular disease may preferentially affect the juxtaglomerular apparatus. Second, diabetic autonomic neuropathy may reduce neural stimulation of the juxtaglomerular apparatus.[49,287–289,312,357,370] Third, inactive forms of renin, called "big renin," may be released and not generate angiotensin II.[97] Fourth, decreased renal prostaglandin synthesis in these patients may reduce renin generation.[284]

Patients with primary hyporeninemic hypoaldosteronism and mild hyperkalemia do not require specific therapy. Volume contraction should be avoided because reduced renal distal tubule sodium delivery exacerbates both the hyperkalemia and acidosis. If hyperkalemia and/or metabolic acidosis are severe, then medical intervention is necessary. Patients whose ECF volume is expanded often respond to potent diuretics.[90,92] Exogenous mineralocorticoids, such as fludrocortisone, can further mitigate hyperkalemia and acidosis although supraphysiologic doses may be required as a result of relative renal mineralocorticoid resistance.[90,287]

Hyperkalemia will exacerbate markedly the metabolic acidosis. Reduction of potassium levels with mineralocorticoids, Na^+/K^+ exchange resins, or diuretics increases renal NH_4^+ excretion and improves or reverses the hyperchloremic acidosis.[100,243,345]

A number of drugs interfere with at various levels with the renin-angiotensin II-aldosterone axis and may induce hyperkalemic renal tubular acidosis. Inhibition of renal prostaglandin synthesis reduces renin secretion and can produce the syndrome.[272] By blockade of either conversion of angiotensin I to angiotensin II (ACE inhibitors) or the action of angiotensin (angiotensin receptor-1 antagonists), these widely used drugs can decrease adrenal aldosterone secretion. However, these drugs will increase renin levels markedly. The aldosterone deficiency that is produced is not complete. For the ACE inhibitors, an escape phenomenon has been described after prolonged use (i.e., angiotensin II production becomes again renin dependent). The incomplete aldosterone deficiency and the ACE-inhibitor escape phenomenon provide the rationale for combined use of these drugs in heart failure, hypertension and in intervention strategies to retard progression of renal insufficiency. Hyperkalemia and metabolic acidosis do not usually develop when these drugs are administered alone. However, these drugs are clinically important causes of hyperkalemia when given to patients with decreased renal function and when given in combination with other drugs that also interfere with the renin-angiotensin-aldosterone axis and aldosterone action (Fig. 59.23).

Abnormal Cortical Collecting Duct ("Renal Resistance to Mineralocorticoids")

Genetic Causes

Hyperkalemic RTA of genetic origin is most frequently observed in pseudohypoaldosteronism type I occurring in young children without other apparent renal pathology.[12] The disease is characterized by salt-wasting, hyperkalemia and metabolic acidosis in the presence of markedly elevated plasma renin activity and aldosterone concentrations. In the autosomal-dominant form of pseudohypoaldosteronism type I (MIM 177735), mineralocorticoid resistance is limited to the kidneys and is caused by heterozygous mutations in the gene encoding the mineralocorticoid receptor.[137]

In the autosomal-recessive form of pseudohypoaldosteronism type I (MIM 264350) aldosterone resistance is generalized, affecting all major

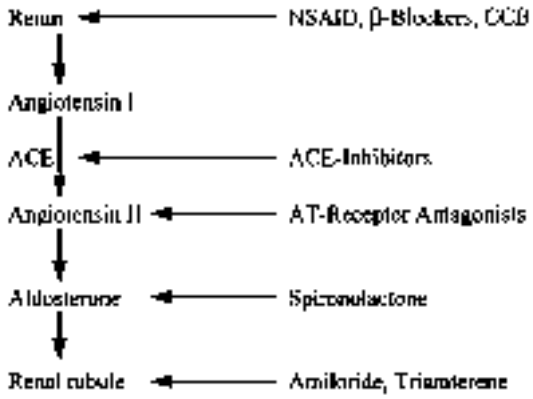

FIGURE 59.23 Commonly used drugs that interfere with synthesis or action of component of the renin-angiotensin-aldosterone axis. NSAID, nonsteroidal anti-inflammatory drugs.

mineralocorticoid-sensitive tissues (kidney, colon, sweat and salivary glands). Aldosterone resistance is due to homozygous, loss of function mutations in the alpha, beta or gamma subunits of the amiloride-sensitive, epithelial sodium channel (ENaC).[68] This recessive form of pseudohypoaldosteronism type I manifests with lifelong severe salt-wasting, while the dominant form is characterized by a milder defect. Renal salt wasting improves with advancing age in these patients. This disorder can be effectively treated with generous exogenous salt supplements. The syndrome usually becomes less severe as these children mature.[99] However, even after electrolytes become normal and salt supplements can be reduced, aldosterone levels remain very high and these individuals remain relatively resistant to mineralocorticoid effects and are very sensitive to any aldosterone blockade.

Another distinct group of mineralocorticoid-resistant patients present with hyperkalemic, hyperchloremic acidosis, expanded ECF volume, hypertension, low to normal renin and aldosterone levels, and a diminished response to the kaliuretic effects of exogenous mineralocorticoids. Renin and aldosterone levels increase when volume is reduced by diuretics or salt restriction. This syndrome was first described in several children by Gordon and co-workers[148] and is called pseudohypoaldosteronism type II or Gordon's syndrome. Schambelan et al.[311] suggested almost 30 years ago that a renal distal tubule "chloride shunt"—that is, increased NaCl reabsorption in the thick limb and early distal tubule leading to impaired K^+ and H^+ secretion—could explain the features of this disorder. Thus, pseudohypoaldosteronism type II exhibits a clinical phenotype directly opposite of Gitelman's syndrome, which is characterized by hypotension, salt wasting, and metabolic alkalosis, and is due to mutations in the thiazide-sensitive NaCl cotransporter NCC. NCC gain of function mutation, a reasonable candidate mechanism for this syndrome, was, however, excluded. Rather, this syndrome was shown to be the consequence of mutations in two of the four known WNK (with no lysine kinases) kinase genes, WNK1 and WNK4 located on chromosomes 12 and 17, respectively.[378] WNK1 and WNK4 are predominantly expressed in the distal convoluted tubule and collecting duct. WNK4 downregulates the activity of ion transport pathways expressed in these nephron segments, such as the apical thiazide-sensitive Na^+-Cl^- cotransporter and apical secretory K^+ channel ROMK (which will become less active), as well as upregulates paracellular chloride transport and phosphorylation of tight junction proteins such as claudins. WNK4 mutations behave as a loss of function for the Na^+–Cl^- cotransporter (which will become more active) and a gain of function with regard to ROMK and claudins. These dual effects of WNK4 mutations fit with proposed mechanisms for developing electrolyte and acid–base abnormalities and hypertension in PHA-II and point to WNK4 as a multifunctional regulator of diverse ion transporters.[132] WNK1, an aldosterone-inducible protein, interacts with WNK4 by mechanisms that are not yet well characterized. The mutation in WNK1 results in gain of function and inhibition of WNK4, thereby activating NCC.[382] WNK1 also stimulates Na^+ transport via EnaC.[113] Via this process, a gain of function mutation would be expected to result in hypertension, but also hypokalemia and metabolic alkalosis, which are not observed in pseudohypoaldosteronism type II. More information on the precise roles and interactions of WNK1 and WNK4 is needed and the results will greatly affect our understanding of the regulation of distal ion and H^+ transport and of blood pressure regulation.

Acquired Forms of Hyperkalemic Distal RTA

Most commonly, renal tubular damage can lead to destruction of mineralocorticoid target cells within the kidney with impaired secretion of potassium and protons.[66,232,264,308,355] Due to the cell damage by a variety of pathological processes, apparent renal mineralocorticoid resistance is present. Patients with systemic lupus erythematosus,[91,204] obstructive uropathy,[20] sickle cell disease,[22,93] allergic drug reactions,[73] and damaged renal transplants[24,288] may develop impaired collecting duct function and renal tubule mineralocorticoid resistance. Many of these patients have multiple distal tubule defects in association with the mineralocorticoid resistance. Juxtaglomerular destruction can produce hyporeninemic hypoaldosteronism in addition to the mineralocorticoid resistance. Classic distal renal tubular acidosis may also coexist with decreased mineralocorticoid responsiveness probably reflecting wide-spread damage to the collecting ducts, both cortical and medullary.

Renal mineralocorticoid resistance may have a pharmacologic basis (Fig. 59.23). The spironolactones, competitive inhibitors of aldosterone, bind to specific receptors and block transport of aldosterone into the cell nucleus. These drugs have a potent effect when the prevailing mineralocorticoid level is high. They are less effective when mineralocorticoids are low and are ineffective in adrenalectomized individuals. Spironolactone reduces Na^+ reabsorption, H^+ secretion, and K^+ secretion in the distal tubule and may generate hyperkalemic hyperchloremic acidosis in those individuals dependent on high mineralocorticoid activity to maintain H^+ and K^+ balance (e.g., patients with cirrhosis).[131,182]

Amiloride and triamterene are diuretics that block distal tubule electrogenic Na^+ transport.[342] However,

their effect is independent of mineralocorticoid activity and the diuretic effect occurs even in adrenalectomized individuals.[228] Amiloride blocks the Na^+ channels on the luminal membrane of distal tubule cells. Reduced electrogenic Na^+ transport decreases the lumen-negative voltage, reducing H^+ and K^+ secretion.[152] Hence a voltage-dependent acidification and K + secretory defect develops.[152] Triamterene has similar effects although its mechanism of action is not identical to amiloride.

Cyclosporine A is frequently associated with hyperkalemia. Although it was initially believed that this drug produced hyporeninemic hypoaldosteronism, subsequent studies have shown relatively normal aldosterone levels.[5] These patients probably develop renal resistance to the effect of aldosterone. Cyclosporine may also block other steps in the renin-angiotensin-aldosterone axis.[5,336]

Gastrointestinal Hyperchloremic Acidosis

Large quantities of H^+ and HCO_3^- continuously cycle through the gastrointestinal tract. Basal gastric HCl secretion is about 10 mEq/hr (0−50 mEq/liter). Acid secretion can increase to 50 mEq/hr after appropriate stimulation.[119] At this time, the gastric HCl concentration may reach 150 mEq/liter. Most of the HCl secreted by the stomach is neutralized by HCO_3^- secreted by the pancreas and liver. These organs can secrete up to 250 mEq/day of HCO_3^-. Some HCl is also neutralized by small intestine ion transport. The small intestine epithelium contains $Na^+/H+$ cation exchangers, which secrete H^+ and absorb Na^+ from the lumen, and Cl^-/HCO_3^- anion exchangers, which secrete HCO_3^- and absorb Cl^- from the lumen. When these two ion exchangers operate together, the net result is NaCl absorption and H_2CO_3 secretion. However, Na^+/H^+ exchange predominates in the jejunum while Cl^-/HCO_3^- exchange is more active in the duodenum and ileum.[358]

Normally, the small intestine delivers between 600 and 1500 ml/day of relatively HCO_3^--rich fluid to the colon. The colon absorbs most of this fluid and electrolyte load. A Cl^-/HCO_3^- anion exchanger in the colon reduces stool $[Cl^-]$ to low levels. Sodium is absorbed in exchange for H^+ and for K^+. However, the HCO_3^- is largely decomposed by organic acids produced by colonic bacterial metabolism. Acetic, butyric, propionic, lactic, and other acids are produced when these bacteria ferment carbohydrates delivered to the colon. H^+ from these acids combines with HCO_3^- in the lumen to form H_2CO_3 (which dehydrates to H_2O and CO_2). The organic acid anions remain in stool as Na^+ and K^+ salts and represent decomposed HCO_3^-. In consequence, stool water usually has an acid pH reaction.

Diarrhea markedly increases the loss of stool water and stool base. If the sum of stool $[HCO_3^-]$ and decomposed $[HCO_3^-]$ is equal to the $[HCO_3^-]$p, then diarrhea should produce volume depletion without severe acid−base derangements. More commonly, the sum of $[HCO_3^-]$ and decomposed $[HCO_3^-]$ in watery stool is between 30 and 80 mEq/liter.[352] Decomposed $[HCO_3^-]$ usually exceeds $[HCO_3^-]$ and the stool pH is often acid. Despite its acid pH, the large quantity of decomposed HCO_3^- in stool results in a metabolic acidosis.

Diarrhea leads to ECF contraction and stimulation of the renin-angiotensin-aldosterone axis. Hyperchloremic acidosis develops due to the loss of stool HCO_3^- and decomposed HCO_3^- with much less chloride loss. The volume depletion also stimulates dietary chloride retention. Hypokalemia develops due to the large amount of K^+ that is lost in stool (30−65 mEq/liter). Colonic K^+ secretion, which is largely driven by the negative electrical voltage in the colon lumen, is further stimulated by high aldosterone levels.

Under normal circumstances, the kidneys should be able to compensate for stool alkali losses by increasing renal net acid excretion. However, patients with severe diarrhea often also have impaired renal function. In addition to a decreased GFR, low Na^+ delivery to the distal renal tubule due to volume contraction will reduce renal acid excretion. In consequence, reduced renal acid excretion usually contributes to the development of metabolic acidosis in patients with diarrhea.[189]

Many patients with diarrhea also develop a component of anion gap metabolic acidosis. This is usually due to lactic acidosis, which occurs as a result of volume depletion. Volume contraction may also elevate protein and phosphate concentrations, which will elevate the anion gap.[368] Uremic acidosis can occur when vascular collapse produces renal failure.

Hypokalemic hyperchloremic acidosis secondary to diarrhea may generate a relatively alkaline urine pH (>6.0) at a time maximal renal acidification should exist. The reason for the relatively high urine pH is the dramatic increase in renal ammoniagenesis and ammonium excretion that develops in these patients. The dual stimuli of chronic metabolic acidemia and hypokalemia markedly augment ammoniagenesis and renal ammonia excretion. The high urine NH_4^+ levels drive up the urine pH. When a relatively alkaline urine is noted in a patient with hypokalemic hyperchloremic acidosis, this should suggest a diagnosis of renal tubular acidosis. The key differential finding is a high urine $[NH_4^+]$ or a negative urinary anion gap in patients with diarrhea and normal renal acidification and a low $[NH_4^+]$ or a positive urinary anion gap in those with

distal RTA. This issue is further discussed in Diagnosis of Proximal and Hypokalemic Distal Tubular Acidosis.

The [HCO_3^-] in pancreatic and biliary secretions ranges from 50 to 100 mEq/liter. Normally, this HCO_3^- neutralizes gastric HCl or is absorbed by the jejunum, resulting in no net systemic acid–base effects. However, if these secretions are removed from the body, then hyperchloremic acidosis results. This can occur in patients with pancreatic or biliary fistulas. Consequently, patients with pancreas transplants with bladder drainage develop hyperchloremic metabolic acidosis even with normal renal function and require large amounts of base supplements.[268] This and other disadvantages of bladder diversion (reflux pancreatitis, chemical cystitis, hyperinsulinemia) have lead to the increasing use of a more physiologic drainage procedure that is either enteric or portal vein drainage. These procedures eliminate loss of HCO_3^- and metabolic acidosis with comparable perioperative complication rates.[213]

Several compounds can accelerate gastrointestinal HCO_3^- loss and produce hyperchloremic metabolic acidosis. Cholestyramine, a nonabsorbed anion exchange resin used to treat hyperlipidemia, biliary pruritis, and several other disorders, is ingested as a chloride salt. In the GI tract, Cl^- released from the resin exchanges with HCO_3^-. The resin-bound HCO_3^- is excreted in the stool. The chloride released from the resin is absorbed via the Cl^-/HCO_3^- anion exchanger. The modest HCO_3^- loss and Cl^- gain usually produced by cholestyramine ingestion is generally handled by increased renal acid and Cl^- excretion. However, young children and adults with renal insufficiency or reduced renal acid excretion can develop hyperchloremic acidosis when they ingest cholestyramine.[201,304]

As mentioned earlier, ingestion of $CaCl_2$ produces hyperchloremic acidosis[281] and can be used experimentally as an acid load to study renal acidification.

Gastrointestinal–Ureteral Connections

When urine enters the gastrointestinal tract, or a segment of intestine is interposed into the urine stream, hypokalemic hyperchloremic metabolic acidosis often develops. As discussed previously, the small intestine and colon contain Cl^-/HCO_3^- exchangers. When isotonic saline is instilled into the colon, the [Cl^-] progressively falls and [HCO_3^-] increases as a result of this exchange.[84,202] Potassium also diffuses into the colon lumen due to its lumen-negative voltage. Similarly, if chloride-rich urine enters the colon or ileum, the Cl^- is absorbed and HCO_3^- secreted. Urine NH_4^+ will also be absorbed by the intestine either together with Cl^- or in exchange for N_4^+.[109,257] This further reduces the acid load present in urine. Large quantities of ammonia (and HCO_3^-) will be generated in the intestine by bacterial hydrolysis of urea. If this NH_4^+ is absorbed without HCO_3^-, systemic acidification also results. Urea conversion to NH_4^+ and HCO_3^- elevates the pH of the fluid and increases the fraction of ammonia in the NH_3 unionized form. Although absorption of NH_3 will not produce acidosis, it can lead to hyperammonemic encephalopathy in these patients.[202]

Chronic renal insufficiency, resulting from obstructive uropathy and interstitial nephritis, occurs commonly in patients whose urinary tracts are diverted into GI segments. This contributes to the metabolic acidosis that develops. Distal tubule acidification mechanisms may be especially susceptible to such damage.

Ureterosigmoidostomy, one of the earliest forms of surgical urinary diversion, results in prolonged colon exposure to urine. This provides ample opportunity for Cl^-/HCO_3^- exchange, NH_4^+ absorption, and K^+ secretion. Consequently, hypokalemic hyperchloremic acidosis occurs commonly in these patients.[246,337] These electrolyte abnormalities are exacerbated by constipation, which increases urine–colon contact time, and are reduced by incontinence, which decreases contact time. Ureterosigmoidostomy is now only occasionally used and the ureteral anastomosis is then placed into the distal rectosigmoid to minimize contact time.[64]

Isolated loops of ileum, or less commonly jejunum, can be used as urine bladder substitutes. These loops have several advantages in comparison with ureterosigmoidostomy. Fecal contamination of the urinary tract is avoided and intestine–urine contact time is reduced because urine is externally drained into a urostomy bag.[255] However, if a long bowel segment is used, or if stomal stenosis develops, then contact time increases and severe hypokalemic hyperchloremic acidosis can develop.[109,234] Jejunal segments may generate less K^+ wasting than ileal loops.[144] When hypokalemic metabolic acidosis develops, $NaHCO_3$, other $NaHCO_3$ precursors, and potassium salts are used to correct acid–base and electrolyte abnormalities. Recent studies suggest that pharmacologic inhibition of cyclic AMP, an intestinal secretogogue, may reduce the severity of these electrolyte abnormalities. Both nicotinic acid and chlorpromazine have been used in this fashion.[257]

Postchronic Hypocapnia

Posthypocapnic hyperchloremic acidosis develops when patients with chronic respiratory alkalosis stop hyperventilating. Chronic hypocapnia decreases renal NH_4^+ and titrable acid excretion and induces a transient $NaHCO_3$ diuresis. This continues until a new lower steady-state plasma [HCO_3^-] is established when

acid balance is restored. In humans, compensation decreases the plasma [HCO_3^-] by about 0.4 mEq/liter for each 1-mm Hg reduction in CO_2 tension, which results in a near normal arterial pH.[209] The renal compensatory response also generates mild ECF volume contraction and stimulates retention of dietary NaCl.[138] Consequently, hyperchloremia develops. However, the increase in chloride does not equal the HCO_3^- reduction and the difference produces a slight increase in the anion gap,[208] comprised mainly of organic acid anions, especially lactate.

If respiratory alkalosis recedes and the pCO_2 increases toward normal, then renal net acid excretion must increase to normalize acid–base status. Sodium must also be retained together with the HCO_3^-. To the extent that the low [HCO_3^-] and high [Cl^-] persist, this represents a hyperchloremic metabolic acidosis. The resulting metabolic acidosis is transient and probably dependent on the severity of preexisting hypocapnia.[138]

HCl and HCl Precursors

Infusion or ingestion of HCl and compounds that can be metabolized to HCl produces hyperchloremic metabolic acidosis. For example, ingested NH_4Cl is metabolized by the liver to urea and HCl. Similarly, chloride salts of metabolizable organic cations can be converted to HCl. They include basic amino acids such as histidine, arginine, lysine, and hydroxylysine, which are generally prepared as HCl salts. HCl is liberated when the amino acids are metabolized to neutral products, to CO_2 and H_2O, or are incorporated into proteins.[168]

Intravenous hyperalimentation solutions include neutral, acidic, and basic amino acid salts. When the quantities of Cl^-- and Na^+-containing amino acid salts are balanced, their acid–base impact is neutral. However, some synthetic amino acid solutions contain a higher concentration of chloride-containing amino acid salts, which represents a net HCl load. Hyperchloremic acidosis can develop, especially in young children and patients with impaired renal function.[120,168] This hyperchloremic acidosis is efficiently prevented by adding bicarbonate precursors, such as sodium acetate to the currently used solutions. Failure to supply thiamine to parenterally fed patients induced severe lactic acidosis.[363]

Chloride gas inhalation can also produce hyperchloremic acidosis because when Cl2 gas is hydrated it generates HCl.[346]

Dilution Acidosis

Diluting a solution of nonbicarbonate nonvolatile buffers with saline or water proportionately reduces the concentration of the acids and conjugate bases. This has a minimal effect on the solution's pH:

$$pH = pKa + \log base/X\text{: }acid/X = pKa + \log base\text{:}acid$$

where X = water or saline. However, diluting the HCO_3^-/pCO_2 buffer pair in an open system produces a different result. While [HCO_3^-] falls, the pCO_2 is maintained at baseline levels because it is continuously replenished. A fall in [HCO_3^-] with a stable pCO_2 reduces the pH.

Similarly, the pH of separated whole blood, maintained at a pCO_2 of 40 mm Hg, will fall sharply if the blood is diluted with saline.[135] However, the pH reduction produced by dilution is much less when intact animals are expanded to an equivalent degree.[135,302] Stabilization of the pH in the intact animal is due to the interaction of the HCO_3^-/pCO_2 pair with non-HCO_3^- buffers, such as hemoglobin and phosphate, as well as other extracellular and intracellular buffers. These buffers accept H^+ and generate HCO_3^- to prevent a marked reduction in pH:

$$NaB + H_2CO_3 \rightarrow HB + NaHCO_3$$

ECF volume expansion will decrease proximal tubule HCO_3^- reabsorption and this may contribute to development of metabolic acidosis. However, this effect is relatively small in humans. In consequence, the plasma [HCO_3^-] falls only about 2 mEq/liter following ECF volume expansion in humans.[135]

Mild expansion metabolic acidosis could also occur in patients with the syndrome of inappropriate antidiuretic hormone secretion. A proportionate decrease in plasma [Na^+], [Cl^-], and [HCO_3^-] should result in acidosis. However, the [HCO_3^-] generally remains normal in these patients. In part, this is due to the buffer interactions discussed previously. An additional factor is direct stimulation of adrenal aldosterone secretion produced by hyponatremia.[75] The higher aldosterone levels accelerate distal tubular H^+ secretion (HCO_3^- generation) to offset the reduction in [HCO_3^-]. ADH may also modulate renal acid excretory capacity directly by virtue of its inhibitory effect on HCO_3^- reabsorption in the thick ascending limb[146] and its stimulation of sodium reabsorption in the collecting duct.[316]

Summary: Treatment of Metabolic Acidosis

Generally, the metabolic acidoses can be divided into those resulting from a chronic underexcretion of acid (i.e., uremic and distal renal tubular acidosis), chronic wasting of bicarbonate (i.e., proximal RTA or diarrhea), and acute net overproduction of acids (i.e., ketoacidosis, lactic acidosis).

Patients with chronic acidosis owing to decreased acid excretion can often be readily treated with exogenous sodium bicarbonate. The daily bicarbonate requirements should be relatively modest because it would only be necessary to offset normal net acid production rates of 70–100 mEq/day. In addition to normalization of acid–base parameters, the correction of the acidosis will stop skeletal dissolution, reverse hyperventilation, and improve the overall state of well-being. The specifics of therapy in patients with distal renal tubular acidosis, the mineralocorticoid-deficiency states, and uremic acidosis have been discussed in the appropriate previous sections.

When acute or chronic acidosis results from a loss of bicarbonate salts, exogenous sodium bicarbonate may also prove effective. This is apparent in patients with acute and chronic diarrhea, pancreatic fistulas, and various gastrointestinal–ureteral connections. However, patients with proximal RTA are resistant to exogenous bicarbonate therapy and usually require an alternative therapy.

A third category includes those metabolic acidoses associated with an acute accumulation of strong acids that overwhelms normal renal acid excretory capacity. Ketoacidosis, lactic acidosis, and the toxin-associated acidoses fall into this group. In these individuals, bicarbonate therapy is often inappropriate and ineffective. The therapeutic thrust must be directed toward an understanding and reversal of the underlying pathophysiology. With ketoacidosis, insulin and fluid therapy will reverse the acidosis, but bicarbonate administration is ineffective alone and perhaps deleterious. Lactic acidosis reflects a basic underlying disturbance in mitochondrial oxygenation, which mandates immediate therapy. The low bicarbonate and pH do not necessarily require therapy with exogenous bicarbonate unless these levels become very low. In these acidoses, the accumulating anions represent potential bicarbonate; therefore, rebound metabolic alkalosis may occur following exogenous bicarbonate administration.

If the pH is below 7.2, and certainly if it is near 7.0, and the underlying process cannot be reversed immediately, sodium bicarbonate infusion may be necessary to prevent development of fatal acidemia. When the acidosis is severe, reductions in HCO_3^- produce disproportionately large reductions in pH. For example, if the HCO_3^- concentration is 4 mEq/liter and the pCO_2 is 12 mm Hg, the pH will be 7.15. At this point, respiratory compensation is almost maximal. A further reduction in HCO_3^- of only 2 mEq/liter will cause the pH to plummet to 6.84.

To calculate exogenous bicarbonate requirements, a distribution space of approximately 50% body weight is a good first approximation. However, much larger quantities of bicarbonate may be necessary, especially when accumulating acids, such as lactic acid or ketoacids, are rapidly being generated. Under such circumstances, the HCO_3^- distribution space may exceed 100% of body weight. In some patients with chronic lactic acidosis, the lactic acid generation rate may be accelerated by bicarbonate infusions so that no net beneficial effect results.[121] Whenever sodium bicarbonate therapy is used, its adverse effects must be anticipated and, if possible, avoided. Sodium bicarbonate is usually administered as a hypertonic solution that produces hypernatremia, hyperosmolality, ECF volume expansion, and pulmonary congestion. When large quantities of sodium bicarbonate are administered, adequate water must be provided to avoid severe hypertonicity. Although the effects of infused bicarbonate on the plasma potassium concentration are small, physicians should be cautious if hypokalemia already exists. Further reductions in plasma potassium concentrations might produce profound hypokalemia, resulting in muscle weakness or even respiratory muscle paralysis. When sodium bicarbonate is administered to a patient with a high concentration of potential bicarbonate (i.e., lactate or ketoacids), reversal of the underlying disturbance may result in development of a rebound metabolic alkalosis.[372]

Acknowledgments

The authors thank Henry N. Hulter for the many suggestions to improve this chapter and Billy Krapf for secretarial assistance.

References

[1] Abelow BJ, Holford TR, Insogna KL. Cross-cultural association between dietary animal protein and hip fracture. Calcif Tissue Int 1992;50:14–8.
[2] Adrogue HJ, Madias NE. Changes in plasma potassium concentration during acid–base disturbances. Am J Med 1981; 71:456–67.
[3] Adrogue HJ, Chap Z, Ishida T, Field J. Role of the endocrine pancreas in the kalemic response to acute metabolic acidosis in conscious dogs. J Clin Invest 1985;75:798–808.
[4] Addae SK, Lotspeich WD. Relation between glutamine utilization and production in metabolic acidosis. Am J Physiol 1968;215:269–77.
[5] Adu D, Turney J, Michael J, McMaster P. Hyperkalemia in cyclosporine treated allograft recipients. Lancet 1983;2:370–3.
[6] Agroyannis B, Koutsikos D, Tranatos-Exarchou H, Yatzidis H. Erythrocytosis in type I renal tubular acidosis with nephrocalcinosis. Nephrol Dial Transplant 1992;7:365–6.
[7] Albright F, Burnett CH, Parson W, Reifenstein EC, Roos A. Osteomalacia and late rickets. Medicine 1946;25:399–479.
[8] Alper S. Genetic diseases of acid–base transporters. Annu Rev Physiol 2002;64:899–923.
[9] Alpern RJ, Sakhaee K. The clinical spectrum of chronic metabolic acidosis: homeostatic mechanisms produce significant morbidity. Am J Kidney Dis 1997;29:291–302.

[10] Amanzadeh J, Gitomer WL, Zerwekh JE, Preisig PA, Moe OW, Pak C, et al. Effect of high protein diet on stone-forming propensity and bone loss in rats. Kidney Int 2003;64:2142–9.
[11] Ambühl PM, Amemyia M, Danczkay M, Lötscher M, Kaissling B, Moe OW, et al. Chronic metabolic acidosis increases NHE_3 protein abundance in rat kidney. Am J Physiol 1996;271: F917–25.
[12] Armanini D, Kuhnle U, Strasser T, Dorr H, Butenandt I, Weber PC, et al. Aldosterone receptor deficiency in pseudohypoaldosteronism. N Engl J Med 1985;313:1178–81.
[13] Arrief AI, Leach W, Park R, Lazarowitz VC. Systemic effects of NaHCO3 in experimental lactic acidosis in dogs. Am J Physiol 1982;242:586–91.
[14] Arruda JAL, Mascimento L, Arevalo G, Baranowski RL, Cubria A, Carrasquillo C, et al. Bicarbonate reabsorption in chronic renal failure. Studies in man and the rat. Pflugers Arch 1978;376:193–9.
[15] Aurga S, Wehrli S, Kaissling B, Moe OW, Preisig PA, Pajor AM, et al. Chronic metabolic acidosis increases NaDC-a mRNA and protein abundance in rat kidney. Kidney Int 2000;58:206–15.
[16] Ballmer PE, Mc Nurlan MA, Hulter HN, Anderson SE, Garlick PJ, Krapf R. Chronic metabolic acidosis decreases albumin synthesis and induces negative nitrogen balance in humans. J Clin Invest 1995;95:39–45.
[17] Basir MA, Bhatia J, Brudno DS, Kleinman LI. Effects of carbicarb and sodium bicarbonate on hypoxic lactic acidosis in newborn pigs. J Invest Med 1996;44:70–4.
[18] Batlle DC. Segmental characterization of defects in collecting tubule acidification. Kidney Int 1986;30:546–54.
[19] Batlle DC, Hizon M, Cohen E, Gutterman C, Gupta R. The use of the urinary anion gap in the diagnosis of hyperchloremic metabolic acidosis. N Engl J Med 1988;318:594–9.
[20] Batlle DC, Itsarayoungyven K, Arruda JAL, Kurtzman NA. Hyperkalemic hyperchloremic metabolic acidosis in sickle cell hemoglobinopathies. Am J Med 1982;72:188–92.
[21] Batlle DC, Kurtzman NA. The defect in distal (type I) renal tubular acidosis. In: Gonick HC, Buckalew Jr VM, editors. Renal Tubular Disorders: Pathophysiology Diagnosis and Management. New York: Marcel Dekker; 1985. p. 281–305.
[22] Batlle DC, Mozes MF, Manaligod J, Arruda JAL, Kurtzman NA. The pathogenesis of hyperchloremic metabolic acidosis associated with kidney transplantation. Am J Med 1981;70:786–96.
[23] Batlle DC, Subatini S, Kurtzman NA. On the mechanism of toluene-induced renal tubular acidosis. Nephron 1988;49:210–8.
[24] Batlle DC, Shehy JT, Roseman MK, Arruda JAL, Kurtzman NA. Clinical and pathophysiologic spectrum of acquired distal renal tubular acidosis. Kidney Int 1981;20:389–96.
[25] Bailey JL, Wang X, England BK, Price SR, Ding X, Mitch WE. The acidosis of chronic renal failure activates muscle proteolysis in rats by augmenting transcription of genes encoding proteins of the ATP-dependent ubiquitin-proteasome pathway. J Clin Invest 1996;97:1447–53.
[26] Bailey JL, Wang X, Price SR. The balance between glucocorticoids and insulin regulates muscle proteolysis via the ubiquitin–proteasome pathway. Miner Electrolyte Metab 1999; 25:220–3.
[27] Baum M, Cano A, Alpern RJ. Glucocorticoids stimulate Na/H antiporter in OKP cells. Am J Physiol 1993;264:F1027–31.
[28] Bendavid C, Kleta R, Long R, Ouspenskaia M, Muenke M, Haddad D, et al. FISH diagnosis of the common 57-kb deletion in CTNS causing cystinosis. Hum Genet 2004;115:510–4.
[29] Bennett JS, Bond J, Singer I, Gottlieb AJ. Hypouricemia in Hodgkin's disease. Ann Intern Med 1972;76:751–6.
[30] Bennett IL, Freeman HC, Mitchell GL, Cooper MN. Acute methyl alcohol poisoning: a review based on experience in an outbreak of 323 cases. Med (Baltimore) 1953;32:431–63.
[31] Bersin RM, Arieff AI. Improved hemodynamic function during hypoxia with carbicarb, a new agent for the treatment of metabolic acidosis. Am J Physiol 1989;77:227–33.
[32] Better OS, Chaimowitz C, Naveh Y, Stein A, Nahir AM, Barzilai A, et al. Syndrome of incomplete renal tubular acidosis after cadaver kidney transplantation. Ann Intern Med 1969;71:39–46.
[33] Bihari D, Gimson AES, Lindridge J, Williams R. Lactic acidosis in fulminant hepatic failure: some aspects of pathogenesis and prognosis. J Hepatol 1985;1:405–16.
[34] Blackshear PJ, Holloway PAH, Alberti KG. The metabolic effects of sodium dichloracetate in the starved rat. Biochem J 1974;142:279–86.
[35] Block JB, Bronson WR, Bell W. Metabolic abnormalities of lactic acid in Burkitt type lymphoma with malignant effusions. Ann Intern Med 1966;65:101–8.
[36] Boettger T, Hübner CA, Maier H, Rust MB, Beck FX, Jentsch TJ. Deafness and renal tubular acidosis in mice lacking the K-Cl co-transporter Kcc4. Nature 2002;416:874–8.
[37] Booth BE, Tsai HC, Morris Jr RC. Metabolic acidosis in vitamin-D deficient chick. Metabolism 1977;26:1099–105.
[38] Boubaker K, Flepp M, Sudre P. Hyperlactatemia and antiretroviral therapy. Clin Infect Dis 2001;33:1931–7.
[39] Bouissou F, Barthe P, Pierragi MT. Severe idiopathic nephrotic syndrome with tubular dysfunction (report on nine pediatric cases). Clin Nephrol 1980;14:135–41.
[40] Boudry JF, Stoner LC, Burg MB. The effect of lumen pH on potassium transport in renal cortical collecting tubules. Am J Physiol 1976;230:239–44.
[41] Boyd RE, Brennan PT, Deng J-F, Rochester DF, Spyker DA. Strychnine poisoning. Am J Med 1983;74:507–12.
[42] Brenes LG, Sanchez MI. Impaired urinary ammonium excretion in patients with isolated proximal tubular acidosis. J Am Soc Nephrol 1993;4:1073–8.
[43] Brenes LG, Brenes JN, Hernandez MM. Familial proximal renal tubular acidosis. A distinct clinical entity. Am J Med 1977;63:244–52.
[44] Brennan TS, Klahr S, Hamm LL. Citrate transport in rabbit nephron. Am J Physiol 1986;251:F683–9.
[45] Brenner RJ, Spring DB, Sebastian A, McSherry EM, Genat HK, Palubinskas AJ, et al. Incidence of radiographically evident bone disease nephrocalcinosis and nephrolithiasis in various types of renal tubular acidosis. N Engl J Med 1982;307:217–21.
[46] Brent J, Mc Martin K, Phlipps S, Burkart KK, Donovan JW, Wells M, et al. Fomepizole for treatment of methanol poisoning. N Engl J Med 2001;344:424–9.
[47] Brent J, Mc Martin K, Philips S, Burkhart KK, Donovan JW, Wells M, et al. Fomepizole for the treatment of ethylene glycol poisoning. N Engl J Med 1999;340:832–8.
[48] Breslau NA, Brinkley L, Hill KD, Pak CYC. Relationship of animal protein rich diet to kidney stone formation and calcium metabolism. J Clin Endocrinol Metab 1988;66:140–6.
[49] Brezis M, Litvin Y. Syndrome of hyporeninemic hypoaldosteronism. Study of two cases and review of the literature. Isr J Med Sci 1977;13:1013–21.
[50] Brown MT, Cunningahm MJ, Ingelfinger JR, Becker AN. Progressive sensorineural hearing loss in association with distal renal tubular acidosis. Arch Otolaryngol Head Neck Surg 1993;119:458–60.
[51] Bruce LJ, Cope DL, Jones GK, Schofield AE, Burley M, Povey S, et al. Familial distal renal tubular acidosis is associated with

mutations in the red cell anion exchanger (Band 3, AE1) gene. J Clin Invest 1997;100:1693–701.
[52] Bruce RA, Jones JW, Strait GB. Anaerobic metabolic responses to acute maximal exercise in male athletes. Am Heart J 1964;67:643–50.
[53] Brüngger M, Hulter HN, Krapf R. Effect of chronic metabolic acidosis on the growth hormone/IGF-1 endocrine axis: new cause of growth hormone insensitivity in humans. Kidney Int 1997;51:216–21.
[54] Brüngger M, Hulter HN, Krapf R. Effect of chronic metabolic acidosis on thyroid hormone homeostasis in humans. Am J Physiol 1997;272:F648–53.
[55] Buckalew Jr VM, McCurdy DK, Ludwig GD, Chaykin LB, Elkinton JR. The syndrome of incomplete renal tubular acidosis. Am J Med 1968;45:32–42.
[56] Buehler JH, Berns AS, Webster Jr JR, Addington WW, Cugell DW. Lactic acidosis from carboxyhemoglobinemia after smoke inhalation. Ann Intern Med 1975;82:803–5.
[57] Bushinsky DA. Net calcium efflux from live bone during chronic metabolic but not respiratory acidosis. Am J Physiol 1989;256:F836–842.
[58] Bushinsky DA, Kreiger NS, Geisser DI, Grossman EB, Coe FL. Effects of pH on bone calcium and proton fluxes in vitro. Am J Physiol 1983;245:F204–9.
[59] Bushinsky DA, Nalbantian-Brandt C, Favus MJ. Elevated Ca++ does not inhibit the 1,25(OH)2D response to phosphorus restriction. Am J Physiol 1989;256:F285–9.
[60] Bushinsky DA, Smith SB, Gavrilov KL, Gavrilov LF, Li J, Levi-Setti R. Acute acidosis-induced alteration in bone bicarbonate and phosphate. Am J Physiol Renal Phys 2002;283:F1091–7.
[61] Bushinsky DA, Smith SB, Gavrilov KL, Gavrilov LF, Li J, Levi-Setti R. Chronic acidosis-induced alteration in bone bicarbonate and phosphate. Am J Physiol Renal Phys 2003;285:F532–9.
[62] Bushinsky DA, Frick KK. The effects of acid on bone. Curr Opin Nephrol Hypertens 2000;9:369–79.
[63] Cade R, Spooner G, Juncose L, Fuller T, Tarrant D, Raulerson D, et al. Chronic renal vein thrombosis. Am J Med 1977;63:387–97.
[64] Caprilli R, Frieri G, Latella G, Gallucci M, Bracoi U. Electrolyte and acid–base imbalance in patients with rectosigmoid bladder. J Urol 1986;135:148–50.
[65] Carlisle EJF, Donnelly SM, Vasuvattakul S, Kamel KS, Tobe S, Halperin MD. Glue-sniffing and distal renal tubular acidosis: Sticking to the facts. J Am Soc Nephrol 1991;1: 1019–27.
[66] Carroll HJ, Farber SJ. Hyperkalemia and hyperchloremic acidosis in chronic pyelonephritis. Metabolism 1964;13:808–17.
[67] Chan YL. Adrenergic control of bicarbonate absorption in the proximal convoluted tubule of the rat kidney. Pflugers Arch 1980;388:159–64.
[68] Chang SS, Grunder S, Hanukoglu A, Rösler A, Mathew PM, Hanukoglu I, et al. Mutations of the epithelial sodium channel cause salt wasting with hyperkalemic acidosis, pseudohypolaldosteronism type 1. Nat Genet 1996;12:248–53.
[69] Chapman BJ, Proudfoot AT. Adult salicylate poisoning: deaths and outcome in patients with high plasma salicylate concentrations. Q J Med 1989;72:699–707.
[70] Chisolm JJ, Harrison HC, Eberlein WR, Harrison HE. Aminoaciduria, hypophosphatemia, and rickets in lead poisoning. Am J Dis Child 1955;89:159–68.
[71] Clarkson TW, Kench JE. Urinary excretion of amino acids by nonabsorbing heavy metals. Biochem J 1956;62:361–72.
[72] Cogan MG, Rector Jr FC. Proximal reabsorption during metabolic acidosis in the rat. Am J Physiol 1982;242:F499–507.
[73] Cogan MG, Arieff AI. Sodium wasting, acidosis and hyperkalemia induced by methicillin interstitial nephritis. Evidence for selective distal tubular dysfunction. Am J Med 1978;4: 500–7.
[74] Cogan MG, Maddox DA, Warnock DG, Lin ET, Rector Jr FC. Effect of acetazolamide on bicarbonate reabsorption in the proximal tubule of the rat. Am J Physiol 1979;237:F447–54.
[75] Cohen JJ, Hulter HN, Smithline N, Melby JC, Schwartz WB. The critical role of the adrenal gland in the renal regulation of acid–base equilibrium during chronic hypotonic expansion. Evidence that chronic hyponatremia is a potent stimulus to aldosterone secretion. J Clin Invest 1976;58: 1201–8.
[76] Cohen JJ, Madias NE, Wolf CF, Schwartz WB. Regulation of acid–base equilibrium in chronic hypocapnia. Evidence that the response of the kidney is not geared at the defense of extracellular $[H^+]$. J Clin Invest 1976;57:1483–9.
[77] Cohen RD, Iles RA. Lactic acidosis: Some physiological and clinical considerations. Clin Sci Mol Med 1977;53:405–10.
[78] Cohn DW, Hruska KA, Klahr S, Hammerman MR. Increased Na–H exchange in brush border vesicles from dogs with renal failure. Am J Physiol 1982;243:F293–9.
[79] Conn JW, Rovner DR, Cohen EL, Annderson Jr JE. Inhibition of heparinoid of aldosterone biosynthesis in man. J Clin Endocrinol Metab 1966;26:527–32.
[80] Cotton EK, Fahlberg VI. Hypoglycemia with salicylate poisoning. Am J Dis Child 1964;108:171–3.
[81] Cox M, Sterns RH, Singer I. The defense against hyperkalemia. The roles of insulin and aldosterone. N Engl J Med 1979;299:525–32.
[82] Cutler Jr GB, Laue L. Congenital adrenal hyperplasia due to 21-hydroxylase deficiency. N Engl J Med 1990;323:1806–13.
[83] Dafnis E, Spohn M, Lonis B, Kurtzman NA, Sabatini S. Vanadate causes hypokalemic distal renal tubular acidosis. Am J Physiol 1992;262:F449–53.
[84] D'Agostino A, Leadbetter WF, Schwartz WB. Alterations in the ionic composition of isotonic saline solution instilled into the colon. J Clin Invest 1953;32:444–8.
[85] Dai LJ, Friedman PA, Quamme GA. Acid–base changes alter Mg^{++} uptake in mouse distal convoluted tubule cells. Am J Physiol 1997;272:F759–66.
[86] Davidoff F. Effects of guanidine derivates on mitochondrial function. I. Phenethylbiguanidine inhibition of respiration in mitochondria from guinea pig and rat tissue. J Clin Invest 1968;47:2331–43.
[87] De Brabander N, Wojciechowski M, De Decker K, de Weerdt A, Jorens PG. Fomepizole as a therapeutic strategy in paediatric methanol poisoning. Eur J Pediatr 2005;164:158–61.
[88] Dedmon RE, Wrong O. The excretion of organic anion in renal tubular acidosis with particular reference to citrate. Clin Sci 1962;22:19–32.
[89] De Franco PE, Haragsim L, Schmitz PG, Bastani B. Absence of vacuolar H + ATPase pump in the collecting duct of a patient with hypokalemic distal reanl tubular acidosis and Sjögren's syndrome. J Am Soc Nephrol 1995;6:295–301.
[90] DeFronzo RA. Hyperkalemia and hyporeninemic hypoaldosteronism. Kidney Int 1980;17:118–34.
[91] DeFronzo RA, Cooke CR, Goldberg M, Cow M, Myers AF, Agus ZS. Impaired renal tubular potassium secretion in systemic lupus erythematosus. Ann Intern Med 1977;86:268–71.
[92] DeFronzo RA, Goldberg M, Cooke CR, Barker C, Grossmann RA, Agus ZS. Investigations into the mechanisms of hyperkalemia following renal transplantation. Kidney Int 1977;11:357–65.
[93] DeFronzo RA, Taufield PA, Black H, McPhedran P, Cooke CR. Impaired renal tubular potassium secretion in sickle cell disease. Ann Intern Med 1979;90:310–6.

[94] DeFronzo RA, Felig P, Ferranini E, Wahren J. Effect of graded doses of insulin on splanchnic and peripheral potassium metabolism in man. Am J Physiol 1980;238:E421–7.
[95] Degenhart HJ, Frankena L, Visser JKA, Cost WS, van Seters AP. Further investigation of a new hereditary defect in the biosynthesis of aldosterone: evidence for a defect in 18-hydroxylation of corticosterone. Acta Physiol Pharmacol Neerl 1967;14:88–90.
[96] DeLeiva A, Christlich AR, Melby JC, Graham CA, Day RP, Luetscher JA, et al. Big renin and biosynthetic defect of aldosterone in diabetes mellitus. N Engl J Med 1976;295:639–43.
[97] Denning H, Dill DB, Talbott IH. Bilanzuntersuchung einer Salmiakazidose. Naunyn Arch Exp Pathol Pharm 1929; 144:297–310.
[98] De Sousa RC, Harrington JT, Ricanati ES, Skelrot JW, Schwartz WB. Renal regulation of acid–base equilibrium during chronic administration of acid. J Clin Invest 1974;53:465–76.
[99] Dillon MJ, Leonard JV, Buckler JM, Ogilvie D, Liddystone D. Pseudohypoaldosteronism. Arch Dis Child 1980;55:427–34.
[100] DiTella PJ, Sodhi B, McCreary J, et al. Mechanism of the metabolic acidosis of selective mineralocorticoid deficiency. Kidney Int 1987;14:466–77.
[101] Domrongkitchaiporn S, Pongskul C, Sirikulchayanonta V, Leeprasert V, Onghiphadhanakul B, Radinahamed B, et al. Bone histology and bone mineral density after correction of acidosis indistal renal tubular acidosis. Kidney Int 2002;62: 2160–6.
[102] Dorhout-Mees EJ, Machado M, Slatopolsky E, Klar S, Bricker NS. The functional adaptation of the diseased kidney. III. Ammonium excretion. J Clin Invest 1966;45:289–96.
[103] Douglas JB, Healy JK. Nephrotoxic effects of amphotericin B, including renal tubular acidosis. Am J Med 1969;46:154–62.
[104] Dubose Jr TD. Hydrogen ion secretion by the collecting duct as a determinant of the urine to blood PCO_2 gradient in alkaline urine. J Clin Invest 1982;69:145–56.
[105] Dubose Jr TD, Caflish CR. Validation of the difference in urine and blood CO_2 tension during bicarbonate loading as an index of distal nephron acidification in experimental models of distal renal tubular acidosis. J Clin Invest 1985;75:1116–23.
[106] Dumoulin A, Lapostolle F, Adnet F, Muzynski J, Baud FJ. Acidosis and hyperlactatemia in acute sodium valproate poisoning. Presse Med 1997;26:555–7.
[107] Ehlers SM, Petzel RA, Brown DC. Ventilatory response in lactic acidosis and diabetic ketoacidosis. Effect of coexistent shock, respiratory disease and severe acidosis. Miner Electrolyte Metab 1980;3:200–6.
[108] Eiam-Ong S, Dafnis E, Spohn M, Kurtzman NA, Sabatini S. H/K-ATPase in distal tubular acidosis: urinary tract obstruction, lithium, and amiloride. Am J Physiol 1993;265:F875–80.
[109] Eiseman B, Bricker EM. Electrolyte absorption following ureteroenterostomy into an isolated intestinal segment. Ann Surg 1952;136:761–9.
[110] Elkinton JR, Huth EJ, Webster Jr GD, McCance RA. The renal excretion of hydrogen ion in renal tubular acidosis. I. Quantitative assessment of the response to ammonium chloride as an acid load. Am J Med 1960;29:544–75.
[111] El-Mallakh RS, Bryan RK, Masi T, Kelly CE, Rakowski KJ. Long-term low dose glucocorticoid therapy associated with remission of overt renal tubular acidosis in Sjögren's syndrome. Am J Med 1985;79:501–14.
[112] Fawcett J, Hsu FW, Tsao T, Rabkin R. Effect of metabolic acidosis on the insulin-like growth factor-1 system and cathepsins B and L gene expression in the kidney. J Lab Clin Med 2000;36: 468–75.
[113] Fejes-Toth N, Snyder PM, Fejes-Toth G. The kidney-specific WK1 isoform is induced by aldosterone and stimulates epithelial sodium channel–mediated Na^+ transport. Proc Natl Acad Sci U S A 2004;101:17434–9.
[114] Ferris T, Kasgarian M, Levitin H, Brandt I, Epstein FH. Renal tubular acidosis and renal potassium wasting acquired as a result of hypercalcemic nephropathy. N Engl J Med 1961;265:924–8.
[115] Field M, Block MB, Levin R, Rall DP. Significance of blood lactate elevations among patients with acute leukemia and other nephroplastic proliferative disorders. Am J Med 1966;40: 528–47.
[116] Fields ALA, Wolmana SL, Halperin ML. Chronic lactic acidosis in a patient with cancer. Therapy and metabolic consequences. Cancer 1981;47:2026–9.
[117] Finch CA, Gollnick PD, Hlastala MP, Miller LR, Dillmann E, Mackler B. Lactic acidosis as a result of iron deficiency. J Clin Invest 1979;64:129–37.
[118] Finkel PN, Kronenberg K, Pesce AJ, Pollack VE, Pirani CC. Adult Fanconi syndrome amyloidosis and marked κ–light chain proteinuria. Nephron 1973;10:1–24.
[119] Fordtran JS, Walsh JH. Gastric acid secretion rate and buffer content of the stomach after eating. J Clin Invest 1973; 52:645–57.
[120] Friendman AL, Chesney RW, Trygstaad C. Autosomal dominant idiopathic Fanconi syndrome with early renal failure. Am J Med Genet 1978;2:225–32.
[121] Fraley DS, Adler S, Bruns F, Segal D. Metabolic acidosis after hyperalimentation with casein hydrolysate. Ann Intern Med 1978;88:352–4.
[122] Fraley DS, Adler S, Bruns FJ, Zett B. Stimulation of lactate production by administration of bicarbonate in a patient with a solid neoplasm and lactic acidosis. N Engl J Med 1980; 303:1100–2.
[123] Franch HA, Raissi S, Wang X, Zheng B, Bailey JL, Price SR. Acidosis impairs insulin receptor substrate-1 associated phosphoinositide 3-kinase signaling in muscle cells: consequences on proteolysis. Am J Physiol Renal Physiol 2004;287:F700–6.
[124] Frassetto L, Morris Jr RC, Sebastian A. Potassium bicarbonate reduces urinary nitrogen excretion in postmenopausal women. J Clin Endocrinol Metab 1997;82:254–9.
[125] Frassetto L, Morris Jr RC, Sebastian A. Effect of age on blood acid–base composition in adult humans: role of age-related renal functional decline. Am J Physiol 1996;271:F1114–22.
[126] Frommer JP, Agus JC. Acute ethylene glycol intoxication. Am J Nephrol 1982;2:1–5.
[127] Fulop M, Drapkin A. Potassium-depleted syndrome secondary to nephropathy apparently caused by "outdated tetracycline.". N Engl J Med 1965;272:986–9.
[128] Fulop M, Dreyer N, Tannenbaum H. The ventilatory response in diabetic ketoacidosis. Clin Sci Mol Med 1974;45:539–49.
[129] Gabow PA, Anderson RJ, Potts DE, Schrier RW. Acid–base disturbances in the salicylate-intoxicated adult. Arch Intern Med 1978;138:1481–4.
[130] Gabow PA, Clay K, Sullivan JB, Lepoff R. Organic acids in ethylene glycol intoxication. Ann Intern Med 1986;105:16–20.
[131] Gabow PA, Moore S, Schrier RW. Spironolactone-induced hyperchloremic acidosis in cirrhosis. Ann Intern Med 1979;90:338–40.
[132] Gamba G. Role of WNK kinases in regulating tubular salt and potassium transport and in the development of hypertension. Am J Renal Physiol 2005;288:F245–52.
[133] Ganote CE, Peterson DR, Carone FA. The nature of d-serine induced nephrotoxicity. Am J Pathol 1974;77:269–82.

[134] Garella S. Extracorporal techniques in the treatment of exogenous intoxications. Kidney Int 1988;33:735–54.
[135] Garella S, Chang BS, Kahn SI. Dilution acidosis and contraction alkalosis: review of a concept. Kidney Int 1975;8:279–83.
[136] Garibotto G, Sofia A, Robaudo C, Saffioti S, Sala MR, Verzola D, et al. Kidney protein dynamics and ammoniagenesis in humans with chronic metabolic acidosis. J Am Soc Nephrol 2004;15:1606–15.
[137] Geller DS, Rodriguez-Soriano J, Vallo A, Schiffer S, Bayer M, Chang SS, et al. Mutations in the mineralocorticoid receptor gene cause autosomal dominant pseudohypoaldosteronism. Nat Genet 1998;19:279–81.
[138] Gennari FJ, Goldstein MB, Schwartz WB. The nature of the renal adaptation to chronic hypocapnia. J Clin Invest 1972;51:1722–30.
[139] Gerst PH, Fleming WH, Malm JR. Increased susceptibility of the heart to ventricular fibrillation during metabolic acidosis. Circ Res 1966;19:63–70.
[140] Gold LW, Massry SG, Arieff AI, Coburn JW. Renal bicarbonate wasting during phosphate depletion. J Clin Invest 1973; 52:2556–62.
[141] Golding PL. Renal tubular acidosis in chronic liver disease. Postgrad Med J 1975;51:5.
[142] Goldstein MB, Bear R, Richardson RMA, Mardsen PA, Halperin ML. The urine anion gap: a clinically useful index of ammonium excretion. Am J Med Sci 1986;292:198–202.
[143] Goldsweig HG, Brissond ML, Davidman M. Proximal tubular dysfunction associated with Burkitt's lymphoma. Cancer 1978;41:568–77.
[144] Golimbu M, Morales P. Jejunal conduits: technique and complications. J Urol 1975;113:787–95.
[145] Gonick HC. Trace metals and the kidney. Miner Electrolyte Metab 1978;1:107–20.
[146] Good DW. Inhibition of bicarbonate absorption by peptide hormones and cyclic adenosine monophosphate in rat medullary thick ascending limb. J Clin Invest 1990;85:1006–13.
[147] Goodman AD, Lemann Jr C, Lennon EJ, Relman AS. Production, excretion and net balance of fixed acids in patients with renal acidosis. J Clin Invest 1965;44:495–506.
[148] Gordon RD. Syndrome of hyperkalemia and hypertension with normal glomerular filtration rate. Hypertension 1986;8: 93–102.
[149] Greenberg AJ, McNamara H, McCrory WW. Metabolic balance studies in primary renal tubular acidosis: effects of acidosis on external calcium and phosphorus balance. J Pediatr 1967; 69:610–8.
[150] Greene NM. Effect of epinephrine on lactate, pyruvate and excess lactate production in normal human subjects. J Lab Clin Med 1961;58:682–6.
[151] Groggel GC, Border WA, Westernfelder C. The kidney in hypergammaglobulinemia disorders. Am J Kidney Dis 1987;9:172–95.
[152] Gross JB, Kokko JP. Effects of aldosterone and potassium-sparing diuretics on electrical potential differences across the distal nephron. J Clin Invest 1977;59:82–9.
[153] Gross JM. Fanconi syndrome (adult type) developing secondary to the ingestion of outdated tetracycline. Ann Intern Med 1963;58:523–8.
[154] Guignard JP, Torrado A. Proximal renal tubular acidosis in vitamin D deficiency rickets. Acta Paediatr Scand 1973; 62:543–6.
[155] Haeussinger D, Gerok W. Hepatocyte heterogeneity in glutamate uptake by isolated perfused rat liver. Eur J Biochem 1983;136:421–5.
[156] Haeussinger D, Gerok W. Hepatocyte heterogeneity in ammonia metabolism. Chem Biol Interact 1984;48:191–4.
[157] Halperin ML, Kamel KS. D-lactic acidosis: turning sugars into acids in the gastrointestinal tract. Kidney Int 1996;49:1–8.
[158] Halperin ML, Chen CB, Cheema-Dhadli S, West ML, Junga RL. Is urea formation regulated primarily by acid–base balance in vivo? Am J Physiol 1986;250:F605–12.
[159] Halperin ML, Hammeke M, Josse RG, Jungas RL. Metabolic acidosis in the alcoholic: a pathophysiologic approach. Metabolism 1983;32:308–15.
[160] Halperin ML, Goldstein MB, Haig A, Johnson MD, Stinebaugh BJ. Studies on the pathogenesis of type I (distal) renal tubular acidosis as revealed by the urinary pCO_2 tensions. J Clin Invest 1974;53:669–77.
[161] Harrington TM, Lemann J. The metabolic production and disposal of acid and alkali. Med Clin N Am 1970;54:1543–54.
[162] Harrison HE, Harrison HC. Experimental production of renal glycosuria, phosphaturia and amino-aciduria by injection of maleic acid. Science 1954;120:606–8.
[163] Harrison JF, Blainey JD. Adult Fanconi syndrome with monoclonal abnormality of immunoglobulin light chains. J Clin Pathol 1967;20:42–8.
[164] Hart GR, Anderson RJ, Crumpler CP, Shulkin A, Reed G, Knochel JP. Epidemic classical heat stroke: clinical characteristics and course of 28 patients. Med (Baltimore) 1982;61: 189–97.
[165] Heaney RP. Protein intake and bone health: the influence of belief systems on the conduct of nutritional science. Am J Clin Nutr 2001;73:5–6.
[166] Rizzoli R, Bonjour JP. Dietary protein and bone health. J Bone Miner Res 2004;19:527–31.
[167] Heffner JE, Sahn SA. Salicylate-induced pulmonary edema. Clinical features and prognosis. Ann Intern Med 1981; 95:405–9.
[168] Heird WC, Dell RB, Driscoll JM, Grebin B, Winters RW. Metabolic acidosis resulting from intravenous alimentation mixtures containing synthetic amino acids. N Engl J Med 1972;287:943–8.
[169] Henger A, Tutt P, Riesen WF, Hulter HN, Krapf R. Acid–base and endocrine effects of aldosterone and angiotensin II inhibition in metabolic acidosis in human patients. J Lab Clin Med 2000;136:379–89.
[170] Hood VL, Keller U, Haymond MW, Kury D. Systemic pH modifies ketone body production rates and lipolysis in humans. Am J Physiol 1990;259:E321–34.
[171] Hood VL, Schubert C, Keller U, Müller S. Effect of systemic pH on pHi and lactic acid generation in exhaustive forearm exercise. Am J Physiol 1988;255:F479–85.
[172] Hoopes RR, Shrimpton AE, Knohl SJ, Hueber P, Hoppe B, Matyus J, et al. Dent disease with mutations in OCLR1. Am J Hum Genet 2005;76:260–7.
[173] Hosch M, Muser J, Hulter HN, Krapf R. Ureagenesis: evidence for lack of hepatic regulation of acid–base equilibrium in humans. Am J Renal Physiol 2003;286:F94–9.
[174] Houillier P, Borensztein P, Bichara M, Paillard M, Prigent A. Chronic neutral phosphate supplementation induces sustained renal metabolic alkalosis. Kidney Int 1992;41:1182–91.
[175] Huckabee WE. Relationships of pyruvate and lactate during anaerobic metabolism. III. Effect of breathing low-oxygen gases. J Clin Invest 1958;37:264–71.
[176] Hulter HN, Halloran BP, Toto RD, Peterson C. Long-term control of plasma calcitriol concentrations in dogs and humans: dominant role of plasma calcium concentration in experimental hyperparathyroidism. J Clin Invest 1986;76:695–702.

[177] Hulter HN, Peterson JC. Acid–base homeostasis during chronic PTH excess in humans. Kidney Int 1985;28:187–92.
[178] Hulter HN, Sebastian A, Toto RD, Bonner EL, Ilnicki LP. Renal and systemic acid–base effects of the chronic administration of hypercalcemia-producing agents: calcitriol, PTH and intravenous calcium. Kidney Int 1985;21:445–58.
[179] Hulter HN. Effects and interrelationships of PTH, Ca^{++}, vitamin D and Pi in acid–base homeostasis. Am J Physiol 248; F739–F752.
[180] Hulter HN. Hypophosphaturia impairs the renal defense against metabolic acidosis. Kidney Int 1984;26:302–7.
[181] Hulter HN, Licht JH, Bonner EL, Glynn RD, Sebastian A. Effects of glucocorticoid steroids on renal and systemic acid–base metabolism. Am J Physiol 1980;239:F30–43.
[182] Hulter HN, Bonne Jr EL, Glynn RD, Sebastian A. Renal and systemic acid–base effects of chronic spironolactone administration. Am J Physiol 1981;240:F381–7.
[183] Hulter HN, Ilnicki LP, Harbottle JA, Sebastian A. Impaired renal H^+ secretion and NH3 production in mineralocorticoid-deficient glucocorticoid-replete dogs. Am J Physiol 1977;326: F136–46.
[184] Humphrey SH, Nash Jr DA. Lactic acidosis complicating sodium nitroprusside therapy. Ann Intern Med 1978;88:58–9.
[185] Huth EJ, Mayock RL, Kerr RM. Hyperthyroidism associated with renal tubular acidosis: discussion of possible relationship. Am J Med 1959;26:818–26.
[186] Igarashi T, Sekine T, Inatomi J, Seki G. Unraveling the molecular pathogenesis of isolated proximal renal tubular acidosis. J Am Soc Nephrol 2002;13:2171–7.
[187] Igarashi T, Shibuya K, Kaoshita S, Higahihara E, Kawato H. Renal cyst formation as a complication of primary distal renal tubular acidosis. Nephron 1991;59:75–9.
[188] Isozaki U, Mitch WE, England BK, Price SR. Protein degradation and increased mRNA encoding proteins of the ubiquitin-proteasome proteolytic pathway in BC3H1 myocytes require interaction between glucocorticoids and acidification. Proc Natl Acad Sci U S A 1996;93:1967–71.
[189] Izraeli S, Rachmel A, Frishberg Y, Ereman A, Flasterstein B, Nitzan M, et al. Transient renal acidification during acute infantile diarrhea: the role of urinary sodium. J Pediatr 1990;117:711–6.
[190] Jehle AW, Forgo J, Biber J, Lederer E, Krapf R, Murer H. Acid-induced stimulation of Na/Pi-cotransport in OK cells. Am J Physiol 1997;273:F396–403.
[191] Jenkins AD, Dousa TP, Smith LH. Transport of citrate across renal brush border membrane: effects of dietary acid and alkali loading. Am J Physiol 1985;249:F590–5.
[192] Jonsson S, O'Meara M, Young JB. Acute cocaine poisoning. Am J Med 1983;75:1061–4.
[193] Karet FE. Inherited distal renal tubular acidosis. J Am Soc Nephrol 2002;13:2178–84.
[194] Karet FE, Gainza FJ, Gyory AZ, Unwin RJ, Wrong O, Tanner MJA, et al. Mutations in the chloride-bicarbonate exchanger gene AE1 cause autosomal dominant but not autosomal recessive distal renal tubular acidosis. Proc Natl Acad Sci U S A 1998;95:6337–42.
[195] Keller U, Mall T, Walter M, Bertel O, Mihatsch M, Ritz R. Pheochromocytoma with lactic acidosis. BMJ 1978;2: 606–7.
[196] Keyvan-Laigarni H, Tannenberg A. Methanol intoxication—comparison of peritoneal dialysis and hemodialysis treatment. Arch Intern Med 1974;134:293–6.
[197] Khanna A, Simoni J, Hacker C, Duran MJ, Wesson DE. Increased endothelin acitivty mediates augmented distal nephron acidification induced by dietary protein. J Am Soc Neprhol 2004;15:2266–75.
[198] Kinsella J, Cujdik T, Sacktor B. Na/H exchange activity in renal brush border membrane vesicles in response to metabolic acidosis: the role of glucocorticoids. Proc Natl Acad Sci U S A 1984;81:630–4.
[199] Kittanakom S, Cordat E, Akkarapatumwong V, Yenchitsomanus PT, Reithmeier RA. Trafficking defects of a novel autosomal recessive distal renal tubular acidosis mutant (S773P) of the human kidney anion exchanger (kAE1). J Biol Chem 2004;279:40960–71.
[200] Kleger GR, Turgay M, Imoberdorf R, McNurlan MA, Garlick PJ, Ballmer PE. Acute metabolic acidosis decreases muscle protein synthesis but not albumin syntheis in humans. Am J Kidney Dis 2001;38:1199–207.
[201] Kleinman PK. Chloestyramine and metabolic acidosis. N Engl J Med 1974;290:861.
[202] Koch M, McDougal WS. The pathophysiology of hyperchloremic metabolic acidosis after urinary diversion through intestinal segments. Surgery 1985;:561–70.
[203] Kotler DP, Tierney AR, Wang J, Peterson RN. Magnitude of body-cell mass depletion and the timing of death. Am J Clin Nutr 1989;50:444–7.
[204] Kozeny GA, Barr W, Bansal VK, Vertuno LL, Fresco R, Robinson J, et al. Occurrence of renal tubular dysfunction in lupus nephritis. Arch Intern Med 1987;147:891–5.
[205] Kerstetter JE, O'Brien KO, Caseria DM, Wall DE, Insogna KL. The impact of dietary protein on calcium absorption and kinetic measures of bone turnover in women. J Clin Endocrinol Metab 2005;90:26–31.
[206] Krapf R, Glatz M, Hulter HN. Neutral phosphate administration generates and maintains renal metabolic alkalosis and hyperparathyroidism. Am J Physiol 1995;268: F802–7.
[207] Krapf R, Vetsch R, Vetsch W, Hulter HN. Chronic metabolic acidosis increases the serum concentration of 1,25-dihydroxyvitamin D in humans by stimulating its production rate. Critical role of acidosis-induced renal hypophosphatemia. J Clin Invest 1992;90:2456–63.
[208] Krapf R, Hulter HN. Renal response to chronic hypocapnia: qualitative differences between dogs and humans? Clin Chem 1992;38:444–5.
[209] Krapf R, Beeler I, Hertner D, Hulter HN. Chronic respiratory alkalosis. The effect of sustained hyperventilation on renal regulation of acid–base equilibrium. N Engl J Med 1991;324: 1394–401.
[210] Krapf R, Schaffner T, Iten PX. Abuse of germanium associated with fatal lactic acidosis. Nephron 1992;62:351–6.
[211] Kreisberg RA, Owen OWC, Siegal AM. Ethanol-induced hyperlactatemia: inhibition of lactate utilization. J Clin Invest 1971;50:164–74.
[212] Krieger NS, Frick KK, Bushinsky DA. Cortisol inhibits acid-induced bone resorption. J Am Soc Nephrol 2002;13:2534–9.
[213] Kuo PC, Johnson LB, Schweitzer EJ, Bartlett ST. Simultaneous pancreas-kidney transplantation—a comparison of enteric and bladder drainage of exocrine pancreatic secretions. Transplantation 1997;63:238–43.
[214] Kurtz I, Maher T, Hulter HN, Schambelan M, Sebastian A. Effect of diet on plasma acid–base composition in normal humans. Kidney Int 1983;24:670–80.
[215] Laghmani K, Preisig PA, Moe OW, Yanagisawa M, Alpern RJ. Enothelin-1/endothelin-B receptor–mediated increases in NHE3 acitivity in chronic metabolic acidosis. J Clin Invest 2001;107:1563–9.
[216] Lameire N, Mathys E. Influence of progressive salt restriction on urinary bicarbonate wasting in uremic acidosis. Am J Kidney Dis 1987;8:151–8.

[217] Langman CB. Calcitriol metabolism during chronic metabolic acidosis. Semin Nephrol 1989;9:65–71.
[218] Lee SW, Russell J, Avioli V. 25-hydroxycholecalciferol: conversion inhibited by systemic acidosis. Science 1977;195:994–6.
[219] Lee DBN, Drinkard JP, Rosen VJ, Gonick HC. The adult fanconi syndrome. Med (Baltimore) 1972;51:107–38.
[220] Leehey D, Gantt C, Lim V. Heparin-induced hypoaldosteronism. Report of a case. JAMA 1981;246:2189–90.
[221] Lemann Jr J, Wilz DR, Brenes LG. Acid, calcium and phosphate balances in proximal renal tubular acidosis. Kidney Int 1976;10:561.
[222] Lemann Jr J, Litzow JR, Lennon EJ. Studies on the mechanism by which chronic metabolic acidosis augments urinary calcium excretion in man. J Clin Invest 1967;46:1318–28.
[223] Lemann Jr J, Litzow JR, Lennon EJ. The effects of chronic acid loads in normal man: further evidence for the participation of bone mineral in the defense against chronic metabolic acidosis. J Clin Invest 1966;45:1608–14.
[224] Lemann Jr J, Bushinsky DA, Hamm LL. Bone buffering of acid and base in humans. Am J Physiol Renal Physiol 2003;54: F811–32.
[225] Lennon EJ, Lemann Jr J, Litzow JR. The effects of diet and stool composition on the net external acid balance of normal subjects. J Clin Invest 1966;45:1601–7.
[226] Levine DL, Chou SY, Ferder LF, Liebman PH, Porush JG. The effect of plamsa bicarbonate levels on proximal tubule sodium reabsorption in NH_4Cl-loaded dogs. J Clin Lab Med 1976;87:804–12.
[227] Li S, Sato S, Yang X, Preisig PA, Alpern RJ. Pyk 2 activation is integral to acid stimulation of sodium/hydrogen exchanger 3. J Clin Invest 2004;114:1782–9.
[228] Licata AA, Bou E, Bartter FC, Cox J. Effects of dietary protein on urinary calcium in normal subjects and in patients with nephrolithiasis. Metabolism 1979;28:895–900.
[229] Lloyd SE, Pearce SH, Fisher SE, Steinmeyer K, Swappbach B, Scheinman SJ. A common molecular basis for three inherited kidney diseases. Nature 1996;379:445–9.
[230] Lotspeich WD. Renal hypertrophy in metabolic acidosis and its relation to ammonia excretion. Am J Physiol 1965;208: 1135–42.
[231] Luft FC. Lactic acidosis update for critical care clinicians. J Am Soc Nephrol 2001;12:S15–9.
[232] Luke RG, Allison MEM, Davidson JF, Duguid WP. Hyperkalemia and renal tubular acidosis due to renal amyloidosis. Ann Intern Med 1969;70:1211–7.
[233] Maclean AJ, Hayslett JP. Adaptive changes in ammonia excretion in renal insufficiency. Kidney Int 1980;17:595–606.
[234] Madsen PO. The etiology of hyperchloremic acidosis following urointestinal anastamosis: an experimental study. J Urol 1964;92:448–54.
[235] Madias NE, Adrogue HG, Cohen JJ. Maladaptive renal response to secondary hypercapnia in chronic metabolic alkalosis. Am J Physiol 1980;238:F283–9.
[236] Madison LL, Lochner A, Wulff J. Ethanol-induced hypoglycemia. II. Mechanism of suppression of hepatic gluconeogenesis. Diabetes 1967;16:252–8.
[237] Madison LL, Mebane D, Unger RH, Lochner A. The hypoglycemic action of ketones. II. Evidence for a stimulatory feedback of ketones on the pancreatic beta cells. J Clin Invest 1964;43:408–15.
[238] Maher T, Schambelan M, Kurtz I, Hulter HN, Jones JW, Sebastian A. Amelioration of metabolic acidosis by dietary potassium restriction in hyperkalemic patients with chronic renal insufficiency. J Lab Clin Med 1984;103:432–45.
[239] Mahlbacher K, Sicuro A, Gerber H, Hulter HN, Krapf R. Growth hormone corrects acidosis induced negative nitrogen balance and renal phosphate depletion and attenuates renal magnesium wasting in humans. Metabolism 1999;48:763–70.
[240] Mahnensmith R, Thier SO, Cooke CR, Broadus de Fronzo RA. Effect of acute metabolic acidemia on renal electrolyte transport in man. Metab Clin Exp 1979;28:831–42.
[241] Malnic G, Klose RM, Giebisch G. Micropuncture study of distal tubular potassium and sodium transport in rat nephron. Am J Physiol 1966;211:529–47.
[242] Maniar S, Laouari D, Dechaux M, Motel V, Uyvert JP, Mathian B, et al. In vivo unaltered muscle protein synthesis in experimental chronic metabolic acidosis. Kidney Int 1994;46:1705–12.
[243] Matsuda O, Nonoguchi H, Tomita K, Shiigai T, Ida T, Shinohara S, et al. Primary role of hyperkalemia in the acidosis of hyporeninemic hypoaldosteronism. Nephron 1988;49:203–9.
[244] Maurer M, Reisen W, Muser J, Hulter HN, Krapf R. Neutralization of Western diet inhibits bone resorption independently of K intakte and reduces cortisol secretion in humans. Am J Renal Physiol 2003;284:F32–40.
[245] May RC, Kelly RA, Mitch WE. Metabolic acidosis stimulates protein breakdown from skeletal muscle. J Clin Invest 1986;77:614–21.
[246] McConnell JB, Murison J, Stewart WK. The role of the colon in the pathogenesis of hyperchloremic acidosis in ureterosigmoid anastomosis. Clin Sci 1979;57:305–12.
[247] McCoy HG, Cipolle RJ, Ehlers SM, Sawchuk RJ, Zaske DE. Severe methanol poisoning. Application of a pharmacokinetic model for ethanol therapy and hemodialysis. Am J Med 1979;67:804–7.
[248] McCurdy DK, Frederic M, Elkinton JR. Renal tubular acidosis due to amphotericin B. N Engl J Med 1968;278:124–30.
[249] McMartin KE, Ambre JJ, Tephly TR. Methanol poisoning in human subjects. Role forformic acid accumulation in the metabolic acidosis. Am J Med 1980;68:414–8.
[250] McSherry E, Morris Jr RC. Attainment and maintenance of normal stature with alkali therapy in infants and children with classic renal tubular acidosis. J Clin Invest 1978;61:509–27.
[251] Medalle R, Webb R, Waterhouse C. Lactic acidosis and associated hypoglycemia. Arch Intern Med 1971;128:273–8.
[252] Melnick JZ, Elshourbagy NA, Moe OW, Preisig PA, Alpern RJ. Adenosine triphosphate lyase mediates hypocitraturia in rats. J Clin Invest 1996;98:2381–7.
[253] Miller PD, Helnig RE, Waterhouse C. Treatment of alcoholic acidosis. The role of dextrose and phosphorus. Arch Intern Med 1978;138:67–72.
[254] Millhorn DE, Eldridge FL, Waldrop TG. Effects of salicylate and 2,4-dinitrophenol on respiration and metabolism. Am J Physiol 1982;53:925–9.
[255] Mitch WE, Medina WE, Grieber S, May RC, England BK, Price SR, et al. Metabolic acidosis stimulates prtoein degradation by activating the adenosine-triphosphate-dependent pathway involving ubiquitin and proteasomes. J Clin Invest 1994;93:2127–33.
[256] Mitchell JH, Wildenthall K, Johnson Jr RL. The effects of acid–base disturbances on cardiovascular and pulmonary function. Kidney Int 1972;1:375–89.
[257] Mohler JL. Metabolic acidosis after bladder replacement: comparison of severity and reversibility in ileal and colonic reservoirs. J Urol 1988;139:628–33.
[258] Molitoris BA, Froment DH, MacKenzie TA, Huffer WH, Alfrey AC. Citrate: a major factor in the toxicity of orally administered aluminum compounds. Kidney Int 1989;36:949–53.

[259] Mookerjee B, Gault MH, Dossetor JB. Hyperchloremic acidosis in early diagnosis of renal allograft rejection. Ann Intern Med 1969;71:47–58.
[260] Morris Jr RC. An experimental renal acidification defect in patients with hereditary fructose intolerance. I. Its resemblance to renal tubular acidosis. J Clin Invest 1968;47:1389–98.
[261] Morris Jr RC, McSherry E, Sherwood LM. Evidence of a pathogenetic role of hyperparathyroidism in the renal tubular dysfunction of patients with Fanconi's syndrome. J Clin Invest 1970;50:68a.
[262] Morrissey JF, Oschoa M, Lotspeich WD, Waterhouse C. Citrate excretion in RTA. Ann Intern Med 1963;58:159–66.
[263] Moss AH, Gabow PA, Kaehny WD, Goodman SI, Haut LL, Haussler MR. Fanconi's syndrome and distal renal tubular acidosis after glue sniffing. Ann Intern Med 1980;92:69–70.
[264] Murphy RV, Coffman EW, Pringle BH, Iseri LT. Studies of sodium and potassium metabolism in salt-losing nephritis. Arch Intern Med 1952;90:750–62.
[265] Nash MA, Torrada AD, Greifer I, Spritzer A, Edelmann Jr CM. Renal tubular acidosis in infants and children. Clinical course, response to treatment, and prognosis. J Pediatr 1972;80:738–48.
[266] Nath KA, Hostetter MK, Hostetter TH. Increased ammoniagenesis as a determinant of progressive renal injury. Am J Kidney Dis 1991;17:654–7.
[267] Nath KA, Hostetter MK, Hostetter TH. Pathophysiology of chronic tubulointerstitial disease in rats: Interaction of dietary acid load, ammonia and complement component C3. J Clin Invest 1985;76:667–75.
[268] Nghiem DD, Gonwa TA, Corry RJ. Metabolic effects of urinary diversion of exocrinesecretions in pancreatic transplantation. Transplantation 1987;43:70–3.
[269] Nicar MJ, Skurla C, Sakhaee K, Pak CYC. Low citrate excretion in nephrolithiasis. Urology 1983;21:8–14.
[270] Nilwarangkur S, Nimmannit S, Chaovakul V, Susaengrat W, Ong-aj-Yooth S, Vasuvattakul S, et al. Endemic primary distal renal tubular acidosis in Thailand. Q J Med 1990;74: 289–301.
[271] Nimmannit S, Malasit P, Chaovakul V, Susaengrat W, Vasuvattakul S, Nilwarangkur S. Pathogenesis of sudden unexplained death (lai tai) and endemic distal renal tubular acidosis. Lancet 1991;338:930–2.
[272] Norby LH, Ramwell P, Weidig J, Slotkoff L, Flambenbaum W. Possible role for impaired renal prostaglandin production in pathogenesis of hyporeninaemic hypoaldosteronism. Lancet 1978;2:1118–22.
[273] Norman ME, Feldman NI, Cohn RM, Roth KS, McCurdy DK. Urinary citrate excretion in the diagnosis of distal renal tubular acidosis. J Pediatr 1978;92:394–400.
[274] Notarianni L. A reassessment of the treatment of salicylate poisoning. Drug Saf 1992;7:292–303.
[275] O'Gorman M, Fivush B, Wise B, Colombani P, Burdick J, Schwarz KB. Proximal renal tubular acidosis secondary to FK506 in pediatric liver transplant patients. Clin Transplant 1995;9:312–6.
[276] Oh MS. A new method for estimating GI-absorption of alkali. Kidney Int 1989;36:915–7.
[277] Oh MS, Carroll HJ, Clemmons JE, Vagnucci AH, Levinson SP, Whange ESM. A mechanism for hyporeninemic hypoaldosteronism in chronic renal disease. Metabolism 1974;23:1157–66.
[278] Oliver J, Koelz AM, Costello J, Bourke E. Acid–base induced alterations in glutamine metabolism and ureogenesis in perfused muscle and liver of the rat. Eur J Clin Invest 1977;7: 445–9.
[279] Ordonez FA, Santos F, martinez V, Garcia E, Fernandez P, Rodriguez J, et al. Resistance to growth hormone and insulin-like growth factor-1 in acidotic rats. Pediatr Nephrol 2000;14:720–5.
[280] Orringer CE, Eustage JC, Wunsch CD, Gardener LB. Natural history of lactic acidosis after grand-mal seizures. A model for the study of an anion-gap acidosis not associated with hyperkalemia. N Engl J Med 1977;297:796–9.
[281] Oster JR, Hotchkiss JL, Carbon M, Farmer M, Vaamonde CA. A short duration renal acidification test using calcium chloride. Nephron 1975;14:281–92.
[282] Oster JR, Moss S, Perez GO, Vaamonde CA. Renal acidification in patients with chronic renal insufficiency: pCO_2 of alkaline urine and response to NH4Cl. Miner Electrolyte Metab 1978;1: 253–62.
[283] Otten J, Vis HL. Acute reversible renal tubular dysfunction following intoxication with methyl-3-chromone. J Pediatr 1968;73:422–5.
[284] Papadoyannakis NJ, Stefanidis CJ, McGeown M. The effect of correction of metabolic acidosis on nitrogen and potassium balance of patients with chronic renal failure. Am J Clin Nutr 1984;40:623–7.
[285] Pares A, Rimola A, Bruguera M, Mas E, Rodes J. Renal tubular acidosis in primary biliary cirrhosis. Gastroenterology 1981;80:681–6.
[286] Peraino RA, Suki WN. Urine HCO-3 augments renal Ca2 + absorption independent of systemic acid–base changes. Am J Physiol 1980;238:F394–8.
[287] Perez GO, Lespier L, Jacobi J, Oster JR, Katz FH, Vaamonde CA, et al. Hyporeninemia and hypoaldosteronism in diabetes mellitus. Arch Intern Med 1977;137:852–5.
[288] Perez GO, Oster JR, Vaamonde CA. Renal acidosis and renal potassium handling in selective hypoaldosteronism. Am J Med 1974;57:809–16.
[289] Perez GO, Seigel L, Schreiner GE. 1 Selective hypoaldosteronism with hyperkalemia. Ann Intern Med 1972;76:757–63.
[290] Pines KL, Mudge GH. Renal tubular acidosis with osteomalacia. Am J Med 1951;11:302–11.
[291] Pitts RF, Lotspeich WD. Bicarbonate and the renal regulation of acid–base balance. Am J Physiol 1946;147:138–54.
[292] Rampini S, Fanconi A, Illig R, Prader A. Effect of hypochlorothiazide on proximal renal tubular acidosis in a with idiopathic "de Toni–Debre–Fanconi syndrome.". Helv Paediatr Acta 1968;23:13–21.
[293] Reaich D, Channon SM, Scrimbeour CM, Goodship THJ. Ammonium chloride induced acidosis increases protein breakdown and amino acid oxidation in humans. Am J Physiol 1992;263:E735–9.
[294] Record CO, Iles RA, Cohen RD, Williams R. Acid–base and metabolic disturbances in fulminant hepatic failure. Gut 1975;16:144–9.
[295] Relman AS. Renal acidosis and renal excretion of acid in health and disease. Adv Intern Med 1964;12:295–347.
[296] Reynolds IB, Bethune JE. Renal tubular acidosis secondary to hyperparathyroidism. Clin Res 1969;17:169.
[297] Ribeiro M, Alloisio N, Almeida H, Gomes C, Texier P, Lemos C, et al. Severe hereditary spherocytosis and distal renal tubular acidosis associated with complete absence of band 3. Blood 2000;96:1602–4.
[298] Richards P, Chamberlain MM, Wrong OM. Treatment of osteoamalacia of renal tubular acidosis by sodium bicarbonate alone. Lancet 1972;ii:994–7.
[299] Ring T, Anderson PT, Knudsen F, Nielsen FB. Salicylate-induced hyperventilation. Lancet 1985;1:1450.

[300] Ritter JM, Doktor HS, Benjamin N. Paradoxical effect of bicarbonate on cytoplasmic pH. Lancet 1990;335:1243–6.
[301] Rodriguez-Soriano J, Boichis H, Stark H, Edelmann Jr CM. Proximal renal tubular acidosis. A defect in bicarbonate reabsorption with normal urinary acidification. Pediatr Res 1967;1:81–98.
[302] Rosenbaum BJ, Makoff DL, Maxwell MH. Acid–base and electrolyte changes induced by acute isotonic saline infusion in the nephrectomized dog. J Lab Clin Med 1969;74:427–35.
[303] Roth GJ, Porte D. Chronic lactic acidosis and acute leukemia. Arch Intern Med 1970;125:317–21.
[304] Runebreg L, Miettinen A, Nikkila EN. Effect of cholestyramine on mineral excretion in man. Acta Med Scand 1972;192:71–6.
[305] Rungroj N, Devonald MAJ, Cuthbert AW, Reimann F, Akkarapatumwong V, Yenchitsomanus P, et al. A novel missense mutation in AE1 causing autosomal dominant distal renal tubular acidosis retains normal transport function but is mistargeted in polarized epithelial cells. J Biol Chem 2004;279:13833–8.
[306] Sanders PW, Herrera GA, Galla JH. Human Bence Jones protein in rat proximal tubule epithelium in vivo. Kidney Int 1987;32:851–61.
[307] Sartorius OW, Roemmelt JC, Pitts RF. The renal regulation of acid–base balance in man. IV. The nature of renal compensation in ammonium chloride acidosis. J Clin Invest 1949; 28:423–33.
[308] Sawyer WH, Solez C. Salt-losing nephritis simulating adrenocortical insufficiency. N Engl J Med 1949;240:210–5.
[309] Scandling JD, Ornt DB. Mechanism of potassium depletion during chronic metabolic acidosis in the rat. Am J Physiol 1987;252:F122–30.
[310] Schambelan M, Sebastian A, Biglieri EG. Prevalence, pathogenesis and functional significance of aldosterone deficiency in hyperkalemic patients with chronic renal failure. Kidney Int 1980;17:89–101.
[311] Schambelan M, Sebastian A, Rector FC. Mineralocorticoid (MC) resistant renal K+ secretory defect: proposed distal chloride shunt. Kidney Int 1978;14:662.
[312] Schambelan M, Stockigt JR, Biglieri M. Isolated hypoaldosteronism in adults. A renin-deficiency syndrome. New Engl J Med 1972;287:573–8.
[313] Schambelan M, Sebastian A, Katuna BA, Arteaga E. Adrenocortical hormone secretory response to chronic NH4CL-induced metabolic acidosis. Am J Physiol 1987;252: E454–60.
[314] Schelling JR, Howard RL, Winter SD, Linas SL. Increased osmolal gap in alcoholic ketoacidosis and lactic acidosis. Ann Intern Med 1990;113:580–2.
[315] Schiess WA, Ayer JL, Lotspeich WD, Pitts RF. The renal regulation of acid–base balance in man. II. Factors affecting the excretion of titratable acid by the normal human subject. J Clin Invest 1948;27:57–64.
[316] Schlatter E. Electrophysiological studies in principal cells of rat cortical collecting tubules. ADH increases the apical membrane Na+ conductance. Pflugers Arch 1987;409:81–92.
[317] Schrock H, Goldstein L. Interorgan relationships for glutamine metabolism in normal and acidotic rats. Am J Physiol 1981;240: E519–25.
[318] Schwartz WB, Hall III PW, Hays RM, Relman AS. On the mechanism of acidosis in chronic renal disease. J Clin Invest 1959;338:39–52.
[319] Schwartz WB, Bank N, Cutler RWP. The influence of urinary ionic strength on the phosphate pK2′ and the determination of titratable acid. J Clin Invest 1959;38:247–56.
[320] Sealey JE, Clark I, Bull MB, Laragh JH. Potassium balance and the control of renin secretion. J Clin Invest 1970;49: 2119–27.
[321] Sebastian A, Harris ST, Ottaway MA, Todd KM, Morris Jr RC. Improved mineral balance and skeletal metabolism in postmenopausal women treated with potassium bicarbonate. N Engl J Med 1994;330:1776–81.
[322] Sebastian A, McSherry E, Morris Jr RC. Renal potassium wasting in renal tubular acidosis (RTA). Its occurrence in types 1 and 2 RTA despite sustained correction of systemic acidosis. J Clin Invest 1971;50:667–78.
[323] Sharpy-Schafer EP, Semple SJG, Halls RW, Howarth S. Venous constriction after exercise: its relation to the acid–base changes in venous blood. Clin Sci 1965;29:397–406.
[324] Shayakul C, Alper SL. Defects in processing and trafficking of the AE+ CL-/HCO_3^- exchanger associated with inherited distal renal tubular acidosis. Clin Exp Nephrol 2004; 8:1–11.
[325] Shechter Y, Ron A. Effect of depletion of bicarbonate or phosphate ions on insulin action in rat adipocytes: further characterization of the receptor-effector system. J Biol Chem 1986;261:14951–4.
[326] Sicuro A, Mahlbacher K, Hulter HN, Krapf R. Effect of growth hormone on renal and systemic acid–base homeostasis in humans. Am J Physiol 1998;274:F650–657.
[327] Siebert DJ, Ebaugh Jr FG. Assessment of tissue anoxemia in chronic anemia by the arterial lactate/pyruvate ratio and excess lactate formation. J Lab Clin Med 1967;69: 177–82.
[328] Simpson AM, Schwartz GJ. Distal renal tubular acidosis with severe hypokalemia, probably caused by colonic H^+/K^+ ATPase. Arch Dis Child 2001;84:504–7.
[329] Simpson DP. Effect of acetazolamide on citrate excretion in the dog. Am J Physiol 1964;206:883–6.
[330] Skinner R, Pearson AD, English MW, Wyllie RA, Coulthard MG, Craft AW. Risk factors for ifosfamide nephrotoxicity in children. Lancet 1996;348:578–80.
[331] Smith AN, Skaug J, Choate KA, Nayir A, Bakkaloglu A, Ozen S, et al. Mutations in ATP6N1B, encoding a new kidney vacuolar proton pump 116 kd subunit, cause recessive distal renal tubular acidosis with preserved hearing. Nat Genet 2000;26: 71–5.
[332] Solomon A, Weiss DT, Kattine A. Nephrotoxic potential of Bence Jones proteins. N Engl J Med 1991;324:1845–51.
[333] Speiser PW, Agdere L, Ueshiba H, White PC, New MI. Aldosterone synthesis in salt-wasting congenital adrenal hyperplasia with complete absence of adrenal 21-hydroxylase. N Engl J Med 1991;324:145–9.
[334] Stacpoole PW. Lactic acidosis: the case against bicarbonate therapy. Ann Intern Med 1986;105:276–9.
[335] Stacpoole PW, Wright EC, Baumgartne TG. A controlled trial of dichloroacetate for treatment of lactic acidosis in adults. N Engl J Med 1992;327:1546–50.
[336] Stahl RA, Kanz L, Mayer B, Schollmeyer P. Hyperchloremic metabolic acidosis with high serum potassium in renal transplant patients. A cyclosporine associated effect. Clin Nephrol 1986;25:245–8.
[337] Stamey TA. The pathogenesis and implications of the electrolyte imbalance in ureterosigmoidostomy. Surg Gynecol Obstet 1956;103:736–58.
[338] Steele TW, Gyorky AZ, Edwards KDG. Renal function in analgesic nephropathy. BMJ 1969;2:213–6.
[339] Steinhart B. Case report: severe ethylene glycol intoxication with normal osmolal gap—"a chilling thought.". J Emerg Med 1990;8:583–5.

[340] Steinmetz PR, Lawson LR. Defect in urinary acidification induced in vitro by amphotericin B. J Clin Invest 1970;49: 596–601.
[341] Stone DK, Seldin DW, Kokko JP, Jacobson HR. Mineralocorticoid modulation of rabbit medullary collecting duct acidification. A sodium-independent effect. J Clin Invest 1983;72:77–83.
[342] Stoner LC, Burg M, Orloff J. Ion transport in cortical collecting tubule: effect of amiloride. Am J Physiol 1974;227:453–9.
[343] Stover EH, Borthwick KJ, Bavalia C, Eady N, et al. Novel ATP6V1B1 and ATP6V0A4 mutations in autosomal recessive distal renal tubular acidosis with new evidence for hearing loss. J Med Genet 2002;39:796–803.
[344] Summitt RC, Etteldorf JN. Salicylate intoxication in children. Experience with peritoneal dialysis and alkalinization of the urine. J Pediatr 1964;64:803–14.
[345] Sutton RA, Wong NL, Dirks JH. Effects of metabolic acidosis and alkalosis on sodium and calcium transport in the dog kidney. Kidney Int 1979;15:520–33.
[346] Szerlip HM, Singer I. Hyperchloremic metabolic acidosis after chlorine inhalation. Am J Med 1984;77:581–2.
[347] Szylman P, Better OS, Chaimowitz C, Rosler A. Role of hyperkalemia in the metabolic acidosis of isolated hypoaldosteronism. N Engl J Med 1975;294:361–5.
[348] Talal N. Sjögren's syndrome, lymphoproliferation, and renal tubular acidosis. Ann Intern Med 1971;74:633–4.
[349] Tannen RL. Relationship of renal ammonia production and potassium homeostasis. Kidney Int 1977;11:453–65.
[350] Tannen RL, Fallas WE, Branckett Jr NC. Incomplete renal tubular acidosis: some clinical and physiological features. Nephron 1975;15:111–23.
[351] Taylor WM, Halperin ML. Regulation of pyruvate dehydrogenase in muscle. Inhibition by citrate. J Biol Chem 1973;248: 6080–3.
[352] Teree TM, Mirabal-Font E, Ortiz A, Wallace WM. Stool losses and acidosis in diarrheal disease of infancy. Pediatrics 1965;36:704–13.
[353] Thorn GW, Koepf GF, Clinton M. Renal failure simulating adrenocortical insufficiency. N Engl J Med 1944; 231:76–85.
[354] Thurston JH, Pollock PG, Warren SK, Jones EM. Reduced brain glucose with normal plasma glucose in salicylate poisoning. J Clin Invest 1970;49:2139–45.
[355] Torres VE, Young Jr WF, Offord KP, Hartery RR. Association of hypokalemia, aldosteronism, and renal cysts. N Engl J Med 1990;322:345–51.
[356] Torres VE, Cowley BD, Branden MG, Yoshida I, Gatoone VH. Long-term ammonium chloride or sodium bicarbonate treatment in two models of polycystic kidney disease. Exp Nephrol 2001;9:171–80.
[357] Tuck ML, Sambhi MP, Levin L. Hyporeninemic hypoaldosteronism in diabetes mellitus. Studies of the autonomic nervous system's control of renin release. Diabetes 1979;28:237–41.
[358] Turnberg LA, Breberdorf FA, Morawski SL, Fordtran JS. Interrelationships of chloride, bicarbonate, sodium and hydrogen transport in the human ileum. J Clin Invest 1970;49: 557–67.
[359] Uribarri J, Oh MS, Carroll HJ. D-lactic acidosis. Medicine 1998;77:73–82.
[360] Uribarri J, Buquing J, Oh MS. Acid–base balance in chronic peritoneal dialysis patients. Kidney Int 1995;47:269–73.
[361] van Ypersele de Strihou C. Importance of endogenous acid production in the regulation of acid–base equilibrium: the role of the digestive tract. Adv Nephrol 1969;:367–85.
[362] Vasile B, Rasulo F, Candiani A, Latronico N. The pathophysiology of propofol infusion syndrome: a simple name for a complex syndrome. Intensive Care Med 2003;29:1417–25.
[363] Velez RJ, Myers R, Guber MS. Severe acute metabolic acidosis (acute beriberi): an avoidable complication of total parenteral nutrition. J Parenter Enteral Nutr 1985;9:216–9.
[364] Villoria JG, Nunez JFM, Miralles JM, DeCastrode D, Pozo S, Romo JMT. Hyporeninemic hypoaldosteronism in diabetic patients with chronic renal failure. Am J Nephrol 1988;8: 127–37.
[365] Wacker EWC, Haynes H, Druyan R, Risher W, Coleman JE. Treatment of ethylene glycol poisoning with ethyl alcohol. JAMA 1965;194:1231–3.
[366] Wang T, Egbert AL, Aronson PS, Giebisch G. Effect of metabolic acidosis on NaCl transport in the proximal tubule. Am J Physiol 1998;274:F1015–9.
[367] Wang W, Geibel J, Giebisch G. Regulation of the small conductance K channels in the apical membrane of rat cortical collecting tubule. Am J Physiol 1990;259:F494–502.
[368] Wanag F, Butler T, Rabban GH, Jones PK. The acidosis of cholera. Contributions of hyper-proteinemia, lactic acidemia and hyperphosphatemia. N Engl J Med 1986;315:1591–5.
[369] Weger M, Deutschmann H, Weger W, Kotanko P, Skrabal F. Incomplete renal tubular acidosis in "primary" osteoporosis. Osteoporos Int 1999;10:325–32.
[370] Weidman P, Reinhart R, Maxwell MH, Row P, Coburn JW, Massry SG. Syndrome of hyporeninemic hypoaldosteronism and hyperkalemia in renal disease. J Clin Endocrinol Metab 1973;36:965–77.
[371] Weinstein B, Irreverre I, Watkin DM. Lung carcinoma, hypouricemia and aminoaciduria. Am J Med 1965;39:520–6.
[372] Whang R. Bicarbonate overshoot: an indication for acetazolamide therapy. South Med J 1975;68:733–4.
[373] Whyte MP, Murphy WA, Fallon MD, Sly WS, Teitelbaum SL, McAlister WH, et al. Osteopetrosis, renal tubular acidosis and basal ganglia calcification in three sisters. Am J Med 1980;69:64–74.
[374] Widmer B, Gerhardt RE, Harrington JT, Cohen JJ. Serum electrolyte and acid–base composition. The influence of graded degrees of chronic renal failure. Arch Intern Med 1979;139:1099–102.
[375] Wiederkehr MR, Kalogiros J, Krapf R. Correction of metabolic acidosis improves thyroid and growth hormone axes in haemodialysis patients. Nephrol Dial Transplant 2004;1995: 1190–7.
[376] Wiederseiner JM, Muser J, Lutz T, Hulter HN, Krapf R. Acute metabolic acidosis: characterization and diagnosis of the disorder and the plasma potassium response. J Am Soc Nephrol 2004;15:1589–96.
[377] Wilson DR, Siddiqui AA. Renal tubular acidosis after kidney transplantation. Ann Intern Med 1973;79:352–61.
[378] Wilson DR, Yendt ER. Treatment of the adult Fanconi syndrome with oral phosphate supplements and alkali. Am J Med 1963;35:487–511.
[379] Wilson ID, Goetz FC. Selective hypoaldosteronism after prolonged heparin administration. Am J Med 1964;36:635–40.
[380] Winters RW, White JS, Hughes MC, et al. Disturbances of acid–base equilibrium in salicylate intoxication. Pediatrics 1959;23:260–85.
[381] Wrong OM. Urinary anion gap in hyperchloremic metabolic acidosis. N Engl J Med 1988;319:585–6.
[382] Yang CL, Angell J, Mitchell R, Ellison DH. WNK kinases regulate thiazide-sensitive Na-Cl cotransport. J Clin Invest 2003;111:1039–45.

[383] Yang SS, Chu P, Lin YF, Chen A, Lin SH. Aristolochic acid–induced Fanconi's syndrome and nephropathy presenting as hypokalemic paralayis. Am J Kidney Dis 2002;39:E14.

[384] Yong JM, Sanderson KV. Photosensitive dermatitis and renal tubular acidosis after ingestion of calcium cyclamate. Lancet 1969;2:1273–5.

[385] Yu TF, Gutman AB. Study of the paradoxical effects of salicylates in intermediate and high dosages on the renal mechanism of excretion of urate in man. J Clin Invest 1959;38: 1298–315.

[386] Yudkin J, Cohen RD. The contribution of the kidney to the removal of a lactic acid load under normal and acidotic conditions in the conscious rat. Clin Sci Mol Med 1975;48:121–31.

This page intentionally left blank

CHAPTER

60

Respiratory Acid–Base Disorders

Nicolaos E. Madias[1] *and Horacio J. Adrogué*[2]

[1]Department of Medicine, Tufts University School of Medicine and Steward St. Elizabeth's Medical Center, Boston, Massachusetts, USA

[2]Department of Medicine, Baylor College of Medicine, The Methodist Hospital, Houston, Texas, USA

The physiologic approach to acid–base disorders views blood pH as determined by the prevailing levels of carbonic acid ($PaCO_2$, the respiratory component) and plasma bicarbonate concentration ($[HCO_3^-]$, the metabolic component), as stipulated by the Henderson equation, $[H^+] = 24 \times PaCO_2/[HCO_3^-]$, the equilibrium relationship of the carbonic acid/bicarbonate system.[2] In this equation, the hydrogen-ion concentration of blood is expressed in nEq/liter, the carbon dioxide tension is expressed in mm Hg and the plasma $[HCO_3^-]$ is expressed in mEq/liter.

In this chapter, we discuss those abnormalities of acid–base equilibrium initiated by a change in blood carbon dioxide tension; such abnormalities are referred to as respiratory disorders.

RESPIRATORY ACIDOSIS

Respiratory acidosis, or primary hypercapnia, is the acid–base disturbance initiated by an increase in CO_2 stores (i.e., carbonic acid) and characterized by an increase in CO_2 tension and acidification of body fluids.[8] Life-threatening acidemia of respiratory origin can occur during severe, acute respiratory acidosis or during respiratory decompensation in patients with chronic hypercapnia.

Respiratory acidosis occurs when carbon dioxide excretion by the lungs lags behind carbon dioxide production, thereby increasing whole-body carbon dioxide stores. Because the sum of PCO_2 and PO_2 is constant in alveolar gas in patients breathing room air (~150 mm Hg at sea level), the development of substantial hypercapnia is by necessity accompanied by equivalent hypoxemia. A simplified form of the alveolar gas equation at sea level and while breathing room air (F_IO_2, 21%) is as follows:

$$P_AO_2 = 150 - 1.25\ PaCO_2$$

where P_AO_2 is alveolar O_2 tension (mm Hg). This equation demonstrates that patients breathing room air cannot reach $PaCO_2$ levels much greater than 80 mmHg because the hypoxemia that would occur at greater values is incompatible with life. Therefore, extreme hypercapnia occurs only during O_2 therapy, and severe CO_2 retention is often the result of uncontrolled O_2 administration.

The level of arterial CO_2 tension ($PaCO_2$) is above 45 mm Hg in patients with simple respiratory acidosis (measured at rest and at sea level).[12] An element of respiratory acidosis may still occur with lower $PaCO_2$ in patients residing at high altitude (e.g., 4000 m or 13,000 ft) or patients with metabolic acidosis, in whom a normal $PaCO_2$ is inappropriately high for this condition. Another special case of respiratory acidosis is the presence of arterial eucapnia, or even hypocapnia, occurring together with severe venous hypercapnia, in patients having an acute, profound decrease in cardiac output but relative preservation of respiratory function. This disorder is known as "pseudorespiratory alkalosis".[7,10,11]

PATHOPHYSIOLOGY

The ventilatory system is responsible for maintaining $PaCO_2$ within normal limits by adjusting alveolar minute ventilation to match the rate of CO_2 production. Clinically relevant conditions that alter CO_2 production are listed in Table 60.1. However, if significant amounts of CO_2 are added to the inspired gas because of

Seldin and Giebisch's The Kidney, Fifth Edition.
DOI: http://dx.doi.org/10.1016/B978-0-12-381462-3.00060-4

© 2013 Elsevier Inc. All rights reserved.

TABLE 60.1 Modifiers of Carbon Dioxide Production

Decrease	Increase
Mechanical ventilation, sedation, muscle relaxants (decreased work of breathing)	Severe dyspnea with use of accessory muscles (increased work of breathing)
Inactivity, sleep	Agitation, seizures, exercise
Hypothermia	Hyperthermia
Fat utilization	Carbohydrate utilization
Weight loss	Weight gain
Hypothyroidism	Hyperthyroidism

TABLE 60.2 Pathogenesis of Respiratory Acidosis

Imbalance between the strength of the respiratory pump and the weight of the respiratory loads caused by either of the following:
Impairment of the respiratory pump
Depressed central drive
Abnormal neuromuscular transmission
Muscle dysfunction
Increased respiratory loads
Ventilation/perfusion mismatch (increased dead space ventilation)
Augmented airway flow resistance
Lung stiffness
Pleural/chest wall stiffness
Augmented ventilatory demand (increased carbon dioxide production)
Failure of carbon dioxide transport
Cardiac arrest, circulatory collapse
Pulmonary embolism (thrombus, fat air)

accidental exposure or experimental design, respiratory acidosis can occur despite the presence of even a substantial increase in alveolar ventilation. The main elements of ventilation are the respiratory pump, which generates a pressure gradient responsible for air flow, and the loads that oppose such action. The strength of the respiratory pump can be evaluated by the pressure gradient generated by the diaphragm, which represents the difference between abdominal and pleural pressures.

The determinants of primary hypercapnia, summarized in Table 60.2, include either an imbalance between the strength of the respiratory pump and the weight of the respiratory loads or a failure of carbon dioxide transport from tissues to the lung. When the respiratory pump is unable to balance the opposing load, respiratory acidosis develops. Higher load can be caused by increased ventilatory demand, augmented airway flow resistance, and stiffness of the lungs or the chest wall. A reduction in pulmonary perfusion can also result in CO_2 retention leading to the condition referred to as "pseudorespiratory alkalosis." Respiratory acidosis is categorized into acute and chronic forms, taking into consideration their usual mode of onset and duration. (Table 60.3 and Table 60.4).

In most clinical settings, the development of respiratory acidosis is multifactorial, and recognition of each of the underlying mechanisms of CO_2 retention allows for effective patient management.

Depressed Pump Secondary to Abnormal Central Drive

The $[H^+]$ of body fluids is the main chemical stimulus for pulmonary ventilation acting on the central chemoreceptors (brainstem) and the peripheral arterial chemoreceptors (carotid and aortic bodies) (8). In normal humans there is a linear relationship between arterial PCO_2 and minute ventilation and the slope becomes steeper in the presence of hypoxemia.[55] In contrast, minute ventilation does not increase until arterial O_2 tension (PaO_2) falls below 60 mmHg, with further increases as hypoxemia worsens; yet, the hypocapnia resulting from the hypoxemia-induced hyperventilation blunts the ventilatory response.[55]

Primary disturbances in the CNS comprise the classic forms of hypercapnia that result from an abnormal respiratory control system. Yet, a faulty respiratory drive is also involved in the development of respiratory failure in other clinical settings that are unrelated to a primary disorder of ventilatory control mechanism. The ventilatory response to hypoxia and hypercapnia in the normal population has a wide range, and genetic factors play a role in this variable response. In addition, an experimentally induced increase in the work of breathing caused by both an increased airway resistance and a decrease in thorax/lung compliance alters the ventilatory drive; this change points to a complex interaction between the mechanical load and the brainstem control of the respiratory muscles. Episodes of apnea occurring in patients with status asthmaticus have been linked to this interaction.[12]

The pathogenesis of upper airway obstruction during sleep includes pharyngeal narrowing during both inspiration (caused by subatmospheric collapsing pressure) and expiration (caused by reduced ventilatory motor output due to central hypopnea).[83]

Depressed Pump Secondary to Abnormal Function of Respiratory Muscles

Inadequate ventilation leading to CO_2 retention may occur whenever the respiratory pump fails to adequately propel air through the respiratory conduits, in

TABLE 60.3 Causes of Acute Respiratory Acidosis

Depressed Central Drive	*Failure of Carbon Dioxide Transport*
General anesthesia	Cardiac arrest, circulatory collapse
Head trauma	Pulmonary embolism (thrombus, fat, air)
Cerebrovascular accident	
Obesity hypoventilation syndrome	*Ventilation/perfusion mismatch*
Cerebral edema	*(increased space ventilation)*
Brain tumor	Acute lung injury
Encephalitis	Multi-lobar pneumonia
Brain-stem lesion	
Abnormal neuromuscular transmission	*Augmented airway flow resistance*
High spinal cord injury	Upper airway obstruction
Guillain-Barré syndrome	Coma-induced hypopharyngeal obstruction
Status epilepticus	Aspiration of foreign body or vomitus
Botulism; tetanus	Laryngospasm
Crisis in myasthenia gravis	Angioedema
Familial periodic paralysis	Inadequate laryngeal intubation
Drugs or toxic agents (e.g., curare, succinylcholine, aminoglycosides, organophosphate poisoning)	Lower airway obstruction
	Status asthmaticus
Muscle dysfunction	Exacerbation of chronic obstructive pulmonary disease
Fatigue	
Hyperkalemia	*Lung stiffness*
Hypokalemia	Atelectasis
Enhanced ventilatory demand	*Pleural/chest wall stiffness*
High carbohydrate diet	Pneumothorax
High carbohydrate dialysate (peritoneal dialysis)	Haemothorax
Sorbent-regenerative hemodialysis	Flail chest
Increased dead space ventilation	Abdominal distension
	Peritoneal dialysis

TABLE 60.4 Causes of Chronic Respiratory Acidosis

Depressed Central Drive	*Ventilation/Perfusion Mismatch*
Central sleep apnea	*(increased dead space ventilation)*
Obesity hypoventilation syndrome	Emphysema
Methadone/heroin addiction	Pulmonary fibrosis
Brain tumor	Pulmonary vascular disease
Bulbar poliomyelitis	
Hypothyroidism	*Augmented airway flow resistance*
	Upper airway obstruction
Abnormal neuromuscular transmission	Tonsillar and peritonsillar hypertrophy
High spinal cord injury	Paralysis of vocal cords
Poliomyelitis	Tumor of the cords or larynx
Multiple sclerosis	Airways stenosis postprolonged intubation
Muscular dystrophy	Thymoma, aortic aneurysm
Amyotrophic lateral sclerosis	Lower airway obstruction
Diaphragmatic paralysis	Chronic obstructive pulmonary disease
Muscle dysfunction	
Myopathic disease (e.g., polymyositis)	*Lung stiffness*
	Severe chronic interstitial lung disease
	Pleural/chest wall stiffness
	Kyphoscoliosis
	Thoracic cage disease
	Thoracoplasty
	Obesity

spite of a normal respiratory drive and the absence of lung disease.[12] Primary disorders of the respiratory muscles and of the motor neurons responsible for pulmonary ventilation are classic examples of this pathophysiologic mechanism. However, an even larger and heterogeneous group of patients exists in which fatigue of the respiratory muscles plays a critical role in the development of respiratory acidosis. Such respiratory muscle fatigue is observed with poor nutrition, certain electrolyte disorders (potassium and phosphate depletion), an obligatory high level of ventilation, decreased compliance of the respiratory system, increased resistance to airflow, and alterations in thoracic configuration. Structural and functional changes in the respiratory muscles, as well as depletion of their energy stores, occur with malnutrition.

Increased Load Secondary to Abnormalities in the Lungs, and Pleural/Chest Wall Stiffness

A reduction in the effective alveolar ventilation (V_A) causes respiratory acidosis in the presence of normal or

even increased total minute ventilation (V_E).[8] The defect responsible for this condition is an increased dead space ventilation (V_D) caused by alveoli that remain ventilated but not perfused and from alveoli with excessive ventilation with respect to heir perfusion. In both cases, an increased ventilation to perfusion ratio (V_A/Q) exists. Advanced chronic obstructive pulmonary disease is the most typical condition in which this pathophysiologic defect dominates the CO_2 retention observed. The maintenance of eucapnia in patients with less advanced disease results from an increased minute ventilation, which compensates for the inefficiency of the CO_2 excretion imposed by the V_A/Q mismatch. Should the airway resistance increase, however, (because of bronchial spasm, edema of the bronchial wall, or retention of secretions), or if the minute ventilation needed to maintain eucapnia is too high, the $PaCO_2$ will increase because of respiratory-muscle fatigue. The expanded V_D in patients with advanced pulmonary disease, pulmonary thromboembolism, and shock, results in ratios of V_D/V_E and V_D/V_T (dead space to tidal volume ventilation) that might be twice the normal value of 0.3; such ratios are frequently associated with CO_2 retention. The nearly linear shape of the CO_2 dissociation curve over the physiologic range greatly facilitates the excretion of carbon dioxide in patients with all types of V_A/Q inequalities, because blood leaving areas with low V_A/Q ratio (that has a relatively high PCO_2) is counterbalanced when mixed with blood traversing high V_A/Q units (that has relatively low PCO_2 values).

Increased Carbon Dioxide Production

Overproduction of CO_2 is seldom the sole cause of CO_2 retention because enhanced V_{CO_2} stimulates ventilation thus increasing CO_2 excretion. Yet, patients with marked reduction in pulmonary reserve and those receiving constant mechanical ventilation might develop respiratory acidosis caused by increased CO_2 production. Relevant clinical conditions characterized by an increased V_{CO2} include physical activity, increased work of breathing by the respiratory muscles, seizures, shivering, fever, and hyperthyroidism. The effect of hyperthermia may be substantial because CO_2 production increases by approximately 13% for each 1°C-increase in body temperature above normal. The administration of large carbohydrate loads, orally or parenterally, is a potentially significant cause of enhanced CO_2 production in patients with hypercapnic respiratory failure. In these cases, a larger portion of fat in the diet might properly supplement caloric intake without imposing the CO_2 burden that results from carbohydrates.[15] Additional causes of CO_2 loading include the infusion of bicarbonate-containing solutions, hemodialysis with sorbent regenerative cartridge systems, and insufflation of the peritoneum with CO_2 during endoscopic procedures.

Failure of Carbon Dioxide Transport

A large reduction in cardiac output and pulmonary blood flow caused by hemorrhage or pharmacologic vasodilation in the presence of constant pulmonary ventilation (i.e., fixed mechanical ventilation) leads to a reduction in $PaCO_2$ and end-tidal PCO_2; the latter is indicative of a reduction in pulmonary CO_2 excretion which results in primary hypercapnia (Figure 60.1). In

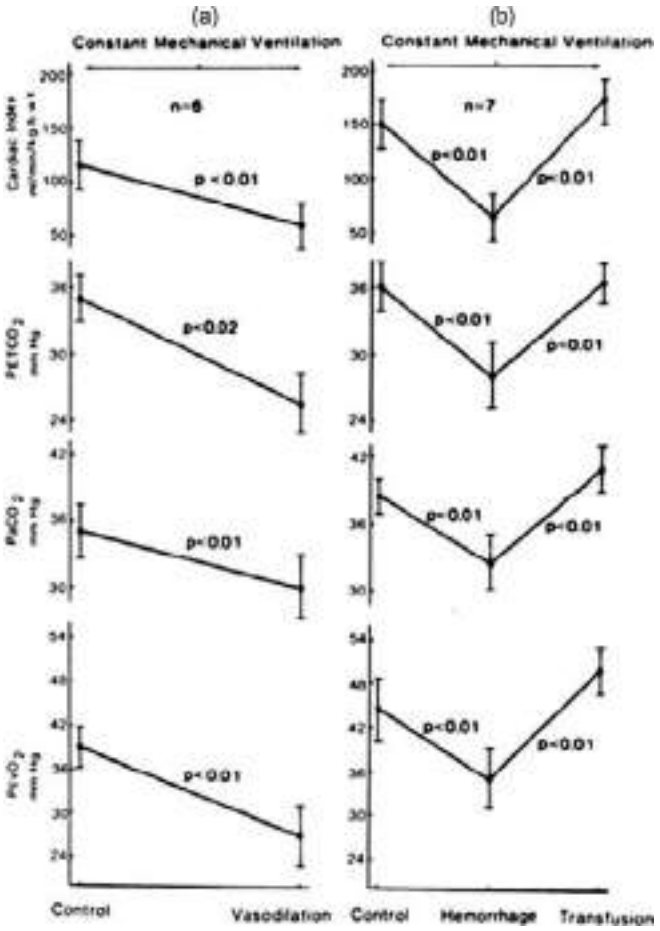

FIGURE 60.1 Reduction in end-tidal PCO_2 ($P_{ET}CO_2$) arterial PCO_2 ($PaCO_2$) and central venous PO_2 ($P_{CV}O_2$) as a result of diminished cardiac index because of pharmacological vasodilation (A) or hemorrahge (B) (changes reversed by transfusion) in the presence of constant pulmonary ventilation in anesthetized dogs. In both cases, arterial hypocapnia occurred in the presence of fixed mechanical ventilation, therefore discounting pulmonary hyperventilation as an obligatory mechanism for its pathogenesis. Moreover, the reduction in $PaCO_2$ was in fact associated with a reduction in pulmonary CO_2 excretion, as indicated by the large and significant decrement in $P_{ET}CO_2$. *(With permission, from Adrogué HJ, Rashad MN, Gorin AB, Yacoub J, Madias NE. Arteriovenous acid–base disparity in circulatory failure: studies on mechanism. Am J Physiol 1989;**257**:F1087–F1093.)*

fact, in states of severe circulatory failure, arterial hypocapnia can coexist with venous and therefore tissue, hypercapnia; however, the body CO_2 stores have been enriched and respiratory acidosis rather than respiratory alkalosis is present. This entity, which we have termed pseudorespiratory alkalosis, develops in patients with profound depression of cardiac function and pulmonary perfusion, but relative preservation of alveolar ventilation, including patients with advanced circulatory failure and those undergoing cardiopulmonary resuscitation.[7,10,11] The severely reduced pulmonary blood flow limits the CO_2 delivered to the lungs for excretion, thereby increasing the venous PCO_2. On the other hand, the increased ventilation-to-perfusion ratio causes a larger than normal decrease of CO_2 per unit of blood traversing the pulmonary circulation, thereby giving rise to arterial eucapnia or frank hypocapnia. A progressive widening of the arteriovenous difference in pH and PCO_2 develops in two settings of cardiac dysfunction, namely, circulatory failure and cardiac arrest. (Figure 60.2).[10] Severe oxygen deprivation prevails in the tissues in these two conditions, and it can be completely disguised by the reasonably preserved arterial oxygen values. Appropriate monitoring of acid–base composition and oxygenation in patients with advanced cardiac dysfunction requires mixed (or central) venous blood sampling in addition to the sampling of arterial blood.[10]

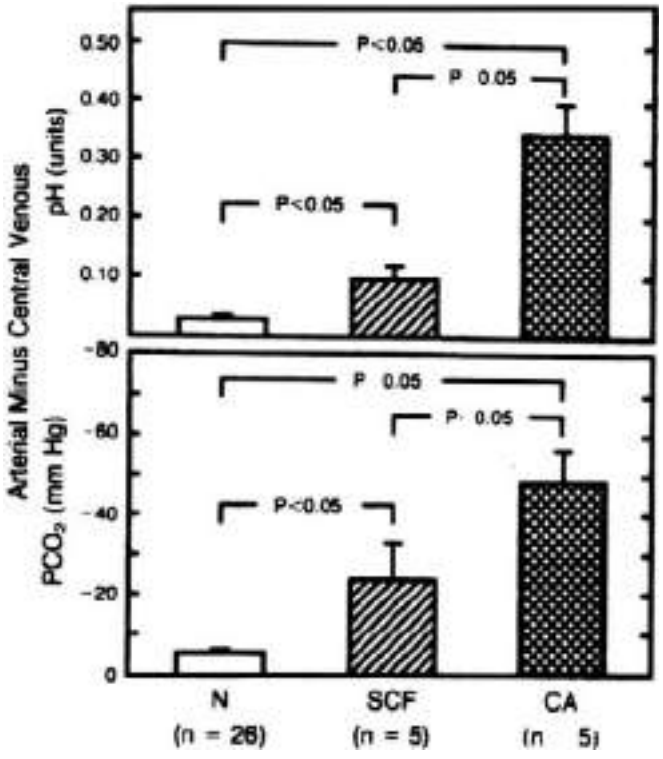

FIGURE 60.2 Arteriovenous differences in pH and PCO_2 in patients with different hemodynamic conditions. Patients with severe circulatory failure or cardiac arrest had a significant widening of the arteriovenous difference in pH and PCO_2. N, normal hemodynamic status; SCF, severe circulatory failure; CA, cardiac arrest in the presence of constant mechanical ventilation. *(With permission, from Adrogué HJ, Rashad MN, Gorin AB, Yacoub J, Madias NE. Assessing acid–base status in circulatory failure: differences between arterial and central venous blood. N Engl J Med 1989;**320**:1312–1316.)*

Secondary Physiologic Response

The secondary increment in plasma $[HCO_3^-]$ observed in acute and chronic hypercapnia is an integral part of the respiratory acidosis.[2] Adaptation to acute hypercapnia elicits an immediate increment in plasma $[HCO_3^-]$ due to titration of non-HCO_3^- body buffers; such buffers generate HCO_3^- by combining with H^+ derived from the dissociation of carbonic acid:

$$CO_2 + H_2O \leftrightarrow H_2CO_3 \leftrightarrow HCO_3^- + H^+$$
$$H^+ + B^- \leftrightarrow HB$$

where B^- refers to the base component and HB refers to the acid component of non-HCO_3^- buffers. This adaptation is completed within 5 to 10 minutes from the increase in $PaCO_2$, and assuming a stable level of hypercapnia, no further change in acid–base equilibrium is detectable for several hours.[22] Observations in unanesthetized normal humans studied in an environmental chamber (inspired CO_2 7 and 10%) reveal a mean $\Delta[HCO_3^-]/\Delta PaCO_2$ slope of 0.1 mEq/L per mm Hg. An essentially identical slope is obtained in humans in whom respiratory acidosis is induced by endogenous hypercapnia.[9]

Moderate hypoxemia does not alter the adaptive response to acute respiratory acidosis. However, studies in dogs have shown that pre-existing hypobicarbonatemia (whether it is caused by metabolic acidosis or chronic respiratory alkalosis) enhances the magnitude of the plasma $[HCO_3^-]$ response to acute hypercapnia; this response is diminished in hyperbicarbonatemic states (whether they are caused by metabolic alkalosis or chronic respiratory acidosis) (Figure 60.3).[4,64]

Although the increment in plasma $[HCO_3^-]$ during acute hypercapnia originates virtually exclusively from body buffering, evidence exists for a renal adjustment even during this early phase of the disorder. A fall in urine pH and a small increase in urine NH_4^+ and titratable acid excretion have been observed within minutes after induction of hypercapnia. Moreover, HCO_3^- reabsorption rate in the proximal convoluted tubule increases in response to acute hypercapnia. Sustained hypercapnia causes an additional, larger increase in plasma $[HCO_3^-]$ owing to stimulation of renal acidification.[5,18,65,87] As a consequence, net acid excretion (largely in the form of NH_4^+) transiently

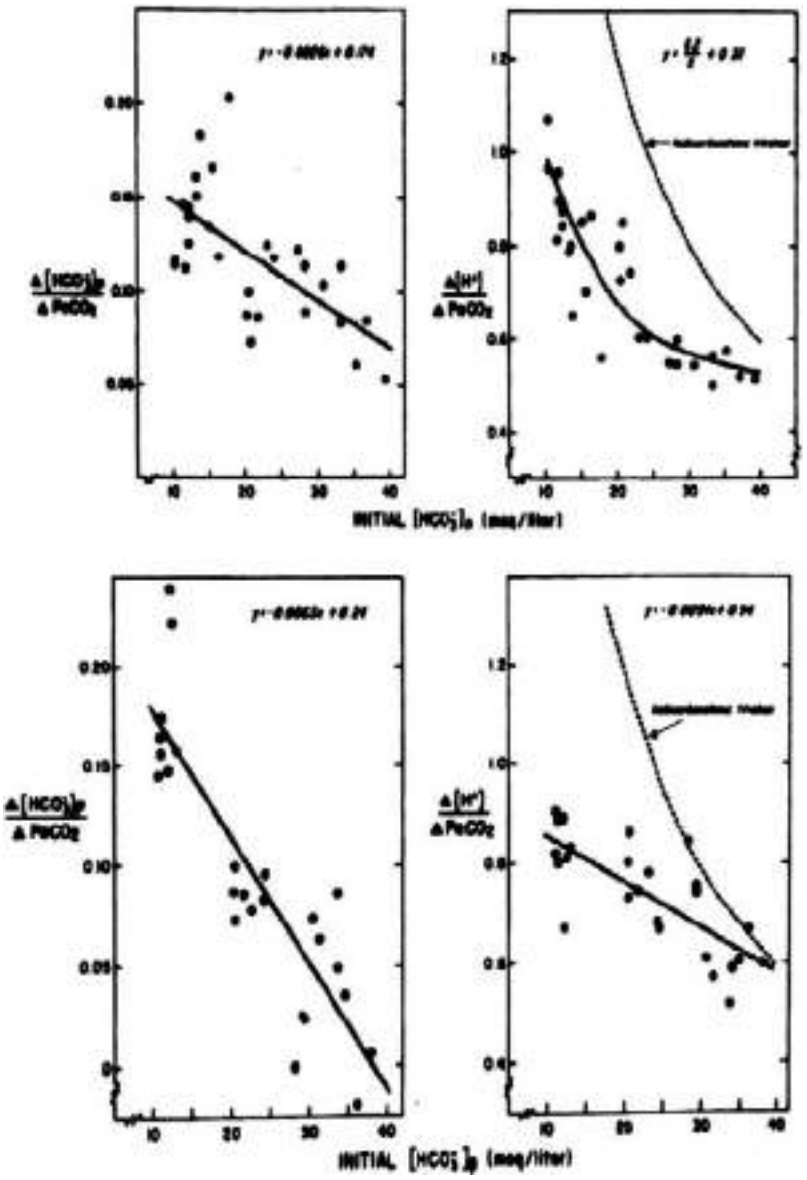

FIGURE 60.3 Influence of chronic metabolic (upper panel) or respiratory (lower panel) acid–base disorders on the acute CO_2 titration curve. Relationship between initial level of $[HCO_3]_P/PaCO_2$ regression line ($\Delta[HCO_3]_P/\Delta PaCO_2$, left) or slope of $[H^+]/PaCO_2$ regression line ($\Delta[H^+]/\Delta PaCO_2$, right) for all acute CO_2 titration studies is shown. Initial level of $[HCO_3]_P$, rather than of $PaCO_2$, is employed as an index of chronic acid–base status of animals with respiratory disorders (lower panel) for reasons of comparison with animals with metabolic acid–base disorders (upper panel). Initial $[HCO_3]_P$ values of 10 and 40 mEq/liter correspond to chronic levels of $PaCO_2$ of about 15 and 100 mm Hg, respectively. Equations describing these functions are shown in respective panels. Slope of each relationship is significantly different from 0. Interrupted line (right), labeled isobicarbonatemic titration, depicts theoretical values for $\Delta[H^+]/\Delta PaCO_2$ that would be obtained if $[HCO_3]_P$ were to remain constant at its chronic level during acute CO_2 titration. *(With permission, from Adrogué HJ, Madias NE. Influence of chronic respiratory acid-base disorders on acute CO_2 titration curve. J Appl Physiol 1985;**58**:1231–1238; and Madias NE, Adrogué HJ. Influence of chronic metabolic acid–base disorders on the acute CO_2 titration curve. J Appl Physiol 1983;**55**:1187–1195).*

exceeds endogenous acid production, effecting negative H^+ balance and generation of new HCO_3^- for the body fluids.[5] Conservation of the new HCO_3^- is ensured by an increased rate of renal HCO_3^- reabsorption, which reflects the hypercapnia-induced increase in H^+ secretory rate. Observations during the provision of exogenous alkali indicate that this increase in renal HCO_3^- reabsorption occurs roughly in parallel with the spontaneous increase in plasma $[HCO_3^-]$. A new steady state emerges for any given level of hypercapnia when the augmented filtered load of HCO_3^- is balanced by the increase in HCO_3^- reabsorption and when net acid excretion returns to the level that offsets daily endogenous acid production. In the new steady state, however, the mix of the net acid constituents differs from the normal baseline: Excretion of NH_4^+ remains increased, but is balanced by increased HCO_3^- excretion and decreased titratable acidity.[5,65] Urine pH is also increased compared to baseline. As HCO_3^- stores are being augmented by the transient increase in net acid excretion, Cl^- stores are correspondingly depleted by a transient increase in renal Cl^- excretion. Chloruresis appears to outstrip net acid excretion during the first 1–2 days of exposure to hypercapnia, the difference being accounted for by an increase in the excretion of Na^+ and K^+. Consequently, some degree of Na^+ and K^+ depletion typically accompanies adaptation to chronic hypercapnia. The hypochloremia that results from the transient chloruresis is sustained by a persistently depressed renal Cl^- reabsorption. In dogs, a new steady state emerges within three to five days. Whether this temporal pattern applies to humans is unknown. In

patients, chronic hypercapnia often reflects gradual deterioration in pulmonary function; consequently, the secondary response might keep pace with the slowing rising $PaCO_2$ without a perceptible delay.[9,65]

Studies in dogs indicate that a highly predictable curvilinear relationship exists between the degree of chronic hypercapnia and the levels at which plasma [HCO_3^-] and blood [H^+] stabilize following full physiological adaptation. Over the range of $PaCO_2$ values between 40 and 90 mm Hg, which would encompass most values encountered clinically, this curvilinear relationship between plasma [HCO_3^-] and $PaCO_2$ is closely approximated by a straight line with a mean $\Delta[HCO_3^-]/\Delta PaCO_2$ slope of 0.3 mEq/L per mm Hg. The corresponding relationship between blood [H^+] and $PaCO_2$ is strikingly linear, [H^+] rising on average by 0.32 nEq/L per mm Hg chronic elevation in $PaCO_2$. Careful observations of patients with chronic hypercapnia as a result of chronic obstructive pulmonary disease allowed estimation of a mean $\Delta[HCO_3^-]/\Delta PaCO_2$ slope of 0.35 mEq/L per mm Hg.[9,23] This slope functions up to a $PaCO_2$ of approximately 70 mm Hg. Beyond that level, the slope of $\Delta[HCO_3^-]/\Delta PaCO_2$ seems to flatten. More recently, a substantially larger slope was reported, but the small number of blood gas measurements, one for each of 18 patients, calls into question the validity of the conclusion reached. Notably, there is no information in humans on the effects of pre-existing metabolic acidosis or metabolic alkalosis on the $\Delta[HCO_3^-]/\Delta PaCO_2$ slope of superimposed chronic hypercapnia. In dogs, the background presence of metabolic disorders alters this slope substantially.

The renal response to chronic hypercapnia is not altered appreciably by dietary Na^+ or Cl^- restriction, moderate K^+ depletion, alkali loading, moderate hypoxemia (PaO_2, 45−55 mm Hg), or adrenalectomy. However, recovery from chronic hypercapnia is crippled by a diet deficient in Cl^-; in this circumstance, despite correction of the level of $PaCO_2$, plasma [HCO_3^-] remains elevated so long as the state of Cl^- deprivation persists, leading to posthypercapnic metabolic alkalosis.[6,26,65,87] On the other hand, moderate potassium depletion does not interfere with full repair of acid−base equilibrium following the return to eucapnia.

Available information implicates essentially the entire nephron and its acidification apparatus in the renal response to chronic hypercapnia. Micropuncture observations in the proximal tubule of the rat indicate that, whereas absolute HCO_3^- reabsorption is increased only mildly in acute hypercapnia, a substantial rise is observed during the chronic phase of the disorder. Total CO_2 absorption was unchanged in microperfused cortical collecting tubules obtained from rabbits exposed to hypercapnia for 3−6 hr, but it was substantially increased in tubules derived from animals that had been exposed to hypercapnia for a 24-hr period. Other microperfusion studies in the rabbit have shown, however, stimulation of acidification in cortical and medullary collecting tubules within 20 min from the onset of hypercapnia. Parallel increases in the rates of the luminal Na^+/H^+ exchanger (presumably the NHE-3) and the basolateral $Na^+/3HCO_3^-$ cotransporter in the proximal tubule have been described; these adaptations reflect an increase in the V_{max} of each transporter but no change in the K_m for sodium.[81] However, other investigators have not been able to reproduce the finding of a stimulated Na^+/H^+ exchanger in chronic hypercapnia.[65] Additionally, several studies have shown that acute or chronic hypercapnia induces exocytotic insertion of H^+-ATPase-containing subapical vesicles to the luminal membrane of both proximal tubule cells and type A intercalated cells of cortical and medullary collecting ducts. Such a redistribution of H^+-ATPase pumps during hypercapnia is not associated with a detectable increase in their quantity in either cortex or medulla. A transient increase in cell calcium appears to be important in this exocytotic event.[85,90] Rat tubule microdissection studies revealed that by 24 hr of hypercapnia, but not at earlier times, the activity of H^+-ATPase along the entire nephron (i.e., proximal tubule, thick ascending limb of Henle, and cortical and medullary collecting tubules) and that of the H^+-K^+-ATPase in the cortical and medullary collecting tubules were increased. Similar increases in the activities of the H^+-ATPase and the H^+-K^+-ATPase were observed in adrenalectomized rats replaced with physiological doses of aldosterone.[41] Further, chronic hypercapnia increases the steady-state abundance of mRNA coding for the basolateral Cl^-/HCO_3^- exchanger (band 3 protein) of type A intercalated cells in rat renal cortex and medulla. Whether this change is translated into increased levels of protein and activity of the exchanger remains unknown.[88]

The signal that triggers the renal acidification response to hypercapnia remains undefined, but present evidence favors the increase in $PaCO_2$ itself rather than the decrease in systemic pH. Indeed, observations in dogs indicate that a decrement in systemic pH is not a prerequisite to the augmentation of renal HCO_3^- reabsorption required for sustaining the secondary hyperbicarbonatemia characteristic of chronic hypercapnia.[65,66] Subsequent *in vitro* studies in rabbit proximal tubule have provided plausible validation of these whole-animal observations. Much more work is required in this area as well as the role of the filtered HCO_3^- load, and that of changes in hemodynamics and hormonal factors (such as stimulated β-adrenergic tone, renin-angiotensin-aldosterone system, cortisol, and arginine vasopressin).

There is currently no information on the impact of graded degrees of chronic renal insufficiency on the

renal acidification response to respiratory acidosis. In a patient with hyporeninemic hypoaldosteronism, hyperkalemia, and an eGFR on the order of 20–25 ml/min/1.73 m^2, the secondary response to chronic hypercapnia was suppressed; correction of the hyperkalemia allowed expression of an essentially normal secondary response. These events were ascribed to the fact that the renal response to chronic hypercapnia largely entails stimulation of ammoniagenesis and increased ammonium excretion, processes that are impaired by hyperkalemia. This case also suggests that in the absence of hyperkalemia, advanced renal insufficiency would be required to adversely impact this response. Obviously, patients with end-stage renal disease cannot mount a renal response to chronic hypercapnia and, thus, they are more subject to severe acidemia. The degree of acidemia is more pronounced in patients receiving hemodialysis rather than peritoneal dialysis because the former treatment maintains, on average, a lower plasma [HCO_3^-].[65]

Plasma Electrolyte Composition during Respiratory Acidosis

Mild hypernatremia ($\Delta[Na^+]$, 2–4 mEq/liter) is typically seen in both acute and chronic hypercapnia.[22] Hypochloremia is a consistent finding in chronic hypercapnia, and it reflects both a shift of chloride into erythrocytes and a loss of chloride in the urine during the adaptive process.[86,87] Plasma potassium concentration increases (by only approximately 0.1 mEq/liter for each 0.1 unit fall in pH) during acute hypercapnia, probably because of a shift of this ion out of cells;[3] plasma potassium does not change appreciably during chronic hypercapnia. Hyperphosphatemia is a characteristic feature of acute hypercapnia and probably reflects a release of phosphate from tissues; a rise in plasma phosphate is not observed during chronic hypercapnia. Consistent changes in plasma calcium and magnesium have not been noted in response to hypercapnia in limited observations in humans. Plasma lactate and pyruvate concentrations fall during acute hypercapnia, but they are not significantly altered by chronic hypercapnia, even in the presence of moderately severe hypoxemia. No appreciable changes in plasma unmeasured anions occur in either acute or chronic hypercapnia.

CEREBROSPINAL FLUID COMPOSITION DURING RESPIRATORY ACIDOSIS

Because carbon dioxide diffuses readily across the blood brain-barrier, increases in $PaCO_2$ are rapidly reflected in the CSF, producing a prompt increase in CSF [H^+].[55] Experimental and clinical studies have demonstrated a narrowed CSF-arterial PCO_2 difference during respiratory acidosis that has been attributed to the associated increase in cerebral blood flow. With persistent hypercapnia, CSF [HCO_3^-] increases progressively, so that the rise in CSF [H^+] is ameliorated. Studies in dogs exposed to 12% CO_2 showed that the steady-state pH decrements were virtually identical in blood and CSF.

Intracellular pH during Respiratory Acidosis

Increases in extracellular PCO_2 both *in vivo* and *in vitro* exert a prompt acidifying effect on intracellular pH.[8,54] Efforts at estimating the magnitude of intracellular acidification during acute hypercapnia using the "whole-body" DMO method have yielded variable results. *In vivo* estimates of intracellular pH of various tissues (using the DMO method or ^{31}P-NMR spectroscopy) have yielded variable responses to acute hypercapnia. Whereas intracellular pH falls in skeletal muscle and kidney by a magnitude similar to that in the extracellular compartment, smaller changes or no changes in intracellular pH have been noted in cardiac muscle, cerebral cortex, and liver (54). Renal intracellular pH returns to the normal level during the chronic phase of respiratory acidosis. There is currently no information regarding the impact of chronic hypercapnia on the intracellular acidity of other tissues.

PATHOPHYSIOLOGIC EFFECTS AND CLINICAL MANIFESTATIONS OF RESPIRATORY ACIDOSIS

Because clinical hypercapnia almost always occurs in association with hypoxemia, it is often difficult to determine whether a specific manifestation is the consequence of the elevated $PaCO_2$ or the reduced PaO_2. Nevertheless, one should bear in mind several characteristic manifestations of neurologic or cardiovascular dysfunction to diagnose the condition accurately and to treat it effectively.

Neurologic

Hypercapnia causes vasodilation and increased cerebral perfusion when autoregulation pathways of cerebral blood flow are intact.[79] This effect amounts to approximately 6% blood flow increase per 1 mm Hg rise in PCO_2, and is less pronounced in women than in men presumably because of differences in prostaglandin levels. Maximal hypercapnic vasodilation occurs at

PCO_2 levels of about 80 mm Hg.[79] Experimental studies in humans demonstrated increases in cerebral blood flow up to 200% in response to hypercapnia. Aging impairs the vasodilatory response, an effect that may be dependent on a lower concentration of oxyhemoglobin or on derangements in the arterial wall.

The precise mechanism of CO_2-induced cerebral vasodilation in humans remains undefined.[24] The increase in cerebral blood flow appears to originate from the associated acidosis, because normalization of pH by administering bicarbonate reverses the vasodilation. Studies in healthy volunteers demonstrated that hypercapnia increased cerebral release of nitric oxide accompanied by an increase in venous-arterial difference for nitrite. In contrast hypoxemia (FiO_2 10 and 12%) caused a net cerebral uptake of nitrite.[76] Release of CNP (C-natriuretic peptide) was also observed in hypercapnia.[76] Animal studies have shown that two mechanisms, namely, activation of K_{ATP} channels in vascular smooth muscle and release of nitric oxide participate in hypercapnic vasodilation.[79] Conversely, some studies in humans have shown that CO_2-induced cerebral vasodilation is independent of nitric oxide.[52] Animal studies have also demonstrated that hypercapnia increases optic disc PO_2 and this effect is prevented with systemic nitric oxide synthase inhibition; thus, nitric oxide seems to mediate CO_2-vasodilation in retinal arterioles.[77]

It is a widely held view that hypercapnia should be avoided in patients suffering from ischemic brain injury because it may lead to uncontrolled intracranial hypertension.[24] However, recently published experimental studies in rats have demonstrated that moderate to severe hypercapnia ($PaCO_2$ 60−100 mm Hg) is neuroprotective after transient global cerebral ischemia-reperfusion injury; this protection was proposed to be mediated by a hypercapnia-induced promotion of survival of neurons by modulating apoptosis-regulating proteins. In contrast, rats exposed to very severe hypercapnia ($PaCO_2$ 100−120 mm Hg) had increased brain injury and more cerebral edema.[93] Whether a similar response occurs in humans remains unknown.[24]

Most of the important clinical manifestations of hypercapnia result from its effects on the central nervous system (CNS).[17,41] Factors that influence the CNS disturbances in respiratory acidosis are the magnitude of the hypercapnia, the rapidity with which it develops the severity of the acidemia, and the degree of attendant hypoxemia. Acute hypercapnia is often associated with marked anxiety, severe breathlessness, disorientation, confusion, incoherence, and combativeness. The alterations in the level of consciousness observed in hypercapnia are accompanied by reductions in brain glutamate and aspartate and increases in glutamine and gammaaminobutyric acid (GABA). In unusually severe hypercapnia, stupor or coma can result.[41] Hypercapnic coma characteristically occurs in patients with acute exacerbations of chronic respiratory insufficiency, who are treated injudiciously with "high-flow" oxygen. Motor disturbances, including tremor, myoclonic jerks, and asterixis, are frequent accompaniments of both acute and chronic hypercapnia. Sustained myoclonus and seizure activity can also develop. Signs and symptoms of increased intracranial pressure (pseudotumor cerebri) are occasionally evident in patients with either acute or chronic hypercapnia, and they appear to be related to the vasodilating effects of CO_2 on cerebral blood vessels.[17,41] Headache is a frequent complaint. Blurring of the optic discs and frank papilledema can be found when hypercapnia is severe.[12] The plantar response can be extensor. It is not surprising, given this broad range of possible CNS findings, that respiratory acidosis often is diagnosed erroneously as a cerebral vascular accident or as an intracranial tumor.

Cardiovascular

Animal studies in cardiac myocytes and in intact isolated hearts have demonstrated that the decrease in tissue pH observed in ischemia, if maintained during reperfusion, may have a protective effect against irreversible tissue injury. The large decrease in tissue pH is accounted for by the combined effects of respiratory and metabolic acidosis in association with hypoxia.[53,57] This protection has been called the "pH paradox" since the rapid correction of acidosis observed during reperfusion precipitates irreversible tissue injury.[21] Correction of ischemia induced-acidosis during reperfusion increases cytosolic free calcium that leads to cellular injury. Administration of inhibitors of Na^+/H^+ exchange have been shown to prevent a rapid rise in tissue pH during reperfusion and this effect ameliorates ischemia/reperfusion injury.[21]

An assessment of myocardial contractility and blood flow in response to short term moderate respiratory acidosis and alkalosis have been reported in anesthetized patients with coronary artery disease. It was concluded that changes in $PaCO_2$ lead to hemodynamic effects largely due to alterations in systemic vascular resistance rather than by alterations in myocardial contractility.[56]

The hemodynamic consequences of respiratory acidosis can reflect a variety of mechanisms, including a depressing effect on myocardial contractility, systemic vasodilation resulting from an action of hypercapnia on vascular smooth muscle, stimulation of the sympathetic nervous system leading to increased plasma catecholamine levels, and blunting of receptor responsiveness to catecholamines.[8] The composite effect of

these inputs is such that acute hypercapnia of mild to moderate degree is usually characterized by warm, flushed skin, a bounding pulse, diaphoresis, increased cardiac output, and normal or increased blood pressure.[12] On the other hand, severe hypercapnia might be attended by decreases in both cardiac output and blood pressure. The vasodilatory effect of acute hypercapnia is most apparent in the cerebral circulation, where blood flow increases in direct relation to the level of $PaCO_2$. Chronic respiratory acidosis is associated with normal cardiac output and blood pressure, unless a complicating disorder such as cor pulmonale supervenes. Cerebral blood flow remains increased in chronic hypercapnia, but the increment appears to be less than that occurring in comparable levels of acute hypercapnia.

Cardiac arrhythmias occur frequently in patients with either acute or chronic hypercapnia, especially those receiving digitalis as therapy for cor pulmonale.[50] Particularly common are supraventricular tachyarrhythmia's with ventricular rates of 120–160 beats/min. Yet the role of the elevated $PaCO_2$ *per se* in the generation of cardiac arrhythmias is unclear. Indeed, remarkably little cardiac irritability occurs in extreme hypercapnia in the absence of accompanying hypoxemia and, by way of contrast, rapid restoration of normal $PaCO_2$ from very high levels is known to trigger cardiac arrhythmias, including those of ventricular origin.[50] Of interest is the reported striking increase in myocardial PCO_2 (e.g., up to 346 mmHg) and $[H^+]$ (e.g., 440 nEq/liter, pH 6.38) after ventricular fibrillation. Such hypercapnia greatly reduces cardiac resuscitability.[78] Because bicarbonate administration can aggravate PCO_2 leading to further circulatory depression, this agent should be used with caution in the presence of respiratory acidosis.

Respiratory

The normally dry alveolar space results from active sodium transport across the epithelial barrier mediated by the Na, K-ATPase.[89] A reduced alveolar fluid reabsorption caused by mechanical stress, endothelial activation, or hypoxia can lead to pulmonary edema. Hypercapnia, independent of acidosis, has been shown to impair alveolar fluid reabsorption by decreasing Na, K-ATPase activity in the alveolar epithelial cells.[89] This CO_2-induced effect results from stimulation of Na, K-ATPase endocytosis. Recent investigations have demonstrated that in rat lungs, hypercapnia leads to extracellular signal-regulated kinase (ERK) activation which in turn may mediate the CO_2-induced Na,K-ATPase down regulation and endocytosis.[92]

Complex shifts in the oxyhemoglobin dissociation curve occur during hypercapnia, because increased $PaCO_2$ tends to shift the curve to the right (Bohr effect), and acidemia (by decreasing intracellular 2,3-DPG) tends to shift the curve to the left.[34,51] Further complexity is introduced if chronic hypoxemia is present, because of an augmented intracellular 2,3-DPG level, which tends to shift the curve to the right. In addition to the effects of hypercapnia on P_{50}, erythropoietin production in response to hypoxia is inhibited by respiratory acidosis.

Contradictory evidence has been obtained about the effects of acute hypercapnia on pulmonary vascular resistance and pulmonary artery pressure; some studies indicate an increase in these parameters, whereas others have failed to demonstrate any significant effect.[12,27] Respiratory acidosis does not significantly influence the pulmonary vasoconstriction in response to hypoxia whereas respiratory alkalosis blunts this response. Diaphragm performance decreases during respiratory acidosis in anesthetized dogs, but such an effect was not observed in other skeletal muscles.

Immune Response

Respiratory acidosis elicits an inhibitory response of the immune system that has been described as a "double-edged sword" since it combines morbid effects as well as potentially salutary actions.[35] Hypercapnia was shown to inhibit bacterial growth but these effects occur at extremely high levels of PCO_2 that are not encountered in clinical practice. A reduction in cytokine signaling between immune cells and of neutrophil and macrophage production of proinflammatory cytokines including TNF-α1, IL-1β, IL-8, and IL-6 occurs in respiratory acidosis; conversely, the complement system is activated.[35]

The impairment in the cellular immune response observed in respiratory acidosis is complex and involves reduction of phagocyte migration, chemotaxis, and adhesion; decreased phagocytic ability; reduction of oxidant-mediated bacterial killing; and altered mechanisms of neutrophil death.[32] It appears that at least some of the effects of hypercapnia on the immune response are dependent on acidemia and not on the level of PCO_2 *per se*.[48]

Whereas the actions described above can be characterized as harmful, the effects of respiratory acidosis on tissue injury caused by infection or inflammation have elements that appear salutary.[31] Animal studies have shown that the severity of lung injury caused by bacterial pneumonia is ameliorated by respiratory acidosis. Similarly, the severity of septic shock and lung injury in systemic sepsis has been shown to be reduced by hypercapnia.[35] Buffering of experimentally induced respiratory acidosis does not have beneficial effects and may worsen tissue injury in bacterial pneumonia.[48]

Renal and Metabolic

Mild to moderate hypercapnia results in renal vasodilation, but acute increments in $PaCO_2$ to levels above 70 mm Hg induce renal vasoconstriction and hypoperfusion. A role for angiotensin II in the renal vasoconstriction observed during acute respiratory acidosis in the company of hypoxemia was documented in conscious dogs. Acute hypercapnia stimulates renin secretion by augmenting β-adrenergic tone and leads to increased plasma cortisol and aldosterone levels. Additionally, acute hypercapnia stimulates antidiuretic hormone release and reduces renal sodium and water excretion as a result of the hormonal changes described and the augmented renal adrenergic activity.[8] Salt and water retention commonly attends sustained hypercapnia, especially in the presence of cor pulmonale. Although metabolic demands may be augmented by the associated sympathetic surge, respiratory acidosis decreases the uptake of glucose in the tissues by inducing insulin resistance and inhibits anaerobic glycolysis by depressing 6-phosphofructokinase activity.[1] This effect can have grave consequences during hypoxia, since glycolysis becomes the main source of energy.

Skeletal

Decreased pH of respiratory or metabolic origin produces net calcium loss from cultured bone, but this response is less intense in respiratory acidosis.[28,29] The relatively mild calcium efflux of respiratory acidosis appears to be mediated exclusively by physicochemical dissolution without involving cell-mediated processes. Conversely, metabolic acidosis produces larger calcium efflux because of the additive effects of inhibition of osteoblastic bone formation and stimulation of osteoclastic bone resorption.[28,29]

DIAGNOSIS OF RESPIRATORY ACIDOSIS

In general, one should never rely on clinical examination alone to assess the adequacy of alveolar ventilation.[12] Whenever carbon dioxide retention is suspected, blood gas determinations should be obtained. Indeed, accurate laboratory data are a prerequisite for establishing the diagnosis of respiratory acidosis. Differentiating between acute and chronic hypercapnia can be a difficult task. Neither the level of hypercapnia nor the magnitude of the associated hypoxemia is particularly helpful. Of course, if the presence of complicating acid–base disorders can be excluded, the acid–base parameters themselves can be of assistance; acute hypercapnia is associated with a lower plasma bicarbonate and blood pH than is chronic hypercapnia of the same magnitude. Nonetheless, the utility of this criterion is limited by the frequent uncertainty about the coexistence of additional acid–base disturbances, the individual variability in the secondary physiologic responses to hypercapnia, and the fact that insufficient time from the onset of hypercapnia might have elapsed for full expression of the adaptive responses. In the end, clinical information must be relied on for distinguishing between acute and chronic respiratory acidosis as well as for establishing the underlying etiology.

MANAGEMENT OF RESPIRATORY ACIDOSIS

As previously noted, carbon dioxide retention, whether acute or chronic, is always associated with hypoxemia in patients breathing room air. In fact, hypoxemia, not hypercapnia or acidemia, is the most critical factor that determines morbidity and mortality of patients with acute or chronic respiratory acidosis. Therefore, the greatest emphasis should be placed on ensuring adequate oxygenation. In addition to the maintenance of appropriate oxygenation, the goals of treatment both of acute and chronic respiratory acidosis should include prevention of severe acidemia and amelioration of the hypercapnia.[6,8]

Administering Oxygen

Since oxygen administration promotes the development of CO_2 retention both in patients with acute and chronic respiratory acidosis, this therapeutic tool must be applied with caution.[16] The primary goal of oxygen therapy is to secure a PaO_2 of 60 to 70 mm Hg or an oxygen saturation of 90 to 93%. Higher levels of PaO_2 achieved with the use of very rich inspired oxygen mixtures increase the risk of worsening hypercapnia without adding significantly to the blood oxygen content.

Venturi masks should be used when possible as they yield a precise fraction of inspired oxygen (FiO_2) and provide a flow that exceeds the full ventilatory requirements.[42] Available Venturi masks deliver an FiO_2 of 24, 28, 31, 35, 40, or 60%. The design of the valve ensures that a specific proportion of oxygen and air are mixed and delivered to the patient. Other methods of oxygen delivery can be used, particularly when higher levels of FiO_2 are required. Nasal cannulae, more comfortable devices that permit oral feedings, can provide flow rates of up to 6 liters/min with an associated FiO_2 of approximately 40%. When using nasal cannula, the oxygen flow rate should be increased by 1 liter/min at a time in most instances

since it is difficult to predict the FiO_2 with this device. Simple face masks using flow rates of 6–10 liters/min can provide FiO_2 of up to 55%, but large fluctuations in FiO_2 are observed. Non-rebreathing masks can provide FiO_2 of up to 90%. The use of positive end expiratory pressure (PEEP) or continuous positive airway pressure (CPAP) can enhance the effect of a given level of oxygen administration in patients with pulmonary edema or diffuse pulmonary disease.

As indicated above, supplemental oxygen may lead to the development or worsening of hypercapnia, and this risk of oxygen therapy is even higher in patients with chronic obstructive pulmonary disease (COPD).[16] The major determinants of CO_2 retention in response to supplemental oxygen in patients with COPD, in order of importance, include an increase in dead space ventilation and ventilation/perfusion (V_A/Q) mismatch due to attenuation of hypoxic pulmonary vasoconstriction, decreased binding affinity of hemoglobin for CO_2 in the presence of increased O_2 saturation (Haldane effect), and decreased minute ventilation caused by depressed respiratory drive.[12,16] Abrupt removal of supplemental oxygen in patients who develop CO_2 retention during oxygen therapy may cause a reduction in PaO_2 to levels lower than that at the start of oxygen administration. Consequently, this practice should be avoided since it can lead to more severe tissue hypoxia and acidemia.

One should always be mindful of the risk of oxygen toxicity, which increases as a function of the level of FiO_2 and the time of exposure. As a rule, the lowest possible FiO_2 that achieves the desired hemoglobin saturation should be used, and oxygen support that results in an FiO_2 greater than 30–40% should be withdrawn as soon as feasible.

Assisted Ventilation

Development or worsening of acidemia (e.g., pH less than 7.20) or marked obtundation during oxygen therapy is an indication for mechanical ventilation, although noninvasive positive pressure ventilation (NPPV) might help avoid the need for endotracheal intubation.

Noninvasive Positive Pressure Ventilation

This form of assisted ventilation consists of the mechanical delivery of breaths via a tightly fitting nasal or full facial mask. The salutary effects of NPPV consist of increasing alveolar ventilation, reducing work of breathing and therefore providing rest to the respiratory muscles, and decreasing the rate of intubation.[12] The ventilator might deliver only inspiratory pressure (i.e., pressure support mode or PSV), or pressure might be applied during the entire respiratory cycle (i.e., bilevel positive airway pressure). The latter has become the preferred mode of NPPV used in COPD patients (the "Bi PAP" ventilator is commonly used for this purpose) because it produces greater improvements in blood gases and reduces the work of breathing more effectively than PSV alone. The high success rate of NPPV is well documented in patients with acute respiratory failure caused by decompensated COPD or acute cardiogenic pulmonary edema. Yet, it appears that NPPV can be effectively used in other conditions, including the immunocompromised patient (in whom intubation carries a higher risk of pulmonary infection), in postoperative respiratory failure, after coronary artery bypass grafting or lung resection, as an adjunct to extubation, and to avoid reintubation of previously mechanically intubated patients. A lower incidence of nosocomial infections, especially pneumonia, in comparison with standard mechanical ventilation likely explains the lower mortality associated with NPPV. Contraindications to the use of NPPV are cardiovascular instability (e.g., hypotension, serious arrhythmias, myocardial ischemia), craniofacial trauma or burns, inability to protect the airway, and the likely need for emergent intubation.

In patients with chronic respiratory acidosis, assisted ventilation should be avoided if adequate oxygenation can be attained by conservative therapy (PaO_2 on the order of 60–70 mmHg and hemoglobin oxygen saturation of 90–93%). As a general rule, if the patient is alert, able to cough, and can cooperate with the treatment program, mechanical ventilation is usually not necessary. Noninvasive positive pressure ventilation is an effective modality for selected patients with acute exacerbations of COPD. Candidates for the use of NPPV are patients with a respiratory rate of 25 per minute or greater accompanied by moderate to severe respiratory distress and acidemia or hypercapnia (pH <7.35 or $PaCO_2 >45$ mm Hg).

Mechanical Ventilation (Invasive, Including Airway Intubation) and Permissive Hypercapnia

Acute respiratory failure accounts for about two-thirds of all patients requiring mechanical ventilation. Causes of acute respiratory failure include ARDS, severe heart failure, fulminant pneumonia, sepsis, trauma, and the postoperative state. The remaining one-third of patients require ventilator assistance because of exacerbations of COPD or neuromuscular disorders, or after developing coma.

The objectives of mechanical ventilation are to reverse progressive respiratory acidosis or life-threatening hypoxemia unresponsive to conservative management and to decrease the work of breathing.

The most widely used mode of mechanical ventilation is assist-control ventilation, in which the ventilator delivers a preset tidal volume when triggered by the patient's inspiratory effort or independently if such an effort does not occur within a preselected time. Another widely used modality is pressure-support ventilation in which 16–30 breaths per minute are delivered to augment the patient's spontaneous respiratory effort by a preset level of pressure (rather than volume).

Traditionally, the goal of treatment with mechanical ventilation had been to restore $PaCO_2$ and arterial blood pH to a level close to the normal values of 40 mm Hg and 7.40, respectively, regardless of the tidal volumes and airway pressures needed.[13] However, it is now clear that large tidal volumes with excessively high airway pressures (e.g., plateau levels higher than 25–35 cm of H_2O) often lead to alveolar overdistension and barotrauma. Therefore, an alternative approach that uses a protective ventilation strategy and allows $PaCO_2$ to rise, called "permissive hypercapnia" (or controlled mechanical hypoventilation), has been introduced.[13,20] In this form of treatment, lower tidal volumes (5 to 7 ml/kg or less) and peak inspiratory pressures are used. As expected, $PaCO_2$ rises but rarely exceeds 80 mm Hg, and blood pH can decrease to as low as 7.00 to 7.10, while blood oxygenation is secured.[20,38] Permissive hypercapnia has been reported to have salutary effects in animal models of cerebral ischemia-reperfusion injury and in lung injury secondary to bacterial infection (see Pathophysiologic Effects and Clinical Manifestations of Respiratory Acidosis).

The increased respiratory drive associated with permissive hypercapnia can cause extreme discomfort, making sedation necessary. Because the patient commonly requires neuromuscular blockade as well, accidental disconnection from the ventilator can cause sudden death. Furthermore, after the neuromuscular blocking agent is discontinued, there might be weakness or paralysis for several days or weeks. There are several contraindications to the use of permissive hypercapnia, including cerebrovascular disease, brain edema, increased intracranial pressure, convulsions, depressed cardiac function, cardiac arrhythmias, and severe pulmonary hypertension. Importantly, most of these entities can develop as adverse effects of permissive hypercapnia itself, especially when hypercapnia is associated with substantial acidemia. In fact, some experimental evidence indicates that correction of acidemia attenuates the adverse hemodynamic effects of permissive hypercapnia.[30] It appears prudent, although still controversial, to keep the blood pH at approximately 7.30 by administering intravenous alkali when controlled hypoventilation is prescribed.[6]

If mechanical ventilation is deemed necessary in patients with chronic respiratory acidosis, the goal should be to increase minute ventilation sufficiently to maintain blood pH and $PaCO_2$ at levels that are close to the patient's chronic baseline values. Because acute alkalemia reduces P_{50}, a rapid increase in blood pH should be avoided in the management of patients with acute exacerbations of chronic respiratory acidosis. Such an alkalemia can be observed with aggressive normalization of $PaCO_2$ via mechanical ventilation or after alkali administration. Because these patients commonly have an associated cardiac or cerebrovascular insufficiency, they cannot augment cardiac output or regional perfusion to overcome the higher oxygen binding affinity of hemoglobin. When employing assisted ventilation, blood gases should be measured frequently to prevent or correct both overventilation and underventilation. In general, as long as adequate oxygenation can be maintained, $PaCO_2$ should be reduced toward the chronic baseline over many hours to a few days.

Improving Pulmonary Function

Measures directed against all possible reversible factors responsible for the respiratory acidosis should be undertaken. Pulmonary infections should be treated aggressively, and direct examination of bronchial secretions and cultures should guide such therapy. Bronchodilators, administered by inhalation, orally, subcutaneously, or intravenously, are the main therapeutic tool for patients with COPD.[69] The most relevant bronchodilators include β-agonists and anticholinergics; theophylline is used less often. Inhaled glucocorticoids, systemic glucocorticoids, and mucoactive agents are often used as adjunct therapy in COPD and other causes of respiratory acidosis. Reversal of the hypercapnia, acidemia, and hypoxemia will usually improve cardiac dysfunction and pulmonary hypertension.[12] Excluding the case of cor pulmonale in association with low cardiac output, administration of digitalis appears to be of no value in the treatment of the depressed cardiac contractility accompanying severe respiratory acidosis. Close monitoring of the patient's fluid status is crucial, because volume overload increases pulmonary capillary pressure and predisposes to the development of pulmonary edema. Diuretics should be used, as needed. In appropriate settings, the use of intermittent ultrafiltration/hemodialysis or continuous arteriovenous or venovenous hemofiltration may be required. Nutritional support is of crucial importance in order to minimize reduction in the strength and endurance of the respiratory muscles and depression in the body's immunity. Administering a larger proportion of nonprotein calories as fat emulsions might aid the weaning process from ventilatory support by decreasing the rate of CO_2 production in comparison with isocaloric amounts of carbohydrate.[15]

Alkali Therapy

The presence of a component of metabolic acidosis has traditionally been the primary indication for alkali therapy in patients with respiratory acidosis. However, in patients maintained on mechanical ventilation, in whom permissive hypercapnia is utilized resulting in blood pH values below 7.20, some clinicians recommend the use of sodium bicarbonate to ameliorate the acidemia.[30] In fact, correction of acidemia attenuates the adverse hemodynamic effects of permissive hypercapnia. As explained before, it appears prudent, although still controversial, to keep the blood pH at approximately 7.30 by administering intravenous alkali when controlled hypoventilation is prescribed.[6]

Alternative forms of alkali, which do not augment CO_2 generation as much as bicarbonate does, but are effective in ameliorating acidemia include Carbicarb® and THAM (Tromethamine).[25,61,63] Carbicarb is an equimolar mixture of sodium carbonate and sodium bicarbonate. Because carbonate is a stronger base, it is used in preference to bicarbonate for buffering hydrogen ions generating bicarbonate rather than carbon dioxide in the process ($CO_3^{2-} + H^+ \rightarrow HCO_3^-$). In addition, the carbonate ion can react with carbonic acid, therby consuming carbon dioxide ($CO_3^{2-} + H_2CO_3^- \rightarrow 2HCO_3^-$). Yet, the interaction of bicarbonate with hydrogen ions still generates CO_2. Thus, Carbicarb limits but does not eliminate the generation of carbon dioxide.[6,19] Clinical experience with Carbicarb is limited, and this product is not yet commercially available for clinical use.

THAM (tris [hydroxymethyl] aminomethane) is a synthetic buffer available as a 0.3-N solution, which at a pH of 7.20–7.40 has a buffer capacity equivalent to that of normal blood.[25] A distinct property of THAM is its capacity to buffer both metabolic acids ($THAM + H^+ \rightarrow THAM^+$) and carbonic acid ($THAM + H_2CO_3 \rightarrow THAM^+ + HCO_3^-$). Because THAM freely penetrates cells it can be an effective intracellular buffer. Indeed, *in vitro* and *in vivo* studies have indicated that both extracellular and intracellular pH rise after THAM administration; *in vitro* studies have shown that THAM exerts a positive inotropic effect on the ischemic myocardium. When used in the experimental treatment of head injury, it reduces brain edema. THAM has been proposed as a substitute for bicarbonate in treating the acidemia of respiratory acidosis because of its theoretical potential to decrease $PaCO_2$.

The effects of THAM in patients with acute respiratory distress syndrome (ARDS) undergoing permissive hypercapnia has been investigated.[91] Permissive hypercapnia of two hours duration and $PaCO_2$ of 80 mm Hg increased cardiac output and decreased systemic vascular resistance. Mean pulmonary artery pressure increased and mean arterial pressure decreased significantly only in the untreated group (pH-uncorrected group). Myocardial contractility decreased in both groups but significantly less (approximately 10%) in the pH-corrected group with THAM.

However, correction of acidemia with this compound leads to CO_2 retention because of pH-mediated depression of ventilation. In addition, serious adverse effects have been reported with the use of THAM, including hyperkalemia, hypoglycemia, and widespread organ necrosis.[6]

In the absence of a complicating element of metabolic acidosis and with the possible exception of the severely acidemic patient with intense generalized bronchoconstriction undergoing mechanical ventilation (see previous discussion), there is no role for alkali administration (i.e., $NaHCO_3$, Carbicarb, THAM) in chronic respiratory acidosis.

MIXED ACID–BASE DISORDERS ASSOCIATED WITH RESPIRATORY ACIDOSIS

Complicating acid–base disorders occur with surprising frequency in patients with acute or chronic respiratory acidosis and often present a considerable challenge to the clinician. What follows is a brief account of the most common mixed acid–base disorders in which respiratory acidosis is a component.

Respiratory Acidosis and Metabolic Acidosis

Clinical examples of this entity include untreated cardiopulmonary arrest, circulatory failure in patients with COPD, severe renal failure associated with hypercapnic respiratory failure, various intoxications, and hypokalemic (or less frequently hyperkalemic) paralysis of respiratory muscles in patients with diarrhea or renal tubular acidosis.[8] In patients with this mixed disturbance, increasing ventilation to reduce $PaCO_2$ can be of great value in rapidly bringing blood pH, and presumably intracellular pH, into a safe range. Therefore, consideration should be given to intubating and mechanically ventilating patients with metabolic acidosis, who retain CO_2, or those with moderate to severe respiratory acidosis, who also develop an element of metabolic acidosis. Despite the potential disadvantages of bicarbonate administration, and considering the profound impact of severe acidemia on cardiovascular function as well as the lack of suitable alternatives, we recommend the judicious administration of sodium bicarbonate in selected patients with metabolic and respiratory acidosis who have a blood pH less than 7.10.[8] However, alkali

therapy must be used with great caution in these patients, because of the substantial risk of further respiratory depression leading to life-threatening hypoxemia and worsened hypercapnia. In patients with metabolic acidosis and respiratory acidosis who also have fluid excess, congestive heart failure, or severe renal failure, administration of any sodium containing alkali might be potentially harmful. Consequently, dialysis utilizing bicarbonate containing dialysate might be a reasonable option. With this treatment modality, not only can large quantities of alkali be delivered, but significant amounts of fluid can also be removed.

Respiratory Acidosis and Metabolic Alkalosis

This combination represents one of the most frequently observed mixed acid–base disorders. Deviation of blood pH toward alkalinity commonly occurs in patients with respiratory acidosis because of several complicating events and medications.[8] Patients with COPD frequently develop gastritis, peptic ulcer disease, or gastrointestinal bleeding as a result of taking xanthines and corticosteroids, and possibly due to the underlying disease itself. Metabolic alkalosis resulting from ingestion of absorbable antacids and/or vomiting is prevalent. Chronic administration of corticosteroids can induce potassium depletion and metabolic alkalosis. Further, prescription of diuretics for treatment of cor pulmonale or other disorders can also generate metabolic alkalosis. Critically ill patients with respiratory failure caused by ARDS and, occasionally, those with profound hypokalemia also might develop this mixed acid–base disorder. Rapid correction of CO_2 retention via mechanical ventilation in patients with long-standing hypercapnia and secondary hyperbicarbonatemia can cause transient alkalemia, a condition commonly referred to as "posthypercapnic metabolic alkalosis." In the absence of the clinical history, simple review of the blood gas values might lead to the erroneous diagnosis of primary metabolic alkalosis. If the patient's chloride intake remains adequate, urinary excretion of the excess bicarbonate will repair the hyperbicarbonatemia in one to three days. On the other hand, unavailability of chloride will perpetuate the state of posthypercapnic alkalosis.

The management of patients with mixed respiratory acidosis and metabolic alkalosis requires a combination of measures aimed at correcting the coexisting disorders. Acetazolamide can produce large bicarbonate losses in the form of the sodium and potassium salt. The pharmacologic effect of acetazolamide substantially diminishes once the elevated plasma [HCO_3^-] is returned toward normal. Plasma potassium should be closely monitored, especially if potassium depletion was initially present, and appropriate supplementation should be provided. On occasion, the administration of an acidifying agent is required. An alternative therapeutic approach in patients with renal failure is the use of either hemodialysis with a "low bicarbonate" concentration in the dialysate or of hemofiltration along with saline replacement. Effective management of the superimposed element of metabolic alkalosis will usually result in a significant decline in the $PaCO_2$ level and improvement of the patient's hypoxemia.

Respiratory Acidosis, Metabolic Acidosis, and Metabolic Alkalosis

This triple disorder might be encountered during cardiopulmonary resuscitation when an element of metabolic alkalosis caused by alkali administration is superimposed on preexisting respiratory acidosis and metabolic (lactic) acidosis. Similarly, this mixed disturbance is observed in severely ill patients with COPD and CO_2 retention, who might develop simultaneously metabolic alkalosis (usually caused by diuretics and a chloride restricted diet) and metabolic acidosis (commonly lactic acidosis caused by hypoxemia, hypotension, or sepsis). The management of this triple acid–base disorder demands application of therapeutic measures aimed at each individual component.

RESPIRATORY ALKALOSIS

The acid–base disturbance initiated by a decrease in CO_2 stores (i.e., carbonic acid) and characterized by a decrease in CO_2 tension is termed respiratory alkalosis, or primary hypocapnia, and entails alkalinization of body fluids.[60] The level of $PaCO_2$ is less than 35 mm Hg in patients with simple respiratory alkalosis, who are at rest and at sea level. An element of respiratory alkalosis can still occur with higher levels of $PaCO_2$ in patients with metabolic alkalosis in whom a normal $PaCO_2$ is inappropriately low for this primary metabolic disorder.

PATHOPHYSIOLOGY

The presence of hypocapnia signifies excessive alveolar ventilation relative to the prevailing CO_2 production, thereby leading to negative CO_2 balance, which may result from increased alveolar ventilation, decreased CO_2 production, or both. Primary hypocapnia might also originate from the extrapulmonary elimination of CO_2, as indicated above. In the vast majority

of cases, however, primary hypocapnia reflects alveolar hyperventilation due to increased ventilatory drive or the use of mechanical ventilation. Increased ventilatory drive might result from signals arising from the lung, peripheral chemoreceptors (carotid and aortic), brainstem chemoreceptors, or influences originating in other centers of the brain.[62] The response of the brainstem chemoreceptors to CO_2 can be augmented by systemic diseases (e.g., liver disease, sepsis), pharmacologic agents, volition, and other influences. Hypoxemia is a major stimulus of alveolar ventilation, but PaO_2 values lower than 60 mm Hg are required to elicit consistently this effect. Not uncommonly, alveolar hyperventilation is the result of maladjusted mechanical ventilators. Further, it is common practice to deliberately induce respiratory alkalosis during general anesthesia in patients with critical elevation of intracranial pressure or brain injury, or in neonatal respiratory failure, especially when pulmonary vascular resistance is exceedingly high. Potential mechanisms of respiratory alkalosis due to decreased CO_2 production in the presence of constant alveolar ventilation (i.e., mechanical ventilation) include a reduction in physical activity (e.g., sedation, skeletal muscle paralysis) or a reduction in the basal metabolic rate (e.g., hypothermia, hypothyroidism). In states of severe circulatory failure, arterial hypocapnia can coexist with venous, and therefore with tissue, hypercapnia; however, the body CO_2 stores have been enriched, and respiratory acidosis rather than respiratory alkalosis is present. This entity, which we have termed pseudorespiratory alkalosis, has been examined in the section on respiratory acidosis.

Respiratory alkalosis is the most frequent acid–base disorder encountered, since it occurs in normal pregnancy and with high-altitude residence. It is also the most common acid–base abnormality in critically ill patients, occurring either as the simple disorder or as a component of mixed disturbances;[7] indeed, in such patients, its presence may represent a grave prognostic sign, especially if $PaCO_2$ levels are below 20–25 mm Hg. Table 60.5 lists the major causes of respiratory alkalosis. Most are associated with the abrupt appearance of hypocapnia, but in many instances the process might be sufficiently prolonged to permit full, chronic adaptation to occur. Consequently, no attempt has been made to separate these conditions into acute and chronic categories.

The mechanisms by which the processes listed in Table 60.5 lead to hyperventilation differ markedly.[62] Hypoxia stimulates ventilation through activation of peripheral chemoreceptors and might result in hypocapnia if CO_2 excretion is unimpeded. Such situations of hypoxia include decreased inspired oxygen tension (e.g., high-altitude residence) and conditions producing increased venous admixture and marked

TABLE 60.5 Causes of Acute Respiratory Alkalosis

Hypoxemia or tissue hypoxia
Decreased inspired O_2 tension
High altitude
Bacterial or viral pneumonia
Aspiration of food, foreign body, or vomitus
Laryngospasm
Drowning
Cyanotic heart disease
Severe anemia
Left shift deviation of HbO_2 curve
Hypotension
Severe circulatory failure
Pulmonary edema
Pseudorespiratory alkalosis
Central nervous system stimulation
Voluntary
Pain
Anxiety-hyperventilation syndrome
Psychosis
Fever
Subarachnoid hemorrhage
Cerebrovascular accident
Meningoencephalitis
Tumor
Trauma
Pulmonary diseases with stimulation of chest receptors
Pneumonia
Asthma
Pneumothorax
Hemothorax
Flail chest
Acute respiratory distress syndrome
Cardiogenic and noncardiogenic pulmonary edema
Pulmonary embolism
Pulmonary fibrosis
Drugs and hormones
Respiratory stimulants (doxapram, nikethamide, ethamivan, progesterone, medroxyprogesterone)

(*Continued*)

TABLE 60.5 (*Continued*)

Salicylates
Nicotine
Xanthines
Dinitrophenol
Pressor hormones (epinephrine, norepinephrine, angiotensin II)
Miscellaneous
Exercise
Pregnancy
Gram-positive septicemia
Gram-negative septicemia
Hepatic failure
Mechanical hyperventilation
Heat exposure
Recovery from metabolic acidosis
Hemodialysis with acetate dialysate

ventilation/perfusion inequality (e.g., bronchopulmonary disease, pulmonary edema). A reduction in PaO_2 below 60 mm Hg is required for hyperventilation to develop. Hypotension, especially when associated with sepsis, often causes respiratory alkalosis even in the absence of a reduced PaO_2. This phenomenon occurs because the stimulus to peripheral chemoreceptor activation is decreased oxygen delivery rather than decreased PaO_2. Severe anemia (hemoglobin level lower than 30% of normal) can lead to respiratory alkalosis by the same mechanism. As noted above, severe circulatory failure in the presence of substantial pulmonary ventilation can give rise to "pseudorespiratory alkalosis," a distinct pattern of arteriovenous acid–base disparity characterized by arterial hypocapnia and alkalemia in association with venous (and tissue) hypercapnia and acidemia.[10,11]

Central-nervous-system–mediated hypocapnia can result from a wide variety of causes. Respiratory alkalosis can certainly be produced through voluntary hyperventilation. The anxiety-hyperventilation syndrome can result in severe hypocapnia and alkalemia leading to the development of chest oppression, circumoral numbness, and paresthesias in the extremities. Early recognition is important because appropriate measures might produce prompt relief. Various neurologic diseases of vascular, infectious, traumatic, or neoplastic origin can also produce hypocapnia, presumably by enhancing stimulatory inputs to ventilation or by interrupting normal inhibitory pathways.

A number of pharmacologic agents can induce hyperventilation and respiratory alkalosis.[62] Aspirin and other salicylates in doses exceeding a few grams per day can produce primary hypocapnia by direct stimulation of medullary chemoreceptors. In cases of salicylate intoxication, respiratory alkalosis often coexists with metabolic acidosis that arises from accumulation of organic acids. Nikethamide, a respiratory stimulant acting directly on the respiratory center of the brainstem and, in addition, increasing the center's sensitivity to CO_2 and activating peripheral chemoreceptors, has been used in the treatment of CO_2-retaining disorders; however, the results obtained with this drug as well as other ventilatory stimulants (e.g., ethamivan, doxapram, almitrine, progesterone, and medroxyprogesterone) have been modest at best. Other drugs known to stimulate alveolar ventilation include nicotine, dinitrophenol, xanthines, and pressor hormones (epinephrine, norepinephrine, and angiotensin II).[62] Progesterone and medroxyprogesterone are also respiratory stimulants that are presumed to act centrally. This property of progesterone is most likely responsible for the $PaCO_2$ of normal women being lower by 2–3 mm Hg than that of normal men, and for the chronic hypocapnia characteristic of normal pregnancy (see later discussion). Progesterone is considered to be the basis of the hyperventilation that occurs during the luteal phase of the normal menstrual cycle ($\Delta PaCO_2$ of approximately 3–6 mm Hg) that is attended by a rise in blood pH and a fall in renal acid excretion. In fact, in both pregnant and nonpregnant women, the $PaCO_2$ value is inversely related to the blood progesterone level.

Patients with a variety of pulmonary disorders, including interstitial lung disease, pneumonia, pulmonary embolism, and pulmonary edema, can develop respiratory alkalosis as a result of stimulation of pulmonary receptors that signal the brainstem through ascending pathways in the vagus nerve; these receptors might be triggered by irritants (nociceptive receptors), pulmonary expansion or collapse (stretch receptors), or pulmonary capillary congestion (juxtacapillary or J receptors).[12] Accompanying hypoxemia, acting on peripheral arterial chemoreceptors, might also play a contributory role. Measurable increases in alveolar ventilation appear early in pregnancy and, subsequently, are augmented further. On average, $PaCO_2$ falls to approximately 34 mm Hg in the first trimester, to about 32 mm Hg in the second trimester, and to approximately 28 mm Hg in the third trimester, when circulating progesterone attains its highest levels. The associated changes in plasma bicarbonate and therefore pH are consistent with adaptation to chronic respiratory alkalosis.

Septicemia due to either gram-positive or gram-negative organisms commonly results in respiratory alkalosis. Whereas the concomitant hypoxemia and

circulatory failure might account for the genesis of hypocapnia in gram-positive sepsis, direct stimulation of central chemoreceptors by bacterial toxins has been shown to account, at least in part, for the respiratory alkalosis of gram-negative sepsis.[7]

Hepatic failure represents an important cause of respiratory alkalosis. The specific mechanisms responsible for the hyperventilation remain uncertain, but the extent of hypocapnia correlates best with the level of blood ammonia.

Mechanical hyperventilation might induce respiratory alkalosis if the mechanical apparatus is improperly adjusted.[80] This complication can be avoided only by assessing acid–base status frequently in patients undergoing assisted or controlled ventilation. Abrupt cessation of mechanical hyperventilation, especially in anesthetized patients or those who had received sedatives, might result in critical hypoxemia due to apnea or severe respiratory depression; the prevailing low level of $PaCO_2$ fails to provide a stimulus for ventilatory drive and apnea or depressed respiration will persist until $PaCO_2$ rises sufficiently to stimulate ventilation. This mechanism may account for a substantial number of cardiorespiratory arrests during recovery from general anesthesia. Despite claims to the contrary, cessation of voluntary hyperventilation might also result in severe hypoxemia due to depressed ventilation or apnea.

Heat exhaustion, heat stroke, fever, hyperthyroidism, and delirium tremens might also produce respiratory alkalosis by mechanisms that remain undefined. Finally, a postmetabolic-acidosis hypocapnia can develop following rapid correction of a large bicarbonate deficit by alkali administration; this persistent hyperventilation, which can last for 24–48 hours, is attributed to a delay in correcting the acidity at the central chemoreceptor site.

Secondary Physiologic Response

Hypocapnia elicits adaptive decrements in plasma $[HCO_3^-]$ that should be viewed as an integral part of the respiratory alkalosis and serve to ameliorate the resulting alkalemia.[44,58] An immediate decrement in plasma $[HCO_3^-]$ occurs in response to hypocapnia. This acute adaptation is complete within 5 to 10 minutes from the onset of hypocapnia, and no further detectable changes in acid–base equilibrium occur for a period of several hours, establishing an operational "acute steady state".[9] The acute adaptation is accounted for principally by alkaline titration of the body's non-HCO_3^- buffers and, to a lesser extent, by increased production of organic acids, notably lactic acid. When hypocapnia is sustained, renal adjustments cause an additional decrease in plasma $[HCO_3^-]$ further ameliorating the resulting alkalemia.[44]

The adjustment in acid–base equilibrium following the induction of acute hypocapnia results entirely from nonrenal mechanisms. Evidence indicates that approximately one third of the total buffering response can be ascribed to red cell and extracellular protein buffering, the remainder being attributed to tissue buffering.

Figure 60.4 depicts the 95% confidence limits for plasma $[HCO_3^-]$ and blood $[H^+]$ in uncomplicated acute respiratory alkalosis of graded severity. These limits represent the range of responses within which acid–base equilibrium would be expected to fall if an acute reduction in $PaCO_2$ were the only factor disturbing plasma acidity. The data from which these limits were calculated were obtained during the course of acute "whole body" titration experiments using passive hyperventilation of anesthetized human subjects undergoing minor surgical procedures.[14] The acute, secondary change in plasma $[HCO_3^-]$ is substantially greater in magnitude than that observed during acute hypercapnia of comparable degree, falling by approximately 0.2 mEq/liter for each 1-mm Hg acute decrement in $PaCO_2$; thus, a reduction in plasma bicarbonate of some 3–4 mEq/liter occurs within minutes after $PaCO_2$ is lowered to 20–25 mm Hg. The resulting change in plasma $[H^+]$, however, is strikingly

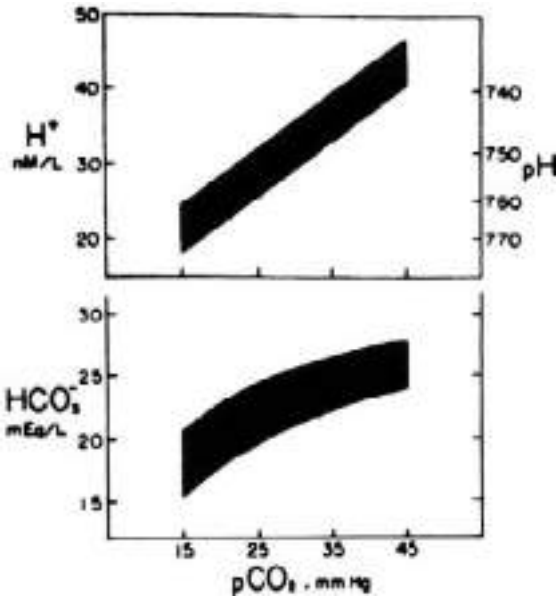

FIGURE 60.4 **Ninety-five percent confidence limits for plasma bicarbonate concentration (lower panel) and plasma hydrogen-ion concentration (upper panel) in acute respiratory alkalosis.** The limits were calculated from data obtained in anesthetized patients who were passively hyperventilated during minor surgical procedures. *(With permission, from Arbus GS, Hebert LA, Levesque PR, Etsten BE, Schwartz WB. Characterization and clinical application of the "significance band" for acute respiratory alkalosis. N Engl J Med 1969;**280**:117–223).*

similar to that observed during acute hypercapnia. On average, plasma $[H^+]$ decreases by approximately 0.75 nEq/liter for each 1-mm Hg acute reduction in $PaCO_2$. Thus, acute adaptation to a $PaCO_2$ of 20 mm Hg in a subject with a normal acid–base equilibrium at baseline will yield, on average, a plasma $[HCO_3^-]$ of 20 mEq/liter and a $[H^+]$ of 24 nEq/liter (pH 7.62).[9]

If hypocapnia persists, plasma $[HCO_3^-]$ falls further as a consequence of renal adaptive responses, which entail a dampening of $[H^+]$ secretion by the renal tubule. As a result, transient suppression of net acid excretion occurs, largely manifested by a fall in ammonium excretion and, early on, by an increase in bicarbonate excretion. Transient bicarbonaturia and a rise in urinary pH occur when hypocapnia develops abruptly but not in response to gradually evolving hypocapnia. These changes in net acid excretion, in turn, lead to positive hydrogen-ion balance and a reduction in the body's bicarbonate stores. Maintenance of the resulting hypobicarbonatemia is ensured by gradual suppression in the rate of renal bicarbonate reabsorption, itself a reflection of the hypocapnia-induced decrease in the tubular hydrogen-ion secretory rate.[44,65]

The adaptive acid retention during sustained hypocapnia is normally accompanied by a loss of sodium into the urine; the resultant extracellular fluid loss is responsible for the hyperchloremia that typically attends chronic respiratory alkalosis. When a new steady state emerges, renal net acid excretion returns to control levels and the altered anionic picture of the extracellular fluid, namely, hypobicarbonatemia and hyperchloremia, is maintained by reduced bicarbonate reabsorption and enhanced chloride reabsorption.

Micropuncture and microperfusion studies have documented suppressed proximal and distal acidification during hypocapnia, including decreased proximal HCO_3^- reabsorption, increased proximal Cl^- reabsorption, and decreased formation and delivery of NH_4^+ and titratable acidity. Reduced proximal HCO_3^- reabsorption has also been demonstrated by micropuncture in chronic hypocapnia, but distal acidification has not been examined with these techniques in the chronic phase of the disorder.[65]

Regarding the cellular mechanisms mediating the down-regulation of renal acidification during chronic hypocapnia, parallel decreases in the rates of the luminal Na^+/H^+ exchanger (Fig 60.5) and the basolateral $Na^+/3HCO_3^-$ cotransporter in the proximal tubule have been found reflecting a decrease in the V_{max} of each transporter, but no change in the K_m for sodium.[49,81] Moreover, hypocapnia induces endocytotic retrieval of H^+-ATPase pumps from the luminal membrane of the proximal tubule cells as well as type A intercalated cells of cortical and medullary collecting tubules.[65] In rat tubule microdissection studies, the

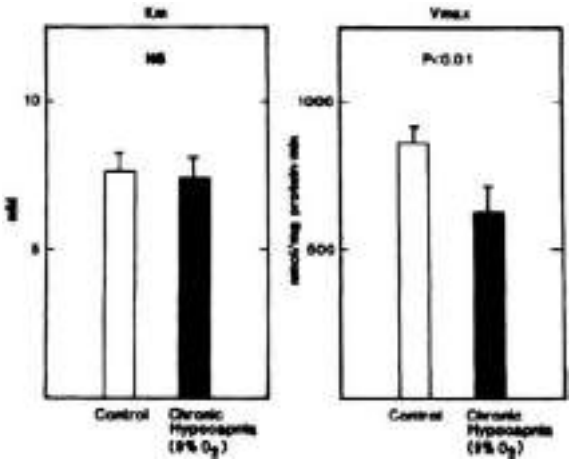

FIGURE 60.5 Kinetic characteristics of rabbit renal cortical brush-border membrane vesicle Na^+-H^+ exchanger in animals adapted to chronic hypocapnia (9% O_2) (shaded bars) or in paired, contemporaneous controls (open bars). Data on Km for sodium are depicted on the left and those on Vmax on the right. Data represent means ± SE for seven paired sets of rabbits. Chronic hypocapnia resulted in a significant decrease in the Vmax of the exchanger, whereas the Km for sodium remained unaltered. *(From ref., 49 with permission).*

activity of the H^+-ATPase along the entire nephron (i.e., proximal tubule, thick ascending limb of Henle, and cortical and medullary collecting tubules) and that of the H^+-K^+-ATPase in the cortical and medullary collecting tubules were decreased by 6 hr of hypocapnia and thereafter. The inhibitory effect of hypocapnia on the H^+-ATPase and the H^+-K^+-ATPase appears to be independent of potassium and aldosterone.[43] No information exists on potential effects of chronic hypocapnia on the basolateral Cl^-/HCO_3^- exchanger (band 3 protein) of type A intercalated cells or the apical Cl^-/HCO_3^- exchanger (pendrin) of type B intercalated cells.

Evidence indicates that the renal adaptation to persistent hypocapnia is mediated not by changes in plasma or "whole-body" intracellular pH but by some direct effect of reduced $PaCO_2$ itself.[33,68] Thus, animals in which plasma $[HCO_3^-]$ had been substantially reduced prior to adaptation to sustained hypocapnia (by means of the chronic administration of a large HCl load) evidenced the same renal response to a primary reduction in $PaCO_2$ as normal, even though the net effect of such adaptation was an overt fall in plasma pH (Fig 60.6).[33]

Approximately two to three days are required for the completion of the renal response to hypocapnia. Limited data in humans (patients subjected to chronic hypocapnia, high-altitude dwellers, volunteers studied at high altitude or at simulated altitude) have indicated that plasma $[HCO_3^-]$ decreases, on average, by approximately 0.4 mEq/liter for each 1-mm Hg chronic

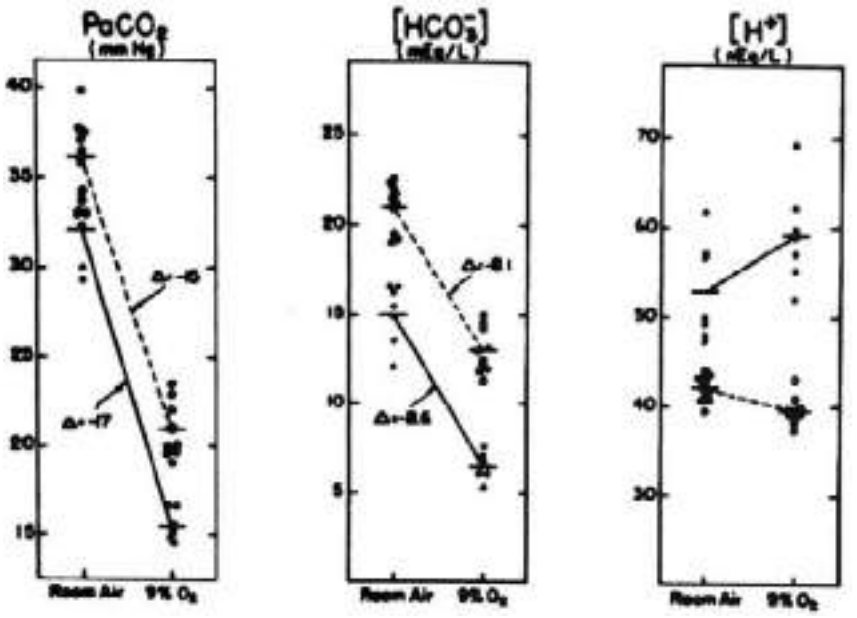

FIGURE 60.6 Changes in plasma bicarbonate concentration and hydrogen-ion concentration during prolonged exposure to hypocapnia in normal dogs (dashed lines) and in dogs with chronic HCL-acidosis (solid lines). Similar decrements in $PaCO_2$ in the two groups produced nearly equivalent reductions in plasma bicarbonate concentration, despite divergent effects on hydrogen-ion concentration. *(From ref., 33 with permission).*

decrease in $PaCO_2$. Despite the similarity in the magnitude of the secondary response of plasma bicarbonate to chronic hypocapnia between dogs and humans, the resultant impact on blood $[H^+]$ is substantially disparate. Whereas in the dog, blood $[H^+]$ falls by only 0.17 nEq/liter for each 1-mm Hg chronic reduction in $PaCO_2$, the corresponding decrease in humans is on the order of 0.4 nEq/liter.[58] The main reason for this discrepancy is the higher baseline level of plasma $[HCO_3^-]$ in humans (24 to 25 mEq/liter vs. 21 mEq/liter in the dog).

Plasma Electrolyte Composition during Respiratory Alkalosis

Mild hyponatremia ($\Delta[Na^+]$, 2–4 mEq/liter) has been noted in acute hypocapnia,[14,58] but plasma sodium concentration remains normal during chronic hypocapnia. Hyperchloremia, a consistent finding in respiratory alkalosis, reflects largely the chloride shift from erythrocytes during the acute state and the volume contraction accompanying the renal response during the chronic stage.[44] Plasma potassium concentration decreases (by approximately 0.1–0.4 mEq/liter for each 0.1-unit rise in pH) during acute hypocapnia.[3] The mechanism of hypokalemia in acute respiratory alkalosis most likely involves both a shift of potassium into the cells and transient kaliuresis accompanying bicarbonaturia that lasts only hours and becomes more evident when hypocapnia develops abruptly.[3] By contrast, a study in normal volunteers with acute respiratory alkalosis caused by voluntary hyperventilation revealed development of mild hyperkalemia that appeared to be mediated by enhanced alpha-adrenergic activity.[59] No appreciable changes in plasma potassium occur during chronic hypocapnia in the dog or in patients at sea level. On the other hand, a persistent reduction in plasma potassium concentration (on the order of 0.5 mEq/liter) was detected in human subjects during chronic hypocapnia induced by exposure to high altitude ($\Delta PaCO_2$ 8 mm Hg). Mild hypophosphatemia is a characteristic feature of acute hypocapnia and reflects translocation of phosphate into cells, but no consistent changes in plasma phosphate have been noted in chronic hypocapnia. Despite the hypophosphatemia, acute respiratory alkalosis decreases the fractional excretion of phosphate, and this response is blunted by β-adrenoreceptor blockers. Mild reduction in ionized calcium occurs in acute hypocapnia because of an alkalemia-induced increase in protein binding of serum calcium. Although this decrease could not account by itself for the tetany and seizures that occasionally attend acute hypocapnia, it might play a contributory role. Serum total calcium and magnesium concentrations remain normal during persistent hypocapnia. A more recent study concluded that chronic hypocapnia induces impaired renal tubular responsiveness to PTH and defective PTH secretion (as defined by the failure of the hormone's levels to rise in response to the prevailing decrease in serum ionized calcium).

A mild and transient elevation in plasma lactate concentration occurs during acute hypocapnia that results from stimulation of 6-phosphofructokinase activity, and there is no appreciable change in plasma lactate during chronic hypocapnia.[44] Plasma unmeasured

anions do not change notably in acute hypocapnia, but small increases (on the order of 3 mEq/liter for a 20-mm Hg chronic reduction in $PaCO_2$) have been observed in chronic respiratory alkalosis; the source of this increase remains unidentified.

Cerebrospinal Fluid Composition during Respiratory Alkalosis

Cerebrospinal fluid (CSF) hydrogen-ion and bicarbonate concentrations fall in parallel with those of arterial blood during induction of acute hypocapnia;[37] the magnitude of the reduction in hydrogen-ion concentration in the CSF of the dog is similar to that observed in the arterial blood. The fall in CSF bicarbonate concentration is accompanied by an increase in CSF chloride concentration that accounts for 75% of the change in the level of bicarbonate, and a mild rise in CSF lactate concentration that accounts for the remaining 25%. Several investigators have noted a widening of the CSF−arterial PCO_2 difference during acute hypocapnia resulting from a lesser fall of PCO_2 in CSF than in blood; this effect is thought to be secondary to the decrease in cerebral blood flow associated with hypocapnia.

Studies of the response of CSF acidity during chronic hypocapnia have shown reductions in CSF hydrogen ion and bicarbonate concentrations similar to those of arterial blood (37).

Intracellular pH during Respiratory Alkalosis

"Whole-body" intracellular hydrogen-ion concentration, as assessed by the DMO (5, 5-dimethyl-2, 4-oxazolidinedione) method, has been found to fall in parallel with extracellular hydrogen-ion concentration when healthy human subjects hyperventilate voluntarily to achieve a $PaCO_2$ of 15−20 mm Hg. Similar results have been obtained from studies in dog and rat muscle and rat brain. On the other hand, ^{31}P-nuclear magnetic resonance (NMR) spectroscopy has revealed much smaller changes in canine heart intracellular pH in response to acute hypocapnia as compared with the extracellular compartment.[55] The response of intracellular acidity to chronic hypocapnia has not been studied.

PATHOPHYSIOLOGIC EFFECTS AND CLINICAL MANIFESTATIONS OF RESPIRATORY ALKALOSIS

Neurologic

A variety of clinical manifestations frequently occur in acute hypocapnia, but these are seldom evident in the chronic phase of the disorder. A rapid decrement in $PaCO_2$ to half normal values or lower is typically accompanied by numbness and paresthesias of the extremities, chest oppression, circumoral numbness, lightheadedness, and mental confusion. Muscle cramps, increased deep-tendon reflexes, carpopedal spasm, and generalized seizures occur infrequently.[62] The neurologic manifestations of acute respiratory alkalosis have been attributed largely to the attendant cerebral hypoperfusion, although additional factors have been implicated, including alkalemia, the pH-induced shift to the left of the oxyhemoglobin dissociation curve, and the decrements in the level of ionized calcium and potassium. Cerebral vasoconstriction and reduced cerebral blood flow have been well documented during acute hypocapnia;[62] in severe cases, cerebral blood flow might reach values lower than 50% of normal. In addition, cerebral vasoconstriction leads to decreases in cerebral blood volume, thereby lowering intracranial pressure. A characteristic electroencephalographic picture consisting of generalized slowing and high-voltage wave forms has been reported. Brain and CSF lactate concentrations have been found to increase by amounts greater than those in the systemic circulation and to remain slightly increased during persistent hypocapnia. Increased synthesis of lactate is consequent to cerebral hypoxia resulting from the intense vasoconstricting effects of hypocapnia and, probably, to alkalemia-induced acceleration of anaerobic glycolysis. Some evidence indicates that cerebral blood flow returns to normal in chronic respiratory alkalosis.

Respiratory alkalosis and hypoxemia are observed in acute mountain sickness (AMS) and high-altitude cerebral edema, conditions characterized by cerebral swelling. Evaluation of self-identified AMS-susceptible and non-AMS-susceptible volunteers demonstrated as early as 40 minutes after development of hypoxemia, increases in cerebral blood volume and brain tissue volume occur, and CSF is shifted into the venous circulation decreasing CSF volume; the latter is a compensatory mechanism to maintain normal intracranial pressure.[40] These findings did not differ in the two study groups. Of note is the clinical observation that administration of acetazolamide ameliorates the central nervous system impairment observed in AMS.

Hypocapnia can have deleterious effects on the brain of premature infants, patients with traumatic brain injury, acute stroke, or general anesthesia, and after cardiopulmonary bypass or sudden exposure to very high altitude.[36,38,45,47,74] The mechanisms of brain injury may include cerebral ischemia; antioxidant-glutathione depletion caused by augmented production of cytotoxic excitatory amino acids; increases in anaerobic metabolism, cerebral oxygen demand,

neuronal dopamine, and brain excitability; and seizure activity.[62] Hypocapnia in premature infants can lead to white-matter damage, including cystic changes, periventricular leukomalacia, and secondary cerebral bleeding. If sepsis is present, the brain damage is enhanced by the release of lipopolysaccharide, interleukin-1β, and tumor necrosis factor α. Long-term neurologic sequelae can develop when immature brains are exposed to $PaCO_2$ levels of less than 15 mm Hg for even short periods.[62] Furthermore, abrupt correction of hypocapnia in these patients leads to cerebral vasodilation, which might cause reperfusion injury or intraventricular hemorrhage.

The effects of acute hypocapnia without hypoxemia to decrease cerebral blood flow and intracranial pressure have been used as a therapeutic tool in reducing brain edema due to a variety of causes, including meningitis, encephalitis, head trauma, and neurosurgical procedures.[70,71,72] Unfortunately, in most instances, the derived benefit is limited in magnitude and short-lived. Hypocapnia had been recommended as a therapeutic measure to produce a favorable redistribution of cerebral blood-flow during focal cerebral ischemia of acute onset. Yet, experimental data suggest that, rather than reducing the area of the critically ischemic brain, hypocapnia might increase the size of the region at risk.[36] Deliberate induction of hypocapnia in patients with traumatic brain injury or acute stroke has actually resulted in worse outcomes; consequently, some experts recommend against this therapeutic approach.

The rationale for the use of hypocapnia (i.e., $PaCO_2$ of 20 to 25 mm Hg) during general anesthesia includes depression of spontaneous ventilation, and reduced requirements of muscle relaxants, analgesics, and sedatives.[62] However, acute hypocapnia during general anesthesia can be followed by impaired cerebral function for up to six days, especially in older patients, and this complication outweighs the potential benefits.

Cardiovascular and Renal

Myocardial contractility assessed in isolated perfused hearts initially increases but rapidly returns to control levels in acute respiratory alkalosis. The switch from the state of augmented contractility is not dependent on the activity of the myocardial Na^+/H^+ exchanger or the Cl^-/HCO_3^- exchanger since blockers of these transporters (amiloride, SITS) did not prevent the biphasic mechanical response. Changes in both cytosolic pH and calcium concentration appear to play a major role in this response.[75] In the isolated rat heart, primary hypocapnia enhances postischemic calcium gain, an effect that is considered nonsalutary. Although acute hypocapnia does not lead to cardiac arrhythmias in normal volunteers, it appears that it contributes to the generation of both atrial and ventricular tachyarrhythmias in patients with ischemic heart disease; such arrhythmias are frequently resistant to standard forms of therapy. Acute respiratory alkalosis impairs myocardial oxygenation by a dual effect that includes increased myocardial oxygen demand and decreased myocardial oxygen supply. The higher oxygen demand is caused by increased contractility and a rise in systemic vascular resistance, whereas the decreased oxygen supply results from reduced coronary flow caused by vasoconstriction as well as increases in platelet count and aggregation.

Chest pain and ischemic ST-T wave changes have been observed in acutely hyperventilating subjects with no evidence of fixed lesions on coronary angiography. The pathogenesis of these manifestations remains unknown, although myocardial ischemia secondary to hypocapnia-induced vasoconstriction and an alkalemia-induced shift to the left of the oxyhemoglobin dissociation curve have been proposed. Indeed, acute hypocapnia has been shown to induce coronary artery spasm and Prinzmetal's angina in susceptible patients.

Hypocapnia produces variable effects on regional blood flows. Acute respiratory alkalosis decreases myocardial, cerebral, dermal, and renal blood flows, but it increases muscle blood flow. Insufficient data exist with regard to the effects of persistent hypocapnia on the distribution of blood flow, but it appears that dermal and renal blood flows remain depressed, whereas muscle and liver perfusion is increased. For reasons that remain unknown, chronic hypocapnia leads to increased responsiveness of the kidney to antidiuretic hormone administration; water retention exceeds that of normocapnic animals, resulting in the rapid development of hyponatremia.

Respiratory

A primary decrease in $PaCO_2$ and the attendant increase in pH characteristic of acute respiratory alkalosis cause a shift to the left in the oxyhemoglobin dissociation curve (Bohr effect), resulting in an impediment of oxygen unloading to the tissues but an enhancement of oxygen loading in the lungs.[52] During chronic alkalosis, however, these effects are offset by a shift of the curve to the right produced by an increased concentration of 2, 3-diphosphoglycerate (2, 3-DPG) in the erythrocytes.[52] In spite of the impediment of oxygen unloading to the tissues in acute hypocapnia, oxygen consumption was found to increase by approximately 12% in anesthetized and paralyzed patients during hyperventilation-induced alkalosis. The mechanism of this response remains undetermined.

Adverse effects of hypocapnia can involve the airways, lung compliance, alveolar-capillary permeability, and pulmonary vasculature.[27,84] Acute respiratory alkalosis causes bronchoconstriction, an increase in airway resistance, and a decrease in lung compliance. Experimental observations have shown that hypocapnia leads to bronchospasm and airway edema; yet the effects of hypocapnia on alveolar-capillary permeability are incompletely defined. Studies utilizing the isolated buffer-perfused rabbit lung have concluded that respiratory alkalosis leads to direct lung injury and also potentiates lung injury induced by ischemia-reperfusion. Additional studies in rats using the isolated perfused lung model have shown that respiratory alkalosis independently of pH level decreases alveolar fluid reabsorption; this effect was associated with decreased Na,K-ATPase activity at the basolateral membrane of distal air spaces.[73] Thus, it appears that hypocapnia increases pulmonary capillary permeability, worsens intrapulmonary shunt and systemic oxygenation, and has a negative effect on acute lung injury.

DIAGNOSIS OF RESPIRATORY ALKALOSIS

Evaluation of the patient's history, physical examination, and ancillary laboratory data, including blood gas determinations, is required to establish the diagnosis of respiratory alkalosis. The presence of respiratory alkalosis, especially the chronic form, is frequently missed; physicians often misinterpret the electrolyte pattern of hyperchloremic hypobicarbonatemia as indicative of normal anion gap metabolic acidosis. If the patient's acid–base profile reveals hypocapnia in association with alkalemia, at least an element of respiratory alkalosis must be present. Yet hypocapnia might be associated with a normal or an acidic pH due to the concomitant presence of additional acid–base disorders. One should also note that mild degrees of chronic hypocapnia leave blood pH within the high normal range. Once the diagnosis of respiratory alkalosis is made, a search for its cause should be carried out. The diagnosis of respiratory alkalosis can have important clinical implications, since it often provides a clue to the presence of an unrecognized, serious disorder or signals the gravity of a known underlying disease.

MANAGEMENT OF RESPIRATORY ALKALOSIS

Accumulated evidence over the past few years indicates that the widely held view that hypocapnia poses little risk to health under most conditions is not accurate. In fact, substantial hypocapnia in hospitalized patients, whether spontaneous or deliberately induced, can be associated with transient or permanent damage in the brain and the respiratory and cardiovascular systems.[36,38,45,46,72,82] Furthermore, rapid correction of severe hypocapnia leads to vasodilation of ischemic areas, resulting in reperfusion injury in the brain and lung. Consequently, severe hypocapnia must be prevented whenever possible, and if present, abrupt correction should be avoided. Severe alkalemia caused by acute primary hypocapnia requires corrective measures that depend on whether serious clinical manifestations are present. Such measures can be directed at reducing plasma [HCO_3^-], increasing $PaCO_2$, or both. Even if baseline plasma [HCO_3^-] is moderately decreased, reducing it further can be particularly rewarding in this setting, as this maneuver combines effectiveness with relatively little risk. For patients with the anxiety-hyperventilation syndrome, in addition to reassurance or sedation, re-breathing into a closed system (e.g., a paper bag) might prove helpful by interrupting the vicious cycle that can result from the reinforcing effects of the symptoms of hypocapnia. Respiratory alkalosis resulting from severe hypoxemia requires oxygen therapy. The oral administration of 250–500 mg of acetazolamide (Diamox) can be beneficial in the management of signs and symptoms of AMS.[47] Of course, patients undergoing mechanical ventilation lend themselves to an effective correction of hypocapnia (whether due to maladjusted ventilator or other causes) by resetting the device.

MIXED ACID–BASE DISORDERS ASSOCIATED WITH RESPIRATORY ALKALOSIS

Respiratory alkalosis is frequently associated with other acid–base disorders. We describe here some of the more common clinical examples of mixed acid–base disturbances in which respiratory alkalosis is a component.

Respiratory Alkalosis and Metabolic Acidosis

This mixed acid–base disorder is commonly encountered during the rapid correction of severe metabolic acidosis. During treatment, plasma [HCO_3^-] often returns toward normal more swiftly than the secondary hypocapnia (originally induced by the acidosis) can abate. As a consequence, the degree of hypocapnia often remains inappropriately large with respect to the then-current decrement in plasma [HCO_3^-] for a period

of several hours or more; blood [H^+] during such intervals is often normal or even frankly low.

Patients with salicylate intoxication commonly manifest elements of both metabolic acidosis and respiratory alkalosis, reflecting the independent effects of the salicylate molecule on both cellular metabolism (uncoupling of oxidative phosphorylation) and ventilation (stimulation of central chemoreceptors). Patients with gram-negative sepsis can also develop this mixed disturbance, reflecting the frequent occurrence of primary hyperventilation, on the one hand, and of lactic acidosis and/or renal failure, on the other. This combination also occurs occasionally in the setting of combined hepatic and renal failure. Additionally, patients undergoing "high-mass-transfer" hemodialysis with acetate dialysate can develop mixed respiratory alkalosis and metabolic acidosis; the former reflects rapid loss of CO_2 into the dialysate, and the latter reflects the removal of bicarbonate by the dialyzer at a rate faster than the body's alkali stores can be replenished by tissue metabolism of the circulating acetate.

It should be noted that patients with sustained respiratory alkalosis of recent onset, in whom renal adaptation to hypocapnia is as yet incomplete (i.e., if hypocapnia has been present for only a day or so), might have acid–base values indistinguishable from those characteristic of patients with this mixed disturbance. Other laboratory data and relevant historical information should serve to differentiate between these alternatives.

Respiratory Alkalosis and Metabolic Alkalosis

Although these two disturbances do not often coexist, when they do, blood [H^+] might, of course, be driven to extremely low levels.[67] Patients with hepatic insufficiency, who frequently have persistent hyperventilation, might develop this combination of acid–base disturbances if they are treated with potent diuretics or if they lose gastric fluid. Pregnant patients who develop metabolic alkalosis from any cause will exhibit this mixed acid–base disorder because they typically feature chronic hypocapnia. Similarly, patients with an underlying metabolic alkalosis might develop such a picture if ventilation is stimulated (e.g., pulmonary embolus, pulmonary edema, sepsis).

Because adaptation to chronic hypocapnia requires renal function, severe alkalemia can develop in patients with end stage renal disease receiving dialysis therapy. Considering that peritoneal dialysis therapy maintains plasma [HCO_3^-] within the normal range regardless of the prevailing $PaCO_2$, patients receiving this treatment are at particular risk of alkalemia.[7]

This mixed disturbance can be diagnosed readily if the level of $PaCO_2$ is less than normal and if plasma [HCO_3^-] is frankly elevated. The disorder should be treated as a medical emergency, because extreme alkalemia carries a grave prognosis.[7] With the exception of patients undergoing mechanical ventilation (and the consequent ability to increase $PaCO_2$ promptly), measures should be taken to rapidly reduce the elevated plasma [HCO_3^-].

References

[1] Adrogué HJ, Chap Z, Okuda Y, Michael L, Hartley C, Entman M, et al. Acidosis-induced glucose intolerance is not prevented by adrenergic blockade. Am J Physiol 1988;255: E812–23.

[2] Adrogué HJ, Gennari FJ, Galla JH, Madias NE. Assessing acid–base disorders. Kidney Int 2009;76:1239–47.

[3] Adrogué HJ, Madias NE. Changes in plasma potassium concentration during acute acid–base disturbances. Am J Med 1981;71:456–67.

[4] Adrogué HJ, Madias NE. Influence of chronic respiratory acid–base disorders on acute CO_2 titration curve. J Appl Physiol 1985;58:1231–8.

[5] Adrogué HJ, Madias NE. Renal acidification during chronic hypercapnia in the conscious dog. Pflügers Arch 1986;406:520–8.

[6] Adrogué HJ, Madias NE. Management of life-threatening acid–base disorders (First of two parts). N Engl J Med 1998;338: 26–34.

[7] Adrogué HJ, Madias NE. Management of life-threatening acid–base disorders (Second of two parts). N Engl J Med 1998;338: 107–11.

[8] Adrogué HJ, Madias NE. Respiratory acidosis. In: Gennari FJ, Adrogué HJ, Galla JH, Madias NE, editors. Acid–base disorders and their treatment. Boca Raton, FL: Taylor & Francis Group; 2005. p. 597–639.

[9] Adrogué HJ, Madias NE. Secondary responses to altered acid-base status: the rules of engagement. J Am Soc Nephrol 2010;21: 920–3.

[10] Adrogué HJ, Rashad MN, Gorin AB, Yacoub J, Madias NE. Assessing acid–base status in circulatory failure: differences between arterial and central venous blood. N Engl J Med 1989;320:1312–6.

[11] Adrogué HJ, Rashad MN, Gorin AB, Yacoub J, Madias NE. Arteriovenous acid–base disparity in circulatory failure: studies on mechanism. Am J Physiol 1989;257:F1087–93.

[12] Adrogué HJ, Tobin MJ. Blackwell's basics of medicine: respiratory failure. Boston: Blackwell Science; 1997.

[13] Amato MBP, Barbas CSV, Medeiros DM, et al. Effect of a protective-ventilation strategy on mortality in the acute respiratory distress syndrome. N Engl J Med 1998;338: 347–54.

[14] Arbus GS, Hebert LA, Levesque PR, Etsten BE, Schwartz WB. Characterization and clinical application of the "significance band" for acute respiratory alkalosis. N Engl J Med 1969;280: 117–23.

[15] Askanazi J, Rosenbaum SH, Hyman AI, Silverberg PA, Milic-Emili J, Kinney JM. Respiratory changes induced by the large glucose loads of total parenteral nutrition. JAMA 1980;243: 1444–7.

[16] Aubier M, Murciano D, Mili J, et al. Effects of the administration of O_2 on ventilation and blood gases in patients with chronic

obstructive pulmonary disease during acute respiratory failure. Am Rev Respir Dis 1980;122:747–54.
[17] Austen FK, Carmichael MW, Adams RD. Neurological manifestations of chronic pulmonary insufficiency. N Engl J Med 1957;257:579–90.
[18] Bengele HH, McNamara ER, Schwartz JH, Alexander EA. Acidification adaptation along the inner medullary collecting duct. Am J Physiol 1988;255:F1155–9.
[19] Bersin RM, Arieff AI. Improved hemodynamic function during hypoxia with Carbicarb, a new agent for the management of acidosis. Circulation 1988;77:227–33.
[20] Bidani A, Tzouanakis AE, Cardenas VJ, Zwischenberger JB. Permissive hypercapnia in acute respiratory failure. JAMA 1994;272:957–62.
[21] Bond JM, Chacon E, Herman B, Lemasters JJ. Intracellular pH and Ca^{2+} homeostasis in the pH paradox of reperfusion injury to neonatal rat cardiac myocytes. Am J Physiol 1993;265: C129–37.
[22] Brackett Jr NC, Cohen JJ, Schwartz WB. Carbon dioxide titration curve of normal man: effect of increasing degrees of acute hypercapnia on acid–base equilibrium. N Engl J Med 1965;272: 6–12.
[23] Brackett Jr NC, Wingo CF, Muren O, Solano JT. Acid–base response to chronic hypercapnia in man. N Engl J Med 1969;280:124–30.
[24] Brambrink A, Orfanakis A. "Therapeutic hypercapnia" after ischemic brain injury. Is there a potential for neuroprotection? Anesthesiology 2010;112:274–6.
[25] Brasch H, Thies E, Iven H. Pharmacokinetics of TRIS (hydroxymethyl-) aminomethane in healthy subjects and in patients with metabolic acidosis. Eur J Clin Pharmacol 1982;22:257–64.
[26] Brijker F, Heijdra YF, van den Elshout FJJ, Folgering H. Discontinuation of furosemide decreases $PaCO_2$ in patients with COPD. Chest 2002;121:377–82.
[27] Brimioulle S, Lejeune P, Vachiery JL, Leeman M, Melot C, Naeije R. Effects of acidosis and alkalosis on hypoxic pulmonary vasoconstriction in dogs. Am J Physiol 1990;258: H347–53.
[28] Bushinsky DA. Stimulated osteoclastic and suppressed osteoblastic activity in metabolic but not respiratory acidosis. Am J Physiol 1995;268:C80–8.
[29] Bushinsky DA, Lam BC, Nespeca R, Sessler NE, Grynpas MD. Decreased bone carbonate content in response to metabolic, but not respiratory, acidosis. Am J Physiol 1993;265:F530–6.
[30] Cardenas Jr VJ, Zwischenberger JB, Tao W, et al. Correction of blood pH attenuates changes in hemodynamics and organ blood flow during permissive hypercapnia. Crit Care Med 1996;24:827–34.
[31] Chonghaile MN, Higgins BD, Costello J, Laffey JG. Hypercapnic acidosis attenuates lung injury induced by established bacterial pneumonia. Anesthesiology 2008;109:837–48.
[32] Coakley RJ, Taggart C, Greene C, McElvaney NG, O'Neil SJ. Ambient pCO_2 modulates intracellular pH, intracellular oxidant generation, and interleukin-8 secretion in human neutrophils. J Leukoc Biol 2002;71:603–10.
[33] Cohen JJ, Madias NE, Wolf CJ, Schwartz WB. Regulation of acid–base equilibrium in chronic hypocapnia: evidence that the response of the kidney is not geared to the defense of extracellular $[H^+]$. J Clin Invest 1976;57:1483–9.
[34] Crandall ED, O'Brasky JE. Direct evidence for participation of rat lung carbonic anhydrase in CO_2 reactions. J Clin Invest 1978;62:618–22.
[35] Curley G, Contreras M, Nichol AD, Higgins BD, Laffey JG. Hypercapnia and acidosis in sepsis: a double-edged sword? Anesthesiology 2010;112:462–72.
[36] Darby JM, Yonas H, Marion DW, Latchaw RE. Local "inverse steal" induced by hyperventilation in head injury. Neurosurgery 1988;23:84–8.
[37] Dempsey JA, Forster HV, Gledhill N, DoPico GA. Effects of moderate hypoxemia and hypocapnia on CSF $[H^+]$ and ventilation in man. J Appl Physiol 1975;38:665–74.
[38] Domino KB, Lu Y, Eisenstein BL, Hlastala MP. Hypocapnia worsens arterial blood oxygenation and increases V_A/Q heterogeneity in canine pulmonary edema. Anesthesiology 1993;78: 91–9.
[39] Dries DJ. Permissive hypercapnia. J Trauma 1995;39:984–9.
[40] Dubowitz DJ, Dyer EAW, Theilmann RJ, Buxton RB, Hopkins SR. Early brain swelling in acute hypoxia. J Appl Physiol 2009; 107:244–52.
[41] Dulfano MJ, Ishikawa S. Hypercapnia: mental changes and extrapulmonary complications. An expanded concept of the "CO_2 intoxication" syndrome. Ann Intern Med 1965;63:829–41.
[42] Durrington HJ, Flubacher M, Ramsay CF, et al. Initial oxygen management in patients with an exacerbation of chronic obstructive pulmonary disease. QJM 2005;98:499–504.
[43] Eiam-Ong S, Laski ME, Kurtzman NA, Sabatini S. Effect of respiratory acidosis and respiratory alkalosis on renal transport enzymes. Am J Physiol 1994;267:F390–9.
[44] Gennari FJ, Goldstein MB, Schwartz WB. The nature of the renal adaptation to chronic hypocapnia. J Clin Invest 1972;51: 1722–30.
[45] Graham EM, Apostolou M, Mishra OP, Delivoria-Papadopoulos M. Modification of the N-methyl-D-asparate (NMDA) receptor in the brain of newborn piglets following hyperventilation induced ischemia. Neurosci Lett 1996;218:29–32.
[46] Graziani LJ, Gringlas M, Baumgart S. Cerebrovascular complications and neurodevelopmental sequelae of neonatal ECMO. Clin Perinatol 1997;24:655–75.
[47] Hackett PH, Roach RC. High-altitude illness. N Engl J Med 2001;345:107–14.
[48] Higgins BD, Costello J, Contreras M, Hassett P, O'Toole D, Laffey JG. Differential effects of buffered hypercapnia versus hypercapnic acidosis on shock and lung injury induced by systemic sepsis. Anesthesiology 2009;111:1317–26.
[49] Hilden SA, Johns CA, Madias NE. Adaptation of rabbit renal cortical Na^+-H^+ exchange activity in chronic hypocapnia. Am J Physiol 1989;257:F615–22.
[50] Holford FD, Mithoefer JC. Cardiac arrhythmias in hospitalized patients with chronic obstructive pulmonary disease. Am Rev Respir Dis 1973;108:879–85.
[51] Hsia CCW. Respiratory function of hemoglobin. N Engl J Med 1998;338:239–47.
[52] Ide K, Worthley M, Anderson T, et al. Effects of the nitric oxide synthase inhibitor L-NMMA on cerebrovascular and cardiovascular responses to hypoxia and hypercapnia in humans. J Physiol 2007;584:321–32.
[53] Kapur S, Wasserstrom JA, Kelly JE, Kadish AH, Aistrup GL. Acidosis and ischemia increase cellular Ca^{2+} transient alternans and repolarization alternans susceptibility in the intact rat heart. Am J Physiol Heart Circ Physiol 2009;296:H1491–512.
[54] Katz LA, Swain JA, Portman MA, Balaban RS. Intracellular pH and inorganic phosphate content of heart in vivo: a ^{31}P-NMR study. Am J Physiol 1988;255:H189–96.
[55] Kazemi H, Johnson DC. Regulation of cerebrospinal fluid acid–base balance. Physiol Rev 1986;66:953–1037.
[56] Kazmaier S, Weyland A, Buhre W, Stephan H, Rieke H, Flloda K, et al. Effects of respiratory alkalosis and acidosis on myocardial blood flow and metabolism in patients with coronary artery disease. Anesthesiology 1998;89:831–7.

[57] Kette F, Weil MH, Gazmuri RJ, Msee JB, Rackow EC. Intramyocardial hypercarbic acidosis during cardiac arrest and resuscitation. Crit Care Med 1993;21:901–6.
[58] Krapf R, Beeler I, Hertner D, Hulter HN. Chronic respiratory alkalosis: the effect of sustained hyperventilation on renal regulation of acid–base equilibrium. N Engl J Med 1991;324: 1394–401.
[59] Krapf R, Caduff P, Wagdi P, Staubli M, Hulter HN. Plasma potassium response to acute respiratory alkalosis. Kidney Int 1995;47:217–24.
[60] Krapf R, Hulter HN. Respiratory alkalosis. In: Gennari FJ, Adrogué HJ, Galla JH, Madias NE, editors. Acid–base disorders and their treatment. Boca Raton: Taylor & Francis; 2005. p. 641–79.
[61] Kucera RR, Shapiro JI, Whalen MA, Kindig NB, Filley GF, Chan L. Brain pH effects of $NaHCO_3$ and Carbicarb in lactic acidosis. Crit Care Med 1989;17:1320–3.
[62] Laffey JG, Kavanagh BP. Hypocapnia. N Engl J Med 2002;347:43–53.
[63] Leung JM, Landow L, Franks M, et al. Safety and efficacy of intravenous Carbicarb in patients undergoing surgery: comparison with sodium bicarbonate in the treatment of mild metabolic acidosis. Crit Care Med 1994;22:1540–9 (erratum *Crit Care Med* 1995;23:420)
[64] Madias NE, Adrogué HJ. Influence of chronic metabolic acid–base disorders on the acute CO_2 titration curve. J Appl Physiol 1983;55:1187–95.
[65] Madias NE, Adrogué HJ. Cross-talk between two organs: how the kidney responds to disruption of acid–base balance by the lung. Nephron Physiol 2003;93:61–6.
[66] Madias NE, Adrogué HJ, Horowitz GL, Cohen JJ, Schwartz WB. A redefinition of normal acid–base equilibrium in man: CO_2 tension as a key determinant of normal plasma bicarbonate concentration. Kidney Int 1979;16:612–8.
[67] Madias NE, Cohen JJ, Adrogué HJ. Influence of acute and chronic respiratory alkalosis on preexisting chronic metabolic alkalosis. Am J Physiol 1990;258:F479–85.
[68] Madias NE, Schwartz WB, Cohen JJ. The maladaptive renal response to secondary hypocapnia during chronic HCl acidosis in the dog. J Clin Invest 1977;60:1393–401.
[69] Man SF, McAlister FA, Anthonisen NR, Sin DD. Contemporary management of chronic obstructive pulmonary disease: clinical applications. JAMA 2003;290:2313–6.
[70] Marion DW, Firlik A, McLaughlin MR. Hyperventilation therapy for severe traumatic brain injury. New Horiz 1995;3: 439–47.
[71] Marion DW, Spiegel TP. Changes in the management of severe traumatic brain injury:1991-1997. Crit Care Med 2000; 28:16–8.
[72] Muizelaar JP, Marmarou A, Ward JD, et al. Adverse effects of prolonged hyperventilation in patients with severe head injury: a randomized clinical trial. J Neurosurg 1991;75: 731–9.
[73] Myrianthefs PM, Briva A, Lecuona E, Dumasius V, Rutschman DH, Ridge KM, et al. Hypocapnic but not metabolic alkalosis impairs alveolar fluid reabsorption. Am J Resp Crit Care Med 2005;171:1267–71.
[74] Nevin M, Colchester AC, Adams S, Pepper S. Evidence for involvement of hypocapnia and hyperfusion in aetiology of neurological deficit after cardiopulmonary bypass. Lancet 1987;2:1493–5.
[75] Panagiotopoulos S, Daly MJ, Nayler WG. Effect of acidosis and alkalosis on postischemic Ca gain in isolated rat heart. Am J Physiol 1990;258:H821–8.
[76] Peebles KC, Richards AM, Cell L, McGrattan K, Murrell CJ, Ainslie PN. Human cerebral arteriovenous vasoactive exchange during alterations in arterial blood gases. J Appl Physiol 2008;105:1060–8.
[77] Petropoulos IK, Pournaras JA, Stangos AN, Pournaras CJ. Effect of systemic nitric oxide synthase inhibition on optic disc oxygen partial pressure in normoxia and in hypercapnia. Invest Opthal Visual Science 2009;50:378–84.
[78] Planta IV, Weil MH, Planta MV, Gazmuri RJ, Duggal C. Hypercarbic acidosis reduces cardiac resuscitability. Crit Care Med 1991;19:1177–82.
[79] Pollock JM, Deibler AR, Whitlow CT, Tan H, Kraft RA, Burdette JH, et al. Hypercapnia-induced cerebral hyperperfusion: an underrecognized clinical entity. Am J Neurorad 2009; 30:378–85.
[80] Riphagen S, Bohn D. High frequency oscillatory ventilation. Intensive Care Med 1999;25:1459–62.
[81] Ruiz OS, Arruda JAL, Talor Z. Na-HCO_3^- cotransport and Na-H antiporter in chronic respiratory acidosis and alkalosis. Am J Physiol 1989;256:F414–20.
[82] Safar P, Xiao F, Radovsky A, et al. Improved cerebral resuscitation from cardiac arrest in dogs with mild hypothermia plus blood flow promotion. Stroke 1996;27:105–13.
[83] Sankri-Tarbichi AG, Rowley JA, Badr MS. Expiratory pharyngeal narrowing during central hypocapnic hypopnea. Am J Resp Crit Care Med 2009;179:313–9.
[84] Schreiber MD, Heymann MA, Soifer SJ. Increased arterial pH, not decreased $PaCO_2$, attenuates hypoxia-induced pulmonary vasoconstriction in newborn lambs. Pediatr Res 1986;20: 113–7.
[85] Schwartz GJ, Al-Awqati Q. Carbon dioxide causes exocytosis of vesicles containing H^+ pumps in isolated perfused proximal and collecting tubules. J Clin Invest 1985;75:1638–44.
[86] Schwartz WB, Brackett Jr. NC, Cohen JJ. The response of extracellular hydrogen ion concentration to graded degrees of chronic hypercapnia: the physiologic limits of defense of pH. J Clin Invest 1965;44:291–301.
[87] Schwartz WB, Hays RM, Polak A, Haynie GD. Effects of chronic hypercapnia on electrolyte and acid–base equilibrium. II. Recovery, with special reference to the influence f chloride intake. J Clin Invest 1961;40:1238–49.
[88] Teixeira Da Silva Jr JC, Perrone RD, Johns CA, Madias NE. Rat kidney band 3 mRNA modulation in chronic respiratory acidosis. Am J Physiol 1991;260:F204–9.
[89] Vadasz I, Dada LA, Briva A, Trejo HE, Welch LC, Chen J, et al. AMP-activated protein kinase regulates CO_2-induced alveolar epithelial dysfunction in rats and human cells by promoting Na,K-ATPase endocytosis. J Clin Invest 2008;118: 752–62.
[90] Verlander JW, Madsen KM, Tischer CC. Effect of acute respiratory acidosis on two populations of intercalated cells in rat collecting duct. Am J Physiol 1987;253:F1142–56.
[91] Weber T, Tschernich H, Sitzwohl C, Ullrich R, Germann P, Zimpfer M, et al. Tromethamine buffer modifies the depressant effect of permissive hypercapnia on myocardial contractility in patients with acute respiratory distress syndrome. Am J Respir Crit Care Med 2000;162:1361–5.
[92] Welch LC, Lecuona E, Briva A, Trejo HE, Dada LA, Sznajder JI. Extracellular signal-regulated kinase (ERK) participates in the hypercapnia-induced Na, K-ATPase downregulation. FEBS Lett 2010. [Epub ahead of print].
[93] Zhou Q, Cao B, Niu L, Cui X, Yu H, Liu J, et al. Effects of permissive hypercapnia on transient global cerebral ischemia-reperfusion injury in rats. Anesthesiology 2010;112:288–97.

CHAPTER

61

Mechanisms and Disorders of Magnesium Metabolism

Karl P. Schlingmann and Martin Konrad

University Children's Hospital, Pediatric Nephrology, Münster, Germany

INTRODUCTION

Body magnesium homeostasis depends on the balanced regulation of intestinal magnesium absorption and renal magnesium conservation. Renal magnesium handling is a filtration–reabsorption process, as there is little evidence of secretion along the nephron segments (Fig 61.1). About 80% of the total plasma magnesium (0.65–1.2 mM) is filtered through the glomeruli. Of the ultrafilterable magnesium (0.5–0.9 mM), 15–20% is reabsorbed by the convoluted and straight portions of the proximal tubule. The thick ascending limb (TAL) of the loop of Henle, specifically the cortical segment, plays a major role in reclaiming filtered magnesium (55–70%), whereas only 5–10% are reabsorbed in the distal convoluted tubule (DCT). However, the DCT provides the selective regulation of magnesium reabsorption and plays an important role in determining the final urinary excretion.[1] About 3–5% of the filtered load normally appear in the urine. Magnesium transport in both the TAL and DCT responds to changes in magnesium to effect sensitive control of magnesium balance.

PHYSIOLOGY OF RENAL MAGNESIUM HANDLING

Glomerular Filtration

Approximately 70% of plasma magnesium is in the ionic form, Mg^{2+}.[2] The remaining magnesium is bound to circulating proteins (essentially albumin) or is complexed with citrate, oxalate, and phosphate anions. About 80% of the total serum magnesium is ultrafilterable through the glomerular membrane that varies with the amount bound to nonfilterable proteins.[3]

Proximal Tubule

Physiology of Proximal Tubule Magnesium Reabsorption

In the adult, proximal tubule magnesium reabsorption rate (15–20%) is considerably less than the fractional reabsorption of sodium and calcium.[3] In neonates, the proximal tubule reabsorbs about 70% of the filtered magnesium that is the same as the fractional reabsorption of sodium and calcium.[4] Clearly, the permeability of the proximal tubule changes during development so that more magnesium is delivered to the loop of Henle in the adult. This maturation in segmental handling of magnesium should be taken into consideration when assessing renal magnesium handling in very young children. Proximal tubule magnesium transport in adults is thought to be active and transcellular in nature, whereas it is probably passive in the immature individual occurring through the paracellular pathway entrained with water movement.

Various hormones alter magnesium reabsorption within the proximal tubule.[5] They do so by influencing salt and water transport, and thus luminal magnesium concentration. Reabsorption is load dependent, so that transport is greater with elevated luminal magnesium concentrations. Extracellular volume expansion or anything that retards salt and water transport results in diminished fluid absorption and greater magnesium delivery into the loop of Henle and the DCT. The increase in distal delivery is normally reclaimed in these nephron segments but may be large enough to cause an increase in urinary magnesium excretion and hypermagnesiuria.[6]

Seldin and Giebisch's The Kidney, Fifth Edition.
DOI: http://dx.doi.org/10.1016/B978-0-12-381462-3.00061-6

© 2013 Elsevier Inc. All rights reserved.

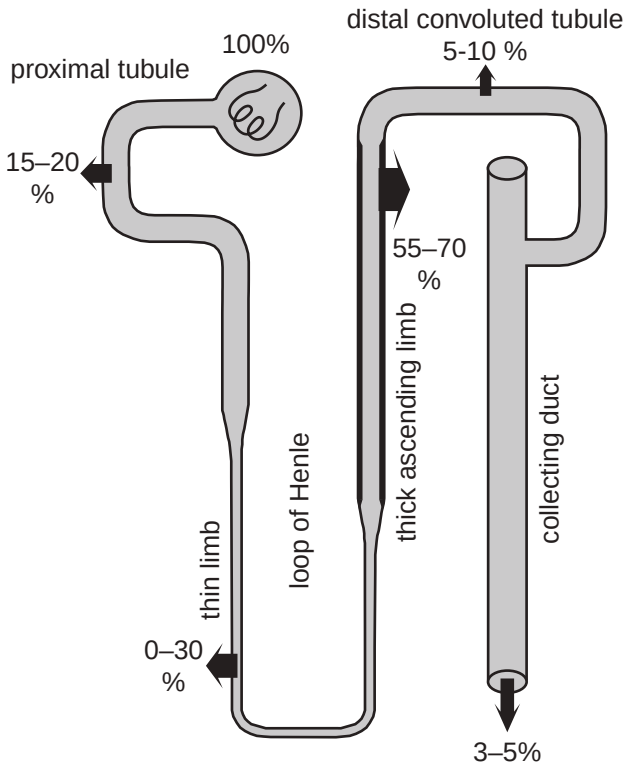

FIGURE 61.1 Summary of segmental magnesium reabsorption along the nephron.

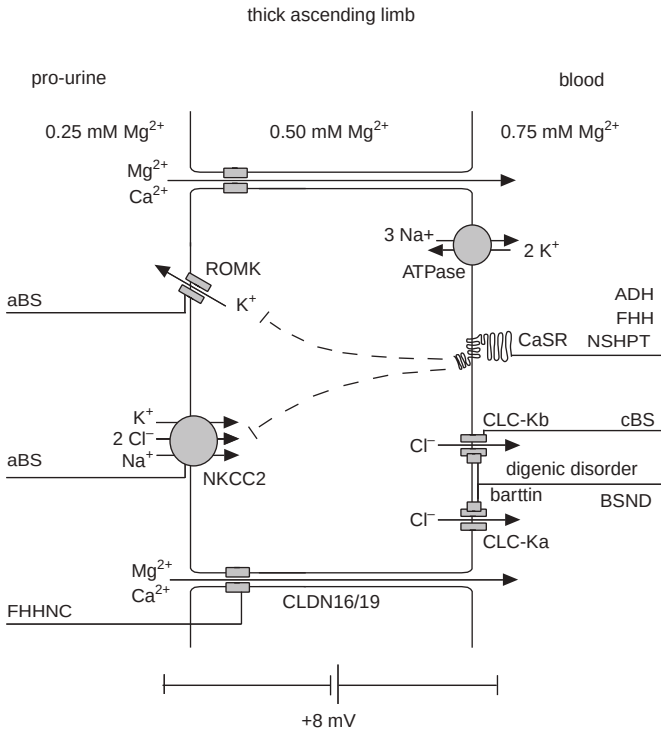

FIGURE 61.2 **Schematic model of magnesium reabsorption in the cTAL of Henle's loop.** The membrane proteins influencing magnesium reabsorption are indicated. Magnesium reabsorption is passive and occurs through the paracellular pathway. Furosemide diminishes Mg^{2+} absorption by inhibiting NKCC2 and transepithelial voltage. Peptide hormones (PTH, calcitonin, glucagon, AVP) enhance magnesium reabsorption in the cTAL by increasing the transepithelial voltage and magnesium permeability of the paracellular pathway.[5] The sites of genetic diseases associated with magnesium reabsorption in the cTAL are indicated: aBS, cBS, antenatal Bartter syndrome with sensorineural deafness (BSND/digenic disorder), FHHNC, ADH, FHH, and NSHPT.

Loop of Henle

Physiology of Loop of Henle Magnesium Reabsorption

The thin descending limb is able to reclaim significant amounts of filtered magnesium. Inference from micropuncture data of the differences in magnesium delivery to the late proximal tubule and the hairpin turn of rat juxtamedullary nephrons indicate that a significant fraction of the filtered magnesium, on the order of 30%, is reclaimed along the descending limb in the concentrating kidney.[7] The amount of magnesium absorption is associated with water transport in the descending limb. Accordingly, magnesium reabsorption is considerably diminished during forced diuresis when water reabsorption is negligible in this segment.[5] The TAL reabsorbs the predominant portion of the magnesium, amounting to some 70% of the filtered load. Moreover, de Rouffignac and colleagues have shown that it is the cortical thick ascending limb (cTAL), not the medullary segment (mTAL), that reabsorbs magnesium.[8] They have further reported that transepithelial magnesium absorption is passive moving from lumen to the interstitial space through the paracellular pathway (Fig 61.2), consistent with earlier observations.[9] The driving force for magnesium movement is the positive luminal transepithelial voltage generated by K^+ recycling across the apical membrane (Fig 61.2). Any influence that alters transepithelial voltage or the permeability of the paracellular pathway will alter magnesium reabsorption in the cTAL.[5] The voltage in the TAL is dependent on apical 70-pS K^+ channel (ROMK) activity and Na−K−2Cl cotransport that control current flow across the apical membrane of the TAL cell. Sodium exits by the basolateral Na−K−ATPase and chloride through basolateral ClC-Ka and ClC-Kb members of the chloride channel family (ClC). Functional expression of ClC-Ka and ClC-Kb channels requires the coexpression of barttin, an essential β-subunit of the channels.[10] As barttin controls ClC-Ka and ClC-Kb activity, it importantly influences salt absorption in the TAL.[11,12] Changes in their transport rates will affect the transepithelial voltage and thus the magnesium absorption. The permeability of the paracellular pathway also plays an important role in determining transepithelial magnesium transport. Paracellular Mg^{2+} movement is influenced by electrostatic charges of

TABLE 61.1 Coordinate Controls of Magnesium Transport in the Loop of Henle and the Diastal Convoluted Tubule

	TAL	DCT
Peptide hormones (PTH, Calcitonin, Glucagon, Vasopressin, Insulin)	↑	↑
Prostaglandins (PGE_2)	↓	↑
Aldosterone	↑	↑
1,25-$(OH)_2$-vitamin D_3	?	↑
Magnesium restriction	↑	↑
Hypermagnesemia	↓	↓
Hypercalcemia	↓	↓
Extracellular volume expansion	↓	↑
Metabolic acidosis	↓	↓
Metabolic alkalosis	↑	↑
Phosphate depletion	↓	↓
Potassium depletion	↓	↓

proteins comprising this route.[3] Moreover, there appears to be selectivity of the pathway to divalent cations.[6] Paracellular proteins of the claudin family of tight junction proteins claudin-16 and claudin-19 have been identified in the TAL and are involved in controlling magnesium and calcium permeability of the paracellular pathway.[13,14] This notion is supported by the phenotype resulting from mutations in the encoding genes *CLDN16* and *CLDN19*. Affected individuals present with massive calcium and magnesium wasting due to defective reabsorption in the cTAL.[13,14]

In humans, the claudin family comprises at least 22 proteins with a molecular weight between 20 and 27 kDa. They consist of four transmembrane helices, two extracellular loops, and intracellular N- and C-termini. While the first loop is believed to influence paracellular charge selectivity, the second is probably responsible for the interaction between opposing claudins of adjacent cells. In association with occludin, claudins polymerize into linear fibrils that ultimately alter ion selectivity and permeability of tight junctions.[15] Claudins have been shown to be differentially expressed along the nephron[16,17] and to be regulated by receptor-mediated activation.[18–20]

Control of Loop of Henle Magnesium Reabsorption

HORMONAL CONTROLS

A large number of hormones stimulate magnesium reabsorption in the loop of Henle (Table 61.1). Included are peptide hormones such as parathyroid hormone (PTH), calcitonin, glucagon, and arginine vasopressin (AVP).[5] Adrenergic agonists, isoproterenol, and insulin also increase magnesium transport.[3] Mineralocorticoids stimulate NaCl absorption and in turn transepithelial voltage in the loop and by inference increase magnesium reclamation in this segment.[1] Prostaglandins, on the other hand, diminish both salt and magnesium conservation in the cTAL.[5] All of these hormonal responses are mediated by changes in transepithelial voltage by altering apical K^+ recycling and Na−K−2Cl cotransport and the paracellular permeability by modifying tight junctions proteins.[21]

NONHORMONAL CONTROLS

The extracellular Ca^{2+}-sensing receptor (CaSR) importantly influences divalent cation transport in the TAL.[1,22–24] Activation of the CaSR decreases hormone-dependent cAMP release by inhibition of adenylyl cyclase. CaSR activation has been reported to reduce the activity of the 70-pS K^+ channel, and thus potassium recycling and Na−K−2Cl cotransport leading to diminished transepithelial voltage.[23] Though putatively acting through this mechanism, it does not affect salt reabsorption much.[8,25–27] A number of studies have shown that elevated calcium and magnesium, as well as the multivalent gadolinium and the calcimimetic NPS R-467, inhibit the hormonal stimulation of intercellular calcium and magnesium movement at any given voltage, suggesting that the CaSR may also have an effect on paracellular pathways, again perhaps acting through the modification of tight junctions.[26–28] CaSRs are expressed at the basolateral membrane of both medullary and cortical TALs so that they respond to increases in divalent cation concentrations in the blood/interstitium rather than luminal Ca^{2+} and Mg^{2+}.[29] This explains earlier findings that increases in plasma calcium or magnesium inhibit calcium and magnesium transport but increases in luminal concentrations do not.[6]

Hypermagnesemia and hypercalcemia have long been known to result in diminished divalent cation reabsorption.[30] Using clearance studies, Wong et al. elevated serum magnesium levels in thyroparathyroidectomized dogs and determined the urinary magnesium excretion rates with elevated filtered magnesium.[31] They showed that elevated filtered magnesium concentration was initially associated with increases in magnesium reabsorption until an apparent tubular maximum, Tm, was attained, beyond which any additional filtered magnesium was excreted in the urine. Micropuncture studies showed that this Tm was the result of increased proximal tubule reabsorption and diminished loop transport, and has been extensively used in the clinical assessment of renal magnesium conservation.[32] The cellular basis for these observations, as revealed by Hebert and colleagues, is the CaSR present at the basolateral membrane of the TAL that inhibits transport upon

elevation of either calcium or magnesium.[23] The concept of a Tm as an index of total renal magnesium conservation is still useful as long as the segmental contribution is considered and the plasma magnesium concentration is not extreme.[33]

Dietary magnesium restriction and hypomagnesemia have been reported to stimulate magnesium absorption within the cTAL.[6,34] Wittner et al. have shown that the increase in magnesium transport is due to an increase in the permeability of the paracellular pathway to magnesium, in keeping with the passive nature of magnesium transport within the loop.[34] Interestingly, calcium absorption in the loop is also increased by magnesium restriction, so the response is not selective to magnesium.[34] Again, we assume that these changes in paracellular magnesium transport involve modification of tight junction proteins including claudin-16 and claudin-19. In support of this notion, Efrati et al. have reported that the amount of *cldn16* transcript is increased in mice with dietary-induced hypomagnesemia.[35]

Loop Diuretics

Furosemide and bumetanide diminish the luminal positive voltage by virtue of their effects on the Na−K−2Cl cotransporter. Because of this, the acute furosemide usage leads to enhanced distal delivery and increased urinary excretion of magnesium.[35] However, with chronic furosemide therapy urinary excretion usually returns to near control levels. This is likely due to enhanced reabsorption in the proximal tubule and DCT. Thus, prolonged use of furosemide does not often lead to renal magnesium wasting.

Distal Convoluted Tubule

Physiology of Distal Convoluted Tubule Magnesium Reabsorption

The DCT plays an essential role in determining the final urinary magnesium excretion since little or no magnesium is reabsorbed beyond this segment.[1] Magnesium transport within the DCT is transcellular and active in nature (Fig 61.3). Magnesium enters the cell through selective ion channels across the apical membrane, driven by the transmembrane negative electrical potential.[36] Apical magnesium entry is the rate-limiting step in reabsorption, and many of the hormonal and nonhormonal controls act at this site. Cellular magnesium is actively extruded at the basolateral membrane, possibly by a sodium-dependent exchange mechanism which is still unresolved at the molecular level.[3] Micropuncture studies and experiments with immortalized mouse DCT (mDCT) cells have shown that magnesium transport in the DCT is dependent on luminal magnesium concentration and apical transmembrane voltage.[36]

Though being far from completely understood, our knowledge of magnesium transport in the DCT has greatly evolved over the recent years. First, the divalent cation channel, TRPM6, had been implicated in renal magnesium absorption based on the observation that mutations in the *TRPM6* gene cause autosomal recessive hypomagnesemia with secondary hypocalcemia (HSH).[37,38] HSH is characterized by very low serum magnesium due to diminished intestinal magnesium absorption and renal magnesium wasting (see section IIA6). TRPM6 is a member of the transient receptor potential melastatin (TRPM) family of cation channels.[39] They are characterized by six transmembrane segments, a highly conserved pore-forming region, and a Pro-Pro-Pro motif following the last transmembrane domain. Unlike the other members of the TRPM family, TRPM6 and its close homologue TRPM7 possess a unique structure in that they have an alpha-kinase domain in the C-terminal region.[39–41] Dorovkov and Ryazanov have shown that this alpha-kinase phosphorylates and activates annexin 1.[42] Annexin 1 plays a

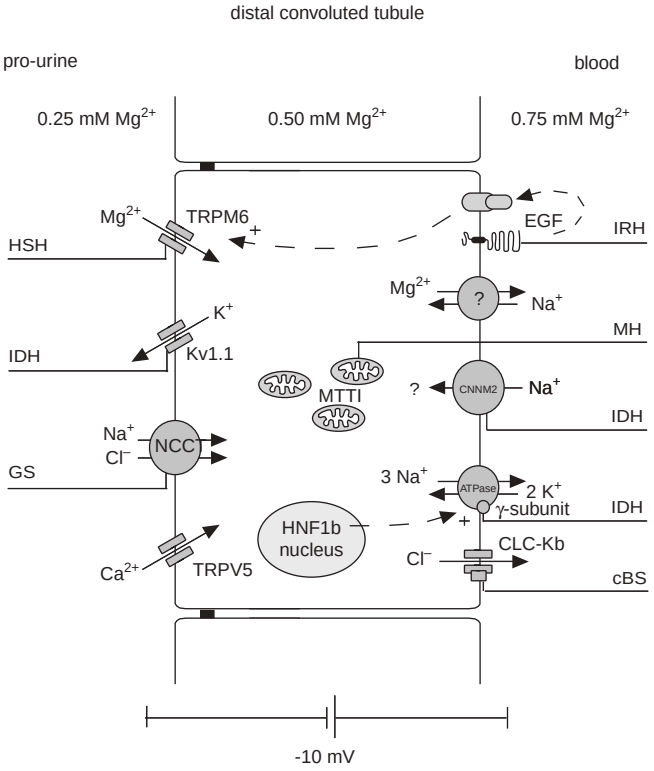

FIGURE 61.3 **Schematic model of magnesium absorption in the DCT.** The membrane proteins influencing magnesium absorption are indicated. Peptide hormones (PTH, calcitonin, glucagon, AVP) enhance magnesium reabsorption in the DCT. The sites of genetic diseases affecting magnesium reabsorption in the DCT are indicated: HSH, IDH, GS, IRH, metabolic hypomagnesemia (MH), cBS.

pleiotropic role in cell proliferation, inflammation, and apoptosis. What this has to do with magnesium transport is not known but Nadler et al. have reported that TRPM7 is essential in cell viability so that it likely plays an important role in cell metabolism.[39] Takezawa et al. have provided evidence that TRPM7 activity is modulated by its own endogenous kinase domain, responding to changes in intracellular levels of cAMP induced by G_i- and G_s-coupled receptors.[43] Earlier it was found that TRPM6 and TRPM7 channels are permeable to calcium and magnesium, are inhibited by increases in intracellular magnesium levels or Mg-ATP,[39] and, although controversial, possibly inactivated by phosphatidylinositol 4,5-bisphosphate hydrolysis.[43,44] TRPM7 is ubiquitously expressed among tissues whereas TRPM6 expression is restricted to few tissues including intestine and kidney.[37] Chubanov et al. have shown that TRPM6 and TRPM7 form heteromultimeric complexes that form functional magnesium permeable channels at the cell surface.[45] Voets et al. have reported that TRPM6 is located along the apical membrane of the small intestine and DCT, transports both magnesium and calcium, and is associated with the divalent cation-binding proteins, parvalbumin, and calbindin-D_{28K}.[46] Whether these binding proteins play a role in regulation of cellular magnesium reabsorption, as they do for calcium, is not known. Several authors have also shown that other divalent ions, such as zinc and cobalt, were also transported by TRPM6, which supports earlier observations demonstrating that TRPM6/TRPM7 are permissive metal ion transporters.[45–47] Nevertheless, magnesium appears to be the preferred substrate so that TRPM6 and TRPM7 are considered as a primary magnesium entry channel.

Control of Distal Convoluted Tubule Magnesium Reabsorption

HORMONAL CONTROLS

A large number of peptide hormones stimulate magnesium absorption within the DCT (Table 61.1). Many of these are the same hormones that influence magnesium transport in the cTAL of Henle's loop. These include PTH, calcitonin, glucagon, and AVP, all of which act through individual receptor-mediated signaling (reviewed in Dai et al.[36]). Renal magnesium conservation seems to be a concerted response to all of these hormones. However, these hormones also stimulate sodium, potassium, and chloride transport in the mTAL, cTAL, and calcium transport in both the cTAL and the distal tubule so that hormonal control is not specific to magnesium.

There is good evidence that vitamin D is important for renal magnesium conservation.[1] Ritchie et al. have demonstrated that $1,25(OH)_2D_3$ increases magnesium entry rates in isolated DCT cells.[48] The response is concentration dependent, involves transcriptional processes necessitating de novo protein synthesis, and does not appear to be related to receptor-mediated cAMP release and stimulation of magnesium uptake.[48] Finally, $1,25(OH)_2D_3$-stimulated magnesium transport is additive to PTH-mediated uptake suggesting that the peptide and steroid hormones regulate magnesium absorption through distinctive intracellular signaling pathways.[36] These studies show that vitamin D_3 metabolites modulate magnesium transport in the DCT independent of other hormonal influences.

Vitamin D_3 administration has often been associated with increases in urinary magnesium and calcium excretion. Vitamin D_3 metabolites increase intestinal absorption of magnesium and calcium so that a positive divalent cation balance may lead to hypermagnesemia and hypercalcemia which in turn diminish magnesium absorption in the loop of Henle through the extracellular CaSR. This may also explain the increase or absence of changes in urinary magnesium excretion following administration of vitamin D_3. The net effect on magnesium balance would thus depend on the relative magnitude of vitamin D_3 actions at the intestinal and renal levels.

Aldosterone enhances hormone-stimulated magnesium entry by potentiating receptor-mediated intracellular signaling, including cAMP formation.[36] Accordingly, acute mineralocorticoids increase magnesium conservation within the DCT in the presence of circulating hormones. Chronic aldosterone administration, on the other hand, generally results in renal magnesium wasting.[36] This has been explained by extracellular volume expansion leading to diminished salt and magnesium reabsorption within the loop of Henle. The potentiation of hormone-mediated magnesium reabsorption in the distal convolute would tend to minimize magnesium loss in hypermineralocorticoidism

Other humoral factors influence renal magnesium conservation such as prostaglandins, insulin, adrenergic agonists, and purinogenic metabolites. Prostaglandin E_2 (PGE_2) is the major arachidonate metabolite synthesized by cyclooxygenase in the mammalian kidney. PGE_2 has a number of diverse actions on the kidney in addition to its ability to influence renal hemodynamics. PGE_2 inhibits salt transport in the mTAL and salt as well as calcium and magnesium absorption within the cTAL and also modulates sodium and water transport in the cortical collecting duct (CCD).[5,49] By its actions in the DCT, prostaglandins may limit magnesium excretion and maintain magnesium balance. Insulin has clearly been shown to have antinatriuretic and antimagnesiuric effects by its actions on the TAL.[5] but insulin also increases magnesium transport in isolated DCT cells.[36] Furthermore, the nephron is richly innervated along its

length from the glomerulus to the collecting tubule. Renal nerve stimulation significantly increases salt and water reabsorption in the proximal tubule, loop of Henle, and distal tubule.[5] Dai and colleagues have shown that isoproterenol increases magnesium transport in DCT cells.[36] It can be concluded from these studies with immortalized mDCT cells that renal nerves and circulating catecholamines play a role in the control of magnesium transport in the DCT.

The interactions of the various peptide and steroid hormones, prostaglandins, and renal innervation are complex.[5] It can be inferred that overall distal magnesium absorption is controlled by all of these influences initiated individually but coming together through shared intracellular signaling pathways.[5] Few studies have been directed at describing these interactions. It is clear that control of renal magnesium handling is orchestrated by many hormones and influences.

The most interesting discovery concerning the hormonal control of tubular magnesium reabsorption stems from the discovery of a mutation in pro-EGF in a family with hereditary magnesium wasting (see below).[50] The mutation impairs the basolateral sorting of epidermal growth factor (EGF) in the DCT. Thereby, binding of EGF to basolaterally expressed EGF receptor (EGFR) is abolished which finally leads to renal magnesium wasting. The supposed mechanism of EGF action is a stimulation of intracellular Src kinase as well as MAP kinase signaling cascades which in turn activate magnesium reabsorption via TRPM6.[51] Thebault and colleagues could show that incubation with EGF leads to an activation of TRPM6-induced currents in HEK293 cells.[51] The authors suggest EGF to be the first selectively acting magnesiotropic hormone as no influence on calcium transport was detected. However, EGF is also known to influence sodium reabsorption in the aldosterone sensitive distal nephron by activation of MAP kinase signaling.[52]

NONHORMONAL CONTROLS

Early in vivo microperfusion studies have demonstrated that elevated extracellular magnesium or calcium also inhibit fractional magnesium transport in superficial rat distal tubules.[6] This has been attributed to the actions of the extracellular CaSR. Riccardi et al. have shown that the CaSR is located on the basolateral membrane of the DCT.[29] Bapty et al. reported that high extracellular magnesium or calcium concentrations inhibit hormone-stimulated magnesium uptake in immortalized mDCT cells.[36,53] These studies clearly indicate that hypermagnesemia and hypercalcemia per se can modify hormone regulation of active, transcellular magnesium transport within the DCT leading to increased magnesium excretion.

The CaSR in the loop of Henle and also in the DCT provides a negative feedback mechanism to mitigate the over exuberant responses of PTH. PTH stimulates calcium and magnesium reabsorption within both nephron segments leading to a rise in serum divalent cation concentrations. Increments in serum calcium and magnesium feedback at the parathyroid gland to inhibit secretion of PTH and at the kidney tubule to inhibit calcium and magnesium transport in the cTAL and the DCT (Fig 61.4). Both extrarenal and intrarenal feedback mechanisms involve the same CaSR located in the parathyroid gland and on renal epithelial cells, respectively. There is evidence that the scenario for PTH feedback may also apply to other calcium- and magnesium-conserving hormones such as vitamin D.[36] Vitamin D metabolites enhance magnesium uptake in isolated DCT cells through a genomic mechanism involving transcriptional/translational processes requiring 2−3 hours following the addition of the hormone.[48] Elevation of extracellular calcium abolishes $1,25(OH)_2D_3$ stimulation indicating that the CaSR may modify gene expression in DCT cells. In order to determine whether elevated extracellular calcium inhibits $1,25(OH)_2D_3$ responses through the CaSR, Dai and coworkers preincubated the cells with a specific antibody to the CaSR protein before treating them with high calcium and $1,25(OH)_2D_3$.[36] The antibody prevented the effect of calcium on $1,25(OH)_2D_3$-induced magnesium uptake, clearly demonstrating a receptor-mediated response.[36] Accordingly, excess $1,25(OH)_2D_3$ increases distal calcium and magnesium transport leading to elevated serum concentrations and activation of the CaSR that provides a negative feedback on divalent cation reabsorption. The CaSR plays an important additional role in mineral metabolism: The CaSR also inhibits water reabsorption in the collecting duct so that excess luminal calcium does not accumulate to form calcareous concretions.[23] There, the CaSR is expressed both at the luminal and basolateral membrane. Therefore, it not only senses interstitial divalent cation concentrations but also intraluminal or urinary cation levels. CaSR activation results in a reduction of autosomal-dominant hypoparathyroidism (ADH)-mediated Aquaporin-2 incorporation into the apical membrane and consecutively a reduced water permeability of the inner medullary collecting duct (IMCD) (citation). The net effect is a concomitant increase in volume flow along with a rise in calcium and magnesium excretion which minimizes the risk of stone formation.[23]

Distal Diuretics

The distal diuretics, hydrochlorothiazide, and amiloride increase magnesium uptake in DCT cells.[36] These agents inhibit sodium chloride cotransport and sodium channels (ENaC), respectively, leading to

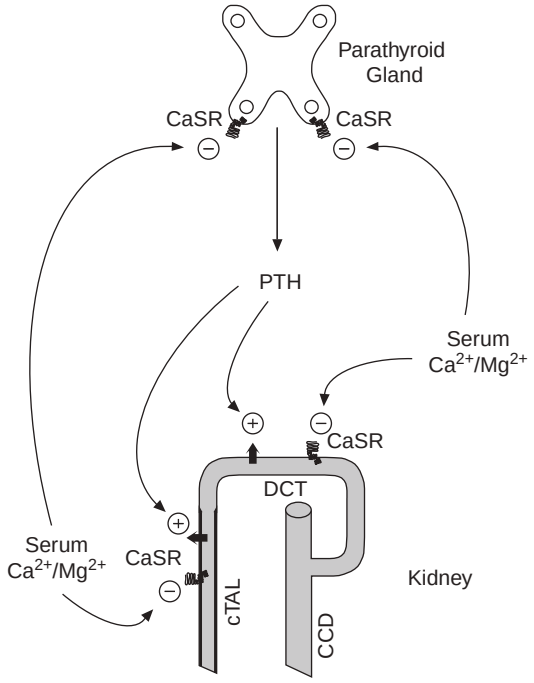

FIGURE 61.4 The extracellular CaSR modulates PTH-stimulated Ca^{2+} and Mg^{2+} reabsorption at renal and extrarenal levels.

diminished intracellular chloride concentration and hyperpolarization of the apical membrane. The increased apical membrane voltage stimulates magnesium entry and transepithelial transport. Although amiloride has clearly been shown to be a magnesium-sparing diuretic, chronic hydrochlorothiazide usage may lead to renal magnesium wasting.[1] The cellular mechanisms for the chronic hydrochlorothiazide effects are unclear but may involve hypokalemia, which can jeopardize renal magnesium conservation.[36,54]

Overall Regulation of Renal Magnesium Handling

In addition to hormonal controls and CaSR-mediated regulation of magnesium reabsorption in TAL and DCT, magnesium transport in these parts of the nephron is regulated in response to altered magnesium status (Table 61.1). A reduction in serum magnesium levels directly results in a decrease in filtered load and consecutively a diminished magnesium flow through the distal nephron. To elucidate the response of the distal nephron to changes in magnesium status, different techniques have been applied including (1) animal studies using magnesium restricted diets and inbred strains with high or low magnesium status, (2) micropuncture and microperfusion studies, and (3) in-vitro experiments with distal tubular cell lines. The discovery of new genes and their encoded proteins involved in paracellular and transcellular magnesium transport in TAL and DCT, respectively, now enables us to investigate the adaptive changes at the molecular level. Classic microperfusion studies in microdissected nephron segments had indicated an increased fractional reabsorption of magnesium in the TAL in rats maintained on a low magnesium diet for only 6 hours, when there is a maximum decline in renal magnesium excretion, but serum magnesium levels are still normal.[55] Calcium and sodium reabsorption rates during this adaptive response remained unchanged. An analogue response was also described for the DCT and furthermore demonstrated in isolated mDCT cells.[56] An inhibition of this adaptive process by pretreatment of cells with cycloheximide, an inhibitor of protein synthesis, implicated genetically controlled mechanisms.[36] More recent studies now identified putative underlying mechanisms of changes in renal tubular magnesium handling in response to magnesium restriction or excess. Efrati and colleagues demonstrated changes in claudin-16 expression in the TAL in mice fed diets with differing magnesium content.[57] Two further studies in mice fed magnesium restricted diets could show that one mechanism underlying the upregulation of renal magnesium conservation in the DCT is an increased expression of TRPM6.[58,59] Contrariwise, Groenestege and colleagues demonstrated that a magnesium enriched diet results in an increase in urinary magnesium, but also calcium wasting.[58] They also found that TRPM6 expression was not dependent on $1,25(OH)_2$-vitamin D or PTH but upregulated by estrogens.[58]

Similarly, hormonal responses are serially organized to regulate magnesium transport in both TAL and DCT. This may be beneficial in that perturbing influences acting in either the loop or distal tubule that can be balanced by homeostatic responses in the other segment. The antenatal Bartter syndrome (aBS) typifies this serial control in magnesium conservation. It results from mutational changes in sodium chloride cotransport in the TAL leading to defective salt absorption (Fig 61.2). Patients with this condition are characterized by volume depletion, hyperreninemia, secondary hyperaldosteronism, hypokalemia, and metabolic alkalosis (see below). Despite defective TAL function, few of these patients demonstrate hypomagnesemia, presumably due to increased reclamation of magnesium in the DCT not affected by the TAL defect.[60–62] In this case, DCT function compensates for diminished TAL reabsorption even though the hormonal controls are similar.

PATHOPHYSIOLOGY OF RENAL MAGNESIUM HANDLING

Genetic Magnesium-Wasting Diseases

Hereditary hypomagnesemia comprises a set of rare genetically determined disorders primarily or secondarily affecting renal magnesium handling. Over the past years, numerous genetic defects in genes encoding components of the renal tubular salt and electrolyte transport machinery or regulating factors have been described (Table 61.2). The spectrum ranges from the most frequent variant, the Gitelman syndrome (GS) with a primary defect in salt reabsorption in the DCT to rare disorders discovered in single patients or families only. The following sections try to summarize essential data from a multitude of research studies published over the last years. Defects primarily or solely affecting renal magnesium handling are preceded by a paragraph on renal salt wasting disorders (Bartter syndrome).

Hypomagnesemia Associated with Abnormal Renal Salt Handling

Tubular salt reabsorption affects the membrane potential of tubular epithelial cells and is involved in the generation of the transepithelial potential, both of which are a prerequisite for the processes of magnesium reabsorption along the different segments of the nephron. Salt-wasting disorders with hypokalemia and metabolic alkalosis, also known as Bartter-like syndromes, impair tubular reabsorption of sodium chloride in different parts of the distal nephron. The renal conservation of magnesium is secondarily affected to a varying extent according to the nephron segment affected in each of the Bartter-like syndromes.

BARTTER SYNDROME

ANTENATAL BARTTER SYNDROME The aBS is caused by mutations either in the furosemide-sensitive Na−K−2Cl cotransporter (NKCC2) or in the ROMK K^+ channel, which cooperate in the apical uptake of sodium chloride in the TAL.[63–66] The defect in sodium chloride reabsorption caused by mutations in either protein reduces the lumen-positive transepithelial voltage and thus impairs passive paracellular reabsorption of calcium and magnesium in this part of the nephron.

aBS is characterized by massive polyuria that manifests in utero with the development of polyhydramnios which in turn results in premature birth in most patients.[67] Postnatally, affected children rapidly develop massive salt wasting and subsequent hypokalemic metabolic alkalosis. In addition, hypercalciuria and nephrocalcinosis occur in virtually all patients. In contrast, disturbances in magnesium homeostasis are not commonly observed in aBS (64). The lack of renal magnesium wasting despite pronounced hypercalciuria is explained by increased distal tubular salt reabsorption, especially via an upregulation of salt reabsorption in the DCT which also leads to enhanced magnesium conservation. The relationship between sodium, calcium, and magnesium handling in the DCT will be discussed in more detail below, as exactly the opposite association is observed in GS, that is, diminished sodium and magnesium transport but increased calcium reabsorption. aBS is characterized by increased prostaglandin E synthesis that might also contribute to an improved magnesium reabsorption in the DCT, as demonstrated in a mDCT cell line.[36]

ANTENATAL BARTTER SYNDROME WITH SENSORINEURAL DEAFNESS The most severe variant of the Bartter-like syndromes is caused by a defect in basolateral chloride extrusion along the distal nephron. Mutations in the activating β-subunit of renal chloride channels ClC-Ka and ClC-Kb or combined mutations of the two chloride channels themselves were identified as the underlying genetic defects.[10,68,69]

Both chloride channels mediate the basolateral extrusion of chloride from tubular epithelial cells in TAL and DCT. In addition, ClC-Ka provides the major route for chloride reabsorption in the ascending thin limb where it is expressed at the apical as well as basolateral membrane. Whereas isolated ClC-Kb defects lead to the clinical picture of classic Bartter syndrome (cBS) (see below), mutations in ClC-Ka have not been described so far in humans. Disruption of ClC-Ka in mice leads to a diabetes insipidus-like phenotype.[70]

Renal salt and water losses are even more severe than in aBS. Patients often require long-term parenteral fluid replacement. The excessive salt wasting is explained by the combined impairment of ClC-Ka- and ClC-Kb-mediated salt reabsorption in both the loop of Henle and in the DCT. Unlike in aBS, hypercalciuria and nephrocalcinosis are uncommon; instead patients often show progressive renal failure of unknown origin.[71]

Serum magnesium levels have been found to be reduced in BSND with values around 0.5 mmol/L.[72] A possible explanation is a combined impairment of paracellular divalent transport in the TAL as well as of active transcellular magnesium reabsorption in the DCT, which results in pronounced renal magnesium wasting and hypomagnesemia. In later stages, however, the impairment of renal function counteracts further magnesium wasting.[72]

CLASSIC BARTTER SYNDROME (CBS) cBS is caused by mutations in the *CLCNKB* gene coding for the chloride channel ClC-Kb.[73,74] The ClC-Kb protein is expressed in the TAL and DCT, where it mediates

TABLE 61.2 Genetic Defects in Genes Encoding Components of the Renal Tubular Salt and Electrolyte Transport Machinery or Regulating Factors

Disorder	OMIM	Gene	Protein	S-Mg^{2+}	S-Ca^{2+}	U-Mg^{2+}	U-Ca^{2+}	Nephrocalcinosis	Additional Findings
Antenatal Bartter syndrome (aBS)	601678 241200	*SLC12A1* *KCNJ1*	NKCC2 ROMK (Kir1.1)	N	N	?	↑↑	Yes	Polyhydramnios, Salt wasting, Hypokalemic alkalosis
Bartter syndrome with sensorineural deafness (BSND)	602522 613090	*BSND* *CLCNKA* + *CLCNKB*	Barttin ClC-Ka + ClC-Kb	↓	N	?	N to ↑	No	Polyhydramnios, Salt wasting, Hypokalemic alkalosis, Deafness
Classic bartter syndrome (cBS)	607364	*CLCNKB*	ClC-Kb	N to ↓	N	N to ↑	variable	rare	Failure to thrive, Salt wasting, Hypokalemic alkalosis
Gitelman syndrome (GS)	263800	*SLC12A3*	NCCT	↓	N	↑	↓	No	Mild salt wasting, Hypokalemic alkalosis, Chondrocalcinosis
EAST/SeSAME syndrome	612780	*KCNJ10*	Kir4.1	↓	N	↑	↓	No	Salt wasting, Epilepsy, Ataxia, Mental retardation, Deafness
Autosomal-dominant hypocalcemia (ADH)	146200	*CASR*	CaSR	↓	↓	↑	↑ to ↑↑	Yes	(Salt wasting, Hypokalemic alkalosis)
Familial hypocalciuric hypercalcemia (FHH)	145980	*CASR*	CaSR	N	↑	↓	↓	No	
Neonatal severe hyperparathyroidism (NSHPT)	239200	*CASR*	CaSR	N to ↑	↑↑↑	↓	↓	No	Skeletal deformities, Extraosseous calcifications, Muscle wasting, Mental retardation
Familial hypomagnesemia with hypercalciuria and nephroclacinosis (FHHNC)	248250 248190	*CLDN16* *CLDN19*	Claudin-16 Claudin-19	↓	N	↑↑	↑↑	Yes	Urinary tract infections, Polyuria/polydipsia, Nephrolithiasis, Chronic renal failure, (eye abnormalities)
Hypomagnesemia with secondary hypocalcemia (HSH)	602014	*TRPM6*	TRPM6	↓↓↓	↓	↑	N	No	Defect in intestinal magnesium uptake
Isolated dominant hypomagnesemia (IDH)	154020	*FXYD2*	γ-subunit	↓	N	↑	↓	No	
Isolated dominant hypomagnesemia (IDH)	160120	*KCNA1*	Kv1.1	↓↓	N	↑	N	No	Episodic ataxia, Myokymia
Isolated dominant hypomagnesemia (IDH)	613882	*CNNM2*	cyclin M2	↓	N	↑	N to ↓	No	
Isolated recessive hypomagnesemia (IRH)	611718	*EGF*	EGF	↓	N	↑	N	No	
Mitochondrial hypomagnesemia (MH)	500005	*MTTI*	tRNA-ILE	↓	N	↑	↓	No	Hypercholesterolemia, Hypertension
Renal Cysts and Diabetes Syndrome (RCAD)	137920	*HNF1B*	HNF1β	↓	N	↑	↓	No	Diabetes (MODY5), Renal dysplasia

chloride efflux from epithelial cells to the interstitium. The clinical picture of cBS varies widely with a spectrum ranging from a phenotype similar to aBS in rare cases to a phenotype almost indistinguishable from GS.[75,76] However, the majority of patients develop hypokalemia, hypochloremia, and failure to thrive during the first year of life, as described by Bartter and coworkers in their initial report.[60] Prenatal onset and nephrocalcinosis as seen in aBS are unusual. A possible explanation for the greater variability in the clinical picture of cBS compared to aBS might be the broad expression pattern of ClC-Kb that appears to be particularly critical for electrolyte handling in the DCT segment.

Hypomagnesemia is detected in up to 50% of affected individuals.[72] Some cBS patients present with combined hypomagnesemia and hypocalciuria, a phenotypic signature of defects in the DCT. Thus, one can assume that in cBS disturbed reabsorption of sodium chloride in distal nephron segments impairs the renal conservation of magnesium.

GITELMAN SYNDROME

The most frequent inherited salt losing tubular disorder affecting renal magnesium handling is the GS. GS is caused by mutations in the thiazide-sensitive sodium-chloride cotransporter NCCT[65,77] which is exclusively expressed at the apical membrane of the DCT. The cardinal features of GS are persistent hypokalemia and metabolic alkalosis with hypomagnesemia and hypocalciuria.[78–81] These findings, which are now considered to be characteristic for disturbances in DCT function, are also seen in other disorders affecting renal magnesium conservation (see below). Although a salt-wasting disorder, salt and water losses in these patients are usually less pronounced than in aBS because the urinary concentrating ability is largely preserved.[76] Patients usually present during childhood or adolescence with symptoms of muscle weakness or overt tetany related to profound hypomagnesemia. However, many "asymptomatic" patients have been reported, and GS is frequently diagnosed following measurement of electrolytes for various other reasons than hypomagnesemia (e.g., preoperative workup). Nevertheless, a large clinical study demonstrated that GS significantly affects quality of life.[82] None of these 50 patients were truly asymptomatic. Salt craving, nocturia, and paresthesia were among the most frequent symptoms.

Mechanisms of enhanced calcium absorption and reduced magnesium transport secondary to disturbed NCCT-mediated salt reabsorption are not fully understood. These features are characteristic for GS but other disorders affecting salt and divalent electrolyte reabsorption in the DCT may result in similar findings (see below). The transport of calcium and magnesium in the DCT is transcellular and active in nature, consisting of an apical entry through a selective ion channel (TRPV5 and TRPM6, respectively) and selective active basolateral extrusion (Fig 61.3). Although Ca^{2+}/Na^{+} exchange has been identified, the molecular nature of the basolateral magnesium transport protein is still unknown, but several studies point to a sodium-coupled exchange mechanism.[1] Paracellular transport of either calcium or magnesium is not observed in the DCT. Accordingly, the notion of Reilly and Ellison is not tenable. They postulated that DCT cells could potentially switch to electrogenic reabsorption of sodium via the apical sodium channel ENaC that would reverse transepithelial voltage to lumen negative that in turn might drive magnesium into the lumen.[83] The hypocalciuria was thought to result from a reduction in NaCl entry into DCT cells leading to hyperpolarization which in turn could increase passive apical calcium entry and basolateral sodium−calcium exchange.

A more satisfying explanation has been advanced by Loffing and colleagues. Immunohistochemical studies in NCCT knockout mice point to the involvement of distinct segments of the distal tubule.[84,85] In NCCT −/− mice, the early portion of the DCT undergoes apoptosis and is almost completely absent with marked decreases in NCCT and TRPM6 expression. In contrast, the late DCT and the connecting tubule (CNT) remain largely intact with retained expression of the epithelial sodium channel ENaC and the epithelial calcium channel TRPV5. Therefore, active transcellular magnesium reabsorption could be impaired simply by loss of early DCT cells in GS patients. Concerning the hypocalciuria, recent studies point to involvement of increased calcium reabsorption upstream to the DCT.[54] The volume contraction in NCCT −/− mice led to a decrease in GFR and an increased fractional reabsorption of sodium, but also calcium already in the proximal tubule where magnesium is poorly reabsorbed. This effect on calcium reabsorption is completely reversed by salt and fluid repletion in these animals. Moreover, Nijenhuis et al. reported that hydrochlorothiazide administration resulted in hypocalciuria in TRPV5 −/− mice showing that active distal tubular calcium reabsorption is not required.[54] As mentioned above, TRPM6 was downregulated in the NCCT knockout mice, which explains the urinary magnesium wasting.[54]

EAST/SESAME SYNDROME

Recently, a complex syndrome combining epilepsy, ataxia, sensorineural deafness, and renal salt wasting was described by two independent groups (for which they introduced the acronyms EAST or SeSAME syndrome).[86,87] Patients present early in infancy with

generalized tonic–clonic seizures, speech and motor delay, severe ataxia, intention tremor, dysdiadochokinesis, severe hearing impairment, and renal salt wasting.

The renal phenotype includes RAAS stimulation, hypokalemic alkalosis, largely preserved urinary concentrating ability, hypomagnesemia and hypocalciuria resembling the above mentioned DCT signature. All patients required high dose potassium and magnesium supplementation (Bockenhauer NEJM),[86] some patients were additionally treated with aldosterone antagonists to narrow potassium losses.[87]

Autosomal-recessive EAST/SeSAME syndrome was shown to be caused by loss-of-function mutations in *KCNJ10*, coding for Kir4.1, a member of the inwardly rectifying potassium channel family.[86,87] Kir4.1 expression was demonstrated in glial cells in several parts of the brain including the spinal cord and in the stria vascularis of the inner ear explaining the observed central nervous phenotype and deafness in affected individuals. In kidney, Kir 4.1 is expressed in DCT, CT as well as in CCD,[88] however its presence was also suggested in TAL.[89] Kir4.1 is localized at the basolateral membrane of distal nephron segments and supposed to function in collaboration with Na–K–ATPase as it allows for a recycling of potassium ions entering the tubular cells in countermove for the extruded sodium.[87] In addition, diminished Kir4.1 function leads to a depolarization of the basolateral membrane and consecutively to a reduction in the driving force for basolateral anion channels as well as sodium coupled exchangers.[90] This decreased basolateral membrane potential could also affect the putative electrogenic Na^+/Mg^{2+} exchanger and possibly explain the observed magnesium wasting in EAST syndrome. Interestingly, the renal phenotype of Kir4.1 −/− mice had not been thoroughly studied until the description of human disease. The re-evaluation of Kir4.1 −/− mice by Bockenhauer and colleagues however clearly demonstrated renal salt wasting leading to significant growth retardation.[86] The concurrent findings of hypomagnesemia and hypocalciuria, also observed in mice, argue for a defect in renal salt reabsorption predominantly in the DCT.

Disorders of Calcium-Sensing Receptor

The extracellular CaSR/Mg^{2+}-sensing receptor (plays an essential role in magnesium and calcium homeostasis by influencing not only PTH secretion in the parathyroid gland but also by directly regulating the rate of magnesium and calcium reabsorption in the kidney. It was first cloned by Brown and colleagues in 1993.[23] Along the distal nephron, the CaSR is expressed basolaterally in TAL and DCT as well as at both the apical and basolateral membrane of the collecting duct.[29] Activation of the CaSR leads to coordinate changes in renal calcium and magnesium excretion and in water diuresis.[23] Dilution of the urine by decreasing aquaporin expression in the collecting duct is thought to minimize the risk of stone formation in the face of an increase in calcium and magnesium excretion. Several diseases associated with both activating and inactivating mutations in the CaSR gene have been described. As alterations in CaSR activity also affect renal magnesium handling, they are presented in this chapter with a special focus on magnesium.

AUTOSOMAL-DOMINANT HYPOPARATHYROIDISM

Activating mutations of the CaSR result in ADH. Patients typically manifest during childhood with seizures or carpopedal spasms. Laboratory evaluation reveals the typical combination of hypocalcemia and low PTH levels, but the majority of patients also exhibit significant hypomagnesemia with serum levels around 0.5–0.6 mmol/L.[91,92] Affected individuals are often given the diagnosis of primary hypoparathyroidism on the basis of inadequately low PTH levels despite their hypocalcemia. Serum calcium levels are typically in a range of 6–7 mg/dL. The differentiation from primary hypoparathyroidism is of particular importance because treatment with vitamin D can result in a dramatic increase in calcium excretion and the occurrence of nephrocalcinosis and impairment of renal function in ADH patients. Therefore, therapy with vitamin D or calcium supplementation should be reserved for symptomatic patients with the aim to maintain serum calcium levels just sufficient for the relief of symptoms.[92]

Activating CaSR mutations lead to a lower set-point of the receptor or an increased affinity for extracellular calcium and magnesium. This inadequate activation by physiological extracellular calcium and magnesium levels then results in diminished PTH secretion and decreased reabsorption of both divalent cations mainly in the cTAL. For magnesium, the inhibition of PTH-stimulated reabsorption in the DCT may significantly contribute to an increased renal loss in addition to the effects observed in the TAL.[36,93] Pronounced hypomagnesemia is observed in patients with complete activation of the CaSR at physiologic serum calcium and magnesium concentrations who also exhibit a Bartter-like phenotype.[94,95] In these patients, CaSR activation inhibits TAL-mediated salt and divalent cation reabsorption to an extent that cannot be compensated in later nephron segments.

FAMILIAL HYPOCALCIURIC HYPERCALCEMIA/ NEONATAL SEVERE HYPERPARATHYROIDISM

Familial hypocalciuric hypercalcemia (FHH)/neonatal severe hyperparathyroidism (NSHPT) result from inactivating mutations present in either heterozygous

or homozygous (or compound heterozygous) state, respectively.[96] FHH patients normally present with mild to moderate hypercalcemia, accompanied by few if any symptoms and often do not require treatment (Table 61.2). Urinary excretion rates for calcium and magnesium are markedly reduced, and serum PTH levels are inappropriately high. In addition, affected individuals also show mild hypermagnesemia.[97] In contrast, NSHPT patients with two CaSR mutations is usually present in early infancy with polyuria and dehydration due to severe symptomatic hypercalcemia. Unrecognized and untreated hyperparathyroidism and hypercalcemia result in skeletal deformities, extraosseous calcifications, muscle wasting, and a severe neurodevelopmental deficit. Early treatment with partial-to-total parathyroidectomy therefore seems to be essential for a favorable outcome.[98] Data on serum magnesium in NSHPT are sparse. However, elevations to levels around 50% above normal have been reported.[99]

Familial Hypomagnesemia with Hypercalciuria and Nephrocalcinosis

Familial hypomagnesemia with hypercalciuria and nephrocalcinosis (FHHNC) is caused by mutations in two different members of the claudin family of tight junction proteins, namely claudin-16 and claudin-19.[13,14] Since its first description, at least 80 different patients have been reported, allowing a comprehensive characterization of the clinical spectrum of this disorder and discrimination from other magnesium-losing tubular diseases.[100–103] Due to excessive renal magnesium and calcium wasting, patients develop the characteristic triad of hypomagnesemia, hypercalciuria, and nephrocalcinosis that gave the disease its name. FHHNC patients usually present during early childhood with recurrent urinary tract infections, polyuria/polydipsia, nephrolithiasis, and/or failure to thrive. Signs of severe hypomagnesemia such as cerebral convulsions and muscular tetany are less common. Additional laboratory findings include elevated serum PTH levels before the onset of chronic renal failure (CRF), incomplete distal tubule acidosis, hypocitraturia, and hyperuricemia present in most patients.[104] The prognosis of FHHNC patients is rather poor with progression to CRF early during adolescence. A considerable number of patients already exhibit a markedly reduced GFR (<60 mL/min per 1.73 m^2) at the time of diagnosis. Hypomagnesemia may completely disappear with the decline of GFR due to reduction in filtered magnesium limiting urinary magnesium excretion.

Whereas the renal phenotype is almost identical in carriers of *CLDN16* and *CLDN19* mutations, ocular involvement including severe myopia, nystagmus, or chorioretinitis are much more prominent in patients with *CLDN19* mutations.[14,101,105,106]

In addition to continuous magnesium supplementation, therapy aims at the reduction of calcium excretion by using thiazides to prevent the progression of nephrocalcinosis and stone formation. The degree of renal calcification has been correlated with progression of CRF.[101] However, therapeutic strategies do not seem to significantly influence the progression of renal failure. Supportive therapy is important for the protection of kidney function and should include provision of sufficient fluids and effective treatment of stone formation and bacterial colonization. As expected, renal transplantation is performed without evidence of recurrence because the primary defect resides in the kidney.

Using a positional cloning approach, Simon et al. could identify a new gene (*CLDN16*, formerly *PCLN1*), which is mutated in patients with FHHNC.[13] *CLDN16* codes for claudin-16 or paracellin-1, a member of the claudin family. More than 20 claudins identified so far comprise a family of ~22 kD proteins with four transmembrane segments, two extracellular domains, and intracellular N and C termini. The individual composition of tight junction strands with different claudins confers the characteristic properties of different epithelia regarding paracellular permeability and/or transepithelial resistance. In this context, a crucial role has been attributed to the first extracellular domain of the claudin proteins, which is extremely variable in number and position of charged amino acid residues.[107] Individual charges have been shown to influence paracellular ion selectivity suggesting that claudins positioned on opposing cells forming the paracellular pathway provide charge-selective pores within the tight junction complex.

The C terminus is remarkable for a consensus threonine-X-valine PDZ-binding domain which is possibly involved in protein–protein interactions and targeting of the paracellin-1 protein to tight junction strands. The longest possible open reading frame of the human cDNA encodes a protein of 305 amino acids with a cytoplasmic N-terminus of 73 amino acids. This structure is in contrast to all other claudins, which share a very short N-terminus of only six or seven amino acids. Interestingly, there is a second in-frame start codon within a suitable Kozak consensus sequence at position Met71 that is analogous to the translation start site of all other claudins. Sequence comparison of the human cDNA with other species and the results of mutation analyses, which identified a common insertion/deletion polymorphism (165_166*del*GG*ins*C) that would lead to a shift of the reading frame (R55fs71X), argue for the second translation initiation start site being used in vivo.[102,108]

The majority of mutations reported thus far in FHHNC are simple missense mutations affecting the transmembrane domains and the extracellular loops

with a particular clustering in the first extracellular loop containing the ion selectivity filter. Within this domain, patients originating from Germany and Eastern European countries exhibit a common mutation (L151F) due to a founder effect.[102] Defects in *CLDN16* have also been shown to underlie the development of a chronic interstitial nephritis in Japanese cattle that rapidly develop CRF shortly after birth.[109] Interestingly, affected animals typically show hypocalcemia but no hypomagnesemia, which might be explained by advanced CRF present at the time of examination. The fact that, in contrast to the point mutations identified in human FHHNC, large deletions of *CLDN16* are responsible for the disease in cattle, might explain the more severe phenotype with early-onset renal failure. However, *Cldn16* knockout mice do not display renal failure during the first months of life.[110] In FHHNC patients, progressive renal failure is generally thought to more likely be a consequence of massive urinary calcium wasting and nephrocalcinosis. A study of a large cohort of FHHNC patients showed that the presence of *CLDN16* mutations leading to a complete loss-of-function on both alleles display a younger age at manifestation as well as a more rapid decline in renal function compared to patients with at least one allele with residual claudin-16 function.[111] These findings support the theory that a complete lack of claudin-16 is associated with a more severe phenotype whereas a residual function delays the progression of CRF.

There is evidence from family analyses that carriers of heterozygous *CLDN16* mutations may also present with clinical symptoms. Two independent studies describe a high incidence of hypercalciuria, nephrolithiasis, and nephrocalcinosis in first-degree relatives of FHHNC patients.[101,102] A subsequent study also found a tendency toward mild hypomagnesemia in family members with heterozygous *CLDN16* mutations.[112] Thus, one might speculate that *CLDN16* mutations are involved in idiopathic hypercalciuric stone formation.

Recently, a homozygous *CLDN16* mutation (T303G) affecting the C-terminal PDZ domain has been identified in two families with isolated hypercalciuria and nephrocalcinosis without disturbances in renal magnesium handling.[113] Interestingly, the hypercalciuria disappeared during follow-up and urinary calcium levels reached normal values beyond puberty. Transient transfection of MDCK cells with the CLDN16 (T303G) mutant revealed localization of the mutant paracellin-1 in the apical membrane, whereas wildtype paracellin-1 was correctly targeted. It still remains to be determined why this type of misrouting is associated with transient isolated hypercalciuria without increased magnesium excretion.

Molecular genetic studies in FHHNC patients with a severe ocular involvement lead to the identification of mutations in a second member of the claudin family, claudin-19 (encoded by *CLDN19*).[14] Claudin-19 is expressed together with claudin-16 predominantly in the TAL. Tight-junction strands in this part of the renal tubule also express claudin-10 and claudin-18.[114] These other claudins are able to maintain the barrier function of the tight junction complex also in the absence of claudin-16 and -19; however, claudin-16 and -19 depleted tight junctions displayed a loss in cation permselectivity (Hou et al. PNAS 2009).[114] Unfortunately, it remains an unanswered question so far, if claudin-16 and -19 directly take part in the formation of a paracellular pore structure selective for magnesium and calcium or if they are simply involved in generating the cation selectivity of the tight junction complex required for maintaining the lumen-positive potential in the TAL (Hou, Goodenough 2010).[115] In this context, it is interesting to note that claudin-16 as well as claudin-19 deficient mice also display increased renal losses of sodium as well as potassium in addition to the disturbance in renal magnesium and calcium handling.[114]

Patients with claudin-19 defects display a renal phenotype indistinguishable from patients with defective claudin-16 function,[14] however, the ocular phenotype also observed in patients with claudin-16 defects is much more severe. The molecular basis for the phenomenon is the expression of claudin-19 specifically in different layers of the retina.[14] Patients show a misdevelopment of the optic disc leading to severe visual impairment and the development of horizontal nystagmus.

Hypomagnesemia with Secondary Hypocalcemia

HSH is an autosomal recessive disorder caused by mutations in the *TRPM6* gene coding for TRPM6, a member of the transient receptor potential (TRP) cation channel family.[37,38] Since its first description by Paunier and colleagues in 1968,[116] at least 50 HSH kindreds have been described.[38,117–119] Patients uniformly manifest in early infancy with generalized convulsions refractory to anticonvulsant treatment or other symptoms of increased neuromuscular excitability such as muscle spasms or tetany. Laboratory evaluation at initial presentation reveals severely reduced serum magnesium levels of around 0.2 mmol/L. Severe hypomagnesemia is accompanied by hypoparathyroidism with barely detectable PTH levels and consecutive hypocalcemia with serum calcium levels around 1.6 mmol/L. The unexpected finding of hypoparathyroidism is thought to result from an inhibition of PTH synthesis and secretion in the presence of extreme hypomagnesemia.[98,120,121] In addition, PTH-induced release of calcium from bone is substantially impaired in hypomagnesemia as magnesium depletion interferes with the generation of cAMP in response to PTH.[98] The hypocalcemia is resistant to treatment with calcium or vitamin D.

Treatment in HSH consists of immediate administration of magnesium, usually via the intravenous route at a dose of 0.1 − 0.2 mmol (equivalent to 25-50 mg) per kilogram of body weight, up to a maximum of 8 mmol (equivalent to 2 g).[62,119] Administration of magnesium alone rapidly leads to relief of clinical symptoms, normocalcemia, and normalization of PTH levels. Acute parenteral therapy is followed by lifelong high-dose oral magnesium supplementation.[122] In the majority of patients, organic magnesium salts such as aspartate or citrate are used. Daily requirements of up to 4 mmol/kg of body weight per day (16 times the recommended daily allowance) have been described,[123] although an average daily requirement of around 1 mmol/kg of body weight per day seems to be sufficient in most HSH patients. Whether these large variations reflect different individual requirements or whether they are the consequence of differences in therapeutic strategies remains to be determined. Adolescent patients usually tolerate oral magnesium to a lesser extent than infants and younger children, who on average receive larger amounts per kilogram of body weight. While gastrointestinal complaints are clearly aggravated with rising amounts of oral magnesium in the same patient, the susceptibility to diarrhea shows marked interindividual variability.

The laxative action of magnesium salts administered in therapeutic doses often leads to pronounced gastrointestinal side effects that occasionally necessitate considering alternative routes of administration such as intravenous or subcutaneous injections. Splitting of oral doses can reduce fluctuations of serum magnesium levels and peak urinary excretion and also alleviate diarrhea. Additional intramuscular magnesium injections might be necessary to reduce oral intake. A regimen consisting of daily intramuscular injections given over a 20-year period has been described.[123] Ultimately, the authors used continuous nocturnal administration via nasogastric tube as a therapeutic alternative to improve quality of life. In another HSH patient, hypomagnesemic seizures only ceased after implantation of a subcutaneous pump system that provides continuous magnesium infusions.[124]

Delay in diagnosis may lead to neurological deficits or may even be fatal as seizures are refractory to anticonvulsive treatment. Several HSH patients with severe mental retardation due to recurrent seizures have been reported. The laboratory evaluation of serum magnesium levels should therefore represent an indispensable part of the workup in infantile seizures. After correction of hypomagnesemia, serum levels should be closely monitored to prevent recurrence of symptoms in the presence of hereditary magnesium deficiency.

Contrasting all other known forms of hereditary hypomagnesemia, pathophysiologic studies in affected patients using radioactive magnesium isotopes pointed to a primary defect in intestinal magnesium absorption.[125] The presence of an additional renal phenotype in HSH was controversial until magnesium-loading studies clearly demonstrated a renal magnesium leak.[126] With rising serum magnesium levels during substitution, renal magnesium loss, which is barely detectable at initial presentation, becomes evident demonstrating a decreased renal threshold for magnesium.[38] Despite remaining hypomagnesemic with serum levels around 0.6 mmol/L, HSH patients display inadequately high fractional excretions for magnesium in a range of 2-4%.[37] Assuming intact renal magnesium conservation, fractional excretions rates would be expected to drop below 1% in the presence of hypomagnesemia.[33]

A positional candidate gene approach enabled the identification of mutations in the *TRPM6* gene as the underlying defect in HSH.[37,38] *TRPM6* codes for a member of the TRP family of cation channels. The TRP protein superfamily comprises more than 20 related cation channels playing important roles in a wide variety of physiological processes such as phototransduction, sensory physiology, and regulation of smooth muscle tone.[127] The conventional TRP proteins can be allocated to three subfamilies: TRPC, TRPV, and TRPM. Three additional more distantly related subfamilies—TRPML, TRPN, and TRPP—have been defined more recently.[127] All TRP ion channels share the common feature of six transmembrane domains with a putative pore-forming region between the fifth and sixth transmembrane domain and intracellular N- and C-termini. Four TRP protein subunits assemble to form a functional channel complex.

The TRPM subfamily comprises eight members that exhibit a significant diversity in domain structure as well as cation selectivity and activation mechanisms. Three members—TRPM2, TRPM6, and TRPM7—are set apart from all other known ion channels because they harbor enzyme domains in their respective C termini and thus represent prototypes of an intriguing new protein family of enzyme-coupled ion channels. TRPM6 and TRPM7 contain protein kinase domains in their C termini, which bear sequence similarity to elongation factor 2 (eEF-2) serine/threonine kinases.[40,42]

The functional characterization of TRPM7 demonstrated permeability for various cations, including calcium, magnesium, and several trace metals.[128] TRPM7 gating was shown to be regulated by intracellular magnesium and magnesium-nucleotide complexes.[39] Targeted deletion of TRPM7 in cell lines results in intracellular magnesium depletion and growth arrest.[41] Taken together, these data point to the essential role of

ubiquitously expressed TRPM7 for cellular magnesium homeostasis.

The TRPM6 protein is highly homologous to the TRPM7 ion channel. However, contrasting TRPM7, only one group thus far has succeeded in functional expression of TRPM6 in a mammalian cell line.[46]

The authors were able to show channel properties similar to those observed for TRPM7. In contrast, another group clearly demonstrated that heteromultimerization with TRPM7 is essential for correct membrane targeting of TRPM6.[45] In this study, TRPM7-induced currents were significantly increased by coexpression of TRPM6. Heteromultimerization has been previously described for other members of the TRP family.[129] The detection of TRPM6 expression in the DCT, together with the functional studies in HSH patients that clearly demonstrated a renal magnesium leak, points to an important role of TRPM6 for active transcellular magnesium reabsorption in the DCT.[37,46] Whether TRPM6 alone or in cooperation with TRPM7 constitutes the apical magnesium channel that was physiologically identified in DCT cells remains to be clarified in future studies.

TRPM6 mutations identified in HSH patients comprise the following classes of mutations: stop mutations and frame shift mutations, both leading to premature stops of translation, as well as splice site mutations, which impede proper mRNA synthesis and presumably lead to absence of the corresponding exon and large exon deletions.[37,38] All of the mentioned mutations that are distributed over the entire TRPM6 protein result in truncated TRPM6 proteins. Only few missense mutations, e.g. S141L in the N terminus and P1017R in the putative pore-forming region of the TRPM6 protein, have been identified so far.[37,117,130] The functional analysis of S141L-TRPM6 demonstrated intracellular retention of the mutant protein upon coexpression with TRPM7 and an abrogation of proper tetrameric TRPM6/TRPM7 complex assembly in the endoplasmic reticulum.[45] In contrast, the P1017R mutant shows a preserved trafficking to the plasma membrane, but obviously interferes with channel gating or permeation mechanisms of the functional ion channel tetramer.[130] Therefore, all HSH mutations functionally characterized thus far result in a complete loss of function of the TRPM6 protein. Obviously, complete lack of TRPM6 ion channel function is required for the development of the typical HSH phenotype. It is intriguing to speculate whether minor changes in TRPM6 function by single point mutations might result in a less severe clinical picture or even in subclinical magnesium deficiency.

The mutational analysis of *TRPM6* also supports the data obtained for TRPM7 pointing to an essential role of the C-terminal kinase domain for ion channel function. While abrogation of TRPM7 kinase activity does not impair ion channel function but leads to a decrease in magnesium mediated channel inhibition, structural absence of the kinase domain leads to a complete suppression of ion channel activity.[41] Similarly, truncating mutations of TRPM6 prior to the kinase domain lead to an obvious loss of ion channel function.

How does an impairment of TRPM6 protein function impede epithelial magnesium transport in the intestine and kidney? The observation that in HSH patients the administration of high oral doses of magnesium are successful in achieving at least subnormal serum magnesium levels supports the existing evidence of two independent transport systems for magnesium in the gastrointestinal tract.[131] TRPM6 probably represents a molecular component of active transcellular magnesium transport. An increased intraluminal magnesium concentration achieved by increased oral intake would enable to compensate for the defect of the active transcellular pathway by increasing absorption via the passive paracellular route.[37,132]

Isolated Dominant Hypomagnesemia

FXYD2 (γ-SUBUNIT)

Isolated dominant hypomagnesemia (IDH) was first linked to a mutation in the *FXYD2* gene on chromosome 11q23 which codes for a γ-subunit of Na−K−ATPase.[133] Only two related families with a *FXYD2* mutation have been described so far.[133,134] The index patients of both families presented with generalized convulsions during childhood, at ages 7 and 13 years, respectively. Serum magnesium levels in the two patients at the time of convulsions were approximately 0.4 mmol/L. One index patient was treated for seizures of unknown origin with antiepileptic drugs until serum magnesium levels were evaluated in adolescence. At that time severe mental retardation was evident. Systematic serum magnesium measurements performed in members of both families revealed low serum magnesium levels of around 0.5 mmol/L in numerous apparently healthy individuals. Consequent pedigree analyses of the two families pointed to an autosomal-dominant mode of inheritance. A genome-wide linkage study mapped the disease locus on Chr 11q23.[135] Detailed haplotype analyses identified a common haplotype segregating in the two families which suggested a common ancestor. Indeed, the mutational screening of the *FXYD2* gene demonstrated the identical mutation G41R in all affected individuals of both family branches.

A ^{28}Mg-retention study in one index patient pointed to a primary renal defect.[134] The intestinal absorption of magnesium was preserved and even stimulated in compensation for the increased renal losses. Urinary

magnesium measurements in affected family members revealed daily magnesium excretions of around 5 mmol per day despite profound hypomagnesemia.[134] In addition, urinary calcium excretions were found to be low in all hypomagnesemic family members, a finding reminiscent of patients presenting with GS. But in contrast to GS, no other associated biochemical findings were reported.

The γ-subunit encoded by *FXYD2* is a member of a family of small single transmembrane proteins that share the common amino acid motif F-X-Y-D. Out of the seven members that differ in tissue specificity, FXYD2 and FXYD4—also called CHIF or channel-inducing factor—are highly expressed along the nephron but display an alternating expression pattern.[136] The γ-subunit comprises two isoforms (named γ-a and γ-b) that are differentially expressed in the kidney. The γ-a isoform is present predominantly in the proximal tubule, and expression of the γ-b isoform predominates in the distal nephron, especially in the DCT and CNT.[137] The ubiquitous Na−K−ATPase is a dimeric enzyme invariably consisting of one α- and one β-subunit. FXYD proteins constitute a third or γ-subunit that represents a tissue-specific regulator of Na−K−ATPase and produces distinct effects on the apparent affinity of the Na−K−ATPase for sodium, potassium, and ATP. The FXYD2 γ-subunit increases the apparent affinity of Na−K−ATPase for ATP while decreasing its sodium affinity.[138] Thus, it might provide a mechanism for balancing energy utilization and maintaining appropriate salt gradients.

Expression studies of the mutant G41R-γ-subunit in mammalian renal tubule cells revealed a dominant negative effect of the mutation leading to retention of the γ-subunit within the cell. Whereas initial data pointed to retention of the entire Na−K−ATPase complex in intracellular compartments, more recent data demonstrate an isolated trafficking defect of the mutant γ-subunit while trafficking of the α/β-complex is preserved.[139] The mutant γ-subunit is obviously retarded in the Golgi complex which points to disturbed post-translational processing. The assumption of a dominant negative effect was first substantiated by the observation that individuals with a large heterozygous deletion of chromosome 11q including the *FXYD2* gene exhibit normal serum magnesium levels.[140] Meanwhile, it could be shown that wildtype γ-subunits oligomerise within the cell before trafficking to the plasma membrane. The G41R-mutant was shown to also oligomerise with itself and the wildtype γ-subunit and obviously prevents proper routing of wildtype γ-subunits to the plasma membrane and incorporation into functional ATPase complexes.[141]

Urinary magnesium wasting together with the expression pattern of the *FXYD2* gene indicate a defect of active transcellular magnesium reabsorption in the DCT in affected individuals. But how can a defect of Na−K−ATPase modulation lead to impaired renal magnesium conservation? One possible explanation is based on changes in intracellular sodium and potassium levels. Meij and colleagues have suggested that diminished intracellular potassium might depolarize the apical membrane resulting in a decrease in magnesium uptake.[133] Alternatively, an increase in intracellular sodium could impair basolateral magnesium transport, which is presumably achieved by a sodium-coupled exchange mechanism. Another explanation is that the γ-subunit is involved not only in Na−K−ATPase function but is also an essential component of a yet-unidentified ATP-dependent transport system specific for magnesium. Like for calcium, both a specific Mg-ATPase and a sodium-coupled exchanger might exist. Further studies are needed to clarify this issue.

Interestingly, *Fxyd2* −/− mice are viable and without observable pathology.[142] The authors state that there are no abnormalities in serum magnesium and urinary excretion of magnesium under physiological conditions. However, a deletion of one or both alleles in mice does not necessarily mimick the effect of the dominant mutation observed in human disease. Experiments with purified Na−K−ATPase from these mice revealed a decrease in thermostability as well as an increased affinity of the enzyme lacking the γ-subunit for sodium which is in accordance with previous studies.[138]

An interesting feature of IDH linked to the *FXYD2*-G41R mutation is the finding of hypocalciuria. One could only speculate that, similar to GS, a defect in Na−K−ATPase function and energy metabolism might lead to an apoptotic breakdown of the early DCT responsible for magnesium reabsorption, while later parts of the distal nephron remain intact. In patients with the FXYD2 mutant, there is no evidence for renal salt wasting and no stimulation of the RAAS. The finding of hypocalciuria despite no apparent volume depletion apparently contradicts theories that favor an increase in proximal tubular calcium reabsorption due to volume depletion in the GS. In fact, these findings instead point to contrary changes in magnesium and calcium reabsorption in the DCT or in different DCT segments.

KCNA1

Genetic heterogeneity in IDH was demonstrated by the identification of a dominant-negative missense mutation in KCNA1 encoding the voltage-gated potassium channel Kv1.1.[143] The phenotype of affected patients originating from a large Brazilian family included recurrent episodes of muscle cramps, tetanic

episodes, tremor, and muscle weakness starting in infancy. Laboratory analyses revealed isolated hypomagnesemia <0.4 mmol/L while urinary magnesium excretions were found to be inadequately elevated pointing to a renal magnesium leak. Interestingly, no alterations in renal calcium handling were observed.

Interestingly, *KCNA1* mutations had been identified before in patients with episodic ataxia with myokymia (OMIM 160120), a neurologic disorder characterized by periodical appearance of incoordination and imbalance as well as myokymia, an involuntary, spontaneous, and localized trembling of muscles.[144] In addition to muscle cramps and tetany attributed to magnesium deficiency, these symptoms were also present in members of the above mentioned Brazilian kindred with hypomagnesemia.

By using a genome-wide SNP-based linkage strategy followed by subsequent conventional sequencing of candidate genes identified a heterozygous mutation in the *KCNA1* gene cosegregating with the disease.[143] The mutation (c.A763G) leads to a nonconservative amino acid exchange (p.N255D) in the encoded Kv1.1 potassium channel. Functional voltage-gated potassium channels of the KCNA family are composed of tetramers. Coexpression of the mutant N255D-Kv1.1 with wildtype channel subunits in HEK293 cells resulted in a significant reduction in current amplitudes compatible with a dominant-negative effect of the mutant. The dominant-negative effect rather seems to be the result of an impaired gating of the potassium channel tetramer as trafficking to the plasma membrane is preserved.[145]

Kv1.1 expression was demonstrated in kidney in colocalization with TRPM6 in the DCT, presumably at the apical membrane. Glaudemans and coworkers propose a model in which Kv1.1 allows for a hyperpolarization of the DCT cell membrane potential as a prerequisite for TRPM6-mediated magnesium entry (Fig 61.3). Thereby, the authors, for the first time, linked magnesium reabsorption in the DCT to potassium secretion and identified a new dependency between renal magnesium and potassium handling at the molecular level.[143]

CNNM2

Another form of IDH was described recently in which mutations in *CNNM2* were discovered.[146] *CNNM2* (or ACDP2) had been identified before by differential gene expression microarray analysis of genes upregulated in face of hypomagnesemia in mice.[147] The authors had demonstrated that the CNNM2 protein is able to induce the transport of different divalent cations including magnesium.[147] Furthermore, the *CNNM2* gene locus had been linked to serum magnesium levels in a genome-wide association study.[148]

Stuiver and colleagues screened *CNNM2* as a candidate gene in patients with unresolved magnesium wasting disorders and identified heterozygous mutations in two unrelated families with IDH.[146] In affected patients, clinical symptoms and time of manifestation seem to be highly variable with symptoms ranging from convulsive episodes in early childhood to muscle weakness, vertigo, and headaches during adolescence. Other heterozygous carriers from both families remained asymptomatic. Serum magnesium levels in affected individuals were in the range of 0.4-0.5 mmol/L and failed to normalize under oral magnesium supplementation. All other serum electrolytes were found to be normal. As data on urinary calcium excretions vary between the described index patients, it remains unclear if the finding of hypocalciuria seen in a number of other inherited magnesium wasting disorders (see above) is also a concomitant feature in patients with *CNNM2* mutations.

The *CNNM2* gene codes for CNNM2 or Cyclin M2, a transmembrane protein expressed in kidney at the basolateral membrane of TAL and DCT, but also expressed in other organs especially the brain.[146] CNNM2 is one of four members of a protein family with a conserved domain structure (for which this family was previously named ancient conserved domain proteins or ACDP family) with sequence similarities to the bacterial CorC protein involved in bacterial magnesium transport.[149]

Whereas a truncating frame-shift mutation was identified in one of the described families, affected individuals of the second family carry a point mutation leading to a nonconservative amino acid exchange at a conserved residue of the CNNM2 protein (T568I).[146] Whereas trafficking of the mutant T568I-CNNM2 protein was preserved in HEK293 cells, patch clamp analyses of mutant and wildtype CNNM2 revealed a significant reduction in magnesium-sensitive, inwardly rectifying sodium currents. In contrast to previous experiments in Xenopus oocytes by Goytain and Quamme,[147] the authors did not observe significant magnesium currents upon over-expression of CNNM2 in HEK293 cells.[146] The localization data together with the functional studies lead to the assumption that CNNM2 might represent a basolateral magnesium sensing mechanism in renal tubular cells rather than being a molecular component of the yet uncharacterized basolateral magnesium extrusion machinery itself. As Stuiver and colleagues identified a truncating mutation as well as a missense mutation in their families, they only speculate on a reduced amount of functional protein as a putative mechanism for the dominant mode of inheritance.[146] Therefore, it remains a subject of further studies how exactly CNNM2 is involved in basolateral magnesium transport processes.

Renal Cysts and Diabetes Syndrome

HNF1β

Hepatocyte nuclear factor 1β (HNF1β) is a transcription factor critical for the development of kidney and pancreas. Heterozygous mutations in *HNF1B* have first been implicated in a subtype of maturity-onset diabetes of the young (MODY5) before an association with developmental renal disease was reported. The renal phenotype is highly variable including enlarged hyperechogenic kidneys, multicystic kidney disease, renal agenesis, renal hypoplasia, cystic dysplasia, as well as hyperuricemic nephropathy. The association with both symptom complexes lead to the term renal cysts and diabetes syndrome. *HNF1B* mutations are present in heterozygous state, either inherited or *de novo*, and comprise point mutations as well as whole-gene deletions.[150] Interestingly, around 50% of affected individuals present with hypomagnesemia due to renal magnesium wasting.[150,151] The degree of hypomagnesemia is usually mild to moderate ($\sim$0.65 mmol/L), and the defect in renal magnesium conservation is accompanied by the occurrence of hypocalciuria. The *HNF1B* gene encodes a transcription factor regulating the expression of numerous renal genes including the *FXYD2* gene which contains several HNF1β-binding sites in its promotor region.[151] In accordance with the phenotype and in silico data, Adalat and colleagues could show that HNF1β was able to stimulate the expression of *FXYD2* in vitro. Therefore, defective FXYD2 transcription represents a putative mechanism explaining renal magnesium wasting in patients with *HNF1B* mutations.

Isolated Recessive Hypomagnesemia

Geven and colleagues initially reported a form of isolated hypomagnesemia in a consanguineous family indicating autosomal recessive inheritance.[152] Two affected girls presented with generalized convulsions during infancy. Unfortunately, late diagnosis resulted in neurodevelopmental deficits in both patients. A thorough clinical and laboratory workup at 4 and 8 years of age, respectively, revealed serum magnesium levels of 0.5 − 0.6 mmol/L with no other associated electrolyte abnormalities. A ^{28}Mg-retention study in one patient pointed to a primary renal defect, while intestinal magnesium uptake was preserved.[152] Both patients exhibited renal magnesium excretions of 3−6 mmol per day despite hypomagnesemia which confirmed renal magnesium wasting whereas calcium excretion rates were in the normal range.

Using a homozygosity mapping strategy, Groenestege and colleagues identified a candidate interval on chromosome 4q.[50] A subsequent screening of candidate genes within this region resulted in the identification of a homozygous point mutation (c. C3209T) in the *EGF* gene leading to a nonconservative amino acid exchange (p.P1070L) in the encoded pro-EGF protein (pro-EGF) in the two sisters.[50] It was further demonstrated the the mutation impairs the basolateral sorting of pro-EGF in the DCT. The EGF hormone is thought to act at the basolateral side of DCT cells via binding to its EGFR to stimulate magnesium reabsorption via TRPM6.[51] The mechanism is described in more detail in the paragraph on hormonal controls of DCT mediated magnesium reabsorption (see above). Despite acting in a paracrine fashion in the DCT, the authors speculate on a role of EGF as a selectively acting magnesiotropic hormone.[50]

Mitochondrial Hypomagnesemia

In 2004, a mutation in the mitochondrial isoleucine tRNA gene, tRNA^{Ile}, or *MTTI* [OMIM 500005], has been discovered in a large Caucasian kindred.[153] An extensive clinical evaluation of this family was prompted after the discovery of hypomagnesemia in the index patient. Pedigree analysis was compatible with mitochondrial inheritance as the phenotype was exclusively transmitted by affected females. The phenotype includes hypomagnesemia, hypercholesterolemia, and hypertension. Of the adults on the maternal lineage, the majority of offspring exhibit at least one of the mentioned symptoms; approximately half of the individuals show a combination of two or more symptoms, and around one-sixth had all three features. Serum magnesium levels of family members in the maternal lineage greatly vary, ranging from $\sim$0.8 to $\sim$2.5 mg/dL (equivalent to $\sim$0.3 to $\sim$1.0 mmol/L) with approximately 50% of individuals being hypomagnesemic.

Hypomagnesemic individuals (serum magnesium $<$0.75 mmol/L) showed higher fractional excretions (median around 7.5%) than their normomagnesemic relatives in the maternal lineage (median around 3%) which clearly pointed to renal magnesium wasting as causative for hypomagnesemia. Interestingly, hypomagnesemia was accompanied by decreased urinary calcium levels, a finding pointing to the DCT as the affected tubular segment. These findings again suggest an association of magnesium and calcium transport in the DCT as discussed above.

The mitochondrial mutation observed in the examined family affects the tRNA^{Ile} gene *MTTI*.[153] The observed nucleotide exchange occurs at the T nucleotide directly adjacent to the anticodon triplet. This position is highly conserved among species and critical for codon−anticodon recognition. The functional consequences of the tRNA defect for mitochondrial function remain to be elucidated in detail. As ATP consumption

along the tubule is highest in the DCT, the authors speculate on an impaired energy metabolism of DCT cells as a consequence of the mitochondrial defect which in turn could lead to disturbed transcellular magnesium reabsorption. Further studies in these patients might help to deliver insight into the mechanism of distal tubular magnesium wasting in these patients.

Acquired Renal Magnesium Wasting Disorders

Cisplatin and Carboplatin

The cytostatic agent cisplatin and the newer antineoplastic drug, carboplatin, are widely used in various protocols for the therapy of solid tumors.[154] Among diverse side effects, nephrotoxicity receives most attention as the major dose-limiting factor.[155] Carboplatin has been reported to have less severe side effects than cisplatin.[156–159] Hypomagnesemia following renal magnesium wasting is regularly observed in patients treated with cisplatin.[154,159,160] The incidence of magnesium deficiency is greater than 30% but increase to over 70% have been observed with longer cisplatin usage and greater accumulated doses.[160]

Cisplatin exerts a direct damage to renal tubular cells and causes proximal as well as distal tubular dysfunction.[155] Acute cisplatin toxicity involves defective mitochondrial function, decreased ATPase activity, altered cell cation content, and altered solute transport. In the distal tubule, the reabsorption of salt and particularly of magnesium are compromised. In rodents, cisplatin leads to an impairment of proximal tubular function, whereas in dogs and humans morphological changes appear predominantly in the DCT and the collecting duct.[161–163] Thus, the interpolation from animal studies concerning cisplatin toxicity may be misleading, but the evidence from both clinical and experimental studies indicate that the drug acts on distal tubular magnesium transport. As there is no magnesium reabsorption within the CCDs, it is likely that actions within the DCT are responsible for the renal magnesium leak. Using micropuncture, Mavichak et al. showed that magnesium reabsorption was diminished in the distal tubule of rats receiving cisplatin.[162] The molecular mechanisms for the acute, apparently selective effects on magnesium remain undefined. It would be of interest to determine if amiloride retains its magnesium-conserving actions in these patients.[1] The effects of cisplatin may persist months or years later—long after the inorganic platinum has disappeared from the renal tissue.[164,165] Whatever cellular mechanisms are involved they must include genetic alterations of magnesium transport. The fact that cisplatin exerts its cytotoxicity binding cellular DNA may be relevant.[154,156] The chronic alterations in distal tubular ion transport comprise a clinical picture reminiscent of GS.[166] Morphological studies in humans with cisplatin nephrotoxicity could demonstrate focal tubular necrosis predominantly in the DCT, a feature also observed in NCCT-deficient mice suggestive for DCT cell apoptosis.[84,167] Therefore, fluid repletion and especially magnesium supplementation with sufficient doses should routinely be prompted to prevent acute and chronic cisplatin nephrotoxicity and the risk of adverse effects from hypomagnesemia.

Aminoglycosides

Aminoglycosides, such as gentamicin, induce renal impairment in up to 35% of patients, dependent on the dose and duration of administration. In addition, aminoglycosides cause hypermagnesiuria and hypomagnesemia.[168] As many as 25% of patients receiving gentamicin will exhibit hypomagnesemia.[168] The hypermagnesiuric response occurs soon after the onset of therapy; it is dose dependent and readily reversible upon withdrawal. As with adults, neonates also display an immediate increase of calcium and magnesium excretion after gentamicin infusion.[169,170] Magnesium wasting is associated with hypokalemia and hypercalciuria that may also lead to diminished plasma calcium concentrations.[171] This would suggest that aminoglycosides affect renal magnesium and calcium transport in the tubular segments where both are reabsorbed. Experimental studies with animals support this notion.[172] The cellular mechanisms are not completely understood, but hypermagnesiuria and hypercalciuria are observed in the absence of histopathological changes.[173] Because gentamicin is a polyvalent cation, it was postulated that it may have effects on the CaSR.[36,174–176] Activation of this receptor by polyvalent cations inhibits the passive reabsorption of magnesium and calcium in the TAL and active hormone-mediated transport in the DCT leading to renal magnesium and calcium wasting.

Calcineurin Inhibitors

The calcineurin inhibitors cyclosporine and tacrolimus (FK506) are widely prescribed as immunosuppressants to organ transplant recipients and in numerous immunologic disorders. Under this therapy, patients are at high risk of developing renal injury and hypertension. Tubular dysfunction with subsequent disturbance of mineral metabolism is another common side effect. Both drugs commonly lead to renal magnesium wasting and hypomagnesemia.[177] These drugs also cause modest hypercalcemia with hypercalciuria and hypokalemia.[177] The hypomagnesemic effect is probably attenuated by the fall in GFR and reduction in filtered magnesium, but this defect appears to be specific

for magnesium.[178] Calcineurin inhibitor therapy is associated with an inappropriately high fractional excretion rate of magnesium, suggesting impaired passive reabsorption in the TAL or active magnesium transport in the DCT.[179]

Chang and colleagues have reported that cyclosporine reduces claudin-16 expression in the TAL.[180] Furthermore, cyclosporine and tacrolimus have been shown to inihibit PTH-stimulated magnesium uptake in a mDCT cell line.[181] Accordingly, Ledeganck and colleagues could show that cyclosporine decreases the renal expression of TRPM6, TRPM7, NCC, and EGF.[182] In contrast to the above mentioned study by Chang et al.,[180] these authors did not find a decrease in claudin-16 or claudin-19 expression in their rat model.[182] In an previous animal study, Nijenhuis et al. had demonstrated that tacrolimus induces a decrease in TRPV5, calbindin-D28k, and TRPM6 at the mRNA level.[183] They could also show a decrease in TRPV5 and calbindin-D28k at the protein level. These effects appeared to be specific, as no morphologic features of tubular toxicity were observed. Finally, Ledeganck and coworkers could demonstrate that the EGF-mediated increase in TRPM6 abundance was abrogated by cyclosporine.[182] As mentioned above, cyclosporine, beyond its effect on magnesium transport in the DCT, downregulates the sodium chloride cotransporter NCCT in the DCT resulting in renal salt wasting.[182]

With respect to magnesium, it is interesting to note that TRPM6 expression in the intestine was not changed upon tacrolimus administration. It is not known whether these drugs act through calcineurin, which is the intracellular receptor for these agents. It is speculated that FK506-binding proteins, which are known to bind and regulate the calcium-permeable transient receptor potential-like cation channels, might be involved because tacrolimus disrupts this binding.[184] In analogy, consider that certain FKBPs might also regulate TRPV5 or TRPM6 expression or activity. Hypomagnesemia has been implicated as a contributor to the nephrotoxicity and arterial hypertension associated with calcineurin inhibitors. Mervaala et al. could demonstrate that the adverse effects of cyclosporine in spontaneously hypertensive rats largely depend on dietary sodium and that these adverse effects can be prevented by magnesium supplementation.[184] Magnesium supplementation also had a beneficial effect on cyclosporine nephrotoxicity in a rat model used by Miura and colleagues.[185]

EGF Receptor Antibodies

The EGF hormone axis has been implicated in renal magnesium handling by the discovery of a homozygous mutation in the *EGF* gene in a family with isolated recessive hypomagnesemia (IRH) (see above).[50] The way for these findings was paved by the observation that anticancer treatments with monoclonal antibodies against the EGFR resulted in renal magnesium wasting and hypomagnesemia.[186] Of note, patients treated with EGFR targeting antibodies (cetuximab, panitumumab) for colorectal cancer usually receive a combination therapy with platinum compounds potentially aggravating the effects on serum magnesium levels. A significant number of patients receiving such a chemotherapeutic regimen show decreasing serum magnesium concentrations over time.[186,187] 24 hour urine collections as well as magnesium loading tests in single patients demonstrated a defect in renal magnesium conservation. Together with the genetic findings in IRH due to a pro-EGF mutation, these findings imply a selective effect of EGFR targeting on transcellular magnesium transport in the DCT. There, TRPM6 mediated magnesium uptake into DCT cells is stimulated by basolaterally secreted EGF via its receptor (EGFR).[50] The initial report of Tejpar and colleagues describes oral as well as intravenous magnesium supplementation in patients with different degrees of hypomagnesemia after cetuximab treatment, however with limited success regarding serum magnesium levels.[186] Subsequent studies investigated the development of hypomagnesemia under EGFR targeting therapy in relation to the antitumor effect and outcome of patients.[188,189] They found that the development of hypomagnesemia is correlated with the tumor response rate and outcome. Patients with a reduction of serum magnesium >50% (!) showed a better tumor response rate and a better overall survival.[189] The authors therefore consider serum magnesium as an easily measurable biomarker for efficacy in colorectal cancer patients treated with cetuximab.

Proton-Pump Inhibitors (PPIs)

Over the last 20 years, PPIs for the reduction of gastric acidity have emerged to one of the most widely prescribed classes of drugs worldwide.[190] Due to the large number of patients, even rare side effects could become apparent that remained undiscovered during initial clinical trials. Hypomagnesemia, clinically apparent as muscle cramps, tetany, nausea, vomiting, but also cerebral convulsions, has been observed in a small but significant number of patients receiving PPIs. It is well conceivable that in a substantially larger number of patients, the relationship between low serum magnesium levels and the use of PPIs remained unrecognized. A recent review summarizing the data from previous publications reveals severely lowered serum magnesium levels below 0.4 mmol/L with concomitant hypocalcemia, a laboratory constellation reminiscent of HSH due to TRPM6 defects.[190] A previous report on hypomagnesemia following PPI treatment had already

described suppressed PTH levels during phases of severe hypomagnesemia as a probable cause of hypocalcemia (as in HSH).[191] Although a number of patients additionally receive diuretics, this finding does not explain the extraordinary degree of magnesium deficiency observed in patients receiving PPIs.

What is the mechanism underlying hypomagnesemia in PPI users? Data regarding urinary magnesium excretions in hypomagnesemic PPI are contradictory. Fractional magnesium excretions were reported to be low in face of profound hypomagnesemia pointing to an intact tubular magnesium reabsorption. However, as observed in HSH patients, a renal magnesium leak might only become apparent if serum magnesium levels reach a certain threshold. An alternative explanation could involve a disturbed intestinal reabsorption of magnesium. Unfortunately, the molecular link between proton-pump inhibition and hypomagnesemia remains unclear so far. In regard of the severe degree of hypomagnesemia, possible molecular mechanisms include an inhibition of TRPM6 leading to a combined intestinal and renal defect, but also a disturbance of ATPases or ATPase-subunits other than gastric H^+-K^+-ATPase involved in epithelial magnesium transport.

In any case, it is recommended to monitor serum magnesium levels patients receiving PPIs, particularly those with concomitant cardiac disease and risk for arrhythmia. Contrariwise, attention should be drawn to the medication list of patients presenting with hypomagnesemia and secondary hypocalcemia due to hypoparathyroidism.

Miscellaneous Agents

A number of antibiotics, tuberculostatics, and antiviral drugs may result in renal magnesium wasting.[33,168] The cellular bases by which these agents lead to abnormal magnesium reabsorption are still largely unknown. Many are associated with general cytotoxicity. Amphotericin B may lead to acquired distal tubular acidosis, which in turn reduces renal magnesium reabsorption.[33] Pamidronate used in the treatment of tumor-associated hypercalcemia has been reported to cause transient hypomagnesemia.[192] The cellular mechanisms are difficult to predict since this drug is used in patients with hypercalcemia that may aggravate renal magnesium wasting.

Metabolic Acidosis

It has long been known that systemic acidosis is associated with renal magnesium wasting. Acute metabolic acidosis produced by infusion of NH_4Cl or HCl leads to significant increases in urinary magnesium excretion.[1,33] Chronic acidosis also leads to urinary magnesium wasting which, as with the acidosis itself, may be partially corrected by the administration of bicarbonate.[1] In contrast to metabolic acidosis, acute and chronic metabolic alkalosis consistently leads to a fall in urinary magnesium excretion.[1]

The cellular basis for the acid-base effects on magnesium transport appears to be diverse. Di Stefano et al. perfused isolated mouse cTAL segments harvested from mice maintained on alkaline drinking water (20 mM sodium bicarbonate) for three days.[193] They showed that alkalosis doubled magnesium absorption from control levels without a change in transepithelial voltage. They interpreted these data to indicate that alkalosis changes the permeability of the paracellular pathway so that magnesium moves passively through the pathway to a greater degree resulting in greater magnesium absorption. The effects of metabolic acidosis were not determined in this study.[193] Nevertheless, these data suggest that pH influences the paracellular pathway perhaps through alteration of claudins. Dai et al. have used an mDCT cell line to determine the effects of extracellular pH changes on cellular magnesium uptake.[36] The results of these experiments showed that acute alkalosis markedly enhances magnesium uptake, whereas acidosis diminishes transport.

Metabolic acidosis of any etiology would be expected to lead to diminished magnesium reabsorption in the distal tubule. Diabetic subjects frequently present with hypomagnesemia and cellular magnesium deficiency.[194–196] This is, in part, due to urinary magnesium wasting.[197] In combination, insulin deficiency and ketoacidosis of uncontrolled diabetes diminish magnesium transport in TAL[198,199] and DCT,[36] resulting in exacerbation of renal magnesium wasting.

Phosphate Restriction and Phosphate Depletion

One of the hallmarks of hypophosphatemia and cellular phosphate depletion is the striking increase in urinary calcium and magnesium excretion.[32,33,36] The hypermagnesiuria may be sufficiently large to lead to overt hypomagnesemia.[200] The increase in divalent ion excretion in both human disease and experimental animal models occurs within hours of dietary phosphate restriction. Three mechanisms have been proposed to account for the increased renal excretion: (1) mobilization of calcium and magnesium from bone, (2) suppression of PTH secretion, and (3) disturbed tubular transport.[36]

It is evident from clearance experiments that the urinary excretion of divalent cations in phosphate-depleted human subjects is inappropriate for the plasma concentration, supporting the notion of defective tubular transport.[200]

Dai et al. have shown that cellular phosphate depletion leads to diminished magnesium uptake in mDCT cells.[201] This observation supports the notion that the DCT may be involved, in part, in decreased

magnesium absorption and increased magnesium excretion associated with hypophosphatemia. The reasons why cellular phosphate depletion leads to diminished magnesium reabsorption are not known.

Cellular Potassium Depletion

Hypokalemia and cellular potassium depletion are associated with diminished magnesium absorption within TAL and DCT that may lead to increased magnesium excretion.[1] The increase in urinary excretion of divalent cations may be explained by the effects of potassium depletion on salt absorption in the TAL. Chloride conservation is impaired in potassium-depleted rats, which may be related to altered basolateral Na−K−ATPase activity resulting in impaired apical NKCC2-mediated sodium chloride cotransport.

To date, there is no direct evidence for changes in magnesium absorption in the TAL with potassium depletion. However, as magnesium and calcium are absorbed by passive mechanisms, it is probable that impaired salt transport can lead to diminished divalent cation absorption in this segment.

Studies using isolated mDCT cells suggest that potassium depletion may have additional effects on magnesium transport in the DCT.[202] Cellular potassium depletion results in the inhibition of magnesium uptake into mDCT cells, as determined by microfluorescence. The exact mechanism for the disturbed magnesium entry is not known, but might involve a diminished potassium excretion via Kv1.1 (KCNA1) as suggested by the discovery of mutant Kv1.1 in a dominantly inherited form of hypomagnesemia (see above).[143] The authors propose a model in which Kv1.1 activity is critical for the establishment and maintenance of the DCT cell membrane potential as a prerequisite for magnesium entry via TRPM6. Further studies are required to fully explain the defective magnesium transport in the DCT associated with cellular potassium depletion.

Experimental and clinical data suggest a close association of serum magnesium, potassium, and phosphate levels. Crook et al. reported a twofold increase in the prevalence of hypophosphatemia (plasma phosphate <0.8 mmol/L) and a sixfold increase in hypokalemia (plasma potassium <3.5 mmol/L) in patients with hypomagnesemia (plasma magnesium <0.70 mmol/L).[203] A trilogy consisting of hypomagnesemia, hypophosphatemia, and hypokalemia was also found in 8% of patients with hypomagnesemia and 17% of patients with severe hypomagnesemia (plasma magnesium <0.50 mmol/L). The evidence suggests that hypokalemia and hypophosphatemia may have profound effects on tubular magnesium transport. Many of the syndromes associated with potassium depletion and phosphate depletion are complicated by concurrent alterations in acid-base balance.[203] There is evidence that acid-base changes have different effects on magnesium transport relative to potassium or phosphate depletion, such that the three disturbances may act in an additive manner to compromise renal magnesium conservation.[36]

References

[1] Quamme GA. Renal magnesium handling: new insights in understanding old problems. Kidney Int 1997;52(5):1180−95.

[2] Quamme GA. Laboratory evaluation of magnesium status. Renal function and free intracellular magnesium concentration. Clin Lab Med 1993;13(1):209−23.

[3] de Rouffignac C, Quamme G. Renal magnesium handling and its hormonal control. Physiol Rev 1994;74(2):305−22.

[4] Lelievre-Pegorier M, Merlet-Benichou C, Roinel N, de Rouffignac C. Developmental pattern of water and electrolyte transport in rat superficial nephrons. Am J Physiol 1983;245(1): F15−21.

[5] De Rouffignac C. Multihormonal regulation of nephron epithelia: achieved through combinational mode? Am J Physiol 1995;269(4 Pt 2):R739−48.

[6] Quamme GA. Control of magnesium transport in the thick ascending limb. Am J Physiol 1989;256(2 Pt 2):F197−210.

[7] Elalouf JM, Roinel N, de Rouffignac C. Effects of dDAVP on rat juxtamedullary nephrons: stimulation of medullary K recycling. Am J Physiol 1985;249(2 Pt 2):F291−8.

[8] Mandon B, Siga E, Roinel N, de Rouffignac C. $Ca2+$, $Mg2+$ and $K+$ transport in the cortical and medullary thick ascending limb of the rat nephron: influence of transepithelial voltage. Pflugers Arch 1993;424(5-6):558−60.

[9] Shareghi GR, Agus ZS. Magnesium transport in the cortical thick ascending limb of Henle's loop of the rabbit. J Clin Invest 1982;69(4):759−69.

[10] Estévez R, Boettger T, Stein V, et al. Barttin is a Cl- channel beta-subunit crucial for renal Cl- reabsorption and inner ear $K+$ secretion. Nature 2001;414(6863):558−61.

[11] Embark HM, Böhmer C, Palmada M, et al. Regulation of CLC-Ka/barttin by the ubiquitin ligase Nedd4-2 and the serum- and glucocorticoid-dependent kinases. Kidney Int 2004;66(5): 1918−25.

[12] Waldegger S, Jeck N, Barth P, et al. Barttin increases surface expression and changes current properties of ClC-K channels. Pflugers Arch 2002;444(3):411−8.

[13] Simon DB, Lu Y, Choate KA, et al. Paracellin-1, a renal tight junction protein required for paracellular $Mg2+$ resorption. Science 1999;285(5424):103−6.

[14] Konrad M, Schaller A, Seelow D, et al. Mutations in the tight-junction gene claudin 19 (CLDN19) are associated with renal magnesium wasting, renal failure, and severe ocular involvement. Am J Hum Genet 2006;79(5):949−57.

[15] Ikari A, Hirai N, Shiroma M, et al. Association of paracellin-1 with ZO-1 augments the reabsorption of divalent cations in renal epithelial cells. J Biol Chem 2004;279(52):54826−32.

[16] Kiuchi-Saishin Y, Gotoh S, Furuse M, Takasuga A, Tano Y, Tsukita S. Differential expression patterns of claudins, tight junction membrane proteins, in mouse nephron segments. J Am Soc Nephrol 2002;13(4):875−86.

[17] Reyes JL, Lamas M, Martin D, et al. The renal segmental distribution of claudins changes with development. Kidney Int 2002;62(2):476−87.

[18] Bruewer M, Hopkins AM, Hobert ME, Nusrat A, Madara JL. RhoA, Rac1, and Cdc42 exert distinct effects on epithelial

barrier via selective structural and biochemical modulation of junctional proteins and F-actin. Am J Physiol Cell Physiol 2004;287(2):C327–35.
[19] Köhler K, Louvard D, Zahraoui A. Rab13 regulates PKA signaling during tight junction assembly. J Cell Biol 2004;165 (2):175–80.
[20] Singh AB, Harris RC. Epidermal growth factor receptor activation differentially regulates claudin expression and enhances transepithelial resistance in Madin-Darby canine kidney cells. J Biol Chem 2004;279(5):3543–52.
[21] Di Stefano A, Wittner M, Nitschke R, et al. Effects of parathyroid hormone and calcitonin on Na+, Cl-, K+, Mg2+ and Ca2 + transport in cortical and medullary thick ascending limbs of mouse kidney. Pflugers Arch 1990;417(2):161–7.
[22] Ba J, Friedman PA. Calcium-sensing receptor regulation of renal mineral ion transport. Cell Calcium 2004;35(3):229–37.
[23] Hebert SC, Brown EM. The extracellular calcium receptor. Curr Opin Cell Biol 1995;7(4):484–92.
[24] Motoyama HI, Friedman PA. Calcium-sensing receptor regulation of PTH-dependent calcium absorption by mouse cortical ascending limbs. Am J Physiol Renal Physiol 2002;283(3): F399–406.
[25] Desfleurs E, Wittner M, Pajaud S, Nitschke R, Rajerison RM, Di Stefano A. The Ca2 +-sensing receptor in the rabbit cortical thick ascending limb (CTAL) is functionally not coupled to phospholipase C. Pflugers Arch 1999;437(5):716–23.
[26] Desfleurs E, Wittner M, Simeone S, et al. Calcium-sensing receptor: regulation of electrolyte transport in the thick ascending limb of Henle's loop. Kidney Blood Press Res 1998;21 (6):401–12.
[27] Di Stefano A, Desfleurs E, Simeone S, Nitschke R, Wittner M. Ca2 + and Mg2 + sensor in the thick ascending limb of the loop of Henle. Kidney Blood Press Res 1997;20(3):190–3.
[28] Frazão JM, Martins P, Coburn JW. The calcimimetic agents: perspectives for treatment. Kidney Int Suppl 2002;80:149–54.
[29] Riccardi D, Hall AE, Chattopadhyay N, Xu JZ, Brown EM, Hebert SC. Localization of the extracellular Ca2 + /polyvalent cation-sensing protein in rat kidney. Am J Physiol 1998;274(3 Pt 2):F611–22.
[30] Massry SG, Coburn JW. The hormonal and non-hormonal control of renal excretion of calcium and magnesium. Nephron 1973;10(2):66–112.
[31] Wong NL, Dirks JH, Quamme GA. Tubular reabsorptive capacity for magnesium in the dog kidney. Am J Physiol 1983;244(1): F78–83.
[32] Kelepouris E, Agus ZS. Hypomagnesemia: renal magnesium handling. Semin Nephrol 1998;18(1):58–73.
[33] Ahmad A, Swaminathan R. Disorders of magnesium metabolism. The kidney: physiology and pathophysiology. New York: Raven Press; 2000. p. 1732-48
[34] Wittner M, Jounier S, Deschênes G, de Rouffignac C, Di Stefano A. Cellular adaptation of the mouse cortical thick ascending limb of Henle's loop (CTAL) to dietary magnesium restriction: enhanced transepithelial Mg2 + and Ca2 + transport. Pflugers Arch 2000;439(6):765–71.
[35] Efrati E, Arsentiev-Rozenfeld J, Zelikovic I. The human paracellin-1 gene (hPCLN-1): renal epithelial cell-specific expression and regulation. Am J Physiol Renal Physiol 2005;288 (2):F272–83.
[36] Dai LJ, Ritchie G, Kerstan D, Kang HS, Cole DE, Quamme GA. Magnesium transport in the renal distal convoluted tubule. Physiol Rev 2001;81(1):51–84.
[37] Schlingmann KP, Weber S, Peters M, et al. Hypomagnesemia with secondary hypocalcemia is caused by mutations in TRPM6, a new member of the TRPM gene family. Nat Genet 2002;31(2):166–70.
[38] Walder RY, Landau D, Meyer P, et al. Mutation of TRPM6 causes familial hypomagnesemia with secondary hypocalcemia. Nat Genet 2002;31(2):171–4.
[39] Nadler MJ, Hermosura MC, Inabe K, et al. LTRPC7 is a Mg. ATP-regulated divalent cation channel required for cell viability. Nature 2001;411(6837):590–5.
[40] Ryazanova LV, Dorovkov MV, Ansari A, Ryazanov AG. Characterization of the protein kinase activity of TRPM7/ ChaK1, a protein kinase fused to the transient receptor potential ion channel. J Biol Chem 2004;279(5):3708–16.
[41] Schmitz C, Perraud AL, Johnson CO, et al. Regulation of vertebrate cellular Mg2 + homeostasis by TRPM7. Cell 2003;114(2):191–200.
[42] Dorovkov MV, Ryazanov AG. Phosphorylation of annexin I by TRPM7 channel-kinase. J Biol Chem 2004;279(49):50643–6.
[43] Takezawa R, Schmitz C, Demeuse P, Scharenberg AM, Penner R, Fleig A. Receptor-mediated regulation of the TRPM7 channel through its endogenous protein kinase domain. Proc Natl Acad Sci U S A 2004;101(16):6009–14.
[44] Runnels LW, Yue L, Clapham DE. The TRPM7 channel is inactivated by PIP(2) hydrolysis. Nat Cell Biol 2002;4(5):329–36.
[45] Chubanov V, Waldegger S, Mederos Y, Schnitzler M, et al. Disruption of TRPM6/TRPM7 complex formation by a mutation in the TRPM6 gene causes hypomagnesemia with secondary hypocalcemia. Proc Natl Acad Sci USA 2004;101(9):2894–9.
[46] Voets T, Nilius B, Hoefs S, et al. TRPM6 forms the Mg2 + influx channel involved in intestinal and renal Mg2 + absorption. J Biol Chem 2004;279(1):19–25.
[47] Gwanyanya A, Amuzescu B, Zakharov SI, et al. Magnesium-inhibited, TRPM6/7-like channel in cardiac myocytes: permeation of divalent cations and pH-mediated regulation. J Physiol 2004;559(Pt 3):761–76.
[48] Ritchie G, Kerstan D, Dai LJ, et al. 1,25(OH)(2)D(3) stimulates Mg2+ uptake into MDCT cells: modulation by extracellular Ca2+ and Mg2 +. Am J Physiol Renal Physiol 2001;280(5): F868–78.
[49] Dai LJ, Bapty B, Ritchie G, Quamme GA. PGE2 stimulates Mg2 + uptake in mouse distal convoluted tubule cells. Am J Physiol 1998;275(5 Pt 2):F833–9.
[50] Groenestege WM, Thébault S, van der Wijst J, et al. Impaired basolateral sorting of pro-EGF causes isolated recessive renal hypomagnesemia. J Clin Invest 2007;117(8):2260–7.
[51] Thebault S, Alexander RT, Tiel Groenestege WM, Hoenderop JG, Bindels RJ. EGF increases TRPM6 activity and surface expression. J Am Soc Nephrol 2009;20(1):78–85.
[52] Falin R, Veizis IE, Cotton CU. A role for ERK1/2 in EGF- and ATP-dependent regulation of amiloride-sensitive sodium absorption. Am J Physiol Cell Physiol 2005;288(5):C1003–11.
[53] Bapty BW, Dai LJ, Ritchie G, et al. Extracellular Mg2(+)- and Ca2(+)-sensing in mouse distal convoluted tubule cells. Kidney Int 1998;53(3):583–92.
[54] Nijenhuis T, Vallon V, van der Kemp AW, Loffing J, Hoenderop JG, Bindels RJ. Enhanced passive Ca2 + reabsorption and reduced Mg2 + channel abundance explains thiazide-induced hypocalciuria and hypomagnesemia. J Clin Invest 2005;115 (6):1651–8.
[55] Shafik IM, Quamme GA. Early adaptation of renal magnesium reabsorption in response to magnesium restriction. Am J Physiol 1989;257(6 Pt 2):F974–7.
[56] Dai LJ, Raymond L, Friedman PA, Quamme GA. Mechanisms of amiloride stimulation of Mg2 + uptake in immortalized

mouse distal convoluted tubule cells. Am J Physiol 1997;272(2 Pt 2):F249–56.
[57] Efrati E, Hirsch A, Kladnitsky O, et al. Transcriptional regulation of the claudin-16 gene by Mg2+ availability. Cell Physiol Biochem 2010;25(6):705–14.
[58] Groenestege WM, Hoenderop JG, van den Heuvel L, Knoers N, Bindels RJ. The epithelial Mg2+ channel transient receptor potential melastatin 6 is regulated by dietary Mg2+ content and estrogens. J Am Soc Nephrol 2006;17(4):1035–43.
[59] Rondón LJ, Groenestege WM, Rayssiguier Y, Mazur A. Relationship between low magnesium status and TRPM6 expression in the kidney and large intestine. Am J Physiol Regul Integr Comp Physiol 2008;294(6):R2001–7.
[60] Bartter FC, Pronove P, Gill JR, Maccardle RC. Hyperplasia of the juxtaglomerular complex with hyperaldosteronism and hypokalemic alkalosis. A new syndrome. Am J Med 1962;33:811–28.
[61] Konrad M, Weber S. Recent advances in molecular genetics of hereditary magnesium-losing disorders. J Am Soc Nephrol 2003;14(1):249–60.
[62] Schlingmann KP, Konrad M, Seyberth HW. Genetics of hereditary disorders of magnesium homeostasis. Pediatr Nephrol 2004;19(1):13–25.
[63] Jeck N, Derst C, Wischmeyer E, et al. Functional heterogeneity of ROMK mutations linked to hyperprostaglandin E syndrome. Kidney Int 2001;59(5):1803–11.
[64] Simon DB, Karet FE, Hamdan JM, DiPietro A, Sanjad SA, Lifton RP. Bartter's syndrome, hypokalaemic alkalosis with hypercalciuria, is caused by mutations in the Na–K–2Cl cotransporter NKCC2. Nat Genet 1996;13(2):183–8.
[65] Simon DB, Nelson-Williams C, Bia MJ, et al. Gitelman's variant of Bartter's syndrome, inherited hypokalaemic alkalosis, is caused by mutations in the thiazide-sensitive Na–Cl cotransporter. Nat Genet 1996;12(1):24–30.
[66] Vargas-Poussou R, Feldmann D, Vollmer M, et al. Novel molecular variants of the Na–K–2Cl cotransporter gene are responsible for antenatal Bartter syndrome. Am J Hum Genet 1998;62 (6):1332–40.
[67] Peters M, Ermert S, Jeck N, et al. Classification and rescue of ROMK mutations underlying hyperprostaglandin E syndrome/ antenatal Bartter syndrome. Kidney Int 2003;64(3):923–32.
[68] Birkenhäger R, Otto E, Schürmann MJ, et al. Mutation of BSND causes Bartter syndrome with sensorineural deafness and kidney failure. Nat Genet 2001;29(3):310–4.
[69] Schlingmann KP, Konrad M, Jeck N, et al. Salt wasting and deafness resulting from mutations in two chloride channels. N Engl J Med 2004;350(13):1314–9.
[70] Matsumura Y, Uchida S, Kondo Y, et al. Overt nephrogenic diabetes insipidus in mice lacking the CLC-K1 chloride channel. Nat Genet 1999;21(1):95–8.
[71] Jeck N, Reinalter SC, Henne T, et al. Hypokalemic salt-losing tubulopathy with chronic renal failure and sensorineural deafness. Pediatrics 2001;108(1):E5.
[72] Jeck N, Schlingmann KP, Reinalter SC, et al. Salt handling in the distal nephron: lessons learned from inherited human disorders. Am J Physiol Regul Integr Comp Physiol 2005;288(4): R782–95.
[73] Konrad M, Vollmer M, Lemmink HH, et al. Mutations in the chloride channel gene CLCNKB as a cause of classic Bartter syndrome. J Am Soc Nephrol 2000;11(8):1449–59.
[74] Simon DB, Bindra RS, Mansfield TA, et al. Mutations in the chloride channel gene, CLCNKB, cause Bartter's syndrome type III. Nat Genet 1997;17(2):171–8.
[75] Jeck N, Konrad M, Peters M, Weber S, Bonzel KE, Seyberth HW. Mutations in the chloride channel gene, CLCNKB, leading to a mixed Bartter-Gitelman phenotype. Pediatr Res 2000;48 (6):754–8.
[76] Peters M, Jeck N, Reinalter S, et al. Clinical presentation of genetically defined patients with hypokalemic salt-losing tubulopathies. Am J Med 2002;112(3):183–90.
[77] Sabath E, Meade P, Berkman J, et al. Pathophysiology of functional mutations of the thiazide-sensitive Na–Cl cotransporter in Gitelman disease. Am J Physiol Renal Physiol 2004;287(2): F195–203.
[78] Bettinelli A, Rusconi R, Ciarmatori S, et al. Gitelman disease associated with growth hormone deficiency, disturbances in vasopressin secretion and empty sella: a new hereditary renal tubular-pituitary syndrome?. Pediatr Res 1999;46(2):232–8.
[79] Károlyi L, Ziegler A, Pollak M, et al. Gitelman's syndrome is genetically distinct from other forms of Bartter's syndrome. Pediatr Nephrol 1996;10(5):551–4.
[80] Gitelman HJ, Graham JB, Welt LG. A new familial disorder characterized by hypokalemia and hypomagnesemia. Trans Assoc Am Physicians 1966;79:221–35.
[81] Peters N, Bettinelli A, Spicher I, Basilico E, Metta MG, Bianchetti MG. Renal tubular function in children and adolescents with Gitelman's syndrome, the hypocalciuric variant of Bartter's syndrome. Nephrol Dial Transplant 1995;10(8):1313–9.
[82] Cruz DN, Shaer AJ, Bia MJ, Lifton RP, Simon DB, Group YGsaBsSCS. Gitelman's syndrome revisited: an evaluation of symptoms and health-related quality of life. Kidney Int 2001;59 (2):710–7.
[83] Reilly RF, Ellison DH. Mammalian distal tubule: physiology, pathophysiology, and molecular anatomy. Physiol Rev 2000;80 (1):277–313.
[84] Loffing J, Vallon V, Loffing-Cueni D, et al. Altered renal distal tubule structure and renal Na(+) and Ca(2+) handling in a mouse model for Gitelman's syndrome. J Am Soc Nephrol 2004;15(9):2276–88.
[85] Schultheis PJ, Lorenz JN, Meneton P, et al. Phenotype resembling Gitelman's syndrome in mice lacking the apical Na+-Cl− cotransporter of the distal convoluted tubule. J Biol Chem 1998;273(44):29150–5.
[86] Bockenhauer D, Feather S, Stanescu HC, et al. Epilepsy, ataxia, sensorineural deafness, tubulopathy, and KCNJ10 mutations. N Engl J Med 2009;360(19):1960–70.
[87] Scholl UI, Choi M, Liu T, et al. Seizures, sensorineural deafness, ataxia, mental retardation, and electrolyte imbalance (SeSAME syndrome) caused by mutations in KCNJ10. Proc Natl Acad Sci U S A 2009;106(14):5842–7.
[88] Ito M, Inanobe A, Horio Y, et al. Immunolocalization of an inwardly rectifying K+ channel, K(AB)-2 (Kir4.1), in the basolateral membrane of renal distal tubular epithelia. FEBS Lett 1996;388(1):11–5.
[89] Tanemoto M, Abe T, Onogawa T, Ito S. PDZ binding motif-dependent localization of K+ channel on the basolateral side in distal tubules. Am J Physiol Renal Physiol 2004;287(6): F1148–53.
[90] Bandulik S, Schmidt K, Bockenhauer D, et al. The salt-wasting phenotype of EAST syndrome, a disease with multifaceted symptoms linked to the KCNJ10 K+ channel. Pflugers Arch 2011;461(4):423–35.
[91] Pollak MR, Brown EM, Estep HL, et al. Autosomal dominant hypocalcaemia caused by a Ca(2+)-sensing receptor gene mutation. Nat Genet 1994;8(3):303–7.
[92] Pearce SH, Williamson C, Kifor O, et al. A familial syndrome of hypocalcemia with hypercalciuria due to mutations in the calcium-sensing receptor. N Engl J Med 1996;335(15):1115–22.
[93] Vargas-Poussou R, Huang C, Hulin P, et al. Functional characterization of a calcium-sensing receptor mutation in severe

autosomal dominant hypocalcemia with a Bartter-like syndrome. J Am Soc Nephrol 2002;13(9):2259–66.
[94] Watanabe S, Fukumoto S, Chang H, et al. Association between activating mutations of calcium-sensing receptor and Bartter's syndrome. Lancet 2002;360(9334):692–4.
[95] Sanda S, Schlingmann KP, Newfield RS. Autosomal dominant hypoparathyroidism with severe hypomagnesemia and hypocalcemia, successfully treated with recombinant PTH and continuous subcutaneous magnesium infusion. J Pediatr Endocrinol Metab 2008;21(4):385–91.
[96] Pollak MR, Brown EM, Chou YH, et al. Mutations in the human Ca(2 +)-sensing receptor gene cause familial hypocalciuric hypercalcemia and neonatal severe hyperparathyroidism. Cell 1993;75(7):1297–303.
[97] Marx SJ, Attie MF, Levine MA, Spiegel AM, Downs RW, Lasker RD. The hypocalciuric or benign variant of familial hypercalcemia: clinical and biochemical features in fifteen kindreds. Medicine (Baltimore) 1981;60(6):397–412.
[98] Cole DE, Quamme GA. Inherited disorders of renal magnesium handling. J Am Soc Nephrol 2000;11 (10):1937–47.
[99] Hunter D, De Lange M, Snieder H, et al. Genetic contribution to bone metabolism, calcium excretion, and vitamin D and parathyroid hormone regulation. J Bone Miner Res 2001;16 (2):371–8.
[100] Benigno V, Canonica CS, Bettinelli A, von Vigier RO, Truttmann AC, Bianchetti MG. Hypomagnesaemia-hypercalciuria-nephrocalcinosis: a report of nine cases and a review. Nephrol Dial Transplant 2000;15(5):605–10.
[101] Praga M, Vara J, González-Parra E, et al. Familial hypomagnesemia with hypercalciuria and nephrocalcinosis. Kidney Int 1995;47(5):1419–25.
[102] Weber S, Schneider L, Peters M, et al. Novel paracellin-1 mutations in 25 families with familial hypomagnesemia with hypercalciuria and nephrocalcinosis. J Am Soc Nephrol 2001;12(9):1872–81.
[103] Wolf MT, Dötsch J, Konrad M, Böswald M, Rascher W. Follow-up of five patients with FHHNC due to mutations in the Paracellin-1 gene. Pediatr Nephrol 2002;17(8):602–8.
[104] Weber S, Hoffmann K, Jeck N, et al. Familial hypomagnesaemia with hypercalciuria and nephrocalcinosis maps to chromosome 3q27 and is associated with mutations in the PCLN-1 gene. Eur J Hum Genet 2000;8(6):414–22.
[105] Nicholson JC, Jones CL, Powell HR, Walker RG, McCredie DA. Familial hypomagnesaemia–hypercalciuria leading to end-stage renal failure. Pediatr Nephrol 1995;9(1):74–6.
[106] Haisch L, Almeida JR, Abreu da Silva PR, Schlingmann KP, Konrad M. The role of tight junctions in paracellular ion transport in the renal tubule: lessons learned from a rare inherited tubular disorder. Am J Kidney Dis 2011;57(2):320–30.
[107] Colegio OR, Van Itallie C, Rahner C, Anderson JM. Claudin extracellular domains determine paracellular charge selectivity and resistance but not tight junction fibril architecture. Am J Physiol Cell Physiol 2003;284(6):C1346–54.
[108] Weber S, Schlingmann KP, Peters M, et al. Primary gene structure and expression studies of rodent paracellin-1. J Am Soc Nephrol 2001;12(12):2664–72.
[109] Ohba Y, Kitagawa H, Kitoh K, et al. A deletion of the paracellin-1 gene is responsible for renal tubular dysplasia in cattle. Genomics 2000;68(3):229–36.
[110] Will C, Breiderhoff T, Thumfart J, et al. Targeted deletion of murine Cldn16 identifies extra- and intrarenal compensatory mechanisms of Ca2 + and Mg2 + wasting. Am J Physiol Renal Physiol 2010.
[111] Konrad M, Hou J, Weber S, et al. CLDN16 genotype predicts renal decline in familial hypomagnesemia with hypercalciuria and nephrocalcinosis. J Am Soc Nephrol 2008;19(1):171–81.
[112] Blanchard A, Jeunemaitre X, Coudol P, et al. Paracellin-1 is critical for magnesium and calcium reabsorption in the human thick ascending limb of Henle. Kidney Int 2001;59(6):2206–15.
[113] Müller D, Kausalya PJ, Claverie-Martin F, et al. A novel claudin 16 mutation associated with childhood hypercalciuria abolishes binding to ZO-1 and results in lysosomal mistargeting. Am J Hum Genet 2003;73(6):1293–301.
[114] Hou J, Renigunta A, Gomes AS, et al. Claudin-16 and claudin-19 interaction is required for their assembly into tight junctions and for renal reabsorption of magnesium. Proc Natl Acad Sci U S A 2009;106(36):15350–5.
[115] Hou J, Goodenough DA. Claudin-16 and claudin-19 function in the thick ascending limb. Curr Opin Nephrol Hypertens 2010;19(5):483–8.
[116] Paunier L, Radde IC, Kooh SW, Conen PE, Fraser D. Primary hypomagnesemia with secondary hypocalcemia in an infant. Pediatrics 1968;41(2):385–402.
[117] Jalkanen R, Pronicka E, Tyynismaa H, Hanauer A, Walder R, Alitalo T. Genetic background of HSH in three Polish families and a patient with an X;9 translocation. Eur J Hum Genet 2006;14(1):55–62.
[118] Walder RY, Shalev H, Brennan TM, et al. Familial hypomagnesemia maps to chromosome 9q, not to the X chromosome: genetic linkage mapping and analysis of a balanced translocation breakpoint. Hum Mol Genet 1997;6(9):1491–7.
[119] Schlingmann KP, Sassen MC, Weber S, et al. Novel TRPM6 mutations in 21 families with primary hypomagnesemia and secondary hypocalcemia. J Am Soc Nephrol 2005;16 (10):3061–9.
[120] Anast CS, Mohs JM, Kaplan SL, Burns TW. Evidence for parathyroid failure in magnesium deficiency. Science 1972;177 (4049):606–8.
[121] Vetter T, Lohse MJ. Magnesium and the parathyroid. Curr Opin Nephrol Hypertens 2002;11(4):403–10.
[122] Shalev H, Phillip M, Galil A, Carmi R, Landau D. Clinical presentation and outcome in primary familial hypomagnesaemia. Arch Dis Child 1998;78(2):127–30.
[123] Cole DE, Kooh SW, Vieth R. Primary infantile hypomagnesaemia: outcome after 21 years and treatment with continuous nocturnal nasogastric magnesium infusion. Eur J Pediatr 2000;159(1-2):38–43.
[124] Aries PM, Schubert M, Müller-Wieland D, Krone W. Subcutaneous magnesium pump in a patient with combined magnesium transport defect. Dtsch Med Wochenschr 2000;125 (33):970–2.
[125] Lombeck I, Ritzl F, Schnippering HG, et al. Primary hypomagnesemia. I. Absorption Studies. Z Kinderheilkd 1975;118 (4):249–58.
[126] Matzkin H, Lotan D, Boichis H. Primary hypomagnesemia with a probable double magnesium transport defect. Nephron 1989;52(1):83–6.
[127] Montell C. Mg2 + homeostasis: the Mg2 + nificent TRPM chanzymes. Curr Biol 2003;13(20):R799–801.
[128] Monteilh-Zoller MK, Hermosura MC, Nadler MJ, Scharenberg AM, Penner R, Fleig A. TRPM7 provides an ion channel mechanism for cellular entry of trace metal ions. J Gen Physiol 2003;121(1):49–60.
[129] Hofmann T, Schaefer M, Schultz G, Gudermann T. Subunit composition of mammalian transient receptor potential channels in living cells. Proc Natl Acad Sci U S A 2002;99(11): 7461–6.

[130] Chubanov V, Schlingmann KP, Wäring J, et al. Hypomagnesemia with secondary hypocalcemia due to a missense mutation in the putative pore-forming region of TRPM6. J Biol Chem 2007;282(10):7656–67.
[131] Schweigel M, Martens H. Magnesium transport in the gastrointestinal tract. Front Biosci 2000;5:D666–77.
[132] Kerstan D, Quamme GA. Physiology and pathophysiology of intestinal absorption of magnesium. In: Massry SG, Morii H, Nishizawa Y, editors. Calcium in Internal Medicine. Surry, UK: Springer-Verlag; 2002. p. 171–83.
[133] Meij IC, Koenderink JB, van Bokhoven H, et al. Dominant isolated renal magnesium loss is caused by misrouting of the Na(+),K(+)-ATPase gamma-subunit. Nat Genet 2000;26 (3):265–6.
[134] Geven WB, Monnens LA, Willems HL, Buijs WC, ter Haar BG. Renal magnesium wasting in two families with autosomal dominant inheritance. Kidney Int 1987;31(5):1140–4.
[135] Meij IC, Saar K, van den Heuvel LP, et al. Hereditary isolated renal magnesium loss maps to chromosome 11q23. Am J Hum Genet 1999;64(1):180–8.
[136] Sweadner KJ, Arystarkhova E, Donnet C, Wetzel RK. FXYD proteins as regulators of the Na,K–ATPase in the kidney. Ann N Y Acad Sci 2003;986:382–7.
[137] Arystarkhova E, Wetzel RK, Sweadner KJ. Distribution and oligomeric association of splice forms of Na(+)-K(+)-ATPase regulatory gamma-subunit in rat kidney. Am J Physiol Renal Physiol 2002;282(3):F393–407.
[138] Arystarkhova E, Donnet C, Asinovski NK, Sweadner KJ. Differential regulation of renal Na,K–ATPase by splice variants of the gamma subunit. J Biol Chem 2002;277(12): 10162–72.
[139] Blostein R, Pu HX, Scanzano R, Zouzoulas A. Structure/function studies of the gamma subunit of the Na,K–ATPase. Ann N Y Acad Sci 2003;986:420–7.
[140] Meij IC, Koenderink JB, De Jong JC, et al. Dominant isolated renal magnesium loss is caused by misrouting of the Na+, K+-ATPase gamma-subunit. Ann N Y Acad Sci 2003;986:437–43.
[141] Cairo ER, Friedrich T, Swarts HG, et al. Impaired routing of wild type FXYD2 after oligomerisation with FXYD2-G41R might explain the dominant nature of renal hypomagnesemia. Biochim Biophys Acta 2008;1778(2):398–404.
[142] Jones DH, Li TY, Arystarkhova E, et al. Na,K–ATPase from mice lacking the gamma subunit (FXYD2) exhibits altered Na+ affinity and decreased thermal stability. J Biol Chem 2005;280(19):19003–11.
[143] Glaudemans B, van der Wijst J, Scola RH, et al. A missense mutation in the Kv1.1 voltage-gated potassium channel-encoding gene KCNA1 is linked to human autosomal dominant hypomagnesemia. J Clin Invest 2009;119(4):936–42.
[144] Browne DL, Gancher ST, Nutt JG, et al. Episodic ataxia/myokymia syndrome is associated with point mutations in the human potassium channel gene, KCNA1. Nat Genet 1994;8(2):136–40.
[145] van der Wijst J, Glaudemans B, Venselaar H, et al. Functional analysis of the Kv1.1 N255D mutation associated with autosomal dominant hypomagnesemia. J Biol Chem 2010;285 (1):171–8.
[146] Stuiver M, Lainez S, Will C, et al. CNNM2, encoding a basolateral protein required for renal Mg2+ handling, is mutated in dominant hypomagnesemia. Am J Hum Genet 2011;88 (3):333–43.
[147] Goytain A, Quamme GA. Functional characterization of ACDP2 (ancient conserved domain protein), a divalent metal transporter. Physiol Genomics 2005;22(3):382–9.
[148] Meyer TE, Verwoert GC, Hwang SJ, et al. Genome-wide association studies of serum magnesium, potassium, and sodium concentrations identify six Loci influencing serum magnesium levels. PLoS Genet 2010;6:8.
[149] Gibson MM, Bagga DA, Miller CG, Maguire ME. Magnesium transport in Salmonella typhimurium: the influence of new mutations conferring Co2+ resistance on the CorA Mg2+ transport system. Mol Microbiol 1991;5 (11):2753–62.
[150] Heidet L, Decramer S, Pawtowski A, et al. Spectrum of HNF1B mutations in a large cohort of patients who harbor renal diseases. Clin J Am Soc Nephrol 2010;5(6):1079–90.
[151] Adalat S, Woolf AS, Johnstone KA, et al. HNF1B mutations associate with hypomagnesemia and renal magnesium wasting. J Am Soc Nephrol 2009;20(5):1123–31.
[152] Geven WB, Monnens LA, Willems JL, Buijs W, Hamel CJ. Isolated autosomal recessive renal magnesium loss in two sisters. Clin Genet 1987;32(6):398–402.
[153] Wilson FH, Hariri A, Farhi A, et al. A cluster of metabolic defects caused by mutation in a mitochondrial tRNA. Science 2004;306(5699):1190–4.
[154] Lajer H, Daugaard G. Cisplatin and hypomagnesemia. Cancer Treat Rev 1999;25(1):47–58.
[155] Yao X, Panichpisal K, Kurtzman N, Nugent K. Cisplatin nephrotoxicity: a review. Am J Med Sci 2007;334(2):115–24.
[156] Boulikas T, Vougiouka M. Recent clinical trials using cisplatin, carboplatin and their combination chemotherapy drugs (review). Oncol Rep 2004;11(3):559–95.
[157] Carrick S, Ghersi D, Wilcken N, Simes J. Platinum containing regimens for metastatic breast cancer. Cochrane Database Syst Rev 2004;(2):CD003374.
[158] English MW, Skinner R, Pearson AD, Price L, Wyllie R, Craft AW. Dose-related nephrotoxicity of carboplatin in children. Br J Cancer 1999;81(2):336–41.
[159] Goren MP. Cisplatin nephrotoxicity affects magnesium and calcium metabolism. Med Pediatr Oncol 2003;41(3):186–9.
[160] Hodgkinson E, Neville-Webbe HL, Coleman RE. Magnesium depletion in patients receiving cisplatin-based chemotherapy. Clin Oncol (R Coll Radiol) 2006;18(9):710–8.
[161] Magil AB, Mavichak V, Wong NL, Quamme GA, Dirks JH, Sutton RA. Long-term morphological and biochemical observations in cisplatin-induced hypomagnesemia in rats. Nephron 1986;43(3):223–30.
[162] Mavichak V, Wong NL, Quamme GA, Magil AB, Sutton RA, Dirks JH. Studies on the pathogenesis of cisplatin-induced hypomagnesemia in rats. Kidney Int 1985;28 (6):914–21.
[163] Swainson CP, Colls BM, Fitzharris BM. Cis-platinum and distal renal tubule toxicity. N Z Med J 1985;98(779):375–8.
[164] Bianchetti MG, Kanaka C, Ridolfi-Lüthy A, Hirt A, Wagner HP, Oetliker OH. Persisting renotubular sequelae after cisplatin in children and adolescents. Am J Nephrol 1991;11(2):127–30.
[165] Markmann M, Rothman R, Reichman B, et al. Persistent hypomagnesemia following cisplatin chemotherapy in patients with ovarian cancer. J Cancer Res Clin Oncol 1991;117 (2):89–90.
[166] Panichpisal K, Angulo-Pernett F, Selhi S, Nugent KM. Gitelman-like syndrome after cisplatin therapy: a case report and literature review. BMC Nephrol 2006;7:10.
[167] Arany I, Safirstein RL. Cisplatin nephrotoxicity. Semin Nephrol 2003;23(5):460–4.
[168] Shah GM, Kirschenbaum MA. Renal magnesium wasting associated with therapeutic agents. Miner Electrolyte Metab 1991;17(1):58–64.

[169] Elliott C, Newman N, Madan A. Gentamicin effects on urinary electrolyte excretion in healthy subjects. Clin Pharmacol Ther 2000;67(1):16–21.
[170] Giapros VI, Cholevas VI, Andronikou SK. Acute effects of gentamicin on urinary electrolyte excretion in neonates. Pediatr Nephrol 2004;19(3):322–5.
[171] Keating MJ, Sethi MR, Bodey GP, Samaan NA. Hypocalcemia with hypoparathyroidism and renal tubular dysfunction associated with aminoglycoside therapy. Cancer 1977;39(4):1410–4.
[172] Garland HO, Birdsey TJ, Davidge CG, et al. Effects of gentamicin, neomycin and tobramycin on renal calcium and magnesium handling in two rat strains. Clin Exp Pharmacol Physiol 1994;21(2):109–15.
[173] Weinberg JM, Harding PG, Humes HD. Alterations in renal cortex cation homeostasis during mercuric chloride and gentamicin nephrotoxicity. Exp Mol Pathol 1983;39(1):43–60.
[174] Kang HS, Kerstan D, Dai L, Ritchie G, Quamme GA. Aminoglycosides inhibit hormone-stimulated Mg2 + uptake in mouse distal convoluted tubule cells. Can J Physiol Pharmacol 2000;78(8):595–602.
[175] McLarnon S, Holden D, Ward D, Jones M, Elliott A, Riccardi D. Aminoglycoside antibiotics induce pH-sensitive activation of the calcium-sensing receptor. Biochem Biophys Res Commun 2002;297(1):71–7.
[176] Ward DT, McLarnon SJ, Riccardi D. Aminoglycosides increase intracellular calcium levels and ERK activity in proximal tubular OK cells expressing the extracellular calcium-sensing receptor. J Am Soc Nephrol 2002;13(6):1481–9.
[177] Rob PM, Lebeau A, Nobiling R, et al. Magnesium metabolism: basic aspects and implications of ciclosporine toxicity in rats. Nephron 1996;72(1):59–66.
[178] Wong NL, Dirks JH. Cyclosporin-induced hypomagnesaemia and renal magnesium wasting in rats. Clin Sci (Lond) 1988;75 (5):509–14.
[179] Lote CJ, Thewles A, Wood JA, Zafar T. The hypomagnesaemic action of FK506: urinary excretion of magnesium and calcium and the role of parathyroid hormone. Clin Sci (Lond) 2000;99 (4):285–92.
[180] Chang CT, Hung CC, Tian YC, Yang CW, Wu MS. Ciclosporin reduces paracellin-1 expression and magnesium transport in thick ascending limb cells. Nephrol Dial Transplant 2007;22 (4):1033–40.
[181] Kim SJ, Kang HS, Jeong CW, et al. Immunosuppressants inhibit hormone-stimulated Mg2 + uptake in mouse distal convoluted tubule cells. Biochem Biophys Res Commun 2006;341(3):742–8.
[182] Ledeganck KJ, Boulet GA, Horvath CA, et al. Expression of renal distal tubule transporters TRPM6 and NCC in a rat model of cyclosporine nephrotoxicity and effect of EGF treatment. Am J Physiol Renal Physiol 2011;301(3):F486–93.
[183] Nijenhuis T, Hoenderop JG, Bindels RJ. Downregulation of Ca (2 +) and Mg(2 +) transport proteins in the kidney explains tacrolimus (FK506)-induced hypercalciuria and hypomagnesemia. J Am Soc Nephrol 2004;15(3):549–57.
[184] Mervaala EM, Müller DN, Park JK, et al. Monocyte infiltration and adhesion molecules in a rat model of high human renin hypertension. Hypertension 1999;33(1 Pt 2):389–95.
[185] Miura K, Nakatani T, Asai T, et al. Role of hypomagnesemia in chronic cyclosporine nephropathy. Transplantation 2002;73 (3):340–7.
[186] Tejpar S, Piessevaux H, Claes K, et al. Magnesium wasting associated with epidermal-growth-factor receptor-targeting antibodies in colorectal cancer: a prospective study. Lancet Oncol 2007;8(5):387–94.
[187] Cao Y, Liao C, Tan A, Liu L, Gao F. Meta-analysis of incidence and risk of hypomagnesemia with cetuximab for advanced cancer. Chemotherapy 2010;56(6):459–65.
[188] Vincenzi B, Santini D, Galluzzo S, et al. Early magnesium reduction in advanced colorectal cancer patients treated with cetuximab plus irinotecan as predictive factor of efficacy and outcome. Clin Cancer Res 2008;14(13):4219–24.
[189] Vincenzi B, Galluzzo S, Santini D, et al. Early magnesium modifications as a surrogate marker of efficacy of cetuximab-based anticancer treatment in KRAS wild-type advanced colorectal cancer patients. Ann Oncol 2011;22(5):1141–6.
[190] Cundy T, Mackay J. Proton pump inhibitors and severe hypomagnesaemia. Curr Opin Gastroenterol 2011;27(2):180–5.
[191] Epstein M, McGrath S, Law F. Proton-pump inhibitors and hypomagnesemic hypoparathyroidism. N Engl J Med 2006;355 (17):1834–6.
[192] Elisaf M, Kalaitzidis R, Siamopoulos KC. Multiple electrolyte abnormalities after pamidronate administration. Nephron 1998;79(3):337–9.
[193] Di Stefano ADE, Moine G. Regulation of Ca2 + and Mg2 + reabsorption in the mouse cortical thick ascending limb of Henle's loop (cTAL) by low magnesium diet and metabolic alkalosis 1995; [p abstract P 015].
[194] Husmann MJ, Fuchs P, Truttmann AC, et al. Extracellular magnesium depletion in pediatric patients with insulin-dependent diabetes mellitus. Miner Electrolyte Metab 1997;23 (2):121–4.
[195] Khan LA, Alam AM, Ali L, et al. Serum and urinary magnesium in young diabetic subjects in Bangladesh. Am J Clin Nutr 1999;69(1):70–3.
[196] Takaya J, Higashino H, Kotera F, Kobayashi Y. Intracellular magnesium of platelets in children with diabetes and obesity. Metabolism 2003;52(4):468–71.
[197] Tosiello L. Hypomagnesemia and diabetes mellitus. A review of clinical implications. Arch Intern Med 1996;156(11):1143–8.
[198] Barbagallo M, Dominguez LJ, Galioto A, et al. Role of magnesium in insulin action, diabetes and cardio-metabolic syndrome X. Mol Aspects Med 2003;24(1-3):39–52.
[199] Guerrero-Romero F, Rodríguez-Morán M. Low serum magnesium levels and metabolic syndrome. Acta Diabetol 2002;39 (4):209–13.
[200] Coburn JW, Massry SG. Changes in serum and urinary calcium during phosphate depletion: studies on mechanisms. J Clin Invest 1970;49(6):1073–87.
[201] Dai LJ, Friedman PA, Quamme GA. Phosphate depletion diminishes Mg2 + uptake in mouse distal convoluted tubule cells. Kidney Int 1997;51(6):1710–8.
[202] Dai LJ, Friedman PA, Quamme GA. Cellular mechanisms of chlorothiazide and cellular potassium depletion on Mg2 + uptake in mouse distal convoluted tubule cells. Kidney Int 1997;51(4):1008–17.
[203] Crook MA. Hypophosphataemia and hypokalaemia in patients with hypomagnesaemia. Br J Biomed Sci 1994;51(1):24–7.

This page intentionally left blank

CHAPTER

62

Calcium Channels

Joost G.J. Hoenderop and René J.M. Bindels

Department of Physiology, Nijmegen Centre for Molecular Life Sciences, Radboud University Nijmegen Medical Centre, The Netherlands

CA^{2+} CHANNELS IN THE KIDNEY

The kidney plays an eminent role in the maintenance of the Ca^{2+} balance by regulating the Ca^{2+} excretion of the body. Renal epithelial cells are unique in their ability to mediate vectorial transport of Ca^{2+} between the luminal and basolateral compartments. The initial step in this process is the Ca^{2+} influx across the luminal membrane. In addition, Ca^{2+} influx is crucial to facilitate Ca^{2+}-dependent signal transduction processes in the renal cell. In general, Ca^{2+} is postulated to enter the epithelial cell via Ca^{2+}-permeable channels present at the plasma membrane under the influence of a steep inwardly-directed electrochemical gradient. In the last decade a series of cation channels, including voltage-dependent and independent channels, has been identified that could facilitate the entry of Ca^{2+} ions in the epithelial cells of the kidney.

Voltage-Dependent Ca^{2+} Channels

Voltage-dependent Ca^{2+} channels have been well characterized in excitable tissues and at least four different types including, L, N, T and P, can be distinguished on the basis of electrophysiological and pharmacological properties.[1] The molecular identity and precise localization of these Ca^{2+} channels along the nephron is not well understood. Previous studies from Yu and colleagues have demonstrated the existence of voltage-dependent Ca^{2+} channels in the kidney (Table 62.1).[2,3] They identified a gene transcript encoding the pore-forming alpha 1-subunit of a Ca^{2+} channel (alpha 1A) in the glomerulus and the distal convoluted tubule (DCT). Skott and coworkers assessed the distribution of the identified alpha(1G)-subunit encoding a voltage-dependent Ca^{2+} channel with T-type characteristics.[4] RT-PCR analysis of microdissected rat nephron segments revealed alpha(1G) expression in DCT, CNT, cortical collecting duct (CCD), and inner medullary collecting duct (IMCD) (Table 62.1). Immunohistochemistry on sections of rat kidneys using an anti-alpha(1G) antibody demonstrated labeling at the apical plasma membrane domains of DCT, CNT and IMCD principal cells. Another study from Bacskai and Friedman examined the parathyroid hormone (PTH)-sensitivity of Ca^{2+} influx in single cultured cells originating from distal renal tubules by measuring the intracellular Ca^{2+} concentration. They found that PTH activates dihydropyridine-sensitive Ca^{2+} channels.[5] Tan and Lau, described a 25 pS, cAMP-sensitive apical Ca^{2+} channel in rabbit kidney CNT cells, that was inhibited by dihydropyridine agonists and depolarization.[6] The properties of these Ca^{2+} channels are largely conferred by their pore-forming alpha1 subunit. In general, voltage-sensitive Ca^{2+} channels are heteromeric, multisubunit proteins, as has been clearly demonstrated for the skeletal muscle and brain channels, and their properties are not only determined by the pore-forming alpha1-subunit itself, but also depend on the presence of regulatory beta subunits. To identify the accessory beta subunit of DCT/CNT Ca^{2+} channels, degenerate primers based on published beta subunit sequences were used to amplify rat kidney cDNA by the polymerase chain reaction (PCR). Alternatively, spliced transcripts of three beta-subunit genes (beta-2,3,4) were identified.[3] Northern blot analysis indicated that beta 4-subunit is preferentially expressed in kidney cortex. Transcripts of all three beta-subunit genes were detected by PCR in microdissected nephron segments, but only the beta 4-subunit was found in DCT/CNT. At present, the physiological significance of these

Seldin and Giebisch's The Kidney, Fifth Edition.
DOI: http://dx.doi.org/10.1016/B978-0-12-381462-3.00062-8

© 2013 Elsevier Inc. All rights reserved.

TABLE 62.1 Characteristics of Ca^{2+} Channels in the Kidney

	Channel Isotype	Selectivity pCa/pNa [125,9]	Segmental distribution
Voltage-dependent Ca^{2+} channels	Alpha 1A	~1000	G, DCT[2]
	Alpha 1G	~1000	DCT, CNT, CD[4]
Other Ca^{2+} permeable channels	TRPC1	1	G, PT, TAL, RV[12,126]
	TRPC3	1.5	G, CD, RV[12,126]
	TRPC4	1.1; 7	G, RV[12,126]
	TRPC5	1.8; 9	G, RV[12,126]
	TRPC6	5	G, CD, RV[12,126]
	TRPV4	6	ATL, TAL, DCT, CNT[29]
	TRPV5	107	DCT, CNT[7]
	TRPV6	130	DCT, CNT, CD[7]
	TRPM3	1.6	CNT, CD[127]
	TRPM6	7	DCT[20]
	TRPP2	5	DCT, CD[128,24]

Ca^{2+} permeable channels that were detected in the kidney are listed in the table. G, glomerulus; PT, proximal tubule; ATL, ascending thin limb of Henle; TAL, thick ascending limb of Henle; DCT, distal convoluted tubule; CNT, connecting tubule; CCD, cortical collecting duct; CD, collecting duct; RV, resistance vessels; n.d., not determined.

voltage-dependent Ca^{2+} channels in transepithelial Ca^{2+} transport remains unclear. Functional Ca^{2+} influx measurements were only performed in non-polarized single cell systems. In addition, pharmacological studies in polarized primary cultures of rabbit CNT and CCD have demonstrated that voltage-dependent Ca^{2+} channel blockers do not inhibit transepithelial Ca^{2+} transport.[7] Additional studies are needed to address the functional relevance of voltage-dependent Ca^{2+} channels in the process of transepithelial Ca^{2+} transport in the kidney.

Other Ca^{2+} Channels

Non-voltage-gated Ca^{2+} channels in the kidney are mainly represented by the transient receptor potential (TRP) superfamily of proteins consisting of Ca^{2+} permeable channels. TRP channels can be divided by sequence homology into at least six subfamilies, designated TRPC (canonical), TRPV (vanilloid), TRPM (melastatin), TRPP (polycystins, PKD-type), TRPA (ankyrin), TRPML (mucolipin), and the more distant subfamily TRPN (no mechano-receptor potential or nomp).[8,7,9,10] Mammalian homologues of the first identified *Drosophila* TRP gene encode a family of at least 20 ion channel proteins (Figure 62.1). Mutations and/or dysfunction of TRP proteins produce many renal diseases, including Mg^{2+} wasting, Ca^{2+}-related disorders and polycystic kidney diseases.

TRPC Channels

TRP channels are widely expressed and facilitate diverse functions, ranging from thermal, tactile, taste, osmolar, and fluid flow sensing to transepithelial ion transport. TRPC1 was the first member of the mammalian TRP family purported to form an ion channel. TRPC channels are ubiquitously expressed in mammalian tissues.[11,9,10] TRPC1, 3, 4, 5 and 6 mRNA and protein expression was detected in freshly isolated rat renal resistance vessels and glomeruli suggesting that these channels may play a role in mediating voltage-independent Ca^{2+} entry to facilitate cellular signal transduction processes.[12] It should be noted that members of the TRPC family are non-selective divalent ion channels (Table 62.1). Interestingly, TRPC1 dysfunction might be important in the development of diabetic nephropathy while TRPC6 seems to be an important target for the treatment of both genetic and acquired glomerular diseases.[13,14] Finally, TRPC3 plays a key role in the influx of Ca^{2+} into principal cells.[15]

TRPM Channels

The discovery and subsequent characterization of members of the TRPM family of cation channels has highlighted new insights into unknown aspects of ion (cellular) homeostasis regulation. The groups of Konrad and Sheffield reported that hypomagnesemia associated with secondary hypocalcemia (HSH) is an autosomal recessive disease that is genetically linked to TRPM6.[16,17] This disease is primarily due to defective intestinal Mg^{2+} absorption and affected individuals show neurologic symptoms of hypomagnesemic hypocalcemia, including seizures and muscle spasms during infancy.[18] Renal Mg^{2+} conservation has been reported to be normal in most patients. In some cases, however, a renal leak has been documented suggesting impaired renal Mg^{2+} reabsorption. Patients studied by Konrad et al. and others showed inappropriately high fractional Mg^{2+} excretion rates with respect to their low serum Mg^{2+} levels.[18] Hypocalcemia is secondary to parathyroid failure resulting from Mg^{2+} deficiency. TRPM6 is a member of the long TRPM family and is similar to TRPM7 (also known as TRP-PLIK[8]), a unique bifunctional protein known as a Mg^{2+} and Ca^{2+}-permeable cation channel with protein kinase activity.[19] TRPM6 has a ~4 fold higher affinity for Mg^{2+} compared to Ca^{2+}, but is clearly permeable for Ca^{2+} (Table 62.1).[20] TRPM6 is exclusively expressed in the early part of the DCT consistent with its role being

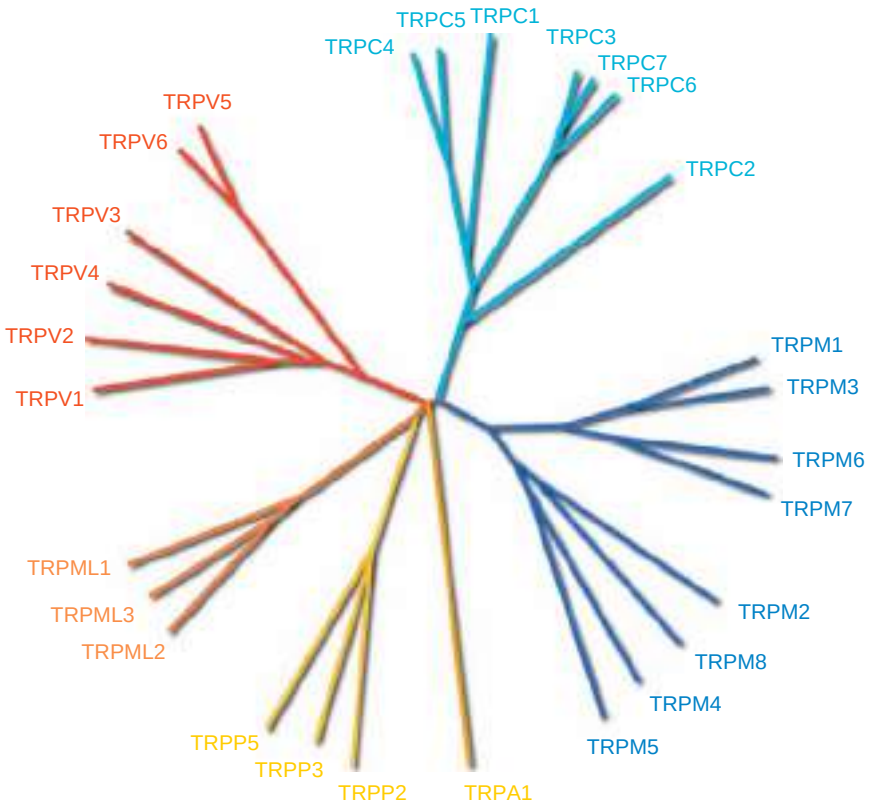

FIGURE 62.1 **Mammalian TRP family tree.** The evolutionary distance between the TRP channels is shown by the total branch lengths in point accepted mutations (PAM) units, which is the mean number of substitutions per 100 residues. The tree was calculated using the neighbor-joining method for human, rat and mouse sequences.[8]

the gatekeeper of active transepithelial Mg^{2+} transport.[18,20] In addition, other TRPM channels have been detected in kidney. Northern and immunoblot analysis demonstrated abundant expression of TRPM3 in human kidney.[21] Functional studies indicated that TRPM3 is permeable for Ca^{2+} and activated by reduction of extracellular osmolarity (Table 62.1).[21] Immunohistochemical localization studies should provide more information about the physiological function of TRPM3 in the kidney.

TRPP Channels

Growing evidence has emerged that polycystins are ion channels or regulators of ion channels. This suggests that autosomal-dominant polycystic kidney disease (ADPKD), which arises from mutations in polycystins, is a form of ion channel disease. ADPKD is a major, inherited nephropathy affecting over 1:1000 of the world wide population.[22,23] The disease is caused by mutations in two genes, PKD1 and PKD2, which encode for the proteins, polycystin-1 and polycystin-2 (TRPP2), respectively. Although disease-associated mutations have been identified in these two proteins, the sequence of molecular events leading to clinical symptoms is still unknown. Polycystin-1 resides in the plasma membrane and it is proposed to function in cell-cell and cell-matrix interactions, whereas TRPP2 is concentrated in the endoplasmic reticulum (Table 62.1). In contrast to the nonselective cation channel TRPP2, TRPP1 is a large, integral membrane protein that structurally resembles a receptor or adhesion molecule. TRPP1 and TRPP2 form a protein complex in cilia, which are microtubule-based organelles that function as cellular mechanosensors. Flow of fluid causes cilia to bend, which in turn results in a TRPP1/TRPP2 complex-dependent increase in intracellular Ca^{2+} levels, directing attention to the regulation of intracellular Ca^{2+} as a possible misstep that participates in cyst formation.[22,23] Immunostaining of human and mouse renal tissues has demonstrated widespread and developmentally regulated TRPP2 expression, with the highest level in thick ascending limb (TAL) and DCT.[24]

TRPV Channels

Plant and colleagues identified TRPV4 as a Ca^{2+}-permeable, non-selective cation channel that exhibits spontaneous activity in isotonic media and is rapidly activated by a decrease in extracellular osmolarity, cell swelling, heat or phorbol esters.[25,26,27] TRPV4 is expressed at high levels in kidney and here subtle changes in osmolarity result in significant changes in the intracellular Ca^{2+} concentration. Here, TRPV4 is candidate for a molecular sensor that confers osmosensitivity.[25,27] Liedtke and Friedman showed that TRPV4

knockout mice have reduced water intake and become more hyperosmolar compared to wild-type littermates.[28] The response to both hyper- and hypoosmolar stimuli was impaired in these knockout mice. Immunohistochemical studies have shown that the expression of this osmotically-responsive cation channel is restricted to water-impermeant nephron segments.[29] The strongest expression of TRPV4 was observed along the basolateral membrane in the ascending thin limb (ATL) and the thick ascending limb (TAL) as was DCT and CNT. TRPV4 was absent from the proximal tubule (PT) and decending thin limb (DTL). These data imply a role for TRPV4 in the response of renal epithelial cells to anisotonicity, particularly in the hypotonic luminal milieu of TAL and DCT, and the potentially hypotonic luminal milieu of the CD.[29]

The most Ca^{2+}-selective channels of the TRP superfamily are the epithelial Ca^{2+} channels TRPV5[30] and TRPV6.[31] These latter channels are predominantly expressed in organs that mediate transepithelial Ca^{2+} transport.[7] Unique properties distinguish them from other TRP channels and studies by several groups have demonstrated that TRPV5 and TRPV6 exhibit all the characteristics being the gatekeepers of active Ca^{2+} transport in kidney and small intestine, respectively. These epithelial Ca^{2+} channels of the TRPV family have been studied in great detail and are, therefore, outlined in the following paragraphs.

EPITHELIAL Ca^{2+} CHANNELS: TRPV5 AND TRPV6

cDNA and Primary Protein Structure

The epithelial Ca^{2+} channel family is restricted to two members and genomic cloning demonstrated that these Ca^{2+} channels are transcribed from distinct genes juxtaposed on human chromosome 7q35, which suggests an evolutionary gene duplication event.[7,32] TRPV5 and TRPV6 are completely conserved in terms of exon size in the coding regions and they share similar intron-exon structures with the other TRP genes. To date, epithelial Ca^{2+} channels have been cloned from several species including pufferfish, rabbit, rat, mouse and human. TRPV5 and TRPV6 exhibit an overall homology of about 75%. Remarkably, several domains in TRPV5/6 are completely conserved within these species including the core structure of the protein consisting of 6 TM segments and the pore region, ankyrin repeats, PDZ motifs and putative protein kinase phosphorylation sites (Figure 62.2).[7] Four TRP-channel subunits will form the functional Ca^{2+} channel. In addition, it was demonstrated that both epithelial channels are high mannose- and complex-glycosylated.[33] PDZ motifs and ankyrin repeat domains are present in a diverse range of receptors and ion channels including other members of the TRPV subfamily. PDZ motifs are recognized by PDZ domains that are modular protein interaction domains playing a role in protein trafficking and protein complex assembly. In general, ankyrins connect ion channels, transporters and cell adhesion molecules to the spectrin-based cytoskeletal elements in distinct membrane domains.[34]

Distribution of TRPV5 and TRPV6

The renal expression profile of TRPV5 has been studied in detail.[7] In different species, it was demonstrated that TRPV5 co-localizes with the Ca^{2+} transport proteins, including calbindin-D_{28K} and the extrusion proteins, the plasma membrane ATPase 1b (PMCA1b) and the Na^{+}-Ca^{2+} exchanger type 1 (NCX1) in the late

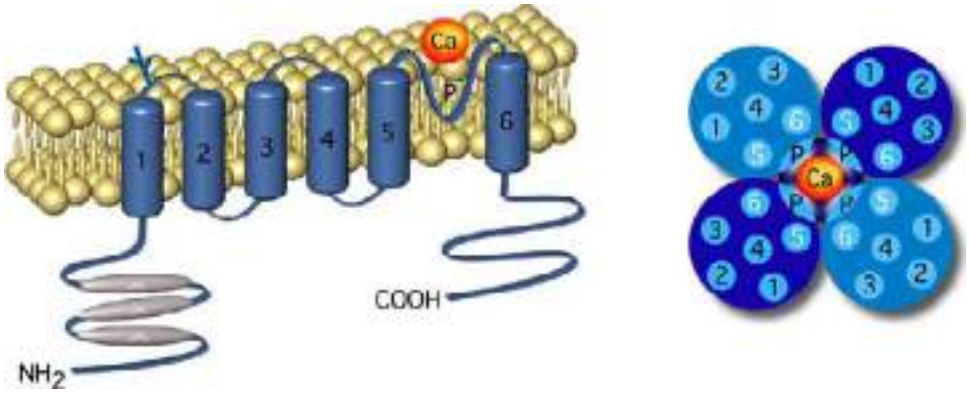

FIGURE 62.2 The epithelial Ca^{2+} channels are ~730 amino acids long with a predicted molecular mass of ~85 kDa. TRPV5 and TRPV6 contain a core domain consisting of 6 TM segments. In addition, a large cytosolic amino- and carboxyl-terminus are present containing ankyrin repeats. Between TM5 and TM6 there is a short hydrophobic stretch predicted to be the pore-forming region of these channels. Four channel subunits will form the functional Ca^{2+} channel.

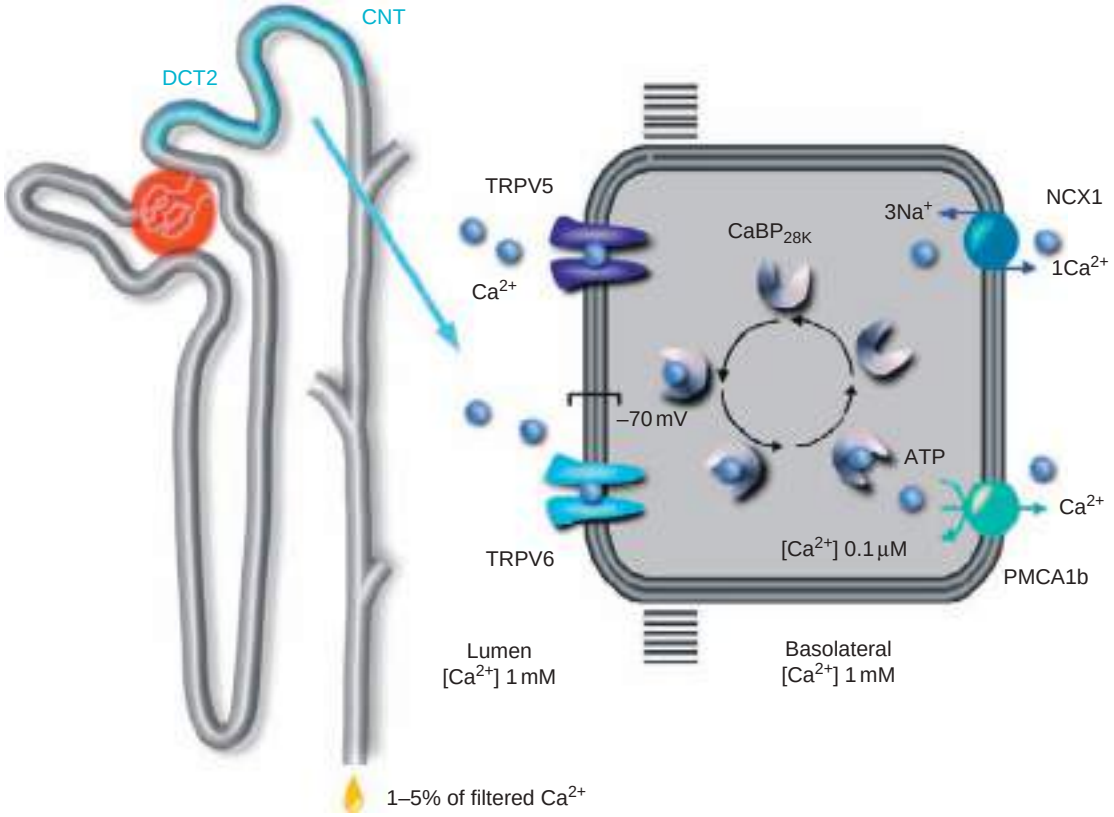

FIGURE 62.3 **Transepithelial Ca^{2+} transport is carried out as a 3-step-process.** Following entry of Ca^{2+} through the (hetero)tetrameric epithelial Ca^{2+} channels, TRPV5 and TRPV6, Ca^{2+} bound to calbindin diffuses to the basolateral membrane. At the basolateral membrane, Ca^{2+} is extruded via a ATP-dependent Ca^{2+}-ATPase (PMCA1b) and a Na^+-Ca^{2+}-exchanger (NCX1). In this way, there is net Ca^{2+} transport from the luminal space to the extracellular compartment. The active form of vitamin D, 1,25-$(OH)_2D_3$, stimulates the individuals steps of transepithelial Ca^{2+} transport by increasing the expression levels of the luminal Ca^{2+} channels, calbindins and the extrusion systems.

DCT (DCT2) and the CNT (Figure 62.3). Transepithelial Ca^{2+} transport is generally envisaged as a three step process consisting of passive entry of Ca^{2+} across the apical membrane, cytosolic diffusion of Ca^{2+} bound to calbindin-D_{28K} and active extrusion of Ca^{2+} across the opposite basolateral membrane via PMCA1b and NCX1. The highest immunocytochemical abundance of TRPV5 was found in DCT2 with a gradual decrease along CNT. A minority of cells along CNT lacked immunopositive staining for TRPV5 and the other Ca_2^+-transporting proteins. These negative cells were identified as intercalated cells.

In contrast to TRPV5, which is mainly expressed in the kidney, TRPV6 shows a more ubiquitous expression pattern. TRPV6 expression was predominantly found in the brush-border membrane of the small intestine where it co-localizes with calbindin-D_{9K} and PMCA1b in agreement with the expected properties being the gatekeeper in active Ca^{2+} absorption.[7,32] Recently, TRPV6 was detected in mouse kidney along the apical domain of DCT2 through inner medullary collecting duct (IMCD). TRPV6 co-localizes with TRPV5 and the other Ca^{2+} transport proteins in DCT2 suggesting a role in Ca^{2+} reabsorption.[35] In addition, the protein is also detected in the intercalated cells and the IMCD that are not involved in transepithelial Ca^{2+} transport pointing to additional functions of TRPV6. Thus, the precise role of this epithelial Ca^{2+} channel in the kidney remains to be established, but given the widespread distribution of TRPV6 throughout the nephron segments functions could include Ca^{2+} reabsorption, Ca^{2+} signaling and others.

Biophysical Properties

In Human Embryonic Kidney (HEK) 293 cells heterogeneously expressing TRPV5, currents through the channel can be activated under conditions of high intracellular Ca^{2+} buffering by hyperpolarizing voltage steps. In divalent cation free solutions, large inward currents are observed, which show a typical time-dependent increase (gating) that remains constant for more than one minute.[36] Outward currents are negligible indicating that the channel is nearly

completely inwardly rectifying. In analogy to voltage-dependent Ca^{2+} channels, permeation through TRPV5/6 can by described by "repulsion" pore models considering a pore consisting of two high affinity binding sites, whereby the double occupation of the two binding sites by either Na^+ or Ca^{2+} provides the "drive" for Ca^{2+} conduction due to mutual repulsion of the two cations or by a three binding-site model in which two low affinity sites flank a high affinity binding site for Ca^{2+}. Importantly, the current through TRPV5 and TRPV6 is carried exclusively by Ca^{2+} at physiological extracellular Ca^{2+} concentrations. In the situation where Ca^{2+} is absent single channel Na^+ currents through TRPV5 can be measured in inside-out patches.[37,38] Given the low conductance of these channels in the presence of extracellular Ca^{2+} reliable single channel measurements are technically not feasible.

A characteristic aspect of currents through the epithelial Ca^{2+} channels is the inactivation at negative membrane potentials. This inactivation is nearly complete if Ca^{2+} is the charge carrier and is significantly delayed when $Ca_2{}^+$ is substituted for Ba^{2+} or other divalents indicating that the process is Ca^{2+}-dependent. Furthermore, currents of monovalent cations through these Ca^{2+} channels do not inactivate. Repetitive stimulation of TRPV5 and TRPV6 currents by short hyperpolarizing pulses consequently result in a decay of the current. The slow recovery from inactivation in divalent cation free solution after the Ca^{2+}-dependent decay is a further typical hallmark of these Ca^{2+} channels. Although the above described structural aspects and basic electrophysiological properties of TRPV5 and TRPV6 are rather similar, some differences exist between these homologous channels including permeability of divalent cations, kinetics of Ca^{2+}-dependent inactivation and recovery from inactivation.[7] For instance, TRPV5 shows a higher permeability for Ba^{2+} compared to TRPV6, e.g., the current ratio I_{Ba}/I_{Ca} is ~0.9 for TRPV5, but only ~0.4 for TRPV6. TRPV6 clearly shows a fast component of inactivation which is less prominent for TRPV5, e.g., time to 10% inactivation at hyperpolarizing steps to−100 mV is ~25 ms for TRPV5 but only ~40 ms for TRPV6. Interestingly, these typical differences could be explained by sequence differences between TRPV5 and TRPV6. Interestingly, the structural determinants of these differences appear not to be located in either the amino- or carboxyl-terminus, but in the intracellular TM2-TM3 linker sequence. Substitution of this TM2−TM3 linker of TRPV6 to TRPV5 confers the kinetic and permeation phenotype of TRPV6 to TRPV5, whereas exchanging the amino- or carboxyl-termini is ineffective.[39] Mutation studies by Suzuki and co-workers demonstrated that a histidine residue at position 587 in the carboxyl-terminus close to TM segment 6 of TRPV6 affect the inactivation behavior of TRPV6.[40] In addition some distinct pharmacological differences exist, e.g., ruthenium red is a 100-fold more potent blocker for TRPV5 than TRPV6 (IC_{50} ~9 μM for TRPV6 but ~100 nM for TRPV5). Furthermore, TRPV5 is approximately four times more sensitive to Cd^{2+} blockage than TRPV6 (IC_{50} ~70 nM for TRPV5 but ~260 nM for TRPV6) .[7]

Ion Selectivity

To date, TRPV5 and TRPV6 are the most Ca^{2+}-selective channels in the TRP superfamily. The unique permeation property in the epithelial Ca^{2+} channels is not conserved in the TRPV subfamily, which shares the highest homology with TRPV5 and TRPV6. TRPV5 and TRPV6 display P_{Ca}/P_{Na} values of more than 100 whereas a permeation sequence of $Ca^{2+} > Ba^{2+} > Sr^{2+} > Mn^{2+}$ has been reported.[41,42,43,36] The permeation profile of monovalent cations is $Na^+ > Li^+ > K^+ > Cs^+$.[41,37,44,43,36]

Nilius and co-workers have demonstrated that the molecular determinants of the Ca^{2+} selectivity and permeation of TRPV5 and TRPV6 reside at a single aspartate residue in the pore-forming region (TRPV5-D542 and TRPV6-D541) (Figure 62.4).[44] Neutralization of these negatively charged amino acid residues affects the high Ca^{2+} selectivity of the epithelial Ca^{2+} channels. These data suggest that high Ca^{2+} selectivity in TRPV5 and TRPV6 depends on a ring of four aspartate residues in the pore region, similar to the ring of four negative residues (aspartates and/or glutamates) in the pore of voltage-dependent Ca^{2+} channels.[45,7,46] Most likely, D542/D541 is the narrowest part of the selectivity filter with a diameter of approximately 5.2 Å and forms part of the high affinity-binding site for Ca^{2+}. A detailed analysis of the structure of the TRPV5 and TRPV6 pores has been recently published (Figure 62.4).[45,46] The amino acid residues facing the pore were determined by cysteine scanning mutagenesis (SCAM). Cysteines introduced in a region preceding D542 for TRPV5, and D541 for TRPV6, displayed a cyclic pattern of reactivity to cysteine reacting agents indicative of a pore helix. This pattern of covalent modification of cysteines supports a KcsA-homology based 3-D model (Figure 62.4). In addition, the pore region of TRPV5 and TRPV6 contains additional negatively charged amino acid residues that only have minor effects on the Ca^{2+} permeation properties. In another study, the role of D542 for blockage of monovalent currents through TRPV5 by Ca^{2+} and Mg^{2+} was supported, however, not for determining Ca^{2+} permeability.[47] However, all of our data including recent findings from concatemers[48] and a detailed

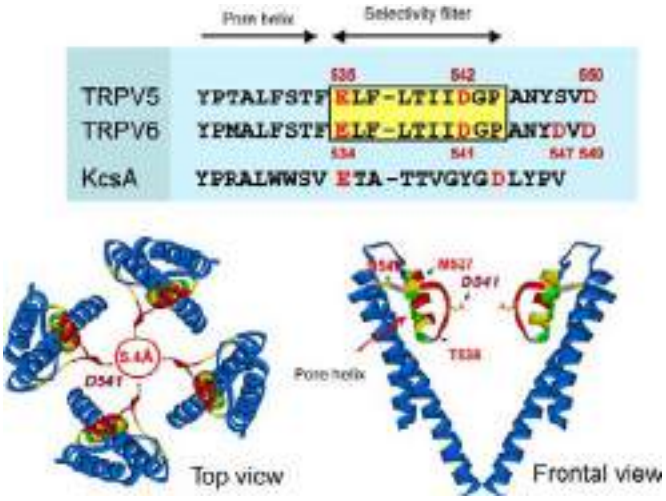

FIGURE 62.4 *Upper part:* Alignment of the pore regions of TRPV5, TRPV6 and the potassium channel KcsA (*NCBI* accession numbers CAB40138 for TRPV5, AAD47636 for TRPV6 and S60172 for KcsA). The boxed sequences represent the putative selectivity filter of the channels. The amino-terminal part of this pore structure likely represents a putative pore helix. *Lower part:* Model for the TRPV6 pore region, based on the KcsA structure. Views of the structure are shown, looking sideways at two opposite subunits (*left*) or looking down from the external solution to the complete homotetrameric channel (*right*). At the narrowest point, formed by the acidic side chain of Asp 541 (orange), the pore has a diameter of 5.4 Å. Blue residues correspond to the residues in TM5 and TM6 (TM1 and TM2 in KcsA), whose accessibility was not tested in this study. Amino acids that were subjected to substituted cysteine accessibility method SCAM analysis (residues P526 to D547) are colored in green, yellow, red or grey: residues in red reacted rapidly to Ag^{+} (reaction rate $>5*10^{6}$ M^{-1} s^{-1}), residues in yellow reacted with Ag^{+} at a rate $<5*10^{6}$ M^{-13} s^{-13}, and residues in green did not show significant reactivity to Ag^{+}. Residues where cysteine substitution resulted in non-functional channels are marked in grey. The figure was prepared using DS ViewerPro 5.0 (Accelrys Inc.), based on the coordinates of KcsA. *Figure adapted from references.*[7,46]

study of TRPV6 pore properties[46] clearly demonstrated that the Ca^{2+} selectivity is determined by D542/D541.

Mechanism of High Ca^{2+} Selectivity

The high Ca^{2+} selectivity of TRPV5 and TRPV6 refers to a mechanism of permeation as proposed previously for voltage-dependent Ca^{2+} channels. In the absence of Ca^{2+}, Mg^{2+} will bind at a site within the pore-region, which is mainly determined by D542/D541. At low driving forces, e.g. less negative membrane potentials, the driving force is not sufficient to displace Mg^{2+} out of the pore and the channel is blocked. At hyperpolarisation, Mg^{2+} will be moved from this high affinity site thereby allowing monovalent cations to permeate the channels. Because of the higher affinity of the binding-site for Ca^{2+} versus Mg^{2+}, Ca^{2+} will outnumber Mg^{2+} at this site and is now blocking the pore for a movement of monovalent cations. If the inward driving force is sufficient enough to remove Ca^{2+} from the high affinity site, a fast inward permeation occurs supported by the low affinity sites, which flank the high affinity Ca^{2+}-binding site. All the data so far support the crucial role of D542/D541 in the channel pore region of TRPV5 and TRPV6 channels.[48]

Rectification and Gating

A predominant inward rectification is a clear hallmark of the TRPV5 and TRPV6 channels besides the high Ca^{2+} selectivity. This inward rectification is only partially due to blockage by Mg^{2+}, which is removed by hyperpolarization. Thus, the most prominent part of rectification remains in the absence of intracellular Mg^{2+} and is not due to blockage by endogenous polyamines. The intrinsic rectification of these channels is, however, dramatically reduced by neutralization of the negatively charged D542/D541 residues indicating that the permeation site is also involved in rectification.[49] In mammalian cells heterogeneously expressing the epithelial Ca^{2+} channels, TRPV5 and TRPV6 are constitutively open at a low intracellular Ca^{2+} concentration and negative membrane voltage.[36] The above described mechanism of removing channel blockage by Ca^{2+} or Mg^{2+} is necessarily part of the gating mechanism.[49] At this moment other mechanisms that might influence gating of TRPV5 and TRPV6 cannot be excluded. Huang and colleagues showed that PIP_2 activates TRPV5 and that activation of TRPV5 by PIP_2 decreases the sensitivity of TRPV5 to inhibition by intracellular Mg^{2+}.[50]

Modulation of the Channel Activity

Intracellular Ca^{2+}

TRPV5 and TRPV6 are controlled by a Ca^{2+}-dependent feedback inhibition. Both Ca^{2+} channels rapidly inactivate during hyperpolarizing voltage steps and this inhibition is reduced when Ca^{2+} is substituted for Ba^{2+} or Sr^{2+} as charge carriers. The inactivation is dependent on the extracellular Ca^{2+} concentration and occurred also in cells buffered intracellularly with BAPTA.[36] In addition, the current disappeared during repetitive activation by short hyperpolarizing pulses. This current decay was significantly diminished when Ca^{2+} was replaced by Ba^{2+} as charge carrier and abolished when extracellular Ca^{2+} was lowered to 1 nM, again indicating that a Ca^{2+}-dependent process inhibits channel activity.[36] Increase of the extracellular Ca^{2+} concentration significantly stimulated the rate of current decay. Ca^{2+} influx is a prerequisite for this phenomenon because the Ca^{2+}-impermeable D542A mutant lacks a monovalent current decay in response

to repetitive stimulation.[44] These findings suggest that the TRPV5/6 channels are down-regulated by Ca^{2+} influx through the channel and thus likely by increasing the Ca^{2+} concentration in a micro-domain near the pore region, thereby inducing feedback inhibition of the channel. This could be a crucial mechanism for the regulation of TRPV5 and TRPV6 under physiological conditions. The inhibition is highly Ca^{2+}-sensitive with calculated affinity values around 100 nM. Considering the high affinity mechanism of Ca^{2+}-dependent TRPV5/6 inhibition, the presence of intracellular Ca^{2+} buffering proteins, such as calbindins, will ultimately determine the channel activity.[51]

Pharmacology

Ruthenium red and econazole are the most effective blockers of the epithelial Ca^{2+} channels identified so far. The inorganic polycationic dye ruthenium red, which binds to phospholipids, inhibits TRPV5 and TRPV6 in a voltage-dependent manner. Transepithelial Ca^{2+} transport in primary cultures of immunodissected rabbit CNT and CCD are inhibited in the same concentration range.[52] Antimycotic imidazoles such as econazole and miconazole are highly effective inhibitors with IC_{50} values of the micromolar range. These compounds block the channels, however, voltage-independently.[53] In addition, TRPV5 and TRPV6 are efficiently blocked by inorganic cations according to the following profile: $Pb^{2+} = Cu^{2+} = Gd^{3+} > Cd^{2+} > Zn^{2+} > La^{3+} > Co^{2+} > Fe^{2+} >> Fe^{3+}$ with IC_{50} values between 1 and 10 μM. Blockers of store-operated Ca^{2+} entry channels (SOC), e.g., SKF965 and 2-aminoethoxydipheny borate (2-APB), are nearly ineffective for TRPV5 and TRPV6.[53,54,55] Another SOC blocker, the adenylcyclase inhibitor MDL 12330A, exerts half-maximal inhibition of TRPV5 at ~20 μM.[53] Xestospongin, a noncompetitive inositol (1,4,5)-trisphosphate receptor antagonist seems, however, to block TRPV6.[56] Blockers of protein tyrosine kinases such as tyrphostin B46 and genistein, CaM antagonists calmidazolium R24571 and trifluoperazine, and voltage-dependent Ca^{2+} channel blockers such as mibefradil, quinidine, nifedipine, niflumic acid and verapamil, have only small or no effects on TRPV5 activity.[53] Interestingly, blockage by ruthenium red and Cd^{2+} is much more sensitive for TRPV5 than TRPV6 which can, therefore, be used to differentiate both Ca^{2+} channels.[33]

pH

Previous studies indicated that acidification of the apical medium inhibits transepithelial Ca^{2+} transport across primary cultures of rabbit CNT and CCD cells.[57] $^{45}Ca^{2+}$-uptake in TRPV5-expressing *Xenopus laevis* oocytes was inhibited by acidification of the incubation medium.[30] Extracellular acidification reduced currents through TRPV5 carried by either monovalent or divalent cations,[58] which was confirmed by Peng and colleagues[59] Additionally, extracellular pH also affected current kinetics, extracellular Mg^{2+} blockage and Ca^{2+} affinity. The gating component of monovalent cation currents through TRPV5 was delayed at alkaline pH and as well as blockage by extracellular Mg^{2+}. For voltage-dependent Ca^{2+} channels and cyclic nucleotide-gated channels, it was found that protonation of a single glutamate residue in the pore region is responsible for the dramatic changes in divalent cation affinity by extracellular pH. A similar mechanism might be applicable for TRPV5 and TRPV6 in which a single aspartate residue in the pore determines the Ca^{2+} permeation and Mg^{2+} blockage of the channel.[44] Extrapolating these findings to the *in vivo* situation, the pH influence could at least in part provide the molecular basis of acidosis-induced calciuresis. Interestingly, the molecular mechanism of TRPV5 blockage by protons is mechanistically understood taking into account the pore structure described above.[45,46] Mutation of the glutamate residue at position 522 to glutamine preceding the pore helix decreased the inhibition of the channel by extracellular protons.[60] Thus, pH sensitivity is mainly mediated by glutamate at position 522 and may act as the "pH sensor" of TRPV5.

Molecular Structure

The molecular architecture of TRPV5 and TRPV6 channels has recently been unraveled.[48] Co-immunoprecipitations and molecular mass determination of TRPV5 and TRPV6 complexes using sucrose gradient sedimentation showed that these channels form homo- and heterotetrameric channel complexes (Figure 62.2).[48] Niemeyer and co-workers identified the third ankyrin repeat being a stringent requirement for physical assembly of TRPV6 subunits.[61] It was proposed that the third ankyrin repeat initiates a molecular zippering process that proceeds past the fifth ankyrin repeat and creates an intracellular anchor that is necessary for functional subunit assembly. Subsequent studies by Chang et al. confirmed the importance of the ankyrin repeats in TRPV5 assembly. Functional studies have shown that ankyrin repeat 1 fulfills a predominant role in the oligomerization of TRPV5.[62]

Interestingly, several studies indicated that certain tissues co-express TRPV5 and TRPV6 which allows oligomerization of these channels *in vivo*. Immunohistochemical studies demonstrated co-expression of TRPV5 and TRPV6 in DCT. Heteromeric complex formation can modify the activity of members of

the TRP family.[63,64] Likewise, hetero-oligomerization of TRPV5 and TRPV6 might influence the functional properties of the Ca^{2+} channel. Because TRPV5 and TRPV6 exhibit different channel kinetics with respect to Ca^{2+}-dependent inactivation, Ba^{2+} selectivity and sensitivity for inhibition by ruthenium red, the influence of the heterotetramer composition on channel properties was investigated.[33] Concatemeric channels were constructed consisting of four TRPV5 and/or TRPV6 subunits configured in a head-to-tail fashion. Differences in the ratio of TRPV5 and TRPV6 subunits in these concatemers showed that the phenotype resembles mixed properties of TRPV5 and TRPV6. Thus, regulation of the relative expression levels of TRPV5 and TRPV6 may be a mechanism to fine-tune the Ca^{2+} transport kinetics in kidney or other TRPV5/6-co-expressing tissues.[33]

The tetrameric organization of TRPV5 and TRPV6 resembles that of the voltage-dependent Ca^{2+} channel and the Shaker potassium channel that are composed of four tandemly associated homologous domains. Clustering of four subunits is assumed to construct an aqueous pore-region centered at the four-fold symmetry axis. This tetrameric architecture of TRPV5/6 implies that four of the aspartic residues (D542, D541) form a negatively charged ring structure that functions as a selectivity filter for Ca^{2+} in analogy with voltage-dependent Ca^{2+} channels.[45,48,46] Protein crystallography of these channels will be the most challenging approach to determine the three-dimensional structure in the near future.

REGULATION OF THE EPITHELIAL Ca^{2+} CHANNELS

Vitamin D

Independent studies consistently demonstrated that the expression of TRPV5 and TRPV6 is tightly controlled by 1,25-$(OH)_2D_3$.[7] First evidence for this vitamin D-sensitivity was observed in vitamin D_3-depleted rats.[65] Decreased 1,25-$(OH)_2D_3$ levels in these animals were supplemented, which was accompanied by normalization of the plasma Ca^{2+} concentration and an increase in renal TRPV5 mRNA and protein expression. In addition, Nijenhuis et al. addressed the 1,25-$(OH)_2D_3$-dependent regulation of TRPV6.[35] Intraperitoneally injection of 1,25-$(OH)_2D_3$ in mice resulted in an increase in TRPV6 mRNA and protein expression in the kidney, however, the effect of this hormone on TRPV5 expression was more robust. The observed vitamin D-dependent regulation of TRPV5 and TRPV6 was further substantiated using many different cell lines and animal knockout models including vitamin D receptor (VDR), 1α-OHase and TRPV5 knockout mice.[66,67,68,69]

Wood and coworkers studied the vitamin D-sensitivity of TRPV6, calbindin-D_{9K} and PMCA1b in Caco-2 cells, which are generally used as model of duodenal cells.[70] A tight correlation between the 1,25-$(OH)_2D_3$-induced expression of TRPV6, calbindin-D_{9K}, PMCA1b and transepithelial Ca^{2+} transport was established in this intestinal cell line. In contrast, Barley et al. could not confirm the generally observed vitamin D-dependent sensitivity of TRPV6 in duodenal biopsies from 20 normal volunteers.[71] However, there was a 10-fold variation between the lowest and the highest level of TRPV6 expression in the human tissues. In addition, the subjects used were a mixed population of men and women of age 25−71 years, which made it difficult to disclose a relationship between TRPV6 expression and vitamin D metabolites. Likewise, cell lines and primary cultures have been established from the distal part of the nephron including DCT and CNT. Measurements of calbindin-D_{28K} expression in control and 1,25-$(OH)_2D_3$-treated renal epithelial cells indicated a direct relationship between 1,25-$(OH)_2D_3$-induced calbindin expression and transepithelial Ca^{2+} transport.[72]

In addition, several genetically modified mouse models including VDR and 1α-OHase knockout mice, in which the vitamin D system has been inactivated, have been created to systematically dissect the genetic regulation of Ca^{2+} transport genes and their functional consequences on transepithelial Ca^{2+} transport. Two groups independently generated 1α-OHase knockout mice that represent a unique animal model for pseudo-vitamin D-deficiency rickets (PDDR) since these mice display undetectable 1,25-$(OH)_2D_3$ concentrations, hypocalcemia, secondary hyperparathyroidism and failure to thrive.[66,68] In addition, the 1α-OHase knockout mice developed distinct histological evidence of rickets and osteomalacia. Interestingly, there was a correlative relationship between the expression level of TRPV5, calbindin-D_{28K} and NCX1 proteins in kidney, TRPV6, calbindin-D_{9K} and PMCA1b in duodenum and the serum Ca^{2+} concentration. Normalization of the plasma Ca^{2+} concentration by 1,25-$(OH)_2D_3$ was associated with a restoration of the expression level of the Ca^{2+} transporters confirming the essential role of these proteins in active 1,25-$(OH)_2D_3$-mediated Ca^{2+} (re)absorption. The concerted regulation of TRPV5/6 and the other Ca^{2+}-transporting proteins guarantees sufficient capacity during high transport rates. Calbindin-D regulates the Ca^{2+} influx across the apical membrane by buffering intracellular Ca^{2+} and thus controlling feedback inhibition of TRPV5/6 channel activity. Analogous observations were made from experiments performed with VDR knockout mice.

Taken together, vitamin D-deficient animal models and epithelial cell lines demonstrated unequivocally the 1,25-$(OH)_2D_3$-sensitivity of TRPV5 and TRPV6. Analysis of putative promoter regions of human and murine TRPV5/6 genes revealed potential vitamin D response elements (VDREs) in line with the previously observed functional data.[65] However, promoter studies are still lacking to further substantiate the existence of functional VDREs in these genes.

Parathyroid Hormone

The parathyroid glands play a key role in maintaining the extracellular Ca^{2+} concentration through their capacity to sense minute changes in the level of blood Ca^{2+}. Early studies using micropuncture and cell preparations demonstrated that PTH stimulates active Ca^{2+} reabsorption in the distal part of the nephron via a dual signaling mechanism involving PKA- and PKC-dependent processes.[73,74] van Abel et al. demonstrated that PTH upregulates TRPV5 expression, which increases active Ca^{2+} reabsorption via a long-term manner. Parathyroidectomized rats displayed a downregulation of TRPV5 protein expression, whereas long-term PTH supplementation restored the expression.[75] In addition, PTH exerts also a short-term effect by rapidly elevating TRPV5 channel activity. Activation of the PTH receptor initiates a signaling pathway, involving cAMP and PKA that rapidly phosphorylates threonine-709 of TRPV5, increasing the channel's open probability and thus promoting Ca^{2+} reabsorption.[76] Altogether, these results suggest that TRPV5 is the molecular target for the short- and long-term PTH-induced stimulation of active Ca^{2+} reabsorption in the distal part of the nephron.

Klotho

Characterization of a mouse that showed a phenotype comparable to human aging led to the identification of the hormone klotho.[77] Klotho is a type-I (single-pass) membrane protein predominantly expressed in tissues involved in Ca^{2+} homeostasis, such as kidney, choroid plexus, and the parathyroid gland. Indeed, there is a growing body of evidence that klotho controls active Ca^{2+} reabsorption in the kidney. Here, klotho is exclusively expressed in DCT2 and CNT, where following extracellular domain shedding, it is secreted into the circulation and the pro-urine. Subsequently, extracellular klotho hydrolyses oligosaccharide chains of N-glycosylated TRPV5, causing channel retention at the plasma membrane and a subsequent increase in TRPV5-mediated Ca^{2+} influx.[78,79] Cha et al. observed a klotho-mediated removal of terminal sialic acids from the N-glycan in TRPV5.[80] This cleavage exposed the underlying galactose-N-acetylglucoseamine disaccharides in TRPV5, so that it can directly interact with a membrane-bound galectin-1, explaining the subsequent plasma membrane retention of TRPV5. Interestingly, treatment with PNGaseF to hydrolyze the entire N-glycan of TRPV5 mimicked the stimulatory effect of klotho, suggesting additional mechanisms besides binding to membrane galectin-1.[78] Thus, there is compelling evidence that klotho is a novel calciotropic hormone that, amongst others, can exert its stimulatory effect on TRPV5 cell surface retention from the pro-urine in the DCT2 and the CNT.[81]

Estrogens and Androgens

Estrogen deficiency after menopause results in bone loss, which is associated with a rise in plasma and urinary Ca^{2+}. *In vivo* studies showed that estrogen deficiency is associated with increased renal Ca^{2+} loss, which can be corrected by estrogen replacement therapy.[82,83] Furthermore, estrogen receptors also reside in proximal and distal tubules within the nephron. However, the underlying mechanism by which estrogen may act on Ca^{2+} reabsorption is still poorly understood. It was demonstrated that estrogen upregulates the expression of TRPV5 in kidney in a 1,25-$(OH)_2D_3$-independent manner.[84] In ovariectomized 1α-OHase knockout mice 17β-estradiol replacement therapy resulted in upregulation of renal TRPV5 mRNA and protein levels, leading to normalization of plasma Ca^{2+} levels. Recent findings suggest that also TRPV6 expression is regulated by estrogen, as duodenal expression of TRPV6 mRNA of 1α-OHase knockout mice and ovariectomized rats is upregulated after 17β-estradiol administration. Van Cromphaut and coworkers reported that renal TRPV5 and duodenal TRPV6 expression is reduced in estrogen receptor alpha (ERalpha) knockout mice and upregulated by estrogen treatment.[85] Furthermore, in lactating mice renal TRPV5 mRNA and duodenal TRPV6 expression levels increased 2 and 13 times, respectively. It is clear that the expression of both epithelial Ca^{2+} channels is influenced by the estrogen status. The mechanism of estrogen-controlled upregulation of epithelial Ca^{2+} channel mRNA remains to be elucidated. Interestingly, Weber et al. recently described an estrogen-responsive element in the promoter sequence of the mouse TRPV6 gene, which was absent in the mouse TRPV5 gene.[86] Finally, it was shown that estradiol can also exert a rapid stimulatory effect on intracellular Ca^{2+} concentration in renal cells involving TRPV5.

Androgens contribute significantly to sex differences observed in renal Ca^{2+} handling by inhibiting the expression of renal Ca^{2+} transport proteins as demonstrated by several experimental findings. Male mice have a greater urinary Ca^{2+} excretion compared to

females, a feature accompanied by a reduced renal expression of Ca^{2+} transport proteins.[87] In addition, orchidectomy (ORX) induced hypocalciuria in male mice, thus resembling a female-like phenotype on renal Ca^{2+} reabsorption. Moreover, testosterone supplementation of ORX mice caused a normalization of their urinary Ca^{2+} excretion, accompanying a decreased expression of renal TRPV5 and calbindin-D_{28K}.[87] Importantly, serum 1,25-$(OH)_2D_3$, PTH, and estrogen levels did not differ between the sham-operated, ORX and testosterone-supplemented ORX mice, suggesting that androgens may directly affect the transcription of the renal Ca^{2+} transporters.

Furthermore, it was demonstrated that TRPV6 expression is suppressed by androgen and was induced by a specific androgen receptor antagonist in human prostate cancer cell line cells, suggesting that the gene is negatively regulated by androgen. TRPV6 was shown to be strongly upregulated in advanced prostate cancer.[88,89] Also in carcinomas of other tissues, such as breast, thyroid, colon and ovary, TRPV6 expression is increased.[90] Thus, TRPV6 might be a marker for tumor progression. Indeed, northern blot analysis, in situ hybridization experiments and immunohistochemistry clearly demonstrated that TRPV6 is highly expressed in prostate cancer cells, whereas in healthy prostate epithelia little or no expression is was found.[91,89] The appearance of TRPV6 correlates positively with tumor grade and TRPV6 might, therefore, be a promising target for the development of drugs against prostate cancer.

Thus, both testosterone and estrogen have opposing regulatory properties in terms of renal transcriptional expression of Ca^{2+} transporters.

Kallikrein

In kidney, tissue kallikrein is secreted into the pro-urine, where it mediates the formation of bradykinin that binds to the type 2 bradykinin receptor. In primary cultures of rabbit CNT cells it has been shown that kallikrein stimulates transcellular Ca^{2+} transport.[92] This stimulatory effect of TK was mediated by the apical bradykinin receptors signaling through the phospholipase C/diacylglycerol/PKC pathway, resulting in phosphorylation of TRPV5 and subsequent delay in its retrieval from the plasma membrane. Additionally, mice lacking tissue kallikrein waste a large amount of Ca^{2+} without any significant alterations in plasma Ca^{2+}, PTH, and vitamin D_3 levels or any detectable changes in the expression of Ca^{2+} transporters in the DCT2 and CNT.[93] These observations together highlight the importance of the regulation of the TRPV5 channel abundance in the plasma membrane by the pro-urine tissue kallikrein.

Dietary Ca^{2+} Content

Several studies described above provide evidence that the epithelial Ca^{2+} channels are regulated by 1,25-$(OH)_2D_3$, it is, however, difficult to distinguish the effects of hypocalcemia from those of vitamin D-deficiency. Therefore, studies were performed in VDR and 1α-OHase knockout mice fed a normal and high rescue Ca^{2+} diet. These mice models are ideal to study the role of dietary Ca^{2+} in the regulation of TRPV5 or TRPV6 independent of 1,25-$(OH)_2D_3$. Intriguingly, the reduced expression level of renal TRPV5 in the 1α-OHase knockout mice was restored by high dietary Ca^{2+} intake and accompanied by normalization of the plasma Ca^{2+} concentration.[94] Importantly, this effect was observed in the absence of 1α-OHase-activity. In contrast, the Ca^{2+}-enriched rescue diet reduced the expression of renal TRPV5 in wild-type mice that exhibit normal serum vitamin D and Ca^{2+} levels. It is known that under physiological conditions, plasma Ca^{2+} acts via a negative feedback mechanism which eventually leads to suppression of the 1α-OHase-activity that decreases Ca^{2+} reabsorption and expression of Ca^{2+} transport proteins. Identical observations were made in VDR knockout mice where TRPV5 and TRPV6 mRNA levels were upregulated by dietary Ca^{2+}.[95] Studies in these knockout mice models revealed that Ca^{2+} supplementation can upregulate gene transcription encoding for Ca^{2+} transporters in the absence of circulating 1,25-$(OH)_2D_3$, but the molecular mechanism of this vitamin D-independent Ca^{2+}-sensitive pathway remains elusive.[94]

Regulation by Auxiliary Proteins

Calmodulin

Calmodulin (CaM) plays a pivotal role as Ca^{2+} sensor in Ca^{2+}-dependent inactivation, thereby facilitating both activation and inactivation of ion channels, including voltage- and ligand-gated Ca^{2+} channels and members of the TRP superfamily. Ca^{2+} binding to CaM is highly cooperative with Ca^{2+} binding first to the carboxyl-terminal EF-hands, which have the highest affinity for Ca^{2+}, followed by Ca^{2+} binding to lower affinity sites located in the amino-terminus. Niemeyer et al. showed that CaM binds to the carboxyl-terminus of human TRPV6 in a Ca^{2+}-dependent manner.[96] In addition, Nilius et al. indicated that the rabbit TRPV5 C-terminal region is also important for the Ca^{2+}-dependent inactivation process.[97] Recently, CaM was shown to bind to the C- and N- tails of TRPV5 and TRPV6 as well as the transmembrane domain of TRPV6 in a Ca^{2+}-dependent fashion (Figure 62.5).[98] Furthermore, electrophysiological measurements of HEK293 cells heterologously co-expressing Ca^{2+}-insensitive CaM

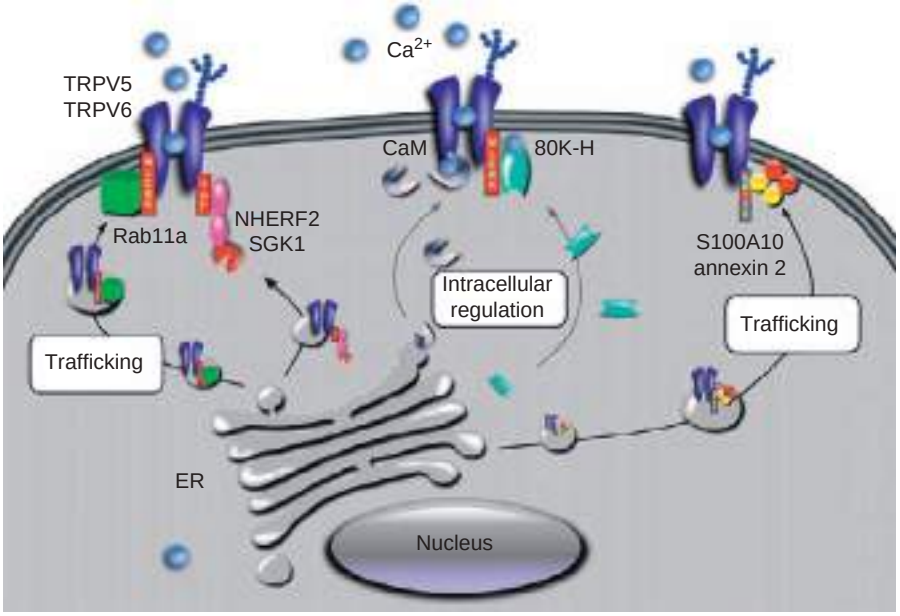

FIGURE 62.5 Integrated model about the regulation of the epithelial Ca^{2+} channels (TRPV5 and TRPV6) by associated protein complexes including calmodulin (CaM), S100A10-annexin 2, Na^+/H^+ exchanger regulating factor 2 (NHERF2), 80K-H, Rab11a. See text for further explanation.

mutants and TRPV6, revealed a significantly reduced inward Ca^{2+} current, whereas no effect of the mutants was demonstrated on currents of TRPV5-expressing cells. It remains, therefore, to be established whether CaM is the general Ca^{2+} sensor or that other processes play a role in the Ca^{2+}-dependent inactivation of TRPV5. Moreover, the high affinity EF-hand Ca^{2+}-binding sites of CaM were demonstrated to contribute primarily to the observed CaM effect upon TRPV6 activity. The C-terminal CaM-binding site of TRPV6 is identical between mouse and rat, but not similarly present in human TRPV6, which might explain the previous observation that CaM binding to human TRPV6 is localized to a different region. Together, these results suggest that CaM positively affects TRPV6 activity.

S100A10-Annexin 2

S100A10 was identified as an associated protein of TRPV5 and TRPV6 by screening a kidney cDNA library using the yeast two-hybrid system. S100A10, which specifically associates with the carboxyl-termini of these epithelial Ca^{2+} channels, is a 97 amino acid protein member of the S100 superfamily that is present in a large number of organisms including vertebrates, insects, nematodes and plants. Several members of the S100 protein family form heteromeric complexes with annexins and S100A10 is often found tightly associated with annexin 2 to form a tetrameric complex. Van de Graaf and co-workers provided evidence of a regulatory role for the S100A10-annexin 2 heterotetramer in TRPV5 and TRPV6 functioning.[52] The association of S100A10 with TRPV5 and TRPV6 was restricted to a short conserved peptide sequence VATTV located in the carboxyl-termini of these channels. The first threonine of this interaction motif was identified as a crucial determinant for binding and channel function. Malfunctioning of these mutant channels was accompanied by a major disturbance in their subcellular localization, indicating that the S100A10-annexin 2 heterotetramer facilitates the translocation of TRPV5 and TRPV6 channels towards the plasma membrane (Figure 62.5). The importance of annexin 2 in this process was demonstrated by a siRNA-based downregulation of annexin 2 that significantly inhibited the currents through TRPV5 and TRPV6 indicating that annexin 2 in conjunction with S100A10 is crucial for TRPV5 activity. Taken together, these findings show that the S100A10-annexin 2 complex is a significant component for the trafficking of the epithelial Ca^{2+} channels and, therefore, the Ca^{2+} homeostasis.

Na^+/H^+ Exchanger Regulating Factor 2

Embark and coworkers recently demonstrated that TRPV5 activity in *Xenopus laevis* oocytes is increased upon co-expression with the Na^+/H^+ exchanger regulating factor 2 (NHERF2) and the serum glucocorticoid inducible kinase (SGK1).[99] In analogy, co-expression of SGK1 with NHERF2 stimulates the activity of the ROMK1, a K^+ channel involved in renal K^+ handling.[100] Coexpression of SGK1 and NHERF2 results in a stabilization of ROMK1 in the plasma membrane, leading to an increased ROMK activity.[101] Whether this mechanism is identical for TRPV5 remains to be established. Using GST pull-down and overlay assays, we demonstrated the specific interaction of NHERF2 with the last three amino acids in the carboxyl-terminus of

TRPV5 (van de Graaf et al., unpublished results). This suggests that the NHERF2/SGK1 protein pair affects TRPV5 in a direct fashion, via protein-protein interaction (Figure 62.5). The last three amino acids of TRPV5 resemble a PDZ motif, which allows binding to a PDZ domain-harboring protein like NHERF2. The concerted action of the NHERF2 and SGK1 proteins increased TRPV5 activity. It is tempting to speculate that the stimulatory effect on TRPV5 trafficking to the plasma membrane reflects SGK1-mediated phosphorylation of TRPV5, but this remains to be demonstrated experimentally.

80K-H

Gkika and colleagues identified 80K-H as a protein involved in the Ca^{2+}-dependent regulation of TRPV5.[102] This latter study demonstrated a specific interaction between 80K-H and TRPV5, co-localization of both proteins in the distal part of the nephron and similar transcriptional regulation by 1,25-$(OH)_2D_3$ and dietary Ca^{2+}. The interaction of 80K-H was localized to a conserved α-helical region of only ~30 amino acids. The interaction between 80K-H and TRPV5 was lost when 5 amino acids (MLERK) at the C terminal end of this region were removed by truncation or mutation into glycines. Furthermore, 80K-H directly bound Ca^{2+} and inactivation of its two EF-hand structures totally abolished the Ca^{2+} binding. Electrophysiological studies using 80K-H mutants showed that three domains of 80K-H (two EF-hand structures, the highly acidic glutamic stretch and the His-Asp-Glu-Leu sequence) are critical determinants for TRPV5 channel activity. Importantly, inactivation of the EF-hand pair reduced the TRPV5-mediated Ca^{2+} current and increased the TRPV5 sensitivity to intracellular Ca^{2+}, accelerating feedback inhibition of channel activity. None of the 80K-H mutants altered the plasma membrane localization of TRPV5 nor the association of 80K-H with TRPV5, suggesting that 80K-H has a direct effect on TRPV5 activity. Taken together, 80K-H act as a novel Ca^{2+} sensor controlling TRPV5 channel activity (Figure 62.5).

Rab11a

Rab11a, a small GTPase involved in trafficking via recycling endosomes, was recently identified as a novel TRPV5- and TRPV6-associated protein.[103] This small GTPase co-localized with TRPV5 and TRPV6 in DCT and CNT. Importantly, the Ca^{2+} channels and Rab11a were here present in vesicular structures underlying the apical plasma membrane. Using a combination of GST pull-down and co-immunoprecipitation assays a direct interaction between Rab11a and the epithelial Ca^{2+} channels (Figure 62.5) was shown, hinting at a novel mechanism of Rab11a-mediated trafficking. Furthermore, it was demonstrated that TRPV5 and TRPV6 preferentially interact with Rab11a in its GDP-bound conformation. Expression of a mutant Rab11a protein, locked in the GDP-bound state, resulted in a marked decrease of channels at the cell surface, indicating a direct role of Rab11a in the trafficking of the Ca^{2+} channels towards the plasma membrane. The interaction of Rab11a was localized to the conserved MLERK domain in the carboxyl-terminus of TRPV5 and TRPV6. 80K-H binding was localized to the same region, suggesting a possible common binding site in TRPV5 and TRPV6 for these two distinct proteins.[102] Mutagenesis of these 5 amino acids abolished channel activity at the plasma membrane by impairing the trafficking to the cell surface. Interestingly, Zobiack and coworkers have demonstrated that the annexin 2-S100A10 complex controls the distribution of Rab11-positive endosomes.[104] Furthermore, annexin 2 was enriched in these endosomes. This suggests that two crucial pathways controlling the cell surface expression of TRPV5 and TRPV6 coincide.

Indeed, the mechanisms underlying TRPV5 endocytosis have been investigated in several studies.[103,105] After reaching the cell surface, the TRPV5 channel was internalized through dynamin- and clathrin-dependent processes. First, TRPV5 appeared in numerous small vesicles, before entering larger vesicles, where it co-localized with Rab11a, a marker for recycling endosomes.[105] The majority of internalized TRPV5 entered the recycling pathway, whereas only a minor part was degraded. TRPV5 channels present in recycling endosomes were able to reach the plasma membrane again through direct interaction with Rab11a. Moreover, the presence of a large and stable recycling pool of TRPV5 channels was demonstrated, as blocking protein biosynthesis did not reduce TRPV5-mediated Ca^{2+} influx. Altogether, the continuous endosomal recycling of internalized TRPV5 channels enables TRPV5 reappearance at with many the plasma membrane providing a synthesis-independent pathway for the apical influx of Ca^{2+}.

WNK

WNK3 and WNK4, members of the With No Lysine (K) family of protein serine/threonine kinases, are also positive regulators of the epithelial Ca^{2+} channels TRPV5 and TRPV6 through enhancing the membrane expression level of the functional channel proteins via a kinase-dependent pathway.[106,107] The kinase domain of WNK3 appeared sufficient to exert the positive effect on TRPV5. Since these WNKs are expressed in the distal part of the nephron, where TRPV5 and TRPV6 are expressed, they might positive regulators of the active Ca^{2+} reabsorption pathway in the kidney.

Regulation by Immunosuppressives and Diuretics

Tacrolimus

Tacrolimus (FK506) is a widely prescribed immunosuppressant drug and is known to induce significant side effects on mineral homeostasis, including increased bone turnover, a negative Ca^{2+} balance and hypercalciuria.[108,109] The kidney plays an essential role in the maintenance of the Ca^{2+} homeostasis by providing the main excretory route. In theory, downregulation of Ca^{2+} transporter proteins in the distal part of the nephron may be involved in the pathogenesis of hypercalciuria during drug treatment. Previous reports showed reduced calbindin-D_{28K} levels during FK506 treatment, suggesting that FK506 could affect active Ca^{2+} transport.[110] In addition, it was demonstrated that FK506 treatment significantly increased urinary Ca^{2+} excretion, accompanied by a down-regulation of the renal mRNA and protein expression of TRPV5.[111] The fact that serum Ca^{2+} concentrations and the glomerular filtration rate did not differ from control animals confirmed that impaired Ca^{2+} reabsorption rather than an increased filtered load caused the hypercalciuria. This data supported the hypothesis that FK506 induces a primary defect of renal active Ca^{2+} reabsorption by specifically down-regulating the proteins involved in active Ca^{2+} transport. The molecular mechanism underlying the downregulation of the epithelial Ca^{2+} channel by FK506 remains elusive. In previous studies, plasma 1,25-$(OH)_2D_3$ was either unaltered or moderately increased, while plasma PTH levels were not affected by similar doses of FK506, which excludes that the reduced Ca^{2+} transport protein expression levels are secondary to decreased circulating levels of calciotropic hormones.

Furosemide

Diuretics such as furosemide are frequently used in the clinical practice. Furosemide is usually administered over a long period of time and is known to disturb Ca^{2+} reabsorption leading to various symptoms including alterations in structure and stability of bone. The molecular mechanism underlying its action on Ca^{2+} reabsorption includes the following events. Furosemide inhibits the Na^+—K^+—$2Cl^-$ (NKCC2) transporter present in the apical membrane of the TALH resulting in a reduction in NaCl reabsorption and K^+ recycling across the apical membrane. This action diminishes the lumen-positive potential that drives the paracellular reabsorption of Ca^{2+} explaining the hypercalciuric action of furosemide. As a consequence the delivery of Ca^{2+} to DCT and CNT is enhanced, which are the primary sites of active Ca^{2+} reabsorption.[7] Indeed, furosemide treatment increased the abundance of the Ca^{2+} transport molecules including TRPV5, TRPV6, calbindin-D_{28K} and calbindin-D_{9K}, in the DCT that could represent a solute load-dependent effect in response to increased calcium delivery and, therefore, serves as a compensatory adaptation in the downstream segment.[112]

Thiazide Diuretics

Thiazide diuretics have, in contrast to loop diuretics, the unique characteristic of decreasing Na^+ reabsorption, while increasing Ca^{2+} reabsorption. In addition, mutations in the thiazide-sensitive Na^+-Cl^- cotransporter (NCC) have been shown to cause Gitelman's syndrome. These patients suffer from hypovolemia, hypokalemic alkalosis, hypomagnesemia and hypocalciuria.[113] Intriguingly, the molecular mechanisms responsible for the hypocalciuria and hypomagnesemia of thiazide administration and Gitelman's syndrome remain elusive. Two hypotheses exist with respect to the Ca^{2+}-sparing effect of thiazides.[7] First, renal salt and water loss due to thiazide treatment result in contraction of the extracellular volume (ECV), which triggers a compensatory increase of proximal Na^+ reabsorption. This would in turn enhance the electrochemical gradient driving passive Ca^{2+} transport in proximal tubule tubular segments.[113,114,115] Early studies by Weinman and Eknoyan already demonstrated that the escape from the chronic effects of chlorothiazide is due to a decrease in the glomerular filtration rate and to an increase in fractional reabsorption in the proximal tubule.[116] Subsequently, Nijenhuis et al. showed in rats that the hydrochlorothiazide (HCTZ)-induced hypocalciuria was accompanied by a significant decrease in body weight compared to controls, illustrating that ECV contraction occurred.[117] Since Na^+ depletion resulted in a similar hypocalciuria, it is likely that the ECV contraction by itself is responsible for the thiazide-induced hypocalciuria. This is further supported by the finding that Na^+ repletion during HCTZ treatment, thereby preventing the ECV contraction, normalized the calciuresis. Second, microperfusion experiments suggested that acute administration of thiazides in the tubular lumen stimulates Ca^{2+} reabsorption in DCT.[118] Subsequently, several molecular mechanisms were postulated to explain this latter stimulatory effect. These included hyperpolarisation of the plasma membrane resulting in increased apical Ca^{2+} entry through TRPV5 and, alternatively, enhanced basolateral Na^+/Ca^{2+} exchange due to a decreased intracellular Na^+ concentration.[114] This last hypothesis was based on substantial co-localization in DCT of

NCC and the proteins involved in active Ca^{2+} transport. However, immunohistochemical studies demonstrated only minor overlap, whereas the Ca^{2+} transporters (i.e., TRPV5, calbindin-D_{28K}, NCX1 and PMCA1b) completely co-localized.[7] Interestingly, it was demonstrated that in the DCT epithelium the Ca^{2+} transport proteins including TRPV5, calbindin-D_{28K} and PMCA1b were decreased in animals treated with high thiazide dosis. In addition, the localization of the NCC protein was shifted from the luminal membrane to the basal membrane. Furthermore, Schultheis et al. generated NCC knockout mice exhibiting hypocalciuria and hypomagnesemia, representing a valuable animal model explaining Gitelman's syndrome.[119] In these mice Ca^{2+} reabsorption was unaltered in the DCT and CNT as indicated by real-time reverse transcription-PCR, Western blotting, and immunohistochemistry for TRPV5 and NCX1 and micropuncture experiments.[120] Micropuncture data indicated that a reduced glomerular filtration and enhanced fractional reabsorption of Na^+ and Ca^{2+} upstream of the DCT provide compensation for the Na^+ transport defect in the DCT and contribute to the hypocalciuria.[120] Taken together, these data support the hypothesis that enhanced proximal tubular Na^+ transport as a consequence of ECV contraction stimulates paracellular Ca^{2+} transport and comprises the molecular mechanism explaining thiazide-induced hypocalciuria. Furthermore, thiazide-induced hypocalciuria could still be elicited in TRPV5 knockout mice, in which active Ca^{2+} reabsorption is virtually abolished.[121] Additional experiments investigating the time dependency of the thiazide effects demonstrated that Ca^{2+} excretion is unaltered during the natriuretic response following HCTZ administration, again indicating that direct stimulation of active Ca^{2+} reabsorption by inhibition of NCC does not occur. In contrast, a profound decrease in urinary Ca^{2+} excretion followed the initial natriuresis and, importantly, paralleled a reduced net Na^+ excretion.[121] Taken together, a long-standing question in physiology and medicine seems resolved indicating that enhanced proximal tubular Na^+ transport as a consequence of ECV contraction, stimulates paracellular Ca^{2+} transport and constitutes the molecular mechanism underlying thiazide-induced hypocalciuria.

Characterization of TRPV5 Knockout Mice

TRPV5 knockout mice have been generated by genetic ablation of TRPV5 to investigate the requirement of TRPV5 functioning in renal and intestinal Ca^{2+} (re)absorption.[67] Interestingly, analysis of 24-hour urine demonstrated that TRPV5 knockout mice exhibit a major calciuresis, since significantly more Ca^{2+} was excreted in the urine compared to wild-type littermates. The urinary Ca^{2+} concentration of the knockout mice reached 20 mM compared to 6 mM for control littermates. Serum analysis demonstrated that TRPV5 knockout mice are normocalcemic, but have significantly elevated 1,25-$(OH)_2D_3$ levels compared to TRPV5 wild-type mice.

As indicated TRPV5 knockout mice display hypercalciuria from impaired active Ca^{2+} reabsorption, but also hyperphosphaturia, polyuria and increased urinary acidification.[67] The latter two adaptations seem highly beneficial because they facilitate the excretion of large quantities of Ca^{2+} by reducing the potential risk of Ca^{2+} precipitations. It has been postulated that a high luminal Ca^{2+} concentration activates the Ca^{2+}-sensing receptor in the apical membrane of the IMCD.[122] The consistent polyuria in hypercalciuric TRPV5 knockout mice, noted by a substantial decrease in urinary osmolality, is caused by downregulation of renal AQP2 water channels, possibly a result of activating the Ca^{2+}-sensing receptor along the luminal membrane of the CD.[123] Furthermore, gene ablation of the collecting duct-specific B1 subunit of H^+-ATPase in TRPV5 knockout mice abolishes enhanced urinary acidification, which resulted in severe tubular precipitations of Ca^{2+}-phosphate in the renal medulla.[123] Thus, in TRPV5 knockout mice, activation of the renal Ca^{2+}-sensing receptor promotes H^+-ATPase-mediated H^+ excretion and downregulation of AQP2, leading to urinary acidification and polyuria, respectively.

To identify the exact defective Ca^{2+} reabsorption site along the nephron in TRPV5 knockout mice *in vivo* micropuncture studies were performed that combine classical and new research tools in a way that promises to yield important new insights into single-nephron function. Quantitative free-flow collections of tubular fluid revealed unaffected Ca^{2+} reabsorption in TRPV5 knockout mice up to the last surface loop of the late proximal tubule. In contrast, mean Ca^{2+} delivery to puncturing sites within the DCT and CNT was significantly enhanced in TRPV5 knockout mice. Because K^+ secretion occurs along these nephron sites the distal luminal potassium concentration was used as an indicator of the distal collection site. Based on the shape of the relationship between distal luminal K^+ concentration and fractional Ca^{2+} delivery it is evident that in contrast to TRPV5 wild-type mice, fractional Ca^{2+} delivery increases with an increased K^+ concentration indicating a defective Ca^{2+} reabsorption in the DCT and CNT which is consistent with the localization of TRPV5.

Remarkably, inactivation of the TRPV5 gene was accompanied by a decrease in the renal calbindin-D_{28K} and NCX1 mRNA expression. Because transepithelial

Ca^{2+} transport in DCT and CNT was abolished in TRPV5 knockout mice, the simultaneous decrease in calbindin-D_{28K} and NCX1 mRNA levels, in the presence of elevated 1,25-$(OH)_2D_3$ levels, suggests a regulatory mechanism primarily controlled by TRPV5. This means that TRPV5 or the Ca^{2+} influx through TRPV5 possibly controls the transcription of the other Ca^{2+} transport genes including calbindin-D_{28K} and NCX1. Although down-regulation of renal calbindin-D_{28K} is secondary to TRPV5 ablation in the TRPV5 knockout mice, the reduced calbindin-D_{28K} level may further augment the severity of the hypercalciuria. In this respect, it is interesting to compare the hypercalciuria in calbindin-D_{28K} and TRPV5 knockout mice. Calbindin-D_{28K} knockout mice fed a regular Ca^{2+} diet displayed a ~2 fold increase in the urinary Ca^{2+} excretion compared to wild-type littermates,[124] whereas TRPV5 knockout mice fed the same Ca^{2+} diet excreted ~6 times more Ca^{2+} in the urine compared to controls.[67] These findings underscore the gatekeeper function of TRPV5 in the process of Ca^{2+} reabsorption.

In general, $Ca_2{}^+$ hyperabsorption by the small intestine is favored as compensation for renal Ca^{2+} wasting. Ca^{2+} absorption was assessed by measuring serum $^{45}Ca^{2+}$ at early time points after oral gavage. A significant increase in the rate of $^{45}Ca^{2+}$ absorption was observed in TRPV5 knockout mice compared to wild-type mice indicating a compensatory role of the small intestine. In addition, TRPV6 and also calbindin-D_{9K} expression levels were significantly up-regulated in TRPV5 knockout mice consistent with this increased Ca^{2+} absorption. These intestinal adaptations likely result from the elevated 1,25-$(OH)_2D_3$ levels observed in TRPV5 knockout mice.

In addition to kidney and intestine, also bone showed a clear phenotype in TRPV5 knockout mice. Microcomputed tomography analyses of the femur demonstrated that trabecular thickness in the femoral head of TRPV5 knockout mice was significantly reduced compared to wild-type mice. Trabecular bone volume, tissue volume and bone fraction were not different between the genotypes. This could not be explained by a difference in trabecular number. Alternatively, it is possible that the trabeculae are longer, i.e., protrude further into the bone marrow cavity and thereby compensate for reduced trabecular thickness. Analyses of the diaphysis showed that cortical bone volume, cortical volume fraction and cortical bone thickness were reduced in TRPV5 knockout versus wild-type mice.

These data from TRPV5 knockout mice unequivocally established that TRPV5 is the gatekeeper in active Ca^{2+} reabsorption. Ablation of the TRPV5 gene seriously disturbs renal Ca^{2+} handling, causing increased 1,25-$(OH)_2D_3$ plasma levels, Ca^{2+} hyperabsorption and reduced bone formation. These deficiencies in Ca^{2+} handling have been reported frequently in patients with idiopathic hypercalciuria, in which TRPV5 dysfunction could contribute to the pathogenesis. Finally, the increased 1,25-$(OH)_2D_3$ levels and effects on bone structure indicate that alterations in TRPV5 may have implications for age-related bone disorders, including osteoporosis.

Acknowledgements

The research projects of the authors were supported by the Dutch Kidney foundation, the Dutch Organization of Scientific Research, the Human Frontiers Science Program and European Science Foundation.

References

[1] Abramowitz J, Birnbaumer L. Physiology and pathophysiology of canonical transient receptor potential channels. Faseb J 2009;23:297–328.
[2] Aicher L, Meier G, Norcross AJ, et al. Decrease in kidney calbindin-D 28 kDa as a possible mechanism mediating cyclosporine A- and FK-506-induced calciuria and tubular mineralization. Biochem Pharmacol 1997;53:723–31.
[3] Andreasen D, Jensen BL, Hansen PB, et al. The alpha(1G)-subunit of a voltage-dependent Ca^{2+} channel is localized in rat distal nephron and collecting duct. Am J Physiol Renal Physiol 2000;279:F997–1005.
[4] Bacskai BJ, Friedman PA. Activation of latent Ca^{2+} channels in renal epithelial cells by parathyroid hormone. Nature 1990;347:388–91.
[5] Barley NF, Howard A, O'Callaghan D, et al. Epithelial calcium transporter expression in human duodenum. Am J Physiol Gastrointest Liver Physiol 2001;280:G285–90.
[6] Bindels RJ, Hartog A, Abrahamse SL, et al. Effects of pH on apical calcium entry and active calcium transport in rabbit cortical collecting system. Am J Physiol 1994;266:F620–7.
[7] Boros S, Bindels RJ, Hoenderop JG. Active Ca^{2+} reabsorption in the connecting tubule. Pflugers Arch 2009;458:99–109.
[8] Cha SK, Ortega B, Kurosu H, et al. Removal of sialic acid involving Klotho causes cell-surface retention of TRPV5 channel via binding to galectin-1. Proceedings of the National Academy of Sciences of the United States of America 2008;105:9805–10.
[9] Chang Q, Hoefs S, van der Kemp AW, et al. The beta-glucuronidase klotho hydrolyzes and activates the TRPV5 channel. Science 2005;310:490–3 [New York, NY].
[10] Chang Q, Gyftogianni E, van de Graaf SF, et al. Molecular determinants in TRPV5 channel assembly. J Biol Chem 2004;279:54304–11.
[11] Chubanov V, Waldegger S, Mederos y Schnitzler M, et al. Disruption of TRPM6/TRPM7 complex formation by a mutation in the TRPM6 gene causes hypomagnesemia with secondary hypocalcemia. Proc Natl Acad Sci U S A 2004;101:2894–9.
[12] Clapham DE. TRP channels as cellular sensors. Nature 2003;426:517–24.
[13] Clapham DE, Runnels LW, Strubing C. The trp ion channel family. Nat Rev Neurosci 2001;2:387–96.
[14] Clapham DE, Montell C, Schultz G, et al. International Union of Pharmacology. XLIII. Compendium of voltage-gated ion channels: transient receptor potential channels. Pharmacol Rev 2003;55:591–6.

[15] Costanzo LS, Windhager EE. Calcium and sodium transport by the distal convoluted tubule of the rat. Am J Physiol 1978;235: F492–506.
[16] Dardenne O, Prud'homme J, Arabian A, et al. Targeted inactivation of the 25-hydroxyvitamin D_3-1(alpha)-hydroxylase gene (CYP27B1) creates an animal model of pseudovitamin D-deficiency rickets. Endocrinology 2001;142:3135–41.
[17] de Groot T, Lee K, Langeslag M, et al. Parathyroid hormone activates TRPV5 via PKA-dependent phosphorylation. J Am Soc Nephrol 2009;20:1693–704.
[18] Delmas P, Padilla F, Osorio N, et al. Polycystins, calcium signaling, and human diseases. Biochem Biophys Res Commun 2004;322:1374–83.
[19] Dodier Y, Banderali U, Klein H, et al. Outer pore topology of the ECaC-TRPV5 channel by cysteine scan mutagenesis. J Biol Chem 2004;279:6853–62.
[20] Du J, Sours-Brothers S, Coleman R, et al. Canonical transient receptor potential 1 channel is involved in contractile function of glomerular mesangial cells. J Am Soc Nephrol 2007;18: 1437–45.
[21] Ellison DH. Divalent cation transport by the distal nephron: insights from Bartter's and Gitelman's syndromes. Am J Physiol Renal Physiol 2000;279:F616–25.
[22] Embark HM, Setiawan I, Poppendieck S, et al. Regulation of the epithelial Ca^{2+} channel TRPV5 by the NHE regulating factor NHERF2 and the serum and glucocorticoid inducible kinase isoforms SGK1 and SGK3 expressed in Xenopus oocytes. Cell Physiol Biochem 2004;14:203–12.
[23] Erler I, Hirnet D, Wissenbach U, et al. Ca^{2+}-selective transient receptor potential V channel architecture and function require a specific ankyrin repeat. J Biol Chem 2004;279:34456–63.
[24] Facemire CS, Mohler PJ, Arendshorst WJ. Expression and relative abundance of short transient receptor potential channels in the rat renal microcirculation. Am J Physiol Renal Physiol 2004;286:F546–51.
[25] Fixemer T, Wissenbach U, Flockerzi V, et al. Expression of the Ca^{2+}-selective cation channel TRPV6 in human prostate cancer: a novel prognostic marker for tumor progression. Oncogene 2003;22:7858–61.
[26] Friedman PA. Codependence of renal calcium and sodium transport. Annu Rev Physiol 1998;60:179–97.
[27] Friedman PA, Coutermarsh BA, Kennedy SM, et al. Parathyroid hormone stimulation of calcium transport is mediated by dual signaling mechanisms involving protein kinase A and protein kinase C. Endocrinology 1996;137:13–20.
[28] Gkika D, Mahieu F, Nilius B, et al. 80K-H as a new Ca^{2+} sensor regulating the activity of the epithelial Ca^{2+} channel transient receptor potential cation channel V5 (TRPV5). J Biol Chem 2004;279:26351–7.
[29] Gkika D, Topala CN, Chang Q, et al. Tissue kallikrein stimulates Ca(2 +) reabsorption via PKC-dependent plasma membrane accumulation of TRPV5. Embo J 2006;25:4707–16.
[30] Goel M, Sinkins WG, Zuo CD, et al. Identification and localization of TRPC channels in the rat kidney. Am J Physiol Renal Physiol 2006;290:F1241–52.
[31] Goel M, Sinkins WG, Zuo CD, et al. Vasopressin-induced membrane trafficking of TRPC3 and AQP2 channels in cells of the rat renal collecting duct. American journal of physiology 2007;293:F1476–88.
[32] Grimm C, Kraft R, Sauerbruch S, et al. Molecular and functional characterization of the melastatin-related cation channel TRPM3. J Biol Chem 2003;278:21493–501.
[33] Hanaoka K, Qian F, Boletta A, et al. Co-assembly of polycystin-1 and -2 produces unique cation-permeable currents. Nature 2000;408:990–4.
[34] Hess P. Calcium channels in vertebrate cells. Annu Rev Neurosci 1990;13:337–56.
[35] Hoenderop JG, Nilius B, Bindels RJ. Molecular mechanisms of active Ca^{2+} reabsorption in the distal nephron. Ann Rev Physiol 2002;64:529–49.
[36] Hoenderop JG, Nilius B, Bindels RJ. Calcium absorption across epithelia. Physiol Rev 2005;85:373–422.
[37] Hoenderop JG, van der Kemp AW, Hartog A, et al. Molecular identification of the apical Ca^{2+} channel in 1, 25-dihydroxyvitamin D_3-responsive epithelia. J Biol Chem 1999;274:8375–8.
[38] Hoenderop JG, Vennekens R, Muller D, et al. Function and expression of the epithelial Ca^{2+} channel family: comparison of the mammalian epithelial Ca^{2+} channel 1 and 2. J Physiol 2001;537:747–61.
[39] Hoenderop JG, Dardenne O, van Abel M, et al. Modulation of renal Ca^{2+} transport protein genes by dietary Ca^{2+} and 1,25-dihydroxyvitamin D_3 in 25-hydroxyvitamin D_3-1a-hydroxylase knockout mice. Faseb J 2002;16:1398–406.
[40] Hoenderop JG, Voets T, Hoefs S, et al. Homo- and heterotetrameric architecture of the epithelial Ca^{2+} channels TRPV5 and TRPV6. Embo J 2003;22:776–85.
[41] Hoenderop JG, Voets T, Hoefs S, et al. Homo- and heterotetrameric architecture of the epithelial Ca^{2+} channels, TRPV5 and TRPV6. Embo J 2003;22:776–85.
[42] Hoenderop JG, Muller D, Van Der Kemp AW, et al. Calcitriol controls the epithelial calcium channel in kidney. J Am Soc Nephrol 2001;12:1342–9.
[43] Hoenderop JG, van Leeuwen JP, van der Eerden BC, et al. Renal Ca^{2+} wasting, hyperabsorption, and reduced bone thickness in mice lacking TRPV5. J Clin Invest 2003;112:1906–14.
[44] Hsu YJ, Dimke H, Schoeber JP, et al. Testosterone increases urinary calcium excretion and inhibits expression of renal calcium transport proteins. Kidney International 2010;77: 601–8.
[45] Jean K, Bernatchez G, Klein H, et al. The role of aspartate residues in Ca^{2+} affinity and permeation of the distal ECaC1 channel. Am J Physiol 2002;282:C665–72.
[46] Jiang Y, Ferguson WB, Peng JB. WNK4 enhances TRPV5-mediated calcium transport: potential role in hypercalciuria of familial hyperkalemic hypertension caused by gene mutation of WNK4. Am J Physiol Renal Physiol 2007;292:F545–54.
[47] Konrad M, Schlingmann KP, Gudermann T. Insights into the molecular nature of magnesium homeostasis. Am J Physiol Renal Physiol 2004;286:F599–605.
[48] Kurosu H, Yamamoto M, Clark JD, et al. Suppression of aging in mice by the hormone Klotho. Science 2005;309:1829–33 [New York, NY].
[49] Lambers TT, Weidema AF, Nilius B, et al. Regulation of the mouse epithelial Ca^{2+} channel TRPV6 by the Ca^{2+}-sensor calmodulin. J Biol Chem 2004;279:28855–61.
[50] Lee CT, Chen HC, Lai LW, et al. Effects of furosemide on renal calcium handling. Am J Physiol Renal Physiol 2007;293: F1231–7.
[51] Lee J, Cha SK, Sun TJ, et al. PIP2 activates TRPV5 and releases its inhibition by intracellular Mg^{2+}. J Gen Physiol 2005;126: 439–51.
[52] Lee N, Chen J, Sun L, et al. Expression and characterization of human transient receptor potential melastatin 3 (hTRPM3). J Biol Chem 2003;278:20890–7.
[53] Liedtke W, Friedman JM. Abnormal osmotic regulation in trpv4-/- mice. Proc Natl Acad Sci U S A 2003;100:13698–703.
[54] Liedtke W, Choe Y, Marti-Renom MA, et al. Vanilloid receptor-related osmotically activated channel (VR-OAC), a candidate vertebrate osmoreceptor. Cell 2000;103:525–35.

[55] Lintschinger B, Balzer-Geldsetzer M, Baskaran T, et al. Coassembly of Trp1 and Trp3 proteins generates diacylglycerol- and Ca^{2+}-sensitive cation channels. J Biol Chem 2000;275: 27799–805.
[56] Loffing J, Vallon V, Loffing-Cueni D, et al. Altered renal distal tubule structure and renal Na^+ and Ca^{2+} handling in a mouse model for Gitelman's syndrome. J Am Soc Nephrol 2004;15: 2276–88.
[57] Lu P, Boros S, Chang Q, et al. The beta-glucuronidase klotho exclusively activates the epithelial Ca2 + channels TRPV5 and TRPV6. Nephrol Dial Transplant 2008;23:3397–402.
[58] Minke B, Cook B. TRP channel proteins and signal transduction. Physiol Rev 2002;82:429–72.
[59] Montell C. Physiology, phylogeny, and functions of the TRP superfamily of cation channels. Sci STKE 2001;90:re1. 2001 Jul 10.
[60] Montell C. Mg^{2+} homeostasis: the Mg^{2+}nificent TRPM chanzymes. Curr Biol 2003;13:R799–801.
[61] Niemeyer BA, Bergs C, Wissenbach U, et al. Competitive regulation of CaT-like-mediated Ca^{2+} entry by protein kinase C and calmodulin. Proc Natl Acad Sci U S A 2001;98:3600–5.
[62] Nijenhuis T, Hoenderop JG, Bindels RJ. Downregulation of Ca^{2+} and Mg^{2+} transport proteins in the kidney explains tacrolimus (FK506)-induced hypercalciuria and hypomagnesemia. J Am Soc Nephrol 2004;15:549–57.
[63] Nijenhuis T, Hoenderop JG, van der Kemp AW, et al. Localization and regulation of the epithelial Ca^{2+} channel TRPV6 in the kidney. J Am Soc Nephrol 2003;14:2731–40.
[64] Nijenhuis T, Hoenderop JG, Loffing J, et al. Thiazide-induced hypocalciuria is accompanied by a decreased expression of Ca^{2+} transporting proteins in the distal tubule. Kidney Int 2003;64:555–64.
[65] Nijenhuis T, Vallon V, van der Kemp AW, et al. Enhanced passive Ca2 + reabsorption and reduced Mg2 + channel abundance explains thiazide-induced hypocalciuria and hypomagnesemia. J Clin Invest 2005;115:1651–8.
[66] Nilius B, Voets T. Diversity of TRP channel activation. Novartis Found Symp 2004;258:140–9 [discussion 149-159, 263-146]
[67] Nilius B, Vennekens R, Prenen J, et al. Whole-cell and single channel monovalent cation currents through the novel rabbit epithelial Ca^{2+} channel ECaC. J Physiol 2000;527:239–48.
[68] Nilius B, Vennekens R, Prenen J, et al. The single pore residue D542 determines Ca^{2+} permeation and Mg^{2+} block of the epithelial Ca^{2+} channel. J Biol Chem 2001;276:1020–5.
[69] Nilius B, Prenen J, Vennekens R, et al. Pharmacological modulation of monovalent cation currents through the epithelial Ca^{2+} channel ECaC1. British J Pharmacol 2001;134:453–62.
[70] Nilius B, Prenen J, Hoenderop JG, et al. Fast and slow inactivation kinetics of the Ca^{2+} channels ECaC1 and ECaC2 (TRPV5 and TRPV6). Role of the intracellular loop located between transmembrane segments 2 and 3. J Biol Chem 2002;277: 30852–8.
[71] Nilius B, Weidema AF, Prenen J, et al. The carboxyl-terminus of the epithelial Ca^{2+} channel ECaC1 is involved in Ca^{2+}-dependent inactivation. Pflugers Arch 2003;445:584–8.
[72] Nordin BE, Need AG, Morris HA, et al. Evidence for a renal calcium leak in postmenopausal women. J Clin Endocrinol Metab 1991;72:401–7.
[73] Palmada M, Embark HM, Yun C, et al. Molecular requirements for the regulation of the renal outer medullary K^+ channel ROMK1 by the serum- and glucocorticoid-inducible kinase SGK1. Biochem Biophys Res Commun 2003;311:629–34.
[74] Panda DK, Miao D, Tremblay ML, et al. Targeted ablation of the 25-hydroxyvitamin D 1alpha -hydroxylase enzyme: evidence for skeletal, reproductive, and immune dysfunction. Proc Natl Acad Sci USA 2001;98:7498–503.
[75] Peng JB, Brown EM, Hediger MA. Apical entry channels in calcium-transporting epithelia. News Physiol Sci 2003;18: 158–63.
[76] Peng JB, Chen XZ, Berger UV, et al. A rat kidney-specific calcium transporter in the distal nephron. J Biol Chem 2000;275: 28186–94.
[77] Peng JB, Chen XZ, Berger UV, et al. Molecular cloning and characterization of a channel-like transporter mediating intestinal calcium absorption. J Biol Chem 1999;274:22739–46.
[78] Peng JB, Chen XZ, Berger UV, et al. Human calcium transport protein CaT1. Biochem Biophys Res Commun 2000;278: 326–32.
[79] Peng JB, Zhuang L, Berger UV, et al. CaT1 expression correlates with tumor grade in prostate cancer. Biochem Biophys Res Commun 2001;282:729–34.
[80] Picard N, Van Abel M, Campone C, et al. Tissue kallikrein-deficient mice display a defect in renal tubular calcium absorption. J Am Soc Nephrol 2005;16:3602–10.
[81] Prince RL, Smith M, Dick IM, et al. Prevention of postmenopausal osteoporosis. A comparative study of exercise, calcium supplementation, and hormone-replacement therapy. N Engl J Med 1991;325:1189–95.
[82] Reid IR. Glucocorticoid osteoporosis–mechanisms and management. Eur J Endocrinol 1997;137:209–17.
[83] Reilly RF, Ellison DH. Mammalian distal tubule: physiology, pathophysiology, and molecular anatomy. Physiol Rev 2000;80: 277–313.
[84] Renkema KY, Velic A, Dijkman HB, et al. The calcium-sensing receptor promotes urinary acidification to prevent nephrolithiasis. J Am Soc Nephrol 2009;20:1705–13.
[85] Rodino MA, Shane E. Osteoporosis after organ transplantation. Am J Med 1998;104:459–69.
[86] Rubtsov AM, Lopina OD. Ankyrins. FEBS Lett 2000;482:1–5.
[87] Sands JM, Naruse M, Baum M, et al. Apical extracellular calcium/polyvalent cation-sensing receptor regulates vasopressin-elicited water permeability in rat kidney inner medullary collecting duct. J Clin Invest 1997;99:1399–405.
[88] Schindl R, Kahr H, Graz I, et al. Store depletion-activated CaT1 currents in rat basophilic leukemia mast cells are inhibited by 2-aminoethoxydiphenyl borate. Evidence for a regulatory component that controls activation of both CaT1 and CRAC (Ca^{2+} release-activated Ca^{2+} channel) channels. J Biol Chem 2002;277:26950–8.
[89] Schlingmann KP, Weber S, Peters M, et al. Hypomagnesemia with secondary hypocalcemia is caused by mutations in TRPM6, a new member of the TRPM gene family. Nat Genet 2002;31:166–70.
[90] Schultheis PJ, Lorenz JN, Meneton P, et al. Phenotype resembling Gitelman's syndrome in mice lacking the apical Na^+-Cl^- cotransporter of the distal convoluted tubule. J Biol Chem 1998;273:29150–5.
[91] Sooy K, Kohut J, Christakos S. The role of calbindin and 1,25dihydroxyvitamin D_3 in the kidney. Curr Opin Nephrol Hypertens 2000;9:341–7.
[92] Strotmann R, Harteneck C, Nunnenmacher K, et al. OTRPC4, a nonselective cation channel that confers sensitivity to extracellular osmolarity. Nat Cell Biol 2000;2:695–702.
[93] Sullivan LP, Wallace DP, Grantham JJ. Epithelial transport in polycystic kidney disease. Physiol Rev 1998;78:1165–91.
[94] Suzuki M, Ohki G, Ishibashi K, et al. A single amino acid mutation results in a rapid inactivation of epithelial calcium channels. Biochem Biophys Res Commun 2002;291:278–85.
[95] Tan S, Lau K. Patch-clamp evidence for calcium channels in apical membranes of rabbit kidney connecting tubules. J Clin Invest 1993;92:2731–6.

[96] Tian W, Salanova M, Xu H, et al. Renal expression of osmotically responsive cation channel TRPV4 is restricted to water-impermeant nephron segments. Am J Physiol Renal Physiol 2004;287:F17–24.

[97] van Abel M, Hoenderop JG, van der Kemp AW, et al. Coordinated control of renal Ca(2+) transport proteins by parathyroid hormone. Kidney International 2005;68:1708–21.

[98] Van Abel M, Hoenderop JG, Dardenne O, et al. 1,25-dihydroxyvitamin D_3-independent stimulatory effect of estrogen on the expression of ECaC1 in the kidney. J Am Soc Nephrol 2002;13:2102–9.

[99] van Baal J, Hoenderop JG, Groenendijk M, et al. Hormone-stimulated Ca^{2+} transport in rabbit kidney: multiple sites of inhibition by exogenous ATP. Am J Physiol 1999;277:F899–906.

[100] Van Baal J, Yu A, Hartog A, et al. Localization and regulation by vitamin D of calcium transport proteins in rabbit cortical collecting system. Am J Physiol 1996;271:F985–93.

[101] van Cromphaut S, Dewerchin M, Hoenderop JG, et al. Active duodenal calcium absorption in vitamin D receptor-knock out mice: functional and molecular aspects. Proc Natl Acad Sci U S A 2001;98:13324–9.

[102] Van Cromphaut SJ, Rummens K, Stockmans I, et al. Intestinal calcium transporter genes are upregulated by estrogens and the reproductive cycle through vitamin D receptor-independent mechanisms. J Bone Miner Res 2003;18:1725–36.

[103] Van Cromphaut SJ, Dewerchin M, Hoenderop JG, et al. Duodenal calcium absorption in vitamin D receptor-knockout mice: functional and molecular aspects. Proc Natl Acad Sci U S A 2001;98:13324–9.

[104] van de Graaf SF, Chang Q, Mensenkamp AR, et al. Direct interaction with Rab11a targets the epithelial Ca^{2+} channels TRPV5 and TRPV6 to the plasma membrane. Molecular and cellular biology 2006;26:303–12.

[105] van de Graaf SF, Rescher U, Hoenderop JG, et al. TRPV5 is internalized via clathrin-dependent endocytosis to enter a Ca^{2+}-controlled recycling pathway. J Biol Chem 2008;283:4077–86.

[106] van de Graaf SF, Hoenderop JG, Gkika D, et al. Functional expression of the epithelial Ca^{2+} channels (TRPV5 and TRPV6) requires association of the S100A10-annexin 2 complex. Embo J 2003;22:1478–87.

[107] Vassilev PM, Peng JB, Hediger MA, et al. Single-channel activities of the human epithelial Ca^{2+} transport proteins CaT1 and CaT2. J Membr Biol 2001;184:113–20.

[108] Vassilev PM, Peng JB, Johnson J, et al. Inhibition of CaT1 channel activity by a noncompetitive IP_3 antagonist. Biochem Biophys Res Commun 2001;280:145–50.

[109] Vennekens R, Prenen J, Hoenderop JG, et al. Pore properties and ionic block of the rabbit epithelial calcium channel expressed in HEK 293 cells. J Physiol 2001;530:183–91.

[110] Vennekens R, Prenen J, Hoenderop JG, et al. Modulation of the epithelial Ca^{2+} channel ECaC by extracellular pH. Pflugers Arch 2001;442:237–42.

[111] Vennekens R, Hoenderop JG, Prenen J, et al. Permeation and gating properties of the novel epithelial Ca^{2+} channel. J Biol Chem 2000;275:3963–9.

[112] Voets T, Janssens A, Droogmans G, et al. Outer pore architecture of a Ca^{2+}-selective TRP channel. J Biol Chem 2004;279:15223–30.

[113] Voets T, Janssens A, Prenen J, et al. Mg^{2+}-dependent gating and strong inward rectification of the cation channel TRPV6. J Gen Physiol 2003;121:245–60.

[114] Voets T, Nilius B, van der Kemp AW, et al. TRPM6 forms the Mg^{2+} influx channel involved in intestinal and renal Mg^{2+} absorption. J Biol Chem 2004;279:19–25.

[115] Voets T, Prenen J, Fleig A, et al. CaT1 and the calcium release-activated calcium channel manifest distinct pore properties. J Biol Chem 2001;276:47767–70.

[116] Walder RY, Landau D, Meyer P, et al. Mutation of TRPM6 causes familial hypomagnesemia with secondary hypocalcemia. Nat Genet 2002;31:171–4.

[117] Weber K, Erben RG, Rump A, et al. Gene structure and regulation of the murine epithelial calcium channels ECaC1 and 2. Biochem Biophys Res Commun 2001;289:1287–94.

[118] Weinman EJ, Eknoyan G. Chronic effects of chlorothiazide on reabsorption by the proximal tubule of the rat. Clin Sci Mol Med 1975;49:107–13.

[119] Wissenbach U, Niemeyer BA, Fixemer T, et al. Expression of CaT-like, a novel calcium-selective channel, correlates with the malignancy of prostate cancer. J Biol Chem 2001;276:19461–8.

[120] Wood RJ, Tchack L, Taparia S. 1,25-Dihydroxyvitamin D_3 increases the expression of the CaT1 epithelial calcium channel in the Caco-2 human intestinal cell line. BMC Physiology 2001;1:1–11.

[121] Yeh BI, Sun TJ, Lee JZ, et al. Mechanism and molecular determinant for regulation of rabbit transient receptor potential type 5 (TRPV5) channel by extracellular pH. J Biol Chem 2003;278:51044–52.

[122] Yoder BK, Hou X, Guay-Woodford LM. The polycystic kidney disease proteins, polycystin-1, polycystin-2, polaris, and cystin, are co-localized in renal cilia. J Am Soc Nephrol 2002;13:2508–16.

[123] Yu AS, Hebert SC, Brenner BM, et al. Molecular characterization and nephron distribution of a family of transcripts encoding the pore-forming subunit of Ca^{2+} channels in the kidney. Proc Natl Acad Sci USA 1992;89:10494–8.

[124] Yu AS, Boim M, Hebert SC, et al. Molecular characterization of renal calcium channel beta-subunit transcripts. Am J Physiol 1995;268:F525–31.

[125] Yun CC. Palmada M, Embark HM, et al. The serum and glucocorticoid-inducible kinase SGK1 and the Na^+/H^+ exchange regulating factor NHERF2 synergize to stimulate the renal outer medullary K^+ channel ROMK1. J Am Soc Nephrol 2002;13:2823–30.

[126] Zhang W, Na T, Peng JB. WNK3 positively regulates epithelial calcium channels TRPV5 and TRPV6 via a kinase-dependent pathway. Am J Physiol Renal Physiol 2008;295:F1472–84.

[127] Zhuang L, Peng JB, Tou L, et al. Calcium-Selective Ion Channel, CaT1, is apically localized in gastrointestinal tract epithelia and is aberrantly expressed in human malignancies. Lab Invest 2002;82:1755–64.

[128] Zobiack N, Rescher U, Ludwig C, et al. The annexin 2/S100A10 complex controls the distribution of transferrin receptor-containing recycling endosomes. Mol Biol Cell 2003;14:4896–908.

This page intentionally left blank

CHAPTER

63

The Calcium-Sensing Receptor

Edward M. Brown[1], *Steven C. Hebert*[2], *Daniela Riccardi*[3] *and John P. Geibel*[2]

[1]Brigham and Women's Hospital and Harvard Medical School, Boston, Massachusetts, U.S.A.
[2]Yale University School of Medicine, New Haven, Connecticut, U.S.A.
[3]Cardiff University, Cardiff, Wales

Cell surface sensors for extracellular Ca^{2+} and Mg^{2+}[51] provide an important mechanism for the regulation of diverse physiological processes by extracellular divalent mineral ions.[53,190,402] These ion sensors function as "calciostats" for Ca^{2+} and/or Mg^{2+} that not only regulate divalent mineral metabolism at the level of the whole organism but also control a variety of other cellular processes (e.g., salt and water handing in various epithelia and cell proliferation-differentiation) in terrestrial and aquatic animals, as well as in plants.[51,177,301] This chapter will focus on the role of the extracellular calcium-sensing receptor (CaSR) in the mammalian parathyroid, kidney, and other tissues participating in divalent mineral ion homeostasis. The unique properties of the mammalian CaSR include: (1) Having extracellular Ca^{2+} and Mg^{2+} as its primary physiological ligands, establishing that ions can function as first messengers. (2) Responding with a millimolar EC_{50}, close to the normal plasma ionized Ca^{2+} concentration, but several orders of magnitude higher than that for ligands of other G protein–coupled receptors. (3) Possessing a remarkable ability to detect small deviations from the normal ionized calcium concentration of 1.1–1.3 mM, making it an ideal sensor for Ca^{2+}, functioning as a "calciostat."

The identification of inherited disorders due to activating or inactivating mutations of the CaSR, basic research in CaSR biology, the development of CaSR-active compounds (calcimimetics), and the results from clinical trials of calcimimetics have established the biological roles of this receptor in mineral ion homeostasis and have suggested roles of the CaSR in several non-Ca^{2+} homeostatic processes,[1,147,201] (also see reviews[147,402]). The reader is referred to Chapter 65 and other chapters in the section, "Regulation and Disorders of Calcium Homeostasis," for additional information and background.

LIGAND BINDING: THE CaSR IS A Ca^{2+}/Mg^{2+} AND AN "EXTRACELLULAR ENVIRONMENT" SENSOR

The CaSR is a member of class C of the G protein–coupled receptor (GPCR) superfamily. Class C receptors include the extracellular Ca^{2+}-sensing receptors (CaSRs and perhaps GPRC6A), the metabotropic glutamate receptors, the GABAB receptors, the V3R pheromone receptors, the T1R taste receptors, and several orphan receptors (RAIG1, GPRC6B-5D, and GABABL).[40]

CaSR Agonists

The CaSR can be activated by Ca^{2+}, Mg^{2+} and certain other polycations (e.g., Gd^{3+}, polylysine, polyarginine, and neomycin[49,52,349]). These agonists are referred to as type I agonists as they can directly and independently activate the receptor (Fig. 63.1). CaSR activity can also be modulated by other substances or conditions that function by modifying the EC_{50} for extracellular Ca^{2+} (up or down); allosteric activators of the CaSR of this type are referred to as type II allosteric activators (Fig.63.1). Thus, type II activators require the presence

Seldin and Giebisch's The Kidney, Fifth Edition.
DOI: http://dx.doi.org/10.1016/B978-0-12-381462-3.00063-X

© 2013 Elsevier Inc. All rights reserved.

of extracellular Ca^{2+} and function as allosteric modifiers of Ca^{2+} affinity. Currently identified physiological type II agonists include polyamines (e.g., spermine),[349] L-amino acids (especially aromatic amino acids),[90] extracellular pH,[347] and extracellular ionic strength, primarily changes in NaCl concentration in a physiological context.[192,301,348] Increases in polyamine[349] or amino acid concentrations,[89] or isosmotic reductions in ionic strength[301,348] reduce the EC_{50} (increase the affinity) for extracellular Ca^{2+}. At a constant ionized Ca^{2+} concentration, these changes in the concentrations of type II agonists will increase activation of the CaSR. As a consequence, CaSR responses to changes in concentrations of divalent minerals or type I agonists must be viewed in the setting of a specific "extracellular environment" (i.e., presence or absence of polyamines and L-amino acids, pH, and ionic strength). Interestingly, the CaSR appears to have initially evolved as a salinity sensor in marine species where these organisms used the effects of ionic strength (salinity) on activation of the receptor by the Ca^{2+}/Mg^{2+} present in salt water to regulate tissue responses for salinity adaptation.[301] With the evolution of land-based tetrapods and the loss of the ocean reservoir of Ca^{2+}/Mg^{2+}, we see the first appearance of the parathyroid glands and parathyroid hormone (PTH), which are required for divalent mineral regulation of the internal "ocean" represented by the extracellular fluids (ECFs) of terrestrial organisms. Currently identified CaSR-active small molecules (calcimimetics and calcilytics) are used in the treatment of certain disorders of calcium homeostasis. They function as allosteric activators and antagonists, respectively, of the CaSR via the type II mechanism and therefore, require extracellular Ca^{2+} to act (Fig. 63.1).[46,307]

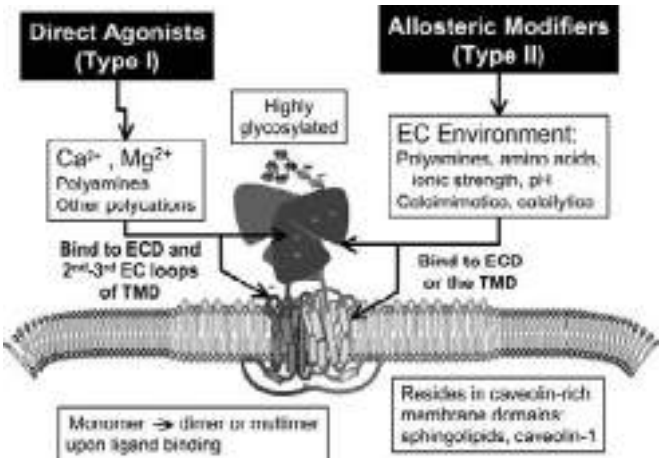
Direct Agonists (Type I)
Allosteric Modifiers (Type II)
Highly glycosylated
EC Environment:
Polyamines, amino acids, ionic strength, pH
Calcimimetics, calcilytics
Ca2+, Mg2+
Polyamines
Other polycations
Bind to ECD and 2nd-3rd EC loops of TMD
Bind to ECD or the TMD
Resides in caveolin-rich membrane domains: sphingolipids, caveolin-1
Monomer → dimer or multimer upon ligand binding

FIGURE 63.1 Schematic representation of the dimeric calcium-sensing receptor (CaSR) localized to caveolin-rich membrane domains. ECD, extracellular domain; TMD, transmembrane domain containing 7 α-helical membrane-spanning segments. Activators/agonists of the receptor can either be type I, which don't require the presence of Ca^{2+} to activate the CaSR, or as type II allosteric modifiers that potentiate the action of Ca^{2+}, which must be present at a concentration of ~1 mM for a type II agent to activate the receptor. Polyamines, such as spermine, act primarily in the type II mode, but can also serve as weak type I agonists. See text for discussion.

Ligand Binding to the CaSR

Class C GPCR receptors have a large (hundreds of residues) N-terminal extracellular domain (ECD) that is joined to the canonical 7-transmembrane (7-TM) domain typical of GPCRs. The ECDs of the class C-related metabotropic glutamate receptors[242,410] or the distantly related bacterial periplasmic nutrient-binding proteins (e.g., the maltose-binding protein (MBP))[397] form a bilobed structure that has a ligand binding region within the central cleft between these lobes (Fig. 63.2A). Following ligand binding, there is a

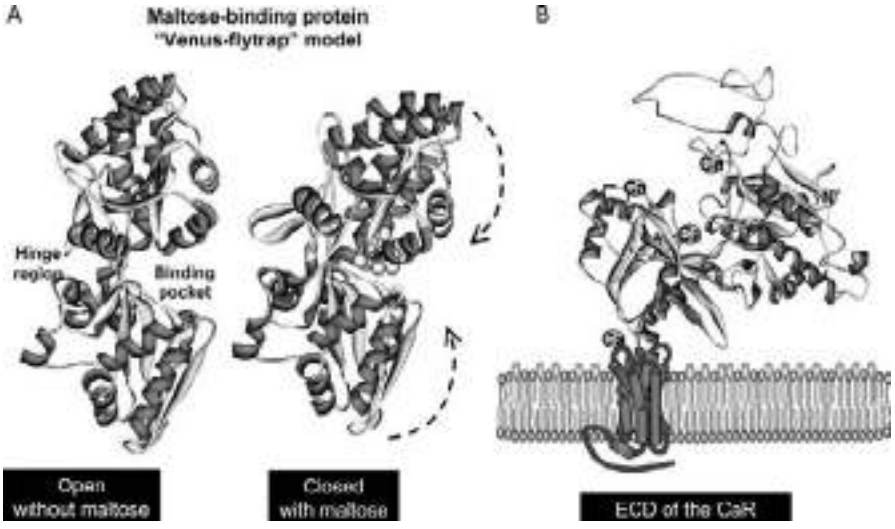

FIGURE 63.2 The Venus flytrap model of the extracellular domain of one monomer of the calcium-sensing receptor (CaSR). A: Structures of the bacterial periplasmic maltose-binding protein in the absence and present of ligand (yellow structure). Note the closing of the lobes around the ligand upon ligand binding (dashed arrows). B: Structural model of the human CaSR made by threading the human sequence through the extracellular domain of mGluR. Note the bilobed structure that is similar to the bacterial maltose-binding protein. Potential calcium interacting sites are shown. The best characterized of these is in the crevice between the two lobes of the VFT, which faces upward and to the left at about 10 o'clock. Structure colors: red = α helices; blue = β strands.

conformational change in the ECD, which results in the two lobes moving toward one another to enclose the ligand (Fig. 63.2A, Venus-flytrap model). This molecular motion in the ECD is thought to be translated into conformational changes in the 7-TM domain, leading to G-protein activation.[242,410]

The ligand-binding sites on class-C receptors, including the CaSR, are located on the ECD and, to a lesser extent, in the 7-TM domains.[39,242,410] While an x-ray crystal structure of the ECD of the CaSR has not been obtained, the ECD can be modeled[207,213,331] on the basis of the known structure of several metabotropic glutamate receptors.[410] This structural model is shown in Fig. 63.2B with the location of potential Ca^{2+}-interacting regions composed of negatively charged amino acid residues. In addition, three serine residues (S-147, S-169, and S-170) and proline-823 in the ECD are crucial for maximal responsiveness to extracellular Ca^{2+}.[205,389,451] Receptor activation by Ca^{2+} is greatly reduced by removal of the ECD, emphasizing the importance of negatively charged acidic (and other) residues in the ECD for the binding of polyvalent cations.[39,176,183,204,205,357,410] Additional acidic residues in the second and third extracellular loops in the 7-TM domain have also been suggested to participate in Ca^{2+}-binding interactions.[176,183,205,206,353] In contrast, the response to calcimimetics is retained when the ECD is removed from the CaSR,[183] indicating that these type II activators bind at a different site than does Ca^{2+}. Observations indicate that the critical sites for interaction of calcimimetics with the CaSR are located in the 7-TM domain, primarily the TM6−TM7 region,[206,331,353] with Glu837, at the outer end of TM7, serving as an "anchor" by binding the amino group in the aliphatic linker between the two hydrophobic ends of the molecule. In addition, negative allosteric modulators of the CaSR (calcilytics) have been identified that exhibit a binding site in the 7-TM domain of the CaSR that overlaps with but is not identical to that for the calcimimetics.[331]

The Concept of Superagonism for Agonist Binding to the Class C Receptors

As described previously, type II agonists (including calcimimetics) of the CaSR can act as allosteric enhancers or positive allosteric modulators.[339,382] It is clear that most GPCRs possess allosteric binding sites that can be recognized by small-molecule ligands.[279] GPCR class-C receptors, including the CaSR,[11,218,430] form dimers (or even multimers), and this intermolecular interaction is believed to play an important role in allosteric activation.[40,339] Type I ligand binding enhances dimerization of the CaSR associated with formation of intermolecular disulfide linkages.[13,155,352,430] Thus, most of the receptors on plasma membranes of cells are in the dimeric (and multimeric) form,[14] since cell surface CaSRs are exposed to millimolar concentrations of extracellular Ca^{2+}. Although the intermolecular disulfide links between ECDs are not essential for dimerization,[452] they play an important structural role and help to maintain the receptor in its inactive state in the absence of agonist. Initial dimerization takes place in the endoplasmic reticulum, and this interaction may be necessary for the receptor's transport to the cell surface.[337] Once on the cell surface, intermolecular interactions between CaSR monomers are essential for normal function of this receptor.[15] Specifically, in the presence of agonist, dimerization of the CaSR and other class C receptors appears to enhance downstream cellular signaling, providing "superagonism".[382] This dimer-driven superagonism, which can also be thought of a positive cooperativity, likely accounts for the ability of type II agonists (e.g., L-amino acids) to activate the receptor by an allosteric mechanism[298] and the remarkable ability of this receptor to detect small changes in ionized Ca^{2+} from the normal plasma Ca^{2+} of 1.1-1.3 mM (Ca^{2+}-Ca^{2+} allosteric enhancing effect). Given that the Hill coefficient of the dimeric CaSR is 3−4, it is likely that there are at least 2 binding sites for calcium on each of the two monomers,[213] resulting in the substantial degree of positive cooperativity needed for the receptor's exquisite sensitivity to small changes in Ca^{2+}. An intact COOH-terminus on the CaSR is also required for cell surface expression.[68,351]

Complex Signaling: the Receptor is Promiscuous

CaSR coupling to G-protein has been referred to as promiscuous, since type I ligands activate one or more of several G proteins (e.g., $G\alpha_{q11}$, $G\alpha_{i2-i3}$).[53,210,429] As with most GPCRs, the COOH-terminal tail of the CaSR and one or more intracellular loops are crucial for signal transduction.[68,351] The CaSR-generated cytosolic signal is a complex of phospholipase activation (PLC, $cPLA_2$, PLD) and the generation of diverse cellular second messengers (see[201,210,429] for reviews), $G\alpha_{q11}$–mediated PLC activation $\rightarrow\uparrow IP_3\rightarrow\uparrow$cytosolic Ca^{2+} concentration ($Ca^{2+}{}_i$) and $Ca^{2+}{}_i$ oscillations as well as $\rightarrow\uparrow DAG\rightarrow\uparrow PKC$; $G\alpha_i$-mediated $\rightarrow\downarrow$cAMP; $\uparrow$intracellular $Ca^{2+}\rightarrow\uparrow$phosphodiesterase (PDE)$\rightarrow\downarrow$cAMP; cytosolic (c)$PLA_2$ activation$\rightarrow\uparrow$arachidonic acid (AA)$\rightarrow\uparrow P_{450}\rightarrow\uparrow$20-HETE; phosphatidylinositol 3-kinase (PI3K)$\rightarrow PIP_3$; MAP kinases, such as ERK1/2, c-Jun activated N-terminal kinase (JNK), and p38 MAPK; filamin scaffolding of $G\alpha_q\rightarrow\uparrow$Lbc RhoGEF$\rightarrow\uparrow$Rho A GTPase leading to activation of a serum response element (SRE) and $G\alpha_{12/13}\rightarrow\uparrow$PLD$\rightarrow\uparrow$phosphatidic acid

(PA).[42,150,178,195,208,229,230,285,336,441,448] It remains unclear in many cases how this second messenger "soup" and related intracellular signaling pathways integrate to modulate cellular functions, such as PTH secretion or renal responses to extracellular Ca^{2+}. The ability of the CaSR to be modulated by such a wide variety of agonists and extracellular conditions likely accounts for its multifunctional nature in regulating divalent mineral balance as well as in modulating diverse cellular functions seemingly unrelated to mineral homeostasis. Examples of the latter include CaSR effects on salt and water transport by the kidney[186] and gastrointestinal epithelia.[147] The CaSR also provides proliferation-differentiation-apoptosis signals to certain epithelial cells (e.g., keratinocytes in the skin, mammary gland cells and colonocytes).[26,50,222]

BINDING PARTNERS OF THE CaSR

Several proteins have been shown to interact with the CaSR and can exert important effects on its function or trafficking. The receptor-activity-modifying proteins (RAMPs), RAMP-1 and RAMP-3, participate in the translocation of the CaSR to the plasma membrane in some cell types.[37] The CaSR on the cell surface exhibits little desensitization when exposed repeatedly to elevated levels of Ca^{2+}_o, at least in parathyroid cells. This resistance to desensitization is the consequence, at least in part, of its interaction with the large, actin-binding scaffold protein, filamin-A,[450] and is likely important to make sure that the CaSR is expressed at sufficient levels on the cell surface to enable it to continuously monitor and maintain a constant level of Ca^{2+}_o. Additional binding partners of the CaSR comprise the K^+ channels, Kir4.1 and Kir4.2, caveolin-1, and the E3 ubiquitin ligase, dorfin.[209] The functional consequences of these interactions remain to be fully elucidated, but Kir4.1 and Kir4.2 colocalize with the CaSR in the basolateral membrane of the distal nephron, and co-expression of the CaSR with these two channels in *X. laevis* oocytes decreases channel activity.[211] Dorfin likely participates in regulating the proteasomal degradation of the receptor.[209]

REGULATION OF CaSR GENE EXPRESSION

Several factors upregulate the expression of the CaSR gene; these include elevated levels of Ca^{2+}_o[447] and calcimimetics,[287] both of which act by stimulating the CaSR, $1,25(OH)_2D_3$ (through vitamin D responsive elements (VDRE) in the CaSR's two promoters, which reside within alternatively spliced regions of the first exon (exons 1A and B)),[60] the cytokines interleukin-1β[308] and interleukin-6,[61] and the chemokines MCP-1 and SDF-1α (which likely traffic intracellular receptor to the cell surface in the short term).[315] Because the CaSR also upregulates the VDR gene and activation of each gene upregulates its own expression,[268,287] there potentially could be synergistic interactions between the VDR and CaSR. For example, activation of the CaSR upregulates its own expression and that of the VDR; upregulation of the latter could potentiate vitamin D signaling via increased VDR occupancy (even without a change in the level of $1,25(OH)_2D_3$), thereby further stimulating CaSR expression and action, and so forth. Factors that downregulate CaSR gene expression include PTH and a high phosphate diet.[361] A reduction in CaSR expression also occurs in both primary (1°) hyperparathyroidism (HPT) and secondary (2°) HPT (e.g., in the setting of renal insufficiency) through incompletely defined mechanisms,[92,119,122,233,398] although a reduction in circulating $1,25(OH)_2D_3$ levels likely contributes in the setting of chronic kidney disease by decreasing CaSR gene expression.

OVERVIEW OF THE CaSR'S ROLE IN Ca^{2+} HOMEOSTASIS

The response of the Ca^{2+}_o homeostatic system to hypocalcemia illustrates the tightly integrated functions of the three key elements of the Ca^{2+}_o homeostatic system: (1) the CaSR, the principal sensor of Ca^{2+}_o, (2) the tissues that mediate the fluxes of Ca^{2+} into and out of the extracellular fluid (ECF) (e.g., bone, kidney and intestine), and (3) the calciotropic hormones regulating these fluxes (PTH, $1,25(OH)_2D_3$ and Ca^{2+}_o itself, serving its "hormone-like" role via the CaSR). Further details can be found in chapter 65. Hypocalcemia evokes PTH secretion by the parathyroid glands. The hypocalcemia-induced increase in the circulating PTH level exerts three key homeostatic actions on the kidney: (1) enhancing distal tubular reabsorption of Ca^{2+}, (2) promoting phosphaturia, and (3) stimulating the synthesis of 1,25-dihydroxyvitamin D_3 ($1,25(OH)_2D_3$) from its largely inactive precursor, 25-hydroxyvitamin D_3. Hypocalcemia also directly stimulates $1,25(OH)_2D_3$ production in the proximal tubule by an action that is likely CaSR-mediated.[409,433] The stimulation of renal Ca^{2+} retention by PTH takes place both in the cortical thick ascending limb of Henle's loop (CTAL)[186] and in the distal convoluted tubule (DCT),[10,139] as described in detail later.[43,104] Consequently, there is a "resetting" of Ca^{2+} reabsorption by the kidney, producing a shift to the right in the curve relating serum to urinary Ca^{2+} concentration so that more Ca^{2+} is reabsorbed at any given level of Ca^{2+}_o.[323] Elevated circulating

concentrations of $1,25(OH)_2D_3$ enhance: (1) gastrointestinal absorption of Ca^{2+}, (2) reabsorption of Ca^{2+} in the DCT,[199,200] and (3) release of skeletal Ca^{2+} in conjunction with the bone resorptive action of PTH. $1,25(OH)_2D_3$ also inhibits PTH production and its own synthesis in the proximal tubule via the VDR, as noted earlier.[48,300] The resultant translocation of Ca^{2+} into the extracellular fluid from GI tract and bone, combined with greater renal tubular reabsorption of Ca^{2+}, will, except when there is severe Ca^{2+} deficiency, restore Ca^{2+}_o to normal.

A more recently discovered hormone that regulates both calcium and phosphate homeostasis as well as the interactions between these homeostatic systems is fibroblast growth factor (FGF)-23. It is released principally by osteocytes (osteoblasts encased in bone during bone formation) in response to $1,25(OH)_2D_3$ and hyperphosphatemia,[221,384,387] and its exerts a potent phosphaturic action on the proximal tubule. FGF-23 inhibits both $1,25(OH)_2D_3$ production and PTH secretion, providing negative feedback control of $1,25(OH)_2D_3$ synthesis and the phosphaturic action of PTH. This rapidly developing field is reviewed elsewhere in this volume and in recent reviews.[221,384,387]

CaSR FUNCTION IN PARATHYROID

As just noted, the regulation by Ca^{2+}_o of PTH secretion by the parathyroid chief cells is a key component of the Ca^{2+}_o homeostatic system.[48,190] The molecular mechanism by which Ca^{2+}_o performs this feat was deduced by the cloning of the CaSR in 1993 in the laboratories of Brown and Hebert.[51] The CaSR senses the extracellular ionic activity of the divalent minerals, Ca^{2+} and Mg^{2+}, and translates this information, via the complex array of cellular signaling pathways described previously, to modify PTH secretion,[196,307] preproPTH mRNA levels via changes in its stability,[248,302] and parathyroid gland hyperplasia.[88,419] Genetic studies have demonstrated that the activity of this receptor determines the steady-state plasma calcium concentration in humans by regulating key elements in the calcium homeostatic system.[310,383]

CaSR Regulates PTH Secretion

The level and constancy of plasma ionized Ca^{2+} are set in large part by regulating the release of Ca^{2+} from bone via the actions of secreted PTH and $1,25(OH)_2D_3$ as well as by modulation of the Ca^{2+} excretion by the kidney, and, indirectly via the action of $1,25(OH)_2D_3$, intestinal calcium absorption, as noted above.[48,190] Figure 63.3 shows the typical inverse relationship between PTH secretion and plasma Ca^{2+}. In contrast there is a direct relationship between urinary Ca^{2+} excretion and plasma Ca^{2+} (Fig. 63.4). These effects of plasma ionized Ca^{2+} on PTH secretion and renal Ca^{2+} excretion are mediated by the CaSR. The role of the CaSR in divalent mineral homeostasis has been established by the identification and characterization of inherited hyper- or hypocalcemic disorders that result from CASR gene mutations (the official designation of the gene for the human CaSR is in all capital letters and italicized) (chromosome 3q13.3–21; Fig. 63.5).[48,174,182,324,404] *In vitro* studies in mammalian cells expressing normal or mutant CaSR proteins have confirmed that these receptor mutations alter the Ca^{2+} EC_{50} of the CaSR (CaSR

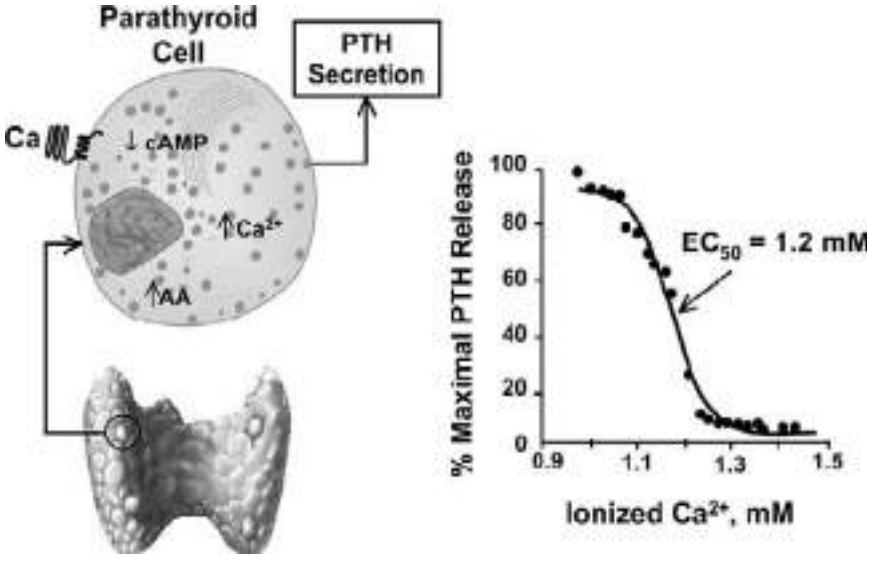

FIGURE 63.3 Inverse relationship between ionized serum calcium and parathyroid hormone (PTH) secretion. PTH secretion is maximal at low ionized calcium; raising calcium reduces secretion via several intracellular signaling pathways, including decreased levels of cAMP and increases in the products of PLA_2 and PLC action. Ionized calcium sensing by the parathyroid gland is mediated by the calcium-sensing receptor (CaSR). The EC_{50} for calcium-sensing by the gland is shown (1.2 mM Ca^{2+}_o); at normal ambient levels of Ca^{2+}_o, the gland is about 70–75% suppressed.

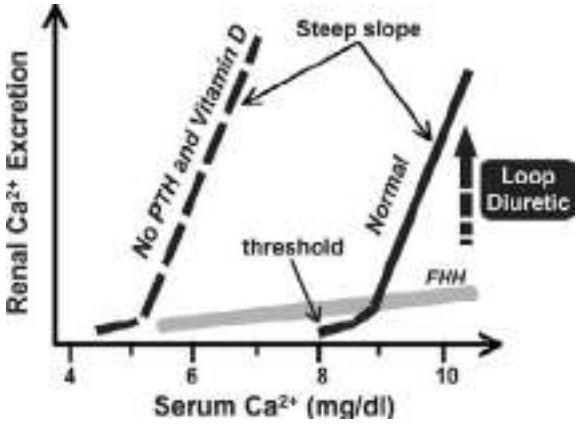

FIGURE 63.4 Direct relationship between serum calcium and renal calcium excretion demonstrating the calcium-sensing ability of the nephron (solid black curve). Note the steep relationship after reaching a threshold serum calcium concentration. In individuals with calcium-sensing receptor (CaSR)–inactivating mutations (FHH, familial hypocalciuric hypercalcemia), the relationship (solid gray line) is flatter than normal. This defect in the relationship is not due to a disturbance in calcium transport function of the thick ascending limb since loop diuretics can markedly increase calcium excretion in FHH. In the absence of parathyroid hormone and vitamin D, the threshold of serum calcium at which calcium excretion begins is reduced but the steep relationship between serum calcium and renal calcium excretion remains. The latter is due to the action of the CaSR.

refers to the CaSR protein).[13,252,292,325] Loss-of-function mutations in one or both of the CASR alleles result in hypercalcemic disorders due to upward resetting of the CaSR EC_{50} for ionized Ca^{2+} in both the parathyroid gland and kidney.[48,83,404] Autosomal dominant hypercalcemia, in which one CASR allele has an inactivating mutation, typically presents as a benign hypercalcemic disorder called familial hypocalciuric hypercalcemia (type 1 FHH; OMIM 145980, known as HHC1) or as symptomatic hypercalcemia in neonatal hyperparathyroidism (NHPT).[326] Two phenotypically similar conditions (HHC2, OMIM 145981; and HHC3, OMIM 600740) are linked to the long[256] and short arms of chromosome 19,[185] respectively, but the responsible genes have not yet been identified. Neonatal severe hyperparathyroidism (NSHPT) results from consanguineous unions in FHH families in which both alleles have inactivating mutations[48,274] or, occasionally, in families in which the two parents have different inactivating mutations (i.e., producing a compound heterozygous infant).[237] Infants with NSHPT exhibit severe hypercalcemia frequently necessitating total parathyroidectomy.[48,404] The hypercalcemia in these loss-of-function CaSR disorders is usually associated with reduced renal Ca^{2+} excretion,[246,275] rather than the increased Ca^{2+} excretion that is observed in other hypercalcemic states (e.g., 1° HPT and malignant hypercalcemia).[403] The abnormal renal response in FHH demonstrates the important role of the CaSR in the hypercalciuric response to hypercalcemia.

Homozygous CaSR knockout mice exhibit marked parathyroid hyperplasia and hyperparathyroidism and die soon after birth due to severe hypercalcemia (Fig. 63.5).[196] Support for the role of PTH in causing the severe and lethal hypercalcemia came form the observations that the lethal mouse phenotype can be rescued by knocking out the PTH gene[238] or by deletion of the *Gcm2* gene, which is the "master gene" needed for development of the parathyroid glands.[412] Studies carried out in the mice with knockout of PTH and/or the CaSR have documented the crucial role of CaSR-regulated PTH secretion as a "floor" preventing hypocalcemia, while the CaSR-mediated upregulation of renal Ca^{2+} excretion and stimulation of calcitonin secretion are an effective "ceiling" limiting increases in serum calcium in response to dietary or other forms of calcium load.[225] Indeed, the PTH knockout mice defend against hypercalcemia just as well as the wild type mice, even though they lack PTH and the ability to suppress it while hypercalcemic.

Autosomal dominant, gain-of-function (activating) mutations in the CaSR result in an opposite shift in plasma ionized calcium (i.e., hypocalcemia) due to downward resetting of the receptor EC_{50} (autosomal dominant hypocalcemia (ADH); OMIM 146200).[341] In some individuals with severe activating mutations, a renal salt wasting disorder with hypercalciuria has been observed that mimics the hyperprostaglandin E_2 syndrome (type V Bartter syndrome).[415,432] The latter confirms the important role of the CaSR in regulating renal Ca^{2+} handling and clearly demonstrates the importance of the CaSR in regulating salt transport in the thick ascending limb (TAL).[187] CASR gene polymorphisms also appear to contribute to the normal variation in steady-state plasma ionized Ca^{2+} concentration, at least in certain populations.[87,383] CaSR-activating or -inhibiting autoantibodies can result in autoimmune hypoparathyroidism[227,231] or an acquired syndrome mimicking FHH, called autoimmune hypocalciuric hypercalcemia, respectively.[232,270,317] Mice with an activating mutation in the CaSR exhibit a phenotype similar to that in patients with ADH.[203] All these various lines of evidence convincingly document the key role of the CaSR in mediating the effects of Ca^{2+} on PTH secretion.

In addition to reducing the secretion of PTH, activation of the CaSR increases the degradation of full length, biologically active PTH1-84 to PTH7-84 and smaller carboxyterminal fragments, thereby decreasing the secretion of intact PTH further still during hypercalcemia and, conversely, increasing it in the setting of hypocalcemia.[413]

CaSR Regulates Expression of the preproPTH Gene

Elevated levels of Ca^{2+}_o and calcimimetics not only inhibit PTH secretion but also decrease the levels of the mRNA encoding preproPTH;[302,365] this action of the calcimimetics proves the mediatory role of the CaSR in regulating preproPTH gene expression. The CaSR-mediated alteration in the level of preproPTH mRNA is the result of a change in preproPTH mRNA stability rather than in gene transcription per se. $1,25(OH)_2D_3$, in contrast, acts by a direct inhibitory action on the transcription of this gene.[391] Naveh-Many, Silver and coworkers have clarified the molecular mechanisms by which Ca^{2+}_o and the CaSR control the stability of preproPTH mRNA. Exposing parathyroid cells to elevated levels of Ca^{2+} activates the CaSR and, through a pathway that involves stimulation of calmodulin (CaM) and protein phosphatase 2B, post-translationally modifies and reduces the binding of the preproPTH mRNA stabilizing factor, AU-rich factor (AUF-1), to an AU-rich element in the 3′ untranslated region (UTR) of the preproPTH mRNA.[248] The loss of AUF-1 from this binding site permits a second, destablizing protein, K-homology splicing regulator protein (KSRP), to bind to the same site. KSRP subsequently interacts with and is activated by the peptidyl-prolyl isomerase, Pin-1, and, pari passu, recruits the endoribonuclease, PMR1, which is part of the RNA-cleaving exosome. PMR-1 then degrades prepro-PTH mRNA by cleaving it internally.[303,304]

CaSR Regulates Parathyroid Cellular Proliferation

Studies in humans with NSHPT[115] or in mice homozygous for knock out of the *Casr* gene (the symbols for mouse genes are italicized with only the first letter capitalized)[196] have proven the CaSR's importance in regulating parathyroid cellular proliferation. In both cases, marked parathyroid cellular proliferation and glandular enlargement ensue despite severe hypercalcemia, documenting that the CaSR has an essential role in tonically inhibiting parathyroid cellular proliferation. Studies in uremic rat models[94,95] have illuminated the mechanisms by which high dietary intake of Ca^{2+}, acting via the CaSR, controls parathyroid proliferation. Induction of the cyclin dependent kinase inhibitor, $p21^{WAF1}$, and downregulation of the growth factor, TGF-α, and its receptor, the epidermal growth factor receptor (EGFR), both of which are upregulated in this setting, are key components of this mechanism.[95] 1,25 $(OH)_2D_3$ appears to act in a similar way to inhibit parathyroid cellular proliferation in similar experimental models.[96] An additional mechanism that may participate in stimulation of parathyroid growth during hypocalcemia is an endothelin-1-mediated stimulation of parathyroid cellular growth.[217] Similar studies are difficult to perform in non-uremic animals owing to their much slower rate of parathyroid proliferation, but it seems likely that similar mechanisms participate. Reduced expression of p21 and another cyclin dependent kinase inhibitor, p27, may also participate in the dysregulation of parathyroid growth in both primary (1°) and secondary (2°) hyperparathyroidism (HPT).[57] The second messenger pathway(s) that link the CaSR to the regulation of parathyroid proliferation have not yet been clarified.

Interactions of Vitamin D and the CaSR in the Regulation of Parathyroid Function

A large body of data has stressed the importance of vitamin D in reducing expression of the preproPTH gene and parathyroid proliferation. What is the relative importance of the VDR and CaSR in controlling parathyroid function? The CaSR clearly regulates the secretion of PTH over a time frame from seconds to minutes or longer and is the dominant regulator of acute changes in secretory rate. Over a longer time frame of three weeks, vitamin D deficiency and hypocalcemia both modulate preproPTH mRNA levels in the rat, although hypocalcemia of ~6 mg/dl more powerfully stimulates preproPTH gene expression than does vitamin D deficiency.[300]

Recent studies utilizing mouse knockout models, however, have provided surprising results regarding the relative importance of the VDR and CaSR in controlling parathyroid gland function *in vivo*. As noted before, homozygous knock out of exon 5 of the CaSR causes striking hyperparathyroidism with marked elevations in both PTH and parathyroid gland size, which clearly cannot be compensated by the remaining VDR gene.[196] This mouse model, if anything, likely underestimates the consequences of loss of the CaSR on parathyroid function, since knock out of exon 5 of the CaSR produces, in some tissues, an alternatively spliced CaSR that lacks exon 5 (which encodes part of the CaSR ECD) and can seemingly still signal.[370] Thus the VDR apparently has limited ability to offset loss of the CaSR in this animal model. In contrast, studies of mice with knockout of the VDR[250] have demonstrated that the CaSR effectively compensates for loss of the vitamin D receptor with regard to the control of parathyroid function. That is, while VDR-/- mice develop strikingly elevated levels of PTH and marked parathyroid enlargement on a standard diet,[156] administering a calcium-rich "rescue" diet normalizes both serum Ca^{2+} and PTH levels.[156,250] Thus hypocalcemia *per se* rather

than vitamin D deficiency is seemingly the dominant contributor to the elevated PTH levels. In addition, if the rescue diet is begun early in life, it completely prevents the parathyroid enlargement in the VDR-/- mice, showing that hypocalcemia per se rather than loss of the VDR was also a critical contributor to parathyroid growth in this setting. Subsequently, Meir, et al. created mice with knockout of the VDR only in the parathyroid glands.[286] In this way, the actions of the VDR on the parathyroid could be separated from systemic alterations in mineral ion homeostasis, e.g., owing to loss of the VDR in kidney and intestine. The mice with parathyroid-specific VDR ablation manifest only modest (~30%) elevations in serum PTH but do not exhibit any change in the number of proliferating parathyroid cells and have normal serum calcium concentrations.[286] Thus, while administering exogenous $1,25(OH)_2D_3$ clearly suppresses preproPTH gene transcription and parathyroid proliferation *in vivo* and *in vitro*, vitamin D seemingly has only a limited role in regulating parathyroid function *in vivo* under normal physiological conditions. These results should not be taken, however, to mean that $1,25(OH)_2D_3$ has no useful therapeutic role, especially in the 2° HPT of renal insufficiency (see below and elsewhere in this volume). Finally, it would be interesting to investigate CaSR signaling efficiency in the parathyroid in mice with deficient VDR signaling to determine to what extent compensatory alterations in the CaSR and/or its downstream signaling components contribute to the phenotypes observed with global or parathyroid-specific knockout of the VDR.

CaSR AND C-CELL FUNCTION

Studies in CaSR knock out mice have documented the mediatory role of the receptor in high Ca^{2+}_o-stimulated CT secretion by showing blunting of high Ca^{2+}-induced CT secretion in response to elevated levels of Ca^{2+}_o in CaSR +/− mice[141] and near total loss of Ca^{2+}-elicited CT secretion in CaSR-/-PTH-/- mice.[225] A plausible model for how the CaSR stimulates CT secretion[281] involves CaSR-induced activation of a nonselective cation channel, which causes cellular depolarization, thereby stimulating voltage-sensitive calcium channels and causing the increase in Ca^{2+}_i that activates exocytosis. Although CT is a potent hypocalcemic hormone in rodents, it has a much more modest, if any, hypocalcemic action in normal humans.

CaSR AND KIDNEY FUNCTION

The kidney plays key roles in Ca^{2+} and Mg^{2+} homeostasis by providing the major route for divalent mineral excretion from the body. Thus, it should not be surprising that variations in serum Ca^{2+} and Mg^{2+} affect many aspects of renal function. For instance, an increase in serum Ca^{2+} reduces glomerular filtration rate, inhibits renin secretion by the juxtaglomerular ^{JG} cells,[137] and induces renal vasoconstriction.[136] The kidney regulates the renal excretion of Ca^{2+} and Mg^{2+} by modulating the tubular reabsorption of these divalent cations along the nephron. The cellular mechanisms mediating mineral ion transport across the various nephron segments from proximal tubule (PT) to collecting duct (CD) are detailed elsewhere in this book (see Chapter 65). The cellular distribution of the CaSR in the kidney coincides with crucial aspects of Na^+, water and divalent mineral transport along the nephron that enables this receptor to modify a range of transport process key to the "safe" excretion of these minerals (i.e., in the absence of stones or nephrocalcinosis). The CaSR is apical in the PT[359] and inner medullary collecting ducts (IMCDs)[379] and basolateral in the TAL,[359] distal convoluted tubule (DCT),[359] and macula densa cells.[359] This differential cellular polarization of the CaSR permits $Ca^{2+}{}_o$ to be sensed in the initial glomerular filtrate in the PT and the final urine in the IMCD, while concurrently responding to changes in serum Ca^{2+} in segments critical for regulated Ca^{2+}/Mg^{2+} absorption (TAL and DCT).[186]

Evidence of a role for plasma Ca^{2+} concentration in determining renal Ca^{2+} excretion comes from examining the relationship between these parameters. Beyond a specific threshold of plasma Ca^{2+}, urinary Ca^{2+} excretion rises steeply with increasing serum Ca^{2+} concentrations (Fig. 63.4) (for reviews see[186,243,244]). Calciotropic hormones, such as PTH and calcitonin, as well as vitamin D, do not modify the steep relationship between plasma Ca^{2+} and urine Ca^{2+} excretion, but instead shift the threshold for the curve to the right such that urinary Ca^{2+} loss occurs at a higher than normal plasma Ca^{2+} Fig. 63.4.[243,244] The steepness of the relationship between urinary Ca^{2+} excretion and plasma Ca^{2+} is, however, lost when the function of the CaSR is impaired as happens in individuals with inactivating mutations of this receptor.[8] The most compelling evidence supporting the role of the CaSR in sensing Ca^{2+}_o and regulating urinary Ca^{2+} excretion comes from such genetic "experiments-in-nature." As discussed earlier in this chapter, individuals heterozygous for inactivating mutations in the CaSR (FHH) are hypercalcemic but have absolute or relative hypocalciuria (i.e., inappropriately low for the prevailing serum calcium concentration).[115,275,403] In contrast, individuals with activating mutations (ADH) are hypocalcemic but exhibit relative or absolute hypercalciuria.[48] Abnormal Ca^{2+}_osensing by the kidney CaSR can account for these abnormal patterns of renal Ca^{2+} excretion.[403]

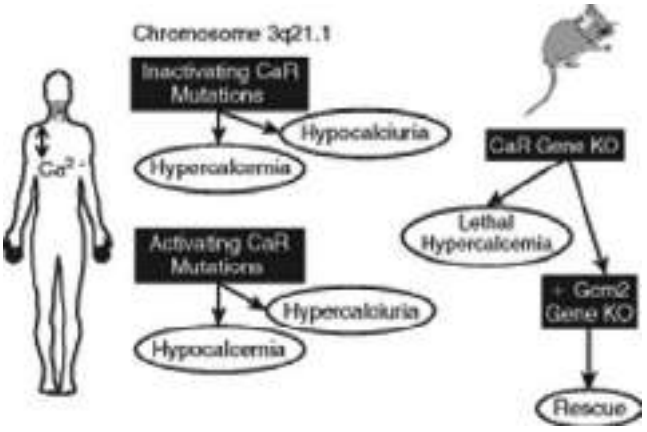

FIGURE 63.5 A: Mutations of the calcium-sensing receptor (CaSR) on chromosome 3q13.3-21 alter the steady-state serum ionized calcium concentration and the calcium-sensing ability of the kidney (serum calcium−urine calcium excretion relationship; Fig. 63.4). Receptor inactivating mutations give rise to hypercalcemia and hypocalciuria while activating mutations result in the opposite phenotype. B: In mice, knocking out the Casr gene results in a lethal phenotype from severe hypercalcemia and hyperparathyroidism within a few days after birth. The severe phenotype can be rescued by deleting the Gcm2 gene, which is required for development of the parathyroid gland. These double-knockout mice have low circulating levels of PTH that is secreted from thymus but is not under the control of the CaSR. See text for discussion.

While our understanding of the function of the CaSR in the kidney is still advancing (see[10,186,358] for reviews), some aspects of CaSR function have been determined for several nephron segments actively involved in the reabsorption of Ca^{2+} and Mg^{2+} as well as Na^+ and water. The reabsorption pattern of Ca^{2+} and Mg^{2+} and the localization of the CaSR along the nephron are shown in Fig. 63.6. In the following sections, we provide a summary of our understanding of the CaSR's functions in specific nephron segments.

CaSR in the Proximal Tubule

For some time, there has been both *in vivo*[409,433] and *in vitro*[30] evidence that Ca^{2+}_o directly modulates the 1-hydroxylation of 25-hydroxyvitamin D_3 in the PT. To avoid the confounding impact of Ca^{2+}_o-induced alterations in circulating PTH levels *in vivo*, Treschel et al. and Weisinger et al. used thyroparathyroidectomized rats infused with PTH to "clamp" the circulating PTH level.[409,433] Changes in $1,25(OH)_2D_3$ levels were then assessed during alterations in serum Ca^{2+}. The steep inverse sigmoidal relationship between Ca^{2+}_o and $1,25(OH)_2D_3$ levels that was observed[433] was reminiscent of the relationship of PTH to Ca^{2+}_o *in vivo* and *in vitro*. Similar results were obtained *in vitro* utilizing an SV40-transformed human PT cell line, that is, enhanced $1,25(OH)_2D_3$ synthesis at low Ca^{2+}_o and inhibition at high Ca^{2+}_o.[30] Recent data supports the CaSR's role in mediating the direct effects of Ca^{2+}_o on the 1-hydroxylation of 25-hydroxyvitamin D_3. Maiti and Beckman utilized the PT cell line, HK-2G, in which high Ca^{2+}_o inhibits CYP27B1 expression,[17] to show that high Ca^{2+} upregulates VDR expression[268] by a p38 MAPK-dependent mechanism.[269] Knocking down the CaSR with siRNA obviated the high Ca^{2+}_o-elicited increase in VDR, showing the latter was CaSR-mediated.[269] However, use of siRNA to document that the CaSR mediated the concomitant inhibition of CYP27B1 expression was not reported.[17] It has also not yet been shown that the high Ca^{2+}_o-induced, CaSR-mediated increase in VDR expression in the PT by itself can account for the reduced expression of CYP27B1.

Furthermore, $1,25(OH)2D_3$ regulates CaSR expression in the kidney: One study in vitamin D−deficient rats found a 90% increase in CaSR expression in the kidneys of $1,25(OH)2D_3$-replete animals,[45] and vitamin D replete rats showed a similar increase in response to $1,25(OH)2D_3$.[60] Vitamin D-responsive elements (VDREs) in the CASR and *Casr* genes and provide a mechanism whereby $1,25(OH)2D_3$ upregulates CaSR expression in parathyroid, thyroid C-cell, and kidney.[60] As noted earlier, since $1,25(OH)2D_3$ upregulates its own expression as well as that of the CaSR, and the CaSR upregulates its own expression and that of the VDR, there could be synergistic interactions between the effects of Ca^{2+}_o, acting via the CaSR, and $1,25(OH)_2D_3$ on the PT and elsewhere in the kidney. CaSR expression in the PT is reduced by PTH and dietary phosphate loading.[361]

Transcripts for the CaSR are present in the regions where PTH/PTHrP mRNA is expressed in the proximal convoluted (PCT) and straight tubule (PST) (as well as in glomerulus, CTAL, DCT and cortical CD).[360] High Ca^{2+}_o inhibits PTH-induced cAMP accumulation in the PCT and CTAL.[278,399] This action could explain, at least in part, the inhibition by the CaSR of PTH-stimulated phosphate excretion. Thus the CaSR directly modulates the action of PTH on the PT (and of renal Ca^{2+} reabsorption in the TAL) in addition to its central, inhibitory effect on PTH secretion. The CaSR protein is in the subapical compartments of the PT,[359] where it mediates some of the effects of high Ca^{2+} on PTH-induced cAMP production.[278] We have hypothesized a role for the receptor in the transport of phosphate and/or in the regulation of a local ionic homeostasis, bypassing systemic levels of calciotropic hormones (see following paragraphs).[358]

McKinney and coworkers[283] reported that luminal and peritubular perfusion of rabbit PCT with high Ca^{2+}_o (5 mM) modulated water and HCO_3^- reabsorption. Because a large fraction of Na^+ transport in PT

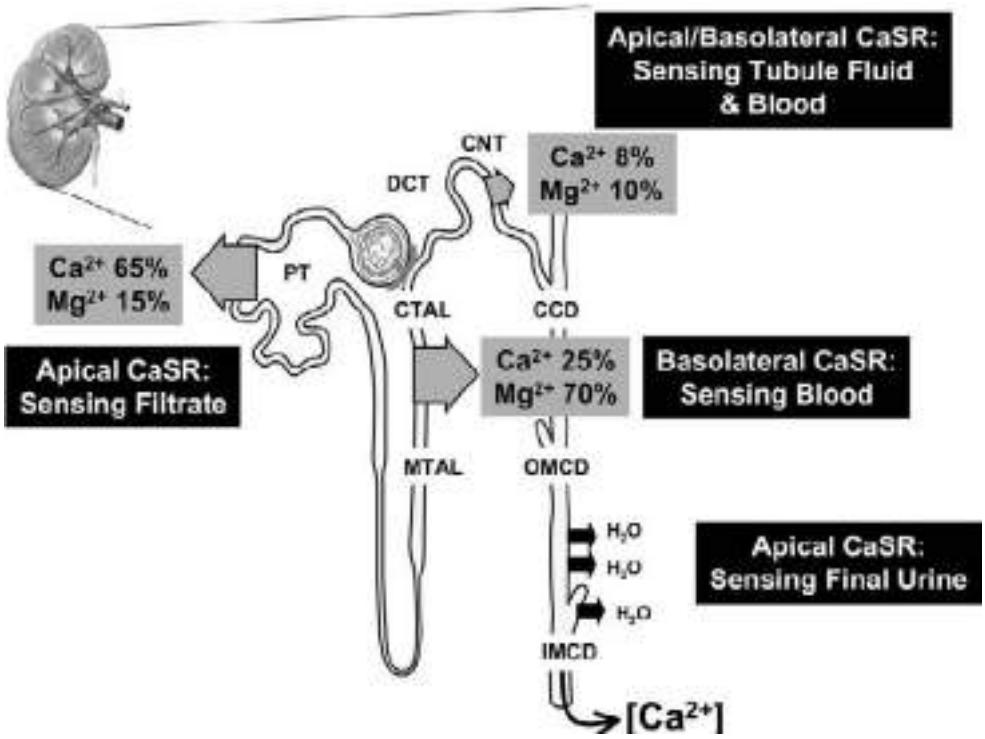

FIGURE 63.6 Schematic representation of fractional reabsorption of calcium and magnesium along the nephron together with the localization of the calcium-sensing receptor (CaSR). The CaSR not only responds to calcium in the blood–interstitium (basolateral localization), but in many nephron segments, the receptor may be modulated by calcium/magnesium in the tubule fluid (apical localization). See text for discussion.

depends on basolateral Na^+, K^+-ATPase (NKA), NKA activity provides an index of solute reabsorption. Preliminary studies by Hebert's group have suggested that increases in Ca^{2+}_o reduce NKA activity by 20 to 35% in a rabbit PT cell line. This magnitude of NKA inhibition is similar to that observed with dopamine, a known regulator of PT solute and volume transport. Modulation of PT NKA by CaSR activation would enable filtered (i.e., luminal) Ca^{2+} to regulate Ca^{2+} delivery to distal nephron segments. In contrast, since only 15% of filtered Mg^{2+} is reabsorbed in the PT (in contrast to the 50–60% of Ca^{2+} reabsorbed proximally), activation of the CaSR in the PT would be expected to have little effect of Mg^{2+} homeostasis.

CaSR in the Thick Ascending Limb of Henle

About 25% of filtered calcium is reabsorbed along the TAL (Fig. 63.6).[139] It is well established that increases in extracellular Ca^{2+} and Mg^{2+} inhibit Cl^- transport in TAL.[100,108,109,344,345] Increases in plasma, but not urinary, Ca^{2+} (or Mg^{2+}) concentrations directly modulate NaCl and mineral ion transport in the rat loop of Henle,[105,344,345] consistent with CaSR expression on basolateral membranes of the TAL.[359,360] Since most divalent mineral reabsorption mediated by the TAL occurs in CTAL,[105,138,140,271] the effect of plasma Ca^{2+} on renal Ca^{2+} (Mg^{2+}) handling relates to changes in interstitial ionized Ca^{2+} and Mg^{2+} surrounding the CTAL. In medullary thick ascending limb (MTAL) and CTAL the lumen-positive transepithelial voltage generated by NaCl reabsorption[58] drives most divalent mineral reabsorption via the paracellular route in mouse,[105,109] rat,[271] and rabbit.[36,104] In addition, a portion of Ca^{2+} absorption in the CTAL (at least in the mouse) may also traverse the transcellular route (see Chapter 65).[140] A number of hormones (e.g., vasopressin, parathyroid hormone, glucagon, calcitonin), coupled to Gαs-linked receptors, increase cellular cAMP accumulation[103,104,189] thereby stimulating NaCl and divalent mineral reabsorption through both paracellular and transcellular routes.[103,104] As we shall see in the following paragraphs, the CaSR uses a variety of mechanisms and second-messenger pathways to modulate NaCl reabsorption, and thereby divalent mineral absorption, in the TAL.

Both genetic experiments-of-nature and acquired disorders have established that the CaSR is a significant regulator of functionally coupled salt and divalent mineral transport in the TAL. Activating mutations of the CaSR are generally associated with autosomal

dominant hypocalcemia (see preceding sections)[341]; however, certain activating mutations of the CaSR have been found in individuals presenting with the phenotypic picture of Bartter syndrome combined with the typical hypocalcemic hypercalciuria present with activating CaSR mutations.[415,432] Bartter syndrome is a set of renal salt- and Ca^{2+}- and Mg^{2+}-wasting disorders due to low or absent ion transport in the TAL.[355] Mutations in several salt transporter genes or in genes encoding transporter regulatory proteins in the TAL cause Bartter syndrome.[187] It is now clear that the CaSR is one of these regulatory proteins. In addition, an acquired Bartter-like phenotype has also been observed in certain individuals receiving the aminoglycosides, gentamicin or amikacin,[82] likely reflecting aminoglycoside antibiotic-induced activation the CaSR in the TAL.[284,431]

At least three second-messenger pathways appear to be involved in CaSR-mediated regulation of transport in the TAL:[16,139,189,358] (1) the CaSR→↑PLA_2→↑AA →↑P_{450} →↑20-HETE pathway; (2) the CaSR→↓AC/↑PDE→↓cAMP pathway; and (3) the CaSR→↑TNF →↑COX-2→↑PGE_2 pathway. A second-messenger pathway commonly coupled to CaSR stimulation is $G\alpha_q$ activation of phospholipase C, release of IP_3 and a rise in Ca_i^{2+} via release of Ca_o^{2+} from internal stores (CaSR→↑PLC→↑IP_3→↑Ca_i^{2+} pathway).[13,51,229] Increasing Ca_o^{2+} does lead to rises in Ca_i^{2+} in the rabbit, rat, and mouse TAL[67,107,320,427] but there are divergent data regarding whether this increase in Ca_i^{2+} is functionally coupled to the $G\alpha_{q/11}$→↑PLC pathway.[107,427] The rise in intracellular Ca^{2+} appears to take place via extracellular entry in the rabbit,[107] but in the mouse CTAL CaSR agonists do induce a rise in Ca_i^{2+} from a thapsigargin-sensitive pool.[320] In the rat, increases in Ca_o^{2+} produce a concentration-dependent increase in IP_3 implicating the classical CaSR→↑PLC→↑IP_3→↑Ca_i^{2+} pathway.[102] Regardless of the mechanism, an important conclusion is that CaSR activation in the TAL gives rise to an increase in Ca_i^{2+}.

The CaSR→↑PLA_2→↑AA→↑P_{450}→↑20-HETE pathway couples CaSR activation to regulation of apical K^+ channels in the TAL (Fig. 63.7).[427,428] Since the apical 30-pS and 70-pS recycling K^+ channels are crucial for maintaining NaCl transport by both the CTAL and MTAL,[168,189,191] inhibition of this channel would decrease NaCl, Ca^{2+} and Mg^{2+} transport. Ca_o^{2+} and the other CaSR agonists, activate phospholipase A2 (PLA_2) releasing arachidonic acid (AA), which can be metabolized by a CYP4A P_{450}-hydroxylase to generate 20-HETE (the CaSR→↑PLA_2→↑AA→↑P_{450}→↑20-HETE pathway).[127,137,426,427,428] 20-HETE inhibits the 70-pS (but not the 30-pS) apical K^+ channel in inside-out membrane patches.[426] In contrast, AA can inhibit the 30-pS (ROMK1) K^+ channel activity independently of

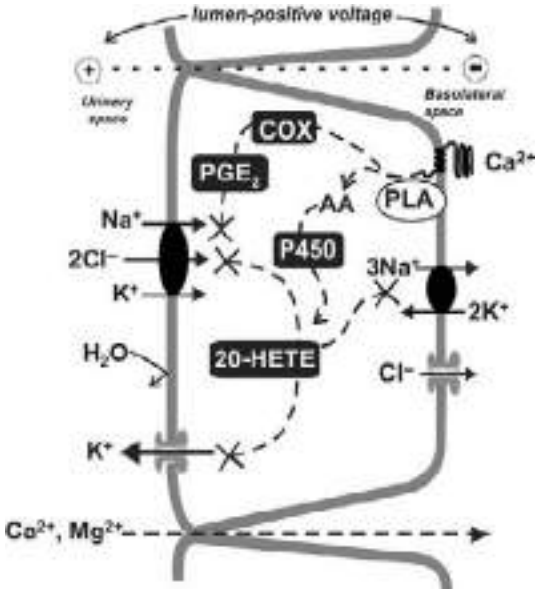

FIGURE 63.7 The PLA_2→↑AA→↑P_{450}→↑20-HETE and the CaSR→↑TNF→↑COX-2→↑PGE_2 pathways couple calcium-sensing receptor (CaSR) activation to regulation of salt and divalent mineral handling in the thick ascending limb. See text for discussion.

the generation of AA metabolites.[263,264] Thus, both the 30-pS and 70-pS K^+ channels in the apical membranes of TAL can be inhibited by components of the CaSR→↑PLA_2→↑AA→↑P_{450}→↑20-HETE pathway. This pathway has also been implicated in the inhibition of salt transport in the CTAL by angiotensin II (Ang II)[161,262] and bradykinin.[170] This effect of Ang II is mediated, at least in part, by P_{450}→↑20-HETE–mediated inhibition of the 70-pS K^+ channel.[262] In addition, this pathway has been implicated in the effect of a K^+-deficient diet to reduce apical 70-pS K^+ channel activity.[172] In fact, K^+ depletion enhances the Ca_o^{2+}-induced inhibition of the 70-pS K^+ channel.[173] Finally, exogenous AA can inhibit adenylate cyclase activity in CTAL by a pertussis toxin–sensitive mechanism[130]; this would modulate the effects of Gαs-coupled hormones on NaCl transport, and thereby divalent mineral absorption.

The CaSR→↓AC/↑PDE→↓cAMP pathway also couples CaSR activation to regulation of salt transport in the TAL (Fig. 63.8). Increases in Ca_o^{2+} reduce vasopressin-stimulated cAMP production in isolated mouse[399,400] and rat[100] TAL segments by inhibiting adenylate cyclase (AC) activity and increasing nucleotide degradation in the TAL.[100,101] Small increases in Ca_o^{2+} (0.5 to > 1.5 mM) produce a modest decrease in cAMP production but a major increase in phosphodiesterase (PDE)-dependent cAMP degradation. Studies on cyclic nucleotide-generating secretagogues in rat and mouse colon support the potent effect of the CaSR to increase PDE activity and suggest that a rise in Ca_o^{2+}

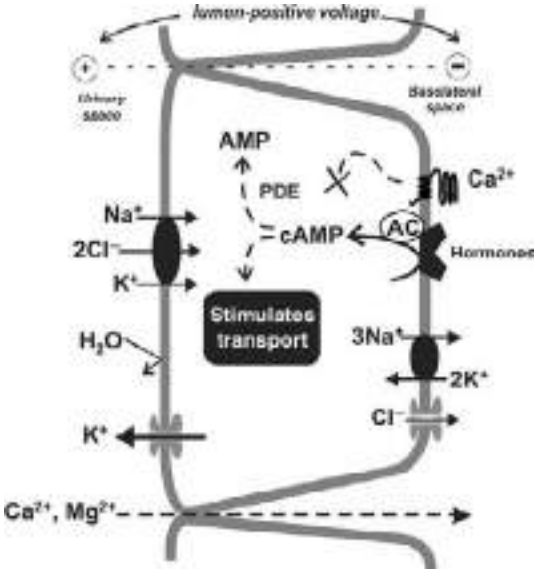

FIGURE 63.8 The CaSR→↓cAMP/↑PDE→↓cAMP pathway couples CaSR activation to regulation of salt and divalent mineral transport in the thick ascending limb (TAL). See text for discussion.

is crucial for activation of PDE.[146] Larger (non-physiological) increases in Ca^{2+}_o (> 1.5 mM) produce an even greater decrease in cAMP production in the TAL.[101] The CaSR agonist-induced rise in Ca^{2+}_i is also crucial for the latter, probably by modulating a Ca^{2+}-inhibitable adenylate cyclase isoform in the TAL (AC types 5 and 6).[64,65,100,193] The mechanism for CaSR-mediated modulation of cAMP has been studied in detail in HEK cells,[150] where CaSR stimulation reversed or prevented cAMP accumulation by activating a pertussis-sensitive $G\alpha_i$ and by increasing Ca^{2+}_i. Low-frequency, but not high-frequency, Ca^{2+}_i oscillations correlated with CaSR-mediated reductions in cAMP. Certain hormones, like PTH, also may enhance the paracellular permeability for Ca^{2+} and Mg^{2+}, at least in mouse CTAL.[439] The CaSR regulates both the active transcellular and passive paracellular reabsorption in mouse CTAL.[297] It should be noted that in bovine parathyroid cells extracellular Ca^{2+} decreases cAMP accumulation by a pertussis toxin-sensitive mechanism, implicating functional coupling of the parathyroid CaSR to $G\alpha_{i2}$.[76] However, in rat TAL, pertussis toxin has no effect on cAMP accumulation induced by increasing Ca^{2+}_o to 2.5 mM.[101]

The CaSR is also expressed in MTAL where it regulates NaCl reabsorption and alters the countercurrent mechanism crucial for urinary concentrating ability. This CaSR effect in MTAL could be important for regulating the concentration of divalent minerals in the final urine, ensuring that divalent minerals are excreted in a less concentrated urine, and thereby, reducing the risk of stone formation or nephrocalcinosis.[190] Information on the effects of CaSR agonists on transport processes in MTAL is inferential. It seems likely that the CaSR in MTAL also functions via the CaSR→↑PLA_2→↑AA→↑P_{450}→↑20-HETE pathway as well as by reducing cAMP,[128] based on a number of studies in MTAL showing that 20-HETE inhibits salt transport[120,121,282,453] by reducing Na^+-K^+-$2Cl^-$ cotransport,[6,282] Na^+-K^+-ATPase,[63,121,282] and apical 70-pS K^+ channel activities.[426]

The CaSR→↑TNF→↑COX-2→↑PGE_2 pathway also participates in CaSR-mediated regulation of salt transport by the TAL (Fig. 63.7). CaSR agonists increase cyclooxygenase-2 (COX-2) expression and COX-2−dependent synthesis of prostaglandin E_2 (PGE_2) in primary cultured MTAL cells.[126,128] CaSR-mediated increases in TNF production in rat MTAL cells depend on activation of PLC and a downstream calcineurin- and NFAT-(nuclear factor of activated T cells) dependent pathway.[423] The increase in COX-2 associated with CaSR stimulation depends, at least in part, on a rise in TNF levels and a TNF autocrine feedback on MTAL cells.[126,128,423] Since PGE_2 reduces NaCl transport by TAL,[97] this CaSR-linked, cytokine-mediated mechanism may contribute to regulating NaCl and divalent mineral handling by CTAL and MTAL. PGE_2 also inhibits the 70-pSK^+ channel in TAL by reducing vasopressin-stimulated cAMP accumulation and by a PKC-dependent pathway.[255] It has been suggested that variations in the local interstitial ionic Ca^{2+} concentration could influence COX-2 activity and PGE_2 production along the TAL from outer medulla to cortex[127] A clinical consequence of the CaSR→↑TNF→↑COX-2→↑PGE_2 pathway can be seen in chronic hypercalcemia where high urinary PGE_2 excretion results from upregulated COX-2 expression.[272] The influence of Ca^{2+}_o on salt transport in TAL via the CaSR→↑TNF→↑COX-2→↑PGE_2 pathway also provides one mechanism for the PGE_2-dependent renal polyuria and salt loss occurring in chronic hypercalcemia.[330]

The integrated effect of stimulation of the CaSR→↑TNF→↑COX-2→↑PGE_2, CaSR→↑PLA_2→↑AA→↑P_{450}→↑20-HETE and CaSR→↓AC/↑PDE→↓cAMP pathways in TAL is a "loop diuretic"−like effect of activation of the CaSR by its agonists. This diuretic effect likely accounts for the observation that increasing serum ionized Ca^{2+} concentration in healthy men by ~25% results in about a 1.5-fold increase in Na^+ excretion[117] and the diuresis and natriuresis that accompanies hypercalcemic states. Chronic hypercalcemia, induced in rats either by PTH[425] to vitamin D,[424] also downregulates several Na^+ transporters, including the Na^+-K^+-$2Cl^-$ cotransporter. While it seems likely that the CaSR mediates these effects, at least in part, this has not been studied experimentally. These

latter two studies also point out that reduced expression of Na^+ transporters in several nephron segments, in addition to TAL, may contribute to the solute and volume depletion observed in some hypercalcemic patients. In addition, this integrated effect of CaSR activity on the TAL and its consequent loop diuretic-like effect may participate in the influence of calcium intake on blood pressure.[171,280,394] The possible impact of molecular variations in the CaSR in Na^+ balance, blood pressure and other processes, such as colonic neoplasia, are currently under investigation.[181,220]

Reabsorption of Ca^{2+} in MTAL and CTAL through the paracellular pathway is accompanied by little water flow since this tubular epithelium has a low water permeability due to the lack of apical aquaporins.[189,309] Thus, we might anticipate that the resultant rise in Ca^{2+} concentration at the basolateral surface of the TAL would activate the CaSR and immediately reduce further NaCl and Ca^{2+} reabsorption. The CaSR, however, has a built in mechanism (Fig. 63.9), whereby increasing ionic strength reduces the receptor's sensitivity (increases the EC_{50}) to extracellular Ca^{2+} by an allosteric mechanism.[188,348] The reduction in CaSR activation at higher ionic strength (NaCl concentration) translates to less inhibition of ion reabsorption. The obvious advantage is that both Na^+ and Ca^{2+} contribute toward their final reabsorption and accumulation at the basolateral membrane of this nephron segment via regulated activity of the CaSR.

As discussed previously, Ca^{2+} and Mg^{2+} reabsorption by the TAL are coupled. This might seem

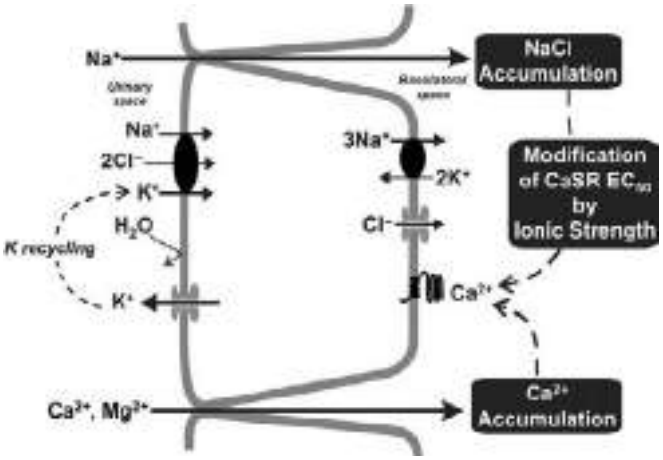

FIGURE 63.9 Role of the allosteric modifying effect of ionic strength in modulating calcium-sensing receptor (CaSR) function in the medullary thick ascending limb. Both Na^+ and Ca^{2+} contribute to their final reabsorption and accumulation at the basolateral membrane of this nephron segment via regulated activity of the CaSR. See text for discussion.

contradictory since normal plasma concentrations of Mg^{2+} are well below the EC_{50} values for CaSR activation by these divalent cations *in vitro*. However, genetic diseases in humans in which the CaSR gene is mutated indicate that the CaSR is also involved in Mg^{2+}_o homeostasis (i.e., serum Mg^{2+} is high-normal or mildly elevated in FHH). While it is still unclear how this is achieved, Mg^{2+}_o might enhance receptor sensitivity to Ca^{2+}_o (a calcimimetic-like effect).[53] However, the tubule Mg^{2+} concentration at TAL can be twice that in the initial glomerular filtrate, owing to the limited reabsorption of Mg^{2+} in the PT compared with other ions such as Na^+, Cl^-, and Ca^{2+}. This increase in Mg^{2+} concentration and delivery to the TAL would enhance Mg^{2+} reabsorption via the paracellular pathway and give rise to higher interstitial Mg^{2+} concentrations near the basolateral membrane. The high basolateral Mg^{2+} concentration may be sufficient to activate the basolateral CaSR in CTAL and suppress reabsorption of further magnesium.

The EC_{50} for Ca^{2+} stimulation of the CaSR can be modified by extracellular pH,[347] suggesting that the receptor might also act as a pH sensor along the nephron. An analogous role for the CaSR has recently be documented in the stomach.[125,158] Thus, not only Ca^{2+}_o, but also the state of acid–base balance could influence salt and water transport along the nephron by modulating the CaSR's activity. Although direct evidence is not available, several mechanisms responsible for NH_4^+ or HCO_3^- transport could be affected by the CaSR, which could, therefore, alter acid-base balance. The TAL actively reabsorbs NH_4^+[160,234,235,236] by transcellular and paracellular pathways.[110] The bulk of transcellular absorption depends on Na^+-K^+(NH_4^+)-$2Cl^-$ cotransporter activity where NH_4^+ instead of K^+ is transported with Na^+ and Cl^-.[160] Paracellular NH_4^+ transport depends on the transepithelial voltage just like the transport of Ca^{2+} or Mg^{2+}. Similar to the influence of the CaSR on divalent mineral absorption, stimulating CaSR (high Ca^{2+}_o and/or pH) may reduce NH_4^+ absorption by the TAL. Therefore, the activity of the CaSR could influence net urinary acid excretion by modulating the accumulation of ammonium/ammonia in the renal medulla. The TAL also reabsorbs HCO_3^- and this transport can be inhibited by angiotensin II via the $PLA_2 \rightarrow \uparrow AA \rightarrow \uparrow P_{450} \rightarrow \uparrow$20-HETE pathway.[161] Similarly, activation of this same pathway by the CaSR would likely reduce HCO_3^- absorption.

Finally, macula densa cells express substantial CaSR immunoreactivity on their basolateral side.[359] Although the receptor's function in this region has not been investigated, indirect evidence suggests that the CaSR could sense changes in Ca^{2+}_o and, accordingly, regulate tubuloglomerular feedback.

CaSR in the DCT

The DCT reabsorbs about 10% of filtered Ca^{2+} by an active transcellular mechanism, as Ca^{2+} movement through the intercellular spaces is negligible because of the markedly low permeability of the tight junctional membranes to Ca^{2+} (see Chapter 65).[138,139] In this nephron segment, Ca^{2+} absorption is inversely proportional to Na^+ absorption[54,93] and strongly regulated by calciotropic factors (PTH, vitamin D). Ca^{2+} absorption is a three-step process. First, apical Ca^{2+} entry occurs down its electrochemical gradient through the Ca^{2+}-selective channel, TRPV5 (see Chapter 65).[197] Second, Ca^{2+} must diffuse across the cell, presumably bound to the Ca^{2+}-binding proteins, calbindins D_{9K} and D_{28K}. Finally, basolateral efflux of Ca^{2+} into the bloodstream is uphill and requires energy achieved by means of a plasma membrane Ca^{2+}-ATPase (PMCA) and the Na^+/Ca^{2+} exchanger (NCX1).[28,138,139,257,266] 1,25 $(OH)_2D_3$ acts in the DCT to increase active Ca^{2+} reabsorption by upregulating the expression of the key molecules participating in transcellular Ca^{2+} transport, including TRPV5, calbindins-D_{9K} and D_{28K}, NCX1, and PMCA1B. The role of vitamin D in regulating this pathway was shown unequivocally using 1 α(OH)ase-/- mice, which lack any endogenous 1,25$(OH)_2D_3$.[198] Repleting these mice with 1,25$(OH)_2D_3$ increases the expression of TRPV5, calbindin-D_{28K}, calbindin-D_{9K}, NCX1 and PMCA1B.

The CaSR is expressed basolaterally, intracellularly, and occasionally apically in a punctate, vesicle-like pattern in DCT.[359,360] What role does it play in modulating Ca^{2+} transport in this nephron segment? Interestingly, restoring normocalcemia and normophosphatemia in the 1 α(OH)ase$^{-/-}$ mice with a high Ca^{2+} high phosphate, lactose-containing "rescue" diet upregulated the expression of TRPV5, calbindin D_{28K}, NCX1 and PMCA1b.[198] These effects of Ca^{2+} supplementation likely reflect direct actions of Ca^{2+} on the same cell type(s) upon which 1,25$(OH)_2D_3$ acts in the DCT. In fact, earlier studies[118] had shown that 1,25$(OH)_2D_3$ and/or elevated medium Ca^{2+}upregulated the expression of calbindin-D_{28K} in primary chicken kidney cells, likely by acting upon the same calbindin-D_{28K}-containing cells. The rescue diet, however, did not fully normalize renal Ca^{2+} handling in the VDR-/- mice, as urinary Ca^{2+} excretion in the VDR-/- mice was twice that in normal mice ingesting the same rescue diet.[251] Therefore, dietary Ca^{2+}-induced upregulation of several components of the transcellular pathway for Ca^{2+} absorption does not completely compensate for loss of the VDR.

A recent study demonstrated that raising Ca^{2+}_o enhanced Ca^{2+} reabsorption in DCT, in contrast to the CaSR-mediated inhibition of Ca^{2+} reabsorption in CTAL.[407] In this study, the CaSR and TRPV5 were co-expressed in the same cells, and activating the CaSR on the apical membrane increased TRPV5 activity, with a resultant rise in Ca^{2+}_i by means of a PKC-dependent phosphorylation of amino acid residues S299 and S654 in TRPV5. This stimulation of the activity of TRPV5 was suppressed by a dominant negative CaSR, proving the receptor's involvement. What is the purpose of a CaSR-dependent stimulation of Ca^{2+} reabsorption in DCT? Topala, et al.[407] suggested that this provides a local feedback mechanism for adjusting Ca^{2+} reabsorption in DCT as a function of the prevailing urinary Ca^{2+} concentration, perhaps mitigating the risk of Ca^{2+}-containing stones when the urine reaching the DCT has an excessively high Ca^{2+} concentration.

The DCT, along with the CTAL, is also an important nephron segment for Mg^{2+} conservation, which occurs through TRPM6, an apical Mg^{2+} channel homologous to TRPV5.[153] The CaSR is expressed in the mouse DCT cell line, MDCT, and cAMP production stimulated by hormones signaling through Gαs activation (PTH, AVP, calcitonin and glucagon) is inhibited by CaSR agonists.[18,19] Moreover, aminoglycosides can inhibit PTH-stimulated Mg^{2+} uptake in these cells likely by activating the CaSR.[224] Additionally, the ability of 1,25 $(OH)_2D_3$ to stimulate Mg^{2+} uptake into MDCT cells is abrogated by elevated Ca^{2+}_o and Mg^{2+}_o.[362] This latter effect of divalent minerals is abolished by pretreatment with CaSR antibodies or antisense CaSR mRNA oligonucleotides.

CaSR in Collecting Duct

Cortical Collecting Duct (CCD)

In the CCD, CaSR protein is cytosolic and at the basolateral membrane of some, but not all, α-intercalated cells,[359] suggesting a potential role for extracellular divalent minerals in preventing stone formation by regulating urinary acidification when tubular Ca^{2+} concentrations are critically high (see below). Indeed, in a recent elegant study performed utilizing the hypercalciuric TRPV5 knockout mouse model, homozygous knockout of TRPV5 produced the expected hypercalciuria, but it was not accompanied by kidney stones.[356] However, the mice manifested marked urinary acidification and increased urine flow. Moreover, when TRPV5-/- mice were bred with mice lacking the B1 subunit of the H^+-ATPase, they exhibited severe nephrocalcinosis, which was lethal within the first 3 months of life, suggesting that urinary acidification was a compensatory mechanism ensuring adequate solubility of urinary Ca^{2+}. Exposing outer medullary collecting ducts from TRPV5-/- mice to the CaSR agonists, Ca^{2+} and neomycin, stimulated H^+ secretion via H^+-ATPase, accompanied by downregulation of aquaporin-2

(AQP2),[356] resulting in not only acidification but also polyuria. The latter would reduce the urinary Ca^{2+} concentration by diluting it in a greater volume. The further CaSR-mediated inhibition of urinary concentrating ability that occurs in the IMCD is described below. These actions of the CaSR on urinary acidification were not observed in the double knockout TRPV5-/-/B1-/- mice. These experiments show that CaSR activation promotes urinary acidification and a reduction in water reabsorption in the TRPV5-/- mice, two mechanisms reducing the urinary concentration and increasing the solubility of the calcium salts, primarily calcium-phosphate salts, that caused nephrocalcinosis in the TRPV5-/-/B1-/- mice. It should be noted that the solubility of calcium oxalate stones, the most common type of stone in humans, has less pH dependence than do calcium-phosphate stones, and urinary acidification mediated by the CaSR in the setting of hypercalciuria might have less impact on calcium oxalate stone formation. Nevertheless, the elaboration of more dilute urine would be beneficial in the latter setting.

Inner Medullary Collecting Duct

In the IMCD, the CaSR is expressed in the same endosomes in which the vasopressin-activated AQP2 water channels reside[379] (Fig. 63.10). Vasopressin-activated V2 receptors on the basolateral membrane of IMCD cells produce cyclic AMP accumulation in these cells. Cyclic AMP activates protein kinase A (PKA), which, in turn, phosphorylates AQP2 (and certainly other proteins) leading to movement of these endosomes to the apical plasma membrane.[142,226] The increase in water permeability of the apical membrane enhances transtubular movement of water driven by the interstitium-to-luminal osmotic gradient. The result of these events is an increase in final urine osmolality. Since the AQP2-containing endosomes also contain CaSR protein, insertion of these endosomes into the apical membrane increases surface expression of both AQP2 and CaSR. Activation of the CaSR by increases in tubular Ca^{2+} concentrations reduces vasopressin-stimulated increases in water permeability in the *in vitro*-perfused IMCD,[379] presumably due to reduced trafficking of AQP2 to the luminal membrane during CaSR activation.[343] Since CaSR stimulation can reduce cAMP accumulation in TAL cells, a similar CaSR-mediated reduction in cAMP in IMCD might account for the reduction in water permeability. Vasopressin-enhanced water permeability in the IMCD is also virtually absent in dihydrotachysterol-induced chronic hypercalcemia.[378] A reduction in AQP2 protein expression and activation of the CaSR contribute to this effect.

A consequence of these effects of CaSR stimulation in the IMCD is regulation of the concentration of ionized Ca^{2+} in final urine. Since the EC_{50} for Ca^{2+}_o stimulation of the CaSR is modified by pH, ionic strength, polyamines, and amino acids (a calcimimetic-like effect, see[402] for review), many tubule fluid constituents in the IMCD can influence receptor activity and its consequences on IMCD water permeability. Ca^{2+} solubility in the tubule fluid or crystal growth may be influenced by many factors altering the CaSR's EC_{50} for Ca^{2+} (see Chapter 68). Moreover, Ca^{2+} delivery to the IMCD is increased whenever the CaSR is stimulated in the TAL. If luminal Ca^{2+} increases in the terminal IMCD above a certain level determined by the integration of factors influencing the CaSR, the enhanced CaSR stimulation in IMCD will alter reabsorption to limit further increases in Ca^{2+} concentration. This influence of Ca^{2+} on water transport in IMCD provides an example of physiological "trade-off" where water conservation is sacrificed to ensure uneventful excretion of divalent cations in a soluble form in terrestrial vertebrates.

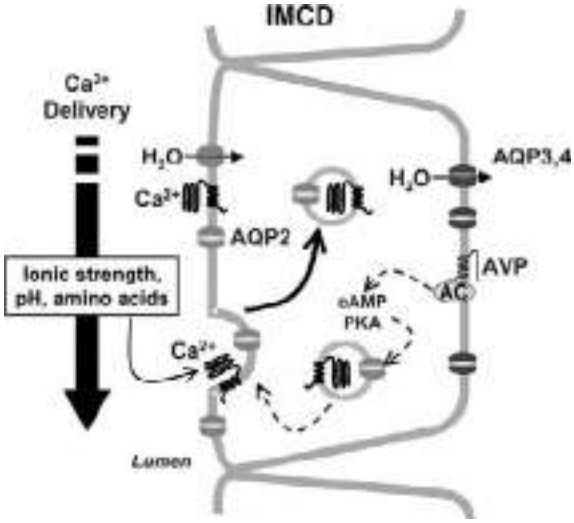

FIGURE 63.10 In the inner medullary collecting duct (IMCD), the calcium-sensing receptor (CaSR) is expressed in the same endosomes in which the vasopressin-activated aquaporin-2 (AQP2) water channels are expressed. Activation of the CaSR by increases in tubular fluid Ca^{2+} concentrations reduce vasopressin-stimulated increases in water permeability by modulating the trafficking of AQP2. Since the EC_{50} for Ca^{2+}_o stimulation of the CaSR is modified by pH, ionic strength, polyamines, and amino acids, many constituents of the tubule fluid in the terminal collecting duct can influence receptor activity and its consequences on IMCD water permeability. See text for discussion.

CaSR and Renin Secretion

Renin plays important roles in sodium, volume and blood pressure homeostasis: Hypovolemia is sensed by the juxtaglomerular (JG) cells of the afferent arteriole in

the kidney, which, in turn, increases renin secretion. Renin converts circulating angiotensinogen to angiotensin II, a potent endogenous pressor that also increases production of the sodium-retaining hormone, aldosterone, by the adrenal zona glomerulosa.[180] The elevation in blood pressure stimulated by angiotensin II combined with the sodium retention promoted by aldosterone tends to normalize sodium and volume homeostasis. It has been known for several decades that elevating Ca^{2+}_o inhibits renin release by the JG cells.[137] Only more recently, however, has it been demonstrated convincingly that the CaSR is expressed by JG cells[316] and mediates the inhibition of renin release by high Ca^{2+}_o.[267] The role that CaSR-mediated regulation of renin secretion plays in normal blood pressure and volume homeostasis is not currently understood. The capacity to modulate renin secretion pharmacologically, e.g., using a CaSR antagonist, could potentially be of therapeutic benefit in high renin forms of hypertension.

Developmental Regulation of Renal CaSR Expression

In the newborn, reduced responsiveness of the kidney to vasopressin and PTH could potentially reflect effects of the CaSR on these aspects of renal function. In the developing rat kidney, there is little prenatal expression of the CaSR, except in large tubules and branching ureteric buds of developing nephrons.[73] CaSR mRNA and protein increase markedly during the first postnatal week, principally due to expression of the receptor in the developing TAL and, to a lesser extent, in the CD. The receptor's level of expression remains nearly constant after postnatal day 14. Thus it is possible that some of the previously described changes in renal handling of divalent cations and water in the perinatal and immediate postnatal periods are related, in part, to the increasing levels of CaSR expression and its resultant inhibitory effects on the actions of PTH and antidiuretic hormone on the developing nephron.

CaSR AND THE SKELETON

Our understanding of the CaSR's roles in bone and cartilage has lagged behind that in parathyroid and kidney, as a result, in part, of controversy as to whether the receptor is actually present in cartilage and bone cells, to say nothing of its biological relevance there. Some studies have provided unequivocal evidence for the receptor's presence in cartilage or chondrocytic cell lines[69,70] and/or in bone,[70] as well as in osteoblastic cell lines, osteoclasts and related cell lines. Others, however, have not (for review, see[405]). The following discussion is a summary of the current state of this field, which ultimately may be relevant to bone disease encountered in patients with kidney disease and the therapy thereof. While the CaSR-related, class C GPCR, GPRC6A,[240,434] which responds to extracellular Ca^{2+}, amino acids (especially basic amino acids), and calcimimetics,[84,85,240,333,435] has been suggested to participate in extracellular Ca^{2+}-sensing in bone,[334] additional study will be required to establish its importance, if any, in bone and to determine if GPRC6A and CaSR interact in these cells

The CaSR in Cartilage

The chondrocytic cell line, RCJ3.1C5.18, expresses easily detectable levels of CaSR mRNA and protein.[72] When these cells are incubated with elevated levels of Ca^{2+}_o, there is suppression of the early differentiation marker, aggrecan, and enhanced expression of several markers of terminal differentiation, namely osteopontin, osteonectin and osteocalcin, as well as increased synthesis of cartilagenous matrix, another indication of enhanced differentiation.[72] Several of these effects of the CaSR were potentiated by overexpressing the wild type CaSR or inhibited by transfecting the cells with a CaSR with defective signaling capacity, suggesting a mediatory role for the receptor. Growth plate cartilage also expresses the CaSR.[70] Initial studies of cartilage in mice with homozygous knock out of exon 5 of the CaSR revealed rickets,[145] suggesting that the receptor might be required for normal cartilage development. However, when these severely hyperparathyroid mice were "rescued" by knock out of the PTH gene (CaSR-/-PTH-/-)[238] or of the key parathyroid transcription factor, Gcm-2 (CaSR-/-Gcm-/-),[412] there was no apparent cartilage phenotype, and the CaSR's role in cartilage, if any, was questioned.

Additional studies at about the same time, however, demonstrated that keratinocytes from CaSR-/- mice could generate a variant CaSR with exon 5 spliced out.[411] This finding raised the possibility that skeletal expression of the "exon 5-less" CaSR in the original CaSR-/- mice might, in fact, possess biological activity capable of rescuing the CaSR-/-PTH-/- and $CaSR^{-/-}$Gcm-/- mice from any skeletal consequences of losing the full length CaSR. In fact, chondrocytes from CaSR-/- mice had the same cellular responses to Ca^{2+}_o seen in wild type chondrocytes,[370] presumably owing to the presence of a biologically active CaSR lacking exon 5. However, it has not yet been possible to directly document biological activity of the exon 5-less CaSR when it is expressed in heterologous cell systems.

To study further the biological actions of the CaSR in bone using knock out mouse models, Chang, et al. developed mice in which exon 7 of the CaSR was "floxed" by inserting loxP sites flanking this exon.[71] Mating of these mice with mice expressing the Cre recombinase only in a particular tissue of interest owing to the recombinase being driven by a suitable promoter specific for that tissue, results in recombinase-mediated excision of the floxed exon and recombination of the ends of the remaining gene. As a result, transcription and translation now produces a truncated CaSR protein lacking exon 7. Mice with exon 7 of the CaSR floxed were mated with mice expressing the Cre recombinase only in chondrocytes to examine the consequences of knocking out the CaSR in cartilage. Exon 7 encodes the entire CaSR transmembrane domain and C-tail, and when the CaSR gene lacks exon 7, it can only generate the CaSR's ECD in a soluble form, which would be released extracellularly and presumably be incapable of signaling.[71] Chondrocyte-specific CaSR deletion resulted in death of embryos by day 13,[71] an unexpectedly severe phenotype in view of the multiple hormonal or other factors regulating chondrocyte development and function. Subsequent use of an inducible Cre recombinase made it possible to delete exon 7 of the CaSR on days 16–18 of embryonic life, i.e., subsequent to when the embryos died in the previous model. This maneuver produced viable embryos, which nevertheless displayed delayed development of their growth plates. These data suggested, therefore, a critical, non-redundant role(s) for the CaSR in cartilage development.

The CaSR in Osteoblasts

Initially, some,[70,442,443] but not all,[335] studies found the CaSR in intact bone, primary osteoblasts in culture and osteoblastic cell lines (for review, see[405]). In osteoblastic cells expressing the CaSR, high Ca^{2+}_o has actions that would be expected to stimulate bone formation. These include promoting proliferation of pre-osteoblasts,[75] enhancing expression of the mRNAs that encode osteoblast differentiation markers, such as Cbfa-1, osteocalcin, osteopontin, and collagen 1, and stimulating mineralized nodule formation.[113]

Studies in the mice with global knock out of exon 5 of the CaSR revealed, in addition to the rickets alluded to above, severe hyperparathyroid bone disease resulting from loss of the CaSR in the parathyroid, which complicated interpretation of the impact of losing the CaSR on osteoblast function per se. Studies in "rescued" CaSR-/-PTH-/-[238] and CaSR-/-Gcm-/-[412] mice, however, showed little or no difference in their bone histology and histomorphometry from that observed in control mice, suggesting that the CaSR does not have an important role in the formation and turnover of the skeleton. However, conditional knock out of exon 7 of the CaSR in osteoblasts utilizing osteoblast-specific Cre's produced mice exhibiting poor postnatal growth and skeletal development, with small poorly mineralized skeletons.[71] Most of these mice experienced long bone and rib fractures and died by 3 weeks of age. Their bones had reduced levels of both early and late markers of osteoblast differentiation, including type 1 collagen, insulin-like growth factor-1 (IGF-1, a key osteoblast growth factor), alkaline phosphatase, and osteocalcin. There was also a higher than normal rate of osteoblast apoptosis. These results suggest key roles for the CaSR in promoting proliferation, differentiation and survival of osteoblasts as well as in enhancing mineralization of the skeleton.[71] They also have the important implication that a calcimimetic with some specificity for osteoblasts might have potential utility as a bone anabolic agent.

The CaSR in Osteoclasts

As with osteoblasts, some studies failed to detect the CaSR in osteoclasts,[385] while others found it in cell lines considered to be models of osteoclast precursors (e.g., RAW 264.7),[288] in multinucleated osteoclasts differentiated from these precursors *in vitro* and in at least some mature osteoclasts in bone sections.[113] Available evidence suggests that while the CaSR serves a permissive role in osteoclastogenesis *in vitro*, high Ca^{2+}_o concentrations also directly suppress osteoclast activity and enhance their apoptosis.[288] Therefore, if the CaSR has similar actions *in vivo*, a calcimimetic targeting both osteoblasts and osteoclasts specifically might not only stimulate bone formation but also inhibit bone resorption, although an *in vitro* investigation that did not detect CaSR transcripts in osteoclasts or their precursors did not observe any functional effect of a calcimimetic on these cells.[385] Clearly more work is necessary to determine the CaSR's role, if any, in osteoclasts *in vivo*. The effects of Ca^{2+}_o on osteoclast function have also been suggested to result from an entirely different Ca^{2+}_o-sensing mechanism (for review,[449]).

THE CaSR AND THE GASTROINTESTINAL TRACT

Roles of the CaSR in the Stomach

In the stomach, the CaSR is expressed in the mucus-secreting surface epithelium,[291,376] the parietal cells in the gastric crypts,[78,148,291] and in the gastrin-secreting G-cells.[55,56] It directly stimulates acid secretion[148] and

also does so indirectly by stimulating gastrin secretion,[55] which, in turn, promotes secretion of histamine from gastric ECL cells. The latter acts directly on parietal cells to stimulate gastric acid secretion.[147] Although gastric acid secretion might not seem relevant to Ca^{2+} homeostasis, both calcium carbonate and calcium phosphate salts are more soluble under acidic conditions ($CaCO_3$ will not dissolve above pH 5.0). Therefore, an acidic environment in the stomach will promote the availability and, subsequently in the small intestine, the absorption of free luminal Ca^{2+}.[147] Recent work has suggested that the CaSR in the stomach senses not only Ca^{2+} but also amino acids and pH.[125,159] Thus the receptor likely integrates several types of signals that impact its functions in the stomach. The response to amino acids may promote the secretion of acid needed to stimulate the gastric phase of protein digestion, while the response of the CaSR to pH could represent, at least in part, the long-sought pH sensor needed for the feedback regulation of acid secretion, stimulating it when pH is high and inhibiting it when pH is low.

Roles of the CaSR in the Small Intestine

The CaSR is present in the small intestine,[74] likely in the same cells expressing the VDR (although this has not yet been formally proven) as well as in cell lines of intestinal origin.[143] However, its functions in the intestine are incompletely characterized. Available data suggest that it can act together with vitamin D to enhance the expression of the various components of the transcellular calcium transport system or substitute, at least in part, for the actions of $1,25(OH)_2D_3$ in certain instances. For example, in organ cultures of fetal rat duodenum, not only $1,25(OH)_2D_3$ but also elevated levels of Ca^{2+}_o increase the expression of the mRNA for calbindin-D_{9K}.[41] Subsequently, van Abel, et al. demonstrated that administering the rescue diet described earlier to 1α(OH)ase-/- mice normalized serum Ca^{2+} concentration concomitant with statistically significant, >10-fold increases in the intestinal expression of TRPV6 and calbindin-D_{9K},[414] similar to the effect of dietary rescue in the kidneys of these mice. While not formally proven, these actions of calcium are likely to be CaSR-mediated. Thus elevated levels of Ca^{2+} can apparently substitute, at least partially, for a lack of vitamin D in maintaining sufficient levels of expression of key elements of the intestinal transcellular Ca^{2+} transport system, suggesting a vitamin D-independent role for Ca^{2+}_o in regulating its own absorption in the intestine. An additional function of the CaSR in the small intestine may be to promote digestion via the capacity of cholecystokinin (CCK)-secreting endocrine cells to secrete CCK in response to calcium[247] or upon exposure to peptides[299] or aromatic amino acids.[194] The secreted cholecystokinin, in turn, would stimulate pancreatic enzyme secretion and enhance small intestinal digestion of ingested nutrients.

Roles of the CaSR in the Colon

Although the proximal small intestine is often thought of as the predominant site for intestinal calcium absorption, substantial absorption also occurs in the cecum of the large intestine by a vitamin D-responsive mechanism.[124] The cloning of the apical intestinal calcium uptake channel, TRPV6, provided a molecular basis for regulated calcium absorption in the cecum, as this channel was expressed at robust levels in this segment of the large bowel.[328] An additional function of the CaSR in the large intestine, which is apparently uninvolved in calcium homeostasis per se, is to inhibit the secretion of fluid by the crypts, particularly when stimulated by cAMP.[146] This action has been suggested to represent a potential target for the treatment of diarrheal disease, such as cholera (e.g., with a calcimimetic).[146] Finally, the CaSR expressed in the colon regulates the growth and differentiation of cells within the colonic crypt, promoting cellular differentiation and inhibiting cell growth.[329,438] It does so by mechanisms that include: (1) upregulation of cyclin-dependent kinase inhibitors such as p21, (2) promotion of E-cadherin expression and suppression of beta-catenin expression,[66] (3) increased local levels of $1,25(OH)_2D_3$[329] (which also enhances differentiation and inhibits proliferation), and (4) reduction in c-myc expression.[222] These actions of the CaSR may contribute to the reduction in the risk of colonic adenomas[181] or colon cancer observed with increased dietary intake of calcium in many but not all studies[20,144,223] (for reviews, see[329,395]).

MODULATION OF THE CaSR IN 2° HPT

The ability of ionized Ca^{2+} to modulate PTH secretion is reduced in secondary hyperparathyroidism (2° HPT).[53,163,167,371] Unlike primary hyperparathyroidism (1° HPT), there is no major right shift in the set point for extracellular Ca^{2+} in 2° HPT during the phase when there is diffuse hyperplasia, although an elevated set-point can occur in severe 2° HPT or 3° HPT (i.e., when hypercalcemia supervenes, which often requires parathyroidectomy).[163] Moreover, no inactivating mutations in the CaSR have been identified as is the case for FHH.[106,202] However, CaSR mRNA and protein expression are significantly

reduced in all forms of hyperparathyroidism, including in 2° HPT.[123,154,184,233,445,446] The magnitude of the decrease in CaSR expression is associated with the degree of parathyroid proliferation[445]: The larger the parathyroid gland, the lower the CaSR protein expression.[59]

In the rat 5/6 nephrectomy model, parathyroid gland hyperplasia is also associated with a reduction in CaSR expression,[293] and both parathyroid hyperplasia and the change in CaSR expression and function are abrogated by a low-phosphate diet.[44,364] While a significant negative correlation between CaSR mRNA expression, glandular weight and PTH secretion has been observed in the rabbit,[21] gland proliferation precedes downregulation of the CaSR.[363] Nevertheless, the CaSR knockout mouse exhibits marked parathyroid gland hyperplasia, showing that the CaSR can indeed influence chief cell proliferation.[196] However, it is clear that the interplay among serum PTH, CaSR expression, and gland hyperplasia is complex since the elevated PTH level in 5/6 nephrectomy rats is reversed after an isogenic kidney transplant without upregulation of CaSR mRNA.[249]

Calcimimetics are Type II Allosteric Enhancers: Role in 2° HPT

Calcimimetics are small, lipophilic organic molecules that function as allosteric enhancers (superagonists) of the CaSR. Thus, calcimimetics are type II agonists that left-shift the ionized Ca^{2+}-PTH secretion curve in parathyroid glands (lower the EC_{50} for ionized Ca^{2+}) without affecting the minimal or maximal responses (Fig. 63.1). As type II agonists, calcimimetics have no effect on PTH secretion in the absence of extracellular Ca^{2+}. In 5/6 nephrectomized and normal rats, calcimimetics cause a dose-dependent decrease in serum PTH and ionized Ca^{2+}.[88,134,306] A first-generation calcimimetic, NPS R-568, was shown to reduce PTH secretion *in vitro* and *in vivo*,[7,133] but it was entirely metabolized by the hepatic P_{450} system and exhibited suboptimal pharmacokinetics in certain individuals. Second-generation calcimimetics (e.g., cinacalcet HCl) overcame this problem in metabolism of the drug (see following sections). Calcimimetics have been shown to reduce PTH secretion in 1° HPT,[321,388,392] 2° HPT,[31,164,165,254,314,346] and parathyroid carcinoma.[393] While calcimimetics can produce a transient increase in calcitonin secretion from thyroidal C cells,[131,306] the dose of calcimimetic that suppresses PTH secretion is at least 10-fold lower than required to alter calcitonin secretion.[131] This apparent specificity of calcimimetics for parathyroid as opposed to other cell types examined to date is an important factor enabling targeted therapy of various forms of hyperparathyroidism.

Calcimimetics reduce plasma Ca^{2+}.[132,321,392,393] The fall in plasma Ca^{2+} is clearly not due to increased renal excretion of Ca^{2+}, given that it occurs in nephrectomized rats,[131] but instead results from the left shift in the relationship between serum Ca^{2+} and PTH. In mild 1° HPT calcimimetics acutely and chronically lower serum PTH and normalize serum Ca^{2+} without increasing urine Ca^{2+} excretion in most patients.[321,392] Activation of the kidney CaSR would be expected to increase urinary Ca^{2+} excretion at any given level of serum Ca^{2+}, and thus the lack of effect of calcimimetics on renal Ca^{2+} excretion in 1° HPT suggests that at doses that reduce the parathyroid set-point, these agents do not exert a calciuric effect owing to their direct renal action. In 1° HPT, a reduced filtered load of Ca^{2+}, decreased bioavailability of the drug in the kidney, or lower calcimimetic sensitivity of the renal, relative to the parathyroid, CaSR have been suggested as the causes of any apparent effect of calcimimetics on the kidney.[131] However, like parathyroidectomy, the calcimimetic NPS R-467 prevents furosemide-induced nephrocalcinosis in rats,[319] suggesting that the reduction in PTH is an important indirect factor in the modulation of renal Ca^{2+} handling in this model. The calcimimetic, cinacalcet HCl (also known as AM 073, KRN 1493, NPS 1493; Cinacalcet HCl, Sensipar in the United States; Mimpara in the European Union), which exhibits good bioavailability and pharmacodynamics,[241,306] lowers serum PTH and serum Ca^{2+} in hemodialysis[31,165,253,254,314,346] and peritoneal dialysis[254] patients with 2° HPT. On the basis of findings from randomized, double-blind studies, cinacalcet HCl was approved for the treatment of secondary HPT.[31,86,112,134,162,305,366]

In the 5/6 nephrectomy model of chronic renal failure in the rat, calcimimetics prevent parathyroid hyperplasia when given at the time of renal mass reduction[419,422] and reduce gland mass when given after the development of diffuse hyperplasia.[88,293,294] These changes in parathyroid gland mass are associated with an increase CaSR and VDR expression[287,372] as well as a reduction in parathyroid cell proliferation.[418] The effects of extracellular Ca^{2+} on parathyroid cell proliferation in culture have been variable[421]; however, parathyroid cells in culture can exhibit a rapid decrease in CaSR expression complicating interpretation of these studies.[290] R-467 suppressed DNA synthesis by 35% in one study,[375] while Ca^{2+} had the opposite effect in cultured parathyroid cells derived from uremic patients that continue to express the CaSR.[374] While the mechanisms for the disparate effects of extracellular Ca^{2+} and calcimimetics remain to be defined,[111,375,421] the downstream mediators of CaSR action on parathyroid gland proliferation–differentiation are under investigation.[91,390] The

CaSR-mediated activation of the mitogen-activated protein kinases (MAPKs; ERK1/2) appears to be linked to the inhibition of PTH secretion.[91,230]

Calcimimetics, the Ca × Pi Product, and Cardiovascular Risk in Dialysis Patients

The elevation of the serum calcium × phosphate product (Ca × Pi) commonly occurring in dialysis patients predisposes them to vascular and tissue calcification and contributes importantly to their increased risk of cardiovascular events.[29,166] Also, plasma PTH levels, as well as those of Pi and calcium, impact on patient survival. As a "uremic toxin",[276,277] the effects of PTH are believed to occur through an alteration in myocardial function and of microvessel thickness.[4,5,33,34] In addition, high Pi concentrations increase vascular calcification,[151,295] an effect that is exacerbated by an elevation in serum calcium concentration.[444] These events are of relevance if one considers that, until the calcimimetics became available, all maneuvers aimed at reducing PTH levels yielded an increase in plasma ionized calcium and of the Ca × Pi product. Indeed, treatment of 2° HPT with $1,25(OH)_2D_3$ or its analogues, while generally initially effective in reducing serum PTH, the calcemic and the phosphatemic effects of vitamin D can ultimately enhance the abnormal mineral metabolism and exacerbate vascular calcification, although retrospective studies have suggested a reduction in overall mortality with vitamin D therapy.[401] In contrast, cinacalcet HCl generally lowers serum Ca^{2+}, serum phosphate, and the serum Ca × Pi product modestly (by ~15%)[32,253,254,346] and decreases both vascular and soft tissue calcification in uremic rats treated with calcitriol,[259] suggesting that this calcimimetic could potentially lower morbidity and mortality due to cardiovascular complications. In the rat uremic model, NPS R-568 treatment has been shown to diminish cardiovascular changes associated with chronic renal failure (cardiac interstitial fibrosis, capillary length density, and arteriolar wall thickness).[312] It is unclear whether calcimimetics reduce cardiovascular risk in animal models by lowering plasma PTH and/or through a direct effect on blood vessels. Evidence that the CaSR is present in rat and porcine blood vessels and that activation of the receptor by high calcium or calcimimetics results in vasodilatation has been demonstrated.[313,437] Also, in uremic rats, but not in sham-operated animals, the calcimimetic R-568 causes a marked and sustained antihypertensive effect.[311] While these animal studies support the potential for a beneficial effect of calcimimetics on cardiovascular risk in chronic renal failure in humans, this latter possibility is currently under investigation. A small meta analysis of four randomized, double-blind, placebo-controlled clinical trials utilizing cinacalcet or placebo in patients who were already being treated with vitamin D and phosphate binders assessed the impact of cinacalcet therapy on end-points other than serum mineral ions and PTH.[98] The results indicated that, relative to patients not receiving cinacalcet who were receiving standard care, patients treated with cinacalcet had a >90% decrease in the rate of parathyroidectomy and about a 40% reduction in hospitalizations for cardiovascular events. The study was not sufficiently powered, however, to determine the effect of the drug on "hard" cardiovascular end-points, such as myocardial infarction or death. Two randomized controlled studies have recently been completed that address this latter point, the ADVANCE ("A randomized study to evaluate the effects of cinacalcet plus low dose vitamin D on vascular calcification in subjects with chronic kidney disease (CKD) receiving hemodialysis") and EVOLVE studies (EValuation Of Cinacalcet HCl Therapy to Lower cardioVascular Events).[79] The results of the ADVANCE trial showed that Cinacalcet produced modest but statistically significant reductions in some indices of vascular (e.g., volume of coronary artery calcification) and valvular (i.e., aortic valve) calcification.[350a] The second of these has as its primary end-points all-cause mortality and first nonfatal cardiovascular event in 3800 chronic dialysis patients treated with a flexible regimen of traditional therapies, and, in addition, receiving either cinacalcet or placebo.[79] While not yet published, the initial results from the EVOLVE trial did not show any reduction in overall cardiovascular mortality in the Cinacalcet-treated patients (www.amgen.com/media/media_pr_detail.jsp?releaseID=1703773).

The severity of osteitis fibrosa is directly proportional to the severity of the 2° HPT and the magnitude of PTH overproduction. While high and sustained elevations in serum PTH in hyperparathyroidism cause osteitis fibrosa, smaller and transient increases in PTH, e.g., those produced by a subcutaneous injection of PTH1-34 or PTH1-84 for the treatment of osteoporosis, have a net anabolic effect on bone.[152] PTH secretion in healthy individuals exhibits complex fluctuations—a circadian rhythm as well as an ultradian rhythm of several PTH pulses per hour.[381] These serum PTH rhythms are generally preserved in chronic renal failure and correlate with serum Ca^{2+}, serum phosphate, and bone metabolism.[135,381] Chronic suppression of PTH secretion with vitamin D analogues in 2° HPT is associated with inhibition of the ultradian and circadian rhythms of PTH, which may contribute to the low bone turnover disease of chronic renal failure.[381] However, while calcimimetics appear to induce a circadian rhythm in serum PTH, interestingly, they do not increase bone mass in ovariectomized rats.[289] In the rat 5/6 nephrectomy model of 2° HPT, NPS R-568 halts the

progression of, and reverses osteitis fibrosa cystica.[420] This response of bone is consistent with the PTH-lowering effect of calcimimetics.[88,132,306] In the rat uremic model, daily intermittent NPS R-568 induces an exaggerated circadian fluctuation in PTH and stabilizes cortical and cancellous bone mass.[215,289]

OTHER APPLICATIONS OF CALCIMIMETICS IN CKD

Recurrent HPT after Parathyroidectomy for Severe 2° or 3° HPT in Patients with End Stage Renal Disease

Some dialysis patients progress from severe 2°, albeit normocalcemic, HPT to a state called "tertiary" (3°) HPT, in which there is frank PTH-dependent hypercalcemia, as noted above.[179,214,340] The progression from 2° to 3° HPT usually occurs coincident with a transition from polyclonal parathyroid hyperplasia to nodular hyperplasia, in which each nodule represents a separate monoclonal growth, behaving functionally like a parathyroid adenoma.[110] Nodular parathyroid glands show an increase in set-point similar to that observed with adenomas in 1° HPT. There is reduced expression of both the CaSR and VDR in this setting, which likely contribute to the associated functional abnormalities.[110] The genetic defects in the parathyroid nodules of patients with 3° HPT, however, usually differ from those seen in parathyroid adenomas.[9,214]

In dialysis patients with 2° or 3° HPT who cannot be adequately controlled by phosphate binders and vitamin D analogues or develop hypercalcemia, subtotal parathyroidectomy may be necessary (or, in some centers, total parathyroidectomy with reimplantation of a small amount of the patient's own parathyroid tissue).[340] Even following initially successful surgery, however, there is a risk of recurrence of HPT ranging from about 10% at three years to 30% after seven years. Cinacalcet might provide a non-surgical approach to the problem of recurrent HPT. In one off-label study (i.e., using the drug in an application not yet formally approved by the FDA) utilizing the drug in this setting in a small number of patients (N = 6), there were substantial reductions in mean PTH (1388 to 435 pg/ml), serum calcium (9.6 to 8.3 mg/dl), serum phosphorus (5.5 to 31.3 mg/dL) and Ca × Pi product (53 to 31 mg^2/dL^2).[258] In additional case reports, cinacalcet has effectively lowered serum calcium to or toward normal in this setting. While the results to date are encouraging, additional experience in CKD patients with recurrent HPT after prior parathyroid surgery is clearly needed to further validate the application of calcimimetics to these patients.

Patients with CKD Prior to the Institution of Dialysis Therapy

There are very limited data on the use of cinacalcet in patients with CKD not yet requiring dialysis.[81] In an off-label, placebo-controlled investigation of 404 patients (75% taking cinacalcet and 25% placebo), cinacalcet reduced PTH by 43% (vs −1.1% in controls) and serum calcium by 8.9% (vs +0.8%), and elevated serum phosphorus by 21% (vs +6.8%), producing a 21% rise in the Ca × Pi product. However, the Ca × Pi product also increased (by 17%) in the placebo group and was 40 mg^2/dL^2 or less in both groups, well within the National Kidney Foundation (NKF) guidelines for this parameter guidelines.[81] There is currently no consensus with regard to whether the drug should be used in this setting. However, given the capacity of cinacalcet to inhibit parathyroid cellular proliferation, it might limit parathyroid hyperplasia in this group; of patients, especially if it were possible to accurately measure parathyroid volume non-invasively. Moreover, in patients with stage 3 and 4 CKD having unusually large elevations in serum PTH, it might make it possible to lower PTH to levels within the NKF guidelines (35–70 pg/mL in stage 3 and 70–110 pg/mL in stage 4). Finally, further studies could determine whether cinacalcet slows the progression of renal failure in stages 3 and 4 CKD, as it does in experimentally-induced renal insufficiency in animal models.[312,338]

Hypercalcemia and HPT Following Renal Transplantation

Renal transplantation is followed by the development of PTH-dependent hypercalcemia in about 10% of patients[22] and persistent, albeit normocalcemic, HPT in additional patients. Hypercalcemia and/or an elevated Ca × Pi product following renal transplantation have been associated with increased mortality and elevated risk of losing the transplanted kidney.[116] Owing to the limited capacity of hyperplastic parathyroid glands to involute, ~50% of patients who are hypercalcemic immediately following transplantation remain so after 12 months. Several studies have utilized cinacalcet to treat hypercalcemia in the post renal transplant period. The largest study carried out to date used the drug off-label in 48 transplant patients who were hypercalcemic or had persistent 2° HPT,[157] but this study did not have an untreated control group. 91% of the hypercalcemic patients became normocalcemic and 70% of the initially normocalcemic patients reached a target PTH of 75 to 125 pg/mL. 10 patients developed hypocalcemia. In several other studies, comparable decrements in PTH and serum calcium were observed

in frankly hypercalcemic patients following renal transplantation.[260]

Some studies have reported hypercalciuria in this setting in patients treated with cinacalcet,[35] which has the potential to damage the transplanted kidney, or the development of modest decreases in renal function.[239] Most reports, however, have not encountered hypercalciuria, and, in those describing reductions in renal function, they were modest (~10% increase in serum creatinine) and were reversible after discontinuing the drug.[239] Increases in bone mineral density have taken place during treatment of patients with cinacalcet following renal transplantation (e.g., in the femoral neck[408]). While this effect of the drug would be very beneficial in such patients, caution is warranted in ascribing this effect to cinacalcet, as control groups were lacking in these two studies.

One study reported that 8 of 9 hypercalcemic renal transplant patients whose serum calcium normalized during treatment for 12 months with cinacalcet remained normocalcemic after cessation of the treatment.[239] Given the absence of a control group, it's unclear whether cinacalcet improved the outcome in these patients, although spontaneous resolution of hypercalcemia in this situation has been estimated to be only ~50%. Thus the drug has the potential to hasten resolution of hypercalcemia and reduce the need for parathyroidectomy post-renal transplant, but further studies are needed in this regard. A recent investigation found that discontinuing cinacalcet therapy before renal transplantation did not adversely impact graft survival.[216] This finding and the stable renal function seen in most patients receiving cinacalcet post renal transplantation are noteworthy, since parathyroidectomy following renal transplantation can be associated with reduction in graft function.[216]

OTHER APPLICATIONS OF CALCIMIMETICS

Parathyroid Carcinoma

Silverberg et al. utilized cinacalcet to treat 29 hypercalcemic patients with inoperable parathyroid cancer.[393] This use of the drug and its application to treating patients with severe hyperparathyroidism who are unable to undergo parathyroid surgery are the only FDA-approved uses of Cinacalcet, in addition to treatment of 2° HPT in stage 5 CKD, in the U.S. The drug has been approved for treatment of 1° HPT in Europe. The mean serum Ca^{2+} in these patients decreased from 14.1 mg/dL to 12.4 mg/dL, with 62% of the patients demonstrating a 1 mg/dL or greater reduction.[393] The patients with the highest initial serum Ca^{2+} showed the largest reduction in serum Ca^{2+} during treatment. While the proportion of patients achieving normocalcemia during treatment with cinacalcet was not explicitly stated, the graphical depiction of the data suggests it to be about 10%.

Serum PTH concentrations, which were measured before the first daily dose of the drug in the morning, did not decline significantly (−4.6%). This observation may reflect the fact that the circulating half-life of cinacalcet is such that serum PTH has increased from its nadir at 2-4 hours following the most recent dose to a level approaching the baseline PTH value by 12-24 hours following the last dose of the drug.[321] Ideally, while measuring the area under the PTH curve over a 24-hour period would provide a more accurate reflection of the integrated impact of cinacalcet on parathyroid function, this is impractical in routine clinical practice. Treatment with cinacalcet did not produce any alteration in quality of life as measured with the SF-36 instrument. Thus at least some biochemical control of hypercalcemia is achievable with cinacalcet in the majority of patients with parathyroid cancer over a time frame of months or longer, but the drug's impact in the longer-term management of this disease, including survival, is not clear at present.

Other Forms of 1° HPT

Cinacalcet has been utilized off-label in patients with 1° HPT in two settings: (1) Mild 1° HPT, as an approach to lowering the serum Ca^{2+} and/or PTH concentrations,[322] and (2) persistent, "intractable" 1° HPT in subjects with a history of failed parathyroid surgery or in those in whom parathyroid surgery is contraindicated.[273] Prior the development of calcimimetics, no medical therapy was available that effectively reduced serum Ca^{2+} on a long-term basis in 1° HPT. In most instances, the CaSR in 1° HPT does not contain the inactivating mutations that are the cause of FHH; thus the calcimimetics are acting upon an inherently normal CaSR.

A placebo-controlled study examined the consequences of treatment with cinacalcet for up to 5 years in patients with mild 1° HPT.[322] After one year, 73% of the patients treated with cinacalcet showed normalization their serum Ca^{2+} concentration, compared with 5% in the placebo group. PTH declined modestly in the cinacalcet-treated group (−7.6%), although the level achieved was significantly lower than in the placebo group. Patients who have undergone successful surgery for 1° HPT demonstrate an increase of ~10% in their BMD over the one to two years after surgery[322]; In contrast, BMD in patients treated with cinacalcet did not rise, although it remained stable over the five years of the study. Thus the drug does not bring about a

true "medical parathyroidectomy".[322] Approximately 20–30% of the patients treated with cinacalcet withdrew from the study during the first year, and an additional 25% withdrew during the last four years, at least in part due to nausea and vomiting, which was present in ~30% of patients; 16% of the placebo group experienced nausea during the first 12 months.[322]

Seventeen patients with intractable 1° HPT, which was of considerably greater severity than in the study just described (mean serum Ca^{2+} of 12.7 mg/dL vs. 10.7 mg/dL, respectively), were treated for a mean of 270 days with cinacalcet. The drug brought about a 1 mg/dL or greater reduction in serum Ca^{2+} in 88% of the patients, and 53% achieved normocalcemia.[273] Cinacalcet has recently been approved for use in treating such patients when they are not candidates for surgery. In summary, off-label treatment of 1° HPT with cinacalcet is costly (several hundred dollars per month depending on the dose) and cannot be considered to be the equivalent of a surgical parathyroidectomy, at least with regard to the skeleton. Furthermore, follow-up of these patients on a regular basis, with the related medical expense, would be required. Therefore, the drug's role in the treatment of 1° HPT other than in patients with parathyroid cancer and those with severe 1° HPT remains unclear. Most likely its use in the United States in mild 1° HPT will be limited to off-label use in subjects unable or unwilling to undergo parathyroidectomy.

Other Forms of Hyperparathyroidism

Cinacalcet has demonstrated some efficacy in several other types of PTH-dependent hypercalcemia. All of these exhibit an elevation in set-point for $Ca^{2+}{}_o$-regulated PTH release, which normalizes or, or returns toward normal, during treatment with calcimimetic, with an associated reduction in serum Ca^{2+}.

One such condition is lithium-induced hypercalcemia. PTH-dependent hypercalcemia occurs in 10–20% of patients being treated with lithium for psychiatric disorders, principally bipolar disorder, although the prevalence of this complication differs widely from <10% to >50% in different series.[380] Lithium-treated patients consistently exhibit an increase in set-point for Ca^{2+}_o-regulated PTH release when studied *in vivo*,[175,350] which likely reflects some direct, but as yet unknown, pharmacological effect of the drug on the parathyroid gland.[47] Some subjects with lithium-induced hyperparathyroidism harbor a parathyroid adenoma if they are subjected to parathyroid surgery, while others have multigland parathyroid hyperplasia. Lithium also decreases renal Ca^{2+} excretion, and can produce a clinical and biochemical presentation of acquired, hypocalciuric, PTH-dependent hypercalcemia resembling FHH.

The therapy of lithium-induced hypercalcemia/hyperparathyroidism can be challenging, because psychiatrists are often reluctant to stop lithium treatment in patients who develop hypercalcemia, which is accompanied by some risk of aggravating the underlying psychiatric disorder. Many such patients have relatively mild hypercalcemia and can be followed expectantly without surgery in a manner similar to that proposed for the follow up of asymptomatic 1° HPT.[27] Several individual case reports or small case series have described off-label treatment of lithium-induced HPT with cinacalcet. Serum calcium concentration declined from an average of 10.8 to 10.0 mg/dL in three patients in one study[169] and from 10.9 to 10.1 in two additional patients.[396] Thus, in subjects with lithium-induced HPT in whom parathyroid surgery is indicated, but the patient refuses or surgery is contraindicated for other reasons, cinacalcet potentially provides an additional mode of treatment.

Familial Hypocalciuric Hypercalcemia

FHH is in most cases a benign clinical condition without long-term sequellae, as noted earlier. Occasional families with FHH, however, exhibit a more severe clinical picture, including neonatal hyperparathyroidism combined with overt bone disease, hypercalcemia that is more severe than the norm in FHH, pancreatitis, or even renal stone disease.[12,182,327] Some such patients have undergone parathyroid surgery,[62,327] providing a rationale for using a calcimimetic as a alternative, medical therapy in these atypical cases. Most FHH mutations demonstrate some capacity for "rescue" of their function by a calcimimetic *in vitro*, providing a rationale for the drug having a Ca^{2+}_o-lowering effect *in vivo*.[212,261,451] There are several reports of FHH being treated off-label with cinacalcet. In one, the drug reduced serum calcium concentration from ~11.4 mg/dL to an average of 9.7 after 12 months of therapy.[406] In another, treatment reduced serum PTH from 148 to 32 pg/ml (normal 7–75) and serum ionized calcium from 1.48 to 1.23 (normal 1.13–1.34).[3] Therefore, the use of a calcimimetic in unusually severe or atypical cases of FHH could: (1) help to assess whether symptoms (such as pancreatitis) are related to the hypercalcemia, and (2) provide an alternative to surgery in the rare case in which the latter was felt to be indicated.

Phosphate-Wasting Disorders

A novel application of treatment with cinacalcet is to alleviate the hypophosphatemia occurring in patients with excessive circulating levels of the phosphaturic hormone, FGF-23.[23,221,228,296] The hypophosphatemia, principally by decreasing the Ca × Pi product, reduces

the structural integrity of bone, producing the characteristic bowing of the lower extremities and other bony abnormalities that are characteristic of the rickets that occurs in the growing skeleton of children.[245] In adults who develop phosphate wasting after growth of the skeleton is complete, hypophosphatemia produces osteomalacia (poorly mineralized bone), in association with bone pain and, in some cases, fractures.[25] Two diseases caused by FGF-23 excess are X-linked hypophosphatemia (XLH) and tumor-induced osteomalacia (TIO).[24,221,367,440] The first is caused by inactivation of the gene encoding PHEX (phosphate-regulating gene with homologies to endopeptidases on the X-chromosome), an endopeptidase whose substrate in unknown, but by an unknown mechanism increases production of FGF-23 by osteocytes.[114,221,436] TIO results from increased synthesis of FGF-23 by tumors of mesenchymal origin, usually benign, which are currently called phosphaturic mesenchymal tumors of the mixed connective tissue type.[219]

Treating patients with either XLH and TIO involves phosphate supplementation combined with administration of $1,25(OH)_2D_3$.[38,221] The latter increases gastrointestinal phosphate absorption and mitigates the 2° HPT caused the transient hypocalcemia that follows administration of phosphate. In spite of treatment with $1,25(OH)_2D_3$, however, 2° (and rarely 3°) HPT may develop, exacerbating the hypophosphatemia owing to PTH-induced phosphaturia.[368] It is the latter complication that prompted the utilization of cinacalcet off-label in XLH[2] and TIO.[149] Administering a single dose of cinacalcet and 20 mg/kg phosphate to eight subjects with XLH produced a decrease in serum PTH (from 34 to 23 pg/ml) and a substantial increase in TmP/GFR (tubular maximum for phosphate corrected for GFR) from 1.7 to 2.5.[2] Chronically administering cinacalcet to two patients with TIO greatly decreased PTH (from 20 to <10 pg/ml in one patient and 24 to <10 pg/ml the other),[149] substantially improved serum phosphate (from 2.8 to 3.7 mg/dL and from 2.8 to 3.4 mg/dL, respectively) and permitted a lowering of the dose of phosphate administered.[149] Thus these preliminary studies suggest a possible role for calcimimetics as an adjunct to supplementation with phosphate and $1,25(OH)_2D_3$ in patients with XLH or TIO, thereby mitigating 2° HPT, enhancing renal phosphate reabsorption, increasing serum calcium $\times$ phosphate product and leading to improved mineralization of bone.

Calciphylaxis

Calciphylaxis (sometimes called calcific uremic arteriolopathy) is a rare but potentially life-threatening condition encountered predominantly in patients with chronic renal insufficiency, particularly those with end stage renal disease receiving dialysis treatment.[99,265,373] Patients present with cutaneous necrosis of variable extent that is painful and can progress and become life-threatening. There is thrombosis of the small cutaneous blood vessels in association with calcification of the media of the vessel wall, which causes skin necrosis.[99,265,373] One of the strongest predictors of the development of calciphylaxis is hyperphosphatemia, associated with the high Ca $\times$ Pi product characteristic of patients with ESRD. While an elevated level of PTH per se is not thought to be a risk factor for calciphylaxis (e.g., the very low incidence of calciphylaxis in PHPT), some consider it a tissue sensitizer predisposing to development of the condition in the presence of other factors initiating the disease, i.e., in ESRD.[99,265,373]

Therapy of calciphylaxis is empiric and suboptimal. In addition to local care of skin ulcers, measures designed to reduce serum phosphorus (and the Ca $\times$ Pi product) using non-calcium-based phosphate binders are a cornerstone of treatment.[99,265,373] Bisphosphonates and the administration of sodium thiophosphate have improved healing of skin lesions in some cases, by an uncertain mechanism(s). Some reports have found that parathyroidectomy prolongs life in individuals with calciphylaxis,[373] providing a rationale for therapy with cinacalcet off-label as a pharmacological approach to lowering serum PTH. This use of cinacalcet has been described in about a dozen articles, mostly single case reports {for example, see[318,342,354,369,386,416]}. While uncontrolled, these studies have shown some efficacy of cinacalcet in treating calciphylaxis, although the use of several other therapies (e.g., bisphosphonates, sodium thiosulfate) concurrently makes it difficult to definitively attribute the observed therapeutic benefit to the calcimimetic. Regardless, the apparent benefit of cinacalcet in these cases affords a rationale for its use in additional patients in this difficult-to-treat condition with its substantial morbidity and mortality.

SUMMARY AND PERSPECTIVES

The field of Ca^{2+}_o-sensing and the CaSR has progressed rapidly since the cloning of the CaSR in 1993. Three major areas of investigation have been: (1) clarifying the CaSR's role in maintaining Ca^{2+}_o homeostasis, (2) identifying and characterizing disorders of Ca^{2+}_o-sensing, and (3) developing CaSR-based therapeutics, especially calcimimetics. Much has been learned about how the CaSR regulates PTH secretion, preproPTH gene expression, and parathyroid cellular proliferation. There is also much greater understanding of how the receptor

regulates the functions of various nephron segments, especially those that relate to the kidney's diverse, key roles in mineral ion homeostasis. The latter include CaSR-mediated control of the 1-hydroxylation of 25-hydroxvitamin D and phosphate handling in the proximal tubule, control of monovalent and divalent cation transport in the TAL, modulation of Ca^{2+} reabsorption in the DCT, regulation of acid secretion, especially in the CCD, and modulation of water reabsorption in both the CCD and IMCD. The relevance of these latter two actions to calcium metabolism have only been elucidated with the recognition that the receptor integrates tubular Ca^{2+} reabsorption with acid secretion and urinary concentration to ensure safe passage of Ca^{2+} salts during their journey through the distal segments of the nephron. Previously unsuspected roles of the CaSR have also emerged in other tissues participating in Ca^{2+}_o homeostasis, especially in bone and intestine. In the former, the CaSR now appears to play critical non-redundant roles of the development, growth and turnover of the skeleton and arguably plays a more fundamental role than vitamin D and the VDR, since loss of the VDR can be compensated nearly completely by provision of normal circulating levels of mineral ions. Finally our understanding of the CaSR's roles in the GI tract is rapidly evolving. The receptor not only promotes the availability of Ca^{2+} in a soluble, readily absorbable form in the stomach, but its ability to sense other components of the ECF, especially pH and amino acids, likely permit it to integrate signals related not only to Ca^{2+} per se but also to other nutrients, especially proteins, and to facilitate the digestion of the latter.

The identification and characterization of inherited diseases of Ca^{2+}_o-sensing, such as familial hypocalciuric hypercalcemia and neonatal severe hyperparathyroidism, as the consequences of inactivating CaSR mutations and autosomal dominant hypoparathyroidism, with or without the features of Bartter's syndrome, as the result of activating CaSR mutations has both clarified the pathophysiology of the CaSR and formally proven its biological relevance. Subsequent studies have uncovered a variety of acquired abnormalities of Ca^{2+}_o-sensing involving the CaSR and its downstream signaling pathways, inactivating or activating antibodies to the CaSR, and alterations in the expression/function of the receptor in 1°, 2° and 3° HPT. The existence of disorders of Ca^{2+}_o-sensing led naturally to the recognition that such disorders might be amenable to treatment with CaSR-based therapeutics, especially the "calcimimetic", allosteric CaSR activators. The first such agent to reach the clinic was cinacalcet HCl, which has been so far only been approved in this country for the treatment of severe 2° HPT in patients receiving dialysis therapy for end stage renal disease, for the therapy of severe hypercalcemia in parathyroid cancer, and for treating severe 1° HPT when surgery is not an option. However, there are a number of currently "off-label" applications where the drug may be useful, such as for treating: (1) hypercalcemia post-renal transplant, (2) recurrent severe hyperparathyroidism after parathyroidectomy in patients with renal failure, (3) lithium-induced hypercalcemia, (4) "severe" or complicated cases of FHH, and (5) the phosphate wasting and iatrogenic 2° HPT in patients with FGF-23 excess.

Although touched on only briefly here, one largely uncharted areas for future investigation are the CaSR's roles in tissues seemingly totally uninvolved on Ca^{2+}_o homeostasis. The receptor regulates myriad cellular processes, a few examples being the growth, differentiation and apoptosis of a variety of cells types[53,129,417] and a variety of processes in the central and peripheral nervous system.[77,80,332,377,417] Further clarification of these roles with not only elucidate important biological questions but may also offer new applications of CaSR-based therapeutics.

CONFLICT OF INTEREST

E.M.B. is an inventor on patents related to the calcium-sensing receptor and calcium receptor active compounds and is receiving royalties on calcimimetics. J.P.G. and D.R. have grants from Amgen.

References

[1] Adams GB, Chabner KT, Alley IR, Olson DP, Szczepiorkowski ZM, Poznansky MC, et al. Stem cell engraftment at the endosteal niche is specified by the calcium-sensing receptor. Nature 2006;439:599–603.

[2] Alon US, Levy-Olomucki R, Moore WV, Stubbs J, Liu S, Quarles LD. Calcimimetics as an adjuvant treatment for familial hypophosphatemic rickets. Clin J Am Soc Nephrol 2008;3:658–64.

[3] Alon US, VandeVoorde RG. Beneficial effect of cinacalcet in a child with familial hypocalciuric hypercalcemia. Pediatr Nephrol 25:1747–50.

[4] Amann K, Neususs R, Ritz E, Irzyniec T, Wiest G, Mall G. Changes of vascular architecture independent of blood pressure in experimental uremia. Am J Hypertens 1995;8:409–17.

[5] Amann K, Tornig J, Flechtenmacher C, Nabokov A, Mall G, Ritz E. Blood-pressure-independent wall thickening of intramyocardial arterioles in experimental uraemia: evidence for a permissive action of PTH. Nephrol Dial Transplant 1995;10:2043–8.

[6] Amlal H, Legoff C, Vernimmen C, Paillard M, Bichara M. Na^+-K^+(NH_4^+)-$2Cl^-$ cotransport in medullary thick ascending limb: control by PKA, PKC, and 20-HET. Am J Physiol 1996;271:C455–63.

[7] Antonsen JE, Sherrard DJ, Andress DL. A calcimimetic agent acutely suppresses parathyroid hormone levels in patients with chronic renal failure. Rapid communication. Kidney Int 1998;53:223–7.

[8] Attie MF, Gill Jr J, Stock JL, Spiegel AM, Downs Jr RW, Levine MA, et al. Urinary calcium excretion in familial hypocalciuric hypercalcemia. Persistence of relative hypocalciuria after induction of hypoparathyroidism. J Clin Invest 1983;72:667–76.

[9] Aucella F, Morrone L, Stallone C, Gesualdo L. The genetic background of uremic secondary hyperparathyroidism. J Nephrol 2005;18:537–47.

[10] Ba J, Friedman PA. Calcium-sensing receptor regulation of renal mineral ion transport. Cell Calcium 2004;35:229–37.

[11] Bai M. Dimerization of G-protein-coupled receptors: roles in signal transduction. Cell Signal 2004;16:175–86.

[12] Bai M, Pearce SH, Kifor O, Trivedi S, Stauffer UG, Thakker RV, et al. *In vivo* and in vitro characterization of neonatal hyperparathyroidism resulting from a de novo, heterozygous mutation in the Ca^{2+}-sensing receptor gene: normal maternal calcium homeostasis as a cause of secondary hyperparathyroidism in familial benign hypocalciuric hypercalcemia. J Clin Invest 1997;99:88–96.

[13] Bai M, Quinn S, Trivedi S, Kifor O, Pearce SHS, Pollak MR, et al. Expression and characterization of inactivating and activating mutations in the human $Ca^{2+}{}_o$-sensing receptor. J Biol Chem 1996;271:19537–45.

[14] Bai M, Trivedi S, Brown EM. Dimerization of the extracellular calcium-sensing receptor (CaR) on the cell surface of CaR-transfected HEK293 cells. J Biol Chem 1998;273:23605–10.

[15] Bai M, Trivedi S, Kifor O, Quinn SJ, Brown EM. Intermolecular interactions between dimeric calcium-sensing receptor monomers are important for its normal function. Proc Natl Acad Sci U S A 1999;96:2834–9.

[16] Bailly C, Imbert-Teboul M, Roinel N, Amiel C. Isoproterenol increases Ca, Mg, and NaCl reabsorption in mouse thick ascending limb. Am J Physiol 1990;258:F1224–31.

[17] Bajwa A, Forster MN, Maiti A, Woolbright BL, Beckman MJ. Specific regulation of CYP27B1 and VDR in proximal versus distal renal cells. Arch Biochem Biophys 2008;477:33–42.

[18] Bapty BW, Dai LJ, Ritchie G, Canaff L, Hendy GN, Quamme GA. Mg^{2+}/Ca^{2+} sensing inhibits hormone-stimulated Mg^{2+} uptake in mouse distal convoluted tubule cells. Am J Physiol 1998;275:F353–60.

[19] Bapty BW, Dai LJ, Ritchie G, Jirik F, Canaff L, Hendy GN, et al. Extracellular Mg^{2+}- and Ca^{2+}-sensing in mouse distal convoluted tubule cells. Kidney Int 1998;53:583–92.

[20] Baron JA, Beach M, Mandel JS, van Stolk RU, Haile RW, Sandler RS, et al. Calcium supplements and colorectal adenomas. Polyp Prevention Study Group. Ann N Y Acad Sci 1999;889:138–45.

[21] Bas S, Aguilera-Tejero E, Bas A, Estepa JC, Lopez I, Madueno JA, et al. The influence of the progression of secondary hyperparathyroidism on the set point of the parathyroid hormone-calcium curve. J Endocrinol 2005;184:241–7.

[22] Bergua C, Torregrosa JV, Fuster D, Gutierrez-Dalmau A, Oppenheimer F, Campistol JM. Effect of cinacalcet on hypercalcemia and bone mineral density in renal transplanted patients with secondary hyperparathyroidism. Transplantation 2008;86: 413–7.

[23] Berndt T, Kumar R. Novel mechanisms in the regulation of phosphorus homeostasis. Physiology (Bethesda) 2009;24: 17–25.

[24] Berndt TJ, Schiavi S, Kumar R. "Phosphatonins" and the regulation of phosphorus homeostasis. Am J Physiol Renal Physiol 2005;289:F1170–82.

[25] Bhan A, Rao AD, Rao DS. Osteomalacia as a result of vitamin D deficiency. Endocrinol Metab Clin North Am 39:321–31 [table of contents].

[26] Bikle DD, Ng D, Tu CL, Oda Y, Xie Z. Calcium- and vitamin D-regulated keratinocyte differentiation. Mol Cell Endocrinol 2001;177:161–71.

[27] Bilezikian JP, Khan AA, Potts Jr. JT. Guidelines for the management of asymptomatic primary hyperparathyroidism: summary statement from the third international workshop. J Clin Endocrinol Metab 2009;94:335–9.

[28] Biner HL, Arpin-Bott MP, Loffing J, Wang X, Knepper M, Hebert SC, et al. Human cortical distal nephron: distribution of electrolyte and water transport pathways. J Am Soc Nephrol 2002;13:836–47.

[29] Blacher J, Guerin AP, Pannier B, Marchais SJ, London GM. Arterial calcifications, arterial stiffness, and cardiovascular risk in end-stage renal disease. Hypertension 2001;38:938–42.

[30] Bland R, Walker EA, Hughes SV, Stewart PM, Hewison M. Constitutive expression of 25-hydroxyvitamin D3-1alpha-hydroxylase in a transformed human proximal tubule cell line: evidence for direct regulation of vitamin D metabolism by calcium. Endocrinology 1999;140:2027–34.

[31] Block GA, Martin KJ, de Francisco AL, Turner SA, Avram MM, Suranyi MG, et al. Cinacalcet for secondary hyperparathyroidism in patients receiving hemodialysis. N Engl J Med 2004;350:1516–25.

[32] Block GA, Zaun D, Smits G, Persky M, Brillhart S, Nieman K, et al. Cinacalcet hydrochloride treatment significantly improves all-cause and cardiovascular survival in a large cohort of hemodialysis patients. Kidney Int 78:578–89.

[33] Bogin E, Levi J, Harary I, Massry SG. Effects of parathyroid hormone on oxidative phosphorylation of heart mitochondria. Miner Electrolyte Metab 1982;7:151–6.

[34] Bogin E, Massry SG, Harary I. Effect of parathyroid hormone on rat heart cells. J Clin Invest 1981;67:1215–27.

[35] Borchhardt KA, Heinzl H, Mayerwoger E, Horl WH, Haas M, Sunder-Plassmann G. Cinacalcet increases calcium excretion in hypercalcemic hyperparathyroidism after kidney transplantation. Transplantation 2008;86:919–24.

[36] Bourdeau JE, Burg MB. Voltage dependence of calcium transport in the thick ascending limb of Henle's loop. Am J Physiol 1979;236:F357–64.

[37] Bouschet T, Martin S, Henley JM. Receptor-activity-modifying proteins are required for forward trafficking of the calcium-sensing receptor to the plasma membrane. J Cell Sci 2005;118:4709–20.

[38] Brame LA, White KE, Econs MJ. Renal phosphate wasting disorders: clinical features and pathogenesis. Semin Nephrol 2004;24:39–47.

[39] Brauner-Osborne H, Jensen AA, Sheppard PO, O'Hara P, Krogsgaard-Larsen P. The agonist-binding domain of the calcium-sensing receptor is located at the amino-terminal domain. J Biol Chem 1999;274:18382–6.

[40] Brauner-Osborne H, Wellendorph P, Jensen AA. Structure, pharmacology and therapeutic prospects of family C G-protein coupled receptors. Curr Drug Targets 2007;8:169–84.

[41] Brehior A, Perret C, Thomasset M. 1,25-dihydroxycholecalciforol and calcium regulate the calbindin-D9K (CaBP 9K) gene expression in fetal rat duodenal organ culture. J Bone Miner Res 1989;4(Suppl. 1):S292.

[42] Breitwieser GE. Calcium sensing receptors and calcium oscillations: calcium as a first messenger. Curr Top Dev Biol 2006;73:85–114.

[43] Wittner M, Mandon B, Roinel N, de Rouffignac C, Di Stefano A. Hormonal stimulation of Ca^{2+} and Mg^{2+} transport in the cortical thick ascending limb of Henle's loop of the mouse: evidence for a change in the paracellular pathway permeability. Pflugers Arch 1993;423(5–6):387–96.

[44] Brown AJ, Ritter CS, Finch JL, Slatopolsky EA. Decreased calcium-sensing receptor expression in hyperplastic parathyroid glands of uremic rats: role of dietary phosphate. Kidney Int 1999;55:1284–92.

[45] Brown AJ, Zhong M, Finch J, Ritter C, McCracken R, Morrissey J, et al. Rat calcium-sensing receptor is regulated by vitamin D but not by calcium. Am J Physiol 1996;270:F454–60.
[46] Brown EM. Clinical utility of calcimimetics targeting the extracellular calcium-sensing receptor (CaSR). Biochem Pharmacol 80:297–307.
[47] Brown EM. Lithium induces abnormal calcium-regulated PTH release in dispersed bovine parathyroid cells. J Clin Endocrinol Metab 1981;52:1046–8.
[48] Brown EM. Clinical lessons from the calcium-sensing receptor. Nat Clin Pract Endocrinol Metab 2007;3:122–33.
[49] Brown EM, Butters R, Katz C, Kifor O. Neomycin mimics the effects of high extracellular calcium concentrations on parathyroid function in dispersed bovine parathyroid cells. Endocrinology 1991;128:3047–54.
[50] Brown EM, Chattopadhyay N, Vassilev PM, Hebert SC. The calcium-sensing receptor (CaR) permits Ca^{2+} to function as a versatile extracellular first messenger. Recent Prog Horm Res 1998;53:257–80.
[51] Brown EM, Gamba G, Riccardi D, Lombardi M, Butters R, Kifor O, et al. Cloning and characterization of an extracellular Ca^{2+}-sensing receptor from bovine parathyroid. Nature 1993;366: 575–80.
[52] Brown EM, Katz C, Butters R, Kifor O. Polyarginine polylysine, and protamine mimic the effects of high extracellular calcium concentrations on dispersed bovine parathyroid cells. J Bone Miner Res 1991;6:1217–25.
[53] Brown EM, MacLeod RJ. Extracellular calcium sensing and extracellular calcium signaling. Physiol Rev 2001;81:239–97.
[54] Brunette MG, Mailloux J, Lajeunesse D. Calcium transport through the luminal membrane of the distal tubule. I. Interrelationship with sodium. Kidney Int 1992;41:281–8.
[55] Buchan AM, Meloche RM. Signal transduction events involved in bombesin-stimulated gastrin release from human G cells in culture. Can J Physiol Pharmacol 1994;72:1060–5.
[56] Buchan AM, Squires PE, Ring M, Meloche RM. Mechanism of action of the calcium-sensing receptor in human antral gastrin cells. Gastroenterology 2001;120:1128–39.
[57] Buchwald PC, Akerstrom G, Westin G. Reduced p18INK4c, $p21CIP_1/WAF_1$ and $p27KIP_1$ mRNA levels in tumours of primary and secondary hyperparathyroidism. Clin Endocrinol (Oxf) 2004;60:389–93.
[58] Burg MB, Green N. Function of the thick ascending limb of Henle's loop. Am J Physiol 1973;224:659–68.
[59] Canadillas S, Canalejo A, Santamaria R, Rodriguez ME, Estepa JC, Martin-Malo A, et al. Calcium-sensing receptor expression and parathyroid hormone secretion in hyperplastic parathyroid glands from humans. J Am Soc Nephrol 2005;16:2190–7.
[60] Canaff L, Hendy GN. Human calcium-sensing receptor gene. Vitamin D response elements in promoters P1 and P2 confer transcriptional responsiveness to 1,25-dihydroxyvitamin D. J Biol Chem 2002;277:30337–50.
[61] Canaff L, Zhou X, Hendy GN. The proinflammatory cytokine, interleukin-6, up-regulates calcium-sensing receptor gene transcription via Stat1/3 and Sp1/3. J Biol Chem 2008;283: 13586–600.
[62] Carling T, Szabo E, Bai M, Ridefelt P, Westin G, Gustavsson P, et al. Familial hypercalcemia and hypercalciuria caused by a novel mutation in the cytoplasmic tail of the calcium receptor [see comments]. J Clin Endocrinol Metab 2000;85: 2042–7.
[63] Carroll MA, McGiff JC, Ferreri NR, Ibraham NG, Songu-Mize E, Schwartzman M. Peptide stimulation of cytochrome P_{450}-related arachidonate metabolism in renomedullary cells: formation of Na^+ -K^+ ATPase inhibitor. Adv Prostaglandin Thromboxane Leukot Res 1985;15:427–30.
[64] Chabardes D, Firsov D, Aarab L, Clabecq A, Bellanger AC, Siaume-Perez S, et al. Localization of mRNAs encoding Ca^{2+}-inhibitable adenylyl cyclases along the renal tubule. Functional consequences for regulation of the cAMP content. J Biol Chem 1996;271:19264–71.
[65] Chabardes D, Imbert-Teboul M, Elalouf JM. Functional properties of Ca^{2+}-inhibitable type 5 and type 6 adenylyl cyclases and role of Ca^{2+} increase in the inhibition of intracellular cAMP content. Cell Signal 1999;11:651–63.
[66] Chakrabarty S, Radjendirane V, Appelman H, Varani J. Extracellular calcium and calcium sensing receptor function in human colon carcinomas: promotion of E-cadherin expression and suppression of beta-catenin/TCF activation. Cancer Res 2003;63:67–71.
[67] Champigneulle A, Siga E, Vassent G, Imbert-Teboul M. Relationship between extra- and intracellular calcium in distal segments of the renal tubule. Role of the Ca^{2+} receptor RaKCaR. J Membr Biol 1997;156:117–29.
[68] Chang W, Chen TH, Pratt S, Shoback D. Amino acids in the second and third intracellular loops of the parathyroid Ca^{2+}-sensing receptor mediate efficient coupling to phospholipase C. J Biol Chem 2000;275:19955–63.
[69] Chang W, Tu C, Bajra R, Komuves L, Miller S, Strewler G, et al. Calcium sensing in cultured chondrogenic RCJ3.1C5.18 cells. Endocrinology 1999;140:1911–9.
[70] Chang W, Tu C, Chen T-H, Komuves L, Oda Y, Pratt S, et al. Expression and signal transduction of calcium-sensing receptors in cartilage and bone. Endocrinology 1999;140:5883–93.
[71] Chang W, Tu C, Chen TH, Bikle D, Shoback D. The extracellular calcium-sensing receptor (CaSR) is a critical modulator of skeletal development. Sci Signal 2008;1 [ra1].
[72] Chang W, Tu C, Pratt S, Chen TH, Shoback D. Extracellular Ca (2 +)-sensing receptors modulate matrix production and mineralization in chondrogenic RCJ3.1C5.18 cells. Endocrinology 2002;143:1467–74.
[73] Chattopadhyay N, Baum M, Bai M, Riccardi D, Hebert SC, Harris HW, et al. Ontogeny of the extracellular calcium-sensing receptor in rat kidney. Am J Physiol 1996;271: F736–43.
[74] Chattopadhyay N, Cheng I, Rogers K, Riccardi D, Hall A, Diaz R, et al. Identification and localization of extracellular Ca^{2+}-sensing receptor in rat intestine. Am J Physiol 1998;274: G122–30.
[75] Chattopadhyay N, Yano S, Tfelt-Hansen J, Rooney P, Kanuparthi D, Bandyopadhyay S, et al. Mitogenic action of calcium-sensing receptor on rat calvarial osteoblasts. Endocrinology 2004;145:3451–62.
[76] Chen C, Barnett J, Congo D, Brown E. Divalent cations suppress 3′,5′-adenosine monophosphate accumulation by stimulating a pertussis toxin-sensitive guanine nucleotide-binding protein in cultured bovine parathyroid cells. Endocrinology 1989;124: 233–9.
[77] Chen W, Bergsman JB, Wang X, Gilkey G, Pierpoint CR, Daniel EA, et al. Presynaptic external calcium signaling involves the calcium-sensing receptor in neocortical nerve terminals. PLoS One 5:e8563.
[78] Cheng I, Qureshi I, Chattopadhyay N, Qureshi A, Butters RR, Hall AE, et al. Expression of an extracellular calcium-sensing receptor in rat stomach. Gastroenterology 1999;116: 118–26.
[79] Chertow GM, Pupim LB, Block GA, Correa-Rotter R, Drueke TB, Floege J, et al. Evaluation of cinacalcet therapy to lower cardiovascular events (EVOLVE): rationale and design overview. Clin J Am Soc Nephrol 2007;2:898–905.
[80] Chiarini A, Dal Pra I, Marconi M, Chakravarthy B, Whitfield JF, Armato U. Calcium-sensing receptor (CaSR) in human brain's pathophysiology: roles in late-onset Alzheimer's disease (LOAD). Curr Pharm Biotechnol 2009;10:317–26.

[81] Chonchol M, Locatelli F, Abboud HE, Charytan C, de Francisco AL, Jolly S, et al. A randomized, double-blind, placebo-controlled study to assess the efficacy and safety of cinacalcet HCl in participants with CKD not receiving dialysis. Am J Kidney Dis 2009;53:197–207.

[82] Chrispal A, Boorugu H, Prabhakar AT, Moses V. Amikacin-induced type 5 Bartter-like syndrome with severe hypocalcemia. J Postgrad Med 2009;55:208–10.

[83] Christensen SE, Nissen PH, Vestergaard P, Heickendorff L, Brixen K, Mosekilde L. Discriminative power of three indices of renal calcium excretion for the distinction between familial hypocalciuric hypercalcaemia and primary hyperparathyroidism: a follow-up study on methods. Clin Endocrinol (Oxf) 2008;69:713–20.

[84] Christiansen B, Wellendorph P, Brauner-Osborne H. Activity of L-alpha-amino acids at the promiscuous goldfish odorant receptor 5.24. Eur J Pharmacol 2006;536:98–101.

[85] Christiansen B, Wellendorph P, Brauner-Osborne H. Known regulators of nitric oxide synthase and arginase are agonists at the human G-protein-coupled receptor GPRC6A. Br J Pharmacol 2006;147:855–63.

[86] Coburn JW, Maung HM. Calcimimetic agents and the calcium-sensing receptor. Curr Opin Nephrol Hypertens 2000;9: 123–32.

[87] Cole DE, Peltekova VD, Rubin LA, Hawker GA, Vieth R, Liew CC, et al. A986S polymorphism of the calcium-sensing receptor and circulating calcium concentrations [see comments]. Lancet 1999;353:112–5.

[88] Colloton M, Shatzen E, Miller G, Stehman-Breen C, Wada M, Lacey D, et al. Cinacalcet HCl attenuates parathyroid hyperplasia in a rat model of secondary hyperparathyroidism. Kidney Int 2005;67:467–76.

[89] Conigrave AD, Mun HC, Brennan SC. Physiological significance of L-amino acid sensing by extracellular Ca^{2+}-sensing receptors. Biochem Soc Trans 2007;35:1195–8.

[90] Conigrave AD, Mun HC, Lok HC. Aromatic L-amino acids activate the calcium-sensing receptor. J Nutr 2007;137: 1524S–7S [discussion 1548S]

[91] Corbetta S, Lania A, Filopanti M, Vincentini L, Ballare E, Spada A. Mitogen-activated protein kinase cascade in human normal and tumoral parathyroid cells. J Clin Endocrinol Metab 2002;87:2201–5.

[92] Corbetta S, Mantovani G, Lania A, Borgato S, Vicentini L, Beretta E, et al. Calcium-sensing receptor expression and signalling in human parathyroid adenomas and primary hyperplasia. Clin Endocrinol (Oxf) 2000;52:339–48.

[93] Costanzo LS, Windhager EE. Calcium and sodium transport by the distal convoluted tubule of the rat. Am J Physiol 1978;235:F492–506.

[94] Cozzolino M, Brancaccio D, Gallieni M, Galassi A, Slatopolsky E, Dusso A. Pathogenesis of parathyroid hyperplasia in renal failure. J Nephrol 2005;18:5–8.

[95] Cozzolino M, Lu Y, Finch J, Slatopolsky E, Dusso AS. p21WAF1 and TGF-alpha mediate parathyroid growth arrest by vitamin D and high calcium. Kidney Int 2001;60:2109–17.

[96] Cozzolino M, Lu Y, Sato T, Yang J, Suarez IG, Brancaccio D, et al. A critical role for enhanced TGF-alpha and EGFR expression in the initiation of parathyroid hyperplasia in experimental kidney disease. Am J Physiol Renal Physiol 2005;289: F1096–102.

[97] Culpepper RM, Andreoli TE. Interactions among prostaglandin E_2, antidiuretic hormone, and cyclic adenosine monophosphate in modulating Cl^- absorption in single mouse medullary thick ascending limbs of Henle. J Clin Invest 1983;71:1588–601.

[98] Cunningham J, Danese M, Olson K, Klassen P, Chertow GM. Effects of the calcimimetic cinacalcet HCl on cardiovascular disease, fracture, and health-related quality of life in secondary hyperparathyroidism. Kidney Int 2005;68:1793–800.

[99] Dauden E, Onate MJ. Calciphylaxis. Dermatol Clin 2008;26:557–68 [ix]

[100] De Jesus Ferreira MC, Bailly C. Extracellular Ca^{2+} decreases chloride reabsorption in rat CTAL by inhibiting cAMP pathway. Am J Physiol 1998;275:F198–203.

[101] de Jesus Ferreira MC, Helies-Toussaint C, Imbert-Teboul M, Bailly C, Verbavatz JM, Bellanger AC, et al. Co-expression of a Ca^{2+}-inhibitable adenylyl cyclase and of a Ca^{2+}- sensing receptor in the cortical thick ascending limb cell of the rat kidney. Inhibition of hormone-dependent cAMP accumulation by extracellular Ca^{2+}. J Biol Chem 1998;273:15192–202.

[102] Chakravarti B, Chattopadhyay N, Brown EM. Signaling through the extracellular calcium-sensing receptor (CaSR). Adv Exp Med Biol 2012;740:103–42.

[103] De Rouffignac C. Multihormonal regulation of nephron epithelia: achieved through combinational mode? Am J Physiol 1995;269:R739–48.

[104] De Rouffignac C, Di Stefano A, Wittner M, Roinel N, Elalouf JM. Consequences of differential effects of ADH and other peptide hormones on thick ascending limb of mammalian kidney [editorial]. Am J Physiol 1991;260:R1023–35.

[105] de Rouffignac C, Quamme G. Renal magnesium handling and its hormonal control. Physiol Rev 1994;74:305–22.

[106] Degenhardt S, Toell A, Weidemann W, Dotzenrath C, Spindler KD, Grabensee B. Point mutations of the human parathyroid calcium receptor gene are not responsible for non-suppressible renal hyperparathyroidism. Kidney Int 1998;53:556–61.

[107] Desfleurs E, Wittner M, Pajaud S, Nitschke R, Rajerison RM, Di Stefano A. The Ca^{2+}-sensing receptor in the rabbit cortical thick ascending limb (CTAL) is functionally not coupled to phospholipase C. Pflugers Arch 1999;437:716–23.

[108] Desfleurs E, Wittner M, Simeone S, Pajaud S, Moine G, Rajerison R, et al. Calcium-sensing receptor: regulation of electrolyte transport in the thick ascending limb of Henle's loop. Kidney Blood Press Res 1998;21:401–12.

[109] Di Stefano A, Desfleurs E, Simeone S, Nitschke R, Wittner M. Ca^{2+} and Mg^{2+} sensor in the thick ascending limb of the loop of Henle. Kidney Blood Press Res 1997;20:190–3.

[110] Drueke T, Martin D, Rodriguez M. Can calcimimetics inhibit parathyroid hyperplasia? Evidence from preclinical studies. Nephrol Dial Transplant 2007;22:1828–39.

[111] Drueke TB. Cell biology of parathyroid gland hyperplasia in chronic renal failure. J Am Soc Nephrol 2000;11:1141–52.

[112] Drueke TB, Ritz E. Treatment of secondary hyperparathyroidism in CKD patients with cinacalcet and/or vitamin D derivatives. Clin J Am Soc Nephrol 2009;4:234–41.

[113] Dvorak MM, Siddiqua A, Ward DT, Carter DH. Physiological changes in extracellular calcium concentration directly control osteoblast function in the absence of calciotropic hormones. Proc Natl Acad Sci U S A 2004;101:5140–5.

[114] Econs MJ, Francis F. Positional cloning of the PEX gene: new insights into the pathophysiology of X-linked hypophosphatemic rickets. Am J Physiol 1997;273:F489–98.

[115] Egbuna OI, Brown EM. Hypercalcaemic and hypocalcaemic conditions due to calcium-sensing receptor mutations. Best Pract Res Clin Rheumatol 2008;22:129–48.

[116] Egbuna OI, Taylor JG, Bushinsky DA, Zand MS. Elevated calcium phosphate product after renal transplantation is a risk factor for graft failure. Clin Transplant 2007;21:558–66.

[117] El-Hajj Fuleihan GE-H, Seifter J, Scott J, Brown EM. Calcium-regulated renal calcium handling in healthy men:

relationship to sodium handling. J Clin Endocrinol Metab 1998;83:2366–72.
[118] Enomoto H, Hendy GN, Andrews GK, Clemens TL. Regulation of avian calbindin-D28K gene expression in primary chick kidney cells: importance of posttranscriptional mechanisms and calcium ion concentration. Endocrinology 1992;130:3467–74.
[119] Eren PA, Turan K, Berber I, Canbakan M, Kara M, Tellioglu G, et al. The clinical significance of parathyroid tissue calcium sensing receptor gene polymorphisms and expression levels in end-stage renal disease patients. Clin Nephrol 2009; 72:114–21.
[120] Escalante B, Erlij D, Falck JR, McGiff JC. Effect of cytochrome P_{450} arachidonate metabolites on ion transport in rabbit kidney loop of Henle. Science 1991;251:799–802.
[121] Escalante B, Erlij D, Falck JR, McGiff JC. Ion transport inhibition in the medullary thick ascending limb of Henle's loop by cytochrome P_{450}-arachidonic acid metabolites. Adv Prostaglandin Thromboxane Leukot Res 1991;21A:209–12.
[122] Farnebo F, Enberg U, Grimelius L, Backdahl M, Schalling M, Larsson C, et al. Tumor-specific decreased expression of calcium sensing receptor messenger ribonucleic acid in sporadic primary hyperparathyroidism. J Clin Endocrinol Metab 1997;82:3481–6.
[123] Farnebo F, Hoog A, Sandelin K, Larsson C, Farnebo LO. Decreased expression of calcium-sensing receptor messenger ribonucleic acids in parathyroid adenomas. Surgery 1998;124:1094–8 [discussion 1098-9].
[124] Favus MJ, Kathpalia SC, Coe FL. Kinetic characteristics of calcium absorption and secretion by rat colon. Am J Physiol 1981;240:G350–4.
[125] Feng J, Petersen CD, Coy DH, Jiang JK, Thomas CJ, Pollak MR, et al. Calcium-sensing receptor is a physiologic multimodal chemosensor regulating gastric G-cell growth and gastrin secretion. Proc Natl Acad Sci U S A 107:17791–6.
[126] Ferreri NR, An SJ, McGiff JC. Cyclooxygenase-2 expression and function in the medullary thick ascending limb. Am J Physiol 1999;277:F360–8.
[127] Ferreri NR, McGiff JC, Carroll MA, Quilley J. Renal COX-2 cytokines and 20-HETE: tubular and vascular mechanisms. Curr Pharm Des 2004;10:613–26.
[128] Ferreri NR, McGiff JC, Vio CP, Carroll MA. TNFalpha regulates renal COX-2 in the rat thick ascending limb (TAL). Thromb Res 2003;110:277–80.
[129] Finney BA, del Moral PM, Wilkinson WJ, Cayzac S, Cole M, Warburton D, et al. Regulation of mouse lung development by the extracellular calcium-sensing receptor, CaR. J Physiol 2008;586:6007–19.
[130] Firsov D, Aarab L, Mandon B, Siaume-Perez S, Rouffignac SD, Chabardes D. Arachidonic acid inhibits hormone-stimulated cAMP accumulation in the medullary thick ascending limb of the rat kidney by a mechanism sensitive to pertussis toxin. Pfleugers Arch 1995;429:636–46.
[131] Fox J, Lowe SH, Conklin RL, Petty BA, Nemeth EF. Calcimimetic compound NPS R-568 stimulates calcitonin secretion but selectively targets parathyroid gland Ca(2+) receptor in rats. J Pharmacol Exp Ther 1999;290:480–6.
[132] Fox J, Lowe SH, Petty BA, Nemeth EF. NPS R-568: a type II calcimimetic compound that acts on parathyroid cell calcium receptor of rats to reduce plasma levels of parathyroid hormone and calcium. J Pharmacol Exp Ther 1999;290:473–9.
[133] Fox J, Petty B, Nemeth EF. A first generation calcimimetic compond (NpsR-568) that acts on parathyroid cell calcium receptor: a novel approachfor hyperparathyroidism. J Bone Miner Res 1993;8(Suppl. 1):S181 [(Abstract].
[134] Franceschini N, Joy MS, Kshirsagar A. Cinacalcet HCl: a calcimimetic agent for the management of primary and secondary hyperparathyroidism. Expert Opin Investig Drugs 2003;12: 1413–21.
[135] Fraser WD, Ahmad AM, Vora JP. The physiology of the circadian rhythm of parathyroid hormone and its potential as a treatment for osteoporosis. Curr Opin Nephrol Hypertens 2004;13:437–44.
[136] Fray JC, Lush DJ, Park CS. Interrelationship of blood flow, juxtaglomerular cells, and hypertension: role of physical equilibrium and Ca. Am J Physiol 1986;251:R643–62.
[137] Fray JC, Park CS, Valentine AN. Calcium and the control of renin secretion. Endocr Rev 1987;8:53–93.
[138] Friedman PA. Codependence of renal calcium and sodium transport. Annu Rev Physiol 1998;60:179–97.
[139] Friedman PA. Calcium transport in the kidney. Curr Opin Nephrol Hypertens 1999;8:589–95.
[140] Friedman PA, Gesek FA. Cellular calcium transport in renal epithelia: measurement, mechanisms, and regulation. Physiol Rev 1995;75:429–71.
[141] Fudge NJ, Kovacs CS. Physiological studies in heterozygous calcium sensing receptor (CaSR) gene-ablated mice confirm that the CaSR regulates calcitonin release in vivo. BMC Physiol 2004;4:5.
[142] Fushimi K, Sasaki S, Marumo F. Phosphorylation of serine 256 is required for cAMP-dependent regulatory exocytosis of the aquaporin-2 water channel. J Biol Chem 1997;272: 14800–4.
[143] Gama L, Baxendale-Cox LM, Breitwieser GE. Ca^{2+}-sensing receptors in intestinal epithelium. Am J Physiol 1997;273: C1168–75.
[144] Garland C, Shekelle RB, Barrett-Connor E, Criqui MH, Rossof AH, Paul O. Dietary vitamin D and calcium and risk of colorectal cancer: a 19-year prospective study in men. Lancet 1985;1:307–9.
[145] Garner SC, Pi M, Tu Q, Quarles LD. Rickets in cation-sensing receptor-deficient mice: an unexpected skeletal phenotype. Endocrinology 2001;142:3996–4005.
[146] Geibel J, Sritharan K, Geibel R, Geibel P, Persing JS, Seeger A, et al. Calcium-sensing receptor abrogates secretagogue-induced increases in intestinal net fluid secretion by enhancing cyclic nucleotide destruction. Proc Natl Acad Sci USA 2006;103:9390–7.
[147] Geibel JP, Hebert SC. The functions and roles of the extracellular Ca^{2+}-sensing receptor along the gastrointestinal tract. Annu Rev Physiol 2009;71:205–17.
[148] Geibel JP, Wagner CA, Caroppo R, Qureshi I, Gloeckner J, Manuelidis L, et al. The stomach divalent ion sensing receptor (SCAR) is a modulator of gastric acid secretion. J Biol Chem 2001;15:15.
[149] Geller JL, Khosravi A, Kelly MH, Riminucci M, Adams JS, Collins MT. Cinacalcet in the management of tumor-induced osteomalacia. J Bone Miner Res 2007;22:931–7.
[150] Gerbino A, Ruder WC, Curci S, Pozzan T, Zaccolo M, Hofer AM. Termination of cAMP signals by Ca^{2+} and G(alpha)i via extracellular Ca^{2+} sensors: a link to intracellular Ca^{2+} oscillations. J Cell Biol 2005;171:303–12.
[151] Giachelli CM, Jono S, Shioi A, Nishizawa Y, Mori K, Morii H. Vascular calcification and inorganic phosphate. Am J Kidney Dis 2001;38:S34–7.
[152] Girotra M, Rubin MR, Bilezikian JP. Anabolic skeletal therapy for osteoporosis. Arq Bras Endocrinol Metabol 2006;50:745–54.
[153] Glaudemans B, Knoers NV, Hoenderop JG, Bindels RJ. New molecular players facilitating Mg^{2+} reabsorption in the distal convoluted tubule. Kidney Int 77:17–22.

[154] Gogusev J, Duchambon P, Hory B, Giovannini M, Goureau Y, Sarfati E, et al. Depressed expression of calcium receptor in parathyroid gland tissue of patients with hyperparathyroidism. Kidney Int 1997;51:328–36.
[155] Goldsmith PK, Fan GF, Ray K, Shiloach J, McPhie P, Rogers KV, et al. Expression, purification, and biochemical characterization of the amino- terminal extracellular domain of the human calcium receptor. J Biol Chem 1999;274:11303–9.
[156] Goltzman D, Miao D, Panda DK, Hendy GN. Effects of calcium and of the Vitamin D system on skeletal and calcium homeostasis: lessons from genetic models. J Steroid Biochem Mol Biol 2004;89-90:485–9.
[157] Gomez Marques G, Obrador Mulet A, Vilar Gimeno A, Pascual Felip MJ, Alarcon Zurita A, Molina Guasch M, et al. Treatment with cinacalcet of secondary hyperparathyroidism after renal transplantation. Transplant Proc 2009;41:2139–43.
[158] Goo T, Akiba Y, Kaunitz JD. Mechanisms of intragastric pH sensing. Curr Gastroenterol Rep
[159] Goo T, Akiba Y, Kaunitz JD. Mechanisms of Intragastric pH Sensing. Curr Gastroenterol Rep 12:465–70.
[160] Good DW. Ammonium transport by the thick ascending limb of Henle's loop. Annu Rev Physiol 1994;56:623–47.
[161] Good DW, George T, Wang DH. Angiotensin II inhibits HCO_3 absorption via a cytochrome P_{450}-dependent pathway in MTAL. Am J Physiol 1999;276:F726–36.
[162] Goodman WG. Calcimimetic agents and secondary hyperparathyroidism: rationale for use and results from clinical trials. Pediatr Nephrol 2003;18:1206–10.
[163] Goodman WG, Belin T, Gales B, Juppner H, Segre GV, Salusky IB. Calcium-regulated parathyroid hormone release in patients with mild or advanced secondary hyperparathyroidism. Kidney Int 1995;48:1553–8.
[164] Goodman WG, Frazao JM, Goodkin DA, Turner SA, Liu W, Coburn JW. A calcimimetic agent lowers plasma parathyroid hormone levels in patients with secondary hyperparathyroidism. Kidney Int 2000;58:436–45.
[165] Goodman WG, Hladik GA, Turner SA, Blaisdell PW, Goodkin DA, Liu W, et al. The Calcimimetic agent AMG 073 lowers plasma parathyroid hormone levels in hemodialysis patients with secondary hyperparathyroidism. J Am Soc Nephrol 2002;13:1017–24.
[166] Goodman WG, London G, Amann K, Block GA, Giachelli C, Hruska KA, et al. Vascular calcification in chronic kidney disease. Am J Kidney Dis 2004;43:572–9.
[167] Goodman WG, Quarles LD. Development and progression of secondary hyperparathyroidism in chronic kidney disease: lessons from molecular genetics. Kidney Int 2008;74:276–88.
[168] Greger R. Ion transport mechanism in thick ascending limb of Henle's loop of mammalian nephron. Physiol Rev 1985;65:760–97.
[169] Gregoor PS, de Jong GM. Lithium hypercalcemia, hyperparathyroidism, and cinacalcet. Kidney Int 2007;71:470.
[170] Grider JS, Falcone JC, Kilpatrick EL, Ott CE, Jackson BA. P_{450} arachidonate metabolites mediate bradykinin-dependent inhibition of NaCl transport in the rat thick ascending limb. Can J Physiol Pharmacol 1997;75:91–6.
[171] Griffith LE, Guyatt GH, Cook RJ, Bucher HC, Cook DJ. The influence of dietary and nondietary calcium supplementation on blood pressure: an updated metaanalysis of randomized controlled trials. Am J Hypertens 1999;12:84–92.
[172] Gu R, Wei Y, Jiang H, Balazy M, Wang W. Role of 20-HETE in mediating the effect of dietary K intake on the apical K channels in the mTAL. Am J Physiol Renal Physiol 2001;280: F223–30.
[173] Gu RM, Wei Y, Jiang HL, Lin DH, Sterling H, Bloom P, et al. K depletion enhances the extracellular Ca^{2+}-induced inhibition of the apical K channels in the mTAL of rat kidney. J Gen Physiol 2002;119:33–44.
[174] Gunn IR, Gaffney D. Clinical and laboratory features of calcium-sensing receptor disorders: a systematic review. Ann Clin Biochem 2004;41:441–58.
[175] Haden ST, Stoll AL, McCormick S, Scott J, Fuleihan GE-H. Alteraions in parathyroid dynamics in lithium-treated subjects. J Clin Endocrinol Metab 1997;82:2844–8.
[176] Hammerland LG, Krapcho KJ, Garrett JE, Alasti N, Hung BC, Simin RT, et al. Domains determining ligand specificity for Ca^{2+} receptors. Mol Pharmacol 1999;55:642–8.
[177] Han S, Tang R, Anderson LK, Woerner TE, Pei ZM. A cell surface receptor mediates extracellular Ca^{2+} sensing in guard cells. Nature 2003;425:196–200.
[178] Handlogten ME, Huang C, Shiraishi N, Awata H, Miller RT. The Ca^{2+}-sensing receptor activates cytosolic phospholipase A2 via a Gqalpha-dependent ERK-independent pathway. J Biol Chem 2001;276:13941–8.
[179] Harach HR, Jasani B. Parathyroid hyperplasia in tertiary hyperparathyroidism: a pathological and immunohistochemical reappraisal. Histopathology 1992;21:513–9.
[180] Harrison-Bernard LM. The renal renin-angiotensin system. Adv Physiol Educ 2009;33:270–4.
[181] Hartman TJ, Albert PS, Snyder K, Slattery ML, Caan B, Paskett E, et al. The association of calcium and vitamin D with risk of colorectal adenomas. J Nutr 2005;135:252–9.
[182] Hauache OM. Extracellular calcium-sensing receptor: structural and functional features and association with diseases. Braz J Med Biol Res 2001;34:577–84.
[183] Hauache OM, Hu J, Ray K, Xie R, Jacobson KA, Spiegel AM. Effects of a calcimimetic compound and naturally activating mutations on the human Ca^{2+} receptor and on Ca^{2+} receptor/metabotropic glutamate chimeric receptors. Endocrinology 2000;141:4156–63.
[184] Haven CJ, van Puijenbroek M, Karperien M, Fleuren GJ, Morreau H. Differential expression of the calcium sensing receptor and combined loss of chromosomes 1q and 11q in parathyroid carcinoma. J Pathol 2004;202:86–94.
[185] Heath Hd Jackson CE, Otterud B, Leppert MF. Genetic linkage analysis in familial benign (hypocalciuric) hypercalcemia: evidence for locus heterogeneity. Am J Hum Genet 1993;53: 193–200.
[186] Hebert SC. Extracellular calcium-sensing receptor: implications for calcium and magnesium handling in the kidney. Kidney Int 1996;50:2129–39.
[187] Hebert SC. Bartter syndrome. Curr Opin Nephrol Hypertens 2003;12:527–32.
[188] Hebert SC. Calcium and salinity sensing by the thick ascending limb: a journey from mammals to fish and back again. Kidney Int Suppl 2004;S28–33.
[189] Hebert SC, Andreoli TE. Control of NaCl transport in the thick ascending limb. Am J Physiol 1984;246:F745–56.
[190] Hebert SC, Brown EM, Harris HW. Role of the Ca^{2+}-sensing receptor in divalent mineral ion homeostasis. J Exp Biol 1997;200:295–302.
[191] Hebert SC, Desir G, Giebisch G, Wang W. Molecular diversity and regulation of renal potassium channels. Physiol Rev 2005;85:319–71.
[192] Hebert SC. Calcium and salinity sensing by the thick ascending limb: a journey from mammals to fish and back again. Kidney Int 2004;(Suppl.):S28–33.
[193] Helies-Toussaint C, Aarab L, Gasc JM, Verbavatz JM, Chabardes D. Cellular localization of type 5 and type 6 ACs in collecting duct and regulation of cAMP synthesis. Am J Physiol Renal Physiol 2000;279:F185–94.

[194] Hira T, Nakajima S, Eto Y, Hara H. Calcium-sensing receptor mediates phenylalanine-induced cholecystokinin secretion in enteroendocrine STC-1 cells. Febs J 2008;275:4620–6.
[195] Hjalm G, MacLeod RJ, Kifor O, Chattopadhyay N, Brown EM. Filamin-A binds to the carboxyl-terminal tail of the calcium-sensing receptor, an interaction that participates in CaR-mediated activation of mitogen-activated protein kinase. J Biol Chem 2001;276:34880–7.
[196] Ho C, Conner DA, Pollak MR, Ladd DJ, Kifor O, Warren HB, et al. A mouse model of human familial hypocalciuric hypercalcemia and neonatal severe hyperparathyroidism [see comments]. Nat Genet 1995;11:389–94.
[197] Hoenderop JG, Bindels RJ. Epithelial Ca^{2+} and Mg^{2+} channels in health and disease. J Am Soc Nephrol 2005;16:15–26.
[198] Hoenderop JG, Dardenne O, Van Abel M, Van Der Kemp AW, Van Os CH, St-Arnaud R, et al. Modulation of renal Ca^{2+} transport protein genes by dietary Ca^{2+} and 1,25-dihydroxyvitamin D3 in 25-hydroxyvitamin D3-1alpha-hydroxylase knockout mice. Faseb J 2002;16:1398–406.
[199] Hoenderop JG, Nilius B, Bindels RJ. Molecular mechanism of active Ca^{2+} reabsorption in the distal nephron. Annu Rev Physiol 2002;64:529–49.
[200] Hoenderop JG, van der Kemp AW, Urben CM, Strugnell SA, Bindels RJ. Effects of vitamin D compounds on renal and intestinal Ca^{2+} transport proteins in 25-hydroxyvitamin D3-1alpha-hydroxylase knockout mice. Kidney Int 2004;66:1082–9.
[201] Hofer AM, Brown EM. Extracellular calcium sensing and signalling. Nat Rev Mol Cell Biol 2003;4:530–8.
[202] Hosokawa Y, Pollak MR, Brown EM, Arnold A. Mutational analysis of the extracellular Ca^{2+}-sensing receptor gene in human parathyroid tumors. J Clin Endocrinol Metab 1995;80:3107–10.
[203] Hough TA, Bogani D, Cheeseman MT, Favor J, Nesbit MA, Thakker RV, et al. Activating calcium-sensing receptor mutation in the mouse is associated with cataracts and ectopic calcification. Proc Natl Acad Sci USA 2004;101:13566–71.
[204] Hu J, Hauache O, Spiegel AM. Human Ca^{2+} receptor cysteine-rich domain. Analysis of function of mutant and chimeric receptors. J Biol Chem 2000;275:16382–9.
[205] Hu J, McLarnon SJ, Mora S, Jiang J, Thomas C, Jacobson KA, et al. A region in the seven-transmembrane domain of the human Ca^{2+} receptor critical for response to Ca^{2+}. J Biol Chem 2005;280:5113–20.
[206] Hu J, Reyes-Cruz G, Chen W, Jacobson KA, Spiegel AM. Identification of acidic residues in the extracellular loops of the seven-transmembrane domain of the human Ca^{2+} receptor critical for response to Ca^{2+} and a positive allosteric modulator. J Biol Chem 2002;277:46622–31.
[207] Hu J, Spiegel AM. Naturally occurring mutations in the extracellular Ca^{2+}-sensing receptor: implications for its structure and function. Trends endocrinol metabol 2003;14:282–8.
[208] Huang C, Hujer KM, Wu Z, Miller RT. The Ca^{2+}-sensing receptor couples to Galpha12/13 to activate phospholipase D in Madin-Darby canine kidney cells. Am J Physiol Cell Physiol 2004;286:C22–30.
[209] Huang C, Miller RT. The calcium-sensing receptor and its interacting proteins. J Cell Mol Med 2007;11:923–34.
[210] Huang C, Miller RT. Novel Ca receptor signaling pathways for control of renal ion transport. Curr Opin Nephrol Hypertens 2010;19:106–12.
[211] Huang C, Sindic A, Hill CE, Hujer KM, Chan KW, Sassen M, et al. Interaction of the Ca^{2+}-sensing receptor with the inwardly rectifying potassium channels Kir4.1 and Kir4.2 results in inhibition of channel function. Am J Physiol Renal Physiol 2007;292:F1073–81.
[212] Huang Y, Breitwieser GE. Rescue of calcium-sensing receptor mutants by allosteric modulators reveals a conformational checkpoint in receptor biogenesis. J Biol Chem 2007;282:9517–25.
[213] Huang Y, Zhou Y, Yang W, Butters R, Lee HW, Li S, et al. Identification and dissection of Ca^{2+}-binding sites in the extracellular domain of Ca^{2+}-sensing receptor. J Biol Chem 2007.
[214] Imanishi Y, Tahara H, Palanisamy N, Spitalny S, Salusky IB, Goodman W, et al. Clonal chromosomal defects in the molecular pathogenesis of refractory hyperparathyroidism of uremia. J Am Soc Nephrol 2002;13:1490–8.
[215] Ishii H, Wada M, Furuya Y, Nagano N, Nemeth EF, Fox J. Daily intermittent decreases in serum levels of parathyroid hormone have an anabolic-like action on the bones of uremic rats with low-turnover bone and osteomalacia. Bone 2000;26:175–82.
[216] Jadoul M, Banos A, Zani VJ, Hercz G. The effects of discontinuing cinacalcet at the time of kidney transplantation. NDT Plus 3:37–41.
[217] Jara A, von Hoveling A, Jara X, Burgos ME, Valdivieso A, Mezzano S, et al. Effect of endothelin receptor antagonist on parathyroid gland growth, PTH values and cell proliferation in azotemic rats. Nephrol Dial Transplant 2006;21:917–23.
[218] Jensen AA, Hansen JL, Sheikh SP, Brauner-Osborne H. Probing intermolecular protein-protein interactions in the calcium-sensing receptor homodimer using bioluminescence resonance energy transfer (BRET). Eur J Biochem 2002;269:5076–87.
[219] Jonsson KB, Zahradnik R, Larsson T, White KE, Sugimoto T, Imanishi Y, et al. Fibroblast growth factor 23 in oncogenic osteomalacia and X-linked hypophosphatemia. N Engl J Med 2003;348:1656–63.
[220] Jung J, Foroud TM, Eckert GJ, Flury-Wetherill L, Edenberg HJ, Xuei X, et al. Association of the calcium-sensing receptor gene with blood pressure and urinary calcium in African-Americans. J Clin Endocrinol Metab 2009;94:1042–8.
[221] Juppner H. Novel regulators of phosphate homeostasis and bone metabolism. Ther Apher Dial 2007;11(Suppl 1):S3–22.
[222] Kallay E, Bajna E, Wrba F, Kriwanek S, Peterlik M, Cross HS. Dietary calcium and growth modulation of human colon cancer cells: role of the extracellular calcium-sensing receptor. Cancer Detect Prev 2000;24:127–36.
[223] Kallay E, Wrba F, Cross HS. Dietary calcium and colon cancer prevention. Forum Nutr 2003;56:188–90.
[224] Kang HS, Kerstan D, Dai L, Ritchie G, Quamme GA. Aminoglycosides inhibit hormone-stimulated Mg^{2+} uptake in mouse distal convoluted tubule cells. Can J Physiol Pharmacol 2000;78:595–602.
[225] Kantham L, Quinn SJ, Egbuna OI, Baxi K, Butters R, Pang JL, et al. The calcium-sensing receptor (CaSR) defends against hypercalcemia independently of its regulation of parathyroid hormone secretion. Am J Physiol Endocrinol Metab 2009;297:E915–23.
[226] Katsura T, Gustafson CE, Ausiello DA, Brown D. Protein kinase A phosphorylation is involved in regulated exocytosis of aquaporin-2 in transfected LLC-PK1 cells. Am J Physiol 1997;272:F817–22.
[227] Kemp EH, Gavalas NG, Krohn KJ, Brown EM, Watson PF, Weetman AP. Activating autoantibodies against the calcium-sensing receptor detected in two patients with autoimmune polyendocrine syndrome type 1. J Clin Endocrinol Metab 2009;94:4749–56.
[228] Kiela PR, Ghishan FK. Recent advances in the renal-skeletal-gut axis that controls phosphate homeostasis. Lab Invest 2009;89:7–14.

[229] Kifor O, Diaz R, Butters R, Brown EM. The Ca^{2+}-sensing receptor (CaR) activates phospholipases C, A2, and D in bovine parathyroid and CaR-transfected, human embryonic kidney (HEK293) cells. J Bone Miner Res 1997;12:715–25.

[230] Kifor O, MacLeod RJ, Diaz R, Bai M, Yamaguchi T, Yao T, et al. Regulation of MAP kinase by calcium-sensing receptor in bovine parathyroid and CaR-transfected HEK293 cells. Am J Physiol Renal Physiol 2001;280:F291–302.

[231] Kifor O, McElduff A, LeBoff MS, Moore Jr. FD, Butters R, Gao P, et al. Activating antibodies to the calcium-sensing receptor in two patients with autoimmune hypoparathyroidism. J Clin Endocrinol Metab 2004;89:548–56.

[232] Kifor O, Moore Jr. FD, Delaney M, Garber J, Hendy GN, Butters R, et al. A syndrome of hypocalciuric hypercalcemia caused by autoantibodies directed at the calcium-sensing receptor. J Clin Endocrinol Metab 2003;88:60–72.

[233] Kifor O, Moore Jr. FD, Wang P, Goldstein M, Vassilev P, Kifor I, et al. Reduced immunostaining for the extracellular Ca^{2+}-sensing receptor in primary and uremic secondary hyperparathyroidism [see comments]. J Clin Endocrinol Metab 1996;81:1598–606.

[234] Kikeri D, Sun A, Zeidel ML, Hebert SC. Cell membranes impermeable to NH_3. Nature 1989;339:478–80.

[235] Kikeri D, Sun A, Zeidel ML, Hebert SC. Cellular $NH_4^+/K+$ transport pathways in mouse medullary thick limb of Henle. Regulation by intracellular pH. J Gen Physiol 1992;99:435–61.

[236] Knepper MA. NH_4+ transport in the kidney. Kidney Int Suppl 1991;33:S95–102.

[237] Kobayashi M, Tanaka H, Tsuzuki K, Tsuyuki M, Igaki H, Ichinose Y, et al. Two novel missense mutations in calcium-sensing receptor gene associated with neonatal severe hyperparathyroidism. J Clin Endocrinol Metab 1997;82:2716–9.

[238] Kos CH, Karaplis AC, Peng JB, Hediger MA, Goltzman D, Mohammad KS, et al. The calcium-sensing receptor is required for normal calcium homeostasis independent of parathyroid hormone. J Clin Invest 2003;111:1021–8.

[239] Kruse AE, Eisenberger U, Frey FJ, Mohaupt MG. Effect of cinacalcet cessation in renal transplant recipients with persistent hyperparathyroidism. Nephrol Dial Transplant 2007;22: 2362–5.

[240] Kuang D, Yao Y, Lam J, Tsushima RG, Hampson DR. Cloning and characterization of a family C orphan G-protein coupled receptor. J Neurochem 2005;93:383–91.

[241] Kumar GN, Sproul C, Poppe L, Turner S, Gohdes M, Ghoborah H, et al. Metabolism and disposition of calcimimetic agent cinacalcet HCl in humans and animal models. Drug Metab Dispos 2004;32:1491–500.

[242] Kunishima N, Shimada Y, Tsuji Y, Sato T, Yamamoto M, Kumasaka T, et al. Structural basis of glutamate recognition by a dimeric metabotropic glutamate receptor. Nature 2000;407: 971–7.

[243] Kurokawa K. Nephrology forum: calcium-regulating hormones and the kidney. Kidney Int 1987;32:760–71.

[244] Kurokawa K. The kidney and calcium homeostasis. Kidney Int 1994;45(Suppl. 44):S97–105.

[245] Land C, Schoenau E. Fetal and postnatal bone development: reviewing the role of mechanical stimuli and nutrition. Best Pract Res Clin Endocrinol Metab 2008;22:107–18.

[246] Law Jr WM, Heath III H. Familial benign hypercalcemia (hypocalciuric hypercalcemia). Clinical and pathogenetic studies in 21 families. Ann Int Med 1985;105:511–9.

[247] Layer P, Hotz J, Eysselein VE, Jansen JB, Lamers CB, Schmitz-Moormann HP, et al. Effects of acute hypercalcemia on exocrine pancreatic secretion in the cat. Gastroenterology 1985;88:1168–74.

[248] Levi R, Ben-Dov IZ, Lavi-Moshayoff V, Dinur M, Martin D, Naveh-Many T, et al. Increased parathyroid hormone gene expression in secondary hyperparathyroidism of experimental uremia is reversed by calcimimetics: correlation with post-translational modification of the transacting factor AUF1. J Am Soc Nephrol 2006;17:107–12.

[249] Lewin E, Garfia B, Recio FL, Rodriguez M, Olgaard K. Persistent downregulation of calcium-sensing receptor mRNA in rat parathyroids when severe secondary hyperparathyroidism is reversed by an isogenic kidney transplantation. J Am Soc Nephrol 2002;13:2110–6.

[250] Li YC, Amling M, Pirro AE, Priemel M, Meuse J, Baron R, et al. Normalization of mineral ion homeostasis by dietary means prevents hyperparathyroidism, rickets, and osteomalacia, but not alopecia in vitamin D receptor-ablated mice. Endocrinology 1998;139:4391–6.

[251] Li YC, Bolt MJ, Cao LP, Sitrin MD. Effects of vitamin D receptor inactivation on the expression of calbindins and calcium metabolism. Am J Physiol Endocrinol Metab 2001;281:E558–64.

[252] Lietman SA, Tenenbaum-Rakover Y, Jap TS, Yi-Chi W, De-Ming Y, Ding C, et al. A novel loss-of-function mutation, Gln459Arg, of the calcium-sensing receptor gene associated with apparent autosomal recessive inheritance of familial hypocalciuric hypercalcemia. J Clin Endocrinol Metab 2009;94:4372–9.

[253] Lindberg JS, Culleton B, Wong G, Borah MF, Clark RV, Shapiro WB, et al. Cinacalcet HCl an oral calcimimetic agent for the treatment of secondary hyperparathyroidism in hemodialysis and peritoneal dialysis: a randomized, double-blind, multicenter study. J Am Soc Nephrol 2005;16:800–7.

[254] Lindberg JS, Moe SM, Goodman WG, Coburn JW, Sprague SM, Liu W, et al. The calcimimetic AMG 073 reduces parathyroid hormone and calcium × phosphorus in secondary hyperparathyroidism. Kidney Int 2003;63:248–54.

[255] Liu HJ, Wei Y, Ferreri NR, Nasjletti A, Wang WH. Vasopressin and PGE_2 regulate activity of apical 70 pS K^+ channel in thick ascending limb of rat kidney. Am J Physiol Cell Physiol 2000;278:C905–13.

[256] Lloyd SE, Pannett AA, Dixon PH, Whyte MP, Thakker RV. Localization of familial benign hypercalcemia, Oklahoma variant (FBHOk), to chromosome 19q13. Am J Hum Genet 1999;64:189–95.

[257] Loffing J, Loffing-Cueni D, Valderrabano V, Klausli L, Hebert SC, Rossier BC, et al. Distribution of transcellular calcium and sodium transport pathways along mouse distal nephron. Am J Physiol Renal Physiol 2001;281:F1021–7.

[258] Lomonte C, Antonelli M, Losurdo N, Marchio G, Giammaria B, Basile C. Cinacalcet is effective in relapses of secondary hyperparathyroidism after parathyroidectomy. Nephrol Dial Transplant 2007;22:2056–62.

[259] Lopez I, Aguilera-Tejero E, Mendoza FJ, Almaden Y, Perez J, Martin D, et al. Calcimimetic R-568 decreases extraosseous calcifications in uremic rats treated with calcitriol. J Am Soc Nephrol 2006;17:795–804.

[260] Lopez V, Toledo R, Sola E, Gutierrez C, Sujan S, Rodriguez MA, et al. Treatment with cinacalcet in 29 kidney transplant patients with persistent hyperparathyroidism. Transplant Proc 2009;41:2394–5.

[261] Lu JY, Yang Y, Gnacadja G, Christopoulos A, Reagan JD. Effect of the calcimimetic R-568 on correcting inactivating mutations in the human calcium-sensing receptor. J Pharmacol Exp Ther 2009.

[262] Lu M, Zhu Y, Balazy M, Reddy KM, Falck JR, Wang W. Effect of angiotensin II on the apical K^+ channel in the thick ascending limb of the rat kidney. J Gen Physiol 1996;108:537–47.

[263] Macica CM, Yang Y, Hebert SC, Wang WH. Arachidonic acid inhibits activity of cloned renal K^+ channel, ROMK1. Am J Physiol 1996;271:F588–94.

[264] Macica CM, Yang Y, Lerea K, Hebert SC, Wang W. Role of the NH_2 terminus of the cloned renal K^+ channel, ROMK1, in arachidonic acid-mediated inhibition. Am J Physiol 1998;274: F175–81.

[265] Madden J.J, Jr. Bailey A, and Spear M. Calciphylaxis: a review. Plast Surg Nurs 30:195–7.

[266] Magyar CE, White KE, Rojas R, Apodaca G, Friedman PA. Plasma membrane Ca^{2+}-ATPase and NCX1 Na^+/Ca^{2+} exchanger expression in distal convoluted tubule cells. Am J Physiol Renal Physiol 2002;283:F29–40.

[267] Maillard MP, Tedjani A, Perregaux C, Burnier M. Calcium-sensing receptors modulate renin release in vivo and in vitro in the rat. J Hypertens 2009.

[268] Maiti A, Beckman MJ. Extracellular calcium is a direct effecter of VDR levels in proximal tubule epithelial cells that counterbalances effects of PTH on renal Vitamin D metabolism. J Steroid Biochem Mol Biol 2007;103:504–8.

[269] Maiti A, Hait NC, Beckman MJ. Extracellular calcium-sensing receptor activation induces vitamin D receptor levels in proximal kidney HK-2G cells by a mechanism that requires phosphorylation of p38alpha MAPK. J Biol Chem 2008;283:175–83.

[270] Makita N, Sato J, Manaka K, Shoji Y, Oishi A, Hashimoto M, et al. An acquired hypocalciuric hypercalcemia autoantibody induces allosteric transition among active human Ca-sensing receptor conformations. Proc Natl Acad Sci U S A 2007;104:5443–8.

[271] Mandon B, Siga E, Roinel N, De Rouffignac C. Ca^{2+}, Mg^{2+} and K^+ transport in the cortical and medullary thick ascending limb of the rat nephron: influence of traasepithelial voltage. Pfluegers Arch 1993;424:558–60.

[272] Mangat H, Peterson LN, Burns KD. Hypercalcemia stimulates expression of intrarenal phospholipase A2 and prostaglandin H synthase-2 in rats. Role of angiotensin II AT1 receptors. J Clin Invest 1997;100:1941–50.

[273] Marcocci C, Chanson P, Shoback D, Bilezikian J, Fernandez-Cruz L, Orgiazzi J, et al. Cinacalcet reduces serum calcium concentrations in patients with intractable primary hyperparathyroidism. J Clin Endocrinol Metab 2009;94: 2766–72.

[274] Marx S, Attie M, Spiegel A, Levine M, Lasker R, Fox M. An association between neonatal severe primary hyperparathyroidism and familial hypocalciuric hypercalcemia in three kindreds. N Engl J Med 1982;306:257–84.

[275] Marx SJ, Attie MF, Levine MA, Spiegel AM, Downs Jr RW, Lasker RD. The hypocalciuric or benign variant of familial hypercalcemia: clinical and biochemical features in fifteen kindreds. Medicine (Baltimore) 1981;60:397–412.

[276] Massry SG, Goldstein DA. The search for uremic toxin(s) "X" "X" = PTH. Clin Nephrol 1979;11:181–9.

[277] Massry SG, Smogorzewski M. Mechanisms through which parathyroid hormone mediates its deleterious effects on organ function in uremia. Semin Nephrol 1994;14:219–31.

[278] Mathias RS, Brown EM. Divalent cations modulate PTH-dependent 3',5'-cyclic adenosine monophosphate production in renal proximal tubular cells. Endocrinology 1991;128: 3005–12.

[279] May LT, Avlani VA, Sexton PM, Christopoulos A. Allosteric modulation of G protein-coupled receptors. Curr Pharm Des 2004;10:2003–13.

[280] McCarron DA. Diet and blood pressure–the paradigm shift. Science 1998;281:933–4.

[281] McGehee DS, Aldersberg M, Liu KP, Hsuing S, Heath MJ, Tamir H. Mechanism of extracellular Ca^{2+} receptor-stimulated hormone release from sheep thyroid parafollicular cells. J Physiol (Lond) 1997;502:31–44.

[282] McGiff JC, Quilley J. 20-HETE and the kidney: resolution of old problems and new beginnings. Am J Physiol 1999;277: R607–23.

[283] McKinney TD, Myers P. Effect of calcium and phosphate on bicarbonate and fluid transport by proximal tubules in vitro. Kidney Int 1982;21:433–8.

[284] McLarnon S, Holden D, Ward D, Jones M, Elliott A, Riccardi D. Aminoglycoside antibiotics induce pH-sensitive activation of the calcium-sensing receptor. Biochem Biophys Res Commun 2002;297:71–7.

[285] McNeil SE, Hobson SA, Nipper V, Rodland KD. Functional calcium-sensing receptors in rat fibroblasts are required for activation of SRC kinase and mitogen-activated protein kinase in response to extracellular calcium. J Biol Chem 1998;273:1114–20.

[286] Meir T, Levi R, Lieben L, Libutti S, Carmeliet G, Bouillon R, et al. Deletion of the vitamin D receptor specifically in the parathyroid demonstrates a limited role for the receptor in parathyroid physiology. Am J Physiol Renal Physiol 2009;297:F1192–8.

[287] Mendoza FJ, Lopez I, Canalejo R, Almaden Y, Martin D, Aguilera-Tejero E, et al. Direct upregulation of parathyroid calcium-sensing receptor and vitamin D receptor by calcimimetics in uremic rats. Am J Physiol Renal Physiol 2009;296: F605–13.

[288] Mentaverri R, Yano S, Chattopadhyay N, Petit L, Kifor O, Kamel S, et al. The calcium sensing receptor is directly involved in both osteoclast differentiation and apoptosis. Faseb J 2006;20:2562–4.

[289] Miller MA, Fox J. Daily transient decreases in plasma parathyroid hormone levels induced by the calcimimetic NPS R-568 slows the rate of bone loss but does not increase bone mass in ovariectomized rats. Bone 2000;27:511–9.

[290] Mithal A, Kifor O, Kifor I, Vassilev P, Butters R, Krapcho K, et al. The reduced responsiveness of cultured bovine parathyroid cells to extracellular Ca^{2+} is associated with marked reduction in the expression of extracellular Ca^{2+}-sensing receptor messenger ribonucleic acid and protein. Endocrinology 1995;136: 3087–92.

[291] Mitsuma T, Rhue N, Kayama M, Mori Y, Adachi K, Yokoi Y, et al. Distribution of calcium sensing receptor in rats: an immunohistochemical study. Endocr Regul 1999;33:55–9.

[292] Mittelman SD, Hendy GN, Fefferman RA, Canaff L, Mosesova I, Cole DE, et al. A hypocalcemic child with a novel activating mutation of the calcium-sensing receptor gene: successful treatment with recombinant human parathyroid hormone. J Clin Endocrinol Metab 2006;91:2474–9.

[293] Mizobuchi M, Hatamura I, Ogata H, Saji F, Uda S, Shiizaki K, et al. Calcimimetic compound upregulates decreased calcium-sensing receptor expression level in parathyroid glands of rats with chronic renal insufficiency. J Am Soc Nephrol 2004;15: 2579–87.

[294] Mizobuchi M, Ogata H, Hatamura I, Saji F, Koiwa F, Kinugasa E, et al. Activation of calcium-sensing receptor accelerates apoptosis in hyperplastic parathyroid cells. Biochem Biophys Res Commun 2007;362:11–6.

[295] Moe SM, Chen NX. Pathophysiology of vascular calcification in chronic kidney disease. Circ Res 2004;95:560–7.

[296] Mossetti G, Rendina D, De Filippo G, Zampa G, Strazzullo P. [Phosphatonins: novel insights and clinical perspectives]. G Ital Nefrol 2009;26:171–80.

[297] Motoyama HI, Friedman PA. Calcium-sensing receptor regulation of PTH-dependent calcium absorption by mouse cortical ascending limbs. Am J Physiol Renal Physiol 2002;283: F399–406.

[298] Mun HC, Culverston EL, Franks AH, Collyer CA, Clifton-Bligh RJ, Conigrave AD. A double mutation in the extracellular Ca^{2+}-sensing receptor's venus flytrap domain that selectively disables L-amino acid sensing. J Biol Chem 2005;280:29067–72.

[299] Nakajima S, Hira T, Eto Y, Asano K, and Hara H. Soybean beta 51-63 peptide stimulates cholecystokinin secretion via a calcium-sensing receptor in enteroendocrine STC-1 cells. Regul Pept 159:148-55.

[300] Naveh-Many T, Silver J. Regulation of parathyroid hormone gene expression by hypocalcemia, hypercalcemia and vitamin D in the rat. J Clin Invest 1990;86:1313–9.

[301] Nearing J, Betka M, Quinn S, Hentschel H, Elger M, Baum M, et al. Polyvalent cation receptor proteins (CaRs) are salinity sensors in fish. Proc Natl Acad Sci USA 2002;99:9231–6.

[302] Nechama M, Ben-Dov IZ, Silver J, Naveh-Many T. Regulation of PTH mRNA stability by the calcimimetic R568 and the phosphorus binder lanthanum carbonate in CKD. Am J Physiol Renal Physiol 2009;296:F795–800.

[303] Nechama M, Peng Y, Bell O, Briata P, Gherzi R, Schoenberg DR, et al. KSRP-PMR1-exosome association determines parathyroid hormone mRNA levels and stability in transfected cells. BMC Cell Biol 2009;10:70.

[304] Nechama M, Uchida T, Mor Yosef-Levi I, Silver J, Naveh-Many T. The peptidyl-prolyl isomerase Pin1 determines parathyroid hormone mRNA levels and stability in rat models of secondary hyperparathyroidism. J Clin Invest 2009;119: 3102–14.

[305] Nemeth EF. Calcimimetic and calcilytic drugs: just for parathyroid cells? Cell Calcium 2004;35:283–9.

[306] Nemeth EF, Heaton WH, Miller M, Fox J, Balandrin MF, Van Wagenen BC, et al. Pharmacodynamics of the type II calcimimetic compound cinacalcet HCl. J Pharmacol Exp Ther 2004;308:627–35.

[307] Nemeth EF, Steffey ME, Hammerland LG, Hung BC, Van Wagenen BC, DelMar EG, et al. Calcimimetics with potent and selective activity on the parathyroid calcium receptor. Proc Natl Acad Sci U S A 1998;95:4040–5.

[308] Nielsen PK, Rasmussen AK, Butters R, Feldt-Rasmussen U, Bendtzen K, Diaz R, et al. Inhibition of PTH secretion by interleukin-1 beta in bovine parathyroid glands in vitro is associated with an up-regulation of the calcium-sensing receptor mRNA. Biochem Biophys Res Commun 1997;238: 880–5.

[309] Nielsen S, Frokiaer J, Marples D, Kwon TH, Agre P, Knepper MA. Aquaporins in the kidney: from molecules to medicine. Physiol Rev 2002;82:205–44.

[310] O'Seaghdha CM, Yang Q, Glazer NL, Leak TS, Dehghan A, Smith AV, et al. Common variants in the calcium-sensing receptor gene are associated with total serum calcium levels. Hum Mol Genet.

[311] Odenwald T, Nakagawa K, Hadtstein C, Roesch F, Gohlke P, Ritz E, et al. Acute blood pressure effects and chronic hypotensive action of calcimimetics in uremic rats. J Am Soc Nephrol 2006;17:655–62.

[312] Ogata H, Ritz E, Odoni G, Amann K, Orth SR. Beneficial effects of calcimimetics on progression of renal failure and cardiovascular risk factors. J Am Soc Nephrol 2003;14:959–67.

[313] Ohanian J, Gatfield KM, Ward DT, Ohanian V. Evidence for a functional calcium-sensing receptor that modulates myogenic tone in rat subcutaneous arteries. Am J Physiol Heart Circ Physiol 2004.

[314] Ohashi N, Uematsu T, Nagashima S, Kanamaru M, Togawa A, Hishida A, et al. The calcimimetic agent KRN 1493 lowers plasma parathyroid hormone and ionized calcium concentrations in patients with chronic renal failure on haemodialysis both on the day of haemodialysis and on the day without haemodialysis. Br J Clin Pharmacol 2004;57:726–34.

[315] Olszak IT, Poznansky MC, Evans RH, Olson D, Kos C, Pollak MR, et al. Extracellular calcium elicits a chemokinetic response from monocytes in vitro and in vivo. J Clin Invest 2000;105: 1299–305.

[316] Ortiz-Capisano MC, Ortiz PA, Garvin JL, Harding P, Beierwaltes WH. Expression and function of the calcium-sensing receptor in juxtaglomerular cells. Hypertension 2007;50:737–43.

[317] Pallais JC, Kifor O, Chen YB, Slovik D, Brown EM. Acquired hypocalciuric hypercalcemia due to autoantibodies against the calcium-sensing receptor. N Engl J Med 2004;351:362–9.

[318] Pallure V, Comte C, Leray-Mouragues H, Dereure O. Cinacalcet as first-line treatment for calciphylaxis. Acta Derm Venereol 2008;88:62–3.

[319] Pattaragarn A, Fox J, Alon US. Effect of the calcimimetic NPS R-467 on furosemide-induced nephrocalcinosis in the young rat. Kidney Int 2004;65:1684–9.

[320] Paulais M, Baudouin-Legros M, Teulon J. Functional evidence for a Ca^{2+}/polyvalent cation sensor in the mouse thick ascending limb. Am J Physiol 1996;271:F1052–60.

[321] Peacock M, Bilezikian JP, Klassen PS, Guo MD, Turner SA, Shoback D. Cinacalcet hydrochloride maintains long-term normocalcemia in patients with primary hyperparathyroidism. J Clin Endocrinol Metab 2005;90:135–41.

[322] Peacock M, Bolognese MA, Borofsky M, Scumpia S, Sterling LR, Cheng S, et al. Cinacalcet treatment of primary hyperparathyroidism: biochemical and bone densitometric outcomes in a five-year study. J Clin Endocrinol Metab 2009;94: 4860–7.

[323] Peacock M, Robertson WG, Nordin BE. Relation between serum and urinary calcium with particular reference to parathyroid activity. Lancet 1969;1:384–6.

[324] Pearce SH. Clinical disorders of extracellular calcium-sensing and the molecular biology of the calcium-sensing receptor. Ann Med 2002;34:201–6.

[325] Pearce SH, Bai M, Quinn SJ, Kifor O, Brown EM, Thakker RV. Functional characterization of calcium-sensing receptor mutations expressed in human embryonic kidney cells. J Clin Invest 1996;98:1860–6.

[326] Pearce SH, Trump D, Wooding C, Besser GM, Chew SL, Grant DB, et al. Calcium-sensing receptor mutations in familial benign hypercalcemia and neonatal hyperparathyroidism. J Clin Invest 1995;96:2683–92.

[327] Pearce SH, Wooding C, Davies M, Tollefsen SE, Whyte MP, Thakker RV. Calcium-sensing receptor mutations in familial hypocalciuric hypercalcaemia with recurrent pancreatitis. Clin Endocrinol (Oxf) 1996;45:675–80.

[328] Peng J-B, Chen XZ, Berger UV, Vassilev PM, Tsukaguchi H, Brown EM, et al. Molecular cloning and characterization of a channel-like transporter mediating intestinal calcium absorption. J Biol Chem 1999;274:22739–46.

[329] Peterlik M, Grant WB, Cross HS. Calcium, vitamin D and cancer. Anticancer Res 2009;29:3687–98.

[330] Peterson LN, McKay AJ, Borzecki JS. Endogenous prostaglandin E_2 mediates inhibition of rat thick ascending limb Cl reabsorption in chronic hypercalcemia. J Clin Invest 1993;91: 2399–407.

[331] Petrel C, Kessler A, Dauban P, Dodd RH, Rognan D, Ruat M. Positive and negative allosteric modulators of the Ca^{2+}-sensing receptor interact within overlapping but not identical binding

sites in the transmembrane domain. J Biol Chem 2004;279: 18990–7.
[332] Phillips CG, Harnett MT, Chen W, Smith SM. Calcium-sensing receptor activation depresses synaptic transmission. J Neurosci 2008;28:12062–70.
[333] Pi M, Chen L, Huang MZ, Zhu W, Ringhofer B, Luo J, et al. GPRC6A null mice exhibit osteopenia, feminization and metabolic syndrome. PLoS One 2008;3:e3858.
[334] Pi M, Faber P, Ekema G, Jackson PD, Ting A, Wang N, et al. Identification of a novel extracellular cation-sensing G-protein-coupled receptor. J Biol Chem 2005;280:40201–9.
[335] Pi M, Hinson TK, Quarles L. Failure to detect the extracellular calcium-sensing receptor (CasR) in human osteoblast cell lines. J Bone Miner Res 1999;14:1310–9.
[336] Pi M, Spurney RF, Tu Q, Hinson T, Quarles LD. Calcium-sensing receptor activation of rho involves filamin and rho-guanine nucleotide exchange factor. Endocrinology 2002;143: 3830–8.
[337] Pidasheva S, Grant M, Canaff L, Ercan O, Kumar U, Hendy GN. Calcium-sensing receptor dimerizes in the endoplasmic reticulum: biochemical and biophysical characterization of CASR mutants retained intracellularly. Hum Mol Genet 2006;15:2200–9.
[338] Piecha G, Kokeny G, Nakagawa K, Koleganova N, Geldyyev A, Berger I, et al. Calcimimetic R-568 or calcitriol: equally beneficial on progression of renal damage in subtotally nephrectomized rats. Am J Physiol Renal Physiol 2008;294:F748–57.
[339] Pin JP, Kniazeff J, Liu J, Binet V, Goudet C, Rondard P, et al. Allosteric functioning of dimeric class C G-protein-coupled receptors. Febs J 2005;272:2947–55.
[340] Pitt SC, Sippel RS, Chen H. Secondary and tertiary hyperparathyroidism, state of the art surgical management. Surg Clin North Am 2009;89:1227–39.
[341] Pollak MR, Brown EM, Estep HL, McLaine PN, Kifor O, Park J, et al. Autosomal dominant hypocalcaemia caused by a Ca^{2+}-sensing receptor gene mutation. Nat Genet 1994;8:303–7.
[342] Prey S, Sparsa A, Durox H, Allot V, Pommepuy I, Salem A, et al. [Calciphylaxis treated by cinacalcet: a medical alternative to parathyroidectomy]. Rev Med Interne 2009;30:186–9.
[343] Procino G, Carmosino M, Tamma G, Gouraud S, Laera A, Riccardi D, et al. Extracellular calcium antagonizes forskolin-induced aquaporin 2 trafficking in collecting duct cells. Kidney Int 2004;66:2245–55.
[344] Quamme GA. Control of magnesium transport in the thick ascending limb. Am J Physiol 1989;256:F197–210.
[345] Quamme GA, de Rouffignac C. Epithelial magnesium transport and regulation by the kidney. Front Biosci 2000;5:D694–711.
[346] Quarles LD, Sherrard DJ, Adler S, Rosansky SJ, McCary LC, Liu W, et al. The calcimimetic AMG 073 as a potential treatment for secondary hyperparathyroidism of end-stage renal disease. J Am Soc Nephrol 2003;14:575–83.
[347] Quinn SJ, Bai M, Brown EM. pH Sensing by the calcium-sensing receptor. J Biol Chem 2004;279:37241–9.
[348] Quinn SJ, Kifor O, Trivedi S, Diaz R, Vassilev P, Brown E. Sodium and ionic strength sensing by the calcium receptor. J Biol Chem 1998;273:19579–86.
[349] Quinn SJ, Ye CP, Diaz R, Kifor O, Bai M, Vassilev P, et al. The Ca^{2+}-sensing receptor: a target for polyamines. Am J Physiol 1997;273:C1315–23.
[350] Racke F, McHenry CR, Wentworth D. Lithium-induced alterations in parathyroid cell function: insight into the pathogenesis of lithium-associated hyperparathyroidism. Am J Surg 1994;168:462–5.
[350a] Raggi P, Chertow GM, Torres PU, Csiky B, Naso A, Nossuli K, et al.; ADVANCE Study Group. The ADVANCE study: a randomized study to evaluate the effects of **cinacalcet** plus low-dose vitamin D on vascular calcification in patients on hemodialysis. Nephrol Dial Transplant 2011;26:1327–39.
[351] Ray K, Fan GF, Goldsmith PK, Spiegel AM. The carboxyl terminus of the human calcium receptor. Requirements for cell-surface expression and signal transduction. J Biol Chem 1997;272:31355–61.
[352] Ray K, Hauschild BC, Steinbach PJ, Goldsmith PK, Hauache O, Spiegel AM. Identification of the cysteine residues in the amino-terminal extracellular domain of the human Ca^{2+} receptor critical for dimerization. Implications for function of monomeric Ca^{2+} receptor. J Biol Chem 1999;274: 27642–50.
[353] Ray K, Northup J. Evidence for distinct cation and calcimimetic compound (NPS 568) recognition domains in the transmembrane regions of the human Ca^{2+} receptor. J Biol Chem 2002;277:18908–13.
[354] Raymond CB, Wazny LD. Sodium thiosulfate, bisphosphonates, and cinacalcet for treatment of calciphylaxis. Am J Health Syst Pharm 2008;65:1419–29.
[355] Reinalter SC, Jeck N, Peters M, Seyberth HW. Pharmacotyping of hypokalaemic salt-losing tubular disorders. Acta Physiol Scand 2004;181:513–21.
[356] Renkema KY, Velic A, Dijkman HB, Verkaart S, van der Kemp AW, Nowik M, et al. The calcium-sensing receptor promotes urinary acidification to prevent nephrolithiasis. J Am Soc Nephrol 2009;20:1705–13.
[357] Reyes-Cruz G, Hu J, Goldsmith PK, Steinbach PJ, Spiegel AM. Human Ca^{2+} receptor extracellular domain. Analysis of function of lobe I loop deletion mutants. J Biol Chem 2001;276:32145–51.
[358] Riccardi D, Brown EM. Physiology and pathophysiology of the calcium-sensing receptor in the kidney. Am J Physiol Renal Physiol 298:F485–99.
[359] Riccardi D, Hall AE, Chattopadhyay N, Xu JZ, Brown EM, Hebert SC. Localization of the extracellular Ca^{2+}/polyvalent cation-sensing protein in rat kidney. Am J Physiol 1998;274: F611–22.
[360] Riccardi D, Lee WS, Lee K, Segre GV, Brown EM, Hebert SC. Localization of the extracellular Ca^{2+}-sensing receptor and PTH/PTHrP receptor in rat kidney. Am J Physiol 1996;271: F951–6.
[361] Riccardi D, Traebert M, Ward DT, Kaissling B, Biber J, Hebert SC, et al. Dietary phosphate and parathyroid hormone alter the expression of the calcium-sensing receptor (CaR) and the Na + -dependent Pi transporter (NaPi-2) in the rat proximal tubule. Pflugers Arch 2000;441:379–87.
[362] Ritchie G, Kerstan D, Dai LJ, Kang HS, Canaff L, Hendy GN, et al. 1,25(OH)(2)D(3) stimulates Mg^{2+} uptake into MDCT cells: modulation by extracellular Ca^{2+} and Mg^{2+}. Am J Physiol Renal Physiol 2001;280:F868–78.
[363] Ritter CS, Finch JL, Slatopolsky EA, Brown AJ. Parathyroid hyperplasia in uremic rats precedes down-regulation of the calcium receptor. Kidney Int 2001;60:1737–44.
[364] Ritter CS, Martin DR, Lu Y, Slatopolsky E, Brown AJ. Reversal of secondary hyperparathyroidism by phosphate restriction restores parathyroid calcium-sensing receptor expression and function. J Bone Miner Res 2002;17:2206–13.
[365] Ritter CS, Pande S, Krits I, Slatopolsky E, Brown AJ. Destabilization of parathyroid hormone mRNA by extracellular Ca^{2+} and the calcimimetic R-568 in parathyroid cells: role of cytosolic Ca and requirement for gene transcription. J Mol Endocrinol 2008;40:13–21.
[366] Ritz E. Calcimimetics–fooling the calcium receptor. Pediatr Nephrol 2005;20:15–8.

[367] Ritz E, Haxsen V, Zeier M. Disorders of phosphate metabolism–pathomechanisms and management of hypophosphataemic disorders. Best Pract Res Clin Endocrinol Metab 2003;17: 547–58.
[368] Rivkees SA, El-Hajj Fuleihan G, Brown EM, Crawford JD. Tertiary hyperparathyroidism during high phosphate therapy of familial hypophosphatemic rickets. J Clin Endocrinol Metab 1992;75:1514–8.
[369] Robinson MR, Augustine JJ, Korman NJ. Cinacalcet for the treatment of calciphylaxis. Arch Dermatol 2007;143: 152–4.
[370] Rodriguez L, Tu C, Cheng Z, Chen TH, Bikle D, Shoback D, et al. Expression and functional assessment of an alternatively spliced extracellular Ca^{2+}-sensing receptor in growth plate chondrocytes. Endocrinology 2005;146:5294–303.
[371] Rodriguez M, Nemeth E, Martin D. The calcium-sensing receptor: a key factor in the pathogenesis of secondary hyperparathyroidism. Am J Physiol Renal Physiol 2005;288:F253–64.
[372] Rodriguez ME, Almaden Y, Canadillas S, Canalejo A, Siendones E, Lopez I, et al. The calcimimetic R-568 increases vitamin D receptor expression in rat parathyroid glands. Am J Physiol Renal Physiol 2007;292:F1390–5.
[373] Rogers NM, Teubner DJ, Coates PT. Calcific uremic arteriolopathy: advances in pathogenesis and treatment. Semin Dial 2007;20:150–7.
[374] Roussanne MC, Gogusev J, Hory B, Duchambon P, Souberbielle JC, Nabarra B, et al. Persistence of Ca^{2+}-sensing receptor expression in functionally active, long-term human parathyroid cell cultures. J Bone Miner Res 1998;13:354–62.
[375] Roussanne MC, Lieberherr M, Souberbielle JC, Sarfati E, Drueke T, Bourdeau A. Human parathyroid cell proliferation in response to calcium, NPS R-467, calcitriol and phosphate. Eur J Clin Invest 2001;31:610–6.
[376] Rutten MJ, Bacon KD, Marlink KL, Stoney M, Meichsner CL, Lee FP, et al. Identification of a functional Ca^{2+}-sensing receptor in normal human gastric mucous epithelial cells. Am J Physiol 1999;277:G662–70.
[377] San Gabriel A, Uneyama H, Maekawa T, Torii K. The calcium-sensing receptor in taste tissue. Biochem Biophys Res Commun 2009;378:414–8.
[378] Sands JM, Flores FX, Kato A, Baum MA, Brown EM, Ward DT, et al. Vasopressin-elicited water and urea permeabilities are altered in IMCD in hypercalcemic rats. Am J Physiol 1998;274: F978–85.
[379] Sands JM, Naruse M, Baum M, Jo I, Hebert SC, Brown EM, et al. Apical extracellular calcium/polyvalent cation-sensing receptor regulates vasopressin-elicited water permeability in rat kidney inner medullary collecting duct. J Clin Invest 1997;99:1399–405.
[380] Saunders BD, Saunders EF, Gauger PG. Lithium therapy and hyperparathyroidism: an evidence-based assessment. World J Surg 2009;33:2314–23.
[381] Schmitt CP, Homme M, Schaefer F. Structural organization and biological relevance of oscillatory parathyroid hormone secretion. Pediatr Nephrol 2005;20:346–51.
[382] Schwartz TW, Holst B. Ago-allosteric modulation and other types of allostery in dimeric 7TM receptors. J Recept Signal Transduct Res 2006;26:107–28.
[383] Scillitani A, Guarnieri V, De Geronimo S, Muscarella LA, Battista C, D'Agruma L, et al. Blood ionized calcium is associated with clustered polymorphisms in the carboxyl-terminal tail of the calcium-sensing receptor. J Clin Endocrinol Metab 2004;89:5634–8.
[384] Shaikh A, Berndt T, Kumar R. Regulation of phosphate homeostasis by the phosphatonins and other novel mediators. Pediatr Nephrol 2008;23:1203–10.
[385] Shalhoub V, Grisanti M, Padagas J, Scully S, Rattan A, Qi M, et al. In vitro studies with the calcimimetic, cinacalcet HCl, on normal human adult osteoblastic and osteoclastic cells. Crit Rev Eukaryot Gene Expr 2003;13:89–106.
[386] Sharma A, Burkitt-Wright E, Rustom R. Cinacalcet as an adjunct in the successful treatment of calciphylaxis. Br J Dermatol 2006;155:1295–7.
[387] Shimada T, Hasegawa H, Yamazaki Y, Muto T, Hino R, Takeuchi Y, et al. FGF-23 is a potent regulator of vitamin D metabolism and phosphate homeostasis. J Bone Miner Res 2004;19:429–35.
[388] Shoback DM, Bilezikian JP, Turner SA, McCary LC, Guo MD, Peacock M. The calcimimetic cinacalcet normalizes serum calcium in subjects with primary hyperparathyroidism. J Clin Endocrinol Metab 2003;88:5644–9.
[389] Silve C, Petrel C, Leroy C, Bruel H, Mallet E, Rognan D, et al. Delineating a Ca^{2+} binding pocket within the venus flytrap module of the human calcium-sensing receptor. J Biol Chem 2005;280:37917–23.
[390] Silver J, Levi R. Cellular and molecular mechanisms of secondary hyperparathyroidism. Clin Nephrol 2005;63: 119–26.
[391] Silver J, Naveh-Many T, Mayer H, Schmelzer HJ, Popovtzer MM. Regulation by vitamin D metabolites of parathyroid hormone gene transcription in vivo in the rat. J Clin Invest 1986;78:1296–301.
[392] Silverberg SJ, Bone 3rd HG, Marriott TB, Locker FG, Thys-Jacobs S, Dziem G, et al. Short-term inhibition of parathyroid hormone secretion by a calcium-receptor agonist in patients with primary hyperparathyroidism. N Engl J Med 1997;337: 1506–10.
[393] Silverberg SJ, Rubin MR, Faiman C, Peacock M, Shoback DM, Smallridge RC, et al. Cinacalcet hydrochloride reduces the serum calcium concentration in inoperable parathyroid carcinoma. J Clin Endocrinol Metab 2007;92:3803–8.
[394] Slama M, Susic D, Frohlich ED. Prevention of hypertension. Curr Opin Cardiol 2002;17:531–6.
[395] Slattery ML, Wolff RK, Herrick JS, Caan BJ, Samowitz W. Calcium, vitamin D, VDR genotypes, and epigenetic and genetic changes in rectal tumors. Nutr Cancer 62:436–42.
[396] Sloand JA, Shelly MA. Normalization of lithium-induced hypercalcemia and hyperparathyroidism with cinacalcet hydrochloride. Am J Kidney Dis 2006;48:832–7.
[397] Spurlino JC, Lu GY, Quiocho FA. The 2.3-A resolution structure of the maltose- or maltodextrin-binding protein, a primary receptor of bacterial active transport and chemotaxis. J Biol Chem 1991;266:5202–19.
[398] Sudhaker Rao D, Han ZH, Phillips ER, Palnitkar S, Parfitt AM. Reduced vitamin D receptor expression in parathyroid adenomas: implications for pathogenesis. Clin Endocrinol (Oxf) 2000;53:373–81.
[399] Takaichi K, Kurokawa K. High Ca^{2+} inhibits peptide hormone-dependent cAMP production specifically in thick ascending limbs of Henle. Miner Electr Metab 1986;12:342–6.
[400] Takaichi K, Kurokawa K. Inhibitory guanosine triphosphate-binding protein-mediated regulation of vasopressin action in isolated single medullary tubules of mouse kidney. J Clin Invest 1988;82:1437–44.
[401] Teng M, Wolf M, Lowrie E, Ofsthun N, Lazarus JM, Thadhani R. Survival of patients undergoing hemodialysis with paricalcitol or calcitriol therapy. N Engl J Med 2003; 349:446–56.
[402] Tfelt-Hansen J, Brown EM. The calcium-sensing receptor in normal physiology and pathophysiology: a review. Crit Rev Clin Lab Sci 2005;42:35–70.
[403] Thakker RV. Disorders of the calcium-sensing receptor. Biochim Biophys Acta 1998;1448:166–70.

[404] Thakker RV. Diseases associated with the extracellular calcium-sensing receptor. Cell Calcium 2004;35:275–82.
[405] Theman TA, Collins MT. The role of the calcium-sensing receptor in bone biology and pathophysiology. Curr Pharm Biotechnol 2009;10:289–301.
[406] Timmers HJ, Karperien M, Hamdy NA, de Boer H, Hermus AR. Normalization of serum calcium by cinacalcet in a patient with hypercalcaemia due to a de novo inactivating mutation of the calcium-sensing receptor. J Intern Med 2006; 260:177–82.
[407] Topala CN, Schoeber JP, Searchfield LE, Riccardi D, Hoenderop JG, Bindels RJ. Activation of the Ca^{2+}-sensing receptor stimulates the activity of the epithelial Ca^{2+} channel TRPV5. Cell Calcium 2009;45:331–9.
[408] Toro Prieto FJ, Bernal Blanco G, Navarro Garcia M, Cabello Chaves V, Garciajimenez R, Pereira Palomo P, et al. Calcimimetics and bone mineral density in renal transplant patients with persistent secondary hyperparathyroidism. Transplant Proc 2009;41:2144–7.
[409] Treschel U, Eisman JA, Fischer JA, Bonjour J-P, Fleisch H. Calcium-dependent parathyroid hormone-independent regulation of 1,25-dihydroxyvitamin D. Am J Physiol 1980;239: E119–24.
[410] Tsuchiya D, Kunishima N, Kamiya N, Jingami H, Morikawa K. Structural views of the ligand-binding cores of a metabotropic glutamate receptor complexed with an antagonist and both glutamate and Gd^{3+}. Proc Natl Acad Sci USA 2002;99:2660–5.
[411] Tu CL, Oda Y, Komuves L, Bikle DD. The role of the calcium-sensing receptor in epidermal differentiation. Cell Calcium 2004;35:265–73.
[412] Tu Q, Pi M, Karsenty G, Simpson L, Liu S, Quarles LD. Rescue of the skeletal phenotype in CasR-deficient mice by transfer onto the Gcm2 null background. J Clin Invest 2003;111: 1029–37.
[413] Valle C, Rodriguez M, Santamaria R, Almaden Y, Rodriguez ME, Canadillas S, et al. Cinacalcet reduces the set point of the PTH-calcium curve. J Am Soc Nephrol 2008;19:2430–6.
[414] van Abel M, Hoenderop JG, van der Kemp AW, van Leeuwen JP, Bindels RJ. Regulation of the epithelial Ca^{2+} channels in small intestine as studied by quantitative mRNA detection. Am J Physiol Gastrointest Liver Physiol 2003;285:G78–85.
[415] Vargas-Poussou R, Huang C, Hulin P, Houillier P, Jeunemaitre X, Paillard M, et al. Functional characterization of a calcium-sensing receptor mutation in severe autosomal dominant hypocalcemia with a Bartter-like syndrome. J Am Soc Nephrol 2002;13:2259–66.
[416] Velasco N, MacGregor MS, Innes A, MacKay IG. Successful treatment of calciphylaxis with cinacalcet-an alternative to parathyroidectomy? Nephrol Dial Transplant 2006;21: 1999–2004.
[417] Vizard TN, O'Keeffe GW, Gutierrez H, Kos CH, Riccardi D, Davies AM. Regulation of axonal and dendritic growth by the extracellular calcium-sensing receptor. Nat Neurosci 2008;11: 285–91.
[418] Wada M, Furuya Y, Sakiyama J, Kobayashi N, Miyata S, Ishii H, et al. The calcimimetic compound NPS R-568 suppresses parathyroid cell proliferation in rats with renal insufficiency. Control of parathyroid cell growth via a calcium receptor. J Clin Invest 1997;100:2977–83.
[419] Wada M, Furuya Y, Sakiyama J-i, Kobayashi N, Miyata S, Ishii H, et al. The calcimimetic compound NPS R-568 suppresses parathyroid cell proliferation in rats with renal insufficiency. J Clin Invest 1997;100:2977–83.
[420] Wada M, Ishii H, Furuya Y, Fox J, Nemeth EF, Nagano N. NPS R-568 halts or reverses osteitis fibrosa in uremic rats [see comments]. Kidney Int 1998;53:448–53.
[421] Wada M, Nagano N. Control of parathyroid cell growth by calcimimetics. Nephrol Dial Transplant 2003;18(Suppl 3): iii13–7.
[422] Wada M, Nagano N, Furuya Y, Chin J, Nemeth EF, Fox J. Calcimimetic NPS R-568 prevents parathyroid hyperplasia in rats with severe secondary hyperparathyroidism. Kidney Int 2000;57:50–8.
[423] Wang D, Pedraza PL, Abdullah HI, McGiff JC, Ferreri NR. Calcium-sensing receptor-mediated TNF production in medullary thick ascending limb cells. Am J Physiol Renal Physiol 2002;283:F963–70.
[424] Wang W, Kwon TH, Li C, Frokiaer J, Knepper MA, Nielsen S. Reduced expression of Na-K-2Cl cotransporter in medullary TAL in vitamin D-induced hypercalcemia in rats. Am J Physiol Renal Physiol 2002;282:F34–44.
[425] Wang W, Li C, Kwon TH, Miller RT, Knepper MA, Frokiaer J, et al. Reduced expression of renal Na+ transporters in rats with PTH-induced hypercalcemia. Am J Physiol Renal Physiol 2004;286:F534–45.
[426] Wang W, Lu M. Effect of arachidonic acid on activity of the apical K+ channel in the thick ascending limb of the rat kidney. J Gen Physiol 1995;106:727–43.
[427] Wang W, Lu M, Balazy M, Hebert SC. Phospholipase A2 is involved in mediating the effect of extracellular Ca^{2+} on apical K^+ channels in rat TAL. Am J Physiol 1997;273: F421–9.
[428] Wang WH, Lu M, Hebert SC. Cytochrome $P\text{-}_{450}$ metabolites mediate extracellular Ca(2 +)-induced inhibition of apical K^+ channels in the TAL. Am J Physiol 1996;271:C103–11.
[429] Ward DT. Calcium receptor-mediated intracellular signalling. Cell Calcium 2004;35:217–28.
[430] Ward DT, Brown EM, Harris HW. Disulfide bonds in the extracellular calcium-polyvalent cation-sensing receptor correlate with dimer formation and its response to divalent cations in vitro. J Biol Chem 1998;273:14476–83.
[431] Ward DT, Maldonado-Perez D, Hollins L, Riccardi D. Aminoglycosides induce acute cell signaling and chronic cell death in renal cells that express the calcium-sensing receptor. J Am Soc Nephrol 2005;16:1236–44.
[432] Watanabe S, Fukumoto S, Chang H, Takeuchi Y, Hasegawa Y, Okazaki R, et al. Association between activating mutations of calcium-sensing receptor and Bartter's syndrome. Lancet 2002;360:692–4.
[433] Weisinger JR, Favus MJ, Langman CB, Bushinsky D. Regulation of 1,25-dihydroxyvitamin D3 by calcium in the parathyroidectomized, parathyroid hormone-replete rat. J Bone Miner Res 1989;4:929–35.
[434] Wellendorph P, Brauner-Osborne H. Molecular cloning, expression, and sequence analysis of GPRC6A, a novel family C G-protein-coupled receptor. Gene 2004;335:37–46.
[435] Wellendorph P, Hansen KB, Balsgaard A, Greenwood JR, Egebjerg J, Brauner-Osborne H. Deorphanization of GPRC6A: a promiscuous L-alpha-amino acid receptor with preference for basic amino acids. Mol Pharmacol 2005;67: 589–97.
[436] Wesseling-Perry K. FGF-23 in bone biology. Pediatr Nephrol 25:603–8.
[437] Weston AH, Absi M, Ward DT, Ohanian J, Dodd RH, Dauban P, et al. Evidence in favor of a calcium-sensing receptor in arterial endothelial cells: studies with calindol and Calhex 231. Circ Res 2005;97:391–8.

[438] Whitfield JF. The calcium-sensing receptor—a driver of colon cell differentiation. Curr Pharm Biotechnol 2009;10:311—6.
[439] Wittner M, Mandon B, Roinel N, de Rouffignac C, Di Stefano A. Hormonal stimulation of Ca^{2+} and Mg^{2+} transport in the cortical thick ascending limb of Henle's loop of the mouse: evidence for a change in the paracellular pathway permeability. Pflugers Arch 1993;423:387—96.
[440] Woznowski M, Quack I, Stegbauer J, Buchner N, Rump LC, Schieren G. Oncogenic osteomalacia, a rare paraneoplastic syndrome due to phosphate wasting—a case report and review of the literature. Clin Nephrol 2008;70:431—8.
[441] Wu Z, Tandon R, Ziembicki J, Nagano J, Hujer KM, Miller RT, et al. Role of ceramide in Ca^{2+}-sensing receptor-induced apoptosis. J Lipid Res 2005;46:1396—404.
[442] Yamaguchi T, Chattopadhyay N, Kifor O, Ye C, Vassilev PM, Sanders JL, et al. Expression of extracellular calcium-sensing receptor in human osteoblastic MG-63 cell line. Am J Physiol Cell Physiol 2001;280:C382—93.
[443] Yamaguchi T, Kifor O, Chattopadhyay N, Brown EM. Expression of extracellular calcium (Ca^{2+}_o)-sensing receptor in the clonal osteoblast-like cell lines, UMR-106 and SAOS-2. Biochem Biophys Res Commun 1998;243:753—7.
[444] Yang H, Curinga G, Giachelli CM. Elevated extracellular calcium levels induce smooth muscle cell matrix mineralization in vitro. Kidney Int 2004;66:2293—9.
[445] Yano S, Sugimoto T, Tsukamoto T, Chihara K, Kobayashi A, Kitazawa S, et al. Association of decreased calcium-sensing receptor expression with proliferation of parathyroid cells in secondary hyperparathyroidism. Kidney Int 2000;58: 1980—6.
[446] Yano S, Sugimoto T, Tsukamoto T, Chihara K, Kobayashi A, Kitazawa S, et al. Decrease in vitamin D receptor and calcium-sensing receptor in highly proliferative parathyroid adenomas. Eur J Endocrinol 2003;148:403—11.
[447] Yarden N, Lavelin I, Genina O, Hurwitz S, Diaz R, Brown EM, et al. Expression of calcium-sensing receptor gene by avian parathyroid gland in vivo: relationship to plasma calcium. Gen Comp Endocrinol 2000;117:173—81.
[448] Young SH, Rozengurt E. Amino acids and Ca^{2+} stimulate different patterns of Ca^{2+} oscillations through the Ca^{2+}-sensing receptor. Am J Physiol Cell Physiol 2002;282: C1414—22.
[449] Zaidi M, Adebanjo OA, Moonga BS, Sun L, Huang CL. Emerging insights into the role of calcium ions in osteoclast regulation. J Bone Miner Res 1999;14:669—74.
[450] Zhang M, Breitwieser GE. High affinity interaction with filamin A protects against calcium-sensing receptor degradation. J Biol Chem 2005;280:11140—6.
[451] Zhang Z, Jiang Y, Quinn SJ, Krapcho K, Nemeth EF, Bai M. L-phenylalanine and NPS R-467 synergistically potentiate the function of the extracellular calcium-sensing receptor through distinct sites. J Biol Chem 2002;277:33736—41.
[452] Zhang Z, Sun S, Quinn SJ, Brown EM, Bai M. The extracellular calcium-sensing receptor dimerizes through multiple types of intermolecular interactions. J Biol Chem 2001;276: 5316—22.
[453] Zou AP, Drummond HA, Roman RJ. Role of 20-HETE in elevating loop chloride reabsorption in Dahl SS/Jr rats. Hypertension 1996;27:631—5.

CHAPTER

64

Renal Calcium Metabolism

José F. Bernardo[1] *and Peter A. Friedman*[2]

[1]Renal-Electrolyte Division, Department of Medicine, University of Pittsburgh, Pittsburgh, USA
[2]Department of Pharmacology and Chemical Biology, University of Pittsburgh, Pittsburgh, USA

INTRODUCTION

Calcium supports diverse physiological roles as a structural element in bone and as a molecular trigger for second messenger signaling. To achieve this, homeostatic mechanisms regulate intracellular calcium at submicromolar levels, whereas extracellular calcium is in the millimolar range. The fact that intricate regulatory processes have evolved than enable ion concentrations to be maintained over several orders of magnitude underscores the importance of the varied biological functions of calcium in signal transduction, cell permeability, excitation-secretion and excitation-contraction coupling, and cell fertilization on the one hand, and maintenance of skeletal integrity on the other.

CALCIUM CHEMISTRY

An adaptable coordination sphere, which facilitates binding to the irregular geometry of proteins, makes calcium particularly well suited for its biological roles. The ability to cross-link two proteins requires an ion with a high coordination number (which dictates the number of electron pairs that can be formed) and is generally six to eight for calcium.[1] Such cross-linking of osseous structural proteins is enhanced at the relatively high calcium concentrations that are found in extracellular fluid. The variable bond length of the calcium ion permits formation of more extensive cross-linking involved in membrane stabilization by facilitating lipid polymorphism and formation of hexagonal arrays. Moreover, unlike disulfide or sugar-peptide cross-links, calcium linking is readily reversible. Despite these virtues, were intracellular free calcium (Ca^{2+}_i) of the same order as its extracellular concentration, the proper functioning of a variety of proteins and macromolecules would be impaired. Thus, from an evolutionary perspective, it is advantageous to maintain low concentrations of intracellular calcium.

The corollary of the benefits accruing from the physical characteristics of calcium at high extracellular concentrations defines a nearly ideal set of attributes that are desirable at submicromolar intracellular concentrations. By virtue of its low intracellular levels, changes of calcium activity can function as first or second messengers to activate effector targets. The fact that calcium can be rapidly bound and released, together with the high affinity and selectivity of many proteins for calcium, enhance its ability to regulate ion channels, calcium-dependent enzymes, and so on. Another advantage of low free intracellular calcium concentrations is that microcrystallization and precipitation of calcium phosphate is avoided. The evolution of high-energy phosphate compounds such as ATP may be selectively favored because they circumvent the microcrystallization and precipitation of calcium phosphate.

Serum Calcium

In adult humans, the calcium concentration of extracellular fluid averages 10 mg/dl (=5 mEq/l, 2.5 mM). Plasma calcium exists as three distinct chemical forms: protein-bound, complexed (but diffusible), and ionized. The relations between the various forms of calcium are shown schematically in Fig. 64.1. Forty percent of the serum calcium is bound to plasma proteins, with albumin accounting for some 90% of this.

Seldin and Giebisch's The Kidney, Fifth Edition.
DOI: http://dx.doi.org/10.1016/B978-0-12-381462-3.00064-1

© 2013 Elsevier Inc. All rights reserved.

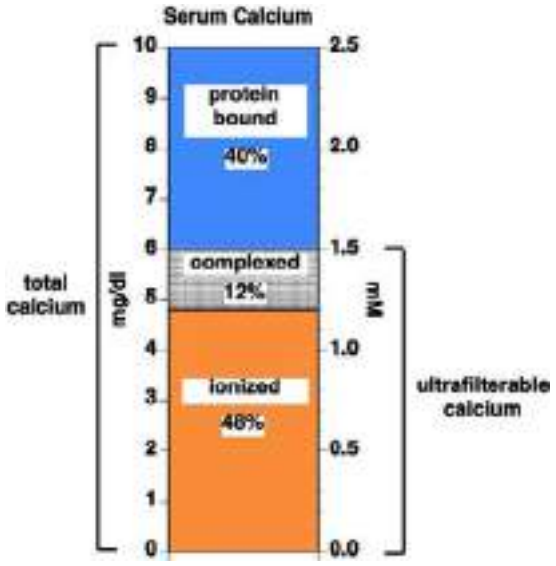

FIGURE 64.1 **Chemical forms of calcium in serum.** Calcium concentrations are expressed as mg/dl on the left-hand axis and as mM on the right. The total serum calcium concentration, 10 mg/dl or 2.5 mM, can be divided into three pools, protein-bound, that complexed with small anions, and ionized calcium. The latter two moieties, i.e., complexed and ionized, represent the calcium that is filtered at the glomerulus and subject to tubular reabsorption as it passes through the nephron.

Smaller percentages are bound, though with greater affinity, to ß-globulin, α_2-globulin, α_1-globulin, and γ-globulin. Ten percent of the serum calcium is complexed with small polyvalent anions. Calcium complexes are formed by ion pairing with phosphate and citrate and, to a lesser extent, with bicarbonate, and sulfate. The degree of complexation depends upon the concentrations of ionized calcium, the complexing anion, and the ambient pH. The different moieties of calcium are important because only diffusible calcium, i.e., the free plus complexed calcium, is filtered at the glomerulus and crosses cell membranes. A comprehensive discussion of the biologically relevant forms of calcium and their interrelations is available elsewhere.[2]

The ultrafilterable, or ionized fractions, of calcium as summarized above are affected by changes in the total serum calcium concentration, blood pH, plasma protein concentration, and the concentration of complexing anions. Increases in total serum calcium concentrations are usually accompanied by concomitant elevations in the concentration of ultrafilterable calcium, at least up to a total concentration of about 4 mM. Above this concentration, the ultrafilterable fraction declines such that increases of ultrafilterable calcium no longer parallel elevations of total calcium concentration. Reduction in calcium ultrafiltration with hypercalcemia has been postulated to result from the formation of insoluble $Ca_3(PO_4)_2$ protein complexes. This idea is supported by the finding that ultrafilterable phosphate concentrations also decline.[3] Conversely, hypocalcemia is generally associated with a fall in calcium ultrafiltration.[4]

Changes in the concentration of serum proteins are usually accompanied by parallel changes in the total serum calcium concentration so that the ultrafilterable fraction remains constant.[5,6,7] In severe hypoproteinemia, however, the ultrafilterable fraction increases.[4,8]

The concentration of ionized Ca^{2+} varies inversely with blood pH. Acidemia increases ionized Ca^{2+} concentrations, whereas alkalemia causes decreases.[5,7,8] Increases in the serum concentration of complexing anions, such as phosphate, citrate, sulfate, or bicarbonate, reduce the ionized Ca^{2+} concentration by sequestering Ca^{2+}.

The amount of calcium in the extracellular fluid represents a dynamic balance between intestinal absorption, renal reabsorption, and osseous resorption. Symptoms of hypocalcemia vary in relation to the ionized serum calcium concentration. Mild reductions of calcium are associated with paresthesias and muscle cramps; more severe decreases of calcium may induce seizures. Increases of plasma calcium, on the other hand, have been implicated in attenuation of the renal effects of parathyroid hormone (PTH), the antidiuretic action of vasopressin, and reduced renal concentrating capacity. A schematic representation of calcium balance, for an adult human, is shown in Fig. 64.2. Assuming a daily dietary calcium intake of 1,000 mg, net intestinal absorption amounts to about 200 mg, with the remaining 800 mg excreted in the feces. In balance, net intestinal absorption is matched by urinary excretion, while calcium accretion and loss from bone are equal. Thus, approximately 200 mg of calcium are excreted daily. In adults, net calcium balance is effectively zero, suggesting that in the absence of a calcium challenge such as lactation, the kidneys represent the dominant regulatory site of calcium metabolism.[9,10]

The renal responses to alterations of extracellular calcium are transduced by the calcium-sensing receptor (CaSR), which is expressed prominently at the sites of PTH and vasopressin action in the kidney.[11,12]

CALCIUM TRANSPORT ALONG THE NEPHRON

General Considerations, Calcium Clearance

Maintenance of extracellular calcium balance requires the daily urinary excretion of 200 mg of

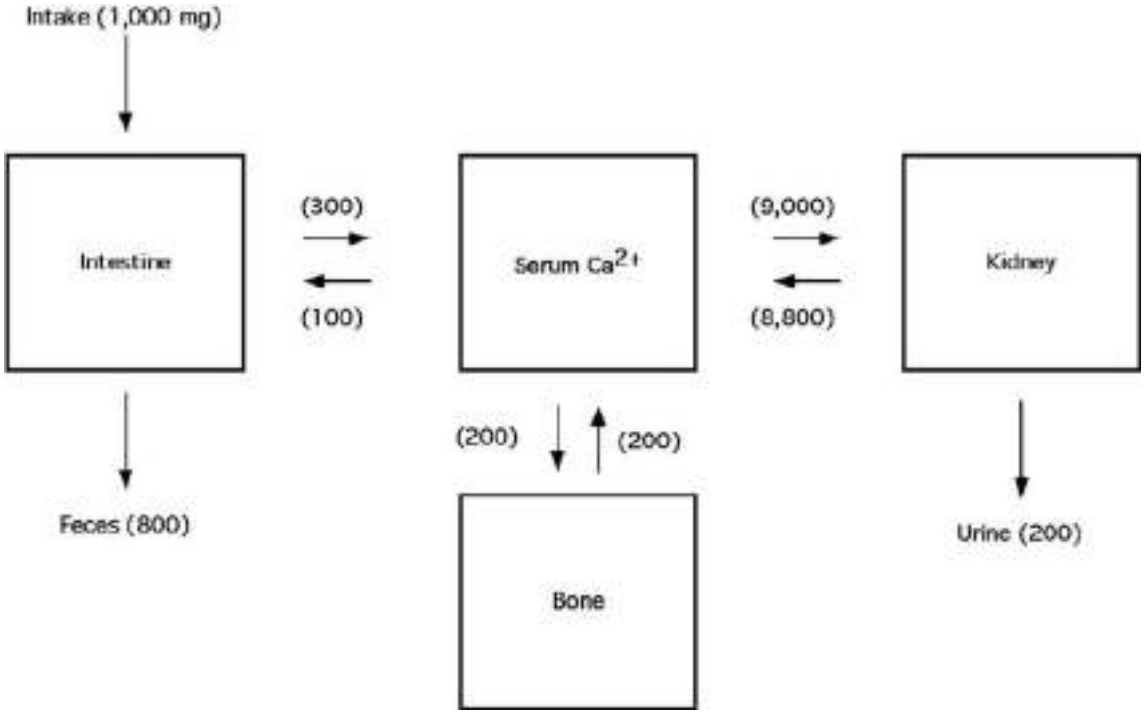

FIGURE 64.2 **Extracellular calcium balance in the adult human.** Numeric values for calcium intake, excretion, and fluxes are in mg/day, approximated for a 70 kg individual, original data from ref. [254].

calcium. The amount of calcium excreted equals the difference between that filtered and reabsorbed:

calcium excreted = filtered load − calcium reabsorbed

or,

$$U_{Ca^{2+}}V = (GFR \times P^{uf}_{Ca^{2+}}) - TCa^{2+}$$

where $U_{Ca^{2+}}$ is the concentration of calcium in the urine, V is the rate of urine flow, GFR is the glomerular filtration rate, $P^{uf}_{Ca^{2+}}$ is the concentration of ultrafilterable calcium in plasma (filtered load being the production of GFR and plasma ultrafiltrable calcium), and $T_{Ca^{2+}}$ is the rate of net Ca^{2+} reabsorption.

Unlike phosphate or magnesium, which exhibit saturable reabsorptive kinetics (i.e., a tubule reabsorption maximum, T^m), most studies[9,13–15] suggest that calcium does not display such behavior. However, some evidence for a calcium $T^m(T^m_{Ca^{2+}})$ has been advanced.[16,17] The $T^m_{Ca^{2+}}$ is conventionally determined by measuring calcium excretion as a function of the plasma calcium, or ultrafilterable calcium, concentration. Two explanations have been proposed for the apparent failure of calcium excretion to saturate at elevated serum calcium concentrations. It has been argued that, *in vivo*, only a limited excursion of ultrafilterable plasma calcium concentrations can be tolerated and that within this range the filtered load of calcium may be less than the $T^m_{Ca^{2+}}$.[14] It has also been postulated that since the bulk of calcium absorption is passive and may be accomplished by a combination of diffusion and solvent drag, no $T^m_{Ca^{2+}}$ exists.

Calcium is reabsorbed throughout its passage along the nephron. As detailed below and shown schematically in Fig. 64.3, 60–70% of the filtered calcium is reabsorbed by proximal tubules, an additional 20% by thick ascending limbs, and 5–10% by distal tubules. Final adjustments of calcium excretion are achieved in collecting ducts, where transport may be absorptive or secretory. The net result of these processes is that only 0.5–1.5% of the filtered calcium is normally excreted in the voided urine.

The interested reader is referred to several excellent monographs for more comprehensive treatments of calcium homeostasis and clearance[2,18] micropuncture[19] and isolated tubule studies[20] of renal calcium transport.

Glomerular Filtration

The renal disposition of calcium begins with its ultrafiltration across the capillaries of the glomerulus. The ultrafilterable forms of calcium include ionized Ca^{2+} and calcium complexed to small anions. Calcium bound to plasma proteins is not filtered. The calcium

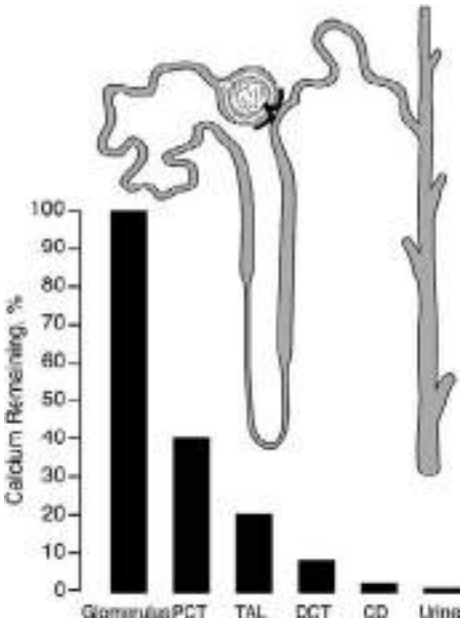

FIGURE 64.3 **Renal calcium absorption.** The figure represents a stylized view of the nephron and the graph depicts the percentage of filtered calcium remaining at the glomerulus, proximal convoluted tubule (PCT), thick ascending limb (TAL) of Henle's loop, distal convoluted tubule (DCT), collecting duct (CD), or in the final urine.

concentration in the ultrafiltrate, measured by directly sampling tubular fluid from Bowman's space is 1.31 mM, or 63% of that in plasma.[21–23] This value compares favorably to that of ultrafiltrate prepared with artificial membranes.[8,23–25]

Glomerular ultrafiltration is a passive process, driven by the net hydraulic and osmotic pressure gradient across the capillary membranes. The glomerulus is generally not considered a site of regulation of calcium absorption or homeostasis. However, it should be borne in mind that PTH depresses the glomerular ultrafiltration coefficient K_f, which may thereby diminish single nephron filtration rates and contribute to the hormone's calcium-sparing action (cf. Hypercalcemia[26,27]). mRNA transcripts for the type 1 PTH receptor (PTH1R)[28,29] and type 2 PTH receptor (PTH2R) are expressed in glomeruli.[30,31]

Proximal Convoluted Tubule

Following its ultrafiltration across the glomerular capillaries, calcium is reabsorbed throughout the nephron. As shown in Fig. 64.3, the majority of the filtered calcium is recovered by the proximal tubules. The proximal nephron of both superficial and juxtamedullary tubules consists of three ultrastructurally distinct segments: S_1, S_2, and S_3.[32] Operationally, however, calcium transport has been characterized in the microscopically recognized proximal convoluted tubules, corresponding primarily to the S_1 segment, and to a lesser extent in superficial proximal straight tubules (*pars recta*), S_2 segments.

Sixty to Seventy percent of the filtered calcium is absorbed by the end of the proximal convoluted tubule. Using *in vivo* micropuncture techniques, Lassiter and colleagues,[22] and subsequently others,[33,34] demonstrated that two-thirds of the filtered calcium is reabsorbed by the end of the accessible proximal convolution in the rat. Somewhat less complete absorption, 37–45%, obtains in the rabbit.[35,36] Remarkably, in the hamster, which exhibits the most robust calcium-sparing effect of PTH, calcium absorption by proximal tubules is negligible.[37] This observation underscores the primacy of distal segments in regulating final calcium excretion.

In general, random collections of proximal tubule fluid samples under control conditions result in tubular fluid to glomerular filtrate calcium ratios, $(TF/GF)_{Ca^{2+}}$ between 1.0 and 1.2. Based on these findings it is commonly held that the concentration of calcium within the proximal tubular fluid remains essentially identical to that of glomerular filtrate or ultrafilterable plasma (UF) calcium,[22,38] i.e., that calcium transport along the length of the proximal convoluted tubule proceeds essentially as an isoosmotic process. These observations, in turn, have been interpreted as indicating that the bulk of calcium absorption is energetically passive. However, a detailed examination of calcium absorption along the length of the accessible superficial proximal tubule revealed that $(TF/GF)_{Ca^{2+}}$ increases from a value close to unity at the earliest micropuncture locations to a value of about 1.2, still relatively early in the nephron, and stayed constant for the remaining accessible portions of the proximal nephron.[39] The cause of the elevated $(TF/GF)_{Ca^{2+}}$ ratios is unclear but may have its origin in molecular sieving of calcium at the luminal pole of the tight junctions as calcium absorption lags behind that of water. Alternatively, the presence of nontransported, anionically complexed calcium within the lumen might contribute to or account for the elevated values of $(TF/GF)_{Ca^{2+}}$. Inasmuch as the proximal tubule transepithelial voltage is about −2.5 mV, these findings are consistent with the idea that a component of proximal calcium transport may be energetically active since it proceeds against an electrochemical gradient.

Proximal Straight Tubule

Because proximal straight tubules (*pars rectae*) do not extend to the surface of the kidney and are not amenable to conventional micropuncture techniques, calcium

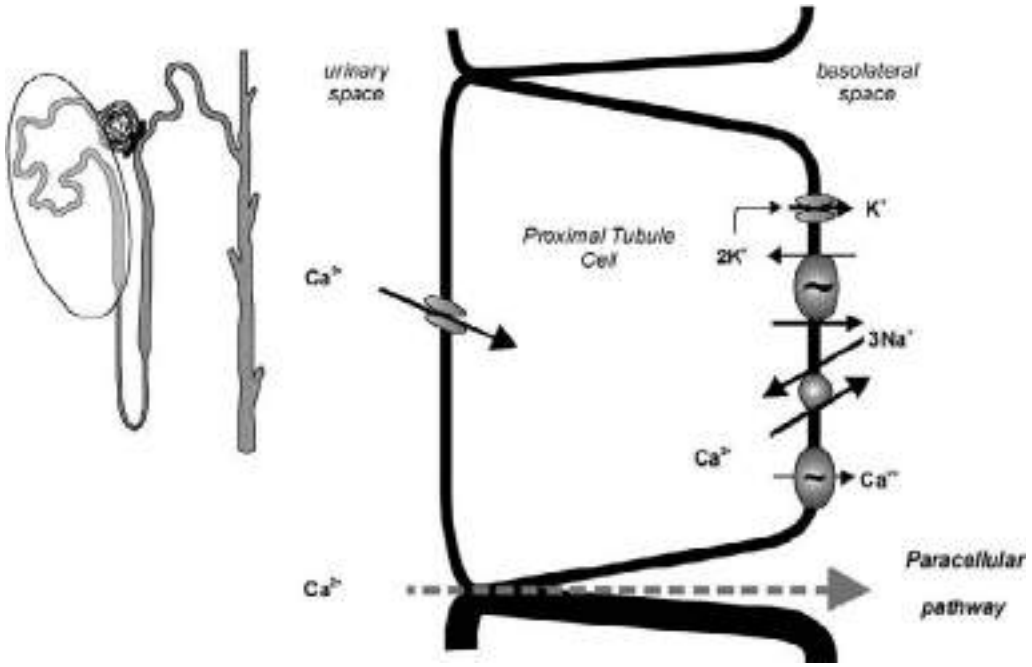

FIGURE 64.4 **Model of proximal tubular calcium absorption.** The inset shows the portion of the nephron referred to in the cell model. In proximal tubules, the majority of calcium is absorbed by passive mechanisms through the paracellular pathway. Evidence supports the presence of a small component of active, transcellular calcium transport.

transport by this segment has been less thoroughly studied than in proximal convoluted tubules. Indirect estimates of calcium reabsorption derived from the difference between the calcium concentration of fluid samples obtained from late proximal convoluted tubules and those from the tip of the loop of Henle suggested that 10% of the filtered calcium is recovered by proximal straight tubules.[22,40,41] This approach necessitates obtaining proximal samples from a superficial nephron, while the samples from the loop of Henle are taken from the tip of a juxtamedullary nephron. Nonetheless, direct *in vitro* microperfusion studies of proximal straight tubules substantiated the conclusion that proximal straight tubules absorb 10% of the filtered calcium.[42,43]

Mechanisms of Proximal Tubule Calcium Transport

Calcium absorption by proximal tubules may be mediated by a combination of passive and active transport mechanisms. The transepithelial absorption of calcium can be conceptually described by the following relation:

calcium absorption = passive transport + active transport

where passive absorption is the sum of diffusion and solvent drag. These relations can be expressed formally as:[44]

$$J_{Ca^{2+}} = \underbrace{\frac{P_{Ca^{2+}}\left(\Delta C_{Ca^{2+}} + \frac{Zi}{RT}\overline{C}_{Ca^{2+}}\Delta\psi\right)}{\text{diffusion}}}_{} + \underbrace{\frac{(1-\sigma_{Ca^{2+}})\overline{C}_{Ca^{2+}}J_v}{\text{solvent drag}}}_{} + \underbrace{\frac{J^{active}_{Ca^{2+}}}{\text{active transport}}}_{}$$

where, $P_{Ca^{2+}}$ is the apparent calcium permeability, $\Delta C_{Ca^{2+}}$ is the transepithelial calcium concentration difference ([lumen-to-bath] − [bath-to-lumen]), z_i is the valence, R the gas constant, T the absolute temperature, $C_{Ca^{2+}}$ is the average transmural calcium concentration across the tubule ([lumen-to-bath + bath-to-lumen]/2), $\Delta\Psi$ is the transepithelial voltage, σCa^{2+} is the reflection coefficient for calcium, J_v is the net fluid absorption, and $J\{^{active}_{Ca^{2+}}\}$ is the metabolically active, transcellular calcium transport.

Most evidence suggests that proximal tubule calcium transport is passive, i.e., energetically independent, and occurs primarily by diffusion and solvent drag. These mechanisms imply that calcium absorption proceeds primarily by the paracellular route (Fig. 64.4) through the lateral intercellular space between adjoining cells. By contrast, active transport is a two-step process, wherein calcium enters the cell across apical plasma membranes and is then extruded across basolateral plasma membranes. Basolateral efflux occurs against a steep electrochemical gradient and is powdered by the hydrolysis of ATP by the Na-K-ATPase. A general schematic representation of

these processes in proximal tubules is shown in Fig. 64.4.

It should be noted that, although small by comparison with paracellular calcium absorption, active cellular absorption by proximal tubules amounts to some 20 μmol/min,[45] which, in fact, is approximately twice that of the distal nephron, where calcium absorption is entirely cellular.

The mechanism of calcium transport by the S_2 segment of the proximal straight tubule resembles that of the proximal convoluted tubule. Studies using isolated perfused rabbit S_2 proximal tubules, under experimental conditions designed to minimize net fluid movement and the electrochemical gradient for Ca^{2+}, generally are consistent with the idea that passive driving forces are the major determinant of calcium absorption.[42,46] However, evidence for a significant amount of active calcium transport has been reported.[43] Sacks and Bourdeau[47] showed that when passive driving forces across isolated S_2 segments of rabbit proximal straight tubules were experimentally manipulated, the direction and rate of net calcium flux were predicted by the magnitude of the imposed electrochemical gradient. Thus, passive diffusion appears to be the major mechanism of transport in proximal straight tubules.

The presence of active, transcellular calcium absorption by proximal tubules, no matter how slight its magnitude, necessitates specific transport proteins in apical plasma membranes to admit calcium and others in basolateral membranes to mediate its extrusion. As far as is presently known, cellular calcium entry is mediated by calcium channels. Support for the presence of such channels takes the form of electrophysiological[48–51] and pharmacological[51–60] evidence. The molecular identity of such proximal tubule calcium channels is unknown but appears not to be TrpV5 or TrpV6.[61] Basolateral calcium efflux in energetically dependent. Two proteins capable of mediating such transport are the plasma membrane Ca^{2+}-ATPase (PMCA) or the NCX Na^+/Ca^{2+} exchanger. Proximal tubule cells express PMCA1 and PMCA4 isoforms, which may serve as the primary mechanism of cellular Ca^{2+} efflux.[62] Proximal tubules also express the NCX1 Na^+/Ca^{2+} exchanger.[63] The relative contribution of NCX1 and PMCA1/4 to cellular calcium absorption is not known.

In summary, proximal tubules exhibit high calcium permeability and low transepithelial electrical resistance. Most calcium absorption proceeds through passive mechanisms and traverses the paracellular pathway (Fig. 64.4). The majority of passive absorption is diffusive, with an additional slight contribution by solvent drag. The active component constitutes 20% of the total calcium absorption and proceeds through a transcellular pathway that involve entry through apical membrane calcium channels and exit across basolateral membranes that is mediated by isoforms of the plasma membrane Ca^{2+}-ATPase and/or the Na^+/Ca^{2+} exchanger.

Descending and Ascending Thin Limbs

Limited information is available on calcium transport and permeability of thin descending limbs of Henle's loop. The few studies failed to uncover evidence for net calcium movement (absorptive or secretory) (summarized in [39]). When single rabbit descending thin limbs were perfused *in vitro*, (TF/UF) Ca^{2+} and (TF/P) inulin increased proportionately.[41] This would allow calcium to accumulate in the tubular fluid. Furthermore, these studies revealed a remarkably low permeability to calcium; about one-tenth that of proximal convoluted tubules.

Thin ascending limbs of Henle's loop also exhibit low calcium permeability and are not a site of net calcium transport.[64] The low permeability of thin ascending limbs is particularly striking in view of its comparatively high permeability to sodium and chloride.[65] In single, microperfused thin ascending limbs of the hamster, removal of luminal calcium had no effect on the concentration of intracellular free calcium,[66] consistent with the low permeability.

In summary, calcium transport by thin descending limbs and thin ascending limbs contributes little to the overall reabsorptive process because of the low Ca^{2+} permeability and absence of active calcium transport by these segments.

Thick Ascending Limb

Approximately 20–25% of the filtered calcium is reabsorbed by thick ascending limbs of Henle's loop. Thick ascending limbs are comprised of medullary and cortical portions. This division is relevant because appreciable functional and species differences attend calcium transport and its hormonal regulation by these nephron segments. Calcium is absorbed by both medullary and cortical portions of thick ascending limbs, though to differing degrees. It is unclear if the gradual changes in cellular architecture between medullary and cortical portions of the thick ascending limb are related to differences in the mechanism or magnitude of calcium transport. The distinguishing feature of calcium transport in thick ascending limbs is the presence of parallel paracellular and cellular transport pathways (Fig. 64.5). Under resting conditions, calcium absorption is energetically passive and proceeds through the paracellular pathway driven primarily by the lumen electropositive transepithelial voltage resulting from

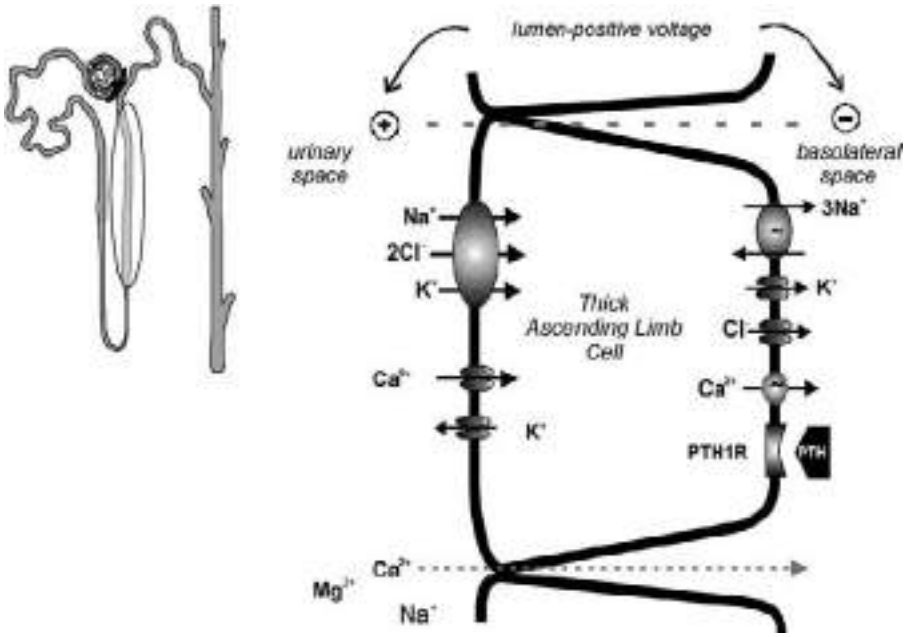

FIGURE 64.5 **Model of calcium absorption in thick ascending limbs.**The inset shows the portion of the nephron referred to in the cell model. Calcium absorption proceeds through both an active, transcellular pathway and by passive mechanisms through the paracellular pathway. Resting, i.e., basal absorption is passive and is driven by the ambient electrochemical gradient for calcium. Calcitropic hormones such as PTH and calcitonin (not shown) stimulate active cellar calcium absorption in cortical and medullary thick ascending limbs, respectively, as detailed in the accompanying text. Other hormones, such as vasopressin, that stimulated Na^+ absorption by the Na-K-2Cl cotransporter, cause parallel elevations of calcium absorption by increasing the transepithelial voltage and the driving force for passive calcium absorption. Conversely, the loop diuretics bumetanide and furosemide, by inhibiting Na-K-2Cl cotransport, decrease the transepithelial voltage and diminish passive calcium absorption with an attendant increase in calcium excretion.

the absorption of Na^+. The greater the rate of Na^+ absorption, the larger the voltage, and the consequent rate of Ca^{2+} absorption. Conversely, lower rates of Na^+ absorption, following the administration of loop-acting diuretics, for instance, the lower the extent of Ca^{2+} absorption. Thus, in the absence of hormonal stimulation, Ca^{2+} and Na^+ absorption parallel one another in thick ascending limbs as they do in proximal tubules.

The pattern of parallel Ca^{2+} and Na^+ absorption is disrupted, however, by PTH and by calcitonin. Thick ascending limbs express the parathyroid hormone receptor and the calcitonin receptor. The distribution of these receptors, as deduced by the ability of their respective ligands to induce cAMP accumulation,[67] varies importantly between medullary and cortical ascending limbs and across species. Table 64.1 summarizes representative findings for humans and the mouse. Direct studies of the effect of PTH and calcitonin on calcium transport by isolated cortical and medullary thick limbs established that these peptides stimulate active, transcellular calcium absorption.[39] Thus, resting calcium absorption proceeds through the paracellular pathway through tight junctions, and active calcium absorption follows a transcellular route.

TABLE 64.1 PTH and Calcitonin Receptor Distribution in Thick Ascending Limbs

Species	Segment	PTHR	CTR
Human	CAL	++	+++
	MAL	++	++
Mouse	CAL	++++	+
	MAL	0	0

Distribution and abundance of parathyroid hormone receptor (PTHR) and calcitonin receptor (CTR) are scaled based on relative stimulation of adenylyl cyclase.[255,256]

Moreover, whereas passive calcium transport in thick limbs parallels Na^+ movement, active calcium cellular calcium transport is inversely related to cellular sodium absorption. The reason for this is that apical membrane calcium influx is voltage dependent. Cellular Na^+ entry depolarizes the cell, thereby reducing the driving force for Ca^{2+} entry, and conversely decreased Na^+ influx hyperpolarizes the transmembrane voltage and increases Ca^{2+} influx. These complex relations between voltage and paracellular vs. cellular calcium movement makes it difficult to assess

the relative contribution of cellular and paracellular calcium transport to the net absorption, especially under physiological conditions or in clinical settings.

Notably, other peptide hormone receptors, including those for ADH and glucagon, are also expressed in thick ascending limbs. Their activation is not accompanied by changes of calcium absorption. This may be explained by the requirement for activation of both adenylyl cyclase and phospholipase C, which occurs with PTH and calcitonin but not ADH or glucagon, for stimulation of cellular calcium transport in cortical ascending limbs.[68]

Bartter's Syndrome and Calcium Transport by Thick Ascending Limbs

Mutations in the *Slc12a1* (Na-K-2Cl cotransporter),[69] the *KCNJ1* (ROMK apical K^+ channel),[70] and *CLCNKB*, (the human homolog of the ClC-K2 basolateral Cl^- channel)[71] genes have been described in a number of families with Bartter's syndrome. The syndrome is characterized by salt wasting, hypokalemic alkalosis and, in the classic and antenatal variants, accompanied by hypercalciuria.[72] Loss of Na-K-2Cl cotransporter function by gene mutation results in a clinical presentation similar to that of inhibition of cotransporter activity by loop diuretics, viz., salt wasting, volume depletion, hypokalemic metabolic alkalosis, and hypercalciuria. These findings underscore the parallel nature of sodium and calcium absorption by thick ascending limbs.

Distal Convoluted Tubules

Distal convoluted tubules absorb 8–10% of the filtered calcium. Although modest in overall magnitude, distal tubules are the most important site for renal calcium economy because they are the site of the key regulatory influence of PTH on calcium absorption. Calcitonin, and $1,25(OH)_2D_3$ also participate in regulating calcium absorption by distal tubules. The other notable feature of calcium absorption by distal tubules is that it proceeds entirely through a transcellular pathways (Fig. 64.8) and is inversely related to sodium absorption. Thus, thiazide diuretics dissociate calcium and sodium movement by inhibiting sodium transport, thereby promoting calcium absorption.

The superficial distal nephron is composed of three tubule segments, the distal convoluted tubule, the connecting tubule, and the cortical collecting tubule, each composed of distinct cell types.[73] The distal convoluted tubule begins at the macula densa and, in most species, ends gradually as a transition to connecting tubules.[74] Although it is generally thought that distal convoluted tubules consist of a single cell type, the distal convoluted tubule cell, intercalated cells may be found, particularly in the later one-third of the tubule. In humans, intercalated cells may be present throughout the distal convoluted tubule.[75] Distal convoluted tubule can be functionally divided in to DCT1 and DCT2 portions. The former expresses the NaCl cotransporter, whereas the latter expresses both the NaCl cotransporter and the epithelial Na channel, ENaC.[76] Connecting tubules consist of connecting tubule cells and intercalated cells. The cortical collecting duct is comprised of principal and of alpha or beta intercalated cells. These different cell types and relevant when considering calcium transport and its hormonal regulation. The distribution of calcium-transporting or regulating proteins in mouse distal nephron sites has been elegantly analyzed.[77] The findings are included in the relevant following sections.

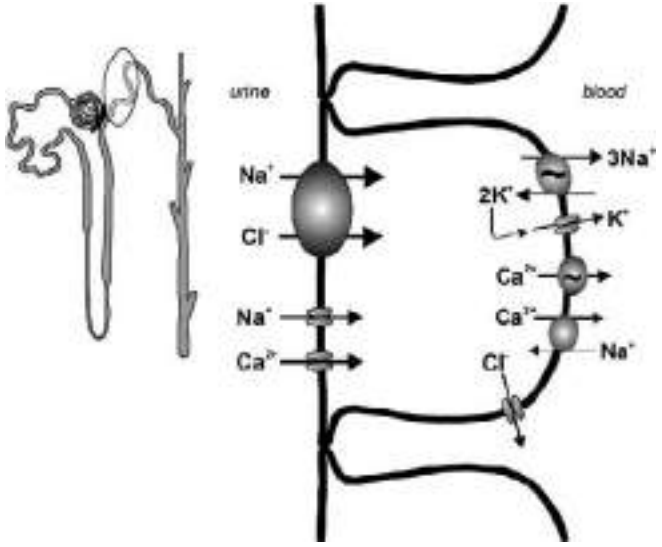

FIGURE. 64.6 **Calcium and sodium absorption by distal convoluted tubules.** The inset highlights this portion of the nephron. The cell model shows two apical membrane Na^+ entry mechanisms, the thiazide-diuretic-inhibitable Na-Cl cotransporter and the amiloride-blockable, epithelial Na channel, ENaC. Calcium enters the cell across apical membranes through dihydropyridine-sensitive calcium channels. Basolateral calcium efflux is thought to be mediated by the plasma membrane Ca^{2+}-ATPase (PMCA) and the Na^+/Ca^{2+} exchanger. In distal convoluted tubules, both basal and stimulated calcium absorption follows a transcellular path.

Pioneering stop-flow studies first demonstrated that calcium was absorbed by distal tubules. Direct examination of calcium transport along the length of the accessible surface distal tubule confirmed these conclusions.[22] 10% of calcium delivered to distal convoluted tubules is absorbed by the end of the accessible surface portion of distal tubules. Since the $(TF/UF)_{Ca2+}$ ratio is less than unity and the transepithelial voltage is lumen-negative,[78,79] calcium

absorption proceeds against both chemical and electrical gradients and, hence, is active. Detailed information on permeability coefficients and related biophysical parameters of distal calcium transport can ben found in previous editions.[39]

Cellular Mechanisms of Distal Tubule Calcium Transport

Calcium absorption by distal convoluted tubules proceeds entirely by active, transcellular absorption (Fig. 64.7). In this regard it is conspicuously different from proximal tubule calcium absorption, which is primarily if not entirely passive and paracellular in nature, or calcium absorption by thick ascending limbs, which is mediated by hybrid transcellular and paracellular mechanisms.

The salient features of cellular calcium transport by distal convoluted tubule cells are summarized schematically in Fig. 64.6. Entry across apical cell membranes occurs through calcium channels[80–84] and basolateral efflux is mediated by a combination of Na^+/Ca^{2+} exchange and Ca^{2+}-ATPase. It is now generally accepted that TrpV5 calcium channels are responsible for apical calcium entry (see Chapter 62, Calcium Channels).[85] TrpV5, was cloned and localized to apical membranes of distal convoluted tubules.[77,86,87] TrpV5 is a homotetramer that is constitutively active, has a 77 pS single channel conductance.[88] Some aspects of the biology of TrpV5 remain to be resolved. For instance, TrpV5 is insensitive to dihydropyridine or phenylalkylamine calcium channel blockers[89,90] that have been shown to inhibit calcium absorption by distal convoluted tubules and DCT cells.[91,92] Recent findings suggest that PTH stimulates Ca^{2+} entry by PKA-mediated phosphorylation of TrpV5.[93] The mechanism whereby thiazide diuretics inhibit calcium entry by TrpV5 channels is uncertain. A heteromeric, dihydropyridine sensitive calcium channel that incorporates ß$_3$-subunits[94,95] has also been described. It is stimulated by PTH,[91] thiazide[96] and amiloride[97] diuretics, but is refractory to furosemide.[95] Its molecular identity is unknown.

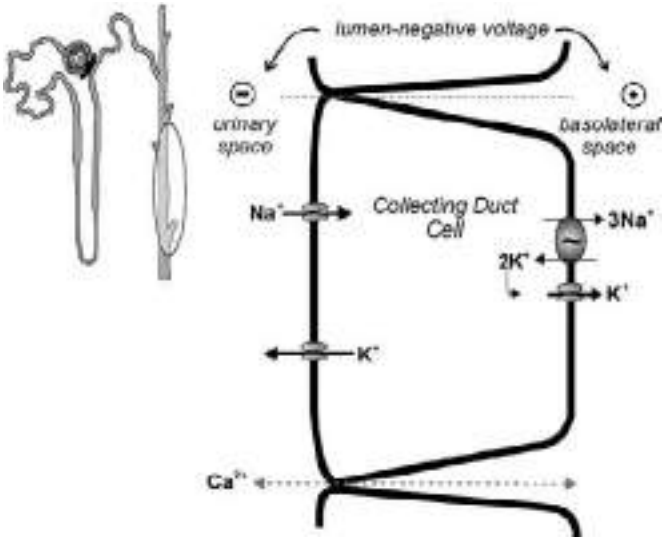

FIGURE 64.7 **Calcium transport by collecting ducts.** This nephron segment is shown in the shaded area of the inset. Collecting ducts are not thought to be a primary site of calcium transport. Studies suggest that calcium movement is small in magnitude and thermodynamically passive. Transport may be absorptive or secretory, driven by the lumen-negative transepithelial voltage.

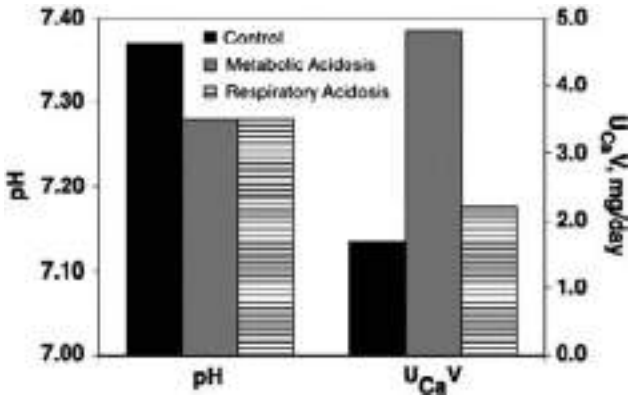

FIGURE 64.8 **Effects of metabolic or respiratory acidosis on serum pH and urinary calcium excretion in rats** *(Redrawn from ref. [171]).*

TRPV5-null mice exhibit a comparable hypocalciuric response to thiazides as do wild-type normal mice.[98] Because the pharmacological site of thiazide action is the distal nephron, Nijenhuis concluded that thiazide diuretics indirectly stimulate paracellular proximal tubular calcium reabsorption by contracting the extracellular fluid volume. The clinical implication of this finding is that patients with recurrent kidney stones must restrict dietary sodium to enhance the volume-depleting action of thiazides to maximize the hypocalciuric effect.

The Klotho gene encodes a type I single-pass transmembrane protein that is associated with TrpV5. Secreted Klotho, a beta-glucuronidase, hydrolyzes extracellular sugar residues on TRPV5, thereby inhibiting internalization of TRPV5 and increasing the abundance of TRPV5 on the cell surface.[99] The net result of this action is to increase TRPV5-mediated calcium influx and renal calcium absorption. Klotho-deficient mice exhibit higher calcium excretion than do wild-type mice.[100]

Distal convoluted tubules express several isoforms each of the Ca^{2+}-ATPase[101,102] (PMCA) and the Na^+/Ca^{2+} exchange (NCX).[103–106] NCX1 is

extensively expressed on basolateral membranes of DCT1 of mouse[107] and DCT2 of rat[108] distal convoluted and connecting tubules. PMCA isoforms display a comparable pattern of distribution.[103] NCX1 operates in forward and reverse modes. In the forward direction, NCX1 mediates calcium efflux that is coupled to sodium influx in a ratio of 3 Na^+ exchanged for 1 Ca^{2+} ion. Operating in this fashion, NCX1 is thus electrogenic.[109] Other exchanger modes and stoichiometries have been reported.[110] Given the membrane hyperpolarization induced by PTH,[91,111] it would be expected that calcium extrusion mediated by NCX1 would be accelerated in response to PTH action, thereby coordinating symmetric increases of apical calcium entry and basolateral efflux, accounting to the hypercalcemic actions of PTH.

The $K_m^{Ca^{2+}}$ for renal Na^+/Ca^{2+} exchange is 0.1–10 μM, within the range of free intracellular Ca^{2+} (Ca_i^{2+}) stimulated by PTH, calcitonin, and thiazide diuretics.[96–112] The K_m is comparable to that of the PMCA,[113–116] whereas the V_{max} of the PMCA is 20–40 times greater than that for Na^+/Ca^{2+} exchange. Assuming that $[Na^+]_i$ is 17.5 mM[117] and Ca_i^{2+} is 120–300 nM,[118] the Na^+/Ca^{2+} exchanger operates in the forward direction at no more than 4–10% of its maximal velocity. Under the same conditions, the PMCA functions at 30–70% of its V_{max}. Thus, under resting conditions, PMCA activity would account for 85% of basolateral calcium efflux and Na^+/Ca^{2+} exchange would mediate only 15%. Based on these considerations, it is reasonable to imagine that resting calcium efflux is mediated by the PMCA and that in response to PTH, thiazide or amiloride diuretics that hyperpolarize distal tubules, the rate of forward electrogenic Na^+/Ca^{2+} exchange increases and accounts for the bulk of calcium efflux.

Gitelman's Syndrome and Distal Tubule Calcium Transport

Gitelman and Welt[119] described a variant of Bartter's syndrome exhibiting salt wasting, hypokalemia, and hypermagnesuria but that was uniquely associated with decreased calcium excretion.[119,120] Gitelman's syndrome is due to inactivating mutations of the apical membrane Na-Cl cotransporter gene, *Slc12a3*, which is located on human chromosome 16. The hypocalciuria of Gitelman's syndrome can be understood from the model of distal tubular calcium absorption depicted in Fig. 64.6. Since the direction and magnitude of sodium and calcium absorption are inversely related in distal convoluted tubules, impaired or diminished apical Na-Cl cotransport enhances calcium absorption. Thus, the disordered mineral ion metabolism accompanying Gitelman's syndrome reinforces the conclusions drawn regarding the cellular mechanisms of distal calcium absorption and the inverse relations between calcium and sodium transport by distal tubules.[109]

Connecting Tubules

Connecting tubules represent a structural and functional transition from distal convoluted tubules to collecting ducts. In superficial nephrons, connecting tubules are short and connect distal convoluted tubules to collecting ducts. Connecting tubules of deep nephrons form an arcade before draining into a collecting duct. The ratio of superficial to deep connecting tubules varies between species (cf. Chapter 20). Notably, whereas distal convoluted tubules consist of a single cell type, the principal cell, connecting tubules are comprised of principal cells and intercalated cells. As in distal convoluted tubules, principal cells mediate calcium absorption. α-intercalated cells secrete protons by a combination of the vacuolar H^+-ATPase and by the gastric-type H/K-ATPase.[121–123] Operationally, cellular calcium absorption is similar to that in distal convoluted tubules: it proceeds by a transcellular route and is stimulated by PTH and thiazide diuretics. Calcium movement by connecting tubules has recently been reviewed in depth.[124] The presence of calcium-transporting principal cells and proton-absorbing intercalated cells may be responsible for the association of hypercalciuria and metabolic acidosis, which has been traced to connecting tubules.[125]

Experimentally metabolic acidosis induced by NH_4Cl or acetazolamide decreased renal TRPV5 and calbindin-D_{28K} mRNA and protein expression in wild-type but not in TRPV5-null mice.[126] Thus, downregulation of renal calcium transport proteins may be the mechanism responsible for hypercalciuria associated with metabolic acidosis. Conversely, chronic metabolic alkalosis increased the expression of calcium transport proteins accompanied by diminished calcium excretion in wild-type mice. This effect persisted in TRPV5-null animals. Additional factors may also contribute to the hypocalciuric effect of metabolic alkalosis.

Collecting Tubules

Cortical collecting tubules only modestly participate in overall calcium homeostasis. Calcium transport is small in magnitude and may be absorptive or secretory. Calcium flux varies directly with the magnitude and direction of the transepithelial voltage.[127] At spontaneous transepithelial voltages (−40 to −50 mV), a

small net secretory flux is observed. Secretory calcium transport could play a role in regulating calcium excretion when long-term changes of transepithelial voltage occur, for instance, as an adaptive response to changes in mineralocorticoid status.[128] A conceptual model of calcium transport by collecting tubules is shown in Fig. 64.7.

Inner medullary collecting ducts absorb calcium and may be responsible for recovery of as much as 1.4% of the filtered load.[129] Calcium absorption by inner medullary collecting ducts is insensitive to PTH. Other reports failed to find evidence to support measurable calcium transport by this nephron segment.[130,131]

TABLE 64.2 Factors Regulating Renal Calcium Transport

Tubule Segment	Fractional Reabsorption	⇓Calcium Reabsorption	⇑Calcium Reabsorption
Proximal Tubule	61%	Volume contraction, phosphate loading,	Volume expansion, phosphate depletion, hypercalcemia, PTH, acetazolamide
Descending thin limb	9%		osmotic diuretics
Thick ascending limb	20%	PTH, calcitonin	furosemide, bumetanide
Distal convoluted tubule	5%	PTH, calcitonin, thiazide diuretics, amiloride, phosphate loading, alkalosis, mineralocorticoid depletion	acidosis
Collecting duct	3%		
Excreted in Urine	<1%		

REGULATION OF RENAL CALCIUM TRANSPORT

A variety of physiological, pathological, hormonal, and pharmacological factors influence tubular calcium reabsorption. The most important of these are enumerated in Table 64.2 and considered below.

Parathyroid Hormone

PTH is the most important physiologic regulator of renal tubular calcium transport, and its actions are covered in detail in Chapter 65. PTH increases renal calcium reabsorption and lowers urinary calcium excretion. In the complete absence of the hormone or in PTH deficiency states, there is diminished tubular reabsorption and hypercalciuria. The stimulatory effect of PTH on calcium transport is limited to distal nephron segments. Paradoxically, PTH decreases calcium absorption by proximal tubules; the calcium-sparing action is due entirely to its effects on cortical thick ascending limbs, distal convoluted tubules, and, in some species, connecting tubules.

Mechanism of PTH Effects on Renal Calcium Transport

It was long held that the calcium-sparing action of PTH was mediated exclusively by the adenylyl cyclase–cAMP–protein kinase A (PKA) axis. This conclusion was based on the following evidence: PTH enhanced the urinary excretion of cAMP formed *de novo* in the kidney (nephrogenous cAMP); administration of exogenous cAMP analogs or forskolin mimicked the effect of PTH in a variety of preparations; and the nephron locations at which PTH activates adenylyl cyclase correlated well with the sites of its physiologic actions. We know now that PTH effects on renal calcium transport, at least in distal tubules, require activation of both PKA and protein kinase C (PKC).[68] It should be borne in mind that PTH-induced formation of nephrogenous cAMP occurs in proximal tubules, where the hormone has little effect on calcium absorption, and is mainly related to the phosphaturic action of PTH. The discrepancy between the necessity and sufficiency of PKA in activating renal calcium transport may be due to non-specific, crossover effects that occur upon addition of high concentrations of forskolin or of exogenous cAMP analogues.[132,133] cAMP-dependent but PKA-independent actions of PTH in some instances may be mediated by EPAC,[134] an exchange protein that is cAMP-dependent and activates PKC.[135]

Functional studies[136] and the molecular cloning of the PTH receptor[137,138] revealed that in addition to activating adenylyl cyclase, PTH activates phosphatidylinositol specific phospholipase C (PI-PLC). PTH stimulation of distal calcium absorption requires activation of PKA and PKC.[68] It should be mentioned that emerging evidence points to the ability of PTH receptors to activate additional signaling pathways involving phospholipase A_2,[139,140] phospholipase D,[68,141] and MAP kinase.[142–144]

The PTH receptor mediates the effects of both PTH and of the PTH-related peptide (PTHrP) and is

therefore designated the Type 1 PTH/PTHrP receptor (PTH1R). A second Type 2 PTH receptor (PTH2R), which responds uniquely to PTH and not PTHrP has also been identified.[145,146] The PTH2R is not thought to be expressed in renal tubular epithelial cells but in vascular cells of the kidney and has not yet been implicated in renal calcium transport.

The PTH1R may activate PKA and PKC. In some cases occupancy of the PTH1R activates only one signaling pathway. For instance, in keratinocytes,[147–149] cardiac myocytes,[150,151] lymphocytes[152–154] and vascular smooth muscle cells[155] reasonable evidence suggests that the PTH1R activates phospholipase C and PKC, PLC but not adenylyl cyclase and PKA. Under certain circumstances, one pathway may be preferentially activated at low concentrations of PTH, while both pathways are stimulated at higher concentrations.[156] These and other cell-specific signaling pathways initiated upon activation of the PTH1R appear to be determined by Na/H exchanger regulatory factor, a cytoplasmic adapter protein.[157]

Extracellular Fluid Volume

Extracellular volume expansion increases calcium excretion, whereas extracellular volume contraction decreases calcium excretion. These effects are brought about indirectly through alterations of proximal tubule function. Calcium transport in proximal tubules is passive and coupled to sodium and water absorption; changes in proximal salt and water absorption cause parallel changes of calcium transport. Hence, by reducing proximal salt absorption, extracellular fluid volume expansion inhibits calcium absorption and increases calcium excretion, whereas volume contraction augments proximal salt absorption, thereby enhancing calcium absorption and decreasing calcium excretion.[130,158] Because of the sheer magnitude of proximal solute absorption, even slight alterations of extracellular fluid volume exert profound effects on calcium absorption. These are commonly ignored or misconstrued when explaining the calcium-sparing actions of drugs such as thiazide diuretics, which reduce extracellular fluid volume. Nonetheless, a number of studies[159,160] provide evidence that the natriuretic effects of volume expansion can only be partially explained by diminished proximal solute reabsorption and point to the presence of distal effects of volume expansion.

Acute extracellular volume expansion decreases ionized calcium concentrations in plasma, with an attendant stimulation of PTH secretion.[161] Increased serum PTH levels, in turn, by directly stimulating calcium absorption by distal convoluted tubules, further reduce calcium excretion.

Acid–Base Balance

Metabolic acidosis increases calcium excretion,[125,162–165] whereas metabolic alkalosis decreases calcium excretion[166–168] at any given plasma calcium concentration. By displacing calcium bound to albumin, acidosis increases the ionized and ultrafilterable calcium in plasma, without affecting the total calcium concentration.[169] Chronic acidosis does not alter resting PTH levels. Further, the changes of renal calcium transport do not require the presence of the parathyroid glands[125,170]and, thus, are not due to secondary changes in serum PTH levels.

The hypercalciuria associated with metabolic acidosis is thought to be caused by reduced distal tubule calcium absorption. The effect is specific for calcium and dissociates the normal parallel relations between renal sodium and calcium absorption, a hallmark of distal tubular regulatory actions. The decline of proximal bicarbonate reabsorption associated with the acidosis decreases fractional calcium reabsorption and augments calcium excretion. Administration of bicarbonate can reverse decreased distal tubule calcium transport.[125,164] The mechanism by which this occurs is uncertain but may be indirect and involve increasing bicarbonate delivery to distal tubules, where bicarbonate is not absorbed and may complex calcium, resulting in greater excretion. However, the effect of bicarbonate to augment distal tubule calcium absorption may also be direct and proceed independent of systemic acid–base status.[125,163]

The effects of respiratory acid–base disturbances on calcium excretion are not as well studied as those of metabolic origin. Respiratory acidosis variably affects renal calcium excretion. As shown in Fig. 64.8, for a comparable fall of blood pH, calcium excretion was unchanged with chronic respiratory acidosis, whereas calcium excretion increased during chronic metabolic acidosis.[171] These findings imply that reductions of pH, per se, do not account for the changes in urinary calcium excretion that accompany chronic metabolic acidosis. In contrast, Chronic respiratory acidosis increased fractional urinary calcium excretion in the dog.[172] Here, serum pH declined to 7.2 after one week of breathing 10% CO_2, while serum PTH and ionized calcium were unchanged but absolute and fractional calcium excretion rose by 50 and 75%, respectively, in the absence of a change in the filtered calcium.

Phosphate Depletion

Chronic phosphate depletion causes striking increases in calcium excretion.[173–175] Although hypophosphatemia, per se, reduces PTH levels, which

contributes to the diminished calcium absorption, the effect of phosphate depletion is independent of PTH.[176] Proximal tubule absorption of both sodium and calcium is reduced proportionately,[177] and calcium absorption is impaired in thick ascending limbs or early distal tubules.[178,179] Acute phosphate infusion reduced calcium excretion to control levels without affecting proximal tubular absorption.[177] In another study,[179] PTH or phosphate infusion partially corrected the renal calcium wasting. Thus, the distal calcium absorptive defect was sensitive to phosphate infusion but was independent of PTH since infusion of PTH failed to alter urinary calcium excretion. It is not known how phosphate augments distal calcium transport.

Hypercalcemia

Hypercalcemia has several effects on the renal calcium handling. It has been noted repeatedly that calcium infusion reduces GFR.[26,180,181] Hypercalcemia causes a fall in the glomerular ultrafiltration coefficient, K_f, resulting in a decrease in both single-nephron and whole-kidney GFR;[26,27,182] these effects do not occur in the absence of PTH. Both the PTH1R and PTH2R are expressed on glomerular cells.[29,31,183] It would be attractive to attribute the calcium-dependent effects of the calcium-sensing receptor (CaSR). However. immunolocalization studies of the CaSR failed to detect protein expression[184] even though cDNA transcripts were reported[28] in the rat glomerulus.

Calcium infusion increases both calcium and sodium excretion,[185] in part due to inhibition of isoösmotic solute absorption by proximal tubules.[180] However, urinary calcium excretion increases to a greater extent than does sodium excretion, suggesting both a specific inhibitory effect of hypercalcemia on calcium transport and, by inference, that this effect occurs in distal tubules, where calcium and sodium absorption can be dissociated. Evidently, in intact animals, elevations of serum calcium are accompanied by suppression of PTH secretion,[180] which decreases calcium absorption at hormone-sensitive sites in cortical thick ascending limbs and particularly distal convoluted tubules. However, hypercalcemia also directly inhibits calcium absorption by thick ascending limbs of Henle's loop.[186,187]

Hypercalcemia suppresses PTH-stimulated cAMP formation specifically in thick ascending limbs. Increasing extracellular calcium from 1 to 5 mM inhibited cAMP production in response to PTH and calcitonin in dissected cortical thick ascending limbs of Henle, but not in proximal convoluted tubules.[188] High calcium also inhibited cAMP production stimulated by forskolin. The mechanism of this inhibitory effect was unclear at the time. It is now appreciated that these effects are mediated by the CaSR.

CaSR

Significant insights in to the regulation of calcium metabolism followed the cloning of the extracellular calcium-sensing receptor (CaSR) by Brown et al.[11] The CaSR is located mainly in the parathyroid glands and on renal tubules. In the parathyroid glands, calcium binding activates the receptor and inhibits PTH secretion. The CaSR colocalizes with the PTH1R in cortical thick ascending limbs and distal convoluted tubules,[184] suggesting a regulatory role on the effects of PTH. Consistent with these observations, graded elevations of extracellular calcium progressively inhibit PTH-stimulated cAMP formation by mouse cortical thick limb and distal convoluted tubule cells. Raising basolateral, but not luminal calcium concentration directly suppressed PTH-stimulated cellular and paracellular calcium absorption by single perfused cortical thick ascending limbs.[189] The CaSR is also expressed at other nephron sites, where it participates in regulating proximal phosphate transport[190] and vasopressin-dependent hydroösmsis in collecting ducts.[191]

The clinical relevance of the CaSR to renal calcium transport has been established by identifying hyper- and hypocalcemic disorders resulting from CaSR mutations: familial hypocalciuric hypercalcemia and neonatal severe hyperparathyroidism result from inactivating CaSR mutations, while an autosomal dominant form of hypocalcemia is caused by activating mutations.[192,193] In addition to effects of mutations on CaSR activation or inactivation, an acquired form of hypocalciuric hypercalcemia and multiple autoimmune disorders arising from the presence of specific antibodies against the CaSR.[194] In ESRD patients, Rodriguez et al. assessed the role of the CaSR in the pathogenesis of secondary hyperparathyroidism.[195] CaSR expression was reduced by 60% in hyperplastic glands as compared with normal parathyroid tissue and it was worst in patients with nodular hyperplasia, a condition associated with refractory secondary hyperparathyroidism.

Clinical Hypercalcemia

Primary hyperparathyroidism accounts for the majority of hypercalcemia seen in the outpatient setting.[196] Epidemiological data point to a decreasing prevalence of primary hyperparathyroidism.[197] The overall age and gender-adjusted rate declined from 82.5 per 100,000 person-years in 1974–1982 to 21.6 per 100,000 from 1993–2001. This trend over several

decades suggests a change in the epidemiology of the disease. The authors speculate that a factor besides the introduction of automated serum calcium testing explains the peak incidence in the 1970s. They hypothesize that the factor could have been the previous widespread use of x-rays in the 1940–1950s as diagnostic and therapeutic tool (head and neck radiation) for acne and thymic enlargement.

Surgery remains the preferred choice for adenoma-related primary hyperparathyroidism. Minimally invasive parathyroidectomy is a procedure that evolved as a result of the technological advance in preoperative and intraoperative localization tools to guide parathyroid surgery and is now commonly performed at several centers. Based on review of medical charts of 352 patients that underwent parathyroidectomy for primary hyperparathyroidism, an intraoperative PTH level 10-min after gland excision with a 50% decrease from the pre-incision PTH levels provided the most reliable evidence of a successful surgical procedure, while avoiding unnecessary parathyroid exploration.[198] The calcium sensing receptor mimetic cinacalcet (Sensipar) is available for patients for whom parathyroidectomy is not an option. Patients with primary hyperparathyroidism treated with cinacalcet for five years maintained normal serum calcium levels with reduced plasma PTH, increased serum phosphate and alkaline phosphatase.[199] No significant effects were noted on bone mineral density. Although not presently approved by the FDA for routine treatment of primary hyperparathyroidism, these and other positive outcomes will likely result in approval.

Humoral hypercalcemia of malignancy (HHM) related to PTH-independent factors such as PTH-related protein (PTHrP) is the other major etiological origin of hypercalcemia.[200] Recently, severe hyperparathyroidism has been described in association to ectopic production of PTH by a metastatic neuroendocrine pancreatic tumor.[201,202] This is an extremely rare cause of HHM, and in several cases there was clear demonstration that the tumor cell expressed the PTH gene as a mechanism of hypercalcemia. In the report of VanHouten there was hypomethylation and increased expression of an otherwise normal PTH gene, leading to the suggestion that the tumor cell expressed a transcription factor capable of interacting with a portion of the PTH gene promoter and then activate PTH gene expression.[202] This biological presentation also has been described in a patient with hepatocellular carcinoma, where the tumor cell secreted intact bioactive PTH.[203] Notably, these extremely rare presentations should not alter the clinical evaluation of patients with humoral hypercalcemia of malignancy.[204]

A secondary and often overlooked cause of hypercalcemia is Milk Alkali Syndrome.[205] Milk Alkali Syndrome consists of hypercalcemia, metabolic alkalosis, and renal insufficiency. Although originally described in middle-aged men consuming milk and antacids for treatment of peptic ulcer disease, it is now most commonly found in older women taking calcium supplements for osteoporosis. Increasing numbers of pregnant women with Milk Alkali Syndrome have been reported. The pathogenesis of the hypercalcemia is complicated and includes various components including excessive calcium intake combined with a failure to suppress $1,25(OH)_2$-vitamin D levels, and other factors.[206] Hypercalcemia and alkalosis generally resolve quickly upon cessation of calcium intake. Ancillary treatment with furosemide, bisphosphonates, or calcitonin is no longer recommended.[205]

Renal Osteodystrophy

The therapeutic control of hyperparathyroidism and bone health, unfortunately, may induce hypercalcemia and vascular calcification in patients with chronic kidney disease. Cardiovascular disease causes more than 60% of deaths among patients with end stage renal disease (ESRD); and the annual cardiovascular mortality rate is significantly higher (by more than an order of magnitude) than in the non-ESRD population, especially among individuals younger than 70.[207] Hyperphosphatemia, hypercalcemia, and the calcium-phosphorus (Ca x P) product are associated with increased mortality, particularly to cardiovascular causes. Goodman et al.[208] reported a high prevalence of coronary artery calcification among young adults receiving dialysis, especially those who were on supportive dialysis for longer than 10 years. More recent findings reveal that vascular calcification itself, as evaluated with x-ray films or ultrasound, is linked to aortic stiffness and reduced patient survival.[209]

A persistent question remains as to whether the use of calcium-based phosphate binders and/or vitamin D to prevent hyperparathyroidism leads to a high calcium burden and vascular calcification. To this end, non-calcium based agents such as Sevelamer and lanthanum salts have been added to the therapeutic armamentarium.

Diuretics

All diuretics, with the notable exception of the thiazides, increase calcium excretion. The magnitude of the calciuric effect varies with the nephron site of action of the particular agent and its associated efficacy. At one extreme, drugs such as acetazolamide that act on proximal tubules have little effect on net calcium excretion. At the other extreme, loop diuretics, the most efficacious diuretics, exert profound effects on calcium

excretion. By contrast, thiazide diuretics decrease calcium excretion. The actions of diuretics on renal calcium excretion and transport are considered below in some detail.

Carbonic Anhydrase Inhibitors

Acetazolamide and related carbonic anhydrase inhibitors block proximal tubule bicarbonate absorption by producing a limiting intra-luminal pH gradient, against which H^+ ions cannot be exchanged for Na^+. Acetazolamide increases urinary sodium excretion with slight, if any, effect on calcium excretion.[210–214] Acetazolamide elicits similar reductions of proximal tubule sodium and calcium absorption.[210] However, although sodium excretion increased while urinary calcium excretion was unchanged, calcium absorption by thick ascending limbs and distal tubules must have been enhanced in a compensatory manner. This would be consistent with the load dependence of calcium transport by thick limbs and especially distal tubules. It is not known whether acetazolamide increases calcium absorption directly or whether the effect is secondary to increased bicarbonate delivery to distal tubules.[125] Nonetheless, acetazolamide caused a relatively greater increase of sodium than of calcium excretion in the isolated perfused dog kidney.[214] These results would favor a direct action of acetazolamide on renal calcium transport.

Loop Diuretics

The major diuretics acting in the loop of Henle are furosemide, bumetanide, piretanide, torsemide, which are sulfamyl anthranilic acid derivatives, and ethacrynic acid, a phenoxyacetic acid,[215] which is now infrequently used. Loop diuretics block sodium absorption by thick ascending limbs, thereby diminishing the driving force for calcium absorption and an attendant and substantial increase of urinary calcium excretion. The magnitude of the natriuresis generally, but not always,[214,216–219] parallels the calciuresis. These deviations may arise from the PTH status at the time the diuretic was administered or other events that regulate calcium or sodium transport at more downstream nephron sites.

Loop diuretics block apical membrane Na-K-2Cl cotransport by thick ascending limbs, where calcium absorption is largely passive, and driven by the lumen-positive transepithelial voltage[187,220] (Fig. 64.5). The positive voltage arises from the secretion of cellular K^+ into the tubular lumen and from the cation permselectivity of the tight junctions. By inhibiting Na-K-2Cl cotransport, loop diuretics decrease intracellular chloride and sodium.[221] The basolateral membrane possesses Cl^- and K^+ conductances,[222] which determine the membrane voltage. Hence, upon blockade of chloride entry, the cytosolic Cl^- activity falls to its equilibrium level[221] and both apical and basolateral membranes hyperpolarize.[223] Thus, the hyperpolarization of both cell membranes upon administration of furosemide is accompanied by depolarization of the transepithelial voltage. These oppositely oriented changes of the transepithelial voltage and the cell membrane potential may exert complicated offsetting effects on calcium transport by thick ascending limbs. The variable effects on calcium and sodium excretion caused by loop diuretics may be related to the magnitude and balance of the inhibitory action of the diuretics on passive calcium absorption and the stimulatory effect on active calcium absorption. The net effect of these competing actions is determined by the relative magnitude of paracellular vs. cellular transport pathways and the extent of drug-induced blockade of Na-K-2Cl cotransport in medullary thick ascending limbs, where there is no cellular calcium absorption, and cortical thick ascending limbs, where the aforementioned considerations suggest that cellular calcium transport may mitigate the degree of blockade of passive paracellular calcium absorption. It should be borne in mind that the passive route clearly dominates overall calcium absorption by thick ascending limbs,[220,224] consistent with the view that furosemide administration usually does not dissociate urinary calcium and sodium excretion.

Thiazide Diuretics

About 5–7% of the filtered sodium and calcium is reabsorbed by distal convoluted tubules. Thiazide diuretics, which block Na-Cl cotransport in distal convoluted tubules, have the unique characteristic of concomitantly decreasing calcium excretion while increasing sodium excretion. The hypocalciuric effect of thiazide diuretics forms the basis for their usefulness in treating idiopathic hypercalciuria.

A model incorporating the generally accepted cellular mechanisms responsible for NaCl and Ca^{2+} absorption by distal convoluted tubule cells is shown in Fig. 64.6. Two sodium entry mechanisms coexist in distal convoluted tubules; an electroneutral Na-Cl cotransporter that is found in early (DCT1) and late (DCT2) distal convoluted tubules and the amiloride-sensitive epithelial Na^+ channel (ENaC) that is restricted to DCT2.[77,225–228] The transport of each Na^+ by the Na-Cl cotransporter is coupled in an electroneutral fashion to the influx of one Cl^- ion. Thiazide diuretics inhibit NaCl reabsorption in distal convoluted tubules.[229–231] As discussed earlier, Ca^{2+} entry in distal convoluted tubules is mediated by TrpV5 and perhaps other calcium-permeable channels that are activated by membrane hyperpolarization. Maneuvers that inhibit

Na^+ entry hyperpolarize the membrane, augmenting the driving force of Ca^{2+} entry.

Initial thiazide administration may not decrease calcium excretion proportionally to the increase in sodium excretion. However, with chronic administration, thiazides cause a sustained reduction in calcium excretion,[213,232–234] that is accompanied by a modest but persistent increase of serum calcium.[213,232,234] The mediating role of PTH on the calcium-sparing effect of thiazide diuretics has been disputed. On balance, it seems that the acute hypocalciuric effects of thiazide diuretics require adequate PTH levels.[235] However, it has been noted that circulating PTH levels actually fall, rather than rise, during thiazide administration.[236,237] Furthermore, acute thiazide administration to thyroparathyroidectomized rats[231,238] or humans[239] produces comparable dissociation of calcium and sodium clearances as in normal subjects. Prolonged administration of polythiazide to thyroparathyroidectomized rats diminished calcium excretion without changing sodium excretion or body weight. Conversely, a permissive role for PTH in the stimulatory effect of thiazide diuretics on rabbit connecting tubules has also been noted.[240] Studies of direct action of thiazide diuretics on calcium absorption by distal convoluted tubules[241] and immortalized distal convoluted tubule cells[96] establishes that chlorothiazide directly stimulates calcium transport. Thus, the stimulatory effect of thiazide diuretics on calcium transport is both direct and independent of PTH.

Extracellular fluid volume contraction may contribute to thiazide-induced decreases of calcium excretion by enhancing proximal tubule solute absorption. This is pointedly illustrated by recent studies in TrpV5-null mice[98] as described earlier.

Potassium-Sparing Diuretics

The mechanism of Na^+ reabsorption by principal cells of cortical collecting ducts is shown in Fig. 64.7. Na^+ enters the cell across the apical plasma membrane down its electrochemical gradient through highly selective epithelial Na^+ channels (ENaC). These channels are inhibited by two chemically distinct drugs; amiloride and triamterene. Amiloride is a pyrazinoylguanidine derivative, whereas triamterene is a chemically unrelated aryl pteridine; both are weak organic bases. As a consequence of their ability to block ENaC, they hyperpolarize the cell. By contrast, spironolactone, an aldosterone analogue that is also a potassium-sparing diuretic, has an entirely different mechanism of action, and depolarizes the cell.[242] The ability of amiloride and triamterene to hyperpolarize the luminal membrane of cells expressing ENaC and possessing apical Ca^{2+} channels activated by hyperpolarization may augment calcium absorption and diminish calcium excretion. Spironolactone, which depolarizes the membrane potential, would not be expected to exhibit such an effect.

Like thiazides, the K-sparing diuretics amiloride[243–250] and triamterene[246] dissociate sodium and calcium excretion. The calcium-sparing actions of amiloride and thiazides are additive in dogs[246] and humans,[244] a likely consequence of their separate sites[229] or mechanisms[96,97] of action on the distal tubule. Amiloride directly stimulates calcium transport by distal convoluted tubules.[97] In the aforementioned studies, amiloride blocked Na^+ entry and hyperpolarized the membrane voltage, which activated calcium entry through dihydropyridine-sensitive Ca^{2+} channels. As far as is presently known, TrpV5 channels are not affected and do not mediate the calcium-sparing action of these drugs.

Triamterene also blocks ENaC[251] and, therefore, should exhibit a calcium-sparing action. However, whereas amiloride decreased fractional calcium excretion in the dog, triamterene did not,[246] i.e., the dissociation of sodium and calcium clearances by triamterene was due to its effect on sodium elimination. In humans, however, triamterene increased calcium excretion[252,253] with a concomitant fall in sodium elimination.[253] In another study, triamterene had no effect on calcium excretion but increased magnesium excretion.[218] Thus, there is uncertainty as to whether triamterene affects renal calcium excretion with no obvious explanation for the difference with amiloride.

Acknowledgements

Original studies and the preparation of this review were supported by NIH grant R01 DK-054171.

References

[1] Williams RJP. Calcium chemistry and its relation to biological function. Symp Soc Exp Biol 1976;30:1–17.
[2] Walser M. Divalent cations: physicochemical state in glomerular filtrate and urine and renal excretion. In: Orloff J, Berliner RW, editors. Handbook of physiology, section 8: renal physiology. 1st ed. Washington, DC: American Physiological Society; 1973. p. 555–86.
[3] Cuche JL, Ott CE, Marchand GR, Diaz-Buxo JA, Knox FG. Intrarenal calcium in phosphate handling. Am J Physiol 1976;230:790–6.
[4] Terepka AR, Dewey PA, Toribara TY. The ultrafiltrable calcium of human serum. II. Variations is disease states and under experimental conditions. J Clin Invest 1957;37:87–98.
[5] Loeb RF. The effect of pure protein solutions and of blood serum on the diffusibility of calcium. J Gen Physiol 1926;8:451–61.
[6] Marshall RW. Plasma fractions. In: Nordin BEC, editor. Calcium, phosphate and magnesium metabolism. Edinburgh: Churchill Livingston; 1976. p. 162–85.

[7] Peterson NA, Feigen GA, Crimson JM. Effect of pH on interaction of calcium ions with serum proteins. Am J Physiol 1961;201:386–92.
[8] Hopkins T, Howard JE, Eisenberg H. Ultrafiltration studies on calcium and phosphorous in human serum. Bull Johns Hopkins Hosp 1952;91:1–21.
[9] Peacock M, Robertson WG, Nordin BEC. Relation between serum and urinary calcium with particular reference to parathyroid activity. Lancet 1969;1:384–6.
[10] Stewart AF. Hypercalcemic and hypocalcemic states. In: Seldin DW, Giebisch G, editors. The kidney: physiology and pathophysiology. 2nd ed. New York: Raven Press, Ltd.; 1992. p. 2431–60.
[11] Brown EM, Gamba G, Riccardi D, Lombardi M, Butters R, Kifor O, et al. Cloning and characterization of an extracellular Ca^{2+}-sensing receptor from bovine parathyroid. Nature 1993;366: 575–80.
[12] Brown EM, Hebert SC. A cloned Ca^{2+}-sensing receptor: a mediator of direct effects of extracellular Ca^{2+} on renal function? J Am Soc Nephrol 1995;6:1530–40.
[13] Chen Jr. PS, Neuman WF. Renal excretion of calcium by the dog. Am J Physiol 1955;180:623–31.
[14] Marshall DH. Calcium and phosphate kinetics. In: Nordin BEC, editor. Calcium, phosphate and magnesium metabolism. Edinburgh: Churchill Livingston; 1976. p. 257–87.
[15] Thompson DD. Renal excretion of calcium and phosphate. Arch Intern Med 1959;103:832–8.
[16] Copp DH, McPherson GD, McIntosh HW. Renal excretion of calcium in man: estimation of Tm-Ca. Metabolism 1960;9: 680–5.
[17] Poulos PP. The renal tubular reabsorption and urinary excretion of calcium by the dog. J Lab Clin Med 1957;49:253–7.
[18] Parfitt AM, Kleerekoper M. The divalent ion homeostatic system - physiology and metabolism of calcium, phosphorus, magnesium, and bone. In: Maxwell MH, Kleeman CR, editors. Clinical disorders of fluid and electrolyte metabolism. 3rd ed. New York: McGraw-Hill Book Company; 1980. p. 269–398.
[19] Sutton RAL, Dirks JH. Renal handling of calcium. Fed Proc 1978;37:2112–9.
[20] Ng RCK, Peraino RA, Suki WN. Divalent cation transport in isolated tubules. Kidney Int 1982;22:492–7.
[21] Harris CA, Baer PG, Chirito E, Dirks JH. Composition of mammalian glomerular filtrate. Am J Physiol 1974;227:972–6.
[22] Lassiter WE, Gottschalk CW, Mylle M. Micropuncture study of renal tubular reabsorption of calcium in normal rodents. Am J Physiol 1963;204:771–5.
[23] Le Grimellec C, Poujeol P, de Rouffignac C. ^{3}H-Inulin and electrolyte concentrations in Bowman's capsule in rat kidney. Comparison with artificial ultrafiltration. Pflugers Arch 1975; 354:117–31.
[24] Loken HF, Havel RJ, Gordan GS, Whittington SL. Ultracentrifugal analysis of protein-bound and free calcium in human serum. J Biol Chem 1960;235:3654–8.
[25] Toribara TY, Terepka AR, Dewey PA. The ultrafiltrable calcium of human serum. I. Ultrafiltration methods and normal values. J Clin Invest 1957;36:738–48.
[26] Humes HD, Ichikawa I, Troy JL, Brenner BM. Evidence for a parathyroid hormone-dependent influence of calcium on the glomerular ultrafiltration coefficient. J Clin Invest 1978;61: 32–40.
[27] Ichikawa I, Humes HD, Dousa TP, Brenner BM. Influence of parathyroid hormone on glomerular ultrafiltration in the rat. Am J Physiol 1978;234:F393–401.
[28] Riccardi D, Lee WS, Lee K, Segre GV, Brown EM, Hebert SC. Localization of the extracellular Ca^{2+}-sensing receptor and PTH/PTHrP receptor in rat kidney. Am J Physiol 1996;271: F951–6.
[29] Yang TX, Hassan S, Huang YNG, Smart AM, Briggs JP, Schnermann JB. Expression of PTHrP, PTH/PTHrP receptor, and Ca^{2+}-sensing receptor mRNAs along the rat nephron. Am J Physiol 1997;272:F751–8.
[30] Endlich N, Endlich K. cAMP pathway in podocytes. Microsc Res Tech 2002;57(4):228–31.
[31] Usdin TB, Bonner TI, Harta G, Mezey E. Distribution of parathyroid hormone-2 receptor messenger ribonucleic acid in rat. Endocrinology 1996;137:4285–97.
[32] Maunsbach AB. Observations on the segmentation of the proximal tubule in the rat kidney: comparison of results from phase contrast, fluorescence and electron microscopy. J Ultrastructure Res 1966;16:239–58.
[33] Agus ZS, Gardner LB, Beck LH, Goldberg M. Effects of parathyroid hormone on renal tubular reabsorption of calcium, sodium, and phosphate. Am J Physiol 1973;224:1143–8.
[34] Edwards BR, Baer PG, Sutton RAL, Dirks JH. Micropuncture study of diuretic effects on sodium and calcium reabsorption in the dog nephron. J Clin Invest 1973;52:2418–27.
[35] Wong NLM, Quamme GA. Association of calcium and sodium handling in the rabbit nephron. A micropuncture study. Renal Physiol Biochem 1990;13:306–13.
[36] Wong NLM, Whiting SJ, Mizgala CL, Quamme GA. Electrolyte handling by the superficial nephron of the rabbit. Am J Physiol 1986;250:F590–5.
[37] Harris CA, Burnatowska MA, Seely JF, Sutton RAL, Quamme GA, Dirks JH. Effects of parathyroid hormone on electrolyte transport in the hamster nephron. Am J Physiol 1979;236: F342–8.
[38] Le Grimellec C, Roinel N, Morel F. Simultaneous Mg, Ca, P, K, Na and Cl analysis in rat tubular fluid. I. During perfusion of either inulin or ferrocyanide. Pflugers Arch 1973;340: 181–96.
[39] Friedman PA. Renal calcium metabolism. In: Alpern RJ, Hebert SC, editors. Seldin and Giebisch's the kidney: physiology and pathophysiology. 4th ed. San Diego: Elsevier; 2008. p. 1851–90.
[40] de Rouffignac C, Morel F, Roinel N. Micropuncture study of water and electrolyte movements along the loop of Henle in Psammomys with special reference to magnesium, calcium and phosphorus. Pflugers Arch 1973;344:309–26.
[41] Jamison RL, Frey NR, Lacy FB. Calcium reabsorption in the thin loop of Henle. Am J Physiol 1974;227:745–51.
[42] Bourdeau JE. Calcium transport across the pars recta of cortical segment 2 proximal tubules. Am J Physiol 1986;251:F718–24.
[43] Rouse D, Ng RCK, Suki WN. Calcium transport in the pars recta and thin descending limb of Henle of rabbit perfused in vitro. J Clin Invest 1980;65:37–42.
[44] Ullrich KJ, Fromter E, Murer H. Prinzipien des epithelialen transportes in niere und darm. Klin Wochenschr 1979;57: 977–91.
[45] Ullrich KJ, Rumrich G, Kloss S. Active Ca^{2+} reabsorption in the proximal tubule of the rat kidney. Dependence on sodium- and buffer transport. Pflugers Arch 1976;364:223–8.
[46] Ng RCK, Rouse D, Suki WN. Calcium transport in the rabbit superficial proximal convoluted tubule. J Clin Invest 1984;74:834–42.
[47] Sacks P, Bourdeau JE. Ca^{2+} absorption in the pars recta of cortical S2 rabbit proximal tubules: role of diffusion. Am J Physiol 1989;257:F262–7.
[48] O'Neil RG, Leng L. Osmo-mechanically sensitive phosphatidylinositol signaling regulates a Ca^{2+} influx channel in renal epithelial cells. Am J Physiol 1997;273:F120–8.

[49] Suzuki M, Taniguchi JA. Ca^{2+} channel in renal epithelial cells introduced by parathyroid hormone. Miner Electrolyte Metab 1995;21:35–9.
[50] Zhang MIN, O'Neil RG. A regulated calcium channel in apical membranes of renal proximal tubule cells. Am J Physiol 1996;271:C1757–64.
[51] Zhang MIN, O'Neil RG. An L-type calcium channel in renal epithelial cells. J Membr Biol 1996;154:259–66.
[52] Almeida AR, Bunnachak D, Burnier M, Wetzels JF, Burke TJ, Schrier RW. Time-dependent protective effects of calcium channel blockers on anoxia- and hypoxia-induced proximal tubule injury. J Pharmacol Exp Ther 1992;260:526–32.
[53] Brunette MG, Leclerc M, Couchourel D, Mailloux J, Bourgeois Y. Characterization of three types of calcium channel in the luminal membrane of the distal nephron. Can J Physiol Pharmacol 2004;82(1):30–7.
[54] Burke TJ, Joseph JK, Bunnachak D, Almeida A, Wetzels JFM, Yu L, et al. Induced alterations in calcium uptake rate in normoxic rat proximal tubules. Ren Fail 1995;17:503–15.
[55] Cejka J-C, Le Maout S, Bidet M, Tauc M, Poujeol P. Activation of calcium influx by ATP and store depletion in primary cultures of renal proximal cells. Pflugers Arch 1994;427:33–41.
[56] McCarty NA, O'Neil RG. Calcium signaling in cell volume regulation. Physiol Rev 1992;72:1037–61.
[57] Rose UM, Bindels RJ, Jansen JW, van Os CH. Effects of Ca^{2+} channel blockers, low Ca^{2+} medium and glycine on cell Ca^{2+} and injury in anoxic rabbit proximal tubules. Kidney Int 1994;46:223–9.
[58] Rose UM, Bindels RJM, Vis A, Jansen JWCM, van Os CH. The effect of L-type Ca^{2+} channel blockers on anoxia-induced increases in intracellular Ca^{2+} concentration in rabbit proximal tubule cells in primary culture. Pflugers Arch 1993;423:378–86.
[59] Tanaka H, Smogorzewski M, Koss M, Massry SG. Pathways involved in PTH-induced rise in cytosolic Ca^{2+} concentration of rat renal proximal tubule. Am J Physiol 1995;268:F330–7.
[60] Wetzels JFM, Yu L, Wang X, Kribben A, Burke TJ, Schrier RW. Calcium modulation and cell injury in isolated rat proximal tubules. J Pharmacol Exp Ther 1993;267:176–80.
[61] Nijenhuis T, Hoenderop JG, van der Kemp AWCM, Bindels RJ. Localization and regulation of the epithelial Ca^{2+} channel TRPV6 in the kidney. J Am Soc Nephrol 2003;14(11):2731–40.
[62] White KE, Gesek FA, Nesbitt T, Drezner MK, Friedman PA. Molecular dissection of Ca^{2+} efflux in immortalized proximal tubule cells. J Gen Physiol 1997;109:217–28.
[63] Dominguez JH, Juhaszova M, Kleiboeker SB, Hale CC, Feister HA. Na^{+}-Ca^{2+} exchanger of rat proximal tubule: gene expression and subcellular localization. Am J Physiol 1992;263: F945–50.
[64] Rocha AS, Magaldi JB, Kokko JP. Calcium and phosphate transport in isolated segments of rabbit Henle's loop. J Clin Invest 1977;59:975–83.
[65] Hebert SC. Nephron heterogeneity. In: Windhager EE, editor. Renal physiology. New York: Oxford University Press; 1992. p. 875–925.
[66] Takahashi N, Kondo Y, Ito O, Igarashi Y, Omata K, Abe K. Cytosolic Ca^{2+} dynamics in hamster ascending thin limb of Henle's loop. Am J Physiol 1995;268:F1148–53.
[67] Morel F, Doucet A. Hormonal control of kidney functions at the cell level. Physiol Rev 1986;66:377–468.
[68] Friedman PA, Coutermarsh BA, Kennedy SM, Gesek FA. Parathyroid hormone stimulation of calcium transport is mediated by dual signaling mechanisms involving PKA and PKC. Endocrinology 1996;137:13–20.
[69] Simon DB, Karet FE, Hamdan JM, Di Pietro A, Sanjad SA, Lifton RP. Bartter's syndrome, hypokalaemic alkalosis with hypercalciuria, is caused by mutations in the Na-K-2Cl cotransporter. Nat Genet 1996;13:183–8.
[70] Simon DB, Karet FE, Rodriguez-Soriano J, Hamdan JH, DiPietro A, Trachtman H, et al. Genetic heterogeneity of Bartter's syndrome revealed by mutations in the K^{+} channel, ROMK. Nat Genet 1996;14:152–6.
[71] Simon DB, Bindra RS, Mansfield TA, Nelson-Williams C, Mendonca E, Stone R, et al. Mutations in the chloride channel gene, *CLCNKB*, cause Bartter's syndrome type III. Nat Genet 1997;17:171–8.
[72] Clive DM. Bartter's syndrome: the unsolved puzzle. Am J Kidney Dis 1995;25:813–23.
[73] Kriz W, Kaissling B. Structural organization of the mammalian kidney. In: Seldin DW, Giebisch G, editors. The kidney: physiology and pathophysiology. 2nd ed. New York: Raven Press, Ltd; 1992. p. 707–77.
[74] Kriz W, Kaissling B, Pszolla M. Morphological characterization of the cells in Henle's loop and the distal tubule. In: Vogel HG, Ullrich KJ, editors. New aspects of renal function. Amsterdam: Excerpta Medica; 1978. p. 67–78.
[75] Tisher CC, Bulger RE, Trump BF. Human renal ultrastructure: III. The distal tubule in healthy individuals. Lab Invest 1968;18:655–68.
[76] Obermüller N, Bernstein P, Velázquez H, Reilly R, Moser D, Ellison DH, et al. Expression of the thiazide-sensitive Na-Cl cotransporter in rat and human kidney. Am J Physiol 1995;269: F900–10.
[77] Loffing J, Loffing-Cueni D, Valderrabano V, Klausli L, Hebert SC, Rossier BC, et al. Distribution of transcellular calcium and sodium transport pathways along mouse distal nephron. Am J Physiol Renal Physiol 2001;281(6):F1021–7.
[78] Hayslett JP, Boulpaep EL, Kashgarian M, Giebisch G. Electrical characteristics of the mammalian distal tubule: Comparison of Ling-Gerard and macroelectrodes. Kidney Int 1977;12:324–31.
[79] Wright FS. Increasing magnitude of electrical potential along the renal distal tubule. Am J Physiol 1971;220:624–38.
[80] Bacskai BJ, Friedman PA. Activation of latent Ca^{2+} channels in renal epithelial cells by parathyroid hormone. Nature 1990;347:388–91.
[81] Matsunaga H, Stanton BA, Gesek FA, Friedman PA. Epithelial Ca^{2+} channels sensitive to dihydropyridines and activated by hyperpolarizing voltages. Am J Physiol 1994;267:C157–65.
[82] Müller D, Hoenderop JGJ, Meij IC, Van den Heuvel LPJ, Knoers NVAM, Den Hollander AI, et al. Molecular cloning, tissue distribution, and chromosomal manning of the human epithelial Ca^{2+} channel (ECAC1). Genomics 2000;67(1):48–53.
[83] Poncet V, Merot J, Poujeol P. A calcium-permeable channel in the apical membrane of primary cultures of the rabbit distal bright convoluted tubule. Pflugers Arch 1992;422:112–9.
[84] Vennekens R, Prenen J, Hoenderop JGJ, Bindels RJM, Droogmans G, Nilius B. Pore properties and ionic block of the rabbit epithelial calcium channel expressed in HEK 293 cells. Journal of Physiology 2001;530(2):183–91.
[85] Hoenderop JG, Nilius B, Bindels RJ. Calcium absorption across epithelia. Physiol Rev 2005;85(1):373–422.
[86] Peng J-B, Chen X-Z, Berger UV, Vassilev PM, Brown EM, Hediger MA. A rat kidney-specific calcium transporter in the distal nephron. J Biol Chem 2000;275(36):28186–94.
[87] Vennekens R, Hoenderop JG, Prenen J, Stuiver M, Willems PH, Droogmans G, et al. Permeation and gating properties of the novel epithelial Ca^{2+} channel. J Biol Chem 2000;275:3963–9.
[88] Nilius B, Vennekens R, Prenen J, Hoenderop JG, Bindels RJ, Droogmans G. Whole-cell and single channel monovalent cation currents through the novel rabbit epithelial Ca^{2+} channel ECaC. J Physiol 2000;527(Pt 2):239–48.

[89] Hoenderop JGJ, van der Kemp AWCM, Hartog A, van de Graaf SFJ, van Os CH, Willems PHGM, et al. Molecular identification of the apical Ca^{2+} channel in 1, 25-dihydroxyvitamin D_3-responsive epithelia. J Biol Chem 1999;274:8375–8.

[90] Peng JB, Chen XZ, Berger UV, Vassilev PM, Tsukaguchi H, Brown EM, et al. Molecular cloning and characterization of a channel-like transporter mediating intestinal calcium absorption. J Biol Chem 1999;274:22739–46.

[91] Gesek FA, Friedman PA. On the mechanism of parathyroid hormone stimulation of calcium uptake by mouse distal convoluted tubule cells. J Clin Invest 1992;90:749–58.

[92] Kauker ML, Zawada ET, Kauker LM, Roman RJ, Rosivall L. Evidence for distal tubular inhibition of calcium efflux by nisoldipine in the SHR rat. Exp Nephrol 1997;5:384–9.

[93] de Groot T, Lee K, Langeslag M, Xi Q, Jalink K, Bindels RJ, et al. Parathyroid hormone activates TRPV5 via PKA-dependent phosphorylation. J Am Soc Nephrol 2009;20(8):1693–704.

[94] Barry ELR, Gesek FA, Yu ASL, Lytton J, Friedman PA. Distinct calcium channel isoforms mediate parathyroid hormone and chlorothiazide-stimulated calcium entry in transporting epithelial cells. J Membr Biol 1998;161:55–64.

[95] Bernardo JF, Magyar CE, Sneddon WB, Friedman PA. Impaired renal calcium absorption in mice lacking calcium channel $ß_3$ subunits. Can J Physiol Pharmacol 2009;87 (7):522–30.

[96] Gesek FA, Friedman PA. Mechanism of calcium transport stimulated by chlorothiazide in mouse distal convoluted tubule cells. J Clin Invest 1992;90:429–38.

[97] Friedman PA, Gesek FA. Stimulation of calcium transport by amiloride in mouse distal convoluted tubule cells. Kidney Int 1995;48:1427–34.

[98] Nijenhuis T, Vallon V, van der Kemp AW, Loffing J, Hoenderop JG, Bindels RJM. Enhanced passive Ca^{2+} reabsorption and reduced Mg^{2+} channel abundance explains thiazide-induced hypocalciuria and hypomagnesemia. J Clin Invest 2005;115(6):1651–8.

[99] Chang Q, Hoefs S, van der Kemp AW, Topala CN, Bindels RJ, Hoenderop JG. The ß-glucuronidase klotho hydrolyzes and activates the TRPV5 channel. Science 2005;310(5747):490–3.

[100] Tsuruoka S, Nishiki K, Ioka T, Ando H, Saito Y, Kurabayashi M, et al. Defect in parathyroid-hormone-induced luminal calcium absorption in connecting tubules of Klotho mice. Nephrol Dial Transplant 2006;21(2762):2767.

[101] Brunette MG, Blouin S, Chan M. High affinity Ca^{2+}-Mg^{2+} ATPase in the distal tubule of the mouse kidney. Can J Physiol Pharmacol 1987;65:2093–8.

[102] Doucet A, Katz AI. High-affinity Ca-Mg-ATPase along the rabbit nephron. Am J Physiol 1982;242:F346–52.

[103] Magyar CE, White KE, Rojas R, Apodaca G, Friedman PA. Plasma membrane Ca^{2+}-ATPase and NCX1 Na^+/Ca^{2+} exchanger expression in distal convoluted tubule cells. Am J Physiol Renal Physiol 2002;283:F29–40.

[104] Ramachandran C, Brunette MG. The renal Na^+/Ca^{2+} exchange system is located exclusively in the distal tubule. Biochem J 1989;257:259–64.

[105] White KE, Gesek FA, Friedman PA. Structural and functional analysis of Na^+/Ca^{2+} exchange in distal convoluted tubule cells. Am J Physiol 1996;271:F560–70.

[106] Yu ASL, Hebert SC, Lee S-L, Brenner BM, Lytton J. Identification and localization of renal Na^+-Ca^{2+} exchanger by polymerase chain reaction. Am J Physiol 1992;263:F680–5.

[107] Campean V, Kricke J, Ellison D, Luft FC, Bachmann S. Localization of thiazide-sensitive Na(+)-Cl(−) cotransport and associated gene products in mouse DCT. Am J Physiol Renal Physiol 2001;281(6):F1028–35.

[108] Bachmann S, Bostanjoglo M, Schmitt R, Ellison DH. Sodium transport-related proteins in the mammalian distal nephron - distribution, ontogeny and functional aspects. Anat Embryol (Berl) 1999;200(5):447–68.

[109] Friedman PA. Codependence of renal calcium and sodium transport. Annu Rev Physiol 1998;60:179–97.

[110] Eisner DA, Lederer WJ. Na:Ca exchange: stoichiometry and electrogenicity. Am J Physiol 1985;248:C189–202.

[111] Tan S, Lau K. Patch-clamp evidence for calcium channels in apical membranes of rabbit kidney connecting tubules. J Clin Invest 1993;92:2731–6.

[112] Gesek FA, Friedman PA. Calcitonin stimulates calcium transport in distal convoluted tubule cells. Am J Physiol 1993;264: F744–51.

[113] Gmaj P, Murer H. Calcium transport mechanisms in epithelial cell membranes. Miner Electrolyte Metab 1988;14:22–30.

[114] Jayakumar A, Cheng L, Liang CT, Sacktor B. Sodium gradient-dependent calcium uptake in renal basolateral membrane vesicles: effect of parathyroid hormone. J Biol Chem 1984;259: 10827–33.

[115] Scoble JE, Mills S, Hruska KA. Calcium transport in canine renal basolateral membrane vesicles. Effects of parathyroid hormone. J Clin Invest 1985;75:1096–105.

[116] van Heeswijk MPE, Geertsen JAM, van Os CH. Kinetic properties of the ATP-dependent Ca^{2+} pump and Na^+/Ca^{2+} exchange system in basolateral membranes from rat kidney cortex. J Membr Biol 1984;79:19–31.

[117] Yoshitomi K, Fromter E. How big is the electrochemical potential difference of Na^+ across rat renal proximal tubular cell membranes *in vivo*? Pflugers Arch 1985;405(Suppl. 1):S121–6.

[118] Friedman PA, Gesek FA. Cellular calcium transport in renal epithelia: measurement, mechanisms, and regulation. Physiol Rev 1995;75:429–71.

[119] Gitelman HJ, Graham JB, Welt LG. A new familial disorder characterized by hypokalemia and hypomagnesemia. Trans Assoc Am Physicians 1966;79:221–35.

[120] Bettinelli A, Bianchetti MG, Girardin E, Caringella A, Cecconi M, Appiani AC, et al. Use of calcium excretion values to distinguish two forms of primary renal tubular hypokalemic alkalosis: Bartter and Gitelman syndromes. J Pediatr 1992;120:38–43.

[121] Fejes-Toth G, Naray-Fejes-Toth A, Velazquez H. Intrarenal distribution of the colonic H,K-ATPase mRNA in rabbit. Kidney Int 1999;56(3):1029–36.

[122] Kim J, Kim YH, Cha JH, Tisher CC, Madsen KM. Intercalated cell subtypes in connecting tubule and cortical collecting duct of rat and mouse. J Am Soc Nephrol 1999;10(1):1–12.

[123] Tsuruoka S, Schwartz GJ. Mechanisms of HCO^-_3 secretion in the rabbit connecting segment. Am J Physiol Renal Physiol 1999;277(4 Pt 2):F567–74.

[124] Boros S, Bindels RJ, Hoenderop JG. Active Ca^{2+} reabsorption in the connecting tubule. Pflugers Arch 2009;458(1):99–109.

[125] Sutton RAL, Wong NLM, Dirks JH. Effects of metabolic acidosis and alkalosis on sodium and calcium transport in the dog kidney. Kidney Int 1979;15:520–33.

[126] Nijenhuis T, Renkema KY, Hoenderop JG, Bindels RJ. Acid–base status determines the renal expression of Ca^{2+} and Mg^{2+} transport proteins. J Am Soc Nephrol 2006;17(3):617–26.

[127] Bourdeau JE, Hellstrom-Stein RJ. Voltage-dependent calcium movement across the cortical collecting duct. Am J Physiol 1982;242:F285–92.

[128] O'Neil RG. Aldosterone regulation of sodium and potassium transport in the cortical collecting duct. Semin Nephrol 1990;10:365–74.

[129] Bengele HH, Alexander EA, Lechene CP. Calcium and magnesium transport along the inner medullary collecting duct of the rat. Am J Physiol 1980;239:F24–9.
[130] Agus ZS, Chiu PJS, Goldberg M. Regulation of urinary calcium excretion in the rat. Am J Physiol 1977;232:F545–9.
[131] Greger R, Lang F, Oberleithner H. Distal site of calcium reabsorption in the rat nephron. Pflugers Arch 1978;374:153–7.
[132] Friedman PA, Gesek FA. Calcium transport in renal epithelial cells. Am J Physiol 1993;264:F181–98.
[133] Jiang H, Shabb JB, Corbin JD. Cross-activation: overriding cAMP/cGMP selectivities of protein kinases in tissues. Biochem Cell Biol 1992;70:1283–9.
[134] Fujita T, Meguro T, Fukuyama R, Nakamuta H, Koida M. New signaling pathway for parathyroid hormone and cyclic AMP action on extracellular-regulated kinase and cell proliferation in bone cells. Checkpoint of modulation by cyclic AMP. J Biol Chem 2002;277(25):22191–200.
[135] Gloerich M, Bos JL. Epac: defining a new mechanism for cAMP action. Annu Rev Pharmacol Toxicol 2010;50:355–75.
[136] Hruska KA, Moskowitz D, Esbrit P, Civitelli R, Westbrook S, Huskey M. Stimulation of inositol trisphosphate and diacylglycerol production in renal tubular cells by parathyroid hormone. J Clin Invest 1987;79:230–9.
[137] Abou-Samra AB, Jüppner H, Force T, Freeman MW, Kong XF, Schipani E, et al. Expression cloning of a common receptor for parathyroid hormone and parathyroid hormone-related peptide from rat osteoblast-like cells: a single receptor stimulates intracellular accumulation of both cAMP and inositol trisphosphates and increases intracellular free calcium. Proc Natl Acad Sci USA 1992;89:2732–6.
[138] Jüppner H, Abou-Samra AB, Freeman M, Kong XF, Schipani E, Richards J, et al. A G protein-linked receptor for parathyroid hormone and parathyroid hormone-related peptide. Science 1991;254:1024–6.
[139] Mandel LJ, Derrickson BH. Parathyroid hormone inhibits Na^+-K^+ ATPase through G_q/G_{11} and the calcium-independent phospholipase A_2. Am J Physiol 1997;272: F781–8.
[140] Ribeiro CP, Dubay GR, Falck JR, Mandel LJ. Parathyroid hormone inhibits Na^+-K^+-ATPase through a cytochrome *P*-450 pathway. Am J Physiol 1994;266:F497–505.
[141] Somermeyer MG, Knauss TC, Weinberg JM, Humes HD. Characterization of Ca^{2+} transport in rat renal brush-border membranes and its modulation by phosphatidic acid. Biochem J 1983;214:37–46.
[142] Quamme G, Pelech S, Biber J, Murer H. Abnormalities of parathyroid hormone-mediated signal transduction mechanisms in opossum kidney cells. Biochim Biophys Acta 1994;1223: 107–16.
[143] Swarthout JT, Lemker JF, Wilhelm D, Dieckmann A, Angel P, Partridge NC. Parathyroid hormone regulation of mitogen activated protein kinases in osteoblastic cells. J Bone Miner Res 1997;12:S162.
[144] Verheijen MHG, Defize LHK. Parathyroid hormone activates mitogen-activated protein kinase via a cAMP-mediated pathway independent of Ras. J Biol Chem 1997;272:3423–9.
[145] Usdin TB. Evidence for a parathyroid hormone-2 receptor selective ligand in the hypothalamus. Endocrinology 1997;138: 831–4.
[146] Usdin TB, Gruber C, Bonner TI. Identification and functional expression of a receptor selectively recognizing parathyroid hormone, the PTH2 receptor. J Biol Chem 1995;270: 15455–8.
[147] Orloff JJ, Ganz MB, Ribaudo AE, Burtis WJ, Reiss M, Milstone LM, et al. Analysis of PTHrP binding and signal transduction mechanisms in benign and malignant squamous cells. Am J Physiol 1992;262:E599–607.
[148] Orloff JJ, Kats Y, Urena P, Schipani E, Vasavada RC, Philbrick WM, et al. Further evidence for a novel receptor for amino-terminal parathyroid hormone-related protein on keratinocytes and squamous carcinoma cell lines. Endocrinology 1995;136:3016–23.
[149] Whitfield JF, Chakravarthy BR, Durkin JP, Isaacs RJ, Jouishomme H, Sikorska M, et al. Parathyroid hormone stimulates PKC but not adenylate cyclase in mouse epidermal keratinocytes. J Cell Physiol 1992;150:299–303.
[150] Rampe D, Lacerda AE, Dage RC, Brown AM. Parathyroid hormone: an endogenous modulator of cardiac calcium channels. Am J Physiol 1991;261:H1945–50.
[151] Schlüter KD, Weber M, Piper HM. Parathyroid hormone induces PKC but not adenylate cyclase in adult cardiomyocytes and regulates cyclic AMP levels via PKC-dependent phosphodiesterase activity. Biochem J 1995;310:439–44.
[152] Atkinson MJ, Hesch RD, Cade C, Wadwah M, Perris AD. Parathyroid hormone stimulation of mitosis in rat thymic lymphocytes is independent of cyclic AMP. J Bone Miner Res 1987;2:303–9.
[153] Klinger M, Alexiewicz JM, Linker-Israeli M, Pitts TO, Gaciong Z, Fadda GZ, et al. Effect of parathyroid hormone on human T cell activation. Kidney Int 1990;37:1543–51.
[154] Whitfield JF, MacManus JP, Youdale T, Franks DJ. The roles of calcium and cyclic AMP in the stimulatory action of parathyroid hormone on thymic lymphocyte proliferation. J Cell Physiol 1971;78:355–68.
[155] Wu S, Pirola CJ, Green J, Yamaguchi DT, Okano K, Jueppner H, et al. Effects of N-terminal, midregion, and C-terminal parathyroid hormone-related peptides on adenosine 3′,5′-monophosphate and cytoplasmic free calcium in rat aortic smooth muscle cells and UMR-106 osteoblast-like cells. Endocrinology 1993;133:2437–44.
[156] Takasu H, Guo J, Bringhurst FR. Human and rat PTH/PTHrP receptors display different signal selectivity for hPTH(1-31) and hPTH(1-30) in stably transfected LLC-PK1 cells. J Bone Miner Res 1997;12:S444.
[157] Weinman EJ, Hall RA, Friedman PA, Liu-Chen LY, Shenolikar S. The association of NHERF adaptor proteins with G protein-coupled receptors and receptor tyrosine kinases. Annu Rev Physiol 2006;68:491–505.
[158] Walser M. Calcium clearance as a function of sodium clearance in the dog. Am J Physiol 1961;200:1099–104.
[159] Knox FG, Schneider EG, Willis LR, Strandhoy JW, Ott CE. Effect of volume expansion on sodium excretion in the presence and absence of increased delivery from superficial proximal tubules. J Clin Invest 1973;52:1642–6.
[160] Morgan T, Berliner RW. A study by continuous microperfusion of water and electrolyte movements in the loop of Henle and distal tubule of the rat. Nephron 1969;6:388–405.
[161] Schneider EG, Goldsmith RS, Arnaud CD, Knox FG. Role of parathyroid hormone in the phosphaturia of extracellular fluid volume expansion. Kidney Int 1975;7:317–24.
[162] Lemann Jr. J, Litzow JR, Lennon EJ. The effects of chronic acid loads in normal man: further evidence for the participation of bone mineral in the defense against chronic metabolic acidosis. J Clin Invest 1966;45:1608–14.
[163] Lemann Jr. J, Litzow JR, Lennon EJ. Studies of the mechanism by which chronic metabolic acidosis augments urinary calcium excretion in man. J Clin Invest 1967;45:1318–28.
[164] Stacy BD, Wilson BW. Acidosis and hypercalciuria: renal mechanisms affecting calcium, magnesium and sodium excretion in the sheep. J Physiol (Lond) 1970;210:549–64.

[165] Williamson BJ, Freeman S. Effect of acute changes in acid-base balance on renal calcium excretion in dogs. Am J Physiol 1957;191:384–7.
[166] Bushinsky DA, Kittaka MK, Weisinger JR, Langman CB, Favus MJ. Effects of chronic metabolic alkalosis on Ca^{2+}, PTH and $1,25(OH)_2D_3$ in the rat. Am J Physiol 1989;257: E578–82.
[167] Edwards NA, Hodgkinson A. Metabolic studies in patients with idiopathic hypercalciuria. Clin Sci 1965;29:143–57.
[168] Marone CC, Wong NLM, Sutton RAL, Dirks JH. Effects of metabolic alkalosis on calcium excretion in the conscious dog. J Lab Clin Med 1983;101:264–73.
[169] Moore EW. Ionized calcium in normal serum, ultrafiltrates, and whole blood determined by ion-exchange electrodes. J Clin Invest 1970;49:318–34.
[170] Marone CC, Sutton RAL. Effects of furosemide on calcium and sodium excretion during acute metabolic acidosis and alkalosis in the rat. Miner Electrolyte Metab 1980;4:62–7.
[171] Lau K, Rodriguez Nichols F, Tannen RL. Renal excretion of divalent ions in response to chronic acidosis: evidence that systemic pH is not the controlling variable. J Lab Clin Med 1987;109:27–33.
[172] Canzanello VJ, Bodvarsson M, Kraut JA, Johns CA, Slatopolsky E, Madias NE. Effect of chronic respiratory acidosis on urinary calcium excretion in the dog. Kidney Int 1990;38:409–16.
[173] Coburn JW, Massry SG. Changes in serum and urinary calcium during phosphate depletion: studies on mechanisms. J Clin Invest 1970;49:1073–87.
[174] Lotz M, Zisman E, Bartter FC. Evidence for a phosphorus-depletion syndrome in man. N Engl J Med 1968;278:409–15.
[175] Young VR, Lofgreen GP, Luick JR. The effects of phosphorus depletion, and of calcium and phosphorus intake, on the endogenous excretion of these elements by sheep. Br J Nutr 1966;20:795–805.
[176] Grabie M, Lau K, Agus ZS, Goldberg M, Goldfarb D. Role of parathyroid hormone in the hypercalciuria of chronic phosphate depletion. Miner Electrolyte Metab 1978;1:279–87.
[177] Goldfarb S, Westby GR, Goldberg M, Agus ZS. Renal tubular effects of chronic phosphate depletion. J Clin Invest 1977;59: 770–9.
[178] Lau K, Agus ZS, Goldberg M, Goldfarb S. Renal tubular sites of altered calcium transport in phosphate depleted rats. J Clin Invest 1979;64:1681–7.
[179] Wong NLM, Quamme GA, O'Callaghan TJ, Sutton RAL, Dirks JH. Renal tubular transport in phosphate depletion: a micropuncture study. Can J Physiol Pharmacol 1980;58: 1063–71.
[180] Edwards BR, Sutton RAL, Dirks JH. Effect of calcium infusion on renal tubular reabsorption in the dog. Am J Physiol 1974;227:13–8.
[181] Le Grimellec C, Roinel N, Morel F. Simultaneous Mg, Ca, P, K, Na and Cl analysis in rat tubular fluid. During acute Ca plasma loading. Pflugers Arch 1974;346:171–88.
[182] Marchand GR. Effect of parathyroid hormone on the determinants of glomerular filtration in dogs. Am J Physiol 1985;248: F482–6.
[183] Lee KC, Brown D, Ureña P, Ardaillou N, Ardaillou R, Deeds J, et al. Localization of parathyroid hormone parathyroid hormone-related peptide receptor mRNA in kidney. Am J Physiol 1996;270:F186–91.
[184] Riccardi D, Hall AE, Chattopadhyay N, Xu JZ, Brown EM, Hebert SC. Localization of the extracellular Ca^{2+} polyvalent cation-sensing protein in rat kidney. Am J Physiol Renal Physiol 1998;274:F611–22.
[185] Massry SG, Coburn JW, Chapman LW, Kleeman CR. Role of serum Ca, parathyroid hormone, and NaCl infusion on renal Ca and Na clearances. Am J Physiol 1968;214:1403–9.
[186] Quamme GA. Effect of hypercalcemia on renal tubular handling of calcium and magnesium. Can J Physiol Pharmacol 1982;60:1275–80.
[187] Shareghi GR, Agus ZS. Magnesium transport in the cortical thick ascending limb of Henle's loop of the rabbit. J Clin Invest 1982;69:759–69.
[188] Takaichi K, Kurokawa K. High Ca^{2+} inhibits peptide hormone-dependent cAMP production specifically in thick ascending limbs of Henle. Miner Electrolyte Metab 1986;12:342–6.
[189] Motoyama HI, Friedman PA. CaSR regulation of PTH-dependent calcium absorption by mouse cortical ascending limbs. Am J Physiol Renal Physiol 2002;283:F399–406.
[190] Ba J, Brown D, Friedman PA. CaSR regulation of PTH-inhibitable proximal tubule phosphate transport. Am J Physiol Renal Physiol 2003;285(6):F1233–43.
[191] Sands JM, Naruse M, Baum M, Jo I, Hebert SC, Brown EM, et al. Apical extracellular calcium/polyvalent cation-sensing receptor regulates vasopressin-elicited water permeability in rat kidney inner medullary collecting duct. J Clin Invest 1997;99:1399–405.
[192] Egbuna OI, Brown EM. Hypercalcaemic and hypocalcaemic conditions due to calcium-sensing receptor mutations. Best Pract Res Clin Obstet Gynaecol 2008;22(1):129–48.
[193] Riccardi D, Brown EM. Physiology and pathophysiology of the calcium-sensing receptor in the kidney. Am J Physiol Renal Physiol 2010;298(3):F485–499.
[194] Brown EM. Anti-parathyroid and anti-calcium sensing receptor antibodies in autoimmune hypoparathyroidism. Endocrinol Metab Clin North Am 2009;38(2):437–45.
[195] Rodriguez M, Nemeth E, Martin D. The calcium-sensing receptor: a key factor in the pathogenesis of secondary hyperparathyroidism. Am J Physiol Renal Physiol 2005;288(2):F253–64.
[196] Silverberg SJ, Bilezikian JP. Primary hyperparathyroidism. In: Rosen CJ, editor. Primer on metabolic bone diseases and disorders of mineral metabolism. 7th ed. Washington, DC: American Society for Bone and Mineral Research; 2008. p. 302–6.
[197] Wermers RA, Khosla S, Atkinson EJ, Achenbach SJ, Oberg AL, Grant CS, et al. Incidence of primary hyperparathyroidism in Rochester, Minnesota, 1993-2001: an update on the changing epidemiology of the disease. J Bone Miner Res 2006;21(1): 171–7.
[198] Chiu B, Sturgeon C, Angelos P. Which intraoperative parathyroid hormone assay criterion best predicts operative success? A study of 352 consecutive patients. Arch Surg 2006;141(5): 483–7.
[199] Peacock M, Bolognese MA, Borofsky M, Scumpia S, Sterling LR, Cheng S, et al. Cinacalcet treatment of primary hyperparathyroidism: biochemical and bone densitometric outcomes in a five-year study. J Clin Endocrinol Metab 2009;94(12):4860–7.
[200] Stewart AF. Clinical practice. Hypercalcemia associated with cancer. N Engl J Med 2005;352(4):373–9.
[201] Abraham P, Ralston SH, Hewison M, Fraser WD, Bevan JS. Presentation of a PTHrP-secreting pancreatic neuroendocrine tumour, with hypercalcaemic crisis, pre-eclampsia, and renal failure. Postgraduate Medical Journal 2002;78(926):752–3.
[202] VanHouten JN, Yu N, Rimm D, Dotto J, Arnold A, Wysolmerski JJ, et al. Hypercalcemia of malignancy due to ectopic transactivation of the parathyroid hormone gene. J Clin Endocrinol Metab 2006;91(2):580–3.
[203] Mahoney EJ, Monchik JM, Donatini G, De Lellis R. Life-threatening hypercalcemia from a hepatocellular carcinoma

secreting intact parathyroid hormone: localization by sestamibi single-photon emission computed tomographic imaging. Endocr Pract 2006;12(3):302–6.
[204] Martin KJ, Goldfarb S. Hypercalcemia in renal bone disease. Nephrology Self-Assessment Program 2007;6(2):80–4.
[205] Picolos MK, Lavis VR, Orlander PR. Milk-alkali syndrome is a major cause of hypercalcaemia among non-end-stage renal disease (non-ESRD) inpatients. Clin Endocrinol 2005;63(5): 566–76.
[206] Felsenfeld AJ, Levine BS. Milk alkali syndrome and the dynamics of calcium homeostasis. Clin J Am Soc Nephrol 2006;1(4):641–54.
[207] Anderson S, Halter JB, Hazzard WR, Himmelfarb J, Horne FM, Kaysen GA, et al. Prediction, progression, and outcomes of chronic kidney disease in older adults. J Am Soc Nephrol 2009;20(6):1199–209.
[208] Goodman WG, Goldin J, Kuizon BD, Yoon C, Gales B, Sider D, et al. Coronary-artery calcification in young adults with end-stage renal disease who are undergoing dialysis. N Engl J Med 2000;342(20):1478–83.
[209] Blacher J, Guerin AP, Pannier B, Marchais SJ, London GM. Arterial calcifications, arterial stiffness, and cardiovascular risk in end-stage renal disease. Hypertension 2001;38(4): 938–42.
[210] Beck LH, Goldberg M. Effects of acetazolamide and parathyroidectomy on renal transport of sodium, calcium, and phosphate. Am J Physiol 1973;224:1136–42.
[211] Freeman S, Jacobsen AB. Acute effects of acetazolamide (Diamox) on plasma urinary electrolytes of dogs with special reference to calcium. Am J Physiol 1957;191:388–92.
[212] McNabb WR, Noormohamed FH, Brooks BA, Lant AF. Renal actions of piretanide and three other "loop" diuretics. Clin Pharmacol Ther 1984;35:328–37.
[213] Seitz H, Jaworski ZF. Effect of hydrochlorothiazide on serum and urinary calcium and urinary citrate. Can Med Assoc J 1964;90:414–20.
[214] Stier Jr. CT, Itskovitz HD. Renal calcium metabolism and diuretics. Annu Rev Pharmacol Toxicol 1986;26:101–16.
[215] Friedman PA, Hebert SC. Site and mechanism of diuretic action. In: Seldin DW, Giebisch G, editors. Diuretic agents: clinical physiology and pharmacology. San Diego: Academic Press; 1997. p. 75–111.
[216] Duarte CG. Effects of ethacrynic acid and furosemide on urinary calcium, phosphate and magnesium. Metabolism 1968;17:867–76.
[217] Sotorník I, Schück O, Sríbrná J. The influence of diuretics on renal calcium excretion. Experientia 1969;25:591–2.
[218] Walker BR, Hoppe RC, Alexander F. Effect of triamterene on the renal clearance of calcium, magnesium, phosphate, and uric acid in man. Clin Pharmacol Ther 1972;13:245–50.
[219] White MG, van Gelder J, Eastes G. The effect of loop diuretics on the excretion of Na^+, Ca^{2+}, Mg^{2+}, and Cl^-. J Clin Pharmacol 1981;21:610–4.
[220] Bourdeau JE, Burg MB. Voltage dependence of calcium transport in the thick ascending limb of Henle's loop. Am J Physiol 1979;236:F357–64.
[221] Greger R, Oberleithner H, Schlatter E, Cassola AC, Weidtke C. Chloride activity in cells of isolated perfused cortical thick ascending limbs of rabbit kidney. Pflugers Arch 1983;399: 29–34.
[222] Greger R, Schlatter E. Properties of the basolateral membrane of the cortical thick ascending limb of Henle's loop of rabbit kidney. A model for secondary active chloride transport. Pflugers Arch 1983;396:325–34.
[223] Greger R, Weidtke C, Schlatter E, Wittner M, Gebler B. Potassium activity in cells of isolated perfused cortical thick ascending limbs of rabbit kidney. Pflugers Arch 1984;401:52–7.
[224] Friedman PA. Basal and hormone-activated calcium absorption in mouse renal thick ascending limbs. Am J Physiol 1988;254:F62–70.
[225] Duc C, Farman N, Canessa CM, Bonvalet JP, Rossier BC. Cell-specific expression of epithelial sodium channel a, b, and g subunits in aldosterone-responsive epithelia from the rat: localization by in situ hybridization and immunocytochemistry. J Cell Biol 1994;127:1907–21.
[226] Gamba G, Saltzberg SN, Lombardi M, Miyanoshita A, Lytton J, Hediger MA, et al. Primary structure and functional expression of a cDNA encoding the thiazide-sensitive, electroneutral sodium-chloride cotransporter. Proc Natl Acad Sci USA 1993;90:2749–53.
[227] Gesek FA, Friedman PA. Sodium entry mechanisms in distal convoluted tubule cells. Am J Physiol 1995;268:F89–98.
[228] Plotkin MD, Kaplan MR, Verlander JW, Lee WS, Brown D, Poch E, et al. Localization of the thiazide sensitive Na-Cl cotransporter, rTSCl, in the rat kidney. Kidney Int 1996;50: 174–83.
[229] Costanzo LS. Localization of diuretic action in microperfused rat distal tubules: Ca and Na transport. Am J Physiol 1985;248: F527–35.
[230] Ellison DH, Velázquez H, Wright FS. Thiazide-sensitive sodium chloride cotransport in early distal tubule. Am J Physiol 1987;253:F546–54.
[231] Quamme GA, Wong NLM, Sutton RAL, Dirks JH. Interrelationships of chlorothiazide and parathyroid hormone: a micropuncture study. Am J Physiol 1975;229:200–5.
[232] Brickman AS, Massry SG, Coburn JW. Changes in serum and urinary calcium during treatment with hydrochlorothiazide: studies on mechanisms. J Clin Invest 1972;51:945–54.
[233] Jorgensen FS. The effect of bendroflumethiazide (Centyl) on the renal excretion of calcium and sodium in normal, parathyroidectomized, thyroidectomized and thyroparathyroidectomized rats. Acta Pharmacol Toxicol 1971;30:296–307.
[234] Parfitt AM. The interactions of thiazide diuretics with parathyroid hormone and vitamin D. Studies in patients with hypoparathyroidism. J Clin Invest 1972;51:1879–88.
[235] Popovtzer MM, Subryan VL, Alfrey AC, Reeve EB, Schrier RW. The acute effect of chlorothiazide on serum-ionized calcium. Evidence for a parathyroid hormone-dependent mechanism. J Clin Invest 1975;55(6):1295–302.
[236] Coe FL, Canterbury JM, Firpo JJ, Reiss E. Evidence for secondary hyperparathyroidism in idiopathic hypercalciuria. J Clin Invest 1973;52:134–42.
[237] Stote RM, Smith LH, Wilson DM, Dube WJ, Goldsmith RS, Arnaud CD. Hydrochlorothiazide effects on serum calcium and immunoreactive parathyroid hormone concentrations. Studies in normal subjects. Ann Intern Med 1972;77:587–91.
[238] Costanzo LS, Weiner IM. On the hypocalciuric action of chlorothiazide. J Clin Invest 1974;54:628–37.
[239] Costanzo LS, Moses AM, Rao K, Weiner IM. Dissociation of calcium and sodium clearances in patients with hypoparathyroidism by infusion of chlorothiazide. Metabolism 1975;24:1367–73.
[240] Shimizu T, Nakamura M, Yoshitomi K, Imai M. Interaction of trichlormethiazide or amiloride with PTH in stimulating calcium absorption in the rabbit connecting tubule. Am J Physiol 1991;261:F36–43.
[241] Costanzo LS, Windhager EE. Calcium and sodium transport by the distal convoluted tubule of the rat. Am J Physiol 1978;235:F492–506.

[242] Horisberger JD, Giebisch G. Potassium-sparing diuretics. Ren Physiol 1987;10:198–220.
[243] Alon U, Chan JC. Effects of hydrochlorothiazide and amiloride in renal hypophosphatemic rickets. Pediatrics 1985;75:754–63.
[244] Alon U, Costanzo LS, Chan JC. Additive hypocalciuric effects of amiloride and hydrochlorothiazide in patients treated with calcitriol. Miner Electrolyte Metab 1984;10:379–86.
[245] Bentur L, Alon U, Berant M. Hypercalciuria in chronically institutionalized bedridden children: frequency, predictive factors and response to treatment with thiazides. Int J Pediatr Nephrol 1987;8:29–34.
[246] Costanzo LS, Weiner IM. Relationship between clearances of Ca and Na: effect of distal diuretics and PTH. Am J Physiol 1976;230:67–73.
[247] Leppla D, Browne R, Hill K, Pak CYC. Effect of amiloride with or without hydrochlorothiazide on urinary calcium and saturation of calcium salts. J Clin Endocrinol Metab 1983;57: 920–4.
[248] Maschio G, Tessitore N, D'Angelo A, Fabris A, Pagano F, Tasca A, et al. Prevention of calcium nephrolithiasis with low-dose thiazide, amiloride and allopurinol. Am J Med 1981;71:623–6.
[249] Ravenscroft PJ, Hall GR, Ahokas JT, Emmerson BT, Tobert JA. Indacrinone: modification of diuretic, uricosuric, and kaliuretic actions by amiloride. Clin Pharmacol Ther 1980;28:45–51.
[250] Ryan MP, Devane J, Ryan MF, Counihan TB. Effects of diuretics on the renal handling of magnesium. Drugs 1984;28(Suppl. 1):167–81.
[251] Busch AE, Suessbrich H, Kunzelmann K, Hipper A, Greger R, Waldegger S, et al. Blockade of epithelial Na^+ channels by triamterenes—underlying mechanisms and molecular basis. Pflugers Arch 1996;432:760–6.
[252] Hänze S, Seyberth H. Untersuchungen zur wirkung der diuretica furosemid, etacrynsaure und triamteren auf die renale magnesium- und calciumaussecheidung. Klin Wochenschr 1967;45:313–4.
[253] Pecchini F, Savi M, Carrara GC, Andreucci VE. Effeto del triamterene sulla calciuria. G Clin Med 1967;48:1140–8.
[254] Wilkinson R. Absorption of calcium, phosphorous and magnesium. In: Nordin BEC, editor. Calcium, phosphate and magnesium metabolism. Edinburgh: Churchill Livingston; 1976. p. 36–112.
[255] Brunette MG, Chabardes D, Imbert-Teboul M, Clique A, Montégut M, Morel F. Hormone-sensitive adenylate cyclase along the nephron of genetically hypophosphatemic mice. Kidney Int 1979;15:357–69.
[256] Chabardès D, Gagnan-Brunette M, Imbert-Teboul M, Gontcharevskaia O, Montégut M, Clique A, et al. Adenylate cyclase responsiveness to hormones in various portions of the human nephron. J Clin Invest 1980;65:439–48.

This page intentionally left blank

CHAPTER

65

The Hormonal Regulation of Calcium Metabolism

Peter J. Tebben[1] *and Rajiv Kumar*[2]

[1]Departments of Internal Medicine and Pediatric and Adolescent Medicine, Divisions of Endocrinology, Diabetes, Metabolism, Nutrition and Pediatric Endocrinology and Metabolism, Mayo Clinic, Rochester, Minnesota, USA

[2]Departments of Internal Medicine and Biochemistry and Molecular Biology, Divisions of Nephrology & Hypertension and Endocrinology, Diabetes, Metabolism, Nutrition, Mayo Clinic, Rochester, Minnesota, USA

INTRODUCTION

Calcium plays a vital role in several biological processes.[1] It is an important constituent bone mineral,[2] and is necessary for normal neuromuscular transmission, muscular contractility, cellular signaling, enzyme function, and blood coagulation. Hence, the appropriate control of calcium homeostasis is vital to the well-being of the organism. A persistently negative calcium balance results in hyperparathyroidism and bone demineralization and contributes to the pathogenesis of osteomalacia and the development of osteoporosis with attendant vertebral and appendicular fractures.[3,4] Severe calcium deficiency results in tetany and, in extreme cases, grand mal seizures. The deposition of excess calcium at ectopic sites occurs in several diseases such as nephrolithiasis, arteriosclerosis, valvular calcification, and calciphylaxis.[3] Therefore, an appreciation of how calcium is normally absorbed, excreted and regulated is important in understanding the pathophysiology of disease.

Calcium homeostasis is a tightly controlled process involving several tissues, hormones, and proteins. The hormones 1α,25-dihydroxyvitamin D (1α,25$(OH)_2$D), parathyroid hormone (PTH), and calcitonin contribute to the regulation of calcium metabolism.[5–7] These three hormones have specific roles in several tissues including the intestinal mucosa, bone, and renal tubular cells. They work in concert with each other through complex interactions to maintain extracellular fluid calcium concentrations in the normal range. In this chapter, we will discuss the physiological role of each of these hormones in calcium homeostasis.

CALCIUM BALANCE

Many tissues are dependent on the maintenance of extracellular calcium concentrations within the physiological range for proper function. If extracellular calcium concentrations are significantly altered or disrupted, tissue and organ dysfunction may result (see above). Bone is the major reservoir of calcium, containing about 99% of total body calcium stores, and provides a significant buffer to maintain extracellular calcium concentrations within the normal range if calcium intake declines or calcium losses occur.[2] The maintenance of serum calcium concentrations in the face of significant overall deficits in calcium balance occurs at the expense of bone integrity. Serum calcium concentrations (range 8.9–10.1 mg/dL in adults) are age dependent, and small differences in circulating concentrations occur as a result of gender.[3,8] Table 65.1 shows normal serum calcium concentrations in males and females measured at the Mayo Clinic. Serum calcium is comprised of protein-bound calcium (40%); complexed calcium, i.e., calcium complexed to ions such as citrate, sulfate, and phosphate (13%); and ionized calcium (47%).[9,10] Total serum calcium concentrations are dependent upon circulating concentrations of albumin and to a smaller extent upon circulating concentration of globulins.[11–17] The biologically active fraction of serum calcium is ionized (normal range 4.8–5.7 mg/dL in adults) and, at a normal serum pH of 7.4, is approximately 47% of total serum calcium. The percentage of ionized calcium changes with pH—an alkaline pH causing a reduction in free ionized

Seldin and Giebisch's The Kidney, Fifth Edition.
DOI: http://dx.doi.org/10.1016/B978-0-12-381462-3.00065-3

© 2013 Elsevier Inc. All rights reserved.

TABLE 65.1 Concentrations at Mayo Clinic

Serum Calcium Concentrations			
Males		Females	
Age (years)	Concentration (mg/dL)	Age (years)	Concentration (mg/dL)
1–14	9.6–10.6	1–11	9.6–10.6
15–16	9.5–10.5	12–14	9.5–10.4
17–18	9.5–10.4	15–18	9.1–10.3
19–21	9.3–10.3	≥19	8.9–10.1
≥22	8.9–10.1		
Age- and Sex-Specific Serum Ionized Calcium Concentrations			
1–19	5.1–5.9	1–17	5.1–5.9
≥20	4.8–5.7	≥18	4.8–5.7

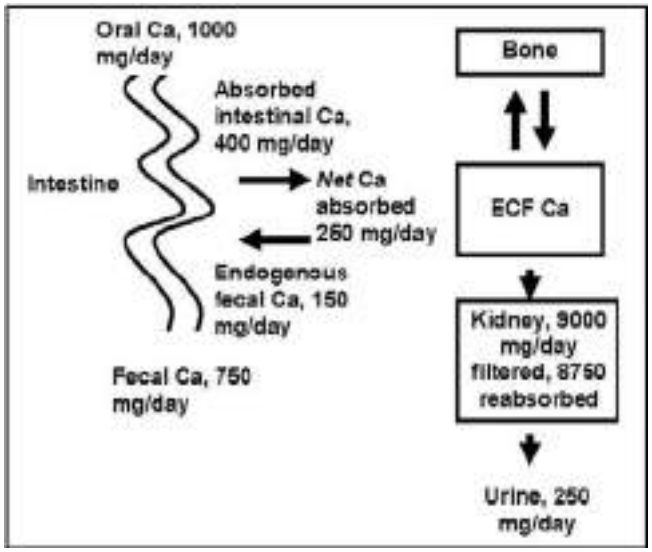

FIGURE 65.1 **Calcium homeostasis in a normal human adult.**

calcium concentrations and an acid pH causing an increase in ionized calcium concentrations. The relationships between ionized calcium, total calcium, albumin and pH are defined by the following equation:[9]

$$[\text{CaProt}] = \{0.2111[\text{Alb}]\} - \left\{(0.42)\frac{[Alb]}{47.3}(7.42 - \text{pH})\right\}$$

CaProt = protein − bound calcium, mmoles/L.

A 1-gram/deciliter change in serum albumin concentration is associated with a 0.8-milligram/deciliter change in total serum calcium. Since globulins bind calcium less avidly than does albumin, a 1-gram/deciliter change in globulins results in a 0.16-milligram/deciliter change in total serum calcium.[11–17] It should be noted that changes in the concentrations of serum proteins are generally not associated with changes in the percentage of ionized calcium present in the circulation. Also, it is worth remembering that the amount of calcium filtered at the glomerulus of the kidney is a sum of the ionized calcium concentration and the complex calcium concentration (approximately 60% of total serum calcium concentration).

Under normal circumstances of neutral calcium balance in the adult human, net intestinal absorption of calcium is equal to urinary calcium (Figure 65.1).[18] Calcium flux into and out of bone is well balanced with equal amounts of calcium being deposited and resorbed. Over a 24-hour period, a typical human adult ingests about 1000 mg of elemental calcium. Approximately 40% of ingested calcium is absorbed in the intestine and enters the bloodstream. Both active and passive processes are involved in the absorption of calcium from the intestine.[19] When the intestinal lumen calcium concentrations are <10 millimoles/liter, active processes play a major role in calcium absorption.[19,20] However, when calcium concentrations in the intestinal lumen exceed 10 millimoles/liter, passive processes become operative in the absorption of calcium.[21] About 150 mg of calcium are excreted into the gastrointestinal tract each day, predominantly in pancreatic and intestinal secretions ("endogenous fecal calcium"),[22] for a net calcium absorption of about 250 mg per day. The kidney filters about 9000 mg of calcium each day in the glomeruli and reabsorbs the majority of filtered calcium in the proximal and distal nephron, resulting in a net loss of about 250 mg from the kidney in the urine.[23–26] A majority of calcium is reabsorbed in the proximal tubule along with sodium (approximately 70 to 85%). The remainder of filtered calcium is reabsorbed in the thick ascending limb of the loop of Henle and in the distal convoluted tubule, largely as a result of the activity of the sodium-calcium exchanger and plasma membrane calcium pump (PMCA). In states of calcium balance, urinary calcium approximates the amount of calcium absorbed in the intestine.

The following sections will describe how the vitamin D endocrine system, PTH, and calcitonin alter calcium homeostasis in various tissues including the intestine, kidney, and bone.

VITAMIN D ENDOCRINE SYSTEM

Nomenclature

The synthesis of the active form of vitamin D, 1α,25-dihydroxyvitamin D, requires sequential metabolic processing of precursor sterols in several tissues such as the skin, liver and kidney. The term vitamin D refers to both vitamin D_2 and vitamin D_3 (Figure 65.2).[27]

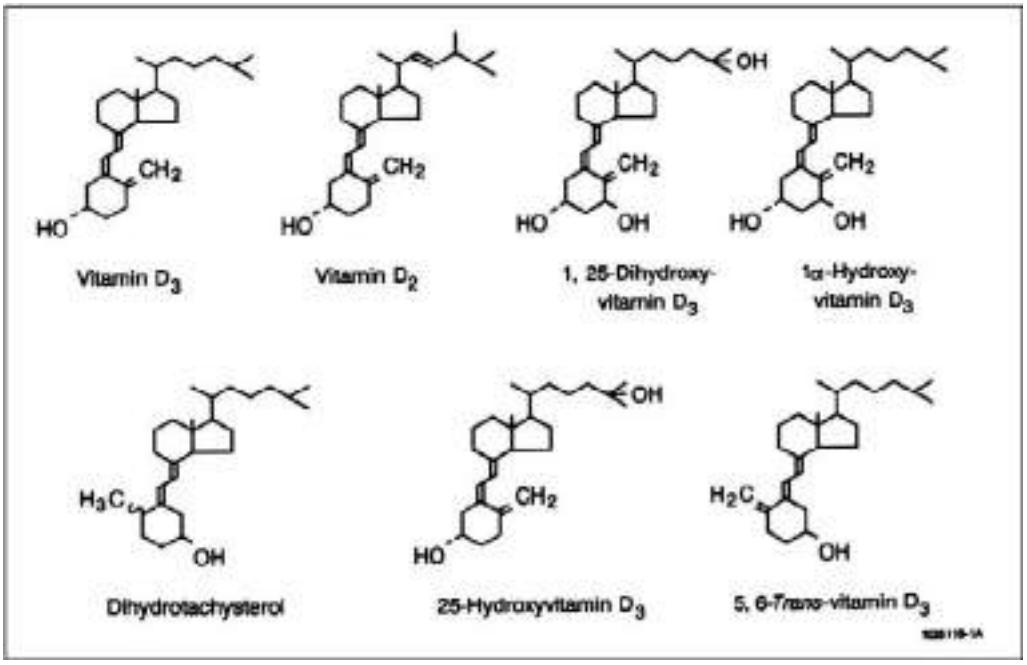

FIGURE 65.2 **Structures of vitamin D_3, vitamin D_2 and other vitamin D metabolites and analogs.**[27]

The metabolic processing of both these forms of vitamin D is similar for practical purposes in mammals, although vitamin D_2 is considerably less active in birds than is vitamin D_3. For the purposes of this chapter, it is appropriate to assume that the metabolic transformations that occur with vitamin D_3 also occur with vitamin D_2. Vitamin D_2 is derived from the plant sterol, ergosterol, whereas, vitamin D_3 is derived from 7-dehydrocholesterol, a byproduct of steroid metabolism. In non-vitamin D supplemented individuals, a majority of circulating vitamin D is in the form of vitamin D_3 or cholecalciferol. Medicinal vitamin D preparations available in the United States today may contain either vitamin D_2 or vitamin D_3. Individuals taking large amounts of vitamin D_2 supplements have elevated concentrations of vitamin D_2 and its 25-hydroxylated metabolite, 25-hydroxyvitamin D_2.[3]

Formation of Vitamin D

In the early 1900s, Huldshinsky[28] and Chick[29] in Vienna showed that exposure of rachitic children to ultraviolet light cured their bone disease. Steenbock and Hart showed that ultraviolet irradiation of animals would put them into positive calcium balance.[30] Later, Steenbock and Black clearly demonstrated that ultraviolet light-induced antirachitic activity in the fat-soluble portion of foods and skin.[31] Hess and Weinstock made similar observations.[32] Building on these observations, Askew and his coworkers isolated vitamin D_2.[33] Windaus and his colleagues showed that 7-dehydrocholesterol was converted to vitamin D_3, and subsequent work showed that this process occurred *in vivo* in normal skin.[34–39] 7-dehydrocholesterol is not directly converted to vitamin D_3 in the skin but rather is first converted to pre-vitamin D_3 that undergoes thermal isomerization to vitamin D_3 (Figure 65.3). Several other, biologically inert, side-products such as lumisterol and tachysterol are produced during the photolysis of 7-dehydrocholesterol. Vitamin D_3 has a higher affinity for the vitamin D binding protein (VDBP) than does pre-vitamin D_3, and the binding of vitamin D_3 to VDBP following its formation in the skin facilitates the removal of the vitamin from skin.[40] Vitamin D_2 and vitamin D_3 are converted in the liver to 25-hydroxyvitamin D_2 and 25-hydroxyvitamin D_3 by the hydroxyvitamin D 25-hydroxylase without significant product inhibition of the enzyme, and consequently circulating 25-hydroxyvitamin D concentrations reflect the amount of vitamin D ingested and the amount of vitamin D formed in the skin. In accord with the earlier observation showing that sunlight exposure enhanced the formation of vitamin D_3 in the skin, several groups have shown that serum 25-hydroxyvitamin D_3 concentrations are lower during and immediately after the winter months than in the summer.[41–51] In the absence of dietary vitamin D supplementation, exposure to ultra-violet B radiation plays an essential role in vitamin D production.

Following conversion of 7-dehydrocholesterol to vitamin D_3 in the skin, vitamin D_3 is transported in the plasma bound to VDBP.[52–54] Any vitamin D_2 ingested

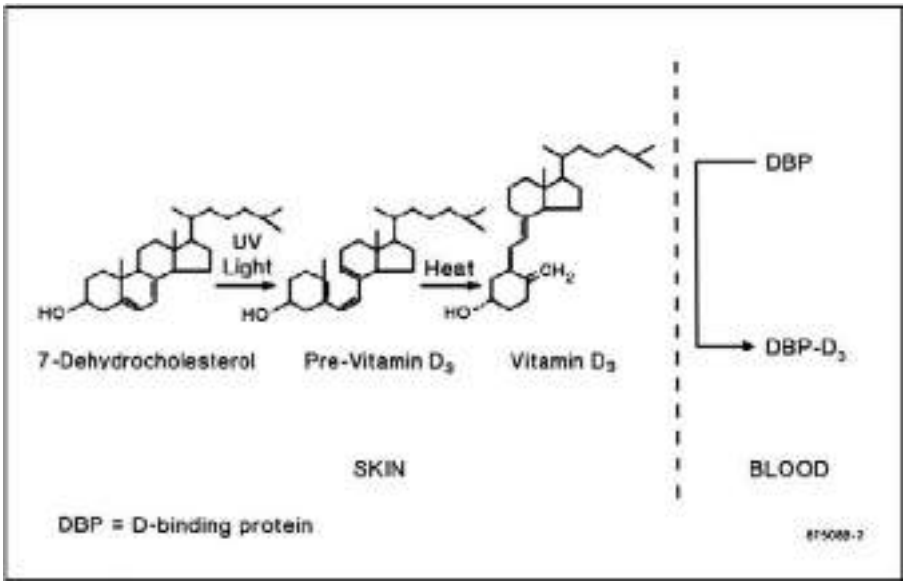

FIGURE 65.3 **The photolysis of 7-dehydrocholesterol to vitamin D_3 via the intermediate, pre-vitamin D_3.**

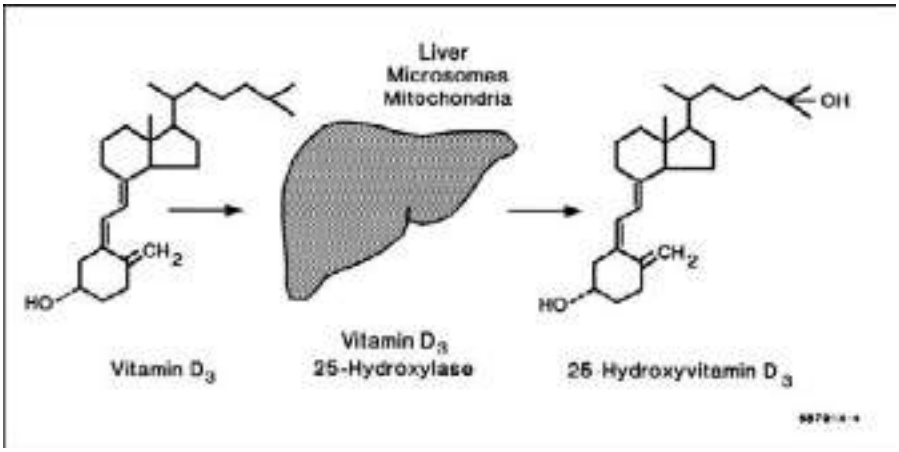

FIGURE 65.4 **The conversion of vitamin D_3 to 25-hydroxyvitamin D_3 in the liver.**

in the diet is also bound to VDBP following absorption in the intestine. Vitamin D_2 and vitamin D_3 are delivered to the liver for hydroxylation by the multicomponent, cytochrome P-450 containing enzyme, vitamin D 25-hydroxylase, which is present in the liver microsomes as well as in mitochondria[55–73] (Figure 65.4). Hepatic conversion of vitamin D_3 to 25-hydroxyvitamin D_3 is not tightly regulated due to a lack of product inhibition of the microsomal vitamin D_3 25-hydroxylase. Several cytochrome P-450s have been cloned and shown to metabolize vitamin D_3 to 25-hydroxyvitamin D_3, including several microsomal cytochrome P-450s and one mitochondrial cytochrome P-450.[74–80] 25-hydroxyvitamin D is the serum metabolite generally measured to determine vitamin D sufficiency or insufficiency in an individual. Accurate determinations of both 25-hydroxyvitamin D_2 and 25-hydroxyvitamin D_3 are obtained using high-performance liquid chromatography methods and mass-spectrometry based methods and such methods are preferred to those using protein binding or antibody binding assays.[81–88]

25-Hydroxyvitamin D_3 is not biologically active except in large concentrations, and it must be metabolized further in the kidney to the bioactive form of vitamin D, 1α,25-dihydroxyvitamin D_3[61,89–98] (Figure 65.5). The 25-hydroxyvitamin D_3-1α-hydroxylase, the enzyme responsible for the conversion of 25-hydroxyvitamin D_3 to 1α,25-dihydroxyvitamin D_3, is a multicomponent, cytochrome P-450 containing enzyme in the mitochondria of renal proximal tubular cells.[99–106] Although the kidney is the primary site of 25-hydroxyvitamin D_3-1α-hydroxylase activity, several other cell types have been shown to have 1α-hydroxylase activity.[107–117] It had previously been thought that the proximal tubule epithelial cells were the only renal cells with 25-hydroxyvitamin D_3 1α-hydroxylase activity. However, several investigators have clearly shown that this enzyme is present and active in several

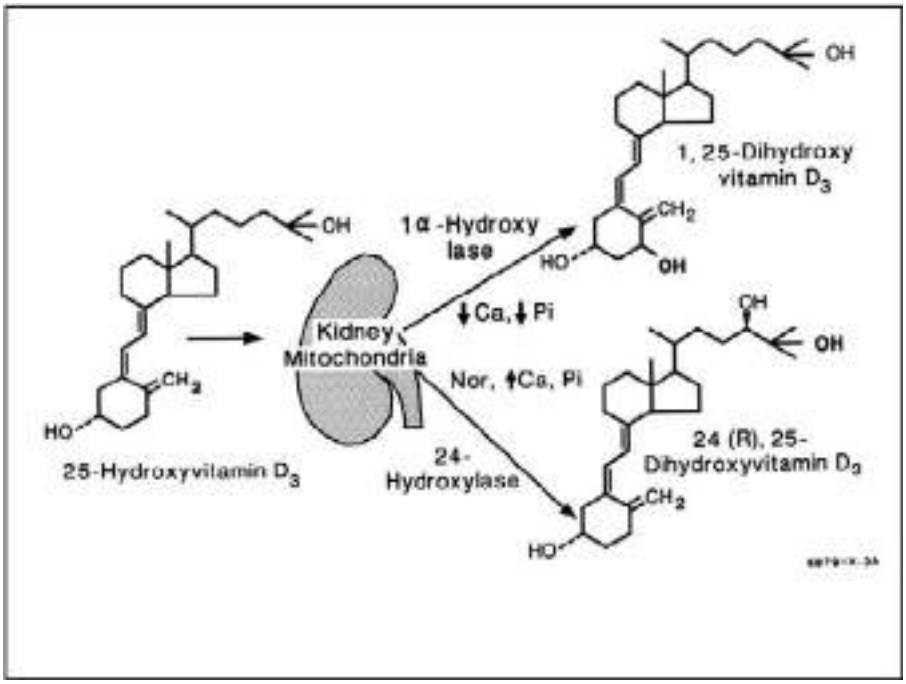

FIGURE 65.5 **The metabolism of 25-hydroxyvitamin D_3 to 1α,25-dihydroxyvitamin D_3 in the kidney.**

segments of the renal tubule.[118–120] The key factors regulating 25-hydroxyvitamin D-1α-hydroxylase production and activity are depicted in Table 65.2. Parathyroid hormone is a potent stimulator of 25-hydroxyvitmain D-1α-hydroxylase and is discussed in detail in the subsequent sections.[6,119,121] In addition to parathyroid hormone, low serum calcium, and low serum phosphorus also stimulate 25-hydroxyvitamin-1α-hydroxylase activity. 1α,25-dihydroxyvitamin D_3 provides a negative feedback through the vitamin D receptor (VDR). VDR-knockout mice have very high concentrations of 1α,25-dihydroxyvitamin D_3.

Recently, other proteins referred to as "phosphatonins" that induce renal phosphate loss have been shown to inhibit renal 25-hydroxyvitamin-1α-hydroxylase activity and 1α,25-hydroxyvitamin D_3 production.[122–126] Two such proteins include fibroblast growth factor 23 (FGF23) and secreted frizzled related protein 4 (sFRP4). Both of these proteins are able to inhibit renal tubule phosphate reabsorption which leads to hypophosphatemia. Despite the hypophosphatemia, which is a potent stimulator of 25-hydroxyvitamin-1α-hydroxylase activity, FGF23 and sFRP4 are capable of preventing the conversion of 25-hydroxyvitamin D_3 to 1α,25-dihydroxyvitamin D_3.[127] FGF23 and sFRP4 are over-expressed in tumors that cause oncogenic osteomalacia, a condition characterized by hypophosphatemia, hyperphosphaturia, and inappropriately low serum 1α,25-dihydroxyvitamin D_3 concentrations.[128] These biochemical abnormalities, including the low 1α,25-dihydroxyvitamin D_3 levels, completely resolve after removal of the offending

TABLE 65.2 Effect of Increased Level or Activity of Various Factors on $1,25(OH)_2D_3$ Concentration or 1α-Hydroxylase Activity

Factor	Animals	Humans	References
Parathyroid hormone	↑	↑	10, 168, 299, 348–355
Serum inorganic phosphorus	↓	↓	356–359
$1α,25(OH)_2D_3$	↓	↓	360, 299
Calcium (direct)	?	↓	133, 361
Calcitonin	↑,↓,0	↑	3, 299, 168, 355, 362, 363
Hydrogen ion	↓	0	364, 365, 348
Sex steroids	↑	↑	366, 367
Prolactin	↑	0	368–370
Growth hormone and insulin-like growth factor-1	↑	↑,↓,0	371–376
Glucocorticoids	↓,0	↑,↓,0	87, 377–380
Thyroid hormone	?	↓[a]	381–383
Fibroblast growth factor 23	↓	?	384, 385
Frizzled related protein 4	↓	?	122
Pregnancy	↑	↑[a]	386, 387

[Modified from Kumar R[6]]

[a] *Effects may be secondary to changes in calcium, phosphorus or parathyroid hormone.*

↑, Stimulation or increase; ↓, suppression or decrease; 0, no effect; ?, unknown effect.

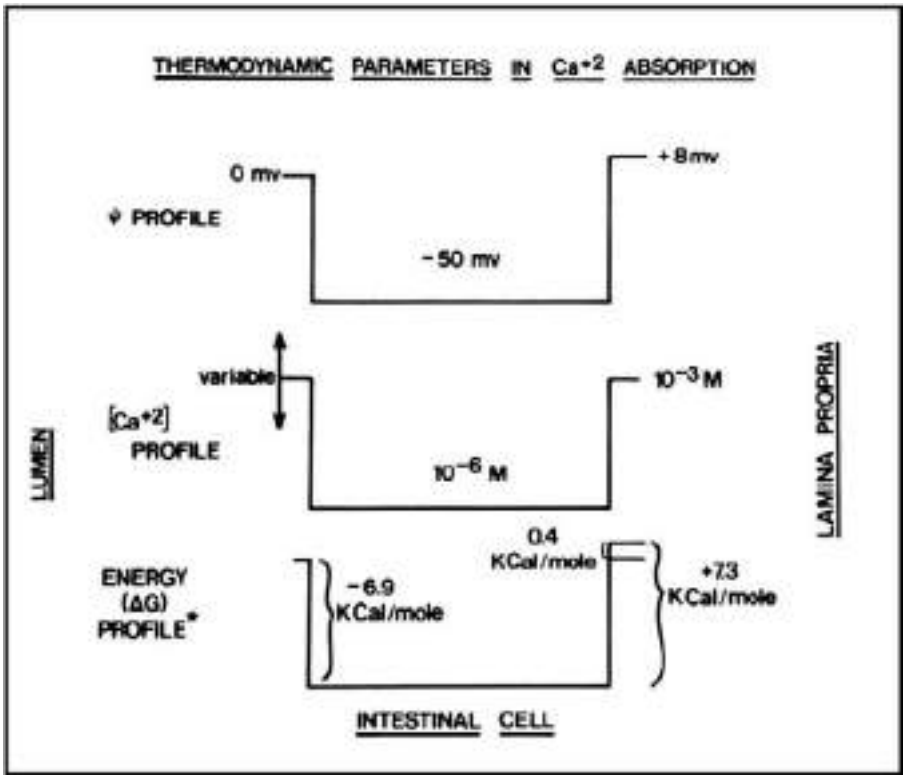

FIGURE 65.6 **Thermodynamic parameters in intestinal calcium absorption.** Estimated thermodynamic patterns relative to the intestinal absorption of calcium. Note the down-hill gradient in the transfer of Ca^+ from the lumen into the enterocyte and the requirement for energy in the extrusion of Ca^+ in the parenteral direction. (*Wasserman R.H. et al.*[19]).

tumor.[129] These proteins appear to play an important role in mineral and vitamin D metabolism.[130]

Mechanism of Action of Vitamin D in Intestine

Calcium is absorbed by the intestine (predominantly in the duodenum and proximal small intestine) by two mechanisms, a passive paracellular mechanism and an active transcellular one. The movement of calcium across the apical border of the intestinal cell into the cell is down a concentration gradient (the interior of the intestinal cell has a calcium concentration in the high nanomolar range) and an electrical gradient (the interior of the cell is electronegative relative to the lumen). It does not require the expenditure of energy. However, the movement of calcium out of the intestinal cell at the basolateral membrane is against an electrical and concentration gradient and requires the expenditure of energy (Figure 65.6). Essential to the process of active calcium transport are several vitamin D dependent proteins, each with a specific function. Vitamin D-dependent calcium transport proteins found in the intestinal epithelial cells include the epithelial calcium channel (ECaC), calbindin D_{9K}, and the plasma membrane calcium pump (PMCA). These proteins work in concert to transport calcium from the intestinal lumen, through the brush border membrane, across the intracellular space to the plasma membrane surface and finally out of the cell into the extra-cellular fluid and plasma (Figure 65.7).

The actions of vitamin D in the intestine play an integral role in the maintenance of plasma calcium concentrations within a narrow range in the face of wide fluctuations in dietary calcium intake. When there is an abundance of dietary calcium, a substantial portion can be absorbed passively through the paracellular route. However, when dietary calcium intake declines and plasma calcium concentrations fall, several adaptive responses occur including the production and release of PTH from the parathyroid gland (Figure 65.8). The parathyroid gland is able to sense and respond to slight changes in extracellular calcium concentrations through the calcium sensing receptor (CaSR).[131,132] In addition to the direct effects on calcium homeostasis in bone and the kidney (discussed below), PTH enhances intestinal calcium absorption indirectly by increasing 1α,25-dihydroxyvitamin D_3 production in the proximal tubule cells of the kidney. Bland et al. have also demonstrated that, in vitro, 25-hydroxyvitamin D-1α-hydroxylase activity is regulated by extracellular calcium concentrations independent of PTH.[133] They showed that human proximal tubule cells cultured in a low calcium environment resulted in a significant increase in 1α-hydroxylase activity and this activity was significantly reduced when cultured in a high calcium environment.

The response in the intestine to low dietary calcium intake is to increase the proportion of ingested calcium

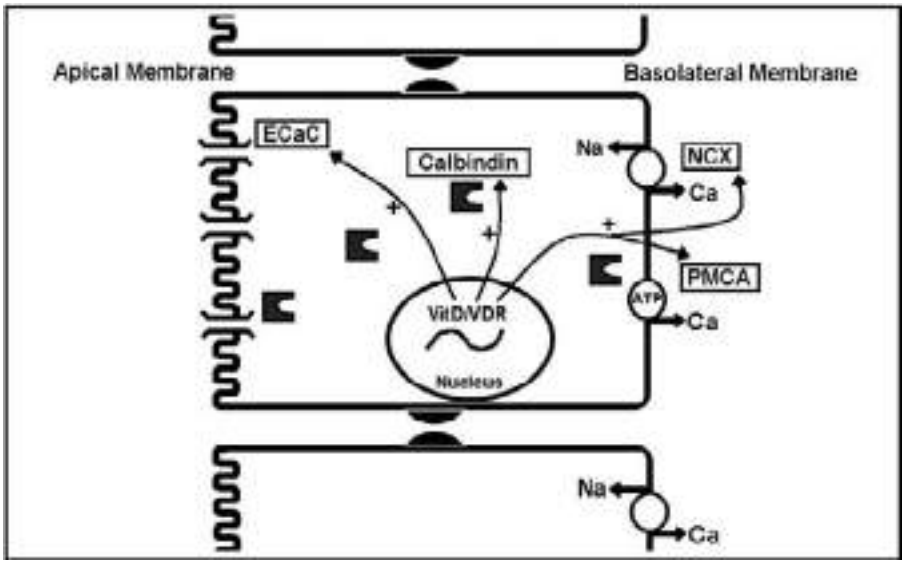

FIGURE 65.7 **Diagram of Epithelial Calcium Transport.** Transcellular transport of calcium ions proceeds from the lumen (intestinal or renal tubular) through the epithelial calcium channel (ECaC) in the apical membrane, across the cytoplasm bound to Calbindin D_{28K} (kidney) or Calbindin D_{9K} (intestine), and subsequently passes through the basolateral membrane through the sodium-calcium exchanger (NCX) or the plasma membrane calcium ATP-ase (PMCA).

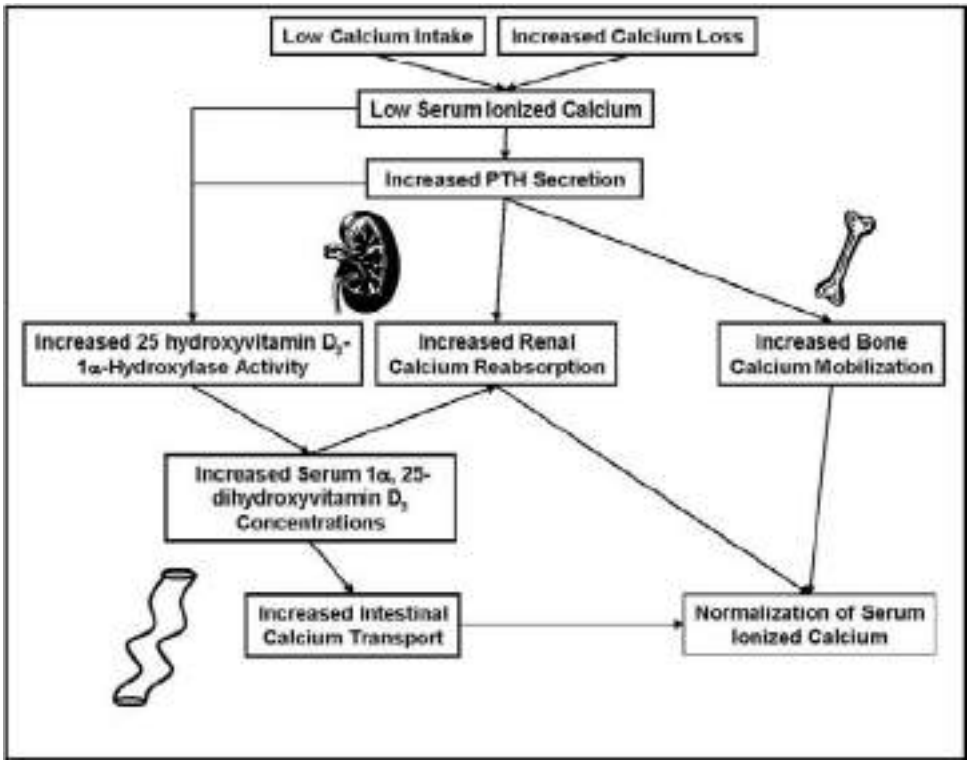
Low Calcium Intake
Increased Calcium Loss
Low Serum Ionized Calcium
Increased PTH Secretion
Increased 25 hydroxyvitamin D3-1α-Hydroxylase Activity
Increased Renal Calcium Reabsorption
Increased Bone Calcium Mobilization
Increased Serum 1α, 25-dihydroxyvitamin D3 Concentrations
Increased Intestinal Calcium Transport
Normalization of Serum Ionized Calcium

FIGURE 65.8 **Physiological response to hypocalcemia.**

that is subsequently absorbed. This is accomplished by increasing the synthesis and activity of several vitamin D responsive calcium transport proteins in the intestinal epithelial cell. The first step of calcium entry from the intestinal lumen to the interior of the cell is accomplished by the ECaC located on the apical surface of the intestinal brush border epithelium.[134–137] When present in the apical cell wall, ECaC facilitates the entry of calcium ions into the intracellular space. Two forms of ECaC ($ECaC_1$ and $ECaC_2$) are found in the intestine and both are vitamin D responsive. Vitamin D enhances ECaC mRNA expression through the vitamin D receptor (VDR).[138–140] Bouillon et al. has demonstrated in VDR-KO mice that the VDR is necessary for effective regulation of several proteins involved in intestinal calcium transport including ECaC.[140,141] Van Abel et al. have shown that 25-hydroxyvitamin D_3 1α,25-hydroxylase-KO mice also

have lower expression of ECaC than wild-type mice which was corrected with the administration of 1α,25-dihydroxyvitmain D_3.[142] Although the stimulatory effect of vitamin D on calcium transport protein production in the intestine is clear, it is unclear what the direct effect of calcium may be on ECaC expression.[141,142] Regardless of the difference in response to a high calcium diet between the VDR-KO and 25-hydroxyvitamin D_3 1α-hydroxylase-KO mice, these studies would suggest that ECaC expression is regulated by vitamin D-dependent and vitamin D-independent mechanisms.

After calcium ions have entered the enterocyte, they must be transported across the cell to the basolateral membrane, where they will subsequently be transported out of the cell. This is accomplished by the calbindins which are found both in intestinal epithelial cells and in renal tubule cells. In humans, calbindin D_{9K} is responsible for transcellular transport in the intestine and calbindin D_{28K} in the renal epithelium.[143–148] Human calbindin D_{9K} is a 79 amino acid protein encoded on the X chromosome.[145] Hisham at al. identified a putative vitamin D response element in the 5′-flanking region of the calbindin D_{9K} gene in the rat.[149] It has clearly been shown that calbindin D_{9K} mRNA and protein expression is diminished in the face of vitamin D deficiency and that 1α,25-dihydroxyvitamin D_3 administration will increase this expression in various animal models of vitamin D deficiency.[150–152] Basal expression and response to 1α,25-dihydroxyvitamin D_3 treatment changes with age in both rats and humans.[147,148,150,153] Basal expression is lower and the increase in calbindin D_{9K} in response to a given amount of 1α,25-dihydroxyvitamin D_3 is diminished. Although 1α,25-dihydroxyvitamin D_3 appears to be the major stimulus for calbindin D_{9K} in the intestine, dietary calcium may have a direct effect on its expression.[140,152]

The increased expression of ECaC and calbindin D_{9K} likely enhance the capacity of the enterocyte to transport calcium from the intestinal lumen to the intracellular space and subsequently to the basolateral membrane. However, their ability to increase calcium absorption in the face of low dietary calcium intake is dependent on the plasma membrane calcium pump (PMCA). The PMCA represents the final step in active calcium transport across the intestinal mucosa and is the single vitamin D responsive protein in the intestine that is energy dependent. Because it is energy dependent, the PMCA is able to transport calcium across the basolateral membrane against a concentration and electrical gradient. Without the PMCA, calcium absorption through the intestinal epithelial cell could not take place in a state of low calcium intake and low intestinal lumen calcium concentrations. Several isoforms of the protein have been identified with PMCA-1 being the major form found in the human duodenum.[154,155] The PMCA is found in the basolateral membrane and actively transports calcium ions out of the cell into the interstitial space against a concentration gradient.[156] Several investigators have shown that PMCA expression is decreased in the absence of, or increased by, the addition of 1α,25-dihydroxyvitamin D_3.[157–162]

Vitamin D plays an integral role in the absorption of calcium across the intestinal mucosa. Several key proteins involved in this process are directly regulated by 1α,25-dihydroxyvitamin D_3 as demonstrated by numerous experimental conditions and in many species. VDR-KO and 25-hydroxyvitamin D 1α-hydroxylase-KO mice have proven to be useful animal models in elucidating the role of vitamin D in intestinal calcium transport. In both of these models, significantly lower concentrations of all three transport proteins when compared to their wild-type counterparts have been described. In addition, intestinal calcium transport is lower in these KO models, demonstrating their importance in calcium transport. Lending further evidence to the importance of 1α,25-dihydroxyvitamin D_3 in intestinal calcium transport is the excellent correlation between increased ECaC, calbindin D_{9K}, and PMCA expression with improved calcium absorption in vitamin D deficient animals when 1α,25-dihydroxyvitamin D_3 is replaced. This is an effect that is apparent in young as well as older animals. However, the effects of 1α,25-dihydroxyvitamin D_3 on transport protein expression are blunted with age. This may at least partly explain the age-related decline in intestinal calcium absorption.

Mechanism of Action of Vitamin D in Kidney

Calcium handling in the kidney is similar to that in the intestine. There are both vitamin D-dependent and vitamin D-independent mechanisms at work. Reabsorption can take place through a passive paracellular route or an active vitamin D dependent transcellular route. About 55% of plasma calcium is ultra-filterable with about 98% being reabsorbed in the tubule.[163] The kidney plays a unique role in the hormonal regulation of calcium in that it is the primary site of conversion of 25-hydroxyvitamin D_3 to the active form of the hormone 1α,25-dihydroxyvitamin D_3. This was first discovered by Fraser and Kodicek when 1α,25-dihydroxyvitamin D_3 production was noted to be diminished after nephrectomy.[94,164] Although the kidney is the major site of 25-hydroxyvitamin D_3 1α-hydroxylase activity, several other cell types are capable of converting 25-hydroxyvitamin D_3 to 1α,25-dihydroxyvitamin D_3.[108,109,112,117,165] It has been known for some time that the proximal tubule epithelial cell exhibited 25-hydroxyvitamin D_3 1α-hydroxylase

activity.[166–170] However, the presence of 25-hydroxyvitamin D-1α-hydroxylase mRNA and protein has more recently been described by Zehnder et al. in more distal portions of the tubule including the distal convoluted tubule, cortical collecting duct, thick ascending limb of loop of Henle, and Bowman's capsule.[119,120] The significance of 25-hydroxyvitamin D-1α-hydroxylase expression and activity in these distal portions of the nephron is not completely known. One could speculate there is a paracrine effect of vitamin D in these portions of the tubule since vitamin D-dependent calcium transport takes place in the distal nephron.

As previously mentioned, a state of hypocalcemia will lead to increased 1α,25-dihydroxyvitamin D_3 production in the kidney that is stimulated by higher PTH concentrations and probably by the hypocalcemia itself. Several vitamin D responsive proteins that are essentially analogous to those described in the intestine are present in the renal tubule cells. The up-regulation of these proteins by vitamin D helps defend against hypocalcemia and the maintenance of plasma calcium within the normal range in the face of low calcium intake or increased bone or soft tissue calcium deposition.

The first step in renal calcium transcellular transport involves the epithelial calcium channel. ECaCs have been described by Hoenderop et al. in the renal tubule apical membrane[136] and are felt to be responsible for uptake of luminal calcium ions to the intracellular compartment. Of the two forms of ECaCs, ECaC-1 expression appears to be limited to the kidney whereas ECaC-2 is found in several other tissues.[171–174] Human ECaC-1 is encoded on the long arm of chromosome 7 and has several putative vitamin D response elements.[175] ECaC mRNA and protein is up-regulated in vitamin D deficient animals after supplementation with 1α,25-dihydroxyvitamin D_3.[137–139,176,189] When measured by quantitative PCR in the VDR-KO mouse model, ECaC-1 concentrations are decreased in the kidney when compared to wild-type littermates.[174] However, in the same study, Weber et al. demonstrated that ECaC-1 could be increased by giving the animals a high calcium rescue diet. This would suggest that renal ECaC-1 is regulated by vitamin D dependent and vitamin D independent mechanisms.

Extensive work has been done regarding the role and regulation of the calcium binding protein calbindin D_{28K} in the kidney. It is felt that calbindin D_{28K} acts as an intracellular calcium transporter from the apical membrane to the basolateral membrane similar to the action of calbindin D_{9K} in the intestine. Calbindin D_{28K} is expressed not only in the kidney but also in neural tissue.[144,177] However, only renal concentrations seem to be impacted by exposure to 1α,25-dihydroxyvitamin D_3.[177] Within the renal tubule, calbindin D_{28K} is found mainly in the distal portions of the nephron and co-localizes with other vitamin D responsive proteins involved in transepithelial calcium transport.[23,178,179] In contrast to the ECaC and PMCA which are located in the apical and basolateral membranes, respectively, calbindin D_{28K} is found in the cytosolic compartment.[180] Several groups have clearly shown that renal calbindin D_{28K} is regulated by vitamin D.[150,177,181–191] Vitamin D deficient or replete animals given 1α,25-dihydroxyvitamin D_3 significantly increase the expression of calbindin D_{28K} mRNA and protein. This effect is also seen in vitro when cultured renal tubule epithelial cells are exposed to 1α,25-dihydroxyvitamin D_3.[180–184] Although 1α,25-dihydroxyvitamin D_3 is a potent stimulator of renal calbindin expression, changes in calcium, phosphorus, and magnesium also impact its expression. Huang and Christakos showed a lack of effect of a high calcium diet in vivo in vitamin D deficient animals on mRNA levels of calbindin D_{28K}.[190] However, Clemens et al. showed that 1α,25-dihydroxyvitamin D_3 induction of calbindin D_{28K} was enhanced by exposure of the cells to a higher calcium concentration.[184] Renal calbindin production also appears to be increased when exposed to a low phosphorus diet and decreased when exposed to a diet rich in magnesium.[177,190–193]

When plasma calcium concentrations are low, the filtered amount of calcium in the glomerulus is also diminished, and the kidney must increase the proportion of calcium that is reabsorbed in order to maintain normal calcium balance. This process cannot take place without the ATP-dependent PMCA. Multiple forms of the PMCA have been described with ubiquitous distribution.[194–198] As in the intestine, the renal PMCA localizes to the basolateral plasma membrane.[196] Along with the sodium-calcium exchanger (NCX), the PMCA is responsible for transporting calcium ions out of the renal epithelial cell into the interstitial space and eventually into the blood. The NCX itself cannot transport calcium across a concentration or electrical gradient as can the PMCA. Renal PMCA mRNA and protein are up-regulated by exposure to 1α,25-dihydroxyvitamin D_3 in vivo and in vitro.[189,199,200] Hoenderop et al. performed an experiment comparing homozygous 25-hydroxyvitamin D_3-1α-hydroxylase knock-out mice with heterozygotes (controls).[189] When on a normal calcium diet, homozygous mice had lower levels of ECaC-1, calbindin D_{28K}, and NCX concentrations when measured by real time PCR. However, PMCA concentrations were not different between the two groups. When given 1α,25-dihydroxyvitamin D_3, both the homo- and heterozygous mice increased expression of all of the calcium transporting proteins including PMCA. This would suggest that 1α,25-dihydroxyvitamin D_3 may not be necessary for basal mRNA levels to

be present but the protein is highly responsive to 1α,25-dihydroxyvitamin D_3.

PARATHYROID HORMONE

Endocrine System

Parathyroid hormone is an 84 amino acid peptide produced and secreted by the parathyroid glands and is an important regulator of extracellular calcium concentrations. PTH secretion from the parathyroid gland is stimulated by hypocalcaemia and inhibited when exposed to elevated calcium levels. In turn, PTH regulates serum calcium concentrations through direct mechanisms in the kidney (enhanced calcium reabsorption) as well as in bone (release of mineral from bone). Since PTH is a potent stimulator of 1α-hydroxylase activity resulting in higher 1α,25-dihydroxyvitamin D_3 concentrations, it also exerts its effects on calcium metabolism indirectly through the vitamin D endocrine system described above. The following section will outline the regulation of PTH synthesis and secretion as well as its effects on calcium homeostasis in the kidney and in bone.

Regulation of Parathyroid Hormone

SYNTHESIS AND SECRETION

The chief cells of the parathyroid gland are responsible for the synthesis, storage, and release of parathyroid hormone. PTH is the product of a larger molecule, pre-pro-parathyroid hormone. The pre-sequence is cleaved in the endoplasmic reticulum resulting in pro-PTH. The pro-sequence is subsequently removed in the Golgi apparatus, leaving the final 84 residues that constitute the secreted and active form of PTH.[201] The release of preformed PTH from secretory vesicles is most acutely affected by extracellular calcium concentrations. Figure 65.9 depicts the steep inverse sigmoidal relationship between calcium concentrations and PTH release. A minimal increase in extracellular ionized calcium will inhibit PTH release. Likewise, a slight decrease in plasma ionized calcium is a potent stimulus for PTH synthesis and secretion.[202–209]

The parathyroid cell is able to detect these small changes in calcium concentrations by means of the calcium sensing receptor (CaSR) located on the cell surface.[131,132,210] The CaSR is not only expressed on the surface of parathyroid cells but also in the kidney, bone, intestine, and several other tissues.[211–231] Mutations in the CaSR have contributed to our understanding of its importance in normal calcium homeostasis. In humans, both activating and inactivating mutation is the CaSR have been described.[232–244] Inactivating mutations result in the condition Familial Hypocalciuric Hypercalcemia (FHH) in which serum calcium levels are increased as a result of a higher calcium set point required to inhibit PTH secretion. Similar clinical features have been described in patients with acquired disease due to inactivating antibodies against the CaSR.[191,246] In both of these diseases, the CaSR has become less sensitive to the effects of extracellular calcium and thus higher concentrations are required to inhibit PTH secretion. The opposite scenario has also been described in which activating mutations in the CaSR or antibodies against the CaSR result in inherited or acquired hypoparathyroidism, respectively.[247,248] These are conditions in which the CaSR is more sensitive to extracellular ionized calcium concentrations and PTH secretion is inhibited at lower calcium levels.

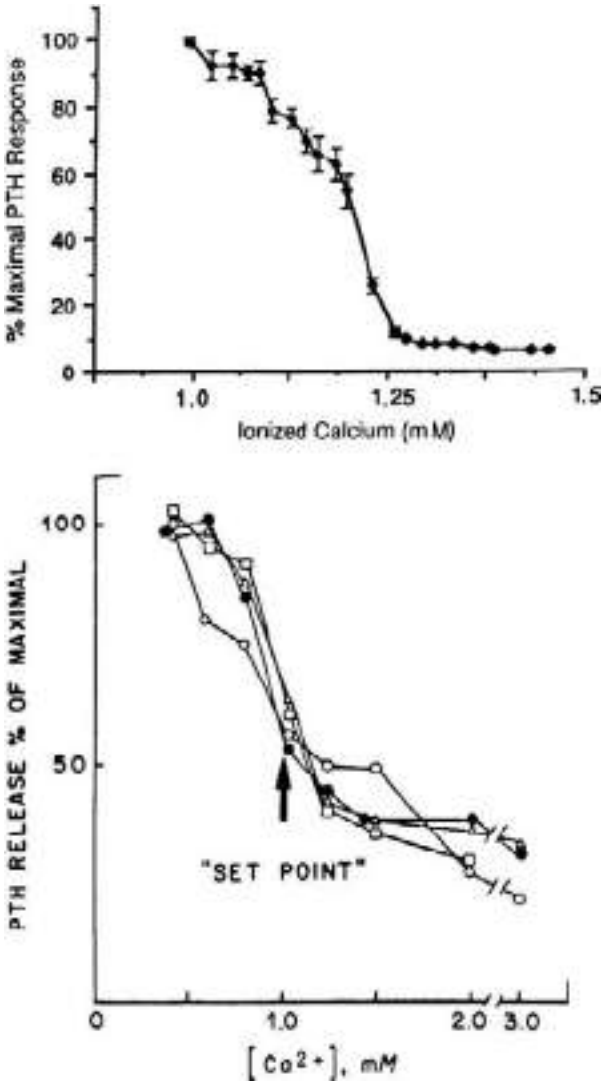

FIGURE 65.9 **Relationship between ionized calcium concentration and parathyroid hormone secretion.** *Reprinted with permission (From Brown, E.M.[202]).*

Several investigators have also shown that cells from parathyroid adenomas and hyperplastic parathyroid glands in patients with primary and secondary hyperparathyroidism have fewer detectable calcium sensing receptors than normal parathyroid tissue.[249] These clinical scenarios point to the critical role of the CaSR in the regulation of PTH secretion in response to calcium concentrations in humans.

Parathyroid hormone secretion is also regulated by 1α,25-dihydroxyvitamin D_3 through the VDR.[250–255] The response to vitamin D on PTH secretion is not as rapid as the acute changes seen with fluctuations in extracellular calcium concentrations detected by the CaSR. Vitamin D acts as a negative feedback on PTH secretion as a means to prevent hypercalcemia. When faced with hypocalcemia, preformed PTH is rapidly secreted from the parathyroid cell and acts in the kidney to increase 1α-hydroxylase activity. The result is increased conversion of 25-hydroxyvitamin D_3 to 1α,25-dihydroxyvitamin D_3. Vitamin D response elements (VDRE) have been identified in the 5′ flanking region of the parathyroid gene and serve to inhibit PTH gene transcription resulting in decreased hormone synthesis.[253,256] In addition to inhibiting PTH secretion by means of the CaSR, extracellular calcium concentrations also influence PTH secretion indirectly by altering VDR expression. Brown et al. fed three groups of rats a vitamin D deficient diet along with either a low, normal, or high calcium diet. Parathyroid tissue VDR mRNA concentrations were approximately sixfold higher in the vitamin D deficient rats fed a high calcium diet.[257] Up-regulation of the VDR in parathyroid cells by higher extracellular calcium concentrations has been observed by others, both *in vivo* and *in vitro*, showing the integrated control of PTH secretion by calcium ion concentration and vitamin D.[258] These findings would suggest that the negative feedback of vitamin D on the parathyroid gland is augmented by higher calcium concentrations, adding yet another layer of control in the regulation of normal calcium homeostasis.

Several other factors also play a role in PTH secretion including serum phosphorus concentrations, magnesium and certain amino acids.[259–271]

Parathyroid Hormone and Kidney

The parathyroid hormone receptor (PTHr) is a G-protein coupled receptor found in a diverse array of tissues including the kidney and bone where it plays an integral part in calcium homeostasis.[272–282] Using RT-PCR and in-situ hybridization techniques, the PTHr has been identified in several portions of the nephron including the glomeruli, proximal convoluted tubule, proximal straight tubule, medullary and cortical thick ascending limb, and the distal convoluted tubule.[283–285] PTH serves different functions in mineral metabolism along the nephron including decreasing phosphate reabsorption (primarily in the proximal portion), facilitating calcium reabsorption (distal portion), and enhanced conversion of 25-hydroxyvitamin D_3 to 1α,25-dihydroxyvitamin D_3.

The direct effect of PTH on transcellular reabsorption of filtered calcium takes place primarily in the distal nephron and uses some of the same machinery as vitamin D regulated calcium transport. Calcium entry into the renal tubule epithelial cell through calcium channels is enhanced in the presence of PTH.[286–290] Friedman et al. demonstrated that this process is dependent on both protein kinase A (PKA) and protein kinase C (PKC) signaling pathways and calcium transport could be prevented with specific inhibitors of PKA or PKC.[288]

Using a murine distal convoluted tubule cell line, Gesek and Friedman demonstrated a dose-dependent calcium uptake by PTH that was inhibited by a dihydropyridine calcium channel blocker.[291] They also demonstrated in the same study that hyperpolarization of the cell was responsible for the calcium uptake and the hyperpolarization was due to chloride efflux. They proposed that the principal mechanism by which PTH induced calcium reabsorption in the distal tubule was through activation of chloride channels that resulted in epithelial cell hyperpolarization. This hyperpolarization sets up a favorable gradient for transcellular calcium transport, thereby facilitating its reabsorption from the distal tubule.

In addition, it has also been shown that distal tubule cells exposed to PTH have increased sodium dependent calcium transport.[292,293] These findings demonstrate the synergistic effects of PTH and vitamin D on calcium reabsorption in the kidney. As outlined in the sections above, there are several vitamin D dependent calcium transport proteins in the distal portions of the nephron. Several of these proteins are utilized or their activity is up-regulated in the presence of PTH.

PTH not only has direct effects on renal tubular calcium transport but also exerts indirect effects through the vitamin D system. PTH is a potent stimulator of 25-hydroxyvitamin D_3 1α-hydroxylase activity in the kidney leading to higher 1α,25-dihydroxyvitamin D_3 concentrations.[245,294–297] Using a luciferase reporter, Brezna et al. demonstrated that PTH stimulates 1α,25-dihydroxyvitamin D_3 production through a promoter in the 1α-hydroxylase gene.[298] Vitamin D then serves to increase extracellular calcium concentrations by the mechanisms describe above.

In states of renal dysfunction, the effects of PTH on the kidney can be dramatically reduced. Its ability to promote phosphate loss in the proximal tubule and reabsorb calcium in the distal tubule can be diminished

despite high circulating levels of PTH. The up-regulatory effect of PTH on 25-hydroxyvitamin D_3 1α-hydroxylase activity is significantly reduced in renal failure.[299] These findings in renal failure are probably (at least partially) due to the decreased number of PTHr found in renal tubular cells in humans and in animal models of chronic renal insufficiency.[300–303]

Parathyroid Hormone and Bone

Calcium metabolism in bone regulated by PTH is complex and involves both osteoblasts and osteoclasts. The effects of PTH on osteoclasts had been thought to be primarily indirect since they do not normally contain PTH receptors. However, osteoclasts from patients with secondary hyperparathyroidism do express PTHr mRNA and protein suggesting a possible direct effect of PTH on ostoeclasts in the disease state.[276] In addition, Dempster et al. have demonstrated increased bone resorption by normal human osteoclasts derived from peripheral monocytes grown on bone slices when exposed to PTH.[304] This effect was seen in the absence of osteoblasts.

When discussing the role of PTH on calcium homeostasis, the main effect in bone is to release calcium ion into the extracellular compartment to maintain normal ionized calcium concentrations. Osteoclasts are the cells responsible for bone resorption and release of mineral. The stimulation of osteoclastogenesis by osteoblasts is by way of the receptor activator of nuclear factor-κB ligand (RANKL), osteoprotegerin (OPG), RANK system (Figure 65.10). RANKL production by osteoblasts is stimulated by PTH and OPG is inhibited by PTH.[305] RANKL induces osteoclast differentiation and activation through the RANK receptor.[306,307] OPG acts by binding to RANKL thus inhibiting osteoclast activation through the RANK receptor.[308,309] Since PTH has positive and negative effects on the production of RANKL and OPG, respectively, its effects on resorption are through two separate yet integrated mechanisms. Once osteoclasts have been activated by PTH through this indirect mechanism, bone resorption ensues and calcium is released.

It should be noted, though, that the type of exposure to PTH (intermittent vs. continuous) will determine the net calcium flux in bone. It is clear that continuous exposure to elevated concentrations of PTH, as in primary hyperparathyroidism, results in a net flux of calcium out of bone resulting in decreased bone mineral content and hypercalcemia. This effect can be reversed with parathyroidectomy.[310–313] In contrast, osteoporotic patients treated with intermittent daily doses of PTH 1-34 have substantial increases in bone mineral content.[314–316] Despite daily treatment with PTH 1-34,

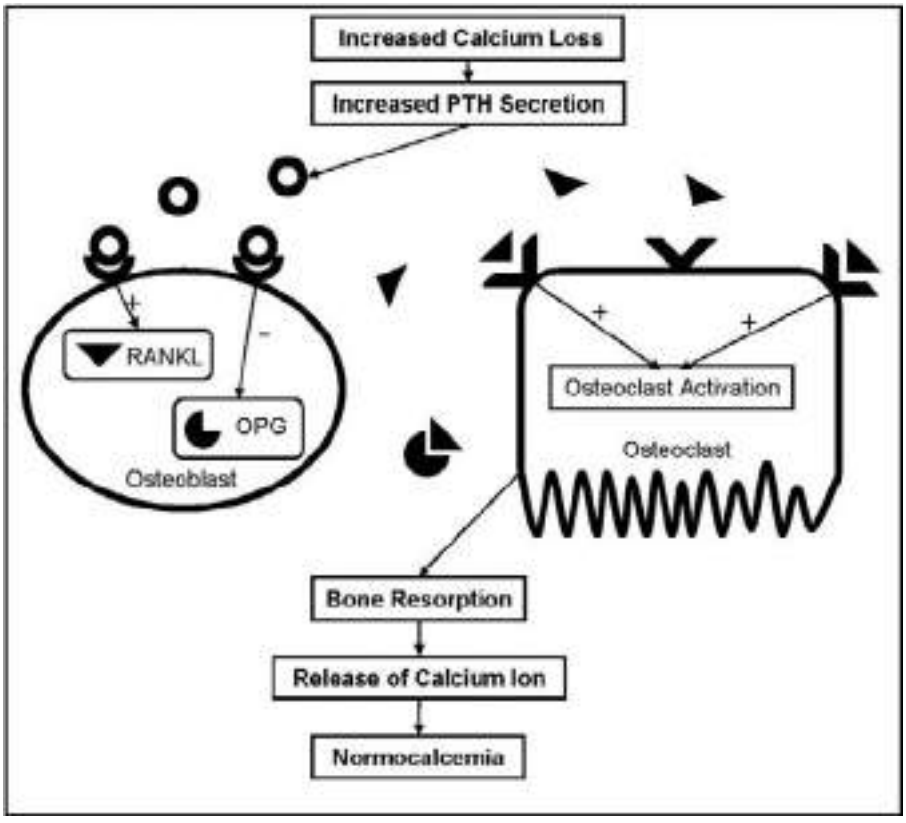

FIGURE 65.10 **Activation of bone resorption by parathyroid hormone.** Parathyroid hormone stimulates the release of calcium from bone indirectly through the osteoblast. When PTH receptors on the osteoblast are activated, they stimulate the production of receptor activator of nuclear factor-κB ligand (RANKL). Osteoprotegerin (OPG) production in the osteoblast is inhibited by PTH. OPG acts to antagonize the action of RANKL by serving as a decoy receptor for RANKL. This allows RANKL to bind its receptor, RANK, which in turn activates the osteoclast thus initiating bone resorbtion and calcium release.

these patients are generally not hypercalcemic and, if so, only transiently. The reason for the discrepancy in the effect on bone metabolism between continuous versus intermittent exposure to PTH is not completely understood.

CALCITONIN

Calcitonin is a 32 amino acid protein encoded on the short arm of chromosome 11 found in the C-cells of the thyroid gland.[317,318] While calcitonin has been used pharmacologically to treat hypercalcemia and osteoporosis, its role in normal calcium physiology is not clear. Under experimental conditions, calcitonin clearly has been shown to affect several aspects of calcium homeostasis. However, in disease states in which calcitonin concentrations are significantly altered, there appears to be little if any effect on calcium metabolism.

The release of calcitonin is stimulated by hypercalcemia and is regulated by extracellular calcium concentrations detected by the CaSR. The presence of the CaSR on the C-cells of the thyroid gland has been clearly demonstrated.[319–321] Fudge and Kovacs used a CaSR heterozygous knock-out mouse to study the effects of calcium administration on calcitonin levels. Despite higher calcium concentrations, the calcitonin levels were lower in the CaSR heterozygous knock-out mice than wild-type mice providing evidence of the importance of the CaSR in the secretion of calcitonin.[322]

The actions of calcitonin are mediated through the calcitonin receptor encoded on chromosome 7q21.3.[323] The calcitonin receptor is found in many tissues including the kidney and bone.[324–331] Under experimental conditions, calcitonin has been shown to have several effects in the kidney that may directly or indirectly affect calcium metabolism. Calcitonin is a known stimulator of 25-hydroxyvitamin D_3 1α-hydroxylase activity thus increasing 1α,25-dihydroxyvitamin D_3 concentrations which will have independent effects on calcium metabolism.[299,332] Several studies also show a direct effect of calcitonin on calcium uptake in renal distal tubule cells. Calcium uptake is enhanced through similar mechanisms as PTH dependent calcium reabsorption. Hyperpolarization due to increased chloride conductance and activation of the NCX appear to play an important role.[333–336] The relative effect of calcitonin on vitamin D production and calcium reabsorption in the kidney is likely minimal in comparison to PTH.

In bone, calcitonin exerts its effects primarily on the osteoclast. In mouse bone marrow culture, calcitonin dose dependently reduced the number of tartrate-resistant acid phosphatase positive cells suggesting that osteoclastogenesis can be inhibited by calcitonin.[337] Osteoclastic bone resorption and release of calcium can be inhibited by exposure of these cells to calcitonin.[338,339] This anti-osteoclast activity of calcitonin can be transient, likely due to a rapid and sustained decrease in calcitonin receptor abundance after calcitonin exposure.[340,341] This calcitonin receptor down-regulation is at least be partially abrogated by exposure of the cells to 1α,25-dihydroxyvitamin D_3.[342]

Despite these findings, the importance of calcitonin in normal calcium homeostasis is uncertain. Patients undergoing thyroidectomy or radioiodine ablation of the thyroid gland for Graves' disease have lower basal and calcium stimulated calcitonin concentrations but no difference in bone mineral density.[343] Another study of patients post thyroidectomy suggested a decrease in bone density in men but reported normal concentrations of calcium, PTH, and osteocalcin.[344] The commonly seen transient hypocalcemia after thyroidectomy has been postulated to be due to a transient rise in calcitonin shortly after surgery. However, there is conflicting evidence as to whether or not the rise in calcitonin is coincident with, or after, the fall in calcium is seen.[345,346] The fall in serum calcium frequently seen after thyroidectomy is more likely due to transient hypoparathyroidism. It has also been noted that patients with medullary thyroid cancer and significantly elevated calcitonin concentrations are not hypocalcemic. Hurley et al. performed a study comparing patients with medullary thyroid cancer (MTC) to patients post thyroidectomy. At baseline and after calcium infusion, calcitonin concentrations were significantly higher in the MTC group compared to the thyroidectomy and control groups. However, there were no differences in serum calcium, phosphorus, or PTH concentrations.[347]

When used in pharmacologic doses or under experimental conditions, calcitonin appears to be involved in calcium homeostasis through several different mechanisms including increased vitamin D production, renal calcium reabsorption, and inhibition of osteoclast function.

CONCLUSION

Most tissues in the body are dependent on calcium for normal function. If extracellular calcium concentrations are not maintained within the normal range, significant pathology may result depending on the duration and severity of the abnormality. Perturbations in calcium homeostasis can result in severe morbidity including osteoporotic fractures, renal failure, and seizures. Due to the consequences associated with abnormalities in calcium metabolism, it is not surprising there are several highly integrated mechanisms in place to defend against hypocalcemia and hypercalcemia.

Assuming there is adequate vitamin D intake or exposure to UVB radiation, the hormonal regulation of calcium is able to maintain eucalcemia despite wide fluctuations in dietary calcium intake. Vitamin D, PTH, and calcitonin work in concert in the intestine, kidney, and in bone to assure normal calcium balance.

References

[1] Adams JS, Clemens TL, Parrish JA, Holick MF. Vitamin-D synthesis and metabolism after ultraviolet irradiation of normal and vitamin-D-deficient subjects. N Engl J Med 1982;306:722–5.

[2] Adams ND, Garthwaite TL, Gray RW, Hagen TC, Lemann Jr J. The interrelationships among prolactin, 1,25-dihydroxyvitamin D, and parathyroid hormone in humans. J Clin Endocrinol Metab 1979;49:628–30.

[3] Adams ND, Gray RW, Lemann Jr J. The calciuria of increased fixed acid production in humans: evidence against a role for parathyroid hormone and 1,25(OH)2-vitamin D. Calcif Tissue Int 1979;28:233–8.

[4] Adams ND, Gray RW, Lemann Jr J. The effects of oral $CaCO_3$ loading and dietary calcium deprivation on plasma 1,25-dihydroxyvitamin D concentrations in healthy adults. J Clin Endocrinol Metab 1979;48:1008–16.

[5] Akeno N, Matsunuma A, Maeda T, Kawane T, Horiuchi N. Regulation of vitamin D-1alpha-hydroxylase and -24-hydroxylase expression by dexamethasone in mouse kidney. J Endocrinol 2000;164:339–48.

[6] Albert B, Johnson A, Lewis J, Raff M, Roberts K, Walter P. Molecular biology of the cell. New York: Garland Science, Taylor and Francis Group; 2002.

[7] Alvarez-Hernandez D, Naves M, Santamaria I, Menarguez J, Torregrosa V, Cannata J. Response of parathyroid glands to calcitriol in culture: is this response mediated by the genetic polymorphisms in vitamin D receptor? Kidney Int Suppl 2003; S19–22.

[8] Anast CS, Winnacker JL, Forte LR, Burns TW. Impaired release of parathyroid hormone in magnesium deficiency. J Clin Endocrinol Metab 1976;42:707–17.

[9] Araya Z, Hosseinpour F, Bodin K, Wikvall K. Metabolism of 25-hydroxyvitamin D3 by microsomal and mitochondrial vitamin D3 25-hydroxylases (CYP2D25 and CYP27A1): a novel reaction by CYP27A1. Biochim Biophys Acta 2003;1632:40–7.

[10] Armbrecht HJ, Boltz MA, Bruns ME. Effect of age and dietary calcium on intestinal calbindin D-9k expression in the rat. Arch Biochem Biophys 2003;420:194–200.

[11] Armbrecht HJ, Boltz MA, Christakos S, Bruns ME. Capacity of 1,25-dihydroxyvitamin D to stimulate expression of calbindin D changes with age in the rat. Arch Biochem Biophys 1998;352:159–64.

[12] Armbrecht HJ, Boltz MA, Kumar VB. Intestinal plasma membrane calcium pump protein and its induction by 1,25(OH)(2)D (3) decrease with age. Am J Physiol 1999;277:G41–7.

[13] Armbrecht HJ, Boltz MA, Wongsurawat N. Expression of plasma membrane calcium pump mRNA in rat intestine: effect of age and 1,25-dihydroxyvitamin D. Biochim Biophys Acta 1994;1195:110–4.

[14] Armbrecht HJ, Hodam TL, Boltz MA. Hormonal regulation of 25-hydroxyvitamin D3-1alpha-hydroxylase and 24-hydroxylase gene transcription in opossum kidney cells. Arch Biochem Biophys 2003;409:298–304.

[15] Askew F, Bourdillon R, Bruce H, Jenkins R, Webster T. The distillation of vitamin D. Proc R Soc B 1931;107:76–90.

[16] Bacskai BJ, Friedman PA. Activation of latent Ca^{2+} channels in renal epithelial cells by parathyroid hormone. Nature 1990;347:388–91.

[17] Bar A, Shani M, Fullmer CS, Brindak ME, Striem S. Modulation of chick intestinal and renal calbindin gene expression by dietary vitamin D3, 1,25-dihydroxyvitamin D3, calcium and phosphorus. Mol Cell Endocrinol 1990;72:23–31.

[18] Barley NF, Prathalingam SR, Zhi P, Legon S, Howard A, Walters JR. Factors involved in the duodenal expression of the human calbindin-D9k gene. Biochem J 1999;341:491–500.

[19] Barry EL, Gesek FA, Yu AS, Lytton J, Friedman PA. Distinct calcium channel isoforms mediate parathyroid hormone and chlorothiazide-stimulated calcium entry in transporting epithelial cells. J Membr Biol 1998;161:55–64.

[20] Berndt T, Craig TA, Bowe AE, Vassiliadis J, Reczek D, Finnegan R, et al. Secreted frizzled-related protein 4 is a potent tumor-derived phosphaturic agent. J Clin Invest 2003;112:785–94.

[21] Bhattacharyya MH, DeLuca HF. Subcellular location of rat liver calciferol-25-hydroxylase. Arch Biochem Biophys 1974;160: 58–62.

[22] Bianda T, Glatz Y, Rbouillon R, Froesch ER, Schmid C. Effects of short-term insulin-like growth factor-I (IGF-I) or growth hormone (GH) treatment on bone metabolism and on production of 1,25-dihydroxycholecalciferol in GH-deficient adults. J Clin Endocrinol Metab 1998;83:81–7.

[23] Bikle DD, Nemanic MK, Gee E, Elias P. 1,25-Dihydroxyvitamin D3 production by human keratinocytes. Kinetics and regulation. J Clin Invest 1986;78:557–66.

[24] Bilezikian JP, Canfield RE, Jacobs TP, Polay JS, D'Adamo AP, Eisman JA, et al. Response of 1alpha, 25-dihydroxyvitamin D3 to hypocalcemia in human subjects. N Engl J Med 1978;299:437–41.

[25] Bindels RJ, Hartog A, Timmermans J, Van Os CH. Active Ca^{2+} transport in primary cultures of rabbit kidney CCD: stimulation by 1,25-dihydroxyvitamin D3 and PTH. Am J Physiol 1991;261: F799–807.

[26] Biner HL, Arpin-Bott MP, Loffing J, Wang X, Knepper M, Hebert SC, et al. Human cortical distal nephron: distribution of electrolyte and water transport pathways. J Am Soc Nephrol 2002;13:836–47.

[27] Bjorkhem I, Hansson R, Holmberg I, Wikvall K. 25-Hydroxylation of vitamin D3 by a reconstituted system from rat liver microsomes. Biochem Biophys Res Commun 1979;90: 615–22.

[28] Bjorkhem I, Holmberg I. Assay and properties of a mitochondrial 25-hydroxylase active on vitamine D3. J Biol Chem 1978;253:842–9.

[29] Bland R, Walker EA, Hughes SV, Stewart PM, Hewison M. Constitutive expression of 25-hydroxyvitamin D3-1alpha-hydroxylase in a transformed human proximal tubule cell line: evidence for direct regulation of vitamin D metabolism by calcium. Endocrinology 1999;140:2027–34.

[30] Bland R, Zehnder D, Hewison M. Expression of 25-hydroxyvitamin D3-1alpha-hydroxylase along the nephron: new insights into renal vitamin D metabolism. Curr Opin Nephrol Hypertens 2000;9:17–22.

[31] Bland R, Zehnder D, Hughes SV, Ronco PM, Stewart PM, Hewison M. Regulation of vitamin D-1alpha-hydroxylase in a human cortical collecting duct cell line. Kidney Int 2001;60: 1277–86.

[32] Blunt JW, DeLuca HF. The synthesis of 25-hydroxycholecalciferol. A biologically active metabolite of vitamin D3. Biochemistry (Mosc) 1969;8:671–5.

[33] Blunt JW, DeLuca HF, Schnoes HK. 25-hydroxycholecalciferol. A biologically active metabolite of vitamin D3. Biochemistry (Mosc) 1968;7:3317–22.

[34] Blunt JW, Tanaka Y, DeLuca HF. The biological activity of 25-hydroxycholecalciferol, a metabolite of vitamin D3. Proc Natl Acad Sci USA 1968;61:1503–6.
[35] Bolt MJ, Wei M, Sitrin MD, Chun Li Y, Cao LP. Regulation of calbindin-D9k expression by 1,25-dihydroxyvitamin D3 and parathyroid hormone in mouse primary renal tubular cells. Arch Biochem Biophys 2002;400:118–24.
[36] Borke JL, Caride A, Verma AK, Penniston JT, Kumar R. Plasma membrane calcium pump and 28-kDa calcium binding protein in cells of rat kidney distal tubules. Am J Physiol 1989;257: F842–9.
[37] Borke JL, Minami J, Verma A, Penniston JT, Kumar R. Monoclonal antibodies to human erythrocyte membrane Ca^{++}-Mg^{++} adenosine triphosphatase pump recognize an epitope in the basolateral membrane of human kidney distal tubule cells. J Clin Invest 1987;80:1225–31.
[38] Borke JL, Minami J, Verma AK, Penniston JT, Kumar R. Co-localization of erythrocyte Ca^{++}-Mg^{++} ATPase and vitamin D-dependent 28-kDa-calcium binding protein. Kidney Int 1988;34:262–7.
[39] Borke JL, Penniston JT, Kumar R. Recent advances in calcium transport by the kidney. Semin Nephrol 1990;10:15–23.
[40] Bouhtiauy I, Lajeunesse D, Brunette MG. The mechanism of parathyroid hormone action on calcium reabsorption by the distal tubule. Endocrinology 1991;128:251–8.
[41] Bouillon R, Muls E, De Moor P. Influence of thyroid function on the serum concentration of 1,25-dihydroxyvitamin D3. J Clin Endocrinol Metab 1980;51:793–7.
[42] Bouillon R, Van Cromphaut S, Carmeliet G. Intestinal calcium absorption: molecular vitamin D mediated mechanisms. J Cell Biochem 2003;88:332–9.
[43] Boyle IT, Gray RW, Omdahl JL, DeLuca HF. Calcium control of the in vivo biosynthesis of 1,25-dihydroxyvitamin D_3: Nicolaysen's endogenous factor. In: Taylor S, editor. Proceeding of the international symposium on endocrinology. London: Heinemann; 1972. p. 468–76.
[44] Brenza HL, DeLuca HF. Regulation of 25-hydroxyvitamin D3 1alpha-hydroxylase gene expression by parathyroid hormone and 1,25-dihydroxyvitamin D3. Arch Biochem Biophys 2000;381:143–52.
[45] Brenza HL, Kimmel-Jehan C, Jehan F, Shinki T, Wakino S, Anazawa H, et al. Parathyroid hormone activation of the 25-hydroxyvitamin D3-1alpha-hydroxylase gene promoter. Proc Natl Acad Sci USA 1998;95:1387–91.
[46] Brown AJ, Zhong M, Finch J, Ritter C, Slatopolsky E. The roles of calcium and 1,25-dihydroxyvitamin D3 in the regulation of vitamin D receptor expression by rat parathyroid glands. Endocrinology 1995;136:1419–25.
[47] Brown EM. Extracellular Ca^{2+} sensing, regulation of parathyroid cell function, and role of Ca^{2+} and other ions as extracellular (first) messengers. Physiol Rev 1991;71:371–411.
[48] Brun P, Dupret JM, Perret C, Thomasset M, Mathieu H. Vitamin D-dependent calcium-binding proteins (CaBPs) in human fetuses: comparative distribution of 9K CaBP mRNA and 28K CaBP during development. Pediatr Res 1987;21:362–7.
[49] Brustad M, Alsaker E, Engelsen O, Aksnes L, Lund E. Vitamin D status of middle-aged women at 65-71 degrees N in relation to dietary intake and exposure to ultraviolet radiation. Public Health Nutr 2004;7:327–35.
[50] Buchan AM, Squires PE, Ring M, Meloche RM. Mechanism of action of the calcium-sensing receptor in human antral gastrin cells.[see comment]. Gastroenterology 2001;120:1128–39.
[51] Buckle RM, Care AD, Cooper CW, Gitelman HJ. The influence of plasma magnesium concentration on parathyroid hormone secretion. J Endocrinol 1968;42:529–34.
[52] Burgos-Trinidad M, Ismail R, Ettinger RA, Prahl JM, DeLuca HF. Immunopurified 25-hydroxyvitamin D 1 alpha-hydroxylase and 1,25-dihydroxyvitamin D 24-hydroxylase are closely related but distinct enzymes. J Biol Chem 1992;267:3498–505.
[53] Butler SJ, Payne RB, Gunn IR, Burns J, Paterson CR. Correlation between serum ionised calcium and serum albumin concentrations in two hospital populations. Br Med J (Clin Res Ed) 1984;289:948–50.
[54] Cai Q, Hodgson SF, Kao PC, Lennon VA, Klee GG, Zinsmiester AR, et al. Brief report: inhibition of renal phosphate transport by a tumor product in a patient with oncogenic osteomalacia. [see comment]. N Engl J Med 1994;330:1645–9.
[55] Calvo MS, Heath III H. Acute effects of oral phosphate-salt ingestion on serum phosphorus, serum ionized calcium, and parathyroid hormone in young adults. Am J Clin Nutr 1988;47:1025–9.
[56] Calvo MS, Kumar R, Heath III H. Elevated secretion and action of serum parathyroid hormone in young adults consuming high phosphorus, low calcium diets assembled from common foods. J Clin Endocrinol Metab 1988;66:823–9.
[57] Canaff L, Petit JL, Kisiel M, Watson PH, Gascon-Barre M, Hendy GN. Extracellular calcium-sensing receptor is expressed in rat hepatocytes. Coupling to intracellular calcium mobilization and stimulation of bile flow. J Biol Chem 2001;276:4070–9.
[58] Caride AJ, Chini EN, Homma S, Dousa TP, Penniston JT. mRNAs coding for the calcium-sensing receptor along the rat nephron: effect of a low-phosphate diet. Kidney Blood Press Res 1998;21:305–9.
[59] Caride AJ, Chini EN, Yamaki M, Dousa TP, Penniston JT. Unique localization of mRNA encoding plasma membrane Ca^{2+} pump isoform 3 in rat thin descending loop of Henle. Am J Physiol 1995;269:F681–5.
[60] Caride AJ, Filoteo AG, Enyedi A, Verma AK, Penniston JT. Detection of isoform 4 of the plasma membrane calcium pump in human tissues by using isoform-specific monoclonal antibodies. Biochem J 1996;316:353–9.
[61] Carre M, Ayigbede O, Miravet L, Rasmussen H. The effect of Prednisolone upon the metabolism and action of 25-hydroxy- and 1,25-dihydroxyvitamin D3. Proc Natl Acad Sci USA 1974;71:2996–3000.
[62] Castillo L, Tanaka Y, DeLuca HF, Sunde ML. The stimulation of 25-hydroxyvitamin D3-1 alpha-hydroxylase by estrogen. Arch Biochem Biophys 1977;179:211–7.
[63] Cetani F, Lemmi M, Cervia D, Borsari S, Cianferotti L, Pardi E, et al. Identification and functional characterization of loss-of-function mutations of the calcium-sensing receptor in four Italian kindreds with familial hypocalciuric hypercalcemia. Eur J Endocrinol 2009;160:481–9.
[64] Chang W, Tu C, Chen TH, Komuves L, Oda Y, Pratt SA, et al. Expression and signal transduction of calcium-sensing receptors in cartilage and bone. Endocrinology 1999;140:5883–93.
[65] Chattopadhyay N. Biochemistry, physiology and pathophysiology of the extracellular calcium-sensing receptor. Int J Biochem Cell Biol 2000;32:789–804.
[66] Chattopadhyay N, Cheng I, Rogers K, Riccardi D, Hall A, Diaz R, et al. Identification and localization of extracellular Ca^{2+}-sensing receptor in rat intestine. Am J Physiol 1998;274:G122–30.
[67] Chattopadhyay N, Mithal A, Brown EM. The calcium-sensing receptor: a window into the physiology and pathophysiology of mineral ion metabolism. Endocr Rev 1996;17:289–307.
[68] Chattopadhyay N, Ye C, Singh DP, Kifor O, Vassilev PM, Shinohara T, et al. Expression of extracellular calcium-sensing receptor by human lens epithelial cells [erratum appears in *Biochem Biophys Res Commun*. 1997 Aug 18;237(2):481] Biochem Biophys Res Commun 1997;233:801–5.

[69] Chen J, Zhang J, Lin S. Down-regulation of PTH/PTHrP receptor in the kidney of patients with renal impairment. Chin Med J (Engl) 1998;111:24–7.
[70] Chen ML, Boltz M, Christakos S, Armbrecht HJ. Age-related alterations in calbindin-D28K induction by 1,25-dihydroxyvitamin D3 in primary cultures of rat renal tubule cells. Endocrinology 1992;130:3295–300.
[71] Cheng I, Klingensmith ME, Chattopadhyay N, Kifor O, Butters RR, Soybel DI, et al. Identification and localization of the extracellular calcium-sensing receptor in human breast. J Clin Endocrinol Metab 1998;83:703–7.
[72] Cheng I, Qureshi I, Chattopadhyay N, Qureshi A, Butters RR, Hall AE, et al. Expression of an extracellular calcium-sensing receptor in rat stomach. Gastroenterology 1999;116:118–26.
[73] Chick H, Palzell E, Hume E. Studies of rickets in Vienna 1919–1922 *[Special Report No 77]* Medical research council. Vienna: Medical Research Council; 1923.
[74] Clemens TL, Adams JS, Henderson SL, Holick MF. Increased skin pigment reduces the capacity of skin to synthesise vitamin D3. Am J Clin Nutr 1994;60:619–30.
[75] Clemens TL, McGlade SA, Garrett KP, Craviso GL, Hendy GN. Extracellular calcium modulates vitamin D-dependent calbindin-D28K gene expression in chick kidney cells. Endocrinology 1989;124:1582–4.
[76] Coltrera MD, Potts Jr JT, Rosenblatt M. Identification of a renal receptor for parathyroid hormone by photoaffinity radiolabeling using a synthetic analogue. J Biol Chem 1981;256:10555–9.
[77] Condamine L, Menaa C, Vrtovsnik F, Vztovsnik F, Friedlander G, Garabedian M. Local action of phosphate depletion and insulin-like growth factor 1 on in vitro production of 1,25-dihydroxyvitamin D by cultured mammalian kidney cells [erratum appears in J Clin Invest 1995 Jan;95(1):following 434] J Clin Invest 1994;94:1673–9.
[78] Conigrave AD, Mun HC, Delbridge L, Quinn SJ, Wilkinson M, Brown EM. L-amino acids regulate parathyroid hormone secretion. J Biol Chem 2004;279:38151–9.
[79] Cornish J, Callon KE, Bava U, Kamona SA, Cooper GJ, Reid IR. Effects of calcitonin, amylin, and calcitonin gene-related peptide on osteoclast development. Bone 2001;29:162–8.
[80] Craviso GL, Garrett KP, Clemens TL. 1,25-Dihydroxyvitamin D3 induces the synthesis of vitamin D-dependent calcium-binding protein in cultured chick kidney cells. Endocrinology 1987;120:894–902.
[81] D'Souza-Li L, Canaff L, Janicic N, Cole DE, Hendy GN. An acceptor splice site mutation in the calcium-sensing receptor (CASR) gene in familial hypocalciuric hypercalcemia and neonatal severe hyperparathyroidism. Hum Mutat 2001;18:411–21.
[82] D'Souza-Li L, Yang B, Canaff L, Bai M, Hanley DA, Bastepe M, et al. Identification and functional characterization of novel calcium-sensing receptor mutations in familial hypocalciuric hypercalcemia and autosomal dominant hypocalcemia. J Clin Endocrinol Metab 2002;87:1309–18.
[83] Darwish HM, DeLuca HF. Identification of a 1,25-dihydroxyvitamin D3-response element in the 5′-flanking region of the rat calbindin D-9k gene. Proc Natl Acad Sci USA 1992;89:603–7.
[84] De Beur SM, Finnegan RB, Vassiliadis J, Cook B, Barberio D, Estes S, et al. Tumors associated with oncogenic osteomalacia express genes important in bone and mineral metabolism. J Bone Miner Res 2002;17:1102–10.
[85] de Vernejoul MC, Horowitz M, Demignon J, Neff L, Baron R. Bone resorption by isolated chick osteoclasts in culture is stimulated by murine spleen cell supernatant fluids (osteoclast-activating factor) and inhibited by calcitonin and prostaglandin E2. J Bone Miner Res 1988;3:69–80.
[86] DeLuca HF. Historical perspective. In: Feldman D, Pike JW, Glorieux FH, editors. Vitamin D. 2nd ed. Boston: Academic Press; 2005. p. 3–14.
[87] DeLuca HF, Schnoes HK. Metabolism and mechanism of action of vitamin D. Annu Rev Biochem 1976;45:631–66.
[88] DeLuca HF, Schnoes HK. Vitamin D: recent advances. Annu Rev Biochem. 1983;52:411–39.
[89] Demay MB, Kiernan MS, DeLuca HF, Kronenberg HM. Sequences in the human parathyroid hormone gene that bind the 1,25-dihydroxyvitamin D3 receptor and mediate transcriptional repression in response to 1,25-dihydroxyvitamin D3. Proc Natl Acad Sci USA 1992;89:8097–101.
[90] Dempster DW, Hughes-Begos CE, Plavetic-Chee K, Brandao-Burch A, Cosman F, Nieves J, et al. Normal human osteoclasts formed from peripheral blood monocytes express PTH type 1 receptors and are stimulated by PTH in the absence of osteoblasts. J Cell Biochem 2005;95:139–48.
[91] den Dekker E, Hoenderop JG, Nilius B, Bindels RJ. The epithelial calcium channels, TRPV5 & TRPV6: from identification towards regulation. Cell Calcium. 2003;33:497–507.
[92] Diaz L, Arranz C, Avila E, Halhali A, Vilchis F, Larrea F. Expression and activity of 25-hydroxyvitamin D-1 alpha-hydroxylase are restricted in cultures of human syncytiotrophoblast cells from preeclamptic pregnancies. J Clin Endocrinol Metab 2002;87:3876–82.
[93] Drezner MK, Neelon FA, Haussler M, McPherson HT, Lebovitz HE. 1,25-Dihydroxycholecalciferol deficiency: the probable cause of hypocalcemia and metabolic bone disease in pseudohypoparathyroidism. J Clin Endocrinol Metab 1976;42:621–8.
[94] Dusso AS, Finch J, Brown A, Ritter C, Delmez J, Schreiner G, et al. Extrarenal production of calcitriol in normal and uremic humans. J Clin Endocrinol Metab 1991;72:157–64.
[95] Eastell R, Yergey AL, Vieira NE, Cedel SL, Kumar R, Riggs BL. Interrelationship among vitamin D metabolism, true calcium absorption, parathyroid function, and age in women: evidence of an age-related intestinal resistance to 1,25-dihydroxyvitamin D action. J Bone Miner Res 1991;6:125–32.
[96] Ebeling PR, Yergey AL, Vieira NE, Burritt MF, O'Fallon WM, Kumar R, et al. Influence of age on effects of endogenous 1,25-dihydroxyvitamin D on calcium absorption in normal women. Calcif Tissue Int 1994;55:330–4.
[97] Edwards RM, Contino LC, Gellai M, Brooks DP. Parathyroid hormone-1 receptor down-regulation in kidneys from rats with chronic renal failure. Pharmacology 2001;62:243–7.
[98] Ejima E, Fujiyama K, Kiriyama T, Ide A, Sera N, Tominaga T, et al. Parathyroidectomy for primary hyperparathyroidism induces positive uncoupling and increases bone mineral density in cancellous bones. Clin Endocrinol (Oxf) 2000;52:203–9.
[99] Eskildsen PC, Lund B, Sorensen OH, Bishop JE, Norman AW. Acromegaly and vitamin D metabolism: effect of bromocriptine treatment. J Clin Endocrinol Metab 1979;49:484–6.
[100] Esvelt RP, Schnoes HK, DeLuca HF. Vitamin D3 from rat skins irradiated in vitro with ultraviolet light. Arch Biochem Biophys 1978;188:282–6.
[101] Eyles DW, Smith S, Kinobe R, Hewison M, McGrath JJ. Distribution of the vitamin D receptor and 1 alpha-hydroxylase in human brain. J Chem Neuroanat 2005;29:21–30.
[102] Fatemi S, Ryzen E, Flores J, Endres DB, Rude RK. Effect of experimental human magnesium depletion on parathyroid hormone secretion and 1,25-dihydroxyvitamin D metabolism. J Clin Endocrinol Metab 1991;73:1067–72.
[103] Favus MJ, Walling MW, Kimberg DV. Effects of 1,25-dihydroxycholecalciferol on intestinal calcium transport in cortisone-treated rats. J Clin Invest 1973;52:1680–5.

[104] Feher JJ, Wasserman RH. Intestinal calcium-binding protein and calcium absorption in cortisol-treated chicks: effects of vitamin D3 and 1,25-dihydroxyvitamin D3. Endocrinology 1979;104:547–51.
[105] Feldman RS, Krieger NS, Tashjian Jr AH. Effects of parathyroid hormone and calcitonin on osteoclast formation in vitro. Endocrinology 1980;107:1137–43.
[106] Ferment O, Garnier PE, Touitou Y. Comparison of the feedback effect of magnesium and calcium on parathyroid hormone secretion in man. J Endocrinol 1987;113:117–22.
[107] Finkelstein JS, Hayes A, Hunzelman JL, Wyland JJ, Lee H, Neer RM. The effects of parathyroid hormone, alendronate, or both in men with osteoporosis. N Engl J Med 2003;349: 1216–26.
[108] Firsov D, Bellanger AC, Marsy S, Elalouf JM. Quantitative RT-PCR analysis of calcitonin receptor mRNAs in the rat nephron. Am J Physiol 1995;269:F702–9.
[109] Fogh-Andersen N, Bjerrum PJ, Siggaard-Andersen O. Ionic binding, net charge, and Donnan effect of human serum albumin as a function of pH. Clin Chem 1993;39:48–52.
[110] Fraher LJ, Hendy GN, Chung UI, Kisiel M, Natale BV, Hodsman AB, et al. Nuclear localization of the type 1 PTH/PTHrP receptor in rat tissues. J Bone Miner Res 2000;15:1033–44.
[111] Fraser DR, Kodicek E. Regulation of 25-hydroxycholecalciferol-1-hydroxylase activity in kidney by parathyroid hormone. Nature New Biol 1973;241:163–6.
[112] Fraser DR, Kodicek E. Unique biosynthesis by kidney of a biological active vitamin D metabolite. Nature 1970;228:764–6.
[113] Freichel M, Zink-Lorenz A, Holloschi A, Hafner M, Flockerzi V, Raue F. Expression of a calcium-sensing receptor in a human medullary thyroid carcinoma cell line and its contribution to calcitonin secretion. Endocrinology 1996;137:3842–8.
[114] Friedman PA, Coutermarsh BA, Kennedy SM, Gesek FA. Parathyroid hormone stimulation of calcium transport is mediated by dual signaling mechanisms involving protein kinase A and protein kinase C. Endocrinology 1996;137:13–20.
[115] Friedrich M, Diesing D, Cordes T, Fischer D, Becker S, Chen TC, et al. Analysis of 25-hydroxyvitamin D3-1alpha-hydroxylase in normal and malignant breast tissue. Anticancer Res 2006;26:2615–20.
[116] Fudge NJ, Kovacs CS. Physiological studies in heterozygous calcium sensing receptor (CaSR) gene-ablated mice confirm that the CaSR regulates calcitonin release in vivo. BMC Physiology 2004;4:5.
[117] Gagnon AM, Simboli-Campbell M, Welsh JE. Induction of calbindin D-28 K in madin-darby bovine kidney cells by 1,25(OH) 2D3. Kidney Int 1994;45:95–102.
[118] Garabedian M, Holick MF, Deluca HF, Boyle IT. Control of 25-hydroxycholecalciferol metabolism by parathyroid glands. Proc Natl Acad Sci USA 1972;69:1673–6.
[119] Garfia B, Canadillas S, Canalejo A, Luque F, Siendones E, Quesada M, et al. Regulation of parathyroid vitamin D receptor expression by extracellular calcium. J Am Soc Nephrol 2002;13:2945–52.
[120] Garrett JE, Tamir H, Kifor O, Simin RT, Rogers KV, Mithal A, et al. Calcitonin-secreting cells of the thyroid express an extracellular calcium receptor gene. Endocrinology 1995;136: 5202–11.
[121] Gartenberg F, Jacobs TP, Shane E, Siris E, Staron RB, McMahon DJ, et al. Increased bone mineral density after parathyroidectomy in primary hyperparathyroidism. J Clin Endocrinol Metab 1995;80:729–34.
[122] Gertner JM, Horst RL, Broadus AE, Rasmussen H, Genel M. Parathyroid function and vitamin D metabolism during human growth hormone replacement. J Clin Endocrinol Metab 1979;49:185–8.
[123] Gesek FA, Friedman PA. Calcitonin stimulates calcium transport in distal convoluted tubule cells. Am J Physiol 1993;264: F744–51.
[124] Gesek FA, Friedman PA. On the mechanism of parathyroid hormone stimulation of calcium uptake by mouse distal convoluted tubule cells. J Clin Invest 1992;90:749–58.
[125] Ghazarian JG, DeLuca HF. 25-Hydroxycholecalciferol-1-hydroxylase: a specific requirement for NADPH and a hemoprotein component in chick kidney mitochondria. Arch Biochem Biophys 1974;160:63–72.
[126] Ghazarian JG, Jefcoate CR, Knutson JC, Orme-Johnson WH, DeLuca HF. Mitochondrial cytochrome p450. A component of chick kidney 25-hydrocholecalciferol-1alpha-hydroxylase. J Biol Chem 1974;249:3026–33.
[127] Ghijsen WE, Van Os CH. 1 alpha, 25-Dihydroxy-vitamin D-3 regulates ATP-dependent calcium transport in basolateral plasma membranes of rat enterocytes. Biochim Biophys Acta 1982;689:170–2.
[128] Glendenning P, Ratajczak T, Dick IM, Prince RL. Calcitriol upregulates expression and activity of the 1b isoform of the plasma membrane calcium pump in immortalized distal kidney tubular cells. Arch Biochem Biophys 2000;380:126–32.
[129] Gordon CM, DePeter KC, Feldman HA, Grace E, Emans SJ. Prevalence of vitamin D deficiency among healthy adolescents. Arch Pediatr Adolesc Med 2004;158:531–7.
[130] Gray RW, Wilz DR, Caldas AE, Lemann Jr J. The importance of phosphate in regulating plasma 1,25-OH_2-vitamin D levels in humans: studies in healthy subjects in calcium-stone formers and in patients with primary hyperparathyroidism. J Clin Endocrinol Metab 1977;45:299–306.
[131] Habener JF, Potts Jr JT. Relative effectiveness of magnesium and calcium on the secretion and biosynthesis of parathyroid hormone in vitro. Endocrinology 1976;98:197–202.
[132] Haddad JG, Matsuoka LY, Hollis BW, Hu YZ, Wortsman J. Human plasma transport of vitamin D after its endogenous synthesis. J Clin Invest 1993;91:2552–5.
[133] Hall AK, Norman AW. Regulation of calbindin-D28K gene expression by 1,25-dihydroxyvitamin D3 in chick kidney. J Bone Miner Res 1990;5:325–30.
[134] Hanai H, Ishida M, Liang CT, Sacktor B. Parathyroid hormone increases sodium/calcium exchange activity in renal cells and the blunting of the response in aging. J Biol Chem 1986;261: 5419–25.
[135] Hansson R, Holmberg I, Wikvall K. 25-Hydroxylation vitamin D3 and side chain hydroxylations of 5 beta-cholestane-3 alpha, 7 alpha, 12 alpha-triol by purified rabbit and rat liver microsomal cytochromes P-450. J Biol Chem 1981;256:4345–9.
[136] Hatem S, Hoyaux D, De Decker V, Appelboom T, Pochet R, Steinfeld S. Expression of calcium-sensing receptor in human minor salivary glands. Clin Exp Rheumatol 2002;20:576.
[137] Haussler MR, Myrtle JF, Norman AW. The association of a metabolite of vitamin D3 with intestinal mucosa chromatin in vivo. J Biol Chem 1968;243:4055–64.
[138] Heaney RP, Recker RR. Determinants of endogenous fecal calcium in healthy women. J Bone Miner Res 1994;9:1621–7.
[139] Hebden C, Smalt R, Chambers T, Pondel MD. Multiple promoters regulate human calcitonin receptor gene expression. Biochem Biophys Res Commun 2000;272:738–43.
[140] Hemmingsen C, Staun M, Lewin E, Nielsen PK, Olgaard K. Effect of vitamin D metabolites and analogs on renal and intestinal calbindin-D in the rat. Calcif Tissue Int 1996;59: 371–6.

[141] Hemmingsen C, Staun M, Olgaard K. The effect of 1,25-vitamin D3 on calbindin-D and calcium-metabolic variables in the rat. Pharmacol Toxicol 1998;82:118–21.
[142] Hemmingsen C, Staun M, Olgaard K. Effects of magnesium on renal and intestinal calbindin-D. Miner Electrolyte Metab 1994;20:265–73.
[143] Hendy GN, D'Souza-Li L, Yang B, Canaff L, Cole DE. Mutations of the calcium-sensing receptor (CASR) in familial hypocalciuric hypercalcemia, neonatal severe hyperparathyroidism, and autosomal dominant hypocalcemia. Hum Mutat 2000;16:281–96.
[144] Henry HL. Regulation of the hydroxylation of 25-hydroxyvitamin D3 in vivo and in primary cultures of chick kidney cells. J Biol Chem 1979;254:2722–9.
[145] Henry HL. Regulation of the synthesis of 1,25-dihydroxyvitamin D3 and 24,25-dihydroxyvitamin D3 int he kidney cell culture. In: Kumar R, editor. Vitamin D: Basic and clinical aspects. Boston: Nijhoff; 1984. p. 152–74.
[146] Hess A, Weinstock M. Antirachitic properties imparted to lettuce and to growing wheat light ultraviolet irradiation. Proc Soc Exp Biol Med 1924;22:5–6.
[147] Higashi T, Shimada K, Toyo'oka T. Advances in determination of vitamin D related compounds in biological samples using liquid chromatography-mass spectrometry: a review. J Chromatogr B Analyt Technol Biomed Life Sci 2010;878:1654–61.
[148] Hoenderop JG, Dardenne O, Van Abel M, Van Der Kemp AW, Van Os CH, St-Arnaud R, et al. Modulation of renal Ca^{2+} transport protein genes by dietary Ca^{2+} and 1,25-dihydroxyvitamin D3 in 25-hydroxyvitamin D3-1alpha-hydroxylase knockout mice. FASEB J 2002;16:1398–406.
[149] Hoenderop JG, De Pont JJ, Bindels RJ, Willems PH. Hormone-stimulated Ca^{2+} reabsorption in rabbit kidney cortical collecting system is cAMP-independent and involves a phorbol ester-insensitive PKC isotype. Kidney Int 1999;55:225–33.
[150] Hoenderop JG, Muller D, Van Der Kemp AW, Hartog A, Suzuki M, Ishibashi K, et al. Calcitriol controls the epithelial calcium channel in kidney. J Am Soc Nephrol 2001;12:1342–9.
[151] Hoenderop JG, Nilius B, Bindels RJ. Epithelial calcium channels: from identification to function and regulation. Pflugers Arch 2003;446:304–8.
[152] Hoenderop JG, Nilius B, Bindels RJ. Molecular mechanism of active Ca2+ reabsorption in the distal nephron. Annu Rev Physiol 2002;64:529–49.
[153] Hoenderop JG, van der Kemp AW, Hartog A, van de Graaf SF, van Os CH, Willems PH, et al. Molecular identification of the apical Ca^{2+} channel in 1, 25-dihydroxyvitamin D3-responsive epithelia. J Biol Chem 1999;274:8375–8.
[154] Hoenderop JG, van der Kemp AW, Urben CM, Strugnell SA, Bindels RJ. Effects of vitamin D compounds on renal and intestinal Ca^{2+} transport proteins in 25-hydroxyvitamin D3-1alpha-hydroxylase knockout mice. Kidney Int 2004;66:1082–9.
[155] Hofbauer LC, Heufelder AE. Clinical review 114: hot topic. The role of receptor activator of nuclear factor-kappaB ligand and osteoprotegerin in the pathogenesis and treatment of metabolic bone diseases. J Clin Endocrinol Metab 2000;85:2355–63.
[156] Hofbauer LC, Heufelder AE. Role of receptor activator of nuclear factor-kappaB ligand and osteoprotegerin in bone cell biology. J Mol Med 2001;79:243–53.
[157] Holick MF. The cutaneous photosynthesis of previtamin D3: a unique photoendocrine system. J Invest Dermatol 1981;77: 51–8.
[158] Holick MF, Garabedian M, DeLuca HF. 1,25-dihydroxycholecalciferol: metabolite of vitamin D3 active on bone in anephric rats. Science 1972;176:1146–7.
[159] Holick MF, MacLaughlin JA, Clark MB, Holick SA, Potts Jr JT, Anderson RR, et al. Photosynthesis of previtamin D3 in human skin and the physiologic consequences. Science 1980;210:203–5.
[160] Holick MF, Schnoes HK, DeLuca HF. Identification of 1,25-dihydroxycholecalciferol, a form of vitamin D3 metabolically active in the intestine. Proc Natl Acad Sci USA 1971;68:803–4.
[161] Holick MF, Schnoes HK, DeLuca HF, Suda T, Cousins RJ. Isolation and identification of 1,25-dihydroxycholecalciferol. A metabolite of vitamin D active in intestine. *Biochemistry* (Mosc) 1971;10:2799–804.
[162] Holmberg I, Berlin T, Ewerth S, Bjorkhem I. 25-Hydroxylase activity in subcellular fractions from human liver. Evidence for different rates of mitochondrial hydroxylation of vitamin D2 and D3. Scand J Clin Lab Invest 1986;46:785–90.
[163] Holmberg I, Kristiansen T, Sturen M. Determination of 25-hydroxyvitamin D3 in serum by high performance liquid chromatography and isotope dilution-mass spectrometry. Scand J Clin Lab Invest 1984;44:275–82.
[164] Hoppener JW, Steenbergh PH, Zandberg J, Bakker E, Pearson PL, Geurts van Kessel AH, et al. Localization of the polymorphic human calcitonin gene on chromosome 11. Hum Genet 1984;66:309–12.
[165] Horst RL, Shepard RM, Jorgensen NA, DeLuca HF. The determination of the vitamin D metabolites on a single plasma sample: changes during parturition in dairy cows. Arch Biochem Biophys 1979;192:512–23.
[166] Horwood NJ, Elliott J, Martin TJ, Gillespie MT. Osteotropic agents regulate the expression of osteoclast differentiation factor and osteoprotegerin in osteoblastic stromal cells. Endocrinology 1998;139:4743–6.
[167] Hosseinpour F, Ibranovic I, Tang W, Wikvall K. 25-Hydroxylation of vitamin D3 in primary cultures of pig hepatocytes: evidence for a role of both CYP2D25 and CYP27A1. Biochem Biophys Res Commun 2003;303:877–83.
[168] House MG, Kohlmeier L, Chattopadhyay N, Kifor O, Yamaguchi T, Leboff MS, et al. Expression of an extracellular calcium-sensing receptor in human and mouse bone marrow cells. J Bone Miner Res 1997;12:1959–70.
[169] Howard A, Legon S, Spurr NK, Walters JR. Molecular cloning and chromosomal assignment of human calbindin-D9k. Biochem Biophys Res Commun 1992;185:663–9.
[170] Howard A, Legon S, Walters JR. Human and rat intestinal plasma membrane calcium pump isoforms. Am J Physiol 1993;265:G917–25.
[171] Howard A, Legon S, Walters JR. Plasma membrane calcium pump expression in human placenta and small intestine. Biochem Biophys Res Commun 1992;183:499–505.
[172] Howard GA, Turner RT, Sherrard DJ, Baylink DJ. Human bone cells in culture metabolize 25-hydroxyvitamin D3 to 1,25-dihydroxyvitamin D3 and 24,25-dihydroxyvitamin D3. J Biol Chem 1981;256:7738–40.
[173] Huang YC, Christakos S. Modulation of rat calbindin-D28 gene expression by 1,25-dihydroxyvitamin D3 and dietary alteration [erratum appears in Mol Endocrinol 1988;2:1236] Mol Endocrinol 1988;2:928–35.
[174] Huldshinsky K. Heilung von rachitis durch kunstliche hohensonne. Deut Med Wochschr 1919;45:712–3.
[175] Hurley DL, Tiegs RD, Wahner HW, Heath III H. Axial and appendicular bone mineral density in patients with long-term deficiency or excess of calcitonin. N Engl J Med 1987;317:537–41.
[176] Ikegame M, Rakopoulos M, Martin TJ, Moseley JM, Findlay DM. Effects of continuous calcitonin treatment on osteoclast-like cell development and calcitonin receptor expression in

mouse bone marrow cultures. J Bone Miner Res 1996;11: 456–65.
[177] Inaba M, Okuno S, Imanishi Y, Nishizawa Y, Morii H. Magnesium deficiency enhances secretion of parathyroid hormone in normal and 5/6-nephrectomized uremic rats. J Endocrinol Invest 1992;15:135–42.
[178] Iqbal SJ, Giles M, Ledger S, Nanji N, Howl T. Need for albumin adjustments of urgent total serum calcium. Lancet 1988;2:1477–8.
[179] Itami A, Kato M, Komoto I, Doi R, Hosotani R, Shimada Y, et al. Human gastrinoma cells express calcium-sensing receptor. Life Sci 2001;70:119–29.
[180] Jastrup B, Mosekilde L, Melsen F, Lund B, Sorensen OH. Serum levels of vitamin D metabolites and bone remodelling in hyperthyroidism. Metabolism 1982;31:126–32.
[181] Jobert AS, Fernandes I, Turner G, Coureau C, Prie D, Nissenson RA, et al. Expression of alternatively spliced isoforms of the parathyroid hormone (PTH)/PTH-related peptide receptor messenger RNA in human kidney and bone cells. Mol Endocrinol 1996;10:1066–76.
[182] Johnson MA, Davey A, Park S, Hausman DB, Poon LW, Georgia Centenarian S. Age, race and season predict vitamin D status in African American and white octogenarians and centenarians. J Nutr Health Aging 2008;12:690–5.
[183] Jonsson KB, Zahradnik R, Larsson T, White KE, Sugimoto T, Imanishi Y, et al. Fibroblast growth factor 23 in oncogenic osteomalacia and X-linked hypophosphatemia.[see comment]. N Engl J Med 2003;348:1656–63.
[184] Juppner H, Hesch RD. Parathormone receptor binding and the influence of membrane degradation of the hormone. J Immunoassay 1980;1:39–55.
[185] Juttmann JR, Visser TJ, Buurman C, de Kam E, Birkenhager JC. Seasonal fluctuations in serum concentrations of vitamin D metabolites in normal subjects. Br Med J (Clin Res Ed) 1981;282:1349–52.
[186] Kameda T, Mano H, Yamada Y, Takai H, Amizuka N, Kobori M, et al. Calcium-sensing receptor in mature osteoclasts, which are bone resorbing cells. Biochem Biophys Res Commun 1998;245:419–22.
[187] Kawashima H, Torikai S, Kurokawa K. Calcitonin selectively stimulates 25-hydroxyvitamin D3-1 alpha-hydroxylase in proximal straight tubule of rat kidney. Nature 1981;291:327–9.
[188] Keating Jr FR, Jones JD, Elveback LR, Randall RV. The relation of age and sex to distribution of values in healthy adults of serum calcium, inorganic phosphorus, magnesium, alkaline phosphatase, total proteins, albumin, and blood urea. J Lab Clin Med 1969;73:825–34.
[189] Kendrick NC, Bishop CW, DeLuca HF. Multiple forms of vitamin D-dependent calcium-binding protein in rat kidney. J Biol Chem 1984;259:12691–5.
[190] Khanal RC, Nemere I. Regulation of intestinal calcium transport. Annu Rev Nutr 2008;28:179–96.
[191] Kifor O, Moore Jr FD, Delaney M, Garber J, Hendy GN, Butters R, et al. A syndrome of hypocalciuric hypercalcemia caused by autoantibodies directed at the calcium-sensing receptor. J Clin Endocrinol Metab 2003;88:60–72.
[192] Kip SN, Strehler EE. Vitamin D3 upregulates plasma membrane Ca^{2+}-ATPase expression and potentiates apico-basal Ca^{2+} flux in MDCK cells. Am J Physiol Renal Physiol 2004;286: F363–9.
[193] Klibanski A, Arnold AL, Toth TL, Hornstein MD, Neer RM, Finkelstein JS. Prevention of estrogen deficiency-related bone loss with human parathyroid hormone-(1-34): a randomized controlled trial. JAMA 1998;280:1067–73.
[194] Komoto I, Kato M, Itami A, Shimada Y, Doi R, Hosotani R, et al. Expression and function of the calcium-sensing receptor in pancreatic islets and insulinoma cells. Pancreas 2003;26:178–84.
[195] Komuves L, Oda Y, Tu CL, Chang WH, Ho-Pao CL, Mauro T, et al. Epidermal expression of the full-length extracellular calcium-sensing receptor is required for normal keratinocyte differentiation. J Cell Physiol 2002;192:45–54.
[196] Kragh-Hansen U, Vorum H. Quantitative analyses of the interaction between calcium ions and human serum albumin. Clin Chem 1993;39:202–8.
[197] Kremer R, Goltzman D. Parathyroid hormone stimulates mammalian renal 25-hydroxyvitamin D3-1 alpha-hydroxylase in vitro. Endocrinology 1982;110:294–6.
[198] Krisinger J, Strom M, Darwish HM, Perlman K, Smith C, DeLuca HF. Induction of calbindin-D 9k mRNA but not calcium transport in rat intestine by 1,25-dihydroxyvitamin D3 24-homologs. J Biol Chem 1991;266:1910–3.
[199] Kronenberg HM, Bringhurst FR, Segre GV, Potts Jr JT. Parathyroid hormone biosynthesis and metabolism. In: Bilezikian JP, editor. The parathyroids: Basic and clinical concepts. New York: Raven Press; 1994. p. 125–37.
[200] Kumar R. Calcium disorders. In: Kokko J, Tannen R, editors. Fluids and electrolytes. 3rd ed. Philadelphia: Saunders; 1996. p. 391–419.
[201] Kumar R. Calcium transport in epithelial cells of the intestine and kidney. J Cell Biochem 1995;57:392–8.
[202] Kumar R. Metabolism of 1,25-dihydroxyvitamin D3. Physiol Rev. 1984;64:478–504.
[203] Kumar R. Vitamin D metabolism and mechanisms of calcium transport. J Am Soc Nephrol 1990;1:30–42.
[204] Kumar R, Cohen WR, Epstein FH. Vitamin D and calcium hormones in pregnancy. N Engl J Med 1980;302:1143–5.
[205] Kumar R, Cohen WR, Silva P, Epstein FH. Elevated 1,25-dihydroxyvitamin D plasma levels in normal human pregnancy and lactation. J Clin Invest 1979;63:342–4.
[206] Kumar R, Merimee TJ, Silva P, Epstein FH. The effect of chronic growth hormone excess or deiciency on plasma 1,25-dihydroxyvitamin D levels in man. In: Norman AW, Schaefer K, von Herrath D, Grigoleit HG, Coburn JW, De Luca HF, Mawer EB, Suda T, editors. Proceedings of the fourth workshop on vitamin D. Elmsford, New York: de Gruyter; 1979. p. 1005–9.
[207] Kumar R, Riggs BL. Vitamin D in the therapy of disorders of calcium and phosphorus metabolism. Mayo Clin Proc 1981;56:327–33.
[208] Kumar R, Schaefer J, Grande JP, Roche PC. Immunolocalization of calcitriol receptor, 24-hydroxylase cytochrome P-450, and calbindin D28k in human kidney. Am J Physiol 1994;266:F477–85.
[209] Lagunova Z, Porojnicu AC, Lindberg F, Hexeberg S, Moan J. The dependency of vitamin D status on body mass index, gender, age and season. Anticancer Res 2009;29:3713–20.
[210] Lajeunesse D, Bouhtiauy I, Brunette MG. Parathyroid hormone and hydrochlorothiazide increase calcium transport by the luminal membrane of rabbit distal nephron segments through different pathways. Endocrinology 1994;134:35–41.
[211] Langub MC, Monier-Faugere MC, Qi Q, Geng Z, Koszewski NJ, Malluche HH. Parathyroid hormone type 1 receptor and human osteoclasts.[comment]. J Bone Miner Res 2001;16: 448–56.
[212] Lawson DE, Fraser DR, Kodicek E, Morris HR, Williams DH. Identification of 1,25-dihydroxycholecalciferol, a new kidney hormone controlling calcium metabolism. Nature 1971;230: 228–30.

[213] Lee GS, Choi KC, Park SM, An BS, Cho MC, Jeung EB. Expression of human Calbindin-D(9k) correlated with age, vitamin D receptor and blood calcium level in the gastrointestinal tissues. Clin Biochem 2003;36:255–61.

[214] Lee K, Brown D, Urena P, Ardaillou N, Ardaillou R, Deeds J, et al. Localization of parathyroid hormone/parathyroid hormone-related peptide receptor mRNA in kidney. Am J Physiol 1996;270:F186–91.

[215] Lee SK, Goldring SR, Lorenzo JA. Expression of the calcitonin receptor in bone marrow cell cultures and in bone: a specific marker of the differentiated osteoclast that is regulated by calcitonin. Endocrinology 1995;136:4572–81.

[216] Lerner UH, Ransjo M, Klaushofer K, Horandner H, Hoffmann O, Czerwenka E, et al. Comparison between the effects of forskolin and calcitonin on bone resorption and osteoclast morphology in vitro. Bone 1989;10:377–87.

[217] Lienhardt A, Bai M, Lagarde JP, Rigaud M, Zhang Z, Jiang Y, et al. Activating mutations of the calcium-sensing receptor: management of hypocalcemia. J Clin Endocrinol Metab 2001;86:5313–23.

[218] Lietman SA, Tenenbaum-Rakover Y, Jap TS, Yi-Chi W, De-Ming Y, Ding C, et al. A novel loss-of-function mutation, Gln459Arg, of the calcium-sensing receptor gene associated with apparent autosomal recessive inheritance of familial hypocalciuric hypercalcemia. J Clin Endocrinol Metab 2009;94:4372–9.

[219] Liu BA, Gordon M, Labranche JM, Murray TM, Vieth R, Shear NH. Seasonal prevalence of vitamin D deficiency in institutionalized older adults. J Am Geriatr Soc 1997;45:598–603.

[220] Loffing J, Loffing-Cueni D, Valderrabano V, Klausli L, Hebert SC, Rossier BC, et al. Distribution of transcellular calcium and sodium transport pathways along mouse distal nephron. Am J Physiol Renal Physiol 2001;281:F1021–7.

[221] Lopez I, Rodriguez M, Felsenfeld AJ, Estepa JC, Aguilera-Tejero E. Direct suppressive effect of acute metabolic and respiratory alkalosis on parathyroid hormone secretion in the dog. J Bone Miner Res 2003;18:1478–85.

[222] Lowery WD, Thomas Jr CG, Awbrey BJ, Rosenstein BD, Talmage RV. The late effect of subtotal thyroidectomy and radioactive iodine therapy on calcitonin secretion and bone mineral density in women treated for Graves' disease. Surgery 1986;100:1142–9.

[223] Lund B, Sorensen OH, Bishop JE, Norman AW. Stimulation of 1,25-dihydroxyvitamin D production by parathyroid hormone and hypocalcemia in man. J Clin Endocrinol Metab 1980;50:480–4.

[224] Madhok TC, DeLuca HF. Characteristics of the rat liver microsomal enzyme system converting cholecalciferol into 25-hydroxycholecalciferol. Evidence for the participation of cytochrome p-450. Biochem J 1979;184:491–9.

[225] Madhok TC, Schnoes HK, DeLuca HF. Incorportion of oxygen-18 into the 25-position of cholecalciferol by hepatic cholecalciferol 25-hydroxylase. Biochem J 1978;175:479–82.

[226] Magyar CE, White KE, Rojas R, Apodaca G, Friedman PA. Plasma membrane Ca^{2+}-ATPase and NCX1 Na^{+}/Ca^{2+} exchanger expression in distal convoluted tubule cells. Am J Physiol Renal Physiol 2002;283:F29–40.

[227] Mahaffee DD, Cooper CW, Ramp WK, Ontjes DA. Magnesium promotes both parathyroid hormone secretion and adenosine 3',5'-monophosphate production in rat parathyroid tissues and reverses the inhibitory effects of calcium on adenylate cyclase. Endocrinology 1982;110:487–95.

[228] Mathias RS, Mathews CH, Machule C, Gao D, Li W, Denbesten PK. Identification of the calcium-sensing receptor in the developing tooth organ. J Bone Miner Res 2001;16:2238–44.

[229] Matsuoka LY, Wortsman J, Haddad JG, Hollis BW. In vivo threshold for cutaneous synthesis of vitamin D3. J Lab Clin Med 1989;114:301–5.

[230] Matusiak D, Murillo G, Carroll RE, Mehta RG, Benya RV. Expression of vitamin D receptor and 25-hydroxyvitamin D3-1 (alpha)-hydroxylase in normal and malignant human colon. Cancer Epidemiol Biomarkers Prev 2005;14:2370–6.

[231] Mayer GP, Hurst JG. Comparison of the effects of calcium and magnesium on parathyroid hormone secretion rate in calves. Endocrinology 1978;102:1803–14.

[232] Mayer GP, Hurst JG. Sigmoidal relationship between parathyroid hormone secretion rate and plasma calcium concentration in calves. Endocrinology 1978;102:1036–42.

[233] McElduff A, LeBoff MS, Moore Jr FD, Butters R, Gao P, Cantor TL, et al. Activating antibodies to the calcium-sensing receptor in two patients with autoimmune hypoparathyroidism. J Clin Endocrinol Metab 2004;89:548–56.

[234] McKinney K, Breitkopf CR, Berenson AB. Association of race, body fat and season with vitamin D status among young women: a cross-sectional study. Clin Endocrinol (Oxf) 2008;69:535–41.

[235] McNeil L, Hobson S, Nipper V, Rodland KD. Functional calcium-sensing receptor expression in ovarian surface epithelial cells. Am J Obstet Gynecol 1998;178:305–13.

[236] McNeil SE, Hobson SA, Nipper V, Rodland KD. Functional calcium-sensing receptors in rat fibroblasts are required for activation of SRC kinase and mitogen-activated protein kinase in response to extracellular calcium. J Biol Chem 1998;273:1114–20.

[237] Mehrotra M, Gupta SK, Tiwari S, Agarwal A, Kumar K, Awasthi PK, et al. Effect of oophorectomy on expression of calcium sensing receptor mRNA in rat duodenal mucosa. Indian J Exp Biol 2003;41:41–6.

[238] Menaa C, Vrtovsnik F, Friedlander G, Corvol M, Garabedian M. Insulin-like growth factor I, a unique calcium-dependent stimulator of 1,25-dihydroxyvitamin D3 production. Studies in cultured mouse kidney cells. J Biol Chem 1995;270:25461–7.

[239] Mirzaei S, Krotla G, Knoll P, Koriska K, Kohn H. Possible effect of calcitonin deficiency on bone mass after subtotal thyroidectomy. Acta Med Austriaca 1999;26:29–31.

[240] Miyashiro K, Kunii I, Manna TD, de Menezes Filho HC, Damiani D, Setian N, et al. Severe hypercalcemia in a 9-year-old Brazilian girl due to a novel inactivating mutation of the calcium-sensing receptor. J Clin Endocrinol Metab 2004;89:5936–41.

[241] Moore EW. Ionized calcium in normal serum, ultrafiltrates, and whole blood determined by ion-exchange electrodes. J Clin Invest 1970;49:318–34.

[242] Moore PR, Mawer EB, Houghton D, Freemont AJ, Hutchison AJ, Gokal R, et al. Down-regulation of human osteoblast PTH/PTHrP receptor mRNA in end-stage renal failure. Kidney Int 2000;58:1440–9.

[243] Muller D, Hoenderop JG, Meij IC, van den Heuvel LP, Knoers NV, den Hollander AI, et al. Molecular cloning, tissue distribution, and chromosomal mapping of the human epithelial Ca^{2+} channel (ECAC1). Genomics 2000;67:48–53.

[244] Muller D, Hoenderop JG, Merkx GF, van Os CH, Bindels RJ. Gene structure and chromosomal mapping of human epithelial calcium channel. Biochem Biophys Res Commun 2000;275:47–52.

[245] Murayama A, Takeyama K, Kitanaka S, Kodera Y, Kawaguchi Y, Hosoya T, et al. Positive and negative regulations of the renal 25-hydroxyvitamin D3 1alpha-hydroxylase gene by parathyroid hormone, calcitonin, and 1alpha,25(OH)2D3 in intact animals. Endocrinology 1999;140:2224–31.

[246] Myrtle JF, Haussler MR, Norman AW. Evidence for the biologically active form of cholecalciferol in the intestine. J Biol Chem 1970;245:1190–6.
[247] Nakajima K, Yamazaki K, Kimura H, Takano K, Miyoshi H, Sato K. Novel gain of function mutations of the calcium-sensing receptor in two patients with PTH-deficient hypocalcemia. Intern Med 2009;48:1951–6.
[248] Navarro JF, Mora C, Macia M, Garcia J. Serum magnesium concentration is an independent predictor of parathyroid hormone levels in peritoneal dialysis patients. Perit Dial Int 1999;19:455–61.
[249] Naveh-Many T, Marx R, Keshet E, Pike JW, Silver J. Regulation of 1,25-dihydroxyvitamin D3 receptor gene expression by 1,25-dihydroxyvitamin D3 in the parathyroid in vivo. J Clin Invest 1990;86:1968–75.
[250] Neer RM, Arnaud CD, Zanchetta JR, Prince RL, Gaich GA, Reginster JY, et al. Effect of parathyroid hormone (1–34) on fractures and bone mineral density in postmenopausal women with osteoporosis. N Engl J Med 2001;344:1434–41.
[251] Nijenhuis T, Hoenderop JG, van der Kemp AW, Bindels RJ. Localization and regulation of the epithelial Ca^{2+} channel TRPV6 in the kidney. J Am Soc Nephrol 2003;14:2731–40.
[252] Nishikawa T, Ishikawa H, Yamamoto S, Koshihara Y. A novel calcitonin receptor gene in human osteoclasts from normal bone marrow. FEBS Lett 1999;458:409–14.
[253] Nissen PH, Christensen SE, Heickendorff L, Brixen K, Mosekilde L. Molecular genetic analysis of the calcium sensing receptor gene in patients clinically suspected to have familial hypocalciuric hypercalcemia: phenotypic variation and mutation spectrum in a Danish population. J Clin Endocrinol Metab 2007;92:4373–9.
[254] Nomura R, Sugimoto T, Tsukamoto T, Yamauchi M, Sowa H, Chen Q, et al. Marked and sustained increase in bone mineral density after parathyroidectomy in patients with primary hyperparathyroidism; a six-year longitudinal study with or without parathyroidectomy in a Japanese population. Clin Endocrinol (Oxf) 2004;60:335–42.
[255] Nordenstrom E, Westerdahl J, Bergenfelz A. Recovery of bone mineral density in 126 patients after surgery for primary hyperparathyroidism. World J Surg 2004;28:502–7.
[256] Norman DA, Fordtran JS, Brinkley LJ, Zerwekh JE, Nicar MJ, Strowig SM, et al. Jejunal and ileal adaptation to alterations in dietary calcium: changes in calcium and magnesium absorption and pathogenetic role of parathyroid hormone and 1,25-dihydroxyvitamin D. J Clin Invest 1981;67:1599–603.
[257] Okamoto Y, DeLuca HF. Separation of two forms of chick 1,25-dihydroxyvitamin D3 and 25-hydroxyvitamin D3 24-hydroxylase. Proc Soc Exp Biol Med 1994;205:52–5.
[258] Okano T, Tsugawa N, Morishita A, Kato S. Regulation of gene expression of epithelial calcium channels in intestine and kidney of mice by 1alpha,25-dihydroxyvitamin D3. J Steroid Biochem Mol Biol 2004;89-90:335–8.
[259] Okazaki T, Igarashi T, Kronenberg HM. 5′-flanking region of the parathyroid hormone gene mediates negative regulation by 1,25-(OH)2 vitamin D3. J Biol Chem 1988;263:2203–8.
[260] Omdahl J, Holick M, Suda T, Tanaka Y, DeLuca HF. Biological activity of 1,25-dihydroxycholecalciferol. Biochemistry (Mosc) 1971;10:2935–40.
[261] Omdahl JL. Interaction of the parathyroid and 1,25-dihydroxyvitamin D3 in the control of renal 25-hydroxyvitamin D3 metabolism. J Biol Chem 1978;253:8474–8.
[262] Omdahl JL, Gray RW, Boyle IT, Knutson J, DeLuca HF. Regulation of metabolism of 25-hydroxycholecalciferol by kidney tissue in vitro by dietary calcium. Nature New Biol 1972;237:63–4.
[263] Orrell DH. Albumin as an aid to the interpretation of serum calcium. Clin Chim Acta 1971;35:483–9.
[264] Orwoll E, Kane-Johnson N, Cook J, Roberts L, Strasik L, McClung M. Acute parathyroid hormone secretory dynamics: hormone secretion from normal primate and adenomatous human tissue in response to changes in extracellular calcium concentration. J Clin Endocrinol Metab 1986;62:950–5.
[265] Pahuja DN, De Luca HF. Thyroid hormone and vitamin D metabolism in the rat. Arch Biochem Biophys 1982;213:293–8.
[266] Pallais JC. Acquired hypocalciuric hypercalcemia due to autoantibodies against the calcium-sensing receptor. N Engl J Med 2004;351:362–9.
[267] Palmer G, Bonjour JP, Rizzoli R, Manen D. Positive and negative control of the expression of parathyroid hormone (PTH)/PTH-related protein receptor via proximal promoter P3 in human osteoblast-like cells. J Clin Endocrinol Metab 2000;85:3376–82.
[268] Palmer G, Bonjour JP, Rizzoli R, Manen D. Sequence and activity of parathyroid hormone/parathyroid hormone-related protein receptor promoter region in human osteoblast-like cells. Gene 1998;218:49–56.
[269] Pannabecker TL, Chandler JS, Wasserman RH. Vitamin-D-dependent transcriptional regulation of the intestinal plasma membrane calcium pump. Biochem Biophys Res Commun 1995;213:499–505.
[270] Pedersen JI, Ghazarian JG, Orme-Johnson NR, DeLuca HF. Isolation of chick renal mitochondrial ferredoxin active in the 25-hydroxyvitamin D3-1alpha-hydroxylase system. J Biol Chem 1976;251:3933–41.
[271] Peng JB, Hediger MA. A family of calcium-permeable channels in the kidney: distinct roles in renal calcium handling. Curr Opin Nephrol Hypertens 2002;11:555–61.
[272] Perez Jurado LA, Li X, Francke U. The human calcitonin receptor gene (CALCR) at 7q21.3 is outside the deletion associated with the Williams syndrome. Cytogenet Cell Genet 1995;70:246–9.
[273] Perwad F, Zhang MY, Tenenhouse HS, Portale AA. Fibroblast growth factor 23 impairs phosphorus and vitamin D metabolism in vivo and suppresses 25-hydroxyvitamin D-1alpha-hydroxylase expression in vitro. Am J Physiol Renal Physiol 2007;293:F1577–83.
[274] Pidasheva S, D'Souza-Li L, Canaff L, Cole DE, Hendy GN. CASRdb: calcium-sensing receptor locus-specific database for mutations causing familial (benign) hypocalciuric hypercalcemia, neonatal severe hyperparathyroidism, and autosomal dominant hypocalcemia. Hum Mutat 2004;24:107–11.
[275] Pike JW, Parker JB, Haussler MR, Boass A, Toverud SV. Dynamic changes in circulating 1,25-dihydroxyvitamin D during reproduction in rats. Science 1979;204:1427–9.
[276] Ponchon G, DeLuca HF. Metabolism and biological activity of vitamin D. Calcif Tissue Res 1970;(Suppl):43–4.
[277] Ponchon G, Deluca HF. Metabolites of vitamin D3 and their biologic activity. J Nutr 1969;99:157–67.
[278] Ponchon G, DeLuca HF. The role of the liver in the metabolism of vitamin D. J Clin Invest 1969;48:1273–9.
[279] Ponchon G, Kennan AL, DeLuca HF. Activation" of vitamin D by the liver. J Clin Invest 1969;48:2032–7.
[280] Popken JL, Brooks RA, Foy RB. Atomic absorption analysis of selected metals associated with serum protein fractions. Am J Med Technol 1974;40:260–4.
[281] Poskitt EM, Cole TJ, Lawson DE. Diet, sunlight, and 25-hydroxy vitamin D in healthy children and adults. Br Med J 1979;1:221–3.
[282] Prosser DE, Jones G. Enzymes involved in the activation and inactivation of vitamin D. Trends Biochem Sci 2004;29:664–73.

[283] Przepiorka D, Baylin SB, McBride OW, Testa JR, de Bustros A, Nelkin BD. The human calcitonin gene is located on the short arm of chromosome 11. Biochem Biophys Res Commun 1984;120:493–9.

[284] Quarles LD. Extracellular calcium-sensing receptors in the parathyroid gland, kidney, and other tissues. Curr Opin Nephrol Hypertens 2003;12:349–55.

[285] Raisz LG, Trummel CL, Holick MF, DeLuca HF. 1,25-dihydroxycholecalciferol: a potent stimulator of bone resorption in tissue culture. Science 1972;175:768–9.

[286] Rakopoulos M, Ikegame M, Findlay DM, Martin TJ, Moseley JM. Short treatment of osteoclasts in bone marrow culture with calcitonin causes prolonged suppression of calcitonin receptor mRNA. Bone 1995;17:447–53.

[287] Raman A. The calcium fractions of normal serum. Clin Biochem 1971;4:141–6.

[288] Ramirez JA, Goodman WG, Gornbein J, Menezes C, Moulton L, Segre GV, et al. Direct in vivo comparison of calcium-regulated parathyroid hormone secretion in normal volunteers and patients with secondary hyperparathyroidism. J Clin Endocrinol Metab 1993;76:1489–94.

[289] Rasmussen H, Wong M, Bikle D, Goodman DB. Hormonal control of the renal conversion of 25-hydroxycholecalciferol to 1,25-dihydroxycholecalciferol. J Clin Invest 1972;51:2502–4.

[290] Rasschaert J, Malaisse WJ. Expression of the calcium-sensing receptor in pancreatic islet B-cells. Biochem Biophys Res Commun 1999;264:615–8.

[291] Riccardi D, Brown EM. Physiology and pathophysiology of the calcium-sensing receptor in the kidney. Am J Physiol Renal Physiol 2010;298:F485–99.

[292] Riccardi D, Lee WS, Lee K, Segre GV, Brown EM, Hebert SC. Localization of the extracellular Ca^{2+}-sensing receptor and PTH/PTHrP receptor in rat kidney. Am J Physiol 1996;271: F951–6.

[293] Rost CR, Bikle DD, Kaplan RA. In vitro stimulation of 25-hydroxycholecalciferol 1 alpha-hydroxylation by parathyroid hormone in chick kidney slices: evidence for a role for adenosine 3′,5′-monophosphate. Endocrinology 1981;108:1002–6.

[294] Rude RK, Oldham SB, Sharp Jr CF, Singer FR. Parathyroid hormone secretion in magnesium deficiency. J Clin Endocrinol Metab 1978;47:800–6.

[295] Russell J, Ashok S, Koszewski NJ. Vitamin D receptor interactions with the rat parathyroid hormone gene: synergistic effects between two negative vitamin D response elements. J Bone Miner Res 1999;14:1828–37.

[296] Saito H, Kusano K, Kinosaki M, Ito H, Hirata M, Segawa H, et al. Human fibroblast growth factor-23 mutants suppress Na^+-dependent phosphate co-transport activity and 1alpha,25-dihydroxyvitamin D3 production. J Biol Chem 2003;278:2206–11.

[297] Sakaki T, Kagawa N, Yamamoto K, Inouye K. Metabolism of vitamin D3 by cytochromes P450. Front Biosci 2005;10:119–34.

[298] Sauveur B, Garabedian M, Fellot C, Mongin P, Balsan S. The effect of induced metabolic acidosis on vitamin D3 metabolism in rachitic chicks. Calcif Tissue Res 1977;23:121–4.

[299] Sawada N, Sakaki T, Ohta M, Inouye K. Metabolism of vitamin D_3 by human CYP27A1. Biochem Biophys Res Commun 2000;273:977–84.

[300] Sawers JS, Kellett HA, Brown NS, Beckett GJ, Seth J, Sinclair IS, et al. Does calcitonin cause hypocalcaemia after thyroidectomy? Br J Surg 1982;69:456–8.

[301] Schiavi SC, Kumar R. The phosphatonin pathway: new insights in phosphate homeostasis. Kidney Int 2004;65:1–14.

[302] Schipani E, Karga H, Karaplis AC, Potts Jr JT, Kronenberg HM, Segre GV, et al. Identical complementary deoxyribonucleic acids encode a human renal and bone parathyroid hormone (PTH)/PTH-related peptide receptor. Endocrinology 1993;132:2157–65.

[303] Schuessler M, Astecker N, Herzig G, Vorisek G, Schuster I. Skin is an autonomous organ in synthesis, two-step activation and degradation of vitamin D_3: CYP27 in epidermis completes the set of essential vitamin D_3-hydroxylases. Steroids 2001;66:399–408.

[304] Schuster I, Egger H, Bikle D, Herzig G, Reddy GS, Stuetz A, et al. Selective inhibition of vitamin D hydroxylases in human keratinocytes. Steroids 2001;66:409–22.

[305] Seeman E, Kumar R, Hunder GG, Scott M, Heath III H, Riggs BL. Production, degradation, and circulating levels of 1,25-dihydroxyvitamin D in health and in chronic glucocorticoid excess. J Clin Inves.t 1980;66:664–9.

[306] Sherwood LM, Herrman I, Bassett CA. Parathyroid hormone secretion in vitro: regulation by calcium and magnesium ions. Nature 1970;225:1056–8.

[307] Sherwood LM, Mayer GP, Ramberg Jr CF, Kronfeld DS, Aurbach GD, Potts Jr JT. Regulation of parathyroid hormone secretion: proportional control by calcium, lack of effect of phosphate. Endocrinology 1968;83:1043–51.

[308] Shimada T, Hasegawa H, Yamazaki Y, Muto T, Hino R, Takeuchi Y, et al. FGF-23 is a potent regulator of vitamin D metabolism and phosphate homeostasis. J Bone Miner Res 2004;19:429–35.

[309] Shimada T, Kakitani M, Yamazaki Y, Hasegawa H, Takeuchi Y, Fujita T, et al. Targeted ablation of Fgf23 demonstrates an essential physiological role of FGF23 in phosphate and vitamin D metabolism. J Clin Invest 2004;113:561–8.

[310] Shimada T, Mizutani S, Muto T, Yoneya T, Hino R, Takeda S, et al. Cloning and characterization of FGF23 as a causative factor of tumor-induced osteomalacia. Proc Natl Acad Sci USA 2001;98:6500–5.

[311] Shimizu T, Yoshitomi K, Nakamura M, Imai M. Effects of PTH, calcitonin, and cAMP on calcium transport in rabbit distal nephron segments. Am J Physiol 1990;259:F408–14.

[312] Shinki T, Ueno Y, DeLuca HF, Suda T. Calcitonin is a major regulator for the expression of renal 25-hydroxyvitamin D_3-1alpha-hydroxylase gene in normocalcemic rats. Proc Natl Acad Sci USA 1999;96:8253–8.

[313] Shinkyo R, Sakaki T, Kamakura M, Ohta M, Inouye K. Metabolism of vitamin D by human microsomal CYP2R1. Biochem Biophys Res Commun 2004;324:451–7.

[314] Shiohara M, Mori T, Mei B, Brown EM, Watanabe T, Yasuda T. A novel gain-of-function mutation (F821L) in the transmembrane domain of calcium-sensing receptor is a cause of severe sporadic hypoparathyroidism. Eur J Pediatr 2004;163:94–8.

[315] Silver J, Naveh-Many T, Mayer H, Schmelzer HJ, Popovtzer MM. Regulation by vitamin D metabolites of parathyroid hormone gene transcription in vivo in the rat. J Clin Invest 1986;78:1296–301.

[316] Silver J, Russell J, Sherwood LM. Regulation by vitamin D metabolites of messenger ribonucleic acid for preproparathyroid hormone in isolated bovine parathyroid cells. Proc Natl Acad Sci USA 1985;82:4270–3.

[317] Somjen D, Katzburg S, Stern N, Kohen F, Sharon O, Limor R, et al. 25 hydroxy-vitamin D_3-1alpha hydroxylase expression and activity in cultured human osteoblasts and their modulation by parathyroid hormone, estrogenic compounds and dihydrotestosterone. J Steroid Biochem Mol Biol 2007; 107:238–44.

[318] Somjen D, Weisman Y, Kohen F, Gayer B, Limor R, Sharon O, et al. 25-hydroxyvitamin D_3-1alpha-hydroxylase is expressed in human vascular smooth muscle cells and is upregulated by

parathyroid hormone and estrogenic compounds. Circulation 2005;111:1666–71.
[319] Sommer S, Berndt T, Craig T, Kumar R. The phosphatonins and the regulation of phosphate transport and vitamin D metabolism. J Steroid Biochem Mol Biol 2007;103:497–503.
[320] Song Y, Kato S, Fleet JC. Vitamin D receptor (VDR) knockout mice reveal VDR-independent regulation of intestinal calcium absorption and ECaC2 and calbindin D9k mRNA. J Nutr 2003;133:374–80.
[321] Spanos E, Colston KW, Evans IM, Galante LS, Macauley SJ, Macintyre I. Effect of prolactin on vitamin D metabolism. Mol Cell Endocrinol 1976;5:163–7.
[322] Speer G, Toth M, Niller HH, Salamon D, Takacs I, Miheller P, et al. Calcium metabolism and endocrine functions in a family with familial hypocalciuric hypercalcemia. Exp Clin Endocrinol Diabetes 2003;111:486–90.
[323] St-Arnaud R, Messerlian S, Moir JM, Omdahl JL, Glorieux FH. The 25-hydroxyvitamin D 1-alpha-hydroxylase gene maps to the pseudovitamin D-deficiency rickets (PDDR) disease locus. J Bone Miner Res 1997;12:1552–9.
[324] Stauffer TP, Guerini D, Carafoli E. Tissue distribution of the four gene products of the plasma membrane Ca^{2+} pump. A study using specific antibodies. J Biol Chem 1995;270: 12184–90.
[325] Staun M, Paerregaard A, Krasilnikoff PA. Measurement of calbindin-D9K in small intestinal biopsy specimens of children. J Pediatr Gastroenterol Nutr 1991;12:328–31.
[326] Steenbock H, Black A. Fact-soluble vitamins. XVII. The induction of growth-promoting and calcifying properties in a ration by exposure to ultraviolet light. J Biol Chem 1924;61: 405–22.
[327] Steenbock H, Hart E. The influence of function on the lime requirements of animals. J Biol Chem 1913;14:1913.
[328] Stellinga-Boelen AA, Wiegersma PA, Storm H, Bijleveld CM, Verkade HJ. Vitamin D levels in children of asylum seekers in the Netherlands in relation to season and dietary intake. Eur J Pediatr 2007;166:201–6.
[329] Suda T, DeLuca HF, Schnoes H, Blunt JW. 25-hydroxyergocalciferol: a biologically active metabolite of vitamin D2. Biochem Biophys Res Commun 1969;35:182–5.
[330] Suda T, DeLuca HF, Schnoes HK, Blunt JW. The isolation and identification of 25-hydroxyergocalciferol. Biochemistry (Mosc) 1969;8:3515–20.
[331] Suda T, Takahashi N, Udagawa N, Jimi E, Gillespie MT, Martin TJ. Modulation of osteoclast differentiation and function by the new members of the tumor necrosis factor receptor and ligand families. Endocr Rev 1999;20: 345–57.
[332] Takahashi N, Akatsu T, Sasaki T, Nicholson GC, Moseley JM, Martin TJ, et al. Induction of calcitonin receptors by 1 alpha, 25-dihydroxyvitamin D_3 in osteoclast-like multinucleated cells formed from mouse bone marrow cells. Endocrinology 1988;123:1504–10.
[333] Takatsuki K, Hanley DA, Sherwood LM. Effects of magnesium ion on parathyroid hormone secretion in vitro. Calcif Tissue Int 1980;32:201–6.
[334] Tanaka Y, Castillo L, DeLuca HF. Control of renal vitamin D hydroxylases in birds by sex hormones. Proc Natl Acad Sci USA 1976;73:2701–5.
[335] Tanaka Y, Deluca HF. The control of 25-hydroxyvitamin D metabolism by inorganic phosphorus. Arch Biochem Biophys 1973;154:566–74.
[336] Tanaka Y, DeLuca HF, Omdahl J, Holick MF. Mechanism of action of 1,25-dihydroxycholecalciferol on intestinal calcium transport. Proc Natl Acad Sci USA 1971;68:1286–8.
[337] Targovnik JH, Rodman JS, Sherwood LM. Regulation of parathyroid hormone secretion in vitro: quantitative aspects of calcium and magnesium ion control. Endocrinology 1971;88:1477–82.
[338] Tauc M, Bidet M, Poujeol P. Chloride currents activated by calcitonin and cAMP in primary cultures of rabbit distal convoluted tubule. J Membr Biol 1996;150:255–73.
[339] Tebben PJ, Kumar R. Vitamin D and the kidney. In: Feldman D, Pike JW, Glorieux FH, editors. Vitamin D. 2nd ed. Burlington, MA: Academic Press; 2005. p. 515–36.
[340] Teegarden D, Meredith SC, Sitrin MD. Determination of the affinity of vitamin D metabolites to serum vitamin D binding protein using assay employing lipid-coated polystyrene beads. Anal Biochem 1991;199:293–9.
[341] Thode J, Juul-Jorgensen B, Bhatia HM, Kjaerulf-Nielsen M, Bartels PD, Fogh-Andersen N, et al. Comparison of serum total calcium, albumin-corrected total calcium, and ionized calcium in 1213 patients with suspected calcium disorders. Scand J Clin Lab Invest 1989;49:217–23.
[342] Tian J, Smogorzewski M, Kedes L, Massry SG. Parathyroid hormone-parathyroid hormone related protein receptor messenger RNA is present in many tissues besides the kidney. Am J Nephrol 1993;13:210–3.
[343] Tian J, Smogorzewski M, Kedes L, Massry SG. PTH-PTHrP receptor mRNA is downregulated in chronic renal failure. Am J Nephrol 1994;14:41–6.
[344] Tikellis C, Xuereb L, Casley D, Brasier G, Cooper ME, Wookey PJ. Calcitonin receptor isoforms expressed in the developing rat kidney. Kidney Int 2003;63:416–26.
[345] Tjellesen L, Christiansen C. Vitamin D metabolites in normal subjects during one year. A longitudinal study. Scand J Clin Lab Invest 1983;43:85–9.
[346] Tolcos M, Tikellis C, Rees S, Cooper M, Wookey P. Ontogeny of calcitonin receptor mRNA and protein in the developing central nervous system of the rat. J Comp Neurol 2003;456:29–38.
[347] Tortelote GG, Valverde RH, Lemos T, Guilherme A, Einicker-Lamas M, Vieyra A. The plasma membrane Ca^{2+} pump from proximal kidney tubules is exclusively localized and active in caveolae. FEBS Lett 2004;576:31–5.
[348] Trechsel U, Bonjour JP, Fleisch H. Regulation of the metabolism of 25-hydroxyvitamin D_3 in primary cultures of chick kidney cells. J Clin Invest 1979;64:206–17.
[349] Trummel CL, Raisz LG, Blunt JW, Deluca HF. 25-Hydroxycholecalciferol: stimulation of bone resorption in tissue culture. Science 1969;163:1450–1.
[350] Tsai KS, Wahner HW, Offord KP, Melton III LJ, Kumar R, Riggs BL. Effect of aging on vitamin D stores and bone density in women. Calcif Tissue Int 1987;40:241–3.
[351] Tsurukai T, Udagawa N, Matsuzaki K, Takahashi N, Suda T. Roles of macrophage-colony stimulating factor and osteoclast differentiation factor in osteoclastogenesis. J Bone Miner Metab 2000;18:177–84.
[352] Turner RL. Mammalian 25-hydroxyvitamin D 1-a-hydroxylase: measurement and regulation. In: Kumar R, editor. Vitamin D: Basic and clinical aspects. Boston: Nijhoff; 1984. p. 175–96.
[353] Urena P, Kong XF, Abou-Samra AB, Juppner H, Kronenberg HM, Potts Jr JT, et al. Parathyroid hormone (PTH)/PTH-related peptide receptor messenger ribonucleic acids are widely distributed in rat tissues. Endocrinology 1993;133:617–23.
[354] Urena P, Kubrusly M, Mannstadt M, Hruby M, Trinh MM, Silve C, et al. The renal PTH/PTHrP receptor is downregulated in rats with chronic renal failure. Kidney Int 1994;45:605–11.
[355] Urist MR. Fundamental and clinical bone physiology. Philadelphia: J. B. Lippincott; 1980.

[356] van Abel M, Hoenderop JG, van der Kemp AW, van Leeuwen JP, Bindels RJ. Regulation of the epithelial Ca^{2+} channels in small intestine as studied by quantitative mRNA detection. Am J Physiol Gastrointest Liver Physiol 2003;285:G78–85.

[357] Van Cromphaut SJ, Dewerchin M, Hoenderop JG, Stockmans I, Van Herck E, Kato S, et al. Duodenal calcium absorption in vitamin D receptor-knockout mice: functional and molecular aspects. Proc Natl Acad Sci USA 2001;98:13324–9.

[358] Varghese Z, Fernando R, Powas SH, Moorhead JF, Varghese S. Analysis of rat vitamin D-dependent calbindin-D28k gene expression. Clin Nephrol 1999;51:263–71.

[359] Wada S, Udagawa N, Nagata N, Martin TJ, Findlay DM. Physiological levels of calcitonin regulate the mouse osteoclast calcitonin receptor by a protein kinase Alpha-mediated mechanism. Endocrinology 1996;137:312–20.

[360] Ward BK, Magno AL, Davis EA, Hanyaloglu AC, Stuckey BG, Burrows M, et al. Functional deletion of the calcium-sensing receptor in a case of neonatal severe hyperparathyroidism. J Clin Endocrinol Metab 2004;89:3721–30.

[361] Wasserman RH, Chandler JS, Meyer SA, Smith CA, Brindak ME, Fullmer CS, et al. Intestinal calcium transport and calcium extrusion processes at the basolateral membrane. J Nutr 1992;122:662–71.

[362] Wasserman RH, Fulmer CS, Shimura F. Calcium absorption and the molecular effects of vitamin D 3. In: Kumar R, editor. Vitamin D: Basic and clinical aspects. Boston: Nijhoff; 1984. p. 233–302.

[363] Wasserman RH, Smith CA, Brindak ME, De Talamoni N, Fullmer CS, Penniston JT, et al. Vitamin D and mineral deficiencies increase the plasma membrane calcium pump of chicken intestine. Gastroenterology 1992;102:886–94.

[364] Watson CG, Steed DL, Robinson AG, Deftos LJ. The role of calcitonin and parathyroid hormone in the pathogenesis of postthyroidectomy hypocalcemia. Metabolism 1981;30:588–9.

[365] Weber HP, Gray RW, Dominguez JH, Lemann Jr J. The lack of effect of chronic metabolic acidosis on 25-OH-vitamin D metabolism and serum parathyroid hormone in humans. J Clin Endocrinol Metab 1976;43:1047–55.

[366] Weber K, Erben RG, Rump A, Adamski J. Gene structure and regulation of the murine epithelial calcium channels ECaC1 and 2. Biochem Biophys Res Commun 2001;289:1287–94.

[367] White P, Cooke N. The multifunctional properties and characteristics of vitamin D-binding protein. Trends Endocrinol Metab 2000;11:320–7.

[368] Wilkins R. Absorption of calcium, phosphorus and magnesium. New York: Churchill Livingstone; 1976.

[369] Windaus A, Linsert O, Luttringhaus A, Weidlich G. Crystalline-vitamin D 2. Annalen de Chemie 1932;492:226–41.

[370] Windaus A, Schenck F, von Weder F. Uber das antirachitisch wirksame bestrahlungs-produkt aus 7-dehydro-cholesterin. Hoppe-Selyers Z Physiol Chem 1936;241:100–3.

[371] Wongsurawat N, Armbrecht HJ. Calcitonin stimulates 1,25-dihydroxyvitamin D production in diabetic rat kidney. Metabolism 1991;40:22–5.

[372] Yamaguchi T, Chattopadhyay N, Kifor O, Ye C, Vassilev PM, Sanders JL, et al. Expression of extracellular calcium-sensing receptor in human osteoblastic MG-63 cell line. Am J Physiol Cell Physiol 2001;280:C382–93.

[373] Yamasaki T, Izumi S, Ide H, Ohyama Y. Identification of a novel rat microsomal vitamin D3 25-hydroxylase. J Biol Chem 2004;279:22848–56.

[374] Yamauchi M, Sugimoto T, Yamaguchi T, Yano S, Wang J, Bai M, et al. Familial hypocalciuric hypercalcemia caused by an R648stop mutation in the calcium-sensing receptor gene. J Bone Miner Res 2002;17:2174–82.

[375] Yang T, Hassan S, Huang YG, Smart AM, Briggs JP, Schnermann JB. Expression of PTHrP, PTH/PTHrP receptor, and Ca^{2+}-sensing receptor mRNAs along the rat nephron. Am J Physiol 1997;272:F751–8.

[376] Yano S, Brown EM, Chattopadhyay N. Calcium-sensing receptor in the brain. Cell Calcium 2004;35:257–64.

[377] Yano S, Sugimoto T, Tsukamoto T, Chihara K, Kobayashi A, Kitazawa S, et al. Decrease in vitamin D receptor and calcium-sensing receptor in highly proliferative parathyroid adenomas. Eur J Endocrinol 2003;148:403–11.

[378] Yoon PS, DeLuca HF. Purification and properties of chick renal mitochondrial ferredoxin. Biochemistry (Mosc) 1980;19: 2165–71.

[379] Yoon PS, DeLuca HF. Resolution and reconstitution of soluble components of rat liver microsomal vitamin D_3-25-hydroxylase. Arch Biochem Biophys 1980;203:529–41.

[380] Yoon PS, Rawlings J, Orme-Johnson WH, DeLuca HF. Renal mitochondrial ferredoxin active in 25-hydroxyvitamin D_3 1 alpha-hydroxylase. Characterization of the iron-sulfur cluster using interprotein cluster transfer and electron paramagnetic resonance spectroscopy. Biochemistry (Mosc) 1980;19:2172–6.

[381] Yoshida N, Yoshida T, Nakamura A, Monkawa T, Hayashi M, Saruta T. Calcitonin induces 25-hydroxyvitamin D_3 1alpha-hydroxylase mRNA expression via protein kinase C pathway in LLC-PK1 cells. J Am Soc Nephrol 1999;10:2474–9.

[382] Yoshida T, Yoshida N, Monkawa T, Hayashi M, Saruta T. Dietary phosphorus deprivation induces 25-hydroxyvitamin D (3) 1alpha-hydroxylase gene expression. Endocrinology 2001;142:1720–6.

[383] Zehnder D, Bland R, Walker EA, Bradwell AR, Howie AJ, Hewison M, et al. Expression of 25-hydroxyvitamin D_3-1alpha-hydroxylase in the human kidney. J Am Soc Nephrol 1999;10:2465–73.

[384] Zehnder D, Evans KN, Kilby MD, Bulmer JN, Innes BA, Stewart PM, et al. The ontogeny of 25-hydroxyvitamin D_3 1alpha-hydroxylase expression in human placenta and decidua. Am J Pathol 2002;161:105–14.

[385] Zelinski JM, Sykes DE, Weiser MM. The effect of vitamin D on rat intestinal plasma membrane CA-pump mRNA. Biochem Biophys Res Commun 1991;179:749–55.

[386] Zhang MY, Wang X, Wang JT, Compagnone NA, Mellon SH, Olson JL, et al. Dietary phosphorus transcriptionally regulates 25-hydroxyvitamin D-1alpha-hydroxylase gene expression in the proximal renal tubule. Endocrinology 2002;143:587–95.

[387] Zuo Q, Claveau D, Hilal G, Leclerc M, Brunette MG. Effect of calcitonin on calcium transport by the luminal and basolateral membranes of the rabbit nephron. Kidney Int 1997;51:1991–9.

CHAPTER

66

Disorders of Calcium Metabolism

Cristina Dumitru[1] *and John Wysolmerski*[2]

[1]TAC S120 Section of Endocrinology and Metabolism, Yale School of Medicine, New Haven, Connecticut, USA
[2]TAC S131 Section of Endocrinology and Metabolism, Yale School of Medicine, New Haven, Connecticut, USA

INTRODUCTION

An adult human contains about 1000 g of calcium, the majority of which (~99%) is found in bone.[1] Calcium serves two principal physiologic functions. The first involves the production of calcium-phosphate hydroxyapatite crystals that bind to organic matrix and provide the unique mineralized structure of bones and teeth. The calcified nature of these tissues allows for mastication and enables bones to protect internal organs, to bear weight, and to function as the levers on which muscles act during locomotion. The second function is metabolic. Soluble calcium ions in the extracellular fluid (ECF) and cytosol are critical for a large number of enzymatic reactions, signaling cascades, and electrical membrane potentials that are necessary for normal cellular functions. Only 1% of total body calcium is contained within the ECF and soft tissues. Of the total circulating calcium, the ionized fraction is generally estimated to be approximately 50%, with the remainder of the total serum calcium bound to serum proteins, primarily albumin, and to a lesser extent complexed with anions, such as citrate or sulfate.[1] Only the ionized fraction of total serum calcium is physiologically important, and this component is regulated on a minute-to-minute basis. Clinical laboratories can measure either total serum calcium or ionized calcium routinely. However, accurate measurement of ionized calcium requires that the specimen be obtained anaerobically and analyzed promptly. Therefore, total serum calcium is most often used as an indirect assessment of the ionized calcium fraction.

The two functions of calcium described in the previous paragraph are interrelated, as skeletal calcium exchanges with ECF calcium. In this way, bones serve as a sink for excess calcium as well as a reservoir of calcium for metabolic needs. Given the large quantitative differences in the size of the two calcium pools, only about 1% of skeletal calcium is in active equilibrium with the ECF at any given time under normal physiologic conditions. A complicated homeostatic system involving multiple organs and hormones regulates the calcium concentration of the ECF as well as the calcium content of the skeleton. The organs involved include the parathyroid glands, the kidneys, the skeleton, and the gut. The hormones that coordinate the calcium regulating functions of these organs are parathyroid hormone (PTH), vitamin D, PTH-related protein (PTHrP) and calcitonin. Abnormalities in these organs, the hormones, or their receptors can all cause disturbances in calcium metabolism and lead to either hypercalcemia or hypocalcemia. In this chapter, we first review the individual components contributing to the regulation of circulating calcium levels. Second we examine the integrated control of calcium homeostasis. Finally, we discuss the most common causes of hypercalcemia and hypocalcemia.

REGULATORS OF CALCIUM HOMEOSTASIS

The Calcium Sensing Receptor

The maintenance of calcium homeostasis requires that a variety of cells within the body have the ability to measure the extracellular ionized calcium concentration of the ECF. This is accomplished primarily through the actions of a 7 transmembrane-spanning G protein-coupled receptor (GPCR) known as the calcium sensing receptor (CaSR).[2–5] The CaSR is a member of subfamily C of GPCRs and is related to the

Seldin and Giebisch's The Kidney, Fifth Edition.
DOI: http://dx.doi.org/10.1016/B978-0-12-381462-3.00066-5

© 2013 Elsevier Inc. All rights reserved.

metabotropic glutamate, pheromone and taste receptors. Evolutionarily, it is descended from periplasmic binding proteins in bacteria that serve as nutrient receptors.[3,6] The human *CaSR* gene is located on chromosome 3q13.3−21 and consists of 7 exons and two distinct promoter regions.[3,5] Expression of the *CaSR* gene is widespread although it is highest in organs that are involved in the regulation of calcium homeostasis, such as the parathyroid glands, the C-cells of the thyroid gland, kidney and bone. The regulation of CaSR mRNA production has not been as extensively studied as other aspects of its physiology, but gene expression has been shown to respond to calcium, vitamin D and cytokines such as interleukin 1β and interleukin 6.[7−10] Regulation of the CaSR and vitamin D receptor are interrelated. Calcium and vitamin D both upregulate *CaSR* gene expression.[11−13] Activation of the CaSR also upregulates expression of the vitamin D receptor (VDR), which, in turn, amplifies the effects of vitamin D on CaSR expression.[12,14] These interactions may be particularly important in the parathyroid to allow for synergistic activity of calcium and vitamin D in regulating PTH gene expression and secretion.

In humans, the mature CaSR encompasses 1078 amino acids. It has a large extracellular domain of 612 amino acids that is heavily glycosylated and serves as the calcium-binding domain.[3−5] The CaSR operates as a homodimer, which forms as the result of disulfide bonds between cysteines 129 and 131 of each monomer.[11,15] The resulting extracellular portions of the complex have been suggested to approximate a Venus flytrap based on molecular modeling derived from the crystal structure of the related metabotropic glutamate receptors. Binding of calcium to clusters of acidic residues within the extracellular domain causes closure of the extracellular "flytrap" motif and this leads to conformational changes that activate intracellular signaling.[6,16] The intracellular portion of the receptor has been shown to couple to $G_{q/11}$, G_i, $G_{12/13}$ and in some instances to G_s.[3,11,17,18] Most commonly, the receptor has been described to activate intracellular calcium transients and MAPK signaling cascades.[3,11] The CaSR also interacts with several other cytoplasmic and/or membrane proteins, including caveolin, filamin, potassium channels (Kir4.1 and Kir4.2) and receptor activating proteins (RAMP) 1 and 3, all of which can modulate downstream receptor signaling.[19] Finally, the receptor has been shown to heterodimerize with several metabotropic glutamate receptor isoforms and GABA receptor isoforms to generate unique hybrid receptors.[20,21] Therefore, like other GPCRs, the CaSR can signal through a variety of pathways and there is likely to be considerable cell type-specific variation in its signaling.

In addition to calcium, the CaSR binds and signals in response to a variety of other cations and positively charged organic molecules such as magnesium, gadolinium, polyamines and aminoglycoside antibiotics.[3,5,11] These molecules can activate the receptor in the absence of calcium and are known as Type 1 ligands. Other ligands, known as Type 2 agonists, have no activity independent of calcium, but instead can modify the sensitivity of the receptor to calcium. These include L-amino acids and small-molecule, allosteric activators and inhibitors known as calcimimetics or calcilytics.[3,5,11] L-amino acids bind to the extracellular domain of the receptor in physiologic concentrations and may help to coordinate protein and calcium metabolism.[22] Calcimimetics and calcylitics bind to the transmembrane domain of the receptor and stabilize the active or inactive conformations of the receptor respectively.[23,24] These compounds have been developed as drugs; cinacalcet (Sensipar) is commercially available for the treatment of hyperparathyroidism in chronic kidney disease (CKD) while calcilytics are currently in clinical trials.[25,26] The CaSR has also been shown to respond to alterations in pH, osmolality and salinity.[3] Therefore, although its actions are critical to the regulation of calcium homeostasis, the CaSR actually is a multifunctional sensor for varied alterations in the extracellular milieu.

The CaSR is expressed widely throughout the body. It has been implicated in a variety of actions including calcium and other ion transport, the regulation of cellular proliferation and differentiation, and hormone secretion. We will limit our discussion to its functions in the three tissues of greatest importance to calcium homeostasis, the parathyroid gland, the kidney and bone. The reader is referred to other more comprehensive reviews for discussion of its many other functions.[3,5]

Parathyroid Gland: The parathyroid gland expresses high levels of the CaSR, which regulates three important aspects of parathyroid physiology: *parathyroid hormone* (*PTH*) gene expression, PTH secretion and parathyroid cell proliferation.[4,27] Signaling from the CaSR leads to a reduction in PTH mRNA.[27,28] This effect may, in part, be indirect and mediated by changes in the sensitivity of suppression of *PTH* gene expression by vitamin D. However, there is also a specific calcium response element in the *PTH* gene promoter located 3.6 kB upstream from the transcription start site that acts to inhibit transcription.[27] In addition, as described in more detail in the Section on PTH, CaSR signaling destabilizes PTH mRNA and shortens its half-life.[28] Both effects result in a reduction of PTH synthesis.

The predominant effect of CaSR activation on PTH production is inhibition of PTH secretion.[3,4,27] Activation of the CaSR leads to a prompt suppression of PTH

release, an effect that involves coupling to $G_{q/11}$ and G_i, and the generation of intracellular calcium transients after receptor activation.[3,27] The control of PTH secretion by extracellular calcium is reviewed in more detail in the section on PTH, but genetic experiments in mice have shown that the coupling of PTH secretion to changes in extracellular calcium is completely dependant on the presence of the CaSR on parathyroid cells.[29,30] Furthermore, the number of functional receptors defines the dose-response relationship between extracellular calcium and PTH secretion by parathyroid cells. Reduced numbers of receptors are found in some patients with familial hypocalciuric hypercalcemia as well as in chronic kidney disease (CKD) and in parathyroid adenomas.[4,27,29,30] In each instance, the parathyroid cells become partially resistant to the ability of extracellular calcium to suppress PTH secretion properly.

The CaSR also regulates parathyroid gland mass, and null mutations in the *CaSR* gene result in parathyroid hyperplasia.[4,27,29,30] Part of this effect is indirect and is mediated by the ability of CaSR signaling to enhance parathyroid sensitivity to vitamin D. However, experiments in mice deficient in the VDR or 1 α-hydroxylase (CYP27B1) have demonstrated a direct effect of CaSR signaling on parathyroid hyperplasia as well.[31,32] The molecular details of how CaSR affects cell proliferation and/or hypertrophy are not yet well described.

The Kidney: Experiments performed prior to the identification of the CaSR had suggested that extracellular calcium had direct effects on renal calcium handling that were independent of any effects of PTH.[33] However, the identification of the CaSR and the recognition of its expression throughout the renal tubule have led to the elucidation of an integrated and intrinsic response of the kidney to changes in circulating calcium levels. In fact, recent experiments in mice have suggested that CaSR-mediated alterations in renal calcium handling may be the principal defense against hypercalcemia, while PTH-mediated responses have a more potent effect on the correction of hypocalcemia.[34] When activated by hypercalcemia, the CaSR affects different portions of the nephron to increase calcium excretion, and to acidify the urine and impair renal concentrating ability in order to protect against nephrocalcinosis or nephrolithiasis in the face of the resulting hypercalciuria.

The CaSR promotes renal calcium excretion through several actions. In the thick ascending loop of Henle (TAL), the CaSR is expressed on the basolateral surface and activation of the receptor leads to inhibition of paracellular and transcellular NaCl and divalent cation reabsorption.[11] These effects are primarily mediated by inhibition of the activity of the renal outer medullary potassium channel (ROMK) and the apical Na^+-K^+-$2Cl^-$ cotransporter, NKCC2, which reduces the net lumen positive charge and lowers the electrochemical driving force for paracellular calcium, sodium and magnesium transport.[35,36] In addition, CaSR signaling results in the degradation of claudin 16, which promotes paracellular transport of calcium and magnesium.[37] Activation of the CaSR also inhibits PTH-mediated calcium reabsorption in the CTAL by inhibiting uptake of calcium across the apical membrane and in the CTAL and distal convoluted tubule by inhibiting the activity of the basolateral calcium pump, PMCA1b, which is necessary for extrusion of calcium from the cell into the ECF.[11,38,39]

Concurrent with its effects on calcium excretion, the CaSR also increases acid and water excretion by the kidney, both of which help to maintain the solubility of calcium salts in the urine and prevent the precipitation of the excreted calcium. Activation of the CaSR in the collecting ducts leads to inhibition of the H^+-ATPase, which results in increased acid secretion.[40] Recent genetic studies have underscored the importance of urine acidification in protecting against stone formation in response to hypercalciuria, at least in mice.[40] Hypercalcemia is also well known to inhibit renal concentrating ability.[11] Stimulation of apical membrane CaSRs in the inner medullary collecting duct inhibits vasopressin induced aquaporin 2 (AQ2) insertion into the apical membrane and reduces the transcellular reabsorption of water.[41] In chronic states of hypercalcemia, the CaSR also downregulates AQ2 expression via post-transcriptional mechanisms.[42]

In addition to the direct effects of the CaSR on renal calcium handling, it also inhibits CYP27B1 activity in the proximal tubule.[11,12] This results in lower levels of 1,25 $(OH)_2$-vitamin D (the active form of the hormone), which will also inhibit calcium absorption from the diet, the release of calcium from bone and calcium reabsorption in the distal tubule, all of which would help to lower circulating calcium concentrations.

The Skeleton: Studies in cell lines and in genetically altered mice suggest that the CaSR also affects bone cells independent of its effects on PTH secretion or 1,25 $(OH)_2$-vitamin D production.[29,43] Osteoclasts, osteoblasts, osteocytes, growth plate chondrocytes and bone marrow immune cells have all been found to express the CaSR.[3,5] Selective knockout of the receptor in osteoblasts has been shown to have profound effects on bone growth and mineralization due to impaired osteoblast activity.[29] Studies in cell culture suggest that CaSR signaling may affect both osteoblast proliferation and differentiation.[44] Low levels of CaSR signaling appear to promote osteoclast differentiation but high levels of calcium have been found to inhibit osteoclast function and cause osteoclast apoptosis.[45,46] The regulation of bone cell function by the CaSR is an evolving

issue and, at present, it is unclear whether the actions the CaSR on osteoclasts and osteoblasts are important in the acute regulation of systemic calcium metabolism. It is certainly possible that the CaSR might regulate the mobilization of calcium from the bone interstitial fluid in ways reminiscent of its actions on ion transport in other sites.

Parathyroid Hormone

The principal regulator of the minute-to-minute calcium concentration is parathyroid hormone. PTH is secreted by the four parathyroid glands, which arise from the third and fourth branchial arches during embryogenesis and normally reside near the posterior capsule of the four poles of the thyroid gland. However, extra or ectopic parathyroid glands or small rests of parathyroid tissue are commonly found from the angle of the jaw to the mediastinum, along the path of embryonic migration of the thymus and parathyroid glands. This can be an important consideration in hyperparathyroid states that require surgical intervention (see below).

Human PTH is encoded by a single gene located on chromosome 11 (11p15). The gene contains three exons; the first codes for the 5′ untranslated portion of the mRNA, the second encompasses most of the pre-pro sequences and the third encodes the actual protein sequence of the secreted hormone.[47–49] The *PTH* gene is a member of a small gene family that also includes the *parathyroid hormone-related protein (PTHrP)* and the *tubuloinfundibular peptide of 39 amino acids (TIP39)* genes.[48] Each of these genes has a similar exon/intron structure and all three bind related receptors with overlapping specificities (see below).[50] The *PTH* and *PTHrP* genes likely arose from a common ancestor and lower vertebrates have multiple *PTH* and *PTHrP* genes.

PTH is initially synthesized as pre-pro-parathyroid peptide and undergoes post-translational modification to produce the active hormone. The 25-residue pre-sequence and the 6-residue pro-sequence are cleaved during the initial production of PTH, yielding the mature, 84-amino acid, full-length protein (PTH 1-84).[51] Full-length PTH is the biologically active form of the hormone. It has a very short half-life (minutes) in the circulation and is degraded by the liver and kidney, which generates circulating carboxy-terminal (C-terminal) fragments. These fragments are cleared by the kidney but may accumulate in the circulation in renal failure.[52]

Three factors, calcium, 1,25 dihydroxyvitamin D and phosphate, have been shown to modulate PTH mRNA levels and/or PTH secretion.[53] Parathyroid cells express high levels of the CaSR, which allow them to respond to small changes in the circulating calcium concentration.[54] Changes in extracellular calcium lead to reciprocal changes in PTH secretion (see below) and gene expression.[53,54] The mechanisms through which CaSR signaling affects *PTH* gene expression are not well described. Although a negative calcium regulatory element has been identified in the *PTH* gene promoter region, it is currently thought that the primary effect of CaSR signaling is post transcriptional.[53] PTH mRNA contains AU-rich elements in the 3′ untranslated region (UTR), which regulate its stability. In the setting of low extracellular calcium concentrations, specific proteins bind to these elements and protect the mRNA from degradation. Activation of CaSR signaling displaces these factors and shortens the half-life of PTH mRNA.[55]

A steep inverse sigmoidal relationship exists between PTH secretion and the extracellular ionized calcium concentration and is defined by four parameters (Figure 66.1). The first is the maximum secretory rate of the parathyroid glands. The second is the slope of the curve at the midpoint. The third is the parathyroid gland's "set point," or calcium concentration at which PTH secretion is half maximal. The final parameter is the basal, nonsuppressible rate of PTH secretion. The steep part of the curve encompasses the physiologic range for extracellular calcium, over which small changes in the concentration of ionized calcium elicit dramatic changes in the rate of PTH secretion.[56] Because of this steep slope, ionized calcium concentrations are maintained in a very narrow physiologic range. A great deal of data in both genetically altered mice and in humans with genetic disorders of calcium sensing have demonstrated the primary importance of the CaSR in controlling PTH secretion.[3,56] For example, mice with either global deletion or parathyroid-specific disruption of the *CaSR* gene have very high levels of circulating parathyroid hormone, which are not suppressed by severe hypercalcemia.[29,30] The same is true of humans with null mutations in the *CaSR* gene.[57] Furthermore, in both mice and humans, heterozygous disruption of the *CaSR* gene results in a milder form of hyperparathyroidism, demonstrating a dose effect between parathyroid CaSR levels and the sensitivity of PTH to calcium-mediated suppression.[29,30,57] Conversely, humans with activating mutations in the *CaSR* gene present with hypoparathyroidism characterized by a failure to secrete PTH in response to hypocalcemia.[58]

The molecular mechanisms by which CaSR signaling inhibits PTH secretion are not completely understood. Binding of calcium to the CaSR activates downstream signaling pathways that, in turn, suppress PTH secretion.[3,56] It is clear that activation of both $G\alpha_q$ and $G\alpha_{11}$ is necessary for suppression of PTH secretion since parathyroid specific disruption of the genes for

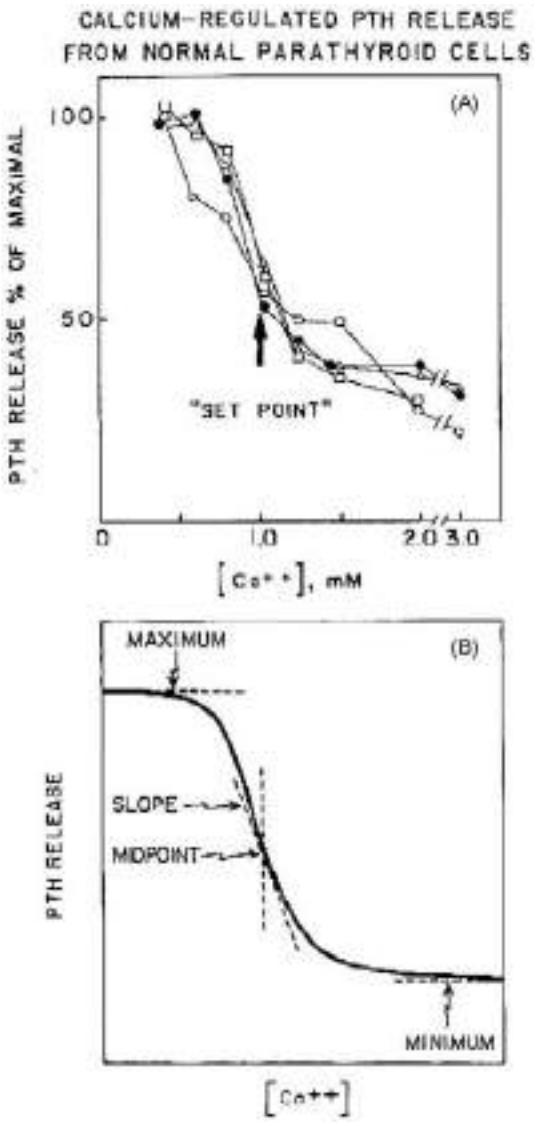

FIGURE 66.1 (A) The inverse sigmoidal relationship between increasing concentrations of extracellular calcium and PTH secretion from dispersed normal parathyroid cells in culture. (B) This relationship can be defined by the maximal rate of PTH secretion, the slope of the curve at the mid-point, the set point (point at half-maximal PTH secretion) and the minimal rate of PTH secretion. *(Reproduced with permission from Brown, EM. 1983. Four-parameter model of the sigmoidal relationship between parathyroid hormone release and extracellular calcium concentration in normal and abnormal parathyroid tissue. J Clin Endocrinol Metab 56:572–581.)*

both of these G-proteins phenocopies the disruption of the *CaSR* gene itself.[59] However, it is not clear how specific signaling events downstream of these G-proteins actually inhibit the secretion of PTH.

Vitamin D will be discussed in more detail below. The active form of vitamin D, 1,25 $(OH)_2$ vitamin D, acts on parathyroid cells to inhibit PTH production, both by increasing circulating calcium levels and by inhibiting *PTH* gene transcription directly.[51,53] This effect is thought to be a result of reduced transcription of the *PTH* gene due to the binding of 1,25 dihydroxyvitamin D to the vitamin D receptor (VDR), which in turn binds to vitamin D response elements in the 5′ flanking region of the *PTH* gene.[60] Vitamin D receptors are abundant in parathyroid tissue and their levels are modulated by calcium and 1,25 $(OH)_2$ vitamin D itself.[53] Activation of the CaSR increases the expression of the VDR in parathyroid cells and 1,25 $(OH)_2$ vitamin D increases the expression of the CaSR, thereby mutually sensitizing the parathyroid glands to negative feedback in states of vitamin D or calcium excess. In CKD and in parathyroid adenomas, expression of both the VDR and the CaSR is reduced, likely contributing to increased PTH production.[61–63]

Phosphate stimulates PTH production and hyperphosphatemia is an important contributor to the development of secondary hyperparathyroidism in patients with chronic kidney disease.[61,64] Some of these effects may be related to the drop in ionized calcium that attends any increase in circulating phosphate, but phosphate also exerts independent effects on PTH mRNA stability.[64] Similar to the effects of low calcium, elevations in serum phosphate lead to the binding of a protein complex to the 3′UTR of PTH mRNA that inhibits its degradation.[55,64] Changes in serum phosphate may also affect PTH indirectly via the actions of fibroblast growth factor 23 (FGF-23), which is secreted from osteocytes (see Chapter 68). The parathyroids respond to FGF-23 but, somewhat paradoxically, FGF-23 has been described to reduce PTH gene expression and secretion,[65–67] even though it also lowers circulating phosphate levels. Therefore, it is possible that the actions of FGF-23 on the parathyroid cells may counterbalance the direct effects of phosphate on PTH gene expression. As discussed in Chapters 69 and 91, FGF-23 levels are elevated in CKD, although it is not known whether these elevated levels contribute to the dysregulation of PTH secretion in these patients. Our understanding of the regulation of parathyroid function by FGF-23 is an evolving area that will require further research for clarification.

PTH binds and activates the Type 1 PTH/PTHrP receptor (PTH1R), a GPCR that is shared with PTHrP.[50,68] It is a member of the B subfamily of GPCRs, which also includes the secretin and calcitonin receptors.[50,69] Two other PTH receptors are also included within this group. The PTH2R is primarily a receptor for TIP39. PTH can bind weakly to this receptor and activate it, but it is not known if this represents a physiological interaction.[50,69] PTHrP cannot activate the PTH2R. There is also a third PTH receptor (PTH3R) documented in zebra fish, but it does not appear to be present within the human genome.[50,69] Thus, as with the PTH peptide family, it appears that evolution has reduced the diversity of PTH receptors.

The amino-terminal portion of PTH [PTH(1–34)] is necessary and sufficient for full activation of the PTH1R. Amino acids in the C-terminal portion of this PTH fragment are thought to bind to the extracellular, amino-terminal portion of the PTH1R, while the amino-terminus of PTH(1–34) binds to the juxtamembrane portion of the PTH1R in order to activate downstream signaling (Figure 66.2).[69,70] The PTH1R has been shown to activate both the cAMP/protein kinase A (PKA) pathway and the phospholipase C/protein kinase C/calcium transient pathway. There is also evidence that the receptor activates phospholipase D and MAPK signaling.[50,69] MAPK activation can occur either through a PLC/PKC-dependant pathway or via a G-protein independent pathway that involves arrestins.[71,72] Many of the classic biological functions of PTH appear to be mediated to a great extent by the cAMP/PKA pathway, which requires the first two amino acids of PTH for activation.[50,69] Less is known about the biological role of the other signaling pathways.

The PTH1R is highly expressed within the skeleton and kidney, the two classic target organs for PTH action. However, it is also widely expressed in many other cells throughout body.[50,69] The receptor at these sites may primarily serve as a PTHrP receptor. However, circulating PTH could theoretically activate these receptors and may therefore affect physiological processes other than calcium and bone metabolism, especially in the setting of hyperparathyroidism.

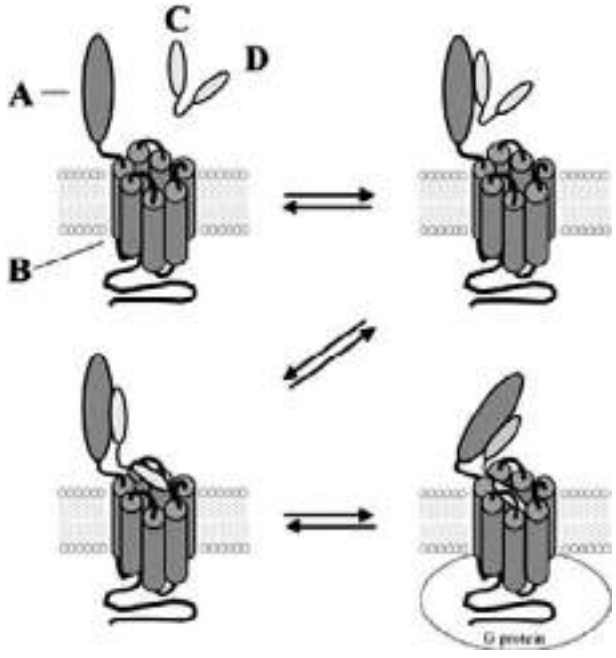

FIGURE 66.2 Model for binding of amino-terminal PTH to the PTHR1. The C-terminal end of PTH (1–34) (C) binds first to the extracellular N-terminal portion of the receptor (B). Subsequently, the amino-terminal portion of PTH 1–34 (D) binds to the J-domain of the receptor. This results in a conformational change of the receptor such that it takes on a more closed shape, which increases its affinity for G-proteins and leads to their activation. *(Reproduced with permission from Potts JT. 2008. Parathyroid hormone: past and present. J Endocrinol 187: 311–325.)*

PTH is the principal hormone that coordinates calcium homeostasis on a minute-to-minute basis. It does this through its actions on the kidney and on bone cells. Below, we discuss the actions of PTH on these two organs in detail.

Kidney: PTH regulates the renal handling of calcium, phosphate, sodium and hydrogen ions.[73] It also regulates the conversion of 25-hydroxyvitamin D to 1,25-dihydroxyvitamin D.[73] The PTH1R is expressed at different sites along the nephron, including the glomerulus, proximal tubules, the cortical ascending limbs and the distal convoluted tubules. In the proximal and thick ascending limbs the receptor is expressed on both the basolateral surface and the luminal surfaces of cells.[74,75]

PTH was originally recognized for its actions to promote urinary phosphate excretion.[73] Approximately 90% of plasma phosphate is filtered by the glomerulus and 80% is actively reabsorbed, primarily by the proximal convoluted tubules. The regulated step in phosphate reabsorption is entry of phosphate across the luminal membrane of the proximal tubule cells though two related sodium-phosphate co-transporters known as NPT2a and NPT2c.[73,76] PTH inhibits phosphate uptake into these cells by triggering the withdrawal of NPT2a from the apical membrane into intracellular vesicles, which leads to proteolytic degradation of the transporter.[73,77–80] Interestingly, activation of the luminal or basolateral PTH1R pool appears to stimulate different signaling pathways, yet both cause internalization of NPT2a. The basolateral receptors increase intracellular cAMP. At the luminal surface, the PTH1R is associated with a scaffolding protein known as NHERF1, which favors the activation of the PKC pathway over the cAMP pathway.[81,82] NHERF1 has also been shown to bind to NPT2a and it has been suggested that dissociation of NHERF1 from NPT2a is necessary to allow internalization of NPT2a in response to PTH.[73,83,84]

PTH increases calcium reabsorption by the kidney. This occurs through the stimulation of active transcellular calcium transport across epithelial cells in the cortical segment of the thick ascending loop of Henle and in the distal convoluted tubule.[73] In distal tubule cells PTH stimulates cAMP/PKA signaling and phospholipase D, both of which are necessary to mediate calcium transport.[85–90] These signaling cascades lead to hyperpolarization of the membrane potential, which stimulates the entry of calcium across the apical membrane as well as its extrusion via sodium/calcium exchange across the basolateral membrane.

PTH acts on the proximal tubule to stimulate the conversion of 25 (OH) vitamin D to 1,25 $(OH)_2$ vitamin D, which is the active form of vitamin D.[50,51,73,91] In this way, PTH indirectly stimulates calcium absorption from the gut and activates bone cell activity. The increase in 1,25 $(OH)_2$ vitamin D is the result of stimulation of both *CYP27B1* gene expression and activity (the enzyme responsible for hydroxylation of vitamin D at the C-1 position).[73,92,93] The effects of PTH on CYP27B1 activity are opposed by the CaSR and by 1,25 $(OH)_2$ vitamin D itself.[12,94,95] PTH also inhibits the degradation of 1,25 $(OH)_2$ vitamin D by decreasing CYP24A1 (24-hydroxylase) activity in the proximal tubule and thus inhibiting vitamin D catabolism.[96,97]

PTH inhibits acid secretion in the proximal tubule and can produce a mild compensated hyperchloremic acidosis.[73] This is the result of phosphorylation of the Na^+/H^+ exchanger (NHE3) by PKA downstream of the PTH1R.[80,98] While this results in reduced bicarbonate and sodium reabsorption by the proximal tubule, the distal tubules compensate by increasing both sodium and bicarbonate absorption. As a result, there is little change in serum bicarbonate concentrations or pH, although chronic elevations in PTH can be associated with mild hyperchloremia.

The skeleton: PTH increases bone turnover although the net effect on bone depends on the pattern of PTH exposure. Continuous PTH exposure causes net bone catabolism, which is seen in states of hyperparathyroidism. In contrast, intermittent PTH exposure has an anabolic effect on the skeleton, which has been exploited pharmacologically in the treatment of osteoporosis. Below, we will discuss the actions of PTH on the three main cell types in bone, osteoclasts, osteoblasts and osteocytes.

PTH stimulates bone resorption due to an increase in the production of new osteoclasts as well as an increase in the activity of existing osteoclasts.[51,73,99,100] Neither osteoclasts nor their precursors express the PTH1R, so these effects result from paracrine interactions between osteoclasts and cells within the osteoblast lineage, which do express the PTH1R. Osteoclast differentiation, activity and survival are regulated by two cytokines, colony-stimulating factor 1 (MCSF, CSF1) and receptor-activator of NFκB ligand (RANKL).[101,102] CSF1 is produced by stromal/osteoblast cells and acts through its receptor c-fms to induce early monocyte/macrophage precursors to enter the osteoclast lineage.[101,102] RANKL is also produced by cells in the stromal/osteoblast lineage and acts through its receptor, receptor-activator of NFκB (RANK) to promote the differentiation of osteoclast precursors into mature osteoclasts, to increase the bone-resorbing activity of mature osteoclasts and to lengthen the life-span of active osteoclasts.[73,100–102] RANKL can also be bound by a secreted decoy receptor known as osteoprotegerin (OPG), which inhibits osteoclast formation and activity, and promotes osteoclast apoptosis.[73,100–102] Therefore, the RANKL/OPG ratio is an important determinant of osteoclastic activity. PTH increases the secretion of CSF1 and RANKL, and suppresses the secretion of OPG raising the RANKL/OPG ratio.[73,99–103] These alterations in local cytokines increase osteoclast numbers and activity, and stimulate bone resorption.

The direct effects of PTH on osteoblast function are complicated and vary depending on the duration of exposure to PTH as well as the state of differentiation of the cells. The reader is referred to more in-depth reviews for a detailed discussion of the specific effects of PTH on osteoblasts.[73,99–104] Continuous and intermittent PTH both increase osteoblast numbers and rates of bone formation *in vivo*.[73,99–104] This does not appear to be due to cell proliferation as most data suggest that PTH inhibits the proliferation of committed osteoblast precursors and mature osteoblasts.[100,105–107] Intermittent exposure to PTH favors the commitment of mesenchymal precursors to the osteoblast lineage and stimulates osteoblast differentiation.[73,100,108–111] In addition, intermittent PTH administration may convert previously quiescent bone lining cells into active osteoblasts.[112] In contrast, prolonged, continuous exposure to PTH inhibits full osteoblast differentiation.[73,91,100] These alternative effects on osteoblast differentiation may help to explain why net anabolic activity differs between continuous and intermittent PTH exposure.

The PTH1R is expressed on osteocytes and PTH inhibits osteocyte apoptosis and suppresses osteocyte production of sclerostin, an important inhibitor of Wnt signaling in bone.[104,113–116] Experiments in mice suggest that activation of the osteocyte PTH1R influence the activity of osteoblasts and osteoclasts on bone surfaces, demonstrating that these cells may help to coordinate bone turnover in response to PTH.[115] C-terminal fragments of PTH also affect osteocytes by binding to a specific, although as yet uncharacterized, C-terminal PTH receptor. Activation of this receptor may antagonize PTH1R actions, which could theoretically contribute to the skeletal resistance to PTH described in CKD, since decreases in GFR increase the concentration of circulating C-terminal PTH fragments.[116]

Vitamin D

Vitamin D is a steroid hormone that contributes to the development and maintenance of cartilage and bone as well as the regulation of calcium and phosphate metabolism. It exerts a myriad of other effects, including the regulation of the immune response, the control of epithelial cell proliferation and the regulation

of cell differentiation. Here we will limit our discussion to its actions on calcium homeostasis.

The biological activity of vitamin D is mediated by 1,25 $(OH)_2$ vitamin D3, which circulates in pM concentrations.[117] The production of active vitamin D is tightly regulated and is the net result of a series of photochemical and enzymatic steps that involve several tissues throughout the body. The first step in vitamin D synthesis is the formation of pre-vitamin D3 from 7-dehydrocholesterol. This reaction occurs in the plasma membrane of keratinocytes and is catalyzed by ultraviolet B light between the wavelengths of 290 and 315 nM.[118] Previtamin D3 is thermodynamically unstable and in a temperature dependant fashion is converted into vitamin D3, which is shed into the ECF and binds to vitamin D binding protein (DBP) in the circulation.[117] The quantity of vitamin D3 formed in the skin depends on the duration and intensity of sunlight exposure and is inhibited by sunscreen, clothing and skin pigmentation. Thus, people with darker skin and those living at latitudes farther from the equator synthesize less vitamin D, and in the Northern hemisphere, there is less vitamin D synthesis in winter months.[119–122] These racial, geographical and seasonal factors all contribute to the patterns of vitamin D deficiency observed in the human population.

Vitamin D3 can be stored in fat and in the liver. As noted above, it circulates bound to DBP and it is hydroxylated at the C-25 position in order to form 25 (OH) vitamin D.[117] This reaction occurs in the liver and is the sum of the actions of several cytochrome p450 enzymes, although the most important appears to be the microsomal enzyme, CYP2R1.[123] Production of 25 (OH) vitamin-D is controlled by substrate availability, so the measurement of circulating 25 (OH) vitamin D is the most reliable clinical indicator of total body vitamin D stores. 25 (OH) vitamin D circulates in nM concentrations, and is also bound to DBP.[117]

The active hormone, 1,25 $(OH)_2$ vitamin D is formed in the kidney under tight regulation by PTH, phosphate, FGF-23 and calcium concentrations.[117] 25 (OH) vitamin D is filtered into the urine and is reabsorbed together with DBP by megalin and cubulin, which are found in the apical membrane of the proximal tubule cells.[124,125] Hydroxylation of 25 (OH) vitamin D is catalyzed by CYP27B1, which is a cytochrome P450 enzyme found within the inner mitochondrial membrane.[126–128] The proximal tubule also expresses 24 hydroxylase activity mediated by CYP24A1 which generates 24, 25 $(OH)_2$ vitamin D and calcitroic acid, the main inactive metabolites of 25 (OH) vitamin D and 1,25$(OH)_2$ vitamin D, respectively.[129,130] CYP24A1 antagonizes the actions of CYP27B1 both by shunting away its substrate and by inactivating its product. The synthesis of 1,25 $(OH)_2$ vitamin D is regulated primarily by altering the expression of CYP27B1 and CYP24A1 in a reciprocal fashion. PTH, low calcium, low phosphate and calcitonin act to stimulate 1,25 $(OH)_2$ vitamin D production, while high calcium, high phosphate, FGF23 and 1,25 $(OH)_2$ vitamin D, itself, inhibit production.[117] In tissues outside the kidney, CYP27B1 and CYP24A1 expression, and 1,25 $(OH)_2$ production are also regulated by a number of growth factor and cytokine pathways as well as by toll-like receptor signaling.[117]

Vitamin D acts as a classical steroid hormone and regulates gene expression by binding to the vitamin D receptor (VDR), a ligand-activated transcription factor that is a member of the large superfamily of steroid hormone receptors.[117,131,132] The active receptor is a heterodimer between the VDR and the retinoic acid X (RXR) receptor. Like other steroid hormone receptors the activated VDR recruits a number of co-factors to specific sequences within target genes in order to form a multiprotein complex that includes chromatin remodeling activity and transcriptional activators or repressors.[131,132] The activity of vitamin D and the VDR depends on the particular makeup of this protein complex and, like other steroid hormone/receptor complexes, is cell-type and target gene specific. We will not review the details of gene regulation by the VDR further. The interested reader is referred to more comprehensive discussions of this topic.[117,131,132]

Vitamin D acts on all the components of calcium homeostasis and controls the acquisition of calcium from the environment as well as modulating the sensitivity of several organs to calcium and PTH. Below, we review the actions of vitamin D on calcium-regulating organs.

The Intestine: Vitamin D deficiency and genetic disruption of the vitamin D receptor cause hypocalcemia, secondary hyperparathyroidism, rickets, osteomalacia, and growth retardation.[117] All of these disturbances can be rescued by the administration of a high calcium and lactose diet that increases vitamin D-independent gut calcium absorption or by selective, transgenic replacement of intestinal VDR expression in VDR-knockout mice.[133,134] Therefore, it has become clear that the dominant actions of vitamin D on calcium and bone metabolism are to support the absorption of calcium and phosphorus from the diet. Calcium is absorbed from the intestine through a saturable, transcellular process that is prominent in the proximal small intestine and a non-saturable, paracellular process that is more prominent in the ileum and colon.[135] Vitamin D has its greatest effects on increasing transcellular transport, although it can also increase paracellular calcium absorption. Vitamin D has traditionally been thought to increase transcellular calcium transport in enterocytes by increasing the production of proteins involved

in calcium entry across the apical membrane (TRPV6), calcium translocation through the cytoplasm (calbindin D_{9k}, calbindin D_{28k}) and calcium extrusion across the basolateral membrane (PMCA1b).[136–143] However, recent knockout mouse models of TRPV6 and calbindin D_{9k} have suggested that the standard model of vitamin D-mediated transcellular calcium transport may be overly simplistic.[144–146] Vitamin D signaling also upregulates the expression of claudin 2 and claudin 12, both of which modulate the permeability of tight junctions to calcium and, thus, likely regulate paracellular calcium transport.[147]

It should be noted that vitamin D also increases intestinal phosphate absorption.[135] This is caused by increases in the apical expression of NPT2b, a sodium-phosphate co-transporter related to the phosphate transporters expressed in the proximal renal tubule.[148,149] However, the exact molecular mechanisms by which vitamin D regulates NPT2b expression and phosphate absorption remain to be defined.

The kidney: In addition to serving as the site of 1,25 $(OH)_2$ vitamin D synthesis, the kidney is also a target of vitamin D actions.[117,150] The VDR is expressed at highest levels in distal tubule cells but is also expressed at lower levels in the proximal tubule.[151] The net effect of vitamin D on the kidney appears to be the regulation of its own synthesis in a short feedback loop in the proximal tubule and the enhancement of calcium reabsorption in the distal convoluted tubule. In the proximal tubule Vitamin D inhibits the production of CYP27B1 and enhances the production of CYP24A1 acting to inhibit further production of 1,25 $(OH)_2$ vitamin D.[117,150] As in the intestine, vitamin D acts on the distal tubule to regulate the production of several proteins involved in transcellular calcium reabsorption. It upregulates the expression of TRPV5 and TRPV6, the two apical calcium entry channels; Calbindin D_{9k} and Calbindin $_{28k}$, which are involved in cytoplasmic calcium translocation; and PMCA1b, which transports calcium out of the cell across the basolateral membrane.[150] It also has been shown to increase PTHR1 expression in the distal tubule and to enhance the effects of PTH on distal tubular calcium reabsorption.[150]

Bone: The vitamin D receptor is expressed in cells of the osteoblast lineage but not in mature osteoclasts. The classic presentation of vitamin D deficiency in children is growth retardation and rickets, while in adults it can result in osteomalacia.[117] However, as noted previously, when VDR-knockout mice were treated with a high calcium "rescue" diet that normalized calcium, phosphate and PTH levels, these bone phenotypes disappeared, suggesting that the dominant effects of vitamin D on bone were indirect.[133] However, a close examination of $VDR^{-/-}$, $CYP27B1^{-/-}$ and double knockout, $VDR^{-/-}$, $CYP27B1^{-/-}$ mice on rescue diets demonstrated that loss of vitamin D function reduced the numbers of osteoblasts and osteoblast progenitors *in vivo*, which is consistent with many studies *in vitro* that have documented effects of vitamin D on osteoblast gene expression, osteoblast proliferation and osteoblast differentiation.[32,117] However, in the presence of adequate amounts of dietary calcium and phosphate, the direct effects of vitamin D on osteoblast function are subtle and may differ depending on the stage of osteoblast differentiation. The indirect effects of vitamin D on osteoclasts are more straightforward. 1,25 $(OH)_2$ vitamin D increases osteoblast expression of RANKL and decreases the production of OPG by osteoblasts.[152,153] By increasing the RANKL/OPG ratio, vitamin D increases the production of osteoclasts and of bone turnover. This effect of vitamin D is clinically apparent in states of 1,25 $(OH)_2$ vitamin D overproduction or in the setting of excess ingestion of vitamin D, where bone resorption is excessive despite the suppression of PTH secretion.

Parathyroid gland: The parathyroid glands are rich in VDR expression and 1,25 $(OH)_2$ vitamin D inhibits transcription of the PTH gene.[60,154–156] This appears to be a direct effect of the VDR on the PTH gene promoter. Vitamin D also regulates PTH production indirectly by increasing CaSR expression in the parathyroids and by increasing systemic calcium levels.[9] As noted previously, CaSR signaling increases VDR expression in the parathyroids, so vitamin D and calcium act synergistically to suppress PTH secretion.[53] Therefore, states of vitamin D deficiency may sensitize the gland to low calcium levels and increase the PTH response to hypocalcemia. This may contribute to the development of parathyroid hyperplasia and secondary hyperparathyroidism in CKD. However, in mice, it appears that calcium remains the most important factor regulating parathyroid gland growth and PTH secretion. Meir and colleagues disrupted the VDR specifically in parathyroid cells and found that while CaSR levels were decreased, PTH secretion was only modestly increased and that serum calcium levels remained normal.[157] These data suggest that the VDR may have a limited role in regulating parathyroid function at baseline.

Parathyroid Hormone-Related Protein

The *PTHrP* and *PTH* genes share structural elements and sequence homology suggesting that they arose through duplication of a common ancestor.[158–161] The portion of both genes encoding the amino-terminal segments of PTH and PTHrP are highly conserved such that the peptides share 8 of the first 13 amino acids and a high degree of predicted secondary structure over the next 21 amino acids. Beyond this, however, the two

genes share little similarity. PTHrP mRNA is expressed in almost every organ at some time during its development or functioning. Many different hormones and growth factors regulate PTHrP mRNA levels. As with PTH, the CaSR regulates *PTHrP* gene expression in many different cell types.[162,163] Another common observation is that mechanical forces induce *PTHrP* gene expression in many sites.[159]

Like PTH, PTHrP binds to and activates the PTH1R. Most studies *in vitro* suggest that this receptor binds PTHrP and PTH with equal affinity and that both peptides trigger identical signaling events.[50,159] However, the human PTH1R may respond somewhat differently to PTH and PTHrP. It appears that PTH and PTHrP demonstrate differences in their ability to stabilize alternate conformational states of the receptor, so that the duration of cAMP production is shorter for PTHrP (1–36) than for PTH (1–34).[164] This may explain why human subjects subjected to continuous infusion of the two peptides for 72 hours, were found to become hypercalcemic with lower doses of PTH 1–34 than PTHrP (1–36) and had lower 1,25 $(OH)_2$ vitamin D production when infused with PTHrP.[165] These studies may also help to explain differences in the biochemical profiles of HHM and hyperparathyroidism (see below).

In addition to being secreted, PTHrP can also be transported into the nucleus of many different cell types.[166,167] The function(s) of nuclear PTHrP is unclear, but replacement of the endogenous mouse PTHrP gene with a mutant version encoding a protein that cannot enter the nucleus causes widespread cellular senescence, growth retardation and early death.[168] This experiment suggests that nuclear PTHrP is of fundamental importance in many cell types.

PTHrP has been suggested to have many functions. The reader is referred to more comprehensive reviews for a complete discussion.[159,169] Here, we will highlight two areas where PTHrP has been documented to have physiological effects in intact organisms.

Cartilage and bone: A series of genetic experiments in mice and genetic disorders in humans have demonstrated that amino-terminal PTHrP acts through the PTH1R to coordinate the rate of chondrocyte differentiation in order to maintain the orderly growth of long bones during development.[170–173] PTHrP is produced by immature chondrocytes at the top of the growth plate in response to another molecule known as Indian Hedgehog (IHH) secreted by differentiating hypertrophic chondrocytes. PTHrP, in turn, acts on its receptor located on proliferating and prehypertrophic cells to slow their rate of differentiation into hypertrophic cells. Therefore, IHH and PTHrP define a local negative feedback loop that regulates the rate of chondrocyte differentiation (see Figure 66.3).[173] PTHrP is also found in other cartilaginous sites such as the costal cartilage and the hyaline cartilage lining the joint space, where it appears to prevent the inappropriate encroachment of bone into these structures.[174,175]

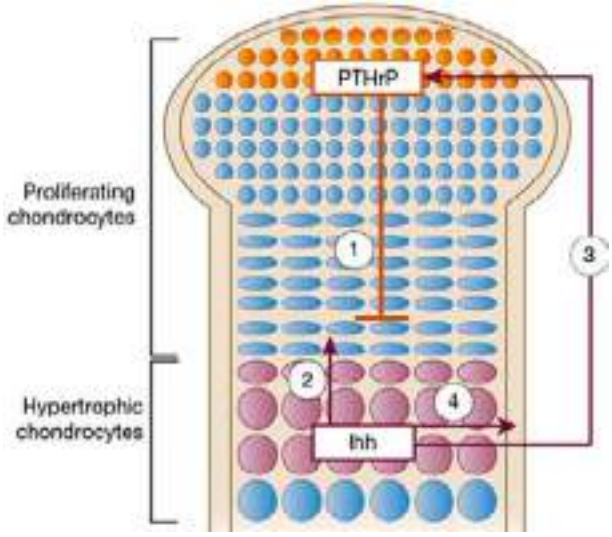

FIGURE 66.3 PTHrP and Indian hedgehog (Ihh) act as part of a negative feedback loop regulating chondrocyte proliferation and differentiation. The chondrocyte differentiation program proceeds from undifferentiated chondrocytes at the end of the bone, to proliferative chondrocytes within the columns and then to prehypertrophic and terminally differentiated hypertrophic chondrocytes nearest the primary spongiosum. PTHrP is made by undifferentiated and proliferating chondrocytes at the ends of long bones. It acts through the PTH1R on proliferating and prehypertrophic chondrocytes to delay their differentiation, maintain their proliferation and delay the production of Ihh, which is made by hypertrophic cells (1). Ihh, in turn, increases the rate of chondrocyte proliferation (2) and stimulates the production of PTHrP at the ends of the bone (3). Ihh also acts on perichondrial cells in order to generate osteoblasts of the bone collar (4). *(Reproduced with permission from Kronenberg HM. 2003. Developmental regulation of the growth plate. Nature 423:332–336.)*

PTHrP also affects bone cells *in vivo*. Heterozygous PTHrP-null mice develop osteopenia with increasing age.[176] In addition, selective deletion of the PTHrP gene from osteoblasts causes decreased bone mass, reduced bone formation, reduced mineral apposition and a reduction in the formation and survival of osteoblasts.[177] These data suggest that PTHrP acts as an important local anabolic factor in the skeleton.

Mammary gland: PTHrP has important functions during breast development, it is involved in regulating systemic calcium metabolism during lactation and it contributes to the pathophysiology of breast cancer.

The mammary gland forms as a bud-like invagination of epidermal cells that grow into a specialized mesenchyme.[178] The epithelial cells of the embryonic mammary bud produce PTHrP, which interacts with the PTH1R expressed on surrounding mesenchymal cells. This interaction is necessary for the outgrowth of the duct system.[179] In both mice and humans,

disruptions of PTHrP signaling cause a failure of breast development past this early bud stage.[180]

PTHrP is also produced by breast epithelial cells during lactation and large quantities are secreted into milk.[181,182] The function of PTHrP in milk is unknown, but it is secreted from the lactating breast into the circulation, where it participates in the regulation of systemic calcium metabolism. The maternal skeleton is an important source of calcium for milk production and the lactating breast secretes PTHrP into the circulation to increase bone resorption.[182] This is the only time in which PTHrP exerts a documented systemic endocrine effect on normal calcium and bone metabolism.

CALCITONIN

Calcitonin is produced by the C-cells of the thyroid gland in humans and by the ultimobranchial body in other animal species. Calcitonin is encoded by the *CALC1* (also referred to as *CALCA*) gene, a member of a family of genes that also encode islet amyloid protein, calcitonin gene related peptide (CGRP), and the precursor of adrenomedullin. Alternative splicing of the CALC1 transcript also yields a homologous peptide, calcitonin gene-related peptide (CGRP), which is produced in the nervous system.[183] Similar to parathyroid cells, C-cells express the CaSR on their cell surface and are sensitive to small changes in extracellular fluid calcium concentrations. Increases in serum calcium levels within the normal physiologic range lead to the secretion of calcitonin.[184]

The calcitonin receptor is a GPCR[185] that is expressed at high levels on osteoclasts. Activation of the calcitonin receptor inhibits osteoclast motility, causes their retraction from the bone surface, and acutely inhibits their ability to resorb bone.[186–188] However, these effects are short-lived, because calcitonin signaling causes a reduction in the number of calcitonin receptors and rapid development of calcitonin resistance.[189] In humans, calcitonin does not appear to be essential for minute-to-minute calcium homeostasis, but it may contribute to the conservation of total body calcium, especially with aging and/or during periods of calcemic stress such as pregnancy or lactation.[190] Experiments in knockout mice suggest that the disruption of calcitonin signaling results in an impaired ability to recover from hypercalcemia, and excessive bone loss during lactation.[191,192]

INTEGRATED REGULATION OF CALCIUM METABOLISM

The various hormones and organ systems discussed in the previous sections all cooperate in order to regulate the ECF ionized calcium concentration and maintain it in a relatively narrow physiologic range. As mentioned previously, it has been suggested that increases in PTH secretion from the parathyroid gland serve as the principal defense against hypocalcemia but that the direct effects of calcium on the kidney CaSR may be more important in returning calcium to the normal range in the face of hypercalcemia. However, this construct has not been validated in human subjects. Even, if this is the case, it is clear that the entire interconnected homeostatic system responds to either hypocalcemia or hypercalcemia.

As illustrated in Figure 66.4, a fall in the ECF calcium level below the physiologic range is rapidly sensed by the parathyroid gland CaSR. Reduced signaling from this receptor then leads to the secretion of more PTH from the parathyroid glands, which, in turn activates the release of calcium and phosphate from the skeleton. There is a rapid release of calcium and phosphate from the bone interstitial fluid followed by an increase in bone resorption that releases calcium

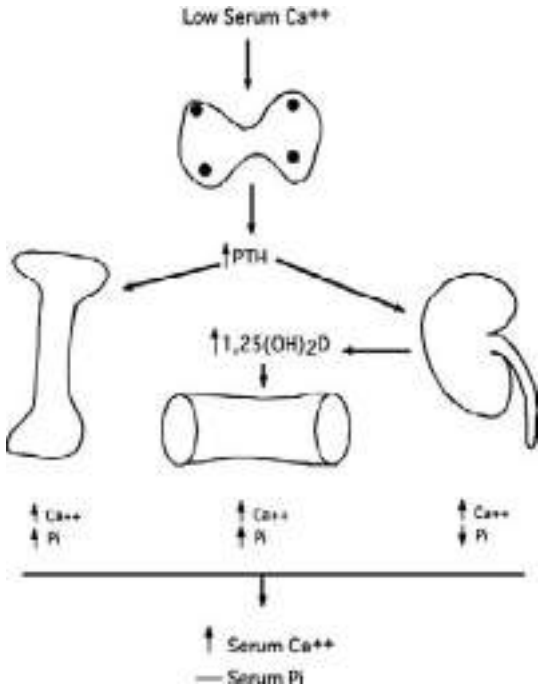

FIGURE 66.4 Integrated response to hypocalcemia. A decrease in the ionized calcium concentration in the ECF is sensed by the CaSR on the parathyroid glands, which leads to increased secretion of PTH. In turn, PTH causes release of calcium from bone and reclamation of calcium from the urine. If the hypocalcemic stimulus is prolonged, PTH induces an increase in the production of 1,25 OH_2 vitamin D from the kidney, which increases calcium absorption from the GI tract. While PTH leads to an increase in the release of phosphate from the skeleton and an indirect increase in GI absorption from the diet, it causes renal excretion of phosphate allowing an increase in the serum calcium levels without changing systemic phosphate levels.

and phosphate from stores within the mineralized portion of bone. In the kidney, PTH increases the reabsorption of calcium from the urine but decreases the reabsorption of phosphate. Presumably, this serves to dispose of the phosphate released from the skeleton and prevents any rise in serum phosphate, which could otherwise inhibit a rise in serum calcium by inducing the precipitation of calcium phosphate salts in soft tissues. In addition to the actions of PTH, reduced CaSR signaling within the kidney also leads to an increase in net calcium reabsorption independent of changes in PTH. Combined, these alterations in parathyroid, skeletal and kidney function return the calcium concentration back to normal and feedback to restrict further PTH release. When hypocalcemia is prolonged, PTH also stimulates the renal production of 1,25 $(OH)_2$ vitamin D, which increases intestinal calcium absorption. When hypocalcemia is no longer present then the system can reset back to its baseline activity. However, if there is a chronic hypocalcemic stress, then long-term elevations in PTH and 1,25 $(OH)_2$ vitamin D may be required to maintain the calcium level within the normal range.

In the presence of hypercalcemia, the various components in the system react in an opposite fashion in order to lower ECF calcium levels. A rise in the ionized calcium level acts on the CaSR in the kidney to trigger an increase in calcium excretion in the urine. As noted previously, this is associated with increased water excretion as well. Increased activation of the parathyroid CaSR suppresses PTH secretion, which, in turn, leads to a reduction in bone resorption and reduced production of 1,25 $(OH)_2$ vitamin D. Hypercalcemia also increases the catabolism of 1,25 $(OH)_2$ vitamin D. When calcium levels return to normal, these various adaptations are reversed and calcium excretion is halted. Normal renal function is critical for the system to be able to maintain a normal calcium in the setting of a chronic excess of calcium entering the ECF, for example in vitamin D excess or in states of pathological bone resorption. If renal function declines and the ability to excrete calcium in the urine is compromised, hypercalcemia will persist.

HYPERCALCEMIA

A list of disorders causing hypercalcemia is provided in Table 66.1. Although there are many potential causes of an elevated calcium level, most patients with hypercalcemia (>90%) are afflicted with either primary hyperparathyroidism or by malignancy-associated hypercalcemia (MAHC).[193,194] Therefore, we will discuss these disorders at some length and only briefly describe the other causes. It is important to keep

TABLE 66.1 Causes of Hypercalcemia

Hyperparathyroidism
Idiopathic primary hyperparathyroidism (PHP)
Familial
MEN type 1 or MEN type 2a
ESRD/tertiary hyperparathyroidism
Familial hypocalciuric hypercalcemia (FHH)
Malignancy associated hypercalcemia (MAHC)
Osteolytic metastases (LOH)
PTHrP and other humoral mediators (HHM)
Endocrinopathies
Adrenal insufficiency
Hyperthyroidism
Acromegaly
VIPoma
Pheochromocytoma
Medications
Vitamin D intoxication
Vitamin A intoxication
Thiazides
Lithium
Milk–alkali syndrome
Excess thyroid hormone
Tamoxifen
Growth hormone
Aminophylline
Granulomatous disease
Sarcoidosis
Tuberculosis
Silicone-induced granulomas
Disseminated candidiasis
Disseminated cytomegalovirus
Pneumocystis carinii pneumonia
Miscellaneous causes
Immobilization
Dehydration
Aluminum toxicity
William's syndrome
Rhabdomyolysis recovery
Idiopathic hypercalcemia of infancy
Jansen's metaphyseal chondrodysplasia

in mind that elevations in the total calcium level can occur in the absence of changes in ionized calcium levels. This is defined as *pseudohypercalcemia*, and occurs in the setting of abnormalities in serum proteins or severe thrombocytosis (platelet counts >700,000).[195] In these setting an ionized calcium level should be obtained to confirm the diagnosis of hypercalcemia before other diagnostic tests are performed.

Clinical Presentation of Hypercalcemia

Patients with mild hypercalcemia (<1 mg/dL above normal) are usually asymptomatic unless they have preexisting cerebral dysfunction. The severity of hypercalcemic symptoms is related both to the degree of elevation in the ionized calcium level and to the rapidity with which the calcium level rises. The higher the calcium and the faster its level rises, the more severe will be the symptoms. When present, symptoms are caused by dehydration secondary to urinary losses of calcium, water, and other electrolytes and to an increase in membrane potential caused by the elevation in ECF ionized calcium concentration (see Table 66.2). Dehydration develops because an increase in the filtered load of calcium leads to hypercalciuria, which is associated with the loss of sodium, anions and water. In addition, as discussed previously, hypercalcemia causes nephrogenic diabetes insipidus due to the stimulation of the CaSR in the collecting ducts of the kidney.[196] Consequently, patients with hypercalcemia frequently report symptoms of polyuria and polydipsia. If significant dehydration ensues, hypercalcemia can worsen quickly because any impairment of glomerular filtration reduces the ability of the kidneys to excrete excess calcium. Patients with moderate to severe hypercalcemia often complain of nausea and vomiting, symptoms likely related to dehydration as well as to the effects of the hypercalcemia on central nervous system function. Because hypercalcemia tends to hyperpolarize membranes, a range of neurologic and neuromuscular signs and symptoms can occur. Patients with mild hypercalcemia often complain of fatigue, depressed affect, and asthenia. With further increases in serum calcium, these complaints progress to impaired concentration and memory, difficulty with cognitive function, stupor, and coma. Muscle weakness can be seen, which can occasionally progress to flaccid paralysis if hypercalcemia becomes severe.[197] Gastrointestinal motility is impaired; this commonly results in constipation and likely contributes to nausea and vomiting. Occasionally, pancreatitis may be the cause of abdominal pain in patients with hypercalcemia.[198,199] Finally, cardiovascular function can be impaired, as manifested by bradycardia and sensitivity to the effects of digitalis. Electrocardiographic changes include shortening of the QT interval, varying degrees of atrioventricular block, and bradyarrhythmias or tachyarrhythmias if the hypercalcemia is severe.[200,201]

TABLE 66.2 Symptoms and Signs of Hypercalcemia

Signs and Symptoms	Acute	Chronic
Gastrointestinal	Anorexia	Dyspepsia
	Nausea	Constipation
	Vomiting	
Cardiac	Bradycardia	Hypertension
	Short QT interval	Digitalis sensitivity
	First degree atrioventricular block	Increased mean carotid intima-media thickness
		Cardiac calcifications,
		Ventricle hypertrophy
		Diastolic dysfunction
Renal	Polyuria	Nephrolithiasis
	Polydipsia	Nephrocalcinosis
Neurologic and psychiatric	Irritability, Psychosis	Depression
	Confusion, Disorientation,	Insomnia
	Forgetfulness	Decreased deep tendon reflexes
	Lethargy, Stupor, Coma	
Musculoskeletal	Bone pain	Hyperuricemia
	Weakness	Gout
	Arthralgia	Pseudo gout
		Pathologic fractures

Primary Hyperparathyroidism

Primary hyperparathyroidism (PHP) is caused by excess production of PTH by the parathyroid glands and is characterized by simultaneous elevations in circulating calcium and PTH levels. Most commonly it is caused by benign adenomas of one or sometimes two parathyroid glands. Less commonly, it is caused by diffuse parathyroid hyperplasia in the setting of the familial endocrine neoplasia syndromes (MEN1 and MEN2). Rarely, it is caused by primary disorders of calcium sensing or by parathyroid carcinoma. Primary hyperparathyroidism is currently estimated to have an incidence between 1 in 500 and 1 in 1000 persons.[202] After the age of 50 years, women are more frequently

affected then men; the female-to-male ratio in that age group is 3:1.[203] Although the onset of hyperparathyroidism can occur at any age, it is more common in older individuals, and the peak incidence is in the sixth decade.[204] Apart from the genetic disorders mentioned above, the only other known risk factor is exposure to external neck irradiation during childhood.

The most common cause of primary hyperparathyroidism is the growth of single or multiple adenomas (more than 75–80%).[205] The typical parathyroid adenoma appears as a collection of chief cells surrounded by a rim of normal tissue at the outer perimeter of the gland. These are clonal neoplasms, whose size and degree of PTH secretion tend to remain remarkably stable over multiple years.[206] One of the features of the neoplastic cells is blunted feedback of PTH secretion by calcium as compared to normal parathyroid cells. The cells in an adenoma have reduced expression of both the CaSR and the VDR as compared to normal cells and the degree of loss of feedback inhibition has been suggested to correlate with the degree of loss of CaSR and/or VDR expression.[207,208] However, it is unclear whether these alterations in VDR and CaSR are drivers of the abnormal proliferation of the original clone of abnormal cells or whether they occur secondary to proliferation of the cells. Approximately 20 to 40% of adenomas have been reported to overexpress cyclin D1, a cell-cycle regulatory protein that can act as a dominant oncogene.[209] An additional 25 to 30% of sporadic adenomas have been reported to have somatic mutations in the multiple endocrine neoplasia 1 (MEN1; menin) tumor suppressor gene on chromosome 11.[210] Approximately 15% of patients with hyperparathyroidism have diffuse enlargement of all four parathyroid glands caused by chief cell hyperplasia.[211] The most common cause of four-gland hyperplasia is long-standing CKD, which leads to chronic hypocalcemia, hyperphosphatemia, and low serum $1,25(OH)_2$ vitamin D levels, all of which stimulate parathyroid cell growth.[212] This hyperplasia can eventually lead to hypercalcemia, so-called tertiary hyperparathyroidism. Most cases of inherited parathyroid hyperplasia result from one of the two MEN syndromes. Hyperparathyroidism is a prominent feature of the MEN1 syndrome, which is caused by mutations in the menin gene, a tumor suppressor.[213] In contrast, hyperparathyroidism associated with the MEN2 syndrome is usually mild and occurs in fewer affected individuals. MEN2 has been shown to be caused by mutations in the *ret* proto-oncogene.[214,215] Both syndromes have an autosomal dominant mode of inheritance. Hyperplasia in these syndromes can be asynchronous, with unequal enlargement of the individual glands over time that gives the misimpression of single-gland disease.[216] Approximately 0.5% of all patients with hyperparathyroidism have parathyroid carcinoma. Typically, these patients have severe hypercalcemia and hyperparathyroidism that recurs following initial therapy.[217] It can be very difficult to distinguish a parathyroid carcinoma from an adenoma by pathologic evaluation alone, but local tissue invasion, local lymph node involvement, and the presence of mitotic figures are clues to the diagnosis. Parathyroid carcinoma occurs with increased frequency in a rare genetic syndrome known as *hyperparathyroid jaw-tumor syndrome*, which is characterized by primary hyperparathyroidism in association with mesenchymal tumors of the mandible.[218] This syndrome was found to be caused by mutations in the *HRPT2* gene encoding the tumor suppressor, parafibromin, and emerging data suggest that mutations in this gene may also cause a significant proportion of sporadic cases of parathyroid carcinoma.[219]

Clinical presentation: The clinical manifestations of primary hyperparathyroidism are variable. They include the characteristic symptoms of hypercalcemia (see Table 66.2) as well as the variable occurrence of skeletal, renal and other organ complications. Historically primary hyperparathyroidism was a rare, severe disease with significant morbidity and mortality. However, as general biochemical screening became popular, it was appreciated that most patients with this disorder had very mild symptoms and many were asymptomatic.[206]

Von Recklinghausen first described osteitis fibrosa cystica in 1891.[220] In the early twentieth century it was linked to hyperparathyroidism when Mandl reported clinical improvement after removal of a parathyroid adenoma from a patient with severe bone disease.[221] The skeletal involvement seen in primary hyperparathyroidism results from a generalized increase in osteoclastic bone resorption, which is accompanied by fibrovascular marrow replacement and increased osteoblastic activity. On radiography, osteitis fibrosa cystica is defined by the following features (see Figure 66.5): (1) generalized demineralization of bone, with coarsening of the trabecular pattern; (2) Subperiosteal resorption, most evident in the phalanges of the hands, resulting in an irregular, serrated appearance to the subperiosteal cortex or even extensive cortical resorption; (3) Bone cysts containing a brownish serous or mucoid fluid predominantly in the central medullary portions of the shafts of the metacarpal bones, pelvis and ribs, which may expend into and disrupt the overlying cortex; (4) Osteoclastomas composed of numerous multinucleated osteoclasts ("giant cells") admixed with stromal cells and matrix, found frequently in trabecular portions of the jaw, long bones, and ribs forming so called "brown tumors;" and (5) Pathologic fractures. Classic osteitis fibrosa cystica is

FIGURE 66.5 Osteitis fibrosa cystica. Hand films from a patient with primary hyperparathyroidism showing the typical findings of parathyroid bone disease. Note the general appearance of osteopenia as well as the erosion of the periosteal surface most prominently seen in the first digit. Also note the cystic dilatation of the distal metacarpals and the mottled appearance of the 5th metacarpal.

now uncommon, occurring in less than 5% of patients. However, primary hyperparathyroidism can also cause more typical osteoporosis and recent data suggest that over 50% of otherwise asymptomatic patients with hyperparathyroidism eventually develop progressive bone loss and are at risk for osteoporosis.[222] Thus, bone mineral density should be measured in all patients with hyperparathyroidism. Cortical bone is more sensitive to the effects of hyperparathyroidism, so bone mineral density in the distal forearm and hip is typically more severely affected than is bone mineral density in the spine.

Up to 20% of patients with primary hyperparathyroidism present with kidney stones, which makes this the most common complication.[223] Primary hyperparathyroidism accounts for fewer than 5% of all calcium kidney stones, but these patients are more likely to have recurrent or severe stone disease. Nephrocalcinosis, or the diffuse deposition of calcium phosphate complexes in the renal parenchyma, is seen less commonly. The most common stone type seen in hyperparathyroidism is calcium oxalate.[224] However, stones of mixed chemical composition (calcium oxalate and calcium phosphate) are often observed. The risk factors for stone disease in patients with hyperparathyroidism are hypercalciuria (>4 mg/kg calcium excretion over 24 hours), which results from hypercalcemia and the increased filtered load of calcium, which triggers the kidney CaSR and overrides the increased distal absorption of calcium mediated by the continuous PTH stimulation.[11] PTH also inhibits bicarbonate reabsorption in the proximal renal tubule resulting in a mild hyperchloremic metabolic acidosis and relatively alkaline urine. Precipitation of calcium phosphate is favored under alkaline conditions, which likely contributes to the formation of calcium phosphate stones and nephocalcinosis. Classically, severe hyperparathyroidism is associated with progressive renal impairment, but it is unclear whether mild hyperparathyroidism directly impairs GFR. In the majority of patients followed conservatively renal function remains stable.

In addition to complications involving bone and the kidney, primary hyperparathyroidism has been associated with a variety of other conditions, which may be related to either hypercalcemia or elevated PTH levels. These are listed in Table 66.3. The issue of whether primary hyperparathyroidism increases the risk for peptic ulcer disease and pancreatitis remains controversial.[225] Peptic ulcer disease was part of the original description of hyperparathyroidism, although this may have represented patients with undiagnosed MEN1 and Zollinger-Ellison syndrome. Although hyperparathyroidism is associated with a higher risk of hypertension, successful surgery does not often correct blood pressure. However, a series of studies have

TABLE 66.3 Potential Complications of Primary Hyperparathyroidism

Renal	Nephrolithiasis
	Nephrocalcinosis
	Impairment of renal function: - decreased creatinine clearance
	Impaired concentrating and acidifying ability
Skeleton	Osteitis fibrosa cystica
	Osteopenia/Osteoporosis
	Increased fracture risk
Cardiovascular	Hypertension
	Left Ventricular Hypertrophy
	Abnormal cardiac calcifications
	Increased cardiac mortality
Malignancy	Increased risk in severe cases

offered suggestive findings that primary hyperparathyroidism is associated with an overall increase in cardiovascular disease.[226]

Diagnosis: The diagnosis of hyperparathyroidism is made by documenting simultaneous elevations in the circulating levels of calcium and PTH in a patient with normal renal function. Plasma intact PTH concentrations, as measured by immunoradiometric assay, will be above the normal range in 90% of cases. In the remaining 10%, the PTH will be inappropriately normal for the degree of hypercalcemia.[227] Plasma 1,25 $(OH)_2$ vitamin D concentrations are increased or normal in most cases of primary hyperparathyroidism. Low 1,25 $(OH)_2$ vitamin D levels may be seen with coexisting vitamin D deficiency or in cases of severe hypercalcemia.[228] Patients with hyperparathyroidism also may have slightly low or low−normal serum phosphorus concentrations, and mild hyperchloremic metabolic acidosis. Alkaline phosphatase levels can be elevated in patients with overt bone disease. Once hyperparathyroidism is diagnosed, patients should be screened for end-organ complications. Renal ultrasonography or spiral computed tomography scans should be used to determine whether the patient has kidney stones. Bone mineral density measurements should be done to detect skeletal disease, preferably using dual energy x-ray absorptiometry, at the spine, hip, and wrist. A 24-hour urine collection should be performed to determine whether hypercalciuria is present.

Management of primary hyperparathyroidism: Surgery is the only curative therapy available for patients with primary hyperparathyroidism. All symptomatic patients or patients with complications of primary hyperparathyroidism such as renal stones or fractures should be referred to an experienced parathyroid surgeon for consideration of parathyroidectomy. Parathyroidectomy is successful and curative for 90−97% of patients when performed by an experienced surgeon.[229] Traditionally, this involved bilateral neck exploration, during which the surgeon identified all four parathyroid glands before resecting the abnormal gland. However, minimally invasive parathyroidectomy has been replacing traditional neck exploration. This requires preoperative localization of the adenoma. Technetium-99 m−sestamibi scans, ultrasonography, 4-dimensional CT scans and magnetic resonance imaging can all be used as preoperative localization studies.[229] A minimally invasive approach is not appropriate for parathyroid hyperplasia because the surgeon must remove either three and one half parathyroid glands or all four glands with autotransplantation of some parathyroid tissue to the forearm. Complications of parathyroid surgery include damage to the recurrent laryngeal nerve and permanent hypoparathyroidism.[230] Activity of the unaffected parathyroid glands is suppressed by the hypercalcemia associated with hyperparathyroidism, and the remaining glands take several days to recover normal secretory activity after removal of the adenoma. This can result in postoperative hypocalcemia in the first 24 to 48 hours. If significant bone disease is present, the influx of calcium into the skeleton as it heals following parathyroidectomy can lengthen the duration and increase the severity of hypocalcemia. This phenomenon is known as the hungry bones syndrome.

The widespread use of routine biochemical screening has led to the increased detection of asymptomatic primary hyperparathyroidism in which patients present with mild hypercalcemia, minimal or no symptoms and no end-organ damage. Studies examining the natural history of long-standing mild, asymptomatic primary hyperparathyroidism have suggested that most patients remain stable and do not develop progressive disease over the course of 10 years. However, the most recent studies suggest that up to 59% of initially asymptomatic patients developed more than a 10% decline in bone mineral density at one or more sites between 10 and 15-years of observation.[231] In addition, concern lingers over the possibility of excess vascular disease and cancer in these patients as well as over the subtle neurocognitive effects ascribed to hyperparathyroidism in some studies. However, it should be noted that the results of three different randomized trials of surgery versus medical follow-up in this patient population have not shown a definitive improvement in neurocognitive symptoms after surgery.[232−234] Therefore, there is much debate over the proper treatment of these patients since it is not clear that surgical correction of their hyperparathyroidism will provide clear benefit. Given ongoing uncertainty about this topic, a group of international experts met in 2008 to review and update guidelines for parathyroidectomy first formulated by an NIH consensus conference in 1990.[235] Table 66.4 lists the criteria for surgery in otherwise asymptomatic patients, and Table 66.5 provides the guidelines for managing nonsurgical patients as suggested by the 2008 International Workshop. These guidelines are not rigid, and each patient must be approached with his or her unique circumstances in mind. In addition, patients who do not undergo surgical treatment should have annual measurements of serum calcium and serum creatinine and should have bone density measurements every year or every other year. If patients demonstrate worsening of hypercalcemia, deterioration of renal function, or progressive bone loss, they should be referred for surgery.

There are no proven medical treatments for primary hyperparathyroidism, but several adjunct medical

TABLE 66.4 Guidelines for Surgery in Asymptomatic Primary Hyperparathyroidism from 2008 International Consensus Conference

Serum calcium (> upper limit of normal) 1.0 mg/dl (0.25 mmol/liter)
Creatinine clearance (calculated) reduced to <60 ml/min
BMD decrease with T-score < − 2.5 at any site and/or previous fracture fragility
Age less than 50 years
Uncertain prospects for adequate medical monitoring

TABLE 66.5 Non-Surgical Management of Primary Hyperparathyroidism

Monitor serum calcium and creatinine annually and bone density (hip, spine, and forearm) every one to two years.[248,246]
In patients with osteopenia and risk factors for fracture or with frank osteoporosis, who are not candidates for surgery, medical therapy with bisphosphonates to preserve bone mass is recommended.[349,246]
Avoid factors that can aggravate hypercalcemia, including thiazide diuretic and lithium carbonate therapy, volume depletion, prolonged bed rest or inactivity, and a high calcium diet (>1000 mg/day).
Encourage physical activity to minimize bone resorption.
Promote adequate hydration to minimize the risk of nephrolithiasis.
Maintain a moderate calcium intake (1000 mg/day). Calcium restriction (eg, <800 mg/day) is probably warranted when the serum calcitriol concentration is high.[248]
Maintain moderate vitamin D intake (400 to 600 IU daily) and treat coexisting vitamin D deficiency with careful monitoring of urinary calcium excretion.[350]

therapies can be useful for patients in need of treatment but who are not considered surgical candidates due to substantial comorbidities, or for those who opt not to proceed with definitive surgery. Maintenance of hydration and physical activity are important in all patients. Bisphosphonates and estrogen replacement therapy have been shown to prevent bone loss and even increase bone mass in patients with hyperparathyroidism. Finally, cinacalcet has been shown to lower serum calcium levels in patients with primary hyperparathyroidism. This drug is an allosteric activator of the CaSR and directly inhibits PTH release by parathyroid adenomas. Cinacalcet demonstrated efficacy in controlling serum calcium in a 1-year randomized clinical trial in patients with this disease.[236] Normalization of serum calcium continued for up to 5 years of therapy in an open-label extension of this trial.[237] However, cinacalcet does not normalize PTH levels or prevent bone loss, so it should not be considered a routine long-term treatment for patients who should otherwise have surgery.

Familial Hypocalciuric Hypercalcemia

Familial Hypocalciuric Hypercalcemia (FHH), also called familial benign hypercalcemia is another form of PTH-dependant hypercalcemia that results from abnormalities in calcium sensing. FHH is caused by loss-of-function mutations of the *CaSR* gene and is inherited in an autosomal dominant pattern in families.[57] The mutations cause a shift in the parathyroid cell's set point for calcium, such that higher than normal levels of blood calcium are needed to suppress PTH secretion. Likewise, abnormal function of the CaSR in the kidney impairs renal calcium excretion and results in hypocalciuria, despite chronic hypercalcemia. Heterozygosity for the mutated *CaSR* gene results in a mild clinical disorder, but homozygotes or compound heterozygotes with two mutant CaSR alleles present with severe primary hyperparathyroidism at birth and require prompt parathyroid surgery for survival. This entity is known as neonatal severe hyperparathyroidism.[57] Finally autoimmune hypocalciuric hypercalcemia (AHH) can be caused by auto antibodies directed against the CaSR that interfere with its function.[238,239]

Clinically, FHH is characterized by lifelong hypercalcemia, which is usually mild but can be as high as 12 mg/dl in some patients. The PTH level is usually slightly elevated or in the upper half of the normal range. The patients are usually asymptomatic and do not manifest end-organ complications of primary hyperparathyroidism. However, in rare instances there have been reports of chondrocalcinosis and pancreatitis in certain families.[240] Phosphate measurements are low, as in primary hyperparathyroidism and magnesium levels are high−normal or slightly elevated. Urine calcium is usually low, although there is much overlap with patients with mild primary hyperparathyroidism. It can be challenging to distinguish between primary hyperparathyroidism and FHH in individual patients. However, the distinction is important since patients with FHH are not helped by surgery. In fact, recurrent hypercalcemia in the first week after surgery is a clinical clue to the correct diagnosis. The most valuable clue to differentiate between the two diagnoses is the occurrence of hypercalcemia in first-degree relatives that is consistent with an autosomal dominant pattern. Documentation of prior normal calcium in the patient under consideration strongly argues against FHH. Finally the ratio of calcium clearance (ClCa) to creatinine clearance (ClCr) has been used to differentiate patients with FHH from those with primary hyperparathyroidism. Calculation can be made using the following formula: Clca/Clcr = [CAu x CRs]/[CAs x CRu]. A ratio of 0.01 or less suggests FHH and separates FHH from primary hyperparathyroidism with modest overlap. However, since primary

hyperparathyroidism is much more common than FHH, most patients with values near the cutoff ClCa/ClCr ratio of 0.01 have primary hyperparathyroidism and not FHH.

The mainstay of therapy for FHH is to prevent the patient from having an unnecessary parathyroidectomy. With the exception of rare patients with pancreatitis, long-term studies suggest that these patients have a benign course.[241]

PARATHYROID-INDEPENDENT HYPERCALCEMIA

This category of disorders represents a heterogeneous collection of causes of hypercalcemia not directly involving the parathyroids. As expected, PTH secretion is appropriately suppressed in response to an elevated ionized calcium level. By far the most common group of affected patients have malignancy-associated hypercalcemia, which will be discussed in some detail. The other causes are found in Table 66.1, only some of which will be discussed below.

Malignancy-Associated Hypercalcemia

Hypercalcemia is a common complication of malignancy, occurring in up to 20 to 30% of patients with cancer sometimes during the course of their disease. Most episodes of hypercalcemia occur with advanced disease and patients with malignancy-associated hypercalcemia (MAHC) usually have a poor prognosis with some studies suggesting up to 50% 30-day mortality.[242] There are two generally recognized forms of this disorder, one in which hypercalcemia is the result of tumor secretion of a humoral factor (usually PTHrP) and one which is the result of extensive bone metastases. Effective pharmacologic therapy has improved the short-term management of these disorders but only effective treatment of the underlying neoplasm can completely resolve the hypercalcemia and significantly influence the long-term prognosis. Although mechanisms in given patients may be varied, in all cases, excessive bone resorption plays a pivotal role in the pathogenesis.

The more common of the two types of MAHC is humoral hypercalcemia of malignancy or HHM. This syndrome generally occurs in patients with few or no bone metastases and resembles primary hyperparathyroidism. Patients with HHM have high blood calcium levels, low blood phosphate levels, and high urinary cAMP levels but suppressed iPTH levels. In 1941, Fuller Albright first proposed the existence of a PTH-like humoral factor and work in the 1980s led to the identification of PTHrP as the cause of HHM.[243] As discussed earlier, PTHrP normally does not circulate, but in patients with cancer, it enters the bloodstream and acts on the PTH1R in bone and kidney to increase bone resorption and cause hypercalcemia. As compared to patients with primary hyperparathyroidism, patients with HHM have low 1,25 $(OH)_2$ vitamin D levels and low levels of bone formation.[244] However, acute infusions of PTHrP into animals increase CYP27B1 activity and increase osteoblast activity, so these differences in HHM still remain unexplained.[245] They may be related to the secretion of other factors by the tumors, to the elevated calcium levels or to differences in how the human PTH1R is activated by PTHrP as compared to PTH. In addition to PTHrP, some non-Hodgkin's lymphomas (usually of B cell origin), produce large amounts of 1,25 $(OH)_2$ vitamin D and can cause hypercalcemia due to activation of bone resorption by vitamin D.[246,247]

The second form of MAHC is due to excessive peritumoral bone resorption in the setting of extensive skeletal metastases and is referred to as local osteolytic hypercalcemia (LOH). LOH occurs most commonly in patients with multiple myeloma and breast cancer. This syndrome is caused by the recruitment and activation of normal osteoclasts that surround the tumor cells and cause local osteolysis. This is though to be the result of secretion of paracrine factors by the tumor cells that stimulate osteoclast differentiation and activity.[248] Myeloma cells secrete numerous cytokines and chemokines that are capable of stimulating bone resorption, including MIP1, lymphotoxin (TNF-β), and interleukins 1β, 3, and 6.[249,250] These factors lead to increased expression of RANKL by marrow stromal cells and osteoblasts and to stimulation of osteoclast formation and activity.[251] Myeloma cells also secrete inhibitors of the Wnt signaling pathway, which also suppresses bone formation.[252] Breast cancer cells secrete PTHrP in quantities that may not reach the circulation to cause HHM, but instead increase local osteoclast activity, again by activating the RANKL/RANK system.[253] Breast cancer cells have also been shown to secrete IL-8 and IL-11, both of which may contribute to local osteoclast activity.[254]

Granulomatous Disease

Hypercalcemia has historically been associated with sarcoidosis, but can also occur in other granulomatous conditions such as tuberculosis, silicone-induced granulomas, and disseminated candidiasis. Approximately 10–20% of patients with sarcoidosis will develop hypercalcemia and 50% will experience hypercalciuria.[255] In patients with the acquired immune

deficiency syndrome (AIDS), hypercalcemia due to granuloma formation has been reported in disseminated cytomegalovirus (CMV) infection and in *Pneumocystis carinii* pneumonia.[256,257] Hypercalcemia in these conditions appears to be vitamin D mediated, since activated macrophages in granulomatous tissue express CYP27B1 and have been shown to be an extra renal source of 1,25 $(OH)_2$ Vitamin D.[258] Increased intestinal absorption of calcium seems to be a major cause of the hypercalcemia. The affected patients may be especially likely to develop hypercalcemia after (1) sunlight exposure, which increases the production of 25 (OH) Vitamin D; or (2) diets enriched in vitamin D and calcium, which increase intestinal absorption of calcium. Glucocorticoids are effective in the treatment of this type of hypercalcemia due to their effects to inhibit gastrointestinal calcium absorption and to suppress production of 1,25 $(OH)_2$ Vitamin D by the granulomas.[259]

Milk-Alkali Syndrome

A study from the University of Oklahoma reported that milk-alkali syndrome due to calcium carbonate ingestion had become the third most common cause of hypercalcemia in hospitalized patients, representing 16% of hospital admissions for hypercalcemia over a 3-year survey.[260] This syndrome results from the ingestion of large amounts of calcium and absorbable alkali. It was first described in the 1930s as a complication of ulcer therapy that consisted of large quantities of milk together with sodium bicarbonate. It continued to be seen commonly in the era before the introduction of H_2-blockers when peptic ulcer disease was often treated with up 20–60 grams of calcium carbonate per day. With the introduction of nonabsorbable antacids and then H_2-blockers and proton pump inhibitors, this syndrome became rare. However, it has become more common again due to the increasing use of calcium carbonate to treat or prevent osteoporosis.

The classic triad defining milk-alkali syndrome consists of hypercalcemia, systemic alkalosis and renal insufficiency. Hypercalcemia is often severe and symptomatic, with presenting values commonly between 15–20 mg/dl. Renal dysfunction can vary from mild to severe and nephrocalcinosis often exists if the syndrome has been present for some time. Other sites of soft tissue calcification, as evidenced by band keratopathy, are common as well. In the older literature, patients were generally reported to be hyperphosphatemic, but in more recent series, phosphate levels have been reported to be normal or low. This most likely reflects the shift from milk, which has a high phosphate content, as a source of calcium to calcium carbonate, which does not. Although some confusion existed in the original literature, recent measurements using modern assays have documented that PTH levels are suppressed.[260,261] The diagnosis of the syndrome requires a careful history especially of over-the-counter medication use.

The pathophysiology of milk-alkali syndrome is not fully understood, but most likely represents a viscous cycle set up by the ingestion of large amounts of calcium in the setting of volume contraction, systemic alkalosis and progressive renal insufficiency. It is unclear what the threshold for the induction of hypercalcemia from oral calcium is, but it may be as low as 2–3 grams of calcium daily. This varies with renal function and also between different subjects. By suppressing PTH and leading to volume contraction, hypercalcemia can limit the kidney's ability to excrete bicarbonate. In turn, systemic alkalosis can impair the renal excretion of calcium and favors the precipitation of calcium phosphate in the kidney and other soft tissues. The development of nephrocalcinosis then leads to progressive renal dysfunction that contributes to the inability to excrete calcium and bicarbonate. Because of volume contraction and the induction of systemic alkalosis, vomiting can precipitate the syndrome. Likewise, the use of thiazide diuretics is a risk factor due to these drugs' ability to interfere with calcium excretion and to cause volume contraction. The biochemical abnormalities are usually reversible with the discontinuation of oral calcium and alkali, and with rehydration followed by forced saline diuresis. If renal failure is severe, making vigorous hydration difficult, hemodialysis against a low calcium bath has also been effective in lowering calcium levels. If the syndrome is acute, hypercalcemia and renal dysfunction resolve promptly and completely. In this setting, there can be rebound hypocalcemia and secondary hyperparathyroidism. In more chronic cases, especially if severe nephrocalcinosis is present, recovery takes longer and renal function may not completely normalize.[262]

Endocrine Disorders

Hypercalcemia occurs in endocrine conditions other than hyperparathyroidism. Mild elevations in circulating calcium can be seen in patients with hyperthyroidism, adrenal insufficiency and pheochromocytoma. Thyroid hormone and catecholamines can stimulate osteoclastic bone resorption directly.[263] In addition, pheochromocytomas often secrete PTHrP.[264] The mechanism for hypercalcemia in adrenal insufficiency is uncertain. In all instances, hypercalcemia resolves with successful treatment of the underlying disorder.

Immobilization

Immobilization due to prolonged bed rest or weightlessness is associated with disordered calcium homeostasis. All immobilized patients develop hypercalciuria but hypercalcemia only occurs in those with a preexisting state of high bone turnover. This is most commonly seen in adolescents with a growing skeleton, particularly those with spinal cord injuries and quadriplegia. Immobilization-associated hypercalcemia in adults is associated with Paget's disease, thyrotoxicosis, primary hyperparathyroidism, and malignancy. Hypercalcemia occurs because of increased osteoclastic bone resorption and decreased osteoblastic bone formation. Prolonged immobilization can lead to osteopenia and nephrolithiasis. Serum PTH and 1,25 $(OH)_2D_3$ concentrations are suppressed, and hypercalcemia and hypercalciuria resolve with resumption of weight bearing.[265] Several studies have reported success in decreasing hypercalcemia and hypercalciuria with the use of bisphosphonates and calcitonin.[266]

Medication-Induced Hypercalcemia

Hypercalcemia is a common complication of therapy with vitamin D preparations. Hypercalcemia of vitamin D intoxication appears to be multifactorial, resulting primarily from a combination of increased GI absorption of calcium and increased bone resorption.[267] Classically, patients with vitamin D intoxication present with hypercalcemia, hyperphosphatemia, and markedly elevated levels of 25 (OH) vitamin D. Because PTH levels are appropriately suppressed, and because vitamin D and hypercalcemia both exert negative feedback on CYP27B1 in the proximal tubules, 1,25 $(OH)_2$ vitamin D levels are usually either normal or only slightly elevated.[268] The amount of vitamin D required to produce hypercalcemia has been estimated to be in excess of 25,000 to 50,000 IU per week. Therefore, it is unusual to see vitamin D intoxication from over-the-counter nutritional supplements. However, there have been reports of hypercalcemia due to poor quality control in the manufacture of these supplements.[269] There have also been outbreaks of vitamin D intoxication resulting from the accidental over supplementation of vitamin D into cow's milk by commercial dairies. Nevertheless, the majority of cases of hypercalcemia occur in patients treated with pharmacological doses of vitamin D or its analogues for the therapy of hypoparathyroidism, malabsorption or renal osteodystropy. The most frequent setting in which vitamin D use leads to hypercalcemia remains the treatment of secondary hyperparathyroidism complicating renal osteodystrophy. Treatment of vitamin D intoxication involves discontinuation of the vitamin D compound, volume expansion and calciuresis. If hypercalcemia is severe or refractory to the above, treatment with glucocorticoids and/or bisphosphonates may be necessary. The duration of hypercalcemia after the withdrawal of the vitamin D source depends on the biological half-life of the compound used.

Chronic lithium therapy is associated with modest increases in parathyroid gland size, which can lead to elevated levels of PTH and calcium.[270] Usually, after lithium therapy is stopped, the blood calcium and PTH levels normalize within several months. Rarely, however, persistent hyperparathyroidism may require parathyroidectomy. Lithium has been described to interfere with the function of CaSR and it increases the set point for PTH secretion in isolated parathyroid cells *in vitro*.[271]

Thiazide diuretics increase proximal tubular calcium reabsorption and may exacerbate hypercalcemia from other causes, such as primary hyperparathyroidism, sarcoidosis, or any other cause of a high, fixed calcium load.[272] Thiazides usually do not cause hypercalcemia in isolation.

Excess ingestion of vitamin A (retinol) results in a syndrome of dry skin, pruritus, pseudotumor cerebri, bone pain, and occasionally hypercalcemia.[273] Hypercalcemia occurs only with the ingestion of 10 times the Recommended Dietary Allowance (RDA) of 5000 IU/day. It can also result from ingestion of isotretinoin (13-cis-retinoic acid [Accutane]) and tretinoin (all-trans-retinoic acid [Retin-A]), which are used to treat acne and acute promyelocytic leukemia. Bones can show characteristic periosteal calcification on radiographs. The hypercalcemia is probably caused by the action of retinoids to stimulate bone resorption.[274]

Renal failure: Hypercalcemia can occur in acute and chronic renal failure but by different mechanisms. Hypercalcemia has been described during the diuretic phase of acute renal failure associated with rhabdomyolysis.[275] In most cases, hypocalcemia occurs during the acute phase of renal failure, and as renal function improves, hypercalcemia occurs. Although the mechanism responsible for the increase in serum calcium in patients with acute rhabdomyolysis is unknown, there are a number of theories. During the early phase of acute rhabdomyolysis the increase in serum phosphorus due to impaired glomerular filtration will lead to a fall in the serum calcium. As serum phosphorus falls during the diuretic phase of acute renal failure, calcium and phosphate salts that have been deposited in soft tissues may be liberated, causing transient hypercalcemia. Alternatively, excessive release of 25 (OH) vitamin D from injured muscle occurs as a result of acute rhabdomyolysis and may lead to increased substrate available for conversion to 1,25 $(OH)_2$ vitamin D as the

kidneys recover. Llach et al. have suggested that the hypercalcemia during the early diuretic phase was due to 1,25$(OH)_2$ vitamin D, which, in turn, was due to increased circulating PTH concentrations.[275]

Hypercalcemia is a common occurrence in patients with chronic renal failure on hemodialysis and can result from hyperparathyroidism, vitamin D intoxication, calcium antacid over ingestion, immobilization, aluminum toxicity or combinations of these factors. In addition, hypercalcemia is particularly common in the first year following renal transplantation. Renal bone disease and related disorders of mineral homeostasis are discussed in greater detail in Chapter 91.

Treatment of Hypercalcemia

The effective treatment of hypercalcemia requires the identification and correction of the underlying pathophysiology. Thus, the treatment for symptomatic primary hyperparathyroidism is surgical removal of the adenoma, and the treatment for malignancy-associated hypercalcemia is the eradication of the underlying neoplasm. Likewise, drugs implicated in hypercalcemia should be discontinued, endocrinopathies should be treated and immobilized patients should be mobilized. However, it is not always possible to fully correct the underlying condition and, sometimes, acute elevations in calcium can be life threatening. Therefore, here we review treatments that can be used to lower circulating calcium levels.

Moderate to severe elevations in serum calcium (above 12−13 mg/dl) usually are symptomatic and acute elevations above 15−16 mg/dl are often associated with an altered level of consciousness progressing to coma and multiple organ dysfunction. In addition, pre-renal azotemia caused by volume depletion can lead to rapidly escalating serum calcium levels in these situations. Therefore, treatments to lower calcium levels acutely should be instituted promptly once serum calcium reaches 13 mg/dl or higher. Principles of management include volume repletion, enhancement of renal calcium excretion, and inhibition of bone resorption.

As reviewed earlier, hypercalcemia leads to renal solute and water losses and all patients with significant hypercalcemia are volume contracted. Dehydration, in turn, limits the ability of the kidney to dispose of excess calcium. Therefore, restoration of the ECF deficit with 0.9% saline should be the first treatment for moderate to severe hypercalcemia. In severe hypercalcemia, this can require the infusion of isotonic saline at rates of 200 to 300 mL/hour, and it should be accompanied by close monitoring of electrolytes and cardiovascular status.[276] Once volume depletion is corrected, treatment with loop diuretics can be initiated to induce natriuresis, which further increases renal calcium excretion. Rehydration and forced saline diuresis can result in lowering of the serum calcium up to 1 to 1.5 mg/dL. In addition, this therapy helps to prevent progressive renal insufficiency and prevents calcium from rising further due to impairments in renal calcium excretion. It also is necessary to garner the full therapeutic effect of therapies directed at inhibiting bone resorption.

Increased bone resorption is a major contributing mechanism responsible for the hypercalcemia of primary hyperparathyroidism and most malignancies. Therefore, inhibition of bone resorption is an effective way to decrease the extracellular calcium concentration before disease-specific therapy is established. The advent of powerful bisphosphonates and more recently therapies directed against the RANKL/RANK cytokine system, has improved the treatment of hypercalcemia significantly, and in the setting of malignancy has enabled the chronic outpatient treatment of MAHC in at least some patients.

Calcitonin is the most rapidly acting antiresorptive agent. It acts directly on osteoclasts to inhibit bone resorption and also lowers renal calcium reabsorption. It can be given in doses of 4 to 8 IU/kg subcutaneously or intramuscularly every 6 to 12 hours.[276] This treatment can lower serum calcium by 1 to 2 mg/dL within several hours, but tachyphylaxis to calcitonin occurs within 24 to 48 hours, probably due to downregulation of calcitonin receptors. Calcitonin use can be particularly effective in the setting of severe hypercalcemia while waiting for the more sustained hypocalcemic effect of administered bisphosphonates to occur. In this regard, it has been shown that calcitonin use with bisphosphonates lowers calcium concentrations more quickly and effectively than either alone.[277]

Bisphosphonates are analogs of pyrophosphates. They have a high affinity for hydroxyapatite and concentrate at the bone surface in areas of high bone turnover. All bisphosphonates inhibit osteoclast function.[278] Non-nitrogen containing compounds, such as etidronate, tiludronate, and clodronate, do so by producing toxic analogs of ATP that cause cell death. Nitrogen-containing compounds, such as pamidronate, alendronate, risedronate and zoledronate, interfere with protein prenylation by inhibiting farnesyl pyrophosphatase, an enzyme in the HMG-CoA reductase pathway.[279] Bisphosphonates, in general, are poorly absorbed and are most effective in treating hypercalcemia when given intravenously. Pamidronate can be given as an intravenous infusion of 60 or 90 mg, which begins to lower serum calcium after 24 to 72 hours and leads to a nadir of calcium within five to six days.[276] Up to 70% of patients with MAHC given Pamidronate

achieve a normalization of calcium lasting up to 18 days. Zoledronate is the other bisphosphonate commonly used to lower calcium levels acutely. Intravenous infusions of 4 to 8 mg of zoledronate result in the normalization of calcium within three to five days in approximately 90% of patients with MAHC, with a duration of response lasting for up to 32 days. In a head-to-head trial, zoledronate resulted in more rapid and more durable remission of hypercalcemia in patients with MAHC than did pamidronate.[280]

Activation of the RANKL/RANK signaling pathway is a final common mechanism for most conditions of excess bone resorption. Therefore, as one might expect, pharmacological blockade of this pathway is particularly effective at inhibiting bone resorption and lowering calcium levels. Denosumab is a fully humanized monoclonal antibody that binds to RANKL and blocks its ability to interact with the RANK receptor. In this manner it mimics the actions of OPG, the natural inhibitor of RANKL signaling. While Denosumab is not formally approved specifically for the treatment of hypercalcemia, it has been shown to reduce the incidence of skeletal related events (including hypercalcemia) when given prophylactically to patients with established bone metastases.[281] Given that it is currently the most potent anti-resorptive agent available, it is likely to be quite effective for the treatment of hypercalcemia and may be especially useful in patients with underlying renal disease, given the potential renal toxicity of intravenous bisphosphonates.[282]

In addition to the above agents, two other classes of drugs can be useful in specific instances. Calcimimetics such as Cinacalcet have been successful in reducing hypercalcemia in trials of patients with primary hyperparathyroidism.[283] Medical therapy in this setting may be helpful in preparation for surgery or in patients that are not surgical candidates. Also, Cinacalcet has been documented to reduce calcium levels in patients with parathyroid carcinoma.[25,284] Glucocorticoids can be effective in hypercalcemic patients with hematologic malignancies, such as multiple myeloma or lymphoma, as well as in patients with granulomatous disorders such as sarcoidosis. They most likely are effective due to their ability to suppress local cytokine and 1,25 $(OH)_2$ vitamin D production.

HYPOCALCEMIA

Hypocalcemia is defined as a total serum calcium concentration of less than 8.4 mg/dl (2.1 mmol/liter) or an ionized calcium concentration of less than 4.48 mg/dl (1.12 mmol/liter). It is important to remember that the total calcium in serum includes both the free and the protein bound fraction. The most common cause of a low total calcium level in hospitalized patients is a reduction in the serum albumin level and, in those patients, ionized calcium levels are normal. Therefore, to make a diagnosis of hypocalcemia based on a total serum calcium level, one must have access to a concurrent measurement of serum albumin. Total serum calcium levels can be corrected for low albumin levels using the following simple formula:

Corrected Calcium Level $= (0.8 \times (4.0\ g/dL - Serum\ Albumin) + Serum\ Calcium$. However, this correction is not always accurate in individual patients, especially those with critically illness. Therefore, if the diagnosis of hypocalcemia is clinically important, an ionized calcium level should be measured to confirm the diagnosis.

Clinical Presentation of Hypocalcemia

The clinical presentation of hypocalcemia depends on the degree and the duration of the low calcium levels. Mild hypocalcemia (within 1 mg/dl below the normal range) is usually asymptomatic. More severe degrees of hypocalcemia can cause varying degrees of neuromuscular irritability, including perioral paresthesias, tingling of the fingers and toes, and spontaneous or latent tetany. Tetany can be elicited by percussion of the facial nerve, which results in contractions of the ipsilateral facial muscle (Chvostek's sign), or by inflating a blood pressure cuff for three to five minutes, which results in carpal spasm (Trousseau's sign). Alterations in membrane potential can present as electrocardiographic abnormalities, which include prolonged QT intervals and marked QRS and ST-segment changes that may mimic acute myocardial ischemia or conduction abnormalities. In severe hypocalcemia or during rapid changes in serum calcium, grand mal seizures or laryngospasm also are possible.[1]

Chronic hypocalcemia is often associated with a milder presentation and may be asymptomatic. However, if chronic hypocalcemia is accompanied by hyperphosphatemia as in PTH deficiency, calcification of the basal ganglia and occasional extrapyramidal disorders may be found. Similar types of calcium deposits can also occur in the lens and lead to cataract formation. When long-standing hypocalcemia is associated with hypophosphatemia as in vitamin D deficiency, growth plate abnormalities (rickets) can occur in children and defects in the mineralization of new bone (osteomalacia) can occur in both adults and children.

Causes of Hypocalcemia

Table 66.6 lists the numerous causes of hypocalcemia. These disorders can be divided into two broad

TABLE 66.6 Causes of Hypocalcemia

Inadequate PTH production/hypoparathyroidism
Iatrogenic
• Neck irradiation • Surgically induced
Infiltrative/Destructive Diseases
• Hemochromatosis • Sarcoidosis • Iron overload due to transfusion dependence in thalassemia • Wilson's disease • Amyloidosis • Metastatic carcinoma
Neonatal
• 2° to maternal hyperparathyroidism • 2° to maternal FHH
Autoimmune
Genetic or developmental disorders
• DiGeorge Syndrome • Activating calcium-sensing receptor mutation • Hypoparathyroidism, Deafness, and Renal Anomalies Syndrome (HDR) • Hypoparathyroidism-Retardation-Dysmorphism (HRD) • Mitochondrial gene defects
Functional hypoparathyroidism
• Magnesium depletion • Magnesium excess • Pseudohypoparathyroidism
Inadequate vitamin D production and action
• Nutritional deficiency • Lack of sunlight exposure • Malabsorption • Post-gastric bypass surgery • End-stage liver disease and cirrhosis • Chronic kidney disease • Vitamin D-dependent rickets type 1 and type 2
Miscellaneous Etiologies
Neonatal hypocalcemia
Hyperphosphatemia
• Phosphate retention in acute or chronic renal failure • Excess phosphate absorption caused by enemas, oral supplements • Massive phosphate release caused by tumor lysis or crush injury
Drugs
• Foscarnet • Intravenous bisphosphonate therapy—especially in patients with vitamin D insufficiency or deficiency
Rapid transfusion of large volumes of citrate-containing blood
Acute critical illness
"Hungry bone syndrome"
• Post-thyroidectomy for Grave's disease • Post-parathyroidectomy
Osteoblastic metastases
Acute pancreatitis
Rhabdomyolysis
Mitochondrial gene defects

groups: (1) those in which hypocalcemia is the result of lack of parathyroid hormone or resistance to parathyroid hormone; and (2) those in which the hypocalcemia occurs despite a normal parathyroid response. The most common cause of hypocalcemia is CKD, especially when creatinine clearance decreases below 30 ml/minute. Progressive renal insufficiency is associated with a complex of metabolic derangements including hyperphosphatemia, low 1,25 $(OH)_2$ vitamin D levels and skeletal resistance to the action of PTH, that lead to chronic hypocalcemia.[285,286] The development of metabolic bone disease in CKD is discussed in more detail in Chapter 91. Below, we will discuss a subset of the disorders listed in Table 66.6 found in patients without a history of CKD.

Hypoparathyroidism

Hypoparathyroidism may be caused by inherited or acquired diseases of the parathyroid gland that result in the impaired synthesis and/or secretion of PTH. Pseudohypoparathyroidism refers to PTH resistance which results in functional hypoparathyroidism, a phenomenon that can also be caused by magnesium deficiency.

Congenital or genetic disorders causing hypoparathyroidism: Congenital hypoparathyroidism has been associated with specific mutations in the signal peptide sequence of the PTH gene, which prevents the appropriate processing and secretion of prepro-PTH.[287] Congenital hypoparathyroidism can also present as part of a syndrome including renal dysplasia and sensorineural hearing loss (HDR), which has been related to mutations in the GATA3 gene.[288–291] Hypoparathyroidism due to defective embryogenesis or parathyroid gland agenesis becomes evident in the neonatal period and is often associated with other branchial cleft abnormalities. The most common of these is the DiGeorge syndrome, which can include absence of the thymus with immunodeficiency, facial abnormalities, and major vascular and cardiac defects.[292,293] Mutations in the glial cell missing B

(GCMB) gene can cause isolated parathyroid gland agenesis.[294–296] Mutations in the CaSR gene can also result in hypoparathyroidism.[297–301] Autosomal dominant hypocalcemia (ADH) is a mirror image of FHH and is caused by activating mutations in the CaSR gene.[275,302] Patients with ADH present with mild to moderate hypocalcemia, hyperphosphatemia, high renal calcium excretion and a low (but measureable) PTH level. Patients with ADH often also present with hypomagnesemia and hypermagnesuria. Some kindreds also present with a picture consistent with Type V Barters (hypokalemia and alkalosis) thought to be due, in part, to the effects of the CaSR on sodium absorption in the thick ascending limb of the Loop of Henle.[303]

Hypoparathyroidism can also develop as the result of autoimmune attack on the parathyroid glands. This can occur in the context of the polyglandular autoimmune syndrome type I. Polyglandular autoimmune (PGA) syndromes are constellations of multiple endocrine gland insufficiencies. PGA Type I is an autosomal recessive disorder with a minor female predominance caused by mutations to the autoimmune regulator (*AIRE*) gene, which codes a nuclear transcription factor involved in the deletion of self-reactive T-cells in the thymus.[304,305] Hypoparathyroidism in PGA type I most commonly occurs in childhood or adolescence and is associated with chronic mucocutaneous candidiasis and primary adrenal insufficiency. Primary hypogonadism, diabetes mellitus, pernicious anemia, vitiligo and autoimmune thyroid disease also occur in this syndrome, although usually after the onset of hypoparathyroidism.

Acquired hypoparathyroidism: Autoimmune hypoparathyroidism can also occur later in life without other autoimmune manifestations. The pathophysiology of this entity is not well understood although autoantibodies against the CaSR are present in almost 30% cases of acquired hypoparathyroidism. How, or if these autoantibodies contribute to the destruction of the parathyroid glands is not known.[306,307]

Most commonly acquired hypoparathyroidism is the result of thyroid, parathyroid, or radical neck surgery.[287] It may be transient, intermittent or permanent. Transient hypoparathyroidism may be due to changes in blood supply to or removal of one or more parathyroid glands during surgery, whereas intermittent hypoparathyroidism is due to decreased parathyroid reserve. Transient hypoparathyroidism may also occur after removal of a parathyroid adenoma as a result of temporary suppression of the remaining parathyroid tissue by the chronically elevated calcium levels caused by the adenoma. It resolves as the remaining glands resume normal function. Some patients with severe hyperparathyroidism develop "hungry bone syndrome" after parathyroidectomy.[308] This syndrome can cause prolonged hypocalcemia and results from the combination of the large influx of calcium and phosphate into healing bones and the relative hypoparathyroidism induced by the preexisting hypercalcemia and/or surgical manipulation of the parathyroid glands. Permanent hypoparathyroidism occurs in patients in whom all parathyroid glands are inadvertently removed/damaged during surgery. They typically become hypocalcemic within 24 hours and remain hypoparathyroid for the duration of their lifetime. Whereas transient hypoparathyroidism occurs in up to 20 percent of patients after surgery for thyroid cancer, permanent hypoparathyroidism occurs in only 0.8 to 3.0 percent of patients after total thyroidectomy.[309]

Acquired hypoparathyroidism can also occur as a result of infiltrative diseases such as hemochromatosis or Wilson's disease.[287] The parathyroid glands can also be destroyed by metastatic tumors and by external radiation to the neck or radioactive iodine therapy for Graves' disease.

Severe magnesium deficiency is a cause of functional hypoparathyroidism as it impairs PTH secretion and causes resistance to the action of PTH in bone and kidneys. Interestingly severe hypermagnesemia can also lead to hypocalcemia due to inhibition of PTH secretion. Parathyroid function is corrected by the return of magnesium levels into the normal range.[310–312]

Diagnosis and treatment: Hypoparathyroidism is suspected in patients with hypocalcemia and hyperphosphatemia in the setting of normal renal function. The diagnosis is confirmed by the finding of a low or low-normal PTH level. Patients will usually also have a low 1,25 $(OH)_2$ Vitamin D level. The presence of cataracts or basal ganglia calcification suggests that the hypocalcemia has been long-standing.

Most patients with hypoparathyroidism require lifelong calcium and vitamin D supplementation. The goals of therapy in patients with hypoparathyroidism are to relieve symptoms and to raise and maintain the serum calcium concentration in the low-normal range. The main complication of treatment for hypoparathyroidism is the development of hypercalciuria and nephrocalcinosis or nephrolithiasis, which put the patient at risk for renal insufficiency.[313] This is the result of the loss of distal tubular calcium reabsorption in the absence of PTH. A large rise in the urinary calcium excretion in the setting of therapy for hypoparathyroidism should raise the possibility of ADH, since chronic activation of the CaSR in the renal tubule will make patients intolerant of the usual therapy with vitamin D and calcium.[287] Therefore, the careful monitoring of urinary and serum calcium are essential and the dose of calcium and vitamin D should be reduced if

urinary calcium excretion is elevated (≥4 mg/kg in 24 hours) or if the serum calcium level is within the normal range. The use of a thiazide diuretic, can also help to decrease urinary calcium excretion in some patients.[272] Ongoing studies suggest that recombinant human PTH or PTH analogues may provide better correction of serum calcium levels without the same risk of hypercalcuria.[314] However, the use of PTH for this purpose has been hampered by its short half-life and expense. In addition, the long-term safety of PTH has not been established, particularly in growing children who may be at greater risk of osteosarcoma. Nevertheless, multiple daily injections of PTH 1-36 have been reported to be helpful in the short-term management of patients with post-operative hypocalcemia that has been difficult to treat with standard therapy.[315,316]

Pseudohypoparathyroidism

Pseudohypoparathyroidism (PHP) is a heterogeneous syndrome characterized by functional hypoparathyroidism, increased serum PTH concentrations and peripheral resistance to the biologic actions of PTH.[317] In 1998, a Japanese epidemiologic study estimated the prevalence of pseudohypoparathyroidism to be 3.4 cases per 1 million people.[318] No information is available regarding the prevalence of PHP in the rest of the world. PHP occurs approximately twice as frequently in females as in males. Patients with PHP often have a number of somatic abnormalities, which are referred to collectively as Albright's hereditary osteodystrophy. These include short stature, round facies, thick neck, barrel chest, subcutaneous ossifications, bradydactyly with disproportional shortening of the fourth and fifth metacarpals/metatarsals, obesity and mild mental retardation.[319] Several variants of PHP have been identified, which result from different abnormalities in the imprinting and tissue-specific expression of the *GNAS1* gene encoding the alpha subunit of the stimulatory G protein ($G\alpha_s$). The three different forms of the disease are PHP type 1a, pseudopseudohypoparathyroidism (pseudo-PHP) and PHP type 1b.[320]

Pseudohypoparathyroidism type Ia is caused by heterozygous loss-of-function mutations in the *GNAS1* gene. This presents as an autosomal dominant disorder but *GNAS1* is an imprinted gene and the presentation of this disorder is determined by whether the subject inherits the mutation from his or her mother or father.[321] Patients who inherit the mutant *GNAS1* gene from their father present with pseudo-PHP and patients who inherit it from their mother exhibit PHP. This is because expression of the paternal allele of GNAS is silenced, or imprinted, in a variety of tissues including the proximal renal tubule. Therefore, if a patient inherits a GNAS mutation from his or her mother, then he or she will have only the paternal allele to rely on. However, as a result of imprinting, many tissues will inactivate that allele and effectively be *GNAS*-null. These patients will present with AHO (Albright's hereditary osteodystrophy), which results from reduced GNAS expression during development, biochemical hypoparathyroidism and PTH resistance. These patients classically have a decreased response of the proximal tubule to PTH, which can be characterized by a diminished nephrogenous cAMP response to PTH administration.[322] In addition, due to the importance of $G\alpha_s$ and cAMP signaling downstream of many peptide hormones, patients with pseudohypoparathyroidism type 1a often manifest mild resistance to other hormones such as TSH, LH and FSH as well.[323] In contrast, if the patient inherits a GNAS mutation in the paternal allele, he or she will still suffer from AHO because of the developmental consequences of having only one normal *GNAS* allele. However, imprinting of the mutant allele will leave other adult tissues with their normal complement of one normal *GNAS* allele. These patients do not manifest PTH or other hormone resistance, they have normal serum calcium and phosphate levels and they have a normal nephrogenous cAMP response to PTH. These patients are referred to as having pseudo-pseudohypoparathyroidism.[324]

Patients with pseudohypoparathyroidism type Ib lack the phenotype of AHO and exhibit hormone resistance that is limited to the action of PTH in the kidney. These patients have been described to carry mutations in far upstream regulatory elements of the GNAS gene that are thought to be involved in the control of paternal GNAS gene methylation and its silencing in the kidney.[325,326] Because the PTH resistance is limited to the kidney, these patients are at risk for skeletal complications (osteoporosis or osteitis fibrosa cystica) due to chronic elevations in PTH, despite their biochemical profile of hypoparathyroidism and renal PTH resistance.[327]

Another less well-defined group of patients present with biochemical hypoparathyroidism and an insufficient phosphaturic response to PTH, but have an appropriate nephrogenous cAMP response to PTH and normal $G\alpha_s$ activity. This disorder is termed pseudohypoparathyroidism type II and may be due to intracellular resistance to the effects of cAMP, most likely caused by a defect in cAMP-dependent protein kinase.[328,329]

Laboratory findings in patients with PHP are similar to those seen in patients with hypoparathyroidism and include hypocalcemia, hyperphosphatemia, and a decreased serum $1,25(OH)_2D_3$ concentration. The important feature that distinguishes PHP from hypoparathyroidism is an increased instead of decreased

serum PTH concentration. The Ellsworth-Howard test can be used to classify the type of pseudohypoparathyroidism.[330] PTH is administered to the fasting patient after control serum and urine samples are obtained. Serum and urine are then collected during the first and second half-hours, and the second and third hours after the PTH infusion. Samples are analyzed for cAMP, phosphorus and creatinine. In normal subjects and in hypoparathyroid patients PTH induces a 10- to 20-fold increase in urinary cAMP excretion. In patients with pseudohypoparathyroidism type I (a and b) the response is markedly diminished. Patients with pseudohypoparathyroidism type II have a normal cAMP response, but an abnormal phosphaturic response to PTH. Classification of the type of pseudohypoparathyroidism has no impact on therapy. Management of the hypocalcemic PHP patient is similar to that of the hypoparathyroid patient and involves the administration of calcium and vitamin D. However, due to the intrinsic defects in PTH response, treatment with PTH will not be effective in raising calcium or lowering phosphate levels.

Vitamin D–Related Disorders

Vitamin D deficiency is common in the general population and is especially prevalent in patients without much exposure to sunlight, for example in institutionalized patients, the elderly, shut-ins, and those with chronic medical illness. In fact, one survey of inpatients in Boston suggested that up to 57% of patients admitted to a general medical ward were vitamin D deficient.[331] Even in a random sample of healthy adolescents, vitamin D deficiency was present in more than 24% of subjects.[332]

As discussed previously, levels of vitamin D vary with the season so that the prevalence of vitamin D deficiency is elevated in winter months. The prevalence of vitamin D deficiency is also greatly affected by the definition of a normal vitamin D level. This has been a controversial topic for several years.[333] Historically, the lower end of the normal range had been defined by the presence of secondary hyperparathyroidism and was set at a circulating 25 (OH) vitamin D level of 15 ng/ml. However, based on a series of epidemiological studies examining parameter such as fracture rates, PTH levels and falls, it was suggested that vitamin D levels should be over 30 ng/ml.[334] However, a recent review of this literature by the Institute of Medicine suggested that 20 ng/ml was a more accurate reflection of the lower end of the normal range.[335] This conversation will undoubtedly continue, but most patients with mild vitamin D deficiency do not demonstrate frank hypocalcemia, presumably because the serum calcium level is supported by increased PTH secretion. Overt hypocalcemia due to vitamin D deficiency is unlikely to occur in patients with levels over 15–20 ng/ml, unless they are also severely calcium deficient or they are on medications that lower bone resorption such as bisphosphonates.[336]

When it does occur, the primary mechanism of hypocalcemia in vitamin D deficiency is decreased intestinal absorption of calcium. In distinction to hypoparathyroidism, vitamin D deficiency is accompanied by hypophosphatemia and increased renal phosphate clearance as a result of secondary hyperparathyroidism. That compensatory response is a consequence of the hypocalcemic stimulus to PTH secretion as well as the stimulation of PTH gene expression and parathyroid cell proliferation by low vitamin D levels. The secondary hyperparathyroidism results in increased calcium mobilization from the skeleton, increased renal reabsorption of calcium, and increased renal 1α-hydroxylation of 25 (OH) vitamin D. Therefore, in all but the most severe vitamin D deficiency, circulating 1,25 $(OH)_2$ vitamin D levels are actually normal or elevated even though 25 (OH) vitamin D levels are low.[337]

Most patients with hypocalcemia and Vitamin D deficiency suffer from a deficiency of vitamin D synthesis and/or malabsorption. Malabsorption is an important cause of vitamin D deficiency in all age groups. Fat malabsorption from any cause or short-bowel syndrome can result in enteric losses of vitamin D. Fat malabsorption should be ruled out in patients with very low 25 (OH) vitamin D levels (<10–15 ng/dL). A number of medications cause vitamin D deficiency. Anticonvulsant medications and antituberculosis therapy are classic examples of medication that accelerate the hepatic inactivation of vitamin D.[338]

Impaired 1-alpha hydroxylation of 25(OH) vitamin D: The most common cause of a defect in 1 alpha-hydroxylase activity is CKD. Impaired 1α-hydroxylation is observed once the creatinine clearance decreases to approximately 30 to 40 mL/minute. Deficiency of 1,25 $(OH)_2$ vitamin D as a result of CKD most likely contributes to the disordered mineral metabolism and parathyroid hyperplasia that are characteristic of longstanding CKD.[339,340] This topic will be discussed in more detail in Chapter 91.

A form of congenital rickets can result from autosomal recessive, loss-of-function mutations in the *CYP27B1* gene.[127] This disorder is known as pseudovitamin D deficiency Rickets or Vitamin D-Dependent Rickets Type 1. Biochemically, this disorder is characterized by hypocalcemia and secondary hyperparathyroidism. The only metabolic abnormalities that differentiate it from dietary vitamin D

deficiency are the presence of normal or elevated levels of 25 (OH) vitamin D and very low levels of 1,25 $(OH)_2$ vitamin D, despite the elevated PTH levels. The disease is inherited in an autosomal recessive fashion and patients present in infancy with rickets, osteomalacia, and seizures, which resolve with therapeutic replacement of 1α-hydroxylated metabolites of vitamin D.[341]

Target organ resistance to 1,25-dihydroxyvitamin: Hereditary vitamin D-resistant rickets (HVDRR, also known as vitamin D-dependent rickets, Type 2) is characterized by resistance to biological effects of calcitriol due to inactivating mutations in the VDR gene.[342,343] This disorder is inherited in an autosomal recessive fashion and patients present with hypocalcemia, hypophosphatemia, secondary hyperparathyroidism and elevated levels of 1,25 $(OH)_2$ vitamin D. The presentation varies but most patients with HVDRR present in infancy or in adolescence with hypophosphatemia, rickets, seizures and, in some families, alopecia totalis.[344,345] Patients require lifelong therapy with large doses of vitamin D3, 1,25 $(OH)_2$ vitamin D and calcium. Therapeutic efficacy is variable and depends on the amount of residual VDR function contained within the mutant receptor. If loss of VDR activity is complete, than calcium infusions along with high doses of oral calcium are necessary to provide enough calcium to heal the rickets and/or maintain adequate bone mineralization.[346]

A variety of other conditions can cause mild to moderate hypocalcemia and these are listed in Table 66.6.

Treatment of Hypocalcemia

A calcium concentration, corrected for albumin, of less than 7.5 mg/dl in a patient with or without symptoms is an indication for treatment. The serum calcium should be increased back into the range (>7.5−8.0 mg/dl) in which symptoms and complications do not occur. Long term objectives are to prevent skeletal deformity and osteomalacia and to resolve secondary hyperparathyroidism while preventing hypercalciuria and hypercalcemia. When treating a pediatric population, the normal growth and development of bones is the priority with the same careful follow up to avoid complications.

Acute management: Severe hypocalcemia may be associated with life-threatening symptoms, in which case urgent treatment with parenteral calcium is indicated.[1] Patients who require immediate attention may exhibit a positive Chvostek's or Trousseau's sign, seizures, papilledema, hypotension, and prolonged ST segment and QT intervals on EKG. This is most likely to occur when the onset of hypoparathyroidism is abrupt. It may also occur in the patient with widespread osteoblastic metastases, tumor lysis, acute pancreatitis, or hungry bone syndrome. In any of those settings, the hypocalcemia is usually of acute onset and associated with significant symptoms. Hence, the calcium concentration should be corrected rapidly. In the case of overt tetany, 10 to 20 ml of calcium gluconate (90 mg of elemental calcium in 10 ml), diluted in 50 to 100 ml of 5% dextrose should be infused intravenously over 10 minutes. Continuous cardiac monitoring is important particularly if the patient is receiving digoxin as serious cardiac arrhythmias may occur. When managing recurrent symptomatic hypocalcemia, a continuous infusion of calcium gluconate should be instituted to provide 10 to 15 mg/kg of elemental calcium over approximately six to eight hours. Calcium chloride can also be used but is more irritating at the site of venous access. If hypocalcemia is likely to persist, therapy should be initiated early with oral calcium supplements (1 to 2 grams of elemental calcium) and calcitriol (0.5 to 1.0 micrograms) daily. Hypomagnesemia, if present, should be corrected with magnesium sulfate intramuscularly or intravenously. Intramuscular injections may be painful, in which case a continuous infusion of 48 mEq of magnesium for 24 hours may be administered. Magnesium therapy should continue for several days in order to restore intracellular magnesium and should be extended as long as the cause of hypomagnesemia is present. The dose of magnesium should be reduced by 50% in patients with renal insufficiency, and the serum magnesium concentration should be followed closely.

Chronic treatment: Most patients with chronic hypocalcemia will require both calcium (1 to 2 g elemental) and vitamin D to maintain a serum calcium concentration in the low normal range. A variety of vitamin D preparations are available and they vary in biologic activity, cost, and duration of effect. Calcitriol can be used for treatment of all chronic hypocalcemic states as it is the biologically active form of vitamin D. The principal advantages of calcitriol are its rapid onset and short duration of action, which minimizes the risk and duration of hypercalcemia in case of unintentional overdose. Calcitriol is the optimal modality in patients with hypoparathyroidism, pseudohypoparathyroidism, and renal failure, as these states are characterized by a deficiency of 1,25 $(OH)_2$ vitamin D. Nevertheless, treatment with high doses of cholecalciferol, ergocalciferol, or calcifediol can increase serum concentrations of 25-hydroxyvitamin D sufficiently to act directly on the vitamin D receptor. Calcidiol binds to the vitamin D receptor, but with far lower affinity than that of 1,25 $(OH)_2$ vitamin D3. These preparations also have a longer duration of action than calcitriol and can result in

prolonged hypercalcemia should overdosage occur.[347] In patients with vitamin D malabsorption causing the hypocalcemia, it would be appropriate to treat with the parent vitamin D compound, ergocalciferol. In severe liver disease, since the formation of 25-hydroxyvitamin D is impaired, calcifediol may be used. Vitamin D requirements may change as a consequence of concomitant administration of anticonvulsants, thiazide diuretics, oral contraceptives, and antacids, or the presence of electrolyte disturbances such as hypomagnesemia or hyperphosphatemia. Requirements may also change during pregnancy due to increased levels of DBP and the production of calcitriol by the placenta.[348] 1 to 2 g of elemental calcium given together with vitamin D should be sufficient to meet the goals of therapy in most patients. As discussed before, the dose of calcium should be adjusted to maintain the total serum calcium concentration in the low normal range (8.0 to 9.0 mg/dl) with the 24-hour urinary calcium excretion not to exceed 4 mg/kg/day to prevent hypercalciuria, nephrolithiasis, nephrocalcinosis and renal impairment. In patients with hypoparathyroidism, addition of a thiazide diuretic may decrease vitamin D requirements by decreasing urinary excretion of calcium, especially when used in combination with moderate salt restriction. Diet recommendations are also important to facilitate achieving treatment objectives. Foods that are high in phosphate, such as dairy products, should be limited to avoid hyperphosphatemia, which may cause soft tissue calcification and impair the efforts to raise serum calcium levels.

References

[1] Wysolmerski J, Insogna KL. The parathyroid glands, hypercalcemia, and hypocalcemia. In: Goldman L, Schafer A, editors. Goldman's cecil medicine. 24th ed. Philadelphia: Elsevier Saunders; 2012. p. 1591–601.

[2] Brown EM, Gamba G, Riccardi D, et al. Cloning and characterization of an extracellular Ca(2+)-sensing receptor from bovine parathyroid. Nature 1993;366(6455):575–80.

[3] Brown EM, MacLeod RJ. Extracellular calcium sensing and extracellular calcium signaling. Physiol Rev 2001;81(1):239–97.

[4] Chattopadhyay N, Mithal A, Brown EM. The calcium-sensing receptor: a window into the physiology and pathophysiology of mineral ion metabolism. Endocr Rev 1996;17(4):289–307.

[5] Riccardi D, Kemp P. The calcium-sensing receptor beyond extracelluar calcium homeostasis: conception, development, adult physiology, and disease. Annu Rev Physiol 2012;74:271–97.

[6] Felder CB, Graul RC, Lee AY, Merkle HP, Sadee W. The venus flytrap of periplasmic binding proteins: an ancient protein module present in multiple drug receptors. AAPS PharmSci 1999;1(2):E2.

[7] Canaff L, Zhou X, Hendy GN. The proinflammatory cytokine, interleukin-6, up-regulates calcium-sensing receptor gene transcription via Stat1/3 and Sp1/3. J Biol Chem 2008;283(20):13586–600.

[8] Canaff L, Hendy GN. Calcium-sensing receptor gene transcription is up-regulated by the proinflammatory cytokine, interleukin-1beta. Role of the NF-kappaB PATHWAY and kappaB elements. J Biol Chem 2005;280(14):14177–88.

[9] Canaff L, Hendy GN. Human calcium-sensing receptor gene. Vitamin D response elements in promoters P1 and P2 confer transcriptional responsiveness to 1,25-dihydroxyvitamin D. J Biol Chem 2002;277(33):30337–50.

[10] Chakrabarty S, Wang H, Canaff L, Hendy GN, Appelman H, Varani J. Calcium sensing receptor in human colon carcinoma: interaction with Ca(2+) and 1,25-dihydroxyvitamin D(3). Cancer Res 2005;65(2):493–8.

[11] Riccardi D, Brown EM. Physiology and pathophysiology of the calcium-sensing receptor in the kidney. Am J Physiol Renal Physiol 2010;298(3):F485–99.

[12] Maiti A, Beckman MJ. Extracellular calcium is a direct effecter of VDR levels in proximal tubule epithelial cells that counterbalances effects of PTH on renal Vitamin D metabolism. J Steroid Biochem Mol Biol 2007;103(3-5):504–8.

[13] Yarden N, Lavelin I, Genina O, et al. Expression of calcium-sensing receptor gene by avian parathyroid gland in vivo: relationship to plasma calcium. Gen Comp Endocrinol 2000;117(2):173–81.

[14] Canadillas S, Canalejo R, Rodriguez-Ortiz ME, et al. The up-regulation of the parathyroid VDR expression by extracellular calcium is mediated by the ERK1/2-MAPK signaling pathway. Am J Physiol Renal Physiol 2010.

[15] Fan GF, Ray K, Zhao XM, Goldsmith PK, Spiegel AM. Mutational analysis of the cysteines in the extracellular domain of the human Ca^{2+} receptor: effects on cell surface expression, dimerization and signal transduction. FEBS Lett 1998;436(3):353–6.

[16] Silve C, Petrel C, Leroy C, et al. Delineating a Ca^{2+} binding pocket within the venus flytrap module of the human calcium-sensing receptor. J Biol Chem 2005;280(45):37917–23.

[17] Mamillapalli R, VanHouten J, Zawalich W, Wysolmerski J. Switching of G-protein usage by the calcium-sensing receptor reverses its effect on parathyroid hormone-related protein secretion in normal versus malignant breast cells. J Biol Chem 2008;283(36):24435–47.

[18] Mamillapalli R, Wysolmerski J. The calcium-sensing receptor couples to Galpha(s) and regulates PTHrP and ACTH secretion in pituitary cells. J Endocrinol 2010;204(3):287–97.

[19] Huang C, Miller RT. The calcium-sensing receptor and its interacting proteins. J Cell Mol Med 2007;11(5):923–34.

[20] Chang W, Tu C, Cheng Z, et al. Complex formation with the Type B gamma-aminobutyric acid receptor affects the expression and signal transduction of the extracellular calcium-sensing receptor. Studies with HEK-293 cells and neurons. J Biol Chem 2007;282(34):25030–40.

[21] Gama L, Wilt SG, Breitwieser GE. Heterodimerization of calcium sensing receptors with metabotropic glutamate receptors in neurons. J Biol Chem 2001;276(42):39053–9.

[22] Wellendorph P, Brauner-Osborne H. Molecular basis for amino acid sensing by family C G-protein-coupled receptors. Br J Pharmacol 2009;156(6):869–84.

[23] Brown EM. Clinical utility of calcimimetics targeting the extracellular calcium-sensing receptor (CaSR). Biochem Pharmacol 2010;80(3):297–307.

[24] Trivedi R, Mithal A, Chattopadhyay N. Recent updates on the calcium-sensing receptor as a drug target. Curr Med Chem 2008;15(2):178–86.

[25] Block GA, Martin KJ, de Francisco AL, et al. Cinacalcet for secondary hyperparathyroidism in patients receiving hemodialysis. N Engl J Med 2004;350(15):1516–25.
[26] Ward DT, Riccardi D. New concepts in calcium-sensing receptor pharmacology and signalling. Br J Pharmacol 2012;165(1): 35–48.
[27] Chen RA, Goodman WG. Role of the calcium-sensing receptor in parathyroid gland physiology. Am J Physiol Renal Physiol 2004;286(6):F1005–11.
[28] Levi R, Ben-Dov IZ, Lavi-Moshayoff V, et al. Increased parathyroid hormone gene expression in secondary hyperparathyroidism of experimental uremia is reversed by calcimimetics: correlation with posttranslational modification of the trans acting factor AUF1. J Am Soc Nephrol 2006;17(1):107–12.
[29] Chang W, Tu C, Chen TH, Bikle D, Shoback D. The extracellular calcium-sensing receptor (CaSR) is a critical modulator of skeletal development. Sci Signal 2008;1(35): [ra1].
[30] Ho C, Conner DA, Pollak MR, et al. A mouse model of human familial hypocalciuric hypercalcemia and neonatal severe hyperparathyroidism. Nat Genet 1995;11(4):389–94.
[31] Li YC, Amling M, Pirro AE, et al. Normalization of mineral ion homeostasis by dietary means prevents hyperparathyroidism, rickets, and osteomalacia, but not alopecia in vitamin D receptor-ablated mice. Endocrinology 1998;139(10):4391–6.
[32] Panda DK, Miao D, Bolivar I, et al. Inactivation of the 25-hydroxyvitamin D 1alpha-hydroxylase and vitamin D receptor demonstrates independent and interdependent effects of calcium and vitamin D on skeletal and mineral homeostasis. J Biol Chem 2004;279(16):16754–66.
[33] Takaichi K, Kurokawa K. High Ca^{2+} inhibits peptide hormone-dependent cAMP production specifically in thick ascending limbs of Henle. Miner Electrolyte Metab 1986;12(5-6): 342–6.
[34] Kantham L, Quinn SJ, Egbuna OI, et al. The calcium-sensing receptor (CaSR) defends against hypercalcemia independent of its regulation of parathyroid hormone secretion. Am J Physiol Endocrinol Metab 2009.
[35] Gamba G, Friedman PA. Thick ascending limb: the Na(+):K(+):2Cl (-) co-transporter, NKCC2, and the calcium-sensing receptor, CaSR. Pflugers Arch 2009;458(1):61–76.
[36] Wang W, Lu M, Balazy M, Hebert SC. Phospholipase A2 is involved in mediating the effect of extracellular Ca^{2+} on apical K^+ channels in rat TAL. Am J Physiol 1997;273(3 Pt 2): F421–9.
[37] Ikari A, Okude C, Sawada H, et al. Activation of a polyvalent cation-sensing receptor decreases magnesium transport via claudin-16. Biochim Biophys Acta 2008;1778(1):283–90.
[38] Blankenship KA, Williams JJ, Lawrence MS, McLeish KR, Dean WL, Arthur JM. The calcium-sensing receptor regulates calcium absorption in MDCK cells by inhibition of PMCA. Am J Physiol Renal Physiol 2001;280(5):F815–22.
[39] Motoyama HI, Friedman PA. Calcium-sensing receptor regulation of PTH-dependent calcium absorption by mouse cortical ascending limbs. Am J Physiol Renal Physiol 2002;283(3): F399–406.
[40] Renkema KY, Velic A, Dijkman HB, et al. The calcium-sensing receptor promotes urinary acidification to prevent nephrolithiasis. J Am Soc Nephrol 2009;20(8):1705–13.
[41] Sands JM, Naruse M, Baum M, et al. Apical extracellular calcium/polyvalent cation-sensing receptor regulates vasopressin-elicited water permeability in rat kidney inner medullary collecting duct. J Clin Invest 1997;99(6):1399–405.
[42] Sands JM, Flores FX, Kato A, et al. Vasopressin-elicited water and urea permeabilities are altered in IMCD in hypercalcemic rats. Am J Physiol 1998;274(5 Pt 2):F978–85.
[43] Liu J, Lv F, Sun W, et al. The abnormal phenotypes of cartilage and bone in calcium-sensing receptor deficient mice are dependent on the actions of calcium, phosphorus, and PTH. PLoS Genet 2011;7(9):e1002294.
[44] Dvorak MM, Siddiqua A, Ward DT, et al. Physiological changes in extracellular calcium concentration directly control osteoblast function in the absence of calciotropic hormones. Proc Natl Acad Sci USA 2004;101(14):5140–5.
[45] Mentaverri R, Yano S, Chattopadhyay N, et al. The calcium sensing receptor is directly involved in both osteoclast differentiation and apoptosis. FASEB J 2006;20(14):2562–4.
[46] Kameda T, Mano H, Yamada Y, et al. Calcium-sensing receptor in mature osteoclasts, which are bone resorbing cells. Biochem Biophys Res Commun 1998;245(2):419–22.
[47] Naveh-Maney T, Silver J, Kronenberg H. Parathyroid hormone: molecular biology. In: 3rd ed. Bilezikian J, Raisz L, Martin T, editors. Principals of bone biology, vol. 1. San Diego, CA: Academic Press; 2008. p. 577–93.
[48] Nissenson R, Juppner H. Parathyroid hormone. In: Rosen C, editor. Primer on the metabolic bone diseases and disorders of mineral metabolism. 7th ed. Washington, DC: American Society for Bone and Mineral Research; 2008. p. 123–7.
[49] Potts JT. Parathyroid hormone: past and present. J Endocrinol 2005;187(3):311–25.
[50] Gensure RC, Gardella TJ, Juppner H. Parathyroid hormone and parathyroid hormone-related peptide, and their receptors. Biochem Biophys Res Commun 2005;328(3):666–78.
[51] Nissenson R, Juppner H. Parathyroid hormone. Primer on the Metab Bone Dis and Disord of Miner Metab 2008;:123–7.
[52] Endres DB, Villanueva R, Sharp Jr CF, Singer FR. Measurement of parathyroid hormone. Endocrinol Metab Clin North Am 1989;18(3):611–29.
[53] Naveh-Maney T, Silver J, Kronenberg H. Parathyroid hormone: molecular biology. Princ of Bone Biol 2008;1:577–93.
[54] Hofer AM, Brown EM. Extracellular calcium sensing and signalling. Nat Rev Mol Cell Biol 2003;4(7):530–8.
[55] Moallem E, Kilav R, Silver J, Naveh-Many T. RNA-Protein binding and post-transcriptional regulation of parathyroid hormone gene expression by calcium and phosphate. J Biol Chem 1998;273(9):5253–9.
[56] Brown EM. Calcium receptor and regulation of parathyroid hormone secretion. Rev Endocr Metab Disord 2000;1(4):307–15.
[57] Pollak MR, Brown EM, Chou YH, et al. Mutations in the human Ca(2+)-sensing receptor gene cause familial hypocalciuric hypercalcemia and neonatal severe hyperparathyroidism. Cell 1993;75(7):1297–303.
[58] Pollak MR, Brown EM, Estep HL, et al. Autosomal dominant hypocalcaemia caused by a Ca(2+)-sensing receptor gene mutation. Nat Genet 1994;8(3):303–7.
[59] Wettschureck N, Lee E, Libutti SK, Offermanns S, Robey PG, Spiegel AM. Parathyroid-specific double knockout of Gq and G11 alpha-subunits leads to a phenotype resembling germline knockout of the extracellular Ca^{2+} -sensing receptor. Mol Endocrinol 2007;21(1):274–80.
[60] Okazaki T, Igarashi T, Kronenberg HM. 5′-flanking region of the parathyroid hormone gene mediates negative regulation by 1,25-(OH)2 vitamin D3. J Biol Chem 1988;263(5):2203–8.
[61] Goodman WG, Quarles LD. Development and progression of secondary hyperparathyroidism in chronic kidney disease: lessons from molecular genetics. Kidney Int 2008;74(3): 276–88.
[62] Saidak Z, Mentaverri R, Brown EM. The role of the calcium-sensing receptor in the development and progression of cancer. Endocr Rev 2009;30(2):178–95.

[63] Yano S, Sugimoto T, Tsukamoto T, et al. Decrease in vitamin D receptor and calcium-sensing receptor in highly proliferative parathyroid adenomas. Eur J Endocrinol 2003;148(4): 403–11.
[64] Silver J, Naveh-Many T. Phosphate and the parathyroid. Kidney Int 2009;75(9):898–905.
[65] Ben-Dov IZ, Galitzer H, Lavi-Moshayoff V, et al. The parathyroid is a target organ for FGF23 in rats. J Clin Invest 2007;117 (12):4003–8.
[66] Bergwitz C, Juppner H. Regulation of phosphate homeostasis by PTH, vitamin D, and FGF23. Annu Rev Med 2010;61:91–104.
[67] Lavi-Moshayoff V, Wasserman G, Meir T, Silver J, Naveh-Many T. PTH increases FGF23 gene expression and mediates the high FGF23 levels of experimental kidney failure: a bone parathyroid feedback loop. Am J Physiol Renal Physiol 2010;299(4):F882–9 [Epub].
[68] Juppner H, Abou-Samra AB, Freeman M, et al. A G protein-linked receptor for parathyroid hormone and parathyroid hormone-related peptide. Science 1991;254(5034):1024–6.
[69] Gardella T, Juppner H, Brinhurst FR, Potts J. Receptors for parathyroid hormone (PTH) and PTH-related protein. Princ of Bone Biol 2008;1:555–76.
[70] Castro M, Nikolaev VO, Palm D, Lohse MJ, Vilardaga JP. Turn-on switch in parathyroid hormone receptor by a two-step parathyroid hormone binding mechanism. Proc Natl Acad Sci USA 2005;102(44):16084–9.
[71] Gesty-Palmer D, Chen M, Reiter E, et al. Distinct beta-arrestin- and G protein-dependent pathways for parathyroid hormone receptor-stimulated ERK1/2 activation. J Biol Chem 2006;281 (16):10856–64.
[72] Rey A, Manen D, Rizzoli R, Caverzasio J, Ferrari SL. Proline-rich motifs in the parathyroid hormone (PTH)/PTH-related protein receptor C terminus mediate scaffolding of c-Src with beta-arrestin2 for ERK1/2 activation. J Biol Chem 2006;281(50): 38181–8.
[73] Bisello A, Friedman P. PTH and PTHrP actions on kidney and bone. Princ of Bone Biol 2008;1:665–712.
[74] Amizuka N, Lee HS, Kwan MY, et al. Cell-specific expression of the parathyroid hormone (PTH)/PTH-related peptide receptor gene in kidney from kidney-specific and ubiquitous promoters. Endocrinology 1997;138(1):469–81.
[75] Ba J, Brown D, Friedman PA. Calcium-sensing receptor regulation of PTH-inhibitable proximal tubule phosphate transport. Am J Physiol Renal Physiol 2003;285(6):F1233–43.
[76] Tenenhouse HS. Phosphate transport: molecular basis, regulation and pathophysiology. J Steroid Biochem Mol Biol 2007;103 (3-5):572–7.
[77] Bacic D, Lehir M, Biber J, Kaissling B, Murer H, Wagner CA. The renal Na+/phosphate cotransporter NaPi-IIa is internalized via the receptor-mediated endocytic route in response to parathyroid hormone. Kidney Int 2006;69(3):495–503.
[78] Kempson SA, Lotscher M, Kaissling B, Biber J, Murer H, Levi M. Parathyroid hormone action on phosphate transporter mRNA and protein in rat renal proximal tubules. Am J Physiol 1995;268(4 Pt 2):F784–91.
[79] Keusch I, Traebert M, Lotscher M, Kaissling B, Murer H, Biber J. Parathyroid hormone and dietary phosphate provoke a lysosomal routing of the proximal tubular Na/Pi-cotransporter type II. Kidney Int 1998;54(4):1224–32.
[80] Zhang Y, Norian JM, Magyar CE, Holstein-Rathlou NH, Mircheff AK, McDonough AA. In vivo PTH provokes apical NHE3 and NaPi2 redistribution and Na-K-ATPase inhibition. Am J Physiol 1999;276(5 Pt 2):F711–9.
[81] Sneddon WB, Syme CA, Bisello A, et al. Activation-independent parathyroid hormone receptor internalization is regulated by NHERF1 (EBP50). J Biol Chem 2003;278(44): 43787–96.
[82] Mahon MJ, Donowitz M, Yun CC, Segre GV. Na(+)/H(+) exchanger regulatory factor 2 directs parathyroid hormone 1 receptor signalling. Nature 2002;417(6891):858–61.
[83] Hernando N, Deliot N, Gisler SM, et al. PDZ-domain interactions and apical expression of type IIa Na/P(i) cotransporters. Proc Natl Acad Sci USA 2002;99(18):11957–62.
[84] Wade JB, Liu J, Coleman RA, et al. Localization and interaction of NHERF isoforms in the renal proximal tubule of the mouse. Am J Physiol Cell Physiol 2003;285(6):C1494–503.
[85] Bacskai BJ, Friedman PA. Activation of latent Ca^{2+} channels in renal epithelial cells by parathyroid hormone. Nature 1990;347 (6291):388–91.
[86] Gesek FA, Friedman PA. On the mechanism of parathyroid hormone stimulation of calcium uptake by mouse distal convoluted tubule cells. J Clin Invest 1992;90(3):749–58.
[87] Friedman PA, Coutermarsh BA, Kennedy SM, Gesek FA. Parathyroid hormone stimulation of calcium transport is mediated by dual signaling mechanisms involving protein kinase A and protein kinase C. Endocrinology 1996;137(1): 13–20.
[88] Friedman PA, Gesek FA, Morley P, Whitfield JF, Willick GE. Cell-specific signaling and structure-activity relations of parathyroid hormone analogs in mouse kidney cells. Endocrinology 1999;140(1):301–9.
[89] Singh AT, Gilchrist A, Voyno-Yasenetskaya T, Radeff-Huang JM, Stern PH. G alpha12/G alpha13 subunits of heterotrimeric G proteins mediate parathyroid hormone activation of phospholipase D in UMR-106 osteoblastic cells. Endocrinology 2005;146 (5):2171–5.
[90] Bouhtiauy I, Lajeunesse D, Brunette MG. The mechanism of parathyroid hormone action on calcium reabsorption by the distal tubule. Endocrinology 1991;128(1):251–8.
[91] Lee M, Partridge NC. Parathyroid hormone signaling in bone and kidney. Curr Opin Nephrol Hypertens 2009;18(4): 298–302.
[92] DeLuca HF. Overview of general physiologic features and functions of vitamin D. Am J Clin Nutr 2004;80(6 Suppl.): 1689S–96S.
[93] Dusso AS, Brown AJ, Slatopolsky E. Vitamin D. Am J Physiol Renal Physiol 2005;289(1):F8–28.
[94] Maiti A, Hait NC, Beckman MJ. Extracellular calcium-sensing receptor activation induces vitamin D receptor levels in proximal kidney HK-2G cells by a mechanism that requires phosphorylation of p38alpha MAPK. J Biol Chem 2008;283(1): 175–83.
[95] Murayama A, Takeyama K, Kitanaka S, et al. Positive and negative regulations of the renal 25-hydroxyvitamin D3 1alpha-hydroxylase gene by parathyroid hormone, calcitonin, and 1alpha,25(OH)2D3 in intact animals. Endocrinology 1999;140 (5):2224–31.
[96] Barletta F, Dhawan P, Christakos S. Integration of hormone signaling in the regulation of human 25(OH)D3 24-hydroxylase transcription. Am J Physiol Endocrinol Metab 2004;286(4): E598–608.
[97] Matsumoto T, Kawanobe Y, Ogata E. Regulation of 24,25-dihydroxyvitamin D-3 production by 1,25-dihydroxyvitamin D-3 and synthetic human parathyroid hormone fragment 1-34 in a cloned monkey kidney cell line (JTC-12). Biochim Biophys Acta 1985;845(3):358–65.
[98] Zhao H, Wiederkehr MR, Fan L, Collazo RL, Crowder LA, Moe OW. Acute inhibition of Na/H exchanger NHE-3 by cAMP. Role of protein kinase a and NHE-3 phosphoserines 552 and 605. J Biol Chem 1999;274(7):3978–87.

[99] Datta NS, Abou-Samra AB. PTH and PTHrP signaling in osteoblasts. Cell Signal 2009;21(8):1245–54.
[100] Kousteni S, Bilezikian J. Cellular actions of parathyroid hormone. Princ of Bone Biol 2008;1:639–57.
[101] Nakashima T, Takayanagi H. Osteoclasts and the immune system. J Bone Miner Metab 2009;27(5):519–29.
[102] Yavropoulou MP, Yovos JG. Osteoclastogenesis—current knowledge and future perspectives. J Musculoskelet Neuronal Interact 2008;8(3):204–16.
[103] Goltzman D. Studies on the mechanisms of the skeletal anabolic action of endogenous and exogenous parathyroid hormone. Arch Biochem Biophys 2008;473(2):218–24.
[104] de Paula FJ, Rosen CJ. Back to the future: revisiting parathyroid hormone and calcitonin control of bone remodeling. Horm Metab Res 2010;42(5):299–306.
[105] Onyia JE, Bidwell J, Herring J, Hulman J, Hock JM. *In vivo*, human parathyroid hormone fragment (hPTH 1-34) transiently stimulates immediate early response gene expression, but not proliferation, in trabecular bone cells of young rats. Bone 1995;17(5):479–84.
[106] Qin L, Li X, Ko JK, Partridge NC. Parathyroid hormone uses multiple mechanisms to arrest the cell cycle progression of osteoblastic cells from G1 to S phase. J Biol Chem 2005;280 (4):3104–11.
[107] Wang YH, Liu Y, Rowe DW. Effects of transient PTH on early proliferation, apoptosis, and subsequent differentiation of osteoblast in primary osteoblast cultures. Am J Physiol Endocrinol Metab 2007;292(2):E594–603.
[108] Ishizuya T, Yokose S, Hori M, et al. Parathyroid hormone exerts disparate effects on osteoblast differentiation depending on exposure time in rat osteoblastic cells. J Clin Invest 1997;99 (12):2961–70.
[109] Midura RJ, Su X, Morcuende JA, Tammi M, Tammi R. Parathyroid hormone rapidly stimulates hyaluronan synthesis by periosteal osteoblasts in the tibial diaphysis of the growing rat. J Biol Chem 2003;278(51):51462–8.
[110] Pettway GJ, Schneider A, Koh AJ, et al. Anabolic actions of PTH (1-34): use of a novel tissue engineering model to investigate temporal effects on bone. Bone 2005;36(6):959–70.
[111] Valenta A, Roschger P, Fratzl-Zelman N, et al. Combined treatment with PTH (1-34) and OPG increases bone volume and uniformity of mineralization in aged ovariectomized rats. Bone 2005;37(1):87–95.
[112] Dobnig H, Turner RT. Evidence that intermittent treatment with parathyroid hormone increases bone formation in adult rats by activation of bone lining cells. Endocrinology 1995;136 (8):3632–8.
[113] Bellido T, Ali AA, Gubrij I, et al. Chronic elevation of parathyroid hormone in mice reduces expression of sclerostin by osteocytes: a novel mechanism for hormonal control of osteoblastogenesis. Endocrinology 2005;146(11):4577–83.
[114] Keller H, Kneissel M. SOST is a target gene for PTH in bone. Bone 2005;37(2):148–58.
[115] O'Brien CA, Plotkin LI, Galli C, et al. Control of bone mass and remodeling by PTH receptor signaling in osteocytes. PLoS One 2008;3(8):e2942.
[116] Divieti PP. PTH and osteocytes. J Musculoskelet Neuronal Interact 2005;5(4):328–30.
[117] Bikle D, Adams J, Christakos S. Vitamin D: production, metabolism, mechanisms of action, and clinical requirements. Primer on the metabolic bone diseases and disorders of mineral metabolism. 7th ed. Washington, DC: The American Society for Bone and Mineral Research; 2008141–149.
[118] MacLaughlin JA, Anderson RR, Holick MF. Spectral character of sunlight modulates photosynthesis of previtamin D3 and its photoisomers in human skin. Science 1982;216(4549): 1001–3.
[119] Clemens TL, Adams JS, Henderson SL, Holick MF. Increased skin pigment reduces the capacity of skin to synthesise vitamin D3. Lancet 1982;1(8263):74–6.
[120] Matsuoka LY, Ide L, Wortsman J, MacLaughlin JA, Holick MF. Sunscreens suppress cutaneous vitamin D3 synthesis. J Clin Endocrinol Metab 1987;64(6):1165–8.
[121] Matsuoka LY, Wortsman J, Dannenberg MJ, Hollis BW, Lu Z, Holick MF. Clothing prevents ultraviolet-B radiation-dependent photosynthesis of vitamin D3. J Clin Endocrinol Metab 1992;75(4):1099–103.
[122] Webb AR, Kline L, Holick MF. Influence of season and latitude on the cutaneous synthesis of vitamin D3: exposure to winter sunlight in Boston and Edmonton will not promote vitamin D3 synthesis in human skin. J Clin Endocrinol Metab 1988;67 (2):373–8.
[123] Cheng JB, Motola DL, Mangelsdorf DJ, Russell DW. De-orphanization of cytochrome P450 2R1: a microsomal vitamin D 25-hydroxilase. J Biol Chem 2003;278(39):38084–93.
[124] Nykjaer A, Dragun D, Walther D, et al. An endocytic pathway essential for renal uptake and activation of the steroid 25-(OH) vitamin D3. Cell 1999;96(4):507–15.
[125] Nykjaer A, Fyfe JC, Kozyraki R, et al. Cubilin dysfunction causes abnormal metabolism of the steroid hormone 25(OH) vitamin D(3). Proc Natl Acad Sci USA 2001;98(24): 13895–900.
[126] Monkawa T, Yoshida T, Wakino S, et al. Molecular cloning of cDNA and genomic DNA for human 25-hydroxyvitamin D3 1 alpha-hydroxylase. Biochem Biophys Res Commun 1997;239 (2):527–33.
[127] St-Arnaud R, Messerlian S, Moir JM, Omdahl JL, Glorieux FH. The 25-hydroxyvitamin D 1-alpha-hydroxylase gene maps to the pseudovitamin D-deficiency rickets (PDDR) disease locus. J Bone Miner Res 1997;12(10):1552–9.
[128] Takeyama K, Kitanaka S, Sato T, Kobori M, Yanagisawa J, Kato S. 25-Hydroxyvitamin D3 1alpha-hydroxylase and vitamin D synthesis. Science 1997;277(5333):1827–30.
[129] Ohyama Y, Noshiro M, Okuda K. Cloning and expression of cDNA encoding 25-hydroxyvitamin D3 24-hydroxylase. FEBS Lett 1991;278(2):195–8.
[130] Tanaka Y, Castillo L, DeLuca HF. The 24-hydroxylation of 1,25-dihydroxyvitamin D3. J Biol Chem 1977;252(4): 1421–4.
[131] Haussler M, Whitfield GK, Haussler C, Hsieh J, Jurutkfa P. Nuclear Vitamin D receptor: natural ligands, molecular structure-function, and transcriptional control of vital genes. In: Feldman D, Pike J, Adams J, editors. Vitamin D. 3rd ed. Waltham, MA: Academic Press; 2011. p. 137–70.
[132] Pike J, Meyer M, Lee S. The Vitamin D receptor: biochemical, molecular, biological, and genomic era investigations. In: Feldman D, Pike J, Adams J, editors. Vitamin D. 3rd ed. Waltham, MA: Academic Press; 2011. p. 97–136.
[133] Amling M, Priemel M, Holzmann T, et al. Rescue of the skeletal phenotype of vitamin D receptor-ablated mice in the setting of normal mineral ion homeostasis: formal histomorphometric and biomechanical analyses. Endocrinology 1999;140(11): 4982–7.
[134] Xue Y, Fleet JC. Intestinal vitamin D receptor is required for normal calcium and bone metabolism in mice. Gastroenterology 2009;136(4):1317–27 [e1311-1312].
[135] Fleet JC, Schoch R. Molecular mechanisms for regulation of intestinal calcium and phosphate absorption by Vitamin D. In: Feldman D, Pike J, Adams JS, editors. Vitamin D. 3rd ed. Wlatham, MA: Academic Press; 2011. p. 349–62.

[136] Bronner F, Pansu D, Stein WD. An analysis of intestinal calcium transport across the rat intestine. Am J Physiol 1986;250(5 Pt 1):G561–9.
[137] Cai Q, Chandler JS, Wasserman RH, Kumar R, Penniston JT. Vitamin D and adaptation to dietary calcium and phosphate deficiencies increase intestinal plasma membrane calcium pump gene expression. Proc Natl Acad Sci USA 1993;90 (4):1345–9.
[138] Feher JJ, Fullmer CS, Wasserman RH. Role of facilitated diffusion of calcium by calbindin in intestinal calcium absorption. Am J Physiol 1992;262(2 Pt 1):C517–26.
[139] Meyer MB, Zella LA, Nerenz RD, Pike JW. Characterizing early events associated with the activation of target genes by 1,25-dihydroxyvitamin D3 in mouse kidney and intestine in vivo. J Biol Chem 2007;282(31):22344–52.
[140] Song Y, Peng X, Porta A, et al. Calcium transporter 1 and epithelial calcium channel messenger ribonucleic acid are differentially regulated by 1,25 dihydroxyvitamin D3 in the intestine and kidney of mice. Endocrinology 2003;144(9):3885–94.
[141] Van Cromphaut SJ, Dewerchin M, Hoenderop JG, et al. Duodenal calcium absorption in vitamin D receptor-knockout mice: functional and molecular aspects. Proc Natl Acad Sci USA 2001;98(23):13324–9.
[142] Wasserman RH, Smith CA, Brindak ME, et al. Vitamin D and mineral deficiencies increase the plasma membrane calcium pump of chicken intestine. Gastroenterology 1992;102(3):886–94.
[143] Wasserman RH, Taylor AN. Vitamin d3-induced calcium-binding protein in chick intestinal mucosa. Science 1966;152 (3723):791–3.
[144] Kutuzova GD, Sundersingh F, Vaughan J, et al. TRPV6 is not required for 1alpha,25-dihydroxyvitamin D3-induced intestinal calcium absorption in vivo. Proc Natl Acad Sci USA 2008;105(50):19655–9.
[145] Benn BS, Ajibade D, Porta A, et al. Active intestinal calcium transport in the absence of transient receptor potential vanilloid type 6 and calbindin-D9k. Endocrinology 2008;149 (6):3196–205.
[146] Kutuzova GD, Akhter S, Christakos S, Vanhooke J, Kimmel-Jehan C, Deluca HF. Calbindin D(9k) knockout mice are indistinguishable from wild-type mice in phenotype and serum calcium level. Proc Natl Acad Sci U S A 2006;103(33):12377–81.
[147] Fujita H, Sugimoto K, Inatomi S, et al. Tight junction proteins claudin-2 and -12 are critical for vitamin D-dependent Ca^{2+} absorption between enterocytes. Mol Biol Cell 2008;19(5): 1912–21.
[148] Marks J, Srai SK, Biber J, Murer H, Unwin RJ, Debnam ES. Intestinal phosphate absorption and the effect of vitamin D: a comparison of rats with mice. Exp Physiol 2006;91(3):531–7.
[149] Xu H, Bai L, Collins JF, Ghishan FK. Age-dependent regulation of rat intestinal type IIb sodium-phosphate cotransporter by 1,25-(OH)(2) vitamin D(3). Am J Physiol Cell Physiol 2002;282 (3):C487–93.
[150] Tebben P, Kumar R. Vitamin D and the kidney. In: Feldman D, Pike JW, Adams JS, editors. Vitamin D. 3rd ed. Waltham, MA: Academic Press; 2011. p. 471–91.
[151] Kawashima H, Kurokawa K. Localization of receptors for 1,25-dihydroxyvitamin D3 along the rat nephron. Direct evidence for presence of the receptors in both proximal and distal nephron. J Biol Chem 1982;257(22):13428–32.
[152] Takeda S, Yoshizawa T, Nagai Y, et al. Stimulation of osteoclast formation by 1,25-dihydroxyvitamin D requires its binding to vitamin D receptor (VDR) in osteoblastic cells: studies using VDR knockout mice. Endocrinology 1999;140 (2):1005–8.
[153] Kearns AE, Khosla S, Kostenuik PJ. Receptor activator of nuclear factor kappaB ligand and osteoprotegerin regulation of bone remodeling in health and disease. Endocr Rev 2008;29(2):155–92.
[154] Naveh-Many T, Marx R, Keshet E, Pike JW, Silver J. Regulation of 1,25-dihydroxyvitamin D3 receptor gene expression by 1,25-dihydroxyvitamin D3 in the parathyroid in vivo. J Clin Invest 1990;86(6):1968–75.
[155] Russell J, Lettieri D, Sherwood LM. Suppression by 1,25(OH) 2D3 of transcription of the pre-proparathyroid hormone gene. Endocrinology 1986;119(6):2864–6.
[156] Silver J, Russell J, Sherwood LM. Regulation by vitamin D metabolites of messenger ribonucleic acid for preproparathyroid hormone in isolated bovine parathyroid cells. Proc Natl Acad Sci U S A 1985;82(12):4270–3.
[157] Meir T, Levi R, Lieben L, et al. Deletion of the vitamin D receptor specifically in the parathyroid demonstrates a limited role for the receptor in parathyroid physiology. Am J Physiol Renal Physiol 2009;297(5):F1192–8.
[158] Mangin M, Webb AC, Dreyer BE, et al. An identification of a cDNA encoding a parathyroid hormone-like peptide from a human tumor asociated with humoral hypercalcemia of malignancy. Proc Natl Acad Sci U S A 1988;85:597–601.
[159] Philbrick WM, Wysolmerski JJ, Galbraith S, et al. Defining the roles of parathyroid hormone-related protein in normal physiology. Physiol Rev 1996;76:127–73.
[160] Klein RF, Strewler GJ, Leung SC, Nissenson RA. Parathyroid hormone-like adenylate cyclase-stimulating activity from a human carcinoma is associated with bone-resorbing activity. Endocrinology 1987;120(2):504–11.
[161] Suva LJ, Winslow GA, Wettenhall RE, et al. A parathyroid hormone-related protein implicated in malignant hypercalcemia: cloning and expression. Science 1987;237:893–6.
[162] Chattopadhyay N. Effects of calcium-sensing receptor on the secretion of parathyroid hormone-related peptide and its impact on humoral hypercalcemia of malignancy. Am J Physiol Endocrinol Metab 2006;290(5):E761–70.
[163] VanHouten J, Dann P, McGeoch G, et al. The calcium-sensing receptor regulates mammary gland parathyroid hormone-related protein production and calcium transport. J Clin Invest 2004;113(4):598–608.
[164] Dean T, Vilardaga JP, Potts Jr JT, Gardella TJ. Altered selectivity of parathyroid hormone (Pth) and Pth-related protein for distinct conformations of the Pth/Pthrp receptor. Mol Endocrinol 2007.
[165] Horwitz MJ, Tedesco MB, Sereika SM, et al. Continuous PTH and PTHrP infusion causes suppression of bone formation and discordant effects on 1,25(OH)2 vitamin D. J Bone Miner Res 2005;20(10):1792–803.
[166] Fiaschi-Taesch NM, Stewart AF. Minireview: parathyroid hormone-related protein as an intracrine factor–trafficking mechanisms and functional consequences. Endocrinology 2003;144(2):407–11.
[167] Jans DA, Thomas RJ, Gillespie MT. Parathyroid hormone-related protein (PTHrP): a nucleocytoplasmic shuttling protein with distinct paracrine and intracrine roles. Vitam Horm 2003;66:345–84.
[168] Miao D, Su H, He B, et al. Deletion of the mid- and carboxyl regions of PTHrP produces growth retardation and early senescence in mice. J Bone Mineral Res 2005;20:S14.
[169] Strewler GJ. The physiology of parathyroid hormone-related protein. N Engl J Med 2000;342(3):177–85.
[170] Lanske B, Karaplis AC, Lee K, et al. PTH/PTHrP receptor in early development and Indian hedgehog-regulated bone growth. Science 1996;273:663–6.

[171] Schipani E, Lanske B, Hunzelman JL, et al. Targeted expression of constitutively active receptors for parathyroid hormone and parathyroid hormone-related peptide. Proc Natl Acad Sci USA 1996;94:13689–94.
[172] Weir EC, Philbrick WM, Amling M, Niff LA, Baron R, Broadus AE. Targeted overexpression of parathyroid hormone-related peptide in chondrodysplasia and delayed endochondrial bone formation. Proc Natl Acad Sci U S A 1996;93:10240–5.
[173] Kronenberg HM. PTHrP and skeletal development. Ann N Y Acad Sci 2006;1068:1–13.
[174] Chen X, Macica C, Nasiri A, Judex S, Broadus AE. Mechanical regulation of PTHrP expression in entheses. Bone 2007;41 (5):752–9.
[175] Chen X, Macica CM, Dreyer BE, et al. Initial characterization of PTH-related protein gene-driven lacZ expression in the mouse. J Bone Miner Res 2006;21(1):113–23.
[176] Amizuka N, Karaplis AC, Henderson JE, et al. Haploinsufficiency of parathyroid hormone-related peptide (PTHrP) results in abnormal postnatal bone development. Dev Biol 1996;175(1):166–76.
[177] Miao D, He B, Jiang Y, et al. Osteoblast-derived PTHrP is a potent endogenous bone anabolic agent that modifies the therapeutic efficacy of administered PTH 1-34. J Clin Invest 2005;115(9):2402–11.
[178] Robinson GW. Cooperation of signalling pathways in embryonic mammary gland development. Nat Rev Genet 2007;8 (12):963–72.
[179] Hens JR, Wysolmerski JJ. Key stages of mammary gland development: molecular mechanisms involved in the formation of the embryonic mammary gland. Breast Cancer Res 2005;7 (5):220–4.
[180] Wysolmerski JJ, Cormier S, Philbrick WM, et al. Absence of functional type 1 parathyroid hormone (PTH)/PTH-related protein recpetors in humans is associated with abnormal breast development and tooth impaction. J Clin Endocrinol Metab 2001;86(4):1788–94.
[181] Budayr AA, Halloran BR, King JC, Diep D, Nissenson RA, Strewler GJ. High levels of a parathyroid hormone-like protein in milk. Proc Natl Acad Sci U S A 1989;86:7183–5.
[182] VanHouten JN, Dann P, Stewart AF, et al. Mammary-specific deletion of parathyroid hormone-related protein preserves bone mass during lactation. J Clin Invest 2003;112(9): 1429–36.
[183] Lou H, Cote GJ, Gagel RF. The calcitonin exon and its flanking intronic sequences are sufficient for the regulation of human calcitonin/calcitonin gene-related peptide alternative RNA splicing. Mol Endocrinol 1994;8(12):1618–26.
[184] Austin LA, Heath III H, Go VL. Regulation of calcitonin secretion in normal man by changes of serum calcium within the physiologic range. J Clin Invest 1979;64(6):1721–4.
[185] Gorn AH, Lin HY, Yamin M, et al. Cloning, characterization, and expression of a human calcitonin receptor from an ovarian carcinoma cell line. J Clin Invest 1992;90(5):1726–35.
[186] Bruzzaniti A, Baron R. Molecular regulation of osteoclast activity. Rev Endocr Metab Disord 2006;7(1-2):123–39.
[187] Shyu JF, Shih C, Tseng CY, et al. Calcitonin induces podosome disassembly and detachment of osteoclasts by modulating Pyk2 and Src activities. Bone 2007;40(5):1329–42.
[188] Zaidi M, Datta HK, Moonga BS, MacIntyre I. Evidence that the action of calcitonin on rat osteoclasts is mediated by two G proteins acting via separate post-receptor pathways. J Endocrinol 1990;126(3):473–81.
[189] Suzuki H, Nakamura I, Takahashi N, et al. Calcitonin-induced changes in the cytoskeleton are mediated by a signal pathway associated with protein kinase A in osteoclasts. Endocrinology 1996;137(11):4685–90.
[190] Hu M, Gagel R. Calcitonin gene family of peptides. Princ of Bone Biol 2008;1:813–36.
[191] Davey RA, Turner AG, McManus JF, et al. Calcitonin receptor plays a physiological role to protect against hypercalcemia in mice. J Bone Miner Res 2008;23(8):1182–93.
[192] Woodrow JP, Sharpe CJ, Fudge NJ, Hoff AO, Gagel RF, Kovacs CS. Calcitonin plays a critical role in regulating skeletal mineral metabolism during lactation. Endocrinology 2006;147 (9):4010–21.
[193] Weber CJ, Sewell CW, McGarity WC. Persistent and recurrent sporadic primary hyperparathyroidism: histopathology, complications, and results of reoperation. Surgery 1994;116 (6):991–8.
[194] Burt ME, Brennan MF. Incidence of hypercalcemia and malignant neoplasm. Arch Surg 1980;115(6):704–7.
[195] van Dijk JM, Sonnenblick M, Weissberg N, Rosin A. Pseudohypercalcemia and hyperviscosity with neurological manifestations in multiple myeloma. Isr J Med Sci 1986;22 (2):143–4.
[196] Hebert SC, Brown EM, Harris HW. Role of the Ca(2+)-sensing receptor in divalent mineral ion homeostasis. J Exp Biol 1997;200(Pt 2):295–302.
[197] Patten BM, Bilezikian JP, Mallette LE, Prince A, Engel WK, Aurbach GD. Neuromuscular disease in primary hyperparathyroidism. Ann Intern Med 1974;80(2):182–93.
[198] Rasmussen K. [Pancreatitis and hypercalcemia]. Nord Med 1964;71:560–1.
[199] Khoo TK, Vege SS, Abu-Lebdeh HS, Ryu E, Nadeem S, Wermers RA. Acute pancreatitis in primary hyperparathyroidism: a population-based study. J Clin Endocrinol Metab 2009;94(6):2115–8.
[200] Ahmed R, Kiya F, Kitano K, Takagi H, Hashiba K. Effects of combined changes in serum calcium and potassium on QT interval. A study by Holter electrocardiographic monitoring during hemodialysis. Jpn Heart J 1987;28(6):813–28.
[201] Kiewiet RM, Ponssen HH, Janssens EN, Fels PW. Ventricular fibrillation in hypercalcaemic crisis due to primary hyperparathyroidism. Neth J Med 2004;62(3):94–6.
[202] Wermers RA, Khosla S, Atkinson EJ, Hodgson SF, O'Fallon WM, Melton III LJ. The rise and fall of primary hyperparathyroidism: a population-based study in Rochester, Minnesota, 1965-1992. Ann Intern Med 1997;126(6):433–40.
[203] Shelby H. Age and sex-related incidence of primary hyperparathyroidism. World J Surg 2008;32(5):800.
[204] Wagner B, Begic-Karup S, Raber W, Schneider B, Waldhausl W, Vierhapper H. Prevalence of primary hyperparathyroidism in 13387 patients with thyroid diseases, newly diagnosed by screening of serum calcium. Exp Clin Endocrinol Diabetes 1999;107(7):457–61.
[205] Bilezikian JP. Hypercalcemia. Curr Ther Endocrinol Metab 1994;5:511–4.
[206] Shlapack MA, Rizvi AA. Normocalcemic primary hyperparathyroidism-characteristics and clinical significance of an emerging entity. Am J Med Sci 2012;343(2):163–6.
[207] Corbetta S, Mantovani G, Lania A, et al. Calcium-sensing receptor expression and signalling in human parathyroid adenomas and primary hyperplasia. Clin Endocrinol 2000;52 (3):339–48.
[208] Sudhaker Rao D, Han ZH, Phillips ER, Palnitkar S, Parfitt AM. Reduced vitamin D receptor expression in parathyroid adenomas: implications for pathogenesis. Clin Endocrinol 2000;53 (3):373–81.

[209] Imanishi Y, Hosokawa Y, Yoshimoto K, et al. Primary hyperparathyroidism caused by parathyroid-targeted overexpression of cyclin D1 in transgenic mice. J Clin Invest 2001;107(9):1093–102.
[210] Chandrasekharappa SC, Guru SC, Manickam P, et al. Positional cloning of the gene for multiple endocrine neoplasia-type 1. Science 1997;276(5311):404–7.
[211] Rogers HM, Keating Jr FR. Primary hypertrophy and hyperplasia of the parathyroid glands as a cause of hyperparathyroidism. Am J Med 1947;3(4):384–401.
[212] Castleman B, Mallory TB. Parathyroid hyperplasia in chronic renal insufficiency. Am J Pathol 1937;13(4):553–74 [557].
[213] Guru SC, Goldsmith PK, Burns AL, et al. Menin, the product of the MEN1 gene, is a nuclear protein. Proc Natl Acad Sci USA 1998;95(4):1630–4.
[214] Ponder BA, Smith D. The MEN II syndromes and the role of the ret proto-oncogene. Adv Cancer Res 1996;70:179–222.
[215] Miya A, Yamamoto M, Morimoto H, et al. Expression of the ret proto-oncogene in human medullary thyroid carcinomas and pheochromocytomas of MEN 2A. Henry Ford Hosp Med J 1992;40(3-4):215–9.
[216] DeLellis RA, Mazzaglia P, Mangray S. Primary hyperparathyroidism: a current perspective. Arch Pathol Lab Med 2008;132(8):1251–62.
[217] De Wesselow OL, De Wardener HE. Carcinoma of the parathyroid gland with hyperparathyroidism. Lancet 1949;1(6559):820–3.
[218] Pepe J, Cipriani C, Pilotto R, et al. Sporadic and hereditary primary hyperparathyroidism. J Endocrinol Invest 2011;34(7 Suppl.):40–4.
[219] Shane E, Bilezikian JP. Parathyroid carcinoma: a review of 62 patients. Endocr Rev Spring 1982;3(2):218–26.
[220] F vR. Die Fibrose oder deformirende Ostitis, die Osteomalacie und die osteoplastische Carcinose in ihren gegense- itigen Beziehungen. Festschriftfir Rudolph Virchow. Berlin. 1891.
[221] Sharpe HS. Hyperparathyroidism associated with osteitis fibrosa cystica. Can Med Assoc J 1939;40(2):164–5.
[222] Lowe H, McMahon DJ, Rubin MR, Bilezikian JP, Silverberg SJ. Normocalcemic primary hyperparathyroidism: further characterization of a new clinical phenotype. J Clin Endocrinol Metab 2007;92(8):3001–5.
[223] Rejnmark L, Vestergaard P, Mosekilde L. Nephrolithiasis and renal calcifications in primary hyperparathyroidism. J Clin Endocrinol Metab 2011;96(8):2377–85.
[224] Koide T, Yoshioka T, Oka T, Sonoda T. Promotive effect of urine from patients with primary hyperparathyroidism on calcium oxalate crystal aggregation in an in vitro whole urine system. J Urol 1988;140(6):1571–4.
[225] Abboud B, Daher R, Boujaoude J. Digestive manifestations of parathyroid disorders. World J Gastroenterol 2011;17(36):4063–6.
[226] Nilsson IL, Yin L, Lundgren E, Rastad J, Ekbom A. Clinical presentation of primary hyperparathyroidism in Europe–nationwide cohort analysis on mortality from nonmalignant causes. J Bone Miner Res 2002;17(Suppl. 2):N68–74.
[227] Hollenberg AN, Arnold A. Hypercalcemia with low-normal serum intact PTH: a novel presentation of primary hyperparathyroidism. Am J Med 1991;91(5):547–8.
[228] Shaker JL, Krawczyk KW, Findling JW. Primary hyperparathyroidism and severe hypercalcemia with low circulating 1,25-dihydroxyvitamin D. J Clin Endocrinol Metab 1990;71(5):1305–9.
[229] Eisenberg H, Pallotta J, Sacks B, Brickman AS. Parathyroid localization, three-dimensional modeling, and percutaneous ablation techniques. Endocrinol Metab Clin North Am 1989;18(3):659–700.
[230] Pino Rivero V, Keituqwa Yanez T, Pardo Romero G, Trinidad Ruiz G, Marcos Garcia M, Blasco Huelva A. [Complications of thyroid and parathyroid surgery. Retrospective study and review of the literature]. An Otorrinolaringol Ibero Am 2003;30(6):607–14.
[231] Rubin MR, Bilezikian JP, McMahon DJ, et al. The natural history of primary hyperparathyroidism with or without parathyroid surgery after 15 years. J Clin Endocrinol Metab 2008;93(9):3462–70.
[232] Ambrogini E, Cetani F, Cianferotti L, et al. Surgery or surveillance for mild asymptomatic primary hyperparathyroidism: a prospective, randomized clinical trial. J Clin Endocrinol Metab 2007;92(8):3114–21.
[233] Bollerslev J, Jansson S, Mollerup CL, et al. Medical observation, compared with parathyroidectomy, for asymptomatic primary hyperparathyroidism: a prospective, randomized trial. J Clin Endocrinol Metab 2007;92(5):1687–92.
[234] Rao DS, Phillips ER, Divine GW, Talpos GB. Randomized controlled clinical trial of surgery versus no surgery in patients with mild asymptomatic primary hyperparathyroidism. J Clin Endocrinol Metab 2004;89(11):5415–22.
[235] Khan A, Grey A, Shoback D. Medical management of asymptomatic primary hyperparathyroidism: proceedings of the third international workshop. J Clin Endocrinol Metab 2009;94(2):373–81.
[236] Peacock M, Bilezikian JP, Klassen PS, Guo MD, Turner SA, Shoback D. Cinacalcet hydrochloride maintains long-term normocalcemia in patients with primary hyperparathyroidism. J Clin Endocrinol Metab 2005;90(1):135–41.
[237] Peacock M, Bolognese MA, Borofsky M, et al. Cinacalcet treatment of primary hyperparathyroidism: biochemical and bone densitometric outcomes in a five-year study. J Clin Endocrinol Metab 2009;94(12):4860–7.
[238] Kifor O, Moore Jr FD, Delaney M, et al. A syndrome of hypocalciuric hypercalcemia caused by autoantibodies directed at the calcium-sensing receptor. J Clin Endocrinol Metab 2003;88(1):60–72.
[239] Pallais JC, Kifor O, Chen Y-B, Slovik D, Brown EM. Acquired hypocalciuric hypercalcemia due to autoantibodies against the calcium-sensing receptor. N Engl J Med 2004;351(4):362–9.
[240] Volpe A, Guerriero A, Marchetta A, Caramaschi P, Furlani L. Familial hypocalciuric hypercalcemia revealed by chondrocalcinosis. Joint Bone Spine 2009;76(6):708–10.
[241] Pearce SH, Wooding C, Davies M, Tollefsen SE, Whyte MP, Thakker RV. Calcium-sensing receptor mutations in familial hypocalciuric hypercalcaemia with recurrent pancreatitis. Clin Endocrinol 1996;45(6):675–80.
[242] Ralston SH, Gallacher SJ, Patel U, Campbell J, Boyle IT. Cancer-associated hypercalcemia: morbidity and mortality. Clinical experience in 126 treated patients. Ann Intern Med 1990;112(7):499–504.
[243] Broadus AE, Mangin M, Ikeda K, et al. Humoral hypercalcemia of cancer. Identification of a novel parathyroid hormone-like peptide. N Engl J Med 1988;319(9):556–63.
[244] Stewart AF, Horst R, Deftos LJ, Cadman EC, Lang R, Broadus AE. Biochemical evaluation of patients with cancer-associated hypercalcemia: evidence for humoral and nonhumoral groups. N Engl J Med 1980;303(24):1377–83.
[245] Cornish J, Callon KE, Lin C, Xiao C, Moseley JM, Reid IR. Stimulation of osteoblast proliferation by C-terminal fragments of parathyroid hormone-related protein. J Bone Miner Res 1999;14(6):915–22.

[246] Seymour JF, Gagel RF. Calcitriol: the major humoral mediator of hypercalcemia in Hodgkin's disease and non-Hodgkin's lymphomas. Blood 1993;82(5):1383–94.
[247] Mundy GR, Luben RA, Raisz LG, Oppenheim JJ, Buell DN. Bone-resorbing activity in supernatants from lymphoid cell lines. N Engl J Med 1974;290(16):867–71.
[248] Yagiz K, Rittling SR. Both cell-surface and secreted CSF-1 expressed by tumor cells metastatic to bone can contribute to osteoclast activation. Exp Cell Res 2009;315(14):2442–52.
[249] Choi SJ, Cruz JC, Craig F, et al. Macrophage inflammatory protein 1-alpha is a potential osteoclast stimulatory factor in multiple myeloma. Blood 2000;96(2):671–5.
[250] Pfeilschifter J, Chenu C, Bird A, Mundy GR, Roodman GD. Interleukin-1 and tumor necrosis factor stimulate the formation of human osteoclastlike cells in vitro. J Bone Miner Res 1989;4 (1):113–8.
[251] Heider U, Zavrski I, Jakob C, et al. Expression of receptor activator of NF-kappaB ligand (RANKL) mRNA in human multiple myeloma cells. J Cancer Res Clin Oncol 2004;130 (8):469–74.
[252] Tian E, Zhan F, Walker R, et al. The role of the Wnt-signaling antagonist DKK1 in the development of osteolytic lesions in multiple myeloma. N Engl J Med 2003;349(26):2483–94.
[253] Guise TA, Yin JJ, Taylor SD, et al. Evidence for a causal role of parathyroid hormone-related protein in the pathogenesis of human breast cancer-mediated osteolysis. J Clin Invest 1996;98 (7):1544–9.
[254] Bendre MS, Montague DC, Peery T, Akel NS, Gaddy D, Suva LJ. Interleukin-8 stimulation of osteoclastogenesis and bone resorption is a mechanism for the increased osteolysis of metastatic bone disease. Bone 2003;33(1):28–37.
[255] Harrell GT, Fisher S. Blood chemical changes in Boeck's Sarcoid with particular reference to protein, calcium and phosphatase values. J Clin Invest 1939;18(6):687–93.
[256] Ahmed B, Jaspan JB. Case report: hypercalcemia in a patient with AIDS and pneumocystis carinii pneumonia. Am J Med Sci 1993;306(5):313–6.
[257] Zaloga GP, Chernow B, Eil C. Hypercalcemia and disseminated cytomegalovirus infection in the acquired immunodeficiency syndrome. Ann Intern Med 1985;102(3):331–3.
[258] Barbour GL, Coburn JW, Slatopolsky E, Norman AW, Horst RL. Hypercalcemia in an anephric patient with sarcoidosis: evidence for extrarenal generation of 1,25-dihydroxyvitamin D. N Engl J Med 1981;305(8):440–3.
[259] Kimberg DV, Baerg RD, Gershon E, Graudusius RT. Effect of cortisone treatment on the active transport of calcium by the small intestine. J Clin Invest 1971;50(6):1309–21.
[260] Beall DP, Scofield RH. Milk-alkali syndrome associated with calcium carbonate consumption. Report of 7 patients with parathyroid hormone levels and an estimate of prevalence among patients hospitalized with hypercalcemia. Medicine (Baltimore) 1995;74(2):89–96.
[261] Bullimore DW, Miloszewski KJ. Raised parathyroid hormone levels in the milk alkali syndrome: an appropriate response? Postgrad Med J 1987;63(743):789–92.
[262] Beall DP, Henslee HB, Webb HR, Scofield RH. Milk-alkali syndrome: a historical review and description of the modern version of the syndrome. Am J Med Sci 2006;331(5):233–42.
[263] Mundy GR, Shapiro JL, Bandelin JG, Canalis EM, Raisz LG. Direct stimulation of bone resorption by thyroid hormones. J Clin Invest 1976;58(3):529–34.
[264] Mune T, Katakami H, Kato Y, Yasuda K, Matsukura S, Miura K. Production and secretion of parathyroid hormone-related protein in pheochromocytoma: participation of an alpha-adrenergic mechanism. J Clin Endocrinol Metab 1993;76(3): 757–62.
[265] Stewart AF, Adler M, Byers CM, Segre GV, Broadus AE. Calcium homeostasis in immobilization: an example of resorptive hypercalciuria. N Engl J Med 1982;306(19):1136–40.
[266] Varache N, Audran M, Clochon P, et al. Aminohydroxypropylidene bisphosphonate (AHPrBP) treatment of severe immobilization hypercalcaemia in a young patient. Clin Rheumatol 1991;10(3):328–32.
[267] Vieth R. The mechanisms of vitamin D toxicity. Bone Miner 1990;11(3):267–72.
[268] Manitius A, Levitin H, Beck D, Epstein FH. On the mechanism of impairment of renal concentrating ability in hypercalcemia. J Clin Invest 1960;39:693–7.
[269] Araki T, Holick MF, Alfonso BD, et al. Vitamin D intoxication with severe hypercalcemia due to manufacturing and labeling errors of two dietary supplements made in the United States. J Clin Endocrinol Metab 2011;96(12):3603–8.
[270] Mak TW, Shek CC, Chow CC, Wing YK, Lee S. Effects of lithium therapy on bone mineral metabolism: a two-year prospective longitudinal study. J Clin Endocrinol Metab 1998;83 (11):3857–9.
[271] Wallace J, Scarpa A. Similarities of Li+ and low Ca^{2+} in the modulation of secretion by parathyroid cells in vitro. J Biol Chem 1983;258(10):6288–92.
[272] Porter RH, Cox BG, Heaney D, Hostetter TH, Stinebaugh BJ, Suki WN. Treatment of hypoparathyroid patients with chlorthalidone. N Engl J Med 1978;298(11):577–81.
[273] Smith FR, Goodman DS. Vitamin A transport in human vitamin A toxicity. N Engl J Med 1976;294(15):805–8.
[274] Oreffo RO, Teti A, Triffitt JT, Francis MJ, Carano A, Zallone AZ. Effect of vitamin A on bone resorption: evidence for direct stimulation of isolated chicken osteoclasts by retinol and retinoic acid. J Bone Miner Res 1988;3(2):203–10.
[275] Llach F, Felsenfeld AJ, Haussler MR. The pathophysiology of altered calcium metabolism in rhabdomyolysis-induced acute renal failure. Interactions of parathyroid hormone, 25-hydroxycholecalciferol, and 1,25-dihydroxycholecalciferol. N Engl J Med 1981;305(3):117–23.
[276] Stewart AF. Clinical practice. Hypercalcemia associated with cancer. N Engl J Med 2005;352(4):373–9.
[277] Thiebaud D, Jacquet AF, Burckhardt P. Fast and effective treatment of malignant hypercalcemia. Combination of suppositories of calcitonin and a single infusion of 3-amino 1-hydroxypropylidene-1-bisphosphonate. Arch Intern Med 1990;150(10):2125–8.
[278] Zaidi M, Blair HC, Moonga BS, Abe E, Huang CL. Osteoclastogenesis, bone resorption, and osteoclast-based therapeutics. J Bone Miner Res 2003;18(4):599–609.
[279] van beek E, Lowik C, van der Pluijm G, Papapoulos S. The role of geranylgeranylation in bone resorption and its suppression by bisphosphonates in fetal bone explants in vitro: a clue to the mechanism of action of nitrogen-containing bisphosphonates. J Bone Miner Res 1999;14(5):722–9.
[280] Major P, Lortholary A, Hon J, et al. Zoledronic acid is superior to pamidronate in the treatment of hypercalcemia of malignancy: a pooled analysis of two randomized, controlled clinical trials. J Clin Oncol 2001;19(2):558–67.
[281] Coleman RE. Bone cancer in 2011: prevention and treatment of bone metastases. Nat Rev Clin Oncol 2012;9(2):76–8.
[282] Lewiecki EM, Miller PD, McClung MR, et al. Two-year treatment with denosumab (AMG 162) in a randomized phase 2 study of postmenopausal women with low BMD. J Bone Miner Res 2007;22(12):1832–41.

[283] Shoback DM, Bilezikian JP, Turner SA, McCary LC, Guo MD, Peacock M. The calcimimetic cinacalcet normalizes serum calcium in subjects with primary hyperparathyroidism. J Clin Endocrinol Metab 2003;88(12):5644–9.
[284] Silverberg SJ, Rubin MR, Faiman C, et al. Cinacalcet hydrochloride reduces the serum calcium concentration in inoperable parathyroid carcinoma. J Clin Endocrinol Metab 2007;92 (10):3803–8.
[285] Spodick DH. Classic chronic renal failure: hyperkalemia and hypocalcemia. Am J Geriatr Cardiol 2005;14(6):336–7.
[286] Massry SG, Arieff AI, Coburn JW, Palmieri G, Kleeman CR. Divalent ion metabolism in patients with acute renal failure: studies on the mechanism of hypocalcemia. Kidney Int 1974;5 (6):437–45.
[287] Rubin M, Levine M. Hypoparathyroidism and pseudohypoparathyroidism. In: Rosen C, editor. Primer on the metabolic bone diseases and disorders of mineral metabolism. 7th ed. Washington, DC: The American Society for Bone and Mineral Research; 2008. p. 354–61.
[288] Ali A, Christie PT, Grigorieva IV, et al. Functional characterization of GATA3 mutations causing the hypoparathyroidism-deafness-renal (HDR) dysplasia syndrome: insight into mechanisms of DNA binding by the GATA3 transcription factor. Hum Mol Genet 2007;16(3):265–75.
[289] Chiu WY, Chen HW, Chao HW, Yann LT, Tsai KS. Identification of three novel mutations in the GATA3 gene responsible for familial hypoparathyroidism and deafness in the Chinese population. J Clin Endocrinol Metab 2006;91 (11):4587–92.
[290] Nesbit MA, Bowl MR, Harding B, et al. Characterization of GATA3 mutations in the hypoparathyroidism, deafness, and renal dysplasia (HDR) syndrome. J Biol Chem 2004;279(21): 22624–34.
[291] Gaynor KU, Grigorieva IV, Nesbit MA, et al. A missense GATA3 mutation, Thr272Ile, causes the hypoparathyroidism, deafness, and renal dysplasia syndrome. J Clin Endocrinol Metab 2009;94(10):3897–904.
[292] Lichtner P, Konig R, Hasegawa T, Van Esch H, Meitinger T, Schuffenhauer S. An HDR (hypoparathyroidism, deafness, renal dysplasia) syndrome locus maps distal to the DiGeorge syndrome region on 10p13/14. J Med Genet 2000;37(1):33–7.
[293] Greenberg F. Hypoparathyroidism and the DiGeorge syndrome. N Engl J Med 1989;320(17):1146–7.
[294] Sticht H, Hashemolhosseini S. A common structural mechanism underlying GCMB mutations that cause hypoparathyroidism. Med Hypotheses 2006;67(3):482–7.
[295] Mannstadt M, Bertrand G, Muresan M, et al. Dominant-negative GCMB mutations cause an autosomal dominant form of hypoparathyroidism. J Clin Endocrinol Metab 2008;93 (9):3568–76.
[296] Bowl MR, Mirczuk SM, Grigorieva IV, et al. Identification and characterization of novel parathyroid-specific transcription factor glial cells missing homolog B (GCMB) mutations in eight families with autosomal recessive hypoparathyroidism. Hum Mol Genet 2010;19(10):2028–38.
[297] Sarin R, Tomar N, Ray D, Gupta N, Sharma YD, Goswami R. Absence of pathogenic calcium sensing receptor mutations in sporadic idiopathic hypoparathyroidism. Clin Endocrinol (Oxf) 2006;65(3):359–63.
[298] Watanabe T, Minagawa M. [Familial hypoparathyroidism due to activating mutations in the calcium-sensing receptor gene]. Nihon Rinsho 2002;60(2):331–7.
[299] Yamamoto M, Akatsu T, Nagase T, Ogata E. Comparison of hypocalcemic hypercalciuria between patients with idiopathic hypoparathyroidism and those with gain-of-function mutations in the calcium-sensing receptor: is it possible to differentiate the two disorders? J Clin Endocrinol Metab 2000;85 (12):4583–91.
[300] De Luca F, Ray K, Mancilla EE, et al. Sporadic hypoparathyroidism caused by de Novo gain-of-function mutations of the Ca(2+)-sensing receptor. J Clin Endocrinol Metab 1997;82 (8):2710–5.
[301] Baron J, Winer KK, Yanovski JA, et al. Mutations in the Ca (2 +)-sensing receptor gene cause autosomal dominant and sporadic hypoparathyroidism. Hum Mol Genet 1996;5 (5):601–6.
[302] Okazaki R, Chikatsu N, Nakatsu M, et al. A novel activating mutation in calcium-sensing receptor gene associated with a family of autosomal dominant hypocalcemia. J Clin Endocrinol Metab 1999;84(1):363–6.
[303] Vargas-Poussou R, Huang C, Hulin P, et al. Functional characterization of a calcium-sensing receptor mutation in severe autosomal dominant hypocalcemia with a Bartter-like syndrome. J Am Soc Nephrol 2002;13(9):2259–66.
[304] Gardner JM, Fletcher AL, Anderson MS, Turley SJ. AIRE in the thymus and beyond. Curr Opin Immunol 2009;21(6):582–9.
[305] Alimohammadi M, Bjorklund P, Hallgren A, et al. Autoimmune polyendocrine syndrome type 1 and NALP5, a parathyroid autoantigen. N Engl J Med 2008;358(10):1018–28.
[306] Li Y, Song YH, Rais N, et al. Autoantibodies to the extracellular domain of the calcium sensing receptor in patients with acquired hypoparathyroidism. J Clin Invest 1996;97(4): 910–4.
[307] Kifor O, McElduff A, LeBoff MS, et al. Activating antibodies to the calcium-sensing receptor in two patients with autoimmune hypoparathyroidism. J Clin Endocrinol Metab 2004;89(2): 548–56.
[308] Brasier AR, Nussbaum SR. Hungry bone syndrome: clinical and biochemical predictors of its occurrence after parathyroid surgery. Am J Med 1988;84(4):654–60.
[309] Hundahl SA, Cady B, Cunningham MP, et al. Initial results from a prospective cohort study of 5583 cases of thyroid carcinoma treated in the united states during 1996. U.S. and German thyroid cancer study group. An American college of surgeons commission on cancer patient care evaluation study. Cancer 2000;89(1):202–17.
[310] Scott ME. Resistant hypoparathyroidism and magnesium depletion. Lancet 1973;1(7810):1005.
[311] Rude RK, Oldham SB, Singer FR. Functional hypoparathyroidism and parathyroid hormone end-organ resistance in human magnesium deficiency. Clin Endocrinol (Oxf) 1976;5 (3):209–24.
[312] Homer L. Hypoparathyroidism requiring massive amounts of medication, with apparent response to magnesium sulfate. J Clin Endocrinol Metab 1961;21:219–23.
[313] Kanis JA, Russell RG. Rate of reversal of hypercalcaemia and hypercalciuria induced by vitamin D and its 1alpha-hydroxylated derivatives. Br Med J 1977;1(6053):78–81.
[314] Bilezikian JP, Khan A, Potts Jr JT, et al. Hypoparathyroidism in the adult: epidemiology, diagnosis, pathophysiology, target-organ involvement, treatment, and challenges for future research. J Bone Miner Res 2011;26(10):2317–37.
[315] Nogueira EL, Costa AC, Santana A, et al. Teriparatide efficacy in the treatment of severe hypocalcemia after kidney transplantation in parathyroidectomized patients: a series of five case reports. Transplantation 2011;92(3):316–20.
[316] Puig-Domingo M, Diaz G, Nicolau J, Fernandez C, Rueda S, Halperin I. Successful treatment of vitamin D unresponsive hypoparathyroidism with multipulse subcutaneous infusion of teriparatide. Eur J Endocrinol 2008;159(5):653–7.

[317] Favus MJ. American society for bone and mineral research. Primer on the metabolic bone diseases and disorders of mineral metabolism. 6th ed. Washington, DC: American Society for Bone and Mineral Research; 2006.
[318] Nakamura Y, Matsumoto T, Tamakoshi A, et al. Prevalence of idiopathic hypoparathyroidism and pseudohypoparathyroidism in Japan. J Epidemiol 2000;10(1):29–33.
[319] Albright FBC, Smith PH. Pseudohypoparathyroidism: an example of seabright-bantam syndrome: report of three cases. Endocrinology 1942;30:922–32.
[320] Bastepe M. The GNAS locus and pseudohypoparathyroidism. Adv Exp Med Biol 2008;626:27–40.
[321] Wilson LC, Oude Luttikhuis ME, Clayton PT, Fraser WD, Trembath RC. Parental origin of Gs alpha gene mutations in albright's hereditary osteodystrophy. J Med Genet 1994;31 (11):835–9.
[322] Chase LR, Melson GL, Aurbach GD. Pseudohypoparathyroidism: defective excretion of 3′,5′-AMP in response to parathyroid hormone. J Clin Invest 1969;48(10): 1832–44.
[323] Levine MA, Downs Jr RW, Moses AM, et al. Resistance to multiple hormones in patients with pseudohypoparathyroidism. Association with deficient activity of guanine nucleotide regulatory protein. Am J Med 1983;74(4):545–56.
[324] Levine MA, Ahn TG, Klupt SF, et al. Genetic deficiency of the alpha subunit of the guanine nucleotide-binding protein Gs as the molecular basis for albright hereditary osteodystrophy. Proc Nat Acad Sci Usa 1988;85(2):617–21.
[325] Juppner H, Schipani E, Bastepe M, et al. The gene responsible for pseudohypoparathyroidism type Ib is paternally imprinted and maps in four unrelated kindreds to chromosome 20q13.3. Proc Natl Acad Sci U S A 1998;95(20):11798–803.
[326] Liu J, Litman D, Rosenberg MJ, Yu S, Biesecker LG, Weinstein LS. A GNAS1 imprinting defect in pseudohypoparathyroidism type IB. J Clin Invest 2000;106(9):1167–74.
[327] Murray TM, Rao LG, Wong MM, et al. Pseudohypoparathyroidism with osteitis fibrosa cystica: direct demonstration of skeletal responsiveness to parathyroid hormone in cells cultured from bone. J Bone Miner Res 1993;8(1):83–91.
[328] Silve C. Pseudohypoparathyroidism syndromes: the many faces of parathyroid hormone resistance. Eur J Endocrinol 1995;133(2):145–6.
[329] Drezner M, Neelon FA, Lebovitz HE. Pseudohypoparathyroidism type II: a possible defect in the reception of the cyclic AMP signal. N Engl J Med 1973;289(20): 1056–60.
[330] Audran M, Alix E, Jallet P, Renier JC. [The effects of synthetic 1-34 fragment of human PTH on kidney and bone receptors in man. Use of the Ellsworth-Howard test]. Rev Rhum Mal Osteoartic 1982;49(8-9):599–608.
[331] Thomas MK, Lloyd-Jones DM, Thadhani RI, et al. Hypovitaminosis D in medical inpatients. N Engl J Med 1998;338(12):777–83.
[332] Gordon CM, DePeter KC, Feldman HA, Grace E, Emans SJ. Prevalence of vitamin D deficiency among healthy adolescents. Arch Pediatr Adolesc Med 2004;158(6):531–7.
[333] Saintonge S, Bang H, Gerber LM. Implications of a new definition of vitamin D deficiency in a multiracial us adolescent population: the national health and nutrition examination survey III. Pediatrics 2009;123(3):797–803.
[334] Binkley N, Ramamurthy R, Krueger D. Low vitamin D status: definition, prevalence, consequences, and correction. Endocrinol Metab Clin North Am 2010;39(2):287–301 [table of contents]
[335] Ross AC, Manson JE, Abrams SA, et al. The 2011 report on dietary reference intakes for calcium and vitamin D from the institute of medicine: what clinicians need to know. J Clin Endocrinol Metab 2011;96(1):53–8.
[336] Premaor MO, Alves GV, Crossetti LB, Furlanetto TW. Hyperparathyroidism secondary to hypovitaminosis D in hypoalbuminemic is less intense than in normoalbuminemic patients: a prevalence study in medical inpatients in southern Brazil. Endocrine 2004;24(1):47–53.
[337] Schmidt-Gayk H, Bouillon R, Roth HJ. Measurement of vitamin D and its metabolites (calcidiol and calcitriol) and their clinical significance. Scand J Clin Lab Invest Suppl 1997;227:35–45.
[338] Brodie MJ, Boobis AR, Hillyard CJ, et al. Effect of rifampicin and isoniazid on vitamin D metabolism. Clin Pharmacol Ther 1982;32(4):525–30.
[339] Patel NM, Gutierrez OM, Andress DL, Coyne DW, Levin A, Wolf M. Vitamin D deficiency and anemia in early chronic kidney disease. Kidney Int 2010;77(8):715–20.
[340] Seeherunvong W, Abitbol CL, Chandar J, Zilleruelo G, Freundlich M. Vitamin D insufficiency and deficiency in children with early chronic kidney disease. J Pediatr 2009;154 (6):906–911 e901.
[341] Kitanaka S, Murayama A, Sakaki T, et al. No enzyme activity of 25-hydroxyvitamin D3 1alpha-hydroxylase gene product in pseudovitamin D deficiency rickets, including that with mild clinical manifestation. J Clin Endocrinol Metab 1999;84 (11):4111–7.
[342] Yagi H, Ozono K, Miyake H, Nagashima K, Kuroume T, Pike JW. A new point mutation in the deoxyribonucleic acid-binding domain of the vitamin D receptor in a kindred with hereditary 1,25-dihydroxyvitamin D-resistant rickets. J Clin Endocrinol Metab 1993;76(2):509–12.
[343] Malloy PJ, Weisman Y, Feldman D. Hereditary 1 alpha,25-dihydroxyvitamin D-resistant rickets resulting from a mutation in the vitamin D receptor deoxyribonucleic acid-binding domain. J Clin Endocrinol Metab 1994;78(2): 313–6.
[344] Burnett CH, Dent CE, Harper C, Warland BJ. Vitamin D-resistant rickets. Analysis of twenty-four pedigrees with hereditary and sporadic cases. Am J Med 1964;36:222–32.
[345] Fraher LJ, Karmali R, Hinde FR, et al. Vitamin D-dependent rickets type II: extreme end organ resistance to 1,25-dihydroxy vitamin D3 in a patient without alopecia. Eur J Pediatr 1986;145(5):389–95.
[346] Balsan S, Garabedian M, Larchet M, et al. Long-term nocturnal calcium infusions can cure rickets and promote normal mineralization in hereditary resistance to 1,25-dihydroxyvitamin D. J Clin Invest 1986;77(5):1661–7.
[347] Vieth R. Vitamin D toxicity, policy, and science. J Bone Miner Res 2007;22(Suppl. 2):V64–8.
[348] Zerwekh JE, Breslau NA. Human placental production of 1 alpha,25-dihydroxyvitamin D3: biochemical characterization and production in normal subjects and patients with pseudohypoparathyroidism. J Clin Endocrinol Metab 1986;62 (1):192–6.
[349] Khan AA, Bilezikian JP, Kung AW, et al. Alendronate in primary hyperparathyroidism: a double-blind, randomized, placebo-controlled trial. J Clin Endocrinol Metab 2004;89 (7):3319–25.
[350] Oyajobi BO. Multiple myeloma/hypercalcemia. Arthritis Res Ther 2007;9(Suppl. 1):S4.

This page intentionally left blank

CHAPTER

67

Pathogenesis and Treatment of Nephrolithiasis

Fredric L. Coe[1], *Andrew Evan*,[2] *and Elaine Worcester*[1]

[1]University of Chicago School of Medicine, Chicago, Illinois, USA

[2]Indiana University, Indianapolis, Indiana, USA

Stone forming patients are labeled by the stones they form. The largest group form calcium stones (calcium oxalate (CaOx), calcium phosphate (CaP), or a mixture of both); others form stones containing primarily uric acid (UA), struvite (infection stones), or cystine. The pathogenesis of each stone type differs; clinical evaluation, therefore, begins with analysis of all available stones. A large fraction of the common calcium stone formers have no systemic disease but do excrete more calcium than the average person, an inherited trait (idiopathic hypercalciuria, IH) that probably reflects the simple fact that risk of calcium stones increases with rate of urine calcium excretion. These "idiopathic" calcium stone formers (ICSF) produce stones mainly of CaOx crystals, and are by far the most common kind of patient a physician will encounter in practice. All ICSF studied thus far exhibit the same renal histopathology and surgical anatomy, and appear to form their stones via a single highly defined pathway, and therefore represent what amounts to a well-defined specific disease. By contrast, idiopathic calcium stone formers whose stones contain over 50% CaP (IPSF) have renal histopathology, surgical anatomy, and mechanisms of stone production that differ radically from those of ICSF, though they share IH as a common physiological trait. Patients with calcium stones due to systemic diseases such as primary hyperparathyroidism, distal renal tubular acidosis (RTA), ileostomy, small bowel resection, and obesity bypass procedures exhibit renal histopathologies, mechanisms of stone production, and treatments that are specific to the underlying disease. Despite their heterogeneity, all stone diseases share formation of unwanted solid phase crystals that produce similar clinical syndromes. As well, crystals nucleate and grow according to natural laws one can use in clinical practice.

STONES, CLINICAL PRESENTATION, AND NATURAL HISTORY

Crystals form in urine of virtually all healthy people, but among those destined for stone disease they are coarser and larger, and cause a syndrome of pain and hematuria which often eludes diagnosis for some time, the crystals being dispersed or not looked for. As perhaps a second stage, though the continuity may be more apparent than real, crystals become so large and dense they form a gravel or sand-like material whose passage is gritty and evident. Such attacks of gravel with or without bleeding are usually recognized by patients and diagnosed as a kind of stone problem. Certainly the conventional passage of a formed stone is a step beyond gravel, if only because the formed stone may lodge along the urinary tract and demand a procedure to remove it. Pain is usual though not invariant, as is bleeding. Finally, stones and plaques of crystal may form along the calyces and papillary tips, forming the radiographic pattern of nephrocalcinosis that may or may not be associated with stone passage, gravel, or crystalluria with hematuria. Thus is stone disease divided into at least four great divisions as seen by patients and doctors, though all arise in similar ways.

Nature of Stones and Crystals

Formed stones are a complex of proteins interlaid with crystals, like a kind of disordered mineralized

Seldin and Giebisch's The Kidney, Fifth Edition.
DOI: http://dx.doi.org/10.1016/B978-0-12-381462-3.00067-7

© 2013 Elsevier Inc. All rights reserved.

TABLE 67.1 Percent of Stones in Which a Given Crystal Type is Found

Crystal Type	US Population[a]	US Veterans[b]
Calcium oxalate monohydrate	43	63
Calcium oxalate dihydrate	61	42
Apatite	62	23
Brushite	2	2
Struvite	16	11
Uric acid	9	9
Cystine	1	0.4
Ammonium acid urate	0.4	1

[a]*Herring LC. Observations on the analysis of ten thousand urinary calculus.* J Urol. *1962;88:545–555.*
[b]*Mandel NS, Mandel GS. Urinary tract stone disease in the United States veteran population, II: geographical analysis of variations in composition.* J Urol *1989;142:1516–1521; Mandel NS, Mandel GS. Urinary tract stone disease in the United States veteran population, I: geographical frequency of occurrence.* J Urol. *1989;142:1513–1515.*

tissue. The matrix proteins include Tamm-Horsfall protein (THP), osteopontin, albumin, prothrombin fragments, and other urine proteins. The crystals are most often CaOx, monohydrate (COM) or dihydrate (COD)[1,2,3] (Table 67.1), often admixed with CaP species such as apatite (APA) and brushite (BR), less often admixed with UA. In a smaller number of patients (12% of 2011 patients seen in the University of Chicago Kidney Stone Clinic with stone analyses), stones are predominantly or completely composed of CaP[4,5]; CaP stones are more common in women. In another 7% of our patients, stones were predominantly UA. Uncommon stones (each seen in fewer than 2% of patients) include those of cystine, struvite, ammonium acid urate, and drugs (Table 67.1). Because each kind of stone crystal evidences a particular disorder of urine supersaturation, stone analysis is the bedrock of clinical practice. Repeated stones all deserve analysis, as urine chemistry changes with time, and a change in composition may signal a need for change of treatment.

Clinical Presentation

Renal Colic

The pain from passage of a stone begins as a discomfort, often not called a pain, and progresses over 30 minutes or so to a plateau of extreme severity, which remains constant thereafter unless medications are given or the stone moves. The pain of a stone in the renal pelvis and upper ureter is over the lateral and anterior abdomen on one side, in a broad band from the ribs downward, and is not well localized. As the stone moves down, the pain moves in parallel, toward the bladder, and a downward moving pain is sure evidence of stone movement. At the uretero-vesical junction, stones often lodge and produce urinary frequency and urgency, dysuria, and hematuria, the complex easily misdiagnosed as urinary infection if symptoms begin there. This latter is common with small stones that easily pass the upper ureter but stick at the bladder junction, and give their first symptoms there. When the stone passes into the bladder, obstruction is relieved and pain disappears on the instant, with a speed unlike any other known pain.

The character of colic is not describable. All attest to severity surpassing any other pain that afflicts humankind, but poets and writers alike fall silent when asked to describe it. What little we have been offered suggests a deep boring and hot sensation, but no more detail than that. Colic is diagnosed by its curious timing, progress, peculiar intensity, and magical disappearance. On the left side, colic can resemble diverticulitis, except the latter causes constipation, whereas colic causes diarrhea and vomiting. On the right it mimics biliary colic, but is too lateral, too severe, too detached from eating, and unnatural in its downward progress. We[6] have constructed long lists of differential diagnosis, but find the problem pointless, because no one mistakes renal colic, for long, as anything other than what it is.

Radiography of Stones

CaOx and CaP stones tend to be small (1–10 mm), bright, and circumscribed. UA stones are famously radiolucent on routine radiography, but can be easily visualized by computed tomography (CT) scan done without contrast infusion. Cystine stones are only faintly visible on routine x-rays, so that we often underestimate size, but CT is ideal for them. A struvite stone, being an amalgam of magnesium ammonium and calcium phosphate crystals and much protein that is made by waves of bacterial overgrowth, naturally appears like a gnarled root. Ultrasound detects stones, but is less sensitive for small stones and does not show anatomy well compared with CT.[7] Because noncontrast CT gives an excellent view of the renal pelvis and of whether there is obstruction, it is our preferred mode of visualization. Protocols using lower doses of radiation are under investigation to evaluate their diagnostic accuracy, and may become preferred in order to limit radiation exposure.

Stones pass in inverse proportion to their size,[8] although time to passage may require four to six weeks.[9] Below 5 mm, passage is common, while ureteral stones greater than 7 mm in diameter pass spontaneously less than 50% of the time. Above 10 mm, passage is unlikely. Stones in the distal ureter are more likely to pass than those located more proximally. Large stones in the renal pelvis grow at leisure and can gradually fill up the collecting system. Such behavior is

more usual for struvite, UA and cystine stones, but CaOx stones do attain such stature occasionally. A stone that fills at least two calyces is called a stag horn stone, although this old and picturesque name is better reserved for stones that fill all of the calyces, and have the shape of a stag's horns.

Urinalysis

Given that crystals are coarse and often symptom producing, one might think that urinalysis is valuable in clinical practice of stone prevention, but our experience is the opposite. It is true that one can teach urine crystal morphology in a stone clinic, and the appearances of crystals under the microscope are beguiling, especially under polarized light, but the impact on diagnosis is modest. In addition, a single sample of urine may not represent the daily average. However, at least one study shows that persistent crystalluria in a first morning urine while on treatment is correlated with relapse.[10]

COM crystals are small dumbbell shapes that can superficially resemble red blood cells. The more dramatic COD is bipyramidal, as shown in all usual atlases. UA forms a reddish dust, because it absorbs uricine, a bilirubin metabolite and is an indication of low urine pH. Calcium phosphates are often small, and called "amorphous," though they are in fact crystalline if seen under higher magnification. Calcium phosphates form whenever urine pH is much above 6.5, and may be irrelevant to stone formation or not depending on how well the spot urine pH represents that of the average 24-hour urine. Crystals occur in casts, and such casts have no established significance. Cystine crystals are found in urine of most cystinuric patients, and have little significance as the cool temperature of the room as compared with the body can allow crystals that are not present *in vivo*. Of course, they may be the first clue as to the correct diagnosis. Perhaps the most valuable finding is a urine pH above eight, which suggests infection with urea hydrolyzing bacteria, and requires follow up with urine culture. Overall, we hesitate to seem skeptical of urinalysis, given its preeminence in nephrology, but in the stone clinic it is more of aesthetic visual than clinical interest.

NATURAL HISTORY

Epidemiology

In the United States, 11% of men and 5.6% of women will report having formed a stone by their seventh decade; the risk is about three times higher in whites compared with African Americans, but has increased in both groups as well as both sexes over the past three decades.[11] Although this may reflect, in part, improved radiologic detection of asymptomatic stones, a true increase in stone formation seems likely based on hospitalization rates. Obesity is associated with increased risk for stone formation, which rises with body mass index and waist circumference, especially in women.[12]

Stone formation is associated with an increased risk of chronic kidney disease, although the mechanism is not known.[13] There also appears to be an increased risk of hypertension among stone formers,[14] and an attendant increase in risk of cardiovascular disease.[15]

There is a significant genetic component to stone formation. In studies comparing stone rates in male twins, the concordance rate for stones was 32% in monozygotic compared with 17% in dizygotic twins.[16] Similarly, in a longitudinal cohort of adult men, those with a family history of stones were 2.5 times more likely to form a first stone over eight years of follow-up than those without.[17] A number of rare monogenic diseases are known which predispose to stone formation.[18] However, most of the genetic predisposition appears to be polygenic, and is strongly influenced by environmental triggers, as seen in diseases such as hypertension and diabetes.

Recurrence

Following a first stone you may confidently predict that 50% of patients will form at least one more stone after eight years and 75% will recur by 15 years.[19] In those with more than one stone, recurrence occurs sooner; approximately 45% of such ICSF will have a new stone within three years. Once recurrent, stones maintain a one- to two-year interval between themselves in the average patient, although the spread is very wide. We have tried in vain to properly characterize high-velocity stone formers.[20] When we have analyzed the stone history of patients with many stones we find the rate of stones per year surprisingly constant and that stone number increases pari passu with how long people wait from their first stone to obtaining preventative treatment. On the other hand, we find many patients in whom a single stone episode will yield a collection of dozens or perhaps hundreds of small stones passed within hours or days, whereas for most people an episode is no more than a single stone. We have never understood how batches of stones are made and passed within a day's span.

PRIMARY PROCESS OF CRYSTALLIZATION

Solid phase begins as the association of ions or molecules in solution reduce the energy of bonds with

water molecules so much that they leave the solution as so-called solid-phase nuclei. For calcium and oxalate, or calcium and phosphate, the association involves formation of dissolved salts; for uric acid and cystine, the molecules associate with themselves, mainly by hydrophobic forces. In either case, for practical purposes, one finds that nuclei form as some critical concentration is reached.

The Notion of Supersaturation

An ideal formal statement of the critical concentrations for nucleation is to compare salt or molecular concentrations of a solution to those at the solubility, any excess being called the supersaturation (SS), and implying the solution is carrying more than it can hold. This naive idea gives the right sense of SS, in begging the question of what is meant by "more than it can hold." If crystals of a salt are incubated for some time, usually 48 hours, with a solution that is initially free of the salt, the concentrations of salt in solution will increase until the crystals no longer dissolve. This concentration is called the solubility and is empirically determined, being otherwise unknowable. A solution that contains the solubility concentration is called saturated. Values for CaOx, calcium monohydrogen phosphate (BR) (a commonly measured initial phase of calcium phosphate), and undissociated UA are (in μM/l) 6.2, 0.39, and 520, respectively.

If one slowly adds calcium and oxalate to a saturated solution it will remain clear. The salt concentration will rise above solubility, and the solution is called supersaturated. The level of SS may be expressed as the ratio of the concentration of the dissolved salt to its solubility. The solution is metastable in that the extra salt, CaOx, for example, will crystallize out and bring the solution to solubility given any of a number of perturbations. The most obvious is to add seed crystals of, for example, CaOx, which will grow until equilibrium is restored. Seeds of CaP, or UA, which are "heterogeneous," will also promote formation of CaOx nuclei on their surfaces and deplete the system back to solubility. The same is true for cell debris and aggregated proteins. If one continues to add calcium and oxalate, but not a solid seed, SS will rise to a critical point called the upper limit of metastability (ULM),[21] which is an empirical limit at which CaOx nuclei will form spontaneously, and bring the solution back down to solubility.

Actual values for SS and the ULM can be determined in human urine (Fig. 67.1). For CaP (Fig. 67.1, open circles) the SS values of normal urine range from 0.1 to 5, versus 2 to 20 for CaOx (Fig. 67.1, stars). The ULM can be determined by adding sodium oxalate to aliquots of the urine, to achieve a CaOx ULM, or calcium chloride, to obtain the CaP ULM. Among healthy individuals, the ULM is strongly dependent upon, but considerably above, the SS,[22] as shown by the position of all points above the line of identity. ULM values range from two- to 11-fold above SS for CaP and 11- to 50-fold for CaOx. How ULM varies with SS is not understood, but that it does so reflects a highly protective set of mechanisms that appear to be aimed at defense against renal crystallization.

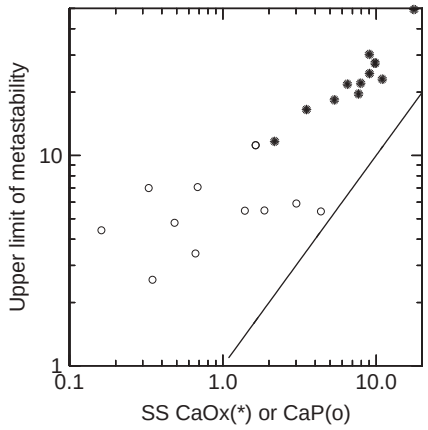

FIGURE 67.1 Relationship between upper limit of metastability (ULM, y-axis) and urine supersaturation (x-axis) for calcium oxalate (stars) and calcium phosphate (open circles). The diagonal line is the line of identity. ULM rises with supersaturation for both phases. Values are from normal individuals.

Relationship of Supersaturation to Stone Composition

As measured clinically SS represents two or three days of urine measurement out of a lifetime, and one wonders to what extent such a slim sampling can be useful in predicting formation of solid phases over the months to years that stones begin and grow in the renal collecting system. In fact, SS appears to be a very robust measure of long-term crystallization forces. Among men and women whose stones were predominantly CaOx (Fig. 67.2), COM SS was above corresponding same-sex normal values, whereas CaP and UA SS values were not. Among patients whose stones were predominantly CaP (Fig. 67.2), CaP SS was above same-sex normal values, whereas COM SS was not. Naturally, because higher urine pH favors CaP SS and reduces UA SS, UA SS is lower than normal in this group. Among patients with UA stones, UA SS is above normal and COM SS is not. Overall, even when measured only a few times, urine SS reflects at least the main components of stones, and therefore one must conclude that renal physiology acts to maintain SS at a reasonably stable level in most stone formers,

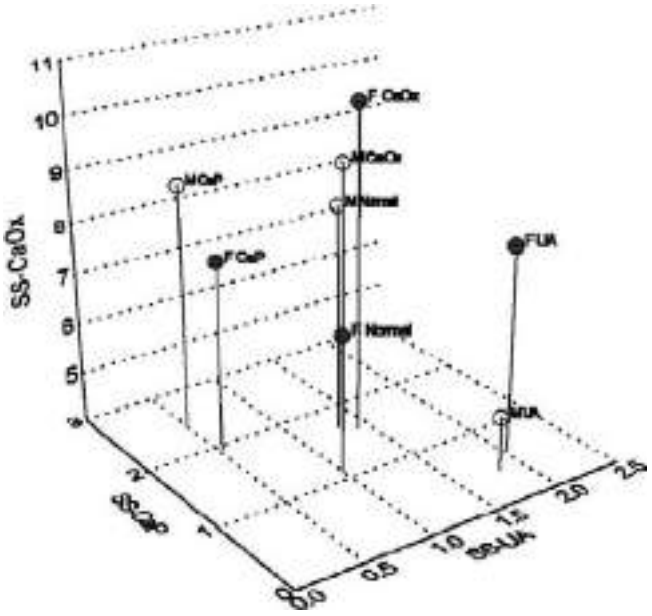

FIGURE 67.2 Supersaturation (SS) versus stone composition. SS for calcium oxalate (CaOx) (z-axis), calcium phosphate (CaP) (y-axis) and uric acid (UA) (x-axis) in females (closed symbols) are low for normals and correspond to stone composition in stone forming females. For males (open symbols), the same is true except that healthy individuals are more similar to stone-forming patients. *(Reprinted with permission from ref.[23])*

and that a few urine samples give a strong insight into long-term, stone-forming tendencies of a patient.

The normal values we used to compare with patient data show a marked sex difference. Whereas healthy women have urine COM SS below that of stone-forming women (Fig. 67.2), COM SS in urine of men is nearly at the levels of patients and is much higher than among healthy women. This occurs mainly because, being larger, men have higher traffics of calcium and oxalate into urine than women, but share with them virtually the same daily urine volume.[23] The finding accords well with the epidemiological observation that male stone formers outnumber female stone formers, and further support the value of even sparse SS measurements to characterize the stone forming impulse of an individual.

Given the general rule that stone composition follows SS, one may ask about the exceptions. When individual urine samples fail to show SS corresponding to stone composition, or show SS not reflected in stone composition, can one use such a discrepancy clinically? We[24] found two types of exception. Sometimes SS elevation is present but the predicted mineral phase is absent from all analyzed stones (Type 1). This occurs mainly when urine volumes are very low and multiple SS values are high. The phenomenon suggests some important renal mechanisms that reduce crystallization. Type 2 discrepancies are solid phase in stones without a relevant SS in the urine. Here, we have found very high urine volume is the rule, and assume that matters have changed with the patients after passing a stone, so that fluid intake increased and a past SS was abolished. These exceptions are a kind of sporadic accent on a general backdrop of correspondence, and we propose that a break in correspondence has clinical use in pointing to increased urine volume, especially, which may not hold long term.

CONTROL OF SUPERSATURATION

Given that SS is the driving force for crystallization, and that direct experiments document a strong link between SS measurements made clinically and stone mineral composition, as well as gender differences in stone forming potential, the regulation of SS and the factors that influence it are clearly at the center of stone pathophysiology. One might at this point illustrate SS values from healthy men and women, and how they vary with factors such as urine volume, pH and mineral traffic, but our interest is what happens among patients with stones. The following figures are therefore made from our measurements of three 24-hour urine samples obtained prior to any treatment among 4500 patients with documented stone formation. As best is possible, they convey some sense of what one encounters in such a population.

Effects of Water Reabsorption

For CaOx, reduced urine volume raises SS markedly (Fig. 67.3), although even at the highest urine flows SS remains above 1, indicating near universal SS in human urine samples over 24 hours. Put another way, crystals of CaOx are unlikely to dissolve in human urine once formed, and anything that provokes nucleation of CaOx is apt to cause a stone to grow given enough time and provided other defenses do not prevent such from happening. For CaP (Fig. 67.4), volume also matters, but the tilt of the graph and spread of the points make clear how much less dramatic the effect. Also note that levels of SS for CaP in urine are much lower than for CaOx, and half of all samples are below one, indicating that CaP phases need not persist even if initially formed. For UA volume effects are also quite marked (not shown). As in the case of CaP, over half of urines are under-saturated. Overall, urine volume of two liters is a useful point to observe. Above this point, further reduction of SS is possible, but the number of urines thins, because one reaches the limits of plausible behavior. Below one liter, high SS is the rule and increase becomes very important. This supports the

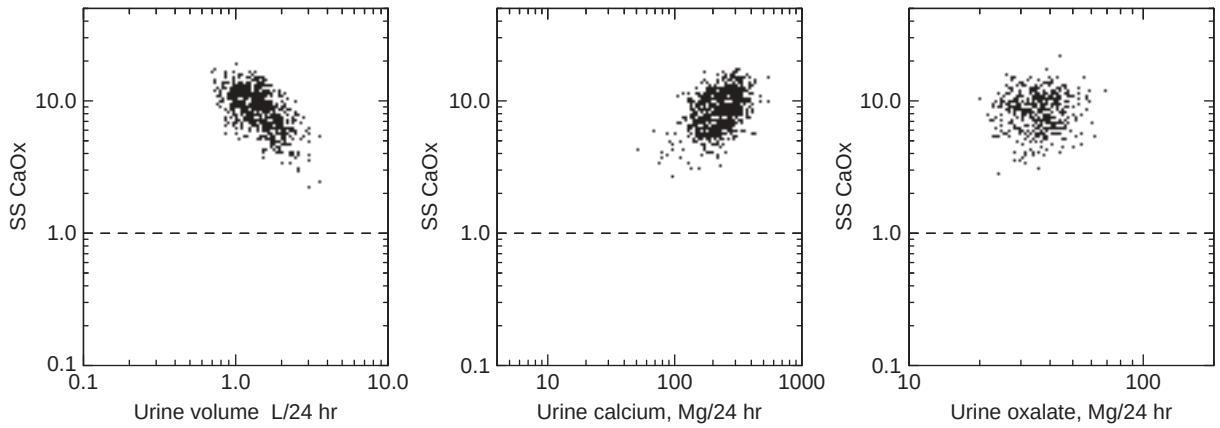

FIGURE 67.3 Determinants of urine calcium oxalate (CaOx) supersaturation (SS). Calcium oxalate SS, y-axis of each panel, varies strongly with urine volume (left panel), moderately with urine calcium excretion (middle panel), and modestly with urine oxalate excretion (right panel). Each point is a single 24-hour urine sample from a patient with nephrolithiasis.

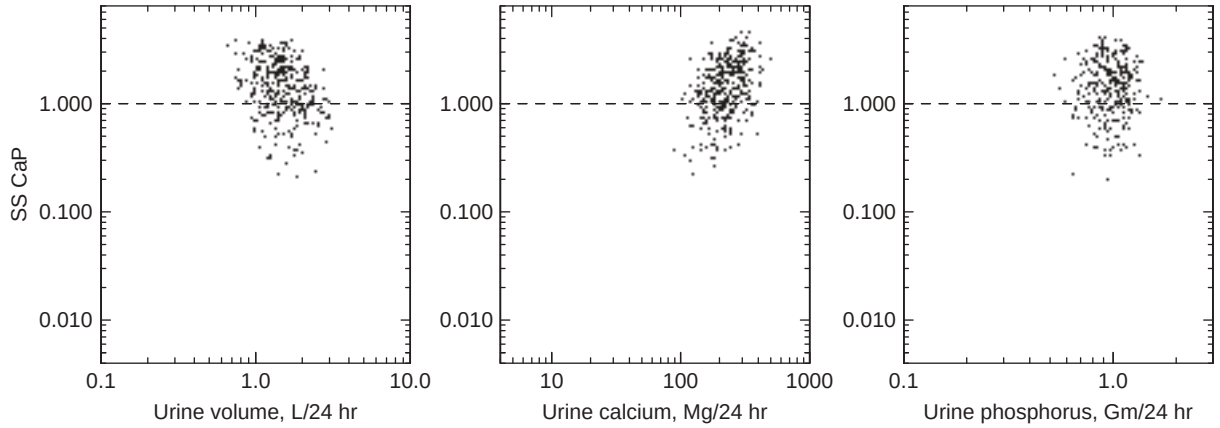

FIGURE 67.4 Determinants of urine calcium phosphate (CaP) supersaturation (SS). Same as Fig. 68.3 except SS values are for calcium phosphate, and urine phosphorus is shown in the right panel in place of urine oxalate excretion.

clinical maxim of two l/day as a goal for urine volume, while less than one l/day is a serious problem. Of interest, the normal person has a urine volume of 1.4 ± 0.05 liters as an average,[25] yet does not make stones. Urine volume obviously varies over the course of the day, and is lowest overnight, which is the time of day associated with the highest levels of SS.[26] This should be kept in mind when advising patients to increase fluid intake.

Effects of Relevant Urinary Solute Traffic

For CaOx, urine calcium excretion is a main controller of SS (Fig. 67.3); therefore, it should be unsurprising that hypercalciuric states are the most prevalent clinical causes of stone disease. Rather than using hard cut-points for diagnosing hypercalciuria, urine calcium should be thought of as a graded risk factor more like blood pressure, and like blood pressure in relation to stroke, higher is worse than lower.[27] As well, and perhaps like the stroke analogy, the spread of SS about any urine calcium point shows how many other factors must be interacting. One is volume, and the rest are not defined on this presentation. Urine oxalate excretion (Fig. 67.3) has none of the effect of calcium, the graph being almost spherical. This fact is incontrovertible, yet *in vitro*, and for theoretical reasons, urine oxalate concentration ought to exert a controlling influence equal to that of calcium.[28] The reason is that the range of oxalate excretion is modest, and the effects offset by other factors such as volume and calcium. For CaP matters are similar but with less sharpness (Fig. 67.4). Urine calcium excretion has a striking effect, as for CaOx; volume affects SS modestly, and urine phosphorus excretion virtually not at all. For UA, volume influences SS rather more than for CaP and a bit less dramatically than for CaOx, and UA excretion is utterly without effect.

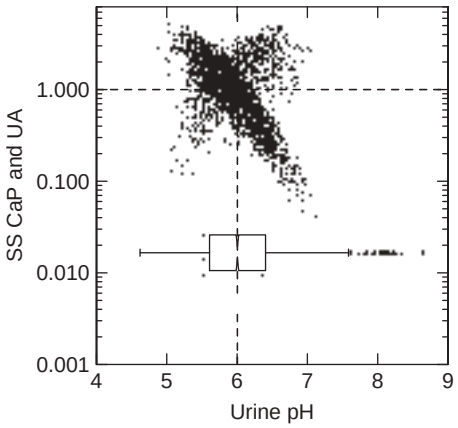

FIGURE 67.5 Relationship between urine pH and supersaturation (SS) for uric acid (UA) and calcium phosphate (CaP). The dashed horizontal line represents the border between supersaturated (above 1) and undersaturated urines. The figure provides evidence for a natural pH optimum to minimize UA (points descending downward to the right) and CaP (points ascending upward to the right) SS. The two SS data sets pass through a dual minimum at about pH 6; the median of the pH distribution for all urine samples in the set is precisely at the dual minimum (dashed vertical line). The horizontal notched box is a nonparametric representation of the median and one quartile on either side of the distribution of urine pH values shown as an oval of tiny dots about the notched box.

Effects of Urine pH on Supersaturation

What really matters in the case of CaP and UA SS is urine pH (Fig. 67.5); in a sense the link between SS and mineral content of these two solid phases reflects stability of 24-hour average urine pH. Above pH 6, virtually no urine is supersaturated with UA, and below 5.3 virtually all are supersaturated. For CaP, the effect is less exacting, perhaps because calcium concentration plays an important role, but SS does not occur below pH 5.3. For CaOx, pH has little effect on SS. That it has any reflects increasing calcium complexation with phosphorus and citrate at higher pH levels, so urine calcium ion falls. As noted before, virtually all urines are supersaturated with CaOx.

Regulation of Urine pH in Relation to Supersaturation

We have no desire to duplicate here detailed materials elsewhere in this volume concerning acid excretion and control of renal acid base balance. However, we have something to add of potential value, offering a perspective usually not considered. Constraints of solubility must have affected renal adaptation to water conservation and mechanisms for maintenance of blood pH, because the solubility laws are prebiological. More compelling, a urine pH near 6 would seem almost a necessary choice for the normal state, because the human design includes excretion of both considerable amounts of calcium, phosphorus, and UA. When plots of CaP and UA SS as a function of urine pH are combined as in Fig. 67.5, a pH about 6 is clearly near a double SS minimum. Among our samples, the mean and median pH were 6.005, a value that represents the actual compromise reached between net acid excretion, ammonium ion excretion, and reabsorption of filtered organic anions such as citrate. This pH effectively removes UA SS as a characteristic of the 24-hour urine.

Daily acid production, from formation of sulfuric acid during protein metabolism, is balanced by proton titration of urine phosphorus, and ammonium excretion. The amounts of urine phosphorus are set mainly by diet intake, although acid loading leads to bone mineral resorption with extra phosphorus availability. Titration of urine phosphorus to the dihydrogen form removes phosphorus from interaction with calcium, which is how low pH lowers CaP SS. Falling pH titrates urate to the dihydrogen form (pK 5.35), which has a limited solubility of 98 mg/l in urine. To keep urine pH near 6, as clearly occurs, ammonia formation in response to acid load must be nicely balanced with phosphorus excretion and proton secretion, otherwise urine pH would run too high or too low. We presume evolution has favored this compromise pH, and suggest the subject may be worth serious experimental attention.

Organic anion reabsorption is increased by acid loading and depressed by alkali loading so that response to alkaline ash diet by the kidney need not result in as great an increase of urine pH as would be required by excretion of bicarbonate as the sole response. Citrate, the most well known of the urine anions, binds urine calcium in a soluble salt, so that increase of pH that does occur is offset by reduced calcium ion activity.[29] The effects of other urine anions on calcium complexation and urine free calcium ion activity are not known. Acid loading lowers urine anions and therefore favors calcium ion activity increase, but abolishes calcium phosphate SS through titration of monohydrogen phosphate to the dihydrogen form. The total response of urine anions to acid-base balance change strongly suggests an evolved defense against CaP crystallization.

Other Effects

Urine SS is influenced by the free-ion activities of the relevant ligands that make up the stone-forming material. As such, it is reduced by high ionic strength that reduces activity coefficients, and therefore very low urine sodium and potassium concentrations raise SS, all other factors being held constant. Oxalate forms

salts with magnesium, sodium, and other urine ions, and the ion activities of each of its ligands affect CaOx SS. Likewise, calcium forms phosphate, sulfate, oxalate, citrate, and other salts, so its free-ion activity also varies with multiple ligand concentrations. Even so, the effects of raw calcium excretion are dramatic, and clinically evident, whereas effects of magnesium and sodium are usually not so because the range of values encountered in clinical practice is too narrow to permit important effects. This is a critical point. Clinical reality concerns what actually happens. Some uncommon patients, for example, because of bowel disease, have almost no urine sodium, or magnesium; among their ranks are a few in whom sodium administration or magnesium loading will lower SS and improve stone prevention. We have emphasized volume, pH, and excretion of calcium because they act generally, and with considerable effect, in most patients.

Relationships between Supersaturation and Upper Limit of Metastability

As first described, the ULM would seem a property of solution, as is SS, and between them no obvious connections come to immediate mind. However, we have already shown how among healthy people ULM and SS seem linked (Fig. 67.1), and this also occurs in patients with stones[30,31] but to a lesser extent than in non-stone formers. Among healthy women and men, ULM for CaP and for CaOx rises with SS, as seen in Fig 67.1. Among patients with stones the distance above the line of identity, which essentially gauges the defense against crystal formation, is reduced compared with that of healthy individuals. That the ULM to SS distance is smaller for CaP than CaOx, in healthy individuals and patients, suggests that CaP is more likely to form as an initial phase, making a starter template on which CaOx can overgrow.

INHIBITORS OF CRYSTALLIZATION AND CELL CRYSTAL INTERACTIONS

Urine certainly slows formation and growth of CaOx and CaP crystals, and we presume that at least late nephron tubule fluid must do the same. We do not know which molecules are primarily responsible for this phenomenon or if defects of inhibition cause stone disease. Perhaps the best evidence for a pathogenetic role of reduced inhibition is the low ULM to SS distance already alluded to in stone formers versus healthy individuals, and the molecules responsible for that effect are unknown. Presently we do not use measurements of individual inhibitors or of urine inhibition in clinical practice. If a commercially practical ULM measurement could be produced, this type of assay might be found useful in predicting the course of treated stone formers, perhaps, but that is mere speculation. At the moment, and when we first wrote this chapter, the whole matter of inhibitors is of mainly theoretical interest.

Calcium Oxalate Molar Ratio

We have found that the calcium/oxalate molar ratio correlated strongly with the ULM for CaOx.[22] However calcium and oxalate molarity both correlate strongly with SS and therefore with ULM so we are concerned that inferences from regression analysis may be misleading.

Citrate

Because it binds calcium in a soluble complex, citrate is clearly a protection against stone formation, and low citrate a risk factor for stones. At urine concentrations of mM levels, citrate can reduce crystal aggregation.[32] *In vitro*, citrate inhibits CaOx growth by 33% at 0.5 mM, and inhibits CaP crystallization at concentrations between 0.5 and 2 mM.[33] Adding 2 to 3 mM of citrate to urine decreases the number and size of crystal particles that form when calcium and oxalate are added to increase SS. In urine, citrate increases the ULM for CaP.[34] These data support the role of citrate as a treatment for calcium stones in patients with hypocitraturia.

Pyrophosphate and Phytate

A long and complex history of unfulfilled promise shadows these small and potent molecules. At 16 μM, pyrophosphate inhibits growth of CaOx crystals *in vitro*, and urine levels of it average 20 to 40 μM.[35] Urine levels of pyrophosphate can vary over a 10-fold range, as well, so clinical events could arise from its deficiency. On the other hand, dialysis of urine does not much reduce growth inhibition effects, suggesting extreme molecular redundancy, and efforts to raise urine pyrophosphate by giving oral orthophosphate supplements do not reduce stone formation significantly. Another small molecule of related character, phytate, inhibits brushite and apatite crystallization; but whereas pyrophosphate inhibited apatite most effectively, phytate inhibited brushite crystallization most effectively.[36] Perhaps modern methods for quantifying these molecules could be important in understanding why some patients with CaP stones produce apatite, others brushite crystals.

Macromolecules and Small Molecules Combined

In addition to the small molecules described above, urine contains a variety of macromolecules, including proteins and glycosaminoglycans, which are active against crystals, and could, in the aggregate, explain the extraordinary ability of urine to prevent crystal growth, aggregation, and nucleation. Presently we recognize at least 10 molecules that have anti-crystal properties, but the links between them and clinical stone disease are tenuous and suggestive: THP,[32,37] chondroitin sulfate,[38] citrate,[39] calgranulin,[40] osteopontin,[41,42] bikunin (inter-α-trypsin inhibitor),[43] prothrombin F1 fragment,[44] heparan sulfate,[45] the complement inhibitor CD59,[46] and inorganic pyrophosphate.[47] These molecules can inhibit to various degrees the nucleation, growth and aggregation of CaOx and CaP crystals, and their ability to bind to cells, at concentrations found in urine. A few studies suggest impaired inhibition may play a role in certain stone formers.

Such a system implies extreme redundancy, perhaps an intentional result of evolutionary biology, perhaps fortunate chance. We omit discussion here of the specialized molecular structures involved in crystal inhibition, but recent work using cystine crystals suggests that understanding the molecular basis of crystal inhibition may eventually lead to the ability to design effective inhibitors for some types of stones.[48]

DISORDERS OF CALCIUM STONE FORMATION

Idiopathic Calcium Stones: Metabolic Abnormalities

Most calcium stone formers have no systemic disease, and most diagnostic evaluation and treatment concerns urine abnormalities that can increase SS, the established driving force for crystal nucleation and growth: high calcium and oxalate excretions, low citrate excretion, high urine pH and low volume. Calcium excretion of patients (Fig. 67.6, upper right panel) frequently exceeds the upper 95th percentiles for normal women (indented) and normal men. Deviations are less marked but still obvious for oxalate and citrate excretions (lower panels). Urine volume of patients overlaps with normals (upper middle panel). Urine pH of CaP stone formers exceeds normals, that of UA stone formers (discussed in a later section) is below normal.

Idiopathic Hypercalciuria (IH)

Pathogenesis

The common definition of IH is urine calcium excretion (mg/day) above 250 in women and 300 in men, values at about the 80th percentiles for healthy

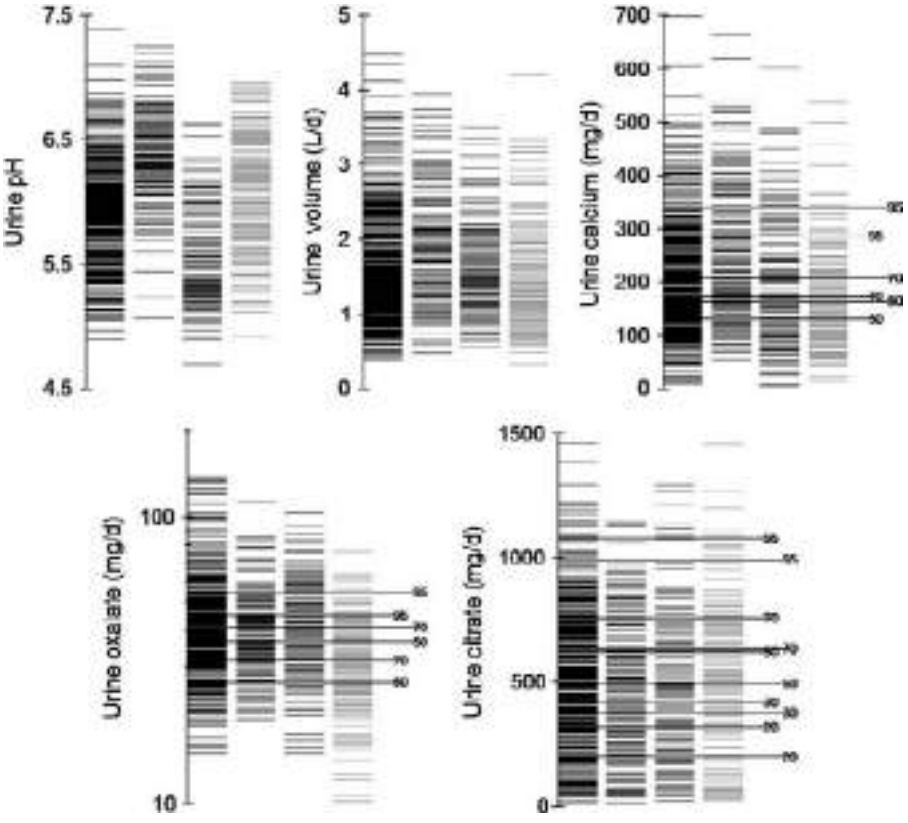

FIGURE 67.6 Urine stone risk factors. Values among normal subjects (right bar in each panel), and (from right to left) uric acid, calcium phosphate, and calcium oxalate stone formers. Percentiles for normal women (indented pins) and men are shown for reference. Each horizontal stripe represents one person.

individuals (Fig. 67.6); serum calcium is not elevated, and known causes of hypercalciuria such as hyperthyroidism, Cushing's syndrome, excess vitamin D intake, sarcoidosis, glucocorticoid use or other systemic diseases are absent. IH is found in 30–60% of ICSF.

Like hypertension, IH is familial, being found in about 50% of first-degree relatives of probands for both sexes.[49] Although IH is clearly genetic, studies of the monogenic hypercalciuric states, in which nephrocalcinosis and/or stones may be found, have not cast much light on pathogenesis of IH, although they offer intriguing clues.[50] Dent's disease appears to drive hypercalciuria via increased calcitriol levels, as in IH. Bartter syndromes involve defects of thick ascending limb calcium transport. Autosomal dominant hypocalcemic hypercalciuria arises from a gain of function mutation in the cell surface calcium receptor (CaSR), and stones and hypercalciuria are abetted mainly by vitamin D and calcium repletion to control hypocalcemia. Familial hypomagnesemia is caused by defects of paracellin-1. However, studies of patients with IH have not found a significant contribution to pathogenesis by mutations in these genes, nor by mutations in the vitamin D receptor (VDR), or the distal tubule apical calcium channel TRPV5. Patients with IH represent one end of the natural distribution of calcium excretion, and hypercalciuria results from the interplay of genetic endowment with environmental triggers.

The extra urine calcium in IH comes from diet, bone or both. In five studies (Fig. 67.7, left panel), one of them containing three separate comparisons[51] calcium absorption by IH patients exceeded normal.[51–55] High levels of serum calcitriol are common in IH (Fig. 67.7, right panel),[53,54,56–64] and this hormone could raise calcium absorption rates. However, many patients with IH have high gut calcium absorption rates with normal calcitriol levels. In this, they resemble an inbred rat colony whose members absorb calcium at high rates because of an over expression of the VDR by intestine.[65] By inference, some human IH could arise in such a way, and one study presents evidence supporting this mechanism.[60]

Another feature of IH compatible with calcitriol stimulation of target tissues is a tendency for bone mineral to be lost during low-calcium diet challenge.[59] In both normal subjects and patients with IH, urine calcium rises as gut calcium absorption (calculated as [diet calcium-fecal calcium]) increases,[66] but patients with IH excrete more calcium than do normal subjects at any level of net calcium absorption, and their urine calcium often exceeds the amount of dietary calcium absorbed. This latter is of great clinical importance, since it means that bone mineral is being lost in the urine, and implies that renal calcium conservation must be impaired. Administration of oral calcitriol to normal subjects can replicate features of IH, particularly the tendency to go into negative calcium balance on a low calcium diet.[67]

Numerous cross sectional studies have found that bone mineral density (BMD) is often decreased in IH[57,68] and BMD correlates inversely with the level of urine calcium.[56] In a prospective study, 46 subjects with hypercalciuria had BMD re-measured after three years of follow-up, and urine calcium excretion was predictive of the change in femoral z score—the higher the urine calcium excretion, the greater the drop in femoral neck mineral density.[69] Risk of fracture is increased in IH as well, as documented by a 19-year

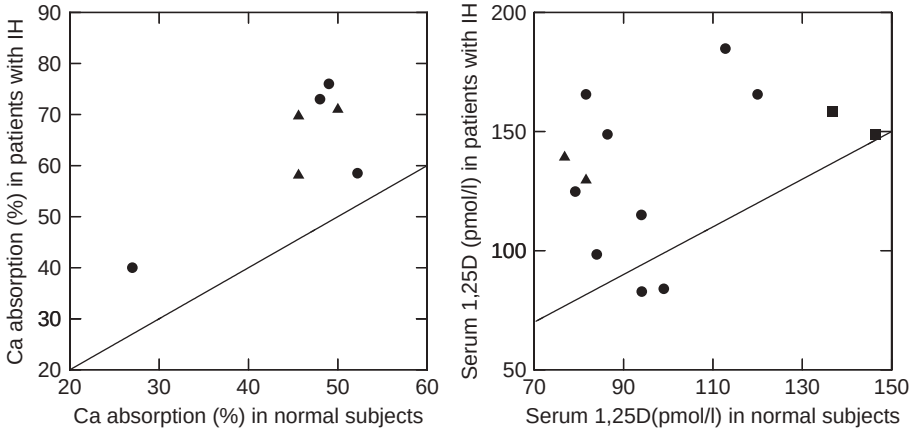

FIGURE 67.7 Intestinal calcium absorption (left panel) and serum calcitriol levels (right panel) in patients with idiopathic hypercalciuria (IH) and healthy individuals. Each solid point is a study and represents a plot of the mean of patients with IH against the mean of healthy individuals in that same study. Triangles and squares depict multiple patient group comparisons within a single publication. The clustering of points above the diagonal lines of identity illustrates the elevation of absorption and calcitriol among IH patients versus normal subjects. Triangles in the left panel are from,[51] circles are from.[52–55] In the right panel, triangles are from,[54] squares are from,[56] circles are from the remaining references in the text.

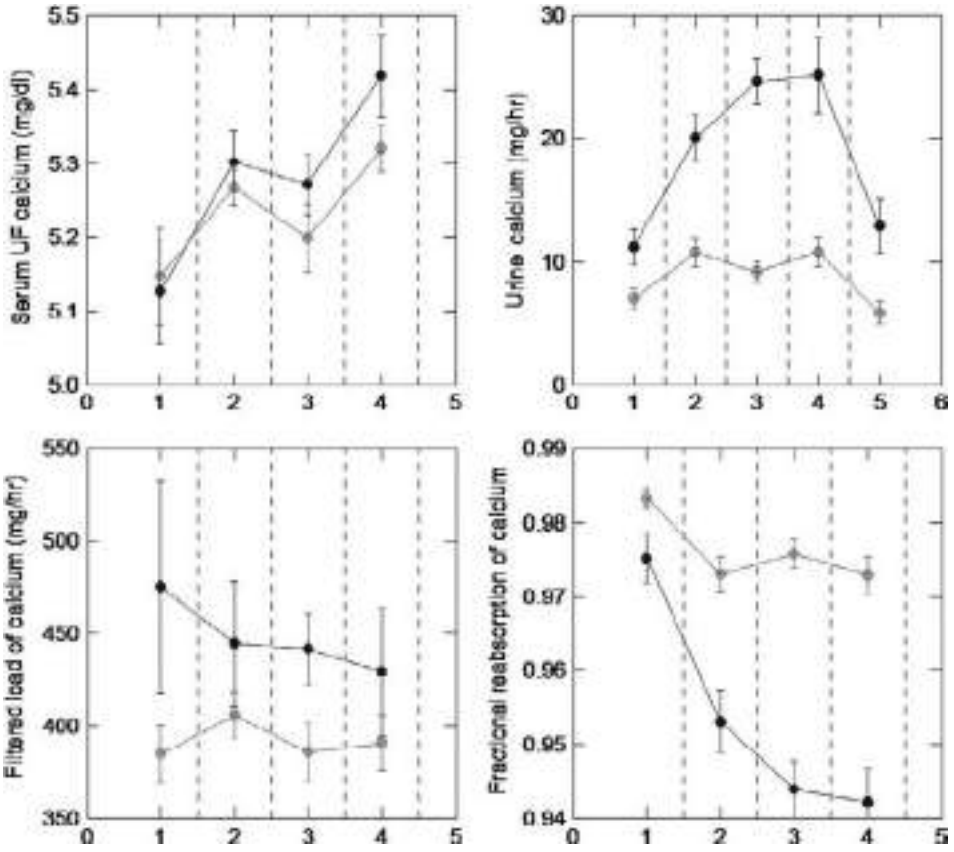

FIGURE 67.8 Calcium handling in patients with idiopathic hypercalciuria (IH) (black circles) and controls (grey circles) fasting and with meals. Serum ultrafilterable calcium increased with meals, but values did not differ between IH and control (upper left panel); neither did the filtered load of calcium (lower left panel). Urine calcium of IH increased far more than control (upper right panel), and fractional calcium reabsorption of IH was significantly less than control (lower right panel). Therefore, response of IH to feeding was an abnormally marked decrease in tubule calcium reabsorption. *(Reprinted with permission from ref.[73])*

follow-up of a cohort in Rochester, Minnesota, which found a four-fold increase in vertebral fractures among stone formers.[70] Abnormal bone histomorphometry has been found in eight studies of IH to date, with generally increased resorption, low bone formation, and a mineralization defect.[71] The mechanisms are still unclear, but a recent report[72] found increased bone expression of receptor activator of nuclear factor kappaB ligand and osteoprotegerin in patients with IH versus control subjects.

How the extra calcium gets into the urine is now reasonably well known. Potential models were increased filtered load from post-prandial increase of serum calcium, reduced renal tubule calcium reabsorption, or both; in fact, reduced tubule reabsorption mediates hypercalciuria.[73] Fasting and with meals, fractional excretion of calcium by IH exceeds controls, but ultra-filterable calcium concentrations and calcium filtered loads do not differ (Fig. 67.8). Using endogenous lithium clearance as a marker, proximal tubule (PT) reabsorption falls with meals more in subjects with IH than in normal subjects,[74] and the delivery of calcium out of PT is crudely proportional to the magnitude of urine calcium excretion (Fig. 67.9); the increased sodium (Na) delivered out of PT is quantitatively reabsorbed distally, so that no difference was seen in Na excretion on the controlled diet. Whether

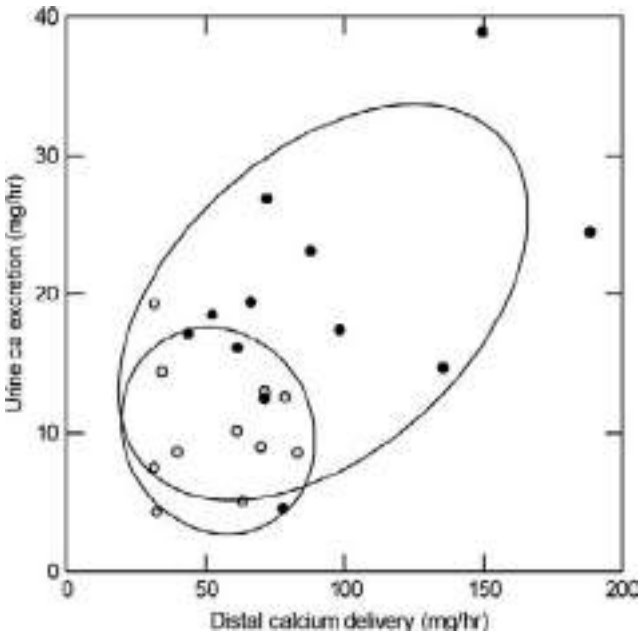

FIGURE 67.9 Relationship between distal calcium delivery and absolute urine calcium excretion in stone formers with IH (black symbols) and controls (gray symbols). Distal delivery is higher in subjects with IH, and calcium excretion rises with distal delivery, but excretion is higher in IH versus controls at comparable deliveries. *(Reprinted with permission from ref.[74])*

other tubule sites also participate in the decreased calcium reabsorption seen in IH is still unknown. This work sheds light on the mechanisms for two successful treatments for recurrent calcium stones; both low sodium diet and thiazide, which reduce urine calcium in IH, could work, in part, by raising PT reabsorption.

Although IH involves accelerated calcium transport in gut, kidney and bone, diet plays a role in promoting calcium loss in these subjects. For example, feeding 100 gm. of glucose reduces renal calcium reabsorption to a much greater extent in IH than in normal subjects, contributing to the negative calcium balance in these patients.[75] High salt intake is also associated with increased calcium in the urine.[76] However, higher dietary calcium intake was associated with decreased risk of stone formation in epidemiologic studies.[77] Because of that, and the risk of bone mineral loss on low calcium intakes,[59] low calcium diet is no longer used for treatment of kidney stones.

Treatment

Having said what one can about pathogenesis and how much is left to discover, therapy is rather well developed and well tested. Most current treatments to prevent stones have as their goal lowering urine SS. A general consensus exists that, in the absence of systemic disease, a first calcium stone can be treated conservatively with increased fluid. A randomized trial in such patients showed a significant decrease in recurrent stones in those patients who increased urine output to over two liters daily.[78] Water is the optimal beverage, but a variety of fluids can be used, if those that are high in sugar or sodium are avoided.

In patients who relapse, additional therapy should be added to fluid intake. Diet modification is one strategy. A randomized trial tested the hypothesis that a diet with a normal calcium intake (30 mmol/day) but low in sodium (50 mmol) and animal protein (52 gm/day) would prevent stones better than a low calcium-low oxalate diet in hypercalciuric men.[79] After 5 years of follow up, significantly fewer men on the normal calcium diet had recurrent stones compared to those on low calcium diet (20 vs. 38%, $p = 0.04$). A second trial of low protein diet for stone prevention was negative, but sodium was not restricted in that study.[80] A diet study has not been done in women, or replicated in other sites. In the United States, the DASH-sodium diet, originally created to lower blood pressure, has many of the features of the study diet used to prevent stones, after elimination of nuts, and was associated with fewer stone episodes in epidemiologic studies,[81] but no trial has validated it as a method of stone prevention.

As a kind of byproduct of their original design, thiazide-type diuretics reduce urine calcium loss and stone recurrence. The mechanism of the reduced calcium loss is probably increased PT calcium reabsorption, with shunting of re-absorbed calcium into bone, as opposed to urine[82] and the effect lasts as long as the drug is taken. Three prospective controlled trials of thiazide have been carried out for three years each (Fig. 67.10)[83–85] and yielded the same result: placebo-treated patients (open symbols) relapsed at a higher rate than corresponding thiazide-treated patients (closed symbols), the effect reaching statistical significance by the end of year three. Being protective of bone in a disease that can deplete bone of its mineral, and protective against stones in recurrent stone formers, thiazide is the primary treatment for IH. Our preference is for chlorthalidone, because it is long acting and used once daily, although hydrochlorothiazide and indapamide have also been used successfully. Very low doses of 12.5 mg can be effective, and we often begin there; 25 mg is effective for most people. Kaliuresis with potassium depletion is staved off with reduced sodium (100 mEq daily is a good goal) and increased potassium intake, or with amiloride 5 to 10 mg every morning or a potassium supplement.

We are often asked what to do when someone who is in need of stone prevention from IH cannot take thiazide. Use of the diet detailed above, with careful follow-up to ensure compliance, can be helpful. Amiloride alone will not work. Since oral glucose raises urine calcium in IH, avoidance of sugar loads is prudent. Often thiazide side effects arise from too high a dose. Sometimes "drug allergies" are a myth or may be overcome by change to another molecular variant.

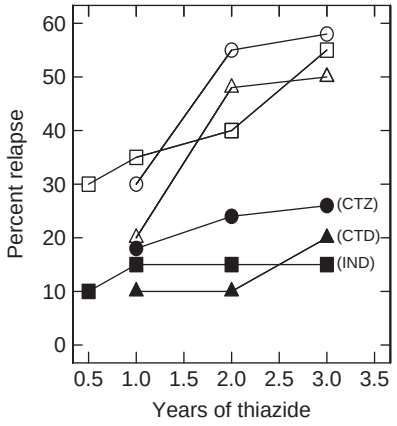

FIGURE 67.10 Three trials of thiazide for reduction of calcium stone recurrence. The percentage of patients with relapse (y-axis) was much reduced in those receiving active drug (filled symbols) vs placebo (open circles). All three trials were randomized, double blind, and prospective. CTZ, hydrochlorothiazide, 25 mg twice daily;[85] CTD, chlorthalidone 25 or 50 mg daily;[84] IND, indapamide, 2.5 mg daily.[83] All three trials showed significant differences between controls and active drug treatment.

Low Urine Citrate

Stone formers, especially females, excrete less citrate than healthy people of the same sex[86] (Fig. 67.6). Citrate inhibits nucleation and growth of calcium crystals, and binds calcium in a soluble complex[39] thereby reducing SS values. The administration of alkali may also have beneficial effects on the skeleton,[87] and can lower urine calcium,[88] although long term data on these effects in stone formers is absent.

The cause of hypocitraturia is usually not apparent. Urine citrate excretion is positively correlated with net GI alkali absorption,[89] which in most cases is provided by fruits and vegetables, and inadequate intake of these foods results in hypocitraturia in some idiopathic stone formers. Filtered citrate is mainly reabsorbed in PT, and citrate in urine is that which escapes reabsorption.[29] Reabsorption is decreased by alkali and increased by acid loads[90] and potassium depletion.[91] Administration of potassium citrate results in metabolism of most of the absorbed citrate to bicarbonate, which allows more filtered citrate to escape reabsorption in PT; urine pH also rises. If only citric acid is administered, a transient increase in urine citrate will occur as citrate that escaped metabolism in the liver is filtered, but metabolized citrate will titrate the ingested proton and no net gain of alkali will occur. Therefore, potassium citrate or bicarbonate will raise urine citrate, but citric acid will not. This may account for the inconsistent results with administration of lemon juice as a substitute for potassium citrate.

Treatment

What is the best course of action for physicians? We propose measuring citrate as part of every 24-hour urine analysis for stone diagnosis, and raising it when it is low, using a potassium citrate salt. Two trials[92,93] document efficacy of supplemental potassium citrate in reducing stone recurrence in hypocitraturic calcium stone formers (Fig. 67.11). Dosing should be about 2/3 of urine ammonia excretion. Care should be taken to monitor urine pH, and avoid raising it significantly above 6.2, as CaP SS may increase, and lead to worsened, not improved, stone formation. When thiazide is used for hypercalciuria, and the inevitable fall occurs in blood potassium, urine citrate will fall, and a small but useful trial[94] has shown that potassium citrate snuffs out the otherwise stubborn recurrences of stones, presumed to form because of urine citrate deficiency. Given a reasonable action, no physician needs to despair at the incomplete understanding evident in this tiny area of science. Nor, given better science, is a better treatment likely to be found.

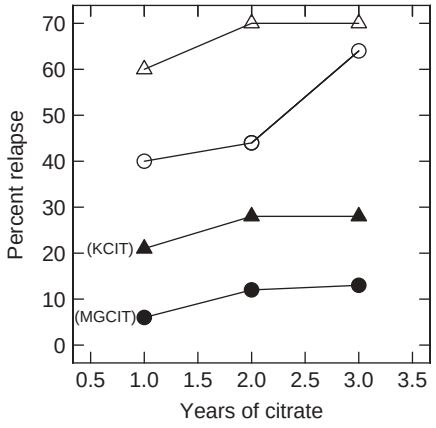

FIGURE 67.11 Two trials of citrate for reduction of calcium stone recurrence. The percent of patients with relapse (y-axis) was much reduced in those receiving active drug (filled symbols) vs placebo (open circles). The two trials were randomized, double blind, and prospective. KCIT, potassium citrate 20 mEq three times daily;[92] MGCIT, potassium-magnesium citrate, two tablets twice daily.[93] Both trials showed significant differences between controls and active drug treatment.

High Urine Oxalate

Urine oxalate may arise from endogenous production in the liver, as an end-product of glyoxalate, amino acid and ascorbic acid metabolism, and from GI absorption of preformed oxalate.[95] Dietary oxalate is absorbed mainly in the colon, and normally about 10% of ingested oxalate is absorbed. Oxalate from both sources has only one fate—renal excretion. Under ordinary circumstances, approximately half of urine oxalate is derived from the diet, and the other half is endogenously produced.[96] Recent experiments using mice in whom the oxalate transporter SLC26A6 was knocked out have led to the understanding that oxalate is also secreted into the gut,[97] and increased urine oxalate may also result from a drop in gut secretion; this has not yet been documented in humans.

Higher urine oxalate values are often encountered in stone formers versus normal subjects (Fig. 67.6) and should be given proper attention. Mild hyperoxaluria (values from 40 to 60 mg/d) may result from a diet high in oxalate[98] or more commonly from a diet low in calcium,[99] as well as from protein loads. Ascorbic acid intake may also contribute significantly to urine oxalate. Oxalate degrading bacteria are normally present in the gut, and absence of such flora may also lead to increased gut oxalate absorption.[100]

Recent work suggests that renal oxalate handling may differ between stone formers and normal subjects.[101] In calcium stone formers on a low oxalate diet, urine oxalate was higher than among a group of normal subjects on the same diet. Plasma oxalate levels did not differ between the two groups, but while

oxalate reabsorption was seen in the normal subjects, oxalate secretion was frequently seen in the stone patients, at similar levels of plasma oxalate. This suggests that control of oxalate transport in the kidney may provide stability of plasma oxalate levels.

Very high levels of urine oxalate, of 80 mg/d or more, occur because of small bowel malabsorption or primary oxalate over-production (see below). These are very serious conditions that can damage kidneys and demand a high level of clinical attention.

This strangely combative area of nephrolithiasis hardly deserves the attention it has had if one maintains a purely clinical perspective. The idea that changes in urine oxalate influence CaOx SS more than corresponding changes in urine calcium has been shown to be incorrect.[28] As we have shown, the range of urine oxalate excretions is much smaller than that for urine calcium or volume so oxalate increase as a cause of stones is modest in practice.

Treatment

Patients with dietary hyperoxaluria should restrict dietary oxalate sources, avoid ascorbic acid supplementation, and ensure a normal calcium intake (800–1200 mg/day) from food. A recent three month pilot study showed that in a group of stone patients with mild hyperoxaluria, urine oxalate fell significantly more with a low sodium, low animal protein, normal calcium (1200 mg) diet compared with a low oxalate diet.[102] This is consistent with findings that stone patients do not appear to have higher oxalate intakes than normal subjects.[103]

High Urine Uric Acid

One of us was not altogether wrong in 1973 describing a tendency toward high urine uric acid excretion (750 and 800 mg/d, women and men, respectively) among patients who formed calcium stones.[104] High levels of uric acid in urine salt out CaOx salts[105] and reduce their solubility. This could foster CaOx overgrowths on Randall's plaque. Allopurinol, in one prospective controlled trial,[106] reduced CaOx stone recurrence, adding a critical support to a supposed pathogenetic mechanism.

Treatment

The source of the extra urine uric acid is usually diet that contains above a pound of beef, chicken and fish—combined—daily. Treatment could be as simple as reducing the total to two-thirds pound, not what one would imagine as a low-protein diet. No diet trial has been undertaken. Allopurinol is effective by trial, but can cause toxic epidermolysis. If stones are persistent and surgically active, diet is of no avail, and high urine uric acid is the main problem, then 100 to 300 mg of the drug daily is reasonable.

IDIOPATHIC CALCIUM STONES: PATHOLOGY

Idiopathic Calcium Oxalate Stone Formation: Role of Interstitial Plaque

These most common stone formers have so distinctive a pattern of clinical presentation, altered physiology, renal histopathology and mechanisms for stone formation they deserve a special place and an extensive presentation. No other kind of patient shares their distinctive features. Like all idiopathic calcium stone formers they have no systemic disease, and display a high prevalence of IH. Their stones are predominantly CaOx in composition and form as overgrowths on the renal papillae.

During percutaneous nephrolithotomy (PNL) or ureteroscopy (URS) stones are found firmly attached to the papillary tips over regions of interstitial apatite plaque, which appear visually as white sub-urothelial deposits (Fig. 67.12, panels A and B). Plaque forms in the basement membranes of thin limbs of Henle's loop[107] (Fig. 67.12, panel C) as micro-particles within which alternating lamina of crystal and an organic matrix form a tree-ring pattern (Fig. 67.12 panels D and E). Particles fuse together in the papillary interstitium to form a syncytium (Fig. 67.12, panel D) in which islands of crystals float in an organic sea. The material accumulates beneath the basement membranes of inner medullary collecting ducts (IMCD) (Fig. 67.12, panel F) and Bellini ducts (BD), and under the urothelium, where it appears as white plaque. The plaque crystal is biological apatite, and the organic layers contain osteopontin[108] and the third heavy chain of the inter alpha trypsin inhibitor,[109] both known inhibitors of CaOx and CaP nucleation and growth. In 30 consecutive ICSF, minute inspection of serial sections from papillary biopsies revealed no crystals in any epithelial compartment, only interstitial plaque.[110]

In a large prospective trial, all stones of sequential ICSF were identified during PNL and classified as being attached or not to the papillary surface.[111] For all attached stones, intra-operative imaging (Fig. 67.13) was used to test if the attachment was on plaque. The results, allowing for unattached stones, and some variation in ascertainment, showed that 75.4% (95% CI = 58–93%) of stones were attached to plaque. Since plaque occupies only 5–10% of total papillary area this is a very large deviation from chance. When studied via IR spectroscopy and digital image reconstruction, virtually all unattached stones showed evidence of having grown attached to plaque: an apatite

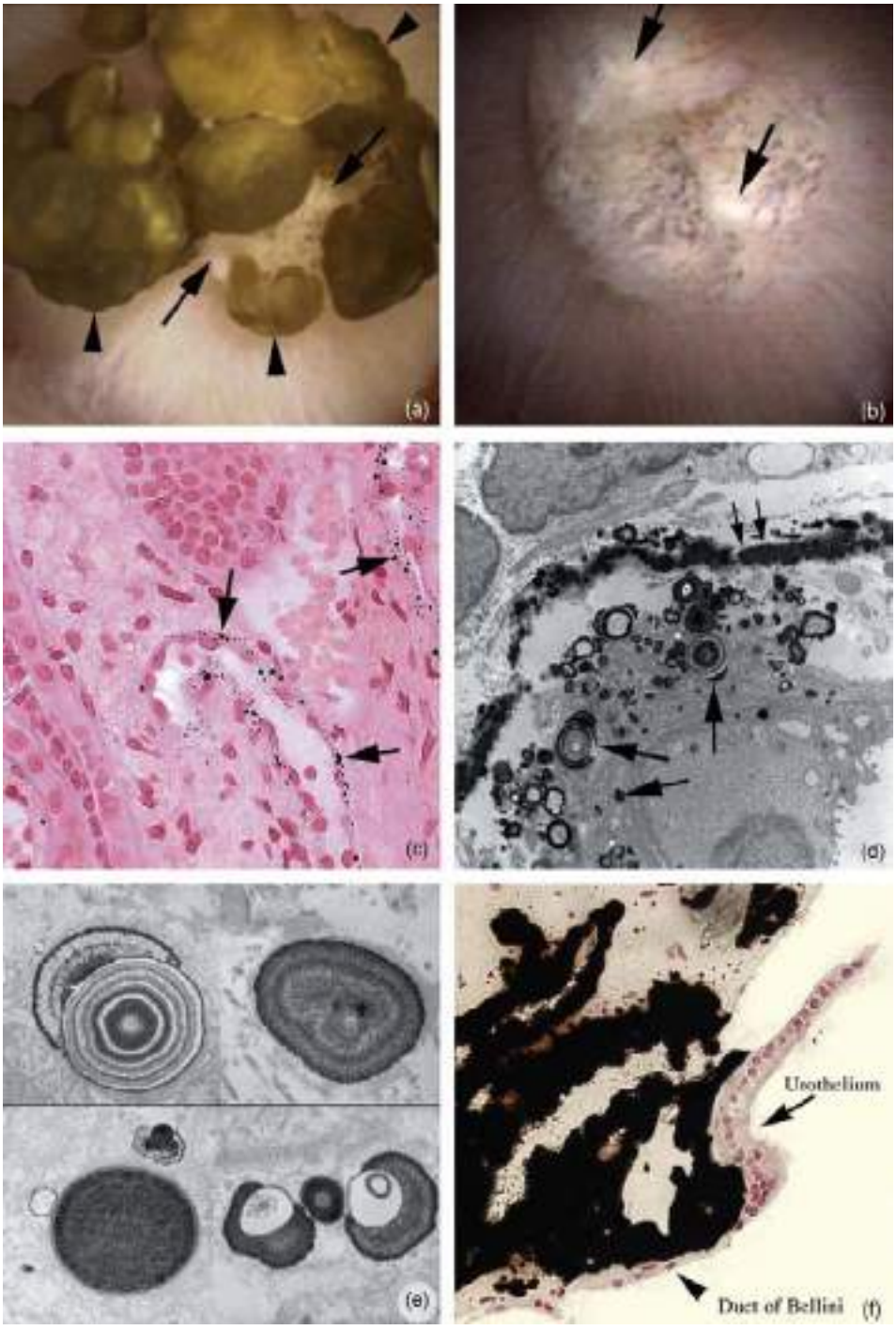

FIGURE 67.12 Digital endoscopic and histologic characteristics of sites of Randall's plaque in ICSF. Panel A is an example of a papilla from an ICSF patient video recorded at the time of stone removal by percutaneous nephrolithotomy revealing a number of small CaOx stones (arrowheads) attached to the tip of the renal papilla. These stones are near or upon regions of irregular whitish plaque material (arrows), more easily seen following removal of the stones (panel B, arrows). These sites of plaque are sub-urothelial in location and represent mineral deposits that first appear as very small spherical structures embedded in the basement membranes of the thin loops of Henle (arrows, panel C) and nearby interstitial space. Because of the location of these crystalline structures, they are termed interstitial deposits or Randall's plaque. By transmission electron microscopy (TEM), the interstitial deposits are seen as individual multilayered spherical structures of varying sizes (arrows, panel D) embedded in the basement membranes of the thin loops of Henle while forming a syncytium in which islands of crystals float in an organic sea (double arrow, panel D). Higher magnification TEM micrographs (panel E) reveal each deposit to be made of alternating light (crystalline material) and electron dense (matrix material) rings. Extensive accumulation of crystalline deposits around the loops of Henle spread into the nearby interstitial space extending to the urothelial lining of the urinary space (panel F).

attachment site often with adherent tubule fragments.[112] In ICSF, the amount of papillary surface covered by plaque correlates strongly with numbers of stones formed, corrected statistically for age and duration of stone disease.[113]

Growth on Plaque

A 0.5 mm CaOx stone (Fig. 67.14, panel (A)) was excised during surgery en bloc with its underlying attachment site (Fig. 67.14, panel (B)).[114] The urinary surface of the stone attachment site occupies the upper half of panel C and the left upper quadrant of panel (D) of Fig. 67.14. Presumably, and via an unknown sequence of events, the integrity of the urothelium was breached at this region of the papillum (Fig. 67.14, panel (C), arrow), exposing sub-urothelial plaque to urine. The exposed surface of plaque, where the stone was attached, is covered by a ribbon of alternating

FIGURE 67.13 An attached stone before and after removal. A 3-mm stone (arrow, panel A) lying on an upper pole lateral papillum of an ICSF patient is visualized by a digital endoscope before removal and after removal (panel B). The region where the stone was attached contains sites of interstitial plaque (arrow, panel B). The removed stone has a white patch (arrow, insert to panel B) on its tissue or attachment surface.

organic (black) and crystal (white) layers (Fig. 67.14, panel (D)). The inner boundary layer covering where plaque was exposed (Fig. 67.14, panel (D)) contains Tamm Horsfall protein (Fig. 67.14, panel (F)) and is therefore of urine origin; osteopontin (Fig. 67.14, panel (E)) is also present. The inset at upper right in panel d shows, at higher magnification, crystals oriented perpendicular to the plane of the organic layers. On the outer boundary of the ribbon (*) large rafts of crystals have grown out of the ribbon plane into what was the urinary space and extend outward forming the base of the stone. A double arrow points to large crystals just beneath the ribbon boundary.

From this picture, one infers that following exposure of plaque to urine the plaque surface was covered with organic molecules of urine origin—the inner boundary layer. Driven by urine SS, crystals nucleated in this layer and were covered by more matrix in which new nuclei formed; this process was repeated to make the lamination of the ribbon. Eventually, crystallization escaped from matrix control and expanded to form the base of a new stone.

The crystal in the ribbon and stone base is apatite, not CaOx. In the stone itself, one finds no CaOx until about 70 microns into the stone body, quite remote from the base. This means that CaOx stone formation depends upon deposition of plaque, exposure of plaque to urine via disruption of urothelium, a presumably spontaneous covering of the exposed plaque surface by urine molecules adsorbed onto the matrix of the plaque, nucleation of apatite driven by urine CaP SS, and subsequent waves of matrix covering, apatite nucleation, and eventually escape from the ribbon to form the apatite stone base. More apatite accumulates but eventually, perhaps because of the balance of urine SS values, CaOx comes to predominate. As an alternative, formation of apatite may eventually reduce local pH in the stone interior, favoring CaOx; this idea has no support as yet from experiments. Presently we have no information about what causes urothelial disruption, but the processes of apatite nucleation and plaque formation have been studied reasonably well.

Apatite Nucleation

It would appear that formation of CaOx stones depends upon nucleation and growth of apatite driven by urine CaP SS, so one might ask if CaP SS of ICSF exceeds normal. In fact it does. In a GCRC controlled study (Fig. 67.15) CaP SS (lower right panel) of ICSF (grey bars) exceeds normal (cross hatched bars).[26] Normal controls did not achieve SS values above 1, whereas the SF invariably exceeded 1 (dashed line on graph). Surprisingly, the highest CaP SS values were overnight. Urine calcium molarity of ICSF (upper left panel) far exceeded controls; this difference reflects IH in ICSF coupled with virtually identical urine volumes between the groups (lower middle panel). Urine pH values (lower left panel) and urine phosphate excretions (not shown) did not differ. The critical role of an initial apatite deposit over exposed plaque coupled with the ability of IH to produce marked CaP SS means that clinicians need to control both CaP and CaOx SS in ICSF, a hitherto non-intuitive idea.

The importance of apatite nucleation also raises a possible link between urine citrate levels and CaOx stone formation. Citrate inhibits nucleation and growth of apatite at concentrations of 0.5 to 2 mM/l, levels found in normal urine. If indeed the primary nucleation over exposed plaque is apatite, low urine citrate excretion could foster CaOx stone formation by

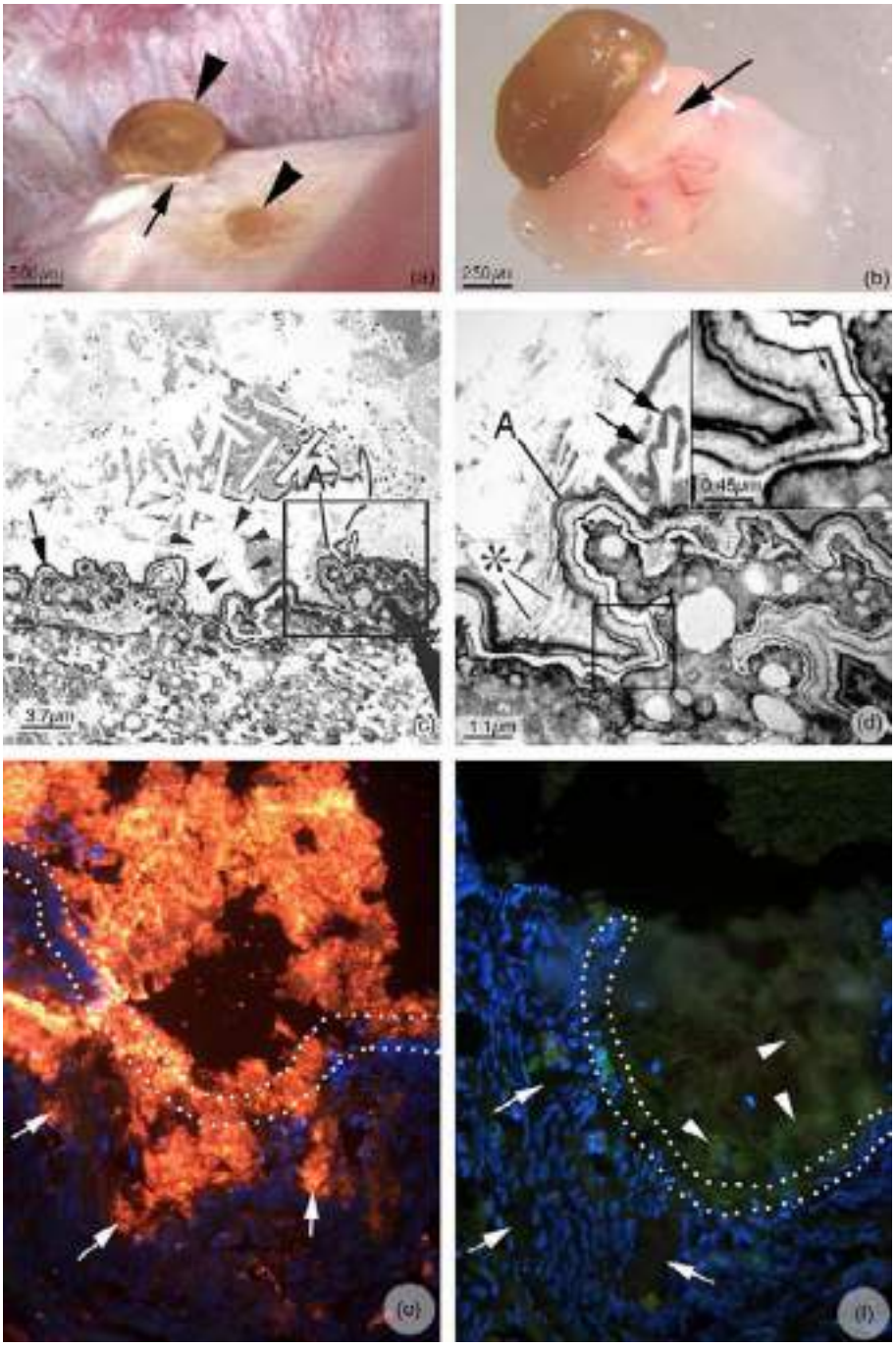

FIGURE 67.14 Endoscopic and ultrastructural analysis of a stone from an ICSF patient. By digital intraoperative endoscopy, small stones (arrowheads) are seen adhered to a papillum (panel A). A distinct region of Randall's plaque is visible just under the stone at the tip of the arrow. During PNL, the larger of the two stones seen in panel A was removed with a biopsy instrument such that the stone-plaque-tissue complex remained intact (panel B, arrow pointing to Randall's plaque region seen in panel A). Panel C is a TEM micrograph at the stone-plaque-tissue interface. The upper portion of the micrograph shows the stone while the lower portion shows interstitial plaque within the papillary tissue. An arrow marks the plaque boundary which has the unique appearance of a multilayered ribbon. Rafts of large crystals (always coated with matrix material) appear to grow out of the ribbon and into what was the urinary space (now the base of a stone). One particular crystal (outlined in arrowheads) is seen attached to the outer matrix layer of the ribbon. Panel D is a higher magnification image of the square seen in panel C. The ribbon-like structure is clearly seen as nine separate layers. The inset (upper right hand corner) reveals five thin black organic lamina that alternate with four white lamina. In the thickest of the white lamina, one can see tiny thin spicules that run perpendicular to the ribbon and have the appearance of multiple voids that contain tightly packed crystals (small arrows, inset). Small (asterisk) and large (arrows) coated crystals are seen inserted into the outer matrix layer of the ribbon. By immuno-histochemistry (panel E) osteopontin was detected in both the stone and interstitial plaque (white arrows) while sites of Tamm-Horsfall protein (panel F) were only seen in the stone (white arrowheads). The dotted white line delineates the interface region. See color plate section at the back of the book.

removing an important inhibitor. Likewise, increase of citrate by potassium alkali administration could reduce CaOx stone formation presuming that increase of urine pH did not offset the benefits of increased citrate inhibition.

Apical Collecting Duct Calcium Receptor (CaSR) Does Not Protect Against Supersaturation

That urine volume can be the same in the ICSF and controls, especially overnight when calcium molarity in ICSF reaches nearly 6 mM/L (Fig. 67.15, compare upper left and lower middle panels), does not accord with the concept, arising in rodents, that the apical collecting duct CaSR protects against stones by reducing water reabsorption when calcium excretion rises.[26] But our data are perfectly predictable from what is otherwise known. The human CaSR, *in vitro*, has an EC50 of about 6 mM/l at the pH and ionic strength of urine.[115] At a total concentration of 6 mM/L, urine contains only about 3 mM/l of calcium ion, the remaining

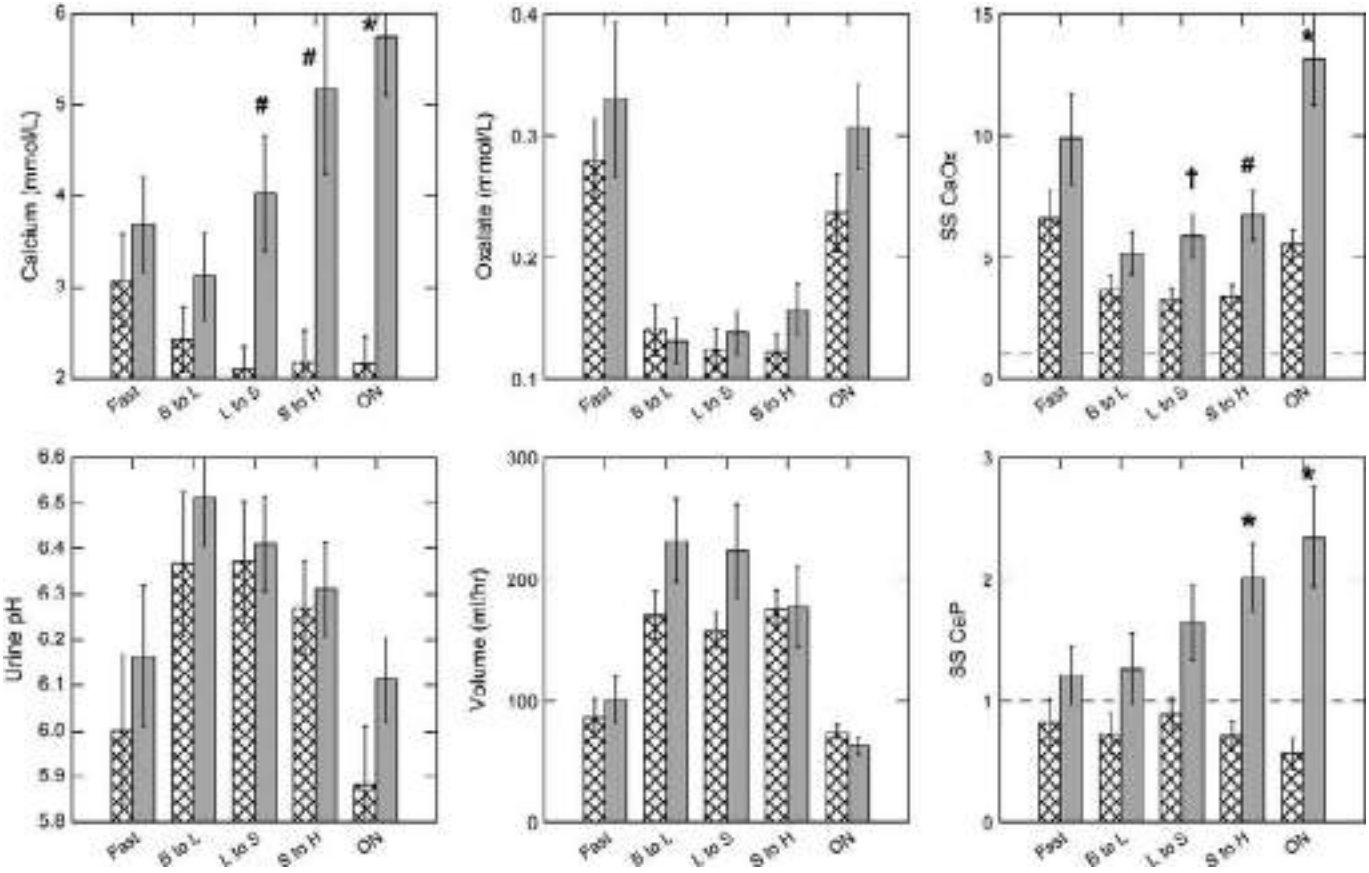

FIGURE 67.15 Urine SS for CaOx and CaP throughout the day in IH and normals. CaOx SS (*top right*) and CaP SS (*bottom right*) are shown during fasting and in the periods from breakfast to lunch (B to L), lunch to supper (L to S), supper to home (S to H), and overnight (ON). Horizontal lines indicate SS of 1. Concentrations of urine calcium (*top left*) and oxalate (*top middle*), as well as urine pH (*bottom left*) and urine flow rate (*bottom middle*), during the same periods are indicated. Cross-hatched bars, normal subjects (N); gray bars, IH. Values are means ± SE adjusted for repeated measures. Significant differences between IH and N by time period: $^{*}P < 0.001$, $^{\#}P < 0.01$, $^{\dagger}P < 0.05$. *(Reprinted with permission from ref. [15])*

calcium being complexed with phosphate, oxalate, sulfate, citrate and other anions. Possibly, the CaSR of stone formers is less sensitive than normal, because reduction of urine calcium excretion in enuretic children with IH may reduce nocturnal urine volume,[116] but this matter has not been addressed. For the moment one may suggest that modest nocturia might be valuable in treatment of very active stones in ICSF.

How Plaque Forms

The fraction of papillary surface covered by plaque (Fig. 67.16) varies directly with urine calcium excretion and inversely with urine volume and pH;[117] a multivariate score using all three variables accounts for much of the variation. How these three variables link mechanistically to plaque is a research matter, but one mechanism is well supported enough to warrant presentation.

Plaque forms in the basement membranes of thin limbs, which are mingled with capillaries in the papilla in a ratio of 4:1, capillaries predominant (Fig. 67.17). Thin limb fluid, in all animal micro-puncture studies, has a high SS with respect to CaP,[118] because water extraction raises calcium concentration above blood levels, and phosphate and bicarbonate to or above blood level. But because the epithelium has very low calcium permeability, entry into the basement membrane from the lumen could be easily over-balanced by diffusive losses into the interstitium.

Such losses are reduced by calcium delivery from the capillaries. The descending vasa recta pass downward through the inner stripe of the outer medulla (OM) in bundles surrounded by a ring of thick ascending limbs (Fig. 67.17) that enrich the OM interstitium with calcium by reabsorbing calcium without water. The descending vas carries this extra calcium down into the papillum, where counter-current trapping helps to keep it there. Vasopressin regulates medullary thick ascending limb (mTAL) reabsorption, therefore low 24 hour urine volumes, which must reflect correspondingly higher vasopressin levels, and more

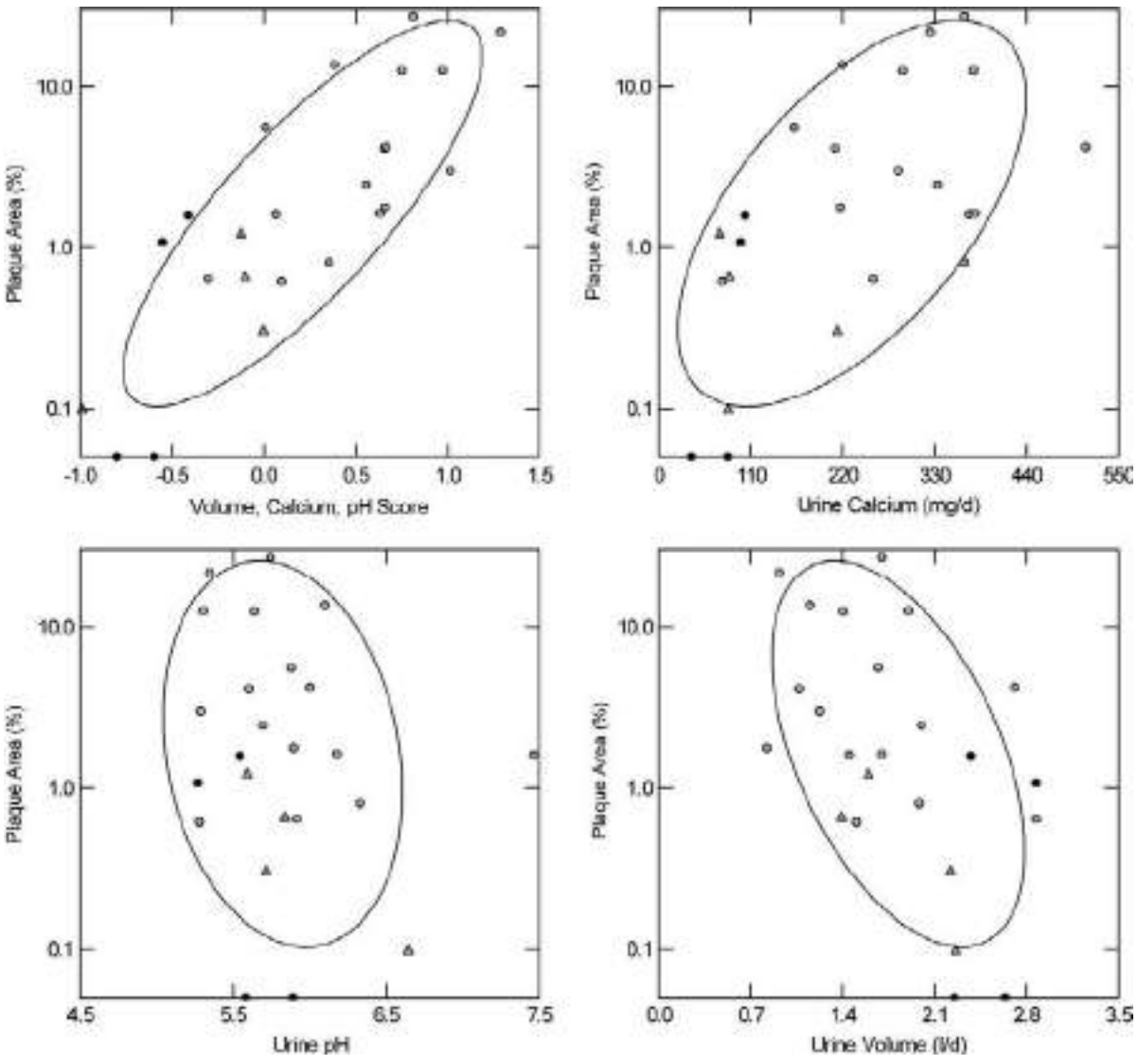

FIGURE 67.16 Relationships between plaque surface coverage and urine composition. Fraction of papillary surface covered by plaque, as determined from intra-operative digital imaging (y-axis of all 4 panels), varies with urine calcium (upper right panel), and inversely with urine pH and volume (bottom panels). A multi-variable score using all three variables accounted for much of the variation in plaque coverage (upper left panel). ICSF are open circles, controls (N) are closed circles; triangles are patients with obesity bypass procedures. *(Redrawn from ref.[117])*

efficient solute trapping, would correlate with plaque abundance. The fact that a few 24 hour urine volumes can correlate so well as they do with plaque that accumulates over years suggests that fluid intake must be strongly habitual and reasonably constant in any one person.

IH increases delivery of calcium out of PT (Fig 67.9), and thin loop segments reabsorb negligible amounts of calcium, so this increase of delivery reaches the mTAL which reabsorbs calcium mainly via electro-chemical equilibria. An increase of delivery will therefore increase absolute calcium reabsorption into the medullary interstitium and thence into the blood in the descending vas recta bundles. They in turn will carry a more calcium-enriched blood than normal down to the capillaries of the papillary tips, directly opposite to the thin limb basement membranes. The result will be increased plaque via local increase in CaP SS, and a tendency for plaque abundance to parallel urine calcium.

The implications of vas "wash down" of calcium into the papillary interstitium are clinically meaningful. Low sodium diet and thiazide might be expected to reduce plaque formation as well as stones because they can increase PT reabsorption. Reduced protein intake, by reducing endogenous acid load from oxidation of sulfur on methionine and cystine, would also increase PT reabsorption. High water intake will not only reduce urine SS but will reduce vasopressin levels and

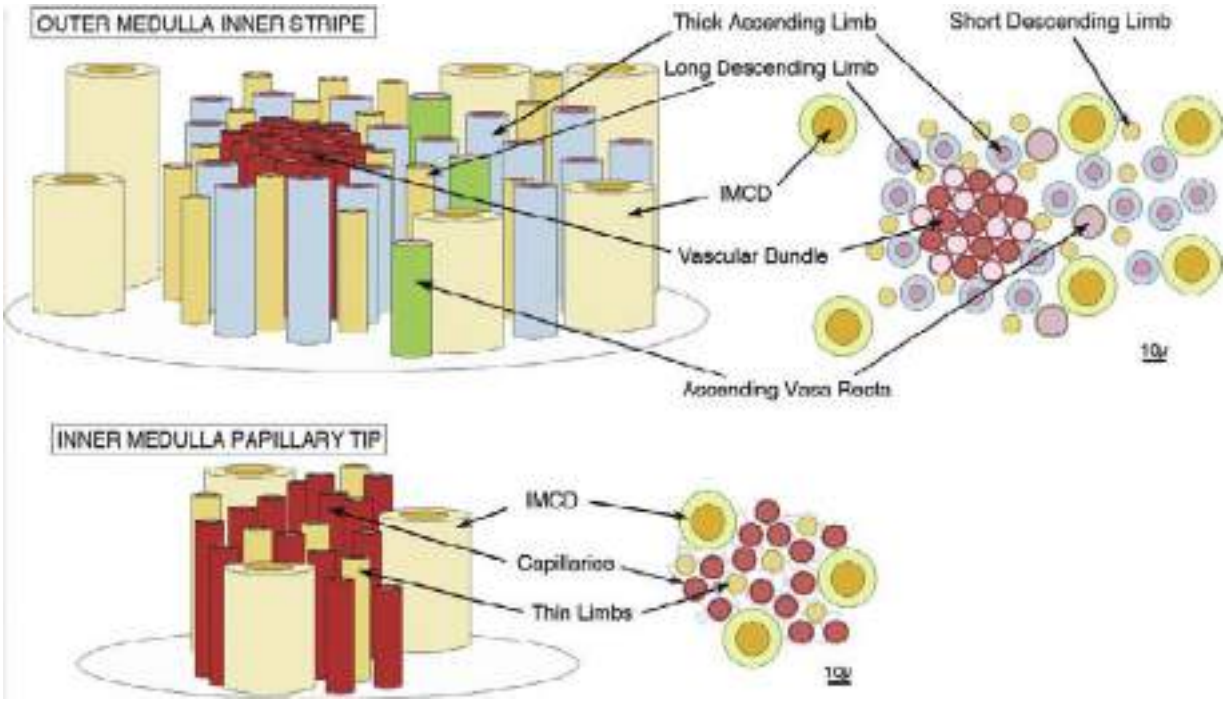

FIGURE 67.17 Physiology of vas wash-down for plaque formation. In the inner stripe of the OM (upper panel), vascular bundles (descending are solid circles, ascending are clear) are surrounded by medullary thick ascending limbs of the long nephrons (mTAL) which reabsorb NaCl and calcium without water. In IH PT can deliver more calcium than normal to mTAL with each meal, raising the absolute rate of mTAL calcium reabsorption above normal. Running downward inside the ring of mTAL, vas blood will be enriched in calcium, and increase inner medulla interstitial [Ca] in the region of thin loops favoring apatite nucleation there. Counter current trapping will help retain the extra calcium. mTAL CaSR is down-regulated by the high ionic strength in OM so it does not shut off continued reabsorption. Short descending thin limbs from mid and outer cortical nephrons travel downward within medullary rays, whose basic unit is a quartet of IMCD with an internal loose bundle of short descending limbs. This arrangement removed water reabsorption by short limbs from diluting the interstitium around the descending vas recta bundles.

therefore mTAL reabsorption and, to the extent that vas wash-down is true, plaque formation.

The Idiopathic CaOx Stone Former as a Unique Clinical Phenotype

The ICSF phenotype is so distinctive as to be unique. Apart from IH, which is not a disease, but merely a selection of people from the high tail of human calcium excretion, there is no systemic illness. Stones are over 50% CaOx. In over 30 instances thus far, kidneys always reveal a singular appearance: normal papillae except for interstitial plaque; no crystals in any epithelial compartments. Stones grow on the outside of the papillae, over regions of interstitial plaque that have been exposed to the urine via disruption of the urothelial membrane. The process of overgrowth begins with an initial apatite layer. Plaque itself forms in basement membranes of thin limbs of Henle's loop and the mechanism appears to involve the basic physiology of IH itself coupled with the peculiar anatomy of the inner stripe of the outer medulla. This physiology and anatomy links plaque formation to the magnitude of IH via changes in PT calcium reabsorption, and to urine volume via both effects of high urine flow to wash solutes out of the deep medulla, and reduction by high water intakes of vasopressin, that drives mTAL calcium reabsorption in the inner stripe.

No other kind of stone former observed thus far manifests the clinical and histopathological characteristics of the ICSF, and we believe, therefore, that ICSF should be set apart into their own category. Because the links between the final disease, stones, and the physiology and histopathology of the condition are reasonably well understood, because treatments to prevent the stones are effective and act through reasonably well defined pathways of pathogenesis, and because the prime mover, IH, is established as heritable, ICSF appear to satisfy all the criteria of a unique disease of stone formation.

Idiopathic Calcium Phosphate (Brushite, BR) Stone Formers

Clinical and Histopathological Features

Like ICSF in their metabolic derangements except for a tendency for high urine pH, the stones they form

contain above 50% CaP. They produce significant amounts of interstitial (white) plaque, but also have a second type of plaque (yellow plaque) which represents plugging of IMCD with apatite crystal.[119] Yellow plaque is seen on the papillary surface as linear yellow streaks, very different from the white plaque of the ICSF (Fig. 67.18, arrows, panel c). Scattered IMCD and BD are massively dilated with apatite plugs (Fig. 67.18, panel a). Epithelial cells of plugged IMCD and BD are mostly dead (Fig. 67.18, panel b) and interstitial fibrosis is severe (Fig. 67.18, panels e and f). Here and there plugs extend out of hugely dilated BD into the urinary space (Fig. 67.18, panels a and b). The papillae are distorted and abnormal, pitted, scarred, and flattened (Fig. 67.18, panel a).

The plugs and stones appear to have a common cause in an elevated urine pH. Among a large series of stone formers for whom stone composition has been determined, the fraction of stone crystal that is CaP rises in synchrony with the urine pH (Fig. 67.19).[4] The higher pH increases CaP SS and therefore the risk of CaP crystallization. Once the process of apatite plugging and consequent cell injury begins, lumen pH of individual IMCD could rise creating a vicious cycle, and if wide-spread the process would further increase urine pH.

Even as new research tests these ideas about pathogenesis, we will be left with the problem of what comes first. The phosphate content of kidney stones in the United States has been rising for decades,[4] and during that time use of extracorporeal shockwave lithotripsy (ESWL) and of potassium alkali for stone treatment both have become common practice. In fact, the number of ESWL procedures per patient, corrected for number of stones, age, sex, and duration of stone disease, rises progressively with the number of ESWL procedures.[4] Possibly, terminal IMCD and BD injury from ESWL or increase of urine pH from potassium citrate treatments initiate CaP crystallization, which then leads to a cycle of further cell injury and crystal plugging. Obstructive uropathy can reduce acidification, and stones are nothing if not a cause of recurrent obstruction. Possibly high urine pH is like IH, an hereditary trait. In patients who converted from making stones composed mainly of CaOx to those composed of CaP, urine pH was significantly higher when they were still making CaOx stones, compared with patients who did not convert.[120] The increased urine pH in patients with idiopathic CaP stones is not accompanied by abnormal serum pH or bicarbonate, although some such patients have abnormalities of acidification on provocative testing with ammonium chloride.[121] This appears to be part of the incomplete RTA syndrome.

How Brushite Stones Form

At surgery mature stones are not often found attached to protruding apatite plugs, nor are they found on the rather scanty plaque. They are usually free in the renal pelvis and calyces. The plug extensions into the urine are like nascent stones in that their further growth is dependent entirely on urine SS and inhibitors, and plugs could break off and grow into clinically relevant stones. This is untested. Possibly stones form in free solution.

Idiopathic Calcium Oxalate and Calcium Phosphate Stone Formers in Practice

As clinicians, we take heed of stone analysis with brushite or CaP even above 20%, because the kidneys can be involved in a significant tubular disease. In such patients we are liberal with thiazide and water, and reduced diet sodium and protein, but stingy with potassium alkali which could increase urine pH and CaP SS. We need a trial of potassium alkali in CaP stone formers, because this reasonable approach may be wrong. Citrate inhibits CaP crystallization, so alkali could be more beneficial than harmful.

PNL and URS are increasingly being used for stone removal, and during such procedures urologists can observe if papillae are affected with plaque alone, or with ductal plugging and papillary retraction. The former implies that water, reduced salt and protein, thiazide and potassium alkali all are reasonable treatment measures. The latter implies that alkali may not be ideal and that measures to prevent stone recurrence should be, perhaps, more urgent and aggressively pursued, as the disease may be more damaging. While not as yet accepted practice, use of observations during stone surgery to guide medical intervention is reasonable and practical in many cases, and can be recommended as an adjunct to medical stone prevention.

CALCIUM STONES ARISING FROM SYSTEMIC DISEASES

In these patients, stones are a manifestation of a systemic disease that, itself, warrants diagnosis and treatment. In each case where we have adequate information, the systemic disease has produced a specific renal histopathology and set of urine stone forming abnormalities which arise from disease-specific and often complex pathophysiology. The whole approach to patients with systemic stone forming disease differs radically, therefore, from that used for idiopathic stone formers.

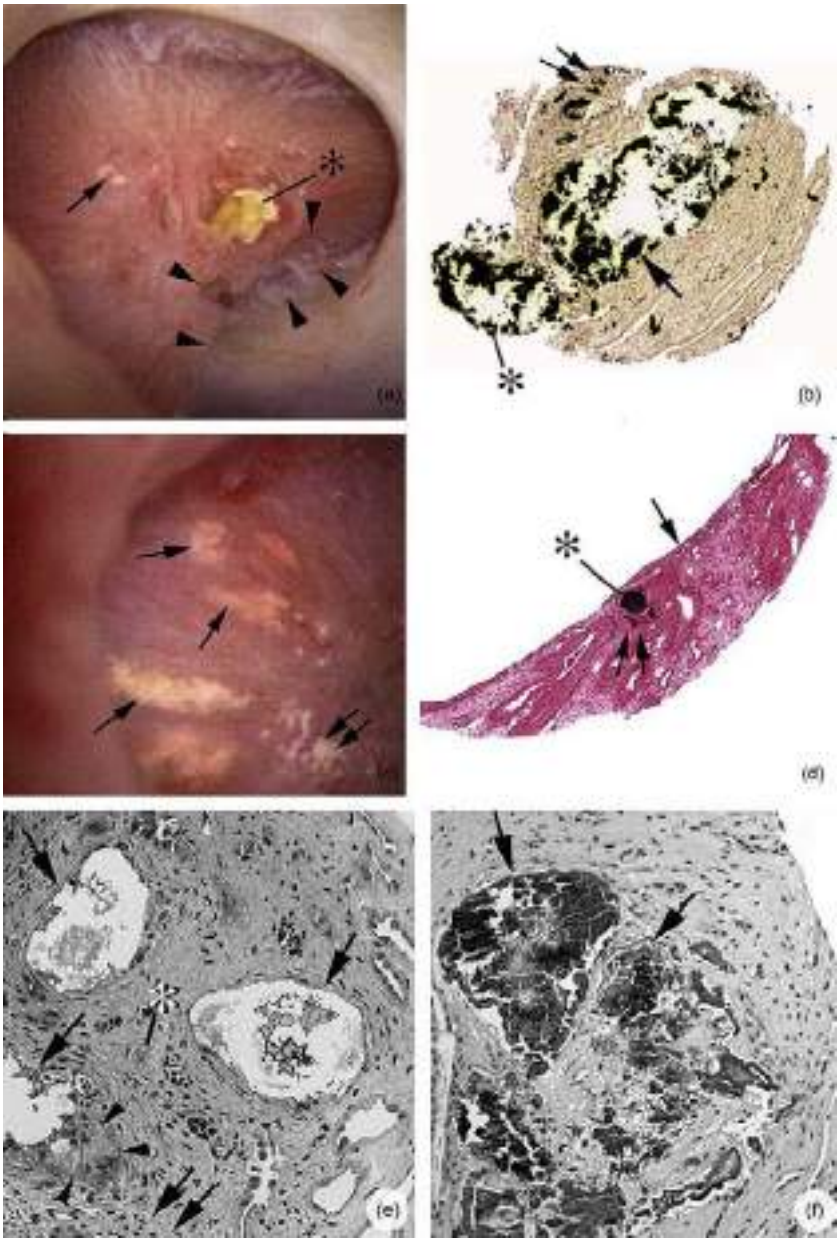

FIGURE 67.18 Endoscopic and histologic images from brushite (BR) stone formers**.** Panel a shows an example of a papillum from a BR patient that was video recorded at the time of stone removal. Papillae from BR patients often showed depressions (arrowheads) near the papillary tip and flattening, a phenomenon not seen in CaOx stone formers. Like CaOx patients, the papilla from BR stone formers possessed sites of Randall's plaque (arrow), though less in amount. In addition, these papillae possessed sites of yellowish crystalline deposits at the openings of ducts of Bellini (asterisk). The ducts were usually enlarged and occasionally filled with a crystalline material that protruded from the duct that might serve as a site for stone attachment. Panel b shows crystal deposition in a papillary biopsy stained by the Yasue method. Note crystal deposits protruding from the duct of Bellini (*) and in the lumens of an associated inner medullary collecting duct (IMCD) and of a nearby loop of Henle (arrows). The crystal deposits greatly expanded the lumen of these tubules and induced cell injury to complete cell necrosis of the tubular epithelium. A cuff of interstitial inflammation and fibrosis accompanied sites of intra luminal deposition. Panel c shows sites of yellow plaque on the papillum of a BR stone former. Yellowish mineral deposition (single arrows) was found within lumens of IMCD just beneath the urothelium; these deposits are called yellow plaque. Deposits ranged from large areas of crystal deposition in collecting tubules that formed a spoke and wheel-like pattern around the circumference of the papilla to small, single sites of yellowish material in focal regions of a collecting duct lumen. Histologic analysis of sites of yellow plaque (panel d) confirms that these crystal deposits are in IMCD (asterisk) positioned just beneath the urothelial lining (arrow). The double arrow shows a site of interstitial plaque like that seen in idiopathic CaOx stone formers**.** Light micrograph in panel e shows extensive interstitial fibrosis (double arrow), tubular atrophy (asterisk), loss of tubular lining cells (single arrows) and giant cell formation (arrowheads), while panel f shows a region of heavy mineral deposition (single arrows) at the site of extensive tubular injury and fibrosis. These changes were never seen in CaOx stone formers. See color plate section at the back of the book.

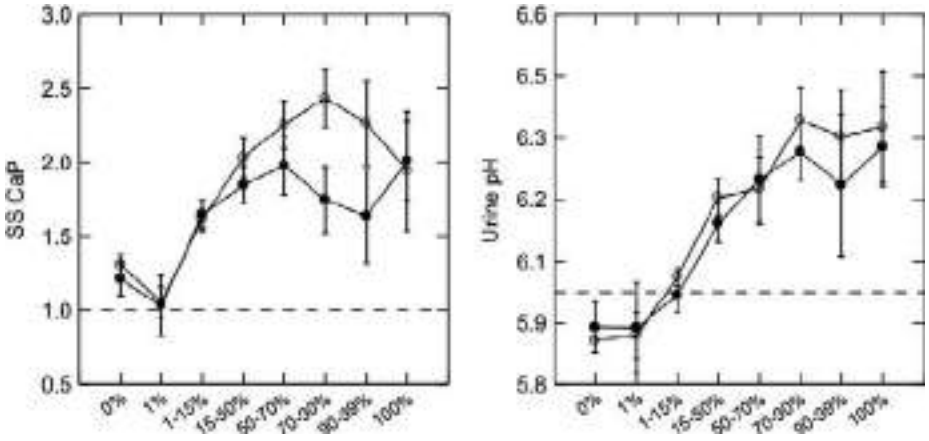

FIGURE 67.19 Correspondence beween percentage of CaP in stones and urinary CaP SS and pH. As expected, CaP SS rose with stone CaP percent (left panel, y- and x-axis, respectively), among men (gray circles) and women (black circles). Values are mean ± SEM. Urine pH also rose progressively (right panel) which would increase CaP SS. *(Reprinted with permission from ref.[4])*

Primary Hyperparathyroidism (PHPT).

Pride of place goes to this disease, even though only 5% of stone patients have it.[25] Before most other causes were known about, PHPT was recognized as a curable cause, and surgeons in the better centers were regularly performing curative neck dissections. The disease arises from neoplasia of one or more parathyroid glands, leading to solitary adenoma in 85% of patients and multiple gland enlargements in the remainder. Malignant neoplasm of the parathyroid glands is rare as a cause of stones. Here, we focus specifically on the stone disease and factors producing stones, leaving details of parathyroid hormone regulation and actions to the appropriate chapters.

Because the main actions of parathyroid hormone (PTH)—increased renal production of calcitriol, increased bone mineral turnover, and increased renal tubule calcium reabsorption—all raise serum calcium, an elevated blood calcium level is always found, if one looks for it properly. The problem is that the elevation can be mild, and because normal values for serum calcium depend on the analytical methods used to measure it, and the methods in use are numerous and variable, the true normal may often not be known by a physician.

PHPT is easily confused with IH because hypercalciuria is prominent and hypercalcemia subtle, often below 11 mg/dl. Although serum phosphorus is generally low, because PTH reduces renal phosphate reabsorption, this trait is also common in ICSF, for unknown reasons. The PTH elevation may also be subtle, but the failure of PTH to be suppressed by elevated serum calcium strongly suggests PHPT. The high urine calcium raises SS with CaOx and CaP, which are the proximate mechanism for stone formation. The hypercalciuria is a direct effect of increased calcium absorption by intestine, driven by calcitriol excess, and bone mineral loss, driven by PTH. One often hears that stones in this disease are more enriched with calcium phosphate salts than is usual, but our patients for whom we have complete stone analysis show only a subtle increase, and only in men.[25]

The renal histopathology of primary hyperparathyroidism combines that of ICSF and IPSF (Fig. 67.20).[122] CaOx stones grow on plaque, and many BD are plugged with apatite crystals (Fig. 67.20). Because PHPT is a marked hypercalciuric state, plaque is not a surprise, although the exact pathophysiology is not defined as yet. Likewise, that urine pH and CaP SS are somewhat higher in PHPT than ICSF,[25] presumably accounts for plugging. Observed at PNL or URS, the combination of apatite tubule plugging with CaOx stones growing on plaque can be of diagnostic use, and suggest the correct diagnosis when hypercalcemia is subtle and PHPT might be mistaken for ICSF or IPSF. Although this combined pathology also occurs in bowel diseases, their presence is almost always obvious.

Given distinctive hypercalcemia and hypercalciuria, PHPT is not difficult to diagnose. Serum PTH is reduced by all hypercalcemic states due to vitamin D excess, primary bone mineral loss from tumor invasion or rapidly progressive osteoporosis, or mediated via the PTH-related peptide found in malignant neoplasms, so one asks not whether PTH levels are high but simply whether PTH levels are not subnormal. If normal or high, PTH values confirm the presence of PHPT in a person with both hypercalcemia and hypercalciuria, and little more needs be done before curative surgery.

Given normal or low urine calcium, however, the possibility exists of familial hypocalciuric hypercalcemia (FHH), a hereditary disorder of the calcium receptor in parathyroid and renal tubule cells. Such patients may have stones and come to attention for them, but should not be considered for parathyroid surgery. Stones will be due to another condition. Family

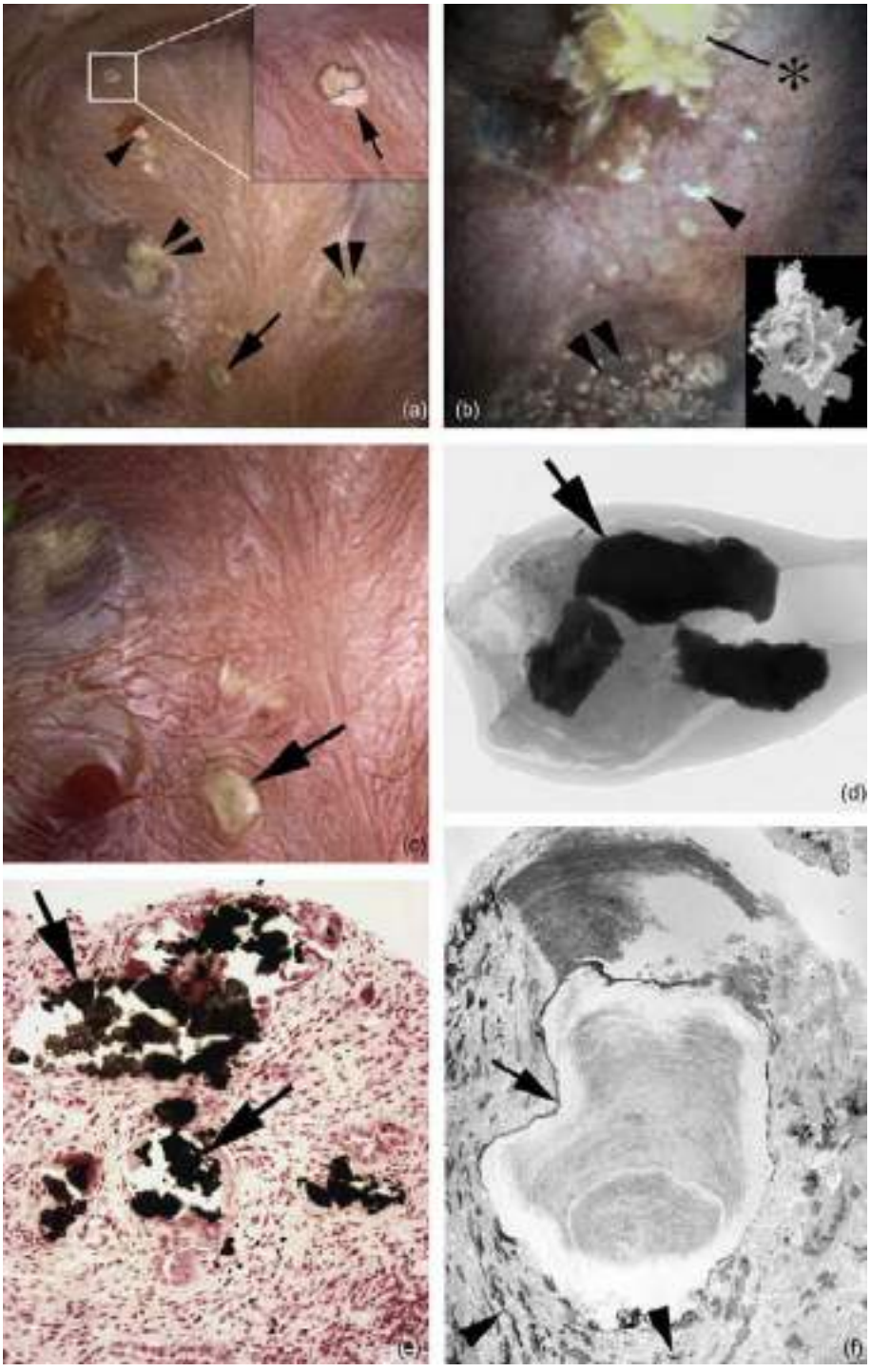

FIGURE 67.20 Endoscopic and histologic images of stone-forming patients with primary hyperparathyroidism (PHPT). Digital endoscopic and histopathologic characteristics of renal papilla from patients with PHPT include a combination of features seen in ICSF and IPSF patients. Patients may have attached stones (see small stone within white outlined square in panel A and enlarged insert where stone is outlined and region of white plaque indicated by arrow; also see asterisk in panel B) at sites of Randall's plaque (single arrowheads, panels A & B) and dilated openings of ducts of Bellini with protruding plugs (single arrow, panel A and C) on the same papilla. Attached stones were composed of CaOx and apatite (see micro-CT insert in panel B). Suburothelial yellow plaque was noted across the papilla and varied in size from small to rather large deposits (double arrowheads, panels A & B). The very large size of some of the intraluminal deposits was confirmed by micro-CT (arrow, panel D). Yasue stained sections and TEM micrographs revealed the massive sites of intraluminal plugs filling the lumens of IMCD (arrows, panels E & F) associated with a loss of all lining cells. A cuff of interstitial fibrosis (arrowheads, panel F) surrounds the plugged tubules. See color plate section at the back of the book.

members can be screened for hypercalcemia as the trait is autosomal dominant with 100% penetrance. Guise and Mundy offer a convenient formula for evaluating urine calcium to diagnose FHH.

Other confusions may arise from lithium treatment, which can induce a state of parathyroid over activity, and use of thiazide, which may raise blood calcium yet leave incompletely treated an independent hypercalciuric state, thus creating a factitious semblance of PHPT. Distinguishing sporadic hyperparathyroidism and its familial forms from the multiple endocrine neoplasia syndromes is usually unnecessary, as stone patients tend to have simple hyperparathyroidism. However, the details of the multiple endocrine neoplasia (MEN) syndromes are discussed in other chapters and may be of interest.

Surgical excision of the abnormal gland(s) is curative for stones, in our work as well as that of others. Postoperatively, serum calcium returns to normal, and urine calcium falls markedly, although it may remain mildly elevated, for unknown reasons. SS for both CaOx and CaP drops and stone formation decreases. The surgery is never intended to confirm the diagnosis, which can be made using serum calcium, urine calcium, and PTH values, but to cure the disease. Proper surgery identifies all parathyroid glands in the neck, to ensure that all abnormal tissue is removed, leaving normal glands untouched. If all parathyroid tissue is removed, creating hypoparathyroidism, a new and difficult stone-forming condition may be produced, because patients lose the effects of PTH to raise renal calcium reabsorption. When supplemental calcium is given by mouth to raise blood calcium to an acceptable level, urine calcium levels rise steeply, and stones form.

Renal Tubular Acidosis

Inherited or acquired forms of distal RTA (Type I RTA) raise urine pH and urine calcium, decrease urine citrate, and produce CaP stones. At surgery, interstitial plaque is not above normal abundance and stones are not found growing on what little is present (Fig. 67.21).[123] Tubule plugging is very widespread (Fig. 67.21) with attendant fibrosis and tissue damage. As in IPSF and PHPT the origin of the CaP stones is not clear: detachment of protruding plugs or free solution crystallization. Diagnosis is from reduced serum bicarbonate with alkaline urine pH, and often hypokalemia showing the importance of blood screening for all stone formers. Treatment with potassium citrate can correct acidosis and reduce hypercalciuria, but careful follow-up is required to ensure that urinary SS for CaP falls. Persistent hypercalciuria after acidosis has been corrected can be treated as for IH, with thiazide.

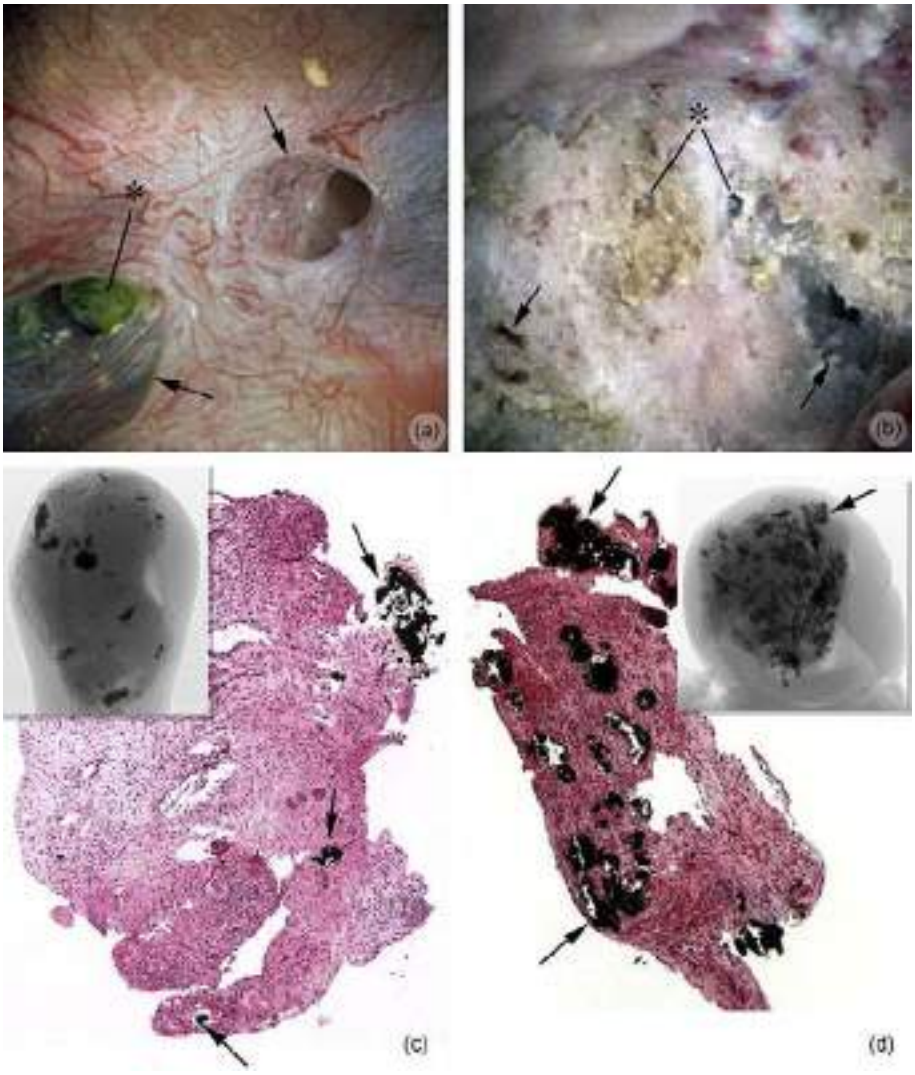

FIGURE 67.21 Endoscopic and histologic images of stone-forming patients with distal tubular acidosis (dRTA). These stone-forming patients have a range of papillary abnormalities. Papillae may be normal apart from an occasional dilated duct of Bellini (arrows, panel A) and yellow plaque representing apatite mineral plugs (asterisk, panel A) within IMCD. Panel B shows the most extensive papillary damage with retraction, loss of normal architecture, multiple dilated ducts of Bellini that produce a pitted appearance (arrows), some with protruding mineral deposits (asterisks), and a whitish thickened membrane appearance. Papillary biopsies also reveal a range of histopathology. The Yasue stained section seen in panel C shows minimal IMCD plugging (black material at arrows); micro-CT (insert) examination of the biopsy sample confirms the intra-luminal location and sparseness of crystal deposits. Yasue stained papillary biopsy seen in panel D shows diffuse IMCD plugging (arrows) encased in extensive interstitial fibrosis. The micro-CT micrograph (insert) confirms the location and density of intra-luminal deposits (arrows).

Patients with RTA are at risk of loss of renal function, presumably secondary to severe nephrocalcinosis and recurrent bouts of stone formation.[124]

Bowel Diseases

Small Bowel Resection

Loss of small bowel results in a constellation of abnormal physiologies sometimes referred to as enteric hyperoxaluria: small-bowel malabsorption coupled with the presence of at least some colon that receives small-bowel effluent and through which excess oxalate enters the blood. Typical settings are Crohns disease, or small-bowel resection or bypass, the latter in treatment of obesity or hypercholesterolemia;[125] pancreatic insufficiency or sprue may cause a similar picture. In all cases, treatment is difficult. Oxalate absorption is mediated by many transporter assemblages,[126] and unabsorbed fatty acids in all of these conditions appear to increase colonic oxalate absorption.[127] Reduced colonic reabsorption of water and salts leads to diarrhea with loss of alkali in the stool, and consequent low urine citrate from systemic bicarbonate losses.[125,128] The resulting urine, high in oxalate and low in volume and citrate, is ideal for stone production.

The renal histopathology in small bowel resection from inflammatory bowel disease is like that of PHPT in combining apatite tubule plugging with CaOx stone overgrowth on plaque (Fig. 67.22).[129] Plaque abundance exceeds that seen in PHPT whereas the amount of plugging is less. The plugs contain mainly apatite, with a scattering of CaOx. Mechanisms for plaque include low urine volume and pH. Plugging with apatite would not be expected given the low urine pH and absence of CaP SS. Urine CaOx SS is quite high, however, and possibly crystals of CaOx form as an initial

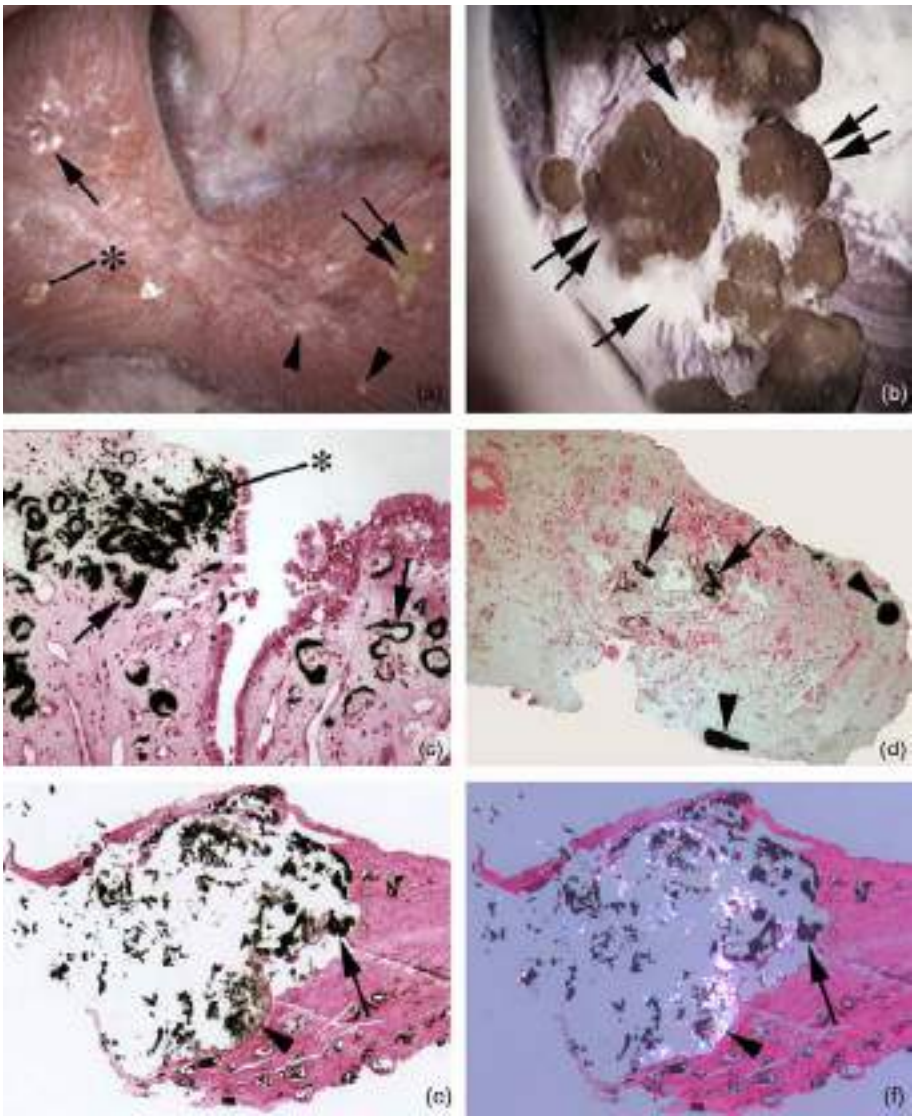

FIGURE 67.22 Endoscopic and histologic images of crystalline deposits in patients with small bowel resection with CaOx stone disease. In panel A papillae from these stone-forming patients are seen to have both attached stones (double arrow) on white plaque (single arrow) and protruding plugs (asterisk) from dilated openings of ducts of Bellini while others have large amount of white plaque (single arrow, panel B) with numerous attached stones (double arrow, panel B). Sites of yellow plaque (arrowheads) are seen in panel A. Yasue stained sections from papillary biopsies show large areas of interstitial plaque (arrows, panel C) surrounding the thin loops of Henle and extending to the base of the urothelial cells (asterisk, panel C). Areas of interstitial plaque (arrows, panel D) and plugged IMCD (arrowheads, panel D) are found in the same biopsy sample at varying amounts. The mineral type was apatite in these tubules. Other biopsy samples showed large deposits in IMCD to be a mixture of apatite (non-birefringent material at arrow, panels E and F) and CaOx crystals (birefringent material at arrowhead, panels E and F). See color plate section at the back of the book.

nucleation and injure cells. Injury could impair acidification, so tubule fluid pH rises and apatite forms in individual tubules. This conjecture requires experimental testing. Stones are generally CaOx and uric acid. The former grow on plaque; the latter presumably form in free solution, but this has not as yet been proven experimentally. Despite low pH, uric acid has not to date been found in tubule plugs.

The usual treatment measures are reasonable, but mediocre in use. Low-fat diet reduces delivery of fatty acids to the colon, but may impair nutrition in someone with small-bowel disease, so its use is marginal in many situations. Low oxalate diet is not difficult to prescribe, especially because vegetables and citrus fruits may already have been reduced because of intolerance. Cholestyramine, 2 to 4 g with each meal, is the measure we have found most effective, but the agent is unpleasant and cumbersome. Being a resin that can adsorb both oxalate and the offending bile and fatty acids,[18] it needs to be swallowed toward the end of a meal so it will migrate along with the food and take up the anions from it. Patients do not like to do this, and often miss doses. The resin has a taste many find objectionable. Even so, we have used it with some success, as have others.[130,131] Finally there is oral calcium, also taken toward the end of each meal. The calcium is intended to precipitate oxalate in the bowel lumen, and may do so if taken with good timing. Reasonable outcomes for stone prevention were published long ago;[132] there are no trials.

Obesity Bypass Procedures and Bariatric Surgery

Both jejuno-ileal bypass and modern bariatric surgery, particularly the Roux-en-Y or duodenal switch type of procedures, lead to hyperoxaluria in significant numbers of patients;[133] gastric banding does not appear to carry this risk.[134] Among bypass patients, papillary plaque abundance is normal (Fig. 67.23).[107] Stones are never attached to the papillary surfaces, but are found free in the renal pelvis. Scattered tubule plugs are apatite admixed with traces of CaOx.[110]

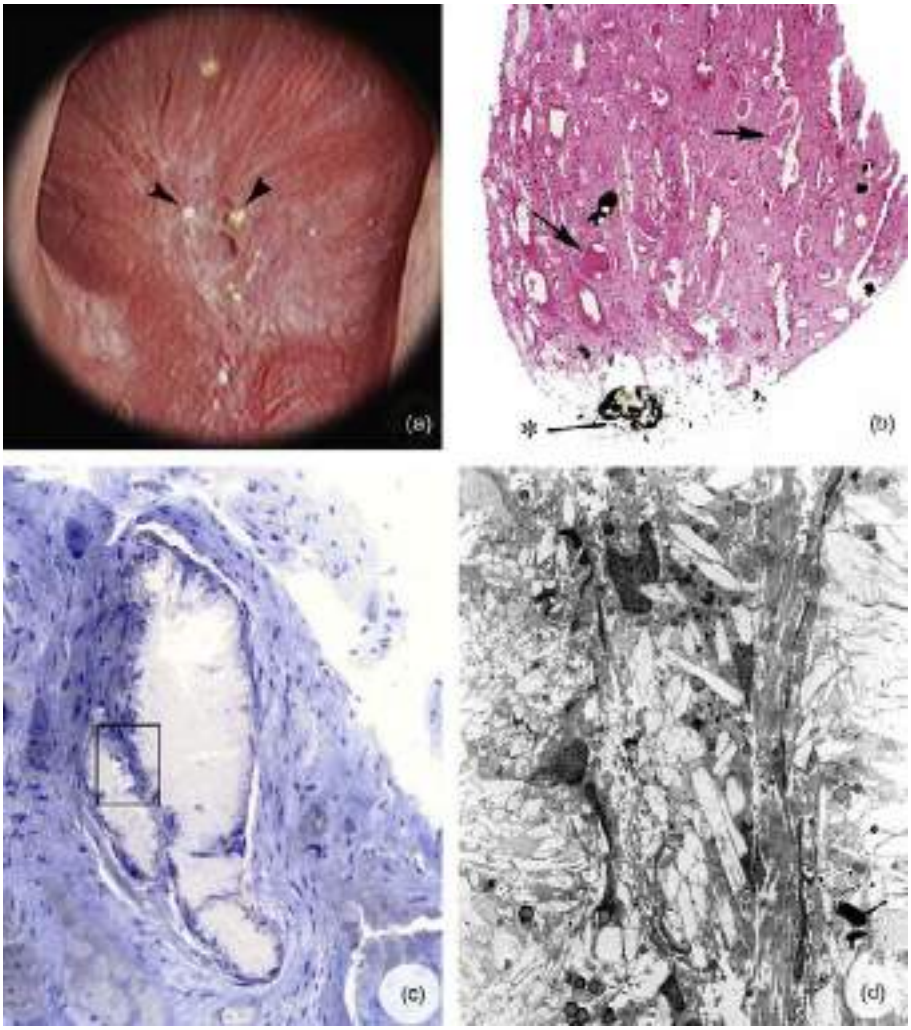

FIGURE 67.23 Endoscopic and histologic images from a stone forming patient who underwent intestinal bypass surgery for obesity. Panel A is an example of a papilla from an intestinal bypass stone former that was video recorded at the time of stone removal. Distinct sites of Randall's plaque were not found, instead, several nodular-appearing structures (arrowheads) were noted near the openings of the ducts of Bellini. Panel B is a low magnification light microscopic image of a papillary biopsy specimen from an intestinal bypass stone former showing crystalline deposits (asterisk) only in the lumens of a few IMCD or ducts of Bellini. No sites of interstitial crystalline deposit were seen. Note dilated collecting ducts (arrows) with cast material and regions of fibrosis around crystal-deposits-filled collecting ducts. Panel C is a light microscopic image showing a collecting duct completely filled with crystalline material. Panel D is an electron microscopic image of a region of the collecting duct seen in panel C (see rectangle). No cellular detail remains; only crystalline material is found. See color plate section at the back of the book.

Although hyperoxaluric, bypass patients maintain high urine volumes and have rather modest CaOx SS;[125] perhaps for this reason deposits are modest. Likewise high urine volumes with low normal pH would predict little plaque. Stones themselves can be abundant and their origin is uncertain; free solution crystallization is a real possibility. We do not have tissue from bariatric patients as yet. Presumably they will be like the bypass patients. Both categories of obesity surgery have the same underlying physiology and treatments are the same as for enteric hyperoxaluria from bowel resection. In some cases, severe hyperoxaluria may lead to tissue deposition of oxalate with acute or chronic renal failure.[135]

Ileostomy

Unlike small bowel resection and bypass procedures, there is no colon and therefore no hyperoxaluria. Instead volume depletion and bicarbonate wasting predominate, causing very scanty and acidic urine. From this one would predict considerable interstitial plaque, and that is indeed found (Fig. 67.24).[136] CaOx stones grow on the plaque as expected. Because of very low urine pH, uric acid SS is marked, but CaP SS is absent, so one might expect stones to contain uric acid and no CaP; this is true. However, tubule plugging is marked (Fig. 67.24) and the crystals in plugs are a mixture of apatite and the sodium and ammonium salts of uric acid; all three crystals are stable at high, not low pH. This discordance between crystal type and urine SS must arise from local acidification defects in the individual tubules as crystals are a form of pH indicator. Mechanisms are as yet unknown. Treatment is well established: maintain fluid intake as possible, use supplemental alkali as tolerated. Management is very complex as these can be sick and fragile patients. Of note, acute dehydration episodes can produce acute kidney injury from many causes: falling blood pressure, uric acid plugging of ureters, and acute uric acid nephropathy.[137]

Primary Hyperoxaluria

These rare autosomal recessive enzyme defects cause very high oxalate excretion rates, above 80 mg daily and typically in the range of 150 to 300 mg daily, due to overproduction of oxalate in the liver. Stones often begin in childhood, and renal failure is common as well. The high production of oxalate after kidneys fail can promote systemic oxalate deposition in heart and skin and blood vessels, and sudden bursts of oxalate into the tubule fluid of a renal transplant can destroy the organ.[138] Stone disease is CaOx, and may be very severe.

The usual type (type I: MIM 604285) is absence or ineffectiveness of the enzyme alanine/glyoxalate aminotransferase (AGT), that converts glyoxalate to glycine.[95] Without it, glyoxalate amounts increase, which is converted to oxalate by lactate dehydrogenase. In 40% of cases, the enzyme is not absent but is misdirected from its proper peroxisomal location to mitochondria, within which it cannot function except at a minimal level. Liver tissue has 3% to 40% of normal enzyme activity but full immunoreactivity, and the latter shows the improper location. The remainder lacks the enzyme because of one or more mutations in its structure. While the kidneys are functioning, one can diagnose this condition by high urine glyoxylate and glycolate levels as well as high oxalate levels. When renal failure has occurred, study of liver tissue remains definitive, however genetic diagnosis is becoming available, and may obviate the need for biopsy in many cases.[139]

In kidneys, plaque is absent (Fig. 67.25). Tubules are plugged with CaOx admixed with apatite. The numbers of plugged tubules approximate those seen in RTA, but deposits extend higher up in the nephron than usual in stone diseases, involving the thin loops and PT. Interstitial fibrosis also far exceeds that seen in any other stone disease.

Treatment can begin with large fluid intake and pyridoxine, 25 to 100 mg daily, the dosing raised by doubling depending on response. Pyridoxine is a cofactor for AGT, and patients with mutations associated with mitochondrial translocation seem to be the ones that respond.[138] Orthophosphate supplements and potassium citrate have also been reported as effective[140] but without controlled trials. Renal failure is common and is treated by combined liver–kidney transplantation.[141] Transplant nephrologists should beware of this condition, which can sneak by if stone history is slighted, especially if native biopsy was not performed. Management of transplantation is discussed in Chapter 94.

Type II hyperoxaluria (MIM 260000, 604296) is rare. The defect is loss of glyoxylate reductase/hydroxypyruvate reductase (GRHPR), leading to oxalate and L-glyceric acid overproduction. Treatment is the same as that for type I except that pyridoxine is not likely to be useful and renal failure is not as common.[142]

Recently, mutations in an uncharacterized gene, DHDPSL, on chromosome 10, have been associated with a third type of PH, now termed PH III. This autosomal recessive disorder is associated with presentation of stones in childhood, and preservation of renal function with conservative treatment appears to be the norm in the 9 families described thus far.[143]

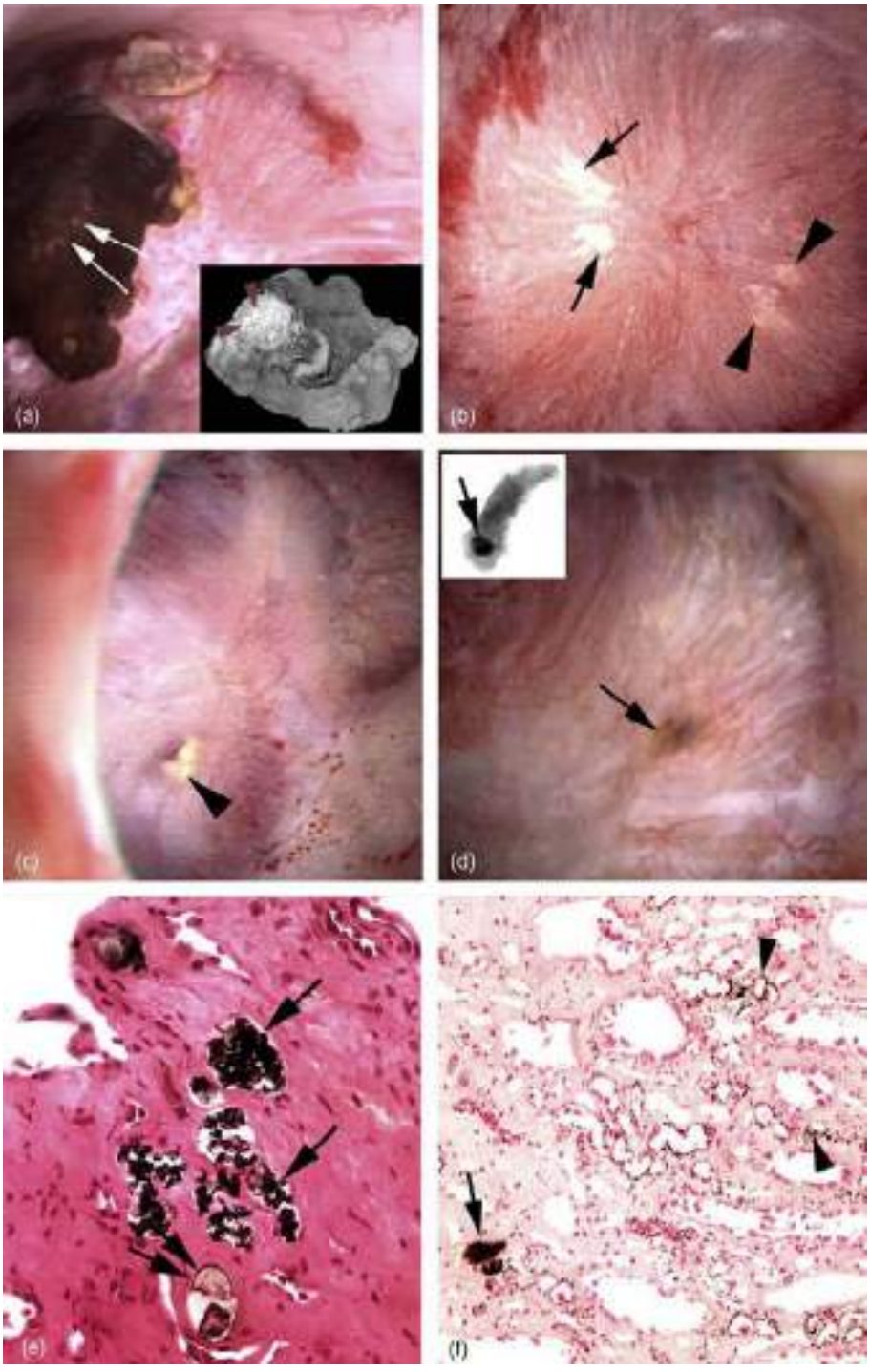

FIGURE 67.24 Endoscopic and histologic views of papillae from ileostomy stone patients. Papillary morphology as viewed by digital endoscope varied from normal (panels A and B) to retracted (panel C) and with attached stones (double white arrow, panel A) near white plaque (arrows, panel B) and/or protruding plugs from ducts of Bellini (arrowhead, panel C) with yellow plaque (arrowheads, panel B). Attached stones when removed and examined by micro-CT showed regions of apatite on their tissue surface (arrowheads, insert in panel A). By endoscopy, large intraluminal deposits were noted as dark spots on the papillary surface (arrow, panel D) which were confirmed by micro-CT (arrow in insert of panel D). Intraluminal plugging of IMCD and ducts of Bellini was more prominent than attached stones. Yasue stained papillary biopsy samples revealed numerous dilated IMCD and ducts of Bellini filled with Yasue-positive deposits (arrows panels E & F) and Yasue-negative deposits (double arrow, panel E). The Yasue-positive material was apatite while the Yasue-negative material was sodium and ammonium salts of uric acid. Sites of interstitial plaque were noted in the basement membrane of thin loops of Henle (arrowheads, panel F). See color plate section at the back of the book.

URIC ACID (AND OTHER PURINES) IN STONES

We have already pointed out that urine pH controls uric acid SS (Fig. 67.5), and at a pH of above 6.2 SS does not occur. For this reason, alkali sufficient to raise urine pH will abolish uric acid crystallization. That patients with uric acid stones have low urine pH is evident from Fig. 67.6. Mechanisms creating the low pH have been advanced in the past few years. A crucial factor appears to be insulin resistance[144,145] which reduces renal ammonia production.[144] This accounts for the well-known links between uric acid stones and diabetes.[146] Mere obesity seems important in that urine pH falls as body weight, adjusted for urine creatinine (an index of obesity) rises.[147] Metabolic syndrome,

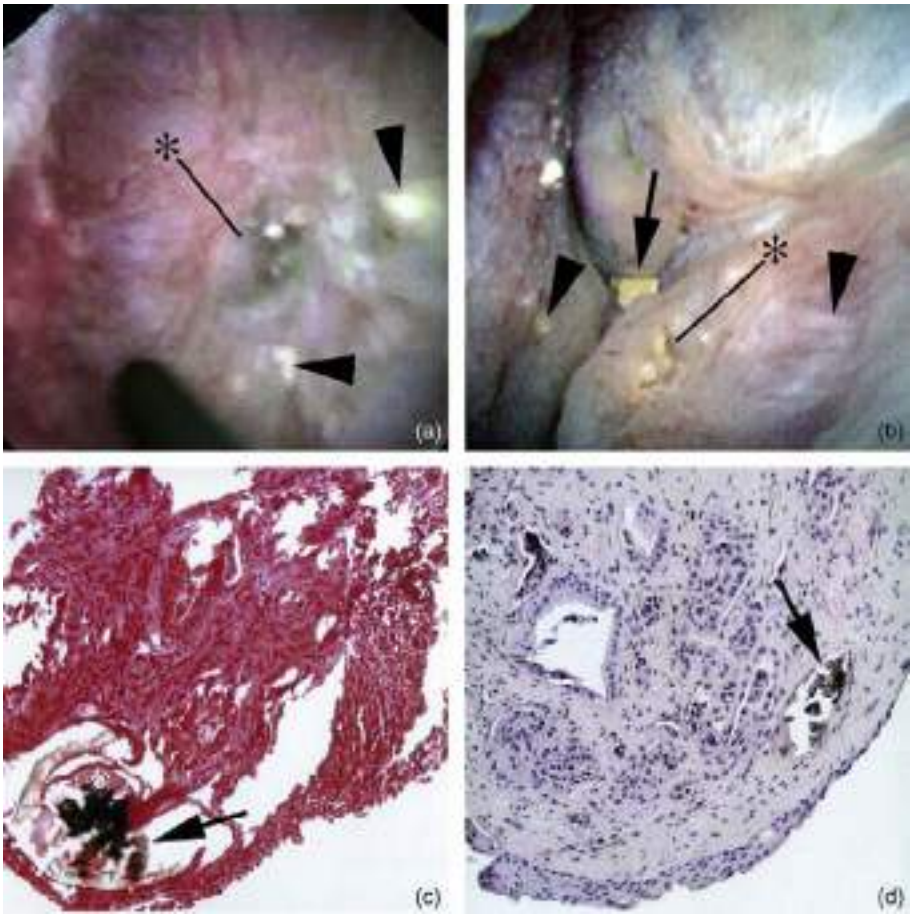

FIGURE 67.25 Endoscopic and histologic images of stone-forming patients with primary hyperoxaluria. Endoscopic examination at time of stone removal reveals normal appearing papilla with dilated openings of ducts of Bellini (asterisks, panels A and B) containing mineral as well as protruding plugs with attached stone (large arrow, panel B). Regions of yellow plaque were numerous (arrowheads, panels A and B) but no white plaque was noted. Histopathology showed intraluminal plugging in IMCD (arrow, panel D) and ducts of Bellini (arrow, panel C). All mineral deposits were found to be CaOx with only a small amount of apatite. See color plate section at the back of the book.

characterized by insulin resistance, is also associated with decreased 24-hour urine pH. Chronic diarrhea causes uric acid stones, as already pointed out in our discussion of ileostomy.

Potassium alkali salts are best because they avoid sodium loads, with their attendant disadvantages of volume expansion and high blood pressure. But diabetes or age occasionally impairs potassium excretion in this group of patients. In some instances, potassium retention reduces ammonia excretion producing the low pH (Type 4) RTA. For such patients a sodium alkali salt is needed. We find that 25 mEq twice daily of citrate or bicarbonate is sufficient for most people, a few requiring a third dose. Unlike CaOx, uric acid can dissolve at pH values attainable in human urine, and stones may well shrink. More often, large ones lose outer mass, and their constituent fragments become unglued and begin to pass.

The syndromes of uric acid crystallization merit comment as they differ from those of calcium stones. Given a sudden delivery of uric acid into the renal tubules, from lysis of tumors, a uricosuric drug, or a sudden fall in urine volume in someone with a low urine pH, crystals of uric acid may form in renal tubules, and cause acute renal failure—so-called acute uric acid nephropathy. Hydration and alkali may reverse this condition; in the case of uric acid overproduction, such as tumor lysis syndrome, rasburicase, recombinant urate oxidase, is the most effective treatment.[148] Another outcome of sudden uricosuria or fall in pH or volume is formation of sludge made from a mass of uric acid crystals that obstructs both ureters and leads to obstructive renal failure. Less dramatic, uric acid crystals may pass with pain and bleeding, yet being radiolucent and prone to disperse in the bladder the crystals may never be seen. The easiest syndrome to diagnose is uric acid gravel, which passes as a gritty material and is orange-red from adsorbed pigment. Management of obstructive uropathy and prevention of tumor lysis syndrome are discussed elsewhere in this volume. Finally, uric acid stones were described as radiolucent in years past, being so on routine abdominal flat-plate radiographs and intravenous pyelography. With CT scanning uric acid stones look identical to calcium stones; however, they may be distinguished by their lower density by Hounsfield units.[149]

The rare hereditary uric acid overproduction states, such as Lesch-Nyhan syndrome, should be considered when uric acid stones present in childhood. 2,8-dihydroxyadenine urolithiasis occurs in patients

with a deficiency of adenine phosphoribosyltransferase (APRT, MIM 102600) and may cause renal failure as well as stones. Other rare purine stones include ammonium acid urate stones, which are associated with diarrheal syndromes and laxative abuse, and with hypokalemia. Correction of the potassium depletion and control of diarrhea are therapeutic.

CYSTINURIA AND CYSTINE STONES

The two genes responsible for cystinuria (Table 67.2) encode the light and heavy subunits of the dibasic amino acid transporter that normally reabsorbs the majority of filtered cystine in PT.[150] Modern classification of cystinuria is type I or non-I (Table 67.2) depending on the gene defect, if known, or the urine cystine of heterozygotes in the family. Cystinuria causes stones via simple supersaturation because of the poor solubility of cystine in urine, and clinical presentation does not differ between the two types, nor does the treatment. Presentation is often in childhood, and the disease is associated with very frequent stone formation and need for procedures. Cystine stones do not fragment will with extracorporeal shock wave lithotripsy, and this, combined with the large size to which cystine stones often grow, means that these patients often need percutaneous approaches for stone removal.

Among seven patients with typical cystinuria and passage of cystine stones, papillary morphology varies from nearly normal to massively scarred (Fig. 67.26).[151] Bellini ducts are plugged with cystine, as one would expect, but IMCD are plugged with massive deposits of apatite, which one might not expect, and apatite deposits can be found even in the thin limbs of Henle (Fig. 67.26, panels C and D**)**. We suspect the process here resembles that in IPSF in that lumen pH rises and initiates a vicious cycle of apatite crystallization and cell injury. The initiating event may be obstruction by cystine deposits in the BD. The well-known reduction of renal function in cystinuria patients[152] could well reflect the plugging and cell destruction illustrated here. Alternatively, these patients might lose function simply because they have an inherited PT transport disorder; this matter has not been studied to date.

Cystine solubility is about 1 mM/l of urine (243 mg/l) and rises with pH.[153] Supersaturation is best measured directly, if possible, because simple calculations from molarity and urine pH are not accurate.[154] However, direct measurements are complex and may not be available.[155] In general, a urine volume between 3.5 and 5 liters daily will dissolve the urine cystine of many patients. In others, one must raise pH using potassium citrate, 25 mEq two to three times daily, to about 7. Reduction of diet sodium and protein can reduce urine cystine excretion modestly.

When volume, citrate, and diet measures are in place, how can one tell if treatment is adequate apart from waiting for more stones? We usually re-measure total urine cystine and calculate if the urine volume will dissolve it at the pH of the 24-hour sample or, if possible, measure supersaturation directly. If stones continue, or when patients do not maintain volume or pH high enough, we use drugs, which are limited in value by side effects. D-penicillamine and alpha-mercaptopropionylglycine (tiopronin) form mixed disulfides with cysteine, thereby reducing cystine, the cysteine homodimer.[156] Dosing of either is reasonably simple. D-penicillamine comes in 125- and 250-mg tablets, providing 0.83 and 1.6 mM of drug, respectively. Given 4 to 8 mM of cystine excretion daily, 125 or 250 mg four times a day is reasonable depending on the divergence between total cystine excretion and total urine volume. For example, given 4 mM cystine excretion per day in someone who will not raise urine volume above 2 liters per day, the former dose of 125 mg four times daily should complex about 2.4 mM, or close to the extra cystine. For alpha-mercaptopropionylglycine the dose size is 100 mg giving 0.61 mM of the drug. Both drugs have similar side effects but the incidence is lower with

TABLE 67.2 Cystinuria

Disease	MIM	Inheritance	Locus/ Gene	Gene Product	Functions	Location	Phenotype
Cystinuria type A (type I)	104614	Autosomal recessive	2p16.3/ SLC3A1	rBAT	Heavy unit of heteromeric aa transporter	Proximal tubule, S3	Heterozygotes: Normal urine cystine excretion
Cystinuria type B (usually type non-I)	604144	Incompletely autosomal recessive	19q13.1/ SLC7A9	b0, + AT	Light subunit of heteromeric aa transporter	Proximal tubule, S1 and S2	Heterozygotes: Elevated urine cystine excretion

(From *Coe FL, Evan A, Worcester E. Kidney stone disease. J Clin Invest. 2005;115:2598–2608, with permission.)*
aa, amino acids; MIM, Mendelian Inheritance in Man; S1, S2, S3, segments 1–3 of the proximal tubule.

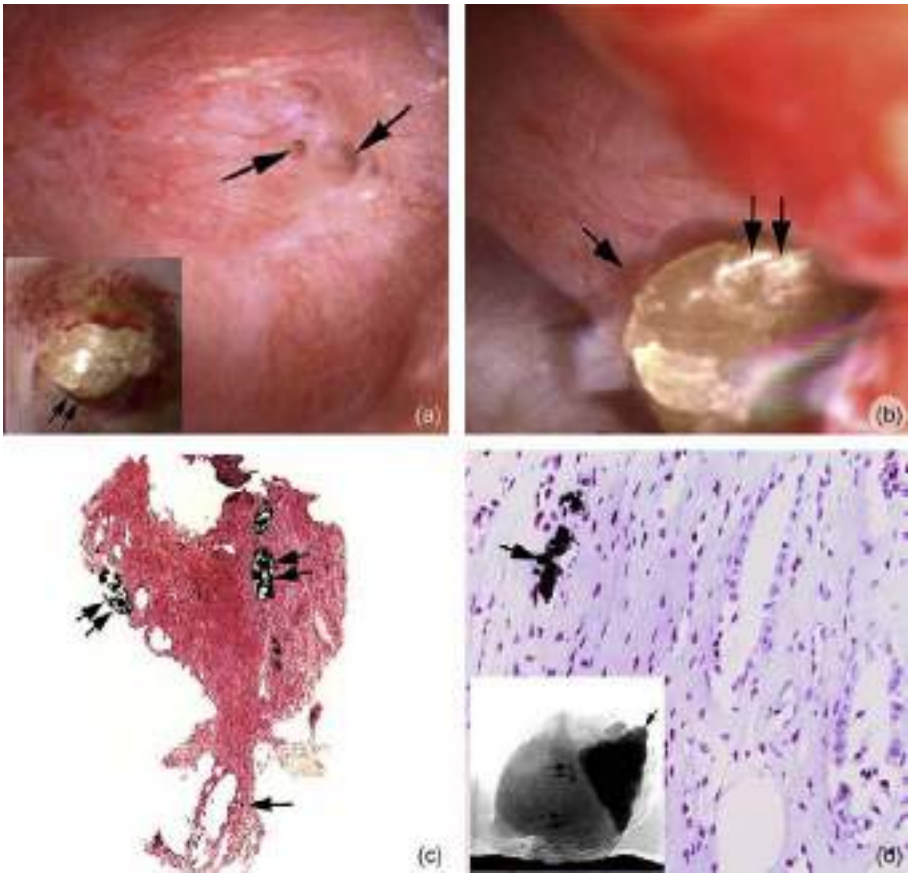

FIGURE 67.26 Endoscopic and histologic views of papillae from cystine stone patients. Papillary morphology as seen through the endoscope varies from normal to flattened with greatly enlarged openings (arrows, panel A) of the ducts of Bellini. Some dilated ducts of Bellini contained protruding plugs (insert panel A) of crystalline material (double arrow). In addition, small sites of suburothelial Randall's plaque were noted. Occasionally, large masses of crystalline material were seen at the time of PNL to lie under the urothelium at a site marked by dilated ducts of Bellini and upon unroofing the urothelium during the biopsy procedure (single arrow in panel B), deposits were exposed that were located within a tubular lumen (double arrow in panel B). The deposits were determined to be cystine. The papillary histopathology of the cystine patients also showed variation from normal to regions of plugging, dilation and injury of IMCD (double arrows in panel C). Intraluminal plugging with crystals was noted in thin loops of Henle (single arrow in panels C and D), and IMCD (double arrows in panel C). The insert in panel D shows a 3-D reconstructed micro-CT image of a papillary biopsy and the arrow indicates the site of the protruding plug like that seen in the insert in panel A. The large, dense triangular deposit was determined to be cystine. Surrounding this large deposit are several smaller regions of mineral (double arrow) that are consistent with apatite. Panel D is a paraffin section from the lower half of the biopsy seen by micro-CT and shows Yasue positive material in a thin loop of Henle (arrow). See color plate section at the back of the book.

tiopronin, which is our drug of choice. Adequate therapy can prevent new stone formation and may be able to decrease the size of existing stones if supersaturation is lowered adequately.

Cystine stones are hard to see with routine radiographs, having only sulfur as a heavy atom, sparsely distributed in the molecule and crystals. CT scanning resolves the stones perfectly. Some cystine stones become coated with calcium salts, particularly if pH of the urine has been raised in someone who is also hypercalciuric; such "eggshell" stones will not dissolve and can be hard to fracture. Some writers recommend screening all cystinurics for routine metabolic stones because they harbor such disorders no less frequently than other people. All stones should be analyzed to be sure they do not contain additional phases that might need individual treatment. The lemon-yellow color of cystine is no guarantee that no more lies inside.

PLAQUE AND DEPOSITS IN ALL FORMS OF STONE DISEASE: AN INTEGRATION

Quantities of Plaque and Deposits

In biopsy samples, using high resolution micro-CT analysis, deposits can be quantified as number/cubic mm of tissue and mean size of deposit. Plaque abundance can be quantified as the fraction of papillum covered using intra-operative digital imaging. For the

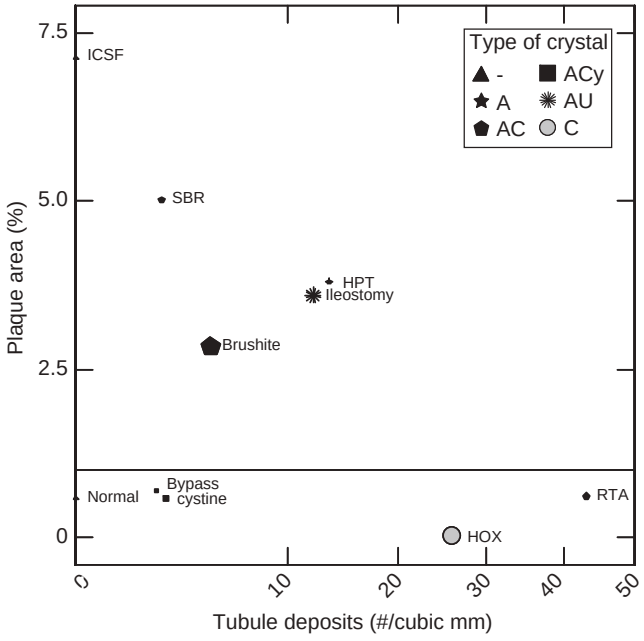

FIGURE 67.27 Papillary plaque surface area (*y*-axis) versus tubule deposit density (*x*-axis) in nine stone forming conditions (ICSF, brushite, small bowel resection (SBR), hyperparathyroidism (HPT), ileostomy, obesity bypass, cystine, primary hyperoxaluria (HOX), renal tubular acidosis (RTA)) and normal subjects. Size of symbol gauges mean size of individual deposits. Deposit density and size are from micro-CT analysis. The *horizontal line* represents the upper boundary of plaque abundance in normal renal tissue. Type of crystal in deposits: *A* apatite, *C* CaOx, *Cy* cystine, *U* sodium and ammonium urate crystals, *dash* no deposits, shown as *triangles* for normal and ICSF. *(Reprinted with permission from: Coe FL, Evan AP, Lingeman JE, Worcester EM. Plaque and deposits in nine human stone diseases. Urol Res 38:239-247, 2010).*

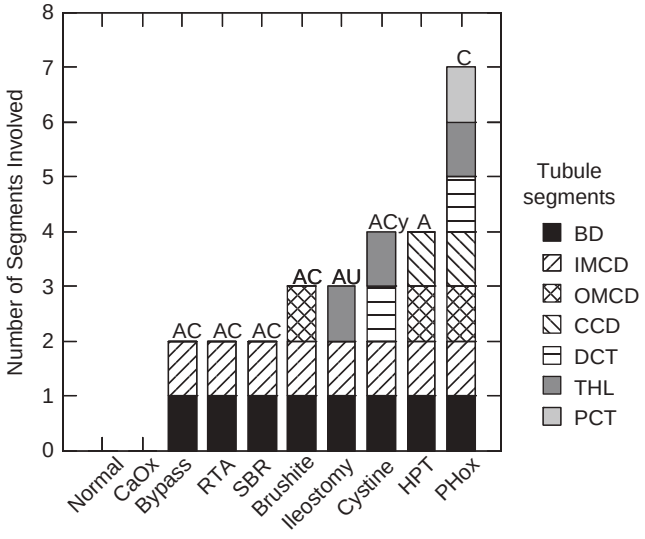

FIGURE 67.28 Renal tubule segments containing crystal deposits in 9 stone forming conditions and normal subjects. Abbreviations as in Fig. 27. *BD*, Bellini ducts; *IMCD, OMCD and CCD*, inner and outer medullary and cortical collecting ducts; *DCT*, distal convoluted tubule; *tHL*, thin limbs of Henle's loop; *PCT*, proximal tubule. *(Reprinted with permission from: Coe FL, Evan AP, Lingeman JE, Worcester EM. Plaque and deposits in nine human stone diseases. Urol Res 38:239-247, 2010).*

nine diseases with tissue analysis, 4 have no more than normal amounts of plaque (Fig. 67.27): obesity bypass, cystinuria, primary hyperoxaluria and RTA. ICSF are unique in having abundant plaque without any deposits, and normal subjects, of course, have trivial plaque and no deposits. Primary hyperoxaluria and RTA have the most deposits, and primary hyperparathyroidism, IPSF (brushite), ileostomy and small bowel resection have high amounts of both deposits and plaque. As noted in the symbols and legend, apatite is the most common crystal in deposits, accompanied by CaOx; cystine and urate species are unique to cystinuria and ileostomy, respectively.

Abundance and deposit size tell, however, only part of the story. In obesity bypass, RTA and small bowel resection, deposits are limited to the BD and IMCD (Fig. 67.28), in other words to the most terminal nephron segments. They extend into the outer medullary collecting ducts in IPSF (brushite), primary hyperparathyroidism and primary hyperoxaluria, essentially by contiguity. In primary hyperparathyroidism they extend even further, into the cortical collecting ducts, and in ileostomy and cystinuria they involve the thin limbs and distal tubule (DCT). Primary hyperoxaluria is unique in that deposits invade the entire nephron. The stone diseases therefore form a spectrum along three axes: deposit density, deposit size, and deposit extent, which are often discordant from one another. Exactly why this happens is not clear except perhaps for the extreme invasiveness of primary hyperoxaluria, which floods the nephron with oxalate, lifelong.

Physiological Correlates of Plaque

The effects of urine calcium excretion, volume, and pH on plaque abundance found among ICSF, obesity bypass, and normal subjects (Fig. 67.16) can be reproduced in the nine separate conditions we have data for. A multivariable score derived from these three measurements separates the conditions into two groups (Fig. 67.29, left panel): low plaque states (lower left) and high plaque states (upper right). The five high plaque states are to the lower right on the middle panel of the figure, because of having higher urine calcium molarities (x axis) and lower pH values vs. the 4 low plaque states: plaque increases with the ratio of calcium to water excretion and falls with pH. When urine volume is plotted against urine calcium excretion (right panel) the high plaque states are at higher urine calcium excretions for a given urine volume (downward and to the right of the low plaque states). So the effects

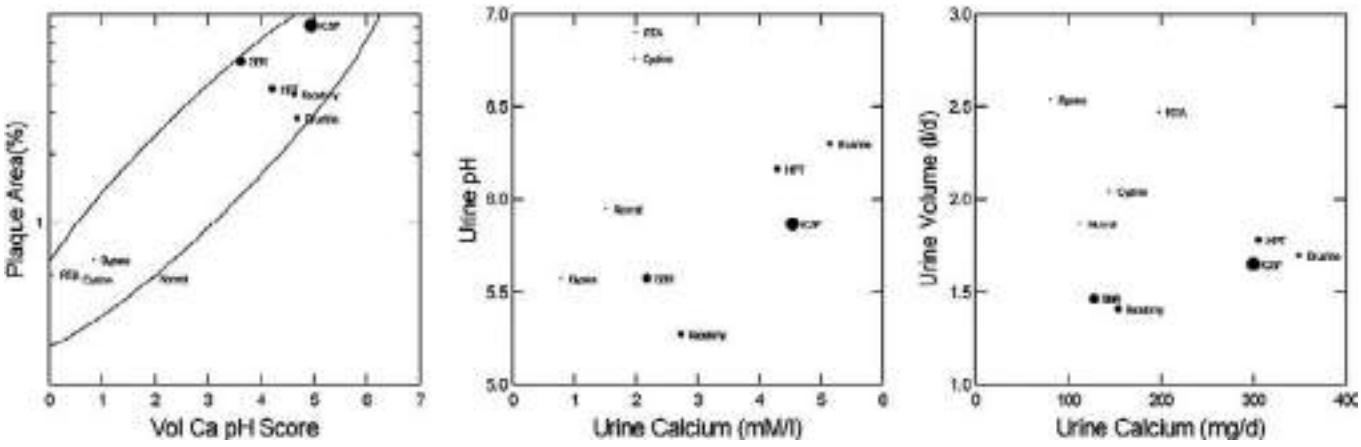

FIGURE 67.29 Determinants of plaque surface area in 8 stone forming conditions and normal subjects. Relationship between urine volume and calcium excretion (*right panel*) and urine pH and urine calcium molarity (*middle panel*); abbreviations as in Fig. 68.27. *Size of symbol* denotes plaque surface area. Note clustering of high (*large symbols*) plaque states to the lower right of both panels and marked separation from low plaque states. A score incorporating volume, urine calcium and urine pH predicts plaque coverage well across all stone forming conditions studied so far. *(Reprinted with permission from: Coe FL, Evan AP, Lingeman JE, Worcester EM. Plaque and deposits in nine human stone diseases. Urol Res 38:239-247, 2010).*

of high calcium and low water excretion and pH to promote plaque can be duplicated among normals and eight separate stone forming diseases, meaning the relationships are robust.

INFECTION (STRUVITE) STONES

Magnesium ammonium phosphate crystals, literally the solid phase of a triple salt, were described by Struve, who found them in caves, and gave his name to them: struvite.[157] These stones form only when the kidneys are colonized by bacteria that possess the enzyme urease, which hydrolyzes urea to ammonia and CO_2. The ammonia raises pH by accepting protons; HCO_3 is produced as the CO_2 dissolves in the alkaline urine, raising local levels of bicarbonate and eventually of carbonate ions. Protons are removed from phosphate as well, raising local concentrations of PO_4^{-3} as ammonia converts to ammonium ion. In the micro-environment of bacterial colonies, struvite crystallizes out of solution along with calcium carbonate to make large branched stones that often fill multiple calyces in a staghorn conformation.

The bacteria involved are usually *Proteus*, *Klebsiella*, *Pseudomonas*, and *Enterobacter* species, never *Escherichia coli*, and appear to colonize the urine mainly after multiple episodes of antibiotic treatment for routine infections. Once in place, the stones and their bacteria cannot be treated with antibiotics, as they act like all infected foreign bodies. The bacteria lodge in and stick to the stone, and antibiotics cannot penetrate into the depths of the crystal masses to kill all of the organisms. Resistance evolves easily under such circumstances. The only treatment option is surgical.

We have found two clinical divisions of struvite stone patients.[158] One forms struvite stones with at least some CaOx in them. These patients are men and women and harbor the conventional set of metabolic causes of stones. They usually report having passed stones, and their renal function is only slightly below normal, as is the case with most stone formers.[124] The second type is mainly women, in whom a large stone is found on radiograph, the latter often obtained in evaluation of infection or bleeding or pain. The stones contain no CaOx, and the patients have no usual metabolic cause of stones. Renal function is frequently reduced by a small amount. In either case, the stone must be removed and the infection treated.

A third kind of patient presents with acquired or hereditary deformity of the urinary system or a spinal cord injury with subsequent bladder dysfunction and need for chronic catheterization. Abnormal drainage, catheter infections, and dead space in distorted anatomy promote bacterial lodgment and colonization and eventuate in struvite stones. This last category of patient is in the purview of surgical urology and rehabilitation medicine and requires unusually complex management. In cases where complete removal of stone material is not possible, aceto-hydroxamic acid may be used to inhibit urease and prevent stone growth.[159,160] However, many patients exhibit serious side effects, including deep vein thrombosis and headache, limiting the use of this agent.

When surgery is undertaken for infection stones, the goal must be removal of all fragments, for all parts of the stone are infected and can grow back. We cannot

dwell, here, on details of surgery, but this kind of work is best left to centers with high levels of experience and instrumentation. Antibiotic treatment after complete removal of the stones should be with bactericidal agents with the intent to sterilize the urinary tract and prevent re-growth. Given a successful removal of the foreign bodies, this is a reasonable goal. Prevention of struvite stones depends on proper and judicious treatment of the many urinary tract infections that stone passage and removal engender, a matter covered elsewhere in this volume.

FINAL THOUGHTS

Stone patients are sometimes approached with therapeutic nihilism, as though further stone formation was inevitable. However, experience has shown that stone recurrence is highly preventable. Treatment aimed at lowering urinary SS with respect to the stone matrix by correcting metabolic abnormalities uncovered using 24 hour urines for evaluation has been shown to decrease stone recurrence over decades.[161] Such treatment can markedly lower the need for procedures for stone removal as well. Careful follow-up is required, to confirm that urine SS remains low and to modify the treatment regime—fluids, diet and medications—as needed to maintain the lowest possible SS. With such attention, prevention of stones is attainable over long time periods.

Acknowledgment

Supported in part by National Institutes of Health grant NIDDK PO156788.

References

[1] Abate N, Chandalia M, Cabo-Chan Jr. AV, Moe OW, Sakhaee K. The metabolic syndrome and uric acid nephrolithiasis: novel features of renal manifestation of insulin resistance. Kidney Int 2004;65:386–92.
[2] Asplin JR. Evaluation of the kidney stone patient. Semin Nephrol 2008;28:99–110.
[3] Asplin JR. Hyperoxaluric calcium nephrolithiasis. Endocrinol Metab Clin North Am 2002;31:927–49.
[4] Asplin JR, Arsenault D, Parks JH, Coe FL, Hoyer JR. Contribution of human uropontin to inhibition of calcium oxalate crystallization. Kidney Int 1998;53:194–9.
[5] Asplin JR, Bauer KA, Kinder J, Muller G, Coe BJ, Parks JH, et al. Bone mineral density and urine calcium excretion among subjects with and without nephrolithiasis. Kidney Int 2003;63:662–9.
[6] Asplin JR, Donahue S, Kinder J, Coe FL. Urine calcium excretion predicts bone loss in idiopathic hypercalciuria. Kidney Int 2006;70:1463–7.
[7] Asplin JR, Mandel NS, Coe FL. Evidence of calcium phosphate supersaturation in the loop of Henle. Am J Physiol 1996;270: F604–13.
[8] Asplin JR, Parks JH, Chen MS, Lieske JC, Toback FG, Pillay SN, et al. Reduced crystallization inhibition by urine from men with nephrolithiasis. Kidney Int 1999;56:1505–16.
[9] Asplin JR, Parks JH, Coe FL. Dependence of upper limit of metastability on supersaturation in nephrolithiasis. Kidney Int 1997;52:1602–8.
[10] Asplin JR, Parks JH, Nakagawa Y, Coe FL. Reduced crystallization inhibition by urine from women with nephrolithiasis. Kidney Int 2002;61:1821–9.
[11] Atmani F, Khan SR. Role of urinary bikunin in the inhibition of calcium oxalate crystallization. J Am Soc Nephrol 1999;10 (Suppl. 14):S385–8.
[12] Barcelo P, Wuhl O, Servitge E, Rousaud A, Pak CY. Randomized double-blind study of potassium citrate in idiopathic hypocitraturic calcium nephrolithiasis. J Urol 1993;150:1761–4.
[13] Bataille P, Achard JM, Fournier A, Boudailliez B, Westeel PF, El Esper N, et al. Diet, Vitamin D and vertebral mineral density in hypercalciuric calcium stone formers. Kidney Int 1991;39: 1193–205.
[14] Belostotsky R, Seboun E, Idelson GH, Milliner DS, Becker-Cohen R, Rinat C, et al. Mutations in DHDPSL are responsible for primary hyperoxaluria type III. Am J Hum Genet 2010;87: 392–9.
[15] Bergsland KJ, Coe FL, Gillen DL, Worcester EM. A test of the hypothesis that the collecting duct calcium-sensing receptor limits rise of urine calcium molarity in hypercalciuric calcium kidney stone formers. Am J Physiol Renal Physiol 2009;297:F1017–23.
[16] Bergsland KJ, Kelly JK, Coe BJ, Coe FL. Urine protein markers distinguish stone-forming from non-stone-forming relatives of calcium stone formers. Am J Physiol Renal Physiol 2006;291: F530–6.
[17] Bergsland KJ, Zisman AL, Asplin JR, Worcester EM, Coe FL. Evidence for net renal tubule oxalate secretion in patients with calcium kidney stones. Am J Physiol Renal Physiol 2011;300: F311–8.
[18] Bergstralh EJ, Monico CG, Lieske JC, Herges RM, Langman CB, Hoppe B, et al. Transplantation outcomes in primary hyperoxaluria. Am J Transplant 2010;10:2493–501.
[19] Birge SJ, Peck WA, Berman M, et al. Study of calcium absorption in man: a kinetic analysis and physiologic model. J Clin Invest 1969;48:1705–13.
[20] Bisaz S, Felix R, Neuman WF, Fleisch H. Quantitative determination of inhibitors of calcium phosphate precipitation in whole urine. Miner Electrolyte Metab 1978;1:74–83.
[21] Borghi L, Meschi T, Amato F, Briganti A, Novarini A, Giannini A. Urinary volume, water and recurrences of idiopathic calcium nephrolithiasis: a 5-year randomized prospective study. J Urol 1996;155:839–43.
[22] Borghi L, Meschi T, Guerra A, Novarini A. Randomized prospective study of a nonthiazide diuretic, indapamide, in preventing calcium stone recurrences. J Cardiovasc Pharmacol 1993;22(Suppl. 6):S78–86.
[23] Borghi L, Schianchi T, Meschi T, Guerra A, Allegri F, Maggiore U, et al. Comparison of two diets for the prevention of recurrent stones in idiopathic hypercalciuria. N Engl J Med 2002;346:77–84.
[24] Brennan S, Hering-Smith K, Hamm LL. Effect of pH on citrate reabsorption in the proximal convoluted tubule. Am J Physiol 1988;255:F301–306s.
[25] Broadus AE, Insogna KL, Lang R. A consideration of the hormonal basis and phosphate leak hypothesis of absorptive hypercalciria. J Clin Endocrinol Metab 1984;58:161–9.

[26] Chillaron J, Font-Llitjos M, Fort J, Zorzano A, Goldfarb DS, Nunes V, et al. Pathophysiology and treatment of cystinuria. Nat Rev Nephrol 2010;6:424–34.
[27] Coe FL. Renal Colic and Flank Pain. In: Text Book of nephrology, edited by Massry S and Glassock RJ. 1995, pp. 567–573.
[28] Coe FL, Clark C, Parks JH, Asplin JR. Solid phase assay of urine cystine supersaturation in the presence of cystine binding drugs. J Urol 2001;166:688–93.
[29] Coe FL, Evan A, Worcester E. Kidney stone disease. J Clin Invest 2005;115:2598–608.
[30] Coe FL, Favus MJ, Crockett T, Strauss AL, Parks JH, Porat A, et al. Effects of low-calcium diet on urine calcium excretion, parathyroid function and serum 1,25(OH)2D3 levels in patients with idiopathic hypercalciuria and in normal subjects. Am J Med 1982;72:25–32.
[31] Coe FL, Parks JH. Hyperoxaluric states. In: Coe FL, Parks JH, editors. Nephrolithiasis: pathogenesis and treatment. Chicago: Year Book Medical Publishers; 1988. p. 172–204.
[32] Coe FL, Parks JH, Bushinsky DA, Langman CB, Favus MJ. Chlorthalidone promotes mineral retention in patients with idiopathic hypercalciuria. Kidney Int 1988;33:1140–6.
[33] Coe FL, Parks JH, Moore ES. Familial idiopathic hypercalciuria. N Engl J Med 1979;300:337–40.
[34] Coe FL, Raisen L. Allopurinol treatment of uric-acid disorders in calcium-stone formers. Lancet 1973;1:129–31.
[35] Coll DM, Varanelli MJ, Smith RC. Relationship of spontaneous passage of ureteral calculi to stone size and location as revealed by unenhanced helical CT. AJR Am J Roentgenol 2002;178:101–3.
[36] Curhan GC, Willett WC, Rimm EB, Stampfer MJ. A prospective study of dietary calcium and other nutrients and the risk of symptomatic kidney stones. N Engl J Med 1993;328:833–8.
[37] Curhan GC, Willett WC, Rimm EB, Stampfer MJ. Family history and risk of kidney stones. J Am Soc Nephrol 1997;8:1568–73.
[38] Curhan GC, Willett WC, Speizer FE, Stampfer MJ. Twenty-four-hour urine chemistries and the risk of kidney stones among women and men. Kidney Int 2001;59:2290–8.
[39] Danpure CJ. Oxalate metabolism and the primary hyperoxalurias. In: Rao NP, Kavanagh JP, Preminger GM, editors. Urinary tract stone disease. London: Springer-Verlag; 2011. p. 195–206.
[40] Daudon M, Hennequin C, Boujelben G, Lacour B, Jungers P. Serial crystalluria determination and the risk of recurrence in calcium stone formers. Kidney Int 2005;67:1934–43.
[41] De Yoreo J, Qiu R, Hoyer JR. Molecular modulation of calcium oxalate crystallization. Am J Physiol Renal Physiol 2006;291: F1123–32.
[42] Ettinger B, Citron JT, Livermore B, Dolman LI. Chlorthalidone reduces calcium oxalate calculous recurrence but magnesium hydroxide does not. J Urol 1988;139:679–84.
[43] Ettinger B, Pak CY, Citron JT, Thomas C, ms-Huet B, Vangessel A. Potassium-magnesium citrate is an effective prophylaxis against recurrent calcium oxalate nephrolithiasis. J Urol 1997;158:2069–73.
[44] Ettinger B, Tang A, Citron JT, Livermore B, Williams T. Randomized trial of allopurinol in the prevention of calcium oxalate calculi. N Engl J Med 1986;315:1386–9.
[45] Evan AE, Lingeman JE, Coe FL, Miller NL, Bledsoe SB, Sommer AJ, et al. Histopathology and surgical anatomy of patients with primary hyperparathyroidism and calcium phosphate stones. Kidney Int 2008;74:223–9.
[46] Evan AP, Bledsoe S, Worcester EM, Coe FL, Lingeman JE, Bergsland KJ. Renal inter-alpha-trypsin inhibitor heavy chain 3 increases in calcium oxalate stone-forming patients. Kidney Int 2007;72:1503–11.
[47] Evan AP, Coe FL, Gillen D, Lingeman JE, Bledsoe S, Worcester EM. Renal intratubular crystals and hyaluronan staining occur in stone formers with bypass surgery but not with idiopathic calcium oxalate stones. Anat Rec (Hoboken) 2008;291:325–34.
[48] Evan AP, Coe FL, Lingeman JE, Shao Y, Matlaga BR, Kim SC, et al. Renal crystal deposits and histopathology in patients with cystine stones. Kidney Int 2006;69:2227–35.
[49] Evan AP, Coe FL, Lingeman JE, Shao Y, Sommer AJ, Bledsoe SB, et al. Mechanism of formation of human calcium oxalate renal stones on Randall's plaque. Anat Rec (Hoboken) 2007;290: 1315–23.
[50] Evan AP, Coe FL, Rittling SR, Bledsoe SM, Shao Y, Lingeman JE, et al. Apatite plaque particles in inner medulla of kidneys of calcium oxalate stone formers: osteopontin localization. Kidney Int 2005;68:145–54.
[51] Evan AP, Lingeman J, Coe F, Shao Y, Miller N, Matlaga B, et al. Renal histopathology of stone-forming patients with distal renal tubular acidosis. Kidney Int 2007;71:795–801.
[52] Evan AP, Lingeman JE, Coe FL, Bledsoe SB, Sommer AJ, Williams Jr. JC, et al. Intra-tubular deposits, urine and stone composition are divergent in patients with ileostomy. Kidney Int 2009;76:1081–8.
[53] Evan AP, Lingeman JE, Coe FL, Parks JH, Bledsoe SB, Shao Y, et al. Randall's plaque of patients with nephrolithiasis begins in basement membranes of thin loops of Henle. J Clin Invest 2003;111:607–16.
[54] Evan AP, Lingeman JE, Coe FL, Shao Y, Parks JH, Bledsoe SB, et al. Crystal-associated nephropathy in patients with brushite nephrolithiasis. Kidney Int 2005;67:576–91.
[55] Evan AP, Lingeman JE, Worcester EM, Bledsoe SB, Sommer AJ, Williams Jr. JC, et al. Renal histopathology and crystal deposits in patients with small bowel resection and calcium oxalate stone disease. Kidney Int 2010;78:310–7.
[56] Favus MJ, Karnauskas AJ, Parks JH, Coe FL. Peripheral blood monocyte vitamin D receptor levels are elevated in patients with idiopathic hypercalciuria. J Clin Endocrinol Metab 2004;89:4937–43.
[57] Gambaro G, Vezzoli G, Casari G, Rampoldi L, D'Angelo A, Borghi L. Genetics of hypercalciuria and calcium nephrolithiasis: from the rare monogenic to the common polygenic forms. Am J Kidney Dis 2004;44:963–86.
[58] Gault MH, Chafe LL, Morgan JM, Parfrey PS, Harnett JD, Walsh EA, et al. Comparison of Patients with idiopathic calcium phosphate and calcium oxalate stones. Medicine 1991;70:345–58.
[59] Goldfarb DS, Coe FL, Asplin JR. Urinary cystine excretion and capacity in patients with cystinuria. Kidney Int 2006;69: 1041–7.
[60] Goldfarb DS, Fischer ME, Keich Y, Goldberg J. A twin study of genetic and dietary influences on nephrolithiasis: a report from the Vietnam Era Twin (VET) Registry. Kidney Int 2005;67: 1053–61.
[61] Gomes SA, dos Reis LM, Noronha IL, Jorgetti V, Heilberg IP. RANKL is a mediator of bone resorption in idiopathic hypercalciuria. Clin J Am Soc Nephrol 2008;3:1446–52.
[62] Grases F, Ramis M, Costa-Bauza A. Effects of phytate and pyrophosphate on brushite and hydroxyapatite crystallization. Urol Res 2000;28:136–40.
[63] Grases F, Genestar C, Conte A, March P, Costa-bauza A. Inhibitory effect of pyrophosphate, citrate, magnesium and chondroitan sulfate in calcium oxalate urolithiasis. Br J Urol 1989;64:235–7.
[64] Gray RW, Wilz DR, Caldas AE, Lemann Jr. J. The importance of phosphate in regulating plasma 1,25-(OH)2-vitamin D levels in humans: studies in healthy subjects in calcium-stone formers and in patients with primary hyperparathyroidism. J Clin Endocrinol Metab 1977;45:299–306.

[65] Greischar A, Nakagawa Y, Coe FL. Influence of urine pH and citrate concentration on the upper limit of metastability for calcium phosphate. J Urol 2003;169:867–70.
[66] Griffith DP, Khonsari F, Skurnick JH, James KE. A randomized trial of acetohydroxamic acid for the treatment prevention of infection-induced urinary stones in spinal cord injury patients. J Urol 1988;140:318–24.
[67] Grover PK, Ryall RL, Marshall VR. Effect of urate on calcium oxalate crystallization in human urine: evidence for a promotory role of hyperuricosuria in urolithiasis. Clin Sci 1990;79:9–15.
[68] Hamm LL, Alpern RJ. Regulation of acid-base balance, citrate, and urine pH. In: Coe FL, Favus MJ, Pak CYC, Parks JH, Preminger GM, editors. Kidney stones: medical and surgical management. Philadelphia: Lippincott-Raven; 1996. p. 289–302.
[69] Hatch M, Freel RW. Intestinal transport of an obdurate anion: oxalate. Urol Res 2005;33:1–16.
[70] Haussler MR, Baylink J, Hughes MR, et al. The assay of 1,25-dihydroxyvitamin D3: physiologic and pathologic modulation of circulating hormone levels. Clin Endocrinol Metab 1976;5:1512–652.
[71] Heilberg IP, Weisinger JR. Bone disease in idiopathic hypercalciuria. Curr Opin Nephrol Hypertens 2006;15:394–402.
[72] Herring LC. Observations on the analysis of ten thousand urinary calculus. J Urol 1962;88:545–55.
[73] Hess B, Nakagawa Y, Coe FL. Inhibition of calcium oxalate monohydrate crystal aggregation by urine proteins. Am J Physiol 1989;257:F99–106.
[74] Hiatt RA, Ettinger B, Caan B, Quesenberry CP, Duncan D, Citron JT. Randomized controlled trial of low animal protein, high fiber diet in the prevention of recurrent calcium oxalate kidney stones. Am J Epidemiol 1996;144:25–33.
[75] Holmes RP, Goodman HO, Assimos DG. Contribution of dietary oxalate to urinary oxalate excretion. Kidney Int 2001;59:270–6.
[76] Hoppe B, Beck BB, Milliner DS. The primary hyperoxalurias. Kidney Int 2009;75:1264–71.
[77] Howard SC, Jones DP, Pui CH. The tumor lysis syndrome. New England J Med 2011;364:1844–54.
[78] Jehle S, Zanetti A, Muser J, Hulter HN, Krapf R. Partial neutralization of the acidogenic Western diet with potassium citrate increases bone mass in postmenopausal women with osteopenia. J Am Soc Nephrol 2006;17:3213–22.
[79] Jiang Z, Asplin JR, Evan AP, Rajendran VM, Velazquez H, Nottoli TP, et al. Calcium oxalate urolithiasis in mice lacking anion transporter Slc26a6. Nat Genet 2006;38:474–8.
[80] Kaplan RA, Haussler MR, Deftos LJ, Bone H, Pak CY. The role of 1 alpha, 25-dihydroxyvitamin D in the mediation of intestinal hyperabsorption of calcium in primary hyperparathyroidism and absorptive hypercalciuria. J Clin Invest 1977;59:756–60.
[81] Kathpalia SC, Favus MJ, Coe FL. Evidence for size and charge permselectivity of rat ascending colon. Effects of ricinoleate and bile salts on oxalic acid and neutral sugar transport. J Clin Invest 1984;74:805–11.
[82] Kaufman DW, Kelly JP, Curhan GC, Anderson TE, Dretler SP, Preminger GM, et al. Oxalobacter formigenes may reduce the risk of calcium oxalate kidney stones. J Am Soc Nephrol 2008;19:1197–203.
[83] Kim SC, Coe FL, Tinmouth WW, Kuo RL, Paterson RF, Parks JH, et al. Stone formation is proportional to papillary surface coverage by Randall's plaque. J Urol 2005;173:117–9.
[84] Kok DJ, Papapoulos SE, Blomen LJ, Bijvoet OL. Modulation of calcium oxalate monohydrate crystallization kinetics in vitro. Kidney Int 1988;34:346–50.
[85] Kristensen C, Parks JH, Lindheimer M, Coe FL. Reduced glomerular filtration rate and hypercalciuria in primary struvite nephrolithiasis. Kidney Int 1987;32:749–53.
[86] Kuo RL, Lingeman JE, Evan AP, Paterson RF, Parks JH, Bledsoe SB, et al. Urine calcium and volume predict coverage of renal papilla by Randall's plaque. Kidney Int 2003;64:2150–4.
[87] Laerum E, Larsen S. Thiazide prophylaxis of urolithiasis: a double-blind study in general practice. Acta Med Scand 1984;215:383–9.
[88] Lemann Jr. J, Piering WF, Lennon EJ. Possible role of carbohydrate-induced calciuria in calcium oxalate kidney-stone formation. N Engl J Med 1969;280:232–7.
[89] Lemann Jr. J, Worcester EM, Gray RW. Hypercalciuria and stones. Am J Kidney Dis 1991;17:386–91.
[90] Lieske JC, Leonard R, Swift H, Toback FG. Adhesion of calcium oxalate monohydrate crystals to anionic sites on the surface of renal epithelial cells. Am J Physiol 1996;270:F192–9.
[91] Lingeman J, Kahnoski R, Mardis H, Goldfarb DS, Grasso M, Lacy S, et al. Divergence between stone composition and urine supersaturation: clinical and laboratory implications. J Urol 1999;161:1077–81.
[92] Liu Y, Mo L, Goldfarb DS, Evan AP, Liang F, Khan SR, et al. Progressive renal papillary calcification and ureteral stone formation in mice deficient for Tamm-Horsfall protein. Am J Physiol Renal Physiol 2010;299:F469–78.
[93] Maalouf NM, Cameron MA, Moe OW, Sakhaee K. Novel insights into the pathogenesis of uric acid nephrolithiasis. Curr Opin Nephrol Hypertens 2004;13:181–9.
[94] Maalouf NM, Sakhaee K, Parks JH, Coe FL, ms-Huet B, Pak CY. Association of urinary pH with body weight in nephrolithiasis. Kidney Int 2004;65:1422–5.
[95] Madore F, Stampfer MJ, Rimm EB, Curhan GC. Nephrolithiasis and risk of hypertension. Am J Hypertens 1998;11:46–53.
[96] Maierhofer WJ, Gray RW, Cheung HS, Lemann Jr. J. Bone resorption stimulated by elevated serum 1,25-(OH)2-vitamin D concentrations in healthy men. Kidney Int 1983;24:555–60.
[97] Malluche HH, Tschoepe W, Ritz E, Meyer-Sabellek W, Massry SG. Abnormal bone histology in idiopathic hypercalciuria. J Clin Endocrinol Metab 1980;50:654–8.
[98] Mandel NS, Mandel GS. Urinary tract stone disease in the United States veteran population. II. Geographical analysis of variations in composition. J Urol 1989;142:1516–21.
[99] Mandel NS, Mandel GS. Urinary tract stone disease in the United States veteran population. I. Geographic frequency of occurence. J Urol 1989;142:1513–5.
[100] Melton LJ, Crowson CS, Khosla S, Wilson DA, O'Fallon WM. Fracture risk among patients with urolithiasis: a population-based cohort study. Kidney Int 1998;53:459–64.
[101] Miller OF, Kane CJ. Time to stone passage for observed ureteral calculi: a guide for patient education. J Urol 1999;162:688–90.
[102] Miller NL, Gillen DL, Williams Jr. JC, Evan AP, Bledsoe SB, Coe FL, et al. A formal test of the hypothesis that idiopathic calcium oxalate stones grow on Randall's plaque. BJU Int 2009;103:966–71.
[103] Miller NL, Williams Jr. JC, Evan AP, Bledsoe SB, Coe FL, Worcester EM, et al. In idiopathic calcium oxalate stone-formers, unattached stones show evidence of having originated as attached stones on Randall's plaque. BJU Int 2010;105:242–5.
[104] Milliner DS, Eickholt JT, Bergstralh EJ, Wilson DM, Smith LH. Results of long-term treatment with orthophosphate and pyridoxine in patients with primary hyperoxaluria. N Engl J Med 1994;331:1553–8.

[105] Monico CG, Rossetti S, Schwanz HA, Olson JB, Lundquist PA, Dawson DB, et al. Comprehensive mutation screening in 55 probands with type 1 primary hyperoxaluria shows feasibility of a gene-based diagnosis. J Am Soc Nephrol 2007;18:1905–14.
[106] Muller D, Hoenderop JG, Vennekens R, Eggert P, Harangi F, Mehes K, et al. Epithelial Ca(2 +) channel (ECAC1) in autosomal dominant idiopathic hypercalciuria. Nephrol Dial Transplant 2002;17:1614–20.
[107] Nakagawa Y, Asplin JR, Goldfarb DS, Parks JH, Coe FL. Clinical use of cystine supersaturation measurements. J Urol 2000;164:1481–5.
[108] Nelson WK, Houghton SG, Milliner DS, Lieske JC, Sarr MG. Enteric hyperoxaluria, nephrolithiasis, and oxalate nephropathy: potentially serious and unappreciated complications of Roux-en-Y gastric bypass. Surg Obes Relat Dis 2005;1:481–5.
[109] Nicar MJ, Hill K, Pak CY. A simple technique for assessing the propensity for crystallization of calcium oxalate and brushite in urine from the increment in oxalate or calcium necessary to elicit precipitation. Metabolism 1983;32:906–10.
[110] Nicar MJ, Peterson R, Pak CY. Use of potassium citrate as potassium supplement during thiazide therapy of calcium nephrolithiasis. J Urol 1984;131:430–3.
[111] Nouvenne A, Meschi T, Guerra A, Allegri F, Prati B, Fiaccadori E, et al. Diet to reduce mild hyperoxaluria in patients with idiopathic calcium oxalate stone formation: a pilot study. Urology 2009;73:725–30.
[112] Pak CY, Fuller C, Sakhaee K, Zerwekh JE, Adams BV. Management of cystine nephrolithiasis with alpha-mercaptopropionylglycine. J Urol 1986;136:1003–8.
[113] Pak CY, ms-Huet B, Poindexter JR, Pearle MS, Peterson RD, Moe OW. Rapid communication: relative effect of urinary calcium and oxalate on saturation of calcium oxalate. Kidney Int 2004;66:2032–7.
[114] Pak CY, Peterson R, Sakhaee K, Fuller C, Preminger G, Reisch J. Correction of hypocitraturia and prevention of stone formation by combined thiazide and potassium citrate therapy in thiazide-unresponsive hypercalciuric nephrolithiasis. Am J Med 1985;79:284–8.
[115] Pak CYC, East DA, Sanzenbacher LJ, et al. Gastrointestinal calcium absorption in nephrolithiasis. J Clin Endocrinol Metab 1972;35:261–70.
[116] Parks JH, Coe FL. Evidence for durable kidney stone prevention over several decades. BJU Int 2009;103:1238–46.
[117] Parks JH, Coe FL. An increasing number of calcium oxalate stone events worsens treatment outcome. Kidney Int 1994;45:1722–30.
[118] Parks JH, Coe FL. Urine citrate and calcium in calcium nephrolithiasis. Adv Exp Med Biol 1986;208:445–9.
[119] Parks JH, Coe FL, Evan AP, Worcester EM. Urine pH in renal calcium stone formers who do and do not increase stone phosphate content with time. Nephrol Dial Transplant 2009;24:130–6.
[120] Parks JH, Coe FL, Evan AP, Worcester EM. Clinical and laboratory characteristics of calcium stone-formers with and without primary hyperparathyroidism. BJU Int 2009;103:670–8.
[121] Parks JH, Coward M, Coe FL. Correspondence between stone composition and urine supersaturation in nephrolithiasis. Kidney Int 1997;51:894–900.
[122] Parks JH, Worcester EM, Coe FL, Evan AP, Lingeman JE. Clinical implications of abundant calcium phosphate in routinely analyzed kidney stones. Kidney Int 2004;66:777–85.
[123] Parks JH, Worcester EM, O'Connor RC, Coe FL. Urine stone risk factors in nephrolithiasis patients with and without bowel disease. Kidney Int 2003;63:255–65.
[124] Penniston KL, Kaplon DM, Gould JC, Nakada SY. Gastric band placement for obesity is not associated with increased urinary risk of urolithiasis compared to bypass. J Urol 2009;182:2340–6.
[125] Pillay SN, Asplin JR, Coe FL. Evidence that calgranulin is produced by kidney cells and is an inhibitor of calcium oxalate crystallization. Am J Physiol 1998;275:F255–61.
[126] Quinn S, Bai M, Brown E. pH sensing by the calcium-sensing receptor. J Biol Chem 2004;36:37241–9.
[127] Rendina D, Mossetti G, Viceconti R, Sorrentino M, Castaldo R, Manno G, et al. Association between vitamin D receptor gene polymorphisms and fasting idiopathic hypercalciuria in recurrent stone-forming patients. Urology 2004;64:833–8.
[128] Rennie D. Guano in the renal pelvis (editorial). N Engl J Med 1979;300:361–2.
[129] Rimer JD, An Z, Zhu Z, Lee MH, Goldfarb DS, Wesson JA, et al. Crystal growth inhibitors for the prevention of L-cystine kidney stones through molecular design. Science 2010;330:337–41.
[130] Rule AD, Bergstralh EJ, Melton III LJ, Li X, Weaver AL, Lieske JC. Kidney stones and the risk for chronic kidney disease. Clin J Am Soc Nephrol 2009;4:804–11.
[131] Rule AD, Roger VL, Melton III LJ, Bergstralh EJ, Li X, Peyser PA, et al. Kidney stones associate with increased risk for myocardial infarction. J Am Soc Nephrol 2010;21:1641–4.
[132] Sakhaee K, Williams RH, Oh MS, Padalino P, ms-Huet B, Whitson P, et al. Alkali absorption and citrate excretion in calcium nephrolithiasis. J Bone Miner Res 1993;8:789–94.
[133] Schwille PO, Rumenapf G, Wolfel G, Kohler R. Urinary pyrophosphate in patients with recurrent urolithiasis and in healthy controls: a re evaluation. J Urol 1988;140:239–45.
[134] Sebastian A, Morris Jr. RC. Improved mineral balance and skeletal metabolism in postmenopausal women treated with potassium bicarbonate. N Engl J Med 1994;331:279.
[135] Shen FH, Baylink DJ, Nielsen RL, Sherrard DJ, Ivey JL, Haussler MR. Increased serum 1,25-dihydroxyvitamin D in idiopathic Hypercalciuria. J Lab Clin Med 1977;90:955–62.
[136] Shum DKY, Gohel MDI. Separate effects of urinary chondroitin sulphate and heparan sulphate on the crystallization of urinary calcium oxalate: differences between stone formers and normal control subjects. Clin Sci 1993;85:33–9.
[137] Sinha MK, Collazo-Clavell ML, Rule A, Milliner DS, Nelson W, Sarr MG, et al. Hyperoxaluric nephrolithiasis is a complication of Roux-en-Y gastric bypass surgery. Kidney Int 2007;72:100–7.
[138] Smith LH. Hyperoxaluric states. In: Coe FL, Favus MJ, editors. Disorders of bone and mineral metabolism. New York: Raven Press; 1992. p. 707–28.
[139] Smith LH, Fromm H, Hoffman AF. Acquired hyperoxaluria, nephrolithiasis and intestinal disease. N Engl J Med 1972;286:1371.
[140] Stamatelou KK, Francis ME, Jones CA, Nyberg LM, Curhan GC. Time trends in reported prevalence of kidney stones in the United States: 1976-1994. Kidney Int 2003;63: 1817–23.
[141] Stapleton AMF, Ryall RL. Blood coagulation proteins and urolithiasis are linked: crystal matrix protein is the F1 activation peptide of human prothrombin. Brit J Urol 1995;75: 712–9.
[142] Sutherland JW, Parks JH, Coe FL. Recurrence after a single renal stone in a community practice. Miner Electrolyte Metab 1985;11:267–9.
[143] Taylor EN, Curhan GC. Determinants of 24-hour urinary oxalate excretion. Clin J Am Soc Nephrol 2008;3:1453–60.
[144] Taylor EN, Stampfer MJ, Curhan GC. Diabetes mellitus and the risk of nephrolithiasis. Kidney Int 2005;68:1230–5.
[145] Taylor EN, Stampfer MJ, Curhan GC. Obesity, weight gain, and the risk of kidney stones. JAMA 2005;293:455–62.

[146] Taylor EN, Stampfer MJ, Mount DB, Curhan GC. DASH-style diet and 24-hour urine composition. Clin J Am Soc Nephrol 2010;5:2315–22.
[147] Trinchieri A, Lizzano R, Castelnuovo C, Zanetti G, Pisani E. Urinary patterns of patients with renal stones associated with chronic inflammatory bowel disease. Arch Ital Urol Androl 2002;74:61–4.
[148] Valenti G, Laera A, Gouraud S, Pace G, Aceto G, Penza R, et al. Low-calcium diet in hypercalciuric enuretic children restores AQP2 excretion and improves clinical symptoms. Am J Physiol Renal Physiol 2002;283:F895–903.
[149] von Unruh GE, Voss S, Sauerbruch T, Hesse A. Dependence of oxalate absorption on the daily calcium intake. J Am Soc Nephrol 2004;15:1567–73.
[150] Webster KE, Cramer SD. Genetic basis of primary hyperoxaluria type II. Mol Urol 2000;4:355–64.
[151] Weise WJ, Serrano FA, Fought J, Gennari FJ. Acute electrolyte and acid-base disorders in patients with ileostomies: a case series. Am J Kidney Dis 2008;52:494–500.
[152] Williams JJ, Rodman JS, Peterson CM. A randomized double blind study of acetohydroxamic acid in struvite nephrolithiasis. N Engl J Med 1984;311:760–4.
[153] Wills MR, Zisman E, Wortsman J, Evens RG, Pak CY, Bartter FC. The measurement of intestinal calcium absorption by external radioisotope counting: application to study of nephrolithiasis. Clin Sci 1970;39:95–106.
[154] Worcester EM, Coe FL. New insights into the pathogenesis of idiopathic hypercalciuria. Semin Nephrol 2008;28:120–32.
[155] Worcester EM, Coe FL, Evan AP, Bergsland KJ, Parks JH, Willis LR, et al. Evidence for increased postprandial distal nephron calcium delivery in hypercalciuric stone-forming patients. Am J Physiol Renal Physiol 2008;295:F1286–94.
[156] Worcester EM, Coe FL, Evan AP, Parks JH. Reduced renal function and benefits of treatment in cystinuria vs other forms of nephrolithiasis. BJU Int 2006;97:1285–90.
[157] Worcester EM, Evan AP, Coe FL. Disorders of renal calcium handling, urinary stones and nephrocalcinosis. In: Warrell D, Cox T, Firth J, editors. Oxford textbook of medicine. Oxford, U.K: Oxford University Press; 2010.
[158] Worcester EM, Gillen DL, Evan AP, Parks JH, Wright K, Trumbore L, et al. Evidence that postprandial reduction of renal calcium reabsorption mediates hypercalciuria of patients with calcium nephrolithiasis. Am J Physiol Renal Physiol 2007;292:F66–75.
[159] Worcester EM, Parks JH, Evan AP, Coe FL. Renal function in patients with nephrolithiasis. J Urol 2006;176:600–3.
[160] Yao J, Kathpalia P, Bushinsky DA, Favus MJ. Hyperresponsiveness of vitamin D receptor gene expression to 1,25-dihydroxyvitamin D3. A new characteristic of genetic hypercalciuric stone-forming rats. J Clin Invest 1998;101:2223–32.
[161] Zarse CA, McAteer JA, Tann M, Sommer AJ, Kim SC, Paterson RF, et al. Helical computed tomography accurately reports urinary stone composition using attenuation values: in vitro verification using high-resolution micro-computed tomography calibrated to fourier transform infrared microspectroscopy. Urology 2004;63:828–33.

This page intentionally left blank

CHAPTER

68

Proximal Tubular Handling of Phosphate

Heini Murer, Ian C. Forster, Nati Hernando, Jürg Biber

Institute of Physiology, University of Zürich-Irchel, Zürich, Switzerland

INTRODUCTION

The renal capacity to reabsorb inorganic phosphate ions ($H_2PO_4^-/HPO_4^{2-}$; abbreviated as Pi) is a major determinant of whole-body Pi homeostasis, which is required for normal cellular functions (e.g., energy metabolism and signaling mechanisms) and bone growth and remodeling. Consequently, urinary excretion of Pi is tightly controlled according to the body needs by a variety of hormones, diets, and metabolic factors.[1–4] Diverse pathophysiological conditions and genetic diseases that are manifested by an altered renal reabsorption of Pi have been described[6,7,40,50,185] (see also Chapter 69).

The basic concepts of the renal handling of Pi and the regulation of renal Pi excretion have been reviewed in a number of articles[1–5,12,177] to which the reader is referred for original publications not cited in this chapter. Here we will focus on sodium-dependent Pi cotransporters that are responsible for renal reabsorption of Pi and we will address the cellular mechanisms involved in the regulation of these cotransporter proteins.

PROXIMAL TUBULAR REABSORPTION OF PHOSPHATE

Under normal physiological and dietary conditions, approximately 80% of the filtered Pi is reabsorbed in the proximal tubules. Studies on isolated perfused proximal tubules and brush border membrane vesicles (BBMVs) isolated from the superficial or the deep kidney cortex indicated that the rates of Na-dependent Pi transport in convoluted tubules are approximately threefold higher than rates observed in straight tubules, which suggests intranephronal heterogeneity along the proximal segments S1, S2, and S3. In addition, there is evidence of an internephronal heterogeneity as the fractional delivery of Pi to the early distal tubules of juxtamedullary nephrons is smaller compared with that of superficial nephrons.[1]

There is no Pi reabsorption in the segments of the loop of Henle and Pi reabsorption along the distal part of the nephron remains controversial. Taking different methodological approaches and species differences into account, it appears that up to 10% of the filtered load may be handled by distal tubular segments, yet the molecular mechanisms are still unknown.

Apical Entry Step

Studies performed with isolated proximal tubules and BBMVs showed that the apical uptake of Pi is strictly dependent on the presence of sodium ions (i.e., occurs via secondary active, sodium-dependent transport mechanism(s): Na/Pi-cotransport). Furthermore, in all experimental systems, Na/Pi-cotransport activity is modulated by the extracellular pH, with higher uptake rates observed at more alkaline pH.[12]

Assuming a membrane potential of ≈ -65 mV, a stochiometry of overall Na/Pi cotransport of at least two sodium ions per one Pi ion and a concentration gradient for sodium of 10:1, the intracellular accumulation of Pi is found to be >100:1 (intra- versus extracellular). However, as indicated by nuclear magnetic resonance (NMR) studies, the intracellular Pi concentration may be assumed to be in the range of 0.7 to 1.8 mM.[55] As this concentration of Pi is far below the thermodynamic equilibrium, it follows that the driving

Seldin and Giebisch's The Kidney, Fifth Edition.
DOI: http://dx.doi.org/10.1016/B978-0-12-381462-3.00068-9

© 2013 Elsevier Inc. All rights reserved.

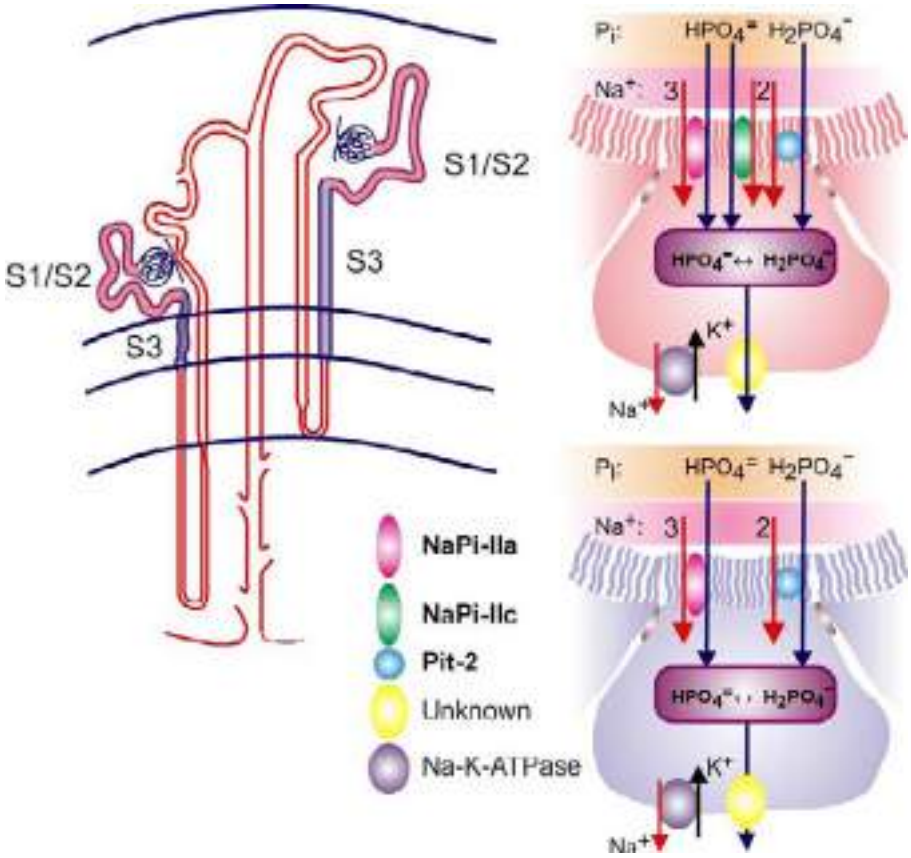

FIGURE 68.1 Na/Pi-cotransporters localized in the proximal tubular cells. In adults, uptake of filtered phosphate in the apical brush border membrane has been shown to be mediated mainly by NaPi-IIa and NaPi-IIc in the S1/S2 segments (pale pink) and NaPi-IIa in the S3 segments (pale blue). They transport preferably divalent Pi with different Na:Pi stoichiometries, as indicated. In addition PiT-2 is found in S1, S2 and S3 and transports preferably monovalent Pi. Its contribution to overall Pi transport is unclear, but has been shown to show a different regulatory time course from the SLC34 proteins in rodents. Furthermore, NaPi-IIa and NaPi-IIc represents the major target for the regulation of proximal tubular Pi reabsorption (see text). Compensation for Na^+ loading and altered membrane potential due to electrogenic transport by NaPi-IIa and PiT-2 is mediated by the Na-K-ATPase in the basolateral membrane. The basolateral Pi exit pathway has still not been identified.

forces for the apical entry step(s) of Pi are always in excess. Therefore, changes of the transport rates (due to changes on either the number of transport units or their kinetic properties. e.g., K_m) offer possibilities for an efficient regulation of the apical uptake of Pi. In fact, there is ample evidence showing that most regulatory factors that influence the overall proximal tubular Pi transport capacity (TmPi/GFR-tubular maximum for Pi reabsorption per unit of glomerular filtration rate) alter the abundance of apical Na/Pi-cotransporters.

Basolateral Exit of Phosphate

Exit of Pi at the basolateral side of the proximal tubular cell occurs down the electrochemical gradient of Pi. Transport of Pi through the basolateral membrane is not well understood and the corresponding Pi transporter proteins have not been identified. To maintain the intracellular Pi concentration high enough to sustain the intracellular metabolism, basolateral exit mechanisms are regarded as "controlled leak" pathways. Different mechanisms for the basolateral exit of Pi have been proposed, such as a phosphate/anion (bicarbonate) exchange or a sodium-independent, pathway.[12]

GENE PRODUCTS INVOLVED IN PROXIMAL TUBULAR PHOSPHATE REABSORPTION

Several mammalian membrane proteins have been cloned, which, after expression in oocytes of *Xenopus laevis*, mediate Na/Pi cotransport. These Na/Pi-cotransporters have been grouped into type I, type II, and type III Na/Pi-cotransporters and more recently were assigned to the solute carrier (SLC) families 17 (type I), 20 (type III), and 34 (type II).[16–19] Studies with Npt2 knockout mice and analysis of patients with hereditary hypophosphatemic rickets with hypercalciuria (HHRH) indicated that the type II Na/Pi-cotransporters are of major importance for proximal tubular reabsorption of Pi.[20,21,36,87] One member of the SLC20 family, PiT-2, has been localized at the BBM of proximal tubules as well, however its role in renal handling of Pi is however less clear.[23,25,37] Na/Pi-cotransporters localized at the apical membrane of proximal tubular cells are indicated in Figure 68.1.

The type I Na/Pi-cotransporter (NaPi-I, SLC17A1) was originally identified on the basis of its Na/Pi cotransport activity after expression in oocytes. Moreover, a number of findings have questioned its role in the renal handling of Pi-I besides acting as a

Na/Pi-cotransporter: i) NaPi-1 also exhibits anion channel activity; ii) Na/Pi-cotransport mediated by NaPi-I is not dependent on the pH; and iii) alterations of the renal handling of Pi could not be correlated with changes of NaPi-I protein content.[12,24]

The Type ll Na/Pi-Cotransporter Family SLC34

The Na/Pi-cotransporter family SLC34 comprises three members: type IIa/NaPi-IIa (SLC34A1), type IIb/NaPi-IIb (SLC34A2), and type IIc/NaPi-IIc (SLC34A3) NaPi-IIa and NaPi-IIc are expressed in the kidneys. Expression of NaPi-IIb has not been reported in the kidney but in a number of other epithelial and epithelial-like tissues, for example in small intestine, liver, testes and lung.[143] In the small intestine NaPi-IIb protein is localized at the apical membrane of enterocytes and, as demonstrated with a conditional mouse knock-out model, is involved in reabsorption of dietary Pi.[89,116]

NaPi-IIa (SLC34A1) has been cloned from renal tissues of different species. The human (NPT2; chromosome 5q35) and mouse genes (Npt2; chromosome 13) are approximately 16 kb in length and are arranged into 13 exons and 12 introns.[17–19,143] In promoter constructs analyzed so far, elements for transcriptional regulations by bicarbonate/CO_2 tension, vitamin D, and Pi deficiency have been detected. However, the physiological significance of transcriptional regulation of NaPi-IIa gene expression has not been established unequivocally.[12]

By reverse transcriptase-polymerase chain reaction (RT-PCR) and *in situ* hybridizations, expression of NaPi-IIa mRNA has been detected exclusively in the proximal tubules. This was confirmed by immunohistochemical analysis, which demonstrated that NaPi-IIa protein is restricted to the BBM of proximal tubular cells. By immunogold electron microscopy it was shown that NaPi-IIa cotransporters are evenly distributed along the whole length of the microvilli.[12,28] Under Pi balanced dietary conditions the abundance of the NaPi-IIa protein is usually stronger in proximal tubules of juxtamedullary nephrons and decreases gradually along the tubular axes.

NaPi-IIa consists of approximately 635 amino acids. On immunoblots this protein is detected between 80 and 100 kDa. Interestingly, after denaturation in the presence of reducing agents, two bands of approximately 45 and 50 kDa are observed, which is likely due to a proteolytic cleavage between the N-glycosylation sites contained within the extracellular loop between the transmembrane regions TM5 and TM6 (see Figure 68.2).[29] Separate expression of the cleavage products in oocytes of *X. laevis* oocytes did not result in Na/Pi cotransport activity, whereas after coexpression of both parts, Na/Pi cotransport could be restored[30,147] indicating that proteolytically cleaved NaPi-IIa-cotransporters are functional. Whether a fraction of the NaPi-IIa protein content in apical membranes is proteolytically processed *in vivo* or if cleavage occurs during the isolation of proximal tubular BBMV, is currently not known.

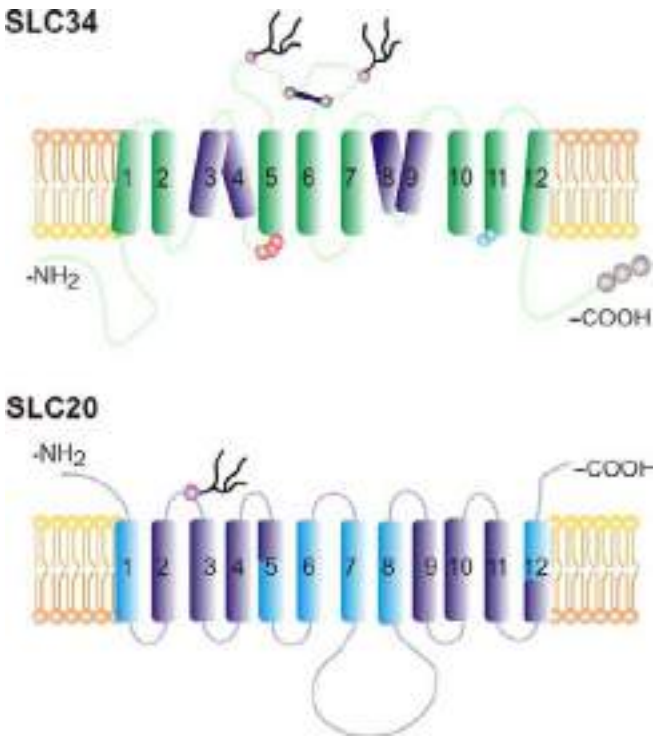

FIGURE 68.2 Topology models Na/Pi-cotransporters. Upper: SLC34 proteins (NaPi-IIa, NaPi-IIc) are predicted to comprise 12 transmembrane helices and intracellular N- and C-termini. A large extracellular loop between helices 5 and 6 contains two N-glycosylation sites (in NaPi-IIa) and a disulfide bridge, essential for correct function. The two halves of the protein, comprising helices 1–5 and 6–12 contain inverted repeat regions that include two putative re-entrant domains (purple: helices 3,4 and 8,9) that are thought to associate and form the transport pathway. In NaP_i-IIa, the dibasic KR motif (brown) was shown to be necessary for the responsiveness to parathyroid hormone. At the C-terminus, interaction with the PDZ proteins NHERF1 and PDZK1 occurs via the TRL C-terminal PDZ-binding motif (red). Three residues (AAD motif) responsible for conferring electrogenicity and a 3:1 Na:Pi stoichiometry for NaPi-IIa are also indicated (red). Lower: SLC20 proteins (PiT-1,2) are predicted to comprise 12 transmembrane helices and extracellular N- and C-termini. Two conserved inverted repeat domains are indicated (purple). There is one confirmed N-glycosylation site in the first extracellular loop of PiT-2.

Expression of NaPi-IIc (SLC34A3) has been detected in kidney, heart, spleen, and placenta. In kidneys, the largest amount of NaPi-IIc protein was detected in weaning animals; in adult mice, the abundance of this cotransporter is markedly decreased. On the basis of

these observations, NaPi-IIc has been referred as a "growth related Na/Pi-cotransporter".[167,174] In mouse and rat kidneys, NaPi-IIc was localized at the BBM of S1 and S2 segments but was not observed at the luminal membrane of S3 segments.[127]

Type III Na/Pi-Cotransporters Family SLC20

The retroviral receptors Glvr-1 (PiT-1) and Ram-1 (PiT-2) have been shown to induce Na/Pi-cotransport in oocytes of *X. laevis* and were assigned to the SLC20 Na/Pi-cotransporter protein family.[16,103]

Transcripts of PiT-1 and PiT-2 have been detected in many tissues, including kidney, small intestine, liver, lung, striated muscle, heart, and brain. In kidneys, expression of PiT-1/2 mRNA was observed in the cortex and medulla. It has been estimated that SLC20 mRNA accounts for only approximately 0.5% of total renal Na/Pi-cotransporter mRNA.[10]

In addition to NaPi-IIa and NaPi-IIc, PiT-2 (SLC20A2) has also been localized at the proximal tubular apical membrane as well[23,37] (Figure 68.1). No other nephron localization for PiT-2 is known so far. Although, by *in-situ* hybridization, PiT-1 mRNA has been detected throughout the entire renal tissue,[10] the localization of the PiT-1 protein remains to be determined.

Relative Roles of Na/Pi-Cotransporters in Renal Handling of Pi

Studies performed with knock-out mouse models and analysis of hereditary human diseases with hypophosphatemia suggested that the relative roles of NaPi-IIa and NaPi-IIc in renal reabsorption of Pi in rodents and humans might differ. In mice (and possibly all rodents) NaPi-lla appears to be of major importance whereas in humans the relative roles of NaPi-IIa and NaPi-IIc are less clear.

Mouse Studies

A central role of NaPi-IIa in the renal handling of Pi was demonstrated with mice in which the Npt2 (NaPi-IIa) gene was ablated.[20,22,36] Npt2 deficient mice show massive renal loss of Pi and consequently hypophosphatemia, as well as hypercalciuria due to elevated levels of 1,25-$(OH)_2$VitD3. Flux measurements performed with isolated BBMVs demonstrated that, compared with BBMV's of control mice, Na/Pi uptake was reduced by 70 to 80%. The remaining 20 to 30% of Na/Pi-cotransport activity was attributed to an up-regulation of NaPi-IIc.[163] In contrast, NaPi-IIc deficient mice did not develop hypophosphatemia or phosphaturia, and Na/Pi-cotransport in isolated BBMVs was unchanged.[176] NaPi-IIc$^{-/-}$ mice showed hypercalcemia and hypercalciuria due to elevated levels of 1,25-$(OH)_2$VitD3 suggesting a role of NaPi-IIc in calcium metabolism. In BBMVs isolated from kidneys of NaPi-IIa/NaPi-IIc double knock out mice still residual Na/Pi-cotransport was observed that is likely due to PiT-2. However, the overall role of PiT-2 in renal handling of Pi remains to be determined.

Human Studies

In a genome-wide study of a large prospective cohort NaPi-IIa has been found to be associated with serum concentration of Pi.[35] In fact, several mutations in the NaPi-IIa gene have been described in patients with hypercalciuria and elevated urinary Pi excretion. However, in all carriers, NaPi-IIa mutations were heterozygous and could not be correlated with hyperphosphaturia.[68,157] On the other hand, a homozygous duplication in the NaPi-IIa gene (I154_V160 dup) causes autosomal recessive Fanconi's syndrome and hypophosphytemic rickets.[148] Complete loss of function of this mutant due to the missorting of the mutated NaPi-IIa was observed in *in-vitro* studies. Compared to NaPi-IIa, a more critical role of NaPi-IIc in Pi homeostasis in humans has been become evident. In patients with HHRH several mutations have been mapped in the SLC34A3 gene.[21,104] Thus, these findings indicate that the function of NaPi-IIc in humans likely remains more important during adulthood compared to mice and may not be strongly dependent on growth.

Transport Mechanisms

SLC 34

Once correctly targeted to the membrane, NaPi-IIa/c transport characteristics are influenced only by changes in membrane potential (for NaPi-IIa) and external pH (for both NaPi-IIa and NaPi-IIc). So far, no evidence exists of post-translational modification of their kinetic properties. With constant pH and membrane potential, the transport capacity is therefore a direct function of the number of proteins present in the membrane. SLC34 protein membrane abundance is influenced by a variety of physiologically important regulatory factors (see below). NaPi-IIa and NaPi-IIc Na/Pi cotransport kinetics have been characterized in Sf9 cells and in *Xenopus* oocytes (by tracer uptake and electrophysiology).[14,46–48,53,54,67,69] Transport is Na^+-dependent and displays an apparent affinity constant for Pi typically <0.1 mM and an apparent affinity constant for Na^+ in the range 40−60 mM. Arsenate is the only other substrate known to be transported by the type IIa Na^+/Pi-cotransporters.[51]

It was established by means of heterologous expression in *Xenopus* oocytes that NaPi-IIa and NaPi-IIc preferentially transport divalent Pi (HPO_4^{2-}).[52,53,67] An important mechanistic difference between NaPi-IIa and NaPi-IIc is that transport activity for NaPi-IIa is electrogenic, whereas for NaPi-IIc it is electroneutral. Electrogenic NaPi-IIa translocates one net positive charge per transport cycle and the transport rate increases with membrane hyperpolarization, whereas electroneutral NaPi-IIc is insensitive to membrane potential and no net charge is translocated. This functional distinction is reflected in their respective Na^+:Pi stoichiometries- 3:1 for NaPi-IIa and 2:1 for NaPi-IIc.[52–54,67] It also follows that the theoretical Pi concentrating capacity is approximately 100-fold higher for NaPi-IIa, which, however implies a greater energetic cost to the cell resulting from Na^+ and charge accumulation. The preference for divalent Pi explains, in part, the strong dependence on external pH that would result from the titration of Pi species. In addition, protons can act directly on the transporter protein by competing with Na^+ binding and modulating conformational changes associated with the empty carrier states.[47,48]

The loading of NaPi-IIa and NaPi-IIc proteins with substrates is proposed to be ordered. Biophysical studies (presteady-state analysis and voltage clamp fluorometry) have established that two Na^+ ions bind sequentially and cooperatively before phosphate.[14,56] A third Na^+ binding transition precedes a rate-limiting reorientation of the fully loaded carrier. The order of substrate release at the cytosol is unknown. For NaPi-IIc, one of the two Na^+ ions, which confers electrogenicity to NaPi-IIa, can still interact with the protein but is not cotransported.[67]

Transport by NaPi-IIa and NaPi-IIc is blocked by the competitive inhibitor phosphonoformic acid or foscarnet (PFA) with a reported inhibition constant $\approx 0.4–0.6$ mM.[46,182] PFA itself is not transported. Several other inhibitors of type IIb Na/Pi-cotransporters with significantly lower inhibitory constants than PFA have been reported.[59] These possibly act in a noncompetitive manner on NaPi-II proteins and a phosphophloretin compound was reported to exhibit inhibition at micromolar concentrations[32] although its efficacy on heterologously expressed NaPi-II-cotransporters is unknown.

In addition to the cotransport-related current, two other currents related to the expressed protein can be observed for the electrogenic NaPi-IIa under voltage clamp: a cation leak that is active in the absence of Pi, and presteady-state currents. The leak is proposed to be mediated by the translocation of a single Na^+ ion per cycle at a rate <10% of the cotransport mode.[61] It is unlikely to have physiological consequences, because Pi is normally present at sufficiently high concentrations to ensure that cotransport mode dominates and it is not observed in the electro-neutral NaPi-IIc.[52] However, naturally occurring mutations in NaPi-IIc are reported to result in a significant Na^+-leak, which illustrates how minor changes in the amino acid composition can have profound effects on function and important clinical consequences for phosphate homeostasis.[104] Presteady-state current relaxations, induced by rapid changes in membrane voltage reflect nonlinear charge movements associated with the electrogenic NaPi-IIa.[47,48] Detailed study of their properties led to the identification and quantification of voltage-dependent steps in the transport cycle (namely the voltage-dependent reorientation of the empty carrier and the first Na^+ binding step) and estimations of the transport or turnover rate (number of Pi molecules translocated per second per protein), to be $\approx 10\ s^{-1}$ (e.g., see Table 2 in Ref 67).

SLC20

The two known mammalian isoforms of SLC20 proteins (PiT-1, SLC20A1 and PiT-2, SLC20A2) were originally identified as retroviral receptors Glvr-1 and Ram-1, respectively. They were later shown to be Na^+-coupled Pi transporters and the electrogenicity and basic kinetics of transport characterized.[103] It became apparent from these and other studies, e.g.,[63,64] that SLC20 proteins were functionally distinct from SLC34 transporters and the differences were underscored in an electrophysiological characterization of PiT-1 transport kinetics.[9] The most important kinetic parameter that distinguishes SLC20 from SLC34 proteins is that the former preferentially transport monovalent Pi ($H_2PO_4^-$) with a 2:1 Na^+:Pi stoichiometry.[9] Like SLC34 proteins, the apparent affinities for Pi and Na^+ are also typically $\leq 100\ \mu M$ and ≈ 50 mM, respectively. Another kinetic property that distinguishes SLC34 and SLC20 proteins is the weaker sensitivity to pH in the latter case: for PiT-1 the maximum transport rate is relatively constant over a 3 pH units and the apparent Pi affinity decreases only at pH <6. The preference for monovalent Pi and insensitivity of transport kinetics to reduced pH would allow SLC20 proteins to transport Pi under conditions where SLC34 proteins are functionally compromised. Unlike SLC34 proteins that are considered exclusively Na^+ driven, it was shown that Li^+ can replace Na^+ as the driving cation for PiT-1, albeit with a reduced transport rate.[9] Furthermore, in the absence of Na^+, lowering pH from 7.5 to 6.0 induces significant Pi uptake in *Xenopus* oocytes that expressed PiT-2. It has been proposed that H^+ may also substitute for Na^+ for this isoform.[64,66] PFA is a weak inhibitor of PiT-1,2 mediated transport activity[66] and to date no specific inhibitors for SLC20 have been

reported. Kinetic studies suggest that Na^+ is the first ion to interact followed by a random binding of Na^+ and Pi.[9] Finally, in contrast to SLC34 proteins in which the final translocation of substrates is assumed electroneutral, this partial reaction of the transport cycle may confer electrogenicity to PiT-1,2.[67]

Structure-Function Relationships

SLC 34

The current model of the secondary structure of the type II Na/Pi-cotransporter is depicted in Figure 68.2 and predicts 12 transmembrane domains (TMDs) and cytoplasmically oriented N- and C-termini, the intracellular localization of which has been verified by epitope tagging and *in vitro* glycosylation assays.[8] In this model, TMDs 1 to 5 are separated, from TMDs 6 to 12 by a large extracellular loop that contains two N-glycosylation sites. This loop also contains one essential disulfide bridge; a second bridge has also been proposed that possible links TMD 5 to TMD 11.[70] Both bridges are thought to be important for defining final folding of the membrane-bound protein. The large extracellular loop and the N- and C-termini represent the greatest source of variation between species.[18] The C-termini is important for targeting and protein-protein interactions. For example, the TRL motif in the C-terminus plays a role as a PDZ binding motif and a KR motif located in an intracellular linker region (Figures 68.2 and 68.3) is critical for PTH sensitivity (see below). In contrast, the central "core" of TMDs shows a high degree of residue similarity or identity, and is largely conserved even in bacterial homologs, which suggests its importance in defining the transport characteristics.[18,19] Given that the electrogenic (NaPi-IIa) and electroneutral (NaPi-IIc) isoforms share the same substrate specificities and preference for divalent Pi,[67] this suggests that structural features that determine substrate recognition and translocation are similar. Substituted cysteine accessibility mutagenesis assays have provided additional insight into the membrane topology and strongly suggest that the transport pathway is likely formed by two inverted repeat segments comprising TMDs 3 and 4 and TMDs 7 and 8.[71–73] It was also established that the NaPi-IIa functional unit is a monomer[31] although evidence from biochemical studies[75] and using the split ubiquitin approach[101] and freeze fracture of *Xenopus* oocyte membranes containing the expressed transporter[77] suggest that dimerization is likely. Close comparison of the NaPi-IIa and NaPi-IIc sequences has revealed one region between the predicted TMD3 and TMD4 that contains specific residues important for conferring electrogenicity and defining the transport stoichiometry.[52]

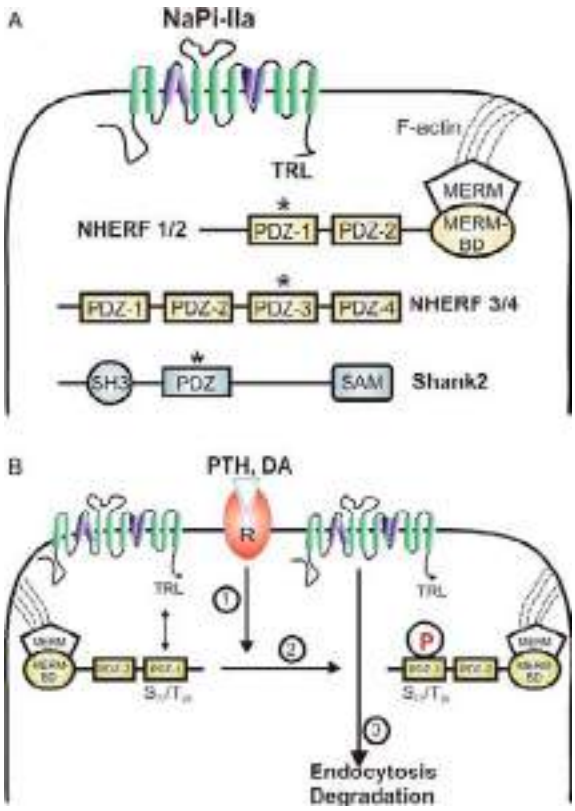

FIGURE 68.3 A: Interaction of NaPi-IIa with PDZ-proteins. NaPi-IIa interacts with the 4 members of the NHERF family (NHERF1–4) as well as with Shank2E. All these proteins are located at the brush border membrane (BBM) or in close proximity. The asterisks indicate which PDZ domains are engaged in association with NaPi-IIa. Other domains are: The Src Homology 3 (SH3), Merlin-Ezrin-Radixin-Moesin (MERM), MERM-binding domain (MERM-BD) and sterile alpha motif (SAM). B: The association of NaPi-IIa with NHERF1 is regulated by several hormones through a mechanism that involves phosphorylation of NHERF1. Parathyroidhormne (PTH) as well as dopamine (DA) treatment induces endocytosis of NaPi-IIa without altering the expression of NHERF1. Binding of these hormones to their receptors (R) triggers an intracellular signal (step 1) that leads to phosphorylation of two residues located within the first PDZ-domain of NHERF1: serine-77 and threonine-95 (step 2). This phosphorylation destabilizes the association of NaPi-IIa with NHERF1, thus allowing the removal of NaPi-IIa from the brush border membrane (step 3); in contrast, NHERF1 remains anchored to the apical cytoskeleton via its MERM-binding domain. Internalized NaPi-IIa is finally degraded in lysosomes.

The functional importance of these residues was confirmed experimentally.[52,78]

SLC20

Like SLC34 proteins, their current topology is predicted to comprise 12 TMDs but with extracellular N- and C-terminal tails (Figure 68.2). Also like SLC34 cotransporters, the structure of SLC20 proteins contains an inverted repeat architecture. This topology is

suggested by bioinformatic predictions, epitope tagging, cysteine scanning and *in vitro* glycosylation studies, e.g.,[67,79,132] Several studies have focussed on identifying the viral receptor domains, which has led to further insight into the secondary structure of PiT's.[81,82] For example, the large intracellular domain and associated TMDs have been removed and shown not to be required for retroviral recognition,[81] although it is unknown if the transport function was compromised. PiT-1 and PiT-2 differ in the location of their virus binding sites: for PiT-2 this has been identified in the first extracellular loop, whereas that for PiT-1, has been suggested to be in the fourth extracellular loop[81,82,88] (Figure 68.2).

PROTEIN-PROTEIN INTERACTIONS OF TYPE II NA/PI-CO-TRANSPORTERS

Intracellular sorting, hormonal regulation and stability at the plasma membrane of a given protein may be controlled via its association with interacting partners. By Yeast-two hybrid screens several proteins have been identified that interact with NaPi-IIa and NaPi-IIc. No proteins that may interact with the PiT-2 transporter have been identified so far.

NaPi-IIa Associated Proteins

NaPi-IIa interacts, among others, with several PDZ domain-containing proteins, namely the four members of the NHERF family[76,84,91,101] and Shank2E[26] (Figure 68.3). Importantly, these five proteins are located either at the renal proximal BBM (NHERF1, NHERF3 and Shank2E) or in its close proximity (NHERF2, NHERF4).[84,159]

PDZ domains are modules involved in protein-protein interactions, and are widely expressed across philia (for review see [62]). They consist of 80 to 100 amino acids distributed in six β strands (βA−βF) and two α helices (αA−αB). PDZ domains typically bind to the C-terminus (PDZ-binding motif) of their interacting partners, via a conserved motif (R/K-XXX-G-ϕ-G-ϕ, where X is any amino acid and ϕ is a hydrophobic residue) located between helix αB and strand βB. NHERF1 and NHERF2 consist of two PDZ domains and a C-terminal sequence that interacts with actin-binding proteins from the Ezrin-Radisin-Moesin (ERM) family[65,159] (Figure 68.3). NHERF3 and NHERF4 contain 4 PDZ domains but lack the ERM-binding domain, whereas Shank2E contains six ankyrin repeats, one SH3 domain and a single PDZ domain (Figure 68.3). The presence of multiple interacting domains within each of these proteins, together with their ability to form homo or heterodimers, opens the possibility for the formation of multiprotein complexes that can bring together regulatory and target proteins. Indeed, in addition to NaPi-IIa and several other renal transporters, NHERF1 and NHERF2 also interact with other proteins involved in Pi homeostasis, such as the parathyroid hormone receptor (PTHR), phospholipase Cβ and small G-proteins.[90] Similarly, NHERF3 interacts with several renal transporters as well as with the Ste20-related serine/threonine protein kinase (SLK) and the Dual-specific A-kinase anchoring protein 2 (D-AKAP2).[76] Shank2 associates with several renal transporters and with the F-binding proteins cortactin, α-fodrin, and Abp1.[92]

Biochemical studies indicated that the interaction of NaPi-IIa with PDZ-proteins requires the presence of the last three amino acid residues (TRL) and involves particular PDZ domains within the NHERFs.[91] NaPi-IIa interacts with the first PDZ domain of NHERF1, and this interaction is hormonally regulated by a mechanism that involves phosphorylation of NHERF1 (see below).[94,95,113,114] The absence of NHERF1, or preventing its association with NaPi-IIa, leads to mislocalization of the cotransporter.[86,93,171] Thus, NHERF1 deficient mice are characterized by hyperphosphaturia due to reduced expression of NaPi-IIa in the BBM.[86] As the proximal BBM is heavily enriched in actin, the molecular mechanism by which NHERF1 controls the apical expression of NaPi-IIa may rely on the ability of NHERF1 to bind to the actin cytoskeleton via its ERM-binding domain.[159] Despite being phosphaturic, NHERF1 deficient mice are normophosphatemic,[86] suggesting a compensatory extra-renal mechanism. Normal phosphaturia and normal apical expression of NaPi-IIa has been observed in NHERF2$^{-/-}$ mice.[98,159]

NHERF3, previously known as PDZK1, also colocalizes with NaPi-IIa at the BBM of proximal tubules.[76] Unlike NHERF1, NHERF3 does not have a domain able to bind to the actin cytoskeleton. However, its presence at the proximal BBM may be explained by its ability to heterodimerize with NHERF1.[76,91] Nevertheless, the physiological role of the interaction of NHERF3 with NaPi-IIa remains unknown, since the absence of NHERF3 does not affect neither the expression nor the regulation of NaPi-IIa.[11,99]

NaPi-IIc Associated Proteins

NaPi-IIc interacts with NHERF1 and NHERF3, but not with the other PDZ-proteins that associate with NaPi-IIa.[135] However, NaPi-IIc does not contain a typical C-terminal PDZ-binding motif, and the molecular domains involved in the interactions are different from those of NaPi-IIa. In contrast to NaPi-lla,[99] chronic

adaptation of NaPi-llc to a low Pi-diet is impaired in PDZK1 deficient mice.[49]

REGULATION OF PROXIMAL TUBULAR REABSORPTION OF PI

The extent of the renal proximal tubular reabsorption of Pi is regulated by a variety of hormones, diets, and metabolic factors and several hereditary and acquired disorders have been shown to result in disturbances of renal clearance of Pi.[1,2,4,6,12,177] Most physiological and pathophysiological alterations of proximal Pi reabsorption can be explained by changes of apical Na/Pi-cotransport activity that is due to an alteration of abundances of Na/Pi-cotransporters NaPi-IIa, NaPi-IIc and PiT-2. Alternative modes for the regulation of Na/Pi-cotransporters, such as by changes of the membrane lipid composition (see below), have been proposed as well.

A reduction of the number of type II Na/Pi-cotransporters is achieved by endocytic retrieval at the intermicrovillar clefts (Figure 68.3). Endocytosis of NaPi-IIa occurs by receptor-mediated endocytosis involving clathrin-coated vesicles.[28] Results obtained with kidney-specific megalin knockout mice are also in accord with this notion. In proximal tubules of these mice, the endocytotic machinery was severely impaired and the apical abundance and rate of endocytosis of NaPi-IIa were reduced.[102] In contrast to NaPi-IIa, NaPi-IIb (transfected into OK cells) is not regulated by PTH. On the basis of chimera constructs made between the NaPi-IIa and the NaPi-IIb proteins, a dibasic amino-acid motif (RK or RR) contained in an intracellular loop (Figure 68.2) was identified and demonstrated to be required for the PTH responsiveness of NaPi-IIa.[184] A yeast two-hybrid screen performed against this intracellular loop identified PEX19, a peroxisomal farnesylated protein, as an additional NaPi-IIa associated protein.[151] Although PEX19 interacts with AP2, it remains to be shown if PEX19 provides a link between NaPi-IIa and the endocytotic machinery.

After its internalization, NaPi-IIa is associated with early endosomes and subsequently routed to lysosomes and degraded.[12,28] In contrast, although initially associated with clathrin-coated vesicles, internalized NaPi-IIc has not been detected in the early endosomes and was not degraded in the lysosomes.[105] Therefore, it was proposed that, under acute regulatory conditions, internalized NaPi-IIc, in contrast to the NaPi-IIa isoform, may be able to recycle back to the membrane.

Little is known about the recovery of NaPi-IIa proteins after PTH-induced internalization and lysosomal degradation. In a study performed with rats, it was shown that after PTH stimulation, the recovery of urinary excretion of Pi and the apical abundance of the NaPi-IIa did not parallel in time. Three hours after PTH injection, renal Pi excretion was normalized, whereas the abundance of the NaPi-IIa protein was still reduced.[139] Based on in vitro experiments, *de novo* protein synthesis is required for the recovery of NaPi-IIa.[12]

Parathyroid Hormone

Although the main signal activating parathyroid hormone (PTH) secretion is a reduction in the circulating levels of calcium, there is also evidence suggesting that the parathyroid gland responds to changes in circulating Pi.[5] PTH reduces renal reabsorption of Pi by inhibiting proximal Na/Pi-cotransport. PTH receptors (PTHR) belong to the family of G-protein coupled receptors, and within the renal proximal tubule are localized at the apical and basolateral membranes.[109,164] Binding of PTH to the apical PTHR results predominantly in an activation of PLC and subsequent stimulation of protein kinase C (PKC) pathways. In contrast, binding of PTH to basolateral receptors leads preferentially to activation of adenyl cyclase, and via cyclic AMP (cAMP), to stimulation of protein kinase A (PKA). The effect of basolateral PTHR on Pi transport may be modulated by the calcium sensing receptor.[110]

The phosphaturic effect of PTH is achieved by promoting endocytosis of NaPi-IIa followed by its lysosomal degradation, thus resulting in a reduced amount of cotransporters at the BBM.[12,28,77] This effect is detected within minutes upon PTH administration, and was reproducible in different animal and cellular models. In isolated proximal tubules, agonist binding to apical and basolateral PTHR results in internalization and degradation of NaPi-IIa, which suggests that activation of both PKC and PKA pathways trigger endocytosis of NaPi-IIa.[28,164] However, recent studies using modified PTH analogs indicate that PKA signaling represents the predominant pathway.[13] Both signaling cascades seem to involve MAP kinases ERK1/2.[28] PTH also seems to reduce the apical abundance of NaPi-IIc and PiT-2.[105,127] However, both effects are considerably slower than the regulation of NaPi-IIa. Although endocytosed NaPi-IIc undergoes degradation, this process does not take place in lysosomes.[105] Thus, it appears that upon removal from the BBM NaPi-IIa and NaPi-IIc are not targeted to the same intracellular compartment.

PTH does not induce internalization of the NaPi-IIa interacting proteins NHERF1 and NHERF3.[93] This suggests that the association of NaPi-IIa with these partners may be hormonally regulated by an on/off mechanism. NHERF1 and NHERF3 are

phosphorylated in basal conditions.[93,159] Several kinases, including GRK6A, PKC, PKA and Cdc2, are known to phosphorylate NHERF1. Moreover, incubation with PTH or pharmacological stimulation of PKA and PKC results in NHERF1 hyperphosphorylation. Serine-77 and threonine-95 were identified as the residues phosphorylated in response to PTH.[94,95,113] Both amino acids are located within the first PDZ domain of NHERF1, i.e., the domain engaged in interaction with NaPi-IIa. This modification destabilizes the association of NaPi-IIa with NHERF1, allowing the retrieval of the cotransporter from the BBM.[114] Current data suggest that NaPi-IIa is not a phosphoprotein, either in basal conditions or upon PTH administration.[93]

NHERF1 interacts with apical PTHR as well as with PLCβ.[43,115] The presence of an apical complex consisting of NHERF1, PTHR and PLCβ plays a critical role on the regulation of NaPi-IIa. Thus, endocytosis of NaPi-IIa after stimulation of apical PTHR is impaired in proximal tubules of NHERF1-deficient mice.[117] This effect could not be explained by a general impairment of the endocytic machinery, since the internalization of the NaPi-IIa in response to pharmacological activation of PKC or PKA was normal. Instead, it seems to be due to the inability of the NHERF1-deficient tubules to properly activate PLC in response to PTH administration.

NHERF1 and NHERF3 also interact with the PKA anchoring proteins ezrin and D-AKAP2, respectively.[76,91] However, such a close spatial arrangement of PKA with NaPi-IIa appears not to be required for the regulation of the cotransporter, since the endocytosis of NaPi-IIa induced via the PKA signaling pathway is normal in NHERF1 as well as PDZK1-deficient mice.[99,117]

Dopamine

The cells of the proximal tubule have the ability to produce dopamine (DA), and this intrarenal production is stimulated in response to high dietary Pi.[15,118,119] The DA receptors are G-protein coupled receptors that act by stimulating (D1-like) or inhibiting (D2-like) adenylyl cyclase.[120] DA exerts a phosphaturic effect which, as in the case of PTH, is achieved by reducing the expression of NaPi-IIa at the BBM.[121] Pharmacological experiments in isolated proximal tubules indicated that agonist binding to apical (but not to basolateral) D1-like receptors results in internalization of NaPi-IIa.[121] Furthermore, this effect was blunted by PKA inhibitors but not by inhibitors of PKC or ERK1/2. This suggests that PTH and dopamine down-regulate NaPi-IIa via independent pathways.

Similar to the PTHR, D1-like receptors interact with NHERF1 and this interaction seems to be crucial for the DA-induced downregulation of NaPi-IIa.[94] Indeed DA failed to downregulate NaPi-IIa in NHERF1-deficient mice, an observation that associates with the inability of DA to stimulate either cAMP accumulation or PKC activity.[94] Furthermore, DA administration results in phosphorylation of NHERF1 at the same sites than PTH does (serine-77 and threonine-95).[113] Thus, endocytosis of NaPi-IIa in response to either PTH or DA requires previous destabilization of the association between the cotransporter and NHERF1.

Phosphatonins

Hereditary and acquired disorders such as X-linked hypophosphatemia (XHL), autosomal hypophosphatemic rickets [ADHR), and oncogenic hypophosphatemic osteomalacia (OHO) show hypophosphatemia due to increased renal wasting of Pi.[6,7] These disorders led to the identification of several factors (phosphatonins) such as fibroblast growth factor-23 (FGF23), secreted frizzled related protein-4 (sFRP4), and matrix extracellular phosphoglycoprotein (MEPE).[42,80,122,129,168]

FGF23 is produced and secreted in bones by osteoblasts/osteocytes.[124] Both serum concentrations of Pi and 1.25-$[OH]_2$VitD3 stimulate secretion of FGF23.[27,60,97,125,126,128] The phosphaturic effect of FGF23 is explained by reduction of the apical abundances of NaPi-IIa and NaPi-IIc. Accordingly, FGF23 deficient mice are hyperphosphatemic and show elevated serum levels of 1,25-$[OH]_2$VitD3.[108,128] As expected, FGF23 transgenic mice show phosphaturia that correlates with reduced amounts of both NaPi-IIa and NaPi-IIc proteins.[134] Similarly, overexpression of FGF23 and *in vitro* treatment of isolated proximal tubules reduce the abundances of NaPi-IIa, NaPi-IIc and PiT2.[22,131,178] Cellular mechanisms leading to altered abundances of apical Na/Pi-cotransporters by FGF23 are not known. Klotho is required as a cofactor for the cellular effect of FGF23 via its receptor FGFR1c.[111,131,134,192] Additionally to its function as a cofactor, Klotho may act directly on Na/Pi-cotransporters by modifying sugar residues and thereby altering transport rates.[96]

Injection of sFRP-4 elicits a decrease of NaPi-IIa abundance and an increase of Pi excretion.[137] Observed altered phosphorylation of beta-catenin indicates a mechanism involving Wnt-signaling pathway upstream to down-regulation of NaPi-IIa by sFRP-4.[137]

MEPE, a member of the SIBLING (short integrin-binding ligand interacting glycoprotein) protein family, is primarily expressed in bone cells. The phosphaturic action of MEPE is paralleled by a decrease of NaPi-IIa protein abundance.[138]

Atrial Natriuretic Factor/Nitric Oxide

The atrial natriuretic factor (ANF) and nitric oxide (NO) have been described to regulate proximal

tubular Na/Pi-cotransport.[1,4,12,177] Studies on isolated tubules demonstrated that these factors lead to a reduction (via endocytosis) of the content of NaPi-IIa in the apical membrane, via an activation of protein kinase G.[140]

Dietary Phosphate Content

The dietary content of Pi is a potent regulator of proximal tubular Pi reabsorption and its effect has been extensively studied by micropuncture/microperfusion experiments and using isolated BBMVs.[38,153] The content of Pi in the diet provokes altered rates of apical Na/Pi-cotransport; no changes of the apparent K_m value for Pi have been described. To a large extent, this adaptive phenomenon is independent of PTH, 1.25-$[OH]_2$VitD3, growth hormone, or plasma calcium.[4,12] The effects of changes in the dietary content of Pi on the rate of apical Na/Pi-cotransport and the abundances of Na/Pi-cotransporters are observed within two to four hours (acute adaptation).[141,142,153] The physiological signaling mechanisms involved in this adaptive phenomenon are poorly understood. It remains to be shown if hypophosphatemia is sensed directly by the proximal tubules or eventually at other sites such as in the central nervous system[149] or in the small intestine.[116,144] Of interest, after gavage of Pi to the upper small intestine of rats, urinary excretion of Pi increased within 15 minutes and was independent of PTH, FGF23 and altered serum Pi concentration. Based on these observations it has been postulated that a (yet unknown) phosphaturic factor is released from small intestinal mucosa due to an activation of one or more phosphate sensing mechanisms.[100,144]

Intake of diets of different contents of Pi alters the abundances of NaPi-IIa, NaPi-IIc and PiT-2, yet with different half-times of responses.[23,25] The fastest response is observed for NaPi-IIa ($t_{1/2} \approx 1$ hr), followed by PiT-2 ($t_{1/2} \approx 8$ hrs) and NaPi-IIc ($t_{1/2}2 \approx 24$ hrs). The acute (within two hours) upregulation of NaPi-IIa was shown to be independent of protein synthesis,[12] and an important role of the microtubules has been suggested on the basis of the blockage of the adaptive response by colchicine.[12] High-Pi diet leads to an internalization of NaPi-IIa, which is followed by degradation in the lysosomes.[12] High-Pi diet also promotes an internalization of the NaPi-IIc, however no lysosomal degradation of the NaPi-IIc protein was observed.[39]

In agreement with the role of NHERF1 in the apical positioning of NaPi-IIa, upregulation of this cotransporter by low-Pi diet was slightly impaired in NHERF1-deficient mice.[146] Although NaPi-IIa strongly interacts with NHERF3 (PDZK1), its adaptation to dietary Pi is not impaired in NHERF3 $^{-/-}$ mice.[99] In contrast, dietary regulation of NaPi-IIc is blunted in the absence of NHERF3.[49]

In adult mice, adaptation of the NaPi-IIa protein to a low-Pi diet was not paralleled by a change of the NaPi-IIa mRNA, whereas in weaning animals, an increase of NaPi-IIa mRNA has been reported. In contrast, NaPi-IIc mRNA has been shown to be upregulated by a low-Pi diet in all development stages.[45] Enhanced transcription of type II Na/Pi-cotransporter mRNA induced by a low-Pi diet may be explained by an enhanced binding of the transcription factor TFE3 to a phosphate response element contained within the promoter regions of the NaPi-IIa and NaPi-IIc gene.[150] In a mouse model deficient in the phosphatase calcineurin Aα, the level of NaPi-IIa mRNA was reduced and the adaptive effect of a low-Pi diet was blunted.[155]

Regulation by Lipids/Potassium Depletion

In addition to changes in the number of NaPi-IIa proteins, alterations in the proximal tubular Pi reabsorption, such as those observed after adaptation by a low-Pi diet or potassium depletion, have been proposed to correlate with changes in the membrane lipid composition including cholesterol, shingomyelin, and glycoshingolipids.[44,130,142,145,156] Furthermore, thyroid hormone status was shown to modulate Na/Pi-cotransport and the cholesterol/phospholipids ratio in proximal tubular apical membranes.[165]

Potassium depletion provokes increased urinary excretion of Pi, and BBMVs isolated from potassium-depleted rats exhibited decreased Na/Pi-cotransport. Decreased Na/Pi-cotransport in BBMV's was explained by a reduction of the abundance of NaPi-IIc and PiT-2, but not of NaPi-IIa protiens. Paradoxically, the abundance of NaPi-IIa is upregulated by potassium depletion.[37]

Fasting/Diabetes

Fasting increases urinary Pi excretion, which is due to a decrease of tubular reabsorption of Pi. Northern blot analysis indicated that fasting for 48 hours did not result in a decrease of renal expression of NaPi-IIa or NaPi III mRNA.[154]

Insulin stimulates BBM Na/Pi-cotransport.[5,12,106,177] In agreement, proximal Pi reabsorption was reduced in streptotocin-induced diabetes, though without changes of NaPi-IIa or type III Na/Pi-cotransporters mRNAs.[160] Moreover, no change of the NaPi-IIa protein abundance in BBMV was detected. In rats treated with streptotocin, the adaptive response to a low-Pi diet on the amount of NaPi-IIa was blunted indicating that

insulin may have a permissive effect on the response of NaPi-IIa to changes of the dietary content.[160]

Ontogeny/Aging

During ontogenesis and aging, transport rates in renal BBMv and the relative abundances of NaPi-IIa and NaPi-IIc are altered.[161,179] In kidneys of newborn rats, expression of the NaPi-IIa was only observed in functional, juxtamedullary nephrons and was absent in the undifferentiated structures (S-shaped bodies) of the outer cortex. During suckling, the distribution of NaPi-IIa is uniform throughout the cortex and correlates with the formation of differentiated brush borders. In kidneys of weaning rats, the expression pattern changed to a pattern similar to that observed in adults. Since during these transitions no changes of NaPi-IIa mRNA have been detected, it was suggested that the ontogenic changes on the expression of NaPi-IIa are due to posttranscriptional mechanisms.[57,133] Expression of NaPi-IIc is not observed in suckling animals; instead it is expressed predominantly in weaning animals and is markedly reduced in adults.[174]

Acidosis

Metabolic acidosis leads to an increased urinary Pi excretion, which is related to a reduction of proximal tubular apical Na/Pi-cotransport. As this effect was dependent on intact adrenal glands, an involvement of corticosteroids has been suggested.[1,2,34]

In rats fed a normal-Pi diet, metabolic acidosis provoked a decrease of the content of the NaPi-IIa protein as well as of mRNA.[166] In mice, fed a normal-Pi diet, metabolic acidosis results in a decrease of the content of NaPi-IIa and NaPi-IIc mRNA. However, both transporters were upregulated at the protein level.[112,162] Increased urinary excretion under metabolic acidotic conditions may be explained, at least in part, by the sensitivity of type II Na/Pi-cotransporters to luminal pH -values.[47,169]

Intoxication by Heavy Metals

In kidneys of rats injected with cadmium for two or more weeks, reduced Na/Pi cotransport correlated with a decrease of NaPi-IIa. Despite morphological changes of the microvillar structures, the abundance of aquaporin-1 and the Na/sulfate cotransporter NaSi-1 were not affected, indicating that exposure to cadmium results in a selective loss of NaPi-IIa.[85,170] On the other hand, a direct effect of heavy metals, including cisplatin,[172] on NaPi-IIa cannot be excluded as SH groups may play an important role in the Na/Pi-cotransport.[74]

Mice that were injected with cadmium, showed increased levels of FGF23 and increased urinary excretion of Pi that correlated with a decreased abundance of NaPi-IIc, but, interestingly, not of NaPi-IIa proteins.[173]

GENETIC ALTERATIONS LEADING TO IMBALANCE OF PI HOMEOSTASIS

Mutations of SLC34 Cotransporters

As reported above, studies performed in mice models clearly indicated that the bulk of the renal reabsorption of Pi in adults can be attributed to NaPi-IIa, whereas the contribution of NaPi-IIc is by far quantitatively smaller. However, in 2006 three independent groups reported an unexpected association between mutations on NaPi-IIc with hypophosphatemic rickets with hypercalciuria (HHRH) in humans[21,187,193] (Table 68.1). This association has been strengthened by more recent publications describing additional mutations on NaPi-IIc in patients affected by HHRH. Although mutations on NaPi-IIa were identified in patients with nephrolithiasis and osteoporosis, their implication on the development of hypophosphatemia in humans is controversial.[68,157] A recent report described inactivating mutations of NaPi-IIa in patients with autosomal recessive Fanconi syndrome and hypophosphatemic rickets (ARFS)[148] (Table 68.1).

Mutations of FGF23

In the last years it has become clear that FGF23 and its co-receptor Klotho are major regulators of Pi homeostasis. Mutations in FGF23 were identified as the cause for autosomal dominant hypophosphatemic rickets (ADHR)[7,42,168] (Table 68.1). FGF23 is inactivated by proteolytic cleavage at a conserved site (RXXR). Mutations resulting in ADRH affect the two arginine located within the proteolytic site. Substitution of either arginine prevents the degradation of FGF23, thus resulting in elevated levels of intact FGF23 in plasma, which despite the mutation retains its phosphaturic effect.[190] Transgenic mice expressing proteolytic resistant FGF23, or animals in which the mutated FGF23 was incorporated by injection of naked DNA, recapitulate the phenotype of ADHR.[33,175] These studies showed that the hypophosphatemia is due to hyperphosphaturia caused by FGF23-induced downregulation NaPi-IIa and NaPi-IIc.

Mutations on FGF23 resulting in low circulating levels of the intact protein have been described in patients with familial tumoral calcinosis with hyperphosphatemia (FTC)[41] (Table 68.1). These mutations lead either to intracellular retention or reduced

TABLE 68.1 Genetic Alterations Leading to Imbalance of Pi Homeostasis

Syndrom	Gene	Serum Pi	PTH	1,25(OH)2-VD	FGF23
HHRH	SLC34A3	Low	Low	High	Normal-low
ARFS and HR	SLC34A1	Low	Normal	Low	Normal
Nephrolitiasis osteoporosis	SLC34A1	Low	Normal	High	
ADHR	FGF23 (gain)	Low	Normal	Inappropiately normal	High
FTC	FGF23 (loss)	High	Normal-low	Normal	Low
FTC	Klotho (loss)	High	High	High	High
HRH	Klotho (gain)	Low	High	Normal	High
XLH	PHEX	Low	Normal	Inappropiately normal	High
ARHR	DMP1	Low	Normal	Inappropiately normal	High
TIO		Low			High
FD/MAS	GNAS	Low			High
FTC	GALNT3	High	Low	Inappropiately normal	Low

Mutations on the genes encoding transporters (SLC34A1 and SLC34A3) or regulatory proteins (FGF23, Klotho, PHEX, DMP1, GNAS or GALNT3) have been reported in patients with different hypophosphatemic syndromes. HHRH: hypophosphatemic rickets with hypercalciuria; ARFS and HR: autosomal recessive Fanconi syndrome and hypophosphatemic rickets; ADHR: autosomal dominant hypophosphatemic rickets; FTC: familial tumoral calcinosis with hyperphosphatemia; HRH: hypophosphatemic rickets and hyperparathyroidism; XLH: X-linked hypophosphatemia; ARHR: autosomal recessive hypophosphatemic rickets; TIO: tumor-induced osteomalacia; FD/MAS: fibrous dysplasia/McCune-Albright syndrome.

proteolytic stabilty of FGF23. In agreement with the human data, FGF23 deficient mice have increased expression of NaPi-IIa and severe hyperphosphatemia.[108,128]

Mutations of Klotho

A mutation in Klotho was found in a patient with FCT who presented hyperphosphatemia despite elevated FGF23[136] (Table 68.1). The mutated Klotho is proposed to have a reduced expression at the plasma membrane, thus preventing the FGF23 phosphaturic effect. An interchromosomal translocation resulting in increased levels of Klotho was reported in a patient with hypophosphatemic rickets and hyperparathyroidism[181] (Table 68.1). Surprisingly, FGF23 was also elevated explaining the hypophosphatemic status.

Hypophosphatemic Syndromes Related to Elevated FGF23

Elevated FGF23 has been reported in several other hypophosphatemic syndromes with clinical features similar to those of ADHR, including X-linked hypophosphatemia (XHL), autosomal recessive hypophosphatemic rickets (ARHR), tumor-induced osteomalacia (TIO) and fibrous dysplasia/McCune-Albright syndrome (FD/MAS) (for review see [168]) (Table 68.1). However, the primary cause of all these pathologies affects genes other than FGF23 itself.

XLH, or familial vitamin D resistant rickets, is caused by mutations in the phosphate regulating gene with homology to endopeptidases on the X-chromosome (PHEX).[183] This gene encodes a metalloprotease produced in the bone. The high levels of FGF23 found in patients with XLH,[83] led to the proposal of FGF23 being a substrate of PHEX. Although this direct connection remains controversial, the hypophosphatemia in Phex-deficient mice (Hyp mice)[185] is corrected by ablation of FGF23, supporting the notion that FGF23 acts downstream of PHEX.[108]

ARHR is caused by mutations in the dentin matrix acidic phosphoprotein 1 (DMP1), a protein highly expressed in bone.[186,188] The phenotype of Dmp1-deficient mice is also reverted by ablation of FGF23, suggesting that the hypophosphatemia is attributable to the high circulating FGF23.[158]

TIO, also known as oncogenic osteomalacia, is an acquired hypophosphatemic disorder characterized by tumors. It was recognized early on that these tumors express a factor able to inhibit Pi transport when applied to renal proximal cells in culture and to induce phosphaturia in mice.[189] Indeed, there were these findings what led to the proposal of a circulating factor/s (phosphatonins) controlling renal excretion of Pi. Later on it was found that the concentration of FGF-23 is high in TIO patients and that surgical removal of tumors corrects renal Pi wasting and restores FGF23 levels.[83,129,191] The molecular mechanism underlying

the increased production of FGF23 in these tumors remains unknown. Several other proteins are highly expressed by tumoral tissues, including DMP1, FGF7, sFRP4, and MEPE (for review see [134]).

FD/MAS, are rare diseases that result from activating mutations on the α subunit of stimulatory G-protein (GNAS). Both syndromes can present with hypophosphatemia due to elevated expression of FGF23.

Hyperphosphatemic Syndromes Related to Reduced FGF23

In addition to mutations on FGF23 or Klotho, FTC caused by reduced FGF23 also associates with mutations in GALNT3.[107] GALNT3 is a glycosyl transferase that glycosylates FGF23 within the proteolytic site, rendering it more resistant to the proteolytic processing. Patients with GALNT3 mutations and Galnt3-deficient mice are hyperphosphatemic, had increased FGF23 expression in bone but low circulating levels of intact peptide.[107,180]

Acknowledgments

The authors express their thanks to the many former and present colleagues with whom they have had the pleasure to collaborate. Furthermore, the continuous financial support by the Swiss National Fonds is acknowledged.

References

[1] Berndt TJ, Knox FG. Renal regulation of phosphate excretion. In: Seldin DW, Giebisch G, editors. The kidney, physiology and pathophysiology. New York: Raven Press; 1992. p. 2511–32.
[2] Bonjour JP, Caverzasio J. Phosphate transport in the kidney. Rev Physiol Biochem Pharmacol 1984;100:161–214.
[3] Dennis VW. Phosphate metabolism: contribution of different cellular compartments. Kidney Int 1996;49:938–42.
[4] Knox FG, Haramati A. Renal regulation of phosphate excretion. In: Seldin GW, Giebisch G, editors. The kidney: physiology and pathophysiology. New York: Raven Press; 1985. p. 1351–96.
[5] Silver J, Naveh-Many T. Phosphate and the parathyroid. Kidney Int 2009;75:898–905.
[6] Bielesz B, Klaushofer, Oberbauer R. Renal phosphate loss in hereditary and acquired disorders of bone mineralization. Bone 2004;35:1229–39.
[7] Farrow EG, White KE. Recent advances in renal phosphate handling. Nature Rev 2010;6:207–17.
[8] Radanovic T, Gisler SM, Biber J, Murer H. Topology of the type IIa Na/Pi cotransporter. J Membr Biol 2006;212:41–9.
[9] Ravera S, Virkki LV, Murer H, Forster IC. Deciphering PiT transport kinetics and substrate specificity using electrophysiology and flux measurements. Am J Physiol 2007;293:C606–20.
[10] Tenenhouse HS, Roy S, Martel J, Gauthier C. Differential expression, abundance, and regulation of Na-phosphate cotransporter genes in murine kidneys. Am J Physiol 1998;275: F527–34.
[11] Kocher O, Pal R, Roberts M, Cirovic C, Gilchrist A. Targeted disruption of the PDZK1 gene by homolgous recombination. Mol Cell Biol 2003;23:1175–80.
[12] Murer H, Kaissling B, Forster I, Biber J. Cellular mechanisms in proximal tubular handling of phosphate. In: Seldin DW, Giebisch G, editors. The kidney, physiology and pathophysiology. New York: Lippincott Williams & Wilkins; 2000. p. 1869–84.
[13] Nagai S, Okazaki M, Segawa H, Bergwitz C, Dean T, Potts JT, et al. Acute down-regulation of sodium-dependent phosphate transporter NPT2a involves predominantly the cAMP/PKA pathway as revealed by signaling-selective parathyroid hormone analogs. J Biol Chem 2011;286:1618–826.
[14] Forster IC, Loo DD, Eskandari S. Stoichiometry and Na^+ binding cooperativity of rat and flounder renal type II Na^+-P_i cotransporters. Am J Physiol 1999;276:F644–9.
[15] Friedlander G, Amiel C. Autocrine/paracrine control of renal phosphate transport. Kidney Int 1996;57:S148–53.
[16] Collins JF, Bai L, Ghishan FK. The SLC20 family of proteins: dual functions as sodium-phosphate cotransporters and viral receptors. Pflugers Arch 2004;447:647–52.
[17] Murer H, Hernando N, Forster I, Biber J. Proximal tubular phosphate reabsorption. Physiol Rev 2000;80:1373–409.
[18] Werner A, Dehmet L, Nalbant P. Na-dependent phosphate cotransporters: the NaPi protein families. J Exp Biol 1998;201: 135–42.
[19] Werner A, Kinne RK. Evolution of the Na-Pi cotransport systems. Am J Physiol 2001;280:R301–12.
[20] Beck L, Karaplis AC, Amizuka N, Hewson AS, Ozawa H, Tenenhouse HS. Targeted inactivation of Npt2 in mice leads to severe renal phosphate wasting, hypercalciuria and skeletal abnormalities. Proc Natl Acad Sci (USA) 1998;95:5372–7.
[21] Bergwitz C, Roslin NM, Tieder M, Loredo-Osti JC, Bastepe M, Abu-Zahra H, et al. SLC34A3 mutations in patients with hereditary hypophosphatemic rickets with hypercalciuria predict a key role for the sodium-phosphate cotransporter NaPi-IIc in maintaining phosphate homeostasis. Am J Hum Genet 2006;78: 179–92.
[22] Tomoe Y, Segawa H, Shiozawa K, Kaneko I, Tominaga R, Hanabusa E, et al. Phosphaturic action of fibroblast growth factor 23 in Npt2 null mice. Am J Physiol 2010;298:F1341–50.
[23] Villa-Bellosta R, Ravera S, Sorribas V, Stange G, Levi M, Murer H, et al. The Na^+-Pi-cotransporter PiT-2 (SLC20A2) is expressed in the apical membrane of rat renal proximal tubules and regulated by dietary Pi. Am J Physiol 2009;296:F691–9.
[24] Busch AE, Biber J, Murer H, Lang F. Electrophysiological insights of type I and II Na/Pi transporters. Kidney Int 1996;49:986–7.
[25] Moe OW. PiT-2 coming out of the pits. Am J Physiol 2009;296: F689–690.
[26] McWilliams RR, Breusegem SY, Brodsky KF, Kim E, Levi M, Doctor RB. Shank2E binds NaPi cotransporter at the apical membrane of proximal tubule cells. Am J Physiol 2005;289: C1042–51.
[27] Saito H, Kusano K, Kinosaki M, Ito H, Hirata M, Segawa H, et al. Human fibroblast growth factor-23 mutants suppress Na^+-dependent phosphate co-transport activity and 1alpha,25-dihydroxyvitamin D3 production. J Biol Chem 2003;278:2206–11.
[28] Bacic D, Wagner CA, Hernando N, Kaissling B, Biber J, Murer H. Novel aspects in regulated expression of the renal type IIa Na/Pi cotransporter. Kidney Int 2004;66:S5–12.
[29] Biber J, Custer M, Magagnin S, Hayes G, Werner A, Lötscher M, et al. Renal Na/Pi-cotransporters. Kidney Int 1995;49:981–5.
[30] Ehnes C, Forster IC, Köhler K, Biber J, Murer H. Functional studies on a split type II Na/Pi cotransporter. J Membr Biol 2002;188:227–36.

[31] Köhler K, Forster I, Lambert G, Biber J, Murer H. The functional unit of the renal type IIa Na/Pi cotransporter is a monomer. J Biol Chem 2000;275:26113–20.
[32] Peerce BE, Peerce B, Clarke RD. Phosphophloretin sensitivity of rabbit renal NaPi-IIa and NaPi-Ia. Am J Physiol 2004;286: F955–64.
[33] Segawa H, Kawakami E, Kaneko I, Kuwahata M, Ito M, Kusano K, et al. Effect of hydrolysis-resistant FGF23-R179Q on dietary phosphate regulation of the renal type-II Na/Pi transporter. Pflugers Arch 2003;446:585–92.
[34] Prabhu S, Levi M, Dwarakanath V, Arar M, Biber J, Murer H, et al. Effect of glucocorticoids on neonatal rabbit renal cortical sodium-inorganic phosphate messenger RNA and protein abundance. Pediatr Res 1997;41:20–4.
[35] Kestenbaum B, Glazer NL, Köttgen A, Felix JF, Hwang SJ, Liu Y, et al. Common genetic variants associate with serum phosphorous concentration. J Am Soc Nephrol 2010;21:1223–32.
[36] Tenenhouse HS. Regulation of phosphorous homeostasis by the type IIa Na/phosphate cotransporter. Ann Rev Nutr 2005;25:10.1–10.18.
[37] Breusegem SY, Takahashi H, Giral-Arnal H, Wang X, Jiang T, Verlander JW, et al. Differential regulation of the renal sodium-phosphate cotransporters NaPi-IIa, NaPi-IIc, and PiT-2 in dietary potassium deficiency. Am J Physiol 2009;297: F350–61.
[38] Tenenhouse HS, Martel J. Renal adaptation to phosphate deprivation: lessons from the X-linked Hyp mouse. Pediatr Nephrol 1993;7:312–8.
[39] Segawa H, Yamanaka S, Ito M, Kuwahata M, Shono M, Yamamoto T, et al. Internalization of renal type IIc Na-Pi cotransporter in response to a high-phosphate diet. Am J Physiol 2005;288:F587–96.
[40] Knochel JP. The clinical and physiological implications of phosphorus deficiency. In: Seldin DW, Giebisch G, editors. The kidney, physiology and pathophysiology. New York: Raven Press; 1992. p. 2533–62.
[41] Larsson T, Yu X, Davis SI, Draman MS, Mooney SD, Cullen MJ, et al. A novel recessive mutation in fibroblast growth factor-23 causes familial tumoral calcinosis. J Clin Endocrinol Metab 2005;90:2424–7.
[42] Quarles LD. FGF23, PHEX, and MEPE regulation of phosphate homeostasis and skeletal mineralization. Am J Physiol 2003;285: E1–9.
[43] Mahon MJ, Donowitz M, Yun CC, Segre GV. Na^+/H^+ exchanger regulatory factor 2 directs parathyroid hormone 1 receptor signalling. Nature 2002;417:858–61.
[44] Inoue M, Digman MA, Cheng M, Breusegem SY, Halaihel N, Sorribas V, et al. Partitioning of NaPi cotransporter in cholesterol-, sphingomyelin-, and glycosphingolipid-enriched membrane domains modulates NaPi protein diffusion, clustering and activity. J Biol Chem 2004;279:49160–71.
[45] Madjdpour C, Bacic D, Kaissling B, Murer H, Biber J. Segment specific expression of sodium-phosphate cotransporters NaPia and -IIc and interacting proteins in mouse renal proximal tubules. Pflugers Arch 2004;448:402–10.
[46] Busch AE, Wagner CA, Schuster A, Waldegger S, Biber J, Murer H, et al. Properties of electrogenic P_i transport by a human renal brush border Na^+/P_i transporter. J Am Soc Nephrol 1995;6:1547–51.
[47] Forster IC, Biber J, Murer H. Proton-sensitive transitions of renal type II Na^+-coupled phosphate cotransporter kinetics. Biophys J 2000;79:215–30.
[48] Forster I, Hernando N, Biber J, Murer H. The voltage dependence of a cloned mammalian renal type II Na^+/P_i cotransporter (NaPi-2). J Gen Physiol 1998;112:1–18.
[49] Giral H, Lanzano L, Caldas Y, Blaine J, Verlander JW, Lei T, et al. Role of PDZK1 protein in apical membrane expression of renal sodium-coupled phosphate transporters. J Biol Chem 2011;286:15032–42.
[50] Rasmussen H, Tenenhouse HS. Mendelian hypophosphatemias. In: Scriver CR, Beaudet AL, Sly WS, Valle D, editors. The metabolic and molecular bases of inherited disease. New York: McGraw-Hill; 1995. p. 3717–45.
[51] Villa-Bellosta R, Sorribas V. Role of rat sodium/phosphate cotransporters in the cell membrane transport of arsenate. Toxicol Appl Pharmacol 2008;232:125–34.
[52] Bacconi A, Virkki LV, Biber J, Murer H, Forster IC. Renouncing electrogenicity is not free of charge: switching on electrogenicity in a Na^+-coupled phosphate cotransporter. Proc Nat Acad Sci (USA) 2005;102:12606–11.
[53] Forster IC, Virkki LV, Bossi E, Murer H, Biber J. Electrogenic kinetics of a mammalian intestinal Na^+/P_i-cotransporter. J Membrane Biol 2006;212:177–90.
[54] Virkki LV, Forster IC, Biber J, Murer H. Substrate interactions in the human type IIa sodium-phosphate cotransporter (NaPi-IIa). Am J Physiol 2005;288:F969–81.
[55] Freeman D, Bartlett S, Radda G, Ross B. Energetics of sodium transport in the kidney: Saturation transfer ^{31}P-NMR. Biochim Biophys Acta 1983;762:325–36.
[56] Virkki LV, Murer H, Forster IC. Voltage clamp fluorometric measurements on a type II Na^+-coupled P_i cotransporter: shedding light on substrate binding order. J Gen Physiol 2006;127:539–55.
[57] Taufiq S, Collins JF, Gishan FK. Posttranscriptional mechanisms regulate ontogenic changes in rat renal sodium-phosphate transporter. Am J Physiol 1997;272:R134–41.
[58] Villa-Bellosta R, Sorribas V. Different effects of arsenate and phosphonoformate on Pi transport adaptation in opossum kidney cells. Am J Physiol 2009;297:C516–25.
[59] Weinstock J. Inhibitors of sodium-dependent phosphate transport. Expert Opinion Therapeutic Patents 2004;14:3.
[60] Perward F, Zhang MYH, Tenenhouse HS, Portale AA. Fibroblast growth factor 23 impairs phosphorus and vitamin D metabolism in vivo and suppresses 25-hydroxyvitamin D 1α-hydroxylase expression in vitro. Am J Physiol 2007;293: F1577–83.
[61] Andrini O, Ghezzi C, Murer H, Forster IC. The leak mode of type II Na-Pi cotransporters. Channels 2008;2:346–57.
[62] Jemth P, Gianni S. PDZ domains: folding and binding. Biochemistry 2007;46:8701–8.
[63] Bai L, Collins JF, Ghishan FK. Cloning and characterization of a type III Na-dependent phosphate cotransporter from mouse intestine. Am J Physiol 2000;279:C1135–43.
[64] Bottger P, Hede SE, Grunnet M, Hoyer B, Klaerke DA, Pedersen L. Characterization of transport mechanisms and determinants critical for Na^+-dependent Pi symport of the PiT family paralogs human PiT1 and PiT2. Am J Physiol 2006;291:C1377–87.
[65] Reczek D, Berryman M, Bretscher A. Identification of EBP50: a PDZ-containing phosphoprotein that associates with members of the ezrin-radixin-moesin family. J Cell Biol 1997;139:169–79.
[66] Villa-Bellosta R, Bogaert YE, Levi M, Sorribas V. Characterization of phosphate transport in rat vascular smooth muscle cells. Implications for vascular calcification. Arterioscler Thromb Vasc Biol 2007;27:1030–6.
[67] Virkki LV, Biber J, Murer H, Forster IC. Phosphate transporters: a tale of two solute carrier families. Am J Physiol 2007;293: F643–54.
[68] Lapointe J-Y, Tessier J, Paquette Y, Wallendorff B, Coady M, Pichette V, et al. NPT2a gene variation in calcium nephrolithiasis with renal phosphate leak. Kidney Int 2006;69:2261–7.

[69] Radanovic T, Murer H, Biber J. Expression of the Na/P_i-cotransporter type IIb in Sf9 cells: functional characterization and purification. J Membrane Biol 2003;194:91–6.
[70] Köhler K, Forster IC, Stange G, Biber J, Murer H. Transport function of the renal type IIa Na^+/P_i cotransporter is codetermined by residues in two opposing linker regions. J Gen Physiol 2002;120:693–703.
[71] Ghezzi C, Murer H, Forster IC. Substrate interactions of the electroneutral Na^+-coupled inorganic phosphate cotransporter [NaPi-IIc]. J Physiol 2009;587:4293–307.
[72] Lambert G, Forster IC, Stange G, Köhler K, Biber J, Murer H. Cysteine mutagenesis reveals novel structure-function features within the predicted third extracellular loop of the type IIa Na^+/P_i cotransporter. J Gen Physiol 2001;117:533–46.
[73] Lambert G, Traebert M, Hernando N, Biber J, Murer H. Studies on the topology of the renal type II NaPi-cotransporter. Pflugers Arch 1999;437:972–8.
[74] Köhler K, Forster IC, Stange G, Biber J, Murer H. Essential cysteine residues of the type IIa Na^+/P_i cotransporter. Pflugers Archiv 2003;446:203–10.
[75] Delisle MC, Giroux S, Vachon V, Boyer C, Potier M, Beliveau R. Molecular size of the functional complex and protein subunits of the renal phosphate symporter. Biochemistry 1994;33:9105–9.
[76] Gisler SM, Pribanic S, Bacic D, Forrer P, Gantenbein A, Sabourin LA, et al. PDZK1, I: a major scaffolder in brush borders of proximal tubular cells. Kidney Int 2003;64:1733–45.
[77] Forster IC, Hernando N, Biber J, Murer H. Proximal tubular handling of phosphate: A molecularperspective. Kidney Int 2006;70:1548–59.
[78] Virkki LV, Forster IC, Bacconi A, Biber J, Murer H. Functionally important residues in the predicted 3rd transmembrane domain of the type IIa sodium-phosphate cotransporter (NaPi-IIa). J Membrane Biol 2005;206:227–38.
[79] Farrell KB, Tusnady GE, Eiden MV. New structural arrangement of the extracellular regions of the phosphate transporter SLC20A1, the receptor for gibbon ape leukemia virus. J Biol Chem 2009;284:29979–87.
[80] Schiavi SC, Kumar R. The phosphatonin pathway: new insights in phosphate homeostasis. Kidney Int 2004;65:1–14.
[81] Bottger P, Pedersen L. The central half of Pit2 is not required for its function as a retroviral receptor. J Virol 2004;78:9564–7.
[82] Feldman SA, Farrell KB, Murthy RK, Russ JL, Eiden MV. Identification of an extracellular domain within the human PiT2 receptor that is required for amphotropic murine leukemia virus binding. J Virol 2004;78:595–602.
[83] Jonsson KB, Zahradnik R, Larsson T, White KE, Sugimoto T, Imanishi Y, et al. Fibroblast growth factor 23 in oncogenic osteomalacia and X-linked hypophosphatemia. N Engl J Med 2003;348:1656–63.
[84] Biber J, Gisler SM, Hernando N, Wagner CA, Murer H. PDZ interactions and proximal tubular phosphate reabsorption. Am J Physiol 2004;287:F871–5.
[85] Herak-Kramberger CM, Spindler B, Biber J, Murer H, Sabolic I. Renal type II Na/Pi cotransporter is strongly impaired whereas the Na/sulfate cotransporter and aquaporin 1 are unchanged in cadmium treated rats. Pflugers Arch 1996;432:336–44.
[86] Shenolikar S, Voltz JW, Minkoff CM, Wade JB, Weinman EJ. Targeted disruption of the mouse NHERF-1 gene promotes internalization of proximal tubule sodium-phosphate cotransporter type IIa and renal phosphate wasting. Proc Natl Acad Sci (USA) 2002;99:11470–5.
[87] Miyamoto KI, Haito-Sugino S, Kuwahara S, Ohi A, Nomura K, Ito M, et al. Sodium-dependent phosphate cotransporters: lessons from gene knockout and mutation studies. J Pharmaceutical Sciences 2011;: Epub ahead of print
[88] Johann SV, van Zeijl M, Cekleniak J, O'Hara B. Definition of a domain of GLVR1 which is necessary for infection by gibbon ape leukemia virus and which is highly polymorphic between species. J Virol 1993;67:6733–6.
[89] Sabbagh Y, O'Brien SP, Song W, Boulanger JH, Stockmann A, Arbeeny C, et al. Intestinal npt2b plays a major role in phosphate absorption and homeostasis. J Am Soc Nephrol 2009;20:2348–58.
[90] Weinman EJ, Hall RA, Friedman PA, Liu-Chen LY, Shenolikar S. The association of NHERF adaptor proteins with G protein-coupled receptors and receptor tyrosine kinases. Annu Rev Physiol 2006;68:491–505.
[91] Gisler SM, Stagliar I, Traebert M, Bacic D, Biber J, Murer H. Interaction of the type IIa Na/Pi cotransporter with PDZ proteins. J Biol Chem 2001;276:9206–13.
[92] Boeckers TM, Bockmann J, Kreutz MR, Gundelfinger ED. ProSAP/Shank proteins - a family of higher order organizing molecules of the postsynaptic density with an emerging role in human neurological disease. J Neurochem 2002;81:903–10.
[93] Deliot N, Hernando N, Horst-Liu Z, Gisler SM, Capuano P, Wagner CA, et al. Parathyroid hormone treatment induces dissociation of type IIa Na-Pi cotransporter-Na^+/H^+ exchanger regulatory factor-1 complexes. Am J Physiol 2005; 289:C159–67.
[94] Weinman EJ, Biswas R, Steplock D, Douglass TS, Cunningham R, Shenolikar S. Sodium-hydrogen exchanger regulatory factor 1 (NHERF-1) transduces signals that mediate dopamine inhibition of sodium-phosphate co-transport in mouse kidney. J Biol Chem 2010;285:13454–60.
[95] Weinman EJ, Biswas RS, Peng G, Shen L, Turner CL, Xiafei E, et al. Parathyroid hormone inhibits renal phosphate transport by phosphorylation of serine 77 of sodium-hydrogen exchanger regulatory factor-1. J Clin Invest 2007;117:3412–20.
[96] Hu MC, Shi M, Zhang J, Pastor J, Nakatani T, Lanske B, et al. Klotho: a novel phosphaturic substance acting as an autocrine enzyme in the renal proximal tubule. FASEB J 2010;24: 3438–50.
[97] Shimada T, Hasegawa H, Yamazaki Y, Muto T, Hino R, Takeuchi Y, et al. FGF-23 is a potent regulator of vitamin D metabolism and phosphate homeostasis. J Bone Mineral Res 2004;19:429–35.
[98] Cunningham R, et al. Urine electrolyte, mineral, and protein excretion in NHERF-2 and NHERF-1 null mice. Am J Physiol 2008;294:F1001–7.
[99] Capuano P, Bacic D, Stange G, Hernando N, Kaislling B, Pal R, et al. Expression and regulation of the renal Na/phosphate cotransporter NaPi IIa in a mouse model deficient for the PDZ protein PDZK1. Pflugers Arch 2005;499:392–402.
[100] Bergwitz C, Jüppner H. Phosphate sensing. Adv Chronuic Kidney Dis 2011;18:132–44.
[101] Gisler SM, Kittanakom S, Fuster D, Wong V, Bertic M, Radanovic T, et al. Monitoring protein-protein interactions between the mammalian integral membrane transporters and PDZ-interacting partners using a modified split-ubiquitin membrane yeast two-hybrid system. Mol Cell Proteomics 2008;7:1362–77.
[102] Bachmann S, Schlichting U, Geist B, Mutig K, Petsch T, Bacic D, et al. Kidney-specific inactivation of the megalin gene impairs trafficking of renal inorganic sodium phosphate cotransporter NaPi IIa. J Am Soc Nephrol 2004;15:892–900.
[103] Kavanaugh MP, Kabat D. Identification and characterization of a widely expressed phosphate transporter/retrovirus receptor family. Kidney Int 1996;49:959–63.

[104] Jaureguiberry G, Carpenter TO, Forman S, Juppner H, Bergwitz C. A novel missense mutation in SLC34A3 that causes hereditary hypophosphatemic rickets with hypercalciuria in humans identifies threonine 137 as an important determinant of sodium-phosphate cotransport in NaPi-IIc. Am J Physiol 2008;295:F371–9.

[105] Segawa H, Yamanaka S, Onitsuka A, Tomoe Y, Kuwahata M, Ito M, et al. Parathyroid hormone-dependent endocytosis of renal type IIc Na-Pi cotransporter. Am J Physiol 2007;292: F395–403.

[106] Seifert SA, Hsiao SC, Murer H, Biber J, Kempson SA. Renal endosomal phosphate (Pi) transport in normal and diabetic rats and response to chronic Pi deprivation. Cell Biochem Funct 1997;15:9–14.

[107] Frishberg Y, Topaz O, Bergman R, Behar D, Fisher D, Gordon D, et al. Identification of a recurrent mutation in GALNT3 demonstrates that hyperostosis-hyperphosphatemia syndrome and familial tumoral calcinosis are allelic disorders. J Mol Med 2005;83:33–8.

[108] Sitara D, Razzaque MS, Hesse M, Yoganathan S, Taguchi T, Erben RG, et al. Homozygous ablation of fibroblast growth factor-23 results in hyperphosphatemia and impaired skeletogenesis, and reverses hypophosphatemia in Phex-deficient mice. Matrix Biol 2004;23:421–32.

[109] Amizuka N, Lee HS, Kwan MY, Arazani A, Warshawsky H, Hendy GN, et al. Cell-specific expression of the parathyroid hormone PTH/PTH-related peptide receptor gene in kidney from kidney-specific and ubiquitous promoters. Endocrinology 1997;138:469–81.

[110] Ba J, Brown D, Friedman PA. Calcium-sensing receptor regulation of PTH-inhibitable proximal tubule phosphate transport. Am J Physiol 2003;285:F1233–43.

[111] Urakawa I, Yamazaki Y, Shimada T, Iijima K, Hasegawa H, Okawa K, et al. Klotho converts canonical FGF receptor into a specific receptor for FGF23. Nature 2007;444:770–4.

[112] Nowik M, Picard N, Stange G, Capuano P, Tenenhouse HS, Biber J, et al. Renal phosphaturia during metabolic acidosis revisited: molecular mechanisms for decreased renal phosphate reabsorption. Pflugers Arch 2008;457:539–49.

[113] Weinman EJ, Steplock D, Zhang Y, Biswas R, Bloch RJ, Shenolikar S. Cooperativity between the phosphorylation of Thr95 and Ser77 of NHERF-1 in the hormonal regulation of renal phosphate transport. J Biol Chem 2010;285:25134–8.

[114] Weinman EJ, Steplock D, Shenolikar S, Blanpied TA. Dynamics of PTH-induced disassembly of Npt2a/NHERF-1 complexes in living OK cells. Am J Physiol 2011;300:F231–5.

[115] Mahon MJ, Segre GV. Stimulation by parathyroid hormone of a NHERF-1-assembled complex consisting of the parathyroid hormone I receptor, phospholipase Cbeta, and actin increases intracellular calcium in opossum kidney cells. J Biol Chem 2004;279:23550–8.

[116] Marks J, Debnam ES, Unwin RJ. Phosphate homeostasis and the renal-gastrointestinal axis. Am J Physiol 2010;299:F285–96.

[117] Capuano P, Bacic D, Roos M, Gisler SM, Stange G, Biber J, et al. Defective coupling of apical PTH receptors to phospholipase C prevents internalization of the Na^+-phosphate cotransporter NaPi-IIa in Nherf1-deficient mice. Am J Physiol 2007;292:C927–34.

[118] Berndt TJ, Khraibi AA, Thothathri V, Dousa TP, Tyce GM, Knox FG. Effect of increased dietary phosphate intake on dopamine excretion in the presence and absence of the renal nerves. Miner Electrolyte Metab 1994;20:158–62.

[119] Weinman EJ, Biswas R, Steplock D, Wang P, Lau YS, Desir GV, et al. Increased renal dopamine and acute renal adaptation to a high-phosphate diet. Am J Physiol 2011;300:F1123–9.

[120] Wang X, Villar VA, Armando I, Eisner GM, Felder RA, Jose PA. Dopamine, kidney, and hypertension: studies in dopamine receptor knockout mice. Pediatr Nephrol 2008;23:2131–46.

[121] Bacic D, Capuano P, Buam M, Zhang J, Stange G, Biber J, et al. Activation of dopamine D1-like receptors induces acute internalization of the renal Na/phosphate cotransporter NaPi IIa in mouse kidney and OK-cells. Am J Physiol 2004;288: F740–7.

[122] Berndt T, Kumar R. Phosphatonins and the regulation of phosphate homeostasis. Annu Rev Physiol 2007;69:341–59.

[123] Ghezzi C, Meinild AK, Murer H, Forster IC. Voltage- and substrate-dependent interactions between sites in putative reentrant domains of a Na^+-coupled phosphate cotransporter. Pflugers Arch 2011;461:645–63.

[124] Feng JQ, Ye L, Schiavi S. Do osteocytes contribute to phosphate homeostasis? Curr Opin Nephrol Hypertens 2009; 18:285–91.

[125] Burnett SM, Gunawardene SC, Bringhurst FR, Jüppner H, Lee H, Finkelstein JS. Regulation of C-terminal and intact FGF-23 by dietary phosphate in men and women. J Bone Miner Res 2006;21:1187–96.

[126] Ferrari SL, Bonjour JP, Rizzoli R. Fibroblast growth factor-23 relationship to dietary phosphate and renal phosphate handling in healthy young men. J Clin Endocrinol Metab 2005;90:1519–24.

[127] Picard N, Capuano P, Stange G, Mihailova M, Kaissling B, Murer H, et al. Acute parathyroid hormone differentially regulates renal brush border membrane phosphate cotransporters. Pflugers Arch 2010;460:677–87.

[128] Shimada T, Kakitani M, Yamazaki Y, Hasegawa H, Takeuchi Y, Fujita T, et al. Targeted ablation of Fgf23 demonstrates an essential physiological role of FGF23 in phosphate and vitamin D metabolism. J Clin Invest 2004;113:561–8.

[129] Shimada T, Mizutani S, Muto T, Yoneya T, Hino R, Takeda S, et al. Cloning and characterization of FGF23 as a causative factor of tumor-induced osteomalacia. Proc Natl Acad Sci [USA] 2001;98:6500–5.

[130] Levi M, Baird BM, Wilson PV. Cholesterol modulates rat renal brush border membrane phosphate transport. J Clin Invest 1990;85:231–7.

[131] Baum M, Schiavi S, Dwarakanath V, Quigley R. Effect of fibroblast growth factor-23 on phosphate transport in proximal tubules. Kidney Int 2005;68:1148–53.

[132] Salaun C, Rodrigues P, Heard JM. Transmembrane topology of Pit-2, a phosphate transporter-retrovirus receptor. J Virol 2001;75:5584–92.

[133] Traebert M, Lötscher M, Aschwanden R, Ritthaler T, Biber J, Murer H, et al. Distribution of the sodium phosphate transporter (NaPi 2) during the postnatal ontogeny of the rat kidney. J Am Soc Nephrol 1999;10:1407–15.

[134] Gattineni J, Baum M. Regulation of phosphate transport by fibroblast growth factor 23 [FGF23]: implications for disorders of phosphate metabolism. Pediatr Nephrol 2010;25:591–601.

[135] Villa-Bellosta R, Barac-Nieto M, Breusegem SY, Barry NP, Levi M, Sorribas V. Interactions of the growth-related type IIc renal sodium/phosphate cotransporter with PDZ proteins. Kidney Int 2008;73:456–64.

[136] Ichikawa S, Imel EA, Kreiter ML, Yu X, Mackenzie DS, Sorenson AH, et al. A homozygous missense mutation in human Klotho causes severe tumoral calcinosis. J Clin Invest 2007;117:2684–91.

[137] Berndt TJ, Bielesz B, Craig TA, Tebben PJ, Bacic D, Wagner CA, et al. Secreted frizzled-related protein-4 reduces sodium-phosphate cotransporter abundance and activity in proximal tubule cells. Pflügers Arch 2006;451:579–87.

[138] Dobbie H, Unwin RJ, Faria NJR, Shirley DG. Matrix extracellular phosphoglycoprotein causes phosphaturia in rats by inhibiting tubular phosphate reabsorption. Nephrol Dial Tranplant 2008;23:730–3.
[139] Friedlander MM, Wald H, Dranitzky-Elhalel M, Levi M, Popovtzer MM. Recovery of renal tubule phosphate reabsorption despite reduced levels of sodium-phosphate transporter. Eur J Endocrinol 2004;151:797–801.
[140] Bacic D, Hernando N, Traebert M, Lederer E, Völkl H, Biber J, et al. Regulation of the renal IIa Na/Pi cotransporter by cGMP. Pflugers Arch 2001;443:306–13.
[141] Levine BS, Ho LD, Pasiecznik K, Coburn JW. Renal adaptation to phosphorous deprivation: characterization of early events. J Bone Miner Res 1986;1:33–40.
[142] Levine BS, Knibloe KA, Golchini K, Hashimoto S, Kurtz I. Renal adaptation to dietary phosphate deprivation: Role of proximal tubule brush border membrane fluidity. Am J Physiol 1991;260:F613–8.
[143] Murer H, Forster I, Biber J. The sodium phosphate cotransporter family SLC34. Pflugers Arch 2004;447:763–7.
[144] Berndt T, Thomas LF, Craig TA, Sommer S, Li X, Bergstralh EJ, et al. Evidence for a signaling axis by which intestinal phosphate rapidly modulates renal phosphate reabsorption. Proc Natl Acad Sci (USA) 2007;104:11085–90.
[145] Molitoris BA, Alfrey AC, Harris RA, Simon FR. Renal apical membrane cholesterol and fluidity in regulation of phosphate transport. Am J Physiol 1985;249:F12–9.
[146] Weinman EJ, Boddeti A, Cunningham R, Akom M, Wang F, Wang Y, et al. NHERF-1 is required for renal adaptation to a low phosphate diet. Am J Physiol 2003;285:F1225–32.
[147] Kohl B, Wagner CA, Huelseweh B, Busch A, Werner A. The Na-phosphate cotransport system (NaPi II) with a cleaved protein backbone: implications on function and membrane insertion. J Physiol 1998;508:341–50.
[148] Magen D, Berger L, Coady MJ, Ilivitzki A, Militianu D, Tieder M, et al. A loss-of-function mutation in NaPi-lla and renal fanconi's syndrome. N Engl J Med 2010;362:1102–9.
[149] Mulroney SE, Woda CB, Halaihel N, Louie B, McDonnell K, Schulkin J, et al. Central control of renal sodium-phosphate [NaPi 2] transporters. Am J Physiol 2004;286:F647–52.
[150] Moz Y, Silver J, Naveh-Many T. Characterization of a cis-acting element in the renal NaPi 2 cotransporter mRNA that determines mRNA stability. Am J Physiol 2003;284: F663–70.
[151] Ito M, Iidawa S, Izuka M, Haito S, Segawa H, Kuwahata M, et al. Interaction of a farnesylated potein with renal type IIa Na/Pi cotransporter in response to parathyroid hormone and dietary phosphate. Biochem J 2004;377:607–16.
[152] Levi M, Jameson DM, van der Meer BW. Role of BBM lipid composition and fluidity in impaired renal Pi transport in aged rats. Am J Physiol 1989;256:F85–94.
[153] Levi M, Kempson SA, Lötscher M, Biber J, Murer H. Molecular regulation of renal phosphate transport. J Membrane Biol 1996;154:1–9.
[154] Li H, Onwochei M, Ruch RJ, Xie Z. Regulation of rat Na/Pi cotransporter-1 gene expression: the roles of glucose and insulin. Am J Physiol 1996;271:E1021–8.
[155] Moz Y, Levi R, Lavi V, Cox KB, Molkentin JD, Silver J, et al. Calcineurin A is central to the expression of the renal type II Na/Pi cotransporter gene and to the regulation of renal phosphate transport. J Am Soc Nephrol 2004;15:2972–80.
[156] Zajicek HK, Wang H, Puttaparthi K, Halaihel N, Markovich D, Shayman J, et al. Glycosphingolipids modulate renal phosphate transport in potassium deficiency. Kidney Int 2001;60: 694–704.
[157] Prie D, Huart V, Bakouh N, Planelles G, Dellis O, Gérard B, et al. Nephrolithiasis and osteoporosis associated with hypophosphatemia caused by mutations in the type 2a sodium-phosphate cotransporter. N Engl J Med 2002;347:983–91.
[158] Liu S, Zhou J, Tang W, Menard R, Feng JQ, Quarles LD. Pathogenic role of Fgf23 in Dmp1-null mice. Am J Physiol 2008;295:E254–61.
[159] Shenolikar S, Voltz JW, Cunningham R, Weinman EJ. Regulation of ion transport by the NHERF family of PDZ proteins. Physiology 2004;19:362–9.
[160] Abraham MI, Woods RE, Breedlove DK, Kempson SA. Renal adaptation to low-phosphate diet in diabetic rats. Am J Physiol 1992;262:F731–6.
[161] Caverzasio J, Bonjour J-P, Murer H, Fleisch H. Renal Pi transport in young growing and adult rats: Comparative studies in brush border membrane vesicles (BBMV) and in whole kidney. Pflugers Arch 1982;394:217–21.
[162] Stauber A, Radanovic T, Stange G, Murer H, Wagner CA, Biber J. Regulation of intestinal phosphate transport. II: Metabolic acidosis stimulates Na-dependent phosphate absorption and expression of Na/Pi cotransporter NaPi IIb in small intestine. Am J Physiol 2005;288:501–6.
[163] Tenenhouse HS, Martel J, Gauthier C, Segawa H, Miyamoto K. Differential effects of Npt2a gene ablation and X-linked Hyp mutation on renal expression of Npt2c. Am J Physiol 2003;285: F1271–8.
[164] Traebert M, Volkl H, Biber J, Murer H, Kaissling B. Luminal and contraluminal action of 1-34 and 3-34 PTH peptides on renal type IIa Na-P[i] cotransporter. Am J Physiol 2000;278: F792–8.
[165] Prasad R, Kumar V. Thyroid hormones stimulate Na-Pi transport activity in rat renal brush-border membranes: role of membrane lipid composition and fluidity. Mol Cell Biochem 2005;268:75–82.
[166] Ambühl PM, Zajicek HK, Wang H, Puttaparthi K, Levi M. Regulation of renal phosphate transport by acute and chronic metabolic acidosis in the rat. Kidney Int 1998;53:1288–98.
[167] Ohkido I, Segawa H, Yanagida R, Nakamura M, Miyamoto K. Cloning, gene structure and dietary regulation of the type IIc Na/Pi cotransporter in the mouse kidney. Pflugers Arch 2003;446:106–15.
[168] Strom TM, Juppner H. PHEX, FGF23, DMP1 and beyond. Curr Opin Nephrol Hypertens 2008;17:357–62.
[169] Villa-Bellosta R, Sorribas V. Compensatory regulation of the sodium/phosphate cotransporters NaPi-IIc (SCL34A3) and Pit-2 (SLC20A2) during Pi deprivation and acidosis. Pflugers Arch 2010;459:499–508.
[170] Condron RJ, Schroen CJ, Marshall AT. Morphometric analysis of renal proximal tubules in cadmium treated rats. J Submicrosc Cytol Pathol 1994;26:51–8.
[171] Hernando N, Déliot N, Gisler SM, Lederer E, Weinman EJ, Biber J, et al. PDZ-domain interactions and apical expression of type IIa Na/Pi-cotransporters. Proc Natl Acad Sci [U S A] 2002;99:11957–62.
[172] Courjault-Gautier F, Le Grimellec C, Giocondi MC, Toutain HJ. Modulation of sodium-coupled uptake and membrane fluidity by cisplatin in renal proximal tubular cells in primary culture and brush border membrane vesicles. Kidney Int 1995;47: 1048–56.
[173] Aranami F, Segawa H, Furutani J, Kuwahara S, Tominaga R, Hanabusa E, et al. Fibroblast growth factor 23 mediates the phosphaturic actions of cadmium. J med Invest 2010;57: 95–108.
[174] Segawa H, Kaneko I, Takahashi A, Ito M, Kuwahata M, Ohkido I, et al. Growth-related renal type II Na/Pi cotransporter. J Biol Chem 2002;277:19665–72.

[175] Shimada T, Urakawa I, Yamazaki Y, Hasegawa H, Hino R, Yoneya T, et al. FGF-23 transgenic mice demonstrate hypophosphatemic rickets with reduced expression of sodium phosphate cotransporter type IIa. Biochem Biophys Res Commun 2004;314:409–14.

[176] Segawa H, Onitsuka A, Kuwahata M, Hanabusa E, Furutani J, Kaneko I, et al. Type IIc sodium-dependent phosphate transporter regulates calcium metabolism. J Am Soc Nephrol 2009;20:104–13.

[177] Silve C, Friedlander G. Renal regulation of phosphate excretion. In: Seldin GW, Giebisch G, editors. The kidney: physiology and pathophysiology. New York: Lippincott Williams & Wilkins; 2000. p. 1885–904.

[178] Larsson T, Marsell R, Schipani E, Ohlsson C, Ljunggren O, Tenenhouse HS, et al. Transgenic mice expressing fibroblast growth factor 23 under the control of the alpha1[I] collagen promoter exhibit growth retardation, osteomalacia, and disturbed phosphate homeostasis. Endocrinology 2004;145: 3087–94.

[179] Spitzer A, Barac-Nieto M. Ontogeny of renal phosphate transport and the process of growth. Pediatr Nephrol 2001; 16:763–71.

[180] Ichikawa S, Sorenson AH, Austin AM, Mackenzie DS, Fritz TA, Moh A, et al. Ablation of the Galnt3 gene leads to low-circulating intact fibroblast growth factor 23 (Fgf23) concentrations and hyperphosphatemia despite increased Fgf23 expression. Endocrinology 2009;150:2543–50.

[181] Brownstein CA, Adler F, Nelson-Williams C, Iijima J, Li P, Imura A, et al. A translocation causing increased alpha-klotho level results in hypophosphatemic rickets and hyperparathyroidism. Proc Natl Acad Sci (USA) 2008;105:3455–60.

[182] Szczepanska-Konkel M, Yusufi AN, VanScoy M, Webster SK, Dousa TP. Phosphonocarboxylic acids as specific inhibitors of Na^+-dependent transport of phosphate across renal brush border membrane. J Biol Chem 1986;261:6375–83.

[183] Francis F, Hennig S, Korn B, Reinhardt R, de Jonge P, Poustka A, et al. A gene (PEX) with homologies to endopeptidases is mutated in patients with X-linked hypophosphatemic rickets. The HYP Consortium. Nat Genet 1995;11:130–136.

[184] Karim-Jimenez Z, Hernando N, Biber J, Murer H. A dibasic motif involved in parathyroid hormone-induced down-regulation of the type IIa NaPi cotransporter. Proc Natl Acad Sci (USA) 2000;97:12896–901.

[185] Tenenhouse HS, Murer H. Disorders of renal tubular phosphate transport. J Am Soc Nephrol 2003;14:240–7.

[186] Feng JQ, Ward LM, Liu S, Lu Y, Xie Y, Yuan B, et al. Loss of DMP1 causes rickets and osteomalacia and identifies a role for osteocytes in mineral metabolism. Nat Genet 2006; 38:1310–5.

[187] Lorenz-Depiereux B, Benet-Pages A, Eckstein G, Tenenbaum-Rakover Y, Wagenstaller J, Tiosano D, et al. Hereditary hypophosphatemic rickets with hypercalciuria is caused by mutations in the sodium-phosphate cotransporter gene SLC34A3. Am J Hum Genet 2006;78:193–201.

[188] Lorenz-Depiereux B, Bastepe M, Benet-Pages A, Amyere M, Wagenstaller J, Muller-Barth U, et al. DMP1 mutations in autosomal recessive hypophosphatemia implicate a bone matrix protein in the regulation of phosphate homeostasis. Nat Genet 2006;38:1248–50.

[189] Cai Q, Hodgson SF, Kao PC, Lennon VA, Klee GG, Zinsmiester AR, et al. Brief report: inhibition of renal phosphate transport by a tumor product in a patient with oncogenic osteomalacia. N Engl J Med 1994;330:1645–9.

[190] Shimada T, Muto T, Urakawa I, Yoneya T, Yamazaki Y, Okawa K, et al. Mutant FGF-23 responsible for autosomal dominant hypophosphatemic rickets is resistant to proteolytic cleavage and causes hypophosphatemia in vivo. Endocrinology 2002;143:3179–82.

[191] White KE, Jonsson KB, Carn G, Hampson G, Spector TD, Mannstadt M, et al. The autosomal dominant hypophosphatemic rickets (ADHR) gene is a secreted polypeptide overexpressed by tumors that cause phosphate wasting. J Clin Endocrinol Metab 2001;86:497–500.

[192] Gattineni J, Bates C, Twombley K, Dwarakanath V, Robinson ML, Goetz R, et al. FGF23 decreases renal NaP-2a and NaPi-2c expression and induces hypophosphatemia in vivo predominantly via FGF receptor 1. Am J Physiol 2009;297: F282–291 svf

[193] Ichikawa S, Sorenson AH, Imel EA, Friedman NE, Gertner JM, Econs MJ. Intronic deletions in the SLC34A3 gene cause hereditary hypophosphatemic rickets with hypercalciuria. J Clin Endocrinol Metab 2006;91:4022–7.

CHAPTER

69

Clinical Disturbances of Phosphate Homeostasis

Theresa J. Berndt and Rajiv Kumar

Mayo Clinic, Rochester, Minnesota, USA

THE IMPORTANCE OF PHOSPHORUS IN BIOLOGICAL SYSTEMS

Phosphorus is the sixth most abundant element in the body and is essential for energy-consuming metabolic processes of cells. Approximately 85% of phosphate in the body is present in bones, 14% in cells from soft tissues, and 1% in extracellular fluids.[1] Phosphorus plays an important role in a number of biological processes, and is an exceptionally important component of hy droxyapatite, the major component of bone mineral.[2] In addition, phosphorus is present in nucleic acids, bioactive signaling proteins, phosphorylated enzymes, and cell membranes.[3–6] A prolonged deficiency of phosphorus and inorganic phosphate results in serious biological problems, including bone mineralization resulting in osteomalacia or rickets, abnormal erythrocyte, leukocyte and platelet function, impaired cell membrane integrity that can result in rhabdomyolysis, and impaired cardiac function.[7] Therefore, the maintenance of appropriate phosphorus homeostasis is critical for the well-being of the organism.

THE REGULATION OF PHOSPHATE BALANCE

Phosphorus exists in plasma almost entirely as inorganic phosphate.[1,7,8] The adult animal or human maintains phosphate balance through a series of complex hormonally and locally regulated metabolic adjustments. In states of neutral phosphate balance, net accretion equals net output. The major organs involved in the absorption, excretion, and reabsorption of phosphate are the intestine and the kidney (Fig. 69.1).[9,10] Furthermore, the movement of phosphorus between the extracellular fluid and bone and soft tissue also plays an important role in the maintenance of normal serum phosphate concentrations. A normal diet adequate in phosphorus normally contains $\approx$1500 mg of phosphorus. Approximately 1100 mg of ingested dietary phosphate is absorbed in the proximal intestine, predominantly in the jejunum. About 200 mg of phosphorus is secreted into the intestine via pancreatic and intestinal secretions, giving a net phosphorus absorption of approximately 900 mg/24 hours. Phosphorus that is not absorbed in the intestine or is secreted into the intestinal lumen eventually appears in the feces. Absorbed phosphorus enters the extracellular fluid pool and moves in and out of bone (and to a smaller extent in and out of soft tissues) as needed ($\approx$200 mg). Approximately 900 mg of phosphorus (equivalent to the amount absorbed in the intestine) is excreted in the urine.

A number of hormones such as parathyroid hormone (PTH) and $1\alpha,25(OH)_2D_3$ are involved in the control of phosphorus metabolism.[11] Concentrations of these hormones are regulated by phosphorus in a manner that is conducive to the maintenance of normal phosphate. Other peptide factors and hormones, such as growth hormone and insulin-like growth factor 1, alter phosphorus balance, although their circulating concentrations are not directly controlled by ambient phosphorus concentrations. The "phosphatonins," fibroblast growth factor 23 (FGF-23), and secreted frizzled related protein-4 (sFRP-4) that induce a state of negative phosphate balance directly by inhibiting renal phosphate reabsorption in the proximal tubule and indirectly by inhibiting the synthesis of $1\alpha,25(OH)_2D_3$

Seldin and Giebisch's The Kidney, Fifth Edition.
DOI: http://dx.doi.org/10.1016/B978-0-12-381462-3.00069-0

© 2013 Elsevier Inc. All rights reserved.

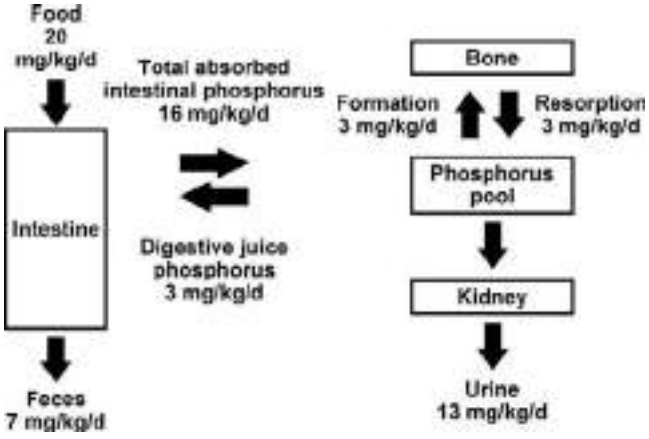

FIGURE 69.1 **Phosphorus metabolism.** *(From Schiavi SC, Kumar R. The phosphatonin pathway: new insights in phosphate homeostasis. Kidney Int 2004;65:1–14, with permission.)*

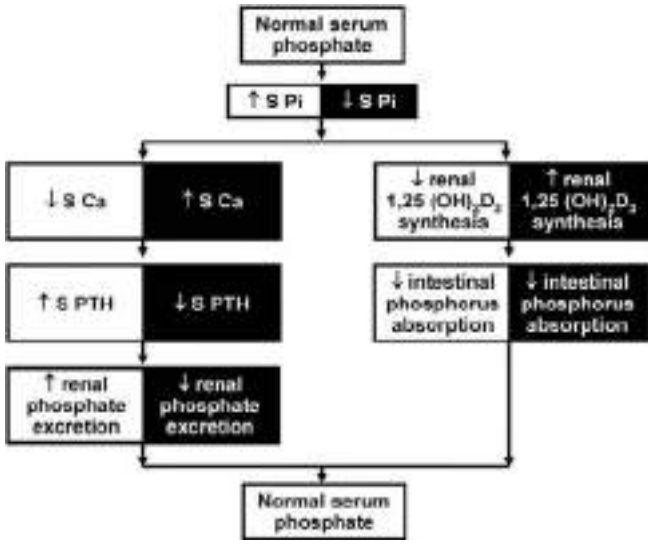

FIGURE 69.2 **Influence of phosphatate (Pi) on parathyroid hormone (PTH) and vitamin D synthesis and activity.** *(From Schiavi SC, Kumar R. The phosphatonin pathway: new insights in phosphate homeostasis. Kidney Int 2004;65:1–14, with permission.)*

and reducing the intestinal absorption of phosphorus, also play a key role in the regulation of phosphate balance.[12–16] Two factors, fibroblast growth factor 7 (FGF-7) and matrix extracellular phosphoglycoprotein (MEPE), have been shown to inhibit phosphate transport in renal epithelial cells in culture and, in the case of matrix extracellular phosphorus glycoprotein, to induce phosphaturia in mice.[17,18] FGF7 and MEPE, however, have not been demonstrated to prevent compensatory increases in serum $1\alpha,25(OH)_2D_3$ concentrations seen in hypophosphatemic states or to directly inhibit 25-hydroxyvitamin D 1α-hydroxylase activity.

Parathyroid hormone, by virtue of its phosphaturic effect in the kidney, decreases overall phosphate retention, whereas $1\alpha,25(OH)_2D_3$ increases phosphate retention by enhancing the efficiency of phosphorus absorption in the intestine and in the kidney.[19–31] It should be noted that parathyroid hormone has two opposing effects. As noted previously, parathyroid hormone increases urinary phosphate excretion. At the same time, it also increases the synthesis of $1\alpha,25(OH)_2D_3$ by stimulating the activity of the 1α-hydroxylase enzyme in the kidney. In turn, $1\alpha,25(OH)_2D_3$ increases the efficiency of phosphorus absorption in the intestine and kidney.[28–30,32–35] The phosphatonins, in contrast, increase renal phosphate excretion and inhibit 25-hydroxyvitamin D 1α-hydroxylase activity, thereby further decreasing the retention of phosphorus.[12,15,36,37]

Figure 69.2 shows the physiological changes known to occur with low or high dietary intakes of phosphate. A decrease in serum phosphate concentrations results in increased ionized calcium concentrations, decreased parathyroid hormone secretion, and a subsequent decrease in renal phosphate excretion. At the same time, by parathyroid hormone-independent mechanisms, there is an increase in renal 25-hydroxyvitamin D 1α-hydroxylase activity, increased $1\alpha,25(OH)_2D_3$ synthesis, and increased phosphorus absorption in the intestine and reabsorption in the kidney.[20–31,35,38] Conversely, with elevated phosphate intake, there are decreased calcium concentrations, increased parathyroid hormone release from the parathyroid gland, and increased renal phosphate excretion. Increased serum phosphate concentrations inhibit renal 25-hydroxyvitamin D 1α-hydroxylase and decrease $1\alpha,25(OH)_2D_3$ synthesis. Reduced $1\alpha,25(OH)_2D_3$ concentrations decrease intestinal phosphorus absorption as well as renal phosphate reabsorption. All of these factors tend to bring serum phosphate concentrations back into the normal range.

THE PHYSIOLOGY OF PHOSPHATE IN THE KIDNEY

In conditions of phosphate deprivation, the kidney rapidly increases tubular phosphate reabsorption and reduces urinary phosphate excretion to negligible levels in order to preserve phosphate balance.[39,40,42–56] In infants and children, phosphate reabsorption is high so as to maintain a positive phosphate balance required for growth.[57–59] Conversely, decreased phosphate reabsorption has been demonstrated in the elderly.[60–63] Phosphate is freely filtered at the glomerulus. Under conditions of normal dietary phosphate intake, and in the presence of intact parathyroid glands, approximately 20% of the filtered phosphate load is excreted.

The other 80% of the filtered load of phosphate is reabsorbed by the renal tubules.

The proximal tubules are the major sites of phosphate reabsorption along the nephron. There is little phosphate reabsorption between the late proximal tubule and the early distal tubule in animals with intact parathyroid glands.[44,64–71] However, in the absence of parathyroid hormone, phosphate is avidly reabsorbed between the late proximal tubule and early distal tubule, reflecting phosphate reabsorption by the proximal straight tubule (Fig. 69.3).[66] Phosphate transport rates are approximately three times higher in the proximal convoluted than in the proximal straight tubules.[72] Renal phosphate handling is characterized by intranephronal heterogeneity, reflecting segmental differences in phosphate handling within an individual nephron as well as internephronal heterogeneity.[44,67,72,73]

The uptake of phosphate is mediated by sodium-phosphate cotransporters that are located at the apical border of proximal tubule cells (NaPi IIa and NaPi IIc).[74–97] The structure and physiology of these phosphate transport molecules have been extensively reviewed, and the reader is directed to other publications in this regard.[82–90] The sodium-phosphate cotransporters are highly homologous and are predicted to have similar structures. Mice with ablation of the NaPi IIa gene exhibit renal phosphate wasting, and it is estimated that the NaPi IIa transporter is responsible for approximately 85% of proximal tubular phosphate transport which contributes to the adaptive increase in tubular phosphate transport in animals fed a low-phosphate diet (Fig. 69.4).[98,99]

FACTORS REGULATING RENAL PHOSPHATE EXCRETION

Dietary Phosphate and Renal Phosphate Reabsorption

The influence of dietary phosphate intake on the urinary excretion of phosphate has been known for many years.[40–56,100] The reabsorption of phosphate is decreased in animals fed a high-phosphate diet, whereas animals with a low intake of phosphate reabsorb almost 100% of the filtered load of phosphate. These changes in phosphate reabsorption are associated with parallel changes in the abundance of NaPi IIa and IIc transporters.[101,102] The dietary intake of phosphate can differ considerably depending on the ingestion of foods containing varying amounts of phosphate.

Although dietary phosphate deprivation results in marked changes in the plasma concentrations of several hormones (Fig. 69.2) that contribute to the increases in phosphate reabsorption, the enhanced tubular reabsorption can also be demonstrated independent of changes in these hormones.[103–106] The mechanism of upregulation of Na/Pi cotransport in OK cells by low-Pi media involves two regulatory mechanisms: an

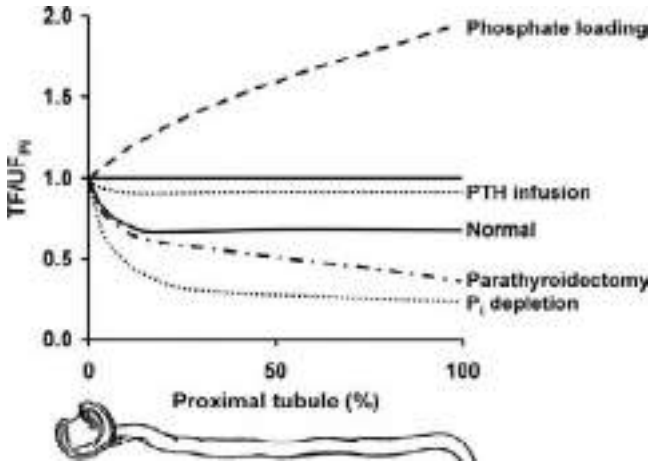

FIGURE 69.3 The generation of tubule fluid/ultrafiltrate phosphate (UFPi) ratios below 1.0 along the proximal convoluted tubule is due to more avid reabsorption of phosphate than isotonic fluid for most circumstances. Diet and parathyroid hormone are the major factors that affect phosphate transport. *(From Berndt T, Knox F. Renal regulation of phosphate excretion. In: Seldin DAG (ed.). The Kidney: Physiology and Pathophysiology. New York: Raven Press, 1992:2511–2532, with permission.)*

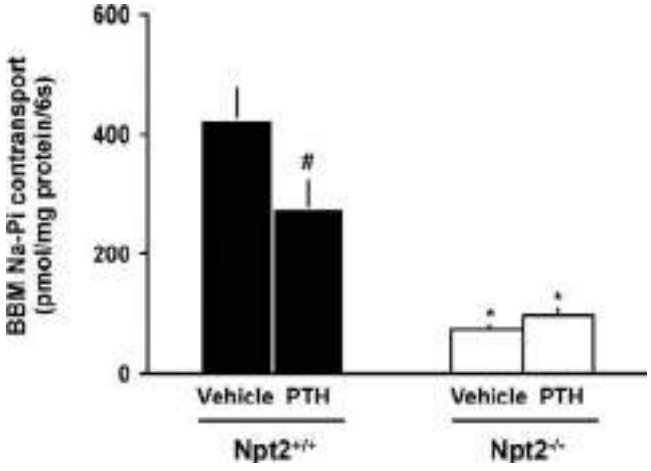

FIGURE 69.4 Effect of parathyroid hormone (PTH) on brush border membrane Na-Pi cotransport in Npt2 +/+ and Npt2 −/− mice. Anesthetized mice were injected with vehicle or PTH (10 μg/100 g BW) and killed 2 hours later. Renal brush border membranes vesicles were prepared from kidney cortex, and transport of Pi was assayed. Effect of PTH in Npt2 + / + mice, $p < 0001$; affect of genotype in PTH-treated mice, $p < 0041$. *(From Zhao N, Tenenhouse HS. Npt2 gene disruption confers resistance to the inhibitory action of parathyroid hormone on renal sodium-phosphate cotransport. Endocrinology 2000;141:2159–2165, with permission).*

immediate (early) increase (after two hours) in the expression of Na/Pi cotransporter, independent of mRNA synthesis or stability, and a delayed (late) effect (after 4–6 hours), resulting in an increase in NaPi-4 mRNA abundance (Fig. 69.5).[105,107] Although the changes in phosphate reabsorption in response to a low- or high-phosphate meal are demonstrable within two hours, there are not always concomitant alterations in plasma phosphate concentrations. Thus, the sensing mechanism that initiates the renal adaptations in phosphate reabsorption to the changes in phosphate intake is speculative. The enhanced phosphate reabsorption of short-term phosphate deprivation has been linked to decreased intrarenal synthesis of dopamine and/or stimulation of beta adrenoreceptors, since infusion of dopamine or propranolol restores the phosphaturic response to PTH in short-term (less than three days) phosphate deprivation.[108–110] The concept of central control of phosphate homeostasis was suggested since decreased dietary phosphate intake upregulated the NaPi IIa expression in the brain and increased phosphate intake downregulated the expression of NaPi IIa in the brain.[111] In this study, increasing cerebrospinal fluid phosphate concentrations in the presence of low plasma phosphate concentrations reversed the adaptations to feeding a low-phosphate diet, suggesting that the phosphate concentration in the brain regulates not only central but also renal expression of NaPi IIa transporters. Studies using cultured renal proximal tubular cells provide persuasive evidence of an intrinsic ability of these cultured cells to increase phosphate transport when exposed to a low phosphate concentration in the medium.[103–106] In addition to the factors that play a role in enhancing or decreasing phosphate reabsorption in the proximal nephron in response to changes in dietary phosphate noted previously, it should be remembered that alterations in serum phosphate concentrations also alter $1\alpha,25(OH)_2D_3$ synthesis and serum concentrations.[45,112–115] Infusions of $1\alpha,25(OH)_2D_3$ increase the renal reabsorption phosphate, predominantly in the proximal nephron.[20–27,31] Since the proximal tubule is a major site of phosphate reabsorption, it is the primary site for the tubular adaptation to changes in dietary phosphate intake. The enhanced phosphate reabsorption along the nephron during phosphate deprivation in specific nephron subsegments is dependent on the length and severity of phosphate deprivation.

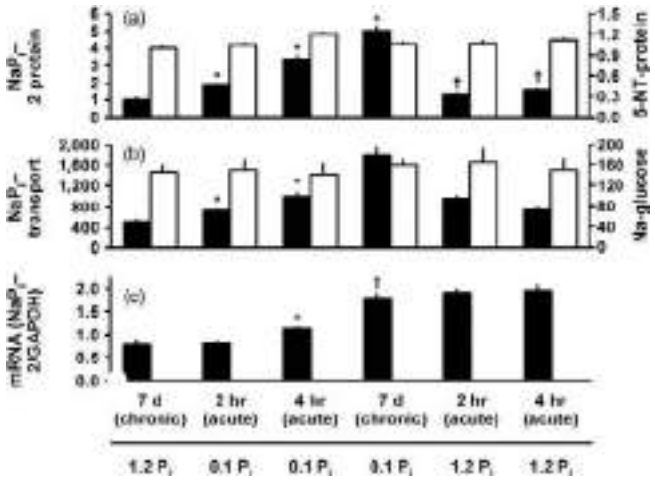

FIGURE 69.5 Pi-deprivation dependent alterations in (A) rat type II transporter (NaPi-2) protein content, (B) rat brush border membrane Na/Pi cotransport activity, and (C) specific rat type II transporter mRNA content (NaPi-2). Rats were fed for 7 days with a diet containing high Pi (1.2 Pi) and were exposed for different time periods to low Pi (0.1 Pi). Rats chronically adapted to low Pi have been re-fed with high Pi for two or four hours. A: Black small square, Na/Pi transport; white square, 5-NT-protein. B: Black small square, Na/Pi transport; white square, Na-glucose. *(From Murer H, Lotscher M, Kaissling B, Levi M, Kempson SA, Biber J. Renal brush border membrane Na/Pi-cotransport: molecular aspects in PTH-dependent and dietary regulation. Kidney Int 1996;49:1769–1773, with permission.)*

Parathyroid Hormone and Renal Phosphate Reabsorption

Plasma-ionized calcium levels are a critical determinant of PTH secretion. A fall in plasma-ionized calcium increases PTH secretion and an elevation of plasma-ionized calcium above normal levels decreases PTH secretion. Parathyroidectomy decreases renal phosphate excretion and, conversely, injection of PTH increases urinary phosphate excretion.[116–120] Micropuncture studies show that PTH decreases and parathyroidectomy increases phosphate reabsorption along the proximal tubule (Fig. 69.3).[65–69,121] The proximal straight tubule is an important site of PTH modulation of phosphate transport and may be critical in the final regulation of phosphate excretion.[64,70,73,122] Parathyroid hormone maintains phosphate homeostasis as a result of its regulation of the sodium phosphate cotransporters in the kidney. Renal sodium-phosphate cotransporters are reduced in number along the apical borders of proximal tubular cells following the administration of parathyroid hormone 1 through 34 but not by the administration of parathyroid hormone 3 through 34.[94,95] The renal sodium-phosphate cotransporters NaPi IIa have been shown to be internalized and degraded within the lysosomes.[84,89,123,124] Disruption of the NaPi IIa gene in mice resulted in increased excretion of phosphate compared to wildtype mice and a resistance to the phosphaturic response to PTH, although the cyclic adenosine monophosphate

(cAMP) response is normal (Fig. 69.4).[125] Under conditions where the phosphaturic effect of PTH is blunted or absent, such as short-term phosphate deprivation or acute respiratory alkalosis, the inhibitory effect of PTH on phosphate reabsorption by the proximal convoluted tubule remains intact. However, this increased delivery of phosphate is blunted by enhanced reabsorption by the proximal straight tubule.[73,122,70] These studies suggest that the regulation of phosphate reabsorption by PTH in the proximal convoluted and proximal straight tubule subsegments may be mediated by different mechanisms. It should be noted that parathyroid hormone has two opposing effects. As noted previously, parathyroid hormone increases urinary phosphate excretion. At the same time, it also increases the synthesis of $1\alpha,25(OH)_2D_3$ by stimulating the activity of the 25-hydroxyvitamin D_3 1α-hydroxylase enzyme in the kidney.[126–128]

Vitamin D and Renal Phosphate Reabsorption

A complex interrelationship exists between vitamin D and PTH. Both hormones play important roles in calcium and phosphate regulation.[129–134] Decreases in plasma ionized calcium levels increase PTH levels and PTH also stimulates the renal conversion of $25(OH)_2D_3$ to $1,25(OH)_2D_3$ by the 25-hydroxyvitamin D_3 1α-hydroxylase located in the proximal tubule of the kidney.[126–128,135–137] Dietary phosphate deprivation or hypophosphatemia induces 25-hydroxyvitamin D_3 1α-hydroxylase.[34,112–115,138] Mice or rats, but not pigs, fed a low-phosphate diet show a decrease in the activity of the 25-hydroxyvitamin D_3 24-hydroxylase (a renal enzyme involved in the catabolism of $1,25(OH)_2D_3$) compared with rats fed a normal phosphate diet within 24 hours of phosphate restriction.[139–141] Vitamin D modestly decreases renal phosphate excretion, and its primary effect is to enhance phosphate transport in the intestine.[20–27,31] Vitamin D receptor (VDR)-mutant mice exhibit decreased serum phosphate, however, phosphate transport by renal cortical brush border membranes, phosphate excretion or NaPi IIa or NaPi IIc mRNA levels were not different between VDR-null or wildtype mice, while NaPi IIa protein expression and NaPi IIa cotransporter immunoreactive signals were slightly but significantly decreased in the $VDR^{-/-}$ mice compared with the wildtype mice.[102] When VDR knockout mice were fed a low-phosphate diet, serum phosphate concentrations were more markedly decreased in the VDR knockout mice than in the wildtype mice. Other studies performed in vitamin D receptor and 25-hydroxyvitamin D 1α-hydroxylase null mutant mice show that both these knockout mice adapt to phosphate deprivation with increased NaPi IIa protein in a manner similar to that found in wildtype mice.[142] However, when these mice were fed a high-phosphate diet, phosphate excretion was less in the vitamin D receptor and 25-hydroxyvitamin D 1α-hydroxylase null mutant mice compared to the wildtype mice. In vitamin D-deprived rats, NaPi IIa transporter protein and mRNA were reported to be decreased in juxtamedullary but not superficial renal cortical tubules compared with normal rats.[143]

Insulin, Growth Hormone, Insulin-Like Growth Factor, and Renal Phosphate Reabsorption

Insulin decreases plasma phosphate and phosphate excretion in human and animal models.[144–148] This enhanced renal phosphate reabsorption can be demonstrated in the absence of changes in blood glucose, PTH, and phosphate levels or urinary sodium excretion. Initial micropuncture studies by DeFronzo et al.[145] demonstrate enhanced phosphate reabsorption in hyperinsulinemic dogs. Conversely, somatostatin infusion decreases plasma insulin levels and increases phosphate excretion.[149] Growth hormone decreases phosphate excretion and has been postulated to contribute to increased phosphate reabsorption and positive phosphate balance demonstrated in growing animals.[60,61] Administration of a growth hormone antagonist for 4 days to immature rats suppressed growth in these rats and was associated with increased phosphate excretion and a decreased transport capacity for phosphate reabsorption.[150,151] Subsequent studies performed in juvenile rats in which growth hormone was suppressed showed increase phosphate excretion to levels comparable to adult rats as a result of decreased NaPi IIa expression, demonstrating the important role for growth hormone in the enhanced phosphate reabsorption in developing animals.[152] Hammerman et al.[153] demonstrated that growth hormone administration increased phosphate uptake by brush border membrane vesicles prepared from kidneys of adult dogs. These effects of growth hormone on phosphate reabsorption may also be due to insulin-like growth factor-1 (IGF-1).[154–161] Growth hormone stimulates the renal synthesis and release of IGF-1.[154] The addition of IGF-1 to cultured renal opossum kidney cells stimulates sodium-dependent phosphate transport.[157] A selective increase in sodium-dependent phosphate uptake was detectable after 15 minutes and is maximal at five hours. Chronic administration of IGF-1 infused by osmotic mini-pump for six days significantly increased the maximal tubular reabsorption of phosphate in the presence and absence of PTH and enhanced phosphate transport by renal brush border membranes.[158]

Renal Nerves, Catecholamines, Dopamine, and Serotonin

Acute renal denervation increases urinary phosphate excretion independent of parathyroid hormone.[109,162–166] Numerous studies have demonstrated that acute renal denervation or the administration of catecholamines alters phosphate reabsorption.[109,162–175] The increase in urinary phosphate excretion after acute renal denervation could be due to both increased production of dopamine and decreased α- or β-adrenoreceptor activity, since acute renal denervation has been shown to initially increase renal dopamine excretion and almost completely abolish norepinephrine and epinephrine levels in the kidney.[176,177] Epinephrine decreases plasma phosphate, presumably by shifting phosphate from the extracellular into the intracellular space. The hypophosphatemic response to isoproterenol infusion is blocked by propranolol, suggesting involvement of the beta adrenoreceptors. Infusion of isoproterenol markedly enhances renal phosphate reabsorption in normal rats and in hypophosphatemic mice.[173,178] The enhanced phosphate reabsorption and attenuated phosphaturic response to PTH observed in acute respiratory alkalosis and phosphate deprivation is blocked by infusion of propranolol, suggesting a possible role for stimulation of β-adrenoreceptors in these conditions. Stimulation of α-adrenoreceptors by the addition of epinephrine to cultured opossum kidney cells blunts the PTH-induced increase in cAMP levels and the inhibition of phosphate transport.[179] Stimulation of α2-adrenoreceptors *in vivo* has also been demonstrated to attenuate the phosphaturic response to PTH.[109] Dopamine infusion and the infusion of L-DOPA or glupopa, dopamine precursors, increase phosphate excretion in the absence of PTH.[180–182] Dopamine administration has been reported to decrease phosphate transport in cultured opossum kidney cells and rabbit proximal straight tubules.[172,183–188] Studies suggest that dopamine may be a proximal tubular paracrine substance in the regulation of phosphate reabsorption. The enzyme that converts L-DOPA to dopamine is located exclusively in the proximal convoluted and straight tubules, also the primary sites of phosphate reabsorption. Increasing dietary phosphate intake increases urinary dopamine excretion and phosphate excretion.[189] Inhibition of endogenous dopamine synthesis by the administration of carbidopa to rats resulted in decreased dopamine and phosphate excretion, suggesting a role for endogenous dopamine in phosphate regulation.[168,177] A potential paracrine role for dopamine in phosphate regulation was strengthened by studies performed in opossum kidney cells that demonstrated that the addition of dopamine or L-DOPA selectively decreased phosphate uptake (Fig. 69.6). Furthermore, phosphate-replete OK cells produced more dopamine from L-DOPA than phosphate-deprived cells.[185] Administration of dopamine to phosphate-deprived or respiratory alkalotic rats increases phosphate excretion and enhances the phosphaturic response to PTH.[108,109] Subsequent studies in opossum kidney cells performed by several laboratories demonstrated that increasing dopamine synthesis inhibits phosphate transport by multiple mechanisms including activation of DA1 and DA2 receptors.[184,187,188] More recent studies performed using mouse kidney slices, perfused proximal tubules, and opossum kidney cells examined the effect of dopamine on NaPi IIa expression and localization using DA1 and DA2 agonists.[183] In these studies, dopamine induced the internalization of NaPi IIa by activation of luminal DA1 receptors. Renal proximal tubules also synthesize serotonin from 5-hydroxytryptophan by the same enzyme that converts L-DOPA to dopamine. Incubation of opossum kidney cells with either serotonin or 5-hydroxytryptophan enhanced phosphate transport and raises the possibility that serotonin may also be involved in the physiological regulation of renal phosphate transport.[180,186,190,191]

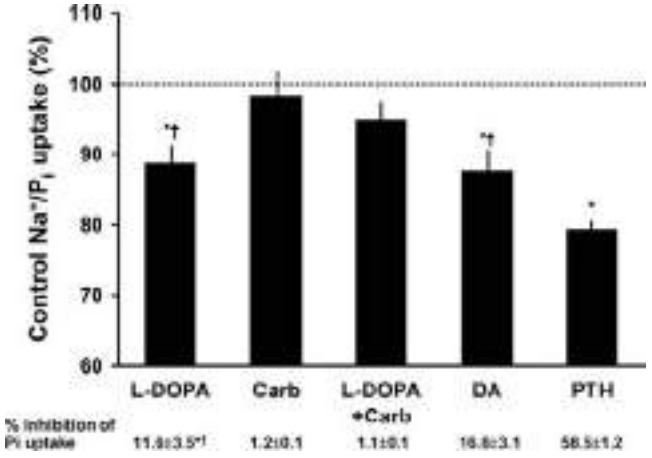

FIGURE 69.6 Effects of incubation either with 250 μM L-DOPA, 250 μM carbidopa (Carb), with combination of both, with exogenous dopamine (DA, 10 μM) or with parathyroid hormone (PTH 2 U/ml) on Na + -Pi cotransport in opossum kidney (OK) cell monolayers. Effects of exogenous and endogenous agents on Na + -Pi cotransport are expressed as % difference (decrease) from basal values denoted by dotted line. *Significant differences ($p < 05$, paired t test) from controls. † Significant difference ($p < 05$) compared with values from PTH. Each bar denotes mean ± SE of four independent experiments, each performed in triplicate. *(From Glahn RP, Onsgard MJ, Tyce GM, Chinnow SL, Knox FG, Dousa TP. Autocrine/paracrine regulation of renal Na(+)-phosphate cotransport by dopamine. Am J Physiol 1993;264: F618–622, with permission.)*

The Phosphatonins and Renal Phosphate Reabsorption

The term "phosphatonin" was introduced to describe a factor or factors responsible for the inhibition of renal phosphate reabsorption and altered 25-hydroxyvitamin D 1α-vitamin D regulation observed in patients with tumor-induced osteomalacia.[192] Cai et al.[193] described a patient with tumor-induced osteomalacia in whom the biochemical characteristics of hypophosphatemia, renal phosphate wasting and reduced 1α,25(OH)2D disappeared following removal of the tumor. A similar biochemical phenotype exists in patients with X-linked hypophosphatemic rickets (XLH) and the animal model, the Hyp mouse.[194–199] Several investigators have shown the presence of circulating factors in the serum of Hyp mice that inhibit sodium-dependent phosphate transport in the kidney.[200–202] Further studies demonstrated that patients with the disease, autosomal dominant hypophosphatemic rickets (ADHR), had activating mutations within the fibroblast growth factor homolog, fibroblast growth factor 23 (FGF-23).[203] Its persistence in the circulation resulted in the biochemical phenotype of hypophosphatemia, renal phosphate wasting and low 1α,25$(OH)_2$D concentrations.[203,204] Studies using serial analysis of gene expression (SAGE) identified additional genes that were overexpressed in tumors associated with tumor-induced osteomalacia.[205] Some studies have identified several new factors that also play a role in the regulation of phosphorus transport and homeostasis.[12–16,36,206–210] These include the "phosphatonins," FGF-23, and sFRP-4 that induce a state of negative phosphate balance directly by inhibiting renal phosphate reabsorption in the proximal tubule and indirectly by inhibiting the synthesis of 1α,25$(OH)_2D_3$ and reducing the intestinal absorption of phosphorus.[12–16,36,206–210] Two factors, fibroblast growth factor 7 (FGF-7) and MEPE have been shown to inhibit phosphate transport in renal epithelial cells in culture and, in the case of matrix extracellular phosphorus glycoprotein, to induce phosphaturia in mice.[18,211] FGF-7 and MEPE, however, have not been demonstrated to prevent compensatory increases in serum 1α,25$(OH)_2D_3$ concentrations seen in hypophosphatemic states or to directly inhibit 25-hydroxyvitamin D 1α-hydroxylase activity. In contrast, the phosphatonins increase renal phosphate excretion and inhibit 25-hydroxyvitamin D 1α-hydroxylase activity, thereby further decreasing the retention of phosphorus.

Fibroblast Growth Factor-23

As noted previously, FGF-23 was initially postulated to be the factor responsible for autosomal dominant hypophosphatemic rickets.[203] A mutation in the FGF-23 gene resulted in expression of a FGF-23 protein that was resistant to proteolysis and with a prolonged half-life and biopotency.[204,212–216] Recombinant FGF-23 produced hypophosphatemia when administered intraperitoneally to mice.[37] Serum calcium concentrations did not change following the administration of the peptide. When Chinese hamster ovary cells were transfected with an FGF-23 expression plasmid and cells were implanted in nude mice, the animals became hypophosphatemic and the fractional excretion of phosphate was increased within 10 days. Alkaline phosphatase concentrations increased in the serum consistent with changes in bone mineralization. Radiologic evidence of rickets in the long bones and histological evidence of rachitic changes were observed after several weeks. There was a decrease in the amount of messenger RNA for the 25-hydroxyvitamin D 1α-hydroxylase. In support of these studies, Bowe et al. demonstrated that recombinant FGF-23 inhibited sodium-dependent phosphate transport in opossum kidney cells.[206] Furthermore, intravenous infusion of recombinant FGF-23 into mice caused a rapid, dose-dependent increase in the fractional excretion of phosphate with little or no change in sodium excretion (Fig. 69.7).[15] These studies suggest that FGF-23 has direct actions on renal phosphate transport. The role of FGF-23 in modulating plasma phosphate concentrations and 25 hydroxyvitamin D 1α-hydroxylase levels was further supported by the generation of FGF-23 null mutant mice.[217] These mice had reduced growth rate and died 10 to 14 weeks after birth. Serum phosphate concentrations were elevated within 10 days after birth and serum calcium concentrations became moderately elevated 2 weeks after birth. Interestingly, these mice developed increased renal 25-hydroxyvitamin D 1α-hydroxylase messenger RNA levels and associated increases in serum 1α,25$(OH)_2$D concentrations. A moderate increase in serum calcium concentrations was also observed that could be a consequence of the increased 1α,25$(OH)_2$D concentrations and increased intestinal calcium transport. Parathyroid hormone concentrations were diminished in the homozygous mutant mice only at 9 weeks of age. Long bones displayed abnormal mineralization and reduced growth plate. The TmP/GFR was significantly increased in FGF-23 in null mutant animals. Conversely, transgenic mice overexpressing FGF-23 have reduced serum phosphate concentrations, increased phosphate excretion, and reduced renal sodium-phosphate cotransporter, NaPi IIa.[218,219] In addition to changes in phosphate homeostasis, chronic overexpression of FGF-23 has also been linked to disturbances in vitamin D metabolism, calcium homeostasis and increased PTH levels.[212] The exact interaction and the relative contribution of FGF-

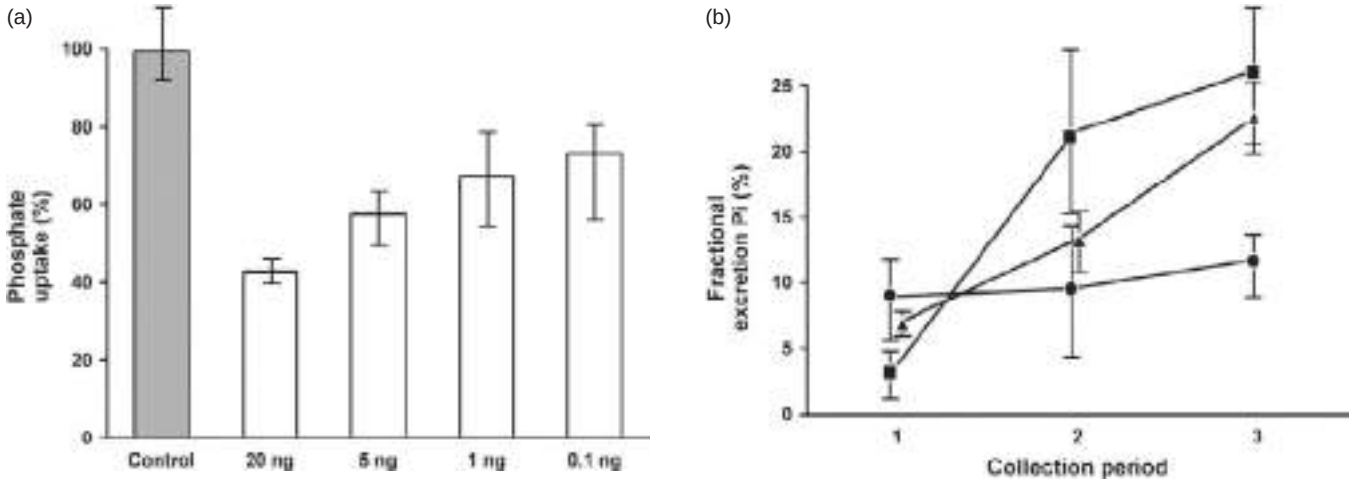

FIGURE 69.7 **Effect of fibroblast growth factor-23 (FGF23) on phosphate transport.** (a) In vitro effects of FGF23 on inorganic phosphorus transport (Pi) in opossum kidney cells. (b) FGF23 effects on the percent fractional Pi excretion. Mice were infused for 2 hours with vehicle (circle), 0.5 μg FGF23/2 hours (triangle), or 5 μg FGF23/2 hours (square). *(From Schiavi SC, Kumar R. The phosphatonin pathway: new insights in phosphate homeostasis. Kidney Int 2004;65:1–14, with permission.)*

23, PTH, and vitamin D on phosphate homeostasis in these models of chronic FGF-23 excess remains unknown.

The role of FGF-23 in the physiologic regulation of phosphate homeostasis has been addressed by studies to determine the effect of dietary phosphate intake on serum FGF-23 levels. In healthy humans, the effects of phosphate loading and deprivation have shown modest or no changes in circulating FGF-23 concentrations. In one study, an increased phosphate intake slightly increased serum FGF-23.[220] In contrast, other studies in humans did not demonstrate an effect of dietary phosphate intake on serum FGF-23 levels.[221] In rats with renal failure, an increase in dietary phosphate has been shown to increase FGF-23 concentrations in the serum.[222] Future studies are necessary to determine the source of FGF-23 and how its expression is regulated.

The mechanism of action of FGF-23 on phosphate transport is currently unknown. Limited *in vitro* binding studies suggest that FGF23 may bind to FGFR-Fc fusion proteins.[223] Furthermore, tyrosine kinase inhibitors that are known to inhibit signaling through FGFRs block the effect of FGF-23 on sodium-dependent phosphate opossum kidney cells. These results raise the possibility that FGF-23 may signal through one of the known FGFRs.

Secreted Frizzled Related Protein-4

sFRP-4 was among the most consistently overexpressed genes found associated with oncogenic osteomalacia. To assess whether sFRP-4 has phosphatonin activity, it was expressed by recombinant methods in COS or insect cells.[36] Increasing concentrations of the recombinant protein were added to opossum kidney cells to determine whether it inhibits sodium-dependent phosphate transport. We observed that sFRP-4 inhibited sodium-dependent phosphate transport in opossum kidney cells in a dose-dependent manner at concentrations in the pg/ml range. When infused into rats, sFRP-4 increased renal phosphate excretion at 2 and 8 hours following initiation of the sFRP-4 infusion (Fig. 69.8).[36,15] Minimal changes in sodium excretion were seen and calcium excretion did not change. Interestingly, the effects of sFRP-4 were also demonstrated in parathyroidectomized rats, thus demonstrating that parathyroid hormone was not essential for the phosphaturic effect of sFRP-4. During an 8-hour intravenous infusion of sFRP-4, serum phosphate concentrations decreased and phosphate excretion increased. However, no change in 25-hydroxyvitamin D 1α-hydroxylase messenger RNA concentrations was noted in the kidney. The infusion of sFRP-4 was associated with a decrease in β-catenin concentrations in renal cells and an increase in phosphorylated β-catenin, thereby demonstrating that sFRP-4 may act as an antagonist against Wnt molecules in the kidney. Additionally, sFRP-4 was detected in the plasma of healthy subjects and in patients with tumor-induced osteomalacia, although the current assay did not detect elevated levels associated with tumor-induced osteomalacia. Thus, the data published to date suggest that sFRP-4 is a phosphatonin. Details concerning the mechanism by which FRP-4s inhibits renal

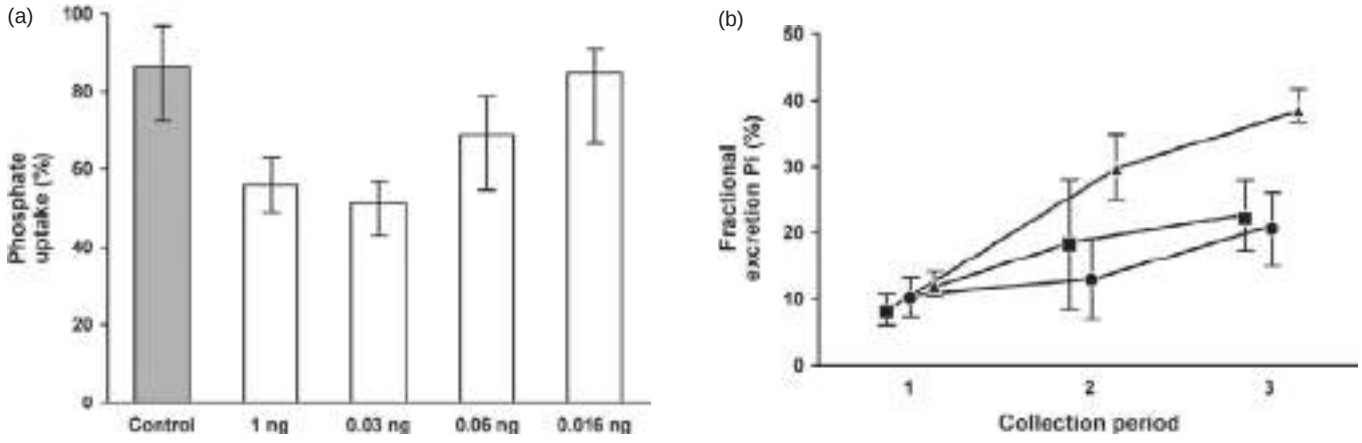

FIGURE 69.8 (a) Effect of frizzled-related protein-4 (FRP4) on phosphate transport. In vitro effects of FRP4 on inorganic phosphorus transport (Pi) in opossum kidney cells. (b) FRP4 effects on the percent fractional Pi excretion. Mice were infused for 2 hours with vehicle (circle), 0.05 μg FRP4/2 hours (square), or 0.5 μg FRP4/2 hours (triangle). *(From Schiavi SC, Kumar R. The phosphatonin pathway: new insights in phosphate homeostasis. Kidney Int 2004;65:1–14, with permission.)*

phosphate reabsorption and its relationship to FGF-23 will need to be elucidated in the future. Studies performed in mice in which the sFRP-1 gene was deleted demonstrate that these mice exhibit enhanced trabecular bone formation in adult mice. In these studies, plasma phosphate concentrations were significantly increased by 29% in male mice at 18 to 20 weeks of age, consistent with the possibility that sFRP proteins modulate renal phosphate reabsorption.[224]

Matrix Extracellular Phosphoglycoprotein

Matrix extracellular phosphoglycoprotein (MEPE) is also among the most abundantly overexpressed mRNA species found in tumors associated with renal phosphate wasting and osteomalacia.[18,205,225] Recently, MEPE has been expressed in insect cells and administered to mice *in vivo*.[18] The protein causes renal phosphate wasting and a reduction in serum phosphate concentrations *in vivo*. Additionally, there is inhibition of sodium-dependent phosphate uptake noted in opossum kidney cells exposed to the protein. MEPE also inhibits bone mineralization *in vitro* and MEPE null mice have increased bone mineralization.[226] This suggests that it may play a role in the pathogenesis of X-linked hypophosphatemic rickets in which there is phosphate wasting and evidence for a mineralization defect that is independent of low phosphate concentrations in the extracellular fluid.[227] Recent evidence suggests that concentrations of this substance are increased in the serum of patients with X-linked hypophosphatemic rickets.[207] It has been suggested that MEPE is a substrate for PHEX[228,229] and that PHEX prevents proteolysis of MEPE and release of a protease-resistant MEPE-ASARM peptide, an inhibitor of mineralization (minhibin). Phex may be acting to interfere with the actions of other enzymes that degrade extracellular matrix proteins. PHEX and MEPE form a nonproteolytic protein interaction via the MEPE carboxy-terminal ASARM motif. The ASARM peptide is believed to inhibit mineralization *in vivo*. The binding of MEPE and ASARM peptide by PHEX may explain why loss of functional osteoblast-expressed PHEX results in defective mineralization in Hyp. MEPE concentrations have been measured in normal humans and concentrations of the protein appear to correlate with bone mineral density and serum phosphate concentrations.[230]

Fibroblast Growth Factor 7

A recent report has shown that FGF-7 is overexpressed in tumors associated with osteomalacia and renal phosphate wasting.[17,211] FGF-7 protein inhibited sodium-dependent phosphate transport in opossum kidney cells. Anti–FGF-7 antibodies attenuated the inhibitory effect of tumor supernatants on sodium-dependent phosphate transport. Only low concentrations of FGF-23 were present in the supernatant medium of tumor cells. At present it is not known if FGF-7 circulates in plasma, whether it alters 25-hydroxyvitamin D 1α-hydroxylase levels or whether it is elevated in the plasma of subjects with tumor induced osteomalacia. Nevertheless, the report does point to the complexity of factors involved in the pathogenesis of tumor induced osteomalacia.

ACUTE AND CHRONIC HYPOPHOSPHATEMIA

Hypophosphatemia is a commonly seen condition in the hospital setting. By definition, this is a decrease in serum phosphate concentrations below those seen in a normal healthy population. Serum phosphate concentrations vary with age, being higher in young individuals than in adults. Table 69.1 shows concentrations of serum phosphorus in males and females of different ages as determined at the Mayo Clinic.

Hypophosphatemia does not necessarily imply an overall deficiency of phosphate, since serum phosphate concentrations can change as a result of redistribution of phosphate from serum and extracellular fluid into bone and soft tissues. When the underlying disorder causing the redistribution resolves, serum phosphate concentrations returned to normal. Hypophosphatemia can be the result of decreased intake or absorption of phosphorus, a redistribution of phosphate from the serum into cells, or decreased renal phosphate reabsorption.[11] Table 69.2 shows the causes and mechanisms of hypophosphatemia. Severe hypophosphatemia, often requiring therapy with phosphate, occurs in the following conditions: acute renal failure (especially when there has been significant tissue damage and necrosis), chronic alcoholism and alcohol withdrawal, dietary deficiency and therapy with phosphate-binding antacids, hyperalimentation, neuroleptic malignant syndrome, recovery from diabetic ketoacidosis, recovery from exhaustive exercise, after kidney transplantation, respiratory alkalosis, severe thermal burns, therapeutic hyperthermia, Reye syndrome, after major surgery, periodic paralysis, acute malaria, drug therapy with ifosamide or cisplatin, acetaminophen intoxication, or cytokine infusions with tumor necrosis factor or interleukin-2.[11]

Hypophosphatemia can cause a variety of clinical disorders. Red cell, leukocyte, and platelet dysfunction has been described.[11] In red cells, hypophosphatemia is associated with a decline in 2,3-diphosphoglycerate and adenosine triphosphate.[11] Structural defects in the red cell resulting in hemolysis have been described.[231,232] In severe hypophosphatemia, leukocyte chemotaxis, phagocytosis, and bactericidal activity are depressed.[233] Platelet dysfunction manifests by thrombocytopenia, an increase in platelet diameter, accelerated platelet disappearance, impaired clot retraction, and hemorrhage into the skin and intestine has been described.[234] Central nervous system dysfunction has been described in patients with severe hypophosphatemia. Patients may manifest irritability, weakness, numbness, paresthesias, confusion, obtundation, seizures and coma.[235] Rhabdomyolysis has been described in severe hypophosphatemia, especially in the context of alcoholism.[236–238] Myofibrillar damage has been observed in severe hypophosphatemia.[239] A reversible cardiomyopathy has been described in experimental animals and patients with severe hypophosphatemia.[11,240] Also, dysfunction can also cause weakness of the diaphragm and has, in some instances, been described to result in respiratory insufficiency.[57,241–250] In some instances, dietary phosphorus deprivation and severe hypophosphatemia have been associated with an osteolytic syndrome.[11] A number of other less well-defined abnormalities have been described in patients with hypophosphatemia, but the precise cause-and-effect relationship remains to be firmly established.[11]

TABLE 69.1 Normal Serum Phosphorus Concentrations in Humans at Mayo Clinic

Males		Females	
Age, y	Concentration, mg/dl	Age, y	Concentration, mg/dl
1–4	4.3–5.4	1–7	4.3–5.4
5–13	3.7–5.4	8–13	4.0–5.2
14–15	3.5–5.3	14–15	3.5–4.9
16–17	3.1–4.7	16–17	3.1–4.7
>18	2.5–4.5	>18	2.5–4.5

Pathophysiology of Hypophosphatemia in Clinical Disorders

An examination of the pathophysiology of hypophosphatemia in various clinical disorders is instructive because it brings to light various mechanisms that are normally involved in the regulation of serum phosphate concentrations. This is particularly the case in the emerging area of inherited rickets and acquired forms of rickets due to tumors. Here, new substances have been isolated and identified that play an important role in the pathophysiology of the syndromes and that might also play an important role in the regulation of phosphate concentrations under normal circumstances.

Respiratory Alkalosis

In the clinical setting, the most common cause of acute hypophosphatemia is respiratory alkalosis (see previous sections), which causes a rapid redistribution of phosphate from the serum into the intracellular space, resulting in a marked decrease in plasma phosphate (Fig. 69.9).[11,251–256] Since respiratory alkalosis decreases the plasma phosphate concentration, it is

TABLE 69.2 Causes of Moderate Hypophosphatemia

Pseudohypophosphatemia	Cellular Uptake Syndromes
Mannitol	Recovery from hypothermia
Bilirubin	Burkitt lymphoma
Acute leukemia	Histiocytic lymphoma
	Acute myelomonocytic leukemia
Decreased dietary intake	Acute myelogenous leukemia
	Chronic myelogenous leukemia in blast crisis
Decreased intestinal absorption	Treatment of pernicious anemia
Vitamin D deficiency	Erythropoietin therapy
Malabsorption	Erythrodermic psoriasis
Steatorrhea	Hungry bone syndrome
Secretory diarrhea	After parathyroidectomy
Vomiting	Acute leukemia
PO43 − binding antacids	
	Increased excretion into the urine
Shift from serum into cells	Hyperparathyroidism
Respiratory alkalosis	Renal tubule defects
Sepsis	Fanconi syndrome
Heat stroke	X-linked hypophosphatemic rickets
Neuroleptic malignant syndrome	Hereditary hypophosphatemic rickets with hypercalciuria
Hepatic coma	Polyostotic fibrous dysplasia
Salicylate poisoning	Neurofibromatosis
Gout	Kidney transplantation
Panic attacks	Oncogenic osteomalacia
Psychiatric depression	Recovery from hemolytic-uremic syndrome
	Aldosteronism
Hormonal effects	Licorice ingestion
Insulin	Volume expansion
Glucagon	Inappropriate secretion of antidiuretic hormone
Epinephrine	Mineralocorticoid administration
Androgens	Corticosteroid therapy
Cortisols	Diuretics
Anovulatory hormones	Aminophylline therapy
Nutrient effects	
Glucose	
Fructose	
Glycerol	
Lactate	
Amino acids	
Xylitol	

Source: Popovtzer MM, Knochel JP, Kumar R. Disorders of calcium phosphorus, vitamin D, parathyroid hormone activity. In: Schrier RW, ed. Renal and Electrolyte Disorders. *Philadelphia: Lippinco.*

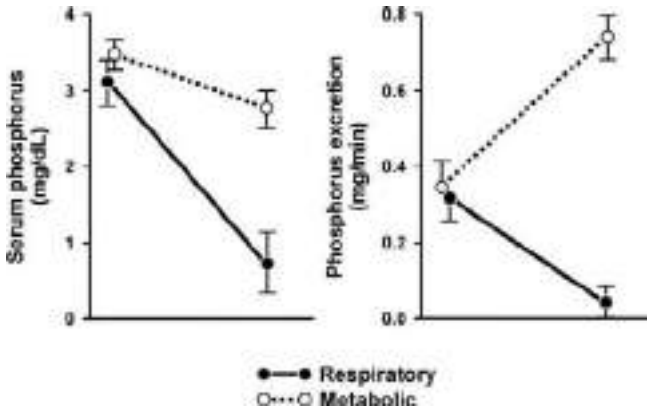

FIGURE 69.9 Respiratory alkalosis may depress serum phosphorus concentration markedly in normal subjects and cause virtual disappearance of phosphorus from urine. Serum phosphorus falls only slightly with the same degree of alkalosis produced by infusion of $NaHCO_3$ and is associated with an increase of phosphaturia. *(From Mostellar ME, Tuttle EP Jr. Effects of alkalosis on plasma concentration and urinary excretion of inorganic phosphate in man. J Clin Invest 1964;43:138–149, with permission.)*

likely that changes in the filtered load of phosphate contribute to the changes in phosphate excretion. However, a direct effect of respiratory alkalosis changes on renal phosphate reabsorption has also been demonstrated in the absence of changes in the filtered load of phosphate.[73,257–259] The effects of acute respiratory alkalosis on plasma phosphate and on phosphate reabsorption are due to the decrease in PCO_2 rather than the concomitant changes in blood pH. The effects of respiratory alkalosis on phosphate homeostasis are mediated, in part, by release of catecholamines.[108,260,261]

Sepsis

Sepsis is associated with hypophosphatemia.[262–268] In septic patients with hypophosphatemia, 80% of these patients had very high levels of tumor necrosis

factor (TNF) and interleukin-6.[263,269,270] Injection of various interleukins and TNFα in experimental animals and in humans decreased plasma phosphate, suggesting a role for inflammatory cytokines in the hypophosphatemic effect of sepsis.[269–275]

Refeeding Syndrome

The earliest descriptions of hypophosphatemia with refeeding were described in starved patients in war time. This syndrome is frequently observed in clinical settings in patients after prolonged fasting, massive weight loss after gastric surgery, chronic alcoholism, chronic malnutrition, oncology patients, and anorexia nervosa.[276–284] Hypophosphatemia is observed after either parenteral or enteral refeeding and is mediated by changes in carbohydrate metabolism, decreased insulin concentrations and increased glucagon levels.

Alcohol Withdrawal

Hypophosphatemia commonly occurs in the context of alcohol withdrawal. It affects approximately 50% of patients with alcoholism, requiring hospitalization.[7,11] The etiology of hypophosphatemia is multifactorial in patients admitted for alcoholism. Poor nutritional intake, magnesium deficiency which can result in hypophosphatemia as a result of renal phosphate wasting[285–289] and alcohol-induced abnormalities in tubular function[290] probably all contribute to the pathogenesis of hypophosphatemia in such patients. Abstinence from alcohol is generally associated with the recovery from hypophosphatemia.

Renal Transplantation

Hypophosphatemia has frequently been reported in transplant patients with concomitant decreased bone mineral density.[291] This hypophosphatemia is the result of decreased renal reabsorption of phosphate and is thought to be due, in part, to elevated PTH levels as a result of prior renal failure and the administration of glucocorticoids. However, some transplant patients exhibit increased phosphate excretion even when kidney function and PTH levels are normal.[292] A recent study examined the mechanism and time course of the post-transplant hypophosphatemia.[293] In this study, early (two weeks to one month) transplantation patients exhibited hypophosphatemia and phosphaturia, compared with control subjects or late (9–12 months) post-transplantation patients. Serum from these patients with hypophosphatemia inhibited phosphate transport by opossum kidney cells, suggesting the presence of a circulating phosphatonin substance.[294] Serum FGF-23 levels are known to be markedly increased in patients with chronic renal failure; however, they are not significantly increased following renal transplantation.[295–297]

Tumor-Induced Osteomalacia

This syndrome is associated with chronic hypophosphatemia and osteomalacia that is corrected following removal of the tumor. Initial experiments performed in patients with tumor-induced osteomalacia (TIO) were the first to describe "phosphatonins" as a circulating factor from the serum of these patients that inhibits phosphate transport in opossum kidney cells.[193] Numerous reports now show that serum FGF-23 is elevated in some, but not all, patients with oncogenic or tumor-induced osteomalacia.[206,296,298–302] Removal of the tumor is generally associated with a reduction in serum FGF-23 concentrations, and there is a temporal association between the reduction in serum FGF-23 concentrations, the increase in serum phosphate concentrations, a decrease in renal phosphate wasting and an increase in serum $1\alpha,25(OH)_2D_3$ concentrations.[296,301,302] In some patients, FGF-23 concentrations are not greatly increased and do not dramatically decrease following tumor removal.[296] The increase in serum FGF-23 concentrations is consistent with the overexpression of messenger RNA and protein for FGF-23 within the tumors themselves. Recently, venous sampling has demonstrated a gradient between FGF-23 concentrations in tumor venous effluent and FGF-23 concentrations in peripheral blood, suggesting that elevations of serum FGF-23 are due to direct secretion from the tumors.[301] As described previously, several phosphatonin molecules, including secreted frizzled related protein-4, MEPE, and fibroblast growth factor-7, have all been isolated from tumors from patients with TIO. Increased serum or renal concentrations of these proteins result in decreased renal phosphate reabsorption which contributes to the subsequent hypophosphatemia and osteomalacia.

Autosomal Dominant Hypophosphatemic Rickets

Autosomal dominant hypophosphatemic rickets (ADHR) is an inherited disorder of phosphate homeostasis characterized by decreased renal phosphate reabsorption and hypophosphatemia linked to chromosome 12p13.[303] These biochemical abnormalities are associated with bone pain, muscle weakness, poor growth, and evidence of rickets and osteomalacia.[304] Individuals with this disease present with renal phosphate wasting and inappropriately normal serum $1\alpha,25(OH)_2D$ concentrations.[304] As noted earlier, mutations in the FGF-23 gene within a pro-convertase processing site were identified as the cause for autosomal dominant hypophosphatemic rickets.[203] These mutations appear to prevent processing of FGF-23 in mice and enhances the *in vivo* biological potency resulting in increased serum concentration of FGF-23, decreased serum phosphate concentrations and low $1\alpha,25(OH)_2D$

concentrations.[212,214] When transgenic mice expressing human FGF-23 were generated, these mice exhibited hypophosphatemic rickets suggesting that increased expression of FGF-23 may play a role in this disease syndrome.[204]

X-Linked Hypophosphatemic Rickets

X-linked hypophosphatemic rickets (XLH) is the most common inherited cause of rickets.[192,305–307] XLH (and murine model of this diseases, Hyp mouse and the Gy mouse) is an inherited X-linked dominant disorder characterized by hypophosphatemia, normocalcemia and an inappropriately low concentration of serum $1\alpha,25(OH)_2D$.[305–309] Many studies have demonstrated that in XLH there is decreased renal phosphate reabsorption.[305–307] This defect in phosphate reabsorption was demonstrated to be due to a humoral factor, since parabiosis performed between a normal and Hyp mouse causes hypophosphatemia in the normal mouse, and this effect is reversible.[200,201] These results are further supported by cross renal transplantation experiments.[202] When a kidney from a Hyp mouse is transplanted into a normal mouse, phosphate wasting is no longer observed. Conversely, transplantation of a kidney from a normal mouse into a Hyp mouse results in phosphate wasting by the normal transplanted kidney. These data are consistent with a circulating hypophosphatemic substance in the circulation of Hyp mice. The addition of Hyp mouse serum to primary renal cells selectively inhibits phosphate uptake, and the Hyp serum inhibits phosphate transport to a greater extent than normal serum, indicating the presence of a factor in Hyp mouse serum that inhibits phosphate uptake.[310] Positional cloning efforts have shown that PHEX (phosphate regulating endopeptidase on the X-chromosome) is the mutant gene responsible for XLH.[311] The same gene is mutated in mice with the Hyp and Gy mutations (in the Gy mouse there is a deletion of the adjacent spermine gene as well).[311–314] Since the mutant gene in this syndrome is a protease, it has been thought that a lack of proteolytic activity results in comparing degradation of a hypophosphatemic substance. With the identification of FGF-23 as a hypophosphatemic peptide responsible for phosphate wasting in patients with autosomal dominant hypophosphatemic rickets, and the elevation of FGF-23 in some patients with tumor-induced osteomalacia, considerable effort has been expended to determine whether FGF-23 concentrations are elevated in patients with XLH and whether FGF-23 is a substrate for PHEX. The evidence for elevated FGF-23 expression in patients with X-linked hypophosphatemic rickets is conflicting. Jonsson and coworkers describe elevated serum FGF-23 concentrations in many subjects,[296] whereas Weber and colleagues reported only modestly increased or normal concentrations of FGF-23.[210] In the Hyp mouse, preliminary reports suggest that FGF-23 serum concentrations are elevated and neutralization of FGF-23 with an antibody ameliorates hypophosphatemia and rickets.[315] These data are consistent with the premise that PHEX processes FGF-23 either directly or indirectly under normal circumstances. The inactivation of FGF-23 by PHEX has been demonstrated by some, but not all investigators.[206,316,317] Inactivation of PHEX, as occurs in individuals with XLH and in Hyp mice, would reduce FGF-23 degradation and cause renal phosphate wasting and hypophosphatemia.

Fibrous Dysplasia/McCune-Albright Syndrome

Fibrous dysplasia is a genetic, noninherited disease caused by somatic activating missense mutations of GNAS1 that affects the skeleton or with endocrine and cutaneous abnormalities, McCune-Albright syndrome.[318–322] Phosphate wasting is observed in approximately 50% of these patients and is associated with defects in bone mineralization.[323–327] Riminucci and coworkers examined the concentrations of FGF-23 in the plasma of patients with fibrous dysplasia, some of whom have hypophosphatemia.[328] These investigators demonstrated that those patients who had low phosphate concentrations had elevated FGF-23 concentrations in the blood, whereas those who had normal phosphate concentrations did not have elevations in FGF-23.

Humoral Hypercalcemia of Malignancy and Hyperparathyroidism

Patients with humoral hypercalcemia of malignancy or primary hyperparathyroidism have elevated serum calcium concentrations, hypophosphatemia, and altered serum $1\alpha,25(OH)D_3$ concentrations. Of note, in patients with primary hyperparathyroidism, $1\alpha,25(OH)D_3$ concentrations are increased. Whereas, in patients with humoral hypercalcemia of malignancy serum, $1\alpha,25(OH)D_3$ concentrations are inappropriately low for the degree of hypophosphatemia that these patients manifest.[329] It is possible that increased circulating FGF-23 could contribute to the hypophosphatemia seen in individuals with these disorders. Recently, serum FGF-23 has been shown to be elevated five- to 10-fold in patients with humoral hypercalcemia of malignancy.[330] Interestingly, the elevations in FGF-23 are not correlated with the concentrations of serum phosphorus. It is possible that a low serum $1\alpha,25(OH)D3$ concentration seen in the patients with humoral hypercalcemia of malignancy could have been due to the increased FGF-23 concentrations. Patients with primary hyperparathyroidism have slightly elevated FGF-23 concentrations that do not change after parathyroidectomy.[331]

ACUTE AND CHRONIC HYPERPHOSPHATEMIA

Hyperphosphatemia occurs in renal failure and tumoral calcinosis. Patients with hyperphosphatemia generally have no symptoms as a result of this disorder. The consequences of hyperphosphatemia include the deposition of calcium in phosphate in soft tissues such as skin, blood vessels, and heart, and the development of secondary hyperparathyroidism as a result of hypocalcemia.

Renal Failure

Hyperphosphatemia and secondary hyperparathyroidism are common complications of chronic renal failure and end-stage renal disease.[11,332,333] The causes of hyperphosphatemia and chronic renal failure are multifactorial. In patients with renal failure, retention of phosphate as a result of reduced glomerular filtration is the primary cause for hyperphosphatemia. While in the early stages of chronic renal failure, an increase in serum phosphate concentrations can be overcome by an increased rate of parathyroid hormone release (which occurs as a result of hypocalcemia and perhaps directly due to the effect of phosphate on the parathyroid gland). As renal failure progresses with further nephron damage, hyperphosphatemia becomes chronic and fixed.[334–344] Parathyroid hormone concentrations remained chronically elevated. At the same time, a reduction in the synthesis of $1\alpha,25(OH)D_3$ occurs as a result of hyperphosphatemia and reduced nephron mass.[11,332,333] This causes a reduction in calcium absorption in the intestine, a negative calcium balance, and further hyperparathyroidism. A reduction in $1\alpha,25(OH)D_3$ concentrations also results in an increase in parathyroid hormone synthesis on account of the absence of inhibition of parathyroid hormone synthesis by $1\alpha,25(OH)D_3$.[11,332,333] Chronically elevated concentrations of parathyroid hormone cause bone disease in these patients.

Tumoral Calcinosis

Tumoral calcinosis is an unusual disorder associated with hyperphosphatemia, elevated $1\alpha,25(OH)_2D_3$ concentrations, and a reduced excretion of phosphorus in the urine. The phenotype seen in this disorder is the opposite of that seen in tumor-induced osteomalacia and in the inherited forms of rickets. It has been speculated that a deficiency of phosphatonin activity could account for this disorder. Two distinct abnormalities have been elucidated in patients with tumoral calcinosis. In some families with tumoral calcinosis, a defect in the activity of an O-linked glycosylating enzyme, GALNT3,[345] has been observed. Interestingly, serum FGF-23 concentrations are high in these patients. It is uncertain from the published report if the serum FGF-23 concentrations were measured using an assay that detects intact FGF-23 or FGF-23 fragments as well as the intact molecule. It is possible that there could be defects in the processing of FGF-23 as a result of a failure in glycosylation of the molecule or as a result of the chronic hyperphosphatemia seen in these patients. Another report suggests that the hyperostosis–hyperphosphatemia syndrome is an allelic disorder similar to tumoral calcinosis.[346] No reports of FGF-23 concentrations in this syndrome are available.

In a second family, mutational analyses identified a homozygous S71G mutation in FGF-23 in the TC patients which was not found in control alleles.[347] These individuals had low normal levels of intact FGF-23. It has been suggested that the mutation stabilizes full-length FGF-23.

In summary, the study of patients with various clinical disorders of phosphate metabolism has yielded rich insights into the handling of phosphate in the kidney and other organs.

References

[1] Fleisch H. Homeostasis of inorganic phosphate. In: Urist MR, editor. Fundamental and clinical bone physiology. Philadelphia: JB Lippincott; 1980. p. 268–82.

[2] Neuman W. Bone material and calcification mechanisms. In: Urist MR, editor. Fundamental and clinical bone physiology. Philadelphia: JB Lippincott; 1980. p. 83–107.

[3] Cohen P. The structure and regulation of protein phosphatases. Ann Rev Biochem 1989;58:453–508.

[4] Hubbard SR, Till JH. Protein tyrosine kinase structure and function. Annu Rev Biochem 2000;69:373–98.

[5] Hunter T, Cooper JA. Protein-tyrosine kinases. Annu Rev Biochem 1985;54:897–930.

[6] Krebs EG, Beavo JA. Phosphorylation-dephosphorylation of enzymes. Annu Rev Biochem 1979;48:923–59.

[7] Knochel JP. The pathophysiology and clinical characteristics of severe hypophosphatemia. Arch Intern Med 1977;137:203–20.

[8] Knochel JP. The clinical and physiological implications of phosphorus deficiency. In: Seldin DW, Giebisch G, editors. The kidney: physiology and pathophysiology. New York: Raven Press; 1992. p. 2533–62.

[9] Marxhall DH, Nordin BE, Speed R. Calcium, phosphorus and magnesium requirement. Proc Nutr Soc 1976;35:163–73.

[10] Nordin BE, Bulusu L. Plasma-phosphate and tubular reabsorption of phosphate. Lancet 1970;1:998.

[11] Popovtzer MM, Knochel JP, Kumar R. Disorders of calcium phosphorus, vitamin D, parathyroid hormone activity. In: Schrier RW, editor. Renal and electrolyte disorders. Philadelphia: Lippincott-Raven; 1997. p. 241–319.

[12] Berndt T, Schiavi S, Kumar R. The "phosphatonins" and the regulation of phosphorus homeostasis. Am J Physiol Renal Physiol 2005;289:F1170–1182.

[13] Kumar R. Phosphatonin—a new phosphaturetic hormone? (lessons from tumour-induced osteomalacia and X-linked hypophosphataemia). Nephrol Dial Transplant 1997;12:11–3.
[14] Kumar R. Tumor-induced osteomalacia and the regulation of phosphate homeostasis. Bone 2000;27:333–8.
[15] Schiavi SC, Kumar R. The phosphatonin pathway: new insights in phosphate homeostasis. Kidney Int 2004;65:1–14.
[16] Schiavi SC, Moe OW. Phosphatonins: a new class of phosphate-regulating proteins. Curr Opin Nephrol Hypertens 2002; 11:423–30.
[17] Carpenter TO, Ellis BK, Insogna KL, Philbrick WM, Sterpka J, Shimkets R. FGF7 - an inhibitor of phosphate transport derived from oncogenic osteomalacia-causing tumors. J Clin Endocrinol Metab 2005;90:1012–20.
[18] Rowe PS, Kumagai Y, Gutierrez G, Garrett IR, Blacher R, Rosen D, et al. MEPE has the properties of an osteoblastic phosphatonin and minhibin. Bone 2004;34:303–19.
[19] Berndt T, Knox F. Renal regulation of phosphate excretion. In: Seldin DAG, editor. The kidney: physiology and pathophysiology. New York: Raven Press; 1992. p. 2511–32.
[20] Bonjour JP, Caverzasio J. Phosphate transport in the kidney. Rev Physiol Biochem Pharmacol 1984;100:161–214.
[21] Bonjour JP, Preston C, Fleisch H. Effect of 1,25-dihydroxyvitamin D3 on the renal handling of Pi in thyroparathyroidectomized rats. J Clin Invest 1977;60:1419–28.
[22] Fleisch H, Bonjour JP, Rizzoli R, Hugi K. Effect of vitamin D metabolites on calcium and phosphate metabolism. Contrib Nephrol 1978;13:96–103.
[23] Georgaki H, Puschett JB. Acute effects of a "physiological" dose of 1,25-dihydroxy vitamin D3 on renal phosphate transport. Endocr Res Commun 1982;9:135–43.
[24] Knox FG, Haramati A. Renal regulation of phosphate excretion. In: Seldin DW, Giebisch G, editors. The kidney: physiology and pathology. New York: Raven Press; 1985. p. 1351–96.
[25] Muhlbauer RC, Bonjour JP, Fleisch H. Tubular handling of Pi: localization of effects of 1,25(OH)2D3 and dietary Pi in TPTX rats. Am J Physiol 1981;241:F123–128.
[26] Puschett JB, Fernandez PC, Boyle IT, Gray RW, Omdahl JL, DeLuca HF. The acute renal tubular effects of 1,25-dihydroxycholecalciferol. Proc Soc Exp Biol Med 1972;141:379–84.
[27] Puschett JB, Kuhrman MS. Renal tubular effects of 1,25-dihydroxy vitamin D3: interactions with vasopressin and parathyroid hormone in the vitamin D-depleted rat. J Lab Clin Med 1978;92:895–903.
[28] Tanaka Y, DeLuca HF. Role of 1,25-dihydroxyvitamin D3 in maintaining serum phosphorus and curing rickets. Proc Natl Acad Sci U S A 1974;71:1040–4.
[29] Tanaka Y, Frank H, DeLuca HF. Biological activity of 1,25-dihydroxyvitamin D3 in the rat. Endocrinology 1973;92: 417–22.
[30] Tanaka Y, Frank H, DeLuca HF. Role of 1,25-dihydroxycholecalciferol in calcification of bone and maintenance of serum calcium concentration in the rat. J Nutr 1972;102:1569–77.
[31] Troehler U, Bonjour JP, Fleisch H. Effect of 1,25-dihydroxycholecalciferol on the extra-renal handling of inorganic phosphate in thyroparathyroidectomized but not in intact rats. Adv Exp Med Biol 1984;178:87–91.
[32] Rizzoli R, Fleisch H, Bonjour JP. Role of 1,25-dihydroxyvitamin D3 (1,25-(OH)2D3) on intestinal inorganic phosphate (Pi) absorption in rats with normal vitamin D supply. Calcif Tissue Res 1977;22(Suppl):561–2.
[33] Rizzoli R, Fleisch H, Bonjour JP. Role of 1,25-dihydroxyvitamin D3 on intestinal phosphate absorption in rats with a normal vitamin D supply. J Clin Invest 1977;60:639–47.
[34] Tanaka Y, Deluca HF. The control of 25-hydroxyvitamin D metabolism by inorganic phosphorus. Arch Biochem Biophys 1973;154:566–74.
[35] Tanaka Y, Frank H, DeLuca HF. Intestinal calcium transport: stimulation by low phosphorus diets. Science 1973;181:564–6.
[36] Berndt T, Craig TA, Bowe AE, Vassiliadis J, Reczek D, Finnegan R, et al. Secreted frizzled-related protein 4 is a potent tumor-derived phosphaturic agent. J Clin Invest 2003;112:785–94.
[37] Shimada T, Mizutani S, Muto T, Yoneya T, Hino R, Takeda S, et al. Cloning and characterization of FGF23 as a causative factor of tumor-induced osteomalacia. Proc Natl Acad Sci U S A 2001;98:6500–5.
[38] Rizzoli R, Caverzasio J, Fleisch H, Bonjour JP. Parathyroid hormone-like changes in renal calcium and phosphate reabsorption induced by Leydig cell tumor in thyroparathyroidectomized rats. Endocrinology 1986;119:1004–9.
[39] Barrett PQ, Gertner JM, Rasmussen H. Effect of dietary phosphate on transport properties of pig renal microvillus vesicles. Am J Physiol 1980;239:F352–9.
[40] Caverzasio J, Bonjour JP. Mechanism of rapid phosphate (Pi) transport adaptation to a single low Pi meal in rat renal brush border membrane. Pflugers Arch 1985;404:227–31.
[41] Caverzasio J, Brown CD, Biber J, Bonjour JP, Murer H. Adaptation of phosphate transport in phosphate-deprived LLC-PK1 cells. Am J Physiol 1985;248:F122–7.
[42] Caverzasio J, Danisi G, Straub RW, Murer H, Bonjour JP. Adaptation of phosphate transport to low phosphate diet in renal and intestinal brush border membrane vesicles: influence of sodium and pH. Pflugers Arch 1987;409:333–6.
[43] Caverzasio J, Murer H, Fleisch H, Bonjour JP. Phosphate transport in brush border membrane vesicles isolated from renal cortex of young growing and adult rats. Comparison with whole kidney data. Pflugers Arch 1982;394:217–21.
[44] Haramati A, Haas JA, Knox FG. Adaptation of deep and superficial nephrons to changes in dietary phosphate intake. Am J Physiol 1983;244:F265–269.
[45] Haramati A, Knox FG. Relationship between plasma phosphate and renal handling of phosphate: studies with low phosphate diet and nicotinamide. Adv Exp Med Biol 1982;151:41–6.
[46] Levine BS, Ho K, Hodsman A, Kurokawa K, Coburn JW. Early renal brush border membrane adaptation to dietary phosphorus. Miner Electrolyte Metab 1984;10:222–7.
[47] Levine BS, Ho LD, Pasiecznik K, Coburn JW. Renal adaptation to phosphorus deprivation: characterization of early events. J Bone Miner Res 1986;1:33–40.
[48] Muhlbauer RC, Bonjour JP, Fleisch H. Tubular localization of adaptation to dietary phosphate in rats. Am J Physiol 1977;233: F342–348.
[49] Pastoriza-Munoz E, Mishler DR, Lechene C. Effect of phosphate deprivation on phosphate reabsorption in rat nephron: role of PTH. Am J Physiol 1983;244:F140–149.
[50] Shah SV, Kempson SA, Northrup TE, Dousa TP. Renal adaptation to a low phosphate diet in rats. J Clin Invest 1979;64: 955–66.
[51] Steele TH. Interactions of starvation and selective phosphorus depletion on renal phosphate reabsorption. Ren Physiol 1982;5:44–52.
[52] Steele TH. Renal response to phosphorus deprivation: effect of the parathyroids and bicarbonate. Kidney Int 1977;11:327–34.
[53] Steele TH, DeLuca HF. Influence of dietary phosphorus on renal phosphate reabsorption in the parathyroidectomized rat. J Clin Invest 1976;57:867–74.
[54] Stoll R, Kinne R, Murer H, Fleisch H, Bonjour JP. Phosphate transport by rat renal brush border membrane vesicles:

influence of dietary phosphate, thyroparathyroidectomy, and 1,25-dihydroxyvitamin D3. Pflugers Arch 1979;380:47–52.
[55] Trohler U, Bonjour JP, Fleisch H. Inorganic phosphate homeostasis. Renal adaptation to the dietary intake in intact and thyroparathyroidectomized rats. J Clin Invest 1976;57:264–73.
[56] Wen SF, Boynar Jr JW, Stoll RW. Effect of phosphate deprivation on renal phosphate transport in the dog. Am J Physiol 1978;234:F199–206.
[57] Agusti AG, Torres A, Estopa R, Agustividal A. Hypophosphatemia as a cause of failed weaning: the importance of metabolic factors. Crit Care Med 1984;12:142–3.
[58] Brodehl J, Gellissen K, Weber HP. Postnatal development of tubular phosphate reabsorption. Clin Nephrol 1982;17:163–71.
[59] Vainsel M. Tubular reabsorption of phosphate in normal children and in children with rickets. Rev Eur Etud Clin Biol 1972;17:656–62.
[60] Corvilain J, Abramow M. Effects of growth hormone on tubular transport of phosphate in normal and parathyroidectomized dogs. J Clin Invest 1964;43:1608–12.
[61] Corvilain J, Abramow M. Some effects of human growth hormone on renal hemodynamics and on tubular phosphate transport n man. J Clin Invest 1962;41:1230–5.
[62] Kiebzak GM, Sacktor B. Effect of age on renal conservation of phosphate in the rat. Am J Physiol 1986;251:F399–407.
[63] Sorribas V, Lotscher M, Loffing J, Biber J, Kaissling B, Murer H, et al. Cellular mechanisms of the age-related decrease in renal phosphate reabsorption. Kidney Int 1996;50:855–63.
[64] Awazu M, Berndt TJ, Knox FG. Effect of phosphate infusion on proximal tubule phosphate reabsorption in phosphate-deprived and respiratory alkalotic rats. Miner Electrolyte Metab 1987;13:393–6.
[65] Goldfarb S, Beck LH, Agus ZS, Goldberg M. Dissociation of tubular sites of action of saline, PTH and DbCAMP on renal phosphate reabsorption. Nephron 1978;21:221–9.
[66] Greger R, Lang F, Marchand G, Knox FG. Site of renal phosphate reabsorption. Micropuncture and microinfusion study. Pflugers Arch 1977;369:111–8.
[67] Haramati A, Haas JA, Knox FG. Nephron heterogeneity of phosphate reabsorption: effect of parathyroid hormone. Am J Physiol 1984;246:F155–158.
[68] Harris CA, Burnatowska MA, Seely JF, Sutton RA, Quamme GA, Dirks JH. Effects of parathyroid hormone on electrolyte transport in the hamster nephron. Am J Physiol 1979;236: F342–348.
[69] Knox FG, Haas JA, Berndt T, Marchand GR, Youngberg SP. Phosphate transport in superficial and deep nephrons in phosphate-loaded rats. Am J Physiol 1977;233:F150–153.
[70] Rybczynska A, Hoppe A, Knox FG. Effect of propranolol on phosphate reabsorption by superficial nephron segments in response to parathyroid hormone in phosphate-deprived rats. J Am Soc Nephrol 1990;1:200–4.
[71] Strickler JC, Thompson DD, Klose RM, Giebisch G. Micropuncture study of inorganic phosphate excretion in the rat. J Clin Invest 1964;43:1596–607.
[72] Dennis VW, Woodhall PB, Robinson RR. Characteristics of phosphate transport in isolated proximal tubule. Am J Physiol 1976;231:979–85.
[73] Berndt TJ, Knox FG. Nephron site of resistance to phosphaturic effect of PTH during respiratory alkalosis. Am J Physiol 1985;249:F919–922.
[74] Bacic D, Wagner CA, Hernando N, Kaissling B, Biber J, Murer H. Novel aspects in regulated expression of the renal type IIa Na/Pi-cotransporter. Kidney Int Suppl 2004;:S5–12.
[75] Biber J, Custer M, Magagnin S, Hayes G, Werner A, Lotscher M, et al. Renal Na/Pi-cotransporters. Kidney Int 1996;49:981–5.
[76] Biber J, Custer M, Werner A, Kaissling B, Murer H. Localization of NaPi-1, a Na/Pi cotransporter, in rabbit kidney proximal tubules, II: localization by immunohistochemistry. Pflugers Arch 1993;424:210–5.
[77] Biber J, Murer H. A molecular view of renal Na-dependent phosphate transport. Ren Physiol Biochem 1994;17:212–5.
[78] Biber J, Murer H, Forster I. The renal type II Na + /phosphate cotransporter. J Bioenerg Biomembr 1998;30:187–94.
[79] Custer M, Meier F, Schlatter E, Greger R, Garcia-Perez A, Biber J, et al. Localization of NaPi-1, a Na-Pi cotransporter, in rabbit kidney proximal tubules. I. mRNA localization by reverse transcription/polymerase chain reaction. Pflugers Arch 1993;424: 203–9.
[80] Karim-Jimenez Z, Hernando N, Biber J, Murer H. A dibasic motif involved in parathyroid hormone-induced down-regulation of the type IIa NaPi cotransporter. Proc Natl Acad Sci U S A 2000;97:12896–901.
[81] Lambert G, Traebert M, Hernando N, Biber J, Murer H. Studies on the topology of the renal type II NaPi-cotransporter. Pflugers Arch 1999;437:972–8.
[82] Murer H. Homer Smith Award. Cellular mechanisms in proximal tubular Pi reabsorption: some answers and more questions. J Am Soc Nephrol 1992;2:1649–65.
[83] Murer H, Biber J. Control of proximal tubular apical Na/Pi cotransport. Exp Nephrol 1996;4:201–4.
[84] Murer H, Biber J. Membrane traffic and control of proximal tubular sodium phosphate (Na/Pi)-cotransport. Wien Klin Wochenschr 1997;109:441–4.
[85] Murer H, Biber J. Molecular mechanisms of renal apical Na/phosphate cotransport. Annu Rev Physiol 1996;58:607–18.
[86] Murer H, Biber J. Renal sodium-phosphate cotransport. Curr Opin Nephrol Hypertens 1994;3:504–10.
[87] Murer H, Forster I, Hilfiker H, Pfister M, Kaissling B, Lotscher M, et al. Cellular/molecular control of renal Na/Pi-cotransport. Kidney Int 1998;65:S2–10.
[88] Murer H, Hernando N, Forster I, Biber J. Molecular aspects in the regulation of renal inorganic phosphate reabsorption: the type IIa sodium/inorganic phosphate co-transporter as the key player. Curr Opin Nephrol Hypertens 2001;10: 555–61.
[89] Murer H, Hernando N, Forster I, Biber J. Proximal tubular phosphate reabsorption: molecular mechanisms. Physiol Rev 2000;80:1373–409.
[90] Murer H, Lotscher M, Kaissling B, Biber J. Molecular mechanisms in the regulation of renal proximal tubular Na/phosphate cotransport. Kidney Blood Press Res 1996;19:151–4.
[91] Pfister M, Forgo J, Ziegler U, Biber J, Murer H. cAMP-dependent and -independent downregulation of type II Na-Pi cotransporters by PTH. Am J Physiol 1999;276:F720–5.
[92] Pfister MF, Lederer ED, Forgo J, Ziegler U, Lotscher M, Quabius ES, et al. Parathyroid hormone-dependent degradation of type II Na + /Pi cotransporters. J Biol Chem 1997;272: 20125–30.
[93] Pfister MF, Ruf I, Stange G, Ziegler U, Lederer ED, Biber J, et al. Parathyroid hormone leads to the lysocomal degradation of the renal type II Na/Pi cotransporter. Proc Natl Acad Sci U S A 1998;95:1909–14.
[94] Traebert M, Roth J, Biber J, Murer H, Kaissling B. Internalization of proximal tubular type II Na-P(i) cotransporter by PTH: immunogold electron microscopy. Am J Physiol Renal Physiol 2000;278:F148–154.
[95] Traebert M, Volkl H, Biber J, Murer H, Kaissling B. Luminal and contraluminal action of 1-34 and 3-34 PTH peptides on renal type IIa Na-P(i) cotransporter. Am J Physiol Renal Physiol 2000;278:F792–798.

[96] Werner A, Kempson SA, Biber J, Murer H. Increase of Na/Pi-cotransport encoding mRNA in response to low Pi diet in rat kidney cortex. J Biol Chem 1994;269:6637–9.
[97] Werner A, Moore ML, Mantei N, Biber J, Semenza G, Murer H. Cloning and expression of cDNA for a Na/Pi cotransport system of kidney cortex. Proc Natl Acad Sci USA 1991;88: 9608–12.
[98] Beck L, Karaplis AC, Amizuka N, Hewson AS, Ozawa H, Tenenhouse HS. Targeted inactivation of Npt2 in mice leads to severe renal phosphate wasting, hypercalciuria, skeletal abnormalities. Proc Natl Acad Sci U S A 1998;95:5372–7.
[99] Hoag HM, Martel J, Gauthier C, Tenenhouse HS. Effects of Npt2 gene ablation and low-phosphate diet on renal Na (+)/phosphate cotransport and cotransporter gene expression. J Clin Invest 1999;104:679–86.
[100] Steele TH, Stromberg BA, Underwood JL, Larmore CA. Renal resistance to parathyroid hormone during phosphorus deprivation. J Clin Invest 1976;58:1461–4.
[101] Ritthaler T, Traebert M, Lotscher M, Biber J, Murer H, Kaissling B. Effects of phosphate intake on distribution of type II Na/Pi cotransporter mRNA in rat kidney. Kidney Int 1999;55:976–83.
[102] Segawa H, Kaneko I, Yamanaka S, Ito M, Kuwahata M, Inoue Y, et al. Intestinal Na-P(i) cotransporter adaptation to dietary P (i) content in vitamin D receptor null mice. Am J Physiol Renal Physiol 2004;287:F39–47.
[103] Barac-Nieto M, Alfred M, Spitzer A. Phosphate depletion in opossum kidney cells: apical but not basolateral or transepithelial adaptions of Pi transport. Exp Nephrol 2001;9:258–64.
[104] Biber J, Forgo J, Murer H. Modulation of Na + -Pi cotransport in opossum kidney cells by extracellular phosphate. Am J Physiol 1988;255:C155–161.
[105] Markovich D, Verri T, Sorribas V, Forgo J, Biber J, Murer H. Regulation of opossum kidney (OK) cell Na/Pi cotransport by Pi deprivation involves mRNA stability. Pflugers Arch 1995;430:459–63.
[106] Reshkin SJ, Forgo J, Biber J, Murer H. Functional asymmetry of phosphate transport and its regulation in opossum kidney cells: phosphate "adaptation." Pflugers Arch 1991;419:256–62.
[107] Murer H, Lotscher M, Kaissling B, Levi M, Kempson SA, Biber J. Renal brush border membrane Na/Pi-cotransport: molecular aspects in PTH-dependent and dietary regulation. Kidney Int 1996;49:1769–73.
[108] Berndt TJ, Tucker RR, Kent PD, Streiff PC, Tyce GM, Knox FG. Dopamine enhances the phosphaturic effect of PTH during acute respiratory alkalosis. J Lab Clin Med 1999;134:616–22.
[109] Isaac J, Berndt TJ, Chinnow SL, Tyce GM, Dousa TP, Knox FG. Dopamine enhances the phosphaturic response to parathyroid hormone in phosphate-deprived rats. J Am Soc Nephrol 1992;2:1423–9.
[110] Rybczynska A, Hoppe A, Knox FG. Propranolol restores phosphaturic effect of PTH in short-term phosphate deprivation. Am J Physiol 1990;258:R120–123.
[111] Mulroney SE, Woda CB, Halaihel N, Louie B, McDonnell K, Schulkin J, et al. Central control of renal sodium-phosphate (NaPi-2) transporters. Am J Physiol Renal Physiol 2004;286: F647–652.
[112] Gray RW. Control of plasma 1,25-$(OH)_2$-vitamin D concentrations by calcium and phosphorus in the rat: effects of hypophysectomy. Calcif Tissue Int 1981;33:485–8.
[113] Gray RW, Garthwaite TL. Activation of renal 1,25-dihydroxyvitamin D3 synthesis by phosphate deprivation: evidence for a role for growth hormone. Endocrinology 1985;116:189–93.
[114] Gray RW, Haasch ML, Brown CE. Regulation of plasma 1,25-$(OH)_2$-D3 by phosphate: evidence against a role for total or acid-soluble renal phosphate content. Calcif Tissue Int 1983;35:773–7.
[115] Gray RW, Napoli JL. Dietary phosphate deprivation increases 1,25-dihyroxyvitamin D3 synthesis in rat kidney *in vitro*. J Biol Chem 1983;258:1152–5.
[116] Beutner EH, Munson PL. Time course of urinary excretion of inorganic phosphate by rats after parathyroidectomy and after injection of parathyroid extract. Endocrinology 1960;66: 610–6.
[117] Foulks JG, Perry FA. Renal excretion of phosphate following parathyroidectomy in the dog. Am J Physiol 1959;196:554–60.
[118] Kuntziger H, Amiel C, Roinel N, Morel F. Effects of parathyroidectomy and cyclic AMP on renal transport of phosphate, calcium, and magnesium. Am J Physiol 1974;227:905–11.
[119] Talmage RV, Kraintz FW. Progressive changes in renal phosphate and calcium excretion in rats following parathyroidectomy or parathyroid administration. Proc Soc Exp Biol Med 1954;87:263–7.
[120] Talmage RV, Kraintz FW, Buchanan GD. Effect of parathyroid extract and phosphate salts on renal calcium and phosphate excretion after parathyroidectomy. Proc Soc Exp Biol Med 1955;88:600–4.
[121] Lorentz WB. Effect of parathyroid hormone on renal tubular permeability. Am J Physiol 1976;231:1401–7.
[122] Rybczynska A, Berndt TJ, Hoppe A, Knox FG. Site of restoration of the effect of PTH by propranolol in respiratory alkalosis. Kidney Int 1990;38:258–62.
[123] Hernando N, Forgo J, Biber J, Murer HPTH. Induced downregulation of the type IIa Na/P(i)-cotransporter is independent of known endocytic motifs. J Am Soc Nephrol 2000;11:1961–8.
[124] Keusch I, Traebert M, Lotscher M, Kaissling B, Murer H, Biber J. Parathyroid hormone and dietary phosphate provoke a lysosomal routing of the proximal tubular Na/Pi-cotransporter type II. Kidney Int 1998;54:1224–32.
[125] Zhao N, Tenenhouse HS. Npt2 gene disruption confers resistance to the inhibitory action of parathyroid hormone on renal sodium-phosphate cotransport. Endocrinology 2000;141: 2159–65.
[126] Boyle IT, Gray RW, DeLuca HF. Regulation by calcium of *in vivo* synthesis of 1,25-dihydroxycholecalciferol and 21,25-dihydroxycholecalciferol. Proc Natl Acad Sci U S A 1971;68: 2131–4.
[127] DeLuca HF. The kidney as an endocrine organ for the production of 1,25-dihydroxyvitamin D3, a calcium-mobilizing hormone. N Engl J Med 1973;289:359–65.
[128] Garabedian M, Holick MF, Deluca HF, Boyle IT. Control of 25-hydroxycholecalciferol metabolism by parathyroid glands. Proc Natl Acad Sci U S A 1972;69:1673–6.
[129] DeLuca HF, Schnoes HK. Metabolism and mechanism of action of vitamin D. Annu Rev Biochem 1976;45:631–66.
[130] DeLuca HF, Schnoes HK. Vitamin D: recent advances. Annu Rev Biochem 1983;52:411–39.
[131] Habener JF, Rosenblatt M, Potts Jr. JT. Parathyroid hormone: biochemical aspects of biosynthesis, secretion, action, and metabolism. Physiol Rev 1984;64:985–1053.
[132] Kumar R. The metabolism and mechanism of action of 1,25-dihydroxyvitamin D3. Kidney Int 1986;30:793–803.
[133] Kumar R. The metabolism of 1,25-dihydroxyvitamin D3. Endocr Rev 1980;1:258–67.
[134] Kumar R. Metabolism of 1,25-dihydroxyvitamin D3. Physiol Rev 1984;64:478–504.
[135] Kawashima H, Kurokawa K. Metabolism and sites of action of vitamin D in the kidney. Kidney Int 1986;29:98–107.
[136] Kawashima H, Torikai S, Kurokawa K. Localization of 25-hydroxyvitamin D3 1 alpha-hydroxylase and 24-hydroxylase

along the rat nephron. Proc Natl Acad Sci USA 1981;78: 1199–203.
[137] Wark JD, Larkins RG, Eisman JA, Wilson KR. Regulation of 25-hydroxy-vitamin D-1 alpha-hydroxylase in chick isolated renal tubules: effects of prostaglandin E2, frusemide and acetylsalicylic acid. Clin Sci (Lond) 1981;61:53–9.
[138] Gray RW. Effects of age and sex on the regulation of plasma 1,25-$(OH)_2$-D by phosphorus in the rat. Calcif Tissue Int 1981;33:477–84.
[139] Engstrom GW, Horst RL, Reinhardt TA, Littledike ET. Effect of dietary phosphorus levels on porcine renal 25-hydroxyvitamin D-1 alpha- and 24R-hydroxylase activities and plasma 1,25-dihydroxyvitamin D3 concentration. J Anim Sci 1985;60: 1005–11.
[140] Tanaka Y, DeLuca HF. Rat renal 25-hydroxyvitamin D3 1- and 24-hydroxylases: their *in vivo* regulation. Am J Physiol 1984;246:E168–173.
[141] Tenenhouse HS, Meyer Jr RA, Mandla S, Meyer MH, Gray RW. Renal phosphate transport and vitamin D metabolism in X-linked hypophosphatemic Gy mice: responses to phosphate deprivation. Endocrinology 1992;131:51–6.
[142] Capuano P, Radanovic T, Wagner CA, Bacic D, Kato S, Uchiyama Y, et al. Intestinal and renal adaptation to a low-Pi diet of type II NaPi cotransporters in vitamin D receptor- and 1alphaOHase-deficient mice. Am J Physiol Cell Physiol 2005;288:C429–434.
[143] Taketani Y, Segawa H, Chikamori M, Morita K, Tanaka K, Kido S, et al. Regulation of type II renal Na + -dependent inorganic phosphate transporters by 1,25-dihydroxyvitamin D3. Identification of a vitamin D-responsive element in the human NAPi-3 gene. J Biol Chem 1998;273:14575–81.
[144] DeFronzo RA, Cooke CR, Andres R, Faloona GR, Davis PJ. The effect of insulin on renal handling of sodium, potassium, calcium, and phosphate in man. J Clin Invest 1975;55:845–55.
[145] DeFronzo RA, Goldberg M, Agus ZS. The effects of glucose and insulin on renal electrolyte transport. J Clin Invest 1976;58:83–90.
[146] Feld S, Hirschberg R. Growth hormone, the insulin-like growth factor system, and the kidney. Endocr Rev 1996;17:423–80.
[147] Hammerman MR. Interaction of insulin with the renal proximal tubular cell. Am J Physiol 1985;249:F1–11.
[148] Hammerman MR, Rogers S, Hansen VA, Gavin III JR. Insulin stimulates Pi transport in brush border vesicles from proximal tubular segments. Am J Physiol 1984;247:E616–624.
[149] Lau K, Guntupalli J, Eby B. Effects of somatostatin on phosphate transport: evidence for the role of basal insulin. Kidney Int 1983;24:10–5.
[150] Haramati A, Mulroney SE, Lumpkin MD. Regulation of renal phosphate reabsorption during development: implications from a new model of growth hormone deficiency. Pediatr Nephrol 1990;4:387–91.
[151] Mulroney SE, Lumpkin MD, Haramati A. Antagonist to GH-releasing factor inhibits growth and renal Pi reabsorption in immature rats. Am J Physiol 1989;257:F29–34.
[152] Woda CB, Halaihel N, Wilson PV, Haramati A, Levi M, Mulroney SE. Regulation of renal NaPi-2 expression and tubular phosphate reabsorption by growth hormone in the juvenile rat. Am J Physiol Renal Physiol 2004;287:F117–123.
[153] Hammerman MR, Karl IE, Hruska KA. Regulation of canine renal vesicle Pi transport by growth hormone and parathyroid hormone. Biochim Biophys Acta 1980;603:322–35.
[154] Caverzasio J, Bonjour JP. Growth factors and renal regulation of phosphate transport. Pediatr Nephrol 1993;7:802–6.
[155] Caverzasio J, Bonjour JP. [IGF-1 and phosphate homeostasis during growth]. Nephrologie 1992;13:109–13.
[156] Caverzasio J, Bonjour JP. Influence of recombinant IGF-I (somatomedin C) on sodium-dependent phosphate transport in cultured renal epithelium. Prog Clin Biol Res 1988;252: 385–6.
[157] Caverzasio J, Bonjour JP. Insulin-like growth factor I stimulates Na-dependent Pi transport in cultured kidney cells. Am J Physiol 1989;257:F712–7.
[158] Caverzasio J, Montessuit C, Bonjour JP. Stimulatory effect of insulin-like growth factor-1 on renal Pi transport and plasma 1,25-dihydroxyvitamin D3. Endocrinology 1990;127:453–9.
[159] Hirschberg R, Brunori G, Kopple JD, Guler HP. Effects of insulin-like growth factor I on renal function in normal men. Kidney Int 1993;43:387–97.
[160] Hirschberg R, Ding H, Wanner C. Effects of insulin-like growth factor I on phosphate transport in cultured proximal tubule cells. J Lab Clin Med 1995;126:428–34.
[161] Quigley R, Baum M. Effects of growth hormone and insulin-like growth factor I on rabbit proximal convoluted tubule transport. J Clin Invest 1991;88:368–74.
[162] Mann KJ, Dousa DM, Kerrigan RJ, Berndt TJ, Knox FG. Acute renal denervation decreases tubular phosphate reabsorption. Miner Electrolyte Metab 1992;18:354–8.
[163] Mann KJ, Rybczynska A, Berndt TJ, Hoppe A, Tyce GM, Knox FG. Renal denervation enhances the phosphaturic effect of parathyroid hormone. Miner Electrolyte Metab 1991;17:16–20.
[164] Szalay L, Bencsath P, Takas L. Effect of splanchincotomy on the renal excretion of inorganic phosphate in the anaesthetized dog. Pflugers Arch 1977;367:283–6.
[165] Szalay L, Colindres RE, Jackson R, Gottschalk CW. Effects of chronic renal denervation in conscious restrained rats. Int Urol Nephrol 1986;18:3–18.
[166] Szenasi G, Bencsath P, Lehoczky E, Takacs L. Tubular transport and urinary excretion of phosphate after renal denervation in the anesthetized rat. Am J Physiol 1981;240:F481–486.
[167] Cuche JL, Marchand GR, Greger RF, Lang RC, Knox FG. Phosphaturic effect of dopamine in dogs. Possible role of intrarenally produced dopamine in phosphate regulation. J Clin Invest 1976;58:71–6.
[168] Debska-Slizien A, Ho P, Drangova R, Baines AD. Endogenous renal dopamine production regulates phosphate excretion. Am J Physiol 1994;266:F858–867.
[169] Goto F. The effects of dopamine on renal excretion of sodium, phosphate and cyclic AMP in thyroparathyroidectomized dogs. Endocrinol Jpn 1979;26:649–54.
[170] Isaac J, Berndt TJ, Knox FG. Role of dopamine in the exaggerated phosphaturic response to parathyroid hormone in the remnant kidney. J Lab Clin Med 1995;126:470–3.
[171] Isaac J, Berndt TJ, Thothathri V, Tyce GM, Knox FG. Catecholamines and phosphate excretion by the remnant kidney. Kidney Int 1993;43:1021–6.
[172] Kaneda Y, Bello-Reuss E. Effect of dopamine on phosphate reabsorption in isolated perfused rabbit proximal tubules. Miner Electrolyte Metab 1983;9:147–50.
[173] LeClaire M, Berndt TJ, Knox FG. Isoproterenol infusion increases the maximal tubular capacity of phosphate reabsorption. Ren Physiol Biochem 1992;15:134–40.
[174] Leme CE, Liberman B, Wajchenberg BL. Effect of norepinephrine, propranolol and phentolamine on the phosphaturic action of bovine parathyroid extract in man. Nephron 1973;11: 365–72.
[175] Sacktor B, Kinsella JL. Hormonal effects on sodium cotransport systems. Ann N Y Acad Sci 1985;456:438–44.
[176] Baines AD. Effects of salt intake and renal denervation on catecholamine catabolism and excretion. Kidney Int 1982;21: 316–22.

[177] Debska-Slizien A, Ho P, Drangova R, Baines AD. Endogenous dopamine regulates phosphate reabsorption but not NaK-ATPase in spontaneously hypertensive rat kidneys. J Am Soc Nephrol 1994;5:1125–32.

[178] Thornton LR, Meyer MH, Meyer Jr. RA. Isoproterenol increases renal tubular reabsorption of phosphate in X-linked hypophosphatemic (Hyp) mice. Miner Electrolyte Metab 1999;25:204–9.

[179] Cheng L, Liang CT, Precht P, Sacktor B. Alpha-2-adrenergic modulation of the parathyroid hormone-inhibition of phosphate uptake in cultured renal (OK) cells. Biochem Biophys Res Commun 1988;155:74–82.

[180] de Toledo FG, Beers KW, Berndt TJ, Thompson MA, Tyce GM, Knox FG, et al. Opposite paracrine effects of 5-HT and dopamine on Na(+)-Pi cotransport in opossum kidney cells. Kidney Int 1997;52:152–6.

[181] de Toledo FG, Thompson MA, Bolliger C, Tyce GM, Dousa TP. gamma-L-glutamyl-L-DOPA inhibits Na(+)-phosphate cotransport across renal brush border membranes and increases renal excretion of phosphate. Kidney Int 1999;55: 1832–42.

[182] Sadiq S, Berndt TJ, Nath KA, Knox FG. Effect of gamma-L-glutamyl-L-dopa on phosphate excretion. J Lab Clin Med 2000;135:52–6.

[183] Bacic D, Capuano P, Baum M, Zhang J, Stange G, Biber J, et al. Activation of dopamine D1-like receptors induces acute internalization of the renal Na + /phosphate cotransporter NaPi-IIa in mouse kidney and OK cells. Am J Physiol Renal Physiol 2005;288:F740–747.

[184] Baines AD, Drangova R. Does dopamine use several signal pathways to inhibit Na-Pi transport in OK cells?. J Am Soc Nephrol 1998;9:1604–12.

[185] Glahn RP, Onsgard MJ, Tyce GM, Chinnow SL, Knox FG, Dousa TP. Autocrine/paracrine regulation of renal Na (+)-phosphate cotransport by dopamine. Am J Physiol 1993;264:F618–622.

[186] Hafdi Z, Couette S, Comoy E, Prie D, Amiel C, Friedlander G. Locally formed 5-hydroxytryptamine stimulates phosphate transport in cultured opossum kidney cells and in rat kidney. Biochem J 1996;320(Pt 2):615–21.

[187] Lederer ED, Sohi SS, McLeish KR. Dopamine regulates phosphate uptake by opossum kidney cells through multiple counter-regulatory receptors. J Am Soc Nephrol 1998;9:975–85.

[188] Perrichot R, Garcia-Ocana A, Couette S, Comoy E, Amiel C, Friedlander G. Locally formed dopamine modulates renal Na-Pi co-transport through DA1 and DA2 receptors. Biochem J 1995;312(Pt 2):433–7.

[189] Berndt TJ, MacDonald A, Walikonis R, Chinnow S, Dousa TP, Tyce GM, et al. Excretion of catecholamines and metabolites in response to increased dietary phosphate intake. J Lab Clin Med 1993;122:80–4.

[190] Berndt TJ, Liang M, Tyce GM, Knox FG. Intrarenal serotonin, dopamine, and phosphate handling in remnant kidneys. Kidney Int 2001;59:625–30.

[191] Gross JM, Berndt TJ, Knox FG. Effect of serotonin receptor antagonist on phosphate excretion. J Am Soc Nephrol 2000;11:1002–7.

[192] Econs MJ, Drezner MK. Tumor-induced osteomalacia—unveiling a new hormone. N Engl J Med 1994;330:1679–81.

[193] Cai Q, Hodgson SF, Kao PC, Lennon VA, Klee GG, Zinsmiester AR, et al. Brief report: inhibition of renal phosphate transport by a tumor product in a patient with oncogenic osteomalacia. N Engl J Med 1994;330:1645–9.

[194] Drezner MK. Hypophosphatemic rickets. Endocr Dev 2003;6: 126–55.

[195] Drezner MK. The role of abnormal vitamin D metabolism in X-linked hypophosphatemic rickets and osteomalacia. Adv Exp Med Biol 1984;178:399–404.

[196] Econs MJ, Feussner JR, Samsa GP, Effman EL, Vogler JB, Martinez S, et al. X-linked hypophosphatemic rickets without "rickets." Skeletal Radiol 1991;20:109–14.

[197] Econs MJ, Samsa GP, Monger M, Drezner MK, Feussner JR. X-Linked hypophosphatemic rickets: a disease often unknown to affected patients. Bone Miner 1994;24:17–24.

[198] Polisson RP, Martinez S, Khoury M, Harrell RM, Lyles KW, Friedman N, et al. Calcification of entheses associated with X-linked hypophosphatemic osteomalacia. N Engl J Med 1985;313:1–6.

[199] Posillico JT, Lobaugh B, Muhlbaier LH, Drezner MK. Abnormal parathyroid function in the X-linked hypophosphatemic mouse. Calcif Tissue Int 1985;37:418–22.

[200] Meyer Jr RA, Meyer MH, Gray RW. Parabiosis suggests a humoral factor is involved in X-linked hypophosphatemia in mice. J Bone Miner Res 1989;4:493–500.

[201] Meyer Jr RA, Tenenhouse HS, Meyer MH, Klugerman AH. The renal phosphate transport defect in normal mice parabiosed to X-linked hypophosphatemic mice persists after parathyroidectomy. J Bone Miner Res 1989;4:523–32.

[202] Nesbitt T, Coffman TM, Griffiths R, Drezner MK. Crosstransplantation of kidneys in normal and Hyp mice. Evidence that the Hyp mouse phenotype is unrelated to an intrinsic renal defect. J Clin Invest 1992;89:1453–9.

[203] ADHR Consortium. Autosomal dominant hypophosphataemic rickets is associated with mutations in FGF23. *Nat Genet* 2000;26:345–348.

[204] Shimada T, Muto T, Urakawa I, Yoneya T, Yamazaki Y, Okawa K, et al. Mutant FGF-23 responsible for autosomal dominant hypophosphatemic rickets is resistant to proteolytic cleavage and causes hypophosphatemia *in vivo*. Endocrinology 2002;143:3179–82.

[205] De Beur SM, Finnegan RB, Vassiliadis J, Cook B, Barberio D, Estes S, et al. Tumors associated with oncogenic osteomalacia express genes important in bone and mineral metabolism. J Bone Miner Res 2002;17:1102–10.

[206] Bowe AE, Finnegan R, Jan de Beur SM, Cho J, Levine MA, Kumar R, et al. FGF-23 inhibits renal tubular phosphate transport and is a PHEX substrate. Biochem Biophys Res Commun 2001;284:977–81.

[207] Bresler D, Bruder J, Mohnike K, Fraser WD, Rowe PS. Serum MEPE-ASARM-peptides are elevated in X-linked rickets (HYP): implications for phosphaturia and rickets. J Endocrinol 2004;183:R1–9.

[208] Rowe PS, Kumagai Y, Gutierrez GE, Garrett IR, Blacher R, Rosen D, et al. MEPE has the properties of an osteoblastic phosphatonin and minhibin. Bone 2004;34:303–19.

[209] Strewler GJ. FGF23, hypophosphatemia, and rickets: has phosphatonin been found? Proc Natl Acad Sci U S A 2001;98:5945–6.

[210] Weber TJ, Liu S, Indridason OS, Quarles LD. Serum FGF23 levels in normal and disordered phosphorus homeostasis. J Bone Miner Res 2003;18:1227–34.

[211] Carpenter TO, Ellis BK, Insogna KL, Philbrick WM, Sterpka J, Shimkets R. Fibroblast growth factor 7: an inhibitor of phosphate transport derived from oncogenic osteomalacia-causing tumors. J Clin Endocrinol Metab 2005;90:1012–20.

[212] Bai X, Miao D, Li J, Goltzman D, Karaplis AC. Transgenic mice overexpressing human fibroblast growth factor 23 (R176Q) delineate a putative role for parathyroid hormone in renal phosphate wasting disorders. Endocrinology 2004;145: 5269–79.

[213] Bai XY, Miao D, Goltzman D, Karaplis AC. The autosomal dominant hypophosphatemic rickets R176Q mutation in fibroblast growth factor 23 resists proteolytic cleavage and enhances *in vivo* biological potency. J Biol Chem 2003;278:9843–9.

[214] White KE, Carn G, Lorenz-Depiereux B, Benet-Pages A, Strom TM, Econs MJ. Autosomal-dominant hypophosphatemic rickets (ADHR) mutations stabilize FGF-23. Kidney Int 2001;60:2079–86.

[215] White KE, Evans WE, O'Riordan JLH, Speer MC, Econs MJ, Lorenz-Depiereux B, et al. Autosomal dominant hypophosphataemic rickets is associated with mutations in FGF23. Nat Genet 2000;26:345–8.

[216] White KE, Jonsson KB, Carn G, Hampson G, Spector TD, Mannstadt M, et al. The autosomal dominant hypophosphatemic rickets (ADHR) gene is a secreted polypeptide overexpressed by tumors that cause phosphate wasting. J Clin Endocrinol Metab 2001;86:497–500.

[217] Shimada T, Kakitani M, Yamazaki Y, Hasegawa H, Takeuchi Y, Fujita T, et al. Targeted ablation of Fgf23 demonstrates an essential physiological role of FGF23 in phosphate and vitamin D metabolism. J Clin Invest 2004;113:561–8.

[218] Larsson T, Marsell R, Schipani E, Ohlsson C, Ljunggren O, Tenenhouse HS, et al. Transgenic mice expressing fibroblast growth factor 23 under the control of the alpha1(I) collagen promoter exhibit growth retardation, osteomalacia, and disturbed phosphate homeostasis. Endocrinology 2004;145:3087–94.

[219] Shimada T, Urakawa I, Yamazaki Y, Hasegawa H, Hino R, Yoneya T, et al. FGF-23 transgenic mice demonstrate hypophosphatemic rickets with reduced expression of sodium phosphate cotransporter type IIa. Biochem Biophys Res Commun 2004;314:409–14.

[220] Ferrari SL, Bonjour JP, Rizzoli R. Fibroblast growth factor-23 relationship to dietary phosphate and renal phosphate handling in healthy young men. J Clin Endocrinol Metab 2005;90:1519–24.

[221] Larsson T, Nisbeth U, Ljunggren O, Juppner H, Jonsson KB. Circulating concentration of FGF-23 increases as renal function declines in patients with chronic kidney disease, but does not change in response to variation in phosphate intake in healthy volunteers. Kidney Int 2003;64:2272–9.

[222] Saito H, Maeda A, Ohtomo S, Hirata M, Kusano K, Kato S, et al. Circulating FGF-23 is regulated by 1alpha,25-dihydroxyvitamin D3 and phosphorus *in vivo*. J Biol Chem 2005;280:2543–9.

[223] Yamashita T, Konishi M, Miyake A, Inui K, Itoh N. Fibroblast growth factor (FGF)-23 inhibits renal phosphate reabsorption by activation of the mitogen-activated protein kinase pathway. J Biol Chem 2002;277:28265–70.

[224] Bodine PV, Zhao W, Kharode YP, Bex FJ, Lambert AJ, Goad MB, et al. The Wnt antagonist secreted frizzled-related protein-1 is a negative regulator of trabecular bone formation in adult mice. Mol Endocrinol 2004;18:1222–37.

[225] Rowe PS, de Zoysa PA, Dong R, Wang HR, White KE, Econs MJ, et al. MEPE, a new gene expressed in bone marrow and tumors causing osteomalacia. Genomics 2000;67:54–68.

[226] Gowen LC, Petersen DN, Mansolf AL, Qi H, Stock JL, Tkalcevic GT, et al. Targeted disruption of the osteoblast/osteocyte factor 45 gene (OF45) results in increased bone formation and bone mass. J Biol Chem 2003;278:1998–2007.

[227] Xiao ZS, Crenshaw M, Guo R, Nesbitt T, Drezner MK, Quarles LD. Intrinsic mineralization defect in Hyp mouse osteoblasts. Am J Physiol 1998;275:E700–708.

[228] Guo R, Rowe PS, Liu S, Simpson LG, Xiao ZS, Darryl Quarles LD. Inhibition of MEPE cleavage by Phex. Biochem Biophys Res Commun 2002;297:38–45.

[229] Rowe PS, Garrett IR, Schwarz PM, Carnes DL, Lafer EM, Mundy GR, et al. Surface plasmon resonance (SPR) confirms that MEPE binds to PHEX via the MEPE-ASARM motif: a model for impaired mineralization in X-linked rickets (HYP). Bone 2005;36:33–46.

[230] Jain A, Fedarko NS, Collins MT, Gelman R, Ankrom MA, Tayback M, et al. Serum levels of matrix extracellular phosphoglycoprotein (MEPE) in normal humans correlate with serum phosphorus, parathyroid hormone and bone mineral density. J Clin Endocrinol Metab 2004;89:4158–61.

[231] Jacob HS, Amsden T. Acute hemolytic anemia with rigid red cells in hypophosphatemia. N Engl J Med 1971;285:1446–50.

[232] Klock JC, Williams HE, Mentzer WC. Hemolytic anemia and somatic cell dysfunction in severe hypophosphatemia. Arch Intern Med 1974;134:360–4.

[233] Craddock PR, Yawata Y, Van Santen L, Gilberstadt S, Silvis S, Jacob HS. Acquired phagocyte dysfunction. A complication of the hypophosphatemia of parenteral hyperalimentation. N Engl J Med 1974;290:1403–7.

[234] Yawata Y, Hebbel RP, Silvis S, Howe R, Jacob H. Blood cell abnormalities complicating the hypophosphatemia of hyperalimentation: erythrocyte and platelet ATP deficiency associated with hemolytic anemia and bleeding in hyperalimented dogs. J Lab Clin Med 1974;84:643–53.

[235] Knochel J, Montanari A. Central Nervous System Manifestations of Hypophosphatemia and Phosphorus Depletion. Boston: Little, Brown; 1992.

[236] Ellinas PA, Rosner F. Rhabdomyolysis and hypophosphatemia. Am J Med 1993;94:449–50.

[237] Knochel JP. Hypophosphatemia and rhabdomyolysis. Am J Med 1992;92:455–7.

[238] Singhal PC, Kumar A, Desroches L, Gibbons N, Mattana J. Prevalence and predictors of rhabdomyolysis in patients with hypophosphatemia. Am J Med 1992;92:458–64.

[239] Ferguson ER, Blachley JD, Carter NW, Knochel JP. Derangements of muscle composition, ion transport, and oxygen consumption in chronically alcoholic dogs. Am J Physiol 1984;246:F700–709.

[240] Fuller TJ, Nichols WW, Brenner BJ, Peterson JC. Reversible depression in myocardial performance in dogs with experimental phosphorus deficiency. J Clin Invest 1978;62:1194–200.

[241] Affarah H, Salti I, Feisal KA. Hypophosphatemia as a possible cause of acute respiratory failure. J Med Liban 1980;31:229–34.

[242] Brown EL, Jenkins BA. A case of respiratory failure complicated by acute hypophosphataemia. Anaesthesia 1980;35:42–5.

[243] Fiaccadori E, Coffrini E, Fracchia C, Rampulla C, Montagna T, Borghetti A. Hypophosphatemia and phosphorus depletion in respiratory and peripheral muscles of patients with respiratory failure due to COPD. Chest 1994;105:1392–8.

[244] Furlan AJ, Hanson M, Cooperman A, Farmer RG. Acute areflexic paralysis: association with hyperalimentation and hypophosphatemia. Arch Neurol 1975;32:706–7.

[245] Gravelyn TR, Brophy N, Siegert C, Peters-Golden M. Hypophosphatemia-associated respiratory muscle weakness in a general inpatient population. Am J Med 1988;84:870–6.

[246] Knochel JP. The clinical status of hypophosphatemia: an update. N Engl J Med 1985;313:447–9.

[247] Newman JH, Neff TA, Ziporin P. Acute respiratory failure associated with hypophosphatemia. N Engl J Med 1977;296:1101–3.

[248] Rie MA. Hypophosphatemia and diaphragmatic contractility. N Engl J Med 1986;314:519–20.

[249] Ritz E. Acute hypophosphatemia. Kidney Int 1982;22:84–94.
[250] Varsano S, Shapiro M, Taragan R, Bruderman I. Hypophosphatemia as a reversible cause of refractory ventilatory failure. Crit Care Med 1983;11:908–9.
[251] Brautbar N, Leibovici H, Massry SG. On the mechanism of hypophosphatemia during acute hyperventilation: evidence for increased muscle glycolysis. Miner Electrolyte Metab 1983;9:45–50.
[252] Gadisseux P, Sica DA, Ward JD, Becker DP. Severe hypophosphatemia after head injury. Neurosurgery 1985;17:35–40.
[253] Mostellar ME, Tuttle Jr. EP. Effects of alkalosis on plasma concentration and urinary excretion of inorganic phosphate in man. J Clin Invest 1964;43:138–49.
[254] Paleologos M, Stone E, Braude S. Persistent, progressive hypophosphataemia after voluntary hyperventilation. Clin Sci (Lond) 2000;98:619–25.
[255] Srinivasagam D, Seshadri MS, Peter JV, Cherian AM, Charles D, Kanagasabapathy AS. Prevalence & pathogenesis of hypophosphatemia in ventilated patients. Indian J Med Res 1992;96:87–90.
[256] Watt JW, Silva P. Respiratory alkalosis and associated electrolytes in long-term ventilator dependent persons with tetraplegia. Spinal Cord 2001;39:557–63.
[257] Haramati A, Nienhuis D. Renal handling of phosphate during acute respiratory acidosis and alkalosis in the rat. Am J Physiol 1984;247:F596–601.
[258] Hoppe A, Metler M, Berndt TJ, Knox FG, Angielski S. Effect of respiratory alkalosis on renal phosphate excretion. Am J Physiol 1982;243:F471–475.
[259] Krapf R, Jaeger P, Hulter HN. Chronic respiratory alkalosis induces renal PTH-resistance, hyperphosphatemia and hypocalcemia in humans. Kidney Int 1992;42:727–34.
[260] Hoppe A, Rybczynska A, Knox FG, Angielski S. Beta-receptors in resistance to phosphaturic effect of PTH in respiratory alkalosis. Am J Physiol 1988;255:R557–562.
[261] Tucker RR, Berndt TJ, Thotharthri V, Newcome J, Joyner MJ, Knox FG. Propranolol blocks the hypophosphaturia of acute respiratory alkalosis in human subjects. J Lab Clin Med 1996;128:423–8.
[262] Antachopoulos C, Papassotiriou I. Hypophosphatemia in meningococcal sepsis. Pediatr Nephrol 2004;19:1435–6.
[263] Barak V, Schwartz A, Kalickman I, Nisman B, Gurman G, Shoenfeld Y. Prevalence of hypophosphatemia in sepsis and infection: the role of cytokines. Am J Med 1998;104:40–7.
[264] Chesney PJ, Davis JP, Purdy WK, Wand PJ, Chesney RW. Clinical manifestations of toxic shock syndrome. JAMA 1981;246:741–8.
[265] Chesney RW, Chesney PJ, Davis JP, Segar WE. Renal manifestations of the staphylococcal toxic-shock syndrome. Am J Med 1981;71:583–8.
[266] Elisaf M, Theodorou J, Pappas H, Siamopoulos KC. Acid–base and electrolyte abnormalities in febrile patients with bacteraemia. Eur J Med 1993;2:404–7.
[267] Kay MA, McCabe ED. Escherichia coli sepsis and prolonged hypophosphatemia following exertional heat stroke. Pediatrics 1990;86:307–9.
[268] Riedler GF, Scheitlin WA. Hypophosphataemia in septicaemia: higher incidence in gram-negative than in gram-positive infections. Br Med J 1969;1:753–6.
[269] del Giglio A, Zukiwski AA, Ali MK, Mavligit GM. Severe, symptomatic, dose-limiting hypophosphatemia induced by hepatic arterial infusion of recombinant tumor necrosis factor in patients with liver metastases. Cancer 1991;67:2459–61.
[270] Mavligit GM, Zukiwski AA, Charnsangavej C, Carrasco CH, Wallace S, Gutterman JU. Regional biologic therapy. Hepatic arterial infusion of recombinant human tumor necrosis factor in patients with liver metastases. Cancer 1992;69:557–61.
[271] Kozeny GA, Nicolas JD, Creekmore S, Sticklin L, Hano JE, Fisher RI. Effects of interleukin-2 immunotherapy on renal function. J Clin Oncol 1988;6:1170–6.
[272] Quan W, Ramirez M, Taylor C, Vinogradov M, Quan F, Khan N. High-dose continuous infusion plus pulse interleukin-2 and famotidine in metastatic kidney cancer. Cancer Biother Radiopharm 2005;20:36–40.
[273] Quan W, Ramirez M, Taylor WC, Vinogradov M, Khan N, Jackson S. High-dose continuous infusion plus pulse interleukin-2 and famotidine in melanoma. Cancer Biother Radiopharm 2004;19:770–5.
[274] Sarmiento UM, Riley JH, Knaack PA, Lipman JM, Becker JM, Gately MK, et al. Biologic effects of recombinant human interleukin-12 in squirrel monkeys (Sciureus saimiri). Lab Invest 1994;71:862–73.
[275] Webb DE, Austin III HA, Belldegrun A, Vaughan E, Linehan WM, Rosenberg SA. Metabolic and renal effects of interleukin-2 immunotherapy for metastatic cancer. Clin Nephrol 1988;30: 141–5.
[276] Bowling TE, Silk DB. Refeeding remembered. Nutrition 1995;11:32–4.
[277] Brooks MJ, Melnik G. The refeeding syndrome: an approach to understanding its complications and preventing its occurrence. Pharmacotherapy 1995;15:713–26.
[278] Fisher M, Simpser E, Schneider M. Hypophosphatemia secondary to oral refeeding in anorexia nervosa. Int J Eat Disord 2000;28:181–7.
[279] Kohn MR, Golden NH, Shenker IR. Cardiac arrest and delirium: presentations of the refeeding syndrome in severely malnourished adolescents with anorexia nervosa. J Adolesc Health 1998;22:239–43.
[280] Marik PE, Bedigian MK. Refeeding hypophosphatemia in critically ill patients in an intensive care unit: a prospective study. Arch Surg 1996;131:1043–7.
[281] Melchior JC. From malnutrition to refeeding during anorexia nervosa. Curr Opin Clin Nutr Metab Care 1998;1:481–5.
[282] Mezoff AG, Gremse DA, Farrell MK. Hypophosphatemia in the nutritional recovery syndrome. Am J Dis Child 1989;143: 1111–2.
[283] Vaszar LT, Culpepper-Morgan JA, Winter SM. Refeeding syndrome induced by cautious enteral alimentation of a moderately malnourished patient. Gastroenterologist 1998;6:79–81.
[284] Weinsier RL, Krumdieck CL. Death resulting from overzealous total parenteral nutrition: the refeeding syndrome revisited. Am J Clin Nutr 1981;34:393–9.
[285] Elisaf M, Merkouropoulos M, Tsianos EV, Siamopoulos KC. Pathogenetic mechanisms of hypomagnesemia in alcoholic patients. J Trace Elem Med Biol 1995;9:210–4.
[286] Paunier L. Effect of magnesium on phosphorus and calcium metabolism. Monatsschr Kinderheilkd 1992;140:S17–20.
[287] Welt LG. Experimental magnesium depletion. Yale J Biol Med 1964;36:325–49.
[288] Whang R, Oei TO, Aikawa JK, Watanabe A, Vannatta J, Fryer A, et al. Predictors of clinical hypomagnesemia. Hypokalemia, hypophosphatemia, hyponatremia, and hypocalcemia. Arch Intern Med 1984;144:1794–6.
[289] Whang R, Welt LG. Observations in experimental magnesium depletion. J Clin Invest 1963;42:305–13.
[290] De Marchi S, Cecchin E, Basile A, Bertotti A, Nardini R, Bartoli E. Renal tubular dysfunction in chronic alcohol abuse: effects of abstinence. N Engl J Med 1993;329:1927–34.
[291] Rojas E, Carlini RG, Clesca P, Arminio A, Suniaga O, De Elguezabal K, et al. The pathogenesis of osteodystrophy after

renal transplantation as detected by early alterations in bone remodeling. Kidney Int 2003;63:1915–23.
[292] Levi M. Post-transplant hypophosphatemia. Kidney Int 2001;59:2377–87.
[293] Green J, Debby H, Lederer E, Levi M, Zajicek HK, Bick T. Evidence for a PTH-independent humoral mechanism in post-transplant hypophosphatemia and phosphaturia. Kidney Int 2001;60:1182–96.
[294] Nakanishi S, Kazama JJ, Nii-Kono T, Omori K, Yamashita T, Fukumoto S, et al. Serum fibroblast growth factor-23 levels predict the future refractory hyperparathyroidism in dialysis patients. Kidney Int 2005;67:1171–8.
[295] Imanishi Y, Inaba M, Nakatsuka K, Nagasue K, Okuno S, Yoshihara A, et al. FGF-23 in patients with end-stage renal disease on hemodialysis. Kidney Int 2004;65:1943–6.
[296] Jonsson KB, Zahradnik R, Larsson T, White KE, Sugimoto T, Imanishi Y, et al. Fibroblast growth factor 23 in oncogenic osteomalacia and X-linked hypophosphatemia. N Engl J Med 2003;348:1656–63.
[297] Kazama JJ, Sato F, Omori K, Hama H, Yamamoto S, Maruyama H, et al. Pretreatment serum FGF-23 levels predict the efficacy of calcitriol therapy in dialysis patients. Kidney Int 2005;67:1120–5.
[298] John MR, Wickert H, Zaar K, Jonsson KB, Grauer A, Ruppersberger P, et al. A case of neuroendocrine oncogenic osteomalacia associated with a PHEX and fibroblast growth factor-23 expressing sinusidal malignant schwannoma. Bone 2001;29:393–402.
[299] Larsson T, Zahradnik R, Lavigne J, Ljunggren O, Juppner H, Jonsson KB. Immunohistochemical detection of FGF-23 protein in tumors that cause oncogenic osteomalacia. Eur J Endocrinol 2003;148:269–76.
[300] Nelson AE, Bligh RC, Mirams M, Gill A, Au A, Clarkson A, et al. Clinical case seminar: Fibroblast growth factor 23—a new clinical marker for oncogenic osteomalacia: case reports. J Clin Endocrinol Metab 2003;88:4088–94.
[301] Takeuchi Y, Suzuki H, Ogura S, Imai R, Yamazaki Y, Yamashita T, et al. Venous sampling for fibroblast growth factor-23 confirms preoperative diagnosis of tumor-induced osteomalacia. J Clin Endocrinol Metab 2004;89:3979–82.
[302] Yamazaki Y, Okazaki R, Shibata M, Hasegawa Y, Satoh K, Tajima T, et al. Increased circulatory level of biologically active full-length FGF-23 in patients with hypophosphatemic rickets/osteomalacia. J Clin Endocrinol Metab 2002;87:4957–60.
[303] Econs MJ, McEnery PT, Lennon F, Speer MC. Autosomal dominant hypophosphatemic rickets is linked to chromosome 12p13. J Clin Invest 1997;100:2653–7.
[304] Econs MJ, McEnery PT. Autosomal dominant hypophosphatemic rickets/osteomalacia: clinical characterization of a novel renal phosphate-wasting disorder. J Clin Endocrinol Metab 1997;82:674–81.
[305] Fraser D, Scriver CR. Familial forms of vitamin D-resistant rickets revisited. X-linked hypophosphatemia and autosomal recessive vitamin D dependency. Am J Clin Nutr 1976;29:1315–29.
[306] Scriver CR. The William Allan Memorial Award address: On phosphate transport and genetic screening. "Understanding backward—living forward" in human genetics. Am J Hum Genet 1979;31:243–63.
[307] Scriver CR, Tenenhouse HS. X-linked hypophosphataemia: a homologous phenotype in humans and mice with unusual organ-specific gene dosage. J Inherit Metab Dis 1992;15:610–24.
[308] Eicher EM, Southard JL, Scriver CR, Glorieux FH. Hypophosphatemia: mouse model for human familial hypophosphatemic (vitamin D-resistant) rickets. Proc Natl Acad Sci U S A 1976;73:4667–71.
[309] Lyon MF, Scriver CR, Baker LR, Tenenhouse HS, Kronick J, Mandla S. The Gy mutation: another cause of X-linked hypophosphatemia in mouse. Proc Natl Acad Sci U S A 1986;83:4899–903.
[310] Lajeunesse D, Meyer Jr RA, Hamel L. Direct demonstration of a humorally-mediated inhibition of renal phosphate transport in the Hyp mouse. Kidney Int 1996;50:1531–8.
[311] A gene (PEX) with homologies to endopeptidases is mutated in patients with X-linked hypophosphatemic rickets. The HYP Consortium. *Nat Genet* 1995;11:130–136.
[312] Lorenz B, Francis F, Gempel K, Boddrich A, Josten M, Schmahl W, et al. Spermine deficiency in Gy mice caused by deletion of the spermine synthase gene. Hum Mol Genet 1998;7:541–7.
[313] Meyer Jr RA, Henley CM, Meyer MH, Morgan PL, McDonald AG, Mills C, et al. Partial deletion of both the spermine synthase gene and the Pex gene in the X-linked hypophosphatemic, gyro (Gy) mouse. Genomics 1998;48:289–95.
[314] Strom TM, Francis F, Lorenz B, Boddrich A, Econs MJ, Lehrach H, et al. Pex gene deletions in Gy and Hyp mice provide mouse models for X-linked hypophosphatemia. Hum Mol Genet 1997;6:165–71.
[315] Aono Y, Shimada T, Yamazaki Y, Hino R, Takeuchi Y, Fujita T, et al. The neutralization of FGF-23 ameliorates hypophosphatemia and rickets in Hyp mice. J Bone Miner Res 2003;18:S16.
[316] Campos M, Couture C, Hirata IY, Juliano MA, Loisel TP, Crine P, et al. Human recombinant endopeptidase PHEX has a strict S1′ specificity for acidic residues and cleaves peptides derived from fibroblast growth factor-23 and matrix extracellular phosphoglycoprotein. Biochem J 2003;373:271–9.
[317] Guo R, Liu S, Spurney RF, Quarles LD. Analysis of recombinant Phex: an endopeptidase in search of a substrate. Am J Physiol Endocrinol Metab 2001;281:E837–847.
[318] Albright F, Butler AM, Hampton AO, Smith P. Syndrome characterized by osteitis fibrosa disseminata, areas of pigmentation and endocrine dysfunction with precocious puberty in females. N Engl J Med 1937;216:727–46.
[319] Lichtenstein L. Polyostotic fibrous dysplasia. Arch Surg 1938;36:874–9.
[320] Lichtenstein L, Jaffe HL. Fibrous dysplasia of bone: a condition affecting one, several or many bones, the graver cases of which may present abnormal pigmentation of skin, premature sexual development, hyperthyroidism and still other extraskeletal abnormalities. Arch Pathol 1942;33:777–97.
[321] McCune DJ, Bruch H. Progress in pediatrics: osteodystrophia fibrosa. Am J Dis Child 1937;54:806–48.
[322] Weinstein LS, Shenker A, Gejman PV, Merino MJ, Friedman E, Spiegel AM. Activating mutations of the stimulatory G protein in the McCune-Albright syndrome. N Engl J Med 1991;325:1688–95.
[323] Bianco P, Riminucci M, Majolagbe A, Kuznetsov SA, Collins MT, Mankani MH, et al. Mutations of the GNAS1 gene, stromal cell dysfunction, and osteomalacic changes in non-McCune-Albright fibrous dysplasia of bone. J Bone Miner Res 2000;15:120–8.
[324] Collins MT, Chebli C, Jones J, Kushner H, Consugar M, Rinaldo P, et al. Renal phosphate wasting in fibrous dysplasia of bone is part of a generalized renal tubular dysfunction similar to that seen in tumor-induced osteomalacia. J Bone Miner Res 2001;16:806–13.
[325] Corsi A, Collins MT, Riminucci M, Howell PG, Boyde A, Robey PG, et al. Osteomalacic and hyperparathyroid changes

in fibrous dysplasia of bone: core biopsy studies and clinical correlations. J Bone Miner Res 2003;18:1235–46.
[326] Dachille RD, Goldberg JS, Wexler ID, Shons AR. Fibrous dysplasia-induced hypocalcemia/rickets. J Oral Maxillofac Surg 1990;48:1319–22.
[327] Ryan WG, Nibbe AF, Schwartz TB, Ray RD. Fibrous dysplasia of bone with vitamin D resistant rickets: a case study. Metabolism 1968;17:988–98.
[328] Riminucci M, Collins MT, Fedarko NS, Cherman N, Corsi A, White KE, et al. FGF-23 in fibrous dysplasia of bone and its relationship to renal phosphate wasting. J Clin Invest 2003;112:683–92.
[329] Stewart AF, Horst R, Deftos LJ, Cadman EC, Lang R, Broadus AE. Biochemical evaluation of patients with cancer-associated hypercalcemia: evidence for humoral and nonhumoral groups. N Engl J Med 1980;303:1377–83.
[330] Singh RJ, Kumar R. Fibroblast growth factor 23 concentrations in humoral hypercalcemia of malignancy and hyperparathyroidism. Mayo Clin Proc 2003;78:826–9.
[331] Tebben PJ, Singh RJ, Clarke BL, Kumar R. Fibroblast growth factor 23, parathyroid hormone, and 1alpha,25-dihydroxyvitamin D in surgically treated primary hyperparathyroidism. Mayo Clin Proc 2004;79:1508–13.
[332] McCarthy JT, Kumar R. Behavior of the vitamin D endocrine system in the development of renal osteodystrophy. Semin Nephrol 1986;6:21–30.
[333] McCarthy JT, Kumar R. Renal osteodystrophy. Endocrinol Metab Clin North Am 1990;19:65–93.
[334] Bricker NS, Bourgoignie J, Weber H, Schmidt RW, Slatopolsky E. Pathogenesis of the uremic state: a new perspective. Adv Nephrol Necker Hosp 1972;2:263–76.
[335] Coburn J, Kanis J, Popovtzer M, Ritz E, Slatopolsky E, Fleisch H. Pathophysiology and treatment of uremic bone disease. Calcif Tissue Int 1983;35:712–4.
[336] Cozzolino M, Brancaccio D, Gallieni M, Galassi A, Slatopolsky E, Dusso A. Pathogenesis of parathyroid hyperplasia in renal failure. J Nephrol 2005;18:5–8.
[337] Slatopolsky E, Bricker NS. The role of phosphorus restriction in the prevention of secondary hyperparathyroidism in chronic renal disease. Kidney Int 1973;4:141–5.
[338] Slatopolsky E, Brown A, Dusso A. Pathogenesis of secondary hyperparathyroidism. Kidney Int Suppl 1999;73:S14–19.
[339] Slatopolsky E, Delmez JA. Pathogenesis of secondary hyperparathyroidism. Miner Electrolyte Metab 1995;21:91–6.
[340] Slatopolsky E, Dusso A, Brown AJ. The role of phosphorus in the development of secondary hyperparathyroidism and parathyroid cell proliferation in chronic renal failure. Am J Med Sci 1999;317:370–6.
[341] Slatopolsky E, Hruska K, Rutherford WE. Current concepts of parathyroid hormone and vitamin D metabolism: perturbations in chronic renal disease. Kidney Int Suppl 1975;:90–6.
[342] Slatopolsky E, Lopez-Hilker S, Dusso A, Brown A, Delmez J, Martin K. Renal osteodystrophy: past and future. Contrib Nephrol 1990;78:38–45 [discussion, 45–36].
[343] Slatopolsky E, Rutherford WE, Hruska K, Martin K, Klahr S. How important is phosphate in the pathogenesis of renal osteodystrophy? Arch Intern Med 1978;:848–52 [138(Spec No):)]
[344] Slatopolsky E, Rutherford WE, Martin K, Hruska K. The role of phosphate and other factors on the pathogenesis of renal osteodystrophy. Adv Exp Med Biol 1977;81:467–75.
[345] Topaz O, Shurman DL, Bergman R, Indelman M, Ratajczak P, Mizrachi M, et al. Mutations in GALNT3, encoding a protein involved in O-linked glycosylation, cause familial tumoral calcinosis. Nat Genet 2004;36:579–81.
[346] Frishberg Y, Topaz O, Bergman R, Behar D, Fisher D, Gordon D, et al. Identification of a recurrent mutation in GALNT3 demonstrates that hyperostosis-hyperphosphatemia syndrome and familial tumoral calcinosis are allelic disorders. J Mol Med 2005;83:33–8.
[347] Larsson T, Yu X, Davis SI, Draman MS, Mooney SD, Cullen MJ, et al. A novel recessive mutation in fibroblast growth factor-23 causes familial tumoral calcinosis. J Clin Endocrinol Metab 2005;90:2424–7.

This page intentionally left blank

CHAPTER

70

Glucose Reabsorption in The Kidney

Charles S. Hummel and Ernest M. Wright

Department of Physiology, The David Geffen School of Medicine at UCLA, Los Angeles, California, USA

OVERVIEW OF GLUCOSE HOMEOSTASIS

Glucose is the major fuel source to the body's tissues, and it comes in various forms in the diet: simple sugar, disaccharides, polysaccharides, and starch. It is utilized in both oxidative and non-oxidative metabolic pathways, it provides a substrate for triglyceride synthesis in adipose tissue, and it is enzymatically polymerized into glycogen for storage in muscle and the liver. Glucose is synthesized endogenously in the liver and kidneys by gluconeogenesis. Its plasma concentration is maintained within narrow limits, 4–10 mM (70–110 mg/dL), with many hormonal influences. Pathological alterations in glucose homeostasis are most often identified with diabetes.

GLUCOSE TRANSPORTERS IN GLUCOSE HOMEOSTASIS

The transport of glucose across biological membranes is a critical step regulating its concentration in plasma. There are two major classes of proteins responsible for glucose transport.

Facilitated GLUcose Transporters (GLUTs) bind to glucose and translocate it across membranes in an energy-independent fashion: they require a glucose concentration gradient to drive net transport; hence they *facilitate* the *diffusion* of glucose. The GLUTs belong to the *SLC2A* gene family, part of the larger Membrane Facilitators Superfamily (MFS).[1] There are currently 14 identified GLUT genes within the human body, for example, the protein coded by the *SLC2A2 gene*, GLUT2, allows glucose to be reabsorbed in the kidney by facilitating diffusion across basolateral membranes, and mutations in this gene are responsible for the Fanconi-Bickel Syndrome (FBS, OMIM 227810).[2]

Sodium-dependent GLucose Transporters (SGLTs) bind Na^+ ions and glucose, transporting them across the membrane in an *energy-dependent* fashion: the Na^+ electrochemical potential gradient, maintained by the Na^+/K^+ ATPase, drives the transport of glucose into cells. This allows non-metabolized glucose analogs to accumulate in tissues in excess of the plasma concentration and so they are crucial for the reabsorption of glucose in the kidneys and the intestinal absorption of dietary glucose. SGLTs belong to the *SLC5A* gene family, part of the Sodium Solute Symporter (SSS) superfamily of proteins.[3,4] Although the amino acid sequences are quite different among members of the SSS family, the atomic structures reveal common features that suggest similar transport mechanisms.[5–7]

As with the GLUTs, SGLT genes are expressed throughout the body.[3,4,8] However, mRNA expression profiles offer only hints of physiological function, and establishing *functional* roles for SGLTs in the body's tissues has proven to be non-trivial.

CELLULAR AND MOLECULAR PHYSIOLOGY OF SGLTS

SGLT1 was the first identified and is the most extensively studied Na^+/D-glucose co-transporter.[4] It was cloned in 1987 by expression cloning,[9] and it is responsible for the intestinal absorption of D-glucose and D-galactose from the diet. Through a combination of biophysics, immunohistochemistry, molecular genetics, and freeze fracture electron microscopy, it was established that either defective translation, post-

Seldin and Giebisch's The Kidney, Fifth Edition.
DOI: http://dx.doi.org/10.1016/B978-0-12-381462-3.00070-7

© 2013 Elsevier Inc. All rights reserved.

translational trafficking, or function of SGLT1 leads to glucose-galactose malabsorption (GGM, OMIM # 182380; online, Mendelian Inheritance in Man, http://www.ncbi.nlm.nih.gov/OMIM). GGM is an extremely rare, autosomal recessive disease, in which patients experience life-threatening osmotic diarrhea starting in the first few days of life. Failure to absorb sugars broken down from the lactose in mother's milk or infant formula leads to profuse, watery diarrhea that abates only when sources of glucose or galactose are eliminated from the diet. As long as GGM is identified and appropriate dietary modifications are made, patients lead relatively normal and healthy lives.[10] Its expression cloning and detailed characterization, in addition to the molecular details of GGM, firmly established hSGLT1 as crucial to glucose and galactose absorption in the gut. On the other hand patients with GGM have only a mild renal glycosuria (see below).

There are four other members of the SLC5A gene family that are capable of transporting glucose, SGLT2, SGLT4, SGLT5 and SGLT6.[11] Human SGLT3, which is expressed in gut neuronal cells, depolarizes the cell upon exposure to glucose, is believed to be a glucose sensor and not a transporter.[12–14] hSGLT6 is a Na^+/myo-inositol co-transporter which also is a low affinity glucose transporter and it is now referred to as hSMIT2.[3,4] hSGLT2 (SLC5A2) is abundantly expressed in the kidney but mRNA is also found in liver, heart, brain and muscle. This is believed to be the transporter responsible for the bulk of glucose reabsorption in kidney and mutations in the gene are associated with renal glucosuria (see below). In addition to D-mannose, hSGLT4 has also been shown to transport D-glucose, fructose, and 1,5-anhydro-D-glucitol.[15] Its mRNA has been detected in small intestine, kidney, liver, lung and brain, where it may be important in maintaining stores of mannose for protein glycosylation. SGLT5, exclusively expressed in the human kidney cortex, is a mannose and fructose sodium cotransporter with a higher affinity and turnover than for glucose.[16] Its cellular location and function within the cortex is as yet unknown.

SGLTS AND RENAL GLUCOSE REABSORPTION

180 g/day of D-glucose is filtered across the glomerulus into the kidney in humans, yet less than <1% of this filtered load ends up in the urine in healthy persons. What is responsible for the efficient reabsorption of glucose, and where is this accomplished within the kidney?

In what has been described as one of the most important contributions to renal physiology,[17] Wearn and Richards developed the free-flow micropuncture technique in 1924.[18] In their first study on frog nephrons, they detected plasma levels of sodium and glucose in the "glomerular urine" but not in the "bladder urine," proving "beyond doubt that the reabsorption of these substances must take place in the renal tubules." By introducing oil blocks and perfusing pipettes in subsequent work, specific tubular regions were quantitatively perturbed and analyzed.[19] With such a novel approach, they showed that nearly all glucose was reabsorbed within the proximal tubule, and this could be blocked by phlorizin.[20]

Micropuncture and single nephron analyses were subsequently adapted for the study of mammalian kidneys, demonstrating that, in rats, glucose reabsorption occurred in the proximal tubule with sensitivity to phlorizin.[21,22] It was previously established that intravenous administration of phlorizin inhibited renal glucose reabsorption in humans by up to 100%.[23]

In 1970, using sensitive fluorometric-enzymatic methods for measuring D-glucose and inulin, as well as Lissamine green for more precisely locating nephron segment puncture sites and tubular transit times, detailed studies of glucose reabsorption could be performed in rat nephrons.[24] These free-flow micropuncture studies demonstrated that ≈98% of D-glucose reabsorption occurred within the PT, and most reabsorption occurred within the first 3 mm from the glomerulus (Figure 70.1); no measurable net glucose reabsorption occurred distal to the PT. A follow-up study showed that glucose competed with [^{3}H]-phlorizin for the same (and at that time) as-yet-unknown "binding site" in isolated brush borders of rat kidney, with reversibility, stereospecificity (D-glucose over L-glucose), and Na^+-dependence.[25] Renal D-glucose reabsorption was attributed to active Na^+/sugar cotransport, similar to and consistent with Crane's hypothesis that Na^+-dependent transport drives intestinal absorption of D-glucose and D-galactose, which he articulated in a groundbreaking 1960 presentation in Prague.[26]

Barfuss and Schafer expanded on these early studies by making quantitative estimates of D-glucose absorption in isolated, perfused segments of early and late PT from rabbit nephrons.[27] They found that in early segments, maximal [^{14}C]-D-glucose absorption (J_{max}) was high, with a relatively low affinity for glucose (K_m ≈ 2 mM). In comparison, later segments showed a 10-fold reduction in J_{max}, with higher affinity for glucose (K_m ≈ 0.4 mM). From this, they concluded there were at least two distinct systems of glucose reabsorption in the proximal tubule. Detailed studies using PT brush border membrane vesicles from human and rabbit kidneys showed more evidence of two transport systems: an early, low affinity (K_m glucose = 6 mM) transporter

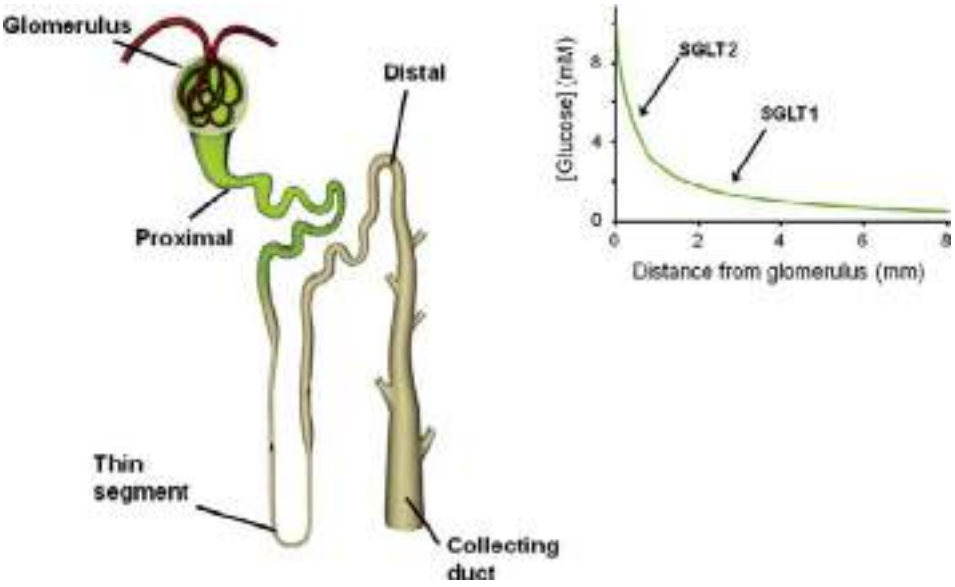

FIGURE 70.1 **Glucose reabsorption in the proximal tubule.** As shown in this simulation of the findings in Frohnert et al. (1970) the reabsorption of the bulk of filtered glucose occurs in the proximal tubule of the kidney. Under normal conditions, some 80% of the tubular glucose is reabsorbed within the first 2 mm of convoluted PT (S1, 2 segment), where SGLT2 is the predominantly expressed isoform. In later portions of PT (S3 segment), SGLT1 is believed to "mop up" the remaining tubular glucose.

with 1:1 Na^+:D-glucose stoichiometry and a later, high affinity (K_m glucose = 0.3 mM) transporter with 2:1 stoichiometry.[28–31]

After the two renal sodium glucose cotransporters were characterized, attention turned to their molecular identification In 1992, low-stringency hybridization screening of human kidney cDNA libraries, using rabbit and human SGLT1 sequences as probes, led to the identification of a clone bearing 59% DNA sequence identity to hSGLT1.[28] When cRNA of the clone was injected into *Xenopus* oocytes, [^{14}C]-α-methyl-D-glucopyranoside (αMDG, a SGLT-specific glucose analog) accumulation was 2- to 3-fold higher than that observed in water-injected oocytes. αMDG transport was Na^+-dependent and phlorizin-sensitive, sugar affinity was low compared to hSGLT1, D-galactose was not a substrate, and Na^+:glucose stoichiometry was 1:1.[32] In the same study, Na^+/glucose co-transport was also reported to be electrogenic and voltage-dependent, although the magnitude of maximal currents observed under voltage-clamp were <1% of those seen in hSGLT1-injected oocytes; but they were 2-fold larger than currents from control (H_2O-injected) oocytes. From this, Kanai and colleagues concluded it was not possible to claim hSGLT2 is a high capacity transporter *per se*, but rather its high level of mRNA in early PT segments—measured by *in situ* hybridization—might correspond to abundant protein expression at the luminal membrane; and hSGLT2 proteins as an *ensemble* might operate with a high capacity for glucose reabsorption. They further suggested that hSGLT1's 2:1 Na^+:glucose coupling, which endows it with greater accumulative power than a transporter with 1:1 stoichiometry, along with its high affinity for glucose, allows it to salvage the remaining tubular glucose in the late PT.

Subsequent studies of rat SGLT2 demonstrated substrate specificity (i.e., lack of D-galactose transport) and an additional estimate of 1:1 Na^+:glucose coupling.[33] *In situ* hybridization and northern blot analyses revealed SGLT2 message predominantly in outer kidney cortex while SGLT1 was found within inner cortical and outer medullary regions. Based on: (1) previous work showing the bulk of glucose reabsorption occurs in the early PT, (2) fluxes in isolated tubules showing evidence of two transport systems, and (3) spatial differences in SGLT1 and 2 mRNA expression, it was concluded that SGLT2 is *the* major Na^+/D-glucose cotransporter in the kidney.

Recently our biophysical characterization of cloned human SGLT1 and SGLT2 expressed in HEK293 cells confirmed and extended the previous oocyte studies:[34] the apparent glucose affinities ($K_{0.5}$) were much more similar than expected, 1.8 and 4.9 mM for SGLT1 and SGLT2; Galactose was a poor substrate for SGLT2 with a $K_{0.5}$ greater than 100 mM; and phlorizin was a more potent blocker of SGLT2 than SGLT1 with a Ki of 11 vs 140 nanomolar. The higher affinity of SGLT2 for phlorizin was mostly due to a slower off rate.

There are several reports on SGLT protein localization within the rat kidney. In the first, SGLT1 and GLUT1 antibodies were tested in various sections—inner medulla, outer medulla-inner segment, outer medulla-outer segment, and cortex. SGLT1 immunoblotting revealed signal in cortical and outer medullary regions, whereas GLUT1 signal was observed in inner and outer medulla but not cortex.[35]

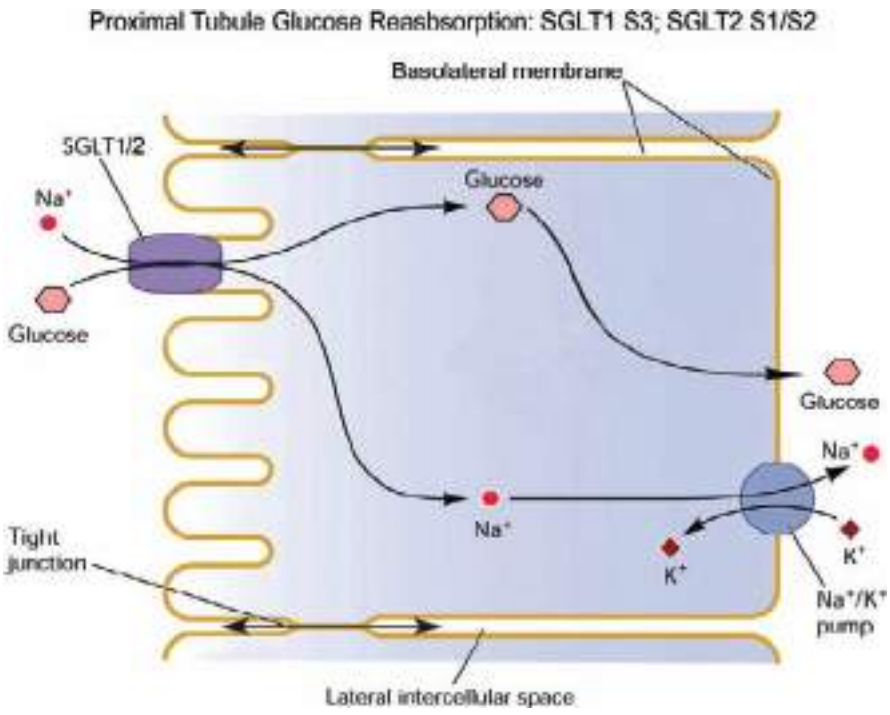

FIGURE 70.2 **Cellular mechanism of SGLTs in glucose reabsorption in the proximal tubule.** A schematic of how SGLT1 and 2 mediate the intestinal absorption, or renal reabsorption, of glucose. The Na^+ electrochemical potential gradient is maintained by the Na^+/K^+ pump, powers glucose accumulation by SGLTs from tubular lumen into cells; glucose subsequently moves down its concentration gradient across the basolateral membrane via GLUT2 (GLUT1 may be involved as well) into the interstitium and then blood. Both SGLT1 and 2 operate in similar fashion at a cellular level, though there are differences in function at the molecular level.

Immuno-fluorescent, -peroxidase, and -gold staining identified SGLT1 signal in all segments—S1, 2, and 3—of PT on apical membrane surfaces, whereas GLUT1 reactivity was observed on basolateral membrane surfaces of S3 PT as well as more inner (outer and inner medullary) regions. A second study examined SGLT1 and GLUT2 distribution;[36] in cortex, SGLT1 (on apical membranes) and GLUT2 (on basolateral membranes) showed co-reactivity in 40% of tubules. Moreover, SGLT1 signal was found in the majority of cortical PTs, based on co-staining with the PT marker, anti-γ-GTP. In a third study SGLT1 was localized on the brush border membrane of the proximal tubule with increasing intensity from the S1 to the S3 segments.[37] There was substantial intracellular staining in the cells of the S1 segment and, surprisingly, there was SGLT-related staining in the apical domains of the macula densa and adjacent cortical parts of the thick ascending limb of Henle. Apart from the fact that different SGLT1 antibodies were used in these studies there is no simple explanation for these subtle differences in SGLT1 distribution. So far there is only one paper reporting on the immunolocation of SGLT2 in the rodent kidney.[38] Here there was specific SGLT2 antibody staining of apical membranes of the early proximal convoluted tubule of the mouse and this was not observed in the $SGLT2^{-/-}$ mice.

Overall, we may conclude that there are two SGLT genes expressed in the kidney, SGLT2 in the brush border membrane of the early proximal tubule and SGLT1 in the brush border membrane of the late proximal tubule. Furthermore the localization of SGLTs to the apical membrane and GLUTs to the basolateral membrane provides plausible cellular mechanisms for glucose reabsorption in kidney (Figure 70.2). However, for human kidney there still are no immunocytochemical studies of SGLT2 and SGLT1 distribution and no physiological studies on isolated tubules.

While the atomic structure of human SGLTs is not yet known, the structure of a bacterial homolog vSGLT with 32% amino acids identity to hSGLT1 has been solved and refined to 2.7 Å (Figure 70.3).[5–7] As expected from biochemical studies the structure contains 14 transmembrane helices, and we also find one galactose molecule bound to the center of the protein occluded from the aqueous solutions on each side of the membrane. The most notable features of the structure are: i) the inverted repeat (TM1−5 and TM6−10) forming the core of the protein. While these repeats can be superimposed there is no amino acid homology between them; ii) there are two discontinuous membrane helices, TM1 and TM6, at the core of the sugar binding sites; and iii) hydrophobic gates occlude the sugar from the external solutions, external gates, M73, Y87 and F424 and the internal gate Y263. The pyranose sugar ring is stacked against the aromatic ring of the inner gate. Molecular dynamic studies show that after

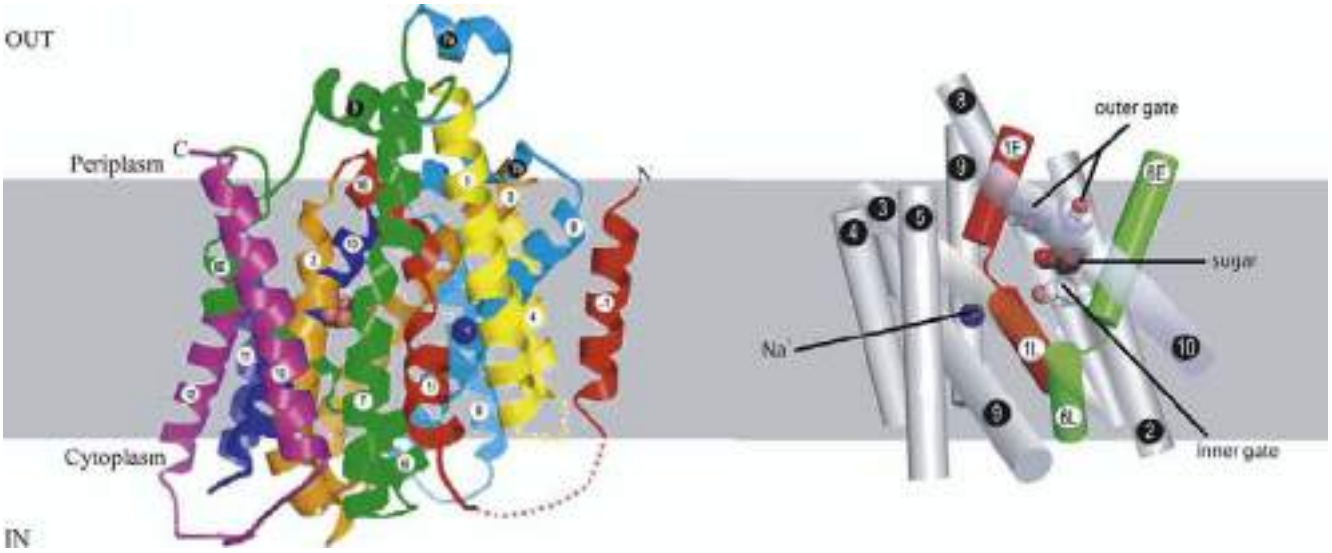

FIGURE 70.3 **The structure of the bacterial SGLT homolog vSGLT.** A side view of the 3-D structure of vSGLT in the membrane. The structure contains 14 transmembrane spanning helices (-1 to 13) with sugar bound in the center occluded from the external solutions. The structure consists of two inverted repeats (TM1-5 and TM6-10) with one TM helix in each repeat containing an unwound region in the middle of the membrane. A simpler model is shown on the right to illustrate the position of the sugar, the outer and internal hydrophobic gates, and the presumed location of the sodium binding site (blue sphere). *(Figure is modified from ref. [5,6,11].) Note: homology models of hSGLT1 show conservation of the sugar and sodium binding sites and the external and internal gates.*[39]

sodium release into the cytoplasm the tyrosine side chain rotates to a different position to allow the release of sugar to the cytoplasm.[7]

The high amino acid identity between vSGLT and hSGLT1, including the conservation of the sugar and sodium coordinating residues and the gates, has facilitated the generation and testing of a hSGLT homology model.[39] Mutation of the glucose binding residues produces profound reductions in the apparent sugar affinity ($K_{0.5}$), e.g. the mutation E102C increases the glucose $K_{0.5}$ from 0.5 to >100 mM. Evidence was also obtained for the opening of the external gates by external sodium, i.e., external methanethiosulfonate reagents and dyes only reached cysteine mutants in the sugar binding site when sodium was present in the external medium, and this access was blocked by sugar and phlorizin. This provides direct evidence that sodium/glucose cotransport is controlled by the coordinated opening and closing of the external and internal gates. Much structural work remains to be done to fully understand the atomic mechanism of transport.

GENETIC ABLATION OF SGLTS

Studies of transgenic mice deficient in SGLT2 ($SGLT2^{-/-}$) and SGLT1 ($SGLT1^{-/-}$) have shed new light on the relative roles of SGLT2 and 1 in renal glucose reabsorption *in vivo*.[38,40–42] In each of the three $SGLT2^{-/-}$ studies, absolute urinary glucose excretion was 60–70% of the filtered load in knock-out ($SGLT2^{-/-}$) mice, compared with 0% in WT mice. This implies that SGLT2 is of major importance in renal glucose reabsorption, but in the absence of functional SGLT2, there is still significant renal glucose reabsorption.

In the first study, detailed micropuncture experiments of cortical (i.e., *superficial*) nephrons were performed.[38] Early proximal convoluted tubular collections demonstrated 80% reabsorption of the filtered glucose load in WT mice, compared with 0% in $SGLT2^{-/-}$ mice. In later PT collections, the fractional reabsorption was 90% in wild type mice and 20% in knock-outs. It was also found that the filtered glucose load was proportional to the rate of excretion in knock-out mice, but independent of the load in WT. A major role for SGLT2 in glucose reabsorption was clearly established by this work; yet there was a significant discrepancy between superficial cortical fluid collections, which suggested SGLT2 is responsible for ≥80% of glucose reabsorption, and whole kidney glucose excretion measurements suggesting SGLT2 was responsible for 60% of glucose reabsorption. The results of this study make clear the importance of considering nephron heterogeneity in defining the role of Na^+/D-glucose co-transporters in renal glucose reabsorption.

A second study looked at mice deficient in SGLT2 and how they handled streptozotocin-induced diabetes.[42] Interestingly, $SGLT2^{-/-}$ mice showed

dramatically increased mortality—70% compared with 10% in wild type—due to sepsis from pyelonephritis. From this work, new questions about the safety of hSGLT2 inhibitors have emerged, which warrant further study.

In a third study, the SGLT2$^{-/-}$ strain used by Vallon et al.[41] was crossed with *db/db*—diabetic, obese, hyperlipidemic—mice. The resulting double transgenics had better glycemic control in both the fed and fasting states, they were less obese, and they displayed improved pancreatic β-cell health—increased cell mass (60%) and reduced cell death—compared with *db/db* mice alone.[41] Also, single transgenic (SGLT2$^{-/-}$) mice fed a high fat diet were protected from developing hyperglycemia, hyperinsulinemia, and glucose intolerance, when compared with their wild-type littermates on the same diet.

Taken together, these studies suggest that SGLT2 plays a significant role in glucose reabsorption, and genetically ablating SGLT2 can result in dramatic improvement of hyperglycemia and associated sequelae in T2DM. Indeed these knock-out studies are consistent with using SGLT2 inhibitors as a viable insulin-independent approach to treating type 2 diabetes mellitus (see below). It is also clear that there are significant compensatory mechanisms of glucose reabsorption in the absence of SGLT2, capable of reabsorbing up to 40% of the filtered load. What are the molecular players behind such compensation? One possibility is that hSGLT1 serves a robust role in the absence of SGLT2.

In awake SGLT1$^{-/-}$ mice the urinary glucose concentration was significantly increased (from ~0 to 20 mM) and the fractional reabsorption was reduced 3% in the absence of any apparent changes in SGLT2 mRNA or protein expression.[40] Micropuncture experiments on the last surface loop of proximal convoluted tubules showed that there was an increase in both the delivery and concentration of glucose in SGLT1$^{-/-}$ mice relative to wild-type mice: from 2 to 4 pmole/min and from 0.4 to 0.8 mM. These studies suggest that SGLT1 in the late proximal tubule does play a role in mopping up the last remaining glucose in the glomerular filtrate. As expected the most obvious phenotype of the SGLT1$^{-/-}$ mice is glucose-galactose-malabsorption, but the surprise is that unlike human GGM this phenotype only develops after weaning.

GENETICS OF RENAL GLYCOSURIA

Familial renal glycosuria (FRG, OMIM # 233100 and 182381) is an autosomal recessive condition characterized by urinary glucose excretion with normal plasma glucose levels, oral glucose tolerance tests, and plasma insulin levels. Patients absorb glucose and galactose normally, and they have no known defects in glucose utilization in tissues.[43] Long before any of the SGLT genes were identified, work was well underway to characterize FRG. In 1969, renal glucose titrations on two families with hereditary renal glycosuria showed that affected individuals typically had a lowered threshold (F_{mingG}) for glycosuria and reduced T_{max} (characteristic of "type A FRG"), and in one instance an exaggerated splay (characteristic of "type B FRG").[44] Importantly, sugar fluxes in jejunal mucosa samples demonstrated no difference in hexose transport between FRG patients and normal controls, i.e. intestinal glucose absorption was unaffected in FRG. There were also hints that inheritance of glycosuria was autosomal recessive, conflicting with the dogma of the time that FRG was inherited in autosomal dominant fashion. Further pedigree and physiological analyses of three generations from a single family established autosomal recessive inheritance as well as an intermediate phenotype of mild glycosuria in heterozygote family members.[45]

In more recent years, given the proposed role for hSGLT2 in renal glucose reabsorption,[32,33] researchers analyzed the gene encoding hSGLT2 (*SLC5A2*) and found it was associated with hereditary glycosuria.[46] Further studies confirmed *SLC5A2*'s involvement in a single individual with glycosuria,[47] and across multiple families, many with consanguineous unions.[48,49] In patients with either homozygous or compound heterozygous SGLT2 mutations, glucose excretion ranged from 15 to 200 g/day; and, consistent with previous hypotheses,[45] heterozygote family members frequently displayed glycosuria of ≤4 g/day. Follow-up studies of patients with combined severe glycosuria and aminoaciduria revealed a novel missense mutation in hSGLT2,[50] and aminoaciduria has been described in another case report of a patient with FRG.[51] The aminoaciduria was not immediately explained and was believed due to the severity of glycosuria rather than an intrinsic defect in amino acid reabsorption.

Analyses of *SLC5A2* mutations in families with FRG have revealed several noteworthy trends. First, most mutations identified in FRG are private: in 23 families with FRG, 21 unique mutations were observed;[49] and in another large analysis, 17 families yielded 20 unique mutations.[48] One mutation, a splice-site mutation ("IVS 7 + 5 g >a"), was observed in nine different families, with index cases showing either homozygosity or compound heterozygosity with this mutation; it was speculated that due to the high prevalence of this mutation, the region encoding the splice-site is a mutational "hot spot." Second, many of the mutations producing pronounced glycosuria (>20 g/d) are predicted to result

in either premature stop codons (by point or frameshift mutations) or deletions/insertions resulting in truncated proteins. There is precedent for this in GGM, where mutations in SGLT1 resulted in proteins which were non-functional or failed to traffic to the plasma membrane.[10]

There is significant heterogeneity in urinary glucose excretion among individuals with FRG. In patients homozygous or compound heterozygous for mutations in *SLC5A2*, excretion ranged from 10 to 200 g/d; some of this may be due to the difference between mutations resulting in partially-functional hSGLT2 protein versus those which produce non-functional or non-trafficked protein. However, in at least one instance, two members of the same family with the same compound heterozygous genotype (R137H, Δ358-8) had remarkably different excretion profiles: 200 g/d for the first index case, and 80 g/day for the second.[49] Such a finding hints at major differences in compensatory mechanisms of renal reabsorption in the setting of partially or completely impaired hSGLT2 function.

In general, FRG patients have no other phenotypic findings other than increased urinary glucose excretion: they do not suffer from hypoglycemia or any other impairment in glucose homeostasis, they do not have alterations in electrolyte excretion or significant changes in volume status, and long-term follow-up of one patient with severe glycosuria showed no alterations in renal function.[52] That said, in one recent study, elevated urinary glucose excretion was linked to mild diuresis in two patients with severe glycosuria: plasma renin activity and serum aldosterone were elevated to 3–4-fold above normal, suggesting volume and/or electrolyte loss accompanies glycosuria.[48] Among the group of mutation analyses and clinical case report data, FRG appears to be linked exclusively to mutations in hSGLT2 further cementing its significant role in glucose reabsorption in the kidney.

A second genetic disorder of renal glucose reabsorption is the rare Fanconi-Bickel Syndrome (FBS) (MIM 227810) linked to mutations in the facilitated glucose transporter 2 (GLUT2).[53] A major part of renal glucose reabsorption—facilitated diffusion of glucose across the basolateral membrane—is impaired (Figure 70.2). Interestingly, GLUT2 does not appear to be essential for intestinal glucose absorption in mice and in FBS patients (see [54]). FBS is described as a glycogen storage disease with hepatic and renal overload. Symptoms include hypoglycemia, hypergalactosemia, failure to thrive, and hypophosphatemic rickets. In addition, patients show generalized aminoaciduria and metabolic acidosis. With frequent carbohydrate feeds, phosphate and bicarbonate supplementation, patients lead relatively normal lives, although they are short in stature.[53,55]

DIABETES MELLITUS: A DISEASE OF HYPERGLYCEMIA

Diabetes mellitus (DM) is by far the most significant disease of disordered glucose homeostasis, in terms of severity, global disease burden, and costs to society. Often referred to as one disease, diabetes comprises a heterogeneous group of disorders, in which plasma glucose levels are elevated both in the fasting and postprandial state; and it frequently accompanies other metabolic derangements. Type 1 diabetes (T1DM) typically expresses early in life (childhood to early adulthood) and it is caused by the destruction of pancreatic β islet cells leading to an absolute deficiency in insulin secretion. Patients require exogenous insulin to properly handle high post-prandial glucose loads, and they are prone to hypoglycemia and ketoacidosis in the fasting state. Although T1DM is believed to be caused by some combination of infection, autoimmune mechanism, genetics, and environmental factors, no clear etiologic agent has been implicated.[56]

Type 2 diabetes mellitus (T2DM) was historically described as "adult-onset" diabetes mellitus; however this description is no longer relevant as T2DM can affect individuals in early adolescence. This is in part due to the rampant obesity epidemic that has plagued the developed world in recent decades. T2DM is a disease of diminished tissue insulin sensitivity (or diminished β-cell insulin output, i.e., a relative insulin deficiency), and it is linked with obesity, the consumption of foods high in refined sugars and fat, a sedentary lifestyle, and numerous genetic factors.[57,58,59] One in three American adults is projected to have diabetes by 2050,[60] and yet current oral hypoglycemic medications (e.g., biguanides, sulfonylureas, and thiazolidinediones) all have potentially significant side effects and high long-term failure rates.[61] Glycemic control is linked significantly to the incidence of microvascular and macrovascular complications,[62] and thus developing more effective and safer ways to ameliorate fasting and post-prandial hyperglycemia is of critical importance in the treatment of T2DM. One such target with significant interest from the pharmaceutical industry is glucose reabsorption in the kidney by hSGLT2.

BLOCKING RENAL GLUCOSE REABSORPTION AS A TREATMENT FOR DIABETES

Long before the renal SGLTs were identified, the relationship between intravenous phlorizin administration and glycosuria was established. Human studies in the 1930s showed that, at high enough doses, phlorizin

induced renal glucose excretion of ≈100%.[23,63] In the more recent past, phlorizin was shown to diminish hyperglycemia and normalize insulin sensitivity in several diabetic rat models.[64–66] Yet phlorizin was deemed unsuitable as a treatment: it has limited bioavailability due to lactase-hydrolase cleavage in the intestines, and there were concerns it would cause diarrhea by inhibiting hSGLT1.

Based on the promising results from studies of phlorizinized humans and diabetic rodents, while also considering phlorizin's limited oral bioavailability, the Tanabe Seiyaku Company's Discovery Research Laboratory initiated a program to develop renal SGLT inhibitors as antidiabetics.[67] Starting with phlorizin they synthesized the O-glycoside T-1095 (hSGLT1 $IC_{50} = 20\ \mu M$, hSGLT2 $IC_{50} = 2\ \mu M$) and T-1095A (hSGLT1 $IC_{50} = 200$ nM, hSGLT2 $IC_{50} = 50$ nM)[68] (Figure 70.4). T-1095 included a methyl acetate group on carbon 5 of the glucose ring which resulted in enhanced oral bioavailability, and it could be cleaved to its more potent form—T-1095A—in plasma. The relatively low SGLT2:SGLT1 specificity of T-1095A allowed it to inhibit both renal transporters *in vivo*, as does phlorizin. The drug showed efficacy in animal models: diabetic (streptozotocin-induced or C57BL/KsJ-db/db) rats showed dose-dependent reductions in blood glucose. With long term administration, plasma glucose and glycosylated hemoglobin (HbA_{1C}) levels were reduced and glucose tolerance test performance improved.[68] Importantly, the progression of diabetic nephropathy slowed significantly.[69]

In the decade that followed, numerous candidate SGLT2 inhibitors emerged, five are in advanced Phase III clinical trials[70–72] and one, dapagliflozin, has been submitted to FDA and EMA for clinical approval. The discovery and extensive studies of dapagliflozin (Figure 70.4) marked a significant turning point in the development of hSGLT2 inhibitors. Chemists at Bristol-Meyers Squibb started first by reducing the O-glycoside linkage in phlorizin to a C-C bond between sugar and the aglycone's phenyl ring 1; this was designed to prevent enzymatic cleavage by intestinal lactase-hydrolase. Then, through a structure-activity relationship (SAR) optimization scheme they settled on an aglycone notable for a C4 chlorine substitution in ring 1, which was connected to a second ring by a single methylene (-CH2-) linker. The resulting compound (Figure 70.4) showed remarkable potency ($IC_{50} = 1$ nM) and specificity (1200:1) for hSGLT2 over hSGLT1.[73] In rats, a 10 mg/kg-body weight dose of dapagliflozin produced the same 24 hour glycosuric effect (2000 mg glucose excreted per 200 g body weight) as a 300 mg/kg dose of T-1095A.[68,73]

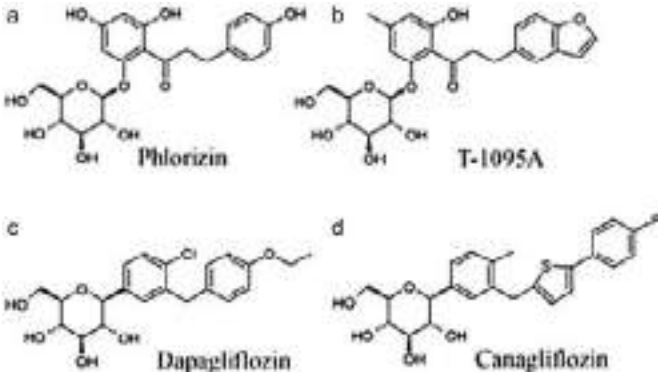

FIGURE 70.4 **Structures of SGLT inhibitors.** (a) Phlorizin is the canonical SGLT inhibitor; (b) T-1095A was the first inhibitor synthesized based on the structure of phlorizin. (c) and (d) Dapagliflozin and Canagliflozin are selective hSGLT2 inhibitors in phase III clinical trials.

Since its discovery, a number of studies have been published on dapagliflozin's performance in animals and humans. It increased urinary glucose excretion in healthy rats and reduced hyperglycemia in diabetic animals;[74] and in diabetic and obese rats it improved glycemic control and pancreatic β-cell morphology and function.[75] In healthy human subjects, dapagliflozin induced dose-dependent urinary glucose excretion of up to 50% of the filtered load.[76] In diabetic patients the results were also impressive: glycemic control improved in patients taking dapagliflozin over a short period,[77] it significantly reduced hyperglycemia and lowered HbA_{1C} in patients with poorly-controlled diabetes.[78] It also worked as part of combination therapies, both with insulin and/or insulin sensitizers[79] and the standard first-line T2DM pharmacotherapy metformin,[80] successfully normalizing markers of diabetic disease extent.

Overall, dapagliflozin has been shown to reduce fasting and post-prandial glucose levels by 20%, lower HbA_{1C} to below 7%, induce weight loss (≈2% of body weight), and it can be administered as *once daily* oral drug therapy. Importantly, every published study to date has demonstrated that dapagliflozin does not cause hypoglycemia—a serious side effect of many anti-diabetes drugs currently in clinical use. It has also shown hints of efficacy in the management of hypertension: it causes mild diuresis and a reduction of ≈5 mm Hg in systolic blood pressure.[80] Side effects reported in greater frequency than in patients receiving placebo were genital infections and symptoms/signs of urinary tract infections.[78–80] This is undoubtedly connected to increased urinary glucose, and it will likely be explored in long-term clinical studies of dapagliflozin (i.e. phase IV clinical trials). At the time of this writing, dapagliflozin was rejected by the FDA owing to concerns about an increase risk of bladder and breast cancer, but it just received (April 2012) a favorable

review from the EMA Committee for Medicinal Products for Human Use. It is anticipated that dapagliflozin (Forxiga) will be the first to market anti-diabetes pharmacotherapy targeting hSGLT2.

Other SGLT2 inhibitors in advanced Phase III trials include empagliflozin[81] and canagliflozin (Figure 70.4). Both are C-aryl glycosides that reduced fasting blood glucose and improved glucose tolerance in high-fat diet fed KK (HF-KK) mice, and it increased urinary glucose excretion in both HF-KK and normal mice and Zucker Diabetic Fatty (ZDF) rats.[82,83] In recently-published phase I clinical studies in healthy human subjects, canagliflozin reduced the renal threshold for urinary glucose excretion (UGE), and single-ascending dose studies demonstrated a maximum 24 hour UGE of 70 g.[84] In addition, normal subjects given $\geq$200 mg doses of canagliflozin before breakfast showed lower plasma glucose levels (10−20%) and reduced insulin secretion ($\leq$50%) compared with persons receiving placebo.

Lexicon has developed a non-specific SGLT inhibitor using L-xylose linked by a C-aryl bond to the aglycone of dapagliflozin, LX4211. This has Ki's of 1.1 nM (hSGLT2) and 36 nM (hSGLT1).[85] LX4211 blocked up to $\approx$50% of glucose reabsorption in diabetic/obese mice.[86] In an early phase 2 clinical trial of 36 diabetic subjects, LX4211 caused urinary glucose excretion of up to 60 g/day, reduced HbA_{1C} by $\approx$0.7% as well as plasma fructosamine, compared with placebo, and lowered fasting (by 50 mg/dL) and post-prandial glucose. Surprisingly, the Lexicon non-specific SGLT inhibitor does not appear to be more effective than the specific SGLT2 inhibitors in blocking renal glucose reabsorption, with a maximum of 50% inhibition.

Although the race is well under way to develop drugs specifically targeting hSGLT2, there are unresolved questions about what role hSGLT2, hSGLT1 and other proteins play in renal glucose reabsorption. Since dapagliflozin, which *in vitro* blocks 100% of D-glucose transport by hSGLT2, inhibits glucose reabsorption *in vivo* by $\leq$50%[76] there may be other significant components involved in renal glucose reabsorption. At the same time, there are lingering questions about precisely *how* inhibitors interact with Na^+/D-glucose cotransporters. For example, little dapagliflozin is detected in the urine,[87,88] suggesting its interaction with the renal hSGLTs may be unique: it is plausible it is an irreversible inhibitor of hSGLT2, it may block glucose transport from the cytoplasmic surface of hSGLT2.

While there have been few mechanistic studies of SGLT2 inhibitors we have characterized the interaction of dapagliflozin and several of its structural homologs with hSGLT1 and hSGLT2.[89] Dapagliflozin and 4-fluoro-4-deoxy-dapagliflozin (F-dapagliflozin) block hSGLT2-mediated αMDG accumulation, as well as D-glucose-coupled Na^+ currents, in cells with high (Ki = 6 nM) potency; furthermore, a D-galactose derivative of dapagliflozin (galacto-dapagliflozin) was also a potent inhibitor (Ki = 25 nM). In comparison, hSGLT1 a 10^2- to 10^5-fold higher concentrations of dapaglifozin and its derivatives was required to block hSGLT1. The SGLT2 and SGLT1 OFF-rates for dapagliflozin and derivatives were compared with those for phlorizin. For hSGLT1, dapagliflozin, F-dapagliflozin, and galacto-dapagliflozin all dissociated very rapidly ($t_{1/2,Off}$ = 1 s); whereas for hSGLT2, dapagliflozin does not readily dissociate, F-dapagliflozin ($t_{1/2,Off}$ = 170 s) dissociated slowly and galacto-dapagliflozin came off rapidly ($t_{1/2,Off}$ = 20 s). These findings indicate that the blockers bind to the external surface of the SGLTs and that the relative potency between SGLT1 and SGLT2 largely depends on the rate of dissociation from the protein. The pharmacokinetics of renal SGLT2 inhibitors leaves many unresolved questions about their mode of action. For example: (1) in the face of high binding to serum proteins, >90%, and the low rate of appearance of the unmodified drugs in the urine, do they inhibit from the tubular lumen as in the case of phlorizin?; (2) what explains the observations that the SGLT drugs only inhibit glucose reabsorption by ~50%, while phlorizin inhibits 100%; and 3) what explains the long lasting effect, in excess of 24 hours, of one oral dose given the high amount of drug metabolism?

CONCLUSIONS

Considerable advances have been made over the past two decades in understanding the physiology of glucose reabsorption by the kidney. It is clear that the SGLTs and GLUTs play central roles in the complete reabsorption of the filtered glucose in the proximal tubule, and mutations in these genes largely account for the glucosuria observed in patients with Familial Renal Glucosuria, Fanconi-Bickel Syndrome, and Glucose-Galactose-Malabsorption. However, questions still remain about possible compensatory changes in mice and men with "ablation" of SGLT2. Contrary to common perceptions, glucose reabsorption from the glomerular filtrate is not essential for life. The clinical studies with the SGLT inhibitors have clearly established that in healthy subjects the loss of 80 grams of glucose to the urine has no remarkable adverse effects and in diabetic patients there is a "normalization" of glucose homeostasis. The added benefit with the use of these drugs in diabetics is the sustained loss in weight, up to 6 kg over three years. While the development of SGLT inhibitors as antidiabetic drugs may or may not

turn out to be a clinical success, this has indeed produced a resurgence in interest in the physiology of glucose handling by the kidney.

Acknowledgments

We are grateful to our past and present colleagues for their contributions to our understanding of the biology SGLTs and to financial support from the National Institutes of Health (DK19567, 0–34; DK0077133, 0–4; and the National Research Service Award DK082153 to CH).

References

[1] Thorens B, Mueckler M. Glucose transporters in the 21st Century. Am J Physiol Endocrinol Metab 2010;298:E141–5.
[2] Santer R, Groth S, Kinner M, Dombrowski A, Berry GT, Brodehl J, et al. The mutation spectrum of the facilitative glucose transporter gene SLC2A2 GLUT2 in patients with Fanconi-Bickel syndrome. Hum Genet 2002;110:21–9.
[3] Wright E, Turk E. The sodium/glucose cotransport family SLC5. Pflügers Archiv Eur J Physiol 2004;447:510–8.
[4] Wright EM, Loo DD, Hirayama BA. Biology of human sodium glucose transporters. Physiol Rev 2011;91:733–94.
[5] Abramson J, Wright EM. Structure and function of Na^+-symporters with inverted repeats. Curr Opin Struct Biol 2009;19: 425–32.
[6] Faham S, Watanabe A, Besserer GM, Cascio D, Specht A, Hirayama BA, et al. The crystal structure of a sodium galactose transporter reveals mechanistic insights into Na + /sugar symport. Science 2008;321:810–4.
[7] Watanabe AC, S, Chaptal, V, Rosenberg, JM, Wright, EM, Grabe, M, and Abramson, J, The mechanism of sodium and substrate release from the binding pocket of vSGLT. Nature 2010;468:988–91.
[8] Nishimura M, Naito S. Tissue-specific mRNA expression profiles of human ATP-binding cassette and solute carrier transporter superfamilies. Drug Metab Pharmacokinet 2005;20: 452–77.
[9] Hediger MA, Coady MJ, Ikeda TS, Wright EM. Expression cloning and cDNA sequencing of the Na + /glucose co-transporter. Nature 1987;330:379–81.
[10] Wright EM, Martin MG, Turk E. Familial glucose-galactose malabsorption and hereditary renal glycosuria. In: Scriver CR, Beaudet AL, Sly WS, Valle D, Childs B, Kinzler KW, Vogelstein B, editors. The metabolic & molecular bases of inherited disease. McGraw-Hill; 2001. p. 4891–908.
[11] Wright EM, Loo, Donald DF, Hirayama, Bruce A. Biology of Human Sodium Glucose Transporters. Physiol Rev 2011;91: 733–94.
[12] Bianchi L, Diez-Sampedro A. A single amino acid change converts the sugar sensor SGLT3 into a sugar transporter. PLoS One 2010;5:e10241.
[13] Diez-Sampedro A, Hirayama BA, Osswald C, Gorboulev V, Baumgarten K, Volk C, et al. A glucose sensor hiding in a family of transporters. Proc Natl Acad Sci U S A 2003;100:11753–8.
[14] Voss AA, Diez-Sampedro A, Hirayama BA, Loo DD, Wright EM. Imino sugars are potent agonists of the human glucose sensor SGLT3. Mol Pharmacol 2007;71:628–34.
[15] Tazawa S, Yamato T, Fujikura H, Hiratochi M, Itoh F, Tomae M, et al. SLC5A9/SGLT4, a new Na + -dependent glucose transporter, is an essential transporter for mannose, 1,5-anhydro-D-glucitol, and fructose. Life Sciences 2005;76:1039–50.
[16] Grempler R, Augustin R, Froehner S, Hildebrandt T, Simon E, Mark M, et al. Functional characterisation of human SGLT-5 as a novel kidney-specific sodium-dependent sugar transporter. *FEBS Lett* 586: 248–253.
[17] Sands JM. Micropuncture: unlocking the secrets of renal function. Am J Physiol Renal Physiol 2004;287:F866–7.
[18] Wearn JT, Richards AN. Observations on the composition of glomerular urine, with particular reference to the problem of reabsorption in the renal tubules. Am J Physiol – Leg Content 1924;71:209–27.
[19] Richards AN, Walker AM. Methods of collecting fluid from known regions of the renal tubules of amphibia and of perfusing the lumen of a single tubule. Am J Physiol – Leg Content 1936;118:111–20.
[20] Walker AM, Hudson CL. The reabsorption of glucose from the renal tubule in amphibia and the action of phlorizin upon it. Am J Physiol – Leg Content 1936;118:130–43.
[21] Walker AM, Bott PA, Oliver J, MacDowell MC. The collection and analysis of fluid from single nephrons of the mammalian kidney. Am J Physiol – Leg Content 1941;134:580–95.
[22] Walker AM, Oliver J. Methods for the collection of fluid from single glomeruli and tubules of the mammalian kidney. Am J Physiol – Leg Content 1941;134:562–79.
[23] Chasis H, Jolliffe N, Smith HW. The action of phlorizin on the excretion of glucose, xylose, sucrose, creatinine and urea by man. J Clin Invest 1933;12:1083–90.
[24] Frohnert PP, Hohmann B, Zwiebel R, Baumann K. Free flow micropuncture studies of glucose transport in the rat nephron. Pflugers Arch 1970;315:66–85.
[25] Frasch W, Frohnert PP, Bode F, Baumann K, Kinne R. Competitive inhibition of phlorizin binding by D-glucose and the influence of sodium: a study on isolated brush border membrane of rat kidney. Pflügers Archiv Eur J Physiol 1970;320: 265–84.
[26] Crane RK, Miller D, Bihler L. The restrictions on possible mechanisms of intestinal active transport of sugars. In: Kleinzeller A, Kotyk A, editors. Membrane Transport and Metabolism. Academic Press, Inc.; 1961.
[27] Barfuss DW, Schafer JA. Differences in active and passive glucose transport along the proximal nephron. Am J Physiol 1981;241:F322–32.
[28] Wells RG, Pajor AM, Kanai Y, Turk E, Wright EM, Hediger MA. Cloning of a human kidney cDNA with similarity to the sodium-glucose cotransporter. Am J Physiol 1992;263:F459–65.
[29] Turner RJ, Moran A. Further studies of proximal tubular brush border membrane D-glucose transport heterogeneity. J Membr Biol 1982;70:37–45.
[30] Turner RJ, Moran A. Heterogeneity of sodium-dependent D-glucose transport sites along the proximal tubule: evidence from vesicle studies. Am J Physiol 1982;242:F406–14.
[31] Turner RJ, Silverman M. Sugar uptake into brush border vesicles from normal human kidney. Proc Natl Acad Sci U S A 1977;74:2825–9.
[32] Kanai Y, Lee WS, You G, Brown D, Hediger MA. The human kidney low affinity Na + /glucose cotransporter SGLT2. Delineation of the major renal reabsorptive mechanism for D-glucose. J Clin Invest 1994;93:397–404.
[33] You G, Lee W-S, Barros EJG, Kanai Y, Huo T-L, Khawaja S, et al. Molecular Characteristics of Na^+-coupled Glucose Transporters in Adult and Embryonic Rat Kidney. J Biol Chem 1995;270:29365–71.
[34] Hummel CS, Lu C, Loo DD, Hirayama BA, Voss AA, Wright EM. Glucose transport by human renal Na^+/D-glucose cotransporters SGLT1 and SGLT2. Am J Physiol Cell Physiol 2011;300: C14–21.

[35] Takata K, Kasahara T, Kasahara M, Ezaki O, Hirano H. Localization of Na^+-dependent active type and erythrocyte/HepG2-type glucose transporters in rat kidney: immunofluorescence and immunogold study. J Histochem Cytochem 1991;39:287–98.

[36] Cramer SC, Pardridge WM, Hirayama BA, Wright EM. Colocalization of GLUT2 glucose transporter, sodium/glucose cotransporter, and gamma-glutamyl transpeptidase in rat kidney with double-peroxidase immunocytochemistry. Diabetes 1992;41:766–70.

[37] Balen D, Ljubojevic M, Breljak D, Brzica H, Zlender V, Koepsell H, et al. Revised immunolocalization of the Na^+-D-glucose cotransporter SGLT1 in rat organs with an improved antibody. Am J Physiol Cell Physiol 2008;295:C475–89.

[38] Vallon V, Platt KA, Cunard R, Schroth J, Whaley J, Thomson SC, et al. SGLT2 mediates glucose reabsorption in the early proximal tubule. J Am Soc Nephrol 2011;22:104–12.

[39] Sala-Rabanal M, Hirayama BA, Loo DD, Chaptal V, Abramson J, Wright EM. Bridging the gap between structure and kinetics of human SGLT1. Am J Physiol-Cell Physiol 2012;302:C1293–305.

[40] Gorboulev V, Schurmann A, Vallon V, Kipp H, Jaschke A, Klessen D, et al. Na + -D-glucose Cotransporter SGLT1 is Pivotal for Intestinal Glucose Absorption and Glucose-Dependent Incretin Secretion. Diabetes 61:187–196.

[41] Jurczak MJ, Lee HY, Birkenfeld AL, Jornayvaz FR, Frederick DW, Pongratz RL, et al. SGLT2 deletion improves glucose homeostasis and preserves pancreatic beta-cell function. Diabetes 2011;60:890–8.

[42] Ly JP, Onay T, Sison K, Sivaskandarajah G, Sabbisetti V, Li L, et al. The Sweet Pee model for Sglt2 mutation. J Am Soc Nephrol 2011;22:113–23.

[43] Wright E. Diseases of renal glucose handling. In: Lifton R, Somlo S, Giebisch GH, Seldin DW, editors. Genetic diseases of the kidney. Elsevier, Inc.; 2009. p. 131–40.

[44] Elsas LJ, Rosenberg LE. Familial renal glycosuria: a genetic reappraisal of hexose transport by kidney and intestine. J Clin Invest 1969;48:1845–54.

[45] Elsas LJ, Busse D, Rosenberg LE. Autosomal recessive inheritance of renal glycosuria. Metabolism 1971;20:968–75.

[46] Santer R, Kinner M, Schneppenheim R, Hillebrand G, Kemper M, Ehrich J, et al. The molecular basis of renal glucosuria: Mutations in the gene for a renal glucose transporter SGLT2. J Inherit Metab Dis 2000;23:178.

[47] van den Heuvel LP, Assink K, Willemsen M, Monnens L. Autosomal recessive renal glucosuria attributable to a mutation in the sodium glucose cotransporter SGLT2. Hum Genet 2002;111:544–7.

[48] Calado J, Sznajer Y, Metzger D, Rita A, Hogan MC, Kattamis A, et al. Twenty-one additional cases of familial renal glucosuria: absence of genetic heterogeneity, high prevalence of private mutations and further evidence of volume depletion. Nephrol Dial Transplant 2008;23:3874–9.

[49] Santer R, Kinner M, Lassen CL, Schneppenheim R, Eggert P, Bald M, et al. Molecular analysis of the SGLT2 gene in patients with renal glucosuria. J Am Soc Nephrol 2003;14:2873–82.

[50] Magen D, Sprecher E, Zelikovic I, Skorecki K. A novel missense mutation in SLC5A2 encoding SGLT2 underlies autosomal-recessive renal glucosuria and aminoaciduria. Kidney Int 2005;67:34–41.

[51] Sankarasubbaiyan S, Cooper C, Heilig CW. Identification of a novel form of renal glucosuria withoverexcretion of arginine, carnosine, and taurine. Am J Kidney Dis 2001;37:1039–43.

[52] Scholl-Burgi S, Santer R, Ehrich JH. Long-term outcome of renal glucosuria type 0: the original patient and his natural history. Nephrol Dial Transplant 2004;19:2394–6.

[53] Santer R, Schneppenheim R, Suter D, Schaub J, Steinmann B. Fanconi-Bickel syndrome–the original patient and his natural history, historical steps leading to the primary defect, and a review of the literature. Eur J Pediatr 1998;157:783–97.

[54] Wright EM. Diseases of renal glucose handling. In: Lifton R, editor. In genetic diseases of the kidney. Elsevier; 2008. p. 1130–40.

[55] Mohandas Nair K, Sakamoto O, Jagadeesh S, Nampoothiri S. Fanconi-Bickel Syndrome. Indian J Pediatr 2011.

[56] van Belle TL, Coppieters KT, von Herrath MG. Type 1 diabetes: etiology, immunology, and therapeutic strategies. Physiol Rev 2011;91:79–118.

[57] Ingelsson E, Langenberg C, Hivert M-F, Prokopenko I, Lyssenko V, Dupuis J, et al. Detailed physiologic characterization reveals diverse mechanisms for novel genetic loci regulating glucose and insulin metabolism in humans. Diabetes 2010;59:1266–75.

[58] Staiger H, Machicao F, Fritsche A, Haring H-U. Pathomechanisms of Type 2 Diabetes Genes. Endocr Rev 2009;30:557–85.

[59] Zimmet P, Alberti KG, Shaw J. Global and societal implications of the diabetes epidemic. Nature 2001;414:782–7.

[60] Boyle J, Thompson T, Gregg E, Barker L, Williamson D. Projection of the year 2050 burden of diabetes in the US adult population: dynamic modeling of incidence, mortality, and prediabetes prevalence. Population Health Metrics 2010;8:29.

[61] Kahn SE, Haffner SM, Heise MA, Herman WH, Holman RR, Jones NP, et al. Glycemic durability of rosiglitazone, metformin, or glyburide monotherapy. N Engl J Med 2006;355:2427–43.

[62] Stratton IM, Adler AI, Neil HA, Matthews DR, Manley SE, Cull CA, et al. Association of glycaemia with macrovascular and microvascular complications of type 2 diabetes UKPDS 35: prospective observational study. BMJ 2000;321:405–12.

[63] Shannon JA, Smith HW. The excretion of inulin, xylose, and urea by normal and phlorizinized man. J Clin Invest 1935;14:393–401.

[64] Blondel O, Bailbe D, Portha B. Insulin resistance in rats with non-insulin-dependent diabetes induced by neonatal 5 days streptozotocin: evidence for reversal following phlorizin treatment. Metabolism 1990;39:787–93.

[65] Rossetti L, Shulman GI, Zawalich W, DeFronzo RA. Effect of chronic hyperglycemia on in vivo insulin secretion in partially pancreatectomized rats. J Clin Invest 1987;80:1037–44.

[66] Rossetti L, Smith D, Shulman GI, Papachristou D, DeFronzo RA. Correction of hyperglycemia with phlorizin normalizes tissue sensitivity to insulin in diabetic rats. J Clin Invest 1987;79:1510–5.

[67] Tsujihara K, Hongu M, Saito K, Inamasu M, Arakawa K, Oku A, et al. Na^+-glucose cotransporter inhibitors as antidiabetics. I. Synthesis and pharmacological properties of 4′-dehydroxyphlorizin derivatives based on a new concept. *Chem Pharm Bull Tokyo* 1996;44:1174–80.

[68] Oku A, Ueta K, Arakawa K, Ishihara T, Nawano M, Kuronuma Y, et al. T-1095, an inhibitor of renal Na^+-glucose cotransporters, may provide a novel approach to treating diabetes. Diabetes 1999;48:1794–800.

[69] Arakawa K, Ishihara T, Oku A, Nawano M, Ueta K, Kitamura K, et al. Improved diabetic syndrome in C57BL/KsJ-db/db mice by oral administration of the Na^+-glucose cotransporter inhibitor T-1095. Br J Pharmacol 2001;132:578–86.

[70] Chao EC, Henry RR. SGLT2 inhibition—a novel strategy for diabetes treatment. Nat Rev Drug Discov 2010;9:551–9.
[71] Kipnes MS. Sodium-glucose cotransporter 2 inhibitors in the treatment of Type 2 diabetes: a review of Phase II and III trials. Science 2011.
[72] Liu j, Lee T. SGLT2 Inhibitors for type 2 diabetes. Annu Rep Med Chem 2011;46:103–15.
[73] Meng W, Ellsworth BA, Nirschl AA, McCann PJ, Patel M, Girotra RN, et al. Discovery of dapagliflozin: a potent, selective renal sodium-dependent glucose cotransporter 2 SGLT2 inhibitor for the treatment of type 2 diabetes. J Med Chem 2008;51: 1145–9.
[74] Han S, Hagan DL, Taylor JR, Xin L, Meng W, Biller SA, et al. Dapagliflozin, a selective SGLT2 inhibitor, improves glucose homeostasis in normal and diabetic rats. Diabetes 2008;57:1723–9.
[75] Macdonald FR, Peel JE, Jones HB, Mayers RM, Westgate L, Whaley JM, et al. The novel sodium glucose transporter 2 inhibitor dapagliflozin sustains pancreatic function and preserves islet morphology in obese, diabetic rats. Diabetes, Obes Metab 2010;12:1004–12.
[76] Komoroski B, Vachharajani N, Boulton D, Kornhauser D, Geraldes M, Li L, et al. Dapagliflozin, a novel SGLT2 inhibitor, induces dose-dependent glucosuria in healthy subjects. Clin Pharmacol Ther 2009;85:520–6.
[77] Komoroski B, Vachharajani N, Feng Y, Li L, Kornhauser D, Pfister M. Dapagliflozin, a novel, selective SGLT2 inhibitor, improved glycemic control over 2 weeks in patients with type 2 diabetes mellitus. Clin Pharmacol Ther 2009;85:513–9.
[78] Ferrannini E, Jimenez Ramos S, Salsali A, Tang W, List JF. Dapagliflozin monotherapy in type 2 diabetic patients with inadequate glycemic control by diet and exercise: a randomized, double-blind, placebo-controlled, phase III trial. Diabetes Care 2010;33:2217–24.
[79] Wilding JP, Norwood P, T'Joen C, Bastien A, List JF, Fiedorek FT. A study of dapagliflozin in patients with type 2 diabetes receiving high doses of insulin plus insulin sensitizers: applicability of a novel insulin-independent treatment. Diabetes Care 2009;32:1656–62.
[80] Bailey CJ, Gross JL, Pieters A, Bastien A, List JF. Effect of dapagliflozin in patients with type 2 diabetes who have inadequate glycaemic control with metformin: a randomised, double-blind, placebo-controlled trial. Lancet 2010;375:2223–33.
[81] Aires I, Calado J. BI-10773, a sodium-glucose cotransporter 2 inhibitor for the potential oral treatment of type 2 diabetes mellitus. Curr Opin Investig Drugs 2010;11:1182–90.
[82] Grempler R, Thomas L, Eckhardt M, Himmelsbach F, Sauer A, Sharp DE, Bakker RA, Mark M, Klein T, and Eickelmann P. Empagliflozin, a novel selective sodium glucose cotransporter-2 SGLT-2 inhibitor: characterisation and comparison with other SGLT-2 inhibitors. Diabetes Obes Metab.
[83] Nomura S, Sakamaki S, Hongu M, Kawanishi E, Koga Y, Sakamoto T, et al. Discovery of canagliflozin, a novel c-glucosidewith thiophene ring, as sodium-dependent glucose cotransporter 2 inhibitor for the treatment of type 2 diabetes mellitus[1]. *J Med Chem*: null-null 2010.
[84] Sha S, Devineni D, Ghosh A, Polidori D, Chien S, Wexler D, et al. Canagliflozin, a novel inhibitor of sodium glucose co-transporter 2, dose-dependently reduces calculated renal threshold for glucose excretion and increases urinary glucose excretion in healthy subjects. Diabetes Obes Metab 2011.
[85] Freiman J, Ruff DA, Frazier K, Combs K, Turnage A, Shadoan M, et al. LX4211, an SGLT2 inhibitor, shows rapid and significant improvement in glycemic control over 4 weeks in patients with type 2 diabetes mellitus. Endocrine Reviews 2010;31:S1692.
[86] Goodwin NC, Mabon R, Harrison BA, Shadoan MK, Almstead ZY, Xie Y, et al. Novel l-Xylose derivatives as selective sodium-dependent glucose cotransporter 2 SGLT2 Inhibitors for the treatment of type 2 diabetes. J Med Chem 2009;52:6201–4.
[87] Kasichayanula S, Chang M, Hasegawa M, Liu X, Yamahira N, LaCreta FP, et al. Pharmacokinetics and pharmacodynamics of dapagliflozin, a novel selective inhibitor of sodium-glucose co-transporter type 2, in Japanese subjects without and with type 2 diabetes mellitus. Diabetes Obes Metab 2011; 13:357–65.
[88] Obermeier M, Yao M, Khanna A, Koplowitz B, Zhu M, Li W, et al. In vitro characterization and pharmacokinetics of dapagliflozin BMS-512148, a potent sodium-glucose cotransporter type II inhibitor, in animals and humans. Drug Metab Dispos 2010;38:405–14.
[89] Hummel C, Lu C, Liu J, Loo DDF, Chezzi C, Hirayama BA, et al. Structural selectivity of Human SGLT Inhibitors. Am J Physiol 2011.

CHAPTER

71

Kidney Transport of Amino Acids and Oligopeptides, and Aminoacidurias

Simone M.R. Camargo[1], *Victoria Makrides*[1], *Robert Kleta*[2] *and François Verrey*[1]

[1]Institute of Physiology and Zürich Center for Integrative Human Physiology (ZIHP), University of Zurich, Zurich, Switzerland.

[2]University College London, London, U.K.

FILTRATION AND REABSORPTION OF AMINO ACIDS AND OLIGOPEPTIDES

Reabsorption of amino acids is a fundamental and evolutionarily well-conserved mechanism that involves active transcellular transport by specialized transporter proteins localizing to both luminal and basolateral tubular epithelial cell membranes. Approximately 50 g (450 mmol) of free amino acids are filtered daily into the primary urine by human kidney glomeruli. By reabsorbing these amino acids, kidney tubules prevent their loss in the urine. In addition, amino acid metabolism by kidney tubules plays an important role in whole body amino acid homeostasis. Di- and tripeptides are also efficiently reabsorbed from the primary urine with uptake, to a large extent, followed by intracellular hydrolysis to free amino acids and subsequent basolateral export.

Depending on the amino acid, plasma concentration of free amino acids and consequently in the ultrafiltrate varies from low μmol/l up to nearly 1 mmol/l (Table 71.1). For most amino acids reabsorption is ~99.5% efficient and therefore the fractional excretion is less than 0.5% of filtered load. In humans, serine, glycine, histidine, and taurine are notable exceptions for which a higher fraction is lost in the urine (Table 71.1). For several amino acids, a variable fractional excretion is observed, for example, tending to increase when the filtered load increases.[1,2] The filtered load also depends on the glomerular fluid filtration rate (GFR), which itself is influenced by factors like circadian rhythm, orthostasis, and extracellular volume. Interestingly, by a mechanism not yet understood, renal plasma flow (RPF) and GFR are increased by a high protein diet or infusion of free amino acids.[3] The involvement of glucagon, NO or tubuloglomerular feedback have been suggested as possible mechanisms.[4,5] As discussed in later sections, differences in the fractional excretion observed for individual amino acids may result from the various selective transporters' (relative) expression levels, kinetics, ion dependence, and axial localization along the nephron.

Evidence that amino acid reabsorption along the nephron is axially heterogeneous was first derived from clinical observations. Specifically, lesions of the early proximal kidney tubule were observed in Fanconi syndrome, a condition characterized by glucosuria, phosphaturia, and aminoaciduria. Since glucose and phosphate were already known to be reabsorbed in proximal tubules, it was inferred that this nephron segment is also the main site of amino acid reabsorption.[6] The hallmark experiments confirming the role of proximal tubules were carried out using micropuncture and microinjection.[7–9] Quantification revealed approximately 80% of filtered amino acids are reabsorbed in the first half of the proximal convoluted tubule (S1 segment) whereas less than 1% remains in the tubular fluid at the end of the straight portion (S3 segment) of the proximal tubule.[10]

Concerning the later tubular segments, it was demonstrated by free flow micropuncture that no additional active amino acid transport takes place along the

Seldin and Giebisch's The Kidney, Fifth Edition.
DOI: http://dx.doi.org/10.1016/B978-0-12-381462-3.00071-9

© 2013 Elsevier Inc. All rights reserved.

TABLE 71.1 Plasma and Urine Concentration and Fractional Excretion of Amino Acids in Human Adults

Amino acid	Plasma concentration μM (range)[1]	Urine concentration (mmol/mol creatinine, 24 hours)[2]	Fractional excretion (%)[3]
Alanine	146–494	9–98	0.44
Arginine	28–108	0–8	0.77
Aspartic acid	2–9	5–50	1.96[+]
Asparagine	26–92	10–65	1.54[$]
Citrulline*	10–58	1–22	
Cystine	24–54	2–12	
Glutamic acid	6–62	0–21	0.68
Glutamine	340–798	11–42	0.71
Glycine	100–384	17–146	2.4
Histidine	68–108	49–413	6.52
Isoleucine	39–90	30–186	0.51
Leucine	98–205	1–9	0.26
Lysine	119–243	2–16	0.92
Methionine	13–37	2–53	0.66
Ornithine*	36–135	1–5	0.32[$]
Phenylalanine	42–74	1–5	0.69
Proline	97–297	3–13	0.047[$]
Serine	78–166	0–9	2.19
Taurine*	18–95	18–89	6.55[+]
Threonine	92–197	13–587	1.04
Tryptophan	25–65	6–74	
Tyrosine	26–78	3–14	1.38
Valine	172–335	3–36	0.2

[1]*Shih V. Amino acid analysis. In: Blau N DM, Blaskovics ME, ed. Physician's guide to the laboratory diagnosis of metabolic disease. London: Chapman Hall Medical, 1996:13–30.*
[2]*Venta R. Year-long validation study and reference values for urinary amino acids using a reversed-phase HPLC method. Clin Chem 2001; 47:575–83.*
[3]*Tietze I.N, Sorensen S.S, Eiskjaer H, Thomsen K, Pedersen E.B. Tubular handling of amino acids after intravenous infusion of amino acids in healthy humans Nephrol Dial Transplant 1992;7:493–500.*
[+] *Silbernagl S. Renal handling of amino acids and oligopeptides Contrib Nephrol 1981;24:18–29.*
[$]*Liu W, Lopez JM, VanderJagt DJ, Glew RH, Fry DE, Schermer C, et al. Evaluation of aminoaciduria in severely traumatized patients. Clin Chim Acta 2002; 316:123–8.*
[*]*Non-proteinogenic*

loop of Henle.[7] Furthermore, it was shown by microinjection[11] and microinfusion experiments[12,13] that with the exception of taurine, amino acids delivered into the early loops of superficial distal nephrons are recovered quantitatively from the final urine. Taken together, these experiments indicated that there is no significant amino acid reabsorption beyond the proximal tubule. One caveat is that a quantitative difference exists between the amino acid fractional delivery values for superficial nephrons reported above and the urinary amino acid fractional excretion. This difference was suggested to be due to the differential absorptive capacity of superficial and deep nephrons.[14]

FROM "TRANSPORT SYSTEMS" TO TRANSPORTERS

The transport of free amino acids and small peptides was intensively studied during the second half of the last century thanks to the availability of radiolabeled amino acids and sensitive analytical quantification techniques such as paper chromatography and liquid chromatography. Erythrocyte and cell culture models, as well as tissue and organ experimental systems, in particular small intestine and kidney, were used. From the latter epithelial organs, brush border membrane vesicles were produced that allowed measurement of luminal transports in the presence of defined solutes at their trans-side, i.e., inside vesicles. Prior to the molecular identification of transport proteins, the so-called "transport systems" were functionally defined by amino acid selectivity, stereospecificity, ion-(sodium, chloride, potassium), or proton dependence, thermodynamic properties (equilibrative or concentrative) and transport type (co-transport = symport (S), exchange = antiport (A) or facilitated diffusion = uniport (U).[15–17] These "transport systems" were named according to functional properties with letters corresponding to the main/first described amino acid substrate, e.g., system A (L-alanine), N (L-asparagine), L (L-leucine), and ASC (L-alanine, L-serine and L-cysteine). In general, capital letters denoted sodium-dependent (except systems L and T) and lowercase sodium-independent systems (e.g., $b^{0,+}$). The transport of basic or acidic amino acids was identified by a plus or a minus symbol (e.g., system y^+L and X^-_{AG}) and the letter B used for systems with a broad amino acid selectivity (for example B^0, $B^{0,+}$).

A new era started with the molecular identification of transporters, which was made possible by the complementary techniques of DNA cloning and cellular over-expression.[18–22] Currently, about 50 amino acid and peptide transporters have been molecularly described. Researchers identifying new amino acid transporters have generally named them according to the "rules" previously used to describe transport systems[15] on occasion resulting in multiple names for the same transporter. The human genome organization (HUGO) proposed a new classification scheme for the genes of solute carriers (SLC) based on sequence homology.[19] This system is now in use for other

vertebrate species as well. The SLC gene nomenclature is increasingly used also to name the encoded transport proteins (Table 71.2). The molecular identification of transporters has allowed their detailed functional characterization using cellular overexpression systems, in particular *Xenopus laevis* oocytes. Additionally, the availability of cDNA allowed measurement of mRNA expression in tissues, initially by Northern blot analysis, and later by real time quantitative RT-PCR (qPCR) and microarray chips. Furthermore, specific antibodies could be generated and used to localize transport proteins at the tissue, cellular and subcellular levels. Noteworthy, the molecular identification of transporters has resulted in the identification of genetic defects underlying several hereditary amino acid transport-related diseases, in particular causing aminoacidurias (discussed in later sections).

More recently, to address questions about the functional role of amino acid transporters in a physiological context, knockout mice (conventional, tissue-specific and/or conditional) and transgenic mice and rats have been generated. Urine analysis, determination of amino acid fractional excretion, microperfusion, isolated tubule perfusion and other techniques are therefore once again valuable tools for phenotyping genetically-modified animals to increase understanding of the physiological roles of amino acid transporters. In addition, the structure-function relationship of amino acid transporters can be probed using truncated and chimeric constructs, cysteine scanning and so on.[23–25] Specifically questions could be addressed concerning accessibility of residues, substrate and ion binding sites, allosteric binding domains, tertiary and quaternary structure, and protein interactions. Currently, using bacterial homologues of mammalian transporters, the three dimensional structures of GltPh (PDB 1XFH), a homologue of sodium-dependent glutamate transporters (SLC1 family), and of $LeuT_{Aa}$ (PDB 2A65), a homologue of B^0AT1/SLC6A19 (SLC6 family), and PEPT(So) (PDB 2XUT), a homolog of the mammalian peptide transporters (SLC15 family) have been solved[26–28] adding a new level to our understanding of the structure-function relationships of these molecular machines.

FUNCTIONAL SCHEMA OF AMINO ACID REABSORPTION BY PROXIMAL TUBULE EPITHELIAL CELLS

The reabsorption of amino acids by kidney proximal tubules is a transcellular process involving passage across two membranes, namely from the tubular lumen into an epithelial cell, and from the cytoplasm to the extracellular space, for diffusion back into the circulation.

A summary of the current knowledge concerning the arrangement of transporters involved in transepithelial amino acid reabsorption by kidney proximal tubule cells is proposed in the model shown in Figure 71.1 (modified from Verrey et al., 2009).[29] The luminal influx of amino acids is mediated by a set of secondary active transporters driven by the co-transport of Na^+ or H^+ and by one heteromeric amino acid transporter that functions as an antiporter, ($b^{0),+}$AT-rBAT (SLC7A9-SLC3A1).

Transporter selectivity for amino acids overlaps to some extent though generally with different affinities for common substrates. For example, neutral amino acids, which represent > 80% of the free plasma amino acids, are all transported with different apparent affinities and transport rates by the luminal transporter B^0AT1 (SLC6A19) [30–32] (Fig. 71.1). Some amino acids are also transported by the heterodimeric amino acid transporter, $b^{0,+}$-rBAT (SLC7A9–SLC3A1). However, the main function of this exchanger is the import of cationic amino acids and cystine. Furthermore, $b^{0,+}$-rBAT cannot substitute for B^0AT1 since as an obligatory amino acid exchanger (antiporter) it does not contribute to the overall net amino acid import (see sections on specific transporters below).[33–35] The imino and neutral amino acid transporters, SIT1, PAT1 and PAT2 also display overlapping substrate selectivity with B^0AT1. SIT1 (SLC6A20) is an SLC6 family member expressed in the proximal tubule, which in addition to mediating a very efficient L-proline transport, transports other neutral amino acids.[36–38] PAT2 (SLC36A2) and PAT1 (SLC36A1), SLC36 family proton co-transporter(s), also transport L-proline and small neutral amino acids.[39,40] Estimation of the relative contribution of each transporter to the actual transport of a given amino acid is very difficult, since this depends not only on the apparent affinity ($K_{0.5}$) and V_{max} (expression level and transport rate) of each involved transporter and on the amino acid concentration (for the given amino acid), but also on the presence of competing amino acids and compounds. An additional complication is the role of co-transported and/or exchanged substrates, which depending on the transporter are ions, protons, or amino acids. The concentration of co-substrate(s) on both sides of the membrane determines availability and driving force, and thus determines their impact on the amino acid transport rate. Furthermore, in the case of transports driven by an electrical gradient, membrane potential plays an important role.

The majority of the transporters involved in amino acid reabsorption in the kidney are localized along the first two (S1 and S2) proximal tubule segments where

TABLE 71.2 Kidney Amino Acid Transporter Proteins, Slc Names and the Corresponding Transport Systems[1]

Protein name[2]	Slc name[3]	System	Main Substrates	Ion dependency	Transport type	Kidney tubule localization
APICAL SURFACE LOCALIZATION						
B^0AT1	Slc6a19	B	Neutral AA	Na^+	S	S1 >S2
B^0AT3	Slc6a18		Neutral AA	Na^+, Cl^-	S	S2, S3
$b^{0,+}$-rBAT	[4]Slc7a9-Slc3a1	$b^{0,+}$	R,K,ornithine, cystine	-	A	S1 >S2 (rBAT also S3)
PAT2	Slc36a2	IMINO	P,G,A, MeAIB	H^+	S	S1 >S2
SIT1	Slc6a20		P, MeAIB	Na^+, Cl^-	S	S1-3
EAAC1/ EAAT3	Slc1a1	X^-_{AG}	L or D-D, L-E	Na^+, H^+-S; K^+-A	S/A	S2, S3 >S1
PEPT1	Slc15a1	peptide	di- tri-peptides	H^+	S	S1 >S2
PEPT2	Slc15a2					S3
Taut1	Slc6a6		taurine, hypotaurine, and β-alanine	Na^+, Cl^-	S	Collecting duct
BASOLATERAL SURFACE LOCALIZATION						
LAT2-4F2	Slc7a8-Slc3a2	L	Neutral AA, but not P, BCH	-	A	S1 >S2
LAT4	Slc43a2		L,I,M,F,BCH	-	U	(4F2hc also S3)
y + LAT1-4F2	Slc7a6-Slc3a2	y^+L	K,R,Q,H,M,L	Na^+ for neutral AA	A	S1 >S2
TAT1	Slc16a10	T	F,Y,W	-	U	S1 >S2
Snat3 / SN1	Slc38a3	N	Q,N,H	Na^+-S; H^+-A	S/A	S3, (S2)
AGT1 / XAT2	Slc7a13-Slc3a2	x^-	L-D, L-E	-	A?	S3, distal convoluted tubule
UNKOWN SUBCELLULAR LOCALIZATION						
Asc1-4F2	Slc7a10	asc	G,A,S,C,T	-	A	Loop of Henle, distal and collecting duct
Asc2	Slc7a12&		S,G,A,T,L,F,Y	-		Collecting ducts

[1],[17,58,85,124,133] *Camargo SM, Bockenhauer D, Kleta R. Aminoacidurias: Clinical and molecular aspects.* Kidney Int. *Apr 2008;73(8):918-925; Verrey F, Closs EI, Wagner CA, Palacin M, Endou H, Kanai Y. CATs and HATs: the SLC7 family of amino acid transporters. Pflugers Arch. Feb 2004;447(5):532–542.*

[2]*The most common names are indicated.*

[3]*Slc names correspond to the gene symbols given by the HUGO gene nomenclature committee.*

[4]*Members of the heterodimeric amino acid transporter (HAT) family are associated to glycoproteins (heavy chains) rBAT (Slc3a1), 4F2hc (Slc3a2) or unknown (&); AA, amino acids (indicated in single letter code); S, symport = co-transport with ion; A, antiport = obligatory exchange against AA or ion; U, uniport = facilitated diffusion pathway. S1-S3, segments of the proximal kidney tubule.*

most of the amino acid reabsorption occurs. However, some high affinity luminal co-transporters are localized predominantly in the S3 proximal tubule segment, downstream of lower affinity transporters. This is the case for the high affinity Na^+-Glucose co-transporter SGLT1 (Slc5a1), which is expressed downstream of low affinity SGLT2 (Slc5a2).[45] Additionally, the high affinity oligopetide transporter PEPT2 (Slc15a2) and the high affinity neutral amino acid transporter B^0AT3 (SLCA18) are expressed downstream of PEPT1 (Slc15a1) and B^0AT1 (Slc6a19), respectively.[45,50] This sequential distribution of low and high affinity transporters along the proximal tubule is suggested to optimize recovery from the ultrafiltrate by permitting absorption of residual solutes and of solutes that have diffused back into the tubular fluid via the relatively leaky paracellular pathway. The various secondary active amino acid transporters expressed in the luminal plasma membrane are all described below in short sections.

The basolateral transport of amino acids is not as well understood as the luminal amino acid influx. This is due to several reasons, a trivial one being that

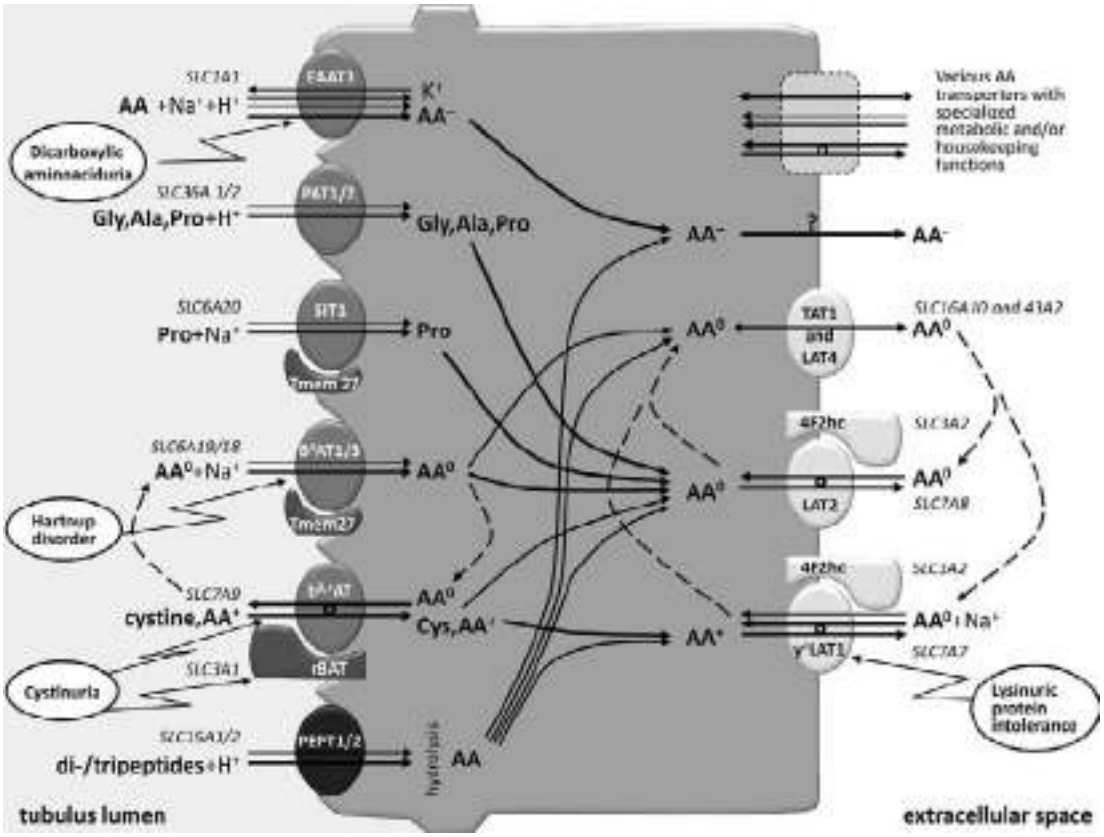

FIGURE 71.1 Cellular model for the reabsorption of amino acids across a proximal kidney tubule cell. Names of the involved transporters and their human gene are indicated. Most of them have been shown to be expressed mainly in the early segments of mouse proximal tubule (S1 and S2), with the exception of SIT1 that is expressed all along the proximal tubule, and of B0AT3 and EAAT3, which are expressed mainly in the later proximal tubule (S2 and S3). AA^0 neutral amino acid, AA^- anionic amino acid, AA^+ cationic amino acid, Tmem27 (collectrin).

measuring efflux is technically more demanding than measuring influx. The central issue is that the role of basolateral amino acid transport is more complex than that of luminal amino acid uptake. Whereas apical transport aims at clearing the filtered amino acids from the urinary fluid, basolateral transport in addition to transporting the cellular amino acid content into the extracelluar space, also maintains a physiological intracellular amino acid concentration. This is a task that basolateral amino acid transporters of tubular cells have in common with those of non-polarized cells. Indeed, intracellular amino acids are required to fulfil cellular housekeeping tasks and as substrates for amino acid metabolism. Therefore, a relatively stable amino acid gradient from the tubular cells towards the extracellular fluid has to be maintained.

Specifically, some amino acids display similar concentrations within and outside of the cells, while others display an asymmetric distribution. This is particularly evident for anionic amino acids that, despite carrying a charge that should drive efflux, are present at higher concentrations in the cytosol than in the extracellular space.[46,47] Likewise, in some cells cationic AAs, whose charge should drive influx, are none-the-less not more concentrated in cytosol than in plasma. Two transporters in amino acid transporting epithelial cells that play important roles in the control of various neutral and cationic amino acid intracellular concentrations are the heterodimeric exchangers (antiporters) LAT2-4F2hc (SLC7A8-SLC3A2, neutral amino acid antiporter) and y^+LAT1-4F2hc (SLC7A7-SLC3A2, antiporter exchanging intracellular cationic amino acids for extracellular neutral amino acids and Na^+). As obligatory exchangers (antiporters), these transporters can only mediate net vectorial transport of those amino acid substrates that are exchanged for co-substrates recycled back through the membrane by unidirectional amino acid efflux pathway(s).[48] To date, two facilitated diffusion pathway transporters (uniporters), which mediate the directional transport of substrates along their concentration gradient, are proposed to fulfil this function in the basolateral membrane of kidney proximal tubule cells. Specifically, we have shown that the aromatic amino acid uniporter TAT1 (Slc16a10) is present

in the proximal kidney tubule basolateral membranes. Using the *Xenopus laevis* oocyte expression system we demonstrated TAT1 is capable of recycling amino acids to drive the efflux of other substrates by the antiporter LAT2-4F2hc.[49] However, the TAT1 knockout mouse does not show the dramatic changes in urinary amino acid concentrations expected if TAT1 alone recycles amino acids activating efflux via the exchangers LAT2-4F2hc and y^+LAT1-4F2hc (unpublished data). Another candidate for the recycling function is LAT4 (SLC43A2), which we have shown also cooperates with LAT2 in the *Xenopus laevis* oocyte expression system.[49] More work is needed to understand the controlled efflux of amino acids through the basolateral membrane of transporting epithelia.

Finally, it can be hypothesized that given the narrow substrate selectivity of the uniporters known to date, some players that drive net transport of neutral, anionic, and imino acids at the basolateral membrane are not, as yet, molecularly identified.

TRANSPORTERS INVOLVED IN THE LUMINAL UPTAKE OF AMINO ACIDS AND OLIGOPEPTIDES

Neutral Amino Acids

B^0AT1 (SLC6A19) is the major neutral amino acid transporter. It is a *symporter* that co-transports Na^+ and a broad range of neutral amino acids (all proteogenic ones) with low affinity (millimolar range).[30,31] Unlike many other members of the SLC6 family, B^0AT1 is not Cl^- dependent, and does not transport biogenic amines nor related osmolites.[50,31] B^0AT1 mRNA was found to be highly expressed in kidney proximal tubule and small intestine. In both mice and humans B^0AT1 is expressed in the brush border membrane of early proximal kidney tubules (S1).[51,42] Another interesting feature of B^0AT1 is its interaction with two tissue specific accessory proteins. In kidney, B^0AT1 interacts with the accessory protein, collectrin (*Tmem27*), and in intestine with the angiotensin converting enzyme 2 (*Ace2*). Tmem27 is a type I transmembrane protein that appears to interact non-covalently with B^0AT1. The collectrin (Tmem27 or *coll*) knockout mouse lacks renal B^0AT1 although intestinal expression is normal. Furthermore, *tmem27* knockout animals display a massive neutral aminoaciduria without glucosuria or phosphaturia pointing to Tmem27 being the specific obligatory subunit of B^0AT1 in the kidney.[52–54] In the intestine, where Tmem27 is not expressed, B^0AT1 interacts with Ace2. The Ace2 knockout mouse, which has normal kidney expression of B^0AT1, lacks intestinal B^0AT1 expression and displays impaired intestinal neutral amino acid transport.[32] The B^0AT1 knockout mouse, which does not express B^0AT1 in either kidney or intestine, has a reduced bodyweight. Consistent with B^0AT1 being the major Na^+-dependent neutral amino acid transporter of small intestine and kidney proximal tubule luminal membranes, brush-border vesicles prepared from both tissue sources lack Na^+-dependent neutral amino acid uptake. Furthermore, they do not show any compensatory increase in peptide transport and have normal expression of both accessory proteins, namely Tmem27 and Ace2.[55]

B^0AT3 is structurally and functionally related to SLC6A19 (B^0AT1). It is highly expressed in apical membranes of kidney proximal tubules with a complementary axial expression vs. B^0AT1, namely with a higher expression in the later S2 and S3 segments. The SLC6A18 gene is localized on chromosome 5p15 in tandem with the SLC6A19 gene and the two protein products share ~50% identity.[42] Functionally, B^0AT3 transports a broad range of neutral amino acids in a Na^+ and Cl^- dependent manner with a substrate specificity similar to B^0AT1, but with higher affinities (micromolar range). As for B^0AT1, B^0AT3 requires the accessory protein Tmem27 for renal expression.[43,44,52] B^0AT3 appears to reabsorb residual tubular amino acids, i.e. amino acids not reabsorbed in early proximal kidney tubule segments by B^0AT1 and/or which have leaked back into the lumen via a paracellular route.[56] Although, in a *slc6a18* knockout mouse model an abnormal excretion of several neutral amino acids (especially glycine) was observed,[43,57] this transporter appears not to play a functional role in humans since a large fraction of the population displays a nonsense single nucleotide polymorphism with no associated phenotype.[58]

Imino and Small Neutral Amino Acids

PAT1 and PAT2 (SLC36A1 and 2) co-transport small neutral amino acids or imino acids with protons. Their functional description was rendered more complicated by the fact that the proton gradient across the luminal membrane of proximal tubule cells depends on the activity of the sodium−proton exchanger NHE3. Therefore, PAT-mediated transport was first erroneously considered to be Na^+-dependent. Both PAT1 and PAT2 mRNAs were detected in kidneys but are mainly expressed in other tissues. PAT1 mRNA was found for instance in small intestine, brain, and colon, while PAT2 in lungs, heart, testis, muscles, and spleen.[39] These two transporters have a similar substrate selectivity that includes L- and D-proline, hydroxyproline, glycine, sarcosine, L, D, and β-alanine, D-serine, D-cysteine, betaine, α-(methylamino)isobutyric acid, and

GABA. Compared with PAT1, PAT2 prefers L- over D-alanine, does not distinguish between L- or D-serine and has a ten-fold lower affinity for GABA.[40] The major functional difference between these two transporters is that PAT1 displays a low affinity for its substrates (millimolar range), whereas PAT2 is a high affinity transporter (micromolar range). The PAT2 protein was shown to localize at the apical membrane of the early proximal tubule portion in human kidney.[59] Although, PAT1 protein has been localized to the brush border membranes of intestinal enterocytes, in mouse kidney proximal tubule cells only a subapical membrane expression has been shown.[44] No report of a knockout mouse model for either PAT1 or PAT2 has been published.

SIT1 (SLC6A20) functions as a symporter, co-transporting with high affinity (micromolar range) L-proline, methylaminoisobutyrate (MeAIB), methyl-proline, or hydroxyproline with Na^+ and Cl^-. Thus, together with PAT2 and possibly PAT1, SIT1 represents the so called "imino system." Unlike PAT1 and -2, SIT1 does not transport glycine or β-alanine.[36,38] The mRNA of SIT1 is highly expressed in small intestine, kidney, lungs, spleen, testis, and brain, and the protein has been shown to localize to the luminal brush border membrane of the entire proximal kidney tubule and of the small intestine.[42] SIT1 has been suggested to interact with the accessory protein Tmem27, since Tmem27 knockout animals showed a much reduced expression of SIT1 in the kidney.[52] Co-expression experiments in *Xenopus* oocytes show that SIT1 can functionally interact with the accessory proteins Tmem27 and Ace2. SIT1 was also shown to co-localize with Ace2 in human small intestine brush border membranes (Vuille-dit-Bille, Camargo and Verrey, unpublished data). As yet, no knockout mouse model for SIT1 (*slc6a20*) has been reported.

Cationic Amino Acids and L-Cystine

rBAT (SLC3A1) and $b^{0,+}$AT (SLC7A9) form together a heterodimeric amino acid transporter (HAT).[60] It is composed of the type II glycoprotein (heavy subunit) rBAT and the catalytic subunit (light subunit) $b^{0,+}$AT, that are covalently linked by a disulfide bridge.[61,62] The light chain, which contains 12 putative transmembrane domains, is the active subunit and confers substrate specificity. Both subunits are primarily expressed in kidney and intestine where they localize to the brush border membrane of proximal tubules or small intestine enterocytes.[62,63] When over-expressed in an epithelial cell model (MDCK cells) rBAT and $b^{0,+}$AT co-localize in the apical membrane, while in the absence of rBAT, $b^{0,+}$AT is retained intracellularly, demonstrating rBAT is essential for cell surface expression of $b^{0,+}$AT.[64,65] The rBAT and $b^{0,+}$AT heterodimer mediates the obligatory exchange of large neutral (notably cystine) against dibasic (arginine, lysine, ornithine) amino acids.[34] Mouse models generated by the ablation of the heavy or light chains excrete higher levels of cystine and dibasic amino acids in the urine.[66–68]

Anionic Amino Acids

EAAC1/EAAT3 (SLC1A1) functions as a high affinity symporter and antiporter. It co-transports L-glutamate, L- or D-aspartate with Na^+ and H^+ from the tubule lumen into the cell in exchange for K^+ that is transported to the outside. The transporter is highly expressed in the later portion of kidney proximal tubules (S2, S3 >S1) and in distal convoluted tubule, the brush border of ileal enterocytes, and in various subpopulations of neurons.[20,69] EAAC1/EAAT3 is the only anionic amino acid transporter thus far detected in the apical membrane of proximal tubule cells. EAAT3 was shown to have an allosteric negative modulator, the glutamate transport associated protein (GTRAP3–18). GTRAP3–18, which interacts with the carboxy-terminal end of the transporter, is a membrane-associated protein expressed in the same tissues as EAAT3 that has been shown to retard the exit of EAAT3 from the endoplasmatic reticulum.[70,71] The ablation of Slc1a1 in a mouse model induced a marked urinary excretion of L-glutamate and aspartate, which was not compensated for by other transporters.[72]

Oligopeptides

PEPT1 and PEPT2 (SLC15A1 and 2) are members of the PEPtide Transporter family. These symporters use the proton gradient as the driving force to transport small peptides derived from protein degradation into the cells. PEPT1 and PEPT2 have a broad selectivity accepting all dipeptides and tripeptides composed of the 20 proteinogenic amino acids. The substrate affinity and localization of the two orthologs diverge; PEPT1 has a low affinity (millimolar range) and is expressed in small intestine, kidney, extra hepatic biliary duct and brain, while PEPT2 has a higher affinity (micromolar range) and is expressed in the kidneys, brain, lungs, eyes, and mammary glands. Both transporters are complementarily expressed on apical proximal tubule membranes. The low affinity PEPT1 is highly expressed in the early segments of the proximal tubule and the high affinity PEPT2 in the more distal portion of the proximal tubule (S3). Importantly, PEPTs

transport a large number of other molecules, in particular drugs from several important classes such as β-lactamate antibiotics (cephalosporins and penicillins). The transport of sartans and ACE inhibitors is still debated.

Knockout mouse models for both transporters have been generated. Both are viable and have a mild phenotype. The clearance of the non-metabolized peptide glycylsarcosine was not different in a PEPT1 knockout mouse compared with wild type animals, while the intestinal absorption of this substrate was drastically reduced. In contrast, glycylsarcosine clearance was twofold higher in PEPT2 knockout mice than in wild type littermates suggesting that the high affinity PEPT2 is responsible for the majority of peptide reabsorption in the kidneys.[73–75]

TRANSPORTERS INVOLVED IN BASOLATERAL EFFLUX OF AMINO ACIDS

Neutral Amino Acids

LAT2 (SLC7A8) and 4F2*hc* (SLC3A2) form a heterodimeric amino acid transporter (HAT) with a broad selectivity for neutral amino acids that functions as an obligatory exchanger. Interestingly its extracellular affinity is quite high (micromolar range) whereas its intracellular affinity for the same substrates is approximately 1000-fold lower.[47] LAT2 is highly expressed in small intestine, kidney, brain, muscles, lungs, bladder, and pancreas.[63,76,77] It localizes to the basolateral membrane of proximal tubule epithelial cells with the highest expression in the early portion (S1). In contrast, the glycoprotein heavy chain subunit 4F2hc, which functions as chaperone assisting in the plasma membrane targeting of LAT2, has a ubiquitous localization. Knockout mice for *Slc7a8* present elevated urinary excretion of glycine, L-serine, L-threonine, L-glutamine, L-leucine, and L-valine. The same amino acids, with the addition of L-lysine, were elevated in the serum of animals. Even though Slc7a8 is highly expressed in the placenta and brain, mice were viable and have only a moderate impairment of movement coordination.[78]

TAT1 (SLC16A10), the T-type aromatic amino acid transporter is by sequence homology a member of the monocarboxylate transporter (MCT) family and functions as a low affinity symmetric uniporter (facilitated diffusion pathway) for aromatic amino acids, L-dopa and iodothyronines.[79,80] TAT1 is highly expressed in the kidneys, small intestine, colon, liver, stomach, heart muscle and testis and localizes to the basolateral membrane of epithelial cells in small intestine and kidney. It is abundant in the early S1 and S2 segments of kidney proximal tubules. The functional interaction of TAT1 and LAT2-4F2 for mediating neutral amino acid efflux is described above in the section on a functional schema of amino acid reabsorption. A TAT1 knockout model has been generated but no functional data has been published yet (F. Verrey, personal communication).

LAT4 (SLC43A2) is a recently identified member of the Slc43 family that is not yet fully characterized. Similar to TAT1, LAT4 functions as a Na^+-independent, facilitative diffusion pathway (uniporter) with narrow substrate selectivity. Branched chain amino acids, L-methionine and phenylalanine are transported with low affinity. It is expressed in kidney, spleen, heart, brain, small intestine, and testis.[81] In situ hybridization data indicates the transporter is expressed in distal nephron segments, namely the distal tubule and collecting duct but our preliminary data indicate that LAT4 mRNA is substantially expressed in proximal tubules (Mariotta, Camargo and Verrey, unpublished data). A LAT4 knockout has been generated but no functional data is yet available (F. Verrey, personal communication).

SNAT3, SN1 (SLC38A3), previously designated as system N, is a sodium dependent glutamine transporter expressed in brain, retina, liver, kidney, pancreas, and adipose tissue. In the kidney, it localizes to the basolateral membrane of later proximal tubules (S3).[82,83] SNAT3/SN1 transports L-glutamine, histidine, L-asparagine and also alanine with low affinity (low millimolar range).[84] The transport is coupled to Na^+ co-transport and proton counter transport. The transport direction has been shown to be reversible.[85] Although extracellular pH influences SNAT3 transport activity, it is primarily the glutamine gradient that determines the direction of transport. The role of SNAT3 in pH control and during metabolic acidosis is discussed below in the section on amino acid metabolism. The SNAT3 knockout in mice is lethal between postnatal days 10 to 14 (C.Wagner, personal communication;[86]).

Cationic Amino Acids

y^+LAT1 (SLC7A7) and 4F2*hc* (SLC3A2) form a heterodimeric amino acid transporter (HAT) that under physiological conditions primarily transports dibasic amino acids out of cells in exchange for the influx of neutral amino acids and Na^+.[87] Under experimental conditions an inverted exchange can be measured revealing a high extracellular affinity for cationic amino acids, similar to the affinity for neutral amino acids. The intracellular affinities are however not

known. The glycoprotein heavy chain subunit 4F2*hc* is ubiquitously expressed, while y^+LAT1 is highly expressed in intestine, kidney, lungs, and leukocytes.[63,87,88] Similar to $b^{0,+}$AT-rBAT, y^+LAT1-4F2*hc* localizes to kidney proximal tubules (S1 >S2 ≫S3) and small intestine enterocytes (jejunal and ileal). However, in contrast to $b^{0,+}$AT-rBAT expression is on the basolateral membranes representing an efflux pathway for cationic amino acids taken up apically by $b^{0,+}$AT-rBAT (see Figure 71.1).[48,63] The 4F2*hc* heavy chain subunit, analogously to rBAT, functions as a chaperone assisting in the plasma membrane sorting of y^+LAT1.[48,87,89] The ablation of the *slc7a7* gene results in intrauterine growth retardation and a low rate survival.[90]

Anionic Amino Acids

AGT1 (SLC7A13) is a member of the heterodimeric amino acid transporter family but its accessory protein (heavy chain), which is neither rBAT nor 4F2hc, remains unknown. The function of AGT1 was tested in *Xenopus* oocytes using fusion proteins with the heavy chains 4F2hc or rBAT. AGT1 fusion proteins were shown to transport L-glutamate and L-aspartate with high affinity (micromolar range) independent of Na^+ and Cl^-. It has not been demonstrated whether it functions like other heterodimeric amino acid transporters as obligatory exchanger. AGT1 appears to be expressed exclusively in the kidney where it localizes to the basolateral membrane of the straight part of the proximal tubules (S3) and also to the distal convoluted tubule. Apparently expression is specifically in tubule segments where the luminal transporter for anionic amino acids EAAT3 is also expressed.[91] This axial localization of basolateral AGT1 suggests its involvement in the transcellular reabsorption of L-glutamate and L-aspartate. If AGT1 functions as obligatory exchanger, a net efflux of these amino acids would imply that substrates that recycle out of the cell via facilitated diffusion pathways must be taken up in exchange. Since AGT1 uptake was only tested at low amino acids concentrations (20 μM), and since competition with 2 mM of some neutral amino acids, e.g. L-cysteine, substantially inhibited the L-aspartate uptake this possibility is not excluded. Additional experiments in an expression system and especially a knockout animal model of *slc7a13* would help in solving this open question.

Amino Acid Transporters in More Distal Segments of the Nephron

Only low amounts of amino acids reach the loop of Henle and the distal nephron segments. As mentioned, beyond the proximal tubule, with the exception of taurine uptake, no substantial amino acid reabsorption was detected by micropuncture and microinjection. Of the amino acid transporters involved in reabsorption described above, only the anionic amino acid transporters EAAT3 (luminal) and AGT1 (basolateral) have been detected in the distal nephron, specifically in the distal convoluted tubule. This suggests that basolateral transporters expressed in later kidney tubule segments primarily fulfill housekeeping functions. Some of these transporters for which localization studies have been performed, are listed below.

Asc-1 (SLC7A10) and 4F2hc (SLC3A2) form a heterodimeric transporter expressed in brain, lung, kidney, and intestine, which functions as antiporter, although possibly not exclusively. Asc1-4F2hc mediates the Na^+-independent transport of small neutral amino acids (Gly, Ala, Ser, Cys, Thr) with high extracellular apparent affinity (micromolar range) and, to some extent, efflux of large neutral amino acids.[92] In kidney, Asc-1 mRNA was shown to be expressed in the loop of Henle, the distal tubule, and the collecting duct. The presence of this transporter in distal nephron segments suggests a role in housekeeping functions rather than for amino acid reabsorption. The *slc7a10* knockout mouse ($asc^{-/-}$) shows a severe brain phenotype with tremor and seizures and early postnatal death. The heterozygous animal was also characterized, and Asc-1 was suggested to be the major D-serine transporter in the brain. The renal function of these knockout animals has not been analyzed.[93,94]

Asc2 (SLC7A12) is a heterodimeric transporter that does not interact with rBAT or 4F2 (Slc3a1 or 2), the accessory proteins (heavy chains) of other Slc7 family members. Asc2 expressed in *Xenopus* oocytes as fusion protein with rBAT and 4F2hc, displayed an amino acid selectivity and affinity similar to Asc1. It was shown to function as a Na^+ and Cl^--independent exchanger. It is expressed in muscles, placenta, spleen, brain, and kidney, where it localizes to the cortical and the outer- and inner medullary collecting ducts. Its subcellular localization has not been conclusively demonstrated,[95] but its axial localization and functional characteristics suggest a housekeeping role.

TauT1 (SLC6A6) is a member of the Na^+-Cl^- neurotransmitter and amino acid transporter family and co-transports taurine, hypotaurine, and β-alanine with high affinity (low micromolar range) together with sodium and chloride.[96] TauT1 is expressed in kidney, intestine, retina, brain, liver, muscles, and placenta. In the kidney, it is expressed in the outer and the inner medulla and the protein was shown to localize apically in the inner medulla collecting duct. Its expression

increases after a salt load, leading to an increased taurine concentration within medullary cells.[97,98] The knockout animals (taut$^{-/-}$) excrete taurine, display hypotaurinemia, but do not show defective antidiuresis upon water deprivation. However, these knockout mice display an impaired ability to lower urine osmolality and to increase urinary water excretion. The latter defect is considered to result from an extrarenal role of taurine transport in the regulation of vasopressin secretion.

Renal Amino Acid Metabolism

The contribution of the kidney to whole body amino acid homeostasis is not only via proximal tubule reabsorption but also due to renal metabolism and interorgan exchange of amino acids and their metabolites.[99] For example, the kidney is the major site for glutamine and proline disposal from arterial blood, and for serine and arginine de novo production and an important source of other amino acids.[100] To illustrate, a 70 kg man produces ~3–4 g serine daily, ~2 g/day arginine, and ~1 g/day tyrosine, as well as lesser amounts (<1 g/day) of threonine, lysine, and leucine.[99] Amino acid supply to the kidney (achieved by reabsorption of amino acids from primary filtrate and the arteriole blood flow) is supplemented by the relatively high renal turnover rate of reabsorbed proteins. Amino acid metabolism in the kidney has local and systemic effects on diverse physiological processes including pH regulation, vasodilation, and urea cycle regulation. Furthermore, renal disease such as acute or chronic renal insufficiency alters kidney protein balance, amino acid metabolism, and nitrogen release thereby contributing to physiological responses throughout the body.[100–102]

Glutamine/Glutamate Renal Transport Metabolism

In the kidney glutamine metabolism contributes to pH regulation through glutamine-glutamate metabolism, ammonia and ammonium formation and excretion, and bicarbonate regeneration.[99] Renal glutamine uptake accounts for ~10–15% of the whole body daily flux (~70 g/day) while urinary excretion accounts for less than 1% of daily renal uptake. Approximately 80% of the taken up glutamine is metabolized by the mitochondrial phosphate-dependent glutaminase in the proximal tubule and a further 10% is metabolized in the distal tubule by γ-glutamyl transferase. Glutaminase activity produces glutamate and ammonia. The majority (70%) of the ammonia is released into the renal vein and the remainder excreted in urine. Urinary glutamate release is considerably less than 1% of renal glutamine uptake. Rather, glutamate is transaminated to alanine and α-ketoglutarate, which can be utilized in the krebs cycle, or further degraded by the glutamate dehydrogenase pathway to ammonia and more α-ketoglutarate. α-Ketoglutarate can also be converted by phosphoenolpyrvate carboxykinase in the gluconeogenic pathway to glucose and two bicarbonate ions. Renal production indeed contributes nearly 25% to the total body gluconeogenesis with 80% of gluconeogesis from glutamine. Ammonia released in the acidotic primary urine is protonated to ammonium helping to increase the H^+ excretion.[83,103] However, unlike the hepatic glutaminase, which is inhibited by low pH and stimulated by ammonia, the renal enzyme is inhibited by both ammonia and glutamate. Since glutamine is rate-limiting for ammonia production and under normal conditions nearly all glutamine is reabsorbed from the urine, to boost ammonia production during metabolic acidosis, glutamine uptake from the blood must increase. Therefore, metabolic acidosis strongly stimulates arterial glutamine uptake and renal metabolism by increasing the expression of basolateral glutamine transporter SNAT3 (SLC38A3) and the activity and expression of glutamine-glutamate pathway enzymes.[104–106]

Arginine, Citrulline and NO

As the primary source of L-arginine (not targeted for immediate urea production) the kidney plays a major role in whole body arginine homeostasis. In addition to protein biosynthesis, arginine is a precursor for creatine, nitric oxide (NO), and (after decarboxylation to agmatine guanidine) other polyamine metabolites. The rate limiting step in L-arginine synthesis is the production of L-citrulline by small intestine metabolism of glutamine.[107] Daily kidneys reabsorb more than 80% or about 1.5 g of L-citrulline from primary urine and release ~2–4 g of L-arginine to the renal vein, of which 5–15% is from de novo synthesis.[108] L-arginine production from L-citrulline is catalyzed by two enzymes. First, argininosuccinate synthetase (ASS) in an ATP consuming step produces adenylocitrulline, which is coupled the amino group of aspartate forming aminosuccinic acid. Subsequent hydrolysis by argininosuccinate lyase (ASL) yields arginine and fumarate. Biosynthetic activity is greatest in proximal tubule S1 cells, and sharply diminishes by the S2 to S3 segments. Citrulline uptake is mediated most likely by B^0AT1 and $b^{0,+}AT$ apically and organic anion transporter OAT1 (SLC22A6) basolaterally.[109,110] In S3 segments protein catabolism produces the arginine derivative asymmetrical dimethylargineine (AMDA), which is

metabolized to L-citrulline by mitochondrial *NG, NG*-dimethylaminohydrogenase, boosting arginine production modestly. The kidney accounts for ~40% of the total body breakdown of AMDA.

Along with de novo L-arginine synthesis, 3.1 g (~8 mmol) of L-arginine are filtered and reabsorbed by human kidneys daily. Proximal tubule cells metabolize ~10% of L-arginine content by three mitochondrial pathways: (1) conversion into guanidinoacetic acid (by cortical arginine:glycine amidinotransferase (GAT)), which is exported into the blood stream for eventual creatine production; (2) hydrolysis by arginase II ((AII) with a complementary distribution to ASS and ASL in PCT) into ornithine and urea; and (3) a low level of decarboxylation by arginine decarboxylase (ADC) to agmatine and CO_2.[107] AII activity increases from the cortex to the inner medulla.[111] Additionally, nitric oxide synthetase (NOS) enzymes metabolize L-arginine to nitric oxide and citrulline—which in the presence of ASS, ASL and aspartate can be recycled to L-arginine.[111] All three isoforms of nitric oxide synthetase, the endothelial, neuronal and inducible (eNOS, nNOS and iNOS respectively) are expressed in various kidney regions and structures, and compete with arginase for L-arginine. Metabolism for creatine production consumes the majority of the L-arginine metabolized in the kidney, while AII, ACD, and NOS enzymes use only a small proportion of renal supplies. Both the subcellular compartmentalization and the heterogeneous distribution in renal cortical vs. medullary zones of L-arginine synthesis and degradation pathways allow kidney to simultaneously contribute to arginine plasma supply, and ornithine, NO, and urea synthesis.[99,101,111]

Aromatic Amino Acids: Phenylalanine and Tyrosine

The kidney accounts for ~40% of the whole body activity of phenylalanine 4-hydroxlase which catalyzes the synthesis of the conditionally essential amino acid L-tyrosine from L-phenylalanine. The total body turnover of L-phenylalanine and L-tyrosine is ~10 g and 7 g per day, respectively. Kidneys, which take up 0.5-1 g L-phenylalanine and release ~1 g per day L-tyrosine, account for ~15% of whole body tyrosine flux.[99] Kidney is a major contributor to the net release of L-tyrosine to the bloodstream, unlike liver, the rate of renal de novo production combined with L-tyrosine release due to protein catabolism (a combined ~7 μmol/min) is greater than disposal rate (~1.8 μmol/min).[112] These rates are altered in patients with chronic kidney disease (CDK) such that tyrosine hydroxylation is decreased. In these patients, L-tyrosine deficiency can develop, emphasizing the importance of renal L-tyrosine synthesis.

Glycine and Serine

In the proximal tubule, 1.5 g of L-glycine are reabsorbed daily and metabolized to L-serine. Glycine decarboylase complex and serine hydroxymethyltransferase catalyze synthesis of one serine, bicarbonate, and ammonia moiety from each two glycine cleaved, accounting for ~30% of renal serine and ~10% of renal ammonia production. The hydrolysis of glutathione by γ-glutamyltranspeptidase in kidney proximal tubule brush border membranes is a further source of glycine. Kidneys also synthesize serine via conversion of L-glutamine, L-glutamate, and L-aspartate to L-serine via the phosphorylated intermediate pathway. Overall, the renal serine production of 3−4 g/day while representing only ~5−7% of total body turnover is equal to the normal daily serine dietary intake.[99]

Protein, Oligopeptide and Glutathione Metabolism

Amino acid supply to the kidney is supplemented by the relatively high renal turnover rate of reabsorbed proteins. Although the gomerular filtration barrier limits the distribution of proteins in the primary filtrate low concentrations are present. Furthermore, in the post absorptive state kidney protein degradation is ~45% greater than synthesis. A number of exopeptidases have been identified in proximal tubule brush border membranes and cytosol. The most abundant is the broad spectrum aminopeptidase N. For dipeptides, in comparison to liver, small intestine (ileum, jujenum) and muscle, kidney exhibits the highest level of hydrolase activity.[113] As much as 10% of all body L-leucine originating from protein degradation comes from the kidneys. In total ~7 g of proteins per day are degraded by the kidneys. Considering kidneys weigh ~1% of total skeletal muscle and <13% of the splanchnic organs, human kidneys contribute disproportionally towards total body protein degradation and synthesis (~10% of the total for each measure).[114] Much of this involves assimilation and/or production of circulating plasma low molecular weight oligopeptides. As an example of the contribution of renal metabolism to oligopeptide metabolism we consider the case of glutathione (glutamyl-cysteine-glycine). Glutathione (GSH) is efficiently taken up by kidney with ~80% plasma GSH absorbed during a single pass. Meanwhile 30% is absorbed from the primary filtrate, the majority (>60%) is absorbed from the plasma by Na^+-dependent and Na^+-independent basolateral

transporter(s). OAT3 (SLC22A6), OAT1 (SLC22A8) and NaC_2 (SLC3A3) all of which are expressed on basolateral membranes have been suggested as candidates.[115] Within cells, DIC (SLC25A10) and OGC (SLC25A11) are responsible for the majority (>80%) of renal mitochondrial GSH transport. On the luminal membrane efflux is carried out by OAT1a1 (SLCo1A1), Mrp2/Abcc2 and Mrp4/Abcc4 transporters.[115] GSH synthesis and degradation pathways are segregated spatially with synthesis occurring in the cytoplasm by sequential glutmate-cysteine ligase and GSH synthetase (ATP-dependent) activities. Whereas in kidney degradation is catalyzed extracellularly by activity of the proximal tubule brush border membrane localized integral membrane proteins, γ-glutamyltransferase (cleaves γ-glutamyl peptide bond between L-glutamyl L-cysteinyl) and dipeptidase (hydrolyzes L-cysteinyl-glycyl peptide bond).[115] Analysis of knockout animals indicates the contribution of PEPT2 reabsorption of gly-cys for renal synthesis of GSH.[116]

AMINOACIDURIAS

Aminoacidurias, which are characterized by the abnormal excretion of specific amino acids in the urine, can be caused by metabolic or transport defects. In contrast to metabolic diseases, in which one or more enzymes involved in the synthesis or catabolism of amino acids is defective, transport disorders result from deficient amino acid transport from the nephron lumen into the proximal tubule epithelial cells or from cells to the extracellular space. Transport diseases are caused by mutations in the genes encoding the membrane proteins responsible for the mostly active transport of amino acids. Clinical consequences of specific aminoacidurias can arise from either a deficiency of particular amino acid(s) (urinary loss), or the precipitation of certain amino acid(s) (e.g. cystine) in the urine. Amino acids deficiencies can also be caused by decreased absorption in the intestine, since many of these transporters are also expressed in the enterocytes of the small intestine and are responsible for substantial amino acid absorption.[117]

The association of a disease with an amino acid transport defect was first suggested a century ago.[118,119] Since then, several diseases due to transport defects have been described. Progress in diagnosing aminoacidurias was greatly facilitated by the advent of reliable and sensitive chromatography methods.[120,121] The molecular characterization of the amino acid transporters has also contributed greatly to advances in genetic diagnoses.[18,55,29] For the purpose of this review the specific aminoacidurias identified so far (see Table 71.3) are classified by the chemical properties of the amino acids abnormally excreted (i.e., neutral, basic (cationic), acidic (anionic), or iminoaciduria).

Basic Aminoacidurias

Cystinuria (OMIM #220100)

Mutations in either interacting subunit gene *SLC3A1* (rBAT) or neutral and basic amino acid transporter encoding gene *SLC7A9* ($b^{0,+}AT$) cause cystinuria.[35,122] Cystinuria, due to mutations in *SLC3A1* (chromosomal locus 2p21), is an autosomal recessive trait with heterozygous parents unaffected. In contrast, mutations in *SLC7A9* (chromosomal locus 19q13.11) lead to a mild to moderately abnormal urinary amino acid pattern in most obligate heterozygotes (e.g., parents) and thus

TABLE 71.3 Aminoacidurias Genetically Elucidated in Human

Aminoaciduria	Gene	Protein	Chromosome	Hallmark (Elevation of Individual AA in Urine)
Cystinuria A	*SLC3A1*	rBAT	2p21	Cystine, Lysine, Arginine, Ornithine
Cystinuria B	*SLC7A9*	$b^{0,+}AT$	19q13.11	Cystine, Lysine, Arginine, Ornithine
Lysinuric protein intolerance	*SLC7A7*	y^+LAT1	14q11.2	Lysine, Arginine, Ornithine
Hartnup disorder	*SLC6A19*	B^0AT1	5p15.33	Neutral amino acids
				Proline
Iminoglycinuria*	*SLC36A2*	PAT2	5q33.1	Hydroxyproline
				Glycine
Dicarboxylic aminoaciduria	*SLC1A1*	EAAT3/EAAC1	9p24	Aspartate
				Glutamate

**Pending independent confirmation.*
According to HUGO (www.genenames.org) and NCBI build 36.

can be seen as an autosomal dominant trait. The initial nomenclature, based on the excretion status of obligate heterozygotes (cystinuria types I, II (non-I), III (non-I)), has been "replaced" by a more meaningful system linked to the genotype.[123] Mutations in *SLC3A1* cause cystinuria type A, mutations in *SLC7A9* cause cystinuria type B, and mutations in both genes ("compound" heterozygotes) cause cystinuria type AB. Disease severity is apparently the same for cystinuria types A and B. The average prevalence is 1 in 7000 births, and to date 133 mutations in *SLC3A1* and 95 mutations in *SLC7A9* have been identified. Reported mutations include nonsense, missense, splicing, frameshift, and large sequence rearrangements.[124]

CLINICAL FINDINGS

Patients with cystinuria often present with nephro- or urolithiasis at almost any age with a clear preference in childhood due to elevated urinary cystine. Kidney stones are radio opaque, although less than calcium containing ones, and easily diagnosed by ultrasound examinations. Stones in the bladder are also often found. The presence of bladderstones in childhood should always prompt consideration of cystinuria. Early diagnosis is important since it allows for the prevention or reduction of kidney stones. Diagnostically, urinary levels of dibasic amino acids L-lysine, L-arginine, and L-ornithine, and most prominently of cystine are elevated (e.g., cystine can be up to 50-times normal). Plasma levels of these amino acids in general are at the lower end of the normal range. Clinical problems arise only from the elevated urinary cystine, which due its low solubility, precipitates within the urinary tract forming cystine stones. Urine microscopy reveals characteristic and pathognomonic hexagonal crystals. The cyanide-nitroprusside urinary test is also used, but is not considered specific.

TREATMENT

Treatment is non-specific and consists mostly of a high fluid intake to keep the urinary cystine below the solubility threshold of about 1000 μmol/l (at pH <7). As cystine solubility increases with pH, alkalization of urine, typically with potassium citrate, can be used. Chelation with D-penicillamine or mercaptopropionylglycine, while highly effective, is rarely used due to serious side effects. Overall, treatment is cumbersome and some patients lose kidney function at some time due to recurrent nephro- and urolithiasis.

Lysinuric Protein Intolerance (OMIM #222700)

Lysinuric protein intolerance (LPI) is caused by mutations in *SLC7A7*, which similar to cystinuria, is a member of the heterodimeric amino acid transporter family (HAT). The mutations causing this autosomal recessive disorder have, in contrast to cystinuria, been identified exclusively in the light subunit *SLC7A7* (chromosomal locus 14q11.2).[125,126] *SLC7A7-SLC3A2* mediates the transport of dibasic amino acids from intracellular to basolateral compartments. The incidence of LPI is very low, but in some populations reaches up to 1:50,000 births. Currently, a total of 50 different LPI causative mutations of *SLC7A7* have been described.[127] Most of the LPI-causative mutations consist of missense, nonsense or small deletions, whereas larger deletions, insertions, or splice-site mutations are less frequent.

CLINICAL FINDINGS

Patients affected by this disorder in general come to medical attention early in life with several significant problems including a failure to thrive and intellectual impairment. Episodes of diarrhea and hyperammonemia coincide with increased protein intake (hence the name). Ammonia typically rises quickly postprandially and may normalize within hours. This makes documentation of hyperammonemia difficult due to timing of blood draw, if not suspected. Apparently, hyperammonemia is caused by an interruption of the urea cycle due to a lack of required intermediates (e.g., ornithine). Patients unfortunately also develop interstitial pneumonia in the form of an alveolar proteinosis, hepatomegaly and liver cirrhosis, severe osteopenia and bone marrow involvement. Renal insufficiency can develop due to glomerulonephritis of suspected immunological etiology. Phenotypic variability and the lack of a specific clinical presentation have caused misdiagnosis variously as disorders of urea cycle, lysosomal storage diseases such as Niemann-Pick type B and Gaucher disease, celiac disease, or autoimmune disorders.[128] Episodes of diarrhea following protein intake can point towards the correct diagnosis.

Elevations of urinary dibasic amino acids, L-lysine, L-arginine, and L-ornithine are diagnostic and more pronounced than in cystinuria; urinary cystine levels in contrast to cystinuria are almost normal (elevated only 2−3 times the norm). In contrast to cystinuria, plasma levels of L-lysine, L-arginine, and L-ornithine tend to be below the norm. Orotic acid and homocitrulline are also elevated and can be of diagnostic value for discrimination from urea cycle defects.

The significance of the clinical picture in LPI can be explained by a more severe loss and reduced intestinal absorption of dibasic amino acids, in comparison to cystinuria, leading to an inefficient urea cycle resulting in hyperammonemia. Obviously, a defect in the basolateral export of dibasic amino acids (as in LPI) has more severe consequences than a defect in the luminal membrane (as in cystinuria). This is attributed to the fact that a large fraction of the nutritional amino acids,

including dibasic amino acids, are (re)absorbed as di- and tripeptides that are then hydrolyzed intracellularly before being transported out of the cell through the basolateral membrane. Some of the unique immunological features of this disease are probably related to the expression profile of *SLC7A7* (y^+LAT1), which is much broader than that of *SLC3A1*/*SLC7A9* (rBAT/$b^{0,+}$AT).[129]

TREATMENT

Treatment is symptomatic and consists of protein restriction, as for other urea cycle disorders, and in this case in supplementation with citrulline. Citrulline is a precursor for both arginine and ornithine, thus can partially restore the defective functions of the urea cycle.

Neutral Aminoacidurias

Hartnup Disorder (OMIM #234500)

Cloning of the human *SLC6A19* gene (chromosomal locus 5p15.33) led to the identification of a deleterious splice site mutation in members of the British Hartnup family, in which the disorder was originally described.[130] Hartnup disorder is an autosomal-recessive disorder with an incidence of 1 to 15,000 live births. In addition to the original Hartnup mutation, 21 further deletions, missense, nonsense and splice site mutations in the *SLC6A19* gene causing the disorder have been identified.[32–133] Mutations in genes encoding the renal and intestinal B^0AT1 accessory proteins, Tmem27 (*tmem27*) and Ace2 (*ace2*) respectively, are not responsible for the disorder. Both tmem27 and ace2 genes are located in the X chromosome, and so far no patients with an X-linked neutral aminoaciduria have been observed.

CLINICAL FINDINGS

First recognized in the 1950s in London/UK as a defect of neutral amino acid transport, Hartnup disorder became an example of how diet can unveil the signs and symptoms of a multifaceted disease. The protein-restricted diet imposed on the population (World War II, and post-war) revealed the defective (re)absorption of amino acids characteristic of Hartnup disorder. The symptoms are variable and patients can present with the pellagra-like signs (including light-sensitive dermatitis), intermittent cerebellar ataxia and psychosis-like symptoms. The variability of the symptoms might be due to the high frequency of compound heterozygosity, and/or to the differential interactions of specific mutations with intestinal and renal accessory proteins, and/or dietary habits.

Diagnostically, elevated urinary neutral amino acids are the first indication of the disorder and are observed in all Hartnup patients. L-glutamine, alanine, tryptophan, tyrosine, serine and the branched chain amino acids can reach values five to ten fold higher than reference. Proline and glycine excretion are not increased. Plasma amino acids levels are usually in the normal range.

The neutral aminoaciduria resulting from Hartnup disorder must be differentiated from a generalized aminoaciduria, which is an obligate diagnostic hallmark of a renal Fanconi syndrome. The most common cause of renal Fanconi syndrome in childhood is cystinosis, a treatable lysosomal storage disorder.

TREATMENT

Currently patients from "protein supersaturated" countries are often recognized only by newborn screening programs, as they are asymptomatic. The question remains whether these patients should or need to be treated. Patients with pellagra-like symptoms are treated with niacin oral replacement, which reverses the clinical features of the disorder. Pellagra and the neurological symptoms are thought to be caused by deficiency of tryptophan, since this is a precursor of niacin and serotonin.

Iminoacidurias

Iminoglycinuria (OMIM #242600)

Mutations in multiple genes have been suggested to be the cause of iminoglycinuria. Identified by sequencing of candidate genes, encoding glycine and imino acid transporters, namely *SLC36A2* (PAT2), *SLC6A20* (SIT1), *SLC6A19* (B^0AT1), and *SLC6A18* (B^0AT3) in patients with glycinuria and iminoglycinuria, a complex combination of mutations and polymorphisms was found and suggested to cause the disorder.[59] However, this hypothesis is controversial. *SLC6A18* (B^0AT3) and *SLC6A19* (B^0AT1) have a broad substrate spectrum. Therefore genetic defects should cause a general neutral aminoaciduria and not solely the abnormal excretion of proline and/or glycine.[32,43,52] The imino transporter SIT1 encoded by the gene *SLC6A20* located at chromosomal locus 3p21.31 is another candidate. However, preliminary genetic studies found no linkage with the region encoding *SLC6A20* (SIT1) (chromosomal locus 3p21.31) and disease,[134] whereas when tested in an exogenous expression system SIT1 mutations (found in iminoglycinuria patients) did decrease transport activity.

Mutations in genes encoding the glycine and L-proline transporters, PAT1 (*SLC36A1*) and 2 (*SLC36A2*), are additional disease candidates. The *SLC36A2* (PAT2) gene seems to be the best candidate while analysis of the *SLC36A1* (PAT1) chromosome

locus (5q33.1) failed to uncover a linkage with the disorder.[134] The incidence of iminoglycinuria is 1:10,000 births.

CLINICAL FINDINGS

Patients with present with elevated urinary levels of glycine, proline, and hydroxyproline. Interestingly, obligate heterozygotes may also display glycinuria.

Patients diagnosed by newborn screening programs should be subsequently confirmed, since iminoglycinuria can occur in normal neonates, presumably reflecting tubular immaturity. Several reports have linked iminoglycinuria with other diseases. However this finding may have been biased due to ascertainment errors resulting from the specific populations screened (e.g., mental health institutions). As for other aminoacidurias, the fractional excretion of all respective amino acids should be analyzed to exclude urinary losses due to elevated plasma levels. Such as occurs in the metabolic disorder hyperprolinemia, in which, due to significantly elevated plasma proline levels, urine findings can mimic iminoglycinuria by exceeding urinary reabsorption capacity.

TREATMENT

At the present time, iminoglycinuria is considered an incidental finding and no treatment is necessary. Whether constant urinary glycine, proline, and hydroxyproline losses have an impact on health is not known.

Acidic Aminoaciduria

Dicarboxylic Aminoaciduria (OMIM 222730)

Dicarboxylic aminoaciduria is an autosomal recessive disorder with an incidence of 1:35,000 births, as estimated from a 25-year screening program in Quebec, Canada.[135] The cause of dicarboxylic aminoaciduria was identified as mutations in the *SLC1A1* gene (chromosomal locus 9p24) encoding the glutamate and aspartate transporter EAAC1/EAAT3.[136–138] In two pedigrees missense and deletion mutations were identified in homozygotes.

CLINICAL FINDINGS

A few patients with an excess urinary excretion of acidic amino acids, i.e., aspartate and glutamate, otherwise lacking clinical symptoms, have been reported.[139,140] The patients with the identified *SLC1A1* mutations presented high urinary glutamate and aspartate and one of them also displayed symptoms of an obsessive compulsive disorder.

PERSPECTIVES

Following the molecular identification of most amino acid transporters, current research aims at understanding their role in mediating and controlling the flux of amino acids between different body compartments, in particular as regards amino acid homeostasis in the extracellular space (milieu intérieur) and their role for the function of organs and cells. A step forward in this direction requires that kinetic, regulatory and expression data of transporters be integrated in the understanding of physiological regulatory networks controlling body and cellular amino acid metabolism. Such integrated analysis of the physiological networks will be necessary to understand the contribution of kidney proximal tubule transport and metabolic functions to body amino acid homeostasis in health and disease. This integrated view shall lead towards a better understanding of the complex pathophysiology and symptoms of genetic diseases such as lysinuric protein intolerance (LPI) and of acquired diseases.

Acknowledgments

The laboratory of F. Verrey is supported by the Swiss National Foundation grant 31-130471.

References

[1] Sorensen SS, Lauridsen IN, Thomsen K, Pedersen EB. Effect of two regimens of intravenous amino acid infusion on renal haemodynamics, renal tubular function and sodium and water homeostatic hormones in healthy humans. Nephrol Dial Transplant 1991;6:410–9.

[2] Tietze IN, Sorensen SS, Eiskjaer H, Thomsen K, Pedersen EB. Tubular handling of amino acids after intravenous infusion of amino acids in healthy humans. Nephrol Dial Transplant 1992;7:493–500.

[3] Castellino P, Coda B, DeFronzo RA. Effect of amino acid infusion on renal hemodynamics in humans. Am J Physiol 1986;251: F132–40.

[4] Premen AJ. Potential mechanisms mediating postprandial renal hyperemia and hyperfiltration. FASEB J 1988;2:131–7.

[5] Sallstrom J, Carlstrom M, Olerud J, et al. High-protein-induced glomerular hyperfiltration is independent of the tubuloglomerular feedback mechanism and nitric oxide synthases. Am J Physiol Regul Integr Comp Physiol 2010;299:R1263–8.

[6] Brown JL, Samiy AH, Pitts RF. Localization of amino-nitrogen reabsorption in the nephron of the dog. Am J Physiol 1961;200: 370–2.

[7] Eisenbach GM, Weise M, Stolte H. Amino acid reabsorption in the rat nephron. Free flow micropuncture study. Pflugers Arch 1975;357:63–76.

[8] Silbernagl S. Tubular reabsorption of L-glutamine studied by free-flow micropuncture and microperfusion of rat kidney. Int J Biochem 1980;12:9–16.

[9] Silbernagl S, Deetjen P. Molecular specificity of the L-arginine reabsorption mechanism. Microperfusion studies in the proximal tubule of rat kidney. Pflugers Arch 1973;340:325–34.

[10] Silbernagl S. Renal transport of amino acids. Klin Wochenschr 1979;57:1009–19.
[11] Bergeron M, Vadeboncoeur M. Microinjections of L-leucine into tubules and peritubular capillaries of the rat. II. The maleic acid model. Nephron 1971;8:367–74.
[12] Gunther R, Silbernagl S, Deetjen P. Maleic acid induced aminoaciduria, studied by free flow micropuncture and continuous microperfusion. Pflugers Arch 1979;382:109–14.
[13] Silbernagl S, Volker K, Dantzler WH. Cationic amino acid fluxes beyond the proximal convoluted tubule of rat kidney. Pflugers Arch 1994;429:210–5.
[14] Silbernagl S. Renal handling of amino acids and oligopeptides. Contrib Nephrol 1981;24:18–29.
[15] Christensen HN. Role of amino acid transport and countertransport in nutrition and metabolism. Physiol Rev 1990;70: 43–77.
[16] Murer H, Evers J, Kinne R. Polarity of proximal tubular epithelial cells in relation to transepithelial transport. Curr Probl Clin Biochem 1976;6:173–89.
[17] Stevens BR, Ross HJ, Wright EM. Multiple transport pathways for neutral amino acids in rabbit jejunal brush border vesicles. J Membr Biol 1982;66:213–25.
[18] Broer S. Amino acid transport across mammalian intestinal and renal epithelia. Physiol Rev 2008;88:249–86.
[19] Hediger MA, Romero MF, Peng JB, Rolfs A, Takanaga H, Bruford EA. The ABCs of solute carriers: physiological, pathological and therapeutic implications of human membrane transport proteins Introduction. Pflugers Arch 2004;447: 465–8.
[20] Kanai Y, Hediger MA. Primary structure and functional characterization of a high-affinity glutamate transporter. Nature 1992;360:467–71.
[21] Palacin M, Estevez R, Bertran J, Zorzano A. Molecular biology of mammalian plasma membrane amino acid transporters. Physiol Rev 1998;78:969–1054.
[22] Verrey F, Jack DL, Paulsen IT, Saier Jr MH, Pfeiffer R. New glycoprotein-associated amino acid transporters. J Membr Biol 1999;172:181–92.
[23] Franca R, Veljkovic E, Walter S, Wagner CA, Verrey F. Heterodimeric amino acid transporter glycoprotein domains determining functional subunit association. Biochem J 2005;388: 435–43.
[24] Jiang J, Amara SG. New views of glutamate transporter structure and function: advances and challenges. Neuropharmacology 2011;60:172–81.
[25] Rudnick G. Serotonin transporters—structure and function. J Membr Biol 2006;213:101–10.
[26] Newstead S, Drew D, Cameron AD, et al. Crystal structure of a prokaryotic homologue of the mammalian oligopeptide-proton symporters, PepT1 and PepT2. EMBO J 2011;30: 417–26.
[27] Yamashita A, Singh SK, Kawate T, Jin Y, Gouaux E. Crystal structure of a bacterial homologue of Na^+/Cl^--dependent neurotransmitter transporters. Nature 2005;437:215–23.
[28] Yernool D, Boudker O, Jin Y, Gouaux E. Structure of a glutamate transporter homologue from Pyrococcus horikoshii. Nature 2004;431:811–8.
[29] Verrey F, Singer D, Ramadan T, Vuille-dit-Bille RN, Mariotta L, Camargo SM. Kidney amino acid transport. Pflugers Arch 2009;458:53–60.
[30] Bohmer C, Broer A, Munzinger M, et al. Characterization of mouse amino acid transporter B0AT1 (slc6a19). Biochem J 2005;389:745–51.
[31] Camargo SM, Makrides V, Virkki LV, Forster IC, Verrey F. Steady-state kinetic characterization of the mouse B0AT1 sodium-dependent neutral amino acid transporter. Pflugers Arch 2005;451:338–48.
[32] Camargo SM, Singer D, Makrides V, et al. Tissue-specific amino acid transporter partners ACE2 and collectrin differentially interact with hartnup mutations. Gastroenterology 2009;136: 872–82.
[33] Bertran J, Werner A, Moore ML, et al. Expression cloning of a cDNA from rabbit kidney cortex that induces a single transport system for cystine and dibasic and neutral amino acids. Proc Natl Acad Sci USA 1992;89:5601–5.
[34] Chillaron J, Estevez R, Mora C, et al. Obligatory amino acid exchange via systems b0 + -like and y^+L-like. A tertiary active transport mechanism for renal reabsorption of cystine and dibasic amino acids. J Biol Chem 1996;271:17761–70.
[35] Feliubadalo L, Font M, Purroy J, et al. Non-type I cystinuria caused by mutations in SLC7A9, encoding a subunit (b^0, + AT) of rBAT. Nat Genet 1999;23:52–7.
[36] Kowalczuk S, Broer A, Munzinger M, Tietze N, Klingel K, Broer S. Molecular cloning of the mouse IMINO system: an Na^+- and Cl^--dependent proline transporter. Biochem J 2005; 386:417–22.
[37] Ristic Z, Camargo SM, Romeo E, et al. Neutral amino acid transport mediated by ortholog of imino acid transporter SIT1/SLC6A20 in opossum kidney cells. Am J Physiol Renal Physiol 2006;290:F880–7.
[38] Takanaga H, Mackenzie B, Suzuki Y, Hediger MA. Identification of mammalian proline transporter SIT1 (SLC6A20) with characteristics of classical system imino. J Biol Chem 2005;280:8974–84.
[39] Boll M, Foltz M, Rubio-Aliaga I, Kottra G, Daniel H. Functional characterization of two novel mammalian electrogenic proton-dependent amino acid cotransporters. J Biol Chem 2002;277: 22966–73.
[40] Kennedy DJ, Gatfield KM, Winpenny JP, Ganapathy V, Thwaites DT. Substrate specificity and functional characterisation of the H^+/amino acid transporter rat PAT2 (Slc36a2). Br J Pharmacol 2005;144:28–41.
[41] Daniel H, Rubio-Aliaga I. An update on renal peptide transporters. Am J Physiol Renal Physiol 2003;284:F885–92.
[42] Romeo E, Dave MH, Bacic D, et al. Luminal kidney and intestine SLC6 amino acid transporters of B0AT-cluster and their tissue distribution in Mus musculus. Am J Physiol Renal Physiol 2006;290:F376–83.
[43] Singer D, Camargo SM, Huggel K, et al. Orphan transporter SLC6A18 is renal neutral amino acid transporter B0AT3. J Biol Chem 2009;284:19953–60.
[44] Vanslambrouck JM, Broer A, Thavyogarajah T, et al. Renal imino acid and glycine transport system ontogeny and involvement in developmental iminoglycinuria. Biochem J 2010;428: 397–407.
[45] Wright EM. Renal Na^+-glucose cotransporters. Am J Physiol Renal Physiol 2001;280:F10–8.
[46] Filho JC, Bergstrom J, Stehle P, Furst P. Simultaneous measurements of free amino acid patterns of plasma, muscle and erythrocytes in healthy human subjects. Clin Nutr 1997;16: 299–305.
[47] Meier C, Ristic Z, Klauser S, Verrey F. Activation of system L heterodimeric amino acid exchangers by intracellular substrates. EMBO J 2002;21:580–9.
[48] Bauch C, Forster N, Loffing-Cueni D, Summa V, Verrey F. Functional cooperation of epithelial heteromeric amino acid transporters expressed in madin-darby canine kidney cells. J Biol Chem 2003;278:1316–22.
[49] Ramadan T, Camargo SM, Herzog B, Bordin M, Pos KM, Verrey F. Recycling of aromatic amino acids via TAT1 allows efflux of

neutral amino acids via LAT2-4F2hc exchanger. Pflugers Arch 2007;454:507–16.
[50] Broer A, Klingel K, Kowalczuk S, Rasko JE, Cavanaugh J, Broer S. Molecular cloning of mouse amino acid transport system B0, a neutral amino acid transporter related to Hartnup disorder. J Biol Chem 2004;279:24467–76.
[51] Kowalczuk S, Broer A, Tietze N, Vanslambrouck JM, Rasko JE, Broer S. A protein complex in the brush-border membrane explains a Hartnup disorder allele. Faseb J 2008;22:2880–7.
[52] Danilczyk U, Sarao R, Remy C, et al. Essential role for collectrin in renal amino acid transport. Nature 2006;444:1088–91.
[53] Kleta R, Gahl WA. Collecting evidence: the case of collectrin (Tmem27) and amino acid transport. Am J Physiol Renal Physiol 2007;292:F531–2.
[54] Malakauskas SM, Quan H, Fields TA, et al. Aminoaciduria and altered renal expression of luminal amino acid transporters in mice lacking novel gene collectrin. Am J Physiol Renal Physiol 2007;292:F533–44.
[55] Broer S, Palacin M. The role of amino acid transporters in inherited and acquired diseases. Biochem J 2011;436:193–211.
[56] Parks LD, Barfuss DW. Transepithelial transport and metabolism of glycine in S1, S2, and S3 cell types of the rabbit proximal tubule. Am J Physiol Renal Physiol 2002;283:F1208–15.
[57] Quan H, Athirakul K, Wetsel WC, et al. Hypertension and impaired glycine handling in mice lacking the orphan transporter XT2. Mol Cell Biol 2004;24:4166–73.
[58] Eslami B, Kinboshi M, Inoue S, Harada K, Inoue K, Koizumi A. A nonsense polymorphism (Y319X) of the solute carrier family 6 member 18 (SLC6A18) gene is not associated with hypertension and blood pressure in Japanese. Tohoku J Exp Med 2006;208:25–31.
[59] Broer S, Bailey CG, Kowalczuk S, et al. Iminoglycinuria and hyperglycinuria are discrete human phenotypes resulting from complex mutations in proline and glycine transporters. J Clin Invest 2008;118:3881–92.
[60] Palacin M, Nunes V, Font-Llitjos M, et al. The genetics of heteromeric amino acid transporters. Physiol (Bethesda) 2005;20:112–24.
[61] Nakamura E, Sato M, Yang H, et al. 4F2 (CD98) heavy chain is associated covalently with an amino acid transporter and controls intracellular trafficking and membrane topology of 4F2 heterodimer. J Biol Chem 1999;274:3009–16.
[62] Pfeiffer R, Loffing J, Rossier G, et al. Luminal heterodimeric amino acid transporter defective in cystinuria. Mol Biol Cell 1999;10:4135–47.
[63] Dave MH, Schulz N, Zecevic M, Wagner CA, Verrey F. Expression of heteromeric amino acid transporters along the murine intestine. J Physiol 2004;558:597–610.
[64] Bauch C, Verrey F. Apical heterodimeric cystine and cationic amino acid transporter expressed in MDCK cells. Am J Physiol Renal Physiol 2002;283:F181–9.
[65] Reig N, Chillaron J, Bartoccioni P, et al. The light subunit of system b(0,+) is fully functional in the absence of the heavy subunit. Embo J 2002;21:4906–14.
[66] Feliubadalo L, Arbones ML, Manas S, et al. Slc7a9-deficient mice develop cystinuria non-I and cystine urolithiasis. Hum Mol Genet 2003;12:2097–108.
[67] Font-Llitjos M, Feliubadalo L, Espino M, et al. Slc7a9 knockout mouse is a good cystinuria model for antilithiasic pharmacological studies. Am J Physiol Renal Physiol 2007;293:F732–40.
[68] Peters T, Thaete C, Wolf S, et al. A mouse model for cystinuria type I. Hum Mol Genet 2003;12:2109–20.
[69] Shayakul C, Kanai Y, Lee WS, Brown D, Rothstein JD, Hediger MA. Localization of the high-affinity glutamate transporter EAAC1 in rat kidney. Am J Physiol 1997;273:F1023–9.
[70] Butchbach ME, Lai L, Lin CL. Molecular cloning, gene structure, expression profile and functional characterization of the mouse glutamate transporter (EAAT3) interacting protein GTRAP3-18. Gene 2002;292:81–90.
[71] Ruggiero AM, Liu Y, Vidensky S, et al. The endoplasmic reticulum exit of glutamate transporter is regulated by the inducible mammalian Yip6b/GTRAP3-18 protein. J Biol Chem 2008;283:6175–83.
[72] Peghini P, Janzen J, Stoffel W. Glutamate transporter EAAC-1-deficient mice develop dicarboxylic aminoaciduria and behavioral abnormalities but no neurodegeneration. EMBO J 1997;16:3822–32.
[73] Hu Y, Smith DE, Ma K, Jappar D, Thomas W, Hillgren KM. Targeted disruption of peptide transporter Pept1 gene in mice significantly reduces dipeptide absorption in intestine. Mol Pharm 2008;5:1122–30.
[74] Ocheltree SM, Shen H, Hu Y, Keep RF, Smith DE. Role and relevance of peptide transporter 2 (PEPT2) in the kidney and choroid plexus: in vivo studies with glycylsarcosine in wild-type and PEPT2 knockout mice. J Pharmacol Exp Ther 2005;315:240–7.
[75] Shen H, Ocheltree SM, Hu Y, Keep RF, Smith DE. Impact of genetic knockout of PEPT2 on cefadroxil pharmacokinetics, renal tubular reabsorption, and brain penetration in mice. Drug Metab Dispos 2007;35:1209–16.
[76] Nishimura M, Naito S. Tissue-specific mRNA expression profiles of human ATP-binding cassette and solute carrier transporter superfamilies. Drug Metab Pharmacokinet 2005;20:452–77.
[77] Rossier G, Meier C, Bauch C, et al. LAT2, a new basolateral 4F2hc/CD98-associated amino acid transporter of kidney and intestine. J Biol Chem 1999;274:34948–54.
[78] Braun D, Wirth EK, Wohlgemuth F, et al. Aminoaciduria, but normal thyroid hormone levels and signaling, in mice lacking the amino acid and thyroid hormone transporter Slc7a8. Biochem J 2011;439:249–55.
[79] Kim DK, Kanai Y, Chairoungdua A, Matsuo H, Cha SH, Endou H. Expression cloning of a Na+-independent aromatic amino acid transporter with structural similarity to H+/monocarboxylate transporters. J Biol Chem 2001;276:17221–8.
[80] Ramadan T, Camargo SM, Summa V, et al. Basolateral aromatic amino acid transporter TAT1 (Slc16a10) functions as an efflux pathway. J Cell Physiol 2006;206:771–9.
[81] Bodoy S, Martin L, Zorzano A, Palacin M, Estevez R, Bertran J. Identification of LAT4, a novel amino acid transporter with system L activity. J Biol Chem 2005;280:12002–11.
[82] Mackenzie B, Erickson JD. Sodium-coupled neutral amino acid (System N/A) transporters of the SLC38 gene family. Pflugers Arch 2004;447:784–95.
[83] Moret C, Dave MH, Schulz N, Jiang JX, Verrey F, Wagner CA. Regulation of renal amino acid transporters during metabolic acidosis. Am J Physiol Renal Physiol 2007;292:F555–66.
[84] Fei YJ, Sugawara M, Nakanishi T, et al. Primary structure, genomic organization, and functional and electrogenic characteristics of human system N 1, a Na+- and H+-coupled glutamine transporter. J Biol Chem 2000;275:23707–17.
[85] Broer A, Albers A, Setiawan I, et al. Regulation of the glutamine transporter SN1 by extracellular pH and intracellular sodium ions. J Physiol 2002;539:3–14.
[86] Ruderisch N, Virgintino D, Makrides V, Verrey F. Differential axial localization along the mouse brain vascular tree of luminal sodium-dependent glutamine transporters Snat1 and Snat3. J Cereb Blood Flow Metab 2011;31:1637–47.

[87] Pfeiffer R, Rossier G, Spindler B, Meier C, Kuhn L, Verrey F. Amino acid transport of y + L-type by heterodimers of 4F2hc/CD98 and members of the glycoprotein-associated amino acid transporter family. Embo J 1999;18:49–57.

[88] Torrents D, Estevez R, Pineda M, et al. Identification and characterization of a membrane protein (y + L amino acid transporter-1) that associates with 4F2hc to encode the amino acid transport activity y + L. A candidate gene for lysinuric protein intolerance. J Biol Chem 1998;273:32437–45.

[89] Kleemola M, Toivonen M, Mykkanen J, Simell O, Huoponen K, Heiskanen KM. Heterodimerization of y(+)LAT-1 and 4F2hc visualized by acceptor photobleaching FRET microscopy. Biochim Biophys Acta 2007;1768:2345–54.

[90] Sperandeo MP, Annunziata P, Bozzato A, et al. Slc7a7 disruption causes fetal growth retardation by downregulating Igf1 in the mouse model of lysinuric protein intolerance. Am J Physiol Cell Physiol, All Economy Clthes Shops 2007;293:C191–8.

[91] Matsuo H, Kanai Y, Kim JY, et al. Identification of a novel Na + -independent acidic amino acid transporter with structural similarity to the member of a heterodimeric amino acid transporter family associated with unknown heavy chains. J Biol Chem 2002;277:21017–26.

[92] Fukasawa Y, Segawa H, Kim JY, et al. Identification and characterization of a Na(+)-independent neutral amino acid transporter that associates with the 4F2 heavy chain and exhibits substrate selectivity for small neutral D- and L-amino acids. J Biol Chem 2000;275:9690–8.

[93] Rutter AR, Fradley RL, Garrett EM, et al. Evidence from gene knockout studies implicates Asc-1 as the primary transporter mediating d-serine reuptake in the mouse CNS. Eur J Neurosci 2007;25:1757–66.

[94] Xie X, Dumas T, Tang L, et al. Lack of the alanine-serine-cysteine transporter 1 causes tremors, seizures, and early postnatal death in mice. Brain Res 2005;1052:212–21.

[95] Chairoungdua A, Kanai Y, Matsuo H, Inatomi J, Kim DK, Endou H. Identification and characterization of a novel member of the heterodimeric amino acid transporter family presumed to be associated with an unknown heavy chain. J Biol Chem 2001;276:49390–9.

[96] Ramamoorthy S, Kulanthaivel P, Leibach FH, Mahesh VB, Ganapathy V. Solubilization and functional reconstitution of the human placental taurine transporter. Biochim Biophys Acta 1993;1145:250–6.

[97] Bitoun M, Levillain O, Tappaz M. Gene expression of the taurine transporter and taurine biosynthetic enzymes in rat kidney after antidiuresis and salt loading. Pflugers Arch 2001;442:87–95.

[98] Yu MJ, Pisitkun T, Wang G, Shen RF, Knepper MA. LC-MS/MS analysis of apical and basolateral plasma membranes of rat renal collecting duct cells. Mol Cell Proteomics 2006;5:2131–45.

[99] van de Poll MC, Soeters PB, Deutz NE, Fearon KC, Dejong CH. Renal metabolism of amino acids: its role in interorgan amino acid exchange. Am J Clin Nutr 2004;79:185–97.

[100] Garibotto G, Sofia A, Robaudo C, et al. Kidney protein dynamics and ammoniagenesis in humans with chronic metabolic acidosis. J Am Soc Nephrol 2004;15:1606–15.

[101] Garibotto G, Sofia A, Saffioti S, Bonanni A, Mannucci I, Verzola D. Amino acid and protein metabolism in the human kidney and in patients with chronic kidney disease. Clin Nutr 2010;29:424–33.

[102] Ottonello L, Gnerre P, Bertolotto M, et al. Leptin as a uremic toxin interferes with neutrophil chemotaxis. J Am Soc Nephrol 2004;15:2366–72.

[103] Nowik M, Lecca MR, Velic A, Rehrauer H, Brandli AW, Wagner CA. Genome-wide gene expression profiling reveals renal genes regulated during metabolic acidosis. Physiol Genomics 2008;32:322–34.

[104] Busque SM, Wagner CA. Potassium restriction, high protein intake, and metabolic acidosis increase expression of the glutamine transporter SNAT3 (Slc38a3) in mouse kidney. Am J Physiol Renal Physiol 2009;297:F440–50.

[105] Treberg JR, Clow KA, Greene KA, Brosnan ME, Brosnan JT. Systemic activation of glutamate dehydrogenase increases renal ammoniagenesis: implications for the hyperinsulinism/hyperammonemia syndrome. Am J Physiol Endocrinol Metab 2010;298:E1219–25.

[106] Wagner CA. Metabolic acidosis: new insights from mouse models. Curr Opin Nephrol Hypertens 2007;16:471–6.

[107] Brosnan ME, Brosnan JT. Renal arginine metabolism. J Nutr 2004;134:2791S–5S discussion 2796S-2797S.

[108] Gropper SSS, Jack L, Groff James L. Advanced nutrition and human metabolism. 5th ed. Belmont: Wadsworth Pub Co; 2009.

[109] Mitsuoka K, Shirasaka Y, Fukushi A, et al. Transport characteristics of L-citrulline in renal apical membrane of proximal tubular cells. Biopharm Drug Dispos 2009;30:126–37.

[110] Nakakariya M, Shima Y, Shirasaka Y, Mitsuoka K, Nakanishi T, Tamai I. Organic anion transporter OAT1 is involved in renal handling of citrulline. Am J Physiol Renal Physiol 2009;297:F71–9.

[111] Levillain O. Expression and function of arginine-producing and consuming-enzymes in the kidney. Amino Acids 2011.

[112] Moller N, Meek S, Bigelow M, Andrews J, Nair KS. The kidney is an important site for in vivo phenylalanine-to-tyrosine conversion in adult humans: A metabolic role of the kidney. Proc Natl Acad Sci U S A 2000;97:1242–6.

[113] Adibi SA. Renal assimilation of oligopeptides: physiological mechanisms and metabolic importance. Am J Physiol 1997;272:E723–36.

[114] Tessari P, Garibotto G, Inchiostro S, et al. Kidney, splanchnic, and leg protein turnover in humans. Insight from leucine and phenylalanine kinetics. J Clin Invest 1996;98:1481–92.

[115] Lash LH. Renal glutathione transport: Identification of carriers, physiological functions, and controversies. Biofactors 2009;35:500–8.

[116] Frey IM, Rubio-Aliaga I, Siewert A, et al. Profiling at mRNA, protein, and metabolite levels reveals alterations in renal amino acid handling and glutathione metabolism in kidney tissue of Pept2$^{-/-}$ mice. Physiol Genomics 2007;28:301–10.

[117] Scriver CR, Mahon B, Levy HL, et al. The Hartnup phenotype: Mendelian transport disorder, multifactorial disease. Am J Hum Genet 1987;40:401–12.

[118] Garrod AE. The Croonian lectures on inborn errors of metabolism. Lectures III. Lancet 1908;172:124–48.

[119] Garrod AE. The Croonian lectures on inborn errors of metabolism. Lectures IV. Lancet 1908;172:214–20.

[120] Dent CE. A study of the behaviour of some sixty amino-acids and other ninhydrin-reacting substances on phenol-collidine filter-paper chromatograms, with notes as to the occurrence of some of them in biological fluids. Biochem J 1948;43:169–80.

[121] Spackman DH, Stein WH, Moore S. Automatic recording apparatus for use in the chromatography of amino acids. Anal Chem 1958;30:1190–206.

[122] Calonge MJ, Gasparini P, Chillaron J, et al. Cystinuria caused by mutations in rBAT, a gene involved in the transport of cystine. Nat Genet 1994;6:420–5.

[123] Dello Strologo L, Pras E, Pontesilli C, et al. Comparison between SLC3A1 and SLC7A9 cystinuria patients and carriers:

a need for a new classification. J Am Soc Nephrol 2002;13: 2547–53.
[124] Chillaron J, Font-Llitjos M, Fort J, et al. Pathophysiology and treatment of cystinuria. Nat Rev Nephrol 2010;6:424–34.
[125] Borsani G, Bassi MT, Sperandeo MP, et al. SLC7A7, encoding a putative permease-related protein, is mutated in patients with lysinuric protein intolerance. Nat Genet 1999;21:297–301.
[126] Torrents D, Mykkanen J, Pineda M, et al. Identification of SLC7A7, encoding y + LAT-1, as the lysinuric protein intolerance gene. Nat Genet 1999;21:293–6.
[127] Sebastio G, Sperandeo MP, Andria G. Lysinuric protein intolerance: reviewing concepts on a multisystem disease. Am J Med Genet C Semin Med Genet 2011;157:54–62.
[128] Sperandeo MP, Andria G, Sebastio G. Lysinuric protein intolerance: update and extended mutation analysis of the SLC7A7 gene. Hum Mutat 2008;29:14–21.
[129] Broer S. Lysinuric protein intolerance: one gene, many problems. Am J Physiol Cell Physiol 2007;293:C540–541.
[130] Kleta R, Romeo E, Ristic Z, et al. Mutations in SLC6A19, encoding B^0AT1, cause Hartnup disorder. Nat Genet 2004;36:999–1002.
[131] Cheon CK, Lee BH, Ko JM, Kim HJ, Yoo HW. Novel mutation in SLC6A19 causing late-onset seizures in Hartnup disorder. *Pediatr Neurol* 42:369–371.
[132] Seow HF, Broer S, Broer A, et al. Hartnup disorder is caused by mutations in the gene encoding the neutral amino acid transporter SLC6A19. Nat Genet 2004;36:1003–7.
[133] Zheng Y, Zhou C, Huang Y, Bu D, Zhu X, Jiang W. A novel missense mutation in the SLC6A19 gene in a Chinese family with Hartnup disorder. Int J Dermatol 2009;48:388–92.
[134] Kleta R, Tinloy B, Aydin HI, et al. Iminoglycinuria. Unexpected molecular findings. J Am Soc Nephrol 2006;17: 819A (Abstract)
[135] Auray-Blais C, Cyr D, Drouin R. Quebec neonatal mass urinary screening programme: from micromolecules to macromolecules. J Inherit Metab Dis 2007;30:515–21.
[136] Bailey CG, Ryan RM, Thoeng AD, et al. Loss-of-function mutations in the glutamate transporter SLC1A1 cause human dicarboxylic aminoaciduria. J Clin Invest 2011;121: 446–53.
[137] Kanai Y, Hediger MA. The glutamate/neutral amino acid transporter family SLC1: molecular, physiological and pharmacological aspects. Pflugers Arch 2004;447:469–79.
[138] Smith CP, Weremowicz S, Kanai Y, Stelzner M, Morton CC, Hediger MA. Assignment of the gene coding for the human high-affinity glutamate transporter EAAC1 to 9p24: potential role in dicarboxylic aminoaciduria and neurodegenerative disorders. Genomics 1994;20:335–6.
[139] Melancon SB, Dallaire L, Lemieux B, Robitaille P, Potier M. Dicarboxylic aminoaciduria: an inborn error of amino acid conservation. J Pediatr 1977;91:422–7.
[140] Swarna M, Rao DN, Reddy PP. Dicarboxylic aminoaciduria associated with mental retardation. Hum Genet 1989;82: 299–300.

This page intentionally left blank

CHAPTER

72

Organic Anion and Cation Transporters in Renal Elimination of Drugs

Gerhard Burckhardt[1] *and Hermann Koepsell*[2]

[1]Center of Physiology and Pathophysiology, University Medicine Gottingen, Göttingen, Germany

[2]Institute of Anatomy and Cell Biology and Institute of Molecular Plant Physiology and Biophysics, University of Wurzburg, Würzburg, Germany

INTRODUCTION

The kidneys efficiently excrete endogenous and exogenous organic anions and cations, including widely used drugs and potentially toxic compounds. At pH 7.4, organic anions carry one or more negative charges, and organic cations one or more positive charges, respectively. Many exogenous organic anions and cations undergo secretion in renal proximal tubules, involving uptake across the basolateral membrane into tubule cells and release across the apical (lumenal, brush-border) membrane into the lumen. For organic anions, uptake from the blood takes place against an opposing inside negative membrane potential whereas, for organic cations, the inside negative electrical potential difference has to be overcome during their release into the lumen. Thus, secretion requires the input of cellular energy. In this chapter, we shall focus on proximal tubular organic anion and organic cation transporters being involved in drug secretion.

ORGANIC ANION TRANSPORT SYSTEMS

Characteristics of Organic Anion Secretion in Proximal Tubules

Initial experiments revealed proximal tubules as the principle site of organic anion secretion in various species (for earlier literature see[1,2]). In most of these studies, *p*-aminohippurate (PAH) served as a model organic anion, and the substrate specificity of the so-called PAH transport system in the basolateral membrane was extensively tested by stop-flow competition experiments with rat kidneys *in situ*. This system preferred amphiphilic compounds carrying one negative charge or two negative charges separated 6–7 Å by a hydrophobic moiety and being able to form multiple hydrogen bridges.[3] The "PAH transport system" turned out to interact with a multitude of chemically unrelated molecules including many drugs.

PAH uptake across the basolateral membrane occurred by an exchange against intracellular α-ketoglutarate.[4,5] Thereby, PAH uptake is a tertiary active process, with the Na^+,K^+-ATPase establishing the extracellular-to-intracellular Na^+ gradient (primary active process), the sodium-dicarboxylate cotransporter utilizing this Na^+ gradient for intracellular α-ketoglutarate enrichment (secondary active process), and the PAH/α-ketoglutarate exchanger using the intracellular-to-extracellular α-ketoglutarate gradient for PAH uptake against the inside negative membrane potential (tertiary active process; see also Figure 72.1). In addition, α-ketoglutarate absorbed from the primary urine or derived from metabolism can drive PAH uptake.[6] The arrangement of three co-operating transporters is conserved among species including man. As opposed, earlier experiments on

Seldin and Giebisch's The Kidney, Fifth Edition.
DOI: http://dx.doi.org/10.1016/B978-0-12-381462-3.00072-0

© 2013 Elsevier Inc. All rights reserved.

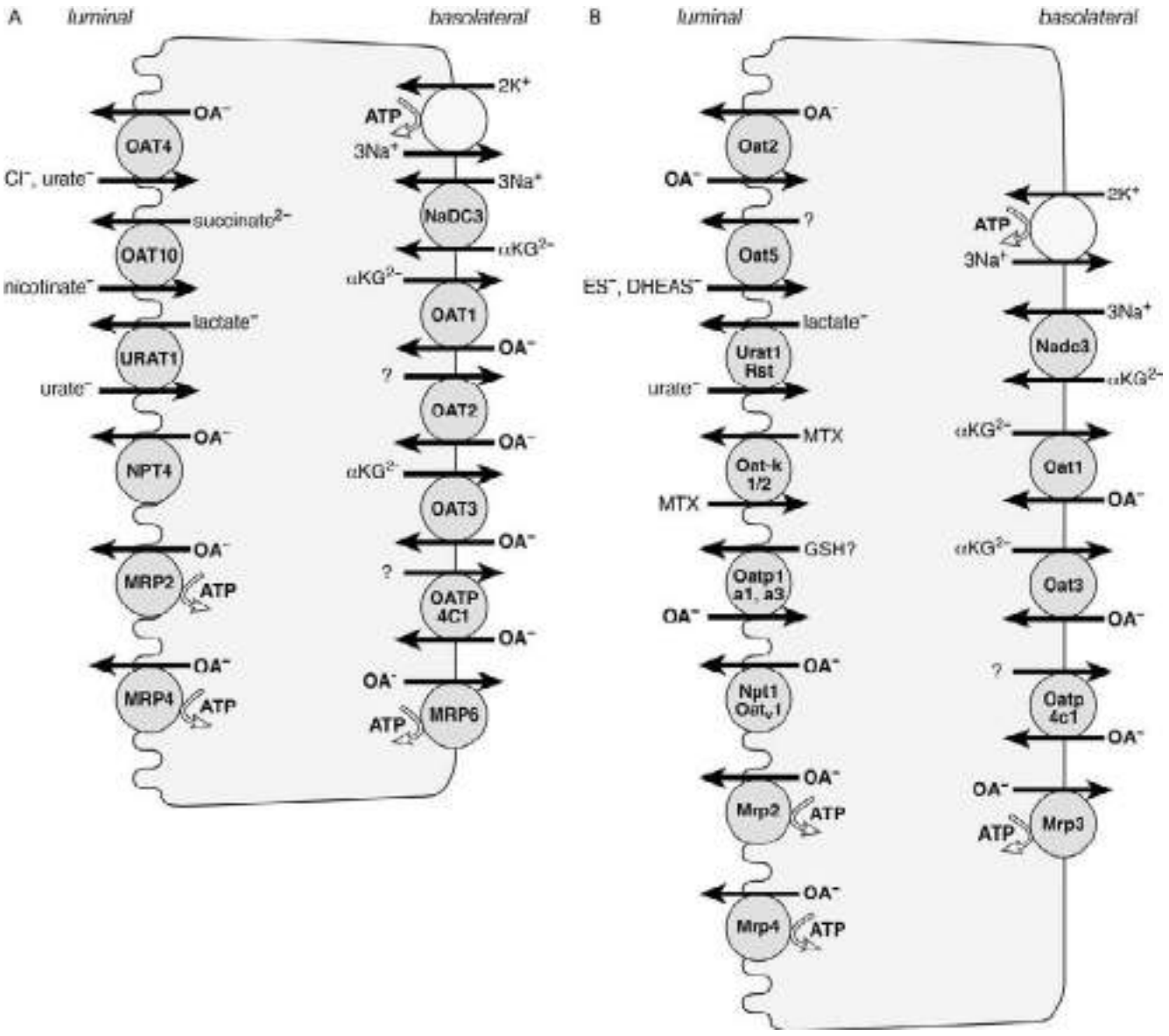

FIGURE 72.1 Organic anion transporters in human (A) and rat (B) renal proximal tubule cells. Lumen (urine) side is left, interstitial (blood) side is right. Transporters are symbolized by circles. Abbreviations: αKG^{2-}, α-ketoglutarate; $DHEAS^-$, dihydroepiandrosterone sulfate; ES^-, estrone-3-sulfate; GSH, glutathione; MTX, methotrexate; OA^-, organic anion.

PAH release across the apical membrane revealed species differences.[1]

With the advent of molecular cloning and heterologous expression techniques, several proximal tubular transporters for organic anions have been characterized. Figure 72.1A shows transporters that are involved in the secretion of anionic drugs and toxins, or are targets of drugs, in the human proximal tubule. These include OAT1, OAT2, OAT3, OATP4C1, and MRP6 in the basolateral cell membrane, and OAT4, OAT10, URAT1, NPT4, MRP2, and MRP4 in the apical membrane. In rodent proximal tubules, Oat1, Oat3, Oatp4c1, and Mrp3 were found in the basolateral membrane, and Oat2, Oat5, Urat1, Oat-K1/2, Oatp1a1, Npt1/Oat_v1, Mrp2, and Mrp4 in the apical membrane (Figure 72.1B). Thereby, both cell sides contain antiporters (OATs/Oats, URAT1/Urat1, OATP4C1/Oatp4c1), ATP-driven systems (MRPs/Mrps) and a voltage-driven system (NPTs/Npts). Taken together, the picture of organic anion transport became more complicated than it was anticipated from earlier *in vivo* and *in vitro* functional studies.

DRUG TRANSPORTERS IN THE BASOLATERAL MEMBRANE OF PROXIMAL TUBULE CELLS

The Organic Anion Transporter 1 (OAT1/Oat1; *SLC22A6/Slc22a6*)

The Organic Anion Transporter 1 (humans, OAT1; other species, Oat1) was cloned from man, monkey, pig (p), rabbit (rb), rat (r), and mouse (m).[7–9] OAT1/Oat1 is the member A6/a6 of family *SLC22/Slc22*, that consist of at least 25 different genes.[10] The gene coding for OAT1 was located to chromosome 11q12.3 paired with that of OAT3.[10,11] OAT1 mRNA is expressed in kidneys, and to a small extent also in brain and other tissues.[12–14] In rats, mRNA expression rose from day 10 after birth and reached a maximum in adult animals[15] whereas, in mice, Oat1 mRNA did not rise before day 25 after birth.[16] Importantly, gender differences were observed in adult rats and mice with higher Oat1 mRNA expression in male animals.[15,16]

Immunohistochemical studies localized OAT1/Oat1 protein to the basolateral membrane of proximal tubules of human, monkey, rat and mouse kidneys.[7–9] In humans, OAT1 was found along the complete proximal tubule whereas rOat1 was highest in the S2 segment. Immunohistochemistry in adult rats revealed more Oat1 protein in male than in female animals.[17,18] Whether gender differences are present in humans is not known (for reviews on gender differences see[8,18]).

The expression of human OAT1 was under positive control of hepatocyte nuclear factors 1α (HNF-1α) and 4α (HNF-4α).[8] An increased expression of rOat1 was found after treatment of kidney slices or proximal tubules with insulin and epidermal growth factor as well as after bile duct ligation in rats whereas, in several other circumstances such as fever, endotoxinemia, renal insufficiency, ischemia-reperfusion, and ureter obstruction, the abundance of rOat1 was—at least transiently—decreased (reviewed in[8,9]). A down-regulation of Oat1 expression most probably decreases the renal excretion of anionic drugs. In this regard, it is interesting that inhibition of COX-2 attenuated the endotoxin-induced down-regulation of rOat1.[19]

Short-term down-regulation involves a protein kinase C (PKC) activity-dependent endocytosis of OAT protein.[20] Thereby, the protein itself is not phosphorylated,[21] but possibly ancillary proteins such as caveolin 2.[22] The appearance of immunoreactive rOat1 in vesicles beneath the basolateral membrane after mercury treatment of rats suggests that endocytosis of Oat1 may occur also *in vivo*.[23]

Several non-synonymous single nucleotide polymorphisms have been described for human OAT1 (summarized in[9,24]). Except for the amino acid change R50H which led to changes in the K_m for adefovir, cidofovir and tenofovir, other amino acid exchanges did not result in altered transport function, at least for the tested substrates.

Following heterologous expression, OAT1/Oat1 proved to be a *p*-aminohippurate (PAH)/α-ketoglutarate antiporter with *in vitro* affinities for PAH between 5 and 50 μM (range, 3.1 to 430 μM[8,25]). A prototypical, though not OAT1-specific inhibitor is probenecid with K_i or IC_{50} values between 1.4 and 18.6 μM.[8,25] Numerous compounds were tested as possible substrates of OAT1/Oat1 either by checking their inhibition of the uptake of labeled PAH (or other labeled or fluorescent substrates), or by direct demonstration of transport of labeled test compounds (results compiled in[7,8,25]). Among endogenous substrates of OAT1/Oat1 are, e.g., medium-chain fatty acids, α-ketoglutarate, cAMP and cGMP, prostaglandins E_2 and $F_{2\alpha}$, urate, and acidic neurotransmitter metabolites. Drugs interacting with OAT1/Oat1 included β-lactam antibiotics, antiviral drugs, non-steroidal anti-inflammatory drugs, diuretics, ACE inhibitors, angiontensin II receptor 1-antagonists, and methotrexate. Furthermore, OAT1/Oat1 interacted with uremic toxins, environmental toxins, and carcinogens. Thus, OAT1/Oat1 covers a wide substrate spectrum, is involved in renal drug handling, and contributes to nephrotoxicity. The interaction of several compounds with the same transporter, OAT1/Oat1, can lead to drug-drug interaction during renal excretion, alter pharmacokinetics and cause potentially serious side effects (for examples see[26,27]).

For mouse Oat1, a quantitative structure-activity relationship was determined.[28] For mono-anions, interaction with mOat1 increased (or K_i decreased) with increasing mass and hydrophobicity, e.g., with the chain length of fatty acids. For di-anions, steric and electrostatic factors became the main determinants of affinity. For transport velocity, other factors seemed important because no correlation was found between V_{max} and K_m or K_i.[28] In general, QSAR on mOat1 was in agreement with earlier data obtained for PAH transport in rat kidney *in situ*.[3] Mutational studies on OAT1/Oat1 were performed to find out residues important for transport function: amino acid residues surrounding the putative substrate binding site of human OAT1 include R466 (transmembrane helix TMH11), K382 (TMH8), Y353, Y354 (both in TMH7), and F374 (TMH8) (summarized in[9]). R466 is also important for the interaction of OAT1 with chloride that increases the V_{max} of the transporter, but has no effect on its affinity towards PAH.[29]

An Oat1 knockout mouse was generated which did not show any gross abnormalities.[30] The clearance of PAH, furosemide, bendroflumethiazide, and a number

of endogenous hydroxyl-substituted short chain fatty acids was decreased.[30,31] Thus, mOat1 contributes to the renal excretion of diuretics and of hitherto unknown endogenous metabolites.

The Organic Anion Transporter 2 (OAT2/Oat2; *SLC22A7/Slc22a7*)

OAT2/Oat2 was cloned from man, rat, and mouse.[7–9] The gene for human OAT2 is located on chromosome 6p21.1.[10] In humans and male rats, the expression of OAT2/Oat2 mRNA was high in liver and low in kidneys. In female rats, Oat2 expression in kidneys exceeded its expression in liver.[13,14] In male mice, message for Oat2 was expressed in kidneys, but hardly in liver whereas, in female mice, message was found both in liver and kidneys. Immunolocalization studies revealed human OAT2 at the basolateral membrane of proximal tubule cells.[32] In rat and mouse kidneys, Oat2 appeared to be present in the apical membrane of proximal tubule cells and exhibited a higher expression in female animals.[33] Thus there are gender and species differences in Oat2 expression.

In liver and kidneys, OAT2/Oat2 expression was under positive control of HNF-1α and HNF-4α.[34,35] In diabetic rats and in cisplatin-treated mice, a decreased renal Oat2 expression was found.[36,37] As regards single nucleotide polymorphisms, three non-synonymous SNPs were reported the functional consequence of which is unknown (see[9]).

Due to conflicting results in the literature,[7,8,25] it is unclear whether OAT2/Oat2 interacts with and is driven by dicarboxylates. High affinities of human and rat OAT2/Oat2 were reported for prostaglandin E_2 and prostaglandin $F_{2\alpha}$. Other endogenous substrates of OAT2 are nucleobases, nucleosides and nucleotides such as adenine, adenosine, GMP, GDP, GTP, cGMP, and cAMP.[38] Urate was transported by OAT2 with an apparent K_m of 1.17 mM, suggesting that OAT2 contributes to proximal tubular urate secretion.[39] Among drugs, some diuretics (hydrochlorothiazide, furosemide), pravastatin, sartanes (losartan and telmisartan), cephalosporins, erythromycin, histamine receptor-2 blockers, NSAIDs, and uricosurics (probenecid, benzbromarone) interacted with OAT2. High affinities were reported for antineoplastic drugs (methotrexate, fluorouracil, taxol).[7,8]

In humans, the basolateral localization of OAT2 would favour a role in organic anion (urate) and drug excretion whereas, in rodents, the apical location of Oat2 is hard to reconcile with secretion. Thus, more information is needed to fully appreciate the function of OAT2/Oat2.

THE ORGANIC ANION TRANSPORTER 3 (OAT3/Oat3; *SLC22A8/Slc22a8*)

As reviewed in,[7–9] OAT3/Oat3 was cloned from man, monkey, pig, rabbit, rat, and mouse. The gene SLC22A8 is located on chromosome 11q12.3, in direct neighbourhood to the gene of OAT1.[10,11] In all species, the mRNA for OAT3/Oat3 was highest in the kidneys; additional expression was found in brain, liver, skeletal muscle, and adrenals.[12–14] The mRNA levels increased shortly after birth and reached the same levels in mature male and female rats.[15] Based on quantitative mRNA analysis, the expression of OAT3 was threefold higher than that of OAT1, and more than tenfold higher than the expression levels of OAT2 and OAT4.[40] The mRNA levels corresponded to protein expression as tested by Western blotting, indicating that OAT3 is the most abundant OAT isoform in the human kidney.[40]

In immunohistochemistry, OAT3/Oat3 was found at the basolateral membrane of proximal tubules as well as in thick ascending limbs of Henle's loops, connecting tubules and collecting ducts; gender differences were only apparent for rOat3 in proximal tubules with lower expression in female rats (reviewed in[7–9,18]). OAT3/Oat3 was also found in human, rat, and mouse choroid plexus. At this location, OAT3/Oat3 is likely involved in the uptake of organic anions including neurotransmitter metabolites and drugs from the cerebrospinal fluid and their transport into the blood. Indeed, Oat3 knockout mice showed an impaired cerebrospinal fluid-to-blood transport of fluorescent organic anions.[41]

Hepatocyte nuclear factors HNF-1α and HNF-1β induced OAT3 expression and HNF-1α knockouts showed a diminished renal expression of Oat3 (reviewed in[8]). Inhibition of promoter methylation also increased OAT3 expression. As summarized in,[8] OAT3/Oat3 expression is subject to regulation by various factors. Insulin, epidermal growth factor and short term exposure to prostaglandin E_2 increased whereas long term PGE_2 elevation as observed in fever and inflammatory states decreased rOat3. Intracellular cAMP served to increase the OAT3 promoter activity. Several kidney disorders such as ischemia-reperfusion, ureteral obstruction as well as methotrexate and cisplatin treatment decreased rOat3 abundance. Biliary obstruction and 5/6 nephrectomy increased rOat3 protein expression (see[8]).

The existence of several single nucleotide polymorphisms in the promoter and the coding region of human OAT3 have been described (compiled in[9]), including 9 non-synonymous mutations, leading to changes in the amino acid sequence or premature truncation. Three loss-of-function mutations (R149S,

Q239X, I260R) were found in Asian-Americans.[42] The impact of these mutations is unknown.

A widely used test substrate for heterologously expressed OAT3/Oat3 is estrone-3-sulfate with half-maximal transport rates (K_t or K_m) between 2.2 and 21.2 μM.[8] PAH was translocated by OAT3/Oat3, but the affinity was smaller than that of OAT1/Oat1. OAT3/Oat3 is driven by the outwardly directed concentration gradient of α-ketoglutarate. Thus, OAT3/Oat3 is involved in uptake of organic anions from the blood, which fits to its location at the basolateral membrane.

Numerous compounds have been tested as putative substrates of OAT3/Oat3 (results compiled in[7,8,25]). An interaction was demonstrated for endogenous substances such as the second messengers cAMP, cGMP; the vitamin folate; the bile salts cholate and taurocholate; the (sulfated) hormones cortisol, dehydroepiandrosterone sulfate, estrone sulfate; the local hormones prostaglandin E_2 and $F_{2\alpha}$; the purine metabolite urate; and some neurotransmitter metabolites. Highly interesting is the observation that Oat3 knockout mice have a decreased blood pressure.[43] Obviously, intact mOat3 excretes one or more endogenous substances that lower blood pressure. Thymidine could play such a role, because knockout mice had an increased thymidine concentration in blood, and thymidine infusion lowered blood pressure.[43]

Drugs interacting with OAT3/Oat3 comprised ACE inhibitors, angiotensin II receptor blockers, diuretics, statins, antibiotics, antineoplastics, immune suppressants, histamine receptor 2 blockers, and non-steroidal anti-inflammatory drugs.[7,8,25] As compared to OAT1, OAT3/Oat3 has higher affinities for urate, benzylpenicillin, and loop diuretics, suggesting a dominant role in proximal tubular secretion of these compounds. Indeed, Oat3 knockout mice showed a decreased renal excretion of diuretics, benzylpenicillin, quinolones and methotrexate.[31,44]

Chimeras between rat Oat3 and Oat1 revealed that substrate recognition is located in transmembrane helices TMH 6-12, i.e. in the C-terminal part of rOat3. Replacement of the positively charged arginine 454 that is conserved in all OATs, by the acidic amino acid aspartate (R454D) abolished PAH uptake, but did not change the handling of cimetidine.[45] The mutant lysine-370 to alanine (K370A) also was unable to translocate PAH, but still transported cimetidine, indicating that cimetidine interacts with amino acid residues different from those involved in binding and translocation of PAH, and that translocation of PAH requires the presence of cationic amino acid residues in TMH 8 and 11.[45] Aromatic residues in TMH 7 (W334, F335, Y341) and F362 in TMH 8 were found to be important for the translocation of PAH and cimetidine, but not for the transport of estrone sulfate.[46] Whether rOat3 has, as suggested, three parallel transportation paths, one for PAH, one for cimetidine, and one for estrone sulfate, must be clarified in future experiments.

In summary, OAT3/Oat3 has a wider distribution than OAT1/Oat1 along the nephron, operates as an organic anion/α-ketoglutarate exchanger, and handles small and, unlike OAT1/Oat1, also larger and more hydrophobic substrates.

The Organic Anion Transporting Polypeptide 4C1 (OATP4C1/Oatp4c1; *SLCO4C1/Slco4c1*)

OATP4C1 was cloned from human and rat kidneys and in both species, OATP4C1/Oatp4c1 proteins were found in the basolateral membrane of proximal tubule cells.[47] The gene for human OATP4C1 was located on chromosome 5q21.2. In humans, the expression was found in kidneys, liver, and weakly in lungs.[12,13,47] In rats, predominant expression was found in the kidneys and a weaker one in the lungs.[47] Gender differences were not apparent. Thus, OATP4C1 can be regarded as a kidney-specific OATP. Functional tests revealed the transport of the endogenous compounds cAMP, triiodothyronine, thyroxine, but not of cGMP, taurocholate, prostaglandin E_2, estradiol-17β-D-glucuronide, and PAH. Among drugs, digoxin, ouabain, and methotrexate were taken up by OATP4C1.[47,48] It was assumed that the physiological role of OATP4C1/Oatp4c1 is to present thyroid hormones to proximal tubule cells. The extent to which this transporter contributes to the proximal tubular secretion of drugs remains to be determined.

The Multidrug Resistance-Associated Protein 6 (MRP6/Mrp6; *ABCC6/Abcc6*)

MRP6/Mrp6 is a member of the ATP binding cassette (ABC) proteins[49] that is mainly expressed in liver and kidneys.[12,13,26] The murine homologue, mMrp6, showed highest expression in the liver, but was also found in other organs including the skin.[12,49] Within human and mouse kidneys, MRP6/Mrp6 was localized to the basolateral membrane of proximal tubule cells (see[26]). This ATP-driven transporter handled glutathione-conjugates, the endothelin receptor antagonist BQ-123, and conferred low level resistance to epipodophyllotoxins and anthracyclines; probenecid and indomethacin inhibited MRP6.[26,49] Mutations in the second nucleotide binding domain were associated with the connective tissue disease, *Pseudoxanthoma elasticum*, but the exact causal relationship between MRP6 and this disorder is unknown. Given the localization in the basolateral membrane of proximal tubule cells and

the function of an ATP-driven efflux transporter it is unlikely that MRP6 contributes to organic anion secretion.

MRP1 (ABCC1) was found in the basolateral membrane of Henle's loops and collecting ducts, and MRP3 (ABCC3) in distal tubules.[26] In rats, Mrp3 was localized also to the basolateral membrane of proximal tubules. Also these transporters are not likely involved in organic anion secretion but may protect renal tubule cells from cytotoxic compounds.[26]

DRUG TRANSPORTERS IN THE APICAL MEMBRANE OF PROXIMAL TUBULE CELLS

The Organic Anion Transporter 4 (OAT4, *SLC22A11*)

This transporter (reviewed in[7–9]) occurs only in humans. The gene for OAT4 is located on chromosome 11q13, in close neighbourhood to that of URAT1.[10,11] OAT4 expression was highest in the kidneys, lower in placenta, and virtually absent from all other tested organs.[12,14] Immunohistochemical studies revealed the presence of OAT4 in the proximal tubules only where it is located at the apical membrane. Thereby, OAT4 interacts with the scaffolding proteins PDZK1 and NHERF1 through its three C-terminal amino acids.[7] Factors influencing the expression of OAT4 are presently unknown.

Mutational analysis revealed that evolutionary conserved glycine residues at positions 241 and 400 (transmembrane helices 5 and 8, respectively) are functionally important. Replacement of these residues by long aliphatic amino acids abolished transport activity, whereas the glycine-to-alanine mutation (G241A, G400A) reduced transport rates and decreased affinities were observed.[50] Glycine is thought to participate in helix-helix interactions that seem to be important for transport activity of OAT4.

Eight non-synonymous single nucleotide polymorphisms were found, one of which (R48X) is deleterious (reviewed in[9]). The impact of the other amino acid changes on the function of OAT4 is unknown.

Following heterologous expression (for results see[7,8,25]), OAT4 transported estrone-3-sulfate with high affinity (K_t of 1 μM). Other endogenous compounds translocated by OAT4 were urate, the prostaglandins E_2 and $F_{2\alpha}$, and dehydroepiandrosterone sulfate; no inhibition was found with glucuronidated steroids, suggesting that OAT4 only handles sulfated compounds. Cholate, taurocholate, octanoate, and corticosterone inhibited OAT4. Intracellular glutarate *trans*-stimulated estrone-3-sulfate uptake, but did not *cis*-inhibit it when present in the extracellular medium, suggesting different affinities for this dicarboxylate at the inner and outer binding sites.[51] Similar findings for PAH indicate that the internal binding site has a higher affinity to this organic anion than the external binding site. Labeled PAH was not taken up by OAT4, but its efflux was accelerated by estrone-3-sulfate in the medium. It was concluded that OAT may work asymmetrically, taking up estrone-3-sulfate or urate in exchange for intracellular (α-keto)glutarate ("influx mode"). Intracellular organic anions such as PAH are effluxed through OAT4, probably in exchange for external chloride ("efflux mode").[51]

As reviewed in,[7,8,25] OAT4 interacted with β-lactam antibiotics, angiotensin II receptor-1 blockers, methotrexate, diuretics, NSAIDs, and was inhibited by probenecid. The secretion of diuretics such as torasemide can lead to an increased reabsorption of urate due to diuretic/urate antiport at OAT4, explaining the observation that therapy with diuretics can cause hyperuricemia.[52] NPT4 is yet another site for an interaction between diuretics and urate (see later).

Taking together, OAT4 in the apical membrane of proximal tubule cells can contribute to the absorption of estrone sulfate and urate from the primary urine, and to the secretion of anionic drugs. Since OAT4 is not present in rodents it is not possible to learn more about its function from knockout animals.

The Organic Anion Transporter 5 (Oat5, *Slc22a19*)

Oat5 was cloned from rat and mouse in which it was restricted to the kidney and was equally expressed in male and female animals.[53,54] There is no human homologue to Slc22a19.[10] The Oat5 protein was localized to the apical membrane in the late proximal tubule segments. The interaction of Oat5 with dicarboxylates is not yet settled, because conflicting results were reported on the ability of succinate to *trans*-stimulate uptake of estrone-3-sulfate. Endogenous substrates were dehydroepiandrosterone sulfate and estradiol sulfate, but not prostaglandins and urate. A few drugs were tested: furosemide, benzylpenicillin, diclofenac, and ibuprofen inhibited Oat5.[53,54] As long as the driving force for Oat5 is not defined it is not possible to speculate on the role of this transporter in drug secretion or absorption.

The Organic Anion Transporter 10 (OAT10/Oat10; *SLC22A13/Slc22a13*)

OAT10 (previously cloned as orphan transporter ORCTL3) is predominantly expressed in human

kidneys and weakly in brain, heart and colon.[55] The gene is located on chromosome 3p22.2.[10] Western blots showed the rOat10 protein in the apical, but not in the basolateral membrane, and female animals showed a stronger expression of rOat10 than did males.[55] Endogenous substrates of OAT10 were nicotinate, lactate, urate, succinate, and glutathione. Succinate served as counter anion for nicotinate and urate uptake from the lumen. Among the few drugs tested, furosemide, hydrochlorothiazide, sulfinpyrazone, and cyclosporine A inhibited OAT10.[55] It needs to be established whether OAT10 is involved in cyclosporine A-induced nephropathy. The physiological role of OAT10 is probably the uptake of the vitamin nicotinate in small intestine and renal proximal tubule cells.

The Urate Anion Transporter 1 (URAT1/Urat1/Rst; *SLC22A12/Slc22a12*)

URAT1/Urat1/Rst was cloned from human and mouse kidneys (for reviews see[7–9]). The gene for human URAT1 is located on chromosome 11q13.1 adjacent to that of OAT4.[10,11] The highest though not exclusive expression was found in kidneys.[12,14] Human and mouse URAT1/Urat1 were immunolocalized to the apical membrane of proximal tubule cells where they interact with the scaffolding protein PDZK1. Male mice showed a higher expression than female animals, indicating sex differences at least in this species.[18]

Hepatocyte nuclear factor-1α and -1β induced the expression of human and mouse URAT1/Urat1 promoter, and mUrat1 expression was diminished in a HNF-1α knockout mouse. Furthermore, the mUrat1 promoter was found to be hypomethylated, suggesting a tissue-specific epigenetic control (reviewed in[9]).

URAT1 mutations have been linked to familial hypouricemia.[56] Most of the hypouricemic patients in Japan and Korea carry a truncation mutation, W258X. Meanwhile, several more amino acid exchanges have been described (see[9] for a compilation). Some mutations occur also with hyperuricemia and gout, but the molecular mechanism is unknown.[57]

URAT1 expressed in oocytes displayed saturable uptake of urate.[56] Extracellular chloride inhibited, and intracellular chloride *trans*-stimulated urate uptake, indicating that URAT1 can operate as urate/chloride exchanger. Preloading of oocytes with lactate *trans*-stimulated urate uptake, indicating urate/lactate exchange as another transport mode of URAT1.[56] The endogenous compounds L- and D-lactate, acetoacetate, β-hdyroxybutyrate, succinate (but not α-ketoglutarate), and orotate inhibited urate uptake. Exogenous compounds inhibiting URAT1 were the uricosuric drugs probenecid, benzbromarone, losartan; the antiuricosuric drugs pyrazine carboxylate and pyrazine dicarboxylate; the loop diuretics furosemide and bumetanide; the NSAIDs phenylbutazone, salicylate and indomethacin; and the vitamin nicotinate.[56] PAH and estrone sulfate did not affect URAT1.

Also mouse Urat1/Rst transported urate (K_m 1.2 mM) and performed urate/chloride, urate/lactate and urate/pyrazinoate exchange.[58] Uptake of labeled urate was inhibited, when the uricosurics probenecid and benzbromarone, the uremic toxins indoxyl sulfate, indole acetate, hippurate, and a number of acidic neurotransmitter metabolites were present in the medium.[59]

In summary, URAT1/Urat1 is involved in urate absorption from the primary urine. Thereby, urate uptake is driven by exchange against lactate that is transported into the cells by a sodium-lactate symporter in the apical membrane, as has been convincingly demonstrated in a c/ebpδ knockout mouse.[60] This mouse does not express the sodium-coupled lactate transporters Slc5a8 and Slc5a12 in the apical membrane of proximal tubules and excretes lactate and—at unchanged Urat1 expression—urate with the urine. In man, uricosurics inhibit URAT1, and loss-of-function mutations cause an increased urate clearance and a reduction in serum level of urate.

The Voltage-Sensitive Organic Anion Transporter 1 (Oat_v1/Npt1; *Slc17a1*)

Searching for the voltage-driven transporter for PAH and urate in urate-secreting species (rabbits, pigs), Oat_v1 was identified by expression cloning from pig kidneys.[61] The message for $pOat_v1$ was restricted to liver and kidneys. $pOat_v1$ is not a member of the SLC22 family, but showed highest identity to human and rodent NPT1/Npt1 (*SLC17A1*/*Slc17a1*), previously cloned as sodium-dependent phosphate transporters from human, rabbit, and mouse kidneys and located to the apical membrane of the proximal tubule segments S1–S3 (for review see[62]). The human gene for NPT1 was found on chromosome 6p21.3-p23.[62] The expression of mNpt1 was under control of heptatocyte nuclear factor-1α, and HNF-1α knockout mice had greatly diminished proximal tubular Npt1 expression.[63,64] Fasting decreased and streptozotocin-induced diabetes increased renal and hepatic expression of NaPi-1/Npt1 in rats, respectively.[65] Whether gender differences exist is not known.

Human NPT and mouse Npt1/NaPi-1 performed the uptake of radiolabeled organic anions including PAH, urate, estradiol-17β-D-glucuronide, benzylpenicillin, faropenem, and mevalonate.[66–69] Benzylpenicillin, ampicillin, cephalexin, cefazolin,

indomethacin, furosemide, benzoate, lactate, and probenecid inhibited uptake of labeled faropenem by mNpt1.[70] Uptake of labeled PAH by porcine Oat_v1 was inhibited by, e.g., estrone sulfate, penicillin G, salicylate, indomethacin, ibuprofen, diclofenac, furosemide, bumetanide, and probenecid.[61] Organic anion transport was independent of sodium, but was inhibited by increasing chloride concentrations as well as by DIDS and NPPB.[61,66,67,70]

It is likely that organic anion transport through NPT1/Npt1 is electrogenic. Busch et al. observed outward currents upon addition of benzylpenicillin, phenol red and probenecid in *Xenopus laevis* oocytes expressing rbNaPi-1 (Npt1[69]). PAH uptake (K_m 4.4 mM) by $pOat_v1$/pNpt1 was increased at inside positive membrane potentials.[61] More recently, mNpt1 was purified and inserted into proteoliposomes for functional characterization.[68] Both, sodium-dependent phosphate transport and sodium-independent PAH and urate transport were observed, indicating that at least mNpt1 is able to carry out both functions. The affinity of mNpt1 for urate and PAH was similar (K_m 1.1 mM) and uptake was accelerated by a proteoliposome-inside positive membrane potential. Chloride stimulated (whereas it inhibited in other studies) PAH uptake, but was not transported itself. Salicylate, aspirin and acetaminophen, but not other NSAIDs, inhibited PAH and urate transport; radiolabeled aspirin was translocated by reconstituted mNpt1.

The mutation of an arginine residue (R138A) conserved within the SLC17 family abolished transport.[68] A lowered V_{max} was found with the T269I mutation[68] that corresponds to a SNP in human NPT1 gene associated with gout.[71] Taken these data together it is likely that NPT1/Npt1/Oat_v1 is involved in the voltage-driven exit of organic anions including urate, PAH, β-lactam antibiotics, diuretics and some non-steroidal anti-inflammatory drugs.

The Sodium-Phosphate Transporter 4 (NPT4/Npt4; *SLC17A3/Slc17a3*)

Exploring the locus for hereditary hemochromatosis in humans, two genes closely related and juxtapositioned to *SLC17A1* were found on chromosome 6p21.3 and sequenced.[72] One of these genes, *SLC17A3*, was expressed only in liver and kidneys and the gene product was named NPT4. In mice deficient in HNF-1α, the expression of Npt4 in kidneys was reduced, indicating that, like Npt1 (see previous chapter), Npt4 is under control of this hepatic nuclear transcription factor.[63] Npt4 was also isolated from rat kidneys where it was immunolocalized to the apical membrane of proximal tubule cells of the segments S2 and S3; segment S1 following directly the glomerulus did not show any labelling.[73] Human NPT4 was also localized to the apical membrane of proximal tubule cells.[74]

When human NPT4 was expressed in COS cells, a perinuclear localisation was found; the authors speculated that NPT4 is involved in the release of phosphate from the endoplasmic reticulum, and loss of its function should give rise to the glycogen storage disease type 1c.[75] Indeed, a patient with this disease showed a non-synonymous SNP, resulting in a Gly201Arg mutation.[75] The functional consequences of this mutation were, however, not tested.

Single nucleotide polymorphisms of the human *SCL17A3* gene correlated with hyperuricemia.[76] The linkage was not as strong as with SNPs affecting the urate transporter GLUT9 and the breast cancer resistance protein ABCG2[76] and, in later studies, failed to reach statistical significance[77] or were associated with an increase in serum uric acid only in women.[78]

When rat Npt4 was expressed in *Xenopus laevis* oocytes it showed a sodium-dependent phosphate transport.[73] Expression of human NPT4 also in oocytes resulted in the uptake of labelled estrone-3-sulfate, estrone-17β-D-glucuronide, prostaglandin E_2, taurocholate, PAH, bumetanide, and ochratoxin A.[74] Uptake was stimulated by depolarization, and PAH and bumetanide application caused an outward current in voltage-clamped oocytes. PAH uptake was inhibited by the hormones DHEAS, β-estradiol sulfate, estriol, estrone-3-sulfate; the diuretics hydrochlorothiazide, chlorothiazide, trichlormethiazide, bumetanide, furosemide, spironolacton; the NSAIDs diclofenac, ibuprofen and indomethacin; and the common inhibitor probenecid. No interaction with NPT4 was seen for succinate, α-ketoglutarate, lactate, nicotinate, xanthine, and hypoxanthine.

Importantly, labelled urate was transported by NPT4.[74] In Japanese hyperuricemic patients, two mutations (N68H and F304S) were found in NPT4. Expression of these mutants in *Xenopus laevis* oocytes resulted in a decreased urate uptake as compared to oocytes expressing the wildtype NPT4.[74] Thus, it is likely that NPT4 constitutes the voltage-driven exit step for urate secreted into proximal tubules. A decreased function of NPT4 will decrease urate secretion and lead to hyperuricemia.

The Organic Anion Transporting Polypeptides, Subfamily 1A (OATP1A/Oatp1a; *SLCO1A/Slco1a*)

The organic anion transporting polypeptides were grouped into 6 families, OATP1-6.[48,79] The genes (formerly SLC21) have been systematically renamed to

SLCO followed by the number of OATP/Oatp. Human OATP1A2 (SLCO1A2; formerly OATP-A; SLC21A3) was localized to the apical membranes of distal tubules[80] and, hence, is not involved in proximal tubular drug secretion. Of the rat homologues, rOatp1a1 (Slco1a1; formerly Oatp1) and rOatp1a3 (Slco1a3; formerly OAT-K1/K2) have been localized to the apical membrane of proximal tubule cells.[81,82] Oatp1a1 expression in rats and mice was higher in males than in females[83,84] and, in mice, mRNA appeared late in adult animals.[83] Rat Oatp1 transported bile salts, hormones and their conjugates, peptides, drugs, toxins, and even organic cations (reviewed in[48,85,86]). Since it appears that Oatp1 is rather involved in drug uptake across the apical membrane rather than in drug secretion, we do not further consider this transporter in this review.

Oat-K1 and its N-truncated variant Oat-K2 were isolated as rat renal homologues of Oatp1a1 (reviewed in[87]). In the new nomenclature, Oat-K1 was classified as Oatp1a3 (gene Slco1a3; formerly Slc21a4).[79] The message for rOat-K1 was detected exclusively in kidneys and was located to superficial and juxtamedullary proximal straight tubules (S3 segment[82]). Antibodies reacted with a 40 kDa band in rat renal brush-border membranes, indicating the expression of the rOat-K1 protein in the apical membrane.[82] The mRNA for the splice variant rOat-K2 was detected mainly in the S3 segment, but also in proximal convoluted tubules as well as in collecting ducts.[88] When expressed in MDCK cells, rOat-K2 appeared in the apical membrane,[88] suggesting that both transporters are located in the apical membrane.

Rat Oatp1a3/Oat-K1 mediated the sodium-and chloride-independent, bidirectional transport of methotrexate (K_m 2.1 μM) and folate (substrates reviewed in[87]). Further transported substrates were the hormone conjugates dehydroepiandrosterone sulfate, estrone-3-sulfate, estradiol-17β-D-glucuronide; the thyroid hormones triiodothyronine and thyroxin; the bile salt taurocholate; and the mycotoxin ochratoxin A. PAH inhibited methotrexate transport but was not translocated.[89] A series of non-steroidal anti-inflammatory drugs inhibited methotrexate uptake, but were not translocated. Although truncated, rOat-K2 was functional and translocated methotrexate, folate, taurocholate, and prostaglandin E_2. In addition transport of dehydroepiandrosterone sulfate, estrone sulfate, estradiol-17β-D-glucuronide, triiodothyronin, thyroxine, ochratoxin A, and the antiviral drug zidovudine was shown.[87]

Taken together, rat Oatp1a3/Oat-K1 and Oat-K2 interact with endogenous compounds and selected drugs, methotrexate and zidovudine. Oatp3a1/Oat-K1 and K2 were considered important for renal methotrexate secretion.[87,90] The inhibition by NSAIDs could provide an explanation for the toxic accumulation of methotrexate in the body, when co-administered with analgesics.

The Multidrug Resistance Protein 2 (MRP2/Mrp2; *ABCC2/Abcc2*)

The ATP binding cassette (ABC) transporter MRP2/Mrp2 is mainly expressed kidneys, liver, placenta and small intestine (for reviews see[26,49,91,92]). Highest expression was found in human liver and jejunum; in human kidneys, mRNA for MRP2 was moderately expressed as compared to the highly expressed OAT1 and OAT3.[13,93] The human gene, ABCC2, is located on chromosome 10q24.[92,94] In mice, mRNA for Mrp2 was low until day 10 after birth; from day 15 on, the mRNA was higher and did not show statistically significant sex differences in adulthood.[93]

MRP2/Mrp2 is a large protein consisting of 1,545 amino acids arranged in three membrane spanning domains, MSD0, MSD1 and MSD2, with 5, 6, and 6 transmembrane helices (TMH) each, respectively.[49,91] Between MSD1 and MSD2 and carboxyterminal from MSD2 there are two intracellularly located nucleotide binding domains (NBDs). In human MRP2, TMH 6, 9, 16, and 17, and in rMrp2 TMH 11, 14, and 15 are important for function (for literature see[91,95]). In all organs, MRP2 protein was found at the apical membrane. Within human and rat kidneys, MRP2/Mrp2 is located in the proximal tubules in segments S1 to S3 and thus prone to ATP-driven extrusion of its substrates.[96,97]

Several loss-of-function mutations of MRP2 are the cause of the *Dubin-Johnson syndrome* in humans, a rare autosomal-recessive disease with hyperbilirubinemia and deposition of a dark pigment in the liver (for a review of mutations see[95,98]). Mrp2 is absent in two rat strains, the Eisai hyperbilirubinemic rat and the TR$^-$ rat[99,100] that served as models for the Dubin-Johnson syndrome and offered valuable insights into the physiological function of MRP2/Mrp2. More recently, Mrp2 knockout mice were generated which were also hyperbilirubinemic (summarized in[101]). The increased serum levels in bilirubin diglucuronide in MRP2/Mrp2 deficient humans, rats, and mice is due both to an impaired secretion of hepatic bilirubin diglucuronide across the canalicular membrane into the bile and to an increased release of this metabolite through the upregulated Mrp3 and Mrp4 across the sinusoidal membrane into the blood.[101] The functional significance of several other single nucleotide polymorphisms observed in human MRP2 is not yet clear.[98] The SNP 1249G > A that leads to the amino acid exchange

Val417Ile is frequent in Caucasians (22%) and Japanese (13%) and possibly associated with a renal tubulopathy induced by the antiviral drug tenofovir.[102] The SNP -24C > T in the promoter region was found to cause a lower renal MRP2 expression and a decreased excretion of methotrexate.[98,103]

MRP2/Mrp2 is an ATP-driven pump for the endogenous compounds leukotrienes C_4, D_4 and E_4, mono- and bis-glucuronidated bilirubin, estradiol-17β-D-glucuronide, glutathione, glutathione-conjugates, and conjugated bile salts. Exogenous compounds being transported by or interfering with MRP2/Mrp2 include β-lactam antibiotics, statins, NSAIDs, HIV drugs, and a number of anticancer drugs (reviewed in[49,91,92,94,95]). The clinical importance of MRP2 is based on its ability to confer resistance to a number of cytostatic drugs. ln proximal tubules, MRP2/Mrp2 is expected to pump glutathione, glucuronide and sulfate conjugates into the urine, utilizing ATP hydrolysis as energy source. When human MRP2 was expressed in HEK293 cells and inside-out vesicles were prepared from these cells, an ATP-driven uptake of radiolabeled PAH with low affinity was found.[104]

The Multidrug Resistance Protein 4 (MRP4/Mrp4; *ABCC4/Abcc4*)

The mRNA for MRP4/Mrp4 was low in several organs and showed the highest levels in kidneys and prostate.[12,92,93] The human gene for this ABC transporter, *ABCC4*, is located on chromosome 13q32.[94] In mice, the mRNA was present at their birth; at day 15 after birth, a small increase in mRNA levels took place and from day 30 on, expression in female mice exceeded that in male mice considerably, indicating sex differences in adult animals.[93] The female-dominant mMrp4 expression was verified in Western blots.[105] In gonadectomized mice, 5-dehydrotestosterone application decreased mRNA, suggesting that androgens repress the expression of Mrp4.[105] In contrast to mice, rMrp4 showed a male-dominant expression in adult rats.[106] It is unknown whether sex differences exist in human MRP4 expression. In human kidneys, MRP4 was localized to the apical membrane of proximal tubule cells.[107]

Hepatic mMrp4 mRNA expression was regulated through the constitutive androstane receptor (CAR) and the peroxisome proliferator-activated receptor α (PPARα), leading to an increased expression during cholestasis.[108] In mouse kidneys, ischemia-reperfusion injury increased the mRNA, but decreased the Mrp4 protein level, and in rat kidneys, endotoxemia did not change mRNA, but again decreased protein levels, suggesting that a post-translational regulation takes place.[108] Conflicting results have been obtained with Mrp2-deficient TR^- rats with either no change or an increased rMrp4 expresssion; in Mrp2 knockout mice, mMrp4 was upregulated (summarized in[108]).

Several single nucleotide polymorphisms have been reported for the MRP4 gene in Caucasians and Japanese (collected in[98]). Although a number of non-synonymous SNPs lead to amino acid exchanges in conserved regions, no influence on expression and localization of MRP4 was found in liver; functional consequences of these mutations were not studied so far.[98]

MRP4/Mrp4 has only two membrane-spanning domains (MSD1 and MSD2) and lacks MSD0.[49] Thereby, MRP4/Mrp4 is with 1325 amino acids the shortest member of the ABCC family.[108] Morever, MRP4/Mrp4 differs from MRP2/Mrp2 in its ability to transport cyclic nucleotides and nucleoside analogues.[49,108] Cells overexpressing human MRP4 showed a unique resistance to 9-(2-phosphonylmethoxyethyl) adenine (PMEA), 9-(2-phosphonylmethoxyethyl)guanine (PMEG), and azidothymidine (AZT), suggesting that this ATP-driven transporter translocates nucleoside-based antiviral drugs across the cell membrane.[109] Numerous endogenous compounds are substrates of MRP4/Mrp4: cAMP, cGMP, prostaglandins (PGE_1, PGE_2, $PGF_{2\alpha}$), leukotrienes (LTB_4, LTC_4), unconjugated (cholate) and conjugated bile acids, (e.g. taurocholate, glycocholate), conjugated steroids (dehydroepiandrosterone sulfate, estradiol-17βD-glucuronide), folic acid, and glutathione.[94,108] Thereby, cholate, glycocholate, taurocholate, LTB_4 are cotransported with glutathione.[94] In addition, MRP4 turned out as an ATP-driven urate transporter.[110] Since urate transport showed a Hill coefficient of 1.7 it is likely that two molecules of urate may be transported per cycle. Possibly, there are two independent transport sites interacting allosterically.[110] Together with OAT_v1/NPT1 and NPT4, MRP4 is involved in urate secretion in proximal tubules.

Human MRP4 transported a number of drugs including antibiotics (ceftizoxime, cefazolin, cefotaxime, cefmetazole), diuretics (hydrochlorothiazide, furosemide), antihypertensives (enalapril, olmesartan), statins (pravastatin), antivirals (adefovir, tenofovir), and anticancer drugs (methotrexate, topotecan).[94,108] Non-steroidal anti-inflammatory drugs (indomethacin, sulindac), and probenecid inhibited MRP4.[108] The decreased renal excretion of ceftizoxime, adefovir, tenofovir, hydrochlorothiazide, and furosemide in Mrp4 knockout mice proved an important role of Mrp4 in drug secretion.[111–113]

TR^- rats lacking Mrp2 in liver and kidneys, did not show a lower PAH clearance than wildtype rats, suggesting that the contribution of rMrp2 to urinary PAH

excretion is low.[114] Indeed, human MRP4 transported PAH with a K_m of 160 μM, whereas MRP2 exhibited a much lower affinity. ATP-driven PAH transport by MRP4 was sensitive to probenecid, sulfinpyrazone, dipyridamole, and acyclovir. The expression of MRP4 protein (tested by Western blots) was fivefold higher than that of MRP2. Together with the approximately 30 fold higher affinity for PAH, MRP4 should clearly dominate over MRP2 in the efflux of PAH across the apical membrane.[114]

OVERVIEW OF TRANSPORTERS INVOLVED IN TRANSPORT OF SELECTED ANIONIC DRUGS

β-Lactam Antibiotics

Most β-lactam antibiotics are excreted by the kidneys and undergo proximal tubular secretion. Benzylpenicillin (BP in Figure 72.2) is taken up across the basolateral membrane into proximal tubule cells mainly by OAT3, because OAT3 has a higher affinity for this antibiotic than OAT1.[7] Since OAT4, NPT1, and MRP2 interacted with benzylpenicillin, one or more of these transporters may be involved in its exit across the apical membrane.[7,61,67,69,115] However, the quantitative contribution of the apical transporters to overall benzylpenicillin secretion is not clear at present. Most cephalosporines (CS in Figure 72.2) interacted with OAT1 with higher affinity than with OAT3, and OAT2 had a very low affinity, rendering OAT1 the prime candidate for uptake across the basolateral membrane.[7] OAT4 was inhibited by cephalosporines with low affinity, leaving it open whether this transporter contributes much to cephalosporin exit across the apical membrane.[7] A considerably higher affinity for ceftizoxime, cefazolin and cefmetazole strongly suggests that MRP4 is the most important transporter for the release of cephalosporines from tubule cells into the urine.[94,108]

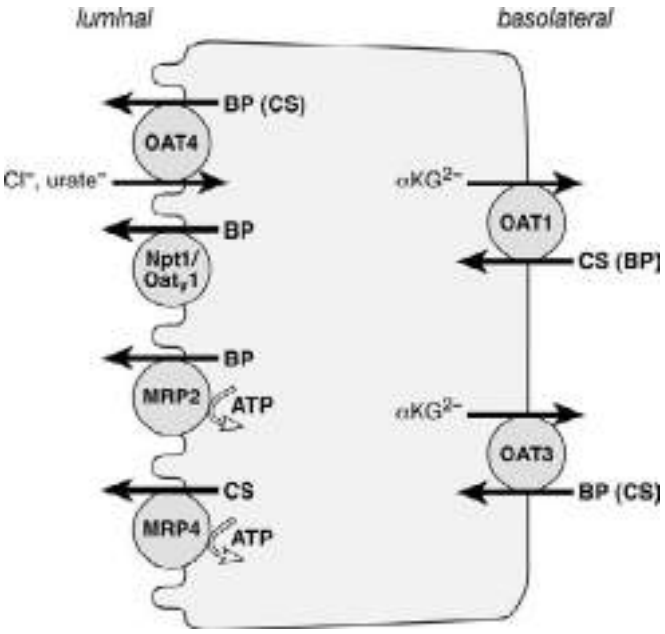

FIGURE 72.2 Proximal tubular secretion of β-lactam antibiotics. The antibiotics are taken up from the bood into the proximal tubule cell by OAT1 and OAT3, both in exchange for intracellular α-ketoglutarate (or another organic anion). Cephalosporines (CS) are preferred by OAT1 whereas benzylpenicillin (BP) shows a higher affinity toward OAT3. At the luminal membrane, OAT4 and MRP2 are involved in benzylpenicillin release, and OAT4 and MRP4 in the release of cephalosporines. In rodents, Npt1/Oat$_v$1 may also export benzylpenicillin.

Antiviral Drugs

Many antiviral drugs (AVD in Figure 72.3) are renally excreted and interact with organic anion transporters, irrespective whether they carry a negative charge, such as adefovir, cidofovir, 9-(-2-phosphonylmethoxyethyl)guanidine (PMEG) and 9-(2-phosphonoethyl) diaminopurine (PMEDAP), or are uncharged, e.g. acyclovir, ganciclovir and zidovudine. Uptake of these drugs across the basolateral membrane is largely mediated by OAT1; only zidovudine was transported also by OAT2 and OAT3[7] (Figure 72.3). Hence, OAT1 is most probably responsible for the dose-limiting, nephrotoxic effects of these compounds. Although OAT4

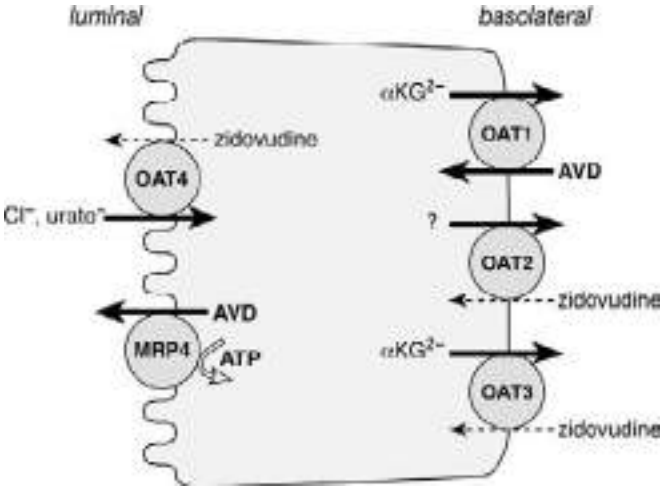

FIGURE 72.3 Proximal tubular secretion of antiviral drugs. OAT1 transports most antiviral drugs (AVD) from the blood into the cell, whereas OAT3 and OAT2 interact only with zidovudine. Once inside the proximal tubule cells, most antiviral drugs leave through MRP4 in the apical membrane. OAT4 may interact with zidovudine.

translocated zidovudine[7] it is more likely that MRP4 is the efflux transporter at the apical membrane, because it afforded a resistance against several antiviral

drugs.[109] In addition, Mrp4 knockout mice accumulated more adefovir and tenofovir in their kidneys and excreted less with the urine.[112]

Non-Steroidal Anti-Inflammatory Drugs (NSAIDs)

Most NSAIDs are preferentially excreted by the liver. However, they interact with renal organic anion transporters, and some of them have been shown to be translocated, i.e., indomethacin by human and rat OAT1/Oat1 and acetylsalicylate and salicylate by rOat1.[7] For all other NSAIDs, an inhibition of OAT1/Oat1 mediated transport was found. In general, the affinity of human OAT1 decreased with increasing hydrophilicity of the NSAIDs.[7] Since labeled acetylsalicylate, indomethacin, and salicylate were transported by rOat2, and salicylate by hOAT3,[7] these transporters may also be involved in uptake of selected NSAIDs from blood into proximal tubule cells. Again, inhibition by various NSAIDs of both transporters were observed.[7]

Interestingly, it has been proposed that NSAIDs should be used to decrease the toxicity of antiviral drugs by drug interaction at OAT1.[116] An interaction at OAT3 was proposed to be involved in the potentially life-threatening accumulation of methotrexate in patients taking NSAIDs (for literature see[117,118]), In this regard, it is important to compare therapeutic plasma levels of NSAIDs with the affinity of OATs. Only the plasma concentrations of salicylate, phenylbutazon, indomethacin, and probenecid are high enough to inhibit OAT3.[119]

NSAIDs were also tested with organic anion transporters present in the apical membrane. OAT4 was inhibited by diclofenac, ibuprofen, ketoprofen, phenylbutazone, but not, or only weakly, by salicylate (see[7]). Oat_v1-mediated transport was inhibited by salicylate, indomethacin, ibuprofen, and diclofenac.[61] The human NPT1 showed a weak transport of labeled indomethacin.[66] Human NPT4 was inhibited by diclofenac, ibuprofen and indomethacin.[74] For rOat-K1, an interaction with indomethacin, ketoprofen, ibuprofen, flufenamate, phenylbutazone, but not of salicylate was reported.[120] Oat-K2, however, did not translocate indomethacin.[88] The competition for Oat-K1 could contribute to the above mentioned methotrexate/NSAID interaction. Several NSAIDs including flurbiprofen, ibuprofen, indomethacin, indoprofen, ketoprofen and diclofenac inhibited MRP4.[121] It is not known, however, whether these compounds inhibit only or are indeed translocated by MRP4. Since methotrexate is translocated by MRP4,[94] inhibition by NSAIDs could contribute to the accumulation of methotrexate in patients treated with analgesics.

In summary, NSAIDs interfere with organic anion transporters in proximal tubule cells. Although renal excretion is not the main route for elimination of most NSAIDs, some of these compounds can inhibit the secretion of other organic anions such as the cytostatic drug methotrexate and cause side effects. On the other hand, NSAIDs may deliberately be used to decrease the nephrotoxicity of, e.g., antiviral drugs during HIV therapy.

Diuretics

Diuretics are secreted in proximal tubules to reach their target salt transporters in the distal tubule from the lumenal side. Among the human basolateral OATs, OAT1 translocated labelled bumetanide and furosemide, OAT2 bumetanide, and OAT3 furosemide; all other diuretics inhibited (see[7] for K_i values). OAT1 possessed a higher affinity for most thiazide diuretics (TZ in Figure 72.4), whereas OAT3 had a higher affinity for loop diuretics (LD in Figure 72.4). Both Oat1 and Oat3 knockout mice showed a decreased renal excretion of furosemide and bendroflumethiazide, strongly suggesting that both transporters are involved in proximal tubular secretion of diuretics.[31]

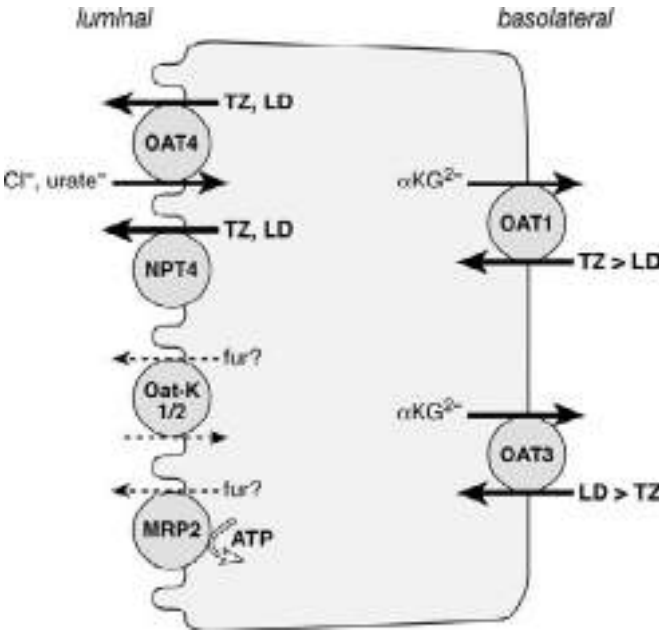

FIGURE 72.4 Transport systems possibly involved in proximal tubular secretion of diuretics. Thiazides (TZ) are preferentially taken up from blood by OAT1 and loop diuretics (LD) by OAT3 in the basolateral membrane. Both classes of diuretics leave the cell across the apical membrane through OAT4, in exchange for urate or chloride ions. NPT4 accomplishes the electrogenic exit of thiazide and loop diuretics. An interaction of furosemide (fur) with OatK-1/2, and MRP2 has been reported but it is not clear whether these transporters are involved in furosemide release.

At the lumenal membrane, it is likely that OAT4 is involved in the efflux of diuretics into the urine. OAT4 transported labeled bumetanide and was inhibited by thiazides and loop diuretics (see[7]). The export of diuretics, e.g., torasemide, in exchange for urate could explain the hyperuricemia observed in antihypertensive monotherapy with diuretics.[52] An interaction of furosemide with rOat-K1[122] and rOat-K2,[88] $pOat_v1$,[61] and hMRP2[115] was reported. However, it is not known whether any of these transporters translocates furosemide and other diuretics across the apical membrane. NPT4, however, is clearly a candidate for the release of diuretics, because thiazides and loop diuretics inhibited NPT4-mediated PAH transport and labelled bumetanide was taken up into NPT4-expressing oocytes.[74] Since extracellular bumetanide induced an outward current it is highly likely that transport is electrogenic. Given the inside negative electrical potential difference across the apical membrane, NPT4, probably acts as an important exit transporter for the negatively charged diuretics.

ORGANIC CATION TRANSPORT SYSTEMS

Characteristics of Organic Cation Transport in Proximal Tubules

In the kidney, organic cations may be ultrafiltrated in the glomeruli and reabsorbed or secreted in renal tubules. Hydrophilic organic cations that do not bind to plasma proteins are readily filtrated and may be reabsorbed in renal tubules. However, most organic cations are not filtrated efficiently because they are relatively hydrophobic and bound to plasma proteins. These organic cations are actively secreted. Reabsorption and secretion of organic cations have been investigated in proximal tubules, distal tubules, and collecting ducts, however, secretion of organic cations in proximal tubules has been studied in most detail.[123] Substrates for organic cation secretion include primary, secondary, tertiary, or quaternary amines that have a positive charge at physiological pH. Organic cations are secreted by a two-step procedure. In the first step, they are taken up across the basolateral membrane by an electrogenic transport system that accepts a variety of structurally different organic cations and uses the electrochemical gradient to accumulate cations intracellularly. The energy provided by the membrane potential is restored by the Na^+,K^+-ATPase. In a second step, organic cations are released across the luminal membrane by a proton/organic cation antiporter that helps to overcome the inside negative membrane potential. This step is energized by an extracellular over intracellular proton concentration difference that is mainly generated by the Na^+/H^+ exchanger. For reabsorption, organic cations are transported across the luminal membrane and leave the cells via a polyspecific transporter in the basolateral membrane. Renal handling of organic cations is dependent on their concentrations in the plasma. For example, in rabbit and dog, choline is secreted at high plasma concentrations, whereas it is reabsorbed at normal plasma concentrations below 25 μM.[124,125]

Figure 72.5 depicts transporters that mediate secretion and reabsorption of organic cations in human renal proximal tubules. The Na^+,K^+-ATPase in the basolateral membrane generates and maintains a high intracellular concentration of potassium, which is the prerequisite for the membrane potential that drives organic cation uptake by the electrogenic organic cation transporters. The extracellular-over-intracellular proton gradient across the luminal membrane generated by the sodium/proton antiporter provides the driving

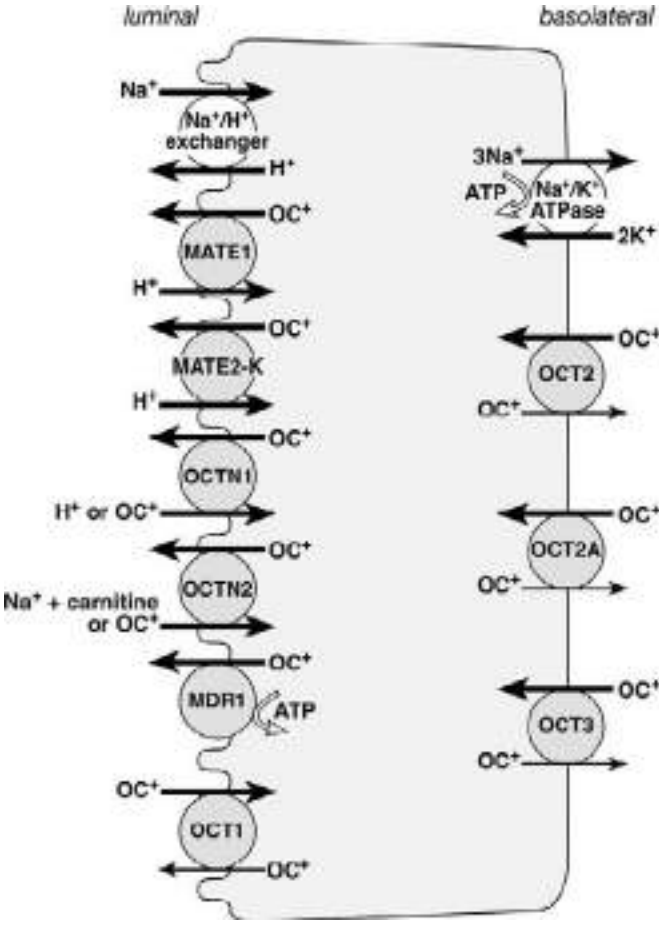

FIGURE 72.5 Transport systems for organic cations in human renal proximal tubule cells. Thick and thin arrows indicate that large and small uptake rates are presumed. OCT2A is a functional active splice variant of OCT2.

force for the proton/organic cation exchangers that mediate the efflux of organic cations into the tubular lumen. Transporters OCT1 (SLC22A1), OCT2 (SLC22A2), OCT3 (SLC22A3), OCTN1 (SLC22A4), and OCTN2 (SLC22A5) belong to the organic cation transporter family *SLC22* which is a member of the major solute facilitator (MFS) superfamily.[125,126] MATE1 (*SLC47A1*) and MATE2-K (*SLC47A2*) are members of the multidrug and toxin extrusion family *SLC47*[123,127] whereas MDR1 (ABCB1) belongs to the ATP-binding cassette transporter family ABC.[128]

Cloning and Functions of OCT1-3/Oct1-3; *SLC22A1-3/Slc22a1-3*

OCT1/Oct1, OCT2/Oct2, and OCT3/Oct3 are electrogenic polyspecific transporters that are expressed in kidney. On the protein level, individual transporter subtypes from different species exhibit cross-species identities of 78 to 95%. Within a given species, the amino acid identities between different subtypes are 67 to 70% between OCT1 and OCT2, 47 to 57% between OCT1 and OCT3, and 49 to 51% between OCT2 and OCT3. In addition to renal excretion and reabsorption, OCT1−3 are critically involved in small intestinal absorption and hepatic excretion of cationic drugs.[123] The OCT-transporters influence the distribution of cationic drugs and endogenous compounds in various tissues, for example in brain and heart.[123,129−131] Species-specific expression and membrane locations of the three OCT subtyes have been observed. In humans, OCT2 is most strongly expressed in kidneys whereas OCT1 and OCT3 are most strongly expressed in liver and adrenal gland, respectively.[123,132]

OCT1/Oct1, OCT2/Oct2, and OCT3/Oct3 have been isolated from rats,[133−135] mice,[136] and humans.[137−139] Oct1 and Oct2 were also cloned from rabbit[140,141] and Oct2 also from pig.[125]

Expression and Main Functions of OCT1/Oct1

In the species tested so far, OCT1/Oct1 is mainly expressed in liver where it is located at the sinusoidal membrane of the hepatocytes.[132,142] In rat, mouse, and rabbit, strong expression of Oct1 was also observed in kidneys whereas relatively small amounts of OCT1 mRNA were detected in human kidney.[123,143] In humans, OCT1 is also expressed in various other organs[123] and in various tumors.[144,145] Using immunohistochemistry, Oct1 protein was localized at the basolateral membranes of S1 and S2 segments of rat proximal tubules,[125] however, in human OCT1 has been recently localized to luminal membranes of proximal and distal tubules.[143] Apical location of OCT1/Oct1 has been also observed in lung bronchial epithelial cells and brain microvessel endothelial cells of rodents and human.[131,146] Human OCT1 transports the endogenous Cyclo(His-Pro) and salsosinol, xenobiotics and drugs ([147] and Table 72.1). Important transported drugs are the antidiabetic metformin; the antineoplastic drugs oxaliplatin, picoplatin and metaiodobenzylguanidine; the antiparasitic drugs furaminidine and pentamidine; and the antiviral drugs acyclovir, ganciclovir, lamuvidine and zalzitabine (Table 72.1). Studies with mice in which either Oct1, Oct2 or Oct3 or Oct1 plus Oct2 were removed indicated the importance of Oct1 and Oct2 for renal secretion of tetraethylammonium (TEA) and of the antidiabetic metformin. In humans with defect mutations in OCT1, increased renal excretion of metformin was observed, suggesting that OCT1 is critically involved in renal reabsorption rather than in excretion of organic cations.[143]

Expression and Main Functions of OCT2/Oct2

In human, rat, mouse, and rabbit, OCT2/Oct2 is most strongly expressed in the kidneys.[123] In addition, OCT2/Oct2 was detected in placenta, thymus, adrenal glands, neurons and microvessel of brain, inner ear, and lung.[123,131,148] In rat and human kidneys, OCT2/Oct2 was localized to the basolateral membrane of proximal tubules.[123] In rat kidneys, where Oct1 is expressed in the S1 and S2 segments, Oct2 was located to the S2 and S3 segments. At variance, in human kidneys, OCT2 is expressed in all three segments of proximal tubules.[123] Uptake measurements of organic cations across the basolateral membrane of isolated proximal tubules from man and rabbit suggest that OCT2/Oct2 is the dominating organic cation transporter in the basolateral membrane of renal proximal tubules in these species.[123] OCT2/Oct2 was localized to apical membranes of the choroid plexus in rat and to apical membranes of bronchial epithelial cells in human and rat.[146,149] Human OCT2 transports various endogenous compounds including choline, the neuromodulators agmatine, Cyclo(His-Pro) and salsolinol, and the neurotransmitters acetylcholine, epinephrine, histamine, norepinephrine and serotonin.[147] Important drugs transported by hOCT2 are the antidiabetic drug metformin; the antineoplastic drugs cisplatin, oxaliplatin, picoplatin, ormaplatin, tetraplatin, transplatin, metaiodobenzylguanidine; the anti-ulcer drugs cimetidine, famotidine, ranitine; the antiviral drugs lamuvidine, zalcitabine; and the anti-parkinson drugs amantadine and memantine (Table 72.1). A pivotal importance of OCT2 for renal secretion of some organic cations in humans can be derived from the finding that the OCT2 substrate cisplatin showed a reduced

TABLE 72.1 Drugs that are Transported by Human Organic Cation Transporters Expressed in Renal Proximal Tubules. IC_{50} values (normal face) and K_m values (bold face) are given in μM.

	Compound	hOCT1	hOCT2	hOCT3	hOCTN1	hOCTN2	MATE1	MATE2-K	MDR1
Antiallergic	Fexofenadine						substrate		substrate
Anesthetic antiarrhythmic	Lidocaine		294	**K_m:139**	0.8				
Antiarrhythmic	Procainamide	15–74	28–406	355–738 substrate	(<500)	(<300)	**K_m: 1230**	**K_m: 1580,** or **4100**	
Antiarrhythmic	Quinidine	5.4–114 substrate	7.1–446	**K_m: 216**	69	<100	29	23	Substrate
Antiarrhythmic vasodilator	Verapamil	1.2–2.9	13–85		8.4 substrate	<50 substrate	28	32 substrate	Substrate
Antibacterial	Cephaloridine				<1000	**K_m:230**			
Antibacterial	Levofloxacin						substrate		
Antibacterial	Tetracycline							substrate	
Anticonvulsanr	Gabapentin[186]				substrate				
Antidiabetic	Metformin	**K_m: 1470–2160**	**K_m: 990–1380**	**K_m: 2260**			**K_m: 780**	**K_m: 1050–1980**	
Antifungal	Salicylic acid						substrate		
Antihypertensive	Captopril							substrate	
Antihypotensive	Etilefrine	447	4009	**K_m: 2800**					
Antineoplastic	Cisplatin	1000–5000	1.5–10000 substrate	1000–5000			1000–5000 substrate	>4000 substrate	
Antineoplastic	Metaiodoben-zylguanidin	substrate	substrate	substrate					
Antineoplastic	Oxaliplatin	substrate	substrate	substrate				substrate[201]	
Antineoplastic	Picoplatin[217]	substrate	substrate	substrate					
Antineoplastic	Topotecan						**K_m: 70**	**K_m: 60**	Substrate
Antimalarial	Quinine	13–52 substrate	3.4–34 substrate	37	2500	<100	substrate	substrate	
Antiparasitic	Furaminidine	**K_m: 6.1**	182	20					
Antiparasitic	Pentamidine	**K_m: 36**	3.8–11	15					
Anti-ulcer	Cimetidine	95–166	**K_m: 67–73**	240	435	<2000	**K_m: 170**	**K_m: 120–370**	Substrate
Anti-ulcer	Famotidine		**K_m: 56**	~20			0.6	9.7	

(*Continued*)

TABLE 72.1 (*Continued*)

	Compound	hOCT1	hOCT2	hOCT3	hOCTN1	hOCTN2	MATE1	MATE2-K	MDR1
Anti-ulcer	Ranitine	22−28	**K_m: 265**	372			25	25	
Antiviral	Acyclovir	**K_m: 151**					**K_m: 2640**	**K_m: 4320**	
Antiviral	Ganciclovir	**K_m: 516**					**K_m: 5120**	**K_m: 4280**	
Antiviral	Lamuvidine	**K_m: 249−1250**	**K_m: 248−1900**	**K_m: 2140**					
Antiviral	Tenofovir	9×10^{-4}	6×10^{-4}	5×10^{-6}			substrate		
Antiviral	Zalcitabine	**K_m: 242**	**K_m: 232**						
Anti-Parkinson	Amantadine	18−236	**K_m: 27**	>1000			112	1167	
Anti-Parkinson	Memantine	3.7−27	**K_m: 34**	236					
Cardioprotective	Mildronate					**K_m: 26**			

nephrotoxicity in patients with a defect mutation of hOCT2.[150]

Expression and Main Functions of OCT3/Oct3

The tissue expression pattern of OCT3/Oct3 is broad.[123,125,147] OCT3/Oct3 is expressed in adrenal gland, uterus, prostate, stomach, liver, placenta, kidneys, heart, small intestine, lung, brain, skin, blood vessels, and thymus. In brain, OCT3/Oct3 is expressed in astrocytes and neurons and is critically involved in central nervous functions.[123,129,130] Human OCT3 has been located to basolateral membranes from placenta epithelium[151] and to luminal membranes of bronchial and intestinal epithelial cells.[123] Like hOCT2, human OCT3 (hOCT3) transports the neuromodulators agmatine, Cyclo(His-Pro) and salsolinol and the neurotransmitters epinephrine, histamine and norepinephrine.[147] hOCT3 transports the anesthetic lidocaine; the antiarrhythmic drug quinidine; the antidiabetic metformin; the antihypotensive drug etilefrine; the antineoplastic drug oxaliplatin; and antiviral drug lamivudine (Table 72.1).

Common Transport Characteristics of OCT1-3/Oct1-3

OCT1-3/Oct1-3 have similar basic functional properties which are species independent as follows.[123] First, they translocate a variety of organic cations with widely differing molecular structures and are inhibited by a large number of additional compounds that are not transported. Substrates and inhibitors of OCTs from human and other species have been compiled in previous reviews.[123,125,147] Second, OCT1-3/Oct1-3 translocate organic cations in an electrogenic manner.[123] Third, OCT1-3 operate independently of Na^+ and Cl^-, and are probably also independent of H^+ gradients.[123,152] Fourth, OCTs/Octs are able to translocate organic cations across the plasma membrane in either direction. In addition to cation influx, cation efflux has been demonstrated for rOCT1, rOCT2, hOCT2, rOCT3, and hOCT3.[123]

For substrates of OCT1-3/Oct1-3 K_m values in the micro- to millimolar range have been determined. Most substrates translocated by OCT1-3/Oct1-3 are organic cations which carry one positive charge or weak bases that are positively charged at physiological pH.[123] Noncharged compounds (for example cimetidine at alkaline pH[153]), organic cations with two positive charges,[154] and the inorganic cation cesium[155] were also transported. Whether OCT1-3/Oct1-3 are also capable to translocate individual organic anions has not been resolved.[156,157] Transported endogenous substrates of human OCTs include the neurotransmitters acetylcholine, dopamine, serotonin, histamine; the neuromodulators Cyclo(His-Pro) and salsolinol[123,158]; and other compounds such as choline, N^1-methylnicotinamide, creatinine, guanidine, and agmatine.[123] Drugs that are transported by human OCTs are indicated in Table 72.1. They include the histamine H_2 receptor antagonists cimetidine and famotidine; the dopamine D2 receptor antagonist pramipexole; the antidiabetic metformin; the anti-arrhythmic drugs quinidine, lidocaine, procainamide, and phenytoin; the anti-parkinson drug memantine and amantadine; the antihypotensive drug etifefrine; and the antineoplastic drugs cisplatin, oxaliplatin and picoplatin. Human OCTs also transport the antiparasitic drugs furamidine and pentamidine and the antiviral drugs acyclovir, ganciclovir, zalcitabine and lamuvidine.[147] Ethidium is an example for a transported toxin.[159] Other organic cations that are transported by human OCTs are tetraethylammonium (TEA), 1-methyl-4-pyridinium (MPP), azidoprocainamide, 4-(4-dimethylamino)styryl-N-methylpyridinium, N-(4,4-azo-n-pentyl)-quinuclidine, tributylammonium azidoprocainamide, and berberine.[123,147] Interestingly, in voltage-clamped oocytes expressing rOct2, it was observed that Cs^+, but not Li^+, Na^+, or K^+, induced inward currents and inhibited rOct2-mediated TEA uptake.[155] This suggested that Cs^{2+} is translocated by rOct2 in addition to organic cations. Table 1 indicates apparent K_m and K_i values of human OCT1, OCT2 and/or OCT3 for drugs. More complete tables of substrates and inhibitors of OCT1, OCT2 and OCT3 of human and other species have been presented in previous reviews.[123,125,147]

Transported substrates of OCTs/Octs exhibit mutual inhibition that can be total at high concentrations of the inhibitory substrates. A variety of cations (for example, tetrapentylammonium, cyanine 863, decynium 22, and disprocynium), noncharged compounds (e.g., corticosterone, deoxycorticosterone, and β-estradiol) and anions (e.g., probenecid and α-ketoglutarate) inhibited OCTs/Octs, but were not transported themselves.[123,147] This indicates that the criteria for selectivity of cation binding to OCTs/Octs and of cation transport are different, implying the limitation of pharmacophore models of OCTs/Octs that were derived from *IC50* values obtained from inhibition experiments.[123]

Ligand Specificities of OCT1-3/Oct1-3

Some substrates and inhibitors have similar affinities for the OCT/Oct subtypes whereas the affinity of several other substrates and inhibitors differs significantly.[123,147] For a given subtype of the OCT/Oct transporters, distinct species differences in affinity for

substrates and inhibitors exist. For example, tetramethylammonium inhibited MPP uptake by OCT1/Oct1 with IC_{50} values (in mM) of 0.9 in rat, 2.0 in mouse, 5.8 in rabbit, and 12.4 in humans.[125] Similarly, corticosterone inhibited MPP uptake by OCT3/Oct3 with IC_{50} values of 4.9 μM in rats versus 0.12 μM in humans.[125] The affinity differences of the OCT/Oct subtypes in individual species can be used to distinguish between cation uptake by the different transporters.[123,125,147] Compounds that interact with two OCT subtypes may be nontransported inhibitors for one subtype and a poorly transported substrate for another. For example, quinine inhibited TEA uptake by rOct1 and rOct2 with IC_{50} values of 4.1 and 23 μM, respectively, and was transported by rOct1, but not by rOct2.[86,160]

Substrate Binding Regions of OCT1-3/Oct1-3

Employing the firstly cloned organic cation transporter from rat (rOct1) as prototype,[133] the outward-open and inward-open substrate binding cleft of this polyspecific transporter has been investigated using site-directed mutagenesis combined with functional characterizations and modeling of tertiary structures.[152,161–165] Conformations of the transporter with the outward-facing and inward-facing substrate binding cleft were modeled and docking of substrates and inhibitors to the clefts was simulated.[165] Functional characterization of the mutants included a comparison of K_m and V_{max} values of different substrates and a comparison of K_i values of substrates and inhibitors. In addition, K_i values of nontransported inhibitors that were either applied to the extracellular or intracellular side of the membrane, were compared.[165,166] Modeling of the tertiary structure of rOct1 was possible since two members of the MFS superfamily, the lactose permease LacY and the glycerol-3-phosphate transporter GlpT from Escherichia coli, had been crystallized and their tertiary structures determined.[167,168] The transporters were crystallized in a conformation with a large inward-open cleft that is formed by eight transmembrane α-helices. The outward-open conformation of rOct1 was modeled by employing a putative rearrangement mechanism for lactose transport by LacY that was proposed on the basis of biochemical data.[152,165,169] Mutagenesis of rOct1 provided evidence for a high quality of the outward-facing and inward-facing structural models. It was shown that mutations of eight amino acids that line the modeled inward-open cleft are involved in substrate recognition and/or translocation (Fig. 72.6). These amino acids are phenylalanine 160 on the predicted second transmembrane α helix (TMH), tryptophan 218, tyrosine 222 and threonine 226 on successive turns of TMH 4, arginine 440, leucine 447, and glutamine 448 in TMH 10, and aspartate 475 in the middle of TMH 11.[161,163,165] Mutations of these amino acids resulted in changed *Km* values for TEA and/or MPP. The selective effect of individual mutants on the K_m value for either TEA or MPP suggests that the binding sites for individual substrates are partially different. Using the nontransported inhibitors corticosterone and tetrabutylammonium (TBuA), the substrate binding region of rOct2 was characterized in its outward-open and inward-facing conformations.[166] The experiments showed that both inhibitors interact from the intracellular as well as from the extracellular side. Interestingly, TBuA had a significantly higher affinity from the outside as compared to the inside, whereas corticosterone had a higher affinity from the inside than from the outside.

Employing a mutant of rOct1 with increased cation induced currents but similar K_m value for TEA and MPP, the effect of point mutations on the inhibition of TEA induced currents by extracellular or intracellular corticosterone was investigated.[165,170] It was observed that mutations of Phe160, Tryp218 and Leu447 changed the affinity for inhibition of cation induced currents by extracellular and intracellular corticosterone whereas replacement of Arg440 by lysine decreased the affinity for inhibition of TEA-induced currents by extracellular corticosterone and reduced the maximal inhibition by extracellular and intracellular corticosterone.[165] Comparing the inhibition of [^{3}H]MPP uptake by extracellular corticosterone in HEK293 cells that were transfected with rOct1 wildtype or rOct1(D475E) it was observed that also this mutation changed the affinity of extracellular and intracellular corticosterone. Importantly Phe160, Tryp218, Arg440, Leu447 and Asp475 are located within the innermost parts of the modeled outward-open and inward-open binding clefts (Figure 72.6).

High-Affinity Binding Sites in OCT1-3/Oct1-3

A comparison of the substrate binding regions in the models of the outward-open and inward-open clefts of rOct1 with sizes of substrates[163] and the partially different amino acids that are relevant for the K_m and/or K_i values of TEA, MPP, corticosterone and/or TBuA suggest that more than one compound can bind at the same time. Using voltage-clamp fluorometry with rOct1 in which phenylalanine 483 in TMH 11 located close to the extracellular surface was replaced by cysteine and labeled with tetramethylrhodamine-6-maleimide (TMRM), high affinity binding sites of organic cations were detected. In oocytes expressing TMRM-labeled rOct1, potential-dependent fluorescence changes were observed which were prevented

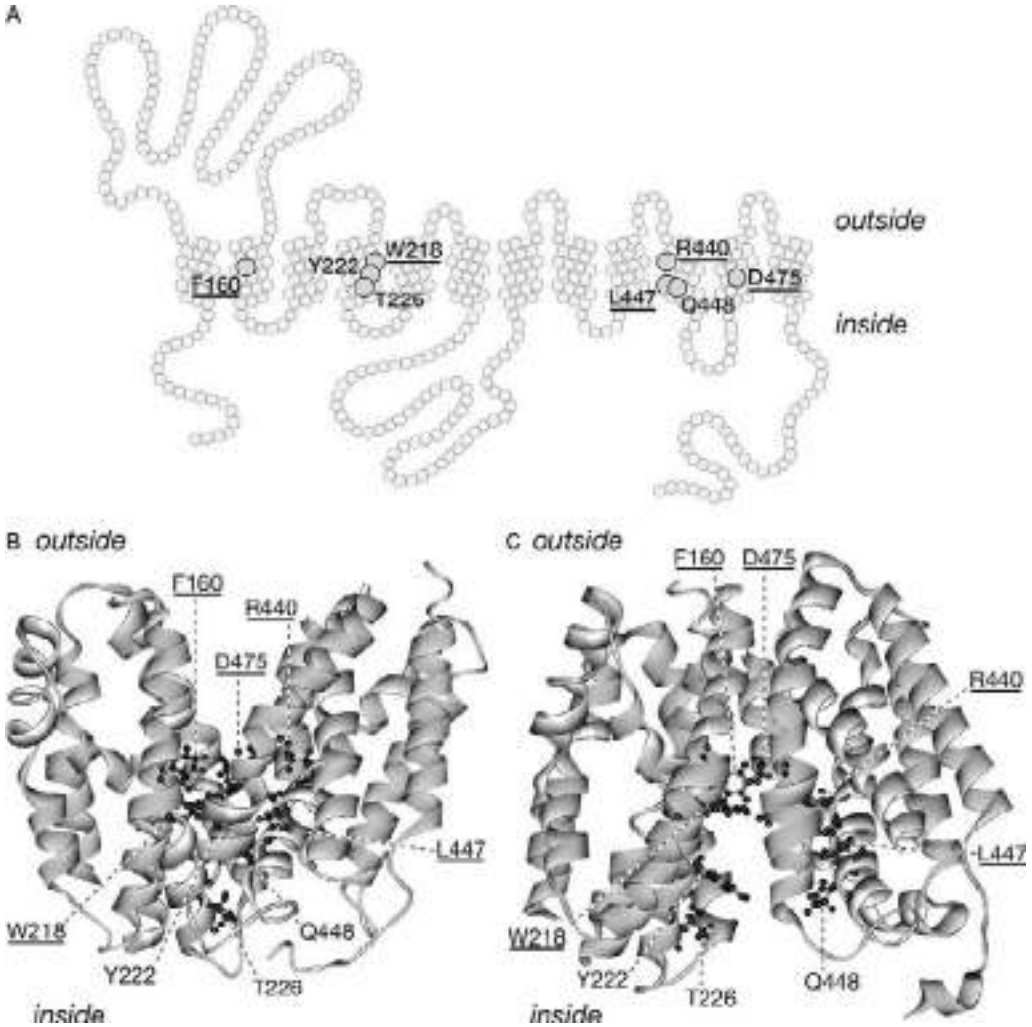

FIGURE 72.6 Structure models of rOct1 with amino acids that are located within the outward-open and inward-open binding clefts. A: Amino-acid sequence and membrane topology model of α-helical transmembrane domains of rOct1. B: Side view of the structural Oct1 model in the outward-facing conformation. A ribbon presentation is shown. **C**: Side view of the inward facing rOct1 model. Mutagenesis experiments showed that the indicated amino acids are critical for affinity and/or selectivity of the substrates TEA and MPP and suggested that extracellular and intracellular corticosterone interacts with the underlined amino acids.

by the substrates TEA, choline and MPP, and by the nontransported inhibitor TBuA. Titrating the substrate effects and the effect of TBuA on fluorescence revealed two affinities of each substrate to rOct1 and three affinities of TBuA to the extracellular side of rOct1. One apparent dissociation constant (K_D) for TBuA (0.3 μM) was similar to the K_i value for inhibition of organic cation transport whereas the other two K_D values (~0.4 nM, ~2 pM) were much lower. These data indicate the existence of two binding sites for the substrates which may be located in the outward-open and/or inward open cleft and three TBuA binding sites in the outward-open cleft. The functional relevance of the high affinity binding sites is not fully understood. So far, for organic cation transport by OCT1-3/Oct1-3 no significant deviation from Michaelis Menten type kinetics has been observed. However, it has been shown that the IC_{50} values determined for the inhibition of organic cation uptake by some drugs were largely different when different substrate concentrations far below the respective K_m value were employed for uptake measurements. For example, for the inhibition of hOCT2 mediated MPP uptake by quinidine IC_{50} values of 446 μM and 13 μM were determined using MPP concentrations of 1 nM or 1 μM for the uptake measurements.[147] High affinity interaction of inhibitors with OCT1-3/Oct1-3 may lead to inhibition of organic cation uptake using low substrate concentrations. For example, the antiviral drug lamivudine inhibited the uptake of 1.3 nM MPP by human OCT1-3 with IC_{50}

values between 8 pM and 20 pM.[171] Thus, high affinity inhibition may be of biomedical importance for drug-drug interaction at OCTs.

Proposed Transport Mechanism of OCT1-3/Oct1-3

Because the OCTs/Octs mediate facilitative diffusion of structurally different compounds and translocate cations in both directions, the question has to be solved whether they are transporters as generally assumed (in which substrate translocation is stoichiometrically linked to structural changes within the protein) or whether they are channels that exhibit short opening times (explaining the relatively low rates of cation translocation) and contain cation-ligand binding sites (explaining the observed saturation at high substrate concentrations). Electrical measurements with Oct2 from rat shed some light on the transport mechanism. In the inside-out configuration, giant patches from oocytes expressing rOct2 clamped to 0 mV yielded K_m values for the efflux of choline and TEA that were similar to the K_m values obtained at the same holding potential for the influx of these substrates into intact oocytes.[172] This suggested symmetric translocation of small cations by rOct2 and is consistent with a symmetric transporter or a channel. Figure 72.7A shows recordings from giant patches with symmetrical choline concentrations and at various membrane potentials. The experiments demonstrated that both inward and outward currents are voltage dependent in a way that is symmetric around the reversal potential. Interestingly, considerably higher currents were observed with 2 mM choline as compared with 10 mM choline on both sides of the membrane. This result would be expected for the simple alternating access model (Fig. 72.7B), but is difficult to reconcile with a channel. The alternating access model predicts electrogenic transport as a result of the sequence of steps (substrate binding to the outside → translocation of the bound substrate to the intracellular side → dissociation of the substrate → reorientation of the empty substrate binding site toward the extracellular side) at low intracellular concentrations of substrate. At high substrate concentrations, this model predicts electroneutral cation exchange, which is not recorded by the electrical measurements. Alternatively, a channel with an inhibitory, low-affinity cation binding site may show a similar decrease of current at high substrate concentrations. Strong evidence in favor of transport was obtained by demonstrating *trans*-stimulation under voltage-clamp conditions. *Trans*-stimulation of MPP uptake by choline into proteoliposomes containing purified rOct1 was observed when the proteoliposomes were clamped to

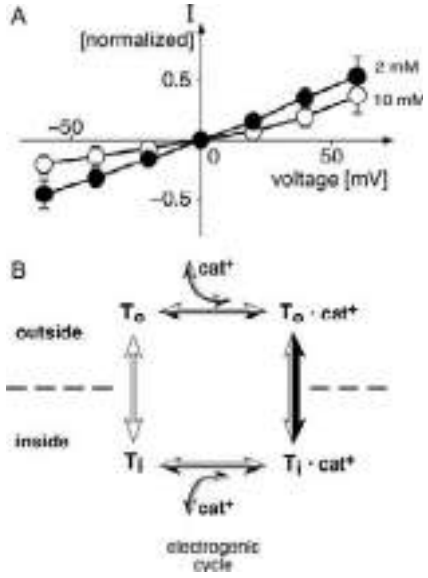

FIGURE 72.7 Characteristics of choline transport by rOct2. A: Current-voltage relation in giant patches of *Xenopus laevis* oocytes expressing rOct2, inside-out configuration with symmetrical choline concentrations of 2 mM or 10 mM; the holding potential between voltage steps was 0 mV. B: Model of a simple transporter, illustrating the individual reaction steps involved in electrogenic cation uniport (closed arrows) and electroneutral cation/cation exchange (open arrows). To and Ti, transporter conformations with the cation-binding site oriented outwardly and inwardly, respectively. Cat^+, monovalent organic cation.

0 mV.[173] *Trans*-stimulation of a transporter is expected if the in-to-out reorientation of the substrate binding site of the loaded carrier occurs more quickly than the reorientation of the empty one (Fig. 72.7B). Finally, a transport mechanism is also supported by the high activation energies which have been determined for rOct2-mediated currents in oocytes observed after addition of tetraethylammonium or cesium to the bath.[155] In oocytes expressing rOct2 clamped to −100 mV, a stoichiometry of 1:1 has been determined for uptake of positive charge and organic cation substrates, demonstrating absence of leakage for inorganic ions under these conditions.[152] In contrast, a surplus of positive charge carried by inorganic ions was translocated together with organic cation substrates at zero membrane potential. Since the potential dependence is consistent with cotranslocation of inorganic ions, but not with leakage, an occluded state during the transport cycle is postulated.

Short-Term Regulations of OCT1-3/Oct1-3

Regulation of transport by OCTs/Octs may influence the excretion of drugs and the exposure of the body to xenobiotics.[123,174] After cloning of OCT1-3/Oct1-3, the

short-term regulation of individual transporters was studied after overexpression of the transporters in epithelial cells. Regulation of human OCT1 (hOCT1), rat Oct1 (rOct1), human OCT2 (hOCT2), and human OCT3 (hOCT3) was investigated in HEK293 cells and CHO cells stably transfected with the individual transporters. The regulation of hOCT1 expressed in HEK293 cells or CHO cells was identical, however, distinct differences in regulation were observed for the three human subtypes and for hOCT1 compared to rOct1. Surprisingly, certain characteristics observed for regulation of 4-[4-(dimethylamino)-styryl]-*N*-methylpyridinium (ASP) transport across the basolateral membrane of human renal proximal tubules were not found for ASP uptake by the individual transporters expressed in HEK293 and CHO cells. This suggests differences between proximal tubular cells and the cell lines used for expression.

Short-term regulation of rOct1 has been investigated in most detail. rOct1-mediated transport of ASP in stably transfected HEK293 cells was stimulated by activators of PKC, PKA, and tyrosine kinase.[174,175] In HEK 293 cells, PKC-dependent stimulation of rOct1 was accompanied by phosphorylation of rOct1. After stimulation of rOct1 by PKC the *IC50* values obtained for inhibition of ASP uptake by TEA, tetrapentylammonium (TPeA), and quinine were decreased by factors of 58, 15, and 2, respectively. Substitution of the individual serine or threonine residues in each of the five putative PKC phosphorylation sites of rOct1 by alanine suppressed the PKC activation. Remarkably, the apparent affinities of TEA, TPeA, and quinine were changed differently in each mutant. After the mutations, no affect of PKC on the apparent affinity of rOct1 for TEA, TPeA, and quinine could be detected.

Taken together, complex, subtype-specific short-term regulations of the organic cation transporters were detected which may involve transporter phosphorylation and binding of regulatory proteins. Thereby functional properties of the transporter and the concentrations of transporters within the plasma membrane may be altered.

Transcriptional Long-Term Regulations of OCT1-3/Oct1-3

The genes encoding human OCT1, OCT2 and OCT3 are located in a cluster on chromosome 6q26−27 together with insulin like growth factor receptor 2 (IGF2R).[125,176] It has been suggested that OCTs and IGF2R are regulated in a coordinated way and that the regulation involves promotor methylation. The promotor of hOCT1 contains two DNA response elements for the hepatocyte nuclear factor-4α (HNF-4α).[177] HNF-4α binds to these response elements and activates transcription of hOCT1. This activation was inhibited by chenodeoxycholic acid via a component (SHP, small heterogenic partner) of the bile-acid inducible transcriptional repressor.[177] Basal transcription of hOCT2 is regulated by upstream stimulating factor 1 (USF1) which binds to a 5E-box regulatory element of hOCT2.[178] Kidney specific expression of hOCT2 versus expression in the liver is regulated by hypomethylation of the promoter including a CpG motif in the E-box.[179] Methylation of the CpG motif prevents binding of USF and down-regulates transcription. In rat kidneys of males expression of rOct2 is higher compared to females. Basolateral uptake of TEA into rat renal proximal tubule cells of male rats was twice as high as in females and correlated with increased levels of rOct2 mRNA and protein.[123] Application of testosterone to female rats resulted in increased expression of rOct2, whereas application of estradiol to male rats decreased the expression of rOct2.[123] Similarly it was shown that levels of Oct2 mRNA in Madin Darby canine kidney (MDCK) cells increased about twofold following exposure to testosterone.[123] Dexamethasone and hydrocortisone had similar effects. In the promotor of rat Oct2 two androgen response elements were identified that are required for the testosterone dependent regulation.[123] The steroid dependent regulation of OCT2/Oct2 is species dependent and may occur on the transcriptional and posttranscriptional level. For example in kidneys of male rabbits the concentration of rbOct2 mRNA was higher compared to female kidneys whereas rbOct2 protein and transport activity in male and female kidneys were similar.[123]

Regulations of OCT1-3/Oct1-3 in Kidney under Pathological Conditions

The expressions of OCTs/Octs in the kidney may be also changed during diseases and after treatments with drugs. For example, in rat renal expression of rOct2 was reduced during chronic renal failure. In 5/6-nephrectomized rats renal clearance of cimetidine was decreased in parallel with the expression of rOct2 protein whereas the expressions of rOct1, rOat1, rOat3, and Na^+,K^+-ATPase were not changed.[123] During diabetes renal expression of OCT1-3/Oct1-3 may be decreased. In rat, streptozotocin induced diabetes was associated with a reduction of renal clearance of N1-methyl-nicotinamide (NMN), basolateral uptake of TEA into renal proximal tubules and renal protein expressions of rOct1, rOct2 and rOct3.[123] During experimental hyperuricemia in rat, renal expression of rOct2 and renal functions were decreased.[123] Rats were made hyperuricemic by feeding with oxonic acid, an inhibitor of uric acid metabolism. After 10 days, plasma uric acid, plasma creatinine, and

blood urea nitrogen levels were significantly increased and TEA uptake in renal slices was decreased. In parallel, renal expression of rOct2 was decreased on mRNA and protein levels whereas expressions of rOct1 and rOct3 remained unchanged. Four days after application of a single dose of cisplatin to mice necrosis of renal proximal tubules and increased blood urea nitrogen levels were observed. In parallel the expression of Oct2 was reduced. The expressions of transporters Oat1, Oat2 and OatpA1 were reduced whereas the expressions of the export transporters Mrp2, Mrp4, Mrp5, Mdr1a, Mdr1b were increased.[37] In rat the renal expression of rOct2 protein was increased after depletion of magnesium.[180] The upregulation may explain why magnesium depletion enhances cisplatin-induced nephrotoxicity.[181]

Expression and Renal Functions of OCTN1/Octn1 (*SLC22A4/Slc22a4*)

OCTN1/Octn1 is another transporter of the *SLC22* family that is expressed in renal proximal tubules. It has been cloned from humans, rats, and mice and has been localized to the brush-border membrane.[182–185] In humans OCTN1 is also expressed in skeletal muscle, trachea, bone marrow, granulocytes, lymphocytes, macrophages and various additional tissues.[123] OCTN1/Octn1 may operate as organic cation/proton exchanger, as organic cation antiporter, as sodium-dependent transporter for zwitterions or as sodium-independent transporter for zwitterions.[123,186] Cations transported by the human transporter (hOCTN1) are TEA, quinidine, pyrilamine and verapamil whereas transported zwitterions are ergothioneine, glycine-betaine, betonicine, stachydrine, gabapentin, and carnitine.[123,186] In patients containing a point mutation in hOCTN1 (Leu503Phe) which leads to a reduced uptake of gabapentin, the excretion of gabapentin in the proximal tubule was decreased.[186] A metabolome analysis of wildtype mice compared with Octn1(-/-) mice indicated a complete deficiency of the naturally occuring antioxidant ergothioneine.[187] OCTN1/Octn1 is critical for ergothioneine absorption in small intestine and for reabsorption of ergothioneine in renal proximal tubules. Mutations in human OCTN1 (hOCTN1) have been associated with rheumatoid arthritis and Crohn's disease.[123] This is supposed to be due to reduced antioxidant effect of ergothioneine because patients with Crohn's disease showed largely reduced blood concentrations of ergothioneine, and Octn1(-/-) mice exhibited greater susceptibility to intestinal inflammation after ischemia.[187] In addition to its role for renal reabsorption or secretion of zwitterions, OCTN1/Octn1 is supposed to contribute to the efflux of organic cations across the luminal membrane of renal proximal tubules.

The proton/organic cation antiporters Mate1 and Mate2-K in the brush-border membrane of renal proximal tubules (Fig. 72.5) are probably the most important extrusion transporters for organic cations,[127] however, OCTN1/Octn1 has a different substrate selectivity and may complement efflux of organic cations.

Expression and Renal Functions of OCTN2/Octn2 (*SLC22A5/Slc22a5*)

OCTN2/Octn2 has been cloned from humans, rats, and mice.[184,188–190] In humans, expression of this transporter has been detected in skeletal muscle, heart, kidney, liver, placenta and many other organs.[123] In kidneys of rats and mice, Octn2 protein was localized to the apical membrane of proximal tubular epithelial cells.[123] Functional characterization revealed that hOCTN2 is a high affinity Na^+-carnitine and Na^+-mildronate cotransporter but can function alternatively as polyspecific and Na^+-independent cation uniporter that translocates for example TEA.[123,191] TEA and L-carnitine interact at the same binding site and/or use the same transport path since carnitine uptake by hOCTN2 was competitively inhibited by TEA, and TEA uptake by hOCTN2 was competitively inhibited by L-carnitine.[123] Na^+-dependent transport of L-carnitine by OCTN2/Octn2 is electrogenic and stereospecific.[123] For human OCTN2, an apparent K_m for L-carnitine of 4 to 5 μM and half-maximal concentrations for Na^+-activation between 2 and 19 mM were determined.[123] hOCTN2 is a polyspecific transporter since Na^+ dependent uptake of L-carnitine by hOCTN2 was inhibited by many organic cations and weak bases (e.g., nicotine, MPP, MPTP, procainamide, quinine, methamphetamine, emetine, clonidine, and cimetidine), zwitterions (e.g. cephaloridine, cefepime, and cefoselis), and noncharged compounds (e.g. corticosterone and aldosterone).[123]

A detailed characterization of the mouse Octn2 (mOctn2) showed that mOctn2 translocates organic cations in either directions across the plasma membrane.[123] L-carnitine uptake was trans-stimulated by intracellular TEA, and TEA efflux was trans-stimulated by extracellular L-carnitine. Studies with juvenile visceral steatosis (jvs) mice that suffer from a homozygous loss-of-function mutation of Octn2 indicated that Octn2 is critically involved in renal excretion of TEA.[123]

Expression, Renal Functions and Regulations of MATE1/Mate1 (*SLC47A1/Slc47a1*)

The *SLC47* family contains two subtypes of H^+-organic cation antiporters called multidrug and toxin extrusion 1 MATE1/Mate1 and kidney specific

MATE2-K/Mate-2K.[127] Human MATE1 was the first cloned and characterized member of the *SLC47* family.[192] Mate1 was also cloned from mouse, rat and rabbit.[127] hMATE1 is strongly expressed in liver, kidney and skeletal muscle, however, the tissue distribution of MATE1 in other species is different.[123] In kidney hMATE1 is located in the brush-border membrane of renal proximal tubules. hMATE1 translocates the model cations TEA, MPP and paraquat as well as fluoroquinolones.[147,193] Transported endogenous compounds are creatinine, estrone sulfate, guanidine and thiamine.[147] hMATE1 transports the antiarrhythmic drugs procainamide and levofloxacin; the antidiabetic drug metformin; the antifungal drug salicylic acid; the antineoplastic drugs cisplatin, oxaliplatin and topotecan; the antimalarial drug quinine; the anti-ulcer drug cimetidine; the antiallergic drug fexofenadine; and the antiviral drugs acyclovir, ganciclovir and tenofovir (Table 72.1). In hMATE1 four glutamate residues within transmembrane domains have been identified that are directly or indirectly involved in binding and/or translocation of TEA and cimetidine.[194] Using double-transfected MDCK cells containing hOCT2 in the basolateral membrane and hMATE1 in the luminal membrane it was shown that the basolateral-to apical transport of metformin as well as intracellular metformin could be inhibited by basolateral application of 1 mM cimetidine.[195] This indicates that both transporters are involved in renal secretion of metformin and may exhibit drug-drug interactions at hMATE1 and hOCT2. Removal of Mate1 in mice (mMate1) proved a potential physiological and pharmacological importance of mMate1 for renal secretion of organic cations.[195] After removal of mMate1 the renal clearance of metformin was reduced by more than 80%. After 5/6 nephrectomy of rats the expression of rMate1 was reduced.[196] Basal transcriptional activity of hMATE1 is regulated by transcription factors Sp1, activating protein-1 and activating protein-2 repressor.[197,198] Recently 10 variants of hMATE1 with reduced expression and/or changed transport function were identified.[199–201]

Expression and Renal Functions of MATE2-K (*SLC47A2*)

MATE2-K was cloned from human (hMATE2-K) and rabbit.[202,203] hMATE-K is predominantly expressed in human kidney. Like hMATE1, hMATE2-K is located in the brush-border membrane of renal proximal tubules and operates as H^+-organic cation antiporter. hMATE2-K transports the endogenous compounds creatinine, estrone sulfate, guanidine, N^1-methylnicotinamide and thiamine.[147] Drugs transported by hMATE2-K are procainamide, verapamil, tetracycline, captopril (antihypertensive), cisplatin, oxaliplatin, topotecan, quinine, cimetidine, acyclovir, ganciclovir and metformin (Table 72.1). For many compounds interacting with hMATE2-K similar affinites have been observed compared to hMATE1. Exceptions are disopyramide, cephradine, desipramine, diltiazem, pramipexole, amantadine, and famotidine (Table 72.1 and[147]). Two variants of hMATE2-K with reduced amounts of transporter protein within the plasma membrane have been identified.[199]

Expression and Renal Functions of MDR1/Mdr1 (ABCB1/Abcb1)

MDR1/Mdr1 or P-glycoprotein is a member of the ATP-binding cassette (ABC) superfamily of transport proteins. It is a polyspecific transporter for hydrophobic solutes including organic cations.[86,123] MDR1/Mdr1 is composed of two homologous halves, each containing six TMHs and an ATP-binding domain. This transporter is infamous for inducing resistance to anticancer drugs in cancer cells; however, it is also found in healthy tissues, including liver, kidney, small intestine, brain and other organs. In kidneys, MDR1/Mdr1 was located to the luminal membrane of proximal tubules in human and mouse.[123] In human kidney, expression of MDR1 was also detected in the mesangium, thick ascending limb of Henle loop, and collecting duct.[123] MDR1/Mdr1 is a primary active transporter that pumps, driven by ATP hydrolysis, compounds of various structures out of cells. Water-soluble substrates are taken up directly from the cytosol, whereas hydrophobic substrates from the cytosol or from the extracellular side partition into the plasma membrane and enter the transporter from the lipid phase.[204] In rat, the involvement of Mdr1 in the renal secretion of digoxin was demonstrated.[123]

Substrates of MDR1/Mdr1 include a large variety of exogenous and endogenous compounds that may be very hydrophobic and may have molecular masses above 1000 Da. The substrates may be amphiphilic or uncharged. They may contain a positive or negative net charge. Human MDR1 transports aldosterone. Drugs that are tranported by human MDR1 are dexamethason and hydrocortisone; the cardiac glycoside digoxin; the antiarrhythmics quinidine, verapamil and propafenone; the antineoplastic compounds colchicine, daunorubicin, doxorubicin, vinblastine, vincristine and topotecan; the antibiotics cefazolin and cefoperazon; the HIV protease inhibitors indinavir, ritonavir and saquinavir; and the immunosuppressant cyclosporine. In addition hMDR1 translocates antihypertensive, anticholinergic, antidepressant, and antihistaminic drugs, antimalaria, antifungal, and antihelminthic agents.[123] For secretion of specific cationic drugs in human

proximal tubules the combined actions of hOCT2 in the basolateral membrane with hMDR1, hMATE-1 and/or hMATE2-K in the brush-border membrane may be required (Fig. 72.5, Table 72.1).

Drug-Drug Interactions at Organic Cation Transporters in Kidney

Drug-drug interactions at organic cation transporters in kidney may influence the excretion of drugs that are secreted in the proximal tubule or the reabsorption of drugs that are ultrafiltrated in the proximal and/or distal tubule. Since significant species differences exist concerning location, selectivity and regulation of the organic cation transporters conclusions about drug-drug interactions in humans should not be drawn from studies in animals. If different drugs are translocated by the same transporter they mutually block their translocation competitively. A nontransported drug may also block binding or translocation of a transported drug. It should be kept in mind that the affinity of nontransported inhibitory drugs to inhibit translocation of different substrates may differ largely at least in case of OCTs/Octs.[147] Drug-drug interactions at individual transporters may be clinically relevant if the respective transporter plays a significant role for the renal excretion or reabsorption of the specific drug and the *in vivo* concentrations of the inhibiting drugs are high enough. Whether transporters are critically involved in renal handling of a specific drug in humans can only be concluded on the basis of studies with patients containing mutated transporters with changed functions. When the critical involvement of a transporter for a specific drug has been determined drug-drug interaction on that transporter may be concluded from clinical studies in which the effects of coapplication of drugs are investigated.

The cytostatic cisplatin is transported by OCT2/Oct2 of human and rodents and it has been shown in rodents that Oct2 is critically involved in renal excretion and nephrotoxicity of cisplatin.[148,205,206] Since the nephrotoxicity of cisplatin was reduced in patients with defect mutations of OCT2, this transporter is also critical for cisplatin nephrotoxicity in humans.[150] In mice, cisplatin nephrotoxicity could be reduced by coapplication of cimetidine suggesting drug-drug interaction of these two substrates at Oct2.[148] Thus cimetidine may be employed to reduce cisplatin nephrotoxicity in humans. Studies in rats also suggest that cisplatin nephrotoxicity in humans can be reduced by coapplication with the antineoplastic drug imatinib which is a high affinity inhibitor of OCTs.[207] Clinical studies suggested interaction of organic cations during renal excretion which may occur at different transporters in the proximal tubule. For example, coapplication of cimetidine which is translocated by hOCT2, hMATE1, hMATE2-K and hMDR1 reduced tubular secretion of metformin which is transported by hOCT1-3, hMATE1 and hMATE2-K,[208] of ranitidine transported by hOCT2,[209] and of procainamide transported by hOCT1, hMATE1 and hMATE2-K.[210]

hOCT2 transports the HIV drug lamuvidine with an apparent K_m value around 1 mM. Lamuvidine inhibited uptake of 12.5 nM MPP 40% with an IC_{50} value of 8 pM.[171] This observation shows that clinically relevant low concentrations of lamuvidine or other cationic drugs may partially inhibit renal secretion of hOCT2 substrates which are present in concentration far below their respective K_m values.

Polymorphisms and Mutations in Organic Cation Transporters

Genetic variants in hOCT, hOCTN and hMATE transporters and hMDR1 may account for interindividual variability of pharmacokinetics of cationic drugs. Geographic, ethnic, and racial differences in the frequency of genetic variants of drug transporters may be reasons for differences in drug response and/or drug toxicity.[147] So far, more than 2000 single-nucleotide polymorphisms (SNPs) for the hOCT, hOCTN and hMATE genes were listed in the databases. Current next-generation sequencing projects aim at the complete sequencing of 1000 human genomes to identify more variants, especially those with low frequencies.[211] Most sequence variants are present in introns and may have no phenotypic consequences. Variants located in the 5′- and 3′-flanking regions may lead to an altered expression level.[132,212] Sequence variants within exons may result in amino acid substitutions. These nonsynonymous or missense variants may affect transport function. The functional effects of missense mutations have to be determined experimentally. They may lead to changed amounts of transport protein in the plasma membrane, to changed regulation, to changed K_m and V_{max} values of transported compounds, and to changes of IC_{50} values of inhibitors. Since the effects on K_m, V_{max} and IC_{50} values may be cation specific, missense mutations may change transporter selectivity. Most non-synonymous variants in human genes encoding OCTs and MATEs that affect function and/or expression have been compiled in a recent review.[147] Some functional relevant missense mutations of hOCTNs have been reported earlier.[123] For recently published functional relevant missense mutations see references.[186,199–201]

It may be very difficult to identify clinical effects of missense mutations. This may be exemplified by the

investigations on effects of hOCT variants on the treatment of the antidiabetic metformin. Metformin is transported by hOCT1, hOCT2 and hOCT3 and variants of hOCT1 and hOCT2 with reduced transport activity for metformin have been identified.[147] A relatively small group of healthy volunteers with defect mutations in hOCT1 showed a blunted reduction of blood glucose after application of metformin.[213] This was explained by reduced uptake of metformin in the liver. At variance no correlation was observed between patients with type 2 diabetes that do not benefit from metformin treatment and patients with hOCT1 variants.[214] Controverse data were also obtained concerning the effects of hOCT2 variants on renal excretion of metformin. In three studies employing 14-26 individuals a decreased renal metformin excretion has been reported in patients with defect mutations in hOCT2.[213,215,216] This observation was not reproduced in a fourth study using 104 patients.[143] This suggests that metformin secretion in the proximal tubule and the role of hOCT2 in this process is not physiologically relevant. Interestingly Tzvetkow and coworkers observed that patients containing hOCT1 variants with reduced transport activity showed an increased renal excretion of metformin.[143] Since hOCT1 was detected in luminal membranes of proximal and distal tubules[143] the authors hypothesized that hOCT1 mediates the first step in the reabsorption of ultrafiltrated metformin and that this reabsorption is physiologically important.

OUTLOOK

After cloning of various polyspecific transporters most systems involved in the secretion and reabsorption of organic anions and cations in human renal proximal tubules have been identified. The relevant modes of operation of these transporters have been defined and admittedly incomplete substrate specificities have been determined. For some transporters the transport mechanism has been tentatively elucidated. Mutagenesis experiments and modeling provided evidence that the OCTs/Octs and, most likely also the other polyspecific transporters contain a large binding region where two or more substrates can bind simultaneously. High and low affinity binding sites were observed which may exhibit mutual allosteric interactions and may inhibit the transport. Most missense mutations in human organic anion and cation transporters leading to functional changes have been identified. Short- and long-term regulations of several transporters have been observed showing that transcription, membrane turnover, substrate selectivity and/or transport activity can be regulated. For short-term regulation some signaling pathways were identified, however, the involved mechanisms are not understood. These observations and species differences concerning substrate selectivities and regulation show that our knowledge derived from individual transporters as well as from knockout mice only provides approximate ideas concerning drug excretion in human proximal tubules *in vivo*. It is a challenge for future investigations to identify the transporters which are critical for secretion and reabsorption of specific drugs in human, to identify the functional consequence of missense mutations, and to determine biomedical relevant drug-drug interactions. These drug-drug interactions may occur at the level of individual transporters (i.e., by competition) or at the cellular level (e.g., by changes of membrane potential). Taken together, we still must follow a long road toward understanding the behavior of drugs in the kidney.

References

[1] Pritchard JB, Miller DS. Mechanisms mediating renal secretion of organic anions and cations. Physiol Rev 1993;73:765–96.

[2] Burckhardt G, Pritchard JB. Organic anion and cation antiporters. In: Seldin DW, Giebisch G, editors. The kidney: physiology and pathophysiology. 3rd ed. Philadelphia: Lippincott Williams & Wilkins; 2000. p. 193–222.

[3] Ullrich KJ. Renal transporters for organic anions and organic cations. Structural requirements for substrates. J Membr Biol 1997;158:95–107.

[4] Shimada H, Moewes B, Burckhardt G. Indirect coupling to Na^+ of *p*-aminohippuric acid uptake into rat renal basolateral membrane vesicles. Am J Physiol Renal Physiol 1987;253:F795–801.

[5] Pritchard JB. Coupled transport of *p*-aminohippurate by rat kidney basolateral membrane vesicles. Am J Physiol Renal Physiol 1988;255:F597–604.

[6] Shuprisha A, Lynch RM, Wright SH, Dantzer V. Real-time assessment of α-ketoglutarate effect on organic anion secretion in perfused rabbit proximal tubules. Am J Physiol Renal Physiol 1999;277:F513–23.

[7] Rizwan AN, Burckhardt G. Organic anion transporters of the SLC22 family: biopharmaceutical, physiological, and pathological roles. Pharm Res 2007;24:450–70.

[8] VanWert AL, Gionfriddo MR, Sweet DH. Organic anion transporters: discovery, pharmacology, regulation and roles in pathophysiology. Biopharm Drug Dispos 2010;31:1–71.

[9] Srimaroeng C, Perry JL, Pritchard JB. Physiology, structure, and regulation of the cloned organic anion transporters. Xenobiotica 2008;38:889–935.

[10] Jacobsson JA, Haitina T, Lindblom J, Fredriksson R. Identification of six putative human transporters with structural similarity to the drug transporter SLC22 family. Genomics 2007;90:595–609.

[11] Eraly SA, Hamilton BA, Nigam SK. Organic anion and cation transporters occur in pairs of similar and similarly expressed genes. Biochem Biophys Res Commun 2003;300:333–42.

[12] Bleasby K, Castle JC, Roberts CJ, et al. Expression profiles of 50 xenobiotic transporter genes in humans and pre-clinical species: a resource for investigations into drug disposition. Xenobiotica 2006;36:963–88.

[13] Hilgendorf C, Ahlin G, Seithel A, Artursson P, Ungell A-L, Karlsson J. Expression of thirty-six drug transporter genes in

human intestine, liver, kidney, and organotypic cell lines. Drug Metab Dispos 2007;35:1333–40.
[14] Nishimura M, Naito S. Tissue-specific mRNA expression profiles of human ATP-binding cassette and solute carrier transporter superfamilies. Drug Metab Pharmacokinet 2005;20: 452–77.
[15] Buist SCN, Cherrington NJ, Choudhuri S, Hartley DP, Klaassen CD. Gender-specific and developmental influences on the expression of rat organic anion transporters. J Pharmacol Exp Ther 2002;301:145–51.
[16] Buist SCN, Klaassen CD. Rat and mouse differences in gender-predominant expression of organic anion transporter (OAT1-3, *SLC22A6-8*) mRNA levels. Drug Metab Dispos 2004;32:620–5.
[17] Ljubojevic M, Herak-Kramberger CM, Hagos Y, et al. Rat renal cortical OAT1 and OAT3 exhibit gender differences determined by both androgen stimulation and estrogen inhibition. Am J Physiol Renal Physiol 2004;287:F124–38.
[18] Sabolic I, Asif AR, Budach WE, Wanke C, Bahn A, Burckhardt G. Gender differences in kidney function. Pflügers Arch - Eur J Physiol 2007;455:397–429.
[19] Höcherl K, Schmidt C, Bucher M. COX-2 inhibition attenuates endotoxin-induced downregulation of organic anion transporters in the renal cortex. Kidney Int 2009;75:373–80.
[20] Wolff NA, Thies K, Kuhnke N, et al. Protein kinase C activation downregulates human organic anion transporter 1-mediated transport through carrier internalization. J Am Soc Nephrol 2003;14:1959–68.
[21] You G, Kuze K, Kohanski RA, Amsler K, Henderson S. Regulation of mOAT-mediated organic anion transport by ocadaic acid and protein kinase C in LLC-PK_1 cells. J Biol Chem 2000;275:10278–84.
[22] Kwak J-O, Kim H-W, Oh K-J, Kim DS, Han KO, Cha SH. Co-localization and interaction of organic anion transporter 1 with caveolin-2 in rat kidney. Exp Mol Med 2005;37:204–12.
[23] Di Giusto G, Anzai N, Ruiz ML, Endou H, Torres AM. Expression and function of Oat1 and Oat3 in rat kidney exposed to mercuric chloride. Arch Toxicol 2009;83:887–97.
[24] Kerb R. Implications of genetic polymorphisms in drug transporters for pharmacotherapy. Cancer Lett 2006;234:4–33.
[25] Burckhardt BC, Burckhardt G. Transport of organic anions across the basolateral membrane of proximal tubule cells. Rev Physiol Biochem Pharmacol 2003;146:95–158.
[26] Masereeuw R, Russel FGM. Therapeutic implications of renal anionic drug transporters. Pharmacol Ther 2010;126:200–16.
[27] Ho RH, Kim RB. Transporters and drug therapy: Implications for drug disposition and disease. Clin Pharmacol Ther 2005;78:260–77.
[28] Kaler G, Truong DM, Khandelwal A, et al. Structural variation governs substrate specificity for organic anion transporter (OAT) homologs. Potential remote sensing by OAT family members. J Biol Chem 2007;282:23841–53.
[29] Rizwan AN, Krick W, Burckhardt G. The chloride dependence of the human organic anion transporter 1 (hOAT1) is blunted by mutation of a single amino acid. J Biol Chem 2007;282: 13402–9.
[30] Eraly SA, Vallon V, Vaughn DA, et al. Decreased renal organic anion secretion and plasma accumulation of endogenous organic anions in OAT1 knockout mice. J Biol Chem 2006;281:5072–83.
[31] Vallon V, Rieg T, Ahn SY, Wu W, Eraly SA, Nigam SK. Overlapping in vitro and in vivo specificities of the organic anion transporters OAT1 and OAT3 for loop and thiazide diuretics. Am J Physiol Renal Physiol 2008;294:F867–73.
[32] Enomoto A, Takeda M, Shimoda M, et al. Interaction of human organic anion transporters 2 and 4 with organic anion transport inhibitors. J Pharmacol Exp Ther 2002;301:797–802.
[33] Ljubojevic M, Balen D, Breljak D, et al. Renal expression of organic anion transporter OAT2 in rats and mice is regulated by sex hormones. Am J Physiol Renal Physiol 2007;292: F361–72.
[34] Maher JM, Slitt AL, Callaghan TN, et al. Alterations in transporter expression in liver, kidney, and duodenum after targeted disruption of the transcription factor HNF1α. Biochem Pharmacol 2006;72:512–22.
[35] Popowski K, Eloranta JJ, Saborowski M, Fried M, Meier PJ, Kullak-Ublick GA. The human organic anion transporter 2 gene is transactivated by hepatocyte nuclear factor-4α and suppressed by bile acids. Mol Pharmacol 2005;67:1629–38.
[36] Manautou JE, Nowicki MT, Aleksunes LM, Sawant SP, Dnyanmote AV, Mehendale HM. Renal and hepatic transporter expression in type 2 diabetic rats. Drug Metab Lett 2008;2:11–7.
[37] Aleksunes LM, Augustine LM, Scheffer GL, Cherrington NJ, Manautou JE. Renal xenobiotic transporters are differentially expressed in mice following cisplatin treatment. Toxicology 2008;250:82–8.
[38] Cropp CD, Komori T, Shima JE, et al. Organic anion transporter 2 (*SLC22A7*) is a facilitative transporter of cGMP. Mol Pharmacol 2008;73:1151–8.
[39] Sato M, Mamada H, Anzai N, Shirasaka Y, Nakanishi T, Tamai I. Renal secretion of uric acid by organic anion transporter 2 (*OAT2*/*SLC22A7*) in human. Biol Pharm Bull 2010;33:498–503.
[40] Motohashi H, Sakurai Y, Saito H, et al. Gene expression levels and immunolocalization of organic ion transporters in human kidney. J Am Soc Nephrol 2002;13:866–74.
[41] Sweet DH, Miller DS, Pritchard JB, Fujiwara Y, Beier DR, Nigam SK. Impaired organic anion transport in kidney and choroid plexus of organic anion transporter 3 (*Oat3* (*Slc22a8*)) knockout mice. J Biol Chem 2002;277:26934–43.
[42] Urban TJ, Sebro R, Hurowitz EH, et al. Functional genomics of membrane transporters in human populations. Genome Res 2006;16:223–30.
[43] Vallon V, Eraly SA, Wikoff WR, et al. Organic anion transporter 3 contributes to the regulation of blood pressure. J Am Soc Nephrol 2008;19:1732–40.
[44] VanWert AL, Srimaroeng C, Sweet DH. Organic anion transporter 3 (Oat3/*Slc22a8*) interacts with carboxyfluoroquinolones, and deletion increases systemic exposure to ciprofloxacin. Mol Pharmacol 2008;74:122–31.
[45] Feng B, Dresser MJ, Shu Y, Johns SJ, Giacomini KM. Arginine 454 and lysine 370 are essential for the anion specificity of the organic anion transporter, rOAT3. Biochemistry 2001;40: 5511–20.
[46] Feng B, Shu Y, Giacomini KM. Role of aromatic transmembrane residues of the organic anion transporter, rOAT3, in substrate recognition. Biochemistry 2002;41:8941–7.
[47] Mikkaichi T, Suzuki T, Onogawa T, et al. Isolation and characterization of a digoxin transporter and its rat homologue expressed in the kidney. Proc Natl Acad Sci USA 2004;101: 3569–74.
[48] Hagenbuch B, Gui C. Xenobiotic transporters of the human organic anion transporting polypeptides (ATP) family. Xenobiotica 2008;38:778–801.
[49] Deeley RG, Westlake C, Cole SPC. Transmembrane transport of endo- and xenobiotics by mammalian ATP-binding cassette multidrug resistance proteins. Physiol Rev 2006;86:849–99.
[50] Zhou F, Tanaka K, Pan Z, Ma J, You G. The role of glycine residues in the function of human organic anion transporter 4. Mol Pharmacol 2004;65:1141–7.
[51] Hagos Y, Stein D, Ugele B, Burckhardt G, Bahn A. Human renal organic anion transporter 4 (hOAT4) operates as an asymmetric urate transporter. J Am Soc Nephrol 2007;18:430–9.

[52] Hagos Y, Bahn A, Vormfelde SV, Brockmöller J, Burckhardt G. Torasemide transport by organic anion transporters contributes to hyperuricemia. J Am Soc Nephrol 2007;18:3101–9.
[53] Anzai N, Jutabha P, Enomoto A, et al. Functional characterization of rat organic anion transporter 5 (*Slc22a19*) at the apical membrane of renal proximal tubules. J Pharmacol Exp Ther 2005;315:534–44.
[54] Youngblood GL, Sweet DH. Identification and functional assessment of the novel murine organic anion transporter Oat5 (*Slc22a19*) expressed in kidney. Am J Physiol Renal Physiol 2004;287:F236–44.
[55] Bahn A, Hagos Y, Reuter S, et al. Identification of a new urate and high affinity nicotinate transporter, hOAT10 (SLC22A13). J Biol Chem 2008;283:16332–41.
[56] Enomoto A, Kimura H, Chairoungdua A, et al. Molecular identification of a renal urate-anion exchanger that regulates blood urate levels. Nature 2002;417:447–52.
[57] Vázquez-Mellado J, Jiménez-Vaca AL, Cuevas-Covarrubias S, Alvarado-Roma V, Pozo-Molina G, Burgos-Vargas R. Molecular analysis of the SLC22A12 (URAT1) gene in patients with primary gout. Rheumatology 2007;46:215–9.
[58] Hosoyamada M, Ichida K, Enomoto A, Hosoya T, Endou H. Function and localization of urate transporter 1 in mouse kidney. J Am Soc Nephrol 2004;15:261–8.
[59] Imaoka T, Kusuhara H, Adachi-Akahane S, et al. The renal-specific transporter mediates facilitative transport of organic anions at the brush border membrane of mouse renal tubules. J Am Soc Nephrol 2004;15:2012–22.
[60] Thangaraju M, Ananth S, Martin PM, et al. c/ebpδ null mouse as a model for a double knock-out of slc5a8 and slc5a12 in kidney. J Biol Chem 2006;281:26769–73.
[61] Jutabha P, Kanai Y, Hosoyamada M, et al. Identification of a novel voltage-driven organic anion transporter present at apical membrane of renal proximal tubule. J Biol Chem 2003;278: 27930–8.
[62] Reimer RJ, Edwards RH. Organic anion transport is the primary function of the SLC17/type I phosphate transporter family. Pflügers Arch - Eur J Physiol 2004;447:629–35.
[63] Cheret C, Doyen A, Yaniv M, Pontoglio M. Hepatocyte nuclear factor 1 a controls renal expression of the Npt1-Npt4 anionic transporter locus. J Mol Biol 2002;322:929–41.
[64] Soumounou Y, Gauthier C, Tenenhouse HS. Murine and human type I Na-phosphate cotransporter genes: structure and promoter activity. Am J Physiol Renal Physiol 2001;281:F1082–91.
[65] Li H, Ren P, Onwochei M, Ruch RJ, Xie Z. Regulation of rat Na^+/P_i cotransporter-1 gene expression: the roles of glucose and insulin. Am J Physiol Endocrinol Metab 1996;271:E1021–8.
[66] Uchino H, Tamai I, Yamashita K, et al. *p*-Aminohippuric acid transport at renal apical membrane mediated by human inorganic phosphate transporter NPT1. Biochem Biophys Res Commun 2000;270:254–9.
[67] Yabuuchi H, Tamai I, Morita K, et al. Hepatic sinusoidal membrane transport of anionic drugs mediated by anion transporter. Npt1 J Pharmacol Exp Ther 1998;286:1391–6.
[68] Iharada M, Miyaji T, Fujimoto T, et al. Type 1 sodium dependent phosphate transporter (SLC17A1 protein) is a Cl-dependent urate transporter. J Biol Chem 2010;285:26107–13.
[69] Busch AE, Schuster A, Waldegger S, et al. Expression of a renal type I sodium/phosphate transporter (NaPi-1) induces a conductance in *Xenopus* oocytes permeable for organic and inorganic anions. Proc Natl Acad Sci USA 1996;93:5347–51.
[70] Uchino H, Tamai I, Yabuuchi H, et al. Faropenem transport across the renal epithelial luminal membrane via inorganic phosphate transporter Npt1. Antimicrob Agents Chemother 2000;44:574–7.
[71] Urano W, Taniguchi A, Anzai N, et al. Sodium-dependent phosphate cotransporter type 1 sequence polymorphisms in male patients with gout. Ann Rheum Dis 2010;69:1232–4.
[72] Ruddy DA, Kronmal GS, Lee VK, et al. A 1.1-Mb transcript map of the hereditary hemochromatosis locus. Genome Res 1997;7:441–56.
[73] Ishibashi K, Matsuzaki T, Takata K, Imai M. Identification of a new member of type I Na/phosphate co-transporter in the rat kidney. Nephron Physiol 2002;94:10–8.
[74] Jutabha P, Anzai N, Kitamura K, et al. Human sodium phosphate transporter 4 (hNPT4/*SLC17A3*) as a common renal secretory pathway for drugs and urate. J Biol Chem 2010;285: 35123–32.
[75] Melis D, Havelaar AC, Verbeek E, et al. NPT4, a new microsomal phosphate transporter: mutation analysis in glycogen storage disease type 1c. J Inherit Metab Dis 2004;27:725–33.
[76] Dehghan A, Köttgen A, Yang Q, et al. Association of three genetic loci with uric acid concentration and risk of gout: a genome-wide association study. Lancet 2008;372:1953–61.
[77] Stark K, Reinhard W, Grassl M, et al. Common polymorphisms influencing serum uric acid levels contribute to susceptibility to gout, but not to coronary artery disease. PloS ONE 2009;4:e7729.
[78] Polasek O, Jeroncic I, Mulic R, et al. Common variants in SLC17A3 gene affect intra-personal variation in serum uric acid levels in longitudinal time series. Croat Med J 2010;51:32–9.
[79] Hagenbuch B, Meier PJ. Organic anion transporting polypeptides of the OATP/SLC21 family: phylogenetic classification as OATP/SLCO superfamily, new nomenclature and molecular/functional properties. Pflügers Arch - Eur J Physiol 2004;447: 653–65.
[80] Lee W, Glaeser H, Smith LH, et al. Polymorphisms in human organic anion-transporting polypeptide 1A2 (OATP1A2). Implications for altered drug disposition and central nervous system drug entry. J Biol Chem 2005;280:9610–7.
[81] Bergwerk AJ, Shi X, Ford AC, et al. Immunologic distribution of an organic anion transport protein in rat liver and kidney. Am J Physiol Gastrointest Liver Physiol 1996;271:G231–8.
[82] Masuda S, Saito H, Nonoguchi H, Tomita K, Inui K-I. mRNA distribution and membrane localization of the OAT-K1 organic anion transporter in rat renal tubules. FEBS Lett 1997;407: 127–31.
[83] Cheng X, Maher J, Chen C, Klaassen CD. Tissue distribution and ontogeny of mouse organic anion transporting polypeptides (OATPS). Drug Metab Dispos 2005;33:1062–73.
[84] Li N, Hartley DP, Cherrington NJ, Klaassen CD. Tissue expression, ontogeny, and inducibility of rat organic anion transporting polypeptide 4. J Pharmacol Exp Ther 2002;301:551–60.
[85] Hagenbuch B, Meier PJ. The superfamily of organic anion transporting polypeptides. Biochim Biophys Acta 2003;1609: 1–18.
[86] Van Montfoort J, Meijer DKF, Groothuis GMM, Koepsell H, Meier PJ. Drug uptake systems in liver and kidney. Curr Drug Metab 2003;4:185–211.
[87] Masuda S. Functional characteristics and pharmacokinetic significance of kidney-specific organic anion transporters, OAT-K1 and OAT-K2, in the urinary excretion of anionic drugs. Drug Metab Pharmacokinet 2003;18:91–103.
[88] Masuda S, Ibaramoto K, Takeuchi A, Saito H, Hashimoto Y, Inui K. Cloning and functional characterization of a new multispecific organic anion transporter, OAT-K2, in rat kidney. Mol Pharmacol 1999;55:743–52.
[89] Masuda S, Takeuchi A, Saito H, Hashimoto Y, Inui K-I. Functional analysis of rat renal organic anion transporter OAT-K1: bidirectional methotrexate transport in apical membrane. FEBS Lett 1999;459:128–32.

[90] Takeuchi A, Masuda S, Saito H, Doi T, Inui K-I. Role of kidney-specific organic anion transporters in the urinary excretion of methotrexate. Kidney Int 2001;60:1058–68.
[91] Jedlitschky G, Hoffmann U, Kroemer HK. Structure and function of the MRP2 (ABCC2) protein and its role in drug disposition. Expert Opin Drug Metab Toxicol 2006;2:351–66.
[92] van de Water F, Masereeuw R, Russel FGM. Function and regulation of multidrug resistance proteins (MRPs) in the renal elimination of organic anions. Drug Metab Rev 2005;37: 443–71.
[93] Maher JM, Slitt AL, Cherrington NJ, Cheng X, Klaassen CD. Tissue distribution and hepatic and renal ontogeny of the multidrug resistance-associated protein (MRP) family in mice. Drug Metab Dispos 2005;33:947–55.
[94] Nies AT, Schwab M, Keppler D. Interplay of conjugating enzymes with OATP uptake transporters and ABCC/MRP efflux pumps in the elimination of drugs. Expert Opin Drug Metab Toxicol 2008;4:545–68.
[95] Choudhuri S, Klaassen CD. Structure, function, expression, genomic organization, and single nucleotide polymorphisms of human ABCB1 (MDR1), ABCC (MRP), and ABCG2 (BCRP) efflux transporters. Int J Toxicol 2006;25:231–59.
[96] Schaub TP, Kartenbeck J, König J, et al. Expression of the conjugate export pump encoded by the *mrp2* gene in the apical membrane of kidney proximal tubules. J Am Soc Nephrol 1997;8:1213–21.
[97] Schaub TP, Kartenbeck J, König J, et al. Expression of the *MRP2* gene-encoded conjugate export pump in human kidney proximal tubules and in renal cell carcinoma. J Am Soc Nephrol 1999;10:1159–69.
[98] Gradhand U, Kim RB. Pharmacogenomics of MRP transporters (ABCC1-5) and BCRP (ABCG2). Drug Metab Rev 2008;40: 317–54.
[99] Büchler M, König J, Brom M, et al. cDNA cloning of the hepatocyte canalicular isoform of the multidrug resistance protein, cMrp, reveals a novel conjugate export pump deficient in hyperbilirubinemic mutant rats. J Biol Chem 1996;271:15091–8.
[100] Paulusma CC, Bosma PJ, Zaman GJ, et al. Congenital jaundice in rats with a mutation in a multidrug resistance-associated protein gene. Science 1996;271:1126–8.
[101] Kruh GD, Belinsky MG, Gallo JM, Lee K. Physiological and pharmacological functions of Mrp2, Mrp3 and Mrp4 as determined from recent studies on gene-disrupted mice. Cancer Metast Rev 2007;26:5–14.
[102] Izzedine H, Hulot JS, Villard E, et al. Association between ABCC2 gene haplotypes and tenofovir-induced proximal tubulopathy. J Infect Dis 2006;194:1481–91.
[103] Haenisch S, Zimmermann U, Dazert E, et al. Influence of polymorphisms of ABCB1 and ABCC2 on mRNA and protein expression in normal and cancerous kidney cortex. Pharmacogenomics 2007;7:56–65.
[104] Leier I, Hummel-Eisenbeiss J, Cui Y, Keppler D. ATP-dependent *para*-aminohippurate transport by apical multidrug resistance protein MRP2. Kidney Int 2000;57:1636–42.
[105] Maher JM, Cheng X, Tanaka Y, Scheffer GL, Klaassen CD. Hormonal regulation of renal multidrug resistance-associated proteins 3 and 4 (Mrp3 and Mrp4) in mice. Biochem Pharmacol 2006;71:1470–8.
[106] Chen C, Klaassen CD. Rat multidrug resistance protein 4 (Mrp4, Abcc4): molecular cloning, organ distribution, postnatal renal expression, and chemical inducibility. Biochem Biophys Res Commun 2004;23:46–53.
[107] Van Aubel RAMH, Smeets PHE, Peters JGP, Bindels RJM, Russel FGM. The *MRP4*/*ABCC4* gene encodes a novel apical organic anion transporter in human kidney proximal tubules: Putative efflux pump for urinary cAMP and cGMP. J Am Soc Nephrol 2002;13:595–603.
[108] Russel FGM, Koenderink JB, Masereeuw R. Multidrug resistance protein 4 (MRP4/ABCC4): a versatile efflux transporter for drugs and signalling molecules. Trends Pharmacol Sci 2008;29:200–7.
[109] Schuetz JD, Connelly MC, Sun D, et al. MRP4: A previously unidentified factor in resistance to nucleoside-based antiviral drugs. Nature Medicine 1999;5:1048–51.
[110] Van Aubel RAMH, Smeets PHE, van den Heuvel JJMW, Russel FGM. Human organic anion transporter MRP4 (ABCC4) is an efflux pump for the purine end metabolite urate with multiple allosteric substrate binding sites. Am J Physiol Renal Physiol 2005;288:F327–33.
[111] Hasegawa M, Kusuhara H, Adachi M, Schuetz JD, Takeuchi K, Sugiyama Y. Multidrug resistance-associated protein 4 is involved in the urinary excretion of hydrochlorothiazide and furosemide. J Am Soc Nephrol 2007;18:37–45.
[112] Imaoka T, Kusuhara H, Adachi M, Schuetz JD, Takeuchi K, Sugiyama Y. Functional involvement of multidrug resistance-associated protein 4 (MRP4/ABCC4) in the renal elimination of the antiviral drugs adefovir and tenofovir. Mol Pharmacol 2007;71:619–27.
[113] Ci L, Kusuhara H, Adachi M, Schuetz JD, Takeuchi K, Sugiyama Y. Involvement of MRP4 (ABCC4) in the luminal efflux of ceftizoxime and cefazolin in the kidney. Mol Pharmacol 2007;71:1591–7.
[114] Smeets PHE, Van Aubel RAMH, Wouterse AC, van den Heuvel JJMW, Russel FGM. Contribution of multidrug resistance protein 2 (MRP2/ABCC2) to the renal excretion of *p*-aminohippurate (PAH) and identification of MRP4 (ABCC4) as a novel PAH transporter. J Am Soc Nephrol 2004;15: 2828–35.
[115] Bakos E, Evers R, Sinkó E, Váradi A, Borst P, Sarkadi B. Interactions of the human multidrug resistance proteins MRP1 and MRP2 with organic anions. Mol Pharmacol 2000; 57:760–8.
[116] Mulato AS, Ho ES, Cihlar T. Nonsteroidal anti-inflammatory drugs efficiently reduce the transport and cytotoxicity of adefovir mediated by the human renal organic anion transporter 1. J Pharmacol Exp Ther 2000;295:10–5.
[117] Inui K-I, Masuda S, Saito H. Cellular and molecular aspects of drug transport in the kidney. Kidney Int 2000;58:944–58.
[118] Mizuno N, Niwa T, Yotsumoto Y, Sugiyama Y. Impact of drug transporter studies on drug discovery and development. Pharmacol Rev 2003;55:425–61.
[119] Takeda M, Khamdang S, Narikawa S, et al. Characterization of methotrexate transport and its drug interactions with human organic anion transporters. J Pharmacol Exp Ther 2002;302: 666–71.
[120] Masuda S, Saito H, Inui K-I. Interactions of nonsteroidal anti-inflammatory drugs with rat renal organic anion transporter, OAT-K1. J Pharmacol Exp Ther 1997;283:1039–42.
[121] Reid G, Wielinga P, Zelcer N, et al. The human multidrug resistance protein MRP4 functions as a prostaglandin efflux transporter and is inhibited by nonsteroidal antiinflammatory drugs. Proc Natl Acad Sci USA 2003;100:9244–9.
[122] Saito H, Masuda S, Inui K-I. Cloning and functional characterization of a novel rat organic anion transporter mediating basolateral uptake of methotrexate in the kidney. J Biol Chem 1996;271:20719–25.
[123] Koepsell H, Lips K, Volk C. Polyspecific organic cation transporters: Structure, function, physiological roles, and biopharmaceutical implications. Pharm Res 2007;24:1227–51.

[124] Koepsell H. Organic cation transporters in intestine, kidney, liver, and brain. Annu Rev Physiol 1998;60:243–66.
[125] Koepsell H, Schmitt BM, Gorboulev V. Organic cation transporters. Rev Physiol Biochem Pharmacol 2003;150:36–90.
[126] Pao SS, Paulsen IT, Saier Jr. MH. Major facilitator superfamily. Microbiol Mol Biol Rev 1998;62:1–34.
[127] Terada T, Inui K-I. Physiological and pharmacokinetic roles of H^+/organic cation antiporters (MATE/SLC47A). Biochem Pharmacol 2008;75:1689–96.
[128] Higgins CF. ABC transporters: from microorganisms to man. Annu Rev Cell Biol 1992;8:67–113.
[129] Vialou V, Balasse L, Callebert J, Launay J-M, Giros B, Gautron S. Altered aminergic neurotransmission in the brain of organic cation transporter 3-deficient mice. J Neurochem 2008;106: 1471–82.
[130] Cui M, Aras R, Christian WV, et al. The organic cation transporter-3 is a pivotal modulator of neurodegeneration in the nigrostriatal dopaminergic pathway. Proc Natl Acad Sci USA 2009;106:8043–8.
[131] Lin C-J, Tai Y, Huang M-T, et al. Cellular localization of the organic cation transporters, OCT1 and OCT2, in brain microvessel endothelial cells and its implication for MPTP transport across the blood-brain barrier and MPTP-induced dopaminergic toxicity in rodents. J Neurochem 2010;114:717–27.
[132] Nies AT, Koepsell H, Winter S, et al. Expression of organic cation transporters OCT1 (SLC22A1) and OCT3 (SLC22A3) is affected by genetic factors and cholestasis in human liver. Hepatology 2009;50:1227–40.
[133] Gründemann D, Gorboulev V, Gambaryan S, Veyhl M, Koepsell H. Drug excretion mediated by a new prototype of polyspecific transporter. Nature 1994;372:549–52.
[134] Kekuda R, Prasad PD, Wu X, et al. Cloning and functional characterization of a potential-sensitive, polyspecific organic cation transporter (OCT3) most abundantly expressed in placenta. J Biol Chem 1998;273:15971–9.
[135] Okuda M, Saito H, Urakami Y, Takano M, Inui K-I. cDNA cloning and functional expression of a novel rat kidney organic cation transporter, OCT2. Biochem Biophys Res Commun 1996;224:500–7.
[136] Schweifer N, Barlow DP. The *Lx1* gene maps to chromosome 17 and codes for a protein that is homologous to glucose and polyspecific transmembrane transporters. Mamm Genome 1996;7:735–40.
[137] Gorboulev V, Ulzheimer JC, Akhoundova A, et al. Cloning and characterization of two human polyspecific organic cation transporters. DNA Cell Biol 1997;16:871–81.
[138] Gründemann D, Schechinger B, Rappold GA, Schömig E. Molecular identification of the corticosterone-sensitive extraneuronal catecholamine transporter. Nature Neurosci 1998;1:349–51.
[139] Zhang L, Dresser MJ, Gray AT, Yost SC, Terashita S, Giacomini KM. Cloning and functional expression of a human liver organic cation transporter. Mol Pharmacol 1997;51: 913–21.
[140] Terashita S, Dresser MJ, Zhang L, Gray AT, Yost SC, Giacomini KM. Molecular cloning and functional expression of a rabbit renal organic cation transporter. Biochim Biophys Acta 1998;1369:1–6.
[141] Zhang X, Evans KK, Wright SH. Molecular cloning of rabbit renal organic cation transporter rbOCT2 and functional comparisons with rbOCT1. Am J Physiol Renal Physiol 2002;283: F124–33.
[142] Meyer-Wentrup F, Karbach U, Gorboulev V, Arndt P, Koepsell H. Membrane localization of the electrogenic cation transporter rOCT1 in rat liver. Biochem Biophys Res Commun 1998;248: 673–8.
[143] Tzvetkov MV, Vormfelde SV, Balen D, et al. The effects of genetic polymorphisms in the organic cation transporters OCT1, OCT2, and OCT3 on the renal clearance of metformin. Clin Pharmacol Ther 2009;86:299–306.
[144] More SS, Li S, Yee SW, et al. Organic cation transporters modulate the uptake and cytotoxicity of picoplatin, a third-generation platinum analogue. Mol Cancer Ther 2010;9: 1058–69.
[145] Zhang S, Lovejoy KS, Shima JE, et al. Organic cation transporters are determinants of oxaliplatin cytotoxicity. Cancer Res 2006;66:8847–57.
[146] Lips KS, Volk C, Schmitt BM, et al. Polyspecific cation transporters mediate luminal release of acetylcholine from bronchial epithelium. Am J Respir Cell Mol Biol 2005;33:79–88.
[147] Nies AT, Koepsell H, Damme K, Schwab M. Organic cation transporters (OCTs, MATEs), in vitro and in vivo evidence for the importance in drug therapy. In: Fromm M, Kim R, editors. Handbook of experimental pharmacology. Berlin, Heidelberg: Springer; 2010.
[148] Ciarimboli G, Deuster D, Knief A, et al. Organic cation transporter 2 mediates cisplatin-induced oto- and nephrotoxicity and is a target for protective interventions. Am J Pathol 2010;176:1169–80.
[149] Sweet DH, Miller DS, Pritchard JB. Ventricular choline transport. J Biol Chem 2001;276:41611–9.
[150] Filipski KK, Mathijssen RH, Mikkelsen TS, Schinkel AH, Sparreboom A. Contribution of organic cation transporter 2 (OCT2) to cisplatin-induced nephrotoxicity. Clin Pharmacol Ther 2009;86:396–402.
[151] Sata R, Ohtani H, Tsujimoto M, et al. Functional analysis of organic cation transporter 3 expressed in human placenta. J Pharmacol Exp Ther 2005;315:888–95.
[152] Schmitt BM, Gorbunov D, Schlachtbauer P, et al. Charge-to-substrate ratio during organic cation uptake by rat OCT2 is voltage-dependent and altered by exchange of glutamate 448 with glutamine. Am J Physiol Renal Physiol 2009;296:F709–22.
[153] Barendt WM, Wright SH. The human organic cation transporter (hOCT2) recognizes the degree of substrate ionization. J Biol Chem 2002;277:22491–6.
[154] Ming X, Ju W, Wu H, Tidwell RR, Hall JE, Thakker DR. Transport of dicationic drugs pentamidine and furamidine by human organic cation transporters. Drug Metab Dispos 2009;37:424–30.
[155] Schmitt BM, Koepsell H. Alkali cation binding and permeation in the rat organic cation transporter rOCT2. J Biol Chem 2005;280:24481–90.
[156] Kimura H, Takeda M, Narikawa S, Enomoto A, Ichida K, Endou H. Human organic anion transporters and human organic cation transporters mediate renal transport of prostaglandins. J Pharmacol Exp Ther 2002;301:293–8.
[157] Harlfinger S, Fork C, Lazar A, Schömig E, Gründemann D. Are organic cation transporters capable of transporting prostaglandins? Naunyn Schmiedebergs Arch Pharmacol 2005;372: 125–30.
[158] Taubert D, Grimberg G, Stenzel W, Schömig E. Identification of endogenous key substrates of the human organic cation transporter OCT2 and their implication in function of dopaminergic neurons. PloS ONE 2007;2:e385.
[159] Lee W-K, Reichold M, Edemir B, et al. Organic cation transporters OCT1, 2 and 3 mediate high affinity transport of the mutagenic vital dye ethidium in the kidney proximal tubule. Am J Physiol Renal Physiol 2009;296:F1504–13.

[160] Arndt P, Volk C, Gorboulev V, et al. Interaction of cations, anions, and weak base quinine with rat renal cation transporter rOCT2 compared with rOCT1. Am J Physiol Renal Physiol 2001;281:F454–68.
[161] Gorboulev V, Volk C, Arndt P, Akhoundova A, Koepsell H. Selectivity of the polyspecific cation transporter rOCT1 is changed by mutation of aspartate 475 to glutamate. Mol Pharmacol 1999;56:1254–61.
[162] Gorboulev V, Shatskaya N, Volk C, Koepsell H. Subtype-specific affinity for corticosterone of rat organic cation transporters rOCT1 and rOCT2 depends on three amino acids within the substrate binding region. Mol Pharmacol 2005;67: 1612–9.
[163] Popp C, Gorboulev V, Müller TD, Gorbunov D, Shatskaya N, Koepsell H. Amino acids critical for substrate affinity of rat organic cation transporter 1 line the substrate binding region in a model derived from the tertiary structure of lactose permease. Mol Pharmacol 2005;67:1600–11.
[164] Gorbunov D, Gorboulev V, Shatskaya N, et al. High-affinity cation binding to organic cation transporter 1 induces movement of helix 11 and blocks transport after mutations in a modeled interaction domain between two helices. Mol Pharmacol 2008;73:50–61.
[165] Volk C, Gorboulev V, Kotzsch A, Müller TD, Koepsell H. Five amino acids in the innermost cavity of the substrate binding cleft of organic cation transporter 1 interact with extracellular and intracellular corticosterone. Mol Pharmacol 2009;76: 275–89.
[166] Volk C, Gorboulev V, Budiman T, Nagel G, Koepsell H. Different affinities of inhibitors to the outwardy and inwardly directed substrate binding site of organic cation transporter 2. Mol Pharmacol 2003;64:1037–47.
[167] Abramson J, Smirnova I, Kasho V, Verner G, Kaback HR, Iwata S. Structure and mechanism of the lactose permease of *Escherichia coli*. Science 2003;301:610–5.
[168] Huang Y, Lemieux MJ, Song J, Auer M, Wang D-N. Structure and mechanism of the glycerol-3-phosphate transporter from Escherichia coli. Science 2003;301:616–20.
[169] Kaback HR, Dunten R, Frillingos S, et al. Site-directed alkylation and the alternating access model for LacY. Proc Natl Acad Sci USA 2007;104:491–4.
[170] Sturm A, Gorboulev V, Gorbunov D, et al. Identification of cysteines in rat organic cation transporters rOCT1 (C322, C451) and rOCT2 (C451) critical for transport activity and substrate affinity. Am J Physiol Renal Physiol 2007;293: F767–79.
[171] Minuesa G, Volk C, Molina-Arcas M, et al. Transport of lamivudine [(-)-b-L-2′,3′-dideoxy-3′-thiacytidine] and high-affinity interaction of nucleoside reverse transcriptase inhibitors with human organic cation transporters 1, 2, and 3. J Pharmacol Exp Ther 2009;329:252–61.
[172] Budiman T, Bamberg E, Koepsell H, Nagel G. Mechanism of electrogenic cation transport by the cloned organic cation transporter 2 from rat. J Biol Chem 2000;275:29413–20.
[173] Keller T, Elfeber M, Gorboulev V, Reiländer H, Koepsell H. Purification and functional reconstitution of the rat organic cation transporter OCT1. Biochemistry 2005;44:12253–63.
[174] Ciarimboli G, Schlatter E. Regulation of organic cation transport. Pflügers Arch - Eur J Physiol 2005;449:423–41.
[175] Ciarimboli G, Koepsell H, Iordanova M, et al. Individual PKC-phosphorylation sites in organic cation transporter 1 determine substrate specificity and transport regulation. J Am Soc Nephrol 2005;16:1562–70.
[176] Zwart R, Sleutels F, Wutz A, Schinkel AH, Barlow DP. Bidirectional action of the *Igf2r* imprint control element on upstream and downstream imprinted genes. Genes Dev 2001;15:2361–6.
[177] Saborowski M, Kullak-Ublick G-A, Eloranta JJ. The human organic cation transporter-1 gene is transactivated by hepatocyte nuclear factor-4a. J Pharmacol Exp Ther 2006;317:778–85.
[178] Asaka J-I, Terada T, Ogasawara K, Katsura T, Inui K-I. Characterization of the basal promoter element of human organic cation transporter 2 gene. J Pharmacol Exp Ther 2007;321:684–9.
[179] Aoki M, Terada T, Kajiwara M, et al. Kidney-specific expression of human organic cation transporter 2 (OCT2/SLC22A2) is regulated by DNA methylation. Am J Physiol Renal Physiol 2008;295:F165–70.
[180] Yokoo K, Murakami R, Matsuzaki T, Yoshitome K, Hamada A, Saito H. Enhanced renal accumulation of cisplatin via renal organic cation transporter deteriorates acute kidney injury in hypomagnesemic rats. Clin Exp Nephrol 2009;13: 578–84.
[181] Lajer H, Kristensen M, Hansen HH, et al. Magnesium depletion enhances cisplatin-induced nephrotoxicity. Cancer Chemother Pharmacol 2005;56:535–42.
[182] Tamai I, Yabuuchi H, Nezu J-I, et al. Cloning and characterization of a novel human pH-dependent organic cation transporter, OCTN1. FEBS Lett 1997;419:107–11.
[183] Wu X, George RL, Huang W, et al. Structural and functional characteristics and tissue distribution pattern of rat OCTN1, an organic cation transporter, cloned from placenta. Biochim Biophys Acta 2000;1466:315–27.
[184] Tamai I, Ohashi R, Nezu J-I, et al. Molecular and functional characterization of organic cation/carnitine transporter family in mice. J Biol Chem 2000;275:40064–72.
[185] Gisler SM, Pribanic S, Bacic D, et al. PDZK1: A major scaffolder in brush-borders of proximal tubular cells. Kidney Int 2003;64:1733–45.
[186] Urban TJ, Brown C, Castro RA, et al. Effects of genetic variation in the novel organic cation transporter, OCTN1, on the renal clearance of gabapentin. Clin Pharmacol Ther 2007;83: 416–21.
[187] Kato Y, Kubo Y, Iwata D, et al. Gene knockout and metabolome analysis of carnitine/organic cation transporter OCTN1. Pharm Res 2010;27:832–40.
[188] Schömig E, Spitzenberger F, Engelhardt M, Martel F, Örding N, Gründemann D. Molecular cloning and characterization of two novel transport proteins from rat kidney. FEBS Lett 1998;425:79–86.
[189] Sekine T, Kusuhara H, Utsunomiya-Tate N, et al. Molecular cloning and characterization of high-affinity carnitine transporter from rat intestine. Biochem Biophys Res Commun 1998;251:586–91.
[190] Wu X, Prasad PD, Leibach FH, Ganapathy V. cDNA sequence, transport function, and genomic organization of human OCTN2, a new member of the organic cation transporter family. Biochem Biophys Res Commun 1998;246:589–95.
[191] Grigat S, Fork C, Bach M, et al. The carnitine transporter *SLC22A5* is not a general drug transporter, but it efficiently translocates mildronate. Drug Metab Dispos 2009;37:330–7.
[192] Otsuka M, Matsumoto T, Morimoto R, Arioka S, Omote H, Moriyama Y. A human transporter protein that mediates the final excretion step for toxic organic cations. Proc Natl Acad Sci USA 2005;102:17923–8.
[193] Ohta K-Y, Imamura Y, Okudaira N, Atsumi R, Inoue K, Yuasa H. Functional characterization of multidrug and toxin extrusion protein 1 as a facilitative transporter for fluoroquinolones. J Pharmacol Exp Ther 2009;328:628–34.

[194] Matsumoto T, Kanamoto T, Otsuka M, Omote H, Moriyama Y. Role of glutamate residues in substrate recognition by human MATE1 polyspecific H^+/organic cation exporter. Am J Physiol Cell Physiol 2008;294:C1074–8.

[195] Tsuda M, Terada T, Ueba M, et al. Involvement of human multidrug and toxin extrusion 1 in the drug interaction between cimetidine and metformin in renal epithelial cells. J Pharmacol Exp Ther 2009;329:185–91.

[196] Nishihara K, Masuda S, Ji L, Katsura T, Inui K-I. Pharmacokinetic significance of luminal multidrug and toxin extrusion 1 in chronic renal failure in rats. Biochem Pharmacol 2007;73:1482–90.

[197] Kajiwara M, Terada T, Asaka J-I, et al. Critical roles of Sp1 in gene expression of human and rat H^+/organic cation antiporter MATE1. Am J Physiol Renal Physiol 2007;293: F1564–70.

[198] Choi HJ, Yee SW, Kim MJ, et al. Identification and characterization of novel polymorphisms in the basal promoter of the human transporter, MATE1. Pharmacogen Genom 2009;19: 770–80.

[199] Kajiwara M, Terada T, Ogasawara K, et al. Identification of multidrug and toxin extrusion (MATE1 and MATE2-K) variants with complete loss of transport activity. J Hum Genet 2009;54:40–6.

[200] Meyer zu, Schwabedissen HE, Verstuyft C, Kroemer HK, Becquemont L, Kim RB. Human multidrug and toxin extrusion 1 (MATE1/SLC47A1) transporter: Functional characterization, interaction with OCT2 (SLC22A2), and single nucleotide polymorphisms. Am J Physiol Renal Physiol 2010; 298:F997–1005.

[201] Chen Y, Teranishi K, Li S, et al. Genetic variants in multidrug and toxic compound extrusion-1, hMATE1, alter transport function. Pharmacogenomics 2009;9:127–36.

[202] Masuda S, Terada T, Yonezawa A, et al. Identification and functional characterization of a new human kidney-specific H^+/organic cation antiporter, kidney-specific multidrug and toxin extrusion 2. J Am Soc Nephrol 2006;17: 2127–35.

[203] Zhang X, Cherrington NJ, Wright SH. Molecular identification and functional characterization of rabbit MATE1 and MATE2-K. Am J Physiol Renal Physiol 2007;293: F360–70.

[204] Higgins CF, Gottesman MM. Is the multidrug transporter a flippase? Trends Biochem Sci 1992;17:18–21.

[205] Ciarimboli G, Ludwig T, Lang D, et al. Cisplatin nephrotoxicity is critically mediated via the human organic cation transporter 2. Am J Pathol 2005;167:1477–84.

[206] Yonezawa A, Masuda S, Nishihara K, Yano I, Katsura T, Inui K-I. Association between tubular toxicity of cisplatin and expression of organic cation transporter rOCT2 (Slc22a2) in the rat. Biochem Pharmacol 2005;70:1823–32.

[207] Tanihara Y, Masuda S, Katsura T, Inui K-I. Protective effect of concomitant administration of imatinib on cisplatin-induced nephrotoxicity focusing on renal organic cation transporter OCT2. Biochem Pharmacol 2009;78:1263–71.

[208] Somogyi A, Stockley C, Keal J, Rolan P, Bochner F. Reduction of metformin renal tubular secretion by cimetidine in man. Br J Clin Pharmac 1987;23:545–51.

[209] van Crugten J, Bochner F, Keal J, Somogyi A. Selectivity of the cimetidine-induced alterations in the renal handling of organic substrates in humans. Studies with anionic, cationic and zwitterionic drugs. J Pharmacol Exp Ther 1986;236: 481–7.

[210] Lai MY, Jiang FM, Chung CH, Chen HC, Chao PD. Dose dependent effect of cimetidine on procainamide disposition in man. Int J Clin Pharmacol Ther Toxicol 1988;26:118–21.

[211] Kaiser J. DNA sequenzing: a plan to capture human diversity in 1000 genomes. Science 2008;319:395.

[212] Hesselson SE, Matsson P, Shima JE, et al. Genetic variation in the proximal promoter of ABC and SLC superfamilies: liver and kidney-specific expression and promoter activity predict variation. PloS ONE 2009;4:e6942.

[213] Shu Y, Brown C, Castro RA, et al. Effect of genetic variation in the organic cation transporter 1, OCT1, on metformin pharmacokinetics. Clin Pharmacol Ther 2008;83:273–80.

[214] Shikata E, Yamamoto R, Takane H, et al. Human organic cation transporter (*OCT1* and *OCT2*) gene polymorphisms and therapeutic effects of metformin. J Hum Genet 2007;52:117–22.

[215] Song IS, Shin HJ, Shim EJ, et al. Genetic variants of the organic cation transporter 2 influence the disposition of metformin. Clin Pharmacol Ther 2008;84:559–62.

[216] Wang Z-J, Yin OQP, Tomlinson B, Chow MSS. OCT2 polymorphisms and in-vivo renal functional consequence: studies with metformin and cimetidine. Pharmacogen Genom 2008;18:637–45.

[217] Burger H, Zoumaro-Djayoon A, Boersma AWM, et al. Differential transport of platinim compounds by the human organic cation transporter hOCT2 (hSLC22A2). Brit J Pharmacol 2010;159:898–908.

This page intentionally left blank

CHAPTER

73

Renal Filtration, Transport, and Metabolism of Albumin and Albuminuria

Erik Ilsø Christensen, Rikke Nielsen and Henrik Birn

Department of Biomedicine, Anatomy, Section of Cell Biology, Aarhus University, Aarhus, Denmark

INTRODUCTION

Albuminuria is one of the oldest yet remains one of the most sensitive and widely used markers of kidney dysfunction. Albumin is the most abundant plasma protein[1] and its urinary excretion is determined by the combined effects of glomerular filtration and renal tubular processing (Fig. 73.1). Dysfunction of both these processes may result in increased excretion of albumin, and glomerular injuries as well as tubular damage have been implicated in the initial events leading to albuminuria. Albuminuria not only indicates acute or chronic renal damage but is also a well established and independent marker of progression in chronic kidney disease (CKD). Interventions aimed at reducing albuminuria have proved effective in ameliorating the continuous loss of renal function in various form of CKD suggesting that albuminuria not only is a marker of kidney disease but in fact involved in the pathophysiology of progression. Experimental evidence points to direct and deleterious effects of albumin on renal tubular cells and identifies a number of downstream mediators initiating inflammation and eventually renal fibrosis.

Gene analyses in human diseases and animal knockout models have identified a number of key molecules regulating glomerular filtration and tubular reabsorption of albumin. In most cases of human disease, however, both the precipitating events and the accelerating mechanisms associated with albuminuria are unknown and may include several, different pathways. The relative importance of the various molecular mechanisms regulating glomerular filtration and tubular handling of albumin remain controversial both in normal physiology and in disease and the evidence for an independent pathogenic role of albumin in the development and progression of renal disease is debated.

This chapter will review the structures controlling glomerular filtration of albumin and discuss the molecular and pathophysiological mechanisms causing changes in glomerular permselectivity. Furthermore, the receptors regulating tubular reuptake of filtered albumin are presented and the possible pathways by which filtered albumin may cause tubular and interstitial damage are discussed in relation to acute and chronic kidney disease.

ALBUMIN

Albumin is an anionic, flexible, heart-shaped, 585-amino acid, single polypeptide chain with a MW ~67 kDa present in plasma at a normal concentration of 35–50 mg/ml. While it is not essential to life, a number of important and very diverse functions have been ascribed to this protein including the maintenance of the oncotic pressure and blood volume, acid/base buffer functions, antioxidant functions, and the transport of a number of different substances including fatty acids, bilirubin, ions such as Ca^{2+} and Mg^{2+}, drugs, hormones, and lipophilic as well as hydrophilic vitamins, e.g., vitamin A, riboflavin, vitamin B6, ascorbic acid, and folate.[1] Albumin undergoes posttranslational modification including glycation, acetylation, methylation, carbamylation and phosphorylation.[2] Albumin is almost exclusively synthesized in the liver at a rate of 10–15 g per day in a healthy person and its normal half life is estimated to 19 days representing the balance between synthesis, transcapillary escape, and catabolism predominantly within muscle, liver and

Seldin and Giebisch's The Kidney, Fifth Edition.
DOI: http://dx.doi.org/10.1016/B978-0-12-381462-3.00073-2

© 2013 Elsevier Inc. All rights reserved.

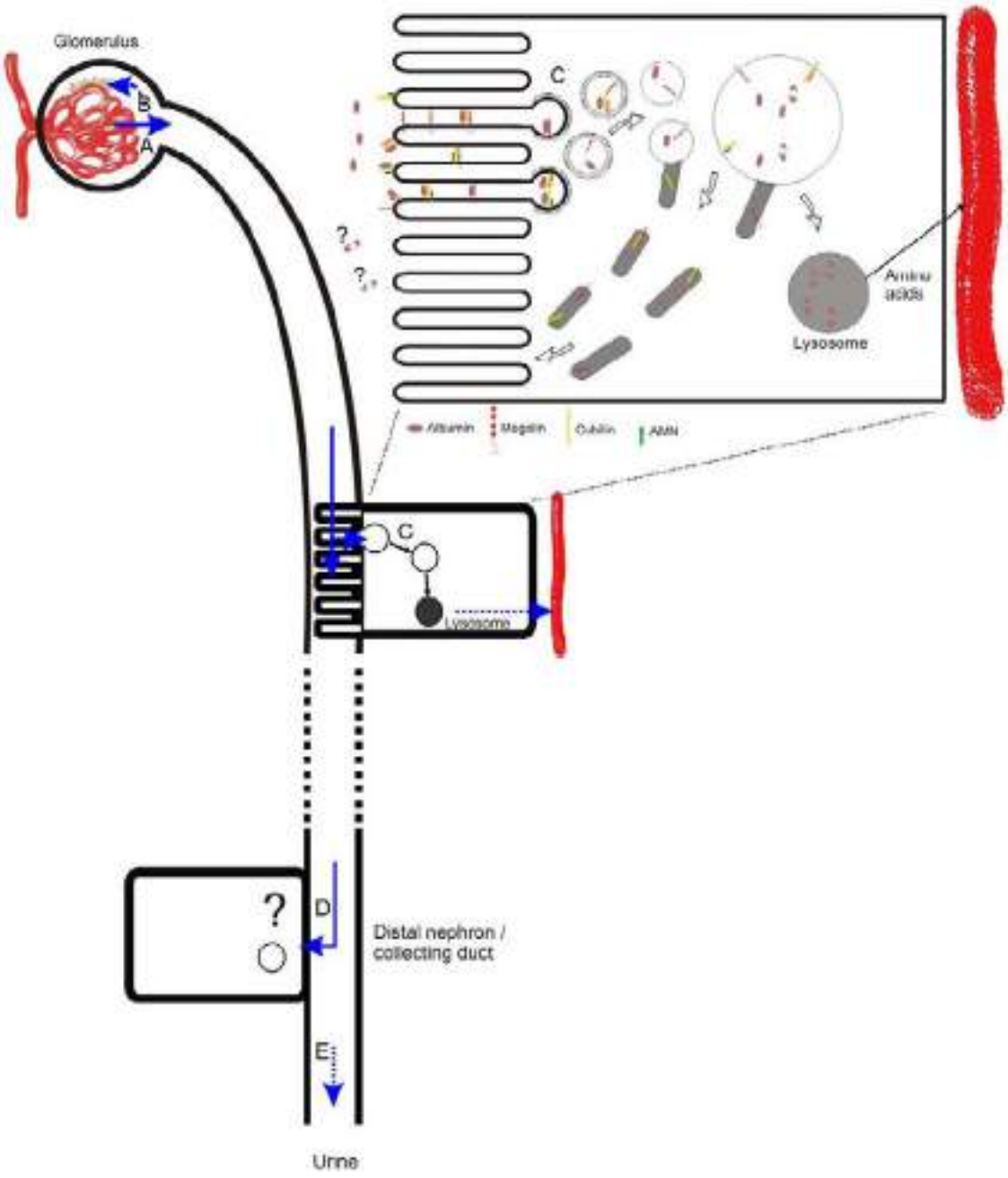

FIGURE 73.1 Renal albumin handling. Plasma albumin is filtered in the glomeruli (A). Filtered albumin may be taken up by podocytes (B) possibly by a megalin mediated process. It is not clear whether albumin is taken up from the subepithelial space or from the urinary space, or both. Filtered albumin is reabsorbed in the proximal tubule by megalin and cubilin/AMN mediated endocytosis (C). Albumin is degraded within the lysosomal compartment and amino acids are released at the basolateral cell surface. Under proteinuric conditions, albumin, not reabsorbed by the proximal tubule, may be taken up by more distal nephron segments or collecting ducts (D) by an unknown mechanism (see also figure 74.6). Depending on the balance between glomerular filtration of albumin and the tubular reabsorptive and degradative capacity, albumin and albumin fragments may be excreted in the urine (E). Urinary albumin fragments have been identified, however, the origin and significance of these remain unclear.

kidney.[1] In kidney diseases such as nephrotic syndrome and end stage renal disease, including well managed patients on peritoneal dialysis, albumin synthesis appears to be increased compensating for increased losses.[1] Normally the albumin gene is silent in the kidney, however, it has recently been shown that the gene is activated in cases of acute kidney failure leading to the renal synthesis of albumin.[3] The local production of albumin is associated with albuminuria, however, the extent to which local synthesis of albumin

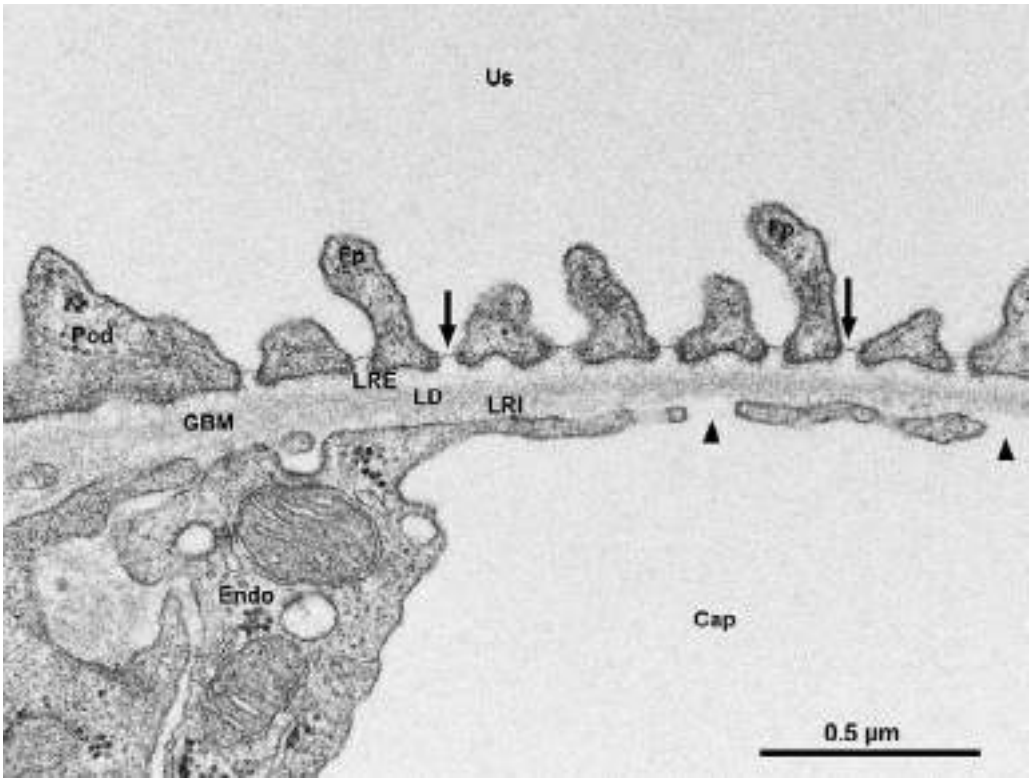

FIGURE 73.2 Electron micrograph of the glomerular filtration barrier. Filtration takes place from the glomerular capillaries (Cap) through the pores (arrowheads) of the endothelial cells (Endo), the glomerular basement membrane (GBM) consisting of the three layers, lamina rara interna (LRI), lamina densa (LD) and lamina rara externa (LRE) and finally through the filtration slit membrane (arrows) between the foot processes (Fp) of the podocytes (Pod) into the urinary space (Us).

contributes to the urinary excretion of albumin is not known.

GLOMERULAR FILTRATION

Glomerular Filtration Barrier

The glomerular filtration barrier is structurally composed of three layers, the capillary endothelial cells, the glomerular basement membrane (GBM) and the podocyte filtration slit membrane (Fig. 73.2). The barrier is freely permeable to water, solutes and small molecules however, increasing size of macromolecules causes increasing restriction to filtration as do negative charge.[4]

The fenestrated endothelium (Fig. 73.2) is unusual since the fenestrae generally are not closed by diaphragms, except as demonstrated in rat where the capillaries which are direct tributaries to the efferent arteriole do indeed have diaphragms closing the fenestrae.[5] The pores in the endothelium appear not to be fully open holes. By special fixation procedures it has been demonstrated that the pores are filled with glycoproteins forming "sieve plugs"[6,7] probably contributing to the endothelial part of the filtration barrier.[8] The endothelial cells have a thick glycocalyx and an even thicker endothelial cell surface coat,[9] which are believed by many authors to contribute significantly to the charge selectivity of the barrier[10] (for a recent review see Haraldsson et al.[4]).

The basement membrane, which in man is about 300 nm thick, consists of three layers, a lamina densa, located between a lamina rara interna facing the endothelial cell and a lamina rara externa, facing the podocyte (Fig. 73.2). In the 1970s the GBM was considered the major contributor to the charge selectivity of the filtration barrier[11–14] (see also Kanwar et al.[15] for references). *In vitro* studies, however, on isolated GBM[16] showed no charge selectivity and removal of charged components of the GBM in mouse knock out studies in general did not change charge selectivity, for discussions see.[15,17] A large variety of both genetic[18] and acquired, albuminuric diseases affect the GBM, e.g., Alport syndrome and diabetes mellitus (see also later).

The third component of the barrier, the podocyte filtration slit membrane (Fig. 73.2), has attracted great interest as a key part of the filtration barrier, especially since the findings that, for example, gene defects of

nephrin (*NPHS1*) induce the congenital nephrotic syndrome of the Finnish type[19] and gene defects of podocin (NPHS2) induce nephrotic syndrome of the non-Finnish type.[20] The porous structure of the filtration slit membrane was first described by Rodewald and Karnowsky[21] measuring the dimensions of the pores to be 4×14 nm. In a recent publication[22] the mean radius of the observed irregular circular or elipsoid pores were measured to be 12.1 nm. In proteinuric rats additional large pores were observed[22] and suggested to contribute to the increased filtration of protein/albumin in pathologic conditions, a finding which awaits confirmation.

An elegant model for the charge restriction has recently been put forward, based on micropuncture experiments in glomeruli of *Necturus maculosus*.[23,24] The authors identified a filtration dependant negative electrical charge in the Bowman's space compared to the capillary lumen, a charge that would allow negatively charged proteins like albumin to be electrophoresed back to the blood and the opposite for positively charged proteins.

There is no doubt that all three structural components of the glomerular filter are necessary for maintaining the barrier, illustrated by the observations that damage to any part eventually leads to albuminuria, that the GBM is synthesized from both the epithelial- and endothelial cells and that vascular endothelial growth factor (VEGF)-A produced by the podocytes influences development and maintenance of the endothelial cells which possesses receptors for VEGF-A, VEGFR-1 and 2.[25]

Glomerular Filtration of Albumin

The amount of albumin normally filtered in the glomeruli has been estimated using various techniques, including micropuncture of rats and dogs, estimating the concentration of albumin in the ultrafiltrate between 1 and 50 μg/ml.[26] This corresponds to a filtered load of albumin between 170 mg and 9 g per 24 h in normal humans. Inhibition of tubular albumin uptake in humans by lysine suggested filtration of at least 281 μg/min, corresponding to ~400 mg/24 h.[27] Similar studies in lysine treated rats resulted in the excretion of 2.5 mg to 25 mg/24 h[28,29] corresponding to 0.7−7 g/24 h in humans. In rat the filtration fraction of albumin was estimated to 0.0006 by micropuncture studies[30] in good agreement with the results mentioned above. This figure was, however, challenged by Comper and colleagues[31−33] who estimated the filtration fraction by two-photon microscopy to be 0.034. As calculated by Gekle[34] this implies a filtration of 225 g/24 h of albumin in humans and the results were immediately questioned by several groups.[34−37] Subsequently, three studies[38−40] have seriously questioned the technical approach applied by Russo et al. Thus, the notion of normal glomerular filtration of such large amounts of albumin remains highly controversial. For an excellent review comparing glomerular permselectivity of ficoll, dextran and globular proteins, see Venturoli and Rippe.[41]

Albumin Uptake in Glomerular Cells

Albumin uptake has been demonstrated *in vivo* in podocytes from human, rat and mouse and *in vitro* in mouse and human podocytes.[42] Accumulation of endocytosed protein in podocytes is also indicated by podocyte vacuolization in proteinuric patients[43] and experimentally, endocytic uptake of tracer proteins in podocytes have been demonstrated *in vivo*.[44,45] The albumin binding receptor megalin (see below) has been identified in rat podocytes[46] and very recently also on human podocytes[47] providing a mechanism for the endocytic uptake of albumin and other proteins. It has been proposed that unless removed, filtered proteins would clog the glomerular filter due to the podocyte slit membrane.[48,49] Such a theoretical clogging of the slit diaphragm may be attenuated by megalin mediated, podocyte endocytosis of trapped protein, including albumin. It should be emphasized that the endocytic uptake of albumin in the podocytes is minimal compared to the subsequent uptake in the proximal tubule (see below).

Tubular Albumin Uptake

Endocytosis of Albumin in the Renal Proximal Tubule

Proximal tubule uptake of albumin by endocytosis was described almost 45 years ago.[50,51] The identification of the receptors megalin, cubilin and amnionless (AMN)[52−54] and subsequent studies of these receptors have now firmly established them as an endocytic complex responsible for the reabsorption of filtered albumin. Megalin has been identfied as an albumin binding protein involved in albumin reabsorption in the proximal tubule *in vivo*.[55] This was later confirmed by the presence of albuminuria in megalin knockout mice[56,57] and in Donnai Barrow patients having mutations in *LRP2* encoding megalin (personal observations). Direct binding of albumin to cubilin was demonstrated estimating a Kd of 0.6 μM[56] and the physiological importance was established by the presence of albuminuria in cubilin knockout mice[58] and in patients with cubilin defects causing Imerslund-Gräsbeck's syndrome/megaloblastic anemia 1,[59] which is an autosomal recessive vitamin B_{12} deficiency disorder caused by malfunction of either cubilin or AMN. AMN has not been shown to

have a direct receptor function, but is a chaperone for cubilin (see later) and lack of AMN has been associated with albuminuria both in humans and in animal models.[56] A recent study further supports the role of cubilin in albumin reabsorption by showing that the SNP I2984V in cubilin is associated with microalbuminuria in the general population.[60]

Renal Expression, Structure and Sorting of Megalin, Cubilin and AMN

Megalin is heavily expressed in the renal proximal tubule brush border, the endocytic compartments, and membrane recycling system.[53,61–63] Megalin is also detectable in lysosomes in small quantities, but after endocytosis the majority of megalin is recycled to the apical membrane via dense apical tubules.[64] Cubilin co-localizes with megalin in the renal proximal tubule[54,65,66] and AMN co-localizes with cubilin.[67] In rats and humans additional expression of megalin in the podocytes has been identified.[46,47] For more information of the expression of the receptors in other epithelia see.[68,69]

Megalin (Fig. 73.3) was identified nearly 30 years ago[46,53] as a large glycosylated protein (600 kDa) belonging to the low density lipoprotein (LDL) receptor family.[70–72] Megalin is a multiligand receptor with four binding clusters in the extracellular domain.[70,72] The binding clusters each contain 7 to 11 complement-type repeats. Structural studies of the LDL receptor and the twelfth repeat in megalin have revealed that each consists of approximately 40 amino acids with 6 cysteines forming 3 disulfide bridges and a C-terminal calcium cage.[73–76] Separation of the binding clusters is obtained by 16 growth factor repeats separated by 8 YWTD spacer regions, which are involved in pH dependent release of ligands.[77] Finally the extracellular domain contains one epidermal growth factor-like repeat which is situated next to the membrane spanning area. The four binding clusters are responsible for the binding of albumin;[55,78] one of the more than 50 ligands which so far has been reported for megalin.[69]

The receptor spans the membrane once and is equipped with a short intracellular tail (209 amino acids) which contains 2 endocytic motifs (NPXY) driving clustering into coated pits and a NPXY-like motif (NQNY) involved in apical sorting of the receptor.[79] Apical sorting is also dependent on the receptor associated protein (RAP),[80] acting as a chaperone[81] and phosphorylation of a PPSP motif in the cytoplasmic tail.[82]

Cubilin (Fig. 73.3) is identical to the intestinal intrinsic factor-B12 receptor[66,83] and is a 460 kDa, peripheral membrane protein. Its structure is dominated by 27 ekstracellular CUB domains (complement c1r/C1s, Uegf (epidermal growth factor-related sea urchin protein)) and bone morphogenic protein 1.[84,85] The CUB domains are involved in ligand binding, but despite the numerous domains only around 15 ligands have been identified[69] including albumin.[56,78] The N-terminus cubilin contains 8 epidermal growth factor (EGF) repeats and a 110 amino acid stretch.[84,85] No transmembrane domain has been identified and sorting

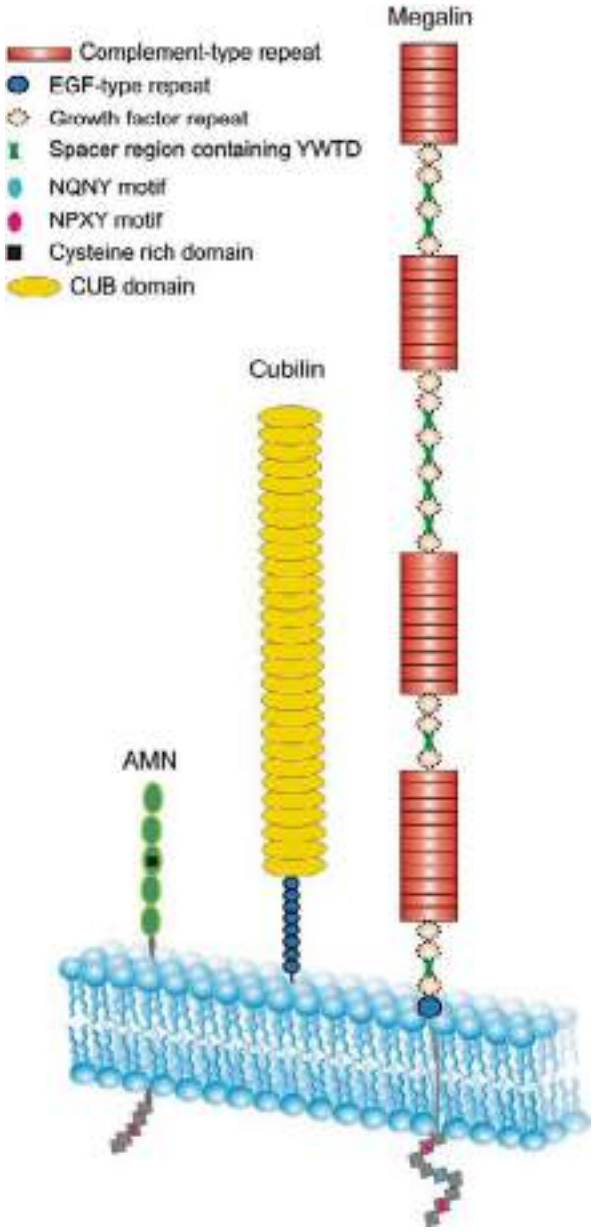

FIGURE 73.3 Schematic illustration of megalin, cubilin and amnionless (AMN). The three receptors co-operate in the proximal tubular uptake of filtered albumin. Cubilin binds albumin, but is dependent on complex formation with megalin and/or AMN to sustain endocytosis. Megalin and AMN contain NPXY motifs necessary for recruitment of the endocytic machinery and initiation of endocytosis. AMN is furthermore involved in translocation of cubilin from the RER to the plasma membrane. *Figure modified from.*[69]

and anchorage of cubilin to the membrane is accomplished through physical interaction with AMN and megalin.[86,67,85] *In vitro* studies showed that sorting relies on interaction of the EGF domains in cubilin with AMN.[87,67] This cooperation between cubilin and AMN is supported by intracellular retention of cubilin in dogs suffering from AMN mutations causing Imerslund-Gräsbeck's syndrome[56,88] and in AMN deficient mice.[89] The apical plasma membrane localization of AMN is in the same manner dependent on intact cubilin as AMN is retained intracellularly both in cubilin deficient mice and in humans with no cubilin expression.[58,90]

Cubilin also associates with megalin through CUB domain 12−17 and 22−27 as well as through the N-terminus[85,86,91] and megalin appears to be important for the stability of cubilin in the membrane as suggested by decreased levels of cubilin in *in vitro* studies and in rabbits producing megalin antibodies[86] as well as by immunocytochemistry in megalin knockout mice.[58,56]

AMN (Fig. 73.3) has a molecular weight ranging from 38−50 kDa[92] and was initially recognized as being involved in normal development of the middle portion of the primitive streak in mice. Mice which lack AMN fail to develop amnion. It has a cytoplasmic tail with the endocytic motif NPXY, a transmembrane domain and N-terminal extracellular domain encompassing approximately 70 amino acids with a cysteine rich region as the only characteristic domain.[52] It should be noted that the above described interdependence of the receptors for normal sorting complicates the endocytic analysis of each receptor separately.

Endocytosis of Albumin Receptors

Endocytosis of megalin is driven by endocytic motifs in the cytoplasmic tail (see above) that mediate the assembly of clathrin and adaptor proteins such as AP-2, Dab2 and ARH.[93,94,95] The significance of Dab2 to the endocytosis of megalin is supported by mutual dependence of megalin and Dab2 for normal localization[96] and the mild, but significant proteinuria observed in Dab2 knockout mice.[97] Dab2 further associates megalin with nonmuscle myosin heavy chain IIA and actin,[98] whereas the adaptor protein GAIP interacting protein C-terminus (GIPC) attaches myosin VI to the complex.[99,100] These interactions are suggested to be important for the post endocytic transport of the complex corroborated by the albuminuria observed in GIPC- and myosin VI knockout mice.[101,100]

Interaction of megalin and cubilin together with their strict co-localization in the proximal tubule suggests that megalin mediates the internalization of cubilin and its ligands.[85] Several *in vitro* studies strengthened this concept such as decreased cubilin endocytosis in megalin compromised cells.[102,103] AMN holds a NPXY motif and it is apparent that in cell cultures lacking megalin, cubilin can work in conjunction with AMN.[67] *In vivo* in the kidney, however, this cooperation is not able to sustain normal endocytosis.[58] The concept of megalin being the motor for albumin endocytosis is supported by a recent study showing that an SNP in the megalin binding area of cubilin is associated with microalbuminuria in the normal population and in diabetics.[60] It has been shown recently, by analysis of the crystal structure of cubilin, that changes in a residue that does not directly interact with intrinsic factor B12 result in Imerslund-Gräsbeck's disease. Thus, a SNP in the megalin binding region might similarily interfere with cubilin association to megalin hindering endocytosis of cubilin-bound albumin.[104]

Regulation of Albumin Receptors

It has generally been assumed that under normal physiological conditions proximal tubule endocytic uptake of albumin is a constitutive process determined only by the receptor expression.[56] Little is known, however, about the regulation of receptor expression in normal physiology. Studies in disease and transgene mice have suggested, that megalin expression may be under influence of the renin-angiotensin system. Angiotensin II decreases megalin expression in a long term proteinuric mouse model induced by renin overexpression.[105] Furthermore, angiotensin II has recently been shown to stimulate trafficking of several sodium transporters and megalin into microvilli.[106] However, in this latter study no apparent decrease in megalin levels was observed. An intrarenal proximal tubular renin-angiotensin system has been suggested[107] and the molecular actions of this system are complex. The role of these components in the direct or indirect regulation of megalin is at present very difficult to deduce. Furthermore, an additional link between angiotensin II and megalin expression has evolved. Transforming growth factor (TGF)-β reduces megalin expression *in vitro*[108] and in a proteinuric hypertensive mouse model the action of TGF-β has been shown to be modulated by angiotensin II receptor antagonists at doses that do not decrease aterial blood pressure. This is believed to be mediated by reestablishment of the equilibrium between TGF-β and bone morphogenic protein 7 (BMP7)/BMP7-inhibitors.[105] Thus, treatment with angiotensin II antagonists might elevate megalin expression through a decrease in BMP7-inhibitors resulting in BMP7 mediated inhibiton of TGF-β. Obviously the effect of angiotensin II on glomerular function in addition to the proposed effect on tubular megalin expression may contribute to the changes in urinary albumin excretion observed with

modulation of this system. In a recently published study it is shown that megalin contains 3 PPAR (peroxisome proliferator-activated receptors) response elements in its promotor region and that megalin expression increases in response to PPAR ligands in mouse kidneys[109] suggesting a direct regulation of megalin expression by PPAR. The physiological significance of this regulation remains to be established, however, PPAR agonists have in a number of studies been shown to be renoprotective in diabetic patients including an amelioration of albuminuria.[110]

RENAL TUBULAR ALBUMIN METABOLISM

Lysosomal Degradation of Albumin

Following proximal tubule endocytic uptake, albumin accumulates within the lysosomal compartment[111,51] where it is degraded.[112] In rats, albumin is reabsorbed within all three segments of the proximal tubule, however, catabolism appears to be slower in the S3 segment.[113] This process is dependent on ATP-mediated acidification of the lysosomal compartment.[114,115] Interference with lysosomal function from increased filtration of albumin has been suggested by experimental induction of albuminuria. This resulted in functional and structural changes in lysosomes[116] and increased activity of lysosomal enzymes such as cathepsin[117] suggesting that albumin overload changes the protein catabolic function of the proximal tubule cell.

It is generally believed that albumin is fully degraded within the lysosomal compartment and that amino acids are returned to the circulation through a basolateral exit mechanism.[118–120] Based on the identification of albumin fragments in normal human and animal urine it has been proposed that albumin fragments resulting from the proximal tubule degradation of proteins are normally excreted at the luminal cell surface.[121–124] Most of these fragments are suggested to be very small with MW <500 Da[125] and apparently undetectable by conventional immune or dye-based assays, however, may be detected either by size exclusion chromatography of injected and processed labeled albumin[126,122] or by the Biuret protein assay.[127] Although cells grown *in vitro* may secrete fragments[126] so far no direct evidence for the tubular generation and luminal secretion of albumin fragments *in vivo* has been published. *In vitro* microperfusion of proximal tubules suggested peritubular, but not luminal release of degradation products[120] and knockout of megalin and cubilin in mice did not change the excretion of urinary albumin fragments showing that receptor mediated endocytosis is not involved in the generation of these.[128] Furthermore, other studies have not confirmed the presence of significant amount of albumin fragments in the urine.[129,130] Thus, the amount, origin and pathophysiologic implication of potential urinary albumin fragments remain to be established.

Transtubular Recovery of Albumin

In addition to the well established endocytic pathway for albumin uptake, the existence of a high capacity pathway for the transtubular transport of very large amounts of intact albumin has been suggested.[131] Such a pathway would be essential for the recovery of $\sim$225 g/24 h of albumin suggested to be filtered in the human kidney if, as proposed by Comper and colleagues, the filtration fraction for albumin is much higher than previously believed.[132]

The transtubular recovery of intact albumin was proposed after the identification of a small, second peak of labeled albumin appearing in the renal vein following bolus injection of labeled albumin into the isolated perfused kidney.[133] Later studies by electron microscopy of endogenous and fluorescent labeled albumin injected into normal rats showing albumin labeled vesicles in the basolateral aspect of the proximal tubule cell and apparent fusion with the basolateral membrane[132,33] were interpreted as evidence of vesicular transcytosis. So far there has been no published, direct evidence for a specific, high capacity, transcellular transport of albumin. In fact, when a high capacity, low affinity mechanism for albumin uptake was identified using isolated, perfused proximal tubules only negligible transtubular transport was found and the uptake was believed to represent non-specific, fluid phase endocytosis.[120]

The proposed high capacity, transtubular albumin retrieval pathway does not involve megalin and cubilin as demonstrated by the fact that inactivation of these receptors in mice leads to albuminuria in the order of 20–40 μg/h[58,56] which is much less than the proposed amount of transcellular albumin transport. Furthermore, inactivation of megalin and cubilin leads to total abolishment of the normal tubular vesicular labeling (Fig. 73.4)[58,56] disputing the existence of an alternative and significant pathway of vesicular albumin uptake.

It has been hypothesized that the transcellular transport of intact albumin may involve the major histocompatibility complex-related Fc receptor (FcRn). FcRn is responsible for the transcytosis of proteins such as IgG across the placental barrier[134] and possibly podocytes.[135] It has been identified in the luminal part of the kidney proximal tubule cells[136] and binds albumin.[137] FcRn knockout mice are hypoalbuminemic and the half live of circulating albumin is reduced.[138] When kidneys from

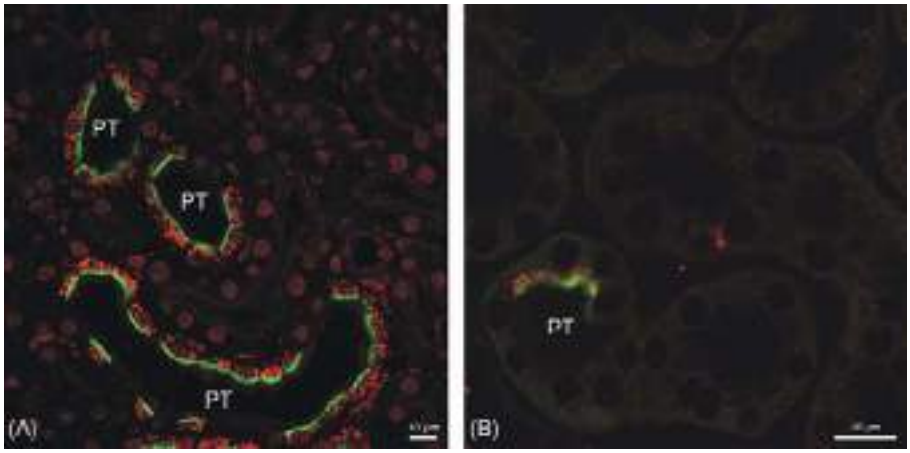

FIGURE 73.4 Immunohistochemical analysis of albumin reabsorption in a mosaic megalin- and a mosaic cubilin knockout mouse showing that both receptors are required for albumin endocytosis. Several proximal tubules (PT) from these mice contain both receptor deficient - and wildtype proximal tubule cells. A. Representative micrograph of a megalin knockout mouse with wildtype cells containing megalin (green) dispersed among megalin deficient cells. All cells contain cubilin (not labeled). Albumin (red) is almost exclusively detected in megalin containing cells indicating that cubilin is unable to sustain endocytosis of albumin without megalin. B. Representative micrograph of a cubilin knockout mouse with wildtype cells containing cubilin (green) dispersed among cubilin deficient cells. All cells contain megalin (not labeled). Albumin (red) is almost exclusively detected in cubilin containing cells suggesting that cubilin is the receptor responsible for binding albumin. See color plate section at the back of the book.

FcRn deficient mice are transplanted into wild type mice the mice become hypoalbuminemic.[139] Although this points to a role for the FcRn in albumin metabolism, no information on the absolute albumin excretion rate in the urine of these mice was given. Furthermore, when FcRn is expressed in Madin-Darby canine kidney (MDCK) cells transcytosis of IgG but not albumin was observed.[140] Finally, albumin binds FcRn preferable at pH 6.5[137] suggesting that the affinity for albumin at the luminal membranes of the proximal tubule is low. In conclusion, although the possibility of transtubular transport of intact albumin cannot be excluded the evidence for the transport of large amount of albumin so far has been indirect. The implication of the FcRn as an additional albumin receptor within the proximal tubule is intriguing, however, needs confirmation.

Albumin Induced Renal Tubular and Interstitial Damage

The concept of proteinuria-induced renal tubular and interstitial damage has been propagated as a major factor causing the progressive loss of renal function in CKD.[141] Albuminuria has been shown to be a major risk-factor for the progression of renal disease and the protective effect of anti-proteinuric treatment has been shown to be correlated to the reduction in proteinuria.[142] Experimental studies have demonstrated the ability of albumin, or albumin bound substances, to induce phenotypic changes in tubular cells and animal models have demonstrated albumin overload induced tubular and interstitial damage (Fig. 73.5).[143,144] In a model based on the amphibian kidney in which some nephrons open into the peritoneal cavity and therefore are selectively exposed to serum or albumin when this is injected intraperitoneally, fibrosis was observed around the exposed tubules.[145,146] Most of the evidence for the direct effects of albumin on renal tubular cells originates from *in vitro* studies in which various renal cell lines are exposed to albumin or derivatives and it is not clear whether the tubular effects of albumin involve the megalin/cubilin receptor complex and whether it is dependent on endocytosis. In fact, studies in analbuminemic rats suggested that albumin itself was not important for the progression of proteinuric, renal disease.[147] Interestingly albumin at low or moderate concentrations may promote *in vitro* cell growth[148,149] possibly by a phosphatidylinositide 3-kinase dependent pathway[150] whereas high concentrations of albumin activates pathways that induce apoptosis, endoplasmic reticulum (ER)-stress, cytokine production and phenotypic changes. Ultimately these changes can cause cell death, local inflammation and fibrosis. Although it is important to recognize that the phenotype of renal cell lines in culture, in particular immortalized cell lines, may not resemble the *in vivo* phenotype, similar changes have been observed in experimental models and human diseases characterized by albuminuria as discussed below.

Apoptosis

Tubular cell apoptosis and atrophy is a marked feature of both acute and chronic, proteinuric renal disease.[151,152] Albumin induces proximal tubule cell apoptosis *in vitro*.[151,153,154] The mechanism by which

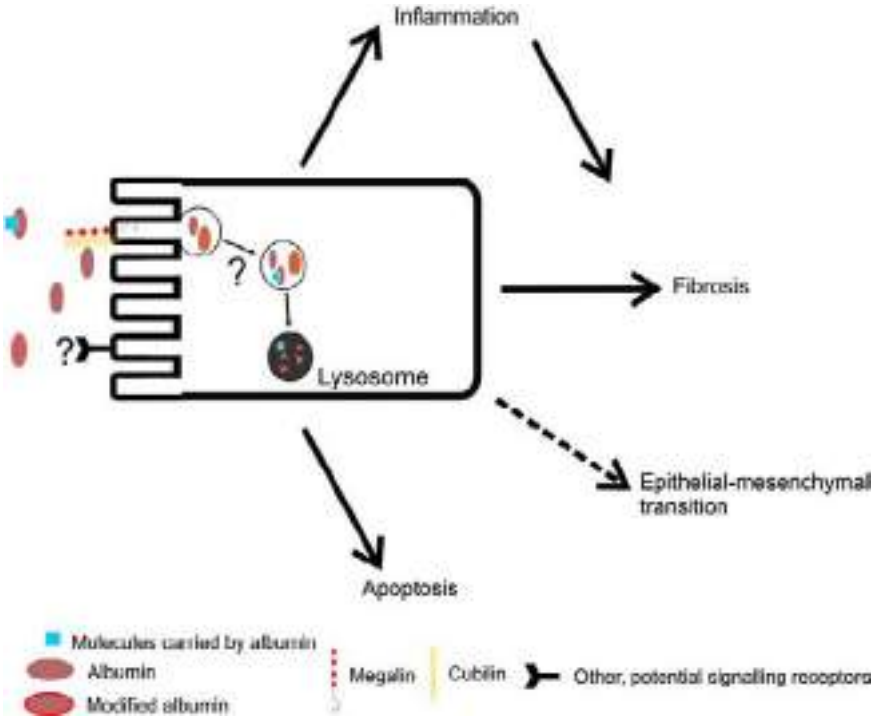

FIGURE 73.5 Effects of albumin on tubular cells. Filtered albumin, whether native or modified, as well as albumin bound substance may affect tubular function and phenotype. Albumin in vitro activates various signaling pathways initiating inflammation fibrosis, apoptosis, and possibly EMT (see text for details). The exact role of the balance between the many pathways in normal physiology is not established, however, experimental studies associated with increased filtration of albumin have demonstrated activation of both apoptosis, inflammation and fibrosis suggesting these mechanism to be involved in the development and progression of renal insufficiency. It is not fully established to which extent all or some of these pathways are dependent on albumin binding to the megalin/cubilin-receptor complex, on endocytosis, and/or on the activation of other potential signaling receptors.

filtered albumin activate downstream mediators of apoptosis is not fully elucidated. Based on *in vitro* studies several pathways have been implicated including both the extrinsic and intrinsic apoptotic pathways. Inactivation of protein kinase C (PKC)-δ both *in vitro* and *in vivo* inhibited albumin and proteinuria induced apoptosis suggesting this acts as an upstream mediator of apoptosis by the intrinsic pathway.[153] Alternatively albumin may induce apoptosis by the stimulation of transmembrane Fas receptor expression that eventually leads to the activation of caspase 8.[155,151] The mechanism by which albumin may induce Fas-receptor expression is not established. Albumin may, by an as yet unknown mechanism, activate mitogen-activated protein kinases ERK1/2 and cause degradation of nuclear factor of kappa light polypeptide gene enhancer in B-cells inhibitor, alpha (IκBα) which then activates activator protein (AP-1) and nuclear factor kappa-light-chain-enhancer of activated B cells (NF-κB), and increases clusterin production. AP-1 stimulates apoptosis whereas NF-κB stimulates inflammation and blocks apoptosis through Bcl. NF-κB dominates initially, however, later clusterin prevents continued NF-κB activation allowing AP-1 and apoptosis to predominate.[154] This complex hypothesis implies a shift in the balance between albumin-induced proinflammatory and proapoptotic pathways which still needs to be established *in vivo*. Other studies have suggested that megalin may associate with protein kinase B (PKB) facilitating the translocation of PKB to the plasma membrane important for its activation by phosphorylation. Both this association as well as the phosphorylation of PKB appear to be inhibited by exposure to albumin. When LL-CPK1 cells are exposed to high concentrations of albumin the amount of both megalin and PKB at the plasmamembrane is reduced. PKB is important for the phosphorylation of Bcl-2-antagonist of cell death protein (Bad) inhibiting the proapoptotic effect of Bad. Thus, albumin induced and megalin dependent decreases in PKB-activation removes the inhibition on the proapoptotic effect of Bad.[148] The possible interaction between these various pathways inducing apoptosis remains unresolved.

ER-Stress

The ER is the site for folding, glycosylation and degradation of newly synthesized proteins involving ER-resident enzymes and chaperones. In ER-stress the demand for protein folding is increased or the process is disrupted leading to an increase in misfolded proteins within the ER.[156] ER-stress induces a physiological response increasing the expression of ER-chaperones as part of the unfolded protein response (UPR). UPR increases the capacity to handle unfolded proteins and slows the transcription of new proteins, however, it may also lead to apoptosis. Increased expression UPR-proteins have been shown both in glomerular and tubular cells in different experimental models of proteinuric kidney disease[156] and markers of ER-stress have been identified in tubular epithelial cells

of human biopsies of various kidney diseases.[157,152] Increased expression of proteins involved in UPR have also been identified in tubular cells exposed to albumin *in vitro* and this has been associated with apoptosis mediated via C/EBP homologous protein (CHOP)[158,152] suggesting another pathway for albumin induced apoptosis. The ER-stress response is believed to allow cells to recover after injury and to be protective against additional damage, however, if prolonged it causes apoptosis.[156] It is not clear how exposure to albumin induces ER-stress and whether this requires accumulation of the protein within the tubular cell.

Interstitial Inflammation and Fibrosis

In vitro studies using proximal tubule cells have shown that albumin exposure induces the expression of a number of inflammatory and fibrogenic mediators, including cytokines such as regulated on activation normal T cell expressed and secreted (RANTES),[159,160] monocyte chemotactic protein (MCP)-1,[161] fractalkine[162] and tumor necrosis factors (TNF)- α,[163] as well as endothelin,[164,165] TGF-β[164] and collagen,[166] and may induce changes in tubular cell expression of surface integrins.[167] These data suggest that albumin and/or bound ligands initiate a series of events that eventually lead to interstitial fibrosis. The exact cascade has not been established, however, proposed intracellular signalling cascades include the activation of NF-κB[168–172] as well as signal transducer and activator of transcription (STAT)[173] factors, possibly through formation of reactive oxygen species,[169,173] a process that may also depend on protein kinase C.[169] There is some evidence to suggest that the process involves the initial endocytic uptake of albumin as renal cell lines with low endocytic activity do not respond to albumin by activation of intracellular pathways and collagen synthesis.[166] Interestingly, differential effects have been observed depending on post-translational modifications of albumin.[146,174] Two studies have evaluated the effect of proteinuria secondary to glomerular damage in megalin deficient mice in which albumin reabsorption is abrogated.[175,176] In one study crescentic glomerulonephritis was induced by injection of anti-glomerular basement membrane serum into conditional megalin knockout mice revealing ~70% deficiency of megalin in proximal tubule cells. Eighteen days after the induction of glomerulonephritis no difference in tubular degeneration or interstitial fibrosis was observed between megalin deficient mice and controls. However, an upregulation of proinflammatory and profibrotic mediators such as inter-cellular adhesion molecule (ICAM)-1, vascular cell adhesion protein (VCAM)-1, and TGF-β was most pronounced in megalin positive tubular cells. In contrast, an increase in apoptosis markers was more pronounced in megalin deficient proximal tubule profiles.[176] In another study heavy proteinuria was induced by injection of an immunotoxin in sensitive mice expressing human CD25 in podocytes.[175] These mice were combined with conditional megalin knockout mice revealing ~60% deficiency of megalin in proximal tubule cells. Ten days after the induction of proteinuria a higher expression of heme-oxygenase-1 and MCP-1 was identified in megalin expressing tubular cells associated with increased apoptosis.[175] None of these studies examined the isolated effect of albumin on proximal tubule cells nor did they assess any megalin independent effects of albumin which itself was blunted by a residual megalin expression of 30–40%. Furthermore, the studies examined the effect of deficient tubular protein uptake less than three weeks after the induction of proteinuria suggesting that they are not optimal models of CKD. Thus, further studies are needed to examine to effect of targeted disruption of the tubular, albumin receptors in animal models of kidney disease allowing for longer follow up.

Epithelial-Mesenchymal Transition (EMT)

The transition of differentiated tubular cells into myofibroblast-like cells producing α-smooth muscle actin and interstitial matrix components leading to progressive fibrosis has been implicated in the progression of kidney fibrosis.[177] Several mediators have been implicated in this process and recently *in vitro* studies have suggested that albumin may induce EMT possibly through activation of the mTOR pathway.[178] Whether this occur *in vivo* following renal injury and whether EMT is in fact induced by protein overload is still controversial.[179]

Effect of Albumin Distal to the Proximal Tubule

There is some suggestion of distal tubular injury associated with albuminuria,[180] however, whether this is a primary or secondary event has not been established. It has been suggested that the filtration of albumin in excess of the capacity for proximal tubule reabsorption, thus leading to the exposure of distal tubule cells to filtered albumin may cause distal tubular cell damage. Apoptosis as well as the increased expression of TGF-β and its receptor have been induced by albumin *in vitro* in renal cells assumed to have a more distal phenotype such as MDCK cells.[181,151,182] *In vitro* these cells were able to endocytose albumin by a clathrin-mediated pathway. How-ever, although endocytic uptake of proteins has been demonstrated in distal tubular/collecting duct cells[183–185] the mechanism of distal tubular endocytosis

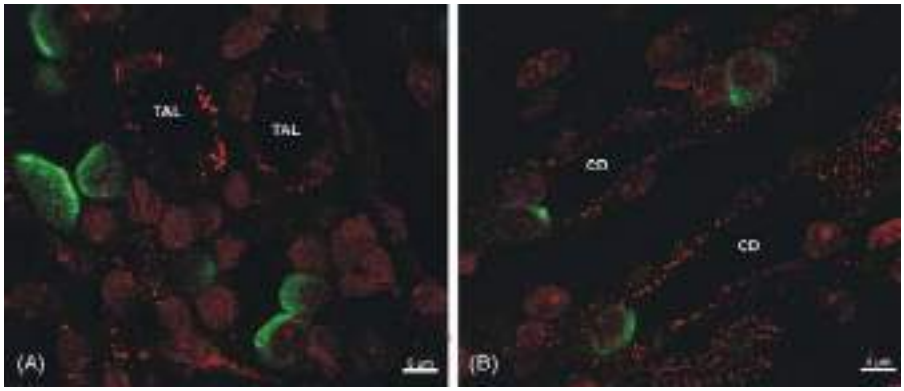

FIGURE 73.6 Immunohistochemical investigation of albumin uptake in renal medulla of a megalin knockout mouse showing that when proximal tubular uptake is disrupted, albumin can be detected in more distal part of the nephron as well as in collecting ducts. A. Micrograph of distal tubule segments (thick ascending limbs, TAL) with visible albumin vesicles (red), next to collecting ducts with intercalated cells positive for H^+-ATP'ase (green). B. Micrograph of collecting duct principal cells positive for albumin (red) and intercalated cell H^+-ATP'ase (green).

in vivo is unresolved[111,186,187] as they do not express megalin or cubilin.[68] See also Figures 73.1 and 73.6 for collecting duct and distal tubular uptake of endogenous albumin in megalin KO mice. Thus, MDCK cells may not be an optimal cell type for the study of the effect of albumin on distal tubule function.

MECHANISMS OF ALBUMINURIA IN DISEASE

Albuminuria denotes the excretion of abnormal and elevated amounts of albumin in the urine. Traditionally albuminuria in the low range of 30 to 300 mg per 24 h has been defined as microalbuminuria although it is unlikely that the 300 mg/24 h limit reflects any abrupt change in pathogenesis. The natural history of albuminuria most likely constitutes a continuum, often fluctuating, as the urinary excretion of albumin, even in healthy people, is determined by a number of factors of which some are not directly related to disease pathology, such as sex, age and physical activity.

Nephrotic syndrome is characterized by the excretion of more than 3 g of albumin/24 h and associated with hypoalbuminemia, hyperlipidemia and edema. Usually this is considered to be due to increased glomerular leak of albumin. Most cases of nephrotic syndrome appear to be acquired, immunemediated diseases, however, within recent years a number of nephrotic conditions have been recognized as the result of single gene defects in podocyte proteins involved in maintenance of the slit diaphragm. Thus, these inherited conditions appear to be the result of changes in the glomerular filtration barrier.[188] In parallel, single gene diseases comprising tubular albuminuria have been shown to be associated with dysfunction of megalin, cubilin and/or AMN (Table 73.1). These include diseases characterized by mutations in the receptor genes, e.g., Donnai Barrow's syndrome (megalin)[189] and Imerslund-Gräsbeck's syndrome (cubilin or AMN).[90] Patients with Imerslund-Gräsbeck's disease have proteinuria in the range of 0.4–1.5 g/24 h[190] reflecting the quantitative significance of cubilin for the tubular reabsorption of filtered albumin. Dent's disease[191] caused by mutations in the gene encoding for the ClC-5[192,193] manifests in decreased levels of megalin and cubilin as demonstrated in a mouse model of Dent's disease[194,195] and in a patient with Dent's disease.[196] Similar mechanisms may be associated with inherited or acquired forms of Fanconi syndrome revealing a protein excretion pattern very similar to that observed in megalin deficient mice.[57]

Clearly most human conditions with albuminuria are not associated with well defined, single gene mutations explaining the phenotype of glomerular or tubular albuminuria. In addition, albuminuria may also be associated with more widespread changes in vascular and organ function as indicated by its association with mortality and cardiovascular disease in large populations. Most primary renal diseases with significant albuminuria are associated with structural changes in the glomeruli signifying that changes in glomerular function are the major contributor to the albuminuria, however, this does not exclude that tubular dysfunction may also be present. In some cases of systemic diseases, such as hypertension and diabetes, tubular dysfunction has been implicated in the early events leading to low grade albumuria as discussed below.

Hypertension and Cardiovascular Disease

Microalbuminuria is an established marker of risk in cardiovascular disease and hypertension.[197] It is traditionally believed that this is due to changes in vascular

TABLE 73.1 Inherited, Single-gene Mutation Diseases with Tubular Albuminuria and Corresponding animal Models

Gene (protein) Affected	Disease	Phenotype	Animal Models
LRP2 (Megalin)	Donnai-Barrow's syndrome[189]	Albuminuria and tubular proteinuria. Cognitive impairment. Hypertelorism, Myopia, Iris coloboma, Sensorineural hearing loss, Agenesis of corpus callosum,	LRP2 gene knock out mice[208] Conditional LRP2 gene knock out mice[209] RAP knockout mice[210]
CUBN (Cubilin)	Hereditary megaloblastic anaemia 1. (Imerslund-Gräsbeck's syndrome)[211]	Albuminuria and tubular proteinuria. Selective intestinal vitamin cobalamin malabsorption. Anemia	Conditional CUBN gene knock out mice[58]
AMN (amnionless)	Hereditary megaloblastic anaemia 1. (Imerslund-Gräsbeck's syndrome)[211]	Similar to above	Inherited selective cobalamin malabsorption in dogs[212]
ClCN5 (chloride channel 5)	Dents disease[191]	Albuminuria and tubular proteinuria. hypercalciuria, nephrolithiasis, nephrocalcinosis. polyuria. Renal failure. Rickets, osteomalacia.	ClCN5 gene knock out mice[195,213]
OCRL (a type II phosphatidylinositol bisphosphate 5-phosphatase)	Lowe syndrome[214]	Albuminuria and tubular proteinuria. Aminoaciduria, hypercalciuria, nephrocalcinosis. polyuria. Renal failure. Cataracts, glaucoma. Mental retardation, reduced muscle tone,	OCRL and Inpp5b gene knock out mice transfected with the human type II phosphoinositide 5-phosphatase encoded by INPP5B[215]
CTNS (cystinosin)	Cystinosis [216]	Fanconi syndrome with tubular proteinuria. Renal failure. Failure to thrive, vomiting, constipation, polyuria, dehydration, rickets. Photophobia, blepharospasm, visual impairment	C57BL/6 CTNS gene knock out mice[217]

and endothelial function.[198] The risk of developing overt kidney disease associated with isolated microalbuminuria is very small.[199] Recently, a single nucleotide polymorphism in the cubilin gene has been associated with microalbuminuria in large populations independent of diabetes and hypertension[60] suggesting that microalbuminuria may in part be a result of differences in receptor function and tubular reabsorptive capacity. Also, experimental observations suggest that tubular dysfunction may contribute to the albuminuria observed in spontaneous hypertensive rats.[200,201] These studies evaluated tubular function indirectly and showed that tubular lysosomal degradation is impaired in hypertension and may be restored by inhibition of the renin angiotensin system. Clearly it is difficult to compare early changes in human hypertensive disease with animal models in particular since long standing, uncontrolled hypertension is known to be associated with renal disease and proteinuria. Thus, the degree of tubular dysfunction in cardiovascular disease with albuminuria remains to be established.

Diabetes

Microalbuminuria in diabetes is associated with increased risk of developing diabetic nephropathy. GBM changes have been identified in diabetes and microalbuminuria but the findings overlap with changes in nonalbuminuric patients.[202] Several studies in humans have suggested that tubular dysfunction in diabetic patients with microalbuminuria may precede increased albumin excretion[124,203] and similar findings have been observed both in animal models[32,204] and *in vitro*.[205] The molecular changes underlying tubular dysfunction have not been clarified but may involve changes in megalin/cubilin mediated uptake.[206,204] Downregulation of megalin has been observed in albuminuric, diabetic rats.[204,207] Increased urinary shedding of megalin and cubilin has been described in microalbuminuric type I diabetic patients.[206] In animal models inhibition of the renin angiotensin system has been shown to improve tubular function[201,207] indicating that regulation of megalin may be affected in diabetic albuminuria and thus providing another potential target for this group of drugs in addition to the effect on blood pressure and glomerular hemodynamics. Interestingly, a single nucleotide polymorphism in the cubilin gene was associated with a small, but significant risk of persistent microalbuminuria in diabetics, but not with severe nephropathy.[60] Thus, while tubular albumin absorption may play a role for the development of microalbuminuria, its role in the development of overt nephropathy is unclear.

In conclusion, the contribution of proximal tubule dysfunction to the albuminuria observed in most proteinuric, human diseases of glomerular or systemic origin is a matter of controversy and still needs to be resolved. Whether tubular dysfunction is a secondary effect simply reflecting the underlying disease, a consequence of albuminuria and/or whether this is part of the pathogenesis and may contribute to the progression also remains to be established. Progress in this area requires introduction of clinical assays to specifically evaluate this aspect of proximal tubule function which will permit the development of specific interventions aimed at restoring tubular function as well.

References

[1] Prinsen BH, de Sain-van der Velden MG. Albumin turnover: experimental approach and its application in health and renal diseases. Clin Chim Acta 2004;347:1–14.

[2] Thongboonkerd V, McLeish KR, Arthur JM, Klein JB. Proteomic analysis of normal human urinary proteins isolated by acetone precipitation or ultracentrifugation. Kidney Int 2002;62:1461–9.

[3] Ware LB, Johnson AC, Zager RA. Renal cortical albumin gene induction and urinary albumin excretion in response to acute kidney injury. Am J Physiol Renal Physiol 2011;300:F628–38.

[4] Haraldsson B, Nystrom J, Deen WM. Properties of the glomerular barrier and mechanisms of proteinuria. Physiol Rev 2008;88: 451–87.

[5] Elger M, Sakai T, Kriz W. The vascular pole of the renal glomerulus of rat. Adv Anat Embryol Cell Biol 1998;139:1–98.

[6] Rostgaard J, Qvortrup K. Electron microscopic demonstrations of filamentous molecular sieve plugs in capillary fenestrae. Microvasc Res 1997;53:1–13.

[7] Rostgaard J, Qvortrup K. Sieve plugs in fenestrae of glomerular capillaries—site of the filtration barrier? Cells Tissues Organs 2002;170:132–8.

[8] Ballermann BJ, Stan RV. Resolved: capillary endothelium is a major contributor to the glomerular filtration barrier. J Am Soc Nephrol 2007;18:2432–8.

[9] Hjalmarsson C, Johansson BR, Haraldsson B. Electron microscopic evaluation of the endothelial surface layer of glomerular capillaries. Microvasc Res 2004;67:9–17.

[10] Friden V, Oveland E, Tenstad O, Ebefors K, Nystrom J, Nilsson UA, et al. The glomerular endothelial cell coat is essential for glomerular filtration. Kidney Int 2011;79:1322–30.

[11] Brenner BM, Hostetter TH, Humes HD. Molecular basis of proteinuria of glomerular origin. N Engl J Med 1978;298:826–33.

[12] Kanwar YS, Farquhar MG. Presence of heparan sulfate in the glomerular basement membrane. Proc Natl Acad Sci USA 1979;76:1303–7.

[13] Kanwar YS, Linker A, Farquhar MG. Increased permeability of the glomerular basement membrane to ferritin after removal of glycosaminoglycans (heparan sulfate) by enzyme digestion. J Cell Biol 1980;86:688–93.

[14] Rennke HG, Cotran RS, Venkatachalam MA. Role of molecular charge in glomerular permeability. Tracer studies with cationized ferritins. J Cell Biol 1975;67:638–46.

[15] Kanwar YS, Danesh FR, Chugh SS. Contribution of proteoglycans towards the integrated functions of renal glomerular capillaries: a historical perspective. Am J Pathol 2007;171: 9–13.

[16] Bolton GR, Deen WM, Daniels BS. Assessment of the charge selectivity of glomerular basement membrane using Ficoll sulfate. Am J Physiol 1998;274:F889–96.

[17] Farquhar MG. The glomerular basement membrane: not gone, just forgotten. J Clin Invest 2006;116:2090–3.

[18] Gubler MC. Inherited diseases of the glomerular basement membrane. Nat Clin Pract Nephrol 2008;4:24–37.

[19] Tryggvason K. Unraveling the mechanisms of glomerular ultrafiltration: nephrin, a key component of the slit diaphragm. J Am Soc Nephrol 1999;10:2440–5.

[20] Boute N, Gribouval O, Roselli S, Benessy F, Lee H, Fuchshuber A, et al. NPHS2, encoding the glomerular protein podocin, is mutated in autosomal recessive steroid-resistant nephrotic syndrome. Nat Genet 2000;24:349–54.

[21] Rodewald R, Karnovsky MJ. Porous substructure of the glomerular slit diaphragm in the rat and mouse. J Cell Biol 1974;60: 423–33.

[22] Gagliardini E, Conti S, Benigni A, Remuzzi G, Remuzzi A. Imaging of the porous ultrastructure of the glomerular epithelial filtration slit. J Am Soc Nephrol 2010;21:2081–9.

[23] Hausmann R, Kuppe C, Egger H, Schweda F, Knecht V, Elger M, et al. Electrical forces determine glomerular permeability. J Am Soc Nephrol 2010;21:2053–8.

[24] Menzel S, Moeller MJ. Role of the podocyte in proteinuria. Pediatr Nephrol 2010.

[25] Eremina V, Baelde HJ, Quaggin SE. Role of the VEGF—a signaling pathway in the glomerulus: evidence for crosstalk between components of the glomerular filtration barrier. Nephron Physiol 2007;106:32–7.

[26] Maack T, Park CH, Camargo MJF. Renal filtration, transport and metabolism of proteins 1992;2:3005–38.

[27] Mogensen CE, Sølling K. Studies on renal tubular protein reabsorption: partial and near complete inhibition by certain amino acids. Scand J Clin Lab Invest 1977;37:477–86.

[28] Tencer J, Frick IM, Oquist BW, Alm P, Rippe B. Size-selectivity of the glomerular barrier to high molecular weight proteins: upper size limitations of shunt pathways. Kidney Int 1998;53:709–15.

[29] Thelle K, Christensen EI, Vorum H, Orskov H, Birn H. Characterization of proteinuria and tubular protein uptake in a new model of oral L-lysine administration in rats. Kidney Int 2006;69:1333–40.

[30] Tojo A, Endou H. Intrarenal handling of proteins in rats using fractional micropuncture technique. Am J Physiol 1992;263:F601–6.

[31] Comper WD, Hilliard LM, Nikolic-Paterson DJ, Russo LM. Disease-dependent mechanisms of albuminuria. Am J Physiol Renal Physiol 2008;295:F1589–600.

[32] Russo LM, Sandoval RM, Campos SB, Molitoris BA, Comper WD, Brown D. Impaired tubular uptake explains albuminuria in early diabetic nephropathy. J Am Soc Nephrol 2009;20: 489–94.

[33] Russo LM, Sandoval RM, McKee M, Osicka TM, Collins AB, Brown D, et al. The normal kidney filters nephrotic levels of albumin retrieved by proximal tubule cells: retrieval is disrupted in nephrotic states. Kidney Int 2007;71:504–13.

[34] Gekle M. Renal albumin handling: a look at the dark side of the filter. Kidney Int 2007;71:479–81.

[35] Christensen EI, Birn H, Rippe B, Maunsbach AB. Controversies in nephrology: renal albumin handling, facts, and artifacts!. Kidney Int 2007;72:1192–4.

[36] de Borst MH. On the origin of albuminuria. Kidney Int 2007;72:1409–10.

[37] Remuzzi A, Sangalli F, Fassi A, Remuzzi G. Albumin concentration in the Bowman's capsule: multiphoton microscopy vs micropuncture technique. Kidney Int 2007;72:1410–1.

[38] Peti-Peterdi J. Independent two-photon measurements of albumin GSC give low values. Am J Physiol Renal Physiol 2009;296: F1255–7.

[39] Peti-Peterdi J, Sipos AA. High-powered view of the filtration barrier. J Am Soc Nephrol 2010;21:1835–41.
[40] Tanner GA. Glomerular sieving coefficient of serum albumin in the rat: a two-photon microscopy study. Am J Physiol Renal Physiol 2009;296:F1258–65.
[41] Venturoli D, Rippe B. Ficoll and dextran vs. globular proteins as probes for testing glomerular permselectivity: effects of molecular size, shape, charge, and deformability. Am J Physiol Renal Physiol 2005;288:F605–13.
[42] Eyre J, Ioannou K, Grubb BD, Saleem MA, Mathieson PW, Brunskill NJ, et al. Statin-sensitive endocytosis of albumin by glomerular podocytes. Am J Physiol Renal Physiol 2007;292:F674–81.
[43] Yoshikawa N, Ito H, Akamatsu R, Hazikano H, Okada S, Matsuo T. Glomerular podocyte vacuolation in focal segmental glomerulosclerosis. Arch Pathol Lab Med 1986;110:394–8.
[44] Farquhar MG, Wissig SL, Palade GE. Glomerular permeability. I. Ferritin transfer across the normal glomerular capillary wall. J Exp Med 1961;113:47–66.
[45] Graham Jr RC, Karnovsky MJ. Glomerular permeability. Ultrastructural cytochemical studies using peroxidases as protein tracers. J Exp Med 1966;124:1123–34.
[46] Kerjaschki D, Farquhar MG. Immunocytochemical localization of the Heymann nephritis antigen (GP330) in glomerular epithelial cells of normal lewis rats. J Exp Med 1983;157:667–86.
[47] Prabakaran T, Nielsen R, Larsen JV, Schwartz Sorensen S, Feldt-Rasmussen U, Saleem MA, et al. Endocytosis of a-galactosidase a in human podocytes in fabry disease is mediated by different receptors. J Am Soc Nephrol 2010;21:566A.
[48] Kanwar YS, Rosenzweig LJ. Clogging of the glomerular basement membrane. J Cell Biol 1982;93:489–94.
[49] Smithies O. Why the kidney glomerulus does not clog: a gel permeation/diffusion hypothesis of renal function. Proc Natl Acad Sci USA 2003;100:4108–13.
[50] Maunsbach AB. Absorption of I^{125}-labeled homologous albumin by rat kidney proximal tubule cells. A study of microperfused single proximal tubules by electron microscopic autoradiography and histochemistry. J Ultrastruct Res 1966;15:197–241.
[51] Maunsbach AB. Albumin absorption by renal proximal tubule cells. Nature 1966;212:546–7.
[52] Kalantry S, Manning S, Haub O, Tomihara-Newberger C, Lee HG, Fangman J, et al. The amnionless gene, essential for mouse gastrulation, encodes a visceral-endoderm-specific protein with an extracellular cysteine-rich domain. Nat Genet 2001;27:412–6.
[53] Kerjaschki D, Farquhar MG. The pathogenic antigen of Heymann nephritis is a membrane glycoprotein of the renal proximal tubule brush border. Proc Natl Acad Sci USA 1982;79: 5557–61.
[54] Sahali D, Mulliez N, Chatelet F, Laurent Winter C, Citadelle D, Sabourin JC, et al. Comparative immunochemistry and ontogeny of two closely related coated pit proteins. The 280-kd target of teratogenic antibodies and the 330-kd target of nephritogenic antibodies. Am J Pathol 1993;142:1654–67.
[55] Cui S, Verroust PJ, Moestrup SK, Christensen EI. Megalin/gp330 mediates uptake of albumin in renal proximal tubule. Am J Physiol 1996;271:F900–7.
[56] Birn H, Fyfe JC, Jacobsen C, Mounier F, Verroust PJ, Orskov H, et al. Cubilin is an albumin binding protein important for renal tubular albumin reabsorption. J Clin Invest 2000;105: 1353–61.
[57] Leheste JR, Rolinski B, Vorum H, Hilpert J, Nykjær A, Jacobsen C, et al. Megalin knockout mice as an animal model of low molecular weight proteinuria. Am J Pathol 1999;155:1361–70.
[58] Amsellem S, Gburek J, Hamard G, Nielsen R, Willnow TE, Devuyst O, et al. Cubilin is essential for albumin reabsorption in the renal proximal tubule. J Am Soc Nephrol 2010;21: 1859–67.
[59] Wahlstedt-Froberg V, Pettersson T, Aminoff M, Dugue B, Grasbeck R. Proteinuria in cubilin-deficient patients with selective vitamin B12 malabsorption. Pediatr Nephrol 2003;18: 417–21.
[60] Boger CA, Chen MH, Tin A, Olden M, Kottgen A, de Boer IH, et al. CUBN is a gene locus for albuminuria. J Am Soc Nephrol 2011;22:555–70.
[61] Chatelet F, Brianti E, Ronco P, Roland J, Verroust P. Ultrastructural localization by monoclonal antibodies of brush border antigens expressed by glomeruli. I. Renal distribution. Am J Pathol 1986;122:500–11.
[62] Christensen EI, Birn H, Verroust P, Moestrup SK. Membrane receptors for endocytosis in the renal proximal tubule. Int Rev Cytol 1998;180:237–84.
[63] Christensen EI, Nielsen S, Moestrup SK, Borre C, Maunsbach AB, De Heer E, et al. Segmental distribution of the endocytosis receptor gp330 in renal proximal tubules. Eur J Cell Biol 1995;66:349–64.
[64] Christensen EI. Rapid membrane recycling in renal proximal tubule cells. Eur J Cell Biol 1982;29:43–9.
[65] Sahali D, Mulliez N, Chatelet F, Dupuis R, Ronco P, Verroust P. Characterization of a 280-kD protein restricted to the coated pits of the renal brush border and the epithelial cells of the yolk sac. Teratogenic effect of the specific monoclonal antibodies. J Exp Med 1988;167:213–8.
[66] Seetharam B, Christensen EI, Moestrup SK, Hammond TG, Verroust PJ. Identification of rat yolk sac target protein of teratogenic antibodies, gp280, as intrinsic factor-cobalamin receptor. J Clin Invest 1997;99:2317–22.
[67] Fyfe JC, Madsen M, Hojrup P, Christensen EI, Tanner SM, de la Chapelle A, et al. The functional cobalamin (vitamin B12)-intrinsic factor receptor is a novel complex of cubilin and amnionless. Blood 2004;103:1573–9.
[68] Christensen EI, Birn H. Megalin and cubilin: multifunctional endocytic receptors. Nat Rev Mol Cell Biol 2002;3:256–66.
[69] Christensen EI, Verroust PJ, Nielsen R. Receptor-mediated endocytosis in renal proximal tubule. Pflugers Arch 2009;458:1039–48.
[70] Hjälm G, Murray E, Crumley G, Harazim W, Lundgren S, Onyango I, et al. Cloning and sequencing of human gp330, a Ca (2+)-binding receptor with potential intracellular signaling properties. Eur J Biochem 1996;239:132–7.
[71] Raychowdhury R, Niles JL, McCluskey RT, Smith JA. Autoimmune target in Heymann nephritis is a glycoprotein with homology to the LDL receptor. Science 1989;244:1163–5.
[72] Saito A, Pietromonaco S, Loo AK, Farquhar MG. Complete cloning and sequencing of rat gp330/"megalin," a distinctive member of the low density lipoprotein receptor gene family. Proc Natl Acad Sci USA 1994;91:9725–9.
[73] Bieri S, Atkins AR, Lee HT, Winzor DJ, Smith R, Kroon PA. Folding, calcium binding, and structural characterization of a concatemer of the first and second ligand-binding modules of the low-density lipoprotein receptor. Biochemistry 1998;37: 10994–1002.
[74] Fass D, Blacklow S, Kim PS, Berger JM. Molecular basis of familial hypercholesterolaemia from structure of LDL receptor module. Nature 1997;388:691–3.
[75] Russell DW, Brown MS, Goldstein JL. Different combinations of cysteine-rich repeats mediate binding of low density lipoprotein receptor to two different proteins. J Biol Chem 1989;264: 21682–8.
[76] Wolf CA, Dancea F, Shi M, Bade-Noskova V, Ruterjans H, Kerjaschki D, et al. Solution structure of the twelfth cysteine-rich ligand-binding repeat in rat megalin. J Biomol NMR 2007;37:321–8.

[77] Davis CG, Goldstein JL, Sudhof TC, Anderson RG, Russell DW, Brown MS. Acid-dependent ligand dissociation and recycling of LDL receptor mediated by growth factor homology region. Nature 1987;326:760–5.
[78] Zhai XY, Nielsen R, Birn H, Drumm K, Mildenberger S, Freudinger R, et al. Cubilin- and megalin-mediated uptake of albumin in cultured proximal tubule cells of opossum kidney. Kidney Int 2000;58:1523–33.
[79] Takeda T, Yamazaki H, Farquhar MG. Identification of an apical sorting determinant in the cytoplasmic tail of megalin. Am J Physiol Cell Physiol 2003;284:C1105–13.
[80] Christensen EI, Gliemann J, Moestrup SK. Renal tubule gp330 is a calcium binding receptor for endocytic uptake of protein. J Histochem Cytochem 1992;40:1481–90.
[81] Birn H, Vorum H, Verroust PJ, Moestrup SK, Christensen EI. Receptor-associated protein is important for normal processing of megalin in kidney proximal tubules. J Am Soc Nephrol 2000;11:191–202.
[82] Yuseff MI, Farfan P, Bu G, Marzolo MPA. Cytoplasmic PPPSP motif determines Megalin's phosphorylation and regulates receptor's recycling and surface expression. Traffic 2007;8: 1215–30.
[83] Seetharam B, Levine JS, Ramasamy M, Alpers DH. Purification, properties, and immunochemical localization of a receptor for Intrinsic Factor-Cobalamin complex in the rat kidney. J Biol Chem 1988;263:4443–9.
[84] Kozyraki R, Kristiansen M, Silahtaroglu A, Hansen C, Jacobsen C, Tommerup N, et al. The human intrinsic factor-vitamin B12 receptor, cubilin: molecular characterization and chromosomal mapping of the gene to 10 p within the autosomal recessive megaloblastic anemia (MGA1) region. Blood 1998;91:3593–600.
[85] Moestrup SK, Kozyraki R, Kristiansen M, Kaysen JH, Rasmussen HH, Brault D, et al. The intrinsic factor-vitamin B12 receptor and target of teratogenic antibodies is a megalin-binding peripheral membrane protein with homology to developmental proteins. J Biol Chem 1998;273:5235–42.
[86] Ahuja R, Yammani R, Bauer JA, Kalra S, Seetharam S, Seetharam B. Interactions of cubilin with megalin and the product of the amnionless gene (AMN): effect on its stability. Biochem J 2008;410:301–8.
[87] Coudroy G, Gburek J, Kozyraki R, Madsen M, Trugnan G, Moestrup SK, et al. Contribution of cubilin and amnionless to processing and membrane targeting of cubilin-amnionless complex. J Am Soc Nephrol 2005;16:2330–7.
[88] He Q, Madsen M, Kilkenney A, Gregory B, Christensen EI, Vorum H, et al. Amnionless function is required for cubilin brush-border expression and intrinsic factor-cobalamin (vitamin B12) absorption *in vivo*. Blood 2005;106:1447–53.
[89] Strope S, Rivi R, Metzger T, Manova K, Lacy E. Mouse amnionless, which is required for primitive streak assembly, mediates cell-surface localization and endocytic function of cubilin on visceral endoderm and kidney proximal tubules. Development 2004;131:4787–95.
[90] Storm T, Emma F, Verroust PJ, Hertz JM, Nielsen R, Christensen EI. A patient with cubilin deficiency. N Engl J Med 2011;364:89–91.
[91] Yammani RR, Seetharam S, Seetharam B. Cubilin and megalin expression and their interaction in the rat intestine: effect of thyroidectomy. Am J Physiol Endocrinol Metab 2001;281: E900–7.
[92] Tanner SM, Aminoff M, Wright FA, Liyanarachchi S, Kuronen M, Saarinen A, et al. Amnionless, essential for mouse gastrulation, is mutated in recessive hereditary megaloblastic anemia. Nat Genet 2003;33:426–9.
[93] Keyel PA, Mishra SK, Roth R, Heuser JE, Watkins SC, Traub LM. A single common portal for clathrin-mediated endocytosis of distinct cargo governed by cargo-selective adaptors. Mol Biol Cell 2006;17:4300–17.
[94] Nagai M, Meerloo T, Takeda T, Farquhar MG. The adaptor protein ARH escorts megalin to and through endosomes. Mol Biol Cell 2003;14:4984–96.
[95] Oleinikov AV, Zhao J, Makker SP. Cytosolic adaptor protein Dab2 is an intracellular ligand of endocytic receptor gp600/megalin. Biochem J 2000;347:613–21.
[96] Nagai J, Christensen EI, Morris SM, Willnow TE, Cooper JA, Nielsen R. Mutually dependent localization of megalin and Dab2 in the renal proximal tubule. Am J Physiol Renal Physiol 2005;289:F569–76.
[97] Morris SM, Tallquist MD, Rock CO, Cooper JA. Dual roles for the Dab2 adaptor protein in embryonic development and kidney transport. EMBO J 2002;21:1555–64.
[98] Hosaka K, Takeda T, Iino N, Hosojima M, Sato H, Kaseda R, et al. Megalin and nonmuscle myosin heavy chain IIA interact with the adaptor protein Disabled-2 in proximal tubule cells. Kidney Int 2009;75:1308–15.
[99] Lou X, McQuistan T, Orlando RA, Farquhar MG.. GAIP, GIPC and Galphai3 are concentrated in endocytic compartments of proximal tubule cells: putative role in regulating megalin's function. J Am Soc Nephrol 2002;13:918–27.
[100] Naccache SN, Hasson T, Horowitz A. Binding of internalized receptors to the PDZ domain of GIPC/synectin recruits myosin VI to endocytic vesicles. Proc Natl Acad Sci USA 2006;103:12735–40.
[101] Gotoh N, Yan Q, Du Z, Biemesderfer D, Kashgarian M, Mooseker MS, et al. Altered renal proximal tubular endocytosis and histology in mice lacking myosin-VI. Cytoskeleton (Hoboken) 2010;67:178–92.
[102] Hammad SM, Barth JL, Knaak C, Argraves WS. Megalin acts in concert with cubilin to mediate endocytosis of high density lipoproteins. J Biol Chem 2000;275:12003–8.
[103] Kozyraki R, Fyfe J, Verroust PJ, Jacobsen C, Dautry-Varsat A, Gburek J, et al. Megalin-dependent cubilin-mediated endocytosis is a major pathway for the apical uptake of transferrin in polarized epithelia. Proc Natl Acad Sci USA 2001;98:12491–6.
[104] Andersen CB, Madsen M, Storm T, Moestrup SK, Andersen GR. Structural basis for receptor recognition of vitamin-B(12)-intrinsic factor complexes. Nature 2010;464:445–8.
[105] Huby AC, Rastaldi MP, Caron K, Smithies O, Dussaule JC, Chatziantoniou C. Restoration of podocyte structure and improvement of chronic renal disease in transgenic mice overexpressing renin. PLoS One 2009;4:e6721.
[106] Riquier-Brison AD, Leong PK, Pihakaski-Maunsbach K, McDonough AA. Angiotensin II stimulates trafficking of NHE3, NaPi2, and associated proteins into the proximal tubule microvilli. Am J Physiol Renal Physiol 2010;298: F177–86.
[107] Pohl M, Kaminski H, Castrop H, Bader M, Himmerkus N, Bleich M, et al. Intrarenal renin angiotensin system revisited: role of megalin-dependent endocytosis along the proximal nephron. J Biol Chem 2010;285:41935–46.
[108] Gekle M, Knaus P, Nielsen R, Mildenberger S, Freudinger R, Wohlfarth V, et al. Transforming growth factor-beta1 reduces megalin- and cubilin-mediated endocytosis of albumin in proximal-tubule-derived opossum kidney cells. J Physiol 2003;552:471–81.
[109] Cabezas F, Lagos J, Cespedes C, Vio CP, Bronfman M, Marzolo MP. Megalin/LRP2 expression is induced by

peroxisome proliferator-activated receptor-alpha and -gamma: implications for PPARs' roles in renal function. PLoS One 2011;6:e16794.
[110] Yang J, Zhang D, Li J, Zhang X, Fan F, Guan Y. Role of PPARgamma in renoprotection in Type 2 diabetes: molecular mechanisms and therapeutic potential. Clin Sci (Lond) 2009;116:17–26.
[111] Bourdeau JE, Carone FA, Ganote CE. Serum albumin uptake in isolated perfused renal tubules. J Cell Biol 1972;54:382–98.
[112] Slattery C, Lee A, Zhang Y, Kelly DJ, Thorn P, Nikolic-Paterson DJ, et al. *In vivo* visualization of albumin degradation in the proximal tubule. Kidney Int 2008;74:1480–6.
[113] Clapp WL, Park CH, Madsen KM, Tisher CC. Axial heterogeneity in the handling of albumin by the rabbit proximal tubule. Lab Invest 1988;58:549–58.
[114] Kamijo Y, Hora K, Tanaka N, Usuda N, Kiyosawa K, Nakajima T, et al. Identification of functions of peroxisome proliferator-activated receptor alpha in proximal tubules. J Am Soc Nephrol 2002;13:1691–702.
[115] Mego JL, Farb RM, Barnes J. An adenosine triphosphate-dependent stabilization of proteolytic activity in heterolysosomes. Evidence for a proton pump. Biochem J 1972;128: 763–9.
[116] Haga HJ, Andersen KJ, Rygh T, Iversen BM, Matre R. Changes in lysosome populations in the rat kidney cortex induced by experimental proteinuria. Int J Biochem 1988;20:793–800.
[117] Olbricht CJ, Irmler H, Gutjahr E, Koch KM. Effect of low-molecular-weight dextran on proteolytic and nonproteolytic lysosomal enzymes in isolated segments of rat proximal tubule. Nephron 1993;64:262–7.
[118] Birn H, Christensen EI. Renal albumin absorption in physiology and pathology. Kidney Int 2006;69:440–9.
[119] Gekle M. Renal tubule albumin transport. Annu Rev Physiol 2005;67:573–94.
[120] Park CH, Maack T. Albumin absorption and catabolism by isolated perfused proximal convoluted tubules of the rabbit. J Clin Invest 1984;73:767–77.
[121] Clavant SP, Greive KA, Nikolovski J, Reeve S, Smith AI, Comper WD. Albumin fragments in normal rat urine are derived from rapidly degraded filtered albumin. Nephrol (Carlton) 2003;8:72–9.
[122] Hilliard LM, Osicka TM, Clavant SP, Robinson PJ, Nikolic-Paterson DJ, Comper WD. Characterization of the urinary albumin degradation pathway in the isolated perfused rat kidney. J Lab Clin Med 2006;147:36–44.
[123] Osicka TM, Comper WD. Protein degradation during renal passage in normal kidneys is inhibited in experimental albuminuria. Clin Sci (Lond) 1997;93:65–72.
[124] Osicka TM, Houlihan CA, Chan JG, Jerums G, Comper WD. Albuminuria in patients with type 1 diabetes is directly linked to changes in the lysosome-mediated degradation of albumin during renal passage. Diabetes 2000;49:1579–84.
[125] Strong KJ, Osicka TM, Comper WD. Urinary-peptide excretion by patients with and volunteers without diabetes. J Lab Clin Med 2005;145:239–46.
[126] Gudehithlu KP, Pegoraro AA, Dunea G, Arruda JA, Singh AK. Degradation of albumin by the renal proximal tubule cells and the subsequent fate of its fragments. Kidney Int 2004;65: 2113–22.
[127] Greive KA, Balazs ND, Comper WD. Protein fragments in urine have been considerably underestimated by various protein assays. Clin Chem 2001;47:1717–9.
[128] Weyer K, Nielsen R, Christensen EI, Birn H. Generation of urinary albumin fragments does not require proximal tubular uptake. J Am Soc Nephrol 2012;23:591–6.
[129] Norden AG, Sharratt P, Cutillas PR, Cramer R, Gardner SC, Unwin RJ. Quantitative amino acid and proteomic analysis: very low excretion of polypeptides >750 Da in normal urine. Kidney Int 2004;66:1994–2003.
[130] Seegmiller JC, Barnidge DR, Burns BE, Larson TS, Lieske JC, Kumar R. Quantification of urinary albumin by using protein cleavage and LC-MS/MS. Clin Chem 2009;55:1100–7.
[131] Comper WD, Russo LM. The glomerular filter: an imperfect barrier is required for perfect renal function. Curr Opin Nephrol Hypertens 2009;18:336–42.
[132] Comper WD, Hilliard LM, Nikolic-Paterson DJ, Russo LM. Disease-dependent mechanisms of albuminuria. Am J Physiol Renal Physiol 2008;295:F1589–600.
[133] Eppel GA, Osicka TM, Pratt LM, Jablonski P, Howden BO, Glasgow EF, et al. The return of glomerular-filtered albumin to the rat renal vein. Kidney Int 1999;55:1861–70.
[134] Firan M, Bawdon R, Radu C, Ober RJ, Eaken D, Antohe F, et al. The MHC class I-related receptor, FcRn, plays an essential role in the maternofetal transfer of gamma-globulin in humans. Int Immunol 2001;13:993–1002.
[135] Akilesh S, Huber TB, Wu H, Wang G, Hartleben B, Kopp JB, et al. Podocytes use FcRn to clear IgG from the glomerular basement membrane. Proc Natl Acad Sci USA 2008;105: 967–72.
[136] Haymann JP, Levraud JP, Bouet S, Kappes V, Hagege J, Nguyen G, et al. Characterization and localization of the neonatal Fc receptor in adult human kidney. J Am Soc Nephrol 2000;11:632–9.
[137] Chaudhury C, Brooks CL, Carter DC, Robinson JM, Anderson CL. Albumin binding to FcRn: distinct from the FcRn-IgG interaction. Biochemistry 2006;45:4983–90.
[138] Kim J, Bronson CL, Hayton WL, Radmacher MD, Roopenian DC, Robinson JM, et al. Albumin turnover: FcRn-mediated recycling saves as much albumin from degradation as the liver produces. Am J Physiol Gastrointest Liver Physiol 2006;290: G352–60.
[139] Sarav M, Wang Y, Hack BK, Chang A, Jensen M, Bao L, et al. Renal FcRn reclaims albumin but facilitates elimination of IgG. J Am Soc Nephrol 2009;20:1941–52.
[140] Tesar DB, Tiangco NE, Bjorkman PJ. Ligand valency affects transcytosis, recycling and intracellular trafficking mediated by the neonatal Fc receptor. Traffic 2006;7:1127–42.
[141] Abbate M, Zoja C, Remuzzi G. How does proteinuria cause progressive renal damage? J Am Soc Nephrol 2006;17:2974–84.
[142] Chiurchiu C, Remuzzi G, Ruggenenti P. Angiotensin-converting enzyme inhibition and renal protection in nondiabetic patients: the data of the meta-analyses. J Am Soc Nephrol 2005;16(Suppl. 1):S58–63.
[143] Eddy AA, Giachelli CM. Renal expression of genes that promote interstitial inflammation and fibrosis in rats with protein-overload proteinuria. Kidney Int 1995;47:1546–57.
[144] Eddy AA, Kim H, Lopez-Guisa J, Oda T, Soloway PD. Interstitial fibrosis in mice with overload proteinuria: deficiency of TIMP-1 is not protective. Kidney Int 2000;58:618–28.
[145] Gross ML, Hanke W, Koch A, Ziebart H, Amann K, Ritz E. Intraperitoneal protein injection in the axolotl: the amphibian kidney as a novel model to study tubulointerstitial activation. Kidney Int 2002;62:51–9.
[146] Gross ML, Piecha G, Bierhaus A, Hanke W, Henle T, Schirmacher P, et al. Glycated and carbamylated albumin is more "nephrotoxic" than unmodified albumin in the amphibian kidney. Am J Physiol Renal Physiol 2011;301:F476–85.
[147] Okuda S, Oochi N, Wakisaka M, Kanai H, Tamaki K, Nagase S, et al. Albuminuria is not an aggravating factor in

experimental focal glomerulosclerosis and hyalinosis. J Lab Clin Med 1992;119:245–53.
[148] Caruso-Neves C, Pinheiro AA, Cai H, Souza-Menezes J, Guggino WB. PKB and megalin determine the survival or death of renal proximal tubule cells. Proc Natl Acad Sci USA 2006;103:18810–5.
[149] Iglesias J, Abernethy VE, Wang Z, Lieberthal W, Koh JS, Levine JS. Albumin is a major serum survival factor for renal tubular cells and macrophages through scavenging of ROS. Am J Physiol 1999;277:F711–22.
[150] Dixon R, Brunskill NJ. Activation of mitogenic pathways by albumin in kidney proximal tubule epithelial cells: implications for the pathophysiology of proteinuric states. J Am Soc Nephrol 1999;10:1487–97.
[151] Erkan E, Garcia CD, Patterson LT, Mishra J, Mitsnefes MM, Kaskel FJ, et al. Induction of renal tubular cell apoptosis in focal segmental glomerulosclerosis: roles of proteinuria and Fas-dependent pathways. J Am Soc Nephrol 2005;16: 398–407.
[152] Wu X, He Y, Jing Y, Li K, Zhang J. Albumin overload induces apoptosis in renal tubular epithelial cells through a CHOP-dependent pathway. OMICS 2010;14:61–73.
[153] Li X, Pabla N, Wei Q, Dong G, Messing RO, Wang CY, et al. PKC-delta promotes renal tubular cell apoptosis associated with proteinuria. J Am Soc Nephrol 2010;21:1115–24.
[154] Takase O, Minto AW, Puri TS, Cunningham PN, Jacob A, Hayashi M, et al. Inhibition of NF-kappaB-dependent Bcl-xL expression by clusterin promotes albumin-induced tubular cell apoptosis. Kidney Int 2008;73:567–77.
[155] Erkan E, De Leon M, Devarajan P. Albumin overload induces apoptosis in LLC-PK(1) cells. Am J Physiol Renal Physiol 2001;280:F1107–14.
[156] Cybulsky AV. Endoplasmic reticulum stress in proteinuric kidney disease. Kidney Int 2010;77:187–93.
[157] Lindenmeyer MT, Rastaldi MP, Ikehata M, Neusser MA, Kretzler M, Cohen CD, et al. Proteinuria and hyperglycemia induce endoplasmic reticulum stress. J Am Soc Nephrol 2008;19:2225–36.
[158] Ohse T, Inagi R, Tanaka T, Ota T, Miyata T, Kojima I, et al. Albumin induces endoplasmic reticulum stress and apoptosis in renal proximal tubular cells. Kidney Int 2006;70:1447–55.
[159] Wang Y, Chen J, Chen L, Tay YC, Rangan GK, Harris DC. Induction of monocyte chemoattractant protein-1 in proximal tubule cells by urinary protein. J Am Soc Nephrol 1997;8: 1537–45.
[160] Zoja C, Donadelli R, Colleoni S, Figliuzzi M, Bonazzola S, Morigi M, et al. Protein overload stimulates RANTES production by proximal tubular cells depending on NF-kappa B activation. Kidney Int 1998;53:1608–15.
[161] Tang S, Leung JC, Abe K, Chan KW, Chan LY, Chan TM, et al. Albumin stimulates interleukin-8 expression in proximal tubular epithelial cells *in vitro* and *in vivo*. J Clin Invest 2003;111: 515–27.
[162] Donadelli R, Zanchi C, Morigi M, Buelli S, Batani C, Tomasoni S, et al. Protein overload induces fractalkine upregulation in proximal tubular cells through nuclear factor kappaB- and p38 mitogen-activated protein kinase-dependent pathways. J Am Soc Nephrol 2003;14:2436–46.
[163] Drumm K, Bauer B, Freudinger R, Gekle M. Albumin induces NF-kappaB expression in human proximal tubule-derived cells (IHKE-1). Cell Physiol Biochem 2002;12:187–96.
[164] Yard BA, Chorianopoulos E, Herr D, van der Woude FJ. Regulation of endothelin-1 and transforming growth factor-beta1 production in cultured proximal tubular cells by albumin and heparan sulphate glycosaminoglycans. Nephrol Dial Transplant 2001;16:1769–75.
[165] Zoja C, Morigi M, Figliuzzi M, Bruzzi I, Oldroyd S, Benigni A, et al. Proximal tubular cell synthesis and secretion of endothelin-1 on challenge with albumin and other proteins. Am J Kidney Dis 1995;26:934–41.
[166] Wohlfarth V, Drumm K, Mildenberger S, Freudinger R, Gekle M. Protein uptake disturbs collagen homeostasis in proximal tubule-derived cells. Kidney Int Suppl 2003:103–9.
[167] Peruzzi L, Trusolino L, Amore A, Gianoglio B, Cirina P, Basso G, et al. Tubulointerstitial responses in the progression of glomerular diseases: albuminuria modulates alpha v beta 5 integrin. Kidney Int 1996;50:1310–20.
[168] Donadelli R, Abbate M, Zanchi C, Corna D, Tomasoni S, Benigni A, et al. Protein traffic activates NF-kB gene signaling and promotes MCP-1-dependent interstitial inflammation. Am J Kidney Dis 2000;36:1226–41.
[169] Morigi M, Macconi D, Zoja C, Donadelli R, Buelli S, Zanchi C, et al. Protein overload-induced NF-kappaB activation in proximal tubular cells requires H(2)O(2) through a PKC-dependent pathway. J Am Soc Nephrol 2002;13:1179–89.
[170] Rangan GK, Wang Y, Tay YC, Harris DC. Inhibition of nuclear factor-kappaB activation reduces cortical tubulointerstitial injury in proteinuric rats. Kidney Int 1999;56:118–34.
[171] Takase O, Marumo T, Hishikawa K, Fujita T, Quigg RJ, Hayashi M. NF-kappaB-dependent genes induced by proteinuria and identified using DNA microarrays. Clin Exp Nephrol 2008;12:181–8.
[172] Wang Y, Rangan GK, Tay YC, Wang Y, Harris DC. Induction of monocyte chemoattractant protein-1 by albumin is mediated by nuclear factor kappaB in proximal tubule cells. J Am Soc Nephrol 1999;10:1204–13.
[173] Nakajima H, Takenaka M, Kaimori JY, Hamano T, Iwatani H, Sugaya T, et al. Activation of the signal transducer and activator of transcription signaling pathway in renal proximal tubular cells by albumin. J Am Soc Nephrol 2004;15: 276–85.
[174] Iglesias J, Levine JS. Albuminuria and renal injury—beware of proteins bearing gifts. Nephrol Dial Transplant 2001;16:215–8.
[175] Motoyoshi Y, Matsusaka T, Saito A, Pastan I, Willnow TE, Mizutani S, et al. Megalin contributes to the early injury of proximal tubule cells during nonselective proteinuria. Kidney Int 2008;74:1262–9.
[176] Theilig F, Kriz W, Jerichow T, Schrade P, Hahnel B, Willnow T, et al. Abrogation of protein uptake through megalin-deficient proximal tubules does not safeguard against tubulointerstitial injury. J Am Soc Nephrol 2007;18:1824–34.
[177] Liu Y. New insights into epithelial-mesenchymal transition in kidney fibrosis. J Am Soc Nephrol 2010;21:212–22.
[178] Lee JY, Chang JW, Yang WS, Kim SB, Park SK, Park JS, et al. Albumin-induced epithelial-mesenchymal transition and ER stress are regulated through a common ROS-c-Src kinase-mTOR pathway: Effect of imatinib mesylate. Am J Physiol Renal Physiol 2011;200:214–22.
[179] Kriz W, Kaissling B, LeHir M. Epithelial-mesenchymal transition (EMT) in kidney fibrosis: fact or fantasy? J Clin Invest 2011;121:468–74.
[180] Cawood TJ, Bashir M, Brady J, Murray B, Murray PT, O'Shea D. Urinary collagen IV and piGST: potential biomarkers for detecting localized kidney injury in diabetes–a pilot study. Am J Nephrol 2010;32:219–25.
[181] Erkan E, Devarajan P, Schwartz GJ. Apoptotic response to albumin overload: proximal vs. distal/collecting tubule cells. Am J Nephrol 2005;25:121–31.

[182] Liu HC, Liao TN, Lee TC, Chuang LY, Guh JY, Liu SF, et al. Albumin induces cellular fibrosis by upregulating transforming growth factor-beta ligand and its receptors in renal distal tubule cells. J Cell Biochem 2006;97:956–68.
[183] Christensen EI, Carone FA, Rennke HG. Effect of molecular charge on endocytic uptake of ferritin in renal proximal tubule cells. Lab Invest 1981;44:351–8.
[184] Madsen KM, Harris RH, Tisher CC. Uptake and intracellular distribution of ferritin in the rat distal convoluted tubule. Kidney Int 1982;21:354–61.
[185] Straus W. Occurence of phagosomes and phago-lysosomes in different segments of the nephron in relation to the reabsorption, transport, digestion and extrusion of intravenously injected horseradish peroxidase. J Cell Biol 1964;21: 295–308.
[186] Cho J, Galaske RG, Arbesman H, van Liew JB. Renal albumin reabsorption in normal and sodium maleate-treated rats. Renal Physiol 1985;8:8–18.
[187] Cortney MA, Sawin LL, Weis DD. Renal tubular protein absorption in the rat. J Clin Invest 1970;49:1–4.
[188] Chiang CK, Inagi R. Glomerular diseases: genetic causes and future therapeutics. Nat Rev Nephrol 2010;6:539–54.
[189] Kantarci S, Al-Gazali L, Hill RS, Donnai D, Black GC, Bieth E, et al. Mutations in LRP2, which encodes the multiligand receptor megalin, cause Donnai-Barrow and facio-oculo-acoustico-renal syndromes. Nat Genet 2007;39:957–9.
[190] Broch H, Imerslund O, Monn E, Hovig T, Seip M. Imerslund-Grasbeck anemia. A long-term follow-up study. Acta Paediatr Scand 1984;73:248–53.
[191] Devuyst O, Thakker RV. Dent's disease. Orphanet J Rare Dis 2010;5:28.
[192] Fisher SE, Black GC, Lloyd SE, Hatchwell E, Wrong O, Thakker RV, et al. Isolation and partial characterization of a chloride channel gene which is expressed in kidney and is a candidate for Dent's disease (an X-linked hereditary nephrolithiasis). Hum Mol Genet 1994;3:2053–9.
[193] Lloyd SE, Pearce SH, Fisher SE, Steinmeyer K, Schwappach B, Scheinman SJ, et al. A common molecular basis for three inherited kidney stone diseases. Nature 1996;379:445–9.
[194] Christensen EI, Devuyst O, Dom G, Nielsen R, Van Der Smissen P, Verroust P, et al. Loss of chloride channel ClC-5 impairs endocytosis by defective trafficking of megalin and cubilin in kidney proximal tubules. Proc Natl Acad Sci USA 2003;100:8472–7.
[195] Piwon N, Gunther W, Schwake M, Bosl MR, Jentsch TJ. CIC-5 Cl^--channel disruption impairs endocytosis in a mouse model for Dent's disease. Nature 2000;408:369–73.
[196] Santo Y, Hirai H, Shima M, Yamagata M, Michigami T, Nakajima S, et al. Examination of megalin in renal tubular epithelium from patients with Dent disease. Pediatr Nephrol 2004;19:612–5.
[197] Weir MR. Microalbuminuria and cardiovascular disease. Clin J Am Soc Nephrol 2007;2:581–90.
[198] Jensen JS, Borch-Johnsen K, Jensen G, Feldt-Rasmussen B. Microalbuminuria reflects a generalized transvascular albumin leakiness in clinically healthy subjects. Clin Sci (Lond) 1995;88:629–33.
[199] Levey AS, de Jong PE, Coresh J, Nahas ME, Astor BC, Matsushita K, et al. The definition, classification and prognosis of chronic kidney disease: a KDIGO Controversies Conference report. Kidney Int 2011;80:17–28.
[200] Hilliard LM, Russo LM, Comper WD. Hypertension-mediated albuminuria is associated with reduced lysosomal activity in the kidney and the heart. Am J Nephrol 2009;29:454–64.
[201] Russo LM, Brammar GC, Jerums G, Comper WD, Osicka TM. The effect of ramipril on albumin excretion in diabetes and hypertension: the role of increased lysosomal activity and decreased transforming growth factor-beta expression. J Hypertens 2003;21:419–28.
[202] Chavers BM, Bilous RW, Ellis EN, Steffes MW, Mauer SM. Glomerular lesions and urinary albumin excretion in type I diabetes without overt proteinuria. N Engl J Med 1989;320: 966–70.
[203] Petrica L, Petrica M, Vlad A, Jianu DC, Gluhovschi G, Ianculescu C, et al. Proximal tubule dysfunction is dissociated from endothelial dysfunction in normoalbuminuric patients with type 2 diabetes mellitus: a cross-sectional study. Nephron Clin Pract 2010;118:c155–64.
[204] Tojo A, Onozato ML, Ha H, Kurihara H, Sakai T, Goto A, et al. Reduced albumin reabsorption in the proximal tubule of early-stage diabetic rats. Histochem Cell Biol 2001;116:269–76.
[205] Ishibashi F. Chronic high glucose inhibits albumin reabsorption by lysosomal alkalinization in cultured porcine proximal tubular epithelial cells (LLC-PK1). Diabetes Res Clin Pract 2006;72:223–30.
[206] Thrailkill KM, Nimmo T, Bunn RC, Cockrell GE, Moreau CS, Mackintosh S, et al. Microalbuminuria in type 1 diabetes is associated with enhanced excretion of the endocytic multiligand receptors megalin and cubilin. Diabetes Care 2009;32:1266–8.
[207] Tojo A, Onozato ML, Kurihara H, Sakai T, Goto A, Fujita T. Angiotensin II blockade restores albumin reabsorption in the proximal tubules of diabetic rats. Hypertens Res 2003;26: 413–9.
[208] Willnow TE, Hilpert J, Armstrong SA, Rohlmann A, Hammer RE, Burns DK, et al. Defective forebrain development in mice lacking gp330/megalin. Proc Natl Acad Sci USA 1996;93: 8460–4.
[209] Leheste JR, Melsen F, Wellner M, Jansen P, Schlichting U, Renner-Muller I, et al. Hypocalcemia and osteopathy in mice with kidney-specific megalin gene defect. FASEB J 2003;17: 247–9.
[210] Willnow TE, Armstrong SA, Hammer RE, Herz J. Functional expression of low density lipoprotein receptor- related protein is controlled by receptor-associated protein *in vivo*. Proc Natl Acad Sci USA 1995;92:4537–41.
[211] Grasbeck R. Imerslund-Grasbeck syndrome (selective vitamin B(12) malabsorption with proteinuria). Orphanet J Rare Dis 2006;1:17.
[212] Fyfe JC, Ramanujam KS, Ramaswamy K, Patterson DF, Seetharam B. Defective brush-border expression of intrinsic factor-cobalamin receptor in canine inherited intestinal cobalamin malabsorption. J Biol Chem 1991;266:4489–94.
[213] Wang SS, Devuyst O, Courtoy PJ, Wang XT, Wang H, Wang Y, et al. Mice lacking renal chloride channel, CLC-5, are a model for Dent's disease, a nephrolithiasis disorder associated with defective receptor-mediated endocytosis. Hum Mol Genet 2000;9:2937–45.
[214] Schurman SJ, Scheinman SJ. Inherited cerebrorenal syndromes. Nat Rev Nephrol 2009;5:529–38.
[215] Bothwell SP, Chan E, Bernardini IM, Kuo YM, Gahl WA, Nussbaum RL. Mouse model for Lowe syndrome/Dent disease 2 renal tubulopathy. J Am Soc Nephrol 2011;22:443–8.
[216] Wilmer MJ, Emma F, Levtchenko EN. The pathogenesis of cystinosis: mechanisms beyond cystine accumulation. Am J Physiol Renal Physiol 2010;299:F905–16.
[217] Nevo N, Chol M, Bailleux A, Kalatzis V, Morisset L, Devuyst O, et al. Renal phenotype of the cystinosis mouse model is dependent upon genetic background. Nephrol Dial Transplant 2010;25:1059–66.

SECTION 4

PATHOPHYSIOLOGY OF RENAL DISEASE

This page intentionally left blank

CHAPTER

74

Physiologic Principles in the Clinical Evaluation of Electrolyte, Water, and Acid–Base Disorders

Daniel Batlle, Sheldon Chen and Syed K. Haque

The Feinberg School of Medicine, Northwestern University, Chicago, Illinois, USA

The kidneys play a fundamental role in the regulation of water and electrolyte excretion as well as in the maintenance of acid base balance. Water and electrolyte homeostasis is accomplished almost exclusively through changes in the volume and composition of urine. Routes of external loss other than from the kidneys play a limited role in regulation, even though they may display some response to the needs of the organism.[1–4] Intake of the various electrolytes and of water can vary extremely widely and almost independently of each other. Balance (used as a synonym for external balance) is the difference between intake and excretion by all routes.[4] Internal balance, on the other hand, means the rate of transfer of a substance between the intra- and extracellular fluids, a concept that has proven especially useful with regard to potassium homeostasis. In this chapter, we will limit the discussion to external balance as we review the physiology underlying the clinical approach to the evaluation of water and electrolyte excretion by the kidneys. No attempt will be made to discuss in-depth specific regulatory mechanisms that are outlined in detail in other chapters. The objective of this chapter is to summarize the rationale and physiologic principles behind the use of urinary indices and clinical tools available in the evaluation of normal and pathophysiologic states related to sodium, water, potassium, and acid–base disturbances.

CONCEPT OF EXTERNAL BALANCE AND STEADY-STATE

The kidney varies the rate of excretion of various solutes to match the input from dietary intake and endogenous production. "Zero balance" or "in balance" both refer to a state in which input equals output.[4,5] Commonly the unit of time is a 24-hour day, and the rate of excretion can only be applied with reasonable certainty to substances that are not metabolized.[4] The term "steady-state" is used to mean a dynamic equilibrium, with the implication that input and output are occurring but are equal.[4] Thus, steady-state, when used with regard to body electrolyte homeostasis refers to zero balance. Humans in a steady-state excrete absorbed ions as well as the metabolic products from their diet.[4] Endogenous production of a substance does not preclude the use of the balance concept. Rather, this production is considered to be a component of intake. For example, water is produced continuously by the metabolism of foodstuffs; this production of water contributes an additional approximate 0.3 L/day to the intake of water from other sources.[4]

The term "steady-state" should not be used to refer to a condition in which both input and output are constant but different. In this case, the body composition is changing progressively, and this clearly represents an unsteady-state.[4] The change in the rate of excretion in

Seldin and Giebisch's The Kidney, Fifth Edition.
DOI: http://dx.doi.org/10.1016/B978-0-12-381462-3.00074-4

© 2013 Elsevier Inc. All rights reserved.

response to a deficit or a surplus of an electrolyte may occur promptly or require a lag period. To reach a steady-state, a variable amount of time is needed for each ion. For example, a water load is excreted within hours, whereas a potassium-deficient diet requires a few days for the renal conservation of potassium to be completed. A low-sodium diet leads to a transient negative sodium balance where sodium excretion exceeds sodium intake in the initial adaptation period (Fig. 74.1).[6] This negative sodium balance reduces extracellular fluid volume (ECFV), which then activates the sodium-conserving mechanisms of the kidney. A high-sodium diet, by transiently resulting in sodium retention, expands ECFV and thereby elicits a signal that deactivates the mechanisms that promote tubular reabsorption of sodium. In both situations, a new steady-state is ultimately reached in which sodium intake and output is equivalent.[5,6] To evaluate the composition of urine in patients, one should first consider their diet. A corollary of this is that there are no "normal" values for the composition of urine, only "expected" ones depending on dietary intake and other stimuli. Because dietary intake fluctuates so greatly (for example, normal dietary intake of sodium may vary from 20 mEq/day to 500 mEq/day), urinary net excretion of sodium varies to match sodium intake. Also, the dietary intake of sodium can be extrapolated from the urine composition of sodium, provided that the patient is in a steady-state. For instance, when a subject is in a steady-state, the finding of 500 mEq of sodium in the urine implies that the subject must have consumed about 500 mEq of sodium in the diet. Likewise, the finding of 20 mEq of sodium in the urine reflects dietary intake of only 20 mEq of sodium. This information is very useful for instance when assessing adherence to dietary instructions in subjects with essential hypertension.

Salt balance is achieved through the integrated action of several factors that regulate sodium reabsorption by the renal tubules.[6] Under normal circumstances, sodium reabsorption by the kidney is determined by the status of the effective arterial blood volume (EABV).[1,7–9] When the EABV decreases, the kidney reabsorbs sodium and chloride, thereby protecting the EABV from contracting further. When the EABV increases, tubular reabsorption decreases, resulting in increased renal salt excretion.[10] Thus, in healthy individuals, sodium balance is directly related to effective arterial blood volume.

When a healthy individual is placed on a low-salt diet, renal NaCl excretion exceeds dietary intake during the initial three to five days (Figure 74.1).[6] The time required to achieve low urine Na^+ and Cl^- varies very little from individual to individual. Age, however, influences this time period, with older individuals taking a longer time to achieve sodium balance.[5] The essential feature of renal salt wasting is ongoing natriuresis, despite a contraction in ECFV to below the lower limit of normal in a normal individual on a salt-free diet. This is clinically evident by an exaggerated decline in blood pressure, sometimes to overtly hypotensive levels or at least manifested by postural hypotension. This fall in blood pressure when coupled with a rise in heart rate upon standing up is a good clinical sign of volume depletion.

In subjects with sodium-retaining states, urinary sodium excretion is usually low but at times it may exceed 200 mEq under certain pathological conditions. For instance, an edematous patient on rigid salt restriction may excrete more than 200 mEq of sodium, but this does not necessarily constitute salt wasting. In this instance, the kidney may be excreting sodium above intake because the mobilization of edema and release of sodium into the circulation.

Now let us consider the situation of a subject who develops acute diarrhea, becomes volume-depleted and maintains an intake of sodium in the normal/high range (250 mEq/day). This subject will avidly reabsorb sodium, reflecting a decrease in EABV despite the high-salt intake and the urinary sodium will be much less than the intake. For instance, urinary sodium could be as low as 10 to 20 mEq a day. This subject is not in a steady-state because of volume depletion from the diarrhea, which provides a potent stimulus for sodium retention. In this case, the extent of sodium excretion does not reflect sodium intake. Accordingly, one should examine the composition of the urine in light of the clinical condition of the subject and the prevailing stimuli.

The concept of the steady-state and appropriate renal response also applies to the excretion of water and solutes other than sodium. For instance, a urinary excretion of 60 mmol of potassium per day may be appropriate for subjects consuming a diet containing 60 mEq of K^+, but would be actually clear evidence potassium wasting in a hypokalemic patient on such diet. Here the hypokalemic stimulus, in someone with normal kidney function, leads to renal retention of potassium as a result of both enhanced reabsorption and decreased potassium secretion.

URINARY CONSTITUENTS AS CLINICAL INDICES: GENERAL CONSIDERATIONS

Urine collected over 24 hours to determine the daily solute excretion is the conventional approach to evaluate external balance of a given solute that is primarily excreted by the kidneys. To the extent that ions such as Na^+ and K^+ are largely excreted by the kidneys one can estimate dietary intake in the steady-state and the

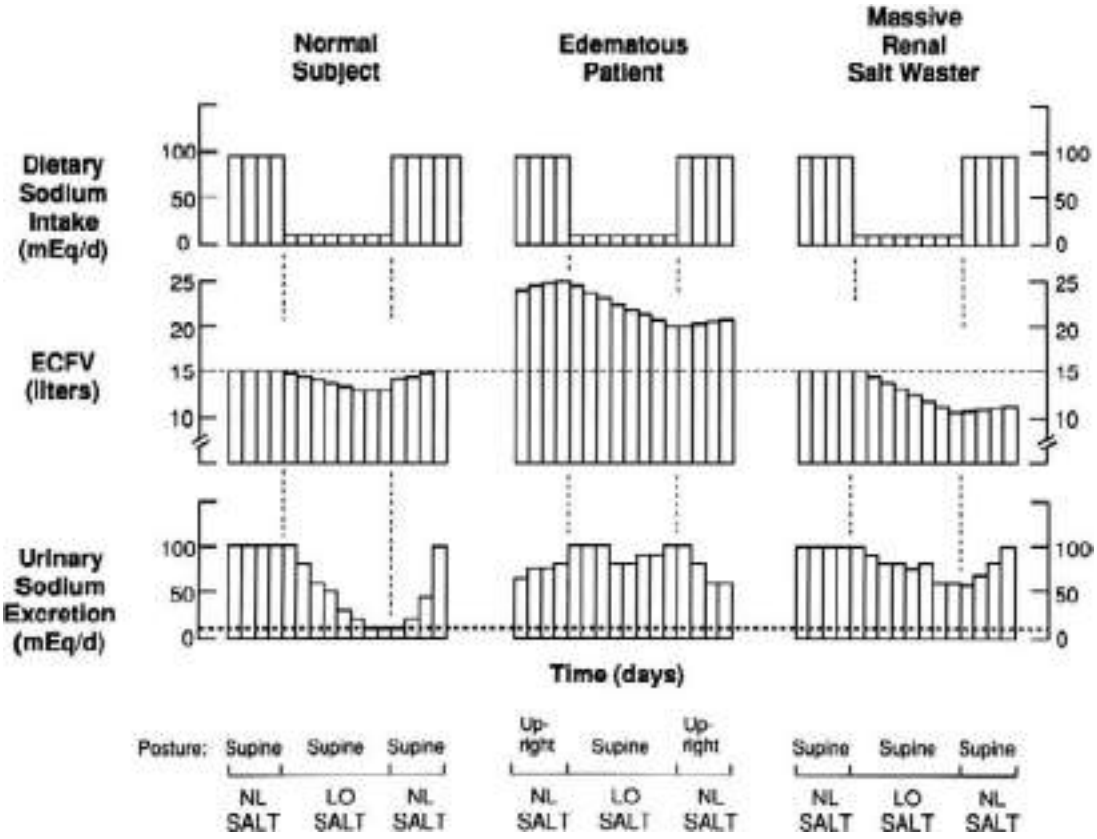
Normal Subject
Edematous Patient
Massive Renal Salt Waster
Dietary Sodium Intake (mEq/d)
ECFV (liters)
Urinary Sodium Excretion (mEq/d)
Time (days)
Posture: Supine Supine Supine Up-right Supine Up-right Supine Supine Supine
NL SALT LO SALT NL SALT NL SALT LO SALT NL SALT NL SALT LO SALT NL SALT

FIGURE 74.1 In the normal subject, a low-salt diet results in a reduction of extracellular fluid volume (ECFV) (middle panel) from a normal value of 15 to about 13 L. At that point, intake (upper panel) and urinary excretion (lower panel) are equal. The subject is in balance. (Horizontal dotted lines represent the basal levels of ECFV (middle panel) and dietary sodium during severe sodium restriction (lower panel).) In the edematous patient, a low-salt diet results in a reduction in ECFV from 25 to 20 L from an initial value of 25 L. Nevertheless, ECFV is still above the normal range and natriuresis continues (lower panel). The patient is in negative sodium balance but is not salt wasting; that is, ECFV remains over expanded. In renal salt wastage, a low-salt diet results in a 5-liter reduction in ECFV with persistent negative sodium balance. This constitutes salt wastage. *(From Toto R, Seldin DW. Salt wastage. In: Seldin DW, Giebisch G, eds. The Kidney: Physiology and Pathophysiology. New York: Raven Press; 1992:2143–63, with permission.)*

kidney response to physiologic and pathophysiologic conditions by measuring the urinary concentrations and calculating the excretion rates when urine volume per unit time is known. In most clinical situations, a random "spot" urine collection is sufficient for the initial evaluation of a patient's condition.[3] Aside from being more convenient and rapid, the spot urine has the advantage that the stimulus is known at the time the urine is collected, and therefore the expected renal response can be predicted. For instance, prior to vigorous volume replacement it is useful to know how the kidneys are responding in terms of avid sodium retention or not.

Since errors are frequent when trying to collect urine accurately, urine creatinine should always be part of the measurement as a way to verify the completeness of the 24-hour collection. The urine creatinine assessment takes advantage of the fact that the kidneys excrete creatinine at a relatively fixed rate depending on the person's muscle mass, a gauge of the daily creatinine input. While excretion of creatinine for an individual is relatively constant over a 24-hour period, provided that the serum creatinine is stable, it might vary depending upon protein intake. Muscular individuals and exercise, both increase creatinine excretion.[11] For clinical purposes, it is generally accepted that a 24-hour urine collection is complete when the total urine creatinine is 20–25 mg per kg body mass for men and 15–20 mg per kg body mass for women.

Urinary Sodium and Chloride as Indices of Volume Status

The medical history and physical examination is always the first step in assessing arterial blood volume at the bedside. The clinical evaluation should be supplemented by the measurement of urine sodium and chloride in spot urine. The kidney has the extraordinary ability to elaborate virtually salt-free urine in the setting of dietary salt deprivation or when extra-renal losses of sodium are sufficient to decrease the EABV.[6] Under

normal circumstances, the kidney excretes sodium and chloride in the urine in an amount equivalent to the dietary intake. As discussed earlier, the kidney modulates sodium excretion and reabsorption in accordance with the status of the EABV.[8,12] When the EABV decreases, the kidney reabsorbs sodium and chloride, thereby protecting the EABV from shrinking further. On the other hand, when the EABV expands, tubular reabsorption of sodium and chloride decreases, resulting in greater urinary excretion of these ions.[5]

In analyzing renal sodium excretion, the existing volume status must always be taken into account, as noted in the earlier discussion regarding renal NaCl excretion in individuals in various clinical settings who were placed on low-salt diets. Further urinary chloride should be concurrently measured with urinary sodium. In volume-depleted states, the simultaneous measurement of urine sodium and chloride provides complementary information regarding the underlying cause, particularly when acid–base status is also altered such as in vomiting or diarrhea.

In states of volume depletion, the urine concentrations of sodium and chloride are both usually below 15 mEq/L, and in volume-replete conditions, they are well above 20 mEq/L (usually above 40 mEq/l). As summarized in Table 74.1, four patterns of urinary sodium and chloride can be encountered.

(1) Low levels of urinary sodium and chloride. This reflects low intake of salt or extrarenal salt losses. This can also be seen after cessation of diuretics when the volume deficit still persists.[13]

(2) Low urinary chloride with normal/high urinary sodium. In a setting of low EABV, this pattern suggests that another anion is present in the urine, usually HCO_3^-, as in the setting of recent vomiting (see following paragraphs). This can also occur in the syndrome of congenital chloridorrhea, which is a syndrome of severe diarrhea, hypokalemia, and often metabolic alkalosis that is caused by a defect in the ileal and colonic chloride–bicarbonate exchange transporter that normally mediates active chloride absorption.[14] In this syndrome, there is appropriate renal response to volume depletion with virtually absent urine chloride, but urinary sodium is elevated because of the high filtered load of bicarbonate which obligates sodium excretion.

(3) Low urinary sodium with normal/high urinary chloride. In a patient with low EABV, as seen in the setting of diarrhea or laxative abuse, this pattern suggests that another cation is being excreted, most often ammonium and rarely potassium.

(4) High excretion of urinary sodium and chloride. In a setting of low EABV, this pattern suggests ongoing diuretic use (both thiazide and loop diuretic) or an intrinsic tubular defect as in Bartter's or Gitelman's syndromes. This pattern is also consistent with salt wastage of any cause with post-obstructive diuresis being a classic example.

TABLE 74.1 Patterns of Urinary Sodium and Chloride in Various Conditions

a. Low urinary sodium and chloride	Salt restriction
	Extrarenal salt losses
	Previous use of diuretics
	Vomiting (maintenance phase)
b. Low urinary chloride but "normal/high" sodium	Vomiting with metabolic alkalosis (generation phase)
	Congenital chloridorrhea
c. Low urinary sodium but "normal/high" chloride	Diarrhea with volume depletion but metabolic acidosis
d. High urinary sodium and chloride	Loop and thiazide Diuretics
	Bartter's and Gitelman's syndromes
	Salt-wasting as seen in postobstructive diuresis and some types of chronic interstitial nephritis

Urinary chloride concentration under physiologic conditions, like urinary sodium, reflects the chloride intake. While urinary sodium and chloride change in the same direction under most circumstances, they may occasionally dissociate (Table 74.1). The most notable situation is patients with vomiting and metabolic alkalosis with volume contraction. In this setting, urinary chloride concentration is low, reflecting the salt-retaining state induced by volume depletion. When the patient is actively vomiting, the increase in plasma bicarbonate and thus filtered bicarbonate might exceed the reabsorptive capacity of the tubules, resulting in bicarbonate excretion. Therefore, bicarbonate is rejected in the proximal tubules and this obligates the excretion of sodium resulting in a sodium bicarbonate diuresis. In this situation, chloride is retained appropriately, reflecting volume contraction. Thus, in a patient with active vomiting, the urine sodium may be high, while chloride concentration is invariably low (Table 74.1).

In the maintenance phase of metabolic alkalosis, however, the ECFV depletion persists even if vomiting has ceased, leading to secondary hyperaldosteronism and sodium retention. Therefore urinary sodium, as well as urinary chloride concentration, can be low after protracted vomiting or nasogastric suction. Similarly, diuretic-induced metabolic alkalosis results in increased urinary concentrations of both sodium and chloride during the generation phase of the metabolic alkalosis when the nephron is under the effects of the

diuretic (Table 74.1). When the diuretic is discontinued, the metabolic alkalosis can be maintained by preexisting volume depletion, decreased glomerular filtration rate (GFR), and secondary hyperaldosteronism, and urinary sodium is usually low. The urinary concentration of chloride, likewise, is appropriately low (< 15 mEq/L), reflecting the persistence of volume depletion and indeed, the administration of saline to restore the volume status to normal results in correction of the metabolic alkalosis.

Under conditions of metabolic acidosis other than the type resulting from renal tubular acidosis, the presence of large amounts of ammonium in the urine obligates the loss of an anion (chloride) resulting in a higher than expected urinary concentration of chloride.[15] The urinary concentration of sodium, however, in this situation will be appropriately low reflecting the intravascular volume depletion.[16,17] This pattern is typically seen in metabolic acidosis caused by diarrhea.[15,18]

In patients with metabolic alkalosis due to Bartter's or Gitelman's syndromes, urinary chloride and sodium concentrations are elevated due to a tubular defect in reabsorption.[19] When these patients become volume-depleted, renal conservation of salt is clearly suboptimal as manifested by relatively high level of urine sodium and chloride.

Spot Urine vs Timed Urine Collections

The 24 hour urine collection remains the proper way to evaluate solute excretion. One can use urine creatinine in a spot urine sample to calculate the urinary sodium/creatinine ratio as a way to estimate 24-hour urinary sodium excretion much in the same way that the urinary albumin/creatinine ratio is used to estimate 24-hour albumin excretion rate. The good linear relationship between the urine sodium/urine creatinine ratio has moreover been used to develop formulas to generate values of 24-hour sodium excretion based on the spot sodium/creatinine ratio. Kawasaki et al.[20] proposed the formula:

$$\text{24-Hour Urinary Sodium (mEq/day)} = 16.3 \times \sqrt{X_{Na}}$$

$$\text{Where } X_{Na} = (\text{Spot } U_{Na}/\text{Spot } U_{Cr}) \times \text{predicted 24 h urinary Cr excretion}$$

$$\text{Predicted 24 h urinary Cr excretion (Male)} = -12.63 \times \text{Age} + 15.12 \times \text{Weight} + 7.39 \times \text{Height} - 79.90 \text{ (mg/day)}$$

$$\text{Predicted 24 h urinary Cr excretion (Female)} = -4.72 \times \text{Age} + 8.58 \times \text{Weight} + 5.09 \times \text{Height} - 74.50 \text{ (mg/day)}$$

Linear correlation between formula-estimated and actual 24-hour urinary sodium was 0.53.[20] Others have reported a similar correlation (r = 0.55).[21]

Interestingly, a strong linear correlation between spot urine Sodium/Creatinine ratio and 24-hour Sodium excretion has been reported when evening spot samples were used but not when morning or random urine samples were used (see Table 74.2 and Figure 74.2).[22] The linear correlation was even better when the evening spot urine Sodium/Creatinine ratio was adjusted for 24-hour creatinine excretion.[22]

It should also be noted that there is a diurnal variation in the excretion of water and electrolytes. A larger amount of the potassium excreted daily occurs close to noon while the rate of excretion of sodium is lowest overnight.[23,24] Ideally, this diurnal variation should be taken into account when interpreting urine tests, but in practice this is rarely done. There is limited information addressing the possible shortcomings of not taking into account the diurnal variation in the interpretation of electrolyte disorders at the bedside using spot urine samples. As noted above, a recent study suggests that spot urine sodium/creatinine ratio when taken in the evening correlates better with 24-Hour Sodium excretion than when taken in the morning.[22] For practical purposes, however, a spot urine sample for electrolytes can be ordered any time of the day when the purpose is to assess a pathophysiologic situation such as volume depletion or renal failure.

Fractional Excretion of Sodium

The fractional excretion of sodium (FE_{Na}) reflects the percent of filtered sodium that is excreted in the urine. The filtered sodium load can be determined from the product of the Glomerular Filtration Rate (GFR) and the Plasma Sodium (P_{Na}). Sodium excretion is equal to the product of the urine sodium (U_{Na}) and the urine

TABLE 74.2 Correlations between Spot Urine Sodium/Creatinine Ratio and 24-Hour Sodium Excretion

Correlation of 24-Hours Sodium Excretion with:	Spot Sodium/Creatinine Ratio: (correlation coefficients)	Predicted 24-Hours Sodium Excretion: (correlation coefficients)
Random Urine Sample	− 0.01	0.17
Morning Urine Sample	0.14	0.31
Evening Urine Sample	0.67	0.86

Source: Mann SJ, Gerber LM et al. Estimation of 24-hour sodium excretion from spot urine samples. J Clin Hypertens. 2010;12(3):174–80.

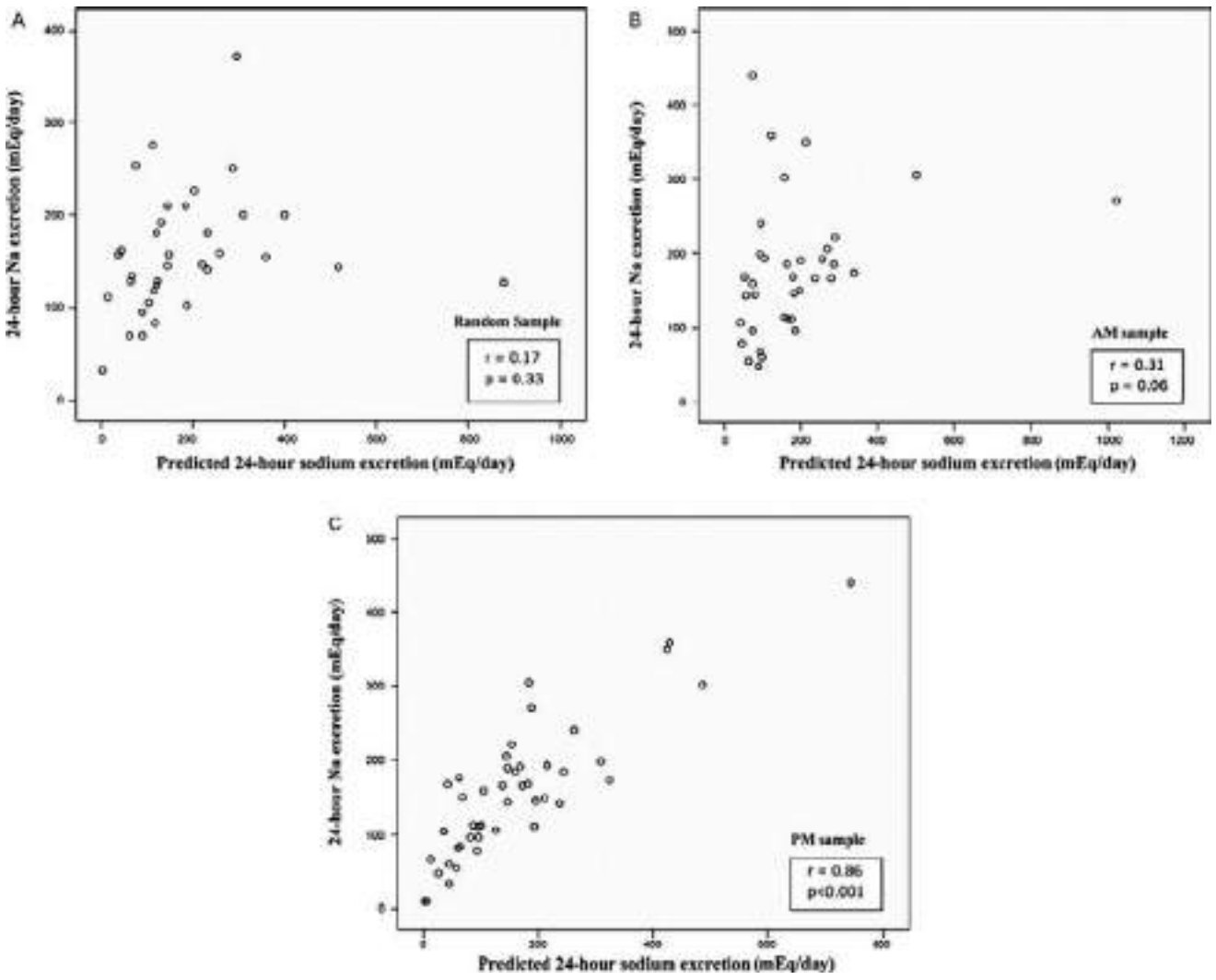

FIGURE 74.2 Correlation between actual 24-hour sodium excretion and sodium excretion predicted from random sample (panel A), morning (AM) sample (panel B), and evening (PM) sample (panel C). *(From Mann SJ, Gerber LM et al. Estimation of 24-hour sodium excretion from spot urine samples. J Clin Hypertens (Greenwich). 2010;12(3):174–80, with permission.)*

flow rate (V). Since GFR is often not available, the FE_{Na} can be derived as follows:

$$FE_{Na}(\%) = (U_{Na} \times V/GFR \times P_{Na}) \times 100 \quad (74.1)$$

Since $GFR = U_{Cr} \times V/P_{Cr}$, the equation for FE_{Na} (%) becomes:

$$FE_{Na}(\%) = ((U_{Na} \times V)/(U_{Cr} \times V/P_{Cr}) \times P_{Na}) \times 100 \quad (74.2)$$

Because V cancels out, it follows that:

$$FE_{Na}(\%) = (U_{Na} \times P_{Cr})/(U_{Cr} \times P_{Na}) \times 100 \quad (74.3)$$

FE_{Na} is usually used to distinguish prerenal disease from acute tubular necrosis (ATN), the two most common causes of acute renal failure.[8,12] In prerenal disease, the reabsorption of almost all of the filtered sodium represents an appropriate response to decreased renal perfusion. When GFR decreases due to renal vasoconstriction with intact tubular function, the FENa is low, usually less than 1%.[25] In ATN, there is an associated tubular dysfunction, with an inability to conserve sodium and thus, the FE_{Na} is high, usually more than 2%. A value between 1 and 2% may be seen with a prerenal disorder or ATN, but typically it is below 1% in prerenal disorders.[26] However, FE_{Na} can be low (<1%) in patients with ischemic ATN, if they are evaluated early in the course, as they make the transition from prerenal disease to postischemic ATN, or if they remain ischemic with established ATN.[16] A low FE_{Na} is appropriate in this setting due to continued renal ischemia and can be achieved because

tubular function is relatively intact early in the course of ATN.[27,28] A clinical setting in which ATN is frequently associated with decreased FE_{Na} is the acute renal failure associated with contrast nephropathy.[29–31] Occasionally, it is also observed in sepsis,[32] myoglobinuria,[33] obstructive uropathy,[34] acute glomerulonephritis,[16,17] and renal allograft rejection.[17] In patients with chronic renal failure, renal vasoconstriction may not be associated with a FE_{Na} less than 1% due to chronic adaptation to an increased single-nephron GFR. Here, there is an adaptive decrease in tubular reabsorption in order to maintain sodium balance, thus making the interpretation of FE_{Na} difficult.[25] One mathematical consideration also complicates the interpretation of FE_{Na}. As the renal failure progresses, the urinary creatinine in the denominator decreases, making the FE_{Na} increase on that basis alone. Thus, a patient can be prerenal, but if the reduction in GFR is severe enough, the FE_{Na} can sometimes be pushed well above 1%. The pre-renal state can still be correctly diagnosed, however, by the gold standard test of seeing if the renal failure reverses with volume repletion. Due to the limitations of using FE_{Na}, the need arises for other indices that could help to clinically distinguish between ATN and pre-renal diseases (see following sections). This is not to say that the other indices are better but provide additional information that may help to assess the overall picture. Table 74.3 provides a summary of the expected values in the differential diagnosis of prerenal vs. acute renal failure.

TABLE 74.3 Urine Indices Used in the Differential Diagnosis of Prerenal and Ischemic Intrinsic Renal Azotemia

Diagnostic Index	Prerenal Azotemia	Ischemic Intrinsic Azotemia
Fractional excretion of Na^+ (%)	<1%	>1%
Urinary Na^+ concentration (mEq/L)	<10	>20
Urinary creatinine/plasma creatinine ratio	>40	<20
Urinary urea nitrogen/plasma urea nitrogen ratio	>8	<3
Urine specific gravity	>1.018	<1.012
Urine osmolality (mOsm/kg H_2O)	>500	<250
Plasma BUN/creatinine ratio	>20	<10–15
Renal failure index, (UNa/(Ucr/Pcr))	<1	>1
Urine sediment	Hyaline casts	Muddy brown granular casts

Fractional Excretion of Urea

Urine sodium and chloride concentrations are difficult to interpret with concurrent diuretic therapy.[35] The ensuing rise in urinary sodium and chloride likewise will raise the FE_{Na} and FE_{Cl} (fractional excretion of chloride) even in patients with pre-renal disease and oliguria. The coexistence of a pre-renal state and natriuretic agents (diuretics) clearly alters the interpretation of FE_{Na} such that despite volume depletion sodium excretion is increased during ongoing use of diuretics.[35] In volume depletion and pre-renal azotemia due to vomiting or nasogastric suction, the ensuing metabolic alkalosis causes bicarbonaturia which increases urinary sodium and hence FE_{Na} at high levels.[36,37] Given the limitations of using FE_{Na}, the need arose for a better marker for differentiating pre-renal conditions from ATN. This has led to the use of the fractional excretion of urea (FE_{Urea}).[37–39]

The FE_{Urea} is calculated using the formula used to calculate the fractional excretion of other electrolytes:

$$FE_{Urea} = (U_{ur} \times P_{cr})/(P_{ur} \times U_{cr}) \times 100 \qquad (74.4)$$

The FE_{Urea} is 50 to 65% in healthy subjects and usually below 35% in pre-renal disease.[39] To distinguish pre-renal states from ATN, the use of FE_{Urea} was evaluated by Carvounis et al.[36] The study consisted of three groups; the first group had 50 patients with pre-renal disease, the second group had 27 patients with prerenal disease who had been given diuretics, and the third group had 25 patients with established ATN. The FE_{Na} was characteristically low (<1%) in the pre-renal group but was substantially higher than 1% in the prerenal group on diuretics and in the ATN group.[36] In contrast, the FE_{Urea} was similar in both the prerenal groups (27.9 and 24.5% in groups 1 and 2, respectively) and significantly different from the ATN group (58.6%, $p < 0001$). While 92% of patients in group 1 had a FE_{Na} <1%, only 48% of patients in group 2 had a low FE_{Na}. By contrast, 89% of patients who were prerenal and on diuretic therapy had a FE_{Urea} below 35%. In the prerenal cases (groups 1 and 2), FE_{Urea} had the best sensitivity and specificity (90 and 96%, respectively), and the best positive and negative predictive values (99 and 75%, respectively). These data suggest that when FE_{Urea} of less than 35% is found, 99% of such cases will be prerenal, including prerenal states with diuretic use.[36]

The clearance of urea reflected by the FE_{Urea} is affected by decreased renal perfusion as seen in prerenal states. In evaluating the relationship of urine volume to urea excretion in humans using diuretic agents, it was found that the percent of filtered urea excreted increased with proximal diuretics (mannitol and acetazolamide) but not with distal agents (mercaptomerin and ethacrynic acid).[36,39,40] This is consistent with the

notion that urea is not reabsorbed significantly in the distal nephron. As most of the diuretics in clinical use work beyond the proximal tubule, FE_{Urea} should not be affected by their use. This is unlike FE_{Na}, which is increased by all forms of diuretics.[36,37,40]

There are situations, however, where FE_{Urea} may not predict the ongoing prerenal status. Such settings should be kept in mind when FE_{Urea} is used. For instance, in states of osmotic diuresis, and with the administration of acetazolamide and mannitol, the proximal tubular absorption of salt and water is reduced, and thus an increased FE_{Urea} is to be expected even in the presence of renal hypoperfusion.[36,40] In other studies, the utility of FE_{Urea} has been questioned.[41,42] It is reasonable, however, to use fractional urea excretion in conjunction with other urinary indices such as FE_{Na} to gain a more complete picture than with either one alone in situations where the clinical picture is not straightforward.

Fractional Excretion of Lithium

Markers of proximal fluid reabsorption can be used to assess proximal tubular sodium reabsorption.[41] Such a marker should be freely filtered at the glomerulus, should be reabsorbed in the same fashion as sodium and water in the proximal tubule, should not be reabsorbed beyond the proximal tubule, should not be secreted, and its plasma levels should not fluctuate significantly in response to hormones and changes in ECFV. Lithium fits this profile with the exception that it is reabsorbed in the loop of Henle as well as in the proximal tubule.

To assess proximal fluid reabsorption, the fractional clearance of endogenous or exogenous lithium can be utilized.[42] The endogenous lithium clearance, despite its clear advantages over the exogenous method, would require very sensitive assays to measure trace amounts of lithium present in the serum and is difficult to use. Thus, it is necessary to give lithium either acutely or for several days prior to measuring lithium clearance or its fractional clearance. The fractional excretion of lithium (FE_{Li}) is approximately 20% in healthy controls and below 10% in prerenal disease regardless of diuretic therapy.[42] In ATN, FE_{Li} is typically higher than 25%.[42]

FE_{Li} is probably a more sensitive index than FE_{Na} in differentiating prerenal states from ATN, especially in patients receiving concomitant diuretics.[41,42] The use of lithium, however, has its own disadvantages. Its use is limited by the necessity of administering exogenous lithium, by the expertise needed to detect lithium levels in urine and by the acute changes in tubular electrolyte handling induced by lithium loading.[42,43] Moreover, concern about the value of fractional Lithium excretion as a marker of proximal tubular fluid delivery has been raised because studies suggesting reabsorption of lithium in the thick ascending limb of the loop of Henle, which could be inhibited by loop diuretics.[44,45] For clinical purposes, lithium clearance is not used but it offers valuable information in clinical physiology studies aimed at assessing segmental sodium handling throughout the nephron. It should be noted, however, that initial studies showed that lithium was reabsorbed almost entirely in the proximal tubule in a fashion similar to that of sodium,[44] thus making lithium the marker of choice for determining proximal reabsorption. However, further studies uncovered a number of problems with using lithium clearance for assessing proximal reabsorption.[46–50] First, lithium undergoes significant reabsorption in the loop of Henle, and to a lesser extent in the distal tubule and collecting duct.[41,44] Amiloride can be used to block the reabsorption of lithium in the distal tubule and collecting duct especially when on a Na restricted diet.[51,52] A second problem with the use of lithium is that in the presence of mineralocorticoid-induced volume expansion and with the administration of inhibitors of prostaglandin synthesis, lithium reabsorption in Henle's loop is increased.[53,54] In the aggregate, lithium clearance is the best available method to assess the delivery of sodium and water out of the proximal tubule, and is reasonably accurate in the steady-state. In states of volume and hormonal perturbations, however, lithium clearance is much less reliable.

Fractional Excretion of Uric acid has also been used, but has been found to be no better or inferior to Fe_{Na} and FE_{Li}.[42,45] A summary of specificity and sensitivity of these various indices in the detection of prerenal vs acute renal failure is provided in Table 74.4.

EVALUATION OF DISORDERS OF WATER EXCRETION

The two variables governing water excretion include the magnitude of interstitial osmolality and the vasopressin-regulated, aquaporin-2 (AQP2)–dependent water transport in the collecting ducts. The interstitial osmolality increases whenever there is an increase in either sodium or urea concentration in the medullary interstitium and this provides the driving force for water absorption from the collecting duct for any given level of arginine vasopressin (AVP).[10] For example, increased protein intake results in higher urea levels, which then enhances the ability of the kidney to concentrate the urine.[55,56]

AVP regulates water permeability by principal cells in the collecting tubule by activating basolateral V2 receptors and this result in the insertion of AQP2 water channels into the apical surface of the cells, which

TABLE 74.4 Specificity and Sensitivity of FE_{na}, FE_{urea} and FE_{UA} at the Detection Limits of Pre-Renal (PR) and Acute Tubular Necrosis (ATN), as determined by the Receiver Operating Characteristic Curve Technique

	FE_{Na}	FE_{Urea}	FE_{UA}
Pre-renal Detection Limit (%)	1.3	15	12
Specificity	78	72	78
Sensitivity	75	93	68
ATN Detection Limit (%)	3.5	25	20
Specificity	61	56	33
Sensitivity	96	96	96

Source: Steinhauslin F, Burnier M, Magnin JL, Munafo A, Buclin T, Diezi J, Biollaz J. Fractional excretion of trace lithium and uric acid in acute renal failure. J Am Soc Nephrol 1994;4:1429–37.

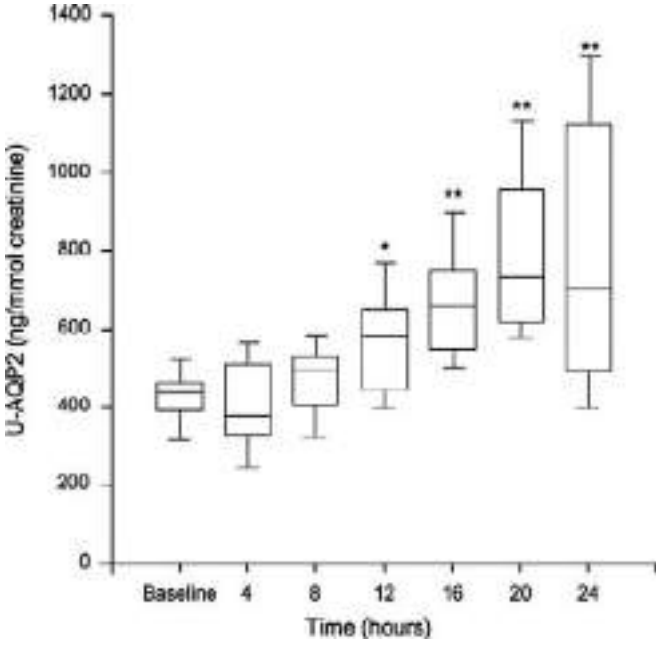

FIGURE 74.3 Urinary (u) aquaporin-2 (AQP2) excretion during 24 hours of water deprivation in 15 healthy subjects. Baseline, 24-hour collection before the experiment; 4 hours, 1200; 8 hours, 1600; 12 hours, 2000; 16 hours, 2400; 20 hours, 0400, 24 hours, 0800 the next morning. Results are medians with 25th, 75th, 10th, and 90th percentiles. $*p < 01$ and $**p < 001$, significant deviation from baseline. *(From Pedersen RH, Bentzen H, Bech JN, Pedersen EB. Effect of water deprivation and hypertonic saline infusion on urinary AQP2 excretion in healthy humans. Am J Physiol Renal Physiol 2001;280:F860–F867, with permission.)*

results in an increase in water permeability.[10,57] Synthesized AVP is released in response to two stimuli: an increase in plasma osmolality and changes in blood volume and pressure.[28] AVP-mediated increases in total AQP2 expression contribute to the long-term regulation of urinary concentration. AVP also increases water reabsorption by the kidney by increasing the expression and activity of the Na^+-K^+-$2Cl^-$ cotransporter and the urea transporter.[58,59] AVP-mediated regulation of AQP2 activity and expression provides by far the main mechanism for regulation of collecting duct water permeability.[60] AVP binding to the V_2 receptor activates a G-protein that increases adenylyl cyclase activity and cyclic adenosine monophosphate (cAMP) function. cAMP-activated protein kinase A then phosphorylates AQP2 and targets it to the apical surface of principal cells, which immediately increases water transport.[57,60]

Measurements of AQP2 protein in the urine correlate with AVP levels, during water deprivation and after AVP administration (Fig. 74.3).[61,62] The critical role of AQP2 in the regulation of water excretion is now widely accepted, but at the clinical level, there is no need currently for measurements of AQP2 in the urine. For practical purposes, the clinical assessment of normal and abnormal handling of water by the kidneys starts with the measurement of plasma and urine osmolality (U_{Osm}).

Plasma and Urine Osmolality

Plasma osmolality is tightly maintained within normal range (275–290 mOsmol/Kg). A 1% increase in plasma osmolality above 280 mOsm/kg triggers corrective response in the form of stimulation of the thirst center and activation of osmoreceptors resulting in the release of AVP.[63] On the other hand, urine osmolality varies greatly, depending on water intake, and therefore should be interpreted in conjunction with measurements of plasma sodium or osmolality. In healthy adults, the urinary osmolality can vary from a minimum of about 50 to a maximum of about 1200 mOsm/kg H_2O. It is to be noted that the concentrating ability tends to fall with age, and the maximum U_{Osm} in an elderly patient may be only 600 to 700 mOsm/kg H_2O.

The urine flow rate is directly proportional to the number of osmoles excreted, and is inversely proportional to the urine osmolality, as expressed below:

$$\text{Urine flow rate (or volume)} = \text{Number of osmoles per day}/\text{urine osmolality} \quad (74.5)$$

Several examples of this relationship are shown in Table 75.5. This table shows the urine volume needed to excrete a given amount of solute, at various levels of urine osmolality. In disorders in which the rate of AVP secretion is very low, and essentially constant, for example, in a patient with central diabetes insipidus (DI), the maximum U_{Osm} may be only 100 mOsm/kg H_2O. In this patient, the daily urine volume would be

12 L if 1200 mOsm of solute are to be excreted, as in a typical Western diet that generates a daily solute load of about 900 to 1200 mOsm. Dietary proteins and NaCl are the precursors of most of the urinary osmoles. In patients on a low-solute diet (0.6 g/kg body weight of protein and 10 mg/kg body weight of sodium), the total solute load may be as low as 300 mOsm. In such cases, only 3 L of urine are required to excrete the solute load, if the U_{Osm} is 100 mOsm/kg H_2O (Table 74.5).

In a healthy subject on a diet that generates 1200 mOsm of solutes, about half of the urine osmoles consists of urea. Because the concentration of urea in the luminal fluid is roughly equal to that in the papillary interstitial component,[64,65] urea will not cause water movement across the luminal membrane in the inner medulla. This renders urea an ineffective osmole. Thus, some authors believe that it is more correct to say that the urine flow rate is proportional to the number of nonurea osmoles (electrolytes, predominantly sodium and chloride in healthy subjects, and ammonium and β-hydroxybutyric acid during prolonged fasting) and to their concentrations in the medullary interstitial compartment.[64,65] Accordingly, the effective osmoles in the urine of a healthy subject on a typical Western diet would be half the total solute load, or about 600 mOsm.[13] The formula given above can therefore be modified as follows:

$$\text{Urine flow rate} = \text{Number of ''effective'' urine osmoles per day} / \text{''effective'' urine osmolality} \quad (74.6)$$

An important caveat to the generalization that urea is an ineffective osmole exists when an electrolyte-poor urine is excreted. In this case, the concentration of urea in the urine is more than that in the papillary interstitial compartment.[65] In this setting, urea becomes an effective osmole and the increase in osmolality from the increase in urea reflects renal water conservation. The rationale for this change in permeability for urea is the fact that the chief goal of the urinary concentrating process is to ensure that a decrease in urine output ensues when ADH acts.[3] For this to occur, effective osmoles must be excreted with water. These effective osmoles, usually NaCl, are replaced by urea when the content of electrolytes in urine is low.[64] This latter situation may apply, for instance, to sodium-retaining states, such as congestive heart failure, where sodium and chloride are avidly reabsorbed in the proximal tubule and therefore, the excretion in the urine is low.

TABLE 74.5 Relationship Between UOsm and Urine Volume

UOsm	Urine Volume (L) if 1200 mOsm of Solutes are to be Excreted	Urine Volume (L) if 300 mOsm of Solutes are to be Excreted
100	12	3
300	4	1
600	2	0.5
1200	1	0.25

A complete analysis of water handling by the kidneys requires the calculation of free water excretion and electrolyte-free water excretion.[66] These calculations offer information about the quantity of water absorbed or excreted by the kidney, information that is not provided by measuring only U_{Osm}.[66] The calculation of electrolyte-free water excretion further dissects out the effect of free water excretion that is independent of urea, and helps predict the trend of plasma sodium.

Free Water Clearance and Electrolyte-Free Water Clearance

The excretion of free water relative to the extent of water intake can be estimated by the free water clearance (FWC), which equals the volume of urinary water (over a period of time) that exceeds the virtual volume that would be required to excrete the solute load in an iso-osmolar fashion. Thus, the FWC reflects the amount of pure water excreted.[66–68] This concept is illustrated in the following example. A patient collects 4 L of urine with a urine osmolarity of 70 mOsm/L. A concurrently measured serum osmolarity is 280 mOsm/L, four times as concentrated as the urine. If the urinary solutes excreted (70 mOsm/L × 4L) were dissolved in just one-fourth of the actual volume of urine, then the urine osmolarity would match the serum osmolarity of 280 mOsm/L. The other 3 L would be pure water to make up the remainder of the 4 L total volume. Hence, the FWC is as follows:

$$\text{FWC} = \text{Actual urine volume (V)} - \text{Iso-osmolar urine volume } (V_{iso}) \quad (74.7)$$

In mathematical terms, the virtual volume of iso-osmolar urine can be calculated by determining how dilute or concentrated the urine is compared with the serum:

$$\text{Volume of iso-osmolar urine } (V_{iso}) = V \times (U_{Osm}/S_{Osm}) \quad (74.8)$$

Where V = urinary volume, U_{Osm} = urine osmolarity, and S_{Osm} = serum osmolarity.

After calculating the iso-osmolar volume (1 L in the example above), the remainder of the total urine

volume should be composed of osmole-free water. This is quantified as FWC in the following equation:

$$\begin{aligned} \text{FWC} &= \text{Actual urine volume (V)} \\ &\quad - \text{Iso-osmolar urine volume } (V_{iso}) \\ &= V - \{V \times (U_{Osm}/S_{Osm})\} \end{aligned} \tag{74.9}$$

This can be rearranged to:

$$= V \times \{(1 - U_{Osm}/S_{Osm})\} \tag{74.10}$$

Lastly, clearance is always expressed in terms of volume per unit of time; in the example above, the FWC is 3 L/24 hours. The time term may be introduced by dividing the FWC by the time over which the urine was collected, or $V \times \{(1 - U_{Osm}/S_{Osm})\}$/time. This becomes the general formula for the FWC (or CH_2O):

$$CH_2O = V \times \{(1 - U_{Osm}/S_{Osm})\}/\text{time} \tag{74.11}$$

Where CH_2O = free water clearance, V = volume of urine, U_{Osm} = urine osmolarity, and S_{Osm} = serum osmolarity.

All osmoles, however, are not equally active. Some osmotically active particles, such as urea, freely cross the cell membrane and therefore do not influence water movement between the extracellular and intracellular compartments.[64] Of these, the predominant species are sodium (especially in the extracellular fluid), potassium (especially in the intracellular fluid), chloride, bicarbonate, and glucose. For simplicity, the cationic particles may be summed and used as a surrogate for the overall tonicity. To reformulate the FWC based on tonicity, the osmoles in the equation above should be replaced by their equivalent tonically active cations. Thus, the ratio of U_{Osm}/S_{Osm} becomes $(U_{Na} + U_K)/S_{Na}$, where U_{Na} and U_K are the urinary sodium and potassium concentrations and S_{Na} is the serum sodium concentration. Serum potassium is usually ignored because it represents an insignificant fraction of the total serum cationic tonicity, but urine potassium must be taken into account because it often constitutes a sizeable portion of the total urinary cationic tonicity. Thus, the FWC equation becomes:

$$C^eH_2O = V \times (1 - (U_{Na} + U_K)/S_{Na}\}/\text{time} \tag{74.12}$$

This equation is also known as the electrolyte-free water clearance (abbreviated C^eH_2O) because it includes only the major electrolytes that contribute to the overall tonicity.

The most noteworthy term in the electrolyte-free water clearance is the ratio of the urinary electrolyte solutes to the main serum electrolyte solute (sodium). It makes intuitive sense that if the urinary electrolyte concentrations are low compared with those of the serum electrolytes, a fair amount of free water is being excreted, consistent with the formula. On the other hand, if the urinary electrolyte concentrations are relatively high and their sum approaches the value of the serum electrolyte concentration, then the term $1 - (U_{Na} + U_K)/S_{Na}$ will have a low value, indicating a reduced electrolyte-free water clearance. A third scenario is also possible in that the sum total of the urinary electrolytes could exceed the serum electrolytes, yielding an electrolyte-free water clearance that is negative. This equates with the reabsorption of water, and in an individual with hyponatremia, predicts further lowering of plasma sodium unless a therapeutic intervention takes place (see following sections).[66]

Volume Status in the Evaluation of Hyponatremia

The evaluation of hyponatremia is often based on volume status as a way to determine the "appropriateness" of AVP secretion.[10,37] Classification of a patient's volume status as hypovolemic, euvolemic, or hypervolemic based on physical examination findings helps to identify the cause of the hyponatremia and to plan its treatment.[66] The recent introduction of vasopressin V_2 antagonists for the treatment of hyponatremia is based on this classification.[66,69]

The principles underlying the evaluation of alterations in water balance are based on: (1) elucidation of factors involved in the generation and maintenance of osmotic pressure, which is exerted by solutes present in the medullary interstitium, i.e., the driving force and (2) assessment of AVP-regulated water permeability of the apical surface of collecting duct principal cells.[28,55,70] Impaired free water excretion may be attributed to changes in one or both of these two variables.[10] In addition, the delivery of fluid to the diluting segments plays a critical role. A decrease in GFR decreases the delivery of both NaCl and water to the ascending limb causing impaired dilution.[28] For instance, in hypothyroidism, hyponatremia results, at least in part, from a decreased GFR and decreased delivery of NaCl and water to the distal tubule. Thiazide diuretics can also cause hyponatremia via a decreased GFR (in addition to other important mechanisms discussed below) if volume contraction is severe. The associated enhancement in proximal fluid reabsorption further limits the delivery of NaCl and water to the diluting segments.

Diuretics are commonly associated with hyponatremia, and the offending agents are almost always thiazides.[10] Thiazide diuretics contribute to impaired water excretion through various mechanisms, including decreased delivery of filtrate to the diluting sites caused by impaired dilution of luminal fluid in the early distal tubule as a result of inhibition of the electroneutral NaCl cotransporter leading to generation of hypertonic urine.[71] Thiazides may also directly

increase the water permeability of inner medullary collecting duct tubules.[72] Increased water intake generally contributes to thiazide-induced hyponatremia.[73]

Any condition that causes an increase in AVP will result in decreased free water excretion. A decrease in intravascular volume is a potent physiologic stimulus for the release of AVP. Intravascular volume depletion may result from true volume depletion seen in conditions like vomiting, diarrhea, blood loss, or a salt-wasting syndrome, or from hypervolemic conditions associated with decreased effective circulating volume (e.g., congestive heart failure, cirrhosis, or nephrotic syndrome). Hyponatremia is often seen in these conditions.[28,74,75] Patients with cirrhosis or congestive heart failure also have a reduced ability to excrete the water load due, in part, to a blunted decrease in urinary AQP2 and AVP levels.[75]

Impaired free water excretion, due to high circulating AVP is usually exacerbated by increased proximal tubular reabsorption of sodium and water and reduced GFR. This results in a decrease in distal delivery of fluid.[74] AVP is usually not measured in the clinical setting but one can assume that levels of this hormone are increased whenever the urine is concentrated.[10] Some studies estimate that as many as 10 to 20% of patients diagnosed with syndrome of inappropriate antidiuretic hormone (SIADH) have AVP levels at the lower limit of detection by radioimmunoassay.[76] It has been suggested that non-AVP ligands (e.g., oxytocin, nitric oxide, and atrial natriuretic peptide (ANP)) may activate AQP2, causing water retention.[10,70,77,78]

The possibility that ANP release may promote AQP2 channel activity could explain, in part, the mechanism underlying hyponatremia associated with some kinds of neurosurgical disease[79] such as in cerebral salt wasting, a syndrome where hyponatremia develops in the setting of cerebral disease or trauma.[80] In contrast to SIADH, cerebral salt wasting is typically characterized by volume depletion. The primary defect here is sodium wasting, which then results in volume-induced stimulation of AVP release. Cerebral salt wasting is associated with increased circulating atrial and brain natriuretic peptides that increase the GFR and decrease proximal sodium reabsorption causing natriuresis and volume depletion.[80,81]

Electrolyte-Free Water Clearance in the Assessment of Hyponatremia

The following example illustrates the use of the electrolyte-free water clearance in a hypothetical patient with hyponatremia before and after treatment with a vasopressin V_2 antagonist (Table 74.6).[66]

TABLE 74.6 Changes in Serum and Urinary Parameters Before and After Therapy with a V2 Antagonist in a Hypothetical Patient

	SNa, mEq/L	SOsm, mOsm/L	UNa, mEq/L	UK, mEq/L	UOsm, mOsm/L	Urine volume, ml
Pretreatment	126	262	100	60	600	1400
Post-treatment	134	280	80	40	400	2000

The electrolyte-free water clearance (C^eH_2O) for this patient before the administration of a vasopressin antagonist is:

$$\begin{aligned} C^eH_2O &= V \times \{1 - (U_{Na} + U_K)/S_{Na}\}/\text{time} \\ &= 1400 \times \{1 - (100 + 60)/126\}/24 \text{ hours} \\ &= -378 \text{ ml}/24 \text{ hours} \end{aligned} \tag{74.13}$$

The free water clearance according to the classical formula is:

$$\begin{aligned} CH_2O &= V \times \{(1 - U_{Osm}/S_{Osm})\}/\text{time} \\ &= 1400 \times \{(1 - 600/262)\}/24 \text{ hours} \\ &= -1806 \text{ ml}/24 \text{ hours} \end{aligned} \tag{74.14}$$

The electrolyte-free water clearance and free water clearance after treatment are as follows:

$$\begin{aligned} C^eH_2O &= V \times \{1 - (U_{Na} + U_K)/S_{Na}\}/\text{time} \\ &= 2000 \times \{1 - (80 + 40)/134\}/24 \text{ hours} \\ &= +209 \text{ ml}/24 \text{ hours} \end{aligned} \tag{74.15}$$

and

$$\begin{aligned} CH_2O &= V \times \{(1 - U_{Osm}/S_{Osm})\}/\text{time} \\ &= 2000 \times \{(1 - 400/280)\}/24 \text{ hours} \\ &= -857 \text{ ml}/24 \text{ hours} \end{aligned} \tag{74.16}$$

Practically speaking, the negative electrolyte-free water clearance pretreatment, which is indicative of renal water retention, predicts that the hyponatremia will worsen unless something is done therapeutically and should alert the clinician to the need for more aggressive treatment. For hyponatremia to improve, water excretion must be increased or sodium needs to be gained in excess of water by the administration of hypertonic saline. The latter, however, is not indicated in asymptomatic subjects with moderate hyponatremia.

The principles discussed in the preceding paragraphs are a guide to the rational treatment of hyponatremia, but the urgency and modality of treatment are determined by the presence and severity of symptoms.[66] Once the electrolyte-free water clearance becomes positive, in the case illustrated by the

aquaretic action of a V_2 antagonist, the correction of hyponatremia can potentially occur.[66] As long as the electrolyte-free water clearance is positive, hyponatremia will improve according to the principle of the steady-state unless the patient's water intake exceeds the water output, C^eH_2O plus insensible and stool losses. Water restriction still is needed but, as the positive electrolyte-free water clearance becomes larger in magnitude, the water restriction can be relaxed. Because the administration of V_2 antagonists "vaptans" increases plasma sodium and thus, it may also increase thirst, one should be cautious not to prescribe too strict a water restriction while using these agents.[66] In fact, while using these agents water restriction should be avoided once the positive free water clearance is established and plasma sodium has increased to a safe range.

The electrolyte-free water clearance and the free water clearance usually agree (qualitatively) in their assessment of the renal capacity to excrete water, but as the example in Table 74.6 shows, the free water clearance can sometimes be deceiving.[66] Before treatment, both the electrolyte-free and free water clearances were negative and predicted exacerbation of hyponatremia, but after treatment with a V_2 antagonist, the electrolyte-free water clearance (C^eH_2O) became positive whereas the FWC remained negative. The FWC stayed negative in value because the U_{Osm} remained greater than the S_{Osm}, likely as a result of the urine urea nitrogen (UUN), which keeps the urine osmolarity at a relatively high level.[66] UUN represents a "liability" for the use of FWC as a tool to interpret renal water handling during hyponatremia because urea is freely permeable across membranes and typically does not affect water movement. The persistence of a negative value for FWC might lead some to believe that water is still being reabsorbed, when in fact the kidneys are excreting free water, as indicated by the positive electrolyte-free water clearance (and supported by the FWC becoming less negative). Thus, to be meaningful, the FWC must be followed longitudinally; any single value in time could be misleading.[66] In contrast, the electrolyte-free water clearance gives a more accurate clinical picture, as it is not affected by the problem of urea being an ineffective osmole. We advocate the use of electrolyte-free water clearance over regular FWC as it helps in assessing whether the kidneys are avidly retaining water and whether hyponatremia is likely to worsen or improve. It also aids in the prescription of an appropriate degree of water restriction and other interventions to treat hyponatremia.[66]

C^eH_2O can be simplified through the use of the urine/plasma electrolyte ratio.[82] When the ratio ($U_{Na} + U_K/S_{Na}$) is below 1.0, C^eH_2O has to be positive, therefore reflecting that electrolyte−free water is being excreted (see Table 74.7). When the ratio is even lower (i.e., <0.5), significant amounts of electrolyte-free water are being excreted.[82] In contrast, no electrolyte-free water is being excreted when the ratio is equal to 1.0 or higher (Table 74.7).

TABLE 74.7 Approach to Raising Plasma Tonicity by Water Restriction

Urine/Plasma Electrolyte Ratio	Insensible H_2O Losses	Expected Net H_2O Loss[a]	Recommended H_2O Consumption
≥1.0	800 mL	−800 mL	0 mL
0.5–1.0	800 mL	−800 to −1300 mL	up to 500 mL
≤0.5	800 mL	−1300 to −1800 mL	up to 1 L

Source: Furst H, Hallows KR, Post J, Chen S, Kotzker W, Goldfarb S et al. The urine/plasma electrolyte ratio: a predictive guide to water restriction. Am J Med Sci 2000; 319:240–4.

[a]*These estimates are based on a U/P ratio, a simplified formulation of CeH2O. They also assume that urine sodium and potassium losses are replaced, that a patient has an average body surface area of 1.73 m2 and eats a normal diet, and calculate for the period during which the next 1 L of urine is excreted.*

Physiologic Principles Guiding Assessment of Polyuric Syndromes

Polyuria is arbitrarily defined as a urine volume of more than 3 L/day in adults and 2 L/m2 in children. Comparing the urine volume in an individual to the average values in a group of subjects, however, is not as physiologically relevant as the urine volume expected for a given stimulus.[83] An individual on a typical diet has an osmole excretion rate of 900 to 1200 mOsm/day. In contrast, the osmole excretion rate in an individual on a low-protein, low-salt diet would be much lower, say 300 mOsm/day. If this individual were capable of maximal urinary concentrating capacity, the U_{Osm} will be 1200 mOsm/kg H_2O, and this subject's expected minimum urine volume would be 0.25 L/day. If this subject has impaired urinary concentrating ability (e.g., a maximal U_{Osm} of about 600 mOsm/kg H_2O) then the minimum urine volume would be 0.5 L/day. This is more than the expected minimum and thus would indicate polyuria due to impaired renal concentrating ability. This example illustrates the inappropriateness of applying data gathered from one population (subjects consuming their usual diet), in defining a condition such as polyuria, to a population with a much lower osmole excretion rate (subjects consuming a low-protein and low-salt diet).[83,84]

Polyuria may be due to a primary surplus of free water (water diuresis) or to the presence of excess osmoles in the urine (osmotic diuresis).[13] To

differentiate the various causes of polyuria, one needs information on urine electrolytes and osmolality. Plasma osmolality should be measured and also calculated from plasma sodium, plasma glucose, and plasma urea. Urine osmolality helps differentiate a water diuresis from an osmotic diuresis. In water diuresis, there is a large volume of dilute urine, with the urine osmolality usually below 250 mOsm/kg H_2O. If the U_{Osm} is more than 300 mOsm/kg H_2O in a polyuric subject, an osmotic diuresis is to be suspected.[13] Further, total solute excretion (calculated on a 24-hour urine collection from the product of the urine osmolarity and the urine output) is normal with a water diuresis (600–900 mOsm/day) but markedly increased (usually more than 1200 mOsm/day) with an osmotic diuresis. In osmotic diuresis, decreased solute reabsorption is the primary abnormality. Glucosuria, high-protein feedings (in which urea acts as the osmotic agent), volume expansion due to saline loading, or impaired sodium reabsorption following the release of bilateral urinary tract obstruction[85–87] are typical examples.

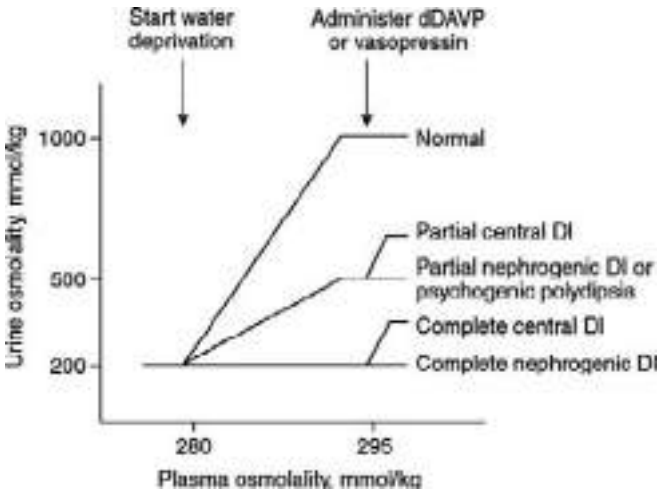

FIGURE 74.4 The diagram shows the typical response after water deprivation in healthy individuals, in patients with complete or partial central diabetes insipidus (DI), in patients with complete or partial nephrogenic DI, and in patients with primary or psychogenic polydipsia. The 200 mmol/kg straight line is for schematic representation because patients with full phenotype (central or nephrogenic DI) have a urine osmolality less than 100 mmol/kg. *(From Sands JM, Bichet DG. Nephrogenic diabetes insipidus. Ann Intern Med 2006;144:186–194, with permission.)*

Direct and Indirect Tests to Evaluate Concentrating Capacity

The three major causes of water diuresis are primary (or psychogenic) polydipsia, central diabetes insipidus (CDI), and nephrogenic diabetes insipidus (NDI). Each of these three disorders is associated with an increase in water output and the excretion of relatively dilute urine. In these cases, urine osmolality can decrease to less than 100 mOsm/kg.[88] With primary polydipsia, the polyuria is an appropriate response to enhanced water intake; in comparison, the water loss is inappropriate with either form of DI. The three disorders can be distinguished from one another by examining the urine osmolality in response to exogenous AVP and to water deprivation (Fig. 74.4).[84,89,90] The fluid deprivation tests provide a standardized approach to interpret urine osmolality, when plasma osmolality is not already elevated. It must be appreciated that there is no need to perform a water restriction test, and, in fact, it is contraindicated clinically when plasma osmolality is above normal.

The first step is to examine plasma sodium. In the polydipsic patient, the plasma sodium is usually in the low range of normal, typically around 135 mmol/L as a result of excessive drinking.[91] On the other hand, in patients with DI, the plasma sodium is in the high-normal range (usually more than 140 mmol/L).[92] A plasma sodium of more than 150 mmol/L is usually not seen in compensated DI, because the initial water loss stimulates the thirst mechanism, thus increasing water intake. In cases where the patients are obtunded or suffering from rare central nervous system (CNS) disorders, where the thirst center is also affected, the patient may have hypo- or adipsia, and thereby develop hypernatremia.

Patients with DI have roughly intact thirst mechanisms and usually do not present with hyperosmolality, but rather, they present with normal plasma osmolality and serum sodium and symptoms of polyuria and polydipsia. In these cases, it is most appropriate to perform a fluid deprivation test.

The water deprivation test can be carried out as an indirect test or by measuring plasma AVP after fluid deprivation.[83] The indirect test has been successfully used in various protocols to make an appropriate diagnosis in most cases (Fig. 74.4).[90] It generally yields interpretable results by the end of the test and does not require sensitive assays for the often unavailable measurement of plasma AVP levels, which are the basis of the direct test.[63] The patient is asked to stop drinking about 12 hours before the test, usually after dinner, and the urine osmolality and volume are measured the following morning. To distinguish central DI from nephrogenic DI, the response to administered AVP (2 to 5 units subcutaneously) or, preferably, the AVP receptor (V_2) agonist desmopressin (DDAVP, 1–2 μg subcutaneously or intravenously) should be assessed. For this, urine osmolality and volume are measured in the two to four hours following AVP administration.

Three different patterns can be observed with the indirect test (fluid deprivation followed by AVP administration):

(1) The urine osmolality does not increase after fluid deprivation (Fig. 74.4).[63,90] This is expected in both complete central and nephrogenic DI despite a modest increase in plasma osmolality caused by the fluid restriction. These two types of DI can be distinguished by administering exogenous AVP. In complete central DI, there is a striking increase in U_{Osm}, between 100 and 800%, with a concomitant fall in urine output.[63,83,93] In complete nephrogenic DI, by contrast, there is an absent response to exogenous AVP (less than 10% increase in U_{Osm}), indicative of total renal resistance to AVP.

(2) The urine osmolality increases after fluid deprivation but only marginally (i.e., less than 50%) (Fig. 74.4).[90] This can be seen in partial nephrogenic DI and in partial central DI. Patients with partial central DI usually achieve a U_{Osm} of 300 mOsm/kg H_2O or higher after AVP administration, while patients with nephrogenic DI typically have a persistently low urine osmolality that rises, but remains well below 300 mOsm/kg H_2O, after exogenous AVP administration.[63,83]

(3) The urine osmolality increases more than 50% after fluid deprivation, usually to above 500 mOsm/kg H_2O (Fig. 74.4).[90] This is observed in primary polydipsia. In this setting, there is no further response to exogenous AVP since endogenous release is intact (provided the patient had been compliant with fluid restriction). It is to be noted that these patients do not reach a normal U_{Osm} of 800 mOsm/kg or more. This is due to impairment of the maximum urinary concentrating ability, resulting from a partial washout of the medullary interstitial gradient, and possibly from downregulation of ADH release and/or renal action during prior protracted water drinking.[94]

Difficulties in interpreting the response to exogenous AVP also can arise in central DI. The water diuresis that occurs in all of these disorders washes out the medullary concentration gradient.[9,84,91,95] In addition, there is a down regulation of kidney AQP2 water channels.[96,97] Thus, the initial increases in urine osmolality in response to administered AVP or dDAVP are not as robust as would be expected.[95] For this reason, plasma AVP levels should be measured to aid in this distinction; hyperosmolar patients with nephrogenic DI will have clearly elevated AVP levels while those with central DI will have undetectable levels (complete central DI) or relatively low AVP levels (partial central DI) relative to the high plasma osmolality.[83]

The measurement of AVP after fluid deprivation has been shown to provide a definite diagnosis in most cases of polyuria and polydipsia, provided the final level of plasma osmolality is above 295 mOsm/kg H2O or the final serum sodium is more than 145 mmol/L.[83] The magnitude of the AVP response to osmotic stimuli is not appreciably diminished by pre-existing chronic overhydration or dehydration.[98] Hence, the relationship of plasma AVP to plasma osmolality is usually within or above normal limits in nephrogenic DI and primary polydipsia. In most cases, nephrogenic DI and primary polydipsia can then be distinguished by measuring urine osmolality before and after the dehydration test and relating these values to the concurrent plasma AVP concentrations. Given the proven usefulness of both the indirect and the direct approaches, a combined fluid deprivation test that synthesizes the crucial aspects of both tests can easily be performed, and in many cases will allow interpretation of both the plasma AVP levels and the response to an AVP challenge. By combining the fluid deprivation test with plasma AVP determinations, greater than 95% of all cases of polyuria and polydipsia can be diagnosed accurately.[83,89]

An unusual situation that mimics central DI is a rare syndrome unique to pregnancy that has been ascribed to increased vasopressinase activity.[99–103] In this situation, the levels of AVP are low because of increased degradation and not a result of lack of production. Since vasopressinase does not degrade synthetic dDAVP, treatment with this analogue is effective. The diagnosis can be made by finding detectable levels of endogenous AVP, which is unlike in severe central DI, and by the increase in urine osmolality seen after exogenous AVP administration or dDAVP, which resembles central DI. These features would not be conclusive if it were not for the clinical setting and the prompt resolution of the symptoms after childbirth.[102–104]

The interpretation of therapeutic responses in the syndromes of DI is best assessed in terms of urine volume in the new steady-state. The clinical response is apparent from the ability to excrete the same daily solute load in a smaller volume of urine.[52] For instance, studies in patients with polyuria due to long-term use of lithium revealed a significant improvement in the urine volume after administration of amiloride (Fig. 74.5).[52] In this study, after weeks on amiloride, urine output decreased, on average, from 4.7 L to about 3.1 L. It should be noted that this has measurable clinical benefit, in terms of decreasing urinary frequency, both at daytime and nighttime. This clinical benefit cannot be assessed by the simple measurement of maximal U_{Osm}, which provides only a qualitative assessment of the renal concentrating ability.

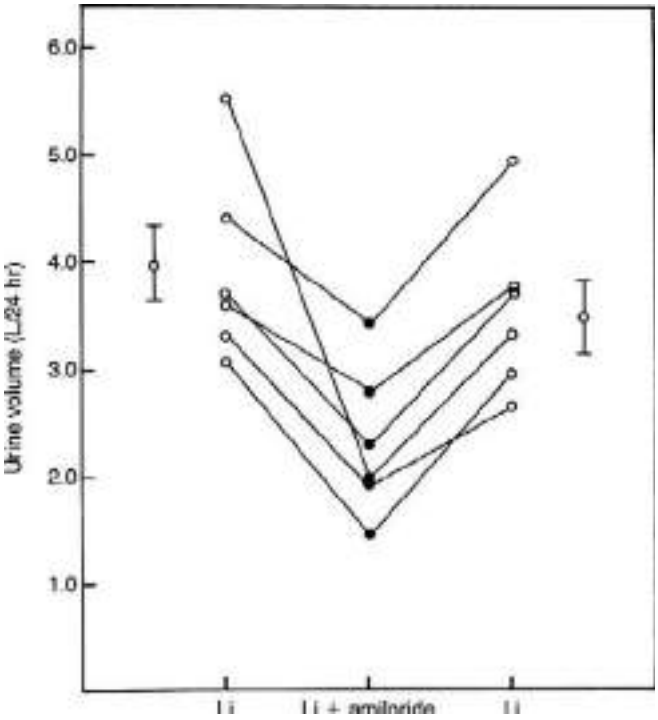

FIGURE 74.5 Twenty-four-hour urine volume in six patients (patients 1, 2, 4, 6, 7, and 9), before, during, and after amiloride administration (20 mg daily). Li, lithium. *(From Batlle DC, von Riotte AB, Gaviria M, Grupp M. Amelioration of polyuria by amiloride in patients receiving long-term lithium therapy. N Engl J Med 1985;312:408–14. Reprinted with permission of Massachusetts Medical Society, © 1985 Massachusetts Medical Society. All rights reserved.)*

EVALUATION OF POTASSIUM DISORDERS

In the steady-state, urinary potassium excretion varies in proportion to dietary intake (median dietary intake is 56 to 84 mEq/day).[105–107] The correlation between dietary potassium intake and urinary potassium content is high ($r = 0.82$).[87] About 90% of ingested potassium is excreted in the urine,[108] with renal excretion varying from10 mEq/day under conditions of potassium deprivation to 700 mEq/day under conditions of potassium loading. Less than 15% of ingested potassium is excreted in the stool (5–15 mEq/day) and a small amount is lost through sweat. It is of interest to note that our modern diet (e.g., saturated fats, oils, cereal grain) is relatively potassium-poor when compared to the potassium-rich diet of our Paleolithic ancestors (e.g., fruits, leafy greens).[109] A list of potassium rich foods is given in Table 74.8.

Approximately 80 to 90% of the filtered potassium is reabsorbed in the proximal tubule and the loop of Henle.[105–107] Of this, approximately 65% is reabsorbed in the proximal tubule and 25% in thick ascending limb of loop of Henle.[98] Potassium is secreted by the principal cells in the cortical collecting tubule via a specific channel called renal outer medullary potassium channel or ROMK.[105,106] In the cortical and outer medullary collecting tubules, the intercalated cells can reabsorb potassium, and thereby counteract the potassium secretion by the principal cells.[110] This process is mediated by an active H^+/K^+-ATPase pump in the luminal membrane, which results in both H^+ secretion and potassium reabsorption.[111,112] The activity of this pump is increased with potassium depletion[111,112] and is reduced with potassium loading.[111]

Tubule flow rate and luminal sodium concentration may independently affect potassium secretion.[113–116] A flow-dependent fall of lumen potassium concentration when delivery of fluid to the distal tubule is increased favors the chemical gradient for potassium secretion.[107,117–119] The relationship between potassium secretion and flow or sodium concentration is initially very steep and then potassium secretion tends to plateau.[107,118,120] While flow rate and sodium concentration may be shown to have independent effects on potassium secretion experimentally, they are usually interdependent on each other. In fact, the increase in distal potassium secretion with increasing flow rate largely depends on the associated increase in sodium concentration in the lumen of the distal tubule which, when reabsorbed via the sodium channel (ENaC), creates a favorable voltage for potassium secretion.[107]

Chronic adaptations take place with either potassium deprivation, surplus, or changes in sodium delivery that involve amplification of both potassium retaining mechanisms (i.e., kaliferic effect) and potassium excretory mechanisms (i.e., kaliuretic effect).[121] When potassium intake is increased, the ability to excrete potassium is greatly enhanced. This adaptive response is evident within one day of increasing potassium intake and persists for one to two days following return to baseline levels of potassium intake. High potassium intake inhibits salt and water reabsorption by the proximal convoluted tubule and/or the thick ascending limb, which results in an increase in sodium delivery and flow rate to distal nephron potassium secretory sites. High potassium intake also stimulates aldosterone which further enhances potassium secretion.[107] Potassium deprivation on the other hand leads to suppression of potassium secretion and enhancement of active tubular potassium absorption, partly as a result of suppression of aldosterone levels due to low serum potassium concentration and also by inhibition of potassium secretion by a decrease in ROMK channel activity in the CCD.[122,123]

TABLE 74.8 High Potassium Foods

Highest (>1000 mg/100 g): (About 1% K+, 10 mEq = 750 gm)	Very High (>500 mg/100 g): (About 0.5% K+, 10 mEq = 750 gm)	High Content (>250 mg/100 g): (About 0.25% K+, 10 mEq = 750 gm)		
Dried figs	Dried Fruits (Dates, Prunes)	**Vegetables**	**Fruits**	**Meats**
Molasses	Nuts	Spinach	Banana	Veal and Beef
Seaweed	Avocados	Tomatoes	Cantaloupe	Pork
	Bran Cereals	Broccoli	Orange	Lamb
	Wheat Germ	Winter Squash	Kiwi	
	Lima Beans	Beets		
		Carrots		
		Cauliflower		
		Potatoes		

The suppression of the normally operating kaliuretic mechanisms, while critical to the adaptation to potassium deprivation, is never sufficient to obliterate potassium secretion completely. This explains why, in humans subjected to dietary potassium deprivation with intake of less than 1 mEq/day, urinary potassium excretion declines but never actually matches intake.[124–126] This decrease in potassium excretion is gradual and reaches a maximum level in five to seven days (Fig. 74.6).[124] While on a high salt intake the initial decline in potassium excretion is blunted (Fig. 74.6). This suggests that the reduction in potassium excretion is not due to increased reabsorption but rather to decrease in potassium secretion which is, in part, sodium dependent.

With potassium restriction, there is a concomitant increase in free water clearance and enhanced diluting capacity consistent with enhancement of the Na^+-K^+-$2Cl^-$ cotransporter activity in the thick ascending loop of Henle, a mechanism that may play an important role in the renal adaptation required for potassium conservation.[127] Potassium secretion in the CCD, however, may not cease completely even with profound degrees of potassium depletion.[128] The adaptation to potassium deprivation is less efficient in terms of renal potassium retention when sodium intake is concurrently increased (Fig. 74.6).[124] This suggests that kaliuresis cannot be turned down quickly if sodium delivery is increased because high intake of sodium favors potassium secretion in the cortical collecting tubule.

Renal potassium wastage is almost always due to enhancement of kaliuretic mechanisms rather than to failure of kaliferic mechanisms.[121] For instance, when mineralocorticoid activity is maintained at a constant level through exogenous administration, in the face of potassium deprivation, a negative potassium balance is seen.[129] Often, several kaliuretic mechanisms may be operating simultaneously (increased distal sodium delivery, increased aldosterone), serving to accentuate the kaliuresis.[121]

Clinical Evaluation of Renal Potassium Handling

The kidney maintains potassium balance primarily by varying the secretion of potassium into the lumen of the distal tubule, according to physiologic needs. Hyperkalemia of renal origin always arises from impaired potassium secretion.[108] The assessment of potassium handling is relatively straightforward since all the potassium that appears in the urine originates from its secretion and this process is restricted to the late distal tubule and CCD, the major site of regulation of potassium secretion.

Many factors influence potassium secretion in the CCD including plasma potassium concentration, dietary potassium intake, flow rate, sodium delivery, transepithelial potential difference, adrenal hormones, and acid–base status.[23] For practical purposes, however, net secretion of potassium in the CCD is critically dependent on and can be best conceptualized and clinically assessed through the interplay of two of these factors: sodium delivery/transport and the level of mineralocorticoid activity.

The interplay between mineralocorticoid activity (aldosterone) and sodium delivery/transport is such that they often, under physiologic conditions, go in opposite directions such that potassium secretion is maintained more or less constant. For instance, when sodium is restricted in the diet, aldosterone goes up

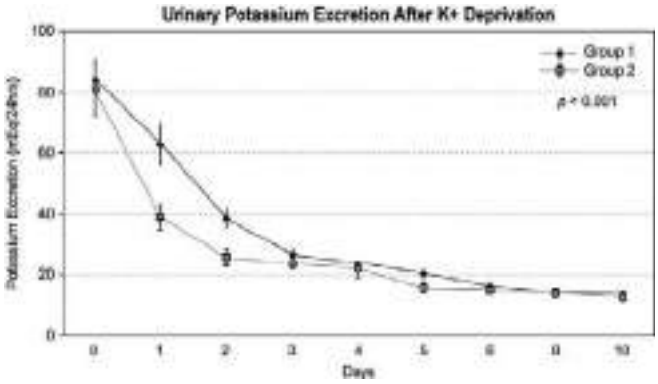

FIGURE 74.6 Urinary potassium excretion (24 hour) in normal volunteers placed on a zero-potassium diet. The upper line (group 1) shows individuals on a high-sodium diet whereas the lower tracing (group 2) depicts individuals on a normal-sodium diet. The initial adaptation to potassium deprivation in the diet is less effective in individuals on a high sodium diet. *(From Cremer EJ, Giricz K, Nakamoto L, Patel S, Schlueter W, Rosa R, Kelani T, Batlle D. Potassium Deprivation in Normal Human Subjects; Impact on Potassium, Sodium, and Acid-Base Balance in Normal Human Subjects. American Society of Nephrology 36th Annual Meeting and Scientific Exposition, 2003, with permission.)*

but sodium delivery goes down and potassium secretion does not change appreciably. Conversely, when sodium is high in the diet, aldosterone is suppressed and sodium delivery increases, resulting in attenuated change in potassium secretion. When both go in the same direction, there are profound changes in potassium secretion, as seen for instance in the syndrome of primary hyperaldosteronism. In this situation, sodium delivery is high and aldosterone is also elevated, resulting in profound potassium wastage and hypokalemia.

The generation of a lumen-negative voltage in the CCD requires an "electrogenic" reabsorption of sodium. The reabsorption of sodium occurs at a faster rate than the reabsorption of its accompanying anion, usually chloride, thereby creating an electric driving force (a "lumen-negative" voltage).[130] Reabsorption of sodium in the CCD occurs by its ion-specific channel (ENaC) in the apical membrane of principal cells. Delivery of sodium to the CCD does not seem to be rate limiting for the secretion of potassium unless when urinary sodium is very low. In other words, provided that urinary sodium is above a critical level of about 20 mEq/L, potassium secretion proceeds provided that there is mineralocorticoid activity. A clinical situation where this is most apparent is chronic liver disease with secondary hyperaldosteronism. In these patients, urinary potassium is very high despite the low urinary sodium.[131]

Potassium channels are not usually rate limiting for the net secretion of potassium.[129] In keeping with this notion, hyperkalemia has not been described as a result of defects in the potassium channel (ROMK). By contrast, interference with the sodium channel often curtails potassium secretion, leading to hyperkalemia. Drugs such as the potassium-sparing diuretics amiloride and triamterene, as well as the antibiotics trimethoprim and pentamidine in their cationic form, block ENaC and hence decrease the lumen-negative driving force for the net secretion of potassium in the CCD.[132,133] These drugs are most effective when urinary sodium is low as they are competitive blockers for sodium uptake. Accordingly, the use of these agents causes hyperkalemia when salt intake is restricted, but is relatively ineffective when salt intake is generous. Conversely, hypokalemia develops when the sodium channel is overactive as seen in Liddle's syndrome, which results from activating mutations in the β or γ subunits of ENaC.[134,135]

Urinary Indices in the Evaluation of Hypokalemia and Hyperkalemia

Urine K^+ Excretion and Spot Urine K^+

Urinary potassium excretion over 24 hours should be sufficient to assess whether the kidney is responding appropriately to the prevailing level of plasma potassium and dietary K^+ intake. If potassium intake is increased slowly, healthy subjects can excrete more than 400 mEq of potassium per day (8 to 10 times normal intake) without a substantial elevation in the plasma potassium concentration.[105–107] Thus, a finding of chronic hyperkalemia invariably reflects the existence of a defect in urinary potassium excretion, since normal renal function would otherwise result in the rapid excretion of the excess potassium.

With potassium depletion of three to five days' duration, 24-hour urinary potassium excretion falls to 10 to 20 mEq/day but never goes below this level (Fig. 74.6).[121,124–126] Thus, in hypokalemia, an appropriately low urinary potassium excretion suggests extrarenal losses (usually from the gastrointestinal tract) or the remote use of diuretics (if the collection has been obtained after the diuretic effect has worn off). In comparison, the excretion of more than 20 mEq of potassium per day indicates a component of renal potassium wasting that is likely the result of inappropriate potassium secretion.

Using a determination of potassium in spot urine may be misleading if urine flow is not taken into account.[13,136] For instance, urinary potassium concentration of 15 mEq/L may be inappropriately high for an individual with hypokalemia who has more than 2 L of urine a day. One can circumvent this by measuring the urine potassium/creatinine ratio or the urine

potassium/osmolality ratio.[13] Measurement of urinary creatinine concentration concurrent with urinary potassium concentration can provide a better measure of actual potassium excretion rate. A potassium-to-creatinine ratio greater than 20 mEq/g has been suggested to indicate the presence of renal potassium wasting.[130]

Similar to the use of spot urine sodium/urine creatinine ratio to estimate 24-H urinary sodium, spot urine potassium/ urine creatinine ratio has also been used to develop formulas to generate values of 24-hour potassium excretion. Kawasaki et al.[20] proposed the formula:

$$\text{24-hour urinary potassium (mEq/day)} = 7.2 \times \sqrt{X_K}$$

where $X_K = (\text{Spot } U_K/\text{Spot } U_{Cr}) \times$ predicted 24 urinary Cr excretion

$$\begin{aligned}&\text{predicted 24 h urinary Cr excretion (Male)}\\ &= -12.63 \times \text{Age} + 15.12 \times \text{Weight} + 7.39 \times \text{Height} - 79.90 \text{ (mg/day)}\\ &\text{predicted 24 h urinary Cr excretion (Female)}\\ &= -4.72 \times \text{Age} + 8.58 \times \text{Weight} + 5.09 \times \text{Height} - 74.50 \text{ (mg/day)}\end{aligned}$$

Linear correlation between formula-estimated and actual 24-hour urinary potassium was 0.44.[20] Thus, the estimation is not precise but maybe of some use in epidemiologic studies where potassium excretion and intake is being estimated using this formula when 24 h potassium excretion is not available.

Fractional Potassium Excretion (FE_K) and Transtubular Potassium Gradient (TTKG)

The fractional excretion of potassium (FE_K) reflects the amount of potassium excreted in relation to the amount of potassium filtered:

$$FE_K\,(\%) = U_K \times V/GFR \times P_K \times 100 \qquad (74.17)$$

When GFR is not available, FE_K can be calculated by the formula that uses plasma and urine creatinine:

$$FE_K\,(\%) = (U_K \times P_{cr})/(P_K \times U_{cr}) \times 100 \qquad (74.18)$$

The FE_K is useful in the evaluation of hyperkalemic syndromes occurring in the setting of chronic kidney disease (CKD). It has the advantage that it takes into account the prevailing GFR, which is usually reduced in patients with chronic hyperkalemia.[137,138]

Often renal hyperkalemia is due to selective aldosterone deficiency or tubular defects in potassium secretion associated with some causes of CKD.[139] In such patients, GFR is usually decreased but higher than 25 ml/min, a level not low enough to account for hyperkalemia. Fractional potassium excretion in these hyperkalemic patients is lower than that of subjects without hyperkalemia and comparable GFR (Fig. 74.7).[137] In the setting of reduced GFR, fractional potassium excretion is useful as it reveals reduced potassium secretion relative to GFR while absolute potassium excretion may be the same as that of normokalemic patients with comparable GFR. Since plasma potassium is elevated, however, absolute potassium excretion relative to the filtered load of potassium is inappropriately low. The following example illustrates this. A patient with a GFR of 25 ml/min has plasma potassium of 6.0 mEq/L and a urinary potassium excretion of 60 mEq/day (Table 74.9). The excretion of potassium may be the same as that of a healthy individual with a GFR of 100 ml/min but plasma potassium of 4.0 mEq/L. Clearly, the excretion in the hyperkalemic patient is low relative to the elevated plasma K^+ and the fractional K^+ excretion does not reflect this because the widely different GFR. Accordingly one needs to compare the FE_K to an individual with a similarly reduced GFR but without hyperkalemia. In this example the hyperkalemic patient has a fractional excretion of 40% which is much lower than that of the normokalemic patient with the same GFR (Table 74.9 and Fig. 74.7).[137]

In the evaluation of hypokalemia, the fractional potassium excretion offers little advantage to simply

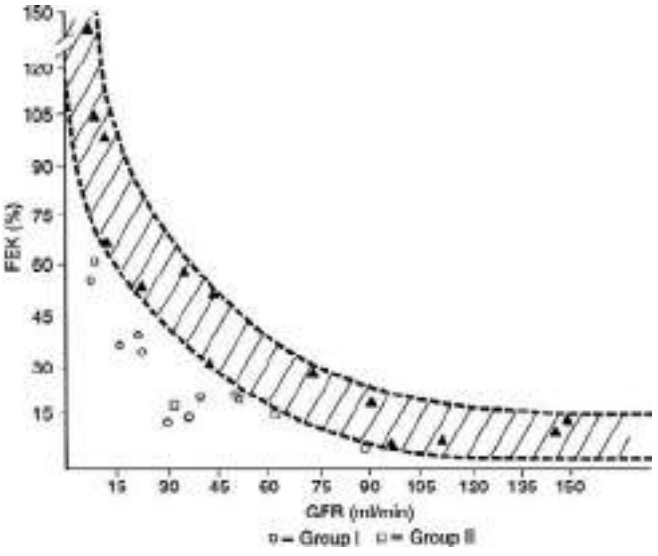

FIGURE 74.7 Relation of fractional excretion of potassium (FEK) to glomerular filtration rate (GFR) under baseline conditions. The area inside the broken lines depicts the normal adaptive increase in FEK observed with a chronic reduction in GFR. Each patient (*open symbols*) had baseline FEK lower than that expected for the corresponding GFR. Open circles denote patients with hyperkalemic distal renal tubular acidosis; open squares represent patients with hyperkalemic metabolic acidosis due to selective aldosterone deficiency. *(From Batlle D, Arruda JAL, Kurtzman NA. Hyperkalemic distal renal tubular acidosis associated with obstructive uropathy. N Engl J Med 1981;304:373–80. Reprinted with permission of Massachusetts Medical Society, © 1981 Massachusetts Medical Society. All rights reserved.)*

TABLE 74.9 Comparison of FE_K with Varying GFR

GFR	Plasma K^+	UK × V	FEK
100	4.0	60	15
25	6.0	60	40
25	4.0	60	60

FEK, fractional excretion of potassium; GFR, glomerular filtration rate.

measuring urinary potassium excretion. A FE_K less than 6% is consistent with appropriate potassium conservation as determined from an analysis of potassium excretion by healthy subjects subjected to dietary potassium deprivation.[125,140,141]

To assess the potassium secretory process in the CCD, the use of the transtubular potassium gradient (TTKG) was introduced.[142] This index is conceptually attractive as it focuses on CCD events where the secretion of potassium is regulated. The first step in the use of this test is to reach an approximation of the K^+ in the lumen of the terminal CCD. This is done by correcting the urinary potassium concentration for the amount of water reabsorbed in the MCD as reflected by dividing urinary potassium concentration by the urine-to-plasma osmolality ratio:

$$K^+CCD = K^+urine/(urine\ osmolality/plasma\ osmolality) \quad (74.19)$$

The TTKG can then be calculated by dividing the K^+CCD by the plasma K^+ as follows:

$$TTKG = \{K^+urine/(urine\ osmolality/plasma\ osmolality)\}/K^+plasma \quad (74.20)$$

The TTKG therefore reflects the driving chemical force for net potassium secretion in the CCD. The validity of this index relies on several assumptions. First, by correcting for water reabsorption in the MCD, it is assumed that most osmoles delivered to the MCD are not reabsorbed in the MCD (i.e., the urine must be at least iso-osmolar with plasma).[142] This assumption is valid except in states of contracted EABV.[3] A second assumption is that potassium is not secreted or reabsorbed in the MCD.[3] This assumption, however, may not be valid in conditions of extreme potassium depletion where net reabsorption of potassium in the MCD can occur and also in conditions of supraphysiologic potassium intake, where potassium secretion in the MCD is seen.[3] A third limitation with the use of the TTKG is that at very high flow rates, the TTKG, if examined in isolation, may falsely underestimate potassium secretion due to lack of equilibration in the cortical distal nephron.[13] With these caveats in mind, the TTKG is a valid clinical tool to assess the driving force for net potassium secretion in the CCD.

Rather than focus on a range of normal values for TTKG, it is more useful clinically to evaluate TTKG in terms of expected values.[136,137,139,142] A large deviation from expected values implies that there is a renal impairment in potassium homeostasis due to either an intrinsic renal defect or because of a normal renal response to an inappropriate stimulus for potassium excretion (e.g., hyperaldosteronism in the presence of hypokalemia).[136] In a study by Ethier et al., expected values for TTKG were derived under stimuli known to modulate potassium excretion, i.e., potassium deprivation, high mineralocorticoid activity and acute potassium loading.[142] On the basis of this study, it was concluded that the value for TTKG should be close to 1.0 in individuals on a low-potassium diet for at least 3 days and that the value for TTKG during hyperkalemia with normal adrenal and renal function should be 10 or higher.[142] Failure to note this high a level with hyperkalemia would imply an intrinsic renal defect or lack of stimulation of potassium secretion (e.g., low aldosterone activity).[130] In a more recent study of hypokalemic patients, TTKG was higher in patients with mineralocorticoid excess (13.3 ± 4.4) and diuretic usage (8.6 ± 1.3) and lower in those with diarrhea (1.6 ± 0.3) than in normal controls, reflecting renal potassium conservation.[136] Another use for TTKG is to follow the renal response to therapy for a potassium disturbance. If a patient with hyperkalemia due to hyporeninemic hypoaldosteronism is to be treated, the TTKG that is initially low (or, at least, inappropriately so) should increase with the administration of fludrocortisones.[143] While the TTKG is an appropriate tool to conceptualize the renal site responsible for hyperkalemia, at the practical level, one can assume that hyperkalemia results from decreased CCD potassium secretion any time that urinary potassium excretion is low in the face of a high level of plasma potassium.

Clinical Approach to Potassium Disorders

In most cases of hypokalemia, the diagnosis is apparent from the clinical history, physical examination and review of medications, such as with diarrhea, vomiting and diuretic use.[136] The physical examination should focus on evidence of volume depletion and the presence or absence of hypertension. A search for possible medications that can alter extrerenal

potassium handling is always in order.[144] Analysis of acid–base status can also be helpful in determining the etiology of hypokalemia. Hypokalemia due to vomiting and nasogastric suction can be associated with metabolic alkalosis. In contrast, diarrhea-related hypokalemia is usually associated with metabolic acidosis. Hypokalemia associated with moderate metabolic alkalosis secondary to diuretic use is common, with volume depletion and secondary hyperaldosteronism playing important roles in the development of hypokalemia.

Determining the cause of hypokalemia can sometimes be challenging, especially in patients who surreptitiously use laxatives or diuretics, as this is often denied by these patients. Laxative abuse is usually associated with metabolic acidosis. Surreptitious vomiting, as in bulimia, and illicit use of diuretics may be seen in weight-conscious individuals. Patients with hypertension and otherwise unexplained hypokalemia should be suspected of having primary hyperaldosteronism. Bartter's and Gitelmann's syndrome are characterized by severe hypokalemia and metabolic alkalosis, which usually manifests in childhood. In these patients, blood pressure is usually low or normal, and hyperreninemia and hyperaldosteronism are present. Renal magnesium wasting results in hypomagnesemia and hypercalciuria is also seen. In Gitelman's syndrome, hypokalemia is usually milder, but hypomagnesemia is more severe and there is no hypercalciuria. Hypomagnesemia induces renal potassium wasting by poorly defined mechanisms, thus magnesium should be measured in all patients with unexplained hypokalemia.[130,145] The hypocalciuria characteristic of Gitelman Syndrome has never been fully explained. An increase in the transepithelial voltage along the thick ascending limb has recently been proposed as the primary stimulus for increased paracellular calcium reabsorption along this segment.[146–148]

With renal potassium losses, reversing the factors promoting kaliuresis is necessary to correct the hypokalaemia (e.g., high-salt intake in a patient receiving diuretics). The use of potassium-sparing drugs such as amiloride or triamterene may be helpful until the potassium deficiency is ultimately amenable to cure (e.g., an adrenal adenoma causing primary hyperaldosteronism).[121] These drugs may also be used as chronic therapy when a surgical cure is not possible (e.g., bilateral adrenal hyperplasia) or in Liddle's syndrome.

The mere finding of chronic hyperkalemia suggests impaired potassium secretion since with normal renal function, an increased potassium burden would lead to rapid excretion of the excess potassium.[108] The urine potassium concentration will be low in the setting of chronic hyperkalemia, as in the syndrome of hyporeninemic hypoaldosteronism, and with drugs that block sodium channels (e.g., trimethoprim and amiloride).[132] The syndrome of hyporeninemic hypoaldosteronism is an important cause of hyperkalemia in patients with a mild to moderate reduction in GFR. As discussed previously, in the setting of CKD, renal potassium secretion is best assessed using the fractional potassium excretion (Fig. 74.7).[137] In patients with chronic hyperkalemia, FE_K is lower than that of normokalemic patients with similar reductions in GFR (Table 74.9 and Fig. 74.7). This is evidence that potassium secretion is impaired in hyperkalemic patients for any given level of GFR.

Acidosis is known to inhibit renal potassium secretion.[149] Renal potassium excretion is inversely related to ammonium excretion, such that potassium excretion is depressed when ammonium excretion is enhanced as in states of metabolic acidosis.[150] In the classic form of RTA, however, renal potassium excretion is increased, leading to severe hypokalemia despite of acidosis. Clearly then, the driving force for hypokalemia in distal RTA cannot be systemic acidosis which would be expected to decrease potassium secretion. The reason for hypokalemia in the classic form of distal RTA remains to be elucidated.[151] The hypokalemia in distal RTA could be readily explained by a permeability defect causing passive potassium secretion, as occurs with amphotericin B administration.[151,152] A permeability defect as a mechanism of distal RTA, however, seems unique to amphotericin B, so alternative explanations are required to explain the potassium wastage mechanism.[151,153]

Enhanced potassium secretion may be driven by secondary hyperaldosteronism which may be a feature of distal RTA.[154,155] Aldosterone oversecretion could be expected due to sodium wastage which has been documented in some patients with distal RTA.[154,155] This may be a reasonable explanation; however, it is unclear why some patients present with striking hypokalemia while others do not. One attractive mechanism that may explain the hypokalemia is the existence of a defect in the renal H^+/K^+-ATPase pump.[156] Renal potassium excretion is determined not only by active potassium secretion localized largely to the distal tubule and cortical collecting tubule, but also by active potassium absorption localized, at least in part, to the outer medullary collecting tubule.[157,158] If the H^+/K^+-ATPase pump in the collecting tubule were defective in distal RTA, one could explain both hypokalemia and metabolic acidosis.

A strong argument against the H^+/K^+-ATPase theory, however, is the finding that severe hypokalemia occurs in all hereditary types of RTA regardless of the molecular defect involved.[151] Hypokalemia is seen in patients in whom the defect is due to a mutation

of the H^+-ATPase, the AE1 (electroneutral anion exchanger) and the carbonic anhydrase-2 genes.[188–193] This suggests that the mechanism of enhanced potassium secretion is not related to a primary H^+/K^+-ATPase defect.[151] Perhaps a concomitant amplification of secretory mechanisms that involve either the potassium channel, ROMK, or the sodium channel, ENaC, is involved in all types of hypokalemic distal RTA.[151]

EVALUATION OF METABOLIC ACIDOSIS

Metabolic acidosis is a process whereby an excess nonvolatile acid load is placed on the body due to excess acid generation or diminished acid removal by normal homeostatic mechanisms.[159,160] Analysis of acid–base disorders begins with the clinical history and assessment of plasma chloride and plasma bicarbonate. The presence or absence of hyperchloremia is a useful clue in the evaluation of metabolic acidosis.[18] When plasma chloride increases out of proportion to sodium (proportional changes in chloride and sodium can be seen with dehydration), either a chronic respiratory alkalosis or a hyperchloremic metabolic acidosis must be present. A blood gas is usually needed to distinguish with certainty between a metabolic acidosis and a chronic respiratory alkalosis. The type of metabolic acidosis present can be initially approached by assessing whether plasma anion gap (AG) is normal or elevated.

Plasma Anion Gap

The anion gap in plasma is used to differentiate hyperchloremic metabolic acidosis (normal AG) from high AG metabolic acidosis.[161] In a pure hyperchloremic metabolic acidosis, there is an increase in plasma chloride equivalent to the fall in plasma bicarbonate, so that the sum of these two anions remains unchanged. The calculation of the plasma anion gap is part of the diagnostic approach as it allows one to classify the disorders into categories of normal anion gap or elevated anion gap. Although these categories can overlap the classification is nevertheless very useful to clinicians.[160] The plasma anion gap in pure hyperchloremic metabolic acidosis is not increased, and may even be slightly reduced due to buffering of protons by proteins. In hyperchloremic metabolic acidosis, hyperchloremia ensues due to enhanced renal chloride retention.[18]

A clinical setting in which the AG may be misleadingly low is hypoalbuminemic states.[162–164] Albumin is negatively charged and makes up a significant portion of unmeasured anions.[165] Therefore, hypoalbuminemia will lead to an underestimation of the size of the AG and potentially to a failure to recognize a clinically important high AG metabolic acidosis. To circumvent this issue, the effect of serum albumin on the plasma AG must be taken into account in the analysis of acid–base disturbances. Figge et al. derived a formula for the plasma AG that takes into account serum albumin, which is based on a mathematical model that has been verified by experiments *in vitro*.[162] This formula is as follows:

$$\text{Albumin-corrected AG} = \text{AG} + 2.5 \times (4.4 - \text{albumin in g/dl}) \quad (74.21)$$

In other words, for each 1-g/dl decrease in serum albumin below 4.4 g/dl, the observed AG underestimates the actual concentration of unmeasured anions by 2.5 mEq/L.[162] This estimation has been shown to correlate more or less with other formulas that take into account the effect of plasma albumin on the anion gap.[165] An alternative is just to accept that hypoalbuminemia leads to a low anion gap and to use this "baseline" anion gap as the basis for comparison with the current anion gap in an acid–base disorder. For example, if a patient with nephrotic syndrome chronically has an albumin of 2.5 g/dl and thus the anion gap is typically around 7, then a current anion gap of 12, though seemingly normal, would constitute an elevated anion gap of 5 units for this patient and should trigger a search for the cause.

A low plasma AG is seen in certain IgG myelomas in which the cationic nature of the paraprotein causes a rise in chloride anions in order to balance the protein's cationic charge.[166] In contrast, the plasma anion gap is normal or even increased in multiple myeloma associated with IgA and IgG paraproteins.[166] IgG paraproteins have isoelectric points that are higher than physiologic pH and are positively charged. The converse takes place with IgA paraproteins, which have isoelectric points below physiologic pH. They behave like anions and when present in large concentrations, the anion gap should increase. In IgA myeloma, however, the AG is usually normal as a result of co-existing hypoalbuminemia, which may reduce an otherwise elevated AG to a normal level. Thus, the interpretation of the plasma AG requires a careful review of all the possible variables that may affect it.

An additional limitation with the use of plasma AG occurs in the detection of mixed metabolic acid–base disturbances.[163] Traditionally, the relationship between changes in the concentration of unmeasured anions (ΔAG) and change in serum bicarbonate concentration (ΔHCO_3^-) helps uncover the presence of a mixed acid–base disorder (typically a high AG metabolic acidosis accompanied by either a metabolic alkalosis or a normal AG metabolic acidosis). Deviation from the presumed 1:1 ratio in this relationship ($\Delta AG/\Delta HCO_3^-$)

that is present in a high AG metabolic acidosis has been used to diagnose these complex acid–base disturbances.[163] When the ΔHCO_3^- (using a mean normal value for bicarbonate of 24 mEq/L) exceeds the ΔAG, a normal AG metabolic acidosis co-exists. Conversely, when the ΔAG exceeds the ΔHCO_3^-, a metabolic alkalosis is present in addition to the high AG metabolic acidosis. Several studies, however, have indicated that there is variability in this ratio, such that a deviation from a 1:1 ratio may not necessarily indicate the presence of a coexisting normal AG acidosis or metabolic alkalosis. This is due to the fact that this 1:1 ratio may be transient and/or depend on the type of metabolic acidosis present.[163,167–171] Studies involving ketoacidosis or lactic acidosis, as well as rarer causes of organic acid accumulation such as toluene poisoning, showed that ratios either greater than 1 or less than 0.8 (the latter being less common) were observed in the absence of an apparent co-existing metabolic alkalosis or normal AG acidosis.[167,168,172–177] This underscores the importance of considering patient history, physical examination, or other laboratory data in accurately defining an acid–base disorder.[163] Nonetheless, the plasma AG, with all the previously mentioned caveats, provides a convenient "starting point" in the evaluation of metabolic acidosis and helps to monitor over time the changes in unmeasured anions such as lactate during therapy for metabolic acidosis in the acute setting.

Urinary Indices in the Evaluation of Metabolic Acidosis

Various urinary indices, including pH and urinary concentrations of sodium, potassium, chloride, and bicarbonate, as well as assessment of the response to provocative tests, can be used, in most cases, to accurately delineate the cause of a metabolic acidosis and its mechanism. Except in patients abusing laxatives, who often deny the practice vehemently, diarrhea as a cause of hyperchloremic metabolic acidosis is evident from the patient's history.

In patients with diarrhea, such as a patient with severe cholera, the acidosis is often more severe than that accounted for by the bicarbonate loss in the stool.[178] The actual bicarbonate concentration of the stools underestimates bicarbonate loss because of the presence in the intestine of organic acids from bacterial products. Titration of intestinal bicarbonate by these acids lowers the final bicarbonate concentration in the stool, resulting in an underestimation of the net alkali loss. Even taking this into consideration, the measured plasma bicarbonate concentration is often much lower than expected from bicarbonate losses due to co-existing lactic acidemia or renal failure, which are common complications of severe cholera.[178]

In addition, volume contraction from diarrhea may be severe enough to inhibit maximal renal tubular acidification. Euvolemic individuals subjected to a chronic acid challenge can increase acid excretion to as much as 200 mEq/day with only a small decrease in plasma bicarbonate. Although studies on renal acid excretion in cholera patients are not available, it seems reasonable to expect that it may not increase maximally, due to the limitation of impaired sodium delivery. This can be inferred from studies of metabolic acidosis in individuals abusing laxatives.[18,179]

Volume depletion in laxative abusers may be unrecognized because these patients have developed compensatory mechanisms and are not overtly hypotensive.[18,179] These patients often come to medical attention due to hypokalemia of unknown etiology. With laxative abuse, hypokalemia is more often seen than hyperchloremic metabolic acidosis and can be severe due to concomitant diuretic abuse and self-induced vomiting. Aldosterone likewise promotes renal potassium loss in these patients. This latter effect may be attenuated despite hyperaldosteronism if distal sodium delivery is impaired from sodium depletion. Urinary sodium availability also affects the ability to lower urine pH.[179] In salt-retaining states with urine sodium below 25 mmol/L, urine pH cannot be maximally lowered (Fig. 74.8).[15] Here, urine pH is a misleading index of distal acidification in that the "intrinsic" renal capacity for distal H^+ secretion is normal once sodium delivery is increased.[15,179] A clue to the diagnosis of laxative abuse is the virtual absence of urinary sodium, which may be less than 1 mEq/day. This, in turn, impairs maximal distal acidification in response to acidemia. When sodium excretion is increased through salt replacement, urine pH falls maximally and acid excretion increases with improvement in the metabolic acidosis (Fig. 74.9).[179]

Whenever a hyperchloremic metabolic acidosis is present without any obvious cause (e.g., diarrhea) and with a relatively normal GFR, distal renal tubular acidosis (RTA) should be suspected. With appropriate suspicion, the diagnosis can usually be confirmed by the findings of an inappropriately low rate of acid excretion and an inappropriately high urine pH.[180] The urine pH is typically inappropriately high in the classic form of RTA (distal or type I RTA) and low in type IV distal RTA (i.e., selective aldosterone deficiency).[138]

Urine Anion Gap

In the presence of metabolic acidosis, ammonium is the most important component of acid excretion. Urinary ammonium (NH_4^+) is usually not measured in the clinical laboratories but can be inferred by

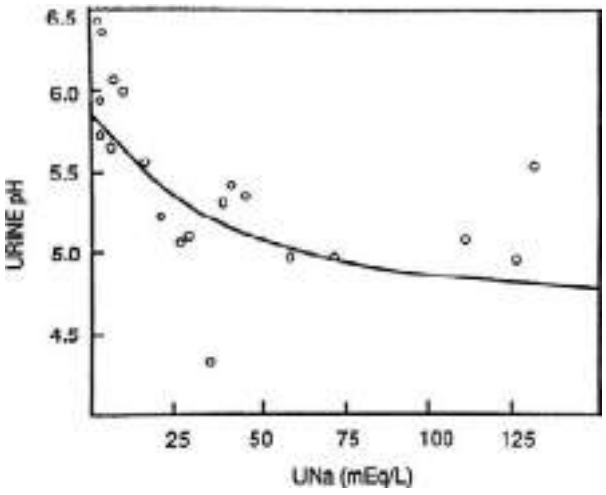

FIGURE 74.8 Urinary pH in relation to urinary sodium concentration in eight patients with diarrhea. Urinary sodium (UNa) was increased by administration of furosemide or sodium chloride. The relation between urinary pH (y-axis) and urinary sodium (x-axis) could be expressed as a curvilinear line, according to the following equation: $y = -0.16 \ln(x) + 5.8$ ($r = 0.75$, $p < .001$). *(From Batlle DC, Hizon M, Cohen E, Gutterman C, Gupta R. The use of the urinary anion gap in the diagnosis of hyperchloremic metabolic acidosis. N Engl J Med 1988;318:594–99. Reprinted with permission of Massachusetts Medical Society, © 1988 Massachusetts Medical Society. All rights reserved.)*

calculating the urine anion gap in patients with a hyperchloremic metabolic acidosis.[15] The principle is similar to that of the plasma anion gap, namely the sum of all anions must equal the sum of all cations. Thus,

$$\{Cl^-\} + \{HCO_3^-\} + \{\text{unmeasured anions}\} = \{Na^+\} + \{K^+\} + \{\text{unmeasured cations}\} \quad (74.22)$$

The unmeasured anions include sulfate, phosphate, and organic anions. Cations not routinely measured include NH_4^+, Ca^{2+}, and Mg^{2+}. NH_4^+ is by far the predominant species in the setting of metabolic acidosis and its excretion can be indirectly estimated through the urinary anion gap (Fig. 74.10).[15] The urine anion gap is calculated from the urine electrolytes by the formula:

$$\text{Urine anion gap} = \{Na^+\} + \{K^+\} - \{Cl^-\} \quad \text{if urine pH is} < 6.5 \text{ or} \quad (74.23)$$

$$\text{Urine anion gap} = \{Na^+\} + \{K^+\} - (\{Cl^-\} + \{HCO_3^-\}) \quad \text{if urine pH is} > 6.5 \quad (74.24)$$

Thus, the urine anion gap provides information regarding the renal response to systemic acidosis.[15,180,181] The urine anion gap will be low (usually a negative value) if there is a decrease in unmeasured anions or an increase in unmeasured cations (e.g., NH_4^+). The urine anion gap will be increased (usually a positive value) if there is an increase in unmeasured anions or a decrease in unmeasured cations (e.g., NH_4^+). Because the concentrations of unmeasured anions in the urine do not change considerably and because NH_4^+ is the major unmeasured cation in the presence of metabolic acidosis, the urine anion gap in this setting provides a rough estimate of urine NH_4^+. It should be noted that the utility of the urine anion gap is limited to the evaluation of metabolic acidosis.[15] In the absence of metabolic acidosis the main determinants of the urine anion gap is the composition of the ingested electrolytes. The urine anion gap can be decreased in diarrhea associated metabolic acidosis, whereas it is typically increased in all syndromes associated with renal tubular acidosis.[15]

Patients with a distal acidification defect (e.g., distal RTA) typically have a positive urine anion gap because of low NH_4^+ excretion, whereas in diarrheal states associated with metabolic acidosis, the urine anion gap is negative, reflecting the fact that NH_4^+ excretion is appropriately increased.[15] Information regarding NH_4^+ excretion from subjects with proximal RTA is limited. The excretion rates of NH_4^+ may not be reduced as compared to those of control subjects.[182–184] For instance, in a study by Brenes et al., the response to a 3-day acid loading test with NH_4Cl was evaluated in eight patients with isolated proximal RTA and in 10 healthy control subjects.[185] In the basal state, all subjects with proximal RTA had rates of NH_4^+ excretion similar to those of the control subjects, suggesting a normal pattern of ammonium renal handling. On the third day of acid loading, however, their NH_4^+ excretion rates were significantly lower than those of controls, demonstrating impairment in maximal urinary NH_4^+ excretion.[185,186] Given this latter finding, it is likely that the urinary anion gap in proximal RTA may not be as negative as in normal people with metabolic acidosis. Although reduced, however, the amount of urinary ammonium may still be sufficient to result in a negative urine anion gap (Table 74.11). Since these previous studies did not provide information on urinary anion gap in proximal RTA, additional data on this parameter are needed from such patients. In distal RTA, the urine anion gap is consistently positive without exception.[15]

Another clinical setting in which the urinary anion gap is useful is with chronic respiratory alkalosis. As with hyperchloremic metabolic acidosis, chronic respiratory alkalosis presents with hyperchloremia and hypobicarbonatemia.[131] Because of these latter findings, a diagnosis of chronic metabolic acidosis is often mistakenly made particularly when blood pH and blood pCO_2 are not available. In reality, many of

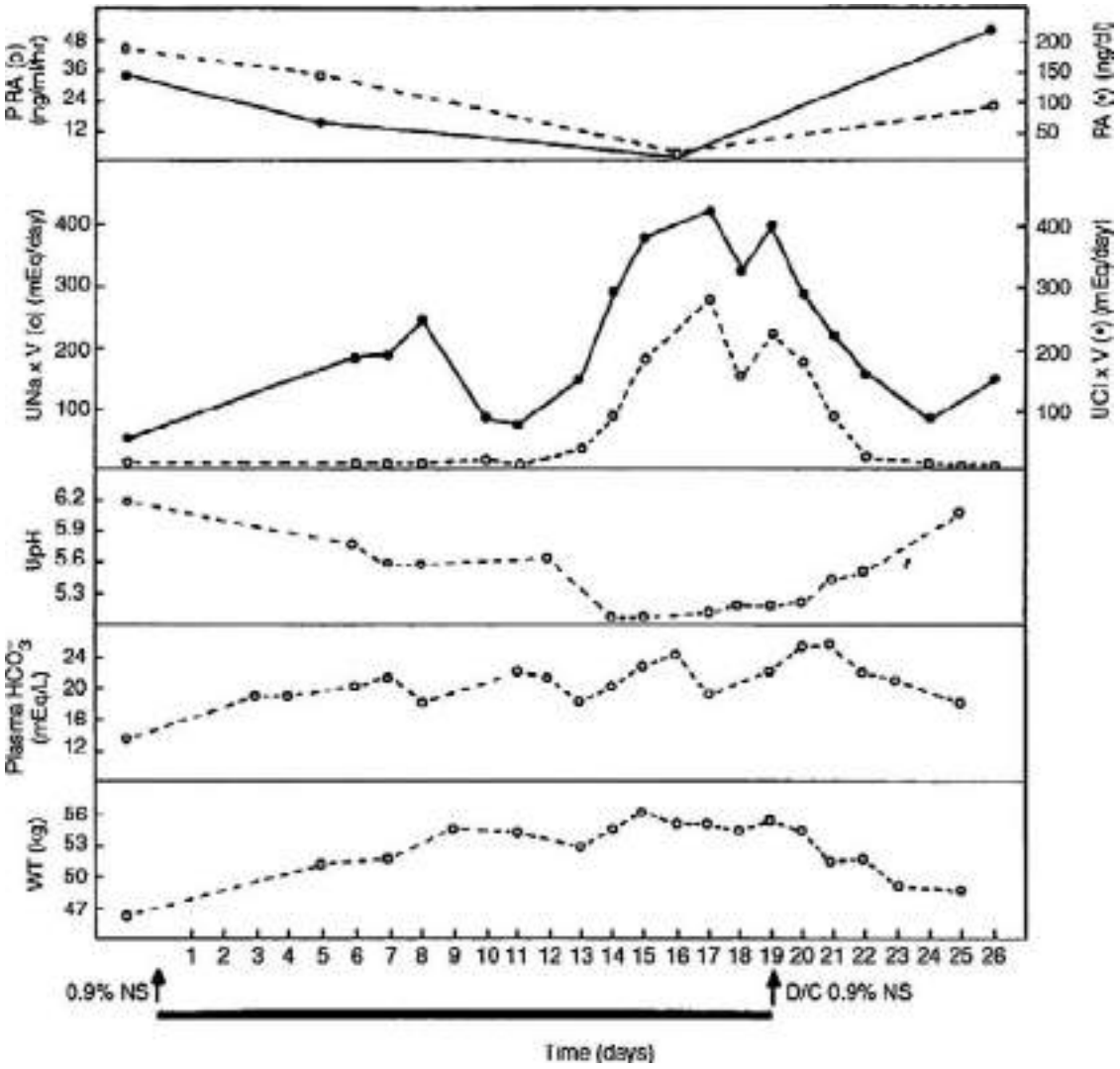

FIGURE 74.9 Effect of daily intravenous saline infusion (0.9% NaCl) on plasma renin activity (PRA), sodium and chloride excretion, urine pH, plasma bicarbonate, and total body weight in a patient who continued to abuse laxatives throughout the observation period. Note the reversible improvement in plasma bicarbonate and the fall in urine pH that occurred during saline administration. *(From Batlle D, von Riotte A, Schlueter W. Urinary sodium in the evaluation of hyperchloremic metabolic acidosis. N Engl J Med 1987;316:140–4. Reprinted with permission of Massachusetts Medical Society, © 1987 Massachusetts Medical Society. All rights reserved.)*

these patients have a chronic respiratory alkalosis but this is not appreciated unless a blood gas is done. The urine anion gap helps to distinguish between a chronic respiratory alkalosis and a chronic metabolic acidosis. A positive urine anion gap in the presence of hyperchloremia and hypobicarbonatemia should suggest a chronic respiratory alkalosis or a renal tubular acidosis (Table 74.10). Because renal tubular acidosis is relatively rare and chronic respiratory alkalosis is frequent in hospitalized patients, we think the urine anion gap is extremely helpful to separate metabolic acidosis from respiratory alkalosis. In chronic respiratory alkalosis, the urine anion gap is positive owing to suppressed ammonium excretion, which serves as an adaptive response to chronic alkalemia. Conversely, the urine anion gap is expected to be decreased (negative) in situations of chronic respiratory acidosis where the formation and excretion of ammonium is increased. Other causes where urine anion gap is increased or decreased are listed in Table 74.11. The acidosis associated with chronic renal failure (or advanced CKD) is largely due to the decrease in ammonium excretion. Normally, an acid load results in a several-fold increase in ammonia excretion with a more modest increase in titratable acid excretion. By contrast, in advanced CKD, despite the prevailing systemic acidosis, there is a failure to increase ammonia

excretion to the levels found in normal subjects with acidosis.[187] Even when factored for GFR, ammonium excretion in patients with advanced CKD fails to increase appropriately.[186,187] Accordingly, the urine anion gap is expected to be increased (positive) with advanced CKD despite the presence of metabolic acidosis (see Table 74.11).

Although, in a qualitative sense, the urinary anion gap roughly reflects urinary ammonium excretion in the setting of hyperchloremic metabolic acidosis, it is not a precise diagnostic index and does have limitations.[15] The urine anion gap is influenced by changes in other unmeasured cations (e.g., calcium and possibly magnesium, the excretion of which are increased during acidosis) or unmeasured anions, or both. For example, the urine anion gap may be decreased (i.e., negative) if the urine contained large amounts of unusual cations such as lithium. Conversely, the gap may be increased (i.e., positive) if the urine contained certain anionic antibiotics such as carbenicillin. In ketoacidosis, the gap is likely to be increased due to the presence of large amounts of ketone anions, despite a high excretion of ammonium.[15,188] In this setting, the urine anion gap would greatly underestimate ammonium excretion. Type of diet and circadian influences can also affect anion excretion and thus influence the urine anion gap.[189] Despite these limitations, the urine anion gap is a useful bedside index of ammonium excretion in a patient with hyperchloremic metabolic acidosis as it helps distinguish metabolic acidosis due to reduced ammonium excretion (i.e., distal RTA) from the acidosis that is due to gastrointestinal bicarbonate losses.

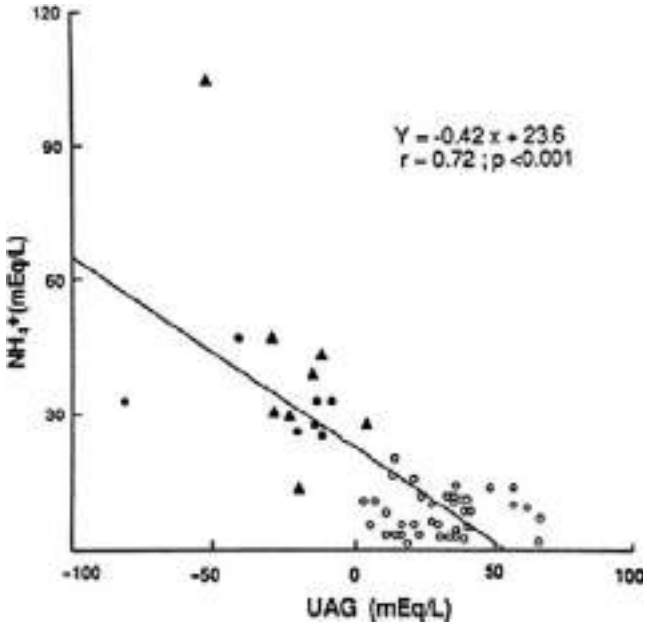

FIGURE 74.10 Urinary ammonium (NH4+) in relation to the urinary anion gap (UAG). Thirty-eight patients with altered distal urinary acidification are represented by open circles; seven normal subjects receiving ammonium chloride, closed circles; and eight patients with hyperchloremic metabolic acidosis associated with diarrhea, triangles. *(From Batlle DC, Hizon M, Cohen E, Gutterman C, Gupta R. The use of the urinary anion gap in the diagnosis of hyperchloremic metabolic acidosis. N Engl J Med 1988;318:594–9. Reprinted with permission of Massachusetts Medical Society, © 1988 Massachusetts Medical Society. All rights reserved.)*

Urine Osmolar Gap

The urine osmolar gap is another method that can be used to indirectly estimate NH_4^+ excretion.[3] The rationale here is that urinary cations (mainly sodium, potassium, and NH_4^+) must be accompanied by an

TABLE 74.11 Conditions where Urinary Anion Gap is Predictably Altered:

1- Increased (Positive) Urine Anion Gap (0 - +50 mEq/l):
• Distal renal tubular acidosis (all types). • Advanced CKD (GFR <20 ml/min). • Chronic respiratory alkalosis. • Vomiting.
2- Decreased (Negative) Urine Anion Gap (0 - − 50 mEq/l):
• Chronic metabolic acidosis from diarrhea. • Proximal renal tubular acidosis. • Chronic respiratory acidosis. • Recovery phase from chronic respiratory alkalosis. • Recovery phase from diabetic Ketoacidosis.

TABLE 74.10 Urine Anion Gap in Various Conditions

	Plasma HCO_3^-	Plasma Chloride	Ammonium	Urine Anion Gap
Metabolic acidosis (diarrhea)	Low	High	High	Negative (0 to −50)
Chronic respiratory alkalosis	Low	High	Low	Positive (0 to +50)
Metabolic acidosis (distal RTA)	Low	High	Low	Positive (0 to +50)
Metabolic acidosis (proximal RTA)	Low	High	Normal or reduced	Unknown*

**Data are limited with respect to use of urine anion gap in proximal RTA. It is possible that the urine anion gap is negative in this setting, reflecting a relatively high rate of ammonium excretion.*
RTA, renal tubular acidosis.

equal number of anions and that the major contributors to urine osmolality are glucose and urea.[3] If all urine components are expressed in mmol/L, the calculated urine osmolality (excluding the portion contributed by NH_4^+ and its anions), is as follows:

$$\text{Calculated urine osmolality} = 2 \times (\text{sodium} + \text{potassium}) + \text{urea} + \text{glucose}$$

The urine osmolar gap is the difference between the calculated and measured urine osmolalities and is assumed to consist of NH_4^+ and its anions. Therefore, urine NH_4^+ concentration is assumed to be equal to half of the urine osmolar gap. One limitation to this estimate is seen with the wide range in the concentration of divalent urine anions, especially sulfate, and of unmeasured urine cations other than NH_4^+ which can be present in variable amounts (e.g., lithium, magnesium, or calcium).[164] Moreover, information on urea and glucose concentrations in urine is usually not available in the usual clinical setting. Thus, it is much easier to use the urine anion gap than the urine osmolar gap to estimate urine NH_4^+.

Minimal Urine pH and Maximal Acid Excretion During Metabolic Acidosis

In addition to measuring urine electrolytes and calculating the urine anion gap, urine pH should be measured to assess the ability of the collecting duct to acidify the urine.[180] Urine pH can be measured during spontaneous metabolic acidosis or after administration of an acidifying salt. It can also be measured following the infusion of sodium sulfate or after giving furosemide. In the presence of systemic acidosis, urine pH should be below 5.5; this would be consistent with appropriate urinary acidification and, thus, exclude distal RTA. The finding of a urinary pH above 5.5 in the setting of systemic acidosis is usually diagnostic of distal RTA, as long as distal Na^+ delivery is adequate. It is important to keep in mind, however, that some patients with RTA have urine pH values below 5.5 during acidosis and still have impaired distal acidification. Many of these patients have hyperkalemia and/or aldosterone deficiency and some have defects in NH_4^+ excretion.[18,138]

Urine pH should be measured in a freshly voided sample in the morning and ideally collected under mineral oil. The presence of mineral oil, however, is not critical, which is contrary to what is traditionally recommended. To rule out a distal acidification defect, inducing only a mild degree of metabolic acidosis is sufficient (i.e., plasma HCO_3^- between 20 and 22 mEq/L). Because the body's homeostatic mechanisms are so efficient, serum HCO_3^- and blood pH can be maintained within the normal range despite ongoing acid challenges such as excessive meat ingestion.[159,190] Unfortunately, there is little information about urinary acidification under these conditions, but it is reasonable to assume that it is appropriately stimulated in terms of enhanced acid excretion. Chronic metabolic acidosis results in decreased citrate excretion.[191,192] A low level of citrate excretion may be a clue to the presence of subclinical or eubicarbonatemic metabolic acidosis.

In normal subjects urine pH is approximately 6.0 for the majority of measurements performed during a 24-hour period.[193] This implies that the urine contains little HCO_3^- and would seem to contradict the view that the kidney maintains acid–base balance in the face of an alkali load by markedly increasing the excretion of HCO_3^-. The traditional formula for net acid excretion is as follows:

$$\text{Net acid excretion} = U_{NH_4^+} + U_{\text{Titratedacid}} - U_{HCO_3^-}(194) \quad (74.26)$$

If bicarbonaturia were the main route for elimination of an alkali load, the expected higher urine pH would, in turn, increase the risk for calcium phosphate stones. Rather than increasing bicarbonaturia, dietary alkali is converted initially to HCO_3^- in the liver and is then titrated through the production of organic acids. Excreting the daily dietary alkali load in the form of organic anions, including citrate, that can be metabolized to HCO_3^- helps to maintain urine pH close to 6.0. In describing the kidney's role in acid–base balance, it is therefore necessary to include the portion of daily dietary alkali load that is excreted in the form of organic anions that can be metabolized to HCO_3^- in the formula for net acid excretion as potential HCO_3^-.[195] A formula for net acid excretion that would take this into account is as follows:

$$\text{Revised net acid excretion} = U_{NH_4^+} + U_{\text{Titratedacid}} - U_{HCO_3^-} - U_{\text{Potential}HCO_3^-}$$

Ammonium Chloride Loading Test

If systemic acidosis is not present, the acidifying agent ammonium chloride can be given orally in a dose of 0.1 g/kg of body weight daily for three to five days or as a single dose of the same cumulative amount.[180] Urine is then collected hourly from two to eight hours. In our experience, the three-day test gives more reliable results and is preferable as it allows time for a maximal increase in NH_4^+ excretion. In healthy subjects, urine pH falls below 5.5 (usually below 5.0) by the first day and continues to remain low.[185] By the third day, ammonium excretion increases at least three- to five-fold. An alternative acidifying agent is calcium chloride (2 mEq/kg of body weight orally), which

TABLE 74.12 Laboratory Workup for Patients Suspected of Having Distal RTA

Tests	Comments
Urine pH	Freshly voided urine collected in mineral oil
	Knowledge of acid–base status needed
	Knowledge of urine $\{Na^+\}$ needed because urine pH does not fall maximally when urine $\{Na^+\}$ <20 mEq/L
	If urine pH <6.3, urine contains little HCO_3^- and proximal RTA unlikely
	If urine pH <5.5, the classic forms of distal RTA can be excluded but not other types such as type IV RTA and some rate-dependent defects
Urine Na^+, K^+, Cl^-	Calculate urine anion gap.[a] Negative value suggests that NH_4^+ excretion is not reduced and tends to rule out distal RTA[b]
Net acid excretion[b]	Calculated as (NH_4^+ excretion + titratable acidity) − HCO_3^- excretion
Other provocative tests[c]	Urine pCO_2 after bicarbonate loading
	Urine pH and acid excretion after furosemide or Na_2SO_4 administration
	Urine pH and urine K^+ excretion after amiloride

Source: Moorthi K, Batlle D. Renal tubular acidosis. In: Gennari FJ, Adrogue HJ, Galla JH, Madias NE (eds). Acid–Base Disorders and Their Treatment. Boca Raton: Taylor & Francis Group; 2005:417–67.
[a]*Urine ($\{Na^+\} + \{K^+\} - \{Cl^-\}$).*
[b]*Blood pH should be #7.35. If metabolic acidosis is not present, give NH_4Cl (0.1 g/kg) for 2 to 3 days.*
[c]*These tests usually are not needed if the diagnosis is clear from history and above tests.*
RTA, renal tubular acidosis.

gives results similar to ammonium chloride. It can be used in patients who cannot tolerate ammonium chloride due to nausea and vomiting or in patients with liver disease in whom ammonium chloride is contraindicated.[18,196] A suggested laboratory workup of a patient suspected of having distal RTA is summarized in Table 74.12.[180]

Provocative Tests of Distal Acidification

These tests involve the use of sodium sulfate or a loop diuretic to assess Na^+-dependent acidification and can provide additional useful mechanistic information.[137,197,198] By increasing distal sodium delivery, these agents enhance the negative transepithelial potential in the collecting duct and thus stimulate both H^+ and K^+ secretion. A reduction in urine pH accompanied by an increase in potassium excretion following the administration of sodium sulfate indicates a normal response to this enhanced electronegative potential[139,180,197] Fig. 74.11).

Normal subjects can lower urine pH maximally, in the absence of systemic acidosis, provided that distal sodium delivery is increased acutely and while collecting tubule sodium reabsorption is stimulated.[197,199–201] The latter requirement can be achieved by either administration of mineralocorticoid or by placing the subject on a low-sodium diet (i.e., 20 mEq daily) for three days, which stimulates aldosterone release. Aldosterone, in turn, enhances distal sodium reabsorption. The sodium sulfate infusion test can therefore be performed following the administration of fludrocortisone (1 mg orally over the 12 hours preceding the sodium sulfate infusion) or after a low salt diet.[197,202]

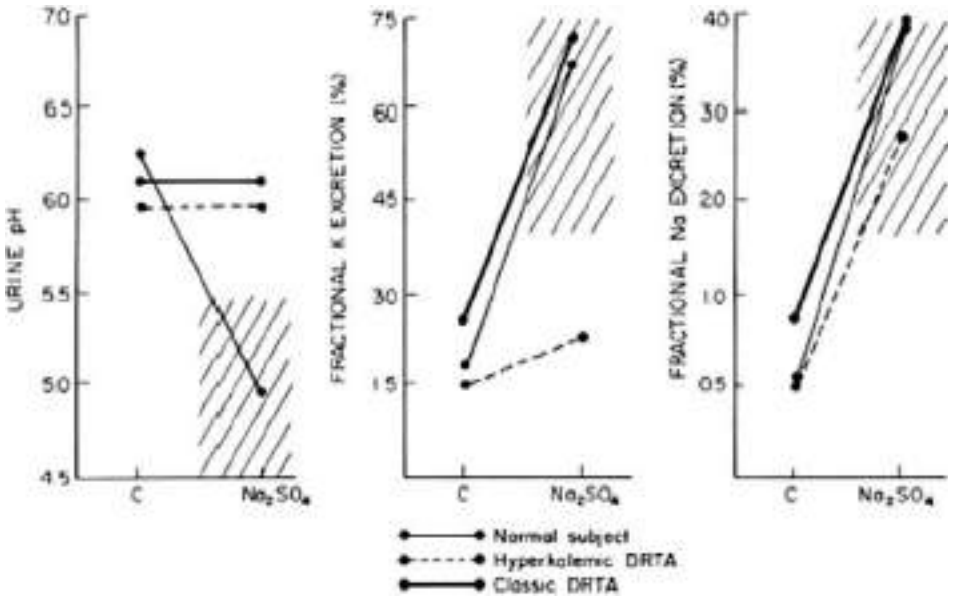

FIGURE 74.11 Response to Na2SO4 in a normal subject, a patient with classic DRTA and a patient with hyperkalemic DRTA. Observe that Na2SO4 fails to lower urine pH and to increase FEK in the patient with hyperkalemic DRTA. In contrast, the patient with classic DRTA increases FEK but cannot lower urine pH normally indicating the presence of an isolated defect for H+ secretion. *(From Batlle, DC. Hyperkalemic hyperchloremic metabolic acidosis associated with selective aldosterone deficiency and distal renal tubular acidosis. Semin Nephrol 1981;1:260–74, with permission.)*

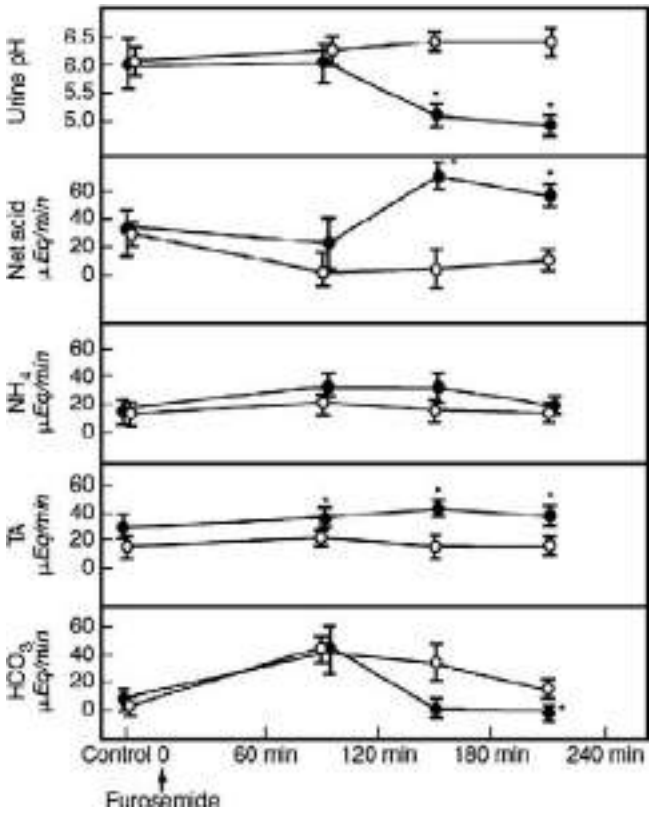

FIGURE 74.12 The effect of furosemide (•) and furosemide + amiloride (o) on urinary acidification in normal subjects. Please note that the lowering effect of furosemide is prevented when amiloride is given concurrently indicating that the effect takes place in the cortical collecting tubule. The asterisk denotes a significant difference between the two experimental conditions. *(From Batlle, DC. Segmental characterization of defects in collecting tubule acidification. Kidney Int 1986; 30:546–54, with permission.)*

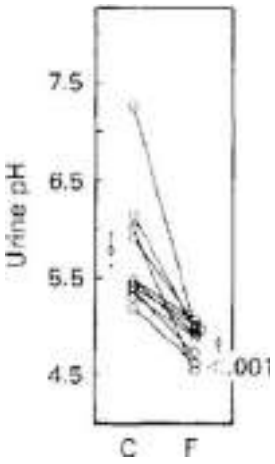

FIGURE 74.13 The effect of Furosemide (F) on urine pH, titratable acid (TA), ammoniurn (NH4), and net acid excretion in ten normal subjects. The data shown in this figure were obtained when urine pH after furosemide was the lowest. C denotes data obtained immediately before furosemide administration. *(From Batlle, DC. Segmental characterization of defects in collecting tubule acidification. Kidney Int 1986; 30:546–54, with permission.)*

When properly performed, the sodium sulfate test results in a fall in urine pH to below 5.5 (usually below 5.0), whether or not systemic acidosis exists. Some subjects may exhibit a late response, so urine collections should continue for two to three hours after the infusion is discontinued. Patients with chronic renal insufficiency also respond normally to sodium sulfate.[202] The increase in acid excretion following sodium sulfate infusion is mainly in the form of NH_4^+. The kaliuretic response that is seen with sodium sulfate administration is also useful in assessing distal potassium secretory capacity (Figure 74.11). Patients with hyperkalemic distal RTA do not increase potassium excretion normally whereas patients with classic distal RTA increase it markedly[137,139,197,199] (Fig. 74.11).

Loop diuretics increase sodium delivery to the collecting duct by blocking NaCl reabsorption in the loop of Henle. Part of the delivered sodium to the distal nephron is reabsorbed in the cortical collecting tubule, which then creates a favorable transepithelial voltage gradient for H^+ and K^+ secretion.[197–199] This interpretation is supported by the finding that the fall in urine pH and the increase in potassium excretion caused by furosemide are obliterated by amiloride (Fig. 74.12).[197,198] Amiloride also mitigates the kaliuretic effect of furosemide. The difference in potassium excretion that is seen, at comparable urine flow rates, when furosemide is given alone and when combined with amiloride demonstrates the significant contribution of the amiloride-sensitive (i.e., Na^+-dependent) component of distal K^+ secretion.[197,198]

The furosemide test is performed by first collecting a urine sample and then giving 40 to 80 mg of furosemide orally.[197] Measurements of urine pH two to four hours following furosemide should give a urine pH below 5.5.[197,198] The test was performed initially without the administration of mineralocorticoid or prior salt restriction to enhance sodium avidity.[197] All subjects responded consistently by lowering urine pH below 5.5 without any prior intervention to enhance avidity for distal sodium reabsorption (Fig. 74.13). More recent studies have used the furosemide test following the administration of mineralocorticoid.[203] While this ensures that distal sodium reabsorption is stimulated we think the furosemide test is reliable even without preexisting minderalocorticoid administration.[197,198] Furosemide when given intravenously[204] or bumetanide administration orally[198] have also been shown to lower urine pH consistently.

The amiloride test is performed by giving 20 mg of amiloride orally following a baseline urine collection

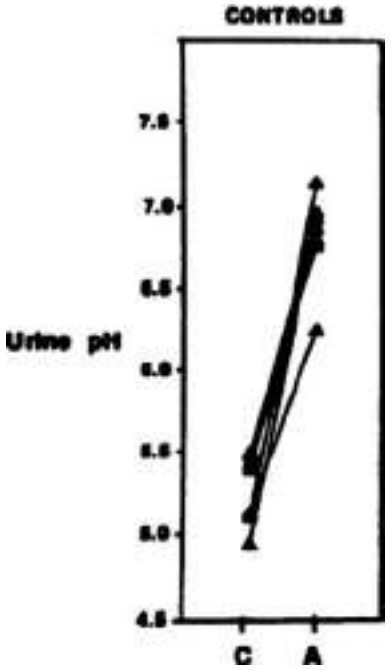

FIGURE 74.14 Effect of amiloride on urine pH in Controls. *(From Schlueter W, Keilani T, Hizon M, Kaplan B, Batlle DC. On the mechanism of impaired distal acidification in hyperkalemic renal tubular acidosis: evaluation with amiloride and bumetanide. J Am Soc Nephrol. 1992 Oct;3 (4):953–64.)*

with hourly urine collections for measurement of pH and electrolyte excretion.[198] Amiloride at low doses blocks apical sodium channels in the cortical collecting duct.[198] Administration of amiloride predictably results in an increase in urine pH and a decrease in urine potassium excretion in normal individuals (Figure 74.14).[198] In patients with a complete voltage-dependent defect, amiloride should not result in a normal increase in urine pH or a further decrease in potassium excretion. A normal response to amiloride (i.e., an increase in urine pH and a decrease in potassium secretion) implies that voltage-dependent H^+ and K^+ secretion is essentially intact.[198] By exclusion then a defect other than a voltage-dependant defect is more likely. It should be noted that for practical purposes, however, the amiloride test is not needed since the presence of hyperkalaemia , in the absence of aldosterone deficiency, suggest a voltage-dependant type of distal RTA.[137]

Another tool to evaluate distal H^+ ion secretion is the assessment of urine PCO_2 in a highly alkaline urine.[205–210] Sodium bicarbonate is given usually intravenously to increase urine bicarbonate concentration to a very high values (urine pH approximately 7.8).[209] This results in a rise in urine PCO_2 to values considerably higher than that prevailing in the blood as a result, at least in part, of H^+ ion secretion in the collecting tubule.[206–210] Normal subjects achieve values of urine PCO_2 higher than 80 mmHg whereas patients with defects in distal acidification fail to increase urine PCO_2 which usually is less than 60 mm of Hg.[209] This test, although cumbersome to execute, is a sensitive test of maximal capacity for collecting tubule H^+ ion secretion. A subnormal rise in urine PCO_2, for example, occurs in patients with incomplete distal RTA.[209]

References

[1] Bekheirnia MR, Schrier RW. Pathophysiology of water and sodium retention: edematous states with normal kidney function. Curr Opin Pharmacol 2006;6(2):202–7.
[2] Schlanger LE, Bailey JL, Sands JM. Electrolytes in the aging. Adv Chronic Kidney Dis 2010;17(4):308–19.
[3] Halperin ML, Kamel KS. Use of the composition of the urine at the bedside: emphasis on physiologic principles to provide insights into diagnostic and therapeutic issues. In: Seldin DW, Giebisch G, editors. The kidney: physiology and pathophysiology. Philadelphia: Lippincott Williams & Wilkins; 2000. p. 2297–327.
[4] Walser M. Phenomenological analysis of electrolyte homeostasis. In: Seldin DW, Giebisch G, editors. The kidney: physiology and pathophysiology. New York: Raven Press; 1992. p. 31–44.
[5] Seldin DW. Sodium balance and fluid volume in normal and edematous states. In: Seldin DW, Giebisch G, editors. The regulation of sodium and chloride balance. New York: Raven Press; 1990. p. 261–92.
[6] Toto R, Seldin DW. Salt wastage. In: Seldin DW, Giebisch G, editors. The kidney: physiology and pathophysiology. New York: Raven Press; 1992. p. 2143–63.
[7] Abraham WT, Schrier RW. Body fluid volume regulation in health and disease. Adv Intern Med 1994;39:23–47.
[8] Epstein FH, Ferguson TB. The effect of the formation of an arteriovenous fistula upon blood volume. J Clin Invest 1955;34 (3):434–8.
[9] Epstein FH, Kleeman CR, Hendrikx A. The influence of bodily hydration on the renal concentrating process. J Clin Invest 1957;36(5):629–34.
[10] Sheridan AM. The clinical application of recent advances in salt and water physiology. Nephrol Rounds 1997;3(4).
[11] Calles-Escandon J, Cunningham JJ, Snyder P, Jacob R, Huszar G, Loke J, et al. Influence of exercise on urea, creatinine, and 3-methylhistidine excretion in normal human subjects. Am J Physiol 1984;246(4 Pt 1):E334–8.
[12] Epstein FH, Post RS, McDowell M. The effects of an arteriovenous fistula on renal hemodynamics and electrolyte excretion. J Clin Invest 1953;32(3):233–41.
[13] Kamel KS, Ethier JH, Richardson RM, Bear RA, Halperin ML. Urine electrolytes and osmolality: when and how to use them. Am J Nephrol 1990;10(2):89–102.
[14] Aichbichler BW, Zerr CH, Santa Ana CA, Porter JL, Fordtran JS. Proton-pump inhibition of gastric chloride secretion in congenital chloridorrhea. N Engl J Med 1997;336(2):106–9.
[15] Batlle DC, Hizon M, Cohen E, Gutterman C, Gupta R. The use of the urinary anion gap in the diagnosis of hyperchloremic metabolic acidosis. N Engl J Med 1988;318(10):594–9.
[16] Miller TR, Anderson RJ, Linas SL, Henrich WL, Berns AS, Gabow PA, et al. Urinary diagnostic indices in acute renal failure: a prospective study. Ann Intern Med 1978;89(1):47–50.

[17] Zarich S, Fang LS, Diamond JR. Fractional excretion of sodium. Exceptions to its diagnostic value. Arch Intern Med 1985;145 (1):108–12.
[18] Batlle D. Hyperchloremic metabolic acidosis. In: Seldin D, Giebisch G, editors. The regulation of acid–base balance. New York: Raven Press; 1989. p. 319–51.
[19] Ariceta G, Rodriguez-Soriano J. Inherited renal tubulopathies associated with metabolic alkalosis: effects on blood pressure. Semin Nephrol 2006;26(6):422–33.
[20] Kawasaki T, Itoh K, Uezono K, Sasaki H. A simple method for estimating 24 h urinary sodium and potassium excretion from second morning voiding urine specimen in adults. Clin Exp Pharmacol Physiol 1993;20(1):7–14.
[21] O'Donnell MJ, Yusuf S, Mente A, Gao P, Mann JF, Teo K, et al. Urinary sodium and potassium excretion and risk of cardiovascular events. JAMA 2011;306(20):2229–38.
[22] Mann SJ, Gerber LM. Estimation of 24-hour sodium excretion from spot urine samples. J Clin Hypertens (Greenwich) 2010;12 (3):174–80.
[23] Tannen RL. Control of potassium excretion. In: Massry SG, Glassock RJ, editors. Textbook of nephrology. Baltimore: Williams & Wilkins; 1983. p. 3.31–48.
[24] Wright FS. Renal potassium handling. Semin Nephrol 1987;7 (3):174–84.
[25] Schrier RW, Wang W, Poole B, Mitra A. Acute renal failure: definitions, diagnosis, pathogenesis, and therapy. J Clin Invest 2004;114(1):5–14.
[26] Steiner RW. Interpreting the fractional excretion of sodium. Am J Med 1984;77(4):699–702.
[27] Brosius FC, Lau K. Low fractional excretion of sodium in acute renal failure: role of timing of the test and ischemia. Am J Nephrol 1986;6(6):450–7.
[28] Leaf A, Cottran R. Acute Renal Failure. New York: Oxford University Press; 1985. p. 168–90.
[29] Carvallo A, Rakowski TA, Argy Jr WP, Schreiner GE. Acute renal failure following drip infusion pyelography. Am J Med 1978;65(1):38–45.
[30] Fang LS, Sirota RA, Ebert TH, Lichtenstein NS. Low fractional excretion of sodium with contrast media-induced acute renal failure. Arch Intern Med 1980;140(4):531–3.
[31] VanZee BE, Hoy WE, Talley TE, Jaenike JR. Renal injury associated with intravenous pyelography in nondiabetic and diabetic patients. Ann Intern Med 1978;89(1):51–4.
[32] Vaz AJ. Low fractional excretion of urine sodium in acute renal failure due to sepsis. Arch Intern Med 1983;143(4):738–9.
[33] Corwin HL, Schreiber MJ, Fang LS. Low fractional excretion of sodium. Occurrence with hemoglobinuric- and myoglobinuric-induced acute renal failure. Arch Intern Med 1984;144(5):981–2.
[34] Hoffman LM, Suki WN. Obstructive uropathy mimicking volume depletion. JAMA 1976;236(18):2096–7.
[35] Sexton C, Seldin DW. Clinical interpretation of laboratory values. In: Kokko J, Tannen RL, editors. Fluids and electrolytes. Philadelphia: WB Saunders Company; 1986. p. 3–62.
[36] Carvounis CP, Nisar S, Guro-Razuman S. Significance of the fractional excretion of urea in the differential diagnosis of acute renal failure. Kidney Int 2002;62(6):2223–9.
[37] Nanji AJ. Increased fractional excretion of sodium in prerenal azotemia: need for careful interpretation. Clin Chem 1981;27 (7):1314–5.
[38] Brady HR, Brenner BM, Lieberthal W. Acute renal failure. In: Brenner BM, editor. The kidney. Philadelphia: WB Saunders; 1996. p. 1200–52.
[39] Kaplan AA, Kohn OF. Fractional excretion of urea as a guide to renal dysfunction. Am J Nephrol 1992;12(1–2):49–54.
[40] Goldstein MH, Lenz PR, Levitt MF. Effect of urine flow rate on urea reabsorption in man: urea as a "tubular marker". J Appl Physiol 1969;26(5):594–9.
[41] Atherton JC, Green R, Hughes S, McFall V, Sharples JA, Solomon LR, et al. Lithium clearance in man: effects of dietary salt intake, acute changes in extracellular fluid volume, amiloride and frusemide. Clin Sci (Lond) 1987;73(6):645–51.
[42] Steinhauslin F, Burnier M, Magnin JL, Munafo A, Buclin T, Diezi J, et al. Fractional excretion of trace lithium and uric acid in acute renal failure. J Am Soc Nephrol 1994;4(7):1429–37.
[43] Olsen NV, Olsen MH, Fogh-Andersen N, Feldt-Rasmussen B, Kamper A, Plum I, et al. Lithium clearance method and the renal response to low-dose dopamine in man: a randomized, controlled study. Clin Sci (Lond) 1993;84(2):237–42.
[44] Dorhout Mees EJ, Beutler JJ, Boer WH, Koomans HA. Does lithium clearance reflect distal delivery in humans? Analysis with furosemide infusion. Am J Physiol 1990;258(4 Pt 2):F1100–4.
[45] Kosmadakis G, Viskaduraki M, Michail S. The validity of fractional excretion of uric acid in the diagnosis of acute kidney injury due to decreased kidney perfusion. Am J Kidney Dis 2009;54(6):1186–7.
[46] Baer L, Platman SR, Kassir S, Fieve RR. Mechanisms of renal lithium handling and their relationship to mineralocorticoids: a dissociation between sodium and lithium ions. J Psychiatr Res 1971;8(2):91–105.
[47] Eknoyan G, Suki WN, Rector Jr FC, Seldin DW. Functional characteristics of the diluting segment of the dog nephron and the effect of extracellular volume expansion on its reabsorptive capacity. J Clin Invest 1967;46(7):1178–88.
[48] Hayslett JP, Kashgarian M. A micropuncture study of the renal handling of lithium. Pflugers Arch 1979;380(2):159–63.
[49] Thomsen K, Holstein-Rathlou NH, Leyssac PP. Comparison of three measures of proximal tubular reabsorption: lithium clearance, occlusion time, and micropuncture. Am J Physiol 1981;241 (4):F348–55.
[50] Thomsen K, Schou M. Renal lithium excretion in man. Am J Physiol 1968;215(4):823–7.
[51] Shalmi M, Jonassen T, Thomsen K, Kibble JD, Bie P, Christensen S. Model explaining the relation between distal nephron Li^+ reabsorption and urinary Na^+ excretion in rats. Am J Physiol 1998;274(3 Pt 2):F445–52.
[52] Batlle DC, von Riotte AB, Gaviria M, Grupp M. Amelioration of polyuria by amiloride in patients receiving long-term lithium therapy. N Engl J Med 1985;312(7):408–14.
[53] Daniel B, Edgar L, Naaz P, Santosh H. Lithium-associated kidney effects. Clinical Nephrotoxins. 3rd ed. New York: Springer; 2008. p. 725–48.
[54] Boer WH, Fransen R, Boer P, de Roos R, Koomans HA. Prostaglandin synthesis inhibition stimulates lithium reabsorption in Henle's loop in rats. Kidney Int 1993;43(2):301–6.
[55] Knepper MA, Gamba G. Urine concentration and dilution. In: Brenner BM, editor. The kidney. Philadelphia: WB Saunders; 2004. p. 599–636.
[56] Noda Y, Sohara E, Ohta E, Sasaki S. Aquaporins in kidney pathophysiology. Nat Rev Nephrol 2010;6(3):168–78.
[57] Robben JH, Knoers NV, Deen PM. Cell biological aspects of the vasopressin type-2 receptor and aquaporin 2 water channel in nephrogenic diabetes insipidus. Am J Physiol Renal Physiol 2006;291(2):F257–70.
[58] Kim GH, Ecelbarger CA, Mitchell C, Packer RK, Wade JB, Knepper MA. Vasopressin increases Na-K-2Cl cotransporter expression in thick ascending limb of Henle's loop. Am J Physiol 1999;276(1 Pt 2):F96–103.
[59] Sands JM. Molecular mechanisms of urea transport. J Membr Biol 2003;191(3):149–63.

[60] Brown D, Nielsen S. Cell biology of vasopressin action. In: Brenner BM, editor. The kidney. Philadelphia: WB Saunders Company; 2000. p. 575–94.
[61] Kanno K, Sasaki S, Hirata Y, Ishikawa S, Fushimi K, Nakanishi S, et al. Urinary excretion of aquaporin-2 in patients with diabetes insipidus. N Engl J Med 1995;332(23):1540–5.
[62] Pedersen RS, Bentzen H, Bech JN, Pedersen EB. Effect of water deprivation and hypertonic saline infusion on urinary AQP2 excretion in healthy humans. Am J Physiol Renal Physiol 2001;280(5):F860–7.
[63] Robinson AG. Disorders of antidiuretic hormone secretion. Clin Endocrinol Metab 1985;14(1):55–88.
[64] Gowrishankar M, Lenga I, Cheung RY, Cheema-Dhadli S, Halperin ML. Minimum urine flow rate during water deprivation: importance of the permeability of urea in the inner medulla. Kidney Int 1998;53(1):159–66.
[65] Soroka SD, Chayaraks S, Cheema-Dhadli S, Myers JA, Rubin S, Sonnenberg H, et al. Minimum urine flow rate during water deprivation: importance of the nonurea versus total osmolality in the inner medulla. J Am Soc Nephrol 1997;8 (6):880–6.
[66] Chen S, Jalandhara N, Batlle D. Evaluation and management of hyponatremia: an emerging role for vasopressin receptor antagonists. Nat Clin Pract Nephrol 2007;3(2):82–95.
[67] Burton R, Theodore P. Clinical physiology of acid–base and electrolyte disorders. McGraw-Hill Companies; 2001.
[68] Shoker AS. Application of the clearance concept to hyponatremic and hypernatremic disorders: a phenomenological analysis. Clin Chem 1994;40(7 Pt 1):1220–7.
[69] Schrier RW, Gross P, Gheorghiade M, Berl T, Verbalis JG, Czerwiec FS, et al. Tolvaptan, a selective oral vasopressin V2-receptor antagonist, for hyponatremia. N Engl J Med 2006;355 (20):2099–112.
[70] Verbalis JG. Whole-body volume regulation and escape from antidiuresis. Am J Med 2006;119(7 Suppl 1):S21–9.
[71] Brater DC. Diuretic therapy. N Engl J Med 1998;339(6):387–95.
[72] Cesar KR, Magaldi AJ. Thiazide induces water absorption in the inner medullary collecting duct of normal and Brattleboro rats. Am J Physiol 1999;277(5 Pt 2):F756–60.
[73] Friedman E, Shadel M, Halkin H, Farfel Z. Thiazide-induced hyponatremia. Reproducibility by single dose rechallenge and an analysis of pathogenesis. Ann Intern Med 1989;110(1):24–30.
[74] Abraham WT, Cadnapaphornchai MA, Schrier RW. Cardiac failure, liver diseases, and the nephrotic syndrome. In: Schrier RW, editor. Diseases of the kidney and urinary tract. Philadelphia: Lippincott Williams & Wilkins; 2001. p. 2465–509.
[75] Pedersen RS, Bentzen H, Bech JN, Nyvad O, Pedersen EB. Urinary aquaporin-2 in healthy humans and patients with liver cirrhosis and chronic heart failure during baseline conditions and after acute water load. Kidney Int 2003;63(4): 1417–25.
[76] Verbalis JG. The syndrome of inappropriate antidiuretic hormone secretion and other hypoosmolar disorders. In: Schrier RW, editor. Diseases of the kidney and urinary tract. Philadelphia: Lippincott Williams & Wilkins; 2001. p. 2511–47.
[77] Bouley R, Breton S, Sun T, McLaughlin M, Nsumu NN, Lin HY, et al. Nitric oxide and atrial natriuretic factor stimulate cGMP-dependent membrane insertion of aquaporin 2 in renal epithelial cells. J Clin Invest 2000;106(9):1115–26.
[78] Chou CL, DiGiovanni SR, Luther A, Lolait SJ, Knepper MA. Oxytocin as an antidiuretic hormone. II. Role of V2 vasopressin receptor. Am J Physiol 1995;269(1 Pt 2):F78–85.
[79] Weinand ME, O'Boynick PL, Goetz KL. A study of serum antidiuretic hormone and atrial natriuretic peptide levels in a series of patients with intracranial disease and hyponatremia. Neurosurgery 1989;25(5):781–5.
[80] Palmer BF. Hyponatremia in patients with central nervous system disease: SIADH versus CSW. Trends Endocrinol Metab 2003;14(4):182–7.
[81] McGirt MJ, Blessing R, Nimjee SM, Friedman AH, Alexander MJ, Laskowitz DT, et al. Correlation of serum brain natriuretic peptide with hyponatremia and delayed ischemic neurological deficits after subarachnoid hemorrhage. Neurosurgery 2004;54 (6):1369–73 [discussion 73–4].
[82] Furst H, Hallows KR, Post J, Chen S, Kotzker W, Goldfarb S, et al. The urine/plasma electrolyte ratio: a predictive guide to water restriction. Am J Med Sci 2000;319(4):240–4.
[83] Zerbe RL, Robertson GL. A comparison of plasma vasopressin measurements with a standard indirect test in the differential diagnosis of polyuria. N Engl J Med 1981;305(26):1539–46.
[84] Alexander CS, Filbin DM, Fruchtman SA. Failure of vasopressin to produce normal urine concentration in patients with diabetes insipidus. J Lab Clin Med 1959;54:566–71.
[85] Bishop MC. Diuresis and renal functional recovery in chronic retention. Br J Urol 1985;57(1):1–5.
[86] Gault MH, Dixon ME, Doyle M, Cohen WM. Hypernatremia azotemia, and dehydration ue to high-protein tube feeding. Ann Intern Med 1968;68(4):778–91.
[87] Howards SS. Post-obstructive diuresis: a misunderstood phenomenon. J Urol 1973;110(5):537–40.
[88] Bankir L. Antidiuretic action of vasopressin: quantitative aspects and interaction between V1a and V2 receptor-mediated effects. Cardiovasc Res 2001;51(3):372–90.
[89] Milles JJ, Spruce B, Baylis PH. A comparison of diagnostic methods to differentiate diabetes insipidus from primary polyuria: a review of 21 patients. Acta Endocrinol (Copenh) 1983;104 (4):410–6.
[90] Sands JM, Bichet DG. Nephrogenic diabetes insipidus. Ann Intern Med 2006;144(3):186–94.
[91] De Wardener HE, Herxheimer A. The effect of a high water intake on the kidney's ability to concentrate the urine in man. J Physiol 1957;139(1):42–52.
[92] Rose BD, Post TW. Regulation of plasma osmolality. In: Rose BD, Post TW, editors. Clinical physiology of acid– base and electrolyte disorders. New York: McGraw-Hill; 2001. p. 285–98.
[93] Miller M, Dalakos T, Moses AM, Fellerman H, Streeten DH. Recognition of partial defects in antidiuretic hormone secretion. Ann Intern Med 1970;73(5):721–9.
[94] Moses AM, Clayton B. Impairment of osmotically stimulated AVP release in patients with primary polydipsia. Am J Physiol 1993;265(6 Pt 2):R1247–52.
[95] Harrington AR, Valtin H. Impaired urinary concentration after vasopressin and its gradual correction in hypothalamic diabetes insipidus. J Clin Invest 1968;47(3):502–10.
[96] Terris J, Ecelbarger CA, Nielsen S, Knepper MA. Long-term regulation of four renal aquaporins in rats. Am J Physiol 1996;271(2 Pt 2):F414–22.
[97] Yamamoto T, Sasaki S, Fushimi K, Ishibashi K, Yaoita E, Kawasaki K, et al. Vasopressin increases AQP-CD water channel in apical membrane of collecting duct cells in Brattleboro rats. Am J Physiol 1995;268(6 Pt 1):C1546–51.
[98] Goldman MB, Luchins DJ, Robertson GL. Mechanisms of altered water metabolism in psychotic patients with polydipsia and hyponatremia. N Engl J Med 1988;318(7):397–403.
[99] Barbey F, Bonny O, Rothuizen L, Gomez F, Burnier M. A pregnant woman with de novo polyuria-polydipsia and elevated liver enzymes. Nephrol Dial Transplant 2003;18(10):2193–6.

[100] Lindheimer MD, Barron WM, Davison JM. Osmoregulation of thirst and vasopressin release in pregnancy. Am J Physiol 1989;257(2 Pt 2):F159–69.
[101] Lindheimer MD, Barron WM, Davison JM. Osmotic and volume control of vasopressin release in pregnancy. Am J Kidney Dis 1991;17(2):105–11.
[102] Nora NA, Hedger R, Batlle DC. Severe acute peripartum hypernatremia. Am J Kidney Dis 1992;19(4):385–8.
[103] Sherer DM, Cutler J, Santoso P, Angus S, Abulafia O. Severe hypernatremia after cesarean delivery secondary to transient diabetes insipidus of pregnancy. Obstet Gynecol 2003;102(5 Pt 2):1166–8.
[104] Bichet DG, Fujiwara TM. The metabolic and molecular bases of inherited disease. In: Scriver CR, Beaudet AL, Sly WS, editors. Nephrogenic diabetes insipidus. New York: McGraw-Hill Companies; 2001. p. 4181–204.
[105] Giebisch G, Wang W. Potassium transport: from clearance to channels and pumps. Kidney Int 1996;49(6):1624–31.
[106] Greger R, Gogelein H. Role of K^+ conductive pathways in the nephron. Kidney Int 1987;31(5):1055–64.
[107] Wright FS, Giebisch G. Regulation of potassium excretion. In: Seldin DW, Giebisch G, editors. The kidney: physiology and pathophysiology. New York: Raven Press; 1992. p. 2209–47.
[108] Sebastian A, Schambelan M. Renal hyperkalemia. Semin Nephrol 1987;7(3):223–38.
[109] Sebastian A, Frassetto LA, Sellmeyer DE, Morris Jr RC. The evolution-informed optimal dietary potassium intake of human beings greatly exceeds current and recommended intakes. Semin Nephrol 2006;26(6):447–53.
[110] Stetson DL, Wade JB, Giebisch G. Morphologic alterations in the rat medullary collecting duct following potassium depletion. Kidney Int 1980;17(1):45–56.
[111] Garg LC, Narang N. Ouabain-insensitive K-adenosine triphosphatase in distal nephron segments of the rabbit. J Clin Invest 1988;81(4):1204–8.
[112] Kraut JA, Hiura J, Besancon M, Smolka A, Sachs G, Scott D. Effect of hypokalemia on the abundance of HK alpha 1 and HK alpha 2 protein in the rat kidney. Am J Physiol 1997;272(6 Pt 2):F744–50.
[113] Good DW, Velazquez H, Wright FS. Luminal influences on potassium secretion: low sodium concentration. Am J Physiol 1984;246(5 Pt 2):F609–19.
[114] Khuri RN, Strieder WN, Giebisch G. Effects of flow rate and potassium intake on distal tubular potassium transfer. Am J Physiol 1975;228(4):1249–61.
[115] Kunau Jr RT, Webb HL, Borman SC. Characteristics of the relationship between the flow rate of tubular fluid and potassium transport in the distal tubule of the rat. J Clin Invest 1974;54 (6):1488–95.
[116] Velazquez H, Wright FS, Good DW. Luminal influences on potassium secretion: chloride replacement with sulfate. Am J Physiol 1982;242(1):F46–55.
[117] Good DW, Wright FS. Luminal influences on potassium secretion: sodium concentration and fluid flow rate. Am J Physiol 1979;236(2):F192–205.
[118] Good DW, Wright FS. Luminal influences on potassium secretion: transepithelial voltage. Am J Physiol 1980;239(3):F289–98.
[119] Wright FS. Flow-dependent transport processes: filtration, absorption, secretion. Am J Physiol 1982;243(1):F1–11.
[120] Malnic G, Klose RM, Giebisch G, Seldin DW. Micropuncture study of renal potassium excretion in the rat. 1964. J Am Soc Nephrol 2000;11(7):1354–69.
[121] Mujais SK, Katz AI. Potassium deficiency. In: Seldin DW, Giebisch G, editors. The kidney: physiology and pathophysiologyl. New York: Raven Press; 1992. p. 2249–78.
[122] Wald H, Garty H, Palmer LG, Popovtzer MM. Differential regulation of ROMK expression in kidney cortex and medulla by aldosterone and potassium. Am J Physiol 1998;275(2 Pt 2): F239–45.
[123] Chu PY, Quigley R, Babich V, Huang CL. Dietary potassium restriction stimulates endocytosis of ROMK channel in rat cortical collecting duct. Am J Physiol Renal Physiol 2003;285(6): F1179–87.
[124] Cremer EJGK, Nakamoto L, Patel S, Schlueter W, Rosa R, Kelani T, et al. Potassium deprivation in normal human subjects; impact on potassium, sodium, and Acid–base Balance in Normal Human Subjects. American Society of Nephrology 36th Annual Meeting and Scientific Exposition. 2003.
[125] Huth EJ, Squires RD, Elkinton JR. Experimental potassium depletion in normal human subjects. II. Renal and hormonal factors in the development of extracellular alkalosis during depletion. J Clin Invest 1959;38(7):1149–65.
[126] Squires RD, Huth EJ. Experimental potassium depletion in normal human subjects. I. Relation of ionic intakes to the renal conservation of potassium. J Clin Invest 1959;38(7):1134–48.
[127] Gallen IW, Rosa RM, Esparaz DY, Young JB, Robertson GL, Batlle D, et al. On the mechanism of the effects of potassium restriction on blood pressure and renal sodium retention. Am J Kidney Dis 1998;31(1):19–27.
[128] Wingo CS, Seldin DW, Kokko JP, Jacobson HR. Dietary modulation of active potassium secretion in the cortical collecting tubule of adrenalectomized rabbits. J Clin Invest 1982;70 (3):579–86.
[129] Halperin ML, Cheema-Dhadli S, Lin SH, Kamel KS. Control of potassium excretion: a Paleolithic perspective. Curr Opin Nephrol Hypertens 2006;15(4):430–6.
[130] Kamel KS, Oh MS, Halperin ML. Bartter's Gitelman's, and Gordon's syndromes. From physiology to molecular biology and back, yet still some unanswered questions. Nephron 2002;92(Suppl 1):18–27.
[131] Ahya SN, Soler MJ, Levitsky J, Batlle D. Acid–base and potassium disorders in liver disease. Semin Nephrol 2006;26 (6):466–70.
[132] Velazquez H, Perazella MA, Wright FS, Ellison DH. Renal mechanism of trimethoprim-induced hyperkalemia. Ann Intern Med 1993;119(4):296–301.
[133] Kleyman TR, Roberts C, Ling BN. A mechanism for pentamidine-induced hyperkalemia: inhibition of distal nephron sodium transport. Ann Intern Med 1995;122(2):103–6.
[134] Frindt G, McNair T, Dahlmann A, Jacobs-Palmer E, Palmer LG. Epithelial Na channels and short-term renal response to salt deprivation. Am J Physiol Renal Physiol 2002;283(4): F717–26.
[135] Rubera I, Loffing J, Palmer LG, Frindt G, Fowler-Jaeger N, Sauter D, et al. Collecting duct-specific gene inactivation of alphaENaC in the mouse kidney does not impair sodium and potassium balance. J Clin Invest 2003;112(4):554–65.
[136] Joo KW, Chang SH, Lee JG, Na KY, Kim YS, Ahn C, et al. Transtubular potassium concentration gradient (TTKG) and urine ammonium in differential diagnosis of hypokalemia. J Nephrol 2000;13(2):120–5.
[137] Batlle DC, Arruda JA, Kurtzman NA. Hyperkalemic distal renal tubular acidosis associated with obstructive uropathy. N Engl J Med 1981;304(7):373–80.
[138] Mitra A, Batlle D. Acid–base and electrolytes disorders. Aldosterone deficiency and resistance. Philadelphia: Saunders; 2002. [413–433]
[139] Batlle DC. Hyperkalemic hyperchloremic metabolic acidosis associated with selective aldosterone deficiency and distal renal tubular acidosis. Semin Nephrol 1981;1:260–74.

[140] Black DA, Milne MD. Experimental potassium depletion in man. Clin Sci 1952;11(4):397–415.
[141] Blahd WH, Bassett SH. Potassium deficiency in man. Metabolism 1953;2:218–24.
[142] Ethier JH, Kamel KS, Magner PO, Lemann Jr J, Halperin ML. The transtubular potassium concentration in patients with hypokalemia and hyperkalemia. Am J Kidney Dis 1990;15 (4):309–15.
[143] Choi MJ, Ziyadeh FN. The utility of the transtubular potassium gradient in the evaluation of hyperkalemia. J Am Soc Nephrol 2008;19(3):424–6.
[144] Salem MM, Rosa RM, Batlle DC. Extrarenal potassium tolerance in chronic renal failure: implications for the treatment of acute hyperkalemia. Am J Kidney Dis 1991;18(4):421–40.
[145] Gennari FJ. Hypokalemia. N Engl J Med 1998;339(7):451–8.
[146] Favre GA, Nau V, Kolb I, Vargas-Poussou R, Hannedouche T, Moulin B. Localization of tubular adaptation to renal sodium loss in gitelman syndrome. Clin J Am Soc Nephrol 2012;7 (3):472–8.
[147] Ellison DH. Adaptation in gitelman syndrome: "we just want to pump you up". Clin J Am Soc Nephrol 2012;7(3):379–82.
[148] Reilly RF, Huang CL. The mechanism of hypocalciuria with NaCl cotransporter inhibition. Nat Rev Nephrol 2011;7(11): 669–74.
[149] Toussaint C, Vereerstraeten P. Effects of blood pH changes on potassium excretion in the dog. Am J Physiol 1962;202: 768–72.
[150] Tannen RL. Effect of potassium on renal acidification and acid–base homeostasis. Semin Nephrol 1987;7(3):263–73.
[151] Batlle D, Moorthi KM, Schlueter W, Kurtzman N. Distal renal tubular acidosis and the potassium enigma. Semin Nephrol 2006;26(6):471–8.
[152] Steinmetz PR, Lawson LR. Defect in urinary acidification induced in vitro by amphotericin B. J Clin Invest 1970;49 (3):596–601.
[153] Batlle DC, Sabatini S, Kurtzman NA. On the mechanism of toluene-induced renal tubular acidosis. Nephron 1988;49 (3):210–8.
[154] Sebastian A, McSherry E, Morris Jr RC. Renal potassium wasting in renal tubular acidosis (RTA): its occurrence in types 1 and 2 RTA despite sustained correction of systemic acidosis. J Clin Invest 1971;50(3):667–78.
[155] Sebastian A, McSherry E, Morris Jr RC. Impaired renal conservation of sodium and chloride during sustained correction of systemic acidosis in patients with type 1, classic renal tubular acidosis. J Clin Invest 1976;58(2):454–69.
[156] Dafnis E, Spohn M, Lonis B, Kurtzman NA, Sabatini S. Vanadate causes hypokalemic distal renal tubular acidosis. Am J Physiol 1992;262(3 Pt 2):F449–53.
[157] Codina J, DuBose Jr TD. Molecular regulation and physiology of the H+,K+-ATPases in kidney. Semin Nephrol 2006;26 (5):345–51.
[158] Wingo CS. Active proton secretion and potassium absorption in the rabbit outer medullary collecting duct. Functional evidence for proton-potassium-activated adenosine triphosphatase. J Clin Invest 1989;84(1):361–5.
[159] Alpern RJ, Sakhaee K. The clinical spectrum of chronic metabolic acidosis: homeostatic mechanisms produce significant morbidity. Am J Kidney Dis 1997;29(2):291–302.
[160] Kraut JA, Madias NE. Metabolic acidosis: pathophysiology, diagnosis and management. Nat Rev Nephrol 2010;6 (5):274–85.
[161] Kraut JA, Madias NE. Differential diagnosis of nongap metabolic acidosis: value of a systematic approach. Clin J Am Soc 1997;7(4):671–9.
[162] Figge J, Rossing TH, Fencl V. The role of serum proteins in acid–base equilibria. J Lab Clin Med 1991;117(6):453–67.
[163] Kraut JA, Madias NE. Serum anion gap: its uses and limitations in clinical medicine. Clin J Am Soc Nephrol 2007;2 (1):162–74.
[164] Sterns RH. Fluid electrolyte and acid–base disturbances. In: Glassock RJ, editor. NephSAP. The American Society of Nephrology; 2004. p. 192–231.
[165] Feldman M, Soni N, Dickson B. Influence of hypoalbuminemia or hyperalbuminemia on the serum anion gap. J Lab Clin Med 2005;146(6):317–20.
[166] De Troyer A, Stolarczyk A, De Beyl DZ, Stryckmans P. Value of anion-gap determination in multiple myeloma. N Engl J Med 1977;296(15):858–60.
[167] Adrogue HJ, Wilson H, Boyd 3rd AE, Suki WN, Eknoyan G. Plasma acid–base patterns in diabetic ketoacidosis. N Engl J Med 1982;307(26):1603–10.
[168] Kim HY, Han JS, Jeon US, Joo KW, Earm JH, Ahn C, et al. Clinical significance of the fractional excretion of anions in metabolic acidosis. Clin Nephrol 2001;55(6):448–52.
[169] Orringer CE, Eustace JC, Wunsch CD, Gardner LB. Natural history of lactic acidosis after grand-mal seizures. A model for the study of an anion-gap acidosis not associated with hyperkalemia. N Engl J Med 1977;297(15):796–9.
[170] Paulson WD. Anion gap-bicarbonate relation in diabetic ketoacidosis. Am J Med 1986;81(6):995–1000.
[171] Uribarri J, Oh MS, Carroll HJ. D-lactic acidosis. A review of clinical presentation, biochemical features, and pathophysiologic mechanisms. Medicine (Baltimore) 1998;77(2): 73–82.
[172] Adrogue HJ, Eknoyan G, Suki WK. Diabetic ketoacidosis: role of the kidney in the acid–base homeostasis re-evaluated. Kidney Int 1984;25(4):591–8.
[173] Brivet F, Bernardin M, Cherin P, Chalas J, Galanaud P, Dormont J. Hyperchloremic acidosis during grand mal seizure lactic acidosis. Intensive Care Med 1994;20(1): 27–31.
[174] Brivet F, Bernardin M, Dormont J. Hyperchloremic acidosis in metabolic acidosis with anion gap excess. Comparison with diabetic ketoacidosis. Presse Med 1991;20(9):413–7.
[175] Carlisle EJ, Donnelly SM, Vasuvattakul S, Kamel KS, Tobe S, Halperin ML. Glue-sniffing and distal renal tubular acidosis: sticking to the facts. J Am Soc Nephrol 1991;1(8): 1019–27.
[176] Oh MS, Carroll HJ, Uribarri J. Mechanism of normochloremic and hyperchloremic acidosis in diabetic ketoacidosis. Nephron 1990;54(1):1–6.
[177] Oster JR, Singer I, Contreras GN, Ahmad HI, Vieira CF. Metabolic acidosis with extreme elevation of anion gap: case report and literature review. Am J Med Sci 1999;317(1): 38–49.
[178] Wang F, Butler T, Rabbani GH, Jones PK. The acidosis of cholera. Contributions of hyperproteinemia, lactic acidemia, and hyperphosphatemia to an increased serum anion gap. N Engl J Med 1986;315(25):1591–5.
[179] Batlle DC, von Riotte A, Schlueter W. Urinary sodium in the evaluation of hyperchloremic metabolic acidosis. N Engl J Med 1987;316(3):140–4.
[180] Moorthi K, Batlle D. Renal tubular acidosis. In: Gennari FJ, Adrogue HJ, Galla JH, Madias NE, editors. Acid–base disorders and their treatment. Boca Raton: Taylor & Francis Group; 2005. p. 417–67.
[181] Salem MM, Batlle D. Metabolic acidosis. In: Massry SG, Glassock RJ, editors. Textbook of nephrology. Baltimore: Williams & Wilkins; 1995. p. 430–49.

[182] Brenes LG, Brenes JN, Hernandez MM. Familial proximal renal tubular acidosis. A distinct clinical entity. Am J Med 1977;63 (2):244–52.
[183] Nash MA, Torrado AD, Greifer I, Spitzer A, Edelmann Jr CM. Renal tubular acidosis in infants and children. Clinical course, response to treatment, and prognosis. J Pediatr 1972;80 (5):738–48.
[184] Rodriguez Soriano J, Boichis H, Stark H, Edelmann Jr CM. Proximal renal tubular acidosis. A defect in bicarbonate reabsorption with normal urinary acidification. Pediatr Res 1967;1 (2):81–98.
[185] Brenes LG, Sanchez MI. Impaired urinary ammonium excretion in patients with isolated proximal renal tubular acidosis. J Am Soc Nephrol 1993;4(4):1073–8.
[186] Lemann Jr J, Adams ND, Wilz DR, Brenes LG. Acid and mineral balances and bone in familial proximal renal tubular acidosis. Kidney Int 2000;58(3):1267–77.
[187] Gauthier P, Simon EE, Lemann J. Acid–base and electrolyte disorder acidosis of chronic renal failure. Philadelphia: Suanders; 2002. p. 207–216
[188] Goldstein MB, Bear R, Richardson RM, Marsden PA, Halperin ML. The urine anion gap: a clinically useful index of ammonium excretion. Am J Med Sci 1986;292(4):198–202.
[189] Oh M, Carroll HJ. Value and determinants of urine anion gap. Nephron 2002;90(3):252–5.
[190] Alpern RJ. Trade-offs in the adaptation to acidosis. Kidney Int 1995;47(4):1205–15.
[191] Crawford MA, Milne MD, Scribner BH. The effects of changes in acid–base balance on urinary citrate in the rat. J Physiol 1959;149:413–23.
[192] Melnick JZ, Preisig PA, Haynes S, Pak CY, Sakhaee K, Alpern RJ. Converting enzyme inhibition causes hypocitraturia independent of acidosis or hypokalemia. Kidney Int 1998;54 (5):1670–4.
[193] Coe FL, Parks J. Pathogenesis and treatment of nephrolithiasis. In: Seldin DW, Giebisch G, editors. The kidney: physiology and pathophysiology. Philadelphia: Lippincott Williams & Wilkins; 2000. p. 1841–67.
[194] Henderson LJ. A critical study of the process of acid excretion. J Biol Chem 1911;9:403–24.
[195] Halperin ML, Cheema Dhadli S, Kamel KS. Physiology of acid–base balance: links with kidney stone prevention. Semin Nephrol 2006;26(6):441–6.
[196] Lash JP, Arruda JA. Laboratory evaluation of renal tubular acidosis. Clin Lab Med 1993;13(1):117–29.
[197] Batlle DC. Segmental characterization of defects in collecting tubule acidification. Kidney Int 1986;30(4):546–54.
[198] Schlueter W, Keilani T, Hizon M, Kaplan B, Batlle DC. On the mechanism of impaired distal acidification in hyperkalemic renal tubular acidosis: evaluation with amiloride and bumetanide. J Am Soc Nephrol 1992;3(4):953–64.
[199] Batlle DC. Sodium-dependent urinary acidification in patients with aldosterone deficiency and in adrenalectomized rats: effect of furosemide. Metabolism 1986;35(9):852–60.
[200] Morris RC, Piel CF, Audioun E. Renal tubular acidosis. Effects of sodium phosphate and sulfate on renal acidification in two patients with renal tubular acidosis. Pediatrics 1965;36(6): 899–904.
[201] Shinoda T, Shiigai T. Sodium sulfate and furosemide loading tests for the diagnosis of renal tubular acidosis. Nihon Rinsho 1985;43(9):1849–54.
[202] Schwartz WB, Jenson RL, Relman AS. Acidification of the urine and increased ammonium excretion without change in acid–base equilibrium: sodium reabsorption as a stimulus to the acidifying process. J Clin Invest 1955;34(5):673–80.
[203] Walsh SB, Shirley DG, Wrong OM, Unwin RJ. Urinary acidification assessed by simultaneous furosemide and fludrocortisone treatment: an alternative to ammonium chloride. Kidney Int 2007;71(12):1310–6.
[204] Rastogi S, Bayliss JM, Nascimento L, Arruda JA. Hyperkalemic renal tubular acidosis: effect of furosemide in humans and in rats. Kidney Int 1985;28(5):801–7.
[205] Halperin ML, Goldstein MB, Haig A, Johnson MD, Stinebaugh BJ. Studies on the pathogenesis of type I (distal) renal tubular acidosis as revealed by the urinary PCO2 tensions. J Clin Invest 1974;53(3):669–77.
[206] DuBose Jr TD. Hydrogen ion secretion by the collecting duct as a determinant of the urine to blood PCO2 gradient in alkaline urine. J Clin Invest 1982;69(1):145–56.
[207] Arruda JA, Nascimento L, Mehta PK, Rademacher DR, Sehy JT, Westenfelder C, et al. The critical importance of urinary concentrating ability in the generation of urinary carbon dioxide tension. J Clin Invest 1977;60(4):922–35.
[208] Garg LC. Lack of effect of amphotericin B on urine-blood pCO2 gradient in spite of urinary acidification defect. Pflugers Arch 1979;381(2):137–42.
[209] Batlle D, Gaviria M, Grupp M, Arruda JA, Wynn J, Kurtzman NA. Distal nephron function in patients receiving chronic lithium therapy. Kidney Int 1982;21(3):477–85.
[210] Donckerwolcke RA, Valk C, van Wijngaarden-Penterman MJ, van Stekelenburg GJ. The diagnostic value of the urine to blood carbon dioxide tension gradient for the assessment of distal tubular hydrogen secretion in pediatric patients with renal tubular disorders. Clin Nephrol 1983;19(5):254–8.

This page intentionally left blank

CHAPTER

75

Biomarkers for Assessment of Renal Function During Acute Kidney Injury

Prasad Devarajan

Nephrology and Hypertension, Cincinnati Children's Hospital Medical Center, University of Cincinnati College of Medicine, Cincinnati, Ohio, USA

BIOMARKERS OF ACUTE KIDNEY INJURY—AN UN-MET NEED

The incidence of acute kidney injury (AKI) is rising globally, and so are the associated morbidity and mortality rates. AKI afflicts 5–7% of all hospitalized patients. In critically ill patients, the overall prevalence of severe AKI requiring renal replacement therapy (RRT) is about 6%, with a mortality rate of 60%.[1] Mortality and morbidity from AKI has not substantially improved in the past few decades despite technological advances in supportive care. AKI is largely asymptomatic, and establishing the diagnosis currently hinges on functional biomarkers such as serial serum creatinine measurements. Unfortunately, serum creatinine is a delayed and unreliable indicator of AKI for a variety of reasons.[2] First, normal serum creatinine is influenced by several non-renal factors such as age, gender, muscle mass, muscle metabolism, medications, hydration status, nutrition status, and tubular secretion. Second, a number of acute and chronic kidney conditions can exist with no increase in serum creatinine due to the concept of renal reserve—it is estimated that greater than 50% of kidney function must be lost before serum creatinine rises. Third, serum creatinine concentrations do not reflect the true decrease in glomerular filtration rate in the acute setting, since several hours to days must elapse before a new equilibrium between the presumably steady state of creatinine production and the decreased excretion of creatinine is established. Fourth, serum creatinine production is diminished in critical illnesses such as sepsis, and measured serum creatinine is often further reduced by hemodilution resulting from standard goal-directed fluid therapies. Fifth, an increase in serum creatinine represents a late indication of a functional change in glomerular filtration rate, which lags behind important structural changes that occur in the kidney during the early damage stage of AKI. The delay in AKI diagnosis imposed by our dependence on serum creatinine changes is a problem, since animal studies have identified several interventions that can prevent and/or treat AKI if instituted early in the disease course, well before the serum creatinine begins to rise.[3] The lack of early biomarkers has hitherto hampered our ability to translate these promising therapies to human AKI. Also lacking are reliable methods to assess efficacy of preventive or therapeutic interventions, and early predictive biomarkers of drug toxicity.

DESIRABLE CHARACTERISTICS OF AKI BIOMARKERS

First, with respect to assay characteristics, AKI biomarkers should be non-invasive and easy to perform at the bedside or in a standard clinical laboratory, using easily accessible samples such as blood or urine, with quick turn-around times. The majority of AKI biomarkers described thus far have been measured in the urine. Urinary diagnostics have several advantages, including the non-invasive nature of sample collection,

Seldin and Giebisch's The Kidney, Fifth Edition.
DOI: http://dx.doi.org/10.1016/B978-0-12-381462-3.00075-6

© 2013 Elsevier Inc. All rights reserved.

the reduced number of interfering proteins, and the potential for the development of patient self-testing kits. However, disadvantages also exist, including the lack of sample from patients with severe oliguria, and potential changes in urinary biomarker concentration induced by hydration status and diuretic therapy. Plasma-based diagnostics have revolutionized many facets of medicine, as exemplified by the use of troponins for the early diagnosis of acute myocardial infarction. On the other hand, plasma biomarkers may be confounded by extra-renal sources as well as by subclinical changes in renal elimination. Thus, in the case of AKI, it is ideal to develop both urinary and plasma biomarkers.

Second, with respect to diagnostic properties, AKI biomarkers should be sensitive to facilitate early detection, with a wide dynamic range that allow for risk stratification. They should also be highly specific for AKI, enable the identification of AKI sub-types and differentiate AKI from chronic kidney disease (CKD). Ideally, biomarkers are also needed to identify the primary location of injury (proximal tubule, distal tubule, interstitium, or vasculature), and discern AKI etiologies (ischemia, toxins, sepsis, or a combination).

Third, with respect to prognostic abilities, AKI biomarkers should allow for risk stratification (duration and severity of AKI), prediction of hard clinical outcomes (need for renal replacement therapy, length of hospital stay, mortality) and monitoring the response to AKI interventions. Biomarkers associated with clear biologic plausibility and known pathophysiologic mechanisms in AKI are most likely to satisfy the desired diagnostic and prognostic characteristics.

Given the limitations of serum creatinine, the search for improved biomarkers of AKI is of intense contemporary interest. During the past decade, an improved understanding of the early pathophysiologic response of the kidney to stress has uncovered a number of genes and proteins that are rapidly induced in the kidney.[3] They have been implicated in the regulation of novel pathways and mechanisms that modulate the kidney injury. Serendipitously, some of these kidney proteins are also detected in the urine and/or plasma, and are emerging as early non-invasive biomarkers of AKI and its clinical outcomes. Table 75.1 lists the desirable characteristics of AKI biomarkers in general, and illustrates the current status of the four most promising novel AKI biomarkers whose bench-to-bedside translation is chronicled in this chapter. Table 75.2 summarizes the biological characteristics of these and other proposed AKI biomarkers. Since NGAL represents the most extensively studied of the novel biomarkers, it will be the primary focus of this chapter.

TABLE 75.1 Desirable Characteristics of Acute Kidney Injury Biomarkers

Property	NGAL	KIM-1	IL-18	L-FABP
Noninvasive (measured in urine or blood)	Yes	Yes	Yes	Yes
Rapid, standardized clinical platforms available	Yes	Yes	No	No
Sensitive to establish an early diagnosis of AKI	Yes	Yes	Yes	Yes
Results available while damage is limitable	Yes	Yes	Yes	Yes
High gradient to allow severity prediction	Yes	Yes	Yes	Yes
Specific to intrinsic AKI (versus pre-renal AKI)	Yes	Unknown	Unknown	Unknown
Discerns AKI from chronic kidney disease	No	No	No	No
Predicts hard clinical outcomes	Yes	Yes	Yes	Yes
Predicts response to therapies	Yes	Unknown	Unknown	Unknown
Associated with a known mechanism	Yes	Yes	Yes	Yes

AKI: acute kidney injury; NGAL: neutrophil gelatinase-associated lipocalin; KIM-1: kidney injury molecule-1; IL-18: interleukin 18; L-FABP: liver type fatty acid binding protein.

NEUTROPHIL GELATINASE-ASSOCIATED LIPOCALIN (NGAL) AS AN AKI BIOMARKER

NGAL Physiology and Pathophysiology

Human NGAL was originally identified as a novel protein isolated from secondary granules of human neutrophils, and subsequently shown to be a 25-kDa protein covalently bound to neutrophil gelatinase. Mature peripheral neutrophils lack NGAL mRNA expression, and NGAL protein is synthesized at the early myelocyte stage of granulopoiesis during formation of secondary granules. NGAL mRNA is normally expressed in a variety of adult human tissues, including bone marrow, prostate, salivary gland, stomach, colon, trachea, lung, liver, and kidney.[2] Several of these tissues are prone to exposure to microorganisms, and constitutively express NGAL protein at low levels. The promoter region of the NGAL gene contains binding sites for a number of transcription factors, including NF-κB. This could explain the constitutive as well as inducible expression of NGAL in several of the non-hematopoietic tissues. Like other lipocalins, NGAL forms a barrel-shaped tertiary structure with a

TABLE 75.2 Biological Characteristics of Promising Acute Kidney Injury Biomarkers

Biomarker	Sample	Origin	Biological Function
NGAL	Urine	Distal tubule, collecting duct	Regulates iron trafficking, promotes tubule cell survival and proliferation, limits tubule cell apoptosis
NGAL	Blood	Liver, lung, neutrophils	Acute phase reactant, marker of organ cross-talk following acute kidney injury
KIM-1	Urine	Proximal tubule	Promotes epithelial regeneration, regulates tubule cell apoptosis
IL-18	Urine	Proximal tubule	Initiates and promotes tubule cell apoptosis and necrosis
L-FABP	Urine	Proximal tubule	Endogenous antioxidant, suppresses tubulointerstitial damage
NAG	Urine	Proximal tubule	Marker of proximal tubule lysosomal enzyme release as a result of damage to proximal tubule
β2-MG	Urine	Systemic and Proximal tubule	Marker of altered glomerular permeability and/or decreased proximal tubular reabsorption due to damage
Albumin	Urine	Systemic and Proximal Tubule	Marker of altered glomerular permeability and/or decreased proximal tubular reabsorption due to damage

NGAL: neutrophil gelatinase-associated lipocalin; KIM-1: kidney injury molecule-1; IL-18: interleukin 18; L-FABP: liver type fatty acid binding protein; NAG: n-acetyl glucosaminidase; β2-MG; beta2-microglobulin.

hydrophobic calyx that binds small lipophilic molecules. The major ligands for NGAL are siderophores, small iron-binding molecules. Teleologically, NGAL comprises a critical component of innate immunity to bacterial infection. Siderophores are synthesized by bacteria to scavenge iron from the surroundings, and use specific transporters to recover the siderophore-iron complex, ensuring their iron supply. The siderophore-chelating property of NGAL therefore renders it as a bacteriostatic agent. Experimental evidence for this role is derived from mice genetically modified to lack the NGAL gene, which renders them more susceptible to Gram-negative bacterial infections and death from sepsis.

On the other hand, siderophores produced by eukaryotes participate in NGAL-mediated iron shuttling that is critical to various cellular responses such as proliferation and differentiation. This property provides a molecular mechanism for the documented role of NGAL in enhancing the epithelial phenotype. During kidney development, NGAL promotes epithelial differentiation of the mesenchymal progenitors, leading to the generation of glomeruli, proximal tubules, Henle's loop, and distal tubules. However, NGAL expression is also markedly induced in injured epithelial cells, including the kidney, colon, liver and lung. This is likely mediated via NF-κB, which is known to be rapidly activated in epithelial cells after acute injuries, and plays a central role in controlling cell survival and proliferation. In the context of an injured mature organ such as the kidney, the biological role of NGAL induction is one of marked preservation of function, attenuation of apoptosis, and an enhanced proliferative response.[4,5] This protective effect is dependent on the chelation of toxic iron from extracellular environments, and the regulated delivery of siderophore and iron to intracellular sites. Not surprisingly, gene expression studies in AKI have demonstrated a rapid and massive upregulation of NGAL mRNA in the distal nephron segments—specifically in the thick ascending limb of Henle's loop and the collecting ducts. The resultant synthesis of NGAL protein in the distal nephron and secretion into the urine comprises the major fraction of urinary NGAL. Although plasma NGAL is freely filtered by the glomerulus, it is largely reabsorbed in the proximal tubules. Thus, any urinary excretion of NGAL is likely only when a kidney disease precludes proximal tubular NGAL reabsorption, and/or induces distal tubular *de novo* NGAL synthesis. With respect to plasma NGAL, the kidney itself does not appear to be a major source. NGAL protein released into the circulation from distant organs such as the liver and lung constitute a distinct systemic pool. Additional contributions to the systemic pool may derive from activated neutrophils, macrophages, and other immune cells. Furthermore, any decrease in GFR would decrease the renal clearance of NGAL, with subsequent accumulation in the systemic circulation in patients with CKD.

Preclinical transcriptome profiling studies identified *Ngal* (also known as lipocalin 2 or *lcn2*) to be one of the most upregulated genes in the kidney very early after acute injury in animal models.[6] Downstream proteomic analyses also revealed NGAL to be one of the most highly induced proteins in the kidney after ischemic or nephrotoxic AKI in animal models.[7,8] The serendipitous finding that NGAL protein was easily detected in the urine soon after AKI in animal studies has inspired a number of translational human studies, and NGAL has emerged as an excellent biomarker in the urine and plasma for early diagnosis, therapeutic monitoring, and prediction of prognosis in common clinical AKI scenarios. The deployment of standardized clinical platforms for the rapid and accurate measurement of NGAL in urine and plasma has further facilitated the

widespread use and validation of NGAL as a biomarker.

NGAL for the Prediction of AKI and its Severity

In a cross-sectional study of adults with established AKI (doubling of serum creatinine) from varying etiologies, a marked increase in urine and serum NGAL was documented by Western blotting when compared to normal controls.[5] Urine and serum NGAL levels correlated with serum creatinine, and kidney biopsies in subjects with AKI showed intense accumulation of immunoreactive NGAL in cortical tubules, confirming NGAL as a sensitive index of established AKI in humans. An explosion of subsequent studies has now implicated NGAL as an early diagnostic biomarker for AKI in several common clinical situations.

Operations involving cardiopulmonary bypass comprise the most frequent major surgical procedure performed in hospitals worldwide. Even a minor degree of post-operative AKI as manifest by only a 0.2−0.3 mg/dl rise in serum creatinine from baseline (which occurs in up to 30% of cardiac surgeries) is associated with a significant increase in mortality and other adverse outcomes. The pathogenesis of cardiac surgery-associated AKI includes ischemia-reperfusion injury, exogenous toxins (contrast media, non-steroidal anti-inflammatory drugs), endogenous toxins (iron released from hemolysis), and inflammation and oxidative stress (from contact with bypass circuit, surgical trauma, and intra-renal inflammatory responses). The predictive value of NGAL has been most extensively studied in this setting (Table 75.3). In single center prospective studies of children who underwent elective cardiac surgery, AKI (defined as a 50% increase in serum creatinine) occurred one to three days after surgery.[9−15] In contrast, NGAL measurements by ELISA revealed a 10-fold or more increase in the urine and plasma, within two to six hours of the surgery in those who subsequently developed AKI. Both urine and plasma NGAL were excellent independent predictors of AKI, with an area under the receiver-operating characteristic curve (AUC-ROC) of >0.9 for the two to six hour urine and plasma NGAL measurements. A recent prospective multicenter study of children undergoing cardiac surgery has confirmed the early peak (within six hours of initiating cardiopulmonary bypass) of urine and plasma NGAL associated with higher odds of developing AKI,[16] but the diagnostic accuracy by AUC-ROC analysis was lower (0.71). These findings have also been confirmed in several prospective single center studies of adults who developed AKI after cardiac surgery, in whom urinary and/or plasma NGAL was significantly elevated by one to six hours after the operation.[17−31] The AUC-ROCs for the prediction of AKI have ranged widely from 0.61 to 0.96. A prospective multicenter study of adults undergoing cardiac surgery has confirmed the early peak of urine and plasma NGAL associated with higher odds of developing AKI,[16] but the diagnostic accuracy by AUC-ROC analysis was only 0.67 to 0.70.[32] The somewhat inferior performance in adult populations may be reflective of confounding variables such as older age groups, pre-existing kidney disease, prolonged bypass times, chronic illness, and diabetes. The predictive performance of NGAL also depends on the definition of AKI employed, as well as on the severity of AKI.[22−24] For example, the predictive value of plasma NGAL post cardiac surgery was higher for more severe AKI (increase in serum creatinine >50%; mean AUC-ROC 0.79) compared to less severe AKI (increase in serum creatinine >25%; mean AUC-ROC 0.65). Similarly, the discriminatory ability of NGAL for AKI increased with increasing severity as classified by RIFLE criteria. Thus, the AUC-ROC improved progressively for discrimination of R (0.72), I (0.79) and F (0.80) category of AKI. Furthermore, the predictive power of urinary NGAL for AKI after cardiac surgery varied with baseline renal function, with optimal discriminatory performance in patients with normal preoperative renal function.[33] Despite these numerous potential variables, a meta-analysis of published studies in all patients after cardiac surgery revealed an overall AUC-ROC of 0.78 for prediction of AKI, when NGAL was measured within 6 hours of initiation of cardiopulmonary bypass and AKI was defined as a >50% increase in serum creatinine.[34] A current analysis of 25 published studies strongly supports the use of NGAL for AKI prediction after cardiac surgery, with an overall sensitivity of 71%, specificity of 78%, and an average AUC of 0.80 (Table 75.3).

AKI is a frequent complication in critically ill patients, and results in a 40−60% mortality rate. This patient population is extremely heterogeneous, and the etiology and timing of AKI is often unclear. Etiologies include sepsis, nephrotoxins, hypotension, kidney ischemia, mechanical ventilation, and multi-organ disease. Even in such heterogeneous settings, urine and plasma NGAL measurements have been shown to represent early biomarkers of AKI (Table 75.4). Initial studies in the pediatric intensive care setting demonstrated that NGAL predicted AKI about two days prior to the rise in serum creatinine, with high sensitivity and AUC-ROCs of 0.68−0.78.[35,36] Several studies have also examined plasma and urine NGAL levels in critically ill adult populations.[37−47] Urine NGAL obtained on admission predicted subsequent AKI in multi-trauma patients with an outstanding AUC-ROC of

TABLE 75.3 NGAL for the Early Prediction of Acute Kidney Injury after Cardiac Surgery

Reference	Patients	AKI Events	Source	AUC	Sensitivity	Specificity	AKI Definition
[9]	71	20	Urine	0.99	100	98	RIFLE R or greater
[17]	81	16	Urine	0.80	73	78	RIFLE R or greater
[13]	196	99	Urine	0.95	82	90	RIFLE R or greater
[18]	72	34	Urine	0.71	67	58	RIFLE R or greater
[19]	426	85	Urine	0.61	39	78	RIFLE R or greater
[21]	50	9	Urine	0.96	90	78	>0.5 mg/dl Creatinine rise
[25]	90	36	Urine	0.65	71	39	>0.3 mg/dl Creatinine rise
[26]	103	13	Urine	0.50	67	11	RIFLE R or greater
[27]	30	15	Urine	0.85	84	80	RIFLE R or greater
[28]	123	46	Urine	0.88	NR	NR	AKIN Criteria
[29]	50	38	Urine	0.77	82	78	AKIN Criteria
[14]	374	112	Urine	0.92	85	86	RIFLE R or greater
[15]	220	60	Urine	0.90	88	83	RIFLE R or greater
[16]	311	53	Urine	0.71	42	85	Doubling of Creatinine
[32]	1219	60	Urine	0.67	46	81	Doubling of Creatinine
[9]	71	20	Plasma	0.90	50	100	RIFLE R or greater
[12]	120	45	Plasma	0.96	84	94	RIFLE R or greater
[22]	100	23	Plasma	0.80	79	78	RIFLE R or greater
[21]	50	9	Plasma	0.80	90	78	>0.5 mg/dl Creatinine rise
[23]	100	46	Plasma	0.77	73	74	AKIN Criteria
[30]	30	8	Plasma	0.98	100	91	RIFLE R or greater
[31]	879	75	Plasma	0.64	39	82	RIFLE R or greater
[14]	374	112	Plasma	0.94	90	88	RIFLE R or greater
[16]	311	53	Plasma	0.56	27	81	Doubling of Creatinine
[35]	1219	60	Plasma	0.70	50	82	Doubling of Creatinine
Total	6670	1147	***Averages***	0.80	71%	78%	

AKI: acute kidney injury; NR: not reported.

0.98.[39] However, in more mixed populations of all critical care admissions, the performance of urine NGAL on admission was more variable, with an AUC-ROC ranging from 0.71 to 0.89 (Table 75.4). In studies of adult intensive care patients, plasma NGAL concentrations on admission constituted a very good to outstanding biomarker for development of AKI within the next two days, with AUC-ROC ranges of 0.79–0.92.[44–47] In the closely related setting of the emergency department, where again the causes of AKI are myriad and timing of the initial insult uncertain, a single measurement of urine NGAL at the time of initial presentation predicted AKI with an outstanding AUC-ROC of 0.95 in a single center study of adult patients.[48] This has now been confirmed in children,[49] as well as in a large multicenter prospective study of adults presenting to the emergency department,[50] in which urine NGAL was predictive of subsequent AKI with an excellent AUC of 0.81. However, it should be noted that patients with septic AKI display the highest concentrations of both plasma and urine NGAL when compared to those with non-septic AKI,[51] a confounding factor that may add to the heterogeneity of the results in the critical care setting. In addition, the predictive power of urinary NGAL for AKI in the critically ill was optimal in patients with normal preoperative renal function.[42] A meta-analysis revealed an overall AUC-ROC of 0.73 for prediction of AKI, when NGAL

TABLE 75.4 NGAL for the Early Prediction of Acute Kidney Injury in Critical Care Settings

Reference	Patients	AKI Events	Source	AUC	Sensitivity	Specificity	AKI Definition
[35]	140	106	Urine	0.78	54	97	RIFLE R or greater
[37]	204	102	Urine	0.89	80	96	RIFLE R or greater
[48]	635	30	Urine	0.95	90	100	RIFLE R or greater
[38]	451	150	Urine	0.71	78	70	AKIN criteria
[39]	31	11	Urine	0.98	91	95	RIFLE R or greater
[40]	44	18	Urine	0.86	71	100	RIFLE R or greater
[41]	632	171	Urine	0.88	89	70	RIFLE R or greater
[42]	529	147	Urine	0.66	40	80	RIFLE R or greater
[49]	252	18	Urine	0.80	NR	NR	RIFLE I or greater
[43]	145	75	Urine	0.87	88	89	RIFLE R or greater
[50]	1635	96	Urine	0.81	68	81	RIFLE R or greater
[36]	143	22	Plasma	0.68	86	39	Creatinine > 2 mg/dl
[44]	88	42	Plasma	0.92	82	97	RIFLE R or greater
[45]	45	24	Plasma	0.79	68	82	RIFLE R or greater
[46]	307	133	Plasma	0.78	73	81	RIFLE R or greater
[47]	661	24	Plasma	0.82	96	51	Creatinine rise > 0.5 mg/dl
[40]	44	18	Plasma	0.85	83	86	RIFLE R or greater
[41]	632	171	Plasma	0.86	82	70	RIFLE R or greater
Total	6618	1358	***Averages***	0.83	78%	82%	

AKI: acute kidney injury; NR: not reported.

was measured within six hours of clinical contact with critically ill subjects and AKI was defined as a >50% increase in serum creatinine.[34] A current analysis of 18 published studies strongly supports the use of NGAL for AKI prediction in the critically ill population, with an overall sensitivity of 77%, specificity of 81%, and an average AUC of 0.83 (Table 75.4).

AKI due to ischemia-reperfusion occurs to some extent almost invariably in deceased donor renal allografts, and even in some live donor transplants, often resulting in varying degrees of early renal dysfunction. AKI leading to delayed graft function (DGF) complicates 4–10% of live donor and 5–50% of deceased donor kidney transplants. In addition to the well-known complications of AKI and dialysis, DGF predisposes the graft to both acute and chronic rejection, is an independent risk factor for suboptimal graft function at one year post transplant, and increases the risk of chronic allograft nephropathy and graft loss. NGAL has been evaluated as a promising biomarker of AKI and DGF (defined as dialysis requirement within the first post-operative week) in patients undergoing kidney transplantation. Protocol biopsies of kidneys obtained one hour after vascular anastomosis revealed a significant correlation between NGAL staining intensity in the allograft and the subsequent development of delayed graft function.[52] In a prospective multicenter study of children and adults, urine NGAL levels in samples collected on the day of transplant identified those who subsequently developed DGF (which typically occurred two to four days later), with an AUC-ROC of 0.9.[53] This has now been confirmed in a larger multi-center cohort, in which urine NGAL measured within six hours of kidney transplantation predicted subsequent DGF with an AUC-ROC of 0.81.[54] In the largest study reported to date, in 176 recipients of deceased donor grafts, 70 developed DGF. Urinary NGAL levels obtained on the first day after kidney transplant predicted prolonged DGF with an AUC-ROC of 0.75.[55]

Several investigators have examined the role of NGAL as a predictive biomarker of AKI following contrast administration.[56–59] In a prospective study of children undergoing elective cardiac catheterization with contrast administration, both urine and plasma NGAL predicted contrast-induced

TABLE 75.5 NGAL for the Early Prediction of Acute Kidney Injury Severity

Reference	Patients	AKI Events	Source	NGAL in RIFLE-R	NGAL in RIFLE-I	NGAL in RIFLE-F
[13]	196	99	Urine	520	1340	1750
[18]	72	34	Urine	NR	NR	6011
[14]	374	112	Urine	150	230	660
[15]	220	60	Urine	120	205	870
[41]	632	171	Urine	323	523	2013
[49]	252	18	Urine	19.5	185	NR
[50]	1635	96	Urine	94	202	490
Urine Total	3381	494	***Averages***	204	448	1981
[22]	100	23	Plasma	176	252	355
[14]	374	112	Plasma	100	222	358
[47]	661	24	Plasma	230	332	804
[2]	120	45	Plasma	175	245	360
Plasma Total	1255	204	***Averages***	170	263	469

AKI: acute kidney injury; NR: not reported; values for NGAL are in ng/ml.

nephropathy (defined as a 50% increase in serum creatinine from baseline) within two hours after contrast administration, with an AUC-ROC of 0.91−0.92.[56] In several studies of adults administered contrast, an early rise in both urine (four hours) and plasma (two hours) NGAL were documented, in comparison with a much later increase in plasma cystatin C levels (8−24 hours after contrast administration), providing further support for NGAL as an early biomarker of contrast nephropathy.[57−59] A meta-analysis revealed an overall AUC-ROC of 0.894 for prediction of AKI, when NGAL was measured within six hours after contrast administration and AKI was defined as a >25% increase in serum creatinine.[34]

Many reports have now demonstrated that early NGAL measurements are predictive of AKI severity, as classified by the standardized RIFLE criteria.[60] The average concentrations of early NGAL measurements correlate with rising RIFLE stage reached, as shown in Table 75.5. These findings support the use of early NGAL measurements for AKI risk prediction and stratification, and hence as a useful tool for triaging of patient care.

NGAL for the Differential Diagnosis of AKI

In the setting of acute illness, up to 60% of patients may have already sustained AKI on presentation, and up to 30% already display an increase in serum creatinine concentrations on initial presentation.[48] Differentiating between volume-responsive prerenal azotemia, intrinsic AKI, and CKD is critical for appropriate triaging and medical management. Recent evidence suggests that NGAL measurements can serve this purpose. In three published studies of urinary measurements done at the time of presentation to the emergency department, NGAL levels were only mildly elevated in patients with prerenal azotemia or CKD, but markedly elevated in those subsequently adjudicated to have intrinsic AKI, with an overall AUC-ROC for intrinsic AKI prediction of 0.86 (Table 75.6).

NGAL for the Prognosis of AKI

A number of studies have demonstrated the utility of early NGAL measurements for predicting the severity and clinical outcomes of AKI. In children undergoing cardiac surgery, early post-operative plasma NGAL levels correlated with duration and severity of AKI, length of hospital stay, and mortality.[12] In a similar cohort, early urine NGAL levels correlated with duration and severity of AKI, length of hospital stay, dialysis requirement, and death.[13] In a multicenter study of children with diarrhea-associated hemolytic uremic syndrome, urine NGAL obtained early during the hospitalization predicted the severity of AKI and dialysis requirement with high sensitivity.[61] Early urine NGAL levels were also predictive of duration of

TABLE 75.6 NGAL for the Differential Diagnosis of Acute Kidney Injury

Reference	Patients	Normal	Prerenal	Intrinsic AKI	CKD	AUC	Sensitivity	Specificity
[48]	635	16	30	416	22	0.95	90	100
[43]	145	NR	22	187	NR	0.87	75	88
[50]	1635	20	60	335	40	0.81	81	68
Averages		18	37	313	31	0.88	82%	85%

AKI: acute kidney injury; CKD: chronic kidney disease; NR: not reported; values for NGAL in normal, prerenal, intrinsic AKI and CKD are in ng/ml. All studies were done with urine NGAL.

TABLE 75.7 NGAL for the Prognosis of Acute Kidney Injury

Reference	Patients	AKI Events	Source	Mortality	Dialysis/Severe AKI	ICU Stay
[28]	123	46	Urine		AUC 0.88	
[32]	1219	60	Urine		Adj OR 5.4	Adj OR 5.6
[16]	311	53	Urine		Adj OR 4.1	Adj OR 5.9
[41]	632	171	Urine		AUC 0.88	
[63]	100	100	Urine	Adj OR 22	Adj OR 40	
[38]	451	83	Urine	Adj OR 2.6		
[32]	1219	60	Plasma		Adj OR 7.6	Adj OR 5.6
[16]	311	53	Plasma		Adj OR 2.2	Adj OR 4.3
[41]	632	171	Plasma		AUC 0.86	
[62]	109	109	Plasma	Adj OR 1.6		

AKI: acute kidney injury; Adj OR: adjusted odds ratio.

AKI (AUC 0.79) in a heterogeneous cohort of critically ill pediatric subjects.[35]

In adults undergoing cardiopulmonary bypass, those who subsequently required renal replacement therapy were found to have the highest urine NGAL values soon after surgery.[17–28] Similar results were documented in the adult critical care setting.[38–42] Collectively, a meta-analysis of the published studies revealed an overall AUC-ROC of 0.78 for prediction of subsequent dialysis requirement, when NGAL was measured within six hours of clinical contact.[34] Furthermore, a number of studies conducted in the cardiac surgery and critical care populations have identified early NGAL measurements as a very good mortality marker, with an overall AUC-ROC of 0.71 in these heterogeneous populations.[34] There is now evidence for the utility of subsequent NGAL measurements in critically ill adults with established AKI. Serum NGAL measured at the inception of renal replacement therapy was shown to be an independent predictor of 28-day mortality, with an AUC of 0.74.[62] Representative publications reporting the adjusted odds ratios for adverse outcomes related to elevated NGAL levels early in the course of critical illnesses are shown in Table 75.7.

Limitations of NGAL as an AKI Biomarker

Published studies to date indicate that NGAL represents a novel predictive biomarker for AKI and its outcomes. However, NGAL appears to be most sensitive and specific in homogeneous patient populations with temporally predictable forms of AKI. Meta-analyses have also identified age as an effective modifier of NGAL's performance as an AKI biomarker,[34] with better predictive ability in children (overall AUC-ROC 0.93) than in adults (AUC-ROC 0.78). Plasma NGAL measurements may be influenced by a number of coexisting variables such as chronic kidney disease (CKD), chronic hypertension, systemic infections, inflammatory conditions, anemia, hypoxia, and malignancies.[2] In the CKD population, both plasma and urine NGAL levels are elevated, and this correlates with the severity of renal impairment. However, it should be noted that the increase in NGAL in these situations is generally

much less than those typically encountered in AKI. Urine NGAL has also been shown to represent an early biomarker for the degree of chronic injury in patients with IgA nephropathy and lupus nephritis, and may be increased in urinary tract infections.[2] However, the levels of urine NGAL in these situations are significantly blunted compared to that typically measured in AKI.

KIDNEY INJURY MOLECULE-1 (KIM-1) AS AN AKI BIOMARKER

Preclinical subtractive hybridization screens identified kidney injury molecule 1 (*Kim-1*) as a gene that is markedly up-regulated in ischemic rat kidneys.[64] Downstream proteomic studies have also shown KIM-1 to be one of the most highly induced proteins in the kidney after AKI in animal models.[65,66] KIM-1 is a transmembrane protein that is not expressed in normal kidney but is specifically upregulated in dedifferentiated proximal tubule cells after ischemic or nephrotoxic AKI. It has been identified as a phosphatidylserine receptor that transforms epithelial cells into phagocytes by recognizing cell surface-specific epitopes expressed by apoptotic tubular epithelia.[67] A proteolytically processed extracellular domain of KIM-1 is detectable in the urine soon after AKI. KIM-1 represents a promising biomarker for the early diagnosis of AKI and its clinical outcomes.[65,66] The recent availability of a rapid urine dipstick test for KIM-1 will facilitate its further evaluation in preclinical and clinical studies.[68]

In hospitalized patients with established AKI, urinary KIM-1 levels predicted adverse clinical outcomes such as dialysis requirement and mortality (69). In children undergoing CPB who developed AKI one to three days post surgery, urine KIM-1 concentrations were significantly increased within 12 hours.[15,25] The AUC for AKI prediction at 12 hours was 0.83. In a cross-sectional study of critically ill adults with AKI, KIM-1 levels were markedly elevated when compared to healthy controls, yielding an AUC-ROC of 0.95.[37] Age-adjusted levels of urinary KIM-1 were significantly higher in patients who died or required dialysis.[37] KIM-1 is also an excellent marker of nephrotoxicity in preclinical studies.[70] Several prospective studies examining KIM-1 as a biomarker of AKI are underway. The current status of KIM-1 as an AKI biomarker is illustrated in Tables 75.8 and 75.9. Urinary KIM-1 is also increased in a number of chronic kidney diseases, and is an independent predictor of chronic graft loss in renal transplant recipients.[71]

TABLE 75.8 Novel Urinary Biomarkers for the Early Diagnosis of Aki

Biomarker	Cardiopulmonary Bypass (CPB)	Contrast Nephropathy	Kidney Transplant (Tx)	ICU or Emergency Room
NGAL	2 hr post CPB 2 days pre AKI	2 hr post contrast 1–2 days pre AKI	6 hr post Tx 2–3 days pre DGF	On admission 2 days pre AKI
IL-18	6 hr post CPB 1–2 days pre AKI	Not increased	6 hr post Tx 2–3 days pre DGF	2 days pre AKI
L-FABP	6 hr post CPB 1–2 days pre AKI	Not tested	Not tested	2 days pre AKI
KIM-1	12 hr post CPB 1–2 days pre AKI	Not tested	Not tested	Not tested

NGAL, neutrophil gelatinase-associated lipocalin. IL-18, interleukin 18. L-FABP, liver-type fatty acid binding protein. KIM-1, kidney injury molecule 1. AKI, defined as a 50% or greater increase in serum creatinine from baseline. DGF, defined as dialysis requirement within the first week after transplant. Times shown are the earliest time points when the biomarker becomes significantly increased from baseline.

TABLE 75.9 Novel Urinary Biomarkers for the Prediction of Aki Outcomes

Biomarker Name	Cardiopulmonary Bypass (CPB)	Kidney Transplant	ICU or Emergency Room
NGAL	Predicts AKI duration, severity, dialysis, death	Predicts AKI duration	Predicts AKI duration, severity, and dialysis
IL-18	Predicts AKI duration, severity, dialysis, death	Predicts AKI duration	Predicts death
L-FABP	Not tested	Not tested	Predicts AKI severity, dialysis, and death
KIM-1	Not tested	Predicts long term graft loss	Not tested

NGAL, neutrophil gelatinase-associated lipocalin. IL-18, interleukin 18. L-FABP, liver-type fatty acid binding protein. KIM-1, kidney injury molecule 1. AKI, defined as a 50% or greater increase in serum creatinine from baseline.

LIVER-TYPE FATTY ACID BINDING PROTEIN (L-FABP) AS AN AKI BIOMARKER

L-FABP is a protein expressed in the proximal tubule of the kidney. Increased expression and urinary excretion have been described in animal models of AKI.[72–74] Although its precise function is unknown, L-FABP in the kidney has been postulated to represent an endogenous antioxidant capable of suppressing tubule-interstitial damage.

In children undergoing CPB who subsequently developed AKI, urine L-FABP concentrations were significantly increased within four to six hours of the surgery.[11,15] The early urinary L-FABP level was an independent risk factor for the development of AKI, with an AUC of 0.81. In hospitalized patients with established AKI, the AUC of urinary L-FABP for prediction of AKI was 0.93.[75] Urinary L-FABP levels in this cohort were significantly higher in patients with poor outcome, defined as the requirement for renal replacement therapy or the composite end point of death or renal replacement therapy. In patients with septic shock and AKI, urinary L-FABP measured at admission was significantly higher in the non-survivors than in the survivors, with an AUC for mortality prediction of 0.99.[76] Thus, emerging data point to L-FABP as a promising urinary biomarker of AKI and its outcomes (Tables 75.8 and 75.9). However, the urinary excretion of L-FABP is also increased in the setting of CKD.[77] Standardized clinical platforms for the measurement of urinary L-FABP are not currently available.

INTERLEUKIN-18 (IL-18) AS AN AKI BIOMARKER

IL-18 is a pro-inflammatory cytokine and a known mediator of inflammation that is induced in the proximal tubule, and activated by caspase-1.[78] It is a pro-apoptotic molecule that has the potential of worsening the functional consequences of AKI. While very small amounts are present in the normal urine, its concentration is dramatically increased soon after AKI in animal and human models.

In a cross-sectional study, urine IL-18 levels were markedly elevated in patients with established AKI, but not in subjects with urinary tract infection, chronic kidney disease, nephrotic syndrome, or prerenal azotemia.[79] Urinary IL-18 was significantly upregulated prior to the increase in serum creatinine in patients with acute respiratory distress syndrome who develop AKI.[80] On multivariate analysis, urine IL-18 levels predicted the development of AKI 24 hours before the rise in serum creatinine, with an AUC of 0.73. In children undergoing CPB who developed AKI, urinary IL-18 levels increased around six hours and peaked at over 25-fold at 12 hours post CPB. The six hour IL-18 measurement predicted subsequent AKI with an AUC of 0.75-0.84.[10,15] In kidney transplantation, urine IL-18 is an excellent predictive biomarker for DGF, with AUCs in the 0.8–0.9 range.[53,54] Urine IL-18 measurements also represent early biomarkers of AKI in the pediatric intensive care setting, being able to predict this complication about two days prior to the rise in serum creatinine.[81] Early urine IL-18 measurements correlated with the severity of AKI as well as mortality. In two recent prospective multicenter studies in children[16] and adults[32] undergoing cardiac surgery, IL-18 have emerged as an excellent predictor of AKI severity as well as poor clinical outcomes (including longer length of hospitalization, and increased risk for dialysis and death. Overall, IL-18 appears to be more specific to ischemic AKI, and largely unaffected by chronic kidney disease or urinary tract infections. However, IL-18 measurements may also be influenced by a number of coexisting variables, such as endotoxemia, immunologic injury and cisplatin toxicity. Furthermore, plasma IL-18 levels are known to be increased in various pathophysiologic states, such as inflammatory arthritis, inflammatory bowel disease, and systemic lupus erythematosus. The current status of IL-18 as an AKI biomarker is illustrated in Tables 75.8 and 75.9. Standardized platforms for the clinical measurement of urinary IL-18 remain to be developed and validated.

AKI BIOMARKER COMBINATIONS

From the above, it is apparent that there is no single perfect AKI biomarker. A combination of biomarkers may be necessary to provide the best diagnostic and prognostic information in a context-specific manner. Recent studies have explored this possibility. In a large prospective multicenter study of a panel of nine biomarkers to predict clinical outcomes in 971 emergency department patients with suspected sepsis, plasma NGAL emerged as the strongest predictor of shock and death.[82] In a secondary analysis of this cohort, an elevated plasma NGAL level at the time of presentation to the emergency department predicted severe AKI with an AUC of 0.82.[47] In a study examining biomarkers for the prediction of AKI following elective cardiac surgery, urinary NGAL concentrations measured at the time of admission to the ICU predicted the subsequent development of AKI with an AUC of 0.77, and outperformed other biomarkers including α1-microglobulin

and cystatin C.[29] In a similar analysis of multiple urinary biomarkers following cardiac surgery, the six-hour post-operative NGAL best predicted severe AKI with an AUC of 0.88.[28]

Serial measurements of multiple urinary biomarkers after pediatric cardiac surgery have revealed a sequential pattern for the appearance of AKI biomarkers,[15] with NGAL and L-FABP being the earliest responders (with two to four hours after initiation of cardiopulmonary bypass) and KIM-1 and IL-18 representing the intermediate responders (increased 6–12 hours after surgery). The importance of determining the temporal sequence of the biomarkers is underscored by the fact that the course of experimental AKI proceeds in four phases: initiation, extension, maintenance, and recovery.[3] The initiation phase is the period during which initial exposure to the ischemic insult occurs, intracellular ATP depletion is profound, and generation of reactive oxygen molecules and labile iron is initiated. Vasodilator, ATP-donor, anti-oxidant, and iron chelation therapies may be especially effective during this phase, and the appearance of the earliest non-invasive biomarkers such as NGAL may be used to trigger such therapies. Prolongation of ischemia followed by reperfusion ushers in the extension phase. Tubules undergo reperfusion-mediated cell death, and the injured endothelial and epithelial cells amplify the inflammatory cascades. This phase probably represents a window of opportunity for early diagnosis with intermediate biomarkers such as L-FABP and IL-18, and active therapeutic intervention with anti-apoptotic and anti-inflammatory strategies. During the maintenance phase, both cell injury and regeneration occur simultaneously. Measures such as growth factors and stem cells that accelerate the endogenous regeneration processes, initiated by later biomarkers with high specificity such as KIM-1, may be most effective during this phase. Current multicenter studies of multiple biomarkers will help determine which combinations best predict AKI and its outcomes in a context-dependent manner. In this rapidly evolving area of study, ongoing functional genomic and proteomic analyses may also reveal additional biomarkers that further advance this field in the near future.[83]

LIMITATIONS OF EXISTING STUDIES EXAMINING AKI BIOMARKERS

Despite the optimism in the field, there are important limitations that exist in the published AKI biomarker literature that must be acknowledged. First, majority of studies reported were from single centers that enrolled small numbers of subjects. Validation of the published results in additional large multicenter studies will be essential. Second, most studies reported to date did not include patients with CKD. This is problematic, not only because it excludes a large proportion of subjects who frequently develop AKI in clinical practice, but also because CKD in itself can result in increased concentrations of AKI biomarkers, thereby representing a confounding variable. Third, only a few studies have investigated biomarkers for the prediction of AKI severity, morbidity, and mortality.

Finally, and perhaps most importantly, the definition of AKI in the published studies was based largely on elevations in serum creatinine, which raises the conundrum of using a flawed outcome variable to analyze the performance of a novel assay. This definition of AKI sets up the biomarker assay for lack of accuracy due to either false positives (true tubular injury but no significant change in serum creatinine) or false negatives (absence of true tubular injury, but elevations in serum creatinine due to pre-renal causes or any of a number of confounding variables that plague this measurement). It will be crucial in future studies to understand the clinical outcomes of subjects who may be prone to AKI and are "biomarker-positive" but "creatinine-negative." Indeed, a recent multicenter pooled analysis of published data on 2322 critically ill children and adults revealed the surprising finding that approximately 20% of patients display early elevations in NGAL concentrations but never develop increases in serum creatinine.[84] Importantly, this sub-group of "NGAL-positive creatinine-negative" subjects encountered a substantial increase in adverse clinical outcomes, including mortality, dialysis requirement, ICU stay, and overall hospital stay. Thus, early NGAL measurements can identify patients with sub-clinical AKI who have an increased risk of adverse outcomes, even in the absence of diagnostic increases in serum creatinine. It is likely that the other structural AKI biomarkers discussed herein will provide similar diagnostic and prognostic stratification, independent of functional markers such as serum creatinine. Since the gold standard for true AKI (tissue biopsy) is highly unlikely to be feasible, it is vital that large enough future studies demonstrate (a) the association between biomarkers and hard outcomes such as dialysis, cardiovascular events, and death, independent of serum creatinine, and (b) that randomization to a treatment for AKI based on high biomarker levels results in an improvement in kidney function and reduction of clinical outcomes. These should be the next challenges to overcome, in order to firmly establish the clinical utility of AKI biomarkers, and to dramatically improve the outcome of AKI.

References

[1] Uchino S, Kellum JA, Bellomo R, et al. Acute renal failure in critically ill patients: a multinational, multicenter study. JAMA 2005;294(7):813–8.

[2] Devarajan P. Neutrophil gelatinase-associated lipocalin: a promising biomarker for human acute kidney injury. Biomarkers Med 2010;4(2):265–80.

[3] Devarajan P. Update on mechanisms of ischemic acute kidney injury. J Am Soc Nephrol 2006;17(6):1503–20.

[4] Mishra J, Mori K, Ma Q, et al. Amelioration of ischemic acute renal injury by neutrophil gelatinase-associated lipocalin. J Am Soc Nephrol 2004;15(12):3073–82.

[5] Mori K, Lee HT, Rapoport D, et al. Endocytic delivery of lipocalin-siderophore-iron complex rescues the kidney from ischemia-reperfusion injury. J Clin Invest 2005;115(3):610–21.

[6] Supavekin S, Zhang W, Kucherlapati R, et al. Differential gene expression following early renal ischemia-reperfusion. Kidney Int 2003;63(5):1714–24.

[7] Mishra J, Ma Q, Prada A, et al. Identification of neutrophil gelatinase-associated lipocalin as a novel urinary biomarker for ischemic injury. J Am Soc Nephrol 2003;14(10):2534–43.

[8] Mishra J, Mori K, Ma Q, et al. Neutrophil Gelatinase-Associated Lipocalin (NGAL): a novel urinary biomarker for cisplatin nephrotoxicity. Am J Nephrol 2004;24(3):307–15.

[9] Mishra J, Dent C, Tarabishi R, et al. Neutrophil gelatinase-associated lipocalin (NGAL) as a biomarker for acute renal injury following cardiac surgery. Lancet 2005;365(9466):1231–8.

[10] Parikh CR, Mishra J, Thiessen-Philbrook H, et al. Urinary IL-18 is an early predictive biomarker of acute kidney injury after cardiac surgery. Kidney Int 2006;70(1):199–203.

[11] Portilla D, Dent C, Sugaya T, et al. Liver fatty acid-binding protein as a biomarker of acute kidney injury after cardiac surgery. Kidney Int 2008;73(4):465–72.

[12] Dent CL, Ma Q, Dastrala S, et al. Plasma NGAL predicts acute kidney injury, morbidity and mortality after pediatric cardiac surgery: a prospective uncontrolled cohort study. Crit Care 2007;11(6):R127.

[13] Bennett M, Dent CL, Ma Q, et al. Urine NGAL predicts severity of acute kidney injury after cardiac surgery: a prospective study. Clin J Am Soc Nephrol 2008;3(3):665–73.

[14] Krawczeski CD, Woo JG, Wang Y, et al. Neutrophil gelatinase-associated lipocalin concentrations predict development of acute kidney injury in neonates and children after cardiopulmonary bypass. J Pediatr 2011;158(6):1009–15.

[15] Krawczeski CD, Goldstein SL, Woo JG, et al. Temporal relationship and predictive value of urinary acute kidney injury biomarkers after pediatric cardiopulmonary bypass. J Am Coll Cardiol 2011;58(22):2301–9.

[16] Parikh CR, Devarajan P, Zappitelli M, et al. Postoperative biomarkers predict acute kidney injury and poor outcomes after pediatric cardiac surgery. J Am Soc Nephrol 2011;22(9): 1737–47.

[17] Wagener G, Jan M, Kim M, et al. Association between increases in urinary neutrophil-associated lipocalin and acute renal dysfunction after adult cardiac surgery. Anesthesiology 2006;105 (3):485–91.

[18] Koyner J, Bennett M, Worcester E, et al. Urinary cystatin C as an early biomarker of acute kidney injury following adult cardiothoracic surgery. Kidney Int 2008;74(8):1059–69.

[19] Wagener G, Gubitosa G, Wang S, et al. Urinary neutrophil-associated lipocalin and acute kidney injury after cardiac surgery. Am J Kidney Dis 2008;52(3):425–33.

[20] Xin C, Yulong X, Yu C, et al. Urine neutrophil gelatinase-associated lipocalin and interleukin-18 predict acute kidney injury after cardiac surgery. Ren Fail 2008;30(9):904–13.

[21] Tuladhar SM, Puntmann VO, Soni M, et al. Rapid detection of acute kidney injury by plasma and urinary neutrophil gelatinase-associated lipocalin after cardiopulmonary bypass. J Cardiovasc Pharmacol 2009;53(3):261–6.

[22] Haase-Fielitz A, Bellomo R, Devarajan P, et al. Novel and conventional serum biomarkers predicting acute kidney injury in adult cardiac surgery-a prospective cohort study. Crit Care Med 2009;37(2):553–60.

[23] Haase M, Bellomo R, Devarajan P, et al. Novel biomarkers early predict the severity of acute kidney injury after cardiac surgery in adults. Ann Thorac Surg 2009;88(1):124–30.

[24] Haase-Fielitz A, Bellomo R, Devarajan P, et al. The predictive performance of plasma neutrophil gelatinase-associated lipocalin (NGAL) increases with grade of acute kidney injury. Nephrol Dial Transplant 2009;24(11):3349–54.

[25] Han WK, Wagener G, Zhu Y, et al. Urinary biomarkers in the early detection of acute kidney injury after cardiac surgery. Clin J Am Soc Nephrol 2009;4(5):873–82.

[26] Liangos O, Tighiouart H, Perianayagam MC, et al. Comparative analysis of urinary biomarkers for early detection of acute kidney injury following cardiopulmonary bypass. Biomarkers 2009;14(6):423–31.

[27] Che M, Xie B, Xue S, et al. Clinical usefulness of novel biomarkers for the detection of acute kidney injury following elective cardiac surgery. Nephron Clin Pract 2010;115(1): c66–72.

[28] Koyner JL, Vaidya VS, Bennett MR, et al. Urinary biomarkers in the clinical prognosis and early detection of acute kidney injury. Clin J Am Soc Nephrol 2010;5(12):2154–65.

[29] Heise D, Rentsch K, Braeuer A, et al. Comparison of urinary neutrophil glucosaminidase-associated lipocalin, cystatin C, and α1-microglobulin for early detection of acute renal injury after cardiac surgery. Eur J Cardiothorac Surg 2011;39(1): 38–43.

[30] Prabhu A, Sujatha DI, Ninan B, Vijayalakshmi MA. Neutrophil gelatinase associated lipocalin as a biomarker for acute kidney injury in patients undergoing coronary artery bypass grafting with cardiopulmonary bypass. Ann Vasc Surg 2010;24(4): 525–31.

[31] Perry TE, Muehlschlegel JD, Liu KY, et al. Plasma neutrophil gelatinase-associated lipocalin and acute postoperative kidney injury in adult cardiac surgical patients. Anesth Analg 2010;110 (6):1541–7.

[32] Parikh CR, Coca SG, Thiessen-Philbrook H, et al. Postoperative biomarkers predict acute kidney injury and poor outcomes after adult cardiac surgery. J Am Soc Nephrol 2011;22(9):1748–57.

[33] McIlroy DR, Wagener G, Lee HT. Neutrophil gelatinase-associated lipocalin and acute kidney injury after cardiac surgery: the effect of baseline renal function on diagnostic performance. Clin J Am Soc Nephrol 2010;5(2):211–9.

[34] Haase M, Bellomo R, Devarajan P, et al. Accuracy of neutrophil gelatinase-associated lipocalin (NGAL) in diagnosis and prognosis in acute kidney injury: a systematic review and meta-analysis. Am J Kidney Dis 2009;54(6):1012–24.

[35] Zappitelli M, Washburn KK, Arikan AA, et al. Urine NGAL is an early marker of acute kidney injury in critically ill children. Crit Care 2007;11(4):R84.

[36] Wheeler DS, Devarajan P, Ma Q, et al. Serum neutrophil gelatinase-associated lipocalin (NGAL) as a marker of acute kidney injury in critically ill children with septic shock. Crit Care Med 2008;36(4):1297–303.

[37] Vaidya VS, Waikar SS, Ferguson MA, et al. Urinary biomarkers for sensitive and specific detection of acute kidney injury in humans. Clin Transl Sci 2008;1(3):200–8.

[38] Siew ED, Ware LB, Gebretsadik T, et al. Urine neutrophil gelatinase-associated lipocalin moderately predicts acute kidney injury in critically ill adults. J Am Soc Nephrol 2009;20(8): 1823–32.
[39] Makris K, Markou N, Evodia E, et al. Urinary neutrophil gelatinase-associated lipocalin (NGAL) as an early marker of acute kidney injury in critically ill multiple trauma patients. Clin Chem Lab Med 2009;47(1):79–82.
[40] Mårtensson J, Bell M, Oldner A, et al. Neutrophil gelatinase-associated lipocalin in adult septic patients with and without acute kidney injury. Intensive Care Med 2010;36(8): 1333–40.
[41] de Geus HR, Bakker J, Lesaffre EM, le Noble JL. Neutrophil gelatinase-associated lipocalin at ICU admission predicts for acute kidney injury in adult patients. Am J Respir Crit Care Med 2011;183(7):907–14.
[42] Endre ZH, Pickering JW, Walker RJ, et al. Improved performance of urinary biomarkers of acute kidney injury in the critically ill by stratification for injury duration and baseline renal function. Kidney Int 2011;79(10):1119–30.
[43] Singer E, Elger A, Elitok S, et al. Urinary neutrophil gelatinase-associated lipocalin distinguishes pre-renal from intrinsic renal failure and predicts outcomes. Kidney Int 2011;80(4): 405–14.
[44] Constantin J-M, Futier E, Perbet S, et al. Plasma neutrophil gelatinase-associated lipocalin is an early marker of acute kidney injury in adult critically ill patients: a prospective study. J Crit Care 2010;25(1):176 [e1-6].
[45] Niemann CU, Walia A, Waldman J, et al. Acute kidney injury during liver transplantation as determined by neutrophil gelatinase-associated lipocalin. Liver Transplant 2009;15(12): 1852–60.
[46] Cruz DN, de Cal M, Garzotto F, et al. Plasma neutrophil gelatinase-associated lipocalin is an early biomarker for acute kidney injury in an adult ICU population. Int Care Med 2010;36 (3):444–51.
[47] Shapiro NI, Trzeciak S, Hollander JE, et al. The diagnostic accuracy of plasma neutrophil gelatinase-associated lipocalin in the prediction of acute kidney injury in emergency department patients with suspected sepsis. Ann Emerg Med 2010;56(1): 52–9 [e1].
[48] Nickolas TL, O'Rourke MJ, Yang J, et al. Sensitivity and specificity of a single emergency department measurement of urinary neutrophil gelatinase-associated lipocalin for diagnosing acute kidney injury. Ann Intern Med 2008;148(11):810–9.
[49] Du Y, Zappitelli M, Mian A, et al. Urinary biomarkers to detect acute kidney injury in the pediatric emergency center. Pediatr Nephrol 2011;26(2):267–74.
[50] Nickolas TL, Schmidt-Ott KM, Canetta P, et al. Diagnostic and prognostic stratification in the emergency department using urinary biomarkers of nephron damage. J Am Coll Cardiol 2012;59 (3):246–55.
[51] Bagshaw SM, Bennett M, Haase M, et al. Plasma and urine neutrophil gelatinase-associated lipocalin in septic versus non-septic acute kidney injury in critical illness. Int Care Med 2010; 36(3):452–61.
[52] Mishra J, Ma Q, Kelly C, et al. Kidney NGAL is a novel early marker of acute injury following transplantation. Pediatr Nephrol 2006;21(6):856–63.
[53] Parikh CR, Jani A, Mishra J, et al. Urine NGAL and IL-18 are predictive biomarkers for delayed graft function following kidney transplantation. Am J Transplant 2006;6(7):1639–45.
[54] Hall IE, Yarlagadda SG, Coca SG, et al. IL-18 and Urinary NGAL predict dialysis and graft recovery after kidney transplantation. J Am Soc Nephrol 2010;21(1):189–97.
[55] Hollmen ME, Kyllonen LE, Inkinen KA, et al. Urine neutrophil gelatinase-associated lipocalin is a marker of graft recovery after kidney transplantation. Kidney Int 2011;79(1):89–98.
[56] Hirsch R, Dent C, Pfriem H, et al. NGAL is an early predictive biomarker of contrast-induced nephropathy in children. Pediatr Nephrol 2007;22(12):2089–95.
[57] Bachorzewska-Gajewska H, Malyszko J, Sitniewska E, et al. Neutrophil-gelatinase-associated lipocalin and renal function after percutaneous coronary interventions. Am J Nephrol 2006;26(3):287–92.
[58] Bachorzewska-Gajewska H, Malyszko J, Sitniewska E, et al. Neutrophil gelatinase-associated lipocalin (NGAL) correlations with cystatin C, serum creatinine and eGFR in patients with normal serum creatinine undergoing coronary angiography. Nephrol Dial Transplant 2007;22(1):295–6.
[59] Ling W, Zhaohui N, Ben H, et al. Urinary IL-18 and NGAL as early predictive biomarkers in contrast-induced nephropathy after coronary angiography. Nephron Clin Pract 2008;108(3): c176–81.
[60] Bellomo R, Ronco C, Kellum JA, et al. Acute renal failure – definition, outcome measures, animal models, fluid therapy and information technology needs: the second international consensus conference of the acute dialysis quality initiative (ADQI) Group. Crit Care 2004;8(4):R204–12.
[61] Trachtman H, Christen E, Cnaan A, et al. Urinary neutrophil gelatinase-associated lipocalcin in D + HUS: a novel marker of renal injury. Pediatr Nephrol 2006;21(7):989–94.
[62] Kumpers P, Hafer C, Lukasz A, et al. Serum neutrophil gelatinase-associated lipocalin at inception of renal replacement therapy predicts survival in critically ill patients with acute kidney injury. Crit Care 2010;14(1):R9.
[63] Yang HN, Boo CS, Kim MG, et al. Urine neutrophil gelatinase-associated lipocalin: an independent predictor of adverse outcomes in acute kidney injury. Am J Nephrol 2010;31(6): 501–9.
[64] Ichimura T, Bonventre JC, Bailly V, et al. Kidney Injury Molecule-1 (KIM-1), a putative epithelial cell adhesion molecule containing a novel immunoglobulin domain, is up-regulated in renal cells after injury. J Biol Chem 1998;273(7):4135–42.
[65] Bonventre JV. Kidney injury molecule-1 (KIM-1): a urinary biomarker and much more. Nephrol Dial Transplant 2009;24: 3265–8.
[66] Bonventre JV, Yang L. Kidney injury molecule-1. Curr Opin Crit Care 2010; [Epub ahead of print].
[67] Ichimura T, Asseldonk EJ, Humphreys BD, et al. Kidney injury molecule-1 is a phosphatidylserine receptor that confers a phagocytic phenotype on epithelial cells. J Clin Invest 2008;118 (5):1657–68.
[68] Vaidya VS, Ford GM, Waikar SS, et al. A rapid urine test for early detection of kidney injury. Kidney Int 2009;76(1):108–14.
[69] Liangos O, Periyanayagam MC, Vaidya VS, et al. Urinary N-acetyl-beta-(D)-glucosaminidase activity and kidney injury molecule-1 level are associated with adverse outcomes in acute renal failure. J Am Soc Nephrol 2007;18:904–12.
[70] Vaidya VS, Ozer JS, Dieterle F, et al. Kidney injury molecule-1 outperforms traditional biomarkers of kidney injury in preclinical biomarker qualification studies. Nat Biotechnol 2010;28: 478–85.
[71] van Timmeren MM, Vaidya VS, van Ree RM, et al. High urinary excretion of kidney injury molecule-1 is an independent predictor of graft loss in renal transplant recipients. Transplantation 2007;84(12):1625–30.
[72] Noiri E, Doi K, Negishi K, et al. Urinary fatty acid-binding protein 1: an early predictive biomarker of kidney injury. Am J Physiol Renal Physiol 2009;296:F669–79.

[73] Yamamoto T, Noiri E, Ono Y, et al. Renal L-type fatty acid-−binding protein in acute ischemic injury. J Am Soc Nephrol 2007;18:2894−902.
[74] Negishi K, Noiri E, Doi K, et al. Monitoring of urinary L-type fatty acid-binding protein predicts histological severity of acute kidney injury. Am J Pathol 2009;174:1154−9.
[75] Ferguson MA, Vaidya VS, Waikar SS, et al. Urinary liver-type fatty acid-binding protein predicts adverse outcomes in acute kidney injury. Kidney Int 2010;77:708−14.
[76] Doi K, Noiri E, Maeda-Mamiya R, et al. Urinary L-type fatty acid-binding protein as a new biomarker of sepsis complicated with acute kidney injury. Crit Care Med 2010;38:2037−42.
[77] Kamijo A, Sugaya T, Hikawa A, et al. Urinary liver-type fatty acid binding protein as a useful biomarker in chronic kidney disease. Mol Cell Biochem 2006;284(1−2):175−82.
[78] Melnikov VY, Ecder T, Fantuzzi G, et al. Impaired IL-18 processing protects caspase-1 deficient mice from ischemic acute renal failure. J Clin Invest 2001;107:1145−52.
[79] Parikh CR, Jani A, Melnikov VY, et al. Urinary interleukin-18 is a marker of human acute tubular necrosis. Am J Kidney Dis 2004;43:405−14.
[80] Parikh CR, Abraham E, Ancukiewicz M, et al. Urine IL-18 is an early diagnostic marker for acute kidney injury and predicts mortality in the intensive care unit. J Am Soc Nephrol 2005;16:3046−52.
[81] Washburn KK, Zappitelli M, Arikan AA, et al. Urinary Interleukin-18 is an Acute Kidney Injury Biomarker in Critically Ill Children. Nephrol Dial Transplant 2008;23:566−72.
[82] Shapiro NI, Trzeciak S, Hollander JE, et al. A prospective, multicenter derivation of a biomarker panel to assess risk of organ dysfunction, shock, and death in emergency department patients with suspected sepsis. Crit Care Med 2009;37:96−104.
[83] Devarajan P, Krawczeski CD, Nguyen MT, et al. Proteomic identification of early biomarkers of acute kidney injury after cardiac surgery in children. Am J Kidney Dis 2010;56: 632−42.
[84] Haase M, Devarajan P, Haase-Fielitz A, et al. The outcome of neutrophil gelatinase-associated lipocalin-positive subclinical acute kidney injury: a multicenter pooled analysis of prospective studies. J Am Coll Cardiol 2011;7(17):1752−61.

CHAPTER

76

Pathophysiology of Acute Kidney Injury

Bruce A. Molitoris[1] *and Asif Sharfuddin*[2]

[1]Indiana Center for Biological Microscopy, Indiana University School of Medicine, and Roudebush VA Medical Center, Division of Nephrology, Department of Medicine, Indianapolis, Indiana, USA

[2]Indiana University School of Medicine, and Roudebush VA Medical Center, Division of Nephrology, Department of Medicine, Indianapolis, Indiana, USA

CLINICAL OVERVIEW

Classifications and Definitions

Acute Kidney Injury (AKI) is a heterogenous syndrome defined by a rapid decline in glomerular filtration rate (GFR) which may lead to accumulation of metabolic waste products and disturbances in fluid, electrolyte and acid-base handling.[1] In the last few years, the previous terminology of Acute Renal Failure (ARF) has largely been abandoned and the new term AKI has been widely adopted in the medical literature. In this chapter, the term AKI will be used to describe the entire spectrum of disorders that share the same physiologic characteristics but may be pathophysiologically distinct.

In 2002, based on the recommendations of the Acute Dialysis Quality Initiatives (ADQI) the staging of AKI was proposed. The RIFLE classification of AKI is divided into three levels of renal dysfunction namely, "*r*isk", "*i*njury" and "*f*ailure" based on either GFR or urine output criteria whichever is more severe. The GFR criteria assesses renal dysfunction by using either changes in serum creatinine or the percentage decline in GFR from baseline GFR. The parameters used have a high sensitivity, are prognostic based on severity of stage, but represent a retrospective analysis.[2,3] Two other very important clinical outcomes are also incorporated into the RIFLE criteria: "*l*oss" of kidney function as defined by persistent AKI with the need for renal replacement therapy (RRT) for more than four weeks, and "*e*nd" stage kidney disease, defined as the need for RRT for greater than three months. These parameters are more strict and therefore have a higher specificity.[2]

Recently, the Acute Kidney Injury Network (AKIN) proposed a modification of the RIFLE criteria with the addition of a $>=$ 0.3 mg/dl increase in serum creatinine to the criteria that define Risk. Because of the linear relationship between GFR and 1/serum creatinine, it should be kept in mind that a small rise in serum creatinine, in the normal or near normal values, corresponds to relatively large decline in GFR. For example, in a steady state, a serum creatinine of 0.8 mg/dl in a young 50 kg female corresponds to a GFR of approximately 100 ml/min, while a serum creatinine of 1.6 mg/dl would reflect in a GFR of 50 ml/min, a decline of nearly 50% in GFR. In the non-steady state of AKI, the serum creatinine value should be considered very carefully, as this is not an equilibrium state. Thus an overestimation of the GFR is made if standard steady state calculations are made using formulas such as Cockroft-Gault or MDRD if the serum creatinine is rising. Hence during the evolution of acute renal dysfunction, serum creatinine underestimates the degree of renal dysfunction, and conversely it underestimates the degree of renal recovery as function recovers. Having said that, the change from baseline and perhaps the rate of rise of creatinine are still potentially useful in the clinical evaluation of GFR decline. Even creatinine clearance (when collection is accurate) suffers from the same limitation as mentioned above, and causes an overestimation of GFR. Determining an accurate GFR in clinical settings is rarely accomplished and perhaps more important would be the determination of whether the GFR is improving or not. Hence one should always remember that to detect AKI, it is *essential to assess the change in creatinine*, and that *across all patients, a single creatinine valuenever corresponds to a given GFR*.[4]

Seldin and Giebisch's The Kidney, Fifth Edition.
DOI: http://dx.doi.org/10.1016/B978-0-12-381462-3.00076-8

© 2013 Elsevier Inc. All rights reserved.

TABLE 76.1 RIFLE and Acute Kidney Injury Network (AKIN) Definition and Staging of Acute Kidney Injury

RIFLE	AKIN
Definition	
An increase in serum creatinine of >50% developing over < 7 days; or a urine output of <0.5 ml/kg/hr for > 6 hours	An increase in serum creatinine of > 0.3 mg/dl or >50% developing over < 48 hours; or a urine output of <0.5 ml/kg/hr for > 6 hours

Staging Criteria

RIFLE Stage	Increase in Serum Creatinine	Urine Output Criteria	Increase in Serum Creatinine	AKIN Stage
Risk	≥ 50%	<0.5 ml/kg/hr for > 6 hours	≥ 0.3 mg/dl; or ≥ 50%	Stage 1
Injury	≥ 100%	<0.5 ml/kg/hr for > 12 hours	≥ 100%	Stage 2
Failure	≥ 200%	<0.5 ml/kg/hr for > 24 hours or anuria for > 12 hours	≥ 200%	Stage 3
Loss	Need for renal replacement therapy for > 4 weeks			
End-stage	Need for renal replacement therapy for > 3 months			

The production rate and volume of distribution of creatinine also affect the plasma creatinine value, while other factors such as medications (e.g. cimetidine) can inhibit distal tubular creatinine secretion and cause a rise in serum creatinine without being secondary to AKI. Abnormalities in liver function, decreased muscle mass and aging decrease the production of creatinine, whereas fever, immobilization, glucocorticoids or muscle trauma increase its production.

Urine output is sensitive to changes in renal hemodynamics, but extremely insensitive to define or differentiate AKI. Oliguria has been defined as urine output of <400 ml/day or <0.3 ml/kg/hour, and has been found to be associated with a higher mortality as compared to non-oliguric ARF.[5] However, severe AKI can exist in non-oliguric states as well, whereas obstructive causes could present with a fluctuating levels of urine output. The RIFLE criteria does employ urine output as markers of risk, injury or failure, though concordance between serum creatinine and urine output criteria has not been established, even with regards to mortality risk.

Acute Kidney Injury: Incidence and Risk Factors

Incidence

The exact incidence of AKI has varied in the past due to the absence, until recently, of a standard definition. It has been estimated that 3% to 20%[6,7] of hospitalized patients and 25% to 67% of ICU patients develop AKI,[8,9] with 5 to 6% of the ICU population requiring renal replacement therapy after developing AKI.[5,10–13] Studies have indicated that there is an increasing incidence of AKI over the last twenty years. Amongst all Medicare patients, Eggers et al. noted that after adjusting for sex, age and ethnicity, AKI rates increased 10% per year from 14 cases per year in 1992 to 36 cases per year in 2001.[14] The CDC noted >20 fold increase in the incidence of AKI for patients hospitalized between 1980–2005 using ICD-9 codes.[14a]

In another multinational, multicenter observational study of 29,269 critically ill patients, 5.7% developed severe AKI and 4.3% received renal replacement therapy.[15] Although there is less confusion with regard to rates of AKI requiring renal replacement therapy, reported rates still vary due to differences in characteristics of patient populations and variability in criteria for the initiation of renal replacement therapy. Population based studies have shown a rate of 2147 cases of AKI per million population.[13]

Risk Factors

An extremely important aspect in trying to prevent AKI is to identify high risk populations and clinical conditions, or high risk situations and procedures to devise strategies to minimize the incidence and impact of AKI. Numerous risk factors have been identifiedin different population groups, some of which are discussed here (Table 76.2). Most studies have found age to be an independent risk factor for the development of AKI. In 2009 the URSDS, reported incidence rates of AKI in the US using three different datasets from 1995 to 2007[15a] and found the largest increase in AKI incidence was seen among older individuals >85 years age. In a large observational cohort study across five academic centers in the United States, the mean age of patients was 59.5 years. Possible reasons why age

TABLE 76.2 Common Risk Factors for Developing Acute Kidney Injury

Risk Factor
Age
Pre-existing Chronic Kidney Disease
Reduced Effective Arterial Volume
Volume Depletion
Nephrotic Syndrome
Congestive Heart Failure
Cirrhosis
Sepsis
Diabetes Mellitus
Drugs
Non-Steroidal Anti-Inflammatory Drugs
Aminoglycosides
Radio-Contrast Agents
Inflammatory States
Trauma
Burns
Sepsis
Post-Surgical State
Post Solid Organ/Allogenic Bone Marrow Transplant
Mechanical Ventilation

could be an independent risk factor includes decreased residual renal function, presence of comorbidities and increased susceptibility to infections.[16,17] Pre-existing renal insufficiency is a major risk factor for the development of AKI in the non-ICU and ICU setting. Even small decrements in systemic hemodynamics can lead to significant alterations in the renal hemodynamics, due to diminished capacity to auto-regulate the response to a decreased perfusion pressure, leading to a reduction in GFR. Increasing levels of risk are associated with more severe baseline chronic kidney disease (CKD). Compared to patients with baseline eGFR >60 ml/min/1.73 m^2, those with eGFR values of 45–59 ml/min/1.73 m^2 had a nearly 2-fold increased risk of developing dialysis-requiring AKI. This risk increased to more than 40-fold among patients with baseline eGFR values <15 ml/min/1.73 m^2. Underlying diabetes mellitus, hypertension, and the presence of proteinuria were also associated with increased the risk for hospital-acquired AKI.[18] CKD patients are at high risk for development of AKI secondary to radio-contrast agents, aminoglycosides, atheroembolism, and cardiovascular surgery.[19,20]

The presence of exo-and endo-toxins increases the risk for AKI. Antibiotics, non-steroidal anti-inflammatory agents, anesthetic agents, contrast media and diuretics are well defined risk factors for AKI. There is a synergestic increase in nephrotoxicity from such agents when there is renal hypoperfusion for any reason. Severe infections, especially in the setting of a surgical procedure are often associated with AKI. AKI complicating trauma is often multifactorial in origin, resulting from a combination of hypovolemia and myoglobin release from muscle tissue. AKI remains a frequent complication of surgery necessitating cardiopulmonary bypass despite off pump techniques.

Etiology

Frequently the cause for AKI is multifactorial, involving more than one insult. However, traditionally the etiology of AKI has been categorized anatomically into pre-renal, renal and post-renal (Figure 76.1).

Prerenal Acute Kidney Injury

The most common cause of AKI is prerenal azotemia and it accounts for about 40–55% of the cases.[5,10,16] It results from kidney hypoperfusion due to a reduced effective arterial volume (EAV). The effective arterial volme is the volume of blood effectively perfusing organs. Conditions causing hypovolemia resulting in a reduced EAV include hemorrhage (traumatic, gastrointestinal, surgical), GI losses (vomiting, diarrhea, nasogastric suction), kidney losses (over-diuresis, diabetes insipidus) and third spacing (pancreatitis, hypoalbuminemia). In addition cardiogenic shock, septic shock, cirrhosis, nephrotic syndrome and anaphylaxis all are pathophysiologic conditions that decrease effective circulating volume, independent of the volume status, resulting in reduced renal blood flow. Pre-renal AKI reverses rapidly once renal perfusion is restored because the renal parenchyma remains uninjured. However, when hypoperfusion is severe, it may result in ischemia leading to acute tubular necrosis.

Pre-renal azotemia has also been divided into volume responsive and volume non-responsive. In volume responsive pre-renal azotemia correction of the patients volume status results in increased kidney perfusion and resolution of the disorder. In volume non-responsive forms, additional intravenous volume is of no help in restoring kidney perfusion and function. Disease processes such as severe congestive heart failure and sepsis may not respond to intravenous fluids as markedly reduced cardiac output or a reduction in total vascular resistance, respectively, prevent volume mediated improvement in kidney perfusion. Therefore

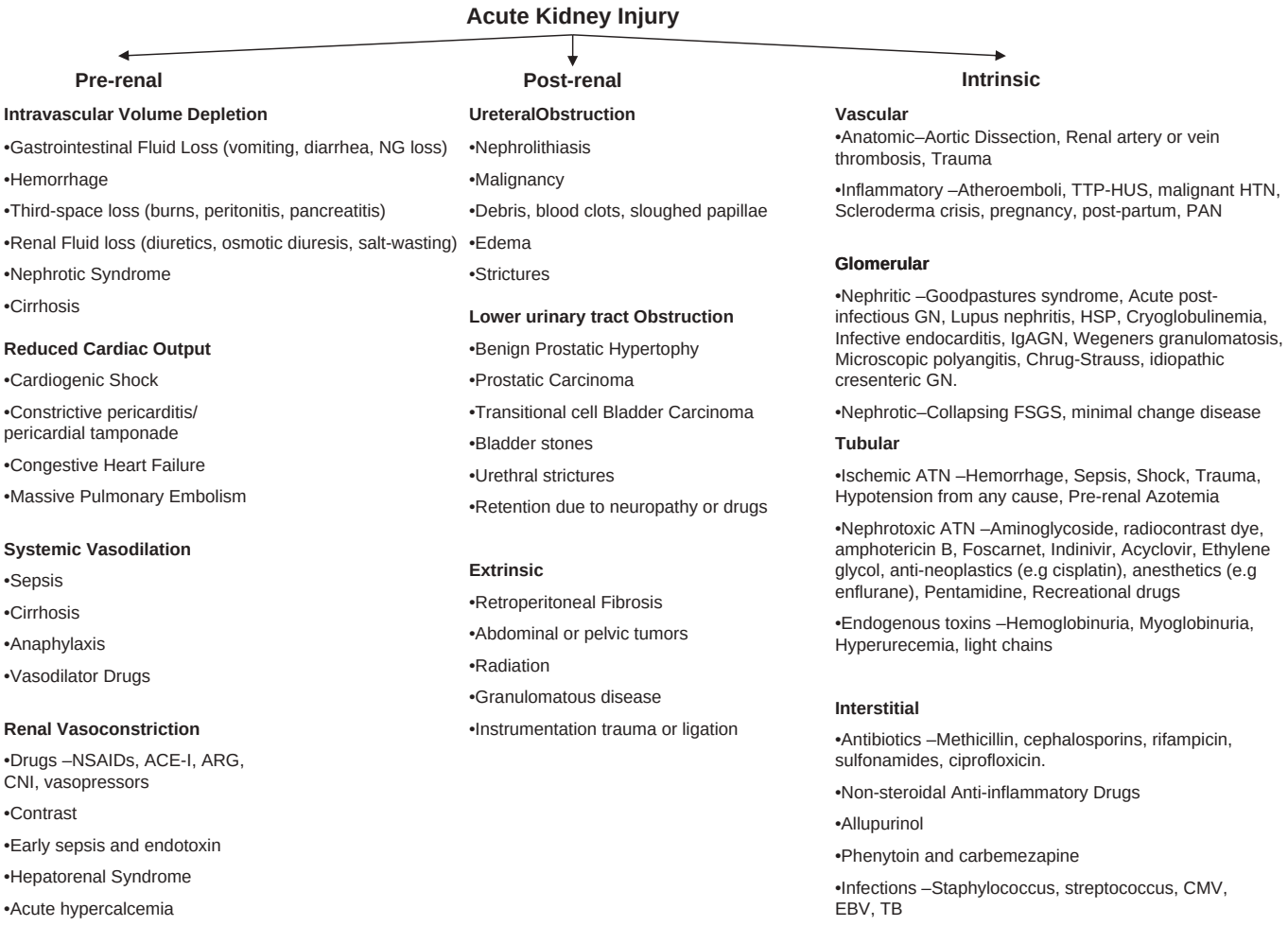

FIGURE 76.1 Etiology of AKI based on anatomical categories (pre/intrinsic/post).

it is essential to understand the mechanism mediating pre-renal azotemia in order to correct it.

Hypovolemia causes a decrease in mean arterial pressure which activates baroreceptors and initiates a cascade of neural and humoral responses. This leads to the activation of sympathetic nervous system that causes increased production of catecholamines especially norepinephrine. The other major consequence is the activation of the renin-angiotgensin-aldosterone (RAAS) system that causes production of angiotensin II (ATII), a very potent vasoconstrictor. There is also an increased release of anti-diuretic hormone (ADH) mediated both by hypovolemia and a rise in extracellular osmolality, that retains water, as well as influencing urea back-diffusion into the papillary interstitium.

In response to volume depletion or states of decreased EAV there is increased intra-renal ATII activity. This increases proximal tubule Na^+ absorption through a complex effect in the glomerulus by preferentially increasing the efferent arterioral resistance. Thus the glomerular hydrostatic pressure is increased and preserves GFR. With severe volume depletion there is greater ATII activity leading to afferent arteriolar constriction, that reduces both renal plasma flow and the filtration fraction.[21] ATII has also been shown to have direct effects on transport in proximal tubule through receptors located in the proximal tubule. It has also been postulated that the proximal tubule can locally produce ATII. Hence under conditions of volume depletion, ATII stimulates a larger fraction of the transport, whereas volume expansion will blunt this response.[22,23]

There is also significantly increased renal sympathetic nerve activity in pre-renal azotemia. Studies have shown that in volume depleted states adrenergic activity independently constricts the afferent arteriole as well as changing the efferent arteriolar resistance through ATII. Renal nerve activity is linked to renin release through β-adrenergic receptors on renin-containing cells while α-a adrenergic influences primarily the vascular resistances within the kidney. In contrast α-2 adrenergic agonists primarily decrease the glomerular ultrafiltration coefficient via ATII. Although vasodilation might be

expected as a result of acute removal of adrenergic activity, a transient increase in ATII is actually seen, along with constancy in GFR and renal blood flow. Even after sub-acute renal denervation renal vascular sensitivity increased to ATII as a result of major up-regulation of ATII receptors. Hence complex effects on the renin-angiotensin activity occur within the kidney secondary to renal adrenergic activity during pre-renal azotemia.[24]

All these systems work together and stimulate vasoconstriction in musculocutaneous and splanchnic circulations, inhibit salt loss through sweat, stimulate thirst and retain salt and water to maintain blood pressure and preserve cardiac and cerebral perfusion. Various compensatory mechanisms preserve glomerular perfusion.[25] Autoregulation is achieved by stretch receptors in afferent arterioles that cause vasodilation in arterioles in response to reduced perfusion pressure. Under physiologic conditions autoregulation works until a mean systemic arterial blood pressure of 75–80 mm Hg. Below this, the glomerular ultrafiltration pressure and GRF decline. Kidney production of prostaglandins, kallikrein and kinins as well as nitric oxide is increased contributing to the vasodilation.[26,27] NSAIDs, by inhibiting prostaglandin production, worsen kidney perfusion in patients with hypoperfusion. Selective efferent arteriolar constriction, which is a result of ATII, helps preserve the intraglomerular pressure andGFR. ACE inhibitors inhibit synthesis of angiotensin II and so disturb this delicate balance in patients with severe reductions in EAV such as severe CHF or bilateral renal artery stenosis and can worsen prerenal azotemia. On the other hand, very high levels of angiotensin II seen in circulatory shock causes constriction of both afferent and efferent arterioles which negates its protective effect.

Although these compensatory mechanisms are protective against acute renal failure, they are overwhelmed in states of severe hypoperfusion. Renovascular disease, hypertensive nephrosclerosis, diabetic nephropathy as well as older age predispose patients to kidney hypoperfusion[28] at lesser degrees of hypotension.

Post-Renal Acute Kidney Injury

Post-renal AKI occurs from either ureteric obstruction or bladder/urethral obstruction. AKI from ureteric obstruction requires that the blockage occur either bilaterally at any level of the ureters, or unilaterally in a patient with a solitary functioning kidney or CKD. Ureteric obstruction can be either intraluminal or external. Bilateral ureteric calculi, blood clots, and sloughed renal papillae can obstruct the lumen, while external compression from tumor or hemorrhage can block the ureters as well. Fibrosis of the ureters intrinsically or of the retroperitoneum can narrow the lumen to the point of complete luminal obstruction. The most common cause for post-renal azotemia is structural or functional obstruction of the bladder neck. Prostatic conditions, therapy with anti-cholinergic agents and a neurogenic bladder can all cause post-renal AKI. Relief of the obstruction usually causes prompt return of GFR if the duration of obstruction has not been excessive. The rate and magnitude of functional recovery is dependent on the extent and duration of the obstruction.[29]

AKI resulting from obstruction usually accounts for less 5% of cases, although in certain settings, e.g., transplant, it can be as high as 6–10%. Clinically the patient can present with pain and oliguria, though these are non-specific. Because of the ease of ultrasonography, its diagnosis is usually straightforward, although a volume depleted patient or a patient with severe reduction in GFR may not show hydronephrosis on radiological assessment. Since initially during the course of the disease GFR is not affected, volume repletion can help with the diagnosis by increasing GFR and urine production into the ureter leading to dilation of the ureter proximal to the obstruction and enhancing ultrasound visualization. Early diagnosis and prompt relief of obstruction remain key goals in preventing long-term parenchymal damage as the shorter the period of obstruction the better the chances for recovery and long-term outcomes. The pathophysiology and treatment of obstructive uropathy are discussed extensively in another chapter.

Intrinsic or Intra-Renal Acute Kidney Injury

It is helpful to divide the causes of intrinsic renal azotemia among categories that delineate the site of the initiating injury. Thus the most useful classification is as follows: (1) Vascular—(a) large renal vessels and (b) renal microvasculature; (2) Glomerular; (3) Tubular and (4) Interstitial. AKI secondary to vasculitides and rapidly progressive glomerulonephritides are discussed elsewhere in the text. Below we shall focus on AKI pathophysiology secondary to tubular and interstitial diseases before going on to discuss ATN in detail.

Interstitial

Acute interstitial nephritis (AIN) represents a frequent cause of acute kidney injury, accounting for 15–27% of renal biopsies performed because of this condition. By and large, drug-induced AIN is currently the commonest etiology of AIN, with antimicrobials and nonsteroidal anti-inflammatory drugs being the most frequent offending agents.[30] Other conditions such as leukemia, lymphoma, sarcoidosis, bacterial infections (e.g., E.coli) and viral infections (e.g., cytomegalovirus) can also cause acute interstitial disease

leading to AKI. The inflammatory cellular infiltrates that characterize AIN, mainly composed of T lymphocytes and macrophages, are a powerful source of cytokines that increase the production of extracellular matrix and the number of interstitial fibroblasts, and induce an amplification process recruiting more inflammatory cells and eosinophils into the interstitium.[31] These are often patchy and present most commonly in the deep cortex and outer medulla and mostly comprised of T-cell and monocytes/macrophages and eosinophils. These infiltrations are always associated with interstitial edema, and sometimes with patchy tubular necrosis that if present is usually in close proximity to areas with extensive inflammatory infiltrates.[32] A few neutrophilic granulocytes may be present as well. The majority of cases of AIN are probably induced by extra-renal antigens being produced by drugs or infectious agents that may be able to induce AIN by: (1) binding to kidney structures, (2) modifying immunogenetics of native renal proteins, (3) mimicking renal antigens, or (4) precipitating as immune-complexes and hence serving as the site of antibody or cellular mediated injury.[33] Medications and specific microbial antigens could elicit an immune reaction after their interstitial deposition (planted antigens). Conversely, tubular cells have the capacity to hydrolyze and process exogenous proteins. In this regard, medications can bind to a normal component of TBM, behaving as a hapten, or can mimic an antigen normally present within the TBM, inducing an immune response directed against this antigen.[34] Immunofluorescence studies in renal biopsies of patients with AIN are generally negative, indicating the absence of antibody-mediated immunity that has a marginal, if any, pathogenic role.[31]

TABLE 76.3 Classification of Various Common Drugs Based on Pathophysiological Categories of AKI

1. **Vasoconstriction/impaired microvasculature hemodynamics (pre-renal)** – NSAID's, ACE-inhibitors,angiotensin receptor blockers, norepinephrine, tacrolimus, cyclosporine,diuretics, cocaine, mitomycin C, estrogen, quinine, interleukin-2, COX-2 inhibitors
2. **Tubular cell toxicity**–Antibiotics – Aminoglycosides, amphotericin B, vancomycin, rifampicin, foscarnet, pentamidine, cephaloridine, cephalothin. Radio-contrast agents, NSAID's, acetaminophen, cyclosporine, cisplatin, mannitol, heavy metals, IVIG, ifosfamide, tenofovir.
3. **Acute Interstitial Nephritis** – Antibiotics – Ampicillin, penicillin G, methicillin, oxacillin, rifampicin, ciprofloxacin, cephalothin, sulfonamides. NSAIDs, aspirin, fenoprofen, naproxen, piroxicam, phenybutazone, radio-contrast agents, thiazinde diuretics, phenytoin, furosemide, allopurinol, cimetidine, omeprazole
4. **Tubular Lumen obstruction** – Sulfonamides, acyclovir, cidofovir, methotrexate, triamterene, methoxyflurane, protease inhibitors, ethylene glycol, indinivir, oral sodium phosphate bowel preparations.
5. **Thrombotic Microangiopathy** – Clopidogrel, cocaine, ticlodipine, cyclosporine, tacrolimus, mitomycin C, oral contraceptives, gemcitibine, bevacizumab.
6. **Osmotic nephrosis** – IVIG, Mannitol, dextrans, hetastarch

Exogenous Nephrotoxins

The kidneys are vulnerable to toxicity as they are the major elimination/metabolizing route of many of these elements and also because epithelial cells reabsorb agents from the interstitium that is exposed to high concentrations of these agents.

RADIOCONTRAST INDUCED NEPHROPATHY (CIN)

CIN is a common complication of radiological or angiographic procedures. The incidence varies from 3–7% in patients without any risk factors, but can be as high as 50% in patients with chronic kidney disease (CKD). Other risk factors include diabetes, intravascular volume depletion, high osmolar contrast, advanced age, proteinuria and anemia.[35,36] The pathophysiology of CIN likely consists of combined hypoxic and toxic renal tubular damage associated with renal endothelial dysfunction and altered microcirculation.[37,38] Initially, radiocontrast injection leads to an abrupt but transient increase in renal plasma flow, GFR and urinary output[39] due to the hyperosmolar radio-contrast agent enhancing solute delivery to the distal nephron and leading to an increased oxygen consumption by enhanced tubular sodium reabsorption. A transient phase vasodilation is followed by a period of sustained vasoconstriction, resulting in hypoxic cell damage mainly to the outer medulla.[40] Renal parenchymal oxygenation decreases especially in the outer medulla as documented in various studies where the cortical PO_2 declined from 40 to 25 mmHg, while the medullary PO_2 fell from 30–26mmHG to 9–15 mmHg.[38,41,42] The renin-angiotensin system is thought to be activated by RC media, while there is also evidence that Ca^{2+} as a second messenger is involved in the renal vasoconstriction.[43] Perturbations in the local vasodilatory system are evident as suggested by aggravation of RCIN in the setting of concomitant NSAID presence, thus highlighting the role of altered renal prostaglandin production in its pathogenesis. Similarly, NO inhibition potentiates the renal damage while L-argninine, a precursor of NO, attenuates the damage implying that a disturbance in NO production likely worsens the decrease in RBF after RC infusion. Increased synthesis and release of endothelin (ET) and adenosine from endothelial cells, combined with suppression of NO production likely results in medullary hypoxia secondary to shunting of blood flow to the cortex. Although experimental animal studies have demonstrated beneficial effects of

using ET-antagonists, their efficacy has not been reproduced in human clinical studies. Video microscopy studies have shown that radiocontrast agents markedly reduced inner medullary papillary blood flow, to the extent of near cessation of RBC movement in papillary vessels, associated with RBC aggregation within the papillary vasa recta.[44] Lastly, mechanical factors such as the viscosity of the radiocontrast agent also plays a role, as the contrast agents increase blood viscosity in the inner medulla which already has hypertonic conditions.[45,46]

Cell-culture studies indicate direct RC media toxicity to proximal tubule cells, which has been observed in human studies where biopsies have shown morphological features of proximal tubular vacuolization, tubular degeneration, and interstitial inflammation and edema. These effects are more pronounced under hypoxic or high-osmolarity conditions. Apoptosis is also induced by RC media in *in vitro* studies.[47] RCIN typically manifests as an acute deline in GFR within 24 to 48 hours after administration with return to baseline by one to two weeks. Urinalysis in these patients can show either findings of pre-renal azotemia with low fractional excretion of sodium, but in severe cases, findings similar to ATN with tubular epithelial cells and coarse granular casts are seen. In human studies, volume expansion is key to prevention but possibly N-acetyl-cysteine or sodium bicarbonate therapy have been shown to be beneficial in reducing RCIN. The reno-protective effects of N-acetlycysteine may be related to improved NO dependent vasodilation and medullary oxygenation in addition to scavenging of free radicals.[37]

ACUTE PHOSPHATE NEPHROPATHY

Oral sodium phosphate containing preparation solutions for colonscopic procedures have recently been identified as a cause for AKI.[48–50] The pathogenesis is related to a transient and significant rise in serum phosphate concentration that occurs simultaneously in the setting of intravascular volume depletion due to the prep agent itself. Intra-tubular precipitation of calcium phosphate salts obstructs the tubular lumen and causes direct tubular damage. Although the complete mechanisms are not fully eludicated, risk factors for acute phosphate nephropathy include pre-existing volume depletion, use of ACE inhibitors and ARBs, CKD, older age, female sex, and higher doses of oral sodium phosphate.[49,50]

Endogenous Nephrotoxins

Myoglobin and hemoglobin are endogenous toxinscommonly associated with ATN. Muscle injury due to insults such as trauma, excessive immobilization, ischemia, inflammatory myopathis, drugs and metabolic disorders, cause the rapid and excessive release of myoglobin.[51] Myoglobin, a 17 kDa hemeproteinis highly filtered by the glomerulus, and enters the proximal tubule epithelial cells through endocytosis and is metabolized. It causes red-brown colored urine with a positive dipstick for heme, but relative absence of red cells. Intravascular hemolysis results in circulating free hemoglobin, which, when it exceeds haptoglobin-binding is filtered, resulting in hemoglobinuria, hemoglobin-cast formation and heme uptake by proximal tubule cells. AKI in rhabdomyolysis is due to a combination of factors including volume depletion, intra-renal vasoconstriction, direct heme-protein mediated cytotoxicity and intraluminal cast formation. The heme center of myoglobin may directly induce lipid peroxidation, generation of isoprostanes and liberation of free iron.[52] Iron is an intermediate accelerator in the generation of free radicals. There is also evidence to suggest increased formation of H_20_2 in rat kidney model of myohemoglobinuria.[53] The subsequent hydroxyl (OH^-) radical plays a vital role in oxidative stress induced AKI through mechanisms discussed in detail later in the chapter. Iron chelators such as deferoxamine and scavengers of reactive oxygen species such as glutathione have been shown to provide protection against myo-hemoglobinuric AKI.[54] Similarly, endothelin antagosists have also been shown to prevent hypofiltration and proteinuria in rats that underwent glycerol induced rhabdomyolysis.[55] These studies implicate the important role of vascular mediators such as endothelin-1, thromboxane A, TNF-α, and F-isoprostance. Others have shown NO supplementation might be beneficial by preventing the heme induced renal vasoconstriction, as heme proteins scavenge nitric oxide.[56,57]

Precipitation of myoglobin with Tamm-Horsfall protein and shed proximal tubule cells leads to cast formation and distal tubular obstruction which is enhanced in acidic urine.[58] In human studies volume expansion and perhaps alkalinaztion of urine to limit cast formation are the preventive measures generally employed as none of the experimental agents used in animal studies have been convincingly beneficial.

Other endogenous nephrotoxins include uric acid and light chains. Excessive light chains, produced in diseases such as multiple myeloma, are filtered, absorbed and then catabolized in proximal tubule cells. The concentration of light chains leaving the proximal portion of the nephron depends on the capacity of the proximal tubule to reabsorb and catabolize them as well as the filtrate concentration. Certain light chains can be directly toxic to the proximal tubules themselves.[59] Light chain-induced cytokine release has been associated with nuclear translocation of NF-κB suggesting that its endocytosis leads to production of

inflammatory cytokines through activation of NF-κB.[60] Once the capacity for proximal tubule uptake is overwhelmed, a light chain load is presented to the distal tubule where upon reaching a critical concentration the light chains aggregate and co-precipitate with Tamm-Horsfall protein and form characteristic light chain casts.[61] Light chains, in the amount seen in plasma cell dyscrasiasts, are also capable of catalyzing the formation of H_2O_2 in cultured HK-2 cells. H_2O_2 stimulates the production of monocytes chemo-attractant protein (MCP-1), a key chemokine involved in monocytes/macrophage recruitment to proximal tubule cells.[62]

Any process reducing GFR such as volume depletion, hypercalcemia or NSAID's will accelerate and aggravate cast formation. It has been proposed that acutely reducing the presented light chain load by plasmapheresis might be beneficial in limiting cast formation and reducing the extent of the AKI in certain select patients.[63] Tumor cell necrosis following chemotherapy can release large amounts of intracellular contents such as uric acid, phosphate and xanthine into the circulation that can potentially lead to AKI. Acute uric acid nephropathy with intratubular crystal obstruction and interstitial nephritis is not seen as commonly as it was in the past mainly due to prophylactic use of allopurinol prior to chemotherapy and or rasburicase to acutely lower the serum uric acid levels.

Other therapeutic agents such as amphotericin B, acyclovir, indinavir, cidofovir, foscarnet, pentamidine, and ifosfamide can all directly cause tubular injury.

MODELS OF ACUTE KIDNEY INJURY

Experimental Models of ARF

Despite a variety of animal and cell culture models of AKI, there remains a need to develop *in vivo* experimental models of ischemic AKI more closely mimicking clinical human AKI for the development of effective therapies.[64,65] Some of the important principles in studying the pathophysiology of AKI in various models include the importance of measuring parameters at multiple appropriate time points and the ability to control physiological functions known to affect kidney function (e.g., temperature, blood pressure, anesthesia, fluid status etc.). A limitation in many experimental models is the lack of co-morbidities such as aged animals, chronic kidney disease, multi-organ failure, pre-existing vascular changes or multiple renal insults, which quite often co-exist in human AKI. We will briefly describe the pros and cons of using these experimental models (Table 76.4).

The warm ischemia-reperfusion renal clamp model is one of the most widely used experimental models in rats and mice because of its simplicity and reproducibility. In rats the inflammatory response, tubular injury and repair, and medullary congestion are similar and probably comparable to human ischemic ATN. However, in human AKI, isolated ischemia is seen rarely seen and neither is there usually complete cessation of blood flow to the kidneys. In this model, important mediators of injury suchreactive oxygen species (ROS) and perioxynitrite species may have a different or delayed role as compared to low oxygen states in hypoperfusion models. Total blood flow cessation also prevents the degradative products of the ischemic kidney from being eliminated. Other factors playing a role in the pathophysiology of AKI such as inflammatory mediators released from gut ischemia, endothelium, smooth vascular muscle cells need to be taken into consideration in any experimental model. Release of bowel proteins into the circulation can act as inflammatory mediators and increase the susceptibility to AKI.[66] The S3 segment of the proximal tubule is almost completely necrosed in such models, a finding not seen very frequently in human ARF. In contrast to animal models, human AKI histological biopsy data are lacking at early time points from the onset of insult.[65] This has made comparison between animal models and human AKI of limited value. Lastly, drug delivery is prevented in total occlusion models, which actually may be of significant value during the peak ischemic insult.

The cold ischemia-warm reperfusion model resembles AKI in human transplants but this model is inadequately studied and difficult experimentally. In the isolated perfused kidney model, the kidney is perfused in *ex vivo* using perfusates either with or without erythrocytes, and employs either ischemic (stopping perfusate) or hypoxic (reduced oxygen tension of erythrocytes) to induce functional impairment. The morphological patterns are different in erythrocyte free and erythrocyte rich perfusates. The latter system is more comparable with what is observed histologically in animal models. Additionally, limitations include exclusion of various inflammatory mediators, neuroendocrine hemodynamic regulation, and systemic cytokine and growth factor interactions known to be present and play a pathophysiologic role in animal models.

Cardiac arrest is a common scenario leading to human ARF. Rabb et al. have described whole body ischemia reperfusion injury model induced by 10 minutes of cardiac arrest, followed by cardiac compression resuscitation, ventilation, epinephrine and fluids, which that lead to a significant rise in SCr and renal tubular injury at 24 hours.[67] One of the unique advantages of this model is the cross talk between vital organs such as the brain, heart, lung and the renal hemodynamics.[68] A hypoperfusion model of AKI using partial aortic clamping was first described by Zager

TABLE 76.4 Comparison of Models of Studying Acute Kidney Injury " + " Minimally Applicable; "++++"Very Applicable

Humans		Animals								Cells	
		Ischemic				Septic			Toxic		
		Warm-Ischemia-reperfusion	Cold-Ischemia-reperfusion	Hypoperfusion/ Cardiac arrest	Isolated Perfused Kidneys	Endotoxin	Cecal Ligation & Puncture	Bacterial Infusion	Contrast/ Pigment/ Glycerol/ Drug	Isolated Proximal Tubule Cells	Cultured Tubular Cells
Simplicity	+	++++	++	++	++	++++	+++	+++	++++	+++	++++
Reproducibility	++	++++	+++	+++	+++	+++	++	+++	+++	+++	+++
Clinical Relevance	++++	++	+++	++++	++	++	++++	+++	+++	+	+
Therapeutic value	+++	++	+++	++++	++	++	+++	+++	+++	+	+
Studying Mechanisms	++	++	++	+++	++	++	+++	+++	+++	+++	+++
Controlling Extrinsic factors	+	+	++	++	+++	++	++	++	++	++++	++++
Isolating single variables	++	+	++	+	+++	+++	++	++	+++	++++	++++
Standardization Value	+	++++	+++	++	+++	+++	++	+++	++	++	+++
Experimental Limitation	++++	+++	+++	+++	++	++	+++	++	++	+	+

et al. may be more representative of human AKI reflecting a state of reduced blood flow to the kidney with systolic blood pressure around 20 mm Hg, resulting in reproducible AKI.[69,70] This was also recently adapted and refined in a study where a novel compound, soluble thrombomodulin, was used to minimize ischemic injury in a partial aortic clamp AKI model.[71]

Toxic models of renal failure employ various known toxins, such as radiocontrast, gentamicin, cisplatin, glycerol and pigments including myoglobin and hemoglobin. Septic models to study AKI include cecal ligation and puncture, endotoxin infusion andbacterial infusion into the peritoneal cavity. The endotoxin model which is simple, inexpensive and suitable to study new pharmacological agents, has certain drawbacks as well. There is variability amongst sources and types of lipopolysaccharide (LPS) endotoxin, rate and method of administration, and it is usually of short duration due to the high mortality associated with the doses required to induce AKI. It also tends to be a vasoconstrictive model and does not recapitulate the hemodynamics nor inflammation of human sepsis.[72] In the cecal ligation and puncture model (CLP), there is considerable similarity with sepsis in humans with acute lung injury, metabolic derangement and systemic vasodilation, accompanied by increased cardiac output initally. However there is some variability depending on the mode and size of cecal perforation. Star et al. have developed a new sepsis model keeping under consideration the following facts: (1) animals should received the same supportive therapy that is standard for ICU patients (i.e., fluid resuscitation and antibiotics); (2) age, chronic co-morbid conditions and genetic heterogeneity vary.[73] Complex animal models of human sepsis that introduce these disease-modifying factors are likely more relevant and may be more pharmacologically relevantthan simple animal models.[73] The zebra fish model developed by Bonventre et al. has the advantages of markedly improved accessibility of the kidney, feasibility of knock-down and upregulation of genes and a short phenotypic readout time, while at the same time possessing the complexity of an organism to study renal injury. These properties may make it a useful inexpensive tool to screen therapeutic agents in the future.[74]

Experimental models of hypoxic acute kidney damage differ morphologically in the distribution of tubular cell injury and tubular segment types differ in their capacity to undergo anaerobic metabolism, mount hypoxia-adaptive responses mediated by hypoxia-inducible factors (HIFs).[75] Hence it is important to keep them in mind the potential pitfalls when evaluating experimental studies or therapeutic interventions using these models. The lack of ability to demonstrate effectiveness of an agent in humans which has been shown to be efficacious in animal models, does not necessarily reflect a flaw with the model. Most often, the agent is administered very late in the course of the human disease, and the patient heterogeneity of the population makes it even more difficult to establish true efficacy.[76]

Role of Biomarkers in AKI

Changes in serum creatinine and/or urine output to diagnose AKI[77] may not be able to identify the early stages of intrinsic kidney injury. Early identification and subsequent early pharmacologic intervention may improve outcomes in AKI. In order to facilitate the early diagnosis of intrinsic injury, multiple biomarkers of tubular injury have been evaluated.[78,79] Biomarkers for AKI include N-acetyl-*B*-D-glucosaminidase (NAG), kidney injury molecule 1 (KIM-1), neutrophil gelatinase-associated lipocalin (NGAL) and interlukin 18 (IL-18), among others.[78,79] In addition, serum cystatin C has been proposed as more sensitive and timely than serum creatinine for detecting changes in GFR, and urinary cystatin C has been proposed as a marker of tubular injury.[78,80,81] Although not utilized yet for routine clinical use, these biomarkers have the potential to provide an early diagnosis of intrinsic AKI and the ability to differentiate pre-renal AKI from intrinsic tubular damage, as well as to provide prognostic information of an episode of AKI. One biomarker or a panel of these biomarkers may eventually provide the necessary early diagnosis to allow therapies to limit kidney damage and promote recovery of kidney function. Please refer to Chapter 75 for a detailed explanation on the role of serum and urinary biomarkers in AKI.

PATHOPHYSIOLOGY OF ACUTE KIDNEY INJURY

Morphological Changes of AKI

Acute Tubular Necrosis (ATN) is the most common form of AKI, and this process of renal tubular injury encompasses more than just cell death followed by repair. It is easier to understand the entire spectrum of injury if one looks at the different compartments involved and the phases they go through (Fig. 76.2).

Tubular Epithelial Cell Injury

Although data regarding which nephron segments in humans with ATN are more severely affected is sparse due to lack of biopsies early in the course of ATN, experimental animal models provide sufficient information to help understand and delineate the

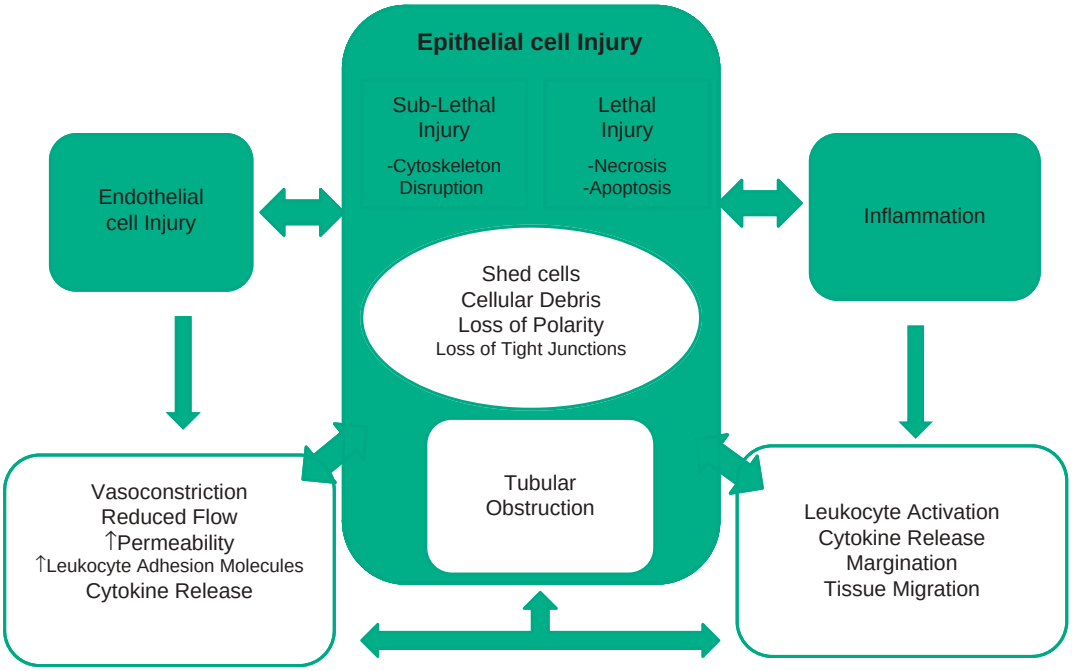

FIGURE 76.2 Overview of pathogenesis in acute kidney injury. The major pathways of impairment of glomerular filtration rate (GFR) in ischemic acute tubular necrosis as a result of vascular and tubular injury (see text for details). *(Source: unpublished figure from Encyclopedia of Intensive Care Medicine. Publisher, Springer. Eds, Vincent, Jean Louise Hall, Jesse B. Ch Epithelial Cell Injury by Asif Sharfuddin and Bruce Molitoris. First Edition due to published March 2012).*

mechanisms of ATN by histological analysis. In ATN the most severe tubular injury takes place within the outer medulla of the kidney, and involves the S3 segment of the proximal tubule (pars recta) and the medullary thick ascending limb (MTAL) of the distal nephron.[82] The S3 segment has limited capacity to undergo anaerobic glycolysis. Secondly, due to its unique primarily venous capillary regional blood flow, there is marked hypoperfusion and congestion in this medullary region post injury that persists even though cortical blood flow may have returned to near normal levels after ischemic injury. Endothelial cell injury and dysfunction are primarily responsible for this phenomenon, known now as the "extension phase" of AKI.[83] The proximal tubule S_1 and S_2 segments are most commonly involved in toxic nephropathy due to their high endocytic rates leading to increased cellular uptake of the toxin.

The apical brush border of proximal tubule cells (PTC) is damaged early resulting in microvilli disruption and detachment from the cell surface forming membrane bound "blebs" released into the tubular lumen. Loss of microvillar surface leads to ineffective enzymatic activity, endocytosis, channel and transporter density resulting in diminished effective transcellular absorption. Patchy detachment and subsequent loss of tubular cells exposing areas of denuded tubular basement and focal areas of proximal tubular dilatation along with the presence of distal tubular casts is also a major pathological findings in ATN.[84] Because the surviving adjacent cells tend to spread out and become flattened, in an attempt to completely or partially cover the denuded epithelium, the appearance is often of a flattened and pauci-cellular epithelium.

Sloughed off tubular cells are also present in the tubular lumen, where they can be overtly necrotic or viable. These cells along with brush border vesicle remnants and cellular debris combine with Tamm-Hosrfall glycoprotein (THP) and form the classical "muddy-brown granular" casts, that have the potential to obstruct the tubular lumen. Cast formation may be potentiated by relative stasis of tubular fluid flow because of the reduction in GFR. On biopsy, these casts may not be captured since they exist within the medulla and actual site of obstruction may be a short segment. However, dilation of tubules proximal due to obstruction is often seen as long as the GFR and regional tubular epithelium are maintained. Eventually decompression of these tubules will occur because of decreased GFR, damage to proximal tubular cells, and persistent reabsorption of tubular fluid in uninjured areas. The injury to the proximal tubule cells in humans is also seen in experimental models of ischemic AKI (Fig. 76.3).

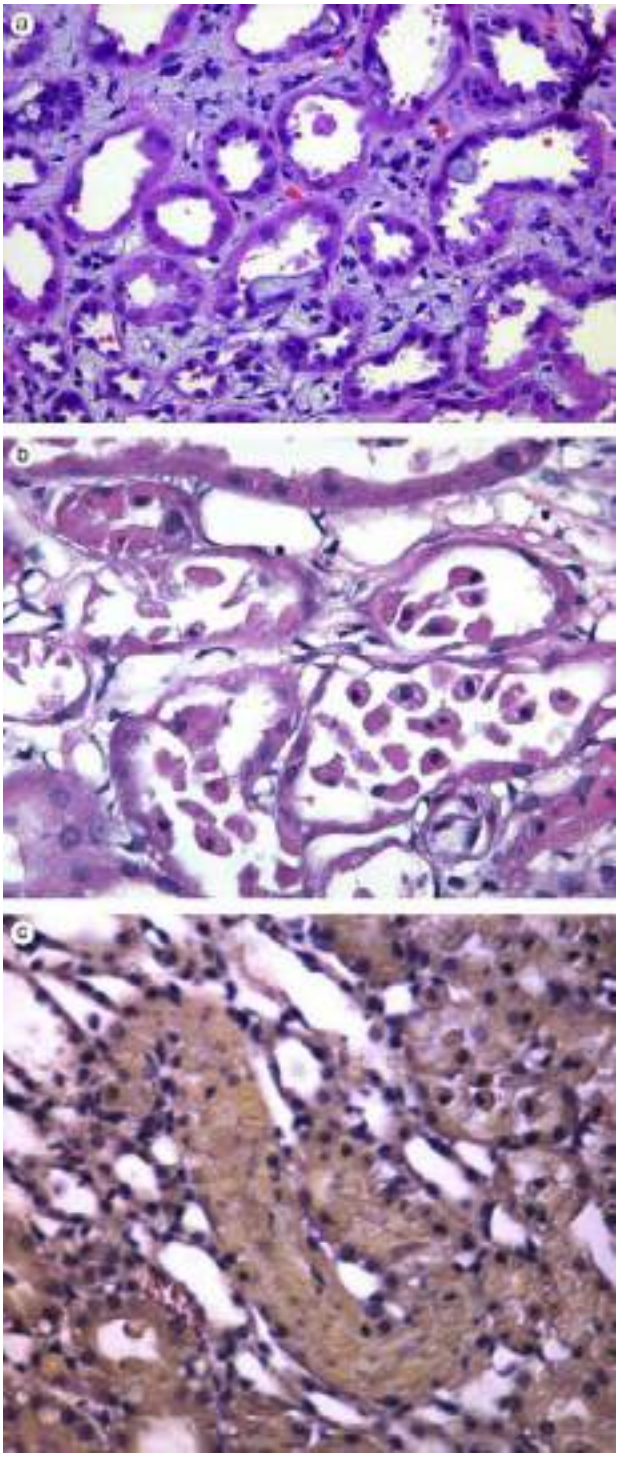

FIGURE 76.3 A. Morphology of acute tubular necrosis in human biopsy specimen. Proximal tubules show loss of brush border, flattening of tubular cells with denuded basement membranes, blebbing of cytoplasm (arrowhead) and vacuolization in a patient with toluene induced acute tubular necrosis. There is also evidence of extensive interstitial edema and expansion with presence of inflammatory cells (arrow). (*Slide courtesy of Dr Carrie Phillips*). B. Morphology of acute tubular necrosis in rat kidney specimen subjected to 60 minutes of hypoperfusion. Areas of detachment of cell and intact cells within the tubular lumen. C. Cellular cast within the tubular lumen. See color plate section at the back of the book.

Apoptotic features are more commonly seen in both proximal and distal tubule cells as compared to necrosis which itself is inconspicuous and restricted to the highly susceptible outer medullary regions. Apart from the proximal tubular cells, the other major epithelial cells of the nephron are those of the medullary thick ascending limb located distally. Apoptotic changes have been detected in human AKI, as shown in distal nephron segments in nephrotoxic acute tubular necrosis. Distal tubular cell apoptosis also occurs in donor biopsies before engraftment, which was predictive of delayed graft function due to acute tubular necrosis.[85] In an *ex vivo* model of hypoxic AKI, inhibition with FG-4497 (specific prolyl-hydroxylase inhibitor which leads to activation of HIF-Aplha) in the isolated perfused kidney led to decreased selective outer medullary distal tubular injury.[86] The course of a tubular cell alterations may take different paths depending on the type and extent of injury as discussed later.

GLOMERULUS

The glomerular tuft collapses in ischemic injury, and some investigators have described the diameter of ischemic endothelial cell fenestrae on average to be larger than that of untreated kidneys.[87] Other human biopsy studies have documented enlargement of juxtaglomerular apparatus during the oligoanuric phase, and thickening and coarsening of foot processes. But these findings have not been confirmed and there still exists a paucity of data on glomerular changes in human ATN in different stages.[87,88] Glomerular epithelial cell injury in ischemic, septic or nephrotoxic injury is not classically seen although some studies have shown thickening and coarsening of foot processes and recently Wagner et al. have shown podocyte specific molecular and cellular changes.[89]

Epithelial Cytoskeletal Abnormalities

Cytoskeletal Alterations

Cellular structure and function are mediated by an interactive and dynamic role of the actin cytoskeleton including but not limited to proximal tubule brush border microvilli structure and function, cell polarity, endocytosis, signal transduction, cell motility, movement of organelles, exocytosis, cellular division and migration, barrier function of the junctional complex, cell-matrix adhesion and signal transduction.[90] Actin is present in globular form (G-actin) that can self-assemble into filamentous (F-actin) to form helical microfilaments. In conjunction with actin-binding proteins, guanosine triphosphatases (GTPases) and adenosine triphophate (ATP), the dynamic process of actin assembly and disassembly is accomplished. The actin

cytoskeleton is present as a layer of microfilaments below the apical plasma membrane, forming the terminal web. The architectural integrity of brush border microvilli is dependent upon extensions of actin filaments from the terminal web to the tip of the individual microvilli.

Under physiologic conditions most actin monomers are ATP-bound, while the bulk of actin found within actin filaments is ADP-bound. The unique binding sites of actin for nucleotides and divalent cations allow conformational changes, apart from its hydrolytic properties that are activated by polymerization. The G-actin ADP complex released on depolymerization (disassembly) undergoes nucleotide exchange with abundant cytosolic ATP, and is then stored as a high energy G-actin ATP intermediate by thymosin-sequestering proteins until needed for polymerization.[91,92] Four groups of actin-binding protein mediate different effects on the actin cytoskeleton including actin sequestering, capping, severing and nucleation. These effects in turn coordinate the continual remodeling of the cytoskeleton and give it the ability to respond to various internal and external stimuli.[93]

Ischemic insults to proximal tubule cells induce a rapid and severe degeneration of the microvillar F-actin core, which in turn mediates the plasma membrane finger-like microvillar structural morphology changes including loss of the apical membrane through blebbing. The degeneration of this F-actin core occurs as a result of ATP depletion leading to depolymerization of microvillar actin. In addition ezrin, an actin binding phosphorylated protein, becomes dephosphorylated during ischemia and the attachment between the microvillar F-actin core and the overlying plasma membrane is lost[94] (Fig. 76.4). The apical membrane is then either exfoliated as "blebs" into the tubule lumen or internalized with the capability of being recycled during cellular recovery. Furthermore, the concentration of F-actin in the cell increases with the formation of large cytosolic aggregates in the perinuclear region and also near the junctional complexes and basolateral membrane. ATP-G-actin levels decrease rapidly during ischemia. Since ADP G-actin cannot be sequestered by thymosin its concentration exceeds a critical threshold resulting in the polymerization in an unregulated fashion.[92]

The actin binding protein family of cofilin, also known as actin depolymerizing factor (ADF), has been shown by Molitoris and colleagues to be a critical mediator in F-actin severing during ischemic injury. In proximal tubule cells (PTC) ADF/cofilin, which when phosphorylated is inactive and does not bind actin, gets rapidly dephosphorylated and therefore activated by renal ischemia. This leads to relocalization from the cytoplasm to the surface membrane, as well as in shed membrane-bound vesicles seen in PTC lumen.[95,96] The mechanism by which disruption of F-actin structure occurs also involves the role of another family of actin

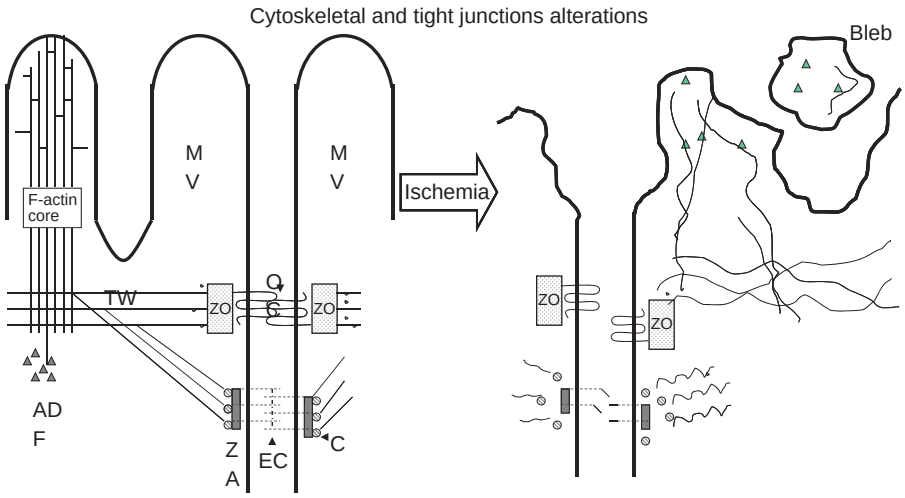

FIGURE 76.4 Cytoskeletal and tight junctions alterations in AKI. Ischemic insult to a proximal tubule cell disrupts actin cytoskeleton and junctional complexes. The orderly arrangement of the actin microfilaments extends from terminal web (TW) into microvilli (MV) as well as interacting with tight junction proteins zonula adherens (ZO), and adherens junction proteins zonula adherens (ZA). Occludin (OC) is transmembrance integral protein of the tight junction forming a multiprotein complex with ZO, controlling paracellular permeability. Severe ATP depletion results in occludin translocating to the cytoplasm, compromising adhesion and permeability. Similarly adherens junction proteins such E-cadherin (EC) and catenins (C) that interact with actin and other junctional components are compromised. ADF or cofilin is activated with ischemia that translocates and gets recruited to apical microvilli and binds to F-actin structures, resulting in severing and depolymerization of F-actin. This leads to subsequent apical membrane disruption and bleb formation.

binding protein called tropomyosin. Under physiologic conditions tropomyosin binds to and stabilizes the F-actin microfilament core in the terminal web, and protects the filaments from ADF/cofilin induced severing and depolymerization. Ashworth et al. have demonstrated that after ischemic injury there is dissociation of tropomyosin from the microfilament core providing access to microfilaments in the terminal web for F-actin binding, severing and depolymerizing actions of ADF/cofilin proteins.[97]

Alterations in the activity of Rho family of GTPases also contributes to changes in actin cytoskeleton associated with ischemia. First, chemical ATP depletion was shown to cause Rho GTPase inactivation.[98] Secondly, GTP depletion during ischemia could also inactivate Rho GTPase function.[99] These two findings, coupled with the finding that cells transfected with a constitutively active form of RhoA during chemical ATP depletion are protected against actin depolymerization, provide evidence of ischemia-induced RhoGTPase inactivation.[100] An additional cytoskeletal component important for cellular polarity and protein trafficking is microtubules. Wald et al. have shown that in reperfused rat proximal tubules non-centrosomal microtubule organizing centers (MTOCs) were fully detached from the cytoskeleton and scattered throughout the cytoplasm at three days after reperfusion when brush borders membranes were mostly reassembled with normal F-actin distribution. At that time microtubules were also fully reassembled but lacked their normal apicobasal orientation, hence demonstrating that the reestablishment of the submembrane F-actin does not seem to be sufficient for a full polarization of the cells.[101] Microtubule formation also occurs by continuous assembly and disassembly of α and β tubulin heterodimer with an intricate polymerization process. Studies indicate that during ischemia α and β tubulin do not participate in microtubule polymerization and their localizations are also different. The fact that GTP levels are depleted by 90% after 30 minutes kidney ischemia in rats supports this assumption of impaired microtubule polymerization.[102]

Epithelial cells are characterized by an asymmetrical distribution of proteins and lipids in the apical and basolateral membrane resulting in surface membrane polarity of these cells. In ischemic ATN this polarity is abolished, but has the potential for re-establishment during recovery. Molitoris et al. have shown evidence to suggest the Na^+K^+-ATPase pump that normally resides in the basolateral membrane of proximal tubule cells, under conditions of chemical anoxia, is redistributed to the apical membrane.[103] This redistribution, which can occur as early as 10 min after ischemia, is another consequence of the disruption of the actin cytoskeleton, which normally maintains the attachment of the Na^+K^+-ATPase to the basolateral membrane.[103–105] Furthermore, both ankyrin and fodrin dissociated from F-actin and each other during ATP depletion.[106] These data were confirmed and indicate wide spread actin cytoskeleton alterations during ATP depletion lead to altered protein-protein interactions.[107] Other nephron segments such as the distal tubule cells, and TAL do not show similar apical redistribution of the Na^+K^+-ATPase. This redistribution results in functional consequences reflected in the loss of unidirectional transport of salt and water across the epithelial cell, resulting in one mechanism of the high fractional excretion of Na^+ seen in patients with ATN (Fig. 76.5).

Junctional Defects and Permeability Alterations

Cell-cell junctional complexes actively participate in the establishment and maintenance of cell polarity, paracellular transport, cytoskeletal interactions, and rearrangements in cellular shape. Ischemia also induces functional changes in the epithelial junctional complexes, which are comprised of at least three structures: adherens junctions (also known as zonula adherens (ZA)), tight junctions (zonula occludens (ZO)) and desmosomes. Tight junctions are located directly apical to the adherens junction, are composed of a growing list of proteins such as occludin, claudin, protein kinase C (PKC), ZO-1 etc., with multiple functions such as adhesion, permeability, structural integrity and paracellular transport of solutes. The actin present in the cortical belt, and in the terminal web, is also linked to the tight junction. Adherens junction, which are located directly below the tight junction, form strong cell–cell adhesion complexes and are composed of proteins such as cadherins and catenins are associated with numerous other junctional and cytoplasmic proteins. They are responsible for adhesion of adjacent cells, regulation of adhesion, and are also linked to the actin cytoskeleton.[108]

In vivo and *in vitro* studies indicate that in early ischemic injury there is an "opening" of the tight junctions as the proteins such as ZO-1 and cingulin become insoluble during ATP depletion, and associate into macromolecular intracellular complexes.[109] This leads to increased permeability of the tight junctions in sublethal injury resulting in back-leakage of glomerular filtrate, which is an important factor in the reduction of GFR as discussed later. If ATP is repleted before lethal injury the permeability defect resolves.[110] PKC signaling regulates both tight junction and adherens junction assembly. Evidence suggest that tight and adherens junction proteins including ZO-1, ZO-2, ZO-3, occludin, vinculin, and p100–p120 are affected by this kinase signaling pathway.[111] It is also likely that disruption of the actin cytoskeleton and reduction in activity of Rho-GTPases also contribute to the changes

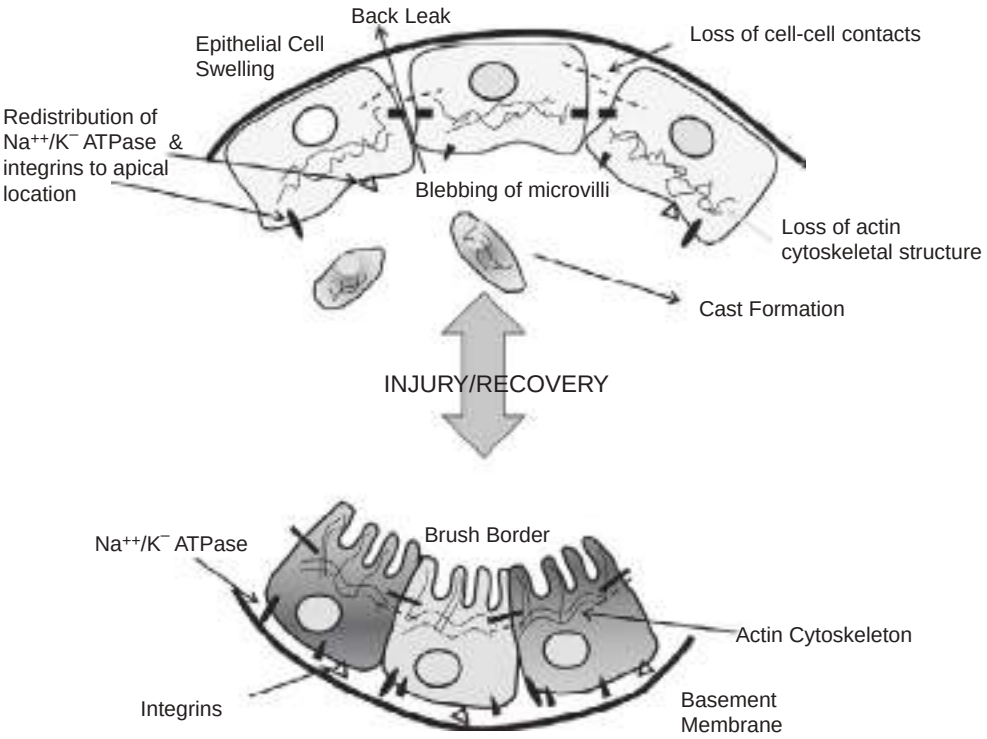

FIGURE 76.5 An overview of sublethal injury to tubular cells. An overview of sublethally injured tubular cells. Na/K/ATPase pumps are normally located at the basolateral membrane. In sublethal ischemia the pumps redistribute to the apical membrane of the proximal tubule. Upon reperfusion, the pumps reverse back to their basolateral location. *(Source: unpublished figure from Encyclopedia of Intensive Care Medicine. Publisher Springer. Eds, Vincent, Jean Louise; Hall, Jesse B. Ch Epithelial Cell Injury by Asif Sharfuddin and Bruce Molitoris. First Edition due to published March 2012.)*

in the tight junction during ischemia.[100] The loss of adherens integrity is in part caused by activation of c-Src which translocates to the adherens junction and tyrosine phosphorylates components such as β-catenin.[112] Nigam et al. have demonstrated the role of tyrosine kinases and phosphatases in the disassociation of adherens junction.[113] The importance of these animal model findings is highlighted by findings in human allografts with ATN where Kwon et al. have shown the same features noted in experimental models of loss of cell polarity and tight junctions.[114]

Epithelial cells also lose their attachment to the underlying extracellular matrix, the mechanism for which has been elucidated as at least being partially due to loss of polarity and redistribution from the basal membrane to the apical membrane of β1-integrins. Integrins are transmembrane proteins normally responsible for the anchoring of epithelial cell to the matrix through actin cytoskeleton and actin-binding proteins.[115] *In vitro* studies of MDCK cells have shown that adherence of these cells to a collagen I substratum is mediated by peripheral actin filaments and adhesion complexes regulated by myosin light chain kinases and adhesion complexes controlled by RhoA.[116] The detachment and loss of tubular cells into the lumen also contributes to the back-leakage of the glomerular filtrate, and at the same time the β1-integrins and E-cadherins might even play a role in mediating the aggregation of these exfoliated cells worsening intraluminal cast formation.

Although the glomerular injury is not as prominent in AKI, Wagner et al. have demonstrated in an *in vivo* rat model that renal ischemia induces podocyte effacement with loss of slit diaphragm and proteinuria owing to rapid loss of interactions between the tight junction proteins Neph1 and ZO-1. Cell culture models using human podocytes further showed that ATP depletion resulted in rapid loss of Neph1 and ZO-1 binding, and redistribution of Neph1 and ZO-1 proteins from the cell membrane to cytoplasm; ATP recovery increased phosphorylation of Neph1 and restored Neph1 and ZO-1 binding and their localization at the cell membrane.[89]

Tubular Obstruction

Tubular obstruction has been noted in ischemic as well as toxic models of injury. Renal tubular epithelial cells can be seen in the urine of patients with AKI,

and can be either alive, apoptotic or necrotic. Micropuncture studies, done over 20 years ago, demonstrated elevation of intratubular pressure early after reperfusion following renal artery occlusion. This is characteristically evident as tubular dilatation, with cast deposition in the distal nephron causing luminal obstruction and back pressure. Although intratubular pressures tend to fall towards normal after 24 hours, the presence of persistent obstruction can be revealed by extracellular volume expansion, which again elevates intratubule pressures. An obstructing cast in the collecting duct could potentially impair the function of multiple nephron units, as many nephrons drain into a single collecting duct.

The term "back-leak" generally implies the passive movement of GFR into the interstitium from the tubular lumen, eventually being recirculated to the systemic vasculature through the venous network. Studies have revealed that if radiolabeled compounds are microinjected into renal tubules after ischemic injury, they can be detected in the contra-lateral kidney. Human studies by Myers et al. provided evidence of transtubular leakage of GFR after ischemic renal failure as well as tubular obstruction, leading to a reduction in measured or effective GFR.[117,118] The presence of areas of open PTC tight junction or denuded basement membrane in electron-microscopy biopsy specimens provides a logical morphological explanation of back-leakage. However, understanding the mechanism responsible for tight junction dysfunction or detachment of tubular cells is key to defining the event of cast formation and tubular obstruction. The integrin superfamily of proteins, located on the basal aspect of the cell, is responsible for the complex cell-matrix adhesion events. The β chains coupled with α chains form β1 integrins, which interact with the actin cytoskeleton and actin-binding proteins such as α-actinin, vinculin and talin. The extracellular domain of the β1 integrins attaches to receptors of proteins such as collagen and fibronectin, which are abundant and constitute the tubular basement membrane. The tri-peptide sequence of arginine-glycine-asparagine (abbreviated as RGD), is a well define receptor for β1 integrin on the extracellular matrix. The loss of polarity causes redistribution of β1 integrins, which become expressed in the apical domain of sublethally injured cell. It was hence hypothesized that administraton of an excess of soluble RGD containing molecules would saturate the extracellular binding site of all exposed β1 integrins within the lumen of the nephron, and thus prevent luminal renal tubular cell-cell adhesion, and this prevent intratubular obstruction. Both intravenous and direct intrarenal infusion of RGD peptides resulted in amelioration of ischemic AKI. It is also possible that the detached tubular cells adhere to Tamm-Horsfall protein (THP) in the distal tubule by RGD sequence peptides. By using dual labeled RGD peptide sequences, it was also discovered that RGD peptides also mapped to intimal surface of vessels in ischemic kidneys.[119] Further studies utilizing RGD peptides in ARF could provide key answers to questions of vascular and epithelial injury in ATN. Recent studies also show a role of the sphingosine-1 phosphate receptor (S1PR) in maintaining structural integrity after AKI. Okusa et al. have shown that S1PRs in the proximal tubule are necessary for stress-induced cell survival, and $S1P_1R$ agonists are renoprotective via direct effects on tubular cells.[120]

MICROVASCULAR INSULT IN AKI—FUNCTIONAL BASIS AND MORPHOLOGICAL CHANGES

Microvasculature and Interstitium

A prominent feature of AKI is interstitial edema, which is in part due to altered endothelial permeability,[121] as well as increased tubular pressure, perhaps via backleak through the wall of injured or distended tubular cells. Solez et al. in 1974 demonstrated there was intravascular leukocyte accumulation following ischemic injury, a finding which is still commonly seen in peritubular capillaries, particularly in the ascending vasa recta in the outer and inner medulla. The pathogenesis and significance of this finding is discussed in detailed later. The peritubular capillaries of the corticomedullary junction and outer medulla are most often affected in ischemic human AKI, exhibiting vascular congestion, accumulation of inflammatory cells and either compression or dilatation of vessels.[122] Subtle and few changes may be seen in larger vessels such as arterioles and arteries. The pathologic profile of interlobular and afferent arteriolar vessels in renal artery clamp experiments shows vacuolization in the muscular layer as early as four hours post-ischemic insult, followed by focal necrosis in the smooth muscle.

Medullary Ischemia

Renal Blood flow (RBF) approximates 20−25% of the total cardiac output, and various forces regulate glomerular filtration as a result of autoregulation of renal blood flow. A small fraction of RBF is delivered to the medulla, while the cortex receives the majority. A relatively hypoxic region thus exists in the medulla with partial pressures of oxygen as low as 20−30 mm Hg. In contrast the partial pressure of oxygen in the cortex is about 80−90 mmHg. It has been known for years that restoration of total RBF to near normal, shortly after an ischemic insult does not prevent the extension or

maintainence phase of AKI. Thus a sequence of endothelial and epithelial cell processes is triggered that are independent of re-establishing total RBF.

The principal determinant of the medullary oxygen requirement is the rate of active Na^+ reabsorption along the mTAL. Therefore, not only the reduction of oxygen delivery, but also the increment of oxygen demand can cause an imbalance. Dehydration, volume depletion and renal hypoperfusion are major stimuli of urine concentration through active sodium reabsorption, which may further exacerbate hypoxic tubular damage. By volume repletion and salt loading, this workload is decreased, obviating the need for urine concentration, and hence able to tilt the balance back to match the oxygen supply. The kidney does have its own protective mechanism known as tubuloglomerular feedback (TGF), the stimulus for which appears to be the sodium concentration of the tubular fluid as sensed by the macula densa of the juxtaglomerular apparatus. Increased sodium sensed in this nephron segment, will in turn activate TGF to reduce the GFR, resulting in reduced metabolic demand placed on the tubule, giving the nephron an optimal oxygen supply versus demand balance. Clinically this results in oliguria, which could be termed as an appropriate physiological response to an insult. When this response system is overwhelmed, due to continued insults such as sever hypoxia, or hypoperfusion, this balance is lost, leading to cell death or necrosis.

Although tubular injury is a major mechanism initiating the decrease in GFR with AKI, the concomitant vascular changes are now being recognized as an important pathophysiologic variable. The glomerular capillary hydraulic pressure is maintained by variations in the preglomerular and postglomerular arteriolar resistances. GFR remains relatively constant despite variations in renal perfusion pressure through the process of autoregulation which includes tubuloglomerular feedback (TF) and myogenic alterations of arteriolar tone. Structurally, resting or basal tone is determined by intrinsic smooth muscle tone, and endothelial cells. Endothelial cells can detect changes in shear stress and mediating responses to altered flow. Basal nitric oxide (NO) activity is an important determinant of resting vascular tone. Responses to extrinsic stimuli are used to measure vascular function, also termed as vascular reactivity. These stimuli can be systemically generated, e.g., ANP, catecholamines, angiotensin II, or locally (paracrine), e.g., thromboxane A2, PGH2, endothelin-1 (ET-1), platelet activating factor (PAF), NO, amongst others. The kidney of all organs has the greatest vasoconstrictor sensitivity to ET-1. Characteristics of tubular fluid also modulate autoregulation of GFR to maintain fluid and electrolyte balance.[123]

It is very important to note that abnormalities in RBF in AKI lead to persistent hypoxia in certain areas of the kidney. Severe hypoperfusion of the outer medulla persists long after the insult which initiated ATN has resolved. As cortical blood flow improves after reperfusion and cortical tubule cells demonstrate repair and regeneration.[124] However, the S3 and MTAL segments of the outer medulla experience ongoing ischemia, thought to be due to "shunting" of oxygen between descending and ascending vasa recta, and vascular congestion in the peritubular capillaries. This contributes to ongoing injury to the S3 PTC and mTALC causing the extension phase of ATN.[125] Studies have also emphasized the role of tubular cell swelling as a cause for vascular congestion, as well as a possibility of compression of capillaries by swollen tubules causing mechanical impediment, limiting reperfusion to the cortico-medullary junction of the kidney.[126] Finally, WBC attachment, especially to the outer stripe venous capillaries and RBC rouleaux formation, leads to reduced and even stagnant flow to that area.

Nitric Oxide in ATN

A variety of vasoactive substances are vasconstrictive mediators of the microcirculation and thought to be major determinants of decreased RBF in AKI. Endothelial cell damage contributes to intra-renal vasoconstriction, by an imbalance of vasodilators and vascoconstrictors. The role of NO in the kidney ranges from homeostatic regulation and integration of tubular, vascular and glomerular functions, to integral cellular functions including energy metabolism, cellular respiration, proliferation and transcription. Specifically NO helps regulate local renal circulation, renal afferent and efferent nerve activity and direct fluid and electrolyte reabsorption in tubules. It is produced in both renal and non-renal vasculaturefrom L-arginine by the Nitric Oxide Synthase (NOS) isoforms, of which the three principal forms are neuronal NOS (nNOS), inducible NOS (iNOS) and endothelial NOS (eNOS).[127] Intrarenal NO is responsible for up to one third of the normal renal blood flow and helps maintain the low renal vascular resistance under physiological conditions. NO also plays a key role in regulating perfusion of the renal medulla and local infusion of NOS inhibitors into animals reduces medullary blood flow and promotes salt retention. Conversely L-arginine infusion increases NO levels and enhances medullary blood flow.[128]

During AKI the production of NO increases in tubular cells as a result of cytokine induced increase in expression of iNOS. Studies by Ling et al. have shown that proximal tubule cells isolated from mice with

iNOS deficiency were resistant to damage by hypoxia, while mice lacking eNOS or nNOS were damaged by hypoxia.[129] Inhibition of eNOS is also known to occur as endothelial dysfunction develops. Furthermore high output NO production by iNOS may suppress the activity of eNOS without changing its abundance. Hence in ischemic AKI, *there is an imbalance of eNOS and iNOS*. Goligorsky et al. have proposed that due to a relative decrease in eNOS, secondary to endothelial dysfunction and damage, there is a loss of anti-thrombogenic properties of the endothelium, hence leading to increased susceptibility to microvascular thrombosis.[130] The decrease also leads to enhanced PMN adhesion, and vasoconstriction. On the other hand, the relative increase in iNOS leads to enhanced PMN motility, induction of tubular epithelial cell injury, loss of vasomotor response and suppression of eNOS.[130] Generation of superoxide and NO in ischemia/reperfusion injury results in the formation of peroxynitrite anion ($ONOO^-$). This metabolite is cytotoxic and is capable of causing lipid peroxidation and DNA damage. Effective scavenging of peroxynitrite by ebselen resulted in amelioration of renal dysfunction and a decrease in nitrotyrosine formation.[131] Hence, apart from oxidative stress, there is a role for nitrosative stress in ensuing loss of kidney function (See section on Reactive Oxygen Species). Selective inhibition, depletion or deletion of iNOS have clearly shown reno-protective effects during ischemia.[129,131] This effect is in part due to rescue of tubular cells from injury by iNOS or its reactive oxidized by products. Administration of L-arginine, NO-donor molsidomine, or the eNOS cofactor tetrahydrobiopterin can preserve medullary perfusion and attenuate acute kidney injury (AKI) induced by ischemia/reperfusion (I/R); conversely the administration of Nω-nitro-L-arginine methyl ester, an NO blocker, has been reported to aggravate the course of AKI following I/R injury.

Certain other forms of AKI, such as rhabdomyolysis, also have their own unique effect on NO balance. This is due to the fact that heme proteins are potent scavengers of NO, and hence when there is an excess of heme proteins, the basal vasodilatory effect of NO is abolished. Since NO has an inhibitory effect of endothelin-1 synthesis (ET-1), there is a surge in ET production thus aggravating the vasoconstriction. It should also be emphasized that both myoglobin and free hemoglobin themselves can induce iNOS thus acting as another pathogen in the AKI associated with rhabdomyolysis.

ROLE OF ENDOTHELIN

The role of endothelin-1 (ET-1) in AKI has been extensively studied. Ischemic and toxic injury increase the expression of pro-ET-1 gene, and the release of mature ET-1 from endothelial cells.[132] ET-1 is the one the most potent vasoconstrictor known, and is produced from a precursor of 38−39 amino acids by the enzyme endothelin-converting enzyme in endothelial cells. It has been shown that ET-1 is detectable in the plasma of human and animals and also in a variety of tissues. The kidney is a major site of ET-1 production and its effect. The major actions of ET-1 are: (1) Hemodynamic-renal vasoconstriction and mesangial cell contraction. (2) Transport: low doses cause diuresis and natriuresis. High doses cause profound anti-natriuretic and anti-diuretic effects.[132] (3) Proliferation: mitogenesis and proliferation of mesangial cells through ET-A receptor stimulation.[132] (4) Inflammation: recruitment and activation of leukocytes.[133]

The renal vasconstrictive effects are produced by vascular smooth muscle cell contraction following activation of ET-A receptor causing a flux of intracellular calcium. The end result is reduction in both RBF and GFR. With the development of various specific ET receptor antagonists there is compelling evidence of its role in ARF. Most ET receptor anatagonists are able to ameliorate the renal injury after ischemic and toxic injury. Jerkic et al. demonstrated that administration of bosentan, a dual ET receptor antagonist, in experimental ischemic AKI resulted in decreased tubular cell injury and increased RBF and GFR.[134] Other toxic injury models such as endotoxin, CsA and myoglobinuric-induced renal failure have all shown to be associated with elevated plasma ET levels.

ENDOTHELIAL CELL INJURY IN AKI

It has been known for over thirty years that endothelial cells in the renal vasculature undergo an early swelling during ischemia leading to a narrowing of the lumen.[135] Evidence of endothelial dysfunction also comes from experiments that have found over expression of ICAM-1 by vascular endothelial cells and enhanced expression of the Arg-Gly-Asp (RGD) peptide binding integrins in ischemic AKI. Using minimally invasive intravital microscopy of the glomerular and peritubular capillaries, Goligorsky et al. have shown endothelial dysfunction andthe no-reflow phenomenon manifested by reversal, deceleration and cessation of blood flow, occurring in a sporadic fashion in pre- and postglomerular capillaries in post-ischemic kidneys.[136]

The integrity of endothelial barrier is also impaired in AKI as shown by *in vitro* studies demonstrating endothelial cell desquamation and formation of gaps between confluent endothelial cells treated with thrombin, while *in vivo* studies in inflammatory states have

provided direct evidence for increased gaps between endothelial cells with increased permeability.[121] The cytoskeletal structure of endothelial cells includes actin filament bundles that form a supportive ring around the periphery, along with the adhesion complexes that provide the integrity of the endothelial layer. Alteration of the normal actin cytoskeleton of endothelial cells *in vitro* has been demonstrated with ATP depletion as a model of ischemic injury and with H_2O_2 as a model of oxidant-mediated reperfusion injury. ATP depletion has been demonstrated to rapidly and reversibly disrupt the normal cortical and basal F-actin structures in endothelial cells resulting in F-actin aggregation and polymerization. Oxidant-mediated endothelial cell injury also has been demonstrated to disrupt the cortical actin band in cultured endothelial cells.[137] The assembly and disassembly of actin filaments is regulated by a large family of actin binding proteins including actin depolymerizing factor (ADF)/cofilin. With ischemic injury, the normal architecture of the actin cytoskeleton is markedly changed along with endothelial cell swelling, impaired cell-cell and cell-substrate adhesion and loss of tight junction barrier functions. ATP depletion of cultured endothelial cells has been shown to induce dephosphorylation/activation of ADF/cofilin in a direct and concentration-dependant fashion. This results in depolymerized and severed actin filaments, seen as filamentous (F) actin aggregates at the basolateral aspects of the cell[138–140] (Fig. 76.6).

Endothelial Permeability Defects

The endothelial barrier serves to separate the inner space of the blood vessel from the surrounding tissue and to control the exchange of cells and fluids between the two. It is defined by a combination of transcellular and paracellular pathways, the latter being a major contributor to the inflammation-induced barrier dysfunction.

Sutton et al. have studied the role of endothelial cells in acute kidney injury by a series of experiments utilizing florescent dextrans and two-photon intra-vital imaging. The increased microvascular permeability observed in acute kidney injury is likely a combination of numerous factors such as: loss of endothelial monolayer, breakdown of perivascular matrix, alterations of endothelial cell contacts and upregulated leukocyte-endothelial interactions. They have shown that 24h after ischemic injury there was loss of localization in vascular endothelial cadherin immunostaining, suggesting severe alterations in the integrity of the adherens junctions of the renal microvasculature.[121] *In vivo* two-photon imaging demonstrated a loss of capillary barrier function within two hours of reperfusion as evidenced by leakiness of high molecular weight dextrans (300,000 Da) into the interstitial space.

Critical constituents of the perivascular matrix, including collagen IV, are known to be substrates of matrix metalloproteinase (MMP)-2 and MMP-9, which are collectively known as gelatinases. Breakdown of barrier function may also be due to matrix metalloproteinase -2 or -9 activation and this up-regulation is temporally correlated with an increase in microvascular permeability.[83,141] In addition, minocycline, a broad based MMP inhibitor, and the gelatinase specific inhibitor ABT-518 both ameliorated the increase in microvascular permeability in this model. Taken together, many findings indicate that the loss of endothelial cells following ischemic injury is not a major contributor to altered microvascular permeability, although renal microvascular endothelial cells are vulnerable to the initiation of apoptotic mechanisms following ischemic injury that can ultimately impact microvascular density[142] (Fig. 76.8).

ENDOTHELIUM AND COAGULATION ABNORMALITIES IN AKI

Endothelial cells have a central role in coagulation through their interaction with protein C mediated by the endothelial cell protein C receptor (EPCR) and thrombomodulin. Protein C is activated by thrombin-mediated cleavage and the rate of this reaction is augmented 1000-fold when thrombin binds to the endothelial cell-surface receptor thrombomodulin. The activation rate of protein C is further increased by approximately 10-fold when EPCR binds protein C and presents it to the thrombin–thrombomodulin complex. Activated protein C acquires antithrombotic and profibrinolytic properties, and participates in numerous anti-inflammatory and cytoprotective pathways to restore normal homeostasis.[143] Activated protein C is also an agonist of protease activated receptor-1.[144] Animal studies have shown pre-treatment with aPC to be beneficial in ameliorating AKI from ischemic or septic injury in rats by inhibiting leukocyte activation through TNF-α, and not by inhibiting coagulation abnormalities.[145,146] It has also shown that both pre -treatment and post-injury treatment with soluble thrombomodulin attenuates renal injury with minimization of vascular permeabilility defects with improvement in capillary renal blood flow.[71]

Injury to endothelial cells could have a role in chronic disease, Basile et al.[89] documented a significant decrease in the density of blood vessels following acute ischemic injury, which led to the phenomenon of "vascular dropout." This phenomenon was verified by Horbelt et al.[90] who found that vascular density was

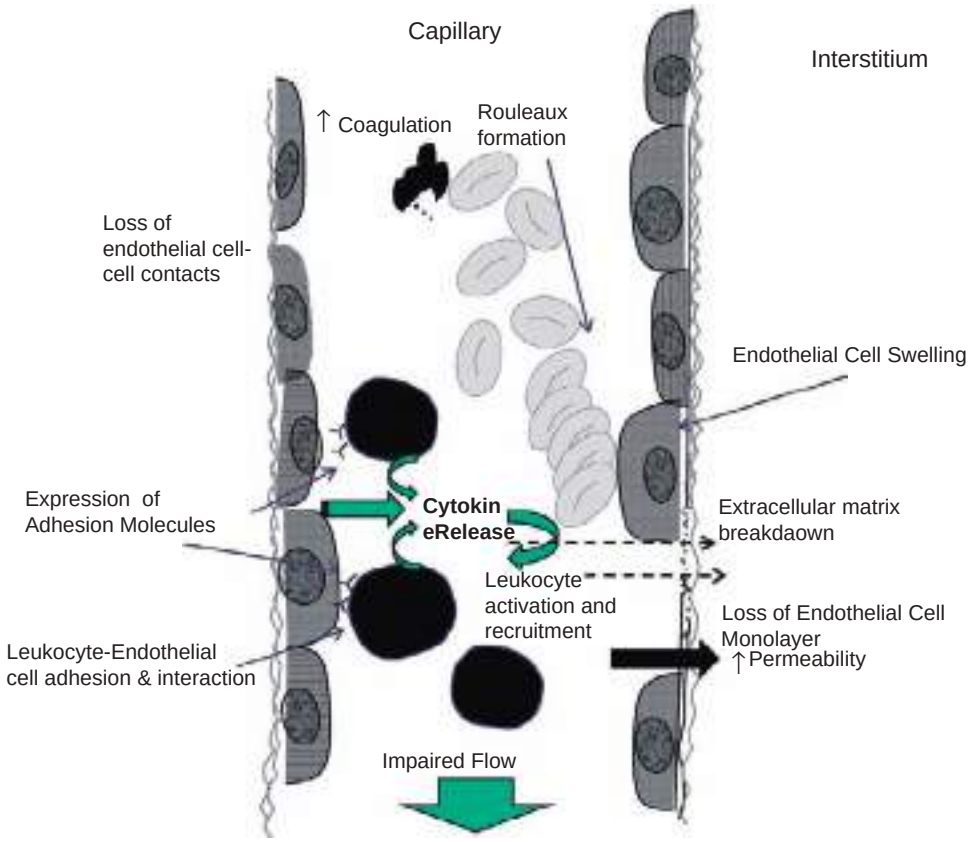

FIGURE 76.6 Endothelial injry in AKI. Key events in endothelial cell activation and injury. Ischemia causes upregulation and expression of genes coding for various cell surface proteins such as E-(endothelial) and P-(platelet) selectin, vascular cell adhesion molecule-1 (VCAM-1), intercellular adhesion molecule-1 (ICAM-1) and reduced thrombomodulin (TM). Activated leukocytes adhere to endothelial cells through these adhesion molecules. Endothelial injury increases the production of endothelin-1 and decreases endothelial derived NOS (eNOS) which serve to induce vasoconstriction and platelet aggregation. The combination of leukocyte adhesion and activation, platelet aggregation and endothelial injury serves as the platform for vascular congestion of the medullary microvasculature. There are permeability defects between endothelial cells as a result of tight and adherens junctional altrerations. *(Source: unpublished figure from Encyclopedia of Intensive Care Medicine. Publisher Springer. Eds, Vincent, Jean Louise; Hall, Jesse B. Ch Endothelial Cell Injury by Asif Sharfuddin and Bruce Molitoris. First Edition March 2012.)*

reduced by almost 45% at four weeks after an ischemic insult. This observation indicates that, unlike renal epithelial tubular cells, the renal vascular system lacks comparable regenerative potential. Ischemia has been shown to inhibit VEGF, while inducing the VEGF inhibitor ADAM-TS 1.[147] The lack of vascular repair was postulated to be due to the reduction in VEGF expression, as administration of VEGF to postischemic rats preserved microvascular density.[148] Vascular dropout might mediate increases in the expression of hypoxia inducible factor (HIF), increase fibrosis, and alters proper hemodynamics, leading to hypertension. Basile et al. have also shown that the poor regenerative potential of endothelial cells and transformation into fibroblasts is in large part owing to the lack of VEGF expression.[149] This may have a critical role in accelerating progression of CKD following initial recovery from ischemia or reperfusion-induced AKI.[150,151] Vascular dropout could predispose individuals to recurrent ischemic events and AKI.[152]

INFLAMMATION IN ACUTE KIDNEY INJURY

Inflammatory Response, Adhesion Molecules and the Role of Leukocytes

Inflammation and recruitment of leukocytes during epithelial injury are now recognized as major mediators of all phases of endothelial and tubular cell injury. Human AKI/ATN biopsies seldom have accumulated neutrophils, as compared to the abundance in experimental animal ischemic studies.[153,154] Neutrophils likely play a modest role as an effector cell in the initiation and extension phases, while T-cells and B-cells

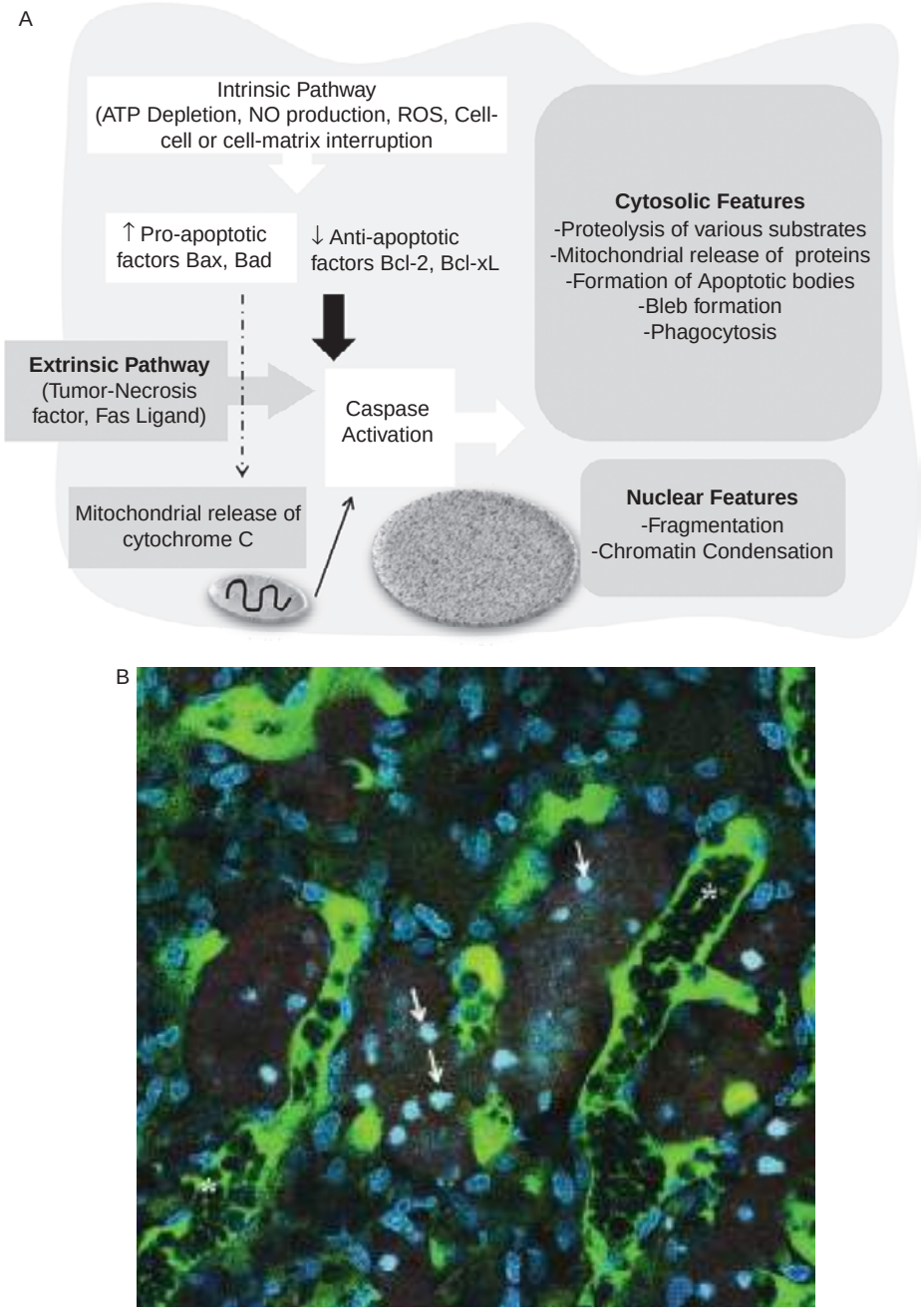

FIGURE 76.7 A. Apoptosis pathways. The cell injury or intrinsic pathway leads to translocation of Bax and other pro-apoptotic proteins from cytosol to the mitochondria, forming pores, causing the release of cytochrome c. Apoptosis-activating factor (APAF) is activated by cytochrome c which binds to and activates procaspase-9. Caspase-3 is activated by activated caspase-9, which along Encyclopedia of Intensive Care Medicine. Publisher Springer. with other downstream caspases induce proteolysis of various cytosolic and nuclear proteins. The death receptor or extrinsic pathway functions primarily by binding of death ligands such as Fas or TNF-α to their cell-surface receptor, resulting in the activation of procaspase-8 to its active form. This occurs through mediation with adaptor proteins such as FADD (Fas ligand associated death domain) and TRADD (TNF-R1 associated death domain). Active caspase-8 activates caspase -3 as well as cleaves proapoptotic protein Bid to its truncated form tBid, that acts visa Bax to induce cytochrome c from the mitochondria. Hence the extrinsic pathway also amplifies the events induced by the intrinsic pathway. *(Source: Adapted from Levine JS, Lieberthal W: Terminal pathways to Cell Death. In Acute Renal Failure: A Companion to Brennor & Rector's The Kidney. 2001, p43; and unpublished figure from Encyclopedia of Intensive Care Medicine. Publisher Springer. Eds, Vincent, Jean Louise; Hall, Jesse B. Ch Epithelial Cell Injury by Asif Sharfuddin and Bruce Molitoris. First Edition 2012.).* B. Live 2 photon imaging of a Sprague-Dawley rat kidney 24 hrs after cecal ligation and puncture. Nuclei are labeled blue with Hoechst. Green represents 500KD FITC dextranwhich labels the vasculature. Red represents 3KD Texas Red dextran that is filtered and labels the tubular lumens. Note apoptotic nuclei which show intense Hoechst staining along with condensation and fragmentation (arrows). Many of these apoptotic nuclei are shed into the lumens of tubules with compromised urine flow. Also noted is the rouleaux formation and congestion in peritubular capillary with lack of blood flow. *(Source: Courtesy of Pierre Dagher, MD, Division of Nephrology, Indiana University School of Medicine.)*

and macrophages probably have major modulatory roles in the extension and repair phases. A complex series of events involving several classes of adhesion molecules including selectins, mucins, integrins, and the Ig superfamily occurs.

Leukocyte recruitment into most organs occurs in a cascade-like fashion. Adherence to the vascular endothelium is a dynamic multifaceted process involving both the leukocyte as well as the endothelial cell. For the leukocyte to be activated to release cytokines it has to receive signals through chemokines circulating in the bloodstream, or through direct contact with the endothelium. Rolling leukocytes can be activated by chemoattractants such as complement C5a and platelet activating factor. Upon activation, leukocyte integrins change their confirmation and bind to endothelial ligands to promote firm adhesion. For neutrophil recruitment β2-intgerin (CD18) seems to be most important. These interactions with the endothelium are mediated through endothelial adhesion molecules that are upregulated during ischemic conditions.[155]

Initially there is slow neutrophil migration mediated by tethering interactions between selectins and their endothelial cell ligands. Singbartl et al. found that platelet P-selectin and not endothelial P-selectin was the main determinant in neutrophil mediated ischemic renal injury.[155] There is also significant protection from both ischemic injury and mortality by blockade of the shared ligand to all three selectins (E-, P- and L-selectin) which seems to be dependent on the presence of a key fucosyl sugar on the selectin ligand.[156,157] In a CLP model of septic azotemia mice gene-deficient for E-selectin or P-selectin or both were completely protected. Selectin-deficient mice revealed unchanged intraperitoneal leukocyte recruitment but altered cytokine levels when compared to wild-type mice.[158] Therefore, it is possible that selectins exert their effects through modulation of systemic cytokine profiles rather than through engagement in leukocyte-endothelial cell interactions.[159]

After the initial rolling, firm adhesion is imparted by interaction between endothelial cell integrins and intercellular adhesion molecule-1 (ICAM-1). Blockade of integrin CD11/CD18, ICAM-1, or deficiency of ICAM-1, were all found to protect from ischemic renal injury.[160] Treatment of humans with anti-ICAM-1 antibodies however did not reduce the rate of delayed graft function or acute rejection following renal transplantation.[161] Alpha-melanocyte-stimulating hormone (α-MSH), a known inhibitor of interleukin-8 (IL-8) and ICAM-1 induction, initially thought to be protective through these mechanisms, was found to be protective independent of inhibition of neutrophil recruitment.[162]

Biopsies of human AKI have demonstrated lymphocytes in ATN, and only recently has the modulatory role of T-cells in the mediation of ischemic injury been established. Rabb et al. in a series of recent experiments showed that T-cell deficient *nu/nu* mice are protected against ischemic injury, along with attenuation of ICAM-1 expression.[163] An early transient increase in T-cells might explain how T-cells could still have a role without being present in histological analysis. Additional evidence that suggests a role of T-cells is derived from studies where blockade of the CD28-B7 co-stimulatory pathway reduced injury, as well as data from STAT-4 deficient mice, which have impaired Th1 phenotype of T-cells, revealing the deleterious role of Th1 phenotypes.[164] There is also now evidence that B-cell deficient mice are protected from ischemic renal injury, while transfer of serum from wild type to B-cell deficient mice restored injury.[165] Macrophage chemoattractants are up-regulated during ischemia, resulting inmigration of macrophages into the outer medulla of the rat kidney. Data from osteopontin knockout mice revealed there was less macrophage infiltration and less fibrosis, even though the course of renal dysfunction was similar to wild type mice. Okusa et al. have also shown recently that although macrophages are required for the full extent of the ischemic renal injury, activation of their adenosine 2A receptors reduces neutrophil accumulation and provides protection against injury, as seen in experiments with macrophage depleted and adenosine 2A receptors deficient mice. The protective effect of adenosine 2A receptor activation is independent of IL-6 and TGF-β mRNA induction.[166]

Macrophages produce proinflammatory cytokines that can stimulate the activity of other leukocytes. Day et al.[111] showed that depletion of macrophages in the kidney and spleen using liposomal clodronate prior to renal ischemia reperfusion injury prevented AKI, whereas adoptive transfer of macrophages reconstituted AKI. This group also showed that agonists of sphingosine-1-phosphate induced lymphopenia, which had a protective effect.[167] However, studies have also shown a lymphocyte independent role of the sphingosine-1 phosphate receptor (S1PR) in maintaining structural integrity after AKI as S1PRs in the proximal tubule are necessary for stress-induced cell survival, and agonists of this receptor are renoprotective via direct effects on tubular cells.[168] Dendritic cells are also thought to have a role in AKI; Dong et al.[114] demonstrated that after AKI, renal dendritic cells produce the proinflammatory cytokines TNF, IL-6, C-C motif chemokine 2, and C-C motif chemokine 5, and that depletion of dendritic cells prior to ischemia substantially reduced the levels of TNF produced in the kidney.[169]

Cytokines in AKI

There is increased renal expression of many proinflammatory cytokines in response to acute ischemic or toxic injury. These include TNF-α, interferon-γ, granulocyte-macrophage colony-stimulating factor (GM-CSF), interleukins 1,2,18, as well as chemokines such as monocytes chemotactic protein-1 (MCP-1), macrophage inflammatory protein-1 (MIP-1), and RANTES. It is also possible that AKI is associated with up-regulation of IL-10, an anti-inflammatory cytokine supported by studies showing protection against AKI in ischemic and cisplatin models of injury by IL-10 administration.[170]

Recent human data suggest the role of both pro-inflammatory as well as anti-inflammatory cytokines in predicting mortality, with higher IL-6, IL-8 and IL-10 plasma levels in non-survivors amongst critically ill patients with AKI. Interestingly, IL-1 and TNF-α were not predictive.[171] Critically ill patients with AKI also have decreased and impaired monocyte cytokine production and elevated plasma cytokine levels in a pattern that closely resembles critically ill patients without AKI, suggesting the very complex role of these cytokines.[172] It is also important to remember that the maximal capacity to produce cytokines in response to stimulation can have considerable inter-individual variation due to genetic pre-determination for their expression.[173] Single nucleotide polymorphisms (SNPs) within the promoter region of these cytokines genes with stable allelic variants have been identified, and in a recent prospective evaluation of these polymorphisms, Jaber et al. found TNF-α and IL-10 gene polymorphismsrelated to the risk of death among patients with ARF who require dialysis. As the list of these cytokine gene polymorphisms grows it is possible that we may be better able to identify patients at higher risk of organ injury.[174]

AKI IN SEPSIS

Sepsis is a common cause for AKI occurring in up to 50% of septic patients with the incidence increasing depending on the severity of the septic shock syndrome.[175–177] When AKI complicates sepsis the mortality can be as high as 70% as compared to AKI without sepsis with a mortality rate ranging from 20–40%.[177]

By using endotoxinor CLP experimental models of sepsis a better understanding is now possible of the intrinsic and complex processes that take place in sepsis related ARF. The primary pathophysiologic renal response to LPS infusion is an alteration in renal hemodynamics with subsequent microvascular damage and relatively mild tubular injury. However, there is substantial variability in LPS response amongst different species and severe AKI typical of ATN is usually not a feature of this model.

The predominant pathogenetic factor in sepsis mediated AKIis renal vasoconstriction mediated through vasoactive hormones that precedes the advent of systemic vasodilation, hypotension and septic shock. Bacteria or endotoxin can induce NO synthase in the systemic circulation leading to nitric oxide-mediated systemic arterial vasodilation. This results in the sensing by the baroreceptors of an underfilled arterial system leading to the increase in sympathetic outflow with the activation of the renin-angiotensin-aldosterone system (RAAS), and also the release of arginine vasopressin from the central nervous system. The combined effects of increased sympathetic tone and RAAS result in intense vasoconstriction with intact tubular function as demonstrated by increased reabsorption of tubular sodium and water. Rats infused with endotoxin show a FENa of less than 1%, eventually leading to pre-renal azotemia.[72] If this prerenal state is not reversed it leads to progressive decrease in sodium reabsorption resulting in a higher FENa, that may progress to an established ATN. Renal denervation studies of mice afforded protection against the decline in GFR during the initial 16 hours of endotoxemia. It is also seen that plasma concentrations of norepinephrine, epinephrine and renin that activate the RAAS are higher in the LPS mice.[178] Such studies indicate the role of vasoactive hormones and neural mediation in early sepsis related AKI.

Endothelin also seems to be indirectly involved in septic AKI,as demonstrated by numerous studies showing a beneficial effect of using non-specific ET antagonists in renal injury during endotoxic shock.[179] ET can also cause a decrease in plasma volume by increasing the "leakiness" of the capillaries.[180] As earlier discussed in the section on nitric oxide, an imbalance exists between iNOS and eNOS in ischemic AKI and a similar pattern is seen in septic AKI as well. Schrier and colleagues investigated the role of NOS in mice given LPS. Due to the lack of specific eNOS inhibitor, a knockout model of eNOS deficient mice was used and found to exhibit increased RVR and higher susceptibility to endotoxemic AKI than wild-type mice despite a higher MAP.[181] Prior studies have revealed down-regulation of eNOS within the kidney and increased expression of iNOS in the renal cortex occurs during the initial 16 hours after exposure to endotoxin. Endothelial cell damage also occurs during sepsis and is associated with microthrombi formation and increased von Willebrand factor (vWF) levels.[182] eNOS production is impaired leading to further imbalance between these two proteins. In humans the use of a non-specific NOS inhibitor was found to increase

mortality in patients with septic shock further substantiating the presence of local and systemic imbalance, as well as between the two isoforms eNOS and iNOS.[183] However, a selective iNOS inhibitorhas been used in a rat model showing protection, but this approach has not been translated in human studies.

In the systemic vasculature upregulated iNOS mediates the arterial vasodilation with a profound and potent effect, causing resistance of the pressor responseto norepinephrine, and angiotensin II. The vascular smooth muscle cell (VSMC) is another key player in systemic vasodilation, as changes in pH or cellular ATP depletion open the ATP-sensitive potassium channels (K-ATP). This causes hyperpolarization of the cell leading to closure of the voltage gated calcium channels, required for the action of the above mentioned pressor hormones. The receptors for these vasoactive hormones might also be down-regulated because of their high endogenous levels. Clinically this is manifested as a poor response of vasopressors such as norepinephrine to raise blood pressure.[176] Arginine vasopressin, an endogenous vasopressor, may help maintain the blood pressure despite the nonresponsiveness of other vasopressore hormones. Some theories behind this hypothesis include: vasopressin-induced inactivation of K-ATP channels, decrease in synthesis of iNOS, and a synergistic mechanism with norepinephrine and angiotensin II, since these three agents share the same intracellular signaling pathway. In sepsis the sites of major arterial vasodilation, such as the splanchnic bed, muscles and skin, have an abundance of the vasopressin receptor V1a. At the glomerular level, vasopressin causes constriction of the efferent arteriole, as compared with norepinephrine which causes afferent arteriolar vasoconstriction, thus making vasopressin a better agent to increase filtration pressure and consequently GFR. Cytokines such as TNF-α, IL-1β, IL-6, and IL-8 are pro-inflammatory and released in response to infectious stimuli. A wide range of effects are seen when levels of these cytokines are elevated during sepsis. These include increased expression of adhesion molecules, increased production of other pro-inflammatory mediators, and activation of various leukocytes. Infusions with TNF-α and IL-1 have produced a similar sepsis like syndrome in animals. Along the same lines, blocking these pro-inflammatory mediators through antibodies has attenuated the shock like state in animal models. However, SIRS or sepsis is not an isolated proinflammatory state.[184] There is also substantial evidence for the presence of anti-inflammatory cytokines IL-10 and IL-13 as well in patients with septic shock. Thus SIRS or sepsis may be more accurately described as a malignant form on intravascular inflammation rather than a mere overexpression of pro- or anti-inflammatory cytokines. The role of TNF-α in endotoxin AKI has been tested in both humans and animals. It has been suggested that TNF-α can cause vasoconstriction even in the absence of iNOS as indicated by knockout mice studies. It is also known that caspases activate both IL-1β an IL-18, along with the resultant upregulation of adhesion molecules. Caspase-1 knockout mice or non-specific capsase inhibitors protect against endotoxemic AKI.[185]

Other mediators of sepsis include the complement cascade and the metabolites of arachidonic acid (PGE2, PGI2, Thromboxane). Thromboxane (TAX) causes platelet and leukocyte aggregation and vasoconstriction. Platelet activating factor (PAF), released by many cells amplifies cytokine production as well as stimulating leukocyte adhesion to endothelial cells. Complement cascades are activated during sepsis, and C5a, a potent complement component with procoagulant properties has been found to be elevated in rodent models of sepsis. Blocking C5a or its receptor has shown some promise in improving survival with sepsis.[175] In sepsis levels of protein C are decreased, and its conversion to activated protein C is also down-regulated.[186] Anti-thrombin III and tissue factor pathway inhibitor are also dramatically reduced. This leads to a procoagulant state resulting in thrombosis of glomerular capillaries and other intra-renal capillary beds causing persistent renal hypoxia to tubules.[187]

Some of the most recent advances in understanding sepsis have involved determining the pathophysiologic roles of NF-κB and Toll-like receptors (TLR). NF-κB is crucial for the maximal expression of many cytokines involved in the pathogenesis of inflammation. It is an intracellular species, resident in the cytosol as a heterodimer and attached to an inhibitory sub-unit called IκB. Activation of NF-κB occurs through loss of IκB which is phosphorylated by serine kinases through oxidant stress pathway mechanisms. The active heterodimer NF-κB then enters the nucleus after undergoing a conformational change, and binds to various promoter sites on the genome stimulating mRNA synthesis of gene coding for most of the pro-inflammatory cytokines such as TNF-α, IL-1β, IL-2, IFN-β, GM-CSF, adhesion molecules such as endothelial-leukocyte adhesion molecule-1, VCAM-1, immuno-receptors such as tissue factor-1, MHC 1 and 2, T-cell receptor 1 and 2, and others proteins such as COX-2.[188]

Toll-like receptors (TLR) are a family of receptors, involved in the innate immunity, that recognize components of bacteria, viruses, parasites and fungi, and induce pro-inflammatory responses by many cells. Nine murine and ten different TLRs have been cloned in humans, each differing in their specificity for microbial components, e.g., LPS, gram-positive cell wall, bacterial DNA and so on. Extracellular matrix breakdown products such as hyaluronan, heparan sulfate,

fibrinogen, or the fibronectin EDA domain can activate TLR4. TLR4 was identified as the receptor for LPS and requires the presence of an extracellular accessory protein called MD-2. CD14, a cell surface receptor, binds LPS complexed with LPS binding protein and transfers the endotoxin to the TLR4 and MD-2 dimer.[189] Each component of this complex is required for effective LPS-induced signaling. The serine kinase required for NF-κB activation occurs via the TLR4 receptor pathway, hence linking the TLR and the transcription factor in the intracellular signaling mechanism. Tubular epithelial cells are among the non-immune cells that express TLR1, -2, -3, -4, and -6, suggesting these TLR might contribute to the activation of immune responses in tubulointerstitial injury.[190]

Upon stimulation with LPS mouse tubular cells in culture upregulate TLR2, -3, and -4 and secrete CC-chemokines such as CCL2/MCP-1 and CCL5/RANTES. These data suggest that tubular TLR expression might be involved in mediating interstitial leukocyte infiltration and tubular injury during bacterial sepsis.[191] TLR4 deficient mice were found to be completely resistant to endotoxin-induced acute renal failure, which was associated with a lack of a systemic TNF-α response. Cross transplantation studies showed that TLR4-deficient recipients of wild-type kidneys developed minimal LPS-induced acute renal failure, whereas wild-type recipients of a TLR4-deficient kidney had severe acute renal injury after exposure to endotoxin.[192] These data strongly indicate a role for extra-renal TLR4 activation in acute renal failure of sepsis. However, they do not support the hypothesis that renal TLR4 expression (e.g., on tubular epithelial cells) plays a major role in sepsis-induced acute renal failure. In contrast, they rather implicate a systemic response to sepsis, involving TLR4 and TNF-α in the development of acute renal failure during sepsis.[190,192] Necrotic tubular cells release potential TLR ligands such as heat shock proteins (HSP) that could activate other tubular cells or resident immune cells in the kidney. Activation of TLR2 and TLR4 on tubular epithelial cells has been shown to specifically stimulate the NF-κB pathway in response to oxidative stress. Furthermore, TLR2 and TLR4 activation on tubular epithelial cells leads to secretion of CC-chemokines indicating a role for these TLR in the initiation of phagocyte influx and immune activation during acute tubular necrosis. Thus TLR activation may be a link between mechanical, toxic, or ischemic tubular cell injury and the onset of an inflammatory "innate" immune response in the pathogenesis of AKI.[190]

The role of ROS has also been recently investigated as a potential mediator of injury in endotoxin-related ARF. Endotoxemia is known to be associated with the generation of oxygen radicals, which may contribute to the renal injury. Exogenous oxygen-radical scavengers were shown to protect against ARF in normotensive endotoxic mice.[193] Furthermore, the early vasoconstrictor response of ARF in sepsis can be potentiated by oxidant-related endothelial cell damage.

Apoptosis and Necrosis

The fate of the epithelial cell after an injury ultimately depends on the extent of the injury. Cells undergoing sublethal injury remain capable of complete functional and structural recovery if the insult is abolished. Severly injured epithelial cells can also become dedifferentiated, express mesenchymal proteins and ultimately repolarize into functional cells with the epithelial phenotype.[194] Cells that suffer a lethal injury either undergo apoptosis or necrosis leading to cell death. In general, the mechanism of cell death induced by an ischemic or cytotoxic insult is determined by the severity and duration of injury.

Morphologically in necrosis there is swelling of cells and organelles and loss of plasma membrane integrity with rupture of cell. The cytosolic contents escape into the surrounding tissue causing injury and reactive inflammation. These cells usually die in contiguous groups. In contrast, apoptotic cells shrink in size, lose microvilli as "blebbing," but have relatively normal plasma membrane and mitochondrial structure. They lose the cell-cell and cell-matrix adhesion early ending up being exfoliated or phagocytosed as single cells. The nuclei in apoptotic cells have a characteristic appearance of chromatin condensation and nuclear fragmentation, resulting in formation of apoptotic bodies. Finally, the apoptotic cell disintegrates into multiple plasma-membrane bound apoptotic bodies that are rapidly phagocytosed by macrophages and neighboring epithelial cells.[195]

Mechanisms of Cell Necrosis

Severe ATP depletion plays a central role in necrosis after ischemic cell injury. The severity and duration of ischemia dictates the fate of the oxygen deprived cell. Weinberg and colleagues have recently discovered novel mechanisms of mitochondrial injury that are a prominent feature of necrosis. Hypoxic tubule cells in suspension undergo a severe and prolonged abnormality in oxidative phosphorylation due to major changes in the complex I function of the mitochondria. It has also been noted that amelioration of mitochondrial dysfunction by improving the cell energy depleted state, caused by hypoxia, was possible through substrates such as α-ketoglutarate plus malate or succinate and aspartate that can be anaerobically metabolized to produce ATP.[196]

Several studies have suggested a role for increased intracellular calcium in the pathogenesis of ATN. Maintainence of low cytosolic (approx 100 nM range) calcium concentrations is crucial to the normal homeostasis of the cell and its organelles. This gradient between extracellular fluid and cytosol is regulated by a complex system of pumps and electrochemical gradients and requires the integrity of membranes and availability of ATP for pump function. The role of calcium in glomerular hemodynamics is discussed elsewhere in the text, while we discuss its role in tubular cell injury.[197]

Numerous studies have shown that ATP depletion leads to a rise in intracellular calcium through impairment of calcium ATPases while inhibition of Na^+/K^+-ATPase activity potentiates calcium entry into cells via the sodium-calcium exchanger. Increased cytosolic calcium during hypoxia causes mitochondrial injury as well as cytoskeletal alterations. High concentrations of Ca^{2+} may alter the inhibitory actions of villin, an actin-binding protein regulating the capacity to sever F-actin or nucleate G-actin, thus leading to cytoskeletal disruption. However this has not been shown to affect loss of brush-border integrity. In the isolated perfused tubule system, actin cytoskeleton alterations seem to be both calcium-dependent and independent, as lethal membrane injury is not a necessary end result of intracellular calcium changes.[198] It is also possible that the interactions between high intracellular Ca^{2+} and the actin cytoskeleton are dynamic and multiplicative and once either is disrputed it leads to a lethal cycle of events resulting in exacerbating the injury.

Phospholipids in the membrane bilayer are substrates for phospholipases, and help maintain the integrity of the cell and its organelles. Because of this crucial role it has long been postulated that activation of phospholipases may play a role in post-ischemic or nephrotoxic tubule cell injury. Enzymes such as phospholipase A2 (PLA2) and calpain are calcium dependent and are activated during ischemic cellular injury. Activation of PLA2 appears to be an important mechanism of plasma and mitochondrial disruption after ischemia, an observation evident from the fact that there is phospholipid degradation that persists after reperfusion.[199] PLA2 activation results in release of fatty acids and lysophospholipids, both of which have been shown by investigators to cause lipid membrane damage. The effect of PLA2 deficiency on renal cells has not yet been examined. Besides the direct hydrolytic action, and generation of possibly toxic free fatty acids, phospholipases also play additional roles through release of eicosanoids which have a vasoactive and chemokine action. The release of arachidonic acid metabolites results in production of lysophospholipids as well as reactive oxygen species, both of which have been shown to contribute to ischemic and nephrotoxic injury.[200,201]

Calpain, which is a cysteine protease, has increased activity in hypoxic conditions that precedes cell membrane damage leading to a further increase in its activity. The role of calpain as a mediator in ischemic rat proximal cell damage, cyclosporine nephrotoxicity and mercuric chloride induced renal injury is evident as pharmacological inhibition elicits cytoprotection in these models.[202] There is also evidence that calpain mediates increased plasma membrane permeability and hydrolysis of cytoskeleton-associated paxillin, vinculin, and talin during renal cell death.[203] The internalization of Na^+/K^+-ATPase from the membrane and the loss of cell polarity could be mediated through calpain induced cleavage of actin-binding proteins such as spectrin, filamin, ankyrin and α-actinin which has been shown indirectly by the use of calpain inhibitors which improved recovery of active Na^+ transport in rabbit renal proximal tubule cells after hypoxia and reoxygenation.[204] All these data tie together the intricate role calpain plays in the ischemic cell damage. Caspases, as discussed in later sections on apoptosis, might also play a role in necrosis when activated, and could well be involved in the pathway leading to this form of cell death.[205]

DNA fragmentation is detected in the kidney cortex as early as 12h after reperfusion, and approximately 40 double-stranded DNA breaks per cell have been shown to be lethal with ineffective DNA repair beyond these levels. Endonucleases generally cleave double stranded (ds) DNA only at sites unprotected by histones. This is evident as the typical "ladder" pattern generated by gel electropheresis of DNA from apoptotic cells. In necrosis there is also release of lysosomal enzymes and proteases that degrade the histones resulting in accessibility of the endonuclease to the entire segment, resulting in shorter segments. This is evident as the typical "smear" pattern seen in gel electropheresis on necrotic cells[206] (Fig. 76.7).

Apoptotic Mechanisms

Unlike necrosis the fundamental biochemical pathways can be divided into a commitment phase and an execution phase, each controlled by various triggers and factors ultimately deciding the fate of the cell. The morphological changes seen, as described above, are the typical apoptotic bodies. Since histones remain intact in apoptosis the activation of specific caspase-activated deoxyribonuclease (CAD) results in cleavage of the dsDNA only at the linking regions between the nucleosomes.[207] But one has to be careful as this does not necessarily reflect apoptosis only and other studies have shown that apoptosis can occur in the absence of inter-nucleosomal cleavage.[208] Similarly, the laddering

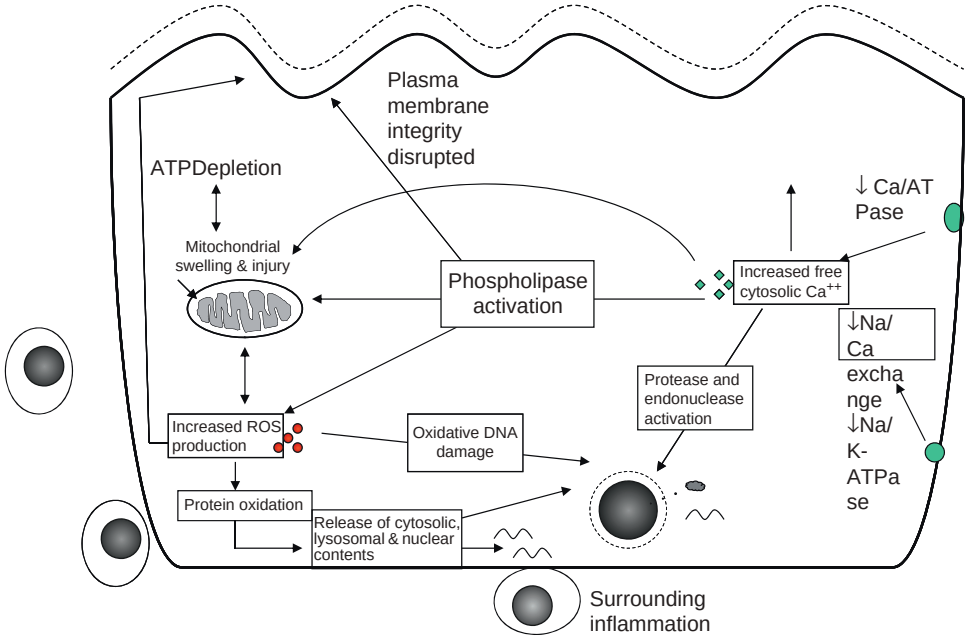

FIGURE 76.8 Pathways of necrosis. Major biochemical pathway of cell necrosis. Severe ATP depletion causes profound mitochondrialinjury which further worsens cellular energy stores and leads to the generation of reactive oxygen species (ROS). Free intracellular calcium levels are increased as a result of decreased pump activity leading to phospholipase activation resulting in disintegration of the plasma membrane as well as further ROS production. High intracellular levels of Ca^{2+}also activate endonucleases damaging DNA, an end-effect which is multifactorial through oxidative damage as well as loss of critical enzymes because of protein oxidation. Cytosolic leaks from the dead cell induce a surrounding inflammatory reaction.

of DNA seen in apoptosis is not specific and can be seen in necrosis or even as an artifact.[209]

Until recently the mode of cell death following ischemia has been related entirely to the severity of ATP depletion. Dagher et al. have shown that ischemia causes depletion of guanosine triphosphate (GTP) as well as ATP in both the ischemic kidney *in vivo* and in cultured renal tubular cells (RTC). They provide seminal evidence that GTP, without substantial ATP depletion, induces apoptosis of RTCs while selective ATP depletion causes necrosis. They also have shown that in animals subjected to acute ischemic renal injury the administration of guanosine maintained renal GTP levels within the normal range without changing the severity of ATP depletion. In addition, guanosine supplementation ameliorated renal dysfunction induced by renal ischemia and appeared to reduce apoptosis of RTCs while having little effect on the amount of necrosis. These studies provide strong evidence that changes in cell GTP as well as ATP stores play an important role in determining the mode of tubular cell death after lethal injury.[210]

CASPASES IN AKI

There is increasing evidence of a role for caspases in hypoxic renal tubular cell injury. Caspases are cysteine proteases that cleave their substrates irreversibly after aspartic acid residues, and can be divided into three major subfamilies. Caspases 1, 4 and 5 do not appear to have any role in apoptosis, rather they have a pro-inflammatory role by activating the cytokines interleukin-1β and interleukin-18. The second group of caspases 3, 6 and 7, are classified as "effector" caspases. Effector caspases are more abundant and catalytically robust than initiator caspases and, by cleaving many cellular proteins, are responsible for the 'execution phase' of apoptosis and for the classic apoptotic phenotype. Caspase 3 activates additional downstream effector caspases. Lastly caspases 2, 8 and 9 are "initiator" caspases and are the first to be activated by pro-apoptotic stimuli. Pro-caspase 8 is activated by interactions between death receptors and their ligands, and pro-caspase 9 by direct injury to cells. Once activated, caspases 8 and 9 both converge on and activate pro-caspase 3, an effector caspase.[185,211]

Caspases are activated by ischemic and cytotoxic insults to cultured RTCsand to the kidney *in vivo*. Furthermore, inhibition of caspases ameliorates ischemia-reperfusion injury in the kidney, and in the heart, brain, liver and gastrointestinal tract. Collectively, these studies provide strong evidence that caspases are important contributors in the pathogenesis of ischemic injury. Conflicting results have been seen when using caspase 1 knockout mice in ischemic renal

injury with two groups reporting less severe injury in caspase 1 -/- mice than in the wild-type controls. This was thought due to a defect in interleukin-18 activation and a consequent reduction in intrarenal inflammation. The other group found no substantive difference in the severity of renal dysfuction or intrarenal inflammation in control and caspase 1 -/- mice following ischemic AKI.[212] Caspase-1 deficient mice were also protected against cisplatin induced renal injury while cold ischemic injury in mice was ameliorated in mice using caspase inhibition.[213,214]

The balance of evidence so far suggests that both groups of caspases are activated by acute renal injury and that both are probably involved in AKI by promoting intrarenal inflammation and by inducing RTC loss by apoptosis.[211] The recent development of potent caspase inhibitors highly specific for the executioner caspases 3 and 7 may provide more effective experimental tools for examining the contribution of RTC apoptosis to the pathogenesis of AKI. Similarly two of the known murine caspases, caspases 11 and 12, are activated only under pathologic conditions of ischemia or stress. Caspase 11 activates caspases 1 and 3 directly inducing both inflammation and apoptosis in an apoptosome-independent manner.[215] The identification of caspases that respond exclusively to pathologic stimuli, however, is of potential therapeutic importance since it suggests the possibility of developing therapeutic interventions that target pathologic cell death without affecting apoptosis.

Caspase inhibition may also protect against lipopolysaccharide—induced AKI—not only by preventing apoptotic cell death but also by inhibiting inflammation. These data raise the possibility that apoptotic kidney cells may actually be a source of this local inflammation, contributing to subsequent non-apoptotic renal injury.[185] Using the cisplatin model of AKI van de Water et al. have shown that α-adducin, a cytoskleletal protein, is a caspase substrate and that it is cleaved by caspase 3 during apoptosis. This is involved in the dismembering of the actin cytoskeleton that is necessary for many of the classic morphological features of apoptosis.[216] Cisplatin has been shown to activate caspases 1, 3, 8 and 9, while caspase inhibition ameliorates cisplatin-induced cell death. Thus, as in ischemic injury, there is evidence that caspase activation is an important contributory factor in the pathogenesis of cisplatin-induced AKI.[217]

MITOCHONDRIA

Apoptosis unlike necrosis is energy requiring and hence a mitochondrial dependent process resulting in release of cytochrome c through mitochondrial pores secondary to ATP depletion and increases in cytosolic Ca^{2+}. Cytochrome c is an essential cofactor for activation of procaspase-9. Molecules such as Bax and Bak are thought to be responsible for the formation of pores.[218] In living cells these changes are prevented by anti-apoptotic members of the Bcl-2 family of proteins. Therefore, the balance between cell survival and apoptosis is determined partly by the relative concentrations of pro-apoptotic and anti-apoptotic Bcl-2 family members. Bcl-2 and Bcl-xL can inhibit the formation of mitochondrial pores and data exist indicating a relative deficiency of Bcl-2 proteins in kidneys subjected to acute injury *in vivo*, while overexpression of Bcl-2 confers resistance of RTC to cisplatin-induced apoptosis.[219] Microinjection of Bcl2_syn into stimulated LLC-PK1 cells significantly reduced the percentage of apoptotic cells detected within four hours, after the treatment. Growth factors might also induce phosphorylation and inactivation of the pro-apoptotic protein Bad and the simultaneous induction of Bcl-xL.[220]

Nuclear Factor κB (NF-κB), an anti-apoptotic transcription factor, is activated by a wide variety of stimuli such as growth factor deprivation, TNF-α, hypoxia, oxidative stress and cisplatin. NF-κB protects against apoptosis through transcriptional induction of anti-apoptotic Bcl-2 family members and through decreased expression of iNOS in tubule cells.[221] The pro-apoptotic transcription factor p53 can be activated by hypoxia, via the hypoxia-inducible transcription factor (HIF-1α), and by other stimuli such as cisplatin, adriamycin, UV light and γ-irradiation.[222] Kelly et al. have demonstrated p53 protein levels increase significantly in both cultured renal tubular cells, as well as *in vivo*, in the medulla 24 h post-ischemia in the renal clamp rat model. This induction was inhibited with the supplementation of guanosine by minimizing cellular GTP depletion. In addition, pfithrin-α, a specific p53 inhibitor prevented apoptosis and protected renal function. The effects of pifithrin-alpha on p53 included inhibition of transcriptional activation of downstream p53 targets, like p21 and Bax, and inhibition of p53 translocation to the mitochondria.[223]

RECEPTOR MEDIATED PATHWAYS

Two receptor classes namely the CD95 (Fas) and the TNF receptor 1 (TNFR-1), when bound to their ligands FasL and TNF-α respectively, lead to activation of caspase 8 and 10 resulting in apoptosis. Tubular cells are normally relatively resistant to FasL and TNF-α induced apoptosis, but when exposed to inflammatory cytokines or to ATP depletion, the expression of Fas/FasLand TNF-α/TNFR-1 is upregulated and the cells become susceptible to Fas and TNF-α mediated apoptosis.[211] So far most of the data are from *in vitro* studies except one study demonstrating that Fas-deficient mice are protected from ischemic AKI.[224]

KINASE MEDIATED PATHWAYS

Several studies now recognize the role of phopatidylinositol 3′ (PI-3) kinase/Akt phosphorylase in the signaling cascade that blocks apoptosis. Akt, a serine/threonine kinase, is activated by PI-3 through phosphorylation, which can bind down stream to the pro-apoptotic Bcl-2 family member Bad and render it dysfunctional. This in turn restores the balance towards greater availability of anti-apoptotic proteins such as Bcl-2 and Bcl-xL. In cisplatin-induced renal tubular injury Shah et al. have shown that suppression of caspase 3 and 9 activation occurs through the PI-3/Akt mediated pathway. Similar results were also obtained in hypoxia-induced RTC's. Akt also induces activation of the pro-survival transcription factor NF-κB.[212,225]

Extracellular signaling kinases (ERK), jun-N-terminal kinase (JNK) and p38 are mitogen activated protein kinases (MAPK), that are responsible with other signal transducing factors for mediating cellular responses involved in apoptosis, survival and cellular repair. Growth factors such as hepatocyte-growth factor (HGF), insulin-like growth factor-1 (IGF-1), epidermal like growth factor (EGF), and vascular endothelial growth factor (VEGF) mediate their actions through ERK1 and ERK2 kinases, which get translocated to the nucleus and activate transcription factors responsible for induction of genes in mitogenic activity. Growth factors also inhibit apoptosis by ERK signaling mediated phosphorylation of the PI-3K, and by effects independent of the PI-3K/Akt pathway. These independent mechanisms include inactivation of Bad, and through activation of the anti-apoptotic transcription factor CREB.[226]

A variety of stimuli of importance in AKI activate JNK, and are well known to promote apoptosis. Bonventre et al. have reported the role of JNK activation after ischemia-reperfusion injury could play a role in the loss of tubular cells.[227] Inhibition of JNK through administration of N-acetly-cysteine points towards a renoprotective mechanism of suppression of this pathway. Another important factor that might decide the fate of the cell depends in part on the relative activation of ERK and inhibition of JNK.[228] Interestingly, increased production of TNF-α by RTCs during ischemia also appears to be mediated by activation of p38.[229] There are also data to suggest that loss of cell-matrix or cell-cell adhesion also leads to apoptosis.

Autophagy, which is the process involved in degradation of a cell's own components through the lysosomal machinery, is now increasingly recognized as perhaps the most frequent cell-death pathway for injured epithelium. Li et al. have demonstrated the important role of autophagy in renal epithelial cells in obstructive uropathy models, while Koesters et al. have shown that transforming growth factor-β expression leads to excessive autophagy in injured tubules.[230,231]

The therapeutic implications of apoptosis in AKI are significant considering the fact that numerous targets are available for modulation. Inhibiting apoptosis seems more of a successful pathway as compared to necrosis where there could be a window of opportunity to tilt the balance towards anti-apoptotic triggers promoting renal cell survival. The initiating caspases are more likely to be effective in preventing cell death than the downstream effector caspases. However, it remains to be seen whether novel therapies can be developed that effectively modulate 'pathologic' apoptosis without interfering with apoptosis required for normal physiologic processes[211] (Fig. 76.8).

Stress Response and the Heat Shock Proteins

A basic cellular defense mechanism against numerous stresses such as fever, trauma or inflammation is the complex heat shock protein (Hsp) system. At baseline in the unstimulated cell they reflect only 2% of the resting cellular protein component. However, they can be induced to up to 20% under conditions of stress. Diverse HSP families of different molecular sizes function as molecular chaperones facilitating the folding of enzymes and other proteins into their functional conformation. After injury, HSPs are believed to facilitate the restoration of normal function by assisting in the refolding of denatured proteins and degradation of irreparably damaged proteins and toxic metabolites, limiting aggregation of damaged peptides and in aiding the appropriate folding of newly synthesized essential polypeptides.[184,232,233] Among the cell-stress pathways activated by renal ischemia the stress proteins Hsp90, Hsp72 and Hsp25 have been studied by several groups of investigators. These proteins are induced after renal I/R injury and their overexpression prior to injury can protect renal epithelia from specific insults and manifestations of *in vitro* injury. Overexpression of Hsp25 has been shown to be protective against actin-based cytoskeleton disruption and some results suggest that 25-kD and 70-kD HSPs induced by ischemic conditioning stabilize the cytoskeletal anchorage of Na^+/K^+ ATPase during repeat renal ischemia.[234,235]

In vivo studies have been subject to greater controversy; initial studies using either an ischemic preconditioning model or cross-tolerance after heat stress induction suggested that heat shock proteins contribute little, if any, protection against ischemic injury in the kidney. However, more recent studies using ischemic or heat preconditioning do suggest a role for either Hsp72 or Hsp25 in protecting against injury from renal ischemia *in vivo*.[232] The apparent conflicting results

from these previous *in vivo* preconditioning studies highlight the potential advantage of studying a model of intrinsic resistance to injury, as recently demonstrated by Basile et al. in the Brown Norway rat, where a preconditioning insult is not required.[236] In the nephrotoxic model recent findings suggest that Hsp72 attenuates cisplatin-nephrotoxicity, and there was evidence of increased Bcl-2/Bax ratio and less apoptosis thus implicating its role in cell death.[237]

Heme Oxygenase

The enzyme heme-oxygenase-1 (HO-1) is responsible for the degradation of heme to bilirubin, carbon monoxide and iron. Its gene is arguably one of the most readily inducible genes responding to numerous stressors including but not limited to hypoxia, hyperthermia, oxidative stress, LPS to name a few. Consequently, induction of HO was described in various forms of AKI including ischemic, endotoxin and nephrotoxic models. A number of studies indicate a protective effect of induction of HO-1 in AKI.[238,239] Prior induction of HO-1 by hemoglobin can reduce endotoxemia-induced renal dysfunction and mortality. Inhibition of HO activity in the intact, disease free kidney reduces medullary blood flow without exerting any effect on cortical blood flow. Overexpression of HO-1 by hemin results in a significant reduction in cisplatin-induced cytotoxicity.[240] TNF-α induced apoptosis in endothelial cells is also attenuated by induction of HO-1. These findings have been supported by studies in which HO-1 deficient mice, in the glycerol-induced AKI model, exhibited marked exacerbation of renal insufficiency and mortality.[241] The protective mechanisms of HO-1 have been extensively studied by Nath et al. who showed over expression of HO-1 in cultured renal epithelial cells induces upregulation of the cell cycle inhibitory protein p21 and confers resistance to apoptosis.[242] Thus the biologic actions HO-1 that appear particularly relevant to AKI include vasodilatory effects, cytoprotective effects, anti-inflammatory actions, anti-apoptotic effects and cellular proliferative effects making it a potentially exploitable expressive enzyme in the prevention and reduction of AKI. Perhaps more importantly it might also benefit in the repair and regeneration of tubular cells.[56,239]

Reactive Oxygen Species and Oxidative Stress

Reactive oxygen species (ROS) have been implicated in the pathogenesis of ischemic and toxic AKI. Three highly reactive ROS, the hydroxyl radical (HO^-), peroxynitrite ($ONOO^-$) and hyperchlorous acid (OCl^-) are discussed here.

The hydroxyl radical (HO^-) is formed from superoxide using the enzyme superoxide dismutase that utilizes ferrous iron as a catalayst. Superoxide is constantly produced by normal cells that are normally protected against the injurous effects of HO^- by numerous scavenging systems. Perioxynitrite ($ONOO^-$), like the HO^- radical, is a potent oxidant formed by the noncatalysed reaction between superoxide and NO. Antioxidants, catalases, and glutathione peroxidases convert the intermediate molecule hydrogen peroxide (H_2O_2) to water. Oxidant stress occurs when there is either a lack of these antioxdants or enzymes or when there is excessive ROS generation.

In ischemic, myoglobinuric or hemoglobinuric renal injury, iron is liberated from storage sites and free iron promotes the generation of HO^-. Other sources of generation include mitochondria where oxygen deprivation leads to "reduction" of the redox state of the electron transport chain, and when reperfusion occurs, free electrons are released capable of increasing superoxide production. A second important source in rats is xanthine oxidase whose production is increased in ischemic and reperfusion and generates superoxide. In the presence of reduced nicotine adenine dinucleotide (NADH) or reduced NAD phosphate (NADPH) the enzymes involved in the metabolism of arachidonic acid produce superoxide. Neutrophils when activated produce superoxide as a result of NADPH oxidase enzyme. Endogenous renal cells, such as tubular epithelial cells, also possess this enzyme which may thus serve as a source of oxidants in ischemia-reperfusion injury. Collectively, an extremely high concentration of ROS can accumulate under pathological conditions overwhelming the scavenging and antioxidant systems as they themselves become suppressed during injury.[243]

ROS damage tissue in a variety of ways. Cells and their organelles—lipids, carbohydrates, proteins, and nucleic acids—can all be affected by ROS. For example, peroxidation of lipids in plasma and intracellular membranes perturbs membrane fluidity, permeability, and ion and solute transport. In response to oxidant stress partially purified membrane fractions from the outer medulla of the kidney display diminished activity, turnover rates, and sulfhydryl content of Na^+K^+-ATPase, accompanied by increased peroxidation of membrane lipid. Cytoskeletal proteins and proteins such as integrins, that facilitate the attachment of cells to the neighboring extracellular matrix, can also be destabilized by ROS. Exposure to hydrogen peroxide rapidly causes single-strand breaks in DNA leading to the activation of the DNA repair enzyme, poly-ADP-ribose polymerase (PARP) resulting in the consumption of NAD* and impaired ATP synthesis. Additionally, hydrogen peroxide compromises

mitochondrial ATP synthesis by inhibiting the ATP-synthetase complex.[243]

Evidence for the role of ROS in AKI comes from both *in vitro* and *in vivo* studies. The generation of ROS during ischemic and postischemic phases is well documented. For example, studies undertaken in renal epithelial cells demonstrate that increased amounts of ROS are generated not only during reoxygenation after hypoxic exposure, but also during the hypoxic phase.[233] Superoxide anion is usually vasoconstrictive-based on its capacity to scavenge nitric oxide, while hydrogen peroxide may exert vasodilatory or vasoconstrictive effects. ROS can also alter the expression or activity of variousvasoactive species, can greatly impair the endothelium, and can profoundly perturb vascular reactivity because of ROS-mediated effects on intracellular calcium handling in smooth muscle cells. ROS can also promote leukocytic adherence to the endothelium. Thus, ROS contribute to many renal vascular and hemodynamic changes observed during the initiation and established phases of ATN: endothelial injury, leukocytic adherence, increased endothelial expression of vasoconstrictive peptides, impaired endothelium-derived vascular relaxation, heightened sensitivity to vasoconstrictors, greater sensitivity to neural stimulation, increased basal vascular tone, and dysfunctional autoregulation.[123]

Oxidative stress can injure plasma and intracellular membranes by activating phospholipases, in particular, phospholipase A_2, present in membrane-bound and cytosolic fractions. ROS can also damage DNA, impair enzymatic processes, and ion pumps, including direct oxidant injury to Na^+/K^+-ATPase and Ca^{2+}-ATPase. That oxidative stress may contribute to inflammatory events in the ischemic kidney is demonstrated by studies of ischemic injury in mice that overexpress oxidant-scavenging genes, such as glutathione peroxidase. Such mice exhibit less ischemic injury to the kidney along with less activation of NF-κB and attenuation in the upregulation of relevant chemokines.[244]

The demonstration in relevant disease models that antioxidant maneuvers exert beneficial effects has stimulated the application of antioxidant therapies to human ATN. Relevant to this is the demonstration that the administration of the thiol-donating antioxidant, N-acetyl-cysteine, reduces the risk of renal insufficiency induced by contrast dye.[245] There have been numerous studies that have illustrated benefits of antioxidants in preventing renal ischemic damage, including superoxide dismutase, catalase, inhibitors of xanthine oxidase, scavengers of HO^- and agents that bind free iron. Unfortunately, the transition from bench research on animals and cells to clinical studies has proven less promising.[246] As gene-deletions and knockout mice models become more available to study the mechanisms of disease, and the effect of therapies, their use in oxidant injury has also been evaluated. Recently it has been shown that PARP ablation preserved ATP levels, renal function, and attenuated the inflammatory response in the setting of IRI in the mouse model.[247]

The capacity of ROS to influence the expression of growth-promoting substances and, in turn, the utilization by growth factors of ROS as signaling species, raises the intriguing possibility that ROS may be also involved in the recovery phase from ATN.[243]

CELLULAR REPAIR, REGENERATION AND RECOVERY

Renal tubular regeneration is one of the most remarkable phenomena in mammalian biology research as it can restore kidney function and structure after ischemic or toxic renal injury. This is clinically evident in the fact that most patients recover from AKI, if the insult is removed within a critical time period, before complete necrosis sets in. Sublethally injured cells initiate the process of repair and regeneration once reperfusion commences. Most sublethally injured cortical PTC cells repair themselves without going through a "dedifferentiated stage." Although exfoliation of cells might not be considered a morphological stage of repair, it is associated with the generation of signals that initiate the process of repair including accumulation of leukocytes, and the integration of growth factors to determine the fate of the epithelial cells. The stage of regeneration in severly injured cells is the "dedifferentiated stage," which is manifested morphologically as the appearance of flattened cells, with a poorly differentiated brush border. In the S3 segment of the proximal tubules, the viable cells exhibit marked increase in proliferation, spreading across the injured denuded basement membrane. Finally, these poorly differentiated cells regain their differentiated character and produce a normal proximal tubule epithelium.

At a cellular and molecular level, recovery from ATN means the re-establishment of the normal cellular architecture and the physiological functions of the renal tubule. This is obviously dependent on cellular ATP repletion once there is adequate oxygen delivery and metabolic substrates.This ATP repletion occurs in a biphasic manner with a rapid initial phase followed by a slow gradual increase to pre-ischemic levels.[248] The reassembly of the cytoskeletal structure occurs with concurrent ATP repletion, restoring the apical microvilli within 24 hours. Na^+/K^+-ATPase is reassociated with basal actin cytoskeleton within 24 hours even though some apical Na^+/K^+/ATPase activity

persists for longer periods of time. The restoration of the lipid polarity lags behind that of the Na^+/K^+-ATPase pump and is complete by 10 days post-ischemia.[249]

Role of Growth Factors

Growth factors have been implicated in the control of both cell differentiation and proliferation.[194] The kidney is a known site of synthesis for several growth factors, including Transforming Growth Factors β (TGF-β), Epidermal Growth factors (EGF), Hepatocyte Growth Factors (HGF), and Insulin-Like Growth Factor I (IGF-1) to name a few. Observations describing changes in the renal expression of these factors after experimentally induced ischemic ARF in rats are abundant, implicating a potential role in the regeneration process. We shall briefly discuss each one and their proposed roles in the process of recovery.

TGF-β

In the later stages of renal repair TGF-ß, a polypeptide growth factor, has the capability to mediate numerous events including as apoptosis, tubulogenesis, cellular hypertrophy and differentiation of regenerating proximal tubule cells. It may also negatively regulate cellular proliferation thereby balancing the activity of pro-mitogenic growth factors. In *in vitro* studies TGF-β stimulates extracellular matrix (ECM) synthesis, cell clustering, tubulogenesis and apoptosis while inhibiting proliferation of renal proximal tubule cells. Within 12 hours of ischemic injury there is enhanced expression of TGF-ß1 mRNA and protein in damaged and regenerating proximal tubules that may remain elevated for up to 14 days post-ischemia. However, overall there is no substantive evidence suggesting that it plays a critical role in the renal tubular repair response as inhibiting TGF-β does not accelerate recovery.[250]

Although fibrosis is generally not evident within the time frame that TGF-β expression returns to baseline values, recent data support the concept that transient TGF-β activity post-ischemia may induce subsequent interstitial fibrosis by promoting the deposition renal fibroblasts. Another important observation is that TGF-β neutralization prevented the loss of renal microvessels and GFR following recovery from AKI.[194,250]

Other Growth Factors

HGF has potent mitogenic activity that is localized in the peritubular endothelial cells. The kidney is both a target and generation site of HGF. Extrarenal and intrarenal HGF mRNA and HGF protein measurements are elevated within six hours of ischemic or toxic ARF, and numerous reports of exogenous administration enhancing recovery of renal function in experimental models are now available.[251] Results from transgenic mice indicate that overexpressing HGF within the proximal tubule cell may ameliorate renal damage induced by ischemia/reperfusion by at least two different processes: enhancement of tubule cell proliferation and protection against cell death.[252]

IGF-1 expression is predominantly located in the medullary collecting duct and to a lesser degree in glomeruli and proximal tubule cells. Like HGF it may be involved in the repair process of the injured kidney. IGF receptors are found throughout the kidney but there are very high concentrations in the basolateral membrane of proximal tubules. Renal artery clamp induced AKI was significantly attenuated by exogenous administration of exogenous IGF-1.[194] IGF administration has also been shown to induce up-regulation of cell-cycle inhibitory protein p21 (discussed later). Human trials using IGF-1 in AKI in the ICU setting or delayed graft function on post-transplant patients have not yet revealed any significant difference versus placebo therapy.[253,254] However, the study in the AKI patients in the ICU setting was started several days after the onset of AKI. This alone could have limited the efficacy of the drug.[254] In the delayed graft function post-transplant study the drug was instituted within five hours of transplant but still lacked any beneficial effect.[253]

Growth Hormone (GH) regulates the expression of IGF-1 and the growth hormone receptor has been found to be down-regulated in experimental ischemic AKI. Exogenous supplementation with high dose GHhowever does not modify the course of experimental ischemic ARF in rats and in human trials critically ill patients recombinant GH was actually found to be associated with higher mortality and morbidity.[255]

EGF is normally produced by the mTAL and distal tubules. The EGF receptor is present in glomeruli, proximal tubule cells, medullary interstitial cells and collecting ducts. It is normally present in the basolateral membrane, but upregulated to the apical membrane during ischemic injury in the proximal tubule cell in rats. Exogenous EGF administration *in vivo* enhances proliferation and or DNA repair, and accelerates recovery of damaged proximal tubules after ischemic or mercuric-chloride-induced damage.[194,256]

VEGF is specific in its action on the endothelial cells and may be involved in neovascularization after injury. It is expressed in glomeruli and collecting duct epithelial cells in adult kidneys while its receptors are in the glomerular endothelium and peritubular capillaries. Recent data suggest that, unlike in other organs, during renal I/R injury VEGF synthesis in kidneys is primarily regulated post-transcriptionally and is interrelated to IL-6 levels.

VEGF treatment ameliorates disease manifestations in several models such as glomerulonephritis, remnant kidney and TMA. However, overall the exact role of VEGF in AKI remains controversial and still needs to be fully evaluated.[257,258]

It is interesting to note that quite a few of the sites of expression of gene involved in the repair and regenerative processes, are localized to the mTAL or peritubular capillarysegments of the nephron. This suggests a possible paracrine signaling mechanism to stimulate regeneration in severely injured cells of the neighboring S3 proximal tubule cells.

Cell-Cycle Regulators

The protein p21 (also known as WAF1, CIP1 or SD11) regulates cell proliferation by inhibiting the cell cycle through the cyclin kinase pathway. It also has been shown to inhibit apoptosis induced by numerous stimuli. Safirstein and colleagues have demonstrated its induction in murine kidneys after ischemia, cisplatin and acute obstruction.[259] By delaying the entry of cells into the cell-cycle, they can reduce cell death from apoptosis or necrosis. In p21 knockout $^{-/-}$ mice subjected to ischemia reperfusion morphologic damage was evident throughout the cortex, where as wild type mice only had damage in the S3 segment of the proximal tubule.[260] As discussed earlier, heme-oxygenase-1 (HO-1) overexpression induces p21 up-regulation. Similarly IGF administration also causes upregulation of p21. Hence all these protective mechanisms are likely linked through delay in cell death by arresting a particular phase of the cell-cycle through p21 protein.[259]

Growth Factor Receptors

To complete the discussion on growth factors the role of their receptors also needs to be considered. A number of studies have shown that the expression of receptors for EGF, HGF, FGF-7 and IGF-1 is enhanced with acute renal injury. For example, histologic analyses show the increase in HGF receptor immunoreactivity is most marked in the most severely damaged nephron segments in the outer medulla. In the injured proximal tubules the receptor is redistributed from an apical location to an intracellular location. The prolonged elevation of this receptor (up to eight days), could mean that even late treatment with exogenous HGF might be beneficial,[261] although there are no data to support this hypothesis.

Acute Kidney Injury

Long-Term Effects and Cross-Talk Amongst Organs

A series of experiments has shown that the post-ischemic kidney has persistent local hypoxia that stimulates pathways leading to progressive interstitial scarring. In post-ischemic animals subjected to bilateral ischemic injury the authors found localization of pimonidazole, which binds to cellular thiols at pO_2 levels of less than 10mmHg, consistently in the outer medullary zone up to five weeks after ischemic insults. In animals undergoing a unilateral nephrectomy followed by ischemic insult this localization was more intense and widely distributed. The rate of interstitial scarring, development of proteinuria and decline in GFR was faster in these animals as compared to those with bilateral injury. Lastly, they found supplementation of L-arginine increased the renal blood flow, reduced hypoxia, and attenuated the secondary manifestations of ischemic damage.[262]

These observations prove that chronic hypoxia does indeed exist long after an ischemic insult and that the hypoxia is more severe in the setting of reduced renal mass resulting in progressive fibrosis that develops following apparent recovery after ischemic injury. Although no study to date has examined the long-term vascular structure and function in ARF among native human kidneys there is evidence from renal allografts, where damage to peritubular capillaries correlates with progressive functional loss.[263] It is possible that loss of peritubular capillary density could contribute to delayed graft function and development of chronic allograft nephropathy. Apart from ischemic injury, numerous factors can cause capillary rarefaction including aging, cyclosporine, angiotensin II, glomerulonephritis and radiation-induced renal injury with altered expression of VEGF.[264] It is also possible that the vascular injury could lead to potential hypertension in the long run as experimental model data suggest reductions in peritubular capillary density are associated with salt-sensitive hypertension, elevated pressure measured at 20 weeks after injury to solitary kidney and greater pressor responsiveness to angiotensin II.[265] Thus it is possible that after recovery from injury a subject could be predisposed toward higher arterial blood pressures with increased Na^+ intake.

CROSS TALK AMONGST ORGANS

AKI is likely a systemic event that can potentially cause alterations in other organs of the body. Kelly et al. have demonstrated the effects of renal ischemia on cardiac tissues.[68] Induction of IL-1, TNF-α, and ICAM-1 mRNA was seen in cardiac tissues as early as six hours post renal ischemic injury, and remained elevated upto 48h post-renal ischemic injury. There was also a significant increase in myeloperoxidase activity in the heart and liver, apart from the kidneys. The increase in cardiac MPO activity could be prevented by administration of anti-ICAM-1 antibody at the time of renal ischemia. At 48 h cardiac function evaluation by

echocardiography also revealed increases in left ventricular end systolic and diastolic diameter and decreased fractional shortening. As little as 15 min of ischemia also resulted in significantly more apoptosis in cardiac tissue.[68] Rabb et al. have shown that renal ischemic injury leads to increase in pulmonary vascular permeability defects which are mediated through macrophages.[266] Furthermore they also showed that in a rat model of bilateral renal ischemic injury or nephrectomy there was down regulation of lung epithelial Na channel, Na^+/K^+-ATPase and aquaporin-5 expression, but not in unilateral ischemic models suggesting the role of uremic toxins in modulating these effects in the lung.[267]

Conversely speaking, other organs also regulate ischemic renal injury. Slutsky et al. have recently demonstrated the role of lung injury in inducing renal damage. They found that in rabbits, injurious lung ventilatory strategies (high tidal volume and low peak end expiratory pressure) alone, were sufficient to induce renal epithelial cell apoptosis. This was further substantiated by the fact that plasma obtained from rabbits that underwent the injurious ventilation strategy induced greater apoptosis in cultured LLC-RK1 cells *in vitro*, suggesting that circulating soluble factors associated with the injurious mechanical ventilation might be involved in this process.[268] Another example of extra-renal organs regulating ischemic acute renal failure is the effect of the brain death on renal transplants. Traumatic brain injury elicits a cytokine and inflammatory response. These cytokines result in renal inflammation in renal transplants from brain dead, but not living donors.[269] The absence of such inflammation may contribute to the success of living unrelated donor renal transplants compared with cadaver transplants that have better immunologic matches.[270]

CLINICAL COURSE & DIAGNOSTIC TESTS IN AKI

Clinical Course

Prerenal azotemia by definition should rapidly reverse upon restoration of renal perfusion. The clinical course of ATN can be divided into four phases: initiation, extension, maintenance, and recovery. During the initiation phase, which can last several hours, the patient is exposed to the insult and parenchymal cell damage is established. Thus the severity of ATN is potentially limitable if this phase can be clinically detected, but unfortunately it is seldom that this duration is long enough or recognized early enough to prevent frank ATN. The recently proposed extension phase by Sutton et al., involves continued hypoxia of the corticomedullary junction secondary to microvascular congestion along with inflammation in this region.[125] As has been described in detail earlier, cellular injury in this region of the outer medulla continues leading to a fall in GFR through continued epithelial cell damage and release of inflammatory cytokines. This phase could represent a window of opportunity to prevent further progression of established ATN.[125] In the maintenance phase of ATN, the GFR remains low and this phase typically lasts between one to two weeks, but can be as long as up to six months. Finally, the recovery phase is heralded by a rise in urine output followed by a decline in serum creatinine. An excessive post-ATN diuresis might result if the recovery of the tubular reabsorptive process lags behind glomerular filtration. The usual diuresis seen after ATN is likely a combination of osmotic diuresis induced by filtration of filtered urea and other solutes, the appropriate excretion of salt and water accumulated during the maintenance phase,[195,271,272] along with a distal concentrating defect that has not yet resolved.

Clinical Features

A detailed history and physical exam is crucial to the diagnosis and management of any form of AKI. Evidence of volume depletion includes symptoms of thirst and dizziness, while physical exam will reveal absolute or orthostatic hypotension, tachycardia, reduced jugular venous distension, dry mucous membranes and decreased skin turgor. Weight loss, increased fluid loss from gastrointestinal, urinary or insensible sources and documentation of hemorrhage all support the evidence of volume depletion as a cause for AKI. One should also carefully review nursing and pharmacy records to identify potential nephrotoxic drugs. Causes of reduced effective arterial blood volume (EABV) such advanced heart failure may reveal their characteristic findings such as elevated jugular venous pressure, bibasilar pulmonary rales or effusions, cardiomegaly, S3 gallop rhythm, liver congestion and peripheral edema. Other patients may demonstrate typical stigmata of chronic liver disease such as ascites, palmar erythema, splenomegaly, jaundice and telangiectasia, serving as important supportive clinical findings for reduced EABV as the cause of AKI. In the ICU setting it is quite often difficult to assess the volume status of a critically ill patient as physical exam is often complicated by edema due to third space losses. In these settings, the use of invasive hemodynamic monitoring using central venous pressure monitoring or Swan-Ganz catheter or both is often quite helpful in determining the EABV in a patient.[273]

Other causes of AKI will have their own diagnostic features in the history and physical exam.

Urinary and Blood Tests

Urinary indices are quick, inexpensive and extremely useful tools to assist in the differential diagnosis of AKI. The fractional excretion of sodium (FENa) is a sensitive index for this purpose and has been substantiated in several reports since it was first reported by Espinel.[274–276] Prerenal azotemia is a state of avid reabsorption of filtered Na^+ and water leading to low urine concentrations of sodium and relatively high urine/plasma (U/P) ratio of osmolality, urea nitrogen, and creatinine resulting generally in a FENa of less than 1%. In contrast, ATN has functional impairment of proximal tubule cells resulting in higher urinary Na^+ concentration, and lower U/P ratios of osmolality, urea nitrogen and creatinine, leading to usually a FENa of >1%. Animal models of AKI that have studied mechanisms of tubular injury, as described earlier in the text, have elucidated the effects of ischemia on the Na^+/K^+-ATPase pumps and co-transporters present in the tubules. However, one should keep in mind that none of them are absolutely specific or sensitive, neither have they altered the management or outcome of ARF. Because the process of AKI is dynamic the timing of urinary testing, effects of diuretics, and the presence of underlying CKD can all alter the mechanisms for Na^+ reabsorption and should be kept in mind when interpreting the results. Similarly, approximately 15% of patients with non-oliguric ischemic or nephrotoxic AKI have a FENa of less than 1% which could represent an early phase or a milder form of injury as has been reported in the course of ARF accompanying rhabdomyolysis, sepsis, radiocontrast nephrotoxicity, ischemia, acute glomerulonephritis, renal allograft rejection, hepatorenal syndrome and NSAID exposure.[277,278] The Na^+ transporting segments in other areas of the nephron, and their function, are probably relatively preserved in such circumstances as compared to the corticomedullary junction and the outer medulla which suffers more localized epithelial cell damage.

A more useful test in settings of chronic kidney disease or in patients who have received a diuretic is measuring the fractional excretion of urea. A low fractional excretion of urea (FE_{UN}) was recently shown to have a high sensitivity (85%), high specificity (92%), and more importantly a high positive predictive value (98%). If a FE_{UN} of 35% or less is found, 98% of such cases will have prerenal azotemia[278] (Table 76.5A and B).

TABLE 76.5A Urine Indices Used in the Differential Diagnosis of Pre-Renal AKI and Acute Tubular Necrosis

Diagnostic Index	Pre-renal AKI	Acute tubular necrosis
Fractional excretion of sodium (%)	<1*	>2*
Urine sodium concentration (meq/L)	<20	>40
Urine creatinine/plasma creatinine ratio	>40	<20
Urine urea nitrogen/plasma urea nitrogen ratio	>8	<3
Urine specific gravity	>1.018	~1.010
Urine osmolality (mOsm/kg H_2O)	>500	~300
Plasma BUN/creatinine ratio	>20	<10–15
Renal failure index, $U_{Na}/(U_{Cr}/P_{Cr})$	<1	>1
Urine sediment	Hyaline casts	Muddy brown granular casts

FE_{Na} may be >1% in prerenal AKI associated with diuretic use and/or the setting of bicarbonaturia or chronic kidney disease; FE_{Na} often <1% in acute tubular necrosis caused by radiocontrast or rhabdomyolysis

Pathophysiologic Basis of Complications of AKI

Hyponatremia and Fluid Overload

Life threatening complications secondary to AKI may arise rapidly in these patients and have to be anticipated to prevent adverse consequences. Careful and frequent monitoring of volume status and electrolytes is essential in deciding the approach to management. Volume overload is a result of salt and water retention and is aggravated by attempts to restore diuresis in oliguric patients as well as obligatory needs such as medications and nutrition.[279] Intravascular volume excess may be particularly dangerous in elderly or heart failure patients. Hyponatremia may be caused by excessive free water ingestion or by the administration of dextrose solutions or hypotonic fluids.

Hyperkalemia

Hyperkaemia is a common and life-threatening complication of AKI, reflecting the decreased GFR, low cortical collecting duct flow rate and decreased distal sodium load. It is compounded by coexisting metabolic acidosis and a hypercatabolic state causing efflux of potassium from the intracellular space. Medications such as ACE-I, NSAID's, digitalis, spirinolactone, beta-blockers and heparin may further aggravate the rise in serum potassium. Electrocardiographic (ECG) abnormalities include peaked, thin, symmetrical T waves which is the earliest change seen, followed by prolongation of PR interval, depressed ST segment and QRS widening. Life-threatening arrhythmias such as ventricular tachycardia, bradycardia, heart block, asystole and ventricular fibrillation may ensue if hyperkalemia is not corrected.[279] In addition, neuromuscular derangements

TABLE 76.5B Urine Sediment in the Differential Diagnosis of Acute Kidney Injury

Normal or few red blood cells or white blood cells
Pre-renal azotemia; Arterial thrombosis or embolism; Pre-glomerular vasculitis
HUS/TTP; Scleroderma crisis
Post-renal AKI
Granular casts
Acute tubular necrosis; Glomerulonephritis or vasculitis ;Interstitial nephritis
Red blood cell casts
Glomerulonephritis or vasculitis; Malignant hypertension
White blood cell casts
Acute interstitial nephritis or exudative glomerulonephritis; pyelonephritis
Marked leukemic or lymphomatous infiltration
Eosinophiliuria (>5%)
Allergic interstitial nephritis (antibiotics >> NSAIDs) ; Atheroembolism
Crystalluria
Acute urate nephropathy ;Calcium oxalate (ethylene glycol intoxication); Acyclovir;
Indinavir
Sulfonamides; Radiocontrast agents
HUS, hemolytic uremic syndrome; TTP, thrombotic thrombocytopenic purpura;
NSAID, non-steroidal anti-inflammatory drugs

such as hyporeflexia, flaccid paralysis, weakness and parasthesias may occur and can be life-threatening if they extend to involve the respiratory or phonation muscles. Certain medications such as cisplatin, amphotericin and aminoglycosides may cause transient early hypokalemia reflecting TAL epithelial injury.[280,281]

Hyperurecemia

AKI patients usually develop a mild degree of hyperuricemia (12−15 mg/dl), as the primary route of elimination of uric acid is glomerular filtration and proximal tubule secretion. Higher levels should raise the suspicion for acute urate nephropathy secondary to tumor lysis syndrome or rhabdomyolysis. Sometimes it is possible to differentiate borderline mixed scenarios by measuring urine uric acid/urine creatinine ratio which is typically less than 0.75 in states of impaired excretion and greater than 1.0 in states of increased uric acid production.[282] The fractional excretion of uric acid can also be helpful in differentiation prerenal AKI (less than 10%) and intrinsic ATN (greater than 15%).[283]

Uremia

Due to the inability to excrete nitrogenous waste products, non-oliguric, non-catabolic AKI patients can exhibit a daily rise in serum BUN and creatinine of 10−20 mg/dl and 0.5−1.0 mg.dl, respectively. Oliguric, catabolic patients exhibit comparably larger daily changes in these values. Manifestations of uremia can vary from vague non-specific symptoms such as lethargy, nausea, confusion, anorexia and restless leg syndrome to severe life threatening signs such as seizures, pericarditis, pericardial effusion with tamponade and coma. Other clinical signs include asterexis, myoclonus, stupor, hyperreflexia, focal neurologic deficits and ileus.[284] The severity of the renal injury generally dictates the severity of these complications.

Acidosis

Due to decreased proximal tubule reabsorption of HCO_3 and the inability of the acutely injured kidney to regenerate bicarbonate through ammoniagenesis, there is progressive accumulation of organic acids such as sulfate and phosphate leading to metabolic acidosis. The main systemic features of metabolic acidosis include Kussmaul respiration, nausea, vomiting, fatigue, lethargy, stupor, coma, decreased myocardial contractility, cardiac arrhythmia, resistance to vasopressor drugs, peripheral arterial vasodilation and insulin resistance. Acidosis may be severe when there are concurrent mechanisms of hydrogen ion generation such as lactic acidosis, liver disease or sepsis which will further exacerbate hyperkalemia, hyperphosphatemia and hyperurecemia.

Calcium and Phosphorus

Hypocalcemia is commonly found in AKI secondary to a combination of these processes: (1) decreased synthesis of 1,25-$(OH_2)D_3$; (2) increased serum phosphate caused by skeletal resistance to PTH as well as reduction in GFR; and (3) deposition of calcium in damaged tissues.[285] Clinical manifestations of hypocalcemia are usually not evident and most patients are asymptomatic. However, in certain cases (e.g., pancreatitis and rhadomyolysis) severe symptomatic hypocalcemia with resultant signs and symptoms such as muscle cramps, seizures, confusion, positive Trousseau and Chvostek signs as well as electrocardiographic features of prolonged QT interval and non-specific T wave changes occur. The same processes that lead to hypocalcemia cause hyperphosphatemia which can be exacerbated in conditions such as rhabdomyolysis and tumor lysis syndrome, active tissue necrosis and hemolysis. Acidosis and hypercatabolism can also cause

shifts of phosphorus from the ICF to ECF space further increasing the serum levels. Metastatic deposition of calcium phosphate occurs usually when the calcium x phosphorus product exceeds 70, further lowering calcium levels.[286]

Magnesium

Oliguric AKI patients commonly will have mild asymptomatic Hypermagnesemia due to the decreased excretion of dietary or medication related (antacid, laxative etc.) magnesium. Severe hypermagnesemia (levels >5mg/dl) is rare even in anuric AKI but when present can lead to hypocalcemia. Certain drugs such as aminoglycosides, amphotericin, cyclosporin and cisplatin can cause hypomagnesemia in non-oliguric AKI due to impaired tubular transport of magnesium.[279] Hypokalemia is aggravated by hypomagnesemia and patients can have symptoms of seizures, cardiac arrhythmias, cramps and neuromuscular instability.

Anemia

Anemia is a common occurrence in AKI and occurs rapidly post injury. It is usually multifactorial with ineffective erythropoiesis, inappropriate erythropoietin (Epo) production and hemolysis being the major contributors. It has been consistently noted there is a rapid decline in erythropoietin levels post AKI and that normalization does not take place till weeks after recovery.[287] Tan et al. also found that in experimental AKI a substantial capacity for Epo production is retained but the sensitivity of the Epo response to blood oxygen availability is significantly reduced.[288] A qualitative platelet dysfunction secondary to uremia also exists in AKI that could serve to exacerbate the anemia by potential blood loss.

Nutrition

One of the most frustrating and troublesome complications of AKI is malnutrition as most patients have a net protein breakdown that sometimes exceeds 200mg/day. Some of the reasons why AKI patients end up in a net negative nitrogen balance include a) anorexia secondary to uremia, b) hypercatabolism, c) loss of essential nutrients through dialysis or drainage fluids and lastly d) restriction of adequate protein intake secondary to volume overload or azotemia[279,289] (Fig. 76.9).

PATHOPHYSIOLOGIC BASIS OF THERAPY OF AKI

Preventive Strategies

One of the main principles behind preventive strategies in ARF is avoidance. In any clinical scenario the use of less or non-nephrotoxic agents should be considered an essential option in considering treatment or diagnostic options. Examples include using non-iodinated contrast agents such as gadolinium or carbon dioxide in radiological procedures. Another example would be to consider non-invasive testing of cardiovascular status to better risk-stratify a patient.

The second principle is of prophylaxis. Aside from using clinical scores to predict high risk patients, other measures can be taken to prevent AKI. The single most important preventive therapy that has been shown consistently to minimize and prevent AKI in high risk settings is optimization of intravascular volume status and hemodynamics. Whether it is post-surgical ATN, burns, hypovolemic shock, nephrotoxicity from numerous agents, infections, restoration of volume prevents the development of experimental or human ATN. A prime example of this is in the setting of radiocontrast nephropathy where it has been demonstrated that prophylactic administration of saline before and after the procedure is effective in minimizing AKI.[290] Along the same line, certain other agents, e.g., oral N-acetylcysteine and recently intravenous sodium bicarbonate, have been added in combination with volume repletion and shown to be further protective than hydration alone.[245,291]

Thirdly, it is imperative to accurately and closely monitor for signs of renal dysfunction if nephrotoxins or other insults have occurred. Using adjunctive testing such as drug monitoring or more frequent serial blood and urine testing perhaps can help in diagnosing early subtle changes of ARF.

Role of Ischemic Pre-Conditioning

A significant amount of data now exists to suggest there may be intrinsic mechanisms brought to bear by the kidney when exposed to a toxic or ischemic insult, that protect it against a subsequent exposure to ischemia. Zager and colleagues performed the first experiments evaluating the effects of prior exposure to ischemia on subsequent susceptibility to ischemic injury. This group focused on early time points after an initial ischemic exposure and concluded that the rat is not more susceptible to a second ischemic episode when timed at or near the peak of functional deficit after the first.[292] Park et al. found that in contrast to what normally occurs after 30 min of bilateral ischemia, when a second period of ischemia of 30 or 35 min duration is imposed 8 days later, there is no subsequent increase in blood urea nitrogen or creatinine, no decrease in glomerular filtration rate, or increase in fractional excretion of sodium. A shorter period of prior ischemia (15 min) was partially protective against subsequent ischemic injury 8 days later.[227] Possible mechanisms include upregulation of certain protective

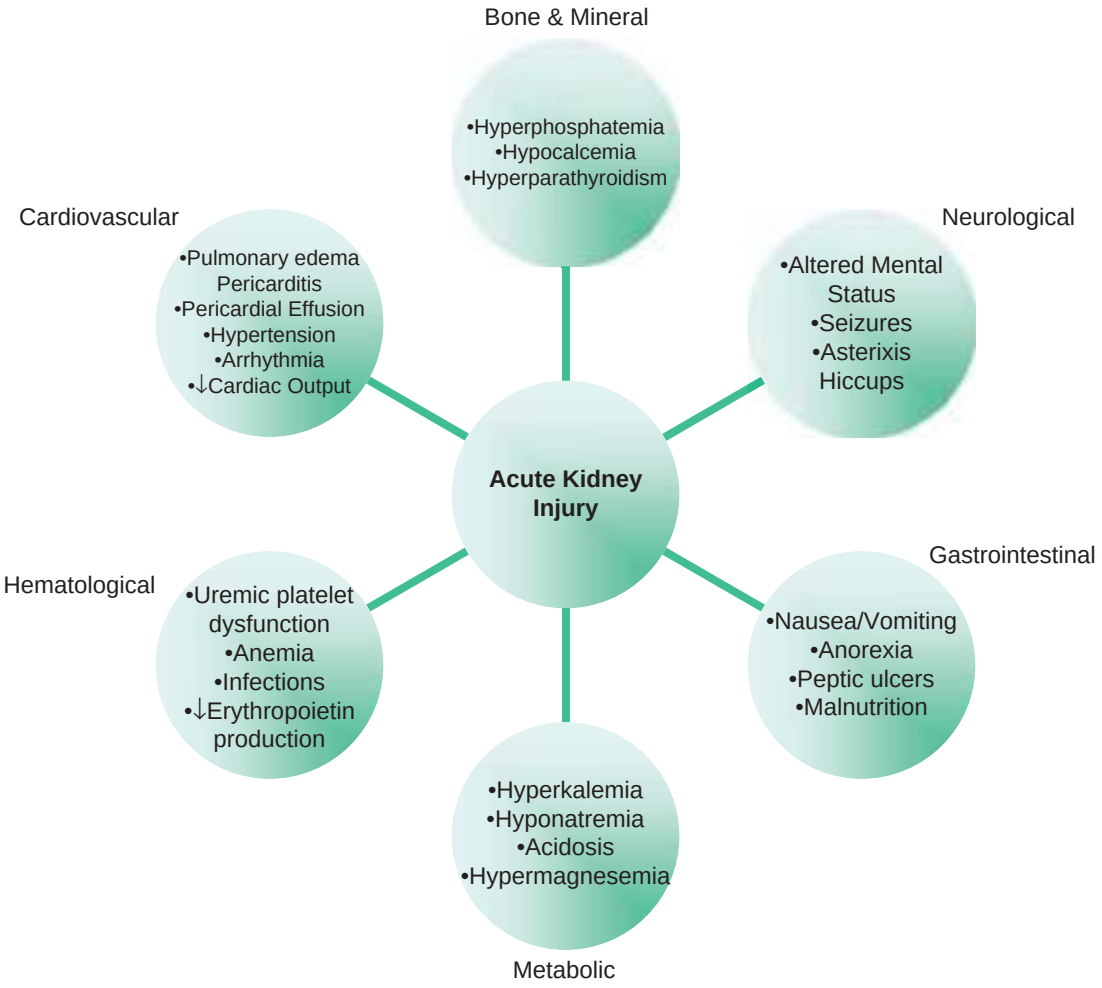

FIGURE 76.9 Common complications of AKI.

proteins such as HSP-25. Post-ischemic HSP-25 levels are much higher in the preconditioned kidney, which may stabilize the actin cytoskeleton post-ischemia and contribute to the alteration in expression of these kinases. There are also data to suggest the protective effect of ischemic preconditioning on ischemia/reperfusion -induced acute renal failure is closely related torenal nitric oxide production following the increase in eNOS expression after the reperfusion and the suppressive effect of ischemic preconditioning on the ischemia/reperfusion-induced renal ET-1 overproduction may be partly involved in the ameliorating effect of ischemic preconditioning.[293] A recent randomized, single-blind, controlled pilot trial of patients undergoing cardiopulmonary bypass-assisted cardiac surgery who received remote ischemic preconditioning by an automated thigh tourniquet of lower extremity ischemia showed an absolute risk reduction of AKI of 0.27 and a significantly reduced relative risk due to preconditioning of 0.43. Hence, remote ischemic preconditioning may prevents acute kidney injury in patients undergoing high risk surgeries.[294] With this understanding, it might be possible to mimic these processes using exogenous influences and hence prevent or alter the course of AKI.

Novel and Potential Therapies

Research in experimental animal models in the last decade has led to the discovery of potentially novel targets for the treatment of AKI. An exhaustive list of agents has been shown to be effective in animal models. We shall discuss a few of the relevant potential therapies that have recently been found to be beneficial.

ERYTHROPOIETIN

Erythropoietin is a glycoprotein hormone that controls the proliferation, differentiation of erythroid progenitor cells, synthesized by fibroblasts that are in direct contact with the capillaries and tubules. Apart

from its role in erythrogenesis, it plays important functions including protection of vascular endothelium from apoptosis and acting as an angiogenic factor. In the kidney, the expression of erythropoietin (Epo) is virtually absent at 24h following ischemic injury. However, erythropoietin receptor expression in the kidney remains well maintained. The role of erythropoietin in cell survival, proliferation, migration and differentiation have been well described recently in various in-vitro models.[295] Thus, its utility as a therapeutic agent in AKI has been under recent investigation. Rabb et al. were the first to show that intravenous administration of Epo in rats rapidly treats anemia associated with AKI as well as significantly improving survival, but they found no effect on renal function as measured by serum creatinine.[296] However, three different authors have shown a beneficial effect of using Epo in the setting of ischemic AKI. Cumulatively, these different studies indicated that pretreatment with Epo decreases ischemia induced renal dysfunction, attenuates mTAL apoptosis, decreases caspase activation and decreases renal leukocyte accumulation.[297–299] There is also evidence to suggest that Epo inhibits the JNK pathway, and induces heat shock protein 70, affording protection against apoptosis.[300,301] Functionally, Epo afforded protection by inhibiting a decline in GFR, prevented reduction of aquaporin 1,2,3 channels, and decreases in Na^+/K^+-ATPase and N^+H^+exchanger 3 pumps.[302] Although the dosing and timing of Epo administration varied amongst these studies there was universal agreement between them showing protective effects in all pre-injury treatment with Epo studies. The effect of using Epo late after ischemic injury has has also been found to be beneficial.[301] Human trials using bio-marker based early intervention strategies however havefound conflicting results of the effect of Epo in reducing the incidence of AKI[303] and its use remains unclear in the setting of AKI.[304] It is possible that it has more benefit in a single injury human scenario such as transplantation where it has shown benefit.[305]

Ichimura et al. demonstrated that injured kidney epithelial cells expressing kidney injury molecule-1 (KIM-1) could assume the attributes of endogenous phagocytes by internalizing apoptotic bodies. KIM-1 was directly responsible for phagocytosis in cultured primary rat tubule epithelial cells, and also in porcine and canine epithelial cell lines. KIM-1 specifically recognized the apoptosis marker phosphatidylserine and oxidized lipoproteins expressed by apoptotic tubular epithelial cells, which led to remodeling and repair of the tubule.[306]

Another protein, the transmembrane glycoprotein NMB (GPNMB), is upregulated 15-fold following ischemic damage in kidney tissue, more than 10-fold in macrophages, and threefold in surviving epithelial cells after injury.[307] Macrophages and epithelial cells expressing GPNMB contained 3 times more apoptotic bodies than cells not expressing GPNMB. Mutation of GPNMB or ablation of inflammatory macrophages prevents normal repair of the kidney. Kidneys from post-ischemic GPNMB-mutant mice exhibited a fivefold increase in apoptotic cellular debris compared with wildtype mice.[307] GPNMB is, therefore, a phagocytic protein that is necessary for recruitment of the autophagy protein LC3 to the phagosome where these proteins are colocalized, and for lysosomal fusion with the phagosome and hence bulk degradation of their content. These studies demonstrate that GPNMB is necessary for crosstalk between the macroautophagy degradation pathway and phagocytosis, and an important component of epithelial repair.[307]

Macrophages also have an important role in repair and recovery. The Wnt pathway ligand Wnt7b is produced by macrophages to stimulate repair and regeneration. When macrophages are ablated from the injured kidney, the canonical Wnt pathway response in kidney epithelial cells is reduced.[308] Furthermore, when Wnt7b is somatically deleted in macrophages, repair of injury is greatly diminished. Injection of the Wnt pathway regulator Dkk2 into accelerates the repair process and indicates a therapeutic option for ischemic AKI. Because Wnt7b is known to stimulate epithelial responses during kidney development, these findings indicate that macrophages are able to rapidly invade an injured tissue and re-establish a developmental program that is beneficial for repair and regeneration.[308]

STEM CELLS

There is emerging data now supporting the role of extra-renal cells in the regenerative process following AKI. Stem cells are undifferentiated cells found in the bone marrow as either hematopoietic stem cells (HSC) or mesenchymal stem cells (MSC). Studies in humans have demonstrated that when female kidneys were transplanted into male recipients who experience post-transplant ATN, Y chromosome-bearing cells were found in the transplanted kidney tubular epithelium.[309] This gives rise to the concept that extra-renal cells participate in the repair or regenerative process post ATN. Igarashi et al. have demonstrated in mice that HSC can differentiate into renal tubular cells after I/R injury.[310] Similar observations were made by Cantley et al. who showed that adult mouse bone marrow stem cells are mobilized by transient ischemia and home specifically to regions of injured tubules,[311] differentiate into renal tubular epithelial cells and appear to constitute the majority of the cells present in the previously necrotic tubules. The loss of stem cells following bone marrow ablation resulted in a greater rise in blood urea

nitrogen after renal ischemia, while stem cell infusion after bone marrow ablation reversed this effect.

The use of pluropotent mesenchymal stem cells (MSC), which can easily be harvested and cultured from bone marrow, in the treatment of ischemic AKI has recently been demonstrated by Westenfelder et al.[312] Animals infused with MSC either immediately or 24 hours after reperfusion had significantly better renal function, lower renal injury and apoptotic scores and higher mitogenic indices than vehicle treated animals. The authors found no or scarce numbers of infused MSC in the renal parenchyma, but did note that the expression of pro-inflammatory genes such as IL-1β, TNF-α, IFN-γ, and iNOS was significantly reduced, while expression of anti-inflammatory gene IL-10 was marked elevated. Expression of known renoprotective growth factors such bFGF, and TGF-α, along with anti-apoptotic protein Bcl-2 were also noted to be enhanced. Hence the authors concluded there was little trans-differentiation of these MSC into tubular or endothelial cells, but rather the action of MSC is probably paracrine in nature. However, another group of investigators have been able to demonstrate the actual presence of green fluorescent protein (GFP) labeled MSC in the tubular epithelial lining as far out as 21 days post glycerol induced ARF in mice.[313] Similarly, Morigi et al. have demonstrated injection of MSC of male bone marrow origin remarkably protected cisplatin-treated syngeneic female mice from renal function impairment and severe tubular injury where these cells localized in the tubular epithelial lining. These data indicate mesenchymal stem cells engrafted in the damaged kidney and differentiated into tubular epithelial cells, thereby restoring renal structure and function.[314]

$CD133^+$ progenitor/stem cells with regenerative potential have also been identified in the human kidney.[315] These cells were able to differentiate into both renal epithelium and endothelium *in vitro*. Mice with glycerol-induced AKI injected with these cells showed improved recovery from tubular damage.[316] MSCs are also present in the kidney and might be derived from the embryonic tissue or bone marrow. Bone-marrow cells can migrate to the kidney and participate in normal tubular epithelial cell turnover and repair after AKI.[317] Lange et al. demonstrated that infusion of MSCs improved recovery of renal function and were predominantly located in glomerular capillaries whereas tubules showed no iron labeling, indicating absent tubular transdifferentiation.[318] Knockdown of VEGF by short interfering RNA reduced effectiveness of MSCs in the treatment of ischemic AKI in a rat model. Animals treated with VEGF-depleted MSCs had reduced microvessel density, indicating that VEGF is an important mediator of the early and late phase of renoprotective action of stem-cell treatment.[319] With the use of genetic fate-mapping techniques and chimeric mice, Humphreys et al. showed that the predominant mechanism of repair following ischemic AKI was regeneration of surviving tubular epithelial cells rather than engraftment of bone marrow stem cells.[320,321] Therefore, the "renotropism" exhibited by progenitor and stem cells could have a huge impact on therapeutic options in the future once their roles are more fully defined.[322]

Hence, although the exact mechanisms of renoprotection using stem cells still remain to be fully elucidated, this is an exciting and active area of research and therapies aimed at enhancing the mobilization, propagation, and/or delivery of bone marrow stem cells to the kidney hold potential as entirely new approaches for the treatment of acute tubular necrosis.

ENDOTHELIAL PROGENITOR CELLS

There is also now emerging evidence of a potential role of using endothelial cells as therapeutic agents. Brodsky and colleagues have shown that rats infused with intact endothelial cells in ischemic AKI have an attenuated renal injury. They were also able to demonstrate actual implantation of the transplanted endothelial cells into the renal microvasculature.[323] They also found that stem cells harvested from a skeletal muscle have a potential to differentiate *ex vivo* into the endothelial lineage and are endowed with the potential to ameliorate acute ischemic renal dysfunction.[324] The concept of restoring vascular supply to damaged or ischemic organs for accelerating their regeneration is well-established.[325] One therapeutic strategy based on this concept is the delivery of angiogenic factors to the site of injury.

Another strategy could be the use of endothelial progenitor cells (EPCs). This heterogeneous group of cells originates from hematopoietic stem cells (HSCs) or their angioblastic subpopulation and MSCs. In the bone marrow, these cells are characterized by surface markers, such as CD34, VEGF-R2 (Flk-1), and an early marker CD133; moreover, circulating EPCs can express markers such as HSC, c-kit and Sca-1. Upon further differentiation, these cells lose CD133 and express VE-cadherin and von Willebrand factor.[326] Data indicate that EPCs are mobilized after acute ischemic injury and are recruited to the kidney, where they can ameliorate AKI through both paracrine effects as well as repair of the injured renal microvasculature.[327] Human HSCs administered systemically 24 h after kidney injury were selectively recruited to injured kidneys of immunodeficient mice and localized prominently in and around the vasculature.[327] This recruitment was associated with repair of the kidney microvasculature and tubule epithelial cells, improved functional recovery, and increased survival. HSCs recruited to the kidney

expressed markers consistent with circulating EPCs and synthesized high levels of proangiogenic cytokines, which promoted proliferation of both endothelial and epithelial cells. Although purified HSPCs acquired endothelial progenitor markers once recruited to the kidney, engraftment of human endothelial cells in the mouse capillary walls was rare, indicating that renal repair mediated by human stem cells is by paracrine mechanisms rather than replacement of vasculature.[112] Targeting the mechanisms to block these dysfunctional intra-cellular processes may be of key therapeutic value in the field on intensive care medicine

CONCLUSION

Major progress has been made in our understanding of molecular and pathophysiological mechanisms of AKI with the literature now rich with fascinating new approaches to treat AKI. We hope that recent advances in proteomics, discovery of newer early biomarkers, improved imaging techniques and sensitive quantitative bioassays will ultimately culminate in better understanding of AKI leading to effective therapies. Clearly, an exciting and dynamic era lies ahead of us in the field.

References

[1] Lameire N, Van Biesen W, Vanholder R. Acute renal failure. Lancet 2005;365(9457):417–30.

[2] Bellomo R, Ronco C, Kellum JA, Mehta RL, Palevsky P. Acute renal failure - definition, outcome measures, animal models, fluid therapy and information technology needs: the second international consensus conference of the acute dialysis quality initiative (ADQI) group. Crit Care 2004;8(4):R204–12.

[3] Hoste E, Clermont G, Kersten A, Lameire N. Clinical evaluation of the new RIFLE criteria for acute renal failure. Crit Care 2004;8:S81.

[4] Lameire N, Hoste E. Reflections on the definition, classification, and diagnostic evaluation of acute renal failure. Curr Opin Crit Care 2004;10(6):468–75.

[5] Liano F, Pascual J. Epidemiology of acute renal failure: a prospective, multicenter, community-based study. madrid acute renal failure study group. Kidney Int 1996;50(3):811–8.

[6] Uchino S, Bellomo R, Goldsmith D, Bates S, Ronco C. An assessment of the RIFLE criteria for acute renal failure in hospitalized patients. Crit Care Med 2006;34(7):1913–7.

[7] Fang Y, Ding X, Zhong Y, et al. Acute kidney injury in a Chinese hospitalized population. Blood Purif ;30(2):120–6.

[8] Thakar CV, Christianson A, Freyberg R, Almenoff P, Render ML. Incidence and outcomes of acute kidney injury in intensive care units: a veterans administration study. Crit Care Med 2009;37(9):2552–8.

[9] Hoste EA, Clermont G, Kersten A, et al. RIFLE criteria for acute kidney injury are associated with hospital mortality in critically ill patients: a cohort analysis. Crit Care 2006;10(3):R73.

[10] Nash K, Hafeez A, Hou S. Hospital-acquired renal insufficiency. Am J Kidney Dis 2002;39(5):930–6.

[11] Soubrier S, Leroy O, Devos P, et al. Epidemiology and prognostic factors of critically ill patients treated with hemodiafiltration. J Crit Care 2006;21(1):66–72.

[12] Mehta RL, Pascual MT, Soroko S, et al. Spectrum of acute renal failure in the intensive care unit: the PICARD experience. Kidney Int 2004;66(4):1613–21.

[13] Ali T, Khan I, Simpson W, et al. Incidence and outcomes in acute kidney injury: a comprehensive population-based study. J Am Soc Nephrol 2007;18(4):1292–8.

[14] Xue JL, Eggers P, Himmelfarb J, Collins AJ. Expenditures associated with acute renal failure in medicare beneficiaries. J Am Soc Nephrol 2004;15:582A.

[14a] Centers for Disease Control and Prevention (CDC). Hospitalization discharge diagnoses for kidney disease - United States, 1980-2005. MMWR Morb. Mortal Wkly 57, 309–312 (2005).

[15] Uchino S, Kellum JA, Bellomo R, et al. Acute renal failure in critically ill patients: a multinational, multicenter study. Jama 2005;294(7):813–8.

[15a] Acute Kidney Injury - United States Renal Data System 2009 Annual Data Report. United States Renal Data System [online], http://www.usrds.org/2009/pdf/V108 09.PDF (2009)

[16] Sesso R, Roque A, Vicioso B, Stella S. Prognosis of ARF in hospitalized elderly patients. Am J Kidney Dis 2004;44(3):410–9.

[17] Yegenaga I, Hoste E, Van Biesen W, et al. Clinical characteristics of patients developing ARF due to sepsis/systemic inflammatory response syndrome: results of a prospective study. Am J Kidney Dis 2004;43(5):817–24.

[18] Hsu CY, McCulloch CE, Fan D, Ordonez JD, Chertow GM, Go AS. Community-based incidence of acute renal failure. Kidney Int 2007;72(2):208–12.

[19] McCullough PA, Sandberg KR. Epidemiology of contrast-induced nephropathy. Rev Cardiovasc Med 2003;4(Suppl. 5): S3–9.

[20] Chertow GM, Lazarus JM, Christiansen CL, et al. Preoperative renal risk stratification. Circulation 1997;95(4):878–84.

[21] Kastner PR, Hall JE, Guyton AC. Control of glomerular filtration rate: role of intrarenally formed angiotensin II. Am J Physiol 1984;246(6 Pt 2):F897–906.

[22] Quan A, Baum M. Regulation of proximal tubule transport by endogenously produced angiotensin II. Nephron 2000;84(2): 103–10.

[23] Schuster VL, Kokko JP, Jacobson HR. Angiotensin II directly stimulates sodium transport in rabbit proximal convoluted tubules. J Clin Invest 1984;73(2):507–15.

[24] Blantz RC. Pathophysiology of pre-renal azotemia. Kidney Int 1998;53(2):512–23.

[25] Badr KF, Ichikawa I. Prerenal failure: a deleterious shift from renal compensation to decompensation. N Engl J Med 1988;319 (10):623–9.

[26] Yared A, Kon V, Ichikawa I. Mechanism of preservation of glomerular perfusion and filtration during acute extracellular fluid volume depletion. Importance of intrarenal vasopressin-prostaglandin interaction for protecting kidneys from constrictor action of vasopressin. J Clin Invest 1985;75(5):1477–87.

[27] Oliver JA, Sciacca RR, Cannon PJ. Renal vasodilation by converting enzyme inhibition. Role of renal prostaglandins. Hypertension 1983;5(2):166–71.

[28] Pascual J, Liano F, Ortuno J. The elderly patient with acute renal failure. J Am Soc Nephrol 1995;6(2):144–53.

[29] Mustonen S, Ala-Houhala IO, Tammela TL. Long-term renal dysfunction in patients with acute urinary retention. Scand J Urol Nephrol 2001;35(1):44–8.

[30] Praga M, Gonzalez E. Acute interstitial nephritis. Kidney Int ;77 (11):956–61.
[31] Neilson EG. Pathogenesis and therapy of interstitial nephritis. Kidney Int 1989;35(5):1257–70.
[32] Kodner CM, Kudrimoti A. Diagnosis and management of acute interstitial nephritis. Am Fam Physician 2003;67(12):2527–34.
[33] Michel DM, Kelly CJ. Acute interstitial nephritis. J Am Soc Nephrol 1998;9(3):506–15.
[34] Rossert J. Drug-induced acute interstitial nephritis. Kidney Int 2001;60(2):804–17.
[35] Persson PB, Hansell P, Liss P. Pathophysiology of contrast medium-induced nephropathy. Kidney Int 2005;68(1):14–22.
[36] Bettmann MA. Contrast medium-induced nephropathy: critical review of the existing clinical evidence. Nephrol Dial Transplant 2005;20(Suppl. 1):i12–17.
[37] McCullough PA. Radiocontrast-induced acute kidney injury. Nephron Physiol 2008;109(4):p61–72.
[38] Liss P, Carlsson PO, Nygren A, Palm F, Hansell P. Et-A receptor antagonist BQ123 prevents radiocontrast media-induced renal medullary hypoxia. Acta Radiol 2003;44(1):111–7.
[39] Nygren A, Ulfendahl HR. Effects of high- and low-osmolar contrast media on renal plasma flow and glomerular filtration rate in euvolaemic and dehydrated rats. A comparison between ioxithalamate, iopamidol, iohexol and ioxaglate. Acta Radiol 1989;30(4):383–9.
[40] Heyman SN, Rosenberger C, Rosen S. Regional alterations in renal haemodynamics and oxygenation: a role in contrast medium-induced nephropathy. Nephrol Dial Transplant 2005;20(Suppl. 1):i6–11.
[41] Heyman SN, Reichman J, Brezis M. Pathophysiology of radiocontrast nephropathy: a role for medullary hypoxia. Invest Radiol 1999;34(11):685–91.
[42] Liss P, Nygren A, Hansell P. Hypoperfusion in the renal outer medulla after injection of contrast media in rats. Acta Radiol 1999;40(5):521–7.
[43] Haller C, Hizoh I. The cytotoxicity of iodinated radiocontrast agents on renal cells *in vitro*. Invest Radiol 2004;39(3):149–54.
[44] Nygren A, Ulfendahl HR, Hansell P, Erikson U. Effects of intravenous contrast media on cortical and medullary blood flow in the rat kidney. Invest Radiol 1988;23(10):753–61.
[45] Ueda J, Nygren A, Sjoquist M, Jacobsson E, Ulfendahl HR, Araki Y. Iodine concentrations in the rat kidney measured by X-ray microanalysis. Comparison of concentrations and viscosities in the proximal tubules and renal pelvis after intravenous injections of contrast media. Acta Radiol 1998;39(1):90–5.
[46] Lancelot E, Idee JM, Couturier V, Vazin V, Corot C. Influence of the viscosity of iodixanol on medullary and cortical blood flow in the rat kidney: a potential cause of Nephrotoxicity. J Appl Toxicol 1999;19(5):341–6.
[47] Hizoh I, Haller C. Radiocontrast-induced renal tubular cell apoptosis: hypertonic versus oxidative stress. Invest Radiol 2002;37 (8):428–34.
[48] Hurst FP, Abbott KC. Acute phosphate nephropathy. Curr Opin Nephrol Hypertens 2009;18(6):513–8.
[49] Markowitz GS, Perazella MA. Acute phosphate nephropathy. Kidney Int 2009;76(10):1027–34.
[50] Markowitz GS, Stokes MB, Radhakrishnan J, D'Agati VD. Acute phosphate nephropathy following oral sodium phosphate bowel purgative: an underrecognized cause of chronic renal failure. J Am Soc Nephrol 2005;16(11):3389–96.
[51] Polderman KH. Acute renal failure and rhabdomyolysis. Int J Artif Organs 2004;27(12):1030–3.
[52] Reeder BJ, Wilson MT. Hemoglobin and myoglobin associated oxidative stress: from molecular mechanisms to disease States. Curr Med Chem 2005;12(23):2741–51.
[53] Holt S, Moore K. Pathogenesis of renal failure in rhabdomyolysis: the role of myoglobin. Exp Nephrol 2000;8(2):72–6.
[54] Zager RA, Burkhart KM. Differential effects of glutathione and cysteine on Fe2 +, Fe3 +, H2O2 and myoglobin-induced proximal tubular cell attack. Kidney Int 1998;53(6): 1661–72.
[55] Karam H, Bruneval P, Clozel JP, Loffler BM, Bariety J, Clozel M. Role of endothelin in acute renal failure due to rhabdomyolysis in rats. J Pharmacol Exp Ther 1995;274(1):481–6.
[56] Hill-Kapturczak N, Chang SH, Agarwal A. Heme oxygenase and the kidney. DNA Cell Biol 2002;21(4):307–21.
[57] Ogawa T, Nussler AK, Tuzuner E, et al. Contribution of nitric oxide to the protective effects of ischemic preconditioning in ischemia-reperfused rat kidneys. J Lab Clin Med 2001;138(1): 50–8.
[58] Sanders PW, Booker BB, Bishop JB, Cheung HC. Mechanisms of intranephronal proteinaceous cast formation by low molecular weight proteins. J Clin Invest 1990;85(2):570–6.
[59] Winearls CG. Acute myeloma kidney. Kidney Int 1995;48(4): 1347–61.
[60] Sengul S, Zwizinski C, Simon EE, Kapasi A, Singhal PC, Batuman V. Endocytosis of light chains induces cytokines through activation of NF-kappaB in human proximal tubule cells. Kidney Int 2002;62(6):1977–88.
[61] Chauveau D, Choukroun G. Bence Jones proteinuria and myeloma kidney. Nephrol Dial Transplant 1996;11(3):413–5.
[62] Wang PX, Sanders PW. Immunoglobulin light chains generate hydrogen peroxide. J Am Soc Nephrol 2007;18(4):1239–45.
[63] Kaplan AA. Therapeutic apheresis for the renal complications of multiple myeloma and the dysglobulinemias. Ther Apher 2001;5(3):171–5.
[64] Lieberthal W, Nigam SK. Acute renal failure. II. Experimental models of acute renal failure: imperfect but indispensable. Am J Physiol Renal Physiol 2000;278(1):F1–12.
[65] Rosen S, Heyman SN. Difficulties in understanding human "acute tubular necrosis": limited data and flawed animal models. Kidney Int 2001;60(4):1220–4.
[66] Adrie C, Adib-Conquy M, Laurent I, et al. Successful cardiopulmonary resuscitation after cardiac arrest as a "sepsis-like" syndrome. Circulation 2002;106(5):562–8.
[67] Burne-Taney MJ, Kofler J, Yokota N, Weisfeldt M, Traystman RJ, Rabb H. Acute renal failure after whole body ischemia is characterized by inflammation and T cell-mediated injury. American journal of physiology-renal fluid & electrolyte physiology 2003;285(1):F87–94.
[68] Kelly KJ. Distant effects of experimental renal ischemia/reperfusion injury. J Am Soc Nephrol 2003;14(6):1549–58.
[69] McDougal G, Compos S, Molitoris BA. Partial aortic clamp. San Diego: Paper presented at: ASN; 2003.
[70] Zager RA. Partial aortic ligation: a hypoperfusion model of ischemic acute renal failure and a comparison with renal artery occlusion. J Lab Clin Med 1987;110(4):396–405.
[71] Sharfuddin AA, Sandoval RM, Berg DT, et al. Soluble thrombomodulin protects ischemic kidneys. J Am Soc Nephrol 2009;20 (3):524–34.
[72] Kikeri D, Pennell JP, Hwang KH, Jacob AI, Richman AV, Bourgoignie JJ. Endotoxemic acute renal failure in awake rats. Am J Physiol 1986;250(6 Pt 2):F1098–1106.
[73] Doi K, Leelahavanichkul A, Yuen PS, Star RA. Animal models of sepsis and sepsis-induced kidney injury. J Clin Invest 2009;119(10):2868–78.
[74] Hentschel DM, Park KM, Cilenti L, Zervos AS, Drummond I, Bonventre JV. Acute renal failure in zebrafish - A novel system to study a complex disease. Am J Physiol Renal Physiol 2004.

[75] Heyman SN, Rosenberger C, Rosen S. Experimental ischemia-reperfusion: biases and myths-the proximal vs. distal hypoxic tubular injury debate revisited. Kidney Int ;77(1):9-16.
[76] Heyman SN, Lieberthal W, Rogiers P, Bonventre JV. Animal models of acute tubular necrosis. Curr Opin Crit Care 2002;8 (6): 526–34.
[77] Murray PT, Devarajan P, Levey AS, et al. A framework and key research questions in AKI diagnosis and staging in different environments. Clin J Am Soc Nephrol 2008;3(3):864–8.
[78] Coca SG, Parikh CR. Urinary biomarkers for acute kidney injury: perspectives on translation. Clin J Am Soc Nephrol 2008;3(2):481–90.
[79] Coca SG, Yalavarthy R, Concato J, Parikh CR. Biomarkers for the diagnosis and risk stratification of acute kidney injury: a systematic review. Kidney Int 2008;73(9):1008–16.
[80] Herget-Rosenthal S, Pietruck F, Volbracht L, Philipp T, Kribben A. Serum cystatin C–a superior marker of rapidly reduced glomerular filtration after uninephrectomy in kidney donors compared to creatinine. Clin Nephrol 2005;64(1):41–6.
[81] Dharnidharka VR, Kwon C, Stevens G. Serum cystatin C is superior to serum creatinine as a marker of kidney function: a meta-analysis. Am J Kidney Dis 2002;40(2):221–6.
[82] Racusen L. The morphologic basis of acute renal failure. Philadelphia: WB Saunders; 2001.
[83] Molitoris BA, Sutton TA. Endothelial injury and dysfunction: role in the extension phase of acute renal failure. Kidney Int 2004;66(2):496–9.
[84] Solez K, Morel-Maroger L, Sraer JD. The morphology of "acute tubular necrosis" in man: analysis of 57 renal biopsies and a comparison with the glycerol model. Medicine (Baltimore) 1979;58(5):362–76.
[85] Oberbauer R, Rohrmoser M, Regele H, Muhlbacher F, Mayer G. Apoptosis of tubular epithelial cells in donor kidney biopsies predicts early renal allograft function. J Am Soc Nephrol 1999;10(9):2006–13.
[86] Rosenberger C, Rosen S, Shina A, et al. Activation of hypoxia-inducible factors ameliorates hypoxic distal tubular injury in the isolated perfused rat kidney. Nephrol Dial Transplant 2008;23(11):3472–8.
[87] Solez K, Racusen LC, Whelton A. Glomerular epithelial cell changes in early postischemic acute renal failure in rabbits and man. Am J Pathol 1981;103(2):163–73.
[88] Bohle A, Christensen J, Kokot F, et al. Acute renal failure in man: new aspects concerning pathogenesis. A morphometric study. Am J Nephrol 1990;10(5):374–88.
[89] Wagner MC, Rhodes G, Wang E, et al. Ischemic injury to kidney induces glomerular podocyte effacement and dissociation of slit diaphragm proteins Neph1 and ZO-1. J Biol Chem 2008;283(51):35579–89.
[90] Molitoris BA. Actin cytoskeleton in ischemic acute renal failure. Kidney Int 2004;66(2):871–83.
[91] Atkinson SJ, Molitoris BA. Cytoskeletal alterations as a basis of cellular injury in acute renal failure. In: Molitoris BA, Finn WF, editors. Acute renal failure: a companion to brenner & rector's the kidney. 1st ed. Philadelphia: WB Saunders; 2001. p. 119–31.
[92] Atkinson SJ, Hosford MA, Molitoris BA. Mechanism of actin polymerization in cellular ATP depletion. J Biol Chem 2004;279 (7):5194–9.
[93] Pollard TD, Borisy GG. Cellular motility driven by assembly and disassembly of actin filaments. Cell 2003;112(4):453–65.
[94] Chen J, Wagner MC. Altered membrane-cytoskeleton linkage and membrane blebbing in energy-depleted renal proximal tubular cells. Am J Physiol Renal Physiol 2001;280(4):F619–27.
[95] Ashworth SL, Sandoval RM, Hosford M, Bamburg JR, Molitoris BA. Ischemic injury induces ADF relocalization to the apical domain of rat proximal tubule cells. Am J Physiol Renal Physiol 2001;280(5):F886–94.
[96] Ashworth SL, Southgate EL, Sandoval RM, Meberg PJ, Bamburg JR, Molitoris BA. ADF/cofilin mediates actin cytoskeletal alterations in LLC-PK cells during ATP depletion. Am J Physiol Renal Physiol 2003;284(4):F852–62.
[97] Ashworth SL, Wean SE, Campos SB, et al. Renal ischemia induces tropomyosin dissociation-destabilizing microvilli microfilaments. Am J Physiol Renal Physiol 2004;286(5): F988–96.
[98] Raman N, Atkinson SJ. Rho controls actin cytoskeletal assembly in renal epithelial cells during ATP depletion and recovery. Am J Physiol 1999;276(6 Pt 1):C1312–24.
[99] Hallett MA, Dagher PC, Atkinson SJ. Rho GTPases show differential sensitivity to nucleotide triphosphate depletion in a model of ischemic cell injury. Am J Physiol Cell Physiol 2003;285(1):C129–38.
[100] Gopalakrishnan S, Raman N, Atkinson SJ, Marrs JA. Rho GTPase signaling regulates tight junction assembly and protects tight junctions during ATP depletion. Am J Physiol 1998;275(3 Pt 1):C798–809.
[101] Wald FA, Figueroa Y, Oriolo AS, Salas PJ. Membrane repolarization is delayed in proximal tubules after ischemia-reperfusion: possible role of microtubule-organizing centers. Am J Physiol Renal Physiol 2003;285(2):F230–40.
[102] Caron A, Desrosiers RR, Beliveau R. Kidney ischemia-reperfusion regulates expression and distribution of tubulin subunits, beta-actin and rho GTPases in proximal tubules. Arch Biochem Biophys 2004;431(1):31–46.
[103] Molitoris BA. Na(+)-K(+)-ATPase that redistributes to apical membrane during ATP depletion remains functional. Am J Physiol 1993;265(5 Pt 2):F693–7.
[104] Molitoris BA, Geerdes A, McIntosh JR. Dissociation and redistribution of Na + ,K(+)-ATPase from its surface membrane actin cytoskeletal complex during cellular ATP depletion. J Clin Invest 1991;88(2):462–9.
[105] Sutton TA, Molitoris BA. Mechanisms of cellular injury in ischemic acute renal failure. Semin Nephrol 1998;18(5):490–7.
[106] Molitoris BA, Dahl R, Hosford M. Cellular ATP depletion induces disruption of the spectrin cytoskeletal network. Am J Physiol 1996;271(4 Pt 2):F790–8.
[107] Woroniecki R, Ferdinand JR, Morrow JS, Devarajan P. Dissociation of spectrin-ankyrin complex as a basis for loss of Na-K-ATPase polarity after ischemia. Am J Physiol Renal Physiol 2003;284(2):F358–64.
[108] Marrs JA, Gopalakrishnan S, Bacallao RL. Tight junction and adherens junction dysfunction during ischemic injury. 1st ed. Philadelphia: WB Saunders; 2001.
[109] Tsukamoto T, Nigam SK. Tight junction proteins form large complexes and associate with the cytoskeleton in an ATP depletion model for reversible junction assembly. J Biol Chem 1997;272(26):16133–9.
[110] Canfield PE, Geerdes AM, Molitoris BA. Effect of reversible ATP depletion on tight-junction integrity in LLC-PK1 cells. Am J Physiol 1991;261(6 Pt 2):F1038–45.
[111] Stuart RO, Nigam SK. Regulated assembly of tight junctions by protein kinase C. Proc Natl Acad Sci U S A 1995;92(13): 6072–6.
[112] Sinha D, Wang Z, Price VR, Schwartz JH, Lieberthal W. Chemical anoxia of tubular cells induces activation of c-Src and its translocation to the zonula adherens. Am J Physiol Renal Physiol 2003;284(3):F488–97.
[113] Tsukamoto T, Nigam SK. Role of tyrosine phosphorylation in the reassembly of occludin and other tight junction proteins. Am J Physiol 1999;276(5 Pt 2):F737–50.

[114] Kwon O, Corrigan G, Myers BD, et al. Sodium reabsorption and distribution of Na + /K + -ATPase during postischemic injury to the renal allograft. Kidney Int 1999;55(3):963–75.
[115] Zuk A, Bonventre JV, Brown D, Matlin KS. Polarity, integrin, and extracellular matrix dynamics in the postischemic rat kidney. Am J Physiol 1998;275(3 Pt 1):C711–31.
[116] Prahalad P, Calvo I, Waechter H, Matthews JB, Zuk A, Matlin KS. Regulation of MDCK cell-substratum adhesion by RhoA and myosin light chain kinase after ATP depletion. Am J Physiol Cell Physiol 2004;286(3):C693–707.
[117] Myers BD, Hilberman M, Spencer RJ, Jamison RL. Glomerular and tubular function in non-oliguric acute renal failure. Am J Med 1982;72(4):642–9.
[118] Alejandro V, Scandling Jr. JD, Sibley RK, et al. Mechanisms of filtration failure during postischemic injury of the human kidney. A study of the reperfused renal allograft. J Clin Invest 1995;95(2):820–31.
[119] Goligorsky MS, Noiri E, Kessler H, Romanov V. Therapeutic effect of arginine-glycine-aspartic acid peptides in acute renal injury. Clin Exp Pharmacol Physiol 1998;25(3-4):276–9.
[120] Bajwa A, Jo SK, Ye H, et al. Activation of Sphingosine-1-Phosphate 1 Receptor in the Proximal Tubule Protects Against Ischemia-Reperfusion Injury. J Am Soc Nephrol 25.
[121] Sutton TA, Mang HE, Campos SB, Sandoval RM, Yoder MC, Molitoris BA. Injury of the renal microvascular endothelium alters barrier function after ischemia. Am J Physiol Renal Physiol 2003;285(2):F191–8.
[122] Klingebiel T, von Gise H, Bohle A. Morphometric studies on acute renal failure in humans during the oligoanuric and polyuric phases. Clin Nephrol 1983;20(1):1–10.
[123] Conger J. Hemodynamic factors in acute renal failure. Adv Ren Replace Ther 1997;4(2 Suppl. 1):25–37.
[124] Prasad PV, Priatna A, Spokes K, Epstein FH. Changes in intrarenal oxygenation as evaluated by BOLD MRI in a rat kidney model for radiocontrast nephropathy. J Magn Reson Imaging 2001;13(5):744–7.
[125] Sutton TA, Fisher CJ, Molitoris BA. Microvascular endothelial injury and dysfunction during ischemic acute renal failure. Kidney Int 2002;62(5):1539–49.
[126] Mason J, Joeris B, Welsch J, Kriz W. Vascular congestion in ischemic renal failure: the role of cell swelling. Miner Electrolyte Metab 1989;15(3):114–24.
[127] Kone BC. Nitric oxide synthesis in the kidney: isoforms, biosynthesis, and functions in health. Semin Nephrol 2004;24 (4):299–315.
[128] Mattson DL, Wu F. Control of arterial blood pressure and renal sodium excretion by nitric oxide synthase in the renal medulla. Acta Physiol Scand 2000;168(1):149–54.
[129] Ling H, Edelstein C, Gengaro P, et al. Attenuation of renal ischemia-reperfusion injury in inducible nitric oxide synthase knockout mice. Am J Physiol 1999;277(3 Pt 2):F383–90.
[130] Goligorsky MS, Brodsky SV, Noiri E. NO bioavailability, endothelial dysfunction, and acute renal failure: new insights into pathophysiology. Semin Nephrol 2004;24(4):316–23.
[131] Noiri E, Nakao A, Uchida K, et al. Oxidative and nitrosative stress in acute renal ischemia. Am J Physiol Renal Physiol 2001;281(5):F948–57.
[132] Kohan DE. Endothelins in the normal and diseased kidney. Am J Kidney Dis 1997;29(1):2–26.
[133] Muller DN, Fiebeler A, Park JK, Dechend R, Luft FC. Angiotensin II and endothelin induce inflammation and thereby promote hypertension-induced end-organ damage. Clin Nephrol 2003;60(Suppl. 1):S2–12.
[134] Jerkic M, Miloradovic Z, Jovovic D, et al. Relative roles of endothelin-1 and angiotensin II in experimental post-ischaemic acute renal failure. Nephrol Dial Transplant 2004; 19(1):83–94.
[135] Johnston WH, Latta H. Glomerular mesangial and endothelial cell swelling following temporary renal ischemia and its role in the no-reflow phenomenon. Am J Pathol 1977;89(1): 153–66.
[136] Yamamoto T, Tada T, Brodsky SV, et al. Intravital videomicroscopy of peritubular capillaries in renal ischemia. Am J Physiol Renal Physiol 2002;282(6):F1150–5.
[137] Hinshaw DB, Burger JM, Armstrong BC, Hyslop PA. Mechanism of endothelial cell shape change in oxidant injury. J Surg Res 1989;46(4):339–49.
[138] Bogatcheva NV, Verin AD. The role of cytoskeleton in the regulation of vascular endothelial barrier function. Microvasc Res 2008;76(3):202–7.
[139] Campos SB, Ashworth SL, Wean S, et al. Cytokine-induced F-actin reorganization in endothelial cells involves RhoA activation. Am J Physiol Renal Physiol 2009;296(3): F487–95.
[140] Suurna MV, Ashworth SL, Hosford M, et al. Cofilin mediates ATP depletion-induced endothelial cell actin alterations. Am J Physiol Renal Physiol 2006;290(6):F1398–407.
[141] Sutton TA, Kelly KJ, Mang HE, Plotkin Z, Sandoval RM, Dagher PC. Minocycline reduces renal microvascular leakage in a rat model of ischemic renal injury. Am J Physiol Renal Physiol 2005;288(1):F91–7.
[142] Horbelt M, Lee SY, Mang HE, et al. Acute and chronic microvascular alterations in a mouse model of ischemic acute kidney injury. Am J Physiol Renal Physiol 2007;293(3): F688–95.
[143] Gupta A, Rhodes GJ, Berg DT, Gerlitz B, Molitoris BA, Grinnell BW. Activated protein C ameliorates LPS-induced acute kidney injury and downregulates renal INOS and angiotensin 2. Am J Physiol Renal Physiol 2007;293(1):F245–54.
[144] Gupta A, Williams MD, Macias WL, Molitoris BA, Grinnell BW. Activated protein C and acute kidney injury: selective targeting of PAR-1. Curr Drug Targets 2009.
[145] Gupta A, Gerlitz B, Richardson MA, et al. Distinct functions of activated protein C differentially attenuate acute kidney injury. J Am Soc Nephrol 2009;20(2):267–77.
[146] Mizutani A, Okajima K, Uchiba M, Noguchi T. Activated protein C reduces ischemia/reperfusion-induced renal injury in rats by inhibiting leukocyte activation. Blood 2000;95 (12):3781–7.
[147] Basile DP, Fredrich K, Chelladurai B, Leonard EC, Parrish AR. Renal ischemia reperfusion inhibits VEGF expression and induces ADAMTS-1, a novel VEGF inhibitor. Am J Physiol Renal Physiol 2008;294(4):F928–36.
[148] Leonard EC, Friedrich JL, Basile DP. VEGF-121 preserves renal microvessel structure and ameliorates secondary renal disease following acute kidney injury. Am J Physiol Renal Physiol 2008;295(6):F1648–57.
[149] Basile DP, Friedrich JL, Spahic J, et al. Impaired endothelial proliferation and mesenchymal transition contribute to vascular rarefaction following acute kidney injury. Am J Physiol Renal Physiol 2011;300(3):F721–33 [Epub 2010 Dec 1]
[150] Basile DP. The endothelial cell in ischemic acute kidney injury: implications for acute and chronic function. Kidney Int 2007;72 (2):151–6.
[151] Okusa MD, Chertow GM, Portilla D. The nexus of acute kidney injury, chronic kidney disease, and world kidney day 2009. Clin J Am Soc Nephrol 2009;4(3):520–2.
[152] Molitoris BA. Contrast nephropathy: are short-term outcome measures adequate for quantification of long-term renal risk?. Nat Clin Pract Nephrol 2008;4(11):594–5.

[153] Miyazawa S, Watanabe H, Miyaji C, Hotta O, Abo T. Leukocyte accumulation and changes in extra-renal organs during renal ischemia reperfusion in mice. J Lab Clin Med 2002;139(5):269–78.
[154] Ysebaert DK, De Greef KE, Vercauteren SR, et al. Identification and kinetics of leukocytes after severe ischaemia/reperfusion renal injury. Nephrol Dial Transplant 2000;15(10):1562–74.
[155] Singbartl K, Ley K. Leukocyte recruitment and acute renal failure. J Mol Med 2004;82(2):91–101.
[156] Burne MJ, Rabb H. Pathophysiological contributions of fucosyltransferases in renal ischemia reperfusion injury. J Immunol 2002;169(5):2648–52.
[157] Nemoto T, Burne MJ, Daniels F, et al. Small molecule selectin ligand inhibition improves outcome in ischemic acute renal failure. Kidney Int 2001;60(6):2205–14.
[158] Singbartl K, Forlow SB, Ley K. Platelet, but not endothelial, P-selectin is critical for neutrophil-mediated acute postischemic renal failure. Faseb J 2001;15(13):2337–44.
[159] Matsukawa A, Lukacs NW, Hogaboam CM, et al. Mice genetically lacking endothelial selectins are resistant to the lethality in septic peritonitis. Exp Mol Pathol 2002;72(1):68–76.
[160] Kelly KJ, Williams Jr. WW, Colvin RB, et al. Intercellular adhesion molecule-1-deficient mice are protected against ischemic renal injury. J Clin Invest 1996;97(4):1056–63.
[161] Salmela K, Wramner L, Ekberg H, et al. A randomized multicenter trial of the anti-ICAM-1 monoclonal antibody (enlimomab) for the prevention of acute rejection and delayed onset of graft function in cadaveric renal transplantation: a report of the European Anti-ICAM-1 renal transplant study group. Transplantation 1999;67(5):729–36.
[162] Jo SK, Yun SY, Chang KH, et al. alpha-MSH decreases apoptosis in ischaemic acute renal failure in rats: possible mechanism of this beneficial effect. Nephrol Dial Transplant 2001;16 (8):1583–91.
[163] Burne-Taney MJ, Rabb H. The role of adhesion molecules and T cells in ischemic renal injury. Curr Opin Nephrol Hypertens 2003;12(1):85–90.
[164] Yokota N, Burne-Taney M, Racusen L, Rabb H. Contrasting roles for STAT4 and STAT6 signal transduction pathways in murine renal ischemia-reperfusion injury. Am J Physiol Renal Physiol 2003;285(2):F319–25.
[165] Burne-Taney MJ, Ascon DB, Daniels F, Racusen L, Baldwin W, Rabb H. B cell deficiency confers protection from renal ischemia reperfusion injury. J Immunol 2003;171(6):3210–5.
[166] Day YJ, Huang L, Ye H, Linden J, Okusa MD. Renal ischemia-reperfusion injury and adenosine 2A receptor-mediated tissue protection: the role of macrophages. Am J Physiol Renal Physiol 2004.
[167] Jo SK, Bajwa A, Awad AS, Lynch KR, Okusa MD. Sphingosine-1-phosphate receptors: biology and therapeutic potential in kidney disease. Kidney Int 2008;73(11):1220–30.
[168] Bajwa A, Jo SK, Ye H, et al. Activation of sphingosine-1-phosphate 1 receptor in the proximal tubule protects against ischemia-reperfusion injury. J Am Soc Nephrol 2010;21(6): 955–65.
[169] Dong X, Swaminathan S, Bachman LA, Croatt AJ, Nath KA, Griffin MD. Resident dendritic cells are the predominant TNF-secreting cell in early renal ischemia-reperfusion injury. Kidney Int 2007;71(7):619–28.
[170] Deng J, Kohda Y, Chiao H, et al. Interleukin-10 inhibits ischemic and cisplatin-induced acute renal injury. Kidney Int 2001;60(6):2118–28.
[171] Simmons EM, Himmelfarb J, Sezer MT, et al. Plasma cytokine levels predict mortality in patients with acute renal failure. Kidney Int 2004;65(4):1357–65.
[172] Himmelfarb J, Le P, Klenzak J, Freedman S, McMenamin ME, Ikizler TA. Impaired monocyte cytokine production in critically ill patients with acute renal failure. Kidney Int 2004;66(6): 2354–60.
[173] Balakrishnan VS, Guo D, Rao M, et al. Cytokine gene polymorphisms in hemodialysis patients: association with comorbidity, functionality, and serum albumin. Kidney Int 2004;65 (4):1449–60.
[174] Jaber BL, Rao M, Guo D, et al. Cytokine gene promoter polymorphisms and mortality in acute renal failure. Cytokine 2004;25(5):212–9.
[175] Riedemann NC, Guo RF, Ward PA. The enigma of sepsis. J Clin Invest 2003;112(4):460–7.
[176] Schrier RW, Wang W. Acute renal failure and sepsis. N Engl J Med 2004;351(2):159–69.
[177] Hoste EA, Lameire NH, Vanholder RC, Benoit DD, Decruyenaere JM, Colardyn FA. Acute renal failure in patients with sepsis in a surgical ICU: predictive factors, incidence, comorbidity, and outcome. J Am Soc Nephrol 2003;14(4): 1022–30.
[178] Wang W, Falk SA, Jittikanont S, Gengaro PE, Edelstein CL, Schrier RW. Protective effect of renal denervation on normotensive endotoxemia-induced acute renal failure in mice. Am J Physiol Renal Physiol 2002;283(3):F583–7.
[179] Albertini M, Clement MG, Hussain SN. Role of endothelin ETA receptors in sepsis-induced mortality, vascular leakage, and tissue injury in rats. Eur J Pharmacol 2003;474(1): 129–35.
[180] Eibl G, Hotz HG, Faulhaber J, Kirchengast M, Buhr HJ, Foitzik T. Effect of endothelin and endothelin receptor blockade on capillary permeability in experimental pancreatitis. Gut 2000; 46(3):390–4.
[181] Wang W, Mitra A, Poole B, et al. Endothelial nitric oxide synthase-deficient mice exhibit increased susceptibility to endotoxin-induced acute renal failure. Am J Physiol Renal Physiol 2004;287(5):F1044–8.
[182] McGill SN, Ahmed NA, Christou NV. Increased plasma von Willebrand factor in the systemic inflammatory response syndrome is derived from generalized endothelial cell activation. Crit Care Med 1998;26(2):296–300.
[183] Lopez A, Lorente JA, Steingrub J, et al. Multiple-center, randomized, placebo-controlled, double-blind study of the nitric oxide synthase inhibitor 546C88: effect on survival in patients with septic shock. Crit Care Med 2004;32(1): 21–30.
[184] Pinsky MR. Pathophysiology of sepsis and multiple organ failure: pro- versus anti-inflammatory aspects. Contrib Nephrol 2004;144:31–43.
[185] Guo R, Wang Y, Minto AW, Quigg RJ, Cunningham PN. Acute renal failure in endotoxemia is dependent on caspase activation. J Am Soc Nephrol 2004;15(12):3093–102.
[186] Jagneaux T, Taylor DE, Kantrow SP. Coagulation in sepsis. Am J Med Sci 2004;328(4):196–204.
[187] Garcia-Fernandez N, Montes R, Purroy A, Rocha E. Hemostatic disturbances in patients with systemic inflammatory response syndrome (SIRS) and associated acute renal failure (ARF). Thromb Res 2000;100(1):19–25.
[188] Cavaillon JM, Fitting C, Adib-Conquy M. Mechanisms of immunodysregulation in sepsis. Contrib Nephrol 2004;144: 76–93.
[189] Perera PY, Mayadas TN, Takeuchi O, et al. CD11b/CD18 acts in concert with CD14 and Toll-like receptor (TLR) 4 to elicit full lipopolysaccharide and taxol-inducible gene expression. J Immunol 2001;166(1):574–81.
[190] Anders HJ, Banas B, Schlondorff D. Signaling danger: toll-like receptors and their potential roles in kidney disease. J Am Soc Nephrol 2004;15(4):854–67.

[191] Tsuboi N, Yoshikai Y, Matsuo S, et al. Roles of toll-like receptors in C-C chemokine production by renal tubular epithelial cells. J Immunol 2002;169(4):2026–33.
[192] Cunningham PN, Wang Y, Guo R, He G, Quigg RJ. Role of Toll-like receptor 4 in endotoxin-induced acute renal failure. J Immunol 2004;172(4):2629–35.
[193] Wang W, Jittikanont S, Falk SA, et al. Interaction among nitric oxide, reactive oxygen species, and antioxidants during endotoxemia-related acute renal failure. Am J Physiol Renal Physiol 2003;284(3):F532–7.
[194] Ichimura T, Bonventre JV. Growth factors, signaling, and renal injury and repair. 1st ed. Philadelphia: WB Saunders; 2001.
[195] Lieberthal W, Koh JS, Levine JS. Necrosis and apoptosis in acute renal failure. Semin Nephrol 1998;18(5):505–18.
[196] Feldkamp T, Kribben A, Roeser NF, et al. Preservation of complex I function during hypoxia-reoxygenation-induced mitochondrial injury in proximal tubules. Am J Physiol Renal Physiol 2004;286(4):F749–59.
[197] Edelstein CL. Calcium-mediated proximal tubular injury-what is the role of cysteine proteases?. Nephrol Dial Transplant 2000;15(2):141–4.
[198] Sogabe K, Roeser NF, Davis JA, Nurko S, Venkatachalam MA, Weinberg JM. Calcium dependence of integrity of the actin cytoskeleton of proximal tubule cell microvilli. Am J Physiol 1996;271(2 Pt 2):F292–303.
[199] Portilla D. Role of fatty acid beta-oxidation and calcium-independent phospholipase A2 in ischemic acute renal failure. Curr Opin Nephrol Hypertens 1999;8(4):473–7.
[200] Bonventre JV, Nemenoff R. Renal tubular arachidonic acid metabolism. Kidney Int 1991;39(3):438–49.
[201] Goto S, Nakamura H, Morooka H, Terao Y, Shibata O, Sumikawa K. Role of reactive oxygen in phospholipase A2 activation by ischemia/reperfusion of the rat kidney. J Anesth 1999;13(2):90–3.
[202] Liu X, Van Vleet T, Schnellmann RG. The role of calpain in oncotic cell death. Annu Rev Pharmacol Toxicol 2004;44:349–70.
[203] Liu X, Schnellmann RG. Calpain mediates progressive plasma membrane permeability and proteolysis of cytoskeleton-associated paxillin, talin, and vinculin during renal cell death. J Pharmacol Exp Ther 2003;304(1):63–70.
[204] Liu X, Rainey JJ, Harriman JF, Schnellmann RG. Calpains mediate acute renal cell death: role of autolysis and translocation. Am J Physiol Renal Physiol 2001;281(4):F728–38.
[205] Edelstein CL, Shi Y, Schrier RW. Role of caspases in hypoxia-induced necrosis of rat renal proximal tubules. J Am Soc Nephrol 1999;10(9):1940–9.
[206] Kaushal GP, Basnakian AG, Shah SV. Apoptotic pathways in ischemic acute renal failure. Kidney Int 2004;66(2):500–6.
[207] Uegaki K, Otomo T, Sakahira H, et al. Structure of the CAD domain of caspase-activated DNase and interaction with the CAD domain of its inhibitor. J Mol Biol 2000;297(5):1121–8.
[208] Schulze-Osthoff K, Walczak H, Droge W, Krammer PH. Cell nucleus and DNA fragmentation are not required for apoptosis. J Cell Biol 1994;127(1):15–20.
[209] Enright H, Nath KA, Hebbel RP. Internucleosomal cleavage of DNA is insufficient evidence to conclude that cell death is apoptotic. Blood 1994;83(7):2005–7.
[210] Dagher PC. Apoptosis in ischemic renal injury: roles of GTP depletion and p53. Kidney Int 2004;66(2):506–9.
[211] Bonegio R, Lieberthal W. Role of apoptosis in the pathogenesis of acute renal failure. Curr Opin Nephrol Hypertens 2002;11(3):301–8.
[212] Kaushal GP. Role of caspases in renal tubular epithelial cell injury. Semin Nephrol 2003;23(5):425–31.
[213] Jani A, Ljubanovic D, Faubel S, Kim J, Mischak R, Edelstein CL. Caspase inhibition prevents the increase in caspase-3, -2, -8 and -9 activity and apoptosis in the cold ischemic mouse kidney. Am J Transplant 2004;4(8):1246–54.
[214] Faubel S, Ljubanovic D, Reznikov L, Somerset H, Dinarello CA, Edelstein CL. Caspase-1-deficient mice are protected against cisplatin-induced apoptosis and acute tubular necrosis. Kidney Int 2004;66(6):2202–13.
[215] Nicholson DW. From bench to clinic with apoptosis-based therapeutic agents. Nature 2000;407(6805):810–6.
[216] van de Water B, Tijdens IB, Verbrugge A, et al. Cleavage of the actin-capping protein alpha -adducin at Asp-Asp-Ser-Asp633-Ala by caspase-3 is preceded by its phosphorylation on serine 726 in cisplatin-induced apoptosis of renal epithelial cells. J Biol Chem 2000;275(33):25805–13.
[217] Safirstein RL. Acute renal failure: from renal physiology to the renal transcriptome. Kidney Int Suppl 2004;91:S62–6.
[218] Kaufmann SH, Hengartner MO. Programmed cell death: alive and well in the new millennium. Trends Cell Biol 2001;11(12):526–34.
[219] Lee RH, Song JM, Park MY, Kang SK, Kim YK, Jung JS. Cisplatin-induced apoptosis by translocation of endogenous Bax in mouse collecting duct cells. Biochem Pharmacol 2001;62(8):1013–23.
[220] Peherstorfer E, Mayer B, Boehm S, et al. Effects of microinjection of synthetic Bcl-2 domain peptides on apoptosis of renal tubular epithelial cells. Am J Physiol Renal Physiol 2002;283(1):F190–6.
[221] Edelstein LC, Lagos L, Simmons M, Tirumalai H, Gelinas C. NF-kappa B-dependent assembly of an enhanceosome-like complex on the promoter region of apoptosis inhibitor Bfl-1/A1. Mol Cell Biol 2003;23(8):2749–61.
[222] Gottifredi V, Shieh SY, Prives C. Regulation of p53 after different forms of stress and at different cell cycle stages. Cold Spring Harb Symp Quant Biol 2000;65:483–8.
[223] Kelly KJ, Plotkin Z, Vulgamott SL, Dagher PC. P53 mediates the apoptotic response to GTP depletion after renal ischemia-reperfusion: protective role of a p53 inhibitor. J Am Soc Nephrol 2003;14(1):128–38.
[224] Nogae S, Miyazaki M, Kobayashi N, et al. Induction of apoptosis in ischemia-reperfusion model of mouse kidney: possible involvement of Fas. J Am Soc Nephrol 1998;9(4):620–31.
[225] Yang CH, Murti A, Pfeffer SR, Kim JG, Donner DB, Pfeffer LM. Interferon alpha /beta promotes cell survival by activating nuclear factor kappa B through phosphatidylinositol 3-kinase and Akt. J Biol Chem 2001;276(17):13756–61.
[226] Scheid MP, Schubert KM, Duronio V. Regulation of bad phosphorylation and association with Bcl-x(L) by the MAPK/Erk kinase. J Biol Chem 1999;274(43):31108–13.
[227] Park KM, Chen A, Bonventre JV. Prevention of kidney ischemia/reperfusion-induced functional injury and JNK, p38, and MAPK kinase activation by remote ischemic pretreatment. J Biol Chem 2001;276(15):11870–6.
[228] Arany I, Megyesi JK, Kaneto H, Tanaka S, Safirstein RL. Activation of ERK or inhibition of JNK ameliorates H(2)O(2) cytotoxicity in mouse renal proximal tubule cells. Kidney Int 2004;65(4):1231–9.
[229] Meldrum KK, Meldrum DR, Hile KL, et al. p38 MAPK mediates renal tubular cell TNF-alpha production and TNF-alpha-dependent apoptosis during simulated ischemia. Am J Physiol Cell Physiol 2001;281(2):C563–70.

[230] Li L, Zepeda-Orozco D, Black R, Lin F. Autophagy is a component of epithelial cell fate in obstructive uropathy. Am J Pathol 2010;176(4):1767–78.
[231] Koesters R, Kaissling B, Lehir M, et al. Tubular overexpression of transforming growth factor-beta1 induces autophagy and fibrosis but not mesenchymal transition of renal epithelial cells. Am J Pathol 2010;177(2):632–43.
[232] Kelly KJ. Stress response proteins and renal ischemia. Minerva Urol Nefrol 2002;54(2):81–91.
[233] Paller MS, Weber K, Patten M. Nitric oxide-mediated renal epithelial cell injury during hypoxia and reoxygenation. Ren Fail 1998;20(3):459–69.
[234] Smoyer WE, Ransom R, Harris RC, Welsh MJ, Lutsch G, Benndorf R. Ischemic acute renal failure induces differential expression of small heat shock proteins. J Am Soc Nephrol 2000;11(2):211–21.
[235] Aufricht C, Bidmon B, Ruffingshofer D, et al. Ischemic conditioning prevents Na,K-ATPase dissociation from the cytoskeletal cellular fraction after repeat renal ischemia in rats. Pediatr Res 2002;51(6):722–7.
[236] Basile DP, Donohoe D, Cao X, Van Why SK. Resistance to ischemic acute renal failure in the Brown Norway rat: a new model to study cytoprotection. Kidney Int 2004;65(6):2201–11.
[237] Zhou H, Kato A, Yasuda H, Odamaki M, Itoh H, Hishida A. The induction of heat shock protein-72 attenuates cisplatin-induced acute renal failure in rats. Pflugers Arch 2003;446 (1):116–24.
[238] Kanakiriya S, Nath KA. Heme oxygenase and acute renal injury. 1st ed. Philadelphia: WB Saunders; 2001.
[239] Kapturczak MH, Wasserfall C, Brusko T, et al. Heme oxygenase-1 modulates early inflammatory responses: evidence from the heme oxygenase-1-deficient mouse. Am J Pathol 2004;165(3):1045–53.
[240] Shiraishi F, Curtis LM, Truong L, et al. Heme oxygenase-1 gene ablation or expression modulates cisplatin-induced renal tubular apoptosis. Am J Physiol Renal Physiol 2000;278(5): F726–36.
[241] Nath KA, Haggard JJ, Croatt AJ, Grande JP, Poss KD, Alam J. The indispensability of heme oxygenase-1 in protecting against acute heme protein-induced toxicity *in vivo*. Am J Pathol 2000;156(5):1527–35.
[242] Inguaggiato P, Gonzalez-Michaca L, Croatt AJ, Haggard JJ, Alam J, Nath KA. Cellular overexpression of heme oxygenase-1 up-regulates p21 and confers resistance to apoptosis. Kidney Int 2001;60(6):2181–91.
[243] Nath KA, Norby SM. Reactive oxygen species and acute renal failure. Am J Med 2000;109(8):665–78.
[244] Ishibashi N, Weisbrot-Lefkowitz M, Reuhl K, Inouye M, Mirochnitchenko O. Modulation of chemokine expression during ischemia/reperfusion in transgenic mice overproducing human glutathione peroxidases. J Immunol 1999;163(10): 5666–77.
[245] Tepel M, Zidek W. N-Acetylcysteine in nephrology; contrast nephropathy and beyond. Curr Opin Nephrol Hypertens 2004;13(6):649–54.
[246] Balakrishnan VS, Blumberg J, Pereira BJ, Jaber BL. Antioxidant and oxidative stress indices in dialysis-dependent acute renal failure. Blood Purif 2003;21(3):213–9.
[247] Zheng J, Devalaraja-Narashimha K, Singaravelu K, Padanilam BJ. Poly(ADP-ribose) polymerase-1 gene ablation protects mice from ischemic renal injury. Am J Physiol Renal Physiol 2005;288(2):F387–98.
[248] Stromski ME, Cooper K, Thulin G, Gaudio KM, Siegel NJ, Shulman RG. Chemical and functional correlates of postischemic renal ATP levels. Proc Natl Acad Sci USA 1986;83(16):6142–5.
[249] Spiegel DM, Wilson PD, Molitoris BA. Epithelial polarity following ischemia: a requirement for normal cell function. Am J Physiol 1989;256(3 Pt 2):F430–6.
[250] Spurgeon KS, Donohoe DL, Basile DP. Transforming growth factor-{beta} in acute renal failure: receptor expression, effects on proliferation, cellularity and vascularization after recovery from injury. Am J Physiol Renal Physiol 2004.
[251] Nagano T, Mori-Kudo I, Kawamura T, Taiji M, Noguchi H. Pre- or post-treatment with hepatocyte growth factor prevents glycerol-induced acute renal failure. Ren Fail 2004;26 (1):5–11.
[252] Fiaschi-Taesch NM, Santos S, Reddy V, et al. Prevention of acute ischemic renal failure by targeted delivery of growth factors to the proximal tubule in transgenic mice: the efficacy of parathyroid hormone-related protein and hepatocyte growth factor. J Am Soc Nephrol 2004;15(1):112–25.
[253] Hladunewich MA, Corrigan G, Derby GC, et al. A randomized, placebo-controlled trial of IGF-1 for delayed graft function: a human model to study postischemic ARF. Kidney Int 2003;64(2):593–602.
[254] Hirschberg R, Kopple J, Lipsett P, et al. Multicenter clinical trial of recombinant human insulin-like growth factor I in patients with acute renal failure. Kidney Int 1999;55(6):2423–32.
[255] Takala J, Ruokonen E, Webster NR, et al. Increased mortality associated with growth hormone treatment in critically ill adults. N Engl J Med 1999;341(11):785–92.
[256] Hammerman MR. Growth factors and apoptosis in acute renal injury. Curr Opin Nephrol Hypertens 1998;7(4):419–24.
[257] Matsumoto M, Makino Y, Tanaka T, et al. Induction of renoprotective gene expression by cobalt ameliorates ischemic injury of the kidney in rats. J Am Soc Nephrol 2003;14 (7):1825–32.
[258] Vannay A, Fekete A, Adori C, et al. Divergence of renal vascular endothelial growth factor mRNA expression and protein level in post-ischaemic rat kidneys. Exp Physiol 2004;89 (4):435–44.
[259] Price PM, Megyesi J, Saf Irstein RL. Cell cycle regulation: repair and regeneration in acute renal failure. Kidney Int 2004;66(2):509–14.
[260] Megyesi J, Andrade L, Vieira Jr. JM, Safirstein RL, Price PM. Positive effect of the induction of p21WAF1/CIP1 on the course of ischemic acute renal failure. Kidney Int 2001;60(6):2164–72.
[261] Liu Y. Hepatocyte growth factor and the kidney. Curr Opin Nephrol Hypertens 2002;11(1):23–30.
[262] Basile DP. Rarefaction of peritubular capillaries following ischemic acute renal failure: a potential factor predisposing to progressive nephropathy. Curr Opin Nephrol Hypertens 2004;13(1):1–7.
[263] Ishii Y, Sawada T, Kubota K, Fuchinoue S, Teraoka S, Shimizu A. Injury and progressive loss of peritubular capillaries in the development of chronic allograft nephropathy. Kidney Int 2005;67(1):321–32.
[264] Choi YJ, Chakraborty S, Nguyen V, et al. Peritubular capillary loss is associated with chronic tubulointerstitial injury in human kidney: altered expression of vascular endothelial growth factor. Hum Pathol 2000;31(12):1491–7.
[265] Basile DP, Donohoe D, Roethe K, Osborn JL. Renal ischemic injury results in permanent damage to peritubular capillaries and influences long-term function. Am J Physiol Renal Physiol 2001;281(5):F887–899.
[266] Kramer AA, Postler G, Salhab KF, Mendez C, Carey LC, Rabb H. Renal ischemia/reperfusion leads to macrophage-mediated increase in pulmonary vascular permeability. Kidney Int 1999;55(6):2362–7.

[267] Rabb H, Wang Z, Nemoto T, Hotchkiss J, Yokota N, Soleimani M. Acute renal failure leads to dysregulation of lung salt and water channels. Kidney Int 2003;63(2):600–6.
[268] Imai Y, Parodo J, Kajikawa O, et al. Injurious mechanical ventilation and end-organ epithelial cell apoptosis and organ dysfunction in an experimental model of acute respiratory distress syndrome. Jama 2003;289(16):2104–12.
[269] Pratschke J, Wilhelm MJ, Laskowski I, et al. Influence of donor brain death on chronic rejection of renal transplants in rats. J Am Soc Nephrol 2001;12(11):2474–81.
[270] Kielar ML, Rohan Jeyarajah D, Lu CY. The regulation of ischemic acute renal failure by extrarenal organs. Curr Opin Nephrol Hypertens 2002;11(4):451–7.
[271] Star RA. Treatment of acute renal failure. Kidney Int 1998;54 (6):1817–31.
[272] Brady HR, Singer GG. Acute renal failure. Lancet 1995;346 (8989):1533–40.
[273] Bellomo R, Cole L, Ronco C. Hemodynamic support and the role of dopamine. Kidney Int Suppl 1998;66:S71–4.
[274] Miller TR, Anderson RJ, Linas SL, et al. Urinary diagnostic indices in acute renal failure: a prospective study. Ann Intern Med 1978;89(1):47–50.
[275] Espinel CH. The FENa test. Use in the differential diagnosis of acute renal failure. Jama 1976;236(6):579–81.
[276] Zarich S, Fang LS, Diamond JR. Fractional excretion of sodium. Exceptions to its diagnostic value. Arch Intern Med 1985;145 (1):108–12.
[277] Anderson RJ. Clinical and laboratory diagnosis of acute renal failure. In: Finn BAMWF, editor. Acute renal failure: a companion to brenner & rector's the kidney. 1st ed. Philadelphia: WB Saunders; 2001. p. 157–68.
[278] Carvounis CP, Nisar S, Guro-Razuman S. Significance of the fractional excretion of urea in the differential diagnosis of acute renal failure. Kidney Int 2002;62(6):2223–9.
[279] Burdmann E, Luis Y. Metabolic and electrolyte disturbances: secondary manifestations. In: Molitoris BA, Finn WF, editors. Acute renal failure: a companion to brennor & rector's the kidney. Philadelphia: Saunders; 2001. p. 169–91.
[280] Molitoris BA. Cell biology of aminoglycoside nephrotoxicity: newer aspects. Curr Opin Nephrol Hypertens 1997;6(4): 384–8.
[281] Blachley JD, Hill JB. Renal and electrolyte disturbances associated with cisplatin. Ann Intern Med 1981;95(5):628–32.
[282] Conger JD. Acute uric acid nephropathy. Med Clin North Am 1990;74(4):859–71.
[283] Steinhauslin F, Burnier M, Magnin JL, et al. Fractional excretion of trace lithium and uric acid in acute renal failure. J Am Soc Nephrol 1994;4(7):1429–37.
[284] Brouns R, De Deyn PP. Neurological complications in renal failure: a review. Clin Neurol Neurosurg 2004;107(1): 1–16.
[285] Akmal M, Bishop JE, Telfer N, Norman AW, Massry SG. Hypocalcemia and hypercalcemia in patients with rhabdomyolysis with and without acute renal failure. J Clin Endocrinol Metab 1986;63(1):137–42.
[286] Giachelli CM. Vascular calcification mechanisms. J Am Soc Nephrol 2004;15(12):2959–64.
[287] Nielsen OJ, Thaysen JH. Erythropoietin deficiency in acute tubular necrosis. J Intern Med 1990;227(6):373–80.
[288] Tan CC, Tan LH, Eckardt KU. Erythropoietin production in rats with post-ischemic acute renal failure. Kidney Int 1996;50 (6):1958–64.
[289] Druml W. Nutritional support in patients with acute renal failure. In: Molitoris BA, Finn WF, editors. Acute renal failure: a companion to brennor & rector's the kidney. Philadelphia: Saunders; 2001. p. 465–89.
[290] Weisbord SD, Palevsky PM. Prevention of contrast-induced nephropathy with volume expansion. Clin J Am Soc Nephrol 2008;3(1):273–80.
[291] Merten GJ, Burgess WP, Gray LV, et al. Prevention of contrast-induced nephropathy with sodium bicarbonate: a randomized controlled trial. Jama 2004;291(19):2328–34.
[292] Zager RA, Jurkowitz MS, Merola AJ. Responses of the normal rat kidney to sequential ischemic events. Am J Physiol 1985;249(1 Pt 2):F148–59.
[293] Yamasowa H, Shimizu S, Inoue T, Takaoka M, Matsumura Y. Endothelial nitric oxide contributes to the renal protective effects of ischemic preconditioning. J Pharmacol Exp Ther 2005;312(1):153–9.
[294] Zimmerman RF, Ezeanuna PU, Kane JC, et al. Ischemic preconditioning at a remote site prevents acute kidney injury in patients following cardiac surgery. Kidney Int ;80(8):861-867.
[295] Westenfelder C. Unexpected renal actions of erythropoietin. Exp Nephrol 2002;10(5-6):294–8.
[296] Nemoto T, Yokota N, Keane WF, Rabb H. Recombinant erythropoietin rapidly treats anemia in ischemic acute renal failure. Kidney Int 2001;59(1):246–51.
[297] Patel NS, Sharples EJ, Cuzzocrea S, et al. Pretreatment with EPO reduces the injury and dysfunction caused by ischemia/reperfusion in the mouse kidney *in vivo*. Kidney Int 2004;66 (3):983–9.
[298] Sharples EJ, Patel N, Brown P, et al. Erythropoietin protects the kidney against the injury and dysfunction caused by ischemia-reperfusion. J Am Soc Nephrol 2004;15(8):2115–24.
[299] Vesey DA, Cheung C, Pat B, Endre Z, Gobe G, Johnson DW. Erythropoietin protects against ischaemic acute renal injury. Nephrol Dial Transplant 2004;19(2):348–55.
[300] Yang CW, Li C, Jung JY, et al. Preconditioning with erythropoietin protects against subsequent ischemia-reperfusion injury in rat kidney. Faseb J 2003;17(12):1754–5.
[301] Johnson DW, Pat B, Vesey DA, Guan Z, Endre Z, Gobe GC. Delayed administration of darbepoetin or erythropoietin protects against ischemic acute renal injury and failure. Kidney Int 2006;69(10):1806–13.
[302] Gong H, Wang W, Kwon TH, et al. EPO and alpha-MSH prevent ischemia/reperfusion-induced down-regulation of AQPs and sodium transporters in rat kidney. Kidney Int 2004;66 (2):683–95.
[303] Endre ZH, Walker RJ, Pickering JW, et al. Early intervention with erythropoietin does not affect the outcome of acute kidney injury (the EARLYARF trial). Kidney Int; 77(11): 1020–1030.
[304] Song YR, Lee T, You SJ, et al. Prevention of acute kidney injury by erythropoietin in patients undergoing coronary artery bypass grafting: a pilot study. Am J Nephrol 2009;30(3): 253–60.
[305] Cassis P, Azzollini N, Solini S, et al. Both darbepoetin alfa and carbamylated erythropoietin prevent kidney graft dysfunction due to ischemia/reperfusion in rats. Transplantation; 92(3): 271–279.
[306] Ichimura T, Asseldonk EJ, Humphreys BD, Gunaratnam L, Duffield JS, Bonventre JV. Kidney injury molecule-1 is a phosphatidylserine receptor that confers a phagocytic phenotype on epithelial cells. J Clin Invest 2008;118(5):1657–68.
[307] Li B, Castano AP, Hudson TE, et al. The melanoma-associated transmembrane glycoprotein Gpnmb controls trafficking of cellular debris for degradation and is essential for tissue repair. FASEB J ;24(12):4767–4781.
[308] Lin SL, Li B, Rao S, et al. Macrophage Wnt7b is critical for kidney repair and regeneration. Proc Natl Acad Sci USA; 107 (9):4194–4199.

[309] Gupta S, Verfaillie C, Chmielewski D, Kim Y, Rosenberg ME. A role for extrarenal cells in the regeneration following acute renal failure. Kidney Int 2002;62(4):1285–90.

[310] Lin F, Cordes K, Li L, et al. Hematopoietic stem cells contribute to the regeneration of renal tubules after renal ischemia-reperfusion injury in mice. J Am Soc Nephrol 2003;14(5): 1188–99.

[311] Kale S, Karihaloo A, Clark PR, Kashgarian M, Krause DS, Cantley LG. Bone marrow stem cells contribute to repair of the ischemically injured renal tubule. J Clin Invest 2003;112(1): 42–9.

[312] Togel F, Hu Z, Weiss K, Isaac J, Lange C, Westenfelder C. Administered mesenchymal stem cells protect against ischemic acute renal failure through differentiation-independent mechanisms. Am J Physiol Renal Physiol 2005.

[313] Herrera MB, Bussolati B, Bruno S, Fonsato V, Romanazzi GM, Camussi G. Mesenchymal stem cells contribute to the renal repair of acute tubular epithelial injury. Int J Mol Med 2004;14 (6):1035–41.

[314] Morigi M, Imberti B, Zoja C, et al. Mesenchymal stem cells are renotropic, helping to repair the kidney and improve function in acute renal failure. J Am Soc Nephrol 2004;15(7): 1794–804.

[315] Gupta S, Verfaillie C, Chmielewski D, et al. Isolation and characterization of kidney-derived stem cells. J Am Soc Nephrol 2006;17(11):3028–40.

[316] Bussolati B, Bruno S, Grange C, et al. Isolation of renal progenitor cells from adult human kidney. Am J Pathol 2005;166(2): 545–55.

[317] De Broe ME. Tubular regeneration and the role of bone marrow cells: 'stem cell therapy'–a panacea? Nephrol Dial Transplant 2005;20(11):2318–20.

[318] Lange C, Togel F, Ittrich H, et al. Administered mesenchymal stem cells enhance recovery from ischemia/reperfusion-induced acute renal failure in rats. Kidney Int 2005;68(4): 1613–7.

[319] Togel F, Zhang P, Hu Z, Westenfelder C. VEGF is a mediator of the renoprotective effects of multipotent marrow stromal cells in acute kidney injury. J Cell Mol Med 2009;13(8B): 2109–14.

[320] Humphreys BD, Bonventre JV. Mesenchymal stem cells in acute kidney injury. Annu Rev Med 2008;59:311–25.

[321] Humphreys BD, Valerius MT, Kobayashi A, et al. Intrinsic epithelial cells repair the kidney after injury. Cell Stem Cell 2008;2 (3):284–91.

[322] Cantley LG. Adult stem cells in the repair of the injured renal tubule. Nat Clin Pract Nephrol 2005;1(1):22–32.

[323] Brodsky SV, Yamamoto T, Tada T, et al. Endothelial dysfunction in ischemic acute renal failure: rescue by transplanted endothelial cells. Am J Physiol Renal Physiol 2002;282(6): F1140–9.

[324] Arriero M, Brodsky SV, Gealekman O, Lucas PA, Goligorsky MS. Adult skeletal muscle stem cells differentiate into endothelial lineage and ameliorate renal dysfunction after acute ischemia. Am J Physiol Renal Physiol 2004;287(4):F621–7.

[325] Reinders ME, Rabelink TJ, Briscoe DM. Angiogenesis and endothelial cell repair in renal disease and allograft rejection. J Am Soc Nephrol 2006;17(4):932–42.

[326] Tongers J, Losordo DW. Frontiers in nephrology: the evolving therapeutic applications of endothelial progenitor cells. J Am Soc Nephrol 2007;18(11):2843–52.

[327] Becherucci F, Mazzinghi B, Ronconi E, et al. The role of endothelial progenitor cells in acute kidney injury. Blood Purif 2009;27(3):261–70.

This page intentionally left blank

CHAPTER

77

Ischemic Renal Disease

Christopher J. Cooper[1], Lance D. Dworkin[2] and William L. Henrich[3]

[1]Department of Medicine, University of Toledo, Toledo, Ohio, USA

[2]Brown University, Providence, Rhode Island, USA

[3]University of Texas Health Science Center at San Antonio, San Antonio, Texas, USA

The intrinsic ability of the kidney to regulate renal blood flow and glomerular filtration rate (GFR) over a wide range of perfusion pressures has fascinated physiologists for decades. These adaptive responses to physiologic and pathologic alterations in renal perfusion, known collectively as renal autoregulation, serve to maintain renal excretory function in settings of decreased renal blood flow, such as in states of volume depletion, hypotension, or reduced cardiac output. Another important and unique setting of renal hypoperfusion is that of renal arterial occlusive disease due to a fixed stenosis, a situation that typically presents with a chronic, gradual, and eventually critical reduction of perfusion. This physiologic stress depends on renal autoregulation to maintain GFR, but the ongoing global renal hypoperfusion appears to eventually produce chronic ischemic injury to the renal parenchyma through mechanisms that are not clearly understood. This latter prospect is clearly a threat to the viability of the kidney and appears to be an important cause of chronic and often irreversible kidney disease. An understanding of the limits, mechanisms, and the pharmacologic manipulation of renal autoregulation is important in this setting because the disordered physiology is silent. Likewise, an understanding of the pathophysiology of chronic ischemic injury is important in designing effective clinical strategies to treat this disorder.

This chapter will focus on the clinically important issue of atherosclerotic renal artery stenosis (RAS) as a cause of ischemic renal disease, also known as ischemic nephropathy (IN). This disorder is recognized more frequently as a cause of end-stage renal disease. The patient population most likely to benefit from revascularization procedures is, however, not clearly defined. However, recently completed clinical trials, in conjunction with ongoing studies, are likely to bring clarity to this clinical conundrum. This chapter will review the clinical presentations of ischemic renal disease, the modalities available for diagnosis, the pathophysiology of renal hypoperfusion and ischemic renal injury, and provide insights into treatment.

ATHEROSCLEROTIC RENAL ARTERY STENOSIS: A COMMON DISORDER WITH INCREASING CLINICAL RECOGNITION AND PUBLIC HEALTH IMPORTANCE

Over the past few decades, the lesions of renal artery stenosis have been more frequently diagnosed in atherosclerotic patients with hypertension or deteriorating renal function. In addition to an increased awareness of the disorder among clinicians, the proliferation of noninvasive diagnostic techniques such as magnetic resonance angiography, computed tomography (CT) angiography, and duplex sonography has fueled this trend. Among the estimated 60 million Americans with hypertension, the prevalence of significant RAS in this population has been estimated at 2 to 5%. Autopsy series done in the 1960s indicate that RAS is common in the elderly. An autopsy study by Holley et al.[74] demonstrated a 27% prevalence of 50% stenoses in patients with a mean age of 64 years, however, the prevalence increased to 62% in individuals greater than 70 years old. Alternatively, a study by Schwartz and White demonstrated a lower prevalence of stenoses $\geq 50\%$: 5% if younger than 65 years, 18% in 65- to 74-year-olds, and 42% if 75 years and older.[156] Kuroda et al.[92] found atherosclerotic RAS of at least 75% luminal area

Seldin and Giebisch's The Kidney, Fifth Edition.
DOI: http://dx.doi.org/10.1016/B978-0-12-381462-3.00077-X

© 2013 Elsevier Inc. All rights reserved.

narrowing in 10% of autopsies of 60-year-old Japanese individuals with a history of stroke, and a 24% prevalence in individuals with carotid stenosis.[92] Importantly, it is likely that these autopsy series overestimate the rate since Edwards et al. have described a prevalence of 6.8% in a prospective U.S. cohort of adults >65 years old when a liberal Duplex velocity threshold of 1.8 meters/second was used during community screening.[48] In aggregate these studies suggest that renal stenoses are rather common, and that the prevalence rises rather dramatically in the elderly and it is undoubtedly true that many of the "50%" stenoses documented at autopsy were hemodyamically irrelevant. This latter point is of importance as more patients are now identified with non-invasive imaging.

As would be expected given the generally diffuse involvement of atherosclerosis, the prevalence of RAS is high when renal angiography is performed on patients who are undergoing angiography for other indications.[60,145] When performed in the evaluation for aortic disease,[19,175] coronary artery disease,[66,80,145] or peripheral arterial occlusive disease,[117,169] the prevalence has ranged from 11 to 42%. The highest prevalence seems to be in patients with peripheral vascular and aortic disease.

The public health importance of kidney disease due to RAS can be gauged by the number of individuals who progress to end-stage renal disease (ESRD) as a result of this disorder. The true prevalence in this population has been difficult to accurately estimate. It is widely believed that clinical diagnosis of IN is often missed and that many individuals who have been labeled as having hypertensive nephrosclerosis as a primary cause of ESRD may actually have suffered IN. On the other hand, the mere presence of RAS in an individual with chronic kidney disease does not prove IN as its etiology. Using the U.S. Renal Data System database, Fatica et al.[50] reviewed the primary causes of ESRD in patients starting ESRD therapy during 1991 to 1997, and they found that the incidence of renovascular disease as a primary cause of ESRD increased from 1.4% of new ESRD cases to 2.1%. The annualized increase was 12.4% per year. This is a greater rate of increase than for ESRD from diabetes mellitus (8.3% per year) and ESRD overall (5.4% per year).[50]

In a report from England, Scoble and colleagues prospectively performed renal arteriography in all new patients with ESRD during an 18-month period in the late 1980s.[157] Atherosclerotic renal artery disease was ultimately believed to be the cause of ESRD in 6% of all patients and in 14% of patients older than 50 years. Appel and coworkers suggest that renovascular disease accounts for 11% of all patients with ESRD older than 50 years and 20% of ESRD cases among whites older than 50 years.[6] Mailloux et al.[106] performed an analysis of patients entering their ESRD program between 1982 and 1985 for possible ischemic nephropathy and estimated a prevalence of 16%. This represented a significant increase from a prevalence of 8% reported among those who entered their program between 1970 and 1982.[106] This was thought to most likely be a reflection of increased awareness of the disease and the rising age of the dialysis population.

Further supporting the public health importance of IN is the clear evidence that this diagnosis imparts a high mortality risk and that patients with ESRD due to IN do poorly on dialysis. Given the frequent coexistent atherosclerotic coronary artery disease in these patients, cardiovascular deaths are common. In a Swedish study of a cohort of patients with RAS lesions exceeding 50%, Johansson and colleagues found a risk ratio (versus age-matched controls) was 3.3 for overall mortality and 5.7 for cardiovascular mortality.[81] Baboolal et al.[8] published a report in 1998 describing the poor outcome of medically treated patients with severe bilateral RAS: such patients had a crude mortality rate at 60 months of 45%. In an analysis of survival of patients who started dialysis from 1970 to 1985 by Mailloux et al.,[105] patients with renovascular disease as the cause of ESRD had very poor survival, a mean survival of 27-months and a 12% 5-year survival rate.

Over the past few decades intraluminal renal artery revascularization has enjoyed tremendous technologic advances and has become a very commonly performed procedure. This is likely in response to the increased awareness of the diagnosis and in hopes of favorably altering its poor prognosis. Among the estimated two to four million cases of renal artery stenosis in the United States, approximately 7000 such procedures are done annually, at an estimated cost of $1.7 billion per year. It remains unclear if the rate of utilization is appropriate, and some experts have suggested that this rate is far too low while others have suggested that it is far too high. Unfortunately, the current body of literature in this area supports only opinion-based rather than firm evidence-based recommendations. Although there is controversy surrounding the management of this disorder and conflicting recommendations from experts regarding treatment, the prevalence of the disorder mandates that clinicians know how to efficiently diagnose the disorder and be familiar with the current understanding of the pathophysiology and natural history of IN.

CLINICAL PRESENTATIONS OF ISCHEMIC NEPHROPATHY

IN can present as one of several clinical manifestations. Mild to moderate kidney disease in a patient

with known renovascular disease should raise suspicion for the presence of ischemic renal disease. These patients tend to be older, have a shorter duration of hypertension, require more medications for blood pressure (BP) control, show other features of diffuse vascular disease, and have a higher incidence of hypertensive retinopathy and vascular bruits than patients with essential hypertension. These patients may develop a progressive decrease in renal size by sonography along with a rising serum creatinine concentration. Ischemic renal disease should also be considered in any elderly patient who presents with unexplained acute or chronic kidney disease, especially if there is evidence of generalized atherosclerosis, even in the absence of hypertension. Development of hypertension later in life (after age 60) or an abrupt loss of blood pressure control in previously well-controlled essential hypertension, with evidence of a decline in renal function, should also raise the suspicion of this entity. Bilateral renovascular disease may be suspected from the occurrence of acute kidney injury following the initiation or intensification of antihypertensive therapy, especially with an angiotensin-converting enzyme (ACE) inhibitor or angiotensin receptor blocker. Nevertheless, the absence of ARF in this setting does not rule out the possibility of ischemic renal disease.[78] A similar reduction in GFR may occur in the setting of intravascular volume depletion, congestive heart failure (CHF), and use of other antihypertensive agents such as vasodilators. A clinical scenario in which the diagnosis of renal artery disease is often suspected is in patients with poorly controlled hypertension, renal insufficiency, and left ventricular hypertrophy who develop acute pulmonary edema rapidly, so-called "flash pulmonary edema." Finally, unstable angina with poorly controlled hypertension may be a presenting complaint, especially when the degree of coronary stenosis seems proportionally less than the severity of the presentation.[87]

The character of the renal disease is nonspecific, with progressive azotemia with mild-to-moderate proteinuria (rarely nephrotic) and a bland urinary sediment. There have been reports of nephrotic-range proteinuria that has been attributed to the development of focal glomerulosclerosis in the kidney contralateral to a unilateral RAS lesion.[4,13,54,82] Rarely the disease may present with acute oligoanuric kidney disease due to progression from a high-grade, compensated lesion to complete or critical obstruction.[139,146,151]

DIAGNOSIS OF ISCHEMIC NEPHROPATHY

Given the large population of atherosclerotic patients and the nonspecific nature of the presentation, the diagnosis of IN is often considered in an extremely large number of patients. A cost-efficient, effective, and safe diagnostic strategy is desirable to identify these patients with IN. This section addresses various tests available. A recommended strategy for diagnosis is then presented.

There is an extensive body of literature and many reviews on the diagnosis of renovascular hypertension (RVH), but there is a relative dearth of data on the diagnosis of IN. To what degree this literature on RVH can be applied to the setting of IN is not clear. The tests that depend on the presence of a high renin state or high angiotensin II (Ang II) tone would not be expected to extrapolate well to the diagnosis of IN given the differences in pathophysiology of the disorders. However, data derived from the RVH literature on the anatomic diagnosis of RAS are useful. A meta-analysis published in 2001 by Vasbinder et al.[179] evaluated the literature on diagnostic tests for renal artery stenosis in patients suspected of having RVH. These authors constructed receiver-operating characteristic (ROC) curves, and these are shown in Figure 77.1. From this analysis they

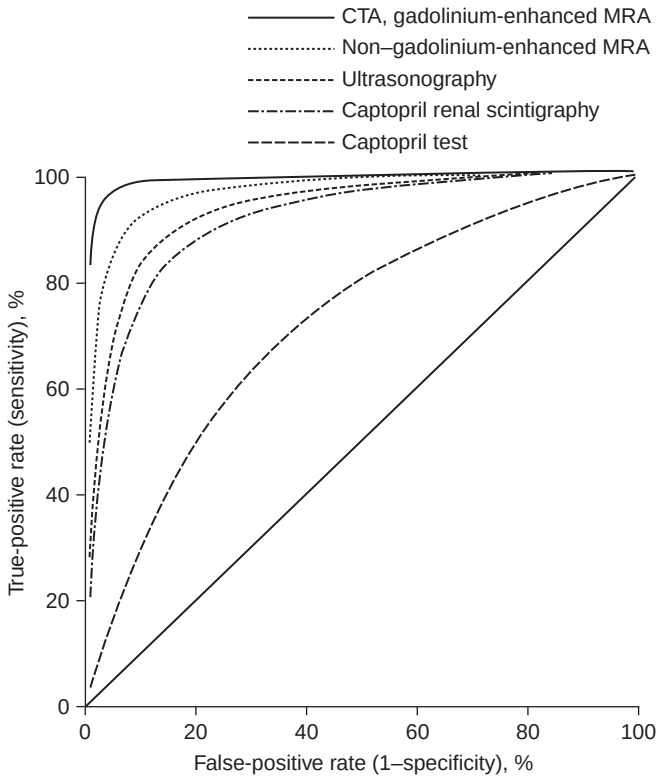

FIGURE 77.1 Summary receiver-operator curves for diagnostic tests in patients suspected of having renovascular hypertension. *(from ref. [179], with permission.)*

concluded that computed tomography angiography (CTA) and gadolinium-enhanced three-dimensional magnetic resonance angiography (MRA) were the most reliable noninvasive tests when compared to the gold standard of renal angiography. The authors also noted that few studies on these tests had been published and recommended further research in this area. In this effort, this same Dutch group later published their results of a prospective study of these two diagnostic modalities compared to intra-arterial DSA in this setting.[180] They found suboptimal diagnostic characteristics of CTA and MRA, with the combined sensitivity and specificity of 64 and 92% for CTA and 62 and 84% for MRA. They concluded that CTA and MRA are not sufficiently sensitive to rule out RAS in hypertensive patients, and they contended that DSA is the diagnostic method of choice.

Angiography

Angiography remains the single most accurate test to diagnose and quantitate renal artery disease. This may be performed with conventional technique but has largely been supplanted by intra-arterial Digital Subtraction Angiography (DSA) technique. Although *intravenous* DSA was once considered as a less invasive alternative to conventional angiography, in that it does not require arterial catheterization, it still requires nephrotoxic radiocontrast which limits its utility in patients with renal insufficiency. In contrast *intra-arterial* DSA can be performed with small volumes of contrast, and it has been reported to have similar sensitivity as conventional angiography.[89] Intra-arterial angiography can be accomplished using carbon dioxide,[67] however, the images are of lesser quality and may create greater uncertainty about lesion severity unless combined with judicious use of iodinated contrast.[103]

Renal angiography during intra-arterial angiography performed for other indications may be a reasonable diagnostic strategy, for example, during evaluation for aortic disease, lower extremity peripheral arterial occlusive disease, or coronary artery disease. When a cardiologist performs a renal angiography during a cardiac catheterization that is done through the femoral approach (pejoratively termed "drive-by" renal angiography), essentially the only incremental risk is that of the minimal volume of contrast needed to visualize the renal arteries. The suprarenal aorta has already been traversed for the coronary study, and therefore the risk for lower extremity and renal embolic sequelae has already been realized. The limitations of noninvasive evaluation for RAS (as discussed previously), the high incidence of incidental RAS in this population,[144] the prolonged phase of silent progression that may result in irreversible renal injury when it finally becomes clinically manifest, and the potential for interrupting the course of IN (to be discussed in the following sections) have been the justification for routinely including this renal artery evaluation during coronary catheterizations done via the femoral approach. Apposing this is the increased contrast exposure resulting from additional angiographic images of the abdominal and scraping of the aorta by the catheters (with an attendant risk of atheroembolization) if selective images of the renal arteries is performed. To balance these risks consensus guidelines were developed and published.[186] The more difficult issue involves the decision of whether to place a renal artery stent during the procedure and this issue requires circumspection, knowledge of the competing risks and benefits of revascularization versus medical management, and informed consent from the patient.

Duplex Ultrasonography

Another anatomic test for RAS that has a role in noninvasive evaluation of RAS is duplex ultrasonography. There are several major advantages of Duplex, namely that it is entirely safe and that the data provides functional information about lesion severity (systolic velocity and turbulence of flow) as well as anatomic information (lesion location). However, as shown in the meta-analysis by Vasbinder, it appears to have inferior diagnostic characteristics compared with MRA and CTA. This technique involves B-mode imaging with a pulsed Doppler beam to measure end-diastolic to peak systolic velocities in the renal artery and aorta. Some centers have reported sensitivity of 92.5 to 98% and specificity of 96 to 98%.[130,143] It is an operator-dependent test, and although diagnostic accuracy is improving, it will require further improvements to become the universal noninvasive test of choice. Obesity, recent food intake, increased bowel gas, and adhesions from prior surgery may limit the quality of images and may hinder diagnostic utility.

Functional Testing for RAS

Given the suboptimal characteristics of these anatomic tests, the functional tests—or "hemodynamic probes" as some authors have called them—may be useful in certain settings. Most rely on the interruption of Ang II–maintained GFR or the lowering of renal perfusion distal to a lesion by inducing controlled

systemic hypotension. Textor et al.[171] have shown that nitroprusside-controlled lowering of arterial blood pressures will decrease GFR in individuals with bilateral RAS, but the logistics preclude using this as a common diagnostic test. Combining the use of captopril with renal scintigraphy, may yield helpful information about blood flow beyond a stenotic lesion in the renal artery. The most commonly used renal scans are the 99mTc-DTPA scan (which estimates GFR) and the 131I-iodohippurate scan (Hippuran) (which estimates renal plasma flow). The 99mTc-mercaptoacetyltriglycine (Mag3) combines the advantages of both of these, and can be used to quantify the relative blood flow to each kidney.[77] However, several studies have demonstrated poor performance of renal scintigraphy for the evaluation of renal artery stenosis.[75,49] In one circumstance, the evaluation of renal function in a patient with an occluded renal artery, scintigraphy may still be useful if it demonstrates significant residual function of the post-occlusion kidney.[44]

Diagnostic Strategies

When one has at least a moderate suspicion of the disease and when a finding of RAS would guide management, many experts feel that an anatomic test for RAS should be pursued. Unless an angiogram is planned for a separate indication (such as to evaluate for coronary artery disease), a noninvasive evaluation is generally a prudent next step. Until recently MRA with gadolinium would be considered, however, in patients with IN and an estimated GFR less than 40 ml/min/1.72m^2 the risk of nephrogenic systemic fibrosis, is prohibitive. If the patient has normal renal function (which is generally not the case when the diagnosis is considered in the evaluation of ischemic nephropathy), CT angiogram is an acceptable alternative. Duplex ultrasonography is a useful alternative since it is entirely non-invasive, safe, and provides information on the functional significance of lesion severity as measured by the flow velocity. If a coronary catheterization or aortic angiography is being done on such a patient, then the angiographer should visualize the renal arteries as part of the study. In selected patients it may be justified to proceed directly to angiography if the pretest suspicion is sufficiently high and the other modalities are contraindicated (MRA or CTA because of contrast concerns) or the images are unlikely to be of diagnostic utility (example: morbid obesity and Duplex ultrasonography). CO_2 may be used as an adjunct to limit the volume of iodinated radiocontrast in individuals at risk for radiocontrast nephropathy.

CLINICAL SIGNIFICANCE OF ATHEROSCLEROTIC RENAL ARTERY STENOSIS

After the diagnosis of a renal artery lesion is secure, the next step is to assess the clinical significance of the lesion in hopes of prospectively identifying patients who will benefit from therapy. In this regard, it is important to have an appreciation of the anatomic natural history, the clinical natural history, and the pathophysiology of the disorder. These issues will be addressed later in the chapter. Several diagnostic tests have been proposed to test the physiologic and clinical significance of a given lesion, and these are reviewed here.

A parameter that may have a role in assessing the clinical significance of a lesion and in guiding the use of invasive revascularization interventions is that of the sonographically measured renal resistance-index value.[140] It has been hypothesized that intrarenal small-vessel disease may limit the benefit of main renal artery revascularization in patients with atherosclerotic RAS, and increased intrarenal renal vascular resistance may be a functional marker of this microvascular disease. The sonographically determined resistance index (RI) is considered a noninvasive measure of intra-renal resistance to blood flow, and it is calculated as follows:

$$\mathrm{RI} = [1 - (\text{end-diastolic velocity}/\text{maximal systolic velocity})] \times 100 \quad (77.1)$$

Radermacher et al.[140] assessed the prognostic value of this parameter among 138 patients who had unilateral or bilateral RAS of at least 50% of the luminal diameter and who underwent angioplasty or surgical revascularization. Their data indicated that a resistive-index value of at least 80 reliably identifies patients in whom angioplasty or surgery will not improve renal function, blood pressure, or kidney survival. Others, such as the group led by Hansen, have demonstrated that a high resistive index was associated with loss of GFR post-revascularization and high long-term mortality, but not with blood pressure response.[39]

Hemodynamic Assessment of RAS

The physiologic tests or "hemodynamic probes" may also have a role in this setting. As will be discussed later in the chapter, GFR is maintained in settings of reduced renal perfusion (such as may be the case with a high-grade RAS lesion) by maintenance of increased efferent arteriolar tone by Ang II. These tests are intended to demonstrate whether there is a drop in GFR distal to a RAS lesion after the pharmacologic interruption with an ACE inhibitor (ACE-I) of Ang

II–maintained efferent arteriolar tone. Safian and Textor suggest using captopril renography with nuclear scans to assess the functional significance of lesions by determining the renal function of the individual kidneys and by determining the dependence of renal function on Ang II.[149] As described above, the practice of using scintigraphy diagnostically though has not been validated. In contrast there is a growing literature about the use of pressure gradients measured during invasive angiography, either at rest or with a pharmacologic agent, to predict outcome of revascularization.[96] These investigators have observed that a higher pressure gradient (>21 mmHg) induced by intra-arterial papaverine was associated with an improvement in blood pressure post-procedure.

Another important issue that must be considered when assessing the clinical significance of an individual lesion is what degree of stenosis is considered hemodynamically significant? The most important consideration is the cross-sectional area through which renal blood flows. Assuming that the stenotic lesion narrows the lumen circumferentially, the luminal can be calculated as the area of a circle by multiplying pi by the square of the radius ($A = \pi r^2$). The severity of stenosis is generally assessed clinically by an estimation of the degree of reduction of luminal diameter (rather than luminal area) on angiographic longitudinal projections. Thus, decreasing a luminal radius or diameter to half would reduce the luminal area to one quarter. A basic understanding of fluid dynamics is also helpful in understanding the flow and pressure effects of the length and degree of stenotic lesions. This rearranged version of Poiseulle's equation shows the relationship of the parameters:

$$P1 - P2 = 8[Q \times n \times 1/\pi \times r^4] \qquad (77.2)$$

where Q = flow, n = viscosity coefficient, r = radius, l = length of narrowing, and P1 − P2 = pressure gradient across the stenosis. Obviously the situation is much more complicated in a physiologic system with distensible blood vessels and with pulsatile, less-than-perfectly laminar flow. Nevertheless, the equation indicates that the radius of the stenosis should be much more hemodynamically important than length of the lesion: a reduction of radius by half would increase the pressure gradient by a factor of 16 while a doubling of the length would increase the gradient by a factor of 2.

With these considerations in mind, it should be noted that autoregulation fails to maintain GFR below SBPs of 75 to 80 mm Hg and that experts have stated that this occurs when reduction of luminal diameter is reduced by 70%. Classic studies on dogs by May et al.[109] in the early 1960s support the contention that the degree of obstruction must exceed 70 to 80% of the cross-sectional luminal area before appreciable pressure gradients develop across a lesion. Using cardiac-gated magnetic resonance cine phase-contrast flow measurements with high temporal resolution in a canine model of renal artery stenosis, Schoenberg and colleagues[153] made more sophisticated descriptions of pulsatile flow profiles and pressure gradients to describe the immediate hemodynamic impact of various degrees of stenosis (as measured by reductions in luminal diameter). As shown in Figure 77.2, the area under the single cardiac-cycle flow-versus-time curve as a measure of mean flow did not substantially decrease until the degree of stenosis reached levels between 70 and 90%. They also showed that trans-stenotic pressure did not significantly

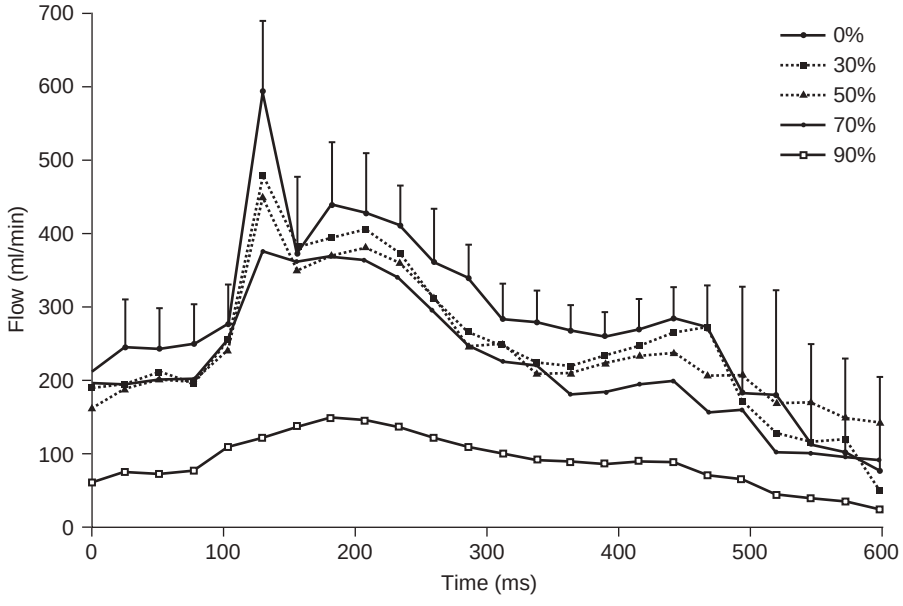

FIGURE 77.2 Hemodynamic changes in the time-resolved flow profiles obtained noninvasively with cardiac-gated magnetic resonance flow measurements. Averaged data of seven dogs are presented. For reasons of clarity, error bars are given only for the normal flow curve (0% stenosis). With increasing degree of stenosis, the early systolic peak declines, followed by a loss of the midsystolic maximum. Whereas the area under curve as a measure of mean flow does not substantially change up to 80% stenosis, the early systolic peak is sensitive to minor stenoses induced in the renal artery. *(from ref. [153], with permission.)*

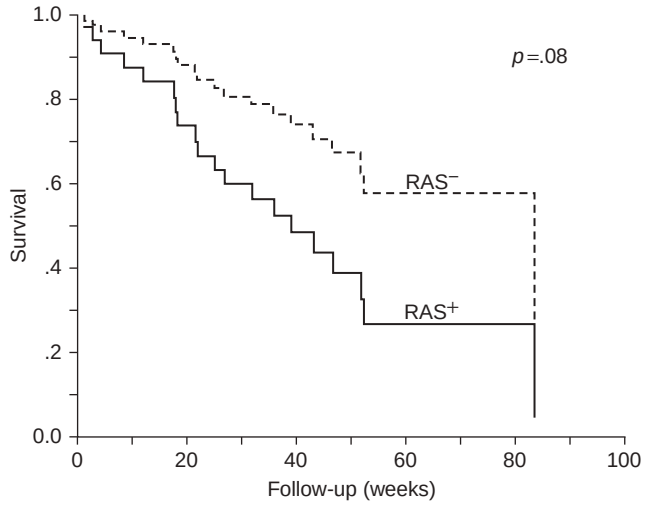

FIGURE 77.3 Cox regression curve of renal survival without end-stage renal disease (ESRD) in renal artery stenosis (RAS)—negative and RAS-positive patients with diabetes, with adjustment for baseline serum creatinine level. *(from ref. [123], with permission.)*

change until the animal was confronted with similarly high degrees of stenosis. As shown in Fig. 77.2, the only significant flow abnormality observed at lesser degrees of stenosis was a gradual loss of the early systolic peak of flow. The ultimate clinical significance of such subtle flow changes is not known. Raising concern that lesser degrees of obstruction may have a long-term deleterious impact, Myers et al.[123] found that subcritical (< 65%) stenosis is a significant risk factor for progressive chronic kidney disease in hypertensive patients with type 2 diabetes mellitus and azotemia (serum creatinine of at least 1.8 mg/dl), as shown in Figure 77.3. This finding raises the possibility that large-vessel RAS may also be a marker for progressive small vessel disease. As described above the pressure gradient across the stenosis may be predictive of the response to revascularization, although this remains somewhat controversial.[96] A concept that has received little attention is the relationship between intrarenal resistance and translesional pressure gradients. For example, it is possible that translesional gradients are lower when post-lesion intra-renal resistance is high. The drop in pressure sensed by the kidney is likely dependent upon the relative degree of obstruction of the renal artery before the kidney and the amount of intra-renal resistance to flow. Whether these factor(s) are dynamic or static, and their relationship within patients and to the response to revascularization has not been explored experimentally.

Assessment of Kidney Size

The global renal atrophy of IN is an important non-invasive marker of the disorder, and its implications on the reversibility and prognosis of disease may be different than that in other chronic renal diseases, where small kidney size is widely considered a marker of irreversibility. Given the distinct pathophysiology of IN, it is not clear when reduced renal size indicates "death" versus "hibernation" of the kidney. Caps et al.[27] elucidated the incidence of renal atrophy when they followed 204 kidneys in 122 subjects prospectively with serial (every 6 months) duplex scans for a mean of 33 months and observed that the 2-year cumulative incidence of renal atrophy (defined as >1 cm reduction in length) was 5.5, 11.7, and 20.8% when the index scan revealed a normal artery, less than 60% stenosis, and greater than or equal to 60% stenosis, respectively. They also found that systolic blood pressure (SBP) above 180 mm Hg and elevations in creatinine also correlated with atrophy.[27] Greco and Breyer contend in their 1997 review of atherosclerotic renal disease that renal atrophy is reversible, and they cite evidence from studies that indicate good renal functional outcomes following surgical revascularization of small kidneys and that indicate that renal size may increase after revascularization.[60] Tubular atrophy and glomerular collapse, which are generally considered reversible, are often seen in IN, and perhaps this could contribute to renal shrinkage in this setting. Alternatively, glomerular sclerosis and interstitial fibrosis could be present, and this pathology is considered irreversible. A renal biopsy could be used to distinguish between these causes of atrophy and gauge prognosis and guide therapy, but this is rarely done in this setting.

Despite the availability of these various anatomic and hemodynamic tests, the current state of the art in predicting which patients with RAS will benefit from invasive revascularization is inadequate. As will be discussed, the literature on treatment of RAS indicates that a substantial proportion of patients with RAS do not benefit from or are harmed by revascularization procedures. To understand why repairing a stenosis in the renal artery might not work, one must have an appreciation of the pathophysiology of IN.

PATHOPHYSIOLOGY OF RENAL UNDERPERFUSION AND ISCHEMIC NEPHROPATHY

The classic experiments of Goldblatt provide insight into the acute physiologic alterations that result in renovascular hypertension following constriction of the renal artery.[57] Goldblatt produced *in vivo* renal artery stenosis by applying a metal clip to partially occlude the renal artery. In the Goldblatt two-kidney—one clip model of renal artery stenosis, the hypertensive state that results is associated with increased renin levels. However, because of pressure natriuresis in the

nonstenotic kidney, volume status is normal. This situation approximates unilateral stenosis in an individual with two functioning kidneys. In contrast, the one clip-one kidney model is characterized by normal renin levels and hypervolemia. Volume expansion persists due to the absence of a compensatory pressure natriuresis in an unaffected contralateral kidney. Further studies have demonstrated that the renin dependence of the two-kidney−one-clip model is not permanent.[21,137] During the first few months following renal artery constriction, renin levels are high and removal of the clip will reverse the hypertensive state (known as phase I). This evolves to a state in which renin declines, but in which hypertension is still reversible (phase II), and finally to a state in which removal of the clip does not reverse the hypertension (phase III). These experiments, along with many subsequent studies, have made it clear that the pathophysiology of renal artery stenosis is at least partly time-dependent, that RAS may result in irreversible renal damage, and that the anatomic correction of RAS lesions does not necessarily correct the underlying pathophysiology. Understanding why this is the case requires an understanding of the physiology of renal autoregulation, the pathophysiology of prolonged states of renal underperfusion, and the causes of nephropathy in the clinical scenarios of renal ischemia.

ADAPTIVE RESPONSES TO RENAL UNDERPERFUSION

The unique positioning and independent control of resistance vessels proximal and distal to the glomerular capillary loops, the afferent and efferent arterioles, provide the kidney with an effective means of regulating the hydraulic forces driving glomerular filtration. An understanding of the hemodynamic effects of Ang II in renal artery occlusion requires some knowledge of the determinants of GFR. A summary of the interactions between these determinants is shown in the Figure 77.4. The rate of filtrate formation depends on several dynamic variables: systemic blood pressure, plasma flow rate (QA), glomerular hydraulic pressure (PGC), and afferent and efferent arteriolar resistance (RA and RE, respectively). In general, the driving force for filtration is PGC, which is determined by the systemic blood pressure, QA and the relative pre- and postglomerular resistances, RA and RE. For any given pressure gradient across the glomerular capillary wall, the absolute rate of filtrate formation also depends on the ultrafiltration coefficient (Kf), which is the product of the capillary surface area and the intrinsic hydraulic permeability of the capillary wall. As renal perfusion pressure declines, the afferent arteriole dilates and total renal vascular resistance declines. This vasodilation appears to be primarily an intrinsic, myogenic response to the decline in perfusion pressure. In addition to the direct effect of reducing perfusion pressure on the afferent arteriole, a decrease in solute delivery to the macula densa region of the distal tubule elicits vasodilation in the afferent arterioles. This communication between the macula densa cells and the afferent arteriole is termed "tubuloglomerular feedback" (TGF). The exact mechanisms responsible for this action are not completely understood. Potential local mediators include adenosine, thromboxanes, and nitric oxide.[20,152,168]

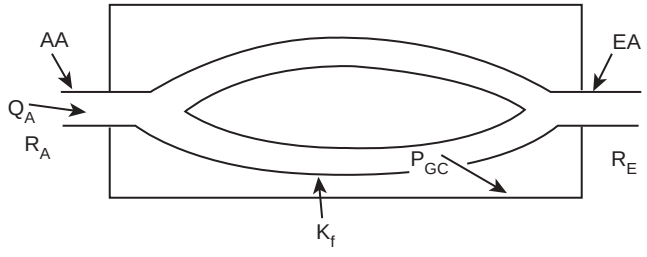

FIGURE 77.4 Determinants of glomerular filtration rate (GFR). AA, afferent arteriole; EA, efferent arteriole; QA, plasma flow rate; PGC, glomerular hydraulic pressure; RA, afferent arteriolar resistance; RE, efferent arteriolar resistance; and Kf, ultrafiltration coefficient.

The most common cause of a reduction in renal artery pressure is low systemic blood pressure. Under circumstances in which systemic blood pressure is reduced, circulating levels of several vasoconstrictive factors, including Ang II, arginine vasopressin (AVP), the sympathetic nervous system, and plasma catecholamines rise, leading to an increase peripheral resistance,. If renal vascular resistance increased in proportion to systemic vascular resistance, renal plasma flow, glomerular capillary pressure, and GFR would fall. However, at least two mechanisms combine to differentially alter the the response of the renal vasculature to a reduction in perfusion pressure and to preserve GFR; increased renal prostaglandin production leading to a reduction in afferent arteriolar resistance and the relative constriction of the efferent arterioles.

Renal prostaglandins are autocoids that are derived from the cyclo-oxygenase (COX) enzyme-catalyzed metabolism of arachadonic acid. Prostaglandins synthesized in the kidney act locally and have minimal systemic effects. They oppose the vasoconstrictive effects of Ang II, AVP, and increased renal nerve activity on the afferent arteriole, resulting in a net reduction in afferent arteriolar resistance in response to decreased renal artery pressure.[3,43] In this regard, prostacyclin and prostaglandin E2 (PGE2) appear to be the

most important renal prostaglandins. The renal prostaglandin system appears to be inactive and insignificant in states of normal renal perfusion, and inhibition of the renal prostaglandin system in health typically has few detectable effects. However, under circumstances in which systemic vascular resistance is increased in order to preserve blood pressure, renal prostaglandin synthesis and release dramatically increase. It is under these circumstances that inhibition of renal prostaglandins would produce deleterious effects on renal perfusion and glomerular filtration. This explains the well-known adverse effect on GFR that has been observed when a nonsteroidal anti-inflammatory drug (NSAID) is administered to patients with conditions that impair renal perfusion such as true volume depletion, effective circulating volume depletion (such as liver failure), and states of low cardiac output (such as CHF).[128,132] Hemodynamically, significant RAS is another condition in which inhibition of prostaglandin synthesis could adversely effect GFR.

The second factor that preserves GFR during reductions in renal artery pressure is preferential constriction of the efferent arterial in response to increased local concentrations of Ang II. The increase in efferent arteriolar resistance is associated with an increase in total renal vascular resistance and a decrease in renal plasma flow; however, because of the downstream location of this resistive force relative to the filtering unit (glomerulus), PGC remains constant tending to maintain GFR. In this manner, the kidney is able to increase the filtration fraction (GFR/renal plasma flow [RPF]) and preserve GFR despite reductions in renal plasma flow, such as occur in states of reduced cardiac output, volume depletion, or renal artery obstruction. There is also evidence that norepinephrine and the renal sympathetic nerves (possibly via Ang II) preferentially constrict the efferent arteriole relative to the afferent arteriole.[14,15,45,47,90]

Given the dependence of P_{GC} and GFR on Ang II during reductions in renal perfusion pressure, it would be expected that pharmacologic interruption of the renin/angiotensin/aldosterone system could have clinically important effects, and this is clearly the case. When ACE-I therapy decreases Ang II production or when angiotensin receptor blockers inhibit Ang II effects in conditions of increased vasoconstrictor tone, efferent resistance may decline leading to clinically important reductions in PGC and GFR. The magnitude of the effect of administration of an ACE-I on GFR depends in large part upon the local Ang II level and on systemic hemodynamics. If ACE-I administration fails to improve systemic hemodynamic parameters such as cardiac output, is associated with a marked decline in systemic blood pressure or is administered in a setting where GFR is markedly dependent on efferent arteriolar constriction, then RE will fall sharply and PGC and GFR will decline. As might be expected, this situation may exist when the blood flow through the renal artery is impaired by a fixed obstruction.

It is important to appreciate that the effects of ACE inhibition in the stenotic or ischemic, underperfused kidney are theoretically different from those in other progressive renal diseases, where renal artery pressure is not is not reduced. In the latter circumstance, glomerular hyperfiltration and glomerular hypertension may contribute to the progressive injury and scarring that leads to loss of function. In that setting, the effect of ACE-I and angiotensin II receptor blocker (ARB) therapy to dilate the efferent arteriole and lower glomerular capillary is beneficial in slowing the rate of progression of chronic diseases such as diabetic renal disease.[2,55,83,101,108,131] The renal protective effects of ACE-I and ARB may also be relevant to the nonstenotic kidney in patients with unilateral ischemic renal disease. ACE-I and ARB therapy may also be useful in reducing the amount of proteinuria in chronic glomerular diseases.[53,68] The chronically ischemic, underperfused kidney distal to an obstructive renal artery lesion, on the other hand, may respond differently to ACE-I therapy if there is dependence on Ang II to maintain a physiologically acceptable GFR.

Pathophysiology of Ischemic Nephropathy

The kidneys receive a blood supply that is three- to fivefold higher than other metabolically active organs such as heart and liver. There appears to be a critical perfusion pressure of about 70 to 80 mm Hg (which generally correlates with a greater than 70% stenosis in a systemically normotensive individual), below which the adaptive physiologic mechanisms described previously are no longer able to sustain GFR. Given that less than 10% of the oxygenated blood flow to the kidney is needed for metabolic requirements of the kidney, it would be expected that reductions in excretory function would occur in an affected kidney well before major ischemic injury develops. The intermediate steps by which this initially reversible decline in GFR then progresses into structural changes in the kidney are not well understood. The pathological changes do not appear to be directly a result of tissue hypoxia, as supported by the following observations: (1) the kidney is endowed with a generous supply of oxygen;[129] (2) as renal artery pressure and GFR decline as a result of decreased perfusion pressure, active transport and solute reabsorption also cease, markedly reducing oxygen utilization by the kidney; (3) measurements of oxygen tension in the renal veins of patients with renal artery stenosis do not demonstrate

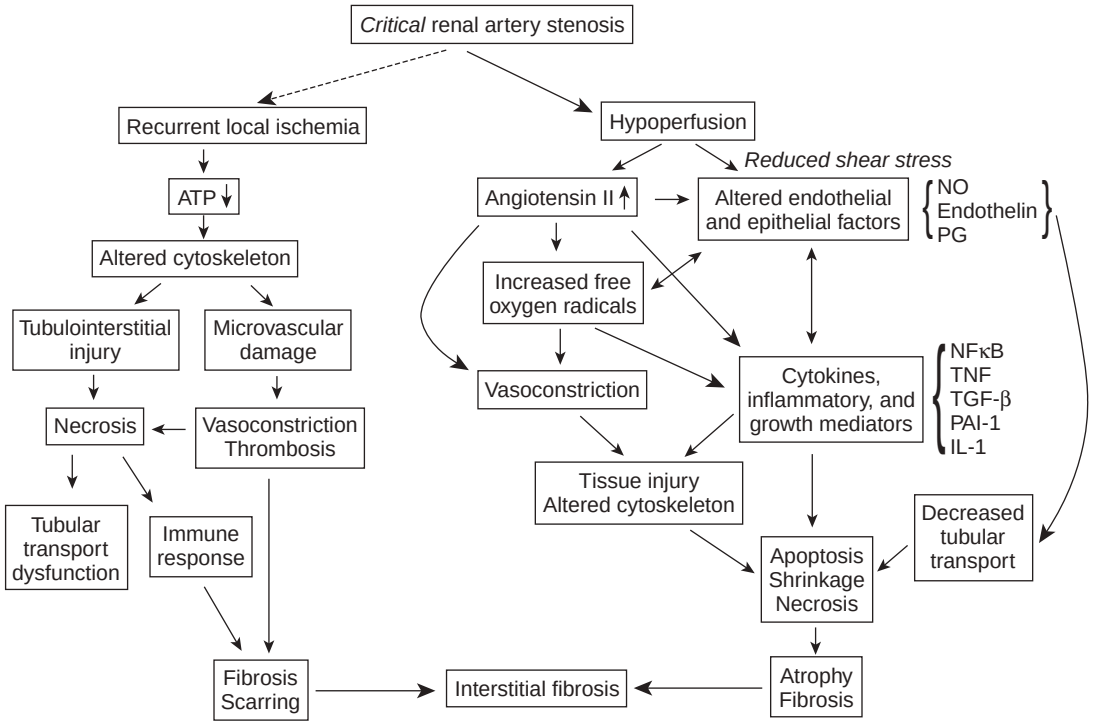

FIGURE 77.5 Summary of proposed interrelated mechanisms by which renal artery stenosis induces kidney injury leading to ischemic nephropathy. *(from 97, with permission.)*

desaturation;[187] (4) there is no augmentation of erythropoietin production from the affected kidney;[187] and (5) IN develops commonly in individuals with atherosclerotic RAS, but rarely develops distal to RAS lesions of similar hemodynamic impact produced by fibromuscular dysplasia (FMD).[97] Based on these observations, it appears that ischemic nephropathy is not simply the result of global hypoxia of the kidney and that other mechanisms are at play.

The precise pathophysiology by which RAS causes IN is not well understood. In addition to or as a result of the ischemia of the kidney, the process probably involves a complex interaction of oxidative, vasoactive, apoptotic, fibrogenic, inflammatory, atheroembolic, and micro-atherosclerotic factors. The relationship and relative importance of these various factors will require further study. An understanding of these mechanisms will be critical in developing optimal treatment strategies and guiding a rational use of medical and invasive interventions. A review by Lerman and Textor[97] addresses in detail the pathophysiology of ischemic nephropathy, and their schematic diagram, shown in Figure 77.5, lists many of these proposed pathways and indicates complex interactions among them. Several of these factors will be addressed in the following sections. The main reason for understanding the IN process in the kidney ipsilateral to renal artery stenosis is that the presence of IN may underlie the failure in renal function and blood pressure to improve after the renal artery obstruction is corrected.

Atherosclerosis

As stated previously, IN develops commonly in individuals with atherosclerotic RAS, but it rarely develops distal to RAS lesions of similar hemodynamic impact produced by FMD.[138] The sparing of patients with FMD, who are generally younger women and otherwise free of atherogenic risk factors, suggest that additional factors related to atherosclerosis [diabetes, hyperlipidemia, platelet activation or atheroembolization] may contribute significantly to kidney injury. Chade et al.[29,30] demonstrated using the porcine model of RAS that hypercholesterolemia superimposed on RAS accelerates the development of fibrosis in the stenotic kidney. Clinically, high resistance to flow in smaller arteries of the kidney (sonographically measured noninvasively by calculating intrarenal resistive index of the segmental arteries) has been shown to be highly predictive of poor renal recovery after successful revascularization,[140] and this may be due to atheromatous intrarenal small vessel disease. Interestingly, in patients with *atherosclerotic* renal disease a combination of vascular sclerosis, interstitial fibrosis, inflammatory cell infiltration, atubular glomeruli, and focal or global glomerulosclerosis is seen when biopsy of the affected kidney is performed.[156] While some of these changes

are seen in animal models of experimentally induced renal stenosis, "this mixture (of changes) cannot be reproduced in animal models.[114]"

Redistribution of Intrarenal Blood Flow

In experimental models of reduced renal artery blood flow, relative blood flow is altered to favor the corticomedullary circulation over more superficial cortical areas.[100] This probably serves to protect the more ischemic medullary parenchyma. The changes in flow distribution are probably mediated by various vasoactive substances such as prostaglandin E2, nitric oxide, urodilatin, endothelin, Ang II, and adenosine. The involvement of this mechanism is supported by findings by Mounier-Vehier et al.,[121] which show that a reduction in ultrasound-measured cortical thickness is an early morphologic marker of atherosclerotic renal disease, one that tends to develop before gross renal length decreases.

Atheroemboli

Histopathologic abnormalities in IN often include evidence of renal cholesterol microembolization, and the cholesterol emboli syndrome can be an obvious complication of angioplasty or surgery. The cholesterol microemboli may lodge in a small artery and impair distal blood flow. The ensuing foreign body reaction causes intimal proliferation, giant cell formation, and further narrowing of the vascular lumen. The microemboli seem to elicit an immune reaction, as hypocomplementemia, eosinophilia, and eosinophiluria are frequently observed with the cholesterol emboli syndrome. Work by Edwards, Hiramoto and others data suggests that a large number of emboli may be released during renal stenting,[46,71] This has led to interest in devices to capture emboli liberated during stenting. As stated above, evidence for spontaneous atheroemboli can be demonstrated with renal biopsy,[156] although the degree to which this contributes to loss of kidney function is not known.

Imbalance of Vasoconstrictors

One of the predominant effects of renal artery stenosis may be activation of the renin-angiotensin-aldosterone axis. The decrease in renal blood flow in animal models of RAS can be blunted by Ang II receptor blockers, suggesting that Ang II plays a role in renal ischemia. On the other hand, effects of Ang II blockade by ACE-Is have also been shown to accentuate the renal atrophic changes in the two-kidney−one-clip model independent of the effects of lowering of systemic blood pressure.[56,172] In addition to Ang II, other potent vasoconstrictors such as thromboxane and endothelin appear to be activated by ischemic insults. The renal vasculature is especially sensitive to the effects of endothelin,[181] which causes afferent and efferent arteriolar vasoconstriction and decreases the filtration coefficient (Kf), producing a net decline in GFR. In experimental models of acute and chronic ischemia (the latter induced by cyclosporine administration), functional and morphologic changes can be blunted by administration of anti-endothelin antibodies.[93] High levels of endothelin have been observed in chronic renal ischemia models as well as in renal hypoperfusion in the setting of hepatorenal syndrome.[120] However, systemic endothelin levels do not appear to be elevated in patients with renovascular disease when compared with patients with essential hypertension,[164] suggesting that if endothelin plays a role in human ischemic renal disease, it must be intrarenal.

Reduced Shear Stress

Under conditions of hypoperfusion, the normal counterbalancing release of vasodilator substances such as prostaglandins and NO may be impaired, thereby accentuating the ischemia.[159,160] One of the reasons for this may be a loss of shear stress due to decreased renal blood flow. Even subtle reductions of perfusion pressure and flow, as demonstrated by Schoenberg (Fig. 77.2),[153] could conceivably initiate injury through this mechanism. It has been shown that shear stress is a major regulatory mechanism for production of nitric oxide.

Oxidative Stress

As discussed previously, hemodynamically significant RAS stimulates the renin-angiotensin system, resulting in increased production of Ang II. It has also been reported that Ang II stimulates the production of reactive oxygen species such as superoxide, probably through the activation of membrane-bound nicotinamide adenine dinucleotide (NADH) or NADPH (nicotinamide adenine dinucleotide phosphate) oxidase.[52,141] The pro-oxidant effects of Ang II may interact with those of coexisting metabolic disorders and hypertension such that a relative increase in reactive oxygen species (especially superoxide) and reduced production of nitric oxide (NO) may be present. This imbalance may promote endothelial dysfunction by a resultant increase in oxidative stress. Lerman et al.[98] demonstrated increased oxidative stress in their pig model of RAS. Higashi et al.[70] demonstrated evidence of excessive oxidative stress in patients with RVH that appeared to reverse after angioplasty and was associated with evidence of endothelial dyfunction that also improved after angioplasty. Minuz et al.[116] showed that oxidative stress, as indicated by measurements of lipid peroxidation products, is increased in patients with renovascular disease and hypertension as compared with patients with essential hypertension.

Furthermore, this appeared to be due to activation of the renin-angiotensin system, and it was associated with an increase in thromboxane A2 biosynthesis, which would be expected to enhance platelet activation. Enhanced platelet aggregation and adhesion could contribute to microvascular renal injury as well as cardiovascular disease associated with this disorder. Additionally, this oxidative stress and reduced NO production may impair endothelium-dependent vasodilation, which may have local and systemic consequences. Locally, the resulting vasoconstriction could increase ischemic tissue injury. Systemically, hypertension could result. Increased free-oxygen radicals could also impact on fibrogenic and inflammatory mediators. Chade et al.[31,32] demonstrated in the porcine model of RAS described previously that chronic blockade of the oxidative stress pathway using antioxidant vitamins improved renal hemodynamics and decreased inflammation and fibrosis in the ischemic kidney.

Fibrogenic Factors

Fibrogenic, trophic, and inflammatory mediators are probably involved in the progression of IN. These may include nuclear factor kappa B (NFκB), tumor necrosis factor (TNF), transforming growth factor beta (TGF-β), interleukin-1 and others. Pathologically, interstitial fibrosis and glomerular sclerosis are often seen in chronically ischemic kidneys. Chade et al.[29,30] demonstrated in pigs increased expression of TGF-β, increased trichrome staining (indicating collagen deposition), as well as more prominent interstitial fibrosis, tubular atrophy, and glomerular sclerosis in kidneys distal to a RAS lesion.

Inflammation

Inflammatory responses to the altered ischemic milieu may also contribute to the renal injury. Histological examination of ischemic kidneys often shows evidence of mononuclear infiltrates, tubulitis, and interstitial fibrosis.[29,174] Immunoglobulin and complement deposition has been noted in the areas of sclerosis in human ischemic kidneys.[189] The inflammatory process is likely initiated by alterations in cellular antigenicity induced by ischemia.[174] Inflammation may then contribute to interstitial fibrosis and atherosclerosis.

Disruption of Cellular Membrane Integrity and Intracellular Milieu

Ischemic injury can result in derangements of cellular membrane pumps responsible for maintenance of the internal milieu. One of the key events in this process may be calcium influx. Anoxic injury results in a rapid increase in cytosolic calcium, which can impair several vital cell functions.[22] This may explain the protective effects of calcium channel blockers in some models of ischemic injury. Mitochondrial calcium uptake impairs oxidative phosphorylation, further reducing cellular adenosine triphosphate (ATP) levels. In the acute kidney injury model, an increase in cytosolic calcium also activates phospholipases and generates toxic oxygen radicals, which can cause further membrane damage.[110,163] Ischemia delays the recovery of adenine nucleotide levels, and leads to depletion of high-energy stores from phosphate bonds in the acute kidney injury model. It has been shown that a decrease in cellular ATP by 50% is associated with severe apical microfilament disruption and cytoplasmic actin polymerization, and these changes can be reversed by increasing the cellular ATP to 70% of control values.[86] Van Why and others have devised an *in vivo* ischemic model, which results in graded ATP depletion. They have shown generation of heat-shock proteins when cellular ATP decreased to 50 to 60% of control values.[178]

Apoptosis

Enhanced renal apoptotic activity is evident within one week of unilateral RAS, but whether there is true cellular reduction or whether it represents a natural compensation for the hyperplastic response after injury is unclear. It appears that enhanced apoptosis is ongoing for several months after an insult, a finding that suggests that apoptosis is necessary for remodeling of tubular structure.[56] Apoptosis occurs primarily in the thick ascending limb after an acute ischemic insult.[155] Tubular atrophy is commonly observed by routine histology and is primarily due to a decrease in cell size. This is accompanied by a decrease in cell organelles and cellular protein content.[24,56] It has been noted that the autophagolysosome activity, which increases degradation of cell organelles, is transiently increased in ischemic kidneys.[24] Apoptosis likely contributes to the global renal atrophy that is observed in IN.

Other Issues Pertinent to the Pathophysiology of IN

The true hemodynamic events in IN likely involve numerous,transient acute reductions superimposed on chronic, progressive and, eventually, a critical reduction in blood flow to the involved kidney.[170] Acute hypoperfusion and chronic, slowly progressive ischemia clearly have different consequences for the kidney. It must be noted that some of the hypotheses discussed above have been derived in large part from data obtained in models of acute ischemic kidney injury or isolated chronic ischemia models that do not adequately incorporate the complex combination of hemodynamic, metabolic, and atherogenic insults that

typically exist in human disease. Lerman et al.[99] developed a swine model of renal artery stenosis, which is induced by the intravascular placement of a local irritant coil in the renal artery, and the gradual and progressive renal artery narrowing in this model resembles human RAS lesion progression and has been useful in elucidating mechanisms of injury. The administration of a high-cholesterol diet has been used to produce an atherogenic milieu in the animals.[29,30] However this model probably does not incorporate repetitive acute ischemic insults, which have been postulated to be important in human IN and appear to provoke delayed, cumulative pro-fibrotic sequelae in the kidney.

Another important issue in the pathophysiology of IN is that renal blood flow may be maintained via collateral arterial supply to a kidney whose flow is impaired by a severely stenotic artery.[60] Presumably, the collateral circulation would be more substantial in settings of a slowly progressive RAS lesion. Collateral arteries may arise from the suprarenal, lumbar, and ureteric vessels. Because of this collateral circulation, renal viability and function may be maintained despite occlusion of the main renal artery.[66] In fact, salvage of renal function by revascularization of dialysis-dependent patients with IN has been associated with the presence of collateral circulation on angiogram.[7,12]

Clinically, it is also important to understand that reductions in systemic blood pressure, even when the reductions are from frankly elevated to normal blood pressures, may further impair perfusion distal to a RAS lesion. When the kidney senses underperfusion, it releases renin thereby activating pressor and sodium-retaining mechanisms (primarily via the renin-angiotensin II–aldosterone system) that induce a state of systemic arterial hypertension in order to restore renal perfusion across the resistance of the stenotic lesion. This process of RAS producing systemic hypertension is known as renovascular hypertension (RVH), and a full discussion of this topic is beyond the scope of this chapter. Due to the risks of uncontrolled hypertension (which is often very severe or malignant in patients with RVH), antihypertensive medications are indicated and generally administered to such patients. Antihypertensive medications are usually effective in achieving a sustained normalization of systemic blood pressures. Interruption of RVH may lower the forward pressure head that pushes blood through the RAS lesion, and consequently worsen the perfusion to the post-stenotic kidney. This perfusion impairment may be severe enough that autoregulation fails to maintain GFR and that ischemic pathologic changes occur. Experimental observations by Michel et al.[115] support this theoretical concern, as they demonstrated much more severe histopathologic changes (glomerular collapse and fibrosis) after 5 weeks of therapy with ACE inhibitor. Discussed below, there is now observational data suggesting a lower rate of dialysis for patients with RAS treated with ACE or ARB, however this may result from better preservation of the contralateral, non-stenotic kidney in patients with unilateral RAS, despite more rapid progression of IN in the post-stenotic kidney.

PATHOLOGY OF THE KIDNEY IN ISCHEMIC NEPHROPATHY

Based on experimental models, biopsy, and autopsy material, several pathological changes of ischemic renal disease have been described.[193] The glomeruli usually are shrunken, with wrinkling of the glomerular tuft and thickening of the Bowman's capsule. Glomerular cysts, which are derived from filtration into an obstructed space due to detachment from the proximal tubule, may be seen. Localized areas of glomerular sclerosis are also common.[111] Renal tubular changes are prominent, showing patchy necrosis and atrophy associated with dimunition in cell size and involution of tubular epithelial cells. Bowman's space may be filled with collagenous material and patchy peritubular inflammatory cell infiltrates are seen. Histological changes of renal atrophy include small glomeruli crowded together among small atrophic tubular cells. Vascular changes due to generalized atherosclerosis as well as preexisting hypertension are also common. These consist of medial thickening of the intrarenal arteries, arteriolar hyalinosis and interlobular fibroelastosis. Evidence of cholesterol embolization is also frequently observed. Electron microscopic examination of the tubular epithelium usually reveals decreased features of differentiation.[24] Proximal tubular cells show loss of brush border, decreased number of mitochondria, and simplification of basement membranes. The antigenic profile of the tubular epithelial cells changes with new expression of keratin and vimentin and changes in surface glycoproteins.[174]

Gross renal atrophy may accompany these histologic findings. Gobe et al.[56] studied the cellular events leading to progressive atrophy in kidneys distal to stenotic

TABLE 77.1 Clinical Syndromes Associated with Renal Artery Stenosis

- Renovascular hypertension
- Acute azotemia following initiation of angiotensin-converting enzyme inhibitors (or ARBs) that resolves with discontinuation
- Heart failure and pulmonary edema
- Ischemic nephropathy
- Asymptomatic/incidental

renal arteries. During the initial phase, tubular cell death resulted from necrosis and apoptosis. During the chronic phase (10–28 days), the gross reduction in kidney size continued while cell death resulted from apoptosis alone and the level of mitosis returned to near normal. Following correction of RAS, they observed hypertrophy and hyperplasia, interpreted as evidence of regeneration. Although diminutive renal size is considered to imply irreversibility in other chronic renal diseases, these findings suggest that there might be some recovery of renal function in chronic ischemic kidneys. However, the clinical experience is that renal function does not usually improve following revascularization of small, shrunken kidneys less than 7 cm in length. Histopathologic findings of glomerular collapse and tubular atrophy would imply a better prospect for improvement than glomerular sclerosis and interstitial fibrosis.

NATURAL HISTORY OF ISCHEMIC NEPHROPATHY

It is now well recognized that obstructive lesions of the renal artery may lead to chronic renal insufficiency and end-stage renal disease (ESRD).[158] These occlusive lesions may progress gradually and may erode renal function over time in a process that is initially silent and then later clinically apparent. This disease has variously been termed "ischemic renal disease," "ischemic nephropathy (IN)," "azotemic renovascular disease," or "hypoperfusion injury." IN is not synonymous with renal artery stenosis, and it is only one of the several often-overlapping clinical syndromes that may result from RAS. Others are listed in Table 77.1. Renovascular hypertension is hypertension caused by RAS and does not necessarily involve renal parenchymal damage: not all patients with IN have hypertension.

TABLE 77.2 Causes of Renal Arterial Occlusive Disease

- Atherosclerosis
- Fibromuscular dysplasia
- Extrinsic compression
- Radiation
- Kinking or suture line edema of renal allograft artery
- Pheochromocytoma
- Neurofibromatosis
- Aortic dissection
- Congenital bands
- Vasculitis
  - –Polyarteritis nodosa
  - –Takayasu arteritis
  - –Kawasaki disease
- –Williams syndrome

It should also be remembered that there are also multiple different disorders that may result in hemodynamically significant obstructive renal artery lesions, and these are listed in Table 77.2. The overwhelming majority of the cases are due to atherosclerotic lesions, and this etiology is the only epidemiologically significant cause of clinically evident IN. Arterial fibrodysplasias (including fibromuscular dysplasia) are the second leading cause of renal arterial occlusive disease; and, although this type of pathology is a potentially correctable cause of secondary hypertension, it very rarely causes ischemic nephropathy. Atherosclerotic lesions typically involve the proximal main renal artery, rarely extending beyond the proximal third of the vessel. In about 75% of cases, significant aortic atherosclerosis is also present. A stenosis of the renal artery due to atherosclerosis may be bilateral in up to 50% of patients.[166] There is a body of literature to support the provocative theory that infectious diseases such as *Chlamydia pneumoniae* infection may contribute to atherosclerotic disease,[5,59,91,122] including that involving the renovascular bed.[176]

To optimally utilize interventions for patients with RAS, it is important to understand the natural history of RAS lesions that are not revascularized. Table 77.3 shows the rates of anatomic lesion progression in various reports in the literature.[60,145] It indicates that progression of the arterial lesion occurs in a substantial percentage, although perhaps a minority, of affected arteries. Depending on the population studied, the length of follow up, the indications for repeated anatomic assessment, and the definition of progression, rates of progression range from 29 to 71% and rates of occlusion range from 3 to 16%. The study by Caps et al.[26] indicated that the risk of progression increases with the degree of occlusion on the index ultrasound: 18% of initially normal renal arteries, 28% of arteries with less than 60 RAS, and 49% of arteries with greater than or equal to 60% RAS demonstrated progression in this prospective study; hypertension (systolic blood pressure >160 mm Hg) and diabetes mellitus also were associated with progression. Importantly, these rates have not been validated in the current era of effective antihypertensive medications, anti-platelet medications, and lipid-lowering medications including statins. As a consequence the rates may over-estimate what is likely to be observed in a compliant, actively managed patient.

Notwithstanding the anatomic progression, an accurate estimate of the much more meaningful outcome of clinically significant chronic kidney disease has been even more elusive. In this regard, the literature is confusing and contradictory. In 1981 Dean et al.[40] reported that 17 (41%) of 41 patients randomly selected for nonoperative management of RAS experienced a

TABLE 77.3 Natural History of Atherosclerotic Renovascular Disease

			Anatomic Result			
Source	**Modality**	**Year**	**No. of Patients**	**Length of Follow-up, mo**	**Progression, %**	**Occlusion, %**
Meaney et al.[112]	Angio	1968	39	6–120	36	8
Wollenweber et al.[188]	Angio	1968	30	12–88	63	—
Dean et al.[40]	Angio	1981	35	6–102	29	11
Schreiber et al.[154]	Angio	1984	85	12–60	44	16
Tollefson[173]	Angio	1991	48	15–180	71	15
Zierler et al.[192]	Duplex	1994	80	6–24	42	11
Caps et al.[26]	Duplex	1998	170	Mean 33	51 (5 y)a	3

(*Adapted from Greco BA, Breyer JA. Atherosclerotic ischemic renal disease.* Am J Kidney Dis *1997;29:167-187.*)
Angio, angiography; Duplex; duplex doppler sonography; Not reported.
a18% of normal renal arteries, 28% if <60% renal artery stenosis (RAS), 49% if >60% RAS. Systolic blood pressure >160 mm Hg and diabetes mellitus were also associated with progression.

deterioration of renal function or loss of renal size despite acceptable blood pressure control by their unspecified standards. In a prospective cohort study published in 1994, Connolly et al.[35] estimated the 2-year renal survival to be 97% with unilateral disease, 82% with bilateral stenosis, and 45% with unilateral stenosis and contralateral occlusion. Their data confirmed the logical expectation that chronic kidney disease is more likely to develop if RAS lesions affect the whole of the functioning renal mass. In a 1998 article by Baboolal et al.,[8] patients with severe bilateral RAS demonstrated a decrease in the median GFR from 39 ml/min to 31 and 24 ml/min at 24 and 60 months, respectively ($p < .05$). Of the 51 patients who underwent angiography, six patients had reached ESRD over a median period of follow-up of 52 months.[8] Two other reports, however, have suggested a more benign course of incidentally discovered RAS; and their findings can be used to support a conservative approach to management of RAS lesions, at least those found incidentally. In 2001, Leertouwer et al.[95] retrospectively evaluated a cohort of 126 patients with incidental RAS of at least 50% on angiograms done in evaluation for extrarenal arterial occlusive disease and found that during a 10-year follow-up amazingly none had required renal replacement therapy and that serum creatinine values were stable, even with bilateral disease. Chabova et al.[28] followed 68 patients with incidental RAS of at least 70% on angiogram for mean of 39 months and reported in 2000 that only four (5.8%) eventually had renal revascularization and 7.4% developed ESRD, with only one case due to vascular occlusive disease. Thus, while it is reasonable to suspect some progression of atherosclerosis will occur in affected renal arteries over time, it is likely that total occlusion of the renal artery occurs in a minority of patients.

It is also important to understand that the progression of IN is dominated by a phase that is essentially clinically silent. During this stage, the disorder would be obscure were it not for a high clinical index of suspicion, the finding of renal asymmetry on abdominal scanning done for other reasons, or the incidental finding on angiography done for other reasons. As illustrated in a review of the subject by Safian and Textor,[149] when the lesions progress asymmetrically, as is usually the case, the relatively uninvolved kidney may maintain normal serum creatinine through compensatory hypertrophy and hyperfiltration (as well as through increased tubular creatinine secretion). As illustrated in their review article, the serum creatinine level does not increase until the individual's disease progresses to involve the other kidney such that the entire renal mass is then rendered ischemic. Of course, an individual with a solitary functioning kidney or an individual whose contralateral kidney is simultaneously injured during the course of RAS progression (for example, by uncontrolled hypertension or by diabetes), the kidney injury would become manifest sooner in its course. Given that the disorder is generally not sought until a workup for clinically apparent chronic kidney disease is undertaken, the prospects for amelioration of established disease are of critical importance in the deciding on whether to pursue invasive revascularization.

Treatment of Ischemic Nephropathy

The optimal treatment strategy of RAS lesions is not clear. Various algorithms have been proposed,[124,136,137,148,170] and there is much controversy among experts regarding which patients should be managed conservatively and which patients should undergo

invasive interventions. The benefits of revascularization may include stabilization of or improvement in renal function. Even salvage from dialysis has been described in such patients (see subsequent sections). However, these benefits are not universally or predictably realized. Furthermore, the vascular interventions have risk(s), and a substantial proportion of patients who undergo revascularization realize no benefit and/or encounter complications. The ability of clinicians to predict which patients will benefit from revascularization is imperfect. The vagaries of the natural history of medically managed RAS—with some reports suggesting a low risk for progression to ESRD—and the uncertainties of the benefits of invasive interventions have left the indications for revascularization controversial. In addition to understanding the pathophysiology, natural history, and diagnostic tests of IN, it is important to be familiar with the literature on treatment so that clinicians may provide informed opinions to patients.

Before reviewing the current literature, some clarifications are appropriate. The definitions of renal functional improvement, stabilization, and improvement vary widely from study to study. Most reports use static measures of renal function (usually serum creatinine or creatinine clearance measures) at the time of intervention and then at certain times after intervention. Outcomes are categorized based on comparisons of the pre- and postintervention measures of static renal function. However, a more meaningful outcome would involve a comparison of dynamic renal function—that is, the stability or rate of change of renal function as measured by the slope of a plot of renal function versus time—before and after interventions. In 2002, Rundback et al.[147] under the auspices of the American Heart Association, published a consensus scientific statement that proposed guidelines for the reporting of renal artery revascularization in clinical trials, and they recommended incorporating a comparison of slope of GFR versus time before and after the intervention, also known as breakpoint analysis, in the reporting of renal outcomes and in defining benefit and failure of treatments. Figure 77.6 shows examples of situations that would be considered benefit and failure. A stabilization or a slowing of the rate of deterioration of renal function would be considered a benefit using this system, but these situations would be considered "no change" or "worsening" in the static comparison system.

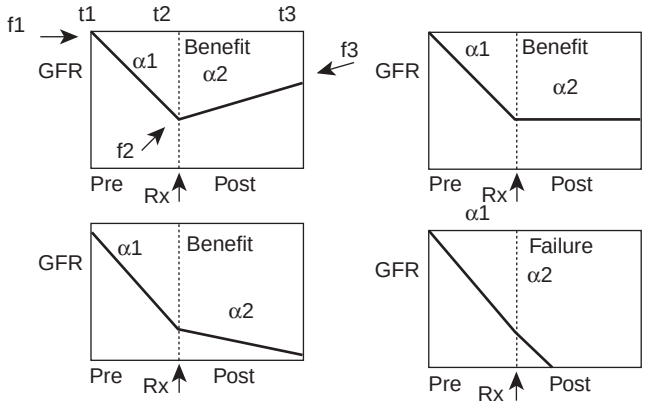

FIGURE 77.6 Breakpoint analysis. α1 indicates slope of GFR before treatment [(f2 − f1)/(t2 − t1)]; α2, slope of GFR after intervention [(f3 − f2)/([t3 − t2)]; Δα, change in slope of GFR after treatment (α2 − α1); f1, value of GFR at a definable time (t1) before intervention; f2, value of GFR at the time of intervention (t2); and f3, value of GFR at a definable follow-up time (t3). *(from ref. 147, with permission.)*

Another important issue to consider when reviewing the literature on RAS is the importance of patient selection for the studies. Important baseline factors include the following: severity of stenosis, degree of threat to renal function imparted by RAS lesions, and severity and acuity of renal dysfunction.

Severity of Stenosis

Stenosis severity can be graded by several measures: minimal luminal diameter, percent stenosis, or by the magnitude of decline in blood pressure measured across the stenosis. Whereas percent stenosis is the most commonly reported measurement, Leesar and others have suggested that minimal luminal diameter and the pressure gradient measured with a pressure sensing 0.014 in guidewire and after a vasodilatory drug are best correlated with clinical outcome.[34,96] Various degrees of stenosis have been used as inclusion criteria in clinical trials and registries, with many studies requiring between 50 and 70% minimal luminal narrowing. The American Heart Association consensus statement on RAS research has recommended that stenosis more than 50% in diameter should be considered the minimum threshold for inclusion in a renal revascularization trial.[147] Given that duplex ultrasound generally categorizes stenoses as greater than 60% diameter stenosis and that it does not have the ability to precisely quantitate the degree of stenosis above this level, this threshold may be used in studies that use this technology. As discussed previously, the hemodynamic consequences of stenotic lesions of less than 70 to 80% are questionable. Only subtle changes in flow patterns have been noted at less critical degrees of narrowing,[153] and these probably have no immediate impact on global oxygenation and no definite effects on renal function.

Degree of Threat to Renal Function Imparted by Renal Artery Stenosis Lesions

Some studies have required that the entire functioning renal mass be threatened by RAS lesions (that is bilateral RAS or unilateral RAS in a solitary functioning kidney), while others have permitted inclusion of

patient with unilateral disease. Obviously there is no risk of symptomatic kidney injury in patients with unilateral disease and a normal non-stenotic kidney. Patients with fibromuscular dysplasia are often included in the studies, however, these patients are also unlikely to develop renal insufficiency as a result of their RAS lesions.

Severity and Acuity of Renal Dysfunction

The degree of renal dysfunction of subjects entering the studies is of critical importance. There may be a "window of opportunity" in which revascularization can produce benefit. In patients with advanced chronic azotemia, renal dysfunction may result from irreversible, intrinsic kidney damage and, therefore not be amenable to treatment by revascularization. Other studies may require that patients have progressive, but not end-stage, renal disease, and such studies would be more likely to show a benefit of interventions if such benefits exist.

Thus, many patients included in these studies (i.e., those with <70% stenosis or those whose whole functioning renal mass was not threatened by RAS lesions or those with nonatherosclerotic RAS) had disease that would not have been expected to cause azotemia. Therefore, one would not expect improvement in renal function in these patients even with successful revascularization, and it could be argued that long-term stability of renal function (and not improvement) would be the desired outcome after revascularization of these patients.

Before proceeding with a discussion of the treatment of ischemic nephropathy, it is worthwhile to briefly address the treatment of renovascular hypertension, as this diagnosis often coexists or is suspected of coexisting in patients with ischemic nephropathy. Separate from the decision whether to offer revascularization with the intention to produce improvement or stabilization of renal function, one must consider whether revascularization should be offered to patients with RAS for the purpose of lowering blood pressures or curing hypertension. Historically, control of blood pressure in RVH had been the major impetus for the development of renal revascularization techniques. However, the accrual over the years of a highly effective armamentarium of antihypertensive drugs that are now capable of inhibiting many blood pressure regulatory pathways has rendered this indication substantially less important. These authors feel that revascularization for the purpose of curing or improving control of hypertension is infrequently indicated in patients with *atherosclerotic* RAS. In such patients, revascularization rarely produces a cure, with studies suggesting cure rates of well less than 10%[17,177,25] which stands in contrast to the treatment of fibromuscular dysplasia where hypertension cure is commonplace.[162] Modern randomized controlled trials indicate that percutaneous transluminal renal artery angioplasty (PTRA) of atherosclerotic RAS is not substantially better in treating hypertension than is medical management in patients with atherosclerotic RAS.[135,177,183] Given the significant risks of the surgical and endovascular procedures, we do not believe that revascularization is indicated in most such patients. Perhaps it could be offered to patients with extremely resistant or severe hypertension, or in those in whom medical therapy is not well tolerated, however even in these settings superiority of medical therapy is not established.

Another group of patients with RVH to whom revascularization should be considered (separate from the indication of treating RVH or IN) includes those who present with heart failure, or "flash pulmonary edema." The latter syndrome has been described in the literature, and it is likely due to labile hypertension, diastolic left ventricular (LV) dysfunction due to chronic hypertension, and sodium retention caused by RAS-induced activation of renin-angiotensin system and renal dysfunction.[133] It is generally accompanied by severely elevated BP (mean SBP of 200 mm Hg in one series). Several retrospective observational studies have suggested that correcting RAS is associated with improvement.[16,42,58,113,134] In a report from Bloch et al.,[16] 17 of 22 patients with bilateral RAS and recurrent pulmonary edema had no further episodes after successful stent placement in one or both renal arteries. The five patients who developed recurrent episodes after stenting were found to have had stent thrombosis or restenosis. However, the use of ACE inhibitors was substantially greater after in these patients after revascularization, and this may also have contributed to the reduced incidence of symptomatic CHF. Currently this represents the only Class I indication for renal artery revascularization in the current AHA guidelines for Peripheral Arterial Disease, although the basis for this recommendation is retrospective observational data and expert consensus that in aggregate is described as level "B" evidence.[72] In fact, there are no randomized controlled trials demonstrating better outcomes in patients with RAS and symptomatic CHF that were revascularized as compared to those treated medically.

MEDICAL MANAGEMENT

As discussed in the section on natural history of IN, the efficacy of medical therapy is not clear. Clearly, anti-atherosclerotic therapies are indicated, such as lipid-lowering therapies, antiplatelet medications, treatment of hyperglycemia, and treatment of

hypertension. The optimal blood pressure in these patients is not known. The low goal of ≤130/80 mmHg that is generally recommended for patients with renal insufficiency may not be optimal for patients with RAS, who may require higher systemic blood pressures to maintain adequate blood flow across a stenosis. Additionally, as discussed previously, ACE-Is and ARBs carry the additional concern that interruption of the ANG II–maintained efferent arteriolar vasoconstriction may cause reductions in glomerular pressure and renal excretory function and as such carry a "black box warning" in their FDA approval. However, recent data suggests that these agents are reasonably safe and more importantly improve outcome. Specifically, observational data from the Province of Ontario analyzed by Hackam et al suggests that treatment of RAS with ACE/ARB is associated with lower CV event rates (10 vs 13%) and need for dialysis (1.5 vs. 2.5%) at the expense of an increased risk of acute kidney injury hospitalizations (1.2 vs. 0.6%).[61] In parallel the use of statins appears to be associated with improved survival, restenosis-free survival after stent revascularization, and lessened lesion progression.[9,33,36,160,161]

Surgical Treatment

It has been shown by many groups that RAS can be successfully revascularized surgically and that renal function may improve or stabilize in some subjects after the intervention. Novick et al.[126] reported on 51 patients with differing anatomies who underwent revascularization procedures. Success was achieved for a wide spectrum of anatomic possibilities, including patients with chronic bilateral arterial occlusion (but good distal runoff), patients with arterial stenosis in a solitary functioning kidney, patients with bilateral high-grade stenosis, and patients with unilateral high-grade disease or occlusion in an atrophic kidney. Overall, improvement occurred in nearly two thirds of patients in the short follow-up period of the study. No control group was included.

Dean et al.[40] reported similar success in a surgical revascularization study. In this study, the authors noted that a renal biopsy to determine kidney viability was usually not helpful and that larger poorly functioning kidneys had the worst prognosis. Successfully revascularized patients with bilateral occlusive disease and moderate azotemia or a serum creatinine above 3.0 mg/dl had the largest fall in serum creatinine after the operation. These results suggest that even patients with advanced disease may benefit from the surgical revascularization. Patent distal vessels without evidence of stenosis are predictive of a good outcome. Successful operative outcomes have also been reported in the circumstance of the totally occluded renal artery with renal parenchyma supplied by collaterals. In a larger series of surgical revascularization from the Cleveland Clinic, Novick et al.[126] reported in 1987 that of the 161 patients, who underwent the procedure, 89% showed improvement or stabilization in renal function and 11 % had progression of chronic kidney disease. As expected, the longer the kidney is occluded, the worse the postoperative function; however, salvage of function after 4 months of renal artery occlusion has been reported. A common limitation of the surgical literature is a lack of a corresponding control group that is treated medically. As a consequence it is oftentimes difficult to understand the absolute or relative

TABLE 77.4 Renal Outcome of Surgical Revascularization in Ischemic Renal Disease

			Renal Function, %				
Source	**Year**	**No. of Patients**	***Improved***	***Stable***	***Worse***	**Mortality, %**	**Duration of Follow-up in Months (Mean, Range)**
Luft et al.[104]	1983	12	67	17	17	17	40 (9–72)
Jamieson et al.[79]	1984	23	65	0	35	17	24 (3–69)
Novick et al.[125]	1987	161	58	31	11	11	39 (6–117)
Hallet et al.[62]	1987	91	22	53	25	7.1	–
Hansen et al.[63]	1992	70	49	36	15	2.5	24 (6–58)
Messina et al.[113]	1992	17	77	12	11	0	29 (7–82)
Bredenberg et al.[18]	1992	40	55	25	20	<3	24(2–60)
Libertino et al.[102]	1992	91	49	35	16	6	35 (6–96)

(*Adapted from Greco BA, Breyer JA. Atherosclerotic ischemic renal disease.* Am J Kidney Dis *1997;29:167-187.*)

advantage and to what degree patient selection plays in the outcomes.

Table 77.4 summarizes the renal outcomes of several of the surgical series that have been reported.[60,145] With the advent of endovascular revascularization techniques, there have been fewer publications on surgical revascularization. These studies are generally reports on the outcomes in different groups, and these are not randomized, controlled trials. Inherent in these studies is some bias in that groups with greater expertise in the procedure are usually the ones reporting results. In contrast, groups with poor outcome probably are less likely to publish results. Therefore, it is not clear that such results are widely achievable. Furthermore, the risk of major vascular surgery in elderly patients with widespread atherosclerosis is a major consideration. It has been generally reported that the major complication rate is 8 to 11% and that the mortality rate is 2 to 8%.[149] These facts have been highlighted in a recent review of a large and contemporary US database of hospital discharge data demonstrating a 10% in-hospital mortality.[118] A follow-up report from this group reanalyzed the dataset to address the effect of hospital volume on outcome. Only a very marginal effect was seen: high-risk patients did no better or worse at high volume centers whereas low risk patients apparently benefited by treatment in a high volume center.[119]

There is a body of literature that reports some dialysis-dependent patients with RAS may benefit from surgical revascularization. Four series from different institutions[7,12,64,85] included 35 patients on maintenance dialysis (including one patient who had been on maintenance dialysis for 13 months) and have demonstrated effective partial recovery of renal function after surgical revascularization, and all patients were able to discontinue dialysis, although the duration of follow-up in these studies is generally short. Serum creatinine levels of some patients returned to normal. Normal renal size, collateral blood flow,[41] nearly normal histology on biopsy, and a rapid pre-ESRD loss of renal function were associated with salvage. In general however, surgical revascularization has been supplanted by percutaneous methods such as angioplasty for FMD and stenting for atherosclerosis, given the prohibitive mortality associated with surgical revascularization.

Renal Artery Angioplasty

Percutaneous transluminal renal angioplasty (PTRA) is a less invasive alternative to surgical revascularization whose utility has largely been relegated to treatment of fibromuscular dysplasia, supplanted by stenting for the treatment of atherosclerotic renal stenoses. There is only one head-to-head comparison of angioplasty and surgical revascularization. In 1993, Weibull et al.[184] demonstrated relative equivalence when PTRA and surgical revascularization were directly compared in a cohort of 58 patients with unilateral RAS. Improved or stable renal function was seen in 83% after PTRA and 72% after surgery.[184] Much of the literature concentrates on renal angioplasty interventions targeted primarily at the treatment of RVH rather than IN. Table 77.5 provides a summary of renal outcomes following PTRA from several studies.[60,145] The complication rates of PTRA are variable. Typical rates of major complications have been reported as 3 to 15%,[60,70,140] and these may include bleeding at the puncture site, pseudoaneurysm of the femoral artery, rupture or thrombosis of the renal artery, dissection of the renal artery or access artery,

TABLE 77.5 Renal Outcome of Percutaneous Renal Angioplasty for Ischemic Renal Disease

			Renal Function Result, %				
Source	**Year**	**No. of Patients**	***Improved***	***Stable***	***Worse***	**Mortality, %**	**Duration of Follow-up in Months (Mean, Range)**
Luft et al.[104]	1983	12	25	42	33	0	8 (1–25)
Sos et al.[165]	1986	55	47	35	18	NA	16 (4–40)
Bell et al.[11]	1987	20	35	50	15	0	18 (1–60)
Martin et al.[107]	1988	79	43	57[a]	—	1	11 (0–42)
Canzanello et al.[25]	1989	69	52[b]	—	48	3	29
O'Donovan et al.[127]	1992	17	53	12	35	29	–
Bonelli et al.[17]	1995	320	27	53	20	2.2	24 (0–157)

(Adapted from Greco BA, Breyer JA. Atherosclerotic ischemic renal disease. Am J Kidney Dis *1997;29:167-187.)*

[a]*Sum of stable and worse.*

[b]*Sum of improved and stable.*

—, Not reported ; NA, not applicable.

the cholesterol emboli syndrome, and radiocontrast nephropathy. Expected mortality rates have been reported to be 1% to 6%.[60,136,145]

In 2000, van Jaarsveld et al.[177] published the results of the Dutch Renal Artery Stenosis Intervention Cooperative (DRASTIC) Study Group, the largest randomized controlled trial to address the use of renal artery angioplasty without stenting. In this study, 106 patients with hypertension who had atherosclerotic renal-artery stenosis and a serum creatinine of 2.3 mg/dl or less were randomly assigned to undergo PTCA (n = 56) or medical therapy (n = 50). RAS was defined as at least 50% stenosis, and patients with a solitary kidney were excluded. Twenty-one percent of the subjects had less than 70% stenosis and only 23% had bilateral RAS. Nine percent of the medical group progressed to total occlusion. Creatinine clearance was better in the PTRA group at 3 months (70 vs. 59 ml/min; p = .03), but the same at 12 months (70 vs. 62 ml/min; p = .11). Twenty-two of the 50 patients in the drug treatment group crossed over to PTRA after 3 months: 14 patients because of persistent hypertension on more than two drugs and eight patients because of an increase of 0.2 mg/dl of the serum creatinine or worsening of the time-activity curve on renal scintigraphy. The results were inconclusive regarding the utility for the treatment of ischemic nephropathy. The study population was small and included many patients who had hemodynamically inconsequential RAS and/or whose whole functioning renal mass was not clearly threatened by the index RAS lesions. Therefore, one would not expect the RAS to cause major renal dysfunction over the follow-up period, thereby lessening the potential benefit of successful revascularization. Even more importantly, the liberal use of rescue revascularization (crossover) followed by an intention-to-treat analysis of the data may have reduced any treatment advantage.

Renal Artery Stenting

Endovascularly deployed stents appear to provide better prospects for restenosis-free long-term patency than angioplasty alone. This is especially true for ostial stenoses which constitute the majority of atherosclerotic stenoses. Stenting achieves higher initial technical success rates, improved immediate patency, and lower restenosis rates in comparison to balloon angioplasty alone. Technical problems with stent placement include malpositioning, embolization of the stent, main renal artery rupture, distal arterial wire perforation, dissection, or branch vessel occlusion. Stents that are coated with and elute antiproliferative medications (such as sirolimus, everolimus, or paclitaxel) have shown success in reducing restenosis rates in coronary arteries.[84,150,167,185] However, there has been only one study of a drug coated "renal" stent, the sirolimus-eluting Genesis stent, which failed to meet its pre-specified performance metrics and work on this platform was abandoned.[190] There is limited data suggesting that drug-eluting coronary stents may have some utility for the treatment of in-stent restenosis but the data remains mixed.[88,191]

Multiple studies on renal artery stenting have been published over the past decade. In the preliminary reports of the U.S. Multicenter Trial, which involved 304 stents placed in 296 renal arteries in 263 patients whose disease was 80% ostial and 98% atherosclerotic, the technical success 95% and the restenosis rate was 32.7% at 6 months. Among 123 patients with serum creatinine above 1.5 mg/dl, renal function improved in 34%, remained stable in 39%, and deteriorated in 27%.[142] In a 1999 review of 10 studies that included 416 stents placed in 379 patients (with 97% of stenoses being atherosclerotic and 80% being ostial), Isles et al.[76] found a 96 to 100% technical success rate and a 16% restenosis at 6 to 12 months. Serum creatinine improved in 26%, stabilized in 48%, and deteriorated in 26% of patients whose renal function was initially impaired (serum creatinine >1.5 mg/dl). In 2000, Leertouwer et al.[94] published a meta-analysis of 14

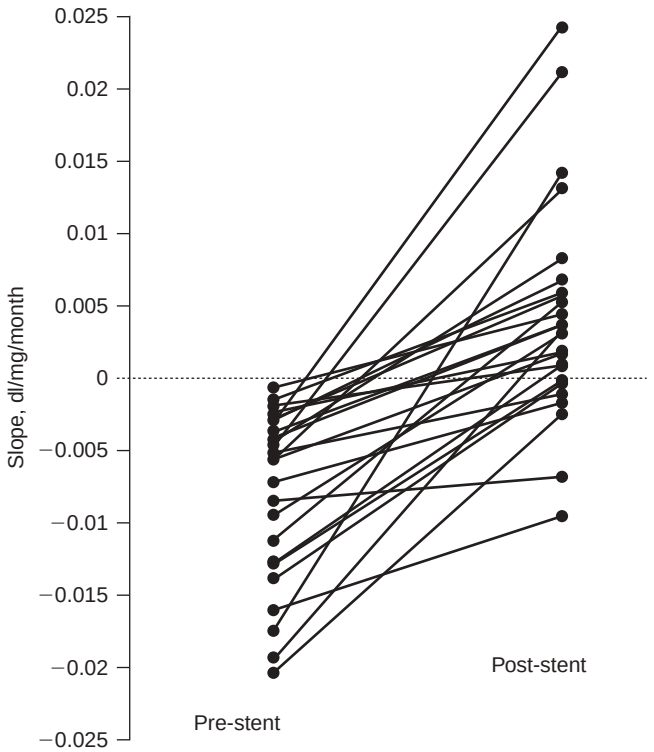

FIGURE 77.7 Slopes of plots of reciprocal of serum creatinine measured before and after renal artery stent deployment in 25 patients with global renovascular disease and chronic renal failure. Negative and positive slopes depict deteriorating and improving renal function, respectively. *(From ref. [182], with permission.)*

studies of stenting in 678 patients compared with ten studies of PTRA in 644 patients. They found that the restenosis rate at 6 to 29 months was 17% after stenting and 26% after PTRA; after stenting, renal function improved in 30%, stabilized in 38%, and worsened in 32%; and the improvement rate was greater after PTRA (38%, $p < .001$). Burket et al.[23] found an early decline in blood pressure after stenting, and a decrease in the number of required medicines to treat hypertension.

Studies by Harden and Watson[65,182] suggest that stenting may improve the outcome of IN, although as is discussed later, a substantial criticism of this work is the absence of a concurrent control group for comparison. The Watson study focused on patients with progressive, but not severe, chronic renal insufficiency and with global high-grade renovascular obstruction.[182] Renal artery stenting was performed in all of the 33 patients studied who had as criteria for inclusion into the analysis progressive renal insufficiency (defined by serum creatinine >1.5 mg/dl [mean, 2.1 mg/dl]), a negative slope of 1/serum creatinine, and more than 70% RAS producing global renovascular obstruction (bilateral renal artery stenosis or unilateral stenosis in the presence of a solitary or single functional kidney). Of 25 patients who had a mean follow-up of 20 months, the mean slope of 1/creatinine improved from −0.0079 to +0.0043 dl/mg per month with preservation of renal size while patient survival was 90%. As shown in Fig. 77.7, stabilization or improvement in renal function was documented in all surviving subjects. There was only one procedure-related complication—a femoral artery hematoma. Although the findings of these studies support the idea of using stenting to treat IN, the lack of a control group limits the strength and interpretability of the conclusions.

More recently two randomized trials have been completed that directly compared medical therapy alone against medical therapy with stenting, the STAR and ASTRAL trials.[1,10] The STAR trial was conducted by a Dutch cooperative group and tested in a cohort of 140 patients whether stenting could reduce by 50% the proportion of patients that experienced a 20% decline in GFR. Unfortunately 28% of patients who were enrolled in the stent arm had no significant renal artery stenosis and were not treated. Not surprisingly, with a substantial false positive rate of enrollment, in addition to what was likely an over-estimation of the likely treatment effect of stenting, the study authors concluded that "confidence bounds…are compatible with both efficacy and harm, so the finding is inconclusive." ASTRAL, published in late 2009, had a much larger enrollment of 806 randomized patients. However ASTRAL also had a high rate of false positive inclusion, approximately 17%, in addition to 5% of subjects in whom stenting was attempted but not completed. There was also selection bias inherent in the study design as patients were entered only if the enrolling center felt that the subject did not definitely require revascularization. Despite this the study demonstrated a trend toward an improvement in the primary endpoint of slope of reciprocal Cr (-0.0713×10^{-3} vs. -0.13×10^{-3} micromole/L/yr, $p = 0.06$). However this difference was neither statistically nor clinically significant, as were the findings of the secondary analyses. From these recent studies we would conclude that: (1) If stenting has an effect on the progression of ischemic nephropathy it is likely modest in size, (2) great caution should be utilized to avoid over-analyzing these results due to the methodologic issues that confound their interpretation: high rates of false + enrollment lack of centralized analysis of critical study measures such as stenosis severity or renal function, and the lack of a consistent, specified medical intervention. Some have criticized the ASTRAL result for an apparently higher than expected rate of complications and lower than expected success rate, however, it is entirely unclear whether the ASTRAL result is better reflective of the "realities of stenting" when compared to single center publications, or whether technical issues were more excessive in this study.

Evolution in technology may modify the future approach to the treatment of renal artery stenosis. Several investigators have now reported retrospective or observational series that suggest that Embolic Protection Devices (EPD) may improve the result of renal artery revascularization, at least as it relates to the preservation of renal function.[47,69,73] Thus far there has been one prospective trial of EPD use, a study that also tested in a two by two factorial design a platelet glycoprotein IIbIIIa inhibitor abciximab, administered in a double-blind fashion.[37] Abciximab overall, and more specifically when administered in conjunction with the EPD, resulted in improved renal function. More surprisingly, the analysis of the embolic debris demonstrated a high rate of platelet-rich emboli captured by the EPD, suggesting that these lesions may be more thrombotic than previously appreciated. Whether more widespread adoption of EPDs or potent platelet inhibitors will generally improve the effect of renal artery stenting is unknown but these results raise the possibility that the net effect of the revascularization procedure is determined by the benefit of improved blood flow balanced by injury due to atheromatous or thrombotic debris.[37]

Currently ongoing is a large prospective, National Institutes of Health–sponsored multicenter randomized trial to test the effect of stenting when added to a background of aggressive medical therapy. Known as CORAL, for Cardiovascular Outcomes in Renal Atherosclerotic Lesions, it began in the spring of 2005

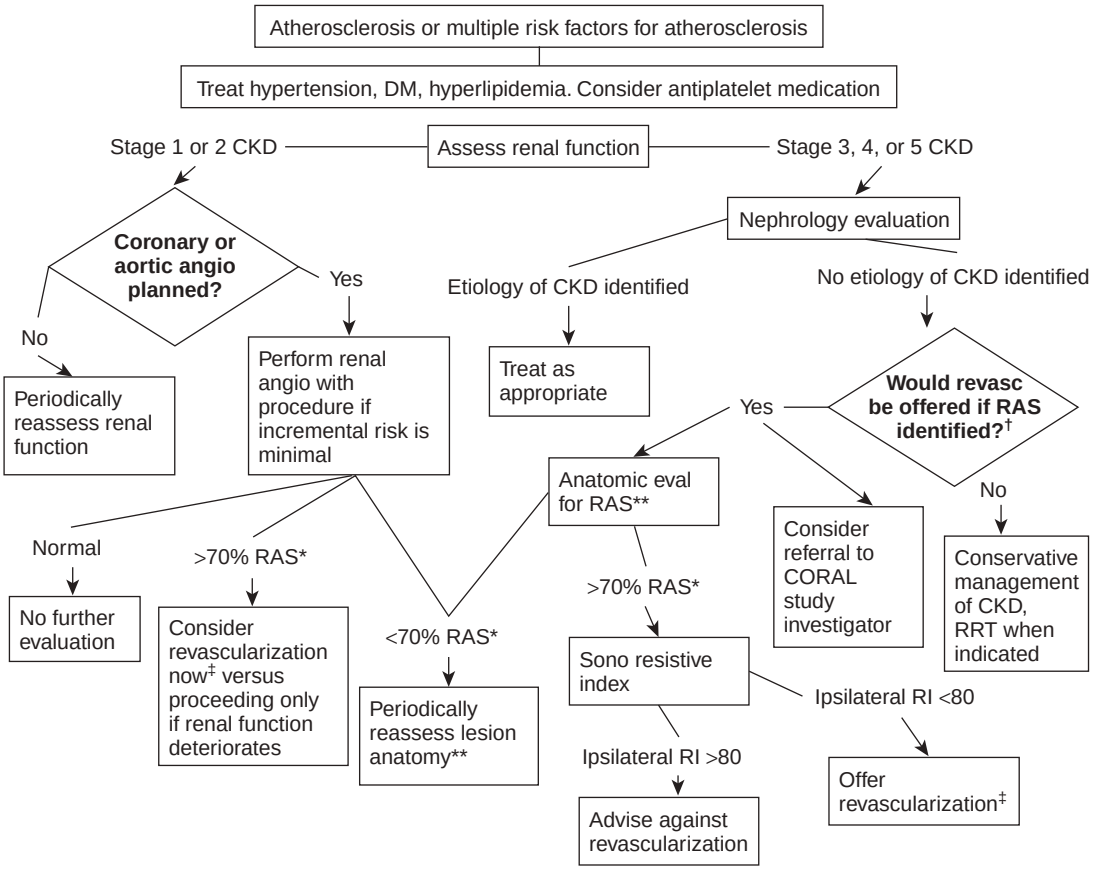
Atherosclerosis or multiple risk factors for atherosclerosis
Treat hypertension, DM, hyperlipidemia. Consider antiplatelet medication
Stage 1 or 2 CKD
Assess renal function
Stage 3, 4, or 5 CKD
Coronary or aortic angio planned?
Yes
No
Periodically reassess renal function
Perform renal angio with procedure if incremental risk is minimal
Nephrology evaluation
Etiology of CKD identified
No etiology of CKD identified
Treat as appropriate
Would revasc be offered if RAS identified?†
Yes
No
Anatomic eval for RAS**
Consider referral to CORAL study investigator
Conservative management of CKD, RRT when indicated
Normal
>70% RAS*
<70% RAS*
>70% RAS*
No further evaluation
Consider revascularization now‡ versus proceeding only if renal function deteriorates
Periodically reassess lesion anatomy**
Sono resistive index
Ipsilateral RI <80
Ipsilateral RI >80
Offer revascularization‡
Advise against revascularization

FIGURE 77.8 *60% if sonoduplex is used as diagnostic modality. **Magnetic resonance angiography (MRA) or computed tomography angiography (CTA) are generally tests of choice. Other options are discussed in text. Also consider renal angiography during cardiac catheterization or aortic angiography if either of these procedures is indicated otherwise in these patients. †Very limited life expectancy, patient preference against revascularization, and advanced longstanding chronic renal insufficiency are factors that may persuade against revascularization and would make further evaluation futile. ‡The renal artery revascularization procedure of choice is generally percutaneous transluminal renal artery angioplasty (PTRA) with stenting. Surgical revascularization could be considered if aortic or other intra-abdominal vascular surgical procedure is indicated for other reasons and if perioperative risk is not prohibitive. CKD, chronic kidney disease, with stages as defined by K/DOQI; RRT, renal replacement therapy; RI, resistive index; RAS, renal artery stenosis; revasc, revascularization.

and will include approximately 1000 patients with hypertension and documented significant RAS.[38] Patients are randomized to medical therapy with or without renal artery stenting with follow up for a composite endpoint of cardiovascular and renal events. It is designed to test the hypothesis that renal artery stenting (along with medical therapy) reduces cardiovascular and renal morbidity and mortality.

Recommended Approach

There are many different reasonable approaches and algorithms for the diagnosis and management of patients with IN, and the recommendations that follow and that are summarized in Figure 77.8 remain opinion-based, as data are not sufficient to make definitive recommendations. In patients at high risk for atherosclerosis or in those with known atherosclerosis, renal function should be monitored and anti-atherosclerotic life style and pharmacologic interventions and risk factor reduction should be used. A high degree of suspicion for coexisting coronary artery disease should be maintained. If renal insufficiency is found, appropriate nephrologic evaluation should be undertaken and this should include an assessment for ischemic nephropathy. In many patients an anatomic evaluation of the renal arteries is warranted to further stratify their stage of disease and expected outcome. Duplex ultrasonography is currently the test of choice since it is entirely non-invasive and involves no nephrotoxic contrast agents, if appropriately trained technologists and interpreting physicians are available. MRA is an alternative in centers where experienced ultrasonagraphers are not available but is limited to patients with an estimated GFR of greater than 40 ml/min, due to the risk of nephrogenic systemic sclerosis with administration of gadolinium to patients with impaired renal function. In

patients with mild renal dysfunction a CTA may be *considered*. At other centers MRA without contrast may become an alternative test.

Once one or more renal artery stenoses are identified medical therapy with aspirin or another anti-platelet agent, a statin and an agent to interrupt the renin-angiotensin system such as an ACE or ARB should be instituted. Renal function as assessed by serum creatinine and serum potassium should be followed carefully during institution of such treatment. In addition careful attention to blood pressure control using agents such as calcium antagonists, combination β- α-adrenergic blockers and diuretics are appropriate. During treatment with medical therapy follow-up of lipids, HbA1c (if appropriate) and blood pressure is of great importance, with titration of medications to achieve guidelines-driven outcomes.

The decision to refer for revascularization should be made with circumspection. Critical in the decision include an objective measure of stenosis severity, recognizing that many of the tomographic imaging studies such as CTA and MRA grossly over-estimate lesion severity. As such, if the patient is referred for an invasive assessment, at a minimum the evaluation of the lesion severity should be done objectively and oftentimes requires measurement of a pressure gradient with an 0.014 inch pressure sensing guidewire to discern if the apparent stenosis is of any functional significance. In parallel to the lesion assessment a critical review should be given to potential benefit for revacularization balanced against the expected risks of the specific patient. In general one can expect a greater potential for improvement in renal function in patients with advanced chronic kidney disease, however this is associated with less renal function reserve and a higher probability of dialysis dependence if complications occur or renal function fails to improve. At this time there is little role for captopril-augmented renal scintigraphy, with the possible exception for the evaluation of the occluded renal artery where the scintigram will occasionally demonstrate a viable kidney that contributes significantly to GFR and that may benefit from surgical revascularization. At this time, given the results of ASTRAL that demonstrate either a small or marginal treatment effect, a compelling case could be made for reserving renal artery revacularization to those patients who have clearly failed medical therapy or are willing to participate in a clinical outcomes trial.

SUMMARY

This chapter was intended to provide an intellectual framework that will improve the clinician's understanding of the complex issues involved in the management of patients with ischemic renal disease. By understanding the mechanisms and limits of renal autoregulation, one can appreciate how the kidney compensates for the renal hypoperfusion that RAS causes. The pharmacologic interference of this process may cause a decrease in renal function although this scenario is less frequent than was once supposed. RAS may cause chronic and or even irreversible renal injury via a complicated pathophysiologic process, and this is an important cause of renal morbidity. The diagnosis of ischemic nephropathy is often difficult but important to make because anti-atherosclerotic medical treatments will likely benefit patients and selected patients may benefit from revascularization. A recommended approach to the diagnosis and treatment of RAS is provided, but it should be noted that the results of ongoing trials may soon alter these recommendations.

References

[1] The Astral Investigators. Revascularization versus medical therapy for renal-artery stenosis. N Engl J Med 2009;361:1953–62.

[2] Randomised placebo-controlled trial of effect of ramipril on decline in glomerular filtration rate and risk of terminal renal failure in proteinuric, non-diabetic nephropathy. The GISEN Group (Gruppo Italiano di Studi Epidemiologici in Nefrologia). Lancet 1997;349:1857–1863.

[3] Aiken JW, Vane JR. Intrarenal prostaglandin release attenuates the renal vasoconstrictor activity of angiotensin. J Pharmacol Exp Ther 1973;184:678–87.

[4] Alkhunaizi AM, Chapman A. Renal artery stenosis and unilateral focal and segmental glomerulosclerosis. Am J Kidney Dis 1997;29:936–41.

[5] Anderson JL, Carlquist JF, Muhlestein JB, Horne BD, Elmer SP. Evaluation of C-reactive protein, an inflammatory marker, and infectious serology as risk factors for coronary artery disease and myocardial infarction. J Am Coll Cardiol 1998;32:35–41.

[6] Appel RG, Bleyer AJ, Reavis S, Hansen KJ. Renovascular disease in older patients beginning renal replacement therapy. Kidney Int 1995;48:171–6.

[7] Ascer E, Gennaro M, Rogers D. Unilateral renal artery revascularization can salvage renal function and terminate dialysis in selected patients with uremia. J Vasc Surg 1993;18:1012–8.

[8] Baboolal K, Evans C, Moore RH. Incidence of end-stage renal disease in medically treated patients with severe bilateral atherosclerotic renovascular disease. Am J Kidney Dis 1998;31: 971–7.

[9] Bates MC, Campbell JE, Stone PA, Jaff MR, Broce M, Lavigne PS. Factors affecting long-term survival following renal artery stenting. Catheter Cardiovasc Interv 2007;69(7):1037–43.

[10] Bax L, Woittiez AJ, Kouwenberg HJ, Mali WP, Buskens E, Beek FJ, et al. Stent placement in patients with atherosclerotic renal artery stenosis and impaired renal function. Ann Intern Med 2009;150:840–8.

[11] Bell GM, Reid J, Buist TA. Percutaneous transluminal angioplasty improves blood pressure and renal function in renovascular hypertension. Q J Med 1987;63:393–403.

[12] Besarab A, Brown RS, Rubin NT, Salzman E, Wirthlin L, Steinman T, et al. Reversible renal failure following bilateral renal artery occlusive disease. Clinical features, pathology, and the role of surgical revascularization. JAMA 1976;235:2838–41.

[13] Bhowmik D, Dash SC, Jain D, Agarwal SK, Tiwari SC, Dinda AK. Renal artery stenosis and focal segmental glomerulosclerosis in the contralateral kidney. Nephrol Dial Transplant 1998;13: 1562–4.
[14] Blantz RC, Gabbai FB. Effect of angiotensin II on glomerular hemodynamics and ultrafiltration coefficient. Kidney Int 1987; (Suppl. 20):S108–11.
[15] Blantz RC, Konnen KS, Tucker BJ. Angiotensin II effects upon the glomerular microcirculation and ultrafiltration coefficient of the rat. J Clin Invest 1976;57:419–34.
[16] Bloch MJ, Trost DW, Pickering TG, Sos TA, August P. Prevention of recurrent pulmonary edema in patients with bilateral renovascular disease through renal artery stent placement. Am J Hypertens 1999;12:1–7.
[17] Bonelli FS, McKusick MA, Textor SC, Kos PB, Stanson AW, Johnson CM, et al. Renal artery angioplasty: technical results and clinical outcome in 320 patients. Mayo Clin Proc 1995;70: 1041–52.
[18] Bredenberg CE, Sampson LN, Ray FS, Cormier RA, Heintz S, Eldrup-Jorgensen J. Changing patterns in surgery for chronic renal artery occlusive diseases. J Vasc Surg 1992;15:1018–23.
[19] Brewster DC, Retana A, Waltman AC, Darling RC. Angiography in the management of aneurysms of the abdominal aorta: its value and safety. N Engl J Med 1975;292:822–5.
[20] Briggs JP, Schnermann JB. Whys and wherefores of juxtaglomerular apparatus function. Kidney Int 1996;49:1724–6.
[21] Brown JJ, Davies DL, Morton JJ, Robertson JI, Cuesta V, Lever AF, et al. Mechanism of renal hypertension. Lancet 1976;1: 1219–21.
[22] Burke TJ, Schrier RW. Pathophysiology of cell ischemia. In: Schrier RW, Gottschalk CW, editors. Diseases of the kidney. Boston: Little, Brown; 1993. p. 1257–86.
[23] Burket MA, Cooper CJ, Kennedy DJ, Brewster PS, Ansel GM, Moore JA, et al. Renal artery angioplasty and stent placement: predictors of a favorable outcome. Am Heart J 2000;139:64–71.
[24] Cantin M, Solymoss B, Benchimol S, Desormeaux Y, Langlais J, Ballak M. Metaplastic and mitotic activity of the ischemic (endocrine) kidney in experimental renal hypertension. Am J Pathol 1979;96:545–65.
[25] Canzanello VJ, Millan VG, Spiegel JE, Ponce PS, Kopelman RI, Madias NE. Percutaneous transluminal renal angioplasty in management of atherosclerotic renovascular hypertension: results in 100 patients. Hypertension 1989;13:163–72.
[26] Caps MT, Perissinotto C, Zierler RE, Polissar NL, Bergelin RO, Tullis MJ, et al. Prospective study of atherosclerotic disease progression in the renal artery. Circulation 1998;98:2866–72.
[27] Caps MT, Zierler RE, Polissar NL, Bergelin RO, Beach KW, Cantwell-Gab K, et al. Risk of atrophy in kidneys with atherosclerotic renal artery stenosis. Kidney Int 1998;53:735–42.
[28] Chabova V, Schirger A, Stanson AW, McKusick MA, Textor SC. Outcomes of atherosclerotic renal artery stenosis managed without revascularization. Mayo Clin Proc 2000;75:437–44.
[29] Chade AR, Rodriguez-Porcel M, Grande JP, Krier JD, Lerman A, Romero JC, et al. Distinct renal injury in early atherosclerosis and renovascular disease. Circulation 2002;106:1165–71.
[30] Chade AR, Rodriguez-Porcel M, Grande JP, Zhu X, Sica V, Napoli C, et al. Mechanisms of renal structural alterations in combined hypercholesterolemia and renal artery stenosis. Arterioscler Thromb Vasc Biol 2003;23:1295–301.
[31] Chade AR, Rodriguez-Porcel M, Herrmann J, Krier JD, Zhu X, Lerman A, et al. Beneficial effects of antioxidant vitamins on the stenotic kidney. Hypertension 2003;42:605–12.
[32] Chade AR, Rodriguez-Porcel M, Herrmann J, Zhu X, Grande JP, Napoli C, et al. Antioxidant intervention blunts renal injury in experimental renovascular disease. J Am Soc Nephrol 2004;15:958–66.
[33] Cheung CM, Patel A, Shaheen S, Cain S, Eddington H, Hegarty J, et al. The effects of statins on the progression of atherosclerotic renovascular disease. Nephron Clin Pract 2007;107:c35–42.
[34] Colyer WR, Cooper CJ, Burket MW, Thomas WJ. Utility of a 0.014 pressure-sensing guidewire to assess renal artery translesional systolic pressure gradients. Cathet Cardiovasc Intervent 2003;59:372–7.
[35] Connolly JO, Higgins RM, Walters HL, Mackie AD, Drury PL, Hendry BM, et al. Presentation, clinical features and outcome in different patterns of atherosclerotic renovascular disease. QJM 1994;87:413–21.
[36] Corriere MA, Edwards MS, Pearce JD, Andrews JS, Geary RL, Hansen KJ. Restenosis after renal artery angioplasty and stenting: incidence and risk factors. J Vasc Surg 2009;50(4):813–9.
[37] Cooper CJ, Haller ST, Colyer W, Steffes M, Burket MW, Thomas WJ, et al. Embolic protection and platelet inhibition during renal artery stenting. Circulation 2008;117(21):2752–60.
[38] Cooper CJ, Murphy TP, Matsumoto A, Steffes M, Cohen DJ, Jaff M, et al. Stent revascularization for the prevention of cardiovascular and renal events among patients with renal artery stenosis and systolic hypertension: rationale and design of the CORAL trial. Am Heart J 2006;152(1):59–66.
[39] Crutchley TA, Pearce JD, Craven TE, Stafford JM, Edwards MS, Hansen KJ. Clinical utility of the resistive index in atherosclerotic renovascular disease. J Vasc Surg 2009;49:148–55.
[40] Dean RH, Kieffer RW, Smith BM, Oates JA, Nadeau JH, Hollifield JW, et al. Renovascular hypertension: anatomic and renal function changes during drug therapy. Arch Surg 1981;116:1408–15.
[41] Dean RH, Lawson JD, Hollifield JW, Shack RB, Polterauer P, Rhamy RK. Revascularization of the poorly functioning kidney. Surgery 1979;85:44–52.
[42] Duclos J, Goecke H, Opazo M. Flash pulmonary edema: when the kidney causes decompensation of the heart. Rev Med Chil 2002;130:1033–6.
[43] Dunn MJ, Hood VL. Prostaglandins and the kidney. Am J Physiol 1977;233:169–84.
[44] Dwyer KM, Vrazas JI, Lodge RS, Humphery TJ, Schlicht SM, Murphy BF, et al. Treatment of acute renal failure caused by renal artery occlusion with renal artery angioplasty. Am J Kidney Dis 2002;40(1):189–94.
[45] Edwards RM. Segmental effects of norepinephrine and angiotensin II on isolated renal microvessels. Am J Physiol 1983;244: F526–34.
[46] Edwards MS, Corriere MA, Craven TE, Pan XM, Rapp JH, Pearce JD, et al. Atheroembolism during percutaneous renal artery revascularization. J Vasc Surg 2007;46:55–61.
[47] Edwards MS, Craven BL, Stafford J, Craven TE, Sauve KJ, Ayerdi J, et al. Distal embolic protection during renal artery angioplasty and stenting. J Vasc Surg 2006;44(1):128–35.
[48] Edwards MS, Craven TE, Burke GL, Dean RH, Hansen KJ. Renovascular disease and the risk of adverse coronary events in the elderly: a prospective, population-based study. Arch Intern Med 2005;165(2):207–13.
[49] Eklöf H, Ahlström H, Magnusson A, Andersson LG, Andrén B, Hägg A, et al. A prospective comparison of duplex ultrasonography, captopril renography, MRA, and CTA in assessing renal artery stenosis. Acta Radiol 2006;47(8):764–74.
[50] Fatica RA, Port FK, Young EW. Incidence trends and mortality in end-stage renal disease attributed to renovascular disease in the United States. Am J Kidney Dis 2001;37:1184–90.
[51] Deleted in press.

[52] Fukui T, Ishizaka N, Rajagopalan S, Laursen JB, Capers Q, Taylor WR, et al. p22phox mRNA expression and NADPH oxidase activity are increased in aortas from hypertensive rats. Circ Res 1997;80:45–51.

[53] Gansevoort RT, Sluiter WJ, Hemmelder MH, de Zeeuw D, de Jong PE. Antiproteinuric effect of blood-pressure-lowering agents: a meta-analysis of comparative trials. Nephrol Dial Transplant 1995;10:1963–74.

[54] Gephardt GN, Tubbs RR, Novick AC, McMahon JT, Pohl MA. Renal artery stenosis, nephrotic-range proteinuria, and focal and segmental glomerulosclerosis. Cleve Clin Q 1984;51:371–6.

[55] Giatras I, Lau J, Levey AS. Effect of angiotensin-converting enzyme inhibitors on the progression of nondiabetic renal disease: a meta-analysis of randomized trials. angiotensin-converting-enzyme inhibition and progressive renal disease study group. Ann Intern Med 1997;127:337–45.

[56] Gobe GC, Axelsen RA, Searle JW. Cellular events in experimental unilateral ischemic renal atrophy and in regeneration after contralateral nephrectomy. Lab Invest 1990;63:770–9.

[57] Goldblatt H, Lynch J, Hanzal R, Summerville W. Studies on experimental hypertension. I. The production of persistent elevation of systolic blood pressure by means of renal ischemia. J Exp Med 1934;59:347–79.

[58] Gray BH, Olin JW, Childs MB, Sullivan TM, Bacharach JM. Clinical benefit of renal artery angioplasty with stenting for the control of recurrent and refractory congestive heart failure. Vasc Med 202;7:275–279.

[59] Grayston JT, Kuo CC, Coulson AS, Campbell LA, Lawrence RD, Lee MJ, et al. Chlamydia pneumoniae (TWAR) in atherosclerosis of the carotid artery. Circulation 1995;92:3397–400.

[60] Greco BA, Breyer JA. Atherosclerotic ischemic renal disease. Am J Kidney Dis 1997;29:167–87.

[61] Hackam DG, Duong-Hua ML, Mamdani M, Li P, Tobe SW, Spence JD, et al. Angiotensin inhibition in renovascular disease: a population-based cohort study. Am Heart J 2008;156(3): 549–55.

[62] Hallett Jr. JW, Fowl R, O'Brien PC, Bernatz PE, Pairolero PC, Cherry Jr. KJ, et al. Renovascular operations in patients with chronic renal insufficiency: do the benefits justify the risks? J Vasc Surg 1987;5:622–7.

[63] Hansen KJ, Ditesheim JA, Metropol SH, Canzanello V, Graves J, Plonk Jr. GW, et al. Management of renovascular hypertension in the elderly population. J Vasc Surg 1989;10: 266–73.

[64] Hansen KJ, Thomason RB, Craven TE, Fuller SB, Keith DR, Appel RG, et al. Surgical management of dialysis-dependent ischemic nephropathy. J Vasc Surg 1995;21:197–209.

[65] Harden PN, MacLeod MJ, Rodger RS, Baxter GM, Connell JM, Dominiczak AF, et al. Effect of renal-artery stenting on progression of renovascular renal failure. Lancet 1997;349(9059): 1133–6.

[66] Harding MB, Smith LR, Himmelstein SI, Harrison K, Phillips HR, Schwab SJ, et al. Renal artery stenosis: prevalence and associated risk factors in patients undergoing routine cardiac catheterization. J Am Soc Nephrol 1992;2:1608–16.

[67] Hawkins Jr. IF, Wilcox CS, Kerns SR, Sabatelli FW. CO2 digital angiography: a safer contrast agent for renal vascular imaging? Am J Kidney Dis 1994;24:685–94.

[68] Hebert LA, Bain RP, Verme D, Cattran D, Whittier FC, Tolchin N, et al. Remission of nephrotic range proteinuria in type I diabetes. collaborative study group. Kidney Int 1994;46: 1688–93.

[69] Henry M, Henry I, Polydorou A, Hugel M. Embolic protection for renal artery stenting. *J Cardiovasc Surg* (Torino) 2008;49(5): 571–89.

[70] Higashi Y, Sasaki S, Nakagawa K, Matsuura H, Oshima T, Chayama K. Endothelial function and oxidative stress in renovascular hypertension. N Engl J Med 2002;346:1954–62.

[71] Hiramoto J, Hansen KJ, Pan XM, Edwards MS, Sawhney R, Rapp JH. Atheroemboli during renal artery angioplasty: an ex vivo study. J Vasc Surg 2005;41(6):1026–30.

[72] Hirsch AT, Haskal ZJ, Hertzer NR, Bakal CW, Creager MA, Halperin JL, et al. ACC/AHA 2005 practice guidelines for the management of patients with peripheral arterial disease (lower extremity, renal, mesenteric, and abdominal aortic). Circulation 2006;113(11):e463–654.

[73] Holden A, Hill A. Renal angioplasty and stenting with distal protection of the main renal artery in ischemic nephropathy: early experience. J Vasc Surg 2003;38(5):962–8.

[74] Holley KE, Hunt JC, Brown Jr. AL, Kincaid OW, Sheps SG. Renal artery stenosis: a clinical-pathologic study in normotensive and hypertensive patients. Am J Med 1964;37: 14–22.

[75] Huot SJ, Hansson JH, Dey H, Concato J. Utility of captopril renal scans for detecting renal artery stenosis. Arch Intern Med 2002;162:1981–4.

[76] Isles CG, Robertson S, Hill D. Management of renovascular disease: a review of renal artery stenting in ten studies. QJM 1999;92:159–67.

[77] Itoh K. 99mTc-MAG3: review of pharmacokinetics, clinical application to renal diseases and quantification of renal function. Ann Nucl Med 2001;15:179–90.

[78] Jackson B, McGrath BP, Matthews PG, Wong C, Johnston CI. Differential renal function during angiotensin converting enzyme inhibition in renovascular hypertension. Hypertension 1986;8:650–4.

[79] Jamieson GG, Clarkson AR, Woodroffe AJ, Faris I. Reconstructive renal vascular surgery for chronic renal failure. Br J Surg 1984;71:338–40.

[80] Jean WJ, al Bitar I, Zwicke DL, Port SC, Schmidt DH, Bajwa TK. High incidence of renal artery stenosis in patients with coronary artery disease. Cathet Cardiovasc Diagn 1994;32: 8–10.

[81] Johansson M, Herlitz H, Jensen G, Rundqvist B, Friberg P. Increased cardiovascular mortality in hypertensive patients with renal artery stenosis. Relation to sympathetic activation, renal function and treatment regimens. J Hypertens 1999;17: 1743–50.

[82] Johnston RJ, Alkhunaizi AM. Unilateral focal segmental glomerulosclerosis with contralateral sparing on the side of renal artery stenosis. AJR Am J Roentgenol 1999;172:35–7.

[83] Kasiske BL, Kalil RS, Ma JZ, Liao M, Keane WF. Effect of antihypertensive therapy on the kidney in patients with diabetes: a meta-regression analysis. Ann Intern Med 1993;118:129–38.

[84] Kastrati A, Mehilli J, von Beckerath N, Dibra A, Hausleiter J, Pache J, et al. Sirolimus-eluting stent or paclitaxel-eluting stent vs balloon angioplasty for prevention of recurrences in patients with coronary in-stent restenosis: a randomized controlled trial. JAMA 2005;293:165–71.

[85] Kaylor WM, Novick AC, Ziegelbaum M, Vidt DG. Reversal of end stage renal failure with surgical revascularization in patients with atherosclerotic renal artery occlusion. J Urol 1989;141:486–8.

[86] Kellerman PS. Exogenous adenosine triphosphate (ATP) preserves proximal tubule microfilament structure and function *in vivo* in a maleic acid model of ATP depletion. J Clin Invest 1993;92:1940–9.

[87] Khosla S, White CJ, Collins TJ, et al. Effects of renal artery stent implantation in patients with renovascular hypertension

presenting with unstable angina or congestive heart failure. Am J Cardiol 1997;80:363–6.
[88] Kiernan TJ, Yan BP, Eisenberg JD, Ruggiero NJ, Gupta V, Drachman D, et al. Treatment of renal artery in-stent restenosis with sirolimus-eluting stents. Vasc Med 2010;15(1):3–7.
[89] Kim D, Porter DH, Brown R, Crivello MS, Silva P, Leeming BW. Renal artery imaging: a prospective comparison of intra-arterial digital subtraction angiography with conventional angiography. Angiology 1991;42:345–57.
[90] Kon V, Yared A, Ichikawa I. Role of renal sympathetic nerves in mediating hypoperfusion of renal cortical microcirculation in experimental congestive heart failure and acute extracellular fluid volume depletion. J Clin Invest 1985;76:1913–20.
[91] Kuo CC, Shor A, Campbell LA, Fukushi H, Patton DL, Grayston JT. Demonstration of Chlamydia pneumoniae in atherosclerotic lesions of coronary arteries. J Infect Dis 1993;167:841–9.
[92] Kuroda S, Nishida N, Uzu T, Takeji M, Nishimura M, Fujii T, et al. Prevalence of renal artery stenosis in autopsy patients with stroke. Stroke 2000;31:61–5.
[93] Lanese DM, Conger JD. Effects of endothelin receptor antagonist on cyclosporine-induced vasoconstriction in isolated rat renal arterioles. J Clin Invest 1993;91:2144–9.
[94] Leertouwer TC, Gussenhoven EJ, Bosch JL, Van Jaarsveld BC, van Dijk LC, Deinum J, et al. Stent placement for renal arterial stenosis: where do we stand? A meta-analysis. Radiology 2000;216:7–85.
[95] Leertouwer TC, Pattynama PM, Berg-Huysmans A. Incidental renal artery stenosis in peripheral vascular disease: a case for treatment? Kidney Int 2001;59:1480–3.
[96] Leesar MA, Varma J, Shapira A, Fahsah I, Raza ST, Elghoul Z, et al. Prediction of hypertension improvement after stenting of renal artery stenosis: comparative accuracy of translesional pressure gradients, intravascular ultrasound, and angiography. J Am Coll Cardiol 2009;53(25):2363–71.
[97] Lerman L, Textor SC. Pathophysiology of ischemic nephropathy. Urol Clin North Am 2001;28:793–803 ix
[98] Lerman LO, Nath KA, Rodriguez-Porcel M, Krier JD, Schwartz RS, Napoli C, et al. Increased oxidative stress in experimental renovascular hypertension. Hypertension 2001; 37:541–6.
[99] Lerman LO, Schwartz RS, Grande JP, Sheedy PF, Romero JC. Noninvasive evaluation of a novel swine model of renal artery stenosis. J Am Soc Nephrol 1999;10:1455–65.
[100] Lerman LO, Taler SJ, Textor SC, Sheedy PF, Stanson AW, Romero JC. Computed tomography-derived intrarenal blood flow in renovascular and essential hypertension. Kidney Int 1996;49:846–54.
[101] Lewis EJ, Hunsicker LG, Bain RP, Rohde RD. The effect of angiotensin-converting-enzyme inhibition on diabetic nephropathy. The collaborative study group. N Engl J Med 1993;329:1456–62.
[102] Libertino JA, Bosco PJ, Ying CY, Breslin DJ, Woods BO, Tsapatsaris NP, et al. Renal revascularization to preserve and restore renal function. J Urol 1992;147:1485–7.
[103] Liss P, Eklöf H, Hellberg O, Hägg A, Boström-Ardin A, Löfberg AM, et al. Renal effects of CO2 and iodinated contrast media in patients undergoing renovascular intervention: a prospective, randomized study. J Vasc Interv Radiol 2005;16 (1):57–65.
[104] Luft FC, Grim CE, Weinberger MH. Intervention in patients with renovascular hypertension and renal insufficiency. J Urol 1983;130:654–6.
[105] Mailloux LU, Bellucci AG, Mossey RT, Napolitano B, Moore T, Wilkes BM, et al. Predictors of survival in patients undergoing dialysis. Am J Med 1988;84:855–62.
[106] Mailloux LU, Napolitano B, Bellucci AG, Vernace M, Wilkes BM, Mossey RT. Renal vascular disease causing end-stage renal disease, incidence, clinical correlates, and outcomes: a 20-year clinical experience. Am J Kidney Dis 1994;24:622–9.
[107] Martin LG, Casarella WJ, Gaylord GM. Azotemia caused by renal artery stenosis: treatment by percutaneous angioplasty. Am J Roentgenol 1988;150:839–44.
[108] Maschio G, Alberti D, Janin G, Locatelli F, Mann JF, Motolese M, et al. Effect of the angiotensin-converting-enzyme inhibitor benazepril on the progression of chronic renal insufficiency. The angiotensin-converting-enzyme inhibition in progressive renal insufficiency study group. N Engl J Med 1996;334: 939–45.
[109] May AG, Van de Berg, DeWeese JA, Rob CG. Critical arterial stenosis. Surgery 1963;54:250–9.
[110] McCoy CE, Selvaggio AM, Alexander EA, Schwartz JH. Adenosine triphosphate depletion induces a rise in cytosolic free calcium in canine renal epithelial cells. J Clin Invest 1988;82:1326–32.
[111] McManus JFA, Lupton CH. Ischemic obsolescence of renal glomeruli: natural history of the lesions and their relation to hypertension. Lab Invest 1960;9:413–34.
[112] Meaney TF, Dustan HP, McCormack LJ. Natural history of renal arterial disease. Radiology 1968;91:881–7.
[113] Messina LM, Zelenock GB, Yao KA, Stanley JC. Renal revascularization for recurrent pulmonary edema in patients with poorly controlled hypertension and renal insufficiency: a distinct subgroup of patients with arteriosclerotic renal artery occlusive disease. J Vasc Surg 1992;15:73–80.
[114] Meyrier A, Buchet P, Simon P, Fernet M, Rainfray M, Callard P. Atheromatous renal disease. Am J Med 1988;85:139–46.
[115] Michel JB, Dussaule JC, Choudat L, Auzan C, Nochy D, Corvol P, et al. Effects of antihypertensive treatment in one-clip, two kidney hypertension in rats. Kidney Int 1986;29:1011–20.
[116] Minuz P, Patrignani P, Gaino S, Degan M, Menapace L, Tommasoli R, et al. Increased oxidative stress and platelet activation in patients with hypertension and renovascular disease. Circulation 2002;106:2800–5.
[117] Missouris CG, Buckenham T, Cappuccio FP, MacGregor GA. Renal artery stenosis: a common and important problem in patients with peripheral vascular disease. Am J Med 1994;96:10–4.
[118] Modrall JG, Rosero EB, Smith ST, Arko III FR, Valentine RJ, Clagett GP, et al. Operative mortality for renal artery bypass in the United States: results from the national inpatient sample. J Vasc Surg 2008;48(2):317–22.
[119] Modrall JG, Rosero EB, Smith ST, Arko III FR, Valentine RJ, Clagett GP, et al. Effect of hospital volume on in-hospital mortality for renal artery bypass. Vasc Endovascular Surg 2009;43 (4):339–45.
[120] Moore K, Wendon J, Frazer M, Karani J, Williams R, Badr K. Plasma endothelin immunoreactivity in liver disease and the hepatorenal syndrome. N Engl J Med 1992;327:1774–8.
[121] Mounier-Vehier C, Lions C, Devos P, Jaboureck O, Willoteaux S, Carre A, et al. Cortical thickness: an early morphological marker of atherosclerotic renal disease. Kidney Int 2002;61: 591–8.
[122] Muhlestein JB, Hammond EH, Carlquist JF, Radicke E, Thomson MJ, Karagounis LA, et al. Increased incidence of Chlamydia species within the coronary arteries of patients with symptomatic atherosclerotic versus other forms of cardiovascular disease. J Am Coll Cardiol 1996;27:1555–61.
[123] Myers DI, Poole LJ, Imam K, Scheel PJ, Eustace JA. Renal artery stenosis by three-dimensional magnetic resonance angiography in type 2 diabetics with uncontrolled hypertension

and chronic renal insufficiency: prevalence and effect on renal function. Am J Kidney Dis 2003;41:351–9.
[124] Novick AC, Fergany A. Renovascular hypertension and ischemic nephropathy. In: Walsh P, editor. Campbell's urology. Philadelphia: WB Saunders; 2002.
[125] Novick AC, Textor SC, Bodie B, Khauli RB. Revascularization to preserve renal function in patients with atherosclerotic renovascular disease. Urol Clin North Am 1984;11:477–90.
[126] Novick AC, Ziegelbaum M, Vidt DG, Gifford Jr. RW, Pohl MA, Goormastic M. Trends in surgical revascularization for renal artery disease: ten years' experience. JAMA 1987;257: 498–501.
[127] O'Donovan RM, Gutierrez OH, Izzo Jr. JL. Preservation of renal function by percutaneous renal angioplasty in high-risk elderly patients: short-term outcome. Nephron 1992;60: 187–92.
[128] Oates JA, FitzGerald GA, Branch RA, Jackson EK, Knapp HR, Roberts LJ. Clinical implications of prostaglandin and thromboxane A2 formation (2). N Engl J Med 1988;319:761–7.
[129] Ofstad J, Aukland K. Renal circulation. In: Seldin D, Geibisch G, editors. The kidney: physiology and pathophysiology. New York: Raven Press; 1985. p. 471–96.
[130] Olin JW, Piedmonte MR, Young JR, DeAnna S, Grubb M, Childs MB. The utility of duplex ultrasound scanning of the renal arteries for diagnosing significant renal artery stenosis. Ann Intern Med 1995;122:833–88.
[131] Parving HH, Hommel E, Jensen BR, Hansen HP. Long-term beneficial effect of ACE inhibition on diabetic nephropathy in normotensive type 1 diabetic patients. Kidney Int 2001;60: 228–34.
[132] Patrono C, Dunn MJ. The clinical significance of inhibition of renal prostaglandin synthesis. Kidney Int 1987;32:1–12.
[133] Pickering TG, Herman L, Devereux RB, Sotelo JE, James GD, Sos TA, et al. Recurrent pulmonary oedema in hypertension due to bilateral renal artery stenosis: treatment by angioplasty or surgical revascularisation. Lancet 1988;2:551–2.
[134] Planken II, Rietveld AP. Rapid onset pulmonary edema (flash edema) in renal artery stenosis. Neth J Med 1998;52:116–9.
[135] Plouin PF, Chatellier G, Darne B, Raynaud A. Blood pressure outcome of angioplasty in atherosclerotic renal artery stenosis: a randomized trial. essai multicentrique medicaments vs angioplastie (EMMA) study group. Hypertension 1998;31: 823–9.
[136] Plouin PF, Rossignol P, Bobrie G. Atherosclerotic renal artery stenosis: to treat conservatively, to dilate, to stent, or to operate? J Am Soc Nephrol 2001;12:2190–6.
[137] Pohl M. Renal artery stenosis, renal vascular hypertension, and ischemic nephropathy. In: Schrier RW, editor. Diseases of the kidney and urinary tract. Philadelphia: Lippincott Williams & Wilkins; 2001. p. 1282–4.
[138] Pohl MA, Novick AC. Natural history of atherosclerotic and fibrous renal artery disease: clinical implications. Am J Kidney Dis 1985;5:A120–30.
[139] Pontremoli R, Rampoldi V, Morbidelli A, Fiorini F, Ranise A, Garibotto G. Acute renal failure due to acute bilateral renal artery thrombosis: successful surgical revascularization after prolonged anuria. Nephron 1990;56:322–4.
[140] Radermacher J, Chavan A, Bleck J, Vitzthum A, Stoess B, Gebel MJ, et al. Use of Doppler ultrasonography to predict the outcome of therapy for renal-artery stenosis. N Engl J Med 2001;344:410–7.
[141] Rajagopalan S, Kurz S, Munzel T, Tarpey M, Freeman BA, Griendling KK, et al. Angiotensin II-mediated hypertension in the rat increases vascular superoxide production via membrane NADH/NADPH oxidase activation: contribution to alterations of vasomotor tone. J Clin Invest 1996;97: 1916–23.
[142] Rees CR, Palmaz JC, Becker GJ, Ehrman KO, Richter GM, Noeldge G, et al. Palmaz stent in atherosclerotic stenoses involving the ostia of the renal arteries: preliminary report of a multicenter study. Radiology 1991;181:507–14.
[143] Riehl J, Schmitt H, Bongartz D, Bergmann D, Sieberth HG. Renal artery stenosis: evaluation with colour duplex ultrasonography. Nephrol Dial Transplant 1997;12: 1608–14.
[144] Rihal CS, Textor SC, Breen JF, McKusick MA, Grill DE, Hallett JW, et al. Incidental renal artery stenosis among a prospective cohort of hypertensive patients undergoing coronary angiography. Mayo Clin Proc 2002;77:309–16.
[145] Rimmer JM, Gennari FJ. Atherosclerotic renovascular disease and progressive renal failure. Ann Intern Med 1993;118: 712–9.
[146] Roche Z, Rutecki G, Cox J, Whittier FC. Reversible acute renal failure as an atypical presentation of ischemic nephropathy. Am J Kidney Dis 1993;22:662–7.
[147] Rundback JH, Sacks D, Kent KC, Cooper C, Jones D, Murphy T, et al. Guidelines for the reporting of renal artery revascularization in clinical trials. American heart association. Circulation 2002;106:1572–85.
[148] Safian RD. Atherosclerotic renal artery stenosis. Curr Treat Options Cardiovasc Med 2003;5:91–101.
[149] Safian RD, Textor SC. Renal-artery stenosis. N Engl J Med 2001;344:431–42.
[150] Sawhney N, Moses JW, Leon MB, Kuntz RE, Popma JJ, Bachinsky W, et al. Treatment of left anterior descending coronary artery disease with sirolimus-eluting stents. Circulation 204;110: 374–379.
[151] Schlanger LE, Haire HM, Zuckerman AM, Loscalzo CE, Mitch WE. Reversible renal failure in an elderly woman with renal artery stenosis. Am J Kidney Dis 1994;23:123–6.
[152] Schnermann J, Briggs J, Kriz W, Moore L, Wright F. Control of glomerular vascular resistance by the tubuloglomerular feedback mechanism. In: Leaf A, Giebisch G, Bolls L, Giorini S, editors. Renal pathophysiology: recent advances. New York: Raven Press; 1980. p. 165–82.
[153] Schoenberg SO, Bock M, Kallinowski F, Just A. Correlation of hemodynamic impact and morphologic degree of renal artery stenosis in a canine model. J Am Soc Nephrol 2000; 11:2190–8.
[154] Schreiber MJ, Pohl MA, Novick AC. The natural history of atherosclerotic and fibrous renal artery disease. Urol Clin North Am 1984;11:383–92.
[155] Schumer M, Colombel MC, Sawczuk IS, Gobe G, Connor J, O'Toole KM, et al. Morphologic, biochemical, and molecular evidence of apoptosis during the reperfusion phase after brief periods of renal ischemia. Am J Pathol 1992;140:831–8.
[156] Schwartz CJ, White TA. Stenosis of renal artery: an unselected necropsy study. Br Med J 1964;5422:1415–21.
[157] Scoble JE, Maher ER, Hamilton G, Dick R, Sweny P, Moorhead JF. Atherosclerotic renovascular disease causing renal impairment: a case for treatment. Clin Nephrol 1989; 31:119–22.
[158] Shanley PF. The Pathology of chronic renal ischemia. Semin Nephrol 1996;16:21–32.
[159] Sigmon DH, Beierwaltes WH. Renal nitric oxide and angiotensin II interaction in renovascular hypertension. Hypertension 1993;22:237–42.
[160] Sigmon DH, Beierwaltes WH. Degree of renal artery stenosis alters nitric oxide regulation of renal hemodynamics. J Am Soc Nephrol 1994;5:1369–77.
[161] Silva VS, Martin LC, Franco RJ, Carvalho FC, Bregagnollo EA, Castro JH, et al. Pleiotropic effects of statins may improve outcomes in atherosclerotic renovascular disease. Am J Hypertens 2008;21:1163–8.

[162] Slovut DP, Olin JW. Fibromuscular dysplasia. N Engl J Med 2004;350:1862–71.
[163] Snowdowne KW, Freudenrich CC, Borle AB. The effects of anoxia on cytosolic free calcium, calcium fluxes, and cellular ATP levels in cultured kidney cells. J Biol Chem 1985;260: 11619–26.
[164] Sorensen SS, Egeblad M, Eiskjaer H, Madsen B, Nielsen CB, Sihm I, et al. Endothelin in renovascular and essential hypertension. Blood Press 1994;3:364–9.
[165] Sos TA, Pickering TG, Sniderman K, Saddekni S, Case DB, Silane MF, et al. Percutaneous transluminal renal angioplasty in renovascular hypertension due to atheroma or fibromuscular dysplasia. N Engl J Med 1983;309:274–9.
[166] Stanley JC, Whitehouse Jr. WM. Occlusive and aneurysmal disease of the renal arterial circulation. Dis Mon 1984;30: 1–62.
[167] Storger H, Grube E, Hofmann M, Schwarz F, Haase J. Clinical experiences using everolimus-eluting stents in patients with coronary artery disease. J Intervent Cardiol 2004;17:387–90.
[168] Stribrna J, Schuck O, Peregrin JH, Krajickova D, Skibova J. Evaluating the outcome of percutaneous transluminal angioplasty in renal graft artery stenosis using the areas under the time curve of glomerular filtration rate and blood pressure. Physiol Res 2000;49:635–41.
[169] Swartbol P, Thorvinger BO, Parsson H, Norgren L. Renal artery stenosis in patients with peripheral vascular disease and its correlation to hypertension: a retrospective study. Int Angiol 1992;11:195–9.
[170] Textor SC. Ischemic nephropathy: where are we now? J Am Soc Nephrol 2004;15:1974–82.
[171] Textor SC, Novick AC, Tarazi RC, Klimas V, Vidt DG, Pohl M. Critical perfusion pressure for renal function in patients with bilateral atherosclerotic renal vascular disease. Ann Intern Med 1985;102:308–14.
[172] Tokuyama H, Hayashi K, Matsuda H, Kubota E, Honda M, Okubo K, et al. Differential regulation of elevated renal angiotensin II in chronic renal ischemia. Hypertension 2002;40(1): 34–40.
[173] Tollefson DF, Ernst CB. Natural history of atherosclerotic renal artery stenosis associated with aortic disease. J Vasc Surg 1991;14:327–31.
[174] Truong LD, Farhood A, Tasby J, Gillum D. Experimental chronic renal ischemia: morphologic and immunologic studies. Kidney Int 1992;41:1676–89.
[175] Valentine RJ, Myers SI, Miller GL, Lopez MA, Clagett GP. Detection of unsuspected renal artery stenoses in patients with abdominal aortic aneurysms: refined indications for preoperative aortography. Ann Vasc Surg 1993;7:220–4.
[176] van der Ven AJ, Hommels MJ, Kroon AA, Kessels A, Flobbe K, van Engelshoven J, et al. Chlamydia pneumoniae *seropositivity and systemic and renovascular atherosclerotic disease*. Arch Intern Med 2002;162:786–90.
[177] Van Jaarsveld BC, Krijnen P, Pieterman H, Derkx FH, Deinum J, Postma CT, et al. The effect of balloon angioplasty on hypertension in atherosclerotic renal-artery stenosis. dutch renal artery stenosis intervention cooperative study group. N Engl J Med 2000;342:1007–14.
[178] Van Why SK, Mann AS, Thulin G, Zhu XH, Kashgarian M, Siegel NJ. Activation of heat-shock transcription factor by graded reductions in renal ATP, *in vivo*, in the rat. J Clin Invest 1994;94:1518–23.
[179] Vasbinder GB, Nelemans PJ, Kessels AG, Kroon AA, de Leeuw PW, van Engelshoven JM. Diagnostic tests for renal artery stenosis in patients suspected of having renovascular hypertension: a meta-analysis. Ann Intern Med 2001;135: 401–11.
[180] Vasbinder GB, Nelemans PJ, Kessels AG, Kroon AA, Maki JH, Leiner T, et al. Accuracy of computed tomographic angiography and magnetic resonance angiography for diagnosing renal artery stenosis. Ann Intern Med 2004;141:674–82.
[181] Vercellotti GM, Tolins JP. Endothelial activation and the kidney: vasomediator modulation and antioxidant strategies. Am J Kidney Dis 1993;21:331–43.
[182] Watson PS, Hadjipetrou P, Cox SV, Piemonte TC, Eisenhauer AC. Effect of renal artery stenting on renal function and size in patients with atherosclerotic renovascular disease. Circulation 2000;102:1671–7.
[183] Webster J, Marshall F, Abdalla M, Dominiczak A, Edwards R, Isles CG, et al. Randomised comparison of percutaneous angioplasty vs continued medical therapy for hypertensive patients with atheromatous renal artery stenosis. Scottish and newcastle renal artery stenosis collaborative group. J Hum Hypertens 1998;12:329–35.
[184] Weibull H, Bergqvist D, Bergentz SE, Jonsson K, Hulthen L, Manhem P. Percutaneous transluminal renal angioplasty versus surgical reconstruction of atherosclerotic renal artery stenosis: a prospective randomized study. J Vasc Surg 1993;18:841–50.
[185] Werner GS, Krack A, Schwarz G, Prochnau D, Betge S, Figulla HR. Prevention of lesion recurrence in chronic total coronary occlusions by paclitaxel-eluting stents. J Am Coll Cardiol 2004;44:2301–6.
[186] White CJ, Jaff MR, Haskal ZJ, Jones DJ, Olin JW, Rocha-Singh KJ, et al. Indications for renal arteriography at the time of coronary arteriography: a science advisory from the American heart association committee on diagnostic and interventional cardiac catheterization, council on clinical cardiology, and the councils on cardiovascular radiology and intervention and on kidney in cardiovascular disease.; American heart association committee on diagnostic and interventional cardiac catheterization, council on clinical cardiology; American heart association council on cardiovascular radiology and intervention; American heart association council on kidney in cardiovascular disease. Circulation 2006;114(17):1892–5.
[187] Wiecek A, Kokot F, Kuczera M, Grzeszczak W, Kiersztejn M. Plasma erythropoietin concentrations in renal venous blood of patients with unilateral renovascular hypertension. Nephrol Dial Transplant 1992;7:221–4.
[188] Wollenweber J, Sheps SG, Davis GD. Clinical course of atherosclerotic renovascular disease. Am J Cardiol 1968;21:60–71.
[189] Yonezawa S, Sato E, Okamoto K. Polyanion, immunoprotein and proteinase inhibitor in ischemic glomerular change. Nephron 1981;28:105–11.
[190] Zähringer M, Sapoval M, Pattynama PM, Rabbia C, Vignali C, Maleux G, et al. Sirolimus-eluting versus bare-metal low-profile stent for renal artery treatment (GREAT Trial): angiographic follow-up after 6 months and clinical outcome up to 2 years. J Endovasc Ther 2007;4:460–8.
[191] Zeller T, Rastan A, Schwarzwälder U, Mueller C, Schwarz T, Frank U, et al. Treatment of instent restenosis following stent-supported renal artery angioplasty. Catheter Cardiovasc Interv 2007;70(3):454–9.
[192] Zierler RE, Bergelin RO, Isaacson JA, Strandness Jr. DE. Natural history of atherosclerotic renal artery stenosis: a prospective study with duplex ultrasonography. J Vasc Surg 1994;19:250–7.
[193] Zollinger HU, Torhorst J, Riede UN, von TV, Geering B, Rohr HP. Incomplete or subinfarction of the kidney (unilateral renal artery stenosis with resultant renal contraction). Histologic, morphometric and electron microscopic investigations. Beitr Pathol 1973;148:15–34.

CHAPTER

78

Pathophysiology and Pathogenesis of Diabetic Nephropathy

Sheldon Chen[1] *and Charbel Khoury*[1] *and Fuad N. Ziyadeh*[2]

[1]Northwestern University, Chicago, U.S.A.

[2]American University of Beirut, Beirut, Lebanon

Diabetic nephropathy is the major cause of end-stage renal disease (ESRD) in the industrialized world. Although the incidence of nephropathy due to type 1 diabetes may not be increasing, type 2 diabetes mellitus, considered 30 years ago a rather benign condition invariably associated with the "normal" aging process, is now the most common single cause of chronic kidney disease in the United States, Japan, and Europe.[1,2] The associated health care costs are massive and not only is diabetic nephropathy a major burden on the quality of life, it also predicts an ominous prognosis despite advances in the medical management of renal and cardiovascular diseases. For instance, the diabetic patient with proteinuria has a two- to fourfold increased risk of morbidity and mortality from cardiovascular diseases.[3] Even with chronic dialysis, the cardiac death rate of diabetic patients is ~50% higher than nondiabetic patients.

The pathophysiology of diabetic nephropathy is complex. Renal injury was initially thought to be caused by hemodynamic alterations (renal hyperperfusion, intraglomerular hypertension, and glomerular hyperfiltration),[4] but there is now clear evidence that these changes are only one aspect of a complex series of metabolic and biochemical alterations caused by disturbed glucose homeostasis.[5] Hyperglycemia is a necessary prerequisite but genetic susceptibility is also crucial for the development of diabetic nephropathy.[6] Several lines of evidence, including familial aggregation, suggest the existence of genes where allelic variation contributes to risk of diabetic nephropathy. Metabolic changes and hemodynamic stress can induce the release of vasoactive peptides, cytokines, and growth factors that can trigger a host of autocrine and/or paracrine effects[7] that eventually mediate the effects of hyperglycemia and nonenzymatically glycated proteins on the functional alterations (hyperperfusion, hyperfiltration) as well as the structural changes (early hypertrophy, excess extracellular matrix deposition, podocyte abnormalities) of diabetic nephropathy.[5,8,9] This chapter will provide a comprehensive review of our current understanding of the pathophysiology of diabetic nephropathy.

EPIDEMIOLOGY

There are approximately 200 million people with diabetes mellitus worldwide, and this number is projected to increase to 366 million by 2030. In the United States, it is estimated that 18.8 million people (or ~6% of the population) have diabetes (ADA statistics webpage found at http://www.diabetes.org/diabetes-basics/diabetes-statistics/), but a significant portion of those with type 2 diabetes have not yet been clinically identified. Up to one third of patients with type 1 diabetes eventually develop nephropathy after ~20 years of diabetes.[10] Among those with type 2 diabetes, the risk of nephropathy is less clear and varies with ethnicity.[1] However, some European studies have suggested that the risk of ESRD in type 2 diabetic patients is almost as high as in type 1 diabetic patients.[2] African Americans, Native Americans, Asians, and Hispanics are more prone to developing both type 2 diabetes and diabetic nephropathy than non-Hispanic whites. The reasons for this difference remain unknown but genetic factors may be implicated. There has been a secular trend of

Seldin and Giebisch's The Kidney, Fifth Edition.
DOI: http://dx.doi.org/10.1016/B978-0-12-381462-3.00078-1

© 2013 Elsevier Inc. All rights reserved.

decreasing prevalence of nephropathy in type 1 diabetic patients,[11,12] presumably because of progressively better management of glycemia and hypertension. Although in type 2 diabetic patients, aggressive early, multi-factorial intervention reduces the frequency of cardiovascular and renal endpoints,[13] there was little evidence of a decreasing incidence of nephropathy in patients with type 2 diabetes.[14–16] As of 2005, however, the incidence of diabetic nephropathy leading to end-stage renal disease seems to be leveling off, but whether that positive trend continues will require additional years of data to confirm[17] (USRDS 2011). The increasing prevalence of type 2 diabetes in the aging population[16] and the better survival of diabetic patients with nephropathy had been the major reasons for the rising numbers of type 2 diabetics with ESRD,[2,18] but incident rates have recently stabilized or are falling in older populations and among whites. The sobering news is that diabetes-related ESRD is increasing among younger minority patients (USRDS 2011). Importantly, the risk of dying from cardiovascular disease is greater than the chance that one may live long enough to develop ESRD. An increasing proportion of diabetic patients can have acute but irreversible renal failure, superimposed on chronic kidney disease, usually after cardiac or septic complications. Administration of radiocontrast media agents or nonsteroidal anti-inflammatory agents may sometimes precipitate renal failure that may not resolve.

According to the US Renal Data System (www.usrds.org, 2004; incidence data from 2002) diabetic nephropathy was the primary diagnosis in 45% of incident patients starting renal replacement therapy (i.e., 148 of 326 patients per million). This was an increase of 221% compared with 1990,[19] (updated for USRDS 2011, incidence data from 2009, diabetic kidney disease accounted for 43% of incident patients, i.e., 154 of 354.8 patients per million). The number of type 2 diabetic patients with ESRD in the United States in 2000 far exceeded that of type 1 (38% and 6% of the total ESRD dialysis population, respectively). This is due to the much higher prevalence of type 2 diabetes in the overall diabetic population (90–95%) as compared with type 1 diabetes (5–10%). Survival of diabetic patients on dialysis is considerably worse than that for nondiabetic patients. Five-year mortality is between 40% and 80% in diabetic patients with ESRD in European countries and the United States. The main causes of death in hemodialyzed diabetic patients are primarily cardiovascular events but infection also plays a significant role.[20,21] Survival rates in dialyzed diabetic patients are much better in Eastern countries such as Japan,[22] presumably related to the lower rate of cardiovascular death in the background population of Japan.

Genetic Risk Factors

The risk of nephropathy is strongly determined by genetic factors and only approximately 30% of patients with type 1 or type 2 diabetes will ultimately develop nephropathy.[23] Genetic factors may directly influence the development of diabetic nephropathy and/or be clustered with genes influencing cardiovascular diseases.[24,25] One support for genetic transmission is an experimental study showing that bone marrow–derived mesangial cell progenitors transmit diabetic nephropathy from donors with type 2 diabetes (*db/db* mice) to naive, normoglycemic recipients.[26] There is ongoing research through genomic screening and candidate gene approaches to better identify genetic loci for diabetic nephropathy susceptibility.[27–30] Although some potential genes have been identified, linkage was only present in defined ethnic subpopulations and not in the majority of patients. An incomplete list of previously implicated genes is shown in Table 78.1. The major problem with such studies is that diabetic nephropathy is a complex disease trait, meaning that several genes are likely involved and the inheritance patterns do not follow simple Mendelian rules. For example, a potential association between polymorphisms in candidate genes and the development and progression of nephropathy has been widely studied.[31–37] These case-control studies are often problematic and clear guidelines for such polymorphism studies have been provided.[38] The complexity of this genetic linkage analysis is exemplified by studies with controversial results investigating the insertion or deletion polymorphism of the angiotensin-converting

TABLE 78.1 Some Genes Implicated in Susceptibility and/or Progression of Diabetic Nephropathy

Gene	Gene Variant
Promoter of RAGE	63-bp deletion (decreased risk)
Histocompatibility antigen	DR3/4
Angiotensin-converting enzyme	D/I
Angiotensinogen	M235T
Aldose reductase	Z + 2 alleles
Transforming growth factor-β1	Leu10Pro, Arg25Pro
Apolipoprotein E	e2 allele
Paraoxonase 1	T107C, Leu54Met
Interleukin-1γ	T105C
Atrial natriuretic peptide	C708T
Glucose transporter 1	Xba1/HacIII
Mannose-binding lectin	YA/YA, XA/YA

RAGE, receptor for advanced glycation end-product.

enzyme (ACE) gene. Discrepancies could be explained by genetic heterogeneity and by small effects in limited cases in most studies (often <200 cases). The current opinion about the role of ACE gene polymorphism is that it may be associated with progression of disease in certain ethnic populations, but it is not a predictor of the development of diabetic nephropathy.[39,40]

The introduction of Genome-Wide Association Studies (GWAS) is projected to bring new insights into the genetics of diabetic nephropathy. After scanning the entire genome, this method tries to identify single nucleotide polymorphisms (SNPs) associated with a particular disease, and thus can pinpoint areas of the genome involved in renal disease for example. So far, 2 GWAS have been conducted on patient populations with diabetic nephropathy.[41] Pezzolesi et al. identified two loci that are significantly associated with renal disease in patients with type 1 diabetes: the FRMD3 (4.1 protein ezrin, radixin, moesin [FERM] domain containing 3) and CARS (cysteinyl-tRNA synthetase). These findings were replicated using samples from the Diabetes Control and Complications Trial (DCCT)/Epidemiology of Diabetes Interventions and Complications (EDIC) study.[42] On the other hand, using a Japanese cohort, Maeda et al. suggest that ELMO1 (engulfment and cell motility 1 gene) and SLC12A3 (solute carrier family 12, member 3) may be associated with type 2 diabetic nephropathy.[43] This was later confirmed by studies on African-American cohorts with type 2 diabetes as well as data from the GoKinD collection which includes Caucasians with type 1 diabetes.[44,45] Because it casts a wide net, GWAS should increase our understanding of the pathology of diabetic nephropathy, and help identify novel therapeutic targets. This powerful method also promises to give clinicians and researchers a better understanding of the differences in disease progression and therapeutic responsiveness, paving the way towards a personalized medical practice.

More recently, the tools of genome-wide association studies have been applied to diabetic nephropathy. This method allows for a comprehensive genetic survey of the entire genome for chromosomal regions that are linked with a specific trait, in this case diabetic nephropathy.[46] A genome scan for diabetic nephropathy in African-Americans identified susceptibility loci on chromosomes 3q, 7p, and 18q.[47] Another scan in Pima Indians, a native American tribe with an alarmingly high incidence of early-onset type 2 diabetes,[48] also identified linkage to diabetic nephropathy on chromosome 7.[49,50] This powerful method, or its derivative technologies, may in the future more clearly identify the genetic risk for developing diabetic nephropathy. However, the genetic findings still need to be sussed out for their functional significance and explained in the larger pathophysiological context.

CLINICAL COURSE OF DIABETIC NEPHROPATHY IN TYPE 1 AND TYPE 2 DIABETES

Five clinical stages characterize the progression of diabetic nephropathy (Fig. 78.1, Table 78.2).[51] These stages are classified on the basis of the values of the glomerular filtration rate (GFR), urinary albumin excretion (UAE), and systemic blood pressure. The discrete structural lesions in the renal parenchyma and vasculature (discussed in subsequent sections) generally become more severe with advancing clinical stages, but the diagnosis of diabetic nephropathy is often made on clinical grounds without the need for renal biopsy except in atypical presentations. The stages are best delineated in the setting of type 1 diabetes because the patient is often young, typically does not have essential hypertension that can cause renal injury, and the onset of diabetes is much more easily pinpointed. In these patients, sustained albuminuria due to diabetic nephropathy rarely develops before the first 10 years of diabetes. On the other hand, if a patient has diabetes for longer than 25 years and has not developed proteinuria, the future risk of developing nephropathy is only about 1% per year.

It should be noted that transient albuminuria can be first detected in human type 1 diabetes when the patient has uncontrolled diabetes or co-existent infections. This feature is not reflective of established diabetic nephropathy because the patient typically reverts to the normoalbuminuric state when the blood glucose is better controlled or an infection is cleared.

The natural history for patients with type 2 diabetes is not as easily characterized as in type 1 patients,[52,53]

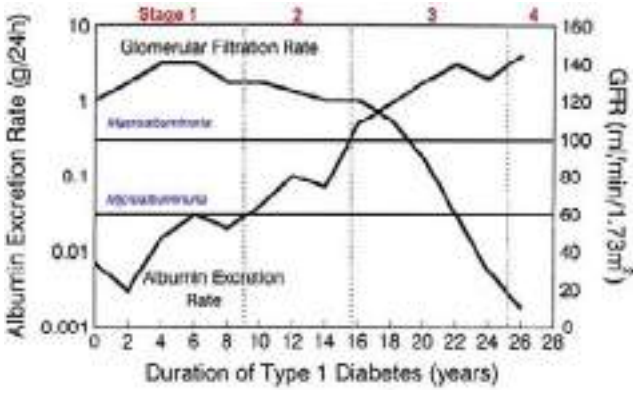

FIGURE 78.1 Five clinical stages characterize the progression of diabetic nephropathy. *(Adapted from Molitch ME. Am J Med 102: 392–398, 1997)*

TABLE 78.2 Clinical Stages of Diabetic Nephropathy

Stage	GFR	UAE	Blood Pressure	Years After Diagnosis
1. Hyperfiltration	Supernormal	<30 mg/d	Normal	0
2. Microalbuminuria	High normal–normal	30–300 mg/d	Rising	5–15
3. Overt proteinuria	Normal-decreasing	>300 mg/d	Elevated	10–20
4. Progressive nephropathy	Decreasing	Increasing	Elevated	15–25
5. ESRD	<15 ml/min	Massive	Elevated	20–30

GFR, glomerular filtration rate; UAE, urinary albumin excretion; ESRD, end-stage renal disease.

because 5% to 20% of these patients have some degree of albuminuria at the time of recognition of diabetes. Unlike type 1 patients, patients with type 2 diabetes commonly have hypertension at presentation and the renal disease in these patients can be attributed to diabetes only in approximately 75% of the cases. A renal biopsy may sometimes be indicated to reach the correct diagnosis. Moreover, due to increased cardiovascular mortality, many type 2 diabetic patients die before they ever progress to ESRD. Nevertheless, longitudinal observations in the Pima Indians have revealed that the course of diabetic nephropathy in type 2 diabetes is very similar to that of type 1 diabetes.[48,54,55] Thus, although it may be debated that diabetic nephropathies due to either type 1 or type 2 diabetes are specific entities, there is convincing evidence that basic pathophysiological mechanisms that eventually lead to nephropathy are essentially similar in types 1 and 2 diabetes.[56–58] However, in type 2 diabetes cases, other noxious factors, being or not related to diabetes mellitus itself, such as hypertension, obesity, dyslipidemia, and macrovascular ischemic renal disease could additionally injure the kidney resulting in complex patterns of nephropathy. The pathophysiological changes prior to the development of type 2 diabetes have been classified as the metabolic syndrome (see subsequent sections).[59]

Stage I

The earliest renal manifestations in type 1 diabetes are nephromegaly and glomerular hypertrophy, which are accompanied by afferent arteriolar vasodilation, renal hyperperfusion (although some find that renal blood flow is reduced[60]), and glomerular hyperfiltration (Fig. 78.1). Microscopically, there is thickening of the glomerular and tubular basement membranes. All these early functional and structural manifestations appear even if the patient is not destined to develop overt diabetic nephropathy. The UAE in this stage is normal (<30 mg/d or <20 μg/min) (Fig. 78.1) but occasionally a transient increase in UAE ("transient microalbuminuria") is present secondary to poor glycemic control or infection. Typically the blood pressure is below the hypertensive range (<140/90 mm Hg). The GFR is increased by 20 to 40% above normal values, with higher levels being frequently achieved when glycemic control is poor. Some studies suggest that patients with more renal hypertrophy or higher degrees of hyperfiltration (GFR >150 ml/min) are at increased risk for the future development of overt nephropathy.[61–64] In patients with type 2 diabetes, this early stage is not readily discernible owing to the increased age but there may be modest degrees of nephromegaly and hyperfiltration.[65]

Stage II

Incipient or latent nephropathy is defined by the appearance of microalbuminuria (UAE of 30–300 mg/day or 20–200 μg/min).[66] Without intervention, UAE increases at the rate of 10% to 20% per year and is almost always accompanied by a steady rise in blood pressure. Hypertension (>140/90 mm Hg) is typically diagnosed one to two years after the appearance of microalbuminuria in type 1 diabetes. Microalbuminuria rarely develops before five years of disease duration (median, 10 years) in type 1 diabetes, but in type 2 diabetes microalbuminuria may be present at the time of diagnosis of hyperglycemia in up to 20% of patients with as many as 40% of patients having elevated blood pressure as well. This may be due to the fact that many of these patients have had impaired glucose tolerance for years before actually being diagnosed with diabetes, or it may reflect another disease causing increased UAE as part of the metabolic syndrome, most notably essential hypertension. Other possible causes of increased UAE in this population include renovascular hypertension, morbid obesity, and sleep apnea. Even during this clinically "silent" phase of the disease, there may be significant mesangial matrix expansion or diffuse glomerulosclerosis, further thickening of the glomerular and tubular

basement membranes, and some degree of podocyte loss. The GFR may remain elevated or may decrease to within the "normal" range (100–120 ml/min) (Fig. 78.1). Longitudinal studies have shown that the patient with microalbuminuria is at greater risk for the development of overt proteinuria (UAE >300 mg/d) compared with patients with normoalbuminuria. For example, type 1 diabetic patients with persistent microalbuminuria have approximately an 80% chance of developing established nephropathy within the ensuing five to seven years.[67,68] In contrast, the percentage of patients with type 2 diabetes who progress to overt proteinuria is significantly lower, in part because of excess mortality due to cardiovascular events.[69] Thus, the predictive value of microalbuminuria in patients with type 2 diabetes is much less clear than in type 1 patients.

Stage III

This stage is characterized by the development of overt proteinuria (total protein excretion >500 mg/day) or macroalbuminuria (UAE >300 mg/d) (Fig. 78.1). In type 1 patients this occurs after an average of 15 years of diabetes. Hypertension is almost always present, and the worse the blood pressure control is, the more rapidly the GFR declines (Fig. 78.4). If a renal biopsy were to be performed, the glomeruli would typically demonstrate diffuse glomerulosclerosis and/or nodular glomerulosclerosis, further podocyte loss with focal areas of foot process effacement, arteriolar hyalinosis in both the afferent and efferent arterioles, and variable degrees of tubulointerstitial fibrosis. Structure–function correlations indicate a highly significant inverse correlation between declining GFR and mesangial expansion.[70] The progressive expansion of the glomerular mesangium causes a reduction in the glomerular filtering surface area. Nephron loss due to tubulointerstitial fibrosis is another major cause of the reduction in GFR. In the untreated patient, the GFR falls at a rate of about 1 ml/min/month, but this rate of fall can vary significantly from patient to patient. As the GFR falls from previously supernormal levels, the serum creatinine may remain in the normal range or be slightly elevated and is therefore not a reliable indicator of the magnitude of disease progression.

Stage IV

After approximately five years of overt nephropathy, untreated patients progress to advanced nephropathy, as characterized by nephrotic-range proteinuria (>3.5 g/d), worsened hypertension that becomes difficult to control, and a progressive decline in GFR (Fig. 78.1). In fact, diabetic nephropathy is the most common cause of the nephrotic syndrome in the adult population. Parenchymal and vascular lesions become more severe. The rate of decline in GFR is steady over a period of months but is variable from patient to patient and depends on the degree of elevation of blood pressure as well as the amount of UAE.

Stage V

The final stage is progressive renal failure reaching ESRD, with the GFR declining to 15 ml/min or lower. The patient may soon need renal replacement therapy to control uremic symptoms or excessive volume expansion. The average time for progression to ESRD from the time of diagnosis of diabetes is about 20 to 25 years, with a more rapid course developing in patients with uncontrolled hypertension and/or heavy proteinuria. Many patients, especially those with type 2 diabetes, never reach ESRD because of the severely increased risk of cardiovascular mortality in this population.

PATHOLOGY OF KIDNEY DISEASE IN DIABETES MELLITUS

Kidney structure is dramatically altered in diabetes in virtually all affected patients (Fig. 78.2, Table 78.3), even those not destined to develop full-blown diabetic nephropathy. The early structural changes include kidney enlargement involving both the tubules and the glomeruli and occurring as early as the first few months after the onset of diabetes.[71] This process involves predominantly hypertrophy (cell enlargement) and, to a much lesser extent, hyperplasia (cellular proliferation).[72–76] The larger glomerular volume and the resultant increase in capillary surface area maintain a higher GFR despite the development of mesangial matrix expansion.

One of the earliest cellular changes in diabetes is mesangial and tubular cell hypertrophy.[76] Insights into the complex mechanisms of growth came mostly from in vitro studies exposing renal cells to high ambient glucose concentrations. After a self-limited and short period of proliferation, glomerular and tubular cells subjected to hyperglycemia *in vitro* or *in vivo* become arrested in the G_1 phase of the cell cycle.[77,78] This G_1-phase arrest is mediated by $p27^{Kip1}$, an inhibitor of cyclin-dependent kinases (CDKI).[78] Another inhibitor, p21, may play a role as well. High glucose, via stimulation of the ERK isoform of the mitogen-activated protein kinases (MAPKs), leads to a posttranscriptional increase in $p27^{Kip1}$ expression because phosphorylation

of serine residues increases the half-life of $p27^{Kip1}$.[79] Deletion of $p27^{Kip1}$ attenuates high-glucose–induced hypertrophy of mesangial cells.[80] In addition, angiotensin II (Ang II) further enhances $p27^{Kip1}$ induction and blockade of Ang II attenuates high-glucose–mediated mesangial cell hypertrophy.[78,81] Treatment of diabetic animals with an ACE inhibitor attenuates $p27^{Kip1}$, but not p21, and reduces renal hypertrophy.[82] Knock out of $p27^{Kip1}$ in mice made diabetic with streptozotocin (STZ) results in less diabetic nephropathy.[83] While cell cycle arrest is essential, it may not be sufficient for the development of hypertrophy. Complementary signals increasing RNA and protein synthesis are needed for the cell to grow. Early in diabetes, renal cells, and especially mesangial cells, activate the mammalian target of rapamycin (mTOR).[84,85] mTORC1 acts mainly on two important downstream targets: the eukaryotic translation initiation factor 4E-binding protein 1 (4EBP1) and the serine/threonine protein kinase p70S6 kinase 1 (S6K1). Phosphorylation of 4EBP1 leads to the release of eIF4E and consequently the initiation of cap-dependent translation of mRNAs. On the other hand S6K1 phosphorylates the 40S ribosomal protein S6, and plays a role in the regulating cellular and organ hypertrophy.[86] In fact inhibition of the mTOR pathway with rapamycin, or the knockdown of S6K1 decrease renal hypertrophy in rodent models of diabetes.[85,87] Moreover rapamycin treatment can reduce basement membrane thickening, mesangial matrix accumulation, as well as renal inflammatory markers, and lead to significantly less albuminuria.[88]

The basement membranes of tubules and glomeruli begin to thicken after two to three years of diabetes (Fig. 78.3). The width of the glomerular basement membrane (GBM) often exceeds 500 nm, or nearly double the control value.[89] There is increased abundance of type IV collagen, laminins, and nidogen/entactin, but other reports have described an increase in the subendothelial content of the novel (restricted) α3(IV) and α4(IV) collagen chains and a relative decrease in the density of the classical (ubiquitous) α1(IV) and α2(IV) collagen chains.[90] There may also be a relative reduction in the other novel α5(IV) collagen chain.[91] Thus, altered assembly of collagen IV chains is one major aspect of the altered composition of the thickened GBM and may partly explain the proteinuria. In fact, thickening of the GBM correlates well with the presence of proteinuria[56,57] and is potentially reversible with insulin therapy and tight glycemic control.[92]

After three to five years of diabetes, expansion of the mesangial regions of the glomerulus begins (Fig. 78.2). The most distinctive lesion of full-blown diabetic glomerulopathy is nodular glomerulosclerosis, frequently termed the "Kimmelstiel-Wilson lesion." Nodules probably form in response to injury produced by microaneurysmal dilation of glomerular capillaries and mesangial lysis. Nodules are present in up to 25% of diabetic patients at postmortem examination. A similar pattern may be seen in other renal diseases, notably light-chain nephropathy and amyloidosis; however, appropriate immunofluorescent staining, electron microscopy, and historical and laboratory information distinguish these conditions from the nodular glomerulosclerosis of diabetes. More prevalent is the diffuse rather than nodular enlargement of the mesangium (diffuse glomerulosclerosis) (Fig. 78.2). Matrix accumulation in the mesangium is the result of increased synthesis and decreased degradation of extracellular matrix molecules, especially fibronectin and the classical collagen chains α1(IV) and α2(IV) and nonfibrillar short-chain collagen VIII.[93] Fibrillary collagens that are not native to the glomerulus (such as collagens type I and III) eventually appear within the expanded mesangium. A small increase in mesangial cell volume may also occur. Mesangial cell proliferation is not considered to be a feature of diabetic nephropathy, although a very modest and self-limited increase in cell number

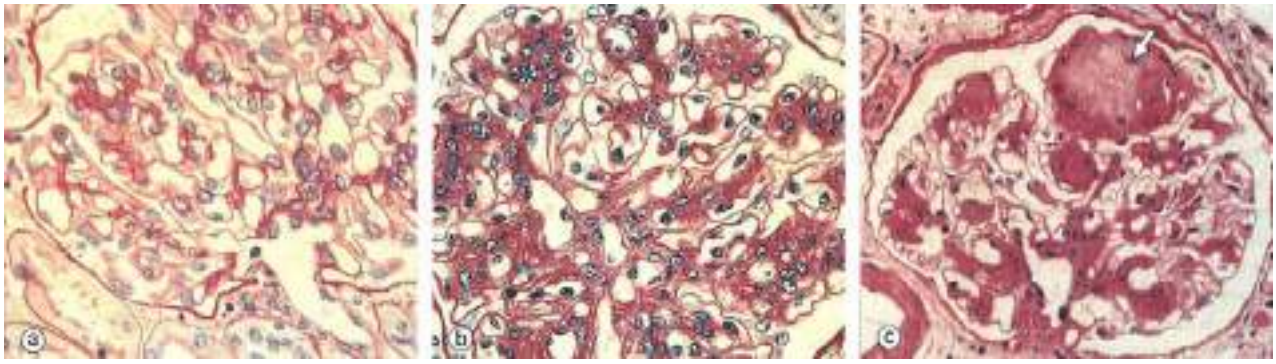

FIGURE 78.2 Appropriate immunofluorescent staining, electron microscopy, and historical and laboratory information distinguish these conditions from the nodular glomerulosclerosis of diabetes. More prevalent is the diffuse rather than nodular enlargement of the mesangium (diffuse glomerulosclerosis). *(From Vora JP, Chattington PD, Ibrahim H. Clinical Manifestations and Natural History of Diabetic Nephropathy. Harcourt Publishers Limited: London, 2000. pp. 6.34.1–6.34.12)*

per glomerulus may perhaps occur as an early accompaniment to glomerular hypertrophy.[76,94] In advanced glomerulosclerosis, mesangial cell number may actually decrease. Globally sclerotic (obsolescent) glomeruli similar to those seen in kidneys with ESRD of any cause can also develop in diabetes. Other glomerular lesions include "capsular drops," which are lens-shaped pieces of sclerosing extracellular matrix adjacent to Bowman capsule, and "fibrin caps," which are homogeneous eosinophilic masses overlying capillary loops.

Although diabetic nephropathy is generally regarded as primarily a glomerular disease, discrete abnormalities of the vasculature and tubulointerstitium also occur.[95,96] One pathognomonic finding is the arteriosclerotic hyalinosis of both the afferent and efferent arterioles. Lesions of the renal tubulointerstitium include chronic interstitial inflammation (with macrophage recruitment), interstitial fibrosis, tubular atrophy, and a predisposition to papillary necrosis. The worsening proteinuria can have adverse effects on the tubules, causing tubular atrophy and inciting interstitial fibrosis. Tubulointerstitial fibrosis is perhaps the best pathologic correlate for the progressive decline in GFR.[95–97] Tubulointerstitial fibrosis and renal arteriosclerosis can be present in patients with type 1 or type 2 diabetes mellitus, but are more prevalent in type 2 diabetic patients. Renal structure is, in fact, heterogeneous in type 2 diabetic patients: only a subset has typical diabetic glomerulopathy, while a substantial proportion has more advanced tubulointerstitial and vascular rather than glomerular lesions, or has normal or near normal renal structure.[98]

TABLE 78.3 Histopathology in Diabetic Nephropathy

Glomerular structural lesions
Glomerular hypertrophy
Glomerular basement membrane thickening
Podocytopenia
Mesangial matrix expansion
Diffuse glomerulosclerosis
Nodular (Kimmelstein-Wilson) glomerulosclerosis
Capsular drop
Fibrin caps
Arteriolosclerosis and hyalinosis (afferent and efferent)
Nonglomerular structural lesions
Tubuloepithelial cell hypertrophy
Tubular basement membrane thickening
Tubular atrophy and interstitial fibrosis
Armanni-Ebstein tubulopathy
Papillary necrosis

THE CENTRAL ROLE OF PODOCYTES IN THE PATHOPHYSIOLOGY OF DIABETIC PROTEINURIA

It is likely that proteinuria is an important predictor of kidney disease as well as of cardiovascular complications.[3,99] In addition, proteinuria is a progression factor because it can aggravate the tubulointerstitial fibrosis and the progression of renal failure.[100] Proteinuria arises because of permeability defects of the glomerular capillary wall that are related to abnormalities in GBM composition and to alterations in the structure and function of the cells lining the GBM (especially the podocytes, and to a lesser extent, the endothelium).[101,102] In diabetic nephropathy there is a marked reduction in the number of anionic moieties such as sialic acid and heparan sulfate proteoglycans (HSPG) in the GBM, and this has been correlated with loss in the charge-permselectivity. Loss of size-permselectivity most likely is due to changes in podocyte function and structure. Podocyte dysfunction is well recognized as a crucial player in the pathogenesis of various progressive nephropathies including

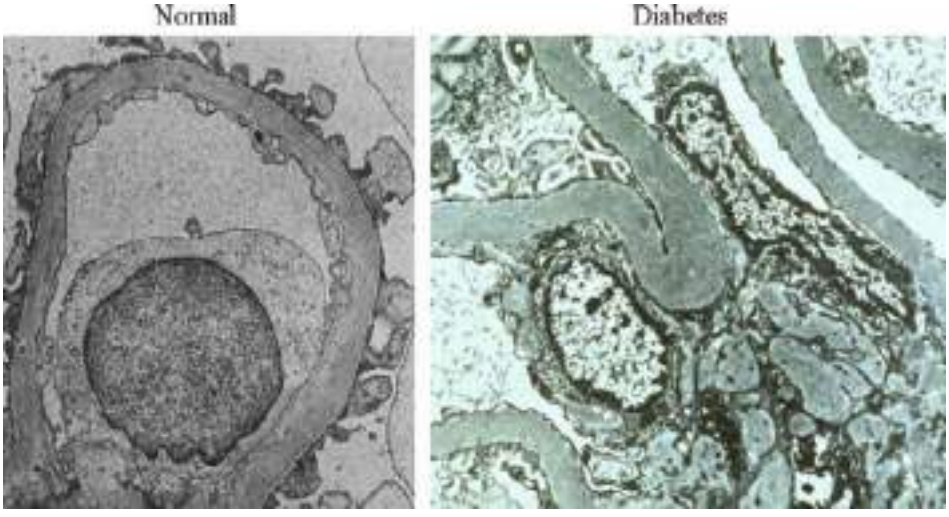

FIGURE 78.3 GBM thickening in diabetes. *(Eelectron micrographs courtesy of Dr. John E. Tomaszewski)*

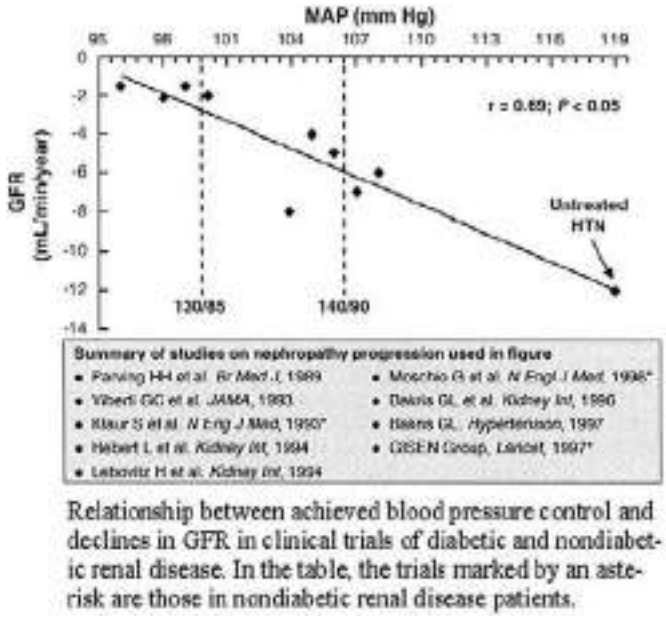
MAP (mm Hg)
95 98 101 104 107 110 113 116 119
GFR (mL/min/year)
0 -2 -4 -6 -8 -10 -12 -14
r = 0.69; P < 0.05
Untreated HTN
130/85
140/90
Summary of studies on nephropathy progression used in figure
Parving HH et al. Br Med J, 1989
Viberti GC et al. JAMA, 1983
Klaur S et al. N Eng J Med, 1950*
Hebert L et al. Kidney Int, 1994
Lebovitz H et al. Kidney Int, 1994
Moschio G et al. N Engl J Med, 1996*
Bakris GL et al. Kidney Int, 1996
Bakris GL. Hypertension, 1997
GISEN Group. Lancet, 1997*

Relationship between achieved blood pressure control and declines in GFR in clinical trials of diabetic and nondiabetic renal disease. In the table, the trials marked by an asterisk are those in nondiabetic renal disease patients.

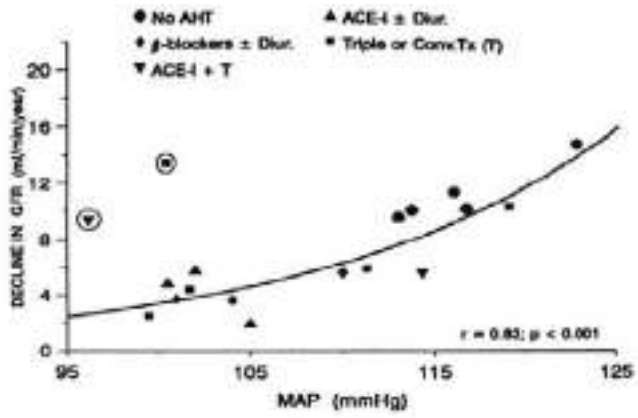

Relationships between mean arterial blood pressure and the rate of decline in GFR in IDDM patients with nephropathy.

FIGURE 78.4 (Left) Relationship between achieved blood pressure and declines in GFR. (Right) Relationships between mean arterial blood pressure and the rate of decline. *(From Bakris GL et al.* Am J Kidney Dis *36: 646–661, 2000, From Deferrari G et al.* Diabetes Metab Rev *13: 51–61, 1997)*

diabetic kidney disease.[103,104] Cross-sectional and longitudinal studies in patients with diabetic nephropathy have described an increase in foot process width in microalbuminuric subjects, and this parameter correlates directly with the UAE.[105] In addition, the number and density of podocytes are markedly reduced (podocytopenia), whether the patient is afflicted with type 1 or type 2 diabetes.[106–109] The decreased number of podocytes per glomerulus in humans is seen early in the course of the disease and is a strong predictor of progressive renal injury.[108,110] Widening or stretching of the remaining podocytes maintains coverage of the GBM but also causes a derangement in the filtration slit diaphragms.[111] Podocytopenia can exacerbate the development of proteinuria because when the GBM is denuded, it comes into contact with Bowman capsule and this promotes synechiae formation, an initial step in the development of glomerulosclerosis.[103] Several experimental studies in diabetic rats have reported a decrease in podocyte number, broadening of the foot processes, and reduction in nephrin protein expression.[112] Consistent with the observed loss of podocytes in diabetes, podocytes can be present in the urine of diabetic patients, especially when the albuminuria progresses from microalbuminuria to macroalbuminuria. Interestingly, treatment with an ACE inhibitor reduces the number of urinary podocytes.[113,114] Nephrin staining,[115] but not CD2AP expression,[116] is extensively reduced in renal biopsy specimens from diabetic patients with nephropathy. When treated with an ACE inhibitor, nephrin expression is restored.[111]

The etiology of podocyte loss in diabetes remains speculative, but two mechanisms can be suggested: cell detachment from the GBM and apoptosis.[104] Loss of cell anchorage to the GBM may result from downregulation of the $\alpha_3\beta_1$ integrin receptor, the principal adhesion complex that attaches the podocyte to the GBM. In fact, the $\alpha_3\beta_1$ integrin is decreased in the podocytes of humans and rats with diabetes.[117,118] Furthermore, high-glucose media in cultured rat or human podocytes decreases the expression of $\alpha_3\beta_1$ integrin;[117,118] this downregulation is perhaps mediated by increased levels of the multifunctional cytokine transforming growth factor-β (TGFβ).[119,120] As will be discussed later, multiple factors in the diabetic state can stimulate the activity of this cytokine, which in turn is responsible for most of the renal manifestations of diabetic kidney disease except perhaps for the proteinuria.[121,122] Addition of Ang II to cultured rat glomerular epithelial cells induces apoptosis of the cells, and this effect is also mediated by the TGFβ system.[123]

There is significant experimental evidence that podocyte-derived vascular endothelial growth factor (VEGF) may mediate the proteinuria of diabetes.[104] Interventional studies in the STZ-diabetic rat or the type 2 diabetic db/db mouse (both models of overexpression of podocyte-derived VEGF) have shown that treatment with neutralizing anti-VEGF antibodies or inhibitors of VEGF signaling significantly ameliorated the albuminuria of diabetes.[124–126] The underlying mechanism is still unclear but it has been postulated that VEGF causes afferent arteriolar vasodilatation via nitric oxide (NO),[127]

increasing plasma flow into the glomerulus, opens the junctions between endothelial cells[128] and maintains endothelial fenestrations,[129] and alters the synthetic program for collagen, integrins, and other matrix components by all three glomerular resident cell types, which can eventually have an impact on protein passage across the glomerular capillary wall.[101,102,129] Research findings provide strong support for an autocrine loop in which the podocyte is a target cell for the effects of podocyte-derived VEGF.[101,104,130]

Serum VEGF levels are significantly increased in patients with type 1[131,132] and type 2[133] diabetes. Perhaps the kidney is one source of serum VEGF. Interestingly, the serum VEGF level and urinary VEGF excretion correlate with the degree of proteinuria among diabetic patients.[131,133] VEGF mRNA and protein are more abundant in the glomeruli, distal tubules, and collecting ducts of diabetic than in normal rats.[134,135] Similar findings are reported in human diabetes.[136,137] Equally important, the expression of VEGF receptors on the glomerular endothelium is elevated in the diabetic kidney.[134,137] In a study on diabetic patients, the extent of VEGF and VEGFR2 staining in the kidney was significantly associated with the presence of marked proteinuria (>2 g/d).[137] Some studies, however, have found a decreased renal VEGF content in advanced diabetic nephropathy with severe glomerulosclerosis (or other severe glomerulopathies).[138,139] This does not necessarily contradict the previous findings because late diabetic glomerulosclerosis with appreciable loss of podocytes may be expected to eventually result in decreased podocyte-derived VEGF expression. Then again, some have found that VEGF mRNA expression is decreased even in early diabetic nephropathy and is associated with peritubular capillary rarefaction.[140] For an in-depth and balanced analysis of the complex field of VEGF as it relates to DN, we refer the reader to a recent review article.[141]

CELLULAR AND MOLECULAR MECHANISMS IN THE PATHOPHYSIOLOGY OF DIABETIC NEPHROPATHY

A host of mediators can be shown to be important in the pathogenesis of diabetic nephropathy (Table 78.4) and these will be reviewed here.

Early Hemodynamic Alterations in the Glomerulus

Altered renal hemodynamics is an early characteristic feature of diabetes in humans as well as animal models.[63,142] It is widely held that glomerular capillary hypertension in diabetes is the major hemodynamic alteration that contributes to progressive glomerular injury.[142,143] The increase in glomerular capillary pressure is accompanied by increased glomerular blood flow, which is caused by afferent arteriolar dilation but with little or no dilation of the efferent arteriole. An imbalance of a variety of vasoactive and growth factors including the renin-angiotensin-aldosterone system (RAAS), atrial natriuretic peptide, insulin-like growth factor-1, endothelin, prostanoids, and eicosanoids has been implicated in diabetic hyperfiltration, but evidence strongly implicates the NO system as the main mediator for afferent arteriolar dilation.[144,145] Three major theories have been put forward to account for the hemodynamic changes in the glomerulus: (1) a primary alteration in vascular function, (2) a primary alteration in tubular function, and (3) a primary growth of the total filtration surface area (part of the hypertrophic response), mediated by endothelial cell proliferation, capillary elongation, and new capillary formation.[146–148]

It has been well characterized that diabetes is associated with impaired autoregulation at the afferent arteriolar level.[149] This vascular theory suggests that vascular smooth cells, mesangial cells, and endothelial

TABLE 78.4 Mediators of Diabetic Renal Disease

- **I.** Genetic predisposition[a]
- **II.** Glomerular hemodynamic stress[a]
- **III.** Metabolic perturbations
  - **A.** Nonenzymatic glycation of circulating or structural proteins
    - Amadori-modified albumin[a]
    - Advanced glycation end-products (AGEs)[a]
  - **B.** Activation of pathways of glucose metabolism
    - GLUT-1 upregulation
    - Polyol pathway[a]
    - Cellular redox state (increased $NADPH/NADP^+$, $NADH/NAD^+$)
    - Hexosamine biosynthetic pathway[a]
    - De novo synthesis of diacylglycerol and stimulation of protein kinase C (PKC)[a] (especially α and β isoforms)
    - Activation of mitogen-activated protein kinase (MAPK)[a] (ERK and p38 isoforms)
    - Oxidative stress[a]
  - **C.** Activation of cytokines and growth factor systems
    - Transforming growth factor-β[a]
    - Connective tissue growth factor
    - Vascular endothelial growth factor
    - Other growth factors (platelet-derived growth factor,[a] insulin-like growth factor-I)
    - Angiotensin II[a]
    - Other vasoactive factors (endothelins,[a] thromboxane,[a] kinins[a])
    - Leptin[a]
    - Chemokines (e.g., macrophage chemoattractant protein-1, RANTES)

[a]*Factors known to stimulate the transforming growth factor-β system.*

cells are primarily responding to a combination of high-glucose concentrations, local autacoids, and systemic signals to alter the normal autoregulatory response to the prevailing systemic pressure. Studies supporting a primary vascular role include impaired calcium transients in afferent arterioles from diabetic rats.[148,150] Numerous groups have found a persistent altered responsiveness to vasoconstrictors of vascular smooth muscle cells and mesangial cells obtained from diabetic rats.[148,151–155] Some of these studies, using mesangial and vascular smooth muscle cells cultured in high glucose or obtained from diabetic rats, have identified protein kinase C (PKC), reactive oxygen species (ROS), and TGF-β to be important mediators of vascular dysfunction.

A case for tubuloglomerular feedback as the initiating factor has been put forward by Blantz and coworkers.[156,157] These investigators have convincingly demonstrated that increased uptake of glucose and sodium in proximal tubular segments may limit sodium delivery to the macula densa, thus inhibiting tubuloglomerular feedback and preventing constriction of the afferent arteriole. Presumably the enzyme ornithine decarboxylase plays an important role in this pathway.[156] Studies in diabetic animals and patients with salt loading lend further evidence to this hypothesis. NaCl restriction would cause a decrease in GFR in the normal situation; however, in animals with long-standing diabetes and in diabetic humans, salt restriction causes a surprising increase in GFR. This salt paradox could be explained by the further decrease in salt delivery to the macula densa and further afferent arteriolar dilation. However, several studies report unimpaired tubuloglomerular feedback in diabetes;[158,159] one group suggested that enhanced tubuloglomerular feedback may mitigate the increase in GFR.[158] It is likely that much of the discrepant results are accounted for by variations in diabetes induction, degree of hyperglycemia, weight loss, insulin levels, and duration of diabetes. Without a standardized experimental approach it is virtually impossible to interpret the various results.

Regardless of the cause of hemodynamic alterations in diabetes, progressive renal injury eventually ensues. One potential scenario to explain this outcome has been put forward by Kriz and coworkers.[160] With increased glomerular capillary pressure, there is stretching of mesangial cells with loss of tethering to the GBM. Loss of tethering may be contributed by altered integrin expression and growth factor production. This would lead to a ballooning of the capillary loop and denuding of the GBM on the epithelial side. Alterations in GBM composition may also play a role. Dropout of podocytes may ensue due to abnormal stretching of podocytes and loss of adherence to the GBM.[161] Furthermore, abnormal stretch may stimulate TGF-β production by mesangial cells, leading to a sclerotic response.[162,163] This scenario would fit with the glomerular volume increase noted in experimental and human diabetes as well as the diffuse mesangial matrix expansion and podocyte dropout.

Enhanced tubular transport of solutes and water is correlated with glomerular hyperfiltration. The elevation in the glomerular transcapillary hydraulic pressure gradient as well as the increase in *glomerular* plasma flow leads to an increase in GFR. This, in turn, enhances the colloid osmotic pressure in postglomerular capillaries, which can facilitate the reabsorption of water and sodium in proximal tubules. These processes provide a mechanistic link between enhanced tubular transport and the primary abnormality of glomerular hyperfiltration. As an alternative explanation, a primary abnormality in sodium reabsorption has been linked to glomerular hyperfiltration.[157] This explanation suggests that an increase in reabsorption of sodium chloride in the proximal tubule or the loop of Henle leads to an increase in GFR by an intact macula densa mechanism. Diabetes-induced hypertrophy of tubules that mediate stimulated sodium chloride reabsorption could be pivotal in this process, again connecting the structural changes with the hemodynamic adaptation in diabetes.[157] Therefore, both mechanisms could explain the increase in tubular reabsorption that occurs in diabetic nephropathy.

Role of Glucose Uptake and Metabolism

Extracellular hyperglycemia may define the diabetic state but it is the high intracellular glucose concentration that appears to be the critical metabolic abnormality that promotes pathological changes in diabetic nephropathy. Renal cells do not require insulin for glucose uptake but instead rely on a family of transmembrane proteins to facilitate glucose transport across the cell membrane. Glucose diffuses down its concentration gradient, and in diabetes, renal intracellular glucose levels rise in proportion to the degree of hyperglycemia. The most widely expressed glucose transporter is the GLUT-1 isoform, a high-affinity, low-capacity, facilitative transporter that typically would be saturated at or near physiological glucose concentrations.[164] GLUT-1 is normally found in the glomerulus and the tubules, but diabetes changes its distribution and cellular expression. While most tissues downregulate GLUT-1 expression in the face of hyperglycemia to protect cells from excess glucose transport and metabolism, some renal cells such as mesangial cells actually upregulate GLUT-1 gene transcription and protein translation when cultured in high-glucose media.[165] This positive feedback

is an apparent maladaptive response in mesangial cells, because the cells can readily take up more glucose from a diabetic environment, resulting in high intracellular glucose concentration that then initiates signaling cascades, which are integral to the pathophysiology of diabetic kidney disease. In fact, mesangial cells that overexpress GLUT-1 demonstrate avid uptake of glucose even when cultured in normal concentrations of glucose; the cells also behave like wild-type mesangial cells incubated in high glucose in that they increase the synthesis of extracellular matrix proteins such as collagens and fibronectin.[166] Interestingly, several relevant factors in the diabetic state in addition to hyperglycemia can upregulate GLUT-1 expression on the surface of mesangial cells.[167] These factors, which include TGF-β, Ang II, and shear stress, can then stimulate net glucose uptake and intracellular metabolism and therefore promote glucotoxicity.[168]

The Polyol Pathway

Metabolic pathways for intracellular metabolism of glucose are myriad. Activation of the polyol pathway has been shown to be important in the development of some complications of diabetes mellitus such as cataracts, retinopathy, and neuropathy, but its involvement in the development of nephropathy remains much less established. Many of the early, but not late, features of diabetic renal disease can be attributed to activation of the polyol pathway. Aldose reductase, the first and rate-limiting enzyme in this pathway, catalyzes the NADPH-dependent reduction of hexose or pentose sugars to their corresponding sugar alcohols, or polyols.[169] Tissues that do not require insulin for glucose uptake (kidney, lens, retina, and peripheral nerves) become subject to relatively greater loads of intracellular glucose. Increased oxidation of sorbitol to fructose via fructose dehydrogenase is coupled to reduction of NAD^+ to NADH, and a more reduced cytosolic ratio of $NADH/NAD^+$ may result in abnormalities of cellular function, including myo-inositol depletion, ROS generation, PKC stimulation, and even TGF-β production.[170–172] Glomerular hyperfiltration in diabetic rats can be ameliorated by the administration of sorbinil, an aldose reductase inhibitor.[173] In a small randomized trial of type 1 normoalbuminuric diabetic subjects, ponalrestat (a carboxylate-containing aldose reductase inhibitor) reduced renal hyperfiltration.[174] Urinary albumin excretion in diabetic rats has also been reduced by aldose reductase inhibitor therapy.[175,176] Feeding sorbinil to diabetic rats has been reported to decrease the width of the GBM,[177] and the stimulation by high glucose of collagen type IV expression in cultured proximal tubular cells can be abolished with sorbinil, although cellular hypertrophy is not prevented.[178] However, the long-term effects of polyol-pathway inhibition on renal extracellular matrix accumulation have not been uniformly favorable. The aldose reductase inhibitor statil did not reduce the magnitude of glomerulosclerosis in diabetic rats after seven months despite normalization of erythrocyte sorbitol levels with this drug.[179]

The sorbitol pathway may also produce metabolites capable of nonenzymatically glycating intracellular proteins (see subsequent sections), which can be further phosphorylated via novel pathways that are activated in diabetes mellitus. Sorbitol-3-phosphate, fructose-3-phosphate, 3-deoxyglucosone, and other unidentified metabolites are increased in erythrocytes of diabetic subjects and could participate in protein glycation and cross-linking.[180,181] Such studies provide an intriguing pathogenetic link between the products of the polyol pathway (or other pathways of glucose metabolism) and the reactions of nonenzymatic glycation.

The Hexosamine Biosynthetic Pathway

Fructose-6-phosphate can be converted to glucosamine-6-phosphate, with glutamine donating its amido group to become glutamate. The final products of the pathway are uridine diphosphate (UDP)-N-acetyl-glucosamine (GlcNAc) and other nucleotide hexosamines. The amination of fructose-6-phosphate is rate limiting and is catalyzed by glutamine: fructose-6-phosphate amidotransferase (GFAT). Interestingly, high glucose, superoxide production, and Ang II can all stimulate GFAT activity in endothelial or mesangial cell cultures.[182,183] Also, the high-glucose-induced stimulation of TGF-β and fibronectin that is observed in mesangial cells is partly mediated by activation of the hexosamine pathway because treatment of the cells with the GFAT inhibitor azaserine or with GFAT antisense oligonucleotides diminishes this stimulation.[183] The mechanism by which increased flux through the hexosamine pathway induces gene transcription is likely through covalent modification of key transcription factors and signaling molecules.[170] For instance, hyperglycemia-induced mitochondrial superoxide overproduction activates the hexosamine pathway, which stimulates Sp1 activity by post-translational O-linked glycosylation at critical serine or threonine sites;[184] this activation of the Sp1 transcription factor then leads to induction of key prosclerotic factors including TGF-β1 and plasminogen activator inhibitor-1 (PAI-1).[184] The hexosamine pathway can also regulate vascular function by inhibiting endothelial NO synthase (eNOS) via O-linked glycosylation modification of a key signaling enzyme, the Akt/PKB.[185]

Signaling through Protein Kinase C

The signaling pathways that mediate some of the effects of hyperglycemia may involve activation of one or more isoforms of PKC. Based on a series of ^{14}C-radiolabeling experiments, the relationship between hyperglycemia and PKC activation has been ascribed to an increased intracellular metabolism of glucose that promotes the de novo formation of diacylglycerol, the major endogenous activator of the classic and novel isoforms of PKC.[186–190] Interestingly, diacylglycerol synthesis may also be linked to the glucose-induced increase in the ratio of $NADH/NAD^+$ that derives from the polyol pathway.[191] PKC activity, measured by the cytosol-to-membrane shift of various classical PKC isoforms, is increased in mesangial and endothelial cells incubated in high-glucose media.[172,186,192,193] Glomeruli from diabetic rodents also display elevated PKC activity and cytosol-to-membrane translocation of diacylglycerol-sensitive PKC isoforms.[194,195] Increased activity of PKC in glomerular mesangial cells may lead to an increase in extracellular matrix expression, such as fibronectin, laminin and type IV collagen.[186,190]

Specific blockade of one particular PKC isoform *in vivo* has been made possible with the engineering of a safe and orally active PKC-β inhibitor Ruboxistaurin (LY333531). In diabetic rats this compound ameliorates the renal hemodynamic abnormalities, decreases the proteinuria, and prevents the glomerular overexpression of TGF-β and the matrix components, fibronectin and type IV collagen.[196,197] A randomized, double-blind, placebo-controlled, pilot study conducted on patients with type 2 diabetes receiving renin-angiotensin system inhibitors showed that the addition of Ruboxistaurin reduced albuminuria relative to the patients' baseline. However, when comparing the treatment and placebo arms of the trial, the changes in the albumin-to-creatinine ratios were not significant.[198] Other PKC isoforms, particularly PKC-α,[199] may also mediate the renal lesions in diabetes, but this possibility will have to await the design of selective isoform inhibitors. The actual molecular targets downstream of PKC activation remain unclear, but they somehow stimulate other signal transduction pathways (such as MAPKs, PI3Kinases and various growth factors). For instance, markedly elevated ambient glucose levels in mesangial cells can activate p38, a MAPK family member, but they do not significantly affect JNK activity. One member of MAPK family, ERK, is markedly activated in mesangial cells cultured under high-glucose conditions and in glomeruli of diabetic rats, and this activation is mediated through a PKC-dependent mechanism.[200] The activated ERK participates in the induction of TGF-β and the production of extracellular matrix.[201]

Oxidative Stress as a Common Initiator

Generation of ROS has received much attention with regard to the initiation of diabetic microvascular complications, including kidney disease.[202] As espoused by Brownlee, increased ROS generation is a consequence of persistent exposure to high glucose and this process involves increased mitochondrial oxidation as well as decreased scavenging of ROS.[170,184] Glycolysis of intracellular glucose results in production of NADH and pyruvate. Mitochondrial NADH and $FADH_2$ provide energy for ATP production through oxidative phosphorylation via the electron transport chain. Electron transfer through the mitochondrial complexes generates ATP synthase via a proton gradient. With increased electron flux, a high-proton gradient, and a high electrochemical potential difference, superoxide generation is enhanced. In response to elevations in extracellular glucose, aortic endothelial cells generate intracellular ROS primarily via mitochondrial NADH and $FADH_2$ that are generated by the tricarboxylic acid cycle from cytosolic pyruvate.[184] Subsequent superoxide generation initiates DNA strand breaks leading to poly (ADP-ribose) polymerase (PARP)–mediated glyceraldehyde phosphate dehydrogenase (GAPDH) inhibition.[203] Inhibition of GAPDH may then mediate PKC activation, hexosamine formation, advanced glycation end products (AGEs) formation, and NF-κB activation.[170] Studies in human mesangial cells have shown a host of similar changes related to mitochondrial ROS generation.[204] An interesting finding is that high-glucose stimulation of mitochondrial ROS mediates COX-2 upregulation in human mesangial cells.[204]

Oxidative stress has been clearly demonstrated in several animal models of diabetic kidney disease. Markers for this state are often reflected in decrements of glutathione or increased urinary 8-isoprostane. Inhibition of ROS with α-lipoic acid[205] or via overexpression of a cytosolic superoxide dismutase[206] prevents diabetic kidney disease in rodent models. Inasmuch as the accumulated data show that mitochondrial generation of ROS occurs in endothelial cells, this mechanism likely plays an important role in the generalized endothelial dysfunction of diabetes, including the development of albuminuria. Apart from mitochondrial ROS, a membrane-bound NADPH oxidase may potentially contribute to high-glucose-induced ROS production.[151] Studies have identified a novel form of NADPH oxidase, NOX-4, in the kidney,[207] which is upregulated in animal models of diabetic kidney disease.[208] The role of NOX-4 in diabetic kidney disease is starting to be uncovered. Administration of antisense oligonucleotides inhibiting NOX-4 have been shown to decrease glomerular hypertrophy, and resulted in decreased fibronectin

expression in renal cortex and notably in the glomeruli.[209] Moreover, NADPH oxidases have been localized to podocyte, and the NOX-1 and NOX-4 isoforms are upregulated in hyperglycemic milieu both *in vitro* and *in vivo*.[210] The accumulation of ROS from mitochondrial and non-mitochondrial pathways in the podocyte builds up into apoptotic signals such as the p38 MAPK pathway.[211] Accordingly oxidative stress could be contributing to the pathological changes in diabetic nephropathy, including podocyte loss and albuminuria. The subcellular source of ROS in diabetic kidney disease remains to be clarified. Also, the role of inhibition of discrete pathways of ROS generation is an exciting area of research that can help dictate future therapies for diabetic nephropathy.

Nonenzymatic Glycation of Proteins

Glycated proteins arise from a condensation reaction, driven by the ambient glucose concentration, in which a free sugar covalently attaches to a protein at reactive NH_2 groups. Glycation proceeds through the formation of a labile Schiff base adduct, which then undergoes an intramolecular Amadori rearrangement to become a stable glucose-modified protein. The reaction occurs slowly, and the degree and duration of hyperglycemia influence the amount of glycated protein. Amadori-modified proteins may further evolve through a series of spontaneous rearrangement, dehydration, and polymerization reactions to become advanced glycation end products (AGEs). Nonenzymatic glycation can be mediated by a large variety of carbohydrates including glucose, and by methylglyoxal and 3-deoxyglucosone. In fact, methylglyoxal and 3-deoxyglucosone are far more reactive than glucose, forming adducts with amino groups of proteins, nucleic acid, and phospholipids up to several thousand times more readily than glucose. Although the chemical reactions involved are nonenzymatic, the production and detoxification of AGE precursors is actually controlled by enzymatic mechanisms. Thus the accelerated formation of glycated proteins in diabetes may result from increased production and/or decreased degradation. A large body of research has been devoted to understanding the role of glycated proteins in the pathogenesis of diabetic complications.

ROLE OF AMADORI-GLYCATED ALBUMIN

A large clinical study found that type 1 diabetic patients who have nephropathy manifest significantly higher levels of Amadori albumin than subjects without nephropathy.[212] The severity of tissue damage in diabetic nephropathy often parallels the localization of glycated proteins in glomeruli. Albumin modified by Amadori-glucose adducts has been linked to the development of diabetic nephropathy through its ability to activate PKC-β, upregulate the TGF-β system, and stimulate expression of extracellular matrix proteins in glomerular cells.[213–215] When PKC-β activity is specifically blocked by the selective inhibitor LY-379196, the increase in type IV collagen synthesis is prevented to the same degree,[214] consistent with the notion that the β isoform plays a predominant role among the PKC isotypes.[197,216] A putative cell-surface receptor is postulated to transduce the observed actions of glycated albumin.

Chronic administration of Fab fragments of an anti-glycated albumin antibody, A717, significantly lowers the plasma glycated albumin concentration in the diabetic *db/db* mouse and produces significantly less urinary albumin excretion.[217] Glomeruli from A717-treated *db/db* mice also showed considerably less mesangial expansion than control mice; this was associated with attenuation of the augmented mRNA levels for α1(IV) collagen and fibronectin.[217]

ROLE OF ADVANCED GLYCATION END PRODUCTS

The Maillard reaction, resulting in AGE production, alters protein structure and molecular surface composition, and this can profoundly change the affected molecule's biochemical properties and surface topology. Virtually any protein can be affected by glycoxidative modifications but particularly long-lived proteins including matrix and structural proteins or intercellular matrix components are prone to form AGEs.[218] The kidney, however, is not only a target of AGEs but also a culprit, as declining renal function is associated with retention in the plasma of high concentrations of these products.[219]

Glucose is a predominant source of reactive sugars for AGE formation but many other sugar molecules can also condense with proteins such as fructose, threose, glucose-6-phosphate, and glyceraldehyde-3-phosphate to produce different AGEs such as N^{ε}-(carboxymethyl)-lysine (CML) and pentosidine. Pentosidine is a cross-linking molecule that covalently bridges distant lysine and arginine residues by a complex C5-sugar ring thereby linking different proteins together or forming intramolecular covalent bonds. Protein adducts arising from this pathway are accordingly termed "advanced lipoperoxidation end products." Compounds such as malondialdehyde,

hydroxynonenal (HNE)-lysine, or acrolein adducts derived from oxidized hydroxy-aminoacids, L-serine or L-threonine, belong to the glycoxidation class of terminally modified proteins. Lipoxidative and glycoxidative pathways may converge, resulting in the same end product, CML, whereas pentosidine is only formed from carbohydrate precursors. In contrast, AGEs such as imidazolone and pyrraline adducts can also be generated independently from oxidative stress.

In the diabetic kidney, progressive tissue damage is closely related to the deposition of AGEs.[220] In an animal model, cellular and molecular growth events typical for progressive diabetic nephropathy can be almost mimicked by chronic intravenous infusion of CML-albumin.[221] AGEs induce connective tissue growth factor (CTGF) expression in the kidney through a TGF-β-mediated effect;[222] CTGF is known to mediate many of the profibrotic effects of TGF-β.[223] Interestingly, AGEs activate the TGF-β−Smad signaling pathway in mesangial cells by autocrine production of Ang II.[224] Pharmacological interventions using AGE-breaking agents or inhibitors of AGE formation such as aminoguanidine, OPB-9195, ALT-946, pyridoxamine and others have been widely used to prevent AGE-induced end-organ damage.[225]

In 1992, Schmidt and her colleagues first discovered a cellular surface receptor that binds AGE-modified proteins with high affinity, which was subsequently termed "receptor for AGE" (RAGE).[226] Subsequent research identified several additional cell surface molecules capable of binding AGE-modified proteins, including macrophage scavenger receptors (MSRs) type A and B1 (CD36), oligosaccharyl transferase-48 termed "AGE receptor 1" (AGE-R1), 80K-H phosphoprotein (AGE-R2), and galectin-3 (AGE-R3), the scavenger receptor. Among these molecules, RAGE has been best characterized. It is a 35-kD protein belonging to the immunoglobulin superfamily whose gene is located on chromosome 6. RAGE is a transmembrane receptor consisting of 394 amino acids with a single hydrophobic transmembrane domain of 19 amino acids and a C-terminal cytosolic tail of 43 amino acids.[227] The extracellular part consists of a terminal V-type and two distinct C-type domains (V-C-C) where V domains bind ligands and the highly charged cytosolic tail mediates activation of intracellular signal transduction pathways. Various mRNA splice variants have been detected that encode truncated proteins with different biological properties. The receptor can bind different AGE-adducts with high affinity, including CML and pentosidine.[228]

In normal human kidney, RAGE protein is found on glomerular podocytes and tubular epithelia by immunohistochemical techniques. In the presence of AGE ligands, susceptible cells can rapidly upregulate RAGE expression (e.g., in podocytes of diabetic kidney). In contrast, RAGE expression in other glomerular cells is generally less inducible.[229] Cellular expression of RAGE can be induced by AGE ligands as well as in the absence of AGEs, such as during inflammatory tissue remodeling or after direct cytokine stimulation by TNF-β. These experimental observations are on RAGE induction readily explained by the presence of NF-κB and SP-1 binding sites in the promoter region of the RAGE gene.

Activation of RAGE triggers multiple intracellular signal transduction cascades depending on the individual cell type.[230] This can include enhanced intracellular oxidant stress and activation of NF-κB by redox-sensitive signaling pathways.[231] AGEs may also inhibit cellular NO production, which is mediated at least in part by downregulation of eNOS and increased NADP(H) oxidase expression, thus linking RAGE activity to chronic endothelial cell dysfunction. RAGE activation can increase RAGE mRNA transcription directly and thus initiate an auto-amplifying loop. RAGE activation can also induce intracellular generation of hydrogen peroxide, which is dependent on the functional integrity of NADPH oxidase.

In diabetic nephropathy, renal expression of RAGE and VEGF increases considerably, including in podocytes.[134] Experimentally, soluble RAGE (sRAGE) has been used extensively as a tool to block RAGE-dependent effects in cultured cells and in experimental animals. Treatment of diabetic *db/db* mice with sRAGE significantly reduces the albuminuria and the glomerular hypertrophy. On the other hand, homozygous RAGE-null mice rendered diabetic do not develop increased renal VEGF and TGF-β expression, indicating a pivotal role for RAGE-dependent activation of these growth factors in the development of diabetic kidney disease.[124]

Renin-Angiotensin-Aldosterone System

Data from animal studies suggest that local angiotensin-generating systems exist in many tissues including the kidney, and these systems may operate independently of the systemic RAAS.[232] Micropuncture and microdialysis experiments in normal rats have demonstrated that proximal tubular and interstitial fluid contain Ang II concentrations in the nanomolar compared with picomolar range in the systemic circulation. These studies suggest that tubular cells possess a RAAS and can produce Ang II. Significant activation of the proximal tubular RAAS is presumed to occur in the diabetic state. Studies in early STZ-induced diabetes have shown enhanced expression of renin mRNA, which contributes to this local

RAAS activation. It is hypothesized that the increased local production of Ang II could contribute to tubulointerstitial injury in diabetes.

Of particular importance is the observation that systemic application of an ACE inhibitor results in almost complete inhibition of systemic Ang II formation but has only little effect on intrarenal Ang II production. Also of interest is that intact Ang II is intracellularly present in endosomes and is derived from receptor-mediated endocytosis that follows Ang II binding to its putative receptor. This could be an important mechanism because it has been demonstrated in certain cells that Ang II may directly go into the nucleus and could regulate gene transcription.[58]

Ang II is metabolized by peptidases such as aminopeptidase A (APA) into angiotensin III and further into angiotensin IV (Ang IV). Ang IV binds to a specific receptor named AT4. This receptor is widely expressed in the kidney including endothelial, proximal tubular, and distal convoluted tubular cells. Ang IV stimulates PAI-1 expression in proximal tubular and endothelial cells through AT4 receptors. Since PAI-1 reduces extracellular matrix turnover, Ang IV may induce renal fibrosis independently of activation of AT1 and AT2 receptors. Moreover, Ang IV-generating enzymes are upregulated in conditions with presumed high levels of Ang II in the kidney such as diabetic nephropathy, likely shifting more Ang II into the degradation pathway to Ang IV.[233]

Drugs interfering with the RAAS are a mainstay of therapy in preventing the progression of diabetic nephropathy as first reported by Zatz and coworkers in experimentally-induced diabetes.[234] Although initially considered to act solely through normalization of systemic and glomerular hypertension, it is now clear that inhibition of the RAAS has many effects, including antifibrotic and anti-inflammatory mechanisms. In fact, Ang II itself induces in renal cells many proinflammatory and profibrogenic cytokines, chemokines, and growth factors.[58] High glucose stimulates expression of renin and angiotensinogen in mesangial and tubular cells.[235,236] This stimulation results in an increase in local Ang II concentrations that may, in turn, through autocrine and paracrine pathways, induce a whole battery of different cytokines and growth factors. Experimental studies indicate that high-glucose–mediated generation of ROS is important in the upregulation of angiotensinogen in proximal tubular cells.[235]

Inhibition of the RAAS significantly reduces proteinuria in diabetic nephropathy as compared with other antihypertensive classes of medications. Treatment with ACE inhibitors or AT1-receptor antagonists attenuate podocyte foot process broadening in STZ-diabetic rats.[113,114] An AT1-receptor antagonist, but not the calcium channel blocker amlodipine, normalized the reduced nephrin expression in podocytes from spontaneously hypertensive rats with superimposed STZ-induced diabetes.[237] Thus, a local increase in Ang II leads to suppression of nephrin expression in podocytes, and thereby can enhance the ultrafiltration of proteins. Podocytes express AT1 and probably AT2 receptors and could respond to stimulation with Ang II. Transgenic rats with targeted overexpression of the AT1-receptor to podocytes showed pseudocysts in podocytes, followed by foot process effacement and local detachments.[238] These changes subsequently progressed to focal segmental glomerulosclerosis.

Podocytes are also a likely site for Ang II generation. It has been previously shown that high ambient glucose concentration induces Ang II formation in podocytes through upregulation of angiotensinogen expression.[239] Furthermore, proteinuria and the transit of proteins through the ultrafiltration barrier likely activate Ang II formation in podocytes. Finally, mechanical stretch could increase Ang II generation in podocytes.[240] Interestingly, Ang II formation as a consequence of mechanical stress appears to be independent of ACE. In this regard, it has been demonstrated that chymase, an Ang II forming enzyme not inhibited by ACE inhibitors, is upregulated in glomeruli of patients with nephropathy due to type 2 diabetes.[241] This observation suggests that local glomerular formation of Ang II in the diabetic state may be partly independent of ACE and may not be abolished by ACE inhibition alone.

Activation of the RAAS may play an important role in macrophage recruitment. Biopsy studies from patients with diabetic nephropathy and investigations in various animal models have revealed the presence of inflammatory cells, especially mononuclear cell infiltrates, in the glomerular and tubulointerstitial compartments.[242] Monocyte chemoattractant protein-1 (MCP-1) is an important chemokine for macrophages/monocytes, and high glucose has been shown to stimulate MCP-1 expression in mesangial cells. In fact, increases in tubular expression of MCP-1 and RANTES, members of the C-C chemokine subfamily with chemoattractant properties for monocytes/macrophages, have been found adjacent to infiltrating immune cells in renal biopsy specimens from patients with diabetic nephropathy.[243,244] The MCP-1 increase could be relevant in another way that does not involve macrophages. MCP-1 directly stimulates matrix expression in mesangial cells[245] and increases cellular motility in podocytes,[246,247] having the associated effect of making a podocyte monolayer more permeable to albumin. Extrapolated to diabetic nephropathy, these MCP-1 effects may abet the process of mesangial matrix expansion and diabetic albuminuria. The proinflammatory transcription factor NF-κB has been detected mainly in tubular cells in biopsy specimens from 11

patients with type 2 diabetes and overt nephropathy, indicating that proteinuria may have contributed to this activation.[243] Activation of the RAAS may play an important role in this process. In animal models of kidney disease there is upregulation of NF-κB in tubular cells that is inhibited by inhibitors of the RAAS.[58,248] Ang II, through an effect mediated by AT2 and not AT1 receptors, increases the mRNA and protein levels of RANTES in cultured glomerular endothelial cells.[249] Intraperitoneal infusion of Ang II into naive rats for 4 days significantly stimulates glomerular influx of macrophages/monocytes as well as the expression of RANTES mRNA and protein in the glomeruli, mainly in endothelial cells and small capillaries.[249] Ang II also stimulates the chemoattractant cytokines MCP-1 and osteopontin in mesangial and tubular cells, which may play a role in glomerular and tubular inflammation associated with proteinuria.[250]

Aldosterone, working independently from the RAAS, may be involved in the development of diabetic nephropathy.[251] The aldosterone antagonist spironolactone attenuates the enhanced TGF-β1 expression and the increased collagen deposition in rats three weeks after STZ administration.[251] In a preliminary study, Schjoedt and colleagues observed that an increased plasma aldosterone level during long-term treatment with an AT1-receptor blocker is associated with a decline in GFR in patients with nephropathy due to type 1 diabetes.[252] These data demonstrate that aldosterone contributes to the progression of diabetic nephropathy despite blockade of the AT1 receptor. Spironolactone decreases proteinuria in patients with type 2 diabetes and early nephropathy.[253] The more selective aldosterone antagonist, eplerenone, also decreases the microalbuminuria in patients with type 2 diabetes independent of its antihypertensive effect.[254] In addition to direct effects on renal cells, aldosterone also potentiates the Ang II-mediated signal processes such as MAPK activation, indicating that Ang II and aldosterone act in concert.[255]

In summary, there are many deleterious effects of the RAAS in the pathophysiology of diabetic nephropathy. Early treatment with drugs that interfere with RAAS activation, especially ACE inhibitors and AT1 receptor blockers, is a major mainstay in the clinical management of the diabetic patient who is at risk of developing nephropathy.

TGF-β is the Common, Downstream Mediator of Diabetic Nephropathy

The cytokine TGF-β has risen to prominence in the past several years as the principal mediator of progressive renal diseases including diabetic nephropathy. TGF-β has been shown to be the final common pathway or mediator that leads to the hypertrophic and prosclerotic changes in diabetic kidney disease, thus fulfilling all of Koch's postulates as a chief etiologic agent of the disease.[122,256,257] TGF-β stimulates the synthesis of key extracellular matrix molecules including type I collagen, type IV collagen, fibronectin, and laminin.[258] TGF-β also decreases matrix degradation by inhibiting proteases as well as activating inhibitors of those proteases (e.g., PAI-1).[259] Additionally, TGF-β promotes cell−matrix interactions by upregulating integrins, the cell-surface receptors for matrix.[260]

The biologic effects of TGF-β in kidney cells, which include cell hypertrophy and stimulation of extracellular matrix production, closely resemble those of hyperglycemia. Almost all of the molecular mediators and intracellular signaling pathways that have been identified in diabetic kidney injury have also been found to stimulate the renal TGF-β activity as an intermediary step (see also Table 78.4). These include high-glucose concentration;[261] early (Amadori) as well as AGE-modified proteins;[215,262] oxidative stress and overproduction of superoxide by the mitochondrial electron-transport chain;[170,202,263] cyclical stretch/relaxation of mesangial cells in culture;[163] de novo synthesis of diacylglycerol and PKC activation;[192,197] stimulation of MAPK, such as ERK;[201] glucosamine overproduction;[183] and high levels of vasoactive substances such as Ang II,[74,264] endothelin,[265] and thromboxane.[266]

Studies in animal models of both type 1 and type 2 diabetes further implicate TGF-β as an important mediator of diabetic kidney disease. TGF-β1 mRNA and protein levels are increased in both the glomerular and tubular compartments of rat and mouse models of diabetes.[267−269] Of particular significance is the finding of concomitant upregulation of the renal TGF-β type II signaling receptor in tubules and glomeruli.[270,271] In almost all renal cell types studied in tissue culture (except perhaps for podocytes), high ambient glucose has been shown to upregulate the expression and bioactivity of TGF-β; these include proximal tubular epithelial cells, glomerular mesangial and endothelial cells, and interstitial fibroblasts.[75,121,122,272] In all renal cells studied, including podocytes, high glucose also upregulates the TGF-β type II receptor.[271,273]

Human studies have also corroborated the important role that the renal TGF-β system plays in the pathogenesis of diabetic nephropathy.[274,275] Glomerular TGF-β1 mRNA is markedly increased[276] and there is net production of TGF-β1 protein by the kidney in diabetic patients.[277] Interestingly, therapy with an ACE inhibitor protects the kidney through a host of mechanisms that also include the lowering of TGF-β1 production.[278] In fact, a decrease in the circulating TGF-β1 level predicts a better long-term preservation of the GFR.[278]

Blocking the activity of the renal TGF-β system in diabetic animals has provided proof-of-concept that the development of renal disease is due to overactivity of this system in diabetes. Neutralizing monoclonal antibodies to TGF-β prevent the glomerular hypertrophy and attenuate the increase in TGF-β1, α1(IV) collagen, and fibronectin mRNAs in STZ-induced diabetes in mice.[279] Also, the antibody therapy in the *db*/*db* mouse, a model of type 2 diabetes, prevents the mesangial matrix expansion (but without affecting the albuminuria).[121] This latter finding may suggest that diabetic proteinuria, unlike the hypertrophic and prosclerotic renal manifestations of diabetes, is mediated by increased podocyte-derived VEGF rather than by TGF-β.[101,121,124,125]

Hypoxia and Diabetic Nephropathy

Clinical studies have provided evidence that even mild anemia (hemoglobin <13.8 g/dl) increases risk for progression in patients with type 2 diabetes and nephropathy.[280] Moreover, treating anemia early in renal failure with erythropoietin slows the decline of renal function.[281] In practice, however, the benefit of erythropoiesis-stimulating agents has not held up to the scrutiny of several large, prospective, randomized controlled trials such as TREAT which showed no renal benefit and no delay in the progression to ESRD with darbepoetin alfa.[286] The exact mechanisms by which anemia increases the risk for progression of diabetic nephropathy are incompletely understood, but a few suggestions could be made. Anemia likely causes renal hypoxia. It has been described in experimental models of chronic renal injury that hypoxia is an important factor aggravating interstitial fibrosis, partly by the induction of factors such as TGF-β and VEGF. The transdifferentiation of tubular epithelial cells into fibroblasts, an important process contributing to tubular atrophy and interstitial fibrosis, is stimulated by cellular hypoxia and mediated, appropriately enough, by hypoxia-inducible factor-1 (HIF-1), a transcription factor that plays a role in regulating genes critical to the adaptation to low oxygen.[282–284] Certain growth factors and cytokines are stimulated by HIF-1 which itself can be increased by Ang II via activation of AT2 receptors, leading to the suppression of SM-20, a dihydrogenase involved in hydroxylation of HIF-1α.[58] Since hydroxylated HIF-1α is rapidly degraded through the proteasome, the Ang II-mediated decrease in hydroxylation leads to stabilization of this important transcription factor. Thus, hypoxia plus Ang II may induce growth factors and signaling pathways with potentially deleterious effects in diabetic nephropathy. On the other hand, erythropoietin application may have additional effects in addition to correcting anemia, and the mobilization of potential progenitor cells by this treatment has become the focus of active research.[285] Certainly, more experiments are necessary to elucidate how anemia may contribute to the development and progression of diabetic nephropathy. Lastly, any well-meaning attempt to correct anemia for the sake of diabetic nephropathy has to be weighed against the not-inconsiderable risk of stroke, hypertension, other cardiovascular event, and possibly increased mortality that seem to arise from the overzealous use of erythropoiesis-stimulating agents.[286–290]

METABOLIC SYNDROME/OBESITY AND RENAL DISEASE

The metabolic syndrome is increasingly being recognized as a major contributor to cardiovascular diseases among large segments of the population worldwide. Although once relegated to a constellation of risk factors that were not considered to play a major role in kidney diseases, analyses in large population groups have identified the metabolic syndrome as a major risk factor for chronic kidney disease. Conversely, chronic kidney disease has also emerged as a key risk factor for predicting cardiovascular disease even in patients with mild renal dysfunction.

The metabolic syndrome is defined as having at least three of the following five parameters: increased waist circumference, elevated triglycerides, decreased high-density lipoproteins (HDLs), elevated blood pressure, and elevated fasting blood glucose.[291] These values have been derived primarily from the white population and will likely need to be redefined for different ethnic groups. It appears that some Asian populations develop the metabolic syndrome with lesser levels of waist circumference,[292] whereas African Americans may exhibit features of insulin resistance without a correlation with visceral adiposity.[293] Values pertaining to blood pressure and fasting blood glucose may also need to be revised as lower levels of pressure and glucose have been associated with increased cardiovascular risk. Other features such as albuminuria and left ventricular hypertrophy may also be added to the definition.[294] The major outcome of the metabolic syndrome is the increased risk these patients have for developing myocardial infarctions, strokes, and diabetes mellitus.

The recognition that the metabolic syndrome is strongly associated with kidney disease has only been appreciated in the past few years.[295] In 2003, a statistical relationship was found between features of the metabolic syndrome and albuminuria using the Third National Health and Nutrition Survey (NHANES III)

cohort.[296,297] In 2004, Chen et al.[298] found that each component of the metabolic syndrome added to the risk of impaired renal function as estimated by four different GFR formulas that are based on the serum creatinine value. The estimated GFR has also been inversely correlated with the development of cardiovascular disease and poor outcome after a major cardiovascular event.[299,300] In addition, even low levels of albuminuria in patients with left ventricular hypertrophy are associated with increased cardiovascular risk.[294] The interplay between heart and kidney, that chronic kidney disease is adversely influenced by chronic heart disease and vice versa, has recently been promulgated as the cardiorenal syndrome.[301] Therefore, it is apparent that there is a very close relationship between the metabolic syndrome, renal dysfunction, and cardiovascular endpoints. However, the mechanisms linking this triad together remain unclear.

The nature of the kidney lesions associated with the metabolic syndrome has not been clearly established. Studies have found that obese individuals (body mass index [BMI] >30) have large kidneys and glomerulomegaly (reviewed in[295]). This appears to be strikingly uniform such that almost 100% of patients with obesity-related kidney disease exhibit glomerulomegaly.[302] In addition, several studies have demonstrated an altered hemodynamic profile in obesity. Thus, obese patients have increased renal blood flow, increased filtration fraction, and mild glomerular hyperfiltration.[303,304] The close resemblance of obesity-related kidney disease to the early features of diabetic kidney disease is intriguing. However, the pathologic lesion in the former is distinct from diabetic nephropathy as there is typically focal and segmental glomerulosclerosis rather than diffuse mesangial matrix expansion or nodular glomerulosclerosis.[302]

The mediators of kidney disease associated with the metabolic syndrome and obesity have not been identified. Using the NHANES data, the fasting blood glucose and systolic blood pressure are the most closely linked to albuminuria and the development of renal insufficiency.[298] Sleep apnea and hypoxia may also contribute to kidney impairment. It is now recognized that visceral adipocytes are a potent source of deleterious factors that could impact renal function. Visceral adipocytes probably produce all components of the RAAS, and this may contribute to systemic hypertension and altered renal hemodynamics.[305,306] Production of leptin, VEGF, endothelin-1, TGF-β, and PAI-1 by adipocytes[307–309] may also contribute to hypertension, altered glomerular blood flow, glomerulomegaly, focal sclerosis, and albuminuria. Production of adipocyte-derived TNF-α may mediate an inflammatory cascade in the kidney that leads to renal dysfunction. Alternatively, the adipocyte-induced regulation of adiponectin may contribute to endothelial dysfunction and renal injury.[295]

Treatment approaches for the metabolic syndrome are only now being addressed. Weight loss and exercise are important cornerstones and greater attention is required to allow physicians to incorporate behavior-altering regimens into their clinical practice. Apart from behavior modification, attention has been paid to the role of PPAR-γ agonists (glitazones) and inhibitors of the RAAS. The glitazones are able to decrease visceral adiposity by inhibiting adipocyte hypertrophy and proliferation.[310] The recognition that both ACE inhibitors and AT1 receptor blockers are able to decrease insulin resistance and lower hemoglobin A1c may in part be due to adipocyte-derived activation of the RAAS.

REGRESSION

One would assume that the morphological alterations of advanced diabetic nephropathy (e.g., glomerulosclerosis, interstitial fibrosis) are not reversible and represent a one-way road to ESRD. Experimental[311] and clinical studies[312] show, however, that this pessimistic scenario is not necessarily true. Several studies indicate that aggressive blood pressure control with agents that interfere with the RAAS leads to remission of overt proteinuria. Fioretto and colleagues performed serial renal biopsy in eight patients with type 1 diabetes and nephropathy who had undergone a successful pancreas transplantation.[312] These investigators found that sustained euglycemia reversed the morphological alterations of diabetic nephropathy, including increased GBM thickness and mesangial matrix expansion, 10 years after receiving the pancreas transplant. The regression of diabetic nephropathy was convincing, but clearly this process takes time. In addition, Perkins et al.[313] showed that the onset of sustained microalbuminuria does not imply an inexorable progression to nephropathy, at least not in patients with type 1 diabetes. This study provides indirect evidence that aggressive management aimed at various risk factors could lead to remission of albuminuria. Since no renal biopsies were performed in this study, it remained unproven whether morphological changes of diabetic nephropathy were also improved. Although the molecular mechanisms surrounding regression are currently incompletely understood, it is possible that induction of metalloproteinases that may degrade the deposited extracellular matrix play a central role in the healing. Nevertheless, there is light at the end of the tunnel and a better understanding of the complex pathophysiology of diabetic nephropathy will likely improve a multipronged approach to induce regression.

SUMMARY AND OUTLOOK

Only a minority of diabetic patients will ever develop diabetic kidney disease. This has been the major impetus to try to identify those genes that are either predisposing to or protective against the development of diabetic kidney disease. Much remains to be understood about the genetic factors that are at play. Another concept that has emerged is that injury to the kidney in susceptible patients may start before diabetes mellitus has fully manifested. Evidence is emerging that the metabolic syndrome can injure the kidney through many different mechanisms in addition to hypertension and hyperglycemia. Although it has been debated for many years whether hemodynamic or metabolic changes are more important in the development of overt diabetic nephropathy, it is now clear that metabolic events can be triggered by hemodynamic stress and thus these processes are interwoven, depicting two sides of one coin. On a molecular level, metabolic pathways activated by hyperglycemia as well as by proteins altered by high blood glucose such as Amadori products and AGEs are key players in the development of diabetic nephropathy. Oxidative stress that is induced by high-glucose–mediated activation of the mitochondrial electron-transport chain is an early event in the development of diabetic complications. A variety of growth factors and cytokines are then induced through complex signal transduction pathways involving PKC, MAPK, and NF-κB. The cytokine TGF-β has emerged as an important downstream mediator for the development of renal hypertrophy and the accumulation of extracellular matrix components. Activation of the RAAS in different kidney compartments by high glucose, mechanical stress, and proteinuria can cause many of the pathophysiological changes associated with diabetic nephropathy. In fact, it has been shown that Ang II is involved in almost every pathophysiological process implicated in the development of diabetic nephropathy (hemodynamic changes, hypertrophy, extracellular matrix accumulation, growth factor/cytokine induction, ROS formation, podocyte damage, proteinuria, interstitial inflammation, and fibrosis). Consequently, blocking the deleterious effects of Ang II is an essential part of every therapeutic regimen to prevent and treat diabetic nephropathy. There is hope that regression of diabetic nephropathy could be achieved under certain circumstances.

References

[1] Remuzzi G, Schieppati A, Ruggenenti P. Clinical practice. Nephropathy in patients with type 2 diabetes. N Engl J Med 2002;346(15):1145–51.

[2] Ritz E, Rychlik I, Locatelli F, Halimi S. End-stage renal failure in type 2 diabetes: a medical catastrophe of worldwide dimensions. Am J Kidney Dis 1999;34(5):795–808.

[3] Hemmelgarn BR, Manns BJ, Lloyd A, et al. Relation between kidney function, proteinuria, and adverse outcomes. JAMA 2010;303(5):423–9.

[4] Zatz R, Meyer TW, Rennke HG, Brenner BM. Predominace of hemodynamic rather than metabolic factirs in the pathogensis of diabetic glomerulopathy. Proc Natl Acad Sci USA 1985; 82:5963–7.

[5] Wolf G, Ritz E. Diabetic nephropathy in type 2 diabetes prevention and patient management. J Am Soc Nephrol 2003;14(5):1396–405.

[6] Freedman BI, Bostrom M, Daeihagh P, Bowden DW. Genetic factors in diabetic nephropathy. Clin J Am Soc Nephrol 2007;2(6):1306–16.

[7] Riser BL, Cortes P, Yee J, et al. Mechanical strain- and high glucose-induced alterations in mesangial cell collagen metabolism: role of TGF-beta. J Am Soc Nephrol 1998;9(5):827–36.

[8] Abboud HE. Growth factors and diabetic nephrology: an overview. Kidney Int Suppl 1997;60:S3–6.

[9] Tsuchida K, Cronin B, Sharma K. Novel aspects of transforming growth factor-Beta in diabetic kidney disease. Nephron 2002;92(1):7–21.

[10] Selby JV, FitzSimmons SC, Newman JM, Katz PP, Sepe S, Showstack J. The natural history and epidemiology of diabetic nephropathy. Implications for prevention and control. JAMA 1990;263(14):1954–60.

[11] Bojestig M, Arnqvist HJ, Hermansson G, Karlberg BE, Ludvigsson J. Declining incidence of nephropathy in insulin-dependent diabetes mellitus. N Engl J Med 1994;330(1):15–8.

[12] Nordwall M, Bojestig M, Arnqvist HJ, Ludvigsson J. Declining incidence of severe retinopathy and persisting decrease of nephropathy in an unselected population of Type 1 diabetes-the linkoping diabetes complications study. Diabetologia 2004;47(7):1266–72.

[13] Gaede P, Vedel P, Larsen N, Jensen GV, Parving HH, Pedersen O. Multifactorial intervention and cardiovascular disease in patients with type 2 diabetes. N Engl J Med 2003;348(5):383–93.

[14] Adler AI, Stevens RJ, Manley SE, Bilous RW, Cull CA, Holman RR. Development and progression of nephropathy in type 2 diabetes: the united kingdom prospective diabetes study (UKPDS 64). Kidney Int 2003;63(1):225–32.

[15] Yokoyama H, Okudaira M, Otani T, et al. Higher incidence of diabetic nephropathy in type 2 than in type 1 diabetes in early-onset diabetes in Japan. Kidney Int 2000;58(1):302–11.

[16] Zimmet P, Alberti KG, Shaw J. Global and societal implications of the diabetes epidemic. Nature 2001;414(6865):782–7.

[17] Friedman EA, Friedman AL. Is there really good news about pandemic diabetic nephropathy? Nephrol Dial Transplant 2007;22(3):681–3.

[18] McBean AM, Li S, Gilbertson DT, Collins AJ. Differences in diabetes prevalence, incidence, and mortality among the elderly of four racial/ethnic groups: whites, blacks, hispanics, and asians. Diabetes Care 2004;27(10):2317–24.

[19] Collins AJ, Kasiske B, Herzog C, et al. Excerpts from the united states renal data system 2003 annual data report: atlas of end-stage renal disease in the united states. Am J Kidney Dis 2003;42(6 Suppl 5):S1–230 [A5-7]

[20] Dikow R, Adamczak M, Henriquez DE, Ritz E. Strategies to decrease cardiovascular mortality in patients with end-stage renal disease. Kidney Int Suppl 2002;80:5–10.

[21] Dikow R, Ritz E. Cardiovascular complications in the diabetic patient with renal disease: an update in 2003. Nephrol Dial Transplant 2003;18(10):1993–8.

[22] Iseki K, Tozawa M, Iseki C, Takishita S, Ogawa Y. Demographic trends in the okinawa dialysis study (OKIDS) registry (1971–2000). Kidney Int 2002;61(2):668–75.
[23] Berger M, Monks D, Wanner C, Lindner TH. Diabetic nephropathy: an inherited disease or just a diabetic complication? Kidney Blood Press Res 2003;26(3):143–54.
[24] Freedman BI, Yu H, Spray BJ, Rich SS, Rothschild CB, Bowden DW. Genetic linkage analysis of growth factor loci and end-stage renal disease in African Americans. Kidney Int 1997;51(3):819–25.
[25] Keller CK, Bergis KH, Fliser D, Ritz E. Renal findings in patients with short-term type 2 diabetes. J Am Soc Nephrol 1996;7(12):2627–35.
[26] Zheng F, Cornacchia F, Schulman I, et al. Development of albuminuria and glomerular lesions in normoglycemic B6 recipients of db/db mice bone marrow: the role of mesangial cell progenitors. Diabetes 2004;53(9):2420–7.
[27] Ek J, Andersen G, Urhammer SA, et al. Mutation analysis of peroxisome proliferator-activated receptor-gamma coactivator-1 (PGC-1) and relationships of identified amino acid polymorphisms to Type II diabetes mellitus. Diabetologia 2001;44(12): 2220–6.
[28] Hansen L, Fjordvang H, Rasmussen SK, et al. Mutational analysis of the coding regions of the genes encoding protein kinase B-alpha and -beta, phosphoinositide-dependent protein kinase-1, phosphatase targeting to glycogen, protein phosphatase inhibitor-1, and glycogenin: lessons from a search for genetic variability of the insulin-stimulated glycogen synthesis pathway of skeletal muscle in NIDDM patients. Diabetes 1999;48(2):403–7.
[29] Hansen L, Urioste S, Petersen HV, et al. Missense mutations in the human insulin promoter factor-1 gene and their relation to maturity-onset diabetes of the young and late-onset type 2 diabetes mellitus in caucasians. J Clin Endocrinol Metab 2000;85 (3):1323–6.
[30] Nielsen EM, Hansen L, Echwald SM, et al. Evidence for an association between the Leu162Val polymorphism of the PPARalpha gene and decreased fasting serum triglyceride levels in glucose tolerant subjects. Pharmacogenetics 2003;13(7): 417–23.
[31] Moller AM, Ek J, Durviaux SM, et al. Hepatocyte nuclear factor-6: associations between genetic variability and type II diabetes and between genetic variability and estimates of insulin secretion. Diabetologia 1999;42(8):1011–6.
[32] Moller AM, Jensen NM, Pildal J, et al. Studies of genetic variability of the glucose transporter 2 promoter in patients with type 2 diabetes mellitus. J Clin Endocrinol Metab 2001;86(5): 2181–6.
[33] Parving HH, Tarnow L, Rossing P. Genetics of diabetic nephropathy. J Am Soc Nephrol 1996;7(12):2509–17.
[34] Pedersen OB, Hansen T, Hansen L, Echwald SM, Urhammer SA. Chasing the genetic determinants of the presumed polygenic forms of type 2 diabetes. Status and perspectives. Ugeskr Laeger 2002;164(16):2163–6.
[35] Pildal J, Lajer M, Hansen SK, et al. Studies of variability in the islet amyloid polypeptide gene in relation to Type 2 diabetes. Diabet Med 2003;20(6):491–4.
[36] Poulsen P, Andersen G, Fenger M, et al. Impact of two common polymorphisms in the PPARgamma gene on glucose tolerance and plasma insulin profiles in monozygotic and dizygotic twins: thrifty genotype, thrifty phenotype, or both? Diabetes 2003;52(1):194–8.
[37] Prabhakar SS. Role of nitric oxide in diabetic nephropathy. Semin Nephrol 2004;24(4):333–44.
[38] Couser WG. Revisions to Instructions to JASN authors regarding articles reporting studies using DNA Arrays, DNA polymorphisms, and randomized controlled clinical trials. J Am Soc Nephrol 2003;14(10):2686–7.
[39] Kunz R, Bork JP, Fritsche L, Ringel J, Sharma AM. Association between the angiotensin-converting enzyme-insertion/deletion polymorphism and diabetic nephropathy: a methodologic appraisal and systematic review. J Am Soc Nephrol 1998;9(9): 1653–63.
[40] Scharplatz M, Puhan MA, Steurer J, Bachmann LM. What is the impact of the ACE gene insertion/deletion (I/D) polymorphism on the clinical effectiveness and adverse events of ACE inhibitors?—Protocol of a systematic review. BMC Med Genet 2004;5:23.
[41] Hindorff L.A., Junkins H.A., Mehta J.P., Manolio T.A. A Catalog of Published Genome-Wide Association Studies. Available at, <www.genome.gov/gwastudies>; 2010 [accessed 29.04.10].
[42] Pezzolesi MG, Poznik GD, Mychaleckyj JC, et al. Genome-wide association scan for diabetic nephropathy susceptibility genes in type 1 diabetes. Diabetes 2009;58(6):1403–10.
[43] Maeda S, Osawa N, Hayashi T, Tsukada S, Kobayashi M, Kikkawa R. Genetic variations associated with diabetic nephropathy and type II diabetes in a Japanese population. Kidney Int Suppl 2007;106:S43–8.
[44] Pezzolesi MG, Katavetin P, Kure M, et al. Confirmation of genetic associations at ELMO1 in the GoKinD collection supports its role as a susceptibility gene in diabetic nephropathy. Diabetes 2009;58(11):2698–702.
[45] Leak TS, Perlegas PS, Smith SG, et al. Variants in intron 13 of the ELMO1 gene are associated with diabetic nephropathy in African Americans. Ann Hum Genet 2009;73(2):152–9.
[46] Baier L, Kovacs P, Wiedrich C, et al. Positional cloning of an obesity/diabetes susceptibility gene(s) on chromosome 11 in Pima Indians. Ann N Y Acad Sci 2002;967:258–64.
[47] Bowden DW, Colicigno CJ, Langefeld CD, et al. A genome scan for diabetic nephropathy in African Americans. Kidney Int 2004;66(4):1517–26.
[48] Nelson RG, Newman JM, Knowler WC, et al. Incidence of end-stage renal disease in type 2 (non-insulin-dependent) diabetes mellitus in Pima Indians. Diabetologia 1988;31(10):730–6.
[49] Imperatore G, Hanson RL, Pettitt DJ, Kobes S, Bennett PH, Knowler WC. Sib-pair linkage analysis for susceptibility genes for microvascular complications among Pima Indians with type 2 diabetes. Pima diabetes genes group. Diabetes 1998;47(5): 821–30.
[50] Lindsay RS, Kobes S, Knowler WC, Bennett PH, Hanson RL. Genome-wide linkage analysis assessing parent-of-origin effects in the inheritance of type 2 diabetes and BMI in Pima Indians. Diabetes 2001;50(12):2850–7.
[51] Mogensen CE, Christensen CK, Vittinghus E. The stages in diabetic renal disease. With emphasis on the stage of incipient diabetic nephropathy. Diabetes 1983;32(Suppl 2):64–78.
[52] DCCT. Retinopathy and nephropathy in patients with type 1 diabetes four years after a trial of intensive therapy. The diabetes control and complications trial/epidemiology of diabetes interventions and complications research group. N Engl J Med 2000;342(6):381-389.
[53] Olivarius Nde F, Andreasen AH, Keiding N, Mogensen CE. Epidemiology of renal involvement in newly-diagnosed middle-aged and elderly diabetic patients. cross-sectional data from the population-based study "Diabetes Care in General Practice," Denmark. Diabetologia 1993;36(10):1007–16.
[54] Myers BD, Nelson RG, Williams GW, et al. Glomerular function in Pima Indians with noninsulin-dependent diabetes mellitus of recent onset. J Clin Invest 1991;88(2):524–30.
[55] Nelson RG, Knowler WC, McCance DR, et al. Determinants of end-stage renal disease in Pima Indians with type 2 (non-

insulin-dependent) diabetes mellitus and proteinuria. Diabetologia 1993;36(10):1087–93.
[56] Caramori ML, Kim Y, Huang C, et al. Cellular basis of diabetic nephropathy: 1. Study design and renal structural-functional relationships in patients with long-standing type 1 diabetes. Diabetes 2002;51(2):506–13.
[57] White KE, Bilous RW. Type 2 diabetic patients with nephropathy show structural-functional relationships that are similar to type 1 disease. J Am Soc Nephrol 2000;11(9):1667–73.
[58] Wolf G. New insights into the pathophysiology of diabetic nephropathy: from haemodynamics to molecular pathology. Eur J Clin Invest 2004;34(12):785–96.
[59] Wagh A, Stone NJ. Treatment of metabolic syndrome. Expert Rev Cardiovasc Ther 2004;2(2):213–28.
[60] Ditzel J, Junker K. Abnormal glomerular filtration rate, renal plasma flow, and renal protein excretion in recent and short-term diabetics. Br Med J 1972;2(5804):13–9.
[61] Rigalleau V, Garcia M, Lasseur C, et al. Large kidneys predict poor renal outcome in subjects with diabetes and chronic kidney disease. BMC Nephrol 2010;11:3.
[62] Mogensen CE, Christensen CK. Predicting diabetic nephropathy in insulin-dependent patients. N Engl J Med 1984;311(2): 89–93.
[63] Rudberg S, Persson B, Dahlquist G. Increased glomerular filtration rate as a predictor of diabetic nephropathy–an 8-year prospective study. Kidney Int 1992;41(4):822–8.
[64] Zerbini G, Bonfanti R, Meschi F, et al. Persistent renal hypertrophy and faster decline of glomerular filtration rate precede the development of microalbuminuria in type 1 diabetes. Diabetes 2006;55(9):2620–5.
[65] Nelson RG, Meyer TW, Myers BD, Bennett PH. Clinical and pathological course of renal disease in non-insulin-dependent diabetes mellitus: the Pima Indian experience. Semin Nephrol 1997;17(2):124–31.
[66] Mogensen CE, Vestbo E, Poulsen PL, et al. Microalbuminuria and potential confounders. A review and some observations on variability of urinary albumin excretion. Diabetes Care 1995;18(4):572–81.
[67] DCCT. Effect of intensive therapy on the development and progression of diabetic nephropathy in the diabetes control and complications trial. Kidney Int 1995;47:1703–20.
[68] Mogensen CE. Microalbuminuria predicts clinical proteinuria and early mortality in maturity-onset diabetes. N Engl J Med 1984;310(6):356–60.
[69] Ritz E, Orth SR. Nephropathy in patients with type 2 diabetes mellitus. N Engl J Med 1999;341(15):1127–33.
[70] Mauer SM, Steffes MW, Ellis EN, Sutherland DE, Brown DM, Goetz FC. Structural-functional relationships in diabetic nephropathy. J Clin Invest 1984;74(4):1143–55.
[71] Fioretto P, Steffes MW, Brown DM, Mauer SM. An overview of renal pathology in insulin-dependent diabetes mellitus in relationship to altered glomerular hemodynamics. Am J Kidney Dis 1992;20(6):549–58.
[72] Seyer-Hansen K. Renal hypertrophy in experimental diabetes mellitus. Kidney Int 1983;23(4):643–6.
[73] Seyer-Hansen K, Hansen J, Gundersen HJ. Renal hypertrophy in experimental diabetes. A morphometric study. Diabetologia 1980;18(6):501–5.
[74] Wolf G, Mueller E, Stahl RA, Ziyadeh FN. Angiotensin II-induced hypertrophy of cultured murine proximal tubular cells is mediated by endogenous transforming growth factor-beta. J Clin Invest 1993;92(3):1366–72.
[75] Wolf G, Sharma K, Chen Y, Ericksen M, Ziyadeh FN. High glucose-induced proliferation in mesangial cells is reversed by autocrine TGF-beta. Kidney Int 1992;42(3):647–56.
[76] Wolf G, Ziyadeh FN. Molecular mechanisms of diabetic renal hypertrophy. Kidney Int 1999;56(2):393–405.
[77] Zhang Y, Shi Y, Liu Y, et al. Growth pattern switch of renal cells and expression of cell cycle related proteins at the early stage of diabetic nephropathy. Biochem Biophys Res Commun 2007;363 (1):159–64.
[78] Wolf G, Schroeder R, Ziyadeh FN, Thaiss F, Zahner G, Stahl RA. High glucose stimulates expression of p27Kip1 in cultured mouse mesangial cells: relationship to hypertrophy. Am J Physiol 1997;273(3 Pt 2):F348–56.
[79] Wolf G, Reinking R, Zahner G, Stahl RA, Shankland SJ. Erk 1,2 phosphorylates p27(Kip1): functional evidence for a role in high glucose-induced hypertrophy of mesangial cells. Diabetologia 2003;46(8):1090–9.
[80] Awazu M, Omori S, Ishikura K, Hida M, Fujita H. The lack of cyclin kinase inhibitor p27(Kip1) ameliorates progression of diabetic nephropathy. J Am Soc Nephrol 2003;14(3): 699–708.
[81] Wolf G, Ziyadeh FN. Renal tubular hypertrophy induced by angiotensin II. Semin Nephrol 1997;17(5):448–54.
[82] Wolf G, Wenzel U, Ziyadeh FN, Stahl RA. Angiotensin converting-enzyme inhibitor treatment reduces glomerular p16INK4 and p27Kip1 expression in diabetic BBdp rats. Diabetologia 1999;42(12):1425–32.
[83] Wolf G, Schanze A, Stahl RA, Shankland SJ, Amann K. p27 (Kip1) Knockout mice are protected from diabetic nephropathy: evidence for p27(Kip1) haplotype insufficiency. Kidney Int 2005;68(4):1583–9.
[84] Sataranatarajan K, Mariappan MM, Lee MJ, et al. Regulation of elongation phase of mRNA translation in diabetic nephropathy: amelioration by rapamycin. Am J Pathol 2007;171(6): 1733–42.
[85] Mori H, Inoki K, Masutani K, et al. The mTOR pathway is highly activated in diabetic nephropathy and rapamycin has a strong therapeutic potential. Biochem Biophys Res Commun 2009;384(4):471–5.
[86] Choo AY, Blenis J. Not all substrates are treated equally: implications for mTOR, rapamycin-resistance and cancer therapy. Cell Cycle 2009;8(4):567–72.
[87] Chen JK, Chen J, Thomas G, Kozma SC, Harris RC. S6 kinase 1 knockout inhibits uninephrectomy- or diabetes-induced renal hypertrophy. Am J Physiol Renal Physiol 2009;297(3):F585–93.
[88] Yang Y, Wang J, Qin L, et al. Rapamycin prevents early steps of the development of diabetic nephropathy in rats. Am J Nephrol 2007;27(5):495–502.
[89] Inoue S, Bendayan M. High-resolution ultrastructural study of the rat glomerular basement membrane in long-term experimental diabetes. Ultrastruct Pathol 1995;19(3):175–85.
[90] Zhu D, Kim Y, Steffes MW, Groppoli TJ, Butkowski RJ, Mauer SM. Glomerular distribution of type IV collagen in diabetes by high resolution quantitative immunochemistry. Kidney Int 1994;45(2):425–33.
[91] Funabiki K, Makita Y, Yamamoto M, et al. Dissociated expression of collagen type IV subchains in diabetic kidneys of KKAy mice. Nephron 1998;80(2):208–13.
[92] Fioretto P, Kim Y, Mauer M. Diabetic nephropathy as a model of reversibility of established renal lesions. Curr Opin Nephrol Hypertens 1998;7(5):489–94.
[93] Hopfer U, Hopfer H, Meyer-Schwesinger C, et al. Lack of type VIII collagen in mice ameliorates diabetic nephropathy. Diabetes 2009;58(7):1672–81.
[94] Osterby R. The number of glomerular cells and substructures in early juvenile diabetes. A quantitative electron microscopic study. Acta Pathol Microbiol Scand A 1972;80(6):785–800.

[95] Bader R, Bader H, Grund KE, Mackensen-Haen S, Christ H, Bohle A. Structure and function of the kidney in diabetic glomerulosclerosis. Correlations between morphological and functional parameters. Pathol Res Pract 1980;167(2–4):204–16.
[96] Ziyadeh FN, Goldfarb S. The renal tubulointerstitium in diabetes mellitus. Kidney Int 1991;39(3):464–75.
[97] Lane PH, Steffes MW, Fioretto P, Mauer SM. Renal interstitial expansion in insulin-dependent diabetes mellitus. Kidney Int 1993;43(3):661–7.
[98] Dalla Vestra M, Saller A, Mauer M, Fioretto P. Role of mesangial expansion in the pathogenesis of diabetic nephropathy. J Nephrol 2001;14(Suppl 4):S51–7.
[99] Mattock MB, Barnes DJ, Viberti G, et al. Microalbuminuria and coronary heart disease in NIDDM: an incidence study. Diabetes 1998;47(11):1786–92.
[100] Remuzzi G, Ruggenenti P, Benigni A. Understanding the nature of renal disease progression. Kidney Int 1997;51(1): 2–15.
[101] Chen S, Kasama Y, Lee JS, Jim B, Marin M, Ziyadeh FN. Podocyte-derived vascular endothelial growth factor mediates the stimulation of alpha3(IV) collagen production by transforming growth factor-beta1 in mouse podocytes. Diabetes 2004;53(11):2939–49.
[102] Chen S, Lee JS, Iglesias-de la Cruz MC, et al. Angiotensin II stimulates alpha3(IV) collagen production in mouse podocytes via TGF-beta and VEGF signalling: implications for diabetic glomerulopathy. Nephrol Dial Transplant 2005;20(7):1320–8.
[103] Pavenstadt H, Kriz W, Kretzler M. Cell biology of the glomerular podocyte. Physiol Rev 2003;83(1):253–307.
[104] Wolf G, Chen S, Ziyadeh FN. From the periphery of the glomerular capillary wall toward the center of disease: podocyte injury comes of age in diabetic nephropathy. Diabetes 2005;54(6):1626–34.
[105] Berg UB, Torbjornsdotter TB, Jaremko G, Thalme B. Kidney morphological changes in relation to long-term renal function and metabolic control in adolescents with IDDM. Diabetologia 1998;41(9):1047–56.
[106] Dalla Vestra M, Masiero A, Roiter AM, Saller A, Crepaldi G, Fioretto P. Is podocyte injury relevant in diabetic nephropathy? Studies in patients with type 2 diabetes. Diabetes 2003;52(4):1031–5.
[107] Pagtalunan ME, Miller PL, Jumping-Eagle S, et al. Podocyte loss and progressive glomerular injury in type II diabetes. J Clin Invest 1997;99(2):342–8.
[108] Steffes MW, Schmidt D, McCrery R, Basgen JM. Glomerular cell number in normal subjects and in type 1 diabetic patients. Kidney Int 2001;59(6):2104–13.
[109] White KE, Bilous RW, Marshall SM, et al. Podocyte number in normotensive type 1 diabetic patients with albuminuria. Diabetes 2002;51(10):3083–9.
[110] Meyer TW, Bennett PH, Nelson RG. Podocyte number predicts long-term urinary albumin excretion in Pima Indians with Type II diabetes and microalbuminuria. Diabetologia 1999;42 (11):1341–4.
[111] Langham RG, Kelly DJ, Cox AJ, et al. Proteinuria and the expression of the podocyte slit diaphragm protein, nephrin, in diabetic nephropathy: effects of angiotensin converting enzyme inhibition. Diabetologia 2002;45(11):1572–6.
[112] Kelly DJ, Aaltonen P, Cox AJ, et al. Expression of the slit-diaphragm protein, nephrin, in experimental diabetic nephropathy: differing effects of anti-proteinuric therapies. Nephrol Dial Transplant 2002;17(7):1327–32.
[113] Gross ML, El-Shakmak A, Szabo A, et al. ACE-inhibitors but not endothelin receptor blockers prevent podocyte loss in early diabetic nephropathy. Diabetologia 2003;46(6):856–68.
[114] Mifsud SA, Allen TJ, Bertram JF, et al. Podocyte foot process broadening in experimental diabetic nephropathy: amelioration with renin-angiotensin blockade. Diabetologia 2001;44(7):878–82.
[115] Doublier S, Salvidio G, Lupia E, et al. Nephrin expression is reduced in human diabetic nephropathy: evidence for a distinct role for glycated albumin and angiotensin II. Diabetes 2003;52(4):1023–30.
[116] Benigni A, Gagliardini E, Tomasoni S, et al. Selective impairment of gene expression and assembly of nephrin in human diabetic nephropathy. Kidney Int 2004;65(6): 2193–200.
[117] Chen HC, Chen CA, Guh JY, Chang JM, Shin SJ, Lai YH. Altering expression of alpha3beta1 integrin on podocytes of human and rats with diabetes. Life Sci 2000;67(19):2345–53.
[118] Kitsiou PV, Tzinia AK, Stetler-Stevenson WG, et al. Glucose-induced changes in integrins and matrix-related functions in cultured human glomerular epithelial cells. Am J Physiol Renal Physiol 2003;284(4):F671–9.
[119] Kagami S, Border WA, Ruoslahti E, Noble NA. Coordinated expression of beta 1 integrins and transforming growth factor-beta-induced matrix proteins in glomerulonephritis. Lab Invest 1993;69(1):68–76.
[120] Kumar NM, Sigurdson SL, Sheppard D, Lwebuga-Mukasa JS. Differential modulation of integrin receptors and extracellular matrix laminin by transforming growth factor-beta 1 in rat alveolar epithelial cells. Exp Cell Res 1995;221(2):385–94.
[121] Ziyadeh FN, Hoffman BB, Han DC, et al. Long-term prevention of renal insufficiency, excess matrix gene expression, and glomerular mesangial matrix expansion by treatment with monoclonal antitransforming growth factor-beta antibody in db/db diabetic mice. Proc Natl Acad Sci U S A 2000;97(14): 8015–20.
[122] Ziyadeh FN. Mediators of diabetic renal disease: the case for TGF-beta as the major mediator. J Am Soc Nephrol 2004;15(Suppl 1):S55–7.
[123] Ding G, Reddy K, Kapasi AA, et al. Angiotensin II induces apoptosis in rat glomerular epithelial cells. Am J Physiol Renal Physiol 2002;283(1):F173–80.
[124] de Vriese AS, Tilton RG, Elger M, Stephan CC, Kriz W, Lameire NH. Antibodies against vascular endothelial growth factor improve early renal dysfunction in experimental diabetes. J Am Soc Nephrol 2001;12(5):993–1000.
[125] Flyvbjerg A, Dagnaes-Hansen F, De Vriese AS, Schrijvers BF, Tilton RG, Rasch R. Amelioration of long-term renal changes in obese type 2 diabetic mice by a neutralizing vascular endothelial growth factor antibody. Diabetes 2002;51(10): 3090–4.
[126] Sung SH, Ziyadeh FN, Wang A, Pyagay PE, Kanwar YS, Chen S. Blockade of vascular endothelial growth factor signaling ameliorates diabetic albuminuria in mice. J Am Soc Nephrol 2006;17(11):3093–104.
[127] van der Zee R, Murohara T, Luo Z, et al. Vascular endothelial growth factor/vascular permeability factor augments nitric oxide release from quiescent rabbit and human vascular endothelium. Circulation 1997;95(4):1030–7.
[128] Suarez S, Ballmer-Hofer K. VEGF transiently disrupts gap junctional communication in endothelial cells. J Cell Sci 2001;114(Pt 6):1229–35.
[129] Esser S, Wolburg K, Wolburg H, Breier G, Kurzchalia T, Risau W. Vascular endothelial growth factor induces endothelial fenestrations in vitro. J Cell Biol 1998;140(4):947–59.
[130] Foster RR, Hole R, Anderson K, et al. Functional evidence that vascular endothelial growth factor may act as an

autocrine factor on human podocytes. Am J Physiol Renal Physiol 2003;284(6):F1263–73.
[131] Chiarelli F, Spagnoli A, Basciani F, et al. Vascular endothelial growth factor (VEGF) in children, adolescents and young adults with Type 1 diabetes mellitus: relation to glycaemic control and microvascular complications. Diabet Med 2000;17(9):650–6.
[132] McLaren M, Elhadd TA, Greene SA, Belch JJ. Elevated plasma vascular endothelial cell growth factor and thrombomodulin in juvenile diabetic patients. Clin Appl Thromb Hemost 1999;5(1): 21–4.
[133] Wasada T, Kawahara R, Katsumori K, Naruse M, Omori Y. Plasma concentration of immunoreactive vascular endothelial growth factor and its relation to smoking. Metabolism 1998;47(1):27–30.
[134] Cooper ME, Vranes D, Youssef S, et al. Increased renal expression of vascular endothelial growth factor (VEGF) and its receptor VEGFR-2 in experimental diabetes. Diabetes 1999;48(11):2229–39.
[135] Tsuchida K, Makita Z, Yamagishi S, et al. Suppression of transforming growth factor beta and vascular endothelial growth factor in diabetic nephropathy in rats by a novel advanced glycation end product inhibitor, OPB-9195. Diabetologia 1999;42(5):579–88.
[136] Cha DR, Kang YS, Han SY, et al. Vascular endothelial growth factor is increased during early stage of diabetic nephropathy in type II diabetic rats. J Endocrinol 2004;183(1):183–94.
[137] Hu KB, Liu ZH, Zhou H, Li LS. Upregulation of VEGF and VEGF receptor in glomeruli associated with marked proteinuria and endothelial damage in patients with type 2 diabetic nephropathy [abstract]. J Am Soc Nephrol 2000;11:A0627.
[138] Bailey E, Bottomley MJ, Westwell S, et al. Vascular endothelial growth factor mRNA expression in minimal change, membranous, and diabetic nephropathy demonstrated by non-isotopic in situ hybridisation. J Clin Pathol 1999;52(10):735–8.
[139] Shulman K, Rosen S, Tognazzi K, Manseau EJ, Brown LF. Expression of vascular permeability factor (VPF/VEGF) is altered in many glomerular diseases. J Am Soc Nephrol 1996;7(5):661–6.
[140] Lindenmeyer MT, Kretzler M, Boucherot A, et al. Interstitial vascular rarefaction and reduced VEGF-A expression in human diabetic nephropathy. J Am Soc Nephrol 2007;18(6):1765–76.
[141] Chen S, Ziyadeh FN. Vascular endothelial growth factor and diabetic nephropathy. Curr Diab Rep 2008;8(6):470–6.
[142] Zatz R, Brenner BM. Pathogenesis of diabetic microangiopathy. The hemodynamic view. Am J Med 1986;80(3):443–53.
[143] Hostetter TH. Hypertrophy and hyperfunction of the diabetic kidney. J Clin Invest 2001;107(2):161–2.
[144] De Vriese AS, Stoenoiu MS, Elger M, et al. Diabetes-induced microvascular dysfunction in the hydronephrotic kidney: role of nitric oxide. Kidney Int 2001;60(1):202–10.
[145] Goligorsky MS. Endothelial cell dysfunction and nitric oxide synthase. Kidney Int 2000;58(3):1360–76.
[146] Li B, Yao J, Kawamura K, et al. Real-time observation of glomerular hemodynamic changes in diabetic rats: effects of insulin and ARB. Kidney Int 2004;66(5):1939–48.
[147] Osterby R, Brekke IB, Gundersen HJ, et al. Quantitative studies of glomerular ultrastructure in human and experimental diabetes. Appl Pathol 1984;2(4):205–11.
[148] Sharma K, Deelman L, Madesh M, et al. Involvement of transforming growth factor-beta in regulation of calcium transients in diabetic vascular smooth muscle cells. Am J Physiol Renal Physiol 2003;285(6):F1258–70.
[149] Hayashi K, Epstein M, Loutzenhiser R, Forster H. Impaired myogenic responsiveness of the afferent arteriole in streptozotocin-induced diabetic rats: role of eicosanoid derangements. J Am Soc Nephrol 1992;2(11):1578–86.
[150] Carmines PK, Ohishi K, Ikenaga H. Functional impairment of renal afferent arteriolar voltage-gated calcium channels in rats with diabetes mellitus. J Clin Invest 1996;98(11): 2564–71.
[151] Hua H, Munk S, Goldberg H, Fantus IG, Whiteside CI. High glucose-suppressed endothelin-1 Ca2 + signaling via NADPH oxidase and diacylglycerol-sensitive protein kinase C isozymes in mesangial cells. J Biol Chem 2003;278(36):33951–62.
[152] Hurst RD, Stevanovic ZS, Munk S, et al. Glomerular mesangial cell altered contractility in high glucose is Ca2 + independent. Diabetes 1995;44(7):759–66.
[153] Mene P, Pugliese G, Pricci F, Di Mario U, Cinotti GA, Pugliese F. High glucose inhibits cytosolic calcium signaling in cultured rat mesangial cells. Kidney Int 1993;43(3):585–91.
[154] Williams B, Schrier RW. Glucose-induced protein kinase C activity regulates arachidonic acid release and eicosanoid production by cultured glomerular mesangial cells. J Clin Invest 1993;92(6):2889–96.
[155] Williams B, Tsai P, Schrier RW. Glucose-induced downregulation of angiotensin II and arginine vasopressin receptors in cultured rat aortic vascular smooth muscle cells. Role of protein kinase C. J Clin Invest 1992;90(5):1992–9.
[156] Thomson SC, Deng A, Bao D, Satriano J, Blantz RC, Vallon V. Ornithine decarboxylase, kidney size, and the tubular hypothesis of glomerular hyperfiltration in experimental diabetes. J Clin Invest 2001;107(2):217–24.
[157] Thomson SC, Vallon V, Blantz RC. Kidney function in early diabetes: the tubular hypothesis of glomerular filtration. Am J Physiol Renal Physiol 2004;286(1):F8–15.
[158] Pollock CA, Lawrence JR, Field MJ. Tubular sodium handling and tubuloglomerular feedback in experimental diabetes mellitus. Am J Physiol 1991;260(6 Pt 2):F946–52.
[159] Thorup C, Ollerstam A, Persson AE, Torffvit O. Increased tubuloglomerular feedback reactivity is associated with increased NO production in the streptozotocin-diabetic rat. J Diabetes Complications 2000;14(1):46–52.
[160] Kriz W, Hosser H, Hahnel B, Simons JL, Provoost AP. Development of vascular pole-associated glomerulosclerosis in the Fawn-hooded rat. J Am Soc Nephrol 1998;9(3):381–96.
[161] Dessapt C, Baradez MO, Hayward A, et al. Mechanical forces and TGFbeta1 reduce podocyte adhesion through alpha3beta1 integrin downregulation. Nephrol Dial Transplant 2009;24(9):2645–55.
[162] Gruden G, Zonca S, Hayward A, et al. Mechanical stretch-induced fibronectin and transforming growth factor-beta1 production in human mesangial cells is p38 mitogen-activated protein kinase-dependent. Diabetes 2000;49(4): 655–61.
[163] Riser BL, Cortes P, Yee J, et al. Mechanical strain- and high glucose-induced alterations in mesangial cell collagen metabolism: role of TGF-beta. J Am Soc Nephrol 1998;9(5):827–36.
[164] Hoffman BB, Ziyadeh FN. Facilitative glucose transport proteins and sodium-glucose co-transporters in the kidney. Curr Opin Nephrol Hypertens 1995;4(5):406–11.
[165] Heilig CW, Brosius 3rd FC, Henry DN. Glucose transporters of the glomerulus and the implications for diabetic nephropathy. Kidney Int Suppl 1997;60:S91–9.
[166] Heilig C, Concepcion L, Riser B, Freytag S. Overexpression of Glut 1 in rat mesangial cells: a new model to simulate diabetes. J Am Soc Neph 1994;5:965 [abstract]
[167] Inoki K, Haneda M, Maeda S, Koya D, Kikkawa R. TGF-beta 1 stimulates glucose uptake by enhancing GLUT1 expression in mesangial cells. Kidney Int 1999;55(5):1704–12.

[168] Mogyorosi A, Ziyadeh FN. GLUT1 and TGF-beta: the link between hyperglycaemia and diabetic nephropathy. Nephrol Dial Transplant 1999;14(12):2827–9.
[169] Kikkawa R, Umemura K, Haneda M, Arimura T, Ebata K, Shigeta Y. Evidence for existence of polyol pathway in cultured rat mesangial cells. Diabetes 1987;36(2):240–3.
[170] Brownlee M. Biochemistry and molecular cell biology of diabetic complications. Nature 2001;414(6865):813–20.
[171] Haneda M, Koya D, Isono M, Kikkawa R. Overview of glucose signaling in mesangial cells in diabetic nephropathy. J Am Soc Nephrol 2003;14(5):1374–82.
[172] Ziyadeh FN, Fumo P, Rodenberger CH, Kuncio GS, Neilson EG. Role of protein kinase C and cyclic AMP/protein kinase A in high glucose-stimulated transcriptional activation of collagen alpha 1 (IV) in glomerular mesangial cells. J Diabetes Complications 1995;9(4):255–61.
[173] Goldfarb S, Ziyadeh FN, Kern EF, Simmons DA. Effects of polyol-pathway inhibition and dietary myo-inositol on glomerular hemodynamic function in experimental diabetes mellitus in rats. Diabetes 1991;40(4):465–71.
[174] Pedersen MM, Christiansen JS, Mogensen CE. Reduction of glomerular hyperfiltration in normoalbuminuric IDDM patients by 6 mo of aldose reductase inhibition. Diabetes 1991;40(5):527–31.
[175] Beyer-Mears A, Ku L, Cohen MP. Glomerular polyol accumulation in diabetes and its prevention by oral sorbinil. Diabetes 1984;33(6):604–7.
[176] Chang WP, Dimitriadis E, Allen T, Dunlop ME, Cooper M, Larkins RG. The effect of aldose reductase inhibitors on glomerular prostaglandin production and urinary albumin excretion in experimental diabetes mellitus. Diabetologia 1991;34 (4):225–31.
[177] Mauer SM, Steffes MW, Azar S, Brown DM. Effects of sorbinil on glomerular structure and function in long-term-diabetic rats. Diabetes 1989;38(7):839–46.
[178] Bleyer AJ, Fumo P, Snipes ER, Goldfarb S, Simmons DA, Ziyadeh FN. Polyol pathway mediates high glucose-induced collagen synthesis in proximal tubule. Kidney Int 1994;45(3): 659–66.
[179] Daniels BS, Hostetter TH. Aldose reductase inhibition and glomerular abnormalities in diabetic rats. Diabetes 1989;38(8): 981–6.
[180] Petersen A, Szwergold BS, Kappler F, Weingarten M, Brown TR. Identification of sorbitol 3-phosphate and fructose 3-phosphate in normal and diabetic human erythrocytes. J Biol Chem 1990;265(29):17424–7.
[181] Szwergold BS, Kappler F, Brown TR. Identification of fructose 3-phosphate in the lens of diabetic rats. Science 1990;247(4941): 451–4.
[182] James LR, Ingram A, Ly H, Thai K, Cai L, Scholey JW. Angiotensin II activates the GFAT promoter in mesangial cells. Am J Physiol Renal Physiol 2001;281(1):F151–62.
[183] Kolm-Litty V, Sauer U, Nerlich A, Lehmann R, Schleicher ED. High glucose-induced transforming growth factor beta1 production is mediated by the hexosamine pathway in porcine glomerular mesangial cells. J Clin Invest 1998;101(1):160–9.
[184] Du XL, Edelstein D, Rossetti L, et al. Hyperglycemia-induced mitochondrial superoxide overproduction activates the hexosamine pathway and induces plasminogen activator inhibitor-1 expression by increasing Sp1 glycosylation. Proc Natl Acad Sci U S A 2000;97(22):12222–6.
[185] Du XL, Edelstein D, Dimmeler S, Ju Q, Sui C, Brownlee M. Hyperglycemia inhibits endothelial nitric oxide synthase activity by posttranslational modification at the Akt site. J Clin Invest 2001;108(9):1341–8.
[186] Ayo SH, Radnik R, Garoni JA, Troyer DA, Kreisberg JI. High glucose increases diacylglycerol mass and activates protein kinase C in mesangial cell cultures. Am J Physiol 1991;261(4 Pt 2):F571–7.
[187] Craven PA, Davidson CM, DeRubertis FR. Increase in diacylglycerol mass in isolated glomeruli by glucose from de novo synthesis of glycerolipids. Diabetes 1990;39(6):667–74.
[188] Craven PA, DeRubertis FR. Protein kinase C is activated in glomeruli from streptozotocin diabetic rats. Possible mediation by glucose. J Clin Invest 1989;83(5):1667–75.
[189] Lee TS, Saltsman KA, Ohashi H, King GL. Activation of protein kinase C by elevation of glucose concentration: proposal for a mechanism in the development of diabetic vascular complications. Proc Natl Acad Sci U S A 1989;86(13):5141–5.
[190] Studer RK, Craven PA, DeRubertis FR. Role for protein kinase C in the mediation of increased fibronectin accumulation by mesangial cells grown in high-glucose medium. Diabetes 1993;42(1):118–26.
[191] Tilton RG, Baier LD, Harlow JE, Smith SR, Ostrow E, Williamson JR. Diabetes-induced glomerular dysfunction: links to a more reduced cytosolic ratio of NADH/NAD+. Kidney Int 1992;41(4):778–88.
[192] Fumo P, Kuncio GS, Ziyadeh FN. PKC and high glucose stimulate collagen alpha 1 (IV) transcriptional activity in a reporter mesangial cell line. Am J Physiol 1994;267(4 Pt 2):F632–8.
[193] Kikkawa R, Haneda M, Uzu T, Koya D, Sugimoto T, Shigeta Y. Translocation of protein kinase C alpha and zeta in rat glomerular mesangial cells cultured under high glucose conditions. Diabetologia 1994;37(8):838–41.
[194] Babazono T, Kapor-Drezgic J, Dlugosz JA, Whiteside C. Altered expression and subcellular localization of diacylglycerol-sensitive protein kinase C isoforms in diabetic rat glomerular cells. Diabetes 1998;47(4):668–76.
[195] DeRubertis FR, Craven PA. Activation of protein kinase C in glomerular cells in diabetes. Mechanisms and potential links to the pathogenesis of diabetic glomerulopathy. Diabetes 1994;43(1):1–8.
[196] Koya D, Haneda M, Nakagawa H, et al. Amelioration of accelerated diabetic mesangial expansion by treatment with a PKC beta inhibitor in diabetic db/db mice, a rodent model for type 2 diabetes. FASEB J 2000;14(3):439–47.
[197] Koya D, Jirousek MR, Lin YW, Ishii H, Kuboki K, King GL. Characterization of protein kinase C beta isoform activation on the gene expression of transforming growth factor-beta, extracellular matrix components, and prostanoids in the glomeruli of diabetic rats. J Clin Invest 1997;100(1):115–26.
[198] Tuttle KR, Bakris GL, Toto RD, McGill JB, Hu K, Anderson PW. The effect of ruboxistaurin on nephropathy in type 2 diabetes. Diabetes Care 2005;28(11):2686–90.
[199] Thallas-Bonke V, Lindschau C, Rizkalla B, et al. Attenuation of extracellular matrix accumulation in diabetic nephropathy by the advanced glycation end product cross-link breaker ALT-711 via a protein kinase C-alpha-dependent pathway. Diabetes 2004;53(11):2921–30.
[200] Haneda M, Araki S, Togawa M, Sugimoto T, Isono M, Kikkawa R. Mitogen-activated protein kinase cascade is activated in glomeruli of diabetic rats and glomerular mesangial cells cultured under high glucose conditions. Diabetes 1997;46 (5):847–53.
[201] Isono M, Cruz MC, Chen S, Hong SW, Ziyadeh FN. Extracellular signal-regulated kinase mediates stimulation of TGF-beta1 and matrix by high glucose in mesangial cells. J Am Soc Nephrol 2000;11(12):2222–30.
[202] Koya D, Hayashi K, Kitada M, Kashiwagi A, Kikkawa R, Haneda M. Effects of antioxidants in diabetes-induced

oxidative stress in the glomeruli of diabetic rats. J Am Soc Nephrol 2003;14(8 Suppl 3):S250–3.
[203] Du X, Matsumura T, Edelstein D, et al. Inhibition of GAPDH activity by poly(ADP-ribose) polymerase activates three major pathways of hyperglycemic damage in endothelial cells. J Clin Invest 2003;112(7):1049–57.
[204] Kiritoshi S, Nishikawa T, Sonoda K, et al. Reactive oxygen species from mitochondria induce cyclooxygenase-2 gene expression in human mesangial cells: potential role in diabetic nephropathy. Diabetes 2003;52(10):2570–7.
[205] Melhem MF, Craven PA, Liachenko J, DeRubertis FR. Alpha-lipoic acid attenuates hyperglycemia and prevents glomerular mesangial matrix expansion in diabetes. J Am Soc Nephrol 2002;13(1):108–16.
[206] DeRubertis FR, Craven PA, Melhem MF, Salah EM. Attenuation of renal injury in db/db mice overexpressing superoxide dismutase: evidence for reduced superoxide-nitric oxide interaction. Diabetes 2004;53(3):762–8.
[207] Geiszt M, Kopp JB, Varnai P, Leto TL. Identification of renox, an NAD(P)H oxidase in kidney. Proc Natl Acad Sci U S A 2000;97(14):8010–4.
[208] Etoh T, Inoguchi T, Kakimoto M, et al. Increased expression of NAD(P)H oxidase subunits, NOX4 and p22phox, in the kidney of streptozotocin-induced diabetic rats and its reversibity by interventive insulin treatment. Diabetologia 2003;46(10): 1428–37.
[209] Gorin Y, Block K, Hernandez J, et al. Nox4 NAD(P)H oxidase mediates hypertrophy and fibronectin expression in the diabetic kidney. J Biol Chem 2005;280(47):39616–26.
[210] Eid AA, Gorin Y, Fagg BM, et al. Mechanisms of podocyte injury in diabetes: role of cytochrome P450 and NADPH oxidases. Diabetes 2009;58(5):1201–11.
[211] Susztak K, Raff AC, Schiffer M, Bottinger EP. Glucose-induced reactive oxygen species cause apoptosis of podocytes and podocyte depletion at the onset of diabetic nephropathy. Diabetes 2006;55(1):225–33.
[212] Schalkwijk CG, Ligtvoet N, Twaalfhoven H, et al. Amadori albumin in type 1 diabetic patients: correlation with markers of endothelial function, association with diabetic nephropathy, and localization in retinal capillaries. Diabetes 1999;48(12): 2446–53.
[213] Cohen MP, Ziyadeh FN. Amadori glucose adducts modulate mesangial cell growth and collagen gene expression. Kidney Int 1994;45(2):475–84.
[214] Cohen MP, Ziyadeh FN, Lautenslager GT, Cohen JA, Shearman CW. Glycated albumin stimulation of PKC-beta activity is linked to increased collagen IV in mesangial cells. Am J Physiol 1999;276(5 Pt 2):F684–90.
[215] Ziyadeh FN, Han DC, Cohen JA, Guo J, Cohen MP. Glycated albumin stimulates fibronectin gene expression in glomerular mesangial cells: involvement of the transforming growth factor-beta system. Kidney Int 1998;53(3):631–8.
[216] Ishii H, Jirousek MR, Koya D, et al. Amelioration of vascular dysfunctions in diabetic rats by an oral PKC beta inhibitor. Science 1996;272(5262):728–31.
[217] Cohen MP, Sharma K, Jin Y, et al. Prevention of diabetic nephropathy in db/db mice with glycated albumin antagonists. A novel treatment strategy. J Clin Invest 1995;95(5): 2338–45.
[218] Almdal T, Norgaard K, Feldt-Rasmussen B, Deckert T. The predictive value of microalbuminuria in IDDM. A five-year follow-up study. Diabetes Care 1994;17(2):120–5.
[219] Cooper ME. Interaction of metabolic and haemodynamic factors in mediating experimental diabetic nephropathy. Diabetologia 2001;44(11):1957–72.
[220] McLennan SV, Martell SK, Yue DK. Effects of mesangium glycation on matrix metalloproteinase activities: possible role in diabetic nephropathy. Diabetes 2002;51(8):2612–8.
[221] Vlassara H, Striker LJ, Teichberg S, Fuh H, Li YM, Steffes M. Advanced glycation end products induce glomerular sclerosis and albuminuria in normal rats. Proc Natl Acad Sci USA 1994;91(24):11704–8.
[222] Zhou G, Li C, Cai L. Advanced glycation end-products induce connective tissue growth factor-mediated renal fibrosis predominantly through transforming growth factor beta-independent pathway. Am J Pathol 2004;165(6):2033–43.
[223] Gore-Hyer E, Shegogue D, Markiewicz M, et al. TGF-beta and CTGF have overlapping and distinct fibrogenic effects on human renal cells. Am J Physiol Renal Physiol 2002;283(4): F707–16.
[224] Fukami K, Ueda S, Yamagishi S, et al. AGEs activate mesangial TGF-beta-Smad signaling via an angiotensin II type I receptor interaction. Kidney Int 2004;66(6):2137–47.
[225] Williams ME. New therapies for advanced glycation end product nephrotoxicity: current challenges. Am J Kidney Dis 2003;41(3 Suppl 1):S42–7.
[226] Schmidt AM, Vianna M, Gerlach M, et al. Isolation and characterization of two binding proteins for advanced glycosylation end products from bovine lung which are present on the endothelial cell surface. J Biol Chem 1992;267(21):14987–97.
[227] Neeper M, Schmidt AM, Brett J, et al. Cloning and expression of a cell surface receptor for advanced glycosylation end products of proteins. J Biol Chem 1992;267(21):14998–5004.
[228] Kislinger T, Fu C, Huber B, et al. N(epsilon)-(carboxymethyl)lysine adducts of proteins are ligands for receptor for advanced glycation end products that activate cell signaling pathways and modulate gene expression. J Biol Chem 1999;274(44):31740–9.
[229] Wendt TM, Tanji N, Guo J, et al. RAGE drives the development of glomerulosclerosis and implicates podocyte activation in the pathogenesis of diabetic nephropathy. Am J Pathol 2003;162(4):1123–37.
[230] Hewitson TD, Kelynack KJ, Tait MG, et al. Pirfenidone reduces in vitro rat renal fibroblast activation and mitogenesis. J Nephrol 2001;14(6):453–60.
[231] Yamagishi S, Inagaki Y, Okamoto T, et al. Advanced glycation end product-induced apoptosis and overexpression of vascular endothelial growth factor and monocyte chemoattractant protein-1 in human-cultured mesangial cells. J Biol Chem 2002;277(23):20309–15.
[232] Wolf G, Ziyadeh FN. The role of angiotensin II in diabetic nephropathy: emphasis on nonhemodynamic mechanisms. Am J Kidney Dis 1997;29(1):153–63.
[233] Thaiss F, Wolf G, Assad N, Zahner G, Stahl RA. Angiotensinase A gene expression and enzyme activity in isolated glomeruli of diabetic rats. Diabetologia 1996;39(3): 275–80.
[234] Zatz R, Dunn BR, Meyer TW, Anderson S, Rennke HG, Brenner BM. Prevention of diabetic glomerulopathy by pharmacological amelioration of glomerular capillary hypertension. J Clin Invest 1986;77(6):1925–30.
[235] Hsieh TJ, Zhang SL, Filep JG, Tang SS, Ingelfinger JR, Chan JS. High glucose stimulates angiotensinogen gene expression via reactive oxygen species generation in rat kidney proximal tubular cells. Endocrinology 2002;143(8):2975–85.
[236] Singh R, Singh AK, Alavi N, Leehey DJ. Mechanism of increased angiotensin II levels in glomerular mesangial cells cultured in high glucose. J Am Soc Nephrol 2003;14(4):873–80.
[237] Bonnet F, Cooper ME, Kawachi H, Allen TJ, Boner G, Cao Z. Irbesartan normalises the deficiency in glomerular nephrin

expression in a model of diabetes and hypertension. Diabetologia 2001;44(7):874–7.
[238] Hoffmann S, Podlich D, Hahnel B, Kriz W, Gretz N. Angiotensin II Type 1 receptor overexpression in podocytes induces glomerulosclerosis in transgenic rats. J Am Soc Nephrol 2004;15(6):1475–87.
[239] Abbate M, Zoja C, Morigi M, et al. Transforming growth factor-beta1 is up-regulated by podocytes in response to excess intraglomerular passage of proteins: a central pathway in progressive glomerulosclerosis. Am J Pathol 2002;161(6):2179–93.
[240] Durvasula RV, Petermann AT, Hiromura K, et al. Activation of a local tissue angiotensin system in podocytes by mechanical strain. Kidney Int 2004;65(1):30–9.
[241] Huang XR, Chen WY, Truong LD, Lan HY. Chymase is upregulated in diabetic nephropathy: implications for an alternative pathway of angiotensin II-Mediated diabetic renal and vascular disease. J Am Soc Nephrol 2003;14(7):1738–47.
[242] Noronha IL, Fujihara CK, Zatz R. The inflammatory component in progressive renal disease–are interventions possible? Nephrol Dial Transplant 2002;17(3):363–8.
[243] Mezzano S, Aros C, Droguett A, et al. NF-kappaB activation and overexpression of regulated genes in human diabetic nephropathy. Nephrol Dial Transplant 2004;19(10):2505–12.
[244] Mezzano S, Droguett A, Burgos ME, et al. Renin-angiotensin system activation and interstitial inflammation in human diabetic nephropathy. Kidney Int Suppl 2003;86:S64–70.
[245] Park J, Ryu DR, Li JJ, et al. MCP-1/CCR2 system is involved in high glucose-induced fibronectin and type IV collagen expression in cultured mesangial cells. Am J Physiol Renal Physiol 2008;295(3):F749–57.
[246] Burt D, Salvidio G, Tarabra E, et al. The monocyte chemoattractant protein-1/cognate CC chemokine receptor 2 system affects cell motility in cultured human podocytes. Am J Pathol 2007;171(6):1789–99.
[247] Lee EY, Chung CH, Khoury CC, et al. The monocyte chemoattractant protein-1/CCR2 loop, inducible by TGF-beta, increases podocyte motility and albumin permeability. Am J Physiol Renal Physiol 2009;297(1):F85–94.
[248] Ruiz-Ortega M, Lorenzo O, Suzuki Y, Ruperez M, Egido J. Proinflammatory actions of angiotensins. Curr Opin Nephrol Hypertens 2001;10(3):321–9.
[249] Wolf G, Ziyadeh FN, Thaiss F, et al. Angiotensin II stimulates expression of the chemokine RANTES in rat glomerular endothelial cells. Role of the angiotensin type 2 receptor. J Clin Invest 1997;100(5):1047–58.
[250] Wolf G, Schneider A, Helmchen U, Stahl RA. AT1-receptor antagonists abolish glomerular MCP-1 expression in a model of mesangial proliferative glomerulonephritis. Exp Nephrol 1998;6(2):112–20.
[251] Fujisawa G, Okada K, Muto S, et al. Spironolactone prevents early renal injury in streptozotocin-induced diabetic rats. Kidney Int 2004;66(4):1493–502.
[252] Schjoedt KJ, Andersen S, Rossing P, Tarnow L, Parving HH. Aldosterone escape during angiotensin II receptor blockade in diabetic nephropathy is associated with enhanced decline in GFR. J Am Soc Nephrol 2003;14: [F-FC027, 027A [abstract]].
[253] Sato A, Hayashi K, Naruse M, Saruta T. Effectiveness of aldosterone blockade in patients with diabetic nephropathy. Hypertension 2003;41(1):64–8.
[254] Hollenberg NK. Aldosterone in the development and progression of renal injury. Kidney Int 2004;66(1):1–9.
[255] Mazak I, Fiebeler A, Muller DN, et al. Aldosterone potentiates angiotensin II-induced signaling in vascular smooth muscle cells. Circulation 2004;109(22):2792–800.
[256] Reeves WB, Andreoli TE. Transforming growth factor beta contributes to progressive diabetic nephropathy. Proc Natl Acad Sci U S A 2000;97(14):7667–9.
[257] Ziyadeh FN. Evidence for the involvement of transforming growth factor-beta in the pathogenesis of diabetic kidney disease: are Koch's postulates fulfilled? Curr Pract Med 1998;1:87–9.
[258] Sharma K, Ziyadeh FN. Biochemical events and cytokine interactions linking glucose metabolism to the development of diabetic nephropathy. Semin Nephrol 1997;17(2):80–92.
[259] Ziyadeh FN, Sharma K. Role of transforming growth factor-beta in diabetic glomerulosclerosis and renal hypertrophy. Kidney Int Suppl 1995;51:S34–6.
[260] Heino J, Ignotz RA, Hemler ME, Crouse C, Massague J. Regulation of cell adhesion receptors by transforming growth factor-beta. Concomitant regulation of integrins that share a common beta 1 subunit. J Biol Chem 1989;264(1):380–8.
[261] Ziyadeh FN, Sharma K, Ericksen M, Wolf G. Stimulation of collagen gene expression and protein synthesis in murine mesangial cells by high glucose is mediated by autocrine activation of transforming growth factor-beta. J Clin Invest 1994;93 (2):536–42.
[262] Yang CW, Vlassara H, Peten EP, He CJ, Striker GE, Striker LJ. Advanced glycation end products up-regulate gene expression found in diabetic glomerular disease. Proc Natl Acad Sci U S A 1994;91(20):9436–40.
[263] Iglesias-De La Cruz MC, Ruiz-Torres P, Alcami J, et al. Hydrogen peroxide increases extracellular matrix mRNA through TGF-beta in human mesangial cells. Kidney Int 2001;59(1):87–95.
[264] Wolf G, Ziyadeh FN, Zahner G, Stahl RA. Angiotensin II-stimulated expression of transforming growth factor beta in renal proximal tubular cells: attenuation after stable transfection with the c-mas oncogene. Kidney Int 1995; 48(6):1818–27.
[265] Nakamura T, Ebihara I, Fukui M, Tomino Y, Koide H. Effect of a specific endothelin receptor A antagonist on mRNA levels for extracellular matrix components and growth factors in diabetic glomeruli. Diabetes 1995;44(8):895–9.
[266] Studer RK, Negrete H, Craven PA, DeRubertis FR. Protein kinase C signals thromboxane induced increases in fibronectin synthesis and TGF-beta bioactivity in mesangial cells. Kidney Int 1995;48(2):422–30.
[267] Nakamura T, Fukui M, Ebihara I, et al. mRNA expression of growth factors in glomeruli from diabetic rats. Diabetes 1993;42(3):450–6.
[268] Sharma K, Ziyadeh FN. Renal hypertrophy is associated with upregulation of TGF-beta 1 gene expression in diabetic BB rat and NOD mouse. Am J Physiol 1994;267(6 Pt 2): F1094–1001.
[269] Yang CW, Hattori M, Vlassara H, et al. Overexpression of transforming growth factor-beta 1 mRNA is associated with up-regulation of glomerular tenascin and laminin gene expression in nonobese diabetic mice. J Am Soc Nephrol 1995;5(8): 1610–7.
[270] Hong SW, Isono M, Chen S, Iglesias-De La Cruz MC, Han DC, Ziyadeh FN. Increased glomerular and tubular expression of transforming growth factor-beta1, its type II receptor, and activation of the Smad signaling pathway in the db/db mouse. Am J Pathol 2001;158(5):1653–63.
[271] Isono M, Mogyorosi A, Han DC, Hoffman BB, Ziyadeh FN. Stimulation of TGF-beta type II receptor by high glucose in mouse mesangial cells and in diabetic kidney. Am J Physiol Renal Physiol 2000;278(5):F830–8.

[272] Rocco MV, Chen Y, Goldfarb S, Ziyadeh FN. Elevated glucose stimulates TGF-beta gene expression and bioactivity in proximal tubule. Kidney Int 1992;41(1):107–14.
[273] Iglesias-de la Cruz MC, Ziyadeh FN, Isono M, et al. Effects of high glucose and TGF-beta1 on the expression of collagen IV and vascular endothelial growth factor in mouse podocytes. Kidney Int 2002;62(3):901–13.
[274] Yamamoto T, Noble NA, Cohen AH, et al. Expression of transforming growth factor-beta isoforms in human glomerular diseases. Kidney Int 1996;49(2):461–9.
[275] Yoshioka K, Takemura T, Murakami K, et al. Transforming growth factor-beta protein and mRNA in glomeruli in normal and diseased human kidneys. Lab Invest 1993;68(2): 154–63.
[276] Iwano M, Kubo A, Nishino T, et al. Quantification of glomerular TGF-beta 1 mRNA in patients with diabetes mellitus. Kidney Int 1996;49(4):1120–6.
[277] Sharma K, Ziyadeh FN, Alzahabi B, et al. Increased renal production of transforming growth factor-beta1 in patients with type II diabetes. Diabetes 1997;46(5):854–9.
[278] Sharma K, Eltayeb BO, McGowan TA, et al. Captopril-induced reduction of serum levels of transforming growth factor-beta1 correlates with long-term renoprotection in insulin-dependent diabetic patients. Am J Kidney Dis 1999;34(5):818–23.
[279] Sharma K, Jin Y, Guo J, Ziyadeh FN. Neutralization of TGF-beta by anti-TGF-beta antibody attenuates kidney hypertrophy and the enhanced extracellular matrix gene expression in STZ-induced diabetic mice. Diabetes 1996;45(4):522–30.
[280] Mohanram A, Zhang Z, Shahinfar S, Keane WF, Brenner BM, Toto RD. Anemia and end-stage renal disease in patients with type 2 diabetes and nephropathy. Kidney Int 2004;66(3): 1131–8.
[281] Gouva C, Nikolopoulos P, Ioannidis JP, Siamopoulos KC. Treating anemia early in renal failure patients slows the decline of renal function: a randomized controlled trial. Kidney Int 2004;66(2):753–60.
[282] Higgins DF, Kimura K, Bernhardt WM, et al. Hypoxia promotes fibrogenesis in vivo via HIF-1 stimulation of epithelial-to-mesenchymal transition. J Clin Invest 2007;117(12): 3810–20.
[283] Kimura K, Iwano M, Higgins DF, et al. Stable expression of HIF-1alpha in tubular epithelial cells promotes interstitial fibrosis. Am J Physiol Renal Physiol 2008;295(4):F1023–9.
[284] Haase VH. Hypoxia-inducible factors in the kidney. Am J Physiol Renal Physiol 2006;291(2):F271–81.
[285] Bahlmann FH, de Groot K, Haller H, Fliser D. Erythropoietin: is it more than correcting anaemia? Nephrol Dial Transplant 2004;19(1):20–2.
[286] Pfeffer MA, Burdmann EA, Chen CY, et al. A trial of darbepoetin alfa in type 2 diabetes and chronic kidney disease. N Engl J Med 2009;361(21):2019–32.
[287] Singh AK, Szczech L, Tang KL, et al. Correction of anemia with epoetin alfa in chronic kidney disease. N Engl J Med 2006;355(20):2085–98.
[288] Besarab A, Bolton WK, Browne JK, et al. The effects of normal as compared with low hematocrit values in patients with cardiac disease who are receiving hemodialysis and epoetin. N Engl J Med 1998;339(9):584–90.
[289] Drueke TB, Locatelli F, Clyne N, et al. Normalization of hemoglobin level in patients with chronic kidney disease and anemia. N Engl J Med 2006;355(20):2071–84.
[290] Palmer SC, Navaneethan SD, Craig JC, et al. Systematic review: erythropoiesis-stimulating agents in patients with chronic kidney disease. Ann Intern Med. May 3.
[291] Park YW, Zhu S, Palaniappan L, Heshka S, Carnethon MR, Heymsfield SB. The metabolic syndrome: prevalence and associated risk factor findings in the US population from the third national health and nutrition examination survey, 1988-1994. Arch Intern Med 2003;163(4):427–36.
[292] Tan CE, Ma S, Wai D, Chew SK, Tai ES. Can we apply the national cholesterol education program adult treatment panel definition of the metabolic syndrome to Asians? Diabetes Care 2004;27(5):1182–6.
[293] Solano MP, Perry AC, Wang X, Ross R, Goldberg RB. Insulin resistance but not visceral adipose tissue is associated with plasminogen activator inhibitor type 1 levels in overweight and obese premenopausal African-American women. Int J Obes Relat Metab Disord 2003;27(1):82–7.
[294] Wachtell K, Ibsen H, Olsen MH, et al. Albuminuria and cardiovascular risk in hypertensive patients with left ventricular hypertrophy: the LIFE study. Ann Intern Med 2003;139(11): 901–6.
[295] Bagby SP. Obesity-initiated metabolic syndrome and the kidney: a recipe for chronic kidney disease? J Am Soc Nephrol 2004;15(11):2775–91.
[296] Palaniappan L, Carnethon M, Fortmann SP. Association between microalbuminuria and the metabolic syndrome: NHANES III. Am J Hypertens 2003;16(11 Pt 1):952–8.
[297] Wrone EM, Carnethon MR, Palaniappan L, Fortmann SP. Association of dietary protein intake and microalbuminuria in healthy adults: Third national health and nutrition examination survey. Am J Kidney Dis 2003;41(3):580–7.
[298] Chen J, Muntner P, Hamm LL, et al. The metabolic syndrome and chronic kidney disease in U.S. adults. Ann Intern Med 2004;140(3):167–74.
[299] Anavekar NS, McMurray JJ, Velazquez EJ, et al. Relation between renal dysfunction and cardiovascular outcomes after myocardial infarction. N Engl J Med 2004;351(13): 1285–95.
[300] Go AS, Chertow GM, Fan D, McCulloch CE, Hsu CY. Chronic kidney disease and the risks of death, cardiovascular events, and hospitalization. N Engl J Med 2004;351 (13):1296–305.
[301] Ronco C, Haapio M, House AA, Anavekar N, Bellomo R. Cardiorenal syndrome. J Am Coll Cardiol 2008;52(19):1527–39.
[302] Kambham N, Markowitz GS, Valeri AM, Lin J, D'Agati VD. Obesity-related glomerulopathy: an emerging epidemic. Kidney Int 2001;59(4):1498–509.
[303] Adelman RD. Obesity and renal disease. Curr Opin Nephrol Hypertens 2002;11(3):331–5.
[304] Chagnac A, Weinstein T, Korzets A, Ramadan E, Hirsch J, Gafter U . Glomerular hemodynamics in severe obesity. Am J Physiol Renal Physiol 2000;278(5):F817–22.
[305] Furuhashi M, Ura N, Takizawa H, et al. Blockade of the renin-angiotensin system decreases adipocyte size with improvement in insulin sensitivity. J Hypertens 2004;22(10): 1977–82.
[306] Rakugi H, Kamide K, Ogihara T. Vascular signaling pathways in the metabolic syndrome. Curr Hypertens Rep 2002;4(2): 105–11.
[307] Fain JN, Madan AK, Hiler ML, Cheema P, Bahouth SW. Comparison of the release of adipokines by adipose tissue, adipose tissue matrix, and adipocytes from visceral and subcutaneous abdominal adipose tissues of obese humans. Endocrinology 2004;145(5):2273–82.
[308] He G, Bruun JM, Lihn AS, Pedersen SB, Richelsen B. Stimulation of PAI-1 and adipokines by glucose in human adipose tissue in vitro. Biochem Biophys Res Commun 2003;310(3):878–83.

[309] Monzillo LU, Hamdy O, Horton ES, et al. Effect of lifestyle modification on adipokine levels in obese subjects with insulin resistance. Obes Res 2003;11(9):1048–54.

[310] Norris AW, Chen L, Fisher SJ, et al. Muscle-specific PPARgamma-deficient mice develop increased adiposity and insulin resistance but respond to thiazolidinediones. J Clin Invest 2003;112(4):608–18.

[311] Chen S, Iglesias-de la Cruz MC, Jim B, Hong SW, Isono M, Ziyadeh FN. Reversibility of established diabetic glomerulopathy by anti-TGF-beta antibodies in db/db mice. Biochem Biophys Res Commun 2003;300(1):16–22.

[312] Fioretto P, Steffes MW, Sutherland DE, Goetz FC, Mauer M. Reversal of lesions of diabetic nephropathy after pancreas transplantation. N Engl J Med 1998;339(2):69–75.

[313] Perkins BA, Ficociello LH, Silva KH, Finkelstein DM, Warram JH, Krolewski AS. Regression of microalbuminuria in type 1 diabetes. N Engl J Med 2003;348(23): 2285–93.

CHAPTER

79

Renal Failure in Cirrhosis

Pere Ginès[1], *Andrés Cárdenas*[2] *and Robert W. Schrier*[3]

[1]Liver Unit, Institut Clinic de Malalties Digestives i Metaboliques, Hospital Clinic, and University of Barcelona, Institut d'Investigacions Biomèdiques August Pi-Sunyer (IDIBAPS), Ciber de Enfermedades Hepáticas y Digestivas (CIBEREHD), Barcelona, Spain

[2]GI Unit, Institut Clinic de Malalties Digestives i Metaboliques, Hospital Clinic, and University of Barcelona, Institut d'Investigacions Biomèdiques August Pi-Sunyer (IDIBAPS), Ciber de Enfermedades Hepáticas y Digestivas (CIBEREHD), Barcelona, Spain

[3]Department of Medicine, University of Colorado Denver, Division of Renal Diseases and Hypertension, Aurora, CO, USA.

Renal failure is a common complication of patients with advanced cirrhosis. Early studies in patients with cirrhosis focused the attention on a distinctive form of renal failure characterized by progressive azotemia associated with marked abnormalities of the systemic arterial circulation and normal renal histology, a condition later known as hepatorenal syndrome (HRS).[1–4] However, HRS is not the only cause of renal failure in cirrhosis. Patients with cirrhosis may develop renal failure due to a variety of clinical conditions, including bacterial infections (with or without septic shock), gastrointestinal bleeding (with or without hypovolemic shock), administration of non steroidal antiinflammatory drugs (NSAIDs), and intrinsic renal diseases, particularly glomerulonephritis associated with hepatitis B or C infection or alcoholic liver disease.[5] Because the approach to management of renal failure in patients with cirrhosis is different according to the etiology of renal failure, it is essential to establish the cause of renal failure before starting any specific therapy. The aim of this chapter is to review the current approach to renal failure in patients with cirrhosis, with particular emphasis on the pathogenesis, diagnosis, and management.

DEFINITION

The diagnosis of renal failure in patients with cirrhosis is established when serum creatinine increases over 1.5 mg/dL (133 μmol/L) which corresponds to a glomerular filtration rate (GFR) of approximately 30 ml/min.[5–7] Although serum creatinine is the most commonly used GFR marker in cirrhosis, it has some limitations[7,8] Serum creatinine may overestimate GFR mainly due either to decreased creatinine production or reduced muscle mass. Additionally, it is considered that baseline serum creatinine below <1.5 mg/dl does not necessarily exclude renal dysfunction.[9–11] Creatinine clearance also overestimates GFR; more so in those with low GFR.[11] There are no data to indicate that creatinine clearance is better or preferred to serum creatinine concentration as a marker of GFR in patients with cirrhosis. In addition, creatinine clearance is difficult to perform because it depends on the adequate collection of urine volume over 24 hours, which in many cases is inadequate, especially in oliguric patients.[11,12] The estimation of GFR with the Cockcroft and Modification of Diet in Renal Disease (MDRD) equations are based on serum creatinine and therefore have

Seldin and Giebisch's The Kidney, Fifth Edition.
DOI: http://dx.doi.org/10.1016/B978-0-12-381462-3.00079-3

© 2013 Elsevier Inc. All rights reserved.

not shown to be very useful in cirrhosis.[13–15] The gold standard for measuring GFR in cirrhosis relies on clearance techniques of exogenous markers.[7,8] Use of these techniques allows the precise estimation of GFR, which helps to classify patients with chronic kidney disease according to categories previously defined by the National Kidney Foundation.[16] Inulin has been the most widely used marker as it is completely filtered by the glomerulus without being secreted, reabsorbed, synthesized, or metabolized by the ducts. Thus, after an intravenous infusion and at a stable concentration in healthy subjects, the amount filtered equals to the amount excreted in urine. However, this method is cumbersome, expensive and not available in all settings. Other markers such as radiolabeled compounds (51Cr-EDTA, 99mTc-DPTA and 125I-iothalamate) or iohexol/iothalamate are useful, but there are expensive, they expose the patient to radiation if used repeatedly, and they have not been specifically or adequately studied in cirrhosis.

The above-mentioned limitation of using serum creatinine as a marker of renal function may require that the current definition undergo reassessment. New proposed criteria including the acute kidney injury and chronic kidney disease definitions may be useful in patients with cirrhosis but these need to be properly studied[6] Given the above, serum creatinine concentration is still considered the method of choice to estimate GFR in cirrhosis in clinical practice. Although a single measurement of serum creatinine alone is probably inadequate for identifying and/or quantifying either acute or chronic renal disease in cirrhosis repeated measurements over time may be useful in indicating variations of GFR in clinical practice.

Etiology and Epidemiology

There are several causes of renal failure in cirrhosis due to a variety of clinical conditions (Table 79.1). These etiologies are classified as: (1) renal failure associated with infections, (2) hypovolemia induced renal failure (3) intrinsic renal diseases, (4) hepatorenal syndrome (HRS), and (5) drug-induced renal failure. In patients with cirrhosis and ascites the one year probability of developing HRS ranges between 18-23% at one year and increases up to 40-50 % at three to five years of follow-up.[17,18] (Figure 79.1). A systematic review of 74 studies showed that the overall median mortality in patients with cirrhosis and renal failure was 67%, with a 58% mortality at 30 days and 63% mortality at one year[19]In an analysis of 562 hospitalized patients with cirrhosis and renal failure, the most frequent cause of renal failure in cirrhosis was that associated with bacterial infections (46%), followed by hypovolemia-induced renal failure (32%), HRS (13%), parenchymal nephropathy (9%), drug-induced renal failure (7.5%), mixed causes (8%) and other causes (2%).[19] Patients with intrinsic renal disease had a 73% survival at three months followed by a 46% survival in those with hypovolemia-related renal failure. Those with renal failure associated with infections and HRS had the lowest three-month survival probability, 31 and 15% respectively.[19] (Figure 79.2).

TABLE 79.1 Main Causes of Renal Failure in Patients with Cirrhosis

1. Infections
   a. Spontaneous bacterial peritonitis
   b. Spontaneous bacteremia
   c. Urinary tract infection, pneumonia, skin infections
2. Hypovolemia-induced renal failure
   a. Vomiting, diarrhea
   b. Gastrointestinal bleeding (with or without shock)
   c. Diuretic-induced
3. Hepatorenal syndrome
4. Intrinsic renal diseases
   a. Glomerulopathies – IgA nephropathy, membranous nephropathy, membranoproliferative glomerulonephritis, polyarteritis nodosa, cryoglobulinemia due to viral hepatitis, or alcohol.
   b. Chronic kidney diseases due to diabetes, hypertension or other causes.
5. Drug induced renal failure
   a. Hemodynamically induced—Nonsteroidal anti-inflammatory agents, ACE Inhibitors, Angiotensin receptor blockers
   b. Acute tubular necrosis- Aminoglycosides, Amphotericin B, Tenofovir, Adefovir
   c. Acute interstitial nephritis- penicillin, rifampin and sulfonamides

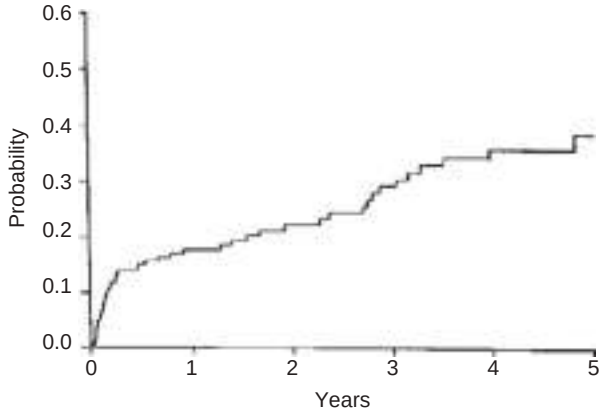

FIGURE 79.1 Probability of developing hepatorenal syndrome in a series of patients with cirrhosis and ascites. *Reproduced with permission from Ref. [17].*

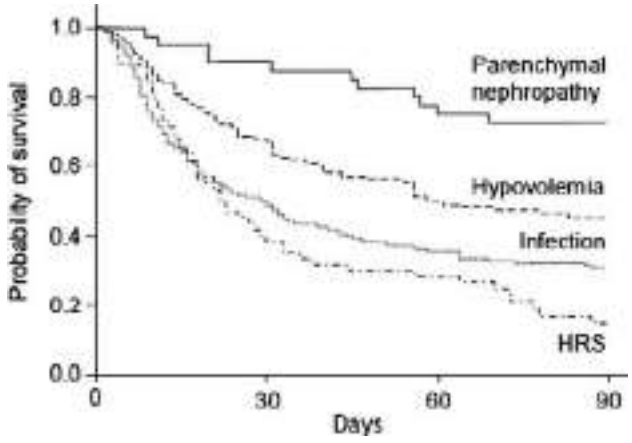

FIGURE 79.2 Survival of patients with renal failure and cirrhosis according to etiology of kidney disease. Patients with intrinsic renal disease had a 73% survival at three months followed by a 46% survival in those with hypovolemia-related renal failure. Those with renal failure associated with infections and HRS which had had the lowest three-month probability, 31% and 15% respectively. *Reproduced with permission from Ref.* [19].

TABLE 79.2 Evaluation of Patients with Cirrhosis and Renal Failure

COMPLETE HISTORY
Infections/ sepsis
NSAID use, high doses of diuretics or other nephrotoxic drugs
Gastrointestinal bleeding
Long-term diabetes, hypertension
Urinary tract obstruction
PHYSICAL EXAMINATION
Volume status
Hemodynamics
Signs of infection or gastrointestinal bleeding
LABORATORY DATA
Serum creatinine, electrolytes, liver tests
Routine urine analysis, urine electrolytes, sediment
24 hr urine volume, sodium, protein, creatinine
Culture—ascites, blood, urine
Renal ultrasound/Doppler

TABLE 79.3 Diagnostic Criteria of Hepatorenal Syndrome in Cirrhosis *

1. Cirrhosis with ascites
2. Serum creatinine > 1.5 mg/dL (133 μmol/L)
3. No improvement of serum creatinine (decrease to a level lower than 1.5 mg/dL (133 μmol/L) (after at least two days off diuretics and volume expansion with albumin (1 g/kg body weight up to a maximum of 100 g/day)
4. Absence of shock
5. No current or recent treatment with nephrotoxic drugs
6. Absence of signs of parenchymal renal disease, as suggested by proteinuria (> 500 mg/day) or hematuria (> 50 red blood cells per high power field), and/or abnormal renal ultrasound.

*From: *Salerno et al. Diagnosis, prevention and treatment of the hepatorenal syndrome in cirrhosis. A consensus workshop of the international ascites club.* Gut *2007;56:1310-8.*

Approach to Renal Failure in Cirrhosis

It is essential to establish the underlying etiology of renal failure before considering further management. That said, there are no specific tests that secure the diagnosis of the different types of renal failure in cirrhosis. In most cases a detailed clinical history, physical exam and assessment of renal function with a thorough evaluation of urine and serum electrolytes will suffice for establishing the cause (Table 79.2). Renal ultrasonography needs to be performed in order to rule out the existence of abnormalities in renal structure suggestive of chronic kidney disease or urinary tract obstruction. Data on urine biomarkers and renal biopsy in the assessment of renal failure in cirrhosis is limited and therefore cannot be routinely recommended in the workup of renal failure in cirrhosis. Since the diagnosis of HRS cannot be made with a specific test, its confirmation is currently made using criteria to exclude other causes of renal failure that can occur in cirrhosis. So, if after an extensive investigation there is no evidence of infection, hypovolemia, administration of nephrotoxic drugs, or intrinsic renal diseases, then HRS should be considered the cause of renal failure. The diagnosis of HRS is based on specific clinical criteria that aim to exclude other causes of renal failure that are not functional, see (Table 79.3) below.

INFECTIONS AND RENAL FAILURE

Bacterial infections are the most common cause of renal failure in cirrhosis. The pathogenesis seems to be related to an impairment of the systemic arterial vasodilation present in cirrhosis due to bacterial products, cytokines or vasoactive mediators that appear in relation with the infection.[21] This occurs mainly in patients that develop spontaneous bacterial peritonitis (SBP) and spontaneous bacteremia, but may occur with any bacterial infection[18,19,22] It is estimated that bacterial infections are present at admission or during hospitalization in 20-60% of patients.[19,22,23] Of these, most are secondary to SBP, other common causes are urinary tract infection, pneumonia and bacteremia[22,23] which are due to both gram negative bacteria and aerobic gram-positive bacteria.[24] Bacterial infections

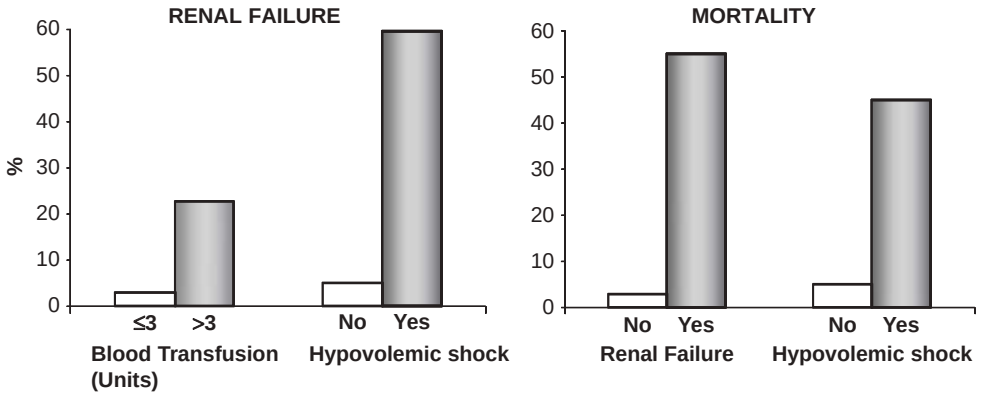

FIGURE 79.3 Renal failure in patients with gastrointestinal bleeding. Left panel: Renal failure according to the number of units of blood transfused and presence or absence of hypovolemic shock (*p < 001). Right panel: In-hospital mortality in patients with cirrhosis and gastrointestinal bleeding according to the development of renal failure and presence or absence of hypovolemic shock (*p < 0.01). *Reproduced with permission from Ref.* [27].

significantly increase mortality in patients with cirrhosis. A meta-analysis of 178 studies estimated that the overall mortality of infected patients with cirrhosis was 38%.[25] The same analysis concluded that the mortality in those with SBP was 43.7% and in those with bacteraemia (1437 patients), the mortality was 42.2%.[25] In any patient with cirrhosis that develops renal failure, the presence of a bacterial infection should be thoroughly sought after. It is important to take into account that signs and symptoms of early bacterial infection may be vague or even absent in some patients with cirrhosis. The mandatory workup consists of a complete blood cell count, liver chemistries, polymorphonuclear cell count in a sample of ascitic fluid, ascitic fluid cultures, urine sediment and culture, abdominal ultrasound, chest X-ray and blood cultures.

HYPOVOLEMIA-INDUCED RENAL FAILURE

Pre-renal renal failure occurs due to a reduction in intravascular volume that causes a drop in renal plasma flow and GFR. In hypovolemia-induced renal failure the major mechanism responsible for renal hypoperfusion is a reduction in intravascular volume which, if severe, may lead to acute tubular necrosis (ATN).[5,6,26] The main causes of hypovolemia in cirrhosis are gastrointestinal bleeding and overdiuresis due to excessive diuretic treatment followed by gastrointestinal fluid losses due to vomiting and/or diarrhea. In most cases, renal function improves after elimination of the precipitating cause and plasma volume expansion. Patients need to be thoroughly questioned about gastrointestinal bleeding, and physical examination should include a rectal exam to rule-out melena, bright red blood per rectum or occult blood if gastrointestinal bleeding is suspected. A naso-gastric tube should be considered if there is a high suspicion of upper GI bleeding. Additionally, if patients were taking diuretics, the type and doses need to be clarified. Patients with cirrhosis and gastrointestinal bleeding require an important reduction in blood volume which in most cases is associated with hypovolemic shock in order to develop renal failure.[27] In moderate to severe cases of GI bleeding (those requiring >3 units of packed red blood cells) there is a 20% chance of developing renal failure. In mild cases this figure drops to less than 5%.[27] When hypovolemic shock develops in patients with cirrhosis and gastrointestinal bleeding there is a 60% probability of developing renal failure and mortality rates are very high (Figure 79.3).

INTRINSIC RENAL DISEASES

Most intrinsic renal diseases are related to common etiologic factors of cirrhosis, including chronic hepatitis B or C infection or alcoholic liver disease. Most encompass kidney diseases secondary to the deposition of circulating immunocomplexes in the glomeruli. The commonest in hepatitis C are membranoproliferative glomerulonephritis, membranous glomerulonephritis and focal segmental glomerular sclerosis.[28] Membranous nephropathy is commonly encountered in patients with hepatitis B and IgA nephropathy in patients with alcoholic cirrhosis.[28] In some patients, the glomerular deposits are mild and do not affect kidney function, whereas in other patients they are so severe that GFR markedly decreases and renal failure develops. In patients with cirrhosis and renal failure due to intrinsic renal diseases, there is usually proteinuria or hematuria. Intrinsic renal disease is considered if there is either proteinuria greater than 500 mg/24-hr, abnormal urine sediment with more than 50 red cells per high power field, or abnormal

renal ultrasound findings in the absence of other causes of renal failure.[6] However some patients with renal failure due to chronic kidney disease may not necessarily meet the definition. Therefore, criteria for this definition are specific but lack sensitivity and thus need to be properly studied.

The role of kidney biopsy in the evaluation of renal failure in cirrhosis is a matter of debate in some centers. Findings demonstrating glomerulosclerosis or significant fibrosis in the renal parenchyma may require the patient receive dialysis or a simultaneous liver–kidney transplant (if being consider for liver transplantation-LT). Limited data indicates that in transvenous renal biopsies in patients with hematuria or proteinuria, various types of lesions may be present. In one retrospective study of 65 patients, renal biopsy showed that glomerular, vascular and tubulointerstitial changes in 77, 69 and 94% of cases respectively.[29] Fibrous endarteritis was the most common renal vascular lesion and pathological changes to different structures were frequently combined. There were no reported complications of transvenous renal biopsy.[29] Another report of 44 liver transplant candidates with renal failure of undetermined etiology that underwent percutaneous renal biopsy revealed that IgA nephropthy and ATN were the most common findings, however there was more than one pathological finding (i.e., interstitial fibrosis, glomerular sclerosis, or membranoproliferative disease) in 64% of patients.[30] A disappointing finding was the development of serious complications (mainly bleeding) requiring intervention in 18% of patients. Therefore the role of renal biopsy in patients with cirrhosis still needs be studied, however a renal biopsy, preferably via transvenous route should be obtained in those patients in whom the diagnosis of HRS is unclear and are being considered for liver transplantation.

HEPATORENAL SYNDROME

HRS is a pre-renal renal failure without any identifiable kidney pathology that occurs in patients with advanced cirrhosis.[31–33] Patients with very advanced liver disease display a profound disturbance in the systemic circulation, characterized by a low arterial blood pressure, high cardiac output and a decreased total systemic vascular resistance. This hemodynamic pattern is due to an intense arterial vasodilation occurring in the splanchnic vascular bed that triggers a neurohormonal response with the activation of the renin- angiotensin-aldosterone system, the sympathetic nervous system and the non-osmotic release of arginine vasopressin (the antidiuretic hormone) aimed at maintaining arterial pressure that eventually leads to vasoconstriction in several vascular beds, particularly the kidneys, decreasing the GFR (Figure 79.4).[5,6] As the disease progresses, splanchnic vasodilation worsens and this creates a vicious cycle that favors further activation of vasoconstrictors (renin, norepinephine and vasopressin) and ongoing renal vasoconstriction that establishes HRS. Although the kidney tries to

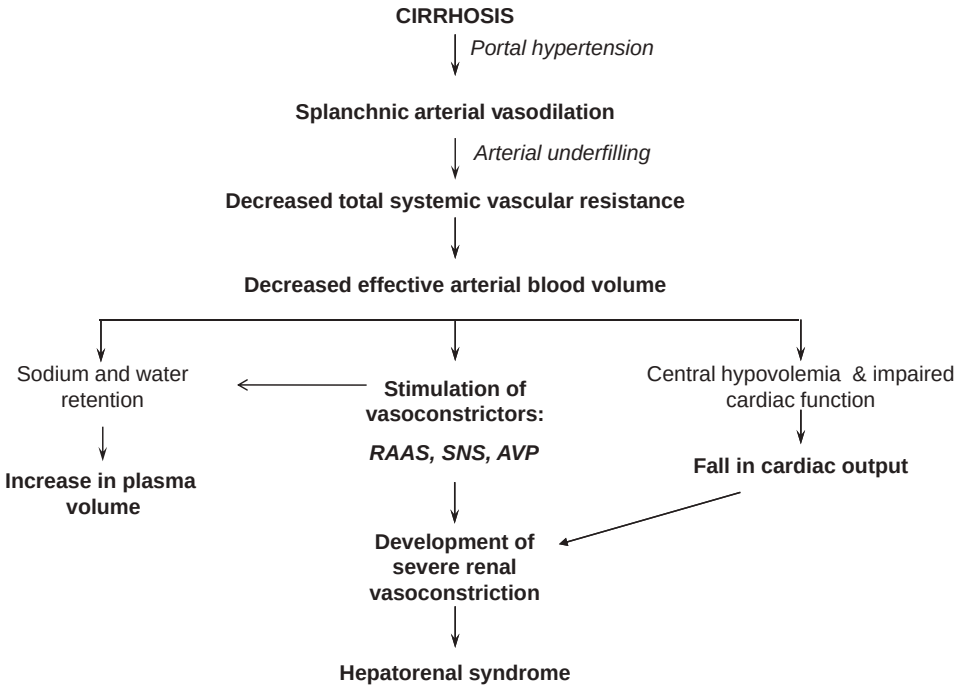

FIGURE 79.4 Proposed pathogenic mechanism of hepatorenal syndrome. Splanchnic vasodilation arising from portal hypertension, an increased plasma volume and a decreased cardiac output seem to play an equally important role in the decreased renal perfusion leading to HRS. The impairment effective arterial blood volume responsible for the activation of vasoconstrictor systems acting on renal circulation is a consequence of both a low systemic vascular resistance causing an abnormal distribution of blood volume and a low cardiac output relative to the markedly dilated arterial bed secondary to cirrhotic cardiomyopathy. (RAAS) Renin-angiotensin-aldosterone system, (SNS) sympathetic nervous system (SNS), and (AVP) arginine vasopressin.

counterbalance the effects of this vasoconstriction with the intrarenal production vasodilators such as prostaglandins, the incessant overproduction of vasoconstrictor factors overcomes their protective role and HRS ensues. In the early stages of cirrhosis there is an increase in cardiac output that compensates for a mild decrease in systemic vascular resistance, but in very advanced cirrhosis there is marked reduction in systemic vascular resistance for which the increased cardiac output cannot compensate for with the development arterial underfilling of circulation. Additionally, in the very advanced stages of cirrhosis cardiac output drops which contributes to decreased effective arterial blood volume and decreased renal perfusion.[34,35] In recent years several studies indicate that adrenal insufficiency (AI) in compensated and decompensated cirrhosis occurs in 26-64% of patients.[36] In those with ascites it might play a role in the pathogenesis of HRS. Normal adrenal function is essential for an adequate response of the arterial circulation to endogenous vasoconstrictors, thus AI could be an important contributory mechanism of circulatory dysfunction associated with renal failure induced by bacterial infections. In one study, adrenal insufficiency was found in 80% of patients with HRS but only in 34% with serum creatinine below 1.5 mg/dL.[37] Another study showed that in patients with cirrhosis, sepsis and adrenal insufficiency treatment with hydrocortisone was associated with a rapid improvement in systemic hemodynamics and a reduction of vasopressor requirements.[38] More studies are needed to clarify the clinical importance of AI in cirrhosis and define the impact of corticosteroid supplementation in patients with liver disease and HRS.

Due to the lack of specific diagnostic markers, the diagnosis of HRS is currently made using criteria to exclude other causes of renal failure that can occur in cirrhosis (Table 79.3).[31–33] There are two types of HRS; in Type 1 HRS renal function deteriorates rapidly with an increase in serum creatinine to a level higher than 2.5 mg/dl in less than two weeks. This type of HRS is associated with a very poor prognosis without treatment with a median survival time of only two weeks if untreated (Figure 79.5).[17,39] In Type 2 HRS there is a steady impairment of renal function and serum creatinine levels usually range between 1.5-2.5 mg/dl. Patients with Type 2 HRS have a median survival time of six months if not transplanted (Figure 79.5).[17,39] Patients with type 2 HRS may go on to develop type 1 HRS, either due to progression of disease or triggering factors such as bacterial infections. Although the differential diagnosis between HRS and ATN remains difficult and the presence of granular casts may be observed in the urine sediments of both HRS and ATN, if renal tubular cells are seen this favors the diagnosis of ATN.[6]

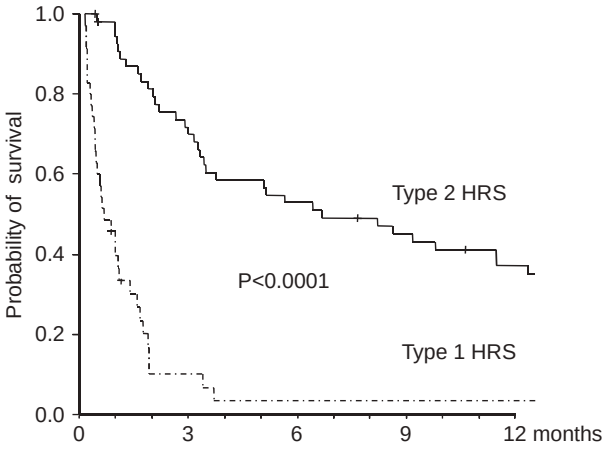

FIGURE 79.5 Probability of survival of patients with cirrhosis according to type of hepatorenal syndrome (HRS). *Reproduced with permission from Ref. [39].*

DRUG-INDUCED RENAL FAILURE

Drug nephrotoxicity in patients with cirrhosis occurs due to medications that cause hemodynamic changes, ATN, and/or acute interstitial nephritis (AIN).[40] Hemodynamically mediated renal failure is mainly caused by NSAIDS and diuretics. These drugs alter the equilibrium between vasodilator and vasoconstrictor factors in the renal circulation. NSAIDs, inhibit the enzymes cycloxygenase-1 and 2 which are responsible for prostaglandin synthesis. Prostaglandins are important renal vasodilators that contribute significantly at maintaining normal renal perfusion. The risk of developing renal failure due to NSAID administration is higher in patients with cirrhosis and ascites and increased activity of the vasoconstrictor systems.[40] Renal failure after NSAID use is followed by a rapid improvement of the GFR to pretreatment values after cessation of the drug in most cases. Diuretic-induced renal failure is usually moderate and reversible after diuretic withdrawal and is related to an imbalance between the fluid loss from the intravascular space caused by diuretic treatment and the passage of fluid from the peritoneal compartment to the general circulation. Drug-induced ATN occurs mainly due to the use of aminoglycosides, amphotericin B or vancomycin. Other drugs used in patients with chronic liver disease undergoing therapy for hepatitis B that may cause renal toxicity are the antivirals adefovir and tenofovir. The specific mechanisms that lead to this toxicity are not completely understood. Thus, it must be taken into account that patients with cirrhosis and renal failure being treated with these drugs may need to switch to

an alternative antiviral such as entecavir. Finally AIN may occur due to antibiotics such as penicillin, rifampin, and sulfonamides as well as with NSAIDs, proton pump inhibitors or allopurinol. In drug-induced AIN there is an inflamatory component that affects the renal tubules and interstitium and occurs as a hypersensitivity reaction to medications. In most cases renal failure will return to normal function after discontinuation of the offending agent.

MANAGEMENT

Successful management of patients with renal failure depends on the prompt recognition of renal failure and of its underlying cause. In general, patients with severe acute renal failure should be admitted to a monitored unit where an appropriate work up and therapy can be performed. If there is any suspicion of an associated bacterial infection, in most cases third-generation cephalosporins are the initial treatment of choice while awaiting cultures.[33] As discussed above, patients with renal failure and severe sepsis may have associated relative AI and may benefit from hydrocortisone administration, however more studies are needed in this area before recommending steroids in this setting. Patients with renal failure and hypovolemia usually respond to volume repletion (saline or colloid) and therapy for gastrointestinal bleeding if present. As mentioned above those with drug- induced renal disease will improve renal function upon discontinuation of the toxic drug. Patients with renal failure that require therapy for large volume ascites or edema should not be treated with spironolactone or furosemide. These patients benefit from large-volume large-volume paracentesis and administration of albumin (8 grams per liter of ascites removed) if necessary (33). Although cirrhotic patients rarely develop renal failure after contrast media for radiological studies, they should undergo standard prophylactic measures such as saline hydration and monitoring of renal function after the procedure.

Patients with Hepatorenal Syndrome

The most important aspect of managing patients with HRS is considering their candidacy for liver transplantation as it is the treatment of choice for individuals with HRS. The main objective of patients with HRS , particularly those awaiting LT, is reversing renal failure in order to provide a successful bridge to transplantation. The best available therapy for HRS other than LT, is the use splanchnic vasoconstrictors plus albumin. Other modalities such as transjugular intrahepatic portosystemic shunts (TIPS), renal replacement therapy and albumin dialysis may be useful in some patients, but data on these approaches is very limited (Figure 79.6).

Vasoconstrictors

The administration of vasoconstrictors is the best medical therapy currently available for the management of HRS. The rationale of this therapy is to improve circulatory function by causing vasoconstriction of the extremely dilated splanchnic arterial bed, which subsequently improves arterial underfilling, reduces the activity of the endogenous vasoconstrictor systems, and increases renal perfusion. The available vasoconstrictors used in HRS are vasopressin analogues (terlipressin) and alpha-adrenergic agonists (noradrenaline or midodrine), which act on V1 vasopressin receptors and α-1 adrenergic receptors, respectively, present in vascular smooth muscle cells (Table 79.4). In most studies, vasoconstrictors have been given in combination with iv albumin to further improve the arterial underfilling (Table 79.4). Most of the published data comes from the use of intravenous terlipressin for type 1 HRS. Non-controlled studies showed response rate of 30-75%.[41–48] Similarly, results from recent randomized controlled studies and systematic reviews indicate that treatment with terlipressin together with albumin is associated with marked improvement of renal function in approximately 40-75% of patients.[49–54]

Although there are no dose-efficacy studies, treatment is typically started with 1 mg/4-6h iv, and the dose is increased up to a maximum of 2 mg/4-6 h after thee days if there is no response to therapy as defined by a reduction of serum creatinine >25% of pre-

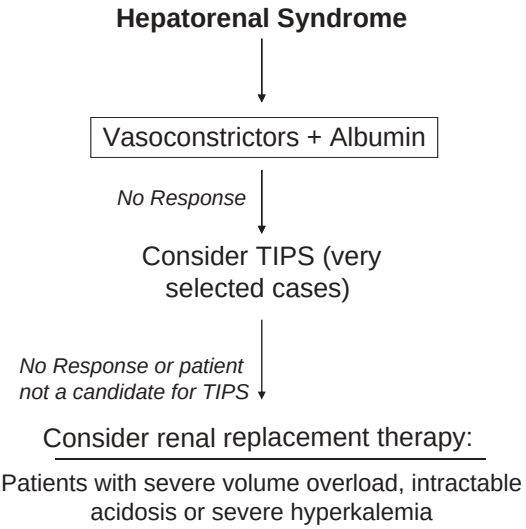
Hepatorenal Syndrome
Vasoconstrictors + Albumin
No Response
Consider TIPS (very selected cases)
No Response or patient not a candidate for TIPS
Consider renal replacement therapy:
Patients with severe volume overload, intractable acidosis or severe hyperkalemia

FIGURE 79.6. Management strategy for patients with hepatorenal syndrome.

TABLE 79.4 Pharmacological Therapies for Hepatorenal Syndrome

VASOCONSTRICTORS
Terlipressin: 1 mg/4-6 hrs intravenously; the dose is increased up to a maximum of 2 mg/4-6 h after 3 days if there is no response to therapy as defined by a reduction of serum creatinine > 25% of pre-treatment values. Response to therapy is considered when there is marked reduction of the high serum creatinine levels, at least below 1.5 mg/dl (133 μmol/L). Treatment is usually given from 5-15 days.
Midodrine and Octreotide: 7.5 mg orally three times daily, increased to 12.5 mg three times daily if needed. Octreotide (100 μg subcutaneously three times daily, increased to 200 μg three times daily if needed).
Norepinephrine: 0.5-3 mg/h as continuous intravenous infusion aimed at increasing mean arterial pressure by 10 mmHg. Treatment is maintained until serum creatinine decreases below 1.5 mg/dl.
ALBUMIN ADMINISTRATION
Concomitant administration of albumin together with vasoconstrictor drugs (1 g/kg body weight at day 1 followed by 20-40 g/day).

treatment values. Response to therapy is considered when there is marked reduction of the serum creatinine levels, at least below 1.5 mg/dl, which is usually associated with increased urine output and improvement of hyponatremia. The incidence of ischemic side effects requiring the discontinuation of treatment is of approximately 7%.[55,56] Two randomized studies have shown that the overall population of patients treated with terlipressin and albumin do not have an improved survival compared to that of patients treated with albumin alone.[50,51] Nonetheless, these studies had a low sample size which could have hindered a survival benefit of treatment. In any case, both studies showed that responders in terms of improvement of renal function after therapy had an improved survival compared to non-responders. Recurrence of HRS after withdrawal of therapy occurs in less than 10% of patients and retreatment with terlipressin is generally effective.[55] Factors associated with poor response include a bilirrubin level ≥10 mg/dL, no increase in mean arterial pressure >5 mmHg or lack of a drop in serum creatinine >0.5 mg/dl at day three of therapy.[57] In addition another study showed that patients with baseline serum creatinine <5.6 mg/dL and receiving >3 days therapy achieved HRS reversal.[58] Finally a systematic review of studies concluded that an increase in mean arterial pressure during vasoconstrictor therapy in patients with HRS was strongly associated with a decrease in serum creatinine which suggests that tailoring therapy to increase the baseline mean arterial pressure is beneficial for these patients.[59] This indicates that less severe renal failure (i.e., lower SCr) and an increase in mean arterial pressure during therapy are associated with a good probability of HRS reversal in those patients treated with terlipressin

Alpha-adrenergic agonists (noradrenaline, midodrine) represent an attractive alternative to terlipressin because of their low cost and wide availability[53,54,60–63] (Table 79.4). However, the information on the efficacy and side effects of alpha-adrenergic agonists in patients with type 1 HRS is still limited. A recent controlled study that compared intravenous terlipressin and albumin vs octreotide/midodrine plus albumin in patients with type 1 HRS.[52] showed that improvement of renal function was significantly better in patients receiving terlipressin and albumin (75%) than in patients treated with midodrine and octreotide and albumin (35 %). This trial specifically compared both treatment regimens and the results indicate that terlipressin is superior to octreotide and midodrine and thus a preferred treatment option for patients with type 1 HRS.[52]

There is limited data on use of vasoconstrictors plus albumin for patients with type 2 HRS. However data from uncontrolled studies suggest that they are effective in decreasing serum creatinine levels in these patients. In two controlled studies, patients with type 2 HRS that received terlipressin plus albumin had a response between 67 and 88%, however few were treated with this strategy in both studies (n = 13) and therefore more studies are needed in order to better define the role of vasoconstrictors plus albumin in the management of type 2 HRS.[51,53]

Transjugular Intrahepatic Portosystemic Shunts (TIPS)

The use of portsosystemic shunts for therapy of HRS has been suggested for years, but the applicability in patients with such advanced liver disease is very limited. Two small studies indicate that the transjugular route with and intrahepatic posrtosystemic shunt (TIPS) may improve GFR as well as reduce the activity of the renin-angiotensin-aldosterone system and the sympathetic nervous system in approximately 60% of patients with type 1 HRS.[64,65] However these studies only included patients with moderate liver failure and excluded those with a history of hepatic encephalopathy, Child-Pugh scores ≥12 or serum bilirubin >5 mg/dL. The applicability of TIPS in patients with type 1 HRS is low because TIPS is considered contraindicated in patients with features of severe liver failure, which are common findings in the setting of type 1 HRS. The use of TIPS in type 2 HRS may improve renal function and reduce the risk of progression to type 1 HRS, but these data would require confirmation in specifically designed studies.[66]

Renal Replacement Therapy and other Dialysis Methods

Renal replacement therapy (RRT), mainly hemodialysis, has been used in the management of patients with type 1 HRS, especially in patients candidates to LT, in an attempt to maintain patients alive until LT is performed or spontaneous improvement in renal function occurs.[67] Unfortunately, the potential beneficial effect of this approach has not been demonstrated in randomized studies comparing RRT to other forms of therapy such as vasoconstrictors. Most patients develop side effects during RRT which include severe arterial hypotension, bleeding, and infections that may contribute to death during treatment. Additionally, indications for RRT (severe fluid overload, acidosis or hyperkalemia) are uncommon in type 1 HRS, at least in the early stages. Other methods such as the use of the molecular readsorbent recirculating system (MARS), an alternative of dialysis that clears albumin-bound substances, including vasodilators, is promising but more data is needed in order to consider it as a therapeutic device for HRS.[60] The results of a recent study using a fractionated plasma separation and adsorption extracorporeal liver support system, Prometheus, suggest that this technique improves survival in patients with type 1 HRS and acute-on-chronic liver failure, however these results require confirmation in larger studies.[68]

LIVER TRANSPLANTATION

It is the treatment of choice for patients with cirrhosis and HRS. Unfortunately a drawback of LT as a treatment modality for type 1 HRS is the very high mortality rates in the waiting list many patients exhibit. This limitation is usually overcome by assigning these patients a high priority for transplantation. Since pretransplant renal failure is an independent risk factor of both short-term and long-term post-transplantation patient and graft survival all efforts should be made to improve renal function in order to obtain a better outcome after transplantation.[70] The reversal of both type 1 and 2 HRS before transplantation may help patients not only reach transplantation, but also reduce the relatively high morbidity after LT characteristic of HRS. An analysis of a cohort of patients with type 1 HRS treated with terlipressin and albumin *vs* albumin alone revealed that among those receiving terlipressin plus albumin, the six month survival rates were 100% for patients that underwent LT.[71] Interestingly the group receiving only albumin and that underwent LT had a survival rate was 94% at six months. The survival rate was significantly better (47%) for those achieving a reversal of HRS versus those not achieving a reversal (4%). In the analysis terlipressin did not confer with a significant posttransplant survival benefit because the six-month survival rate for both groups was similar. What is clear is that LT is beneficial for patients with type 1 HRS regardless of the type of treatment they receive. The advantage of using terlipressin in patients undergoing LT relates mainly to its effect of improving renal function which makes taking care of the patients easier while awaiting LT and, most likely, during the post-transplant period. More studies and a longer follow-up period are still needed to determine whether pre-LT therapy of HRS actually will translate into better post-LT outcomes.

Other management strategies when considering LT in patients with HRS include simultaneous liver-kidney (SLK) transplantation and, LT followed by kidney transplantation. Current criteria for SLK include established end-stage renal disease and dialysis, GFR <30 mL/min and proteinuria >3 grs/day with 24 hour urine protein/creatinine ratio >3, and/or acute kidney injury and a requirement for dialysis at least times per week for more than six weeks.[70] After the introduction of MELD score system for organ allocation in the United States there has been an increase in the use of SLK for patients with cirrhosis and renal failure, which has been associated with a decline in survival after SLK compared to the preceding years.[72–74] Moreover, the outcome of patients with HRS treated with SLK is not better than that of patients with HRS treated with LT alone.[72] In addition, this approach uses kidneys that could be used for patients with chronic renal failure without liver disease, who have prolonged waiting times for renal transplantation. All these factors, together with the fact that renal function in HRS patients usually recovers after LT alone, suggest that SLK is not a good approach for the management of patients with HRS. The only exception may be that of patients with HRS who meet the above criteria for SLK.[70] Performance of LT alone followed by kidney transplantation, if necessary has been advocated by some centers. With this approach, kidney transplantation is performed in patients who undergo LT for HRS and require RRT more than 60 days after LT. Data on this approach is limited to only one study and thus more studies are needed in order to consider this strategy acceptable.[75]

PREVENTION

HRS can be prevented in some clinical settings. In the patients with SBP the risk of HRS is substantial, but it may be prevented with the administration of intravenous albumin (1.5 g/kg at diagnosis of infection and 1 g/kg 48 hours later). This measure prevents

worsening of circulatory dysfunction and the subsequent development of HRS. The rationale for albumin administration is to prevent further arterial underfilling and subsequent activation of vasoconstrictor systems, which usually occur in the setting of SBP in patients with cirrhosis.[76] The incidence of HRS in patients with SBP who receive albumin together with antibiotic therapy is 10%, compared with an incidence of 33% in those not receiving albumin.[76] More importantly, there is improved survival in those receiving albumin (10%) versus those not receiving albumin (29%). In patients with very advanced liver disease the long-term administration of norfloxacin orally (400 mg/day) prevents the development of HRS. In patients with ascitic fluid containing under 15 grams of proteins per liter (1.5 grams per deciliter) and associated liver and/or renal function impairment (bilirubin higher than 3 mg/dL, a Child-Pugh score greater than 10, serum sodium lower than 130 mmol/l and/or serum creatinine greater than 1.2 mg/dL) norfloxacin reduces the risk of HRS and improves survival.[77] The reason why norfloxacin prevents this complications is likely related to its ability to prevent bacterial translocation, suppress proinflammatory cytokines, and improve circulatory function.[78,79] A previous study showed that in patients with acute alcoholic hepatitis the use of pentoxifylline, an inhibitor of tumor necrosis factor-α, (400 mg tid orally for 28 days) reduced the incidence of HRS and mortality (8 and 24%, respectively) with respect to a control group (35 and 46%, respectively), however this has not been confirmed inin further studies. Finally, a large study showed that in the setting of acute alcoholic hepatitis the use of N-acetylcysteine for five days plus prednisolone prevented death due to the hepatorenal syndrome. Mortality at six months was higher in the prednisolone only group compared with N-acetylcysteine group (22 *vs* 9%).[80] These results although promising need confirmation.

Reference

[1] Hecker R, Sherlock S. Electrolyte and circulatory changes in terminal liver failure. Lancet 1956;271:1121–5.

[2] Lancestremere RG, Davidson PL, Earley LE, O'Brien FJ, Papper S. Renal failure in Laennec's cirrhosis. II. Simultaneous determination of cardiac output and renal hemodynamics. J Clin Invest 1962;41:1922–7.

[3] Shear L, Kleinerman J, Gabuzda GJ. Renal failure in patients with Cirrhosis of liver.I. clinical and pathologic characteristics. Am J Med 1965;39(2):184–96.

[4] Schroeder ET, Shear L, Sancetta SM, Gabuzda GJ. Renal failure in patients with Cirrhosis of liver.3. Evaluation of intrarenal blood flow by para-aminohippurate extraction and response to angiotensin. Am J Med 1967;43(6):887–96.

[5] Ginès P, Cárdenas A, Schrier RW. Liver disease and the kidney. In: Schrier RW, editor. Diseases of the kidney and urinary tract 8th ed. 2007. p.2179 –205.

[6] Ginès P, Schrier RW. Renal failure in cirrhosis. N Engl J Med 2009;361:1279–90.

[7] Francoz C, Glotz D, Moreau R, Durand F. The evaluation of renal function and disease in patients with cirrhosis. J Hepatol 2010;52:605–13.

[8] Sherman DS, Fish DN, Teitelbaum I. Assessing renal function in cirrhotic patients: problems and pitfalls. Am J Kidney Dis 2003;41:269–78.

[9] Papadakis MA, Arieff AI. Unpredictability of clinical evaluation of renal function in cirrhosis. Prospective study. Am J Med 1987;82:945–52.

[10] Caregaro L, Menon F, Angeli P, Amodio P, Merkel C, Bortoluzzi A, et al. Limitations of serum creatinine level and creatinine clearance as filtration markers in cirrhosis. Arch Int Med 1994;154:201–5.

[11] Proulx NL, Akbari A, Garg AX, Rostom A, Jaffey J, Clark HD. Measured creatinine clearance from timed urine collections substantially overestimates glomerular filtration rate in patients with liver cirrhosis: a systematic review and individual patient meta-analysis. Nephrol Dial Transplant 2005;20:1617–22.

[12] Cockcroft DW, Gault MH. Prediction of creatinine clearance from serum creatinine. Nephron 1976;16:31–41.

[13] Levey AS, Bosch JP, Lewis JB, Greene T, Rogers N, Roth D. A more accurate method to estimate glomerular filtration rate from serum creatinine: a new prediction equation. Modification of diet in renal disease study group. Ann Int Med 1999;130: 461–70.

[14] Gonwa TA, Jennings L, Mai ML, Stark PC, Levey AS, Klintmalm GB. Estimation of glomerular filtration rates before and after orthotopic liver transplantation: evaluation of current equations. Liver Transplant 2004;10:301–9.

[15] National Kidney Foundation. K/DOQI clinical practice guidelines for chronic kidney disease: evaluation, classification and stratification. Am J Kidney Dis 2002;39(Suppl. 1):S1–266.

[16] Mehta RL, Kellum JA, Shah SV, Molitoris BA, Ronco C, Warnock DG, et al. Acute kidney injury network: report of an initiative to improve outcomes in acute kidney injury. Crit Care 2007;11:R31.

[17] Ginès A, Escorsell A, Ginès P, et al. Incidence, predictive factors, and prognosis of the hepatorenal syndrome in cirrhosis with ascites. Gastroenterology 1993;105:229–36.

[18] Montoliu S, Ballesté B, Planas R, et al. Incidence and prognosis of different types of functional renal failure in cirrhotic patients with ascites. Clin Gastroenterol Hepatol 2010;8: 616–22.

[19] Fede G, D'Amico G, Arvaniti V, Tsochatzis E, Germani G, Georgiadis D, et al. Renal failure and cirrhosis: a systematic review of mortality and prognosis. J Hepatol 2012;56:810–8.

[20] Martin-Llahi M, Guevara M, Torre A, et al. Prognostic importance of the cause of renal failure in patients with cirrhosis. Gastroenterology 2010:1 [Epub ahead of print.].

[21] Tandon P, Garcia-Tsao G. Bacterial infections, sepsis, and multiorgan failure in cirrhosis. Semin Liver Dis 2008;28:26–42.

[22] Fasolato S, Angeli P, Dallagnese L, et al. Renal failure and bacterial infections in patients with cirrhosis: epidemiology and clinical features. Hepatology 2007;45:223–9.

[23] Fernández J, Navasa M, Gómez J, et al. Bacterial infections in cirrhosis: epidemiological changes with invasive procedures and norfloxacin prophylaxis. Hepatology 2002;35:140–8.

[24] Acevedo J, Fernandez J, Castro M, et al. Current recommended empirical antibiotic therapy in patients with cirrhosis and bacterial infection. J Hepatol 2009;50:6A.

[25] Arvaniti V, D'Amico G, Fede G, et al. Infections in patients with Cirrhosis increase mortality 4-fold and should be used in determining prognosis. Gastroenterology 2010;139:1246–56.
[26] Moreau R, Durand F. Renal insufficiency: management prior to transplantation. Liver Transpl 2010;16:S72–6.
[27] Cárdenas A, Ginès P, Uriz J, et al. Renal failure after upper gastrointestinal bleeding in cirrhosis: incidence, clinical course, predictive factors, and short-term prognosis. Hepatology 2001;34: 671–6.
[28] Lhotta K. Beyond hepatorenal syndrome: glomerulonephritis in patients with liver disease. Semin Nephrol 2002;22:302–8.
[29] Trawalé JM, Paradis V, Rautou PE, et al. The spectrum of renal lesions in patients with cirrhosis: a clinicopathological study. Liver Int 2010;30:725–32.
[30] Wadei HM, Geiger XJ, Cortese C, et al. Kidney allocation to liver transplant candidates with renal failure of undetermined etiology: role of percutaneous renal biopsy. Am J Transplant 2008;8:2618–26.
[31] Arroyo V, Ginès P, Gerbes AL, et al. Definition and diagnostic criteria of refractory ascites and hepatorenal syndrome in cirrhosis. International ascites club. Hepatology 1996;23:164–76.
[32] Salerno F, Gerbes A, Wong F, et al. Diagnosis, prevention and treatment of the hepatorenal syndrome in cirrhosis. A consensus workshop of the international ascites club. Gut 2007;56:1310–8.
[33] European Association for the Study of the Liver, Ginès P, Angeli P, Lenz K, et al. EASL clinical practice guidelines. Management of ascites, spontaneous bacterial peritonitis and hepatorenal syndrome in cirrhosis. J Hepatol 2010;53:397–417.
[34] Ruiz-del-Arbol L, Monescillo A, Arocena C, et al. Circulatory function and hepatorenal syndrome in cirrhosis. Hepatology 2005;42:439–47.
[35] Krag A, Bendtsen F, Henriksen JH, Møller S. Low cardiac output predicts development of hepatorenal syndrome and survival in patients with cirrhosis and ascites. Gut 2010;59:105–10.
[36] Fede G, Spadaro L, Tomaselli T, et al. Adrenocortical dysfunction in liver disease: a systematic review. Hepatology 2012. doi:10.1002/hep.25573.
[37] Tsai MH, Peng YS, Chen YC, et al. Adrenal insufficiency in patients with cirrhosis, severe sepsis and septic shock. Hepatology 2006;43:673–81.
[38] Fernández J, Escorsell A, Zabalza M, et al. Adrenal insufficiency in patients with cirrosis and septic shock: effect of treatment with hydrocortisone on survival. Hepatology 2006;44:1288–95.
[39] Alessandria C, Ozdogan O, Guevara M, et al. MELD score and clinical type predict prognosis in hepatorenal syndrome: relevance to liver transplantation. Hepatology 2005;41:1282–9.
[40] Salerno F, Badalamenti S. Drug induced renal failure in cirrhosis. In: Ginès P, Arroyo V, Rodes J, Schrier R, editors. Ascites and renal dysfunction in liver disease. 2nd ed. Oxford: Blackwell Publishing; 2005. p. 372–82.
[41] Uriz J, Ginès P, Cardenas A, et al. Terlipressin plus albumin infusion: an effective and safe therapy of hepatorenal syndrome. J Hepatol 2000;33:43–8.
[42] Moreau R, Durand F, Poynard T, et al. Terlipressin in patients with cirrhosis and type 1 hepatorenal syndrome: a retrospective multicenter study. Gastroenterology 2002;122:923–30.
[43] Ortega R, Ginès P, Uriz J, et al. Terlipressin therapy with and without albumin for patients with hepatorenal syndrome. Efficacy and outcome. Hepatology 2002;36:941–8.
[44] Halimi C, Bonnard P, Bernard B. Effect of terlipressin (Glypressin) on hepatorenal syndrome in cirrhotic patients: results of a multicentre pilot study. Eur J Gastroenterol Hepatol 2002;14:153–8.
[45] Neri S, Pulvirenti D, Malaguarnera M, et al. Terlipressin and albumin in patients with cirrhosis and type I hepatorenal syndrome. Dig Dis Sci 2008;53:830–5.
[46] Triantos CK, Samonakis D, Thalheimer U, et al. Terlipressin therapy for renal failure in cirrhosis. Eur J Gastroenterol Hepatol 2010;22:481–6.
[47] Narahara Y, Kanazawa H, Sakamoto C, Maruyama H, Yokosuka O, Mochida S, et al. The efficacy and safety of terlipressin and albumin in patients with type 1 hepatorenal syndrome: a multicenter, open-label, explorative study. J Gastroenterol 2012;47(3):313–20.
[48] Salerno F, Cazzaniga M, Merli M, Spinzi G, Saibeni S, Italian Association of the Hospital Gastroenterologists (AIGO)investigators, et al. Diagnosis, treatment and survival of patients with hepatorenal syndrome: a survey on daily medical practice. J Hepatol 2011;55(6):1241–8.
[49] Solanki P, Chawla A, Garg R, et al. Beneficial effects of terlipressin in hepatorenal syndrome: a prospective, randomized placebo-controlled clinical trial. J Gastroenterol Hepatol 2003;18: 152–6.
[50] Sanyal A, Boyer T, Garcia-Tsao G, et al. A prospective, randomized, double blind, placebo-controlled trial of terlipressin for type 1 hepatorenal syndrome (HRS). Gastroenterology 2008;134:1360–8.
[51] Martin-Llahi M, Pepin MN, Guevara G, et al. Terlipressin and albumin vs albumin in patients with cirrhosis and hepatorenal syndrome: a randomized study. Gastroenterology 2008;134: 1352–9.
[52] Cavallin M, Merli M, Fasolato S, et al. Terlipressin and albumin vs midodrine plus octreotide and albumin in the treatment of hepatorenal syndrome in patients with cirrhosis: results of a controlled clinical trial by the Italian association for the study of the liver. Hepatology 2011;54:LB-2.
[53] Alessandria C, Ottobrelli A, Debernardi-Venon W, et al. Noradrenalin vs terlipressin in patients with hepatorenal syndrome: a prospective, randomized, unblinded, pilot study. J Hepatol 2007;47:499–505.
[54] Singh V, Ghosh S, Singh B, Kumar P, Sharma N, Bhalla A, et al. Noradrenaline vs. terlipressin in the treatment of hepatorenal syndrome: a randomized study. J Hepatol 2012;:6.
[55] Sagi SV, Mittal S, Kasturi KS, Sood GK. Terlipressin therapy for reversal of type 1 hepatorenal syndrome: a meta-analysis of randomized controlled trials. J Gastroenterol Hepatol 2010;25: 880–5.
[56] Gluud LL, Christensen K, Christensen E, Krag A. Systematic review of randomized trials on vasoconstrictor drugs for hepatorenal syndrome. Hepatology 2010;51:576–84.
[57] Nazar A, Pereira GH, Guevara M, et al. Predictors of response to therapy with terlipressin and albumin in patients with cirrhosis and type 1 hepatorenal syndrome. Hepatology 2010;51: 219–26.
[58] Boyer TD, Sanyal AJ, Garcia-Tsao G, et al. Predictors of response to terlipressin plus albumin in hepatorenal syndrome (HRS) type 1: relationship of serum creatinine to hemodynamics. J Hepatol 2011;55:315–21.
[59] Velez JC, Nietert PJ. Therapeutic response to vasoconstrictors in hepatorenal syndrome parallels increase in mean arterial pressure: a pooled analysis of clinical trials. Am J Kidney Dis 2011;58(6):928–38.
[60] Angeli P, Volpin R, Gerunda G, et al. Reversal of type 1 hepatorenal syndrome with the administration of midodrine and octreotide. Hepatology 1999;29:1690–7.
[61] Wong F, Pantea L, Sniderman K. Midodrine, octreotide, albumin, and TIPS in selected patients with cirrhosis and type 1 hepatorenal syndrome. Hepatology 2004;40:55–64.

[62] Skagen C, Einstein M, Lucey MR, Said A. Combination treatment with octreotide, midodrine, and albumin improves survival in patients with type 1 and type 2 hepatorenal syndrome. J Clin Gastroenterol 2009;43(7):680–5.
[63] Duvoux C, Zanditenas D, Hezode C, et al. Effects of noradrenaline and albumin in patients with type 1 hepatorenal syndrome: a pilot study. Hepatology 2002;36:374–80.
[64] Brensing KA, Textor J, Perz J, et al. Long term outcome after transjugular intrahepatic portosystemic stent-shunt in non-transplant cirrhotics with hepatorenal syndrome: a phase II study. Gut 2000;47:288–95.
[65] Guevara M, Ginès P, Bandi JC, et al. Transjugular intrahepatic portosystemic shunt in hepatorenal syndrome: effects on renal function and vasoactive systems. Hepatology 1998;28: 416–22.
[66] Ginès P, Uriz J, Calahorra B, et al. Transjugular intrahepatic portosystemic shunting versus paracentesis plus albumin for refractory ascites in cirrhosis. Gastroenterology 2002;123: 1839–47.
[67] Gonwa TA, Wadei HM. The challenges of providing renal replacement therapy in decompensated liver cirrhosis. Blood Purif 2012;33:144–8.
[68] Bañares R, Nevens F, Larsen FS, et al. Extracorporeal liver support with the molecular adsorbent recirculating system (MARS) in patients with acute-on-chronic liver failure (AOCLF). The RELIEF trial. J Hepatol 2010;52:1184A.
[69] Kribben A, Gerken G, Haag S, et al. Effects of fractionated plasma separation and adsorption on survival in patients with acute-on-chronic liverfailure. Gastroenterology 2012.
[70] Charlton MR, Wall WJ, Ojo AO, Ginès P, Textor S, International Liver Transplantation Society Expert Panel., et al. Report of the first international liver transplantation society expert panel consensus conference on renal insufficiency after liver transplantation. Liver Transpl 2009;15:S1–34.
[71] Boyer TD, Sanyal AJ, Garcia-Tsao G, et al. Impact of liver transplantation on the survival of patients treated for hepatorenal syndrome type 1. Liver Transpl 2011;17:1328–32.
[72] Jeyarajah DR, Gonwa TA, McBride M, et al. Hepatorenal syndrome: combined liver kidney transplants versus isolated liver transplant. Transplantation 1997;64:1760–5.
[73] Locke JE, Warren DS, Singer AL, et al. Declining outcomes in simultaneous liver-kidney transplantation in the MELD era: ineffective usage of renal allografts. Transplantation 2008;85: 935–42.
[74] Eason JD, Gonwa TA, Davis CL, et al. Proceedings of consensus conference on simultaneous liver kidney transplantation (SLK). Am J Transplant 2008;8:2243–51.
[75] Ruiz R, Barri YM, Jennings LW, et al. Hepatorenal syndrome: a proposal for kidney after liver transplantation (KALT). Liver Transpl 2007;13:838–43.
[76] Sort P, Navasa M, Arroyo V, et al. Effect of intravenous albumin on renal impairment and mortality in patients with cirrhosis and spontaneous bacterial peritonitis. N Engl J Med 1999;341:403–9.
[77] Fernández J, Navasa M, Planas R, et al. Primary prophylaxis of spontaneous bacterial peritonitis delays hepatorenal syndrome and improves survival in cirrhosis. Gastroenterology 2007;133:818–24.
[78] Chin-Dusting JP, Rasaratnam B, Jennings GL, Dudley FJ. Effect of fluoroquinolone on the enhanced nitric oxide-induced peripheral vasodilation seen in cirrhosis. Ann Intern Med 1997;127:985–8.
[79] Rasaratnam B, Kaye D, Jennings G, Dudley F, Chin-Dusting J. The effect of selective intestinal decontamination on the hyperdynamic circulatory state in cirrhosis. A randomized trial. Ann Intern Med 2003;139(3):186–93.
[80] Nguyen-Khac E, Thevenot T, Piquet MA, et al. Glucocorticoids plus N-acetylcysteine in severe alcoholic hepatitis. N Engl J Med 2011;365:1781–9.

CHAPTER

80

Autosomal Dominant Polycystic Kidney Disease

Stefan Somlo[1], *Vicente E. Torres*[2], *Michael J. Caplan*[1]

[1]Yale University School of Medicine, New Haven, Connecticut, USA

[2]Division of Nephrology and Hypertension, Mayo Clinic College of Medicine, Rochester, Minnesota, USA

Autosomal dominant polycystic kidney disease (ADPKD) (MIM 173900) is a systemic disorder characterized by age-dependent occurrence of bilateral, multiple renal cysts as well as a variety of extrarenal manifestations. The latter include cysts in the liver bile ducts, pancreatic ducts, seminal vesicles, and arachnoid membrane, as well as noncystic manifestations, such as intracranial aneurysms and dolichoectasias, aortic root dilatation and aneurysms, mitral valve prolapse, and abdominal wall hernias. Over the past several decades, the study of this disease has yielded remarkable progress and insights. The mutated genes and their respective protein products were identified by positional cloning, the occurrence of multiple somatic mutations were implicated in the molecular pathogenesis, a comprehensive array of orthologous gene animal models have been developed, and a much neglected organelle, the primary cilium, has become the focus of investigation not just in this disease but in a whole panoply of structural kidney diseases as well as more diverse biological processes. There has been improved understanding of the clinical disease and the variation it exhibits, and several directed therapeutic clinical trials based on preclinical and bench investigations are beginning to yield results in patients. Still, the goals of understanding the basic disease mechanisms and finding effective treatments remain a work in progress.

CLINICAL FEATURES OF AUTOSOMAL DOMINANT POLYCYSTIC KIDNEY DISEASE

ADPKD affects between 1 in 400 and 1 in 1000 live births in all ethnic populations worldwide.[1–3] Mutations in either of two genes, *PKD1* or *PKD2*, respectively encoding to protein products called polycystin-1 (PC1) than polycystin-2 (PC2), result in ADPKD. It is the most common single gene disorder that can lead to premature death in man. Approximately 2100 ADPKD patients start renal replacement therapy yearly in the United States. Worldwide yearly incidence rates for end stage renal disease (ESRD) caused by ADPKD in men and women, respectively, are 8.7 and 6.9 per million (1998–2001, United States), 7.8 and 6.0 per million (1998–1999, Europe),[4] and 5.6 and 4.0 per million (1999–2000, Japan).[5] Age-adjusted sex ratios greater than unity (1.2–1.3) suggest a more progressive disease in men than in women. In the United States the incidence of ESRD due to ADPKD has increased by 10.8 percent from 1996–1998 to 2007–2008.[6,7] Similarly, in Denmark ESRD incidence secondary to ADPKD increased from 6.45 per million in 1990–1995 to 7.59 per million in 2002–2007.[8] These trends may be due to improved patient survival before the onset of ESRD.[9] At the same time the age at ESRD in ADPKD patients has increased in both countries.[6,7] In Denmark, age-adjusted male-to-female ratio for onset of ESRD has changed from 1.6 to 1.1, indicating a trend toward similar progression in both genders in recent years.[8]

The diagnosis of ADPKD usually relies on imaging testing (Figure 80.1).[10] Renal ultrasound is commonly used because of cost and safety. Counseling should be done before testing an individual with a family history for the presence of ADPKD. Benefits of testing include certainty regarding diagnosis that may influence family planning, early detection and treatment of disease complications, and identification of genetically unaffected family members for living related-donor renal

Seldin and Giebisch's The Kidney, Fifth Edition.
DOI: http://dx.doi.org/10.1016/B978-0-12-381462-3.00080-X

© 2013 Elsevier Inc. All rights reserved.

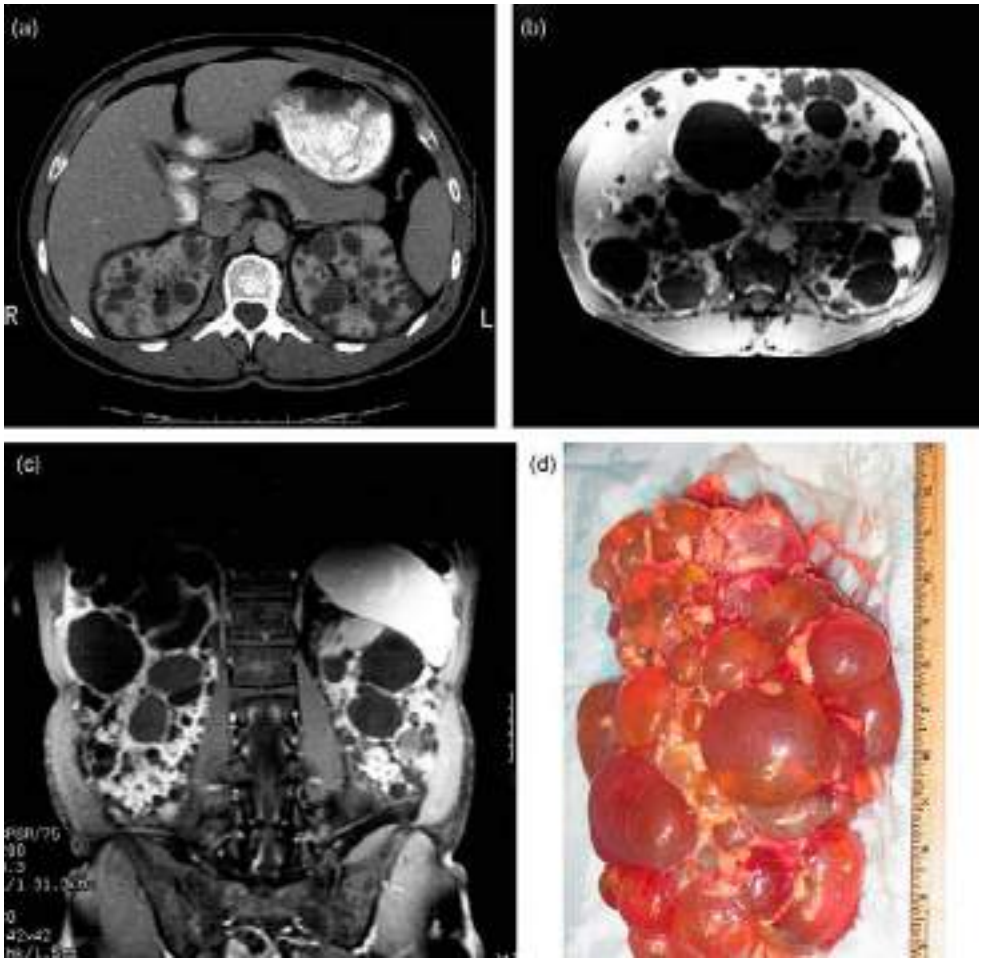

FIGURE 80.1 Radiographic and gross appearance of ADPKD. **a**: Contrast enhanced, axial CT image through the abdomen demonstrating moderate polycystic kidney disease, with numerous bilateral renal cysts, preservation of renal parenchyma, and absence of hepatic cysts. **b,c**: Axial and coronal, gadolinium-enhanced, T1-weighted MR images demonstrating more advanced polycystic kidney and liver disease with marked enlargement of both organs. In both the CT and MR images, cysts appear as hypodense areas within the organ parenchyma. **d**: Nephrectomy specimen from a patient with ADPKD and end-stage renal disease. Cysts permeate the mass of the kidney and the noncystic regions are fibrotic and scarred. *(CT and MRI courtesy of Rex Mahnensmith. Kidney image courtesy of Darren Wallace.)*. See color plate section at the back of the book.

transplantation. The potential for discrimination in terms of health insurability and employment associated with a positive diagnosis has been reduced by the Genetic Information Nondiscrimination Act (GINA) but it does not apply to life, disability or long-term care insurance. Additionally, the psychological burden of knowing affliction by a chronic disease should be considered in the decision to test.

The occurrence and severity of the cystic lesions are highly variable. Cysts have been observed *in utero* and have been detected as incidental findings in 80-year-old patients with otherwise normal blood pressure and kidney function. In genetic terms, the expressivity, or severity, of the phenotype, in this disease is highly variable. By contrast the penetrance is virtually complete if it is expressed as a function of age. Individuals over the age of 30 carrying a causative gene mutation will invariably manifest cysts sufficient for diagnosis when assessed with an appropriately sensitive imaging study. For this reason, the gold standard for diagnosis of ADPKD remains imaging studies of the kidney. The ultrasound criteria, referred to as the modified Ravine criteria,[11] take into account the age-dependent penetrance of the disease by requiring increasing numbers of cysts with increasing age to make the diagnosis. For individuals at 50% risk for the disease (i.e., those with a family history), these criteria include at least two unilateral or bilateral cysts in individuals younger than 30 years; two cysts in each kidney in individuals 30 to 59 years old; and four cysts in each kidney in individuals 60 years or older.[11] In the absence of a family history of ADPKD, bilateral renal enlargement and cysts or the presence of multiple bilateral cysts with hepatic cysts together with the absence of other manifestations

suggesting a different renal cystic disease provide presumptive evidence for the diagnosis of ADPKD.

Revised ultrasound criteria have been proposed to improve the diagnostic performance of ultrasonography in ADPKD[12] (Table 80.1). The presence of at least three (unilateral or bilateral) renal cysts and of two cysts in each kidney have a positive predictive value of 100% in 15 to 39 and 40 to 59 year-old at-risk individuals, respectively. For at-risk individuals ages 60 years and older, four or more cysts in each kidney are required. Although the positive predictive values of these criteria are very high, their sensitivity and negative predictive value are low, particularly when applied to 15- to 59-year-old *PKD2* patients. This is a problem in the evaluation of potential kidney donors where exclusion of the diagnosis is important. Information on the age of ESRD in other affected family members may be helpful in this setting.[13] A history of at least one affected family member with ESRD secondary to ADPKD by age 55 years has 100% positive predictive value for *PKD1*. Conversely, a history of at least one affected family member without ESRD by age ≥ 70 years has 100% positive predictive value for *PKD2*. More strict criteria have therefore been proposed to exclude a diagnosis of ADPKD in an individual at risk from a family with an unknown genotype (Table 80.1). An ultrasound scan finding of normal kidneys or one renal cyst in an individual age 40 years or older has a negative predictive value of 100%. The absence of any renal cyst provides near certainty that ADPKD is absent in at-risk individuals ages 30 to 39 years with a negative predictive value of 98.3%. A negative or indeterminate ultrasound scan result does not exclude ADPKD with certainty in an at-risk individual younger than 30 years of age. In this setting, negative results on magnetic resonance imaging (MRI) or contrast-enhanced computed tomography (CT) provide further assurance, but there are insufficient data to quantify its predictive accuracy. Jointly considering the proposed sonographic criteria, family history information, and findings on high resolution imaging studies routinely obtained during donor evaluations usually allows a determination of disease status in the majority of potential living related kidney donors with high level of certainty.[14]

Genetic testing can be used when the imaging results are equivocal and/or when a definite diagnosis is required in a younger individual, such as a potential living related kidney donor. Prenatal and preimplantation genetic testing are rarely considered for ADPKD.[15] Genetic testing is performed by direct sequence analysis. Direct sequencing yields mutation detection rates of approximately 85%.[16] However, as most mutations are unique and up to one third of *PKD1* changes are predicted to be single amino acid substitution changes, the causative nature of some sequence changes is difficult to prove. Genetic testing can be helpful with *de novo* mutations in the absence of a family history. A unique variant in either *PKD1* or *PKD2* present in the affected child but absent in both parents in the setting of documented maternity and paternity can identify the new mutation.

Natural History of ADPKD

The clinical *sine qua non* for ADPKD is the presence of multiple cysts in both kidneys and the consequent increase in total kidney size. The development of cysts in ADPKD probably starts in the embryo. They

TABLE 80.1 Sonographic Criteria for Diagnosis of ADPKD for Individuals with an Affected First Degree Relative

Family Genotype		Unknown		PKD1*		PKD2†	
Age	**Revised criteria for positive diagnosis**	**PPV**	**SEN**	**PPV**	**SEN**	**PPV**	**SEN**
15–29	≥ 3 cysts, unilateral or bilateral	100	81.7	100	94.3	100	69.5
30–39	≥ 3 cysts, unilateral or bilateral	100	95.5	100	96.6	100	94.9
40–59	≥ 2 cysts in each kidney	100	90.0	100	92.6	100	88.8
≥ 60	≥ 4 cysts in each kidney	100	100	100	100	100	100
	Revised criteria for diagnosis exclusion	**NPV**	**SPEC**	**NPV**	**SPEC**	**NPV**	**SPEC**
15–29	≥ 1 cyst	90.8	97.1	99.1	97.6	83.5	96.6
30–39	≥ 1 cyst	98.3	94.8	100	96.0	96.8	93.8
40–59	≥ 2 cysts	100	98.2	100	98.4	100	97.8

**100% (PPV) if one affected family member has ESRD by age 55 yrs.*
†100% PPV if one affected family member does not have ESRD by age ≥ 70 yrs
PPV, positive predictive value; SEN, sensitivity; NPV, negative predictive value; SPEC, specificity.

continue to form and grow during the remaining life time. Cyst expansion along with associated inflammation, fibrosis, and tubular dropout results in a loss of filtering nephrons, but glomerular filtration rate remains stable for decades thanks to the compensatory capacity of the kidney. During this often-silent phase, mild polyuria due to impaired urinary concentrating capacity, elevated blood pressure, microalbuminuria, and, occasionally, low-grade proteinuria can develop. When enough filtering nephrons have been lost, the glomerular filtration rate (GFR) begins to fall precipitously. Extrarenal manifestations of the disease are rare in childhood. Cysts in the liver usually start later than in the kidney. Patients may seek medical attention at any point in the course of the disease for renal or extrarenal, cyst-related or non−cyst-related manifestations.

The Consortium for Radiologic Imaging Studies of Polycystic Kidney Disease (CRISP) has provided the best clinical information on how cysts develop and grow. Two hundred and forty-one nonazotemic patients have been followed prospectively with yearly magnetic resonance imaging (MRI) examinations to assess kidney and cyst growth.[17] Total kidney volume and cyst volumes increased exponentially. At baseline, total kidney volume was 1060 ± 642 ml, and the mean increase over three years was 204 ml, or 5.3% per year. The rates of change of total kidney and total cyst volumes, and of right and left kidney volumes, were strongly correlated, suggesting that kidney enlargement was due to cyst enlargement. Baseline total kidney volume predicted the subsequent rate of increase in renal volume and was associated with declining GFR in patients with baseline total kidney volume above 1500 ml after the first three years of follow-up. The association between baseline total kidney volume has become increasingly strong with an extended follow-up of eight years, qualifying total kidney volume as a prognostic biomarker in ADPKD.[18]

Renal Manifestations of ADPKD

Hypertension

Hypertension (BP > 140/90 mmHg) is present in approximately 50% of 20-34 year old ADPKD patients with normal renal function and increases to nearly 100% of patients with ESRD.[19] Its development is accompanied by a reduction in renal blood flow, increased filtration fraction, abnormal renal handling of sodium, and extensive remodeling of the renal vasculature.[20,21]

The association between renal size and prevalence of hypertension has supported the hypothesis that stretching and compression of the vascular tree by cyst expansion causes ischemia and activation of the renin−angiotensin system.[22] Whether the classic, circulating renin-angiotensin system is inappropriately activated is controversial.[23,24] There is stronger evidence for the activation of a local intrarenal renin-angiotensin system. Evidence for the latter includes (1) partial amelioration of the reduced renal blood flow, increased renal vascular resistance and increased filtration fraction in the setting of acute or chronic administration of an ACEI;[21,23,25] (2) shift of immunoreactive renin from the juxtaglomerular apparatus to the walls of the arterioles and small arteries;[26,27] (3) ectopic synthesis of renin in the epithelium of dilated tubules and cysts;[27,28] and (4) ACE-independent generation of angiotensin II by a chymase-like enzyme.[29]

It has been suggested that a primary disruption of polycystin protein function in the vasculature may also play a role in the early development of hypertension and renal vascular remodeling. Supportive evidence includes expression of the respective *PKD1* and *PKD2* gene products in vascular smooth muscle[30−32] and endothelium,[33] and enhanced vascular smooth muscle contractility[34] and impaired endothelial dependent vasorelaxation[35] in heterozygous blood vessels. Recent studies have shown that nitric oxide endothelium-dependent vasorelaxation is impaired in small subcutaneous resistance vessels from patients with normal renal function before development of hypertension.[35−37] Other factors proposed to contribute to hypertension in ADPKD include increased sympathetic nerve activity and plasma endothelin-1 levels and insulin resistance.[38]

The diagnosis of hypertension in ADPKD is often made late. Twenty-four hours ambulatory blood pressure monitoring of children or young adults without hypertension may reveal elevated blood pressures and attenuated nocturnal blood pressure dipping and exaggerated blood pressure response during exercise, which may be accompanied by left ventricular hypertrophy and diastolic dysfunction.[39] Early detection and treatment of hypertension is important because cardiovascular disease is the main cause of death and uncontrolled blood pressure increases the risk for proteinuria, hematuria, faster decline of renal function and morbidity and mortality from valvular heart disease and aneurysms.[2,40,41]

Pain

Pain is the most frequent symptom (~60%) reported by adult patients.[42,43] Acute pain may be associated with renal hemorrhage, passage of stones and urinary tract infections. Some patients develop chronic flank pain without identifiable etiology other than the cysts.

VEGF produced by the cystic epithelium[44] may promote angiogenesis, hemorrhage into cysts and gross hematuria. Rarely, a hemorrhagic cyst can rupture into the subcasular or retroperitoneal space. Symptomatic episodes likely underestimate the frequency of cyst

hemorrhage as over 90% of ADPKD patients have hyperdense (CT) or high signal (MRI) cysts reflecting blood or high protein content. Most hemorrhages resolve within two to seven days. If symptoms last longer than one week or if the initial episode occurs after the age of 50 years, investigation to exclude neoplasm should be undertaken.

Approximately 20% of ADPKD patients have kidney stones.[45–47] Their composition is usually uric acid and/or calcium oxalate. Metabolic factors include decreased ammonia excretion, low urinary pH and low urinary citrate concentration. Urinary stasis secondary to the distorted renal anatomy may also play a role. Stones may be difficult to differentiate from cyst wall and parenchymal calcification, which also occur with increased frequency.

As in the general population urinary tract infections affect females more frequently than males. Most are caused by enterobacteriaciae.[48] CT and MRI are sensitive to detect complicated cysts and provide anatomic definition, but the findings are not specific for infection. Nuclear imaging (^{67}Ga or ^{111}In-labeled leukocyte scans) is useful but false negative and positive results are possible. ^{18}fluorodeoxyglucose (^{18}FDG) positron-emission computed tomography (PET/CT) is currently the most helpful imaging modality to detect a cyst infection, but it is not widely available, is expensive, and currently not approved by the Centers for Medicare and Medicaid Services (CMS) for the diagnosis of infection.[49,50] Cyst aspiration should be considered when the clinical setting and imaging are suggestive and blood and urine cultures are negative.

Renal cell carcinoma is a rare cause of pain in ADPKD. It does not occur more frequently than in the general population, but it may present at an earlier age with frequent constitutional symptoms and a higher proportion of sarcomatoid, bilateral, multicentric, and metastatic tumors.[51] A solid mass on ultrasound, speckled calcifications on CT, and contrast enhancement, tumor thrombus and regional lymphadenopathies on CT or MRI should raise the suspicion for a carcinoma.

Renal Failure

The development of renal failure is highly variable. In most patients renal function is maintained within the normal range, despite relentless growth of cysts, until the 4th to 6th decade of life. By the time renal function starts declining, the kidneys usually are markedly enlarged and distorted with little recognizable parenchyma on imaging studies. At this stage, the average rate of GFR decline is approximately 4.4−5.9 mL/min/year.[52] The mutated gene (*PKD1* or *PKD2*) is a significant determinant of the severity of disease and position of the mutation within *PKD1* and possible modifier genes also contribute to the clinical course of ADPKD (see following sections). Other risk factors for a worse prognosis include male gender (particularly in *PKD2*), black race, first episode of hematuria before the age of 30, onset of hypertension before the age of 35, hyperlipidemia, low HDL, and sickle cell trait.[53–55]

Several mechanisms account for renal function decline. The CRISP study has confirmed previous studies suggesting a strong relationship between renal enlargement and functional decline.[17] CRISP has shown that kidney and cyst volumes are the strongest predictors of renal functional decline. CRISP also found that renal blood flow (or vascular resistance) is an independent predictor of functional decline.[56] This points to the importance of vascular remodeling in the progression of the disease and may account for cases where the decline of renal function seems to be out of proportion to the severity of the cystic disease. Angiotensin II, transforming growth factor-β, and reactive oxygen species may contribute to the vascular lesions and interstitial fibrosis by stimulating the synthesis of chemokines, extracellular matrix, and metalloproteinase inhibitors. Other factors such as heavy use of analgesics may contribute to chronic kidney disease (CKD) progression in some patients.

Extrarenal Manifestations of ADPKD

Polycystic Liver Disease

PLD is the most common extrarenal manifestation. It is associated with both *PKD1* and *PKD2* genotypes. The cysts arise by excessive proliferation and dilatation of biliary ductules and peribiliary glands. Estrogen receptors are expressed in the epithelium lining the hepatic cysts and estrogens stimulate hepatic cyst derived cell proliferation.[57] Bile duct cyst growth is also promoted by growth factors and cytokines secreted into the cyst fluid.[63,219]

Hepatic cysts are rare in children. Their frequency increases with age and may have been underestimated by ultrasound and CT studies. Their prevalence by MRI in the CRISP study is 58%, 85 and 94% in 15 to 24, 25 to 34 and 35 to 46 year old participants.[58] Hepatic cysts are more prevalent and hepatic cyst volume is larger in women than in men. Women who have multiple pregnancies or who have used oral contraceptive agents or estrogen replacement therapy have worse disease suggesting an estrogen effect on hepatic cyst growth.[59,60]

Typically, PLD is asymptomatic, but symptoms have become more frequent as the lifespan of ADPKD patients has lengthened with dialysis and transplantation. Symptoms may result from mass effect or from complications related to the cysts. Symptoms typically

caused by massive enlargement of the liver or by mass effect from a single or a limited number of dominant cysts include dyspnea, early satiety, gastroesophageal reflux, and mechanical low back pain. Other complications caused by mass effect include hepatic venous outflow obstruction, inferior vena cava compression, portal vein compression or bile duct compression presenting as obstructive jaundice.[61]

Symptomatic liver cyst complications include cyst hemorrhage, infection and rarely torsion or rupture. The typical presentation of cyst infection is with localized pain, fever, leukocytosis, elevated sedimentation rate and often elevated alkaline phosphatase.[62] It is usually monomicrobial and caused by enterobacteriaceae. MRI is very sensitive for identifying complicated hepatic cysts. On CT scanning, fluid-debris levels within cysts, cyst wall thickening, intracystic gas bubbles, and heterogeneous or increased density have been associated with infection. Radionuclide imaging and more recently ^{18}F-fluorodoxyglucose PET/CT scanning have been used for diagnosis.[63]

Mild dilatation of the common bile duct has been observed in 40% of patients studied by CT and may rarely be associated with episodes of cholangitis.[64] Rare associations of PLD include congenital hepatic fibrosis,[65] adenomas of the ampulla of Vater,[66] and cholangiocarcinoma.[67]

Cysts in other Organs

Seminal vesicles, pancreas, and arachnoid membrane cysts are present in 40% (males), 5%, and 8% of patients, respectively.[68–73] Seminal vesicle cysts rarely result in infertility.[74] Defective sperm motility is another cause of male infertility in ADPKD.[75] Pancreatic cysts are almost always asymptomatic, with very rare occurrences of recurrent pancreatitis and possibly chance associations of intraductal papillary mucinous tumor or carcinoma reported in ADPKD.[76–78] Arachnoid membrane cysts are asymptomatic, but may increase the risk for subdural hematomas.[70,79] Spinal meningeal diverticula may occur with increased frequency and rarely present with intracranial hypotension due to cerebrospinal fluid leak.[80] Ovarian cysts are not associated with ADPKD.[81,82]

Vascular Manifestations

These include intracranial aneurysms and dolichoectasias, thoracic aortic and cervicocephalic artery dissections, and coronary artery aneurysms. They are caused by alterations in the vasculature directly linked to mutations in *PKD1* or *PKD2*. The respective protein products, PC1 and PC2, are expressed in vascular smooth muscle cells (VSMC).[30–32] *Pkd2*$^{+/-}$ VSMCs from mice exhibit increased rates of proliferation and apoptosis and *Pkd2*$^{+/-}$ mice have an increased susceptibility to vascular injury and premature death when induced to develop hypertension.[83,84] Defective structural integrity of blood vessels occur in mice lacking PC1.[85]

Intracranial aneurysms (ICA) occur in approximately 6% of patients with a negative, and 16% of those with a positive family history of aneurysms.[86,87] They are most often asymptomatic. Focal findings such as cranial nerve palsy or seizure result from compression of local structures. The risk of rupture depends on many factors including the size of the aneurysm. Rupture carries a 35–55% risk of combined severe morbidity and mortality.[88] The mean age at rupture is lower than in the general population (39 years versus 51 years). Most patients with ICA have normal renal function and up to 29% will have normal blood pressure at the time of rupture.

Cardiac Manifestations

Mitral valve prolapse occurs in up to 25% of ADPKD patients on echocardiography.[118,184] Aortic insufficiency may occur in association with dilatation of the aortic root.[89] Although these lesions may progress with time, they rarely require valve replacement. Screening echocardiography is not indicated unless a murmur is detected on examination. Clinically inconsequential pericardial effusions are a common incidental finding in ADPKD.[90]

Diverticular Disease

Colonic diverticulosis and diverticulitis are more common in ESRD patients with ADPKD than in those with other renal diseases.[160,198,297] Whether this increased risk extends to patients prior to ESRD is uncertain.[91] There have been reports of extracolonic diverticular disease.[92] It may become clinically significant in a minority of patients. Subtle alterations in polycystin function that may enhance the smooth muscle dysfunction during aging may underlie the development of diverticula.

Isolated Polycystic Liver Disease

Isolated autosomal dominant PLD (ADPLD; MIM 174050) also occurs as a genetically distinct disease in the absence of renal cysts.[93,94] Like ADPKD, ADPLD is genetically heterogeneous, with two genes identified (*PRKCSH* and *SEC63*) accounting for approximately one-third of isolated ADPLD cases. ADPLD often goes undetected even in first-degree relatives of patients with highly symptomatic polycystic liver disease. As in the case of polycystic liver disease associated with ADPKD, isolated ADPLD is more severe in women than in men. Liver function tests remain normal and when symptoms develop, these are related to mass effects or complications such as cyst hemorrhage or infection. Patients with isolated ADPLD may also be at

increased risk for intracranial aneurysms and valvular heart disease.

CILIA AND THE SPECTRUM OF INHERITED CYSTIC DISEASE

Understanding of the clinical spectrum of polycystic kidney diseases as well as clues to the underlying molecular pathogenesis have been significantly advanced by the discovery over the past decade of the central role of cilia in cyst formation in the kidney. The 'cilia hypothesis' for polycystic disorders has been reviewed extensively (e.g., [95–97]). It is now appreciated that defects in cilia-basal body-centriole-related proteins—i.e., those found in the cilial membrane, cilial axoneme, the basal body or pericentriolar region—are varyingly associated with clinical spectrum of disease that can include cystic kidneys, bile duct and pancreatic duct cysts, retinal degeneration and retinitis pigmentosa, *situs inversus* (incorrect left-right body axis), anosmia, infertility, and hydrocephalus.[95,98]

There are two general classes of cilia: the motile "9 + 2" structures and the non-motile '9 + 0' structures that are also referred to as "primary cilia"[99] (Figure 80.2). In the kidney, the apical surface of every tubular epithelial cell, with the exception of mature intercalated cells, is decorated by a single primary cilium, a hair-like structure enclosed by a membrane continuous with the cell membrane and a containing the central axoneme composed of nine peripheral microtubule doublets without a central pair (hence, 9 + 0). The non-motile primary cilium is rooted in the centrosome, the microtubule organizing center of the cell. The centrosome is composed of a mother and a daughter centriole and a cloud of pericentriolar material around the mother centriole. During interphase, the distal end of the mother centriole known as the basal body gives

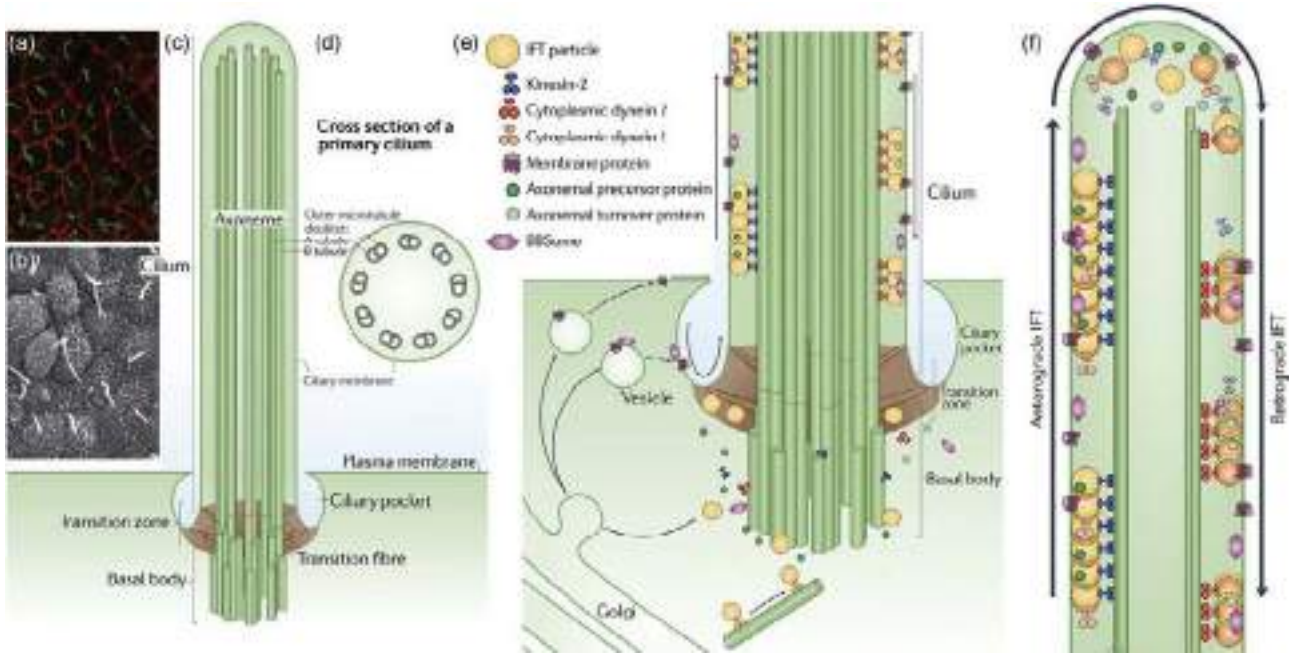

FIGURE 80.2 Structural and functional elements of cilia. **a**: Immunofluorescence image of primary cilia (green) in inner medullary collecting duct (IMCD3) cells; basal bodies, magenta; cell–cell junctions, red. **b:** Scanning electron micrographs of cilia at the mouse embryonic node. **c, d**: Primary cilia differ from motile cilia in that the ciliary axoneme is comprised of nine pairs of microtubules without a central pair (9 + 0). Primary cilium arises from the basal body which is comprised of the centrosome in non-mitotic cells. The base of the cilium has a circumferential invagination of the plasma membrane called the ciliary pocket and is separated from the rest of the cell body by the transition zone. **e**. The transition zone complex, which includes several members of the NPHP, JBTS and MKS protein families, serves to selectively sort proteins that enter and exit the cilium. Proteins pass through the transition zone by either of two processes. Intraflagellar transport (IFT) involves loading of cytoplasmic proteins onto large multiprotein complexes (IFT particles) that move along the outer doublet microtubules beneath the ciliary membrane. Proteins destined for the ciliary membrane (e.g., the polycystins) are synthesized in the endoplasmic reticulum, processed through the Golgi stack and trafficked into vesicles that dock near the ciliary base in a process dependent on the BBSome comprised of proteins associated with BBS. **f**: The IFT particles, comprised of complexes A and B and their cargo, including the BBSome and integral membrane proteins such as polycystins, are moved toward the tip of the cilium by the anterograde motor protein kinesin-2. Once at the tip, the cargo is released and the IFT complexes rearrange so that kinesin-2 is replaced by cytoplasmic dynein-2 which acts as the retrograde motor to carry the particles back to the cell body *(Modified and reprinted by permission from Macmillan Publishers Ltd: Ishikawa H. & Marshall W.F., Ciliogenesis: building the cell's antenna*, Nature Reviews Molecular Cell Biology*, 12:222–234, copyright 2011).*

rise to the primary cilium. Cilia are assembled and maintained by a process called intraflagellar transport (IFT) in which the components of the ciliary axoneme are assembled at the basal bodies into large transport particles called rafts. A region at the base of the cilia composed of transition fibers provides a compartmental demarcation between the cilium and the rest of the cell. Kinesin-2 and cytoplasmic dynein motor proteins mediate the anterograde and retrograde traffic of rafts along the axoneme, respectively. Kinesin-2 forms a heterotrimeric complex composed of two motor subunits KIF3A and KIF3B or KIF3C and a tail-associated nonmotor accessory subunit, KAP3. When the cell prepares to divide in the S-phase, the primary cilium is reabsorbed and each centriole divides into new mother and daughter centrioles that migrate to the poles of the mitotic spindle.

Several lines of complementary evidence converged on cilia as the central organelle in the pathogenesis of ADPKD. Among these were the findings that the PC1 ortholog in *C. elegans* is expressed in cilia[100] and that several mouse models of recessive polycystic kidney disease targeting genes not orthologous to either *PKD1* or *PKD2* exhibited the phenotypic combination of cystic kidney defects and left-right axis abnormalities.[101,102] This is significant because left-right axis determination has been established as a cilia dependent phenotype. The connection was further strengthened when one of these recessive polycystic kidney disease genes, *Tg737* (also called polaris or IFT88), was identified as a component of the intraflagellar transport machinery necessary for ciliary biogenesis.[103] Further direct evidence of the cilia link with ADPKD came with the demonstration of the localization of PC2[104] and PC1[105] in the cilia of kidney epithelia and the discovery that *Pkd2*$^{-/-}$ mice have defects in left-right axis formation.[106] Previous studies in ciliated MDCK cells had shown the mechanical deflection of cilia resulted in cellular calcium transients that could be detected by calcium sensitive fluorescent dyes.[107–109] The discovery that PC1 and PC2 were expressed in cilia coupled with the knowledge that PC2 function as a cation channel (see below)[110] led to the hypothesis that the polycystins were responsible for the cilia-dependent calcium transients observed in cultured cells.[111] This hypothesis was supported by the observation that cells lacking PC1 failed to respond with cellular calcium transients upon deflection of cilia by laminar shear stress under flow.[111] This finding was combined with the discovery that PC2 is required for left-right axis formation led to studies that showed that lateralized PC2-dependent calcium signals played a role in downstream signaling and vertebrate body axis specification.[112] PC2 may be part of a mechanosensory complex that sensed the leftward flow generated by cilial movement in left-right axis formation,[112] although a more complex mechanism for the lateralized nodal calcium signal may be operational.[113]

Subsequently, an ever growing number of genes for human diseases that include cystic changes in the kidney have been identified in their function linked to cilia.[98] These "reverse genetic" discoveries have been complemented by a forward genetic screen using random insertional mutagenesis in zebrafish that resulted in a cystic pronephric kidney phenotype in fish which identified a number of intraflagellar transport related proteins, as well as *Pkd2*, among the target genes.[114] Similarly, in the metanephric mouse kidney, conditional inactivation of the Kif3a component of the heterotrimeric kinesin-2 anterograde motor resulted in loss of cilia and consequent cyst formation during kidney development.[115] Taken together the data support a strong functional connection between defects in cilia structure or function and cyst formation in lumen forming epithelia including kidney tubules, bile ducts and pancreatic ducts.

Recessive Human Ciliopathies

Primary cilia are increasingly implicated in a wide variety of important morphogenic signaling pathways (e.g.,[97,116]) which in turn account for the wide spectrum of clinical features associated with syndromes when cilia function is disturbed.[98,117] Association with cilia, basal body or pericentriolar region has also been reported for the ever expanding groups of genes mutated in recessive "ciliopathy" syndromic disorders with pleiotropic manifestations that include varying degrees and penetrance of kidney cyst formation. These diseases include nephronophthisis (NPHP), Joubert syndrome (JBTS), Meckel-Gruber syndrome (MKS), Bardet-Biedl syndrome (BBS) and oro-facial-digital syndrome (OFD).[118,119] In addition, fibrocystin, the ARPKD gene product is expressed in cilia as well as the apical membrane of distal nephron tubular cells.[120–122]

Subsets of the recessive ciliopathies have coalesced into phenotypic and genetic continuums. NPHP, JBTS, and MKS comprise a phenotypic spectrum roughly proceeding from less severe to more severe, respectively.[118] Manifestations at the NPHP end of the spectrum include kidney and liver fibrosis, kidney cysts and retinal defects. JBTS patients also have cerebellar vermal hypoplasia and cognitive impairment while at the most severe end of the spectrum, MKS patients manifest with occipital encephalocele and are commonly nonviable. BBS shares kidney and retinal defects and in addition is characterized by digital defects, obesity, anosmia and cognitive impairment. Recessive mutations in over thirty genes have been identified among the ciliopathy syndromes.[98,118] Mutations in same genes (e.g., *CEP290*, *NPHP1*, *BBS4*, *MKS1*) give

rise to more than one of clinical syndromes indicating that the phenotypic continuum is mimicked by genotypic overlap. In the most extreme example, mutations in CEP290 has been associated with NPHP, JBTS MKS and BBS.[123] This interrelationship of a spectrum of clinical syndromes with recessive mutations in the same gene likely results from a complex interplay of locus heterogeneity, multiple allelism, modifier gene effects and possibly more complex multigenic inheritance.[98]

Recent work has established that the functional protein complexes composed of the recessive ciliopathy gene products are part of the transition zone and trafficking complexes that determine the molecular composition cilia (Figure 80.2). Mutations in at least nine genes have been associated each with NPHP and JBTS, six genes with MKS, and an additional 14 genes associated with BBS. Extensive cell biological and proteomic analysis has shown that the NPHP, JBTS and MKS associated gene products comprise the transition zone fibers that are critical gatekeepers determining the entrance and exit of components into and out of cilia.[99,124,125] The BBS gene products assemble into the BBSome which functions in the trafficking of integral membrane proteins to and from cilia.[126,127] The other key elements of cilia structure and function are the IFT proteins that, in conjunction with the kinesin and dynein motor proteins, are required to form structurally intact cilia. While mice and fish exhibit polycystic phenotypes with mutations in IFT proteins that result in abnormal or absent cilia, no human diseases with recessive loss of function in IFT genes and absent cilia have been identified possibly because these are embryonically lethal. Taken together, these recent discoveries suggest that recessive ciliopathies result in complex perturbations in the molecular composition of cilia. These findings also define the molecular relationship between the syndromic kidney cystic diseases resulting from ciliopathies with the non-syndromic polycystic kidney diseases, ADPKD and ARPKD. The latter both result from mutations in individual integral membrane proteins that are among the much larger group of client proteins of the BBSome and transition zone complex as they function to determine molecular composition of cilia. Ciliopathy syndromes therefore result from complex perturbations of cilia composition whereas ADPKD and ARPKD result from the discrete absence of individual molecular components of cilia that are not know to otherwise affect delivery or retention of additional ciliary proteins.

GENETICS OF ADPKD

Mutations in at least two genes cause the clinical presentation of ADPKD—a property referred to as genetic heterogeneity. The two genes, *PKD1* located on chromosome 16p13.3 and *PKD2* located on chromosome 4q21, have been isolated by positional cloning.[128–131] The genomic segments occupied by the *PKD1* and *PKD2* genes are of similar size (~45–50 kb), but *PKD1* contains 46 exons that encode ~12 kb of open reading frame, compared to 15 exons and ~3 kb of open reading frame for *PKD2*. Two thirds of the 5′ end of human *PKD1*, both exons and introns, are duplicated multiple times with very high sequence fidelity (>95%) in more proximal regions of chromosome 16.[132–135] *PKD1* accounts for approximately 85% of affected families in European populations, with the remaining 15% resulting from *PKD2* mutations.[136–138] Analysis of the gene locus-dependent clinical phenotypes have highlighted the increased severity of *PKD1*. The mean age of the composite endpoint of death or ESRD is 53 years for *PKD1* and 69.1 years for *PKD2*; both differed significantly from the control population (78 years).[137,139] Given this difference, it is would be expected that the relative prevalence of *PKD2* will increase in patient subgroups stratified based on age of onset of ESRD. In one study, 39.1% of patients reaching ESRD after age 63 had *PKD2* mutations.[140] Using only age of presentation with ESRD as an endpoint, *PKD1* patients have a median age of onset of 54.3 compared with 74.0 for *PKD2* patients.[137,139] The prevalence of hypertension is four-fold lower in *PKD2* compared to *PKD1* and the occurrence of urinary tract infections and hematuria is also reduced in the former compared to *PKD1*.[137,139] The value of these gene locus-based clinical differences in providing specific prognostic information to patients is limited due to the marked intrafamilial and interfamilial variation in clinical manifestations of ADPKD.[141–144]

Molecular Genetic Mechanisms of Cyst Formation in ADPKD

The molecular genetic mechanisms of cyst formation in ADPKD are required to explain two salient clinical features of the disease. The first is to explain why the disease occurs in such a focal manner given that the ADPKD gene mutations are autosomally inherited and all cells in the body carry a mutated allele. The second is to determine the basis of the marked intra-and interfamilial variability in disease severity.

The apparent paradox of the focal nature of ADPKD is highlighted by the observation in microdissection studies of early ADPKD kidneys that localized cystic dilatations occur in kidney tubules that appear otherwise normal despite the presence of the same germline mutation in all the cells.[145] A molecular explanation for this observation has come with the discovery that cyst lining cells from human ADPKD cysts have loss of heterozygosity (LOH) in the chromosomal regions of the

respective *PKD* genes in both kidney tubular[146–149] and bile ductular cysts.[150] The LOH indicates loss of the functional gene from the wild type allele through focal somatic second hit mutations that define cyst formation as a recessive phenotype at the cellular level. The absence of a remnant wild type allele in a subset of cells from a cyst with LOH suggests that the cysts are clonal in origin—i.e., arising from a single cell.[146]

The conclusions from these studies were challenged[151] on the basis of: (1) Immunolocalization studies using anti-PC1 antibodies showing evidence of residual expressed protein in human cysts,[152–155] (2) the relatively low rate of detection of LOH in cysts, (3) the relatively high rate of somatic mutations required to account for the thousands of independent cysts, and (4) the fact that the finding of LOH in cysts established an association, but not a causal link. In retrospect, immunolocalization studies were focused on cellular staining patterns that did not examine cilia expression of the protein; the latter is now thought to be the primary site of PC1 function in ADPKD.[104,105] Additionally, approximately 30% of germline mutations in *PKD1* are predicted to be non-synonymous amino acid substitution mutations[14] which are predicted to yield immunoreactive protein products. If a similar proportion of missense variants occurs among second hit mutations, resulting cysts be positive for PC1 by immunostaining. The relatively low detection rate of LOH in cysts may reflect limitations in comprehensive screening of *PKD1* for pathogenic mutations. Even a decade later, the success rate of *PKD1* mutation detection is still ~85%.[14] When more effective sequence-based mutation detection was applied to cysts from patients with germline *PKD2* mutations, the rate of detection of second hits was the same as the sensitivity of mutation detection suggesting that effectively all cysts had second hits.[156] The rate of somatic mutations required to account for the thousands of cyst that develop in ADPKD are in keeping with the rate of measured HPRT mutation frequencies in kidney epithelial cells ranging from 5×10^{-5} in the first decade to 2.5×10^{-4} after the eighth decade of life.[157]

A variant of the two hit hypothesis was suggested by studies examining kidney cysts from patients with defined *PKD2* mutations. Cyst cells were initially screened for second hit mutations in *PKD2*, followed by screening for *PKD1* mutations in the subset of cysts in which second hit *PKD2* mutations could not be found.[156,158] Evidence of loss of a *PKD1* allele in these latter cysts led to the proposal the trans-heterozygous somatic mutations involving an allele of the *PKD* gene other than the one affected by the germline mutation can give rise to cysts.[156] However, trans-heterozygous mutations are unlikely to be sufficient for cyst formation. Compound heterozygous individuals with bilineal inheritance of a *PKD1* mutation and a *PKD2* mutation show more severe polycystic kidney disease[159] as do trans-heterozygous mice,[160] but the overall severity of phenotype in both man and mouse is within the range observed for individuals with mutations at just one of the gene loci.

Mouse models have established the causal link between second hits in a single *Pkd* gene and cyst formation (Figure 80.3). The occurrence of kidney cysts after embryonic day 14.5 in conventional germline knockout animal models of *Pkd1* and *Pkd2* anticipated a link between homozygous loss of polycystin genes and cyst formation.[161,162] A novel mouse model of *Pkd2* was the first to established a causal relationship between somatic inactivation of the normal allele and cyst formation in adult mice.[163] In this model, a serendipitous modified allele, $Pkd2^{WS25}$, resulted from insertion of a disrupted exon 1 in tandem with the wild type exon1. $Pkd2^{WS25}$ expresses functional PC2 but is prone to genomic rearrangement converting it to either a null or true wild type allele.[163] The dosage of this allele correlates with propensity toward cyst formation and the cyst lining cells in adult mouse kidneys did not express PC2.[163] Subsequently, the conditional Cre-lox system has been used to bypass the embryonic lethality of null mice and achieve homozygous inactivation of *Pkd* genes in a tissue in a selective and temporally controlled manner.[164–168] These studies confirmed that somatic second hit mutations in either *Pkd* gene are sufficient for cyst formation. Similar conditional inactivation approaches have been applied to cilia ablation models targeting genes whose products are required for intraflagellar transport (*Kif3a*, *Ift88*).[115,169] The latter showed that somatic loss of intact cilia also results in a polycystic kidney phenotype. The Cre-lox system offers spatial and temporal control of *Pkd* gene inactivation but has the limitation that inactivation events occur simultaneously in large tracts of cells in either selected nephron segments or along the entire nephron. This is not believed to be the prevalent pattern of inactivation in human disease; in this regard the $Pkd2^{WS25}$ model remains unique in that *Pkd2* inactivation is thought to occur by stochastic mechanism involving individual cells. Interestingly, the molecular events underlying *Pkd2* inactivation in this model are not believed to have a nephron segment specific bias, yet the majority of cysts arise from distal nephron segments.[163,170] More recent mouse studies suggest that collecting duct cyst growth is particularly sensitive to PC1 dosage.[171] These findings have been part of the rationale for the potential benefit of vassopress-2 receptor antagonists in the treatment of ADPKD.[170]

While somatic second hits are sufficient to initiate cyst formation, an increasing number of additional molecular factors affecting progression of polycystic

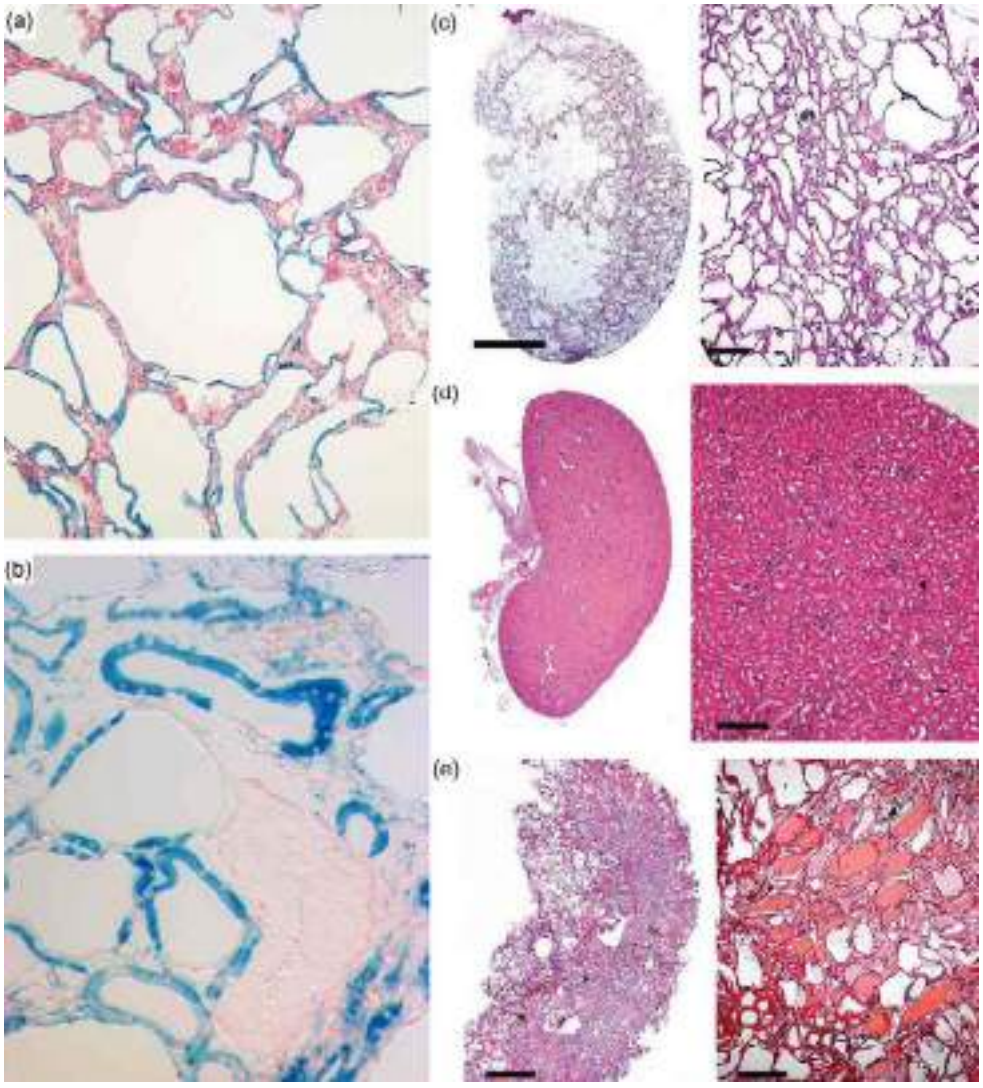

FIGURE 80.3 Mouse models of polycystic kidney disease. **a**: Conditional mouse model of polycystic kidney disease due to homozygous inactivation of Pkd1 in some nephron segments. Cells in the kidney that have undergone inactivation of *Pkd1* are marked by the β-galactosidase expression (blue) from a Cre-recombinase reporter expressing *lacZ*. Tubule segments (*) and glomeruli (*arrowheads*) in which Pkd1 is not inactivated appear normal but are confined to septa between expanding cysts lined by cells stained blue indicating *Pkd1* has been inactivated. **b**: Chimeric mice produced from Pkd1 − / − ES cells aggregated with wild type morulae marked by constitutive lacZ expression show mosaic cyst formation. Cyst lining are comprised of cuboidal wild type cells (*blue staining*) and flat Pkd1 − / − cells that do not express lacZ and are therefore unstained (indicated by arrows). (Images courtesy of Stefan Somlo and Saori Nishio). **c**: Early inactivation of *Pkd1* results in rapidly progressive cyst formation; cystic kidneys postnatal day 19 following inactivation of *Pkd1* on postnatal day 2. **d,e**: Adult inactivation of *Pkd1* results in slowly progressive polycystic kidney disease. Kidneys at 3 months (**d**) following inactivation at 1.5 months show no overt cysts; kidneys at 6 months (**e**) following inactivation at 1.5 months show progressive cyst formation. **d**–**e**: Scale bars, 2 mm (left panels); 100 μm (right panel). *(Modified and reprinted by permission from Macmillan Publishers Ltd: Piontek K et al., A critical developmental switch defines the kinetics of kidney cyst formation after loss of* Pkd1, Nature Medicine, *13:1490–95, copyright 2007.).*

kidney disease have been discovered using *in vivo* model systems. These factors include: (1) The critical role of the timing of second hit mutations with respect to developmental stage, (2) the discovery that reduced dosage of PC1, not just complete absence, is sufficient for graded cystic dilation, (3) the potential role of kidney injury in fostering PKD progression, and (4) the finding that loss of polycystins can exert effects on surrounding cells to promote disease progression. Evidence that timing of polycystin inactivation has a profound impact on the rate of cyst growth came from inducible conditional inactivation mouse models permissive for inactivation of *Pkd* genes either during kidney development or during adult life.[165,169] Using such a model, Piontek et al. showed that inactivating *Pkd1* in the early postnatal period when the mouse kidney is

still undergoing active nephrogenesis resulted in rapid progression of polycystic kidney disease whereas inactivation of *Pkd1* in the post-developmental adult kidney resulted in very slow progression polycystic kidney disease.[165] A similar finding of rapid cyst growth following early inactivation and slow cyst growth following late inactivation was observed in a polycystic model based on cilia ablation following inactivation of *Kif3a*.[169] The discovery of the timing of gene inactivation as a contributing factor to disease progression has led to consideration of the possibility that the majority of somatic second hit mutations in human ADPKD as well as the critical rapid growth phase of cysts occur during embryogenesis.[172] Such a mechanism, if confirmed in patient studies, would potentially have significant implications for the timing of the most effective therapy in ADPKD.

The impact of reduced PC1 dosage, as opposed to complete loss, in polycystic kidney disease has emerged over the past several years. Two animal models expressing hypomorphic (i.e., reduced function) alleles of *Pkd1* showed progressive cyst formation despite the presence of some residual *Pkd1* activity.[173,174] Similarly, loss of the protein bicaudal C results in reduced PC2 expression and cyst formation through de-repression of inhibitory microRNAs.[175] The significant interplay of gene dosage and polycystic kidney disease has, however, best been defined by studies centered on the genes responsible for isolated polycystic liver disease without kidney cysts (ADPLD)—a disease with indistinguishable clinical features from the polycystic liver disease that occurs in ADPKD patients.[176] Heterozygous loss of function mutations in two genes have been identified so far for this dominantly inherited disease: *PRKCSH* and *SEC63*.[177–179] *PRKCSH* encodes the non-catalytic β-subunit of glucosidase II (GIIβ), an *N*-linked glycan processing (glucose trimming) enzyme in the ER.[180–184] The SEC63p protein is highly conserved from yeast to man and functions as part of the ER protein translocation machinery to deliver proteins into and through the ER membrane. The functional unit for this process is the multicomponent translocon (Figure 80.4).[185,186] The activities of the translocon are tightly coordinated with downstream events of protein folding, modification and assembly, thereby providing a direct link between membrane targeting (including the cilial membrane) and protein maturation,[185] and between Sec63p and GIIβ functional pathways.[171,186] While neither protein is expressed in cilia, the connection of these proteins to polycystic kidney diseases is underscored by the finding that *Prkcsh* and *Sec63* conditional mouse models develop kidney cysts in addition to liver cysts by a two hit mechanism when either gene is inactivated in a tissue selective manner.[171] The severity of the polycystic phenotype in the ADPLD gene knockouts can be worsened by reducing the *Pkd1* gene dosage. Increasing *Pkd1* dosage by either genetic or pharmacologic means on the other hand eliminated cyst formation.[171] The ability to modulate severity of polycystic kidney disease in these models by manipulating *Pkd1* dosage establishes PC1 is the rate limiting component of the cystic pathway in both ADPKD and ADPLD. Interestingly, the same study showed that PC1 dosage also affects the severity of the kidney disease Due to mutations in *Pkhd1*, the ARPKD disease gene.[171]

Acute kidney injury following ischemia, nephrotoxin exposure or reduction of renal mass results in markedly augmented progression of cyst formation in animal models based on *Pkd1*, *Pkd2*, *Kif3a* or *Ift88*.[187–192] This is particularly true in adult onset models that otherwise show indolent progression in the absence of injury. These environmental "third hits" have been proposed as an essential part of disease progression in human ADPKD.[193] While it is likely that kidney injury can exacerbate polycystic kidney disease, its contribution to disease progress in human ADPKD is uncertain given that cyst progression also occurs in animal models in the absence of injury.[165,194,195] Finally, evidence is accumulating that there are effects promoting cyst formation that are active in the context of the whole kidney organ and may impact cells that have not lost polycystin expression. Perhaps the most intriguing of these was suggested by a unique chimeric animal model produced by aggregation of $Pkd1^{-/-}$ embryonic stem cells with wild type morulae expressing LacZ as the wild type lineage marker[196] (Figure 80.3). These mice formed kidney cysts commensurate with the degree of $Pkd1^{-/-}$ chimerism. The cyst lining epithelia were mosaic with both $Pkd1^{-/-}$ and $Pkd1^{+/+}$ epithelial cells present in the early stages of cystogenesis. The $Pkd1^{-/-}$ cyst cells appeared flat while the $Pkd1^{+/+}$ cells were cuboidal. Over time, $Pkd1^{-/-}$ cells replaced the $Pkd1^{+/+}$ cells by inducing apoptosis via the c-Jun N-terminal kinase (JNK)-mediated pathway.[196] These findings suggest the possibility that cells that lose PC1 expression induce cystic degeneration followed by programmed cell death in surrounding wild type tubular cells. Another study based on kidney specific inactivation of Pkd1 demonstrated the importance of the immune response mediated by macrophages in the progression of cyst formation in ADPKD.[197] Orthologous gene models of ADPKD based on either *Pkd1* or *Pkd2* show infiltration of alternatively activated macrophages into the pericystic space early in the course of the disease. Pharmacologic depletion of the macrophages markedly slows the rate of growth of kidney cysts in these models.[197] And aggregately, these animal models based on genes orthologous to human ADPKD are providing an increasingly complex and

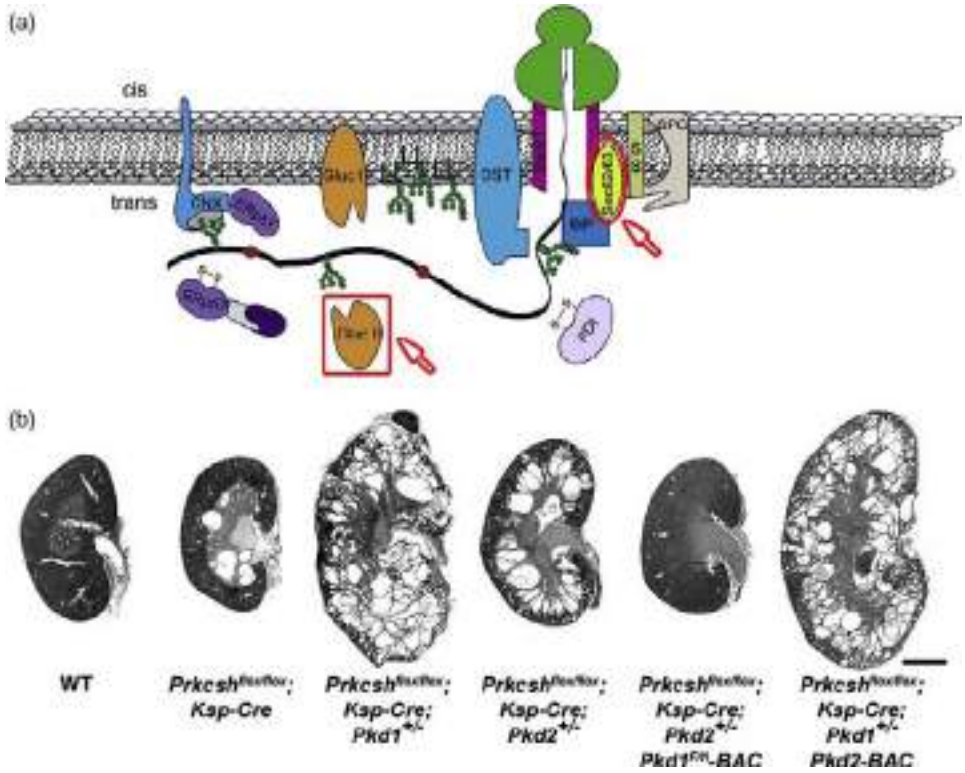

FIGURE 80.4 The inter-relationship of isolated polycystic liver disease (ADPLD) with polycystic kidney disease (ADPKD). **a**: The two known polycystic liver disease gene products, the β subunit of glucosidase-II (GIIβ, indicated as Gluc II, red box) and SEC63 (red oval), are shown in relation to the multicomponent co-translational translocon. GII is an N-linked glycan processing (glucose trimming) enzyme in the ER that plays a major role in regulation of proper folding and maturation of glycoproteins. SEC63 acts as a docking site localizing the ER chaperone BiP to the luminal exit site of the translocon. BiP plays a direct role in gating of the translocation channel and in polypeptide transport via an ATP-dependent reaction that is activated by SEC63. There is a tight interconnection between protein translocation mediated by the multicomponent translocon and protein maturation involving the N-linked glycan processing enzymes, providing a direct link between the functions of the ADPLD gene products. Co-translational maturation events in this pathway include signal peptide cleavage, the transfer and trimming of *N*-linked glycans including the activity of GII, disulfide bond formation, transmembrane domain integration, chaperone binding and protein folding. SPC, signal peptidase complex; SS, signal sequence; PDI, protein disulfide isomerase; OST, oligosaccharyl transferase; Gluc I, glucosidase I; Gluc II, glucosidase II (α and β subunits); CNX, calnexin; CRT, calreticulin. *(Modified and reprinted by permission from Elsevier: ref. [185], copyright 2003.)* **b:** The critical effect of polycystin-1 (PC1) dosage on polycystic disease severity. Inactivation of the APDLD gene *Prkcsh* encoding GIIβ in collecting ducts result in kidney cyst formation due to impaired PC1 biogenesis. The severity of cyst formation is markedly increased by further reducing PC1 with $Pkd1^{+/-}$ background and moderately increased by reducing polycystin-2 (PC2) on the $Pkd2^{+/-}$ background. Over-expression of PC1 using the $Pkd1^{F/H}$-BAC transgene rescues the $Prkcsh^{flox/flox}$;*Ksp-Cre;Pkd2* + / − cystic phenotype; *Pkd2*-BAC has no effect. Ages, P42; scale bar, 2 mm. *(Reprinted by permission from Macmillan Publishers Ltd: Fedeles S et al., A genetic interaction network of five genes for human polycystic kidney and liver diseases defines polycystin-1 as the central determinant of cyst formation,* Nature Genetics, *43:1639–647, copyright 2011.)*

complete picture of the molecular genetic basis for disease progression. These studies also serve to emphasize the importance of using *in vivo* models to validate and refine data obtained from *ex vivo* tissue culture-based systems–ADPKD is after all a disease of three-dimensional organ structure and is most appropriately studied using *in vivo* models.

Molecular Determinants of Disease Progression

Studies have begun to provide clues as to the genetic determinants of disease progression. Interfamilial variation in ADPKD is strongly influenced by gene locus. *PKD1* causes more severe disease than *PKD2*,[139,198] yet the gene products are thought to function in the same genetic and biophysical pathway.[111,199] Either of two explanations can underlie this observed difference: mutation of *PKD1* is inherently a more severe molecular lesion than mutation of *PKD2* or the occurrence of the somatic second hit alterations that precipitate cyst formation more readily affect *PKD1* than *PKD2*. In general, the data support the latter mechanism. Homozygous inactivation of *Pkd1* or *Pkd2*

in the mouse results in similar severity of kidney and pancreatic cystic disease, embryo edema, hemorrhage and embryonic lethality.[161,162] While PC1 is rate limiting in models of dosage reduction, there is an absolute requirement for functional PC2 for PC1 to function normally.[171] Indeed, the *Pkd2*$^{-/-}$ mouse has the additional phenotypic features of randomization of left-right axis formation[106,112] and defects in heart septum formation,[162] neither of which are seen in *Pkd1*$^{-/-}$ mice.[200] Defects of the conotruncus, such as dual outlet right ventricle, have been a variable finding in *Pkd1*$^{-/-}$ mice[201,202] as have defects of bone ossification,[201,203] and vascular integrity.[85] These phenotypes have not been specifically investigated in *Pkd2*$^{-/-}$ mice. In the genetic model organism *Caenorhabditis elegans* (nematode), mutation to either the *Pkd1* ortholog, *lov-1* or the *Pkd2* ortholog, *pkd-2*, results in identical defects in the stereotypical male mating behavior.[204] Doubly mutant *lov-1:pkd-2* worms do not show increased phenotypic severity.[204]

The higher population frequency and increased clinical severity of *PKD1* disease compared to *PKD2* may be explained in large part by a higher frequency, respectively, of germline and somatic mutation affecting *PKD1*. This in turn is certain to be influenced by the four-fold larger coding sequence of *PKD1* compared to *PKD2*. The recent recognition that PC1 is the rate limiting component of the polycystin complex coupled with the significantly higher rate of pathogenic non-synonymous amino acid substitution mutations in PC1 compared to PC2, further suggests that a broader range of mutations in PC1, than in PC2, will result in ADPKD.[14,171] The strongest support for this theory that the frequency of mutation is primarily responsible for the locus specific differences in disease severity comes from the CRISP.[16] At baseline, *PKD1* kidneys had more cysts and were larger than *PKD2* kidneys. However, while the absolute changes in kidney volume were greater for *PKD1* (74.9 mL/year) than for *PKD2* (32.2 mL/year), the relative rates of growth were not significantly different for the two genotypes (5.68% per year vs. 4.82% per year). This suggests that cyst initiation, but not cyst enlargement, is modulated by the disease gene; *PKD1* is more prone to second hits than *PKD2*, but there is no inherent difference in cyst growth potential once second hits occur in either gene.

Most of the several hundred *PKD1* mutations described to date are unique to individual families. This suggests that each mutation essentially arose as a *de novo* event that was fixed in the population since it confers little or no significant reproductive disadvantage.[205] The *de novo* mutation rate for *PKD1* is estimated to range from 1.8×10^{-5} to 6.9×10^{-5} per generation.[206,207] Studies in heterozygous mouse models support these theories. *Pkd2*$^{+/-}$ mice uniformly show loss of PC2 immunoreactivity in cyst linings suggesting that homozygous somatic loss is the underlying cystogenic event; cyst linings in *Pkd1*$^{+/-}$ mice uniformly showed presence of PC2 immunoreactivity allowing for the inference that it was PC1 that was lost in these cysts.[160] In compound heterozygous *Pkd1*$^{+/-}$:*Pkd2*$^{+/-}$ animals, 160 of 171 cysts (93%) showed uniformly positive staining for PC2, 8 (5%) were negative for PC2 and 3 (2%) could not be evaluated. This suggests that in compound heterozygous mice, *Pkd1* was far more often the target of somatic loss *in vivo*.[160]

Genotype-Phenotype Correlations

Genotype-phenotype correlations refer to the association between specific germline mutations (genotype) and the resulting spectrum of disease expression (phenotype). Genotype-phenotype correlations are largely absent in ADPKD with two notable exceptions.[208] The first is the occurrence of contiguous gene deletion syndromes with loss of *PKD1* in conjunction with loss of adjacent *TSC2*, the gene mutated in tuberous sclerosis complex 2. This contiguous gene syndrome results in early onset severe APDKD and clinical features of tuberous sclerosis.[209,210] The second example of genotype-phenotype correlation in ADPKD occurs with recessive inheritance of hypomorphic alleles (i.e., partial, as opposed to complete, loss of function) in either *PKD1*[211,212] or *PKD2*.[213] The phenotype observed in individuals with hypomorphic alleles affecting both copies of the respective *PKD* gene can mimic ARPKD[212] with early-onset polycystic disease manifest by diffuse and more homogeneous, albeit smaller cyst formation.

The marked intrafamilial variation otherwise seen in ADPKD suggest that factors other than the germline mutation determine the course of the disease.[214] This intrafamilial variation was illustrated in a study of dizygotic twins, one of whom developed severe polycystic kidneys *in utero* while the sibling showed a more typical course of adult onset disease.[215] Similarly, in an analysis of age of renal death in 74 parent-offspring pairs, the median difference within the pairs was 0 years, but with a range −26.3 to +27.2 years that followed a normal Gaussian distribution.[216] A systematic analysis of genotype-renal function correlation in 461 affected individuals from 71 ADPKD families with known *PKD2* mutations revealed that the location of *PKD2* mutations did not influence the age of onset of ESRD.[217] This study also found that marked intrafamilial variability in disease severity occurs in *PKD2* as well, with several individuals showing presentation of ESRD before age 50 while affected family members had the typical late onset disease.

Over 90% of mutations in *PKD2* are predicted to be chain terminating loss of function alleles.[14] In *PKD1*, about one third of putative pathogenic variants are predicted to be amino acid substitution or other in-frame variants. Most of the non-truncating mutant alleles are thought to be loss-of-function[218] although missense variants behaving as hypomorphic alleles that result in mild disease expression in the heterozygous state have been identified.[219] Two studies have correlated 5′ location of mutations in *PKD1* with more severe phenotypes. In one study examining 324 patients from 80 families with known *PKD1* mutations, location of the mutations 5′ to the median position correlated significantly with about a 3 year earlier onset of ESRD.[218] In a second study, 51 patients with vascular complications and known *PKD1* mutations were evaluated. The median position of the *PKD1* mutation was significantly further 5′ in the vascular population than in *PKD1* families without vascular complications.[220] Within the vascular population, more severe disease as defined by aneurysmal rupture, early rupture, or more than one vascular case in the family had median mutation locations more 5′ than the *PKD1* vascular population as a whole.[220] These data correspond to a previous report of a smaller number of cases[221] and raises the possibility that the large 5′ extracellular domain of PC1 may act as a dominant factor in aneurysmal complications in ADPKD.

Modifier Effects in ADPKD

Modifier effects, either genetic or environmental, are an alternative explanation to stochastic factors such as second hit timing and frequency for the phenotypic variation seen in ADPKD. The observed intrafamilial variability that argues against strong allelic effects may in fact argue for genetic background effects within families modulating disease expression.[208] A study comparing intrafamilial variation in age to ESRD among siblings to that in monozygotic twins found significant excess variability among the siblings relative to the genetically identical twin pairs.[142] The genetic contribution to intrafamilial disease variability, defined as the proportion of the variance explained by modifier genes (i.e., heritability), was assessed using variance component analysis in two studies. The first examined 406 patients from 66 *PKD1* families and estimated the heritability for creatinine clearance (C_{cr}) among those without ESRD to be 42% and the heritability for ESRD to be 78% among those with ESRD.[222] Although conclusions from this data are limited by power, one possible interpretation that emerges is that genetic factors contribute to differing extents to progression in early stage disease and late stage disease. A second study examined variance of a number of phenotypic traits in 315 affected relatives in 83 *PKD1* families. The heritability for these traits ranged from 18 to 59% of the variance.[223] In this study, modifier genes accounted for 32% of the variance for C_{cr} and 43 to 50% of the variance for age of ESRD,[223] again showing the trend toward more heritability for late stage disease. One putative modifier gene locus was identified in a severely affected *PKD1* family in which affected individuals also carried a heterozygous mutation for HNF-1β,[224] a transcription factor that has been implicated in regulating of *PKD* gene expression.[225,226] A second study analyzing candidate genes as modifiers in a large cohort of ADPKD families identified the canonical Wnt inhibitor Dickkopf 3 as a candidate for modifying ADPKD expression.[227] Much larger studies than these will be required to actually begin to identify modifier loci in genome-wide association studies.[222]

THE PKD GENES AND THEIR PROTEIN PRODUCTS

The *PKD1* and *PKD2* gene products, respectively identified as PC1 (PC1) and PC2 (PC2), were unique and complex when first discovered (Figure 80.5). They have only grudgingly yielded the functional clues that will eventually lead to a full understanding of ADPKD and a successful development of appropriate mechanism-based treatment paradigms.

Polycystin-1

Polycystin-1 (PC1) is an eleven membrane spanning 4302 amino acid protein with a ~3000 amino acid extracellular NH_2-terminus and a ~220 amino acid cytosolic COOH-terminus[129,228] (Fig. 80.5). The extracellular NH_2-terminal domain contains distinct combination protein motifs including leucine-rich repeats, a WSC homology domain, C-type lectin domain, an LDL-A related domain, and 16 immunoglobin-like domains PKD repeats,[129,228,229] a receptor egg jelly (REJ) module containing four fibronectin type III FNIII) domains[230] and a GPCR proteolytic site (GPS motif)[231] within a newly defined GPC autoproteolysis inducing domain (GAIN domain) shift.[232] Additional domains identified either by homology or computational prediction include a PLAT/lipoxygenase homology 2 (LH2) domain between the first and second transmembrane spans[233,234] and a polycystin motif region in the extracellular loop between the sixth and seventh transmembrane spans.[235] The cytoplasmic COOH-terminus of PC1 contains a coiled-coil domain.[236,237] The region of the last five transmembrane spans of PC1 share sequence homology with PC2 (PC2) although there are critical differences in the sequence that suggest that PC1 does not function directly as a channel protein the

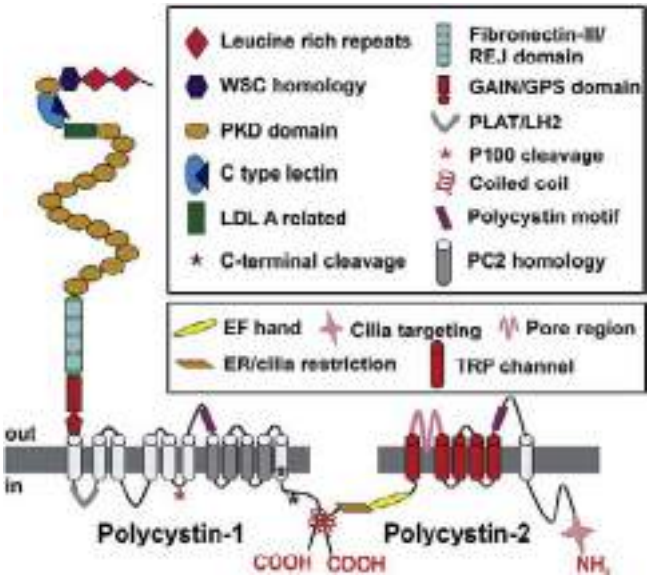

FIGURE 80.5 Schematic representation of the predicted structural domains of polycystin-1 (PC1) and polycystin-2 (PC2). There are a combination of structurally predicted domains and experimentally identified or verified functional domains shown. In PC1, the immunoglobulin-like structure of the PKD domains and the GAIN/GPS domain have been determined by structural studies as have the respective coiled coil domains in the COOH-termini of PC1 and PC2. The interaction of the COOH-terminal coiled coil domains of PC1and PC2 is well established. PC1 undergoes autoproteolytic cleavage at the GPS site to form the extracellular NH_2-terminal fragment and the intramembranous COOH-terminal fragment, which remain non-covalently associated with each other. Additional PC1 cleavage sites have been identified in the COOH-terminus as well as in the intramembranous region. The TRP channel function of PC2 has been shown in several systems to be a nonselective cation channel permeable to Ca^{2+}. The functions of the cilia targeting and the ER/cilia restriction domains in PC2 have defined.

way PC2 does[235] (see Polycystin Channel Function subheading below).

The location and topology of the predicted 11 transmembrane spans of PC1 was demonstrated by experimentally using glycosylation reporter analysis.[238] The NMR solution structure of one the PKD domains, so named because they were first described in PC1, showed the domain to have a β-sandwich fold that belongs to a distinct family uniquely conserved among vertebrate polycystin homologs.[239] Atomic force spectroscopy has shown that PKD domains confer increased tensile strength to the PC1 molecule.[240,241] However, another study found that the PC1 extracellular region is highly extensible and that this extensibility is mainly caused by the unfolding of its immunoglobulin-like PKD domains.[242] Stretching the native PC1 extracellular region results in a sawtooth pattern with equally spaced force peaks resulting from the sequential unfolding of individual PKD domains and domains refold after mechanical force unloading. The tensile properties of the PKD domains is altered by naturally occurring missense mutations found in patients.[243] The PKD domains, along with the WSC homology domain, C-type lectin domain, an LDL-A related domain are thought to be involved in protein-protein or protein-carbohydrate interactions which have led to speculation that PC1 could serve as a receptor for unknown ligands. A mechanosenory role in flow sensation has also been proposed for PC1.[111] PC1 signaling events might be regulated through force driven unfolding/refolding events with or without associated ligand interactions.

PC1 has broad tissue expression, including kidney, brain, heart, bone, and muscle.[244–246] Its expression is developmentally regulated with high levels of expression in developing mouse tissues that subsequently decline.[244,246] The subcellular localization of PC1 in tissues has been difficult to establish likely due to a combination of very low abundance of the native protein and limitations of the antibody reagents. Several studies identified PC1 in the plasma membrane of kidney tubule cells, particularly in the distal nephron segments including collecting ducts.[33,152,247] Within these segments, PC1 appeared at the lateral membrane at sites of intercellular adhesion[248] and at desmosomes.[249] Over-expressed, epitope-tagged full length PC1 has been localized in the lateral membrane.[250] Similar lateral location of a PC1–PC2 complex was reported in kidney tissue over-expressing PC1 as a transgene,[251] although a similar pattern was not reported in epitope tag knockin model.[246] Following the paradigm shift resulting from the discovery of the role of primary cilia in ADPKD and related disorders, much of the emphasis on the subcellular localization of native PC1 has shifted to primary cilia of epithelial cells from the kidney[105,111] and other tissues.[246] Most recently, PC1 has been found to be a component in urinary exosome-like vesicles, whose potential role in the functioning of polycystin signaling and ADPKD is just beginning to be explored.[252]

PC1 Homologous Proteins

With the advent of the sequencing of the human and mouse genomes, four genes encoding proteins structurally related to PC1 have been identified in mammals. PKDREJ contains REJ and GPS motifs in the extracellular part and the PLAT/LH2 domain in the first intracellular loop.[253,254] PKDREJ is only expressed in mammalian testis and mature sperm where it is localized to the plasma membrane and may contribute to transmembrane signaling[255] and controls the timing of fertilization through effects on sperm motility and exocytotic competence.[256] PKD1L1 has two PKD domains,

as well as REJ and GPS motifs in the extracellular region, a PLAT/LH2 domain in the first loop, and a coiled-coil domain in the C-terminal cytoplasmic tail.[257] *Pkd1L1* knockout mice develop defects in left right axis determination,[258] a cilia based phenotype also observed in *Pkd2* knockout mice,[106,112] but absent from *Pkd1* null embryos.[200] Unlike in kidney tissues where PC1 and PC2 are thought to form a receptor channel complex in primary cilia, evidence suggests that in the cilia of the embryonic node responsible for left-right axis determination, Pkd1L1 and PC2 form the signaling complex required for left-right patterning.[259,260] The PKD1L2 and PKD1L3 protein products contain the combination of GPS and PLAT/LH2 domains that uniquely identify all PC1 family members.[235] In addition, both have a C-type lectin domain; PKD1L2 also contains PKD and REJ domains. PKD1L2 and PKD1L3 have transient receptor potential (TRP; see section on PC2 below) ion channel signatures in the last five transmembrane spans that are conserved with PC2 family members suggesting that, unlike PC1, they may possess cation channel functions. A complex of PKD1L3 and a PC2 homolog, PKD2L1, has been identified as a candidate sour taste receptor.[261–263] In addition, this complex has been proposed to function as cerebrospinal fluid chemosensory system that selectively triggers action potentials in response to decreases in extracellular pH.[261] Finally, an overexpression mouse model for Pkd1L2 shows a complex myopathic neuromuscular phenotype[264] that may be related to its function as a cation channel. This data emerging from studies of homologous proteins suggests the possibility that permuted combinations of PC1 and PC2 homologs confer tissue and developmental stage specific functions to polycystin complex and may suggest a broader role for these novel signaling complexes in vertebrate organisms. Understanding the bases for the function of any of these putative receptor-channel complexes may shed considerable mechanistic insight into the functioning of the PC1/PC2 complex that is central to ADPKD.

PC1 Cleavage

The complexity and potential diversity of PC1 function is further amplified by a series of proteolytic events yielding fragments in both the extracellular and intracellular compartments. PC1 undergoes autoproteolytic cleavage at the GPS motif within the GAIN domain to produce an NH_2-terminal fragment (NTF) comprised of the first extracellular domain and a COOH-terminal fragment (CTF) containing the eleven membrane spans and the cytosolic tail[232,265,266] (Figure 80.5). This cleavage process requires an intact REJ module and GAIN domain and likely occurs early in the biosynthetic pathway, probably at the level of the endoplasmic reticulum (ER). The NTF and CTF remain non-covalently associated with each other and functional GPS cleavage is required for PC1 to be able to stimulate spontaneous tubulogenesis of MDCK cells in three dimensional matrix culture.[265] GPS cleavage is conserved in proteins evolutionarily related to PC1[267] and has been reported as an essential step for folding, trafficking, and bioactivity of non-polycystin proteins.[268] The crystal structure of the GAIN domain, which includes the GPS motif at its COOH-terminal region, has recently been solved in two distantly related adhesion-GPCRs which share this domain with the PC1 related proteins in higher organisms.[232] The GPS cleavage process is thought to be necessary for proper trafficking of PC1[269] and for autoinhibitory function in adhesion-GPCRs. GPS cleavage deficient knockin mice show a partial rescue of the *Pkd1* null phenotype suggesting that uncleaved PC1 may behave as hypomorphic allele.[270]

A second intra-membranous cleavage product of PC1 results in the P100 intramembranous fragment with six membrane spanning domains.[271] P100 acts to reduce store operated calcium entry through a mechanism involving the ER calcium sensor protein STIM1.[271] The cytoplasmic tail of PC1 is also cleaved. Two processes have been described that liberate different sized fragments, both of which traffic to the nucleus and affect gene transcription.[272,273] These processes are discussed in detail in the section on C-terminal Cleavage below.

Interactions

The most significant biochemical interaction for PC1 remains its association with PC2. PC1 and PC2 interact through their respective COOH-termini[236,237,274–276] (Figure 80.5). The structural data suggest a stoichiometry of one PC1 molecule and three PC2 molecules in the complex.[276,277] The interaction depends on the integrity of the coiled coil domains in the COOH-termini of PC1 and PC2[237,275] and has been demonstrated using full length PC1 and PC2 constructs. All known pathogenic predicted truncating mutations in either gene result in loss of this interaction.[278] The recognition of this interaction soon after the discovery of the genes led to the hypothesis that PC1 may serve a receptor function that controls the channel activity of PC2 as part of the polycystin signaling complex.

Several other associated complexes for PC1 have been defined although their roles in the pathogenesis of ADPKD are less clear (reviewed in[279]). The extracellular domains of PC1 are capable of *in vitro* homotypic interactions via their PKD domain repeats that may mediate intercellular or intermolecular adhesion as part of polycystin function.[280] In *C. elegans*, the β-subunit of ATP synthase (ATP-2) co-localizes in cilia and

interacts with the PLAT/LH2 domain of the nematode PC1 homolog, LOV-1.[234] Casein kinase II also interacts with LOV-1 and this interaction may regulate trafficking of the *C. elegans* PC2 homolog into cilia in a phosphorylation dependent manner.[281] Interaction with the COOH-terminal domain of PC1 inhibits degradation and results in re-localization of regulators of G protein signaling (RGS7),[282] perhaps fitting with a postulated role for PC1 as an atypical G-protein coupled receptor.[283,284] The cytoplasmic tail of PC1 also interacts with tuberin, the tuberous sclerosis complex 2 (*TSC2*) gene product[285] (see mTOR). PC1 interacts with intermediate filament components including vimentin, cytokeratin 8 and 18 and desmin.[286] PC1 has also been shown to co-localize and complex with the intercellular adhesion molecules E-cadherin and β-catenin suggesting a possible role in stabilization of adherens junctions and the maintenance of the differentiated polarized state of epithelia in kidney tubules.[287,288] PC1 may mediate communication with the extracellular matrix as suggested by co-localization with α2, β1 integrin[289] and interaction with αv,β3 integrin via the COOH-terminal region of the β3 integrin.[290] This diversity of interacting partners highlights the likelihood that PC1 and PC2 (see below) serve a broad array of cellular and tissue functions, not all of which will be related to polycystic kidney disease.

Polycystin-2

From the time of its discovery, polycystin-2 (PC2) was hypothesized to be a cation channel most likely functioning in calcium-based signaling events.[131] PC2 is a 968 amino acid integral membrane protein with six membrane spans and intracellular NH_2- and COOH-termini (Figure 80.5). It belongs to the transient receptor potential (TRP) channel family. TRP channels constitute a family of channel proteins found throughout metazoan evolution that generally function as receptor gated sensory channels. The mammalian TRP channels encompass at least 28 different proteins that are grouped into six subfamilies based the complement of structural motifs in their respective cytosolic NH_2^- and COOH-termini (reviewed in[291,292]). The polycystins belong to the TRPP subfamily and PC2 is also called TRPP2. The last five transmembrane spans bear a strong TRP channel signature and the region between S5 and S6 (transmembrane segments 5 and 6) contains the putative pore region.[235] In addition, the large first extracellular loop between S1 and S2 contains a polycystin motif of unknown function that is highly conserved in all PC1- and PC2-related proteins.[235] The cytoplasmic tail contains a putative calcium binding EF-hand.[131,274,293] The EF hand binds calcium[293] and may have a role in modulating channel activation and inhibition.

PC2 is widely expressed in tissues, particularly the kidney, heart, ovary, testis, vascular smooth muscle, and small intestine.[294,295] In the kidney, PC2 is expressed in all nephron segments, with the possible exception of the thin limbs of the loops of Henle. PC2 is not expressed in the glomerulus. As with PC1, expression in the distal nephron segments may be more robust than in the proximal segments.[163] A domain in the COOH-terminus functions to restrict the membrane location of PC2 to the ER and cilia.[296] At a subcellular level, there is general agreement that both native and heterologously over-expressed PC2 is strongly expressed in the ER membrane of both cultured cells[251,278,296–299] and tissues.[110] The plasma membrane localization of PC2 has been the subject of debate (reviewed in[300]). Native PC2, but not heterologously over-expressed protein, has been reported on the plasma membrane both by anti-native protein antibodies[249,299] and by channel physiology.[301] It has also been proposed that PC2 requires co-assembly with PC1 to traffic to the cell membrane and co-expression of both polycystins results in appearance of a novel plasma membrane cation channel activity.[111,278] Conversely, studies using the C-terminal fragment of PC1 suggested a possible reciprocal role for PC2 in the cellular distribution of PC1.[269,302] There is consensus and strong evidence to show that PC2 is localized to the primary cilia in kidney tissues and cultured epithelial cells.[104,105,112] Native and over-expressed PC2 can be detected in the primary cilium.[303] The NH_2-terminus domain of PC2 containing an RVxP amino acid motif has been identified as both necessary and sufficient for cilia location of type 2 membrane proteins including PC2.[303,304] Trafficking of PC2 to cilia is independent of PC1.[303]

PC2 Homologous Proteins

Two homologs of PC2, PKD2L1 (or PCL) and PKD2L2, have been identified in the mammalian genome.[254,303,305,306] PKD2L1 is expressed in striated muscle (heart and skeletal), brain, spleen, and testis,[306] whereas PKD2L2 is expressed only in testis.[254] PKD2L1 has been shown to function in conjunction with PKD1L3 in sensing sour taste and cerebrospinal fluid pH.[261–263] PC2 is highly conserved in metazoan evolution and homologs have been identified in sea urchin, *C. elegans*, *Drosophila melanogaster* and zebrafish. In sea urchin, the PC2 homolog associates with suREJ3, the PC1 homolog, and both localize to acrosomal region of spermatozoa suggesting a possible role in the ionic channel events that accompany the acrosome reaction during fertilization.[307] In *C. elegans*, mutations in the PC2 homolog result in defects in location-of-vulva and response behavior in the male worms that is indistinguishable from the phenotype seen in LOV-1 (PC1

homolog) mutants.[204] As in mammalian systems, PC2 shows strong expression in the ER membrane and the cilia membrane in *C. elegans*. However, there is little sequence conservation of the cystolic NH_2^- and COOH termini from mammals to invertebrates (*C. elegans* and *Drosophila*) and there appear to be differences in the phosphorylation pattern[281] and trafficking signals[303] with mammalian protein. The PC2 homolog in *Drosophila* is expressed in sperm and knockout in fly results in sperm that retain normal backward motility and ability to fertilize but lose hyperactivation and directed movement required for reaching the female storage organs.[308–310] Flies with a loss of function PC2 allele showed reduced contractility of the visceral smooth muscle cells through a mechanism that requires cooperativity with the ryanodine receptor in regulating intracellular calcium homeostasis.[311] In mammalian systems, PC2 directly interacts with and regulates the activity of the ryanodine receptor[312] and alters smooth muscle cell calcium homeostasis.[83] Finally, zebrafish have proven to be a valuable vertebrate genetic model of polycystic kidney disease. Zebrafish have a pronephric kidney as well as left-right body axis asymmetry and knockdown or mutation of the PC2 homolog in fish results in cystic dilation of the pronephric tubule as well as abnormalities of left-right body axis formation.[114,313,314]

Channel Function

PC2 functions as non-selective cation channel permeable to calcium.[110,278,299,315] The initial studies used a variety of biophysical systems to characterize the channel and this may account for qualitative differences in the channel properties described for PC2. The systems used include co-expressed PC1 and PC2 in CHO-K1 cells studied by patch clamping,[278] the outer membrane of human placental syncytiotrophoblasts and reconstituted purified protein studied in lipid bilayers,[315] ER vesicles prepared from cells overexpressing wild type or mutant PC2 fused to lipid bilayers[110] or epithelial cells in culture treated with chemical chaperones and studied by patch clamp technique.[299] While the channel is non-selective for cations, it does pass calcium and most investigators believe that *in vivo* PC2 function is calcium-based second messenger signaling.[316] PC2 channel activity is stimulated by physiological concentrations of calcium and is inhibited by higher concentrations of calcium that may be achieved locally as a result of PC2 channel activity.[110,315] The critical role of the channel activity in the *in vivo* functioning of PC2 was demonstrated by a pathogenic patient mutation altering a single amino acid (D511V) that resulted in isolated loss of channel activity.[110,317] Aside from biophysical studies, the *in vivo* cellular effects of polycystins have been evaluated by monitoring changes in cellular calcium using fluorescent indicator.[110,111] PC2 can function as an ER calcium release channel.[110] Phosphorylation of PC2 at a casein kinase 2 site, serine 812, modulates channel activity[318] and has a role in trafficking of PC2 between ER, Golgi and plasma membrane compartments.[319] The function of PC2 as a putative mechanosensory channel in cilia[107,111] is discussed in the section on cellular calcium signaling below.

Interactions

The functional association of PC2 with PC1 was discussed in previous sections. PC2 associates with a number of calcium channel proteins. PC2 homomultimerizes with itself via its COOH terminus[236,320,321] as a predicted tetramer.[322] PC2 forms functional heteromeric channels through interaction with at least two other TRP channels, TRPC1[323,324] and TRPV4.[325] In keeping with its putative role in regulating cellular calcium homeostasis via intracellular calcium pools, PC2 interacts directly with the inositol 1,4,5-trisphosphate receptor (IP_3R)[326–328] and also regulates the activity of the ryanodine receptor through direct interaction.[312] PC2 interacts with the ER t-SNARE protein syntaxin-5 which acts to inactivate the channel.[329] Additionally, the mitotic centrosomal kinase Aurora A binds and phosphorylates PC2 at serine 829 and reduces the endoplasmic reticulum calcium release activity of PC2.[330]

Protein interaction screens have yielded several putative PC2 binding partners potentially involved in cytoskeletal interactions. PC2 binds Hax-1 which in turn associates with the F-actin-binding protein cortactin suggesting a link between PKD2 and the actin cytoskeleton.[331] The COOH-terminus of PC2 interacts with CD2AP[332] which also interacts directly with the actin cytoskeleton.[333] PC2 interacts with tropomyosin-1, troponin-1 and alpha-actinin, components of the actin microfilament complex.[334–336] Yeast two hybrid screening also identified mDia1/Drf1 (mammalian Diaphanous or Diaphanous-related formin 1 protein) as a PC2-interacting protein.[337] PC2 and mDia1 co-localize prominently at the mitotic spindles of dividing cells suggesting an association with microtubule cytoskeleton components.

Clues as to regulation of PC2 trafficking have also begun to emerge from studies of associated proteins. In addition to the previously noted co-assembly of PC1 and PC2, a novel interacting protein PIGEA-14 (chibby homolog 1) has been identified that plays a role in PC2 trafficking.[297] PIGEA-14 co-expression with PC2 resulted in translocation of both proteins to the trans-Golgi network, suggesting role for PIGAE-14 in regulating the intracellular location of PC2. PC2 has been proposed to bind to phosphofurin acidic cluster sorting protein (PACS)-1 and PACS-2 via an acidic

cluster in the COOH-terminal domain of PC2 that also contains the serine 812 phosphorylation site.[319] The phosphorylation of PC2 regulates the binding of these adapter proteins that in turn are required for the routing of PC2 between ER, Golgi and plasma membrane compartments.[319] In an attempt to unify the mechanisms of ADPKD with those for autosomal recessive polycystic kidney disease (ARPKD),[338,339] association between PC2 and the *PKHD1* (ARPKD) gene product fibrocystin[340,341] has been investigated. Fibrocystin and PC2 co-localize and co-immumoprecipitate suggesting that they may exist in the same complex[342] and this complex may also include the kinesin-2 anterograde cilia transport motor which may mediate fibrocystin dependent regulation of PC2 channel function.[343] Although direct association was not shown, the *klp-6* gene product in *C. elegans* encoding a kinesin-3 family member functions in the same genetic pathway as the polycystins (i.e., male mating behavior) and is required for localization and function *C. elegans* homolog of PC2 in cilia.[344]

CELLULAR PATHWAYS AFFECTED BY POLYCYSTINS

Anyone inspired to seek a quick primer on the arcane alphabet soup of signaling pathways might consider beginning their quest by perusing the literature documenting the list of cellular activities that may be susceptible to the eclectic influences of the polycystin proteins. This ever-lengthening roster includes the Wnt, mTOR, MAPK-ERK, and AP-1 cascades, and also involves the participation of most of the cell's arsenal of second messenger systems including cAMP, calcium, G proteins and G protein coupled receptors[345] (Figure 80.6). Much remains to be learned concerning the relative importance of the polycystins in modulating the activities of each these pathways and the relative importance of each these pathways in preventing or defining the pathophysiology associated with ADPKD. The number and variety of these pathways testifies to the complexity of the interwoven network of signaling mechanisms that control epithelial morphogensesis and the maintenance of luminal architecture and highlight the central position that the polycystins must occupy in this web.

Wnt Signaling

The canonical Wnt signaling pathway plays a central role in controlling cell proliferation and differentiation.[346] Aberrant Wnt signaling during embryogenesis can lead to axis duplication or dysgenesis of critical body structures,[347,348] and excessive Wnt signaling activity is associated with the malignant transformation and metastatic potential of neoplasms.[349] At the heart of the Wnt pathway is the multifunctional β-catenin protein, which is both a key constituent of the epithelial intercellular adhesive apparatus and an arbiter of a transcriptional pathway that profoundly influences cell proliferation and differentiation.[350,351] The adhesive junctions that alert epithelial cells to the proximity of their neighbors are mediated by the transmembrane calcium-dependent adhesion molecule E-cadherin.[352] The cytoplasmic COOH-terminal tail of E-cadherin binds to several soluble cytosolic proteins, including α-catenin, β-catenin and p120, which together link E-cadherin clustered at sites of cell-cell contact to the subcortical cytoskeleton, which in turns allows cells to exploit their intercellular adhesive junctions in order to organize their membranes into polarized domains.[353] The pool of β-catenin protein that is not bound to E-cadherin is able to enter the nucleus, where it binds to and activates the TCF transcription factor.[346] Many of the genes whose expression is controlled by TCF stimulate cell division, including c-myc, c-jun and cyclin D1.[354] Thus, sequestration of β-catenin at sites of cell-cell contacts prevents it from activating a transcriptional program that results in proliferation. In contrast, loss of cell-cell contact liberates E-cadherin-bound β-catenin, freeing it to pursue its pro-proliferative agenda.

Before β-catenin can enter the nucleus, however, it must negotiate a major hurdle in the form of the cytoplasmic Axin/GSK3/APC complex.[355] The primary purpose of this protein assembly is to capture and phosphorylate free β-catenin and, by so doing, doom it to degradation by the proteasome. Activation of the canonical Wnt signaling cascade leads to inhibition of the GSK3 kinase and hence to an increase in the size of the pool of β-catenin that is free to enter the nucleus and activate TCF-mediated transcription.[346] The Wnt ligands are a family of secreted polypeptides that bind to cell surface receptors composed of a transmembrane protein called Frizzled and a second transmembrane co-receptor that can be any one of several different members of the family of LDL receptor related (LRP) proteins. Ligation of Frizzled by a Wnt protein leads to activation of its cytosolic partner protein Disheveled, which interacts with the Axin/GSK3/APC complex to prevent it from targeting β-catenin for proteasomal destruction.[346] Stimulation of the Frizzled receptor can also elicit several β-catenin-independent effects, including transient elevations in cytosolic calcium concentrations and activation of c-jun kinase (jnk). These additional consequences of Frizzled activation are collectively referred to as non-canonical Wnt signaling.[356,357] Non-canonical Wnt signaling is intimately involved in the establishment of planar cell polarity[357] (see following sections).

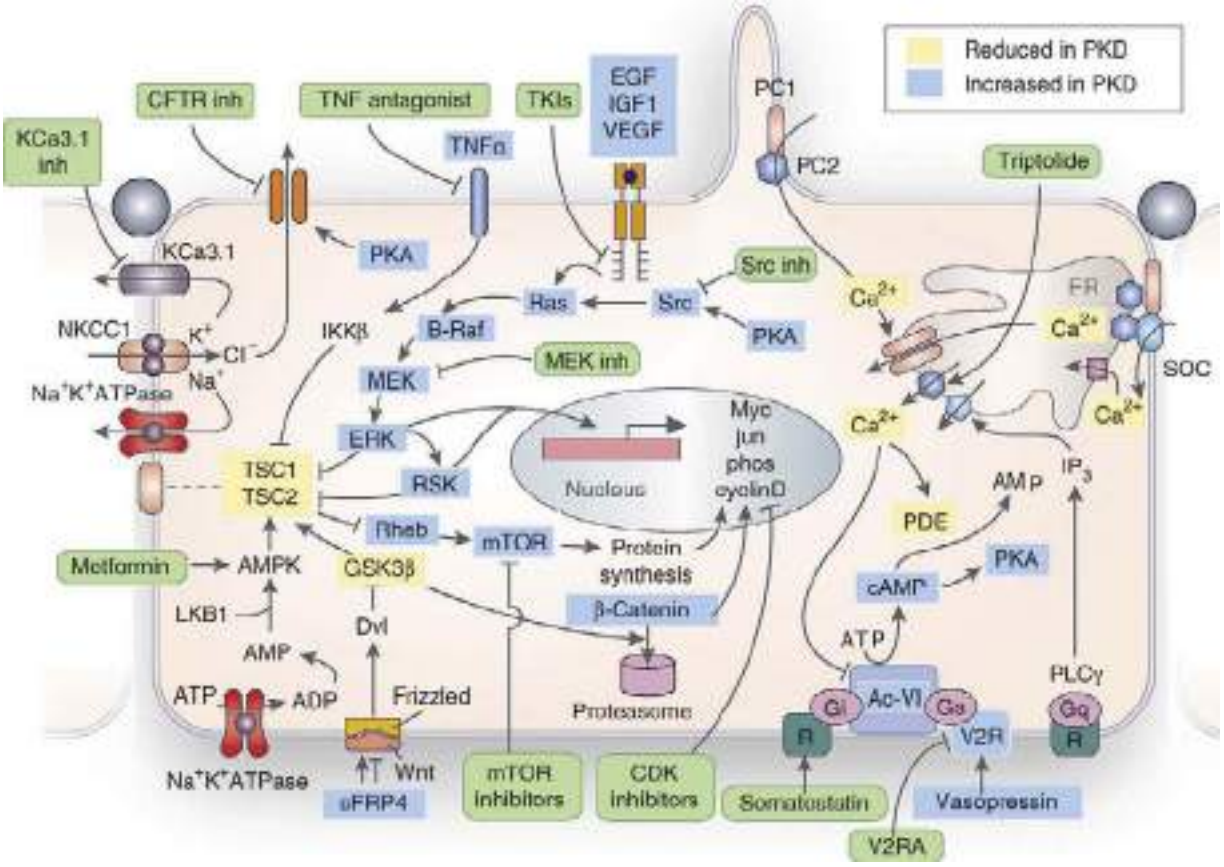

FIGURE 80.6 Signaling pathways associated with polycystin protein functions and PKD. PC1 and PC2 function has been implicated in the up-regulation (blue boxes) or down-regulation (yellow boxes) of a variety of cellular signaling pathways that play important roles in cell growth and differentiation. In the cilium, the polycystin complex appears to participate in flow- or ligand-stimulated calcium entry. Intracellular endoplasmic reticulum (ER) calcium stores are also subject to regulation by the polycystins. Increased concentrations of cAMP, activation of ErbB receptors, and up-regulation of EGF, IGF1, VEGF, and TNF have been described in cells or kidneys with defective polycystin function. Increased cAMP levels contribute to cystogenesis by stimulating chloride and fluid secretion. Activation of tyrosine kinase receptors by ligands present in cystic fluid may contribute to stimulation of MAPK/ERK signaling. Phosphorylation of TSC2 by ERK may lead to the dissociation of TSC2 and TSC1 and lead to the activation of Rheb and mTOR. Up-regulation of TNF or down-regulation of AMPK signaling may also stimulate mTOR signaling through inhibition of the TSC2/TSC1 complex. Activation of AMPK may also blunt cystogenesis through inhibition of CFTR and ERK. Up-regulation of Wnt signaling stimulates mTOR and β-catenin signaling. ERK and mTOR activation promotes G1/S transition and cell proliferation through regulation of cyclin D1. These effects of mutations in polycystin provide the rationale for treatment with V2 receptor antagonists, somatostatin, triptolide; tyrosine kinase, src, MEK, TNF , mTOR, or CDK inhibitors; metformin, and CFTR or KCa3.1 inhibitors (green boxes). AC-VI, adenylate cyclase 6; AMPK, AMP kinase; CDK, cyclin-dependent kinase; ER, endoplasmic reticulum; MAPK, mitogen-activated protein kinase; mTOR, mammalian target of rapamycin; PC1, polycystin-1; PC2, polycystin-2; PDE, phosphodiesterase; PKA, protein kinase A; R, somatostatin sst2 receptor; TSC, tuberous sclerosis proteins tuberin (TSC2) and hamartin (TSC1); V2R, vasopressin V2 receptor; V2RA, vasopressin V2 receptor antagonists. *(Reprinted by permission from Macmillan Publishers Ltd: Harris P.C. & Torres V.E., Autosomal dominant polycystic kidney disease: the last 3 years,* Kidney International, *76:149–168, copyright 2009.)*

Several lines of evidence indicate that the polycystin proteins participate in modulating Wnt signaling and that perturbations of Wnt signaling can lead to renal cystic disease. Studies of genetically manipulated mouse models reveal that either kidney-specific inactivation of the APC gene or expression of constitutively active β-catenin both result in the development of renal cysts that closely resemble those found in ADPKD.[358,359] PC1 can be co-immunoprecipitated in a complex that includes E-cadherin and β-catenin,[287,288,360] indicating that the potential exists for PC1 to exert a direct influence over the stability or extent of membrane bound pool of β-catenin. Overexpression studies employing membrane tethered constructs incorporating the C-terminal of PC1 offer conflicting results. One such study suggests that the membrane tethered C-terminal tail of PC1 can activate Wnt signaling reporters,[361] whereas another study employing similar construct did not detect this activity.[362] The basis for this discrepancy remains to be elucidated. Recent results indicate that the expression of genes associated with activation of the Wnt

pathway is elevated in cystic renal tissue derived from the excised kidneys of ADPKD patients, as compared to the expression levels detected in normal-appearing non-cystic tissue derived from the same kidneys.[363]

A seminal study on inversin, the protein encoded by the gene mutated in nephronophthisis type II, illustrates a fascinating paradigm through which a polypeptide associated with a renal cystic disease can influence signal transduction through both the canonical and non-canonical Wnt pathways. Inversin marks Disheveled for degradation in the proteasome, thus turning off canonical Wnt signaling by preventing Disheveled from inhibiting GSK3.[364] Inversin also enhances manifestations of planar cell polarity that are under the control of the non-canonical Wnt pathway. As discussed in a later section, cleavage of the PC1 COOH-terminal tail releases a fragment that is capable of activating jnk and therefore may be similarly capable of upregulating the non-canonical Wnt pathway.[272] Finally, as discussed below in greater detail, a cleaved COOH-terminal fragment of PC1 can interact directly with the TCF transcription factor and, through this interaction, prevent the TCF transcription factor from activating the expression of genes under the control of the Wnt pathway.[365] Thus, both inversin and PC1 may act through distinct but analogous mechanisms as molecular switches that control the relative strengths of the canonical and non-canonical Wnt signaling pathways. Taken together, these diverse observations suggest that a failure to suppress canonical Wnt signaling and to activate non-canonical Wnt signaling constitutes a plausible mechanism that could account for at least some of the pathogenesis of PKD.[187] In this context, however, it is important to note two recent studies whose results are not consistent with this model. Analysis of mitotic spindle axis, a parameter thought to be related to planar cell polarity, finds that it is not perturbed in advance of cyst formation in mouse models of ADPKD.[366] Furthermore, a study found that the cells lining the cysts that develop in mouse models of ADPKD that have been engineered to express a Wnt/TCF reporter *in vivo* did not demonstrate elevated levels of TCF transcription activity.[367] It remains to be determined whether activation of TCF-mediated transcription is involved in early phases of cyst formation and is terminated by the time that cysts are evident.

Cellular Calcium

PC2 belongs to the TRP family of ion channel proteins.[368] PC2 can function as a non-selective calcium-permeable cation channel at the endoplasmic reticulum and perhaps at the plasma membrane as well.[110,278,315] The importance of the channle activity is suggested by the fact that the disease causing non-synonomous D511V mutation abrogates PC2 channel activity.[110] Functional studies demonstrate that PC2 expression enhances the release of calcium from intracellular stores.[110] PC2 can physically interact directly with the IP3 receptor and, perhaps by virtue of this association, can alter the kinetics of cytoplasmic calcium transients induced by IP3 and by agonists of receptors that signal through IP3.[326]

Seminal studies of MDCK cells performed by Praetorius and Spring illuminated an entirely new perspective on the potential function of the primary cilia that grace the apical surfaces of renal epithelial cells. These investigators found that primary cilia can serve a mechanosensory function and that bending them induces transient elevations of cytosolic calcium concentrations.[107–109,369] Subsequent research using cell lines that lack expression of the polycystin proteins as well as antibodies directed against these proteins' extracellular domains suggests that the PC2 channel activity, as well as polcystin-1 receptor activity, is required for induction of calcium transients in response to ciliary bending.[111] Taken together, these studies gave rise to the hypothesis that cilia on apical surface kidney epithelia sense flow via the PC1/PC2 complex and this flow signal is important in establishing and maintaining kidney tubule lumen morphology *in vivo*. More recently, PC2 has been shown to inhibit the activity of stretch-activated ion channels in smooth muscle cells, indicating a possible role of PC2 in pressure sensing.[370]

The binding of EGF to its receptor initiates elevations in cytosolic calcium concentrations that appear to require participation of the channel activity of PC2.[301] The mechanism responsible for this EGF effect on PC2 channel activity appears to involve a protein called mammalian diaphanous-related formin 1 (mDia1), a member of the formin family of actin and microtubule regulatory proteins whose activity is modulated by the RhoA small GTPase. The mDia protein binds to PC2 and exerts a membrane potential-dependent block on its channel activity. The binding of EGF to its receptor appears to activate RhoA, which in turn releases mDia from PC2 and relieves the associated block of the PC2 channel.[371]

A role for PC2 in governing the size and properties of intracellular calcium stores is suggested by the observation that vascular smooth muscle cells isolated from mice heterozygous for inactivation of the PC2 gene exhibit reduced size of the releasable intracellular calcium pool as well as reduced capacitative calcium entry.[83] PC1 may also modulate the properties of intracellular calcium stores. Over-expression of PC1 in MDCK cells may inhibit capacitative calcium entry and speed calcium re-uptake by the endoplasmic reticulum.[372] While the relationship between these effects of

the polycystins on intracellular calcium stores and the pathophysiology of cystic disease remains to be determined, it is clear that through their involvement in modulating intracellular calcium levels the polycystins impact a physiologically critical second messenger pathway that influences almost every aspect of cellular behavior.

Cyclic AMP

A large body of evidence indicates that fluid secretion into cyst lumens makes use of the same machinery and mechanisms that drive fluid secretion by the well-studied secretory epithelia of the airway, the small intestinal crypt and the shark rectal gland. Chloride accumulates in the cytosol above its electrochemical equilibrium through secondary active transport mediated by a basolateral Na,K,2Cl co-transporter. An apical conductive pathway allows chloride to travel passively down its electrochemical gradient into the cyst lumen and the resultant lumen-negative potential causes sodium to follow paracellularly. The osmotic gradient created by this NaCl transport draws water into the cyst lumen, presumably contributing to the expansion of cyst volume.[373,374] Several studies demonstrate that cAMP levels are elevated in cyst epithelial cells and furthermore that cAMP stimulates cyst fluid and electrolyte secretion.[375,376] The identification, through both functional and cell biological experiments, of CFTR as the apical chloride channel involved in cyst fluid secretion provides a molecular explanation for cAMP's pro-secretory effects.[377,378] The CFTR channel opens in response to protein kinase A-dependent phosphorylation and thus the channel is activated in response to elevations in cytoplasmic cAMP.[379] *In vivo* support for the role of CFTR as a mediator of cyst expansion has come from preclinical studies that showed some efficacy for CFTR inhibitors in reducing cyst formation in an orthologous gene model of *Pkd1*.[380] Additionally, case reports of families in which ADPKD coexists with cystic fibrosis have suggested that individuals with both diseases manifest a milder form of ADPKD,[381,382] although this anecdotal evidence has been challenged.[383] It has also been shown that cAMP acts as a mitogen in ADPKD renal epithelial cells and that this effect may be mediated through stimulation of the B-Raf/MEK/ERK signaling cascade, which is discussed in greater detail later in the chapter.[376,384]

While the involvement of CFTR in cyst fluid secretion provides a plausible connection between cAMP and the production of cyst fluid, it does not explain why cyst epithelial cells manifest high cytosolic cAMP concentrations. It is possible that the perturbations in cytosolic calcium levels discussed in the preceding section may in part account for cAMP dysregulation in cyst cells. Several isoforms of both adenylate cyclase and phosphodiesterase, which generate and degrade cAMP, respectively, are subject to positive or negative regulation by calcium. In fact, recent evidence indicates that the primary cilium contains a cAMP signaling complex that includes two calcium-sensitive isoforms of adenylyl cylclase, AC5 and AC6. This complex also includes protein kinase A as well as A kinase anchoring protein 150, which acts as a scaffold on which components of the cAMP signaling network assemble. This complex interacts with PC2. Loss of PC2 expression or of its channel activity leads to dis-inhibition of AC5 and AC6, resulting in elevated levels of cAMP.[385]

Finally, the polycystin proteins may directly or indirectly alter the activities of G-protein coupled receptors that signal through cAMP. Expression and activity of the V2 vasopressin receptor, for example, is elevated in a number of animal models of PKD.[375,386] As noted in a later section, this fact is being exploited through the development of V2 receptor antagonists as potential therapeutic agents that can potentially slow or prevent cyst fluid accumulation by reducing cytosolic cAMP levels.[386]

G-Protein Coupled Receptor Signaling

While their effects on V2 receptor activity suggest that the polycystins may influence G-protein coupled receptors, other studies suggest that PC1 may itself function as a non-traditional G-protein coupled receptor. The COOH-terminal tail of PC1 contains a short sequence that is capable of activating purified trimeric G proteins.[387] Furthermore, the ability of a membrane tethered construct of the PC1 COOH-terminal tail to activate c-jun kinase and the AP-1 pathway depends upon the involvement of trimeric G-proteins.[284] Expression of PC1 is apparently sufficient to initiate activation of $G\alpha$ subunits and dissociation of the $G\beta$ and γ polypeptides, as detected through measurement of the activities of ion channels whose open probabilities are modulated by $\beta\gamma$ interactions.[283] The presence of PC2 prevented PC1 from exerting this effect on G-proteins. The expression of the membrane tethered C terminal tail of PC1 has been found to activate $G\alpha q$ and thus to increase the activity of phospholipase C (PLC). Increased PLC activity leads to the generation of IP3 and consequently to elevations in cytosolic calcium levels which, in turn, can lead to the activation of the calcium-dependent calcineurin/NFAT-dependent transcription pathway.[388] The NFAT transcription factor governs the expression of genes involved in cell growth and differentiation.[389] Activation of the calcium-sensitive phosphatase calcineurin by sustained elevation of cytosolic calcium levels results in dephosphorylation of NFAT, leading to its nuclear accumulation. Recently, PC1 was shown to bind $G\alpha_{12}$ and

modulate the activity of Gα12/JNK apoptosis pathway.[390] Mutations in $G\alpha_{12}$ or PC1 that eliminate interaction between these proteins also abrogated the PC1 dependent inhibition of $G\alpha_{12}$ stimulated apoptosis.[391]

Thus, PC1 appears to possess the capacity to modulate the activities of trimeric G-proteins and their downstream effectors in much the same manner as traditional seven transmembrane domain G-protein coupled receptors. The nature of the stimuli or ligands that regulate this capacity of PC1 and the relationship of this capacity to the major physiological functions of PC1 remain to be determined.

Mitogen Activated Protein Kinase/Extracellular Regulated Kinase

The mitogen activated protein kinase/extracellular regulated kinase (MAPK/ERK) cascade couples extracellular signals received by a variety of surface receptors, through the activation of small G proteins and the involvement of a variety of adaptors, to the successive phosphorylation of Raf (MAP kinase kinase kinase), MEK (MAP kinase kinase) and MAP kinase/ERK. Activated MAPK/ERK can modulate protein translation and can enter the nucleus to regulate the activities of transcription factors and the cell cycle. The MAPK/ERK pathway receives input from and influences a variety of other signaling pathways, including those associated with G-protein coupled receptors, calcium, cAMP, PKA, PKC, EGF receptor (and other receptor tyrosine kinases) and integrins.[392]

In renal epithelial cells the MAPK/ERK cascade influences a variety of morphogenetic phenomena, including cell spreading, branching and tubulogenesis.[393] In wild type subconfluent cells, PC1 associates with focal adhesion contacts and promotes cell spreading through a mechanism that involves both the ERK cascade as well as the focal adhesion kinase, FAK. The absence of PC1 impedes spreading.[394] Furthermore, the MAPK/ERK cascade is found to be activated in a number of animal models of PKD[384,395] including orthologous gene models for *Pkd1* and *Pkd2*.[166] Studies in cultured human ADPKD cells suggest that ERK activation may be attributable to the high levels of cAMP present in their cytosols, which acts through protein kinase A to activate the MAP kinase kinase kinase B-Raf;[384,396] however, such B-RAf dependent activation was not observed in vivo models based on *Pkd1* and *Pkd2*.[166] It is also worth noting that in the absence of PC2 there is a dramatic increase in the quantity of ERK detectable in the nucleus, suggesting that both of the polycystin proteins participate in providing tonic suppression of the activity of the MAPK/ERK cascade.[397] Clearly, the MAPK/ERK pathway is intimately related to a variety of processes that control epithelial growth and morphogenesis. In light of the numerous observations that the MAPK/ERK cascade is excessively active in a variety of cell and animal models of PKD, efforts are underway to test the potential of inhibitors of the relevant MAPK/ERK cascade kinases to prevent the aberrant cell proliferation and differentiation associated with renal cystic disease.[398]

mTOR

The mTOR (mammalian target of rapamycin) protein is a kinase whose activation leads to increased protein translation and cell growth.[399] Proteins that inhibit the formation of the mRNA cap structure are phosphorylated and inactivated by mTOR. In addition, mTOR phosphorylates and activates ribosomal S6 kinases, which act to enhance the translation of mRNAs that encode proteins involved in translation. Thus, any signal that upregulates mTOR activity produces an enhancement of the cell's capacity to synthesize protein and consequently to increase its size. The mTOR pathway is stimulated by cell surface receptors that signal through PI3 kinase to activate the AKT kinase. Activated AKT phosphorylates the tuberous sclerosis complex, composed of the TSC1 and TSC2 proteins (hamartin and tuberin). The TSC complex acts as a GTPase activating protein (GAP) for the small G protein Rheb. When in the GTP bound state, Rheb acts to enhance mTOR function. Phosphorylation of the TSC complex by AKT inhibits its GAP activity, resulting in elevated levels of GTP bound Rheb and thus in elevated levels of active mTOR kinase.[400]

Since activation of mTOR prepares the cell for additional growth, it is perhaps not surprising that dysregulation of the mTOR pathway that leads to inappropriately high levels of mTOR activation are associated with a variety of neoplastic syndromes. Loss of the TSC complex and its associated Rheb GAP activity, for example, results in loss of suppression of mTOR. Tuberous sclerosis is the hereditary disease caused by inactivating mutations in the genes encoding tuberin and hamartin, and it is characterized by the development of multiple hamartomas as well as renal cysts.[401] It is interesting to note that the TSC2/tuberin gene lies extremely close to the PC1 gene and the two genes have an associated contiguous gene deletion syndrome.[210] Furthermore, PC1 interacts with tuberin through its C-terminus[285,402] and it has been suggested that tuberin may play a role in controlling the trafficking of newly synthesized PC1 to the cell surface. Phosphorylation of TSC2 by ERK leads to dissociation of the TSC1/TSC2 complex and loss of its Rheb GAP activity.[403] This phosphorylation appears to be prevented by PC1.[404] The interaction between PC1 and tuberin also appears to protect tuberin from inactivating phosphorylation by AKT.[405] Thus, the interaction between PC1 and tuberin maintains the Rheb GAP

capacity of the TSC1/TSC2 complex and contributes to the suppression of mTOR activity.

Administration of rapamycin markedly slows cyst development in studies of the Han:SPRD rat model of PKD, suggesting the possibility that inappropriate activation of the mTOR pathway is associated with or in part responsible for the excessive proliferation of renal epithelial cells that characterizes PKD.[406,407] Further support for this hypothesis is provided by studies demonstrating that downstream effectors of the mTOR pathway are inappropriately activated in cyst lining cells.[285] These studies also extend the beneficial effects of rapamycin to two mouse models of polycystic disease.[408] Taken together, these data suggest under normal circumstances the polycystin proteins exert a potentially significant inhibitory influence on the strength of mTOR signaling. It is possible that loss of this mTOR suppression could be responsible for at least some of the hyperplastic component of PKD pathophysiology and human clinical trials using inhibitors of mTOR in ADPKD have been completed (see Prospects for Therapy in ADPKD).

Cell Cycle

As has been noted at several points throughout this chapter, in our current conception of ADPKD the disease is thought to arise, at least in part, as a consequence of inappropriate and excessive proliferation of renal epithelial cells. The clear implication of this model is that ADPKD is associated with the absence of growth suppressive factors that act as brakes on progression through the cell cycle. The nature of these growth suppressive influences is manifold and varied, probably reflecting both direct and indirect consequences of perturbations in the expression or function of the various gene products implicated in renal cystic diseases. In fact, much of the discussion presented in the preceding sections on signaling pathways testifies to the validity of this statement. Essentially all of the signaling pathways that are touched by the polycystin proteins, including Wnt, MAPK/ERK, mTOR, calcium and cAMP are major strands of the intricate net of control elements in which the cell cycle is entangled.

Both of the polycystin proteins themselves exert growth suppressive effects when heterologously expressed, and their absence is associated with increased proliferation. Expression of the full length PC1 protein, for example, activates the JAK-STAT pathway.[194] This in turn leads to upregulation of $p21^{waf1}$, which induces cell cycle arrest. The expression of p21 is reduced by Id2,[409] a helix-loop-helix protein that binds to the COOH-terminal tail of PC2 in a manner that appears to be dependent upon a phosphorylation event presided over by PC1.[410] The absence of either polycystin protein can thus result in the translocation of Id2 to the nucleus, where it can suppress p21 and activate the cell cycle. PC2 null cells derived from the kidneys of $Pkd2^{WS25/-}$ mice proliferate significantly more rapidly than cells derived from the same animals in which the $Pkd2^{WS25}$ allele has undergone recombination to produce a wild type allele.[397] Transfection of a cDNA encoding PC2 into the null cells slows their proliferation to wild type levels. Perhaps somewhat surprisingly, the PC2 null cells manifest unusually extensive branching morphogenesis and tubule formation. This effect is also reversed by expression of wild type PC2. Transfection of these cells with a cDNA encoding the D511V human pathogenic mutant form of PC2 lacking channel activity does not suppress the hyperproliferative phenotype but does reduce tubulogenesis. Thus, the channel activity of the PC2 protein appears to be involved in at least some aspects of growth regulatory functions. PC2 also contributes to growth suppression through a direct physical interaction with eukaryotic translation elongation initiation factor 2a (eIF2a). This translation factor is a substrate for an activating phosphorylation by pancreatic ER-resident eIF2a kinase (PERK). By binding to both eIF2a and PERK, PC2 acts as a signaling scaffold that enhances eIF2a's phosphorylation and consequently decreases cell proliferation.[411]

Finally, it is becoming increasingly clear that the presence of an intact cilium and the appropriate organization of its associated proteins play an important role in regulating the cell cycle.[412] Loss of the cilium appears to be associated with inappropriate cell proliferation in a variety of models. Much remains to be learned about the mechanisms through which the cilium and the receptors expressed within its ensheathing membrane influence the cell cycle. It is interesting to note in this context, however, that in Chlamydomonas several members of the NIMA-related expressed kinases family (Neks) localize to the flagellum.[413,414] The Neks are involved in cell cycle regulation, and mutations in Nek1 and Nek8 account for the pathology found in two mouse models of renal cystic disease.[415]

C-Terminal Cleavage

Until fairly recently, the prevailing view of signal transduction from the cell surface to the nucleus held that extracellular signals received by plasma membrane receptors must undergo an obligate translation into the language of the intracellular second messenger systems before they could exert any influence on events in the nucleus. Revelations from studies of the Drosophila Notch protein and a variety of other transmembrane receptors have led to the definiation of a new signaling paradigm known as regulated

intramembranous proteolysis (RIP). During the course of its postsynthetic processing Notch undergoes proteolytic cleavages that release its extracellular domain, which remains attached to the transmembrane segment via non-covalent interactions. This preparatory cleavage permits Notch to become the substrate for a subsequent intramembraneous cleavage event mediated by γ-secretase that is initiated by the binding of Notch to its ligand Delta, a transmembrane constituent of the plasma membranes of neighboring cells. The fragment released through this final cleavage travels to the nucleus, where it influences transcriptional activities that play a key role in cell fate determination.[416,417] Thus, the C-terminal tail of a membrane protein can itself act as a direct messenger that can carry a signal from the surface to the nucleus without any need for the intercession of traditional second messenger molecules. It has now become clear that such cleavage events are quite common, playing critical roles in a variety of physiological processes, including the unfolded protein response, cholesterol metabolism and the adaptation of pancreatic islet cells to changes in extracellular glucose concentrations.[418]

Both PC1 and fibrocystin undergo cleavages that release COOH-terminal tail fragments capable of entering the nucleus and modulating activities therein.[272,273,419] Two C-terminal tail cleavage fragments have been reported for PC1.[273] The larger of these is approximately 200 amino acid residues in length, apparently comprising the entire extent of the protein's predicted C-terminal tail.[272] This fragment's production is dependent upon the activity of the γ-secretase protease,[365] and it includes the amino acid motif previously identified as a G-protein activation sequence, which is rich in basic residues and appears to be capable of serving as an autonomous nuclear localization motif. Expression of a protein corresponding to this fragment in transfected cells leads to activation of jun kinase and the AP-1 pathway.[272] This fragment can also act as an inhibitor of canonical Wnt signaling by virtue of its ability to bind directly to the TCF transcription factor and impede TCF's interaction with the p300 transcriptional co-activator complex.[420] The cleaved C terminal tail also interacts with the CHOP-10/GADD153 transcription factor and similarly prevents its interaction with p300.[365,421] CHOP is activated as a final step in the endoplasmic reticulum/unfolded protein response pathway and induces the expression of genes that activate apoptotic pathways.[422] Apoptosis has been described in cyst lining epithelial cells and may contribute to cyst formation.[168,410,423–426] Expression of the PC1 tail fragment reduces CHOP activity, as well as the level of apoptotis in *Pkd1*$^{-/-}$ cultured epithelial cells.[365]

The smaller fragment of the PC1 C terminal tail encompasses roughly 17 kDa and does not include the nuclear localization signal that has been identified in the larger fragment. This fragment can interact with STAT6 and the coactivator P100 and is apparently translocated into nuclei by virtue of these associations.[273] The 17 kDa fragment directly activates STAT6, and it activates STAT3 through a mechanism that is dependent upon STAT phosphorylation activated by growth factors or cytokines. The activation of the STAT transcription factors is pro-proliferative and pro-apoptotic. It has been suggested that accumulation of the 17 kDa PC1 fragment in the nucleus may contribute to ADPKD pathogenesis, while inhibition of STAT activity may dramatically slow cyst development.[427,428]

The relationship between these two fragments is currently unclear. It is possible that the smaller fragment is the product of a secondary cleavage of the larger fragment. It is also possible that these fragments arise through separate cleavage mechanisms that respond to and transduce distinct messages. Nuclear accumulation of the PC1 COOH-terminal tail is detected in the renal epithelial cells of transgenic mice that over-express PC1, of mice that manifest kidney specific agenesis of cilia, as well as of wild type mice that have been subjected to ureteral ligation.[272] These data suggest that cleavage and nuclear translocation of the PC1 COOH-terminal tail is suppressed by intact cilia function. Absence of cilia or loss of flow appears to initiate both of the reported PC1 COOH-terminal tail cleavages.[272,273] It is interesting to note that the 17 kDa fragment appears to increase proliferation and apoptosis, whereas the larger fragments appear to suppress these processes. This observation prompts the as yet untested speculation that the two cleavage fragments may participate in distinct phases of the renal epithelial response to injury. According to this model, the early phases of the injury response, which involve apoptosis of epithelial proliferation to replace lost or damaged cells may be mediated at least in part by activation of the cleavage that produces the 17 kDa fragment. Activation of the production of the larger cleavage fragment may accompany the later phases of repair and may serve as a break to prevent repairative proliferation and apoptosis from becoming excessive and potentially pathogenic.

The observations that polcystin-1 and fibrocystin are substrates for COOH-terminal tail cleavage raise a large number of interesting and potentially important questions. Where within the cell do the cleavage events occur? What proteolytic enzymes are responsible? Where are the cleavage sites within the primary structures of PC1 and fibrocystin, and what are the sequence parameters that determine their susceptibility to cleavage? Is the NH_2-terminal GPS cleavage a

prerequisite for PC1 COOH-terminal tail cleavage? How does PC2 expression stimulate PC1 C-terminal tail cleavage?[429] Finally, and perhaps most importantly, do mutations that prevent the cleavage produce a phenotype in cultured renal epithelial cells and in renal tubules *in vivo*? Future research into these and other questions related to COOH-terminal tail cleavages are likely to shed important light on the normal physiological functions of the PC1 and fibrocystin proteins. These studies may also suggest new pathways that can be exploited in the continuing search for novel strategies applicable to the development of therapeutics for renal cystic diseases.

PROSPECTS FOR THERAPY IN ADPKD

A better understanding of pathophysiology and availability of animal models has facilitated the identification of an growing number of potential therapeutic targets and development of preclinical trials. Some candidate drugs are now being tested in clinical trials (Figure 80.6). These include vasopressin V2 receptor antagonists, somatostatin analogs, mTOR inhibitors, c-Src inhibitors and triptolide. The following summarizes the current status of preclinical and clinical trials of various drugs classified by their likely mechanism of action:

Intracellular Calcium Homeostasis and Signaling

Triptolide, the active diterpene in the traditional Chinese medicine Lei Gong Teng, induces cellular calcium release through a PC2−dependent pathway, arrests growth of *Pkd1*$^{-/-}$ cells, and reduces cyst burden in embryonic and kidney-specific conditional *Pkd1* knockout mice.[430,431] TRPV4 activation increases $[calcium]_i$ in *pck* cholangiocytes and inhibits B-Raf and Erk1/2 signaling, cell proliferation, and cyst growth in 3-dimensional-culture. The TRPV4 activator *GSK1016790A* inhibits renal cyst growth and fibrosis.[432] Calcimimetics are allosteric activators of the calcium sensing receptor (CaR). The calcimimetic *R-568* inhibits cyst growth and fibrosis in Cy/+ rats[433] (when administered between 34 and 38 weeks of age) and in *pcy* mice,[434] but had no effect at the concentrations tested on cyst growth in *pck* rats and *Pkd2*$^{WS25/-}$ mice.[435] By coupling to Gq proteins, CaR activates phospholipase C-protein kinase C and mobilizes calcium from intracellular stores. By coupling to Gi proteins, it inhibits adenylyl cyclase-cAMP signaling. The beneficial effects of calcimimetics on PKD are thought to be due to downregulation of cAMP signaling. Inconsistencies in different animal models or at different stages of the disease in the same animal model may be due to the R-568-induced hypocalcemia offseting its effect on intracellular calcium and cAMP.[436] Indeed, inhibition of cyst growth in these studies is associated with a reduction in renal cAMP, whereas cAMP levels remain unchanged when no effect on cyst growth is detected.

Cyclic AMP Signaling

The effect of vasopressin, via V2 receptors, on cAMP levels in the collecting duct, the major site of cyst development in ADPKD, and the role of cAMP in cystogenesis provide a strong rationale for preclinical trials of vasopressin V2 receptor (VPV2R) antagonists. One of these drugs, OPC-31260, has marked effects in terms of reduced levels of cAMP and inhibition of cyst development in models of ARPKD, ADPKD, and nephronophthisis.[386,437,438] Recently, an antagonist with high potency and selectivity for the human VPV2R (tolvaptan) has also been shown to be an effective treatment in the *pck* rat model of ARPKD[439] and the Pkd2 mouse model of ADPKD (V. Torres, unpublished observations). These drugs have no effect on liver cysts, consistent with the absence of VPV2R in the liver. High water intake by itself also exerts a protective effect on the development of PKD in pck rats likely due to suppression of vasopressin.[440] Furthermore, genetic elimination of vasopressin in *pck* rats by breeding these animals with Brattleboro rats yields animals born with normal kidneys that remain relatively free of cysts unless an exogenous VPV2R agonist is administered.[441]

Two three year phase 2 clinical trials with tolvaptan in 63 ADPKD patients have been completed. These trials show this drug to be relatively safe and well tolerated by ADPKD patients. A prospectively designed analysis of annual total kidney volume (TKV) and thrice annual estimated glomerular filtration rate (eGFR) measurements in these patients randomly matched (1:2) to historical controls by gender, hypertension, age and baseline TKV or eGFR shows significant reductions in rates of growth in kidney volume (1.7 versus 5.8% per year) and decline in GFR (−0.71 versus −2.1 mL/min/1.73 m^2 per year).[442] Limitations of the study include small number of patients and utilization of historical controls. A larger, double-blind, placebo controlled trial is currently on-goinig and will be completed in 2012.[443]

Somatostatin acting on SST2 receptors inhibits cAMP accumulation not only in the kidney but also in the liver. Octreotide, a synthetic metabolically stable somatostatin analog, halts the expansion of hepatic cysts from *pck* rats *in vitro* and *in vivo*. Similar effects were observed in the kidneys of the *pck* rat.[444] These observations are consistent with the inhibition of renal growth in a pilot study of long-acting octreotide for human ADPKD[445] and provided support for further clinical trials for ADPKD and ADPLD.[446−448] The latter have shown inhibition of kidney growth and a mean annualized 5% reduction in liver volume.

Limitations of the studies are small number of patients insufficient to adequately assess safety and short duration (6–12 months). Further studies are ongoing. Small-molecule phosphodiesterase activators were shown to to reduce cAMP and inhibit cyst growth in an *in vitro* PKD model.[449] At present the efficacy of these compounds may be limited by their lack of selectivity and potential toxicity *in vivo*.

Chloride Driven Fluid Secretion

Fluid accumulation in the cysts requires chloride secretion by the cystic fibrosis transmembrane conductance regulator (CFTR). CFTR and other transporters required for chloride secretion have received attention as potential therapeutic targets for ADPKD. CFTR inhibitors slow cyst growth in an MDCK cell culture model, in metanephric kidney organ cultures, and in conditional *Pkd1* knockout mice.[380,450] Metformin inhibits MDCK cyst growth and cystic disease in conditional *Pkd1* knockout mice, in part by inhibiting AMPK dependent phosphorylation and activation of CFTR.[451] PPARγ agonists inhibit the expression and apical localization of CFTR, vasopressin-stimulated Cl^- secretion via CFTR in the MDCK cells, and renal and hepatic cyst growth in pck rats.[452,453] Other transporters in addition to CFTR are required for chloride driven fluid secretion into the cysts, the Na-K-2Cl cotransporter for chloride entry at the basolateral cell membrane and Na-K-ATPase and KCa3.1 for recycling of sodium and potassium out of the cell. A KCa3.1 inhibitor, TRAM-34 (an analogue of clotrimazole), inhibits forskolin stimulated transepithelial chloride secretion in filter-grown polarized monolayers of MDCK, NHK, and ADPKD cells, as well as MDCK and ADPKD cell cyst formation and enlargement in collagen gels.[454,455]

Tyrosine Kinase Receptors

Evidence from several laboratories supports an important role of the epidermal growth factor (EGF)/transforming growth factor-alpha (TGF-α)/EGF receptor (EGFR or ErbB1) axis in promoting tubular epithelial cell proliferation and cyst formation.[456] Pharmacologic inhibition of EGFR tyrosine kinase activity inhibits the development of cystic disease in bpk and orpk mice, two autosomal-recessive models of rapidly progressive cystic disease, and in Han:SPRD rats, an autosomal dominant model of slowly progressive renal cystic disease.[457] They had no effect, however in the *pck* rat, an orthologous model of ARPKD, probably because Erb-B2 but not EGFR (Erb-B1) is overexpressed in this model.[458,459] The expression of VEGF and VEGF receptors (VEGFR) is upregulated in the renal and hepatic cystic epithelium. VEGFR-1 and VEGFR-2 ribozyme treatment inhibits cystogenesis and improves renal function in Han:SPRD rats.[460] The VEGF receptor inhibitor SU-5416 reduces cystic development of the liver, but has no effect on renal cyst growth in $Pkd2^{WS25/-}$ mice.[461] Another study suggests that SU-5416 inhibits hepatic cystogenesis in conditional *Pkd2* but not *Pkd1* knockout mice.[462] In contrast with these results, administration of an anti-VEGF antibody (B20.4.1) worsens the cystic disease in Han:SPRD rats[463] and administration of a VEGFR-2 antibody (DC101) at 2 and 4 days of age results in renal cyst formation in CD1 mice.[464]

Src Kinase Inhibitors

Cyclic AMP and receptor tyrosine kinase signaling converge in the activation of c-Src, a nonreceptor tyrosine kinase. c-Src activity is increased in polycystic kidney disease. The Src inhibitor SKI-606 retards cyst growth *pck* rats and *bpk* and *Pkd1* heterozygous mice probably through inhibition of the MAPK (Ras/Raf/MEK/ERK) pathway.[459,465]

Inhibitors of MAPK (Ras/Raf/MEK/ERK) Signaling

PLX5568, a selective small molecule inhibitor of Raf kinases, attenuates cyst enlargement in vitro and in Han:SPRD Cy+/− rats without improving kidney function, presumably due to increased renal fibrosis.[466] Sorafenib, a Raf kinase inhibitor that has activity against receptor tyrosine kinases, including VEGFR and PDGFR, has been found to inhibit cAMP-dependent activation of B-Raf and MEK/ERK signaling, cAMP and/or EGF induced cell proliferation, and growth of human ADPKD cell derived cysts in collagen gels.[467] A MEK inhibitor (PD184352) decreased cyst growth in the slowly progressive *pcy* mouse model of nephronophthisis,[468] whereas a different MEK inhibitor (U0126) failed to affect cystic progression in an acute perinatal *Pkd1* conditional knockout mouse at doses sufficient to reduce phospho-ERK1/2 in cystic kidneys.[166]

mTor Inhibitors

Patients with the contiguous PKD1-TSC2 gene syndrome exhibit a more severe form of PKD than those with ADPKD alone.[469] This observation suggests a convergence of signaling pathways downstream from PC1 and tuberin. mTOR activation in polycystic kidneys and an interaction between PC1 and the tuberous sclerosis protein tuberin have been reported.[285] Preclinical trials of mTOR inhibitors in rodent models of PKD have been mostly encouraging, but differences between rat and mouse studies cast doubt on whether doses of mTOR inhibitors necessary for effectiveness in PKD are feasible in the clinical setting. Tolerated doses and blood levels are much lower in rats than in mice. At doses and blood levels achievable in humans, sirolimus and everolimus are effective in Han:SPRD rats, a

rat model of PKD mainly affecting proximal tubules,[285,406,407,470–472] but not in an orthologous model affecting distal nephrons and collecting ducts.[473] At doses and blood levels higher than those achievable in humans, they are consistently effective in multiple orthologous and non-orthologous mouse models.[408,474,475]

The results of clinical trials have been mostly discouraging, possibly because blood levels capable to inhibit mTOR activity in peripheral blood mononuclear cells are not sufficient to inhibit mTOR activity in the kidney.[476] A randomized, open label, placebo controlled, eighteen month trial (SUISSE) of sirolimus in 100 ADPKD patients with a mean estimated creatinine clearance of 92 ml/min and kidney volumes of 907 (sirolimus) and 1003 (placebo) ml showed no effect on kidney volume or GFR.[477] Doses of sirolimus were low due to toxicity and patient retention was excellent (96% in the sirolimus group). A six-month cross-over trial (SIRENA) of sirolimus in 21 patients with a mean GFR of 77 ml/min/1.73 m^2 and kidney volume of 1874 ml showed less increase in cyst volume on sirolimus compared to placebo, but no effect on GFR.[478] Sirolimus blood levels were higher than in the SUISSE study, but patient retention (71%) was lower. Finally, a randomized, double blinded, placebo controlled, two year trial of everolimus in 433 patients with a mean eGFR of 55 ml/min/1.73 m^2 and kidney volumes of 2028 (everolimus) and 1911 (placebo) ml shows inhibition of kidney growth but a greater decline in eGFR.[479] Limitations of this trial included advanced stage of CKD (6.3% in CKD stage IV) and low patient retention (67% in the everolimus group). All together, these results cast doubt on the role of sirolimus and everolimus in the management of the renal cystic disease in ADPKD, but do not negate completely the importance of mTOR activation in its pathogenesis, nor the possibility that other strategies targeting this pathway could be successful.

Cytokines and Cytokine Receptors

TNFα is one of many cytokines found found in cyst fluids.[480–482] TNF-α, TNFR-I and TNF-α converting enzyme are over-expressed in cystic tissues. The administration of TNF promotes cyst formation in *Pkd2*$^{+/-}$ mice, whereas etanercept had an inhibitory effect.[483] An inhibitor of TNF-α-converting enzyme was shown to ameliorate the polycystic disease in the *bpk* mouse, a recessive non-orthologous model of PKD.[484] The aggravation of PKD by TNFα may be due to its enhancement of the expression of FIP2, a protein that physically interacts with PC2 and prevents its transport to the plasma membrane and primay cilium.[483] Alternatively, TNFα activates IKKβ (inhibitor of κB kinase-β), which physically interacts and phosphorylates hamartin, suppressing TSC1-TSC2 function and activating mTOR.[485]

Arachidonic Acid Signaling

A number of studies have focused on the role of arachidonic acid metabolites and their inhibitors on the progression of PKD. Prostaglandin E2 (PGE2) accumulates in cyst fluids and enhances cAMP production and growth of MDCK cysts in collagen gels.[486] PGE2 may act on four different G protein coupled receptors named E-prostanoid (EP) receptors 1–4. EP2 and EP4 are coupled to G stimulatory proteins and stimulate cAMP formation. EP3 is coupled to G inhibitory protein, inhibits cAMP formation, induces Rho activation and actin polymerization, and antagonizes AVP action. EP1 activation induces inositol 3-phosphate formation and calcium release. Recently, the effects of PGE2 on cAMP formation and cystogenesis, in a three-dimensional cell-culture system of human epithelial cells from normal and ADPKD kidneys, have been shown to be mediated by EP2 receptor activation, thus suggesting a possible role for EP2 receptor antagonists in the treatment of ADPKD.[486] PLA, COX-1 and COX-2 activities and the production of prostacyclin, thromboxane A2 and PGE2 are higher in cystic than wild-type kidneys. Endogenous and steady-state *in vitro* levels of prostanoids were 2–10 times higher in diseased compared with normal kidneys. The administration of the COX-2 inhibitor NS-398 reduced cystic expansion by 18%, interstitial fibrosis by 67%, macrophage infiltration by 33%, cell proliferation by 38%, and presence of oxidized LDL by 59% compared to controls, but had no protective effect on renal function.[487] The production of 20-hydroxyeicosatetraenoic acid (20-HETE), an endogenous cytochrome P450 metabolite of arachidonic acid with mitogenic properties, is markedly increased in microsomes from *bpk* compared to wild-type mice.[488] Daily administration of HET-0016, an inhibitor of 20-HETE synthesis, reduced kidney size by half and doubled survival. Transfection of principal cells isolated from wild-type mice with the cytochrome P450 peptide Cyp4a12 induced a four- to five-fold increase in cell proliferation, which was completely abolished when 20-HETE synthesis was inhibited. These observations suggest that 20-HETE contributes to the proliferation of epithelial cells in the formation of renal cysts and provide another potential target for intervention.

AMP-Activated Protein Kinase (AMPK)

AMPK is an intracellular energy sensor that decreases energy-consuming processes such as secretion, and growth when cellular AMP levels are high and ATP levels are low. AMPK activation inhibits growth through different pathways includeing

inhibition of mTOR and stimulation of the p53/p21 axis. mTORC1 inhibition by AMPK is dependent on Lkb1 signaling from intact cilia and is independent of PC2.[489] AMPK activation also decreases epithelial fluid secretion by directly inhibiting CFTR. Metformin activates AMPK and inhibits the growth of MDCK cysts in collagen gels and renal cyst growth in conditional *Pkd1* knockout mice.[451]

Signal Transducers and Activators of Transcription (Stats)

STATs are a family of transcription factors activated by cytokines and some growth factors that control cell growth, differentiation, and apoptosis. PC1 affects the activity of several STAT transcription factors (STAT1, STAT3, STAT6). STAT3 inhibitors (the anti-parasitic drug pyrimethamine and S3I-201) inhibit cyst formation and growth in conditional *Pkd1* knockout mice.[490] Curcumin, a natural product derived from the plant curcuma longa, inhibits forskolin-induced MDCK cell proliferation, MDCK cystogenesis *in vitro*, and cyst growth in embryonic metanephric organ cultures[491] and conditional *Pkd1* knockout mice,[492] possibly by blocking STAT3 signaling among other mechanisms.

Peroxisome Proliferator Activated Receptors (PPARs)

PPARs are a family of transcription factors that belong to the nuclear receptor superfamily. PPARs form heterodimers with the 9-cis retinoic acid receptor, RXRα. Activation of PPAR:RXRα by PPAR ligands and/or RXRα ligands results in a conformational change, allowing the heterodimers to bind peroxisomal proliferator response elements (PPREs) in target genes and modulate gene transcription. PPARγ is activated by its natural ligands, e.g. prostaglandin J2 and fatty acid derivatives, by conjugated linoleic acid, and by synthetic ligands such as the thiazolidinediones (pioglitazone, troglitazone, and rosiglitazone). Activation of PPARγ causes cell cycle withdrawal by mechanisms that include reduced expression of protein phosphatase 2A, increased phosphorylation, decreased DNA binding and transcriptional activity of the E2F/DP transcription factors, and repressed transcription and enhanced proteasome-dependent degradation of cyclin D1, promotion of terminal differentiation, and induction of apoptosis. Pioglitazone administered to pregnant mice inhibits renal cyst growth, cardiac abnormalities, and subcutaneous edema of $Pkd1^{-/-}$ embryos.[202] Administration of conjugated linoleic acid reduced macrophage infiltration, interstitial inflammation, and interstitial fibrosis in male Han:SPRD Cy +/− rats.[493] N-(4-hydroxyphenyl) retinamide (HPR), a synthetic derivative of retinoic acid, inhibited the growth of ADPKD derived cysts in a three-dimensional collage matrix.[494] Rosiglitazone attenuated PKD progression and prolonged survival in Han:SPRD rats.[495] Pioglitazone inhibited renal and hepatic cyst growth and fibrosis in the *pck* rat model of ARPKD.[453,496] This effect was associated with downregulation of ERK, mTOR and TGFβ signaling and with reduced expression and apical localization of CFTR. Contrary to these favorable results, pioglitazone had no significant effect on cyst growth in *Pkd1* knockout mice.[497]

Histone Deacetylases (HDACs)

Acetylation of histones by histone acetyl transferases increases accessibility of transcription factors to gene promoter regions whereas deacetylation by HDACs has the opposite effect. HDACs also deacetylate specific transcription factors to decrease their DNA binding activity. HDAC1 deacetylates p53 repressing *PKD1* gene transcription.[498] Polycystin signaling increases intracellular calcium and activates protein kinase C which directly or indirectly phosphorylates HDAC5, disrupts its association to myocyte enhancer factor 2C (MEF2C), and releases this transcription factor to affect transcription.[499] HDACs also regulate cellular functions through transcription-independent mechanisms.[500] HDAC6 deacetylates α-tubulin and regulates the stability of microtubules and cilia disassembly during the cell cycle. EGF-induced nuclear localization of β-catenin is regulated by HDAC6-dependent also deacetylates of β-catenin which is important for EGF-induced β-catenin nuclear localization. Valproic acid, an inhibitor of of class I HADCs (HDAC1, HDAC2, HDAC3 and HDAC8) and trichostatin A (TSA), an inhibitor of class II HDACs (HDAC4, HDAC5, HDAC6, HDAC7, HDAC9 and HDAC10) suppress cyst formation and retard renal failure in *Pkd1* and *Pkd2* knockout mice.[499,501]

Cyclins and Cyclin Dependent Kinases (CDK)

Roscovitine (Seliciclib, CYC202), a CDK inhibitor, inhibits cystogenesis and improves renal function in in two non-orhtologous mouse models of PKD (*jck* and *cpk*), acting through transcriptional regulation, blockade of the G1/S phase in the cell cycle, and inhibition of apoptosis.[502] Like PC1, roscovitine increases the levels of p21, which is downregulated in PKD.[503] In polycystic liver disease the expression of miR15a expression is decreased, while that of its target, the cell-cycle regulator cell division cycle 25A (Cdc25A), is upregulated.[504] Cdc25A is a phosphatase that plays an essential role in cell cycle progression by activating CDKs. Menadione lowers the levels of Cdc25A and other cell cycle proteins and inhibits renal and hepatic cyst growth in both *pck* rats and $Pkd2^{WS25/-}$ mice.

Other Targets

Sphingolipids and glycosphingolipids regulate many cellular processes, including proliferation, apoptosis and modulation of cell signaling pathways. Glucosylceramide (GlcCer) and lactosylceramide (LacCer) are elevated by approximately 2–3 fold in ADPKD patients and may stimulate proliferation via the activation of MAPK. The GlcCer synthase inhibitor Genz-123346 suppresses mTOR signaling, induces G1/S cell cycle arrest, and inhibits cystogenesis in mouse models orthologous to human autosomal dominant PKD (*Pkd1* conditional knockout mice) and nephronophthisis (*jck* and *pcy*), but the exact mechanism of action of this drug in PKD is not well understood.[505]

In planning for clinical trials for ADPKD, the use of renal function as the primary outcome becomes an issue. The natural history of ADPKD is characterized by decades of normal renal function, despite progressive enlargement and cystic transformation of the kidneys. By the time the GFR starts to decline, the kidneys are markedly enlarged, distorted, and unlikely to benefit from some treatments that may have been beneficial earlier in the course of the disease. On the other hand, early interventional trials would require unrealistic periods of follow-up if renal function was to be used as the primary outcome. The results of CRISP[17] have shown that the rate of renal growth is a good predictor of functional decline and justify the use of kidney volume as a surrogate marker of disease progression in clinical trials for ADPKD. The continued identification of targets for therapy coupled with the developement of appropriate outcomes for study endpoints portends continued advancement toward developing effective therapy for ADPKD.

References

[1] Torres VE, Harris PC, Pirson Y. Autosomal dominant polycystic kidney disease. Lancet 2007;369:1287–301.

[2] Iglesias CG, Torres VE, Offord KP, Holley KE, Beard CM, Kurland LT. Epidemiology of adult polycystic kidney disease, Olmsted County, Minnesota. Am J Kid Dis 1983;2:630–9.

[3] Torres VE, Holley KE, Offord KP. General features of autosomal dominant polycystic kidney disease. In: Grantham J, Gardner K, editors. Problems in diagnosis and management of polycystic kidney disease. Kansas City: PKD Foundation; 1985. p. 49–69.

[4] Stengel B, Billon S, Van Dijk PC, et al. Trends in the incidence of renal replacement therapy for end-stage renal disease in Europe, 1990-1999. Nephrol Dial Transplant 2003;18(9):1824–33.

[5] Wakai K, Nakai S, Kikuchi K, et al. Trends in incidence of end-stage renal disease in Japan, 1983-2000: age-adjusted and age-specific rates by gender and cause. Nephrol Dial Transplant 2004;19(8):2044–52.

[6] Collins AJ, Foley RN, Herzog C, et al. Excerpts from the US Renal Data System 2009 annual data report. Am J Kidney Dis 2010;55(1 Suppl 1):S1–420 [A426-427]

[7] Schrier RW, McFann KK, Johnson AM. Epidemiological study of kidney survival in autosomal dominant polycystic kidney disease. Kidney Int 2003;63(2):678–85.

[8] Orskov B, Romming Sorensen V, Feldt-Rasmussen B, Strandgaard S. Improved prognosis in patients with autosomal dominant polycystic kidney disease in Denmark. Clin J Am Soc Nephrol 2010;5(11):2034–9.

[9] Patch C, Charlton J, Roderick PJ, Gulliford MC. Use of antihypertensive medications and mortality of patients with autosomal dominant polycystic kidney disease: a population-based study. Am J Kidney Dis 2011;57(6):856–62.

[10] Kielstein R, Sass HM. Genetics in kidney disease: how much do we want to know? Am J Kidney Dis 2002;39(3):637–52.

[11] Ravine D, Gibson RN, Walker RG, Sheffield LJ, Kincaid-Smith P, Danks DM. Evaluation of ultrasonographic diagnostic criteria for autosomal dominant polycystic kidney disease 1. Lancet 1994;343(8901):824–7.

[12] Pei Y, Obaji J, Dupuis A, et al. Unified criteria for ultrasonographic diagnosis of ADPKD. J Am Soc Nephrol 2009;20(1):205–12.

[13] Barua M, Cil O, Paterson AD, et al. Family history of renal disease severity predicts the mutated gene in ADPKD. J Am Soc Nephrol 2009;20(8):1833–8.

[14] Harris PC, Rossetti S. Molecular diagnostics for autosomal dominant polycystic kidney disease. Nature Reviews Nephrol 2010;6(4):197–206.

[15] De Rycke M, Georgiou I, Sermon K, et al. PGD for autosomal dominant polycystic kidney disease type 1. Mol Hum Reprod 2005;11(1):65–71.

[16] Harris PC, Bae KT, Rossetti S, et al. Cyst number but not the rate of cystic growth is associated with the mutated gene in autosomal dominant polycystic kidney disease. J Am Soc Nephrol 2006;17(11):3013–9.

[17] Grantham JJ, Torres VE, Chapman AB, et al. Volume progression in polycystic kidney disease. N Engl J Med 2006;354:2122–30.

[18] Chapman AB, Bost JE, Torres VE, et al. Kidney volume and functional outcomes in autosomal dominant polycystic kidney disease. Clin J Am Soc Nephrol 2012.

[19] Kelleher CL, McFann KK, Johnson AM, Schrier RW. Characteristics of hypertension in young adults with autosomal dominant polycystic kidney disease compared with the general U.S. population. Am J Hypertens 2004;17(11 Pt 1):1029–34.

[20] Torres V, Wilson DM, Offord K, Burnett Jr. J, Romero J. Natriuretic response to volume expansion in polycystic kidney disease. Mayo Clin Proc 1989;64:509–15.

[21] Torres VE, Wilson DM, Burnett JCJ, Johnson CM, Offord KP. Effect of inhibition of converting enzyme on renal hemodynamics and sodium management in polycystic kidney disease. Mayo Clin Proc 1991;66:1010–7.

[22] Gabow PA, Chapman AB, Johnson AM, et al. Renal structure and hypertension in autosomal dominant polycystic kidney disease. Kid Int 1990;38:1177–80.

[23] Chapman AB, Johnson A, Gabow PA, Schrier RW. The renin-angiotensin-aldosterone system and autosomal dominant polycystic kidney disease. N Eng J Med 1990;323:1091–6.

[24] Doulton TW, Saggar-Malik AK, He FJ, et al. The effect of sodium and angiotensin-converting enzyme inhibition on the classic circulating renin-angiotensin system in autosomal-dominant polycystic kidney disease patients. J Hypertens 2006;24(5):939–45.

[25] Watson M, MacNicol A, Allan P, Wright A. Effects of angiotensin-converting enzyme inhibition in adult polycystic kidney disease. Kidney Int 1992;41:206–10.

[26] Graham PC, Lindop GB. The anatomy of the renin-secreting cell in adult polycystic kidney disease. Kidney Int 1988;33 (6):1084–90.
[27] Torres VE, Donovan KA, Scicli G, et al. Synthesis of renin by tubulocystic epithelium in autosomal-dominant polycystic kidney disease. Kidney Int 1992;42(2):364–73.
[28] Loghman-Adham M, Soto CE, Inagami T, Cassis L. The intrarenal renin-angiotensin system in autosomal dominant polycystic kidney disease. Am J Physiol Renal Physiol 2004;287(4):775–88.
[29] McPherson EA, Luo Z, Brown RA, et al. Chymase-like angiotensin II-generating activity in end-stage human autosomal dominant polycystic kidney disease. J Am Soc Nephrol 2004;15 (2):493–500.
[30] Griffin MD, Torres VE, Grande JP, Kumar R. Vascular expression of polycystin. J Am Soc Nephrol 1997;8:616–26.
[31] Torres VE, Cai Y, Chen X, et al. Vascular expression of polycystin 2. J Am Soc Nephrol 2001;12:1–9.
[32] Qian Q, Li M, Cai Y, et al. Analysis of the polycystins in aortic vascular smooth muscle cells. J Am Soc Nephrol 2003;14 (9):2280–7.
[33] Ibraghimov-Beskrovnaya O, Dackowski WR, Foggensteiner L, et al. Polycystin: *In vitro* synthesis, *in vivo* tissue expression, and subcellular localization identifies a large membrane-associated protein. Proc Natl Acad Sci USA 1997;94:6397–402.
[34] Qian Q, Hunter LW, Han YS, et al. Pkd2 + /- vascular smooth muscles develop exaggerated vasocontraction in response to phenylephrine stimulation. JASN 2007;18:485–93.
[35] Wang D, Iversen J, Wilcox CS, Strandgaard S. Endothelial dysfunction and reduced nitric oxide in resistance arteries in autosomal-dominant polycystic kidney disease. Kidney Int 2003;64(4):1381–8.
[36] Clausen P, Feldt-Rasmussen B, Iversen J, Lange M, Eidemak I, Strandgaard S. Flow-Associated dilatory capacity of the brachial artery is intact in early autosomal dominant polycystic kidney disease. Am J Nephrol 2006;26(4):335–9.
[37] Kocaman O, Oflaz H, Yekeler E, et al. Endothelial dysfunction and increased carotid intima-media thickness in patients with autosomal dominant polycystic kidney disease. Am J Kidney Dis 2004;43(5):854–60.
[38] Klein IH, Ligtenberg G, Oey PL, Koomans HA, Blankestijn PJ. Sympathetic activity is increased in polycystic kidney disease and is associated with hypertension. J Am Soc Nephrol 2001;12 (11):2427–33.
[39] Seeman T, Dusek J, Vondrichova H, et al. Ambulatory blood pressure correlates with renal volume and number of renal cysts in children with autosomal dominant polycystic kidney disease. Blood Press Monit 2003;8(3):107–10.
[40] Fick GM, Johnson AM, Hammond WS, Gabow PA. Causes of death in autosomal dominant polycystic kidney disease. J Am Soc Nephrol 1995;5:2048–56.
[41] Ecder T, Chapman A, Brosnahan G, Edelstein C, Johnson A, Schrier R. Effect of antihypertensive therapy on renal function and urinary albumin excretion in hypertensive patients with autosomal dominant polycystic kidney disease. Am J Kid Dis 2000;35(3):427–32.
[42] Bajwa ZH, Sial KA, Malik AB, Steinman TI. Pain patterns in patients with polycystic kidney disease. Kidney Int 2004;66 (4):1561–9.
[43] Bajwa ZH, Gupta S, Warfield CA, Steinman TI. Pain management in polycystic kidney disease. Kidney Int 2001;60 (5):1631–44.
[44] Bello-Reuss E, Holubec K, Rajaraman S. Angiogenesis in autosomal-dominant polycystic kidney disease. Kidney Int 2001;60(1):37–45.
[45] Torres VE, Erickson SB, Smith LH, Wilson DM, Hattery RR, Segura JW. The association of nephrolithiasis and autosomal dominant polycystic kidney disease. Am J Kidney Dis 1988;11 (4):318–25.
[46] Torres VE, Wilson DM, Hattery RR, Segura JW. Renal stone disease in autosomal dominant polycystic kidney disease. Am J Kidney Dis 1993;22:513–9.
[47] Grampsas SA, Chandhoke PS, Fan J, et al. Anatomic and metabolic risk factors for nephrolithiasis in patients with autosomal dominant polycystic kidney disease. Am J Kidney Dis 2000;36 (1):53–7.
[48] Elzinga LW, Bennett WM. Miscellaneous renal and systemic complications of autosomal dominant polycystic kidney disease including infection. In: Watson ML, Torres VE, editors. Polycystic kidney disease, vol I. Oxford: Oxford Medical Publications; 1996. p. 483–99.
[49] Sallee M, Rafat C, Zahar JR, et al. Cyst infections in patients with autosomal dominant polycystic kidney disease. Clin J Am Soc Nephrol 2009;4(7):1183–9.
[50] Jouret F, Lhommel R, Beguin C, et al. Positron-emission computed tomography in cyst infection diagnosis in patients with autosomal dominant polycystic kidney disease. Clin J Am Soc Nephrol 2011;6(7):1644–50.
[51] Keith D, Torres V, King B, Zincki H, Farrow G. Renal cell carcinoma in autosomal dominant polycystic kidney disease (Review). J Am Soc Nephrol 1994;4(9):1661–9.
[52] Klahr S, Breyer J, Beck G, et al. Dietary protein restriction, blood pressure control, and the progression of polycystic kidney disease modification of diet in renal disease study group. J Am Soc Nephrol 1995;5(12):2037–47.
[53] Gabow PA, Johnson AM, Kaehny WD, et al. Factors affecting the progression of renal disease in autosomal- dominant polycystic kidney disease. Kidney Int 1992;41(5):1311–9.
[54] Johnson A, Gabow P. Identification of patients with autosomal dominant polycystic kidney disease at highest risk for end-stage renal disease. J Am Soc Nephrol 1997;8:1560–7.
[55] Yium J, Gabow P, Johnson A, Kimberling W, Martinez-Maldonado M. Autosomal dominant polycystic kidney disease in blacks: clinical course and effects of sickle-cell hemoglobin. J Am Soc Nephrol 1994;4(9):1670–4.
[56] Torres VE, King BF, Chapman A, et al. Magnetic resonance measurements of renal blood flow and disease progression in autosomal dominant polycystic kidney disease. CJASN 2007;2:112–20.
[57] Alvaro D, Mancino MG, Onori P, et al. Estrogens and the pathophysiology of the biliary tree. World J Gastroenterol 2006;12 (22):3537–45.
[58] Bae KT, Zhu F, Guay-Woodford LM, et al. Magnetic resonance imaging evaluation of hepatic cysts in early autosomal dominant polycystic kidney disease. Clin J Am Soc Nephrol 2006;1:64–9.
[59] Gabow P, Johnson A, Kaehny W, Manco-Johnson M, Duley I, Everson G. Risk factors for the development of hepatic cysts in autosomal dominant polycystic kidney disease. Hepatology 1990;11:1033–7.
[60] Shersthra R, McKinley C, Russ P, et al. Postmenopausal estrogen therapy selectively stimulates hepatic enlargement in women with autosomal dominant polycystic kidney disease. Hepatology 1997;26(5):1282–6.
[61] Torres V, Rastogi S, King B, Stanson A, Gross Jr. J, Nagorney D. Hepatic venous outflow obstruction in autosomal dominant polycystic kidney disease. J Am Soc Nephrol 1994;5:1186–92.
[62] Telenti A, Torres V, Gross Jr. J, Van Scoy R, Brown M, Hattery Jr. R. Hepatic cyst infection in autosomal dominant polycystic kidney disease. Mayo Clin Proc 1990;65:933–42.

[63] Bleeker-Rovers CP, de Sevaux RG, van Hamersvelt HW, Corstens FH, Oyen WJ. Diagnosis of renal and hepatic cyst infections by 18-F-fluorodeoxyglucose positron emission tomography in autosomal dominant polycystic kidney disease. Am J Kidney Dis 2003;41(6):18–21.
[64] Ishikawa I, Chikamoto E, Nakamura M, Asaka M, Tomosugi N, Yuri T. High incidence of common bile duct dilatation in autosomal dominant polycystic kidney disease patients. Am J Kidney Dis 1996;27(3):321–6.
[65] Grunfeld JP, Albouze G, Jungers P, et al. Liver changes and complications in adult polycystic kidney disease. Adv Nephrol Necker Hosp 1985;14:1–20.
[66] Serafini FM, Carey LC. Adenoma of the ampulla of Vater: a genetic condition? HPB Surg 1999;11(3):191–3.
[67] Sasaki M, Katayanagi K, Watanabe K, Takasawa K, Nakanuma Y. Intrahepatic cholangiocarcinoma arising in autosomal dominant polycystic kidney disease. Virchows Arch 2002;441 (1):98–100.
[68] Danaci M, Akpolat T, Bastemir M, et al. The prevalence of seminal vesicle cysts in autosomal dominant polycystic kidney disease. Nephrol Dial Transplant 1998;13 (11):2825–8.
[69] Alpern MB, Dorfman RE, Gross BH, Gottlieb CA, Sandler MA. Seminal vesicle cysts: association with adult polycystic kidney disease. Radiology 1991;180(1):79–80.
[70] Wijdicks EF, Torres VE, Schievink WI. Chronic subdural hematoma in autosomal dominant polycystic kidney disease. Am J Kidney Dis 2000;35(1):40–3.
[71] Schievink W, Huston J, Torres V, Marsh W. Intracranial cysts in autosomal dominant polycystic kidney disease. J Neurosurg 1995;83:1004–7.
[72] Alehan FK, Gurakan B, Agildere M. Familial arachnoid cysts in association with autosomal dominant polycystic kidney disease. Pediatrics 2002;110(1 Pt 1):e13.
[73] Nicolau C, Torra R, Bianchi L, et al. Abdominal sonographic study of autosomal dominant polycystic kidney disease. J Clin Ultrasound 2000;28(6):277–82.
[74] Li Vecchi M, Cianfrone P, Damiano R, Fuiano G. Infertility in adults with polycystic kidney disease. Nephrol Dial Transplant 2003;18(1):190–1.
[75] Okada H, Fujioka H, Tatsumi N, et al. Assisted reproduction for infertile patients with 9 + 0 immotile spermatozoa associated with autosomal dominant polycystic kidney disease [published erratum appears in Hum Reprod 1999 Jun;14(6):1166] Hum Reprod 1999;14(1):110–3.
[76] Basar O, Ibis M, Ucar E, et al. Recurrent pancreatitis in a patient with autosomal-dominant polycystic kidney disease. Pancreatology 2006;6(1-2):160–2.
[77] Sakurai Y, Shoji M, Matsubara T, et al. Pancreatic ductal adenocarcinoma associated with Potter type III cystic disease. J Gastroenterol 2001;36(6):422–8.
[78] Naitoh H, Shoji H, Ishikawa I, et al. Intraductal papillary mucinous tumor of the pancreas associated with autosomal dominant polycystic kidney disease. J Gastrointest Surg 2005;9 (6):843–5.
[79] Abderrahim E, Hedri H, Laabidi J, et al. Chronic subdural haematoma and autosomal polycystic kidney disease: report of two new cases. Nephrol (Carlton) 2004;9 (5):331–3.
[80] Schievink W, Torres V. Spinal meningeal diverticula in autosomal dominant polycystic kidney disease. Lancet 1997;26:349.
[81] Stamm ER, Townsend RR, Johnson AM, Garg K, Manco-Johnson M, Gabow PA. Frequency of ovarian cysts in patients with autosomal dominant polycystic kidney disease. Am J Kidney Dis 1999;34(1):120–4.
[82] Heinonen PK, Vuento M, Maunola M, Ala-Houhala I. Ovarian manifestations in women with autosomal dominant polycystic kidney disease. Am J Kidney Dis 2002;40(3):504–7.
[83] Qian Q, Hunter LW, Li M, et al. Pkd2 haploinsufficiency alters intracellular calcium regulation in vascular smooth muscle cells. Hum Mol Genet 2003;12(15):1875–80.
[84] Kip SN, Hunter LW, Ren Q, et al. $[Ca^{2+}]_i$ reduction increases cellular proliferation and apoptosis in vascular smooth muscle cells: relevance to the ADPKD phenotype. Circ Res 2005;96:873–80.
[85] Kim K, Drummond I, Ibraghimov-Beskrovnaya O, Klinger K, Arnaout MA. Polycystin 1 is required for the structural integrity of blood vessels. Proc Natl Acad Sci USA 2000;97(4):1731–6.
[86] Pirson Y, Chauveau D, Torres VE. Management of cerebral aneurysms in autosomal dominant polycystic kidney disease: unruptured asymptomatic intracranial aneurysms. J Am Soc Nephrol 2002;13:269–76.
[87] Irazabal MV, Huston 3rd J, Kubly V, et al. Extended follow-up of unruptured intracranial aneurysms detected by presymptomatic screening in patients with autosomal dominant polycystic kidney disease. Clin J Am Soc Nephrol 2011;6 (6):1274–85.
[88] Inagawa T. Trends in incidence and case fatality rates of aneurysmal subarachnoid hemorrhage in Izumo City, Japan, between 1980-1989 and 1990-1998. Stroke 2001;32(7):1499–507.
[89] Leier CV, Baker PB, Kilman JW, et al. Cardiovascular abnormalities associated with adult polycystic kidney disease. Ann Intern Med 1984;100:683–8.
[90] Qian Q, Hartman RP, King BF, Torres VE. Increased occurrence of pericardial effusion in patients with autosomal dominant polycystic kidney disease. Clin J Am Soc Nephrol 2007;2 (6):1223–7.
[91] Sharp CK, Zeligman BE, Johnson AM, Duley I, Gabow PA. Evaluation of colonic diverticular disease in autosomal dominant polycystic kidney disease without end-stage renal disease. Am J Kidney Dis 1999;34(5):863–8.
[92] Kumar S, Adeva M, King BF, Kamath PS, Torres VE. Duodenal diverticulosis in autosomal dominant polycystic kidney disease. Nephrol Dial Transplant 2006;21 (12):3576–8.
[93] Reynolds DM, Falk CT, Li A, et al. Identification of a locus for autosomal dominant polycystic liver disease, on chromosome 19p13.2-13.1. Am J Hum Genet 2000;67(6):1598–604.
[94] Tahvanainen P, Tahvanainen E, Reijonen H, Halme L, Kaariainen H, Hockerstedt K. Polycystic liver disease is genetically heterogeneous: clinical and linkage studies in eight Finnish families. J Hepatol 2003;38(1):39–43.
[95] Pazour GJ. Intraflagellar transport and cilia-dependent renal disease: the ciliary hypothesis of polycystic kidney disease. J Am Soc Nephrol 2004;15(10):2528–36.
[96] Marshall WF, Nonaka S. Cilia: tuning in to the cell's antenna. Curr Biol 2006;16(15):R604–14.
[97] Goetz SC, Anderson KV. The primary cilium: a signalling centre during vertebrate development. Nat Rev Genet 2010;11 (5):331–44.
[98] Hildebrandt F, Benzing T, Katsanis N. Ciliopathies. N Engl J Med 2011;364(16):1533–43.
[99] Ishikawa H, Marshall WF. Ciliogenesis: building the cell's antenna. Nat Rev Mol Cell Biol 2011;12(4):222–34.
[100] Barr MM, Sternberg PW. A polycystic kidney disease gene homolog required for male mating behavior in *Caenorhabiditis elegans*. Nature 1999;401:386–9.
[101] Mochizuki T, Saijoh Y, Tsuchiya K, et al. Cloning of inv, a gene that controls left/right asymmetry and kidney development. Nature 1998;395(6698):177–81.

[102] Murcia NS, Richards WG, Yoder BK, Mucenski ML, Dunlap JR, Woychik RP. The Oak Ridge Polycystic Kidney (orpk) disease gene is required for left-right axis determination. Development 2000;127(11):2347–55.
[103] Pazour GJ, Dickert BL, Vucica Y, et al. Chlamydomonas IFT88 and its mouse homologue, polycystic kidney disease gene tg737, are required for assembly of cilia and flagella. J Cell Biol 2000;151(3):709–18.
[104] Pazour GJ, San Agustin JT, Follit JA, Rosenbaum JL, Witman GB. Polycystin-2 localizes to kidney cilia and the ciliary level is elevated in orpk mice with polycystic kidney disease. Curr Biol 2002;12(11):R378–80.
[105] Yoder BK, Hou X, Guay-Woodford LM. The polycystic kidney disease proteins, polycystin-1, polycystin-2, polaris, and cystin, are co-localized in renal cilia. J Am Soc Nephrol 2002;13 (10):2508–16.
[106] Pennekamp P, Karcher C, Fischer A, et al. The ion channel polycystin-2 is required for left-right axis determination in mice. Curr Biol 2002;12(11):938–43.
[107] Praetorius HA, Spring KR. Bending the MDCK cell primary cilium increases intracellular calcium. J Membr Biol 2001;184 (1):71–9.
[108] Praetorius HA, Spring KR. The renal cell primary cilium functions as a flow sensor. Curr Opin Nephrol Hypertens 2003;12 (5):517–20.
[109] Praetorius HA, Spring KR. Removal of the MDCK cell primary cilium abolishes flow sensing. J Membr Biol 2003;191 (1):69–76.
[110] Koulen P, Cai Y, Geng L, et al. Polycystin-2 is an intracellular calcium release channel. Nat Cell Biol 2002;4:191–7.
[111] Nauli SM, Alenghat FJ, Luo Y, et al. Polycystins 1 and 2 mediate mechanosensation in the primary cilium of kidney cells. Nat Genet 2003;33(2):129–37.
[112] McGrath J, Somlo S, Makova S, Tian X, Brueckner M. Two populations of node monocilia initiate left-right asymmetry in the mouse. Cell 2003;114(1):61–73.
[113] Tanaka Y, Okada Y, Hirokawa N. FGF-induced vesicular release of Sonic hedgehog and retinoic acid in leftward nodal flow is critical for left-right determination. Nature 2005;435 (7039):172–7.
[114] Sun Z, Amsterdam A, Pazour GJ, Cole DG, Miller MS, Hopkins N. A genetic screen in zebrafish identifies cilia genes as a principal cause of cystic kidney. Development 2004;131 (16):4085–93.
[115] Lin F, Hiesberger T, Cordes K, et al. Kidney-specific inactivation of the KIF3A subunit of kinesin-II inhibits renal ciliogenesis and produces polycystic kidney disease. Proc Natl Acad Sci USA 2003;100(9):5286–91.
[116] Drummond IA. Cilia functions in development. Curr Opin Cell Biol 2012;24(1):24–30.
[117] Quinlan RJ, Tobin JL, Beales PL. Modeling ciliopathies: primary cilia in development and disease. Curr Top Dev Biol 2008;84:249–310.
[118] Harris PC, Torres VE. Polycystic kidney disease. Annu Rev Med 2009;60:321–37.
[119] Lancaster MA, Gleeson JG. The primary cilium as a cellular signaling center: lessons from disease. Curr Opin Genet Dev 2009;19(3):220–9.
[120] Ward CJ, Yuan D, Masyuk TV, et al. Cellular and subcellular localization of the ARPKD protein; fibrocystin is expressed on primary cilia. Hum Mol Genet 2003;12(20):2703–10.
[121] Menezes LF, Cai Y, Nagasawa Y, et al. Polyductin, the PKHD1 gene product, comprises isoforms expressed in plasma membrane, primary cilium, and cytoplasm. Kidney Int 2004;66 (4):1345–55.
[122] Gallagher A, Esquivel E, Briere T, et al. Biliary and pancreatic dysgenesis in mice harboring a mutation in Pkhd1. Am J Pathol 2008;172:417–29.
[123] Coppieters F, Lefever S, Leroy BP, De Baere E. CEP290, a gene with many faces: mutation overview and presentation of CEP290base. Hum Mutat 2010;31(10):1097–108.
[124] Garcia-Gonzalo FR, Corbit KC, Sirerol-Piquer MS, et al. A transition zone complex regulates mammalian ciliogenesis and ciliary membrane composition. Nat Genet 2011;43 (8):776–84.
[125] Sang L, Miller JJ, Corbit KC, et al. Mapping the NPHP-JBTS-MKS protein network reveals ciliopathy disease genes and pathways. Cell 2011;145(4):513–28.
[126] Jin H, White SR, Shida T, et al. The conserved Bardet-Biedl syndrome proteins assemble a coat that traffics membrane proteins to cilia. Cell 2010;141(7):1208–19.
[127] Nachury MV, Seeley ES, Jin H. Trafficking to the ciliary membrane: how to get across the periciliary diffusion barrier? Annu Rev Cell Dev Biol 2010;26:59–87.
[128] The European Polycystic Kidney Disease Consortium. The polycystic kidney disease 1 gene encodes a 14 kb transcript and lies within a duplicated region on chromosme 16. Cell 1994;77:881–94.
[129] Consortium TIPKD. Polycystic kidney disease: the complete structure of the PKD1 Gene and its Protein. Cell 1995;81:289–98.
[130] Consortium TAP. Analysis of the genomic sequence for the autosomal dominant polycystic kidney disease gene (PKD1) predicts the presence of a leucine-rich repeat. Hum Molec Genet 1995;4:575–82.
[131] Mochizuki T, Wu G, Hayashi T, et al. PKD2, a gene for polycystic kidney disease that encodes an integral membrane protein. Science 1996;272(5266):1339–42.
[132] Harris PC, Thomas S, MacCarthy AB, et al. A large duplicated area in the polycystic kidney disease 1 (PKD1) region of chromosome 16 is prone to rearrangement. Genomics 1994;23:321–30.
[133] Watnick T, Piontek K, Cordal T, et al. An unusual pattern of mutation in the duplicated portion of PKD1 is revealed by use of a novel strategy for mutation detection. Hum Mol Genet 1997;6:1473–81.
[134] Peral B, Gamble V, Strong C, et al. Identification of mutations in the duplicated region of the polycystic kidney disease 1 gene (PKD1) by a novel approach. Am J Hum Genet 1997;60 (6):1399–410.
[135] Martin J, Han C, Gordon LA, et al. The sequence and analysis of duplication-rich human chromosome 16. Nature 2004;432 (7020):988–94.
[136] Peters DJM, Sandkuijl LA. Genetic heterogeneity of polycystic kidney disease in Europe. In: Breuining MH, Devoto M, Romeo G, editors. Contributions to nephrology: polycystic kidney disease. Karger: Basel; 1992. p. 128–39.
[137] Torra R, Badenas C, Darnell A, et al. Linkage, clinical features, and prognosis of autosomal dominant polycystic kidney disease types 1 and 2. J Am Soc Nephrol 1996;7 (10):2142–51.
[138] Dicks E, Ravani P, Langman D, Davidson WS, Pei Y, Parfrey PS. Incident renal events and risk factors in autosomal dominant polycystic kidney disease: a population and family-based cohort followed for 22 years [4 presented at Clinical journal of the American Society of Nephrology: CJASN] Clin J Am Soc Nephrol 2006.

[139] Hateboer N, Dijk MA, Bogdanova N, et al. Comparison of phenotypes of polycystic kidney disease types 1 and 2. European PKD1-PKD2 Study Group. Lancet 1999;353(9147): 103–7.
[140] Torra R, Badenas C, Perez-Oller L, et al. Increased prevalence of polycystic kidney disease type 2 among elderly polycystic patients. Am J Kidney Dis 2000;36(4):728–34.
[141] Milutinovic J, Rust PF, Fialkow PJ, et al. Intrafamilial phenotypic expression of autosomal dominant polycystic kidney disease. Am J Kidney Dis 1992;19:465–72.
[142] Persu A, Duyme M, Pirson Y, et al. Comparison between siblings and twins supports a role for modifier genes in ADPKD. Kidney Int 2004;66(6):2132–6.
[143] Hateboer N, Lazarou LP, Williams AJ, Holmans P, Ravine D. Familial phenotype differences in PKD1. Kidney Int 1999;56 (1):34–40.
[144] Pei Y. Practical genetics for autosomal dominant polycystic kidney disease [1 presented at Nephron.Clinical practice] Nephron Clin Pract 2011.
[145] Baert L. Hereditary polycystic kidney disease (adult form): a microdissection study of two cases at an early stage of the disease. Kidney Int 1978;13(6):519–25.
[146] Qian F, Watnick TJ, Onuchic LF, Germino GG. The molecular basis of focal cyst formation in human autosomal dominant polycystic kidney disease type I. Cell 1996;87 (6):979–87.
[147] Brasier JL, Henske EP. Loss of the polycystic kidney disease (PKD1) region of chromosome 16p13 in renal cyst cells supports a loss-of-function model for cyst pathogenesis. J Clin Invest 1997;99(2):194–9.
[148] Torra R, Badenas C, San Millan JL, Perez-Oller L, Estivill X, Darnell A. A loss-of-function model for cystogenesis in human autosomal dominant polycystic kidney disease type 2. Am J Hum Genet 1999;65(2):345–52.
[149] Pei Y, Watnick T, He N, et al. Somatic PKD2 mutations in individual kidney and liver cysts support a "two-hit" model of cystogenesis in type 2 autosomal dominant polycystic kidney disease. J Am Soc Nephrol 1999;10(7):1524–9.
[150] Watnick TJ, Torres VE, Gandolph MA, et al. Somatic mutation in individual liver cysts supports a two-hit model of cystogenesis in autosomal dominant polycystic kidney disease. Mol Cell 1998;2(2):247–51.
[151] Ong AC, Harris PC. Molecular basis of renal cyst formation–one hit or two? Lancet 1997;349(9058):1039–40.
[152] Geng L, Segal Y, Peissel B, et al. Identification and localization of polycystin, the PKD1 gene product. J Clin Invest 1996;98 (12):2674–82.
[153] Ward CJ, Turley H, Ong AC, et al. Polycystin, the polycystic kidney disease 1 protein, is expressed by epithelial cells in fetal, adult, and polycystic kidney. Proc Nat Acad Sci Usa 1996;93(4):1524–8.
[154] Ong AC, Harris PC, Davies DR, et al. Polycystin-1 expression in PKD1, early-onset PKD1, and TSC2/PKD1 cystic tissue. Kidney Int 1999;56(4):1324–33.
[155] Ong AC, Ward CJ, Butler RJ, et al. Coordinate expression of the autosomal dominant polycystic kidney disease proteins, polycystin-2 and polycystin-1, in normal and cystic tissue. Am J Pathol 1999;154(6):1721–9.
[156] Watnick T, He N, Wang K, et al. Mutations of PKD1 in ADPKD2 cysts suggest a pathogenic effect of trans-heterozygous mutations. Nat Genet 2000;25(2):143–4.
[157] Martin GM, Ogburn CE, Colgin LM, Gown AM, Edland SD, Monnat Jr. RJ. Somatic mutations are frequent and increase with age in human kidney epithelial cells. Hum Mol Genet 1996;5(2):215–21.
[158] Koptides M, Mean R, Demetriou K, Pierides A, DeltaS CC. Genetic evidence for a trans-heterozygous model for cystogenesis in autosomal dominant polycystic kidney disease [In Process Citation]. Hum Mol Genet 2000;9(3):447–52.
[159] Pei Y, Paterson AD, Wang KR, et al. Bilineal disease and trans-heterozygotes in autosomal dominant polycystic kidney disease. Am J Hum Genet 2001;68:355–63.
[160] Wu G, Tian X, Nishimura S, et al. Trans-heterozygous Pkd1 and Pkd2 mutations modify expression of polycystic kidney disease. Hum Mol Genet 2002;11(16):1845–54.
[161] Lu W, Peissel B, Babakhanlou H, et al. Perinatal lethality with kidney and pancreas defects in mice with a targetted Pkd1 mutation. Nat Genet 1997;17(2):179–81.
[162] Wu G, Markowitz GS, Li L, et al. Cardiac defects and renal failure in mice with targeted mutations in Pkd2. Nat Genet 2000;24(1):75–8.
[163] Wu G, D'Agati V, Cai Y, et al. Somatic inactivation of Pkd2 results in polycystic kidney disease. Cell 1998;93(2):177–88.
[164] Piontek KB, Huso DL, Grinberg A, et al. A functional floxed allele of Pkd1 that can be conditionally inactivated in vivo. J Am Soc Nephrol 2004;15(12):3035–43.
[165] Piontek K, Menezes LF, Garcia-Gonzalez MA, Huso DL, Germino GG. A critical developmental switch defines the kinetics of kidney cyst formation after loss of Pkd1. Nat Med 2007;13(12):1490–5.
[166] Shibazaki S, Yu Z, Nishio S, et al. Cyst formation and activation of the extracellular regulated kinase pathway after kidney specific inactivation of Pkd1. Hum Mol Genet 2008;17 (11):1505–16.
[167] Lantinga-van Leeuwen IS, Leonhard WN, van der Wal A, Breuning MH, de HE, Peters DJ. Kidney-specific inactivation of the Pkd1 gene induces rapid cyst formation in developing kidneys and a slow onset of disease in adult mice. Hum Mol Genet 2007;16(24):3188–96.
[168] Starremans PG, Li X, Finnerty PE, et al. A mouse model for polycystic kidney disease through a somatic in-frame deletion in the 5′ end of Pkd1. Kidney Int 2008;73 (12):1394–405.
[169] Davenport JR, Watts AJ, Roper VC, et al. Disruption of intraflagellar transport in adult mice leads to obesity and slow-onset cystic kidney disease. Curr Biol 2007;17(18):1586–94.
[170] Torres VE, Wang X, Qian Q, Somlo S, Harris PC, Gattone VH. Effective treatment of an orthologous model of autosomal dominant polycystic kidney disease. Nat Med 2004;10 (4):363–4.
[171] Fedeles SV, Tian X, Gallagher AR, et al. A genetic interaction network of five genes for human polycystic kidney and liver diseases defines polycystin-1 as the central determinant of cyst formation. Nat Genet 2011;43(7):639–47.
[172] Grantham JJ, Cook LT, Wetzel LH, Cadnapaphornchai MA, Bae KT. Evidence of extraordinary growth in the progressive enlargement of renal cysts. Clin J Am Soc Nephrol 2010;5 (5):889–96.
[173] Lantinga-van LI, Dauwerse JG, Baelde HJ, et al. Lowering of Pkd1 expression is sufficient to cause polycystic kidney disease. Hum Mol Genet 2004;13(24):3069–77.
[174] Jiang ST, Chiou YY, Wang E, et al. Defining a link with autosomal-dominant polycystic kidney disease in mice with congenitally low expression of Pkd1. Am J Pathol 2006;168 (1):205–20.
[175] Tran U, Zakin L, Schweickert A, et al. The RNA-binding protein bicaudal C regulates polycystin 2 in the kidney by antagonizing miR-17 activity. Development 2010;137(7):1107–16.
[176] Qian Q, Li A, King BF, et al. Clinical profile of autosomal dominant polycystic liver disease. Hepatology 2003;37(1):164–71.

[177] Li A, Davila S, Furu L, et al. Mutations in PRKCSH cause isolated autosomal dominant polycystic liver disease. Am J Hum Genet 2003;72(3):691–703.
[178] Drenth JP, Te Morsche RH, Smink R, Bonifacino JS, Jansen JB. Germline mutations in PRKCSH are associated with autosomal dominant polycystic liver disease. Nat Genet 2003.
[179] Davila S, Furu L, Gharavi AG, et al. Mutations in SEC63 cause autosomal dominant polycystic liver disease. Nat Genet 2004;36(6):575–7.
[180] Trombetta ES, Simons JF, Helenius A. Endoplasmic reticulum glucosidase II is composed of a catalytic subunit, conserved from yeast to mammals, and a tightly bound noncatalytic HDEL-containing subunit. J Biol Chem 1996;271(44):27509–16.
[181] D'Alessio C, Fernandez F, Trombetta ES, Parodi AJ. Genetic evidence for the heterodimeric structure of glucosidase II. The effect of disrupting the subunit-encoding genes on glycoprotein folding. J Biol Chem 1999;274(36):25899–905.
[182] Ellgaard L, Molinari M, Helenius A. Setting the standards: quality control in the secretory pathway. Science 1999;286 (5446):1882–8.
[183] Treml K, Meimaroglou D, Hentges A, Bause E. The alpha- and beta-subunits are required for expression of catalytic activity in the hetero-dimeric glucosidase II complex from human liver. Glycobiology 2000;10(5):493–502.
[184] Helenius A, Aebi M. Intracellular functions of N-linked glycans. Science 2001;291(5512):2364–9.
[185] Schnell DJ, Hebert DN. Protein translocons: multifunctional mediators of protein translocation across membranes. Cell 2003;112(4):491–505.
[186] Lang SBJ, Fedeles SV, Schorr S, Schirra C, Schäuble N, Jalal C, et al. Differential effects of Sec61α-, Sec62- and Sec63-depletion on transport of polypeptides into the endoplasmic reticulum of mammalian cells. J Cell Sci 2012; [in press].
[187] Patel V, Li L, Cobo-Stark P, et al. Acute kidney injury and aberrant planar cell polarity induce cyst formation in mice lacking renal cilia. Hum Mol Genet 2008;17(11):1578–90.
[188] Takakura A, Contrino L, Zhou X, et al. Renal Injury is a third hit promoting rapid development of adult polycystic kidney disease. Hum Mol Genet 2009;:.
[189] Bastos AP, Piontek K, Silva AM, et al. Pkd1 haploinsufficiency increases renal damage and induces microcyst formation following ischemia/reperfusion. J Am SocNephrol 2009;20(11): 2389–402.
[190] Prasad S, McDaid JP, Tam FW, Haylor JL, Ong AC. Pkd2 dosage influences cellular repair responses following ischemia-reperfusion injury. Am J Pathol 2009;175 (4):1493–503.
[191] Happe H, Leonhard WN, van der Wal A, et al. Toxic tubular injury in kidneys from Pkd1-deletion mice accelerates cystogenesis accompanied by dysregulated planar cell polarity and canonical Wnt signaling pathways. Hum Mol Genet 2009.
[192] Bell PD, Fitzgibbon W, Sas K, et al. Loss of primary cilia upregulates renal hypertrophic signaling and promotes cystogenesis. J Am Soc Nephrol 2011;22(5):839–48.
[193] Zhou J. Polycystins and primary cilia: primers for cell cycle progression. Annu Rev Physiol 2009;71:83–113.
[194] Bhunia AK, Piontek K, Boletta A, et al. PKD1 induces p21 (waf1) and regulation of the cell cycle via direct activation of the JAK-STAT signaling pathway in a process requiring PKD2. Cell 2002;109(2):157–68.
[195] Takakura A, Contrino L, Beck AW, Zhou J. Pkd1 inactivation induced in adulthood produces focal cystic disease. J Am SocNephrol 2008;19(12):2351–63.
[196] Nishio S, Hatano M, Nagata M, et al. Pkd1 regulates immortalized proliferation of rean tubular epithelial cells through p53 induction and JNK activation. J Clin Invest 2005; [in press 2005].
[197] Karihaloo A, Koraishy F, Huen SC, et al. Macrophages promote cyst growth in polycystic kidney disease. J Am Soc Nephrol 2011.
[198] Harris PC, Bae KT, Rossetti S, et al. Cyst number but not the rate of cystic growth is associated with the mutated gene in autosomal dominant polycystic kidney disease [11 presented at] J Am Soc Nephrol 2006.
[199] Hanaoka K, Qian F, Boletta A, et al. Co-assembly of polycystin-1 and -2 produces unique cation-permeable currents. Nature 2000;408(6815):990–4.
[200] Karcher C, Fischer A, Schweickert A, et al. Lack of a laterality phenotype in Pkd1 knock-out embryos correlates with absence of polycystin-1 in nodal cilia. Differentiation 2005;73 (8):425–32.
[201] Boulter C, Mulroy S, Webb S, Fleming S, Brindle K, Sandford R. Cardiovascular, skeletal, and renal defects in mice with a targeted disruption of the Pkd1 gene. Proc Natl Acad Sci USA 2001;98(21):12174–9.
[202] Muto S, Aiba A, Saito Y, et al. Pioglitazone improves the phenotype and molecular defects of a targeted Pkd1 mutant. Hum Mol Genet 2002;11(15):1731–42.
[203] Lu W, Shen X, Pavlova A, et al. Comparison of Pkd1-targeted mutants reveals that loss of polycystin-1 causes cystogenesis and bone defects. Hum Mol Genet 2001;10(21):2385–96.
[204] Barr MM, DeModena J, Braun D, Nguyen CQ, Hall DH, Sternberg PW. The Caenorhabditis elegans autosomal dominant polycystic kidney disease gene homologs lov-1 and pkd-2 act in the same pathway. Curr Biol 2001;11(17):1341–6.
[205] Milutinovic J, Fialkow PJ, Agodoa LY, Phillips LA, Bryant JI. Fertility and pregnancy complications in women with autosomal dominant polycystic kidney disease. Obstet Gynecol 1983;61(5):566–9.
[206] Rossetti S, Strmecki L, Gamble V, et al. Mutation analysis of the entire PKD1 gene: genetic and diagnostic implications. Am J Hum Genet 2001;68(1):46–63.
[207] Dobin A, Kimberling WJ, Pettinger W, Bailey-Wilson JE, Shugart YY, Gabow P. Segregation analysis of autosomal dominant polycystic kidney disease. Genet Epidemiol 1993;10 (3):189–200.
[208] Harris PC, Rossetti S. Determinants of renal disease variability in ADPKD. Adv Chronic Kidney Dis 2010;17(2):131–9.
[209] Sampson JR, Maheshwar MM, Aspinwall R, et al. Renal cystic disease in tuberous sclerosis: the role of the polycystic kidney disease 1 gene. Am J Hum Genet 1997;61:843–51.
[210] Consugar MB, Wong WC, Lundquist PA, et al. Characterization of large rearrangements in autosomal dominant polycystic kidney disease and the PKD1/TSC2 contiguous gene syndrome. Kidney Int 2008;74(11):1468–79.
[211] Rossetti S, Kubly VJ, Consugar MB, et al. Incompletely penetrant PKD1 alleles suggest a role for gene dosage in cyst initiation in polycystic kidney disease. Kidney Int 2009;75(8):848–55.
[212] Vujic M, Heyer CM, Ars E, et al. Incompletely penetrant PKD1 alleles mimic the renal manifestations of ARPKD. J Am Soc Nephrol 2010;21(7):1097–102.
[213] Losekoot M, Ruivenkamp CA, Tholens AP, et al. Neonatal onset autosomal dominant polycystic kidney disease (ADPKD) in a patient homozygous for a PKD2 missense mutation due to uniparental disomy. J Med Genet 2012;49(1):37–40.
[214] Rossetti S, Harris PC. Genotype-phenotype correlations in autosomal dominant and autosomal recessive polycystic kidney disease [5 presented at] J Am Soc Nephrol 2007;2007.
[215] Peral B, Ong AC, San Millan JL, Gamble V, Rees L, Harris PC. A stable, nonsense mutation associated with a case of infantile

onset polycystic kidney disease 1 (PKD1). Hum Mol Genet 1996;5(4):539–42.
[216] Geberth S, Ritz E, Zeier M, Stier E. Anticipation of age at renal death in autosomal dominant polycystic kidney disease (ADPKD)? Nephrol Dial Transplant 1995;10:1603–6.
[217] Magistroni R, He N, Wang K, et al. Genotype-renal function correlation in type 2 autosomal dominant polycystic kidney disease. J Am Soc Nephrol 2003;14(5):1164–74.
[218] Rossetti S, Burton S, Strmecki L, et al. The position of the polycystic kidney disease 1 (PKD1) gene mutation correlates with the severity of renal disease. J Am Soc Nephrol 2002;13(5):1230–7.
[219] Pei Y, Lan Z, Wang K, et al. A missense mutation in PKD1 attenuates the severity of renal disease. Kidney Int 2012;81 (4):412–7.
[220] Rossetti S, Chauveau D, Kubly V, et al. Association of mutation position in polycystic kidney disease 1 (PKD1) gene and development of a vascular phenotype. Lancet 2003;361 (9376):2196–201.
[221] Watnick T, Phakdeekitcharoen B, Johnson A, et al. Mutation detection of PKD1 identifies a novel mutation common to three families with aneurysms and/or Very-Early-Onset disease. Am J Hum Genet 1999;65(6):1561–71.
[222] Paterson AD, Magistroni R, He N, et al. Progressive loss of renal function is an age-dependent heritable trait in type 1 autosomal dominant polycystic kidney disease. J Am Soc Nephrol 2005;16(3):755–62.
[223] Fain PR, McFann KK, Taylor MR, et al. Modifier genes play a significant role in the phenotypic expression of PKD1. Kidney Int 2005;67(4):1256–67.
[224] Bergmann C, Weiskirchen R. It's not all in the cilia, but on the road to it: genetic interaction network in polycystic kidney and liver diseases and how trafficking and quality control matter. J Hepatol 2011.
[225] Verdeguer F, Le CS, Fischer E, et al. A mitotic transcriptional switch in polycystic kidney disease. Nat Med 2010;16 (1):106–10.
[226] Hiesberger T, Bai Y, Shao X, et al. Mutation of hepatocyte nuclear factor-1beta inhibits Pkhd1 gene expression and produces renal cysts in mice. J Clin Invest 2004;113 (6):814–25.
[227] Liu M, Shi S, Senthilnathan S, et al. Genetic variation of DKK3 may modify renal disease severity in ADPK. J Am Soc Nephrol 2010;21(9):1510–20.
[228] Hughes J, Ward CJ, Peral B, et al. The polycystic kidney disease 1 (PKD1) gene encodes a novel protein with multiple cell recognition domains. Nat Genet 1995;10(2):151–60.
[229] Sandford R, Sgotto B, Aparicio S, et al. Comparative analysis of the polycystic kidney disease 1 (PKD!) gene reveals an integral membrane glycoprotein with multiple evolutionary conserved domains. Hum Mol Genet 1997;6:1483–9.
[230] Schroder S, Fraternali F, Quan X, Scott D, Qian F, Pfuhl M. When a module is not a domain: the case of the REJ module and the redefinition of the architecture of polycystin-1. Biochem J 2011;435(3):651–60.
[231] Ponting CP, Hofmann K, Bork P. A latrophilin/CL-1-like GPS domain in polycystin-1. Curr Biol 1999;9(16):R585–8.
[232] Arac D, Boucard AA, Bolliger MF, et al. A novel evolutionarily conserved domain of cell-adhesion GPCRs mediates autoproteolysis. EMBO J 2012;31(6):1364–78.
[233] Bateman A, Sandford R. The PLAT domain: a new piece in the PKD1 puzzle. Curr Biol 1999;9(16):R588–90.
[234] Hu J, Barr MM. ATP-2 interacts with the PLAT domain of LOV-1 and is involved in Caenorhabditis elegans polycystin signaling. Mol Biol Cell 2005;16(2):458–69.
[235] Li A, Tian X, Sung SW, Somlo S. Identification of two novel polycystic kidney disease-1-like genes in human and mouse genomes. Genomics 2003;81(6):596–608.
[236] Qian F, Germino FJ, Cai Y, Zhang X, Somlo S, Germino GG. PKD1 interacts with PKD2 through a probable coiled-coil domain. Nat Genet 1997;16(2):179–83.
[237] Zhu J, Yu Y, Ulbrich MH, et al. Structural model of the TRPP2/PKD1 C-terminal coiled-coil complex produced by a combined computational and experimental approach. Proc Natl Acad Sci USA 2011;108(25):10133–8.
[238] Nims N, Vassmer D, Maser RL. Transmembrane domain analysis of polycystin-1, the product of the polycystic kidney disease-1 (PKD1) gene: evidence for 11 membrane-spanning domains. Biochemistry 2003;42(44):13035–48.
[239] Bycroft M, Bateman A, Clarke J, et al. The structure of a PKD domain from polycystin-1: implications for polycystic kidney disease. EMBO J 1999;18(2):297–305.
[240] Forman JR, Qamar S, Paci E, Sandford RN, Clarke J. The remarkable mechanical strength of polycystin-1 supports a direct role in mechanotransduction. J Mol Biol 2005;349(4):861–71.
[241] Forman JR, Yew ZT, Qamar S, Sandford RN, Paci E, Clarke J. Non-native interactions are critical for mechanical strength in PKD domains. Structure 2009;17(12):1582–90.
[242] Qian F, Wei W, Germino G, Oberhauser A. The nanomechanics of polycystin-1 extracellular region. J Biol Chem 2005;280 (49):40723–30.
[243] Ma L, Xu M, Forman JR, Clarke J, Oberhauser AF. Naturally occurring mutations alter the stability of polycystin-1 polycystic kidney disease (PKD) domains. J Biol Chem 2009;284 (47):32942–9.
[244] Geng L, Segal Y, Pavlova A, et al. Distribution and developmentally regulated expression of murine polycystin. Am J Physiol 1997;272(4 Pt 2):F451–9.
[245] Peters DJM, van de Wal A, Spruit L, et al. Cellular localization and tissue distribution of polycystin-1. J Pathol 1999; 188:439–46.
[246] Wodarczyk C, Rowe I, Chiaravalli M, Pema M, Qian F, Boletta A. A novel mouse model reveals that polycystin-1 deficiency in ependyma and choroid plexus results in dysfunctional cilia and hydrocephalus. PLoS One 2009;4(9):e7137.
[247] Palsson R, Sharma CP, Kim K, McLaughlin M, Brown D, Arnaout MA. Characterization and cell distribution of polycystin, the product of autosomal dominant polycystic kidney disease gene 1. Mol Med 1996;2(6):702–11.
[248] Foggensteiner L, Bevan AP, Thomas R, et al. Cellular and subcellular distribution of polycystin-2, the protein product of the PKD2 gene. J Am Soc Nephrol 2000;11(5):814–27.
[249] Scheffers MS, van der BP, Prins F, et al. Polycystin-1, the product of the polycystic kidney disease 1 gene, co-localizes with desmosomes in MDCK cells. Hum Mol Genet 2000;9 (18):2743–50.
[250] Boletta A, Qian F, Onuchic LF, et al. Biochemical characterization of bona fide polycystin-1 in vitro and in vivo. Am J Kidney Dis 2001;38(6):1421–9.
[251] Newby LJ, Streets AJ, Zhao Y, Harris PC, Ward CJ, Ong AC. Identification, characterization, and localization of a novel kidney polycystin-1-polycystin-2 complex. J Bio Chem 2002;277 (23):20763–73.
[252] Hogan MC, Manganelli L, Woollard JR, et al. Characterization of PKD protein-positive exosome-like vesicles. J Am Soc Nephrol 2009;20(2):278–88.
[253] Hughes J, Ward CJ, Aspinwall R, Butler R, Harris PC. Identification of a human homologue of the sea urchin receptor for egg jelly: a polycystic kidney disease-like protein. Hum Mol Genet 1999;8(3):543–9.

[254] Veldhuisen B, Spruit L, Dauwerse HG, Breuning MH, Peters DJM. Genes homologous to the autosomal dominant polycystic kidney disease genes (PKD1 and PKD2). Eur J Human Genet 1999;7(8):860–72.
[255] Butscheid Y, Chubanov V, Steger K, Meyer D, Dietrich A, Gudermann T. Polycystic kidney disease and receptor for egg jelly is a plasma membrane protein of mouse sperm head. Mol Reprod Dev 2006;73(3):350–60.
[256] Sutton KA, Jungnickel MK, Florman HM. A polycystin-1 controls postcopulatory reproductive selection in mice. Proc Natl Acad Sci U S A 2008;105(25):8661–6.
[257] Yuasa T, Venugopal B, Weremowicz S, Morton CC, Guo L, Zhou J. The sequence, expression, and chromosomal localization of a novel polycystic kidney disease 1-like gene, PKD1L1, in human. Genomics 2002;79(3):376–86.
[258] Vogel P, Read R, Hansen GM, Freay LC, Zambrowicz BP, Sands AT. Situs inversus in Dpcd/Poll-/-, Nme7-/- , and Pkd1l1-/- mice. Vet Pathol 2010;47(1):120–31.
[259] Field S, Riley KL, Grimes DT, et al. Pkd1l1 establishes left-right asymmetry and physically interacts with Pkd2. Development 2011;138(6):1131–42.
[260] Kamura K, Kobayashi D, Uehara Y, et al. Pkd1l1 complexes with Pkd2 on motile cilia and functions to establish the left-right axis. Development 2011;138(6):1121–9.
[261] Huang AL, Chen X, Hoon MA, et al. The cells and logic for mammalian sour taste detection. Nature 2006;442 (7105):934–8.
[262] Ishimaru Y, Inada H, Kubota M, Zhuang H, Tominaga M, Matsunami H. Transient receptor potential family members PKD1L3 and PKD2L1 form a candidate sour taste receptor. Proc Natl Acad Sci U S A 2006;103(33):12569–74.
[263] LopezJimenez ND, Cavenagh MM, Sainz E, Cruz-Ithier MA, Battey JF, Sullivan SL. Two members of the TRPP family of ion channels, Pkd1l3 and Pkd2l1, are co-expressed in a subset of taste receptor cells. J Neurochem 2006;98(1): 68–77.
[264] Mackenzie FE, Romero R, Williams D, et al. Upregulation of PKD1L2 provokes a complex neuromuscular disease in the mouse. Hum Mol Genet 2009;18(19):3553–66.
[265] Qian F, Boletta A, Bhunia AK, et al. Cleavage of polycystin-1 requires the receptor for egg jelly domain and is disrupted by human autosomal-dominant polycystic kidney disease 1-associated mutations. Proc Natl Acad Sci USA 2002;99 (26):16981–6.
[266] Wei W, Hackmann K, Xu H, Germino G, Qian F. Characterization of cis-autoproteolysis of polycystin-1, the product of human polycystic kidney disease 1 gene. J Biol Chem 2007;282(30):21729–37.
[267] Mengerink KJ, Moy GW, Vacquier VD. suREJ3, a polycystin-1 protein, is cleaved at the GPS domain and localizes to the acrosomal region of sea urchin sperm. J Biol Chem 2002;277 (2):943–8.
[268] Krasnoperov V, Lu Y, Buryanovsky L, Neubert TA, Ichtchenko K, Petrenko AG. Post-translational proteolytic processing of CIRL, a natural chimera of cell adhesion protein and G protein-coupled receptor. The role of the GPS motif. J Biol Chem 2002;:.
[269] Chapin HC, Rajendran V, Caplan MJ. Polycystin-1 surface localization is stimulated by polycystin-2 and cleavage at the G protein-coupled receptor proteolytic site. Mol Biol Cell 2010;21 (24):4338–48.
[270] Yu S, Hackmann K, Gao J, et al. Essential role of cleavage of Polycystin-1 at G protein-coupled receptor proteolytic site for kidney tubular structure. Proc Natl Acad Sci U S A 2007;104 (47):18688–93.
[271] Woodward OM, Li Y, Yu S, et al. Identification of a polycystin-1 cleavage product, P100, that regulates store operated Ca entry through interactions with STIM1. PLoS One 2010;5(8): e12305.
[272] Chauvet V, Tian X, Husson H, et al. Mechanical stimuli induce cleavage and nuclear translocation of the polycystin-1 C terminus. J Clin Invest 2004;114(10):1433–43.
[273] Low SH, Vasanth S, Larson CH, et al. Polycystin-1, STAT6, and P100 function in a pathway that transduces ciliary mechanosensation and is activated in polycystic kidney disease. Dev Cell 2006;10(1):57–69.
[274] Celic A, Petri ET, Demeler B, Ehrlich BE, Boggon TJ. Domain mapping of the polycystin-2 C-terminal tail using de novo molecular modeling and biophysical analysis. J Biol Chem 2008;283(42):28305–12.
[275] Giamarchi A, Feng S, Rodat-Despoix L, et al. A polycystin-2 (TRPP2) dimerization domain essential for the function of heteromeric polycystin complexes. EMBO J 2010;29 (7):1176–91.
[276] Yu Y, Ulbrich MH, Li MH, et al. Structural and molecular basis of the assembly of the TRPP2/PKD1 complex. Proc Natl Acad Sci U S A 2009;106(28):11558–63.
[277] Molland KL, Narayanan A, Burgner JW, Yernool DA. Identification of the structural motif responsible for trimeric assembly of the C-terminal regulatory domains of polycystin channels PKD2L1 and PKD2. Biochem J 2010;429 (1):171–83.
[278] Hanaoka K, Qian F, Boletta A, et al. Co-assembly of polycystin-1 and -2 produces unique cation-permeable currents. Nature 2000;408(6815):990–4.
[279] Torres VE, Harris PC. Autosomal dominant polycystic kidney disease: the last 3 years [2 presented at] Kidney Int 2009;:.
[280] Ibraghimov-Beskrovnaya O, Bukanov NO, Donohue LC, Dackowski WR, Klinger KW, Landes GM. Strong homophilic interactions of the Ig-like domains of polycystin-1, the protein product of an autosomal dominant polycystic kidney disease gene, PKD1 [In Process Citation]. Hum Mol Genet 2000;9 (11):1641–9.
[281] Hu J, Bae YK, Knobel KM, Barr MM. Casein kinase II and calcineurin modulate TRPP function and ciliary localization. Mol Biol Cell 2006;17(5):2200–11.
[282] Kim E, Arnould T, Sellin L, et al. Interaction between RGS7 and polycystin. Proc Natl Acad Sci USA 1999;96(11): 6371–6.
[283] Delmas P, Nomura H, Li X, et al. Constitutive activation of G-proteins by polycystin-1 is antagonized by polycystin-2. J Biol Chem 2002;277(13):11276–83.
[284] Parnell SC, Magenheimer BS, Maser RL, Zien CA, Frischauf AM, Calvet JP. Polycystin-1 activation of c-Jun N-terminal kinase and AP-1 is mediated by heterotrimeric G proteins. J Biol Chem 2002;277(22):19566–72.
[285] Shillingford JM, Murcia NS, Larson CH, et al. The mTOR pathway is regulated by polycystin-1, and its inhibition reverses renal cystogenesis in polycystic kidney disease. Proc Natl Acad Sci U S A 2006;103(14):5466–71.
[286] Xu GM, Sikaneta T, Sullivan BM, et al. Polycystin-1 interacts with intermediate filaments. J Biol Chem 2001;276(49): 46544–52.
[287] Huan Y, van Adelsberg J. Polycystin-1, the PKD1 gene product, is in a complex containing E-cadherin and the catenins. J Clin Invest 1999;104(10):1459–68.
[288] Roitbak T, Ward CJ, Harris PC, Bacallao R, Ness SA, Wandinger-Ness A. A polycystin-1 multiprotein complex is disrupted in polycystic kidney disease cells. Mol Biol Cell 2004;15(3):1334–46.

[289] Wilson PD, Geng L, Li X, Burrow CR. The PKD1 gene product, "polycystin-1," is a tyrosine-phosphorylated protein that colocalizes with alpha2beta1-integrin in focal clusters in adherent renal epithelia. Lab Invest 1999;79(10):1311–23.
[290] Woods AJ, White DP, Caswell PT, Norman JC. PKD1/PKCmu promotes alphavbeta3 integrin recycling and delivery to nascent focal adhesions. EMBO J 2004;23(13):2531–43.
[291] Kiselyov K, Soyombo A, Muallem S. TRPpathies. J Physiol 2007;578(Pt 3):641–53.
[292] Nilius B, Owsianik G. The transient receptor potential family of ion channels. Genome Biol 2011;12(3):218.
[293] Petri ET, Celic A, Kennedy SD, Ehrlich BE, Boggon TJ, Hodsdon ME. Structure of the EF-hand domain of polycystin-2 suggests a mechanism for Ca2 + -dependent regulation of polycystin-2 channel activity. Proc Natl Acad Sci U S A 2010;107(20):9176–81.
[294] Markowitz GS, Cai Y, Li L, et al. Polycystin-2 expression is developmentally regulated. Am J Physiol 1999;277(1 Pt 2): F17–25.
[295] Obermuller N, Gallagher AR, Cai Y, et al. The rat Pkd2 protein assumes distinct subcellular distributions in different organs. Am J Physiol 1999;277:F914–25.
[296] Cai Y, Maeda Y, Cedzich A, et al. Identification and characterization of polycystin-2, the PKD2 gene product. JBiolChem 1999;274(40):28557–65.
[297] Hidaka S, Konecke V, Osten L, Witzgall R. PIGEA-14, a novel coiled-coil protein affecting the intracellular distribution of polycystin-2. J Biol Chem 2004;279(33):35009–16.
[298] Scheffers MS, Le H, van der BP, et al. Distinct subcellular expression of endogenous polycystin-2 in the plasma membrane and Golgi apparatus of MDCK cells. Hum Mol Genet 2002;11(1):59–67.
[299] Luo Y, Vassilev PM, Li X, Kawanabe Y, Zhou J. Native polycystin 2 functions as a plasma membrane Ca2 + -permeable cation channel in renal epithelia. Mol Cell Biol 2003;23 (7):2600–7.
[300] Witzgall R. Polycystin-2-an intracellular or plasma membrane channel? Naunyn Schmiedebergs Arch Pharmacol 2005;371 (4):342–7.
[301] Ma R, Li WP, Rundle D, Kong J, Akbarali HI, Tsiokas L. PKD2 functions as an epidermal growth factor-activated plasma membrane channel. Mol Cell Biol 2005;25(18): 8285–98.
[302] Grimm DH, Cai Y, Chauvet V, et al. Polycystin-1 distribution is modulated by polycystin-2 expression in mammalian cells. J Biol Chem 2003;278(38):36786–93.
[303] Geng L, Okuhara D, Yu Z, et al. Polycystin-2 traffics to cilia independently of polycystin-1 by using an N-terminal RVxP motif. J Cell Sci 2006;119(Pt 7):1383–95.
[304] Jenkins PM, Hurd TW, Zhang L, et al. Ciliary targeting of olfactory CNG channels requires the CNGB1b subunit and the kinesin-2 motor protein, KIF17. Curr Biol 2006;16(12): 1211–6.
[305] Nomura H, Turco AE, Pei Y, et al. Identification of PKDL, a novel polycystic kidney disease 2-like gene whose murine homologue is deleted in mice with kidney and retinal defects. J Biol Chem 1998;273(40):25967–73.
[306] Wu GQ, Hayashi T, Park JH, et al. Identification of the human PKD2-related cDNA, *PKD2L*: tissue-specific expression and linkage mapping on chromosome 10q25. Genomics 1998;54 (3):564–8.
[307] Neill AT, Moy GW, Vacquier VD. Polycystin-2 associates with the polycystin-1 homolog, suREJ3, and localizes to the acrosomal region of sea urchin spermatozoa. Mol Reprod Dev 2004;67(4):472–7.
[308] Watnick TJ, Jin Y, Matunis E, Kernan MJ, Montell C. A flagellar polycystin-2 homolog required for male fertility in Drosophila. Curr Biol 2003;13(24):2179–84.
[309] Gao Z, Ruden DM, Lu X. PKD2 cation channel is required for directional sperm movement and male fertility. Curr Biol 2003;13(24):2175–8.
[310] Kottgen M, Hofherr A, Li W, et al. Drosophila sperm swim backwards in the female reproductive tract and are activated via TRPP2 ion channels. PloS one 2011;6(5):e20031.
[311] Gao Z, Joseph E, Ruden DM, Lu X. Drosophila Pkd2 is haploid-insufficient for mediating optimal smooth muscle contractility. J Biol Chem 2004;279(14):14225–31.
[312] Anyatonwu GI, Estrada M, Tian X, Somlo S, Ehrlich BE. Regulation of ryanodine receptor-dependent calcium signaling by polycystin-2. Proc Natl Acad Sci 2007;104(15):6454–9.
[313] Obara T, Mangos S, Liu Y, et al. Polycystin-2 immunolocalization and function in zebrafish. J Am Soc Nephrol 2006;17 (10):2706–18.
[314] Schottenfeld J, Sullivan-Brown J, Burdine RD. Zebrafish curly up encodes a Pkd2 ortholog that restricts left-side-specific expression of southpaw. Development 2007;134(8):1605–15.
[315] Gonzalez-Perrett S, Kim K, Ibarra C, et al. Polycystin-2, the protein mutated in autosomal dominant polycystic kidney disease (ADPKD), is a Ca2 + -permeable nonselective cation channel. Proc Natl Acad Sci 2001;98(3):1182–7.
[316] Delmas P. Polycystins: polymodal receptor/ion-channel cellular sensors. Pflugers Arch 2005;451(1):264–76.
[317] Reynolds DM, Hayashi T, Cai Y, et al. Aberrant splicing in the PKD2 gene as a cause of polycysitic kidney disease. J Am Soc Nephrol 1999;10:2342–51.
[318] Cai Y, Anyatonwu G, Okuhara D, et al. Calcium dependence of polycystin-2 channel activity is modulated by phosphorylation at Ser812. J Biol Chem 2004;279(19):19987–95.
[319] Kottgen M, Benzing T, Simmen T, et al. Trafficking of TRPP2 by PACS proteins represents a novel mechanism of ion channel regulation. EMBO J 2005;24(4):705–16.
[320] Tsiokas L, Kim E, Arnould T, Sukhatme VP, Walz G. Homo- and heterodimeric interactions between the gene products of PKD1 and PKD2. Proc Natl Acad Sci USA 1997;94(13):6965–70.
[321] Somlo S. The PKD2 gene: structure, interactions, mutations, and inactivation. Adv Nephrol Necker Hosp 1999;29 (257–75):257–75.
[322] Ferreira FM, Oliveira LC, Germino GG, Onuchic JN, Onuchic LF. Macromolecular assembly of polycystin-2 intracytosolic C-terminal domain. Proc Natl Acad Sci U S A 2011;108 (24):9833–8.
[323] Tsiokas L, Arnould T, Zhu C, Kim E, Walz G, Sukhatme VP. Specific association of the gene product of PKD2 with the TRPC1 channel. Proc Natl Acad Sci USA 1999;96 (7):3934–9.
[324] Bai CX, Giamarchi A, Rodat-Despoix L, et al. Formation of a new receptor-operated channel by heteromeric assembly of TRPP2 and TRPC1 subunits. EMBO Rep 2008;9(5):472–9.
[325] Kottgen M, Buchholz B, Garcia-Gonzalez MA, et al. TRPP2 and TRPV4 form a polymodal sensory channel complex. J Cell Biol 2008;182(3):437–47.
[326] Li Y, Wright JM, Qian F, Germino GG, Guggino WB. Polycystin 2 interacts with type I inositol 1,4,5-trisphosphate receptor to modulate intracellular Ca2 + signaling. J Biol Chem 2005;280(50):41298–306.
[327] Li Y, Santoso NG, Yu S, Woodward OM, Qian F, Guggino WB. Polycystin-1 interacts with inositol 1,4,5-trisphosphate receptor to modulate intracellular Ca2 + signaling with implications for polycystic kidney disease. J Biol Chem 2009;284 (52):36431–41.

[328] Sammels E, Devogelaere B, Mekahli D, et al. Polycystin-2 activation by inositol 1,4,5-trisphosphate-induced Ca2+ release requires its direct association with the inositol 1,4,5-trisphosphate receptor in a signaling microdomain. J Biol Chem 2010;285(24):18794–805.
[329] Geng L, Boehmerle W, Maeda Y, et al. Syntaxin 5 regulates the endoplasmic reticulum channel-release properties of polycystin-2. Proc Natl Acad Sci USA 2008;105(41):15920–5.
[330] Plotnikova OV, Pugacheva EN, Golemis EA. Aurora A kinase activity influences calcium signaling in kidney cells. J Cell Biol 2011;193(6):1021–32.
[331] Gallagher AR, Cedzich A, Gretz N, Somlo S, Witzgall R. The polycystic kidney disease protein PKD2 interacts with Hax-1, a protein associated with the actin cytoskeleton. Proc Natl Acad Sci USA 2000;97(8):4017–22.
[332] Lehtonen S, Ora A, Olkkonen VM, et al. In vivo interaction of the adapter protein CD2-associated protein with the type 2 polycystic kidney disease protein, polycystin-2. J Biol Chem 2000;275(42):32888–93.
[333] Lehtonen S, Zhao F, Lehtonen E. CD2-associated protein directly interacts with the actin cytoskeleton. Am J Physiol Renal Physiol 2002;283(4):F734–43.
[334] Li Q, Dai Y, Guo L, et al. Polycystin-2 associates with tropomyosin-1, an actin microfilament component. J Mol Biol 2003;325 (5):949–62.
[335] Li Q, Shen PY, Wu G, Chen XZ. Polycystin-2 interacts with troponin I, an angiogenesis inhibitor. Biochemistry 2003;42 (2):450–7.
[336] Li Q, Montalbetti N, Shen PY, et al. Alpha-actinin associates with polycystin-2 and regulates its channel activity. Hum Mol Genet 2005;14(12):1587–603.
[337] Rundle DR, Gorbsky G, Tsiokas L. PKD2 interacts and colocalizes with mDia1 to mitotic spindles of dividing cells: role of mDia1 IN PKD2 localization to mitotic spindles. J Biol Chem 2004;279(28):29728–39.
[338] Guay-Woodford L. Autosomal recessive polycystic kidney disease. In: Flinter F, Saggar-Malik A, editors. The genetics of renal disease. Oxford: Oxford University Press; 2003. p. 239–51.
[339] Zerres K, Mucher G. Autosomal recessive polycystic kidney disease. J Mol Med 1998;76:303–9.
[340] Ward CJ, Hogan MC, Rossetti S, et al. The gene mutated in autosomal recessive polycystic kidney disease encodes a large, receptor-like protein. Nat Genet 2002;30(3):259–69.
[341] Onuchic LF, Furu L, Nagasawa Y, et al. PKHD1, the polycystic kidney and hepatic disease 1 gene, encodes a novel large protein containing multiple immunoglobulin-like plexin-transcription-factor domains and parallel beta-helix 1 repeats. Am J Hum Genet 2002;70(5):1305–17.
[342] Wang S, Zhang J, Nauli SM, et al. Fibrocystin/Polyductin, found in the same protein complex with polycystin-2, regulates calcium responses in kidney epithelia. Mol Cell Biol 2007.
[343] Wu Y, Dai XQ, Li Q, et al. Kinesin-2 mediates physical and functional interactions between polycystin-2 and fibrocystin. Hum Mol Genet 2006;15:3280–92.
[344] Peden EM, Barr MM. The KLP-6 kinesin is required for male mating behaviors and polycystin localization in Caenorhabditis elegans. Curr Biol 2005;15(5):394–404.
[345] Torres VE, Harris PC. Mechanisms of Disease: autosomal dominant and recessive polycystic kidney diseases. Nat Clin Pract Nephrol 2006;2(1):40–55 [quiz 55].
[346] Moon RT. Wnt/beta-catenin pathway. Sci STKE 2005;2005:271 [cm1].
[347] Fagotto F, Funayama N, Gluck U, Gumbiner BM. Binding to cadherins antagonizes the signaling activity of beta-catenin during axis formation in Xenopus. J Cell Biol 1996;132 (6):1105–14.
[348] Heasman J, Crawford A, Goldstone K, et al. Overexpression of cadherins and underexpression of beta-catenin inhibit dorsal mesoderm induction in early Xenopus embryos. Cell 1994;79 (5):791–803.
[349] Giles RH, van Es JH, Clevers H. Caught up in a Wnt storm: Wnt signaling in cancer. Biochim Biophys Acta 2003;1653 (1):1–24.
[350] Brembeck FH, Rosario M, Birchmeier W. Balancing cell adhesion and Wnt signaling, the key role of beta-catenin. Curr Opin Genet Dev 2006;16(1):51–9.
[351] Gottardi CJ, Gumbiner BM. Adhesion signaling: how beta-catenin interacts with its partners. Curr Biol 2001;11(19): R792–4.
[352] Yap AS, Brieher WM, Gumbiner BM. Molecular and functional analysis of cadherin-based adherens junctions. Annu Rev Cell Dev Biol 1997;13:119–46.
[353] Yeaman C, Grindstaff KK, Nelson WJ. New perspectives on mechanisms involved in generating epithelial cell polarity. Physiol Rev 1999;79(1):73–98.
[354] Karim R, Tse G, Putti T, Scolyer R, Lee S. The significance of the Wnt pathway in the pathology of human cancers. Pathology 2004;36(2):120–8.
[355] Hart MJ, de los Santos R, Albert IN, Rubinfeld B, Polakis P. Downregulation of beta-catenin by human Axin and its association with the APC tumor suppressor, beta-catenin and GSK3 beta. Curr Biol 1998;8(10):573–81.
[356] Tada M, Concha ML, Heisenberg CP. Non-canonical Wnt signalling and regulation of gastrulation movements. Semin Cell Dev Biol 2002;13(3):251–60.
[357] Fanto M, McNeill H. Planar polarity from flies to vertebrates. J Cell Sci 2004;117(Pt 4):527–33.
[358] Qian CN, Knol J, Igarashi P, et al. Cystic renal neoplasia following conditional inactivation of apc in mouse renal tubular epithelium. J Biol Chem 2005;280(5):3938–45.
[359] Saadi-Kheddouci S, Berrebi D, Romagnolo B, et al. Early development of polycystic kidney disease in transgenic mice expressing an activated mutant of the beta-catenin gene. Oncogene 2001;20(42):5972–81.
[360] Geng L, Burrow CR, Li HP, Wilson PD. Modification of the composition of polycystin-1 multiprotein complexes by calcium and tyrosine phosphorylation. Biochim Biophys Acta 2000;1535(1):21–35.
[361] Kim E, Arnould T, Sellin LK, et al. The polycystic kidney disease 1 gene product modulates Wnt signaling. J Biol Chem 1999;274(8):4947–53.
[362] Le NH, van der Bent P, Huls G, et al. Aberrant polycystin-1 expression results in modification of activator protein-1 activity, whereas Wnt signaling remains unaffected. J Biol Chem 2004;279(26):27472–81.
[363] Lal M, Song X, Pluznick J, et al. Polycystin-1 C-terminal tail associates with beta-catenin and inhibits canonical Wnt signaling. Hum Mol Genet 2008;17(20):3105–17.
[364] Simons M, Gloy J, Ganner A, et al. Inversin, the gene product mutated in nephronophthisis type II, functions as a molecular switch between Wnt signaling pathways. Nat Genet 2005;37 (5):537–43.
[365] Merrick D, Chapin H, Baggs JE, et al. The gamma-Secretase cleavage product of polycystin-1 regulates TCF and CHOP-Mediated transcriptional activation through a p300-Dependent mechanism. Dev Cell 2012;22(1):197–210.

[366] Nishio S, Tian X, Gallagher AR, et al. Loss of oriented cell division does not initiate cyst formation. J Am Soc Nephrol 2010;21 (2):295–302.
[367] Miller MM, Iglesias DM, Zhang Z, et al. T-cell factor/beta-catenin activity is suppressed in two different models of autosomal dominant polycystic kidney disease. Kidney Int 2011;80 (2):146–53.
[368] Somlo S, Ehrlich B. Human disease: calcium signaling in polycystic kidney disease. Curr Biol 2001;11(9):R356–60.
[369] Praetorius HA, Frokiaer J, Nielsen S, Spring KR. Bending the primary cilium opens Ca2 + -sensitive intermediate-conductance K + channels in MDCK cells. J Membr Biol 2003;191(3):193–200.
[370] Sharif-Naeini R, Folgering JH, Bichet D, et al. Polycystin-1 and -2 dosage regulates pressure sensing. Cell 2009;139(3): 587–96.
[371] Bai CX, Kim S, Li WP, Streets AJ, Ong AC, Tsiokas L. Activation of TRPP2 through mDia1-dependent voltage gating. EMBO J 2008;27(9):1345–56.
[372] Hooper KM, Boletta A, Germino GG, Hu Q, Ziegelstein RC, Sutters M. Expression of polycystin-1 enhances endoplasmic reticulum calcium uptake and decreases capacitative calcium entry in ATP-stimulated MDCK cells. Am J Physiol Renal Physiol 2005;289(3):F521–30.
[373] Riordan JR, Forbush 3rd B, Hanrahan JW. The molecular basis of chloride transport in shark rectal gland. J Exp Biol 1994;196:405–18.
[374] Calvet JP, Grantham JJ. The genetics and physiology of polycystic kidney disease. Semin Nephrol 2001;21 (2):107–23.
[375] Belibi FA, Reif G, Wallace DP, et al. Cyclic AMP promotes growth and secretion in human polycystic kidney epithelial cells. Kidney Int 2004;66(3):964–73.
[376] Yamaguchi T, Pelling JC, Ramaswamy NT, et al. cAMP stimulates the in vitro proliferation of renal cyst epithelial cells by activating the extracellular signal-regulated kinase pathway. Kidney Int 2000;57(4):1460–71.
[377] Brill SR, Ross KE, Davidow CJ, Ye M, Grantham JJ, Caplan MJ. Immunolocalization of ion transport proteins in human autosomal dominant polycystic kidney epithelial cells. Proc Natl Acad Sci U S A 1996;93(19):10206–11.
[378] Sullivan LP, Wallace DP, Grantham JJ. Epithelial transport in polycystic kidney disease. Physiol Rev 1998;78(4):1165–91.
[379] Sheppard DN, Welsh MJ. Structure and function of the CFTR chloride channel. Physiol Rev 1999;79(1 Suppl):S23–45.
[380] Yang B, Sonawane ND, Zhao D, Somlo S, Verkman AS. Small-molecule CFTR inhibitors slow cyst growth in polycystic kidney disease. J Am Soc Nephrol 2008;19(7):1300–10.
[381] O'Sullivan D, Torres V, Gabow P, Thibodeau S, King B, Bergstralh E. Cystic fibrosis and the phenotypic expression of autosomal dominant polycystic kidney disease. Am J Kid Dis 1998;32(6):976–83.
[382] Xu N, Glockner JF, Rossetti S, Babovich-Vuksanovic D, Harris PC, Torres VE. Autosomal dominant polycystic kidney disease coexisting with cystic fibrosis. J Nephrol 2006;19(4):529–34.
[383] Persu A, Devuyst O, Lannoy N, et al. CF gene and cystic fibrosis transmembrane conductance regulator expression in autosomal dominant polycystic kidney disease. J Am Soc Nephrol 2000;11(12):2285–96.
[384] Yamaguchi T, Nagao S, Wallace DP, et al. Cyclic AMP activates B-Raf and ERK in cyst epithelial cells from autosomal-dominant polycystic kidneys. Kidney Int 2003;63 (6):1983–94.
[385] Choi YH, Suzuki A, Hajarnis S, et al. Polycystin-2 and phosphodiesterase 4C are components of a ciliary A-kinase anchoring protein complex that is disrupted in cystic kidney diseases. Proc Natl Acad Sci U S A 2011;108(26):10679–84.
[386] Gattone 2nd VH, Wang X, Harris PC, Torres VE. Inhibition of renal cystic disease development and progression by a vasopressin V2 receptor antagonist. Nat Med 2003;9(10): 1323–6.
[387] Parnell SC, Magenheimer BS, Maser RL, et al. The polycystic kidney disease-1 protein, polycystin-1, binds and activates heterotrimeric G-proteins in vitro. Biochem Biophys Res Commun 1998;251(2):625–31.
[388] Puri S, Magenheimer BS, Maser RL, et al. Polycystin-1 activates the calcineurin/NFAT (nuclear factor of activated T-cells) signaling pathway. J Biol Chem 2004;279 (53):55455–64.
[389] Horsley V, Pavlath GK. NFAT: ubiquitous regulator of cell differentiation and adaptation. J Cell Biol 2002;156(5):771–4.
[390] Yu W, Kong T, Beaudry S, et al. Polycystin-1 protein level determines activity of the Galpha12/JNK apoptosis pathway. J Biol Chem 2010;285(14):10243–51.
[391] Yu W, Ritchie BJ, Su X, Zhou J, Meigs TE, Denker BM. Identification of polycystin-1 and Galpha12 binding regions necessary for regulation of apoptosis. Cell Signal 2011;23 (1):213–21.
[392] Kolch W. Coordinating ERK/MAPK signalling through scaffolds and inhibitors. Nat Rev Mol Cell Biol 2005;6(11):827–37.
[393] Ishibe S, Joly D, Zhu X, Cantley LG. Phosphorylation-dependent paxillin-ERK association mediates hepatocyte growth factor-stimulated epithelial morphogenesis. Mol Cell 2003;12(5):1275–85.
[394] Joly D, Ishibe S, Nickel C, Yu Z, Somlo S, Cantley LG. The polycystin 1-C-terminal fragment stimulates ERK-dependent spreading of renal epithelial cells. J Biol Chem 2006;281 (36):26329–39.
[395] Nagao S, Yamaguchi T, Kusaka M, et al. Renal activation of extracellular signal-regulated kinase in rats with autosomal-dominant polycystic kidney disease. Kidney Int 2003;63 (2):427–37.
[396] Yamaguchi T, Wallace DP, Magenheimer BS, Hempson SJ, Grantham JJ, Calvet JP. Calcium restriction allows cAMP activation of the B-Raf/ERK pathway, switching cells to a cAMP-dependent growth-stimulated phenotype. J Biol Chem 2004;279(39):40419–30.
[397] Grimm DH, Karihaloo A, Cai Y, Somlo S, Cantley LG, Caplan MJ. Polycystin-2 regulates proliferation and branching morphogenesis in kidney epithelial cells. J Biol Chem 2006;281 (1):137–44.
[398] Omori S, Hida M, Fujita H, et al. Extracellular signal-regulated kinase inhibition slows disease progression in mice with polycystic kidney disease. J Am Soc Nephrol 2006;17(6):1604–14.
[399] Sarbassov DD, Ali SM, Sabatini DM. Growing roles for the mTOR pathway. Curr Opin Cell Biol 2005;17(6):596–603.
[400] Mamane Y, Petroulakis E, LeBacquer O, Sonenberg N. mTOR translation initiation and cancer. Oncogene 2006;25(48): 6416–22.
[401] Astrinidis A, Henske EP. Tuberous sclerosis complex: linking growth and energy signaling pathways with human disease. Oncogene 2005;24(50):7475–81.
[402] Kleymenova E, Ibraghimov-Beskrovnaya O, Kugoh H, et al. Tuberin-dependent membrane localization of polycystin-1: a functional link between polycystic kidney disease and the TSC2 tumor suppressor gene. Mol Cell 2001;7(4):823–32.
[403] Ma L, Chen Z, Erdjument-Bromage H, Tempst P, Pandolfi PP. Phosphorylation and functional inactivation of TSC2 by Erk implications for tuberous sclerosis and cancer pathogenesis. Cell 2005;121(2):179–93.

[404] Distefano G, Boca M, Rowe I, et al. Polycystin-1 regulates extracellular signal-regulated kinase-dependent phosphorylation of tuberin to control cell size through mTOR and its downstream effectors S6K and 4EBP1. Mol Cell Biol 2009;29 (9):2359–71.
[405] Dere R, Wilson PD, Sandford RN, Walker CL. Carboxy terminal tail of polycystin-1 regulates localization of TSC2 to repress mTOR. PloS one 2010;5(2):e9239.
[406] Tao Y, Kim J, Schrier RW, Edelstein CL. Rapamycin markedly slows disease progression in a rat model of polycystic kidney disease. J Am Soc Nephrol 2005;16(1):46–51.
[407] Wahl PR, Serra AL, Le Hir M, Molle KD, Hall MN, Wuthrich RP. Inhibition of mTOR with sirolimus slows disease progression in Han:SPRD rats with autosomal dominant polycystic kidney disease (ADPKD). Nephrol Dial Transplant 2006;21(3): 598–604.
[408] Shillingford JM, Piontek KB, Germino GG, Weimbs T. Rapamycin Ameliorates PKD Resulting from Conditional Inactivation of Pkd1. J Am Soc Nephrol 2010;21(3):489–97.
[409] Matsumura ME, Lobe DR, McNamara CA. Contribution of the helix-loop-helix factor Id2 to regulation of vascular smooth muscle cell proliferation. J Biol Chem 2002;277(9): 7293–7.
[410] Li X, Luo Y, Starremans PG, McNamara CA, Pei Y, Zhou J. Polycystin-1 and polycystin-2 regulate the cell cycle through the helix-loop-helix inhibitor Id2. Nat Cell Biol 2005;7 (12):1202–12.
[411] Liang GQ, Yang JW, Wang ZC, Li Q, Tang Y, Chen XZ. Polycystin-2 down-regulates cell proliferation via promoting PERK-dependent phosphorylation of eIF2 alpha. Hum Mol Genet 2008;17(20):3254–62.
[412] Quarmby LM, Parker JD. Cilia and the cell cycle? J Cell Biol 2005;169(5):707–10.
[413] Mahjoub MR, Qasim Rasi M, Quarmby LMA. NIMA-related kinase, Fa2p, localizes to a novel site in the proximal cilia of Chlamydomonas and mouse kidney cells. Mol Biol Cell 2004;15(11):5172–86.
[414] Mahjoub MR, Trapp ML, Quarmby LM. NIMA-related kinases defective in murine models of polycystic kidney diseases localize to primary cilia and centrosomes. J Am Soc Nephrol 2005;16(12):3485–9.
[415] Liu S, Lu W, Obara T, et al. A defect in a novel Nek-family kinase causes cystic kidney disease in the mouse and in zebrafish. Development 2002;129(24):5839–46.
[416] Schroeter EH, Kisslinger JA, Kopan R. Notch-1 signalling requires ligand-induced proteolytic release of intracellular domain. Nature 1998;393(6683):382–6.
[417] Mumm JS, Schroeter EH, Saxena MT, et al. A ligand-induced extracellular cleavage regulates gamma-secretase-like proteolytic activation of Notch1. Mol Cell 2000;5 (2):197–206.
[418] Brown MS, Ye J, Rawson RB, Goldstein JL. Regulated intramembrane proteolysis: a control mechanism conserved from bacteria to humans. Cell 2000;100(4):391–8.
[419] Hiesberger T, Gourley E, Erickson A, et al. Proteolytic cleavage and nuclear translocation of fibrocystin is regulated by intracellular Ca2 + and activation of protein kinase C. J Biol Chem 2006;281(45):34357–64.
[420] Li J, Sutter C, Parker D, Blauwkamp T, Fang M, Cadigan K. CBP/p300 are bimodal regulators of Wnt signaling. EMBO J 2007;26(9):2284–94.
[421] Ohoka N, Hattori T, Kitagawa M, Onozaki K, Hayashi H. Critical and functional regulation of CHOP (C/EBP homologous protein) through the N-terminal portion. J Biol Chem 2007;282(49):35687–94.
[422] Oyadomari S, Mori M. Roles of CHOP/GADD153 in endoplasmic reticulum stress. Cell Death Differ 2004;11(4): 381–9.
[423] Lanoix J, D'Agati V, Szabolcs M, Trudel M. Dysregulation of cellular proliferation and apoptosis mediates human autosomal dominant polycystic kidney disease (ADPKD). Oncogene 1996;13(6):1153–60.
[424] Takiar V, Caplan MJ. Polycystic kidney disease: pathogenesis and potential therapies. Biochim Biophys Acta 2010.
[425] Chapin HC, Caplan MJ. The cell biology of polycystic kidney disease. J Cell Biol 2010;191(4):701–10.
[426] Goilav B. Apoptosis in polycystic kidney disease. Biochim Biophys Acta 2011;1812(10):1272–80.
[427] Olsan EE, Mukherjee S, Wulkersdorfer B, et al. Signal transducer and activator of transcription-6 (STAT6) inhibition suppresses renal cyst growth in polycystic kidney disease. Proc Natl Acad Sci U S A 2011;108(44): 18067–72.
[428] Talbot JJ, Shillingford JM, Vasanth S, et al. Polycystin-1 regulates STAT activity by a dual mechanism. Proc Natl Acad Sci U S A 2011;108(19):7985–90.
[429] Bertuccio CA, Chapin HC, Cai Y, et al. Polycystin-1 C-terminal cleavage is modulated by polycystin-2 expression. J Biol Chem 2009;284(31):21011–26.
[430] Leuenroth SJ, Bencivenga N, Igarashi P, Somlo S, Crews CM. Triptolide reduces cystogenesis in a model of ADPKD. J Am Soc Nephrol 2008;19(9):1659–62.
[431] Leuenroth SJ, Okuhara D, Shotwell JD, et al. Triptolide is a traditional Chinese medicine-derived inhibitor of polycystic kidney disease. Proc Natl Acad Sci U S A 2007;104(11):4389–94.
[432] Gradilone SA, Masyuk TV, Huang BQ, et al. Activation of Trpv4 reduces the hyperproliferative phenotype of cystic cholangiocytes from an animal model of ARPKD. Gastroenterology 2010;139(1):304–314 e302.
[433] Gattone 2nd VH, Chen NX, Sinders RM, et al. Calcimimetic inhibits late-stage cyst growth in ADPKD. J Am Soc Nephrol 2009;20(7):1527–32.
[434] Chen NX, Moe SM, Eggleston-Gulyas T, et al. Calcimimetics inhibit renal pathology in rodent nephronophthisis. Kidney Int 2011;80(6):612–9.
[435] Wang X, Harris PC, Somlo S, Batlle D, Torres VE. Effect of calcium-sensing receptor activation in models of autosomal recessive or dominant polycystic kidney disease. Nephrol Dial Transplant 2009;24(2):526–34.
[436] Torres VE. Type II calcimimetics and polycystic kidney disease: unanswered questions. J Am Soc Nephrol 2009;20 (7):1421–5.
[437] Gattone VH, Maser RL, Tian C, Rosenberg JM, Branden MG. Developmental expression of urine concentration-associated genes and their altered expression in murine infantile-type polycystic kidney disease. Develop Gen 1999;24:309–18.
[438] Torres VE, Wang X, Qian Q, Somlo S, Harris PC, Gattone VH. Effective treatment of an orthologous model of autosomal dominant polycystic kidney disease. Nature Med 2004;10:363–4.
[439] Wang X, Gattone II VH, Harris PC, Torres VE. Effectiveness of vasopressin V2 receptor antagonists OPC-31260 and OPC-41061 on polycystic kidney disease development in the PCK rat. J Am Soc Nephrol 2005;16:846–51.
[440] Nagao S, kazuhiro N, Katsuyama M, et al. Increased water intake decreases progression of polycystic kidney disease in the pck rat. J Am Soc Nephrol 2006;17:228–35.
[441] Wang X, Wu Y, Ward CJ, Harris PC, Torres VE. Vasopressin directly regulates cyst growth in polycystic kidney disease. J Am Soc Nephrol 2008;19(1):102–8.

[442] Higashihara E, Torres VE, Chapman AB, et al. Tolvaptan in autosomal dominant polycystic kidney disease: three years' experience. Clin J Am Soc Nephrol 2011;6 (10):2499–507.
[443] Torres VE, Meijer E, Bae KT, et al. Rationale and design of the TEMPO (Tolvaptan efficacy and safety in management of autosomal dominant polycystic kidney disease and its outcomes) 3-4 study. Am J Kidney Dis 2011;57(5):692–9.
[444] Masyuk TV, Masyuk AI, Torres VE, Harris PC, LaRusso NF. Octreotide inhibits hepatic cystogenesis in a rodent model of polycystic liver disease by reducing cholangiocyte adenosine 3',5'-cyclic monophosphate. Gastroenterology 2007;132 (3):1104–16.
[445] Ruggenenti P, Remuzzi A, Ondei P, et al. Safety and efficacy of long-acting somatostatin treatment in autosomal dominant polcysytic kidney disease. Kidney Int 2005;68:206–16.
[446] van Keimpema L, Nevens F, Vanslembrouck R, et al. Lanreotide reduces the volume of polycystic liver: a randomized, double-blind, placebo-controlled trial. Gastroenterology 2009;137(5):1661–8 [e1661-1662]
[447] Hogan MC, Norby SM. Evaluation and management of pain in autosomal dominant polycystic kidney disease [3 presented at Advances in chronic kidney disease] Adv Chronic Kidney Dis 2010.
[448] Caroli A, Antiga L, Cafaro M, et al. Reducing polycystic liver volume in ADPKD: effects of somatostatin analogue octreotide. Clin J Am Soc Nephrol 2010;5(5):783–9.
[449] Tradtrantip L, Yangthara B, Padmawar P, Morrison C, Verkman AS. Thiophenecarboxylate suppressor of cyclic nucleotides discovered in a small-molecule screen blocks toxin-induced intestinal fluid secretion. Mol Pharmacol 2009;75(1):134–42.
[450] Magenheimer St BS, John PL, Isom KS, et al. Early embryonic renal tubules of wild-type and polycystic kidney disease kidneys respond to cAMP stimulation with cystic fibrosis transmembrane conductance regulator/Na(+),K(+),2Cl(-) Cotransporter-dependent cystic dilation. J Am Soc Nephrol 2006;17(12):3424–37.
[451] Takiar V, Nishio S, Seo-Mayer P, et al. Activating AMP-activated protein kinase (AMPK) slows renal cystogenesis. Proc Natl Acad Sci U S A 2011;108(6):2462–7.
[452] Nofziger C, Brown KK, Smith CD, et al. PPARgamma agonists inhibit vasopressin-mediated anion transport in the MDCK-C7 cell line. Am J Physiol Renal Physiol 2009;297(1):F55–62.
[453] Blazer-Yost BL, Haydon J, Eggleston-Gulyas T, et al. Pioglitazone Attenuates Cystic Burden in the PCK Rodent Model of Polycystic Kidney Disease. PPAR Res 2010;:274376.
[454] Albaqumi M, Srivastava S, Li Z, et al. KCa3.1 potassium channels are critical for cAMP-dependent chloride secretion and cyst growth in autosomal-dominant polycystic kidney disease. Kidney Int 2008;74(6):740–9.
[455] Alper SL. Let's look at cysts from both sides now. Kidney Int 2008;74(6):699–702.
[456] Sweeney Jr. WE, Avner ED. Functional activity of epidermal growth factor receptors in autosomal recessive polycystic kidney disease. Am J Physiol 1998;275(3 Pt 2):F387–94.
[457] Sweeney Jr. WE, Chen Y, Nakanish K, Frost P, Avner ED. Treatment of polycystic kidney disease with a novel tyrosine kinase inhibitor. Kidney Int 2000;57:33–40.
[458] Torres VE, Sweeney Jr. WE, Wang X, et al. Epidermal growth factor receptor tyrosine kinase inhibition is not protective in PCK rats. Kidney Int 2004;66(5):1766–73.
[459] Sweeney Jr. WE, von Vigier RO, Frost P, Avner ED. Src inhibition ameliorates polycystic kidney disease. J Am Soc Nephrol 2008;19(7):1331–41.
[460] Tao Y, Kim J, Yin Y, et al. VEGF receptor inhibition slows the progression of polycystic kidney disease. Kidney Int 2007;72 (11):1358–66.
[461] Amura CR, Brodsky KS, Groff R, Gattone VH, Voelkel NF, Doctor RB. VEGF receptor inhibition blocks liver cyst growth in pkd2(WS25/-) mice. Am J Physiol Cell Physiol 2007;293(1): C419–28.
[462] Spirli C, Okolicsanyi S, Fiorotto R, et al. ERK1/2-dependent vascular endothelial growth factor signaling sustains cyst growth in polycystin-2 defective mice. Gastroenterology 2010;138(1):360–71.
[463] Raina S, Honer M, Kramer SD, et al. Anti-VEGF antibody treatment accelerates polycystic kidney disease. Am J Physiol Renal Physiol 2011;301(4):F773–83.
[464] McGrath-Morrow S, Cho C, Molls R, et al. VEGF receptor 2 blockade leads to renal cyst formation in mice. Kidney Int 2006;69(10):1741–8.
[465] Elliott J, Zheleznova NN, Wilson PD. c-Src inactivation reduces renal epithelial cell-matrix adhesion, proliferation, and cyst formation. Am J Physiol Cell Physiol 2011;301(2):C522–9.
[466] Buchholz B, Klanke B, Schley G, et al. The Raf kinase inhibitor PLX5568 slows cyst proliferation in rat polycystic kidney disease but promotes renal and hepatic fibrosis. Nephrol Dial Transplant 2011;26(11):3458–65.
[467] Yamaguchi T, Reif GA, Calvet JP, Wallace DP. Sorafenib inhibits cAMP-dependent ERK activation, cell proliferation, and in vitro cyst growth of human ADPKD cyst epithelial cells. Am J Physiol Renal Physiol 2010;299(5):F944–51.
[468] Omori S, Hida M, Fujita H, et al. Extracellular signal-regulated kinase inhibition slows disease progression in mice with polycystic kidney disease. J Am Soc Nephrol 2006;17(6):1604–14.
[469] Sampson JR, Maheshwar MM, Aspinwall R, et al. Renal cystic disease in tuberous sclerosis: role of the polycystic kidney disease 1 gene. Am J Hum Genet 1997;61:843–51.
[470] Wu M, Wahl PR, Le Hir M, Wackerle-Men Y, Wuthrich RP, Serra AL. Everolimus retards cyst growth and preserves kidney function in a rodent model for polycystic kidney disease. Kidney Blood Press Res 2007;30(4):253–9.
[471] Wu M, Arcaro A, Varga Z, et al. Pulse mTOR inhibitor treatment effectively controls cyst growth but leads to severe parenchymal and glomerular hypertrophy in rat polycystic kidney disease. Am J Physiol Renal Physiol 2009;297(6):F1597–605.
[472] Zafar I, Belibi FA, He Z, Edelstein CL. Long-term rapamycin therapy in the Han:SPRD rat model of polycystic kidney disease (PKD). Nephrol Dial Transplant 2009;24(8):2349–53.
[473] Renken C, Fischer DC, Kundt G, Gretz N, Haffner D. Inhibition of mTOR with sirolimus does not attenuate progression of liver and kidney disease in PCK rats. Nephrol Dial Transplant 2011;26(1):92–100.
[474] Gattone 2nd VH, Sinders RM, Hornberger TA, Robling AG. Late progression of renal pathology and cyst enlargement is reduced by rapamycin in a mouse model of nephronophthisis. Kidney Int 2009;76(2):178–82.
[475] Spirli C, Okolicsanyi S, Fiorotto R, et al. Mammalian target of rapamycin regulates vascular endothelial growth factor-dependent liver cyst growth in polycystin-2-defective mice. Hepatology 2010;51(5):1778–88.
[476] Canaud G, Knebelmann B, Harris PC, et al. Therapeutic mTOR inhibition in autosomal dominant polycystic kidney disease: what is the appropriate serum level? Am J Transplant 2010;10 (7):1701–6.
[477] Serra AL, Poster D, Kistler AD, et al. Sirolimus and kidney growth in autosomal dominant polycystic kidney disease. N Engl J Med 2010;363(9):820–9.

[478] Perico N, Antiga L, Caroli A, et al. Sirolimus therapy to halt the progression of ADPKD. J Am Soc Nephrol 2010;21(6):1031–40.
[479] Walz G, Budde K, Mannaa M, et al. Everolimus in patients with autosomal dominant polycystic kidney disease. N Engl J Med 2010;363(9):830–40.
[480] Gardner Jr. K, Burnside J, Elzinga L, Locksley R. Cytokines in fluids from polycystic kidneys. Kidney Int 1991;39:718–24.
[481] Nichols MT, Gidey E, Matzakos T, et al. Secretion of cytokines and growth factors into autosomal dominant polycystic kidney disease liver cyst fluid. Hepatology 2004;40(4):836–46.
[482] Zheng D, Wolfe M, Cowley Jr. BD, Wallace DP, Yamaguchi T, Grantham JJ. Urinary excretion of monocyte chemoattractant protein-1 in autosomal dominant polycystic kidney disease. J Am Soc Nephrol 2003;14(10):2588–95.
[483] Li X, Magenheimer BS, Xia S, et al. A tumor necrosis factor-alpha-mediated pathway promoting autosomal dominant polycystic kidney disease. Nat Med 2008;14(8):863–8.
[484] Dell KM, Nemo R, Sweeney Jr. WE, Levin JI, Frost P, Avner ED. A novel inhibitor of tumor necrosis factor-alpha converting enzyme ameliorates polycystic kidney disease. Kidney Int 2001;60(4):1240–8.
[485] Lee DF, Kuo HP, Chen CT, et al. IKKbeta suppression of TSC1 function links the mTOR pathway with insulin resistance. Int J Mol Med 2008;22(5):633–8.
[486] Elberg G, Elberg D, Lewis TV, et al. EP2 receptor mediates PGE2-induced cystogenesis of human renal epithelial cells. Am J Physiol Renal Physiol 2007;293(5):F1622–32.
[487] Sankaran D, Bankovic-Calic N, Ogborn MR, Crow G, Aukema HM. Selective COX-2 inhibition markedly slows disease progression and attenuates altered prostanoid production in Han:SPRD-cy rats with inherited kidney disease. Am J Physiol Renal Physiol 2007;293(3):F821–30.
[488] Park F, Sweeney WE, Jia G, Roman RJ, Avner ED. 20-HETE mediates proliferation of renal epithelial cells in polycystic kidney disease. J Am Soc Nephrol 2008;19(10):1929–39.
[489] Boehlke C, Kotsis F, Patel V, et al. Primary cilia regulate mTORC1 activity and cell size through Lkb1. Nat Cell Biol 2010;12(11):1115–22.
[490] Takakura A, Nelson EA, Haque N, et al. Pyrimethamine inhibits adult polycystic kidney disease by modulating STAT signaling pathways. Hum Mol Genet 2011;20(21):4143–54.
[491] Gao J, Zhou H, Lei T, et al. Curcumin inhibits renal cyst formation and enlargement in vitro by regulating intracellular signaling pathways. Eur J Pharmacol 2011;654(1):92–9.
[492] Leonhard WN, van der Wal A, Novalic Z, et al. Curcumin inhibits cystogenesis by simultaneous interference of multiple signaling pathways: in vivo evidence from a Pkd1-deletion model. Am J Physiol Renal Physiol 2011;300(5):F1193–202.
[493] Scatliff CE, Bankovic-Calic N, Ogborn MR, Aukema HM. Effects of dietary conjugated linoleic acid in advanced experimental polycystic kidney disease. Nephron Exp Nephrol 2008;110(2):e44–8.
[494] Altierei P, Caridi G, Chiesa V, Ponzoni M, Ghiggeri G. N-(4-hydroxyphenyl) retinamide inhibits cystogenesis by polycystic epithelial cell line in vitro. Life Sci 1999;64(22):259–65.
[495] Dai B, Liu Y, Mei C, et al. Rosiglitazone attenuates development of polycystic kidney disease and prolongs survival in Han:SPRD rats. Clin Sci 2010;119(8):323–33.
[496] Yoshihara D, Kurahashi H, Morita M, et al. PPAR-gamma agonist ameliorates kidney and liver disease in an orthologous rat model of human autosomal recessive polycystic kidney disease. Am J Physiol Renal Physiol 2011;300(2):F465–74.
[497] Raphael KL, Strait KA, Stricklett PK, et al. Effect of pioglitazone on survival and renal function in a mouse model of polycystic kidney disease. Am J Nephrol 2009;30(5):468–73.
[498] Van Bodegom D, Saifudeen Z, Dipp S, et al. The polycystic kidney disease-1 gene is a target for p53-mediated transcriptional repression. J Biol Chem 2006;281(42):31234–44.
[499] Xia S, Li X, Johnson T, Seidel C, Wallace DP, Li R. Polycystin-dependent fluid flow sensing targets histone deacetylase 5 to prevent the development of renal cysts. Development 2010;137(7):1075–84.
[500] Li X. Epigenetics and autosomal dominant polycystic kidney disease. Biochim Biophys Acta 2011;1812(10):1213–8.
[501] Cao Y, Semanchik N, Lee SH, et al. Chemical modifier screen identifies HDAC inhibitors as suppressors of PKD models. Proc Natl Acad Sci USA 2009;106(51):21819–24.
[502] Bukanov N, Smith LA, Klinger K, Ledbetter SR, Ibraghimov-Beskrovnaya O. Long lasting arrest of murine polycystic kidney disease with CDK inhibitor R-Roscovitine. Nature 2006.
[503] Park JY, Schutzer WE, Lindsley JN, et al. p21 is decreased in polycystic kidney disease and leads to increased epithelial cell cycle progression: roscovitine augments p21 levels. BMC Nephrol 2007;8:12.
[504] Lee SO, Masyuk T, Splinter P, et al. MicroRNA15a modulates expression of the cell-cycle regulator Cdc25A and affects hepatic cystogenesis in a rat model of polycystic kidney disease. J Clin Invest 2008;118(11):3714–24.
[505] Natoli TA, Smith LA, Rogers KA, et al. Inhibition of glucosylceramide accumulation results in effective blockade of polycystic kidney disease in mouse models. Nat Med 2010;16(7):788–92.

CHAPTER

81

Renal Physiology and Disease in Pregnancy

Kirk P. Conrad and S. Ananth Karumanchi

The urinary system, volume homeostasis, body fluid composition, and osmoregulation are all profoundly altered in normal pregnancy. There are also marked changes in systemic hemodynamics involving cardiac output and blood pressure. Knowledge of these physiological adaptations permits earlier detection and facilitates management of renal disease and hypertension during pregnancy. In the fifth revision of this chapter, the authors revise and update the previous edition coauthored with Marshall Lindheimer, former senior and an original author of the chapter. As before, space limitations lead us to refer on occasion to previous editions of the book especially for details from the older literature.

ANATOMICAL CHANGES

Information about renal anatomy during normal pregnancy is limited, but it appears that the kidney becomes larger. Autopsy studies are obviously scarce, but in one unique and large series[1] combined kidney weights of normotensive women dying during or shortly after gestation were higher than normal values for nonpregnant individuals. However, details about the cause of death, which could have affected kidney weights, were limited. Renal weight also increases during pregnancy in rats, the evidence suggesting that this is due to increased water content, as renal dry weights are similar in gravid and nonpregnant rats.[2,3] In one study in which renal biopsy specimens were obtained from normal gravidas (usually during cesarean section), the light microscopic appearance was described as similar to that in nonpregnant subjects [cited in[4]]. But data from both autopsy material[1] and renal biopsies performed in the last trimester on 12 normal gravidas[5] suggested that glomerular size, but not number of cells, may be increased in pregnant women. Detailed descriptions of the kidneys of normal pregnant women or animals using electron microscopic or immunofluorescence techniques are not available.

Starting in the first trimester, overall renal dimensions—length, width, and thickness—increase and peak during the third trimester at 1 cm above prepregnant values.[6] These changes, documented by ultrasonography and pyelography, translate into an overall increase in renal volume of ~50% by the end of pregnancy[6] (Figure 81.1). Both renal parenchymal and pelvicalyceal volumes enlarge, although the latter typically begins to rise somewhat later during the second trimester. Renal parenchymal volume enlarges most likely due to increases in both vascular and interstitial fluid volume; there is little evidence for cellular hyperplasia or hypertrophy.[7] Renal size and volume estimated by ultrasonography or pyelography in the immediate puerperium are also increased.[4,6] Of interest, roentgenograms performed shortly after delivery and repeated six months later demonstrated that renal length had decreased ~1 cm between the two exams [cited in[4]]. The well-documented dilation of the upper ureter, renal pelvis, and major and minor calyces, which affects the vast majority of gravidas at term, is particularly prevalent on the right side.[7–13] Consequently, urinary stasis and hydronephrosis (either with or without calyceal clubbing) are common physiological occurrences in human pregnancy[14] (Figure 81.2), and usually do not reflect pathologic obstruction. Although the more severe signs of this physiological obstruction resolve at least by 6 weeks after delivery, evidence for urinary stasis persists in many women at 12 weeks postpartum.

Seldin and Giebisch's The Kidney, Fifth Edition.
DOI: http://dx.doi.org/10.1016/B978-0-12-381462-3.00081-1

© 2013 Elsevier Inc. All rights reserved.

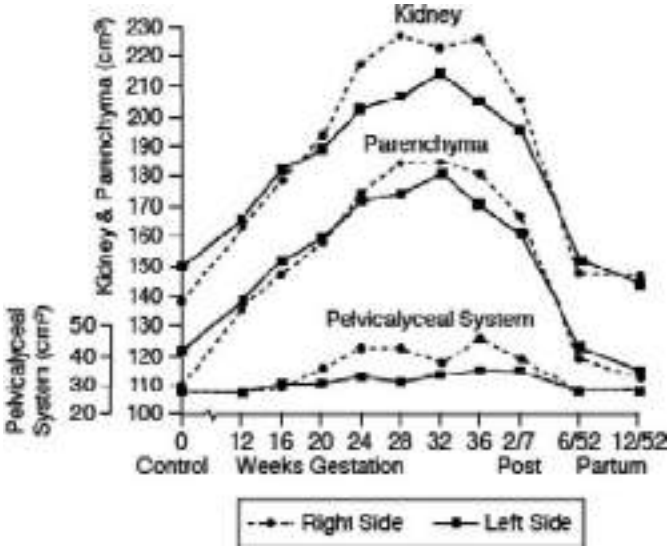

FIGURE 81.1 Quantitative determination by nephrosonography of total renal and pelvicalyceal volumes, as well as the calculated difference of the two, parenchymal volume, in 34 primigravid women throughout pregnancy and in the postpartum period. The volumes were calculated by the ellipsoid formula, volume = length x width x thickness x 0.5233. 2/7, 6/52, and 12/52 designate day 2, and weeks 6 and 12 postpartum, respectively. *[Reproduced with permission from Ref.[6]]*

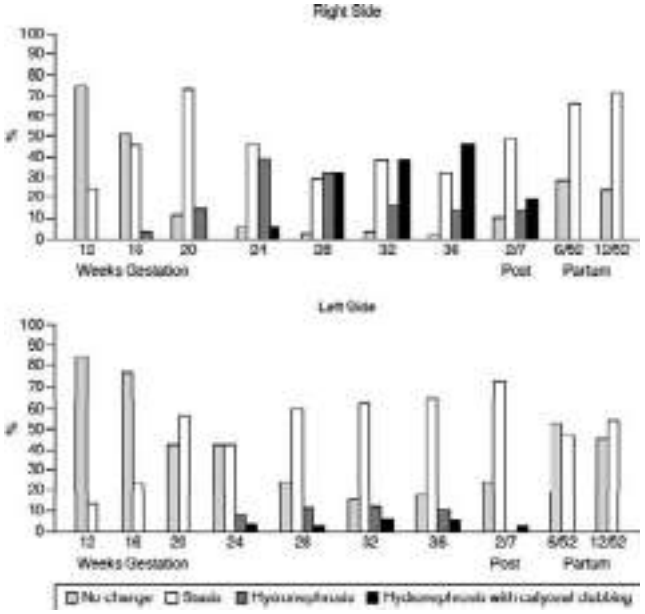

FIGURE 81.2 Qualitative determination by nephrosonography of the right and left upper urinary tracts throughout pregnancy and the postpartum period in the same women as described in Figure 81.1. The percentage of women experiencing changes by nephrosonography is displayed on the ordinate. No change, absence of visible urine in the renal pelvis seen on both longitudinal and/or transverse planes; urinary stasis, slight separation of the renal pelvis observed on both longitudinal and/or transverse planes; hydronephrosis, marked dilation and wide separation of the renal pelvis seen on both longitudinal and/or transverse planes; hydronephrosis with calyceal clubbing, dilation of the renal pelvis accompanied by filling and clubbing of the major and minor renal calyces. 2/7, 6/52, and 12/52 designate day 2, and weeks 6 and 12 postpartum, respectively. *[Reproduced with permission from Ref.[14]]*

The causes of the ureteral dilation are controversial. Both humoral changes and mechanical obstruction have been implicated. Smooth muscle relaxation occurs in several organs during pregnancy, and some authors reported ureteral dilation in nonpregnant humans and animals administered estrogen–progestin derivatives.[9] Ureteral dilation may occur in primates with placentas that secrete hormones but absent fetuses,[4,9] and ultrasonography shows that the ureter dilates before the uterus has enlarged sufficiently to cause obstruction[10,14]; nor is the dilation relieved by prolonged catheterization.[4,9]

The obstructive theory is supported by the observations of marked exacerbation of intraureteral pressure when third trimester gravidas were in a supine or standing position, and significant amelioration upon removal of the obstructive influence of the gravid uterus by placing the subject in the lateral decubitus or knee–chest position, or by cesarean delivery of the fetus.[15] Moreover, the increased pressure was noted only above the pelvic brim.[15,16] These data are supported by the elegant studies of Dure-Smith,[12] who combined *in vivo* and postmortem observations and concluded that ureteral dilation stops at the level of the true bony pelvic brim where the ureter crosses the iliac artery (Figure 81.3). At that junction, one may see a pyelographic filling defect, called the "iliac sign" (Figure 81.3). Although compelling, the data are not conclusive, because Waldeyer's sheath, a connective tissue enveloping the ureters as they enter the true pelvis, hypertrophies during pregnancy and could restrict hormone-induced dilatation below the pelvic brim.

A related theory is that dilation of the ovarian and uterine veins (especially those on the right) during pregnancy obstructs the ureters.[4,8,9,12] The "ovarian vein syndrome" (ureteral colic ascribed to obstruction secondary to enlargement of the ovarian vein) was described in a patient taking oral contraceptives, an observation that combines the humoral and obstructive theories.

Also supporting obstruction as a cause of the physiological dilation is the occurrence of an "overdistention" syndrome in late gestation.[8,17,18,19] This clinical entity caused by exaggerated ureteral dilation is characterized by marked hydronephrosis, abdominal pain, increases in serum creatinine, and in some cases, hypertension.[17,18,20] Some of these patients were successfully managed with ureteral stents, which were removed postpartum without recurrence of signs and

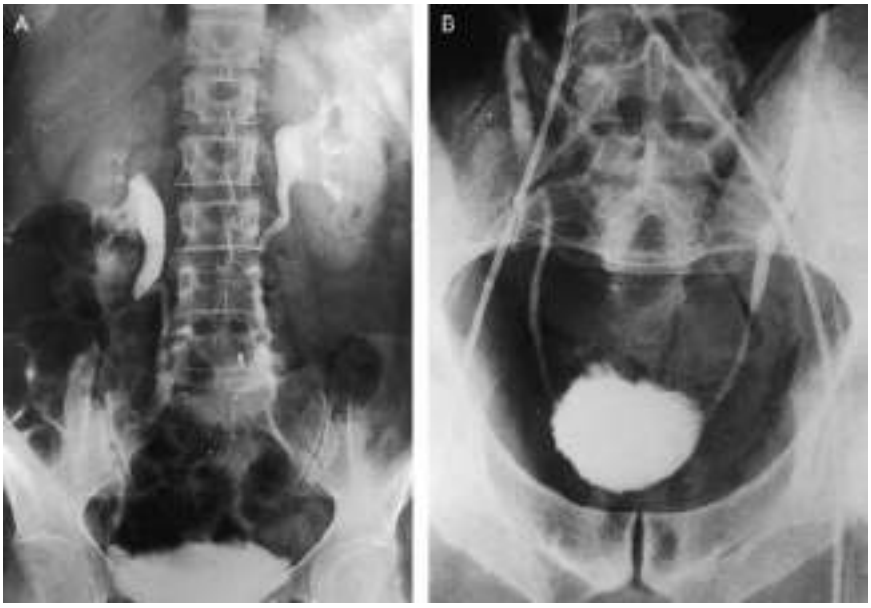

FIGURE 81.3 Intravenous pyelogram (A) demonstrating dilatation of the ureters during pregnancy. Note the sharp cutoff of the ureter at the pelvic brim where it crosses the iliac artery (the iliac sign). Postmortem injection studies (B) showing the relationships of the ureters and iliac arteries at the pelvic brim. The genesis of the iliac sign is shown on the right. *[From Ref.,[12] with permission]*

symptoms.[21] Perhaps the most serious consequences of physiological obstruction during pregnancy are acute urinary retention and nontraumatic rupture of the ureter, but whether these entities reflect extreme instances of physiologic ureteral dilatation or underlying pathology is not clear.[17]

There are other clinical ramifications to the anatomical changes in the urinary tract during pregnancy. First, acceptable norms of kidney size increase by 1 cm if assessed during pregnancy or immediately postpartum, and reductions in renal length noted several months after delivery need not be ascribed to pathological decrements in renal parenchymal mass. Second, ureteral dilation and urinary stasis may contribute to the propensity of women entering pregnancy with benign asymptomatic urinary tract infection to develop frank pyelonephritis (see below). Third, ureteral dilation may result in a higher frequency of vesicoureteral reflux, further predisposing to symptomatic infection, but the presence of increased reflux in gravid women is disputed.[9,16] Finally, the dilated urinary tract may contain substantial urine volumes that can introduce errors in the collection of timed urine volume. This eventuality may be minimized, however, by having the patient hydrated and positioned in lateral recumbency for 1 h prior to starting and again before completing the collection. A modest diuresis minimizes the dead-space error and concurrently ensures that any residual urine in the urinary tract or bladder is dilute and of recent origin.

Ureteral dilation mostly abates by the 12th postpartum week, and therefore imaging of the urinary tract should be deferred to this point, if possible. However, minor but significant dilation may persist in as many as 11% of parous women who have no history of urinary tract infection. This, again, suggests that obstruction may be a significant cause of changes in the ureter during pregnancy.[8,9]

RENAL HEMODYNAMICS

Several carefully conducted serial studies in pregnant women, in which glomerular filtration rate (GFR) and effective renal plasma flow (ERPF) were measured by renal clearances of inulin and *p*-aminohippurate, were conducted during the 1950s and early 1960s. The results convincingly showed that both GFR and ERPF increase during pregnancy, but there was considerable controversy regarding the time course of these changes [reviewed in[9,22–24]]. All concurred that renal hemodynamics rose during the first trimester; the discrepancies concerned late pregnancy, i.e., whether peak increments in GFR and/or ERPF were sustained until term. These divergent results most likely reflect a number of methodological pitfalls, then unappreciated, which can confound the results of renal function tests performed during pregnancy. These potential problems are reviewed in detail elsewhere,[9,22] and here we highlight two of them: the need to impose a high urine flow with hydration, because the dilated ureter introduces dead-space errors, and to position the subject in lateral recumbency. The latter is particularly important in late

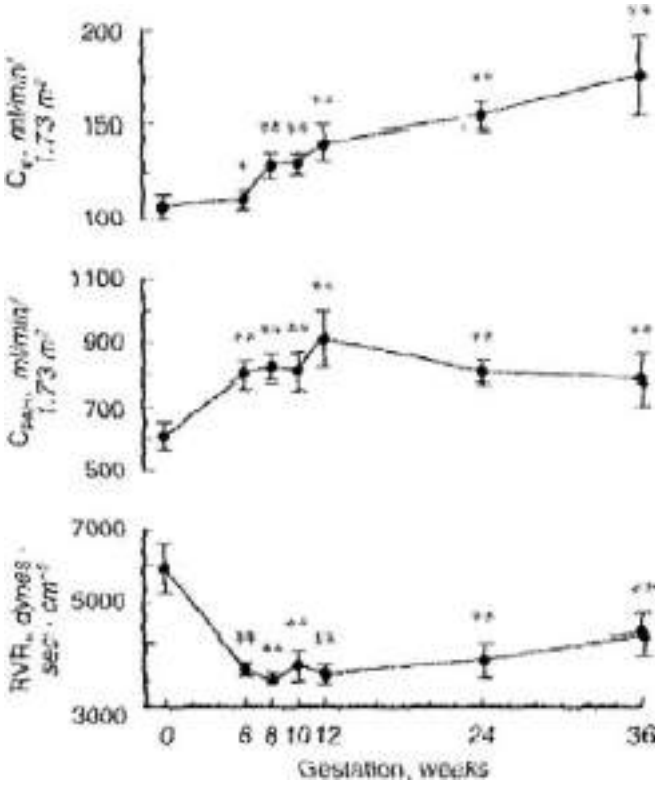

FIGURE 81.4 Renal hemodynamic changes throughout early human pregnancy. Ten women were studied in the midfollicular phase of the menstrual cycle and weeks 6, 8, 10, 12, 24 and 36 of gestation. Renal plasma flow and GFR increased significantly in association with a decrease in renal vascular resistance by week 6 gestation. C_{In}, inulin clearance; C_{PAH}, *p*-aminohippurate clearance; RVR, renal vascular resistance. $^{*}P < 0.05$, $^{**}P < 0.001$ vs midfollicular. Note that authors normalized renal function by body surface area. However, because gestational changes in renal plasma flow and glomerular filtration are functional and not anatomical in nature, such normalization will underestimate true values. *[From Ref.[26] with permission]*

pregnancy, because an upright or supine posture may lead to marked decrements in GFR or ERPF.[9,25]

More recently, investigators reexamined the time course of renal hemodynamic changes in pregnancy, often combining serial 24-h endogenous creatinine clearances with both inulin and *p*-aminohippurate renal clearances and focusing on the first and last few weeks of gestation [22,23,26–31];[24] (Figure 81.4). In some studies, nonpregnant control data were obtained prior to conception and postpartum. Although not all are methodologically flawless, they provide important information summarized as follows: GFR normally increase during the luteal phase of the menstrual cycle,[27,29] continue to rise early in pregnancy, reaching peaks 40–65% above nonpregnant levels by the second trimester. These increments are maintained at least until the 36th gestational week after which a modest decrease in GFR may occur.[28,29] Three months postpartum, GFR values are similar to those measured before pregnancy.

ERPF also increases in the luteal phase of the menstrual cycle and then markedly during gestation reaching values 50–85% above prepregnancy levels during the initial two trimesters[22,23,27,30,31] (Figure 81.4); Near term, however, ERPF seems to decrease ~25%, although it still remains considerably above nongravid values. In general, filtration fraction decreases early in gestation and returns to or towards nonpregnant levels in the last trimester.[22,32]

Given the tremendous increase in GFR and ERPF, the question arises as to whether renal vasodilation is maximal during pregnancy, or whether gravidas possess a "renal functional reserve" similar to that observed during protein loading in nonpregnant subjects. The results of several studies are equivocal. Amino acid infusions consistently increase GFR further in pregnant women, but results of high protein meals are inconclusive.[33–36] Finally, glycine infusions increase GFR in gravid rats.[37]

Mechanisms of Renal Hemodynamic Changes During Pregnancy

Our understanding of mechanism(s) underlying the gestational rise in ERPF and GFR continues to evolve. In part due to both ethical and logistical concerns, most studies designed to determine mechanisms of gestational changes in renal function have utilized animal models as there are several species also known to manifest increases in GFR and ERPF during pregnancy [referenced in[2,9]]. Thus, by applying the renal micropuncture technique to Munich-Wistar rats during midgestation, the period when ERPF and GFR are maximally increased in this species, Baylis[38] demonstrated the gestational rise in single nephron GFR (SNGFR) to be secondary to an increase in glomerular plasma flow, the latter due to a decline in renal vascular resistance. In her rat model, transglomerular hydrostatic pressure difference remained unchanged because there were comparable decreases in both afferent and efferent arteriolar resistances. Plasma oncotic pressure was not significantly different between nonpregnant and midterm pregnant rats and thus not involved in altering SNGFR. Because the animals were in filtration equilibrium, only a minimum value for the ultrafiltration coefficient, K_f could be calculated, which was similar between nonpregnant and midterm pregnant rats; nevertheless, this determinant of glomerular ultrafiltration most likely contributed little to the gestational rise in SNGFR in the gravid rat model. To summarize, SNGFR rises mainly because glomerular plasma flow increases in the gravid rat model.[38]

Whether similar mechanisms occur in pregnant women is unknown as glomerular dynamics cannot be

directly measured. Moreover, human glomeruli may be in filtration disequilibrium, a condition in which alterations in ERPF are predicted to have less impact on GFR.[39] Nevertheless, the parallel increases in ERPF and GFR suggest a similar mechanism governing the rise in GFR in gravid women.

Using an indirect approach, investigators measured the fractional clearance of neutral dextrans ($C_{dextran}/C_{inulin}$) in normal pregnant women serially studied throughout early and late gestation followed by retesting 6 weeks postpartum.[31,40,41] Such data can be analyzed by mathematical models, which incorporate clearance values and plasma oncotic pressures to predict glomerular capillary pressure, the ultrafiltration coefficient (K_f) and glomerular capillary membrane porosity. Permselectivity to neutral dextrans was altered during gestation (Figure 81.5), and the theoretical analysis of the sieving curves, using two different models, suggested that hyperfiltration during pregnancy was mainly due to increments in ERPF with a minor contribution from decreased glomerular oncotic pressure (the latter being greater during late gestation). Membrane porosity appeared to be altered, but comparable to micropuncture studies in rats, there was no evidence of increased glomerular capillary pressure in human pregnancy (Figure 81.5). It should be emphasized, however, that this approach is theoretical in nature being dependent on several assumptions that may or may not be valid.

Further insight into the causes of the altered renal hemodynamics during pregnancy arose from studies in a rat model. Conrad adapted methodologies developed by Gellai and Valtin for measurement of renal function in chronically instrumented, conscious rats and applied them to pregnancy.[42,43] Because physiology is markedly perturbed by anesthesia and surgical stress and the effects of anesthetics and surgical stress can differ in the nonpregnant and pregnant states, studies in chronically instrumented, conscious animals are an essential first step in the investigation of mechanisms underlying maternal circulatory adaptations to pregnancy. Thus, when the same chronically instrumented, conscious rats were serially studied before, during, and after pregnancy, both renal vasodilation and hyperfiltration were observed throughout most of gestation, making it an excellent model to explore the mechanisms underlying these changes.

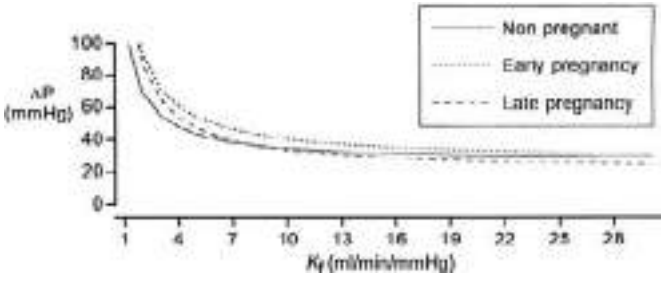

FIGURE 81.5 Theoretical relationship between ultrafiltration coefficient (K_f) and the transglomerular pressure difference (ÄP) in normal pregnancy. Note that over a large range of K_f values, chosen to include those we would expect in humans, there is little change in the ÄP when results during early pregnancy, late gestation, and the nonpregnant state are compared to each other. *[From Ref.[31] with permission]*

The Role of Extracellular Volume

Extracellular and plasma volumes dramatically increase during pregnancy (although most studies suggest after the peak in ERPF and GFR). *Acute* expansion of plasma volume by 10–15% failed to increase the GFR, SNGFR, or glomerular plasma flow in virgin female Munich-Wistar rats.[44] Because volume expansion can suppress tubuloglomerular feedback activity, it could mediate the gestational increases in glomerular plasma flow and SNGFR.[45] However, tubuloglomerular feedback activity was not suppressed in gravid Munich-Wistar rats, rather the mechanism was reset to the higher SNGFR of pregnancy suggesting that volume expansion of pregnancy is actually perceived as "normal." This conclusion supports the "arteriolar underfilling" hypothesis, which states that a *primary* reduction in systemic vascular resistance precedes *secondary* vascular filling during pregnancy; however, the two events are tightly linked and virtually inseparable, although some investigators have discerned a temporal dissociation.[46,47] (Also, see the section Significance of the Volume Changes During Pregnancy.)

Whether *chronic* volume expansion can raise ERPF and GFR to pregnancy levels is difficult to test. Most instances of chronic volume expansion that occur naturally are pathological in nature, for example, congestive heart failure or cirrhosis, and these are conditions where renal function is usually reduced rather than elevated. However, in the rare condition of primary mineralocorticoid excess, which is associated with volume expansion, GFR increases but not to the same degree as observed in pregnancy. Interestingly, chronic administration of either arginine vasopressin (AVP) or oxytocin to chronically instrumented rats permitted water *ad libitum* expands total body water and reduces plasma osmolality (P_{osm}), as well as markedly increases ERPF and GFR.[48,49]Thus, it is possible that chronic volume expansion contributes to the initiation and/or maintenance of elevated ERPF and GFR during pregnancy. Another possibility is that vascular filling consequent to primary arteriolar vasodilation in the kidneys and elsewhere may be permissive for the rise of GFR, in parallel with ERPF.

Maternal Factors in Early Renal Circulatory Adaptations

Mating female rats with vasectomized males produces pseudopregnancy—a condition physiologically mimicking the first half of rat gestation, but in the absence of fetoplacental development. This state reproduces the increases in ERPF and GFR that are observed during early pregnancy.[50,51] Thus, maternal factors alone can induce changes in the renal circulation.

Davison and Noble[29] reported that the 24-h endogenous creatinine clearance increased by 20% during the luteal phase of the menstrual cycle in women. Other investigators corroborated this finding either by using the renal clearance of creatinine,[52,53] 51Cr-EDTA,[53,54] or inulin.[27,55] Furthermore, ERPF measured by the renal clearance of PAH or [^{125}I] hippuran was noted to be increased in two studies[27,54] but not in another.[55] Thus, increases in ERPF and GFR are observed in the luteal phase, albeit to a lesser degree compared to pregnancy. This observation may shed light upon underlying mechanisms, because several hormones that increase during the luteal phase of the menstrual cycle rise even further in early pregnancy (e.g., the ovarian hormones, progesterone, and relaxin, see below).

Sex Steroids

Neither acute nor chronic administration of *estrogen (s)* to humans or laboratory animals influences ERPF or GFR, although the hormone can clearly increase blood flow to other nonreproductive and reproductive organs.[56–60] On the other hand, *progesterone* (or possibly progesterone metabolite(s)[61,62]) may contribute to renal circulatory changes in pregnancy. Chesley and Tepper administered 300 mg/d of progesterone intramuscularly to 10 nonpregnant women for 3 1/2 days and observed a 15% increase in C_{IN} and C_{PAH}. They speculated that longer administration of the hormone might produce larger increases in GFR and ERPF akin to normal gestation.[57] Atallah et al. who studied nine nonpregnant women demonstrated that a rise in circulating progesterone from 7 to 30 ng/mL was associated with a significant rise in endogenous C_{cr} (15%; 103–118 mL/min) 4 h after an i.m. injection of 200 mg of the steroid.[63] By extrapolation, they suggested that pregnancy levels of serum progesterone, which are considerably higher, could account for the 40–65% gestational increase of GFR. Of further interest, studies in male subjects in whom renal function was measured either 3 h after i.m. administration of 310 mmol progesterone or 3 days after 155 mmol progesterone i.m. twice daily revealed significant increases in ERPF (~15% and irrespective of dietary sodium intake), but GFR was unchanged.[64] Finally, subcutaneous injection of 2 mg/kg/d progesterone to intact female rats for 3 days produced a 26% increase in GFR; however, ERPF was not measured in this study.[63] Thus, data from both humans and animals suggest a contribution of progesterone (or its metabolites) to the gestational rises in ERPF and GFR, although definitive evidence is lacking.

Peptide Hormones

Prolactin surges in both pseudopregnant and pregnant rats during the first half of gestation coinciding with the increases in ERPF and GFR. Whether prolactin (or later in pregnancy, *placental lactogen* acting via the same receptor) actually contributes to the increase in renal hemodynamics and GFR during early gestation remains controversial and requires further study.[65]

Relaxin is another hormonal candidate underlying the gestational changes in renal function. In gravid rats and women circulating relaxin arises from the corpus luteum.[66] Human chorionic gonadotropin (hCG) is a major stimulus for relaxin secretion during pregnancy in women.[66]

There was compelling, albeit, circumstantial evidence for considering relaxin a potential mediator of renal vasodilation and hyperfiltration during pregnancy. (i) Circulating relaxin concentrations rapidly increase after conception in women[66] coinciding with the large increases in GFR and ERPF during the first trimester,[29,67]and refs cited above). (ii) Circulating relaxin is detectable during the luteal phase of the menstrual cycle[66,68–70] corresponding with the transient 10–20% increase in GFR and ERPF at that time,[27,29,52–55] and see section *Maternal Factors in Early Renal Circulatory Adaptations*, above. (iii) The early gestational rise in relaxin coincides with another physiological adaptation in human pregnancy, i.e., changes in osmoregulation.[71] These osmoregulatory changes were recapitulated by administering hCG to women in the luteal phase, but not to men suggesting the intermediary role of an ovarian hormone.[72–74] Furthermore, administration of synthetic human relaxin to ovariectomized rats for 7 days produced a significant decline in P_{osm} without changing plasma AVP concentration similar to the osmoregulatory changes noted in normal pregnancy.[75] (iv) Chronic administration of relaxin was reported to reduce blood pressure, [[76] but not confirmed in[77]] and vasoconstrictor responses in the mesenteric circulation of spontaneously hypertensive rats,[76,78] while acute administration increased coronary blood flow and reduced platelet aggregation through nitric oxide (NO) and cGMP,[79,80] thereby implicating a cardiovascular role for the hormone.

Although ERPF and GFR may rise in gravid rats as early as gestational day 5, before circulating relaxin is measurable, there is a jump in renal function between gestational days 8 and 12, when circulating relaxin concentrations surge.[42,66] (The modest increases in GFR

and ERPF that occur during rat gestation before circulating relaxin is detectable on gestational[9] or during pseudopregnancy when circulating relaxin is also undetectable seem to be mediated by other, as yet, undiscovered mechanisms.) Supporting the hypothesis that relaxin mediates the renal circulatory changes of pregnancy, Danielson and colleagues reported that long-term administration of porcine relaxin (pRLX) or of recombinant human relaxin (rhRLX) to chronically instrumented, conscious nonpregnant female rats increased both ERPF and GFR to midgestational levels when renal function peaks in this species.[42,81] The renal circulatory response to relaxin was not contingent upon the ovaries,[81] and intriguingly, was also noted in male rats.[82] Short-term administration of rhRLX to conscious nonpregnant rats also increased GFR and ERPF within 1–2 h.[83] Moreover, myogenic reactivity of small renal arteries isolated from relaxin-treated rats was significantly reduced[84] and comparable to reductions previously reported in small renal arteries isolated from midterm pregnant rats.[85] This phenomenon of reduced myogenic reactivity of small renal arteries has served as a faithful *in vitro* bioassay for the renal vasodilatory changes induced by pregnancy or relaxin treatment of nonpregnant rats.[84,85] Finally, by administering relaxin-neutralizing antibodies or removing circulating relaxin by ovariectomy and maintaining pregnancy with exogenous administration of sex steroids in physiological amounts, the gestational renal hyperfiltration, vasodilation, and reduced myogenic reactivity of small renal arteries isolated from midterm pregnant rats were completely abolished.[86] These experimental manipulations also circumvented the osmoregulatory adaptations of pregnancy.[86] Thus, relaxin is critical to the renal circulatory and osmoregulatory changes of midterm pregnant rats. It may also contribute to these pregnancy adaptations in women.[87]

Endothelium-Derived Relaxing Factors

Endothelium-derived relaxing factors including vasodilatory *prostaglandins* (PGs) and NO have been hypothesized to mediate the gestational increases of ERPF and GFR. The potential intermediary role of PGs has been investigated in gravid animal models and humans. Gestational rises in ERPF and/or GFR were unaffected by administration of PG synthesis inhibitors to chronically instrumented, conscious gravid rats or rabbits.[88–90] Moreover, vasodilatory PG synthesis *in vitro* was not to increased in renal tissues from pregnant animals.[91,92] Although intravenous PG infusion is not physiologically equivalent to locally produced hormone, intravenous infusion of prostacyclin to male human volunteers did not significantly change either ERPF or GFR.[93] In related studies, the cyclooxygenase inhibitor, indomethacin, raised systemic vascular resistance by *only* 5% in pregnant women without significantly affecting either mean arterial pressure or cardiac output, and this increase was trivial compared to the overall decrease in systemic vascular resistance of ~40% observed during normal pregnancy.[94] Similarly, another cyclooxygenase inhibitor, meclofenamate, did not significantly augment systemic vascular resistance in conscious, gravid guinea pigs.[95] Taken together, the results do not support a significant role for vasodilatory PGs in the elevation of ERPF, GFR, and cardiac output, as well as the reduction in both renal and systemic vascular resistances during pregnancy.

Guanosine 3′,5′′-cyclic monophosphate (cGMP) and NO: cGMP, a second messenger of NO may participate in the renal vasodilation and hyperfiltration of pregnancy.[65,96] Because extracellular levels generally reflect intracellular production, plasma levels, urinary excretion, and "metabolic production rate" of cGMP were investigated in conscious rats. All of these variables were increased throughout pregnancy and pseudopregnancy.[65,96,97] Comparable elevations in urinary excretion and plasma concentration of cGMP were reported for human gestation.[98–100] The 24-h urinary excretion of nitrate and nitrite (NO_x), the stable metabolites of NO, also increased during pregnancy and pseudopregnancy in rats consuming a low-NO_x diet, paralleling the rise in urinary cGMP excretion.[97] This gestational rise in urinary NO_x excretion was prevented by chronic administration of nitro-L-arginine methyl ester (L-NAME), an inhibitor of NO synthase, implicating NO as the source. Plasma concentrations of NO_x were also higher in pregnancy, and NO-hemoglobin was detected only in the red blood cells from pregnant, but not from nonpregnant, rats by electron paramagnetic resonance spectroscopy.[97] These results demonstrated that endogenous NO production is increased in gravid rats. Although the tissue source(s) of the gestational increase in NO production was not identified, the possibility that vascular tissues contributed was raised. Plasma levels and urinary excretion of NO_x were also reported to be increased in gravid ewes.[101] Unfortunately, the situation of NO biosynthesis during normal human pregnancy (and in women with preeclampsia) remains controversial.[98,102]

The renal circulation contributes to the overall maternal vasodilatory response of pregnancy. Renal vascular resistance reaches a nadir, and ERPF and GFR peak during midgestation in rats.[42] In chronically instrumented conscious, midterm pregnant and virgin control rats *acutely* administered L-arginine analogs, which inhibit NO synthase, GFR, ERPF, and effective renal vascular resistance converged in the two groups of animals.[102,103] In other words, compared to virgin control rats, the gravid animals responded more

robustly to short-term infusion of NO synthase inhibitors, resulting in a larger decline in GFR and ERPF, and a greater rise in effective renal vascular resistance. Consistent with these *in vivo* data was the inhibition of myogenic reactivity in small renal arteries *ex vivo* isolated from midterm pregnant compared to virgin control rats, which was restored to virgin levels by addition of NO synthase inhibitors to the bath or endothelial removal.[85]

A critical role for NO in renal vasodilation, hyperfiltration, and reduced myogenic reactivity of small renal arteries was also established for relaxin-treated nonpregnant rats again by using L-arginine analogs.[81,84] Thus, NO serves a critical role in the renal circulatory changes of both pregnant and relaxin-treated nonpregnant rats. Although pregnancy and relaxin administration to nonpregnant rats, both elicit renal vasodilation, hyperfiltration and reduced myogenic reactivity of small renal arteries that is dependent upon NO (*vide supra*), unexpectedly the urinary excretion of cGMP and NO metabolites is only increased during pregnancy.[81,96,97] Ironically, therefore, the increased production of cGMP and NO metabolites described initially in rat pregnancy, and which stimulated further interrogation of this vasodilatory pathway, may not be either of vascular origin or of hemodynamic consequence.

Of additional interest is that in one report,[104] but not in another,[105] vasodilatory PGs fulfilled a compensatory role maintaining relative renal hyperfiltration and vasodilation in gravid rats compared to virgin controls during *chronic* NO synthase blockade. In other words, in the setting of chronic NO synthase inhibition, renal function converged in the two groups of rats after short-term infusion of PG synthesis with meclofenamate.[104] PG blockade alone, however, did not affect renal function in conscious virgin or pregnant rats.[88,89,104]

Endothelin and the Endothelial ET_B Receptor Subtype

Paradoxically, *endothelin* (ET) plays a critical role in the renal vasodilation and hyperfiltration of pregnant and relaxin-treated nonpregnant rats. ET is widely recognized as a potent vasoconstrictor through interactions with ET_A and ET_B receptor subtypes on vascular smooth muscle.[106] However, ET also increases intracellular calcium in endothelial cells, thereby stimulating synthesis of prostacyclin, NO, and possibly other relaxing factors through an endothelial ET_B receptor subtype.[107–110] Specific blockade of the ET_B receptor subtype in chronically instrumented, conscious male rats with the pharmacologic antagonist, RES-701-1, induced profound renal vasoconstriction.[111] This unexpected finding indicates a major contribution of endogenous ET in maintaining low renal vascular tone through a RES-701-1 sensitive, endothelial ET_B receptor subtype and tonic stimulation of endothelium-derived relaxing factors and/or restraint of ET production.[107–112] RES-701-1 appears to be relatively selective for the "vasodilator" ET_B receptor subtype on the endothelium.[113] In summary, the RES-701-1 sensitive, endothelial ET_B receptor subtype maintains low renal vascular tone in normal conscious rats most likely through tonic stimulation of NO. However, with ET infusion or in pathophysiological states, ET-mediated vasoconstriction may predominate in the kidney.[113]

A logical extension of these observations in nonpregnant rats is that the endothelial ET_B receptor–NO vasodilatory mechanism is accentuated during pregnancy, thus mediating gestational renal vasodilation and hyperfiltration.[114] Indeed, short-term infusion of RES-701-1 to conscious virgin and gravid rats completely abrogated gestational renal vasodilation and hyperfiltration, thereby producing a convergence of GFR, ERPF, and effective renal vascular resistance in the two groups of animals.[114] As well, the inhibited myogenic reactivity of small renal arteries *ex vivo* isolated from gravid rats was reversed by addition of RES-701-1 or of a mixed $ET_B + ET_A$ antagonist (SB209670), but not a specific ET_A receptor antagonist (BQ123) to the bath.[85] These observations were analogous to those using inhibitors of NO synthase (*vide supra*). Subsequently, the NO/cGMP pathway was suggested to transduce the vasodilatory action of endogenous ET in the renal circulation of pregnant rats.[85,114]

The essential role of the endothelial ET_B receptor subtype in mediating inhibited myogenic reactivity of small renal arteries isolated from pregnant rats was corroborated in the ET_B receptor-deficient rat.[115] Finally, a critical role for the endothelial ET_B receptor subtype in mediating renal vasodilation, hyperfiltration, and reduced myogenic reactivity of small renal arteries was also established for relaxin-treated nonpregnant rats.[82,84]

Vascular Matrix Metalloproteinase-2

Jeyabalan and coworkers[116] proposed that relaxin enhances vascular gelatinase activity during pregnancy that, in turn, mediates renal vasodilation, hyperfiltration, and reduced myogenic reactivity of small renal arteries ultimately through activation of the endothelial ET_B receptor–NO pathway (Figure 81.6). The hypothesis that vascular gelatinase activity plays a pivotal role was founded upon the confluence of several observations: first, the essential role of relaxin, the endothelial ET_B receptor, and NO in pregnancy-mediated renal vasodilation as described above; second, the publications reporting stimulation of matrix metalloproteinase (MMP) expression by relaxin in fibroblasts;[117,118] and third, the ability of vascular MMPs, such as MMP-2, to

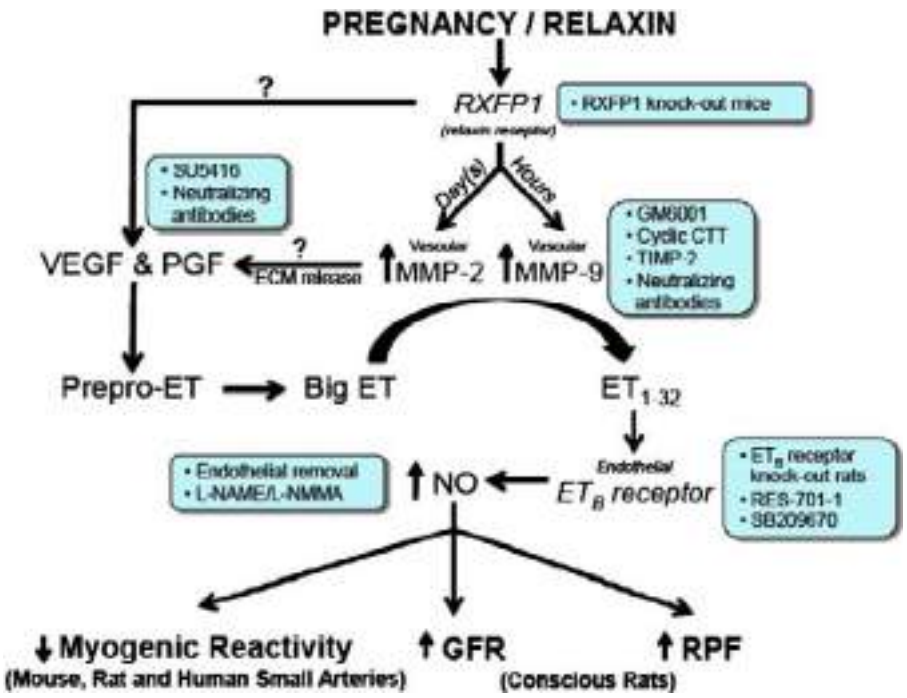

FIGURE 81.6 **Working model for the sustained vasodilatory effect of relaxin.** Depicted are the postulated roles of VEGF and PlGF in mediating the vasodilatory actions of relaxin to be further tested in this grant proposal. The precise localization of VEGF and PGF in the relaxin vasodilatory pathway is currently unknown. Relaxin may increase expression of angiogenic growth factor(s) in the arterial wall and/or release them from the extracellular matrix via MMP-9 or -2. Inhibitors of pregnancy- and/or relaxin-induced vasodilation are shown in the boxes. ET, endothelin; MMP, matrix metalloproteinase; ECM, extracellular matrix; RBF, renal blood flow; GFR, glomerular filtration rate; RFXP, relaxin/insulin-like family peptide receptors; SU5416, vascular endothelial growth factor receptor tyrosine kinase inhibitor; GM6001, a general MMP inhibitor; cyclic CTT, a specific peptide inhibitor of MMP-2; TIMP-2, tissue inhibitor of MMP; RES-701-1, a specific ET_B receptor antagonist; SB209670, a mixed ET_A and ET_B receptor antagonist; L-NAME, nitro-L-arginine methyl ester; L-NMMA, N^G-monomethyl-L-arginine. Note that RFXP2 knockout (in mice), STT (control peptide for cyclic CTT), heat inactivated TIMP-2, BQ-123 (a specific ET_A receptor antagonist), phosphoramidon (an inhibitor of the classical ET-converting enzyme), D-NAME and isotype-matched IgGs (controls for neutralizing antibodies) did not affect the sustained vasodilatory responses to relaxin. *[Reproduced from Ref.[127] with permission]*

hydrolyze big ET at the gly−leu bond to yield ET_{1-32} with activation of ET receptors.[119,120]

The best (if not the only) approach to testing the potential role of MMP-2 in mediating renal vasodilation, hyperfiltration, and inhibited myogenic reactivity of small renal arteries mediated by pregnancy or relaxin is to block MMP-2 production or its activity. Accordingly, short-term infusion of gelatinase inhibitors abrogated relaxin-mediated renal vasodilation and hyperfiltration in conscious rats; moreover, the inhibited myogenic reactivity of small renal arteries isolated from pregnant or relaxin-treated nonpregnant rats was reversed by gelatinase inhibitors *in vitro*.[116] In contrast, there was no effect of the traditional ET-converting enzyme inhibitor, phosphoramidon, which inhibits the processing of big ET to ET_{1-21}.[116] In small renal arteries harvested from relaxin-treated nonpregnant and mid-term pregnant rats, MMP-2 activity is increased by ~50% relative to nonpregnant control arteries.[116,121] Thus, vascular gelatinase activity is not only part of the relaxin-endothelial ET_B receptor−NO vasodilatory pathway, but it is a major locus of regulation by relaxin in this species, because neither endothelial NO synthase nor ET_B receptor abundance is increased by relaxin or pregnancy,[122,123] but not all investigators agree.[124−126]

It is unlikely that vascular MMP-2 and endothelial ET_B receptor−NO are components of separate vasodilatory pathways acting in parallel. If this was the case, then one might predict that after inhibition of either vascular MMP-2 or the endothelial ET_B−NO pathway, compensation of one for the other should be observed. However, no compensation or even partial compensation was noted: each and every inhibitor of the ET_B receptor,[82,84,85,114] NO synthase,[81,84,85,103] or MMP[116] completely abolished the renal circulatory changes during pregnancy or relaxin treatment of nonpregnant rats. Nevertheless, experimental confirmation of a common vasodilatory pathway shared by vascular gelatinase activity and the endothelial ET_B receptor−NO vasodilatory pathway was obtained. That is, small renal arteries isolated from relaxin-treated, ET_B receptor-deficient rats showed upregulation of vascular MMP-2 activity, but failed to show inhibition of myogenic reactivity. This dissociation of the biochemical

and functional consequences of relaxin administration in small renal arteries harvested from ET_B receptor-deficient rats, when taken in the context of the other results (*vide supra*), strongly suggests that vascular gelatinase is in series with, and upstream of, the endothelial ET_B receptor–NO signaling pathway.[116]

To summarize, during pregnancy relaxin accentuates the endothelial ET_B receptor–NO renal vasodilatory pathway by increasing vascular MMP-2 activity (via increases in MMP-2 mRNA and protein[121]). A more recent study also suggests the participation of vascular endothelial growth factor (VEGF) and placental growth factors (PlGF) in the renal vasodilatory pathway of relaxin.[127] Interestingly, higher doses of gelatinase inhibitors also decreased GFR and ERPF, and elevated arterial pressure when administered to control rats, albeit less so than in relaxin-treated rats,[116] whereas phosphoramidon was again without effect.[116] These results suggest that vascular gelatinase activity rather than the traditional ET-converting enzyme may be the main physiological mechanism for big ET processing (and consequent vasodilation) at least in the renal circulation of rats. Possibly, the colocalization of MMP-2 and associated proteins in the caveolae of endothelial cells with the ET_B receptor and eNOS facilitates this interaction (Figure 81.6).

Other factors in addition to relaxin are likely to contribute to gestational renal vasodilation and hyperfiltration especially during late pregnancy, when circulating levels of placental hormones are particularly high. For example, placental growth hormone may contribute.[128] In addition, local factors within the kidneys themselves may participate. Mesangial cell expression of iNOS, the angiotensin (AT)-2, and relaxin receptors was reported to increase during midgestation in rats.[129] Moreover, upregulation of the *n*NOSβ isoform in the renal cortex of midterm pregnancy rats was noted.[130] Intriguingly, Morgan and colleagues observed increased histidine decarboxylase and histamine production in the superficial cortical zone of pregnant mice.[131] Finally, increased renal production of epoxyeicosatrienoic acid may also play a role in renal vasodilation and hyperfiltration of pregnancy.[132]

To conclude, evidence from both animal and human studies suggests that renal hyperfiltration in pregnancy is secondary to increased RPF, the latter resulting from profound decreases in renal vascular resistance. There has been considerable progress in identifying mechanisms responsible for gestational renal vasodilation, and those most promising so far were reviewed in detail above. Of importance, whatever the primary vasodilatory stimulus, it must be a powerful one, for the pregnancy-induced rise in GFR is not restricted to women with two normally functioning kidneys but occurs also in subjects with previously hypertrophied single kidneys (following uninephrectomy) and in transplant recipients.[133,134]

Significance of the Changes in Renal Hemodynamics During Pregnancy

The GFR increase during pregnancy has important clinical consequences. Production of creatinine changes little, so that increases in creatinine clearance lead to a reduction in its plasma level.[4,9,135] This is also true of urea, which may be decreased even further by enhanced protein synthesis. Therefore, levels of creatinine and urea nitrogen decrease from a mean of 0.7 and 12 mg/dl (62 and 4.3 mmol/L), respectively, in the nonpregnant state, to 0.5 and 9 mg/dL (44 and 3.2 mmol/L).[4,9] The implication of these observations is that values considered normal in nonpregnant women may reflect compromised renal function during pregnancy. Concentrations of serum creatinine and urea nitrogen exceeding 0.8 and 13 mg/dL (80 mmol/L and 5 mmol/L), respectively, should alert the clinician to evaluate renal function further.

The augmented filtered load consequent to increased GFR also contributes to the glucosuria, aminoaciduria, and enhanced urinary excretion of water-soluble vitamins that occur during normal pregnancy.[9,23] Urinary protein excretion may double as well, but the greatest increments seem to occur in late gestation, long after changes in renal hemodynamics are maximal.[22,32] Also, there are still discrepancies about whether there are increases in albuminuria during pregnancy, but the majority of studies suggest so.[22,41] It should be borne in mind, though, that many factors affect urinary protein excretion in addition to glomerular filtration, including the pore size and number of fixed charges in the glomerular filtration barrier, and tubular reabsorption rates, a topic discussed elsewhere in this text.

There are also changes, usually increments, in the renal excretion of various low-molecular weight proteins and enzymes during pregnancy. Whether the alterations result from increased filtration and/or changes in tubular handling, or even in production is unclear (see Ref.[22]) for further details and citations). The increments in urinary glucose, amino acids, and proteins mentioned above also have pathophysiological consequences, i.e., the nutrient content of the urine is increased, which may predispose pregnant women to symptomatic urinary tract infection.[4,9] Finally, awareness that the normal limit of urinary protein excretion is increased during gestation to 300 mg/24 h suggests that this event will also occur and may even be exaggerated in women with preexisting kidney disorders, so that increased proteinuria during pregnancy

does not necessarily signify progression or exacerbation of their disease.

RENAL TUBULAR FUNCTION

Glucose, Other Sugars, and Water-Soluble Vitamins

Glucosuria may occur normally during pregnancy. In one study, 30 women with normal glucose tolerance were evaluated serially beginning early in gestation and continuing through the sixth postpartum week (reviewed in Ref.[23]). Daily urinary excretion of glucose was measured by a sensitive and specific enzymatic assay, an important methodological consideration, because excretion of many other reducing substances also increases during pregnancy. All subjects excreted <100 mg/24 h when not pregnant, but during gestation this value was exceeded in 26 women (86%) ranging up to 500 mg in 12, between 0.5 and 1.0 g in 4, and exceeding 1 g/24 h in 10 others. Glucosuria was intermittent and not necessarily related to blood glucose levels or gestational stage. A comparable high incidence of glucosuria in normal pregnancy was reported by others (reviewed in Ref.[9]). Gestational glucosuria reverts to normal within 1 week postpartum.[136]

Renal tubular handling of glucose, including the transport maximum (T_m), threshold, and splay of the titration curve were evaluated during pregnancy. Many reports had weaknesses in experimental design, but there were exceptions. With exquisite attention to methodology, Welsh and Sims[137] assessed the T_m of glucose in normal nonpregnant subjects, nonglycosuric pregnant women, and normoglycemic glycosuric gravidas. The T_m of glucose was lower in the latter group in comparison to the nonglycosuric pregnant subjects, and the authors proposed that gestational glucosuria resulted from increased GFR, and hence filtered load, in women with a low T_m for glucose. Fifteen years later, Davison and colleagues[138] suggested that both the T_m and fractional reabsorption of glucose decrease in all pregnant women. In their study, renal glucose reabsorption was measured in subjects with normal carbohydrate metabolism during and after gestation. Care was taken to avoid extremely high plasma glucose concentrations during infusions, which can affect renal hemodynamics. All women demonstrated lower fractional reabsorption of glucose during pregnancy compared to after delivery. Those most severely glycosuric in pregnancy had the lowest fractional reabsorption rates both during and after gestation; however, they were not glycosuric postpartum because GFR and the filtered load of glucose had decreased substantially. Said otherwise, even if the splay in the glucose titration curve increases or the glucose T_m decreases slightly, the striking gestational increment in GFR and consequent filtered load of glucose remains the major cause of glucosuria in pregnancy.

Gravid rats may also display glucosuria. Renal micropuncture studies in this species reveal that proximal tubular glucose reabsorption is actually enhanced, commensurate with the increment in filtered load; thus, the increased urinary glucose is due mainly to decreased distal tubular reabsorption, and perhaps to changes in epithelial permeability causing backleak in Henle's loop.[139]

Excretion of other sugars, including lactose, fructose, xylose, and fucose, but not arabinose, also increases during pregnancy [citations in Ref.[9]]; lactosuria is present in 50% of gravidas by the end of gestation, when excretion may be as much as 10-fold higher than nongravid women. During pregnancy, certain oligosaccharides are excreted in the urine not found in the urine of nonpregnant women, and thus, they are suspected to be of mammary origin. It should be emphasized, however, that the excretion of these sugars combined is minimal compared to that of glucose, and consequently, they do not amount to a significant nutrient loss to the mother.

The renal excretion of several water-soluble vitamins is also increased during pregnancy including nicotinic, ascorbic, and folic acids.[9] Plasma folate levels actually decrease in pregnancy, and the increased urinary excretion may be largely due to reduced tubular reabsorption rather than enhanced filtered load.

Amino Acids

Urinary excretion of many amino acids rises during pregnancy. In fact, urinary histidine concentration was once used as a method to detect pregnancy, and its disappearance from the urine was noted in preeclampsia.[9] The most detailed studies are by Hytten and Cheyne,[140] who conducted serial measurements in 10 women from early pregnancy through the eighth postpartum week. Renal excretion of glycine, histidine, threonine, serine, and alanine increased early in gestation and urinary losses became substantial near term. In contrast, increments in urinary excretion of lysine, cystine, taurine, tyrosine, phenylalanine, valine, and leucine occurred during the first half of pregnancy, but declined thereafter, and the urinary excretion of asparagine, glutamic acid, and arginine was unchanged during gestation. It is noteworthy that gestational aminoaciduria can reach $\sim$2 g/day, a loss that could adversely affect fetal growth, if protein intake is suboptimal. In some subjects, urinary glycine and histidine excretion exceeded 50% of the filtered load, suggesting a role for inhibition of tubular reabsorptive process. However, these data

reflect 24-h renal clearance measurements, and the little information concerning threshold or T_m during short-term infusion studies is inconclusive.[9]

Uric Acid

Although uric acid production has been described as unchanged during pregnancy,[4,9,22] more recent evidence disputes this conclusion.[141] In either case, gravidas excrete considerably more urate than when they are not pregnant.[22,142,143] The renal clearance of uric acid, typically 6–12 mL/min in nonpregnant women, rises to 12–20 mL/min during pregnancy, and consequently, plasma concentrations decline at least 25% and are only 2.5–4.0 mg/dL in many pregnant women.[9,144] In most centers, 5–5.5 mg/dL is considered to be the normal upper limits for pregnancy,[145] but the upper limit is different depending on the stage of gestation.[144] Circulating urate tends to be higher in women with multiple gestations,[146] displays circadian rhythm with higher and lower levels at morning and night, respectively,[147] and the normal range may be subject to racial variations.[148]

Whereas both the filtered load and absolute tubular reabsorption of urate increase during gestation, most investigators have documented increments in fractional excretion, i.e., the C_{urate}/C_{inulin} ratio is greater in pregnancy than in the nonpregnant state (reviewed in Refs[9] and[22]). However, there have been only two well-monitored serial studies in which investigators determined urate concentrations with specific enzymatic assays, and the results vary. In one study, no difference in fractional clearance of urate during and after pregnancy was reported,[149] whereas in the other,[143] C_{urate}/C_{inulin} increased during the first two trimesters but returned to nonpregnant values in the third.

The peak in renal clearance of urate and the nadir in plasma concentration are observed in early gestation; subsequently, C_{urate} declines and plasma urate levels rise near term.[9,22,143,149] It is not clear whether these findings are confounded by postural artifacts,[9] nonrenal metabolic effects in relation to the oxidant/antioxidant balance during gestation,[141] or possibly by inadvertent inclusion of women with subclinical preeclampsia. In this regard, decrements in the C_{urate}/C_{inulin} or increments in P_{urate} concentrations may precede the clinical manifestations of preeclampsia.[9,22,150]

Potassium Secretion

There are few data on body potassium stores in pregnancy. One study suggests that body stores decline early in gestation and then rise to values ~100 mEq above prepregnancy levels.[151] These findings are consistent with the theoretical considerations that pregnant women should lose potassium in their urine, because they eat and excrete normal quantities of sodium, but manifest very high levels of aldosterone and other potent mineralocorticoids (see below). Furthermore, they develop bicarbonaturia at substantially lower plasma bicarbonate levels than do nonpregnant women. Observations that plasma and serum potassium levels decrease 0.2–0.3 mEq/L between gestational weeks 10 and 28 are also consistent with this formulation.[152]

A more traditional view, however, is that pregnant women do not waste potassium but undergo a cumulative retention of ~350 mEq of the cation, most of which is stored in the products of conception, as well as in the organs of reproduction (Table 81.1).[9,152] Moreover, in striking contrast to nonpregnant women, gravidas are resistant to the kaliuresis provoked by the combination of exogenous mineralocorticoids and a high-sodium diet[153] (Figure 81.7). This remarkable capacity to conserve potassium in the face of high concentrations of potent mineralocorticoids such as aldosterone and deoxycorticosterone (DOC), and the delivery of substantial quantities of sodium to distal nephron sites, may be secondary to the increased circulating levels of progesterone during pregnancy, a view supported by studies in both humans[152,153] and animals[154] but not accepted by all.[155]

Resistance to the kaliuretic influence of mineralocorticoids may benefit gravid women with certain potassium-wasting diseases. On the one hand, excessive potassium loss of primary aldosteronism may be easier to control in gestation (Figure 81.8).[4,9,152,156] On the other, if the kidneys resist kaliuretic stimuli, women with underlying disorders that impair their ability to excrete potassium may be jeopardized by gestation. Finally, there is a rare disorder in which the renal

TABLE 81.1 Storage of Minerals During Pregnancy

Storage site	Sodium, mEq	Potassium, mEq	Calcium, g
Fetus	290	154	28.00
Placenta	57	42	0.65
Amniotic fluid	100	3	Negligible
Uterus	80	50	0.22
Breasts	35	35	0.06
Plasma	140	4	0.12
Red cells	5	24	0.38
Interstitial fluid	240	8	0.25
Total	947	320	29.68

Source: Hytten FE, Leitch I. The Physiology of Human Pregnancy, 2nd ed. Philadelphia: FA Davis; 1971; with permission

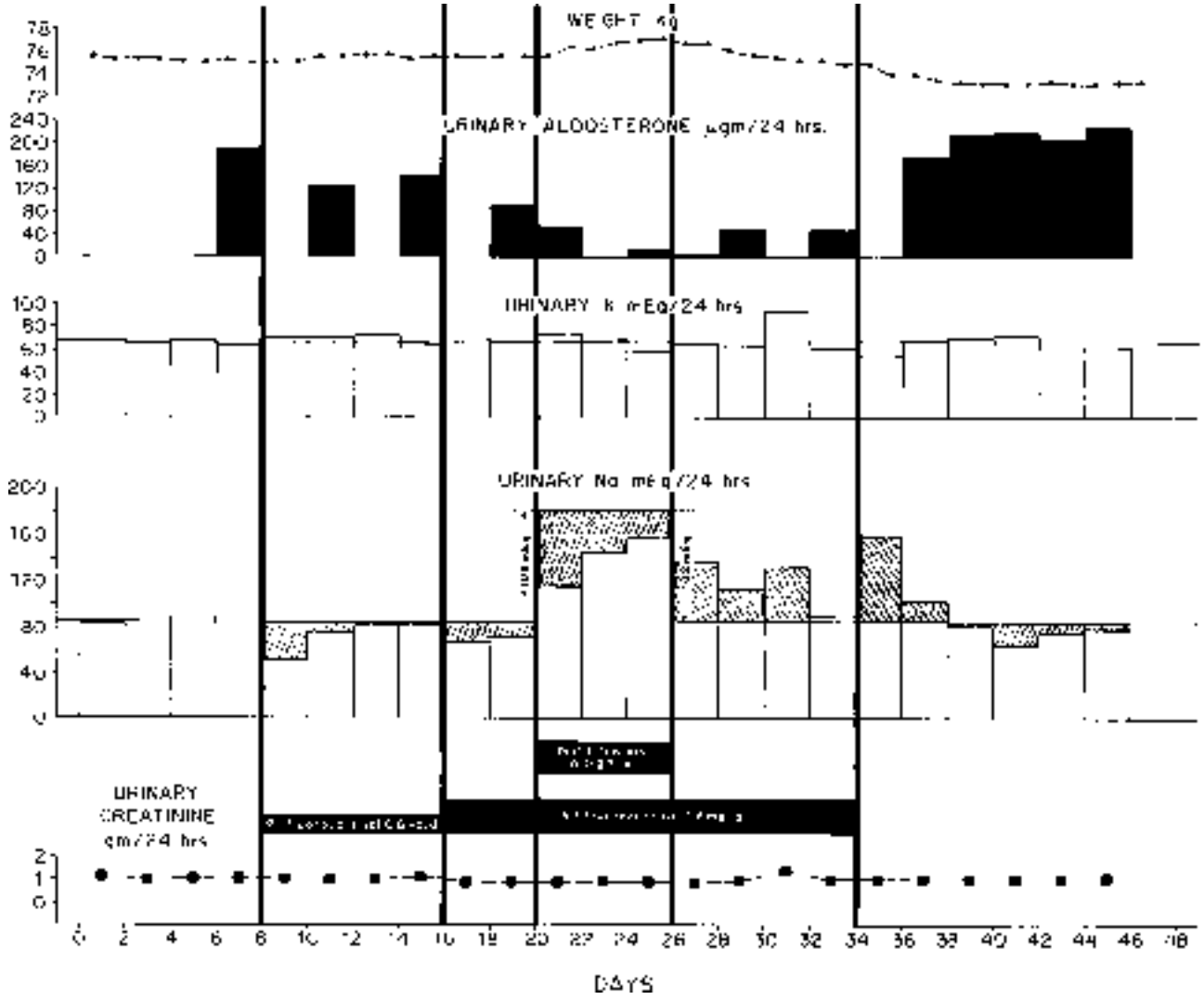

FIGURE 81.7 Effect of a mineralocorticoid (Florinef acetate) in a normal 19-year-old pregnant woman. Oral ingestion of this potent corticoid led to sodium retention, but no kaliuresis was observed even when dietary sodium chloride was abruptly increased during days 20–26 of the study. The high baseline aldosterone excretion is normal for pregnancy. The heavy vertical lines delineate the different treatment periods, and the horizontal lines are the arithmetic means of urinary sodium and potassium excretions during pretreatment (control) days. Note that a kaliuresis occurred only on day 31, but the increased creatinine excretion (asterisk) suggests a collection or measurement error. *[From Ref.,[153] with permission]*

mineralocorticoid receptor is genetically altered in a manner that hormones antagonizing the salt-retaining actions of corticoids become agonist in nature.[157] During pregnancy, progesterone levels increase 100-fold, and women heterozygous for the disorder manifest severe hypertension, renal potassium wasting, and marked hypokalemia, but suppressed aldosterone levels.

Regulation of Acid–Base Balance

Acid–base balance is affected by pregnancy. Blood levels of hydrogen ion decline 2–4 nmol early in gestation, a decrement that is maintained throughout pregnancy,[4,9,158] and arterial (or arterialized capillary) blood pH is typically 7.42–7.44 in gravidas, as compared with 7.38–7.40 in nonpregnant women. This mild alkalemia is respiratory in origin, because pregnant women hyperventilate (believed to be a central effect of progesterone effect), and consequently, their arterial PCO_2 decreases from a nonpregnant mean of 39 to 31 torr during gestation.[4,9,158] Supporting the causal role of progesterone are data showing that arterial PCO_2 also falls 3–4 torr during the luteal phase of the menstrual cycle.[159] These decrements in PCO_2 are compensated by decreases in plasma bicarbonate levels

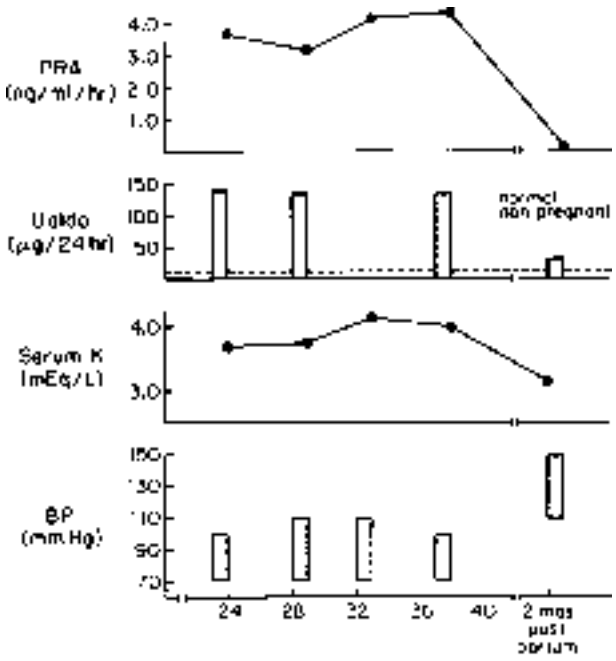

FIGURE 81.8 Plasma renin activity (PRA), urine aldosterone excretion, serum potassium, and blood pressure during pregnancy and 2 months postpartum in a woman with primary aldosteronism. Hypertension and hypokalemia disappeared during pregnancy. *[From Ref.,[156] with permission]*

of ~4 mEq/L, normal values in gestation ranging from 18 to 22 mEq/L,[4,9,158] thereby establishing a blood pH that is only slightly alkalotic.

There have been few studies addressing renal bicarbonate reclamation and regeneration during pregnancy. Lim et al.[158] infused a hypertonic bicarbonate solution in women during the third trimester. The bicarbonate titration curve from that study is shown in Figure 81.9 (left). Despite large filtered loads of bicarbonate, reabsorption continued to increase, and even when plasma levels reached 31 mEq/L, reabsorption virtually matched the filtered load. These results were unexpected, because pregnant women are hypocapnic and have increased extracellular volumes, conditions that should lead to an exaggerated "splay" in the titration curve and/or a decrease in the apparent T_m for bicarbonate. However, a small but persistent bicarbonate leak was noted at lower plasma bicarbonate concentrations during pregnancy than postpartum (Figure 81.9, right). This modest bicarbonaturia was occasionally present at plasma bicarbonate levels as low as 15–16 mEq/L.

Urinary acidification as well as titratable acid and ammonium excretion have been measured in gravid women after being challenged with both acute and chronic administration of NH_4Cl.[4,9,158,160] The results were comparable to those of nonpregnant control subjects. It is noteworthy that the decrement in urine pH and the increases in titratable acid and ammonium excretion occurred even though blood pH decreased only slightly from 7.44 to 7.40. Thus, substantial bicarbonate regeneration can already be demonstrated at a pH higher than in nonpregnant women, and in fact it starts when values are still alkaline relative to the nonpregnant state. Distal hydrogen secretory capacity, as measured by the increment in urinary PCO_2 during the bicarbonaturia that accompanied the hypertonic bicarbonate loading, appeared to be intact during pregnancy.[158] Finally, the decrease in blood pH during exercise is similar in the pregnant and nonpregnant states.[161]

OSMOREGULATION AND RENAL WATER HANDLING

Osmotic Thresholds for AVP Release and Thirst

P_{osm} decreases 8–10 mOsm/kg during normal gestation.[4,9,71,73,74] This decline, which starts in the luteal phase of the menstrual cycle,[27,162] continues through conception and reaches a nadir about gestational week 10, after which it is maintained until term. Only about 1.5 mOsm/kg of the fall can be accounted for by decreases in urea concentration, most of the change resulting from a decline in the concentrations of plasma sodium and its attendant anions.[71] Thus, pregnancy is characterized by a true decrease in effective P_{osm}.

A decrease in P_{osm} of such magnitude in a nonpregnant subject would suppress antidiuretic hormone secretion and result in a state of massive and continuous water diuresis, which does not happen in pregnant women. Rather, gravidas are able to maintain the new, lower P_{osm} within a narrow range, and water loading or fluid restriction, respectively, lead to appropriate dilution and concentration of their urine.[163] These events are made possible because osmotic thresholds for both AVP secretion and thirst decrease by 8–10 mOsm/kg each during gestation, decrements which are already demonstrable during gestational weeks 5–8 and are sustained through term[72,164,165] (Figure 81.10). It should be emphasized that parallel declines in both the osmotic thresholds for AVP release and thirst are required, in order to maintain the new steady state P_{osm} within a narrow range. That is, P_{osm} would rise in the face of persisting circulating levels of AVP at the lower P_{osm} of gestation, if the subject is not simultaneously stimulated to drink water; conversely, considerable polydipsia would be required to maintain a lower P_{osm} in the absence of AVP secretion.

The metabolism of AVP also changes in gestation, hormonal disposal rates rising four-fold between early

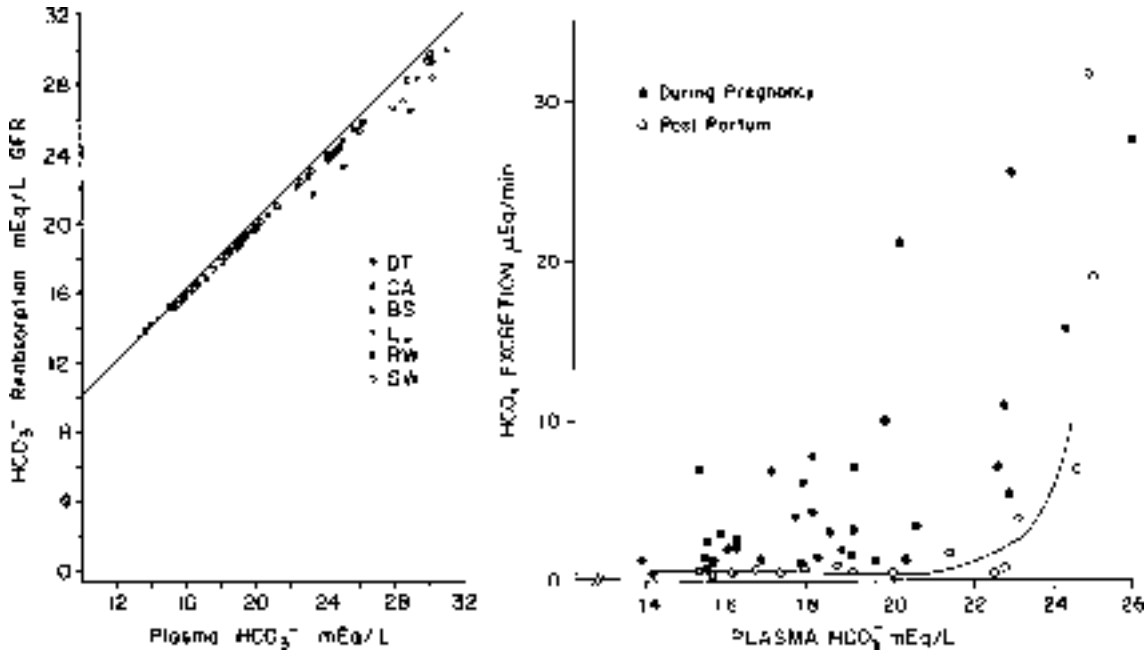

FIGURE 81.9 **Left:** Bicarbonate titration curves in six third-trimester women during slow infusion of 5% $NaHCO_3$ solution. The infusion inadvertently ran faster for a period of 30 min in 1 subject (BS), the only volunteer who displayed a wide splay. **Right**: Bicarbonate excretion as a function of plasma HCO_3 levels in pregnant women (filled circles) and two subjects restudied after delivery (open circles). $THCO_3$ is lower in the pregnant women (mean 18.9 mEq/L), but even when surpassed, the bicarbonaturia is still trivial. *[From Ref.,[158] with permission]*

and midgestation.[164,165] This rather striking increase in the metabolic clearance rate (MCR) of AVP parallels the marked increase in both placental trophoblastic mass and circulating levels of cystine aminopeptidase (vasopressinase).[165,166] Thus, the rise in MCR of AVP is likely due to the extremely high circulating vasopressinase emanating from the placenta, a concept supported by studies showing that the metabolic clearance of 1-deamino 8-D-AVP (DDAVP, Desmopressin), the AVP analogue resistant to inactivation by vasopressinase, does not change in pregnancy[164] (Figure 81.11).

The cause of the osmoregulatory changes in pregnancy is obscure. hCG,[72,167] constitutive NOS,[124,168] and relaxin[75,81] have each been suggested to play etiologic roles. Of further interest, decrements in P_{osm} do not occur in every species[74]; they do so, however in rodents (along with decreases in the osmotic thresholds for AVP release and drinking), and the rat has become the model in which to explore mechanisms responsible for changes that occur in humans.[73,74,169–173] In this latter model, injection of hCG yielded equivocal results (Barron and Lindheimer, unpublished observations), but relaxin lowers P_{osm}, as well as the osmotic threshold for AVP release.[75,81] These data suggest that the osmoregulatory effects of hCG in premenopausal women, ineffective in males, is through stimulation of ovarian relaxin secretion. This hypothesis remains to be explored.

Of interest is a group of investigators[174] that ascribed the decreased P_{osm} in pregnancy to the decreased "effective" circulating volume of pregnancy (so-called "nonosmotic" release mechanism, see below). Ohara et al. suggested that plasma AVP is detectable at low P_{osm} during pregnancy due to nonosmotic release, and gravid rats also manifest upregulation of aquaporin-2 (AQ2) mRNA and protein in apical membranes of the collecting duct, thus abetting water retention and lower body tonicity. However, the mechanism underlying increased AQ2 expression is uncertain, because circulating AVP, although detectable despite the lower P_{osm}, are not elevated above nonpregnant values (as in congestive heart failure). As discussed below, others have accumulated evidence against decreased or "underfill" of the arterial circulation as an explanation for the control of vasopressin secretion during pregnancy. We note here that the observations of Ohara et al may be paradoxical, insofar as an increase in AQ2 might be expected to blunt the animals ability to excrete a water load, yet gravid rats excrete water as well as or better than virgin controls.[172]

Significance of the Osmoregulatory Changes

The physiological significance of the changes in body tonicity, as well as in the osmotic threshold for AVP release and thirst is unclear. They may represent an

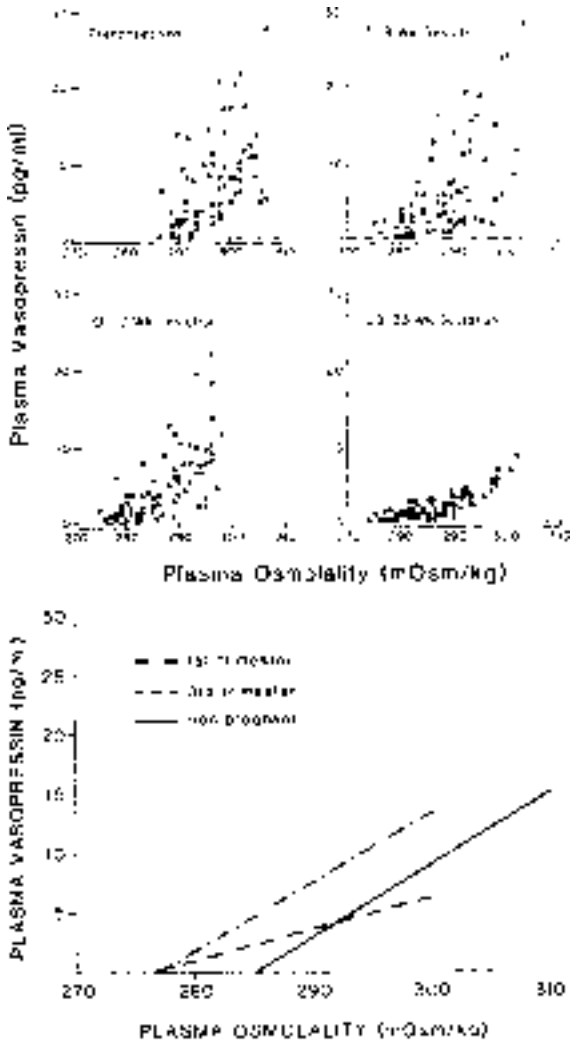

FIGURE 81.10 Relationships of P_{AVP} to P_{osm} during serial hypertonic saline infusions in eight volunteers starting before conception and completed postpartum. Each point in A–D represents individual plasma determinations, and data from the postpartum period, which were similar to these before conception, are not shown. Highly significant mean regression lines from the early pregnancy, the third trimester, and nonpregnant periods demonstrate the marked decrease in the abscissal intercept (which is the apparent osmotic threshold for AVP release) during gestation. The decreased slope ($\Delta P_{AVP}/\Delta P_{osm}$) in the third trimester is discussed in the text. Finally, the osmotic thresholds for thirst in both pregnant and nonpregnant subjects (not shown) were consistently 2–5 mOsm/kg above that for hormone release, and were thus ~10 mOsm/kg lower during pregnancy. *[Modified from Ref.[72]]*

epiphenomenon secondary to hormonal changes of pregnancy, but it is noteworthy that they may facilitate the increments in intravascular and extracellular volume that occur in pregnancy. Some believe the "physiological hypervolemia" of gestation optimizes fetal development, and in this respect, hypoosmolality results in a need for less solute per liter of extracellular water retained, certainly an advantage when sodium is scarce. Another idea is that the retention of water during pregnancy, which is distributed mainly to the intracellular space, creates a reservoir for maintaining extracellular and intravascular volume when water is scarce.

One very clinically relevant consequence of the altered osmoregulation in pregnancy is related to the striking increase in the MCR of AVP. In the past, women with central diabetes insipidus (DI) required increasing amounts of AVP administration during pregnancy. This is no longer the case since virtually all patients are currently managed with DDAVP,[175] which escapes metabolism by circulating placental vasopressinase (*vide supra*). Still there are patients with partial central DI and sufficient hormone secretory capacity to escape detection when nonpregnant, whose disease is unmasked by the marked increase in AVP disposal rates of pregnancy.[176,177] More frequent and dramatic, however, is another syndrome called "transient DI of pregnancy," which presents during the second half of gestation and remits postpartum.[73,74,177–179,180] It is important to recognize this entity as women may become dangerously hypernatremic especially if they undergo cesarean sections using general anesthesia or are water restricted in the delivery suite.[181] These patients have markedly high levels of circulating vasopressinase that may still be above those of normal gestation when measured during the first week of the puerperium.[179,182] Others may have subclinical central DI, their pituitary gland unable to respond to the increases in MCR of AVP during pregnancy. Polyuria in these women is usually unresponsive to large doses of AVP (pitressin), but they concentrate their urine rapidly when treated with DDAVP[179] (Figure 81.12). Some of these patients have hepatic dysfunction usually associated with preeclampsia, but in a few the DI has been associated with acute fatty liver of pregnancy. Thus, it is tempting to speculate that failure of the liver to inactivate vasopressinase, coupled with continuous placental production of large quantities of the enzyme, are causal. Consistent with this reasoning is documentation in one patient of excessive pitocin requirements during labor (vasopressinase destroys oxytocin as well as AVP).[175]

The ability to excrete water during pregnancy can be altered in other ways as well. Changing from lateral recumbency to a supine position decreases urine flow, and quiet standing may be more antidiuretic in pregnant than nonpregnant subjects (reviewed in Refs[4,9,71]). The effect of supine posture is independent of circulating levels of antidiuretic hormone, since it has been noted in a pregnant patient with central DI.[4,9] It should be underscored, however, that these "nonosmotic" influences on water handling are not sufficient, of themselves, to explain the gestational decline in P_{osm}.

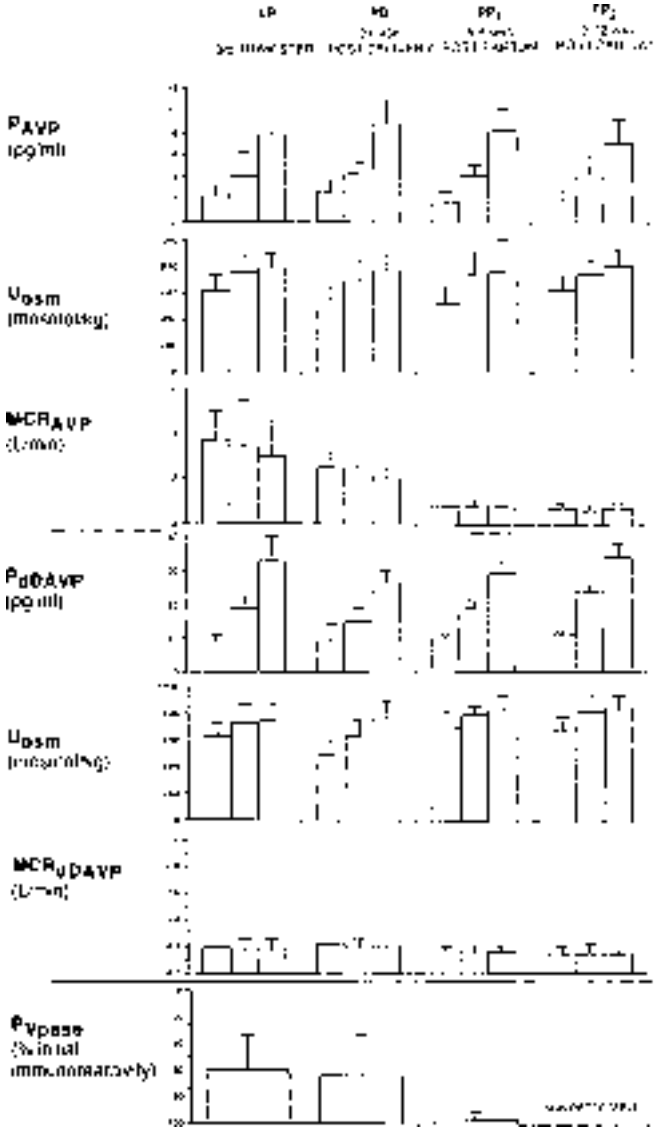

FIGURE 81.11 Plasma levels and metabolic clearance rates (MCRs) of AVP and DDAVP (1-deamino-8-D-AVP) measured serially starting in the third trimester, then 24–48 h postpartum, as well as 5–6 and 10–12 weeks after delivery. Above each bar is one SD. P_{Vpase} = plasma vasopressinase levels. *[From Ref.,[164] with permission]*

No single body position is maintained all day, and in addition the posturally induced antidiuresis rarely retards urine flow sufficiently to account for the chronically reduced P_{osm} (and thus the decreased plasma sodium levels[9,71]) observed in pregnancy.

Nonosmotic Stimulus for AVP Secretion in Pregnancy

The relative contribution of nonosmotic factors to the regulation of AVP secretion during pregnancy is uncertain, but in the nonpregnant human, volume is an important determinant of AVP release: hypovolemia stimulates, whereas hypervolemia blunts hormone secretion. In gestation, absolute blood volume increases markedly, but how the "effective volume" is sensed is a subject of considerable speculation, ([183–186] and discussed below). In this respect, the pregnant rat, which also undergoes a 40–50% increase in plasma volume near term, resets its volume-sensing, vasopressin secretory mechanisms such that the increased volume is sensed as normal.[45,170,187,188] Hypovolemia may decrease the osmotic thresholds for hormone release and thirst (see the chapters by Robertson, MacKnight et al., and Fitzsimons, Vol. 2), and some have ascribed the osmoregulatory changes in human pregnancy to an "underfilling" of the dilated intravascular space, ([184–186] and see below). However, expansion of the central volume by head-out water immersion during the first or last trimester had no effect on either the reduced tonicity or the decreased osmotic thresholds in pregnant women,[167] and P_{osm} could not be restored by overexpansion of volume (produced by administration of exogenous mineralocorticoids) maintained throughout gestation in rats.[170]

Urine Concentration and Dilution

Studies of maximum urinary concentrating capacity (U_{max}) during gestation are reviewed elsewhere[4] [see also Table 81.2 of the first edition of this text,[4] which summarizes data from 255 women in seven publications]. However, there are only three reports that include nonpregnant controls whose mean U_{max} is sufficiently high for valid comparisons. Urine osmolality was lower in the pregnant women in each of these studies, but not significantly so (probably due to the limited number of subjects). In any case, the differences from nonpregnant controls were too small to be of biological significance.

Urinary dilution, too, seems unchanged or only minimally affected by gestation.[4,9] Pregnant women excrete water loads as well as when not pregnant,[163] and gravid rats seem to excrete water more efficiently than virgin controls.[172] The latter observation is of special interest because of the apparent paradoxical observation that AQ2 mRNA and protein are upregulated in the gravid rat.[174] Immunohistochemistry of medullary tissue suggested that the increase in protein was mainly in apical membranes, which should have blunted the animal's ability to excrete water (as would have small undetectable increases in P_{AVP}, which the authors postulated as causing the upregulation). However, this apparent paradox may be resolved, if during the imposition of water loading, the mechanism (s) responsible for the basal increase in AQ2 expression during pregnancy are superseded.[189]

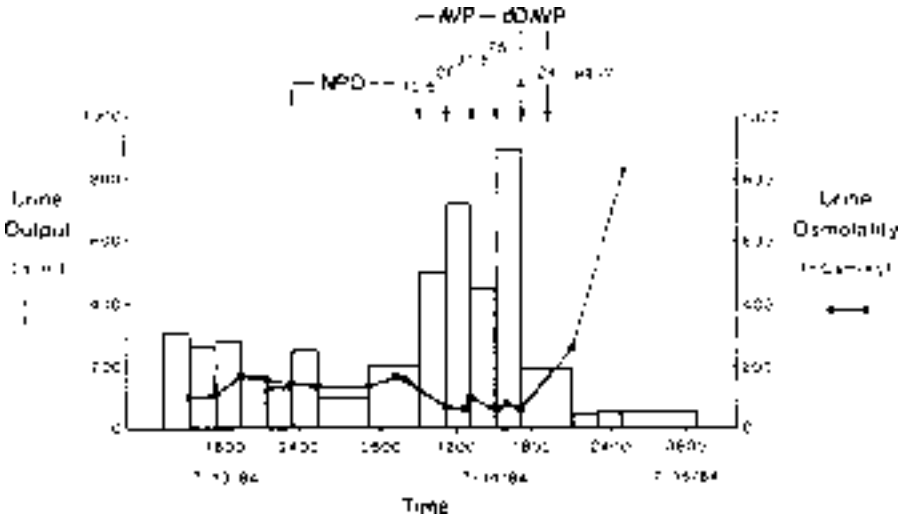

FIGURE 81.12 Urine volume and U_{osm} on postpartum day 6 in a patient who developed DI late in pregnancy and whose polyuria increased in the puerperium (~25 L/24 h). She was unable to concentrate her urine during fluid restriction (NPO), and P_{AVP} was undetectable despite a P_{Na} of 153 mEq/L. DDAVP therapy, however, increased U_{osm} to 800 mOsm/kg. The authors also measured a P_{AVP} of 240 pg/mL 30 min after the last AVP dose (when several thousand pg/mL should have been circulating), but demonstrated that this radioimmunoassay material was not bioactive and probably represented fragments. Finally, vasopressinase level measured 12 days postpartum was 10-fold higher than in women at term. See text for definitions of abbreviations. *[From Ref.,[179] with permission]*

TABLE 81.2 Analysis of Weight Gain

	Increase in Weight, g			
Tissues and Fluids Accounted for	**10 weeks**	**20 weeks**	**30 weeks**	**40 weeks**
Fetus	5	300	1500	3400
Placenta	20	170	430	650
Amniotic fluid	30	350	750	800
Uterus	140	320	600	970
Mammary gland	45	180	360	405
Blood	100	600	1300	1250
Extracellular extravascular fluid	0	30	80	1680
Total	340	1950	5020	9155
Total weight gained	650	4000	8500	12500
Weight not accounted for	310	2050	3480	3345

When investigating urinary diluting capacity in humans, one should be aware that supine posture can interfere with this test. Therefore, studies aimed at detecting minimal urine osmolality or maximum free water clearance should be performed with the patient lying on her side. However, while lateral recumbency is the preferred position for prenatal measurement of most renal functional parameters, this posture interferes with tests of U_{max}. For example, Davison et al.[71] demonstrated that U_{osm} actually decreased in patients dehydrated for 12 h when they assumed a lateral decubitus position for an additional 3 h, but increased when the test was repeated with the subjects sitting quietly. These observations may be explained by fluid mobilization from the extremities during bed rest, which results in either volume suppression of antidiuretic hormone release or in a mild osmotic diuresis. These results demonstrate the importance of upright posture, such as quiet sitting, when tests of maximum urine concentrating ability are performed during pregnancy.

VOLUME HOMEOSTASIS

Factors controlling volume homeostasis in pregnancy are incompletely understood and controversial. At one time, authorities believed that pregnant women retained salt excessively, thus predisposing them to develop hypertension. Sodium intake was curtailed and at times diuretics were prescribed prophylactically. More recently, the gravida was considered a subtle sodium waster, and supplemental salt was even advocated as a means of avoiding preeclampsia (reviewed in Refs.[4,9,150] A third view, to which we subscribe, is that renal sodium handling is similar in pregnant and nonpregnant women. This section summarizes current views on sodium handling and volume homeostasis in normal pregnancy.

Weight Gain

Healthy primigravidas gain ~12 kg during gestation, whereas multiparous women gain about 1 kg less. Most of this gain (~9.5 kg) occurs after the 20th gestational week.[190] Not all of the increase can be accounted for by the products of conception, reproductive tissues, or total body water (discussed below), but 4–6 kg of the added weight may be accounted for by increments

in maternal fat stores.[151,183,190,191] The gain of 12 kg cited above was recorded in pregnant women without any edema or with only leg swelling.[4,190] However, 15% of normal pregnant women may develop generalized edema (including swelling of fingers and face). Their weight gain averaged 14.5 kg, of which 4.9 kg was due to increase in the extracellular-extravascular compartments.

The value of 12 kg is well above averages reported in the older literature. Most surprising, however, is that in the past practitioners tended to regard published averages as upper limits of permissible weight gain, and many pregnant women have been admonished for excessive weight gain and their salt or calorie intake, or both, needlessly restricted. It should be emphasized that some women gain little weight while others may gain twice the average, and gestation proceeds uneventfully in both.

Alterations in Fluid Volume

Most of the weight added in pregnancy represents fluid retention. Total body water has been measured during pregnancy using deuterium, the stable isotope of oxygen [O^{18}], and by bioelectrical impedance.[151,190–194] The results suggest total accumulations of 6–9 L, although they vary due to methodological differences. Of interest, in a serial study starting before conception, Forsum et al.[151] noted higher increments in body fat than other investigators.

The volume of water accumulated in the extracellular compartment remains uncertain due largely to the lack of an ideal tracer for use in pregnant women. Reported estimates vary widely, and there is poor correspondence in those subjects in whom both extracellular and total body water were measured simultaneously. Reports in which thiocyanate was used as the tracer and the gain in extracellular space calculated as 6–7 L appear the most reasonable, since when added to the estimated 1.8–2.5 L of accrued intracellular water, the total approximates that measured directly with deuterium oxide.[4,150,190] Nonetheless, more research in this area will be needed before definitive conclusions can be reached.

Intravascular volume increases during pregnancy due mainly to increases in plasma water and a small increment in red blood cell mass (Table 81.2).[4,9,150,183,195] Plasma volume has been measured in pregnant women by several methods, but usually with Evans blue dye.[9,26,150,195,196] In the earlier literature, values were recorded as increasing until gestational week 30 and then declining. Such studies were in error, because late in gestation the indicator may not attain complete mixing within 10 min, if the subject is positioned in a supine or sitting position. Subsequent studies were performed serially, with the gravidas positioned in lateral recumbency for each measurement, and increases in plasma volume started in the first trimester, accelerated in the second, peaked near gestational week 32, and remained elevated until term.[195,197,198] The maximal gain averages 1,100–1,300 mL, although larger increments may occur when there are multiple fetuses.

Studies in animal models demonstrate increases in both plasma and red cell volume during pregnancy.[2,187] Of interest is an observation that plasma volume increases during early rat gestation even when the animals have a "zero" sodium intake, suggesting that some of the gain can be from internal redistribution of salt and water under this dietary condition.[199,200]

Since expansion of the plasma volume accounts for only 20–30% of the increase in extracellular space, increases in interstitial fluid must be substantial. In his analysis of the distribution of body water during pregnancy, Hytten[190] suggested the following: in women with no edema or leg edema only (~80% of normal gravidas), increments in interstitial fluid average 2.5 L at term, whereas in normotensive women with generalized edema the increase in interstitial fluid reaches ~5 L at term. In normal pregnant women, both with and without edema, the greatest accrual of interstitial fluid occurs in the third trimester, thus lagging somewhat behind the increment in plasma volume.

The mechanisms explaining interstitial fluid volume increases are incompletely understood. Unfortunately, there are but sporadic and/or conflicting data from both animal models and humans.[183,195] Plasma albumin decreases 0.5–1.0 g/dL during pregnancy, but its concentration in interstitial fluid may fall even further; thus, paradoxically, the oncotic pressure difference favors retention of fluid within the capillaries.[195,201,202] However, pregnancy is a vasodilated state (see below), and precapillary resistance is decreased, capillary hydrostatic pressure elevated, and, if the capillary ultrafiltration coefficient is unaltered[203] or higher, more fluid will enter the interstitium, especially if interstitial compliance is increased. In the steady state, there would also be enhanced return of fluid to the intravascular compartment and increased removal of protein through the lymphatics.

There is also speculation that some of the interstitial changes during gestation are due to alterations in the properties of connective tissue ground substance.[4,9,183,190] Thus, although low-molecular weight substances (e.g., cellular nutrients) diffuse readily through this material, fluid is "complexed" and poorly mobilized by diuretics. Furthermore, alterations in interstitial compliance, mediated through humorally induced changes in mucopolysaccharides,

could conceivably influence blood pressure. Data in favor of such a hypothesis are sparse (reviewed in Refs[4,9,183,190]) but provocative, and await further study.

On the one hand, the normal gain in interstitial volume during pregnancy may reduce the safety margin for edema formation in pathological states,[183] thus explaining why previously healthy gravidas may develop pulmonary edema when tocolytic therapy or the development of preeclampsia provokes additional fluid retention. On the other, there is the theoretical advantage of providing a large pool of interstitial fluid, which can be mobilized into the intravascular space when sudden depletion occurs, for example, by hemorrhage. Finally, increased fluid filtration across the capillary may protect the gravida from circulatory overload whose total blood volume is already increased.

In summary, pregnancy is characterized by the accumulation of >7 L of fluid, which is stored not only in the products of conception but also in the maternal intracellular, plasma, and interstitial compartments. In essence, there is maternal "physiologic hypervolemia." However, the volume receptors apparently reset to the hypervolemic state, thus sensing it as normal, and with imposition of salt restriction or diuretic therapy, the maternal response is similar to that observed in salt-depleted nonpregnant subjects (see below).

Renal Sodium Handling

A pregnant woman accrues ~950 mEq of sodium (Table 81.1), which is distributed between the products of conception and the maternal extracellular space (see above). This positive balance occurs gradually throughout gestation with the third trimester being the period of most rapid accumulation; however, the quantity retained is too small to be detected by conventional balance techniques. Renal sodium handling is the primary determinant of volume homeostasis, thus a brief review of the hemodynamic and humoral changes of normal gestation, which might influence urinary sodium excretion follows.

Circulating levels of many antinatriuretic hormones, mainly mineralocorticoids (e.g., aldosterone and DOC) increase during gestation, often markedly (see the previous edition, and Refs,[9,150,195] which provide reviews and monographs with detailed bibliographies). In this regard, the renin–angiotensin system is the control mechanism most studied,[9,195,204] and Figure 81.13 summarizes a detailed study by Wilson et al.[205] in which plasma renin substrate, activity (Plasma renin activity), and urinary sodium and potassium excretion were measured throughout gestation. Note the sequential increases in plasma renin substrate and activity, which start early in gestation. Salt excretion (reflecting intake) was similar during gestation and in the postpartum period, suggesting that inadequate sodium intake does not account for these rises. Moreover, despite these high circulating levels of plasma renin substrate and activity, the renin–angiotensin system responds appropriately to provocative maneuvers, e.g., circulating levels decrease after saline infusion or during a high salt diet, or rise further after the administration of diuretics or when dietary sodium is restricted.[9,195,206–211] Furthermore, inhibition of aldosterone biosynthesis causes a diuresis and subtle signs of volume depletion, the salt loss already apparent when aldosterone excretion, though decreasing, is still considerably above nonpregnant levels.[212] Thus, the renin–angiotensin system does not function autonomously during pregnancy as some have presupposed. Rather, the high circulating levels of aldosterone, which often exceed those measured in nonpregnant patients with primary aldosteronism, are appropriate in pregnancy responding to homeostatic demands.

Nevertheless, physical factors do seem to have a greater influence on renal handling of salt during pregnancy then they do in the nonpregnant state including the antinatriuretic potential of the upright or supine position, and perhaps the vascular changes in the uterus especially in late gestation which has been likened to an arteriovenous shunt.[4,9,150] In pregnancy, therefore, the supine and upright positions are markedly antinatriuretic, and quiet standing may cause greater reductions in sodium excretion in pregnant than in nonpregnant women.[4,9,150] Thus, bed rest in the lateral recumbent position is helpful in the rare instances when a diuretic appears necessary.

Postural influences may also underlie the circadian rhythms of solute and water excretion in pregnant women. Recumbent gravidas typically display patterns of urine flow, creatinine clearance, and aldosterone and electrolyte excretion similar to those of nonpregnant subjects (i.e., daytime peaks and nighttime nadirs). However, ambulation results in more striking changes during pregnancy than in the nonpregnant state, and excretory peaks frequently occur at night (reviewed in Refs[4,9]). On the other hand, nighttime excretion of sodium and solute-free water may be greatest early in pregnancy when postural effects are minimal, suggesting that humoral, rather than mechanical factors are responsible for these changes.[4,9]

Many hormones and autocoids change during pregnancy, which can theoretically enhance renal sodium excretion. These include increased circulating levels of oxytocin, melanocyte stimulating hormone, progesterone, natriuretic peptides, vasodilating PGs, and NO

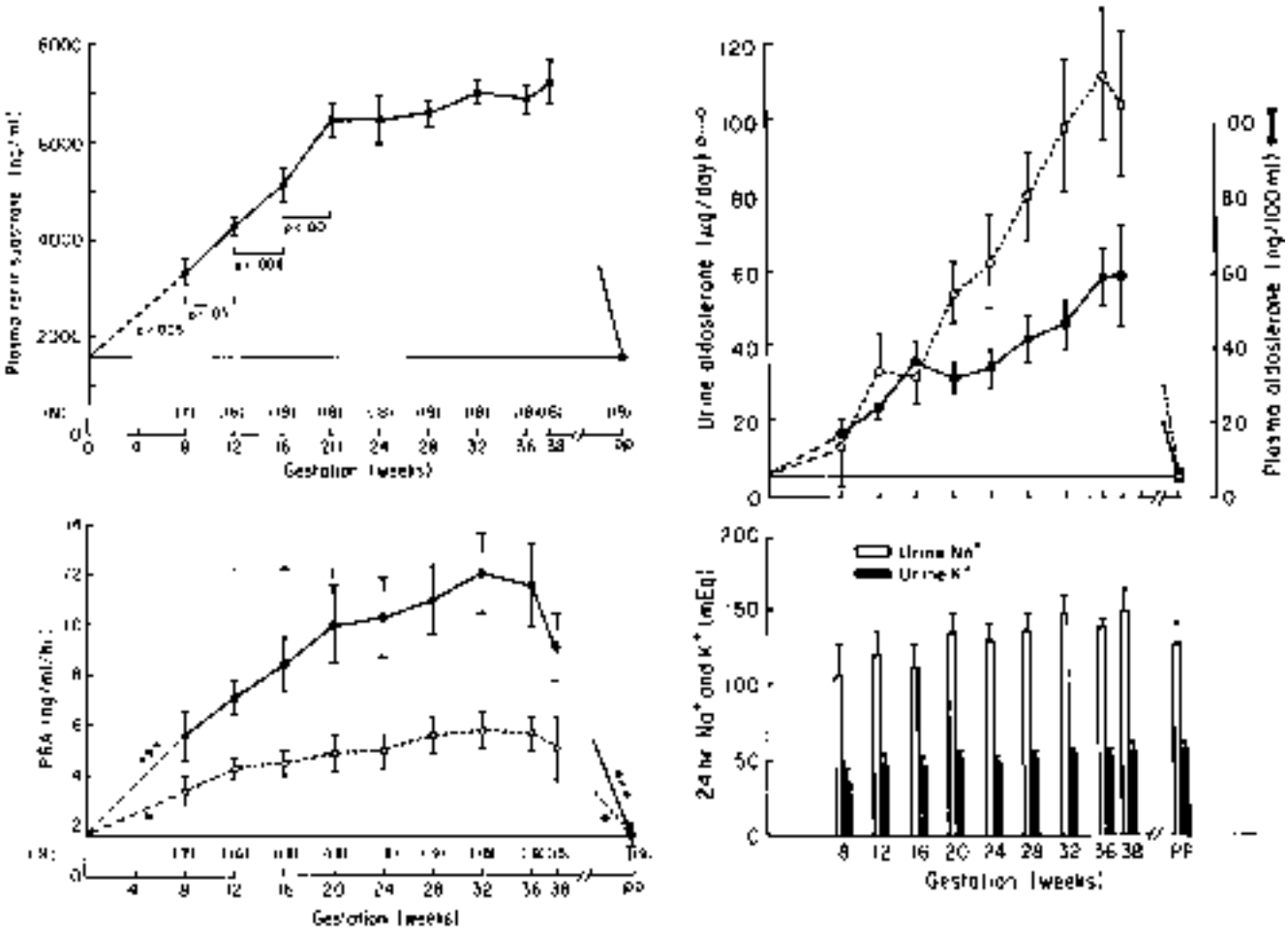

FIGURE 81.13 Sequential changes in plasma renin substrate (A), activity (B), and plasma and urine aldosterone (C) during pregnancy, all related to urine sodium excretion. Dashed line in B represents values normalized to the postpartum substrate levels. *[From Ref.,[156] with permission]*

(for literature reviews see Chapter 100 in the first edition and Refs[9,195,213]). Progesterone levels increase markedly even over those observed during the luteal phase of the menstrual cycle, and binds with higher affinity than aldosterone to the mineralocorticoid receptor prompting investigators to question how aldosterone functions in face of such high circulating levels of progesterone.[214] One possibility may be that progesterone actually contributes to antinatriuresis, as it is the major source of DOC production during pregnancy.[215–218] Because renal steroid 21-hydroxylase activity (the enzyme that converts progesterone to DOC) may be particularly high in pregnancy, a considerable portion of maternal DOC may be produced in the vicinity of the renal receptors whose stimulation enhance sodium reabsorption.[218]

There is considerable literature devoted to the various natriuretic factors and Na^+–K^+ ATPase inhibitors in pregnancy, but their influence on renal sodium excretion during pregnancy is also obscure. In particular, the production of atrial natriuretic peptide (ANP) exceeds increases in metabolic clearance, so that circulating levels are increased.[213,219–221] However, the increments in P_{ANP} are quite modest in relation to the marked increases in extracellular volume that occurs in normal pregnancy. Finally, the renal resistance to the natriuretic effects of atrial peptides described in animal models[222–225] does not seem to occur in human gestation.[221]

Perhaps, the major factor of importance when considering renal salt handling during pregnancy is the profound increase in GFR. Thus, every day more than 10,000 additional milliequivalents of sodium are filtered that must be reabsorbed by the renal tubules, a quantity which greatly exceeds the salt-retaining effects of large amounts of aldosterone, DOC, or estrogens administered experimentally. Quantitatively, the increase in filtered load of sodium is so enormous that

one might anticipate that it would render gravidas more vulnerable to salt and volume depletion. Thus, on the one hand, gravid rats tolerate sodium restriction and adrenalectomy more poorly than do the virgin controls[9,226] but, on the other, all pregnant species including humans are in positive sodium balance, and as noted, many women exhibit edema at some point of their gestation.

Effects of Acute and Chronic Sodium Loads

Whether salt-retaining or salt-losing influences predominate during gestation might be clarified by testing the capacity of pregnant and nonpregnant subjects to excrete saline loads. In the older literature, most studies lack nonpregnant controls.[4,9,150] An exception is that of Chesley and colleagues,[227] who infused 3% saline (410 mEq Na over 30 min) and observed that pregnant subjects excreted the administered sodium as well as the nonpregnant controls despite the fact that they were tested in the supine position and moderately sodium restricted prior to the test. These results, however, were disputed by Weinberger et al.,[211] who observed that gravid subjects given 2 L of isotonic saline over 4 h excreted significantly less sodium than comparably treated nonpregnant controls. More recently, in an extensive and meticulously conducted study in which dietary sodium intake was controlled, and the subjects were evaluated serially during the second and third trimesters and again postpartum, Brown et al.[228] confirmed the original observations of Chesley and coworkers.[227] A similar conclusion was reached in an animal study, in which term pregnant rats excreted acute sodium loads as well as, or better than, virgin littermate controls; however, the animals were anesthetized.[229]

Acute imposition of sodium loads does not necessarily relate to the homeostatic processes involved in sodium balance that occur over the course of an entire gestation. Consequently, several investigators conducted metabolic balance studies in an attempt to assess salt handling over a more prolonged period during pregnancy. Some authors concluded that gravidas have an impaired ability to conserve sodium and may show signs of volume depletion when dietary salt content is too low, whereas others stated that pregnant and nonpregnant subjects withstood challenges to sodium balance in a comparable fashion (reviewed in Refs[4,9]). Bay and Ferris[206] reported that pregnant women achieved balance as rapidly as nonpregnant controls while consuming diets containing as little as 10 mEq of sodium daily. Urinary sodium excretion decreased to similar values in pregnant and nonpregnant subjects 5−7 days after the low salt diet was instituted. These data, however, may lead to different conclusions from those reached by the authors when the following factors are considered: the small daily positive balance of 3−6 mEq in late gestation is too small to be detected by routine metabolic studies, and gravidas appear to excrete all their ingested sodium. Moreover, when gravid subjects are salt restricted, the increased sodium demands of pregnancy should make them resemble patients with cirrhosis or congestive heart failure who virtually eliminate sodium from their urine. Hence, the dietary restriction of 10 mEq daily in the report by Bay and Ferris should have revealed discernible differences in sodium balance between pregnant and control subjects. However, the gravidas in this study actually excreted 1−2 mEq more than the nonpregnant women, failed to gain the 1−2 lb of weight expected during a 7-day period in late gestation, and actually lost >2 lb. Also, plasma aldosterone increased to levels, which are considered high even for pregnant women. Thus the data of Bay and Ferris actually support conclusions contrary to the one they made, i.e., some salt-restricted pregnant women are prone to subtle sodium wasting, and others may achieve balance by invoking compensatory mechanisms such as adrenal steroid production.

In summary, there is a positive, cumulative salt balance during gestation, which amounts to a few milliequivalents of sodium daily. There are many physiological changes during pregnancy that impact sodium balance including the rise in GFR, the effects of physical factors, altered plasma levels of both antinatriuretic and natriuretic hormones, etc., but to what degree each contributes to the overall renal handling of sodium during pregnancy remains uncertain. On the one hand, the vast array and complexity of changing factors during pregnancy that affect sodium balance may render gravid women particularly susceptible to pathological outcomes should a component(s) of this intricate control system be amiss, e.g., the appearance of generalized edema and even obscure hypokalemia occasionally encountered in otherwise normal gravidas. On the other, the vast array and complexity of changing factors in pregnancy may be advantageous and evolutionarily conserved because of the inherent redundancy of mechanisms that can compensate one for the other, in the event that one or more should fail.

Significance of the Volume Changes During Pregnancy

On the one hand, the physiological hypervolemia may be a suboptimal response to the general arterial vasodilation of pregnancy, the so-called “underfill” or “primary arterial dilation” theories. On the other, the volume changes may be a primary event arising from the marked increase in antinatriuretic factors such mineralocorticoids, the so-called “overfill” theory.

However, an intermediate possibility is that volume-sensing mechanisms are continually reset as gestation progresses, and as such, the increments in absolute volume are "sensed" as normal ("normal-fill"). These contrasting hypotheses, previously mentioned in the section on osmoregulation, are clarified further below (see Ref.[183] for extensive review).

Evidence supporting the "underfill" theory is detailed by Schrier[184–186,230] and Duvekot[231] and their respective colleagues, and includes the marked activation of the renin–angiotensin system, substantiated not only by an increase in all of its circulating components (Figure 81.13) but also by the observation that pregnant women manifest exaggerated increases in aldosterone release in response to low-dose infusion of angiotensin II.[232] There is also evidence that the gestational decline in systemic vascular resistance precedes intravascular volume expansion, thus supporting the "primary arterial vasodilation" theory,[26,47,231,233] and administration of angiotensin-converting enzyme (ACE) inhibitors early in pregnancy evokes exaggerated decrements in blood pressure.[230] Finally, as noted, adrenalectomy, sodium restriction, or both, are tolerated more poorly in pregnant animal models.[226]

The "overfill" theory is supported by increases in renal hemodynamics and GFR, *absolute* increments in extracellular and intravascular volumes, elevation in the levels of circulating natriuretic factors and inhibitors of Na^+–K^+ ATPase,[195,213,220,221] and by a report of increased sodium excretory capacity in response to saline infusions.[211] Gravidas also appear more susceptible to complications of volume overload, especially those with underlying cardiac or renal disorders, or those receiving tocolytic therapy with sympathomimetic agents. In addition, they seem to tolerate blood loss better than do nonpregnant women. Finally, the mean circulatory filling pressure measured in gravid rodents has been consistently described as high normal or increased[234–238] as discussed further in Ref.[183]

Evidence for "normal-fill" is supported by animal experiments demonstrating the relationship between intravascular volume depletion and AVP release (detailed in the section on osmoregulation and Refs[74,167,170,187]). Also studies in rats and humans using indices of proximal tubular function such as fractional lithium and free water clearances suggest that sodium and water reabsorption by this nephron segment are unaltered.[239,240] Moreover, with water loading both species dilute their urine normally or better than nonpregnant controls.[71,163,172] Of note here is that failure to dilute the urine normally and excrete water and sodium are major pathophysiological features of hyponatremic patients with cirrhosis or cardiac failure, the prototypic diseases in which absolute extracellular and intravascular volumes are increased while "effective circulating volume" is low. Pregnancy, however, is a physiological condition, and thus salt and water excretory responses to acute sodium and water loads are comparable in pregnant and nonpregnant populations consistent with the concept that pregnancy is a "normal-fill" state (see Refs cited above and[9,227–229]). Finally, as detailed elsewhere,[183,241] circulatory performance during gestation (including the adequate response to exercise) is further evidence that gravidas "sense" their intravascular volume as normal.

In summary, disputes surrounding the true nature of the volume accrual in pregnancy as noted above are yet to be settled, and it may be that all views are correct with each being apropos depending on the stage of gestation, e.g., early primary vasodilation[26,46,47,231,233] followed by rapid compensation to normal-fill, and in some cases, overfill during late gestation due to a predominance of antinatriuretic influences such as physical factors at that time. Settling these controversies should perhaps be a priority, because understanding how the pregnant woman "senses" her volume changes may have wider implications for our understanding and management of gravidas with cardiac disease and hypertensive disorders such as preeclampsia.

RENAL DISORDERS AND GESTATION

This section surveys renal and obstetrical outcomes in pregnancies associated with kidney disease, including acute problems (e.g., urinary tract infection and sudden renal failure), as well as the natural history of gestation in women with chronic renal parenchymal disorders. Once, women in the latter category were advised against conception, while many who had already conceived had their gestations terminated, regardless of renal functional status. Data collected during the past three decades, albeit primarily retrospective, has led to a more rational and optimistic approach to counseling these patients, as well as to guidelines for managing their gestations. Of note, most women with chronic kidney disorders but preserved, or only mildly compromised renal function, can anticipate successful pregnancy outcomes with minimal risk of accelerating their disease.

Patient Evaluation

The approach to gravid women with renal problems is similar to that in nonpregnant populations, although tests which utilize ionizing radiation or radiochemicals should obviously be deferred until after pregnancy unless deemed crucial. Exposures to #5 rads do not

appear to harm the fetus.[242] The effect of the enhanced GFR, as well as alterations in acid-base parameters, and osmoregulation, on normal ranges of circulating creatinine, urea nitrogen, bicarbonate, sodium, and osmoles; blood pH and CO_2 tension were discussed in the previous section and will not be repeated here. Ammonia loading to determine the kidney's ability to excrete protons and achieve a minimal urine pH is rarely performed in pregnancy,[158,197,243] and gravidas may be more susceptible to NH_4Cl-induced nausea than nonpregnant women. When assessing GFR by endogenous creatinine clearance the lower limits of normal should be increased by ~30%. Of note, other endogenous proteins easily measured in clinical labs have recently suggested as better markers of GFR than creatinine levels. One, especially, Cystatin-C has been recommended for use in pregnant women, but its validity for use in pregnancy has been recently questioned.[244,245] Finally, when timed urines are neither practical (e.g., decisions during labor) nor reliable use of the Cockcroft–Gault formula based on preconception body weight can be utilized.[246]

Most, but not all, investigators[247] detect increases in urinary protein excretion in pregnancy.[31,134,248] Accepting the relative imprecision and variabilities of the methods used by hospital laboratories (as well as the fact that certain proteins remain undetected by some and not by other tests), 300 mg/day should be considered the upper limit of protein excretion in pregnancy. There are limited data on normal limits and validity of protein and/or albumin creatinine ratios in gestation. As previously discussed, the fate of urinary albumin excretion is disputed.[22,31,248–256] Even if it does rise, the increments are quite small, and thus use of nonpregnant upper limits of normal is probably permissible. Urine albumin excretion may have predictive value in relation to pregnancy outcome in women with diabetes, and those at high risk for preeclampsia but more research is needed here.

One should recall that as many as 5% of healthy adolescents and young adults manifest postural proteinuria, and this may become apparent or be first detected during pregnancy, especially near term when gravidas tend toward lordosis, a posture that augments urinary protein excretion. Finally, studies of tubular proteinuria, as well as enzymuria in either normal gravidas or those with renal disorders have sporadically appeared [summarized in Refs[4,22,257]]. These measurements are yet to be proved useful in the detection and management of renal disorders in pregnant women.

There have been few attempts to quantitate the urine sediment in pregnancy. Whether or not there is an increase in leukocyturia is unclear, but excretion of red blood cells definitely rises, so that 1–2/RBC per high-power field, considered abnormal in nonpregnant patients is probably acceptable in gravidas.[9,150,160,258] One should be aware, though, that microscopic and even gross hematuria may complicate otherwise uneventful gestations. When this occurs, the differential diagnosis includes all causes of urinary tract bleeding in nonpregnant populations, but often a cause cannot be found and the bleeding subsides postpartum. In some cases, the hematuria may be due to the rupture of small veins around the dilated renal pelvis,[259] the bleeding recurring with subsequent pregnancies. When faced with *de novo* hematuria in a pregnant woman, we follow up the urinalysis with ultrasonographic or magnetic resonance imaging (MRI), deferring more extensive investigations to the postpartum period.

Renal Biopsy

There are few indications to perform percutaneous renal biopsies in pregnant women, although the procedure has the same morbidity as that reported in nonpregnant patients.[260] In 1987, Packham and Fairley[261] described their large experience with renal biopsy during gestation and suggested that most pregnant women with undiagnosed hematuria and/or proteinuria should have antepartum biopsy, claiming that such a policy has important relevance for management and prognosis. We believe that their indications are too broad, and recommend the procedure in only the following instances[260]: (a) sudden deterioration of renal function with no obvious cause present, because certain forms of rapidly progressive glomerulonephritis may respond to aggressive treatment such as steroid pulses and perhaps plasma exchange; and (b) symptomatic nephrotic syndrome remote from term. For the latter, some might consider a therapeutic trial of steroids, but we prefer to determine first whether the lesion is one likely to respond to this treatment before exposing the gravida to it. On the other hand, proteinuria alone in a normotensive woman with well-preserved renal function who has neither marked hypoalbuminemia nor intolerable edema would lead us to examine the patient at more frequent intervals and defer biopsy to the postpartum period. This is because prognosis is determined primarily by the patient's functional status, as reflected in the serum creatinine level or its clearance, and by the presence or absence of hypertension (see below). Our approach to gravidas presenting with asymptomatic microscopic hematuria alone and no pathological findings by ultrasonography is similar. Finally, renal biopsy should not be performed after gestational week 32, because at this stage the decision to deliver is usually made rapidly and independent of biopsy results.

Urinary Tract Infection

Infections of the urinary tract represent the most frequent renal problem encountered during gestation.[9,150,262–264] Although the prevalence of asymptomatic bacteriuria, which ranges between 2% and 10%, is similar to that in nonpregnant populations [exceptions are gravidas with sickle cell trait and diabetes in whom higher rates have been observed[262]], the natural history of covert urinary tract infections differs from that in nongravid women. In the latter, the situation is quite benign, whereas during pregnancy progression to overt cystitis or pyelonephritis occurs in up to 40% of affected gravidas.[9,262–265] It has also been claimed that asymptomatic bacteriuria is associated with increased incidence of anemia, hypertension, and intrauterine growth retardation, as well as "preterm/low-birthweight" infants, but data supporting these assertions are lacking or equivocal.[9,150,262,266–269]

The pathophysiological basis for the increased morbidity noted above can be traced to two of the "physiological" changes in the urinary tract detailed in the preceding sections. There is urinary stasis and ureteral dilatation (sometimes obstructive in origin), and the urine of gravidas has a high nutrient content which supports growth better than that of nonpregnant subjects. Consequently, most authorities believe that all gravidas should be screened at their initial prenatal visit, and women with confirmed positive cultures should be treated, guided by the antibiotic sensitivity of the isolated microorganisms.[9,262,264] Indeed, detection and therapy of asymptomatic infections seems to prevent approximately two-thirds of potential antepartum pyelonephritis.[262] Other investigators,[270–272] however, question the sensitivity and cost-effectiveness of routine screening and suggest that testing be limited to women with a history of recurrent urinary tract infection.

The incidence of bacteriuria increases to ~17% immediately after delivery but decreases again to about 4% if the urine is cultured on day 3 postpartum[273]

Symptomatic Infections

Cystitis or pyelonephritis complicates about 3% of all pregnancies.[262,264] Universal screening for covert bacteriuria does not seem to have decreased the incidence of acute cystitis (1–2%), but appears to be responsible for the decrement in the potentially more serious complication, acute pyelonephritis. Its incidence, once nearly 3%, is now less than 1%, a decline ascribed to prompt treatment once asymptomatic bacteriuria is detected.[262]

Cystitis seems to be a distinct entity with little relationship to covert bacteriuria. The latter is unusual after gestational week 12, whereas most bouts of cystitis appear in the second trimester in women with previously negative screening cultures. Furthermore, it is easier to eradicate, and has a lower recurrence rate, than asymptomatic bacteriuria.[262,264]

Acute pyelonephritis is a potentially more threatening disorder in pregnancy. Most instances, ~70% related to preexisting asymptomatic bacteriuria, but the offending organism may be newly acquired. About 10% of these symptomatic infections in the initial trimester, and the remainder equally divided between the last two trimesters.[262,264] The infecting organisms parallel those cultured in women with asymptomatic bacteriuria (>90% gram-negative rods, primarily *E. coli*).[262–264,272,274] Of importance, gestation seems to decrease tolerance to these pathogens, and gravidas with acute pyelonephritis seem more prone to shock and respiratory distress syndrome, as well as renal, hematological, and liver function abnormalities.[9,262,264,275] Symptomatic infections of the kidney have also been implicated in the etiology of congenital abnormalities, premature delivery, fetal growth retardation, and intrauterine death.[9,150] It is noteworthy that while the infectious attack appears to have little effect on the renal function of nonpregnant patients, acute pyelonephritis in pregnant women may result in transient but marked decrements in GFR.[262,264]

Perinephric abscess, renal carbuncle, and renal cortical abscess are unusual events in pregnancy, but should be considered in cases of occult or resistant infection.[9,262] This is especially true in the immediate puerperium, when focus on uterine and abdominal sources of infection frequently leads physicians to ignore the possibility of the complications noted above.

Management

As of 2011, most authorities would prescribe 7–10 days of antibiotics to treat covert bacteriuria. Such regimens eradicate bacteriuria in 70% of these asymptomatic patients and cure >90% of women with cystitis.[262,264] Shorter courses, currently under investigation, include single dose therapy,[276] an approach, that if proven successful will minimize toxicity, and perhaps identify patients at increased risk for recurrent asymptomatic bacteriuria (the latter who then may benefit from suppressive therapy).[262,264] Also, in 2006 a large WHO randomized trial testing the use of dip sticks to detect significant bacteriuria followed by single day therapy to eradicate it was underway.

While cystitis is treated on an outpatient basis, acute pyelonephritis is preferably treated in a hospital setting, In the latter respect, though, scattered reports claiming successful outpatient management periodically appear.[264,277] Most gravidas with upper tract infections respond with defervescence within 48–72 h,[262,264] but in contrast to gravidas with cystitis or covert bacteriuria, these women have a propensity

toward relapse. Thus, while patients with cystitis or asymptomatic infection warrant a 7–10-day course of the appropriate antibiotic, those with acute pyelonephritis should be treated with therapeutic doses for 2–3 weeks. Subsequently, they should receive continuous suppressive therapy during the remainder of gestation, as well as during the first postpartum weeks, since up to 60% of these patients will have recurrent pyelonephritis if left untreated.[262,264] Some authorities,[274] however, claim that frequent surveillance for recurrent infection, and institution of prompt treatment only when significant bacteriuria is identified, is as effective as suppressive therapy.

Acute Renal Failure

The incidence of acute renal failure (ARF) of sufficient severity to require dialytic therapy is <0.01% in industrialized nations.[278–280] This represents a substantial decline from frequencies reported during the 1960s[278] and is due most likely to liberalization of abortion laws, more aggressive antibiotic therapy, and improvement of prenatal care. Furthermore, maternal mortality associated with ARF, once almost 20%, is now unusual.[278,280,281] These reassuring statistics, however, do not apply to poorer and less industrialized nations, where obstetric patients comprise up to 25% of referrals to dialysis centers, and where ARF continues to cause substantial maternal and fetal mortality.[278,280]

Septic Abortion

Before elective pregnancy termination was legalized, estimates of illegal (usually nonsterile) abortions in the United States were as high as 1 million annually.[278] Approximately 5% of these women became critically ill, and septic shock frequently complicated by renal failure was a leading cause of maternal death. Most of these events took place during the initial trimester, giving ARF in pregnancy a bimodal distribution: one peak in early gestation comprising most cases of septic abortion, and a second after gestational week 35, mainly due to placental abruption, bleeding, and preeclampsia. In countries where access to sterile pregnancy terminations has increased, the initial peak has virtually disappeared.[278,280,281]

The presentation of women with sepsis-related ARF, especially when due to clostridia, can be quite dramatic. Onset may be sudden, from several hours to 1–2 days after the attempted abortion, associated with an abrupt rise in temperature (>40°C), often with vomiting and diarrhea (which may be bloody). Muscle pain may be present, most intensely in the upper limbs, thorax, and abdomen; the latter leading at times to erroneous diagnosis of an intraabdominal inflammatory process (especially when a history of induced abortion is denied or not sought for). Vaginal bleeding may be absent, and clostridia organisms are difficult to culture or detect in the smear, besides being also normally present in the female genital tract. Progression to shock may be rapid, and the patients can manifest a peculiar bronze color due to association of jaundice (secondary to hemolysis) with cutaneous vasodilatation, cyanosis, and pallor. Other features include severe anemia, marked leukocytosis, and severe thrombocytopenia (as part of an intravascular coagulopathy). Hypocalcemia also occurs, and has been reported to be of sufficient severity to provoke tetany. An abdominal roentgenogram may demonstrate air in the uterus or abdomen secondary to gas-forming organisms and/or perforation. Death occurs rapidly in a small percentage of patients, but most respond to antibiotics and volume resuscitation, and survival depends largely on management of the renal failure. (The roles of hyperbaric oxygen, antitoxin, and exchange transfusion, as well as controversies concerning a conservative approach versus early surgical intervention to remove the infected uterus are discussed in most obstetric texts, and in Refs.[278,280,282]

Other Pregnancy-Related Causes

Volume depletion complicating hyperemesis gravidarum, severe vomiting associated with pyelonephritis, and uterine hemorrhage due to a variety of causes (including placenta previa, abruption, failure of the postpartum uterus to contract, lacerations, and perforations) all cause ARF mainly of the tubular necrosis variety.[278,280] Failure to estimate blood loss correctly because the hemorrhage is "concealed" behind the placenta contributes to the development of renal failure in these patients, and such judgment errors can be minimized by the judicial and rapid use of ultrasonic techniques. ARF associated with preeclampsia is discussed in the final section of this chapter.

Cortical Necrosis

Renal cortical necrosis, which was once more frequent in obstetric than in nonpregnant populations,[278,280,283–285] is now rare, its incidence in industrial nations being 1 in 80,000.[279] It presents more commonly in late gestation, when it is often associated with placental abruption and less commonly following retention of a dead fetus. Abruptio placentae should be considered when ARF develops suddenly between gestational weeks 26 through 30, as 45% of the patients in one series[286] had concealed hemorrhage.

Cortical necrosis may involve the whole renal cortex causing irreversible renal failure, but most cases associated with gestation are of the incomplete or "patchy" variety. The latter is characterized by an initial episode

of severe oliguria-anuria, lasting longer than uncomplicated tubular necrosis, followed by a variable return of function.[280,286]

The reason why gravidas are prone to develop cortical necrosis more readily than nonpregnant women is unclear. Many of the patients are older multiparas whose renal biopsies contain evidence of nephrosclerosis, suggesting a kidney vulnerable to whatever the inciting factor may be.[278] There may be severe and prolonged "selective" renal vasospasm causing endothelial damage and local activation of coagulation factors and/or potent vasoconstrictors. Of interest, the Sanarelli-Shwartzman reaction is produced more readily in gravid or postpartum animals than in their nonpregnant controls.[287]

Pregnancy-Specific Complications

There are two very uncommon forms of ARF peculiar to gestation. One is associated with acute fatty liver of pregnancy, and the second, of unknown etiology, occurs postpartum.

Renal failure in association with acute fatty liver is seen mainly near term but can occur shortly after midgestation.[1,9,278,280,288] The earliest manifestations of fatty liver are nausea and vomiting, important clues that may be overlooked or considered functional because the patient is pregnant. Laboratory data will confirm the presence of jaundice and other evidence of hepatic dysfunction.[278,280,289] There is an early rise in ammonia levels, which should be sought for, especially in lethargic patients. Evidence of disseminated intravascular coagulation includes decreased levels of antithrombin III.[289] Serum urate levels are also elevated, often out of proportion to the degree of renal dysfunction.[278] Ultrasonography and computed tomography of the liver also aid in establishing the diagnosis.[278]

The cause of acute fatty liver in pregnancy is unknown. Some signal its frequent association with preeclampsia.[278,290] Reversible urea cycle enzyme abnormalities resembling those in Reye's syndrome have been described.[291,292] Also of interest are women developing acute fatty liver of pregnancy or the microangiopathic hemolytic anemia associated with severe liver abnormalities associated with preeclampsia (see "HELLP syndrome" under preeclampsia below) who harbor a long chain 3-hydroxy acyl-Co-A dehydrogenous deficiency or carry mutations of the enzyme's gene resulting in deficiencies in the fetus.[293,294]

The hepatic lesion, characterized by deposition of fat microdroplets within the hepatocytes is described elsewhere in detail.[1,278,290] The kidney lesion is mild and nonspecific, and the cause of renal failure is obscure. It may be due to hemodynamic changes akin to the "hepatorenal syndrome" in some patients, or to the coagulopathy in others. Of importance, whereas mortality rates for both mother and fetus once exceeded 70% in this disease, and the frequency of accompanying ARF was 60%, these are much less frequent now. Maternal deaths average <10%, and renal dysfunction, when present, is usually mild and rarely requires dialysis.[278] These improved prognoses have been ascribed to earlier recognition of milder forms of the disease, followed by aggressive management, which includes prompt termination of the pregnancy.[278,290]

This second pregnancy-specific condition is characterized by the onset of renal failure in the puerperium after an uneventful gestation and termed *Idiopathic postpartum renal failure*. This disorder was first delineated as a specific clinical entity in the late 1960s.[295–298] By the late 1990s, only several hundred cases had been reported (under a variety of names, including irreversible postpartum renal failure, postpartum hemolytic–uremic syndrome, postpartum malignant nephrosclerosis, and late postpartum intravascular coagulation with ARF).[278,280,295,296,298] Using strict diagnostic criteria, the syndrome is defined by its onset between 1 day and several weeks after delivery. The patient presents with oliguria, or at times anuria, and progresses rapidly to azotemia, often with evidence of microangiopathic hemolytic anemia or a consumption coagulopathy. In the earliest descriptions, blood pressure was often normal, whereas the later literature stressed presentation with severe accelerated hypertension. Extrarenal manifestations have also been described. They involve the cardiovascular (cardiac dilatation and congestive heart failure) and central nervous systems (lethargy, convulsion), and are often disproportionate to the degree of uremia, hypertension, or volume overload.

The cause of this syndrome is unknown. Hypotheses have included an antecedent viral infection, retained placental fragments, or drugs such as ergotamine compounds, oxytocic agents, or oral contraceptives prescribed shortly after delivery. Since some women manifested hypocomplementemia, immunologic causes have been also postulated. Other theories include deficiency of PG production, decreased antithrombin III levels, and endothelial dysfunction perhaps secondary to deficits in NO-dependent endothelium relaxing factor. The pathophysiology of postpartum renal failure has been compared to those disorders currently listed under the "thrombotic microangiopathies" category, including hemolytic–uremic syndrome, thrombotic thrombocytopenic purpura, and for some the hemolysis, elevated liver enzymes, and low platelet (HELLP) syndrome, and even preeclampsia (see below), all disorders characterized by disseminated intravascular coagulation.[297,299] Of interest in this respect is a report of HLA-identical sisters, one of whom developed

postpartum renal failure and the other hemolytic–uremic syndrome associated with contraceptive pill ingestion.[300] Finally, postpartum renal failure has further been compared to the generalized Shwartzman reaction, which, as noted above, develops more readily in pregnant animals.[278,287]

Renal pathology in idiopathic postpartum renal failure has been described in two general categories: changes in the glomerular capillaries resembling those in the hemolytic–uremic syndrome and arteriolar lesions reminiscent of malignant nephrosclerosis or scleroderma.[1,278,301] Immunofluorescence staining shows nonspecific changes: fibrin-like material often present in the mesangium, glomerular capillary walls, and arterioles, and C3 deposits are common, but presence of other immunoglobulins has been rare and inconsistent. It has been suggested that glomerular lesions resembling thrombotic microangiopathy are more apt to be noted in specimens obtained early in the course of the disease, while those demonstrating accelerated nephrosclerosis are seen in biopsy material taken after the disorder becomes chronic. An increased incidence of postbiopsy bleeding has also been reported.[278,280]

Prognosis is guarded, as most women have either succumbed, required chronic dialysis, or have survived with severely reduced renal function. However, rare instances of recovery have been recorded.[278,280] Treatment is aimed at controlling the accelerated hypertension, in conjunction with the usual supportive management for ARF. There are reports of success with early use of anticoagulant therapy such as heparin and fibrinolytic agents (reviewed in Ref.,[254]but the data are not convincing. Similarly, antiplatelet therapy, infusion of fresh blood products including concentrates of antithrombin III, or plasma exchange (used in a variant of postpartum renal failure associated with circulating lupus anticoagulant or antiphospholipid antibodies[302,303] have been advocated and remain to be proven successful[278] Finally, due to a report implicating retained placental fragments with this syndrome, dilatation and curettage may be considered in selected cases.[278]

Miscellaneous Causes

ARF has been provoked by intraamniotic saline administration, amniotic fluid embolism, as well as by diseases or accidents unrelated to the gestation.[278] These include drug ingestion, bacterial endocarditis, and incompatible blood transfusions. Sudden renal failure during gestation has been caused by obstruction secondary to the enlarged uterus,[278,280] various nephritides, collagen disorders,[278,280] and rarely sarcoidosis.[304] The obstructive causes associated with the enlarged uterus, including the overdistention syndrome were described above. Finally, gravidas with underlying renal disease and acute infectious pyelonephritis may be more susceptible to develop acute tubular necrosis, even though they have normal or adequate renal function.[278,280,305] This is especially true when their gestation is complicated by superimposed preeclampsia or another cause of increased blood pressure.[306]

Treatment

Management of ARF during gestation or in the puerperium is similar to that in nonpregnant subjects, but certain points pertinent to obstetric ARF deserve emphasis. As noted, uterine hemorrhage in late pregnancy may be concealed and the blood loss frequently underestimated. Thus, it is important that blood be replaced early, and even that patients be slightly overtransfused in order to forestall the development of acute tubular or cortical necrosis. Either peritoneal dialysis or hemodialysis can be used in obstetric renal failure as detailed elsewhere.[307–311] The former modality is preferred on theoretical grounds, because alterations in fluid and solute levels are more gradual, thus less likely to precipitate hypotension and/or premature contractions.[308–310] If hemodialysis is utilized, the above problems can be minimized by daily treatment for shorter time periods, avoiding high flux technology. Since urea, creatinine, and probably other metabolites that accumulate in uremia cross the placenta, dialysis should be undertaken early in pregnancy, with the aim of maintaining the blood urea nitrogen at <50 mg/dL (18 mmol/L)[308–310,312] In essence, the advantages of early dialysis for nonpregnant patients are even more important for pregnant subjects and make the argument for "prophylactic dialysis" compelling. If the conceptus is near maturity, it should probably be delivered as soon as the mother's condition has been stabilized.

CHRONIC PARENCHYMAL RENAL DISEASE

As noted, the prognosis for pregnant women with chronic renal disease is considerably more optimistic now than two decades ago, a change brought about by a series of studies, primarily retrospective, which date from 1980.[305] These studies, which comprise the gestational history (and in some substantial postpartum follow-ups) of over 1,000 patients whose renal disease was confirmed by biopsy (literature reviewed in Refs[313–316]) permit the following guidelines:

Prognosis, in general, is based on the degree of renal insufficiency at conception, the patients being arbitrarily placed in three categories, those with "mild," "moderate," or "severe" renal dysfunction.

1. Normotensive patients whose function at conception is intact or only mildly decreased, (serum creatinine ≥ 1.4 mg/dL or 125 μmol/L) usually do well (>95% live births, >75% of neonates with weights adequate for gestational age). In addition, gestation has few or no adverse effects on the natural history of their underlying kidney disorder (Figure 81.14[317]). This generalization, however, has to be tempered for certain specific disorders that appear more sensitive to gestation, such as lupus nephropathy and perhaps membranoproliferative glomerulonephritis. There is controversy as to whether or not gestation adversely influences the natural history of IgA nephropathy, focal segmental glomerulosclerosis (FSGS), and reflux nephropathy.[305,318] Authorities agree, however, that women with scleroderma and polyarteritis nodosa (primarily those patients with renal involvement) do very poorly in pregnancy, and counsel such patients against conception or suggest termination to those already pregnant (see below).

Hypertension prior to conception is a substantial risk factor for mother and fetus even when renal function is preserved.[305,314,315,319,320] Controlling the blood pressure leads to pregnancy outcomes similar to those in normotensive women with mild renal dysfunction.[321]

2. The renal prognosis of women whose kidney function is moderately or impaired (serum creatinine ≥ 1.5 mg/dL or ≥ 133 μmol/L) is poorer, but fetal outcome is still quite good (≥90% live births).[316,318] Over one-third of these patients experience renal functional deterioration during pregnancy or in the immediate puerperium which may not revert postpartum, and may at times progress rapidly to end-stage disease. There is also a substantial incidence of severe hypertension (and/or superimposed preeclampsia), and blood pressures can be hectic, and difficult to control.

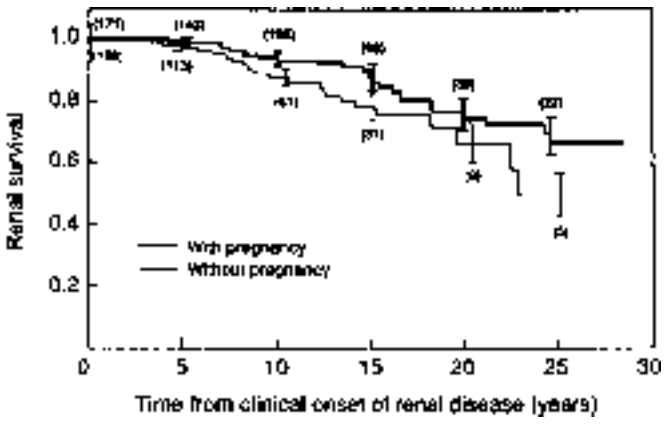

FIGURE 81.14 Kidney survival in women with preexisting chronic glomerulonephritis comparing those who subsequently underwent pregnancies (thick line) compared to those who did not. *[From Ref.,[313] with permission]*

3. Women with severe renal dysfunction [defined here as having a serum creatinine level ≥ 3 mg/dL (≥275 μmol/L)] are often infertile.[309,310] Even when conception occurs, the success rate is low while maternal morbidity is substantial.[308–310,314,315] These are two compelling reasons to discourage pregnancy in such patients.

Finally, we emphasize that the guidelines enumerated above, as well as the discussions of specific diseases that follows, are based primarily on retrospective data. Most of them were obtained from patients with mild disease and there is very little information on pregnant women with moderate and severe renal dysfunction. Thus, confirmation of our views will require large prospective observational trials.

Pathophysiology

Renal Hemodynamics

Pregnant patients with intact or only mildly decreased renal function usually manifest increments in GFR and ERPF often similar to those in normal gravidas[305] [Figure 81.15[170]]. Increases also occur in women with a single kidney due to uninephrectomy and in transplant recipients.[133,134,322] Renal adaptation in the latter two groups is of interest because their GFR and ERPF have already increased substantially prior to conception, due to compensatory morphologic and functional hypertrophy. Increases in renal function, however, appear restricted to patients with only mild dysfunction and GFR does not increase during pregnancy when creatinine levels exceed 1.4 mg/dL (124 μmol/L).[133,134,314,322]

Proteinuria

Urinary protein excretion may increase markedly in pregnant women with parenchymal renal disease.[305] The increments occur most frequently in the second half of pregnancy and do not seem to parallel the changes in renal hemodynamics. In one series[305] which comprised 121 gestations in 89 women the development of, or increase in, abnormal proteinuria was common and occurred in nearly half of all pregnancies. It was severe (≥3 g/24 h) in 39 of the proteinuric women, many of whom manifested substantial edema. Appearance of nephrotic-range proteinuria was associated with virtually every type of renal disease, with the exception of interstitial nephritis, and presented for the first time during gestation in a substantial number of women. Of importance is that these degrees of protein loss were usually well tolerated, had little or no influence on the course of the pregnancy or the natural history of the renal disorder, and fetal outcome was good.

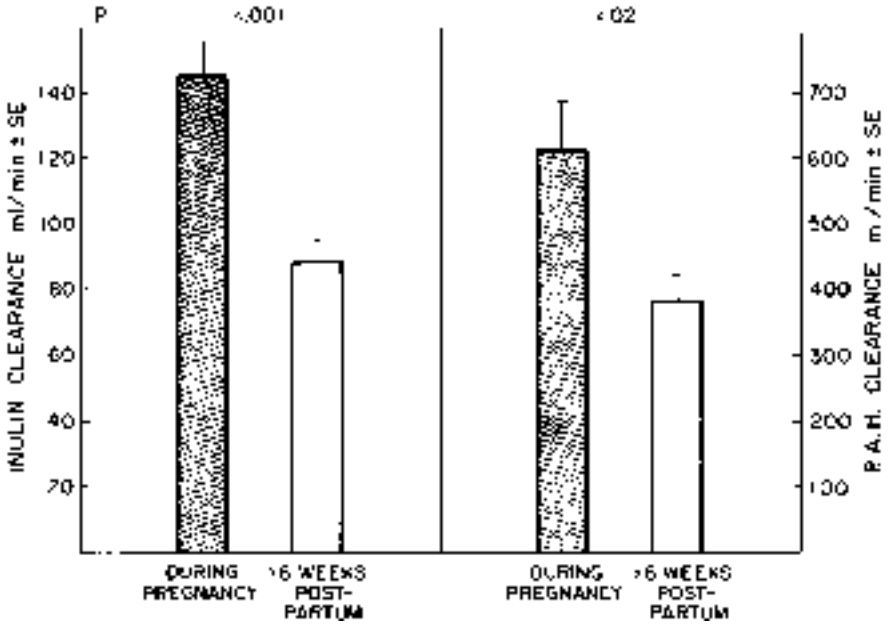

FIGURE 81.15 Two-hour inulin clearance during 19 pregnancies of 16 women with chronic renal disease studied before, during, and after pregnancy. *[From Ref.,[305] with permission]*

Volume Homeostasis

There are sparse data on how renal disease affects the alterations in volume homeostasis and osmoregulation that occur during normal gestation. Of interest, though, is a report[323] suggesting that both blood and plasma volume appear to expand normally even when renal function is moderately decreased, but is markedly attenuated in patients with severe dysfunction.

Blood Pressure

The incidence of hypertension including superimposed preeclampsia associated with pregnancy in women with preexisting kidney disease is universally described as increased, but the specific influence of gestation on the blood pressure in these patients is difficult to assess[310,324] For instance, in one series, where renal function was preserved prior to conception, hypertension complicated 23% of the pregnancies, but blood pressure had been elevated prior to conception in about half the cases. The increments often occurred late in gestation, when it was difficult to distinguish superimposed preeclampsia from an exacerbation of the kidney disease.[325] There are also claims that women with certain specific disorders, such as IgA nephropathy, may have a greater propensity to manifest hypertension during pregnancy (see below). Finally, as noted above, hypertension frequently accelerates or complicates pregnancy when preconception function is moderately or severely compromised.[316] Such patients, of course, have a substantial incidence of high blood pressure prior to conception, and in this respect 79% of the women with moderate and 86% of those with severe insufficiency described by Cunningham et al.[323] developed superimposed preeclampsia.

Specific Disorders

The focus of this text is physiology and pathophysiology. Thus, the section that follows is but a selective summary of gestation in relation to a number of specific renal diseases (Table 81.3); the reader is referred to Ref.[314] regarding more detailed discussions that focus on management.

Glomerulonephritis

Acute poststreptococcal glomerulonephritis during gestation is quite unusual, and the reports in which the diagnosis seems to have been verified are characterized by complete recovery of maternal renal function and a successful pregnancy.[9,150,326,327] Also, a history of "healed" glomerulonephritis in the past has little influence on pregnancy.[9]

Women with most forms of chronic glomerulonephritis (a vague classification encompassing many morphologically distinct entities) have a good renal and fetal prognosis during pregnancy when kidney function is preserved and hypertension is absent or well controlled.[9,305,314,315] There are some exceptions, however: Membranoproliferative glomerulonephritis (where transplacental passage of nephritic factors has been documented[328]) is said by some to be affected

TABLE 81.3 Pregnancy in Women with Underlying Disorders

Renal Disease	Effects
Diabetic nephropathy	Most frequent nephropathy encountered in pregnancy. Gestation does not seem to accelerate functional loss; asymptomatic bacteriuria more frequent; higher incidence of nephrotic-range proteinuria and hypertension after midgestation.
Chronic glomerulonephritis focal glomerulosclerosis (FGS)	Increased incidence of high blood pressure late in gestation, but no adverse effect if renal function is preserved and hypertension absent before gestation. Some disagree, stressing the physiological coagulation changes in pregnancy exacerbate these diseases, especially IgA nephropathy, FGS, and membranoproliferative glomerulonephritis.
SLE	More problems than in most glomerular diseases, but prognosis is more favorable if disease is in remission 6 mo before conception. Poorest maternal and fetal outcomes associated with antiphospholipid antibodies or with lupus anticoagulant.
Scleroderma and periarteritis nodosa	Associated with maternal deaths and poor fetal outcome; reactivation of quiescent scleroderma can occur during pregnancy or puerperium; therapeutic abortion should be considered.
Chronic pyelonephritis (infectious tubulointerstitial disease)	Bacteriuria in pregnancy may lead to acute exacerbations but otherwise is well tolerated. Frequent urine cultures recommended; chronic suppressive antibiotic therapy may be necessary.
Reflux nephropathy	Some controversy; most agree that these patients do well when function is preserved. Frequent urine cultures necessary.
Polycystic kidney disease	Pregnancy uneventful when function preserved; increased tendency for late pregnancy hypertensive complication.
Urolithiasis	The "physiologic" ureteral dilation and stasis of pregnancy do not seem to affect natural history, but infections can be more frequent. Stents have been successfully placed during gestation.
Previous urologic surgery	Other urogenital tract malformations may be present; urinary infections increase, functional decrements have been observed; and cesarean section may be necessary to avoid disruption of the continence mechanism if artificial sphincters or neourethras are present.

Source: Lindheimer MD, Grünfeld J-P, Davison JM. Renal disorders. In: Barron WM, Lindheimer MD, eds. Medical Disorders During Pregnancy, third ed. St. Louis: Mosby; 2000, with permission.

adversely by gestation, but data in the literature appear to us inconclusive. The prognosis of IgA nephropathy is disputed.[314,315] There are claims that gestation provokes accelerated declines in maternal renal function as well as the *de novo* appearance of hypertension, and that both these complications may not remit postpartum. These concerns, however, are not born out by case–control and/or long-term follow-up studies that comprise ~300 patients, published by Jungers and Abe and their respective colleagues.[315,329,330]

Focal Glomerulosclerosis

Another glomerular disease whose prognosis in pregnancy is disputed is FSGS, perhaps because this disorder may have many etiologies, and data are quite limited (#100 patients described in the literature). In one report, hypertension, at times severe, was present in three quarters of the patients and persisted postpartum in 20% these women.[331] Proteinuria increased in most instances, while functional deterioration was recorded in 45% of the patients. On the other hand, it appears that those patients who are normotensive and have preserved renal function prior to conception do well.[314,315] Obviously, considerably more data are required to resolve the dispute.

Collagen Disorders

Systemic lupus erythematosus (SLE) is the most common collagen disorder affecting women of childbearing age.[332] The pregnancy prognosis for women with SLE and renal involvement is complex and is further complicated by the fact that the natural history of this disease is unpredictable whether or not gestation is present.[332,333,334,335,336] An older literature, limited and anecdotal, stressed the adverse affects of pregnancy, but more recently Hayslett,[337] reviewing the results of nine series (comprising 200 patients) published during or after 1980, came to more positive conclusions. When renal function is preserved, the best outcomes are in patients whose systemic disease has been in remission for six or more months before conception. Prognosis is poorer, however, if the disease had been active more recently, presents *de novo* during gestation (where it may be confused with preeclampsia), when there is preexisting hypertension, greater degrees of renal dysfunction, or if a circulating lupus

anticoagulant or antiphospholipid antibody is present. The literature regarding placental transmission of maternal autoantibodies, their relationships to the increased frequency of spontaneous abortion, placental and fetal pathology (especially congenital heart block), and a neonatal lupus syndrome, as well as the poor fetal prognosis associated with circulating lupus anticoagulants and antiphospholipid antibodies, are beyond the scope of this chapter are discussed in Ref.[332]

Contrasting SLE, where gestational prognosis is usually sufficiently benign when kidney function is preserved or only mildly compromised, the outcome of pregnancy in patients with renal scleroderma and periarteritis nodosa is very poor, often because of the associated hypertension which can be malignant in nature.[9,332] Not only is fetal prognosis dismal but most of the reported cases in the older literature, albeit anecdotal and selective, describe maternal deaths. More recently, however, there are descriptions of successful pregnancies (still anecdotal) in patients treated with ACE inhibitors, but the latter drugs are relatively contraindicated for use in pregnancy.[315,332] Thus, we continue to counsel against conception in these last two entities and suggest pregnancy termination when the disease is present in the first trimester.

Diabetes

Diabetic nephropathy is the most common renal disease encountered in obstetric practice. Most reports focus on pregnant women with overt disease, there being only limited data regarding those who have microalbuminuria before conception or early in pregnancy.[338–346,343,347,348–350] There is little evidence of pregnancy adversely affecting the long-term renal prognosis of diabetics whose preconception renal function is preserved, which is surprising given that nephrotic-range proteinuria and hypertension complicate two-thirds of these gestations. However, there is evidence, albeit limited, of rapid functional deterioration in women entering pregnancy with moderate or greater dysfunction.[351,352] Of interest is a report noting that hypothyroidism appears *de novo* during gestation in a significant number of nephrotic diabetics.[353]

Fetal outcome, described as poor in the older literature[9] is presently quite good, 95% of the pregnancies ending successfully. However, there is high incidence of preterm deliveries, often due to termination early in the third trimester, as this is the period when the increases in hypertension and proteinuria occur, and are difficult to differentiate from superimposed preeclampsia.

Miscellaneous Glomerular Diseases

The literature regarding minimal change disease, though limited to less than 200 patients, is quite favorable.[305,315,354] There is also limited experience with membranous nephropathy, but again most patients with preserved renal function do well, though, not surprisingly they have a high incidence of nephrotic-range proteinuria.[9,305,314,315,354] An adverse effect of pregnancy on familial Mediterranean fever with amyloidosis, even when preconception function appears preserved or minimally compromised, has been suggested.[355] The literature regarding vasculitides such as Wegener's granulomatosis, Henoch–Schönlein purpura with renal involvement, and Goodpasture's syndrome is selective and anecdotal.[315,356,357] Regarding the latter disorder is a case report where the disease improved during pregnancy, in which the authors postulated that the placenta, which may share some key antigens with the glomerular basement membrane, provided a large absorptive surface for the autoantibody.[358] Finally data relating to vasculitides like Wegener's granuloses is both limited and anecdotal.[359,360]

Reflux Nephropathy and Other Tubulointerstitial Disorders

Reflux nephropathy is a disease that begins during childhood and thus is present in a substantial number of pregnant women. The natural history of this disorder during pregnancy was once disputed, but two reports[318,361] comprising 697 pregnancies in 290 women with reflux nephropathy were consistent with the dictum that when renal function is preserved and hypertension absent, these gestations do well. However, these patients are prone to urinary tract infection and require special attention during gestation, including frequent urine cultures and prompt treatment when signs of urinary tract infection occur.

Concerning tubulointerstitial disease, most are infectious in nature, and gestational outcome relating to the patient's functional status prior to conception.[305] There are few data concerning renal tuberculosis, which in the older literature appeared to be unaffected by gestation.[9]

Finally, some women who have had major urinary tract reconstructive surgery, especially diversion, may develop reflux during pregnancy.[362] Since such patients have a high incidence of bacteriuria, and the risk of developing obstruction grows as the uterus enlarges, it is gratifying that most authors have reported fairly benign and successful pregnancies (reviewed in Ref.[362]).

Hereditary Disorders

Autosomal Dominant Polycystic Kidney Disease: Patients with polycystic kidney disease have a greater propensity to develop *de novo* late gestational

hypertension or preeclampsia, but pregnancy outcomes are favorable when renal function is preserved and hypertension prior to conception absent.[363,364] There is, however, an increased risk of upper urinary tract infections which can be virulent at times.[365] Also, one group of investigators[363] noted that multiple pregnancies (defined as >three) lead to an earlier onset of kidney failure. However, this may only reflect the influence of pregnancy in women who already had moderate or greater renal dysfunction when they conceived (which is more likely to be the case in older multigravidas).

Though pregnancy does not appear to influence the natural history of the renal disorder, it may have effects on other organs. Liver cysts are said to be larger or more prevalent in parous women, and enlargement of the cysts (increasing their chance of rupturing) may occur during pregnancy.[366] Finally, routine preconception screening of the intracerebral vasculature should be reserved for patients with family histories of clustering for intracranial aneurysms or subarachnoid hemorrhage.[292]

Hereditary Nephritis: This is primarily an X-linked dominant disease (where the majority of carrier females manifest only mild degrees of urinary abnormalities), but ~15% of affected patients have an autosomal dominant or recessive variety.[367,368] Thus, in most women, the disease is clinically silent, but there are exceptions. In addition, the disorder may manifest for the first time during pregnancy (due to observation of hematuria and/or proteinuria when a urinalysis is performed as part of routine prenatal care). However, renal function is usually well preserved and these pregnancies do well, but there is an interesting report of two sisters with the disease, each of whom developed rapidly progressive crescentic glomerulonephritis during their respective pregnancies.[369] Finally, there are variants of hereditary nephritis associated with thrombocytopenia and thrombocytopathy.[367] Such patients are at risk for excessive bleeding during delivery.

Miscellaneous: Patients with *cystinosis* have usually progressed to end-stage renal disease by adolescence, but may conceive while receiving renal replacement therapy. Angiomyolipomas and renal aneurysms may be present in patients with *tuberous sclerosis*, and since the former may bleed and the later rupture during gestation, screening and appropriate interventions are warranted prior to a planned pregnancy.[370] Similarly, women with *von Hippel–Lindau* disease should be screened for silent pheochromocytomas, present in ~25% of such patients, as activation during gestation and especially at delivery has been described.[371,372]

Urolithiasis

The incidence of urolithiasis in pregnancy varies by geographic location, the best estimate being 1 in 1,500 pregnancies [reviewed in Ref.[373]]. This estimate, however, may be too low, due to under-reporting of the disease. Many patients remain undiagnosed until their disease is symptomatic, and in others the symptoms are quite subtle, such as repeat urinary tract infections, and urolithiasis is not considered in the differential diagnosis.

There does not appear to be any increase in either the appearance or recurrence of nephrolithiasis during gestation.[374] This is surprising because normal pregnant women are markedly hypercalciuric and their urinary supersaturation ratios for calcium oxalate and brushite are substantially increased[373,375,376] [Figure 81.16[169]]. There are also increases in magnesium and citrate excretion, but the increments are not enough to counter the strikingly elevated supersaturation ratios.[376] In essence, the combination of supersaturation with the physiologic dilatation, stasis, and perhaps obstruction of the urinary tract, raises the question why stone disease is not more prevalent in

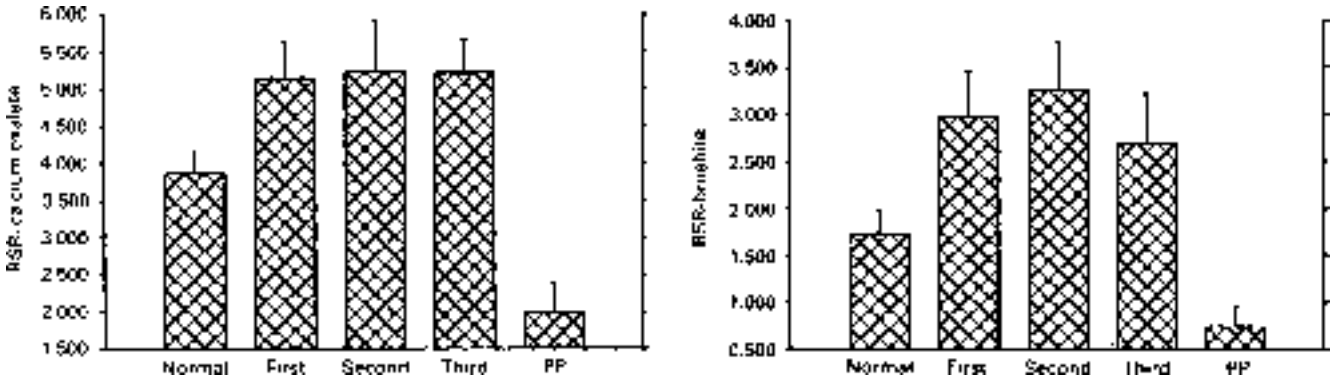

FIGURE 81.16 During pregnancy the relative supersaturation ratios for calcium oxalate (A) and brushite (B) exceed those measured postpartum (PP), as well as values in a population of healthy women (normal) ($p < 0.01$; for both comparisons). *[From Ref.,[376] with permission]*

pregnancy. The answer may be that there is an even greater increment in the urinary excretion of several potent glycoproteins that inhibit stone formation such as nephrocalcin (which inhibits crystal aggregation and growth) and Tamm–Horsfall protein (which decreases aggregation), as well as smaller increases in urinary citrate and magnesium.[373,375,376] In this respect, there is evidence that increments in urinary inhibitors of pathological crystalluria are present as early as the eighth gestational week.[375]

The disease in pregnant women resembles that in nonpregnant patients, ~89% presenting with flank pain, and a similar percentage display either microscopic or macroscopic hematuria.[377] The majority of stones passed during pregnancy contain calcium salts, but some are infective in origin ("struvite").[373] The older literature stressed the dramatic complications associated with obstruction and/or infection, but subsequent studies suggested that gestation has little influence on the course of urolithiasis, with the exception of possible increments in urinary tract infection, and that rates of spontaneous abortion and premature labor may be increased.[373]

The above synopsis relates primarily to women with noninfectious calcium oxalate stones, whose renal function is usually preserved and whose course is relatively benign in the pregnant state. Little is known of the natural history of the more serious "struvite" stones during pregnancy. Similarly, experience with cystinuria is quite limited. One should strive to ensure adequate hydration, especially in early pregnancy when gravidas are frequently nauseous, and to consider withholding *d*-penicillamine during the first 12 gestational weeks.[378]

When nephrolithiasis is suspected, an ultrasound examination of the urinary tract is in order, but when complications suggest the need for surgical intervention, pregnancy should not be a deterrent to the performance of pyelography ([242,373,379] Operative procedures such as open lithotomy and percutaneous nephrostomy, both rigid and flexible ureteroscopy (direct vision) have all been performed during pregnancy, but more currently, placement of a ureteral stent has made it possible to manage gravidas through term with a less invasive technique.[21,291,373,380] Experience with lithotripsy is anecdotal and this procedure should probably be avoided in pregnant women.[381]

Management of Chronic Renal Disease in Pregnancy

Management guidelines similar in most aspects to nonpregnant patients is beyond the scope of this text devoted to physiology and pathophysiology. The reader is referred to reviews elsewhere, especially concerning hemodialysis in pregnancy [382,383 310], Of interest, the kidney, being the source of erythropoietin, makes its replacement necessary, often at creatinine levels when such therapy would not be necessary in the nonpregnant state. The initiation of renal replacement therapy at higher levels of dysfunction that such treatments would be started in nongravid women is also is advocated by some to facilitate better control of volume and electrolytes, and perhaps fetal development. The placenta hydroxylates Vitamin D, while dialysis depletes phosphorous, and one must watch for hypercalcemia, and the fact that pregnancy is a hypercoagulable state may make anticoagulation more difficult. Antihypertensive therapy is discussed below.

Transplantation

The first successful pregnancy in a renal allograft recipient appears to have been reported in 1963,[384] with thousands of such successes noted since. It is estimated that one in every 50 women of childbearing age who have functioning kidney transplants conceive.[322] Often the women were unaware that transplantation had reversed the relative infertility associated with end-stage renal disease[385] and had not been practicing contraception, indicating a failure of physicians to counsel these patients appropriately.

In an extensive literature review published in 1994, Davison (Ref.[386] contains 98 citations) documented 3382 gestations in 2049 gravidas with transplanted kidneys (many more were probably unreported). Most of these patients had received azathioprine and prednisone, experience with cyclosporine, tacrolimus, and mycophenolate being quite limited[309,310,387] (though currently data on women receiving newer immunosuppressants is increasing thanks to effective registries[386,387,388–391,392]). Approximately 35% of these gestations did not proceed beyond the first trimester (but the spontaneous abortion rate of 15% was similar to that in normal pregnant populations). However, of the pregnancies that continued beyond the initial trimester 93% succeeded, both the renal prognosis and the gestational outcome paralleling those with preexisting kidney disease (discussed above). Here, too, the better the renal function prior to conception, the more favorable the outcome. Not surprisingly, the prognosis was better when the allograft came from a living donor.

The success rate may be high but there are many maternal and fetal problems to be dealt with. The incidence of ectopic gestations (which reaches ~0.4%) and hypertension (~30%) are increased, and steroid-induced hyperglycemia, leukopenia, septicemia, uterine rupture, allograft rejection, liver function abnormalities, and maternal death have all been described.[309,322] Women transplanted after renal failure

due to diabetic nephropathy harbor considerable vascular disease and are at particular risk although those with combined renal pancreas-transplant may fare better.[309,322,393,394] Problems for the fetus and neonate include increased incidence of congenital anomalies, premature births, and growth restriction. Serious infections, thrombocytopenia, hypoadrenalism, and hepatic insufficiency affecting the neonate have also been reported.[322]

Most renal allografts recipients experience increments in renal hemodynamics during pregnancy, though smaller than those observed in normal gestation.[134,322] (This occurs despite the presence of but a single functioning kidney, which invariably has undergone some degree of chronic rejection.) Renal volume also increases.[395] On the other hand, functional declines are reported in ~15% of the pregnancies.[322] They occur mainly in late gestation and are transient in nature (rarely due to obstruction).[322,396] The loss, however, may persist, especially when prepregnancy GFR is already compromised.[397] Urinary protein excretion also rises, often to abnormal levels, but in most instances the increase is functional in nature and not related to the health of the allograft.

There is controversy about the effect of pregnancy on long-term allograft survival. In 1993 Salmela et al.[398] suggested that pregnancy might jeopardize the long-term health of the renal allograft. Their small but well designed case–control study showed that women who conceived, even well-preserved renal function, had a lower 10-year graft survival rate (69 versus 100%, $p < 0.005$). This report sent "shock waves" throughout the transplant community, but such alarm proved premature.[399] First, the difference appears due be due mainly to the highly unusual outcome in their control group, who in these same 10 years had no graft failures. In fact the 10-year graft survival statistics of most centers covering all transplant recipients resemble (or may even be poorer than) those of the group of women with allografts who subsequently underwent pregnancy studied by Salmela et al.[398] In addition, their report is at odds with a body of evidence reported both prior to and after their article, which seems to establish that pregnancy has little or no effects on long-term renal allograft survival.[399–405]

Preconception counseling, management of the gestations, and the status of the various immunosuppressive regimens are beyond the scope of this chapter and are discussed in detail elsewhere.[309,387,400] Most recently the American transplantation Association convened a consensus group and issued a report[392] As noted, the natural history of pregnancy in allograft recipients whose immunosuppressive regimens include cyclosporine and even newer drugs is just emerging, the early data seem to support the optimistic conclusions Davison arrived at in his extensive review of the precyclosporine era discussed above[309,387]

Concluding Perspectives

The text devoted to chronic renal disorders stressed that gestation seems well tolerated in of most renal diseases or in allograft recipients[401–405] provided that kidney function was preserved, and hypertension absent or well controlled. Nevertheless, urinary tract infections and preeclampsia seem to occur more often in such patients. In addition gestation did not seem to affect the natural history of their underlying kidney disorder, with certain exceptions. On the other hand, women with greater degrees of renal dysfunction prior to conception have a poorer renal and fetal prognosis. All gravidas with renal disease require close prenatal surveillance, including monitoring of blood pressure and renal function (serum creatinine levels or its clearance). When function deteriorates at any stage of gestation, reversible causes (e.g., urinary tract infection, obstruction, and subtle dehydration) must be considered, but if hypertension accompanies the decrease in GFR, the outlook for the pregnancy is more guarded.

One issue omitted from the discussion of chronic renal disorders was the provocative hypothesis that the increase in glomerular filtration accompanying gestation could have adverse effects on the course of the kidney disease. There is concern, based on evidence derived from animal models, that the hyperfiltration in the residual (intact) nephrons of patients with renal disease (or those with a single kidney after uninephrectomy) is accompanied by increments in glomerular capillary pressure and/or increased mesangial processing of macromolecules that lead to focal glomerular sclerosis and progressive loss of renal function. Hyperfiltration occurs during normal gestation, in gravidas who have renal disease with minimal dysfunction, and in those with single kidneys after uninephrectomy but, fortunately, it does not seem to lead to glomerular injury.

Several long-term follow-up studies have failed to detect increased renal functional loss when women with chronic disorders who had been pregnant were compared to those not known to have conceived.[313,315,330] Davison[406] has performed periodic inulin and *p*-aminohippurate clearances over a span of 17 years in a limited group of parous and nonparous women with and without a variety of renal problems. A small decrease in renal hemodynamics, possibly attributable to pregnancy, occurred in women with a single kidney, and those with chronic renal disease. On the other hand, as noted above, several long-term follow-up studies of 29 women who donated kidneys for transplantation and subsequently

had 39 pregnancies, failed to detect changes in GFR, urinary sediment, or the appearance of hypertension in these donors.[407] Thus the increases in renal hemodynamics seem well tolerated and are not a reason to discourage conception. This opinion is strengthened by data from rat and rabbit animal models though rats with adriamycin nephropathy develop hypertension during gestation.[2,408–416] Finally, preliminary results from pregnant women with underlying kidney disorders, whose authors combine the sieving characteristics of infused dextran with mathematical modeling to assess determinants of ultrafiltration, also suggest that there are no increases in glomerular capillary pressure[31]

HYPERTENSION

The remainder of this chapter is devoted to the hypertensive disorders of pregnancy. Hypertension, the most common medical disorder complicating pregnancy (~5–10% of all gestations) can be a challenging medical problem.[417] Moreover, the hypertensive disorders of pregnancy, primarily the pregnancy-specific disease preeclampsia, remain major causes of morbidity and mortality for mother, fetus, and newborn especially in developing countries. The sections that follow will briefly review the striking alterations of systemic hemodynamics in normal pregnancy, followed by an overview of the classification and diagnosis of the hypertensive disorders of pregnancy with the main focus on preeclampsia, because this disease remains the most potentially ominous of the more common hypertensive disorders encountered during pregnancy. Due to space considerations as well as to the focus of this text (the physiology and pathophysiology of the kidney), we will discuss in more detail the renal alterations associated with high blood pressure in pregnancy, while summarizing the disease effects on other organ systems and management considerations. Readers seeking more details on these topics are referred to the second edition of Chesley's Hypertensive Disorders in Pregnancy,[32] a comprehensive multiauthored text, published in 2009.

CARDIOVASCULAR CHANGES IN NORMAL PREGNANCY

Arterial pressure decreases during normal human pregnancy, the decrements beginning during the luteal phase of the menstrual cycle, continuing after conception, and by midgestation, diastolic levels are ~10 mm Hg below nonpregnant levels. Thereafter, most reports show arterial pressure increasing, gradually approaching nonpregnant levels near term,[27,418–421] and a small increase may occur in the immediate postpartum period.[422] Cardiac output also increases during the luteal phase of the menstrual period, rising further after conception, and peaking some 30–50% above midfollicular values by the end of the first or beginning of the second trimester.[26,27,47,231,423–426] In fact, this early, marked rise in cardiac output is anticipatory in nature, because blood flow and oxygen delivery exceed demands as reflected by the narrowing of the difference in oxygen content between arterial and mixed-venous blood in humans and conscious rats [[427] and citations therein]. Despite some discordance in the older literature, load-independent left ventricular contractility appears to be unaltered during pregnancy.[428–430] A marked decline in systemic vascular resistance initiates the increase in cardiac output and fall in arterial pressure. In essence, normal pregnancy is a profoundly vasodilated state.

Accompanying the early fall in systemic vascular resistance is a rise in arterial compliance.[425,431] The temporal coordination of these two events ensures the maintenance of cardiovascular homeostasis during pregnancy by (i) minimizing the decline in diastolic pressure, (ii) minimizing energy expended by the heart on pulsatile oscillatory work, (iii) preserving steady shear-type (or minimizing oscillatory shear-type) stress at the blood–endothelial interface, and (iv) accommodating increased vascular volume.[425,432] Theoretically, failure or reversal of these compliance changes during pregnancy in the face of the marked massive increase in stroke volume could cause endothelial dysfunction, thereby affecting blood pressure regulation and producing hypertension.[426,433]

The systemic hemodynamic and arterial compliance changes during normal pregnancy in women are also observed in several animal models including sheep,[434,435] rabbits,[436] guinea pigs,[437,438] rats[427,439] and baboons.[46] Of note, long-term relaxin administration to chronically instrumented, conscious rats recapitulates the increase in cardiac output and arterial compliance and reduction in systemic vascular resistance observed during midterm pregnancy in this species.[77,432,440] Thus, in addition to mediating the renal circulatory changes of pregnancy in rats (see section Renal Hemodynamics), relaxin also contributes to the boarder cardiovascular changes in systemic hemodynamic and arterial properties during pregnancy in this species. Whether the hormone plays a similar role in gravid women is presently unknown.

The hormone(s) and distal vasodilatory effector pathway(s) responsible for maternal vasodilation during pregnancy remain uncertain and may vary according to animal species (and possibly by organ circulation and vessel size). Investigators have

emphasized the endothelium in the vascular changes of pregnancy (see section Renal Hemodynamics). Of interest, is that immunoneutralization of relaxin prevented the systemic hemodynamic and global arterial compliance changes during midgestation in conscious rats.[441] Another candidate, calcitonin gene-related peptide (CGRP) hormone, rises in the blood during pregnancy in women.[442] CGRP is a potent vasodilator, and it may contribute to the systemic (and renal) vasodilator responses to pregnancy.[443] Recent evidence also shows increased endothelial angiotensin (AT)-2 receptor expression and AT-2-mediated relaxation of aorta during late pregnancy in rats.[444] Consistent with a potential role of the AT-2 receptor, the midterm decline in systolic blood pressure in midterm pregnant mice was prevented by administration of an AT-2 receptor antagonist.[445] The endothelium produces pressor and vasodilator hormones and autocoids such as PGs, NO and hyperpolarizing factors. Despite initial enthusiasm, the evidence that has emerged is not supportive of a major role for vasodilatory PGs in either women[93,94] or gravid animal models.[88–92,95] However, there is evidence to support a role for NO[102] and hyperpolarizing factors.[102,446,447] An overall refractoriness to the major vasopressors, alpha-adrenergic and vasopressinergic agonists and angiotensin II, has been a consistent finding during pregnancy in women and gravid animal models [reviewed in[22,89,102,241]]. Whether this refractoriness is inherent to the vascular smooth muscle and/or mediated by endothelial vasodilatory factors has not been clearly defined. Interestingly, relaxin administration to conscious, nonpregnant rats mimics pregnancy in this regard, insofar as the renal and systemic vasoconstrictor responses to angiotensin II are attenuated.[77,81,89,103]

Despite the profound decrease in systemic vascular resistance, only a modest decline in arterial pressure is observed during normal pregnancy in both humans and gravid animal models.[27,418,419,421,448] The decline in systemic vascular resistance is mostly offset by a comparable rise in cardiac output, thereby maintaining arterial pressure. (This viewpoint assumes that early pregnancy is a condition of arterial "underfill" or "normal-fill" initiated by primary vasodilation of nonreproductive organs—see section Significance of the Volume Changes During Pregnancy.) At least 4 mechanisms contribute to this reciprocal rise in cardiac output: (i) increased heart rate, (ii) elevated stroke volume, (iii) reduction in ventricular afterload by virtue of the profound decline in systemic vascular resistance and increase in arterial compliance, and (iv) augmentation of active venous tone and/or reduction of passive venous compliance[431] that maintains or even increases left ventricular end diastolic volume or preload[47,233,423,424] despite the marked decline in systemic vascular resistance. As mentioned above, the increase in arterial compliance also buffers the decline in diastolic blood pressure, and this overall cardiovascular picture is recapitulated by administration of relaxin to nonpregnant female (and to male) rats[77,432,440] [and most likely humans, reviewed in[449]].

As pregnancy progresses beyond the first trimester and the expansion of blood volume accelerates, then increases in venous volume are likely to play a larger role in maintaining or increasing the ventricular end diastolic volume, possibly allowing for restoration of the active venous tone and/or reduced passive venous compliance towards nonpregnant values or even for a complete reversal, i.e., reduced active venous tone and/or increased passive venous compliance, in order to accommodate the massive increase in vascular volume at this time. Regrettably, very few studies have focused on the changes in venous function and associated mechanisms, thereby limiting our understanding of the cardiovascular system during normal pregnancy.[450] Finally, ventricular remodeling, so-called "eccentric hypertrophy" also occurs with advancing gestation, thereby contributing to the maintenance of end diastolic volume without increasing end diastolic pressure, and hence cardiac work.[104]

Clinical Significance of the Physiological Decrease in Arterial Pressure During Pregnancy

The physiological decrease in arterial pressure in human pregnancy has clinical implications. The definition of hypertension during gestation has remained 140/90 mm Hg in both contemporary texts and working group recommendations[451,452] but one should consider suspect diastolic levels of 75 mm Hg in the second, and 85 mm Hg in the third trimester, and/or systolic values of 120 mm Hg in mid- and 130 mm Hg in late pregnancy.[419,453,454] In this regard, data from two large epidemiologic studies (comprising >30,000 pregnancies) reveal that diastolic pressures of $\geq$85 mm Hg at any stage of gestation are associated with significant increases of fetal mortality,[453] and there are significant increments in both perinatal mortality and growth restriction when mean arterial pressure exceeds 90 and 95 mm Hg during the second and third trimesters, respectively.[419]

Diagnosis and Classification

Measurement of Blood Pressure

The have been controversies on how measure blood pressure during gestation. These include the positioning of the patient during the measurement (lateral recumbency versus sitting), and which sound should constitute diastolic levels (Korotkoff IV [K_4], muffling,

or V [K_5], disappearance. It is now apparent that the lower levels recorded when the subject lies on her side is merely the difference in hydrostatic pressure when the cuff is positioned substantially above the left ventricle. In addition, an older view that because of their hyperdynamic circulations gravidas often manifest large differences between K_4 and K_5, the latter approaching zero, has been disproved, and K_5 has been established is the sound closest to true diastolic pressure.[455–458] Regarding the definition of hypertension, whether in absolute numbers, (usually 140/90 mm Hg (K_5)), or as increases in pressure (15 mm Hg diastolic and 30 mm Hg systolic, respectively, even when the final value is below 140/90 mm Hg), both had their advocates and through the late 1990s. However, epidemiological data establishing that outcomes are similar no matter what the magnitude of the rise, provided values remain below 140/90 mm Hg, have led to consensus groups to define only $\geq$140/90 mm Hg as the definition of hypertension in pregnancy.[452,459] Nevertheless the National High Blood Pressure Education Program (NHBPEP), stresses that patients with blood pressures below this cutoff who have experienced a 15 and/or 30 mm Hg in diastolic and systolic levels, respectively, be managed as high-risk patients. Of further note these disputes regarding the definition of hypertension are one reason for a host of discordant finding in such areas as epidemiology and outcome research, now hopefully resolved.[460]

Classification

A review of the literature reveals an assortment of terms and schemes, some quite complex and detailed, used to describe the hypertensive disorders of pregnancy. Toxemia, estosis, pregnancy-induced hypertension (PIH), pregnancy-associated hypertension, and preeclamptic toxemia are all utilized to classify the disorder we label as preeclampsia. The reader may be even more confused when the same term (e.g., PIH) is used to include different disorders by various authors. The terminology used in this chapter is that recommended by the Working Group[461] of NHBPEP, modified from that originally proposed by the American College of Obstetricians and Gynecologists' Committee on Terminology in 1972, which is concise and practical. In it, blood pressure in pregnancy is considered in only four categories:

1. Preeclampsia–eclampsia
2. Chronic hypertension of any cause
3. Preeclampsia superimposed on chronic hypertension
4. Gestational hypertension

Preeclampsia (pure or superimposed, categories 1 and 3) poses the greatest threat to fetal survival and is the disorder most often associated with severe maternal complications (including fatalities). The majority of women in the second category have essential hypertension, usually mild in intensity, and their pregnancies usually remain uncomplicated and end successfully. On occasion, however, the high blood pressure is due to specific causes including endocrine tumors, renal artery stenosis, and renal disease,[1,9,48,150,152,462] and some of these women with secondary forms of hypertension do poorly during gestation. Thus, pheochromocytoma, though rare, may present for the first time during gestation and is especially lethal when unsuspected, whereas when diagnosed it can be managed to a successful outcomes, either surgically or pharmacologically (with alpha blockade) depending on the stage of pregnancy.[48,462] Cushing's syndrome, also quite rare, has been associated with exacerbations of the hypertension during pregnancy and poor fetal outcomes,[48,463] and the serious maternal risks associated with scleroderma and periarteritis nodosa were stressed in a previous section. However, not all forms of secondary hypertension have a poor prognosis during gestation. For example, pregnancy may ameliorate the kaliuresis associated with primary aldosteronism[152] (also see Figure 81.7). Finally, both angioplasty and stent placement has been successfully performed on pregnant women with renal artery stenosis.[48]

Gestational hypertension (category 4) is characterized by mild, to moderate, elevation of blood pressure after midgestation, usually near term (though rarely the levels may be higher. The cause of this entity is unclear, but there is evidence that transient hypertension of pregnancy occurs in women destined to have essential hypertension later in life (analogous to women with gestational hyperglycemia who eventually develop type II diabetes).[325] Blood pressure returns to normal during the immediate puerperium,(at which point some relabel the entity "transient hypertension") but these women often have hypertension in subsequent pregnancies. There is an entity entitled late postpartum hypertension, in which women with normotensive gestations develop high blood pressure (usually mild) during a period that ranges from two weeks to six months after delivery.[464,465] Blood pressure remains labile for months but returns to normal values by the end of the first postpartum year. Little is known of this entity, which like transient hypertension of pregnancy, may be a predictor of essential hypertension later in life. Finally, a rare group of patients with activating mineralocorticoid receptor mutations that result in an exaggerated sensitivity to the usually weak mineralocorticoid effect of progesterone have been described.[157] They manifest salt sensitive

hypertension, accompanied by hypokalemia, but virtually undetectable aldosterone levels, most marked during pregnancy as progesterone levels rise.

Preeclampsia–Eclampsia

Epidemiology

Studies designed to determine the incidence of the hypertensive complications of pregnancy, particularly preeclampsia, have several problems. As noted, the presence of diverse classification schemes can be confusing. Equally important, it is very difficult to distinguish clinically between preeclampsia, essential or secondary hypertension, renal disease, and combinations of these separate entities. First, presence of normal blood pressure early in gestation does not necessarily differentiate preeclampsia from other forms of hypertension, as many women with essential hypertension experience decrements in blood pressure to normal values during the first half of pregnancy. Also diseases such as lupus nephropathy, and more rarely pheochromocytoma, as well as an accelerated phase of essential hypertension (actually unusual in pregnancy) may all mimic preeclampsia. These problems are well illustrated by reports in which the etiology of hypertension complicating gestation was established by renal biopsy [nine series cited in Ref.[325]]. In our own study[325] 176 women were biopsied, usually for suspected preeclampsia (Table 81.4). This diagnosis was correct in only 85% of the primiparas and was wrong in most of the multiparas (underscoring the need for caution in interpreting reports in which patients diagnosed as preeclamptic and/or "toxemic" are multiparous).

TABLE 81.4 Renal Pathology in 176 Hypertensive Patients[a]

Diagnosis	No. of Patients	Primigravidas	Multiparas
Preeclampsia[b]	96	79	17
With nephrosclerosis	13	6	7
With renal disease	3	1	2
With both	2	1	1
Nephrosclerosis	19	3	16
With renal disease	4	2	2
Renal disease	31	12	19
Normal histology	8	0	8

Source: Fisher KA, Luger A, Spargo BH, Lindheimer MD. Hypertension in pregnancy: clinical-pathological correlations and remote prognosis. Medicine (Baltimore) 1981;60:267–276.

[a]*Biopsy material (obtained between 1958 and 1976) was considered adequate if it contained eight glomeruli for light microscopic analysis and three for electron microscopic analysis.*

[b]*Only glomerular endotheliosis on biopsy.*

Several other problems, ranging from selected populations to discrepancies between the data and discharge diagnoses are discussed in detail by Ness and Roberts.[466] Thus, the epidemiological literature must be approached with the above reservations in mind, and careful attention should be paid to the different definitions of normalcy, methods used to measure blood pressure, and the quality of the data analyzed.

In view the above limitations it is not surprising that the incidence of preeclampsia in the literature range from 5% to 30%.[9,150,418,419,421,461,467] Of interest, however are data from a number of carefully conducted prospective trials which have mainly focused on normotensive nulliparas (a population where the incidence of preeclampsia is three to five fold higher than in multiparas[150,468,469] reveal the following. Preeclampsia was consistently diagnosed in 4–7% of the "placebo controls," and about twice as many women developed gestational hypertension (ranging from 6–17%).[454,470–472]

There are specific populations at "high risk" to develop pure or superimposed preeclampsia. These include women with diabetes, multifetal gestation, preexisting chronic hypertension or renal disease, and those with a history of preeclampsia in a previous gestation (especially prior to gestational week 36), whose incidence averages 20%.[319] Women with trisomy 13 fetuses also have more preeclampsia, the potential cause of which is discussed below. Presence of nonimmune hydrops fetalis and alpha thalassemia are also associated with more preeclampsia, often before midpregnancy.[9,150]

Finally, the rate of eclampsia has fallen almost 30-fold from the incidence published in the first half of the twentieth century, and is now less the 1 per 1000 births. This no doubt reflects improvement in prenatal care whereby practitioners detect and terminate the pregnancies at-risk in timely fashion, a policy reflected, in part, by an almost two-fold increase in the diagnosis of "severe" preeclampsia during the same period.[150,466]

Clinical Spectrum

Recognition and differentiation of preeclampsia (both "pure"' or superimposed) from other causes of high blood pressure in pregnancy has implications regarding the management of hypertensive gravidas, as this is the disorder most likely to cause serious maternal and fetal complications. However, a precise diagnosis may not always be possible, in which case therapy should be directed toward a presumptive diagnosis of the more serious disorder preeclampsia.

Preeclampsia, characterized by hypertension, proteinuria, edema, and at times coagulation and/or liver function abnormalities, or both, occurs mainly in

nulliparas, usually after the 20th gestational week, and most frequently near term.[9,150,473] The earlier the onset, the less likely it is to be "pure" preeclampsia, and the higher the probability that one is dealing with disease superimposed on underlying essential hypertension or a renal disorder.

Attempts have been made to categorize preeclampsia as "mild" or "severe." The latter is usually defined on the basis of diastolic and systolic levels (≥110 and 160 mm Hg, respectively), the appearance of nephrotic proteinuria, sudden oliguria, or neurologic symptoms (e.g., headache or hyperreflexia), as well as by laboratory tests demonstrating thrombocytopenia and/or abnormal liver function. Since a woman with seemingly mild disease (for instance a teenage gravida with a blood pressure of 140/90 mm Hg and minimal proteinuria) can suddenly convulse, designations such as mild and severe could be misleading. In fact, *de novo* hypertension alone in a third trimester nullipara is sufficient reason to manage such patients as if they were preeclamptics. Of final note, early preeclampsia (onset <34 weeks) is associated with greater morbidity than term preeclampsia.[474] In this respect some suggest subdividing preeclampsia into two groups, in regard to clinical management.[475] This may be misleading, however, as all preeclampsia is potentially explosive.

The eclamptic convulsion, the most dramatic and life-threatening complication of preeclampsia, was once associated with a maternal mortality of 30%, with cerebral hemorrhage as the leading cause of death,[9,150] but improved and aggressive obstetrical management have decreased the occurrence of convulsions and made maternal deaths extremely unusual. Eclampsia is usually preceded by various premonitory signs including headache, visual disturbances, severe epigastric pain, a sensation of constriction of the thorax, apprehension, excitability, hyperreflexia, and hemoconcentration. However, the convulsion can occur suddenly and without warning in a seemingly stable patient with only minimal elevations of blood pressure. It is the capricious nature of this disorder that underlies the need for early hospitalization of women with suspected preeclampsia.

There is a deceptively benign variant of preeclampsia whose initially mild clinical presentation may be misleading. The patient presents with borderline thrombocytopenia, and slightly abnormal liver function tests, normal or minimally elevated blood pressure, and little or no renal dysfunction. However, this form of preeclampsia may rapidly become life threatening when within 24–48 h there is progression to a syndrome characterized by hemolysis with marked evidence of both liver and coagulation abnormalities (transaminases and lactic dehydrogenase increasing to >1,000 IU/dL, platelet counts decreasing to <40,000/mL, with the presence of schistocytes on the blood smear. This complication, termed the HELLP syndrome, constitutes an emergency requiring termination of the pregnancy.[297] Furthermore, although postpartum recovery is usually rapid, the disease could persist for almost a week and some of these patients have undergone plasma exchange.

Finally, there is an uncommon disorder labeled late postpartum eclampsia (hypertension and convulsions that occur 48 h to several weeks after delivery).[476–478] Some of the patients have typical manifestations of preeclampsia and/or eclampsia prodroma, but prophylactic therapy had not been started because of lack of postpartum education, or their presentation at emergency rooms where caregivers are unfamiliar with gestation-related problems.[478] A similar syndrome has been reported in patients administered bromoergocryptine, a drug once utilized to suppress lactation,[479–481] but the evidence for this association was never compelling.

Pathogenic Mechanisms

The etiology of preeclampsia remains unknown, and some[468] suggest the disease has heterogeneous causes. There is evidence of a familial factor, with suggestions that preeclampsia may be inherited as a recessive condition (perhaps with maternal–fetal genotype interactions), or as a dominant one with 50% penetrance.[150,482] There are also ongoing investigations on the roles of angiotensinogen gene polymorphism[483,484] and the gene for 5,10 methylene tetrahydro reductase, an association also linked to hyperhomocysteinemia.[485,486] Detailed discussions of the genetics of preeclampsia can be found in reference.[487] More recently, a small Dutch genetic study suggested that polymorphism in the STOX1 (a member of the winged helix gene family), a paternally imprinted gene has been linked to preeclampsia within a small Dutch cohort.[488]

Considerable research is currently focused on the role of the placenta in the pathogenesis of preeclampsia. This includes determining the mechanisms of pathological changes that occur during the development of the blood supply to the placenta (see below), said to result in a relative hypoxemic environment and to lead to the production of cytokines that enter the maternal circulation and injure the vascular endothelium.[489] Other research focuses on the immune response at the maternal–fetal interface. For instance, placental tissue from preeclamptic pregnancies may express less HLA-G (a nonclassical HLA antigen expressed in normal placental tissues, which may modulate the maternal response to the immunologically "foreign" placenta).[490] Other evidence of pathogenic immune mechanisms include the disease's propensity for nulliparous pregnancies followed by normotensive

subsequent gestations (except if conception is with a new partner), a decreased prevalence in women who have received blood transfusions, required long periods of cohabitation before conceiving, and frequent oral sex, as well description of changes in the placental vasculature that resemble those in the blood vessels in allograft rejection.[491,492] Finally, investigators seeking insight into the cause of preeclampsia have studied a host of factors of placental origin(with a recent emphasis on angiogenic factors, see below).[493]

Pathophysiology of Preeclampsia

Preeclampsia is more than hypertension; it is a systemic disorder with both maternal and fetal manifestations. The disease in the mother includes vasospasm, alterations in many hormonal and autocoid systems which regulate blood pressure and volume control, and coagulation changes. Its physiopathology may also include the failure of mechanisms that deal with oxidative stress, the presence of a proinflammatory state, and an imbalance between pro- and antiangiogenic events. What is important to note is that many of the "nonhypertensive" manifestations of preeclampsia can be life threatening even when hypertension is quite mild.

Blood Pressure

Hypertension in preeclampsia, characteristically labile, represents a reversal the vasodilation of normal pregnancy and is due to increases in peripheral vascular resistance. These are so striking, that blood pressure rises even though cardiac output often falls. There is also a reversal of the resistance of the vasculature to pressor substances characteristic of normal pregnancy (discussed above), the vessels of preeclamptic women being actually hyperresponsive to a variety of pressor peptides and amines, especially to angiotensin II.[156,204] Loss of pressor resistance to the latter may be documented months before the appearance of overt disease.[494]

The cause of the altered vascular reactivity in preeclampsia has been sought for decades but remains obscure. Research has focused on changes in the ratio of vasodilating and vasoconstricting prostanoids (or frank increments in the latter),[495,496] and on the vasoconstricting potential of circulating pressor hormones (angiotensin II and ET), brought about by a number of possible scenarios. These include upregulation of receptors,[156,204,497] loss of resistance by a vasculature damaged by cytokines[489,498] or lipid peroxidases,[489,499] or inhibition of adaptive increments in the production of NO synthase as well as the NO-dependent and independent endothelium-derived relaxing factor.[500,501] Still other investigators focus on gestational alterations in calciotropic hormones, insulin metabolism, and the body stores of calcium and magnesium.[156,502] Most recently agonistic autoantibodies to the angiotensin I receptor have been detected in the blood of preeclamptic (see below) As of 2005, all the above postulates were still unproven.

The Heart

Data describing cardiac performance in preeclampsia is conflicting. This is due to several reasons. First, the investigators often failed to define precisely the study populations and included multiparous women, as well as patients with chronic hypertension and renal disease, all labeled preeclamptics. Many reports describe term and/or intrapartum protocols and the subject studied had often received magnesium sulfate and/or a variety of antihypertensive medications, as well as intravenous solutions of variable solute content. Also, the same data (especially the echocardiographic studies) may be interpreted differently by various groups. Finally, all findings may be correct, reflecting only that the hemodynamic parameters of preeclampsia change as the disease progresses.

Cardiac Performance: Pulmonary edema is a complication of severe preeclampsia, yet the literature is unclear as to whether the disease directly affects the heart or not (reviewed in[429]). In one study[429] focusing on proteinuric nulliparas and appropriately selected pregnant postpartum controls (both groups were restudied one month postpartum), load-independent left ventricular contractility was normal in all groups. Of importance was that if traditional approaches (rather than the load-independent indices) were utilized, some would have interpreted the echocardiographic findings as showing decreased contractility.

A survey of studies designed to determine systemic hemodynamic changes in preeclampsia reveals results that range from high output−low resistance to a low output−high resistance state.[22] This wide and inconsistent spectrum relates both to the problems cited above, and in some instances reflect experimental artifact. We will focus on selected reports where data permits us to focus on nulliparous preeclamptics.

Easterling et al.,[503] in a serial study, using noninvasive echocardiographic techniques, observed an exaggeration of the normally increased cardiac output throughout gestation, as well as greater decreases in peripheral vascular resistance in women who became preeclamptic. The exaggerated Increase in cardiac output, but not the excessive decrement in peripheral vascular resistance, has recently been confirmed in an even larger serial study by Boslo and colleagues.[504] In an a group of term nulliparous preeclamptics (said to have received minimal fluid) Mabie et al.[505] found cardiac output to be normal or slightly increased, while pulmonary capillary wedge pressure (PCWP) was

usually normal. Perhaps the most carefully controlled studies were those by Visser and Wallenburg,[506] in which proteinuric hypertensive women and a small group of normotensive pregnant controls were studied prior to any therapeutic interventions. Using Swan-Ganz pulmonary artery thermodilution techniques they convincingly demonstrated low cardiac output and markedly increased peripheral resistance and low normal PCWP in untreated preeclamptics. They further showed that the profile was variable when subjects had been treated, though on average their cardiac output was similar to that in normotensive gravidas, while peripheral vascular resistance was considerably improved (though still significantly elevated).

The observations described above have several interpretations. The first relates to the heterogeneity of the study designs and populations, with a call for further and more precise research. The second is the intriguing possibility that the older literature "missed" the natural history of cardiac performance in patients destined to develop preeclampsia; an early preclinical period characterized by an exaggeration of the normal increase in cardiac output in gestation as well as an exaggerated decrease in peripheral vascular resistance (the anticipated autoregulatory response). This is followed by a "crossover" to a decreased cardiac output-high peripheral resistance state when the disease manifests near term. If confirmed, though, this would be surprising, given that the increased pressor responsiveness of preeclampsia is detectable at midgestation.[494]

Finally, Hibbard et al. combining echography and modeling techniques studied both preeclamptics and chronic hypertensives with superimposed preeclampsia.[433] They confirmed the decrease in arterial compliance in preeclampsia, demonstrating that a component of the decrease was due to the disease, (in addition to the due to increased blood pressure). They further demonstrated that the first harmonic of the input impedance spectrum was higher, while the data suggested that characteristic impedance was also higher

Liver and Coagulation Abnormalities

Preeclampsia is associated with activation of the coagulation system, although abnormalities are undetectable clinically in most patients.[507] Thrombocytopenia, rarely severe, is the most common finding recorded, whereas increases in platelet activation and size, as well as decrements in their life span, and worsening of the hypercoagulability of normal pregnancy (e.g., reduced antithrombin III, protein S, and protein C) can be detected by special testing in many patients with normal thrombocyte counts.[507] Rarely, however, preeclamptic patients develop evidence of a severe life-threatening coagulopathy, as evidenced by the ominous HELLP syndrome discussed above. Finally, the causes of thrombocytopenia and the hypercoagulability of normal gestation are still unclear.[156,507]

Preeclampsia also affects the liver.[1,508,509] Manifestations of liver involvement include elevation of transaminase and lactic dehydrogenase levels, usually of a mild degree.[510] In fact, preeclampsia is probably the most common cause of mild liver functional abnormalities in pregnancy. However, as described above, the liver can also be the focus of the disease, severe liver failure and disseminated intravascular coagulation combining to threaten both maternal and fetal well-being.[297]

The gross and microscopic hepatic changes in preeclampsia are detailed in the extensive autopsy series of Sheehan and Lynch.[1] In that series the liver appeared normal 40% of the time, and there were occasional petechiae (on the surface or in sections) in another 20%. In the remaining 40%, however, there were confluent petechiae and obvious infarcts. Also described were subcapsular hematomas, some of which had ruptured and were the immediate cause of death. On the other hand, a more recent study in which the liver was assessed laparoscopically, hematomas were quite unusual.[104] Microscopically, there are two characteristic lesions. One is a periportal lesion, manifesting as hemorrhage into the hepatic cellular columns, and the second is the presence of infarction.[1] Also, of interest, also, are results from liver biopsies performed during laparoscopy showing intracellular fatty changes in all patients with preeclampsia, irrespective of the severity of the disease.[104] (Nevertheless, both autopsy and laparoscopy studies are by their nature quite selective). Finally, acute fatty liver of pregnancy, a disorder frequently associated with preeclampsia, was discussed in the ARF section above.

Central Nervous System

Eclampsia, the convulsive phase of preeclampsia, remains a leading cause of maternal death, the proximate causes including disseminated intravascular coagulation-like syndromes, pulmonary edema, aspiration and sepsis, and especially cerebral hemorrhage and edema.[1,150,466] Knowledge of its etiology, however, remains incomplete. Some, noting fibrin deposition in brain at autopsy, relate its cause to the coagulation changes associated with preeclampsia. To others[511] the disease is merely a form of hypertensive encephalopathy, a concept difficult to accept as the convulsion can occur suddenly in women whose systolic levels are consistently below 140 mm Hg. However, vasoconstriction in preeclamptic women can be selective. For example, investigators have demonstrated ultrasonographically the presence of severe cerebral vasospasm in patients with minimal evidence of

peripheral vasoconstriction.[512] They have also suggested that the cause of eclampsia may be heterogeneous, as some patients manifest normal cerebral vascular indices, while others (especially those with mean arterial pressures that exceed the brain's autoregulatory capacity) demonstrate high pressure indexes, and/or perfusion, akin to hypertensive encephalopathy.[513,514] On the other hand, phase contrast velocity imaging techniques combined with MRI consistently fail to demonstrate any changes in cerebral perfusion in severe preeclampsia or eclampsia.[515]

Reports based on cranial axial tomography and MRI (the latter, the preferred diagnostic test) vary but often describe transient abnormalities consistent with localized hemorrhage or edema.[515,516] The edema is said to be vasogenic, and fully reversible, though a recent study has noted "cytotoxic" edema and infarction in up to one forth of the patients.[517] These data, as well as those in the perfusion studies described above are not always easy to interpret; however, as many of the patients had been treated with antihypertensive drugs, magnesium infusions, and especially with considerable fluid administration, raising the possibility that many of these findings may be iatrogenic. Of interest is a disorder termed "reversible posterior leukoencephalopathy syndrome," observed in patients with a variety of medical disorders and in three women with postpartum eclampsia.[518] The disease is life threatening and characterized by accelerated hypertension, severe headaches, altered mental status, cortical blindness, and convulsions, but appears to be reversible with aggressive diuresis and rapid reduction of blood pressure. Review of this article suggests the eclamptic women had been grossly volume overloaded.

The best descriptions of gross and microscopic pathology are in autopsy series of Sheehan and Lynch,[1] as most of these necropsies were performed within two hours of death, thus eliminating most of the postpartum changes that might confound interpretation. Of interest, there was little evidence of brain edema, which led the authors to conclude that cerebral edema was a late, perhaps postseizure event, and not a cause of the convulsion. The major finding was gross evidence of cerebral hemorrhage, not surprisingly present in 60% of the subjects expiring within 48 h of the convulsion. There were also varying degrees of smaller hemorrhages and petechiae observed with the naked eye, and more numerous on histological sections. The petechiae were cited as evidence of vascular disturbances produced by local ischemia. Sheehan & Lynch[1] have produced a series of photomicrographs that we highly recommend to the reader).

The Placenta

Abnormal placentation is believed by many to be the major culprit in the pathophysiology of preeclampsia, if not its proximate cause. This is because uteroplacental ischemia has been used to develop several animal models believed to mimic the disease in humans,[519] and because delivery remains the most successful and probably the only definitive cure in preeclamptic women. Furthermore, the incidence of preeclampsia is increased in women with hydatiform disease (a rapidly growing placenta in the absence of a fetus), and in multifetal gestations (increased placental mass).[9,150] Finally, abnormalities in placentation, which occur between 10 and 20 weeks gestation, may represent the earliest evidence of pathology leading to the disease (reviewed in Ref.[520]), even though maternal signs of preeclampsia do not appear until the late third trimester.

Normal placentation involves the transformation of the spiral arteries from thick-walled, muscular arteries, into sac-like, flaccid uteroplacental vessels that permit delivery of greater volumes of blood at a lower blood pressure than before. This transformation is believed to be accomplished primarily by invasion of trophoblast cells which destroy and replace the endothelium of maternal vessels, and then invade their medial elastic and muscular layers, a process that ensures that the fetus is adequately supplied with oxygen and nutrients. However, in women destined to develop preeclampsia, invasion of the spiral arteries by endovascular trophoblast is incomplete, and it may occur in the decidual but not in the myometrial segments[521] (Figure 81.17). These changes may be focal or diffuse, the result being that many spiral arteries remain muscular, with thick-walled vessels, and blood flow to the placenta is compromised.

Reasons for the failure of spiral artery remodeling are obscure. Of interest are studies by Fisher and associates[520,522] which suggest that in preeclampsia the cytotrophoblast cells fail to mimic a vascular adhesion phenotype and to express adhesion molecules believed to be critical to the process of trophoblastic invasion.[520,522] Differentiation of trophoblasts along the invasive pathway involves alteration in expression of a number of different classes of molecules, including cytokines, adhesion molecules and extracellular matrix molecules, metalloproteinases and class Ib major histocompatibility complex molecule, HLA-G.[523–525] During normal differentiation, invasive trophoblasts alter their adhesion molecule expression from those that are characteristic of epithelial cells (integrin α_6/β_4, α_v/β_5 and E-cadherin) to those of endothelial cells (integrin α_1/β_1, α_v/β_3, PECAM, and VE-cadherin) a process referred to as "pseudovasculogenesis"[526] (Figure 81.17) Both

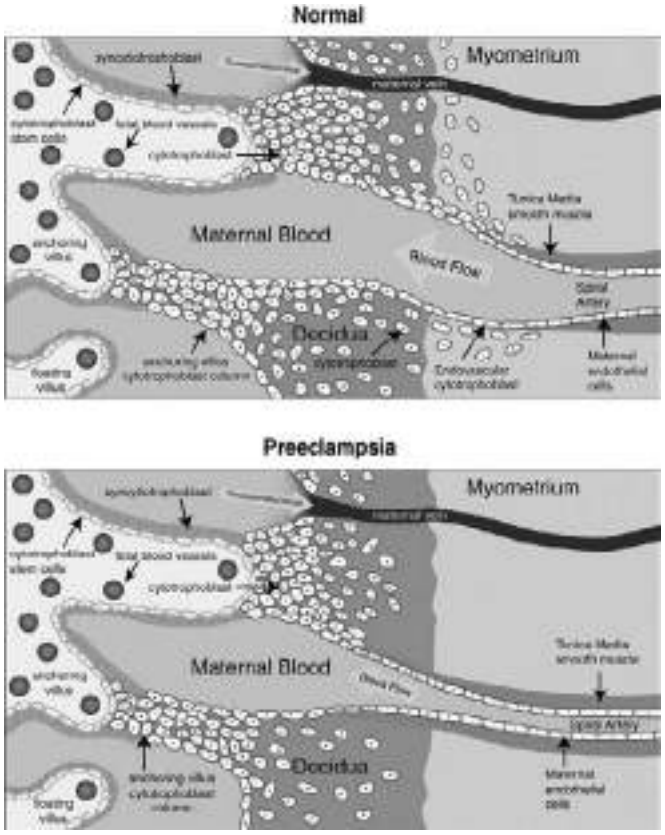

FIGURE 81.17 Cartoon depicting the changes in uteroplacental arteries that take place during normal and preeclamptic gestations. During the process of uterine vascular invasion, the cytotrophoblasts differentiate from an epithelial phenotype to an endothelial phenotype, a process referred to as "pseudovasculogenesis" (Upper Panel). In preeclampsia, cytotrophoblasts fail to adopt an invasive endothelial phenotype. Instead, invasion of the spiral arteries is shallow and they remain small caliber, resistance vessels (Lower Panel). *[Reproduced from Ref.[666] with permission]*

in vitro and *in vivo* studies show that trophoblasts obtained from patients with preeclampsia fail to undergo these alterations of adhesion molecules and pseudovasculogenesis.[522,527] The molecular pathways that regulate pseudovasculogenesis may involve a vast array of transcription factors, growth factors and cytokines.[528]

Another morphologic change in the placentas of preeclamptic women, though believed to be less specific, is an arteriolar lesion termed acute atherosis.[150,520] It is characterized by fibrinoid necrosis of the arterial wall, accumulation of fat-laden macrophages, and perivascular mononuclear cell infiltrates.

Finally, research efforts are in progress to link abnormal placentation early in preeclampsia with circulating markers to predict its occurrence and to explain why symptoms do not occur until late in gestation. The reader is referred to several reviews on the subject [489,520,529]), The reduced placental perfusion may also explain the increased incidence of fetal growth retardation associated with preeclampsia.

Circulating Factors and Endothelial Dysfunction

The increase in blood pressure in preeclampsia has been attributed to generalized endothelial dysfunction that disrupts the appropriate control of vascular tone,[530] Similarly, increased glomerular vascular permeability, and coagulopathy are ascribed to abnormal endothelial expression of procoagulants, while liver dysfunction to hepatic ischemia. In these respects there are considerable data to support the theory that the maternal response in preeclampsia is secondary to generalized endothelial dysfunction. These include studies demonstrating increases during preeclampsia in circulating fibronectin, Factor VIII antigen, and thrombomodulin, all markers of endothelial cell injury decreased production of endothelium-derived vasodilators (e.g., prostacyclins), increased production of vasoconstricting ETs, and enhanced vascular reactivity to angiotensin II.[494,531–535] Of note the characteristic renal lesion of the disease, described in Figure 81.19 is primarily limited to endothelial cells.[325] Finally, serum from preeclamptic women causes endothelial activation in human umbilical vein endothelial cell culture studies *in vitro*.[536]

Identification of circulating factors of placental and/or maternal origin that mediate endothelial dysfunction has been and continues as an area great research activity. There have been reports of alterations in levels of cytokines/growth factors/chemicals such as TNF-α, IL-6, IL-1α, IL-1β, Fas ligand, oxidized lipid products, neurokinin-B and asymmetric dimethylarginine.[537–540] However, there is no evidence that any of these molecules are etiologic. One interesting hypothesis for which some evidence exists, involves excessive exportation" of bits of trophoblastic material from the diseased placenta into the circulation causing the generalized microangiopathy.[541]

Increased sensitivity to angiotensin II, a consistent feature of preeclampsia, may be secondary to increased bradykinin (B2) receptor upregulation in preeclamptic patients.[317] In this respect there is *in vitro* data demonstrating that heterodimerization of B2 receptors with angiotensin II type I receptors (AT1), forms an AT1/B2 heterodimer that shows increased responsiveness to angiotensin. II. It is unclear however whether these alterations observed are of pathophysiological significance or just epiphenomena. Recent studies from the laboratory of a co-author of this chapter (S.A.K.)[542] and others[543,544] have demonstrated an increased placental expression and secretion of sFlt-1 (soluble fms-like tyrosine kinase 1, see below), a naturally occurring circulating VEGF antagonist in patients with preeclampsia. Importantly, when administered exogenously to

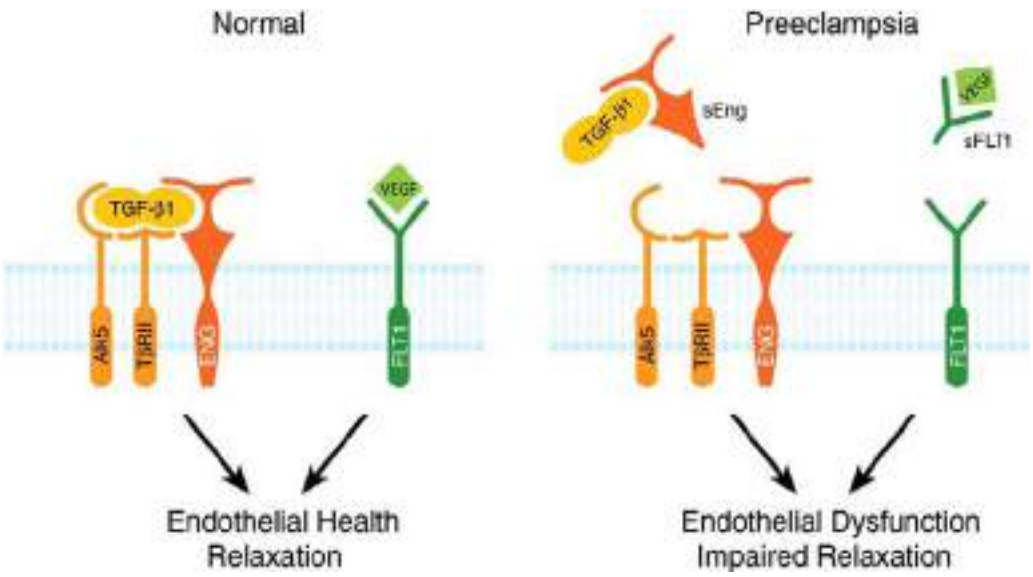

FIGURE 81.18 sFlt1 and sEng causes endothelial dysfunction by antagonizing VEGF and TGF-β1 signaling. There is mounting evidence that VEGF and TGF-β1 are required to maintain endothelial health in several tissues including the kidney and perhaps the placenta. During normal pregnancy, vascular homeostasis is maintained by physiological levels of VEGF and TGF-β1 signaling in the vasculature. In preeclampsia, excess placental secretion of sFlt1 and sEng (two endogenous circulating anti-angiogenic proteins) inhibits VEGF and TGF-β1 signaling respectively in the vasculature. This results in endothelial cell dysfunction, including decreased prostacyclin, NO production, and release of procoagulant proteins. *[Reproduced with permission from Refs[666,667]]*

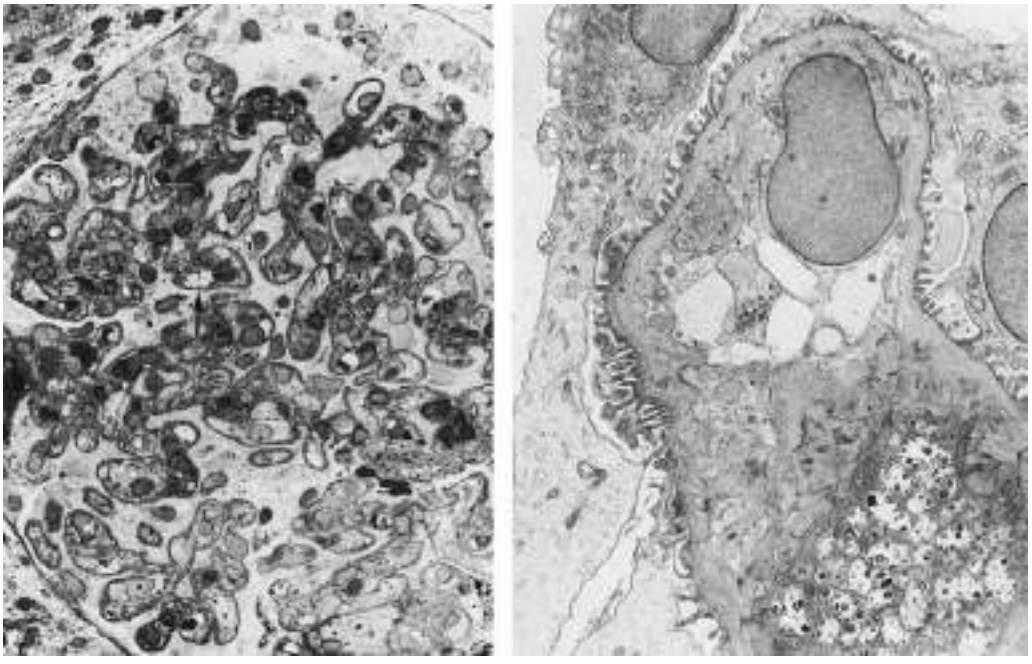

FIGURE 81.19 Light micrograph of glomerulus from a patient with preeclampsia. Capillary lumina are encroached by swollen endothelial and mesangial cells (arrow). **B**: Electron micrograph in the area of a vacuolated tuft demonstrating obliteration of the capillary space. There are also clusters of lysosomal structures which contain myelin-like figures and collections of lipids, most marked in mesangial cells. *(Courtesy of Dr. B.H. Spargo)*

rats, sFlt-1 alone has been shown to be sufficient to induce a preeclampsia-like phenotype.[542] This work has generated considerable enthusiasm for sFlt1 as an important mediator in preeclampsia.

Alterations in Pro and Antiogenic Factors Normal Pregnancy and Preeclampsia

Perhaps the more plausible explanations of genesis of at least two phenotypes of preeclampsia, hypertension and proteinuria are events that lead to an imbalance of pro and anti-angiogenic factors in the circulation of pregnant women. sFlt1 is an anti-angiogenic molecule which antagonizes both VEGF and PlGF. VEGF is important in both angiogenesis (the growth of new blood vessels) and in the maintenance of endothelial cell health in the basal state. Although the function of PlGF is still ill-defined, it appears to act synergistically with VEGF, and may be necessary for wound healing and angiogenesis in ischemic tissues.[545,546] VEGF has a family of receptors, the most important of which are Flt1 (VEGFR1) and Flk1 (VEGFR2).[547] sFlt1 is a truncated form of the Flt1 receptor (see Figure A). It includes the extracellular ligand-binding domain, but not the transmembrane and intracellular domains; it is secreted (hence "soluble") and antagonizes VEGF and PlGF in the circulation by binding and preventing their interaction with their endothelial receptors[548] Although sFlt1 is made in small amounts by other tissues (endothelial cells and monocytes), the placenta seems to the major source of circulating sFlt1 during pregnancy as evidenced by the dramatic fall in circulating concentrations of sFlt1 after the delivery of the placenta.[542]

Circulating sFlt1 levels are increased, while free (unbound) PlGF and free VEGF levels are suppressed, in women with preeclampsia.[542] The increase in sFlt1 precedes the onset of clinical disease by at least five weeks[549–552] and appears to be more pronounced in severe and early-onset preeclampsia.[551,553] In several studies, decreased free PlGF levels were observed before 20 weeks gestation in women who developed preeclampsia later in pregnancy,[551,553–555] though not all investigators have confirmed this finding.[556] Although reduction in free PlGF may be predominantly explained by increased sFlt1 production, some data suggest the fall in PlGF may actually precede the rise in sFlt1, implicating other mechanisms such as decreased PlGF production.[557] Since free PlGF is readily filtered through an intact glomerulus, urinary PlGF is significantly decreased in preeclampsia and measurements of urinary PlGF can also be used for the prediction of preeclampsia.[558]

In vitro studies confirm that excess placental sFlt-1 production induces an anti-angiogenic state in the serum of preeclamptic women that can be rescued by exogenous VEGF and PlGF.[542] Excess sFlt-1 alone, when administered to pregnant rats, induced albuminuria, hypertension and renal pathological changes of glomerular endotheliosis by antagonizing circulating VEGF and PlGF and inducing endothelial dysfunction.[542] Furthermore, a significant percentage of cancer patients receiving VEGF signaling antagonists develop hypertension and proteinuria.[559,560] Even a 50% reduction of renal VEGF production in genetically modified mice resulted in glomerular endotheliosis and proteinuria.[561] These data suggest that excess circulating sFlt-1, by neutralizing VEGF and PlGF, may play a causal role in the pathogenesis of the maternal syndrome in preeclampsia (Figure 81.18).

The role of sFlt-1 in preeclampsia is supported by two clinical studies in a patient population considered high risk for the development of preeclampsia. The genes for sFlt1 and Flt-1 are carried on chromosome 13, and the incidence of preeclampsia in mothers who carry fetuses with trisomy 13 is in fact greatly increased, as compared with all other trisomies or with control pregnant patients.[562] In a more recent study where blood samples were obtained from women with trisomy 13 (in the majority the pregnancy was terminated or ended prior to the final trimester) the ratios of sFlt1/PlGF levels compared to other trisomies or control pregnant women measured during the second trimester were comparable to those observed in pregnant women who subsequently develop preeclampsia.[563] These data suggest a molecular explanation for the increased risk of preeclampsia observed in these patients. Finally, circulating concentrations of sFlt1 were recently reported to be higher in the first versus second pregnancies this accounting for the increased risk of preeclampsia among nulliparous women.[564]

The discussions in this section are detailed because as of 2011 the role of angiogenic factors has become the most exciting research area in the enigmas that historically surrounded understanding preeclampsia.[565] However, there are still unanswered questions to the sFlt-1 story. Although hypoxia of cytotrophoblasts has recently been shown to be a potent inducer of sFlt1 production,[566] the precise mechanisms of excess sFlt-1 production by the preeclamptic placenta are not known. Importantly, the role of sFlt-1 in normal placental development and in placental pseudovasculogenesis is not clear. No coagulation or liver function abnormalities or brain abnormalities (eclampsia) were reported in sFlt-1-treated animals. Finally, sFlt1 may not be altered in some preeclamptic women especially in those labeled mild preeclamptics.[567] Therefore, additional synergistic factors that are elaborated by the placenta may yet be identified that play a role in the pathogenesis of the generalized endothelial

dysfunction noted in preeclampsia. Derangements in other angiogenic molecules have also been observed recently. Levels of endostatin, an anti-angiogenic factor, are also elevated in preeclampsia.[568]

Soluble endoglin (sEng), another anti-angiogenic protein, has also been implicated in the pathogenesis of preeclampsia (see Figure 81.18). The role of this protein in producing preeclampsia phenotypes was evaluated based on the hypothesis that sEng may impair transforming growth factor-beta 1 (TGF-β1) binding to its cell surface receptors and decreasing endothelial NO signaling.[569] sEng is placental in origin, is present in the sera of pregnant women, is elevated in preeclamptic individuals and correlates with disease severity.[570,571] Administration of both sFlt1 and sEng using an adenoviral expression system in rats produces a severe preeclampsia-like animal model with hypertension, proteinuria, glomerular endotheliosis, features of HELLP syndrome and small for gestational age (SGA) pups.[569] The role of sEng in early placentation and its regulation is still not yet known.

Agonistic Antibodies Against AT1 Receptors

Patients with preeclampsia have also been reported to have circulating autoantibodies against the angiotensin receptor -1 (AT1-AA).[572] These autoantibodies are agonistic to the AT1 receptor and have been hypothesized to participate in angiotensin II-induced hypertensive changes noted in preeclamptic patients in preeclamptic patients and in "shallow" placental implantation.[573,574] These autoantibodies have been also shown, *in vitro* to stimulate NADPH oxidase from both trophoblasts and vascular smooth muscle cells, the implication being the antibodies being the antibodies are responsible for the substantial increase in circulating reactive oxygen species in the in preeclampsia.[575] Recently, direct pathogenic role for AT1-AA in preeclampsia has been noted in animal models.[576] However, these antibodies have also been encountered in other examples of vascular injury such as vascular rejection,[577] suggesting that they may be secondary to the generalized microangiopathy of preeclampsia. As of 2011 we could locate no information on the temporal relationship of these autoantibodies with the appearance of preeclampsia. It was also unclear at that time, whether these antibodies synergize with other proteins, such as sFlt-1, to induce systemic endothelial dysfunction or whether they are simply a consequence of the diffuse endothelial injury. Finally, the source of the antigen responsible for these antibodies has not yet been identified.

Oxidative Stress and Inflammation

Oxidative stress, the presence of active oxygen species in excess of available antioxidant buffering capacity, is a prominent feature of preeclampsia. Oxidative stress is known to damage proteins, cell membranes, and DNA and is a potential mediator of endothelial dysfunction. It has been hypothesized that in preeclampsia factors responsible for oxidative stress of placental origin are transferred to the systemic circulation, resulting in oxidative damage to the vascular endothelial cells throughout the body. Proponents of this theory, focus on oxidative stress itself as the link between the placenta and maternal end-organ disease.[578,579]

There are many reports that document increased markers of oxidative stress in both the placentas and circulation of preeclamptic patients.. These include decreased expression of enzymatic antioxidants, abnormally high superoxide generation,, higher levels of lipid peroxidation, and increased production and secretion of isoprostanes, all in the placenta.[580–585] Maternal serum markers include increases in peroxynitrite, protein carbonyls.[586] There are also Increases in volatile organic compounds in alveolar breath,[587] though this is disputed.[588,589]

Animal models and human trials also suggest a role for oxidative stress. One of the major animal models of preeclampsia is produced by infusion of L-NAME (L-nitro-arginine methylester), an inhibitor of NO synthesis, into pregnant rats. This produces a preeclampsia-like syndrome with hypertension, proteinuria, and thrombocytopenia[590,591] A UK study showed that deficiency of selenium, a trace element with antioxidant properties, was associated with an increased risk of preeclampsia.[592] But the most clinically relevant insights come from human trials: if oxidative stress is a key element in preeclampsia, antioxidant treatment might be expected to be beneficial. A randomized controlled trial by Chappell et al randomized showed that supplementation with vitamin C and E decreased preeclampsia in high-risk pregnant women (OR 0.4). PAI-1 and PAI-2, markers of endothelial activation, were also decreased in the treatment group.[593] Similarly, treatment with the antioxidant lycopene was found to decrease the risk of preeclampsia by almost 50% in a small randomized trial.[594] Unfortunately, large randomized controlled trials did not show an effect of antioxidants, vitamin C and vitamin E on the risk of preeclampsia.[595,596] In summary, the data reviewed suggest that oxidative stress while noted in preeclampsia, may not play an important role in the pathogenesis of disease.

The Kidney in Preeclampsia

Renal Morphology

Preeclampsia is accompanied by characteristic morphological alterations in the kidney termed

"glomerular endotheliosis." Detailed descriptions of the renal lesions of preeclampsia, an historical review, a precise of several disagreements in the literature, including whether or not preeclampsia causes focal glomerular sclerosis, and a more complete bibliography can be found elsewhere.[1,473] It is noteworthy that the best information has come from analysis of tissues obtained at necropsy between 1930 and 1950, and renal biopsy series liberally performed from the late 1950 through the mid-1970s. More recently, reasons to perform renal biopsies have become more stringent, with few indications for use of this procedure in routine preeclamptics, either prepartum or in the puerperium (see section on renal disease). The more recent literature, therefore, has focused on more atypical variants of the disease, as biopsies have been performed weeks, and even months following the index pregnancy. We believe that many of these reports have only managed to confuse our understanding of the morphological picture of the disorder, and therefore focus on the older literature in the summary that follows.

The kidneys from women dying after eclampsia are pale and enlarged compared to those of gravidas dying from accidents or other causes, but the variance is such that the differences are not significant.[1] The glomeruli are large and swollen, but not hypercellular. This is due to swelling of the intracapillary cells (mainly endothelial, but mesangial as well), which encroach on the capillary lumina giving the appearance of a bloodless glomerulus (Figure 81.19). This change varies with the severity of the lesion but is usually widespread, involving most of the capillaries in nearly all glomeruli, and the swelling may be of sufficient magnitude that the tuft herniates into the initial segment of the proximal tubule, a phenomenon termed "pouting".[1,325,473,597] On occasion, the mesangium is severely affected, its expanded matrix and enlarged cells extending into the peripheral capillary loops between the endothelial cells and the basement membrane and creating the illusion of "double contours" or "tramtrack." Thrombosis and fibrin-like material, as well as foam cells may be present, and epithelial crescents have been described in rare instances[1,9,325,473,597]

The characteristic glomerular changes of preeclampsia most evident on ultrastructural examination (Figure 81.19) include extensive swelling and vacuolization, primarily of the endothelial cells and to a lesser extent of the mesangial cells, without significant changes elsewhere. The enlarged and reactive cells, which have increased amounts of vacuolated cytoplasm, narrow the capillary lumen and even appear to obliterate it, but result in only moderate widening of the lobular stalks even when mesangial involvement is prominent. Impressive lysosomal changes, especially in material obtained after delivery when the disease is in regression, can also be seen. The basement membrane is not thickened, but may appear so on light microscopy because of the fibrils produced by endothelial and mesangial cells.

Variable densities of amorphous, extracellular debris separate the swollen cells where the capillary lumina are severely narrowed. Occasionally, small subendothelial deposits (thought to represent accumulation of protein) and tactoids of fibrin or a fibrin-like material may be seen. These aberrations may in part be due to the accumulation of several basement membrane proteins including laminin, type IV collagen, tenascin, fibronectin and its receptor, and a proteoglycan in the glomeruli of preeclamptics.[598,599] Moreover, renal biopsies obtained after a prolonged postpartum interval may reveal large cytoplasmic cholesterol clefts in addition to lipid-containing vacuoles.[325,473,597]

Mesangial proliferation, granulated epithelial cells, and nonspecific tubular changes have been described (cited in refs.,[166,167]but this has not been consistent during the 30-year experience at our institution, which includes several hundred biopsies.[325,473,597] Starting in the 1980s there have been more and more reports describing FSGS in association with preeclampsia, some authors claiming that this lesion is a consequence of the disease,[600–605] which would alter the benign prognosis of pure preeclampsia (see above). Presence of FSGS might also suggest that clinicians have not been sufficiently aggressive in controlling the rise in blood pressure, or have utilized antihypertensive agents that failed to decrease glomerular pressure, which might conceivably be high during this disease. Interpretation of our own biopsy material (reviewed in[473,597]) suggests that FSGS, when present, antedated pregnancy or was due to hemodynamic factors present earlier in gestation, conclusions that are consistent with the benign remote prognosis of pure preeclampsia[150,325] (see below). This is because the FSGS lesion, if present, would not likely disappear spontaneously.

Glomerular endotheliosis, which can be superimposed on other preexisting renal lesions, has not been observed by us in biopsies from nonpregnant patients. But others have described similar lesions in a number of nongravid subjects with a variety of glomerular diseases, as well as in certain pregnant women with placental abruption (cited in refs.[9,597]). More recently glomerular endotheliosis has been described in a few renal biopsies from normal third trimester gravidas, but the degree of endothelial swelling was trivial, and even borderline.[5] In the same study, the lesion in preeclamptics was fully developed and glomerular volume markedly increased. Thus we believe, that the glomerular lesion in its fully developed form is distinctive, and that it reverses rapidly after delivery,

the glomeruli resuming a normal appearance within 2–3 weeks.[9,325,473,597] Nevertheless, some authors have attributed abnormalities seen years after the putative disease to residua of the preeclamptic lesion.[9,325,597]

The significance of immunoglobulins and fibrin deposits in the glomerular lesion of preeclamptic patients is disputed, and is discussed in detail elsewhere.[325,473,597] Some authors reported that IgG, IgM, and fibrin are invariably present, but such deposits were found less often by others, including us. Of interest, however, is a report by Packham et al.,[606] in which biopsies performed prior to delivery contained substantially more fibrin deposition than those obtained in the immediate puerperium, suggesting that mobilization of the deposits postpartum occurs more rapidly than was originally appreciated.[606]

Functional Changes

Both GFR and ERPF decrease in preeclampsia.[9,22,150,219] In most studies the former falls more than the latter (32% v 24% in 23 studies reviewed in reference,[94]so that the filtration fraction also decreases. Since the decrement in filtration is <25% and lower in mild cases, the GFR of preeclamptics often remains above values in nonpregnant women, despite morphological evidence of ischemia and an obliterated urinary space. In fact, the decrement may not be appreciated if one is not aware of norms for pregnancy. However, while functional decrements are usually mild or moderate and reverse rapidly after delivery, an occasional preeclamptic patient may progress to ARF, especially when treatment or intervention is neglected, and the long range renal and cardiovascular prognosis of these latter cases is poorer than that associated with acute tubular necrosis in general.[306]

The mechanism(s) responsible for the compromised renal function are unknown. The inciting event may relate both to factors that evoke general vasoconstriction in preeclampsia, and to the morphological changes in the kidney (especially glomerular endotheliosis) described above. Irrespective of the proximal cause, renal vascular resistance is high, which accounts for the reduced renal blood flow. As for the GFR, indirect calculations of renal afferent and efferent arteriolar and of venous resistances suggest that the increment in total renal vascular resistance is primarily due to an increase in the afferent arteriolar resistance.[22,41] This is not unexpected, as the decrement in filtration fraction, albeit consistent is small. Under these circumstances it is tempting to speculate that a reduction in the ultrafiltration coefficient is the explanation for the fall in GFR. In this respect, elegant morphometric studies of renal biopsies in combination with theoretical modeling,[602] and preliminary data from protocols in which glomerular permselectivity to dextrans are used to estimate ultrafiltration coefficient,[607] suggest similar conclusions.

The fractional and absolute clearances of urate also decrease in preeclampsia, and consequently plasma levels of this solute increase [in pregnancy values exceeding 4.5 mg/dL (268 μmol/L) are suspect, while values exceeding 5 mg/dL (297 μmol) are definitely abnormal].[9,22,150] Decrements in urate clearance tend to occur earlier and are more profound than that in GFR, so that the urate/inulin or urate/creatinine clearance ratio is also decreased.

The reasons for the rise in circulating urate and the fall in its renal clearance are also obscure. Certainly, all the changes can be ascribed to decrements in fractional urate clearance. Of interest are studies in the older literature (reviewed in reference[22] and[41]), in which probenecid administration normalized plasma urate levels in preeclamptics, but had little or no effect in normal pregnant women, suggesting that hyperuricemia was primarily due to enhanced tubular reabsorption. Finally, studies whose authors attempted to determine whether there is increased urate production in preeclamptic women yielded conflicting results.[22] Interesting in this respect are recent reports which note that placental xanthene oxidase/dehydrogenase activity may be increased in preeclampsia.[141,608] Finally, recent rodent studies suggest that hyperuricemia may play a pathogenic role by contributing to the vascular damage and hypertension.[609]

Abnormal proteinuria almost always accompanies preeclampsia, and the diagnosis is suspect without this sign (although increased protein excretion may appear later in the course of the disease). The proteinuria may be minimal or severe, is usually nonselective in nature, and its magnitude correlates roughly with the severity of the renal lesion as well as with poor fetal outcome.[325] Of interest, too, is that preeclampsia is the most common cause of nephrotic proteinuria in pregnancy.[325]Tubular proteinuria may also occur in preeclampsia,[22] which is surprising in view of the noninvolvement of the tubules in the morphologic lesion.

Fluid Volumes and Sodium Excretion

Edema was once considered the hallmark of preeclampsia, and salt restriction and/or diuretics figured prominently in preventing or managing the disorder. However, even when interstitial fluid volumes are markedly increased, plasma volume is smaller compared to normal gestation, and severe disease can occur even in the absence of edema (the "dry preeclamptic) [reviewed in[150,195,610,611]]. The reasons for the decrement in plasma volume (which is associated with hypoalbuminemia and hemoconcentration) is unclear, as the decrease precedes any evidence of

hypertension.[160] One major postulate attributes most of the change to increases in capillary permeability.[195,202,203,610] In addition, both proteinuria and liver involvement would be expected to contribute to the hypoalbuminemia.

The ability to excrete sodium may be impaired in preeclamptics but the degree to which this occurs varies.[9,150,195,207,227,610] The reason for the decreased sodium excretory capacity is also poorly understood [reviewed in references[195] and[610]]. The renin–angiotensin–aldosterone system is suppressed or unchanged, while ANP levels are increased and its metabolic clearance unchanged.[195,204,213,219,610] Finally, a literature devoted to cellular sodium transport, including several membrane pumps or their inhibitors, has shed little light on these problems and is reviewed elsewhere.[9,195,610]

Prediction, Prevention, and Remote Prognosis

Prediction

Investigators have sought to identify markers that could provide clues to the cause of preeclampsia (or at least improve its management), to predict the risk of its appearance later in gestation, or to differentiate it from more benign hypertensive complications of pregnancy. In the past a decline in fractional urate clearance, a positive "cold pressor" response, enhanced sensitivity to infused angiotensin II, and demonstration of a rise in blood pressure upon turning from a lateral recumbent to a supine posture (the "roll over" sign) were all heralded as promising tests.[150,612] More recently, studies have focused on autacoids, circulating lipids, oxidant and antioxidant activity, markers of endothelial dysfunction, a host of cytokines, hormones, and circulating proteins (especially those of placental origin such as chorionic gonadotropin, activin, and inhibin), the isoelectric point of albumin, urinary excretion of albumin, and so on.[468,498,612] Unfortunately, the sensitivity and positive predictive value of all these tests are at best modest.

The recent focus on the role of circulating angiogenic proteins in the pathogenesis of preeclampsia, has also raised hope that measurement of these molecules in serum or urine may serve as a screening tool.[550] In retrospective studies, serum sFlt-1 has been reported to have sensitivity of 83% and specificity of 95% between 28 and 32 weeks of pregnancy in predicting preterm preeclampsia[549] Similarly measurement of sFlt-1 between 32 and 36 weeks of pregnancy has been reported to have a 70% sensitivity and 97% specificity for term preeclampsia.[549] A number of studies have also investigated serum PlGF and found that alterations in PlGF occur even as early as first trimester in women destined to develop preeclampsia.[551,554,557,613,614] Recently, a more promising screening strategy has evolved by measuring urinary PlGF levels.[558] In a cross sectional study representing a secondary analysis of stored specimens from a completed prevention trial, Levine et al reported that at 21–32 weeks of gestation, urinary PlGF concentration in the lowest quartile (< 118 pg/mL) was highly predictive of the development of preterm preeclampsia (odds ratio:22.5) and modestly predictive of term preeclampsia (odds ratio:2.2). The ability of sEng to predict preeclampsia has also been evaluated in several studies and found to be particularly useful in early-onset preeclampsia.[570,615] Recently, Kusanovic et al. reported a remarkable performance of delta and slope of PlGF:sEng ratio, (from early pregnancy and midtrimester) with a positive LR of 55.6 (95% CI 36.4–55.6) and 89.6 (95% CI 56.4–89.6), respectively for predicting early-onset preeclampsia.[616] Poon et al. evaluated 7,797 women with singleton pregnancies, during gestational weeks 11–13 using several biomarkers and uterine artery Dopplers. This yielded very good results using an algorithm developed by logistic regression that combined the logs of uterine pulsatility index, mean arterial pressure, PAPP-A, serum free PlGF, body mass index and presence of nulliparity or previous preeclampsia. At a 5% false positive rate, the detection rate for early preeclampsia was 93.1%.[617]

In addition to being useful in the prediction of preeclampsia before the onset of clinical symptoms, angiogenic factors may also prove useful in diagnosing the disease and in distinguishing it from other hypertensive disorders of pregnancy, such as gestational hypertension and chronic hypertension.[618,619] These findings have also been now confirmed on clinical grade automated assays.[620–622] In summary, measurement of circulating angiogenic proteins for the diagnosis and prediction of preeclampsia is still at an early stage but is rapidly evolving. Large prospective trials demonstrating clinical utility are needed.

Prevention

Interventions that could prevent preeclampsia or abort the disease at an early preclinical stage would revolutionize prenatal care. Sodium restriction and/or prescription of prophylactic diuretics were once popular strategies. They were then discarded but were revived in 1985 when a metaanalysis of ~7000 randomized patients suggested that saluretic agents did indeed reduce the incidence of preeclampsia.[623] A careful analysis of the results, however, reveals that there is no difference in the incidence of proteinuric hypertension, the seemingly positive results having been the ability of diuretics to decrease edema or to induce a small decrease in blood pressure.

In the 1990s two new approaches were advocated, each based on plausible hypotheses. The first approach, administration of low-dose aspirin (60−100 mg/day) starting after the gestational week twelve, was based on the postulate that hypertension and coagulation abnormalities in preeclampsia were due to an imbalance in the production of vasodilating and vasoconstricting PGs. The dose of aspirin chosen would inhibit platelet thromboxane synthesis but spare prostacyclin production. Initially, an extremely favorable metaanalysis, primarily based on small series led physicians to routinely prescribe low-dose aspirin prophylactically.[624,625] This optimism proved premature, as a number of large randomized, placebo-controlled trials (several aimed at "high-risk" populations as defined in the epidemiology section above), which included over 30.000 women, have revealed but small effects of aspirin to reduce the incidence of preeclampsia. [454,625,626,627] More recently, a large Cochrane metaanalyses concluded that low-dose aspirin had a modest effect in preventing preeclampsia with a relative risk of preeclampsia of 0.90 (95% CI 0.84−0.97) for aspirin-treated patients.[628] Aspirin prophylaxis should be considered as primary prevention for preeclampsia only in women at high baseline risk in whom the absolute risk reduction will be greatest.

The second approach consisted of dietary calcium supplementation starting in early gestation, based on observations that preeclamptic women are hypocalciuric,[502] and that the incidence of the disease may be greater among populations in which dietary calcium is low,,[629] and on a hypothesis that alterations in calciotropic hormone levels play a role in the genesis of the hypertension.[624,625] Here, too, initial reports were very encouraging, several metaanalyses noting marked and significant reductions in the incidence of preeclampsia (very reminiscent of the aspirin saga) (reviewed in references[624,625]). Again, a carefully conducted, large randomized, and blinded trial comprising >4500 women failed to detect any effects of calcium supplementation on either the incidence of preeclampsia or of improved fetal outcome.[472] The negative results in North America may relate to the virtual absence of severely calcium-deficient diets in that population, in contrast to deficiencies in deprived populations in certain developing nations. More recently in a recent WHO prospective study in women who live in endemic areas of calcium deficiencies, calcium supplementation seems to protect them from adverse pregnancy outcomes including the development of severe preeclampsia.[469]

Are there other promising trials? Enthusiasm for fish oil or its ingredient eicosapentaenoic acid (which are actually surrogates for aspirin in their effects on PGs) appears to have waned.[624,625] However, investigators are contemplating or have started new trials, again based on plausible hypotheses. These include combinations of dietary supplements of L-arginine (the precursor of NO), antioxidants (e.g., vitamin C), and magnesium. Despite the essentially negative results discussed above there are populations where "prophylactic" strategies may improve outcomes. These include subjects with a history of early-onset preeclampsia or who have metabolic abnormalities or risk factors associated with vascular thrombosis. Screening may reveal hyperhomocysteinemia, lupus anticoagulant, antiphospholipid antibodies, activated protein C resistance (factor V Leiden), and protein S deficiency.[630] The presence of these findings increases the likelihood that a preeclampsia-like syndrome will occur in subsequent gestations, and to some is an indication to consider prophylactic treatment with heparin and/or low-dose aspirin.

Remote Prognosis

There is controversy regarding the interpretation of studies designed to determine the remote cardiovascular prognosis of women who experienced preeclampsia or eclampsia. This is not surprising, for as noted, a diagnosis of preeclampsia is suspect when clinical criteria alone are used, although its reliability improves if the population analyzed had their disease when nulliparous, had convulsed (eclampsia), or the diagnosis was confirmed by renal biopsy. Second, data from preeclamptics compared to follow-up information from matched normotensive deliveries lead to different conclusions than those in which the preeclamptic women were compared to the expected prevalence in the general population, matched for race and age at the time of the remote examination. These issues are discussed further below.

In the older literature Chesley[150] reviewed 53 publications with follow-up information on 2637 eclamptics and estimated the prevalence of remote hypertension to be 24% (but the range was enormous).[150] Perhaps the most complete long-term survey after eclampsia is that of Chesley et al.,[150,631] who periodically reexamined 267 of 270 women who survived eclampsia during the years 1931 to 1951. The last report included the years 1973 and 1974,[631] at which time the clinical course of some of these patients had been followed for 40 years! The remote mortality rate in Caucasian women who convulsed during their first gestation was not greater than that of age-matched unselected women from several large epidemiological surveys. In white women who had eclampsia as multiparas and in all black women (this group comprised only 26 patients), the remote mortality was two to five times higher than expected. The prevalence of late

hypertension was also increased in women who had eclampsia as multiparas, which seemed to account for the increment in remote deaths. In contrast, prevalence of hypertension or the distribution of systolic and diastolic blood pressure levels in eclamptic primiparas was similar to that reported for the general population of women in the epidemiological surveys. Prevalence of hypertension was also greater in eclamptic primiparas who manifested high blood pressure in subsequent gestations compared to those who remained normotensive in all later pregnancies. Chesley et al.[150,473] concluded that eclampsia is neither a predictive sign nor a cause of essential hypertension, and that hypertensive pregnancies that follow eclampsia may indicate the probability of later hypertension, but do not cause it. Similar conclusions were reached by Bryans,[632] who studied a group of eclamptic black women, (follow-up averaging 14 years), and by Sibai et al[633] (posteclamptic follow-up seven years).

With preeclampsia, however, the findings are different. A survey of the older literature (reviewed in reference[150,634]) and a number of more recent publications (the latter often combining small numbers of eclamptics with large series of preeclamptic women) consistently reveal an increased remote prevalence of hypertension in women who had preeclampsia.[635–637] It has even been suggested that preeclampsia may have caused the remote hypertension.[634] Of interest in these studies are the following: First, the development of hypertension is far more frequent in women who preeclampsia as multiparas. Second, in the one study where diagnosis was confirmed by renal biopsy (see Table 81.4) two differing outcomes were noted depending upon how the control population was selected.[325] Prevalence of remote hypertension was increased if the authors used age- and race-matched normotensive gravidas as the controls, but was unchanged if they compared the outcome in biopsy-proven preeclamptics to that of age- and race-matched unselected women from the National Survey. Further inspection of the data revealed that the control group of normotensive delivering women had a very low prevalence of remote hypertension, suggesting that normotensive delivery "selects" a population without risk factors for future cardiovascular disease. A number of studies in both the older and more recent literature are consistent with this view.[150,638] However, although favoring the above formulation, we recall a 1964 publication which may some day prove prescient: Epstein[634] followed the clinical course of women with "toxemia" and a group with normotensive deliveries and like others using such controls he observed a higher incidence of remote hypertension in both nulliparous and multiparous preeclamptics. In addition, however, he also measured blood pressure in 74 of the "toxemic" women's siblings, and they displayed a lower prevalence of hypertension, suggesting that the long-term hypertension noted in preeclamptics may have been due to a persistent subtle renal injury.

Women with history of preeclampsia, have also been reported to have increased incidence of dyslipidemias and insulin resistance.[639,640] There are also epidemiological surveys suggesting increased cardiovascular events (including coronary events and strokes) in women with a history of preeclampsia,[474,641,642] that in one study was found uniquely in women with "early" preeclampsia..[474] However, it is unknown whether these represent baseline risk factors in these women at risk for premature preeclampsia or whether they develop as a consequence of preeclampsia More recently it was observed that women with a history of preeclampsia have a slightly higher baseline sFlt-1 concentrations than women with a history of normal pregnancy.[579] Patients with preeclampsia are said to have a decreased long-term incidence of malignancies[643] a provocative observation that is disputed by some.[644] Finally, recurrent preeclampsia has also been associated with increased risk for end-stage renal disease and hypothyroidism in later years, although the absolute risk is relatively low.[645,646]

Management

As already noted this text is devoted to physiology and pathophysiology, and space considerations limit detailed discussions of therapy. The following overview regarding the treatment of preeclampsia–eclampsia and chronic hypertension in pregnancy outlines in brief the management of these conditions and underscores some of the unresolved controversies in this area. For a more comprehensive discussion of treatment the reader is referred to several chapters[48,647,648] in a contemporary text as well as to a report on High Blood Pressure in Pregnancy, issued by the US NHBPEP in 2000[322] as well as periodic updates that are based on that report and published by the American College of Obstetrics and Gynecology.

Preeclampsia–Eclampsia

Due to its capricious and at times explosive nature, suspicion of preeclampsia is sufficient grounds to recommend hospitalization. This approach will diminish the incidence of convulsions, minimize diagnostic error, and improve fetal outcome. Near term, induction of labor is the therapy of choice, whereas attempts to temporize should be made if pregnancy is at an earlier stage.[461] If the latter decision is made, several antihypertensive agents considered safe in pregnancy are available (Table 81.5).[461,648,649] Delivery is indicated at

TABLE 81.5 Drugs for Chronic Hypertension in Pregnancy

Drug (Food and Drug Administration Risk)*	Dose	Concerns or Comments
Preferred agent Methyldopa (B)	0.5–3.0 g/d in two divided doses	Drug of choice according to NHBEP working group; safety after first trimester well documented, including 7-year follow-up evaluation of offspring
Second-line agents† Labetalol (C)	200–1200 mg/d in 2–3 divided doses	May be associated with fetal growth restriction and neonatal bradycardia
Nifedipine (C)	30–120 mg/d of a slow-release preparation	May inhibit labor and have synergistic interaction with magnesium sulfate; small experience with other calcium-entry blockers
Hydralazine (C)	50–300 mg/d in 2–4 divided doses	Few controlled trials, long experience with few adverse events documented, useful only in combination with sympatholytic agent; may cause neonatal thrombocytopenia
β-receptor blockers (C)	Depends on specific agent	May cause fetal bradycardia and decrease uteroplacental blood flow, this effect may be less for agents with partial agonist activity; may impair fetal response to hypoxic stress; risk for growth retardation when started in first or second trimester (atenolol)
Hydrochlorothiazide (C)	25 mg/d	Majority of controlled studies in normotensive pregnant women rather than hypertensive patients, can cause volume depletion and electrolyte disorders; may be useful in combination with methyldopa and vasodilator to mitigate compensatory fluid retention
Contraindicated ACE Inhibitors and AT1-receptor antagonists (D)‡		Leads to fetal loss in animals; human use associated with fetopathy, oligohydramnios, growth restriction, and neonatal anuric renal failure, which may be fatal

U.S. Food and Drug Administration classification.
†*We omit some agents (e.g., clonidine, α-blockers) because of limited data on use for chronic hypertension in pregnancy.*
‡*We would classify in category X during second and third trimesters.*
Note: No antihypertensive drug has been proven safe for use during the first trimester. Drug therapy is indicated for uncomplicated chronic hypertension when diastolic blood pressure is ≥100 mm Hg (Korotkoff V). Treatment at lower levels may be indicated for patients with diabetes mellitus, renal disease, or target organ damage.
NHBPEP, National High Blood Pressure Education Program.

any stage of pregnancy if severe hypertension remains uncontrolled for 24–48 h or at the appearance of certain "ominous" signs such as clotting or liver abnormalities, decreasing renal function, signs of impending convulsions (headache, epigastric pain, and hyperreflexia), or evidence of fetal jeopardy (as evidenced by severe growth retardation and the results of fetal testing).

There is some confusion and even controversy regarding "aggressive" versus "conservative" management of preeclamptic women very remote from term. Contemporary texts stress that such patients warrant termination of their pregnancies, citing a literature that attests the low yield of successful outcomes and, more important, substantial risk of maternal morbidity. Recently, however, this practice has been questioned, the authors proposing an expanded role for "conservative" management of the women, even when they manifest severe disease.[624,650–654] Review of these reports reveals that the case for the conservative approach may be more apparent then real. For example, one group temporizes only as long as blood pressure is reasonably controlled and "ominous" signs and symptoms are absent, precisely what we and others have recommended for decades when suggesting criteria for terminating pregnancy in the face of severe disease (see above). Of interest in this respect is a randomized trial where the investigators[653] assigned patients for either termination or "conservative" management after labeling their disease as severe based on a traditional classification pattern (level of blood pressure and degree of proteinuria), rather than the evolution of the clinical picture over a defined period of time. The positive results in the "conservative" arm are a cogent reminder that when managing women with hypertension in pregnancy we do not treat the diagnosis but the evolving disease.

There is another group which stresses an even more radical form of "conservative" management, a policy that we strongly question. Visser et al.[654] would continue temporization even when patients develop early evidence of the HELLP syndrome (see above). Scrutiny of their results suggests they were inadequately controlled, that there was substantial fetal loss even though they studied patients up to gestational week 34, and that there was evidence of increased maternal

bleeding episodes. Their approach appears too risky to us, and we continue our recommendations that physicians continue to be vigilant, aggressively terminating pregnancies complicated by early-onset preeclampsia using the clinical criteria noted by us above, as well as those by Sibai et al.,[653] who paradoxically entitled their criteria "conservative management." Finally, it should be noted that all of the studies above took place in tertiary care centers with maternal–fetal medicine intensive care units, facilities not readily available to most practitioners.

Sudden Escalating Hypertension and Imminent or Frank Eclampsia

There are controversies on when to treat rapidly rising blood pressure near term or during delivery (usually associated with the presentation of pure or superimposed preeclampsia). There is further debate on how aggressive treatment should be. We adhere to the NHBPEP recommendations,[461] which state that diastolic levels $\geq$105 mm Hg require treatment (though some contemporary texts still recommend $\geq$110 mm Hg). Certain circumstances, such as a teenager whose recent diastolic levels were 70 mm Hg or lower, or any patient demonstrating cerebral signs such as excruciating headache, confusion, or somnolence,[518] warrant treatment at lower levels (Table 81.6).

In the past there was an acrimonious debate about prevention and management of the eclamptic convulsion. Some considered parenteral magnesium the therapy of choice, while others condemned this approach, labeled the drug as ineffective and archaic, and suggested other agents such as phenytoin and diazepam. Still others questioned whether any therapy other than blood pressure control was needed for prophylaxis (see reference,[624,625,655] and previous edition of this text). Several reports of randomized trials appear to have resolved these controversies. In one[656] comprising 1680 patients intravenous magnesium sulfate proved superior to both diazepam and phenytoin in preventing *recurrent* seizures. In another,[657] scheduled to evaluate 4500 women, by comparing magnesium sulfate to phenytoin as *prophylaxis*, the trial was halted after 2123 women had been randomized because seizures were only occurring in the phenytoin arm. In a third,10,141 women underwent a placebo-controlled trial of magnesium, and prophylactic magnesium more than halved the eclampsia rate.[658] Thus magnesium has been demonstrated as the therapy of choice once a convulsion has occurred, and the drug is superior to phenytoin or placebo in preventing eclampsia. (These, and other trials are further reviewed in systematic analyses[627,659] (Table 81.6).

Controversies still exist. Magnesium especially intravenously, is not without hazard, and some contend its risks outweigh those with "mild" preeclampsia and it should be reserved for those with "severe disease" only.[660,661]Trials to settle these questions are needed.

Chronic Hypertension

Most pregnant women with chronic hypertension have the "essential" variety, and their disease is

TABLE 81.6 Drugs for Urgent Control of Severe Hypertension in Pregnancy

Drug (Food and Drug Administration Risk)*	Dose and Route	Concerns or Comments†
Labetalol (C)	20 mg i.v., then 20–80 mg every 20–30 min, up to a maximum of 300 mg; or constant infusion of 1–2 mg/min	Experience in pregnancy less than with hydralazine; probably less risk for tachycardia and arrhythmia than with other vasodilators
Hydralazine (C)	5 mg, i.v. or i.m., then 5–10 mg every 20–40 min; or constant infusion of 0.5–10 mg/h	Drug of choice according to NHBEP working group; long experience of safety and efficacy
Nifedipine (C)	Tablets recommended only: 10–30 mg orally, repeat in 45 min if needed	Possible interference with labor; may interact synergistically with magnesium sulfate
Relatively contraindicated nitroprusside (C)‡	Constant infusion of 0.5–10 μg/kg/min	Possible cyanide toxicity; agent of last resort

*U.S. Food and Drug Administration classification; C indicates that either studies in animals have revealed adverse effects on the fetus (teratogenic, embryocidal, or other) and/or there are no controlled studies in women, or studies in women and animals are not available. Drugs only should be given if the potential benefits justify the potential risk to the fetus.

†Adverse effects for all agents, except as noted, may include headache, flushing, nausea, and tachycardia (primarily caused by precipitous hypotension and reflex sympathetic activation).

‡We would classify in category D: there is positive evidence of human fetal risk, but the benefits of use in pregnant women may be acceptable despite the risk (e.g., if the drug is needed in a life-threatening situation or for a serious disease for which safer drugs cannot be used or are ineffective).

Note: Indicated for acute increase of diastolic blood pressure $\geq$105 mm Hg; goal is a gradual reduction to 90–100 mm Hg.

i.v., intravenously; i.m., intramuscularly; NHBPEP, National High Blood Pressure Education Program.

frequently mild in nature and of recent origin. Over 85% of these gestations are uncomplicated, though outcomes are poorer than those of normotensive populations.[48,150,419,453,662] Albeit small, there is an increased incidence of placental abruption, ARF, cardiac decompensation, and cerebral accidents in the mother, and of growth retardation and (in midtrimester) death of the fetus.[150,461] Such events are mainly associated with superimposed preeclampsia, whose incidence in chronic hypertensives is ~20%.[319] They also tend correlate with the age of the gravida as well as the duration and degree of control of her high blood pressure, many of these complications occurring in women over the age of 30 or in those with evidence of end-organ damage. Extremely obese women with chronic hypertension are at special risk for cardiac decompensation near term, especially if volume loaded during labor. Echocardiography performed earlier in pregnancy will alert the physician to those patients with early evidence of ventricular dysfunction.

The approach to treatment of women with chronic hypertension is also controversial, as some would treat those with mild hypertension and others would not. In this respect randomized studies are needed to resolve this issue. We follow the NHBPEP recommendations,[461] withholding antihypertensive drugs unless diastolic levels are >100 mm Hg (but at lower levels if there is evidence of end-organ damage or specific risk factors such as underlying renal disease). As of 2006 several trials to decide whether mild-moderate hypertension during pregnancy should be treated, Including if such an approach will decrease the incidence of superimposed preeclampsia were in progress. The reader is referred further to two reviews, one focusing on systematic analyses of antihypertensive drugs in pregnancy,[627] the second more philosophical in nature.[663]

Antihypertensive Therapy

Clinicians considering the prescription of antihypertensive drugs to pregnant women should be aware of the following: There have been only a few large randomized multicenter trials. Most studies have been limited in scope, and frequently performed at the request of and with the support of the pharamacological industry. Most published data are from studies where therapy was started after midgestation, when virtually all the risks of provoking congenital malformations have passed. Finally, there are no rigorous animal testing requirements to be met before human trials are undertaken, including standardized means of evaluating the drug effect on the fetus' ability to withstand hypoxic stress, as well as a more complex analysis of morphologic and physiologic variables in the newborn in animal models. This state of affairs should be kept in mind when reviewing the literature on antihypertensive therapy in pregnancy.[663]

Tables 81.5 and 81.6 summarize the status of the more commonly used antihypertensive drugs during gestation, including their pregnancy risk categories (A−D, through X) as defined by the US Food and Drug Administration (see reference[648]). The central adrenergic inhibitor methyldopa remains the preferred drug choice for us because of its long record of use and apparent safety, including evidence from a 7.5 year follow-up study of infants whose mothers received the drug. Beta adrenergic blocking agents are associated with an increased incidence of fetal growth restriction though the effects are minimal, and many clinicians currently use the combined .alpha and beta adrenergic blocker, labetalol.[627,663] Theoretically there may be synergism between magnesium sulfate and calcium channel blocking agents leading to precipitous decreases in blood pressure. In this respect there have been anecdotal report of maternal respiratory arrest, but increased problems do not seem to have appeared in larger surveys.[664] Other comments concerning these agents can be found in Tables 81.5 and 81.6, and the interested reader is referred to references[648] and[627,663] for details on each drug and a summary of randomized trials. We end with the story of ACE inhibitors to underscore why one must be careful when prescribing drugs to pregnant women.

Both captopril and enalapril were originally listed as category C in the Physician's Desk Reference, a designation in which most drugs prescribed to pregnant women fall. While this classification carries some cautionary remarks, most physicians consider Class C drugs as relatively safe. There were reports citing problems in animal models in the early 1980s, but the ACE inhibitors remained Category C medications until 1992. By then mounting evidence that ACE inhibitors used late in pregnancy were associated with renal failure and death in the neonate resulted in the manufacturers being required to print a "black box" warning on the label, and a change to category D in the PDR in 1992 with a similar classification for angiotensin receptor antagonists. More recent data suggest that infants exposed to ACE inhibitors during first trimester were at increased risk for malformations of the cardiovascular system (risk ratio, 3.72; 95 percent confidence interval, 1.89 to 7.30) and the central nervous system (risk ratio, 4.39; 95 percent confidence interval, 1.37 to 14.02).[665] Physicians are taught to do no harm, a cogent reason for continued conservatism when asked to prescribe drugs in pregnancy.

References

[1] Sheehan HL, Lynch JP. Pathology of Toxaemia of pregnancy. Baltimore: Williams and Wilkins; 1973.

[2] Baylis C. Glomerular filtration and volume regulation in gravid animal models. Baillieres Clin Obstet Gynaecol 1994;8(2): 235–64.

[3] Davison JM, Lindheimer MD. Changes in renal haemodynamics and kidney weight during pregnancy in the unanaesthetized rat. J Physiol 1980;301:129–36.

[4] Lindheimer MD, Katz AI. Renal physiology in pregnancy. In: Seldin DW, Geiebisch G, editors. The kidney: physiology and pathophysiology. 1st ed. New York: Raven Press; 1985. p. 2017–41.

[5] Strevens H, Wide-Swensson D, Hansen A, Horn T, Ingemarsson I, Larsen S, et al. Glomerular endotheliosis in normal pregnancy and pre-eclampsia. BJOG 2003;110(9):831–6.

[6] Cietak KA, Newton JR. Serial quantitative maternal nephrosonography in pregnancy. Br J Radiol 1985;58(689):405–13.

[7] Lindheimer MD, Katz AI. Renal physiology in pregnancy. In: Seldin DW, Geiebisch G, editors. The kidney: physiology and pathophysiology. 1st ed. New York: Raven Press; 1985. p. 2017–41.

[8] Rasmussen PE, Nielsen FR. Hydronephrosis during pregnancy: a literature survey. Eur J Obstet Gynecol Reprod Biol 1988;27 (3):249–59.

[9] Lindheimer MD, Katz AI. Renal function and disease in pregnancy. Philadelphia: Lea and Febiger; 1977.

[10] Fried AM, Woodring JH, Thompson DJ. Hydronephrosis of pregnancy: a prospective sequential study of the course of dilatation. J Ultrasound Med 1983;2(6):255–9.

[11] Faundes A, Bricola-Filho M, Pinto e Silva JL. Dilatation of the urinary tract during pregnancy: proposal of a curve of maximal caliceal diameter by gestational age. Am J Obstet Gynecol 1998;178(5):1082–6.

[12] Dure-Smith P. Pregnancy dilatation of the urinary tract. The iliac sign and its significance. Radiology 1970;96(3):545–50.

[13] Conrad KP. Renal changes in pregnancy. Urol Annu 1992; (6):313–40 1992

[14] Cietak KA, Newton JR. Serial qualitative maternal nephrosonography in pregnancy. Br J Radiol 1985;58(689):399–404.

[15] Rubi RA, Sala NL. Ureteral function in pregnant women. 3. Effect of different positions and of fetal delivery upon ureteral tonus. Am J Obstet Gynecol 1968;101(2):230–7.

[16] Mattingly RF, Borkowf HI. Clinical implications of ureteral reflux in pregnancy. Clin Obstet Gynecol 1978;21(3):863–73.

[17] Myers SJ, Lee RV, Munschauser RW. Dilatation and nontraumatic rupture of the urinary tract during pregnancy. A review. Obstet Gynecol 1985;66:809–15.

[18] Nielsen FR, Rasmussen PE. Hydronephrosis during pregnancy: four cases of hydronephrosis causing symptoms during pregnancy. Eur J Obstet Gynecol Reprod Biol 1988;27(3):245–8.

[19] Fainaru O, Almog B, Gamzu R, Lessing JB, Kupferminc M. The management of symptomatic hydronephrosis in pregnancy. BJOG 2002;109(12):1385–7.

[20] Satin S, Seikn GL, Cunningham FG. Reversible hypertension in pregnancy caused by obstructive uropathy. Obstet Gynecol 1993;81:123–5 1993

[21] vanSonnenberg E, Casola G, Talner LB, Wittich GR, Varney RR, D'Agostino HB. Symptomatic renal obstruction or urosepsis during pregnancy: treatment by sonographically guided percutaneous nephrostomy. AJR Am J Roentgenol 1992;158(1):91–4.

[22] Conrad KP, Lindheimer MD. Renal and cardiovascular alterations. In: Lindheimer MD, Roberts JM, Cunningham FG, editors. Chesley's hypertensive disorders in pregnancy. 2nd ed. Stamford: Appleton & Lange; 1999.

[23] Sturgiss SN, Dunlop W, Davison JM. Renal haemodynamics and tubular function in human pregnancy. Baillieres Clin Obstet Gynaecol 1994;8(2):209–34.

[24] Conrad KP. Mechanisms of renal vasodilation and hyperfiltration during pregnancy. J Soc Gynecol Investig 2004;11(7): 438–48.

[25] Chesley LC, Sloan DM. The effect of posture on renal function in late pregnancy. Am J Obstet Gynecol 1964;89:754–9.

[26] Chapman AB, Abraham WT, Zamudio S, Coffin C, Merouani A, Young D, et al. Temporal relationships between hormonal and hemodynamic changes in early human pregnancy. Kidney Int 1998;54(6):2056–63.

[27] Chapman AB, Zamudio S, Woodmansee W, Merouani A, Osorio F, Johnson A, et al. Systemic and renal hemodynamic changes in the luteal phase of the menstrual cycle mimic early pregnancy. Am J Physiol 1997;273(5 Pt 2):F777–82.

[28] Davison JM, Dunlop W, Ezimokhai M. 24-hour creatinine clearance during the third trimester of normal pregnancy. Br J Obstet Gynaecol 1980;87(2):106–9.

[29] Davison JM, Noble MC. Serial changes in 24 hour creatinine clearance during normal menstrual cycles and the first trimester of pregnancy. Br J Obstet Gynaecol 1981;88(1):10–7.

[30] Dunlop W. Serial changes in renal haemodynamics during normal human pregnancy. Br J Obstet Gynaecol 1981;88(1): 1–9.

[31] Roberts M, Lindheimer MD, Davison JM. Altered glomerular permselectivity to neutral dextrans and heteroporous membrane modeling in human pregnancy. Am J Physiol 1996;270(2 Pt 2):F338–43.

[32] Conrad KP, Gaber L, Lindheimer MD. The kidney in normal pregnancy and in preeclampsia. In: Lindheimer MD, Cunningham FG, Roberts JM, editors. Chesley's hypertensive disorders in pregnancy. 3rd ed. Elsevier Press; 2009.

[33] Barron WM, Lindheimer MD. Effect of oral protein loading on renal hemodynamics in human pregnancy. Am J Physiol 1995;269(4 Pt 2):R888–95.

[34] Gaboury CL, Woods LL. Renal reserve in pregnancy. Semin Nephrol 1995;15(5):449–53.

[35] Ronco C, Brendolan A, Bragantini L, Chiaramonte S, Fabris A, Feriani M, et al. Renal functional reserve in pregnancy. Nephrol Dial Transplant 1988;3(2):157–61.

[36] Sturgiss SN, Wilkinson R, Davison JM. Renal reserve during human pregnancy. Am J Physiol 1996;271(1 Pt 2):F16–20.

[37] Baylis C. Effect of amino acid infusion as an index of renal vasodilatory capacity in pregnant rats. Am J Physiol 1988;254(5 Pt 2): F650–6.

[38] Baylis C. The mechanism of the increase in glomerular filtration rate in the twelve-day pregnant rat. J Physiol 1980;305:405–14.

[39] Oken DE. An analysis of glomerular dynamics in rat, dog, and man. Kidney Int 1982;22(2):136–45.

[40] Milne JE, Lindheimer MD, Davison JM. Glomerular heteroporous membrane modeling in third trimester and postpartum before and during amino acid infusion. Am J Physiol Renal Physiol 2002;282(1):F170–5.

[41] Moran P, Lindheimer MD, Davison JM. The renal response to preeclampsia. Semin Nephrol 2004;24(6):588–95.

[42] Conrad KP. Renal hemodynamics during pregnancy in chronically catheterized, conscious rats. Kidney Int 1984;26(1): 24–9.

[43] Gellai M, Valtin H. Chronic vascular constrictions and measurements of renal function in conscious rats. Kidney Int 1979;15 (4):419–26.

[44] Reckelhoff J, Samsell L, Baylis C. Failure of an acute 10–15% plasma volume expansion in the virgin femal rat to mimic the increased glomerular filtration rate (GFR) and altered

glomerular hemodynamics seen at midterm pregnancy. Clin Exp Hyper Pregnancy 1989;B8:533–49.
[45] Baylis C, Blantz RC. Tubuloglomerular feedback activity in virgin and 12-day-pregnant rats. Am J Physiol 1985;249(1 Pt 2): F169–73.
[46] Phippard AF, Horvath JS, Glynn EM, Garner MG, Fletcher PJ, Duggin GG, et al. Circulatory adaptation to pregnancy–serial studies of haemodynamics, blood volume, renin and aldosterone in the baboon (Papio hamadryas). J Hypertens 1986;4 (6):773–9.
[47] Robson SC, Hunter S, Boys RJ, Dunlop W. Serial study of factors influencing changes in cardiac output during human pregnancy. Am J Physiol 1989;256(4 Pt 2):H1060–5.
[48] August P, Lindheimer MD. Chronic hypertension and pregnancy. In: Laragh JH, Brenner BM, editors. Chesley's hypertensive disorders in pregnancy. 2nd ed. Stamford, CT: Appleton & Lange; 1999.
[49] Conrad KP, Gellai M, North WG, Valtin H. Influence of oxytocin on renal hemodynamics and sodium excretion. Ann N Y Acad Sci 1993;689:346–62.
[50] Atherton JC, Bu'lock D, Pirie SC. The effect of pseudopregnancy on glomerular filtration rate and salt and water reabsorption in the rat. J Physiol 1982;324:11–20.
[51] Baylis C. Glomerular ultrafiltration in the pseudopregnant rat. Am J Physiol 1982;243(3):F300–5.
[52] Paaby P, Moller-Petersen J, Larsen CE, Raffn K. Endogenous overnight creatinine clearance, serum beta 2-microglobulin and serum water during the menstrual cycle. Acta Med Scand 1987;221(2):191–7.
[53] Paaby P, Brochner-Mortensen J, Fjeldborg P, Raffn K, Larsen CE, Moller-Petersen J. Endogenous overnight creatinine clearance compared with 51Cr-EDTA clearance during the menstrual cycle. Acta Med Scand 1987;222(3):281–4.
[54] Brochner-Mortensen J, Paaby P, Fjeldborg P, Raffn K, Larsen CE, Moller-Petersen J. Renal haemodynamics and extracellular homeostasis during the menstrual cycle. Scand J Clin Lab Invest 1987;47(8):829–35.
[55] van Beek E, Houben AJ, van Es PN, Willekes C, Korten EC, de Leeuw PW, et al. Peripheral haemodynamics and renal function in relation to the menstrual cycle. Clin Sci (Lond) 1996;91(2): 163–8.
[56] Christy NP, Shaver JC. Estrogens and the kidney. Kidney Int 1974;6(5):366–76.
[57] Chesley LC, Tepper IH. Effects of progesterone and estrogen on the sensitivity to angiotensin II. J Clin Endocrinol Metab 1967;27 (4):576–81.
[58] Nuwayhid B, Brinkman III CR, Woods Jr JR, Martinek H, Assali NS. Effects of estrogens on systemic and regional circulations in normal and renal hypertensive sheep. Am J Obstet Gynecol 1975;123(5):495–504.
[59] Rosenfeld CR, Morriss Jr FH, Battaglia FC, Makowski EL, Meschia G. Effect of estradiol-17beta on blood flow to reproductive and nonreproductive tissues in pregnant ewes. Am J Obstet Gynecol 1976;124(6):618–29.
[60] Magness RR, Phernetton TM, Zheng J. Systemic and uterine blood flow distribution during prolonged infusion of 17beta-estradiol. Am J Physiol 1998;275(3 Pt 2):H731–43.
[61] Everett RB, Worley RJ, MacDonald PC, Gant NF. Modification of vascular responsiveness to angiotensin II in pregnant women by intravenously infused 5alpha-dihydroprogesterone. Am J Obstet Gynecol 1978;131(4):352–7.
[62] Lo F, Kaufman S. Effect of 5 alpha-pregnan-3 alpha-ol-20-one on nitric oxide biosynthesis and plasma volume in rats. Am J Physiol Regul Integr Comp Physiol 2001;280(6): R1902–5.
[63] Atallah AN, Guimaraes JA, Gebara M, Sustovich DR, Martinez TR, Camano L. Progesterone increases glomerular filtration rate, urinary kallikrein excretion and uric acid clearance in normal women. Braz J Med Biol Res 1988;21(1):71–4.
[64] Oparil S, Ehrlich EN, Lindheimer MD. Effect of progesterone on renal sodium handling in man: relation to aldosterone excretion and plasma renin activity. Clin Sci Mol Med 1975;49 (2):139–47.
[65] Conrad KP. Possible mechanisms for changes in renal hemodynamics during pregnancy: studies from animal models. Am J Kidney Dis 1987;9(4):253–9.
[66] Sherwood OD. Relaxin. In: Knobil E, editor. The physiology of reproduction. New York: Raven Press; 1994. p. 861–1009.
[67] Davison JM, Hytten FE. Glomerular filtration during and after pregnancy. J Obstet Gynaecol Br Commonw 1974;81(8): 588–95.
[68] Stewart DR, Celniker AC, Taylor Jr CA, Cragun JR, Overstreet JW, Lasley BL. Relaxin in the peri-implantation period. J Clin Endocrinol Metab 1990;70(6):1771–3.
[69] Johnson MR, Carter G, Grint C, Lightman SL. Relationship between ovarian steroids, gonadotrophins and relaxin during the menstrual cycle. Acta Endocrinol (Copenh) 1993;129 (2):121–5.
[70] Wreje U, Kristiansson P, Aberg H, Bystrom B, von Schoultz B. Serum levels of relaxin during the menstrual cycle and oral contraceptive use. Gynecol Obstet Invest 1995;39 (3):197–200.
[71] Davison JM, Vallotton MB, Lindheimer MD. Plasma osmolality and urinary concentration and dilution during and after pregnancy: evidence that lateral recumbency inhibits maximal urinary concentrating ability. Br J Obstet Gynaecol 1981;88(5): 472–9.
[72] Davison JM, Shiells EA, Philips PR, Lindheimer MD. Serial evaluation of vasopressin release and thirst in human pregnancy. Role of human chorionic gonadotrophin in the osmoregulatory changes of gestation. J Clin Invest 1988;81(3): 798–806.
[73] Lindheimer MD, Barron WM, Davison JM. Osmoregulation of thirst and vasopressin release in pregnancy. Am J Physiol 1989;257(2 Pt 2):F159–69.
[74] Lindheimer MD, Davison JM. Osmoregulation, the secretion of arginine vasopressin and its metabolism during pregnancy. Eur J Endocrinol 1995;132(2):133–43.
[75] Weisinger RS, Burns P, Eddie LW, Wintour EM. Relaxin alters the plasma osmolality-arginine vasopressin relationship in the rat. J Endocrinol 1993;137(3):505–10.
[76] St-Louis J, Massicotte G. Chronic decrease of blood pressure by rat relaxin in spontaneously hypertensive rats. Life Sci 1985;37 (14):1351–7.
[77] Debrah DO, Conrad KP, Jeyabalan A, Danielson LA, Shroff SG. Relaxin increases cardiac output and reduces systemic arterial load in hypertensive rats. Hypertension 2005;46(4):745–50.
[78] Massicotte G, Parent A, St-Louis J. Blunted responses to vasoconstrictors in mesenteric vasculature but not in portal vein of spontaneously hypertensive rats treated with relaxin. Proc Soc Exp Biol Med 1989;190(3):254–9.
[79] Bani D, Bigazzi M, Masini E, Bani G, Sacchi TB. Relaxin depresses platelet aggregation: in vitro studies on isolated human and rabbit platelets. Lab Invest 1995;73 (5):709–16.
[80] Bani-Sacchi T, Bigazzi M, Bani D, Mannaioni PF, Masini E. Relaxin-induced increased coronary flow through stimulation of nitric oxide production. Br J Pharmacol 1995;116(1):1589–94.
[81] Danielson LA, Sherwood OD, Conrad KP. Relaxin is a potent renal vasodilator in conscious rats. J Clin Invest 1999;103(4): 525–33.

[82] Danielson LA, Kercher LJ, Conrad KP. Impact of gender and endothelin on renal vasodilation and hyperfiltration induced by relaxin in conscious rats. Am J Physiol Regul Integr Comp Physiol 2000;279(4):R1298–304.
[83] Danielson LA, Conrad KP. Time course and dose response of relaxin-mediated renal vasodilation, hyperfiltration, and changes in plasma osmolality in conscious rats. J Appl Physiol 2003;95(4):1509–14.
[84] Novak J, Ramirez RJ, Gandley RE, Sherwood OD, Conrad KP. Myogenic reactivity is reduced in small renal arteries isolated from relaxin-treated rats. Am J Physiol Regul Integr Comp Physiol 2002;283(2):R349–55.
[85] Gandley RE, Conrad KP, McLaughlin MK. Endothelin and nitric oxide mediate reduced myogenic reactivity of small renal arteries from pregnant rats. Am J Physiol Regul Integr Comp Physiol 2001;280(1):R1–7.
[86] Novak J, Danielson LA, Kerchner LJ, Sherwood OD, Ramirez RJ, Moalli PA, et al. Relaxin is essential for renal vasodilation during pregnancy in conscious rats. J Clin Invest 2001;107(11): 1469–75.
[87] Smith MC, Conrad KP, Murdoch AP, Danielson LA, Davison JM. Is relaxin necessary to establish a renal response in human pregnancy. Fertil Steril submitted.
[88] Baylis C. Renal effects of cyclooxygenase inhibition in the pregnant rat. Am J Physiol 1987;253(1 Pt 2):F158–63.
[89] Conrad KP, Colpoys MC. Evidence against the hypothesis that prostaglandins are the vasodepressor agents of pregnancy. Serial studies in chronically instrumented, conscious rats. J Clin Invest 1986;77(1):236–45.
[90] Venuto RC, Donker AJ. Prostaglandin E2, plasma renin activity, and renal function throughout rabbit pregnancy. J Lab Clin Med 1982;99(2):239–46.
[91] Conrad KP, Dunn MJ. Renal synthesis and urinary excretion of eicosanoids during pregnancy in rats. Am J Physiol 1987;253 (6 Pt 2):F1197–205.
[92] Brown GP, Venuto RC. Eicosanoid production in rabbit vascular tissues and placentas. Am J Physiol 1990;258(3 Pt 1): E418–22.
[93] Gallery ED, Ross M, Grigg R, Bean C. Are the renal functional changes of human pregnancy caused by prostacyclin? Prostaglandins 1985;30(6):1019–29.
[94] Sorensen TK, Easterling TR, Carlson KL, Brateng DA, Benedetti TJ. The maternal hemodynamic effect of indomethacin in normal pregnancy. Obstet Gynecol 1992;79(5 (Pt 1)): 661–3.
[95] Harrison GL, Moore LG. Blunted vasoreactivity in pregnant guinea pigs is not restored by meclofenamate. Am J Obstet Gynecol 1989;160(1):258–64.
[96] Conrad KP, Vernier KA. Plasma level, urinary excretion, and metabolic production of cGMP during gestation in rats. Am J Physiol 1989;257(4 Pt 2):R847–53.
[97] Conrad KP, Joffe GM, Kruszyna H, Kruszyna R, Rochelle LG, Smith RP, et al. Identification of increased nitric oxide biosynthesis during pregnancy in rats. Faseb J 1993;7(6):566–71.
[98] Conrad KP, Kerchner LJ, Mosher MD. Plasma and 24-h NO(x) and cGMP during normal pregnancy and preeclampsia in women on a reduced NO(x) diet. Am J Physiol 1999;277 (1 Pt 2):F48–57.
[99] Kopp L, Paradiz G, Tucci JR. Urinary excretion of cyclic 3′,5′-adenosine monophosphate and cyclic 3′,5′-guanosine monophosphate during and after pregnancy. J Clin Endocrinol Metab 1977;44(3):590–4.
[100] Sala C, Campise M, Ambroso G, Motta T, Zanchetti A, Morganti A. Atrial natriuretic peptide and hemodynamic changes during normal human pregnancy. Hypertension 1995;25(4 Pt 1):631–6.
[101] Yang D, Lang U, Greenberg SG, Myatt L, Clark KE. Elevation of nitrate levels in pregnant ewes and their fetuses. Am J Obstet Gynecol 1996;174(2):573–7.
[102] Sladek SM, Magness RR, Conrad KP. Nitric oxide and pregnancy. Am J Physiol 1997;272(2 Pt 2):R441–63.
[103] Danielson LA, Conrad KP. Acute blockade of nitric oxide synthase inhibits renal vasodilation and hyperfiltration during pregnancy in chronically instrumented conscious rats. J Clin Invest 1995;96(1):482–90.
[104] Danielson LA, Conrad KP. Prostaglandins maintain renal vasodilation and hyperfiltration during chronic nitric oxide synthase blockade in conscious pregnant rats. Circ Res 1996;79 (6):1161–6.
[105] Baylis C. Cyclooxygenase products do not contribute to the gestational renal vasodilation in the nitric oxide synthase inhibited pregnant rat. Hypertens Pregnancy 2002;21(2): 109–14.
[106] Haynes WG. Endothelins as regulators of vascular tone in man. Clin Sci (Lond) 1995;88(5):509–17.
[107] Yokokawa K, Johnson J, Kohno M, Mandal AK, Yanagisawa M, Horio T, et al. Phosphoinositide turnover signaling stimulated by ET-3 in endothelial cells from spontaneously hypertensive rats. Am J Physiol 1994;267 (3 Pt 2):R635–44.
[108] Hirata Y, Emori T, Eguchi S, Kanno K, Imai T, Ohta K, et al. Endothelin receptor subtype B mediates synthesis of nitric oxide by cultured bovine endothelial cells. J Clin Invest 1993;91(4):1367–73.
[109] Hirata Y, Hayakawa H, Suzuki E, Kimura K, Kikuchi K, Nagano T, et al. Direct measurements of endothelium-derived nitric oxide release by stimulation of endothelin receptors in rat kidney and its alteration in salt-induced hypertension. Circulation 1995;91(4):1229–35.
[110] Tsukahara H, Ende H, Magazine HI, Bahou WF, Goligorsky MS. Molecular and functional characterization of the non-isopeptide-selective ETB receptor in endothelial cells. Receptor coupling to nitric oxide synthase. J Biol Chem 1994;269 (34):21778–85.
[111] Gellai M, Fletcher T, Pullen M, Nambi P. Evidence for the existence of endothelin-B receptor subtypes and their physiological roles in the rat. Am J Physiol 1996;271(1 Pt 2):R254–61.
[112] Kourembanas S, McQuillan LP, Leung GK, Faller DV. Nitric oxide regulates the expression of vasoconstrictors and growth factors by vascular endothelium under both normoxia and hypoxia. J Clin Invest 1993;92(1):99–104.
[113] Gellai M. Physiological role of endothelin in cardiovascular and renal hemodynamics: studies in animals. Curr Opin Nephrol Hypertens 1997;6(1):64–8.
[114] Conrad KP, Gandley RE, Ogawa T, Nakanishi S, Danielson LA. Endothelin mediates renal vasodilation and hyperfiltration during pregnancy in chronically instrumented conscious rats. Am J Physiol 1999;276(5 Pt 2):F767–76.
[115] Novak J, Conrad KP. Small renal arteries isolated from ETB receptor deficient rats fail to exhibit the normal maternal adaptation to pregnancy. Faseb J. [abstract] 2004;18(5 Part I): 205–32.
[116] Jeyabalan A, Novak J, Danielson LA, Kerchner LJ, Opett SL, Conrad KP. Essential role for vascular gelatinase activity in relaxin-induced renal vasodilation, hyperfiltration, and reduced myogenic reactivity of small arteries. Circ Res 2003;93 (12):1249–57.
[117] Palejwala S, Stein DE, Weiss G, Monia BP, Tortoriello D, Goldsmith LT. Relaxin positively regulates matrix

metalloproteinase expression in human lower uterine segment fibroblasts using a tyrosine kinase signaling pathway. Endocrinology 2001;142(8):3405–13.
[118] Unemori EN, Pickford LB, Salles AL, Piercy CE, Grove BH, Erikson ME, et al. Relaxin induces an extracellular matrix-degrading phenotype in human lung fibroblasts in vitro and inhibits lung fibrosis in a murine model in vivo. J Clin Invest 1996;98(12):2739–45.
[119] Fernandez-Patron C, Radomski MW, Davidge ST. Vascular matrix metalloproteinase-2 cleaves big endothelin-1 yielding a novel vasoconstrictor. Circ Res 1999;85(10):906–11.
[120] Fernandez-Patron C, Radomski MW, Davidge ST. Role of matrix metalloproteinase-2 in thrombin-induced vasorelaxation of rat mesenteric arteries. Am J Physiol Heart Circ Physiol 2000;278(5):H1473–9.
[121] Jeyabalan A, Kerchner LJ, Fisher MC, McGuane J, Doty KD, Conrad KP. Matrix metalloproteinase-2 protein in upregulated small arteries from pregnant and relaxin-treated nonpregnant rats. Endocrinology submitted.
[122] Novak J, Rajakumar A, Miles TM, Conrad KP. Nitric oxide synthase isoforms in the rat kidney during pregnancy. J Soc Gynecol Investig 2004;11(5):280–8.
[123] Kerchner LJ, Novak J, Hanley-Yanez K, Doty KD, Danielson LA, Conrad KP. Evidence against the hypothesis that endothelial endothelin B receptor expression is regulated by relaxin and pregnancy. Endocrinology 2005;146 (6):2791–7.
[124] Xu DL, Martin PY, St John J, Tsai P, Summer SN, Ohara M, et al. Upregulation of endothelial and neuronal constitutive nitric oxide synthase in pregnant rats. Am J Physiol 1996;271(6 Pt 2): R1739–45.
[125] Goetz RM, Morano I, Calovini T, Studer R, Holtz J. Increased expression of endothelial constitutive nitric oxide synthase in rat aorta during pregnancy. Biochem Biophys Res Commun 1994;205(1):905–10.
[126] Dschietzig T, Bartsch C, Richter C, Laule M, Baumann G, Stangl K. Relaxin a pregnancy hormone, is a functional endothelin-1 antagonist: attenuation of endothelin-1-mediated vasoconstriction by stimulation of endothelin type-B receptor expression via ERK-1/2 and nuclear factor-kappaB. Circ Res 2003;92(1):32–40.
[127] McGuane JT, Danielson LA, Debrah JE, Rubin JP, Novak J, Conrad KP. Angiogenic growth factors are new and essential players in the sustained relaxin vasodilatory pathway in rodents and humans. Hypertension 2011;57(6):1151–60.
[128] Almeida FA, Pavan MV, Rodrigues CI. The haemodynamic, renal excretory and hormonal changes induced by resting in the left lateral position in normal pregnant women during late gestation. BJOG 2009;116(13):1749–54.
[129] Ferreira VM, Gomes TS, Reis LA, Ferreira AT, Razvickas CV, Schor N, et al. Receptor-induced dilatation in the systemic and intrarenal adaptation to pregnancy in rats. PLoS One 2009;4(3): e4845.
[130] Smith CA, Santymire B, Erdely A, Venkat V, Losonczy G, Baylis C. Renal nitric oxide production in rat pregnancy: role of constitutive nitric oxide synthases. Am J Physiol Renal Physiol 2010;299(4):F830–6.
[131] Morgan TK, Montgomery K, Mason V, West RB, Wang L, van de Rijn M, et al. Upregulation of histidine decarboxylase expression in superficial cortical nephrons during pregnancy in mice and women. Kidney Int 2006;70(2):306–14.
[132] Huang H, Chang HH, Xu Y, Reddy DS, Du J, Zhou Y, et al. Epoxyeicosatrienoic Acid inhibition alters renal hemodynamics during pregnancy. Exp Biol Med (Maywood) 2006;231 (11):1744–52.
[133] Davison JM. Changes in renal function in early pregnancy in women with one kidney. Yale J Biol Med 1978;51(3): 347–9.
[134] Davison JM. The effect of pregnancy on kidney function in renal allograft recipients. Kidney Int 1985;27(1):74–9.
[135] Graves SW, Cook SL, Seely EW. Fluid and electroyte handling in normal pregnancy. J Am Soc Gynecol Invest. [abstract] 1995;2:291.
[136] Davison JM, Lovedale C. The excretion of glucose during normal pregnancy and after delivery. J Obstet Gynaecol Br Commonw 1974;81(1):30–4.
[137] Welsh III GW, Sims EA. The mechanisms of renal glucosuria in pregnancy. Diabetes 1960;9:363–9.
[138] Davison JM, Hytten FE. The effect of pregnancy on the renal handling of glucose. Br J Obstet Gynaecol 1975;82(5): 374–81.
[139] Atherton JC, Green R. Renal tubular function in the gravid rat. Baillieres Clin Obstet Gynaecol 1994;8(2):265–85.
[140] Hytten FE, Cheyne GA. The aminoaciduria of pregnancy. J Obstet Gynaecol Br Commonw 1972;79(5):424–32.
[141] Many A, Hubel CA, Roberts JM. Hyperuricemia and xanthine oxidase in preeclampsia, revisited. Am J Obstet Gynecol 1996;174(1 Pt 1):288–91.
[142] Boyle JA, Campbell S, Duncan AM, Greig WR, Buchanan WW. Serum uric acid levels in normal pregnancy with observations on the renal excretion of urate in pregnancy. J Clin Pathol 1966;19(5):501–3.
[143] Dunlop W, Davison JM. The effect of normal pregnancy upon the renal handling of uric acid. Br J Obstet Gynaecol 1977;84 (1):13–21.
[144] Lind T, Godfrey KA, Otun H, Philips PR. Changes in serum uric acid concentrations during normal pregnancy. Br J Obstet Gynaecol 1984;91(2):128–32.
[145] Lockitch G. The effects of normal pregnancy on common biochemistry and hematology tests. In: Barron WM, Lindheimer MD, editors. Medical disorders during pregnancy. St. Louis: Mosby; 1995. p. 532–45.
[146] Fischer RL, Bianculli KW, Hediger ML, Scholl TO. Maternal serum uric acid levels in twin gestations. Obstet Gynecol 1995;85(1):60–4.
[147] Hill LM, Furness C, Dunlop W. Diurnal variation of serum urate in pregnancy. Br Med J 1977;2(6101):1520.
[148] Barry CL, Royle GA, Lake Y. Racial variation in serum uric acid concentration in pregnancy: a comparison between European, New Zealand Maori and Polynesian women. Aust N Z J Obstet Gynaecol 1992;32(1):17–9.
[149] Semple PF, Carswell W, Boyle JA. Serial studies of the renal clearance of urate and inulin during pregnancy and after the puerperium in normal women. Clin Sci Mol Med 1974;47 (6):559–65.
[150] Chesley LC. Hypertensive disorders in pregnancy. 2nd ed. New York: Appleton-Century-Crofts; 1978.
[151] Forsum E, Sadurskis A, Wager J. Resting metabolic rate and body composition of healthy Swedish women during pregnancy. Am J Clin Nutr 1988;47(6):942–7.
[152] Lindheimer MD, Richardson DA, Ehrlich EN, Katz AI. Potassium homeostasis in pregnancy. J Reprod Med 1987;32 (7):517–22.
[153] Ehrlich EN, Lindheimer MD. Effect of administered mineralocorticoids or ACTH in pregnant women. Attenuation of kaliuretic influence of mineralocorticoids during pregnancy. J Clin Invest 1972;51(6):1301–9.
[154] Mujais SK, Nora NA, Chen Y. Regulation of the renal Na:K pump: role of progesterone. J Am Soc Nephrol 1993;3 (8):1488–95.
[155] Brown MA, Sinosich MJ, Saunders DM, Gallery ED. Potassium regulation and progesterone-aldosterone interrelationships in

human pregnancy: a prospective study. Am J Obstet Gynecol 1986;155(2):349–53.
[156] August P, Lindheimer MD. Pathophysiology of preeclampsia. In: Laragh JH, Brenner BM, editors. Hypertension: pathophysiology, diagnosis, and management. NY: Raven Press; 1995. p. 2407–26.
[157] Geller DS, Farhi A, Pinkerton N, Fradley M, Moritz M, Spitzer A, et al. Activating mineralocorticoid receptor mutation in hypertension exacerbated by pregnancy. Science 2000;289 (5476):119–23.
[158] Lim VS, Katz AI, Lindheimer MD. Acid-base regulation in pregnancy. Am J Physiol 1976;231(6):1764–9.
[159] Takano N, Kaneda T. Renal contribution to acid-base regulation during the menstrual cycle. Am J Physiol 1983;244(3): F320–4.
[160] Gallery ED, Gyory. Urinary concentration, white blood cell excretion, acid excretion, and acid-base status in normal pregnancy: alterations in pregnancy-associated hypertension. Am J Obstet Gynecol 1979;135(1):27–36.
[161] Heenan AP, Wolfe LA. Plasma acid-base regulation above and below ventilatory threshold in late gestation. J Appl Physiol 2000;88(1):149–57.
[162] Vokes TJ, Weiss NM, Schreiber J, Gaskill MB, Robertson GL. Osmoregulation of thirst and vasopressin during normal menstrual cycle. Am J Physiol 1988;254(4 Pt 2):R641–7.
[163] Davison JM, Gilmore EA, Durr J, Robertson GL, Lindheimer MD. Altered osmotic thresholds for vasopressin secretion and thirst in human pregnancy. Am J Physiol 1984;246(1 Pt 2): F105–9.
[164] Davison JM, Sheills EA, Philips PR, Barron WM, Lindheimer MD. Metabolic clearance of vasopressin and an analogue resistant to vasopressinase in human pregnancy. Am J Physiol 1993;264(2 Pt 2):F348–53.
[165] Davison JM, Sheills EA, Barron WM, Robinson AG, Lindheimer MD. Changes in the metabolic clearance of vasopressin and in plasma vasopressinase throughout human pregnancy. J Clin Invest 1989;83(4):1313–8.
[166] Landon MJ, Copas DK, Shiells EA, Davison JM. Degradation of radiolabelled arginine vasopressin (125I-AVP) by the human placenta perfused in vitro. Br J Obstet Gynaecol 1988;95(5): 488–92.
[167] Davison JM, Shiells EA, Philips PR, Lindheimer MD. Influence of humoral and volume factors on altered osmoregulation of normal human pregnancy. Am J Physiol 1990;258(4 Pt 2):F900–7.
[168] Heesch CM, Zheng H, Foley CM, Mueller PJ, Hasser EM, Patel KP. Nitric oxide synthase activity and expression are decreased in the paraventricular nucleus of pregnant rats. Brain Res 2009;1251:140–50.
[169] Barron WM, Durr J, Stamoutsos BA, Lindheimer MD. Osmoregulation and vasopressin secretion during pregnancy in Brattleboro rats. Am J Physiol 1985;248(1 Pt 2):R29–37.
[170] Barron WM, Durr JA, Schrier RW, Lindheimer MD. Role of hemodynamic factors in osmoregulatory alterations of rat pregnancy. Am J Physiol 1989;257(4 Pt 2):R909–16.
[171] Barron WM, Schreiber J, Lindheimer MD. Effect of ovarian sex steroids on osmoregulation and vasopressin secretion in the rat. Am J Physiol 1986;250(4 Pt 1):E352–61.
[172] Dürr JA, Stamoutsos B, Lindheimer MD. Osmoregulation during pregnancy in the rat. Evidence for resetting of the threshold for vasopressin secretion during gestation. J Clin Invest 1981;68(2):337–46.
[173] Koehler EM, McLemore GL, Tang W, Summy-Long JY. Osmoregulation of the magnocellular system during pregnancy and lactation. Am J Physiol 1993;264(3 Pt 2):R555–60.
[174] Ohara M, Martin PY, Xu DL, St John J, Pattison TA, Kim JK, et al. Upregulation of aquaporin 2 water channel expression in pregnant rats. J Clin Invest 1998;101(5):1076–83.
[175] Dürr JA, Lindheimer MD. Diagnosis and management of diabetes insipidus during pregnancy. Endocr Pract 1996;2 (5):353–61.
[176] Baylis PH, Thompson C, Burd J, Tunbridge WM, Snodgrass CA. Recurrent pregnancy-induced polyuria and thirst due to hypothalamic diabetes insipidus: an investigation into possible mechanisms responsible for polyuria. Clin Endocrinol (Oxf) 1986;24(4):459–66.
[177] Hughes JM, Barron WM, Vance ML. Recurrent diabetes insipidus associated with pregnancy: pathophysiology and therapy. Obstet Gynecol 1989;73(3 Pt 2):462–4.
[178] Barron WM, Cohen LH, Ulland LA, Lassiter WE, Fulghum EM, Emmanouel D, et al. Transient vasopressin-resistant diabetes insipidus of pregnancy. N Engl J Med 1984;310 (7):442–4.
[179] Dürr JA, Hoggard JG, Hunt JM, Schrier RW. Diabetes insipidus in pregnancy associated with abnormally high circulating vasopressinase activity. N Engl J Med 1987;316(17):1070–4.
[180] Sherer DM, Cutler J, Santoso P, Angus S, Abulafia O. Severe hypernatremia after cesarean delivery secondary to transient diabetes insipidus of pregnancy. Obstet Gynecol 2003;102(5 Pt 2):1166–8.
[181] Lindheimer MD. Polyuria and pregnancy: its cause, its danger. Obstet Gynecol 2005;105(5 Pt 2):1171–2.
[182] Shah SV, Thakur V. Vasopressinase and diabetes insipidus of pregnancy. Ann Intern Med 1988;109(5):435–6.
[183] Dürr JA, Lindheimer MD. Control of volume and body tonicity. In: Lindheimer MD, Roberts JM, Cunningham FG, editors. Chesley's hypertensive disorders in pregnancy. 2nd ed. Stamford: Appleton & Lange; 1999.
[184] Schrier RW. Pathogenesis of sodium and water retention in high-output and low-output cardiac failure, nephrotic syndrome, cirrhosis, and pregnancy (2). N Engl J Med 1988;319 (17):1127–34.
[185] Schrier RW, Briner VA. Peripheral arterial vasodilation hypothesis of sodium and water retention in pregnancy: implications for pathogenesis of preeclampsia-eclampsia. Obstet Gynecol 1991;77(4):632–9.
[186] Schrier RW, Durr JA. Pregnancy: an overfill or underfill state. Am J Kidney Dis 1987;9(4):284–9.
[187] Barron WM, Stamoutsos BA, Lindheimer MD. Role of volume in the regulation of vasopressin secretion during pregnancy in the rat. J Clin Invest 1984;73(4):923–32.
[188] Koehler EM, McLemore GL, Martel JK, Summy-Long JY. Response of the magnocellular system in rats to hypovolemia and cholecystokinin during pregnancy and lactation. Am J Physiol 1994;266(4 Pt 2):R1327–37.
[189] Jeyabalan A, Conrad KP. Renal physiology and pathophysiology in pregnancy. In: Schrier RW, editor. Renal and electrolyte disorders. 7th ed. Little Brown and Company; 2010.
[190] Hytten FE. Weight gain in pregnancy. In: Hytten FE, Chamberlain G, editors. Clinical physiology in obstetrics. Oxford: Blackwell Scientific; 1980. p. 193–223.
[191] Pipe NG, Smith T, Halliday D, Edmonds CJ, Williams C, Coltart TM. Changes in fat, fat-free mass and body water in human normal pregnancy. Br J Obstet Gynaecol 1979;86 (12):929–40.
[192] Catalano PM, Wong WW, Drago NM, Amini SB. Estimating body composition in late gestation: a new hydration constant for body density and total body water. Am J Physiol 1995;268 (1 Pt 1):E153–8.

[193] Lukaski HC, Siders WA, Nielsen EJ, Hall CB. Total body water in pregnancy: assessment by using bioelectrical impedance. Am J Clin Nutr 1994;59(3):578–85.
[194] Lukaski HC, Hall CB, Siders WA. Assessment of change in hydration in women during pregnancy and postpartum with bioelectrical impedance vectors. Nutrition 2007;23(7-8): 543–50.
[195] Brown MA, Gallery ED. Volume homeostasis in normal pregnancy and pre-eclampsia: physiology and clinical implications. Baillieres Clin Obstet Gynaecol 1994;8(2):287–310.
[196] Zamudio S, Palmer SK, Dahms TE, Berman JC, McCullough RG, McCullough RE, et al. Blood volume expansion, preeclampsia, and infant birth weight at high altitude. J Appl Physiol 1993;75(4):1566–73.
[197] Gallery ED, Hunyor SN, Gyory AZ. Plasma volume contraction: a significant factor in both pregnancy-associated hypertension (pre-eclampsia) and chronic hypertension in pregnancy. Q J Med 1979;48(192):593–602.
[198] Pirani BB, Campbell DM, MacGillivray I. Plasma volume in normal first pregnancy. J Obstet Gynaecol Br Commonw 1973;80(10):884–7.
[199] Baylis C, Munger K. Persistence of maternal plasma volume expansion in midterm pregnant rats maintained on a zero sodium intake: evidence early that early gestational volume expansiondoes not rely on sodium retention. Clin Exp Hypertens 1990;:237–47 1993; B3
[200] Verkeste CM, Slangen BF, Dubelaar ML, van Kreel BK, Peeters LL. Mechanism of volume adaptation in the awake early pregnant rat. Am J Physiol 1998;274(5 Pt 2):H1662–6.
[201] Brown MA, Zammit VC, Mitar DM. Extracellular fluid volumes in pregnancy-induced hypertension. J Hypertens 1992;10(1):61–8.
[202] Oian P, Maltau JM. Calculated capillary hydrostatic pressure in normal pregnancy and preeclampsia. Am J Obstet Gynecol 1987;157(1):102–6.
[203] Brown MA, Zammit VC, Lowe SA. Capillary permeability and extracellular fluid volumes in pregnancy-induced hypertension. Clin Sci (Lond) 1989;77(6):599–604.
[204] Baylis C, Beinder E, Suto T, August P. Recent insights into the roles of nitric oxide and renin-angiotensin in the pathophysiology of preeclamptic pregnancy. Semin Nephrol 1998;18(2): 208–30.
[205] Wilson M, Morganti AA, Zervoudakis I, Letcher RL, Romney BM, Von Oeyon P, et al. Blood pressure, the renin-aldosterone system and sex steroids throughout normal pregnancy. Am J Med 1980;68(1):97–104.
[206] Bay WH, Ferris TF. Factors controlling plasma renin and aldosterone during pregnancy. Hypertension 1979;1(4):410–5.
[207] Brown MA, Nicholson E, Ross MR, Norton HE, Gallery ED. Progressive resetting of sodium-renin-aldosterone relationships in human pregnancy. Clin Exp Hypertens 1987; B5:349–75.
[208] Hsueh WA, Luetscher JA, Carlson EJ, Grislis G, Fraze E, McHargue A. Changes in active and inactive renin throughout pregnancy. J Clin Endocrinol Metab 1982;54(5):1010–6.
[209] Lindheimer MD, del Greco F, Ehrlich EN. Postural effects on Na and steroid excretion, and serum renin activity during pregnancy. J Appl Physiol 1973;35(3):343–8.
[210] Oliver WJ, Neel JV, Grekin RJ, Cohen EL. Hormonal adaptation to the stresses imposed upon sodium balance by pregnancy and lactation in the Yanomama Indians, a culture without salt. Circulation 1981;63(1):110–6.
[211] Weinberger MH, Kramer NJ, Grim CE, Petersen LP. The effect of posture and saline loading on plasma renin activity and aldosterone concentration in pregnant, non-pregnant and estrogen-treated women. J Clin Endocrinol Metab 1977;44(1): 69–77.
[212] Ehrlich EN. Heparinoid-induced inhibition of aldosterone secretion in pregnant women. The role of augmented aldosterone secretion in sodium conservation during normal pregnancy. Am J Obstet Gynecol 1971;109(7):963–70.
[213] Castro LC, Hobel CJ, Gornbein J. Plasma levels of atrial natriuretic peptide in normal and hypertensive pregnancies: a meta-analysis. Am J Obstet Gynecol 1994;171 (6):1642–51.
[214] Quinkler M, Diederich S, Bahr V, Oelkers W. The role of progesterone metabolism and androgen synthesis in renal blood pressure regulation. Horm Metab Res 2004;36 (6):381–6.
[215] Casey ML, MacDonald PC. Metabolism of deoxycorticosterone and deoxycorticosterone sulfate in men and women. J Clin Invest 1982;70(2):312–9.
[216] MacDonald PC, Cutrer S, MacDonald SC, Casey ML, Parker Jr CR. Regulation of extraadrenal steroid 21-hydroxylase activity. Increased conversion of plasma progesterone to deoxycorticosterone during estrogen treatment of women pregnant with a dead fetus. J Clin Invest 1982;69(2):469–78.
[217] Winkel CA, Milewich L, Parker Jr CR, Gant NF, Simpson ER, MacDonald PC. Conversion of plasma progesterone to deoxycorticosterone in men, nonpregnant and pregnant women, and adrenalectomized subjects. J Clin Invest 1980;66 (4):803–12.
[218] Winkel CA, Simpson ER, Milewich L, MacDonald PC. Deoxycorticosterone biosynthesis in human kidney: potential for formation of a potent mineralocorticosteroid in its site of action. Proc Natl Acad Sci U S A 1980;77(12):7069–73.
[219] Irons DW, Baylis PH, Butler TJ, Davison JM. Atrial natriuretic peptide in preeclampsia: metabolic clearance, sodium excretion and renal hemodynamics. Am J Physiol 1997;273(3 Pt 2): F483–7.
[220] Irons DW, Baylis PH, Davison JM. The metabolic clearance of atrial natriuretic peptide during human pregnancy. Am J Obstet Gynecol 1996;175(2):449–54.
[221] Irons DW, Baylis PH, Davison JM. Effect of atrial natriuretic peptide on renal hemodynamics and sodium excretion during human pregnancy. Am J Physiol 1996;271(1 Pt 2): F239–42.
[222] Masilamani S, Castro L, Baylis C. Pregnant rats are refractory to the natriuretic actions of atrial natriuretic peptide. Am J Physiol 1994;267(6 Pt 2):R1611–6.
[223] Olsson K, Karlberg BE, Eriksson L. Atrial natriuretic peptide in pregnant and lactating goats. Acta Endocrinol (Copenh) 1989;120(4):519–25.
[224] Omer S, Mulay S, Cernacek P, Varma DR. Attenuation of renal effects of atrial natriuretic factor during rat pregnancy. Am J Physiol 1995;268(3 Pt 2):F416–22.
[225] Knight S, Snellen H, Humphreys M, Baylis C. Increased renal phosphodiesterase-5 activity mediates the blunted natriuretic response to ANP in the pregnant rat. Am J Physiol Renal Physiol 2007;292(2):F655–9.
[226] Barron WM, Nalbantian-Brandt C, Lindheimer MD. Role of mineralocorticoid in volume homeostasis and pregnancy performance in the rat. Hypertens Preg 1993;250: E352–61.
[227] Chesley LC, Valenti C, Rein H. Excretion of sodium loads by nonpregnant and pregnant normal, hypertensive and preeclamptic women. Metabolism 1958;7(5):575–88.
[228] Brown MA, Gallery ED, Ross MR, Esber RP. Sodium excretion in normal and hypertensive pregnancy: a prospective study. Am J Obstet Gynecol 1988;159(2):297–307.
[229] Katz AI, Lindheimer MD. Renal handling of acute sodium loads in pregnancy. Am J Physiol 1973;225(3):696–9.

[230] August P, Mueller FB, Sealey JE, Edersheim TG. Role of renin-angiotensin system in blood pressure regulation in pregnancy. Lancet 1995;345(8954):896–7.
[231] Duvekot JJ, Cheriex EC, Pieters FA, Menheere PP, Peeters LH. Early pregnancy changes in hemodynamics and volume homeostasis are consecutive adjustments triggered by a primary fall in systemic vascular tone. Am J Obstet Gynecol 1993;169(6):1382–92.
[232] Brown MA, Broughton Pipkin F, Symonds EM. The effects of intravenous angiotensin II upon blood pressure and sodium and urate excretion in human pregnancy. J Hypertens 1988;6 (6):457–64.
[233] Clapp III JF, Capeless E. Cardiovascular function before, during, and after the first and subsequent pregnancies. Am J Cardiol 1997;80(11):1469–73.
[234] Cha SC, Aberdeen GW, Nuwayhid BS, Quillen Jr EW. Influence of pregnancy on mean systemic filling pressure and the cardiac function curve in guinea pigs. Can J Physiol Pharmacol 1992;70(5):669–74.
[235] Davis LE. Vascular pressure-volume relationships in pregnant and estrogen-treated guinea pigs. Am J Physiol 1989;257: R1205–11.
[236] Douglas BH, Harlan JC, Langford HG, Richardson TQ. Effect of hypervolemia and elevated arterial pressure on circulatory dynamics of pregnant animals. Am J Obstet Gynecol 1967;98 (7):889–94.
[237] Goodlin RC, Niebauer MJ, Holmberg MJ, Zucker IM. Mean circulatory filling pressure in pregnant rabbits. Am J Obstet Gynecol 1984;148(2):224–5.
[238] Humphreys PW, Joels N. Effect of pregnancy on pressure-volume relationships in circulation of rabbits. Am J Physiol 1994;267(3 Pt 2):R780–5.
[239] Atherton JC, Bielinska A, Davison JM, Haddon I, Kay C, Samuels R. Sodium and water reabsorption in the proximal and distal nephron in conscious pregnant rats and third trimester women. J Physiol 1988;396:457–70.
[240] Dürr JA, Miller NL, Alfrey AC. Lithium clearance derived from the natural trace blood and urine lithium levels. Kidney Int Suppl 1990;28:S58–62.
[241] McLaughlin MK, Roberts JM. Hemodynamic changes. In: Lindheimer MD, Roberts JM, Cunningham FG, editors. Chesley's hypertensive disorders in pregnancy. Stamford: Appleton & Lang; 1999.
[242] Brendt RL. Effect of embryonic and fetal exposure to x-ray, microwaves, ultrasound, magnetic resonance and isotopes. In: Barron WM, Lindheimer MD, editors. Medical disorders of pregnancy. 2nd ed. St. Louis: Mosby Yearbook; 1995. p. 487–518.
[243] Assali NS, Herzig D, Singh BP. Renal response to ammonium chloride acidosis in normal and toxemic pregnancies. J Appl Physiol 1955;7(4):367–74.
[244] Akbari A, Lepage N, Keely E, Clark HD, Jaffey J, MacKinnon M, et al. Cystatin-C and beta trace protein as markers of renal function in pregnancy. BJOG 2005;112(5):575–8.
[245] Heenan AP, Wolfe LA. Plasma osmolality and the strong ion difference predict respiratory adaptations in pregnant and nonpregnant women. Can J Physiol Pharmacol 2003;81(9): 839–47.
[246] Quadri KH, Bernardini J, Greenberg A, Laifer S, Syed A, Holley JL. Assessment of renal function during pregnancy using a random urine protein to creatinine ratio and Cockcroft-Gault formula. Am J Kidney Dis 1994;24(3):416–20.
[247] Kuo VS, Koumantakis G, Gallery ED. Proteinuria and its assessment in normal and hypertensive pregnancy. Am J Obstet Gynecol 1992;167(3):723–8.
[248] Higby K, Suiter CR, Phelps JY, Siler-Khodr T, Langer O. Normal values of urinary albumin and total protein excretion during pregnancy. Am J Obstet Gynecol 1994;171(4):984–9.
[249] Barr J, Hod M, Erman A, Kaplan B, Ovadia J, Schoenfield A. Microalbuminuria in early pregnancy in normal and high risk patients. Early Pregnancy 1996;2:197–200.
[250] Bernard A, Thielemans N, Lauwerys R, van Lierde M. Selective increase in the urinary excretion of protein 1 (Clara cell protein) and other low molecular weight proteins during normal pregnancy. Scand J Clin Lab Invest 1992;52(8):871–8.
[251] Brown MA, Wang MX, Buddle ML, Carlton MA, Cario GM, Zammit VC, et al. Albumin excretory rate in normal and hypertensive pregnancy. Clin Sci (Lond) 1994;86(3):251–5.
[252] Erman A, Neri A, Sharoni R, Rabinov M, Kaplan B, Rosenfeld JB, et al. Enhanced urinary albumin excretion after 35 weeks of gestation and during labour in normal pregnancy. Scand J Clin Lab Invest 1992;52(5):409–13.
[253] Helkjaer PE, Holm J, Hemmingsen L. Intra-individual changes in concentrations of urinary albumin, serum albumin, creatinine, and uric acid during normal pregnancy. Clin Chem 1992;38(10):2143–4.
[254] Konstantin-Hansen KF, Hesseldahl H, Pedersen SM. Microalbuminuria as a predictor of preeclampsia. Acta Obstet Gynecol Scand 1992;71(5):343–6.
[255] MacRury SM, Pinion S, Quin JD, O'Reilly DS, Lunan CB, Lowe GD, et al. Blood rheology and albumin excretion in diabetic pregnancy. Diabet Med 1995;12(1):51–5.
[256] Taylor AA, Davison JM. Albumin excretion in normal pregnancy. Am J Obstet Gynecol 1997;177(6):1559–60.
[257] Hayashi M, Ueda Y, Hoshimoto K, Ota Y, Fukasawa I, Sumori K, et al. Changes in urinary excretion of six biochemical parameters in normotensive pregnancy and preeclampsia. Am J Kidney Dis 2002;39(2):392–400.
[258] Gallery ED, Ross M, Gyory AZ. Urinary red blood cell and cast excretion in normal and hypertensive human pregnancy. Am J Obstet Gynecol 1993;168(1 Pt 1):67–70.
[259] Danielli L, Korchazak D, Beyar H, Lotan M. Recurrent hematuria during multiple pregnancies. Obstet Gynecol 1987;69(3 Pt 2):446–8.
[260] Lindheimer MD, Davison JM. Renal biopsy during pregnancy: 'to b … or not to b …?'. Br J Obstet Gynaecol 1987;94 (10):932–4.
[261] Packham D, Fairley KF. Renal biopsy: indications and complications in pregnancy. Br J Obstet Gynaecol 1987;94 (10):935–9.
[262] Cunningham FG, Lucas MJ. Urinary tract infections complicating pregnancy. Baillieres Clin Obstet Gynaecol 1994;8 (2):353–73.
[263] Millar LK, Cox SM. Urinary tract infections complicating pregnancy. Infect Dis Clin North Am 1997;11(1):13–26.
[264] Pedler SJ, Orr K. Bacterial, fungal and parasitic infections. In: Barron WM, Lindheimer MD, editors. Medicla disorders of pregnancy. 2nd ed. St. Louis: Mosby; 2000.
[265] Bint AJ, Hill D. Bacteriuria of pregnancy–an update on significance, diagnosis and management. J Antimicrob Chemother 1994;33(Suppl. A):93–7.
[266] Graham JM, Oshiro BT, Blanco JD, Magee KP. Uterine contractions after antibiotic therapy for pyelonephritis in pregnancy. Am J Obstet Gynecol 1993;168(2):577–80.
[267] Meis PJ, Michielutte R, Peters TJ, Wells HB, Sands RE, Coles EC, et al. Factors associated with preterm birth in Cardiff, Wales. II. Indicated and spontaneous preterm birth. Am J Obstet Gynecol 1995;173(2):597–602.
[268] Romero R, Oyarzun E, Mazor M, Sirtori M, Hobbins JC, Bracken M. Meta-analysis of the relationship between

asymptomatic bacteriuria and preterm delivery/low birth weight. Obstet Gynecol 1989;73(4):576–82.
[269] Schieve LA, Handler A, Hershow R, Persky V, Davis F. Urinary tract infection during pregnancy: its association with maternal morbidity and perinatal outcome. Am J Public Health 1994;84(3):405–10.
[270] Campbell-Brown M, McFadyen IR, Seal DV, Stephenson ML. Is screening for bacteriuria in pregnancy worth while? Br Med J (Clin Res Ed) 1987;294(6587):1579–82.
[271] Dempsey C, Harrison RF, Moloney A, Darling M, Walshe J. Characteristics of bacteriuria in a homogeneous maternity hospital population. Eur J Obstet Gynecol Reprod Biol 1992;44 (3):189–93.
[272] Urinary tract infection during pregnancy. Lancet 1985;2 (8448):190–192.
[273] Stray-Pdersen B, Blakstad M, Bergan T. Bacteriuria in the puerperium. Risk factors, screening procedures, and treatment programs. Am J Obstet Gynecol 1990;162(3):792–7.
[274] Lenke RR, VanDorsten JP, Schifrin BS. Pyelonephritis in pregnancy: a prospective randomized trial to prevent recurrent disease evaluating suppressive therapy with nitrofurantoin and close surveillance. Am J Obstet Gynecol 1983;146 (8):953–7.
[275] Hill JB, Sheffield JS, McIntire DD, Wendel Jr GD. Acute pyelonephritis in pregnancy. Obstet Gynecol 2005;105(1):18–23.
[276] Villar J, Lydon-Rochelle MT, Gulmezoglu AM, Roganti A. Duration of treatment for asymptomatic bacteriuria during pregnancy. Cochrane Database Syst Rev 2000;(2):CD000491.
[277] Vazquez JC, Villar J. Treatments for symptomatic urinary tract infections during pregnancy. Cochrane Database Syst Rev 2003;(4):CD002256.
[278] Lindheimer MD, Katz AI, Ganeval D, Grünfeld JP. Acute renal failure in pregnancy. In: Brenner BM, Lazarus JM, editors. Acute renal failure. 3rd ed. New York: Churchill Livingstone; 1993. p. 417–39.
[279] Madias NE, Donohoe JF, Harrington JT. Postischemic acute renal failure. In: Brenner BM, Lazarus JM, editors. Acute renal failure. 2nd ed. New York: Churchill Livingstone; 1988. p. 251–78.
[280] Pertuiset N, Grunfeld JP. Acute renal failure in pregnancy. Baillieres Clin Obstet Gynaecol 1994;8(2):333–51.
[281] Turney JH, Ellis CM, Parsons FM. Obstetric acute renal failure 1956–1987. Br J Obstet Gynaecol 1989;96(6):679–87.
[282] Halpin TF, Molinari JA. Diagnosis and management of clostridium perfringens sepsis and uterine gas gangrene. Obstet Gynecol Surv 2002;57(1):53–7.
[283] Chugh KS, Jha V, Sakhuja V, Joshi K. Acute renal cortical necrosis–a study of 113 patients. Ren Fail 1994;16(1):37–47.
[284] Sheehan HL, Moore LG. Renal cortical necrosis and the kidney of concealed accident hemorrhage. Springfield: Charles C. Thomas; 1953.
[285] Willams TF. Renal cortical necrosis, renal infarction, and hypertension due to renal disease. In: Strauss MD, Welt LG, editors. Diseases of the kidney. 1st ed. Boston: Little Brown; 1963. p. 536–9.
[286] Kleinknecht D, Grunfeld JP, Gomez PC, Moreau JF, Garcia-Torres R. Diagnostic procedures and long-term prognosis in bilateral renal cortical necrosis. Kidney Int 1973;4 (6):390–400.
[287] Conger JD, Falk SA, Guggenheim SJ. Glomerular dynamics and morphologic changes in the generalized Shwartzman reaction in postpartum rats. J Clin Invest 1981;67(5):1334–46.
[288] Fesenmeier MF, Coppage KH, Lambers DS, Barton JR, Sibai BM. Acute fatty liver of pregnancy in 3 tertiary care centers. Am J Obstet Gynecol 2005;192(5):1416–9.
[289] Liebman HA, McGehee WG, Patch MJ, Feinstein DI. Severe depression of antithrombin III associated with disseminated intravascular coagulation in women with fatty liver of pregnancy. Ann Intern Med 1983;98(3):330–3.
[290] Riely CA, Latham PS, Romero R, Duffy TP. Acute fatty liver of pregnancy. A reassessment based on observations in nine patients. Ann Intern Med 1987;106(5):703–6.
[291] Rodriguez PN, Klein AS. Management of urolithiasis during pregnancy. Surg Gynecol Obstet 1988;166(2):103–6.
[292] Wiebers DO, Torres VE. Screening for unruptured intracranial aneurysms in autosomal dominant polycystic kidney disease. N Engl J Med 1992;327(13):953–5.
[293] Ibdah JA, Bennett MJ, Rinaldo P, Zhao Y, Gibson B, Sims HF, et al. A fetal fatty-acid oxidation disorder as a cause of liver disease in pregnant women. N Engl J Med 1999;340 (22):1723–31.
[294] Treem WR, Shoup ME, Hale DE, Bennett MJ, Rinaldo P, Millington DS, et al. Acute fatty liver of pregnancy, hemolysis, elevated liver enzymes, and low platelets syndrome, and long chain 3-hydroxyacyl-coenzyme A dehydrogenase deficiency. Am J Gastroenterol 1996;91(11):2293–300.
[295] Robson JS, Martin AM, Ruckley V, Macdonald MK. Irreversible post-partum renal failure. A new syndrome. Q J Med 1968;37(147):423–35.
[296] Scheer RL, Jones DB. Malignant nephrosclerosis in women post partum. A note on microangiopathic hemolytic anemia. JAMA 1967;201(8):600–4.
[297] Sibai BM, Kustermann L, Velasco J. Current understanding of severe preeclampsia, pregnancy-associated hemolytic uremic syndrome, thrombotic thrombocytopenic purpura, hemolysis, elevated liver enzymes, and low platelet syndrome, and postpartum acute renal failure: different clinical syndromes or just different names?. Curr Opin Nephrol Hypertens 1994;3(4): 436–45.
[298] Wagoner RD, Holley KE, Johnson WJ. Accelerated nephrosclerosis and postpartum acute renal failure in normotensive patients. Ann Intern Med 1968;69(2):237–48.
[299] Kincaid-Smith P. The similarity of lesions and underlying mechanism in preeclamptic toxemia and postpartum renal failure: studies in the acute stage and during follow up. Perspect Nephrol Hypertens 1973;:1013–25 1 Pt 2(0)
[300] Modesto A, Durand D, Orfila C, Suc JM. Syndrome hemolytique uremique chez deux germains HLA identiques. Nephrologie 1984;5:47–8.
[301] Sun NC, Johnson WD, Sung DTW, Woods JD. Idiopathic post partum renal failure: review and report of a successful renal transplanation. Mayo Clinic Proc 1975;50:395–401 [Proceeding].
[302] Kincaid-Smith P, Fairley KF, Kloss M. Lupus anticoagulant associated with renal thrombotic microangiopathy and pregnancy-related renal failure. Q J Med 1988;68(258):795–815.
[303] Kniaz D, Eisenberg GM, Elrad H, Johnson CA, Valaitis J, Bregman H. Postpartum hemolytic uremic syndrome associated with antiphospholipid antibodies. A case report and review of the literature. Am J Nephrol 1992;12(1–2):126–33.
[304] Warren GV, Sprague SM, Corwin HL. Sarcoidosis presenting as acute renal failure during pregnancy. Am J Kidney Dis 1988;12(2):161–3.
[305] Katz AI, Davison JM, Hayslett JP, Singson E, Lindheimer MD. Pregnancy in women with kidney disease. Kidney Int 1980;18 (2):192–206.
[306] Sibai BM, Villar MA, Mabie BC. Acute renal failure in hypertensive disorders of pregnancy. Pregnancy outcome and remote prognosis in thirty-one consecutive cases. Am J Obstet Gynecol 1990;162(3):777–83.

[307] Bagon JA, Vernaeve H, De Muylder X, Lafontaine JJ, Martens J, Van Roost G. Pregnancy and dialysis. Am J Kidney Dis 1998;31(5):756–65.
[308] Hou SH. Pregnancy in women on haemodialysis and peritoneal dialysis. Baillieres Clin Obstet Gynaecol 1994;8 (2):481–500.
[309] Hou S. Fertility and pregnancy in end stage renal disease. In: Brady HR, Wilcox CS, editors. Therapy in nephorology and hypertension: a companion to brenner and rector's the kidney. Philadelphia: WB Saunders; 1998. p. 358–62.
[310] Hou S. Pregnancy in chronic renal insufficiency and end-stage renal disease. Am J Kidney Dis 1999;33(2):235–52.
[311] Okundaye I, Abrinko P, Hou S. Registry of pregnancy in dialysis patients. Am J Kidney Dis 1998;31(5):766–73.
[312] Lew SQ, Watson JA. Urea and creatinine generation and removal in a pregnant patient receiving peritoneal dialysis. Adv Perit Dial 1992;8:131–5.
[313] Jungers P, Houillier P, Forget D, Labrunie M, Skhiri H, Giatras I, et al. Influence of pregnancy on the course of primary chronic glomerulonephritis. Lancet 1995;346(8983):1122–4.
[314] Lindheimer MD, Katz AI. Gestation in women with kidney disease: prognosis and management. Baillieres Clin Obstet Gynaecol 1994;8(2):387–404.
[315] Jungers P, Chauveau D. Pregnancy in renal disease. Kidney Int 1997;52(4):871–85.
[316] Jones DC, Hayslett JP. Outcome of pregnancy in women with moderate or severe renal insufficiency. N Engl J Med 1996;335 (4):226–32.
[317] AbdAlla S, Lother H, el Massiery A, Quitterer U. Increased AT (1) receptor heterodimers in preeclampsia mediate enhanced angiotensin II responsiveness. Nat Med 2001;7(9):1003–9.
[318] Jungers P, Houillier P, Chauveau D, Choukroun G, Moynot A, Skhiri H, et al. Pregnancy in women with reflux nephropathy. Kidney Int 1996;50(2):593–9.
[319] Caritis S, Sibai B, Hauth J, Lindheimer MD, Klebanoff M, Thom E, et al. Low-dose aspirin to prevent preeclampsia in women at high risk. National institute of child health and human development network of maternal-fetal medicine units. N Engl J Med 1998;338(11):701–5.
[320] Sibai BM, Lindheimer M, Hauth J, Caritis S, VanDorsten P, Klebanoff M, et al. Risk factors for preeclampsia, abruptio placentae, and adverse neonatal outcomes among women with chronic hypertension. National institute of child health and human development network of maternal-fetal medicine units. N Engl J Med 1998;339(10):667–71.
[321] Packham DK, Mathews DC, Fairley KF, Whitworth JA, Kincaid-Smith P. Comparison of pregnancy outcome between normotensive and hypertensive women with primary glomerulonephritis. Clin Exp Hypertens 1988;B6:387–99.
[322] Davison JM. Pregnancy in renal allograft recipients: problems, prognosis and practicalities. Baillieres Clin Obstet Gynaecol 1994;8(2):501–25.
[323] Cunningham FG, Cox SM, Harstad TW, Mason RA, Pritchard JA. Chronic renal disease and pregnancy outcome. Am J Obstet Gynecol 1990;163(2):453–9.
[324] Fischer MJ, Lehnerz SD, Hebert JR, Parikh CR. Kidney disease is an independent risk factor for adverse fetal and maternal outcomes in pregnancy. Am J Kidney Dis 2004;43(3):415–23.
[325] Fisher KA, Luger A, Spargo BH, Lindheimer MD. Hypertension in pregnancy: clinical-pathological correlations and remote prognosis. Medicine (Baltimore) 1981;60(4):267–76.
[326] Shepherd J, Shepherd C. Poststreptococcal glomerulonephritis: a rare complicaiton in pregnancy. J Fam Pract 1992;34: 630–2.
[327] Singson E, Fisher KF, Lindheimer MD. Acute poststreptococcal glomerulonephritis in pregnancy: case report with an 18-year follow-up. Am J Obstet Gynecol 1980;137(7):857–8.
[328] Davis III AE, Arnaout MA, Alper CA, Rosen FS. Transfer of C3 nephritic factor from mother to fetus. Is C3 nephritic factor IgG? N Engl J Med 1977;297(3):144–5.
[329] Abe S. Pregnancy in IgA nephropathy. Kidney Int 1991;40 (6):1098–102.
[330] Abe S. The influence of pregnancy on the long-term renal prognosis of IgA nephropathy. Clin Nephrol 1994;41(2):61–4.
[331] Packham DK, North RA, Fairley KF, Ihle BU, Whitworth JA, Kincaid-Smith P. Pregnancy in women with primary focal and segmental hyalinosis and sclerosis. Clin Nephrol 1988;29 (4):185–92.
[332] Lockshin MD, Druzin MD. Rheumatic diseases. In: Barron WM, Lindheimer MD, editors. Medical disorders during pregnancy. 2nd ed. St. Louis: Mosby; 1995.
[333] Huong DL, Wechsler B, Vauthier-Brouzes D, Beaufils H, Lefebvre G, Piette JC. Pregnancy in past or present lupus nephritis: a study of 32 pregnancies from a single centre. Ann Rheum Dis 2001;60(6):599–604.
[334] Tandon A, Ibanez D, Gladman DD, Urowitz MB. The effect of pregnancy on lupus nephritis. Arthritis Rheum 2004;50(12): 3941–6.
[335] Rahman FZ, Rahman J, Al-Suleiman SA, Rahman MS. Pregnancy outcome in lupus nephropathy. Arch Gynecol Obstet 2005;271(3):222–6.
[336] Moroni G, Ponticelli C. The risk of pregnancy in patients with lupus nephritis. J Nephrol 2003;16(2):161–7.
[337] Hayslett JP. The effect of systemic lupus erythematosus on pregnancy and pregnancy outcome. Am J Reprod Immunol 1992;28(3–4):199–204.
[338] Biesenbach G, Zazgornik J. Incidence of transient nephrotic syndrome during pregnancy in diabetic women with and without pre-existing microalbuminuria. BMJ 1989;299 (6695):366–7.
[339] Grenfell A, Brudenell JM, Doddridge MC, Watkins PJ. Pregnancy in diabetic women who have proteinuria. Q J Med 1986;59(228):379–86.
[340] Hayslett JP, Reece EA. Managing diabetic patients with nephropathy and other vascular complications. Baillieres Clin Obstet Gynaecol 1994;8(2):405–24.
[341] Jovanovic R, Jovanovic L. Obstetric management when normoglycemia is maintained in diabetic pregnant women with vascular compromise. Am J Obstet Gynecol 1984;149(6):617–23.
[342] Kitzmiller JL, Brown ER, Phillippe M, Stark AR, Acker D, Kaldany A, et al. Diabetic nephropathy and perinatal outcome. Am J Obstet Gynecol 1981;141(7):741–51.
[343] Miodovnik M, Rosenn BM, Khoury JC, Grigsby JL, Siddiqi TA. Does pregnancy increase the risk for development and progression of diabetic nephropathy? Am J Obstet Gynecol 1996;174(4):1180–9 [discussion 9–91]
[344] Mogensen CE, Klebe JG. Microalbuminuria and diabetic pregnancy. In: Mogensen C, editor. The kidney and hypertension in diabetes. Boston: M. Nijhoff; 1988. p. 223–9.
[345] Reece EA, Winn HN, Hayslett JP, Coulehan J, Wan M, Hobbins JC. Does pregnancy alter the rate of progression of diabetic nephropathy? Am J Perinatol 1990;7(2):193–7.
[346] Sims EAH. Serial studies on renal function in pregnancy complicated by diabetes mellitus. Diabetes 1961;10:190–7.
[347] Biesenbach G, Grafinger P, Stoger H, Zazgornik J. How pregnancy influences renal function in nephropathic type 1 diabetic women depends on their pre-conceptional creatinine clearance. J Nephrol 1999;12(1):41–6.

[348] Dunne FP, Chowdhury TA, Hartland A, Smith T, Brydon PA, McConkey C, et al. Pregnancy outcome in women with insulin-dependent diabetes mellitus complicated by nephropathy. Qjm 1999;92(8):451–4.
[349] How HY, Sibai B, Lindheimer M, Caritis S, Hauth J, Klebanoff M, et al. Is early-pregnancy proteinuria associated with an increased rate of preeclampsia in women with pregestational diabetes mellitus?. Am J Obstet Gynecol 2004;190 (3):775–8.
[350] Irfan S, Arain TM, Shaukat A, Shahid A. Effect of pregnancy on diabetic nephropathy and retinopathy. J Coll Physicians Surg Pak 2004;14(2):75–8.
[351] Kimmerle R, Zass RP, Cupisti S, Somville T, Bender R, Pawlowski B, et al. Pregnancies in women with diabetic nephropathy: long-term outcome for mother and child. Diabetologia 1995;38(2):227–35.
[352] Purdy LP, Hantsch CE, Molitch ME, Metzger BE, Phelps RL, Dooley SL, et al. Effect of pregnancy on renal function in patients with moderate-to-severe diabetic renal insufficiency. Diabetes Care 1996;19(10):1067–74.
[353] Jovanovic-Peterson L, Peterson CM. De novo clinical hypothyroidism in pregnancies complicated by type I diabetes, subclinical hypothyroidism, and proteinuria: a new syndrome. Am J Obstet Gynecol 1988;159(2):442–6.
[354] Abe S. An overview of pregnancy in women with underlying renal disease. Am J Kidney Dis 1991;17(2):112–5.
[355] Livneh A, Cabili S, Zemer D, Rabinovitch O, Pras M. Effect of pregnancy on renal function in amyloidosis of familial Mediterranean fever. J Rheumatol 1993;20(9):1519–23.
[356] Cummins DL, Mimouni D, Rencic A, Kouba DJ, Nousari CH. Henoch-Schonlein purpura in pregnancy. Br J Dermatol 2003;149(6):1282–5.
[357] Koizumi Mea. Scholein-Henoch purpura during pregnancy. Case report. J Obstet Gynaecol 2004;30:371.
[358] Deubner H, Wagnild JP, Wener MH, Alpers CE. Glomerulonephritis with anti-glomerular basement membrane antibody during pregnancy: potential role of the placenta in amelioration of disease. Am J Kidney Dis 1995;25(2):330–5.
[359] Auzary C, Huong DT, Wechsler B, Vauthier-Brouzes D, Piette JC. Pregnancy in patients with Wegener's granulomatosis: report of five cases in three women. Ann Rheum Dis 2000;59 (10):800–4.
[360] Masterson R, Pellicano R, Bleasel K, McMahon LP. Wegener's granulomatosis in pregnancy: a novel approach to management. Am J Kidney Dis 2004;44(4):e68–72.
[361] el-Khatib M, Packham DK, Becker GJ, Kincaid-Smith P. Pregnancy-related complications in women with reflux nephropathy. Clin Nephrol 1994;41(1):50–5.
[362] Vordermark JS, Deshon GE, Agee RE. Management of pregnancy after major urinary reconstruction. Obstet Gynecol 1990;75(3 Pt 2):564–7.
[363] Chapman AB, Johnson AM, Gabow PA. Pregnancy outcome and its relationship to progression of renal failure in autosomal dominant polycystic kidney disease. J Am Soc Nephrol 1994;5 (5):1178–85.
[364] Milutinovic J, Fialkow PJ, Agodoa LY, Phillips LA, Bryant JI. Fertility and pregnancy complications in women with autosomal dominant polycystic kidney disease. Obstet Gynecol 1983;61(5):566–70.
[365] Pison Y, Chauveau D, Grünfeld JP. Autosomal dominant polycystic kidney disease. In: Davison AM, Cameron JS, Grünfeld JP, Kerr D, Ritz E, Winearls CG, editors. Oxford textbook of clinical nephrology. 2nd ed. Oxford: Oxford University Press; 1998. p. 2393–415.
[366] Gabow PA. Autosomal dominant polycystic kidney disease. N Engl J Med 1993;329(5):332–42.
[367] Grünfeld JP, Knebelmann B. Alport's Syndrome. In: Davison AM, Cameron JS, Grünfeld JP, Kerr D, Ritz E, Winearls CG, editors. Oxford textbook of clinical nephrology. Oxford: Oxford University; 1986. p. 2427–37.
[368] Knebelmann B, Antignac C, Gubler NC, Grunfeld JP. A molecular approach to inherited kidney disorders. Kidney Int 1993;44(6):1205–16.
[369] Harris JP, Rakowski TA, Argy Jr WP, Schreiner GE. Alport's syndrome representing as crescentic glomerulonephritis: a report of two siblings. Clin Nephrol 1978;10(6): 245–9.
[370] Torres VE, King BF, Holley KE, Blute ML, Gomez MR. The kidney in the tuberous sclerosis complex. Adv Nephrol Necker Hosp 1994;23:43–70.
[371] Ogasawara KK, Ogasawara EM, Hirata G. Pregnancy complicated by von Hippel-Lindau disease. Obstet Gynecol 1995;85(5 Pt 2):829–31.
[372] Richard S, Chauveau D, Chretien Y, Beigelman C, Denys A, Fendler JP, et al. Renal lesions and pheochromocytoma in von Hippel-Lindau disease. Adv Nephrol Necker Hosp 1994; 23:1–27.
[373] Maikranz P, Lindheimer M, Coe F. Nephrolithiasis in pregnancy. Baillieres Clin Obstet Gynaecol 1994;8(2):375–86.
[374] Coe FL, Parks JH, Lindheimer MD. Nephrolithiasis during pregnancy. N Engl J Med 1978;298(6):324–6.
[375] Davison JM, Nakagawa Y, Coe FC, Lindheimer MD. Increases in both urinary inhibitor activity, and excretion of an inhibitor of crystalluria in pregnancy. A defense against hypercalciuria of normal gestation. Hypertens Preg 1993;12:31–41.
[376] Maikranz P, Holley JL, Parks JH, Lindheimer MD, Nakagawa Y, Coe FL. Gestational hypercalciuria causes pathological urine calcium oxalate supersaturations. Kidney Int 1989;36(1): 108–13.
[377] Stothers L, Lee LM. Renal colic in pregnancy. J Urol 1992;148 (5):1383–7.
[378] Gregory MC, Mansell MA. Pregnancy and cystinuria. Lancet 1983;2(8360):1158–60.
[379] McAleer SJ, Loughlin KR. Nephrolithiasis and pregnancy. Curr Opin Urol 2004;14(2):123–7.
[380] Loughlin KR, Bailey Jr RB. Internal ureteral stents for conservative management of ureteral calculi during pregnancy. N Engl J Med 1986;315(26):1647–9.
[381] Denstedt JD, Razvi H. Management of urinary calculi during pregnancy. J Urol 1992;148(3 Pt 2):1072–4 [discussion 4–5].
[382] Holley JL, Reddy SS. Pregnancy in dialysis patients: a review of outcomes, complications, and management. Semin Dial 2003;16(5):384–8.
[383] Goody AJ, Umans JG. Pregnancy and dialysis. In: Horl W, et al.editor. Replacement of renal function by dialysis. 5th ed. London, UK: Kluwer Academic Pub?; p. 1249.
[384] Murray JE, Reid DE, Harrison JH, Merrill JP. Successful pregnancies after human renal transplantation. N Engl J Med 1963;269:341–3.
[385] Merkatz IR, Schwartz GH, David DS, Stenzel KH, Riggio RR, Whitsell JC. Resumption of female reproductive function following renal transplantation. JAMA 1971;216(11):1749–54.
[386] Davison JM, Redman CW. Pregnancy post-transplant: the establishment of a UK registry. Br J Obstet Gynaecol 1997;104 (10):1106–7.
[387] Armenti VT, Moritz MJ, Davison JM. Medical management of the pregnant transplant recipient. Adv Ren Replace Ther 1998;5(1):14–23.

[388] Di Paolo S, Schena A, Morrone LF, Manfredi G, Stallone G, Derosa C, et al. Immunologic evaluation during the first year of life of infants born to cyclosporine-treated female kidney transplant recipients:analysis of lymphocyte subpopulations and immunoglobulin serum levels. Transplantation 2000;69 (10):2049–54.
[389] Petri M. Immunosuppressive drug use in pregnancy. Autoimmunity 2003;36(1):51–6.
[390] Kainz A, Harabacz I, Cowlrick IS, Gadgil SD, Hagiwara D. Review of the course and outcome of 100 pregnancies in 84 women treated with tacrolimus. Transplantation 2000;70 (12):1718–21.
[391] Armenti VT, Radomski JS, Moritz MJ, Gaughan WJ, McGrory CH, Coscia LA. Report from the National Transplantation Pregnancy Registry (NTPR): outcomes of pregnancy after transplantation. Clin Transpl 2003;:131–41.
[392] McKay DB, Josephson MA, Armenti VT, August P, Coscia LA, Davis CL, et al. Reproduction and transplantation: report on the AST consensus conference on reproductive issues and transplantation. Am J Transplant 2005;5(7): 1592–9.
[393] Ogburn Jr PL, Kitzmiller JL, Hare JW, Phillippe M, Gabbe SG, Miodovnik M, et al. Pregnancy following renal transplantation in class T diabetes mellitus. Jama 1986;255(7):911–5.
[394] Tyden G, Brattstrom C, Bjorkman U, Landgraf R, Baltzer J, Hillebrand G, et al. Pregnancy after combined pancreas-kidney transplantation. Diabetes 1989;38(Suppl. 1):43–5.
[395] Absy M, Metreweli C, Matthews C, Al Khader A. Changes in transplanted kidney volume measured by ultrasound. Br J Radiol 1987;60(714):525–9.
[396] Hartnell GG, Hennessy OF, Williams G. Percutaneous catheter drainage of obstructed transplant kidney in pregnancy. Urology 1985;25(5):522–3.
[397] Sturgiss SN, Davison JM. Perinatal outcome in renal allograft recipients: prognostic significance of hypertension and renal function before and during pregnancy. Obstet Gynecol 1991;78 (4):573–7.
[398] Salmela KT, Kyllonen LE, Holmberg C, Gronhagen-Riska C. Impaired renal function after pregnancy in renal transplant recipients. Transplantation 1993;56(6):1372–5.
[399] Lindheimer MD, Katz AI. Pregnancy in women receiving renal replacement therapy. Kidney 1994;3:135–7 [Editorial]
[400] Davison JM, Lindheimer MD. Renal disorders. In: Creasy RK, Resnik R, editors. Maternal fetal medicine. 4th ed. Philadelphia: WB Saunders; 1999.
[401] Davison JM. Towards long-term graft survival in renal transplantation: pregnancy. Nephrol Dial Transplant 1995;10(Suppl. 1):85–9.
[402] First MR, Combs CA, Weiskittel P, Miodovnik M. Lack of effect of pregnancy on renal allograft survival or function. Transplantation 1995;59(4):472–6.
[403] Rizzoni G, Ehrich JH, Broyer M, Brunner FP, Brynger H, Fassbinder W, et al. Successful pregnancies in women on renal replacement therapy: report from the EDTA Registry. Nephrol Dial Transplant 1992;7(4):279–87.
[404] Sturgiss SN, Davison JM. Effect of pregnancy on long-term function of renal allografts. Am J Kidney Dis 1992;19 (2):167–72.
[405] Sturgiss SN, Davison JM. Effect of pregnancy on the long-term function of renal allografts: an update. Am J Kidney Dis 1995;26(1):54–6.
[406] Davison JM. The effect of pregnancy on longterm renal function in women with chronic renal disease and single kidneys. Clin Exp Hypertens 1989;B8:226 [abstract]
[407] Buszta C, Steinmuller DR, Novick AC, Schreiber MJ, Cunningham R, Popowniak KL, et al. Pregnancy after donor nephrectomy. Transplantation 1985;40(6):651–4.
[408] Podjarny E, Bernheim J, Rathaus M, Pomeranz A, Tovbin D, Shapira J. Adriamycin nephropathy: a model to study effects of pregnancy on renal disease in rats. Am J Physiol 1992;263(4 Pt 2):F711–5.
[409] Baylis C. Immediate and long-term effects of pregnancy on glomerular function in the SHR. Am J Physiol 1989;257(6 Pt 2): F1140–5.
[410] Baylis C, Deng A, Couser WG. Glomerular hemodynamic effects of late pregnancy in rats with experimental membranous glomerulonephropathy. J Am Soc Nephrol 1995;6 (4):1197–201.
[411] Baylis C, Reese K, Wilson CB. Glomerular effects of pregnancy in a model of glomerulonephritis in the rat. Am J Kidney Dis 1989;14(6):456–60.
[412] Baylis C, Wilson CB. Sex and the single kidney. Am J Kidney Dis 1989;13(4):290–8.
[413] Deng A, Baylis C. Glomerular hemodynamic responses to pregnancy in rats with severe reduction of renal mass. Kidney Int 1995;48(1):39–44.
[414] Leaker B, Becker GJ, el-Khatib M, Hewitson TD, Kincaid-Smith P. Repeated pregnancy does not accelerate glomerular sclerosis in rats with subtotal renal ablation. Clin Exper Hypertens 1992; B11:1–23.
[415] Packham DK, Hewitson TD, Whitworth JA, Kincaid-Smith P. Physiological and biochemical effects of pregnancy in uninephrectomized rates. Clin Exp Hypertens 1991;B10:35–48.
[416] Pomeranz M, Podjarny E, Bernheim J, Pomeranz A, Rathaus M, Green J. Effect of recurrent pregnancies on the evolution of adriamycin nephropathy. Nephrol Dial Transplant 1995;10 (11):2049–53.
[417] Sibai B, Dekker G, Kupferminc M. Pre-eclampsia. Lancet 2005;365(9461):785–99.
[418] Christianson RE. Studies on blood pressure during pregnancy. I. Influence of parity and age. Am J Obstet Gynecol 1976;125 (4):509–13.
[419] Friedman EA, Neff RK. Pregnancy hypertension: a systematic evaluation of clinical diagnostic criteria. Littleton: PSG; 1977.
[420] MacGillivray RE, Rose GA, Rowe B. Blood pressure survey in pregnancy. 1969:37;395–407.
[421] Moutquin JM, Rainville C, Giroux L, Raynauld P, Amyot G, Bilodeau R, et al. A prospective study of blood pressure in pregnancy: prediction of preeclampsia. Am J Obstet Gynecol 1985;151(2):191–6.
[422] Walters BN, Thompson ME, Lee A, de Swiet M. Blood pressure in the puerperium. Clin Sci (Lond) 1986;71(5):589–94.
[423] Capeless EL, Clapp JF. Cardiovascular changes in early phase of pregnancy. Am J Obstet Gynecol 1989;161(6 Pt 1):1449–53.
[424] Mabie WC, DiSessa TG, Crocker LG, Sibai BM, Arheart KL. A longitudinal study of cardiac output in normal human pregnancy. Am J Obstet Gynecol 1994;170(3):849–56.
[425] Poppas A, Shroff SG, Korcarz CE, Hibbard JU, Berger DS, Lindheimer MD, et al. Serial assessment of the cardiovascular system in normal pregnancy. Role of arterial compliance and pulsatile arterial load. Circulation 1997;95(10):2407–15.
[426] Hibbard JU, Shroff SG, Lang RM. Cardiovascular changes in preeclampsia. Semin Nephrol 2004;24(6):580–7.
[427] Gilson GJ, Mosher MD, Conrad KP. Systemic hemodynamics and oxygen transport during pregnancy in chronically instrumented, conscious rats. Am J Physiol 1992;263(6 Pt 2): H1911–8.

[428] Geva T, Mauer MB, Striker L, Kirshon B, Pivarnik JM. Effects of physiologic load of pregnancy on left ventricular contractility and remodeling. Am Heart J. 1997;133(1):53–9.
[429] Lang RM, Pridjian G, Feldman T, Neumann A, Lindheimer M, Borow KM. Left ventricular mechanics in preeclampsia. Am Heart J. 1991;121(6 Pt 1):1768–75.
[430] Mone SM, Sanders SP, Colan SD. Control mechanisms for physiological hypertrophy of pregnancy. Circulation 1996;94 (4):667–72.
[431] Edouard DA, Pannier BM, London GM, Cuche JL, Safar ME. Venous and arterial behavior during normal pregnancy. Am J Physiol 1998;274(5 Pt 2):H1605–12.
[432] Conrad KP, Debrah DO, Novak J, Danielson LA, Shroff SG. Relaxin modifies systemic arterial resistance and compliance in conscious, nonpregnant rats. Endocrinology 2004;145 (7):3289–96.
[433] Hibbard JU, Korcarz CE, Nendaz GG, Lindheimer MD, Lang RM, Shroff SG. The arterial system in pre-eclampsia and chronic hypertension with superimposed pre-eclampsia. Bjog 2005;112(7):897–903.
[434] Metcalfe J, Parer JT. Cardiovascular changes during pregnancy in ewes. Am J Physiol 1966;210(4):821–5.
[435] Rosenfeld CR. Distribution of cardiac output in ovine pregnancy. Am J Physiol 1977;232(3):H231–5.
[436] Nuwayhid B. Hemodynamic changes during pregnancy in the rabbit. Am J Obstet Gynecol 1979;135(5):590–6.
[437] Hart MV, Hosenpud JD, Hohimer AR, Morton MJ. Hemodynamics during pregnancy and sex steroid administration in guinea pigs. Am J Physiol 1985;249(2 Pt 2):R179–85.
[438] Curran-Everett D, Morris Jr KG, Moore LG. Regional circulatory contributions to increased systemic vascular conductance of pregnancy. Am J Physiol 1991;261(6 Pt 2):H1842–7.
[439] Slangen BF, Out IC, Verkeste CM, Peeters LL. Hemodynamic changes in early pregnancy in chronically instrumented, conscious rats. Am J Physiol 1996;270(5 Pt 2):H1779–84.
[440] Debrah DO, Conrad KP, Danielson LA, Shroff SG. Effects of relaxin on systemic arterial hemodynamics and mechanical properties in conscious rats: sex dependency and dose response. J Appl Physiol 2005;98(3):1013–20.
[441] Debrah DO, Novak J, Matthews JE, Ramirez RJ, Shroff SG, Conrad KP. Relaxin is essential for systemic vasodilation and increased global arterial compliance during early pregnancy in conscious rats. Endocrinology 2006;147(11):5126–31.
[442] Stevenson JC, Macdonald DW, Warren RC, Booker MW, Whitehead MI. Increased concentration of circulating calcitonin gene related peptide during normal human pregnancy. Br Med J (Clin Res Ed) 1986;293(6558):1329–30.
[443] Yallampalli C, Chauhan M, Thota CS, Kondapaka S, Wimalawansa SJ. Calcitonin gene-related peptide in pregnancy and its emerging receptor heterogeneity. Trends Endocrinol Metab 2002;13(6):263–9.
[444] Stennett AK, Qiao X, Falone AE, Koledova VV, Khalil RA. Increased vascular angiotensin type 2 receptor expression and NOS-mediated mechanisms of vascular relaxation in pregnant rats. Am J Physiol Heart Circ Physiol 2009;296(3):H745–55.
[445] Chen K, Merrill DC, Rose JC. The importance of angiotensin II subtype receptors for blood pressure control during mouse pregnancy. Reprod Sci 2007;14(7):694–704.
[446] Gillham JC, Kenny LC, Baker PN. An overview of endothelium-derived hyperpolarising factor (EDHF) in normal and compromised pregnancies. Eur J Obstet Gynecol Reprod Biol 2003;109(1):2–7.
[447] Luksha L, Nisell H, Kublickiene K. The mechanism of EDHF-mediated responses in subcutaneous small arteries from healthy pregnant women. Am J Physiol Regul Integr Comp Physiol 2004;286(6):R1102–9.
[448] MacGillivray I, Rose GA, Rowe B. Blood pressure survey in pregnancy. Clin Sci 1969;37(2):395–407.
[449] Conrad KP. Unveiling the vasodilatory actions and mechanisms of relaxin. Hypertension 2010;56(1):2–9.
[450] Hibbard JU, Shroff SG, Lindheimer MD. Cardiovascular alterations in normal and preeclamptic pregnancy. In: Lindheimer MD, Cunningham FG, Roberts JM, editors. Chesley's hypertensive disorders in pregnancy. 3rd ed. Elsevier Press; 2009.
[451] Report of the National high blood pressure education program working group on high blood pressure in pregnancy. Am J Obstet Gynecol 2000;183(1):S1–S22.
[452] ACOG practice bulletin. Diagnosis and management of preeclampsia and eclampsia. Number 33, January 2002. Obstet Gynecol 2002;99(1):159–67.
[453] Page EW, Christianson RE. The impact of mean arterial pressure in the middle trimester upon the outcome of pregnancy. Am J Obstet Gynecol 1976;125:740–6.
[454] Sibai BM, Caritis SN, Thom E, Klebanoff M, McNellis D, Rocco L, et al. Prevention of preeclampsia with low-dose aspirin in healthy, nulliparous pregnant women. The National institute of child health and human development network of maternal-fetal medicine units. N Engl J Med 1993;329(17):1213–8.
[455] Blank SG, Helseth G, Pickering TG, West JE, August P. How should diastolic blood pressure be defined during pregnancy? Hypertension 1994;24(2):234–40.
[456] de Swiet M, Shennan A. Blood pressure measurement in pregnancy. Br J Obstet Gynaecol 1996;103(9):862–3.
[457] Johenning AR, Barron WM. Indirect blood pressure measurement in pregnancy: Korotkoff phase 4 versus phase 5. Am J Obstet Gynecol 1992;167(3):577–80.
[458] Shennan A, Gupta M, Halligan A, Taylor DJ, de Swiet M. Lack of reproducibility in pregnancy of Korotkoff phase IV as measured by mercury sphygmomanometry. Lancet 1996;347(8995):139–42.
[459] Brown MA, Lindheimer MD, deSwiet M, van Assche A, Moutquin JM. The classification and diagnosis of the hypertensive disorders of pregnancy: Statement of the International Society for the Study of Hypertension in Pregnancy. Hypertens Preg 2001;20:9–15.
[460] Brown MA, Buddle ML. What's in a name? Problems with the classification of hypertension in pregnancy. J Hypertens 1997;15(10):1049–54.
[461] Group NHBPEPW. Consensus report on high blood pressure in pregnancy. Am J Obstet Gynecol 1990;163: 1689–712.
[462] Greenberg M, Moawad AH, Wieties BM, Goldberg LI, Kaplan EI, Greenberg B, et al. Extraadrenal pheochromocytoma: detection during pregnancy using MR imaging. Radiology 1986;161 (2):475–6.
[463] Aron DC, Schnall AM, Sheeler LR. Cushing's syndrome and pregnancy. Am J Obstet Gynecol 1990;162(1):244–52.
[464] Finnerty Jr FA, Buchholz JH, Guillaudeu RL. A pressor phenomenon associated with the postpartum period. J Am Med Assoc 1957;165(7):778–80.
[465] Piver MS, Corson SL, Bolognese RJ. Hypertension 6 weeks post partum in apparently normal women. A reappraisal and challenge. Obstet Gynecol 1967;30(2):238–41.
[466] Ness RB, Roberts JM. Epidemiology of hypertension. In: Lindheimer MD, Roberts JM, Cunningham FG, editors. Chesley's hypertension in pregnancy. 2nd ed. Stamford: Appleton & Lange; 1999.
[467] Villar J, Say L, Gulmezoglu AM. Eclampsia and pre-eclampsia: a worldwide health problem for 2000 years. In: Critchley H,

McLean A, Poston L, editors. Pre-eclampsia. London: RCOG Press; 2000. p. 189–207.

[468] Ness RB, Roberts JM. Heterogeneous causes constituting the single syndrome of preeclampsia: a hypothesis and its implications. Am J Obstet Gynecol 1996;175(5):1365–70.

[469] Villar J, Abdel-Aleem H, Merialdi M, et al. WHO randomized trial of calcium supplementation among low calcium intake pregnant women. Am J Obstet Gynecol 2005;: [Submitted].

[470] Belizan JM, Villar J, Gonzalez L, Campodonico L, Bergel E. Calcium supplementation to prevent hypertensive disorders of pregnancy. N Engl J Med 1991;325(20):1399–405.

[471] CLASP: a randomised trial of low-dose aspirin for the prevention and treatment of pre-eclampsia among 9364 pregnant women. CLASP (Collaborative Low-dose Aspirin Study in Pregnancy) Collaborative Group. Lancet 1994;343(8898): 619–629.

[472] Levine RJ, Hauth JC, Curet LB, Sibai BM, Catalano PM, Morris CD, et al. Trial of calcium to prevent preeclampsia. N Engl J Med 1997;337(2):69–76.

[473] Gaber LW, Lindheimer MD. Pathology: kidney liver and brain. In: Lindheimer M, Roberts JM, Cunningham FG, editors. Chesley's hypertensive disorders in pregnancy. 2nd ed. Stamford: Appleton & Lange; 1999.

[474] Irgens HU, Reisaeter L, Irgens LM, Lie RT. Long term mortality of mothers and fathers after pre-eclampsia: population based cohort study. BMJ 2001;323(7323):1213–7.

[475] von Dadelszen P, Magee LA, Roberts JM. Subclassification of preeclampsia. Hypertens Pregnancy. 2003;22(2):143–8.

[476] Brown CE, Cunningham FG, Pritchard JA. Convulsions in hypertensive, proteinuric primiparas more than 24 hours after delivery. Eclampsia or some other cause? J Reprod Med 1987;32(7):499–503.

[477] Watson DL, Sibai BM, Shaver DC, Dacus JV, Anderson GD. Late postpartum eclampsia: an update. South Med J. 1983;76 (12):1487–9.

[478] Hirshfield J, Lam C, Karumanchi SA, Lindheimer MD. Late post-partum eclampsia:Examples and review. Obstet Gynecol Surv 2005;: [Submitted]

[479] Katz M, Kroll D, Pak I, Osimoni A, Hirsch M. Puerperal hypertension, stroke, and seizures after suppression of lactation with bromocriptine. Obstet Gynecol 1985;66 (6):822–4.

[480] Postpartum hypertension, seizures, strokes reported with bromocriptine. FDA Drug Bull. 1984;14(1):3–4.

[481] Watson DL, Bhatia RK, Norman GS, Brindley BA, Sokol RJ. Bromocriptine mesylate for lactation suppression: a risk for postpartum hypertension? Obstet Gynecol 1989;74 (4):573–6.

[482] Cooper DW, Brennecke SP, Wilton AN. Genetics of Preeclampsia. Hypertens Preg 1992;12:1–23.

[483] Arngrimsson R, Purandare S, Connor M, Walker JJ, Bjornsson S, Soubrier F, et al. Angiotensinogen: a candidate gene involved in preeclampsia? Nat Genet 1993;4 (2):114–5.

[484] Ward K, Hata A, Jeunemaitre X, Helin C, Nelson L, Namikawa C, et al. A molecular variant of angiotensinogen associated with preeclampsia. Nat Genet 1993;4(1):59–61.

[485] Grandone E, Margaglione M, Colaizzo D, Cappucci G, Paladini D, Martinelli P, et al. Factor V Leiden, C > T MTHFR polymorphism and genetic susceptibility to preeclampsia. Thromb Haemost 1997;77(6):1052–4.

[486] Sohda S, Arinami T, Hamada H, Yamada N, Hamaguchi H, Kubo T. Methylenetetrahydrofolate reductase polymorphism and pre-eclampsia. J Med Genet 1997;34(6):525–6.

[487] Lachmeijer AM, Dekker GA, Pals G, Aarnoudse JG, ten Kate LP, Arngrimsson R. Searching for preeclampsia genes: the current position. Eur J Obstet Gynecol Reprod Biol 2002;105 (2):94–113.

[488] van Dijk M, Mulders J, Poutsma A, Konst AA, Lachmeijer AM, Dekker GA, et al. Maternal segregation of the Dutch preeclampsia locus at 10q22 with a new member of the winged helix gene family. Nat Genet 2005;37(5):514–9.

[489] Conrad KP, Benyo DF. Placental cytokines and the pathogenesis of preeclampsia. Am J Reprod Immunol 1997;37(3):240–9.

[490] Main E, Chiang M, Colbern G. Nulliparous preeclampsia (PE) is associated with placental expression of a variant allele of the new histocompatibility gene HLA-G. Am J Obstet Gynecol 1994;170:289.

[491] Taylor RN. Review: immunobiology of preeclampsia. Am J Reprod Immunol 1997;37(1):79–86.

[492] Ward KW, Lindheimer MD. Genetic factors. In: Lindheimer MD, Roberts JM, Cunningham FG, editors. Chesley's hypertensive disorders in pregnancy. 2nd ed. Stamford: Appleton & Lange; 1999.

[493] Bdolah Y, Sukhatme VP, Karumanchi SA. Angiogenic imbalance in the pathophysiology of preeclampsia: newer insights. Semin Nephrol 2004;24(6):548–56.

[494] Gant NF, Daley GL, Chand S, Whalley PJ, MacDonald PC. A study of angiotensin II pressor response throughout primigravid pregnancy. J Clin Invest 1973;52(11):2682–9.

[495] Fitzgerald DJ, Fitzgerald GA. Eicosanoids in the pathogenesis of preeclampsia. In: Laragh JH, Brenner BM, editors. Hypertension: pathology, diagnosis and management. New York: Raven Press; 1990. p. 1789–807.

[496] McGiff JG, Carrol MD. Magnesium, platelets and the vasculature in preeclampsia-eclampsia. Hypertens Preg 1994;13: 217–26.

[497] Nagai Y, Hara N, Yamaguchi S, Nakanishi K, Masaki K, Tanaka M, et al. Immunohistochemical study of endothelin-1 in preeclamptic nephropathy. Am J Kidney Dis 1997;29(3): 345–54.

[498] Taylor RN, Roberts JM. Endothelial cell dysfunction. In: Lindheimer MD, Roberts JM, Cunningham FG, editors. Chesley's hypertensive disorders in pregnancy. 2nd ed. Stamford: Appleton & Lange; 1999. p. 395–401.

[499] Hubel CA, Roberts JM. Lipid metabolism and oxidative stress. In: Lindheimer MD, Roberts JM, Cunningham FG, editors. Chesley's hypertensive disorders in pregnancy. 2nd ed. Stamford: Appleton & Lange; 1999.

[500] Cockell AP, Poston L. Flow-mediated vasodilatation is enhanced in normal pregnancy but reduced in preeclampsia. Hypertension 1997;30(2 Pt 1):247–51.

[501] Pascoal IF, Lindheimer MD, Nalbantian-Brandt C, Umans JG. Preeclampsia selectively impairs endothelium-dependent relaxation and leads to oscillatory activity in small omental arteries. J Clin Invest 1998;101(2):464–70.

[502] Taufield PA, Ales KL, Resnick LM, Druzin ML, Gertner JM, Laragh JH. Hypocalciuria in preeclampsia. N Engl J Med 1987;316(12):715–8.

[503] Easterling TR, Benedetti TJ, Schmucker BC, Millard SP. Maternal hemodynamics in normal and preeclamptic pregnancies: a longitudinal study. Obstet Gynecol 1990;76(6): 1061–9.

[504] Boslo P, O'Herlihy C, Conroy R, McKenna P. Maternal central hemodynamics in hypertensive disorders of pregnancy. Am J Obstet Gynecol 1998;178(S6):.

[505] Mabie WC, Ratts TE, Sibai BM. The central hemodynamics of severe preeclampsia. Am J Obstet Gynecol 1989;161(6 Pt 1): 1443–8.

[506] Visser W, Wallenburg HC. Central hemodynamic observations in untreated preeclamptic patients. Hypertension 1991;17(6 Pt 2):1072–7.
[507] Baker PN. Platelet and coagulation abnormalities. Stamford, CT: Appleton & Lange; 1999.
[508] Byrd DE, Riely CA. Liver disease in preeclampsia. Gastroenterologist 1996;4(1):65–9.
[509] Minakami H, Oka N, Sato T, Tamada T, Yasuda Y, Hirota N. Preeclampsia: a microvesicular fat disease of the liver? Am J Obstet Gynecol 1988;159(5):1043–7.
[510] Sibai BM, Anderson GD, McCubbin JH. Eclampsia II. Clinical significance of laboratory findings. Obstet Gynecol 1982;59 (2):153–7.
[511] Donaldson JO. The brain in preeclampsia. Hypertens Preg 1994;13:115.
[512] van den Veyver IB, Belfort MA, Rowe TF, Moise KJ. Cerebral vasospasm in eclampsia: transcranial Doppler ultrasound findings. J Maternal Fetal Med 1994;3:9–13.
[513] Belfort M, Whiman I, Grunefeld C. Preeclamptic women with headache are much more likely to have abnormal cerebral perfusin than thse without. Am J Obstet Gynecol 1998;173(S3).
[514] Williams K, Wilson S. Eclampsia occurs with a significan fall in cerebrovascular resistance. Am J Obstet Gynecol 1998;177:S6.
[515] Morriss MC, Twickler DM, Hatab MR, Clarke GD, Peshock RM, Cunningham FG. Cerebral blood flow and cranial magnetic resonance imaging in eclampsia and severe preeclampsia. Obstet Gynecol 1997;89(4):561–8.
[516] Dahmus MA, Barton JR, Sibai BM. Cerebral imaging in eclampsia: magnetic resonance imaging versus computed tomography. Am J Obstet Gynecol 1992;167(4 Pt 1):935–41.
[517] Zeeman GG, Hatab MR, Twickler DM. Increased cerebral blood flow in preeclampsia with magnetic resonance imaging. Am J Obstet Gynecol 2004;191(4):1425–9.
[518] Hinchey J, Chaves C, Appignani B, Breen J, Pao L, Wang A, et al. A reversible posterior leukoencephalopathy syndrome. N Engl J Med 1996;334(8):494–500.
[519] Venuto RC, Lindheimer MD. Animal models. In: Lindheimer MD, Roberts JM, Cunningham FG, editors. Chesley's hypertensive disorders in pregnancy. 2nd ed. Stamford: Appleton & Lange; 1999.
[520] Fisher SJ, Roberts JM. Defects in placentation and placental perfusion. In: Lindheimer MD, Roberts JM, Cunningham FG, editors. Chesley's hypertensive disorders in pregnancy. 2nd ed. Stamford: Appleton & Lange; 1999.
[521] Robertson WB, Brosens I, Dixon G. Maternal uterine vascular lesions in the hypertensive complications of pregnancy. In: Lindheimer MD, Katz AI, Zuspan F, editors. Hypertension in pregnancy. New York: John Wiley; 1976. p. 115–26.
[522] Zhou Y, Damsky CH, Fisher SJ. Preeclampsia is associated with failure of human cytotrophoblasts to mimic a vascular adhesion phenotype. One cause of defective endovascular invasion in this syndrome? J Clin Invest 1997;99 (9):2152–64.
[523] Fisher SJ, Damsky CH. Human cytotrophoblast invasion. Semin Cell Biol 1993;4(3):183–8.
[524] Damsky CH, Fitzgerald ML, Fisher SJ. Distribution patterns of extracellular matrix components and adhesion receptors are intricately modulated during first trimester cytotrophoblast differentiation along the invasive pathway, in vivo. J Clin Invest 1992;89(1):210–22.
[525] Damsky CH, Librach C, Lim KH, Fitzgerald ML, McMaster MT, Janatpour M, et al. Integrin switching regulates normal trophoblast invasion. Development 1994;120(12):3657–66.
[526] Zhou Y, Fisher SJ, Janatpour M, Genbacev O, Dejana E, Wheelock M, et al. Human cytotrophoblasts adopt a vascular phenotype as they differentiate. A strategy for successful endovascular invasion? J Clin Invest 1997;99(9):2139–51.
[527] Zhou Y, Damsky CH, Chiu K, Roberts JM, Fisher SJ. Preeclampsia is associated with abnormal expression of adhesion molecules by invasive cytotrophoblasts. J Clin Invest 1993;91(3):950–60.
[528] Zhou Y, Genbacev O, Fisher SJ. The human placenta remodels the uterus by using a combination of molecules that govern vasculogenesis or leukocyte extravasation. Ann N Y Acad Sci 2003;995:73–83.
[529] Fisher SJ. The placental problem: Linking abnormal cytotrophoblast differentiation to the maternal symptoms of preeclampsia. Reprod Biol Endocrinol 2004;2(1):53.
[530] Roberts JM. Endothelial dysfunction in preeclampsia. Semin Reprod Endocrinol 1998;16(1):5–15.
[531] Mills JL, DerSimonian R, Raymond E, Morrow JD, Roberts II LJ, Clemens JD, et al. Prostacyclin and thromboxane changes predating clinical onset of preeclampsia: a multicenter prospective study. JAMA 1999;282(4):356–62.
[532] Clark BA, Halvorson L, Sachs B, Epstein FH. Plasma endothelin levels in preeclampsia: elevation and correlation with uric acid levels and renal impairment. Am J Obstet Gynecol 1992;166(3):962–8.
[533] Friedman SA, Schiff E, Emeis JJ, Dekker GA, Sibai BM. Biochemical corroboration of endothelial involvement in severe preeclampsia. Am J Obstet Gynecol 1995;172(1 Pt 1):202–3.
[534] Hsu CD, Iriye B, Johnson TR, Witter FR, Hong SF, Chan DW. Elevated circulating thrombomodulin in severe preeclampsia. Am J Obstet Gynecol 1993;169(1):148–9.
[535] Taylor RN, Crombleholme WR, Friedman SA, Jones LA, Casal DC, Roberts JM. High plasma cellular fibronectin levels correlate with biochemical and clinical features of preeclampsia but cannot be attributed to hypertension alone. Am J Obstet Gynecol 1991;165(4 Pt 1):895–901.
[536] Roberts JM, Edep ME, Goldfien A, Taylor RN. Sera from preeclamptic women specifically activate human umbilical vein endothelial cells in vitro: morphological and biochemical evidence. Am J Reprod Immunol 1992;27(3–4): 101–8.
[537] Benyo DF, Smarason A, Redman CW, Sims C, Conrad KP. Expression of inflammatory cytokines in placentas from women with preeclampsia. J Clin Endocrinol Metab 2001;86 (6):2505–12.
[538] Conrad KP, Miles TM, Benyo DF. Circulating levels of immunoreactive cytokines in women with preeclampsia. Am J Reprod Immunol 1998;40(2):102–11.
[539] Savvidou MD, Hingorani AD, Tsikas D, Frolich JC, Vallance P, Nicolaides KH. Endothelial dysfunction and raised plasma concentrations of asymmetric dimethylarginine in pregnant women who subsequently develop pre-eclampsia. Lancet 2003;361(9368):1511–7.
[540] Page NM, Woods RJ, Gardiner SM, Lomthaisong K, Gladwell RT, Butlin DJ, et al. Excessive placental secretion of neurokinin B during the third trimester causes pre-eclampsia. Nature 2000;405(6788):797–800.
[541] Redman CW, Sargent IL. Placental debris, oxidative stress and pre-eclampsia. Placenta 2000;21(7):597–602.
[542] Maynard SE, Min JY, Merchan J, Lim KH, Li J, Mondal S, et al. Excess placental soluble fms-like tyrosine kinase 1 (sFlt1) may contribute to endothelial dysfunction, hypertension, and proteinuria in preeclampsia. J Clin Invest 2003;111 (5):649–58.

[543] Koga K, Osuga Y, Yoshino O, Hirota Y, Ruimeng X, Hirata T, et al. Elevated serum soluble vascular endothelial growth factor receptor 1 (sVEGFR-1) levels in women with preeclampsia. J Clin Endocrinol Metab 2003;88(5):2348–51.

[544] Tsatsaris V, Goffin F, Munaut C, Brichant JF, Pignon MR, Noel A, et al. Overexpression of the soluble vascular endothelial growth factor receptor in preeclamptic patients: pathophysiological consequences. J Clin Endocrinol Metab 2003;88 (11):5555–63.

[545] Luttun A, Tjwa M, Moons L, Wu Y, Angelillo-Scherrer A, Liao F, et al. Revascularization of ischemic tissues by PlGF treatment, and inhibition of tumor angiogenesis, arthritis and atherosclerosis by anti-Flt1. Nat Med 2002;8(8):831–40.

[546] Carmeliet P, Moons L, Luttun A, Vincenti V, Compernolle V, De Mol M, et al. Synergism between vascular endothelial growth factor and placental growth factor contributes to angiogenesis and plasma extravasation in pathological conditions. Nat Med 2001;7(5):575–83.

[547] Dvorak HF. Vascular permeability factor/vascular endothelial growth factor: a critical cytokine in tumor angiogenesis and a potential target for diagnosis and therapy. J Clin Oncol 2002;20 (21):4368–80.

[548] Kendall RL, Thomas KA. Inhibition of vascular endothelial cell growth factor activity by an endogenously encoded soluble receptor. Proc Natl Acad Sci U S A. 1993;90(22):10705–9.

[549] Chaiworapongsa T, Romero R, Kim YM, Kim GJ, Kim MR, Espinoza J, et al. Plasma soluble vascular endothelial growth factor receptor-1 concentration is elevated prior to the clinical diagnosis of pre-eclampsia. J Matern Fetal Neonatal Med 2005;17(1):3–18.

550. Levine RJ, Karumanchi SA. Circulating angiogenic factors in preeclampsia. Clin Obstet Gynecol 2005;48(2):372–86.

[551] Levine RJ, Maynard SE, Qian C, Lim KH, England LJ, Yu KF, et al. Circulating angiogenic factors and the risk of preeclampsia. N Engl J Med 2004;350(7):672–83.

[552] Hertig A, Berkane N, Lefevre G, Toumi K, Marti HP, Capeau J, et al. Maternal serum sFlt1 concentration is an early and reliable predictive marker of preeclampsia. Clin Chem 2004;50 (9):1702–3.

[553] Chaiworapongsa T, Romero R, Espinoza J, Bujold E, Mee Kim Y, Goncalves LF, et al. Evidence supporting a role for blockade of the vascular endothelial growth factor system in the pathophysiology of preeclampsia. Young investigator award. Am J Obstet Gynecol 2004;190(6):1541–7 [discussion 7–50].

[554] Taylor RN, Grimwood J, Taylor RS, McMaster MT, Fisher SJ, North RA. Longitudinal serum concentrations of placental growth factor: evidence for abnormal placental angiogenesis in pathologic pregnancies. Am J Obstet Gynecol 2003;188 (1):177–82.

[555] Torry DS, Wang HS, Wang TH, Caudle MR, Torry RJ. Preeclampsia is associated with reduced serum levels of placenta growth factor. Am J Obstet Gynecol 1998;179(6 Pt 1): 1539–44.

[556] Livingston JC, Chin R, Haddad B, McKinney ET, Ahokas R, Sibai BM. Reductions of vascular endothelial growth factor and placental growth factor concentrations in severe preeclampsia. Am J Obstet Gynecol 2000;183(6):1554–7.

[557] Thadhani R, Mutter WP, Wolf M, Levine RJ, Taylor RN, Sukhatme VP, et al. First trimester placental growth factor and soluble fms-like tyrosine kinase 1 and risk for preeclampsia. J Clin Endocrinol Metab 2004;89(2):770–5.

[558] Levine RJ, Thadhani R, Qian C, Lam C, Lim KH, Yu KF, et al. Urinary placental growth factor and risk of preeclampsia. JAMA 2005;293(1):77–85.

[559] Kabbinavar F, Hurwitz HI, Fehrenbacher L, Meropol NJ, Novotny WF, Lieberman G, et al. Phase II, randomized trial comparing bevacizumab plus fluorouracil (FU)/leucovorin (LV) with FU/LV alone in patients with metastatic colorectal cancer. J Clin Oncol 2003;21(1):60–5.

[560] Yang JC, Haworth L, Sherry RM, Hwu P, Schwartzentruber DJ, Topalian SL, et al. A randomized trial of bevacizumab, an anti-vascular endothelial growth factor antibody, for metastatic renal cancer. N Engl J Med 2003;349(5):427–34.

[561] Eremina V, Sood M, Haigh J, Nagy A, Lajoie G, Ferrara N, et al. Glomerular-specific alterations of VEGF-A expression lead to distinct congenital and acquired renal diseases. J Clin Invest 2003;111(5):707–16.

[562] Tuohy JF, James DK. Pre-eclampsia and trisomy 13. Br J Obstet Gynaecol 1992;99(11):891–4.

[563] Bdolah Y, Palomaki GE, Yaron Y, et al. Circulating angiogenic proteins in trisomy 13. Am J Obstet Gynecol 2005;: [In Press]

[564] Wolf M, Shah A, Lam C, Martinez A, Smirnakis KV, Epstein FH, et al. Circulating levels of the antiangiogenic marker sFLT-1 are increased in first versus second pregnancies. Am J Obstet Gynecol 2005;193(1):16–22.

[565] Lindheimer MD. Unraveling the mysteries of preeclampsia. Am J Obstet Gynecol 2005;193(1):3–4.

[566] Nagamatsu T, Fujii T, Kusumi M, Zou L, Yamashita T, Osuga Y, et al. Cytotrophoblasts up-regulate soluble fms-like tyrosine kinase-1 expression under reduced oxygen: an implication for the placental vascular development and the pathophysiology of preeclampsia. Endocrinology 2004;145 (11):4838–45.

[567] Powers RW, Roberts JM, Cooper KM, Gallaher MJ, Frank MP, Harger GF, et al. Maternal serum soluble fms-like tyrosine kinase 1 concentrations are not increased in early pregnancy and decrease more slowly postpartum in women who develop preeclampsia. Am J Obstet Gynecol 2005;193 (1):185–91.

[568] Hirtenlehner K, Pollheimer J, Lichtenberger C, Wolschek MF, Zeisler H, Husslein P, et al. Elevated serum concentrations of the angiogenesis inhibitor endostatin in preeclamptic women. J Soc Gynecol Investig 2003;10(7):412–7.

[569] Venkatesha S, Toporsian M, Lam C, Hanai J, Mammoto T, Kim YM, et al. Soluble endoglin contributes to the pathogenesis of preeclampsia. Nat Med 2006;12(6):642–9.

[570] Levine RJ, Lam C, Qian C, Yu KF, Maynard SE, Sachs BP, et al. Soluble endoglin and other circulating antiangiogenic factors in preeclampsia. N Engl J Med 2006;355(10):992–1005.

[571] Vaisbuch E, Whitty JE, Hassan SS, Romero R, Kusanovic JP, Cotton DB, et al. Circulating angiogenic and antiangiogenic factors in women with eclampsia. Am J Obstet Gynecol 2011;204(2):152 e1–9 e9.

[572] Wallukat G, Homuth V, Fischer T, Lindschau C, Horstkamp B, Jupner A, et al. Patients with preeclampsia develop agonistic autoantibodies against the angiotensin AT1 receptor. J Clin Invest 1999;103(7):945–52.

[573] Dechend R, Homuth V, Wallukat G, Kreuzer J, Park JK, Theuer J, et al. AT(1) receptor agonistic antibodies from preeclamptic patients cause vascular cells to express tissue factor. Circulation 2000;101(20):2382–7.

[574] Xia Y, Wen H, Bobst S, Day MC, Kellems RE. Maternal autoantibodies from preeclamptic patients activate angiotensin receptors on human trophoblast cells. J Soc Gynecol Investig 2003;10 (2):82–93.

[575] Dechend R, Viedt C, Muller DN, Ugele B, Brandes RP, Wallukat G, et al. AT1 receptor agonistic antibodies from

preeclamptic patients stimulate NADPH oxidase. Circulation 2003;107(12):1632–9.
[576] Zhou CC, Zhang Y, Irani RA, Zhang H, Mi T, Popek EJ, et al. Angiotensin receptor agonistic autoantibodies induce pre-eclampsia in pregnant mice. Nat Med 2008;14(8): 855–62.
[577] Dragun D, Muller DN, Brasen JH, Fritsche L, Nieminen-Kelha M, Dechend R, et al. Angiotensin II type 1-receptor activating antibodies in renal-allograft rejection. N Engl J Med 2005;352 (6):558–69.
[578] Roberts JM. Preeclampsia: what we know and what we do not know. Semin Perinatol 2000;24(1):24–8.
[579] Wolf M, Hubel CA, Lam C, Sampson M, Ecker JL, Ness RB, et al. Preeclampsia and future cardiovascular disease: potential role of altered angiogenesis and insulin resistance. J Clin Endocrinol Metab 2004;89(12):6239–43.
[580] Walsh SW, Vaughan JE, Wang Y, Roberts II LJ. Placental isoprostane is significantly increased in preeclampsia. Faseb J. 2000;14(10):1289–96.
[581] Walsh SW. Maternal-placental interactions of oxidative stress and antioxidants in preeclampsia. Semin Reprod Endocrinol 1998;16(1):93–104.
[582] Wang Y, Walsh SW. Antioxidant activities and mRNA expression of superoxide dismutase, catalase, and glutathione peroxidase in normal and preeclamptic placentas. J Soc Gynecol Investig 1996;3(4):179–84.
[583] Wang Y, Walsh SW. Increased superoxide generation is associated with decreased superoxide dismutase activity and mRNA expression in placental trophoblast cells in pre-eclampsia. Placenta 2001;22(2–3):206–12.
[584] Sikkema JM, van Rijn BB, Franx A, Bruinse HW, de Roos R, Stroes ES, et al. Placental superoxide is increased in pre-eclampsia. Placenta 2001;22(4):304–8.
[585] Zusterzeel PL, Peters WH, De Bruyn MA, Knapen MF, Merkus HM, Steegers EA. Glutathione S-transferase isoenzymes in decidua and placenta of preeclamptic pregnancies. Obstet Gynecol 1999;94(6):1033–8.
[586] Zusterzeel PL, Rutten H, Roelofs HM, Peters WH, Steegers EA. Protein carbonyls in decidua and placenta of pre-eclamptic women as markers for oxidative stress. Placenta 2001;22 (2–3):213–9.
[587] Moretti M, Phillips M, Abouzeid A, Cataneo RN, Greenberg J. Increased breath markers of oxidative stress in normal pregnancy and in preeclampsia. Am J Obstet Gynecol 2004;190 (5):1184–90.
[588] Regan CL, Levine RJ, Baird DD, Ewell MG, Martz KL, Sibai BM, et al. No evidence for lipid peroxidation in severe pre-eclampsia. Am J Obstet Gynecol 2001;185(3):572–8.
[589] Llurba E, Gratacos E, Martin-Gallan P, Cabero L, Dominguez C. A comprehensive study of oxidative stress and antioxidant status in preeclampsia and normal pregnancy. Free Radic Biol Med 2004;37(4):557–70.
[590] Podjarny E, Losonczy G, Baylis C. Animal models of pre-eclampsia. Semin Nephrol 2004;24(6):596–606.
[591] Yallampalli C, Garfield RE. Inhibition of nitric oxide synthesis in rats during pregnancy produces signs similar to those of preeclampsia. Am J Obstet Gynecol 1993;169(5): 1316–20.
[592] Rayman MP, Bode P, Redman CW. Low selenium status is associated with the occurrence of the pregnancy disease pre-eclampsia in women from the United Kingdom. Am J Obstet Gynecol 2003;189(5):1343–9.
[593] Chappell LC, Seed PT, Briley AL, Kelly FJ, Lee R, Hunt BJ, et al. Effect of antioxidants on the occurrence of pre-eclampsia in women at increased risk: a randomised trial. Lancet 1999;354(9181):810–6.
[594] Sharma JB, Kumar A, Malhotra M, Arora R, Prasad S, Batra S. Effect of lycopene on pre-eclampsia and intra-uterine growth retardation in primigravidas. Int J Gynaecol Obstet 2003;81 (3):257–62.
[595] Poston L, Briley AL, Seed PT, Kelly FJ, Shennan AH. Vitamin C and vitamin E in pregnant women at risk for pre-eclampsia (VIP trial): randomised placebo-controlled trial. Lancet 2006;367(9517):1145–54.
[596] Roberts JM, Myatt L, Spong CY, Thom EA, Hauth JC, Leveno KJ, et al. Vitamins C and E to prevent complications of pregnancy-associated hypertension. N Engl J Med 2010;362 (14):1282–91.
[597] Gaber LW, Spargo BH, Lindheimer MD. Renal pathology in pre-eclampsia. Baillieres Clin Obstet Gynaecol 1994;8 (2):443–68.
[598] Foidart JM, Nochy D, Nusgens B, Foidart JB, Mahieu PR, Lapiere CM, et al. Accumulation of several basement membrane proteins in glomeruli of patients with preeclampsia and other hypertensive syndromes of pregnancy. Possible role of renal prostaglandins and fibronectin. Lab Invest 1983;49 (3):250–9.
[599] Shiiki H, Nishino T, Uyama H, Kimura T, Nishimoto K, Hashimoto T, et al. Alterations in extracellular matrix components and integrins in patients with preeclamptic nephropathy. Virchows Arch 1996;427(6):567–73.
[600] Heaton JM, Turner DR. Persistent renal damage following pre-eclampsia: a renal biopsy study of 13 patients. J Pathol 1985;147(2):121–6.
[601] Kida H, Takeda S, Yokoyama H, Tomosugi N, Abe T, Hattori N. Focal glomerular sclerosis in pre-eclampsia. Clin Nephrol 1985;24(5):221–7.
[602] Lafayette RA, Druzin M, Sibley R, Derby G, Malik T, Huie P, et al. Nature of glomerular dysfunction in pre-eclampsia. Kidney Int 1998;54(4):1240–9.
[603] Lee HS, Kim TS. A morphometric study of preeclamptic nephropathy with focal segmental glomerulosclerosis. Clin Nephrol 1995;44(1):14–21.
[604] Nochy D, Heudes D, Glotz D, Lemoine R, Gentric D, Bruneval P, et al. Preeclampsia associated focal and segmental glomerulosclerosis and glomerular hypertrophy: a morphometric analysis. Clin Nephrol 1994;42(1):9–17.
[605] Nochy D, Hinglais N, Jacquot C, Gaudry C, Remy P, Bariety J. De novo focal glomerular sclerosis in preeclampsia. Clin Nephrol 1986;25(3):116–21.
[606] Packham DK, Mathews DC, Fairley KF, Whitworth JA, Kincaid-Smith PS. Morphometric analysis of pre-eclampsia in women biopsied in pregnancy and post-partum. Kidney Int 1988;34(5):704–11.
[607] Moran P, Baylis PH, Lindheimer MD, Davison JM. Glomerular ultrafiltration in normal and preeclamptic pregnancy. J Am Soc Nephrol 2003;14(3):648–52.
[608] Many A, Westerhausen-Larson A, Kanbour-Shakir A, Roberts JM. Xanthine oxidase/dehydrogenase is present in human placenta. Placenta 1996;17(5–6):361–5.
[609] Kang DH, Finch J, Nakagawa T, Karumanchi SA, Kanellis J, Granger J, et al. Uric acid, endothelial dysfunction and pre-eclampsia: searching for a pathogenetic link. J Hypertens 2004;22(2):229–35.
[610] Gallery EDM, Lindheimer MD. Alterations in volume homeostasis. In: Lindheimer MD, Roberts JM, Cunningham FG, editors. Chesley's hypertensive disorders in pregnancy. 2nd ed. Stamford: Appleton & Lange; 1999.
[611] Silver HM, Seebeck MA, Carlson R. Comparison of total volume in normal, preeclamptic, and nonproteinuric gestational hypertensive pregnancy by simultaneous measurement of red

blood cell and plasma volume. Am J Obstet Gynecol 1998;179:87–93.
[612] Friedman SA, Lindheimer MD. Prediction and differential diagnosis. In: Lindheimer MD, Roberts JM, Cunningham FG, editors. Chesley's hypertensive disorders in pregnancy. Stamford: Appleton & Lange; 1999.
[613] Tidwell SC, Ho HN, Chiu WH, Torry RJ, Torry DS. Low maternal serum levels of placenta growth factor as an antecedent of clinical preeclampsia. Am J Obstet Gynecol 2001;184(6):1267–72.
[614] Tjoa ML, van Vugt JM, Mulders MA, Schutgens RB, Oudejans CB, van Wijk IJ. Plasma placenta growth factor levels in midtrimester pregnancies. Obstet Gynecol 2001;98(4):600–7.
[615] Noori M, Donald AE, Angelakopoulou A, Hingorani AD, Williams DJ. Prospective study of placental angiogenic factors and maternal vascular function before and after preeclampsia and gestational hypertension. Circulation 2010;122 (5):478–87.
[616] Kusanovic JP, Romero R, Chaiworapongsa T, Erez O, Mittal P, Vaisbuch E, et al. A prospective cohort study of the value of maternal plasma concentrations of angiogenic and anti-angiogenic factors in early pregnancy and midtrimester in the identification of patients destined to develop preeclampsia. J Matern Fetal Neonatal Med 2009;22 (11):1021–38.
[617] Poon LC, Kametas NA, Maiz N, Akolekar R, Nicolaides KH. First-trimester prediction of hypertensive disorders in pregnancy. Hypertension 2009;53(5):812–8.
[618] Lim JH, Kim SY, Park SY, Yang JH, Kim MY, Ryu HM. Effective prediction of preeclampsia by a combined ratio of angiogenesis-related factors. Obstet Gynecol 2008;111(6): 1403–9.
[619] Salahuddin S, Lee Y, Vadnais M, Sachs BP, Karumanchi SA, Lim KH. Diagnostic utility of soluble fms-like tyrosine kinase 1 and soluble endoglin in hypertensive diseases of pregnancy. Am J Obstet Gynecol 2007;197(1):28 e1–6.
[620] Ohkuchi A, Hirashima C, Suzuki H, Takahashi K, Yoshida M, Matsubara S, et al. Evaluation of a new and automated electrochemiluminescence immunoassay for plasma sFlt-1 and PlGF levels in women with preeclampsia. Hypertens Res 2010;33 (5):422–7.
[621] Sunderji S, Gaziano E, Wothe D, Rogers LC, Sibai B, Karumanchi SA, et al. Automated assays for sVEGF R1 and PlGF as an aid in the diagnosis of preterm preeclampsia: a prospective clinical study. Am J Obstet Gynecol 2010;202(1):40 e1–7 e7.
[622] Verlohren S, Galindo A, Schlembach D, Zeisler H, Herraiz I, Moertl MG, et al. An automated method for the determination of the sFlt-1/PlGF ratio in the assessment of preeclampsia. Am J Obstet Gynecol 2010;202(2): 161 e1- 161 e11
[623] Collins R, Yusuf S, Peto R. Overview of randomised trials of diuretics in pregnancy. Br Med J (Clin Res Ed) 1985;290 (6461):17–23.
[624] Lindheimer MD. Pre-eclampsia-eclampsia 1996: preventable? Have disputes on its treatment been resolved? Curr Opin Nephrol Hypertens 1996;5(5):452–8.
[625] Sibai BM, Cunningham FG. Prevention of preeclampsia-eclampsia. In: Lindheimer MD, Roberts JM, Cunningham FG, editors. Chesley's hypertensive disorders in pregnancy. 2nd ed. Stamford: Appleton & Lange; 1999.
[626] Duley L, Henderson-Smart DJ, Knight M, King JF. Antiplatelet agents for preventing pre-eclampsia and its complications. Cochrane Database Syst Rev 2004;(1): CD004659.
[627] Villar J, Abalos E, Nardin JM, Merialdi M, Carroli G. Strategies to prevent and treat preeclampsia: evidence from randomized controlled trials. Semin Nephrol 2004;24(6):607–15.
[628] Askie LM, Duley L, Henderson-Smart DJ, Stewart LA. Antiplatelet agents for prevention of pre-eclampsia: a meta-analysis of individual patient data. Lancet 2007;369 (9575):1791–8.
[629] Belizan JM, Villar J, Repke J. The relationship between calcium intake and pregnancy-induced hypertension: up-to-date evidence. Am J Obstet Gynecol 1988;158(4):898–902.
[630] Dekker GA, de Vries JI, Doelitzsch PM, Huijgens PC, von Blomberg BM, Jakobs C, et al. Underlying disorders associated with severe early-onset preeclampsia. Am J Obstet Gynecol 1995;173(4):1042–8.
[631] Chesley SC, Annitto JE, Cosgrove RA. The remote prognosis of eclamptic women. Sixth periodic report. Am J Obstet Gynecol 1976;124(5):446–59.
[632] Bryans Jr CI. The remote prognosis in toxemia of pregnancy. Clin Obstet Gynecol 1966;9(4):973–90.
[633] Sibai BM, Sarinoglu C, Mercer BM. Eclampsia. VII. Pregnancy outcome after eclampsia and long-term prognosis. Am J Obstet Gynecol 1992;166(6 Pt 1):1757–61 [discussion 61–3]
[634] Epstein FH. Late vascular effects of toxemia of pregnancy. N Engl J Med 1964;271:391–5.
[635] Carleton H, Forsythe A, Flores R. Remote prognosis of preeclampsia in women 25 years old and younger. Am J Obstet Gynecol 1988;159(1):156–60.
[636] Sibai BM, el-Nazer A, Gonzalez-Ruiz A. Severe preeclampsia-eclampsia in young primigravid women: subsequent pregnancy outcome and remote prognosis. Am J Obstet Gynecol 1986;155(5):1011–6.
[637] Sibai BM, Mercer B, Sarinoglu C. Severe preeclampsia in the second trimester: recurrence risk and long-term prognosis. Am J Obstet Gynecol 1991;165(5 Pt 1):1408–12.
[638] Jonsdotler LS, Agrimsson R, Gierson RT, Sigualdason J, Sigfusson N. Death rates from ischemic heart disease in women with a history of hypertension in pregnancy. Acta Obstet Gynecol Scand 1995;74:772–6.
[639] Hubel CA, Snaedal S, Ness RB, Weissfeld LA, Geirsson RT, Roberts JM, et al. Dyslipoproteinaemia in postmenopausal women with a history of eclampsia. BJOG 2000;107 (6):776–84.
[640] Laivuori H, Tikkanen MJ, Ylikorkala O. Hyperinsulinemia 17 years after preeclamptic first pregnancy. J Clin Endocrinol Metab 1996;81(8):2908–11.
[641] Wilson BJ, Watson MS, Prescott GJ, Sunderland S, Campbell DM, Hannaford P, et al. Hypertensive diseases of pregnancy and risk of hypertension and stroke in later life: results from cohort study. BMJ 2003;326(7394):845.
[642] Smith GC, Pell JP, Walsh D. Pregnancy complications and maternal risk of ischaemic heart disease: a retrospective cohort study of 129,290 births. Lancet 2001;357 (9273):2002–6.
[643] Vatten LJ, Romundstad PR, Trichopoulos D, Skjaerven R. Pre-eclampsia in pregnancy and subsequent risk for breast cancer. Br J Cancer 2002;87(9):971–3.
[644] Mogren I, Stenlund H, Hogberg U. Long-term impact of reproductive factors on the risk of cervical, endometrial, ovarian and breast cancer. Acta Oncol 2001;40 (7):849–54.
[645] Levine RJ, Vatten LJ, Horowitz GL, Qian C, Romundstad PR, Yu KF, et al. Pre-eclampsia, soluble fms-like tyrosine kinase 1, and the risk of reduced thyroid function: nested case-control and population based study. BMJ 2009;339:b4336.

[646] Vikse BE, Irgens LM, Leivestad T, Skjaerven R, Iversen BM. Preeclampsia and the risk of end-stage renal disease. N Engl J Med 2008;359(8):800–9.
[647] Leveno KJ, Cunningham FG. Management of preeclampsia. In: Lindheimer MD, Roberts JM, Cunningham FG, editors. Chesley's hypertensive disorders in pregnancy. 2nd ed. Stamford: Appleton & Lange; 1999.
[648] Umans JG, Lindheimer MD. Antihypertensive treatment. In: Lindheimer MD, Roberts JM, Cunningham FG, editors. Chesley's hypertensive disorders in pregnancy. 2nd ed. Stamford: Appleton and Lange; 1999.
[649] Barron WM. Hypertension. In: Mosby, editor. Medical disorders during pegnancy. St. Louis: Mosby; 1995. p. 1–36.
[650] Chari RS, Friedman SA, O'Brien JM, Sibai BM. Daily antenatal testing in women with severe preeclampsia. Am J Obstet Gynecol 1995;173(4):1207–10.
[651] Schiff E, Friedman SA, Sibai BM. Conservative management of severe preeclampsia remote from term. Obstet Gynecol 1994;84 (4):626–30.
[652] Sibai BM, Akl S, Fairlie F, Moretti M. A protocol for managing severe preeclampsia in the second trimester. Am J Obstet Gynecol 1990;163(3):733–8.
[653] Sibai BM, Mercer BM, Schiff E, Friedman SA. Aggressive versus expectant management of severe preeclampsia at 28 to 32 weeks' gestation: a randomized controlled trial. Am J Obstet Gynecol 1994;171(3):818–22.
[654] Visser W, Wallenburg HC. Temporising management of severe pre-eclampsia with and without the HELLP syndrome. Br J Obstet Gynaecol 1995;102(2):111–7.
[655] Chua S, Redman CW. Are prophylactic anticonvulsants required in severe pre-eclampsia? Lancet 1991;337(8735): 250–1.
[656] Which anticonvulsant for women with eclampsia? Evidence from the Collaborative Eclampsia Trial. Lancet 1995;345 (8963):1455–1463.
[657] Lucas MJ, Leveno KJ, Cunningham FG. A comparison of magnesium sulfate with phenytoin for the prevention of eclampsia. N Engl J Med 1995;333(4):201–5.
[658] Altman D, Carroli G, Duley L, Farrell B, Moodley J, Neilson J, et al. Do women with pre-eclampsia, and their babies, benefit from magnesium sulphate? The Magpie Trial: a randomised placebo-controlled trial. Lancet 2002;359(9321): 1877–90.
[659] Duley L, Henderson-Smart D. Magnesium sulphate versus phenytoin for eclampsia. Cochrane Database Syst Rev 2003;(4): CD000128.
[660] Sibai BM. Magnesium sulfate prophylaxis in preeclampsia: evidence from randomized trials. Clin Obstet Gynecol 2005;48 (2):478–88.
[661] Sibai BM. The magpie trial. Lancet 2002;360(9342):1329 [author reply 31–32]
[662] Rey E, Couturier A. The prognosis of pregnancy in women with chronic hypertension. Am J Obstet Gynecol 1994;171 (2):410–6.
[663] Podymow T, August P, Umans JG. Antihypertensive therapy in pregnancy. Semin Nephrol 2004;24(6):616–25.
[664] Gallery ED. Hypertension in pregnancy. Practical management recommendations. Drugs 1995;49(4):555–62.
[665] Cooper WO, Hernandez-Diaz S, Arbogast PG, Dudley JA, Dyer S, Gideon PS, et al. Major congenital malformations after first-trimester exposure to ACE inhibitors. N Engl J Med 2006;354(23):2443–51.
[666] Lam C, Lim KH, Karumanchi SA. Circulating angiogenic factors in the pathogenesis and prediction of preeclampsia. Hypertension 2005;46(5):1077–85.
[667] Powe CE, Levine RJ, Karumanchi SA. Preeclampsia, a disease of the maternal endothelium: the role of antiangiogenic factors and implications for later cardiovascular disease. Circulation 2011;123(24):2856–69.

This page intentionally left blank

CHAPTER

82

Immune and Inflammatory Glomerular Diseases

Anup Manoharon[1], *Jeffrey R. Schelling*[2], *Matthew Diamond*[1], *Moonja Chung-Park*[3], *Michael Madaio*[1] *and John R. Sedor*[2]

[1]Division of Nephrology, Department of Medicine, Medical College of Georgia, Augusta, Georgia, USA
[2]Department of Medicine, The MetroHealth System and Case Western Reserve University, Cleveland, Ohio, USA
[3]Department of Pathology, The MetroHealth System and Case Western Reserve University, Cleveland, Ohio, USA

GLOMERULONEPHRITIS

Acute glomerulonephritis (AGN) is characterized by the sudden appearance of hematuria, proteinuria, and red blood cell casts, whereas subacute and chronic forms present more indolently. The differential diagnosis is listed in Table 82.1.[1] This discussion will include consideration of the incidence, pathogenesis, pathology, clinical presentation, prognosis and treatment, with emphasis on *primary* forms of the syndrome, including acute post-infectious GN, idiopathic membranoproliferative glomerulonephritis (MPGN) anti-glomerular basement membrane (GBM) disease and IgA nephropathy. Thrombotic microangiopathies will be discussed briefly, since its clinical presentation often mimics that of AGN. Our main focus is on human forms of the disease, and neither the differential diagnosis nor pathophysiology of asymptomatic hematuria or asymptomatic proteinuria is discussed as separate entities, since non-glomerular disease entities may cause them. Nevertheless, these findings may be discovered in patients with less severe forms of diseases discussed below. Furthermore, other diseases may present with features that mimic acute glomerulonephritis and should be considered in the differential diagnosis (Table 82.2). Overall, the history, physical exam, serology and pathology are useful in distinguishing primary renal diseases from systemic diseases with renal manifestations, determining the extent of inflammation and fibrosis, and defining the optimal therapeutic approach.

Acute Post-Streptococcal and Post-Infectious GN

Many infections have been associated with acute GN (e.g., Table 82.3), but acute post-streptococcal glomerulonephritis (APSGN) remains the prototype. It is distinguished by typical clinical presentation, serology, pathology and course. APSGN occurs in episodic/sporadic or in epidemic form; children are affected more often than adults (peak age 2–6y), and males more commonly have overt nephritis despite a higher penetrance in females.[2,3] Group A streptococci account for most cases, and specific subtypes predominate.[4] However other infectious organisms have been associated with the syndrome. Pharyngeal infections dominate in temperate zones, whereas skin infections are more commonly precede disease in the tropics.

Pathogenesis

Three major theories have been proposed with evidence supporting each one. All involve infection with nephritogenic strains (Table 82.4). Unique antigenic determinants are responsible for glomerular localization that leads to alternate complement pathway activation. Amplification of disease occurs initially by anti-streptococcal antibodies binding to glomerular bound antigen, and subsequently by anti-IgG response. The latter results from enzymatic modification of IgG by streptococcal enzymes that lead to altered IgG, production of anti-IgG, localization of the altered IgG in

Seldin and Giebisch's The Kidney, Fifth Edition.
DOI: http://dx.doi.org/10.1016/B978-0-12-381462-3.00082-3

© 2013 Elsevier Inc. All rights reserved.

TABLE 82.1 Major Causes of Acute Nephritis

Low Serum Complement Level*	Normal Serum Complement Level
Systemic Diseases	**Systemic Diseases**
• Systemic Lupus Erythematosus (focal ~75%, diffuse ~90%)*	• Polyarteritis nodosa
• Cryoglobulinemia (~85%)	• Wegener's granulomatosis
• Subacute bacterial endocarditis (~90%)	• Hypersensitivity vasculitis
• "Shunt" nephritis (~90%)	• Henoch-Schonlein purpura
	• Goodpasture's syndrome
	• Visceral abscess
Renal Diseases	Renal Diseases
• Acute poststreptococcal GN (~90%)	• IgG-IgA nephropathy
• Membranoproliferative GN	• Idiopathic RPGN (rapidly progressive GN)
– Type I (~50–80%)**	– Anti-GBM disease
– Type II (~80–90%)	– Pauci-immune*** (no immune deposits)
	– Immune-deposit disease

Table from Madaio, MP, Harrington, JT: The diagnosis of glomerular diseases: Acute GN and the nephrotic syndrome. Arch Intern Med: 161: 25-34, 2001.[1]
**Percentages indicate the approximate frequencies of depressed C3 or hemolytic complement levels during the course of disease*
***Most common pathologic findings associated with hepatitis C infection (see text)*
****Pauci-immune indicates lack of significant glomerular deposition of immunoglobulin by direct immunofluorescence. Many patients have circulating ANCA (see text)*
Normal serum complement levels indicate that production of complement components is keeping up with consumption; it does not exclude participation of complement in the inflammatory process. Repeat measurements useful (2–3x, one week apart) consistently normal serum levels are useful in narrowing the diagnostic possibilities

TABLE 82.2 Disorders Mimicking Acute GN

- Hereditary Nephritis
- Hemolytic-Uremic Syndrome (HUS)
- Thrombotic Thrombocytopenic Purpura (TTP)
- Atheroembolic Renal Disease
- Malignant Hypertension
- Acute Interstitial Nephritis
- Acute Tubular Necrosis

glomeruli, with FcR engagement and complement activation; binding of the latter to glomerular IgG deposits, further exacerbates disease.

Pathology

There is diffuse or focal GN with cellular infiltration and endogenous cellular proliferation.[5–7] Early in the course ("exudative phase") there are neutrophils, eosinophils, lymphocytes and monocytes in capillaries, associated with endothelial and mesangial cell proliferation.[4,6,8,9] Mesangial expansion and lumen occlusion is

TABLE 82.3 Other Infectious Conditions Associated With Glomerular Disease And The Most Commonly Associated Lesions.

Infectious Agent	Pathology
Viral Infections	
Hepatitis B	Membranous GN
	MPGN
	Polyarteritis nodosa
Hepatitis C	MPGN
	Membranous GN
CMV	MPGN
Parovirsus	Proliferative GN
Malaria	
P. faliciparum	Proliferative GN, Membranous GN
P. malaria	MPGN
Schistosomiasis	Proliferative GN
	Occasionally FSGS, Amyloid
Endocarditis	
Streptococcal	Proliferative GN
S. aureus Meth Sens.	
S. aureus Meth Res.	
Others	
Infected A-V Shunts	
Staphlococcal	Proliferative GN, MPGN
Other	
Visceral Abscess	
Many organisms	Proliferative GN
Syphilis	
Adults	Proliferative GN
Children	Membranous GN

TABLE 82.4 Pathogenesis of APSGN: Potential Mechanisms

1. In situ immune complex formation. Cell wall antigens from nephritogenic strains bind to glomeruli, activate complement (alternative pathway) and serve as planted antigen for anti-streptococcal antibodies.[325–329]
2. Molecular Mimicry. Anti-streptococcal antibodies cross-react directly with glomerular antigens.[330–337]
3. Enzymatic modification of IgG. Enzymatic alteration of IgG leads to glomerular localization; Rheumatoid factor binds to glomerular bound IgG.[338–342]
4. Deposition of circulating streptococcal antigen-anti-streptococcal antibody immune complexes (i.e. deposition based on affinity of exposed and complexed streptococcal protein fragments for glomeruli).[343,344]
5. Disease susceptibility/severity influenced by genetic factors.[3,345]

common, and there may be fibrin thrombi;[5] capillary wall thickening is typical. Focal but not diffuse crescents are often seen.[4,10] Over time monocytes replace neutrophils, thereafter the hypercellularity slowly resolves. Acute tubular necrosis, interstitial infiltrates, and vasculitis have been occasionally observed.[11–14]

Initially, IgG and C3 deposits (Figure 82.1) are invariably present within the mesangium and capillary walls,[5,15–18] although the C3 deposits persist longer. Alternative complement pathway proteins predominate, whereas C1q and C4 are often absent.[15–17]

Subepithelial humps (dome-shaped, dense immune deposits) are characteristic on electron microscopy.[15–17] They are prominent in the first month in epithelial slit pores,[17,19–21] associated with nephrotic range proteinuria and persist for one to two months. Their remnants appear as electron-lucent areas.[22] Subendothelial, mesangial and intramembranous deposits are often present and persist after resolution of the humps.[22]

Clinical Presentation; Laboratory Features

The latent period after infection is usually 1–3 weeks after pharyngitis and 3–6 weeks after skin infection.[2] Shorter latent periods suggest an alternative diagnosis. Often a source of infection is not identified. The acute nephritic syndrome usually resolves within a week in children but takes longer in adults, especially those with crescentic GN or nephrotic syndrome. Recurrent episodes are uncommon, however repeated bouts of hematuria may occur during the initial episode. The disease does not usually recur in transplants, although *de novo* disease has been observed.[23]

The laboratory findings provide clues but are not diagnostic. Hematuria, dysmorphic RBCs, and proteinuria are always present, casts are common, and pyuria may be observed in patients with severe inflammation. Nephrotic syndrome occurs in 5% of patients at initial presentation, and is sometimes present with resolution of disease.[24,25] The GFR is typically reduced, and 25% have a serum creatinine >2 mg/dl. Throat or skin cultures may be positive in affected individuals. C3 and CH50 levels are significantly depressed early (>90%) but return to normal at one month.[4,26–29] C4 and C2 are normal. High and persistent titers of C3 nephritic factor suggest MPGN.[28] Hypergammaglobulinemia, cryoglobulinemia and Rheumatoid factor activity may be present but are not diagnostic, whereas Streptozyme antibodies are frequently positive,[2,4,30–32] although also not diagnostic. Antibiotic therapy often prevents the rise in antibody titer but not the disease.

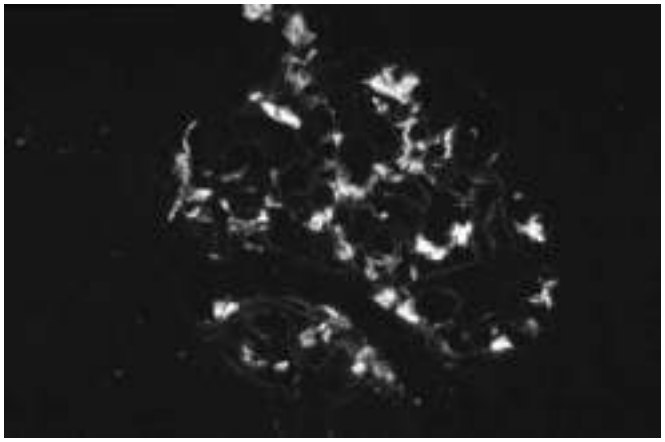

FIGURE 82.1 Post-infectious glomerulonephritis Immunofluorescence microscopy demonstrating relatively discrete granular staining of C3 along all glomerular capillary walls.

Prognosis

Less than 0.5% die of the initial disease and less than 2% die later from disease or develop ESRD.[24,33–43] Children have a better prognosis than adults, and patients older than 40 years with RPGN have the worst prognosis,[36,41,44] although their outcome is better than with other forms of RPGN. There is no difference in outcome between epidemic and sporadic forms. Urinary and histologic abnormalities may persist for years,[45–47] and persistent, heavy proteinuria and/or decreased GFR carry a worse prognosis.[15–17,42,48]

Treatment and Prevention

Therapy is symptomatic, with an emphasis on control of blood pressure and edema. Steroids, immunosuppressive agents, and/or plasmapheresis are generally not indicated, although a short course of steroids may be indicated with crescentic disease (i.e., RPGN). Specific therapy for streptococcal infections is essential and includes treatment of both the patient and any infected family member or close personal contact, to limit spread, e.g., Penicillin G 250 mg q.i.d. or erythromycin 250 mg q.i.d. for 7–10 days. During epidemics, empirical prophylactic treatment of close contacts and family members is recommended.[49]

Anti-GBM Disease and Goodpasture's Syndrome

Anti-GBM disease may occur as a disease limited to the kidney or as part of a pulmonary-renal syndrome (Goodpasture's syndrome).[50,51] The syndrome is rare[52] accounting for approximately 1–2% of all GN[51] and 10–20% of RPGN.[53] Peak incidence occurs in a bimodal distribution in the third and sixth decades,[54] with male predominance in younger patients. Lung hemorrhage is more common in younger men,

smokers[55] and individuals with pulmonary disease,[56] and less common in blacks.[50,57]

Pathogenesis

Genetic susceptibility is suggested by occurrence of disease in siblings and twins,[58,59] and analysis of MHC class II genes demonstrated that some confer susceptibility, while others confer resistance.[60] There is a strong association with HLA-DR2 (and DR15, a subspecificity of DR2), DRB1*1501 and DRB1*1502[61] and a negative association with DR7 and DR1.[60] Clearly, additional factors play a role since approximately one third of Caucasians have the DRB1*1501 allele. An environmental trigger is suggested by temporal and geographic clustering,[62,63] and some have developed disease after prolonged hydrocarbon exposure.[64] A case control study in the North of England suggested that occupational exposure to petroleum-based mineral oils led to higher anti-GBM antibodies.[65] Cigarette smoking has also been associated with the disease, and pulmonary hemorrhage is more common in smokers than in non-smokers.[55]

The onset of either pulmonary inflammation or nephritis may be linked to inflammation;[66–68] 10% of patients with ANCA-mediated vasculitis will develop anti-GBM antibodies,[69–71] and there are case reports of anti-GBM disease in patients with membranous nephropathy.[72–76] These reports suggest that glomerular disease may lead to release of α3(IV) collagen, and initiate an autoimmune response in susceptible individuals.

Anti-GBM antibody-mediated disease may occur following renal transplantation in patients with Alport syndrome,[77–79] as these patients lack α3, α4, α5 type IV chains.[80] Although most patients have a mutation in the coding region for α5(IV), expression of the α3α4α5 complex requires all three chains. These individuals only express the fetal form containing the α1, α2 chains, which is more sensitive to proteolysis and linked to progressive renal failure. Following transplantation with exposure to α3, some patients develop anti-α3(IV) antibodies, presumably due to "foreign" antigen exposure,[81] however, nephritis is uncommon in the transplanted kidney,[82] perhaps because of ongoing immune suppression.

The Goodpasture antigen: α3(IV) collagen.[83,84] Collagen IV is composed of six distinct α chains (α1–α6); each chain contains three domains: a short 7S domain at the N-terminus, a non-collagenous domain (NC1) at the C- terminus, and a long collagenous domain in the middle. The chains assemble into three sets of triple helical protomers: α1α1α2, α3α4α5 or α5α5α6. While the α1 and α2 have a wide distribution, the expression of α3α4α5 is restricted to basement membranes in glomeruli, alveoli, seminiferous tubules, choroid plexus, cochlea and retina.[85] Three dimensional and quaternary organization analyses of the alpha chains revealed head to head association of 2 protomers at the C-terminal, forming an NC1 hexamer. In addition, association of four triple helical 7S domains at the N-terminus forms a tetramer. Supercoiling and looping of the triple helixes and disulfide cross-links between triple helical domains further contribute to the meshwork.[86]

Analysis of antibodies from patients with anti-GBM disease established the non-collagenous domain of the α3 chain (α3 IV NC1) as the autoantigen.[84,85,87–89] Detailed mapping revealed that two conformational epitopes within the N-terminal part of NC1 region (designated E_A and E_B)[90–94] are major targets and account for approximately 90% of autoantibody activity.[95,96] These epitopes are sequestered at the interface between NC1 domains and are relatively inaccessible to autoantibodies.[97] However, when the hexamer structure is denatured, the epitopes are exposed for autoantibody binding. Thus, it has been postulated that "two hits" are required for disease: autoantibody production and exposure of the autoantigen. This may account for the lack of nephritis in some patients with circulating antibodies. Nevertheless, human anti-GBM antibodies have a high affinity for α3(IV) NC1; they bind rapidly to their target antigen and remain tightly bound.[98,99] This property contributes to both the rapidity of disease onset and treatment resistance, once GFR is significantly impaired.

Insights into the pathogenesis have also been derived from animal models. Immunization of normal mice with either recombinant or native antigen induces nephritis,[100,101] however not all strains are susceptible.[102] Disease in rodents is MHC-dependent and both T and B cell responses are required for severe disease expression,[103] although transfer of antibodies alone is capable of inducing nephritis.[104] Nevertheless, T cells are required for severe disease.[105–109] Transfer of α3(IV)-specific CD4 T cells induce nephritis in normal mice,[110] and Th1-related cytokines augment nephritis, whereas Th2 cytokines have a protective effect.[111]

Pathology

The light microscopic findings are typical of crescentic GN.[51,56,112] The majority of patients (>95%) have crescents at the time of biopsy, most often involving over 50% of glomeruli.[113] Tubulointerstitial nephritis is often present.[114] Intense, diffuse linear staining for IgG along the GBM is characteristic (Figure 82.2), and rarely IgA is found. Linear TBM staining may be present. C3 deposits are often found in a discontinuous, linear or granular pattern.[115–117] In the lung, there may be patchy IgG staining, which can be missed, although erythrocytes within disrupted alveoli and hemosiderin-laden macrophages should raise suspicion.[118]

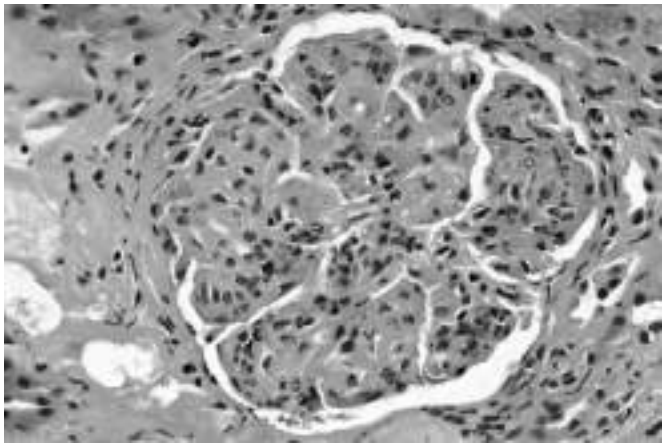

FIGURE 82.2 Antiglomerular basement membrane glomerulonephritis. Immunofluorescence microscopy demonstrating linear staining of IgG along all glomerular capillary walls.

TABLE 82.5 General Characteristics of Apsgn

Age:	Children > Adults (5% < 2y; 5–10% >40y)
Sex:	Male > Female
Site of Infection:	Pharynx (temperate zones); Skin (tropics)
Clinical Features	
edema	85%
gross hematuria	30%
back pain	5%
oliguria (transient)	50%
hypertension	60–80%
nephrotic syndrome	5%
Laboratory	
Urinalysis:	proteinuria, hematuria, casts: 100%
Nephrotic range proteinuria:	~10% over course of disease
Serum Creatinine	≥2 mg/dl –25%
Streptococcal antibody profile (streptozyme):	
>95% positive in patients with pharyngitis	
80% positive in patients with skin infections	
5% false positive rate	
early antibiotic Rx prevents antibody response	
C3, C4 and/or CH50 depressed in >90%	
Hypergammaglobulinemia –90%	
Cryoglobulinemia –75%	

Clinical Presentation

Abrupt onset of renal failure due to rapidly progressive GN is typical.[119] Rarely, patients have a more insidious course with mild symptoms and slow progression over months. Systemic symptoms suggest the possibility of a coexisting vasculitis, whereas, acute onset of hemoptysis raises suspicion of Goodpasture's syndrome. The pulmonary hemorrhage may be life threatening, leading abruptly to respiratory failure, although some patients have a subacute presentation with only fleeting infiltrates on chest x-ray. Unexplained anemia and heme-positive stools may occur after hemoptysis and swallowing blood.

Laboratory findings are typical of acute GN with proteinuria in the non-nephrotic range (< 3 gm/day). GFR is typically reduced at presentation and rapidly deteriorates. Circulating anti-GBM antibodies can be detected in over 90% of cases (i.e., by ELISA), and Western blotting is confirmatory (2–4% false negative).[120] One third of patients also have anti-neutrophil cytoplasmic antibodies (ANCA), with the majority as P-ANCA (i.e., vs. myeloperoxidase MPO).[70,121] These "double positive" patients may develop small vessel vasculitis in organs other than the kidney and lung, and vasculitis may recur after resolution of anti-GBM disease.

Prognosis and Therapy

Untreated, the prognosis is dismal,[51] with death from pulmonary hemorrhage or progressive renal failure prior to the introduction of treatment with corticosteroids, cyclophosphamide and plasma exchange (i.e., patient survival <50%: ESRD >90%)[122] (Table 82.6). Patient and renal survival rates have since improved with early recognition and prompt therapy.[122,123] Patients with an initial creatinine of <6 mg/dl (500 μmol/L) generally have a good prognosis if treated with plasma exchange and immunosuppression,[124] whereas those with a creatinine of >6 mg/dl have a greater likelihood of both ESRD and death. Dialysis-dependent patients are unlikely to recover renal function, particularly if either crescents involve 100% of the glomeruli or there is extensive interstitial fibrosis.[54,56,119,125–128] Aggressive therapy should either be withheld or abbreviated in these patients, as the risks of long-term immunosuppressive therapy outweigh the likelihood of benefit.[128] There are exceptions. A short trial of aggressive therapy may be considered in younger patients with evidence of acute deterioration (e.g., non-oliguric, early active crescent formation) and limited fibrosis on biopsy,[119,129,130] since some of them respond to treatment.

The rationale for plasmapheresis is removal of pathogenic antibodies and other inflammatory mediators.

TABLE 82.6 Therapy for Anti-GBM Antibody Diseases

Oral cyclophosphamide* (2–3 mg/kg/day) OR
IV cyclophosphamide (0.5 g/m^2 BSA)**
IV methylprednisolone (7 mg/kg/day for 3 days)
Prednisone 1 mg/kg/day after IV methylprednisolone***

*rounded down to the nearest 50 mg; reduced to 2 mg/kg/day in patients over 55 y
**for 4–12 months after antibody titers negative; in patients with higher risk for drug toxicity, azathioprine may be substituted as maintenance therapy
***for 4–6 weeks and then tapered off

Despite widespread use, support for efficacy is limited.[122,128,131,132] The standard of care is daily or alternate day 4-liter plasma exchanges for two weeks, with the frequency and duration determined by reduction of anti-GBM antibody titers and clinical response. Lung hemorrhage is an indication for plasmapheresis regardless of the presence and/or severity of renal failure. Corticosteroids and immunosuppressive therapy are required to control the ongoing inflammation and prevent new antibody formation.[122,124,133–138]

Cyclophosphamide is usually continued for 6–12 months, but in patients with higher risk for drug toxicity, azathioprine may be substituted as maintenance therapy. "Double positive" patients (+ ANCA and anti-GBM) present special issues.[139] The patients should receive the same initial treatment, although since their course is more typical of ANCA-associated vasculitis (see Chapter 83), they usually require longer-term maintenance immunosuppression. Those who are dialysis-dependent at presentation, should be considered for a trial of immunosuppression, as some studies suggest that the presence of ANCA is associated with better outcomes,[70] despite an initial need for dialysis,[140] although not all reports have been confirmatory.[139]

Transplantation

Kidney transplantation is an option for patients who have progressed to end stage renal disease. Although linear deposition of IgG along the GBM may be seen in up to 50% of transplanted kidneys, recurrence of nephritis is unusual, unless transplantation is performed in the presence of circulating antibodies.[141–143] Current practice is to delay transplantation for six months after the antibody levels have become undetectable, and this approach results in a 1-year renal survival rate of greater than 90%.

IgA Nephropathy (IgAN)

Initially thought to be a benign form of recurrent hematuria associated with mesangial proliferative GN and IgA deposition, it is now recognized that the clinical and pathologic presentations are diverse, and it may lead to end stage renal disease.[144–146] Most cases are idiopathic, but there is an association with a variety of autoimmune, infectious and chronic inflammatory diseases (Table 82.7).

TABLE 82.7 Secondary causes of IgA Nephropathy[346–358]

GASTROINTESTINAL
Celiac disease/gluten enteropathy
Inflammatory bowel disease (Crohn's disease, ulcerative colitis)
Chronic liver disease (alcoholic and nonalcoholic cirrhosis)
RHEUMATIC
Ankylosing spondylitis
Reiter's syndrome
Rheumatoid arthritis
Sicca syndrome
Uveitis
INFECTION
Human immunodeficiency virus
Leprosy
Toxoplasmosis
Yersinia enterocolitica enteritis
Malignancy
IgA monoclonal gammopathy
Lung cancer
Mycosis fungoides
Pulmonary Disease
Pulmonary hemosiderosis
Dermatitis
Dermatitis Herpetiformis
Psoriasis
VASCULITIS
Henoch-Schonlein Purpura
Behcet's syndrome

Incidence

IgAN is the most common primary GN worldwide with geographic variation,[147] (30–40% Asia; to 5–10% North America).[148–150] The differences are likely due to variations in the actual incidence, screening practices and indications for renal biopsy. It is rare in Blacks[151,152] and more common in Caucasians and Native Americans (Zuni and Navajo tribes).[153] The

disease is typically diagnosed in young adults in the second and third decades of life, and it affects males more commonly than females.[154–156]

Pathogenesis

The precise etiology is unknown, although a variety of factors contribute to the pathogenesis.[157] The key element common to idiopathic and secondary forms appears to be decreased glycosylation of IgA. In normal human sera, IgA1 exists as a monomer or as a polymer, whereas IgA2 is mainly found as a monomer. Patients who develop IgA nephropathy have reduced galactosylation of polymeric IgA1,[30,31] the fraction of polymeric IgA (or IgA complexes) is increased, and there is overrepresentation of IgA1λ.[158–161] There is also an exaggerated response to infectious agents or other stimuli by mucosal lymph, although a specific environmental antigen has not been identified. Many patients have reduced production of polymeric IgA1 within the mucosal immune compartment,[162] but increased numbers of polymeric IgA1 plasma cells in the bone marrow[163] is consistent with systemic involvement.[160,164–166]

Nevertheless, increased IgA levels alone are insufficient to cause disease, since patients with other diseases associated with increased serum IgA (e.g., human immunodeficiency virus infection (HIV), hepatobiliary disease and IgA secreting myeloma) infrequently develop nephritis.[167,168] Thus, either the circulating IgA and IgA-IC among IgAN patients differ qualitatively, or the renal response to IgA deposition is different.[169,170] There is evidence for both of these postulates.[171]

IgA1 has heterogeneous O-glycan moieties in its hinge region, and serum IgA1 from IgAN patients demonstrate altered glycan side chains, with reduced terminal galactose in O-linked oligosaccharides.[172–175] This incomplete galactosylation exposes the terminal sugar, N-acetyl-D galactosamine (GalNAc), generating neo-epitopes that are recognized by naturally occurring IgG and IgA1 antibodies specific for GalNac.[175] It has been suggested that this leads to immune complex formation.[176–178] Additionally, reduced galactosylation results in non-covalent self-aggregation with formation of IgA1-IgA1 complexes.[175,179] This defect is restricted to IgA1 (rather than due to generalized failure of O-glycosylation),[176] and reduced expression or function of the enzyme, core β1,3 galactosyltransferase (C1β3GalT1) that promotes addition of Gal to GalNAc residues, may be responsible. This enzyme is co-dependent on C1β3 galT1specific molecule (cosmc) for its stabilization. In the absence of cosmc, there is a decrease C1β3GalT1 which leads to decreased glycosylation.[180] Another enzyme that can lead to less glycosylation is N-acetyl galactosamine-specific α-2,6 sialyltransferase (ST6GalNacII). If this enzyme acts first on polymeric IgA, then C1β3GalT1 cannot properly glycosylate IgA.[180] In support of this hypothesis, one group reported decreased activity of this enzyme in circulating B cells in IgAN patients.[181]

Other circulating immune complexes have also been implicated,[182,183] including those containing IgA rheumatoid factors,[184] IgA-fibronectin[185] and IgA-soluble FcRI receptors (CD89),[186,187] although their pathogenic role is uncertain.[188,189] Nevertheless, decreased clearance of IgA-containing complexes may contribute to pathogenesis, and this may be especially relevant in patients with liver disease. In this regard, hepatic asialoglycoprotein receptor (ASGP-R)[190,191] and the myeloid FcRI receptor/CD89 are involved in IgA catabolism and clearance of IgA1 immune complexes.[192] Abnormal O-glycosylation or antibodies bound to GalNac may prevent the interaction of IgA with hepatocyte receptors (and monocytes and neutrophils), and therein decreased clearance occurs.

Cellular immunity may also contribute to pathogenesis, with Th2 cytokines (e.g., IL-4 and IL-5) influencing IgA galactosylation.[193–195] In a mouse IgAN model, Th2 bias in response to mucosal infection regulated glycosylation of IgA, and promoted glomerular IgA deposition.[196] Lymphocytes from patients with IgAN produce more IL-4 in response to mitogenic stimulation than controls, and this appears to be more pronounced in patients with severe renal dysfunction. Furthermore, clinical remissions have been associated with more normal IL-4 responses.[194]

Activation of mesangial cells, through cytokine priming, is most likely required for inflammation.[197,198] Nevertheless binding of polymeric, Gal-deficient IgA1 (possibly mediated by transferrin Tfr/CD71 and Fcα/μ receptors) may directly activate mesangial cells.[199–203] A prominent role for IL-6 has also been proposed,[204,205] and this may be especially relevant to patients with liver disease. IL-8, PDGF, TNFα, TGF-β and MCP-1 may also have important roles.[206,207] In any case, either polymeric IgA or aberrantly glycosylated IgA are very efficient at directly activating the complement cascade, either via the alternative or lectin pathways, and this may play a major role.[208–210] Podocyte injury may be involved in progressive disease with proteinuria, as polymeric IgA stimulates podocytes to produce TNF-α.[211]

Several findings suggest that genetic factors contribute to pathogenesis, including familial clustering and a higher risk of disease in identical twins.[212–215] In a large kindred study, linkage analysis revealed an association with 6q22–23 (IgAN1), although since only 60% of patients had IgAN1, other genes are likely involved.[216] Other proposed candidates include MHC, uteroglobin, selectin and angiotensin-1 converting

enzyme genes (DD genotype), however the results have been conflicting.[217–223] Interestingly, a genome-wide search in the ddY murine model revealed that syntenic regions of IgAN1 and selectin genes are major genetic determinants for IgAN.[224]

Pathology

Immunofluorescence (IF) demonstrates prominent deposits of IgA in a diffuse, granular pattern, predominantly within the mesangium (Figure 82.3), and occasionally in the glomerular capillary wall,[225] typically accompanied by C3 and IgG, and less frequently by IgM. There is often a predominance of λ light chains.[226] Light microscopic findings are variable.[225,227] Glomeruli may show mild lesions without mesangial expansion or limited mesangial cell proliferation, mesangioproliferative GN, focal or diffuse proliferative GN, crescents, chronic sclerosing GN, or rarely an MPGN pattern.[227] Electron microscopy typically reveals electron dense deposits, predominantly within the mesangium, although capillary wall deposits are common in more severely affected individuals.

Clinical Presentation

IgAN has many clinical presentations[146,228] (Table 82.9). Recurrent episodes of macroscopic hematuria are more common in younger patients.[229] These episodes often occur within 2–3 days of an upper respiratory tract or other infection. Loin pain may accompany the hematuria, (i.e., due to renal capsular swelling. In 30–40% of patients, the disease is asymptomatic with persistent or intermittent microscopic hematuria or proteinuria discovered incidentally. Acute renal failure occurs in less than 5% due to either crescentic GN,[230] renal tubular obstruction by red blood cells[231] or acute tubular necrosis.[232] Nephrotic syndrome is a less common presentation, although given IgAN's overall prevalence, it accounts for a significant fraction of adults with idiopathic nephrotic syndrome (i.e., 20–25%).

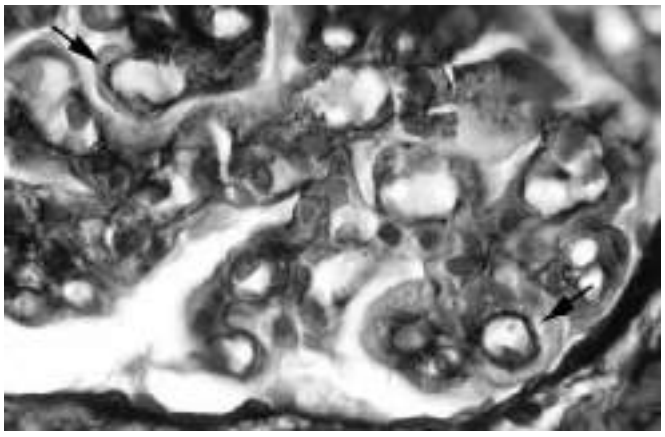

FIGURE 82.3 IgA nephropathy Immunofluorescence microscopy demonstrating intense mesangial staining for IgA.

TABLE 82.8 The Oxford Classification of IgA Nephropathy (2005)[359,360]

Summary of Key Pathological Features
1) Mesangial score
2) Segmental glomerulosclerosis absent (S0) or present (S1)
3) Endocapillary hypercellularity absent (E0) or present (E1)
4) Tubular atrophy/interstitial fibrosis

TABLE 82.9 IgAN Variable Clinical Presentations

Recurrent episodes of gross hematuria (i.e., following infection)
Asymptomatic microscopic hematuria
Acute GN
RPGN with acute renal failure (<5%)
Nephrotic syndrome

Prognosis

Overall prognosis is variable and depends on the severity of clinical and pathologic findings at presentation.[233,234] It has been estimated that ESRD occurs in 15 percent of cases at 10 years and 20–40% percent at 20 years, although this likely reflects selection of patients with more severe disease.[231,235] Some patients have a slow progressive decline in renal function over 10–20 years. Patients with non-nephrotic proteinuria and normal GFR at presentation progress more slowly (e.g., 1–3 ml/min/year). Elevated serum creatinine and heavy proteinuria at either presentation, or within the first year of diagnosis are independent predictors of poor outcome;[236–238] hypertension, glomerulosclerosis, and interstitial fibrosis are others.[228,234,239–244]

Biomarkers and Treatment

Secretory IgA, urinary complement factor H/urine creatinine ratio, serum galactose deficient IgA (HAA-IgA)[245] and urinary ratio of epidermal growth factor and monocyte chemotactic peptide-1 are being investigated as potential biomarkers. No therapeutic approach has consistently been shown to slow progression,[242,246,247] and variations in pathogenesis, pathology, clinical severity, co-morbid conditions and other factors contribute to this limitation. Clinical trials have compared conservative therapy, renin angiotensin aldosterone system (RAAS) blockade, and various immunosuppressive strategies. The consensus is that patients with normal renal function, (including <1 gm of proteinuria, minimal lesion on biopsy, and blood

TABLE 82.10 IgA Adverse Prognosis Factors (overall ESRD 15% at 10y; 20–49% at 20y)

1) Proteinuria >1 g/g creatinine
2) Hypertension
3) Increased creatinine at time of initial diagnosis
4) Hypertriglyceridemia
5) Hyperuricemia
6) Urinary α-1 microglobulin
7) Renal Pathology
   a. Glomerular crescents, interstitial fibrosis
   b. FSP1-positive interstitial fibroblasts
   c. C4d staining on renal biopsy
   d. Intra-arterial IgA staining

pressure of 120/80) do not require treatment. Patients with hypertension, proteinuria (>1 gm/day), reduced GFR, or more severe pathological lesions on biopsy may require treatment. The specific approach remains somewhat controversial. Multiple studies have shown RAAS inhibition (e.g., with ACEI or ARB) slows progression of the disease.[248,249] Although the combination may have additional benefits, acute renal failure may complicate this approach.[250–252] Fish oils, rich in omega 3 fatty acids (ω-3PUFA), eicosapentanoic acid (EPA) and docosahexanoic acid (DHA) may provide anti-inflammatory effects and retard renal progression by competing with arachidonic acid to produce biologically less effective prostaglandins and leukotrienes, and by decreasing platelet aggregation,[253] although clinical trials of efficacy have produced conflicting results.[243,254–257] Nevertheless, given the possible benefit and lack of toxicity, high dose fish oil therapy in combination with ACEI/ARB therapy in patients with proteinuria (>1 g/day) and/or mildly impaired renal function is reasonable.

The efficacy of high dose steroids and other immunosuppressive agents is not certain.[258,259] One prospective multi-center trial randomized IgAN patients (SCr <1.5 mg/dl, proteinuria 1.0–3.5 g/d) to either six months of steroid treatment or supportive therapy.[260] At 6 and 10 years, there was a lower incidence of the doubling of serum creatinine in the steroid group, and this was associated with a decrease in proteinuria.[261] Thus, steroids may be warranted in IgAN patients with heavy proteinuria and relatively normal renal function. Patients with either nephrotic syndrome and histologic findings characteristic of minimal change disease or clinical and pathologic features of RPGN may also benefit from steroid therapy.[262] Other immunosuppressive approaches have been inconclusive.[30,259,263–271] Similarly, removal of the palatine tonsils to reduce serum IgA levels and limit progression[272,273] has not been associated with preservation of renal function.[274,275]

Transplantation

Immunohistologic recurrence develops in as many as 60% of allografts by 10 years and 5–10% of affected allografts are lost to progressive disease.[276–280] Contemporary immunosuppression regimens using MMF have not altered recurrence rates.[281]

Idiopathic MPGN

MPGN or mesangiocapillary GN may be idiopathic or associated with systemic diseases.[282] Pathologically, they share light microscopic features including glomerular capillary wall thickening, hypercellularity and matrix expansion (Figure 82.4). MPGN is further classified as type I, II or III, based on IF and EM patterns.[283–285] This section focuses on primary or idiopathic forms of the disease.

Incidence

Overall these forms represent less than <10% of primary glomerular disease GN,[286–288] although they are somewhat more prevalent in children.

Pathology

MPGN I is characterized by subendothelial and mesangial immune deposits, with IgG and complement deposition predominating. Diffuse thickening of capillary walls is typical, and the loops often have a double-contoured or "tram track" appearance when stained with silver methenamine or periodic acid-Schiff (Figure 82.5). Widespread electron-dense deposits in subendothelial sites are the hallmark of type I disease (Figure 82.6). The hallmark of MPGN type II is the presence of electron dense deposits

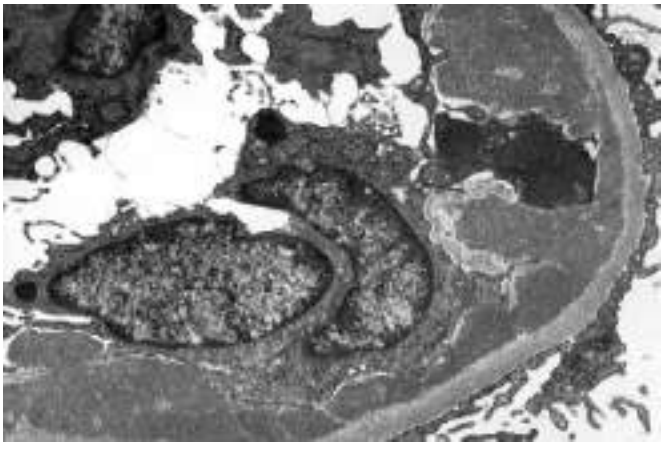

FIGURE 82.4 Membranoproliferative glomerulonephritis (MPGN). Mesangial hypercellularity and increased mesangial matrix with lobular accentuation. There is diffuse thickening of peripheral glomerular capillary walls (H&E, X330).

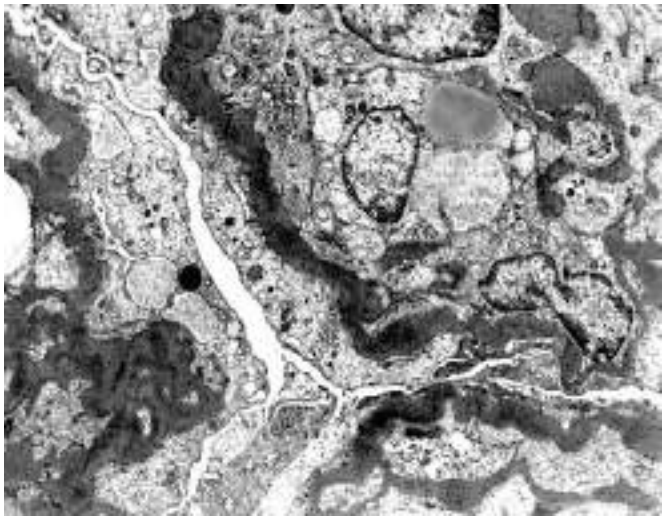

FIGURE 82.5 MPGN Silver stains showing double contoured glomerular capillary walls by enclosing silver-negative subendothelial deposits and mesangial interposition (Jones silver methenamine, X400).

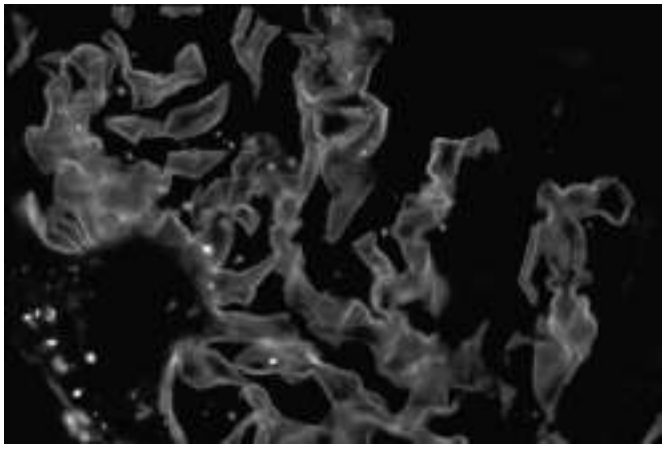

FIGURE 82.6 MPGN, type I Electron micrograph showing large electron-dense subendothelial deposits.

within the lamina densa layer of the GBM that are often visible by conventional eosin and PAS stains (hence the designation Dense Deposit Disease).[289] The dense intramembranous deposits seen by electron microscopy are diagnostic (Figure 82.7) and may involve tubular and vascular basement membranes in the kidney, Bruch's membrane in the eye,[290,291] and sinusoidal membranes in the spleen.[292] The deposits may also be seen within the mesangium and within the basement membranes of Bowman's capsules and tubules.[293] The chemical composition of the electron dense deposits is not known,[294] but they stain with thioflavin T and bind lectin wheat germ agglutinin,

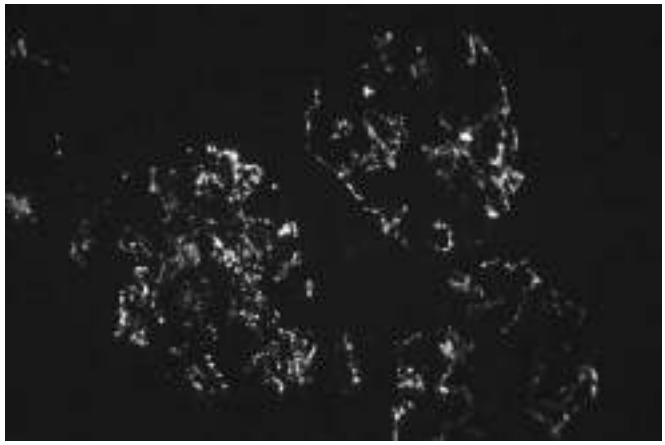

FIGURE 82.7 MPGN, type II Electron micrograph showing intramembranous electron-dense deposits with ribbon-like thickening of glomerular capillary walls. The mesangium is expanded by increased matrix and cells.

suggesting that they are composed of N-acetyl-glucosamine, glycoproteins and lipids rich in unsaturated fatty acids.[295,296] Immunofluorescence reveals intense staining of C3 along capillary walls and within the mesangium. Absence of immunoglobulins is a distinguishing feature of Type II MPGN. By contrast Type III MPGN, also called the Burkholder variant,[297] displays features of MPGN type I and membranous nephropathy, with subepithelial, subendothelial and mesangial deposits.[298] Successive generation of subendothelial and subepithelial deposits disrupt the basement membrane, and concurrent formation of new lamina densa material are often observed.

Pathogenesis

Local activation of the complement cascade is operative in all forms. Catalyst destabilization (e.g., through either acquired antagonism or deficiency in the inhibitory pathway), results in unopposed complement activation in glomeruli. Hypocomplementemia results from local consumption and/or circulating autoantibodies against individual complement components (i.e., nephritic factors).[105,299] Three nephritic autoantibodies[300] have been commonly described in MPGN type 1, including: (1) C4Nef,[301–303] an IgG that stabilizes the C3 convertase, C4b2a, thereby preventing the decay of 2a from C4b2a; (2) C3Nef (see below); and (3) NFt, an autoantibody against C3bBbP that activates the terminal pathway.[303,304] Their precise pathogenic role is uncertain,[299] as they are occasionally detected in either unrelated diseases (e.g., post-streptococcal GN, SLE, meningococcal meningitis)[305–307] or healthy individuals.[307]

Clinical Presentation

MPGN has variable presentations, from microscopic hematuria and sub-nephrotic proteinuria (35%), to nephritic syndrome with mild renal impairment (35%), to an aggressive glomerulonephritis (20%) with rapidly deteriorating renal function, heavy proteinuria, and RBC casts (10%). Laboratory findings often display decreased complement levels [C3, C4, and total complement (CH50)], depending on the variety of MPGN (Table 82.11).

Treatment

Control of hypertension and proteinuria reduction are key, and focus should be on identifying and treating secondary causes of the lesions. For idiopathic disease, treatment is based on disease severity. Patients with sub-nephrotic proteinuria and preserved renal function are treated conservatively. Patients with impaired renal function and/or nephrotic proteinuria can undergo a trial of prednisolone (1 mg/kg/d) for proteinuria reduction.[308] If a response is noted, steroids can be continued at the minimally-effective dose. If there is no response after three months, steroids should be stopped, and a trial of a calcineurin inhibitor or mycophenolate mofetil can be attempted.[309] Patients with rapidly declining renal function, or with crescents on biopsy should be treated as those with other forms of RPGN.

TABLE 82.11 MPGN Pathogenesis

Type I, Immune Complex Formation with Classical Pathway Activation
Antibody Antigen Complexes not well Defined (i.e., in those not Associated with Infections or Cancer)
Three circulating nephritic autoan tibodies[300] commonly described, although their pathogenic role is uncertain as they may be found in other diseases: 1) IgG nephritic factors C4Nef,[301–303] stabilizes C3 convertase, C4b2a, and prevents decay of 2a 2) C3Nef 3) NFt, vs. C3bBbP, activates the terminal pathway[303,304] 4) Persistently low plasma C3, C4–70% type I MPGN (classical pathway) 5) NFt associated with depressed C3, C5, C7, C8, C9 and properdin levels.[284,361–363]
Type II Dense Deposit Disease (by EM; IF C3, no Ig)
Unregulated Renal Complement Activation
1) IgG nephritic factors C3 nephritic factor (C3Nef), 80% patients Autoantibodies vs. C3bBb (rate limiting C3 convertase of the alternative pathway[363] Prolongs half-life of C3 convertase[304,364] preventing physiologic regulation and inactivation by factors H and I,[364] leading to continued activation of C3 (fig 1b). Inflammation may dependent of C5a activation, instead of C5b-9[365] 2) Factor H (fH) dysfunction or deficiency.[366–368] Acquired vs. Hereditary 3) Profoundly low plasma C3, variable C4 levels (alternative pathway)
Type III Type I plus Subepithelial Immune Deposits
low C3 levels, normal C4

TABLE 82.12 MPGN Clinical and Laboratory Features at Presentation

Nephrotic syndrome plus microscopic hematuria (50–60%)
Acute GN (15–30%)
Asymptomatic urinary abnormalities (i.e. proteinuria and hematuria. 20–30%)
Recurrent macroscopic hematuria (< 10%)
Hypertension may be mild or severe
Note that MPGN Type II often presents with acute nephritis and/or macroscopic hematuria, MPGN Type III often presents with more insidious onset
MPGN III low C3 levels, normal C4

Thrombotic Microangiopathies (TMA)

Thrombotic microangiopathy (TMA) is characterized by the syndrome of microangiopathic hemolytic anemia, thrombocytopenia, and variable organ dysfunction due to platelet thrombosis in the microcirculation, which can mimic acute GN.[310] Depending on the predominant distribution of organ involvement, pathologically identical, but clinically separable entities have been designated as: Hemolytic-Uremic Syndrome (HUS) and Thrombotic Thrombocytopenic Purpura (TTP).[311] Since their pathophysiology overlaps, both topics are presented.

Typical HUS commonly affects children under five, is characterized by moderate to severe renal involvement, and is self-limited. It is caused by specific serotypes of *E. coli* or other bacteria that produce Shiga-like toxin.[312] Atypical HUS may be familial or sporadic. The familial forms are associated with genetic abnormalities in complement system proteins. The sporadic forms are often triggered by drugs, malignancy, infection or autoimmune disease that lead to dysregulation of complement system proteins (Table 82.15).

TTP occurs in adults and typically manifests with more neurologic sequelae and variable renal involvement. Prompt recognition of these disorders is essential, as delay in therapy may lead to organ failure or death (i.e., with TTP).

TABLE 82.13 MPGN Pathology

Light microscopy (similar in all forms)
Mesangial expansion and capillary wall thickening [i.e., termed, mesangiocapillary GN[369–371]]. Capillary loops with double-contoured or "tram track" appearance when stained with Jones silver methenamine or periodic acid Schiff (PAS),[283] + /- nodular glomerulosclerosis pattern[284,285]
Immunofluorescence/electron microscopy patterns distinguish the subtypes[284,369] type I, prominent C3 capillary walls and mesangium[358,372] IgG >> IgM C1q + / − C4
EM - subendothelial deposits - type I hallmark; intramembranous dense deposits − type II hallmark).[289]
Increased matrix material (subendothelial)[370,371]
This material is separated from the native GBM by interposed cytoplasmic extensions of mesangial cells and/or infiltrating macrophages, and is responsible for the 'tram track' appearance of the basement membranes seen by light microscopy.

TABLE 82.14 MPGN Pathology

Light microscopy is similar in all forms of MPGN	
mesangiocapillary GN	
-mesangial proliferation and matrix expansion	
-capillary wall thickening (double contour 2° to immune deposits)	
-double contour appearance of capillary loops (2° to immune deposits)	
IF	
Type 1 Type II	**Type III**
IgG ± IgM None	IgG ± IgM C1q, C4, C3 (SEndo/Mes)
EM	
SEndo/Mes Dense Deposits (EM)	SEndo/Mes/Subepith

TABLE 82.15 Systemic Disease and Conditions Associated with TMA

Scleroderma renal crisis
Anti-phospholipid syndrome
Pregnancy[373]
HELLP Syndrome
Postpartum HUS
Human Immunodeficiency Virus (HIV)
Malignancy
Drugs[374]
Mitomycin
Tamoxifen
Cisplatin
Ticlopidine
Quinine
Interferon-α
Calcineurin Inhibitors
Rifampin
Metronidazole
Renal Transplantation[375]
De novo disease
Recurrence of TMA

Incidence

The TMAs occur in 1−4 cases per 1,000,000 people, although it has been reported more frequently in patients with malignancy, HIV infection, or various drug exposures (Table 82.15). As previously mentioned, acquired HUS may be associated with Shiga toxin-producing *E. coli* (or other bacterial) infection and commonly affects infants and children infected with the O157:H7 strain.[313]

Pathophysiology

The involved pathways and distinguishing features of HUS and TTP are summarized in Table 82.16.[312,314–316] TTP is mediated by dysfunction of the metalloprotease ADAMTS13, which degrades large von Wildebrand factor (vWF) multimers.[317] Without this activity, vWF multimers aggregate within vascular lumen, propagating platelet congregation, aggregation, and activation, thus leading to further microthrombosis and sequelae. Low ADAMTS13 activity can result from a constitutive deficiency or acquired circulating IgG autoantibodies to the ADAMTS13 protein.[316]

As mentioned previously, acquired HUS may be associated with Shiga toxin-producing *E. coli* (or other bacterial) infection and commonly affects infants and children infected with the O157:H7 strain. Once thought entirely due to inflammatory cytokine effect on renal endothelial cells,[310] it is now understood that the abnormal regulation of the alternative pathway of the complement cascade augments pathophysiology driving the disorder,[318,319] with excessive activation of C3 leading to formation of the membrane attack complex (C5−9), that in turn, propagates platelet activation and accumulation.

A non-infectious, atypical form of HUS (aHUS) has been identified involving either inherited or acquired defects within the alternative pathway. Initial reports of loss-of-function of regulatory factors (namely, Factor H) appeared in up to 30% of familial cases.[320] Recently,

TABLE 82.16 Distinguishing Pathophysiology of TTP and HUS

TTP
- decreased ADAMTS13 (enzyme that cleaves large vWF multimers)
- large vWF complexes in blood and thrombi, accumulate on the surface of endothelial cells
- fibrinogen in thrombi
- platelet adhesion, aggregation, thrombosis, thrombocytopenia
- microthrombi small vessels
- lack of inflammation or endothelial damage
HUS
- Shiga exotoxin subunit binds to cell surface globotriaosylceramide receptors (e.g., colon, glomerular endothelia)
- Endothelial cells produce TNF-, IL-6, IL-1
- Glomerular endothelial cells produce large vWF multimers
- Fibrin, platelets, microthrombi accumulate
- Microthrombi involving small vessels

a gain-of-function of complement factor B has been identified.[321] Both Factor H and Factor B defects have also been identified in acquired cases. These factors regulate complement activity locally; therefore loss of regulation within the kidney (or other vascular sites) may lead to unregulated complement activation and inflammation.

The genetic form of aHUS is prevalent more in children, where the acquired aHUS manifests more in adults. Systemic disease and conditions associated with TMA are listed in Table 82.15.

Pathology

The histological lesions of TMA are characterized by thickening of arterioles and capillaries, endothelial swelling and detachment, subendothelial accumulation of protein and cell debris, intraluminal platelet thrombi, and partial or complete occlusion of the vessel lumina.[312] These changes can also be seen in other renal pathology, such as scleroderma, malignant nephrosclerosis, and calcineurin inhibitor toxicity. TTP, Shiga toxin-associated HUS and atypical HUS are indistinguishable on microscopy.

Clinical Presentation; Laboratory Features

TMA manifests as a microangiopathic, hemolytic anemia with thrombocytopenia; schistocytes and helmet cells are visualized on peripheral blood smear. Platelet counts vary depending on the syndrome; HUS typically presents with platelet counts between $30-100\times10^9$ cells/L, while TTP is usually manifest by a more severe thrombocytopenia, with $<30\times10^9$ cells/L present. The hemolytic anemia (Coombs' negative) can be severe, with hemoglobins <6.5 g/dl present. Reticulocytosis, hyperbilirubinemia (often indirect), low haptoglobin, and elevated lactate dehydrogenase (LDH) are also present. Hypocomplementemia (especially C3) may be present. The acute kidney injury is more common with HUS and can sometimes mimic RPGN. Clinical presentation varies with HUS typically having more renal manifestations, while TTP displays more neurologic sequelae.

Prognosis and Treatment

Treatment for the TMAs is mostly supportive. Plasma exchange therapy is effective in both TTP and aHUS. Corticosteroids have yielded inconsistent results. Rituximab has had anecdotal success in a few patients with refractory TTP.[322] Recently, the monoclonal C5 antibody eculizumab was effective in a few patients with HUS and aHUS,[323,324] although widespread use requires validation in larger series.

PRIMARY RENAL DISEASES CAUSING NEPHROTIC SYNDROME

The nephrotic syndrome is defined by clinical and laboratory abnormalities common to a variety of primary and secondary kidney diseases, each characterized by increased permeability of the glomerular capillary wall to circulating plasma proteins. The clinical manifestation of filtration barrier dysfunction caused by these disorders is proteinuria (greater than 3.5 g/24 hr) which leads to hypoalbuminemia. Other manifestations such as edema, hyperlipidemia, lipiduria and coagulation disorders occur commonly. This section of the glomerular disease chapter addresses primary or idiopathic kidney diseases, which lead to the nephrotic syndrome. The most common causes of idiopathic nephrotic syndrome, membranous nephropathy, focal and segmental glomerulosclerosis, and minimal change disease are discussed in detail.

Membranous Nephropathy

Membranous nephropathy (MN) is also referred to as membranous glomerulopathy or membranous glomerulonephritis, reflecting morphologic abnormalities of the glomerular basement membrane. MN is one of the most common causes of nephrotic syndrome in adults, comprising an estimated 15–25% of all cases of primary/idiopathic nephrotic syndrome.[376] However, the incidence of FSGS and IgAN is increasing,[376] rivaling MN as the most common etiologies, and

representing a greater cause of nephrotic syndrome than MN in some subpopulations, such as FSGS in African American men.[376–378] MN exists in idiopathic and secondary forms,[379] due to systemic diseases (systemic lupus erythematosus, less commonly mixed connective tissue disease or rheumatoid arthritis), malignancies (lung, colon, gastric and breast carcinomas),[380] infections (hepatitis B and C,[381] syphilis, malaria, schistosomiasis, filariases, leprosy, tuberculosis, parvovirus[382]) and drugs (gold, penicillamine, mercury, probenecid, and perhaps high doses of captopril[383–386]) (Table 82.17). The prevalence of MN varies according to geography, with the highest rates in European-Americans, which exceeds rates in Japan and Australia.[387] However, these data may be biased by biopsy practices, as well as variation in relative frequency of predisposing conditions for secondary MN in each region.[388,389] Idiopathic MN is most common in middle age men,[390–394] rarely occurs in children, and appears to have no racial predilection.[387]

TABLE 82.17 Systemic Diseases Associated with Membranous Nephropathy

CONNECTIVE TISSUE DISEASE
Systemic lupus erythematosus
Mixed connective tissue disease
Rheumatoid arthritis
ADENOCARCINOMAS[380]
Lung
Colon
Stomach
Breast
INFECTIONS
Hepatitis B and C {7940}
Syphilis
Malaria
Schistosomiasis
Filariases
Leprosy
Tuberculosis
Parvovirus[382]
MEDICATIONS
Gold
Penicillamine
Mercury
Probenecid
Captopril[383–386]

Clinical Presentation and Natural History

Approximately 70–80% of patients diagnosed with idiopathic MN present with features of the nephrotic syndrome, including hypoalbuminemia, peripheral edema, and hyperlipidemia,[393,395–403] though this may be an overestimation, since patients with lesser degrees of proteinuria may not be biopsied. Most MN series indicate that at the time of diagnosis, GFR, as determined by serum creatinine, is typically normal or mildly increased, with less than 10% of patients presenting with diminished GFR.[400,403] However, in a study by Shemen et al., wherein GFR was estimated by inulin clearance in 20 patients with MN and heavy proteinuria versus 20 controls, mean GFR was only 58 ml/min/1.73 m^2 in the MN group.[404] Although this study may have enrolled a population with advanced disease, it still highlights that GFR may be abnormal in MN. Patients with MN are generally normotensive,[390,405] with the reported incidence of hypertension at time of diagnosis ranging from 13 to 55%.[387,400]

The natural history of MN can be discerned from untreated controls from therapeutic trials[391,400,406–416] or observational studies,[380,392,393,395,398,417–420] and indicate that the course can be relatively benign in many patients, especially those with sub-nephrotic range proteinuria. In a study of 100 patients with biopsy-proven MN, Schieppati et al. demonstrated that the probability of retaining GFR was 88% at five years and 73% at eight years; 16% developed ESRD over an average of 8 years.[414] Ten year follow-up data from the Ponticelli group showed that 40% of untreated controls developed ESRD.[416] Figures from both of these Italian studies are consistent with those of Pei et al., which demonstrated that 26% of subjects developed chronic kidney disease (defined as GFR <60 ml/min/1.73 m^2) after a mean follow-up interval of 5.8 years.[421] The best outcomes are reported by Kida et al., in a series of 104 Japanese patients, which demonstrated that 80, 70 and 50% of patients had a GFR exceeding 80 ml/min at five, 10 and 15 years, respectively.[402] A comprehensive review by Hogan et al. showed that renal survival probability in untreated patients was 86% at five years, 65% at 10 years and 59% at 15 years.[422] Of patients with MN that experience GFR decline, the course is generally protracted, with a mean time to doubling of creatinine of 30 months in one series[398] and an average of 30 months from presentation to ESRD in another study.[415] More abrupt diminution in GFR should warrant investigation of alternative etiologies of acute kidney injury. MN with fibrocellular crescents (RPGN) has been rarely described,[423] and should be considered in this differential diagnosis.

If proteinuria is used as a surrogate marker of MN disease course, Schiepatti et al. demonstrated partial or complete remission in 65% of subjects at five years,[414] similar to a report from Davison et al., which showed complete remission in 25% of patients at five years.[398] Pooled data from Hogan et al. showed complete remission in 10% at one year, 16% at two years and 22% at three years,[422] consistent with the commonly quoted statement that approximately 25−30% of patients with idiopathic MN spontaneously remit.[387,424] A study from Troyanov et al. demonstrates that dialysis-free renal survival at 10 years is 100% in MN patients with complete proteinuria remission, 90% in those with partial remission (defined as reduction in proteinuria by >50% and to <3.5 g/24 hr), and 45% for those without remission.[425]

Because some patients with MN progress to ESRD, many groups have tried to identify clinical parameters, which predict likelihood of progression. Multiple clinical risk factors have been identified, including massive proteinuria, male gender, advanced age, hypertension, and diminished GFR at clinical presentation. An algorithm has been published, which takes many of these factors into account and yields a quantitative risk for progression.[426] Most,[380,392,398−400,403,415,420,427,428] but not all[414] studies have shown that at the time of diagnosis, patients with non-nephrotic proteinuria have a better prognosis than those with nephrotic range proteinuria. In a biopsy series of 140 patients with MN, initial presentation with more than 10 g proteinuria/24 hours predicted a 60% probability of renal disease progression.[415] Persistent proteinuria of >8 g/24 hr for ≥6 months, >6 g/24 hr for ≥9 months or >4 g/24 hr for ≥18 months was also associated with increased risk of progression to chronic kidney disease.[421]

Most MN case series contain a preponderance of men,[392] suggesting male gender is a risk for more severe disease. Numerous studies have specifically identified male sex as a risk for progression,[394,398,399,403,406,414,415,429] though a few have not.[400,421] Advanced age at time of diagnosis has generally been shown to be associated with risk of progressive GFR decline,[398,400,414,419,430] but not in all reports.[399] Most studies simply evaluated age as a continuous variable, though others defined age >50 years as a categorical risk.[414] Like other glomerular diseases, uncontrolled hypertension has also been shown to be a risk for progression of MN.[399,415,420] A notable exception to this finding is the series from Schiepatti et al.[414] As with most other glomerular diseases, patients presenting with MN and decreased GFR are at risk for progression.[399,400,415,421]

One of the most common complications of MN is thrombosis, venous more commonly than arterial, and particularly involving the renal vein. The incidence of MN-associated renal vein thrombosis is unclear, but estimates for all-cause nephrotic syndrome range from 4% to 62%.[387,431,432] Because many series of renal vein thrombosis contain a disproportionate number of patients with MN,[433−436] it has been suggested that renal vein thrombosis in the context of MN is more common than with other causes of the nephrotic syndrome.[432,437] The classic clinical presentation is acute onset of unilateral flank pain and tenderness, accompanied by gross hematuria and decreased GFR, though a more chronic presentation with indolent features has also been described.[432] Patients with MN and chronic renal vein thrombosis tended to be older and unlikely to progress to ESRD,[436,437] and demonstrate collateral veins on angiographic studies. The purported mechanism is enhanced urinary excretion of anti-thrombotic proteins, but conflicting blood coagulation factor levels have cast doubt on this mechanism.[431,432]

Diagnosis

The diagnosis of MN is made by renal biopsy. However, there are several other supporting laboratory findings. As mentioned previously, nephrotic range proteinuria is present in the majority of patients at the time of diagnosis, and is usually accompanied by other features of the nephrotic syndrome.[393,395−403] Proteinuria of 10 to 20 g per 24 hr is atypical but not unusual.[438] Microscopic hematuria is present in 30 to 50% of patients,[393,403] although gross hematuria is rare.[439] Approximately 90% of patients with MN have a normal or increased GFR at the time of diagnosis.[400,403] Autoantibody titers and complement levels are characteristically normal; low complement levels should raise suspicion of a secondary cause (e.g., lupus nephritis). C5b-9 membrane attack complex has been detected in urine of patients with MN,[440−444] consistent with the conclusion that proteinuria is complement-dependent in the early phases of disease.[445−448]

Since MN can be associated with other systemic diseases, it is advisable to obtain a serologic work-up, particularly if the patient has consistent clinical findings. Appropriate tests could include systemic lupus erythematosus, hepatitis B and C, and syphilis serologies. Because MN is associated with some malignancies, including after the MN diagnosis is established,[449] routinely recommended cancer screens should certainly be performed in patients with MN. Although more extensive screening is often pursued, cost-effectiveness of this strategy, in the absence of suggestive symptoms, is unclear.

Pathology

There are characteristic features on light, IF and EM, which distinguish MN.[386,387,450] Typical histologic findings on light microscopy depend on the stage

(Table 82.18) and duration of the disease (Figure 82.8). There is a lack of hypercellularity. Early on, the basement membranes appear normal, but as the immune deposits increase in size, the basement membrane reaction gives the appearance of spikes. This is best visualized on Masson's trichrome or methenamine silver stains of thinly cut sections. The relatively small deposits often require higher resolution images, which are only achievable with electron microscopy. Light microscopy is also characterized by lack of glomerular or tubulointerstitial inflammatory infiltrates. Fibrocellular crescents are rare, and if present in the context of MN features, often represent concomitant glomerular diseases.[451–456] Similar to other glomerular diseases,[457,458] when tubular atrophy and interstitial fibrosis are observed, these findings portend a poor prognosis in MN.[459,460]

Immunofluorescence microscopy evaluation of kidneys affected by MN reveals granular deposition of immunoglobulins and complement components (IgG [especially IgG4] > C3 > IgM > IgA >> C1q) in a diffuse, granular pattern along glomerular capillary walls.[386,387] The presence of IgA and C1q suggests lupus nephritis,[386,387] though rarely observed in idiopathic MN.[386] Subendothelial, mesangial or/and tubular deposits are rare and if present should raise suspicion of another diagnosis (e.g., lupus). Although C5b-9 staining is not routinely performed in most pathology laboratories, the terminal membrane attack complex characteristically decorates the glomerular capillary wall in MN.[387]

On EM, the pathognomonic finding is glomerular subepithelial, electron-dense deposits by transmission electron microscopy (Figure 82.9). The pathologic stage of disease is based on the size of deposits along with the surrounding basement membrane reaction.[461] This pathology staging scheme has been advocated as a means of assessing prognosis.[427,462] However, most studies have found that pathologic staging does not correlate well with renal outcomes.[380,406,412,415,416,419,420,463,464] The presence of dense deposits within the mesangium is rare with idiopathic MN, but is occasionally observed with secondary forms of MN.[387]

Pathophysiology

The body of evidence indicates that MN lesions result from circulating antibody binding to a resident or planted antigen on podocytes, and proteinuria is complement-dependent. In some cases, DNA, viral and tumor antigens have been identified within immune complexes,[465–470] and it is presumed that these antigens are pathogenic. It has been postulated that these antigens induce an antibody response, and by nature of their physical properties, localize within the basement membrane and podocytes. They persist in the subepithelial location (e.g., due to a physical interaction of the antigen and either the basement membrane or podocyte cell surface) and permit binding of circulating antibodies, (the latter may be facilitated by slightly altered permeability induced by circulating cytokines or chemokines). The antibodies then activate complement, eventually leading to formation of the membrane attack complex (C5b-9),[471] which induces sublethal (or perhaps lethal) injury to podocytes, causing their effacement.[472,473] Clinically, this leads to proteinuria, which is likely mediated through reactive oxygen species generation.[474–477] As the deposits continue to grow, their physical presence also contributes to podocyte foot process effacement.

TABLE 82.18 Pathologic Staging of Membranous Nephropathy Lesions

Pathologic Stage	Histologic Features	Podocyte Foot Process Effacement?
I	Small, diffuse electron-dense immune deposits in a subepithelial (between the GBM and podocyte foot processes) location	Yes
II	Subepithelial "spikes", which are generated by incomplete surrounding of deposits by GBM	Yes
III	Electron-dense deposits appear as intra-membranous due to GBM between the deposit and podocyte foot process	Yes
IV	Deposit loss of electron density, GBM thickened, with pronounced areas of clearing	Yes

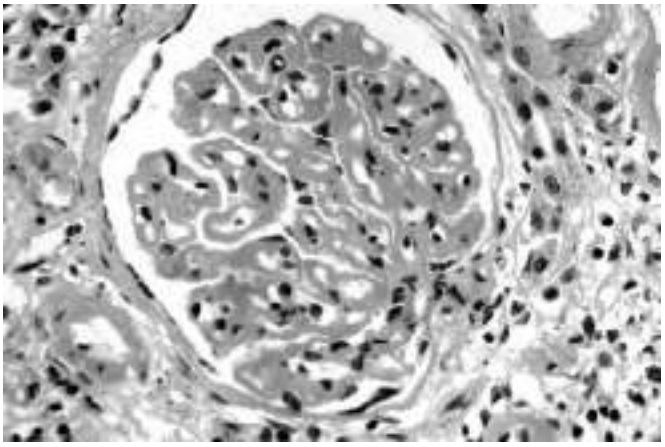

FIGURE 82.8 Membranous glomerulonephritis. All glomerular capillary walls are markedly thickened without significant cellular proliferation (H&E, X320).

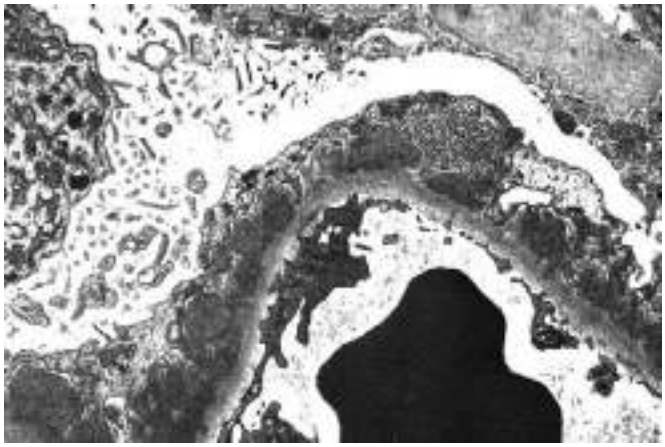

FIGURE 82.9 Membranous glomerulonephritis. Electron micrograph demonstrating multiple electron-dense subepithelial deposits. There is diffuse effacement of overlying epithelial foot processes.

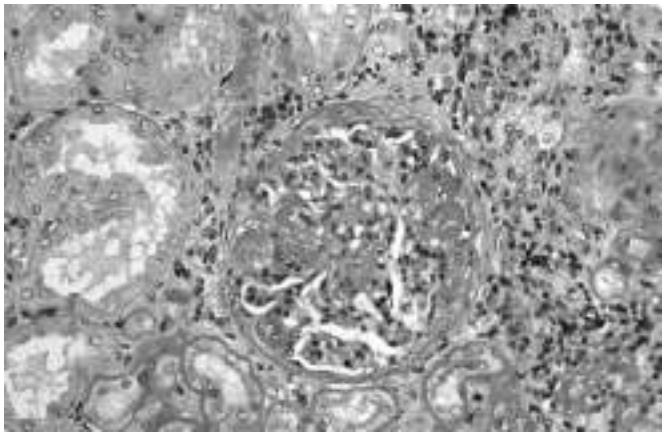

FIGURE 82.10 Focal segmental glomerulosclerosis. Segmental glomerular sclerosis with hyalinosis and partial adhesions to Bowman's capsule. There is patchy tubular loss and interstitial mononuclear cell infiltrate (H&E, X250).

Although C5b-9 staining is not routinely performed in most pathology laboratories, the terminal membrane attack complex is characteristically deposited within the glomerular capillary wall in MN.[387] Since the immune deposits form on the subepithelial side of the basement membrane, chemotactic factors are excreted in the urine and cells are not recruited, nor can they cross an intact GBM. There is podocyte activation and secretion of matrix metalloproteinases,[478,479] which leads to changes in GBM composition. This loss of appropriate extracellular cues then facilitates podocyte apoptosis and detachment,[447] with accompanying cytoskeleton disruption,[480] nephrin-cytoskeleton dissociation[481] and loss of nephrin expression.[482]

Much of the evidence to support pathogenesis is derived from experimental models of MN [e.g., Heymann nephritis[406,483–485]], though translation of these findings to human MN pathophysiology has not always been straightforward. However, in a recent screen of serum from patients with idiopathic MN, a circulating IgG4 subclass autoantibody, which is immunoreactive with the M-type phospholipase A2 receptor, was identified in 70% of samples.[486] The autoantibodies localized to subepithelial deposits in biopsies from MN patients, and antibody titers correlated with disease activity. No immunoreactivity was detected in serum from lupus MN patients, suggesting that the phospholipase A2 receptor is a major antigen for idiopathic MN. Because anti-PLA2 receptor antibodies were not present in all samples, the possibility of other MN antigens exists. Debiec and Ronco described a pregnant patient, who was deficient in neutral endopeptidase (NEP). She developed and transferred anti-NEP antibodies to her baby, who was replete with NEP, and was then born with congenital MN.[487,488] Anti-NEP antibodies were determined to be pathogenic in this case.[489] Antibodies to aldose reductase and manganese superoxide dismutase, both of which are expressed in podocytes, have recently been identified in serum and glomeruli of MN patients.[490]

Genetic Susceptibility

There are rare reports of familial MN.[491–494] Klouda et al. determined that HLA DR3 expression was highly associated with MN,[495] a finding that has subsequently been corroborated in other European populations.[496,497] HLA B18 may also pose a MN risk, and the combination of HLA-DR3, B18 and Bf1 is associated with MN and a rapidly deteriorating clinical course.[498] In studies from Japan, DR2 and DQw1 are more prevalent in patients with MN,[499] and an overall better prognosis for MN in the Japanese has been attributed to genetic differences.[500] Despite these associations between genetic markers and MN, the effect on clinical course is uncertain.

Treatment

The therapy for secondary MN is to treat the underlying disorder or withdraw the offending agent.[379] Because spontaneous remission occurs in approximately one-third of idiopathic MN cases,[501] and most treatment regimens contain drugs with potentially serious side effects, patients with few risk factors for progression, such as women and patients with normal GFR and <3.5 g/d proteinuria should be treated conservatively and monitored closely,[424,426] with an emphasis on anti-hypertensive therapy to control blood pressure and reduce proteinuria, preferably with an ACE inhibitor or angiotensin receptor blocker.[424,502–504]

Diuretics often control edema, and HMG CoA reductase inhibition is recommended for hyperlipidemia.[505,506] Prophylactic anticoagulation therapy to prevent thromboembolism is controversial, and should be reserved for patients with previous events or at high risk for thrombosis.[387,507]

The largest MN trials enrolled subjects with persistent nephrotic range proteinuria and stable GFR, with varying risks for progression. Corticosteroids as a sole agent for reducing proteinuria or preserving GFR are ineffective.[406,407,411,422,508] The Ponticelli group has published extensively about a six-month regimen for idiopathic MN that prescribes methylprednisolone (1 g/d for the first three days of each month) with alternating monthly prednisone (0.5 mg/kg/d) or chlorambucil (0.2 mg/kg/d).[462] At ten years follow-up, renal survival was 92% in the treatment group versus 60% in controls.[416] Because of concern about chlorambucil toxicity, this same group has conducted a randomized trial comparing prednisone combined with cyclophosphamide versus chlorambucil for MN treatment. These studies demonstrated no difference in outcome, and patients in the cyclophosphamide arm experienced fewer side effects,[509] suggesting that cyclophosphamide plus prednisone is also an acceptable choice. In a trial of 94 patients randomized to a six-month regimen with prednisone and cyclophosphamide versus supportive treatment (no immunosuppression), 10-year outcomes for mortality, dialysis-free survival, doubling of serum creatinine and relapse rates were all superior in the experimental group.[510] Another randomized trial involving 42 patients and one-year follow-up, demonstrated that prednisone plus either intravenous cyclophosphamide or cyclosporine was more effective than prednisone alone.[508] These results are consistent with some,[511] but not all studies,[403,408,413,512] though comparisons are difficult because patient populations, entry criteria and treatment regimens differed.[422,513] Nevertheless, in patients with MN that includes the nephrotic syndrome and stable GFR, in addition to supportive therapy, treatment with corticosteroids and an alkylating agent is preferable, particularly if patients have poor prognostic factors for progressive disease.

MN patients presenting with deteriorating GFR represent a special group, since they are at high risk for further progression. However, few trials have been specifically designed to address this subgroup of patients. A retrospective study by Torres et al. demonstrated efficacy of a chlorambucil plus prednisone regimen compared to a historical, untreated control group with equivalent MN progression.[514] Similar results were observed by Warwick et al., though toxicity was significant.[515] Two small studies showed efficacy of oral cyclophosphamide and prednisone in MN subjects with pre-existing, depressed or declining GFR.[516,517] Cattran et al. showed that in MN patients developing GFR decline with conservative therapy, subsequent treatment with cyclosporine slowed progression compared to a placebo control group.[518] More sobering results were obtained in the prospective trial by Falk et al., which demonstrated that prednisone with or without cyclophosphamide did not prevent renal disease progression in a MN cohort with a mean serum creatinine of 2.3 to 2.7 mg/dl and proteinuria greater than 10 g/24 hr,[519] suggesting that salvage therapy may be ineffective, once renal function has deteriorated. Therefore, in patients with serum creatinine exceeding 2.5 to 3.0, though there is no consensus regarding optimum treatment, it would be reasonable to manage conservatively, and prepare for dialysis or transplantation, rather than subjecting these patients to the potential perils of immunosuppressive therapy.

Cyclosporine has been shown to be effective for inducing and sustaining MN remission,[520,521] but concerns about nephrotoxicity render it less desirable for chronic treatment. Among newer agents, mycophenolate mofetil (MMF) and rituximab have been examined in small, mostly uncontrolled trials with MN patients. MMF has the benefit over cyclosporine and other calcineurin inhibitors because of less nephrotoxicity. Miller et al. demonstrated some benefit of MMF in a small study of 16 patients, most of whom had already failed other MN treatments.[522] Similar results were observed in an MMF trial by Choi et al. involving 17 patients with MN.[523] In two recent, small, controlled trials, with 1–2 year follow-up, MMF was no more effective than conservative therapy (no immunosuppression) or cyclophosphamide-containing regimens.[524,525] Rituximab is a chimeric monoclonal antibody, which binds to the B cell CD20 receptor and depletes B cells (but not plasma cells). Remuzzi and Ruggenenti observed that four weekly injections of rituximab conferred a sustained benefit in proteinuria reduction for up to one year in eight patients with MN, who had failed conventional treatment.[526,527] Rituximab, given every two weeks and at six months, may also be effective.[528] In a study of 13 MN patients dependent on MMF, cyclosporine or tacrolimus, four weekly doses of rituximab appeared to enable calcineurin inhibitor withdrawal, with sustained remission at 30 months.[529]

A diagnosis of MN is not a contraindication to renal transplantation. Although there are little outcome data, a recent study of 35 MN patients versus 70 non-MN controls demonstrated no difference in mortality at 10 years, but there was a trend toward decreased allograft survival and a 34% recurrence rate in the MN group.[530] The MN recurrence rate, with associated poor prognosis, was similar in a European transplantation cohort.[531]

Focal Segmental Glomerulosclerosis

Focal segmental glomerulosclerosis (FSGS) describes a histological lesion that is found in patients with idiopathic nephrotic syndrome.[532] FSGS is the most common cause of idiopathic nephrotic syndrome among African Americans. However, patients with FSGS constitute an increasingly larger fraction of idiopathic nephrotic individuals in the general, adult population. A survey of renal biopsies from 1995 to 1997 in adult patients with idiopathic nephrotic syndrome showed that FSGS is the most common lesion, accounting for 35% of all patients and for 50% of cases in African-American patients.[533–535] Focal segmental glomerulosclerosis accounts for approximately 3% of adult cases of end stage renal disease in North America.[535] Persistent non-nephrotic-range proteinuria is associated with good long-term renal survival, but declining glomerular filtration rates characterize patients with persistent nephrotic-range proteinuria. Evidence-based treatment guidelines are now being developed, but as discussed below, many experts recommend corticosteroids as initial therapy in patients with a poor prognosis for renal survival.

TABLE 82.19 Classification of FSGS

PRIMARY
Idiopathic FSGS
Classic
Glomerular tip variant
Collapsing or "malignant" variant
Superimposed on minimal change nephropathy
Familial (caused by mutations in podocyte genes encoding components of the slit diaphragm)
SECONDARY
Sickle-cell disease
Unilateral renal agenesis
HIV infection
Intravenous drug abuse
Vesicoureteral reflux
Diabetes mellitus (rare)
Postinflammatory scarring
Morbid obesity

Diagnosis and Course

Proteinuria, often in the nephrotic range, is the hallmark of FSGS. Hypertension is a presenting feature in approximately one-third of patients, and some degree of renal insufficiency is also present in one-third of patients at the time of diagnosis. Over half the patients with FSGS have hematuria. Proteinuria without hypertension is more common in children than adults with FSGS.[536]

FSGS may be primary (idiopathic) or secondary (Table 82.19). By definition, the term "idiopathic FSGS" is only used if evidence is lacking for other causes of focal glomerulonephritis that could result in focal scarring after healing.

The prognosis and clinical course of idiopathic FSGS are determined primarily by the severity of proteinuria.[537,538] Persistent non-nephrotic-range proteinuria is associated with good long-term renal survival. In contrast, declining glomerular filtration rates characterize patients with persistent nephrotic-range proteinuria. In this latter group of FSGS patients, the prevalence of end-stage renal disease 10 years after initial diagnosis is greater than 50%, and FSGS accounts for approximately 15% of pediatric and 5% of adult cases of end stage renal disease in North America. Patients with HIV-induced FSGS or the collapsing variant of FSGS (see description below) may progress rapidly to end-stage renal disease, often requiring dialysis within several months to 2–3 years after diagnosis, although the outcomes for most HIV patients has improved significantly after introduction of more effective anti-retroviral therapies.[539] The course of secondary forms of FSGS varies according to the severity and activity of the underlying disease.

Pathology

FSGS is a glomerular disease defined by a characteristic histologic pattern of scarring.[540–544] Sclerosis, or scarring, is present in parts (segmental) of some (focal) glomeruli.[543,544] By light microscopy, the typical FSGS lesion demonstrates mesangial collapse, scarring in parts of glomerular capillary tufts and adhesions to Bowman's capsule. However the light microscopic changes are non-specific and can be seen in other renal diseases, including those associated with glomerular inflammation. Immunoglobulin and complement deposition is generally not detected, although IgM and, less frequently, C3 staining can be detected in non-sclerotic glomeruli of some patients with FSGS. Demonstration of abundant immunoglobulin deposits by immunofluorescence should suggest another, superimposed primary or secondary glomerulonephritis. Similar to light microscopy, ultrastructural analysis by electron microscopy shows non-specific changes, predominantly foot process effacement in FSGS patients with heavy proteinuria, but can demonstrate other causes of glomerular disease, which are not apparent by light microscopy. Sometimes the focal, segmental glomerular scar is only identified by electron microscopy.

In addition to this typical lesion, there are additional, structural variants of FSGS that have been recently defined by a Working Group of pathologists.[545] In addition to the lesion described in the preceding paragraph (which is now classified as FSGS, not otherwise specified), the glomerular tip lesion is characterized by swelling, vacuolation, and proliferation of visceral epithelial cells (podocytes) and by sclerosis in the glomerular segments closest to the proximal tubule. Limited evidence suggests that patients with this histology tend to exhibit a more benign course and to be more responsive to steroid therapy compared to patients with classic FSGS. A second variant is characterized by focal or global glomerular capillary collapse and sclerosis with visceral epithelial cell swelling. This lesion is associated with a less favorable prognosis and is identified more commonly in African-American patients and in patients with human immunodeficiency virus (HIV) nephropathy. Additional morphologic variants include the perihilar (perihilar sclerosis and hyalinosis involving >50% of segmentally sclerotic glomeruli) and cellular (at least one glomerulus with segmental endocapillary hypercellularity occluding lumina) patterns. Severe tubulointerstitial disease associated with any of the structural, FSGS lesions correlates with poor long-term renal survival. Because the remission rate after treatment is similar among patients with the histologic variants, response to therapy cannot be predicted on the basis of histology alone.[546]

Pathophysiology

The molecular etiology of the sporadic forms of FSGS has not been determined, but several landmark studies have identified genetic mechanisms of FSGS and nephrotic syndromes, which cluster in families and is often steroid-resistant.[547–551] Mutations in several genes have been linked to familial FSGS, demonstrating the genetic heterogeneity of this disorder. The protein products of the human FSGS and nephrotic syndrome genes identified to date appear necessary for the maintenance of the filtration barrier (specifically the slit diaphragm) by the podocyte. These genes include *NPHS1* (encoding the slit diaphragm protein, nephrin), *NPHS2* (encoding the slit diaphragm protein, podocin), and *ACTN4* (encoding the cytoskeletal protein, α-actinin-4). More recently, mutations in a gene encoding a cation channel (*TRPC6*) have been identified in families with familial glomerulosclerosis. The genetic basis of sporadic FSGS is less well-defined, but mutations in the genes encoding a podocyte-selective transcription factor, *WT1*, and *NPHS2* have been described in approximately 5 and 11% of patients with non-familial, steroid-resistant FSGS. Mutations in the phospholipase C epsilon gene were identified as causing early-onset nephrotic syndrome with end-stage kidney disease.[552] Kidney histology of affected individuals showed diffuse mesangial sclerosis (DMS) as well as FSGS.

The recent discovery that common *APOL1* variants associate with sporadic focal segmental glomerulosclerosis (FSGS) and other non-diabetic kidney diseases in African American patients will likely be a critical turning point in understanding and management of these glomerular diseases.[553] Two genome wide admixture scans had identified a highly significant association on chromosome 22q12 between non-diabetic kidney disease and African ancestry.[554,555] This region contains many genes, and initial investigations focused on non-muscle myosin heavy chain IIA, encoded by *MYH9*, due to its podocyte expression and association with rare, mendelian giant platelet disorders that are also characterized by variably penetrant glomerular diseases. However, attempts to identify the *MYH9* causal variant(s) underlying this association were unsuccessful. Coding variants within the neighboring *APOL1* gene, which is centromeric to *MYH9* on 22q12.3, were shown to account for the association signal.[556] The biology responsible for the association is under intense investigation, but previous work had characterized APOL1 as the trypanosome lytic factor in human serum. Variant APOL1, which encodes the kidney disease risk variants, can kill disease-causing trypanosomes by circumventing the parasite's mechanism to evade lysis. This observation provided a biological explanation for the frequency of the kidney disease associated variants in populations of African ancestry. Similar to sickle cell disease, the parasite killing effect is dominant, requiring a single copy of the risk variant *APOL1* gene, and would be under positive selection in Africa. In contrast, association with kidney disease is best fit by a recessive model.

In addition to genetic factors, accumulating data suggest that steroid-sensitive nephrotic syndrome, as well as a subset of steroid-resistant nephrotic syndrome (particularly those recurring after transplantation) result from circulating a permeability factor(s).[540,557,558] T cells in these patients may promote the production of a circulating factor that alters permeability of the glomerular filtration barrier, but the nature of this factor remains elusive. Serum soluble urokinase receptor (suPAR) is elevated in two-thirds of subjects with primary FSGS, but not in people with other glomerular diseases and a higher concentration of suPAR before transplantation correlates with increased risk for FSGS recurrence after transplantation.[559] As mechanisms responsible for FSGS are better defined, therapy may be tailored for individual patients. The common mechanistic denominator for both the genetic and "acquired" etiologies of FSGS is that these diseases are

podocytopathies, a concept extensively covered in a number of excellent reviews.[540,541,547,551,560]

Treatment

The therapy of FSGS remains controversial, and data for evidence-based decisions are lacking. Most studies of therapy for FSGS patients have employed regimens used for treatment of minimal change nephropathy and have reported variable responses to therapy. However, recent case series, in which FSGS patients were treated with high dose corticosterioids (1 mg/kg/day) for prolonged courses (at least 16 weeks and for as long as 6 months), report response rates of up to 60 to 70% and improved long-term renal survival.[542,561] Many experts recommend a course of corticosteroids be offered to patients with likelihood of progressing to ESRD.

The potential efficacy and side effects of therapy must be considered for each patient. The amount of proteinuria, presence and degree of renal insufficiency, and the extent of scarring on biopsy are appropriate variables to evaluate before administering anti-inflammatory drugs. Non-specific therapy is probably an appropriate first approach in patients with mild proteinuria and normal renal function. Blood pressure should be normalized, if possible, in all hypertensive patients with FSGS. All patients with nephrotic-range proteinuria and FSGS should be treated with angiotensin-converting enzyme (ACE) inhibitors and/or angiotensin receptor antagonists (ARBs), unless otherwise contraindicated. Nephrotic-range proteinuria of any cause is an independent risk factor for progression of chronic renal failure, and ACE inhibitors and AT1 receptor blockers are the most potent anti-proteinuric agents available. Angiotensin stimulates aldosterone synthesis, and small case series suggest that spironolactone, an aldosterone antagonist, also may slow progression in patients with parenchymal renal disease. Hyperlipidemia should be controlled with appropriate medications to lower elevated cholesterol and tryglycerides, if dietary modifications fail to achieve target serum levels. Salt restriction and diuretics should be used to control edema in nephrotic FSGS patients.

Patients with persistent nephrotic proteinuria and renal insufficiency should be considered for more aggressive therapy with corticosteroids or other immunosuppressants. Prednisone, 1 mg/kg/day for at least four months, is now the recommended treatment regimen for patients with FSGS and is usually continued for one to two weeks after induction of remission and then slowly tapered.[561,562] Prolonged prednisone therapy of five to eight months has been advocated by some experts. Some patients, who initially respond to prednisone therapy, may exhibit frequent relapses or become steroid-dependent. Significant tubulointerstitial disease on renal biopsy, an elevated creatinine, and massive proteinuria of more than 10 gm daily suggest that the clinical response to steroid therapy may be poor. Patients with these risk factors may be candidates for early withdrawal from treatment if the steroids are tolerated poorly or cause significant side effects.

High quality evidence for use other immunosuppressive agents in patients with FSGS, who do not respond to corticosteroids alone or who are steroid-dependent or frequently relapse, is limited.[561,562] However, there are a number of reports that alternative immunosuppressive therapy may be beneficial. The North American Nephrotic Syndrome Study Group recently demonstrated, in a randomized controlled trial that steroid-resistant FSGS patients treated with cyclosporine and prednisone had better outcomes compared to patients that were not treated with cyclosporine.[563] Relapse is common when cyclosporine is discontinued, but cyclosporine-treated FSGS patients have a long term decrease in proteinuria and better preservation of GFR. Cyclosporine itself can be nephrotoxic and should be used judiciously. Cyclophosphamide or other cytotoxic drugs can be added to the therapeutic regimen, and small case series suggest that these drugs may induce complete or partial remission in up to 75% of these individuals.[561,562] A NIH-funded, multicenter randomized study of FSGS treatment compared the efficacy of a 12-month course of cyclosporine to a combination of oral pulse dexamethasone and mycophenolate mofetil in children and adults with steroid-resistant primary FSGS and found no difference in proteinuria remission rates.[564] Rituxamab has also been used to treat FSGS in case series and may prevent FSGS recurrence in transplants by regulating sphingomyelinase activity.[565]

Minimal Change Nephropathy

Minimal change disease (MCD), which is also known as minimal change glomerulopathy, nil disease or lipoid nephrosis, is characterized, as the name suggests, by normal histologic appearance by light microscopy. MCD accounts for more than 70% of cases of nephrotic syndrome in children less than 10 years of age, with a decline in incidence in older children. In adults, MCD represents 10 to 15% of cases of idiopathic nephrotic syndrome. Because of the predominance in children, most of the clinical studies have been conducted in pediatric populations.

Clinical Presentation and Natural History

The typical clinical presentation is relatively rapid onset of the nephrotic syndrome, with heavy

proteinuria. In children, hypertension is rare,[566] while in adults, hypertension is variable, but more common.[567] As described later in this chapter, MCD has been associated with infections, malignancies and pharmaceutical agents. Of note, non-steroidal anti-inflammatory agents have been linked to MCD with concomitant tubulointerstitial disease, which is characterized by interstitial lymphocytic infiltrates and pyuria.[568,569] In children, MCD rarely is associated with decreased GFR, whereas a syndrome with combined MCD and acute renal failure has been described in adults.[570] In adults MCD may include episodes of acute kidney injury from low oncotic pressures due to hypoalbuminuria that results in residual renal dysfunction,[571] but rarely progresses to ESRD.

Pathology

As previously mentioned, light microscopy is characteristically normal, with occasional mesangial prominence. In most cases, immunofluorescence microscopy is also negative, although there may be some IgM or complement C3 deposition in a mesangial pattern. The key diagnostic test is electron microscopy (Figure 82.11), which reveals podocyte foot process effacement, and cytoskeletal matting. Although these EM findings are similar in other causes of the nephrotic syndrome, the combination with normal light and immunofluorescence microscopy is diagnostic for MCD.

Pathophysiology

The mechanisms regulating MCD pathogenesis have not been completely defined, though some evidence supports a role for T cell activation, the most compelling being responsiveness to corticosteroid therapy (see below). In addition, evidence exists for a T cell-derived glomerular permeability factor,[572] which is perhaps a lymphokine.[573] The most prominent manifestation of this permeability factor is loss of filtration barrier electrostatic charge, with relative sparing of molecular size selectivity.[574] Overexpression of angiopoietin-like 4 in rat podocytes leads to steroid-sensitive nephrotic syndrome[575]

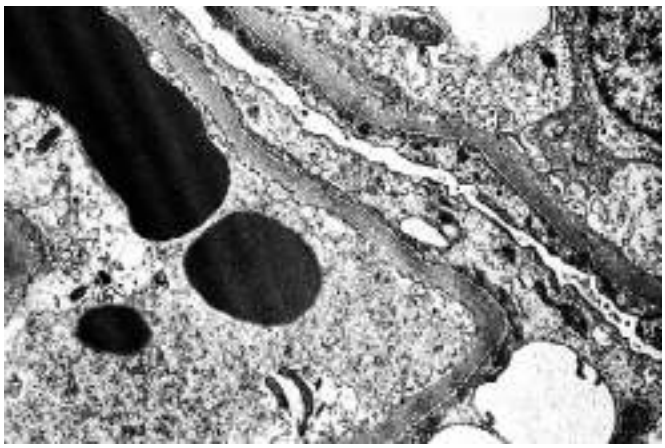

FIGURE 82.11 Minimal change disease. Electron micrograph demonstrating extensive foot process effacement. The glomerular capillary walls appear normal in thickness without any deposits.

Treatment

Standard therapy for MCD is corticosteroids (prednisone 60 mg/m^2/d for children and 1 mg/kg/d for adults). In children, this regimen results in prompt resolution of albuminuria in more than 90% of cases, generally within four to six weeks of initiating treatment. Lack of responsiveness should raise suspicion of alternative pathologies, such as focal and segmental glomerulosclerosis (FSGS), and may warrant repeat biopsy to definitively establish the diagnosis. In children who respond within six weeks, it is recommended to slowly taper the prednisone dose over an additional six weeks. This can be accomplished by decreasing the daily dose or with an alternate day regimen.[572,576,577]

In adults, MCD is also steroid-responsive, though efficacy is generally less, and time of response longer, compared to pediatric patients. In a study by Nalasco et al.,[567] in which 89 adults with MCD were analyzed, remission rates with 60 mg prednisone per day were 60% at 8 weeks, 76% at 16 weeks, and albuminuria eventually resolved in 81% of study subjects. Similar results were obtained in two subsequent, smaller series.[578,579]

Long-term studies indicate that approximately 25% of children achieve permanent remission, 50% relapse frequently (more than one episode per year) and the remaining 25% relapse infrequently.[580] Protocols with alkylating agents cyclophosphamide (2 mg/kg/d for 8 to 12 weeks)[567,574,581,582] or chlorambucil (0.1 to 0.2 mg/kg/d for 8 weeks)[583,584] have an efficacy of approximately 75% in relapsing patients. Because these agents have the potential for serious side effects, such as gonadal dysfunction, malignancy, and infection, protocols containing less toxic immunosuppressive drugs have been developed for relapsing, steroid-dependent and steroid-resistant MCD. In general, cyclosporine has been shown to achieve short term remissions, even in steroid-resistant cases, though long-term remission rates are poor.[585] However, one case series of steroid-dependent and resistant nephrotic syndrome, that included 5 cases of MCD, demonstrated that cyclosporine treatment for a mean of 22 months resulted in good long-term remission.[586] In a randomized trial of eight weeks of cyclophosphamide versus nine months of cyclosporine, involving both adults and children with MCD, both drugs induced remissions, though long-term remission rates were superior in the

cyclophosphamide group.[587] Small studies with newer agents, such as mycophenolate mofetil[588] or rituximab[589] show promise, including the theoretical advantage of less nephrotoxicity compared to cyclosporine, though there is insufficient experience with either drug as alternative treatment for complicated MCD.

Systemic Diseases Associated with the Nephrotic Syndrome

The most common causes of "secondary" nephrotic syndrome, such as diabetic nephropathy (Chapter 78) and lupus nephritis (Chapter 78) are discussed in detail elsewhere. The following section focuses on amyloidosis, multiple myeloma, and nephrotic syndrome associated with infectious diseases, malignancies and drugs.

INFECTIOUS CAUSES OF THE NEPHROTIC SYNDROME

HIV-Associated Nephropathy (HIVAN)

Shortly after the discovery that HIV caused AIDS, several case series of AIDS-related renal disease were reported.[590–592] These reports described a sclerosing glomerular lesion and very poor prognosis. As discussed below, with the advent of effective antiretroviral therapy, the clinical course is now more benign. Furthermore, other nephropathies resulting from HIV infection have been described. Nevertheless, HIVAN is still the most common cause of ESRD among HIV-positive patients, and the third most common cause of ESRD among African Americans in the U.S. between the ages of 20 and 64 (www.usrds.org). The predilection for HIVAN in patients of African descent has been noted in the U.S. and Europe.[593,594] In addition to HIVAN, HIV patients are vulnerable to opportunistic infections (tuberculosis, CMV, fungal) and malignancies (Kaposi's sarcoma, lymphoma), which may lead to glomerular disease.[595]

Clinical Presentation and Natural History

Patients with HIVAN typically present with nephrotic range proteinuria and renal insufficiency. In contrast to most proteinuric renal diseases, hypertension and edema are less common,[596] consistent with the notion that HIVAN involves tubular epithelia and leads to salt-wasting.[594] Kidneys tend to be large and echogenic on ultrasound examination.[597,598] A definitive diagnosis can only be made with a renal biopsy, though recent reports indicate that urinary neutrophil gelatinase-associated lipocalin (NGAL) and growth factors may be sensitive biomarkers for HIVAN.[599,600] Although HIVAN is still typically diagnosed after prolonged exposure to high HIV viral load,[601] it can present early, and rarely at the time of HIV diagnosis.[602,603] The clinical course of HIVAN has become markedly more protracted since introduction of highly active anti-retroviral therapy (HAART) regimens, and should now be considered a cause of chronic, rather than acute kidney injury.

Less commonly, HIV-positive patients can develop thrombotic microangiopathies with renal involvement, such as hemolytic uremic syndrome (HUS). A distinguishing feature is that nephrotic range proteinuria is typically absent,[595] though it can occur due to coexistence of typical HIVAN.[604] Results from small, uncontrolled trials suggest that HIV-associated HUS is resistant to treatment with glucocorticoid hormones, plasmapheresis, immunoglobulin infusion, anti-platelet agents, vincristine or splenectomy.[604–606]

Proliferative glomerulonephritis with immune complex deposition, including with IgA,[607,608] has also been described in HIV-infected patients.[595,609,610] In contrast to African American HIV patients with renal disease, who almost exclusively develop typical HIVAN lesions, HIV-associated immune-mediated GN is observed primarily in Caucasians.[595,609]

Pathology

Although many pathologies have been observed, the classical histologic lesion in HIVAN is a form of focal and segmental glomerulosclerosis called collapsing glomerulopathy, which is characterized by segmental or global glomerular collapse, resulting in widened Bowman's space, and GBM wrinkling[611] (Figure 82.12). Glomerular pathology also includes podocyte hypertrophy and/or hyperplasia,[612,613] which may play a pathophysiologic role. In some cases, robust podocyte proliferation can result in the formation of pseudocrescents. Additional common findings include lymphocytic interstitial infiltrates, tubular microcystic dilation and glomerular endothelial reticular inclusion bodies,[614] though the latter finding is less common since effective anti-retroviral therapies have been widely prescribed. Like most glomerular diseases, tubular atrophy and interstitial fibrosis correlate with progression. Unlike other causes of the nephrotic syndrome, which invariably show podocyte foot process effacement and cytoskeletal rearrangement, podocytes in HIVAN assume a more de-differentiated phenotype, with absence of foot processes, paucity of cytoskeletal elements, and loss of podocyte markers, such as synaptopodin, WT1, podocalyxin and GLEPP1.[612] Immunofluorescence microscopy is typically non-diagnostic, but may show deposition of IgM, C3, and less frequently, C1q.[615]

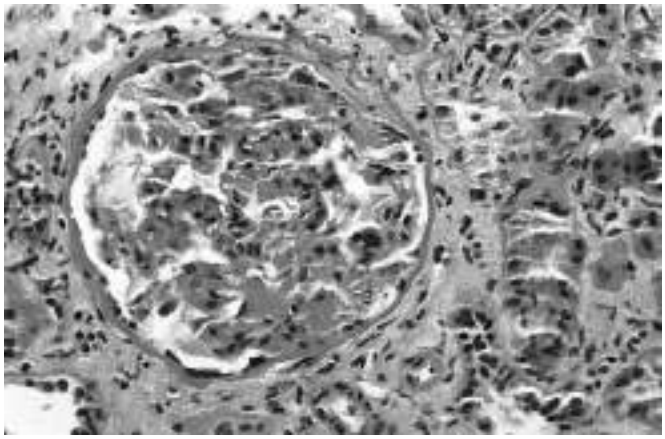

FIGURE 82.12 Collapsing glomerulopathy associated with HIV. Global collapse of glomerular capillary walls with hypertrophy and hyperplasia of podocytes (H&E, X330).

Pathophysiology

Most patients with HIVAN have low CD4 counts,[616] but clinical immunodeficiency is not required for development of HIVAN.[595] HIVAN is caused primarily by infection of resident renal epithelial cells with HIV, which then serve as a viral reservoir. HIV mRNA has been localized to podocytes and tubular epithelial cells from human renal biopsies,[617,618] suggesting that HIV infection is pathogenetic. Furthermore, HIV transgenic mice mimic pathologic findings observed with HIVAN in humans.[619,620] In these animals, the HIV transgene was expressed in epithelial cells prior to demonstrable renal lesions, suggesting a pathophysiologic mechanism involving direct cytopathic effects of HIV, rather than effects from exogenously released cytokines.[621] This conclusion is supported by the observation that HIVAN developed in transgenic kidneys transplanted into wild-type littermates, whereas normal kidneys remained disease free when transplanted into HIV transgenic littermates.[621] Furthermore, transgenic lines that expressed the transgene in extrarenal tissues, but not kidney, did not develop HIVAN pathology.[622] Phylogenetic analysis of HIV sequences from microdissected infected human kidney tubular epithelial cells and circulating blood mononuclear cells revealed evidence of tissue-specific viral evolution, indicating localized kidney HIV replication and existence of renal epithelial cells as HIV reservoirs.[623] Transgenic mice that express HIV accessory proteins, but not the intact virion, also develop typical HIVAN histologic features, indicating that viral proteins, such as nef and vpr, rather than replicating virus, are essential for signaling dysregulation and cytotoxicity.[622,624–626] Neither the specific mechanisms by which HIV gains entry to renal epithelial cells, nor how HIV infection regulates podocyte de-dedifferentiation, collapsing FSGS and other pathologic features is known.

Predisposition for HIV patients of African descent, but living in different environments, as well as HIVAN clustering in African American families, suggests that there may be a genetic component to HIVAN susceptibility.[627] Human mapping studies have implicated a susceptibility region on chromosome 22 that includes the MYH9 and ApoL1 genes,[628] while linkage analysis and expression profiling identified two susceptibility loci in HIV transgenic mice.[629]

Treatment

The current standard of care for HIVAN (as well as for HIV infection, in general) is highly active antretroviral therapy (HAART). Since HAART was introduced in the U.S. 10 years ago, the incidence of ESRD due to HIVAN has only slightly decreased,[630] despite reduction in AIDS-related mortality. Because of the unequivocal benefit of HAART on survival in HIV-infected patients, it is doubtful that a placebo control trial for HIVAN will ever be conducted. Nevertheless, evidence for the efficacy of HAART on HIVAN can be derived from work by Lucas et al., which demonstrated a 60% risk reduction for HIVAN in a large, HIV-infected population followed for 12 years.[631] An uncontrolled, retrospective trial demonstrated that protease inhibitor therapy slowed GFR declines in a small HIVAN cohort,[632] and several case reports or series also document benefit of HAART.[602,618,633,634]

Renal side effects of HAART are fairly common, (reviewed in[635]), including acute kidney injury and crystalluria-induced tubulointerstitial disease with protease inhibitors,[636,637] as well as acute renal and proximal tubule dysfunction with Fanconi syndrome from nucleotide reverse transcriptase inhibitors.[638–642] The latter is due to tubular mitochondrial toxicity.[635]

Two small series have demonstrated benefit of prednisone for the treatment of HIVAN, though many patients relapsed after prednisone was discontinued, and several developed serious infectious complications.[643,644] Because of short-term follow-up, and the potential for complications, larger randomized trials are necessary before prednisone can be recommended as therapy for HIVAN.

HIVAN patients with serum creatinine less than 2.0 mg/dl benefited from ACE inhibitor therapy, as determined by serum creatinine, proteinuria and requirement for renal replacement therapy.[645,646] Renal disease progression was also prevented in HIV transgenic mice treated with angiotensin receptor blockers.[647] In our opinion, ACE inhibitor or ARB therapy is sensible for HIVAN patients with proteinuria, particularly those with concomitant hypertension.

Hepatitis C

Long-term complications of chronic hepatitis C virus (HCV) infection can include glomerular disease, either with or without cryoglobulinemia. The cryoglobulinemia is mixed, with complexes containing HCV virions, anti-HCV immunoglobulins, and rheumatoid factor, which is comprised of IgMκ chains. In populations of patients with mixed essential cryoglobulinemia, approximately 90% will have measurable anti-HCV titers. The exact etiology of the cryoglobulinemia is unknown, but is presumed to be due to B cell proliferation in response to HCV antigenic stimulation.

Clinical Presentation and Natural History

Most patients with renal manifestations of HCV infection have membranoproliferative glomerulonephritis (MPGN) due to type II cryoglobulinemia, which is characterized by polyclonal IgG and anti-globulin IgMκ rheumatoid factor.[648,649] It has been suggested that most cases of idiopathic MPGN are due to underlying viral hepatitis.[650] The exact proportion of HCV-infected patient that develop MPGN is not known, but the risk appears to be greater in subjects with chronic infection and liver disease. In cryoglobulinemic patients, symptoms typically include malaise, weakness, and arthralgia. Common physical findings include hypertension, peripheral edema, palpable purpura and hepatomegaly. Renal involvement is characterized by proteinuria (nephrotic range in approximately 20% of cases), microscopic hematuria and decreased GFR.[648,649,651–655] Serologies commonly reveal detectable serum anti-HCV titer and HCV RNA, elevated liver transaminases (ALT >AST), rheumatoid factor, low C3 and C4 complement levels and cryoglobulinemia.

Pathology

The most common finding is MPGN, especially in patients with cryoglobulinemia, although membranous glomerulopathy, FSGS, mesangial proliferation with IgA deposition, post-infectious, fibrillary and immunotactoid lesions have been reported.[653,654,656] With MPGN, there is typically glomerular tuft lobulation and endothelial cell swelling, GBM splitting, and infiltrates containing lymphocytes, neutrophils and activated macrophages. Mesangial sclerosis is observed in advanced cases. Tubular atrophy and infiltrates are observed with progressive disease. Immunofluorescence generally shows IgG, IgM and C3 in a glomerular capillary pattern, and to a lesser extent, IgA and C1q in mesangium and/or glomerular capillaries. On EM evaluation there are electron-dense deposits, with a fibrillar appearance, in subendothelial, and less commonly, intramembranous or mesangial locations.[648] Mesangial interposition within the GBM has also been described. In the subset of chronic HCV-infected patients with non-cryoglobulinemic MPGN, the histopathology is similar, with the exception that leukocyte infiltrates and the fibrillar pattern of immune complexes are less prominent.

Pathophysiology

The pathophysiologic mechanism regulating HCV infection and glomerular disease is not well established, but presumably is related to immune complex formation with HCV, rheumatoid factor and/or anti-HCV antibodies. The paucity of information is due, in part, to lack of a suitable animal model for HCV-induced renal disease. Currently, chimpanzees are the only model that permits HCV propagation, though studies have been limited to liver pathophysiology and investigation of immune mechanisms.[657]

Treatment

With the assumption that renal manifestations of HCV are related to viral exposure and resulting immune response, therapies have been designed with anti-viral and immunosuppressive agents to suppress viremia and B cell activation, respectively. In small trials in patients with mixed essential cryoglobulinemia, interferon-α treatment resulted in reductions of serologic markers and serum creatinine.[658,659] In several case reports involving patients with chronic HCV infection, cryoglobulinemia and biopsy-proven MPGN, interferon-α administration as a single agent has resulted in modest improvement in GFR and/or proteinuria.[648,660–663] However, these studies uniformly demonstrated that the effect was transient, with high relapse rates of viremia and glomerular disease.

To enhance the anti-viral response, interferon-α is often given in conjunction with ribavirin. This combination therapy has been shown to have some effect, particularly on proteinuria, though complete resolution of glomerular lesions and renal function is exceptional.[664–667] Improvement in GFR and proteinuria is generally associated with successful suppression of HCV viremia.[668] A decision to treat HCV-induced MPGN with combination therapy is complicated by reports of worsening renal function with interferon-α[669,670] and impaired ribavirin clearance in patients with depressed GFR.[671] The duration of anti-viral therapy is dictated by HCV genotypes.[668]

Prior to the realization that most cases of mixed cryoglobulinemia are due to chronic HCV infection, many patients were empirically treated with plasma exchange and immunosuppression (primarily cyclophosphamide and prednisone), with variable success.[652,668] In part due to concerns about the potential for worsening HCV infection, these regimens

are not currently considered first line therapies for cryoglobulinemia or HCV-related MPGN. A recent meta-analysis demonstrated superior reduction of proteinuria with interferon-α-containing regimens compared to immunosuppression with prednisone ± cyclophosphamide.[672] In rare instances of HCV-induced vasculitis with renal involvement, or MPGN with heavy proteinuria and/or rapid decline in GFR, treatment with glucocorticoids and cyclophosphamide should be considered as first-line therapy, though responses have been variable.[668,673]

Finally, humanized anti-CD20 antibodies (rituximab) have been shown to improve the serologic response in cryoglobulinemia,[674] with the rationale that rituximab would reduce B-cell IgM secretion and cryoglobulin formation. However, data regarding effect on HCV-associated glomerular diseases is limited. Two small case series in cryoglobulinemic HCV-related MPGN patients demonstrated that four weekly doses of rituximab reduced proteinuria, but had little effect on serum creatinine.[675,676] Rituximab would theoretically be most effective in conjunction with anti-viral therapy to diminish the stimulus for antibody production; a very recent small trial indicates that this combined approach was indeed effective for resolution of GFR, proteinuria and hematuria in patients with cryoglobulinemia.[677]

Hepatitis B

Hepatitis B virus (HBV) has been most commonly associated with the nephrotic syndrome and a pathologic picture which is predominantly membranous nephropathy.

Clinical Presentation and Natural History

The mode of transmission and clinical course varies between endemic areas, such as Southern Africa, Southeast Asia, and the United States. In endemic regions, HBV is often transmitted from mother to child or between siblings, and the incidence of nephropathy occurs at a 4:1 male:female ratio.[678–680] In the US, HBV-associated glomerular disease affects primarily adults, and the mode of transmission is primarily through sexual contact.[681–683]

Most patients present with proteinuria, often in the nephrotic range. Urinalysis is generally benign, though microscopic hematuria can be seen. Serum hepatic aminotransferase levels may be normal to mildly elevated, consistent with viral carrier status or mild hepatitis. Detection of hepatitis B surface antigen (HBSAg) in serum is helpful diagnostically,[684–692] and hepatitis antigen-containing circulating immune complexes have also been isolated.[688,693] Liver biopsies often reveal chronic active hepatitis, occasionally cirrhosis, and rarely acute hepatitis.[694,695]

Pathology

The most common lesion is membranous nephropathy, although occasional reports of FSGS and MPGN have been described.[678–683,696,697] Rarely, fibrocellular crescents have been associated with membranous lesions.[698,699] Immunofluorescence demonstrates IgG, and less commonly C3, IgM and IgA in a glomerular capillary pattern. EM typically reveals electron-dense deposits in subepithelial locations. Glomerular endothelial tubuloreticular structures,[700] variable detection of HBV antigens within immune deposits,[679,684,686–690,692,701] and electron-dense deposits occasionally in mesangial and subendothelial sites[690] are useful in distinguishing from idiopathic membranous nephropathy.

Pathophysiology

HBSAg, core (HBcAg), e (HBeAg) antigens[702] and viral DNA[680,703] have been detected in glomeruli from biopsies, and circulating immune complexes containing hepatitis viral particles have been detected in HBV-associated glomerular disease,[688,693] thereby implicating viral antigens in pathogenesis.

Treatment

Because spontaneous remission of HBV-related membranous nephropathy is common in children from endemic areas,[694,695] supportive therapy is generally sufficient. Patients with HBV-associated progressive renal disease pose a greater challenge, inasmuch as no therapy has proven unequivocally effective. In small series, glucocorticoid hormones, which are a component of most regimens for idiopathic membranous glomerulopathy, have shown some efficacy in reduction of proteinuria, though a sustained benefit has not been demonstrated, and therapy was associated with enhanced viral replication.[704,705] An initial report, involving five patients, indicated that interferon-α may be effective in reducing HBV viral load and ameliorating associated glomerular disease, as demonstrated by reduction in proteinuria.[706] However, subsequent, larger studies with longer follow-up have produced less optimistic results,[707,708] particularly in those patients with a poor initial response and MPGN histopathology.[708] Case reports with nucleoside analogues, such as adenine arabinoside (vidarabine) or 3TC (lamivudine, Epivir), have shown some promise,[697,709,710] though large trials are necessary before these agents can be confidently recommended for HBV-associated glomerular disease.

Syphilis

Patients with congenital, secondary or latent syphilis have been demonstrated to have associated glomerular disease.[711–722] Typical clinical manifestations are those of the nephrotic syndrome, accompanied by hypertension. In cases of congenital syphilis, a large percentage may have renal involvement.[712] Symptoms, which generally include proteinuria with or without hematuria, appear within weeks after birth. Light microscopic histologic findings are variable, ranging from minimal change disease to proliferative glomerulonephritis with crescents and interstitial infiltrates,[723] although membranous lesions are common. Transmission electron microscopy findings are more consistent, with frequent observation of subepithelial deposits of varying sizes and podocyte foot process effacement. Immunofluorescence microscopic findings typically reveal fine or coarse granular IgG and C3 deposits in a glomerular capillary pattern. Treponemal antigen and antibodies have been detected in glomeruli from biopsies,[711,712] suggesting immune-mediated pathogenesis.

In glomerular disease associated with secondary or latent syphilis, patients usually present with the nephrotic syndrome, though they can be asymptomatic. Serum complement levels are usually normal, though rare cases of hypocomplementemia and circulating complement-containing immune complexes have been described.[720,721] Microscopic pathologic features are similar to that of congenital syphilis, with the most common appearance resembling membranous nephropathy, although minimal change disease is sometimes found. Treponemal antigen and antibodies have been identified in glomeruli from patients with secondary and latent syphilis.[718,720,724]

In all forms of syphilis-associated glomerular disease, response to penicillin therapy is excellent with remission of nephrotic syndrome,[713,723] although residual proteinuria has rarely been observed.

Malaria

Malaria is one of the most common infectious diseases in the world, with an annual incidence of approximately 300-500 million cases.[725] Of the strains of malaria, infection with *P. malariae* (also known as quartan malaria) and *P. falciparum* have been associated with glomerular disease. In cases of falciparum malaria, renal manifestations are rare, but often mild, with hematuria and sub-nephrotic proteinuria, usually with normal GFR.[726,727] Oliguric acute tubular necrosis is the most serious complication of falciparum malaria.[726] One small biopsy series demonstrated that the most common glomerular lesions were mesangial proliferation or MPGN.[728] IgM, C3 and occasionally IgG deposits can be observed, most commonly in a mesangial pattern.[729]

Although quartan malaria is less common than falciparum malaria, renal complications are more frequent. Fortunately, quartan malaria has become a relatively rare cause of glomerular disease in areas where malaria remains endemic.[730] In general nephropathy associated with quartan malaria can be acute, occurring within two to three weeks of infection. This form tends to be mild and transient, with associated features including non-nephrotic proteinuria and glomerular lesions characterized by deposition of IgM, complement and malaria antigens.[725] A more chronic variety, which disproportionately affects children, presents with fever, hypertension, edema, hepatosplenomegaly, nephrotic range proteinuria, and absence of hematuria. Children with the nephrotic syndrome have higher levels of parasitemia compared to infected children without renal involvement. Biopsy series in African children most commonly revealed a variety of pathologic lesions, including focal and diffuse proliferative glomerulonephritis, membranous nephropathy and focal glomerulosclerosis.[731–733] Immunofluorescence microscopy reveals IgG, IgM, C3 and *P. malariae* antigens within glomeruli, suggesting that the pathophysiology is due to immune complex deposition. This mechanism is supported by transmission EM studies demonstrating thickened GBM and intramembranous,[734] fine granular subendothelial or coarse granular subepithelial deposits.[729] Children with quartan malarial renal involvement generally progress to ESRD, with little documented benefit of anti-malarial or immunosuppressive therapies.[735,736]

Schistosomiasis

The most common clinical manifestations of schistosomiasis are cirrhosis, due to *S. mansoni* and *S. japonicum*, and cystitis from *S. haematobium*. However, schistosomiasis has also been identified as a rare cause of glomerular disease. In biopsy series involving patients with coincident *S. mansoni* infection and renal dysfunction, most have MPGN, but membranous glomerulopathy and FSGS have also been observed.[737–739]

A pathology staging systems has been created,[740] with class I lesions demonstrating mesangial proliferation with IgM and C3 deposits, and an associated self-limited clinical course. Stage II lesions occur in the context of symbiotic salmonellosis, and are characterized by glomerular neutrophils and C3 deposition. The accompanying clinical course is typified by fever, vasculitic skin lesions, anemia and rapid onset of the nephrotic syndrome.[741] Combined therapy directed against schistosoma and salmonella is effective.[740]

Stage III and IV lesions occur primarily in patients infected with *S. mansoni* and hepatic fibrosis,[740] with predominance in Caucasian and Hispanic patients. The clinical presentation in stages III and IV includes hypertension, the nephrotic syndrome, hematuria and even red blood cell casts. Extrarenal manifestations often include stigmata of portal hypertension. Class III lesions resemble idiopathic MPGN, with immune complexes comprised of IgG, IgA and C3 in mesangial, subendothelial and subepithelial locations. Stage IV lesions occur most commonly in the African population, and have a focal glomerulosclerosis pattern, which can also be associated with glomerular IgG, IgA and C3 deposition. Schistosomal antigens and antibodies have been detected in eluates from the majority of biopsy samples, as well as within glomerular deposits from human biopsies and animal models,[734,742] strongly suggesting an immune-mediated mechanism of disease. The clinical course tends to be more serious in stages III and IV, often culminating in progression to ESRD. Therapy with anti-parasitic agents directed against *S. mansoni* has been shown to have no effect on the course of kidney disease.[742,743] In a case series of two patients with *S. haematobium* and the nephrotic syndrome, treatment with niridazole resulted in remission of proteinuria.[738]

Stage V glomerular disease is amyloidosis,[744] and it can be caused by infection with either *S. mansoni* or *S. haematobium*. The clinical presentation is similar to stages III and IV, and schistosomiasis-associated amyloidosis is resistant to treatment with glucocorticoid hormones, colchicine or anti-schistosomal agents.

Mycobacterial Diseases

The major mycobacterial diseases with renal manifestations are *M. tuberculosis* and *M. leprae* (leprosy). The epidemiology of tuberculosis is well-chronicled, but leprosy is also a very common problem worldwide, with a prevalence of approximately 12 million cases, 3 million of which are in India.[745] Renal involvement in leprosy often occurs in conjunction with erythema nodosum, and the clinical spectrum can include hematuria, ranging from asymptomatic/microscopic to acute glomerulonephritis, proteinuria, either in the asymptomatic or nephrotic range, and azotemia. In patients with leprosy-associated nephrotic syndrome, the most common renal pathology is amyloidosis.[729,746,747] However, in a large biopsy series of nephrotic syndrome cases in India, 34 of 2827 biopsies revealed membranous nephropathy attributed to infection with *M. tuberculosis* and *M. leprae*.[748] Other lesions include mesangial proliferation, MPGN, focal and diffuse glomerulosclerosis.[729] Immunofluorescence microscopy typically reveals staining with IgM, IgA or fibrin in a mesangial or glomerular capillary pattern. In cases with glomerular deposits, electron microscopy findings include dense deposits in subendothelial and subepithelial locations, as well as GBM thickening and mesangial interposition.[729,749–751] The pathophysiology is most likely due to deposition of immune complexes, which may contain mycobacterial antigens.[749,752–754]

Despite the enormous worldwide prevalence of tuberculosis, associated glomerular disease is relatively uncommon. In biopsy series from third world countries, tuberculosis is one of the most common causes of secondary amyloidosis, with a prevalence ranging as high as 50%.[729,755,756] However, other glomerular lesions have been associated with tuberculosis and the nephrotic syndrome, including minimal change disease and FSGS.[757,758] Several case reports indicate that eradication of tuberculosis infection with antibiotic therapy can result in remission of secondary renal amyloidosis.[759–761]

MALIGNANCY-ASSOCIATED GLOMERULAR DISEASES

Membranous Nephropathy (MN)

Paraneoplastic syndromes including the nephrotic syndrome have rarely been described (in less than 1% of malignancies[762]), most commonly with MN. Estimates for the coincidence of malignancies with documented MN vary widely, but is on the order of 7 to 8%.[763–769] The association between carcinomas of the lung and gastrointestinal tract was first described by Lee et al. in 1966.[763] Since that time, it has been recognized that MN is associated with a variety of carcinomas (Table 82.20). Because most of these malignancies are more common in elderly patients, a new diagnosis of MN in a patient older than age 50 should probably warrant investigation for neoplastic diseases, or at least performance of recommended age-specific cancer screening test.

Clinical Presentation and Natural History

The clinical presentation of malignancy-associated MN is similar to idiopathic MN.[783] A cancer diagnosis precedes the nephrotic syndrome in 30–60% of cases.[782,784] In the remainder, in which the nephrotic syndrome comes first, a cancer diagnosis can usually be established within one year of MN diagnosis,[763,769] though an increased cancer risk extends for up to 15 years.[784] There are reports of MN remission in conjunction with cancer cures[785,786,769] and MN relapse with malignancy recurrence or metastasis.[769,787,788] However, these data linking malignancy with MN

TABLE 82.20 Malignancies Associated with Membranous Nephropathy[767,769–782]

CARCINOMAS
Lung
Colon
Breast
Stomach
Prostate
Rectum
Kidney
Ovary
Pancreas
LEUKEMIA AND LYMPHOMAS
Chronic leukemia
Hodgkin's lymphoma
Non-Hodgkin's lymphoma
Parotid adenolymphoma
OTHER TUMORS
Testicular seminoma
Melanoma
Carcinoid

should be interpreted with caution, since approximately one-third of patients with MN will spontaneously remit, many cancer chemotherapy regimens may independently be effective treatment for MN,[782] and MN resolution does not always parallel malignancy remission.[764,771]

Pathology

Diagnostic renal biopsy findings may be indistinguishable from idiopathic MN. However, additional features, such as glomerular inflammation, mesangial cell proliferation, subendothelial, mesangial, IgA and C1q deposits are suggestive of malignancy-associated MN.[782,783]

Pathophysiology

The pathophysiology of malignancy-associated MN is not well established, but based upon known pathophysiology in idiopathic MN, it has been postulated that tumor antigens are filtered and planted within the subepithelial space, allowing for in situ immune complex formation and complement activation.[762,782] Few cases of documented subepithelial lung and colon cancer antigen deposition have been described.[769,789–792] However, tumor antigen deposition cannot be documented in every case,[764,771] and delineation of relevant epitopes for all tumors precludes definitive testing of an in situ immune complex hypothesis. Alternative hypotheses include cross-reactivity of antitumor antibodies with podocyte and glomerular endothelial cell antigens.[782]

Treatment

Therapy for malignancy-associated MN is generally directed toward the primary malignancy. However, there should be some consideration that immunosuppressive regimens, which have been demonstrated to be beneficial for idiopathic MN, may be detrimental for some cancers. In patients with malignancy-associated nephrotic syndrome, standard supportive care should include angiotensin converting enzyme inhibitor or angiotensin receptor blocker therapy for proteinuria reduction, HMG-CoA reductase therapy for hyperlipidemia, and diuretics for edema. Since there are potential adverse consequences with anticoagulation, and treatment duration is not established, it is unclear whether prophylaxis for thrombosis is warranted.

The magnitude and cost-effectiveness of the workup for malignancy in patients with a preceding MN diagnosis is also controversial. Because malignancy incidence increases with age, it is reasonable for MN patients over 50 years of age to strictly follow screening guidelines for the general population.[782] Symptoms or physical signs suggestive for other malignancies, which would not be diagnosed by standard screening tests, should obviously be pursued with more appropriate studies.

Minimal Change Disease (MCD)

MCD has been observed to accompany lymphomas (Hodgkin's more frequently than non-Hodgkin's),[793–795] leukemia,[794,796] and less commonly, thymoma,[797] renal cell carcinoma,[798] cecal carcinoma[799] or bronchial carcinoma.[800] Onset of the nephrotic syndrome from MCD is generally simultaneous with tumor presentation.[762] Case reports of lymphomas, leukemia, thymoma, mycosis fungoides, and multiple myeloma have also been associated with FSGS.[794,795,801–803]

Proliferative Glomerulonephritis

Membranoproliferative glomerulonephritis (MPGN) with or without fibrocellular crescents has rarely been linked to lymphoma, especially chronic lymphocytic leukemia,[804–806] as well as carcinomas.[807,808] Unlike other malignancy-associated glomerular diseases, MPGN characteristically presents with an active urinary sediment, and often with rapid decline in GFR. The pathophysiology of MPGN, particularly in conjunction with CLL, may be due to cryoglobulinemia.

Vasculitis

The prevalence of ANCA-positive vasculitis and malignancy has been described.[809] An association between malignancies involving respiratory, urinary or GI tract and ANCA-positive rapidly progressive glomerulonephritis (RPGN) has been reported.[810–814] It has been postulated that the tumors stimulate autoantibody generation.

Amyloidosis

Renal amyloidosis has been linked to chronic inflammatory states, which may include some malignancies, especially renal cell carcinoma, Hodgkin's disease, chronic lymphocytic leukemia and adrenal carcinoma.[762,815,816]

DRUG-INDUCED GLOMERULAR DISEASES

Membranous Nephropathy (MN)

Drug-induced MN has been described most commonly with medications prescribed for rheumatoid arthritis, such as oral and parenteral gold, D-penicillamine and bucillamine.[817–822] These drugs have also been linked to minimal change disease (MCD),[820,823,824] though less frequently than with MN. Rare cases of anti-GBM disease and vasculitis due to D-penicillamine have also been reported.[823,825,826] D-penicillamine-induced MN has been associated with HLA-B8/DR3 antigen,[820,827,828] suggesting a genetic predisposition. MN from gold or D-penicillamine generally develops within 6 to 12 months of starting the drugs.[762,782] Decreased GFR is usually not observed. If gold or D-penicillamine are discontinued when MN is diagnosed, proteinuria generally resolves within 12 months.[820,828] However, in a retrospective series of 53 patients with biopsy-proven nephropathy from gold or D-penicillamine, 21 subjects continued therapy for up to 11 months, without adverse effects on GFR, peak proteinuria values, or resolution of proteinuria.[829]

Mercury-containing substances, such as older, infrequently prescribed diuretics, some skin creams, and industrial exposures, have been associated with the nephrotic syndrome, due to MN and MCD.[830–836] When captopril was initially released, high doses were associated with MN.[837–840] Substitution with enalapril resulted in resolution of nephropathy,[841] suggesting that sulfhydryl groups unique to captopril may be a stimulus. Lithium has been associated with a variety of glomerular diseases, including MN and FSGS,[842–844] though the most common glomerular lesion is MCD.[845,846]

Heroin-Induced Focal and Segmental Glomerulosclerosis (FSGS)

An association between chronic heroin use and the nephrotic syndrome was noted over 30 years ago.[847–853] The glomerular lesion most commonly associated with intravenous heroin is FSGS, which occurred predominately in young, African-American men, whereas heroin is associated with MPGN in whites.[854] More recently, it has been demonstrated that the most common etiology of idiopathic nephrotic syndrome in African-American men is FSGS,[855] and MPGN from heroin use coincides with hepatitis C infection,[856] suggesting that heroin use may not be an independent risk for FSGS. Furthermore, the nephrotic syndrome resulting from intravenous drug use is now almost exclusively due to HIV-associated nephropathy. In the original descriptions, heroin-associated FSGS frequently resulted in progression to ESRD, though progression was not inevitable if heroin was discontinued.[762]

In heroin-associated FSGS, glomerular C3 complement and IgM deposits may be observed, though this is likely due to non-specific trapping within areas of sclerosis, and unlikely to be pathophysiologically relevant.[762] Tubulointerstitial inflammation has also been noted. The mechanism of heroin-associated FSGS has never been clearly established, though it has been speculated to be immune-mediated, with heroin metabolites or substances used to cut heroin representing potential antigens. That heroin-related FSGS predominates in African Americans suggests that there may be a genetic predisposition.

Subcutaneous injection of drugs (skin popping), including heroin, can result in chronic infections and abscesses, which are associated with renal amyloidosis.[857–861] One case report demonstrated efficacy of colchicine therapy, as determined by resolution of proteinuria and GFR.[860]

Non-Steroidal Anti-Inflammatory Drug (NSAID)-Induced Minimal Change Disease

NSAIDs have been associated with several different renal abnormalities, including the nephrotic syndrome and allergic interstitial nephritis.[862–864] In contrast to acute renal failure from NSAID-induced vasomotor etiology, the onset of NSAID-mediated nephrotic syndrome occurs from two weeks to over a year after initiation of NSAID use. Clinical features may include hypertension, edema, oliguria and depressed GFR; systemic manifestations of allergic interstitial nephritis, such as fever, rash, and arthralgias are rarely observed. Urinalysis commonly reveals overt proteinuria, microscopic hematuria and pyuria. Unlike allergic interstitial

nephritis from other drugs, eosinophiluria is rarely observed.

Renal biopsies in patients with NSAID-induced nephrotic syndrome reveal MCD, usually in conjunction with interstitial nephritis. Interstitial infiltrates are characteristically comprised of lymphocytes, most commonly cytotoxic T-cells.[865,866]

Proteinuria routinely resolves after NSAID discontinuation, and additional supportive therapy is rarely required.[867] However, complete resolution may require up to one year.[864]

Hemolytic-Uremic Syndrome (HUS) and Thrombotic Thrombocyto-Penic Purpura (TTP)

HUS/TTP has most commonly been associated with infections, but over 50 drugs, particularly cancer chemotherapy drugs, have also been implicated as triggers for HUS/TTP.[868,869] It is difficult to decipher cause and effect in many cases, both because a definitive diagnosis can be elusive, and underlying diseases are also associated with HUS/TTP. However, among chemotherapeutic agents, mitomycin C is best recognized as a cause of HUS/TTP,[869,870] occurring in 5 to 15% of patients receiving a cumulative dose of at least 20 to 30 mg/m^2.[762] The most common clinical presentation is hypertension, hemolytic anemia and acute kidney injury. Despite supportive therapy, which may include hemodialysis, *Staphylococcus* protein A immunoabsorption[871–873] and/or plasmapheresis,[874–876] mortality is extremely high,[877] reflecting concurrent malignancy. Other drugs that have been repeatedly associated with HUS/TTP include cyclosporine A, ticlopidine, quinine, and clopidogrel.[869,878]

The mechanism of drug-induced HUS/TTP has not been established for every agent, but at least for mitomycin C and cyclosporine, both drugs have been postulated to induce formation of circulating immune complexes or autoantibodies,[870,873] which either directly or via an immune-mediated mechanism,[878–880] result in endothelial cell damage. Glomerular capillary endothelial damage may then lead to platelet aggregation and thrombosis.[872]

References

[1] Madaio MP, Harrington JT. The diagnosis of glomerular diseases: acute glomerulonephritis and the nephrotic syndrome. Arch Intern Med 2001;161(1):25–34.

[2] Nissenson AR, Baraff LJ, Fine RN, Knutson DW. Poststreptococcal acute glomerulonephritis: fact and controversy. Ann Intern Med 1979;91(1):76–86.

[3] Rodriguez-Iturbe B, Rubio L, Garcia R. Attack rate of poststreptococcal nephritis in families. A prospective study. Lancet 1981;1(8217):401–3.

[4] Rodriguez-Iturbe B. Acute poststreptoccal glomerulonephritis. In: Schrier R, editor. Diseases of the kidney. Boston: Little Brown; 1993. p. 1929–47.

[5] Feldman H, Mardiney MR, Shuler SE. Immunology and morphology of acute post-streptoccal glomerulonephritis. J Clin Invest 1965;40:283–301.

[6] Kimmelstiel P. The hump-a lesion of acute glomerulonephritis. Bull Pathol 1965;6:187.

[7] Sorof JM, Weidner N, Potter D, Portale AA. Acute poststreptococcal glomerulonephritis in a renal allograft. Pediatr Nephrol 1995;9(3):317–9.

[8] Brenner RM, Peterson J. Postinfectious glomerulonephritis. Nephrology Rounds 2000;3:1–5.

[9] Parra G, Platt JL, Falk RJ, Rodriguez-Iturbe B, Michael AF. Cell populations and membrane attack complex in glomeruli of patients with post-streptococcal glomerulonephritis: identification using monoclonal antibodies by indirect immunofluorescence. Clin Immunol Immunopathol 1984;33(3):324–32.

[10] Gruppe WE. Case records: 6-1975. N Engl J Med 1975;292:307–12.

[11] Bodaghi E, Kheradpir KM, Maddah M. Vasculitis in acute streptococcal glomerulonephritis. Int J Pediatr Nephrol 1987;8(2):69–74.

[12] Earle DP, Jennings RB. Studies of poststreptococcal nephritis and other glomerular diseases. Ann Int Med 1959;51:851–60.

[13] Fordham III CC, Epstein FH, Huffines WD, Harrington JT. Polyarteritis and acute post-streptococcal glomerulonephritis. Ann Intern Med 1964;61:89–97.

[14] Ingelfinger JR, McCluskey RT, Schneeberger EE, Grupe WE. Necrotizing arteritis in acute poststreptococcal glomerulonephritis: report of a recovered case. J Pediatr 1977;91(2):228–32.

[15] Sorger K. Postinfectious glomerulonephritis. Subtypes, clinicopathological correlations, and follow-up studies. Veroff Pathol 1986;125:1–105.

[16] Sorger K, Balun J, Hubner FK, Kohler H, Olbing H, Schulz W, et al. The garland type of acute postinfectious glomerulonephritis: morphological characteristics and follow-up studies. Clin Nephrol 1983;20(1):17–26.

[17] Sorger K, Gessler U, Hubner FK, Kohler H, Schulz W, Stuhlinger W, et al. Subtypes of acute postinfectious glomerulonephritis. Synopsis of clinical and pathological features. Clin Nephrol 1982;17(3):114–28.

[18] Svartman M, Potter EV, Finklea JF. Epidemic scabies and acute glomerulonephritis. Lancet 1972;:249–51.

[19] Fish AJ, Herdman RC, Michael AF, Pickering RJ, Good RA. Epidemic acute glomerulonephritis associated with type 49 streptococcal pyoderma. II. Correlative study of light, immunofluorescent and electron microscopic findings. Am J Med 1970;48(1):28–39.

[20] Lewy JE, Salinas-Madrigal L, Herdson PB, Pirani CL, Metcoff J. Clinico-pathologic correlations in acute poststreptococcal glomerulonephritis. A correlation between renal functions, morphologic damage and clinical course of 46 children with acute poststreptococcal glomerulonephritis. Medicine (Baltimore) 1971;50(6):453–501.

[21] Seegal BC, Andres JA, Hsu KC. Studies on the pathogenesis of acute and progressive glomerulonephritis in man by immunofluorescence and immunoferritin techniques. Fed Proc 1965;24:100.

[22] Tornroth T. The fate of subepithelial deposits in acute poststreptococcal glomerulonephritis. Lab Invest 1976;35(5): 461–74.

[23] Moroni G, Papaccioli D, Banfi G, Tarantino A, Ponticelli C. Acute post-bacterial glomerulonephritis in renal transplant patients: description of three cases and review of the literature. Am J Transplant 2004;4(1):132–6.

[24] Baldwin DS, Gluck MC, Schacht RG, Gallo G. The long-term course of poststreptococcal glomerulonephritis. Ann Intern Med 1974;80(3):342–58.
[25] Hinglais N, Garcia-Torres R, Kleinknecht D. Long-term prognosis in acute glomerulonephritis. The predictive value of early clinical and pathological features observed in 65 patients. Am J Med 1974;56(1):52–60.
[26] Cameron JS, Vick RM, Ogg CS, Seymour WM, Chantler C, Turner DR. Plasma C3 and C4 concentrations in management of glomerulonephritis. Br Med J 1973;3(882):668–72.
[27] Lewis EJ, Carpenter CB, Schur PH. Serum complement component levels in human glomerulonephritis. Ann Intern Med 1971;75(4):555–60.
[28] Madaio MP, Harrington JT. Current concepts. The diagnosis of acute glomerulonephritis. N Engl J Med 1983;309(21): 1299–302.
[29] Sjoholm AG. Complement components and complement activation in acute poststreptococcal glomerulonephritis. Int Arch Allergy Appl Immunol 1979;58(3):274–84.
[30] Maes BD, Oyen R, Claes K, Evenepoel P, Kuypers D, Vanwalleghem J, et al. Mycophenolate mofetil in IgA nephropathy: results of a 3-year prospective placebo-controlled randomized study. Kidney Int 2004;65(5):1842–9.
[31] Stollerman GH, Lewis A, Schultz I, Relationship of immune response to group. A streptococci to the course of acute and chronic recurrent rheumatic fever. Am J Med 1956;20:163–9.
[32] Zaum R, Vogt A, Rodriguez-Iturbe B. Analysis of the immune response to streoricicca proteinase in poststrepococcal disease. Xth lancefield international symposium on streoticiccal diseases, Cologne, Germany: 1987:88.
[33] Drachman R, Aladjem M, Vardy PA. Natural history of an actue glomerulonephritis epidemic in childern. An 11 to 12 year follow up. J Med Sci 1986;18:603.
[34] Garcia R, Rubio L, Rodriguez-Iturbe B. Long-term prognosis of epidemic poststreptococcal glomerulonephritis in Maracaibo: follow-up studies 11–12 years after the acute episode. Clin Nephrol 1981;15(6):291–8.
[35] Kasahara T, Hayakawa H, Okubo S, Okugawa T, Kabuki N, Tomizawa S, et al. Prognosis of acute poststreptococcal glomerulonephritis (APSGN) is excellent in children, when adequately diagnosed. Pediatr Int 2001;43(4):364–7.
[36] Lien JW, Mathew TH, Meadows R. Acute post-streptococcal glomerulonephritis in adults: a long-term study. Q J Med 1979;48(189):99–111.
[37] Nissenson AR, Mayon-White R, Potter EV, Mayon-White V, Abidh S, Poon-King T, et al. Continued absence of clinical renal disease seven to 12 years after poststreptococcal acute glomerulonephritis in Trinidad. Am J Med 1979;67(2):255–62.
[38] Perlman LV, Herdman RC, Kleinman H, Vernier RL. Poststreptococcal glomerulonephritis. A ten-year follow-up of an epidemic. JAMA 1965;194(1):63–70.
[39] Potter EV, Abidh S, Sharrett AR, Burt EG, Svartman M, Finklea JF, et al. Clinical healing two to six years after poststreptococcal glomerulonephritis in Trinidad. N Engl J Med 1978;298(14): 767–72.
[40] Potter EV, Lipschultz SA, Abidh S, Poon-King T, Earle DP. Twelve to seventeen-year follow-up of patients with poststreptococcal acute glomerulonephritis in Trinidad. N Engl J Med 1982;307(12):725–9.
[41] Rodriguez-Iturbe B, Garcia R, Rubio L. Epidemic glomerulonephritis in Maracaibo. Evidence for progression to chronicity. Clin Neph 1976;15:283–301.
[42] Sorger K, Gessler M, Hubner FK, Kohler H, Olbing H, Schulz W, et al. Follow-up studies of three subtypes of acute postinfectious glomerulonephritis ascertained by renal biopsy. Clin Nephrol 1987;27(3):111–24.
[43] Vogl W, Renke M, Mayer-Eichberger D, Schmitt H, Bohle A. Long-term prognosis for endocapillary glomerulonephritis of poststreptococcal type in children and adults. Nephron 1986;44 (1):58–65.
[44] Rodriguez-Iturbe B. Epidemic poststreptococcal glomerulonephritis [clinical conference]. Kidney Int 1984;25(1):129–36.
[45] Berrios X, Lagomarsino E, Solar E, Sandoval G, Guzman B, Riedel I. Post-streptococcal acute glomerulonephritis in Chile–20 years of experience. Pediatr Nephrol 2004;19(3): 306–12.
[46] Buzio C, Allegri L, Mutti A, Perazzoli F, Bergamaschi E. Significance of albuminuria in the follow-up of acute poststreptococcal glomerulonephritis. Clin Nephrol 1994;41(5):259–64.
[47] Lein JW, Keane PM. Limitations of the oral calcium loading test in the management of the recurrent calcareous renal stone former. Am J Kidney Dis 1983;3(1):76–9.
[48] Bhorade MS, Carag HB, Lee HJ, Potter EV, Dunea G. Nephropathy of secondary syphilis. A clinical and pathological spectrum. JAMA 1971;216(7):1159–66.
[49] Zoch-Zwierz W, Wasilewska A, Biernacka A, Tomaszewska B, Winiecka W, Wiercinski R, et al. The course of poststreptococcal glomerulonephritis depending on methods of treatment for the preceding respiratory tract infection. Wiad Lek 2001;54(1–2):56–63.
[50] Salant DJ. Immunopathogenesis of crescentic glomerulonephritis and lung purpura. Kidney Int 1987;32(3):408–25.
[51] Wilson CB, Dixon FJ. Anti-glomerular basement membrane antibody-induced glomerulonephritis. Kidney Int 1973;3(2): 74–89.
[52] Kluth DC, Rees AJ. Anti-glomerular basement membrane disease. J Am Soc Nephrol 1999;10(11):2446–53.
[53] Andrassy K, Kuster S, Waldherr R, Ritz E. Rapidly progressive glomerulonephritis: analysis of prevalence and clinical course. Nephron 1991;59(2):206–12.
[54] Merkel F, Pullig O, Marx M, Netzer KO, Weber M. Course and prognosis of anti-basement membrane antibody (anti-BM-Ab)-mediated disease: report of 35 cases. Nephrol Dial Transplant 1994;9(4):372–6.
[55] Donaghy M, Rees AJ. Cigarette smoking and lung haemorrhage in glomerulonephritis caused by autoantibodies to glomerular basement membrane. Lancet 1983;2(8364):1390–3.
[56] Herody M, Bobrie G, Gouarin C, Grunfeld JP, Noel LH. Anti-GBM disease: predictive value of clinical, histological and serological data. Clin Nephrol 1993;40(5):249–55.
[57] Couser WG. Rapidly progressive glomerulonephritis: classification, pathogenetic mechanisms, and therapy. Am J Kidney Dis 1988;11(6):449–64.
[58] Gossain VV, Gerstein AR, Janes AW. Goodpasture's syndrome: a familial occurrence. Am Rev Respir Dis 1972;105(4):621–4.
[59] D'Apice AJ, Kincaid-Smith P, Becker GH, Loughhead MG, Freeman JW, Sands JM. Goodpasture's syndrome in identical twins. Ann Intern Med 1978;88(1):61–2.
[60] Phelps RG, Rees AJ. The HLA complex in Goodpasture's disease: a model for analyzing susceptibility to autoimmunity. Kidney Int 1999;56(5):1638–53.
[61] Fisher M, Pusey CD, Vaughan RW, Rees AJ. Susceptibility to anti-glomerular basement membrane disease is strongly associated with HLA-DRB1 genes. Kidney Int 1997;51(1):222–9.
[62] Perez GO, Bjornsson S, Ross AH, Aamato J, Rothfield N. A mini-epidemic of Goodpasture's syndrome clinical and immunological studies. Nephron 1974;13(2):161–73.
[63] Kelly PT, Haponik EF. Goodpasture syndrome: molecular and clinical advances. Medicine (Baltimore) 1994;73(4):171–85.
[64] Bombassei GJ, Kaplan AA. The association between hydrocarbon exposure and anti-glomerular basement membrane

antibody-mediated disease (Goodpasture's syndrome). Am J Ind Med 1992;21(2):141–53.
[65] Stevenson A, Yaqoob M, Mason H, Pai P, Bell GM. Biochemical markers of basement membrane disturbances and occupational exposure to hydrocarbons and mixed solvents. QJM 1995;88 (1):23–8.
[66] Guerin V, Rabian C, Noel LH, Droz D, Baron C, Lallemand F, et al. Anti-glomerular-basement-membrane disease after lithotripsy. Lancet 1990;335(8693):856–7.
[67] Umekawa T, Kohri K, Iguchi M, Yoshioka K, Kurita T. Glomerular-basement-membrane antibody and extracorporeal shock wave lithotripsy. Lancet 1993;341(8844):556.
[68] Xenocostas A, Jothy S, Collins B, Loertscher R, Levy M. Anti-glomerular basement membrane glomerulonephritis after extracorporeal shock wave lithotripsy. Am J Kidney Dis 1999;33 (1):128–32.
[69] Wahls TL, Bonsib SM, Schuster VL. Coexistent Wegener's granulomatosis and anti-glomerular basement membrane disease. Hum Pathol 1987;18(2):202–5.
[70] Jayne DR, Marshall PD, Jones SJ, Lockwood CM. Autoantibodies to GBM and neutrophil cytoplasm in rapidly progressive glomerulonephritis. Kidney Int 1990;37(3): 965–70.
[71] Weber MF, Andrassy K, Pullig O, Koderisch J, Netzer K. Antineutrophil-cytoplasmic antibodies and antiglomerular basement membrane antibodies in Goodpasture's syndrome and in Wegener's granulomatosis. J Am Soc Nephrol 1992;2(7): 1227–34.
[72] Moorthy AV, Zimmerman SW, Burkholder PM, Harrington AR. Association of crescentic glomerulonephritis with membranous glomerulonephropathy: a report of three cases. Clin Nephrol 1976;6(1):319–25.
[73] Richman AV, Rifkin SI, McAllister CJ. Rapidly progressive glomerulonephritis. Combined antiglomerular basement membrane antibody and immune complex pathogenesis. Hum Pathol 1981;12(7):597–604.
[74] Kurki P, Helve T, von Bonsdorff M, Tornroth T, Pettersson E, Riska H, et al. Transformation of membranous glomerulonephritis into crescentic glomerulonephritis with glomerular basement membrane antibodies. Serial determinations of anti-GBM before the transformation. Nephron 1984;38(2): 134–7.
[75] Klassen J, Elwood C, Grossberg AL, Milgrom F, Montes M, Sepulveda M, et al. Evolution of membranous nephropathy into anti-glomerular-basement-membrane glomerulonephritis. N Engl J Med 1974;290(24):1340–4.
[76] Meisels IS, Stillman IE, Kuhlik AB. Anti-glomerular basement membrane disease and dual positivity for antineutrophil cytoplasmic antibody in a patient with membranous nephropathy. Am J Kidney Dis 1998;32(4):646–8.
[77] Fleming SJ, Savage CO, McWilliam LJ, Pickering SJ, Ralston AJ, Johnson RW, et al. Anti-glomerular basement membrane antibody-mediated nephritis complicating transplantation in a patient with Alport's syndrome. Transplantation 1988;46(6): 857–9.
[78] Rassoul Z, al-Khader AA, al-Sulaiman M, Dhar JM, Coode P. Recurrent allograft antiglomerular basement membrane glomerulonephritis in a patient with Alport's syndrome. Am J Nephrol 1990;10(1):73–6.
[79] Peten E, Pirson Y, Cosyns JP, Squifflet JP, Alexandre GP, Noel LH, et al. Outcome of thirty patients with Alport's syndrome after renal transplantation. Transplantation 1991;52 (5):823–6.
[80] Kashtan CE, Michael AF. Alport syndrome. Kidney Int 1996;50 (5):1445–63.
[81] Kalluri R, Torre A, Shield III CF, Zamborsky ED, Werner MC, Suchin E, et al. Identification of alpha3, alpha4, and alpha5 chains of type IV collagen as alloantigens for Alport posttransplant anti-glomerular basement membrane antibodies. Transplantation 2000;69(4):679–83.
[82] Netzer KO, Merkel F, Weber M. Goodpasture syndrome and end-stage renal failure–to transplant or not to transplant?. Nephrol Dial Transplant 1998;13(6):1346–8.
[83] Hudson BG, Tryggvason K, Sundaramoorthy M, Neilson EG. Alport's syndrome, Goodpasture's syndrome, and type IV collagen. N Engl J Med 2003;348(25):2543–56.
[84] Turner N, Mason PJ, Brown R, Fox M, Povey S, Rees A, et al. Molecular cloning of the human Goodpasture antigen demonstrates it to be the alpha 3 chain of type IV collagen. J Clin Invest 1992;89(2):592–601.
[85] Derry CJ, Pusey CD. Tissue-specific distribution of the Goodpasture antigen demonstrated by 2-D electrophoresis and western blotting. Nephrol Dial Transplant 1994;9(4):355–61.
[86] Hudson BG. The molecular basis of Goodpasture and Alport syndromes: beacons for the discovery of the collagen IV family. J Am Soc Nephrol 2004;15(10):2514–27.
[87] Saus J, Wieslander J, Langeveld JP, Quinones S, Hudson BG. Identification of the Goodpasture antigen as the alpha 3(IV) chain of collagen IV. J Biol Chem 1988;263(26):13374–80.
[88] Wieslander J, Barr JF, Butkowski RJ, Edwards SJ, Bygren P, Heinegard D, et al. Goodpasture antigen of the glomerular basement membrane: localization to noncollagenous regions of type IV collagen. Proc Natl Acad Sci U S A 1984;81(12): 3838–42.
[89] Kalluri R, Wilson CB, Weber M, Gunwar S, Chonko AM, Neilson EG, et al. Identification of the alpha 3 chain of type IV collagen as the common autoantigen in antibasement membrane disease and Goodpasture syndrome. J Am Soc Nephrol 1995;6 (4):1178–85.
[90] Netzer KO, Leinonen A, Boutaud A, Borza DB, Todd P, Gunwar S, et al. The goodpasture autoantigen. Mapping the major conformational epitope(s) of alpha3(IV) collagen to residues 17–31 and 127–141 of the NC1 domain. J Biol Chem 1999;274(16):11267–74.
[91] Hellmark T, Burkhardt H, Wieslander J. Goodpasture disease. Characterization of a single conformational epitope as the target of pathogenic autoantibodies. J Biol Chem 1999;274(36): 25862–8.
[92] Borza DB, Netzer KO, Leinonen A, Todd P, Cervera J, Saus J, et al. The goodpasture autoantigen. Identification of multiple cryptic epitopes on the NC1 domain of the alpha3(IV) collagen chain. J Biol Chem 2000;275(8):6030–7.
[93] David M, Borza DB, Leinonen A, Belmont JM, Hudson BG. Hydrophobic amino acid residues are critical for the immunodominant epitope of the Goodpasture autoantigen. A molecular basis for the cryptic nature of the epitope. J Biol Chem 2001;276 (9):6370–7.
[94] Gunnarsson A, Hellmark T, Wieslander J. Molecular properties of the Goodpasture epitope. J Biol Chem 2000;275(40):30844–8.
[95] Levy JB, Coulthart A, Pusey CD. Mapping B cell epitopes in Goodpasture's disease. J Am Soc Nephrol 1997;8(11):1698–705.
[96] Hudson BG, Kalluri R, Gunwar S, Noelken ME, Mariyama M, Reeders ST. Molecular characteristics of the goodpasture autoantigen. Kidney Int 1993;43(1):135–9.
[97] Borza DB, Bondar O, Todd P, Sundaramoorthy M, Sado Y, Ninomiya Y, et al. Quaternary organization of the goodpasture autoantigen, the alpha 3(IV) collagen chain. Sequestration of two cryptic autoepitopes by intrapromoter interactions with the alpha4 and alpha5 NC1 domains. J Biol Chem 2002;277 (42):40075–83.

[98] Rutgers A, Meyers KE, Canziani G, Kalluri R, Lin J, Madaio MP. High affinity of anti-GBM antibodies from goodpasture and transplanted alport patients to alpha3(IV)NC1 collagen. Kidney Int 2000;58(1):115–22.

[99] Meyers KE, Kinniry PA, Kalluri R, Neilson EG, Madaio MP. Human goodpasture anti-alpha3(IV)NC1 autoantibodies share structural determinants. Kidney Int 1998;53(2):402–7.

[100] Sado Y, Boutaud A, Kagawa M, Naito I, Ninomiya Y, Hudson BG. Induction of anti-GBM nephritis in rats by recombinant alpha 3(IV)NC1 and alpha 4(IV)NC1 of type IV collagen. Kidney Int 1998;53(3):664–71.

[101] Ryan JJ, Reynolds J, Norgan VA, Pusey CD. Expression and characterization of recombinant rat alpha 3(IV)NC1 and its use in induction of experimental autoimmune glomerulonephritis. Nephrol Dial Transplant 2001;16(2):253–61.

[102] Borza DB, Hudson BG. Of mice and men: murine models of anti-GBM antibody nephritis. Kidney Int 2002;61(5):1905–6.

[103] Kalluri R, Danoff TM, Okada H, Neilson EG. Susceptibility to anti-glomerular basement membrane disease and goodpasture syndrome is linked to MHC class II genes and the emergence of T cell-mediated immunity in mice. J Clin Invest 1997;100 (9):2263–75.

[104] Meyers KE, Allen J, Gehret J, Jacobovits A, Gallo M, Neilson EG, et al. Human antiglomerular basement membrane autoantibody disease in XenoMouse II. Kidney Int 2002;61(5): 1666–73.

[105] West CD. Nephritic factors predispose to chronic glomerulonephritis. Am J Kidney Dis 1994;24(6):956–63.

[106] Salama AD, Chaudhry AN, Ryan JJ, Eren E, Levy JB, Pusey CD, et al. In Goodpasture's disease, CD4(+) T cells escape thymic deletion and are reactive with the autoantigen alpha3(IV) NC1. J Am Soc Nephrol 2001;12(9):1908–15.

[107] Dean EG, Wilson GR, Li M, Edgtton KL, O'Sullivan KM, Hudson BG, et al. Experimental autoimmune Goodpasture's disease: a pathogenetic role for both effector cells and antibody in injury. Kidney Int 2005;67(2):566–75.

[108] Huang XR, Tipping PG, Apostolopoulos J, Oettinger C, D'Souza M, Milton G, et al. Mechanisms of T cell-induced glomerular injury in anti-glomerular basement membrane (GBM) glomerulonephritis in rats. Clin Exp Immunol 1997;109(1): 134–42.

[109] Hopfer H, Maron R, Butzmann U, Helmchen U, Weiner HL, Kalluri R. The importance of cell-mediated immunity in the course and severity of autoimmune anti-glomerular basement membrane disease in mice. Faseb J 2003;17(8):860–8.

[110] Wu J, Hicks J, Borillo J, Glass II WF, Lou YH. CD4(+) T cells specific to a glomerular basement membrane antigen mediate glomerulonephritis. J Clin Invest 2002;109(4):517–24.

[111] Holdsworth SR, Kitching AR, Tipping PG. Th1 and Th2 T helper cell subsets affect patterns of injury and outcomes in glomerulonephritis. Kidney Int 1999;55(4):1198–216.

[112] Senekjian HO, Knight TF, Weinman EJ. The spectrum of renal diseases associated with anti-basement membrane antibodies. Arch Intern Med 1980;140(1):79–81.

[113] Min KW, Gyorkey F, Gyorkey P, Yium JJ, Eknoyan G. The morphogenesis of glomerular crescents in rapidly progressive glomerulonephritis. Kidney Int 1974;5(1):47–56.

[114] Andres G, Brentjens J, Kohli R, Anthone R, Anthone S, Baliah T, et al. Histology of human tubulo-interstitial nephritis associated with antibodies to renal basement membranes. Kidney Int 1978;13(6):480–91.

[115] Briggs WA, Johnson JP, Teichman S, Yeager HC, Wilson CB. Antiglomerular basement membrane antibody-mediated glomerulonephritis and Goodpasture's syndrome. Medicine (Baltimore) 1979;58(5):348–61.

[116] McPhaul Jr JJ, Dixon FJ. Characterization of immunoglobulin G anti-glomerular basement membrane antibodies eluted from kidneys of patients with glomerulonephritis. II. IgG subtypes and in vitro complement fixation. J Immunol 1971;107 (3):678–84.

[117] Weber M, Lohse AW, Manns M, Meyer zum Buschenfelde KH, Kohler H. IgG subclass distribution of autoantibodies to glomerular basement membrane in Goodpasture's syndrome compared to other autoantibodies. Nephron 1988;49 (1):54–7.

[118] Koffler D, Sandson J, Carr R, Kunkel HG. Immunologic studies concerning the pulmonary lesions in Goodpasture's syndrome. Am J Pathol 1969;54(2):293–305.

[119] Walker RG, Scheinkestel C, Becker GJ, Owen JE, Dowling JP, Kincaid-Smith P. Clinical and morphological aspects of the management of crescentic anti-glomerular basement membrane antibody (anti-GBM) nephritis/Goodpasture's syndrome. Q J Med 1985;54(213):75–89.

[120] Westman KW, Bygren PG, Eilert I, Wiik A, Wieslander J. Rapid screening assay for anti-GBM antibody and ANCAs; an important tool for the differential diagnosis of pulmonary renal syndromes. Nephrol Dial Transplant 1997;12(9): 1863–8.

[121] Hellmark T, Niles JL, Collins AB, McCluskey RT, Brunmark C. Comparison of anti-GBM antibodies in sera with or without ANCA. J Am Soc Nephrol 1997;8(3):376–85.

[122] Lockwood CM, Rees AJ, Pearson TA, Evans DJ, Peters DK, Wilson CB. Immunosuppression and plasma-exchange in the treatment of Goodpasture's syndrome. Lancet 1976;1 (7962):711–5.

[123] Peters DK, Rees AJ, Lockwood CM, Pusey CD. Treatment and prognosis in antibasement membrane antibody-mediated nephritis. Transplant Proc 1982;14(3):513–21.

[124] Levy JB, Turner AN, Rees AJ, Pusey CD. Long-term outcome of anti-glomerular basement membrane antibody disease treated with plasma exchange and immunosuppression. Ann Intern Med 2001;134(11):1033–42.

[125] Bouget J, Le Pogamp P, Perrier G, Ramee MP, Rivalan J, Camus C, et al. Anti-basement-membrane antibody mediated, rapidly progressive, glomerulonephritis. Diagnostic and therapeutic strategy based on a retrospective study of 14 cases. Ann Med Interne (Paris) 1990;141(5):409–15.

[126] Daly C, Conlon PJ, Medwar W, Walshe JJ. Characteristics and outcome of anti-glomerular basement membrane disease: a single-center experience. Ren Fail 1996;18(1):105–12.

[127] Savage CO, Pusey CD, Bowman C, Rees AJ, Lockwood CM. Antiglomerular basement membrane antibody mediated disease in the British Isles 1980-4. Br Med J (Clin Res Ed) 1986;292 (6516):301–4.

[128] Flores JC, Taube D, Savage CO, Cameron JS, Lockwood CM, Williams DG, et al. Clinical and immunological evolution of oligoanuric anti-GBM nephritis treated by haemodialysis. Lancet 1986;1(8471):5–8.

[129] Cohen LH, Wilson CB, Freeman RM. Goodpasture syndrome: recovery after severe renal insufficiency. Arch Intern Med 1976;136(7):835–7.

[130] Maxwell AP, Nelson WE, Hill CM. Reversal of renal failure in nephritis associated with antibody to glomerular basement membrane. BMJ 1988;297(6644):333–4.

[131] Simpson IJ, Doak PB, Williams LC, Blacklock HA, Hill RS, Teague CA, et al. Plasma exchange in Goodpasture's syndrome. Am J Nephrol 1982;2(6):301–11.

[132] Johnson JP, Moore Jr J, Austin III HA, Balow JE, Antonovych TT, Wilson CB. Therapy of anti-glomerular basement membrane antibody disease: analysis of prognostic significance of

clinical, pathologic and treatment factors. Medicine (Baltimore) 1985;64(4):219–27.
[133] Madore F, Lazarus JM, Brady HR. Therapeutic plasma exchange in renal diseases. J Am Soc Nephrol 1996;7(3): 367–86.
[134] Lockwood CM, Boulton-Jones JM, Lowenthal RM, Simpson IJ, Peters DK. Recovery from Goodpasture's syndrome after immunosuppressive treatment and plasmapheresis. Br Med J 1975;2(5965):252–4.
[135] Lang CH, Brown DC, Staley N, Johnson G, Ma KW, Border WA, et al. Goodpasture syndrome treated with immunosuppression and plasma exchange. Arch Intern Med 1977;137(8): 1076–8.
[136] Johnson JP, Whitman W, Briggs WA, Wilson CB. Plasmapheresis and immunosuppressive agents in antibasement membrane antibody-induced Goodpasture's syndrome. Am J Med 1978;64(2):354–9.
[137] Jindal KK. Management of idiopathic crescentic and diffuse proliferative glomerulonephritis: evidence-based recommendations. Kidney Int Suppl 1999;70:S33–40.
[138] Bolton WK. Goodpasture's syndrome. Kidney Int 1996;50(5): 1753–66.
[139] Levy JB, Hammad T, Coulthart A, Dougan T, Pusey CD. Clinical features and outcome of patients with both ANCA and anti-GBM antibodies. Kidney Int 2004;66(4): 1535–40.
[140] Segelmark M, Hellmark T, Wieslander J. The prognostic significance in Goodpasture's disease of specificity, titre and affinity of anti-glomerular-basement-membrane antibodies. Nephron Clin Pract 2003;94(3):c59–68.
[141] Cove-Smith JR, McLeod AA, Blamey RW, Knapp MS, Reeves WG, Wilson CB. Transplantation, immunosuppression and plasmapheresis in Goodpasture's syndrome. Clin Nephrol 1978;9(3):126–8.
[142] Wilson CB, Holdsworth SR, Neale TJ. Anti-basement membrane antibodies in immunologic renal disease. Aust N Z J Med 1981;11(Suppl 1):94–100.
[143] Fonck C, Loute G, Cosyns JP, Pirson Y. Recurrent fulminant anti-glomerular basement membrane nephritis at a 7-year interval. Am J Kidney Dis 1998;32(2):323–7.
[144] Koyama A, Igarashi M, Kobayashi M. Natural history and risk factors for immunoglobulin A nephropathy in Japan. Research group on progressive renal diseases. Am J Kidney Dis 1997;29 (4):526–32.
[145] Galla JH. IgA nephropathy. Kidney Int 1995;47(2): 377–87.
[146] Floege J, Feehally J. IgA nephropathy: recent developments. J Am Soc Nephrol 2000;11(12):2395–403.
[147] Geddes CC, Rauta V, Gronhagen-Riska C, Bartosik LP, Jardine AG, Ibels LS, et al. A tricontinental view of IgA nephropathy. Nephrol Dial Transplant 2003;18(8):1541–8.
[148] Levy M, Berger J. Worldwide perspective of IgA nephropathy. Am J Kidney Dis 1988;12(5):340–7.
[149] D'Amico G, Imbasciati E, Barbiano Di Belgioioso G, Bertoli S, Fogazzi G, Ferrario F, et al. Idiopathic IgA mesangial nephropathy. Clinical and histological study of 374 patients. Medicine (Baltimore) 1985;64(1):49–60.
[150] D'Amico G. The commonest glomerulonephritis in the world: IgA nephropathy. Q J Med 1987;64(245):709–27.
[151] Crowley-Nowick PA, Julian BA, Wyatt RJ, Galla JH, Wall BM, Warnock DG, et al. IgA nephropathy in blacks: studies of IgA2 allotypes and clinical course. Kidney Int 1991;39(6): 1218–24.
[152] Jennette JC, Wall SD, Wilkman AS. Low incidence of IgA nephropathy in blacks. Kidney Int 1985;28(6):944–50.
[153] Hoy WE, Hughson MD, Smith SM, Megill DM. Mesangial proliferative glomerulonephritis in southwestern American Indians. Am J Kidney Dis 1993;21(5):486–96.
[154] Schena FP. A retrospective analysis of the natural history of primary IgA nephropathy worldwide. Am J Med 1990;89 (2):209–15.
[155] Clarkson AR, Seymour AE, Thompson AJ, Haynes WD, Chan YL, Jackson B. IgA nephropathy: a syndrome of uniform morphology, diverse clinical features and uncertain prognosis. Clin Nephrol 1977;8(5):459–71.
[156] Colasanti G, Morel Maroger L, D'Amico G. Deposition of fibrin-stabilizing factor (F XIIIA and S), fibrinogen-related antigens, fibrinogen degradation products (FDPd and FDPe) and antihemolytic factor (F VIII) in renal disease: analysis of 161 cases by immunofluorescence microscopy. Clin Nephrol 1987;28(1):28–34.
[157] Barratt J, Feehally J, Smith AC. Pathogenesis of IgA nephropathy. Semin Nephrol 2004;24(3):197–217.
[158] Chui SH, Lam CW, Lewis WH, Lai KN. Light-chain ratio of serum IgA1 in IgA nephropathy. J Clin Immunol 1991;11 (4):219–23.
[159] Lam CW, Chui SH, Leung NW, Li EK, Lai KN. Light chain ratios of serum immunoglobulins in disease. Clin Biochem 1991;24(3):283–7.
[160] Chen N, Nusbaum P, Halbwachs-Mecarelli L, Lesavre P. Light-chain composition of serum IgA1 and i*n vitro* IgA1 production in IgA nephropathy. Nephrol Dial Transplant 1991;6 (11):846–50.
[161] Lai KN, Chui SH, Lai FM, Lam CW. Predominant synthesis of IgA with lambda light chain in IgA nephropathy. Kidney Int 1988;33(2):584–9.
[162] de Fijter JW, Eijgenraam JW, Braam CA, Holmgren J, Daha MR, van Es LA, et al. Deficient IgA1 immune response to nasal cholera toxin subunit B in primary IgA nephropathy. Kidney Int 1996;50(3):952–61.
[163] Harper SJ, Allen AC, Pringle JH, Feehally J. Increased dimeric IgA producing B cells in the bone marrow in IgA nephropathy determined by in situ hybridisation for J chain mRNA. J Clin Pathol 1996;49(1):38–42.
[164] Feehally J. IgA nephropathy—a disorder of IgA production? QJM 1997;90(6):387–90.
[165] Roodnat JI, de Fijter JW, van Kooten C, Daha MR, van Es LA. Decreased IgA1 response after primary oral immunization with live typhoid vaccine in primary IgA nephropathy. Nephrol Dial Transplant 1999;14(2):353–9.
[166] Layward L, Allen AC, Harper SJ, Hattersley JM, Feehally J. Increased and prolonged production of specific polymeric IgA after systemic immunization with tetanus toxoid in IgA nephropathy. Clin Exp Immunol 1992;88(3):394–8.
[167] Emancipator SN, Lamm ME. IgA nephropathy: overproduction or decreased clearance of immune complexes? Lab Invest 1989;61(4):365–7.
[168] Waldherr R, Rambausek M, Duncker WD, Ritz E. Frequency of mesangial IgA deposits in a non-selected autopsy series. Nephrol Dial Transplant 1989;4(11):943–6.
[169] Emancipator SN, Lamm ME. IgA nephropathy: pathogenesis of the most common form of glomerulonephritis. Lab Invest 1989;60(2):168–83.
[170] Allen AC, Willis FR, Beattie TJ, Feehally J. Abnormal IgA glycosylation in Henoch-Schonlein purpura restricted to patients with clinical nephritis. Nephrol Dial Transplant 1998;13(4): 930–4.
[171] Feehally J, Allen AC. Structural features of IgA molecules which contribute to IgA nephropathy. J Nephrol 1999;12 (2):59–65.

[172] Allen A, Feehally J. IgA glycosylation in IgA nephropathy. Adv Exp Med Biol 1998;435:175–83.
[173] Mestecky J, Tomana M, Crowley-Nowick PA, Moldoveanu Z, Julian BA, Jackson S. Defective galactosylation and clearance of IgA1 molecules as a possible etiopathogenic factor in IgA nephropathy. Contrib Nephrol 1993;104:172–82.
[174] Hiki Y, Odani H, Takahashi M, Yasuda Y, Nishimoto A, Iwase H, et al. Mass spectrometry proves under-O-glycosylation of glomerular IgA1 in IgA nephropathy. Kidney Int 2001;59 (3):1077–85.
[175] Tomana M, Novak J, Julian BA, Matousovic K, Konecny K, Mestecky J. Circulating immune complexes in IgA nephropathy consist of IgA1 with galactose-deficient hinge region and antiglycan antibodies. J Clin Invest 1999;104(1): 73–81.
[176] Smith AC, Feehally J. New insights into the pathogenesis of IgA nephropathy. Pathogenesis of IgA nephropathy. Springer Semin Immunopathol 2003;24(4):477–93.
[177] Tomana M, Matousovic K, Julian BA, Radl J, Konecny K, Mestecky J. Galactose-deficient IgA1 in sera of IgA nephropathy patients is present in complexes with IgG. Kidney Int 1997;52(2):509–16.
[178] Kokubo T, Hiki Y, Iwase H, Horii A, Tanaka A, Nishikido J, et al. Evidence for involvement of IgA1 hinge glycopeptide in the IgA1-IgA1 interaction in IgA nephropathy. J Am Soc Nephrol 1997;8(6):915–9.
[179] Mattu TS, Pleass RJ, Willis AC, Kilian M, Wormald MR, Lellouch AC, et al. The glycosylation and structure of human serum IgA1, Fab, and Fc regions and the role of N-glycosylation on Fc alpha receptor interactions. J Biol Chem 1998;273(4):2260–72.
[180] Novak J, Julian BA, Tomana M, Mestecky J. IgA glycosylation and IgA immune complexes in the pathogenesis of IgA nephropathy. Semin Nephrol 2008;28(1):78–87.
[181] Allen AC, Topham PS, Harper SJ, Feehally J. Leucocyte beta 1,3 galactosyltransferase activity in IgA nephropathy. Nephrol Dial Transplant 1997;12(4):701–6.
[182] Hall RP, Stachura I, Cason J, Whiteside TL, Lawley TJ. IgA-containing circulating immune complexes in patients with igA nephropathy. Am J Med 1983;74(1):56–63.
[183] Coppo R, Amore A, Cirina P, Messina M, Basolo B, Segoloni G, et al. Characteristics of IgA and macromolecular IgA in sera from IgA nephropathy transplanted patients with and without IgAN recurrence. Contrib Nephrol 1995;111:85–92.
[184] Schena PF, Pastore A, Sinico RA, Montinaro V, Fornasieri A. Polymeric IgA and IgA rheumatoid factor decrease the capacity of serum to solubilize circulating immune complexes in patients with primary IgA nephropathy. J Immunol 1988;141 (1):125–30.
[185] Jennette JC, Wieslander J, Tuttle R, Falk RJ. Serum IgA-fibronectin aggregates in patients with IgA nephropathy and Henoch-Schonlein purpura: diagnostic value and pathogenic implications. The glomerular disease collaborative network. Am J Kidney Dis 1991;18(4):466–71.
[186] Launay P, Grossetete B, Arcos-Fajardo M, Gaudin E, Torres SP, Beaudoin L, et al. Fcalpha receptor (CD89) mediates the development of immunoglobulin A (IgA) nephropathy (Berger's disease). Evidence for pathogenic soluble receptor-Iga complexes in patients and CD89 transgenic mice. J Exp Med 2000;191(11):1999–2009.
[187] van der Boog PJ, van Zandbergen G, de Fijter JW, Klar-Mohamad N, van Seggelen A, Brandtzaeg P, et al. Fc alpha RI/CD89 circulates in human serum covalently linked to IgA in a polymeric state. J Immunol 2002;168(3):1252–8.
[188] Jackson S. Immunoglobulin-antiimmunoglobulin interactions and immune complexes in IgA nephropathy. Am J Kidney Dis 1988;12(5):425–9.
[189] Miyazaki M, Endoh M, Suga T, Yano N, Kuramoto T, Matsumoto Y, et al. Rheumatoid factors and glomerulonephritis. Clin Exp Immunol 1990;81(2):250–5.
[190] Stockert RJ, Kressner MS, Collins JC, Sternlieb I, Morell AG. IgA interaction with the asialoglycoprotein receptor. Proc Natl Acad Sci U S A 1982;79(20):6229–31.
[191] Roccatello D, Picciotto G, Torchio M, Ropolo R, Ferro M, Franceschini R, et al. Removal systems of immunoglobulin A and immunoglobulin A containing complexes in IgA nephropathy and cirrhosis patients. The role of asialoglycoprotein receptors. Lab Invest 1993;69(6):714–23.
[192] Novak J, Julian BA, Tomana M, Mesteck J. Progress in molecular and genetic studies of IgA nephropathy. J Clin Immunol 2001;21(5):310–27.
[193] Kobayashi I, Nogaki F, Kusano H, Ono T, Miyawaki S, Yoshida H, et al. Interleukin-12 alters the physicochemical characteristics of serum and glomerular IgA and modifies glycosylation in a ddY mouse strain having high IgA levels. Nephrol Dial Transplant 2002;17(12):2108–16.
[194] Scivittaro V, Gesualdo L, Ranieri E, Marfella C, Schewn SA, Emancipator SN, et al. Profiles of immunoregulatory cytokine production in vitro in patients with IgA nephropathy and their kindred. Clin Exp Immunol 1994;96(2):311–6.
[195] Lai KN, Ho RT, Lai CK, Chan CH, Li PK. Increase of both circulating Th1 and Th2 T lymphocyte subsets in IgA nephropathy. Clin Exp Immunol 1994;96(1):116–21.
[196] Chintalacharuvu SR, Nagy NU, Sigmund N, Nedrud JG, Amm ME, Emancipator SN. T cell cytokines determine the severity of experimental IgA nephropathy by regulating IgA glycosylation. Clin Exp Immunol 2001;126(2):326–33.
[197] Fujii K, Muller KD, Clarkson AR, Woodroffe AJ. The effect of IgA immune complexes on the proliferation of cultured human mesangial cells. Am J Kidney Dis 1990;16(3):207–10.
[198] Hiki Y, Kokubo T, Iwase H, Masaki Y, Sano T, Tanaka A, et al. Underglycosylation of IgA1 hinge plays a certain role for its glomerular deposition in IgA nephropathy. J Am Soc Nephrol 1999;10(4):760–9.
[199] Monteiro RC, Van De Winkel JG. IgA Fc receptors. Annu Rev Immunol 2003;21:177–204.
[200] Moura IC, Centelles MN, Arcos-Fajardo M, Malheiros DM, Collawn JF, Cooper MD, et al. Identification of the transferrin receptor as a novel immunoglobulin (Ig)A1 receptor and its enhanced expression on mesangial cells in IgA nephropathy. J Exp Med 2001;194(4):417–25.
[201] Haddad E, Moura IC, Arcos-Fajardo M, Macher MA, Baudouin V, Alberti C, et al. Enhanced expression of the CD71 mesangial IgA1 receptor in Berger disease and Henoch-Schonlein nephritis: association between CD71 expression and IgA deposits. J Am Soc Nephrol 2003;14(2):327–37.
[202] McDonald KJ, Cameron AJ, Allen JM, Jardine AG. Expression of Fc alpha/mu receptor by human mesangial cells: a candidate receptor for immune complex deposition in IgA nephropathy. Biochem Biophys Res Commun 2002;290(1):438–42.
[203] Leung JC, Tsang AW, Chan DT, Lai KN. Absence of CD89, polymeric immunoglobulin receptor, and asialoglycoprotein receptor on human mesangial cells. J Am Soc Nephrol 2000;11 (2):241–9.
[204] Harada K, Akai Y, Kurumatani N, Iwano M, Saito Y. Prognostic value of urinary interleukin 6 in patients with IgA nephropathy: an 8-year follow-up study. Nephron 2002;92 (4):824–6.

[205] Taniguchi Y, Yorioka N, Kumagai J, Katsutani M, Kuratsune M, Amimoto D, et al. Interleukin-6 localization and the prognosis of IgA nephropathy. Nephron 1999;81(1):94–8.
[206] Duque N, Gomez-Guerrero C, Egido J. Interaction of IgA with Fc alpha receptors of human mesangial cells activates transcription factor nuclear factor-kappa B and induces expression and synthesis of monocyte chemoattractant protein-1, IL-8, and IFN-inducible protein 10. J Immunol 1997;159(7):3474–82.
[207] Oortwijn BD, Roos A, Royle L, van Gijlswijk-Janssen DJ, Faber-Krol MC, Eijgenraam JW, et al. Differential glycosylation of polymeric and monomeric IgA: a possible role in glomerular inflammation in IgA nephropathy. J Am Soc Nephrol 2006;17 (12):3529–39.
[208] Hisano S, Matsushita M, Fujita T, Endo Y, Takebayashi S. Mesangial IgA2 deposits and lectin pathway-mediated complement activation in IgA glomerulonephritis. Am J Kidney Dis 2001;38(5):1082–8.
[209] Bogers WM, Stad RK, van Es LA, Daha MR. Immunoglobulin A: interaction with complement, phagocytic cells and endothelial cells. Complement Inflamm 1991;8(5-6):347–58.
[210] Endo M, Ohi H, Ohsawa I, Fujita T, Matsushita M. Complement activation through the lectin pathway in patients with Henoch-Schonlein purpura nephritis. Am J Kidney Dis 2000;35(3):401–7.
[211] Lai KN, Leung JC, Chan LY, Saleem MA, Mathieson PW, Lai FM, et al. Activation of podocytes by mesangial-derived TNF-alpha: glomerulo-podocytic communication in IgA nephropathy. Am J Physiol Renal Physiol 2008;294(4):F945–55.
[212] Scolari F. Inherited forms of IgA nephropathy. J Nephrol 2003;16(2):317–20.
[213] Schena FP. Immunogenetic aspects of primary IgA nephropathy. Kidney Int 1995;48(6):1998–2013.
[214] Julian BA, Quiggins PA, Thompson JS, Woodford SY, Gleason K, Wyatt RJ. Familial IgA nephropathy. Evidence of an inherited mechanism of disease. N Engl J Med 1985;312(4):202–8.
[215] Scolari F, Amoroso A, Savoldi S, Prati E, Scaini P, Manganoni A, et al. Familial occurrence of primary glomerulonephritis: evidence for a role of genetic factors. Nephrol Dial Transplant 1992;7(7):587–96.
[216] Gharavi AG, Yan Y, Scolari F, Schena FP, Frasca GM, Ghiggeri GM, et al. IgA nephropathy, the most common cause of glomerulonephritis, is linked to 6q22-23. Nat Genet 2000;26 (3):354–7.
[217] Fennessy M, Hitman GA, Moore RH, Metcalfe K, Medcraft J, Sinico RA, et al. HLA-DQ gene polymorphism in primary IgA nephropathy in three European populations. Kidney Int 1996;49(2):477–80.
[218] Akiyama F, Tanaka T, Yamada R, Ohnishi Y, Tsunoda T, Maeda S, et al. Single-nucleotide polymorphisms in the class II region of the major histocompatibility complex in Japanese patients with immunoglobulin A nephropathy. J Hum Genet 2002;47(10):532–8.
[219] Kim YS, Kang D, Kwon DY, Park WY, Kim H, Lee DS, et al. Uteroglobin gene polymorphisms affect the progression of immunoglobulin A nephropathy by modulating the level of uteroglobin expression. Pharmacogenetics 2001;11(4): 299–305.
[220] Narita I, Saito N, Goto S, Jin S, Omori K, Sakatsume M, et al. Role of uteroglobin G38A polymorphism in the progression of IgA nephropathy in Japanese patients. Kidney Int 2002;61(5): 1853–8.
[221] Menegatti E, Nardacchione A, Alpa M, Agnes C, Rossi D, Chiara M, et al. Polymorphism of the uteroglobin gene in systemic lupus erythematosus and IgA nephropathy. Lab Invest 2002;82(5):543–6.
[222] Takei T, Iida A, Nitta K, Tanaka T, Ohnishi Y, Yamada R, et al. Association between single-nucleotide polymorphisms in selectin genes and immunoglobulin A nephropathy. Am J Hum Genet 2002;70(3):781–6.
[223] Schena FP, D'Altri C, Cerullo G, Manno C, Gesualdo L. ACE gene polymorphism and IgA nephropathy: an ethnically homogeneous study and a meta-analysis. Kidney Int 2001;60 (2):732–40.
[224] Suzuki H, Suzuki Y, Yamanaka T, Hirose S, Nishimura H, Toei J, et al. Genome-wide scan in a novel IgA nephropathy model identifies a susceptibility locus on murine chromosome 10, in a region syntenic to human IGAN1 on chromosome 6q22-23. J Am Soc Nephrol 2005;16(5):1289–99.
[225] Jennette JC. The immunohistology of IgA nephropathy. Am J Kidney Dis 1988;12(5):348–52.
[226] Lai KN, Chan KW, Mac-Moune F, Ho CP, Yan KW, Lam CW, et al. The immunochemical characterization of the light chains in the mesangial IgA deposits in IgA nephropathy. Am J Clin Pathol 1986;85(5):548–51.
[227] Haas M. Histologic subclassification of IgA nephropathy: a clinicopathologic study of 244 cases. Am J Kidney Dis 1997;29 (6):829–42.
[228] Ibels LS, Gyory AZ. IgA nephropathy: analysis of the natural history, important factors in the progression of renal disease, and a review of the literature. Medicine (Baltimore) 1994;73 (2):79–102.
[229] Hogg RJ. Usual and unusual presentations of IgA nephropathy in children. Contrib Nephrol 1993;104:14–23.
[230] Tumlin JA, Hennigar RA. Clinical presentation, natural history, and treatment of crescentic proliferative IgA nephropathy. Semin Nephrol 2004;24(3):256–68.
[231] Sinniah R. IgA mesangial nephropathy: Berger's disease. Am J Nephrol 1985;5(2):73–83.
[232] Kincaid-Smith P, Ryan GB, Dowling JP, Nicholls K. Acute renal failure in mesangial IgA nephropathy. Contrib Nephrol 1984;40:182–6.
[233] Szeto CC, Lai FM, To KF, Wong TY, Chow KM, Choi PC, et al. The natural history of immunoglobulin a nephropathy among patients with hematuria and minimal proteinuria. Am J Med 2001;110(6):434–7.
[234] Radford Jr MG, Donadio Jr JV, Bergstralh EJ, Grande JP. Predicting renal outcome in IgA nephropathy. J Am Soc Nephrol 1997;8(2):199–207.
[235] Nicholls KM, Fairley KF, Dowling JP, Kincaid-Smith P. The clinical course of mesangial IgA associated nephropathy in adults. Q J Med Spring 1984;53(210):227–50.
[236] D'Amico G. Natural history of idiopathic IgA nephropathy: role of clinical and histological prognostic factors. Am J Kidney Dis 2000;36(2):227–37.
[237] Donadio JV, Bergstralh EJ, Grande JP, Rademcher DM. Proteinuria patterns and their association with subsequent end-stage renal disease in IgA nephropathy. Nephrol Dial Transplant 2002;17(7):1197–203.
[238] Bartosik LP, Lajoie G, Sugar L, Cattran DC. Predicting progression in IgA nephropathy. Am J Kidney Dis 2001;38(4):728–35.
[239] Donadio Jr JV, Grande JP. Immunoglobulin A nephropathy: a clinical perspective. J Am Soc Nephrol 1997;8(8):1324–32.
[240] Beukhof JR, Kardaun O, Schaafsma W, Poortema K, Donker AJ, Hoedemaeker PJ, et al. Toward individual prognosis of IgA nephropathy. Kidney Int 1986;29(2):549–56.
[241] D'Amico G. Influence of clinical and histological features on actuarial renal survival in adult patients with idiopathic IgA nephropathy, membranous nephropathy, and membranoproliferative glomerulonephritis: survey of the recent literature. Am J Kidney Dis 1992;20(4):315–23.

[242] Donadio JV, Grande JP. IgA nephropathy. N Engl J Med 2002;347(10):738–48.
[243] Donadio JV, Bergstralh EJ, Offord KP, Holley KE, Spencer DC. Clinical and histopathologic associations with impaired renal function in IgA nephropathy. Mayo nephrology collaborative group. Clin Nephrol 1994;41(2):65–71.
[244] Katafuchi R, Kiyoshi Y, Oh Y, Uesugi N, Ikeda K, Yanase T, et al. Glomerular score as a prognosticator in IgA nephropathy: its usefulness and limitation. Clin Nephrol 1998;49(1):1–8.
[245] Moldoveanu Z, Wyatt RJ, Lee JY, Tomana M, Julian BA, Mestecky J, et al. Patients with IgA nephropathy have increased serum galactose-deficient IgA1 levels. Kidney Int 2007;71(11):1148–54.
[246] Glassock RJ. The treatment of IgA nephropathy: status at the end of the millenium. J Nephrol 1999;12(5):288–96.
[247] Julian BA. Treatment of IgA nephropathy. Semin Nephrol 2000;20(3):277–85.
[248] Cattran DC, Greenwood C, Ritchie S. Long-term benefits of angiotensin-converting enzyme inhibitor therapy in patients with severe immunoglobulin a nephropathy: a comparison to patients receiving treatment with other antihypertensive agents and to patients receiving no therapy. Am J Kidney Dis 1994;23(2):247–54.
[249] Nakao N, Yoshimura A, Morita H, Takada M, Kayano T, Ideura T. Combination treatment of angiotensin-II receptor blocker and angiotensin-converting-enzyme inhibitor in non-diabetic renal disease (COOPERATE): a randomised controlled trial. Lancet 2003;361(9352):117–24.
[250] Campbell R, Sangalli F, Perticucci E, Aros C, Viscarra C, Perna A, et al. Effects of combined ACE inhibitor and angiotensin II antagonist treatment in human chronic nephropathies. Kidney Int 2003;63(3):1094–103.
[251] Russo D, Minutolo R, Pisani A, Esposito R, Signoriello G, Andreucci M, et al. Coadministration of losartan and enalapril exerts additive antiproteinuric effect in IgA nephropathy. Am J Kidney Dis 2001;38(1):18–25.
[252] Russo D, Pisani A, Balletta MM, De Nicola L, Savino FA, Andreucci M, et al. Additive antiproteinuric effect of converting enzyme inhibitor and losartan in normotensive patients with IgA nephropathy. Am J Kidney Dis 1999;33(5):851–6.
[253] Donadio JV, Grande JP. The role of fish oil/omega-3 fatty acids in the treatment of IgA nephropathy. Semin Nephrol 2004;24 (3):225–43.
[254] Donadio Jr JV, Grande JP, Bergstralh EJ, Dart RA, Larson TS, Spencer DC. The long-term outcome of patients with IgA nephropathy treated with fish oil in a controlled trial. Mayo nephrology collaborative group. J Am Soc Nephrol 1999;10 (8):1772–7.
[255] Donadio Jr JV, Larson TS, Bergstralh EJ, Grande JP. A randomized trial of high-dose compared with low-dose omega-3 fatty acids in severe IgA nephropathy. J Am Soc Nephrol 2001;12 (4):791–9.
[256] Bennett WM, Walker RG, Kincaid-Smith P. Treatment of IgA nephropathy with eicosapentanoic acid (EPA): a two-year prospective trial. Clin Nephrol 1989;31(3):128–31.
[257] Pettersson EE, Rekola S, Berglund L, Sundqvist KG, Angelin B, Diczfalusy U, et al. Treatment of IgA nephropathy with omega-3-polyunsaturated fatty acids: a prospective, double-blind, randomized study. Clin Nephrol 1994;41(4):183–90.
[258] Strippoli GF, Manno C, Schena FP. An "evidence-based" survey of therapeutic options for IgA nephropathy: assessment and criticism. Am J Kidney Dis 2003;41(6):1129–39.
[259] Samuels JA, Strippoli GF, Craig JC, Schena FP, Molony DA. Immunosuppressive treatments for immunoglobulin A nephropathy: a meta-analysis of randomized controlled trials. Nephrology (Carlton) 2004;9(4):177–85.
[260] Pozzi C, Bolasco PG, Fogazzi GB, Andrulli S, Altieri P, Ponticelli C, et al. Corticosteroids in IgA nephropathy: a randomised controlled trial. Lancet 1999;353(9156):883–7.
[261] Pozzi C, Andrulli S, Del Vecchio L, Melis P, Fogazzi GB, Altieri P, et al. Corticosteroid effectiveness in IgA nephropathy: long-term results of a randomized, controlled trial. J Am Soc Nephrol 2004;15(1):157–63.
[262] Alexopoulos E. Treatment of primary IgA nephropathy. Kidney Int 2004;65(1):341–55.
[263] Ballardie FW, Roberts IS. Controlled prospective trial of prednisolone and cytotoxics in progressive IgA nephropathy. J Am Soc Nephrol 2002;13(1):142–8.
[264] Rasche FM, Klotz CH, Czock D, Karges W, Muche R, Jehle PM, et al. Cyclophosphamide pulse therapy in advanced progressive IgA nephropathy. Nephron Clin Pract 2003;93(4):c131–6.
[265] Locatelli F, Pozzi C, Del Vecchio L, Andrulli S, Pani A, Fogazzi G, et al. Combined treatment with steroids and azathioprine in IgA nephropathy: design of a prospetive randomised multicentre trial. J Nephrol 1999;12(5):308–11.
[266] Goumenos DS, Davlouros P, El Nahas AM, Ahuja M, Shortland JR, Vlachojannis JG, et al. Prednisolone and azathioprine in IgA nephropathy—a ten-year follow-up study. Nephron Clin Pract 2003;93(2):C58–68.
[267] Chen X, Chen P, Cai G, Wu J, Cui Y, Zhang Y, et al. [A randomized control trial of mycophenolate mofeil treatment in severe IgA nephropathy]. Zhonghua Yi Xue Za Zhi 2002;82 (12):796–801.
[268] Nowack R, Birck R, van der Woude FJ. Mycophenolate mofetil for systemic vasculitis and IgA nephropathy. Lancet 1997;349 (9054):774.
[269] Pozzi C, Del Vecchio L, Locatelli F. Can immunosuppressive therapy be useful in IgA nephropathy when the "Point of No Return" has already been exceeded? Nephron 2002;92 (3):699–701.
[270] Locatelli F, Pozzi M, Del Vecchio L, Pozzi C. Advanced IgA nephropathy: to treat or not to treat? Nephron Clin Pract 2003;93(4):c119–21.
[271] Scheinman JI, Trachtman H, Lin CY, Langman CB, Chan JC. IgA nephropathy: to treat or not to treat? Nephron 1997;75 (3):251–8.
[272] Xie Y, Nishi S, Ueno M, Imai N, Sakatsume M, Narita I, et al. The efficacy of tonsillectomy on long-term renal survival in patients with IgA nephropathy. Kidney Int 2003;63(5):1861–7.
[273] Xie Y, Chen X, Nishi S, Narita I, Gejyo F. Relationship between tonsils and IgA nephropathy as well as indications of tonsillectomy. Kidney Int 2004;65(4):1135–44.
[274] Rasche FM, Sailer LC, Czock D, Keller F. Tonsillectomy, high dose immunoglobulins, and cyclophosphamide in progressive IgA-nephropathy. Acta Otolaryngol Suppl 2004;(555):32–7.
[275] Matutani S, Honma R, Adachi M, Hotta O. Clinical observation of palatine tonsils with IgA nephropathy. Acta Otolaryngol Suppl 2004;555:58–61.
[276] Frohnert PP, Donadio Jr JV, Velosa JA, Holley KE, Sterioff S. The fate of renal transplants in patients with IgA nephropathy. Clin Transplant 1997;11(2):127–33.
[277] Ohmacht C, Kliem V, Burg M, Nashan B, Schlitt HJ, Brunkhorst R, et al. Recurrent immunoglobulin A nephropathy after renal transplantation: a significant contributor to graft loss. Transplantation 1997;64(10):1493–6.
[278] Bumgardner GL, Amend WC, Ascher NL, Vincenti FG. Single-center long-term results of renal transplantation for IgA nephropathy. Transplantation 1998;65(8):1053–60.

[279] Ponticelli C, Traversi L, Feliciani A, Cesana BM, Banfi G, Tarantino A. Kidney transplantation in patients with IgA mesangial glomerulonephritis. Kidney Int 2001;60(5): 1948–54.
[280] Floege J, Burg M, Kliem V. Recurrent IgA nephropathy after kidney transplantation: not a benign condition. Nephrol Dial Transplant 1998;13(8):1933–5.
[281] Chandrakantan A, Ratanapanichkich P, Said M, Barker CV, Julian BA. Recurrent IgA nephropathy after renal transplantation despite immunosuppressive regimens with mycophenolate mofetil. Nephrol Dial Transplant 2005;20(6):1214–21.
[282] Rennke HG. Secondary membranoproliferative glomerulonephritis. Kidney Int 1995;47(2):643–56.
[283] Habib R, Kleinknecht C, Gubler MC, Levy M. Idiopathic membranoproliferative glomerulonephritis in children. Report of 105 cases. Clin Nephrol 1973;1(4):194–214.
[284] Jackson EC, McAdams AJ, Strife CF, Forristal J, Welch TR, West CD. Differences between membranoproliferative glomerulonephritis types I and III in clinical presentation, glomerular morphology, and complement perturbation. Am J Kidney Dis 1987;9(2):115–20.
[285] Strife CF, McEnery PT, McAdams AJ, West CD. Membranoproliferative glomerulonephritis with disruption of the glomerular basement membrane. Clin Nephrol 1977;7(2): 65–72.
[286] Gonzalo A, et al. Incidence of membranoproliferative glomerulonephritis in a Spanish population. Clin Nephrol. 1986;26 (3):161.
[287] Haas M, Meehan SM, Karrison TG, Spargo BH. Changing etiologies of unexplained adult nephrotic syndrome: a comparison of renal biopsy findings from 1976–1979 and 1995-1997. Am J Kidney Dis 1997;30(5):621–31.
[288] Simon P, et al. Epidemiology of primary glomerular diseases in a French region. Variations according to period and age. Kidney Int 1994;46(4):1192–8.
[289] Kashtan CE, Burke B, Burch G, Gustav Fisker S, Kim Y. Dense intramembranous deposit disease: a clinical comparison of histological subtypes. Clin Nephrol 1990;33(1):1–6.
[290] Colville D, Guymer R, Sinclair RA, Savige J. Visual impairment caused by retinal abnormalities in mesangiocapillary (membranoproliferative) glomerulonephritis type II ("dense deposit disease"). Am J Kidney Dis 2003;42(2):E2–5.
[291] Duvall-Young J, MacDonald MK, McKechnie NM. Fundus changes in (type II) mesangiocapillary glomerulonephritis simulating drusen: a histopathological report. Br J Ophthalmol 1989;73(4):297–302.
[292] Thorner P, Baumal R. Extraglomerular dense deposits in dense deposit disease. Arch Pathol Lab Med 1982;106(12):628–31.
[293] Campbell-Boswell MV, Linder D, Naylor BR, Brooks RE. Kidney tubule basement membrane alterations in type II membranoproliferative glomerulonephritis. Virchows Arch A Pathol Anat Histol 1979;382(1):49–61.
[294] West CD, Witte DP, McAdams AJ. Composition of nephritic factor-generated glomerular deposits in membranoproliferative glomerulonephritis type 2. Am J Kidney Dis 2001;37 (6):1120–30.
[295] Churg J, Duffy JL, Bernstein J. Identification of dense deposit disease: a report for the International study of kidney diseases in children. Arch Pathol Lab Med 1979;103(2):67–72.
[296] Nevins TE. Lectin binding in membranoproliferative glomerulonephritis. Evidence for N-acetylglucosamine in dense intramembranous deposits. Am J Pathol 1985;118(2):325–30.
[297] Burkholder PM, Marchand A, Krueger RP. Mixed membranous and proliferative glomerulonephritis. A correlative light, immunofluorescence, and electron microscopic study. Lab Invest 1970;23(5):459–79.
[298] Abreo K, Moorthy AV. Type 3 membranoproliferative glomerulonephritis: clinicopathologic correlations and long-term follow-up in nine patients. Arch Pathol Lab Med 1982;106(8): 413–7.
[299] Mathieson PW, Peters K. Are nephritic factors nephritogenic? Am J Kidney Dis 1994;24(6):964–6.
[300] Norsworthy P, Davies KA. Complement components and their autoantibodies. Mol Biotechnol 2003;23(3):259–70.
[301] Fujita T, Sumita T, Yoshida S, Ito S, Tamura N. C4 nephritic factor in a patient with chronic glomerulonephritis. J Clin Lab Immunol 1987;22(2):65–70.
[302] Gigli I, Sorvillo J, Halbwachs-Mecarelli L. Regulation and deregulation of the fluid-phase classical pathway C3 convertase. J Immunol 1985;135(1):440–4.
[303] Ohi H, Yasugi T. Occurrence of C3 nephritic factor and C4 nephritic factor in membranoproliferative glomerulonephritis (MPGN). Clin Exp Immunol 1994;95(2):316–21.
[304] Tanuma Y, Ohi H, Hatano M. Two types of C3 nephritic factor: properdin-dependent C3NeF and properdin-independent C3NeF. Clin Immunol Immunopathol 1990;56(2):226–38.
[305] Daha MR, Hazevoet HM, Vanes LA, Cats A. Stabilization of the classical pathway C3 convertase C42, by a factor F-42, isolated from serum of patients with systemic lupus erythematosus. Immunology 1980;40(3):417–24.
[306] Thompson RA, Yap PL, Brettle RB, Dunmow RE, Chapel H. Meningococcal meningitis associated with persistent hypocomplementaemia due to circulating C3 nephritic factor. Clin Exp Immunol 1983;52(1):153–6.
[307] Halbwachs L, et al. Nephritic factor of the classical pathway of complement; immunoglobulin G autoantibody directed against the classical pathway C3 convetase enzyme. J Clin Invest 1980;65(6):1249–56.
[308] Levin A. Management of membranoproliferative glomerulonephritis: evidence-based recommendations. Kidney Int Suppl 1999;70:S41–6.
[309] Jones G, Juszczak M, Kingdon E, Harber M, Sweny P, Burns A. Treatment of idiopathic membranoproliferative glomerulonephritis with mycophenolate mofetil and steroids. Nephrol Dial Transplant 2004;19(12):3160–4.
[310] Ruggenenti P, Noris M, Remuzzi G. Thrombotic microangiopathy, hemolytic uremic syndrome, and thrombotic thrombocytopenic purpura. Kidney Int 2001;60(3):831–46.
[311] Kavanagh D, Richards A, Atkinson J. Complement regulatory genes and hemolytic uremic syndromes. Annu Rev Med 2008;59:293–309.
[312] Noris M, Remuzzi G. Atypical hemolytic-uremic syndrome. N Engl J Med 2009;361(17):1676–87.
[313] Noris M, Remuzzi G. Hemolytic uremic syndrome. J Am Soc Nephrol 2005;16(4):1035–50.
[314] Delvaeye M, Noris M, De Vriese A, Esmon CT, Esmon NL, Ferrell G, et al. Thrombomodulin mutations in atypical hemolytic-uremic syndrome. N Engl J Med 2009;361(4): 345–57.
[315] George JN. Clinical practice. Thrombotic thrombocytopenic purpura. N Engl J Med 2006;354(18):1927–35.
[316] Moake JL. Thrombotic microangiopathies. N Engl J Med 2002;347(8):589–600.
[317] Tsai HM. Pathophysiology of thrombotic thrombocytopenic purpura. Int J Hematol 2010;91(1):1–19.
[318] Monnens L, Molenaar J, Lambert PH, Proesmans W, van Munster P. The complement system in hemolytic-uremic syndrome in childhood. Clin Nephrol 1980;13(4):168–71.

[319] Thurman JM, Marians R, Emlen W, Wood S, Smith C, Akana H, et al. Alternative pathway of complement in children with diarrhea-associated hemolytic uremic syndrome. Clin J Am Soc Nephrol 2009;4(12):1920–4.

[320] Caprioli J, Bettinaglio P, Zipfel PF, Amadei B, Daina E, Gamba S, et al. The molecular basis of familial hemolytic uremic syndrome: mutation analysis of factor H gene reveals a hot spot in short consensus repeat 20. J Am Soc Nephrol 2001;12 (2):297–307.

[321] Kavanagh D, Kemp EJ, Richards A, Burgess RM, Mayland E, Goodship JA, et al. Does complement factor B have a role in the pathogenesis of atypical HUS? Mol Immunol 2006;43 (7):856–9.

[322] Garvey B. Rituximab in the treatment of autoimmune haematological disorders. Br J Haematol 2008;141(2):149–69.

[323] Lapeyraque AL, Malina M, Fremeaux-Bacchi V, Boppel T, Kirschfink M, Oualha M, et al. Eculizumab in severe Shiga-toxin-associated HUS. N Engl J Med 2011;364(26):2561–3.

[324] Nurnberger J, Philipp T, Witzke O, Opazo Saez A, Vester U, Baba HA, et al. Eculizumab for atypical hemolytic-uremic syndrome. N Engl J Med 2009;360(5):542–4.

[325] Bergey EJ, Stinson MW. Heparin-inhibitable basement membrane-binding protein of streptococcus pyogenes. Infect Immun 1988;56(7):1715–21.

[326] Glurich I, Winters B, Albini B, Stinson M. Identification of streptococcus pyogenes proteins that bind to rabbit kidney in vitro and in vivo. Microb Pathog 1991;10(3):209–20.

[327] Nordstrand A, Norgren M, Ferretti JJ, Holm SE. Streptokinase as a mediator of acute post-streptococcal glomerulonephritis in an experimental mouse model. Infect Immun 1998;66(1): 315–21.

[328] Nordstrand A, Norgren M, Holm SE. An experimental model for acute post-streptococcal glomerulonephritis in mice. Adv Exp Med Biol 1997;418:809–11.

[329] Vogt A, Batsford S, Rodriguez-Iturbe B, Garcia R. Cationic antigens in poststreptococcal glomerulonephritis. Clin Nephrol 1983;20(6):271–9.

[330] Becker C, Murphy G. The Experimental induction of glomerulonephritis like that in man by infection with group A Streptococci. J Exp Med 1967;127:1–38.

[331] Fillit H, Damle SP, Gregory JD, Volin C, Poon-King T, Zabriskie J. Sera from patients with poststreptococcal glomerulonephritis contain antibodies to glomerular heparan sulfate proteoglycan. J Exp Med 1985;161(2):277–89.

[332] Kefalides NA, Ohno N, Wilson CB, Fillit H, Zabriski J, Rosenbloom J. Identification of antigenic epitopes in type IV collagen by use of synthetic peptides. Kidney Int 1993;43 (1):94–100.

[333] Kefalides NA, Pegg MT, Ohno N, Poon-King T, Zabriskie J, Fillit H. Antibodies to basement membrane collagen and to laminin are present in sera from patients with poststreptococcal glomerulonephritis. J Exp Med 1986;163(3):588–602.

[334] Khandke KM, Fairwell T, Manjula BN. Difference in the structural features of streptococcal M proteins from nephritogenic and rheumatogenic serotypes. J Exp Med 1987;166 (1):151–62.

[335] Lange CF. Antigenicity of kidney glomeruli: evaluations by antistreptococcal cell membrane antisera. Transplant Proc 1980;12(3 Suppl 1):82–7.

[336] Markowitz AS, Clasen R, Nidus BD, Ainis H. Streptococcal related glomerulonephritis. II. Glomerulonephritis in rhesus monkeys immunologically induced both actively and passively with a soluble fraction from human glomeruli. J Immunol 1967;98(1):161–70.

[337] Markowitz AS, Horn D, Aseron C, Novak R, Battiforia HA. Streptococcal related glomerulonephritis. 3. Glomerulonephritis in rhesus monkeys immunologically induced both actively and passively with a soluble fraction from nephritogenic streptococcal protoplasmic membranes. J Immunol 1971;107(2):504–11.

[338] Grubb A, Grubb R, Christensen P, Schalen C. Isolation and some properties of an IgG Fc-binding protein from group A streptococci type 15. Int Arch Allergy Appl Immunol 1982;67 (4):369–76.

[339] Kronvall G. A surface component in group A, C, and G streptococci with non-immune reactivity for immunoglobulin G. J Immunol 1973;111(5):1401–6.

[340] McIntosh RM, Kaufman DB, McIntosh JR, Griswold W. Glomerular lesions produced by autologous serum and autologous IgG modified by treatment with a culture of a -haemolytic streptooccus. J Med Microbiol 1972;5(1):1–7.

[341] Mosquera J, Katiyar V, Coello J. Neuraminidase Production by Streprococci from Patients with Glomerulonephritis. J infec Dis 1985;151:259–63.

[342] Mosquera J, Rodriguez-Iturbe B. Extracellular Neuraminidase Production of Stepococci Associated with Acute Nephritis. Clin Nephr 1984;21:21–8.

[343] Treser G, Semar M, McVicar M, Franklin M, Ty A, Sagel I, et al. Antigenic streptococcal components in acute glomerulonephritis. Science 1969;163(868):676–7.

[344] Zabriskie JB. The role of streptococci in human glomerulonephritis. J Exp Med 1971;134(3): [Suppl:180s +].

[345] Dodge WF, Spargo BH, Travis LB, Srivastava RN, Carvajal HF, DeBeukelaer MM, et al. Poststreptococcal glomerulonephritis. A prospective study in children. N Engl J Med 1972;286(6): 273–8.

[346] Katz A, Dyck RF, Bear RA. Celiac disease associated with immune complex glomerulonephritis. Clin Nephrol 1979;11 (1):39–44.

[347] Pasternack A, Collin P, Mustonen J, Reunala T, Rantala I, Laurila K, et al. Glomerular IgA deposits in patients with celiac disease. Clin Nephrol 1990;34(2):56–60.

[348] Jennette JC, Ferguson AL, Moore MA, Freeman DG. IgA nephropathy associated with seronegative spondylarthropathies. Arthritis Rheum 1982;25(2):144–9.

[349] Woodroffe AJ. IgA, glomerulonephritis and liver disease. Aust N Z J Med 1981;11(Suppl 1):109–11.

[350] Kalsi J, Delacroix DL, Hodgson HJ. IgA in alcoholic cirrhosis. Clin Exp Immunol 1983;52(3):499–504.

[351] Ramirez G, Stinson JB, Zawada ET, Moatamed F. IgA nephritis associated with mycosis fungoides. Report of two cases. Arch Intern Med 1981;141(10):1287–91.

[352] Woodrow G, Innes A, Boyd SM, Burden RP. A case of IgA nephropathy with coeliac disease responding to a gluten-free diet. Nephrol Dial Transplant 1993;8(12):1382–3.

[353] Nomoto Y, Sakai H, Endoh M, Tomino Y. Scleritis and IgA nephropathy. Arch Intern Med 1980;140(6):783–5.

[354] Andrassy K, Lichtenberg G, Rambausek M. Sicca syndrome in mesangial IgA glomerulonephritis. Clin Nephrol 1985;24 (2):60–2.

[355] Yum MN, Lampton LM, Bloom PM, Edwards JL. Asymptomatic IgA nephropathy associated with pulmonary hemosiderosis. Am J Med 1978;64(6):1056–60.

[356] Nakamoto Y, Asano Y, Dohi K, Fujioka M, Iida H, Kida H, et al. Primary IgA glomerulonephritis and schonlein-henoch purpura nephritis: clinicopathological and immunohistological characteristics. Q J Med 1978;47(188): 495–516.

[357] Helin H, Mustonen J, Reunala T, Pasternack A. IgA nephropathy associated with celiac disease and dermatitis herpetiformis. Arch Pathol Lab Med 1983;107(6):324–7.
[358] Davin JC, Ten Berge IJ, Weening JJ. What is the difference between IgA nephropathy and henoch-schonlein purpura nephritis?. Kidney Int 2001;59(3):823–34.
[359] Cattran DC, Coppo R, Cook HT, Feehally J, Roberts IS, Troyanov S, et al. The Oxford classification of IgA nephropathy: rationale, clinicopathological correlations, and classification. Kidney Int 2009;76(5):534–45.
[360] Roberts IS, Cook HT, Troyanov S, Alpers CE, Amore A, Barratt J, et al. The Oxford classification of IgA nephropathy: pathology definitions, correlations, and reproducibility. Kidney Int 2009;76(5):546–56.
[361] Meyers KE, Finn L, Kaplan BS. Membranoproliferative glomerulonephritis type III. Pediatr Nephrol 1998;12(6):512–22.
[362] Neary J, Dorman A, Campbell E, Keogan M, Conlon P. Familial membranoproliferative glomerulonephritis type III. Am J Kidney Dis 2002;40(1):E1.
[363] Schwertz R, Rother U, Anders D, Gretz N, Scharer K, Kirschfink M. Complement analysis in children with idiopathic membranoproliferative glomerulonephritis: a long-term follow-up. Pediatr Allergy Immunol 2001;12(3):166–72.
[364] Daha MR, Van Es LA. Stabilization of homologous and heterologous cell-bound amplification convertases, C3bBb, by C3 nephritic factor. Immunology 1981;43(1):33–8.
[365] Pickering MC, Warren J, Rose KL, Carlucci F, Wang Y, Walport MJ, et al. Prevention of C5 activation ameliorates spontaneous and experimental glomerulonephritis in factor H-deficient mice. Proc Natl Acad Sci U S A 2006;103(25):9649–54.
[366] Ault BH. Factor H and the pathogenesis of renal diseases. Pediatr Nephrol 2000;14(10–11):1045–53.
[367] Wyatt RJ, Julian BA, Weinstein A, Rothfield NF, McLean RH. Partial H (beta 1H) deficiency and glomerulonephritis in two families. J Clin Immunol 1982;2(2):110–7.
[368] Nasr SH, Valeri AM, Appel GB, Sherwinter J, Stokes MB, Said SM, et al. Dense deposit disease: clinicopathologic study of 32 pediatric and adult patients. Clin J Am Soc Nephrol 2009;4 (1):22–32.
[369] D'Amico G, Ferrario F. Mesangiocapillary glomerulonephritis. J Am Soc Nephrol 1992;2(10 Suppl):S159–66.
[370] Mahieu P. Biochemical structure of glomerular basement membrane in chroni glomerulonephritis. I. Lobular and membranoproliferative glomerulonephritis. Kidney Int 1972;1(2):115–23.
[371] Nagi AH. Histological, ultrastructural and immunofluorescence studies in membranoproliferative glomerulonephritis. J Pathol 1972;106(3):151–4.
[372] Levy M, Gubler MC, Sich M, Beziau A, Habib R. Immunopathology of membranoproliferative glomerulonephritis with subendothelial deposits (Type I MPGN). Clin Immunol Immunopathol 1978;10(4):477–92.
[373] Weiner CP. Thrombotic microangiopathy in pregnancy and the postpartum period. Semin Hematol 1987;24(2):119–29.
[374] Pisoni R, Ruggenenti P, Remuzzi G. Drug-induced thrombotic microangiopathy: incidence, prevention and management. Drug Saf 2001;24(7):491–501.
[375] Ruggenenti P. Post-transplant hemolytic-uremic syndrome. Kidney Int 2002;62(3):1093–104.
[376] Braden GL, Mulhern JG, O'Shea MH, Nash SV, Ucci Jr AA, Germain MJ. Changing incidence of glomerular diseases in adults. Am J Kidney Dis 2000;35(5):878–83.
[377] Bakir AA, Bazilinski NG, Rhee HL, Ainis H, Dunea G. Focal segmental glomerulosclerosis. A common entity in nephrotic black adults. Arch Intern Med 1989;149(8):1802–4.
[378] Korbet SM, Genchi RM, Borok RZ, Schwartz MM. The racial prevalence of glomerular lesions in nephrotic adults. Am J Kidney Dis 1996;27:647–51.
[379] Jefferson JA, Couser WG. Therapy of membranous nephropathy associated with malignancy and secondary causes. Sem Nephrol 2003;23(4):400–5.
[380] Row PG, Cameron JS, Turner DR, Evans DJ, White RH, Ogg CS, et al. Membranous nephropathy. Long-term follow-up and association with neoplasia. Q J Med 1975;44(174):207–39.
[381] Jefferson JA, Johnson RJ. Treatment of hepatitis C-associated glomerular disease. Semin Nephrol 2000;20(3):286–92.
[382] Tanawattanacharoen S, Falk RJ, Jennette JC, Kopp JB. Parvovirus B19 DNA in kidney tissue of patients with focal segmental glomerulosclerosis. Am J Kidney Dis 2000;35 (6):1166–74.
[383] Case DB, Atlas SA, Mouradian JA, Fishman RA, Sherman RL, Laragh JH. Proteinuria during long-term captopril therapy. JAMA 1980;244(4):346–9.
[384] Textor SC, Gephardt GN, Bravo EL, Tarazi RC, Fouad FM, Tubbs R, et al. Membranous glomerulopathy associated with captopril therapy. Am J Med 1983;74(4):705–12.
[385] Sturgill BC, Shearlock KT. Membranous glomerulopathy and nephrotic syndrome after captopril therapy. JAMA 1983;250 (17):2343–5.
[386] Schwartz MM. Membranous glomerulonephritis. In: Heptinstall RH, editor. Pathology of the kidney. 4th ed. Boston/Toronto/London: Little Brown; 1992. p. 559–626.
[387] Falk RJ, Jennette JC, Nachman PH. Primary glomerular diseases. In: Brenner BM, editor. The kidney. 6th ed. Philadelphia: W.B. Saunders; 2000. p. 1284–92.
[388] Takekoshi Y, Tanaka M, Shida N, Satake Y, Saheki Y, Matsumoto S. Strong association between membranous nephropathy and hepatitis-B surface antigenaemia in Japanese children. Lancet 1978;2(8099):1065–8.
[389] Yoshikawa N, Ito H, Yamada Y, Hashimoto H, Katayama Y, Matsuyama S, et al. Membranous glomerulonephritis associated with hepatitis B antigen in children: a comparison with idiopathic membranous glomerulonephritis. Clin Nephrol 1985;23(1):28–34.
[390] Forland M, Spargo BH. Clinicopathological correlations in idiopathic nephrotic syndrome with membranous nephropathy. Nephron 1969;6(4):498–525.
[391] Ehrenreich T, Porush JG, Churg J, Garfinkel L, Glabman S, Goldstein MH, et al. Treatment of idiopathic membranous nephropathy. N Engl J Med 1976;295(14):741–6.
[392] Pierides AM, Malasit P, Morley AR, Willkinson R, Uldall PR, Kerr DN. Idiopathic membranous nephropathy. Q J Med 1977;46(182):163–77.
[393] Noel LH, Zanetti M, Droz D, Barbanel C. Long-term prognosis of idiopathic membranous glomerulonephritis. Study of 116 untreated patients. Am J Med 1979;66(1):82–90.
[394] Hopper Jr J, Trew PA, Biava CG. Membranous nephropathy: its relative benignity in women. Nephron 1981;29(1-2):18–24.
[395] Franklin WA, Jennings RB, Earle DP. Membranous glomerulonephritis: long-term serial observations on clinical course and morphology. Kidney Int 1973;4(1):36–56.
[396] Beregi E, Varga I. Analysis of 260 cases of membranous glomerulonephritis in renal biopsy material. Clin Nephrol 1974;2(6):215–21.
[397] Coggins CH, Frommer JP, Glassock RJ. Membranous nephropathy. Semin Nephrol 1982;2:264.
[398] Davison AM, Cameron JS, Kerr DN, Ogg CS, Wilkinson RW. The natural history of renal function in untreated idiopathic

membranous glomerulonephritis in adults. Clin Nephrol 1984;22(2):61–7.
[399] Tu WH, Petitti DB, Biava CG, Tulunay O, Hopper Jr J. Membranous nephropathy: predictors of terminal renal failure. Nephron 1984;36(2):118–24.
[400] Honkanen E. Survival in idiopathic membranous glomerulonephritis. Clin Nephrol 1986;25(3):122–8.
[401] Abe S, Amagasaki Y, Konishi K, Kato E, Iyori S, Sakaguchi H. Idiopathic membranous glomerulonephritis: aspects of geographical differences. J Clin Pathol 1986;39(11):1193–8.
[402] Kida H, Asamoto T, Yokoyama H, Tomosugi N, Hattori N. Long-term prognosis of membranous nephropathy. Clin Nephrol 1986;25(2):64–9.
[403] Murphy BF, Fairley KF, Kincaid-Smith PS. Idiopathic membranous glomerulonephritis: long-term follow-up in 139 cases. Clin Nephrol 1988;30(4):175–81.
[404] Shemesh O, Ross JC, Deen WM, Grant GW, Myers BD. Nature of the glomerular capillary injury in human membranous glomerulopathy. J Clin Invest 1986;77(3):868–77.
[405] Miller RB, Harrington JT, Ramos CP, Relman AS, Schwartz WB. Long-term results of steroid therapy in adults with idiopathic nephrotic syndrome. Am J Med 1969;46(6):919–29.
[406] [Anonymous]. A controlled study of short-term prednisone treatment in adults with membranous nephropathy. Collaborative study of the adult idiopathic nephrotic syndrome. N Engl J Med 1979;301(24):1301–6.
[407] Cameron JS, Healy MJ, Adu D. The medical research council trial of short-term high-dose alternate day prednisolone in idiopathic membranous nephropathy with nephrotic syndrome in adults. The MRC glomerulonephritis working party. Q J Med 1990;74(274):133–56.
[408] Donadio Jr JV, Holley KE, Anderson CF, Taylor WF. Controlled trial of cyclophosphamide in idiopathic membranous nephropathy. Kidney Int 1974;6(6):431–9.
[409] [Anonymous]. Controlled trial of azathioprine in the nephrotic syndrome secondary to idiopathic membranous glomerulonephritis. Can Med Assoc J 1976;115(12):1209–10.
[410] Kobayashi Y, Tateno S, Shigematsu H, Hiki Y. Prednisone treatment of non-nephrotic patients with idiopathic membranous nephropathy. A prospective study. Nephron 1982;30 (3):210–9.
[411] Cattran DC, Delmore T, Roscoe J, Cole E, Cardella C, Charron R, et al. A randomized controlled trial of prednisone in patients with idiopathic membranous nephropathy. N Engl J Med 1989;320(4):210–5.
[412] Shearman JD, Yin ZG, Aarons I, Smith PS, Woodroffe AJ, Clarkson AR. The effect of treatment with prednisolone or cyclophosphamide-warfarin-dipyridamole combination on the outcome of patients with membranous nephropathy. Clin Nephrol 1988;30(6):320–9.
[413] Suki WN, Chavez A. Membranous nephropathy: response to steroids and immunosuppression. Am J Nephrol 1981;1(1): 11–6.
[414] Schieppati A, Mosconi L, Perna A, Mecca G, Bertani T, Garattini S, et al. Prognosis of untreated patients with idiopathic membranous nephropathy. N Engl J Med 1993;329 (2):85–9.
[415] Donadio Jr JV, Torres VE, Velosa JA, Wagoner RD, Holley KE, Okamura M, et al. Idiopathic membranous nephropathy: the natural history of untreated patients. Kidney Int 1988;33 (3):708–15.
[416] Ponticelli C, Zucchelli P, Passerini P, Cesana B, Locatelli F, Pasquali S, et al. A 10-year follow-up of a randomized study with methylprednisolone and chlorambucil in membranous nephropathy. Kidney Int 1995;48(5):1600–4.
[417] Pollak VE, Rosen S, Pirani CL, Muehrcke RC, Kark RM. Natural history of lipoid nephrosis and of membranous glomerulonephritis. Ann Intern Med 1968;69(6):1171–96.
[418] Hayslett JP, Kashgarian M, Bensch KG, Spargo BH, Freedman LR, Epstein FH. Clinicopathological correlations in the nephrotic syndrome due to primary renal disease. Medicine (Baltimore) 1973;52(2):93–120.
[419] Ramzy MH, Cameron JS, Turner DR, Neild GH, Ogg CS, Hicks J. The long-term outcome of idiopathic membranous nephropathy. Clin Nephrol 1981;16(1):13–9.
[420] MacTier R, Boulton Jones JM, Payton CD, McLay A. The natural history of membranous nephropathy in the West of Scotland. Q J Med 1986;60(232):793–802.
[421] Pei Y, Cattran D, Greenwood C. Predicting chronic renal insufficiency in idiopathic membranous glomerulonephritis. Kidney Int 1992;42(4):960–6.
[422] Hogan SL, Muller KE, Jennette JC, Falk RJ. A review of therapeutic studies of idiopathic membranous glomerulopathy. Am J Kidney Dis 1995;25(6):862–75.
[423] James SH, Lien YH, Ruffenach SJ, Wilcox GE. Acute renal failure in membranous glomerulonephropathy: a result of superimposed crescentic glomerulonephritis. J Am Soc Nephrol 1995;6(6):1541–6.
[424] Cattran D. Management of membranous nephropathy: when and what for treatment. J Am Soc Nephrol 2005;16(5):1188–94.
[425] Troyanov S, Wall CA, Miller JA, Scholey JW, Cattran DC. Idiopathic membranous nephropathy: Definition and relevance of a partial remission. Kidney Int 2004;66(3):1199–205.
[426] Cattran DC, Pei Y, Greenwood CM, Ponticelli C, Passerini P, Honkanen E. Validation of a predictive model of idiopathic membranous nephropathy: its clinical and research implications. Kidney Int 1997;51(3):901–7.
[427] Marx BE, Marx M. Prediction in idiopathic membranous nephropathy. Kidney Int 1999;56(2):666–73.
[428] Hladunewich MA, Troyanov S, Calafati J, Cattran DC. The natural history of the non-nephrotic membranous nephropathy patient. Clin J Am Soc Nephrol 2009;4(9):1417–22.
[429] Harrison DJ, Thomson D, MacDonald MK. Membranous glomerulonephritis. J Clin Pathol 1986;39(2):167–71.
[430] Harvey JM, Howie AJ, Lee SJ, Newbold KM, Adu D, Michael J, et al. Renal biopsy findings in hypertensive patients with proteinuria. Lancet 1992;340(8833):1435–6.
[431] Llach F. Hypercoagulability, renal vein thrombosis, and other thrombotic complications of nephrotic syndrome. Kidney Int 1985;28(3):429–39.
[432] Harris RC, Ismail N. Extrarenal complications of the nephrotic syndrome. Am J Kidney Dis 1994;23(4):477–97.
[433] Llach F, Arieff AI, Massry SG. Renal vein thrombosis and nephrotic syndrome. A prospective study of 36 adult patients. Ann Intern Med 1975;83(1):8–14.
[434] Trew PA, Biava CG, Jacobs RP, Hopper Jr J. Renal vein thrombosis in membranous glomerulonephropathy: incidence and association. Medicine (Baltimore) 1978;57(1):69–82.
[435] Velasquez FF, Garcia PN, Ruiz MN. Idiopathic nephrotic syndrome of the adult with asymptomatic thrombosis of the renal vein. Am J Nephrol 1988;8(6):457–62.
[436] Llach F, Papper S, Massry SG. The clinical spectrum of renal vein thrombosis: acute and chronic. Am J Med 1980;69 (6):819–27.
[437] Wagoner RD, Stanson AW, Holley KE, Winter CS. Renal vein thrombosis in idiopathic membranous glomerulopathy and nephrotic syndrome: incidence and significance. Kidney Int 1983;23(2):368–74.
[438] Mallick NP, Short CD, Manos J. Clinical membranous nephropathy. Nephron 1983;34(4):209–19.

[439] Pruchno CJ, Burns MW, Schulze M, Johnson RJ, Baker PJ, Couser WG. Urinary excretion of C5b-9 reflects disease activity in passive Heymann nephritis. Kidney Int 1989;36(1):65–71.
[440] Schulze M, Donadio Jr JV, Pruchno CJ, Baker PJ, Johnson RJ, Stahl RA, et al. Elevated urinary excretion of the C5b-9 complex in membranous nephropathy. Kidney Int 1991;40 (3):533–8.
[441] Kusunoki Y, Akutsu Y, Itami N, Tochimaru H, Nagata Y, Takekoshi Y, et al. Urinary excretion of terminal complement complexes in glomerular disease. Nephron 1991;59(1): 27–32.
[442] Ogrodowski JL, Hebert LA, Sedmak D, Cosio FG, Tamerius J, Kolb W. Measurement of SC5b-9 in urine in patients with the nephrotic syndrome. Kidney Int 1991;40(6):1141–7.
[443] Coupes BM, Kon SP, Brenchley PE, Short CD, Mallick NP. The temporal relationship between urinary C5b-9 and C3dg and clinical parameters in human membranous nephropathy. Nephrol Dial Transplant 1993;8(5):397–401.
[444] Brenchley PE, Coupes B, Short CD, O'Donoghue DJ, Ballardie FW, Mallick NP. Urinary C3dg and C5b-9 indicate active immune disease in human membranous nephropathy. Kidney Int 1992;41(4):933–7.
[445] Pippin JW, Durvasula R, Petermann A, Hiromura K, Couser WG, Shankland SJ. DNA damage is a novel response to sublytic complement C5b-9-induced injury in podocytes. J Clin Invest 2003;111(6):877–85.
[446] Bijian K, Cybulsky AV. Stress proteins in glomerular epithelial cell injury. Contrib Nephrol 2005;148:8–20.
[447] Nangaku M, Shankland SJ, Couser WG. Cellular response to injury in membranous nephropathy. J Am Soc Nephrol 2005;16 (5):1195–204.
[448] Cunningham PN, Quigg RJ. Contrasting roles of complement activation and its regulation in membranous nephropathy. J Am Soc Nephrol 2005;16(5):1214–22.
[449] Bjorneklett R, Vikse BE, Svarstad E, Aasarod K, Bostad L, Langmark F, et al. Long-term risk of cancer in membranous nephropathy patients. Am J Kidney Dis 2007;50(3):396–403.
[450] Glassock RJ. Diagnosis and natural course of membranous nephropathy. Sem Nephrol 2003;23(4):324–32.
[451] Abreo K, Abreo F, Mitchell B, Schloemer G. Idiopathic crescentic membranous glomerulonephritis. Am J Kidney Dis 1986;8 (4):257–61.
[452] Mitas JA, Frank LR, Swerdlin AR, Johnson DL, Rabetoy GM. Crescentic glomerulonephritis complicating idiopathic membranous glomerulonephropathy. South Med J 1983;76(5): 664–7.
[453] Mathieson PW, Peat DS, Short A, Watts RA. Coexistent membranous nephropathy and ANCA-positive crescentic glomerulonephritis in association with penicillamine. Nephrol Dial Transplant 1996;11(5):863–6.
[454] Dwyer KM, Agar JW, Hill PA, Murphy BF. Membranous nephropathy and anti-neutrophil cytoplasmic antibody-associated glomerulonephritis: a report of 2 cases. Clin Nephrol 2001;56(5):394–7.
[455] Taniguchi Y, Yorioka N, Kumagai J, Ito T, Yamakido M, Taguchi T. Myeloperoxidase antineutrophil cytoplasmic antibody-positive necrotizing crescentic glomerulonephritis and membranous glomerulonephropathy. Clin Nephrol 1999;52(4):253–5.
[456] Meisels IS, Stillman IE, Kuhlik AB. Anti-glomerular basement membrane disease and dual positivity for antineutrophil cytoplasmic antibody in a patient with membranous nephropathy. Am J Kidney Dis 1998;32(4):646–8.
[457] Risdon RA, Sloper JC, De Wardener HE. Relationship between renal function and histological changes found in renal-biopsy specimens from patients with persistent glomerular nephritis. Lancet 1968;2:363–6.
[458] Schainuck LI, Striker GE, Cutler RE, Benditt EP. Structural-functional correlations in renal disease. Hum Pathol 1970;1:631–41.
[459] Wehrmann M, Bohle A, Bogenschutz O, Eissele R, Freislederer A, Ohlschlegel C, et al. Long-term prognosis of chronic idiopathic membranous glomerulonephritis. An analysis of 334 cases with particular regard to tubulo-interstitial changes. Clin Nephrol 1989;31(2):67–76.
[460] Sampson NS, Ryan ST, Enke DA, Cosgrove D, Koteliansky V, Gotwals P. Global gene expression analysis reveals a role for the a_1 integrin in renal pathogenesis. J Biol Chem 2001;276 (36):34182–8.
[461] Ehrenreich T, Churg J. Pathology of membranous nephropathy. In: Sommers SC, editor. Pathology annual 3. New York: Appleton-Century-Crofts; 1968. p. 145.
[462] Ponticelli C, Zucchelli P, Imbasciati E, Cagnoli L, Pozzi C, Passerini P, et al. Controlled trial of methylprednisolone and chlorambucil in idiopathic membranous nephropathy. N Engl J Med 1984;310(15):946–50.
[463] Ponticelli C, Zucchelli P, Passerini P, Cagnoli L, Cesana B, Pozzi C, et al. A randomized trial of methylprednisolone and chlorambucil in idiopathic membranous nephropathy. N Engl J Med 1989;320(1):8–13.
[464] Ponticelli C, Zucchelli P, Passerini P, Cesana B. Methylprednisolone plus chlorambucil as compared with methylprednisolone alone for the treatment of idiopathic membranous nephropathy. The Italian idiopathic membranous nephropathy treatment study group. N Engl J Med 1992;327 (9):599–603.
[465] Winfield JB, Faiferman I, Koffler D. Avidity of anti-DNA antibodies in serum and IgG glomerular eluates from patients with systemic lupus erythematosus. Association of high avidity antinative DNA antibody with glomerulonephritis. J Clin Invest 1977;59(1):90–6.
[466] van Bruggen MC, Kramers C, Walgreen B, Elema JD, Kallenberg CG, van den BJ, et al. Nucleosomes and histones are present in glomerular deposits in human lupus nephritis. Nephrol Dial Transplant 1997;12(1):57–66.
[467] Gamble CN, Reardan JB. Immunopathogenesis of syphilitic glomerulonephritis. Elution of antitreponemal antibody from glomerular immune-complex deposits. N Engl J Med 1975;292 (9):449–54.
[468] Takekoshi Y, Tanaka M, Miyakawa Y, Yoshizawa H, Takahashi K, Mayumi M. Free "small" and IgG-associated "large" hepatitis B e antigen in the serum and glomerular capillary walls of two patients with membranous glomerulonephritis. N Engl J Med 1979;300(15):814–9.
[469] Lai KN, Li PK, Lui SF, Au TC, Tam JS, Tong KL, et al. Membranous nephropathy related to hepatitis B virus in adults. N Engl J Med 1991;324(21):1457–63.
[470] Ronco PM. Paraneoplastic glomerulopathies: new insights into an old entity. Kidney Int 1999;56(1):355–77.
[471] Salant DJ, Belok S, Madaio MP, Couser WG. A new role for complement in experimental membranous nephropathy in rats. J Clin Invest 1980;66(6):1339–50.
[472] Cybulsky AV, Quigg RJ, Salant DJ. The membrane attack complex in complement-mediated glomerular epithelial cell injury: formation and stability of C5b-9 and C5b-7 in rat membranous nephropathy. J Immunol 1986;137(5):1511–6.
[473] Baker PJ, Ochi RF, Schulze M, Johnson RJ, Campbell C, Couser WG. Depletion of C6 prevents development of proteinuria in experimental membranous nephropathy in rats. Am J Pathol 1989;135(1):185–94.

[474] Adler S, Baker PJ, Johnson RJ, Ochi RF, Pritzl P, Couser WG. Complement membrane attack complex stimulates production of reactive oxygen metabolites by cultured rat mesangial cells. J Clin Invest 1986;77(3):762–7.
[475] Shah SV. Evidence suggesting a role for hydroxyl radical in passive Heymann nephritis in rats. Am J Physiol 1988;254(3 Pt 2):F337–44.
[476] Neale TJ, Ullrich R, Ojha P, Poczewski H, Verhoeven AJ, Kerjaschki D. Reactive oxygen species and neutrophil respiratory burst cytochrome b558 are produced by kidney glomerular cells in passive Heymann nephritis. Proc Natl Acad Sci U S A 1993;90(8):3645–9.
[477] Neale TJ, Ojha PP, Exner M, Poczewski H, Ruger B, Witztum JL, et al. Proteinuria in passive Heymann nephritis is associated with lipid peroxidation and formation of adducts on type IV collagen. J Clin Invest 1994;94(4):1577–84.
[478] McMillan JI, Riordan JW, Couser WG, Pollock AS, Lovett DH. Characterization of a glomerular epithelial cell metalloproteinase as matrix metalloproteinase-9 with enhanced expression in a model of membranous nephropathy. J Clin Invest 1996;97(4):1094–101.
[479] Watanabe K, Kinoshita S, Nakagawa H. Gelatinase secretion by glomerular epithelial cells. Nephron 1990;56(4):405–9.
[480] Topham PS, Haydar SA, Kuphal R, Lightfoot JD, Salant DJ. Complement-mediated injury reversibly disrupts glomerular epithelial cell actin microfilaments and focal adhesions. Kidney Int 1999;55(5):1763–75.
[481] Yuan HP, Takeuchi E, Taylor GA, McLaughlin M, Brown D, Salant DJ. Nephrin dissociates from actin, and its expression is reduced in early experimental membranous nephropathy. J Am Soc Nephrol 2002;13(4):946–56.
[482] Doublier S, Ruotsalainen V, Salvidio G, Lupia E, Biancone L, Conaldi PG, et al. Nephrin redistribution on podocytes is a potential mechanism for proteinuria in patients with primary acquired nephrotic syndrome. Am J Pathol 2001;158(5):1723–31.
[483] Border WA. Immune complex detection in glomerular diseases. Nephron 1979;24(3):105–13.
[484] Zager RA, Couser WG, Andrews BS, Bolton WK, Pohl MA. Membranous nephropathy: a radioimmunologic search for anti-renal tubular epithelial antibodies and circulating immune complexes. Nephron 1979;24(1):10–6.
[485] Couser WG. Mechanisms of glomerular injury in immune-complex disease. Kidney Int 1985;28(3):569–83.
[486] Beck Jr LH, Bonegio RG, Lambeau G, Beck DM, Powell DW, Cummins TD, et al. M-type phospholipase A2 receptor as target antigen in idiopathic membranous nephropathy. N Engl J Med 2009;361(1):11–21.
[487] Debiec H, Guigonis V, Mougenot B, Decobert F, Haymann J, Bensman A, et al. Brief report—Antenatal membranous glomerulonephritis due to anti-neutral endopeptidase antibodies. N Engl J Med 2002;346(26):2053–60.
[488] Debiec H, Nauta J, Coulet F, van der BM, Guigonis V, Schurmans T, et al. Role of truncating mutations in MME gene in fetomaternal alloimmunisation and antenatal glomerulopathies. Lancet 2004;364(9441):1252–9.
[489] Ronco P, Debiec H. Molecular pathomechanisms of membranous nephropathy: from Heymann nephritis to alloimmunization. J Am Soc Nephrol 2005;16(5):1205–13.
[490] Prunotto M, Carnevali ML, Candiano G, Murtas C, Bruschi M, Corradini E, et al. Autoimmunity in membranous nephropathy targets aldose reductase and SOD2. J Am Soc Nephrol 2010;21(3):507–19.
[491] Short CD, Feehally J, Gokal R, Mallick NP. Familial membranous nephropathy. Br Med J (Clin Res Ed) 1984;289(6457):1500.
[492] Sato K, Oguchi H, Hora K, Furukawa T, Furuta S, Shigematsu H, et al. Idiopathic membranous nephropathy in two brothers. Nephron 1987;46(2):174–8.
[493] Elshihabi I, Kaye CI, Brzowski A. Membranous nephropathy in two human leukocyte antigen-identical brothers. J Pediatr 1993;123(6):940–2.
[494] Bockenhauer D, Debiec H, Sebire N, Barratt M, Warwicker P, Ronco P, et al. Familial membranous nephropathy: an X-linked genetic susceptibility?. Nephron Clin Pract 2008;108(1):c10–5.
[495] Klouda PT, Manos J, Acheson EJ, Dyer PA, Goldby FS, Harris R, et al. Strong association between idiopathic membranous nephropathy and HLA-DRW3. Lancet 1979;2(8146):770–1.
[496] Muller GA, Muller C, Liebau G, Kompf J, Ising H, Wernet P. Strong association of idiopathic membranous nephropathy (IMN) with HLA-DR 3 and MT-2 without involvement of HLA-B 18 and no association to BfF1. Tissue Antigens 1981;17(3):332–7.
[497] Berthoux FC, Laurent B, le Petit JC, Genin C, Broutin F, Touraine F, et al. Immunogenetics and immunopathology of human primary membranous glomerulonephritis: HLA-A, B, DR antigens; functional activity of splenic macrophage Fc-receptors and peripheral blood T-lymphocyte subpopulations. Clin Nephrol 1984;22(1):15–20.
[498] Short CD, Feehally J, Gokal R, Mallick NP. A major system histocompatability haplotype associated with poor prognosis in idopathic membranous nephropathy. Dis Markers 1983;1:189.
[499] Tomura S, Kashiwabara H, Tuchida H, Shishido H, Sakurai S, Miyajima T, et al. Strong association of idiopathic membranous nephropathy with HLA-DR2 and MT1 in Japanese. Nephron 1984;36(4):242–5.
[500] Abe S, Amagasaki Y, Konishi K, Kato E, Iyori S, Sakaguchi H. Idiopathic membranous glomerulonephritis: aspects of geographical differences. J Clin Pathol 1986;39(11):1193–8.
[501] Polanco N, Gutierrez E, Covarsi A, Ariza F, Carreno A, Vigil A, et al. Spontaneous Remission of Nephrotic Syndrome in Idiopathic Membranous Nephropathy. J Am Soc Nephrol 2010;21:697–704.
[502] Thomas DM, Hillis AN, Coles GA, Davies M, Williams JD. Enalapril can treat the proteinuria of membranous glomerulonephritis without detriment to systemic or renal hemodynamics. Am J Kidney Dis 1991;18(1):38–43.
[503] Gansevoort RT, Heeg JE, Vriesendorp R, De Zeeuw D, De Jong PE. Antiproteinuric drugs in patients with idiopathic membranous glomerulopathy. Nephrol Dial Transplant 1992;7(Suppl 1):91–6.
[504] Rostoker G, Ben Maadi A, Remy P, Lang P, Lagrue G, Weil B. Low-dose angiotensin-converting-enzyme inhibitor captopril to reduce proteinuria in adult idiopathic membranous nephropathy: a prospective study of long-term treatment. Nephrol Dial Transplant 1995;10(1):25–9.
[505] Haas M, Kerjaschki D, Mayer G. Lipid-lowering therapy in membranous nephropathy. Kidney Int 1999;56:S110–2.
[506] Yukawa S, Mune M, Yamada Y, Otani H, Kishino M, Tone Y. Ongoing clinical trials of lipid reduction therapy in patients with renal disease. Kidney Int 1999;56:S141–3.
[507] Glassock RJ. Prophylactic anticoagulation in nephrotic syndrome: a clinical conundrum. J Am Soc Nephrol 2007;18(8):2221–5.
[508] Austin III HA, Illei GG, Braun MJ, Balow JE. Randomized, controlled trial of prednisone, cyclophosphamide, and cyclosporine in lupus membranous nephropathy. J Am Soc Nephrol 2009;20(4):901–11.
[509] Ponticelli C, Altieri P, Scolari F, Passerini P, Roccatello D, Cesana B, et al. A randomized study comparing

methylprednisolone plus chlorambucil versus methylprednisolone plus cyclophosphamide in idiopathic membranous nephropathy. J Am Soc Nephrol 1998;9(3):444–50.

[510] Jha V, Ganguli A, Saha TK, Kohli HS, Sud K, Gupta KL, et al. A randomized, controlled trial of steroids and cyclophosphamide in adults with nephrotic syndrome caused by idiopathic membranous nephropathy. J Am Soc Nephrol 2007;18(6): 1899–904.

[511] Murphy BF, McDonald I, Fairley KF, Kincaid-Smith PS. Randomized controlled trial of cyclophosphamide, warfarin and dipyridamole in idiopathic membranous glomerulonephritis. Clin Nephrol 1992;37(5):229–34.

[512] Alexopoulos E, Sakellariou G, Memmos D, Karamitsos K, Leontsini M, Papadimitriou M. Cyclophosphamide provides no additional benefit to steroid therapy in the treatment of idiopathic membranous nephropathy. Am J Kidney Dis 1993;21 (5):497–503.

[513] Imperiale TF, Goldfarb S, Berns JS. Are cytotoxic agents beneficial in idiopathic membranous nephropathy? A meta-analysis of the controlled trials. J Am Soc Nephrol 1995;5(8):1553–8.

[514] Torres A, Domínguez-Gil B, Carreño A, Hernández E, Morales E, Segura J, et al. Conservative versus immunosuppressive treatment of patients with idiopathic membranous nephropathy. Kidney Int 2002;61(1):219–27.

[515] Warwick GL, Geddes CG, Boulton-Jones JM. Prednisolone and chlorambucil therapy for idiopathic membranous nephropathy with progressive renal failure. Q J Med 1994;87(4):223–9.

[516] Jindal K, West M, Bear R, Goldstein M. Long-term benefits of therapy with cyclophosphamide and prednisone in patients with membranous glomerulonephritis and impaired renal function. Am J Kidney Dis 1992;19(1):61–7.

[517] Bruns FJ, Adler S, Fraley DS, Segel DP. Sustained remission of membranous glomerulonephritis after cyclophosphamide and prednisone. Ann Intern Med 1991;114(9):725–30.

[518] Cattran DC, Greenwood C, Ritchie S, Bernstein K, Churchill DN, Clark WF, et al. A controlled trial of cyclosporine in patients with progressive membranous nephropathy. Canadian glomerulonephritis study group. Kidney Int 1995;47 (4):1130–5.

[519] Falk RJ, Hogan SL, Muller KE, Jennette JC. Treatment of progressive membranous glomerulopathy. A randomized trial comparing cyclophosphamide and corticosteroids with corticosteroids alone. The glomerular disease collaborative network. Ann Intern Med 1992;116(6):438–45.

[520] Cattran DC, Appel GB, Hebert LA, Hunsicker LG, Pohl MA, Hoy WE, et al. Cyclosporine in patients with steroid-resistant membranous nephropathy: a randomized trial. Kidney Int 2001;59(4):1484–90.

[521] Alexopoulos E, Papagianni A, Tsamelashvili M, Leontsini M, Memmos D. Induction and long-term treatment with cyclosporine in membranous nephropathy with the nephrotic syndrome. Nephrol Dial Transplant 2006;21(11):3127–32.

[522] Miller G, Zimmerman III R, Radhakrishnan J, Appel G. Use of mycophenolate mofetil in resistant membranous nephropathy. Am J Kidney Dis 2000;36(2):250–6.

[523] Choi MJ, Eustace JA, Gimenez LF, Atta MG, Scheel PJ, Sothinathan R, et al. Mycophenolate mofetil treatment for primary glomerular diseases. Kidney Int 2002;61(3):1098–114.

[524] Dussol B, Morange S, Burtey S, Indreies M, Cassuto E, Mourad G, et al. Mycophenolate mofetil monotherapy in membranous nephropathy: a 1-year randomized controlled trial. Am J Kidney Dis 2008;52(4):699–705.

[525] Branten AJ, du Buf-Vereijken PW, Vervloet M, Wetzels JF. Mycophenolate mofetil in idiopathic membranous nephropathy: a clinical trial with comparison to a historic control group treated with cyclophosphamide. Am J Kidney Dis 2007;50 (2):248–56.

[526] Remuzzi G, Chiurchiu C, Abbate M, Brusegan V, Bontempelli M, Ruggenenti P. Rituximab for idiopathic membranous nephropathy. Lancet 2002;360(9337):923–4.

[527] Ruggenenti P, Chiurchiu C, Brusegan V, Abbate M, Perna A, Filippi C, et al. Rituximab in idiopathic membranous nephropathy: A one year prospective study. J Am Soc Nephrol 2003;14 (7):1851–7.

[528] Fervenza FC, Cosio FG, Erickson SB, Specks U, Herzenberg AM, Dillon JJ, et al. Rituximab treatment of idiopathic membranous nephropathy. Kidney Int 2008;73:117–25.

[529] Segarra A, Praga M, Ramos N, Polanco N, Cargol I, Gutierrez-Solis E, et al. Successful treatment of membranous glomerulonephritis with rituximab in calcineurin inhibitor-dependent patients. Clin J Am Soc Nephrol 2009;4(6):1083–8.

[530] Moroni G, Gallelli B, Quaglini S, Leoni A, Banfi G, Passerini P, et al. Long-term outcome of renal transplantation in patients with idiopathic membranous glomerulonephritis (MN). Nephrol Dial Transplant 2010.

[531] Cosyns JP, Couchoud C, Pouteil-Noble C, Squifflet JP, Pirson Y. Recurrence of membranous nephropathy after renal transplantation: probability, outcome and risk factors. Clin Nephrol 1998;50(3):144–53.

[532] Madaio MP, Harrington JT. The diagnosis of glomerular diseases: acute glomerulonephritis and the nephrotic syndrome. Arch Intern Med 2001;161(1):25–34.

[533] Haas M, Meehan SM, Karrison TG, Spargo BH. Changing etiologies of unexplained adult nephrotic syndrome: a comparison of renal biopsy findings from 1976–1979 and 1995-1997. Am J Kidney Dis 1997;30(5):621–31.

[534] Braden GL, Mulhern JG, O'Shea MH, Nash SV, Ucci Jr AA, Germain MJ. Changing incidence of glomerular diseases in adults. Am J Kidney Dis 2000;35(5):878–83.

[535] Kitiyakara C, Kopp JB, Eggers P. Trends in the epidemiology of focal segmental glomerulosclerosis. Semin Nephrol 2003;23 (2):172–82.

[536] Korbet SM, Schwartz MM, Lewis EJ. Primary focal segmental glomerulosclerosis: Clinical course and response to therapy. Am J Kidney Dis 1994;23:773–83.

[537] Rydel JJ, Korbet SM, Borok RZ, Schwartz MM. Focal segmental glomerular sclerosis in adults: presentation, course, and response to treatment. Am J Kidney Dis 1995;25(4): 534–42.

[538] Korbet SM, Schwartz MM, Lewis EJ. The prognosis of focal segmental glomerular sclerosis of adulthood. Medicine (Baltimore) 1986;65(5):304–11.

[539] Wyatt CM, Klotman PE. Antiretroviral therapy and the kidney: balancing benefit and risk in patients with HIV infection. Expert Opin Drug Saf 2006;5(2):275–87.

[540] Meyrier A. Mechanisms of disease: focal segmental glomerulosclerosis. Nat Clin Pract Nephrol 2005;1(1):44–54.

[541] Meyrier A. Nephrotic focal segmental glomerulosclerosis in 2004: an update. Nephrol Dial Transplant 2004;19(10): 2437–44.

[542] Korbet SM. Primary focal segmental glomerulosclerosis [Review] [57 refs]. J Am Soc Nephrol 1998;9(7):1333–40.

[543] D'Agati V. The many masks of focal segmental glomerulosclerosis [Review] [143 refs]. Kidney Int 1994;46(4):1223–41.

[544] Falk RJ, Jennette JC, Nachman PH. Primary glomerular disease. In: Brenner BM, editor. The kidney. 6th ed. Philadelphia: W.B. Saunders & Co.; 2000. p. 1263–349.

[545] D'Agati VD, Fogo AB, Bruijn JA, Jennette JC. Pathologic classification of focal segmental glomerulosclerosis: a working proposal. Am J Kidney Dis 2004;43(2):368–82.

[546] Chun MJ, Korbet SM, Schwartz MM, Lewis EJ. Focal segmental glomerulosclerosis in nephrotic adults: presentation, prognosis, and response to therapy of the histologic variants. J Am Soc Nephrol 2004;15(8):2169–77.
[547] Daskalakis N, Winn MP. Focal and segmental glomerulosclerosis. Cell Mol Life Sci 2006;63(21):2506–11.
[548] Daskalakis N, Winn MP. Focal and segmental glomerulosclerosis: varying biologic mechanisms underlie a final histopathologic end point. Semin Nephrol 2006;26(2):89–94.
[549] Pollak MR. Inheirited podocytopathies: recent advances in understanding proteinuric renal disease. 2003.
[550] Somlo S, Mundel P. Getting a foothold in nephrotic syndrome. Nat Genet 2000;24(4):333–5.
[551] Tryggvason K, Patrakka J, Wartiovaara J. Hereditary proteinuria syndromes and mechanisms of proteinuria. N Engl J Med 2006;354(13):1387–401.
[552] Hinkes B, Wiggins RC, Gbadegesin R, Vlangos CN, Seelow D, Nurnberg G, et al. Positional cloning uncovers mutations in PLCE1 responsible for a nephrotic syndrome variant that may be reversible. Nat Genet 2006.
[553] Quaggin SE, George Jr AL. Apolipoprotein L1 and the genetic basis for racial disparity in chronic kidney disease. J Am Soc Nephrol 2011.
[554] Kopp JB, Smith MW, Nelson GW, Johnson RC, Freedman BI, Bowden DW, et al. MYH9 is a major-effect risk gene for focal segmental glomerulosclerosis. Nat Genet 2008;40:1175–84.
[555] Kao WH, Klag MJ, Meoni LA, Reich D, Berthier-Schaad Y, Li M, et al. MYH9 is associated with nondiabetic end-stage renal disease in African Americans. Nat Genet 2008;40(1185): 1192.
[556] Genovese G, Friedman DJ, Ross MD, Lecordier L, Uzureau P, Freedman BI, et al. Association of Trypanolytic ApoL1 Variants with Kidney Disease in African-Americans. Science 2010;329:841–5.
[557] Antignac C. Genetic models: clues for understanding the pathogenesis of idiopathic nephrotic syndrome. J Clin Invest 2002;109(4):447–9.
[558] Savin VJ, McCarthy ET, Sharma M. Permeability factors in focal segmental glomerulosclerosis. Semin Nephrol 2003;23 (2):147–60.
[559] Wei C, El HS, Li J, Fornoni A, Goes N, Sageshima J, et al. Circulating urokinase receptor as a cause of focal segmental glomerulosclerosis. Nat Med 2011;17(8):952–60.
[560] Tryggvason K, Pikkarainen T, Patrakka J. Nck links nephrin to actin in kidney podocytes. Cell 2006;125(2):221–4.
[561] Korbet SM. Treatment of primary focal segmental glomerulosclerosis. Kidney Int 2002;62(6):2301–10.
[562] Meyrier A. Treatment of focal segmental glomerulosclerosis. Expert Opin Pharmacother 2005;6(9):1539–49.
[563] Cattran DC, Appel GB, Hebert LA, Hunsicker LG, Pohl MA, N Amer Nephrotic Syndrome Study Gr, et al. A randomized trial of cyclosporine in patients with steroid-resistant focal segmental glomerulosclerosis. Kidney Int 1999;56(6):2220–6.
[564] Gipson DS, Trachtman H, Kaskel FJ, Greene TH, Radeva MK, Gassman JJ, et al. Clinical trial of focal segmental glomerulosclerosis in children and young adults. Kidney Int 2011;80 (8):868–78.
[565] Fornoni A, Sageshima J, Wei C, Merscher-Gomez S, Aguillon-Prada R, Jauregui AN, et al. Rituximab targets podocytes in recurrent focal segmental glomerulosclerosis. Sci Transl Med 2011;3(85):85ra46.
[566] Lewy JE, Salinas-Madrigal L, Herdson PB, Pirani CL, Metcoff J. Clinico-pathologic correlations in acute poststreptococcal glomerulonephritis. A correlation between renal functions, morphologic damage and clinical course of 46 children with acute poststreptococcal glomerulonephritis. Medicine (Baltimore) 1971;50(6):453–501.
[567] Nolasco F, Cameron JS, Heywood EF, Hicks J, Ogg C, Williams DG. Adult-onset minimal change nephrotic syndrome: a long-term follow-up. Kidney Int 1986;29(6):1215–23.
[568] Warren GV, Korbet SM, Schwartz MM, Lewis EJ. Minimal change glomerulopathy associated with nonsteroidal antiinflammatory drugs. Am J Kidney Dis 1989;13(2):127–30.
[569] Sedor JR, Davidson EW, Dunn MJ. Effects of nonsteroidal antiinflammatory drugs in healthy subjects. Am J Med 1986;81 (2B):58–70.
[570] Jennette JC, Falk RJ. Adult minimal change glomerulopathy with acute renal failure. Am J Kidney Dis 1990;16(5):432–7.
[571] Waldman M, Crew RJ, Valeri A, Busch J, Stokes B, Markowitz G, et al. Adult minimal-change disease: clinical characteristics, treatment, and outcomes. Clin J Am Soc Nephrol 2007;2 (3):445–53.
[572] Mendoza SA, Tune BM. Treatment of childhood nephrotic syndrome. J Am Soc Nephrol 1992;3(4):889–94.
[573] Schnaper HW, Aune TM. Identification of the lymphokine soluble immune response suppressor in urine of nephrotic children. J Clin Invest 1985;76(1):341–9.
[574] Berns JS, Gaudio KM, Krassner LS, Anderson FP, Durante D, McDonald BM, et al. Steroid-responsive nephrotic syndrome of childhood: a long-term study of clinical course, histopathology, efficacy of cyclophosphamide therapy, and effects on growth. Am J Kidney Dis 1987;9(2):108–14.
[575] Clement LC, Avila-Casado C, Mace C, Soria E, Bakker WW, Kersten S, et al. Podocyte-secreted angiopoietin-like-4 mediates proteinuria in glucocorticoid-sensitive nephrotic syndrome. Nat Med 2011;17(1):117–22.
[576] [Anonymous]. Alternate-day versus intermittent prednisone in frequently relapsing nephrotic syndrome. A report of "Arbetsgemeinschaft fur Padiatrische Nephrologie". Lancet 1979;1(8113):401–3.
[577] [Anonymous]. Nephrotic syndrome in children: a randomized trial comparing two prednisone regimens in steroid-responsive patients who relapse early. Report of the international study of kidney disease in children. J Pediatr 1979;95(2):239–43.
[578] Fujimoto S, Yamamoto Y, Hisanaga S, Morita S, Eto T, Tanaka K. Minimal change nephrotic syndrome in adults: response to corticosteroid therapy and frequency of relapse. Am J Kidney Dis 1991;17(6):687–92.
[579] Nakayama M, Katafuchi R, Yanase T, Ikeda K, Tanaka H, Fujimi S. Steroid responsiveness and frequency of relapse in adult-onset minimal change nephrotic syndrome. Am J Kidney Dis 2002;39(3):503–12.
[580] Grupe WE. Childhood nephrotic syndrome: clinical associations and response to therapy. Postgrad Med 1979;65 (5):229–36.
[581] Schulman SL, Kaiser BA, Polinsky MS, Srinivasan R, Baluarte HJ. Predicting the response to cytotoxic therapy for childhood nephrotic syndrome: superiority of response to corticosteroid therapy over histopathologic patterns. J Pediatr 1988;113 (6):996–1001.
[582] Ueda N, Kuno K, Ito S. Eight and 12 week courses of cyclophosphamide in nephrotic syndrome. Arch Dis Child 1990;65 (10):1147–50.
[583] Grupe WE, Makker SP, Ingelfinger JR. Chlorambucil treatment of frequently relapsing nephrotic syndrome. N Engl J Med 1976;295(14):746–9.
[584] Williams SA, Makker SP, Ingelfinger JR, Grupe WE. Long-term evaluation of chlorambucil plus prednisone in the idiopathic nephrotic syndrome of childhood. N Engl J Med 1980;302 (17):929–33.

[585] Niaudet P, Habib R. Cyclosporine in the treatment of idiopathic nephrosis. J Am Soc Nephrol 1994;5(4):1049–56.
[586] Gregory MJ, Smoyer WE, Sedman A, Kershaw DB, Valentini RP, Johnson K, et al. Long-term cyclosporine therapy for pediatric nephrotic syndrome: a clinical and histologic analysis. J Am Soc Nephrol 1996;7(4):543–9.
[587] Ponticelli C, Edefonti A, Ghio L, Rizzoni G, Rinaldi S, Gusmano R, et al. Cyclosporin versus cyclophosphamide for patients with steroid-dependent and frequently relapsing idiopathic nephrotic syndrome: a multicentre randomized controlled trial. Nephrol Dial Transplant 1993;8(12):1326–32.
[588] Choi MJ, Eustace JA, Gimenez LF, Atta MG, Scheel PJ, Sothinathan R, et al. Mycophenolate mofetil treatment for primary glomerular diseases. Kidney Int 2002;61(3):1098–114.
[589] Francois H, Daugas E, Bensman A, Ronco P. Unexpected efficacy of rituximab in multirelapsing minimal change nephrotic syndrome in the adult: first case report and pathophysiological considerations. Am J Kidney Dis 2007;49(1):158–61.
[590] Rao TK, Filippone EJ, Nicastri AD, Landesman SH, Frank E, Chen CK, et al. Associated focal and segmental glomerulosclerosis in the acquired immunodeficiency syndrome. N Engl J Med 1984;310(11):669–73.
[591] Pardo V, Aldana M, Colton RM, Fischl MA, Jaffe D, Moskowitz L, et al. Glomerular lesions in the acquired immunodeficiency syndrome. Ann Intern Med 1984;101(4):429–34.
[592] Gardenswartz MH, Lerner CW, Seligson GR, Zabetakis PM, Rotterdam H, Tapper ML, et al. Renal disease in patients with AIDS: a clinicopathologic study. Clin Nephrol 1984;21(4): 197–204.
[593] Kimmel PL, Barisoni L, Kopp JB. Pathogenesis and treatment of HIV-associated renal diseases: Lessons from clinical and animal studies, molecular pathologic correlations, and genetic investigations. Ann Intern Med 2003;139(3):214–26.
[594] Laradi A, Mallet A, Beaufils H, Allouache M, Martinez F. HIV-associated nephropathy: Outcome and prognosis factors. J Am Soc Nephrol 1998;9(12):2327–35.
[595] Rao TKS. Acute renal failure syndromes in human immunodeficiency virus infection. Semin Nephrol 1998;18(4):378–95.
[596] Lu TC, Ross M. HIV-associated nephropathy: a brief review. Mt Sinai J Med 2005;72(3):193–9.
[597] Bourgoignie JJ, Meneses R, Ortiz C, Jaffe D, Pardo V. The clinical spectrum of renal disease associated with human immunodeficiency virus. Am J Kidney Dis 1988;12(2):131–7.
[598] Carbone L, D'Agati V, Cheng JT, Appel GB. Course and prognosis of human immunodeficiency virus-associated nephropathy. Am J Med 1989;87(4):389–95.
[599] Paragas N, Nickolas TL, Wyatt C, Forster CS, Sise M, Morgello S, et al. Urinary NGAL marks cystic disease in HIV-associated nephropathy. J Am Soc Nephrol 2009;20(8):1687–92.
[600] Soler-Garcia AA, Rakhmanina NY, Mattison PC, Ray PE. A urinary biomarker profile for children with HIV-associated renal diseases. Kidney Int 2009;76(2):207–14.
[601] Winston JA, Klotman ME, Klotman PE. HIV-associated nephropathy is a late, not early, manifestation of HIV-1 infectiont. Kidney In 1999;55(3):1036–40.
[602] Wali RK, Drachenberg CI, Papadimitriou JC, Keay S, Ramos E. HIV-1-associated nephropathy and response to highly-active antiretroviral therapy. Lancet 1998;352(9130):783–4.
[603] Levin ML, Palella F, Shah S, Lerma E, Butter J, Kanwar YS. HIV-associated nephropathy occurring before HIV antibody seroconversion. Am J Kidney Dis 2001;37(5):NIL39–43.
[604] Briggs WA, Tanawattanacharoen S, Choi MJ, Scheel Jr PJ, Nadasdy T, Racusen L. Clinicopathologic correlates of prednisone treatment of human immunodeficiency virus-associated nephropathy. Am J Kidney Dis 1996;28(4):618–21.
[605] Alpers CE, Madias NE, Harrington T, Levey AS, Balakrishnan V. Light at the end of the TUNEL: HIV-associated thrombotic microangiopathy. Kidney Int 2003;63(1):385–96.
[606] Weiner NJ, Goodman JW, Kimmel PL. The HIV-associated renal diseases: Current insight into pathogenesis and treatment. Kidney Int 2003;63(5):1618–31.
[607] Kimmel PL, Phillips TM, Ferreira-Centeno A, Farkas-Szallasi T, Abraham AA, Garrett CT. Brief report: idiotypic IgA nephropathy in patients with human immunodeficiency virus infection. N Engl J Med 1992;327(10):702–6.
[608] Katz A, Bargman JM, Miller DC, Guo JW, Ghali VS, Schoeneman MJ. IgA nephritis in HIV-positive patients: a new HIV-associated nephropathy?. Clin Nephrol 1992;38(2): 61–8.
[609] Nochy D, Glotz D, Dosquet P, Pruna A, Guettier C, Weiss L, et al. Renal disease associated with HIV infection: a multicentric study of 60 patients from Paris hospitals. Nephrol Dial Transplant 1993;8(1):11–9.
[610] Haas M, Kaul S, Eustace JA. HIV-associated immune complex glomerulonephritis with "lupus-like" features: a clinicopathologic study of 14 cases.. Kidney Int 2005;67(4):1381–90.
[611] Valeri A, Barisoni L, Appel GB, Seigle R, D'Agati V. Idiopathic collapsing focal segmental glomerulosclerosis: a clinicopathologic study. Kidney Int 1996;50(5):1734–46.
[612] Barisoni L, Kriz W, Mundel P, D'Agati V. The dysregulated podocyte phenotype: A novel concept in the pathogenesis of collapsing idiopathic focal segmental glomerulosclerosis and HIV-associated nephropathy. J Am Soc Nephrol 1999;10(1): 51–61.
[613] Barisoni L, Mokrzycki M, Sablay L, Nagata M, Yamase H, Mundel P. Podocyte cell cycle regulation and proliferation in collapsing glomerulopathies. Kidney Int 2000;58(1):137–43.
[614] D'Agati V, Suh JI, Carbone L, Cheng JT, Appel G. Pathology of HIV-associated nephropathy: a detailed morphologic and comparative study. Kidney Int 1989;35(6):1358–70.
[615] D'Agati V, Appel GB. HIV infection and the kidney. J Am Soc Nephrol 1997;8(1):138–52.
[616] Atta MG, Choi MJ, Longenecker JC, Haymart M, Wu J, Nagajothi N, et al. Nephrotic range proteinuria and CD4 count as noninvasive indicators of HIV-associated nephropathy. Am J Med 2005;118(11):1288.
[617] Bruggeman LA, Ross MD, Tanji N, Cara A, Dikman S, Gordon RE, et al. Renal epithelium is a previously unrecognized site of HIV-1 infection. J Am Soc Nephrol 2000;11(11):2079–87.
[618] Winston JA, Bruggeman LA, Ross MD, Jacobson J, Ross L, D'Agati VD, et al. Nephropathy and establishment of a renal reservoir of HIV type 1 during primary infection. N Engl J Med 2001;344(26):1979–84.
[619] Dickie P, Felser J, Eckhaus M, Bryant J, Silver J, Marinos N, et al. HIV-associated nephropathy in transgenic mice expressing HIV-1 genes. Virology 1991;185(1):109–19.
[620] Kopp JB, Klotman ME, Adler SH, Bruggeman LA, Dickie P, Marinos NJ, et al. Progressive glomerulosclerosis and enhanced renal accumulation of basement membrane components in mice transgenic for human immunodeficiency virus type I genes. Proc Natl Acad Sci U S A 1992;89:1577–81.
[621] Bruggeman LA, Dikman S, Meng C, Quaggin SE, Coffman TM, Klotman PE. Nephropathy in human immunodeficiency virus-1 transgenic mice is due to renal transgene expression. J Clin Invest 1997;100(1):84–92.
[622] Dickie P, Felser J, Eckhaus M, Bryant J, Silver J, Marinos N, et al. HIV-associated nephropathy in transgenic mice expressing HIV-1 genes. Virology 1991;185(1):109–19.
[623] Marras D, Bruggeman LA, Gao F, Tanji N, Mansukhani MM, Cara A, et al. Replication and compartmentalization of HIV-1

in kidney epithelium of patients with HIV-associated nephropathy. Nat Med 2002;8(5):522–6.
[624] Kajiyama W, Kopp JB, Marinos NJ, Klotman PE, Dickie P. Glomerulosclerosis and viral gene expression in HIV-transgenic mice: Role of *nef*. Kidney Int 2000;58(3):1148–59.
[625] Hanna Z, Kay DG, Rebai N, Guimond A, Jothy S, Jolicoeur P. Nef harbors a major determinant of pathogenicity for an AIDS-like disease induced by HIV-1 in transgenic mice. Cell 1998;95 (2):163–75.
[626] Kaufman L, Collins SE, Klotman PE. The pathogenesis of HIV-associated nephropathy. Adv Chronic Kidney Dis 2010;17 (1):36–43.
[627] Freedman BI, Soucie JM, Stone SM, Pegram S. Familial clustering of end-stage renal disease in blacks with HIV-associated nephropathy. Am J Kidney Dis 1999;34(2):254–8.
[628] Kopp JB, Smith MW, Nelson GW, Johnson RC, Freedman BI, Bowden DW, et al. MYH9 is a major-effect risk gene for focal segmental glomerulosclerosis. Nat Genet 2008;40(10):1175–84.
[629] Papeta N, Chan KT, Prakash S, Martino J, Kiryluk K, Ballard D, et al. Susceptibility loci for murine HIV-associated nephropathy encode trans-regulators of podocyte gene expression. J Clin Invest 2009;119(5):1178–88.
[630] Eggers PW, Kimmel PL. Is there an epidemic of HIV Infection in the US ESRD program? J Am Soc Nephrol 2004;15 (9):2477–85.
[631] Lucas GM, Eustace JA, Sozio S, Mentari EK, Appiah KA, Moore RD. Highly active antiretroviral therapy and the incidence of HIV-1-associated nephropathy: a 12-year cohort study. AIDS 2004;18(3):541–6.
[632] Szczech LA, Edwards LJ, Sanders LL, van der HC, Bartlett JA, Heald AE, et al. Protease inhibitors are associated with a slowed progression of HIV-related renal diseases. Clin Nephrol 2002;57(5):336–41.
[633] Cosgrove CJ, Abu-Alfa AK, Perazella MA. Observations on HIV-associated renal disease in the era of highly active antiretroviral therapy. Am J Med Sci 2002;323(2):102–6.
[634] Saulsbury F. Resolution of organ-specific complications of human immunodeficiency virus infection in children with use of highly active antiretroviral therapy. Clin Infect Dis 2001;32 (3):464–8.
[635] Daugas E, Rougier JP, Hill G. HAART-related nephropathies in HIV-infected patients. Kidney Int 2005;67(2):393–403.
[636] Kopp JB, Miller KD, Mican JAM, Feuerstein IM, Vaughan E, Baker C, et al. Crystalluria and urinary tract abnormalities associated with indinavir. Ann Int Med 1997;127(2):119–25.
[637] Daudon M, Estepa L, Viard JP, Joly D, Jungers P. Urinary stones in HIV-1-positive patients treated with indinavir. Lancet 1997;349(9061):1294–5.
[638] Vittecoq D, Dumitrescu L, Beaufils H, Deray G. Fanconi syndrome associated with cidofovir therapy. Antimicrob Agents Chemother 1997;41(8):1846.
[639] Meier P, Dautheville-Guibal S, Ronco PM, Rossert J. Cidofovir-induced end-stage renal failure. Nephrol Dial Transplant 2002;17(1):148–9.
[640] Kahn J, Lagakos S, Wulfsohn M, Cherng D, Miller M, Cherrington J, et al. Efficacy and safety of adefovir dipivoxil with antiretroviral therapy: a randomized controlled trial. JAMA 1999;282(24):2305–12.
[641] Verhelst D, Monge M, Meynard JL, Fouqueray B, Mougenot B, Girard PM, et al. Fanconi syndrome and renal failure induced by tenofovir: a first case report. Am J Kidney Dis 2002;40 (6):1331–3.
[642] Coca S, Perazella MA. Rapid communication: acute renal failure associated with tenofovir: evidence of drug-induced nephrotoxicity. Am J Med Sci 2002;324(6):342–4.
[643] Smith MC, Austen JL, Carey JT, Emancipator SN, Herbener T, Gripshover B, et al. Prednisone improves renal function and proteinuria in human immunodeficiency virus-associated nephropathy. Am J Med 1996;101(1):41–8.
[644] Eustace JA, Nuermberger E, Choi M, Scheel Jr PJ, Moore R, Briggs WA. Cohort study of the treatment of severe HIV-associated nephropathy with corticosteroids. Kidney Int 2000;58(3):1253–60.
[645] Wei A, Burns GC, Williams BA, Mohammed NB, Visintainer P, Sivak SL. Long-term renal survival in HIV-associated nephropathy with angiotensin-converting enzyme inhibition. Kidney Int 2003;64(4):1462–71.
[646] Burns GC, Paul SK, Toth IR, Sivak SL. Effect of angiotensin-converting enzyme inhibition in HIV-associated nephropathy. J Am Soc Nephrol 1997;8(7):1140–6.
[647] Hiramatsu N, Hiromura K, Shigehara T, Kuroiwa T, Ideura H, Sakurai N, et al. Angiotensin II type 1 receptor blockade inhibits the development and progression of HIV-associated nephropathy in a mouse model. J Am Soc Nephrol 2007;18 (2):515–27.
[648] Johnson RJ, Gretch DR, Yamabe H, Hart J, Bacchi CE, Hartwell P, et al. Membranoproliferative glomerulonephritis associated with hepatitis C virus infection. N Engl J Med 1993;328 (7):465–70.
[649] D'Amico G, Madias NE, Fornasieri A, Ferri C, Sansonno D, Bombardieri S, et al. Renal involvement in hepatitis C infection: cryoglobulinemic glomerulonephritis - discussion. Kidney Int 1998;54(2):650–71.
[650] Meyers CM, Seeff LB, Stehman-Breen CO, Hoofnagle JH. Hepatitis C and renal disease: an update. Am J Kidney Dis 2003;42(4):631–57.
[651] Tarantino A, Campise M, Banfi G, Confalonieri R, Bucci A, Montoli A, et al. Long-term predictors of survival in essential mixed cryoglobulinemic glomerulonephritis. Kidney Int 1995;47(2):618–23.
[652] Fabrizi F, Colucci P, Ponticelli C, Locatelli F. Kidney and liver involvement in cryoglobulinemia. Semin Nephrol 2002;22 (4):309–18.
[653] Markowitz GS, Cheng JT, Colvin RB, Trebbin WM, D'Agati VD. Hepatitis C viral infection is associated with fibrillary glomerulonephritis and immunotactoid glomerulopathy. J Am Soc Nephrol 1998;9(12):2244–52.
[654] Pouteil-Noble C, Maiza H, Dijoud F, MacGregor B. Glomerular disease associated with hepatitis C virus infection in native kidneys. Nephrol Dial Transplant 2000;15(Suppl 8):28–33.
[655] D'Amico G, Colasanti G, Ferrario F, Sinico RA. Renal involvement in essential mixed cryoglobulinemia. Kidney Int 1989;35 (4):1004–14.
[656] Fabrizi F, Pozzi C, Farina M, Dattolo P, Lunghi G, Badalamenti S, et al. Hepatitis C virus infection and acute or chronic glomerulonephritis: an epidemiological and clinical appraisal. Nephrol Dial Transplant 1998;13(8):1991–7.
[657] Fernandez J, Taylor D, Morhardt DR, Mihalik K, Puig M, Rice CM, et al. Long-term persistence of infection in chimpanzees inoculated with an infectious hepatitis C virus clone is associated with a decrease in the viral amino acid substitution rate and low levels of heterogeneity. J Virol 2004;78(18):9782–9.
[658] Ferri C, Marzo E, Longombardo G, Lombardini F, La Civita L, Vanacore R, et al. Interferon-alpha in mixed cryoglobulinemia patients: a randomized, crossover-controlled trial. Blood 1993;81(5):1132–6.
[659] Misiani R, Bellavita P, Fenili D, Vicari O, Marchesi D, Sironi PL, et al. Interferon alfa-2a therapy in cryoglobulinemia associated with hepatitis C virus. N Engl J Med 1994;330 (11):751–6.

[660] Sarac E, Bastacky S, Johnson JP. Response to high-dose interferon-alpha after failure of standard therapy in MPGN associated with hepatitis C virus infection. Am J Kidney Dis 1997;30 (1):113–5.

[661] Moses PL, Krawitt EL, Aziz W, Corwin HL. Renal failure associated with hepatitis C virus infection. Improvement in renal function after treatment with interferon-alpha. Dig Dis Sci 1997;42(2):443–6.

[662] Mazzaro C, Panarello G, Carniello S, Faelli A, Mazzi G, Crovatto M, et al. Interferon versus steroids in patients with hepatitis C virus-associated cryoglobulinaemic glomerulonephritis. Dig Liver Dis 2000;32(8):708–15.

[663] Matsumoto S, Nakajima S, Nakamura K, Etani Y, Hirai H, Shimizu N, et al. Interferon treatment on glomerulonephritis associated with hepatitis C virus. Pediatr Nephrol 2000;15(3-4):271–3.

[664] Garini G, Allegri L, Carnevali L, Catellani W, Manganelli P, Buzio C. Interferon-alpha in combination with ribavirin as initial treatment for hepatitis C virus-associated cryoglobulinemic membranoproliferative glomerulonephritis. Am J Kidney Dis 2001;38(6):E35.

[665] Sabry AA, Sobh MA, Sheaashaa HA, Kudesia G, Wild G, Fox S, et al. Effect of combination therapy (ribavirin and interferon) in HCV-related glomerulopathy. Nephrol Dial Transplant 2002;17(11):1924–30.

[666] Bruchfeld A, Lindahl K, Stahle L, Soderberg M, Schvarcz R. Interferon and ribavirin treatment in patients with hepatitis C-associated renal disease and renal insufficiency. Nephrol Dial Transplant 2003;18(8):1573–80.

[667] Alric L, Plaisier E, Thebault S, Peron JM, Rostaing L, Pourrat J, et al. Influence of antiviral therapy in hepatitis C virus-associated cryoglobulinemic MPGN. Am J Kidney Dis 2004;43 (4):617–23.

[668] Fabrizi F, Lunghi G, Messa P, Martin P. Therapy of hepatitis C virus-associated glomerulonephritis: current approaches. J Nephrol 2008;21(6):813–25.

[669] Ohta S, Yokoyama H, Wada T, Sakai N, Shimizu M, Kato T, et al. Exacerbation of glomerulonephritis in subjects with chronic hepatitis C virus infection after interferon therapy. Am J Kidney Dis 1999;33(6):1040–8.

[670] Suzuki T, Yonemura K, Miyaji T, Suzuki H, Takahira R, Fujigaki Y, et al. Progressive renal failure and blindness due to retinal hemorrhage after interferon therapy for hepatitis C virus-associated membranoproliferative glomerulonephritis. Intern Med 2001;40(8):708–12.

[671] Kamar N, Chatelut E, Manolis E, Lafont T, Izopet J, Rostaing L. Ribavirin pharmacokinetics in renal and liver transplant patients: evidence that it depends on renal function. Am J Kidney Dis 2004;43(1):140–6.

[672] Fabrizi F, Bruchfeld A, Mangano S, Dixit V, Messa P, Martin P. Interferon therapy for HCV-associated glomerulonephritis: meta-analysis of controlled trials. Int J Artif Organs 2007;30 (3):212–9.

[673] Roithinger FX, Allinger S, Kirchgatterer A, Prischl F, Balon R, Haidenthaler A, et al. A lethal course of chronic hepatitis C, glomerulonephritis, and pulmonary vasculitis unresponsive to interferon treatment. Am J Gastroenterol 1995;90(6):1006–8.

[674] Sansonno D, De Re V, Lauletta G, Tucci FA, Boiocchi M, Dammacco F. Monoclonal antibody treatment of mixed cryoglobulinemia resistant to interferon alpha with an anti-CD20. Blood 2003;101(10):3818–26.

[675] Zaja F, De Vita S, Mazzaro C, Sacco S, Damiani D, De Marchi G, et al. Efficacy and safety of rituximab in type II mixed cryoglobulinemia. Blood 2003;101(10):3827–34.

[676] Roccatello D, Baldovino S, Rossi D, Mansouri M, Naretto C, Gennaro M, et al. Long-term effects of anti-CD20 monoclonal antibody treatment of cryoglobulinaemic glomerulonephritis. Nephrol Dial Transplant 2004;19(12):3054–61.

[677] Saadoun D, Resche RM, Sene D, Terrier B, Karras A, Perard L, et al. Rituximab plus peg-interferon-alpha/ribavirin compared with peg-interferon-alpha/ribavirin in hepatitis C-related mixed cryoglobulinemia. Blood 2010;116(3):326–34.

[678] Kleinknecht C, Levy M, Peix A, Broyer M, Courtecuisse V. Membranous glomerulonephritis and hepatitis B surface antigen in children. J Pediatr 1979;95(6):946–52.

[679] Hsu HC, Wu CY, Lin CY, Lin GJ, Chen CH, Huang FY. Membranous nephropathy in 52 hepatitis B surface antigen (HBsAg) carrier children in Taiwan. Kidney Int 1989;36 (6):1103–7.

[680] Wrzolkowa T, Zurowska A, Uszycka-Karcz M, Picken MM. Hepatitis B virus-associated glomerulonephritis: electron microscopic studies in 98 children. Am J Kidney Dis 1991;18 (3):306–12.

[681] Venkataseshan VS, Lieberman K, Kim DU, Thung SN, Dikman S, D'Agati V, et al. Hepatitis-B-associated glomerulonephritis: pathology, pathogenesis, and clinical course. Medicine (Baltimore) 1990;69(4):200–16.

[682] Johnson RJ, Couser WG. Hepatitis B infection and renal disease: clinical, immunopathogenetic and therapeutic considerations. Kidney Int 1990;37(2):663–76.

[683] Lai KN, Li PK, Lui SF, Au TC, Tam JS, Tong KL, et al. Membranous nephropathy related to hepatitis B virus in adults. N Engl J Med 1991;324(21):1457–63.

[684] Takekoshi Y, Tanaka M, Shida N, Satake Y, Saheki Y, Matsumoto S. Strong association between membranous nephropathy and hepatitis-B surface antigenaemia in Japanese children. Lancet 1978;2(8099):1065–8.

[685] Nagy J, Bajtai G, Brasch H, Sule T, Ambrus M, Deak G, et al. The role of hepatitis B surface antigen in the pathogenesis of glomerulopathies. Clin Nephrol 1979;12(3):109–16.

[686] Levy M, Kleinknecht C. Membranous glomerulonephritis and hepatitis B virus infection. Nephron 1980;26(6):259–65.

[687] Slusarczyk J, Michalak T, Nazarewicz-de Mezer T, Krawczynski K, Nowoslawski A. Membranous glomerulopathy associated with hepatitis B core antigen immune complexes in children. Am J Pathol 1980;98(1):29–43.

[688] Wiggelinkhuizen J, Sinclair-Smith C, Stannard LM, Smuts H. Hepatitis B virus associated membranous glomerulonephritis. Arch Dis Child 1983;58(7):488–96.

[689] Hirose H, Udo K, Kojima M, Takahashi Y, Miyakawa Y, Miyamoto K, et al. Deposition of hepatitis B e antigen in membranous glomerulonephritis: identification by F(ab')2 fragments of monoclonal antibody. Kidney Int 1984;26(3):338–41.

[690] Yoshikawa N, Ito H, Yamada Y, Hashimoto H, Katayama Y, Matsuyama S, et al. Membranous glomerulonephritis associated with hepatitis B antigen in children: a comparison with idiopathic membranous glomerulonephritis. Clin Nephrol 1985;23(1):28–34.

[691] Milner LS, Dusheiko GM, Jacobs D, Kala U, Thomson PD, Ninin DT, et al. Biochemical and serological characteristics of children with membranous nephropathy due to hepatitis B virus infection: correlation with hepatitis B e antigen, hepatitis B DNA and hepatitis D. Nephron 1988;49(3):184–9.

[692] Lee HS, Choi Y, Yu SH, Koh HI, Kim MJ, Ko KW. A renal biopsy study of hepatitis B virus-associated nephropathy in Korea. Kidney Int 1988;34(4):537–43.

[693] Kohler PF, Cronin RE, Hammond WS, Olin D, Carr RI. Chronic membranous glomerulonephritis caused by hepatitis

B antigen-antibody immune complexes. Ann Intern Med 1974;81(4):448–51.
[694] Gilbert RD, Wiggelinkhuizen J. The clinical course of hepatitis B virus-associated nephropathy. Pediatr Nephrol 1994;8(1): 11–4.
[695] Levy M, Gagnadoux MF. Membranous nephropathy following perinatal transmission of hepatitis B virus infection—long-term follow-up study. Pediatr Nephrol 1996;10 (1):76–8.
[696] Combes B, Shorey J, Barrera A, Stastny P, Eigenbrodt EH, Hull AR, et al. Glomerulonephritis with deposition of Australia antigen-antibody complexes in glomerular basement membrane. Lancet 1971;2(7718):234–7.
[697] Sakallioglu O, Gok F, Kalman S, Kurekci AE, Gunhan O, Gokcay E. Hepatitis B complicated focal segmental glomerulosclerosis. J Nephrol 2005;18(4):433–5.
[698] Li PK, Lai FM, Ho SS, Wong KC, Lui SF, Lai KN. Acute renal failure in hepatitis B virus-related membranous nephropathy with mesangiocapillary transition and crescentic transformation. Am J Kidney Dis 1992;19(1):76–80.
[699] Lai FM, Li PK, Suen MW, Lui SF, Lai KN. Crescentic glomerulonephritis related to hepatitis B virus. Mod Pathol 1992;5 (3):262–7.
[700] Eknoyan G, Gyorkey F, Dichoso C, Martinez-Maldonado M, Suki WN, Gyorkey P. Renal morphological and immunological changes associated with acute viral hepatitis. Kidney Int 1972;1 (6):413–9.
[701] Knieser MR, Jenis EH, Lowenthal DT, Bancroft WH, Burns W, Shalhoub R. Pathogenesis of renal disease associated with viral hepatitis. Arch Pathol 1974;97(4):193–200.
[702] Ohba S, Kimura K, Mise N, Konno Y, Suzuki N, Miyashita K, et al. Differential localization of s and e antigens in hepatitis B virus-associated glomerulonephritis. Clin Nephrol 1997;48 (1):44–7.
[703] Lai KN, Ho RTH, Tam JS, Lai FM. Detection of hepatitis B virus DNA and RNA in kidneys of HBV- related glomerulonephritis. Kidney Int 1996;50:1965–77.
[704] Lai KN, Tam JS, Lin HJ, Lai FM. The therapeutic dilemma of the usage of corticosteroid in patients with membranous nephropathy and persistent hepatitis B virus surface antigenaemia. Nephron 1990;54(1):12–7.
[705] Lin CY. Clinical features and natural course of HBV-related glomerulopathy in children. Kidney Int Suppl 1991;35: S46–53.
[706] Lisker-Melman M, Webb D, Di Bisceglie AM, Kassianides C, Martin P, Rustgi V, et al. Glomerulonephritis caused by chronic hepatitis B virus infection: treatment with recombinant human alpha-interferon. Ann Intern Med 1989;111(6): 479–83.
[707] Lin CY. Treatment of hepatitis B virus-associated membranous nephropathy with recombinant alpha-interferon. Kidney Int 1995;47(1):225–30.
[708] Conjeevaram HS, Hoofnagle JH, Austin HA, Park Y, Fried MW, Di Bisceglie AM. Long-term outcome of hepatitis B virus-related glomerulonephritis after therapy with interferon alfa. Gastroenterology 1995;109(2):540–6.
[709] Lin CY, Lo SC. Treatment of hepatitis B virus-associated membranous nephropathy with adenine arabinoside and thymic extract. Kidney Int 1991;39(2):301–6.
[710] Kanaan N, Horsmans Y, Goffin E. Lamivudine for nephrotic syndrome related to hepatitis B virus (HBV) infection. Clin Nephrol 2006;65(3):208–10.
[711] Losito A, Bucciarelli E, Massi-Benedetti F, Lato M. Membranous glomerulonephritis in congenital syphilis. Clin Nephrol 1979;12(1):32–7.
[712] Sanchez-Bayle M, Ecija JL, Estepa R, Cambronero MJ, Martinez MA. Incidence of glomerulonephritis in congenital syphilis. Clin Nephrol 1983;20(1):27–31.
[713] Falls Jr WF, Ford KL, Ashworth CT, Carter NW. The nephrotic syndrome in secondary syphilis: report of a case with renal biopsy findings. Ann Intern Med 1965;63(6):1047–58.
[714] Braunstein GD, Lewis EJ, Galvanek EG, Hamilton A, Bell WR. The nephrotic syndrome associated with secondary syphilis. An immune deposit disease. Am J Med 1970;48(5):643–8.
[715] Bhorade MS, Carag HB, Lee HJ, Potter EV, Dunea G. Nephropathy of secondary syphilis. A clinical and pathological spectrum. JAMA 1971;216(7):1159–66.
[716] Hellier MD, Webster AD, Eisinger AJ. Nephrotic syndrome: a complication of secondary syphilis. Br Med J 1971;4 (784):404–5.
[717] Sterzel RB, Krause PH, Zobl H, Kuhn K. Acute syphilitic nephrosis: a transient glomerular immunopathy. Clin Nephrol 1974;2(4):164–8.
[718] O'Regan S, Fong JS, de Chadarevian JP, Rishikof JR, Drummond KN. Treponemal antigens in congenital and acquired syphilitic nephritis: demonstration by immunofluorescence studies. Ann Intern Med 1976;85(3):325–7.
[719] Krane NK, Espenan P, Walker PD, Bergman SM, Wallin JD. Renal disease and syphilis: a report of nephrotic syndrome with minimal change disease. Am J Kidney Dis 1987;9 (2):176–9.
[720] Tourville DR, Byrd LH, Kim DU, Zajd D, Lee I, Reichman LB, et al. Treponemal antigen in immunopathogenesis of syphilitic glomerulonephritis. Am J Pathol 1976;82(3):479–92.
[721] Solling J, Solling K, Jacobsen KU, Olsen S, From E. Circulating immune complexes in syphilitic nephropathy. A case report. Br J Vener Dis 1978;54(1):53–6.
[722] Walker PD, Deeves EC, Sahba G, Wallin JD, O'Neill Jr WM. Rapidly progressive glomerulonephritis in a patient with syphilis. Identification of antitreponemal antibody and treponemal antigen in renal tissue. Am J Med 1984;76(6):1106–12.
[723] Kaschula RO, Uys CJ, Kuijten RH, Dale JR, Wiggelinkhuizen J. Nephrotic syndrome of congenital syphilis. Biopsy studies in four cases. Arch Pathol 1974;97(5):289–96.
[724] Gamble CN, Reardan JB. Immunopathogenesis of syphilitic glomerulonephritis. Elution of antitreponemal antibody from glomerular immune-complex deposits. N Engl J Med 1975;292 (9):449–54.
[725] Eiam-Ong S. Malarial nephropathy. Semin Nephrol 2003;23 (1):21–33.
[726] Boonpucknavig V, Sitprija V. Renal disease in acute Plasmodium falciparum infection in man. Kidney Int 1979;16 (1):44–52.
[727] Eiam-Ong S, Sitprija V. Falciparum malaria and the kidney: a model of inflammation. Am J Kidney Dis 1998;32(3):361–75.
[728] Bhamarapravati N, Boonpucknavig S, Boonpucknavig V, Yaemboonruang C. Glomerular changes in acute plasmodium falciparum infection. An immunopathologic study. Arch Pathol 1973;96(5):289–93.
[729] Boonpucknavig V, Soontornniyomkij V. Pathology of renal diseases in the tropics. Semin Nephrol 2003;23(1):88–106.
[730] Olowu WA, Adelusola KA, Adefehinti O, Oyetunji TG. Quartan malaria-associated childhood nephrotic syndrome: now a rare clinical entity in malaria endemic Nigeria. Nephrol Dial Transplant 2010;25(3):794–801.
[731] Kibukamusoke JW, Hutt MS. Histological features of the nephrotic syndrome associated with quartan malaria. J Clin Pathol 1967;20(2):117–23.
[732] Hendrickse RG, Adeniyi A, Edington GM, Glasgow EF, White RH, Houba V. Quartan malarial nephrotic syndrome.

Collaborative clinicopathological study in Nigerian children. Lancet 1972;1(7761):1143–9.
[733] Boonpucknavig V, Boonpucknavig S, Bhamarapravati N. Plasmodium berghei–infected mice. Focal glomerulonephritis in hyperimmune state. Arch Pathol Lab Med 1979;103 (11):567–72.
[734] Houba V. Immunopathology of nephropathies associated with malaria. Bull World Health Organ 1975;52(2):199–207.
[735] Kibukamusoke JW, Hutt MS, Wilks NE. The nephrotic syndrome in Uganda and its association with quartan malaria. Q J Med 1967;36(143):393–408.
[736] Hendrickse RG, Adeniyi A. Quartan malarial nephrotic syndrome in children. Kidney Int 1979;16(1):64–74.
[737] Rocha H, Cruz T, Brito E, Susin M. Renal involvement in patients with hepatosplenic Schistosomiasis mansoni. Am J Trop Med Hyg 1976;25(1):108–15.
[738] Greenham R, Cameron AH. Schistosoma haematobium and the nephrotic syndrome. Trans R Soc Trop Med Hyg 1980;74 (5):609–13.
[739] Sobh MA, Moustafa FE, el Housseini F, Basta MT, Deelder AM, Ghoniem MA. Schistosomal specific nephropathy leading to end-stage renal failure. Kidney Int 1987;31(4):1006–11.
[740] Barsoum RS. Schistosomiasis and the kidney. Semin Nephrol 2003;23(1):34–41.
[741] Bassily S, Farid Z, Barsoum RS, Soliman LA, Higashi GI, Miner WF. Renal biopsy in Schistosoma-Salmonella associated nephrotic syndrome. J Trop Med Hyg 1976;79(11):256–8.
[742] Sobh MA, Moustafa FE, Sally SM, Deelder AM, Ghoniem MA. Effect of anti-schistosomal treatment on schistosomal-specific nephropathy. Nephrol Dial Transplant 1988;3(6):744–51.
[743] Martinelli R, Noblat AC, Brito E, Rocha H. Schistosoma mansoni-induced mesangiocapillary glomerulonephritis: influence of therapy. Kidney Int 1989;35(5):1227–33.
[744] Barsoum RS, Bassily S, Soliman MM, Ramzy MF, Milad M, Hassaballa AM. Renal amyloidosis and schistosomiasis. Trans R Soc Trop Med Hyg 1979;73(4):367–74.
[745] Seedat YK. Glomerular disease in the tropics. Semin Nephrol 2003;23(1):12–20.
[746] McAdam KP, Anders RF, Smith SR, Russell DA, Price MA. Association of amyloidosis with erythema nodosum leprosum reactions and recurrent neutrophil leucocytosis in leprosy. Lancet 1975;2(7935):572–3.
[747] Prakash J, Singh AK, Saxena RK, Usha. Glomerular diseases in the elderly in India. Int Urol Nephrol 2003;35(2):283–8.
[748] Date A, Raghavan R, John TJ, Richard J, Kirubakaran MG, Shastry JC. Renal disease in adult Indians: a clinicopathological study of 2,827 patients. Q J Med 1987;64(245):729–37.
[749] Shwe T. Immune complexes in glomeruli of patients with leprosy. Lepr Rev 1971;42(4):282–9.
[750] Date A, Thomas A, Mathai R, Johny KV. Glomerular pathology in leprosy. An electron microscopic study. Am J Trop Med Hyg 1977;26(2):266–72.
[751] Chugh KS, Damle PB, Kaur S, Sharma BK, Kumar B, Sakhuja V, et al. Renal lesions in leprosy amongst north Indian patients. Postgrad Med J 1983;59(697):707–11.
[752] Drutz DJ, Gutman RA. Renal manifestations of leprosy: glomerulonephritis, a complication of erythema nodosum leprosum. Am J Trop Med Hyg 1973;22(4):496–502.
[753] Iveson JM, McDougall AC, Leathem AJ, Harris HJ. Lepromatous leprosy presenting with polyarthritis, myositis, and immune-complex glomerulonephritis. Br Med J 1975;3 (5984):619–21.
[754] Bjorvatn B, Barnetson RS, Kronvall G, Zubler RH, Lambert PH. Immune complexes and complement hypercatabolism in patients with leprosy. Clin Exp Immunol 1976;26(3):388–96.
[755] Agarwal SK, Dash SC. Spectrum of renal diseases in Indian adults. J Assoc Physicians India 2000;48(6):594–600.
[756] Rizvi SN, Gulati PD, Vaishnava H. Letter: tuberculosis and renal amyloidosis. Br Med J 1974;4(5945):657.
[757] Lambie SH, Cassidy MJ. Minimal change nephropathy and renal tuberculosis. Clin Nephrol 2003;60(6):439–40.
[758] Thomson PD. Renal problems in black South African children. Pediatr Nephrol 1997;11(4):508–12.
[759] Lowenstein J, Gallo G. Remission of the nephrotic syndrome in renal amyloidosis. N Engl J Med 1970;282(3):128–32.
[760] Sunga Jr MN, Reyes CV, Zvetina J, Kim TW. Resolution of secondary amyloidosis 14 years after adequate chemotherapy for skeletal tuberculosis. South Med J 1989;82(1):92–3.
[761] Castellano I, Gomez-Martino JR, Hernandez MT, Novillo R, Covarsi A. Remission of nephrotic syndrome caused by renal amyloidosis secondary to pulmonary tuberculosis after tuberculostatic treatment. Nefrologia 2001;21(1):88–91.
[762] Appel GB, Radhakrishnan J, D'Agati V. Secondary glomerular disease. In: Brenner BM, editor. The kidney. 6th ed. Philadelphia: W.B. Saunders; 2000. p. 1350–448.
[763] Lee JC, Yamauchi H, Hopper Jr J. The association of cancer and the nephrotic syndrome. Ann Intern Med 1966;64 (1):41–51.
[764] Row PG, Cameron JS, Turner DR, Evans DJ, White RH, Ogg CS, et al. Membranous nephropathy. Long-term follow-up and association with neoplasia. Q J Med 1975;44(174):207–39.
[765] Chavaz A, Mignon F, Morel-Maroger L, Richet G. [Extramembranous glomerulitis. Apropos of 92 cases]. Schweiz Med Wochenschr 1977;107(26):899–907.
[766] Noel LH, Zanetti M, Droz D, Barbanel C. Long-term prognosis of idiopathic membranous glomerulonephritis. Study of 116 untreated patients. Am J Med 1979;66(1):82–90.
[767] Zech P, Colon S, Pointet P, Deteix P, Labeeuw M, Leitienne P. The nephrotic syndrome in adults aged over 60: etiology, evolution and treatment of 76 cases. Clin Nephrol 1982;17 (5):232–6.
[768] Cahen R, Francois B, Trolliet P, Gilly J, Parchoux B. Aetiology of membranous glomerulonephritis: a prospective study of 82 adult patients. Nephrol Dial Transplant 1989;4 (3):172–80.
[769] Burstein DM, Korbet SM, Schwartz MM. Membranous glomerulonephritis and malignancy. Am J Kidney Dis 1993;22 (1):5–10.
[770] da Costa CR, Dupont E, Hamers R, Hooghe R, Dupuis E, Potvliege R. Nephrotic syndrome in bronchogenic carcinoma: report of two cases with immunochemical studies. Clin Nephrol 1974;2(6):245–51.
[771] Couser WG, Wagonfeld JB, Spargo BH, Lewis EJ. Glomerular deposition of tumor antigen in membranous nephropathy associated with colonic carcinoma. Am J Med 1974;57 (6):962–70.
[772] Barton CH, Vaziri ND, Spear GS. Nephrotic syndrome associated with adenocarcinoma of the breast. Am J Med 1980;68 (2):308–12.
[773] Wakashin M, Wakashin Y, Iesato K, Ueda S, Mori Y, Tsuchida H, et al. Association of gastric cancer and nephrotic syndrome. An immunologic study in three patients. Gastroenterology 1980;78(4):749–56.
[774] Stuart K, Fallon BG, Cardi MA. Development of the nephrotic syndrome in a patient with prostatic carcinoma. Am J Med 1986;80(2):295–8.
[775] Beauvais P, Vaudour G, Boccon GL, Levy M. Membranous nephropathy associated with ovarian tumour in a young girl: recovery after removal. Eur J Pediatr 1989;148 (7):624–5.

[776] Hotta O, Taguma Y, Kurosawa K, Sudo K, Takahashi H. Membranous nephropathy associated with nodular sclerosing Hodgkin's disease. Nephron 1993;63(3):347–50.
[777] Schneider BF, Glass WF, Brooks CH, Koenig KG. Membranous glomerulonephritis associated with testicular seminoma. J Intern Med 1995;237(6):599–602.
[778] Nishibara G, Sukemi T, Ikeda Y, Tomiyoshi Y. Nephrotic syndrome due to membranous nephropathy associated with renal cell carcinoma. Clin Nephrol 1996;45(6):424.
[779] Becker BN, Goldin G, Santos R, Glick A, Johnson DH, Breyer JA, et al. Carcinoid tumor and the nephrotic syndrome: a novel association between neoplasia and glomerular disease. South Med J 1996;89(2):240–2.
[780] Kon SP, Fan SL, Kwan JT, Dodd SM, Raftery MJ. Membranous nephropathy complicating adenolymphoma of the parotid (Warthin's tumour). Nephron 1996;73(4):692–4.
[781] Helin K, Honkanen E, Metsaniitty J, Tornroth T. A case of membranous glomerulonephritis associated with adenocarcinoma of pancreas. Nephrol Dial Transplant 1998;13(4): 1049–50.
[782] Jefferson JA, Couser WG. Therapy of membranous nephropathy associated with malignancy and secondary causes. Sem Nephrol 2003;23(4):400–5.
[783] Lefaucheur C, Stengel B, Nochy D, Martel P, Hill GS, Jacquot C, et al. Membranous nephropathy and cancer: epidemiologic evidence and determinants of high-risk cancer association. Kidney Int 2006;70(8):1510–7.
[784] Bjorneklett R, Vikse BE, Svarstad E, Aasarod K, Bostad L, Langmark F, et al. Long-term risk of cancer in membranous nephropathy patients. Am J Kidney Dis 2007;50(3):396–403.
[785] Eagen JW. Glomerulopathies of neoplasia. Kidney Int 1977;11 (5):297–303.
[786] Yamauchi H, Linsey MS, Biava CG, Hopper Jr J. Cure of membranous nephropathy after resection of carcinoma. Arch Intern Med 1985;145(11):2061–3.
[787] Froom DW, Franklin WA, Hano JE, Potter EV. Immune deposits in Hodgkin's disease with nephrotic syndrome. Arch Pathol 1972;94(6):547–53.
[788] Robinson WL, Mitas JA, Haerr RW, Cohen IM. Remission and exacerbation of tumor-related nephrotic syndrome with treatment of the neoplasm. Cancer 1984;54(6):1082–4.
[789] Pascal RR, Iannaccone PM, Rollwagen FM, Harding TA, Bennett SJ. Electron microscopy and immunofluorescence of glomerular immune complex deposits in cancer patients. Cancer Res 1976;36(1):43–7.
[790] Pascal RR, Slovin SF. Tumor directed antibody and carcinoembryonic antigen in the glomeruli of a patient with gastric carcinoma. Hum Pathol 1980;11(6):679–82.
[791] Lewis MG, Loughridge LW, Phillips TM. Immunological studies in nephrotic syndrome associated with extrarenal malignant disease. Lancet 1971;2(7716):134–5.
[792] Costanza ME, Pinn V, Schwartz RS, Nathanson L. Carcinoembryonic antigen-antibody complexes in a patient with colonic carcinoma and nephrotic syndrome. N Engl J Med 1973;289(10):520–2.
[793] Sherman RL, Susin M, Weksler ME, Becker EL. Lipoid nephrosis in Hodgkin's disease. Am J Med 1972;52(5):699–706.
[794] Dabbs DJ, Striker LM, Mignon F, Striker G. Glomerular lesions in lymphomas and leukemias. Am J Med 1986;80(1):63–70.
[795] Watson A, Stachura I, Fragola J, Bourke E. Focal segmental glomerulosclerosis in hodgkin's disease. Am J Nephrol 1983;3 (4):228–32.
[796] Aslam N, Nseir NI, Viverett JF, Bastacky SI, Johnson JP. Nephrotic syndrome in chronic lymphocytic leukemia: a paraneoplastic syndrome? Clin Nephrol 2000;54(6):492–7.
[797] Karras A, de M V, Fakhouri F, Grunfeld JP, Lesavre P. Renal and thymic pathology in thymoma-associated nephropathy: report of 21 cases and review of the literature. Nephrol Dial Transplant 2005;20(6):1075–82.
[798] Auguet T, Lorenzo A, Colomer E, Zamora A, Garcia C, Martinez-Vea A, et al. Recovery of minimal change nephrotic syndrome and acute renal failure in a patient withRenal cell carcinoma. Am J Nephrol 1998;18(5):433–5.
[799] Gandini E, Allaria P, Castiglioni A, d'Amato I, Schiaffino E, Giangrande A. Minimal change nephrotic syndrome with cecum adenocarcinoma. Clin Nephrol 1996;45(4):268–70.
[800] Singer CR, Boulton-Jones JM. Minimal change nephropathy associated with anaplastic carcinoma of bronchus. Postgrad Med J 1986;62(725):213–7.
[801] Ishida I, Hirakata H, Kanai H, Nakayama M, Katafuchi R, Oochi N, et al. Steroid-resistant nephrotic syndrome associated with malignant thymoma. Clin Nephrol 1996;46(5): 340–6.
[802] Cather JC, Jackow C, Yegge J, Hagemeister F, Duvic M. Mycosis fungoides with focal segmental glomerular sclerosis and nephrotic syndrome. J Am Acad Dermatol 1998;38(2 Pt 2):301–5.
[803] Dingli D, Larson DR, Plevak MF, Grande JP, Kyle RA. Focal and segmental glomerulosclerosis and plasma cell proliferative disorders. Am J Kidney Dis 2005;46(2):278–82.
[804] Moulin B, Ronco PM, Mougenot B, Francois A, Fillastre JP, Mignon F. Glomerulonephritis in chronic lymphocytic leukemia and related B-cell lymphomas. Kidney Int 1992;42 (1):127–35.
[805] Feehally J, Hutchinson RM, Mackay EH, Walls J. Recurrent proteinuria in chronic lymphocytic leukemia. Clin Nephrol 1981;16(1):51–4.
[806] Karim M, Hill P, Pillai G, Gatter K, Davies DR, Winearls CG. Proliferative glomerulonephritis associated with mantle cell lymphoma—natural history and effect of treatment in 2 cases. Clin Nephrol 2004;61(6):422–8.
[807] Thorner P, McGraw M, Weitzman S, Balfe JW, Klein M, Baumal R. Wilms' tumor and glomerular disease. Occurrence with features of membranoproliferative glomerulonephritis and secondary focal, segmental glomerulosclerosis. Arch Pathol Lab Med 1984;108(2):141–6.
[808] Walker JF, O'Neil S, Campbell E, Browne O, Doyle G, Carmody M, et al. Carcinoma of the oesophagus associated with membrano-proliferative glomerulonephritis. Postgrad Med J 1981;57(671):592–6.
[809] Pankhurst T, Savage CO, Gordon C, Harper L. Malignancy is increased in ANCA-associated vasculitis. Rheumatology 2004;43(12):1532–5.
[810] Edgar JD, Rooney DP, McNamee P, McNeill TA. An association between ANCA positive renal disease and malignancy. Clin Nephrol 1993;40(1):22–5.
[811] Hruby Z, Bronowicz A, Rabczynski J, Kopec W, Szewczyk Z. A case of severe anti-neutrophil cytoplasmic antibody (ANCA)-positive crescentic glomerulonephritis and asymptomatic gastric cancer. Int Urol Nephrol 1994;26(5):579–86.
[812] Karim MY, Frankel A, Paradinas FJ, Moss J. Anti-neutrophil cytoplasmic antibody-positive crescentic nephritis occurring together with renal cell carcinoma. Nephron 2000;85 (4):368–70.
[813] Baschinsky DY, Baker PB, Niemann TH, Wilmer WA. Pauci-immune ANCA-positive crescentic glomerulonephritis associated with metastatic adenocarcinoma of the lung. Am J Kidney Dis 2000;36(4):E24.
[814] Diez-Porres L, Rios-Blanco JJ, Robles-Marhuenda A, Gutierrez-Molina M, Gil-Aguado A, Vazquez-Rodriguez JJ . ANCA-

associated vasculitis as paraneoplastic syndrome with colon cancer: a case report. Lupus 2005;14(8):632–4.
[815] Kimball KG. Amyloidosis in association with neoplastic disease. Report of an unusual case and clinicopathological experience at memorial center for cancer and allied diseases during eleven years (1948-1958). Ann Intern Med 1961;55:958–74.
[816] Altiparmak MR, Pamuk GE, Pamuk ON. Adrenal carcinoma causing secondary amyloidosis: report of the first case in the literature. Neth J Med 2003;61(4):142–5.
[817] Wilkinson R, Eccleston DW. Nephrotic syndrome induced by gold therapy. Br Med J 1970;2(712):772.
[818] Viol GW, Minielly JA, Bistricki T. Gold nephropathy: tissue analysis by X-ray fluorescent spectroscopy. Arch Pathol Lab Med 1977;101(12):635–40.
[819] Antonovych TT. Gold nephropathy. Ann Clin Lab Sci 1981;11 (5):386–91.
[820] Hall CL. The natural course of gold and penicillamine nephropathy: a longterm study of 54 patients. Adv Exp Med Biol 1989;252:247–56.
[821] Yoshida A, Morozumi K, Suganuma T, Sugito K, Ikeda M, Oikawa T, et al. Clinicopathological findings of bucillamine-induced nephrotic syndrome in patients with rheumatoid arthritis. Am J Nephrol 1991;11(4):284–8.
[822] Nagahama K, Matsushita H, Hara M, Ubara Y, Hara S, Yamada A. Bucillamine induces membranous glomerulonephritis. Am J Kidney Dis 2002;39(4):706–12.
[823] Falck HM, Tornroth T, Kock B, Wegelius O. Fatal renal vasculitis and minimal change glomerulonephritis complicating treatment with penicillamine. Report on two cases. Acta Med Scand 1979;205(1-2):133–8.
[824] Francis KL, Jenis EH, Jensen GE, Calcagno PL. Gold-associated nephropathy. Arch Pathol Lab Med 1984;108(3):234–8.
[825] Matloff DS, Kaplan MM. D-Penicillamine-induced Goodpasture's-like syndrome in primary biliary cirrhosis—successful treatment with plasmapheresis and immunosuppressives. Gastroenterology 1980;78(5 Pt 1):1046–9.
[826] Bienaime F, Clerbaux G, Plaisier E, Mougenot B, Ronco P, Rougier JP. D-Penicillamine-induced ANCA-associated crescentic glomerulonephritis in Wilson disease. Am J Kidney Dis 2007;50(5):821–5.
[827] Speerstra F, Reekers P, van de Putte LB, Vandenbroucke JP, Rasker JJ, de Rooij DJ. HLA-DR antigens and proteinuria induced by aurothioglucose and D-penicillamine in patients with rheumatoid arthritis. J Rheumatol 1983;10(6):948–53.
[828] Moens HJ, Ament BJ, Feltkamp BW, van der Korst JK. Longterm followup of treatment with D-penicillamine for rheumatoid arthritis: effectivity and toxicity in relation to HLA antigens. J Rheumatol 1987;14(6):1115–9.
[829] Hall CL, Tighe R. The effect of continuing penicillamine and gold treatment on the course of penicillamine and gold nephropathy. Br J Rheumatol 1989;28(1):53–7.
[830] Kibukamusoke JW, Davies DR, Hutt MS. Membranous nephropathy due to skin-lightening cream. Br Med J 1974;2 (920):646–7.
[831] Tubbs RR, Gephardt GN, McMahon JT, Pohl MC, Vidt DG, Barenberg SA, et al. Membranous glomerulonephritis associated with industrial mercury exposure. Study of pathogenetic mechanisms. Am J Clin Pathol 1982;77(4):409–13.
[832] Belghiti D, Patey O, Berry JP, Antelin C, Hirbec G, Lagrue G. Lipoid nephrosis of toxic origin. 2 cases. Presse Med 1986;15 (39):1953–5.
[833] Hill GS. Drug-associated glomerulopathies. Toxicol Pathol 1986;14(1):37–44.
[834] Oliveira DB, Foster G, Savill J, Syme PD, Taylor A. Membranous nephropathy caused by mercury-containing skin lightening cream. Postgrad Med J 1987;63(738):303–4.
[835] Meeks A, Keith PR, Tanner MS. Nephrotic syndrome in two members of a family with mercury poisoning. J Trace Elem Electrolytes Health Dis 1990;4(4):237–9.
[836] Li SJ, Zhang SH, Chen HP, Zeng CH, Zheng CX, Li LS, et al. Mercury-induced membranous nephropathy: clinical and pathological features. Clin J Am Soc Nephrol 2010;5(3):439–44.
[837] Hoorntje SJ, Kallenberg CG, Weening JJ, Donker AJ, The TH, Hoedemaeker PJ. Immune-complex glomerulopathy in patients treated with captopril. Lancet 1980;1(8180):1212–5.
[838] Case DB, Atlas SA, Mouradian JA, Fishman RA, Sherman RL, Laragh JH. Proteinuria during long-term captopril therapy. JAMA 1980;244(4):346–9.
[839] Textor SC, Gephardt GN, Bravo EL, Tarazi RC, Fouad FM, Tubbs R, et al. Membranous glomerulopathy associated with captopril therapy. Am J Med 1983;74(4):705–12.
[840] Sturgill BC, Shearlock KT. Membranous glomerulopathy and nephrotic syndrome after captopril therapy. JAMA 1983;250 (17):2343–5.
[841] Webb DJ, Atkinson AB. Enalapril following captopril-induced nephrotic syndrome. Scott Med J 1986;31(1):30–2.
[842] Phan L, Coulomb F, Boudon M, Gallois H, Kleinknecht D. Extramembranous glomerulonephritis induced by lithium. Nephrologie 1991;12(4):185–7.
[843] Santella RN, Rimmer JM, MacPherson BR. Focal segmental glomerulosclerosis in patients receiving lithium carbonate. Am J Med 1988;84(5):951–4.
[844] Kala GK, Mogri M, Weber-Shrikant E, Springate JE. Lithium-induced membranous glomerulonephropathy in a pediatric patient. Pediatr Nephrol 2009;24(11):2267–9.
[845] Richman AV, Masco HL, Rifkin SI, Acharya MK. Minimal-change disease and the nephrotic syndrome associated with lithium therapy. Ann Intern Med 1980;92(1):70–2.
[846] Tam VK, Green J, Schwieger J, Cohen AH. Nephrotic syndrome and renal insufficiency associated with lithium therapy. Am J Kidney Dis 1996;27(5):715–20.
[847] Kilcoyne MM, Gocke DJ, Meltzer JI, Daly JJ, Thomson GE, Hsu KC, et al. Nephrotic syndrome in heroin addicts. Lancet 1972;1 (7740):17–20.
[848] Eknoyan G, Gyorkey F, Dichoso C, Hyde SE, Gyorkey P, Suki WN, et al. Renal involvement in drug abuse. Arch Intern Med 1973;132(6):801–6.
[849] Rao TK, Nicastri AD, Friedman EA. Natural history of heroin-associated nephropathy. N Engl J Med 1974;290(1):19–23.
[850] Treser G, Cherubin C, Longergan ET, Yoshizawa N, Viswanathan V, Tannenberg AM, et al. Renal lesions in narcotic addicts. Am J Med 1974;57(5):687–94.
[851] Llach F, Descoeudres C, Massry SG. Heroin associated nephropathy: clinical and histological studies in 19 patients. Clin Nephrol 1979;11(1):7–12.
[852] Cunningham EE, Brentjens JR, Zielezny MA, Andres GA, Venuto RC. Heroin nephropathy. A clinicopathologic and epidemiologic study. Am J Med 1980;68(1):47–53.
[853] D'Agati V. Pathologic classification of focal segmental glomerulosclerosis. Semin Nephrol 2003;23(2):117–34.
[854] Jaffe JA, Kimmel PL. Chronic nephropathies of cocaine and heroin abuse: a critical review. Clin J Am Soc Nephrol 2006;1 (4):655–67.
[855] Bakir AA, Bazilinski NG, Rhee HL, Ainis H, Dunea G. Focal segmental glomerulosclerosis. A common entity in nephrotic black adults. Arch Intern Med 1989;149(8):1802–4.

[856] do Sameiro FM, Sampaio S, Faria V, Carvalho E. Nephropathy associated with heroin abuse in Caucasian patients. Nephrol Dial Transplant 2003;18(11):2308–13.
[857] Scholes J, Derosena R, Appel GB, Jao W, Boyd MT, Pirani CL. Amyloidosis in chronic heroin addicts with the nephrotic syndrome. Ann Intern Med 1979;91(1):26–9.
[858] Meador KH, Sharon Z, Lewis EJ. Renal amyloidosis and subcutaneous drug abuse. Ann Intern Med 1979;91(4):565–7.
[859] Campistol JM, Montoliu J, Soler-Amigo J, Darnell A, Revert L. Renal amyloidosis with nephrotic syndrome in a Spanish subcutaneous heroin abuser. Nephrol Dial Transplant 1988;3 (4):471–3.
[860] Tan Jr AU, Cohen AH, Levine BS. Renal amyloidosis in a drug abuser. J Am Soc Nephrol 1995;5(9):1653–8.
[861] Bakir AA, Dunea G. Drugs of abuse and renal disease. Curr Opin Nephrol Hypertens 1996;5(2):122–6.
[862] Clive DM, Stoff JS. Renal syndromes associated with nonsteroidal antiinflammatory drugs. N Engl J Med 1984;310(9):563–72.
[863] Abraham PA, Keane WF. Glomerular and interstitial disease induced by nonsteroidal anti-inflammatory drugs. Am J Nephrol 1984;4(1):1–6.
[864] Levin ML. Patterns of tubulo-interstitial damage associated with nonsteroidal antiinflammatory drugs. Semin Nephrol 1988;8(1):55–61.
[865] Stachura I, Jayakumar S, Bourke E. T and B lymphocyte subsets in fenoprofen nephropathy. Am J Med 1983;75(1):9–16.
[866] Bender WL, Whelton A, Beschorner WE, Darwish MO, Hall-Craggs M, Solez K. Interstitial nephritis, proteinuria, and renal failure caused by nonsteroidal anti-inflammatory drugs. Immunologic characterization of the inflammatory infiltrate. Am J Med 1984;76(6):1006–12.
[867] Warren GV, Korbet SM, Schwartz MM, Lewis EJ. Minimal change glomerulopathy associated with nonsteroidal antiinflammatory drugs. Am J Kidney Dis 1989;13(2):127–30.
[868] Murgo AJ. Thrombotic microangiopathy in the cancer patient including those induced by chemotherapeutic agents. Semin Hematol 1987;24(3):161–77.
[869] Medina PJ, Sipols JM, George JN. Drug-associated thrombotic thrombocytopenic purpura-hemolytic uremic syndrome. Curr Opin Hematol 2001;8(5):286–93.
[870] Cantrell Jr JE, Phillips TM, Schein PS. Carcinoma-associated hemolytic-uremic syndrome: a complication of mitomycin C chemotherapy. J Clin Oncol 1985;3(5):723–34.
[871] Mittelman A, Bertram J, Henry DH, Snyder Jr HW, Messerschmidt GL, Ciavarella D, et al. Treatment of patients with HIV thrombocytopenia and hemolytic uremic syndrome with protein A (Prosorba column) immunoadsorption. Semin Hematol 1989;26(2 Suppl 1):15–8.
[872] Snyder Jr HW, Mittelman A, Oral A, Messerschmidt GL, Henry DH, Korec S, et al. Treatment of cancer chemotherapy-associated thrombotic thrombocytopenic purpura/hemolytic uremic syndrome by protein A immunoadsorption of plasma. Cancer 1993;71(5):1882–92.
[873] Mistry B, Kimmel PL, Hetzel PC, Phillips TM, Braden GL. The role of circulating immune complexes and biocompatibility of staphylococcal protein A immunoadsorption in mitomycin C-induced hemolytic uremic syndrome. Am J Kidney Dis 2004;44 (4):e50–8.
[874] Garibotto G, Acquarone N, Saffioti S, Deferrari G, Villaggio B, Ferrario F. Successful treatment of mitomycin C-associated hemolytic uremic syndrome by plasmapheresis. Nephron 1989;51(3):409–12.
[875] Poch E, Almirall J, Nicolas JM, Torras A, Revert L. Treatment of mitomycin-C-associated hemolytic uremic syndrome with plasmapheresis. Nephron 1990;55(1):89–90.
[876] Bosch T, Wendler T. Extracorporeal plasma treatment in thrombotic thrombocytopenic purpura and hemolytic uremic syndrome: a review. Ther Apher 2001;5(3):182–5.
[877] Verweij J, van der Burg ME, Pinedo HM. Mitomycin C-induced hemolytic uremic syndrome. Six case reports and review of the literature on renal, pulmonary and cardiac side effects of the drug. Radiother Oncol 1987;8(1): 33–41.
[878] Zakarija A, Bennett C. Drug-induced thrombotic microangiopathy. Semin Thromb Hemost 2005;31(6):681–90.
[879] Cattell V. Mitomycin-induced hemolytic uremic kidney. An experimental model in the rat. Am J Pathol 1985;121(1):88–95.
[880] Zoja C, Furci L, Ghilardi F, Zilio P, Benigni A, Remuzzi G. Cyclosporin-induced endothelial cell injury. Lab Invest 1986;55 (4):455–62.

CHAPTER

83

Immunologic Mechanisms of Vasculitis

Jonathon W. Homeister[1], *J. Charles Jennette*[1] *and Ronald J. Falk*[2]

[1]Department of Pathology and Laboratory Medicine,
University of North Carolina, Chapel Hill, North Carolina, USA
[2]Department of Medicine, University of North Carolina, Chapel Hill, North Carolina, USA

The kidneys are among the most vascularized tissues of the body. Thus, it is not surprising that they are among the organs most commonly affected by many forms of systemic vasculitis. Vasculitis is inflammation of vessel walls that shares many of the pathophysiologic characteristics of inflammation in any tissue. The seminal pathogenic event is the recruitment and activation of leukocytes in vessel walls with resultant injury. This always involves elements of the innate inflammatory response. In some, if not most, forms of vasculitis, elements of the adaptive immune response also are involved in the induction of the inflammation. This may be an appropriate adaptive immune response (e.g., against rickettsial organisms in the vasculitis of Rocky Mountain spotted fever), an idiosyncratic allergic hypersensitivity response (e.g., in some drug-induced vasculitides), or a maladaptive autoimmune response (e.g., vasculitis caused by antineutrophil cytoplasmic autoantibodies or autoantibodies to capillary basement membrane collagen).

This chapter will review the etiology and pathogenesis of several of the variants of vasculitis that most often affect the kidneys. The focus will be on vasculitides that are not known to be caused by direct invasion of vessel walls by infectious pathogens (i.e., the noninfectious vasculitides). This does not mean that an infection is not involved in the pathophysiology of the vasculitis, only that there is no evidence that the inflammation is directly targeted against intact microbes in the vessel wall. Infection still could be involved indirectly, for example by providing antigens that form pathogenic immune complexes with antibodies or by stimulating a pathogenic autoimmune response. The greatest emphasis will be on vasculitis that predominantly targets small vessels, including glomerular capillaries, because of the frequency and clinical importance of renal involvement in this category of vasculitis.

IMMUNOPATHOLGIC CATEGORIES OF VASCULITIS

Ideally, a classification system for vasculitis would be based on specific etiologies or distinct pathogenic mechanisms especially in a discussion of the pathophysiology of vasculitis. Table 83.1 lists some of the putative etiologies and pathogenic mechanisms for vasculitides that may involve the kidneys. Unfortunately, the etiology and pathogenesis of many forms of vasculitis remain poorly understood and controversial, and thus cannot be used as the sole basis for classification systems that are used for the diagnosis of patients. Instead, categorization of vasculitides is based on a combination of features that includes the types of vessels involved, the pattern of inflammation, the evidence for various immunopathologic processes, and the clinical expression of disease (Table 83.2, Figure 83.1).[56,58,64] The major general subdivisions of vasculitis are large-vessel vasculitis, medium-sized vessel vasculitis, and small-vessel vasculitis. Each subdivision is characterized by a pathologic pattern of inflammatory injury that can be caused by more than one clinicopathologic form of vasculitis and that is a final common pathophysiologic pathway of injury that can result from more than one etiology.

Large-vessel vasculitis affects the aorta or its major arterial branches or both, and is characterized pathologically by chronic inflammation that often includes multinucleated giant cells.[56] Giant cell arteritis and

Seldin and Giebisch's The Kidney, Fifth Edition.
DOI: http://dx.doi.org/10.1016/B978-0-12-381462-3.00083-5

© 2013 Elsevier Inc. All rights reserved.

TABLE 83.1 Categorization of Noninfectious Vasculitis Based on known or Putative Etiologies and Pathogenic Mechanisms

Mediated by Immune Complex Deposition or in Situ Formation
Henoch-Schönlein purpura (IgA vasculitis)
Cryoglobulinemic vasculitis
Lupus vasculitis
Rheumatoid vasculitis
Serum sickness vasculitis (Serum-sickness-associated immune complex vasculitis)
Infection-induced immune complex vasculitis (e.g., hepatitis B and C)
Anti-glomerular basement membrane (anti-GBM) disease
Kawasaki disease (possibly via anti-endothelial antibodies)
Hypocomplementemic urticarial vasculitis (anti-C1q vasculitis)
Mediated by antineutrophil cytoplasmic autoantibodies (ANCAs)
Microscopic polyangiitis
Wegener granulomatosis (Granulomatosis with polyangiitis)
Churg-Strauss syndrome (Eosinophilic granulomatosis with polyangiitis)
Renal-limited vasculitis (pauci-immune crescentic glomerulonephritis)
Cell mediated
Giant cell arteritis
Takayasu arteritis

Takayasu arteritis are the two primary categories. When the kidneys are affected by large-vessel vasculitis, the most commonly involved vessels are the main renal artery and interlobar arteries, and the most common clinical manifestation is renal artery stenosis with renovascular hypertension. The pattern of inflammation in large-vessel vasculitis with a predominance of T lymphocytes, monocytes, and macrophages (including multinucleated giant cells) suggests a type IV cell–mediated immune pathogenesis, however, no exogenous or endogenous (auto) antigen target for a pathogenic T-lymphocyte response has been identified.

Medium-sized vessel vasculitis is necrotizing inflammation of arteries in the absence of involvement of capillaries or venules.[56,58] The primary clinicopathologic categories are polyarteritis nodosa and Kawasaki disease. Although the pathophysiology of these two diseases appears to be quite distinct, both are characterized in the acute phase by arteritis with localized transmural necrosis and infiltration by activated neutrophils and monocytes that cause lytic destruction of the vessel wall.[59,62] Within several days, the acute inflammation and necrosis are replaced predominantly by lymphocytes and macrophages that orchestrate the progressive replacement of the necrosis with fibrosis. In the kidneys, medium-sized vessel vasculitis has a predilection for the lobar and arcuate arteries, but any artery, including the main renal artery, may be involved. Common intrarenal manifestations include pseudoaneurysm formation, thrombosis, infarction, and hemorrhage.

Small-vessel vasculitis is characterized by acute, often necrotizing, inflammation of many small vessels in multiple organs.[58,59] Involvement of glomerular capillaries causing glomerulonephritis is a frequent component of most forms of small-vessel vasculitis, and may be the dominant feature. Involvement of dermal venules causing leukocytoclastic angiitis with palpable purpura also is a frequent feature. Small-vessel vasculitis caused by antiglomerular basement membrane antibodies (anti-GBMs) and antineutrophil cytoplasmic autoantibodies (ANCAs) represent life-threatening forms of small-vessel vasculitis that have a predilection for attacking glomerular and pulmonary capillaries. Although the defining feature of small-vessel vasculitis is the involvement of capillaries and venules, small-vessel vasculitis also may affect small and even medium-sized arteries resulting in a necrotizing arteritis that is histologically indistinguishable from a medium-sized vessel vasculitis such as polyarteritis nodosa.

The kidneys are affected much more often by small-vessel vasculitis than by medium-sized vessel vasculitis or large-vessel vasculitis. Thus, the focus of this chapter will be on the pathophysiology and immunopathology of small-vessel vasculitis. The two major immunopathogenic categories of small-vessel vasculitis are immune complex–mediated vasculitis and antineutrophil cytoplasmic autoantibody (ANCA)–mediated vasculitis. Immune complex vasculitis is characterized immunohistologically by conspicuous localization of immunoglobulin in vessel walls, whereas ANCA vasculitis is characterized by the absence or paucity of immunoglobulin in vessel walls.[58,62,63] Although these two categories of vasculitis have different etiologies, they share many common histologic features and use common inflammatory mediators and pathways. The next section of this chapter will review some of these common inflammatory pathways. The subsequent two sections will review the pathogenic features of immune complex vasculitis and ANCA vasculitis.

BASIC PATHOGENIC EVENTS IN SMALL-VESSEL VASCULITIS

The seminal pathophysiologic event in small-vessel vasculitis is segmental acute inflammation

TABLE 83.2 Names and Definitions of Vasculitis Adopted by the Chapel Hill Consensus Conference on the Nomenclature of Systemic Vasculitis

Large-Vessel Vasculitis[a]	
Giant cell arteritis	Granulomatous arteritis of the aorta and its major branches, with a predilection for the extracranial branches of the carotid artery. Often involves the temporal artery. Usually occurs in patients older than 50 and often is associated with polymyalgia rheumatica.
Takayasu arteritis	Granulomatous inflammation of the aorta and its major branches. Usually occurs in patients younger than 50.
Medium-Sized Vessel Vasculitis[a]	
Polyarteritis nodosa	Necrotizing inflammation of medium-sized or small arteries without glomerulonephritis or vasculitis in arterioles, capillaries, or venules.
Kawasaki disease	Arteritis involving large, medium, and small arteries and associated with mucocutaneous lymph node syndrome. Coronary arteries are often involved. Aorta and veins may be involved. Usually occurs in children.
Small-Vessel Vasculitis[a]	
Wegener's granulomatosis (Granulomatosis with polyangiitis)	Granulomatous inflammation involving the respiratory tract, and necrotizing vasculitis affecting small to medium vessels (e.g., capillaries, venules, arterioles, and arteries). Necrotizing glomerulonephritis is common.
Churg-Strauss syndrome (Eosinophilic granulomatosis with polyangiitis)	Eosinophil-rich and granulomatous inflammation involving the respiratory tract and necrotizing vasculitis affecting small to medium-sized vessels, and associated with asthma and blood eosinophilia
Microscopic polyangiitis	Necrotizing vasculitis with few or no immune deposits affecting small vessels, i.e., capillaries, venules, or arterioles. Necrotizing arteritis involving small and medium-sized arteries may be present. Necrotizing glomerulonephritis is very common. Pulmonary capillaritis often occurs.
Henoch-Schönlein purpura (IgA vasculitis)	Vasculitis with IgA-dominant immune deposits affecting small vessels (i.e., capillaries, venules, or arterioles). Typically involves skin, gut, and glomeruli and is associated with arthralgias or arthritis.
Cryoglobulinemic vasculitis	Vasculitis with cryoglobulin immune deposits affecting small vessels (i.e., capillaries, venules, or arterioles) and associated with cryoglobulins in serum. Skin and glomeruli are often involved.

Source: Jennette JC, Falk RJ, Andrassy K, et al. Nomenclature of systemic vasculitides. Proposal of an international consensus conference. Arthritis Rheum 1994;37:187–192, with permission.

[a]Large artery refers to the aorta and the largest branches directed toward major body regions (e.g., to the extremities and the head and neck); medium-sized artery refers to the main visceral arteries (e.g., renal, hepatic, coronary, and mesenteric arteries); and small artery refers to the distal arterial radicals that connect with arterioles (e.g., renal arcuate and interlobular arteries). Small vessel includes small arteries, arterioles, capillaries, and venules. Note that large and medium-sized vessel vasculitides are confined to arteries. Involvement of capillaries or venules is indicative of small-vessel vasculitis.

of small vessels, often accompanied by necrosis (Figure 83.2).[59,62] Many of the basic inflammatory processes that occur in small-vessel vasculitis also occur in the necrotizing arteritis of medium-sized vessel vasculitis (Figure 83.3). The primary initial effector cells in small-vessel vasculitis are neutrophils and monocytes, although macrophages and T lymphocytes are rapidly recruited in response to the injury and are active participants in the subacute and chronic progression of injury. Targeting of leukocytes to specific vascular segments involves multiple cell adhesive and cell signaling events in both the leukocytes and the vessel walls, particularly the endothelium. Collectively these events (discussed below) comprise a leukocyte adhesion cascade. They have been characterized most thoroughly at sites of physiologic diapedesis of neutrophils and monocytes through small vessels, especially postcapillary venules, as they traffic toward tissue sites of innate and adaptive immune surveillance or sites of immune response to microbial invasion or other pathogenic stimuli.[82,137] The events of the leukocyte adhesion cascade are generally accepted to occur in most tissues. However, recent work has demonstrated that some tissue- and organ-specific variation does occur,[107] although there is no current evidence to suggest that such variation accounts for the vascular and organ predilections of certain of the vasculitides.

In physiologic diapedesis, leukocyte transmigration through vessel walls causes only minor and transient disruption of the vessel wall structure. In vasculitis, the

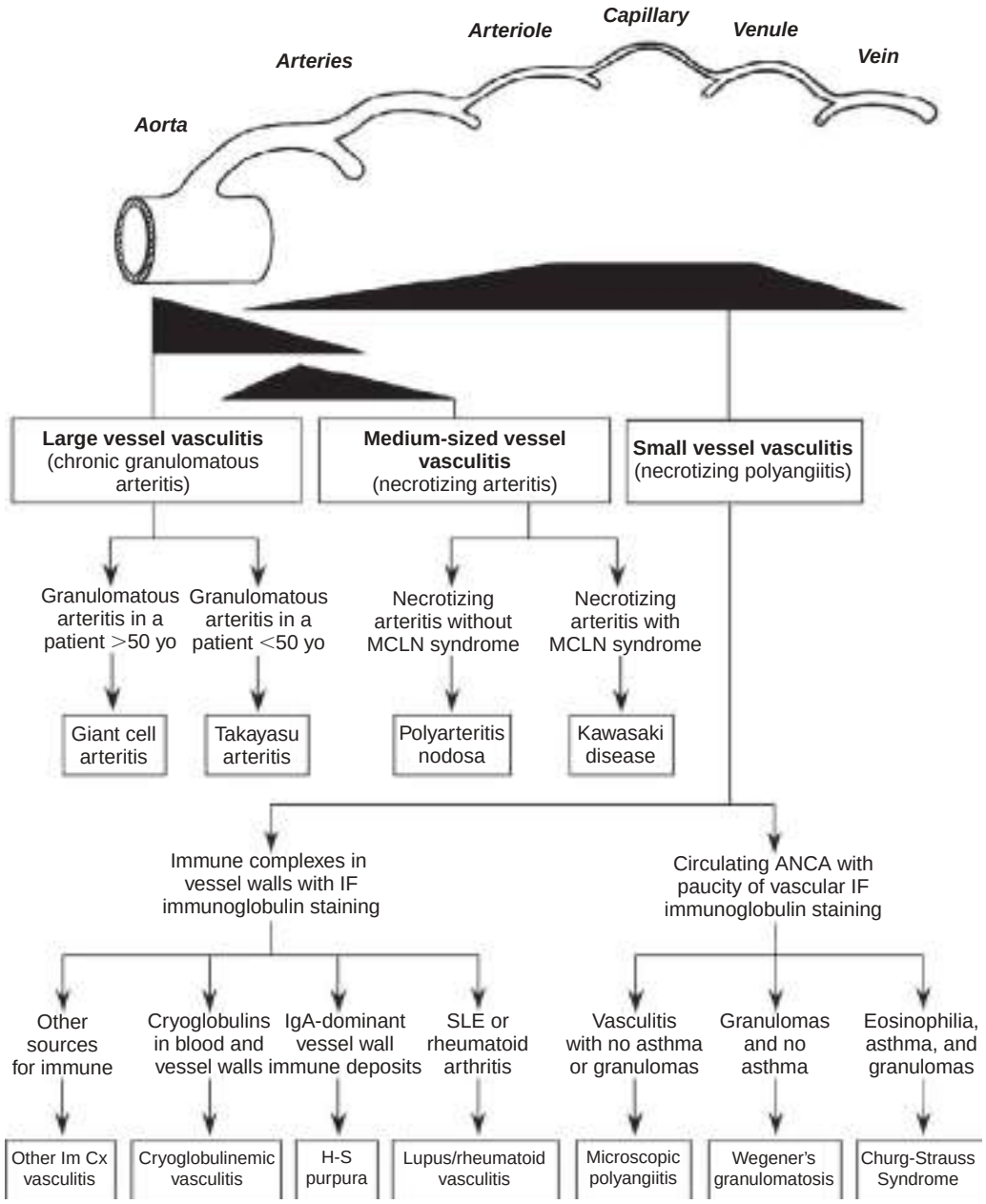

FIGURE 83.1 Diagram depicting the predominant distribution of different forms of vasculitis (black triangles and trapezoid), and an algorithm that provides clinical and pathologic features that can be used to differentiate distinguish different forms of vasculitis.

leukocytes undergo full activation as they attach to and enter the vessel wall rather than waiting until after they have transmigrated into the tissue. Neutrophils survive for only a few minutes, or at most a few hours, at sites of acute inflammation.[62,137] Monocytes transform into activated macrophages after entry into sites of acute inflammation.[54] Activated macrophages release cytokines that modulate the inflammation. For example, macrophages release factors that enhance T-lymphocyte adhesion to nearby venular endothelial cells and induce targeted chemotaxis of T lymphocytes toward the site of the macrophage activation. If the stimulus for acute inflammation does not persist, neutrophils and monocytes are quickly replaced by macrophages and T lymphocytes at the site of small-vessel vasculitis. Thus, sites of small-vessel vasculitis in biopsy specimens, including renal biopsy specimens, often have predominantly macrophages and T

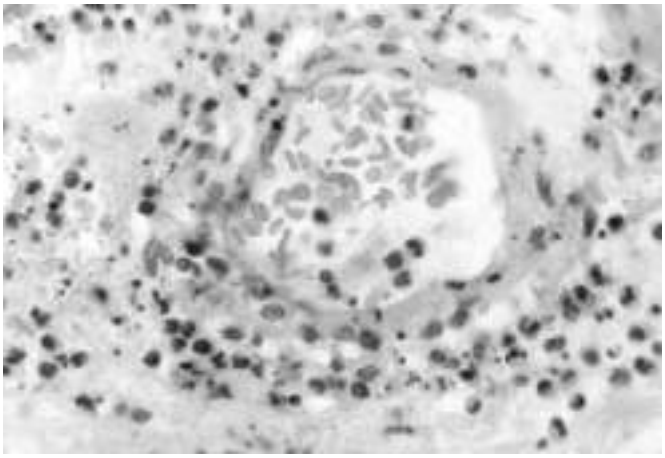

FIGURE 83.2 Leukocytoclastic angiitis with vascular and perivascular infiltration of leukocytes including numerous neutrophils. Note the scattered apoptotic nuclear fragments indicative of leukocytoclasia.

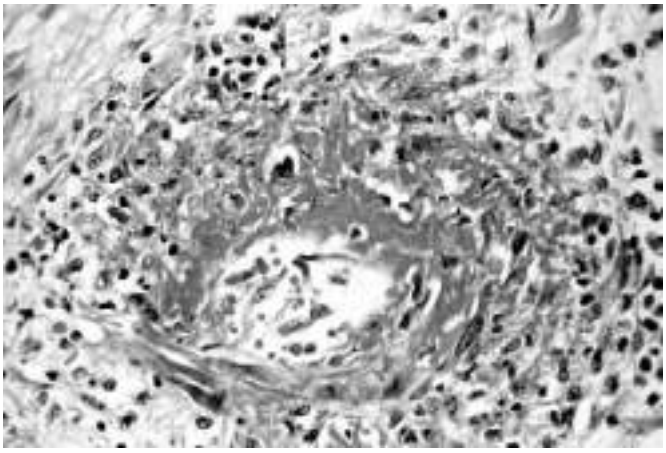

FIGURE 83.3 Necrotizing arteritis affecting an interlobular artery in the kidney. There is segmental fibrinoid necrosis surrounded by infiltrating leukocytes.

lymphocytes in the injured vessels although the initial injury was induced earlier by neutrophils and acutely activated monocytes.

Chemoattractants, Cytokines, and Chemokines

Chemoattractants for neutrophils and monocytes play a central role in mediating vasculitis not only by attracting leukocytes but also by activating leukocytes and endothelial cells to participate in inflammatory events.[22,91,150] Modulation of the expression of adhesion molecules and cytokine/chemokine molecules by endothelial cells, leukocytes in the circulation, and leukocytes in the tissue orchestrates the inflammation at sites of vasculitis. In small-vessel vasculitis, the balance is tipped toward neutrophil recruitment and activation in the acute phase, but within only one or two days the balance shifts toward recruitment of predominantly monocytes and T lymphocytes. However, if the pathogenic process that initiated the initial injury persists, as often is the case, lesions will include a mixture of acute and chronic inflammatory cells for extended periods of time.

Important chemoattractants for neutrophils and monocytes include C5a (which can be generated by activation of either the classical, lectin or alternative complement pathway), leukotriene B4, platelet-activating factor (PAF), and CXC chemokines such as interlukin-8 (IL-8, CXCL8), platelet factor 4 (PF4, CXCL4), GRO1 oncogene (GROα, CXCL1), and stromal cell-derived factor-1 (SDF-1, CXCL12). Progression of vasculitic lesions from an acute to a subacute or chronic phase is mediated primarily by a different set of chemoattractants that preferentially recruit monocytes and T lymphocytes, such as the CC chemokines macrophage inflammatory protein-1α (MIP-1α, CCL3), monocyte chemotactic protein-1 (MCP-1, CCL2), and regulated upon acitivation, normal T-cell expressed, and secreted (RANTES, CCL5). Chemoattractants not only attract leukocytes through direct engagement of ligands on the leukocytes, but also by enhancing the expression and binding of leukocyte adhesion molecules (e.g., β2 and β1 integrins) to their ligands on endothelial cells and elsewhere in the tissue.[150]

Chemokines on the surface of endothelial cells attract leukocytes to the cells in concert with the adhesion molecules reviewed below, and provide a gradient for directional migration toward the intercellular junction (or transcellularly through the endothelial cytoplasm). Once through the endothelium, gradients of bound and free chemokines in the extracellular matrix and interstitial fluid continue to provide directional signals until the leukocyte encounters enough stimulation to undergo full activation. In physiologic diapedesis of leukocytes across postcapillary venules, full activation is not attained until after the leukocyte has migrated away from the vessel wall. In the absence of an adequate pathogenic stimulus in the extravascular compartment, a leukocyte eventually will undergo senescence and apoptosis without becoming activated. In vasculitis, leukocytes are activated as they attach to or enter the vessel wall resulting in inflammatory vascular damage. There are many etiologies for this mural activation, including the presence of infectious organisms in the vessel wall (e.g., *Rickettsia rickettsii* in Rocky Mountain spotted fever), immune complexes in the vessel wall (e.g., cryoglobulins in cryoglobulinemic vasculitis), or activation

by antineutrophil cytoplasmic autoantibodies (e.g., in microscopic polyangiitis).

Leukocyte Recruitment

Leukocyte recruitment into the vessel wall is accomplished by the events of the leukocyte adhesion cascade. This is a multistep process that sequentially involves leukocyte tethering to endothelium followed by leukocyte rolling, activation, arrest, spreading and crawling on the endothelium, and finally paracellular or transcellular migration (diapedesis) across the endothelium[82] (Figure 83.4). Important initial events are the tethering and rolling of leukocytes on the surface of endothelial cells. This allows the leukocytes to sample the endothelial surface for chemokine signals derived from the underlying tissue and for upregulated endothelial adhesion molecules that can modulate rolling and mediate firm adherence. Engagement of these molecules allows static adhesion to the endothelium followed by crawling toward endothelial cell junctions where transmigration between the cells can be accomplished by further engagement of adhesion molecules in the junction.[22] Transmigration through endothelial cells may also occur.[161] Once through the vessel wall, movement into the perivascular interstitial tissue involves chemoattractant gradients and further engagement between integrins and ligands on extracellular matrix molecules.[22,137]

Leukocyte Tethering and Rolling

The first step in the exit of leukocytes from flowing blood within the vessel lumen is margination toward the endothelial surface. The resulting juxtaposition of these cells facilitates capture or tethering of the leukocyte to the endothelial surface. Once tethered, shear stress pushing on the leukocyte, combined with the formation of new adhesive bonds at the downstream leukocyte edge and disruption of adhesive bonds at the upstream leukocyte edge, allows for rolling of the leukocyte along the endothelial surface. The adhesive interactions necessary for leukocyte tethering and rolling are mediated primarily by the binding of selectin adhesion molecules to their ligands.[82,107] E-selectin and P-selectin are expressed on activated endothelium, and P-selectin is also expressed on activated platelets. L-selectin is constitutively expressed on most leukocytes. P-selectin is pre-formed and stored in Weibel-Palade bodies or alpha granules, respectively, and therefore is rapidly translocated to the cell surface quickly in response to mediators released at sites of acute inflammation, such as histamine and thrombin.[88] In contrast, cell surface expression of E-selectin is dependent on RNA and protein synthesis stimulated by inflammatory cytokines such as tumor necrosis factor (TNF) and interleukin-1 (IL-1),[11] and is therefore delayed for several hours after an inflammatory stimulus is received.

A number of selectin ligands (or counter receptors) have been described.[13,63] The best characterized is P-

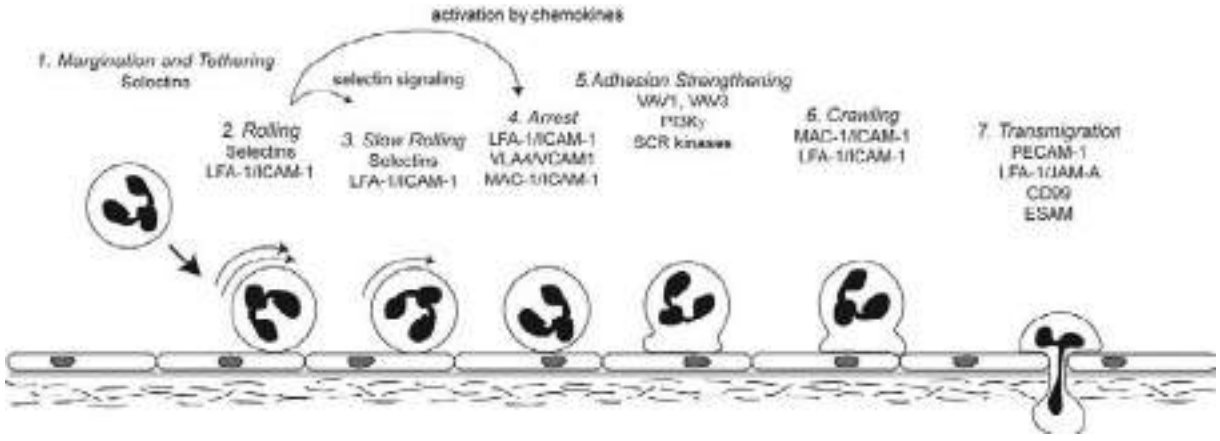

FIGURE 83.4 Diagram depicting the stereotypical events involved in neutrophil diapedesis at a site of inflammation. Activated endothelial cells display upregulated adhesion molecules and bound chemoattractants (e.g., CXC chemokines) that initially induce neutrophil tethering and rolling mediated primarily by interactions between selectins and their ligands (see Table 83.3). This stimulates inside-out signaling events that facilitate the engagement of neutrophil integrins (especially β 2 integrins) with upregulated immunoglobulin superfamily adhesion molecules on endothelial cells (e.g., intercellular adhesion molecule-1, ICAM-1) and result in slow rolling and arrest. Outside-in signaling events strengthen the adhesive interactions by modulating the affinity of the integrins, and facilitate lateral migration toward the inflammatory stimulus. Specialized adhesion molecules at the endothelial cell junctions (e.g., junctional adhesion molecule-1, JAM-1; platelet endothelial cell adhesion molecule-1, PECAM; CD99; endothelial cell-selective adhesion molecule, ESAM) mediate endothelial transmigration. Once through the endothelial barrier, additional leukocyte adhesion molecules (especially β 2 integrins) mediate migration into the extracellular space by engagement of ligands on extracellular matrix (e.g., fibronectin and collagen). The depicted abbreviated adhesion molecules are defined in Table 83.3.

selectin glycoprotein ligand-1 (PSGL-1). PSGL-1 was originally described as a P-selectin ligand but is now known to function as a ligand for all three selectins. It is expressed on most leukocytes, endothelial cells, and platelets. Ligands for E-selectin also include E-selectin ligand -1 (ESL-1) and correctly glycosylated forms of CD44, both of which are expressed on leukocytes. L-selectin ligands include PSGL-1 on other leukocytes, and peripheral node addressins including glycosylation-dependent cell adhesion molecule-1 (GLYCAM-1), podocalyxin, and CD34, which are found on peripheral lymphoid tissue high endothelial venules (HEV).

Binding of the selectins to their ligands is modulated by several molecular features. High affinity selectin binding is dependent on ligand glycosylation, in part requiring the sialyl Lewis X tetrasaccharide as a recognition epitope. The final step in the synthesis of this critical binding epitope is the addition of an α(1,3)-linked fucose, mediated by α(1,3)-fucosyltransferases type VII and IV.[50] L-selectin binding to ligands on peripheral lymph node HEV, or at sites of chronic inflammation, utilize a sulphated version of this epitope, 6-sulph-sialyl Lewis X.[121] Lastly, high affinity binding of P-selectin or L-selectin to PSGL-1 requires sulphation of certain tyrosine residues near the N-terminus of the molecule.[13] The molecular features of the selectins and their ligands result in binding interactions with very high on- and off-rates, allowing bonds to form and break quickly.[85] In addition, shear stress is required and also enhances L-selectin and P-selectin binding. Combined, these binding features result in interactions called catch bonds that are particularly suited to mediating the tethering and rolling of leukocytes on the endothelium.[174]

At sites of small-vessel vasculitis, increased expression of P-selectin and E-selectin on endothelial cells is induced by inflammatory chemokines. Subsequent binding to their ligands on leukocytes allows for and modulates primary leukocyte tethering and rolling. Rolling may also be triggered by secondary tethering.[70,107] In this process, leukocytes previously captured onto the endothelium bind, via their PSGL-1, to L-selectin on other marginated leukocytes and mediate their capture and tethering to the endothelium. The physiologic significance of secondary tethering remains unclear,[76] although it can be observed in vivo.

In addition to selectin-mediated rolling, it is known that some integrin adhesion molecules can mediate and modulate this process. For example, the β_1 integrin very late antigen 4 (VLA4) has been shown to mediate rolling of monocytes and T cells. Similarly, the β2 integrin lymphocyte function-associated antigen 1 (LFA-1) can interact with endothelial intercellular adhesion molecule 1 (ICAM-1) to modulate slow rolling. In this process, neutrophil signaling events triggered by binding to E-selectin result in expression of an intermediate-affinity form of LFA-1 that transiently interacts with endothelial ICAM-1 to decrease rolling velocity. A second β2 integrin, macrophage-1 antigen (MAC-1) can also mediate slow rolling. Thus, the additive ligation of more than one class of adhesion molecule may be required for efficient transition from fast rolling to a state of arrest.

Leukocyte Activation and Arrest

Leukocyte transition from rolling to arrest is the next step in leukocyte transmigration. Leukocyte activation is rapidly triggered by chemokines and other cell activators, and leukocyte arrest is mediated primarily by binding of leukocyte integrin-type adhesion molecules to members of the immunoglobulin superfamily expressed on the endothelium.[70,82,107] Leukocyte rolling facilitates activation by slowing transit time which allows for increased exposure to soluble activating factors and also exposure to endothelial-bound activating factors. Evidence suggests that chemokines that facilitate engagement of integrins and direct endothelial transmigration are bound to glycosaminoglycans (GAGs) or the Duffy antigen/receptor for chemokines (DARC)[90] on the surface of endothelial cells. The type of chemokine that occupies these binding sites depends on the relative availability and concentration of the chemokines. These sites can engage different cytokines depending on the type of leukocyte that is being recruited for a particular physiologic or pathophysiologic process.[91] Thus, if high levels of CXC chemokines are present in the vessel wall, CXC chemokines will occupy the endothelial binding sites and will attract predominantly neutrophils. In contrast, if high levels of CC chemokines are present in the vessel wall, CC chemokine will occupy the endothelial binding sites and will attract predominantly T lymphocytes. Chemokines can reach the luminal surface of endothelial cells by vesicular abluminal-to-luminal transcytosis, or be deposited there by circulating platelets or microparticles, or the exocytosis of intracellular granules derived from other cells.[147]

Integrins with the β_1 or β2 subunit are particularly important in the arrest of neutrophils and monocytes and their recruitment to sites of acute vascular inflammation. These include CD49d/CD29 (VLA-4), CD11a/CD18 (LFA-1), CD11b/CD18 (Mac-1), and CD11c/CD18. The avidity of certain integrins on leukocytes can be rapidly upregulated by chemokines at sites of inflammation[78] and enhance arrest and accumulation of inflammatory cells.[73,137,173] Ligation of specific heterotrimeric G-protein coupled receptors (GPCRs) by

chemokines triggers a complex intracellular signaling cascade that results in integrin transition to intermediate and high affinity forms to promote arrest. This process, termed inside-out signaling, is incompletely understood but is thought to sequentially involve phospholipase C signaling, small GTPase activation, and induction of integrin conformational changes.[82]

Several members of the immunoglobulin superfamily are the ligands on the surface of endothelial cells for the leukocyte integrins. Important examples are the intracellular adhesion molecules (ICAMs) that include ICAM-1, ICAM-2, and ICAM-3. Up-regulation of these ligands, especially ICAM-1, on endothelial cells at sites of vascular inflammation works in concert with the up regulation of integrins on circulating leukocytes to induce leukocyte infiltration at sites of vasculitis. Ligation of CD11a/CD18 (LFA-1) on neutrophils to ICAM-1 on endothelial cells causes adhesion and ligation of CD11b/CD18 (MAC-1) to ICAM-1, promoting arrest and diapedesis.[140] Ligation of β2 integrins to ICAMs is particularly important for neutrophil influx at sites of acute vascular inflammation, whereas lymphocyte recruitment to sites of inflammation depends more on the binding of the β4 integrin VLA-4 (CD49d/CD29) to a different immunoglobulin, vascular cell adhesion molecule-1 (VCAM-1 [CD106]).[22,135]

Many of the leukocyte adhesion cascade processes and events described thus far can contribute to the specificity of leukocyte recruitment and arrest. Specificity can be accounted for by the combinatorial effects of differential expression of integrins and their receptors, differential expression of the chemokines and their receptors, and varied intracellular signaling to regulate integrin function.[82]

ADHESION STRENGTHENING

Recent work[82,107] has begun to delineate events following integrin engagement that are thought to strengthen binding to the endothelium and thereby promote leukocyte recruitment into the inflamed vascular wall. These events are triggered by integrin-mediated outside-in signaling, characterized by ligand-induced integrin conformational changes, and cell surface integrin clustering that result in the recruitment of protein tyrosine kinases (PTKs) and initiation of PTK-dependent signaling pathways.[43] Also, the signaling adaptor molecule paxillin has been shown to bind to the α_4 integrin chain of VLA-4 only in its high-affinity conformation,[120] suggesting that ligand binding initiates outside-in signaling through this adapter protein. In addition, studies have shown that neutrophils lacking phosphatidylinositol 3-kinaseγ (PI3Kγ)[136] or the guanine nucleotide exchange factors VAV1 and VAV3[40] exhibit accelerated detachment. Although these signaling pathways are not fully elucidated, these studies provide evidence that integrin binding events that mediate leukocyte arrest also trigger intracellular signaling processes that stabilize post-arrest leukocyte adhesion.

Leukocyte Crawling and Transmigration

Static leukocyte adhesion to the endothelium is followed by transmigration of the cell across the endothelial barrier. Adherent leukocytes crawl over the endothelial surface (termed lateral migration) to locate a preferred site at which to cross the endothelium. Neutrophil crawling on venular endothelium is dependent MAC-1 and its ligand ICAM-1, and disruption of these binding events results in a delay of transmigration.[108] Crawling is likely to also occur as an integral part of the prominent leukocyte recruitment that occurs on the arterial side of the circulation in the vasculitides.

Once at an endothelial cell junction, neutrophils and monocytes are able to crawl through the junctions between endothelial cells (paracellular transmigration) by progressive engagement and disengagement of a series of adhesion molecules on the surface of the leukocytes with ligands on the junctional surfaces of the endothelial cells.[22,102,130] Platelet/endothelial cell adhesion molecule-1 (PECAM-1) (CD31), an immunoglobulin superfamily member, is expressed on leukocytes and on endothelial cell surfaces and intercellular junctions. Homophilic PECAM-1 adhesion is particularly important for transmigration of leukocytes through intercellular junctions between endothelial cells.[2,22,97] Transmigration of neutrophils and monocytes also involves the interactions of LFA-1, VLA4, or MAC1 on the leukocytes with immunoglobulin superfamily adhesion molecules in the endothelial intercellular junction, JAM-A (junctional adhesion molecule-A), JAM-B, or JAM-C, respectively.[22,82,102] Distal to the PECAM-1-mediated and JAM-mediated events, homophilic binding between CD99 on leukocytes and CD99 in the intercellular junction between endothelial cells takes over to facilitate completion of diapedesis.[22,130] Recent work also shows that endothelial cell-selective adhesion molecule (ESAM) at the endothelial junction facilitates transmigration of neutrophils but not lymphocytes, possibly by activation of the Rho GTPase and destabilization of the tight junction.[151] Leukocytes may also cross the endothelial barrier by a transcellular route through the body of the endothelial cell (transcellular migration). The significance of this route *in vivo*, and the underlying mechanisms involved in this process are currently poorly understood.[82,107]

During the process of diapedesis, there are endothelial cytoskeletal and junctional events that result in localized retraction of endothelial cytoplasm and opening of the intercellular junction. These events result from signals transduced from the ligation of endothelial adhesion molecules (e.g., ICAM-1 and PECAM-1).[22] Endothelial stimulation by inflammatory cytokines and adhesion molecule ligation, activation of membrane bound and interstitial matrix metalloproteinases (MMPs), and release of serine proteinases at the surface of migrating leukocytes cause altered distributions and integrity of junctional adhesion molecules (JAMs), vascular endothelial cadherins, and other junctional complex components so that leukocytes can crawl between endothelial cells into the intima, muscularis, or perivascular interstitium.[22,102,150] Once past the endothelial barrier, leukocyte migration through the underlying lamina and matrix involves progressive engagement of matrix molecules by leukocyte adhesion molecules, especially PECAM-1, β1 integrins (e.g., VLA-4, VLA-5) and carcinoembryonic antigen–related cell adhesion molecules (CEACAMs).[26,100,148]

At sites of vasculitis, the endothelium may be absent because of inflammatory damage. Denudation of endothelium will expose surfaces that contain ligands for neutrophils, monocytes and other inflammatory cells (Table 83.3). At sites of acute necrotizing vasculitis, the lumen often is immediately adjacent to zones of fibrinoid necrosis that contain fibrin that has been generated by the activation of the coagulation cascade by

TABLE 83.3 Adhesion Molecules that Mediate Neutrophil and Monocyte Endothelial Transmigration and Tissue Infiltration at Sites of Vasculitis

Leukocyte Event	Leukocyte Receptor	Endothelial Ligand
Rolling	L-selectin (CD62L)	PSGL-1 (CD162; on leukocytes not endothelium)
	PSGL-1(CD162)	P-selectin (CD62P)
	PSGL-1 (CD162), ESL-1, CD44	E-selectin (CD62E)
	LFA-1 (CD11a/CD18) (β2 integrin)	ICAM-1 (CD54)
	VLA-4 (CD49d/CD29) (β 1 integrin)	VCAM-1 (CD106)
Arrest	LFA-1 (CD11a/CD18) (β 2 integrin)	ICAM-1 (CD54)
	VLA-4 (CD49d/CD29) (β 1 integrin)	VCAM-1 (CD106)
	Mac-1 (CD11b/CD18) (β 2 integrin)	ICAM-1 (CD54)
Crawling	Mac-1 (CD11b/CD18) (β 2 integrin)	ICAM-1 (CD54)
	LFA-1 (CD11a/CD18) (β 2 integrin)	ICAM-1 (CD54)
Transmigration	Mac-1 (CD11b/CD18) (ß2 integrin)	ICAM-1 (CD54)
	LFA-1 (CD11a/CD18) (β 2 integrin)	JAM-A CD321)
	VLA-4 (CD49d/CD29) (β 1 integrin)	JAM-B (CD322)
	Mac-1 (CD11b/CD18) (β 2 integrin)	JAM-C
	PECAM-1 (CD31)	PECAM-1 (CD31)
	MIC2 (CD99)	MIC2 (CD99)
TISSUE LIGAND		
Tissue infiltration	Mac-1 (CD11b/CD18) (β 2 integrin)	Fibrin, fibronectin
	PECAM-1 (CD31)	Basement membrane
	α6β1 integrin (β 1 integrin; CD151)	Laminin
	VLA-4 (CD49d/CD29) (β 1 integrin)	Fibronectin
	VLA-5 (CD49e/CD29) (β 1 integrin)	Fibronectin
	CEACAM (CD66)	Fibronectin

PSGL-1, P-selectin glycoprotein ligand 1; LFA-1, lymphocyte function-associated antigen 1; ICAM-1, intercellular adhesion molecule 1; VLA, very late antigen; VCAM-1, vascular cell adhesion molecule 1; Mac-1, macrophage-1 antigen or complement receptor 3 (CR_3); JAM, junctional adhesion molecule; PECAM-1, platelet endothelial cell adhesion molecule 1; MIC_2, transmembrane glycoprotein $p30/32^{mic2}$; CEACAM, carcinoembryonic antigen-related cell adhesion molecule.

tissue factor and other thrombogenic materials at the site of injury. Mac-1 and other neutrophil and monocyte adhesion molecules can adhere to fibrin and begin the process of activation and migration into the inflamed tissue.[94] Matrix molecules exposed by endothelial denudation, such as fibronectin, laminin, entactin, and collagen also present ligands for leukocyte adhesion molecules, especially β1 integrins such as VLA-4 and VLA-5. Serine proteinases (e.g., elastase) released at the surface of migrating leukocytes act synergistically with β1 integrins and upregulated leukocyte PECAM-1 to allow the leukocytes to migrate into the tissue.[148]

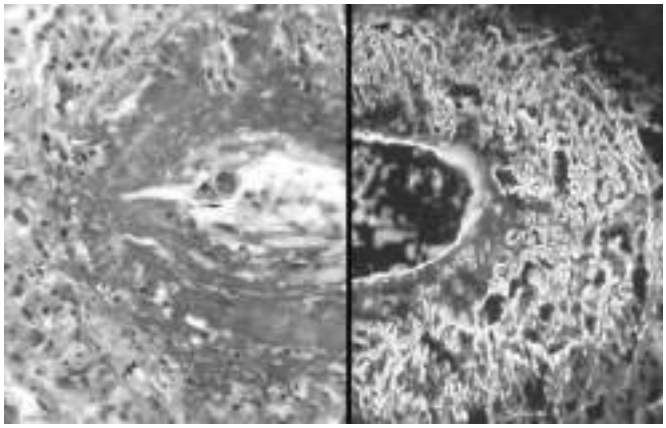

FIGURE 83.5 The *left panel* shows necrotizing arteritis with replacement of the vessel wall by amorphous fibrinoid material (hematoxylin and eosin stain); and the *right panel* shows the staining of fibrinoid necrosis in a artery wall with a fluoresceinated antibody specific for fibrin.

Mechanisms of Tissue Injury

Leukocytes attach to and migrate into the vessel wall at sites of vasculitis, and also undergo concomitant activation. The engagement of leukocyte adhesion molecules sends outside−in activating signals to the leukocyte, stimulating them to release inflammatory mediators. Cytokines and chemokines released by leukocytes, endothelial cells, and tissue cells at the sites of inflammation further amplify leukocyte activation and tissue injury.[150] Neutrophil activation results in the generation of reactive oxygen species and the release by degranulation of lytic and toxic mediators that injure vessel wall components. Production of reactive oxygen species by NADPH oxidase and other cellular sources contributes to vascular tissue injury by causing oxidation of matrix macromolecules as well as cellular molecules including lipids, proteins, and DNA. Neutrophil production of reactive oxygen species may be triggered be mechanisms specific to the pathogenesis of a particular vasculitis, such as engagement of Fcγ receptors in ANCA disease, or by more general inflammatory mediators such as TNFα.[16,38,115]

Other inflammatory events at sites of small-vessel vasculitis include edema, hemorrhage, thrombosis, cell death (both apoptotic and necrotic), and matrix lysis with fibrinoid necrosis. Fibrinoid necrosis results when there is enough destruction to the vessel walls to allow plasma constituents, including the coagulation factors, to seep into vessel walls or the perivascular tissue. Here, the coagulation factors encounter multiple thrombogenic substances, including tissue factor, which results in the generation of fibrin. Fibrin can be demonstrated by immunohistochemistry at sites of fibrinoid necrosis (Figure 83.5). The necrosis of cells and lysis of matrix may erode through the vessel wall into the perivascular tissue resulting in a pseudoaneurysm (often referred to as an aneurysm) (Figure 83.6).[62]

The lysis of matrix in vessel walls and perivascular tissue that results in fibrinoid necrosis is mediated by

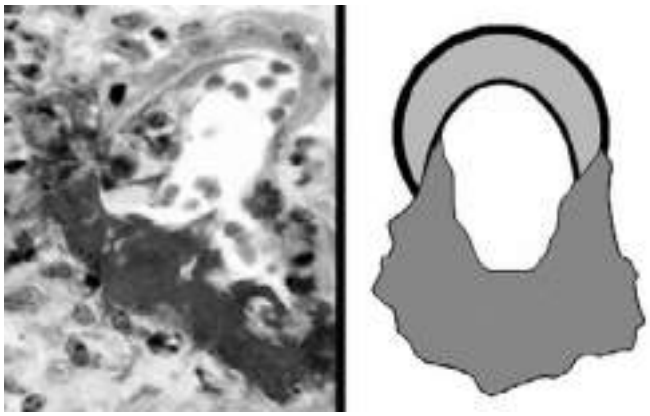

FIGURE 83.6 The *left panel* shows segmental fibrinoid necrosis and pseudoaneurysm formation in a renal interlobular artery (Masson trichrome stain), and the *right panel* illustrates the process diagrammatically.

cytotoxic and lytic enzymes released by leukocyte degranulation, and generated within the inflamed tissue. For example, a number of destructive serine proteinases, such as elastase, proteinase-3, and cathepsin G, are stored in the granules of neutrophils and monocytes and are released when these leukocytes are activated at sites of inflammation.[103] Serine proteinases can be detected at sites of fibrinoid necrosis by immunohistochemistry.[5,101] In addition, matrix metalloproteinase (MMPs), such as collagenase and gelatinase, are produced by leukocytes and tissue cells at sites of inflammation.[81] Most MMPs, which comprise a family of more than 20 endopeptidases, function in the extracellular space, but some are bound to cell membranes (membrane-type MMPs, MT-MMPs). Normally, serine proteinases are held in check by serine proteinase

inhibitors (serpins) and MMPs are held in check by tissue inhibitors of MMPs (TIMPs) (Figure 83.7).[49,81] However, in the microenvironment at sites of necrotizing acute inflammation, this homeostatic balance is tipped in favor of the destructive enzymes.

Serine proteinases, such as elastase, proteinase-3, and cathepsin G, can degrade the constituents of vascular basement membranes, the extracellular matrix of the muscularis of vessels, and perivascular extracellular matrix. Major matrix molecules that can be digested by serine proteinases include collagen, laminin, fibronectin, and proteoglycans.[103,159] Elastase and proteinase-3 also contribute to tissue injury by causing apoptosis and necrosis of cells.[169,170] Elastase also induces leukocytes and endothelial cells to release inflammatory cytokines. Elastase[101] and proteinase-3[5] can be identified by immunohistochemistry at sites or glomerular necrosis in crescentic glomerulonephritis that is a component of ANCA vasculitis.

The potential for tissue injury by serine proteinases is counteracted by serine proteinase inhibitors in the plasma, most important α_1-proteinase inhibitor (α1-antitrypsin), which is produced primarily in the liver.[49] Other serpins are produced to a greater degree at the site of inflammation, for example by neutrophils and macrophages.[49] These include secretory leukocyte protease inhibitor (SLPI) and elafin.[49] α_2-Macroglobulin is a broad-spectrum antiproteinase that inhibits not only serine proteinases but also cysteine proteinases, aspartic proteinases, and MMPs. In the microenvironment at sites of inflammation, inactivation of serine proteinases by serpins is counteracted by the inactivation of serpins by oxidants, such as hypochlorous acid, that are generated by the respiratory bursts of activated neutrophils and monocytes. For example, Donavan and associates have performed in vitro experiments that have demonstrated the ability of oxidants to abolish the inhibitory effect of α_1-antiproteinase on elastase-mediated GBM degradation.[31]

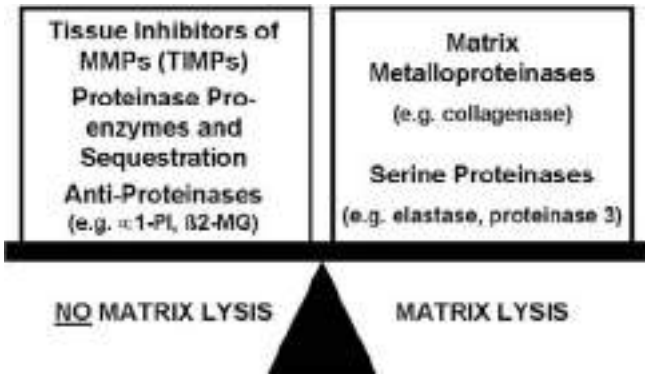

FIGURE 83.7 Diagram depicting the homeostatic balance that exists between matrix metalloproteinases and serine proteinases and the protective mechanisms that hold them at bay until they are needed or until they break free in pathologic processes.

MMPs, including MT-MMPs, can be identified by immunohistochemistry at sites of vascular inflammation.[47] Most MMPs are synthesized by leukocytes and other cells after stimulation by inflammatory cytokines.[81,90,159] However, MMP-8 (collagenase) and MMP-9 (gelatinase) are preformed and stored in the granules of neutrophil and monocyte. Thus, collagenase and gelatinase are released in concert with elastase, proteinase-3, and cathepsin G when neutrophils and monocytes undergo degranulation at sites of acute inflammation. This is a very lytic and toxic brew that can not only degrade the vascular and perivascular extracellular matrix but also can kill the endothelial and smooth muscle cells that comprise the vessel wall.

MMPs are released as proenzymes that must be activated before they can cause tissue injury or remodeling. At sites of inflammation, MMP proenzymes are activated by a variety of inflammatory mediators, including serine proteinases released by leukocyte degranulation, oxidants from leukocyte respiratory bursts, and other MMPs (especially MT-MMPs) that already have undergone activation. The counterbalance that TIMPs provide is counteracted at sites of acute inflammation by neutralization of TIMPs by serine proteinases.[159]

As already discussed, neutrophils and monocytes are important sources of destructive factors that cause injury during acute vasculitis and glomerulonephritis. The innate immune response to tissue injury caused by acute inflammation eventually also recruits T lymphocytes to the sites of acute inflammation. If neutrophil-driven acute inflammation ends, neutrophils disappear through apoptosis or necrosis within a day or two and are replaced by predominantly macrophages and T lymphocytes. In some forms of vasculitis, such as giant cell arteritis and Takayasu arteritis, T lymphocytes may play a dominant role even in the early phase of inflammation. T lymphocytes are able to mediate vascular injury through a variety of mechanisms. T lymphocytes can produce MMPs that degrade matrix.[34] T lymphocytes also release granzymes, which are serine proteinases that are toxic for cells and can digest proteoglycans. Activated T lymphocytes cause matrix degradation indirectly by inducing release of serine proteinases and MMPs by neutrophils and monocytes.

In summary, a broad spectrum of cellular and humoral inflammatory mediator systems are involved in the pathophysiology of inflammation at any site, including vasculitis. These mediators are common to many different pathogenic pathways to vasculitis that are initiated by many different etiologies, some of which are known and others not. The two most common pathways to renal vasculitis are immunoglobulin-

rich immune complex–mediated vasculitis and immunoglobulin-poor pauci-immune antineutrophil cytoplasmic autoantibody (ANCA)–mediated vasculitis. These will be reviewed in the following section.

IMMUNE COMPLEX–MEDIATED VASCULITIS

Basic Pathogenic Events in Immune Complex Vasculitis

In 1942, Arnold Rich observed that patients who were treated intravenously with serum developed systemic vasculitis.[119] Rich hypothesized that the vasculitis was caused by an immunologic response to the serum proteins and he obtained experimental support for this by inducing vasculitis in rabbits by injecting horse serum.[118] In the 1950s and 1960s, many investigators, including Germuth, Dixon, and Cochrane, documented the role for vascular localization of immune complexes containing antigen, immunoglobulin, and complement as a cause for vascular inflammation.[21,41,74,158] This was prompted by the identification by immunofluorescence microscopy of granular deposits of immunoglobulin and complement in the walls of vessels in patients and experimental animals with vasculitis (Figure 83.8).

Numerous experiments demonstrated that immune complexes in vessel walls cause inflammation by activating humoral and cellular inflammatory mediator systems in the blood, including the complement, kinin, and coagulation systems. Activation of humoral inflammatory mediator systems acted in concert with recruitment and activation of leukocytes, especially neutrophils and monocytes, to cause inflammation in the vessel wall. As with systemic immune complex vasculitis in humans (e.g., Henoch-Schönlein purpura or IgA vasculitis, and cryoglobulinemic vasculitis), most animal models of systemic immune complex vasculitis have involvement of glomeruli resulting in an immune complex glomerulonephritis as well as the systemic vasculitis. Of course, glomerulonephritis is in essence a form of vasculitis that is affecting glomerular capillaries.

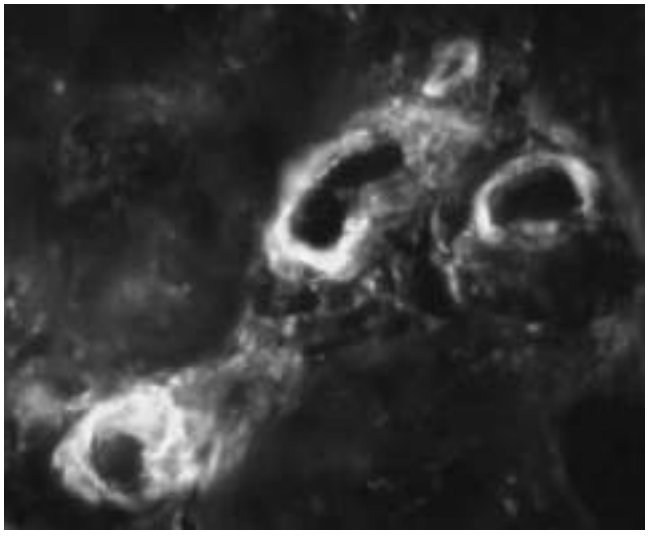

FIGURE 83.8 Granular staining for immunoglobulin A (IgA) in the walls of small dermal vessels in a patient with Henoch-Schönlein purpura (fluoresceinated anti-IgA).

A variety of animal models of immune complex vasculitis have been used to elucidate the pathophysiologic events that cause the vascular inflammation. For example, Kniker and Cochrane used a serum sickness model in rabbits to demonstrate a major role for neutrophils in immune complex vasculitis by ameliorating the vasculitis by depletion of neutrophils.[74] One of the most powerful in vivo experimental systems for dissecting the pathogenic events in immune complex mediated injury is the Arthus reaction.[4,9,20,21,117,166,168] The Arthus reaction mimics the events that take place in a vessel wall at the site of immune complex mediated vasculitis. The classic Arthus reaction involves repeated injection of a foreign antigen into the skin of an experimental animal until circulating antibodies to the antigen develop and react with the antigens at the site of injection to produce immune complex–mediated acute inflammation.[41] However, this process is difficult to control and thus the reverse passive Arthus reaction is a more useful model for investigating the inflammatory events that are induced by immune complexes.[166] This involves local injection of antigen in the tissue at the site of interest along with intravenous injection of the antibody that will form pathogenic immune complexes with the antigen.

Use of the reverse passive Arthus reaction with various knockout mouse strains indicates that immune complex-mediated inflammation involves all of the mediator systems that were discussed in the earlier sections on pathogenic mechanisms that are shared by different forms of vasculitis. Neutrophils are the major effector cells of the acute injury, although mast cells also play a role. Neutrophils are recruited and activated by the interplay of cytokines/chemokines, adhesion molecules, Fcγ receptor engagement, and complement activation.[9,20,117,166–168] There has been controversy over the relative importance of Fc receptor engagement versus complement activation.[9,117] The preponderance of evidence indicates that both are extremely important to the full development of immune complex-mediated inflammation and the two together have a synergist rather than merely additive effect.

Immune complexes that contain antibodies that are capable of activating complement by the classic or alternative pathway can induce acute inflammation. Knockout mouse experiments have demonstrated that the anaphylatoxin C5a, which is generated by the classic, lectin and alternative pathways, is a particularly potent mediator.[9] C5a induces increased vascular permeability, attraction of neutrophils and monocytes, activation of neutrophils and monocytes, and enhanced release of inflammatory cytokines from a number of cell types. C5 knockout mice and C5a receptor knockout mice have a marked reduction in the acute inflammation caused by the reverse passive Arthus reaction.[51] This is in the context of normal immunoglobulin Fc receptors on leukocytes. In addition to C5a, complement activation also generates the anaphylatoxins C3a and C4a, and the cytotoxic membrane attack complex C5b-9. These factors probably play a role in immune complex-mediated vasculitis, but C5a appears to be the dominant complement mediator in immune complex vasculitis.

Immunoglobulins in immune complexes activate complement and they also present their Fc regions for engagement by Fc receptors on leukocytes. Most experimental studies have focused on the importance of the receptors for the gamma heavy chains of IgG (Fcγ receptors) in the pathogenesis of immune complex disease.[117] There are two classes of Fcγ receptors: activating receptors and inhibiting receptors. Both types of receptors are expressed on most leukocytes and thus co-engagement of both types may occur on the same cell. Fcγ receptors occur on neutrophils, monocytes, macrophages, eosinophils, mast cells, and natural killer cells. B lymphocytes have only the inhibitory receptors. In mice, the absence of an activating Fcγ receptor, FcγRIII, results in an impaired Arthus reaction,[48] whereas the absence of an inhibitory Fcγ receptor, FcγRII, results in an enhanced Arthus reaction.[141] Likewise, in a mouse model of anti-GBM disease, which is an example of in situ immune complex-induced inflammation, mice with a deficiency of activating Fcγ receptor develop no disease[105,140] whereas mice with a deficiency of an inhibitory Fcγ receptor develop more severe disease.[140] It is reasonable to conclude that in animals and patients with activating and inhibiting Fc receptors, the outcome of Fc engagement by Fc receptors on leukocytes is the result of the balance between the activating and inhibiting signals to the cell. This in turn is controlled by the number of receptors expressed on the surface and the affinity of the receptors, which is influenced by the cytokines that the leukocyte is exposed to.[79] Thus, once again, there is evidence for a complex interplay between the various mediator systems at sites of inflammation.

Immune complexes in vessel walls must attract leukocytes to the vessel wall and induce them to infiltrate to cause vasculitis. Endothelial and leukocyte adhesion molecules are involved in this process. Once again, the Arthus reaction provides insights into this process. Genetic deficiency of selectins or blockade of selectins with antibodies reduces the severity of the passive reverse Arthus reaction in mice and in particular reduces the number of infiltrating neutrophils.[166,167] Likewise, mice deficient in ICAM-1 have diminished Arthus reaction.[166] Not surprisingly, given their functional redundancy, the absence of a single type of adhesion molecule is not as effective as the absence of multiple types of adhesion molecules in preventing an Arthus reaction. The importance of adhesions molecule in immune complex-mediated vascular inflammation also has been demonstrated in murine glomerulonephritis and alveolar capillaritis that is induced by in situ immune complex formation with anti-GBM antibodies.[98] There is evidence for involvement of selectins, β1 integrins, and β2 integrins. The relative importance of various types of leukocyte adhesion molecules seems to differ among different types of immune complex vascular inflammation.[98] The redundancy of the adhesion molecules and the difference in usage in different diseases presents a problem when contemplating therapeutic strategies that are designed to ameliorate vascular inflammation by blocking leukocyte binding to adhesion molecules.

As in any type of inflammation, cytokines and chemokines and their receptors are very important in orchestrating the inflammatory events in immune complex mediated vasculitis.[98,99,149,168] As with adhesion molecules, there is tremendous redundancy in the cytokines and chemokines that mediate vascular inflammation such that elimination or neutralization of one or a few is not sufficient to completely prevent the inflammation. This has been observed in diverse in vivo experimental systems, including the reverse passive Arthus reaction[168] and rodent models of glomerulonephritis or pulmonary capillaritis.[98] The regulation of immune complex-mediated vasculitis by cytokines includes upregulation and downregulation of inflammatory processes, often through modulation of the activation of leukocyte transcription factor nuclear factor-κB (NF-κB).[121]

The inflammatory events that have been characterized in the Arthus reaction and other experimental models of immune complex-induced vascular inflammation almost certainly occur in all forms of immune complex vasculitis in patients,[20] although there probably are differences in the precise repertoire of mediators that are most important in the various immunopathologic types. For example, cryoglobulinemic vasculitis with a predominance of IgG and IgM in

the vascular immune deposits probably induces somewhat different inflammatory pathways than Henoch-Schönlein purpura vasculitis with a predominance of IgA in the immune deposits.

Hepatitis B-Induced Immune Complex Vasculitis Including Polyarteritis Nodosa

Vascular immune complex deposition has been incriminated in the pathogenesis of clinically and pathologically diverse types of human vasculitis (Table 83.1). The source of the antigen can be exogenous as in serum sickness and vasculitis caused by hepatitis B or endogenous (e.g., an autoantigen) as in cryoglobulinemic vasculitis and lupus vasculitis.

As noted earlier, the first form of human vasculitis in which immune complexes were incriminated in the pathogenesis was serum sickness vasculitis.[119] Vasculitis associated with hepatitis B virus infection was the second well-recognized category of vasculitis caused by a foreign antigen, although in this instance it is being produced internally by the virus. The hepatitis B–associated vasculitis often is thought to mimic idiopathic polyarteritis nodosa, however, the vascular inflammation in patients has a broad spectrum of manifestations that includes necrotizing arteritis as well as small-vessel vasculitis such as leukocytoclastic angiitis in the skin and glomerulonephritis, which most often is a membranous glomerulopathy but may be proliferative or membranoproliferative glomerulonephritis.[44,46,89,109,144,145,154] This broad spectrum of immune complex disease is reminiscent of lupus vascular disease that can range from necrotizing arteritis to small-vessel vasculitis to varied forms of glomerulonephritis[75] and probably results from quantitative and qualitative differences in the amount and composition of circulating and vessel-wall immune complexes in different patients.

Granular deposits of immunoglobulin and complement, and sometimes hepatitis B antigens, have been detected in vessel walls at sites of necrotizing arteritis, cutaneous leukocytoclastic angiitis, and glomerulonephritis.[89,154] HBe antigen has been Identified most often.[145] The complement deposits include C1q, which indicates that the complement system has been activated by the classical pathway with release of the potent inflammatory mediators discussed earlier in this chapter. Thus the pathogenic mechanism could center on the typical sequence of inflammatory events that are set into motion by immune complex formation and complement activation. However, Mason et al. have demonstrated the presence of hepatitis B RNA and DNA as well as surface antigens and core antigens in endothelial cells in patients with extrahepatic disease.[86] They hypothesize that both immune complex formation and viral replication occur in vessel walls and both contribute to the induction of vascular inflammation. This putative role for vascular viral proliferation in the pathogenesis of hepatitis B–associated vasculitis awaits confirmation.

Cryoglobulinemic Vasculitis Including Hepatitis C-Induced Immune Complex Vasculitis

Cryoglobulinemic vasculitis is a small-vessel vasculitis that is caused by the localization of predominantly mixed cryoglobulins in vessel walls.[10,15,39] Clinical manifestations include arthralgias, palpable purpura, and glomerulonephritis. Mixed cryoglobulins are immune complexes and are classified as type II or type III.[123,142] Type II cryoglobulins contain a mixture of monoclonal antibodies with rheumatoid factor activity (usually IgMκ) that is bound to polyclonal immunoglobulin (usually IgG). Type III cryoglobulins are a mixture of more than one polyclonal immunoglobulin, often including one that has rheumatoid activity (usually IgMκ). Some patients have what appears to be a transitional stage between production of polyclonal rheumatoid factor and evolution to a dominant monoclonal rheumatoid factor and are classified as type II–III.[142]

Antibodies with rheumatoid factor activity have specificity for other antibodies, and thus are autoantibodies. Rheumatoid factor antibodies (RFs) often have anti-idiotypic specificity that allows them to bind to the antigen binding region of immunoglobulins (Fab). However, most rheumatoid factor antibodies in cryoglobulinemia can bind to both the Fc and Fab portions of the target immunoglobulins and thus can form more stable and larger immune complexes than anti-idiotypic antibodies that bind to Fab alone.[123] A genetically distinct k light chain is present in RFs in >80% of patients with HCV cryoglobulinemia.[15]

Type I cryoglobulins, which cause vasculitis less often, are not immune complexes because they are composed of monoclonal immunoglobulin, usually IgM and much less commonly IgG. Type I cryoglobulins often are produced by clones of abnormal B cells and often are associated with identifiable lymphoproliferative neoplasms. Aggregates of type I immunoglobulins can accumulate in and occlude the microvasculature resulting in a hyperviscosity syndrome. Less often, these aggregates induce inflammation similar to that caused by types II and III cryoglobulins.

In contrast, type II and type III cryoglobulins are immune complexes with RF antibodies bound to target immunoglobulin acting as antigen. These complexes

activate complement and induce small-vessel vasculitis and glomerulonephritis. The usual histologic expression is a type I membranoproliferative glomerulonephritis with hyaline thrombi (Figure 83.9). The complement activation involves the classical pathway as evidenced by immunostaining for C1q and C_4 along with other complement components in cryoglobulin vascular deposits and by the typical serologic finding of low or undetectable C_4 with normal or near-normal C_3.[39]

Depending on the geographic location, 40 to 90% of patients with mixed cryoglobulinemia have hepatitis C virus (HCV) infection, with the highest incidence in the Mediterranean basin.[100] HCV interacts with B lymphocytes to produce polyclonal B cell activation with a marked increase in the proportion of CD^{5+} lymphocytes, which are the prime suspects in the rheumatoid factor (autoantibody) formation.[25,123] The initial polyclonal activation that produces polyclonal rheumatoid factors and type III cryoglobulins evolves, in some patients, through an intermediate II-III phase into the emergence of a dominant single clone producing monoclonal rheumatoid factor and type II cryoglobulins.[123,142] Type II cryoglobulins from the circulation patients with HCV contain monoclonal IgM rheumatoid factor, polyclonal IgG with specificity for HCV, HCV core protein, and complement component C1q.[123,124] HCV proteins and RNA are present in cryoglobulins, possibly as antigenic components of immune complexes.[15]

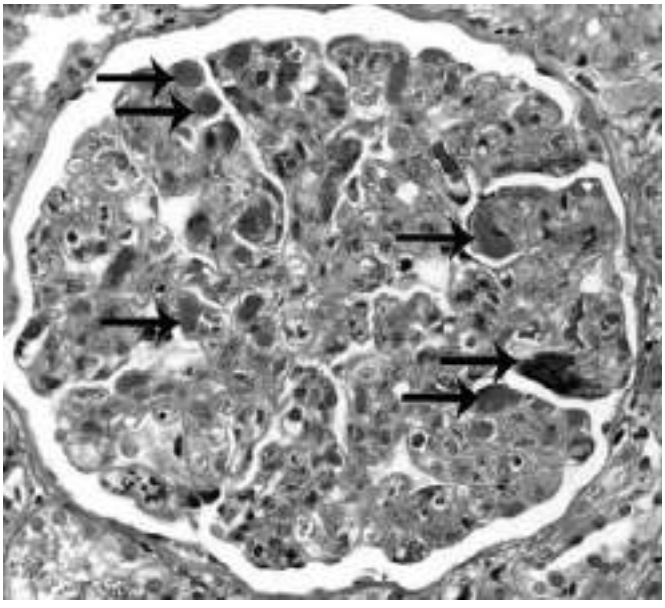

FIGURE 83.9 Glomerulus from a patient with cryoglobulinemic showing numerous hyaline thrombi (arrows) and histologic features of type I membranoproliferative glomerulonephritis.

Mediators of Cryoglobulinemic Vasculitis

Immunostaining of vasculitic lesions in the skin, nerves, kidneys, and elsewhere demonstrate cryoglobulin immune complexes that have the same composition as circulating cryoglobulins, including IgM, IgG, C1q, and HCV proteins.[10,123] In renal biopsy specimens with cryoglobulinemic glomerulonephritis, large intravascular cryoglobulin aggregates appear by light microscopy as hyaline thrombi in glomerular capillaries (Figure 83.9) and by immunofluorescence microscopy as globular staining for IgM and IgG.[10] In addition, there are subendothelial, mesangial and occasionally subepithelial electron dense immune deposits, often with a vague microtubular substructure.[63] The glomerulonephritis most often has a type I membranoproliferative pattern but occasionally can have a focal or diffuse proliferative or mesangioproliferative pattern and rarely a membranous pattern.[10,63] A minority of renal biopsy specimens will have necrotizing vasculitis affecting arterioles or small arteries.[10]

Immunohistology of skin and renal biopsy specimens identifies mediators of inflammation in the glomeruli that implicate many components of the leukocyte-adhesion molecule–cytokine axis that would be expected for immune complex–mediated vasculitis. For example, immunophenotyping of leukocytes in glomeruli affected by cryoglobulinemic glomerulonephritis demonstrates conspicuous infiltration by monocytes and macrophages.[42,116] The infiltrating macrophages express activation markers such as HLA class II molecules.[116] There also is glomerular upregulation of CC chemokine MCP-1 (CCL2), TNF-α, and IL-1α gene and protein expression,[42,116] which would attract and activate neutrophils and monocyte to glomeruli. In a study of cryoglobulinemic glomerulonephritis, endothelial leukocyte adhesion molecule ICAM-1 but not VCAM-1 was upregulated on endothelial cells.[96] However, in a study of small vessels in peripheral nerves from patients with cryoglobulinemic vasculitis, there was greater immunostaining for VCAM-1 compared with ICAM-1.[69] This study also found circulating VCAM-1 in patients with cryoglobulinemia and high levels of circulating VCAM-1 correlated with severe vasculitis.

Animal Models of Cryoglobulinemic Vasculitis

There are good mouse models of cryoglobulinemic vasculitis that have been used to elucidate the pathophysiology of this disease.[45,55,72] An early version used intraperitoneal injection of a mouse rheumatoid factor-producing hybridoma that had been derived from an MRL-lpr/lpr mouse.[45] The pathogenic rheumatoid factor was an IgG3 antibody with specificity

for IgG2a. Intraperitoneal injection of this clone resulted in circulating cryoglobulins and the development of cutaneous leukocytoclastic angiitis and glomerulonephritis that closely mimicked human cryoglobulinemic vasculitis. Monoclonal IgG3 without rheumatoid factor activity self-aggregates to form cryoglobulins but these are not pathogenic immune complexes and mimic glomerular lesions of type I cryoglobulinemia with hyaline thrombus formation but no glomerular inflammation.[55] Depletion of neutrophils from mice that received IgG3 with rheumatoid activity also had hyaline thrombi but no glomerular inflammation, indicating the importance of neutrophils in the mediation of vascular injury.[55] Neutrophils are not conspicuous in renal biopsies of human cryoglobulinemic glomerulonephritis, but one must realize that these are chronic lesions that have been evolving for months or at least weeks prior to renal biopsy, which would favor accumulation of long-lived macrophages. Skin biopsies of acute cryoglobulinemic vasculitis lesions typically show extensive leukocytoclasia indicative of neutrophilic influx and subsequent apoptosis.

A variation on the mouse model uses transgenic expression of the heavy and light chains of the pathogenic IgG_3 without rheumatoid factor activity to cause disease.[72] This model of chronic cryoglobulinemic injury shows the evolution of the glomerulonephritis from a proliferative to a membranoproliferative and eventually a sclerosing pattern and has visceral arteritis rather than cutaneous leukocytoclastic angiitis.

In summary, in both animals and humans, mixed cryoglobulins, which contain rheumatoid factor autoantibodies and target antibodies, cause immune complex–mediated vasculitis with complement activation, cytokine/chemokine secretion, adhesion molecule upregulation, leukocyte infiltration, and inflammatory injury to vessel walls.

Henoch-Schönlein Purpura Vasculitis (IgA Vasculitis)

Henoch-Schönlein purpura is a small-vessel vasculitis caused by immune complexes with IgA-dominant immunostaining.[56,58] Henoch-Schönlein purpura is the most common form of systemic vasculitis in childhood.[126] The mean age at onset is six years and 90% of patients are younger than 10 years. However, Henoch-Schönlein purpura can occur in adults at any age. Virtually all patients with Henoch-Schönlein purpura have palpable purpura caused by dermal leukocytoclastic angiitis. Over three-fourths have arthralgias, two thirds have abdominal pain, and a third to a half have evidence for glomerulonephritis. Glomerulonephritis is more common in older children and adults with Henoch-Schönlein purpura.[126]

The immunopathologic findings in Henoch-Schönlein purpura indicate an immune complex–mediated pathogenesis. Immunostaining of involved and uninvolved small vessel in the skin demonstrates the presence of IgA, C3, C3c, C3d, and fibrin/fibrinogen (Figure 83.8).[29] C_4 and C1q typically are absent; suggesting that the alternative complement activation pathway and not the classical pathway is involved in pathogenesis. This is in contrast to hepatitis B-associated immune complex vasculitis and hepatitis C-associated cryoglobulinemic vasculitis, both of which have conspicuous immunostaining for C_4 and C1q.[39,89] An important feature of the immune deposits is that they contain IgA1 rather than IgA2.[3] Glomerular immune deposits in Henoch-Schönlein purpura glomerulonephritis have the same composition as dermal vascular deposits and are similar to the deposits of IgA nephropathy, although they tend to have more frequent and more intense staining for fibrin/fibrinogen.

The exclusive participation of IgA1 and not IgA2 in the immune deposits of Henoch-Schönlein purpura and IgA nephropathy is in accordance with the hypothesis that the pathogenic immune aggregates of IgA result from abnormal glycosylation of the hinge region of IgA1 molecules.[3,8,77,125,139,140] The heavy chains of IgA1, but not IgA2, contain a praline-rich hinge region between the CH1 and CH2 domains. This hinge region has O-linked glycosylation sites. In fact, IgA1 and IgD are the only immunoglobulin isotypes that contain O-linked glycosylation sites. Multiple studies have demonstrated that most patients with Henoch-Schönlein purpura nephritis or IgA nephropathy have abnormalities in the O-linked glycans of the hinge region, such as diminished galactose or sialic acid or both. One study suggests that patients with Henoch-Schönlein purpura and nephritis have abnormal IgA hinge region glycosylation whereas those with no nephritis do not[29] but this has not been confirmed.

Abnormal IgA1 hinge region glycosylation could lead to the localization of pathogenic complexes of IgA1 in vessel walls by a number of mechanisms. Altered glycosylation can[1] reduce the hepatic clearance of IgA1 by asialoglycan receptors, which have a high affinity of o-linked glycans;[2] cause self-aggregation of circulating and deposited IgA1;[3] increase binding of IgA1 to extracellular matrix, including vascular basement membranes and glomerular mesangium;[4] enhance interactions between IgA1 and inflammatory mediators such as complement and Fcα receptors on leukocytes; and 5) development of IgG antibodies that recognize the aberrant glycosylation.[139,140] An intriguing although conjectural concept is that galactose-deficient hinge region is the target for circulating

antibodies that have been produced in an immune response to infectious pathogens that have α-galactosyl residues on their cell surfaces.[28,143] This might also explain the frequent association of a recent upper respiratory tract infection with the onset of both Henoch-Schönlein purpura and IgA nephropathy.[126] An alternative explanation for this association with infections is that a foreign antigen released by the pathogen is the target of the IgA immune response. In line with this theory, Masuda et al.[87] demonstrated a group A streptococcal antigen, nephritis-associated plasmin receptor, in the mesangial immune deposits of 30% of patients with Henoch-Schönlein purpura nephritis.[87] However, it is possible that the circulating and deposited aggregates of IgA that cause Henoch-Schönlein purpura and IgA nephropathy are not true immune complexes with antibodies specifically bound to antigens, but rather are predominantly homoaggregates of IgA1 with no bound antigens. This concept is supported by the observation that Henoch-Schönlein purpura can develop in patients with IgA1 multiple myelomas that are producing IgA1 paraprotein with abnormal hinge region glycosylation but not in patients with IgA1 multiple myelomas that are producing IgA1 paraprotein with normal hinge region glycosylation.[146]

It is likely that more than one mechanism can result in circulating pathogenic IgA1 complexes, some of which are true immune complexes with bound antigens and other that are homoaggregates of IgA1 without bound antigens. In either instance, the IgA1 complexes localize in the walls of small vessels and the glomerular mesangium and cause inflammatory injury, by alternative pathway complement activation, and by attraction and activation of leukocytes. In addition to IgA and complement, a variety of constituents have been identified in circulating and deposited IgA complexes in IgA nephropathy and Henoch-Schönlein purpura including fibronectin and Fcα receptors (CD89).[79]

The pathogenic importance of fibronectin and CD89 is controversial, but experimental animal data at least support the possibility that they may have a role in pathogenesis.[79,172] Launay et al. created IgA nephropathy in mice with transgenic expression of human CD89.[79] These mice developed circulating CD89 that complexed with IgA, deposited in the mesangium, and caused glomerulonephritis.

IgA-fibronectin aggregates occur in patients with IgA nephropathy and Henoch-Schönlein purpura.[6,60] Uteroglobulin is an anti-inflammatory protein in the plasma with high affinity for fibronectin that prevents the formation of IgA-fibronectin aggregates by binding to fibronectin.[172] Uteroglobin knockout mice and uteroglobulin antisense transgenic mice develop IgA nephropathy,[172] suggesting that reduced uteroglobulin may play a role in human disease. However, Coppo et al.[23,24] determined that patients with IgA nephropathy in fact have increased levels of circulating uteroglobulin and that circulating IgA macromolecular complexes contain both fibronectin and uteroglobulin.[23]

A variety of in vivo and in vitro studies of Henoch-Schönlein purpura and IgA nephropathy demonstrate that the chemokine/cytokine, adhesion molecule, and leukocyte activation pathways typical of immune complex–mediated vasculitis are participating in these diseases. For example, Yang et al.[169,170,171] observed that patients with acute Henoch-Schönlein purpura had increased serum levels of IL-8 and that incubation of endothelial cells with serum from patients with Henoch-Schönlein purpura but not from healthy controls caused increased IL-8 production.[171] Duque et al.[32] demonstrated that mesangial cells exposed to aggregated IgA1 had increased expression of IL-8 and MCP-1 genes and that this was mediated in part by NF-κB activation.[32] In renal biopsy specimens from patients with IgA nephropathy and Henoch-Schönlein purpura, there is increased immunostaining of endothelial cells and mesangial cells for ICAM-1.[95] Thus, there is evidence that the localization of IgA complexes in vessel walls induces the release of cytokines and the upregulation of adhesion molecules that attracts leukocytes and induces injury.

A possible role for IgA antineutrophil cytoplasmic autoantibodies (IgA-ANCA) in Henoch-Schönlein purpura is controversial.[24,104] There is no doubt that some indirect immunofluorescence microscopy assays that use normal neutrophils as substrate and some enzyme immunoassays that use neutrophil proteins as substrate detect increased binding of IgA from patients with Henoch-Schönlein purpura. However, the major issue is whether this is the result of specific recognition of a neutrophil antigen by the antigen binding domain of IgA or is merely the result of nonspecific binding of the abnormal IgA or IgA complexes to the substrate, possibly mediated by the abnormal glycosylation of the IgA or the presence of fibronectin in the complex or some other factor other than the antigen specificity of the IgA.[24] In our judgment, there is no compelling evidence for true IgA-ANCA with specificity for neutrophils proteins in patients with Henoch-Schönlein purpura.

PAUCI-IMMUNE ANTINEUTROPHIL CYTOPLASMIC AUTOANTIBODY VASCULITIS

Pauci-immune small-vessel vasculitis is a necrotizing polyangiitis that can affect capillaries, venules, arterioles, and arteries.[58,59] Glomerular capillaries often

are involved, resulting in a glomerulonephritis that typically has segmental fibrinoid necrosis and crescent formation in the acute phase. Approximately three fourths of patients with pauci-immune necrotizing and crescentic glomerulonephritis also have evidence for involvement of small vessels in other organs. Virtually any organ can be involved. Frequent manifestations are alveolar capillaritis with pulmonary hemorrhage, dermal venulitis with palpable purpura, epineural arteritis with peripheral neuropathy, and inflammation of small arteries and arterioles in abdominal viscera. There are three major clinicopathologic categories of pauci-immune small-vessel vasculitis: microscopic polyangiitis, Wegener's granulomatosis (granulomatosis with polyangiitis), and Churg-Strauss syndrome (eosinophilic granulomatosis with polyangiitis) (Table 83.2; Figure 83.1).[56] The defining feature of Wegener's granulomatosis is necrotizing granulomatous inflammation, most often in the upper or lower respiratory tract. The defining features of Churg-Strauss syndrome are blood eosinophilia and asthma. Microscopic polyangiitis has the systemic vasculitis in the absence of granulomatous inflammation or asthma.

The defining immunopathologic feature common to the pauci-immune small-vessel vasculidities is the absence or paucity of immunohistologic staining of vessels for immunoglobulin. This feature distinguishes pauci-immune small-vessel vasculitis from small-vessel vasculitis that is caused by classical vessel wall immune complex deposition, such as cryoglobulinemic vasculitis or Henoch-Schönlein purpura vasculitis, and from anti-GBM disease with linear staining for IgG along glomerular and pulmonary alveolar capillary basement membranes.[56,58] The absence or paucity of immunoglobulin in the vessel walls does not mean that immunoglobulin is not involved in the pathogenesis of the vasculitis and glomerulonephritis. This does suggest, however, that if immunoglobulin is involved, it is by a mechanism that differs from that of classical immune complex disease. In fact, the data discussed in subsequent sections of this chapter offer compelling evidence that ANCAs are the primary pathogenic factors in the induction of pauci-immune small-vessel vasculitis, at least in those patients who have circulating ANCAs, which is the majority.[115,157] We note, however, that there may be other factors involved in in the pathogenesis of a specific pauci-immune vasculitis. For example, it is becoming increasingly evident that B cells and certain T cell subsets contribute to the development of Wegener's granulomatosis.[155] The possibility that anti-endothelial cell antibodies might contribute to the pathogenesis of pauci-immune vasculitis, either in the presence or absence of ANCAs, has been suggested but is not supported by strong clinical and experimental evidence.

Antineutrophil Cytoplasmic Autoantibodies

Approximately 80% of patients with active, untreated pauci-immune small-vessel vasculitis have circulating ANCAs.[63,64,115,157] ANCAs are specific for proteins in the primary granules of neutrophils and the peroxidase-positive lysosomes of monocytes. In patients with vasculitis or glomerulonephritis, almost all ANCAs are specific for myeloperoxidase (MPO-ANCAs) or proteinase-3 (PR3-ANCAs). Only rare patients have both MPO-ANCAs and PR3-ANCAs.

The preferred method for clinical laboratory detection of ANCAs is enzyme-linked immunosorbent assay (ELISA) using purified MPO and PR3 as target antigen substrate; however, indirect immunofluorescence microscopy assays using normal human neutrophils as substrate often are used as a screening tool.[83,129] When normal, alcohol-fixed neutrophils are used as the substrate, PR3-ANCAs produce a cytoplasmic staining pattern that is referred to as a positive C-ANCA result, whereas MPO-ANCAs produce staining at the periphery of the nucleus (i.e., perinuclear staining) that is referred to as a positive P-ANCA result (Figure 83.10). In vivo, PR3 and MPO are in the same cytoplasmic location in neutrophil primary granules but, in alcohol-fixed neutrophils, the MPO has been solubilized during the substrate preparation and artifactually redistributes to the surface of the nucleus.[17] If a fixative is used for neutrophil preparation that immobilizes proteins by covalent cross linking, such as formalin, PR3-ANCAs and MPO-ANCAs produce an identical staining of the cytoplasm of the neutrophils.

Each of the clinicopathologic phenotypes of pauci-immune small-vessel vasculitis can be associated with PR3-ANCAs (C-ANCAs) or MPO-ANCAs (P-ANCAs), although there are differences in the frequency of these specificities in the different phenotypes (Table 83.4). MPO-ANCAs are most frequent in patients with renal limited disease and PR3-ANCAs are most frequent in Wegener granulomatosis. Microscopic polyangiitis does not have a clear dominance of one antigen specificity over the other. It is important to note that not all patients with pauci-immune small-vessel vasculitis have ANCAs. Patients with ANCA-negative pauci-immune small-vessel vasculitis have disease that is clinically and pathologically identical to the disease in ANCA-positive patients.[33] As discussed in subsequent sections, ANCAs are strongly implicated in the pathogenesis of ANCA-positive small-vessel vasculitis.[115,157] The pathogenesis of ANCA-negative small-vessel vasculitis is unknown. One possibility is that these patients have an autoantibody that can activate neutrophils in the same way as MPO-ANCAs and PR3-ANCAs but this autoantibody is not detected in the current ELISA or indirect immunofluorescence assays.

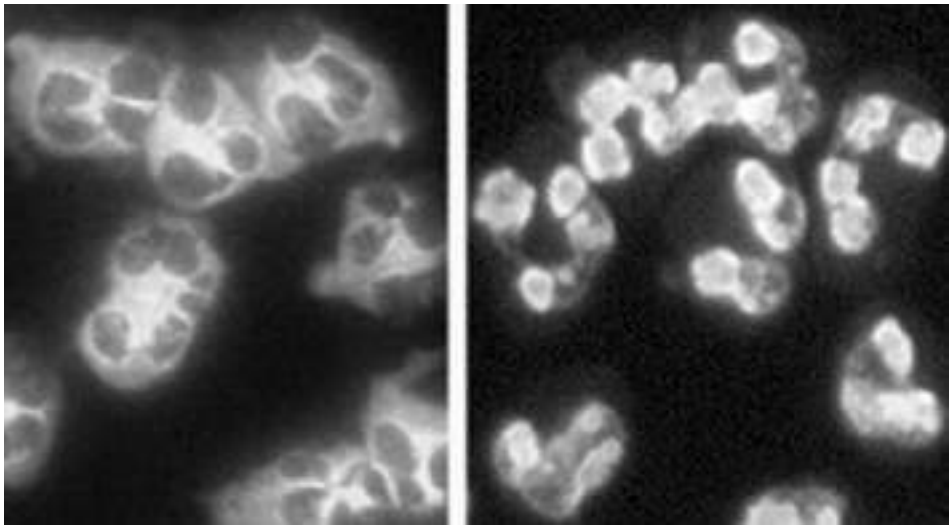

FIGURE 83.10 Immunofluorescence microscopy of alcohol-fixed normal human neutrophils that have been reacted with human PR3–antineutrophil cytoplasmic autoantibody (ANCA) (left) or MPO-ANCA (right) and secondarily stained with fluoresceinated antihuman immunoglobulin G (IgG) resulting in cytoplasmic staining (C-ANCA pattern) or perinuclear staining (P-ANCA pattern), respectively.

TABLE 83.4 Approximate Frequency of ANCA with Specificity for PR3-ANCA or MPO-ANCA in Patients with Active Untreated Renal-Limited Pauci-Immune Crescentic Glomerulonephritis, Microscopic Polyangiitis, Wegener's Granulomatosis, and Churg-Strauss Syndrome

	Renal-Limited Pauci-Immune Crescentic Glomerulonephritis, %	Microscopic Polyangiitis, %	Wegener's Granulomatosis, %	Churg-Strauss Syndrome, %*
PR_3-ANCA	20	40	75	5
MPO-ANCA	70	50	20	40
Negative	10	10	5	55

*75% of Churg Strauss syndrome patients with glomerulnephritis are ANCA positive.
ANCA, antineutrophil cytoplasmic autoantibody; MPO, Myeloperoxidase; PR3, proteinase-3.

Clinical Evidence for the Pathogenicity of ANCA

The high frequency of ANCAs in patients with pauci-immune small-vessel vasculitis raises the possibility that ANCAs are involved in the pathogenesis of this distinctive category of vasculitis. However, this association could be secondary to the vasculitis rather than the cause of the vasculitis. ANCA titer correlate to a degree with the course of ANCA vasculitis and glomerulonephritis,[115] however, this is not a tight correlation. Better clinical evidence for a pathogenic role for ANCAs is the concurrent induction of both MPO-ANCAs and pauci-immune crescentic glomerulonephritis by certain drugs, such as propylthiouracil and hydralazine.[30,93] ANCAs disappear after discontinuation of the drug and the glomerulonephritis remits. More compelling clinical evidence that ANCAs mediated small-vessel vasculitis and glomerulonephritis is the observation that a neonate developed signs and symptoms of glomerulonephritis and pulmonary capillaritis secondary to maternal transfer of MPO-ANCA IgG.[7,131] However, no confirmatory cases of transplacental transmission of disease have been reported. The in vitro and in vivo experimental data discussed in the subsequent sections substantiate the pathogenicity of ANCA IgG and shed light on the mechanisms of injury that are incited by ANCA.

In Vitro Evidence for the Pathogenicity of ANCA

Numerous in vitro studies have demonstrated that both PR3-ANCA and MPO-ANCA IgG can activate neutrophils and monocytes to release mediators of

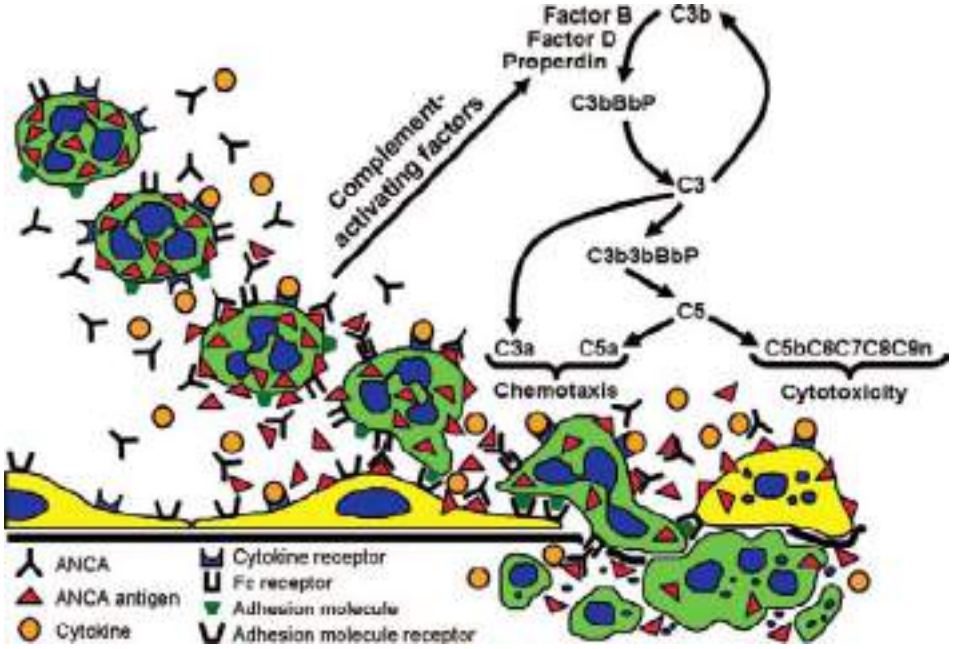

FIGURE 83.11 Diagram depicting induction of vasculitis by antineutrophil cytoplasmic autoantibody (ANCA) immunoglobulin G (IgG). Beginning in the upper left, priming of neutrophils by cytokines results in the expression of ANCA antigens at the cell surface. Neutrophils are activated by both Fc and Fab'2 binding. Activated neutrophils release factors that activate the alternative complement pathway, which amplifies the inflammatory events through further neutrophil recruitment and activation. Activated neutrophils adhere to and destroy endothelial cells and other components of the vessel wall and perivascular tissue. *(From Xiao H, Schreiber A, Heeringa P, Falk RJ, Jennette JC. Alternative complement pathway in the pathogenesis of disease mediated by antineutrophil cytoplasmic autoantibodies. Am J Pathol 2007; 170:52–64 with permission.)*

acute inflammation and injury that are capable of killing endothelial cells (Figure 83.11).[57,65,66,115,127]

One issue to clarify is how antigens that are in cytoplasmic granules can interact with autoantibodies that are in the plasma and interstitial fluid. Although most MPO and PR3 are in the cytoplasm of neutrophils, there appears to be a minor amount of antigen on the surface of circulating neutrophils, although this is controversial, in part because it is difficult to measure surface expression of these antigens without perturbing the cells, which could stimulate them to release the antigens at the surface of the cells. The percentage of circulating cells that have ANCA antigens on their surface may be genetically determined and may be a risk factor for developing ANCA vasculitis.[132,133] There may be a link between increased membrane PR3 expression on neutrophils and expression of CD177 (NB1 glycoprotein).[1] Patients with ANCA disease have epigenetically regulated increased transcription of PR3 and MPO genes in circulating neutrophils, which could result in more ANCA target antigens (MPO and PR_3) available to stimulate the ANCA autoimmune response and more autoantigens available for pathogenic interaction with neutrophils.[19]

In addition to constitutive expression, there is no doubt that circulating neutrophils express more ANCA antigens at their surfaces when they are primed by a variety of proinflammatory factors. These include cytokines, such as tumor necrosis factor alpha (TNFα), and microbial products, such as bacterial formyl peptides. Enhanced expression of small amounts of ANCA-antigens at the surface of neutrophils can be documented in vitro by flow cytometry and by immuno-electron microscopy.[13,34] Thus, viral and bacterial infections could prime circulating neutrophils to interact with ANCAs. Of interest with respect to a possible synergistic role for infections is the observation that the clinical onset and exacerbations of ANCA vasculitis and glomerulonephritis often occur shortly after flulike illnesses.[37]

When neutrophils that have been primed with TNF-α are incubated with ANCA IgG, they are stimulated to release toxic reactive oxygen species and lytic granule enzymes.[13,34] The resultant activation of neutrophils is mediated by both Fc receptor dependent events[78,90] and Fab'2-mediated events.[71,156,160] An essential step in this process is the binding of ANCA IgG to ANCA antigens. Thus, in essence, the neutrophil activation is the result of immune complex formation in the microenvironment of the neutrophil. However, the overall nature of the process by which the ANCA reaction with ANCA antigens results in

neutrophil activation is different from conventional immune complex-mediated disease. This difference is reflected in the paucity of vessel wall accumulation of immune complexes in ANCA vasculitis compared with the overt accumulation of immune complexes in vessel walls in typical immune complex vasculitis. Nevertheless, small amounts of immune complexes probably form in the microenvironment at sites of ANCA-induced inflammation and may contribute to the induction of inflammation. MPO and PR3 are cationic proteins that bind to cells and matrix at sites of neutrophil degranulation. In vitro studies have demonstrated that MPO and PR3 can bind to cultured endothelial cells and that the bound antigens can subsequently bind to MPO-ANCA and PR3-ANCA, respectively.[127]

When neutrophils are activated by ANCA IgG in the presence of endothelial monolayers, the endothelial cells are killed.[36,128] This cytotoxicity can be inhibited with antibodies to β2 integrins,[35] which indicates that close approximation of the activated neutrophils to endothelial cells is required for killing. A role for adhesion molecules in ANCA vasculitis also is supported by the observation that exposure of neutrophils to ANCA IgG causes integrin (CD11a/CD18, CD11b/CD18) and cytokine receptor (CXCR2)- mediated adherence to cultured endothelial cells and endothelial transmigration in an in vitro flow-based adhesion assay.[12,112,113] Stimulation of neutrophils with ANCA IgG causes a conformational change in β2 integrins that enhances ligand binding.[12] Evaluation of renal biopsy specimens from patients with pauci-immune crescentic glomerulonephritis demonstrates upregulation of adhesion molecules in support of their role in leukocyte recruitment. For example, ICAM-1 (CD54), which is the ligand for the β2 integrin CD11a/CD18 (LFA-1), and VCAM-1 (CD106), which is the ligand for the β1 integrin CD49d/CD29 (VLA-4), are upregulated in cellular crescents with increased mRNA and protein.[92] ICAM-1 is expressed to a greater degree than VCAM-1 in glomerular endothelial cells. Thus, ICAM-1 may be more important for initial leukocyte recruitment into glomerular tufts whereas VCAM-1 may be more important for further migration into crescents after capillary wall transmigration.

Monocytes and neutrophils contain MPO and PR3, although these proteins are lost as monocytes transform into macrophages.[17] In vitro studies have demonstrated that ANCA IgG can activate monocytes as well as neutrophils. For example, incubation of monocytes with ANCA IgG induces release of toxic oxygen radicals,[153] monocyte chemoattractant protein-1,[14] and interleukin-8.[114] Thus activation by ANCA IgG could cause activation of both neutrophils and monocytes, which is consistent with the observation that neutrophils and monocytes are the most prevalent leukocytes at sites of acute glomerular injury in ANCA glomerulonephritis.[152] In fact, monocytes/macrophages typically are more conspicuous than neutrophils. However, this could be misleading with respect to the relative importance of these cell types in pathogenesis, because neutrophils are consumed as they cause injury, whereas monocytes transform into macrophages and persist at the site of injury.

In summary, numerous in vitro studies demonstrate that ANCA IgG can activate neutrophils and monocytes and cause them to release toxic products and mediators of inflammation. If this happens in vivo, ANCA IgG could cause vasculitis in humans and in an animal model. As noted earlier, there is clinical evidence to support this.[7,65,131] The following section will describe animal models that also support the pathogenicity of ANCA IgG.[66]

Animal Models of ANCA Glomerulonephritis and Vasculitis

One convincing animal model of ANCA glomerulonephritis and vasculitis uses MPO knockout mice ($MPO^{-/-}$) as a source for pathogenic anti-MPO antibodies and anti-MPO lymphocytes.[66,162,163] To induce this model, $MPO^{-/-}$ mice are immunized with purified mouse MPO. As expected, the $MPO^{-/-}$ mice develop a robust immune response to the mouse MPO because they recognize MPO as a foreign antigen. To induce disease, this anti-MPO reactivity is transferred to mice that do have MPO ($MPO^{+/+}$ mice) in their circulating neutrophils and monocytes. Two different strategies have been used that produce different expressions of disease. One approach involves transfer of anti-MPO lymphocytes and the other transfer of anti-MPO immunoglobulin alone. The lymphocyte transfer model requires that the recipient mice are immune deficient because transfer of autoreactive anti-MPO lymphocytes into immune-competent mice results in a rapid downregulation of the anti-MPO immune response. Transfer of anti-MPO immunoglobulin can be into immune-competent wild type mice or immune-deficient $Rag2^{-/-}$ mice. Both methods of transfer of anti-MPO reactivity into mice with MPO in their circulating neutrophils results in necrotizing and crescentic glomerulonephritis in virtually 100% of recipient mice that receive adequate anti-MPO doses. Some, but not all mice, develop systemic small-vessel vasculitis, including necrotizing arteritis (Figure 83.12) and pulmonary alveolar capillaritis. The disease is relatively mild, with less than 25% of glomeruli involved by necrosis and crescents 6 days after injection of the pathogenic autoantibody. The anti-MPO lymphocyte transfer model causes much

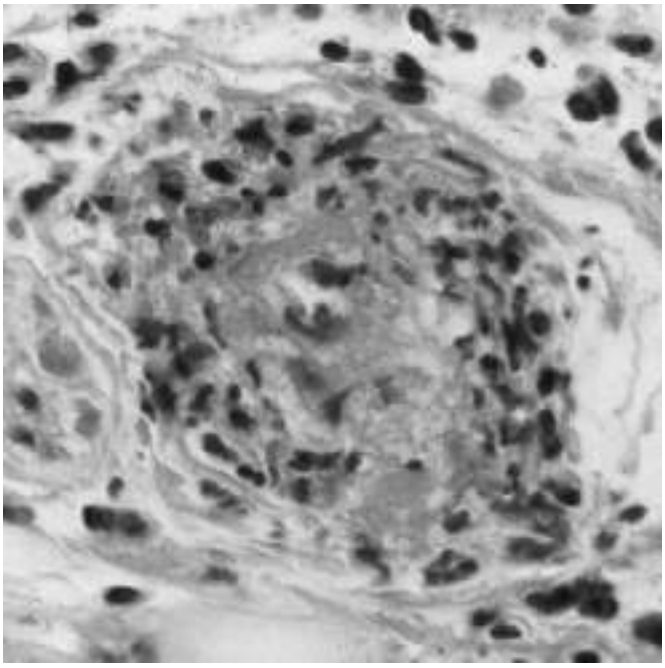

FIGURE 83.12 Necrotizing arteritis in a small artery in the ear of a mouse that received anti-myeloperoxidase IgG. There is a central are of fibrinoid necrosis surrounded by infiltrating leukocytes including neutrophils with leukocytoclasia.

more severe disease with approximately 90% of glomeruli with fibrinoid necrosis and crescents 13 days after lymphocyte transfer. However, the transfer of immune-competent lymphocytes into immune-deficient recipients results in a background of mild to moderate immune complex deposits in glomeruli and thus is not pauci-immune, whereas the transfer of anti-MPO IgG alone causes glomerular necrosis and crescents in the absence of significant glomerular immunoglobulin deposits and thus more closely mimics human pauci-immune ANCA glomerulonephritis.[162]

Induction of ANCA Disease in Mice by Injection of Anti-MPO Lymphocytes

For the lymphocyte transfer experiments, donor $MPO^{-/-}$mice were immunized intraperitoneally with purified murine MPO or bovine serum albumin (BSA) in complete Freund adjuvant.[162] $Rag2^{-/-}$ mice that lack both B-cell and T-cell antigen receptors were used as permissive recipients of the transferred immune-competent lymphocytes. $Rag2^{-/-}$ mice that were injected intravenously with 1×108 or 5×107 anti-MPO splenocytes developed renal insufficiency whereas those that received 1×107 anti-MPO splenocytes, anti-BSA splenocytes, or control splenocytes did not. Postmortem examination of the mice 13 days after the splenocyte transfer revealed glomerular crescents in all mice that received 1×108 or 5×107 anti-MPO splenocytes. $Rag2^{-/-}$ mice that received 1×107 anti-MPO splenocytes, anti-BSA splenocytes, or control splenocytes developed no glomerular crescents or necrosis. In addition to glomerulonephritis, some but not all mice that received 1×108 or 5×107 anti-MPO splenocytes developed hemorrhagic pulmonary capillaritis, necrotizing granulomatous inflammation, and necrotizing arteritis in multiple organs, including lungs, spleen, lymph nodes, and skin. None of the control mice developed vasculitis. Thus, not only does the splenocytes transfer model have crescentic glomerulonephritis as in human ANCA-disease, but also small-vessel vasculitis.

The problematic finding was that all $Rag2^{-/-}$ mice that received the higher doses of splenocytes of any type developed mild to moderate glomerular immune deposits. It appears that the transfer of a competent immune system into immune-deficient $Rag2^{-/-}$ mice caused mild immune complex glomerulonephritis. However, severe necrotizing and crescentic glomerulonephritis develops only after adoptive transfer of anti-MPO splenocytes and not after transfer of anti-BSA or control splenocytes. This observation supports the hypothesis that proinflammatory stimuli augment the induction of glomerulonephritis and vasculitis by increasing the availability of target antigens (e.g., MPO) at the surface of neutrophils. In this instance, the mild to moderate vascular immune complex localization could have acted as the synergistic factor that primed neutrophils to be activated by the anti-MPO antibodies, because, as described later, transfer of anti-MPO IgG alone, which is not accompanied by glomerular immune deposits, causes much less severe glomerulonephritis.

What about anti-MPO T lymphocytes? Are they pathogenic in the absence of anti-MPO antibodies or are they synergistic with factors that augment the injury induced by anti-MPO IgG? The preliminary observations in our experimental model of ANCA disease indicate that anti-MPO T lymphocytes do not play a major role in the pathogenesis of the vascular inflammation.[61] To investigate the respective roles of T cells and B cells, splenocyte preparations with different proportions of anti-MPO T cells and B cells were transferred into $Rag2^{-/-}$ mice. The three different preparations were (1) unfractionated splenocytes (25% T cells, 62% B cells); (2) enriched T cells (79% T cells, 9% B cells); and (3) highly purified T cells ($>$99% T cells). The T-cell enrichment was attained by depletion of B cells by adherence to plastic coated with polyvalent antimouse immunoglobulin antibodies and depletion of monocytes by adherence to nylon columns. The purified T cells were obtained by negative cell sorting using anti-CD19 and anti-MHC class II to selectively exclude remaining B cells and monocytes respectively.

Suspensions of 5×107 cells with the three different proportions of T cells and B cells were administered intravenously to groups of Rag $2^{-/-}$ mice, which lack functional T and B cells of their own. Successful transfer of T lymphocytes with anti-MPO reactivity was confirmed by interferon gamma enzyme-linked immunosorbent spot (ELISpot) assay. Mice that received purified T cells had no detectable anti-MPO antibodies by ELISA whereas the other two groups did. Urine analysis after 12 days showed severe renal disease in mice that received unfractionated splenocytes, mild disease in mice that received preparations enriched for T cells, and no urinary abnormalities in mice that received purified T cells. Pathologic evaluation of kidneys after 13 days demonstrated that administration of unfractionated splenocytes induced crescents and necrosis in approximately 80% of glomeruli whereas splenocytes that had been enriched for T cells caused necrosis and crescents in approximately 5% of glomeruli and pure T cells caused no crescents or necrosis. These data indicate that anti-MPO T cells alone from mice immunized with MPO cannot cause glomerulonephritis in this animal model. This indicates that the B cells in the transferred splenocytes are the critical cell type because they give rise to the ANCA antibody response.

Induction of ANCA Disease in Mice by Injection of Anti-MPO IgG

In contrast to anti-MPO T cells alone, intravenous passive transfer of anti-MPO IgG alone causes pauci-immune crescentic glomerulonephritis and small-vessel vasculitis in either $Rag2^{-/-}$ mice that have no functioning T or B cells of their own, or in immune-competent wild type B6 mice.[162,163] The disease in these mice is pathologically identical to ANCA-associated pauci-immune crescentic glomerulonephritis and vasculitis in humans. All mice (100%) that received adequate doses of anti-MPO IgG developed focal segmental fibrinoid necrosis and crescents in glomeruli whereas no mice that receive control anti-BSA IgG developed glomerular lesions. Immunofluorescence microscopy demonstrates a paucity of immunoglobulin and complement in the glomeruli of mice with anti-MPO IgG induced glomerulonephritis, thus mimicking the pauci-immune feature of human ANCA glomerulonephritis.

Immunoenzyme microscopy of renal tissue for the distribution of neutrophils, macrophages and T lymphocytes demonstrated that induction of glomerulonephritis by injection of anti-MPO IgG is accompanied by glomerular influx of neutrophils and macrophages.[163] Neutrophils were concentrated at sites of segmental necrotizing glomerular injury, and also were identified in Bowman's space in glomeruli with necrosis or crescents. Macrophages were most numerous in crescents. T lymphocytes were not increased in the acute glomerular lesions.

To confirm the importance of neutrophils in the pathogenesis of the glomerulonephritis in this model, NIMP-R14 rat monoclonal antibody that is known to selectively deplete mouse neutrophils in vivo was used.[163] Within one day after a single injection of NIMP-R14 antibody into B6 mice, the number of circulating neutrophils was reduced from 14% of white blood cells to 1%, and remained at this low level for up to five days. This depletion of neutrophils completely protected mice from the development of glomerulonephritis after injection of anti-MPO IgG, which confirms a major pathogenic role for neutrophils.

As noted earlier, in vitro experimental data indicate that ANCAs are more effective at activating neutrophils if the neutrophils have been primed by proinflammatory stimuli. To test this hypothesis in the mouse model of anti-MPO IgG-induced glomerulonephritis, bacterial lipopolysaccharide (LPS) was injected into mice that received anti-MPO.[52] The LPS caused a dose-dependent increase in glomerular necrosis and crescents and increased neutrophil accumulation in glomeruli. The LPS induced increased circulating levels of TNF-α, and treatment with antibodies to TNF-α reversed the enhancement of anti-MPO IgG-induced glomerulonephritis by LPS. These observations suggest that LPS stimulates increased levels of TNF-α that in turn primes neutrophils to interact more effectively with the anti-MPO IgG to induce glomerulonephritis.

Activation of human neutrophils by human ANCA in vitro involves the engagement of Fcγ immunoglobulin receptors (FcγR) on the surface of neutrophils by ANCA IgG after binding to ANCA antigens on the surface of neutrophils.[58,78,90,126] FcγR engagement appears to be more dominant but ANCA Fab'2 binding to ANCA antigens also is important in the activation of neutrophils.[71,156] To evaluate the importance of FcγR in the mouse model of ANCA disease, mice with the absence of certain FcγRs were injected with nephritogenic doses anti-MPO IgG to assess any changes in the induction of glomerulonephritis and vasculitis compared to wild type mice. Preliminary data indicate that mice with an absence of FcγRI and FcγRIII develop no glomerulonephritis.[164] FcγRI$^{-/-}$ mice have reduced incidence of glomerulonephritis with a lower percentage of crescents. FcγRIII$^{-/-}$ mice have little or no reduction in glomerulonephritis. Thus, the preliminary results indicate that the engagement of FcγRI seems to be most important in this model.

In mice, the engagement of FcγR1 and FcγRIII enhances inflammatory and immune events whereas

engagement of FcγRIIb inhibits inflammatory and immune events. Thus FcγRII$^{-/-}$ mice would be hypothesized to have more severe disease in the absence of this anti-inflammatory pathway. Interestingly, when injected with anti-MPO IgG, FcγRIIb$^{-/-}$ mice developed less severe glomerulonephritis than wild type mice, however, they had a higher incidence and greater severity of pulmonary vasculitis.[164] In addition, many of the mice had not only pulmonary capillaritis but also pulmonary necrotizing granulomatous inflammation that closely resembled the necrotizing granulomatous inflammation of patients with Wegener granulomatosis. This observation raises the possibility that the pathophysiologic basis for different clinicopathologic phenotypes of disease in patients (e.g., microscopic polyangiitis versus Wegener granulomatosis) may be dictated by differences in the innate inflammatory response of the patients rather than by differences in the ANCA antibodies or antigens (e.g., different antibody classes or antigen epitope specificity).

Studies in mice with disease induced by not only anti-MPO IgG but also anti-MPO splenocyte transfer, have demonstrated an important role for complement activation.[53,134,165] Anti-MPO IgG induced glomerulonephritis in mice is completely blocked by complement depletion with cobra venom factor.[30] After injection of nephritogenic anti-MPO IgG, C4$^{-/-}$ mice, which have no classic or lectin pathway complement function but normal alternative pathway activity, developed disease comparable to wild type disease; however, C5$^{-/-}$ and factor B$^{-/-}$ mice, which have no alternative pathway function, developed no disease.[165] In vitro, IgG isolated from patients with MPO-ANCA or PR3-ANCA incubated with normal human neutrophils primed with TNF-alpha caused the release of factors that activated complement in serum with generation of C3a.[134,165] In vitro experiments using human material also have shown that neutrophils incubated with ANCA IgG release factors that activate complement, which in turn primes neutrophils for further activation by ANCA.[134] These in vitro event depend on generation of C5a and engagement of C5a receptors on neutrophils.[53,134] Blockade of C5 or C5a ameliorates disease induction in the mouse model, suggesting possible novel therapies in patients.

In summary, this mouse model of ANCA disease that is induced by mouse anti-MPO strongly supports a pathogenic role of ANCA IgG. The experimental animal data also suggest that the induction of disease by ANCA IgG is facilitated and modified by synergistic proinflammatory events, such as cytokine priming of neutrophils, is modulated by engagement of leukocyte Fcγ receptors, and requires amplification of the inflammation by activation of the alternative complement system.[65]

Induction of ANCA Disease in Rats Immunized with Human MPO

Little and associates have induced glomerulonephritis and vasculitis (pulmonary capillaritis) in Wistar-Kyoto rats by immunizing with human MPO resulting in the development of anti-MPO antibodies that cross react with human and rat MPO.[84] Focal segmental pauci-immune glomerulonephritis with crescents developed in 61% of rats and focal pulmonary capillaritis in 41%.

The interaction of leukocytes with the walls of small vessels was directly observed in this model using intravital microscopy of mesenteric vessels. Changes in leukocyte rolling, adherence and transmigration were monitored after application to the mesentery of recombinant CXCL-1, which is a homologue of human interleukin-8, in rats with anti-MPO compared to control rats immunized with human serum albumin. Application of the CXCL-1 to rats with circulating anti-MPO resulted in increased firm adherence and transmigration of leukocytes. This effect could be transferred to unimmunized rats by injection of IgG isolated from the rats that had been immunized with MPO. Induction of circulating anti-MPO by either active immunization or passive transfer also resulted in focal areas of hemorrhage in the mesenteric microvasculature at sites of CXCL-1 application. This animal model provides strong evidence that ANCA IgG can activate leukocytes (presumably neutrophils and monocytes) and induce them to adhere to vessel walls and cause vessel wall injury.

Kain et al.[67] patients with MPO-ANCA and PR3-ANCA have autoantibodies to another neutrophil protein, lysosome-associated membrane protein 2 (LAMP2).[67] LAMP-2 has homology with is a bacterial adhesin FimH. Immunization of rats with FimH induces circulating anti-FimH antibodies that crossreact with LAMP-2, and induces a pauci-immune glomerulonephritis and small vessel vasculitis. The authors postulate that infection of humans by fimbriated bacteria bearing FimH induces an immune response that cross-reacts with LAMP-2 resulting in the mediation of pauci-immune necrotizing glomerulonephritis and vasculitis. To date, no confirmatory reports have been published. Our research group has been unable to reproduce the serologic finding of anti-LAMP-2 antibodies in ANCA patients or the induction of disease in rats by immunization with FimH or LAMP-2.[122]

Immunogenesis of the ANCA Autoimmunity

Clinical and experimental animal data indicate that ANCAs are the major pathogenic factors in ANCA

small-vessel vasculitis. The origin of the ANCA autoimmune response is less clear. Factors that might lead to the ANCA autoimmune response include environmental stimuli (e.g., silica, drugs, and microbial pathogens), dysregulation of granule protein gene expression, autoantigen mimicry, aberrant T cell regulation and immune responses to antisense (complementary) autoantigen peptides.[65] As noted above, autoantigen mimicry by an infectious pathogen is one consideration.

Intriguing observations raise the possibility of a role for peptides that are mimics of not the sense but rather the antisense complementary peptides of the autoantigen, i.e., complementary peptides of PR3 and MPO.[106] Some patients with PR3-ANCA glomerulonephritis and small-vessel vasculitis have not only antibodies to the autoantigen (PR3) but also antibodies to a peptide translated from the antisense DNA strand of PR3 (complementary PR3) or to a mimic of this peptide. Immunization of mice with a complementary PR3 peptide resulted in production of antibodies not only against the complementary PR3 but also against PR3. Both mouse anti-PR3 and anticomplementary PR3, and human anti-PR3 (PR3-ANCA) and anticomplementary PR3 bound to each other, indicating that the anti-PR3 and anticomplementary PR3 have an idiotypic and anti-idiotypic relationship. These findings support the hypothesis that the anti-PR3 autoimmune response could be initiated through an immune response against a peptide that is antisense or complementary to the autoantigen, which in turn induces anti-idiotypic antibodies (autoantibodies) that cross-react with the autoantigen (Figure 83.13). The antisense peptide could arise endogenously by translation of the antisense DNA strand of PR3, or a mimic of this complementary peptide could be introduced into the body as a constituent of an infection microorganism.

Staphylococcus aureus contains a protein that has a sequence that mimics the antisense sequence of PR3. Approximately two thirds of patients with Wegener's granulomatosis have chronic nasal infection with *S. aureus*, and this carriage of *S. aureus* is a risk factor for relapses and prophylactic treatment with antibiotics that eliminate staphylococcal nasal carriage reduces the frequency of relapse.[106] According to the theory proposed by Pendergraft, an antibody response to the S. aureus peptide that mimics a complementary PR3 peptide could result in an anti-idiotypic immune response that cross reacts with the anticomplementary PR3 antibody and with PR3, with the latter being PR3-ANCA. Also in support of this theory that microbial peptide that mimic the complementary peptide of PR3 can induce PR3-ANCA is the association between PR3-ANCA and infection with Ross River virus[138] and *Entamoeba histolytica*.[27] Both of these infectious pathogens contain proteins with amino acid sequences that mimic complementary peptides of PR3.[84]

In summary, one theoretic concept that is supported by substantial clinical and experimental data is that the ANCA autoimmune response is initiated by an appropriate immune response to an antigen introduced into the body by an infectious pathogen. This immune response elicits an anti-idiotypic immune response that includes antibodies that have the capability of cross reacting with self proteins (PR3 or MPO) that have antisense sequences that would produce peptides that

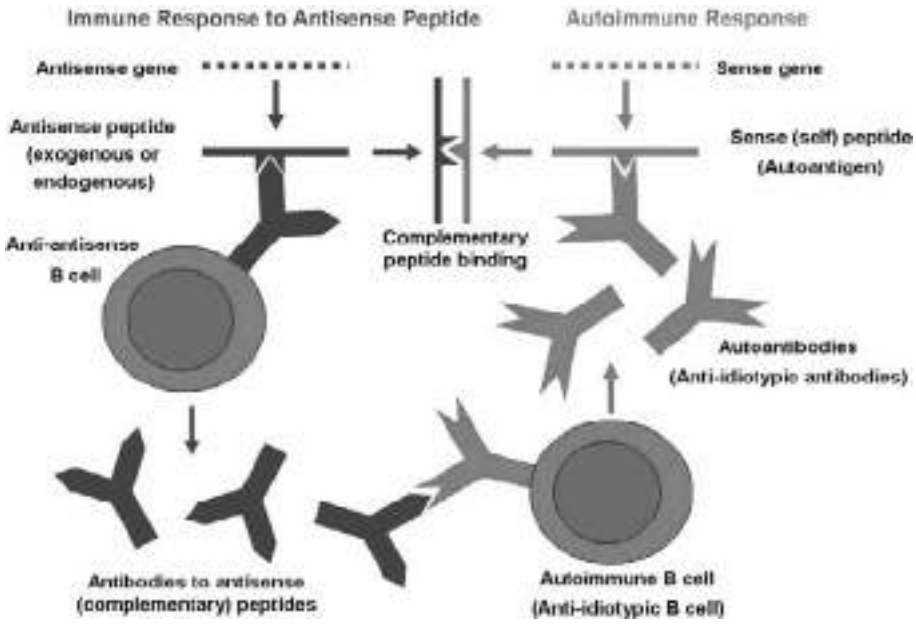

FIGURE 83.13 According to the theory of autoantigen complementarity, an autoimmune response can be initiated by an immune response to an antigen that is either the endogenous product of the antisense strand of the gene for the autoantigen or is an exogenous peptide that mimics this antisense product, possibly derived from an infectious pathogen. This immune response elicits an anti-idiotypic immune response that includes antibodies that have the ability to cross-react with the autoantigen and thus function as autoantibodies.

mimic the microbial peptide that initiated the immune response. These antibodies that cross react with PR3 or MPO are PR3-ANCA or MPO-ANCA respectively. Once in the circulation, these autoantibodies are able to activate neutrophils and monocytes, possibly with synergistic priming from concurrent infections or other processes that result in high levels of circulating cytokines that prime neutrophils and monocytes causing them to express ANCA antigens at the cell surfaces. Activation of neutrophils and monocytes by ANCA IgG causes the cells to adhere to endothelial cells in small vessels and to release inflammatory mediators and destructive products such as oxygen radicals and numerous toxic and lytic enzymes. This results in acute inflammation and necrosis in vessel walls.

References

[1] Abdgawad M, Gunnarsson L, Bengtsson AA, et al. Elevated neutrophil membrane expression of proteinase 3 is dependent upon CD177 expression. Clin Exp Immunol 2010;161:89–97.

[2] Albelda SM, Muller WA, Buck CA, Newman PJ. Molecular and cellular properties of PECAM-1 (endoCAM/CD31): a novel vascular cell-cell adhesion molecule. J Cell Biol 1991;114:1059–68.

[3] Allen AC, Willis FR, Beattie TJ, Feehally J. Abnormal IgA glycosylation in Henoch-Schonlein purpura restricted to patients with clinical nephritis. Nephrol Dial Transplant 1998;13:930–4.

[4] Arthus M. Injections repetees deserum de cheval chez le lapin. V R Soc Biol 1903;55:817–20.

[5] Bajema IM, Hagen EC, de Heer E, van der Woude FJ, Bruijn JA. Colocalization of ANCA-antigens and fibrinoid necrosis in ANCA-associated vasculitis. Kidney Int 2001;60:2025–30.

[6] Baldree LA, Wyatt RJ, Julian BA, Falk RJ, Jennette JC. Immunoglobulin A-fibronectin aggregate levels in children and adults with immunoglobulin A nephropathy. Am J Kidney Dis 1993;22:1–4.

[7] Bansal PJ, Tobin MC. Neonatal microscopic polyangiitis secondary to transfer of maternal myeloperoxidase-antineutrophil cytoplasmic antibody resulting in neonatal pulmonary hemorrhage and renal involvement. Ann Allergy Asthma Immunol 2004;93:398–401.

[8] Barratt J, Feehally J. IgA nephropathy. J Am Soc Nephrol 2005;16:2088–97.

[9] Baumann U, Kohl J, Tschernig T, Schwerter-Strumpf K, Verbeek JS, Schmidt RE, et al. A codominant role of Fc gamma RI/III and C5aR in the reverse Arthus reaction. J Immunol 2000;164:1065–70.

[10] Beddhu S, Bastacky S, Johnson JP. The clinical and morphologic spectrum of renal cryoglobulinemia. Medicine (Baltimore) 2002;81:398–409.

[11] Bevilacqua MP, Pober JS, Mendrick DL, Cotran RS, Gimbrone Jr. MA. Identification of an inducible endothelial-leukocyte adhesion molecule. Proc Natl Acad Sci U S A 1987;84:9238–42.

[12] Calderwood JW, Williams JM, Morgan MD, Nash GB, Savage CO. ANCA induces beta2 integrin and CXC chemokine-dependent neutrophil-endothelial cell interactions that mimic those of highly cytokine-activated endothelium. J Leukoc Biol 2005;77:33–43.

[13] Carlow DA, Gossens K, Naus S, Veerman KM, Seo W, Ziltener HJ. Psgl-1 function in immunity and steady state homeostasis. Immunol Rev 2009;230:75–96.

[14] Casselman BL, Kilgore KS, Miller BF, Warren JS. Antibodies to neutrophil cytoplasmic antigens induce monocyte chemoattractant protein-1 secretion from human monocytes. J Lab Clin Med 1995;126:495–502.

[15] Charles ED, Dustin LB. Hepatitis C virus-induced cryoglobulinemia. Kidney Intern 2009;76:818–24.

[16] Charles LA, Caldas MLR, Falk RJ, Terrell RS, Jennette JC. Antibodies against granule proteins activate neutrophils in vitro. J Leuk Biol 1991;50:539–46.

[17] Charles LA, Falk RJ, Jennette JC. Reactivity of anti-neutrophil cytoplasmic autoantibodies with HL-60 cells. Clin Immunol Immunopath 1989;53:243–53.

[18] Charles LA, Falk RJ, Jennette JC. Reactivity of anti-neutrophil cytoplasmic autoantibodies with mononuclear phagocytes. J Leuk Biol 1992;51:65–8.

[19] Ciavatta DJ, Yang J, Preston GA, et al. Epigenetic basis for aberrant upregulation of autoantigen genes in humans with ANCA vasculitis. J Clin Invest 2010;120:3209–19.

[20] Claudy A. Pathogenesis of leukocytoclastic vasculitis. Eur J Dermatol 1998;8:75–9.

[21] Cochrane CG, Weigle WO, Dixon FJ. The role of polymorphonuclear leukocytes in the initiation and cessation of the Arthus vasculitis. J Exp Med 1959;110:481–94.

[22] Cook-Mills JM, Deem TL. Active participation of endothelial cells in inflammation. J Leukoc Biol 2005;77:487–95.

[23] Coppo R, Chiesa M, Cirina P, Peruzzi L, Amore A, European IgACE Study Group. In human IgA nephropathy uteroglobin does not play the role inferred from transgenic mice. Am J Kidney Dis 2002;40:495–503.

[24] Coppo R, Cirina P, Amore A, Sinico RA, Radice A, Rollino C. Properties of circulating IgA molecules in Henoch-Schonlein purpura nephritis with focus on neutrophil cytoplasmic antigen IgA binding (IgA-ANCA): new insight into a debated issue. Italian group of renal immunopathology collaborative study on henoch-schonlein purpura in adults and in children. Nephrol Dial Transplant 1997;12:2269–76.

[25] Curry MP, Golden-Mason L, Doherty DG, Deignan T, Norris S, Duffy M, et al. Expansion of innate CD5pos B cells expressing high levels of CD81 in hepatitis C virus infected liver. J Hepatol 2003;38:642–50.

[26] Dangerfield J, Larbi KY, Huang MT, Dewar A, Nourshargh S. PECAM-1 (CD31) homophilic interaction up-regulates alpha6-beta1 on transmigrated neutrophils in vivo and plays a functional role in the ability of alpha6 integrins to mediate leukocyte migration through the perivascular basement membrane. J Exp Med 2002;196:1201–11.

[27] Davies DJ, Moran JE, Niall JF, Ryan GB. Segmental necrotising glomerulonephritis with antineutrophil antibody: possible arbovirus aetiology? Br Med J 1982;285:606.

[28] Davin JC, Malaise M, Foidart J, Mahieu P. Anti-alpha-galactosyl antibodies and immune complexes in children with Henoch-Schonlein purpura or IgA nephropathy. Kidney Int 1987;31:1132–9.

[29] Davin JC, Weening JJ. Diagnosis of Henoch-Schonlein purpura: renal or skin biopsy?. Pediatr Nephrol 2003;18:1201–3.

[30] Dolman KM, Gans RO, Vervaat TJ, et al. Vasculitis and antineutrophil cytoplasmic autoantibodies associated with propylthiouracil therapy. Lancet 1993;342:651–2.

[31] Donovan KL, Davies M, Coles GA, Williams JD. Relative roles of elastase and reactive oxygen species in the degradation of human glomerular basement membrane by intact human neutrophils. Kidney Int 1994;45:1555–61.

[32] Duque N, Gomez-Guerrero C, Egido J. Interaction of IgA with Fc alpha receptors of human mesangial cells activates transcription factor nuclear factor-kappa B and induces expression and

synthesis of monocyte chemoattractant protein-1, IL-8, and IFN-inducible protein 10. J Immunol 1997;159:3474–82.
[33] Eisenberger U, Fakhouri F, Vanhille P, Beaufils H, Mahr A, Guillevin L, et al. ANCA-negative pauci-immune renal vasculitis: histology and outcome. Nephrol Dial Transplant 2005;20: 1392–9.
[34] Esparza J, Vilardell C, Calvo J, et al. Fibronectin upregulates gelatinase B (MMP-9) and induces coordinated expression of gelatinase A (MMP-2) and its activator MT1-MMP (MMP-14) by human T lymphocyte cell lines. A process repressed through RAS/MAP kinase signaling pathways. Blood 1999;94:2754–66.
[35] Ewert BH, Becker ME, Jennette JC, Falk RJ. Antimyeloperoxidase antibodies induce neutrophil adherence to cultured human endothelial cells. Ren Fail 1995;17:125–33.
[36] Ewert BH, Jennette JC, Falk RJ. Anti-myeloperoxidase antibodies stimulate neutrophils to damage human endothelial cells. Kidney Int 1992;41:375–83.
[37] Falk RJ, Hogan S, Carey TS, Jennette JC. The clinical course of patients with antineutrophil cytoplasmic autoantibody associated glomerulonephritis and systemic vasculitis. Ann Intern Med 1990;113:656–63.
[38] Falk RJ, Terrell R, Charles LA, Jennette JC. Anti-neutrophil cytoplasmic autoantibodies induce neutrophils to degranulate and produce oxygen radicals. Proc Nat Acad Sci U S A 1990;87:4115–9.
[39] Ferri C, Sebastiani M, Giuggioli D, Cazzato M, Longombardo G, Antonelli A, et al. Mixed cryoglobulinemia: demographic, clinical, and serologic features and survival in 231 patients. Semin Arthritis Rheum 2004;33:355–74.
[40] Gakidis MA, Cullere X, Olson T, Wilsbacher JL, Zhang B, Moores SL, et al. Vav gefs are required for beta2 integrin-dependent functions of neutrophils. J Cell Biol 2004;166: 273–82.
[41] Germuth Jr FG, Senterfit LB, Pollack AD. Immune complex disease. I. Experimental acute and chronic glomerulonephritis. Johns Hopkins Med J 1967;120:225–51.
[42] Gesualdo L, Grandaliano G, Ranieri E, Monno R, Montinaro V, Manno C, et al. Monocyte recruitment in cryoglobulinemic membranoproliferative glomerulonephritis: a pathogenetic role for monocyte chemotactic peptide-1. Kidney Int 1997;51: 155–63.
[43] Giagulli C, Ottoboni L, Caveggion E, Rossi B, Lowell C, Constantin G, et al. The src family kinases hck and fgr are dispensable for inside-out, chemoattractant-induced signaling regulating beta 2 integrin affinity and valency in neutrophils, but are required for beta 2 integrin-mediated outside-in signaling involved in sustained adhesion. J Immunol 2006;177:604–11.
[44] Gower RG, Sausker WF, Kohler PF, Thorne GE, McIntosh RM. Small vessel vasculitis caused by hepatitis B virus immune complexes. Small vessel vasculitis and HBsAG. J Allergy Clin Immunol 1978;62:222–8.
[45] Gyotoku Y, Abdelmoula M, Spertini F, Izui S, Lambert PH. Cryoglobulinemia induced by monoclonal immunoglobulin G rheumatoid factors derived from autoimmune MRL/MpJ-lpr/lpr mice. J Immunol 1987;138:3785–92.
[46] Han SH. Extrahepatic manifestations of chronic hepatitis B. Clin Liver Dis 2004;8:403–18.
[47] Hayashi K, Horikoshi S, Osada S, Shofuda K, Shirato I, Tomino Y. Macrophage-derived MT1-MMP and increased MMP-2 activity are associated with glomerular damage in crescentic glomerulonephritis. J Pathol 2000;191:299–305.
[48] Hazenbos WL, Gessner JE, Hofhuis FM, Kuipers H, Meyer D, Heijnen IA, et al. Impaired IgG-dependent anaphylaxis and Arthus reaction in Fcgamma RIII (CD16) deficient mice. Immunity 1996;5:181–8.
[49] Hiemstra PS. Novel roles of protease inhibitors in infection and inflammation. Biochem Soc Trans 2002;30:116–20.
[50] Homeister JW, Thall AD, Petryniak B, Maly P, Rogers CE, Smith PL, et al. The alpha (1, 3) fucosyltransferases FucT-IV and FucT-VII exert collaborative control over selectin-dependent leukocyte recruitment and lymphocyte homing. Immunity 2001;15:115–26.
[51] Hopken UE, Lu B, Gerard NP, Gerard C. Impaired inflammatory responses in the reverse arthus reaction through genetic deletion of the C5a receptor. J Exp Med 1997;186:749–56.
[52] Huugen D, Xiao H, van Esch A, Falk RJ, Peutz-Kootstra CJ, Buurman WA, et al. Aggravation of anti-myeloperoxidase antibody-induced glomerulonephritis by bacterial lipopolysaccharide: role of tumor necrosis factor-alpha. Am J Pathol 2005;167: 47–58.
[53] Huugen D, van Esch A, Xiao H, et al. Inhibition of complement factor C5 protects against antimyeloperoxidase antibody-mediated glomerulonephritis in mice. Kidney Int 2007;71: 646–54.
[54] Issekutz AC, Issekutz TB. Quantitation and kinetics of blood monocyte migration to acute inflammatory reactions, and IL-1 alpha, tumor necrosis factor-alpha, and IFN-gamma. J Immunol 1993;151:2105–15.
[55] Izui S, Fulpius T, Reininger L, Pastore Y, Kobayakawa T. Role of neutrophils in murine cryoglobulinemia. Inflamm Res 1998;47(Suppl. 3):S145–50.
[56] Jennette JC, Falk RJ, Andrassy K, et al. Nomenclature of systemic vasculitides. Proposal of an international consensus conference. Arthritis Rheum 1994;37:187–92.
[57] Jennette JC, Falk RJ. Pathogenesis of the vascular and glomerular damage in ANCA-positive vasculitis. Nephrol Dial Transplant 1998;13(Suppl. 1):16–20.
[58] Jennette JC, Falk RJ. Small vessel vasculitis. N Engl J Med 1997;337:1512–23.
[59] Jennette JC, Falk RJ. The pathology of vasculitis involving the kidney. Am J Kidney Dis 1994;24:130–41.
[60] Jennette JC, Wieslander J, Tuttle R, Falk RJ. Serum IgA-fibronectin aggregates in patients with IgA nephropathy and Henoch-Schonlein purpura: diagnostic value and pathogenic implications. The glomerular disease collaborative network. Am J Kidney Dis 1991;18:466–71.
[61] Jennette JC, Xiao H, Heeringa P, Hu P, Liu Z, Falk RJ. Adoptive transfer of T lymphocytes alone from MPO knockout mice immunized with MPO can not induce necrotizing and crescentic glomerulonephritis. Kidney Blood Press Res 2003;26:254–5.
[62] Jennette JC. Implications for pathogenesis of patterns of injury in small and medium-sized vessel vasculitis. Cleve Clin J Med 2002;69: [SII–33–38]
[63] Jennette JC, Thomas DB. In: Jennette JC, Olson JL, Schwartz MM, Silva FG, editors. Pauci-immune and Antineutrophil cytoplasmic autoantibody glomerulonephritis and vasculitis in heptinstall's pathology of the kidney. 6th ed. Philadelphia: Lippincott-Raven; 2007. p. 643–74.
[64] Jennette JC, Falk RJ. In: Floege J, Johnson RJ, Feehally J, editors. Renal and systemic vasculitis in comprehensive clinical nephrology. 4th ed. London: Mosby; 2010. p. 292–307.
[65] Jennette JC, Falk RJ, Gasim AH. Pathogenesis of antineutrophil cytoplasmic autoantibody vasculitis. Curr Opin Nephrol Hypertens 2011;20:263–70.
[66] Jennette JC, Xiao H, Falk R, Gasim AM. Experimental models of vasculitis and glomerulonephritis induced by antineutrophil cytoplasmic autoantibodies. Contrib Nephrol 2011;169:211–20.
[67] Kain R, Exner M, Brandes R, et al. Molecular mimicry in pauci-immune focal necrotizing glomerulonephritis. Nat Med 2008;14:1088–96.

[68] Kansas GS. Selectins and their ligands: current concepts and controversies. Blood 1996;88:3259–87.
[69] Kaplanski G, Maisonobe T, Marin V, Gres S, Robitail S, Farnarier C, et al. Vascular cell adhesion molecule-1 (VCAM-1) plays a central role in the pathogenesis of severe forms of vasculitis due to hepatitis C-associated mixed cryoglobulinemia. J Hepatol 2005;42:334–40.
[70] Kelly M, Hwang JM, Kubes P. Modulating leukocyte recruitment in inflammation. J Allergy Clin Immunol 2007;120:3–10.
[71] Kettritz R, Jennette JC, Falk RJ. Crosslinking of ANCA-antigens stimulates superoxide release by human neutrophils. J Am Soc Nephrol 1997;8:386–94.
[72] Kikuchi S, Pastore Y, Fossati-Jimack L, Kuroki A, Yoshida H, Fulpius T, et al. A transgenic mouse model of autoimmune glomerulonephritis and necrotizing arteritis associated with cryoglobulinemia. J Immunol 2002;169:4644–50.
[73] Kishimoto TK, Larson RS, Corbi AL, Dustin ML, Staunton DE, Springer TA. The leukocyte integrins. Adv Immunol 1989;46: 149–82.
[74] Kniker WT, Cochrane CG. Pathogenic factors in vascular lesions of experimental serum sickness. J Exp Med 1965;122:83–98.
[75] Korbet SM, Schwartz MM, Lewis EJ. Immune complex deposition and coronary vasculitis in systemic lupus erythematosus. Report of two cases. Am J Med 1984;77:141–6.
[76] Kunkel EJ, Chomas JE, Ley K. Role of primary and secondary capture for leukocyte accumulation in vivo. Circ Res 1998;82:30–8.
[77] Lau KK, Wyatt RJ, Moldoveanu Z, et al. Serum levels of galactose-deficient IgA in children with IgA nephropathy and Henoch-Schönlein purpura. Pediatr Nephrol 2007;22:2067–72.
[78] Laudanna C, Kim JY, Constantin G, Butcher E. Rapid leukocyte integrin activation by chemokines. Immunol Rev 2002;186:37–46.
[79] Launay P, Grossetete B, Arcos-Fajardo M, Gaudin E, Torres SP, Beaudoin L, et al. Fc alpha receptor (CD89) mediates the development of immunoglobulin A (IgA) nephropathy (Berger's disease). Evidence for pathogenic soluble receptor-IgA complexes in patients and CD89 transgenic mice. J Exp Med 2000;191:1999–2009.
[80] Lawrence MB, Springer TA. Leukocytes roll on a selectin at physiologic flow rates: distinction from and prerequisite for adhesion through integrins. Cell 1991;65:859–73.
[81] Leppert D, Lindberg RL, Kappos L, Leib SL. Matrix metalloproteinases: multifunctional effectors of inflammation in multiple sclerosis and bacterial meningitis. Brain Res Brain Res Rev 2001;36:249–57.
[82] Ley K, Laudanna C, Cybulsky MI, Nourshargh S. Getting to the site of inflammation: The leukocyte adhesion cascade updated. Nature reviews 2007;7:678–89.
[83] Lim LCL, Taylor III JG, Schmitz JL, et al. Diagnostic usefulness of antineutrophil cytoplasmic autoantibody serology: comparative evaluation of commercial indirect fluorescent antibody kits and enzyme immunoassay kits. Am J Clin Pathol 1999;111:363–9.
[84] Little MA, Smyth CL, Yadav R, Ambrose L, Cook HT, Nourshargh S, et al. Anti-neutrophil cytoplasm antibodies directed against myeloperoxidase augment leukocyte-microvascular interactions in vivo. Blood 2005;106:2050–8.
[85] Marshall BT, Long M, Piper JW, Yago T, McEver RP, Zhu C. Direct observation of catch bonds involving cell-adhesion molecules. Nature 2003;423:190–3.
[86] Mason A, Theal J, Bain V, Adams E, Perrillo R. Hepatitis B virus replication in damaged endothelial tissues of patients with extrahepatic disease. Am J Gastroenterol 2005;100:972–6.
[87] Masuda M, Nakanishi K, Yoshizawa N, Iijima K, Yoshikawa N. Group A streptococcal antigen in the glomeruli of children with Henoch-Schonlein nephritis. Am J Kidney Dis 2003;41: 366–70.
[88] McEver RP, Beckstead JH, Moore KL, Marshall-Carlson L, Bainton DF. GMP-140, a platelet alpha-granule membrane protein, is also synthesized by vascular endothelial cells and is localized in Weibel-Palade bodies. J Clin Invest 1989; 84:92–9.
[89] Michalak T. Immune complexes of hepatitis B surface antigen in the pathogenesis of periarteritis nodosa. A study of seven necropsy cases. Am J Pathol 1978;90:619–32.
[90] Middleton J, Neil S, Wintle J, Clark-Lewis I, Moore H, Lam C, et al. Transcytosis and surface presentation of IL-8 by venular endothelial cells. Cell 1997;91:385–95.
[91] Middleton J, Patterson AM, Gardner L, Schmutz C, Ashton BA. Leukocyte extravasation: chemokine transport and presentation by the endothelium. Blood 2002;100:3853–60.
[92] Moon KC, Park SY, Kim HW, Hong HK, Lee HS. Expression of intercellular adhesion molecule-1 and vascular cell adhesion molecule-1 in human crescentic glomerulonephritis. Histopathology 2002;41:158–65.
[93] Morita S, Ueda Y, Eguchi K. Anti-thyroid drug-induced ANCA-associated vasculitis: a case report and review of the literature. Endoc J 2000;47:467–70.
[94] Mosesson MW. Fibrinogen and fibrin structure and functions. J Thromb Haemost 2005;3:1894–904.
[95] Mrowka C, Heintz B, Sieberth HG. VCAM-1, ICAM-1, and E-selectin in IgA nephropathy and Schonlein-Henoch syndrome: differences between tissue expression and serum concentration. Nephron 1999;81:256–63.
[96] Mulder AH, Heeringa P, Brouwer E, Limburg PC, Kallenberg CG. Activation of granulocytes by anti-neutrophil cytoplasmic antibodies (ANCA): a Fc gamma RII-dependent process. Clin Exp Immunol 1994;98:270–8.
[97] Muller WA, Weigl SA, Deng X, Phillips DM. PECAM-1 is required for transendothelial migration of leukocytes. J Exp Med 1993;178:449–60.
[98] Mulligan MS, Johnson KJ, Todd III RF, Issekutz TB, Miyasaka M, Tamatani T, et al. Requirements for leukocyte adhesion molecules in nephrotoxic nephritis. J Clin Invest 1993;91: 577–87.
[99] Mulligan MS, Lentsch AB, Miyasaka M, Ward PA. Cytokine and adhesion molecule requirements for neutrophil recruitment during glycogen-induced peritonitis. Inflamm Res 1998;47:251–5.
[100] Nair KS, Zingde SM. Adhesion of neutrophils to fibronectin: role of the cd66 antigens. Cell Immunol 2001;208:96–106.
[101] Oda T, Hotta O, Taguma Y, et al. Involvement of neutrophil elastase in crescentic glomerulonephritis. Hum Pathol 1997;28:720–8.
[102] Ostermann G, Weber KS, Zernecke A, Schroder A, Weber C. JAM-1 is a ligand of the beta(2) integrin LFA-1 involved in transendothelial migration of leukocytes. Nat Immunol 2002;3:151–8.
[103] Owen CA, Campbell EJ. The cell biology of leukocyte-mediated proteolysis. J Leukoc Biol 1999;65:137–50.
[104] Ozaltin F, Bakkaloglu A, Ozen S, Topaloglu R, Kavak U, Kalyoncu M, et al. The significance of IgA class of antineutrophil cytoplasmic antibodies (ANCA) in childhood Henoch-Schonlein purpura. Clin Rheumatol 2004;23:426–9.
[105] Park SY, Ueda S, Ohno H, Hamano Y, Tanaka M, Shiratori T, et al. Resistance of Fc receptor-deficient mice to fatal glomerulonephritis. J Clin Invest 1998;102:1229–38.

[106] Pendergraft WF, Preston GA, Shah RR, Tropsha A, Jennette JC, Falk RJ. cPR3105-206, a protein complementary to the autoantigen proteinase 3, triggers autoimmunity. Nat Med 2004;10: 72–9.
[107] Petri B, Phillipson M, Kubes P. The physiology of leukocyte recruitment: An in vivo perspective. J Immunol 2008;180: 6439–46.
[108] Phillipson M, Heit B, Colarusso P, Liu L, Ballantyne CM, Kubes P. Intraluminal crawling of neutrophils to emigration sites: A molecularly distinct process from adhesion in the recruitment cascade. J Exp Med 2006;203:2569–75.
[109] Popp Jr JW, Harrist TJ, Dienstag JL, Bhan AK, Wands JR, LaMont JT, et al. Cutaneous vasculitis associated with acute and chronic hepatitis. Arch Intern Med 1981;141: 623–9.
[110] Porges AJ, Redecha PB, Kimberly WT, Csernok E, Gross WL, Kimberly RP. Anti-neutrophil cytoplasmic antibodies engage and activate human neutrophils via Fc gamma RIIa. J Immunol 1994;153:1271–80.
[111] Pudifin DJ, Duursma J, Gathiram V, Jackson TF. Invasive amoebiasis is associated with the development of anti-neutrophil cytoplasmic antibody. Clin Exp Immunol 1994;97:48–51.
[112] Radford DJ, Luu NT, Hewins P, Nash GB, Savage CO. Antineutrophil cytoplasmic antibodies stabilize adhesion and promote migration of flowing neutrophils on endothelial cells. Arthritis Rheum 2001;44:2851–61.
[113] Radford DJ, Savage CO, Nash GB. Treatment of rolling neutrophils with antineutrophil cytoplasmic antibodies causes conversion to firm integrin-mediated adhesion. Arthritis Rheum 2000;43:1337–45.
[114] Ralston DR, Marsh CB, Lowe MP, Wewers MD. Antineutrophil cytoplasmic antibodies induce monocyte IL-8 release. Role of surface proteinase-3, alpha1-antitrypsin, and Fcgamma receptors. J Clin Invest 1997;100:1416–24.
[115] Rarok AA, Limburg PC, Kallenberg CG. Neutrophil-activating potential of antineutrophil cytoplasm autoantibodies. J Leukoc Biol 2003;74:3–15.
[116] Rastaldi MP, Ferrario F, Crippa A, Dell'Antonio G, Casartelli D, Grillo C, et al. Glomerular monocyte-macrophage features in ANCA-positive renal vasculitis and cryoglobulinemic nephritis. J Am Soc Nephrol 2000;11:2036–43.
[117] Ravetch JV, Bolland S. IgG Fc receptors. Annu Rev Immunol 2001;19:275–90.
[118] Rich AR, Gregory JE. The experimental demonstration that periarteritis nodosa is a manifestation of hypersensitivity. Bull Johns Hopkins Hosp 1943;72:65–88.
[119] Rich AR. The role of hypersensitivity in periarteritis nodosa. As indicated by seven cases developing during serum sickness and sulfonamide therapy. Bull Johns Hopkins Hosp 1942;71:123–40.
[120] Rose DM. The role of the alpha4 integrin-paxillin interaction in regulating leukocyte traficking. Exp Mol Med 2006;38:191–5.
[121] Rosen SD. Ligands for l-selectin: Homing, inflammation, and beyond. Annu Rev Immunol 2004;22:129–56.
[122] Roth AJ, Brown MC, Smith RN, et al. Anti-LAMP-2 antibodies are not prevalent in patients with anti-neutrophil cytoplasmic autoantibody (ANCA) disease. J Am Soc Nephrol 2011; [submitted].
[123] Sansonno D, Dammacco F. Hepatitis C virus, cryoglobulinaemia, and vasculitis: immune complex relations. Lancet Infect Dis 2005;5:227–36.
[124] Sansonno D, Lauletta G, Nisi L, Gatti P, Pesola F, Pansini N, et al. Non-enveloped HCV. core protein as constitutive antigen of cold-precipitable immune complexes in type II mixed cryoglobulinaemia. Clin Exp Immunol 2003;133:275–82.
[125] Saulsbury FT. Alterations in the O-linked glycosylation of IgA1 in children with Henoch-Schonlein purpura. J Rheumatol 1997;24:2246–9.
[126] Saulsbury FT. Henoch-Schonlein purpura in children. Report of 100 patients and review of the literature. Medicine (Baltimore) 1999;78:395–409.
[127] Savage CO, Gaskin G, Pusey CD, Pearson JD. Myeloperoxidase binds to vascular endothelial cells, is recognized by ANCA and can enhance complement dependent cytotoxicity. Adv Exp Med Biol 1993;336:121–3.
[128] Savage CO, Pottinger BE, Gaskin G, Pusey CD, Pearson JD. Autoantibodies developing to myeloperoxidase and proteinase 3 in systemic vasculitis stimulate neutrophil cytotoxicity toward cultured endothelial cells. Am J Pathol 1992;141: 335–42.
[129] Savige J, Gillis D, Davies D, et al. International consensus statement on testing and reporting of antineutrophil cytoplasmic antibodies (ANCA). Am J Clin Pathol 1999;111:507–13.
[130] Schenkel AR, Mamdouh Z, Chen X, Liebman RM, Muller WA. CD99 plays a major role in the migration of monocytes through endothelial junctions. Nat Immunol 2002;3:143–50.
[131] Schlieben DJ, Korbet SM, Kimura RE, Schwartz MM, Lewis EJ. Pulmonary-renal syndrome in a newborn with placental transmission of ANCAs. Am J Kidney Dis 2005;45:758–61.
[132] Schreiber A, Busjahn A, Luft FC, Kettritz R. Membrane expression of proteinase 3 is genetically determined. J Am Soc Nephrol 2003;14:68–75.
[133] Schreiber A, Luft FC, Kettritz R. Membrane proteinase 3 expression and ANCA-induced neutrophil activation. Kidney Int 2004;65:2172–83.
[134] Schreiber A, Xiao H, Jennette JC, Schneider W, Luft FC, Kettritz R. C5a receptor mediates neutrophil activation and ANCA-induced glomerulonephritis. J Am Soc Nephrol 2009;20:289–98.
[135] Silber A, Newman W, Sasseville VG, et al. Recruitment of lymphocytes during cutaneous delayed hypersensitivity in nonhuman primates is dependent on E-selectin and vascular cell adhesion molecule 1. J Clin Invest 1994;93:1554–63.
[136] Smith DF, Deem TL, Bruce AC, Reutershan J, Wu D, Ley K. Leukocyte phosphoinositide-3 kinase {gamma} is required for chemokine-induced, sustained adhesion under flow in vivo. J Leukoc Biol 2006;80:1491–9.
[137] Springer TA. Traffic signals on endothelium for lymphocyte recirculation and leukocyte emigration. Annu Rev Physiol 1995;57:827–72.
[138] Stegeman CA, Tervaert JW, Sluiter WJ, Manson WL, de Jong PE, Kallenberg CG. Association of chronic nasal carriage of Staphylococcus aureus and higher relapse rates in Wegener granulomatosis. Ann Intern Med 1994;120:12–7.
[139] Suzuki H, Fan R, Zhang Z, et al. Aberrantly glycosylated IgA1 in IgA nephropathy patients is recognized by IgG antibodies with restricted heterogeneity. J Clin Invest 2009;119:1668–77.
[140] Suzuki Y, Shirato I, Okumura K, Ravetch JV, Takai T, Tomino Y, et al. Distinct contribution of Fc receptors and angiotensin II-dependent pathways in anti-GBM glomerulonephritis. Kidney Int 1998;54:1166–74.
[141] Takai T, Ono M, Hikida M, Ohmori H, Ravetch JV. Augmented humoral and anaphylactic responses in Fc gamma RII-deficient mice. Nature 1996;379:346–9.
[142] Tissot JD, Invernizzi F, Schifferli JA, Spertini F, Schneider P. Two-dimensional electrophoretic analysis of cryoproteins: a report of 335 samples. Electrophoresis 1999;20:606–13.

[143] Tomana M, Novak J, Julian BA, Matousovic K, Konecny K, Mestecky J. Circulating immune complexes in IgA nephropathy consist of IgA1 with galactose-deficient hinge region and antiglycan antibodies. J Clin Invest 1999;104:73–81.

[144] Trepo CG, Zucherman AJ, Bird RC, Prince AM. The role of circulating hepatitis B antigen/antibody immune complexes in the pathogenesis of vascular and hepatic manifestations in polyarteritis nodosa. J Clin Pathol 1974;27:863–8.

[145] Trepo C, Guillevin L. Polyarteritis nodosa and extrahepatic manifestations of HBV infection: the case against autoimmune intervention in pathogenesis. J Autoimmun 2001;16:269–74.

[146] Van Der Helm-Van Mil AH, Smith AC, Pouria S, Tarelli E, Brunskill NJ, Eikenboom HC. Immunoglobulin A multiple myeloma presenting with Henoch-Schonlein purpura associated with reduced sialylation of IgA1. Br J Haematol 2003;122: 915–7.

[147] Von Hundelshausen P, Weber KS, Huo Y, Proudfoot AE, Nelson PJ, Ley K, et al. Rantes deposition by platelets triggers monocyte arrest on inflamed and atherosclerotic endothelium. Circulation 2001;103:1772–7.

[148] Wang S, Dangerfield JP, Young RE, Nourshargh S. PECAM-1, alpha6 integrins and neutrophil elastase cooperate in mediating neutrophil transmigration. J Cell Sci 2005;118(Pt 9):2067–76.

[149] Ward PA, Lentsch AB. Endogenous regulation of the acute inflammatory response. Mol Cell Biochem 2002;234:225–8.

[150] Weber C. Novel mechanistic concepts for the control of leukocyte transmigration: specialization of integrins, chemokines, and junctional molecules. J Mol Med 2003;81:4–19.

[151] Wegmann F, Petri B, Khandoga AG, Moser C, Khandoga A, Volkery S, et al. Esam supports neutrophil extravasation, activation of rho, and vegf-induced vascular permeability. J Exp Med 2006;203:1671–7.

[152] Weidner S, Carl M, Riess R, Rupprecht HD. Histologic analysis of renal leukocyte infiltration in antineutrophil cytoplasmic antibody-associated vasculitis: importance of monocyte and neutrophil infiltration in tissue damage. Arthritis Rheum 2004;50:3651–7.

[153] Weidner S, Neupert W, Goppelt-Struebe M, Rupprecht HD. Antineutrophil cytoplasmic antibodies induce human monocytes to produce oxygen radicals in vitro. Arthritis Rheum 2001;44:1698–706.

[154] Weiss TD, Tsai CC, Baldassare AR, Zuckner J. Skin lesions in viral hepatitis: histologic and immunofluorescent findings. Am J Med 1978;64:269–73.

[155] Wilde B, van Paassen P, Witzke O, Tervaert JW. New pathophysiological insights and treatment of ANCA-associated vasculitis. Kidney Int 2011;79:599–612.

[156] Williams JM, Ben-Smith A, Hewins P, Dove SK, Hughes P, McEwan R, et al. Activation of the G(i) heterotrimeric G protein by ANCA IgG F(ab')2 fragments is necessary but not sufficient to stimulate the recruitment of those downstream mediators used by intact ANCA IgG. J Am Soc Nephrol 2003;14:661–9.

[157] Williams JM, Kamesh L, Savage CO. Translating basic science into patient therapy for ANCA-associated small vessel vasculitis. Clin Sci 2005;108:101–12.

[158] Wilson CB, Dixon FJ. Quantitation of acute and chronic serum sickness in the rabbit. J Exp Med 1971;134:7s–8s.

[159] Witko-Sarsat V, Rieu P, Descamps-Latscha B, Lesavre P, Halbwachs-Mecarelli L. Neutrophils: molecules, functions and pathophysiological aspects. Lab Invest 2000;80:617–53.

[160] Witko-Sarsat V, Reuter N, Mouthon L. Interaction of proteinase 3 with its associated partners: implications in the pathogenesis of Wegener's granulomatosis. Curr Opin Rheumatol 2010;22: 1–7.

[161] Woodfin A, Voisin MB, Nourshargh S. Recent developments and complexities in neutrophil transmigration. Curr Opin Hematol 2010;17:9–17.

[162] Xiao H, Heeringa P, Hu P, Liu Z, Zhao M, Aratani Y, et al. Antineutrophil cytoplasmic autoantibodies specific for myeloperoxidase cause glomerulonephritis and vasculitis in mice. J Clin Invest 2002;110:955–63.

[163] Xiao H, Heeringa P, Liu Z, Huugen D, Hu P, Maeda N, et al. The role of neutrophils in the induction of glomerulonephritis by anti-myeloperoxidase antibodies. Am J Pathol 2005;167: 39–45.

[164] Xiao H, Heeringa P, Schreiber A, Falk RJ, Jennette JC. The role of Fcγ receptors in the induction of glomerulonephritis and pulmonary granulomatous inflammation in mice by anti-myeloperoxidase antibodies (Anti-MPO). J Am Soc Nephrol 2004;15:37A [(abstract)].

[165] Xiao H, Schreiber A, Heeringa P, Falk RJ, Jennette JC. Alternative complement pathway in the pathogenesis of disease mediated by antineutrophil cytoplasmic autoantibodies. Am J Pathol 2007;170:52–64.

[166] Yanaba K, Kaburagi Y, Takehara K, Steeber DA, Tedder TF, Sato S. Relative contributions of selectins and intercellular adhesion molecule-1 to tissue injury induced by immune complex deposition. Am J Pathol 2003;162: 1463–73.

[167] Yanaba K, Komura K, Horikawa M, Matsushita Y, Takehara K, Sato S. P-selectin glycoprotein ligand-1 is required for the development of cutaneous vasculitis induced by immune complex deposition. J Leukoc Biol 2004;76:374–82.

[168] Yanaba K, Mukaida N, Matsushima K, Murphy PM, Takehara K, Sato S. Role of C-C chemokine receptors 1 and 5 and CCL3/macrophage inflammatory protein-1alpha in the cutaneous Arthus reaction: possible attenuation of their inhibitory effects by compensatory chemokine production. Eur J Immunol 2004;34:3553–61.

[169] Yang J, Preston G, Pendergraft W, Segelmark M, Heeringa P, Hogan SL, et al. Internalization of proteinase 3 is concomitant with endothelial cell apoptosis and internalization of myeloperoxidase with generation of intracellular oxidants. Am J Pathol 2001;158:581–92.

[170] Yang JJ, Kettritz R, Falk RJ, Jennette JC, Gaido M. Apoptosis of endothelial cells induced by the neutrophil serine proteases proteinase 3 and elastase. Am J Pathol 1996;149: 1617–26.

[171] Yang YH, Lai HJ, Huang CM, Wang LC, Lin YT, Chiang BL. Sera from children with Active Henoch-Schonlein purpura can enhance the production of interleukin 8 by human umbilical venous endothelial cells. Ann Rheum Dis 2004;63: 1511–3.

[172] Zheng F, Kundu GC, Zhang Z, Ward J, DeMayo F, Mukherjee AB. Uteroglobin is essential in preventing immunoglobulin A nephropathy in mice. Nat Med 1999;5:1018–25.

[173] Zhou X, Gao XP, Fan J, Liu Q, Anwar KN, Frey RS, et al. LPS activation of Toll-like receptor 4 signals CD11b/CD18 expression in neutrophils. Am J Physiol Lung Cell Mol Physiol 2005;288:L655–62.

[174] Zhu C, McEver RP. Catch bonds: Physical models and biological functions. Mol Cell Biomech 2005;2:91–104.

CHAPTER

84

Genetic Abnormalities in Glomerular Function

Yoav Segal[1] *and Clifford E. Kashtan*[2]

[1]Department of Medicine, University of Minnesota, Minneapolis, USA
[2]Department of Pediatrics, University of Minnesota, Minneapolis, USA

INTRODUCTION

The study of inherited diseases arising from single gene defects can provide a wealth of data about the roles that particular proteins normally play in tissue structure and function. The identification of the specific genetic abnormalities underlying several inherited renal disorders has allowed investigators to draw inferences regarding the specific activities of certain glomerular proteins, and the consequences of mutations of these proteins for glomerular function.

In this chapter we will discuss some recent advances in the understanding of genetic kidney diseases that primarily involve the glomerulus. We have organized the chapter according to the site or mechanism of the primary abnormality (Table 84.1): abnormalities of extracellular matrix, storage diseases affecting the glomerulus, primary defects in the slit diaphragm, cytoskeletal defects and defective transcriptional regulation.

DISORDERS OF EXTRACELLULAR MATRIX

Alport Syndrome

The investigation of the molecular biology of Alport syndrome (AS) has provided important insights into the role played by type IV collagen in maintaining the structure and function of the glomerular basement membrane (GBM).The clinical features of AS represent the phenotypic consequences of mutations that alter the expression of type IV collagen in basement membranes.X-linked, autosomal recessive and autosomal dominant forms of AS have been characterized at the gene and protein levels. Absence of three specific isomers of type IV collagen, the α3(IV), α4(IV) and α5(IV) chains, from Alport GBM results early in life in GBM attenuation, manifesting clinically as hematuria. Over time, GBM deficient in these chains undergoes progressive thickening and disorganization, with the development of proteinuria and, ultimately, renal failure.

Clinical Features

Renal Findings: The cardinal finding of AS is hematuria effected males have persistent microscopic hematuria, often first detected during infancy.[1,2] Many also have episodic gross hematuria during the first two decades of life.[2] Boys who are free of hematuria during the first 10 years of life are unlikely to be affected.[2]

Females who are heterozygous for X-linked AS (XLAS) may have intermittent hematuria, and about 7% of obligate female heterozygotes never manifest hematuria.[3] Hematuria appears to be persistent in both males and females with autosomal recessive AS (ARAS). Proteinuria is usually absent in the first few years of life, but develops eventually in all XLAS males, many XLAS females and in both males and females with recessive disease.[2–4] Proteinuria increases progressively with age, and may eventuate in the nephrotic syndrome.[2,5]

Hypertension also increases in incidence and severity with age. Like proteinuria, hypertension is more likely to occur in affected males than in affected females with XLAS, but there are no gender differences in the autosomal recessive form.

End-stage renal disease (ESRD) develops in virtually all affected males with XLAS, but the rate of progression shows significant interkindred variability.[4] Renal

Seldin and Giebisch's The Kidney, Fifth Edition.
DOI: http://dx.doi.org/10.1016/B978-0-12-381462-3.00084-7

© 2013 Elsevier Inc. All rights reserved.

TABLE 84.1 Genetic Abnormalities of Glomerular Function

Disorders of Extracellular Matrix
Alport syndrome
Thin Basement Membrane Nephropathy
HANAC syndrome
Pierson Syndrome
Storage Disorders
Fabry Disease
Other Storage Disorders Associated with Glomerular Dysfunction
Disorders of the Podocyte Slit Diaphragm
Congenital Nephrotic Syndrome of the Finnish Type
Autosomal Recessive Steroid-Resistant Nephrotic Syndrome
Nephrotic Syndrome, Early Onset, Type 3
Disorders of the Podocyte Cytoskeleton
Autosomal Dominant Focal Segmental Glomerulosclerosis
MYH9-related disease (Epstein and Fechtner Syndromes)
Disorders of Podocyte Gene Regulation
Denys-Drash Syndrome and Diffuse Mesangial Sclerosis
Frasier Syndrome
Nail-Patella Syndrome

half-life in men with XLAS is about 25 years.[4] Several authors have observed that the rate of progression to renal failure is fairly constant among affected males within a particular family[6,7] although significant intra-kindred variability in the rate of progression to renal failure has occasionally been reported.[2,8]

Progression to ESRD in females with XLAS was, until recently, considered an unusual event.However, in a landmark study of several hundred XLAS females published in 2003, Jais and colleagues found that about 12% developed ESRD before age 40 (compared with 90% of XLAS males), increasing to 30% by age 60 and 40% by age 80[3] as previously described by Grunfeld et al.[3,9] Both males and females with ARAS appear likely to progress to ESRD during the second or third decade of life.

Hearing Deficit: About 50% of XLAS males display sensorineural deafness by age 25 and by age 40 approximately 90% of XLAS males are deaf.[4] Although it has been clear for some time that the hearing defect in Alport syndrome localizes to the cochlea, histological correlates of deafness in Alport patients have only recently been recognized. Merchant and colleagues found unique and consistent abnormalities in the cochleae of Alport patients, consisting of a zone of separation between the basilar membrane and the cells of the organ of Corti, associated with a cellular infiltrate in the tunnel of Corti and extracellular spaces of Nuel.[10] Electron microscopy showed that the zone of separation occurred between the basement membrane of the organ of Corti and the basilar membrane.These authors speculated that abnormal adhesion of the organ of Corti to the basilar membrane might disrupt the mechanical relationships between outer hair cells and the basilar membrane, resulting in hearing impairment.

Hearing loss in AS is never congenital and usually becomes apparent by late childhood to early adolescence in boys with XLAS.[2] Hearing impairment in members of families with AS is always accompanied by evidence of renal involvement.[2] There is no convincing evidence that deaf males lacking renal disease can transmit AS to their offspring.In females with XLAS hearing loss is less frequent, tends to be less severe and occurs later in life.[3] There do not appear to be gender differences in the incidence or course of deafness in autosomal disease.

In its early stages the hearing deficit is detectable only by audiometry, with bilateral reduction in sensitivity to tones in the 2000 to 8000 Hz range. In affected males the deficit is progressive and eventually extends to other frequencies, including those of conversational speech. Although these males frequently require hearing aids, their deafness tends to stabilize once they develop ESRD.

Ocular Defects: Ocular defects are not unusual in patients with AS, occurring in at least 15 to 30% of patients.[4,11–13] Anterior lenticonus, the conical protrusion of the central portion of the lens into the anterior chamber of the eye, is virtually pathognomonic of AS. Nielsen[14] found that all reported patients with anterior lenticonus who had been adequately examined exhibited evidence of chronic nephritis and sensorineural deafness. Anterior lenticonus is almost entirely restricted to AS families with rapid progression to ESRD (i.e., before age 30) and deafness. Anterior lenticonus is absent at birth, usually appearing during the second to third decade of life.[15] Marked attenuation and fractures of the central portion of the anterior lens capsule have been observed histologically.[16,17]

A variety of other ocular lesions has been reported in patients with AS. Perhaps the most commonly occurring abnormalities are pigmentary changes in the perimacular region, consisting of whitish or yellowish granulations surrounding the foveal area.[13,18–20] Retinal flecks are frequently accompanied by anterior lenticonus but may also occur in the absence of lenticonus. These lesions may arise as a result of abnormalities of Bruch's membrane, the basement membrane that supports the retinal pigment epithelium.[21]

Corneal endothelial vesicles (posterior polymorphous dystrophy) have been observed in AS patients by several investigators,[19,22,23] and may be indicative of abnormalities in Descemet's membrane, the basement membrane underlying the corneal endothelium. Rhys et al. recently described recurrent corneal erosion in AS patients, which they ascribed to abnormalities of the corneal epithelial basement membrane.[24]

Diffuse Leiomyomatosis: The association of AS with leiomyomas of the esophagus and tracheobronchial tree has been reported in approximately 20 families.[25–28] Affected females in these kindreds typically exhibit genital leiomyomas as well, with clitoral hypertrophy and variable involvement of the labia majora and uterus. Symptoms usually appear in late childhood and include dysphagia, post-prandial vomiting, retrosternal or epigastric pain, recurrent bronchitis, dyspnea, cough and stridor. Leiomyomatosis may be suspected by chest X-ray or barium swallow, and confirmed by computed tomography or magnetic resonance imaging.

Arterial Disease: There have been several reports of arterial disease in males with Alport syndrome, including aneurysms of the thoracic and abdominal aorta and the cerebral arterial system.[29–32]

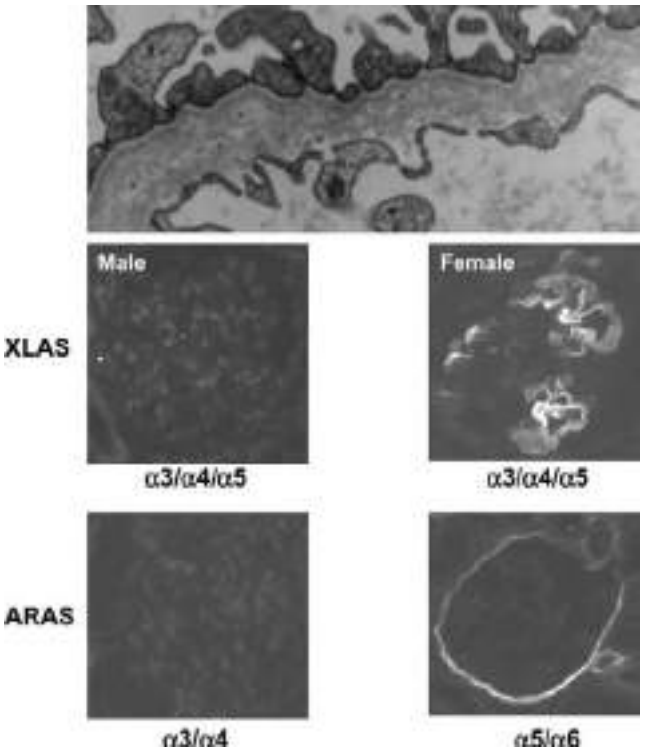

FIGURE 84.1 Glomerular capillary wall ultrastructure and type IV collagen immunostaining in Alport syndrome. The characteristic ultrastructural lesion of Alport syndrome consists of diffuse GBM thickening, scalloping of the epithelial aspect of the GBM, splitting of the lamina densa into multiple layers and dense granular bodies in lucent zones between strands of lamina densa material, all of which are depicted here. There is also variable broadening of podocyte foot processes.In the typical male with X-linked Alport syndrome (XLAS) the type IV collagen network formed by the α3(IV), α4(IV) and α5(IV) chains is completely absent from the kidney.In the typical female heterozygote there is mosaic expression of this network in the kidney. In both males and females with autosomal recessive Alport syndrome (ARAS), the α3α4α5 network is typically absent from GBM, and there is no expression of α3(IV) or α4(IV) chains in Bowman's capsule or tubular basement membranes. However, the α5(IV) and α6(IV) chains are expressed in Bowman's capsule and tubular basement membranes.

Pathology

There are no pathognomonic lesions by light microscopy or direct immunofluorescence in AS. Electron microscopy frequently reveals diagnostic abnormalities. The cardinal ultrastructural feature of the kidney in AS is the variable thickening, thinning, basket-weaving, and lamellation of the GBM (Figures 84.1 and 84.2). Identical morphologic features are apparent in some patients without a family history of nephritis. Such patients may represent new COL4A5 mutations, they may be offspring of asymptomatic female carriers, or may have autosomal recessive disease.

Ultrastructural alterations of GBM were noted in several reports of hereditary nephritis in the 1960s.[1,33–37] The most prominent abnormality is the irregular appearance of the lamina densa, which demonstrates zones of thickening, thinning, and splitting that may be interposed with segments of GBM that appear entirely normal. The abnormalities can affect a portion of a capillary loop, an entire loop, some or all loops, and can even spare individual glomeruli.

The thick segments measure up to 1200 nm, usually have irregular outer and inner contours, and are found more commonly in males than in females. The lamina densa is transformed into a heterogeneous network of membranous strands, which enclose clear electron-lucent areas. The electron-lucent zones may be entirely clear or contain round granules of variable density that measure between 20 and 90 nm in diameter. The origin of these granules is unknown, but Rumpelt has hypothesized that they represent degenerating islands of visceral epithelial cell cytoplasm.[38] Young children and females, and adult males on occasion,[39] may have diffusely attenuated segments of GBM measuring as little as 100 nm or less;in some instances, discontinuities of the GBM have been observed.[2,40]

The specificity of the GBM changes has been questioned.[41] Focal lamina densa splitting and lamellation may be observed in renal biopsies from patients with a variety of glomerular disorders. Clinical correlation and immunofluorescence microscopic examination of all biopsies are necessary when AS is the suspected diagnosis. Diffuse thickening and splitting of the GBM

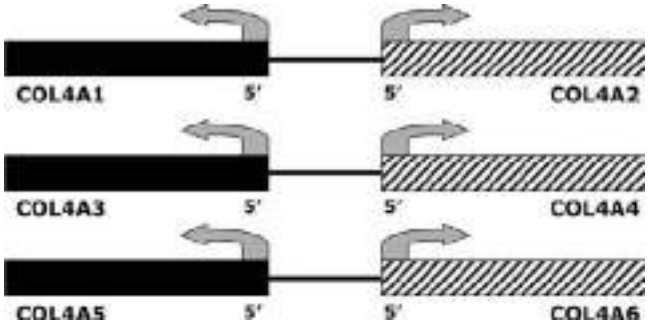

FIGURE 84.2 Type IV collagen genes.The six type IV collagen a chain genes are arranged in pairs on three chromosomes. The 5′ ends of each pair are adjacent to each other, separated by sequences containing regulatory sites.The 5 exons at the 3′ end of each gene encode the carboxyterminal noncollagenous (NC1) domain of the chain. Most of the remaining exons encode the repetitive Gly-X-Y motif of the collagenous portion of the chain.

is strongly suggestive of AS.In the absence of immune deposits, these changes are pathognomonic.

Not all Alport kindreds demonstrate these characteristic ultrastructural features.[42–44] Thick, thin, normal and nonspecifically altered GBM have all been described. Although diffuse attenuation of GBM has been considered the hallmark of "benign familial hematuria" or thin basement membrane nephropathy,[45–47] some patients with this abnormality are members of kindreds with a history of progression to renal failure.[2,42] Thus the signficance of an ultrastructural finding of thin GBMs must be considered in the context of the family history, basement membrane expression of type IV collagen α chains (see below), and genetic information.

Rumpelt described a correlation between the percent of GBM showing splitting of the lamina densa and the degree of proteinuria in AS patients,[5] suggesting that impaired permselectivity may be a functional consequence of the GBM alteration. Kim and colleagues observed that morphometric parameters such as mesangial volume fraction, cortical interstitial volume fraction, and percent global glomerular sclerosis were inversely correlated with creatinine clearance in AS, while creatinine clearance and surface density of peripheral GBM were directly correlated.[48] Similar relationships have been observed in other diseases, such as diabetic nephropathy and membranoproliferative glomerulonephritis (MPGN). However, patients with AS showed significantly greater impairment of filtration for any degree of structural change in comparison with patients with diabetic nephropathy or MPGN. This observation suggests that these morphologic abnormalities only partially account for reductions in creatinine clearance in AS. Decreased conductivity of water across the altered glomerular capillary wall could contribute to the decrement in filtration.

Genetics and Pathophysiology

GENETICS AND BIOCHEMISTRY OF TYPE IV COLLAGEN

Glomerular basement membranes are composed of several major constituents, including type IV collagen, laminin, nidogen and heparan sulfate proteoglycan. The type IV collagen family of proteins comprises six isomeric chains, designated α1−α6(IV),[49,50] (Table 84.2). These chains show extensive sequence homology and share basic structural features, including: (1) a major collagenous domain of about 1400 residues containing the repetitive triplet sequence glycine (Gly)-X-Y, in which X and Y represent a variety of other amino acids. (2) A carboxy-terminal noncollagenous (NC1) domain of about 230 residues. (3) A noncollagenous amino-terminal sequence of 15−20 residues. The major collagenous domain of each chain contains about 20 interruptions of the collagenous triplet sequence, while each noncollagenous domain contains 12 completely conserved cysteine residues which participate in critical disulfide bonds.

Each type IV collagen molecule is a trimer composed of three α chains.The classical type IV collagen trimer isolated from the extracellular matrix of the murine EHS sarcoma has the composition $\alpha1(IV)_2$-$(\alpha2(IV)_1$.[51] Type IV collagen α chains form trimers through

TABLE 84.2 Type IV Collagen Chains

Chain	Gene	Chromosome	Collagenous Domain # Residues (Interruptions)	Noncollagenous Domain # Residues
α1(IV)	*COL4A1*	13	1413 (21)	229
α2(IV)	*COL4A2*	13	1449 (23)	227
α3(IV)	*COL4A3*	2	1410 (23)	233
α4(IV)	*COL4A4*	2	1421 (26)	231
α5(IV)	*COL4A5*	X	1430 (22)	229
α6(IV)	*COL4A6*	X	1417 (25)	228

associations between their carboxy-terminal NC1 domains, accompanied by folding of the collagenous domains into triple helices.[51–53] Variable residues within the NC1 domains confer specificity upon chain-chain associations.[54] Type IV collagen triple helices form networks through several types of intermolecular interaction:end-to-end linkages between the carboxy-terminal domains of two type IV collagen triple helices, covalent interactions between four triple helices at their aminoterminal ends, and lateral associations mediated by binding of the carboxy-terminal domains of one trimer to the collagenous region of another trimer.[55,56] Disulfide bonds involving conserved cysteine residues are critical to the interactions between NC1 domains. These linkages between type IV collagen molecules produce a nonfibrillar, open-network assembly that associates with laminin through interactions mediated by nidogen.[57]

Various integrins mediate cell attachment to type IV collagen.Attachment of glomerular epithelial cells to the α3(IV) chain appears to involve the α3β1 integrin.[58]

The six type IV collagen genes are arranged in pairs on three different chromosomes (Figure 84.2, Table 84.2). The human α1(IV) and α2(IV) chains are encoded by the genes *COL4A1* and *COL4A2*, respectively, on chromosome 13.[59] *COL4A3* and *COL4A4* are located on chromosome 2 and encode the α3(IV) and α4(IV) chains of type IV collagen, respectively,[60] while the α5(IV) and α6(IV) chains are encoded by the *COL4A5* and *COL4A6* genes on the X chromosome.[61,62,63] The 5′ ends of each gene pair are adjacent to each other, separated by sequences of varying length containing motifs involved in the regulation of transcriptional activity.[64–66]

Evidence from a variety of sources indicates the existence of at least three type IV collagen networks in mammalian basement membranes. Studies of the distribution of these networks in basement membranes using monospecific antibodies have revealed a high degree of tissue specificity (Table 84.3). A network composed of heterotrimers with the composition $\alpha1(IV)_2$-α2(IV) is found in all basement membranes, although it is a relatively minor component of mature GBM.A network comprising α3(IV)-α4(IV)-α5(IV) heterotrimers is the predominant collagen in mature GBM, and also occurs in Bowman's capsules and the basement membranes of distal and collecting tubules. The network consisting of $\alpha5(IV)_2$-α6(IV) heterotrimers is present in Bowman's capsule and distal and collecting tubule basement membranes, but is not present in GBM. The epidermal basement membraneand basement membranes surrounding aortic smooth muscles cells (EBM) contains

TABLE 84.3 Type IV Collagen Chain Distribution in Alport Target Organs

Chain	Kidney	Eye	Cochlea	Skin
α1(IV)	All BMs mesangium	All BMs	All BMs	All BMs
α2(IV)	All BMs mesangium	All BMs	All BMs	All BMs
α3(IV)	GBM,	Lens capsule	Inner/outer sulci	None
	BC	Descemet's membrane	Spiral limbus	
	dTBM	Bruch's membrane	Spiral prominence	
		Internal limiting membrane	Basilar memb	
α4(IV)	GBM	Lens capsule	Inner/outer sulci	None
	BC	Descemet's membrane	Spiral limbus	
	dTBM	Bruch's membrane	Spiral prominence	
		Internal limiting membrane	Organ of Corti BM	
α5(IV)	GBM	Lens capsule	Inner/outer sulci	DEJ
	BC	Descemet's membrane	Spiral limbus	
	dTBM	Bruch's membrane	Spiral prominence	
		Internal limiting membrane	Organ of Corti BM	
α6(IV)	BC	Unknown	Unknown	DEJ
	dTBM			

BM: basement membrane; GBM: glomerular basement membrane; BC: Bowman's capsule; dTBM: distal tubular basement membrane; DEJ: dermal-epidermal junction (epidermal basement membrane)

$\alpha1(IV)_2$-$\alpha2(IV)$ and $\alpha5(IV)_2$-$\alpha6(IV)$ networks, but not the $\alpha3(IV)$-$\alpha4(IV)$-$\alpha5(IV)$ network.[67,68]

The $\alpha3(IV)$ chain has been identified as the target of anti-GBM autoantibodies in Goodpasture syndrome.[69–71] The Goodpasture epitope resides in the carboxy-terminal NC1 domain of $\alpha3(IV)$.[72]

ABNORMALITIES OF TYPE IV COLLAGEN GENES AND PROTEINS IN ALPORT SYNDROME

There are three genetic forms of Alport syndrome (Table 84.4).The X-linked form (XLAS), resulting from mutations in *COL4A5*, accounts for about 80% of patients with the disease. About 15% of patients have autosomal recessive Alport syndrome (ARAS), which arises from mutations affecting both alleles of *COL4A3* or *COL4A4*. The heterozygous parents of children with ARAS often have asymptomatic hematuria, although some have normal urinalyses.Finally, approximately 5% of patients have autosomal dominant Alport syndrome (ADAS), due to heterozygous mutations in *COL4A3* or *COL4A4*. Heterozygous mutations in *COL4A3* or *COL4A4* have also been found in families with thin basement membrane nephropathy (see below). It is not yet clear why many, perhaps most, individuals with heterozygous mutations in these genes have asymptomatic hematuria, while others have progressive disease.

XLAS: Several hundred *COL4A5* mutations have been reported in XLAS families.These mutations are distributed throughout the gene, and with few exceptions each mutation is unique. About 20% of reported *COL4A5* mutations are large rearrangements, predominantly deletions.[4,73] Missense mutations account for about 35-40%, about 15% are splice-site mutations, and 25–30% are nonsense mutations or small frame-shifting deletions or insertions that result in premature stop codons.[4,73] About 10 to 15% of *COL4A5* mutations occur as spontaneous events in the proband, explaining why some patients with XLAS lack a family history of the disease.

TABLE 84.4 Molecular Genetics of Alport Syndrome

Affected Inheritance	Locus	Gene Product
X-linked	*COL4A5*	$\alpha5(IV)$
X-linked + leiomyomatosis	*COL4A5* + *COL4A6*	$\alpha5(IV)$ + $\alpha6(IV)$
Autosomal recessive	*COL4A3*	$\alpha3(IV)$
	COL4A4	$\alpha4(IV)$
Autosomal dominant	*COL4A3*	$\alpha3(IV)$
	COL4A4	$\alpha4(IV)$

The association of XLAS with leiomyomatosis of the esophagus and tracheobronchial tree has been reported in several dozen families.[74] Affected members of these families exhibit large deletions that span the adjacent 5′ ends of the *COL4A5* and *COL4A6* genes.[75,76] These deletions involve varying lengths of *COL4A5*, but the *COL4A6* breakpoint is always located in the second intron of the gene.[77–79] Leiomyomatosis does not occur in patients with deletions of *COL4A5* and *COL4A6* that extend beyond intron 2 of *COL4A6*.Mutations of *COL4A6* alone do not appear to cause Alport syndrome, consistent with the absence of the $\alpha6(IV)$ chain from normal GBM.[80]

The great majority of missense *COL4A5* mutations are guanine substitutions in the first or second position of glycine codons that result in the replacement of a glycine residue in the collagenous domain of $\alpha5(IV)$ by another amino acid.[4,73] Such mutations are thought to interfere with the normal folding of the mutant $\alpha5(IV)$ chain into triple helices with other type IV collagen α chains.[81] Glycine lacks a side chain, making it the least bulky of amino acids, and small enough to allow three glycine residues to fit into the interior of a tightly wound triple helix.[82] The presence of a bulkier amino acid in a glycine position presumably creates a kink or an unfolding in the triple helix. Glycine substitutions in the $\alpha1$ chain of type I collagen account for the majority of mutations causing osteogenesis imperfecta, and are common in other genetic disorders of collagen.[83,84] Abnormally folded collagen triple helices exhibit increased susceptibility to proteolytic degradation.[84] The position of the substituted glycine, or the substituting amino acid itself, may influence the effect of the mutation on triple-helical folding, and ultimately the impact of the mutation on the severity of the clinical phenotype.[85]

ARAS: To date, mutations causing ARAS have been found in the *COL4A3* or *COL4A4* gene in several dozen patients.[86–91] Some of these patients are homozygous for their mutations and others are compound heterozygotes. As with *COL4A5*, there appear to be no mutation hot spots in *COL4A3* or *COL4A4*. Although it is possible that ARAS could result from the combination of a mutation in one allele of *COL4A3* and a mutation in one allele of *COL4A4*, no such example has been described. It is worth noting that the mating of two individuals with asymptomatic hematuria due to heterozygous *COL4A3* or *COL4A4* mutations can result in a child who has mutations in both alleles of *COL4A3* or *COL4A4* and, as a result, ARAS.

The reported *COL4A3* and *COLA*4 mutations in ARAS include nonsense, frame-shift, splicing and missense mutations. As with XLAS and other heritable collagen disorders, a common type of mutation in ARAS is a glycine substitution in the collagenous domain of $\alpha3(IV)$ or $\alpha4(IV)$.

ADAS: Heterozygous *COL4A3* and *COL4A4* mutations have been described in several families transmitting Alport syndrome as an autosomal dominant disease.[92–94] It is not clear why some individuals with heterozygous *COL4A3* or *COL4A4* mutations are asymptomatic or exhibit only isolated microhematuria,[86,88,95] while others have a progressive nephropathy. Several possibilities can be proposed: the type and/or site of the mutation may be critical, the presence of certain polymorphisms in these genes may influence the effect of a pathogenic mutation,[94] or a polymorphism or mutation in another gene may modify the effect of the mutation. In some cases, a heterozygous missense mutation in *COL4A3* or *COL4A4* might be more detrimental than a deletion or nonsense mutation, because the mutant chain can then induce the degradation of normal chains with which it forms abnormal trimers (Figure 84.1C).

Genotype-Phenotype Correlations in Alport Syndrome: Male patients with *COL4A5* deletions consistently exhibit sensorineural deafness and progression to ESRD during the second or third decade of life.[4] Most of the missense, nonsense and splicing *COL4A5* mutations described thus far have also been associated with early progression to ESRD in the second or third decade of life and sensorineural deafness. Single amino acid substitutions that alter an mRNA splice site, leading to exon skipping, or small deletions or insertions that shift the transcriptional reading frame, can clearly produce such aberrant protein products that a severe phenotype results. Several missense mutations in *COL4A5* have been associated with late-onset (after the third decade) ESRD and deafness.[4,85] Mutations near the 5′ end of the *COL4A5* gene are associated with earlier onset of ESRD.[96]

The severity of disease in a female heterozygous for a *COL4A5* mutation is probably influenced to some extent by the nature of the mutation, but the extent of inactivation of the X chromosome carrying the normal *COL4A5* allele may be a more important factor. Jais et al. were unable to demonstrate a genotype effect on outcome in XLAS heterozygotes, presumably due to the stronger influence of X-inactivation.[3] Guo et al. described a woman with a severe Alport phenotype (ESRD at age 30), one of whose *COL4A5* alleles carried two missense mutations.[97] Analysis of DNA isolated from the patient's kidney and leukocytes showed inactivation of greater than 90% of the X chromosomes carrying the normal *COL4A5* allele. Other investigators, however, have not been able to confirm that X-inactivation pattern of leukocytes predicts phenotype in XLAS heterozygotes.[98] In a mouse model of X-linked Alport syndrome[99] the relative activity of the X chromosome carrying the mutant *COL4A5* allele determines the outcome of heterozygous females.[100]

Phenotypic information on patients with ARAS is as yet somewhat sparse. Available data indicate that patients with ARAS progress to ESRD before age 30 and have sensorineural deafness, regardless of gender.[87,90,91]

Type IV Collagen in Alport Basement Membranes: Several studies in the 1980s established that the native kidneys of male AS patients failed to bind anti-GBM antibodies from patients with Goodpasture syndrome or from AS patients with post-transplant anti-GBM nephritis.[101–105] These early studies, combined with the observation by Hudson and colleagues that type IV collagen was the target of Goodpasture antibodies,[71] provided the first indication that AS might represent a primary disorder of type IV collagen. The availability of chain-specific antibodies has more recently allowed detailed investigation of the expression of the six type IV collagen α chains in AS basement membranes.

GBM, distal and collecting tubular basement membrane (TBM) and Bowman's capsules of males with XLAS usually lack expression of the α3(IV), α4(IV) and α5(IV) chains, but do express the α1(IV) and α2(IV) chains[106,107] (Table 84.5, Figure 84.3). The α6(IV) chain is not expressed in Bowman's capsule or distal TBM of XLAS males whose basement membranes lack α5(IV) expression.[108,109] Women who are heterozygous for XLAS mutations frequently exhibit mosaicism of GBM expression of the α3(IV), α4(IV) and α5(IV) chains, while expression of the α1(IV) and α2(IV) chains is not

TABLE 84.5 Immunohistochemistry in Alport Syndrome*

	GBM	BC	dTBM	EBM
X-linked (males)				
α3(IV)	−	−	−	normally absent
α4(IV)	−	−	−	normally absent
α5(IV)	−	−	−	−
X-linked (females)*				
α3(IV)	mosaic			normally absent
α4(IV)	mosaic			normally absent
α5(IV)	mosaic			mosaic
Autosomal recessive (males and females)				
α3(IV)	−	−	−	normally absent
α4(IV)	−	−	−	normally absent
α5(IV)	−	+	+	+

**In some AS kindreds, staining of basement membranes for type IV collagen chains is entirely normal.Therefore, a normal result does not exclude a diagnosis of X-linked or autosomal recessive AS.*

***Some heterozygous females have normal basement membrane immunoreactivity for type IV collagen chains. Thus, a normal result does not exclude the carrier state.*

GBM: glomerular basement membrane; BC: Bowman's capsule; dTBM: distal tubular basement membrane; EBM: epidermal basement membrane

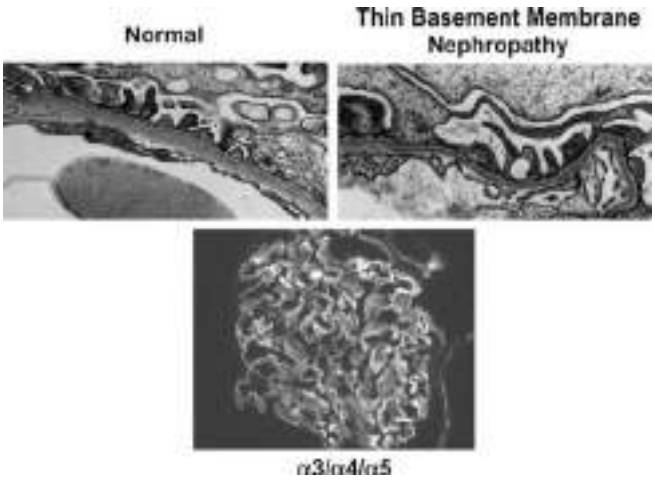

FIGURE 84.3 Glomerular capillary wall ultrastructure and type IV collagen immunochemistry in normal kidneys and in thin basement membrane nephropathy (TBMN). In normal kidneys, the glomerular basement membrane (GBM) has a homogeneous lamina densa, smooth innter (endothelial) and outer (epithelial) surfaces and a constant thickness. In TBMN kidneys, the GBM is diffusely attenuated, with a homogeneous lamina densa. Podocyte foot processes are intact. In both normal and TBMN kidneys, the type IV collagen network formed by the α3(IV), α4(IV) and α5(IV) chains is present in GBM, Bowman's capsule and distal and collecting tubule basement membranes.

affected.[107] The epidermal basement membrane (EBM) normally expresses the α1(IV), α2(IV), α5(IV) and α6 (IV) chains, but not the α3(IV) or α4(IV) chains[107,109,110] (Table 84.5). Most males with XLAS show no EBM expression of α5(IV) or α6(IV), while female heterozygotes frequently display mosaicism[110] (Table 84.5, Figure 84.1). Lens capsules of some males with XLAS do not express the α3(IV), α4(IV) or α5(IV) chains, while expression of these chains appears normal in other patients.[111]

In patients with ARAS, GBMs show no expression of the α3(IV), α4(IV) or α5(IV) chains, but α5(IV) and α6(IV) are expressed in Bowman's capsule, distal TBM and EBM[112] (Table 84.5, Figure 84.3). Therefore, XLAS and ARAS may be distinguishable by immunohistochemical analysis.

It is important to note that immunostaining for type IV collagen is normal in some patients with XLAS and ARAS. Consequently, normal expression of α3(IV), α4 (IV) and α5(IV) chains in basement membranes does not exclude a diagnosis of AS.

The abnormalities of type IV collagen expression observed in AS indicate that a mutation affecting one of the chains involved in the α3(IV)-α4(IV)-α5(IV) network can prevent GBM deposition of the entire network. Similarly, a mutation involving the α5(IV) chain can interfere with basement membrane expression of α5(IV)-α6(IV). Several lines of evidence suggest that the effects of a type IV collagen α chain mutation on the basement membrane expression of its "partner" chains are mediated by post-translational events. Substitution of glycine residues in the α1 chain of type I collagen comprise the majority of mutations causing osteogenesis imperfecta.[113] These mutations impair the folding of α1(IV) chains with α2(IV) chains into trimers, and the resulting trimers exhibit enhanced susceptibility to extracellular proteolytic degradation.[84] By similar means, an α5(IV) chain carrying a glycine substitution could bring about the destruction of normal α3(IV) and α4(IV) chains. Studies of mutations in the α1 chain of type IV collagen in *C. elegans* suggest another possible mechanism. Whether the α1(IV) mutation results in a null allele (deletion or nonsense mutation) or a glycine substitution, the α2(IV) chain accumulates intracellularly and never reaches the basement membrane.[114] Thus, mutations producing null COL4A5 alleles, or α5(IV) proteins that cannot form trimers (due to alterations of the carboxy-terminal domain), or some glycine substitutions, may simply prevent secretion of α3(IV) and α4(IV) chains, which are eventually degraded. Results of *in vitro* studies by Kobayashi and colleagues support the hypothesis that α5(IV) mutations impair the assembly of α3(IV)-α4(IV)-α5(IV) heterotrimers.[81]

Pathogenesis of Basement Membrane Lesions in Alport Syndrome: The tissue pathology of AS arises from abnormalities of basement membrane expression of the α3(IV)-α4(IV)-α5(IV) collagen network. This network is usually absent from or under-expressed in the basement membranes of AS patients, although in the basement membranes of some patients the networks are present but presumably defective in structure and function. The most straightforward demonstration of the consequences of the absence of this network may be anterior lenticonus. Absence or defective expression of these chains results in thinning and mechanical weakness of the anterior lens capsule, which fails to maintain the normal conformation of the lens.[17,111,115] Microhematuria, the first and invariable renal manifestation of AS, may likewise reflect GBM thinning and a tendency to develop focal ruptures early in life, due to the absent or defective expression of the α3-α4-α5(IV) network. Episodic gross hematuria precipitated by infections, which is not uncommon during the first two decades of life, may reflect increased susceptibility of the GBM to proteolysis.[116] On the other hand, the resolution of gross hematuria, which typically occurs by adolescence,[2] may be a function of progressive GBM thickening.[5]

The relentless thickening and lamellation of the Alport GBM features the accumulation of extracellular matrix proteins that are normally absent from GBM, or present in only small amounts. The α1(IV)−α2(IV)

network is highly expressed in the basement membranes of primordial glomeruli, but is normally replaced by the α3(IV)−α5(IV) network at the capillary loop stage of glomerular maturation.[117] In mature glomeruli the α1(IV)−α2(IV) network is confined to the mesangium and the subendothelial region of GBM.[118] This developmental switch fails to occur in Alport glomeruli.[116,119] The α1(IV)−α2(IV) network persists in mature Alport glomeruli and accumulates, spreading from its normal subendothelial location to occupy the full width of GBM.[112,106] Similarly, type V collagen and type VI collagen are normally found in the mesangium and in small quantities in the subendothelial GBM, but are markedly overexpressed in Alport GBM.[106] In addition, laminin chains that are normally confined to the mesangium are expressed in Alport GBM.[120,121] The molecular events that underlie these anomalies in protein expression remain to be elucidated. Whatever the mechanism, glomerulosclerosis in AS may result from the ectopic deposition of certain collagens in GBM.

AS resembles other chronic glomerulopathies in that deterioration of glomerular filtration rate is closely correlated with fibrosis of the renal interstitium.[122] Measurable increases in cortical interstitial volume are unusual in males with XLAS under age 10 years, but progressive expansion of the interstitium frequently occurs during the second decade of life.[122] It is not surprising that at least some of the factors driving interstitial fibrosis in AS are nonspecific, such as increased TGF-β1 activity, monocytic infiltration, epithelial-mesenchymal transformation and enhanced metalloproteinase expression.[123–127] If the pathogenesis of interstitial fibrosis in AS is not specific to the disease, it is conceivable that therapies that interfere with interstitial fibrosis may be of benefit to AS patients, without correcting the primary abnormalities of type IV collagen expression.[128,129]

Diagnosis

Alport syndrome should be considered in the differential diagnosis of patients with persistent microhematuria. Electron microscopic examination of renal tissue remains the most widely available and applied means for diagnosing AS. The presence of diffuse thickening and multilamellation of the GBM predicts a progressive nephropathy, regardless of family history. Unfortunately, ultrastructural information alone does not establish the mode of transmission in a particular family. In a patient with a negative family history, electron microscopy cannot distinguish *de novo* X-linked disease from autosomal recessive disease. In some patients the biopsy findings may be amibiguous, particularly females and young patients of either sex. Furthermore, rare families with progressive nephritis and *COL4A5* mutations in association with thin GBMs have been described, indicating that the classic GBM lesion is not present in all AS kindreds.

In families with a firm diagnosis of AS, evaluation of individuals with newly-recognized hematuria can be limited to ultrasound of the kidneys and urinary tract in most instances. In the absence of tumor or structural anomalies of the urinary tract, a diagnosis other than AS is unlikely. A suspected diagnosis of AS may be confirmed by immunohistochemical methods. Monospecific antibodies directed against type IV collagen α chains are available,[130,131] making it possible to reliably evaluate renal basement membranes for expression of α3(IV), α4(IV) and α5(IV) chains (Table 84.5). Since the α5(IV) chain is normally expressed in the epidermal basement membrane (EBM), examination of skin biopsies by immunofluorescence for expression of α5(IV) is an additional tool for making a diagnosis of AS. Absence of the α5(IV) chain from EBM is diagnostic of XLAS.[132] Given a male patient with a positive family history and clinical features characteristic of AS, examination of skin for α5(IV) expression may obviate the necessity for kidney biopsy. Unfortunately, a normal result does not exclude the diagnosis of AS, since in some XLAS kindreds (about 20%) affected males express α5(IV) in their renal and epidermal basement membranes.Heterozygous females frequently express α5(IV) mosaically in the skin. While clearly mosaic expression of α5(IV) is diagnostic of the carrier state, a normal result does not exclude heterozygosity.

Renal expression of type IV collagen α chains can serve to confirm a diagnosis of AS, and can in addition differentiate XLAS and ARAS (Table 84.5).In most males with XLAS renal basement membranes are devoid of the α3(IV), α4(IV) and α5(IV) chains, while females frequently show mosaic expression of these chains. In most males and females with ARAS the GBM, Bowman's capsule and distal TBM show no expression of the α3(IV) and α4(IV) chains, while α5 (IV) is expressed in Bowman's capsule and distal TBM but not GBM.[112]

The ability to diagnose Alport syndrome by skin biopsy may eventually reduce reliance on kidney biopsy for diagnosis of this disease. Skin biopsy is the initial diagnostic maneuver of choice when kidney biopsy is excessively risky, such as in patients with advanced renal insufficiency.

Genetic analysis provides the only means for reliably diagnosing the carrier state in asymptomatic female members of XLAS kindreds and for making a prenatal diagnosis of AS. There are also clinical situations in which a firm diagnosis of AS cannot be established, or in which it is not possible to determine the mode of transmission, despite careful evaluation of the pedigree and application of the full range of histological methods. In these situations genetic analysis has the

potential to provide information essential for determining prognosis and guiding genetic counseling. Genetic counseling based upon erroneous determination of the mode of inheritance may have unintended consequences.[133]

At the present time, the routine application of molecular analysis is limited by both specific and general problems. First, the sheer size of the type IV collagen loci (>50 exons), combined with the great variety of mutations, many of which are missense alterations of a single base pair, presents a formidable obstacle. Exon-screening methods, such as analysis of single-strand conformational polymorphisms, identify only about 50% of *COL4A5* mutations.[134,135] Detection schemes based on direct sequencing identify have a better detection rate (about 80–90%), but are relatively expensive.[136,137] Consequently, at the time this chapter was written, only a single commercial laboratory offered molecular diagnosis of Alport syndrome (www.genereviews.org).

In the future, automation and miniaturization of DNA analytic techniques may result in a relatively simple, rapid and inexpensive means of assaying a blood or tissue sample for mutations at genetic loci relevant to Alport syndrome, replacing other diagnostic methods. For now, genetic analysis is desirable, but not necessarily available, when there is ambiguity regarding the diagnosis of Alport syndrome or the mode of transmission, or when prenatal testing is desired.

Treatment

Replacement of renal function by transplantation is currently the only "treatment" of proven value for AS. Analysis of data from the North American Pediatric Renal Transplant Cooperative Study (NAPRTCS) documents equivalent allograft survival rates in patients with familial nephritis, in comparison to patients with other diagnoses.[138] However, some AS patients develop anti-GBM nephritis in the renal allograft, usually resulting in graft loss.Data from several transplant centers indicates an incidence of 3–4% in transplanted AS patients.[139–141] These patients are usually male, always deaf, and likely to have reached ESRD before the age of 30.[142] This profile describes the majority of AS patients presenting for renal transplantation, so its predictive value is rather limited. However, AS patients with normal hearing or late progression to ESRD appear to be at very low risk for the development of post-transplant anti-GBM nephritis. Females with XLAS also appear to be in a low-risk category.

The onset of post-transplant anti-GBM nephritis was within the first year following transplantation in approximately 75% of cases. Three-quarters of the allografts failed irreversibly, usually within a few weeks to months after diagnosis.Treatment with plasmapharesis and cyclophosphamide has been of limited benefit. Anti-GBM nephritis has recurred in seven of eight patients who underwent retransplantation. Post-transplant anti-GBM nephritis may recur despite an interval of many years between transplants, and in the absence of detectable circulating anti-GBM antibodies prior to retransplantation.

The target(s) of anti-GBM antibodies in some of these patients has been determined, with variable results. Most patients with XLAS exhibit antibodies that target the carboxy-terminal noncollagenous domain of the α5(IV) chain,[102,141,143,144] but anti-α3(IV) antibodies have also been described.[145] Antibodies against α3(IV) have been observed in ARAS patients with post-transplant anti-GBM nephritis.[143]

It has been proposed that mutations in the *COL4A5* gene that prevent expression of an immunogenic gene product, thereby preventing the establishment of tolerance for α5(IV), might be associated with an increased risk for the development of post-transplant anti-GBM nephritis.[144,103] Of 14 AS patients with post-transplant anti-GBM nephritis examined for a *COL4A5* mutation, seven, or 50%, had complete or partial deletions, compared with a deletion frequency of about 10% in the general AS population (discussed in[142]). Although the sample size is small, the data gathered thus far support the hypothesis that AS patients who develop anti-GBM nephritis after renal transplantation are more likely to carry deletions in the *COL4A5* gene than the AS population at large.

Females who are heterozygous for *COL4A5* mutations would not be expected to be at risk for the development of post-transplant anti-GBM nephritis, since the product of the normal *COL4A5* allele would allow establishment of immunologic tolerance for α5(IV). Nevertheless, post-transplant anti-GBM nephritis has been reported in two females with AS.[87,141] Both of these women were found to have ARAS, due to *COL4A3* mutations.[87,91]

Even if it were to prove true that certain *COL4A5* mutations are associated with a higher risk for the development of post-transplant anti-GBM nephritis, this information would be of limited value in planning transplantation. It is clear that AS males with *COL4A5* deletions can undergo renal transplantation without developing anti-GBM nephritis,[146,147] indicating that other factors, presently unknown, must influence the initiation and elaboration of the immune response to the allograft. At this time it appears that the only way to determine whether a previously untransplanted AS patient will develop post-transplant anti-GBM nephritis is to perform the transplant, although as noted previously certain patients are at very low risk.

Interventions aimed at preventing or slowing the inexorable decline in renal function typical of male AS

are currently under investigation. The role of angiotensin II in the pathogenesis of renal failure in AS is still not well understood. Studies of angiotensin inhibition in AS have involved small numbers of patients with proteinuria serving as their own controls, with relatively short follow-up, and have produced mixed results.[148–151] However, Gross and colleagues found that ramipril therapy initiated prior to the development of proteinuria delayed the onset of proteinuria and renal failure and lengthened survival in a murine model of ARAS.[128,129] Early angiotensin converting enzyme inhibition in dogs with XLAS had no effect on the onset of proteinuria, but did delay ESRD.[152] These observations suggest that angiotensin blockade, initiated early in the course of disease might be beneficial in human AS.

Callis and colleagues found, in an uncontrolled study of eight AS males, that cyclosporine appeared to suppress proteinuria and stabilize renal function, over several years of observation.[153,154] There has yet to be a published report that contradicts these findings. However, the results of trials presented in abstract suggest that patient responses to cyclosporine are variable, and that cyclosporine may accelerate interstitial fibrosis.[155,156] In dogs with XLAS, cyclosporine failed to suppress proteinuria, but treated animals did exhibit a delay in progression to ESRD.[157] At this time, it is the authors' view that the efficacy of cyclosporine as a treatment for AS has not been demonstrated with the degree of certainty needed to overcome concerns about its nephrotoxicity.

Gene transfer approaches aimed at delivering a normal copy of the *COL4A5* gene to glomeruli are currently undergoing investigation in canine models of AS.[158–161]

Thin Basement Membrane Nephropathy (TBMN)

TBMN, like AS, is an inherited disorder of glomerular basement membranes that is characterized clinically by persistent microscopic hematuria and episodic gross hematuria. TBMN differs clinically from AS in several important respects: (1) It is only rarely associated with extrarenal abnormalities. (2) Proteinuria, hypertension and progression to ESRD are unusual. (3) Gender differences in the severity of the signs and symptoms of TBMN are not apparent. (4) Transmission is autosomal dominant in nature.TBMN and early AS may be difficult to distinguish histologically, since diffuse GBM attenuation is characteristic of both. However, the GBM of TBMN patients remains attenuated over time, rather than undergoing the progressive thickening and multilamellation that is pathognomonic of AS.

Clinical Features

Individuals with TBMN typically exhibit persistent microhematuria that is first detected in childhood. In some patients microhematuria is intermittent, and may not be detected until adulthood. Episodic gross hematuria, often in association with upper respiratory infections, is not unusual. The hematuria of TBMN appears to be life-long.It has been estimated that 20–25% of patients referred to a nephrologist for evaluation of persistent hematuria will prove to have thin GBM on renal biopsy.[162]

Overt proteinuria and hypertension are unusual in TBMN, but have been described.[163–166] Some of these patients exhibit focal global glomerulosclerosis on renal biopsy.[164] In occasional adult patients with Alport syndrome the predominant GBM abnormality of is attenuation, rather than thickening and multilamellation. Other glomerular disorders such as IgA nephropathy may occur in patients with TBMN, altering the expected natural history and histopathology of the condition.

Pathology

Light and immunofluorescence microscopy are unremarkable in typical cases of TBMN or thin GBM disease. Most patients with TBMN exhibit diffuse thinning of the GBM as a whole, and of the lamina densa (Figure 84.3). Normal GBM thickness is age- and sex-dependent. Both the lamina densa and the GBM normally increase rapidly in thickness between birth and age two years, followed by gradual thickening throughout childhood, adolescence and into adulthood.[167] GBM thickness of adult men (373 ± 42 nm) exceeds that of adult women (326 ± 45 nm).[168] Thus it is important to consider the age and sex of the patient when evaluating GBM width.Each EM laboratory should establish a consistent technique for measuring GBM thickness, and determine its own means and standard deviations for GBM width, to make comparisons with published data meaningful.

The definition of "thin" GBM in the literature is imprecise, in part because of the use of different techniques to measure GBM width. When an EM laboratory's normal values for GBM width are similar to those of Steffes et al.[168] a cut-off value of 250 nm will accurately separate adults with normal GBM from those with thin GBM. Where the normal values are significantly higher, a cut-off value of 330 nm is appropriate.[169] For children, the cut-off is in the range of 200–250 nm (250 nm is within 2SD of the mean at age 11).[170,167] It is useful to note that the intraglomerular variability in GBM width is small in thin GBM disease.[165] Marked variability in GBM width within a glomerulus, in a patient with persistent microhematuria,

should raise suspicion of Alport syndrome, although focal lamina densa splitting has been described in TBMN.

Genetics and Pathophysiology

TBMN is usually transmitted as an autosomal dominant condition. A negative family history may not be reliable, since patients eventually diagnosed as having TBMN are frequently unaware that they have relatives with hematuria.[171] The first clue to the genetic basis of TBMN was provided by Lemmink and coworkers, who described a large Dutch TBMN kindred in which the disease locus was first mapped to chromosome 2 in the region of the *COL4A3* and *COL4A4* genes, and then affected individuals were found to be heterozygous for a missense mutation in *COL4A4*.[172] Since this landmark work, heterozygous mutations in *COL4A3* or *COL4A4* have been described in numerous TBMN families.[93,95,173,174] However, linkage to the *COL4A3* and *COL4A4* genes has been excluded in other TBMN families, indicating that TBMN is a genetically heterogeneous condition.[175]

To date, immunohistologic studies of type IV collagen in GBM of patients with TBMN or thin GBM disease have failed to uncover any abnormalities in the distribution of any of the six chains. However, it is tempting to speculate that in those kindreds with TBMN due to a heterozygous *COL4A3* or *COL4A4* mutation, a 50% reduction in the GBM α3(IV)$-\alpha$4(IV)$-\alpha$5(IV) network results in lamina densa and GBM thinning and fragility. This reduction is presumably insufficient to trigger the pathophysiologic events that produce the lamina densa splitting and GBM thickening characteristic of Alport syndrome (AS). Immunohistologic evaluation of GBM type IV collagen may be useful in the differentiation of TBMN and AS (see below).

Diagnosis

Patients with persistent, isolated microhematuria are usually candidates for kidney biopsy, once structural urinary tract abnormalities, urinary tract stones and tumors are excluded. If the patient's family history indicates autosomal dominant transmission of hematuria, and there is no history of chronic renal failure, a presumptive diagnosis of TBMN can often be made without kidney biopsy. When family history is negative or unknown, or there are atypical coexisting features such as proteinuria or deafness, renal biopsy may be extremely informative. A finding of thin GBM may be further characterized by examining the distribution of type IV collagen α chains in the kidney. Normal distribution of these chains provides supportive, although not conclusive, evidence for a diagnosis of TBMN (see also preceding section on Alport syndrome).

Treatment

Patients who are given a diagnosis of TBMN should be reassured, but not lost to follow-up examination. The risk of chronic renal insufficiency appears to be small but real.[163–166] Reasonable follow-up would include urinalysis and measurement of blood pressure and renal function every one to two years.

Hereditary Angiopathy with Nephropathy, Aneurysms and Cramps (Hanac Syndrome)

Missense mutations in the *COL4A1* gene encoding the α1 chain of type IV collagen have been associated with autosomal dominant transmission of an angiopathy characterized by nephropathy, aneurysms and muscle cramps in several families.[176] Renal symptoms include hematuria, renal insufficiency and renal cysts. Renal biopsies showed no abnormalities of glomerular basement membrane structure or type IV collagen expression, although basement membranes of Bowman's capsules, tubules and interstitial capillaries showed irregular thickening and lamellation.

Pierson Syndrome

Pierson and colleagues reported familial cases of infantile nephrotic syndrome and distinct ocular abnormalities.[177] The ocular abnormalities were marked by enlargement of the globe (buphthalmos) and reduction in the size and reactivity of the pupils (microcoria). All affected infants died within the first year of life.

Zenker and colleagues reported on consanguineous families with 11 children demonstrating similar clinical features.[178,179] Several of these children were identified by fetal ultrasound, variably demonstrating kidney enlargement and hyperechogenicity, oligohydramnios, placental enlargement and/or pulmonary hypoplasia. Infants surviving to term had congenital nephrotic syndrome, with kidney biopsy or autopsy specimens revealing diffuse mesangial sclerosis.These children also had ocular globe enlargement and microcoria, with sporadic findings of cataract, posterior rupture of the lens capsule (lenticonus) and retinal abnormalities. In additional case reports, affected children had muscular hypotonia, central nervous system hemangioma and genital abnormalities.[180,181] Kidney biopsy specimens from these patients also demonstrated diffuse mesangial sclerosis, as well as marked GBM irregularities. None of these children survived beyond the first year of life.

Zenker and colleagues localized the Pierson syndrome gene to chromosome 3p14–p22 by homozygosity mapping.[182] Identifying the *LAMB2* gene encoding the β2 chain of basement membrane laminin as a

candidate, these workers went on to sequence homozygous and compound heterozygous mutations in five families, including two nonsense mutations, three frameshift mutations and one missense mutation.In one patient, a homozygous nonsense mutation of the *LAMB2* gene was associated with loss of β2 laminin from the GBM.

The β2 chain of laminin is one of four β chains of basement membrane laminin.[183,184,185] Individual laminins are heterotrimeric glycoproteins made up of variable α, β and γ chains, combining in 1:1:1 stoichiometric proportions to form cruciform structural subunits. In turn, laminin subunits self-assemble and generate macromolecular networks within basement membranes, serving myriad roles in overall extracellular matrix organization, determination of basement membrane properties and interactions with adjacent cells. The laminin β2 chain participates in the formation of several distinct αβγ laminins. In particular, laminin-11 comprised of α5β2γ1 is upregulated during development of the kidney glomerulus, in a characteristic mid-gestational switch of laminin and type IV collagen isoforms marking GBM maturation,[117,186]. Partially recapitulating Pierson syndrome, targeted deletion of the mouse *Lamb2* ortholog causes congenital nephrosis, with mesangial hyperceullularity and podocyte foot process injury.[187] Interestingly, laminin β2-deficient mice also demonstrate neuromuscular synapse abnormalities with resulting muscular weakness,[187] a feature with correlates in Pierson syndrome.

The mechanisms by which *LAMB2* mutations give rise to nephrotic syndrome and accelerated kidney disease are uncertain. Ultrastructural abnormalities in Pierson syndrome suggest disruption of GBM structural integrity. Defects in glomerular cell-GBM interactions are also likely, as laminin-11 is a ligand for integrin extracellular matrix receptors,[188,189] most importantly α3β1 integrin mediating glomerular cell attachment to the GBM.[190]

Further discussion on the laminins and their biological roles in kidney and other tissues can be found in several excellent reviews.[183–185,191,192]

STORAGE DISORDERS

Fabry Disease

Fabry disease is an X-linked disorder caused by deficiency of the lysosomal hydrolase enzyme α-galactosidase A (EC 3.2.1.22).Deficient α-galactosidase A (α-Gal A) activity results in accumulation of glycosphingolipid (globotrioacylceramide, or Gb3) in blood vessels and various organs leading to the clinical manifestations of the disease, including chronic renal failure. Also known as Anderson-Fabry disease or angiokeratoma corporis diffusum universale, Fabry disease was first described in 1898 in separate reports by Anderson in England and Fabry in Germany.[193,194] Although the incidence of Fabry disease is approximately 1:40,000, making it a rare cause of renal failure, much is known about the genetic pathophysiology of the disorder. Most importantly Fabry disease has the potential to be effectively treated by enzyme replacement.

Clinical Features

Since Fabry disease is an X-linked disorder, severe clinical manifestations occur in hemizygous males while heterozygous females exhibit a variable but typically less severe course. However, there is increasing recognition of disease-related morbidity in heterozygous females. Data from the Fabry Registry indicated that about 70% of heterozygous females have symptoms of Fabry disease.[195] Although median onset of symptoms was 13 years, and over 80% had a positive family history of Fabry disease, median age of diagnosis was 31 years. Major cerebrovascular, cardiac or renal events occurred in 20% at a median age of 46 years, and proteinuria and reduced glomerular filtration rate were common. These findings illustrate the importance of regular monitoring in females as well as males with Fabry disease.

The clinical features of Fabry disease are summarized in Table 84.6. In hemizygotes (affected males) the initial features of the disease are seen in childhood and early adolescence and consist of paresthesias and pain in the hands and feet with episodic pain crises. The course of the disease is variable but usually leads to end-stage renal disease in the third to sixth decade.

TABLE 84.6 Clinical Manifestations of Fabry Disease

Skin	Angiokeratomas
Nervous system	Painful neuropathy
	Acroparesthesias
	Hypohidrosis
	Stroke
	Dementia
Cardiac	Hypertrophy
	Coronary artery disease
	Cardiomyopathy
Renal	Proteinuria
	Renal failure
Eye	Corneal and lenticular opacities

Myocardial or cerebral infarctions are typically terminal events

The classic skin lesion, angiokeratoma corporis diffusum universale, consists of macules or maculopapules, cherry red to black in color and 1–3 mm in diameter. These lesions first appear in adolescence particularly in the scrotal area, lower back and trunk. There may be up to several dozen lesions. Other skin manifestations include palmar erythema, splinter hemorrhages, and conjunctival or buccal mucosal telangiectasias. One of the most profound and debilitating aspects of the disease is peripheral nerve involvement leading to painful crises, acroparesthesias, and hypohidrosis. Central nervous system involvement includes cerebral infarctions and dementia.Corneal and lenticular opacities occur in all hemizygotes and most heterozygotes.

The most common cardiac manifestation in Fabry disease is coronary artery disease but hypertrophy, congestive heart failure, valvular lesions, and arrythmias are common. A form of the disease limited to the heart has been described and is characterized predominantly by cardiac hypertrophy.[196,197] These patients often have mutations that result in detectable amounts of enzyme. In fact, among 230 consecutive male patients presenting with left ventricular hypertrophy 3% had low plasma α-Gal A activity and may represent cardiac limited variants of the disease.[196]

The earliest renal manifestation is a concentrating defect.Proteinuria, typically in the range of 0.5 to 2 g daily, is first detected in young adulthood.[198,199] Nephrotic-range proteinuria is unusual but may be seen. The urinary sediment is most often bland although some patients exhibit microscopic hematuria. There is increased urinary glycosphingolipid, and urinary myelin bodies, both free and within tubular cells, may be found.[200,201] Classic Maltese crosses can be seen when the urine sediment is examined with a polarizing microscope. Fabry disease has been reported in association with IgA nephropathy[202] and SLE.[203]

End-stage renal disease typically occurs in the third to sixth decade but has been reported in patients less than 20 years old.[198] The clinical course of the renal failure has been described by several investigators. Donati and colleagues followed 12 patients with end-stage renal disease. Eight patients were transplanted and all survived with the longest patient being 66 months post transplant.[204] Three dialysis patients died 9, 11 and 12 months after starting dialysis prompting these investigators to conclude the prognosis was better after transplantation. Nissenson and colleagues described 17 patients (including one woman) with Fabry disease who underwent treatment for end-stage renal disease.[198] Eighty three percent of the patients survived to 33 months and 41% were transplanted.

Pathology

Intracellular glycosphingolipid accumulation is found in most structures of the kidney including glomerular epithelial, endothelial and mesangial cells, tubular epithelial cells, interstitial cells, and blood vessels including endothelial, perithelial and smooth muscle cells.[205,206] During routine processing of paraffin-embedded sections lipids are dissolved by the xylene so that the cells which contained them look like foam cells with empty vacuoles (Figure 84.4). With fresh or fixed-frozen tissue lipids can be identified with fat stains such as Sudan III or oil red O. The glomerular epithelial cells are most prominently affected in the kidney.These cells are filled with small, uniformly sized vacuoles, giving them a foamy appearance (Figure 84.4). Vacuoles are often present in parietal epithelial cells but are not commonly seen in endothelial or mesangial cells. In the later stages of the disease the glomeruli become sclerotic.

Vacuolization of tubular cells is most prominent in the loop of Henle and distal convoluted tubule and is rarely seen in the proximal tubule. Most blood vessels are involved with vacuoles present in endothelium, smooth muscle cells and perithelial cells.In later stages insudative arteriolar changes are observed.[206]

Immunofluorescence is negative except in advanced glomerular sclerosis where non-specific uptake of immunoglobulin or complement can be seen.[206] Glycosphingolipid can be detected with antibodies to trihexosylceramide.[207]

The characteristic lesion of Fabry disease is seen on electron microscopy (Figure 84.8). Stacks or whorls of dense inclusions ranging in diameter from 0.3 to 10 μm (average 3 μm) are found in lysosomes of affected cells. Terms such as onion skin or myelin figures have been used to describe the concentric

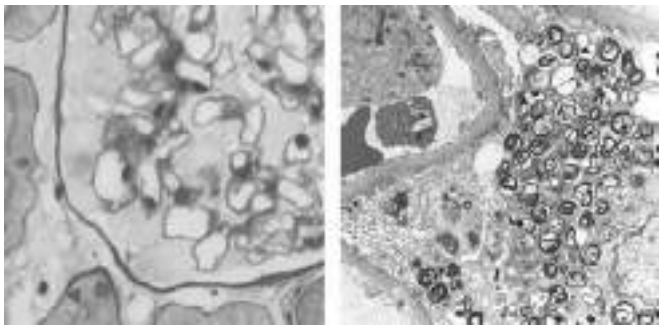

FIGURE 84.4 Renal biopsy findings in Fabry disease. Left: periodic acid-schiff staining demonstrates glomerular cell enlargment, vacuolization and fusion, without capsular adhesions. Right: Electron Microscopy demonstrates glycosphingolipid deposits within podocytes. Micrographs are courtesy of Drs. George Canas and Rahul Koushik.

dense layers of glycosphingolipid deposits.The deposits can also appear as parallel arrays ("zebra bodies").[208] Cells that appear normal on light microscopy can have inclusions.In the glomerulus, deposits are present in every cell type but are less numerous and smaller in endothelial and mesangial cells. Heterozygous females have similar but fewer inclusions. Other intracellular organelles appear normal. Foot process fusion occurs with heavy proteinuria.In the later stages of the disease the glomerular basement membrane becomes wrinkled and thickened and mesangial interposition may occur. These changes are suggestive of glomerular ischemia. Typical inclusions may be present in Bowman's space and tubular lumena, and cells containing glycosphingolipid may be found in the urine and can be used for making the diagnosis of Fabry disease.[200,201]

Genetics and Pathophysiology

The α-Gal A protein has a molecular weight of approximately 50 kDa. It is a homodimeric glycoprotein containing 5 to 15% oligosaccharide chains. Processing includes cleavage of the signal peptide and carbohydrate modifications resulting in the mature 100 kDa enzyme.The mature protein then moves to its site of action in the lysosome. The protein has been crystallized and analyzed in more detail.[209]

α-Gal A cDNA was first isolated in 1986.[210] The coding sequence comprises 1290 bp and codes for a protein of 429 amino acids including a 31 amino acid signal peptide. There are four possible N-glycosylation sites, three of which are used. The α-Gal A gene is located on the long arm of the X chromosome at Xq22.1. The gene is 12 kb in size and contains 7 exons ranging in size from 92 to 291 base pairs.[211] The sequence for the 5′ untranslated region, the signal peptide and the first 33 amino acids of the mature enzyme are contained in exon 1. The gene is *Alu*-rich, containing 12 *Alu* repetitive elements each containing 300 nucleotides that comprise 30% of the gene.[211] Polymorphisms of the α-Gal A gene have been described but are rare.[211,212] These polymorphisms along with other highly polymorphic markers near the α-Gal A gene can be used for diagnosis and carrier detection.[213]

Almost all unrelated families with Fabry disease have different mutations.[211,214–217] The majority of the mutations are single base substitutions in the coding region with two thirds occurring in exons 5 through 7.[212] Other mutations include gene rearrangements such as duplications, deletions, insertions, and RNA processing defects.[218]

Deficiency of α-Gal A leads to progressive intracellular accumulation of neutral glycosphingolipids, particularly those with α-galactosyl moieties, the most abundant of which is globotriaosylceramide (Gb3). Glycosphingolipids are normal constituents of the plasma membrane, the membranes of intracellular organelles, and circulate in association with apolipoproteins, particularly low density lipoprotein.[219] The glycosphingolipids that accumulate in Fabry disease are identical to those found in normal tissue.[220] All tissues except red blood cells accumulate Gb3 with the highest concentrations found in the diseased kidney.[221]

Accumulation of glycosphingolipids, particularly in the CNS and cornea, results from retention of endogenously metabolized glycosphingolipid. The presence of glycosphingolipid in vascular endothelium and smooth muscle may be due to uptake of circulating Gb3.[220] Vascular pathology results from the swollen endothelium narrowing or occluding the vascular lumen.In addition, the endothelium likely serves as an initiator of vascular thrombosis. Whether the renal pathology is entirely secondary to vascular disease or due to glomerular and/or tubular epithelial cell toxicity is unclear. The most prominent early lesion in the kidney is swelling and vacuolization of visceral epithelial cells which likely is the underlying basis for the proteinuria and may be an important factor in the development of glomerular sclerosis.[222]

Classically affected hemizygotes have a large variety of mutations. Patients with mutations that maintain some residual α-Gal A activity tend to have milder phenotypes. Examples include patients with disease confined predominantly to the heart, who most often have missense mutations and express low levels of α-Gal A activity.[223]

Mice in which the α-Gal A gene has been deleted by gene targeting techniques completely lack α-Gal A activity as expected.[224] No clinical phenotype is detectable at 10 weeks of age. However, ultrastructural and histochemical studies, and lipid analysis demonstrate the classic lamellar inclusions in the kidney and accumulation of Gb3 in the liver, kidneys and in cultured fibroblasts. In the kidney the lipid inclusions are first seen in renal tubular cells. Enzyme activity can be restored in cultured embryonic fibroblasts of the deficient mice by transducing the cells with a retrovirus containing the α-Gal A gene, resulting in decreased accumulation of Gb3 in the fibroblasts. Infusion of transduced bone marrow cells corrects the enzyme deficiency and reduces glycosphingolipid stores in α-Gal A-deficient mice.[225]

Diagnosis

Diagnosis of the hemizygote patient can usually be made on clinical grounds with the additional information from slit lamp examination of the eye. The diagnosis should be confirmed by demonstrating decreased to absent α-Gal A activity in serum, leukocytes, cultured skin fibroblasts or biopsied tissue. Atypical variants

may have enzyme activity up to 35% of normal.[220] A dissociation may also exist between serum and tissue enzyme activity.

Heterozygous females have intermediate levels of α-Gal A activity but values may be in the low normal range making measurement of enzyme activity an insensitive way of diagnosing carriers. Alternatives include careful slit lamp eye exam, measuring urinary ceramide digalactoside and trihexoside, or by molecular techniques using restriction fragment length polymorphisms of either the α-Gal A gene or closely linked markers on the X-chromosome.[213] Identification of carriers is particularly relevant when family members are being considered as living kidney donors.[226] Measurement of chorionic villus enzyme level or the enzyme level in cultured amniotic cells is possible.[227]

Treatment

Until recently, clinicians could offer little beyond palliative, symptomatic care to patients with Fabry disease, including carbamazepine and gabapentin, or narcotics, for neuropathic pain, antihypertensive therapy and platelet antagonists. However, the landscape of Fabry therapy has been transformed over the past several years by the introduction of enzyme replacement therapy using recombinant human α-Gal A (agalsidase).

Studies conducted in the 1970s showed that injection of α-Gal A purified from human plasma resulted in transient reduction in plasma Gb3.[228,229] Production of sufficient enzyme for clinical trials was not possible until the advent of recombinant DNA technology. In 2001, Ioannou and colleagues described pre-clinical studies in α-Gal A-deficient mice showing that recombinant human enzyme lowered tissue and plasma Gb3,[230] providing the rationale for human treatment trials.

Phase I/II clinical trials demonstrated that agalsidase produced dose-dependent reductions in plasma, tissue and urine Gb3 in Fabry patients.[231,232] Randomized clinical trials showed that agalsidase administration over 5–6 months resulted in reduced plasma and urine Gb3, amelioration of neuropathic pain, enhanced quality of life, clearing of Gb3 deposits from kidney, heart and skin, and improved cerebral blood flow.[233–235] A multicenter longitudinal study showed that algasidase stabilized renal function in patients with mild to moderate renal impairment at baseline, and reduced left ventricular mass in those with left ventricular hypertrophy at baseline, over one to two years of treatment.[236,237] Agalsidase therapy has been recommended for all affected males and symptomatic carrier females.[238]

Long-term therapeutic outcomes of agalsidase therapy are also promising.[239] Left ventricular mass index remained stable in patients without baseline ventricular hypertrophy and decreased significantly in those with ventricular hypertrophy at the onset of therapy. Pain severity decreased, and quality of life indicators increased, with therapy. Glomerular filtration rate was stabilized by therapy. Trials testing agalsidase therapy against placebo have shown reduced rate of loss of renal function in agalsidase-treated patients, although no effect on proteinuria was observed.[240]

A problem that may affect the long-term efficacy of agalsidase treatment is development of neutralizing antibodies to the enzyme. Linthorst and colleagues found that 11/16 Fabry males developed high titers of neutralizing IgG antibodies to α-Gal A. After six months of treatment, antibody-negative patients had significantly lower urine Gb3 levels compared to antibody-positive patients, suggesting that the antibodies interfered with renal tubular Gb3 clearance.[241] However, the impact of α-Gal A antibodies on the efficacy of agalsidase treatment remains to be determined. A recent analysis found no correlation between anti- α-Gal antibody titers and rate of change in glomerular filtration rate during treatment.[242]

Options for managing end-stage renal failure in Fabry patients include dialysis and transplantation. Initial reports of kidney transplantation for Fabry disease suggested that the allograft might serve to correct the underlying metabolic defect.[243–245] However, kidney transplantation does not improve the systemic manifestations of the disease.[246,247] Graft and patient survival rates for patients with Fabry disease are similar to those in patients with other diagnoses.[248] Glycosphingolipid can accumulate in the transplanted kidney but the deposits are detectable only by electron microscopy predominantly in capillary endothelial cells.[249,250] Loss of the allograft from recurrent disease has not been described. Transplanting the kidney from a heterozygote can result in recurrent disease making donor screening important.[226] Renal allograft recipients with Fabry disease are candidates for agalsidase treatment.[251]

Fabry Disease in Childhood

The signs and symptoms of Fabry disease, particularly pain crises, acroparesthesias, angiokeratomas and corneal opacities, typically have their onset in childhood, although a specific diagnosis is frequently delayed until well into adulthood.[252,253] Albuminuria and characteristic renal histological abnormalities have been described in children and adolescents with Fabry disease.[254,255] Agalsidase therapy in a small number of pediatric patients was associated with clearing of GL-3 from dermal capillary endothelium, and mild or moderate infusion-associated

reactions.[256] In another study, affected children treated with agalsidase resulted in reduced plasma and urine GL-3 levels and decreased pain severity.[257]

OTHER STORAGE DISORDERS ASSOCIATED WITH GLOMERULAR DYSFUNCTION

Glomerular dysfunction may be detected in patients with various inherited storage diseases, associated with accumulation of the storage material in glomerular cells, mesangium or GBM (see Table 84.1). Deficiency of the enzyme lecithin-cholesterol acyltransferase (LCAT) prevents esterification of plasma cholesterol and thus interferes with reverse cholesterol transport from tissues to the liver. The accumulation of free cholesterol in tissues results in a variety of clinical abnormalities, including proteinuria that frequently progresses to ESRD.[258] Light microscopic features of the kidney in LCAT deficiency include mesangial expansion and glomerular capillary wall thickening. The ultrastructural findings are distinctive, consisting of numerous, irregular lucencies in the mesangium and GBM that contain dense granular or membrane-like structures. These lesions regularly recur in renal transplants.

Sialidosis results from deficiency of sialidase, which removes terminal sialic acid residues from sialyl-oligosaccharides released during glycoprotein degradation. Consequently, sialic acid-rich material accumulates in various tissues.Renal involvement, manifested by proteinuria, occurs in type II, or dysmorphic-type, sialidosis.[259] Light and electron microscopy of renal biopsy specimens shows massively swollen podocytes, due to the presence of innumerable thin-walled cytoplasmic vesicles.[260,261] Vesicles may also be seen in mesangial, endothelial and tubular epithelial cells. Material within these vesicles binds the lectin wheat germ agglutinin, confirming the presence of terminal sialic acid moieties. Podocyte detachment has been observed in sialidosis and may be pathogenetically related to the proteinuria.[260,262] Prominent accumulation of storage material in podocytes has also been described in I-cell disease, in which a mixture of mucopolysaccharides, lipids, and oligosaccharides accumulates,[263] and in Hurler syndrome, in which the stored material is mucopolysaccharide.[264]

Although renal disease is not unusual in older patients with glycogen storage disease type 1 (GSD1) due to glucose-6-phosphatase deficiency,[265] it is not clear that the pathologic changes in the kidney arise from storage of glycogen. It has been proposed that proteinuria and glomerulosclerosis in patients with GSD1 result from hyperfiltration injury.

DISORDERS OF THE PODOCYTE SLIT DIAPHRAGM

Congenital Nephrotic Syndrome of the Finnish Type (CNF)

Clinical Features

This autosomal recessive condition is the predominant cause of massive proteinuria in the first month of life. While Finland appears to have the world's highest incidence of CNF (about 1.2 cases/10,000 pregnancies), cases in children of non-Finnish ancestry have been reported from every part of the globe. Fetuses with CNF exhibit proteinuria *in utero*, manifested by elevated levels of α-fetoprotein in the amniotic fluid.[266] Edema frequently appears during the first week of life.[267] Cerebral palsy-like neurological disease has been described in a subset of patients, although the mechanisms of association with CNF are unclear.[268] Infants with CNF eventually develop renal failure, however historically the effects of malnutrition, overwhelming infection and thrombosis frequently resulted in early death, prior to the development of ESRD. Today, with aggressive therapy these children can survive infancy and grow sufficiently to undergo renal transplantation, with excellent rates of patient and graft survival.[269,270] In recent years, the clinical spectrum of glomerular disease due to NPHS1 mutations (see below) has expanded to include childhood- and adult-onset steroid-resistant nephrotic syndrome.[271,272] Furthermore, the heterozygous state may, in some cases, contribute to nephrotic syndrome occurring sporadically.[273,274]

Pathology

Nephrogenesis appears to proceed normally in kidneys of fetuses with CNF.[275] However, histological abnormalities such as focal mesangial hypercellularity, dilatation of Bowman's spaces and renal tubules, and visceral epithelial cell foot process fusion and microvillous transformation, are not unusual in these kidneys. Postnatally, early histological findings include mesangial hypercellularity and matrix expansion. Bowman's spaces and proximal tubules may become cystically dilated.[276,277] After six months, progressive glomerulosclerosis, tubular atrophy and interstitial fibrosis are evident. Immunofluorescence microscopy is typically unremarkable, except for albumin reabsorption droplets in tubular epithelial cells. Electron microscopy shows visceral epithelial

foot process fusion and microvillous transformation, while the GBM typically appears to be structurally normal.Variants on the classical histology have been described.[278]

Genetics and Pathophysiology

For many years efforts to understand the mechanism of proteinuria in CNF focused on the composition on the GBM, particularly proteins contributing to the negative charge of GBM, such as heparan sulfate proteoglycan.[279–282] However, the results of genetic mapping studies carried out in the 1990s, culminating in positional cloning of the *NPHS1* gene encoding nephrin, brought about a dramatic shift in focus to the podocyte slit diaphragm.[283]

Nephrin, an integral membrane protein with a single transmembrane domain and 8 extracellular immunoglobulin-like domains, is expressed at the slit diaphragms between glomerular visceral epithelial cell (podocyte) foot processes[284]; it is the cardinal member of the nephrin family of proteins.[285] The critical role of nephrin in maintaining glomerular permselectivity was confirmed in nephrin-knockout mice, which develop massive proteinuria *in utero* and exhibit absence of podocyte foot processes and slit diaphragms.[286] Nephrin strands from adjacent foot processes appear to interact to form pores in the slit diaphragm.[287] Nephrin interacts with several proteins, including podocin,[288] CD2-associated protein (CD2-AP)[289] and the related adaptor protein CIN85/Ruk_L,[290] ion channels,[291,292] junctional proteins[293,294] and the nephrin analogs Neph1[295] and Neph2.[296] The cytoplasmic tail of nephrin undergoes phosphorylation at several tyrosine residues in a tightly regulated process involving Src family protein kinases.[297–300] Covalent modifications of nephrin and interactions with its binding partners have been implicated in a variety of slit diaphragm functions including barrier formation, turnover, cell signaling and cytoskeletal regulation. Further studies in model systems have shown that nephrin can activate transcription, and that this function is enhanced by the interaction of podocin with the tyrosine-phosphorylated cytoplasmic tail of nephrin.[288,301]

Disease-causing mutations have been identified throughout the *NPHS1* gene, attesting to the functional importance of both the intracellular and extracellular domains of the protein.[302] Two mutations in *NPHS1*, Fin major (nt121delCT) and Fin minor (R1109X), were found to account for >90% of Finnish NPHS1 patients.[283,303]A variety of other mutations in *NPHS1* (>140) have been found in non-Finnish patients.[278,302,304–308] Milder forms of kidney disease may occur in some homozygotes and compound heterozygotes in whom at least one mutation is "mild," resulting in a protein that traffics to the cell membrane and retains partial function.[302,271]

Diagnosis

NPHS1 mutations are the predominant, but not sole, cause of nephrotic syndrome in the first month and account for an estimated 40 to 60% of nephrotic syndrome cases in the first three months of life.[278,309,308] Some infants with clinical CNF have mutations in podocin, the product of the *NPHS2* locus, and a congenital form of focal segmental glomerulosclerosis (FSGS) has been described in patients with *NPHS1* mutations in conjunction with mutations in *NPHS2* (see below).[302] Other conditions that may present with early nephrotic syndrome include congenital infections, renal disorders that typically present in late infancy and childhood, such as minimal change nephrotic syndrome and FSGS, and diffuse mesangial sclerosis (DMS), with or without other features of Denys-Drash syndrome (see below). Features consistent with a diagnosis of CNF include placental enlargement (placental weight greater than 25% of birth weight), positive family history of early nephrotic syndrome and intrauterine proteinuria, indicated by elevated amniotic fluid levels of α-fetoprotein. Hypoalbuminemia is generally severe at presentation (<1 gm/dL).Infants with CNF characteristically maintain a normal GFR through at least the first six months of life, so rapid deterioration of renal function should suggest another diagnosis. Renal biopsy after three to six months will reveal the typical histology of CNF which, while not necessarily specific, differs substantially from the histology of DMS, FSGS and nephropathies associated with congenital infection.The cloning of *NPHS1* and *NPHS2* and the availability of commercial mutation analysis have enhanced diagnostic precision in infants with nephrotic syndrome. Because of the clinical and histological overlap between *NPHS1*- and *NPHS2*-related disease, molecular diagnostic approaches should incorporate analysis of both genes.[302] Screening for less frequent mutations in the *WT1*, *LAMB2* and *PLCE1* genes can be considered in cases in which *NPHS1*/*NPHS2* analysis is non-diagnostic or kidney biopsy demonstrates DMS.

Prenatal diagnosis of CNF due to *NPHS1* mutations is complex.[310] Fetuses with CNF due to *NPHS1* mutations exhibit elevated amniotic fluid α-fetoprotein (AFP) levels during the second trimester.[266] However, amniotic fluid AFP may be elevated in other conditions, such as neural tube defects, and there is overlap between the amniotic fluid AFP levels of fetuses with CNF and healthy carriers of *NPHS1* mutations.[311] Prenatal diagnosis of CNF is greatly facilitated if the disease-causing mutation in the family is known.[312] If the mutation is not known, sequencing of the entire

NPHS1 gene within the required time interval may not be possible. In this situation, the finding of elevated amniotic fluid AFP should prompt a fetal ultrasound to exclude a neural tube defect, followed by serial measurement of amniotic fluid AFP during the second trimester. In fetuses with CNF AFP levels will remain elevated, while levels will decrease in healthy carriers of *NPHS1* mutations.[310]

Treatment

With appropriate management, infants with CNF can thrive sufficiently to allow successful renal transplantation.[269,270] However, such treatment is complex, requiring meticulous attention to nutrition, albumin replacement, correction of hypothyroidism, prophylaxis and prompt recognition and treatment of bacterial sepsis, and prevention of thrombosis. Elective bilateral nephrectomies are performed once the child's real weight reaches about 7 kg. A period of hemo- or peritoneal dialysis for 6−8 weeks allows for optimization of nutrition and normalization of plasma proteins, and then the child undergoes transplantation. While this approach has resulted in excellent rates of patient and graft survival, others have advocated unilateral nephrectomy combined with captopril and indomethacin therapy and later renal transplantation.[313]

Autosomal Recessive Steroid-Resistant Nephrotic Syndrome

Clinical Features

Fuchshuber and colleagues first classified familial autosomal recessive SRNS as a subgroup of idiopathic nephrotic syndrome for genetic mapping studies that culminated in the identification of the *NPHS2* gene and its gene product podocin.[314,315] The defining clinical features included: familial occurrence, childhood-onset of nephrotic syndrome, resistance to steroid therapy, rapid progression to ESRD and absence of recurrence after kidney transplantation. It has since become evident that SRNS due to *NPHS2* mutations is the single most common cause of nephrotic syndrome during the first year of life, accounting for 30 to 40% of cases.[309] Furthermore, 10 to 30% of patients presenting as sporadic cases of childhood-onset SRNS represent homozygous or compound heterozygous offspring of unaffected heterozygous parents, with estimated frequencies dependent on racial and ethnic background.[316,317−320]

Among large cohorts of childhood-onset SRNS, age at presentation has been reported to range from <months to 24 years, with estimated means of 3 to 6 years.[320−322] Age at ESRD has been reported to range from 4 to >27 years, with estimate means of 8 to 10 years. Patients with SRNS and homozygous or compound heterozygous *NPHS2* mutations appear to suffer accelerated progression of disease, in comparison to patients with SRNS but without these mutations.[323,320]

Variable clinical presentations associated with pathogenic *NPHS2* mutations are well described. There are several reports of infantile SRNS demonstrating clinical overlap with CNF; these cases result from *NPHS2* mutations that may be associated with digenic inheritance of *NPHS1* mutations.[324,309,302,325] Familial forms of adult-onset focal glomerulosclerosis also result from *NPHS2* mutations.[326] By comparison to childhood-onset cases, adult-onset cases demonstrate variability in penetrance and clinical course, and association with compound *NPHS2* mutations including common polymorphisms (see below). Viewed in this light, childhood-onset SRNS may represent the most severe manifestation of *NPHS2*-linked glomerular disease, modified by other as yet incompletely undefined genetic and environmental factors.[327] The overall contribution of *NPHS2* mutations to sporadic cases of focal glomerulosclerosis is uncertain but almost certainly lower in adults than children.[328,316,329,330,331,332,326]

Extrarenal manifestations of SRNS associated with *NPHS2* mutations have not been described. Indeed, multisystem findings suggest the likelihood of an alternative primary diagnosis. Additional clinical features of familial SRNS are described below.

Pathology

In familial SRNS, more than 60% of kidney biopsy specimens demonstrate focal glomeruloscerosis as the principal finding.[319,321,333] Variable findings include mesangial expansion, and IgM, IgG and/or complement component deposition. Remaining biopsy specimens generally demonstrate minimal change, although other histological findings have been described.[319]

Genetics and Pathophysiology

Fuchschuber and colleagues first established linkage of a gene for autosomal recessive SRNS in eight families to chromosome 1q-25-q31.[315] Boute and colleagues later reported identification of the *NPHS2* gene and pathogenic mutations in these and several additional families.[314] The *NPHS2* gene spans eight exons over 25 kb, producing a 1853-base pair transcript and a 383-amino acid protein, termed podocin.

Podocin is a member of the prohibitin homology (PHB)-domain family, a family of membrane proteins that associate preferentially with cholesterol-rich lipid rafts in which they play specialized roles.[334] Podocin contains a 104-amino acid amino-terminal intracellular domain, a 17-amino acid amino-terminal-adjacent intramembranous domain

and a 262-amino acid carboxy-terminal intracellular domain; the intramembranous domain mediates attachment to the inner leaflet of the cell membrane and thus confers a hairpin structure.

Several important aspects of podocin function have recently been elucidated. Podocin is expressed in the kidney exclusively, within podocyte foot process plasma membranes at sites of insertion for slit diaphragms.[314,335,289] Podocin forms homo-oligomers and interacts with nephrin and other slit diaphragm proteins within specialized plasma membrane domains, suggesting roles in slit diaphragm formation, maintenance and/or signaling.[288–290] Like other PHB-domain proteins, podocin binding to cholesterol is required for important cellular effects: in particular, podocin regulates the activity of TRPC6 ion channels,[336] calcium-permeable cation channels associated with the slit diaphragm and implicated themselves in inherited glomerular disease (see below). The phenotypes of podocin-mutant mice have confirmed the importance of podocin in slit diaphragm development and maintenance.[337–339]

To date, over 100 *NPHS2* mutations have been identified. The majority are missense mutations, with the remainder nonsense, frameshift and splicing mutations.[319–321,340] Large genetic rearrangements have not been described. *NPHS2* mutations are distributed throughout the gene, with genotype-phenotype correlations suggesting that protein-truncating mutations correlate with earlier onset of disease.[341,320] Disease-associated amino acid-substitutions may alter expression levels and/or intracellular trafficking[301,342–344] and produce disturbances in homo-oligomerization, protein-protein interactions and/or recruitment of nephrin and other slit diaphragm protiens to specialized plasma membrane domains.[301,342,326,336,344] The R229Q variant of podocin has attracted particular attention. Present in various ethnic populations at a frequency of 1-6%, this variant may contribute to disease pathogenesis, most convincingly in the presence of additional genetic mutations.[273,326,327,330,332,345]

Diagnosis

SRNS is a clinicopathological entity diagnosed *a posteriori*. A positive family history can indicate a genetic basis for SRNS.The role of *NPHS2* mutational analysis in the diagnosis and management of nephrotic syndrome is evolving. On the basis of available data, a significant percentage of children and an unknown but much smaller percentage of adults will have *NPHS2* mutations at first presentation with nephrotic syndrome, suggesting that genetic testing may not be useful in adults. Nonetheless, identification of *NPHS2* mutations can minimize patient exposure to ineffective and potentially harmful treatments.Several investigators have advocated genetic testing in familial cases of nephrotic syndrome or concomitant with first-time empiric steroid therapy in non-familial cases.[323,340] Others have argued that knowledge of genetic status serve as an entry criterion for clinical trials.[346] *NPHS2* testing may reveal polymorphisms of uncertain clinical significance, posing challenges in diagnosis and management.

Treatment

Resistance to steroid therapy is a diagnostic feature of SRNS. Criteria for steroid resistance itself have been outlined.[347] Importantly, retrospective studies have now confirmed steroid resistance in large groups of patients with homozygous or compound heterozygous *NPHS2* mutations.[321,319] Partial response patterns with steroid-dependence have also been reported for a small number of patients with heterozygous *NPHS2* mutations.[321]

There are no established treatments for familial SRNS. In retrospective analyses of small groups of patients with *NPHS2* mutations, cytotoxic agents have not been effective.[319,348] Reports on the use of cyclosporine A are limited.[321,348]

Kidney transplantation is the preferred treatment for patients near or at ESRD. Recurrence of proteinuria after kidney transplantation for familial SRNS is infrequent. Weber and colleagues[320] reported the recurrence of proteinuria in only one of 32 patients with pathogenic *NPHS2* mutations, and Ruf and colleagues[319] in only two of 24 patients; in none of these cases were biopsy findings reported. By contrast, Ruf and colleagues reported recurrence of proteinuria in seven of 20 patients (35%) with SRNS but without *NPHS2* mutations. In a contrasting series of reports, Bertelli, Caridi and colleagues reported recurrence of proteinuria in patients with *NPHS2* mutations comparable in frequency to that in patients with SRNS but without *NPHS2* mutations.[348,349] However, several of these patients were *NPHS2* heterozygotes with polymorphisms of unclear significance, raising uncertainty regarding the primary diagnosis. In addition, the majority of patients classified with recurrence of proteinuria underwent empiric treatment for recurrent primary disease without report of biopsy findings.

Winn and colleagues have emphasized caution in selecting first-degree relatives of patients with familial focal glomerulosclerosis as donors for kidney transplantation,[350] suggesting genetic risks for poor outcome in donor and recipient. Outcomes of kidney transplantation in patients with homozygous or compound heterozygous *NPHS2* mutations and related donors have not been reported.

Nephrotic Syndrome, Early-Onset, Type 3

Clinical Features

In 2006, Hinkes et al. described linkage by homozygosity mapping to chromosome 10q23 in seven of 26 consanguineous families with SRNS. Candidate-gene sequencing identified homozygous mutations in the *PLCE1* gene encoding phospholipase Cε, thus the putative cause of NPHS3. Twelve affected children were proteinuric by four years of age and nine progressed to ESRD by age five. Remarkably, two children remitted in association with treatment by steroids or cyclosporine A.[351] Homozygous and compound heterozygous mutations have since been identified in 30% of cases of early-onset SRNS with biopsy findings of diffuse mesangial sclerosis (DMS)[352]; additional case series have also suggested a close association with this specific clinicopathological entity.[353,354] Disease-associated mutations have been identified in unaffected family members as well, indicating that the mutations are incompletely penetrant, perhaps variably expressive,[353,355] and thus confounding on the matter of treatment-responsiveness. Extrarenal manifestations of this disorder have not been described.

Pathology

DMS with its hallmark features, described below in connection with DDS, is the pathological entity most closely associated with NPHS3.Indeed, *PLCE1* mutations are those most frequently identified in DMS.[352] Focal glomerulosclerosis has been described in the balance of NPHS3 cases undergoing biopsy.[351,353]

Genetics and Pathophysiology

Human *PLCE1* is a large gene spanning 34 exons over >300 kb.It encodes at least two major forms of phospholipase Cε—PLCε1a of 2,303 amino acids and PLCε1b of 1,994 amino acids—that arise by alternative splicing of exons 1 and 2 to exon 3 and thus differ at their amino termini.[356–358] The *PLCE1* gene was cloned by homology to other phospholipase C family members. Accordingly, phospholipase Cε serves canonical signaling pathways, hydrolyzing phosphatidyl inositol 4,5-bisphosphate to generate inositol 1,4,5-triphosphate and diacylglycerol, involved respectively in downstream mobilization of intracellular Ca^{2+} stores and activation of protein kinase C Phospholipase Cε is one of 13 known human phospholipase C family members, and is alone in one of six subgroups encompassed by this family.[359]

Like other phospholipase C family members, phospholipase Cε contains core X and Y domains constituting the catalytic domain, and upstream pleckstrin-homology and EF-hand domains.[360] In recent years, it has become evident that phospholipase Cε is otherwise unique, integrating a multitude of signals that emanate from extra- and intracellular-sources and are mediated by major classes of heterotrimeric and monomeric G proteins. As investigated in a variety of cell culture and reconstituted systems, phospholipase Cε: (1) Binds activated Ras family members at a Ras association (RA) site downstream from the catalytic domain; these interactions direct patterns of subcellular localization and enzyme activation, and thus mediate cellular responses to receptor tyrosine kinase stimulation by ligands such as epidermal growth factor and platelet derived growth factor.[356,357,361–363] (2) Binds Rho family members independent of Ras, by which dual modulation of signaling inputs is achieved.[364] (3) Respond to stimulation via G protein-coupled receptors, through Gα subunits $G\alpha_{12/13}$[356,362] or Gβγ subunits,[360] and/or monomeric G-protein signaling intermediates including Rho and Rap.[365,366] (4) Catalyzes, by way of an amino-terminal CDC25 homology domain, guanine nucleotide exchange (GEF), by which GDP bound to G protein is exchanged for GTP, the activity of G proteins is regulated, and the possibilities for autoregulatory pathways expanded.[367]

Phospholipase Cε is in podocytes, where its roles are as yet poorly understood but with preliminary indications of specialized interactions with the IQ motif-containing GTPase-activating protein 1 (IQGAP1), a multifunctional protein implicated in slit diaphragm signaling,[294,351] and B-RAF, a serine/threonine kinase effecting diverse pathways of G protein signaling.[368,369]

Over 20 disease-associated *PLCE1* mutations have been reported, the majority homozygous, truncating mutations. Mutations span the gene and genotype-phenotype correlations are not clearly evident.[353] Inasmuch as mutations have been identified in unaffected individuals, future considerations will include modifier genes and oligogenic inheritance patterns, mechanisms compensating for mutation effects, environmental modifiers, etc., accounting for the multifunctional nature of the protein.

Diagnosis

The frequency of *PLCE1* mutations in childhood-onset SRNS is uncertain. At present, it seems prudent to reserve genetic testing for patients with biopsy findings of DMS, parental consanguinity or early-onset (age<4 years) manifestations with unrevealing *NPHS1*/*NPHS2* testing.The frequency of identified mutations may decrease with age of onset and appears to be negligible among adults.[370,371] Heterozygous mutations have been identified and remain of unclear significance.[371]

DISORDERS OF THE PODOCYTE CYTOSKELETON

Autosomal Dominant Focal Segmental Glomerulosclerosis

At least four loci—FSGS1, FSGS2, FSGS3 and FSGS4—have been implicated in genetic subtypes of focal glomerulosclerosis.By comparison to genetic causes of nephrotic syndrome in early childhood, those at the root of late-onset focal glomerulosclerosis occur in autosomal dominant patterns with perhaps wider variability in penetrance and expressivity. Mutations at these loci are rare.Notwithstanding, studies on these loci have provided insights into biological pathways required for maintenance of glomerular function.

FSGS1: Kaplan and colleagues identified mutations in the *ACTN4* gene encoding α-actinin-4 in three families with autosomal dominant focal glomerulosclerosis.[372] Kidney disease in affected family members was marked by incomplete penetrance, detection of proteinuria during adolescence or adulthood, slow progression of kidney disease and variable progression to ESRD.[372,373] Biopsy findings of focal glomerulosclerosis established the diagnosis in several probands from each of the families. Disease-causing *ACTN4* mutations have since been reported in additional families but not definitively—and not widely—in screening studies of patients with sporadically occurring focal glomerulosclerosis.[328,374,375]

Alpha-actinin-4 is one of four α-actinin family members implicated in filamentous F-actin-binding, cytoskeletal organization and other diverse cellular functions.[376] α-actinins-1 and -4 are expressed primarily in non-muscle cells, and α-actininis-2 and -3 in muscle cells.Identified originally by expression cloning, the *ACTN4* gene on chromosome 19q13 encodes a 3893-base pair transcript and 911-amino acid protein, 86% identical to the cardinal α-actinin-1 family member.[377] Each α-actinin family member contains an amino-terminal head composed of two calponin-homology domains constituting the actin-binding domain, a central rod domain composed of four spectrin repeats, and a carboxy-terminal calcium-binding calmodulin-like domain. The α-actinins homo-dimerize, forming anti-parallel "dumbbells" that bridge F-actin fibers. In recent years, it has become clear that spectrin repeats within the rod domain confer strength and elasticity on α-actinin-mediated cross-links. Moreover, the spectrin repeats can bind a myriad of proteins, both within F-actin filaments and within specialized cellular domains that can include intercellular junctional complexes, focal adhesions at sites of cell-matrix interactions, and cellular processes and protrusions. The body of evidence indicates that the α-actinins are multifunctional, participating in the regulation of diverse cellular behaviors including cell adhesion and motility.

Alpha-actinin-4 but not -1 is present within the kidney glomerulus; its expression and distribution are subject to regulation in experimental glomerular disease.[372,378] Among the small number of disease-causing *ACTN4* mutations reported to date, most are missense mutations within exon 8, altering the actin-binding domain and thus the binding properties of the mutant protein.[372,375,379] Disease-associated α-actinin-4 mutants bind F-actin with higher affinity than the wild-type form, a gain of function offering a tenable explanation for autosomal dominant inheritance.[372,380] Follow-up studies of α-actinin-4 mutants suggest that cellular disease mechanisms are more complicated. In kidney biopsies from FSGS1 patients, and in a variety of model systems, α-actinin-4 mutants aggregate abnormally, undergo rapid degradation and/or fail to traffic to the sites of F-actin filaments, implying that loss-of-function mechanisms distinct from altered actin binding may prevail.[381–384] Homozygous mice rendered deficient in α-actinin-4 by targeted mutagenesis die prematurely with severe glomerular disease, a process mediated at least in part by defects in α-actinin reinforcement of integrin-mediated podocye attachments, further emphasizing the likelihood of loss of function mechanisms.[385,386] Given these multifunctional roles of the α-actinins, it is likely that the effects of *ACTN4* mutations ramify widely through the glomerulus, by mechanisms still incompletely understood.

FSGS2*:* Winn and colleagues described a large New Zealand family with kidney disease segregating in an autosomal dominant pattern.[387,388] Affected individuals presented at a mean age of 33 years with proteinuria and elevation of serum creatinine; more than ten family members evaluated by kidney biopsy demonstrated focal glomerulosclerosis. Extrarenal manifestations of genetic disease were not described. Mapped to chromosome 11q21–q22, the disease gene was eventually identified as *TRPC6* encoding the transient receptor potential C6 ion channel.[389] Reiser et al. simultaneously reported *TRPC6* mutations in five families with autosomal dominant FSGS.[292] Mutations have since been reported in additional families with adult-[390] or childhood-[391] onset of disease, and in sporadic cases from a large Spanish cohort.[392]

TRPC6 is a member of the transient receptor potential (TRP) superfamily of ion channels, and specifically the "canonical" subgroup comprised of seven channels (C1-7) in mammals that share sequence homology with each other and Drosophila orthologues.[393] TRPC6 contains six transmembrane domains within which the fifth and sixth domain putatively form the channel

pore. Both the amino-terminal domain containing ankyrin repeats, and the carboxy-terminal containing a proline-rich region, are intracellular, and offer regulatory sites for channel activity and turnover. TRPC6 forms homo-oligomers and—with other TRPC subgroup members—hetero-oligomers, constituting Ca^{2+}-permeable, non-selective cation channels effecting localized changes in intracellular Ca^{2+}, and thus a variety of cellular processes including cytoskeletal remodeling[394–396] and secondary ion channel activation.[397] TRPC6 is widely expressed.In kidney, it is expressed in glomeruli and tubules and—within glomeruli—in endothelial cells, mesangial cells and the cell body, and primary and foot processes of podocytes.[292,389] TRP channels including TRPC6 are widely recognized as cellular sensors.Like other TRPC subgroup members, TRPC6 is activated by phospholipase C-coupled receptor signaling pathways originating from G protein-coupled receptors and receptor tyrosine kinases.[398] TRPC6 may also be mechanosensitive,[336,399,400] of potential importance to its functions in the glomerulus under conditions of pressurization and mechanical stress. TRPC6 interacts directly with nephrin and podocin in heterologous systems suggesting a specific role(s) in the slit diaphragm.[292]

Disease-causing TRPC6 mutants investigated in heterologous systems operate by gain of function, amplifying Ca^{2+} signals. All but one ("K874X") of seven described to date are missense mutations in the amino- or carboxy-terminus. Mutations variably cause increases in agonist-induced, channel-mediated whole-cell currents[292,389] or Ca^{2+} transients,[390] or delays in wild-type patterns of voltage-dependent channel inactivation.[391] The P112Q mutation within the amino-terminal-most ankyrin repeat increases surface expression of the channel.[389] The mechanisms by which TRPC6 mutants modify cellular processes so as to contribute to disease progression are likely complex and otherwise at an early stage of elucidation.

FSGS3: The importance of the adaptor protein CD2-associated protein (CD2AP) in glomerular function was first demonstrated in a targeted mouse mutant.[401] Homozygous mice with complete CD2AP deficiency developed proteinuria and died prematurely of kidney failure, with histological findings of mesangial hypercellularity, abnormal extracellular matrix accumulation, immunoglobulin deposition, and podocyte foot process effacement. Heterozygotes demonstrated similar findings over a prolonged time course.[402] Since report of the CD2AP mutant mouse strain, additional evidence has implicated CD2AP in human glomerular disease. A heterozygous splicing mutation in the CD2AP gene was identified in two of 45 patients with idiopathic focal glomerulosclerosis.[402] A homozygous truncating mutation was identified in a 10-month-old child with collapsing glomerulopathy.[403] Three heterozygous mutations with functional consequences were identified in an Italian cohort of patients with sporadic idiopathic FSGS.[404]

CD2AP was first identified as an adaptor protein for CD2, a lymphocyte membrane protein that promotes attachment to antigen-presenting cells.[405] A Src homology 3 (Sh3) domain-containing protein, CD2AP is widely expressed and interacts with nephrin and podocin, co-localizing with nephrin at sites of slit diaphragm insertion into podocyte foot processes, and thus implying roles in slit diaphragm development, maintenance and/or signaling.[289,401,406–409] Kim and colleagues have raised the possibility of roles for CDAP in endocytic and protein degradation pathways within glomerular cells, required for protein turnover and maintenance of glomerular architecture;[402] indeed, at least one CD2AP mutation is associated with decreased expression of nephrin and podocin.[404] The action(s) of CD2AP may be mediated in part through actin binding, which is altered by at least one disease-causing mutation.[410,403]

FSGS4: Brown et al. have described pathogenic mutations in the *INF2* gene encoding inverted formin 2, in nine families with autosomal dominant FSGS presenting in adolescence or young adulthood.[411] Kidney biopsy findings in FSGS4 are generally typical of secondary FSGS. One additional family has been reported, in which the proband was a 9 year-old boy presenting with proteinuria.[412]

Inverted formin 2 (INF2) is a member of the formin family, consisting of 15 members in mammals and involved centrally in cytoskeletal remodeling.[413] Like that of other formins, the modular structure of INF2 consists of a diaphanous inhibitory domain (DID), formin homology 1 (FH1) and 2 (FH2) domains that underpin actin filament nucleation and polymerization/depolymerization processes, and a diaphanous autoregulatory domain (DAD) that regulates formin activity largely through inhibtory interactions with the upstream DID. Extrapolating from other formins, INF2 operates as a dimer in which FH2 domains are paired head-to-tail, forming a doughnut structure.Perhaps uniquely among the formins, INF2 severs actin filaments, an activity regulated by DID-DAD interactions.[414,415] INF2 may also be unique among the formins in its endoplasmic reticulum localization[415] and roles in vesicular trafficking.[416]

INF2 is widely expressed and, in the kidney glomerulus, appears to be expressed primarily within podocytes.[411] Disease-causing *INF2* mutations described to date are missense mutations within the DID. In heterologous systems, these mutations alter cellular INF2 distribution from a perinuclear pattern typical of the wild-type protein to a more diffuse pattern. The effects of

these mutations on a multitude of cellular processes including cytoskeletal remodeling and vesicular trafficking are likely manifold and await further investigation.

MYH9-Related Disorders (Epstein and Fechtner Syndromes)

Epstein and Fechtner syndromes are autosomal dominant disorders that share some features with Alport syndrome, including hematuria, progression to ESRD and sensorineural deafness. In addition, patients with these conditions have thrombocytopenia and giant platelets, and Fechtner patients exhibit granulocyte cytoplasmic inclusions known as Döhle-like bodies.[417,418] At least some of these patients have ultrastructural GBM changes that resemble those of Alport syndrome.[419,420] Epstein and Fechtner syndromes are transmitted as autosomal dominant conditions.[418–425]

Until recently Epstein and Fechtner syndromes were considered variants of Alport syndrome. However, recent molecular studies have demonstrated that these disorders have a distinct pathogenesis. First, both disease loci were mapped to chromosome 22q11-13.[427,428] This led directly to the finding that Epstein and Fechtner syndromes, along with two other genetic conditions featuring giant platelets, Sebastian syndrome and May-Hegglin anomaly, and nonsyndromic hereditary deafness DFNA17, result from heterozygous mutations in the gene *MYH9*, which encodes nonmuscle myosin heavy chain IIA (NMMHC-IIA).[429–432]

Clinical Features

Kidney disease is a defining feature of Epstein and Fechtner syndromes but occurs in fewer than 50% of patients with *MYH9* mutations.[431,433–435] It is characterized by variable hematuria, proteinuria and chronic kidney disease, from mild to progressive and leading to ESRD by late adolescence.[424,435–437] Intra-familial differences in kidney disease have been described.[438] Hematological abnormalities are nearly universal in *MYH9*-related disorders and always accompany kidney disease; their clinical features have been reviewed.[439] Sensorineural hearing loss is more frequent than kidney disease and may occur in the absence of other disease manifestations.[429,431,433] Cataracts are a further manifestation of *MYH9*-related disorders.[433,435]

Pathology

Light microscopic findings in Epstein and Fechtner syndromes are non-specific and include glomerulosclerosis and tubulointerstitial fibrosis. Glomerular basement membrane changes seen by electron microscopy have been likened to those in Alport syndrome, with variable thickening, thinning and lamination,[419,420,440–442] but findings of normal-appearing glomerular basement membrane have also been reported.[438,441]

Genetics and Pathophysiology

Three non-muscle myosin class II isoforms are expressed in human tissues, NMMHC-IIA, IIB and IIC.[443] While platelets and granulocytes express the IIA isoform exclusively, the kidney, eye and ear express the IIA isoform as well as at least one additional isoform, an arrangement that likely influences the clinical phenotype of *MYH9*-related diseases.[444] NMMHC-IIA consists of an amino-terminal motor domain that catalyzes the hydrolysis of ATP and binds to actin, and a tail domain that participates in dimer formation.[445] The basic functional unit of NMMHC-IIA is a hexamer in which the dimer is complexed with one pair of essential light chains and one pair of regulatory light chains.[446] Enzymatic activity of NMMHC-IIA is regulated by phosphorylation of regulatory light chain, a target of Rho signaling pathways.[447,448] NMMHC-IIA units assemble at the tail domain as filaments, i.e. bundles, in which motor domains extend outward giving a characteristic "bipolar" array,[449] suited to isometric contraction or net movement of bound actin bundles, and thus constituting major components of the actomyosin motor complex within non-muscle cells. Assembly/disassembly and functions of the actomyosin motor complex are highly regulated, with α-actinin playing an especially important role as an actin cross-linker, alternating with myosin filaments to form a pseudo-sarcomeric unit.[450,451] In contrast to NMMHC-IIB, NMMHC-IIA appears to spend little time bound strongly to actin during its contraction cycle; it has been postulated that this property confers a means of rapid cytoskeletal adaptation to mechanical stress.[452,453]

The mechanisms by which *MYH9* mutations result in glomerular disease are unknown.NMMHC-IIA is expressed in the podocytes of adult kidneys suggesting that absent or defective NMMHC-IIA could adversely affect podocyte function, but the protein is also expressed in mesangial and endothelial cells.[454,455] Extrapolating from work in model cell lines, it is possible to postulate effects on cytoskeletal function, cell-matrix interactions and/or cell-cell interactions.[456–459] Non-muscle myosin is also implicated in extracellular matrix turnover.[460] Within podocytes, NMMHC-IIA function is almost certainly connected to the highly specialized localization and configuration of actomyosin complexes within foot processes.[461,462] To what degree the roles of NMMHC-IIA in kidney overlap

with those in blood cells—themselves at an early stage of elucidation[463]—remains to be determined.

Over 100 mutations in the *MYH9* have been described but not all are independent having arisen spontaneously in different families. Mutations occur in well-described hotspots primarily in the tail domain; most but not all are missense mutations.[433,464,435] Motor domain mutations impair NMMHC-IIA's capacity to move actin,[465] while tail domain mutations compromise filament assembly.[466] Mutations affecting the motor domain of NMMHC-IIA result in severe thrombocytopenia, greater numbers of neutrophil inclusions and development of nephropathy and deafness before age 40, while tail domain mutations are associated with milder degrees of thrombocytopenia, fewer neutrophil inclusions and less severe renal and cochlear involvement.[435] The basis for genotype-phenotype correlations are unknown with possibilities including tolerance for tail mutation effects in kidney and/or overlapping functions of NMMHC-IIB present in kidney but not bood cells.Dominant negative effects of mutant NMMHC-IIA proteins have been recapitulated *in vitro*.[466]

Diagnosis and Treatment

Epstein and Fechtner syndrome are diagnosed primarily on clinical grounds. They are distinguished from Alport syndrome by the accompanying hematologic abnormalities and, in informative families, demonstration of autosomal dominant inheritance. Diagnostic considerations in *MYH9*-related disease presenting chiefly as a blood disorder are reviewed elsewhere.[433] Characteristic patterns of NMMHC-IIA staining in blood cells may be a useful adjunct in diagnosis.[467] *MYH9* gene testing is commercially available.

There are no proven treatments in Epstein and Fechtner syndrome. A study of four patients demonstrated the anti-proteinuric effects of renin-angiotensin inhibitors.[435] Owing to platelet abnormalities, patients with Epstein and Fechtner syndrome may be at increased risk of peri-operative bleeding requiring specialty management.[468]

DISORDERS OF PODOCYTE GENE REGULATION

Denys-Drash Syndrome (DDS) and Frasier Syndromes

Clinical Features

DDS is a constellation of disorders that includes Wilms' tumor, XY gonadal dysgenesis with ambiguous genitalia, and a nephropathy that typically presents as infantile-onset nephrotic syndrome, with rapid progression to renal failure. The association of these disorders was first described by Denys in 1967 and subsequently by Drash in 1971.[469,470] Children with DDS may exhibit the complete constellation of abnormalities, or may exhibit nephropathy and genital abnormalities without Wilms' tumor, or nephropathy and Wilms' tumor without genital abnormalities.[471] Thus the common feature of DDS patients is the nephropathy. Proteinuria is usually documented during infancy and is frequently of nephrotic range. Microhematuria and hypertension are not uncommon. Most patients progress to ESRD by three years of age.

In those patients with a 46XY karyotype, abnormalities of the external genitalia vary from hypospadias with cryptorchidism to clitoral enlargement with labial fusion. External genitalia usually appear normal in those whose karyotype is 46XX. Anomalies of the internal reproductive organs, including atrophy of the vagina and uterus, streak ovaries or dysgenetic testes, may occur with either karyotype. The abnormal gonads of 46XY patients may evolve into gonadoblastoma.

Children with DDS are significantly more likely to have bilateral Wilms' tumor, and are considerably younger when their tumors are identified, than children with sporadic Wilms' tumor.[472] However the histology and behavior of Wilms' tumors associated with DDS are similar to those of sporadic Wilms' tumor.

Pathology

Although a variety of renal histologic abnormalities has been reported in patients with DDS, Habib and her colleagues demonstrated that the common glomerular alteration in these patients is diffuse mesangial sclerosis, or DMS.[473] The glomerular changes of DDS-associated DMS are somewhat variable, depending on the cortical depth of the glomerulus, and therefore its degree of maturation, and the timing of the biopsy or nephrectomy. Juxtamedullary glomeruli show podocyte hypertrophy and mesangial matrix increase without mesangial proliferation. Middle cortical glomeruli show mesangial expansion with obliteration of the capillaries, so that the tuft appears to be a "solidified mass," in Habib's words,[473] covered by a corona of hypertrophied podocytes. Bowman's space is patent and sometimes appears enlarged, although crescents may be present. Finally, glomeruli in the subcapsular zone appear extremely immature, with small tufts containing a few capillary loops, surrounded by podocytes.With time, juxtamedullary glomeruli acquire the appearance of middle cortical glomeruli. This evolution suggests that the formation of glomeruli is initiated more or less normally, but effective maturation is not sustained.

Genetics and Pathophysiology

DDS arises from mutations in WT1, the gene encoding a transcription factor known as the Wilms' tumor

suppressor. The *WT1* gene was identified in 1990, and found to be homozygously deleted in a subset of sporadic Wilms' tumors.[474,475] In 1991, Pelletier and colleagues first reported missense mutations in the WT1 gene in DDS patients.[476]

The *WT1* gene consists of 10 exons. The WT1 protein has four zinc finger domains and a predicted molecular weight of 47 to 49 kDa, according to the presence or absence of two alternatively spliced exons.[477] WT1-expressing cells can generate four *WT1* transcripts, carrying both, one or none of the alternative exons.The first splice consists of a separate exon (exon 5) that encodes a 17-amino acid sequence inserted between the proline-rich amino-terminal domain and the carboxy-terminal zinc finger domains. The second splice results in the insertion of three amino acids—lysine (K), threonine (T) and serine (S)—between zinc fingers 3 and 4. WT1 products containing this second insertion are termed WT1 + KTS, while those lacking it are designated WT1 − KTS. The predominant *WT1* transcript contains both alternative exons, while the least prevalent transcript lacks both exons.

The WT1 protein contains at least two functional domains. The proline-rich amino-terminal domain is essential for transcriptional regulation and also mediates self-association of WT1.[478,479] The carboxy-terminal domain consists of four Cys_2-His_2 zinc finger motifs that mediate binding of WT1 protein to DNA. Zinc fingers 2, 3 and 4 of WT1 exhibit strong homology to the three zinc fingers of the early growth response gene-1 protein product, EGR1,[480,481] and WT1-KTS binds to the consensus binding site for EGR1 (5′-GCG (G/T)GGGCG-3′).[480] However, WT1 binds with 20- to 30-fold greater affinity to a slightly different motif, 5′-GCGTGGGAGT-3′, termed WTE.[482] WT1 + KTS and WT1 − KTS appear to have somewhat different DNA binding specificities,[483] suggesting that alternative splicing of WT1 may be functionally important.

In contrast to EGR1, a potent transcriptional activator, the WT1 protein represses transcription of most of the genes to which it binds.[484] *In vitro* studies have demonstrated WT1-mediated transcriptional repression of the genes encoding IGF-II,[485] IGF-I receptor,[486] PDGF-A chain,[487,488] EGR1,[489] TGF-β1[490] and the EGF-receptor.[491] Transcriptional repression by WT1 may be modulated by other proteins. For example, the ability of WT1 to repress, rather than activate, transcription by binding to the EGR1 consensus site appears to depend upon the presence of the ubiquitously expressed tumor suppressor p53.[492] WT1 is also capable of binding to RNA, and may regulate gene expression by post-transcriptional as well as transcriptional mechanisms.[493]

Introduction of wild-type WT1 into embryonal tumors such as Wilms' tumor and osteosarcoma induces programmed cell death. WT1-induced apoptosis is characterized by repression of EGF-receptor mRNA and protein, and by induction of the cyclin-dependent kinase inhibitor p21, associated with G1 phase arrest.[491,494,495]

WT1 mRNA is expressed during nephrogenesis in the condensed mesenchyme, renal vesicle and podocytes.[496,497] Podocytes of adult kidneys continue to express *WT1* mRNA, but at a reduced level compared to the developing organ.[496,497] In the induced mesenchyme, expression of *WT1* mRNA is preceded by increased expression of the paired-box transcription factors PAX2 and PAX8; the PAX2 and PAX8 proteins have been shown to bind and activate the promoter of the *WT1* gene, and to stimulate expression of endogenous WT1.[498,499] The temporal and spatial pattern of *WT1* mRNA expression is consistent with a role for WT1 in mediating differentiation of nephrogenic mesenchyme to glomerular epithelium, and in maintaining the epithelial phenotype of the podocyte.[484] In this scheme, loss of WT1 function can lead to uncontrolled growth of metanephric blastema cells, resulting in Wilms tumor, as well as aberrant podocyte differentiation. *WT1* mRNA is also expressed in primordial tissue of the gonadal ridge, in ovarian follicular granulosa cells, and in Sertoli cells of the testis.[496,497] Normal maturation of the gonads may also depend upon the functional integrity of WT1. For example, WT1 acts synergistically with the testis-determining factor SRY to activate transcription from promoters containing binding sites for SRY.[500] XY mice lacking KTS + isoforms exhibit reduced expression of *Sry* in the urogenital ridge and a female phenotype.[501]

Most patients with DDS have a mutation in exon 9 of the *WT1* gene affecting the third zinc finger.[502] The predominant abnormality is a missense mutation R394W that abolishes the DNA-binding activity of WT1, as do the less prevalent missense mutations D396B and R366H.[503,504,476] Almost all of these mutations appear to have arised *de novo*, but inheritance of *WT1* mutations has been described.[471]

Wilms' tumors in DDS patients are hemizygous for the mutant *WT1* allele,[476] indicating that the tumors develop through a recessive mechanism. The persistence of nephrogenic rests (undifferentiated mesenchyme) in DDS kidneys[505] likely results from the germline *WT1* mutation. A Wilms' tumor will then result if a somatic mutation ("second hit") of the normal *WT1* allele occurs within a nephrogenic rest, resulting in unrestrained cell proliferation.

In contrast to Wilms' tumor, DMS and gonadal dysgenesis in DDS do not occur by a recessive mechanism, since DDS patients are heterozygous for their WT1 mutations. The dominant effect of DDS mutations could reflect a gain of function by the mutant protein,

but there is no evidence that any of the reported DDS mutations impart new functions to WT1. Rather, it appears that the DDS mutations behave in a dominant-negative fashion, i.e., the mutant protein interferes with the function of the product of the wild-type allele. *WT1* proteins can self-associate *in vitro* and *in vivo*, mediated by domains in the amino-terminal region of the protein.[505,479] The association of mutant and wild-type proteins antagonizes WT1-mediated transcriptional repression.[505,479] The dominant-negative effect of DDS *WT1* mutations helps explain why renal and genital abnormalities are more severe in DDS than in patients with WAGR (*W*ilms-*A*niridia-*G*enital-*R*enal) syndrome, who have one wild-type *WT1* allele, while the other is a null allele due to a deletion or frameshift mutation.

Individuals with typical DDS *WT1* mutations but without the DDS phenotype have been reported. For example, Coppes et al found the R394W mutation in a boy with DDS and in his father, who was phenotypically normal.[471] Another child with this mutation had Wilms' tumor, but normal renal function and histology at age seven.[506] Such cases suggest that there are other factors that influence the penetration or effects of *WT1* mutations Phenotypic variation has been described with other *WT1* mutations as well.[507]

Frasier syndrome is another rare disorder characterized by male pseudohermaphroditism and renal failure.[508] These patients have normal female genitalia and an XY karyotype. Proteinuria appears during childhood, progressing to nephrotic syndrome and chronic renal failure by adolescence or early adulthood. Renal pathologic changes consist of focal and segmental glomerulosclerosis, rather than DMS. Development of Wilms' tumor in patients with Frasier syndrome is rare but has been reported.[509] These patients may not be recognized until they undergo evaluation for primary amenorrhea, and gonadoblastoma is a frequent complication. Screening of exons 8 and 9 of the *WT1* gene in a cohort of Frasier patients showed that they did not carry typical DDS mutations.[510] However, further studies of the *WT1* gene in Frasier patients by Barbaux and colleagues identified mutations in the donor splice site in intron 9, which would be predicted to result in the loss of the WT1 + KTS isoform.[511] The differences between DDS and Frasier syndrome suggest several implications: (1) The WT1 + KTS isoform is particularly important in the testicular differentiation program. (2) Loss of the WT1 + KTS isoform does not prevent nephrogenic mesenchyme from differentiating to the point beyond which evolution into Wilms' tumor is no longer possible. (3) The WT1 − KTS isoforms support podocyte differentiation and function, at least to some extent, resulting in relatively mild renal abnormalities, in comparison to DDS. Intron 9 splice site mutations have been described in male FSGS patients.[512,513] However, *WT1* splice-site mutations appear to be only rarely associated with primary steroid-resistant FSGS, in the absence of genital abnormalities.[512]

Diagnosis and Treatment

DDS should be suspected in children with proteinuria in association with Wilms' tumor and/or ambiguous genitalia, and confirmed by renal biopsy and karyotype analysis. In turn, the presence of DMS in a kidney biopsy should prompt suspicion of DDS. Screening of the *WT1* gene for mutations is as yet available only in research laboratories. Evaluation of DDS patients should include imaging of the internal reproductive organs and, at some point, examination of gonadal histology.

Because of the high risk for development of Wilms' tumor, any remaining renal tissue should clearly be removed once the child develops ESRD (some will have had previous unilateral nephrectomy for Wilms' tumor).[514] Some clinicians favor prophylactic bilateral nephrectomy, or removal of the remaining kidney after excision of a unilateral Wilms, once the diagnosis of DDS has been made, and then proceeding to transplant.[515] Other clinicians prefer to monitor such patients for development of Wilms' tumor in any remaining renal tissue by frequent ultrasound examination, moving to nephrectomy and transplant when ESRD supervenes. Gonadal tissue should be excised in DDS patients with an XY karyotype, because of the frequent occurrence of gonadoblastoma. Gonadectomy is not necessary in those with an XX karyotype. In our experience, children who have been free of Wilms' tumor and off chemotherapy for one year, and who have their gonads removed when indicated, exhibit patient and graft survival rates comparable to our general pediatric renal transplant population.

Nail-Patella Syndrome

Nail-patella syndrome (NPS) is an autosomal dominant disorder consisting of hypoplasia or absence of the patellae, dystrophic nails, dysplasia of the elbows and iliac horns, and renal disease.[516,517]

Clinical Features

Renal Findings: clinically apparent renal disease occurs in less than half of NPS patients.[518,519] The nephropathy is usually benign, with about a 10% risk of progression to ESRD. The clinical signs of NPS nephropathy include microhematuria and mild proteinuria and appear in adolescence or young adulthood. Some patients develop nephrotic syndrome and mild hypertension. The course of the nephropathy may differ substantially in related individuals.

Skeletal Defects: Absence or hypoplasia of the patellae occurs in over 90% of NPS patients[520] and may be associated with effusions and osteoarthritis of the knees. About 80% of patients exhibit osseous processes projecting posteriorly from the iliac wings (iliac horns), which are pathognomonic. Abnormalities of the elbows include aplasia, hypoplasia, and posterior processes at the distal ends of the humeri, and occur in over 90% of patients.[520]

Nails: Nail abnormalities occur inmore than 90% of patients, and tend to be bilateral and symmetric.[520] Fingernails are more commonly affected than toenails. The nails may be absent or dystrophic with discoloration, koilonychia, longitudinal ridges, or triangular lunulae. The latter finding is pathognomonic for NPS.[520]

Pathology

There are no specific light or immunofluorescence microscopic features of the NPS renal lesion. By electron microscopy the GBM, and on occasion the mesangium, exhibits multiple irregular lucencies, producing a "moth-eaten" appearance.[521–524] These lucent areas sometimes appear to contain cross-banded collagen fibrils, which are better seen after staining with phosphotungstic acid. The fibrils tend to be arranged in clusters, with thickening of the adjacent GBM. These fibrils may be observed in the kidneys in the absence of clinically evident renal disease, but they have not been found in extraglomerular basement membranes.

Cross-banded fibrils of type III collagen have been seen in GBM of patients with glomerular disease who lack nail or skeletal abnormalities, sometimes as a familial condition with autosomal recessive inheritance (collagen type III glomerulopathy).[525] Although collagen type III glomerulopathy and NPS appear to be distinct diseases, a recent study identified the collagen fibrils of NPS as type III collagen, suggesting a possible pathogenetic relationship between these disorders.[526]

Pathogenesis

The etiology of NPS was unknown until recently. Targeted disruption in mice of the LIM homeodomain transcription factor gene *Lmx1b* resulted in skeletal defects (hypoplastic nails and absent patellae) as well as renal dysplasia.[527] *LMX1B*, the human homolog of *Lmx1b*, was found to map to chromosome 9q34, where the NPS gene is located, and heterozygous mutations in *LMX1B* were identified in patients with NPS.[528] A variety of mutations in *LMX1B* have been found in NPS patients, including missense, splicing, insertion/deletion and nonsense alterations.[528–530] These findings, along with the results of *in vitro* studies of the transcriptional effects of mixing wild-type and mutant *LMX1B*, suggest that haploinsufficiency of *LMX1B*, rather than a dominant-negative effect, is the cause of NPS.[531,529]

While *LMX1B* appears to be important for normal limb and kidney development, the precise mechanisms for the renal effects of *LMX1B* mutations remain under investigation. LMX1B binds to an enhancer sequence in intron 1 of the mouse and human *COL4A4* genes and stimulates reporter constructs containing this sequence.[532] *Lmx1b*$^{-/-}$ mice exhibit markedly reduced GBM expression of the α3 and α4 chains of type IV collagen.[532] LMX1B binding sites have also been found in the putative regulatory regions of the genes encoding the slit diaphragm proteins podocin and CD2AP, and these genes are down-regulated in *Lmx1b*$^{-/-}$ mice.[533,534] However, Heidet and colleagues were unable to identify any abnormalities in the expression of type IV collagen chains, podocin or CD2AP in the kidneys of NPS patients, although they were able to identify the fibrillar material in NPS GBM as type III collagen.[526]

Treatment

There is no specific therapy for the nephropathy of NPS. Renal transplantation has been performed successfully, without apparent recurrence of the disease in the transplanted kidney. Since NPS is an autosomal dominant disorder, careful evaluation of potential living related kidney donors for features of the disease is essential.

References

[1] Antonovych TT, Deasy PF, Tina LU, D'Albora JB, Hollerman CE, Calcagno PL. Hereditary nephritis:early clinical, functional and morphological studies. Pediatr Res 1969;3:545–56.
[2] Gubler M, Levy M, Broyer M, et al. Alport's syndrome: a report of 58 cases and a review of the literature. Am J Med 1981;70:493–505.
[3] Jais JP, Knebelmann B, Giatras I, et al. X-linked Alport syndrome: natural history and genotype-phenotype correlations in girls and women belonging to to 195 families: a "European Community Alport Syndrome Concerted Action" study. J Am Soc Nephrol 2003;14:2603–10.
[4] Jais JP, Knebelmann B, Giatras I, et al. X-linked Alport syndrome: natural history in 195 families and genotype-phenotype correlations in males. J Am Soc Nephrol 2000;11:649–57.
[5] Rumpelt H-J. Hereditary nephropathy (Alport syndrome): correlation of clinical data with glomerular basement membrane alterations. Clin Nephrol 1980;13:203–7.
[6] Feingold J, Bois E, Chompret A, Broyer M, Gubler MC, Grunfeld JP. Genetic heterogeneity of Alport syndrome. Kidney Int 1985;27:672–7.
[7] Hasstedt SJ, Atkin CL, San Juan AC. Genetic heterogeneity among kindreds with Alport syndrome. Am J Hum Genet 1986;38:940–53.
[8] Renieri A, Meroni M, Sessa A, et al. Variability of clinical phenotype in a large Alport family with gly1143-ser change of collagen a5(IV) chain. Nephron 1994;67:444–9.

[9] Grunfeld J-P, Noel LH, Hafez S, Droz D. Renal prognosis in women with hereditary nephritis. Clin Nephrol 1985;23:267–71.
[10] Merchant SN, Burgess BJ, Adams JC, et al. Temporal bone histopathology in alport syndrome. Laryngoscope 2004;114 (9):1609–18.
[11] Colville D, Savige J, Morfis M, et al. Ocular manifestations of autosomal recessive Alport syndrome. Ophthalmic Genet 1997;18:119–28.
[12] Colville DJ, Savige J. Alport syndrome: a review of the ocular manifestations. Ophthalmic Genet 1997;18:161–73.
[13] Perrin D, Jungers P, Grunfeld JP, Delons S, Noel LH, Zenatti C. Perimacular changes in Alport's syndrome. Clin Nephrol 1980;13:163–7.
[14] Nielsen CE. Lenticonus anterior and Alport's syndrome. Arch Ophthalmol 1978;56:518–30.
[15] Arnott EJ, Crawfurd MDA, Toghill PJ. Anterior lenticonus and Alport's syndrome. Br J Ophthalmol 1966;50:390–403.
[16] Brownell RD, Wolter JR. Anterior lenticonus in familial hemorrhagic nephritis: demonstration of lens pathology. Arch Ophthalmol 1964;71:481–3.
[17] Streeten BW, Robinson MR, Wallace R, Jones DB. Lens capsule abnormalities in Alport's syndrome. Arch Ophthalmol 1987;105:1693–7.
[18] Polack BCP, Hogewind BL. Macular lesions in Alport's disease. Am J Ophthalmol 1977;84:533–5.
[19] Sabates R, Krachmer JH, Weingeist TA. Ocular findings in Alport's syndrome. Ophthalmologica 1983;186:204–10.
[20] Zylbermann R, Silverstone B-Z, Brandes E, Drukker A. Retinal lesion in Alport's syndrome. J Pediatr Ophthalmol 1980;17: 255–60.
[21] Govan JAA. Ocular manifestations of Alport's syndrome: a hereditary disorder of basement membranes. Br J Ophthalmol 1983;67:493–503.
[22] Teekhasaenee C, Nimmanit S, Wutthiphan S, et al. Posterior polymorphous dystrophy and Alport syndrome. Ophthalmology 1991;98:1207–15.
[23] Thompson SM, Deady JP, Willshaw HE, White RHR. Ocular signs in Alport's syndrome. Eye 1987;1:146–53.
[24] Rhys C, Snyers B, Pirson Y. Recurrent corneal erosion associated with Alport's syndrome. Kidney Int 1997;52:208–11.
[25] Cochat P, Guibad P, Garcia Torres R, Roussel B, Guarner V, Larbre F. Diffuse leiomyomatosis in Alport syndrome. J Pediatr 1988;113:339–43.
[26] Garcia Torres R, Guarner V. Leiomiomatosis del esofago, traqueo bronquial y genital asociada con nefropatia hereditaria tipo Alport: un nuevo syndrome. Rev Gastroenterol Mex 1983;70:163–70.
[27] Garcia-Torres R, Cruz D, Orozco L, Heidet L, Gubler MC. Alport syndrome and diffuse leiomyomatosis: clinical aspects, pathology, molecular biology and extracellular matrix studies. A synthesis. Nephrologie 2000;21:9–12.
[28] Roussel B, Birembaut P, Gaillard D, et al. Leiomyomatose aesophagienne familiale associee a un syndrome d'Alport chez un garcon de 9 ans. Helv Paediat Acta 1986;41:359–68.
[29] Kashtan CE, Segal Y, Flinter F, Makanjuola D, Gan JS, Watnick T. Aortic abnormalities in males with Alport syndrome. *Nephrol Dial Transplant*. May 21.
[30] Lyons OTA, St. John ERC, Morales JP, Chan YC, Taylor PR. Ruptured thoracoabdominal aortic aneurysm in a renal transplant patient with Alport's syndrome. Ann Vasc Surg 2007;21:816–8.
[31] Tayel S, Kurczynski TW, Levine M, et al. Marfanoid children. Etiologic heterogeneity and cardiac findings. Am J Dis Child 1991;145(1):90–3.
[32] Vaicys C, Hunt CD, Heary RF. Ruptured intracranial aneurysm in an adolescent with Alport's syndrome—a new expression of type IV collagenopathy. Surg Neurol 2000;54:68–72.
[33] Bohrer N, Churg J, Gribetz D. Glomerulonephritis in two sets of identical twins. Am J Med 1964;36:787–94.
[34] Kinoshita Y, Morita T, Wada J, et al. Hereditary chronic nephritis (Alport) complicated by nephrotic syndrome. Acta Med Biol 1969;17:101–17.
[35] Churg J, Sherman RL. Pathologic characteristics of hereditary nephritis. Arch Pathol 1973;95:374–9.
[36] Hinglais N, Grunfeld J-P, Bois LE. Characteristic ultrastructural lesion of the glomerular basement membrane in progressive hereditary nephritis (Alport's syndrome). Lab Invest 1972;27:473–87.
[37] Spear GS, Slusser RJ. Alport's syndrome:emphasizing electron microscopic studies of the glomerulus. Am J Pathol 1972;69:213–22.
[38] Rumpelt H-J. Alport's syndrome:specificity and pathogenesis of glomerular basement membrane alterations. Pediatr Nephrol 1987;1:422–7.
[39] Yoshikawa N, White RHR, Cameron AH. Familial hematuria: clinicopathological correlations. Clin Nephrol 1982;17:172–82.
[40] Spear GS. Pathology of the kidney in Alport's syndrome. Pathol Annual 1974;9:93–138.
[41] Hill GS, Jenis EH, Goodloe SG. The nonspecificity of the ultrastructural alterations in hereditary nephritis. Lab Invest 1974;31:516–32.
[42] Farboody GH, Valenzuela R, McCormack LJ, Kallaen R, Osborne DG. Chronic hereditary nephritis: a clinicopathologic study of 23 new kindreds and review of the literature. Hum Pathol 1979;10:655–68.
[43] Grunfeld J-P, Bois EP, Hinglais N. Progressive and nonprogressive hereditary nephritis. Kidney Int 1973;4:216–28.
[44] Habib R, Gubler MC, Hinglais N, et al. Alport's syndrome: experience at Hopital Necker. Kidney Int 1982;21:S20–8.
[45] Rogers PW, Kurtzman NA, Bunn SM, White MG. Familial benign essential hematuria. Arch Intern Med 1973;131:257–62.
[46] Tina L, Jenis E, Jose P, Medani C, Papadopoulou Z, Calcagno P. The glomerular basement membrane in benign familial hematuria. Clin Nephrol 1982;17:1–4.
[47] Yoshikawa N, Hashimoto H, Katayama Y, Yamada Y, Matsuo T. The thin glomerular basement membrane in children with hematuria. J Pathol 1984;142:253–7.
[48] Kim KH, Kim Y, Gubler MC, et al. Structural-functional relationships in Alport syndrome. J Amer Soc Nephrol 1995;5:1659–68.
[49] Hudson BG, Reeders ST, Tryggvason K. Type IV Collagen:structure, gene organization, and role in human diseases. J Biol Chem 1993;268:26033–6.
[50] Hudson BG, Trygvasson K, Sundaramoorthy M, Neilson EG. Alport's syndrome, Goodpasture's syndrome, and type IV collagen. N Engl J Med 2003;348:2543–56.
[51] Weber S, Engel J, Wiedemann H, Glanville RW, Timpl R. Subunit structure and assembly of the globular domain of basement membrane collagen type IV. Eur J Biochem 1984;139:401–10.
[52] Dolz R, Engel J, Kuhn K. Folding of collagen IV. Eur J Biochem 1988;178:357–66.
[53] Tsilibary E, Charonis A. The role of the main noncollagenous domain (NC1) in type IV collagen self-assembly. J Cell Biol 1986;103:2467–73.
[54] Boutaud A, Borza DB, Bondar O, et al. Type IV collagen of the glomerular basement membrane: evidence that the chain specificity of network assembly is encoded by the noncollagenous NC1 domains. J Biol Chem 2000;275:30716–24.

[55] Timpl R, Wiedemann H, van Delden V, Furthmayr H, Kuhn K. A network model for the organization of type IV collagen molecules in basement membranes. Eur J Biochem 1981;120:203–11.
[56] Yurchenco PD, Ruben GC. Type IV collagen lateral associations in the EHS tumor matrix: comparison with amniotic and in vitro networks. Am J Pathol 1988;132:278–91.
[57] Aumailley M, Wiedemann H, Mann K, Timpl R. Binding of nidogen and the laminin-nidogen complex to basement membrane collagen type IV. Eur J Biochem 1989;184:241–8.
[58] Krishnamurti U, Chen Y, Michael A, et al. Integrin-mediated interactions between primary /T-SV40 immortalized human glomerular epithelial cells and type IV collagen. Lab Invest 1996;74:650–7.
[59] Boyd CD, Toth-Fejel S, Gadi IK, et al. The genes coding for human pro alpha 1(IV) and pro alpha 2(IV) collagen are both located at the end of the long arm of chromosome 13. Am J Hum Genet 1988;42:309–14.
[60] Mariyama M, Zheng K, Yang-Feng TL, Reeders ST. Colocalization of the genes for the a3(IV) and a4(IV) chains of type IV collagen to chromosome 2 bands q35-q37. Genomics 1992;13:809–13.
[61] Hostikka SL, Eddy RL, Byers MG, Hoyhtya M, Shows TB, Tryggvason K. Identification of a distinct type IV collagen a chain with restricted kidney distribution and assignment of its gene to the locus of X chromosome-linked Alport syndrome. Proc Natl Acad Sci USA 1990;87:1606–10.
[62] Myers JC, Jones TA, Pohjolainen E-R, et al. Molecular cloning of a5(IV) collagen and assignment of the gene to the region of the X chromosome containing the Alport syndrome locus. Am J Hum Genet 1990;46:1024–33.
[63] Sugimoto M, Oohashi T, Ninomiya Y. The genes *COL4A5* and *COL4A6*, coding for basement membrane collagen chains a5(IV) and a6(IV), are located head-to-head in close proximity on human chromosome Xq22 and COL4A6 is transcribed from two alternative promoters. Proc Natl Acad Sci USA 1994;91:11679–83.
[64] Momota R, Sugimoto M, Oohashi T, Kigasawa K, Yoshioka H, Ninomiya Y. Two genes, *COL4A3* and *COL4A4* coding for the human a3(IV) and a4(IV) chains are arranged head-to-head on chromosome 2q36. FEBS Lett 1998;424:11–6.
[65] Poschl E, Pollner R, Kuhn K. The genes for the a1(IV) and a2 (IV) chains of human basement membrane collagen type IV are arranged head-to-head and separated by a bidirectional promoter of unique structure. EMBO J 1988;7:2687–95.
[66] Segal Y, Zhuang L, Rondeau E, Sraer JD, Zhou J. Regulation of the paired type IV collagen genes COL4A5 and COL4A6. Role of the proximal promoter region. J Biol Chem 2001;276 (15):11791–7.
[67] Borza DB, Bondar O, Ninomiya Y, et al. The NC1 domain of collagen IV encodes a novel network composed of the alpha 1, alpha 2, alpha 5, and alpha 6 chains in smooth muscle basement membranes. J Biol Chem 2001;276(30):28532–40.
[68] Seki T, Naito I, Oohashi T, Sado Y, Ninomiya Y. Differential expression of type IV collagen isoforms, alpha5(IV) and alpha6 (IV) chains, in basement membranes surrounding smooth muscle cells. Histochem Cell Biol 1998;110(4):359–66.
[69] Butkowski RJ, Langeveld JPM, Weislander J, Hamilton J, Hudson BG. Localization of the Goodpasture epitope to a novel chain of basement membrane collagen. J Biol Chem 1987;262:7874–7.
[70] Saus J, Wieslander J, Langeveld JPM, Quinones S, Hudson BG. Identification of the Goodpasture antigen as the a3(IV) chain of collagen IV. J Biol Chem 1988;263:13374–80.
[71] Wieslander J, Barr JF, Butkowski R, et al. Goodpasture antigen of the glomerular basement membrane: localization to noncollagenous regions of type IV collagen. Proc Natl Acad Sci USA 1984;81:3838–42.
[72] Kalluri R, Gunwar S, Reeders ST, et al. Goodpasture syndrome: localization of the epitope for the autoantibodies to the carboxyl-terminal region of the a3(IV) chain of basement membrane collagen. J Biol Chem 1991;266:24018–24.
[73] Lemmink HH, Schröder CH, Monnens LAH, Smeets HJM. The clinical spectrum of type IV collagen mutations. Hum Mutat 1997;9:477–99.
[74] Antignac C, Heidet L. Mutations in Alport syndrome associated with diffuse esophageal leiomyomatosis. Contrib Nephrol 1996;117:172–82.
[75] Antignac C, Zhou J, Sanak M, et al. Alport syndrome and diffuse leiomyomatosis: deletions in the 5′ end of the COL4A5 gene. Kidney Int 1992;42:1178–83.
[76] Zhou J, Mochizuki T, Smeets H, et al. Deletion of the paired a5 (IV) and a6(IV) collagen genes in inherited smooth muscle tumors. Science 1993;261:1167–9.
[77] Heidet L, Cohen-Solal L, Boye E, et al. Novel COL4A5/COL4A6 deletions and further characterization of the diffuse leiomyomatosis-Alport syndrome (DL-AS) locus define the DL critical region. Cytogenet Cell Genet 1997;78:240–6.
[78] Heidet L, Dahan K, Zhou J, et al. Deletions of both a5(IV) and a6(IV) collagen genes in Alport syndrome and in Alport syndrome associated with smooth muscle tumors. Hum Mol Genet 1995;4:99–108.
[79] Segal Y, Peissel B, Renieri A, et al. LINE-1 elements at the sites of molecular rearrangements in Alport syndrome-diffuse leiomyomatosis. Am J Hum Genet 1999;64:62–9.
[80] Heiskari N, Zhang X, Zhou J, et al. Identification of 17 mutations in ten exons in the COL4A5 collagen gene, but no mutations found in four exons in COL4A6: a study of 250 patients with hematuria and suspected of having Alport syndrome. J Am Soc Nephrol 1996;7:702–9.
[81] Kobayashi T, Uchiyama M. Characterization of assembly of recombinant type IV collagen alpha3, alpha4, and alpha5 chains in transfected cell strains. Kidney Int 2003;64(6):1986–96.
[82] Piez KA. Molecular and aggregate structures of the collagens. In: Piez KA, Reddi AH, editors. Extracellular Matrix Biochemistry. New York: Elsevier; 1984. p. 1–39.
[83] Kuvaniemi H, Tromp G, Prockop DJ. Mutations in fibrillar collagens (types I, II, III, and XI), fibril-associated collagen (type IV), and network-forming collagen (type X) cause a spectrum of diseases of bone, cartilage, and blood vessels. Hum Mutat 1997;9:300–15.
[84] Prockop DJ. Mutations in collagen genes as a cause of connective-tissue diseases. N Engl J Med 1992;326:540–6.
[85] Gross O, Netzer KO, Lambrecht R, Seibold S, Weber M. Meta-analysis of genotype-phenotype correlation in X-linked Alport syndrome: impact on clnical counseling. Nephrol Dial Transpl 2002;17:1218–27.
[86] Boye E, Mollet G, Forestier L, et al. Determination of the genomic structure of the COL4A4 gene and of novel mutations causing autosomal recessive Alport syndrome. Am J Hum Genet 1998;63:1329–40.
[87] Ding J, Stitzel J, Berry P, Hawkins E, Kashtan C. Autosomal recessive Alport syndrome: mutation in the *COL4A3* gene in a woman with Alport syndrome and posttransplant antiglomerular basement membrane nephritis. J Amer Soc Nephrol 1995;5:1714–7.
[88] Heidet L, Arrondel C, Forestier L, et al. Structure of the human type IV collagen gene *COL4A3* and mutations in autosomal Alport syndrome. J Amer Soc Nephrol 2001;12:97–106.
[89] Knebelmann B, Forestier L, Drouot L, et al. Splice-mediated insertion of an *Alu* sequence in the COL4A3 mRNA causing

autosomal recessive Alport syndrome. Hum Mol Genet 1995;4:675–9.
[90] Lemmink HH, Mochizuki T, van den Heuvel LPWJ, et al. Mutations in the type IV collagen a3 (COL4A3) gene in autosomal recessive Alport syndrome. Hum Mol Genet 1994;3:1269–73.
[91] Mochizuki T, Lemmink HH, Mariyama M, et al. Identification of mutations in the a3(IV) and a4(IV) collagen genes in autosomal recessive Alport syndrome. Nature Genetics 1994;8:77–82.
[92] Ciccarese M, Casu D, Wong FK, et al. Identification of a new mutation in the a4(IV) collagen gene in a family with autosomal dominant Alport syndrome and hypercholesterolaemia. Nephrol Dial Transpl 2001;16:2008–12.
[93] Longo I, Porcedda P, Mari F, et al. COL4A3/COL4A4 mutations: from familial hematuria to autosomal-dominant or recessive Alport syndrome. Kidney Int 2002;61:1947–56.
[94] van der Loop FTL, Heidet L, Timmer EDJ, et al. Autosomal dominant Alport syndrome caused by a COL4A3 splice site mutation. Kidney Int 2000;58:1870–5.
[95] Badenas C, Praga M, Tazon B, et al. Mutations in the COL4A4 and COL4A3 genes cause familial benign hematuria. J Am Soc Nephrol 2002;13:1248–54.
[96] Bekheirnia MR, Reed B, Gregory MC, et al. Genotype-phenotype correlation in X-linked Alport syndrome. J Am Soc Nephrol;21(5):876-883.
[97] Guo C, Van Damme B, Vanrenterghem Y, Devriendt K, Cassiman J-J, Marynen P. Severe Alport phenotype in a woman with two missense mutations in the same COL4A5 gene and preponderant inactivation of the X chromosome carrying the normal allele. J Clin Invest 1995;95:1832–7.
[98] Vetrie D, Flinter F, Bobrow M, Harris A. X inactivation patterns in females with Alport's syndrome: a means of selecting against a deleterious gene? J Med Genet 1992;29:663–6.
[99] Rheault MN, Kren SM, Thielen BK, et al. Mouse model of X-linked Alport syndrome. J Am Soc Nephrol 2004;15 (6):1466–74.
[100] Rheault MN, Kren SM, Hartich LA, et al. X-inactivation modifies disease severity in female carriers of murine X-linked Alport syndrome. Nephrol Dial Transplant 2010;25(3):764–9.
[101] Jeraj K, Kim Y, Vernier RL, Fish AJ, Michael AF. Absence of Goodpasture's antigen in male patients with familial nephritis. Am J Kid Dis 1982;2:626–9.
[102] Kashtan C, Fish AJ, Kleppel M, Yoshioka K, Michael AF. Nephritogenic antigen determinants in epidermal and renal basement membranes of kindreds with Alport-type familial nephritis. J Clin Invest 1986;78:1035–44.
[103] McCoy RC, Johnson HK, Stone WJ, Wilson CB. Absence of nephritogenic GBM antigen(s) in some patients with hereditary nephritis. Kidney Int 1982;21:642–52.
[104] Olson DL, Anand SK, Landing BH, Heuser E, Grushkin CM, Lieberman E. Diagnosis of hereditary nephritis by failure of glomeruli to bind anti-glomerular basement membrane antibodies. J Pediatr 1980;96:697–9.
[105] Savage COS, Pusey CD, Kershaw MJ, et al. The Goodpasture antigen in Alport's syndrome: studies with a monoclonal antibody. Kidney Int 1986;30:107–12.
[106] Kashtan CE, Kim Y. Distribution of the a1 and a2 chains of collagen IV and of collagens V and VI in Alport syndrome. Kidney Int 1992;42:115–26.
[107] Nakanishi K, Yoshikawa N, Iijima K, et al. Immunohistochemical study of a1–5 chains of type IV collagen in hereditary nephritis. Kidney Int 1994;46:1413–21.
[108] Ninomiya Y, Kagawa M, Iyama K, et al. Differential expression of two basement membrane collagen genes, COL4A6 and COL4A5, demonstrated by immunofluorescence staining using peptide-specific monoclonal antibodies. J Cell Biol 1995;130:1219–29.
[109] Peissel B, Geng L, Kalluri R, et al. Comparative distribution of the a1(IV), a5(IV) and a6(IV) collagen chains in normal human adult and fetal tissues and in kidneys from X-linked Alport syndrome patients. J Clin Invest 1995;96:1948–57.
[110] Yoshioka K, Hino S, Takemura T, et al. Type IV Collagen a5 chain: normal distribution and abnormalities in X-linked Alport syndrome revealed by monoclonal antibody. Am J Pathol 1994;144:986–96.
[111] Cheong HI, Kashtan CE, Kim Y, Kleppel MM, Michael AF. Immunohistologic studies of type IV collagen in anterior lens capsules of patients with Alport syndrome. Lab Invest 1994;70:553–7.
[112] Gubler MC, Knebelmann B, Beziau A, et al. Autosomal recessive Alport syndrome: immunohistochemical study of type IV collagen chain distribution. Kidney Int 1995;47:1142–7.
[113] Kuivaniemi H, Tromp G, Prockop DJ. Mutations in collagen genes: causes of rare and some common diseases in humans. FASEB J 1991;5:2052–60.
[114] Gupta MC, Graham PL, Kramer JM. Characterization of a1(IV) collagen mutations in *Caenorhabditis elegans* and the effects of a1 and a2(IV) mutations on type IV collagen distribution. J Cell Biol 1997;137:1185–96.
[115] Ohkubo S, Takeda H, Higashide T, et al. Immunohistochemical and molecular genetic evidence for type IV collagen alpha5 chain abnormality in the anterior lenticonus associated with Alport syndrome. Arch Ophthalmol 2003;121 (6):846–50.
[116] Kalluri R, Shield CF, Todd P, Hudson BG, Neilson EG. Isoform switching of type IV collagen is developmentally arrested in X-linked Alport syndrome leading to increased susceptibility of renal basement membranes to endoproteolysis. J Clin Invest 1997;99:2470–8.
[117] Miner JH, Sanes JR. Collagen IV a3, a4 and a5 chains in rodent basal laminae: sequence, distribution, association with laminins, and developmental switches. J Cell Biol 1994;127:879–91.
[118] Kim Y, Butkowski R, Burke B, et al. Differential expression of basement membrane collagen in membranous nephropathy. Am J Pathol 1991;139:1381–8.
[119] Harvey SJ, Zheng K, Sado Y, et al. Role of distinct type IV collagen networks in glomerular development and function. Kidney Int 1998;54:1857–66.
[120] Abrahamson DR, Prettyman AC, Robert B, St John PL. Laminin-1 reexpression in Alport mouse glomerular basement membranes. Kidney Int 2003;63(3):826–34.
[121] Kashtan CE, Kim Y, Lees GE, Thorner PS, Virtanen I, Miner JH. Abnormal glomerular basement membrane laminins in murine, canine, and human Alport sydnrome: aberrant laminin alpha2 deposition is species independent. J Am Soc Nephrol 2001;12:252–60.
[122] Kashtan CE, Gubler MC, Sisson-Ross S, Mauer M. Chronology of renal scarring in males with Alport syndrome. Pediatr Nephrol 1998;12:269–74.
[123] Cosgrove D, Rodgers K, Meehan D, et al. Integrin alpha1beta1 and transforming growth factor-beta 1 play distinct roles in Alport glomerular pathogenesis and serve as dual targets for metabolic therapy. Am J Pathol 2000;157:1649–59.
[124] Rao VH, Lees GH, Kashtan CE, et al. Increased expression of MMP-2, MMP-9 (type IV collagenases/gelatinases), and MT1-MMP in canine X-linked Alport syndrome (XLAS). Kidney Int 2003;63:1736–48.
[125] Rodgers KD, Rao V, Meehan DT, et al. Monocytes may promote myofibroblast accumulation and apoptosis in Alport renal fibrosis. Kidney Int 2003;63(4):1338–55.

[126] Sayers R, Kalluri R, Rodgers KD, Shield CF, Meehan DT, Cosgrove D. Role for transforming growth factor-beta 1 in Alport renal disease progression. Kidney Int 1999;56:1662–73.
[127] Zeisberg M, Bottiglio C, Kumar N, et al. Bone morphogenic protein-7 inhibits progression of chronic renal fibrosis associated with two genetic mouse models. Am J Physiol Renal Physiol 2003;285(6):F1060–7.
[128] Gross O, Beirowski B, Koepke ML, et al. Preemptive ramipril therapy delays renal failure and reduces renal fibrosis in COL4A3-knockout mice with Alport syndrome. Kidney Int 2003;63(2):438–46.
[129] Gross O, Schulze-Lohoff E, Koepke ML, et al. Antifibrotic, nephroprotective potential of ACE inhibitor vs AT1 antagonist in a murine model of renal fibrosis. Nephrol Dial Transplant 2004;19(7):1716–23.
[130] Kagawa M, Kishiro Y, Naito I, et al. Epitope-defined monoclonal antibodies against type-IV collagen for diagnosis of Alport's syndrome. Nephrol Dial Transpl 1997;12:1238–41.
[131] Kashtan CE. Alport syndrome: is diagnosis only skin deep? Kidney Int 1999;55:1575–6.
[132] van der Loop FTL, Monnens LAH, Schroder CH, et al. Identification of COL4A5 defects in Alport syndrome by immunochemistry of skin. Kidney Int 1999;55:1217–24.
[133] Turco AE, Rossetti S, Bresin E, Corra S. Erroneous genetic risk assessment of Alport syndrome. Lancet 1995;346:1237.
[134] Knebelmann B, Breillat C, Forestier L, et al. Spectrum of mutations in the COL4A5 collagen gene in X-linked Alport syndrome. Am J Hum Genet 1996;59:1221–32.
[135] Renieri A, Bruttini M, Galli L, et al. X-linked Alport syndrome: an SSCP-based mutation survey over all 51 exons of the COL4A5 gene. Am J Hum Genet 1996;58:1192–204.
[136] Inoue Y, Nishio H, Shirakawa T, et al. Detection of mutations in the COL4A5 gene in over 90% of male patients with X-linked Alport's syndrome by RT-PCR and direct sequencing. Am J Kid Dis 1999;34:854–62.
[137] Martin P, Heiskari N, Zhou J, et al. High mutation detection rate in the COL4A5 collagen gene in suspected Alport syndrome using PCR and direct DNA sequencing. J Am Soc Nephrol 1998;9:2291–301.
[138] Kashtan CE, McEnery PT, Tejani A, Stablein DM. Renal allograft survival according to primary diagnosis: a report of the north american pediatric renal transplant cooperative study. Pediatr Nephrol 1995;9:679–84.
[139] Gobel J, Olbricht CJ, Offner G, et al. Kidney transplantation in Alport's syndrome: long-term outcome and allograft anti-GBM nephritis. Clin Nephrol 1992;38:299–304.
[140] Peten E, Pirson Y, Cosyns J-P, et al. Outcome of thirty patients with Alport's syndrome after renal transplantation. Transplantation 1991;52:823–6.
[141] van de Heuvel LPWJ, Schroder CH, Savage COS, et al. The development of anti-glomerular basement membrane nephritis in two children with Alport's syndrome after renal transplantation: characterization of the antibody target. Pediatr Nephrol 1989;3:406–13.
[142] Kashtan CE, Michael AF. Perspectives in clinical nephrology: Alport syndrome. Kidney Int 1996;50:1445–63.
[143] Brainwood D, Kashtan C, Gubler MC, Turner AN. Targets of alloantibodies in Alport anti-glomerular basement membrane disease after renal transplantation. Kidney Int 1998;53:762–6.
[144] Kashtan C, Butkowski R, Kleppel M, First M, Michael A. Posttransplant anti-glomerular basement membrane nephritis in related Alport males with Alport syndrome. J Lab Clin Med 1990;116:508–15.
[145] Hudson BG, Kalluri R, Gunwar S, et al. The pathogenesis of Alport syndrome involves type IV collagen molecules containing the a3(IV) chain: evidence from anti-GBM nephritis after renal transplantation. Kidney Int 1992;42:179–87.
[146] Antignac C, Knebelmann B, Druout L, et al. Deletions in the COL4A5 collagen gene in X-linked Alport syndrome: characterization of the pathological transcripts in non-renal cells and correlation with disease expression. J Clin Invest 1994;93:1195–207.
[147] Ding J, Zhou J, Tryggvason K, Kashtan CE. COL4A5 deletions in three patients with Alport syndrome and posttransplant antiglomerular basement membrane nephritis. J Amer Soc Nephrol 1994;5:161–8.
[148] Adler L, Mathew R, Futterweit S, et al. Angiotensin converting enzyme inhibitor therapy in children with Alport syndrome: effect on urinary albumin, TGF-beta, and nitrite excretion. BMC Nephrol 2002;3(1):2.
[149] Cohen EP, Lemann J. In hereditary nephritis angiotensin-converting enzyme inhibition decreases proteinuria and may slow the rate of progression. Am J Kid Dis 1996;27:199–203.
[150] Proesmans W, Knockaert H, Trouet D. Enalapril in paediatric patients with Alport syndrome: 2 years' experience. Eur J Pediatr 2000;159:430–3.
[151] Proesmans W, Van Dyck M. Enalapril in children with Alport syndrome. Pediatr Nephrol 2004;19(3):271–5.
[152] Grodecki KM, Gains MJ, Baumal R, Osmond DH, Cotter B, Valli VE, et al. Treatment of X-linked hereditary nephritis in Samoyed dogs with angiotensin converting enzyme inhibitor. J Comp Pathol 1997;117:209–25.
[153] Callis L, Vila A, Carrera M, Nieto J. Long-term effects of cyclosporine A in Alport's syndrome. Kidney Int 1999;55:1051–6.
[154] Callis L, Vila A, Nieto J, Fortuny G. Effect of cyclosporin A on proteinuria in patients with Alport's syndrome. Pediatr Nephrol 1992;6:140–4.
[155] Charbit M, Dechaux M, Gagnadoux M, Grunfeld J, Niaudet P. Cyclosporine A therapy in Alport syndrome. J Am Soc Nephrol 2003;14:111A.
[156] Massella L, Rizzoni G. Cyclosporine treatment of young patients with Alport syndrome and proteinuria. J Am Soc Nephrol 2001;12:116A.
[157] Chen D, Jefferson B, Harvey SJ, et al. Cyclosporine A slows the progressive renal disease of Alport syndrome (X-linked hereditary nephritis): results from a canine model. J Am Soc Nephrol 2003;14:690–8.
[158] Harvey SJ, Zheng K, Jefferson B, et al. Transfer of the alpha 5 (IV) collagen chain gene to smooth muscle restores in vivo expression of the alpha 6(IV) collagen chain in a canine model of Alport syndrome. Am J Pathol 2003;162:873–5.
[159] Heikkila P, Parpala T, Lukkarinen O, Weber M, Tryggvason K. Adenovirus-mediated gene transfer into kidney glomeruli using an ex vivo and in vivo kidney perfusion system—first step towards gene therapy of Alport syndrome. Gene Therapy 1996;3:21–7.
[160] Parpala-Sparman T, Lukkarinen O, Heikkila P, Tryggvason K. A novel surgical organ perfusion method for effective ex vivo and in vivo gene transfer into renal glomerular cells. Urol Res 1999;27:97–102.
[161] Tryggvason K, Heikkila P, Pettersson E, Tibell A, Throner P. Can Alport syndrome be treated by gene therapy? Kidney Int 1997;52:1493–9.
[162] Trachtman H, Weiss R, Bennett B, Griefer I. Isolated hematuria in children: indications for a renal biopsy. Kidney Int 1984;25:94–9.
[163] Dische FE, Weston MJ, Parsons V. Abnormally thin glomerular basement membranes associated with hematuria, proteinuria or renal failure in adults. Am J Nephrol 1985;5:103–9.

[164] Nieuwhof CM, de Heer F, de Leeuw P, van Breda Vriesman PJ. Thin GBM nephropathy: premature glomerular obsolescence is associated with hypertension and late onset renal failure. Kidney Int 1997;51:1596–601.
[165] Tiebosch ATMG, Frederik PM, van Breda Vriesman PJC, et al. Thin-basement-membrane nephropathy in adults with persistent hematuria. N Engl J Med 1989;320:14–8.
[166] van Paassen P, van Breda Vriesman PJ, van Rie H, Tervaert JW. Signs and symptoms of thin basement membrane nephropathy: a prospective regional study on primary glomerular disease-The Limburg Renal Registry. Kidney Int 2004;66(3):909–13.
[167] Vogler C, McAdams AJ, Homan SM. Glomerular basement membrane and lamina densa in infants and children: an ultrastructural evaluation. Pediatr Pathol 1987;7:527–34.
[168] Steffes MW, Barbosa J, Basgen JM, Sutherland DER, Najarian JS, Mauer SM. Quantitative glomerular morphology of the normal human kidney. Kidney Int 1983;49:82–6.
[169] Dische FE. Measurement of glomerular basement membrane thickness and its application to the diagnosis of thin-membrane nephropathy. Arch Pathol Lab Med 1992;116:43–9.
[170] Schroder CH, Bontemps CM, Assmann KJM, et al. Renal biopsy and family studies in 65 children with isolated hematuria. Acta Paediatr Scand 1990;79:630–6.
[171] Blumenthal SS, Fritsche C, Lemann J. Establishing the diagnosis of benign familial hematuria: the importance of examining the urine sediment of family members. JAMA 1988;259:2263–6.
[172] Lemmink HH, Nillesen WN, Mochizuki T, et al. Benign familial hematuria due to mutation of the type IV collagen a4 gene. J Clin Invest 1996;98:1114–8.
[173] Buzza M, Wang YY, Dagher H, et al. COL4A4 mutation in thin basement membrane disease previously described in Alport syndrome. Kidney Int 2001;60:480–3.
[174] Buzza M, Wilson D, Savige J. Segregation of hematuria in thin basement membrane disease with haplotypes at the loci for Alport syndrome. Kidney Int 2001;59:1670–6.
[175] Piccini M, Casari G, Zhou J, et al. Evidence for genetic heterogeneity in benign familial hematuria. Am J Nephrol 1999;19:464–7.
[176] Plaisier E, Gribouval O, Alamowitch S, et al. COL4A1 mutations and hereditary angiopathy, nephropathy, aneurysms, and muscle cramps. N Engl J Med 2007;357(26):2687–95.
[177] Pierson M, Cordier J, Hervouuet F, Rauber G. An unusual congenital and familial congenital malformative combination involving the eye and kidney. J Genet Hum 1963;12:184–213.
[178] Hofstaetter C, Neumann I, Lennert T, Dudenhausen JW. Prenatal diagnosis of diffuse mesangial glomerulosclerosis by ultrasonography: a longitudinal study of a case in an affected family. Fetal Diagn Ther 1996;11(2):126–31.
[179] Zenker M, Tralau T, Lennert T, et al. Congenital nephrosis, mesangial sclerosis, and distinct eye abnormalities with microcoria: an autosomal recessive syndrome. Am J Med Genet A 2004;130(2):138–45.
[180] Glastre C, Cochat P, Bouvier R, et al. Familial infantile nephrotic syndrome with ocular abnormalities. Pediatr Nephrol 1990;4(4):340–2.
[181] Swietlinski J, Maruniak-Chudek I, Niemir ZI, Wozniak A, Wilinska M, Zacharzewska J. A case of atypical congenital nephrotic syndrome. Pediatr Nephrol 2004;19(3):349–52.
[182] Zenker M, Aigner T, Wendler O, et al. Human laminin beta 2 deficiency causes congenital nephrosis with mesangial sclerosis and distinct eye abnormalities. Hum Mol Genet 2004;13 (21):2625–32.
[183] Colognato H, Yurchenco PD. Form and function: the laminin family of heterotrimers. Dev Dyn 2000;218(2):213–34.
[184] Miner JH, Yurchenco PD. Laminin functions in tissue morphogenesis. Annu Rev Cell Dev Biol 2004;20:255–84.
[185] Tunggal P, Smyth N, Paulsson M, Ott MC. Laminins: structure and genetic regulation. Microsc Res Tech 2000;51(3):214–27.
[186] Miner JH, Patton BL, Lentz SI, et al. The laminin alpha chains: expression, developmental transitions, and chromosomal locations of alpha1-5, identification of heterotrimeric laminins 8-11, and cloning of a novel alpha3 isoform. J Cell Biol 1997;137 (3):685–701.
[187] Noakes PG, Miner JH, Gautam M, Cunningham JM, Sanes JR, Merlie JP. The renal glomerulus of mice lacking s-laminin/laminin beta 2: nephrosis despite molecular compensation by laminin beta 1. Nat Genet 1995;10(4):400–6.
[188] Delwel GO, de Melker AA, Hogervorst F, et al. Distinct and overlapping ligand specificities of the alpha 3A beta 1 and alpha 6A beta 1 integrins: recognition of laminin isoforms. Mol Biol Cell 1994;5(2):203–15.
[189] Kikkawa Y, Sanzen N, Fujiwara H, Sonnenberg A, Sekiguchi K. Integrin binding specificity of laminin-10/11: laminin-10/11 are recognized by alpha 3 beta 1, alpha 6 beta 1 and alpha 6 beta 4 integrins. J Cell Sci 2000;113(Pt 5):869–76.
[190] Korhonen M, Ylanne J, Laitinen L, Virtanen I. The alpha 1-alpha 6 subunits of integrins are characteristically expressed in distinct segments of developing and adult human nephron. J Cell Biol 1990;111(3):1245–54.
[191] Miner JH. Renal basement membrane components. Kidney Int 1999;56(6):2016–24.
[192] Ryan MC, Christiano AM, Engvall E, et al. The functions of laminins: lessons from in vivo studies. Matrix Biol 1996;15 (6):369–81.
[193] Anderson W. A case of "angio-keratoma". Br J Dermatol 1898;10:113–7.
[194] Fabry J. Ein Beitrag zur Kenntniss der Purpura haemorrhagica nodularis (Purpura papulosa haemorrhagica Hebrae). Arch Dermatol Syph 1898;43:187–200.
[195] Koeberl DD. Age-related efficacy with an AAV vector in Fabry disease mice. Mol Genet Metab 2009;96(3):83–4.
[196] Nakao S, Takenaka T, Maeda M, et al. An atypical variant of Fabry's disease in men with left ventricular hypertrophy. N Engl J Med 1995;333(5):288–93.
[197] Ogawa K, Sugamata K, Funamoto N, et al. Restricted accumulation of globotriaosylceramide in the hearts of atypical cases of Fabry's disease. Hum Pathol 1990;21(10):1067–73.
[198] Nissenson LR, Friedrich KP. Outcome of end-stage renal disease in patients with rare causes of renal failure.Inherited and metabolic disorders. Q J Med 1989;271:1055–62.
[199] Wise D, Wallace HJ, Jellinek EH. Angiokeratoma corporis diffusum. A clinical study of eight affected families. Q J Med 1962;31:177–206.
[200] Chatterjee S, Gupta P, Pyeritz RE, Kwiterovich Jr. PO. Immunohistochemical localization of glycosphingolipid in urinary renal tubular cells in Fabry's disease. Am J Clin Pathol 1984;82(1):24–8.
[201] Desnick RJ, Dawson G, Desnick SJ, Sweeley CC, Krivit W. Diagnosis of glycosphingolipidoses by urinary-sediment analysis. N Engl J Med 1971;284(14):739–44.
[202] Kawamura O, Sakuraba H, Itoh K, et al. Subclinical Fabry's disease occurring in the context of IgA nephropathy. Clin Nephrol 1997;47(2):71–5.
[203] Rosenmann E, Kobrin I, Cohen T. Kidney involvement in systemic lupus erythematosus and Fabry's disease. Nephron 1983;34(3):180–4.
[204] Donati D, Novario R, Gastaldi L. Natural history and treatment of uremia secondary to Fabry's disease: a European experience. Nephron 1987;46:353–9.

[205] Faraggiana T, Churg J, Grishman E, et al. Light- and electron-microscopic histochemistry of Fabry's disease. Am J Pathol 1981;103(2):247–62.
[206] Gubler MC, Lenoir G, Grunfeld JP, Ulmann A, Droz D, Habib R. Early renal changes in hemizygous and heterozygous patients with Fabry's disease. Kidney Int 1978;13(3):223–35.
[207] Fukushima M, Tsuchiyama Y, Nakato T, et al. A female heterozygous patient with Fabry's disease with renal accumulation of trihexosylceramide detected with a monoclonal antibody. Am J Kidney Dis 1995;26(6):952–5.
[208] Dvorak AM, Cable WJ, Osage JE, Kolodny EH. Diagnostic electron microscopy. II. Fabry's disease: use of biopsies from uninvolved skin. Acute and chronic changes involving the microvasculature and small unmyelinated nerves. Pathol Annu 1981;16(Pt 1):139–58.
[209] Murali R, Ioannou YA, Desnick RJ, Burnett RM. Crystallization and preliminary X-ray analysis of human alpha-galactosidase A complex. J Mol Biol 1994;239(4):578–80.
[210] Bishop DF, Calhoun DH, Bernstein HS, Hantzopoulos P, Quinn M, Desnick RJ. Human alpha-galactosidase A: nucleotide sequence of a cDNA clone encoding the mature enzyme. Proc Natl Acad Sci U S A 1986;83(13):4859–63.
[211] Kornreich R, Bishop DF, Desnick RJ. Alpha-galactosidase A gene rearrangements causing Fabry disease. Identification of short direct repeats at breakpoints in an Alu-rich gene. J Biol Chem 1990;265(16):9319–26.
[212] Eng CM, Desnick RJ. Molecular basis of Fabry disease: mutations and polymorphisms in the human alpha-galactosidase A gene. Hum Mutat 1994;3(2):103–11.
[213] Caggana M, Ashley GA, Desnick RJ, Eng CM. Fabry disease: molecular carrier detection and prenatal diagnosis by analysis of closely linked polymorphisms at Xq22.1. Am J Med Genet 1997;71(3):329–35.
[214] Bernstein HS, Bishop DF, Astrin KH, et al. Fabry disease: six gene rearrangements and an exonic point mutation in the alpha-galactosidase gene. J Clin Invest 1989;83(4):1390–9.
[215] Davies JP, Eng CM, Hill JA, et al. Fabry disease: fourteen alpha-galactosidase A mutations in unrelated families from the United Kingdom and other European countries. Eur J Hum Genet 1996;4(4):219–24.
[216] Desnick RJ, Bernstein HS, Astrin KH, Bishop DF. Fabry disease: molecular diagnosis of hemizygotes and heterozygotes. Enzyme 1987;38(1–4):54–64.
[217] Eng CM, Resnick-Silverman LA, Niehaus DJ, Astrin KH, Desnick RJ. Nature and frequency of mutations in the alpha-galactosidase A gene that cause Fabry disease. Am J Hum Genet 1993;53(6):1186–97.
[218] Eng CM, Ashley GA, Burgert TS, Enriquez AL, D'Souza M, Desnick RJ. Fabry disease: thirty-five mutations in the alpha-galactosidase A gene in patients with classic and variant phenotypes. Mol Med 1997;3(3):174–82.
[219] Dawson G, Kruski AW, Scanu AM. Distribution of glycosphingolipids in the serum lipoproteins of normal human subjects and patients with hypo- and hyperlipidemias. J Lipid Res 1976;17(2):125–31.
[220] Desnick RJ, Ioannou YA, Eng CM. a-galactosidase A deficiency: Fabry disease. In: Scriver CR, Beaudet AL, Sly WS, Valle D, editors. The metabolic and molecular basis of inherited disease. New York: McGraw-Hill; 1995. p. 2741–84.
[221] Schibanoff JM, Kamoshita S, O'Brien JS. Tissue distribution of glycosphingolipids in a case of Fabry's disease. J Lipid Res 1969;10:515.
[222] Rennke HG. How does glomerular epithelial cell injury contribute to progressive glomerular damage? Kidney Int 1994;45: S58–63.
[223] Sakuraba H, Eng CM, Desnick RJ, Bishop DF. Invariant exon skipping in the human alpha-galactosidase A pre-mRNA: Ag + 1 to t substitution in a 5'-splice site causing Fabry disease. Genomics 1992;12(4):643–50.
[224] Ohshima T, Murray GJ, Swaim WD, et al. alpha-Galactosidase A deficient mice: a model of Fabry disease. Proc Natl Acad Sci U S A 1997;94(6):2540–4.
[225] Takenaka T, Murray GJ, Qin G, et al. Long-term enzyme correction and lipid reduction in multiple organs of primary and secondary transplanted Fabry mice receiving transduced bone marrow cells. Proc Natl Acad Sci U S A 2000;97(13):7515–20.
[226] Schweitzer EJ, Drachenberg CB, Bartlett ST. Living kidney donor and recipient evaluation in Fabry's disease. Transplantation 1992;54:924–46.
[227] Kleijer WJ, Hussaarts-Odijk LM, Sachs ES, Jahoda MG, Niermeijer MF. Prenatal diagnosis of Fabry's disease by direct analysis of chorionic villi. Prenat Diagn 1987;7(4):283–7.
[228] Brady RO, Tallman JF, Johnson WG, et al. Replacement therapy for inherited enzyme deficiency. Use of purified ceramidetrihexosidase in Fabry's disease. N Engl J Med 1973;289(1):9–14.
[229] Desnick RJ, Dean KJ, Grabowski G, Bishop DF, Sweeley CC. Enzyme therapy in Fabry disease: differential in vivo plasma clearance and metabolic effectiveness of plasma and splenic alpha-galactosidase A isozymes. Proc Natl Acad Sci U S A 1979;76(10):5326–30.
[230] Ioannou YA, Zeidner KM, Gordon RE, Desnick RJ. Fabry disease: preclinical studies demonstrate the effectiveness of alpha-galactosidase A replacement in enzyme-deficient mice. Am J Hum Genet 2001;68(1):14–25.
[231] Eng CM, Banikazemi M, Gordon RE, et al. A phase 1/2 clinical trial of enzyme replacement in Fabry disease: pharmacokinetic, substrate clearance, and safety studies. Am J Hum Genet 2001;68(3):711–22.
[232] Schiffmann R, Murray GJ, Treco D, et al. Infusion of alpha-galactosidase A reduces tissue globotriaosylceramide storage in patients with Fabry disease. Proc Natl Acad Sci U S A 2000;97(1):365–70.
[233] Eng CM, Guffon N, Wilcox WR, et al. Safety and efficacy of recombinant human alpha-galactosidase A-replacement therapy in Fabry's disease. N Engl J Med 2001;345(1):9–16.
[234] Moore DF, Scott LT, Gladwin MT, et al. Regional cerebral hyperperfusion and nitric oxide pathway dysregulation in Fabry disease: reversal by enzyme replacement therapy. Circulation 2001;104(13):1506–12.
[235] Schiffmann R, Kopp JB, Austin 3rd HA, et al. Enzyme replacement therapy in Fabry disease: a randomized controlled trial. JAMA 2001;285(21):2743–9.
[236] Beck M, Ricci R, Widmer U, et al. Fabry disease: overall effects of agalsidase alfa treatment. Eur J Clin Invest 2004;34 (12):838–44.
[237] Kosch M, Koch HG, Oliveira JP, et al. Enzyme replacement therapy administered during hemodialysis in patients with Fabry disease. Kidney Int 2004;66(3):1279–82.
[238] Desnick RJ, Brady R, Barranger J, et al. Fabry disease, an under-recognized multisystemic disorder: expert recommendations for diagnosis, management, and enzyme replacement therapy. Ann Intern Med 2003;138(4):338–46.
[239] Mehta A, Beck M, Elliot P, et al. Enzyme replacement therapy with aglasidase alfa in patients with Fabry's disease: an analysis of registry data. Lancet 2009;374:1986–96.
[240] West M, Nicholls K, Mehta A, et al. Agalsidase alfa and kidney dysfunction in Fabry disease. J Am Soc Nephrol 2009;20 (5):1132–9.
[241] Linthorst GE, Hollak CE, Donker-Koopman WE, Strijland A, Aerts JM. Enzyme therapy for Fabry disease: neutralizing

antibodies toward agalsidase alpha and beta. Kidney Int 2004;66(4):1589–95.
[242] Benichou B, Goyal S, Sung C, Norfleet AM, O'Brien F. A retrospective analysis of the potential impact of IgG antibodies to agalsidase beta on efficacy during enzyme replacement therapy for Fabry disease. Mol Genet Metab 2009;96(1):4–12.
[243] Clarke JT, Guttmann RD, Wolfe LS, Beaudoin JG, Morehouse DD. Enzyme replacement therapy by renal allotransplantation in Fabry's disease. N Engl J Med 1972;287(24):1215–8.
[244] Desnick RJ, Allen KY, Simmons RL, Najarian JS, Krivit W. Treatment of Fabry's disease: correction of the enzymatic deficiency by renal transplantation. J Lab Clin Med 1971;78 (6):989–90.
[245] Philippart M, Franklin SS, Gordon A. Reversal of an inborn sphingolipidosis (Fabry's disease) by kidney transplantation. Ann Intern Med 1972;77(2):195–200.
[246] Spence MW, MacKinnon KE, Burgess JK, et al. Failure to correct the metabolic defect by renal allotransplantion in Fabry's disease. Ann Intern Med 1976;84(1):13–6.
[247] Wilson RE. Transplantation in patients with unusual causes of renal failure. Clin Nephrol 1976;5(2):51–3.
[248] Ojo A, Meier-Kriesche HU, Friedman G, et al. Excellent outcome of renal transplantation in patients with Fabry's disease. Transplantation 2000;69(11):2337–9.
[249] Friedlaender MM, Kopolovic J, Rubinger D, et al. Renal biopsy in Fabry's disease eight years after successful renal transplantation. Clin Nephrol 1987;27(4):206–11.
[250] Mosnier JF, Degott C, Bedrossian J, et al. Recurrence of Fabry's disease in a renal allograft eleven years after successful renal transplantation. Transplantation 1991;51(4):759–62.
[251] Mignani R, Panichi V, Giudicissi A, et al. Enzyme replacement therapy with agalsidase beta in kidney transplant patients with Fabry disease: a pilot study. Kidney Int 2004;65 (4):1381–5.
[252] Desnick RJ, Brady RO. Fabry disease in childhood. J Pediatr 2004;144(5 Suppl):S20–6.
[253] Ramaswami U. Fabry disease during childhood: clinical manifestations and treatment with agalsidase alfa. Acta Paediatr Suppl 2008;97(457):38–40.
[254] Ramaswami U, Whybra C, Parini R, et al. Clinical manifestations of Fabry disease in children: data from the Fabry Outcome Survey. Acta Paediatr 2006;95(1):86–92.
[255] Tondel C, Bostad L, Hirth A, Svarstad E. Renal biopsy findings in children and adolescents with Fabry disease and minimal albuminuria. Am J Kidney Dis 2008;51(5):767–76.
[256] Wraith JE, Tylki-Szymanska A, Guffon N, et al. Safety and efficacy of enzyme replacement therapy with agalsidase beta: an international, open-label study in pediatric patients with Fabry disease. J Pediatr 2008;152(4):563–70 [570 e561]
[257] Schiffmann R, Martin R, Reimschisel T, et al. Four-year prospective clinical trial of agasidase alfa in children with Fabry disease. J Pediatr 2010;156:832–7.
[258] Gjone E. Familial lecithin:cholesterol acyltransferase deficiency—a new metabolic disease with renal involvement. Adv Nephrol Necker Hosp 1981;10:167–85.
[259] Maroteaux P, Humbel R, Strecker G, Michalski JC, Mande RAFP. Un nouveau type de sialidose avec atteinte renale: la nephrosialidose. I. Etude clinique, readiologique et nosologique. Arch Fr Pediatr 1978;35:819–29.
[260] Kashtan CE, Nevins TE, Posalaky Z, Vernier RL, Fish AJ. Proteinuria in a child with sialidosis: case report and histological studies. Pediatr Nephrol 1989;3(2):166–74.
[261] Le Sec G, Stanescu R, Lyon G. Un nouveau type de sialidose avec atteinte renale: la nephrosialidose. II. Etude anatomique. Arch Fr Pediatr 1978;35:830–44.
[262] Sperl W, Gruber W, Quatacker J, et al. Nephrosis in two siblings with infantile sialic acid storage disease. Eur J Pediatr 1990;149(7):477–82.
[263] Castagnaro M, Alroy J, Ucci AA, Jaffe R. Lectin histochemistry and ultrastructure of kidneys from patients with I-cell disease. Arch Pathol Lab Med 1987;111(3):285–90.
[264] Taylor J, Thorner P, Geary DF, Baumal R, Balfe JW. Nephrotic syndrome and hypertension in two children with Hurler syndrome. J Pediatr 1986;108(5 Pt 1):726–9.
[265] Chen YT, Coleman RA, Scheinman JI, Kolbeck PC, Sidbury JB. Renal disease in type I glycogen storage disease. N Engl J Med 1988;318(1):7–11.
[266] Seppala M, Rapola J, Huttunen NP, Aula P, Karjalainen O, Ruoslahti E. Congenital nephrotic syndrome: prenatal diagnosis and genetic counselling by estimation of aminotic-fluid and maternal serum alpha-fetoprotein. Lancet 1976;2(7977):123–5.
[267] Huttunen NP. Congenital nephrotic syndrome of Finnish type. Study of 75 patients. Arch Dis Child 1976;51(5):344–8.
[268] Laakkonen H, Lonnqvist T, Uusimaa J, et al. Muscular dystonia and athetosis in six patients with congenital nephrotic syndrome of the Finnish type (NPHS1). Pediatr Nephrol 2006;21 (2):182–9.
[269] Holmberg C, Antikainen M, Ronnholm K, Ala Houhala M, Jalanko H. Management of congenital nephrotic syndrome of the Finnish type. Pediatr Nephrol 1995;9(1):87–93.
[270] Mahan JD, Mauer SM, Sibley RK, Vernier RL. Congenital nephrotic syndrome: evolution of medical management and results of renal transplantation. J Pediatr 1984;105(4):549–57.
[271] Philippe A, Nevo F, Esquivel EL, et al. Nephrin mutations can cause childhood-onset steroid-resistant nephrotic syndrome. J Am Soc Nephrol 2008;19(10):1871–8.
[272] Santin S, Garcia-Maset R, Ruiz P, et al. Nephrin mutations cause childhood- and adult-onset focal segmental glomerulosclerosis. Kidney Int 2009;76(12):1268–76.
[273] Caridi G, Gigante M, Ravani P, et al. Clinical features and long-term outcome of nephrotic syndrome associated with heterozygous NPHS1 and NPHS2 mutations. Clin J Am Soc Nephrol 2009;4(6):1065–72.
[274] Lahdenkari AT, Kestila M, Holmberg C, Koskimies O, Jalanko H. Nephrin gene (NPHS1) in patients with minimal change nephrotic syndrome (MCNS). Kidney Int 2004;65(5):1856–63.
[275] Rapola J, Sariola H, Ekblom P. Pathology of fetal congenital nephrosis: immunohistochemical and ultrastructural studies. Kidney Int 1984;25(4):701–7.
[276] Huttunen NP, Rapola J, Vilska J, Hallman N. Renal pathology in congenital nephrotic syndrome of Finnish type: a quantitative light microscopic study on 50 patients. Int J Pediatr Nephrol 1980;1(1):10–6.
[277] Sibley RK, Mahan J, Mauer SM, Vernier RL. A clinicopathologic study of forty-eight infants with nephrotic syndrome. Kidney Int 1985;27(3):544–52.
[278] Schoeb DS, Chernin G, Heeringa SF, et al. Nineteen novel NPHS1 mutations in a worldwide cohort of patients with congenital nephrotic syndrome (CNS). Nephrol Dial Transplant 2010;25(9):2970–6.
[279] Ljungberg P, Rapola J, Holmberg C, Holthofer H, Jalanko H. Glomerular anionic charge in congenital nephrotic syndrome of the Finnish type. Histochem J 1995;27(7):536–46.
[280] Van den Heuvel LP, Van den Born J, Jalanko H, et al. The glycosaminoglycan content of renal basement membranes in the congenital nephrotic syndrome of the Finnish type. Pediatr Nephrol 1992;6(1):10–5.
[281] Vermylen C, Levin M, Mossman J, Barratt TM. Glomerular and urinary heparan sulphate in congenital nephrotic syndrome. Pediatr Nephrol 1989;3(2):122–9.

[282] Vernier RL, Klein DJ, Sisson SP, Mahan JD, Oegema TR, Brown DM. Heparan sulfate–rich anionic sites in the human glomerular basement membrane. Decreased concentration in congenital nephrotic syndrome. N Engl J Med 1983;309 (17):1001–9.
[283] Kestila M, Lenkkeri U, Mannikko M, et al. Positionally cloned gene for a novel glomerular protein—nephrin—is mutated in congenital nephrotic syndrome. Mol Cell 1998;1(4):575–82.
[284] Ruotsalainen V, Ljungberg P, Wartiovaara J, et al. Nephrin is specifically located at the slit diaphragm of glomerular podocytes. Proc Natl Acad Sci U S A 1999;96(14):7962–7.
[285] Sellin L, Huber TB, Gerke P, Quack I, Pavenstadt H, Walz G. NEPH1 defines a novel family of podocin interacting proteins. Faseb J 2003;17(1):115–7.
[286] Putaala H, Soininen R, Kilpelainen P, Wartiovaara J, Tryggvason K. The murine nephrin gene is specifically expressed in kidney, brain and pancreas: inactivation of the gene leads to massive proteinuria and neonatal death. Hum Mol Genet 2001;10(1):1–8.
[287] Wartiovaara J, Ofverstedt LG, Khoshnoodi J, et al. Nephrin strands contribute to a porous slit diaphragm scaffold as revealed by electron tomography. J Clin Invest 2004;114 (10):1475–83.
[288] Huber TB, Kottgen M, Schilling B, Walz G, Benzing T. Interaction with podocin facilitates nephrin signaling. J Biol Chem 2001;276(45):41543–6.
[289] Schwarz K, Simons M, Reiser J, et al. Podocin, a raft-associated component of the glomerular slit diaphragm, interacts with CD2AP and nephrin. J Clin Invest 2001;108(11):1621–9.
[290] Tossidou I, Teng B, Drobot L, et al. CIN85/RukL is a novel binding partner of nephrin and podocin and mediates slit diaphragm turnover in podocytes. J Biol Chem 2010;285 (33):25285–95.
[291] Kim EY, Choi KJ, Dryer SE. Nephrin binds to the COOH terminus of a large-conductance Ca2 + -activated K + channel isoform and regulates its expression on the cell surface. Am J Physiol Renal Physiol 2008;295(1):F235–46.
[292] Reiser J, Polu KR, Moller CC, et al. TRPC6 is a glomerular slit diaphragm-associated channel required for normal renal function. Nat Genet 2005;37(7):739–44.
[293] Huber TB, Schmidts M, Gerke P, et al. The carboxyl terminus of Neph family members binds to the PDZ domain protein zonula occludens-1. J Biol Chem 2003;278(15):13417–21.
[294] Lehtonen S, Ryan JJ, Kudlicka K, Iino N, Zhou H, Farquhar MG. Cell junction-associated proteins IQGAP1, MAGI-2, CASK, spectrins, and alpha-actinin are components of the nephrin multiprotein complex. Proc Natl Acad Sci U S A 2005;102(28):9814–9.
[295] Gerke P, Huber TB, Sellin L, Benzing T, Walz G. Homodimerization and heterodimerization of the glomerular podocyte proteins nephrin and NEPH1. J Am Soc Nephrol 2003;14(4):918–26.
[296] Gerke P, Sellin L, Kretz O, et al. NEPH2 is located at the glomerular slit diaphragm, interacts with nephrin and is cleaved from podocytes by metalloproteinases. J Am Soc Nephrol 2005;16(6):1693–702.
[297] Jones N, Blasutig IM, Eremina V, et al. Nck adaptor proteins link nephrin to the actin cytoskeleton of kidney podocytes. Nature 2006;440(7085):818–23.
[298] Jones N, New LA, Fortino MA, et al. Nck proteins maintain the adult glomerular filtration barrier. J Am Soc Nephrol 2009;20(7):1533–43.
[299] Lahdenpera J, Kilpelainen P, Liu XL, et al. Clustering-induced tyrosine phosphorylation of nephrin by Src family kinases. Kidney Int 2003;64(2):404–13.
[300] Verma R, Kovari I, Soofi A, Nihalani D, Patrie K, Holzman LB. Nephrin ectodomain engagement results in Src kinase activation, nephrin phosphorylation, Nck recruitment, and actin polymerization. J Clin Invest 2006;116(5):1346–59.
[301] Huber TB, Simons M, Hartleben B, et al. Molecular basis of the functional podocin-nephrin complex: mutations in the NPHS2 gene disrupt nephrin targeting to lipid raft microdomains. Hum Mol Genet 2003;12(24):3397–405.
[302] Koziell A, Grech V, Hussain S, et al. Genotype/phenotype correlations of NPHS1 and NPHS2 mutations in nephrotic syndrome advocate a functional inter-relationship in glomerular filtration. Hum Mol Genet 2002;11(4):379–88.
[303] Patrakka J, Kestila M, Wartiovaara J, et al. Congenital nephrotic syndrome (NPHS1): features resulting from different mutations in Finnish patients. Kidney Int 2000;58(3):972–80.
[304] Aya K, Shimizu J, Ohtomo Y, et al. NPHS1 gene mutation in Japanese patients with congenital nephrotic syndrome. Nephrol Dial Transplant 2009;24(8):2411–4.
[305] Beltcheva O, Martin P, Lenkkeri U, Tryggvason K. Mutation spectrum in the nephrin gene (NPHS1) in congenital nephrotic syndrome. Hum Mutat 2001;17(5):368–73.
[306] Hildebrandt F, Heeringa SF, Ruschendorf F, et al. A systematic approach to mapping recessive disease genes in individuals from outbred populations. PLoS Genet 2009;5(1):e1000353.
[307] Lenkkeri U, Mannikko M, McCready P, et al. Structure of the gene for congenital nephrotic syndrome of the finnish type (NPHS1) and characterization of mutations. Am J Hum Genet 1999;64(1):51–61.
[308] Machuca E, Benoit G, Nevo F, et al. Genotype-phenotype correlations in non-Finnish congenital nephrotic syndrome. J Am Soc Nephrol 2010;21(7):1209–17.
[309] Hinkes BG, Mucha B, Vlangos CN, et al. Nephrotic syndrome in the first year of life: two thirds of cases are caused by mutations in 4 genes (NPHS1, NPHS2, WT1, and LAMB2). Pediatrics 2007;119(4):e907–19.
[310] Kestila M, Jarvela I. Prenatal diagnosis of congenital nephrotic syndrome (CNF, NPHS1). Prenat Diagn 2003;23(4):323–4.
[311] Patrakka J, Martin P, Salonen R, et al. Proteinuria and prenatal diagnosis of congenital nephrosis in fetal carriers of nephrin gene mutations. Lancet 2002;359(9317):1575–7.
[312] Mannikko M, Kestila M, Lenkkeri U, et al. Improved prenatal diagnosis of the congenital nephrotic syndrome of the Finnish type based on DNA analysis. Kidney Int 1997;51 (3):868–72.
[313] Kovacevic L, Reid CJ, Rigden SP. Management of congenital nephrotic syndrome. Pediatr Nephrol 2003;18(5):426–30.
[314] Boute N, Gribouval O, Roselli S, et al. NPHS2, encoding the glomerular protein podocin, is mutated in autosomal recessive steroid-resistant nephrotic syndrome. Nat Genet 2000;24(4): 349–54.
[315] Fuchshuber A, Jean G, Gribouval O, et al. Mapping a gene (SRN1) to chromosome 1q25-q31 in idiopathic nephrotic syndrome confirms a distinct entity of autosomal recessive nephrosis. Hum Mol Genet 1995;4(11):2155–8.
[316] Caridi G, Bertelli R, Scolari F, Sanna-Cherchi S, Di Duca M, Ghiggeri GM. Podocin mutations in sporadic focal-segmental glomerulosclerosis occurring in adulthood. Kidney Int 2003;64 (1):365.
[317] Chernin G, Heeringa SF, Gbadegesin R, et al. Low prevalence of NPHS2 mutations in African American children with steroid-resistant nephrotic syndrome. Pediatr Nephrol 2008;23 (9):1455–60.
[318] Maruyama K, Iijima K, Ikeda M, et al. NPHS2 mutations in sporadic steroid-resistant nephrotic syndrome in Japanese children. Pediatr Nephrol 2003;18(5):412–6.

[319] Ruf RG, Lichtenberger A, Karle SM, et al. Patients with mutations in NPHS2 (podocin) do not respond to standard steroid treatment of nephrotic syndrome. J Am Soc Nephrol 2004;15 (3):722–32.
[320] Weber S, Gribouval O, Esquivel EL, et al. NPHS2 mutation analysis shows genetic heterogeneity of steroid-resistant nephrotic syndrome and low post-transplant recurrence. Kidney Int 2004;66(2):571–9.
[321] Caridi G, Bertelli R, Di Duca M, et al. Broadening the spectrum of diseases related to podocin mutations. J Am Soc Nephrol 2003;14(5):1278–86.
[322] Ruf RG, Schultheiss M, Lichtenberger A, et al. Prevalence of WT1 mutations in a large cohort of patients with steroid-resistant and steroid-sensitive nephrotic syndrome. Kidney Int 2004;66(2):564–70.
[323] Frishberg Y, Rinat C, Megged O, Shapira E, Feinstein S, Raas-Rothschild A. Mutations in NPHS2 encoding podocin are a prevalent cause of steroid-resistant nephrotic syndrome among Israeli-Arab children. J Am Soc Nephrol 2002;13(2):400–5.
[324] Caridi G, Berdeli A, Dagnino M, et al. Infantile steroid-resistant nephrotic syndrome associated with double homozygous mutations of podocin. Am J Kidney Dis 2004;43 (4):727–32.
[325] Schultheiss M, Ruf RG, Mucha BE, et al. No evidence for genotype/phenotype correlation in NPHS1 and NPHS2 mutations. Pediatr Nephrol 2004;19(12):1340–8.
[326] Tsukaguchi H, Sudhakar A, Le TC, et al. NPHS2 mutations in late-onset focal segmental glomerulosclerosis: R229Q is a common disease-associated allele. J Clin Invest 2002;110 (11):1659–66.
[327] Pereira AC, Pereira AB, Mota GF, et al. NPHS2 R229Q functional variant is associated with microalbuminuria in the general population. Kidney Int 2004;65(3):1026–30.
[328] Aucella F, De Bonis P, Gatta G, et al. Molecular analysis of NPHS2 and ACTN4 genes in a series of 33 Italian patients affected by adult-onset nonfamilial focal segmental glomerulosclerosis. Nephron Clin Pract 2005;99(2):c31–6.
[329] He N, Zahirieh A, Mei Y, et al. Recessive NPHS2 (Podocin) mutations are rare in adult-onset idiopathic focal segmental glomerulosclerosis. Clin J Am Soc Nephrol 2007;2(1):31–7.
[330] Machuca E, Hummel A, Nevo F, et al. Clinical and epidemiological assessment of steroid-resistant nephrotic syndrome associated with the NPHS2 R229Q variant. Kidney Int 2009;75 (7):727–35.
[331] McKenzie LM, Hendrickson SL, Briggs WA, et al. NPHS2 variation in sporadic focal segmental glomerulosclerosis. J Am Soc Nephrol 2007;18(11):2987–95.
[332] Tonna SJ, Needham A, Polu K, et al. NPHS2 variation in focal and segmental glomerulosclerosis. BMC Nephrol 2008;9:13.
[333] Rana K, Isbel N, Buzza M, et al. Clinical, histopathologic, and genetic studies in nine families with focal segmental glomerulosclerosis. Am J Kidney Dis 2003;41(6):1170–8.
[334] Browman DT, Hoegg MB, Robbins SM. The SPFH domain-containing proteins: more than lipid raft markers. Trends Cell Biol 2007;17(8):394–402.
[335] Roselli S, Gribouval O, Boute N, et al. Podocin localizes in the kidney to the slit diaphragm area. Am J Pathol 2002;160 (1):131–9.
[336] Huber TB, Schermer B, Muller RU, et al. Podocin and MEC-2 bind cholesterol to regulate the activity of associated ion channels. Proc Natl Acad Sci U S A 2006;103(46):17079–86.
[337] Mollet G, Ratelade J, Boyer O, et al. Podocin inactivation in mature kidneys causes focal segmental glomerulosclerosis and nephrotic syndrome. J Am Soc Nephrol 2009;20 (10):2181–9.
[338] Philippe A, Weber S, Esquivel EL, et al. A missense mutation in podocin leads to early and severe renal disease in mice. Kidney Int 2008;73(9):1038–47.
[339] Roselli S, Heidet L, Sich M, et al. Early glomerular filtration defect and severe renal disease in podocin-deficient mice. Mol Cell Biol 2004;24(2):550–60.
[340] Karle SM, Uetz B, Ronner V, Glaeser L, Hildebrandt F, Fuchshuber A. Novel mutations in NPHS2 detected in both familial and sporadic steroid-resistant nephrotic syndrome. J Am Soc Nephrol 2002;13(2):388–93.
[341] Hinkes B, Vlangos C, Heeringa S, et al. Specific podocin mutations correlate with age of onset in steroid-resistant nephrotic syndrome. J Am Soc Nephrol 2008;19(2):365–71.
[342] Nishibori Y, Liu L, Hosoyamada M, et al. Disease-causing missense mutations in NPHS2 gene alter normal nephrin trafficking to the plasma membrane. Kidney Int 2004;66(5):1755–65.
[343] Roselli S, Moutkine I, Gribouval O, Benmerah A, Antignac C. Plasma membrane targeting of podocin through the classical exocytic pathway: effect of NPHS2 mutations. Traffic 2004;5 (1):37–44.
[344] Zhang SY, Marlier A, Gribouval O, et al. In vivo expression of podocyte slit diaphragm-associated proteins in nephrotic patients with NPHS2 mutation. Kidney Int 2004;66(3):945–54.
[345] Kottgen A, Hsu CC, Coresh J, et al. The association of podocin R229Q polymorphism with increased albuminuria or reduced estimated GFR in a large population-based sample of US adults. Am J Kidney Dis 2008;52(5):868–75.
[346] Niaudet P. Podocin and nephrotic syndrome: implications for the clinician. J Am Soc Nephrol 2004;15(3):832–4.
[347] ISKDC. Primary nephrotic syndrome in children: clinical significance of histopathologic variants of minimal change and of diffuse mesangial hypercellularity. A Report of the International Study of Kidney Disease in Children. Kidney Int 1981;20(6):765–71.
[348] Caridi G, Bertelli R, Carrea A, et al. Prevalence, genetics, and clinical features of patients carrying podocin mutations in steroid-resistant nonfamilial focal segmental glomerulosclerosis. J Am Soc Nephrol 2001;12(12):2742–6.
[349] Bertelli R, Ginevri F, Caridi G, et al. Recurrence of focal segmental glomerulosclerosis after renal transplantation in patients with mutations of podocin. Am J Kidney Dis 2003;41 (6):1314–21.
[350] Winn MP, Alkhunaizi AM, Bennett WM, et al. Focal segmental glomerulosclerosis: a need for caution in live-related renal transplantation. Am J Kidney Dis 1999;33(5):970–4.
[351] Hinkes B, Wiggins RC, Gbadegesin R, et al. Positional cloning uncovers mutations in PLCE1 responsible for a nephrotic syndrome variant that may be reversible. Nat Genet 2006;38 (12):1397–405.
[352] Gbadegesin R, Hinkes BG, Hoskins BE, et al. Mutations in PLCE1 are a major cause of isolated diffuse mesangial sclerosis (IDMS). Nephrol Dial Transplant 2008;23(4):1291–7.
[353] Boyer O, Benoit G, Gribouval O, et al. Mutational analysis of the PLCE1 gene in steroid resistant nephrotic syndrome. J Med Genet 2010;47(7):445–52.
[354] Ismaili K, Pawtowski A, Boyer O, Wissing KM, Janssen F, Hall M. Genetic forms of nephrotic syndrome: a single-center experience in Brussels. Pediatr Nephrol 2009;24(2):287–94.
[355] Gilbert RD, Turner CL, Gibson J, et al. Mutations in phospholipase C epsilon 1 are not sufficient to cause diffuse mesangial sclerosis. Kidney Int 2009;75(4):415–9.
[356] Lopez I, Mak EC, Ding J, Hamm HE, Lomasney JW. A novel bifunctional phospholipase c that is regulated by Galpha 12 and stimulates the Ras/mitogen-activated protein kinase pathway. J Biol Chem 2001;276(4):2758–65.

[357] Song C, Hu CD, Masago M, et al. Regulation of a novel human phospholipase C, PLCepsilon, through membrane targeting by Ras. J Biol Chem 2001;276(4):2752–7.
[358] Sorli SC, Bunney TD, Sugden PH, Paterson HF, Katan M. Signaling properties and expression in normal and tumor tissues of two phospholipase C epsilon splice variants. Oncogene 2005;24(1):90–100.
[359] Suh PG, Park JI, Manzoli L, et al. Multiple roles of phosphoinositide-specific phospholipase C isozymes. BMB Rep 2008;41(6):415–34.
[360] Wing MR, Houston D, Kelley GG, Der CJ, Siderovski DP, Harden TK. Activation of phospholipase C-epsilon by heterotrimeric G protein betagamma-subunits. J Biol Chem 2001;276 (51):48257–61.
[361] Bunney TD, Harris R, Gandarillas NL, et al. Structural and mechanistic insights into ras association domains of phospholipase C epsilon. Mol Cell 2006;21(4):495–507.
[362] Kelley GG, Reks SE, Smrcka AV. Hormonal regulation of phospholipase Cepsilon through distinct and overlapping pathways involving G12 and Ras family G-proteins. Biochem J 2004;378(Pt 1):129–39.
[363] Song JK, Rhee JS. Enhancement of stability and activity of phospholipase A(1) in organic solvents by directed evolution. Biochim Biophys Acta 2001;1547(2):370–8.
[364] Seifert JP, Zhou Y, Hicks SN, Sondek J, Harden TK. Dual activation of phospholipase C-epsilon by Rho and Ras GTPases. J Biol Chem 2008;283(44):29690–8.
[365] Citro S, Malik S, Oestreich EA, et al. Phospholipase Cepsilon is a nexus for Rho and Rap-mediated G protein-coupled receptor-induced astrocyte proliferation. Proc Natl Acad Sci U S A 2007;104(39):15543–8.
[366] Schmidt M, Evellin S, Weernink PA, et al. A new phospholipase-C-calcium signalling pathway mediated by cyclic AMP and a Rap GTPase. Nat Cell Biol 2001;3(11): 1020–4.
[367] Jin TG, Satoh T, Liao Y, et al. Role of the CDC25 homology domain of phospholipase Cepsilon in amplification of Rap1-dependent signaling. J Biol Chem 2001;276(32): 30301–7.
[368] Chaib H, Hoskins BE, Ashraf S, Goyal M, Wiggins RC, Hildebrandt F. Identification of BRAF as a new interactor of PLCepsilon1, the protein mutated in nephrotic syndrome type 3. Am J Physiol Renal Physiol 2008;294(1):F93–9.
[369] Roskoski Jr. R. RAF protein-serine/threonine kinases: structure and regulation. Biochem Biophys Res Commun 2010;399 (3):313–7.
[370] Gbadegesin R, Zhao S, Charpie J, Brophy PD, Smoyer WE, Lin JJ. Significance of hemolysis on extracorporeal life support after cardiac surgery in children. Pediatr Nephrol 2009;24(3):589–95.
[371] Lowik M, Levtchenko E, Westra D, et al. Bigenic heterozygosity and the development of steroid-resistant focal segmental glomerulosclerosis. Nephrol Dial Transplant 2008;23 (10):3146–51.
[372] Kaplan JM, Kim SH, North KN, et al. Mutations in ACTN4, encoding alpha-actinin-4, cause familial focal segmental glomerulosclerosis. Nat Genet 2000;24(3):251–6.
[373] Mathis BJ, Calabrese KE, Slick GL. Familial glomerular disease with asymptomatic proteinuria and nephrotic syndrome: a new clinical entity. J Am Osteopath Assoc 1992;92(7):875–80 [883-874]
[374] Komatsuda A, Wakui H, Maki N, et al. Analysis of mutations in alpha-actinin 4 and podocin genes of patients with chronic renal failure due to sporadic focal segmental glomerulosclerosis. Ren Fail 2003;25(1):87–93.
[375] Weins A, Kenlan P, Herbert S, et al. Mutational and Biological Analysis of alpha-actinin-4 in focal segmental glomerulosclerosis. J Am Soc Nephrol 2005;16(12):3694–701.
[376] Otey CA, Carpen O. Alpha-actinin revisited: a fresh look at an old player. Cell Motil Cytoskeleton 2004;58(2):104–11.
[377] Honda K, Yamada T, Endo R, et al. Actinin-4, a novel actin-bundling protein associated with cell motility and cancer invasion. J Cell Biol 1998;140(6):1383–93.
[378] Smoyer WE, Mundel P, Gupta A, Welsh MJ. Podocyte alpha-actinin induction precedes foot process effacement in experimental nephrotic syndrome. Am J Physiol 1997;273(1 Pt 2): F150–7.
[379] Lee SH, Weins A, Hayes DB, Pollak MR, Dominguez R. Crystal structure of the actin-binding domain of alpha-actinin-4 Lys255Glu mutant implicated in focal segmental glomerulosclerosis. J Mol Biol 2008;376(2):317–24.
[380] Weins A, Schlondorff JS, Nakamura F, et al. Disease-associated mutant alpha-actinin-4 reveals a mechanism for regulating its F-actin-binding affinity. Proc Natl Acad Sci U S A 2007;104 (41):16080–5.
[381] Yao J, Le TC, Kos CH, et al. Alpha-actinin-4-mediated FSGS: an inherited kidney disease caused by an aggregated and rapidly degraded cytoskeletal protein. PLoS Biol 2004;2(6):e167.
[382] Henderson JM, Al-Waheeb S, Weins A, Dandapani SV, Pollak MR. Mice with altered alpha-actinin-4 expression have distinct morphologic patterns of glomerular disease. Kidney Int 2008;73(6):741–50.
[383] Henderson JM, Alexander MP, Pollak MR. Patients with ACTN4 mutations demonstrate distinctive features of glomerular injury. J Am Soc Nephrol 2009;20(5):961–8.
[384] Michaud JL, Chaisson KM, Parks RJ, Kennedy CR. FSGS-associated alpha-actinin-4 (K256E) impairs cytoskeletal dynamics in podocytes. Kidney Int 2006;70(6):1054–61.
[385] Dandapani SV, Sugimoto H, Matthews BD, et al. Alpha-actinin-4 is required for normal podocyte adhesion. J Biol Chem 2007;282(1):467–77.
[386] Kos CH, Le TC, Sinha S, et al. Mice deficient in alpha-actinin-4 have severe glomerular disease. J Clin Invest 2003;111 (11):1683–90.
[387] Winn MP, Conlon PJ, Lynn KL, et al. Clinical and genetic heterogeneity in familial focal segmental glomerulosclerosis. International collaborative group for the study of familial focal segmental glomerulosclerosis. Kidney Int 1999;55(4):1241–6.
[388] Winn MP, Conlon PJ, Lynn KL, et al. Linkage of a gene causing familial focal segmental glomerulosclerosis to chromosome 11 and further evidence of genetic heterogeneity. Genomics 1999;58(2):113–20.
[389] Winn MP, Conlon PJ, Lynn KL, et al. A mutation in the TRPC6 cation channel causes familial focal segmental glomerulosclerosis. Science 2005;308(5729):1801–4.
[390] Zhu B, Chen N, Wang ZH, et al. Identification and functional analysis of a novel TRPC6 mutation associated with late onset familial focal segmental glomerulosclerosis in Chinese patients. Mutat Res 2009;664(1–2):84–90.
[391] Heeringa SF, Moller CC, Du J, et al. A novel TRPC6 mutation that causes childhood FSG. PLoS One 2009;4(11):e7771.
[392] Santin S, Ars E, Rossetti S, et al. TRPC6 mutational analysis in a large cohort of patients with focal segmental glomerulosclerosis. Nephrol Dial Transplant 2009;24(10):3089–96.
[393] Wu LJ, Sweet TB, Clapham DE. International union of basic and clinical pharmacology. LXXVI. Current progress in the mammalian TRP ion channel family. Pharmacol Rev 2010;62 (3):381–404.
[394] Hofmann T, Schaefer M, Schultz G, Gudermann T. Subunit composition of mammalian transient receptor potential

channels in living cells. Proc Natl Acad Sci USA 2002;99(11): 7461–6.
[395] Moller CC, Wei C, Altintas MM, et al. Induction of TRPC6 channel in acquired forms of proteinuric kidney disease. J Am Soc Nephrol 2007;18(1):29–36.
[396] Tian D, Jacobo SM, Billing D, et al. Antagonistic regulation of actin dynamics and cell motility by TRPC5 and TRPC6 channels. Sci Signal 2010;3(145): [ra77]
[397] Kim EY, Alvarez-Baron CP, Dryer SE. Canonical transient receptor potential channel (TRPC)3 and TRPC6 associate with large-conductance Ca^{2+}-activated K^+ (BKCa) channels: role in BKCa trafficking to the surface of cultured podocytes. Mol Pharmacol 2009;75(3):466–77.
[398] Abramowitz J, Birnbaumer L. Physiology and pathophysiology of canonical transient receptor potential channels. Faseb J 2009;23(2):297–328.
[399] Gottlieb P, Folgering J, Maroto R, et al. Revisiting TRPC1 and TRPC6 mechanosensitivity. Pflugers Arch 2008;455 (6):1097–103.
[400] Spassova MA, Hewavitharana T, Xu W, Soboloff J, Gill DL. A common mechanism underlies stretch activation and receptor activation of TRPC6 channels. Proc Natl Acad Sci U S A 2006;103(44):16586–91.
[401] Shih NY, Li J, Karpitskii V, et al. Congenital nephrotic syndrome in mice lacking CD2-associated protein. Science 1999;286(5438):312–5.
[402] Kim JM, Wu H, Green G, et al. CD2-associated protein haploinsufficiency is linked to glomerular disease susceptibility. Science 2003;300(5623):1298–300.
[403] Lowik MM, Groenen PJ, Pronk I, et al. Focal segmental glomerulosclerosis in a patient homozygous for a CD2AP mutation. Kidney Int 2007;72(10):1198–203.
[404] Gigante M, Pontrelli P, Montemurno E, et al. CD2AP mutations are associated with sporadic nephrotic syndrome and focal segmental glomerulosclerosis (FSGS). Nephrol Dial Transplant 2009;24(6):1858–64.
[405] Dustin ML, Olszowy MW, Holdorf AD, et al. A novel adaptor protein orchestrates receptor patterning and cytoskeletal polarity in T-cell contacts. Cell 1998;94(5):667–77.
[406] Fukasawa H, Bornheimer S, Kudlicka K, Farquhar MG. Slit diaphragms contain tight junction proteins. J Am Soc Nephrol 2009;20(7):1491–503.
[407] Huber TB, Hartleben B, Kim J, et al. Nephrin and CD2AP associate with phosphoinositide 3-OH kinase and stimulate AKT-dependent signaling. Mol Cell Biol 2003;23(14):4917–28.
[408] Li C, Ruotsalainen V, Tryggvason K, Shaw AS, Miner JH. CD2AP is expressed with nephrin in developing podocytes and is found widely in mature kidney and elsewhere. Am J Physiol Renal Physiol 2000;279(4):F785–92.
[409] Palmen T, Lehtonen S, Ora A, et al. Interaction of endogenous nephrin and CD2-associated protein in mouse epithelial M-1 cell line. J Am Soc Nephrol 2002;13(7):1766–72.
[410] Lehtonen S, Zhao F, Lehtonen E. CD2-associated protein directly interacts with the actin cytoskeleton. Am J Physiol Renal Physiol 2002;283(4):F734–43.
[411] Brown EJ, Schlondorff JS, Becker DJ, et al. Mutations in the formin gene INF2 cause focal segmental glomerulosclerosis. Nat Genet 2010;42(1):72–6.
[412] Lee HK, Han KH, Jung YH, et al. Variable renal phenotype in a family with an INF2 mutation. Pediatr Nephrol 2010.
[413] Chesarone MA, DuPage AG, Goode BL. Unleashing formins to remodel the actin and microtubule cytoskeletons. Nat Rev Mol Cell Biol 2010;11(1):62–74.
[414] Chhabra ES, Higgs HN. INF2 Is a WASP homology 2 motif-containing formin that severs actin filaments and accelerates both polymerization and depolymerization. J Biol Chem 2006;281(36):26754–67.
[415] Chhabra ES, Ramabhadran V, Gerber SA, Higgs HN. INF2 is an endoplasmic reticulum-associated formin protein. J Cell Sci 2009;122(Pt 9):1430–40.
[416] Madrid R, Aranda JF, Rodriguez-Fraticelli AE, et al. The formin INF2 regulates basolateral-to-apical transcytosis and lumen formation in association with Cdc42 and MAL2. Dev Cell 2010;18(5):814–27.
[417] Epstein CJ, Sahud MA, Piel CF, et al. Hereditary macrothrombocytopenia, nephritis and deafness. Am J Med 1972;52:299–310.
[418] Peterson LC, Rao KV, Crosson JT, White JG. Fechtner syndrome: a variant of Alport's syndrome with leukocyte inclusions and macrothrombocytopathia. Blood 1985;65:397–406.
[419] Clare NM, Montiel MM, Lifschitz MD, Bannayan GA. Alport's syndrome associated with macrothrombocytopenic thrombocytopenia. Am J Clin Pathol 1979;72:111–7.
[420] Naito I, Nomura S, Inoue S, et al. Normal distribution of collagen IV in renal basement membranes in Epstein's syndrome. J Clin Pathol 1997;50:919–22.
[421] Alving BM, Tarasoff PG, Moore J, Leissenger CA, Fernandez-Bueno C. Successful renal transplantation for Epstein syndrome. Am J Hematol 1986;21:111–3.
[422] Berheim J, Dechavanne M, Bryon PA, et al. Thrombocytopenia, macrothrombocytopathia, nephritis and deafness. Am J Med 1976;61:145–50.
[423] Brivet F, Girot R, Barbanel C, Maier M, Crosnier J. Hereditary nephritis associated with May-Hegglin anomaly. Nephron 1981;29:59–62.
[424] Eckstein JD, Filip DJ, Watts JC. Hereditary thrombocytopenia, deafness, and renal disease. Ann Intern Med 1975;82:639–45.
[425] Hansen MS, Behnke O, Pedersen NT, Videbaek A. Macrothrombocytopenia associated with glomerulonephritis, deafness and aortic cystic medianecrosis. Scand J Hematol 1978;21:197–205.
[426] Parsa KP, Lee DBN, Zamboni L, Glassock RJ. Hereditary nephritis, deafness and abnormal thrombopoiesis: study of a new kindred. Am J Med 1976;60:665–71.
[427] Toren A, Amariglio N, Rozenfeld-Granot G, et al. Genetic linkage of autosomal-dominant Alport syndrome with leukocyte inclusions and macrothrombocytopenia (Fechtner syndrome) to chromosome 22q11-13. Am J Hum Genet 1999;65:1711–7.
[428] Toren A, Rozenfeld-Granot G, Rocca B, et al. Autosomal-dominant giant platelet syndromes: a hint of the same genetic defect as in Fechtner syndrome owing to a similar genetic linkage to chromosome 22q11-13. Blood 2000;96:3447–51.
[429] Lalwani AK, Goldstein JA, Kelley MJ, Luxford W, Castelein CM, Mhatre AN. Human nonsyndromic hereditary deafness DFNA17 is due to a mutation in nonmuscle myosin *MYH9*. Am J Hum Genet 2000;67:1121–8.
[430] Seri M, Cusano R, Gangarossa S, et al. Mutations in MYH9 result in the May-Hegglin anomaly, and Fechtner and Sebastian syndromes. The May-Heggllin/Fechtner Syndrome Consortium. Nat Genet 2000;26(1):103–5.
[431] Seri M, Pecci A, Di Bari F, et al. MYH9-related disease: May-Hegglin anomaly, Sebastian syndrome, Fechtner syndrome, and Epstein syndrome are not distinct entities but represent a variable expression of a single illness. Medicine (Baltimore) 2003;82(3):203–15.
[432] Seri M, Savino M, Bordo D, et al. Epstein syndrome: another renal disorder with mutations in the nonmuscle myosin heavy chain 9 gene. Hum Genet 2002;110(2):182–6.
[433] Althaus K, Greinacher A. MYH9-related platelet disorders. Semin Thromb Hemost 2009;35(2):189–203.

[434] Kunishima S, Matsushita T, Kojima T, et al. Identification of six novel MYH9 mutations and genotype-phenotype relationships in autosomal dominant macrothrombocytopenia with leukocyte inclusions. J Hum Genet 2001;46(12):722–9.
[435] Pecci A, Panza E, Pujol-Moix N, et al. Position of nonmuscle myosin heavy chain IIA (NMMHC-IIA) mutations predicts the natural history of MYH9-related disease. Hum Mutat 2008;29 (3):409–17.
[436] Bepler G, Melhus O, Gunnells JC. Coexpression of May-Hegglin anomaly and hereditary nephritis in a family. South Med J 1994;87(2):202–5.
[437] Yap DY, Tse KC, Chan TM, Lie AK. Epstein syndrome presenting as renal failure in young patients. Ren Fail 2009;31(7):582–5.
[438] Ghiggeri GM, Caridi G, Magrini U, et al. Genetics, clinical and pathological features of glomerulonephritis associated with mutations of nonmuscle myosin IIA (Fechtner syndrome). Am J Kidney Dis 2003;41(1):95–104.
[439] Noris P, Spedini P, Belletti S, Magrini U, Balduini CL. Thrombocytopenia, giant platelets, and leukocyte inclusion bodies (May-Hegglin anomaly): clinical and laboratory findings. Am J Med 1998;104(4):355–60.
[440] Bhatt A, Broxson E, Witte D, Omoloja A. Thrombocytopenia and proteinuria. Nonmuscle myosin heavy-chain-9-related disease (MYH9 RD) or Epstein syndrome (ES). Pediatr Nephrol 2009;24(3):485–8.
[441] Sekine T, Konno M, Sasaki S, et al. Patients with Epstein-Fechtner syndromes owing to MYH9 R702 mutations develop progressive proteinuric renal disease. Kidney Int 2010;78 (2):207–14.
[442] Turi S, Kobor J, Erdos A, Bodrogi T, Virag I, Ormos J. Hereditary nephritis, platelet disorders and deafness-Epstein's syndrome. Pediatr Nephrol 1992;6(1):38–43.
[443] Hodge T, Cope MJ. A myosin family tree. J Cell Sci 2000;113(Pt 19):3353–4.
[444] Marigo V, Nigro A, Pecci A, et al. Correlation between the clinical phenotype of MYH9-related disease and tissue distribution of class II nonmuscle myosin heavy chains. Genomics 2004;83 (6):1125–33.
[445] Sellers JR. Myosins: a diverse superfamily. Biochim Biophys Acta 2000;1496(1):3–22.
[446] Bresnick AR. Molecular mechanisms of nonmuscle myosin-II regulation. Curr Opin Cell Biol 1999;11(1):26–33.
[447] Amano M, Ito M, Kimura K, et al. Phosphorylation and activation of myosin by Rho-associated kinase (Rho-kinase). J Biol Chem 1996;271(34):20246–9.
[448] Sandquist JC, Swenson KI, Demali KA, Burridge K, Means AR. Rho kinase differentially regulates phosphorylation of nonmuscle myosin II isoforms A and B during cell rounding and migration. J Biol Chem 2006;281(47):35873–83.
[449] Adelstein RS, Pollard TD, Kuehl WM. Isolation and characterization of myosin and two myosin fragments from human blood platelets. Proc Natl Acad Sci U S A 1971;68(11):2703–7.
[450] Pellegrin S, Mellor H. Actin stress fibres. J Cell Sci 2007;120(Pt 20):3491–9.
[451] Sanger JW, Sanger JM, Jockusch BM. Differences in the stress fibers between fibroblasts and epithelial cells. J Cell Biol 1983;96(4):961–9.
[452] Ivanov AI, Bachar M, Babbin BA, Adelstein RS, Nusrat A, Parkos CA. A unique role for nonmuscle myosin heavy chain IIA in regulation of epithelial apical junctions. PLoS One 2007;2(7):e658.
[453] Kovacs M, Wang F, Hu A, Zhang Y, Sellers JR. Functional divergence of human cytoplasmic myosin II: kinetic characterization of the non-muscle IIA isoform. J Biol Chem 2003;278 (40):38132–40.
[454] Arrondel C, Vodovar N, Knebelmann B, et al. Expression of the nonmuscle myosin heavy chain IIA in the human kidney and screening for MYH9 mutations in Epstein and Fechtner syndrome. J Am Soc Npehrol 2002;13:65–74.
[455] Marini M, Bruschi M, Pecci A, et al. Non-muscle myosin heavy chain IIA and IIB interact and co-localize in living cells: relevance for MYH9-related disease. Int J Mol Med 2006;17 (5):729–36.
[456] Clark K, Langeslag M, Figdor CG, van Leeuwen FN. Myosin II and mechanotransduction: a balancing act. Trends Cell Biol 2007;17(4):178–86.
[457] Conti MA, Adelstein RS. Nonmuscle myosin II moves in new directions. J Cell Sci 2008;121(Pt 1):11–8.
[458] Deguchi S, Sato M. Biomechanical properties of actin stress fibers of non-motile cells. Biorheology 2009;46(2):93–105.
[459] Vicente-Manzanares M, Ma X, Adelstein RS, Horwitz AR. Non-muscle myosin II takes centre stage in cell adhesion and migration. Nat Rev Mol Cell Biol 2009;10(11):778–90.
[460] Larsen M, Artym VV, Green JA, Yamada KM. The matrix reorganized: extracellular matrix remodeling and integrin signaling. Curr Opin Cell Biol 2006;18(5):463–71.
[461] Drenckhahn D, Franke RP. Ultrastructural organization of contractile and cytoskeletal proteins in glomerular podocytes of chicken, rat, and man. Lab Invest 1988;59(5):673–82.
[462] Ichimura K, Kurihara H, Sakai T. Actin filament organization of foot processes in rat podocytes. J Histochem Cytochem 2003;51(12):1589–600.
[463] Leon C, Eckly A, Hechler B, et al. Megakaryocyte-restricted MYH9 inactivation dramatically affects hemostasis while preserving platelet aggregation and secretion. Blood 2007;110 (9):3183–91.
[464] Pecci A, Panza E, De Rocco D, et al. MYH9 related disease: four novel mutations of the tail domain of myosin-9 correlating with a mild clinical phenotype. Eur J Haematol 2010;84 (4):291–7.
[465] Hu A, Wang F, Sellers JR. Mutations in human nonmuscle myosin IIA found in patients with May-Hegglin anomaly and Fechtner syndrome result in impaired enzymatic function. J Biol Chem 2002;277(48):46512–7.
[466] Franke JD, Dong F, Rickoll WL, Kelley MJ, Kiehart DP. Rod mutations associated with MYH9-related disorders disrupt nonmuscle myosin-IIA assembly. Blood 2005;105(1):161–9.
[467] Kunishima S, Matsushita T, Kojima T, et al. Immunofluorescence analysis of neutrophil nonmuscle myosin heavy chain-A in MYH9 disorders: association of subcellular localization with MYH9 mutations. Lab Invest 2003;83(1):115–22.
[468] Selleng K, Lubenow LE, Greinacher A, Warkentin TE. Perioperative management of MYH9 hereditary macrothrombocytopenia (Fechtner syndrome). Eur J Haematol 2007;79 (3):263–8.
[469] Denys P, Malvaux P, Van Den Berghe H, Tanghe W, Proesmans W. Association of an anatomo-pathological syndrome of male pseudohermaphroditism, Wilms' tumor, parenchymatous nephropathy and XX/XY mosaicism. Arch Fr Pediatr 1967;24(7):729–39.
[470] Drash A, Sherman F, Hartmann WH, Blizzard RM. A syndrome of pseudohermaphroditism, Wilms' tumor, hypertension, and degenerative renal disease. J Pediatr 1970;76(4):585–93.
[471] Coppes MJ, Liefers GJ, Higuchi M, Zinn AB, Balfe JW, Williams BR. Inherited WT1 mutation in Denys-Drash syndrome. Cancer Res 1992;52(21):6125–8.
[472] Jadresic L, Leake J, Gordon I, et al. Clinicopathologic review of twelve children with nephropathy, Wilm's tumor, and genital abnormalities (Drash syndrome). J Pediatr 1990;117 (5):717–25.

[473] Habib R, Loirat C, Gubler MC, et al. The nephropathy associated with male pseudohermaphroditism and Wilms' tumor (Drash syndrome): a distinctive glomerular lesion–report of 10 cases. Clin Nephrol 1985;24(6):269–78.
[474] Call KM, Glaser T, Ito CY, et al. Isolation and characterization of a zinc finger polypeptide gene at the human chromosome 11 Wilms' tumor locus. Cell 1990;60(3):509–20.
[475] Gessler M, Konig A, Bruns GA. The genomic organization and expression of the WT1 gene. Genomics 1992;12(4):807–13.
[476] Pelletier J, Bruening W, Kashtan CE, et al. Germline mutations in the Wilms' tumor suppressor gene are associated with abnormal urogenital development in Denys-Drash syndrome. Cell 1991;67(2):437–47.
[477] Haber DA, Sohn RL, Buckler AJ, Pelletier J, Call KM, Housman DE. Alternative splicing and genomic structure of the Wilms tumor gene WT1. Proc Natl Acad Sci U S A 1991;88 (21):9618–22.
[478] Holmes G, Boterashvili S, English M, Wainwright B, Licht J, Little M. Two N-terminal self-association domains are required for the dominant negative transcriptional activity of WT1 Denys-Drash mutant proteins. Biochem Biophys Res Commun 1997;233(3):723–8.
[479] Moffett P, Bruening W, Nakagama H, et al. Antagonism of WT1 activity by protein self-association. Proc Natl Acad Sci U S A 1995;92(24):11105–9.
[480] Morris JF, Madden SL, Tournay OE, Cook DM, Sukhatme VP, Rauscher 3rd FJ. Characterization of the zinc finger protein encoded by the WT1 Wilms' tumor locus. Oncogene 1991;6 (12):2339–48.
[481] Rauscher 3rd FJ, Morris JF, Tournay OE, Cook DM, Curran T. Binding of the Wilms' tumor locus zinc finger protein to the EGR-1 consensus sequence. Science 1990;250(4985):1259–62.
[482] Nakagama H, Heinrich G, Pelletier J, Housman DE. Sequence and structural requirements for high-affinity DNA binding by the WT1 gene product. Mol Cell Biol 1995;15(3):1489–98.
[483] Bickmore WA, Oghene K, Little MH, Seawright A, van Heyningen V, Hastie ND. Modulation of DNA binding specificity by alternative splicing of the Wilms tumor wt1 gene transcript. Science 1992;257(5067):235–7.
[484] Rauscher 3rd FJ. The WT1 Wilms tumor gene product: a developmentally regulated transcription factor in the kidney that functions as a tumor suppressor. Faseb J 1993;7(10):896–903.
[485] Drummond IA, Madden SL, Rohwer-Nutter P, Bell GI, Sukhatme VP, Rauscher 3rd FJ. Repression of the insulin-like growth factor II gene by the Wilms tumor suppressor WT1. Science 1992;257(5070):674–8.
[486] Werner H, Re GG, Drummond IA, et al. Increased expression of the insulin-like growth factor I receptor gene, IGF1R, in Wilms tumor is correlated with modulation of IGF1R promoter activity by the WT1 Wilms tumor gene product. Proc Natl Acad Sci U S A 1993;90(12):5828–32.
[487] Gashler AL, Bonthron DT, Madden SL, Rauscher 3rd FJ, Collins T, Sukhatme VP. Human platelet-derived growth factor A chain is transcriptionally repressed by the Wilms tumor suppressor WT1. Proc Natl Acad Sci U S A 1992;89(22):10984–8.
[488] Wang ZY, Madden SL, Deuel TF, Rauscher 3rd FJ. The Wilms' tumor gene product, WT1, represses transcription of the platelet-derived growth factor A-chain gene. J Biol Chem 1992;267(31):21999–2002.
[489] Madden SL, Cook DM, Morris JF, Gashler A, Sukhatme VP, Rauscher III FJ. Transcriptional repression mediated by the WT1 Wilms tumor gene product. Science 1991;253 (5027):1550–3.
[490] Dey BR, Sukhatme VP, Roberts AB, Sporn MB, Rauscher 3rd FJ, Kim SJ. Repression of the transforming growth factor-beta 1 gene by the Wilms' tumor suppressor WT1 gene product. Mol Endocrinol 1994;8(5):595–602.
[491] Englert C, Hou X, Maheswaran S, et al. WT1 suppresses synthesis of the epidermal growth factor receptor and induces apoptosis. Embo J 1995;14(19):4662–75.
[492] Maheswaran S, Park S, Bernard A, et al. Physical and functional interaction between WT1 and p53 proteins. Proc Natl Acad Sci U S A 1993;90(11):5100–4.
[493] Caricasole A, Duarte A, Larsson SH, et al. RNA binding by the Wilms tumor suppressor zinc finger proteins. Proc Natl Acad Sci U S A 1996;93(15):7562–6.
[494] Englert C, Maheswaran S, Garvin AJ, Kreidberg J, Haber DA. Induction of p21 by the Wilms' tumor suppressor gene WT1. Cancer Res 1997;57(8):1429–34.
[495] Haber DA, Englert C, Maheswaran S. Functional properties of WT1. Med Pediatr Oncol 1996;27(5):453–5.
[496] Pelletier J, Schalling M, Buckler AJ, Rogers A, Haber DA, Housman D. Expression of the Wilms' tumor gene WT1 in the murine urogenital system. Genes Dev 1991;5(8):1345–56.
[497] Pritchard-Jones K, Fleming S, Davidson D, et al. The candidate Wilms' tumour gene is involved in genitourinary development. Nature 1990;346(6280):194–7.
[498] Dehbi M, Ghahremani M, Lechner M, Dressler G, Pelletier J. The paired-box transcription factor, PAX2, positively modulates expression of the Wilms' tumor suppressor gene (WT1). Oncogene 1996;13(3):447–53.
[499] Dehbi M, Pelletier J. PAX8-mediated activation of the wt1 tumor suppressor gene. Embo J 1996;15(16):4297–306.
[500] Matsuzawa-Watanabe Y, Inoue J, Semba K. Transcriptional activity of testis-determining factor SRY is modulated by the Wilms' tumor 1 gene product, WT1. Oncogene 2003;22 (39):7900–4.
[501] Hammes A, Guo JK, Lutsch G, et al. Two splice variants of the Wilms' tumor 1 gene have distinct functions during sex determination and nephron formation. Cell 2001;106(3):319–29.
[502] Coppes MJ, Huff V, Pelletier J. Denys-Drash syndrome: relating a clinical disorder to genetic alterations in the tumor suppressor gene WT1. J Pediatr 1993;123(5):673–8.
[503] Borel F, Barilla KC, Hamilton TB, Iskandar M, Romaniuk PJ. Effects of Denys-Drash syndrome point mutations on the DNA binding activity of the Wilms' tumor suppressor protein WT1. Biochemistry 1996;35(37):12070–6.
[504] Little M, Holmes G, Bickmore W, van Heyningen V, Hastie N, Wainwright B. DNA binding capacity of the WT1 protein is abolished by Denys-Drash syndrome WT1 point mutations. Hum Mol Genet 1995;4(3):351–8.
[505] Heppe RK, Koyle MA, Beckwith JB. Nephrogenic rests in Wilms tumor patients with the Drash syndrome. J Urol 1991;145(6):1225–8.
[506] Akasaka Y, Kikuchi H, Nagai T, Hiraoka N, Kato S, Hata J. A point mutation found in the WT1 gene in a sporadic Wilms' tumor without genitourinary abnormalities is identical with the most frequent point mutation in Denys-Drash syndrome. FEBS Lett 1993;317(1-2):39–43.
[507] Heathcott RW, Morison IM, Gubler MC, Corbett R, Reeve AE. A review of the phenotypic variation due to the Denys-Drash syndrome-associated germline WT1 mutation R362X. Hum Mutat 2002;19(4):462.
[508] Moorthy AV, Chesney RW, Lubinsky M. Chronic renal failure and XY gonadal dysgenesis: "Frasier" syndrome—a commentary on reported cases. Am J Med Genet Suppl 1987;3:297–302.
[509] Barbosa AS, Hadjiathanasiou CG, Theodoridis C, et al. The same mutation affecting the splicing of WT1 gene is present on Frasier syndrome patients with or without Wilms' tumor. Hum Mutat 1999;13(2):146–53.

[510] Poulat F, Morin D, Konig A, et al. Distinct molecular origins for Denys-Drash and Frasier syndromes. Hum Genet 1993;91 (3):285–6.

[511] Barbaux S, Niaudet P, Gubler MC, et al. Donor splice-site mutations in WT1 are responsible for Frasier syndrome. Nat Genet 1997;17(4):467–70.

[512] Denamur E, Bocquet N, Baudouin V, et al. WT1 splice-site mutations are rarely associated with primary steroid-resistant focal and segmental glomerulosclerosis. Kidney Int 2000;57(5):1868–72.

[513] Tajima T, Sasaki S, Tanaka Y, et al. 46, XY phenotypic male with focal segmental glomerulosclerosis caused by the WT1 splice site mutation. Horm Res 2003;60(6):302–5.

[514] Hu M, Zhang GY, Arbuckle S, et al. Prophylactic bilateral nephrectomies in two paediatric patients with missense mutations in the WT1 gene. Nephrol Dial Transplant 2004;19(1):223–6.

[515] Eddy AA, Mauer SM. Pseudohermaphroditism, glomerulopathy, and Wilms tumor (Drash syndrome): frequency in end-stage renal failure. J Pediatr 1985;106(4):584–7.

[516] Hawkins CF, Smith OE. Renal dysplasia in a family with multiple hereditary abnormalities including iliac horns. *Lancet* 1950;I:803–8.

[517] Mino RA, Mino VH, Livingstone RG. Osseous dysplasia and dystrophy of the nail: review of the literature and report of a case. Am J Roentgenol 1948;6:633–41.

[518] Meyrier A, Rizzo R, Gubler M-C. The nail-patella syndrome: a review. J Nephrol 1990;2:133–40.

[519] Sweeney E, Fryer AE, Mountford RC, Green AJ, McIntosh I. Nail patella syndrome: a study of 123 patients from 43 British families and the detection of 16 novel mutations of *LMX1B*. Am J Hum Genet 2001;699(Suppl):A571.

[520] Bongers EM, Gubler MC, Knoers NV. Nail-patella syndrome. Overview on clinical and molecular findings. Pediatr Nephrol 2002;17(9):703–12.

[521] Ben-Bassat M, Cohen L, Rosenfeld J. The glomerular basement membrane in the nail-patella syndrome. Arch Pathol 1971;92 (5):350–5.

[522] Del Pozo E, Lapp H. Ultrastructure of the kidney in the nephropathy of the nail–patella syndrome. Am J Clin Pathol 1970;54(6):845–51.

[523] Hoyer JR, Michael AF, Vernier RL. Renal disease in nail-patella syndrome: clinical and morphologic studies. Kidney Int 1972;2(4):231–8.

[524] Silverman ME, Goodman RM, Cuppage FE. The Nail-Patella syndrome. Clinical findings and ultrastructural observations in the kidney. Arch Intern Med 1967;120(1):68–74.

[525] Gubler MC, Dommergues JP, Foulard M, et al. Collagen type III glomerulopathy: a new type of hereditary nephropathy. Pediatr Nephrol 1993;7(4):354–60.

[526] Heidet L, Bongers EM, Sich M, et al. In vivo expression of putative LMX1B targets in nail-patella syndrome kidneys. Am J Pathol 2003;163(1):145–55.

[527] Chen H, Lun Y, Ovchinnikov D, et al. Limb and kidney defects in Lmx1b mutant mice suggest an involvement of LMX1B in human nail patella syndrome. Nat Genet 1998;19 (1):51–5.

[528] Dreyer SD, Zhou G, Baldini A, et al. Mutations in LMX1B cause abnormal skeletal patterning and renal dysplasia in nail patella syndrome. Nat Genet 1998;19(1):47–50.

[529] Hamlington JD, Jones C, McIntosh I. Twenty-two novel LMX1B mutations identified in nail patella syndrome (NPS) patients. Hum Mutat 2001;18(5):458.

[530] Knoers NV, Bongers EM, van Beersum SE, Lommen EJ, van Bokhoven H, Hol FA. Nail-patella syndrome: identification of mutations in the LMX1B gene in Dutch families. J Am Soc Nephrol 2000;11(9):1762–6.

[531] Dreyer SD, Morello R, German MS, et al. LMX1B transactivation and expression in nail-patella syndrome. Hum Mol Genet 2000;9(7):1067–74.

[532] Morello R, Zhou G, Dreyer SD, et al. Regulation of glomerular basement membrane collagen expression by LMX1B contributes to renal disease in nail patella syndrome. Nat Genet 2001;27(2):205–8.

[533] Miner JH, Morello R, Andrews KL, et al. Transcriptional induction of slit diaphragm genes by Lmx1b is required in podocyte differentiation. J Clin Invest 2002;109(8):1065–72.

[534] Rohr C, Prestel J, Heidet L, et al. The LIM-homeodomain transcription factor Lmx1b plays a crucial role in podocytes. J Clin Invest 2002;109(8):1073–82.

CHAPTER

85

Cellular Mechanisms of Drug Nephrotoxicity

Robert James Walker[1] *and Zoltán Huba Endre*[2]

[1]Department of Medicine, Dunedin School of Medicine, University of Otago, Dunedin, New Zealand
[2]Christchurch School of Medicine and Health Sciences, University of Otago, Christchurch, New Zealand and Department of Nephrology, Prince of Wales Hospital and Clinical School, University of New South Wales, Sydney, Australia

INTRODUCTION

Nephrotoxins produce acute or chronic kidney failure or functional injury, usually as a result of specific injury to tubular epithelial cells. While these toxins usually produce localized and specific injury to target cells in the kidney by specific mechanisms, many of the final common pathways of cytotoxic injury are shared with ischemia-reperfusion injury. As the latter have been studied more extensively, these are included as part of this review. The common cellular pathways involved lead to cellular adaptation, sublethal or lethal injury, and pathways for regeneration and repair. These events are not confined to the target cells but also involve other cells in the kidney, which may not necessarily reveal apparent injury but which invoke a stress response and/or inflammatory and vascular responses. The role of direct and indirect injury in mediating the phenotypic response to injury is illustrated schematically in Figure 85.1. The parallel response in the cells that are not directly targeted, such as cytokine or growth factor release or release of inflammatory mediators and recruitment of further inflammation together with the response of target cells, are factors that determine the final outcome of toxic injury. The accompanying vascular response may well be pivotal. Thus, the pathophysiology of acute kidney injury includes a complex interplay among specific cellular injury, inflammation, and altered renal hemodynamics. This review will trace the general mechanisms of renal cell injury before focusing on selected specific nephrotoxins that demonstrate these principles of injury. Potentially, all of the cellular events involved in injury leave molecular footprints, which can be used as biomarkers in urine or plasma, Although such biomarkers have been used largely for diagnostic and predicitive purposes, it is through these biomarkers that we may be able to map such events non-invasively. Event specific biomarkers may allow mapping the time course of injury and the recruitment of secondary injury pathways. We will review the development and use of biomarkers in the detection of nephrotoxic injury.

LOCALIZATION OF INJURY

Cellular Susceptibility: General Principles

Renal susceptibility to toxic injury emanates from a combination of nonspecific and specific factors. The major nonspecific factor is high blood flow with the kidney receiving 20–25% of the cardiac output, thus ensuring high delivery rates of circulating toxins. The general principles governing the susceptibility of a particular nephron segment to nephrotoxic or ischemic injury include segmental transport functions, metabolic activity, metabolic reserve, filtered load, and local blood and substrate supply including oxygen. The concentration of a drug or its metabolites will contribute to toxicity, and this will be modified by local tubular reabsorption, secretion, and metabolism, as well as by the local reabsorption of water. Intracellular activating mechanisms and organelle distribution will contribute

Seldin and Giebisch's The Kidney, Fifth Edition.
DOI: http://dx.doi.org/10.1016/B978-0-12-381462-3.00085-9

© 2013 Elsevier Inc. All rights reserved.

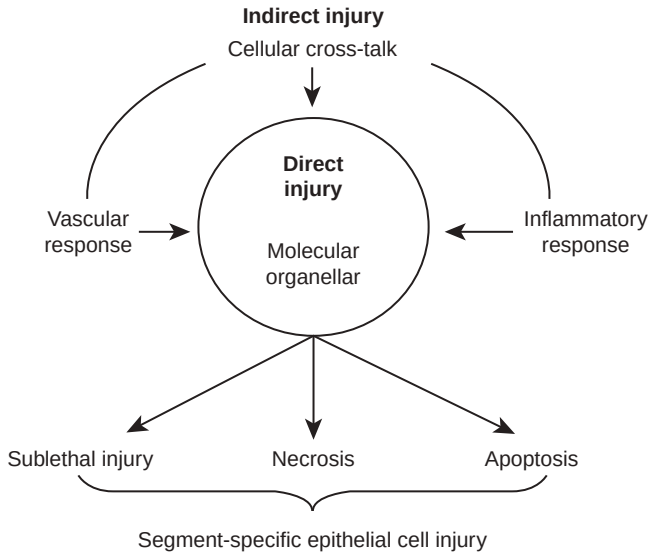

FIGURE 85.1 Determinants of injury outcome. The influence of indirect injury to adjacent structures and of the subsequent vascular and inflammatory response to injury on primary cellular targets of nephrotoxic injury is shown schematically. The phenotypic response to toxic injury is the sum of these responses.

further to toxicity. Because of the heterogeneity of these factors along the nephron, it is not surprising that the pattern of injury differs among nephrotoxins. Toxin delivery to a target site is a sine qua non for toxicity. Protein binding of the potential nephrotoxin will dictate whether the molecule is freely filtered at the glomerulus, dictating early exposure to the luminal aspect of proximal tubular cells or, if highly protein bound, to basolateral transport systems anywhere along the nephron. Thus, there is good correlation between the morphological and functional attributes of each nephron segment and the potential development of nephrotoxicity, especially in the proximal tubule where the greater proportion of specific drug toxicity occurs. Survival after toxicant exposure is also affected by the cycle status of the cell and the extent to which activation of pro- versus anti-apoptotic pathways and pro- versus anti-inflammatory pathways occurs; these factors collectively represent the "stress response" of the cells and are affected by the metabolic state of the cell. The anti-apoptotic and -inflammatory factors may be considered as a type of functional cytoprotective reserve (akin to antioxidant status in the face of oxidant stress), which might account for the differential susceptibility of particular tubular cells.

Renal Blood Flow and Cell Susceptibility

Heterogeneity of renal blood flow (RBF) defines the vascular limits of substrate and toxin delivery. The outer cortex receives 80% of the total RBF, the inner cortex and outer medulla only 15%, the inner medulla 5%, and the papillary region 2%.[38] Renal oxygenation is modified by diffusional shunting of oxygen from arterial to venous vessels running in close approximation. This is most apparent in the vasa recta, so that oxygen tension also falls off sharply at the corticomedullary junction, thereby producing the characteristic low oxygen tensions found in the renal medulla averaging approximately 10 mm Hg.[261] However, preglomerular shunting of oxygen also contributes and reduces cortical oxygenation to below renal vein values.[431] This arrangement is essential for maintenance of the medullary interstitial osmotic gradient generated by the countercurrent multiplier system that allows modulation of water reabsorption for the generation of concentrated or dilute urine. In a teleological sense, the arrangement also provides a selection advantage by creating a zone of borderline oxygenation in the kidney that may be ideal for sensing hypoxia by erythropoietin-producing interstitial cells in cortex. The disadvantage is that any significant reduction in RBF—for example, in shock—can easily lead to hypoxic damage, at least in outer medullary tissues, including "medullary rays" situated in the cortex and containing the S3 proximal tubule and TAL segments arising from glomeruli in the outer and mid-cortical layers.[40] Although both proximal tubular S3 cells and medullary thick ascending limb cells are exposed to a similar risk of hypoxia, only proximal tubular cells undergo early cell death following equivalent hypoxic insults *in vivo*.[119,147,275] This suggests that there are differences in susceptibility to injury between these segments, which may reflect differences in segmental cytoprotective mechanisms as discussed below.

Regulation of regional blood flow may be critical to localization of hypoxic and toxic injury. Autoregulation of cortical blood flow is highly efficient, whereas the extent of autoregulation of medullary blood flow remains controversial. Some studies indicate that medullary blood flow is not efficiently autoregulated, especially during volume expansion.[262,309] Other studies show efficient autoregulation of medullary blood flow under other conditions.[127,183,294] Such disparate observations may arise from different methods of estimating medullary blood flow.[125] Modulation of cortical and medullary blood flow may be critical to the actions of several nephrotoxins, such as iodinated contrast and nonsteroidal anti-inflammatory drugs. Heterogeneity of nitric oxide synthase (NOS) distribution within the kidney influences these regional differences in renal perfusion, and contributes to cytotoxic injury. All three isoforms of NOS are present in the kidney.[457,512] NO from eNOS is involved in regulation and maintenance of blood flow, and NO synthesized by nNOS in the

macula densa is important in the modulation of tubuloglomerular feedback (TGF) and regulation of glomerular filtration rate (GFR).[450] iNOS is present in the tubules of normal rat kidney, predominantly in the medullary thick ascending limb, but its involvement in regulation of kidney function under normal physiological conditions is unclear. Quantitative studies of NOS activity[523] and NO production[550] suggest that the renal medulla is the principal site for basal NO synthesis in the kidney, suggesting an important role of NO in regulation of medullary circulation.[75,76,309]

There is increasing interest in the role of the endothelium in ischemia-reperfusion injury, which may provide some insights into the effects of nephrotoxic injury on the renal vasculature. Endothelial dysfunction and vasoconstrictor hypersensitivity are well-recognized sequelae of ischemic acute renal failure (ARF).[150,151,152,219,278] After ischemia-reperfusion injury loss of GFR arises from a combination of a reduced transcapillary hydraulic pressure gradient (ΔP) during delayed graft function and back leak of the glomerular filtrate presumed secondary to both epithelial injury and tubular obstruction.[3,400] The decrease in ΔP may arise from two mechanisms.[400] The first is a reduction in perfusion pressure secondary to an increase in afferent arteriolar tone as a result of some combination of vasoconstrictor hypersensitivity, endothelial dysfunction impairing the generation of vasodilators, and increased TGF. The afferent arteriole provides the highest contribution to renal vascular resistance and is the key modulatory site for renal autoregulation.[234] The second mechanism is a rise in intratubular pressure arising from actual or functional tubular obstruction. Recent studies[161] confirming the continuing presence of TGF activity after ischemia-reperfusion injury support the postulated contribution from enhanced TGF secondary to reduced sodium and water reabsorption.[306,473] Structural obstruction of the nephron is recognized in ischemic ARF,[414] and functional (high-flow) obstruction causing intratubular pressure increases sufficient to stop filtration have been observed in toxic ARF after p-aminophenol.[190] Endothelial cell dehiscence and microvascular obstruction may also contribute a significant component of this reduction in renal blood flow, as recent studies have observed not only endothelial cell dehiscence, microvascular aggregation, and obstruction, but even reversal of flow.[41,463,528] These observations coupled with evidence of endothelial ICAM1 adhesion molecule upregulation[1] and leukocyte adhesion in the vasa recta[89,91] explain the outer medullary vascular congestion observed consistently after ischemic injury,[307] usually described as the "no-reflow" phenomenon.[257,459]

Iodinated contrast agents may be injurious through modulation of regional blood flow. One of the two principal explanations for genesis of acute renal failure by contrast is induction of vasoconstriction, either directly by high osmolar-contrast agents or by release of endothelin or adenosine or both. Medullary blood flow may be critical, since the potential for regional hypoxia described above predisposes to ischemic injury when both nitric oxide and vasodilator prostaglandin synthesis are blocked.[193] Iodinated contrast reduces NO synthesis in primary cultures of renal artery smooth muscle cells.[412] Injection of radiocontrast results in an immediate decrease in renal blood flow that is counteracted by an increase in renal prostaglandin formation. When prostaglandin synthesis is inhibited by cyclooxygenase inhibitors, prolonged endothelin-mediated renal vasoconstriction is observed.[57] Endothelin antagonists have not been successful in preventing contrast nephropathy.[506] However, the only clinical trial using endothelin antagonists utilized a nonselective endothelin antagonist that promoted both an increase in circulating endothelin of longer duration than the duration of antagonism[185,507] and antagonism of ET-B receptors, which would have suppressed NO production. Subsequent experimental studies have demonstrated protection by ET-A selective antagonists, but it is uncertain whether this protection was hemodynamically mediated.[282]

Modulation of NO also contributes to calcineurin-inhibitor and cisplatin toxicity. Acute dose-dependent vasoconstriction of the renal microcirculation by cyclosporine and tacrolimus is NOS dependent[113,114,509] and reversed by supplementation with l-arginine.[114] Chronic cyclosporine involves downregulation of eNOS, which can be reversed by administration of l-arginine[6,530] or pravastatin.[264] Inhibition of NOS (by 2-amino-4-methylpyridine aggravates experimental cisplatin-induced nephrotoxicity with exaggeration of both histological and metabolic features of cisplatin toxicity including reduction in glutathione[2] -peroxidase activity and elevation of platinum accumulation, but prevents the typical reduction in GSH and increase in malondialdehyde.[418]

Both vasodilator and vasoconstrictor prostaglandins generated by COX from arachidonic acid are critical in the regulation of vascular tone and sodium and water homeostasis in the kidney. Endogenous prostaglandins have been found to modulate the regulatory status of the perfused kidney and there is growing evidence to indicate that COX-2 is involved in the modulation of afferent arteriolar autoregulatory responses.[182,198] The interplay between endogenous vasodilators and vasoconstrictors—for instance, prostaglandins and endothelin—and the increase in vasoconstrictor production when vasodilators are stimulated or vice versa, highlights the important homeostatic effects of local

autoregulation. This is critical in determining regional blood flow and toxicity, but can make interpretation difficult.

CELLULAR TARGETS

Cellular Targets: General

Significant exposure of the kidney to toxicants typically results in ARF. The primary target for most nephrotoxin and ischemic injury are epithelial cells of the proximal tubule.[33,101,274,411] Other renal target cells include endothelial cells—for example, in response to Shiga toxin-2[549] or ischemia.[332] Endothelial cells can also be modified by cytotoxins to sensitize them to other forms of injury. For example, incubation of endothelial cells with calcineurin inhibitors has been shown to increase subsequent adhesion by dendritic cells.[427] Vascular smooth muscle cells can be indirect or direct targets. For instance, impaired vasorelaxation through impaired NO formation characterizes cyclosporine, contrast, and myoglobin toxicity as described. Severe ischemia may injure smooth muscle cells directly.[74] Podocyte injury is critical in the development of several forms of glomerular disease, and is induced experimentally by the nephrotoxin puromycin.[496] Tubular interstitial cells may be targeted by drugs with resultant tubulointerstitial nephritis, glomerular cells to cause proteinuria, and distal tubular cells to cause functional injury manifested as inhibition of transport (e.g., lithium and demeclocycline cause diabetes insipidus, and cotrimoxazole causes hyperkalemia) or structural damage (e.g., with fibrosis induced by lithium or other drugs). Secondary parenchymal injury may result from activation of inflammatory chemokines resulting in an inflammatory response with leukocyte activation and infiltration. This is a critical component of ischemia-reperfusion injury,[33,47,534] but has been inadequately explored in nephrotoxic injury.

Proximal Tubular Characteristics

Most nephrotoxic and ischemic injury involves proximal tubular cells.[32] Proximal tubule dysfunction is primarily responsible for activation of several of the main pathophysiological mechanisms, which leads to loss of GFR in acute renal failure as discussed earlier. The S3 segment of the proximal tubule and the medullary thick ascending limb (MTAL) of the loop of Henle traverse the outer stripe of the outer medulla and medullary rays in close proximity. These are regions of the kidney that are marginally oxygenated because of diffusional shunting of oxygen,[432] and where blood flow is reduced in the setting of ischemic and some toxic injuries.[120,187,307,534] Although both nephron segments have high transport activity and concomitant high metabolic activity, only proximal tubular cells are susceptible to injury causing cell death in most animal models.[119,275] This greater susceptibility probably arises because proximal tubular cells rely principally on fatty acid oxidation for energy,[406,519,520] and have low glycolytic capacity compared with MTAL cells under conditions of oxygen deprivation.[14,417] Thus, the higher glycolytic capacity of MTAL cells allows continued generation of ATP in the setting of rapid ATP depletion resulting from impaired oxidative phosphorylation.[32] There may also be greater cytoprotective reserve in MTAL cells in contrast to proximal tubule cells against early apoptotic injury through early and differential upregulation of anti-apoptotic Bcl-2 family members,[146] and of the protective mitogen-activated kinases (MAP kinase) pathway regulated by extracellular signal kinase (ERK),[96] as will be discussed further below. However, while ATP availability may make distal nephron cells less vulnerable to immediate cell death by necrosis, MTAL cells do undergo sublethal changes and produce various chemokines, cytokines, and growth factors that may have autocrine and/or paracrine effects on the injury and regeneration process of the kidney post-ischemia; MTAL cells may also undergo apoptotic cell death pathways under severe stress conditions.[146,270,271,272]

Transport-Based Selectivity

In the S1 and S2 segments, the proximal tubular cells have well-developed brush borders, a well-developed phagolysosomal system, a large endocytic apparatus with numerous apical vesicles, and mitochondria associated with the basolateral membrane.[477] Functionally, this region is associated with bulk isosmotic solute and fluid reabsorption coupled to the gradient generated by active sodium transport across the basolateral membrane by sodium ATPase and the tubular uptake and metabolism of protein by the endocytic and phagolysosomal systems.[477] The final (S3) segment of the proximal tubule is located in the outer stripe of the outer medulla. The cells are characterized by less well-developed phagolysosomal and endocytic systems, but contain a much greater proportion of smooth endoplasmic reticulum (ER) and peroxisomes.[477] S3 segment cells are the predominant location of the renal mixed-function oxidases, which contribute to both metabolic activation and toxicity of some compounds.

The greater diversity of transport functions in proximal tubule contributes to localization of injury because of preferential accumulation of many toxicants in this segment. For example, halogenated hydrocarbons are

common environmental chemicals present in solvents and pesticides that produce toxicity and ARF after enzymatic conversion to reactive intermediates and cysteine S-conjugates, which are particularly injurious to the S3 segment of proximal tubule,[64,115,116] since the S3 segment has the highest γ-glutamyl transpeptidase and cysteinylglycinase transport activity.[416] Similarly, nephrotoxic heavy metals—including mercury, cadmium, gold, lead, nickel, and chromium—induce injury targeted to the proximal tubule as a result of active transport systems. For example, mercuric chloride conjugates with glutathione[2] and cysteine in the liver and plasma, but accumulates in and is toxic to the S3 segment[456] where the Hg-GSH conjugates are converted into Hg-cysteine conjugates by γ-glutamyl transpeptidase, and then transported intracellularly by the Na-dependent L-alanine, L-serine, and L-cysteine (ASC) systems, and the Na-independent L-system.[538]

The relationship between transport proteins and protection is complex, as illustrated by cadmium-induced injury. Cadmium, a ubiquitous environmental toxin, is absorbed by inhalation or ingestion, and accumulates to produce proximal tubular injury. Cadmium induces the cysteinyl-rich metal-binding protein, metallothionein (MT), an important protective mechanism against many heavy metals.[487] However, MT contributes to cadmium injury since MT-knockout mice are protected against Cd toxicity.[231] Paradoxically, the MT complex facilitates uptake and accumulation by proximal tubular cells, with free cadmium and Cd-MT targeting different subsegments (S3 and S1/S2 segments, respectively) of the proximal tubule *in vivo*.[420] Cd-MT complexes formed in the liver are freely filtered and taken up into proximal tubular cells by endocytosis.[63,420] After endocytosed Cd-MT is degraded by lysosomes, free cadmium is released intracellularly and binds to subcellular targets to produce toxic injury characterized by proteinuria, phosphaturia, glucosuria, aminoaciduria, and polyuria.[419,539] Some protection against cadmium is afforded by pretreatment with cyproterone acetate, which appears to increase transport out of the proximal tubular cells by upregulation of a ZnT-1 transporter gene that encodes for a membrane protein associated with zinc efflux.[468]

Thus, transport systems, including endocytosis, are important in localizing toxicity. Gentamicin localizes to proximal tubule because of selective uptake. Megalin (also known as LRP-2), is a giant multiligand endocytic receptor, abundantly expressed in the apical membrane of proximal tubular epithelial cells, and is known to mediate uptake of β2-microglobulin. Megalin-knockout mice accumulate very little gentamicin compared with wildtype mice, suggesting that megalin-mediated endocytosis is the main mechanism of gentamicin accumulation in proximal tubules.[178,344,428] Even more compelling evidence indicates that megalin mediates MT−heavy metal complexes including MT-Cd.[232] Surface plasmon resonance and flow cytometry studies using overlapping MT peptides and recombinant MT fragments identified the hinge region of MT as a critical site for megalin binding, and suggest that disruption of the hinge motif (SCKKSCC) can inhibit proximal tubular MT uptake and eliminate much of the renal accumulation and toxicity of heavy metals such as cadmium, gold, copper, and also of cisplatinum, which is also transported bound to metallothionin.[232]

Distal tubular cells are also targeted through selective transport mechanisms. Lithium toxicity localizes to the distal nephron because lithium ions enter the cells via the amiloride-sensitive Na channel[16,139] to cause nephrogenic diabetes insipidus by markedly downregulating expressions of AQP2[299,505] and Na,K-ATPase.[256] Through understanding this transport selective toxicity, it was shown that polyuria can be ameliorated by amiloride in patients receiving long-term lithium therapy.[20,24] Similarly, the side effect of closure of luminal apical sodium channels in distal tubular cells—for example, by the antibiotics trimethoprim[492] and pentamidine[235] or by the diuretics triamterine and amiloride—is functional dose-dependent hyperkalemia, as blockade of Na transport reduces the transepithelial voltage and inhibits potassium secretion.

CELL INJURY PATHWAYS

Sublethal Injury

Nephrotoxic or ischemic injury not severe enough to cause cell death can nevertheless produce sublethal injury with significant pathophysiological consequences.[31] Some nephrotoxins produce changes in solute reabsorption as highlighted above for lithium and trimethoprim. Similarly, cadmium and maleic acid toxicity can produce proximal renal tubular acidosis with aminoaciduria, and glycosuria,[16] while amphotericin B can induce a distal renal tubular acidosis with hypomagnesemia and hypokalemia.[102] The factors defining whether sublethal injury produces a higher risk of further injury leading ultimately to cell death or is protective through pre-conditioning (e.g., by upregulation of heme-oxygenase-1) remain of considerable interest in ischemia-reperfusion injury.

Sublethal injury associated with ATP depletion in proximal tubular cells results in impairment of epithelial permeability, loss of functional integrity of tight junctions (zona occludens), loss of cell polarity, and altered localization of cell adhesion molecules and polarized membrane proteins.[31] Proximal tubular cell injury after acute chemical or ischemic insult is

characterized by ATP depletion, mitochondrial and peroxisome dysfunction, impaired solute and ion transport, loss of cell polarity, and cytoskeletal dysfunction. Oxidative damage and ionic and pH changes also contribute to cell injury, but ischemic and chemically induced ATP depletion have been more extensively studied than other mediators of injury.[275,276] The cellular and molecular lesions induced by ATP depletion are duration dependent and have been reviewed recently.[52] The lesions include misfolding and aggregation of membrane and secreted proteins;[248] disruption of the actin-based cytoskeleton;[12,13,331] disturbances in apical–basolateral protein polarization;[134] mislocalization and degradation of protein components of the intercellular junctions;[53,480] upregulation of many genes, including molecular chaperones,[51,248] growth factors and their receptors,[360] and regenerative proteins;[95,199,202] perturbation of integrin-mediated cell adhesion;[151,237,273,553] and induction of cell death by apoptosis or necrosis.[373]

Many of these changes occur very rapidly after the onset of ATP depletion, particularly changes involving the cytoskeleton. The apical microvillar region of proximal tubular cells is particularly sensitive because of the rapid rate of actin polymerization, so that severe but repairable damage occurs within five minutes of ischemia.[330] These changes are not confined to tubular epithelial cells. Rather, renal ischemia rapidly produces characteristic and duration-dependent effects on the actin cytoskeleton of numerous renal cell types, including endothelial[41] and smooth muscle cells, suggesting that the alterations are independent of cell type.[330] Microvascular injury resulting from changes in the endothelial cell actin cytoskeleton—including cell swelling, altered cell–cell attachment and reduced endothelial cell–basement membrane attachment—may play a central role in reduced blood flow to affected microvascular beds secondary to altered vascular reactivity, in increased leukocyte adherence and extravasation, in altered coagulation after endothelial dysfunction, and in increased interstitial edema secondary to increased endothelial permeability.[188] Injury to the vascular endothelium may also contribute to progressive loss of the microvasculature and perhaps via chronic hypoxia through glomerulosclerosis and tubulointerstitial fibrosis to progressive renal disease.[222] Chronic hypoxia induced in part by angiotensin II–mediated vasoconstriction may similarly contribute to chronic cyclosporine nephrotoxicity.[389]

Cell Death: Apoptosis and Necrosis

The responses of renal tubular cells to severe injury include cell death, de-differentiation of viable cells, proliferation, and re-differentiation and restitution of normal epithelium.[442,449,464,470] Cell death pathways are initiated by the same stressors, that initiate adaptive responses, including toxins and ischemia. Where these stressors are of sufficient initial magnitude or there is failure of the adaptive response mechanisms to rescue the cell, cell death is initiated by either apoptosis or necrosis. These responses are intimately related to cell cycle events leading to recovery or cell death (Figure 85.2). Heterogeneity of response in the kidney can result in concurrent apoptosis and necrosis within the same nephron segments following a single injurious influence.[147] The distinction between these modes of death is important in defining therapeutic strategies.[7] A clear distinction between modes of death follows the seminal study by Kerr, Wyllie, and Currie[230] in which they coined the term "apoptosis," and distinguished necrosis and apoptosis using morphological criteria. In necrosis, there is swelling of cell organelles including the mitochondrial matrix, chromatin flocculation, loss of plasma membrane integrity, and rupture of the cell contents into the extracellular space, which invokes an inflammatory response.[228] The mitochondria undergo inner membrane swelling, cristeolysis, and disintegration.[250] Polyribosomes disintegrate and disperse throughout the cytoplasm, and the cisterns of rough ER and Golgi apparatus are dilated and fragmented.[478] In apoptosis, the nuclei undergo chromatin condensation, pyknosis, and karyorrhexis, with the chromatin forming crescents along the periphery of the nuclear membrane.[230,526] The cells then shrink, lose microvillae and cell junctions, and fragment into a series of plasma membrane–bound condensed apoptotic bodies containing small masses of condensed cytoplasm, chromatin, and occasional organelles. Phosphatidylserine residues, normally located on the inner cell membrane surface, are exteriorized prior to cell fragmentation; these signal adjacent viable cells to

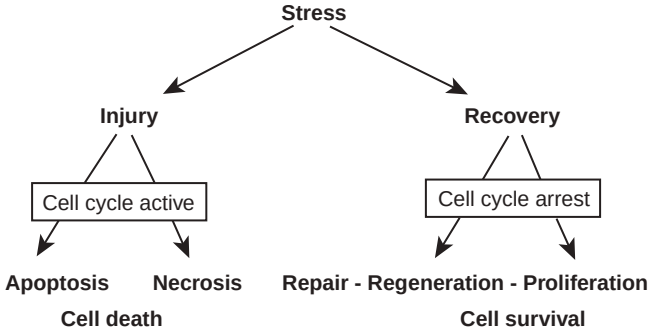

FIGURE 85.2 Injury response and cell cycle activity. The role of cell cycle activity in determining injury outcome is cell-type, toxin, and tissue dependent; the response for the general case is illustrated schematically.

phagocytose the apoptotic bodies without inducing an inflammatory response.[311,454]

To emphasize the distinctions between the catastrophic nature of necrosis in contrast to the orderly, genetically driven process of apoptosis, these are sometimes referred to respectively as "accidental cell death" and "programmed cell death." Despite these distinctions, there is considerable overlap between the cellular pathways involved in apoptosis and necrosis. For example, if a fragmented cell is not phagocytosed—for instance, in *in vitro* culture systems where macrophages are absent, and *in vivo* where phagocytosis is impaired, as in autoimmune disorders[522]—the apoptotic bodies eventually swell and lyse, a process known as secondary necrosis.[229] Consequently, the same insult may produce apoptosis or necrosis depending on severity.[272,274] Studies in animal models which demonstrated that apoptosis is a "normal" feature of ischemia-reperfusion injury *in vivo*,[18,67,82,145,146,362,430,447,448,482,537] have been confirmed in clinical biopsies of transplanted cadaveric kidneys, which are recognized as the best-defined model of human ischemia-reperfusion injury.[49,60,366] These studies have stimulated interest in downregulating apoptosis as a means of ameliorating or preventing acute renal injury,[30,271] a proposal that has now proven successful in experimental ischemia-reperfusion injury with the use of caspase inhibitors[110] and erythropoietin.[439,494]

Adaptive and cell regulatory pathways are initiated simultaneously with cell death pathways at the time of initial cell injury (Fig. 85.2). Thus, injury and recovery are postulated to be part of the same response[177] and involve engagement of the cell cycle.[397] Recovery after injury requires an orderly progression through the cell cycle (reviewed by Price et al.,[397]) which is regulated inter alia by the phosphorylation of substrates by interacting proteins called cyclins and cyclin-dependent kinases (cdk). Transition through so-called regulatory checkpoints G1 (gap-1) and S (DNA synthesis) and G2 and M (mitosis) cannot occur before each phase is completed. Natural inhibitors of cdk's such as p21, the 21-kd protein that inhibits cyclin-dependent kinase 2 (cdk2) activity are increased naturally during G1 to prevent further cycle progression or by the p53 transcription factor after DNA damage[50,88] or by p53-independent mechanisms after acute renal injury.[315] In p21(-/-) mice, both cisplatin and ischemic injury produce more rapid and severe acute renal failure with morphologic damage including necrosis and apoptosis throughout the renal cortex, whereas damage is restricted to the S3 segment of the proximal tubule in wildtype p21(+/+) mice.[313,314] In association with the increase in cell death there is an increase in cell cycle activity in p21(-/-) mice.[312] The corollary to these changes is that increases in p21 expression are associated with suppression of apoptosis after injury, and in preventing p53-induced apoptosis in a variety of cancer types, while reduction of p21 may induce apoptosis in such transformed cells.[157,391] These findings emphasize the importance of coordinated cell cycle control to recovery from acute renal injury with the final outcome dependent on both the severity of injury and the net balance of the cellular responses.[397]

Lethal Injury: Apoptosis

Since apoptosis of renal tubular cells predictably accompanies necrosis[433,434] and mechanisms of necrotic injury, such as ATP depletion and hypoxia, also induce apoptosis in cell culture models,[4,130,167–169,225,274] inhibition of apoptosis may be therapeutic[87] in ameliorating injury after ischemia-reperfusion injury including renal transplantation.[272,482] Intensive investigation of the molecular pathways involved in apoptosis have demonstrated that aspects of necrosis are also actively mediated, and that cytotoxic injury also leads to apoptosis through similar or identical pathways affirming the concept of a continuum of cell injury and death.

Caspases are the molecular executioners of apoptosis.[138,472] The molecular mechanisms of caspase-induced cell death were first elucidated in the nematode *Caenorhabditis elegans*.[489] Caspases are a family of at least 14 highly specific cysteine proteases synthesized as proenzymes (procaspases). They all possess a catalytic cysteine in the active site, require a tetrapeptide recognition sequence with a C-terminus aspartate, cleave target proteins after an aspartate residue, and are hence stylized "c(asp)ases." Procaspases are activated by proteolytic cleavage, usually at caspase substrate sites, which allows autolytic cleavage (e.g., adapter-facilitated self-cleavage by proximity) in a caspase cascade.[471] Caspases are either pro-inflammatory (caspases 1, 4, 5, 11, 13) and involved in maturation of cytokines, such as both interleukin (IL)-1 and IL-18 in the case of caspase-1, or pro-apoptotic.[471] The pro-apoptotic caspases can be divided into initiator caspases (caspases 2, 8, 9, 12) and effector caspases (caspases 3, 6, 7). Initiator caspases are activated by pro-apoptotic stimuli that induce adapter-facilitated self-cleavage. In turn, initiator caspases activate effector caspases that are responsible for cleavage of various physiological substrates including nuclear lamins, cytoskeletal proteins fodrin and gelsolin, actin-signaling protein, p21-activated kinase-2 (PAK2),[42,239,259,303] and caspase-activated DNAase (CAD).[118]

Target cleavage leads to the characteristic molecular and morphological patterns of apoptotic cell death. Lamins are intermediate filament proteins forming the

nuclear lamina underlying the nuclear membrane and responsible for chromatin organization: caspase-induced cleavage leads to collapse and characteristic condensation of nuclear chromatin. Similarly, caspase-induced cleavage of fodrin and gelsolin leads to cell blebbing, while PAK2 cleavage leads to cytoplasmic and nuclear condensation, cellular detachment, and to phosphatidylserine externalization,[302] which is critical for macrophage activation and phagocytosis. CAD activation, through proteolysis of ICAD (inhibitor of caspase-activated DNase), is one of the pathways of endonuclease activation.[118] Endonuclease activation is the final common execution of both apoptotic and necrotic cell death pathways after ischemia-reperfusion injury and results in the generation of unrepairable strand breaks in double-stranded DNA.[482,524] Random digestion of DNA in necrosis produces a smear pattern. Since internucleosomal DNA cleavage is nonrandom, producing DNA fragments that are multiples of ~180 base pairs and characteristic DNA laddering, these strand breaks have long been regarded as an indicator of apoptosis.[525] However, other studies have shown that both apoptosis and necrosis can occur in the absence or in the presence of DNA fragmentation,[73,100,413,483] so it is critical that apoptosis is defined by morphological as well as biochemical criteria. Caspase-independent (CAD-independent) DNA fragmentation occurs via endonuclease G, an endonuclease released from the mitochondrial intermembrane space and responsible mainly for single-strand fragmentation.[265,381] Apoptosis-inducing factor[4] also released from the mitochondrial intermembrane space and induces DNA fragmentation with high molecular weight fragments compared with the smaller fragments generated by caspase-induced deoxyribonuclease.[214,462]

Caspases are activated by mitochondrial or ER-mediated intrinsic pathways or following activation of cell surface receptors, the extrinsic pathway.[223] The extrinsic pathway is activated by triggering of cell death receptors, such as TNF and Fas, cell surface molecules that possess a common piece within their cytoplasmic tails called the death domain (DD).[11,488] Binding of ligands such as FasL to these receptors (e.g., Fas) induces receptor trimerization and formation of a death receptor−ligand complex. Adapter molecules, such as Fas-associated death domain protein or TRADD in the case of TNF, possess both DD and the death sector domain (DED). The death receptor−ligand complex recruits FADD by binding to the DD. FADD in turn recruits procaspase-8 modules through DED interaction and forms the death-inducing signaling complex (DISC) that facilitates activation of caspase-8.[340] Caspase-8 causes autocatalytic activation of further caspase-8 molecules through induced proximity. These translocate to the cytoplasm and directly activate downstream caspases, such as caspase-3, -6, and -7. Alternatively, caspase-8 catalyses the cleavage of cytoplasmic Bid,[256] a death-promoting member of the Bcl-2 superfamily. Truncated Bid (tBid) translocates to the mitochondria, integrates into the outer membrane, and interacts with other Bcl-2 family members to promote release of cytochrome C and other pro-apoptotic factors from the mitochondria, thereby activating caspases of the mitochondrial-dependent pathway.[159] Extrinsic pathway activation is regulated by Fas-associated death domain inhibitory proteins, like cytosolic FLIP (the FADD like IL-1β−converting enzyme inhibitory protein) and cowpox virus protein crm A, which inhibits caspase-8 and downstream caspases.[201,242,243,438,488]

The mitochondria-dependent intrinsic pathway (Figure 85.3) is responsible for most apoptosis, and leads to mitochondrial release of pro-apoptotic factors, including cytochrome C, AIF, and endonuclease G.[213,214,241,461] Intrinsic pathway-activating signals include DNA damage, heat shock, radiation, oxidative stress, glucocorticoids, perturbations in redox balance, ceramide activation of tumor suppressor proteins such as p53, and oncogenes such as c-myc, growth factor withdrawal, and some nephrotoxins.[373] During ischemia-reperfusion and after cisplatin, respiratory chain dysfunction impairs ATP generation. While severe ATP depletion causes necrosis, sustained milder degrees of ATP depletion can trigger apoptosis. One reason for the selective activation of apoptosis with milder degrees of ATP depletion appears to be the relatively greater reduction in the smaller intracellular pool of guanosine triphosphate (GTP), which is in tight equilibrium with ATP.[84] While the GTP: GDP ratio regulates various signaling GTPases such as Ras and Rho, which are regulators of cell proliferation and apoptosis,[174] GTP depletion also triggers an increase in p53, which translocates to the mitochondria and triggers mitochondria-dependent apoptosis.[83,226] In addition to functional changes in mitochondrial energy generation, ischemia produces two structural abnormalities in mitochondria. First, it triggers collapse of the mitochondrial membrane potential ($\Delta\Psi\mu$) following opening of the mitochondrial transition pore in the inner mitochondrial membrane, producing high amplitude swelling and impairing ATP generation early in reflow.[171,172] Second, it triggers leakage of cytochrome c leakage from the inner membrane space into the cytoplasm.[241] Dislocation to the cytoplasm of cytochrome c, an electron shuttle protein, both impairs respiration and facilitates binding of deoxyadenosine triphosphate to the adapter protein apaf-1-cytochrome C-complex, inducing oligomerization to form the high-molecular-weight caspase-activating complex, the apoptosome.[266,551] The apoptosome recruits procaspase-9, which autocatalytically activates and then

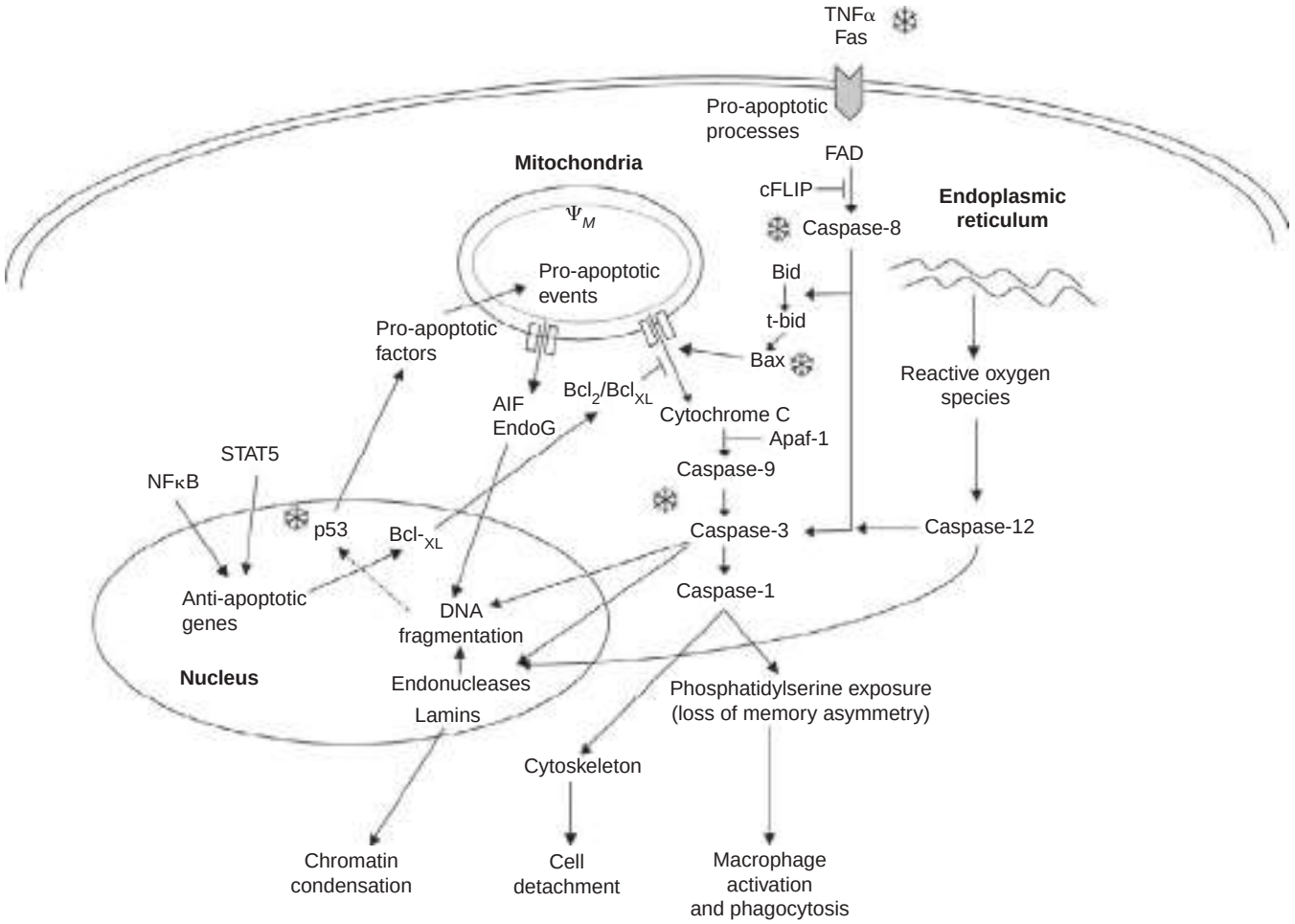

FIGURE 85.3 Extrinsic and intrinsic pathways of apoptosis in nephrotoxic injury. Caspase-dependent fragmentation of DNA follows activation of executioner caspase-3 via either the intrinsic (mitochondrial and endoplasmic reticulum) or extrinsic (Fas/TNF) pathways as shown in schematic form. Caspase-independent fragmentation of DNA follows mitochondrial release of AIF and EndoG and also leads to cell death by apoptosis. Several sites of interaction between the extrinsic and intrinsic pathways are illustrated. Sites of reported activation by cisplatin are marked by the symbol. See text for definitions and detailed explanations.

proteolytically activates caspase-3, triggering execution of apoptosis.[552]

The intrinsic mitochondrial signaling pathway is regulated by members of the Bcl-2 family.[1,87] Mammals possess a large family of Bcl-2 proteins that includes pro-apoptotic as well as anti-apoptotic members. Anti-apoptotic members include the prototype Bcl-2,[491] Bcl-xL, Bcl-w, and Mcl-1. Pro-apoptotic members include Bax, Bak, and Bok. A third class of molecules sharing homology with the Bcl-2 homology-3 (BH3) domain can activate pro-apoptotic members or inactivate antiapoptotic members and include Bin, Bid, Bad, and Bik. The ratio of anti- to pro-apoptotic molecules such as Bcl-2 to Bax is a measure of susceptibility to apoptosis via the intrinsic pathway, perhaps because pro- and anti-apoptotic members of the Bcl-2 family heterodimerize with each other.[1] The precise mechanism by which mitochondrial intermembrane space proteins are released by the actions of Bax and Bak is uncertain. Translocation to the mitochondrion, oligomerization, and insertion of Bax into the outer mitochondrial membrane to form pores or channels, which allow release of intermembrane space proteins, has been proposed.[448] Alternatively, Bax may mediate opening of the mitochondrial permeability transition pore, which then somehow modulates permeability of the outer mitochondrial membrane, perhaps after swelling and rupture.[189] Nevertheless, although there is evidence for these alternatives (see Danial and Korsmeyer[87]), the precise mechanisms remain uncertain. It is clear, however, that anti-apoptotic Bcl-2 family members (such as Bcl-2 and Bcl-xL) block apoptosis-induced release of these intermembrane space proteins, perhaps by stabilizing and preventing opening of the mitochondrial

permeability transition pore.[1,87] Translocation of both pro- and anti-apoptotic Bcl-2 proteins to the mitochondria appears critical: for example, protection against apoptosis in distal tubular cells after oxidative injury was associated with translocation of Bcl-xL to mitochondria within the surviving distal cells, whereas proximal tubular cells showed reduced survival coupled with decreased expression of Bcl-xL, which did not translocate to the mitochondria.[79] After ischemia-reperfusion *in vivo*, rat proximal tubules show a marked increase in Bax expression and apoptosis as well as an expected increase in necrosis.[146] The relevance of these and similar[18] experimental rat studies is clear from similar observations in human kidneys after cadaveric renal transplantation, where increases in apoptosis with ischemia time were associated with increased Bax expression and of cytoplasmic cytochrome C, confirming mitochondrial pathway involvement in the observed apoptosis.[60]

Impairment of mitochondrial outer-membrane integrity allows numerous other proteins normally sequestered in the inner membrane space to enter the cytoplasm.[410] These include caspase-independent death effectors such as the apoptosis-inducing factor (4), mitochondrial pools of co-caspases (such as caspases-2, -3, and -9), the second mitochondrial activator of caspases (Smac),[104] the direct inhibitor of apoptosis proteins (IAPs) binding with low pI (Diablo),[493] and serine protease HtrA2/Omi.[490] AIF translocates to the nucleus triggering chromatin collapse and digestion of DNA as described earlier. IAPs regulate caspase activity by acting as pseudosubstrates. By binding IAPs that inhibit caspases-3, -7, and -9 directly, Smac/Diablo frees these caspases to promote cell death.[410,444]

As shown in Fig. 85.3, there are three potential levels of interaction between the extrinsic and intrinsic apoptotic pathways. Initial activation of caspase-8 via Fas can induce mitochondrial translocation of Bid with resultant cytochrome C release.[292] Second, the transcription factor p53 activates pro-apoptotic Bcl-2 family members and also Fas-dependent apoptosis.[50] Third, the extrinsic and intrinsic pathways converge at caspase-3 activation, the beginning of the execution phase.[472]

Pro-inflammatory caspases are also involved in ischemic renal injury, reflecting our increasing awareness that even apparently purely ischemic renal injury involves significant inflammation.[33] Caspase-1 (previously known as ICE, interleukin-converting enzyme) proteolytically cleaves the precursor forms of both pro-inflammatory cytokines IL-1β, and IL-18.[128] These are increased after ischemia-reperfusion injury, although from a combination of knockout and protection studies, it appears that only the increase in IL-18 plays a significant[317,318] but uncertain[80] role. Cisplatin-induced apoptosis does not involve caspase-1 activation.[224]

Nephrotoxic injury is associated with caspase activation and apoptosis. Cisplatin-induced apoptosis is associated with translocation of Bax to mitochondria, release of cytochrome c, and activation of caspase-9 and -3,[224,253,277,378] while inhibition of these caspases provided partial protection[223] confirming a role for mitochondrial pathway activation. Cisplatin also induces increased expression of TNF-α and Fas and with activation of caspase-8, suggesting a significant contribution to apoptosis from extrinsic pathway activation.[436,481] Similarly, caspase-2 release from human fibroblast mitochondria is associated with cisplatin, etoposide, and UV light−induced apoptosis, which can be prevented by small interfering RNA (SiRNA)-mediated silencing of caspase-2 expression.[252] Since p53 inhibition provides partial protection against cisplatin-induced apoptosis,[78] a role for p53 in cisplatin-induced cell death seems likely.

The ER−specific caspase, caspase-12, appears to be involved in apoptosis following ER stress.[345,408] The ER contains high concentrations of cytochrome P-450 enzymes, which can lead to generation of reactive oxygen metabolites. Microsomal CYP2E1 is the source of reactive oxygen species generation in cisplatin-induced apoptosis.[284] This oxidative stress and mobilization of ER calcium stores precedes procaspase-12 activation, which then leads to apoptosis of LLC-PK1 cells, directly by bypassing caspase-9 and -3, but also partly mediated by caspase-3 activation, perhaps after oxidant injury to the mitochondria and resultant cytochrome C release.[245,285]

Necrosis. While there have been considerable advances over the last decade in our understanding of apoptosis, our understanding of molecular pathways in necrosis has been more selective, beginning with the concept that necrosis is a largely "passive" process secondary to acute ATP depletion. Direct consequences of ATP depletion include impairment of ATP-dependent ion channel transport, disruption of ion gradients, actin cytoskeleton disruption, cell swelling, membrane blebbing, and cell disruption (see recent review by Padanilam[373]). There is now evidence that both forms of cell death include actively mediated steps. Since both necrosis and apoptosis are frequently found together in the same tissue, distinguishing these death modalities may sometimes be difficult.

Classically ischemic, hypoxic or chemical ATP depletion leads to cell death associated with an increase in cell volume, so called "oncosis,"[295] and was presumed to occur because of sodium and water influx and initial potassium ion efflux associated with increased plasma membrane permeability. This general pattern was confirmed using 23Na, 31P, and 87Rb magnetic resonance spectroscopy of intact kidneys.[5,77,409] While the initial sodium influx is balanced

by potassium efflux, increased intracellular sodium will further dissipate ATP by activating Na^+,K^+-ATPase, and severe ATP depletion will lead to failure of pump-leak balance, further sodium influx, and cell swelling.

Further evidence indicates that whether a lethally injured mammalian cell undergoes necrosis or apoptosis may be determined by early activation of cell membrane ion channels. Most cells can regulate their volume by mechanisms called regulatory volume decrease or increase, after osmotic swelling or shrinkage. In contrast, a major hallmark of apoptosis is "normotonic" shrinkage of cells.[293] Apoptotic volume decrease requires active K^+ and Cl^- efflux.[293,367] Necrotic volume increase is initiated by uptake of osmolytes, such as Na^+, Cl^-, and lactate after injury, hypoxia, ischemia, acidosis, or lactacidosis through membrane carriers and through stress-activated nonselective cation channels.[17] Persistence of necrotic volume increase is caused by dysfunction of the regulatory volume decrease mechanism due to impairment of volume-sensitive Cl^- channels under conditions of ATP deficiency or lactacidosis. The role of these ion fluxes in the death phenotype is highlighted by the observation that both lactacidosis-induced dysfunction of regulatory volume decrease and necrotic cell death are prevented by pretreatment of cells with the vacuolating cytotoxin-A (VacA) protein purified from *Helicobacter pylori*, which forms a lactacidosis-resistant anion channel.[367] Similarly, blocking the increase in K^+ and Cl^- conductances following stimulation of either extrinsic or intrinsic pro-apoptotic pathways prevented the biochemical and morphological changes of apoptotic cell death, whereas inhibiting apoptosis by broad-spectrum caspase inhibition did not prevent apoptotic volume decrease.[293]

Stress-activated nonselective cation channels of the transient receptor potential, melastatin-like (TRP) family, such as melastatin-like TRPM2, also known as long transient receptor potential channel-2 (LTRPC2), are dormant in viable cells, but become activated and contribute to necrosis after binding ADP-ribose, or reactive oxygen or nitrogen species.[17,180,310,386,387] LTRPC2 is permeable to both Ca^{2+} and Na^+ after activation, and contributes to Na^+ and Ca^{2+} overload. Since hypoxic and ischemic injury results in oxygen-derived free radical generation,[216,217] such channels explain the earlier observation, that the rate of Na accumulation in the hypoxic kidney was reduced by free radical scavengers.[77] Sodium overload coupled with severe ATP depletion leads to a necrotic outcome. Increased cytosolic calcium further increases ATP depletion by activating Ca^{2+}-ATPase and by producing mitochondrial depolarization (see previous discussion). Even mild oxidative stress can increase cytosolic Ca^{2+} by stimulating release of calcium from intracellular binding sites such as the ER.[527] The role of these TRP channels in nephrotoxic injury is unknown, although the common features of oxidative and mitochondrial injury in cisplatin nephrotoxicity[1] suggest mechanisms likely to activate calcium influx and promote further injury.

Additional molecular events promoting necrosis triggered by ischemia include activation of proteases, phospholipases, endonucleases, poly(ADP-ribose)polymerase (PARP), iNOS, and the protein kinase (PK) family, including PKC and the mitogen-activated protein kinases (MAPK) and the generation of reactive oxygen species.[372] The activated proteases include calpain[181,287,288] and meprin (metallopeptidase from renal tissue),[58,192] both of which mediate further injury. Phospholipases (PL) are activated by phospholipolysis following ischemia. PLA_2 has various isoforms that vary in their dependence on Ca^{2+} for activation. Activation leads to membrane phospholipid breakdown, with potential loss of membrane integrity, generation of inflammatory mediators, and cytotoxicity from lysophospholipids and free fatty acids.[31,394] Separate mention must be made of fatty acids, since β-oxidation of fatty acids is a major energy source in renal cortex.[406,520] Renal peroxisomes and mitochondria utilize identical pathways for β-oxidation of fatty acids, except that peroxisomes, which are single-membrane–bound organelles, do not use carnitine for entry of fatty acids (in contrast to mitochondria where these are involved in transport into the mitochondrial inner matrix).[393] Peroxisome proliferator–activated receptors (PPARs) are members of the nuclear hormone receptor superfamily of ligand-dependent transcription factors. PPARα is expressed predominantly in proximal tubule and medullary thick ascending limb in the kidney and agonists, including fatty acids, eicosanoids, and fibrate drugs, act as ligands and induce fatty acid oxidation.[393] Peroxisomal as well as mitochondrial fatty acid oxidation are inhibited after ischemia-reperfusion and cisplatin injury to the kidney, while administration of PPARα ligands prior to injury was protective.[393,395] Cisplatin attenuates PPARα signaling by reducing the expression of a tissue-specific coactivator of PPARα called PPARγ-coactivator-1 (PGC1) which is also a transcriptional coactivator for other transcription factors including nuclear respiratory factor, which are important in the regulation of oxidative metabolism, cellular respiration, and adaptive thermogenesis.[144] Survival of renal tubular epithelial cells after cisplatin appears to depend on intact PGC-1/PPARα function. PPARα agonists appear to have therapeutic potential for cisplatin-induced ARF. Use of PPARα ligands prevented acute tubular necrosis by ameliorating cisplatin-induced inhibition of mitochondrial medium-chain, acyl-CoA dehydrogenase–mediated fatty acid

oxidation and pyruvate dehydrogenase complex activity.[268] PPARα ligand also protects against cisplatin-induced renal injury by reducing the expression and enzyme activity of proximal tubule endonuclease G.[267]

The PKC family comprises serine-threonine kinases, with 12 isozymes activated by Ca^{2+}, phosphatidyl serines, and diacylglycerol.[372] Activation of PKCs leads to signal transduction via activation of G protein–coupled receptors, tyrosine kinase receptors, and nonreceptor tyrosine kinases.[361] As a result of controlling 70% of the phosphorylating activity in the proximal tubule, PKC regulates numerous physiological functions of the renal epithelium including Na^+,K^+-ATPase activity, gluconeogenesis, and transport of amino acids, glucose, sodium, potassium, chloride, water, organic anions, and cations.[94] PKC isozymes also play a crucial role in the regulation of other major cellular functions, including proliferation and differentiation.[94] After ischemia, the increased Ca^{2+} and phospholipids hydrolysis products induce PKC isoenzymes and activated C-kinase receptor in kidney.[373] PKC induction appears to be protective. Induced PKCα, -βII, and -ζ protect cultured renal cells from oxidant injury and subsequent necrosis.[373] PKC is involved in ischemic preconditioning[258] and heat shock–induced protection.[316]

PKC isoenzymes directly influence mitochondrial function, and are therefore involved in recovery from both ischemic and apoptotic injury to renal cells. For example, while initiation of apoptosis by many agents is preceded by mitochondrial dysfunction and depolarization of the mitochondrial inner membrane, Nowak[365] demonstrated that, in renal proximal tubular cells, cisplatin induces mitochondrial dysfunction associated with hyperpolarization of the mitochondrial membrane, and that these events are mediated by protein kinase C (PKC)-α and extracellular-regulated protein kinase (ERK)1/2. Nowak also demonstrated that PKC-α and ERK1/2 mediate activation of caspase-3 by acting downstream of cytochrome c release from mitochondria, and that ERK1/2 activation by cisplatin occurred through a PKC-α–independent pathway. Nowak subsequently observed[364] that PKC inhibition decreases recovery of physiological function, recovery of PKC activity precedes the return of physiological functions after oxidant injury, and that activation promotes recovery of mitochondrial function and active Na^+ transport. Since oxidant injury–induced *tert*-butylhydroperoxide was associated with recovery of total PKC activity, while that associated with the nephrotoxic cysteine-S conjugate, S-(1,2-dichlorovinyl)-L-cysteine (DCVC), was not, Nowak concluded that the repair of renal function is mediated through PKC-dependent mechanisms, and that cysteine conjugates inhibit renal repair, partly through inhibition of PKC signaling.[364] Subsequently, Nowak observed that serine but not threonine phosphorylation of the beta-subunit of F^1F^1-ATPase was increased during late recovery following DCVC. Inhibition of PKC-α activation decreased this phosphorylation, confirming that PKC-α regulation of repair of mitochondrial function involves phosphorylation of the catalytic subunit of F^1F^1-ATPase.[286]

Repair and regeneration of renal cells after injury is less well studied than the initiation of injury but is known to involve proliferation and migration as well as repair of injured proximal tubular cells, and thus involves growth factors, integrins, and extracellular matrix protein interactions.[146,363] Growth factors administered pre- or post-ischemia–reperfusion injury ameliorate injury and enhance regeneration through their anti-apoptotic, proliferative, and pro-angiogenic actions.[175,176] Insulin-like growth factor (IGF-1) and hepatocyte growth factor may also enhance GFR after injury by increasing NO production, increasing local blood flow and vasodilating renal microvessels.[109,476] However, the utility of growth factors in ARF therapy remains uncertain.[194]

MAP kinases are serine/threonine kinases ubiquitously expressed in mammalian cells and known to be modulated in response to ischemic and toxic stress.[32] MAPK activation is important in determining whether cellular stress leads to proliferation, differentiation, or apoptosis. Three MAPK cascades have been identified, the ERK, JNK, and p38 pathways. Cellular stress, such as toxic injury, induces generation of growth factors and inflammatory cytokines. The ERK pathway is activated by growth factors, vasoactive peptides, and nephrotoxins, including aminoglycosides and cephaloridine[32] via a cytoplasmic-activating protein, MEK1. After activation, ERK proteins translocate to the nucleus, and phosphorylate and activate several Ets-domain transcription factors including Elk-1, SAP1, Ets-1, and Ets-1.[136] ERK activation is involved in cell proliferation and differentiation and appears to be protective in the preconditioned post-ischemic kidney[378] and in distal tubule cells.[8,96] The JNK (c-Jun N-terminal kinase) pathway, also designated as stress-activated protein kinases (SAPK), are activated by genotoxic and osmolar stress, mechanical stretch, shear stress, and the inflammatory cytokines TNFα and IL-1β.[32] They are also activated by ischemia-reperfusion.[392] The p38 pathway is activated by many of the same stimuli that activate JNK/SAPK, but is independently regulated and plays a significant role in inflammatory cytokine production.[32] Activation of the JNK/SAPK and p38 pathways is antiproliferative and can lead to cell death. While the effect of toxins on JNK activation in the kidney is unknown, JNK activation and subsequent apoptosis of hair cells have been implicated in gentamicin

ototoxicity.[531] Activation of ERK in distal tubule cells relative to JNK may contribute to the differential survival of these cells in contrast to proximal tubular cells after ischemia-reperfusion injury[96] and with the renal protection associated with preconditioning.[378]

PARP is a nuclear enzyme that adds ADP-ribose to various proteins including PARP itself after activation by DNA strand breaks. PARP is involved in both DNA repair and gene transcription and acts to open up the condensed structure of chromatin.[308] After injury, activation of PARP leads to consumption of its substrate β-NAD^+. Resynthesis of β-NAD^+ consumes further ATP.[161,301] Whether the cell proceeds to apoptotic or necrotic cell death varies, possibly depending on the degree of initial ATP depletion or on PARP cleavage. While fibroblasts from PARP(-/-) mice are protected from necrosis, TNF-α can still induce death by apoptosis.[163] However, in fibrosarcoma cells, TNF-α can activate PARP and induce death by necrosis.[291] It appears that NAD^+ depletion induced by PARP activation may act as a trigger for AIF translocation from mitochondria to cytoplasm and nucleus to induce chromatin fragmentation.[535] Moderate oxidative stress activates PARP, but it is then inactivated by caspase cleavage, which prevents further ATP depletion and enhances apoptosis.[192]

The inflammatory cascade is initiated by ATP depletion and exacerbated by reperfusion.[369] Endothelial, epithelial, and infiltrating inflammatory cells all participate in and mediate the inflammatory process after ischemia-reperfusion.[443] Endothelial cells express adhesion molecules including ICAM-1, VCAM, P and E selectins, and β2-integrins. ICAM-1 binds to LFA-1 (CD11α/CD18) and Mac-1 (CD11β/CD18) receptors on leucocytes producing recruitment and activation.[398] Involvement of adhesion molecules has been confirmed by blockade of ICAM-1[227] and selectin.[466] Adherent leukocytes release reactive oxygen species, proteases, and other enzymes, and, together with the activated endothelial cells, release inflammatory cytokines such as IL-1, IL-6, IL-8, IL18, TNF-α, chemokines, and MCP-1.[318,465,470] The relative importance of neutrophils, macrophages, and T and B lymphocytes as critical leukocytes in postischemic inflammatory events remains unclear.[33,45,46,48,90,91,233,279,318,534] However, inhibition of various inflammatory pathways, including the CD28-B-7 costimulatory pathway by selectin blockade,[465,466] the melanocortin-stimulated inflammatory gene stimulatory pathway by α-melanocyte−stimulating hormone, α-MSH,[65,66] IL18 cytokine depletion in neutrophil-depleted mice,[318] and of multiple pathways including cell infiltration, ICAM-1 and iNOS upregulation, matrix molecule expression, MAP kinase ERK1/2 activation, and transcription factor activation by cerivastatin,[162] all ameliorate ischemia-reperfusion injury, thus supporting a critical role for inflammation in both necrotic and apoptotic injury.

Overlaps Between Necrosis and Apoptosis

While this review has delineated distinct molecular pathways that are triggered by pro-necrotic or pro-apoptotic events, it is important to emphasize that there is considerable opportunity for intersection and overlap between these pathways after both ischemic and nephrotoxic injury. Mitochondrial and peroxisomal involvement in both pathways appears likely. PARP activation may be crucial as highlighted above. Inflammatory mediators are involved in necrosis, but the observation that inhibition of apoptosis can ameliorate both inflammation and necrosis, for example, by pan-caspase inhibition after ischemia-reperfusion,[81] emphasizes that apoptosis is frequently if not always a normal component of injury previously regarded as pure necrosis. Recruitment of stress-activated pathways and cell cycle proteins may be critical in determining the final outcome after injury. These overlaps highlight new therapeutic opportunities that may be available in the treatment and prevention of nephrotoxic injury.

BIOMARKERS OF NEPHROTOXIC INJURY

While serum creatinine and urea (BUN) have been used routinely to detect and monitor AKI, these conventional biomarkers of renal function only increase beyond the normal range when nearly half of the functional reserve of the kidney has been compromised. Thus, they detect kidney injury only after it is far advanced.[441] They are also slow to respond to change in renal function. Since extrapolations to GFR from serum creatinine require that creatinine is in steady state equilibrium, this requires three to five half lives before such extrapolations are valid. The half-life of creatinine is four hours when GFR is normal[68] and this increases in proportion to any decline in GFR. Thus after the one third decline in GFR required to be diagnosed as having AKI by the corrected RIFLE criteria,[390] creatinine will only reach a steady-state after 12 to 20 hours or longer if the decline is greater. The implication is that at least 12 and, more likely 24 to 48 hours, must elapse before a new creatinine value is a reliable index of changed renal function. This creates an unavoidable delay in diagnosis of and intervention in AKI. In nephrotoxic injury, these delays may be greater since accumulation of drug or injury or both may be needed to induce measurable changes in renal function. In addition, drug-induced kidney injury in

nonclinical animal models is a major cause of elimination of compounds during drug development; these compounds are eliminated from the development process even when it is unclear whether the toxicity would translate to humans. More sensitive biomarkers are needed to enable more reliable diagnosis of nephrotoxin-induced AKI in both clinical and preclinical studies and to facilitate earlier intervention and monitoring.

A biomarker is any parameter that can be objectively measured and evaluated, which acts as an indicator of a normal or pathological process, or of a response to intervention. The identification of biomarkers of renal cellular injury along with the re-discovery and quantitation of the predictive relationship between enzymuria and renal injury[517] have re-kindled widespread interest in the nephrology and diagnostic communities, since these new tools offer the possibility of a paradigm shift in diagnosis of AKI and open the door to early intervention.[121,122,123] These biomarkers are present in urine, plasma and sometimes both. Since plasma or serum biomarkers have many potential sources, urinary biomarkers generally have higher renal specificity and are easily acquired in non-oliguric AKI. Consequently, urinary biomarkers have been the main focus of recent studies. The urinary biomarkers fall into at least five categories: filtered biomarkers where glomerular permeability has increased, filtered biomarkers where renal reabsorption is impaired as a result of tubular injury, pre-formed cellular biomarkers released following injury, upregulated biomarkers, and inflammatory biomarkers released into the urine following recruitment of inflammatory cells.[124] An alternative way of classifying these is as as inflammatory, excreted tubular proteins and surrogate markers of tubular injury, with different mechanisms for increase and significance.[516] At present, the most studied biomarkers are the tubular enzymes GGT, GST and N-acetyl-beta-glucosaminidase (NAG), and the novel induced biomarkers, kidney injury molecule-1, (KIM-1), interleukin 18 (IL-18) and neutrophil gelatinase associated lipocalin (NGAL).[179,322,377] New biomarkers are appearing regularly in the literature, for example, Trefoil factor 3,[536] Clusterin,[98] Netrin-1[508] and Aprotinin.[354] Albumin may have a specific role as a biomarker in AKI since proximal tubular receptor-mediated uptake may be impaired.[347,348,536]

Because nephrotoxic potential is critical in the both safety and commercial decisions regarding the continuation or abandonment of the development of candidate drugs, tubular enzymuria, particularly NAG, GGT, alanine-aminopeptidase, lactate-dehydrogenase and alkaline phosphatase have been widely used by the pharmaceutical industry to assess nephrotoxicity during drug development. However this process has not been regulated until recently. The United States Food and Drug Administration (FDA) and the European Medicines Evaluation Agency (EMEA) have taken an active role together with the pharmaceutical industry in developing a process for context-dependent qualification of biomarkers to improve the drug development and regulatory review process.[154–157] The FDA and the EMEA have also expanded the context in which qualification for biomarkers is determined, and an expedient biomarker-qualification process is currently in place.[98,154,155,156] The Critical Path Institute (C-Path) created the Predictive Safety Testing Consortium (PSTC) as a neutral ground where scientists from 16 pharmaceutical companies and academia could share and test new methods that are more reliable predictors of human safety. The PSTC developed the legal framework needed to share the cost of qualification and to protect intellectual property associated with biomarker qualification and it submits the data to the FDA and EMEA to support the biomarker certification process.[154–156] The first FDA and EMEA review of biomarker qualification data involved biomarkers of renal injury and qualified seven biomarkers as supplemental data for evaluation of nephrotoxicity in nonclinical safety studies.[154] These new biomarkers qualified for specific contexts of use are the urinary concentrations of KIM-1, albumin, total protein, β2-microglobulin, cystatin C, clusterin, and trefoil factor-3. The PSTC submitted data supported claims that three of these urinary biomarkers—total protein, β2-microglobulin, and cystatin C concentrations—could outperform levels of BUN and serum creatinine in detecting and monitoring drug-induced glomerular injury, while four urinary biomarkers—levels of KIM-1, albumin, clusterin, and trefoil factor-3—could either outperform or add value to levels of BUN and serum creatinine in detecting and monitoring certain drug-induced tubular injuries.[154] More recently, renal papillary antigen-1 RPA-1 was qualified as marker of site-specific injury in the collecting duct and clusterin was requalified as a voluntary biomarker for use in detecting drug-induced tubular injury, particularly when signs of regeneration are present. These biomarkers were qualified for use as adjuncts in detecting nephrotoxic injury on a voluntary basis in pre-clinical rat studies while other biomarkers remain "exploratory." The qualification process and need for more data on nephrotoxins and also on reversibility has encouraged much further study, e.g.[98,370,415,536]

From both drug development and safety viewpoints, better biomarkers could enable safer and easier-to-monitor therapies by reducing the margin between efficacy and safety needed for clinical and preclinical applications. Much of the current work involves comparing biomarker performance in preclinical or clinical

contexts. The sensitivity, specificity and time course of biomarkers are critical factors in determining utility in a particular disease. The favored metric for assessing biomarker performance is currently the receiver operator characteristic (ROC) curve analysis. When sensitivity is graphed against (1-specificity), the area under the ROC curve (AUC) (± the confidence interval) defines performance. The AUC for a perfect biomarker is 1.0, for a non-performing biomarker it is 0.50; clinical utility requires a minimum AUC of 0.70, although, realistically, much higher values are needed for clinical utility. Comparison of individual predictors and multivariable models is usually undertaken following the method of DeLong.[92] The prognostic benefit of adding a biomarker to a baseline clinical model is calculated from the net reclassification improvement (NRI) and integrated discrimination Improvement (IDI) indices.[382]

Thus in the detection of histological injury in one study of rat kidney injury induced by ten different nephrotoxins, urinary total protein (ROC AUC 0.86), cystatin C (0.92) and β2-microglobulin (0.89) showed a better diagnostic performance than BUN (0.80) and SCr (0.53) for detecting glomerular injury, while urinary clusterin (ROC AUC 0.88), outperformed BUN (0.79) and SCr (0.73) for detecting proximal tubular injury.[98] Similarly, urinary KIM-1, outperformed the traditional biomarkers SCr, BUN and urinary NAG for the diagnosis of proximal tubular damage, using both using both exclusion and inclusion analysis approaches.[484] For all observed histopathology grades following eight different nephrotoxicants, KIM-1 had the highest AUCs (exclusion analysis, 0.91; inclusion analysis, 0.88), whether compared to SCr (exclusion analysis, 0.73; inclusion analysis, 0.72), BUN (exclusion analysis, 0.79; inclusion analysis, 0.75) or urinary NAG (exclusion analysis, 0.82; inclusion analysis, 0.76). A total of tubular nephrotoxicants, including gentamicin, cisplatin and cyclosporine, and ischaemia-reperfusion injury were examined in that study. Regardless of whether the kidney injury was induced by well-established kidney toxicants or ischemia, urinary KIM-1 outperformed the conventional markers, BUN, SCr and urinary NAG. In addition, the very high ROC-AUC values of 0.91 to 0.99 for urinary Kim-1 demonstrated that urinary KIM-1 measurements were sensitive, specific and accurate in diagnosing either drug-induced or ischaemic kidney injury of various histological types as well as regenerative basophilia when lesions were either subtle with little organ involvement, or very severe with disturbed renal function.[485] KIM-1 was subsequently qualified by the FDA as an early diagnostic biomarker of drug-induced acute kidney tubular alterations in rat toxicology studies, for regulatory decision making as a biomarker used by sponsors on a voluntary basis to demonstrate that drug-induced acute kidney tubular alterations are monitorable in good laboratory practice rat studies (used to support the safe conduct of clinical trials).[485] Urinary KIM-1 was also considered qualified for regulatory decision making as a clinical bridging biomarker for use by sponsors on a voluntary basis in phase 1 and 2 clinical trials for monitoring kidney safety when animal toxicology findings generated a concern for tubular injury.[485]

Using the same approach, the comparative performance, temporal profiles and recovery after gentamicin injury have been published for several candidate urinary biomarkers for kidney injury, including KIM-1, NGAL, osteopontin, glutathione-s transferases, RPA-1, albumin and clusterin.[415] During the evolution of injury, KIM-1, RPA-1, and clusterin best mirrored the histopathologic lesions, while during injury resolution, KIM-1, osteopontin, and BUN best reflected recovery. Based on histopathology, necrosis, or apoptosis scoring, KIM-1 was the best biomarker of overall renal injury.[415] RPA-1 outperformed the other biomarkers using regeneration scores.[415] Clinical studies of KIM-1 have also yielded promising results. FDA/EMEA qualification of KIM-1 as a biomarker for clinical applications will involve a systematic evaluation of diagnostic performance in well-controlled observational and/or interventional clinical protocols using both standard-of-care agents with known nephrotoxic properties and/or exploratory agents with renal safety concerns. As pointed out by the authors, "the opportunity to use the same translational marker, such as Kim-1, for both the preclinical and clinical setting facilitates clinical monitoring of toxicity that has been demonstrated at higher doses in preclinical development or in a single test species when human relevance is suspected.[485]"

An additional potential role of biomarkers reflects their unique role in specific metabolic pathways of cell injury. Detected in serum or urine, their presence should flag recruitment of these specific pathways. Since many recently discovered biomarkers were uncovered by genomic or proteomic strategies, understanding their role in injury can be viewed as linking empirical outcomes to mechanisms. Three examples of novel biomarkers reflecting different injury pathways in AKI are IL-18, KIM-1 and NGAL.

IL-18 is produced in the kidney predominantly by recruited inflammatory cells, probably macrophages[521] but also by activated injured renal parenchymal cells and has a significant role in AKI.[319] Mice deficient in Caspase-1 or IL-18 or wild-type mice treated by IL-18-binding protein are protected from AKI induced by IL-18 injection.[521] KIM-1 is a transmembrane protein express highly expressed in de-differentiated proximal tubular cells in response to injury. It has multiple roles including a role as a phosphatidylserine receptor that

confers a phagocytic phenotype on epithelial cells. This allows these cells to recognize apoptosis cell surface-specific epitopes and thereby enables injured tubular cells to contribute to the clearance of apoptotic cells after AKI.[200] The simultaneous detection of urinary KIM-1 and IL-18 could be regarded as good evidence of significant proximal tubular cell injury leading to cell death and de-differentiation. KIM-1 was the best performing biomarker by histopathology score in models of nephrotoxic injury using cisplatin[475] and gentamicin.[415]

The most highly upregulated biomarker after ischemia-reperfusion injury is NGAL, an acute-phase protein initially found in activated neutrophils but also expressed by a wide range of tissues in response to injury.[460] NGAL participates in host innate immune defence by binding bacterial siderophores to limit bacterial iron acquisition.[135] NGAL forms a complex with iron binding siderophores, which is renoprotective in murine ischemia-reperfusion injury.[335] In the kidney NGAL mRNA expression is only detectable in the distal tubule, including the thick ascending limb of Henle's loop and collecting duct,[376] but the protein is freely filtered and reabsorbed by megalin-mediated transport in the proximal tubule.[197] After ischemia and after cisplatin-induced toxic injury NGAL is detected in a punctate pattern corresponding to endosomes and predominantly in proliferating cell nuclear antigen-positive proximal tubular cells.[321,323] This suggests that proximal tubular NGAL accumulates after injury but that the primary source is the distal tubule belonging to the injured nephrons.[376] Urinary NGAL was recognized immediately as an important biomarker of acute kidney injury,[322] with presence in urine suggesting renal specificity despite the possibility of alternative systemic sources. However, it was confirmed only recently, using cross-transplants between NGAL knockout ($NGAL^{-/-}$) and wild-type C57BL/6 mice ($NGAL^{+/+}$) followed by renal artery clamping, that urinary NGAL definitely originates from the kidney.[376] While urinary NGAL was increased in mice after cisplatin,[323,376] it inexplicably did not appear to increase in some studies in the rat.[475] Interestingly, urinary NGAL had a perfect score (ROC-AUC 1.0) after PAN, a nephrotoxicant that causes marked proteinuria and glomerular morphological changes in rats, similar to those seen in human minimal change nephropathy.[251] Given the potential for albumin and protein to compete with NGAL (and other low molecular weight protein biomarkers) for megalin-mediated transport,[348] the explanation for increased urinary NGAL following PAN may simply be that the proximal reabsorption of NGAL is inhibited.[348] Urinary NGAL has not (yet) been qualified as a nephrotoxicity biomarker, although there is little doubt that both urinary and plasma NGAL have already proven to be a useful as a clinical biomarker of AKI, at least after ischemic injury where it clearly outperforms serum creatinine and blood urea nitrogen.[164–166] Recent clinical studies have demonstrated that in high risk patients screened with urine or serum NGAL and serum creatinine, that creatinine negative but NGAL positive patients were at higher risk of both dialysis and had higher mortality that creatinine negative NGAL negative patients.[164] This also highlights the described delay inherent in using creatinine to make a diagnosis of AKI and suggests that injury biomarkers should be included in the definition of AKI.

In addition to illustrating potential as markers of nephrotoxicity in drug development or in clinical studies, these three biomarkers illustrate the potential for injury biomarkers to provide useful information about timing, location and mechanisms of renal injury in disease. Since NGAL and KIM-1 are produced in different parts of the nephron, the performance of these biomarkers in urine samples should be different as these studies highlight. Recent clinical studies suggest that other factors also modify biomarker performance, including duration of injury and baseline renal function.[122] Further refinements may allow biomarkers to differentiate the specific drug causing renal injury when the patient has been exposed to several potential nephrotoxins. For example urinary levels of regenerating islet-derived protein III beta and gelsolin were increased following gentamicin but not by cisplatin.[132]

Large volumes of data are now needed. Well-designed preclinical and clinical studies that allow biomarker profiles to be followed after different types of AKI, including combinations of as well as individual nephrotoxins and in the presence of various comorbidities that may themselves contribute to biomarker generation or modify biomarker performance.

To illustrate the concepts of drug-induced nephrotoxicity, a number of important drugs with well-defined pathways of injury are discussed in depth.

CYCLOSPORIN A

Since the introduction of cyclosporin A into clinical transplantation in 1978[56] it perhaps more than any other agent, has expanded our understanding of the mechanisms involved in drug-induced nephrotoxicity. Cyclosporin has been shown to modify many different aspects of cellular function, from hormone-receptor activation, second messenger pathways, transcription and translation of mRNA, alterations in protein synthesis and formation, changes in cellular metabolism, cellular repair mechanisms and cell death, the expression of various cytokines and growth factors, and changes

in renal haemodynamics, all of which contribute to the final expression of nephrotoxicity.

Cyclosporin-induced renal functional impairment occurs in all forms of solid organ transplantation, bone marrow transplantation as well as in autoimmune disorders.[173,341] The clinical manifestations of cyclosporin A nephrotoxicity can be classified into two groups, that are not necessarily exclusive. Cyclosporin A induces a marked increase in renal vascular resistance associated with a fall in renal blood flow and a decrease in glomerular filtration rate. These changes are often associated with the development of *de novo* hypertension.[173,341] Cyclosporin A has been shown to modify renal tubular function with impaired distal tubular excretion of potassium and hydrogen ions consistent with a voltage dependent distal renal tubular acidosis,[15,341,344] increased proximal tubular sodium reabsorption with decreased delivery of solute to the distal tubule,[97] and impairment of urinary concentrating ability.[325,342,344]

The clinical presentation of cyclosporin A nephrotoxicity may occur in three different time frames.[218,342] Primary non-function of renal grafts, usually associated with kidneys that have been subjected to prolonged warm ischemia, donor and/or recipient hypotension, or concurrent drug nephrotoxicity.[173,342] Cyclosporin-induced acute alterations in renal haemodynamics augment the damage already sustained by the kidney.[173,342] The acute toxicity is not necessarily associated with an adverse outcome of long-term graft function[173] although this is debated.

At a cellular level the changes in renal haemodynamics are mediated through a variety of hormone-receptor activated pathways, and subsequent intracellular signalling. Cyclosporin A has been shown to enhance the transmembrane Ca^{2+} flux and increase intracellular Ca^{2+} stores in response to agonist stimulation in vascular smooth muscle cells and mesangial cells which leads to enhanced contractility.[320,388] Cyclosporin A has been demonstrated to inhibit activation of protein kinase C (an important component of the second messenger pathway) *in vitro*[500] which also requires Ca^{2+} for its activity. More recent studies have suggested that cyclosporin A inhibits phospholipase A2 directly.[148,453] On this basis it is reasonable to assume that cyclosporin A modulates the hormone receptor activated pathway at several different points with subsequent impairment of cellular function.[499] These alterations in transmembrane signal transduction induced by cyclosporin A have lead Skorecki and colleagues[453] to propose that acute cyclosporin nephrotoxicity is a prototype for a renal membrane signalling disorder.

The acute administration of cyclosporin A causes a dose-dependent increase in renal vascular resistance and a reduction in RBF and GFR in experimental animal and human studies.[338,339] These early changes are functional, with no structural damage evident and are reversible on withdrawl of the drug.[339] In the renal microcirculation, similar reductions were observed.

Baxter et al.[21] have shown that cyclosporin A activates the renin angiotensin system *in vivo* and *in vitro*,.[21,246] Similarly, cyclosporin A has been shown to stimulate and enhance the release of renin from juxtaglomerular cells in culture.[246] Stimulation of mesangial cells by cyclosporin A alone does not modify the release of the vasodilatory prostaglandins or increase in the vasoconstricting prostaglandin thromboxane A_2 (TXA_2). However, cyclosporin A inhibits angiotensin II (AII) stimulated prostaglandin release from mesangial cells,[502] as well as in vascular smooth muscle cells in culture.[247] Exaggerated glomerular thromboxane synthesis has been suggested as a potential mechanism in producing the cyclosporin A induced reductions in GFR. Perico and colleagues[384,395] have shown, *in vivo*, that glomerular synthesis and urinary excretion of thromboxane progressively increase with cyclosporin A therapy. Other studies have demonstrated that the increase in urinary thromboxane excretion is a consequence of intrarenal platelet and macrophage activation probably triggered by cyclosporin induced endothelial damage[27] rather than arising from glomerular mesangial cells.[27,502] The increased release of the vasoconstricting thromboxane from these nonrenal sources could potentate the reduction in glomerular filtration rate associated with cyclosporin A.

Alterations in nitric oxide (NO) and endothelin (ET) have been implicated in cyclosporin-mediated changes in vascular haemodynamics.[28,368] Cyclosporin enhanced release of ET has been implicated as a significant mechanism contributing to cyclosporin-induced vasoconstriction.[385] Cyclosporin has been demonstrated to inhibit NO production by inhibition of inducible nitric oxide synthetase (iNOS) activity, possibly by inhibition of transcription factors in mesangial and vascular smooth muscle cells[305] A number of studies have demonstrated that NO blockade enhances acute cyclosporin nephrotoxicity.[140]

Chan et al.[62] examined endothelial−dependent and independent vascular reactivity in ex vivo studies using aortic rings from rats treated with cyclosporin (5 mg/kg/day) for 7−21 days. They failed to demonstrate impaired endothelial−dependent vasorelaxation but reported enhanced responsiveness to vasoconstricting agents. Therefore, it would seem probable that cyclosporin A induces a decrease in vaso-relaxant mediators (NO, PGI_2, PGE_2) associated with an enhanced response to vasoconstricting agents (AII, ET) which would allow mesangial cell and vascular smooth muscle cell contraction to predominate.[499,502] Subacute

nephrotoxicity frequently occurs in the first six months post transplant,[218,342,343] and it is associated with a slow rise in plasma creatinine or a persistently elevated plasma creatinine compared to azathioprine treated control patients with or without other signs of cyclosporin-induced alterations in renal function.[218,342,344] A significant proportion of patients will have sufficient damage due to interstitial fibrosis that results in irreversible renal impairment.[173,218,342,344] Renal histological changes include an arteriopathy with the development of constrictive intimal proliferation with mucoid thickening and arteriolar hyalinosis, and injury to the proximal tubule with foci of tubular dilatation, epithelial cell degeneration, fine reticulin deposition in the interstitium and giant mitochondria.[129,399] In addition, a significant infiltration of macrophages into the interstitium, associated with an increase in interstitial and tubular cell proliferation has been demonstrated following chronic cyclosporin exposure.[495,533] Activated infiltrating macrophages will amplify the inflammatory and profibrotic response by stimulating fibroblast proliferation and migration as well as increased collagen synthesis. Endothelial cell injury associated with the vascular changes may also be associated with a haemolytic-uremic like syndrome.[342]

Prolonged administration of cyclosporin A, particularly at higher concentrations, has led to the development of chronic nephrotoxicity associated with hypertension, significantly elevated renal vascular resistance and deteriorating renal function that may progress to end stage renal failure.[344] Histopathological changes associated with chronic cyclosporin nephrotoxicity are diffuse interstitial fibrosis or striped interstitial fibrosis with tubular atrophy, an obliterative arteriolopathy and ischaemic changes in some glomeruli.[129,342,346,399]

Lesions characteristic of cyclosporin nephrotoxicity seen in human kidneys have been reproduced in sodium depleted rats treated with cyclosporin.[117] Jackson et al. found that cyclosporin-induced focal areas of tubular atrophy and interstitial fibrosis in the outer cortex and an increase in cell proliferation, the majority of which were located in the interstitium and not the renal tubules.[203] Chronic cyclosporin A administration (12.5 mg/kg/day for 10 weeks) to rats was shown to produce histological injury to the inner stripe of the outer medulla and medullary rays of the kidney[203] similar to that seen in the striped interstitial fibrosis associated with chronic cyclosporin A administration in humans.[346] It is significant that these changes were demonstrated in nephron segments particularly sensitive to limited oxygen availability. Thus hypoxia secondary to cyclosporin-induced vasoconstriction may further potentiate cellular injury. This may also play an important role in the subsequent development of interstitial fibrosis as discussed below in Figure 85.4.

Cyclosporin A has a high lipid solubility and is extensively distributed to extravascular tissues, with the highest concentrations found in fat, liver, and kidney. Metabolism of cyclosporin A is via the cytochrome P-450 dependent mixed function oxidases. Experimentally, cyclosporin A has been shown to significantly inhibit hepatic mixed function oxidases by uncompetitive inhibition.[333] The renal cortex contains similar cytochrome P-450 dependent mixed function oxidases located predominantly in the S3 segment of the proximal tubules which is the main site of histological injury produced by cyclosporin A. Walker et al.[501] have demonstrated that cyclosporin A produces a significant uncompetitive inhibition of renal cortical NADPH cytochrome C reductase, an essential component of the mixed function oxidase enzyme complex.. The combined effect of lower enzyme activity, a greater degree of uncompetitive inhibition and lower enzyme concentrations acting as a rate limiting step, may in part explain the increased propensity for renal tubular damage as compared to hepatocellular damage despite similar tissue concentrations of cyclosporin A in the liver and kidney.[501] Ischaemic damage to the kidney associated with transplantation, coupled with cyclosporin A induced reduction in renal blood flow, would alter oxygen availability and metabolic requirements in

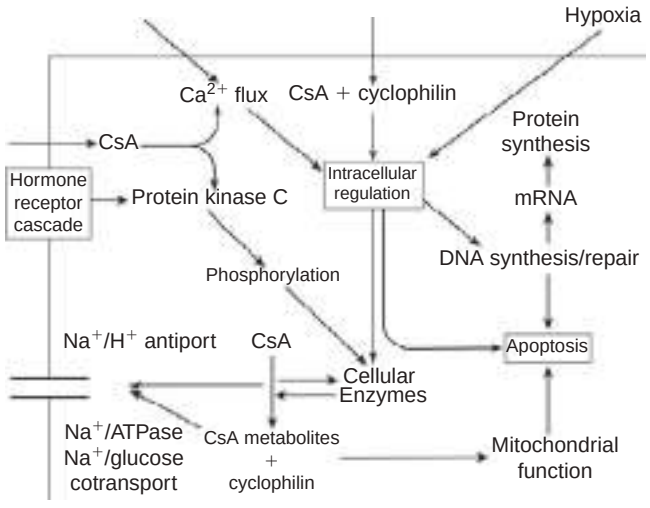

FIGURE 85.4 Potential pathways for the development of cyclosporin-induced interstitial fibrosis. Cyclosporin has been shown to influence the release of a number of cytokines and growth factors within renal vessels, renal tubular epithelial cells, and renal interstitial fibroblasts. With or without cellular injury from other mechanisms (hypoxia and rejection), this can lead to the development of interstitial fibrosis. *(With permission, modified from Walker RJ. Cellular mechanisms of drug nephrotoxicity. In: Seldin DW, Giebisch G, eds. The Kidney: Physiology and Pathophysiology. 3rd ed. New York: Raven Press, 2000:2835–2860.)*

the S3 segment of the nephron. This reduced oxygen gradient would further limit the activity of the renal mixed function oxidases already compromised by the inhibitory effects of cyclosporin.

Cyclosporin A has been shown to reduce renal glutathione content and produce an increase in lipid peroxidation, *in vitro*, in renal cortical microsomes, mitochondria and membrane fractions.[469,501] Cyclosporin A has been shown to generate superoxide through an as-yet-unclarified alteration in cytochrome P450 dependent mixed function oxidase.[435] A reduced availability of glutathione could impair the ability of glutathione peroxidases to metabolise fatty acid peroxides generated by lipid peroxidation. The net effect could be an increase in oxidant injury to renal tubular cells exposed to a hypoxic environment.[499] The hypoxic environment may also impair cellular mechanisms essential for maintaining cell integrity (see below).

Cyclosporin A has been demonstrated to alter cellular macromolecular synthesis in various cell lines in culture[126,500–504] within two hours of exposure to cyclosporin, suggesting that cyclosporin might be altering the normal regulatory mechanisms that control the cellular enzyme systems.[503] At a cellular level cyclosporin has also been shown to modify the intracellular assembly of the renal tubular Na^+ D-glucose cotransporter with subsequent intracellular accumulation of the transporter components.[548] Similarly cyclosporin has been demonstrated to selectively reduce the gluconeogenic capacity of rat proximal tubules via a decrease in phosphoenolpyruvate carboxykinase (PEPCK) activity.[336] This is due to a selective inhibition of renal PEPCK gene transcription and a corresponding reduction in renal PEPCK mRNA. Protein kinase C, a ubiquitous enzyme important in regulating a variety of intracellular functions, can be inhibited by cyclosporin A both *in vivo*, and *in vitro*.[503] These results would suggest a selective inhibition of the activity of a transcription factor(s) required for the expression of specific genes in renal tubules may play a role in cyclosporin-induced nephrotoxicity.[336] The net effect of direct inhibition of various intracellular enzymes or inhibition of gene transcription–translation controlling the synthesis of these enzymes, would be to impair the ability of renal cells to maintain their function and integrity in response to the toxic insult. Histological evidence of cellular damage either apoptosis or necrosis will only be apparent if the toxic injury exceeds the capacity of the cellular mechanisms to respond to the damage or alternatively if the cellular reparative mechanisms are modified by changes in intracellular regulation[499] (Fig. 85.4).

Buss et al.[54] have demonstrated that exposure to cyclosporin directly interferes with renal microsomal protein translation or the regulation of translation. Subsequent studies have shown that cyclosporin binds to cyclophilin A (the intracellular cyclosporin binding protein),[133,467] which is a microsomal peptidyl prolyl cis-trans isomerase, that facilitates protein folding and maturation.[458] Inhibition of cyclophilin A results in an accumulation of unfolded protein which in turns contributes to endoplasmic reticulum stress that further contributes to cellular injury.[374]

Within cells almost all soluble and membrane proteins of the cell are processed or degraded by the endoplasmic reticulum (ER). Proteins enter the ER in an unfolded state as linear polypeptides. In any situation in which an increased burden of unfolded proteins exceeds the ER's ability to deal with them results in a state of ER stress.[32] Pallet and colleagues have provided further evidence supporting the role of cyclophilin A inhibition and ER stress in contributing to tubular injury.[374] If the ER's capability to deal with the increased load of protein via resident enzymes and/or chaperone proteins is exceeded, this may then lead to cellular injury, transformation to a more profibrotic phenotype[374] and cellular death via apoptosis.[32,296]

Cyclosporin has been demonstrated to induce apoptosis in a number of models of cyclosporin toxicity via increased expression of pro-apoptotic mediators. The induction of apoptosis was associated with increased TGFβ synthesis[260] which will further favor the development of interstitial fibrosis. Cyclosporin has been shown to upregulate Fas and Fas ligand expression, p53 expression, alter the ratio of Bax and Bcl-2, and upregulate ICE and caspase 3 activity. This favours the induction of apoptosis leading to tubular cell drop-out and impaired ability to remodel after cyclosporin-induced injury.[186,445,446,529] More recently Justo and colleagues have demonstrated that cyclosporin-induced apoptosis was associated with Bax translocation to the mitochondria and release of cytochrome c that was caspase-independent as well as a caspase-mediated alteration in mitochondrial membrane potential.[215]

Activation of anti-apoptotic pathways offers a possible therapeutic option. Erythropoietin binding to its receptor activates a number of intracellular pathways including the phosphatidyl-inositol 3 phosphate kinase/Akt axis which is a key regulator of cell proliferation and survival. Pallet and colleagues have demonstrated the recombinant human erythropoietin protects against acute cyclosporine nephrotoxicity in part through Akt signaling and inhibition of caspase 3 activation.[375] This would be consistent with other experimental studies that have demonstrated a protective role for EPO in acute kidney injury.[210]

A number of studies have demonstrated a dissociation between cyclosporine–induced changes in GFR and progressive interstitial fibrosis. Angiotensin II has been shown to be an important renal growth factor

independent of its vascular actions. Chronic exogenous AII exposure produces significant renal interstitial proliferation and fibrosis.[211] In addition, renal type I interstitial fibroblasts contain a high density of AII receptors.[547] Experimentally, blockade of the renin - angiotensin system with either AII receptor antagonists or angiotensin converting enzyme inhibitors prevented cyclosporin induced interstitial fibrosis without modification of renal functional parameters.[43,44]

Angiotensin II has been shown to stimulate the release of TGFβ in vascular smooth muscle cells. Furthermore, interactions between TGFβ and PDGF determine the nature of the growth response of cells to AII *in vitro*.[142] Both PDGF and TGFβ are potent fibrogenic growth factors that stimulate fibroblast proliferation, collagen synthesis and alterations in extracellular matrix synthesis. Enhanced renal expression of both PDGF and TGFβ during cyclosporin administration has been demonstrated both experimentally and clinically.[208,209,440] Insulin-like growth factor 1 (IGF1) has also been implicated as a mediator of cyclosporin-induced renal tubular interstitial fibrosis.[208,209]

More recently, the active non-hypercalcemic vitamin D analog, paricalcitriol has been shown to attenuate cyclosporin A induced renal tubular acidosis and fibrosis in an experimental rat model of nephrotoxicity.[379] Park and colleagues propose that the renoprotective effects are due to down regulation of nuclear factor−kappa B (NF-κB) and nitric oxide signalling with subsequent down regulation of TGF β1 signalling pathways.[379] However the role of paricalcitrol on other recognised pathways for CSA-induced nephrotoxicity also need to be explored.

The transmembrane efflux pump P-glycoprotein has been linked to the development of chronic cyclosporin nephrotoxicity. P-glycoprotein is associated with cyclosporin elimination by proximal tubular epithelial cells. Reduced renal expression of tubular P-glycoprotein has been shown to be related a greater degree of cyclosporin nephrotoxicity.[93,240] Recently clinical studies have demonstrated that low levels of renal P-glycoprotein, in the donor kidney leads to decreased cyclosporin clearance and subsequent cyclosporin accumulation and toxicity.[184]

The chronic interstitial fibrosis associated with cyclosporin therapy appears to be related to a complex interplay between cellular regulatory pathways controlling cell death or survival, various cytokines and growth factors whose expression will also be modified degree of cellular injury, as well as by the relative ischemia associated with cyclosporin-induced alterations in renal perfusion as outlined in Figure 85.5.

Thus cyclosporin appears to affect many facets of renal function, from changes in whole-kidney function *in vivo*, to alterations at a subcellular level demonstrated in cell culture models. Despite the large number

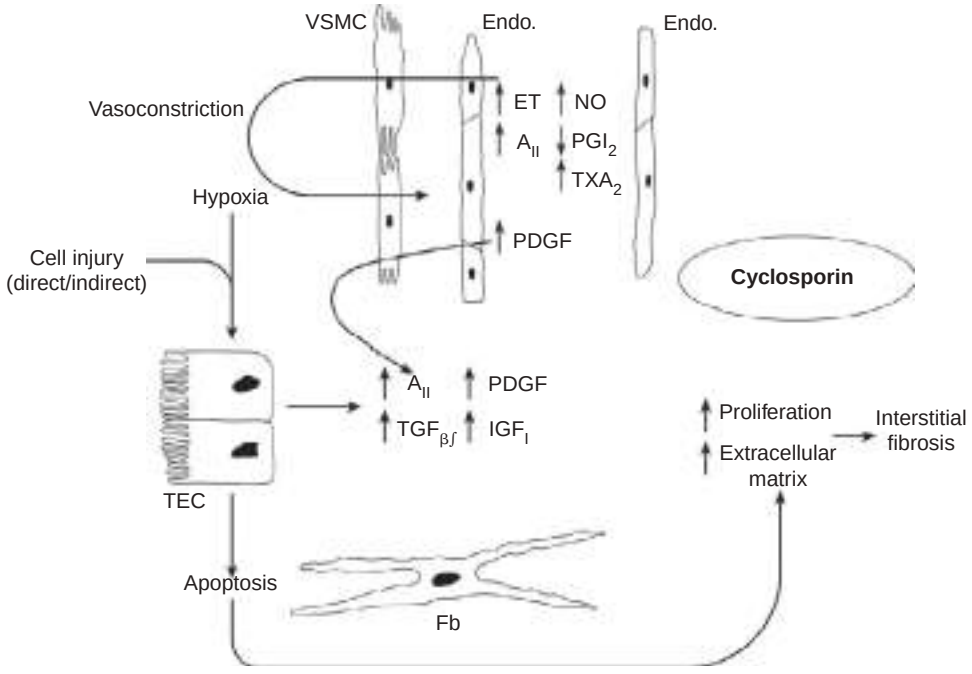

FIGURE 85.5 Diagramatic representation of the interaction of cyclosporin with components of cellular function including hormone receptor cascade and second messenger pathways; transcription, translation, and translocation pathways; apoptotic pathways; and cellular metabolism. *(With permission, modified from Walker RJ, Fawcett JP. Drug nephrotoxicity—cellular mechanisms. In: Jucker E, ed. Progress in Drug Research. Vol. 41. Basel, Birkhauser Verlag AG, 199341:3−45.[499])*

of studies investigating cyclosporin nephrotoxicity, there are still many unanswered questions as to how this unique agent produces the various changes that are manifested in the development of nephrotoxicity.

CISPLATIN

Cisplatin is an antineoplastic agent which acts by inhibiting DNA synthesis.[283] It has been used success fully in solid organ tumours, particularly in testicular germ cell tumours. The clinical use of cisplatin is limited by the development of nephrotoxicity which are manifest clinically as renal tubular defects in potassium, calcium, magnesium and hydrogen ion handling, inability to concentrate the urine and with more severe toxicity, changes in RBF and GFR. The extent of nephrotoxicity has been reduced significantly by the use of appropriate hydration schedules with normal saline.

The high renal concentrations of cisplatin, and subsequent development of nephrotoxicity, are a consequence of renal tubular cell handling predominantly via peritubular uptake and metabolism of cisplatin.[85,86,421,422] Renal clearance of platinum is very efficient, with high clearances at low plasma levels of the drug, due to net tubular secretion in addition to filtration of platinum.[61] Filtration of cisplatin does not appear to be a prerequisite for the initiation of nephrotoxicity; rather, the tubular uptake of cisplatin and metabolites including the basolateral transport of cisplatin and/or metabolites may be important in the generation of nephrotoxicity.[85,325] The kidney specific organic cation transporter 2 (SLC22A) mediates the basolateral uptake of cisplatin and thus its subsequent toxicity. Cisplatin excretion from the cell is via the multidrug and toxin extrusion 1 transporter (MATE1), but the extent to which this may or may not influence intracellular concentrations of cisplatin is less clear.[532]

The current concept of cisplatin nephrotoxicity is that cisplatin uptake by tubular epithelial cells activates complex intracellular signalling pathways including DNA damage response pathways, caspase activation (extrinsic, intrinsic and ER stress pathways), induction of free oxygen radicals along with inactivation of anti-oxidant systems, leading to cell apoptosis and necrosis. This is associated with an intense inflammatory response with TNFα a major mediator further exacerbating tubular cell injury (Figure 85.6).[371]

Morphological studies have shown that cisplatin induces focal damage to the proximal tubules, predominantly confined to the S3 segment located in the outer stripe of the outer medulla.[99,212] The earliest changes of nucleolar segregation, microsomal dispersion and aggregation of smooth endoplasmic reticulum are evident within six hours of cisplatin administration. These

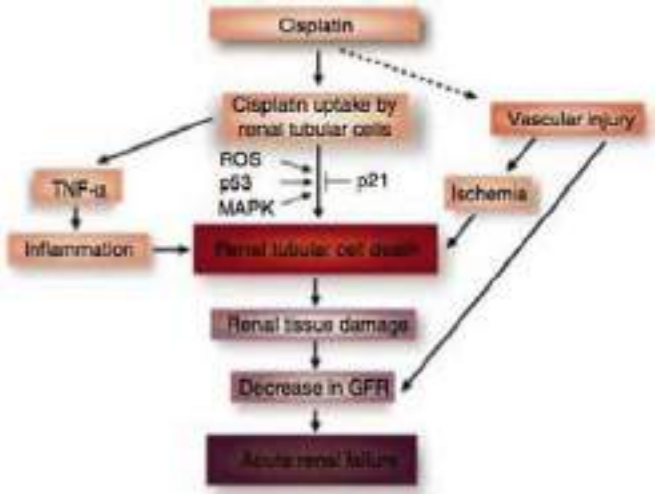

FIGURE 85.6 Overview of the pathophysiological events in cisplatin nephrotoxicity. *(Used with permission from the Nature Publishing Company (Pablo & Dong).*[371])

early changes are consistent with apoptotic changes.[147] Functional changes leading to depression of glomerular filtration rate (GFR) are not apparent until 48 hours post administration, by which stage there is focal loss of the tubular epithelial cells' brush border, cellular swelling, and focal areas of necrosis.[99,212] With established renal failure and maximal nephrotoxicity, there is widespread tubular necrosis, predominantly involving the S3 segment and to a lesser extent, the S1, and S2 segments of the proximal tubule.[99,212]

It has been demonstrated that the cis isomer of the platinum complex is necessary for tumoricidal actions and is also responsible for the development of nephrotoxicity.[85] Unlike other heavy metal-induced nephrotoxicity, the onset of cisplatin toxicity is delayed, with functional changes not readily apparent until 48–72 hours.[149] This suggests that toxicity is not due directly to the effects of the platinum ion but rather to the biotransformation of cisplatin to various platinum metabolites and subsequent binding to intracellular components. The cisplatin metabolites, especially the hydrolysis product $[Pt(NH_2)\ (OH_2)^{2+}]$, when infused into rats at equivalent concentrations to cisplatin, generate greater nephrotoxicity.[85,86]

Within the kidney, cisplatin and metabolites are preferentially localised to the juxtamedullary cortical regions[69,99,324] with a greater degree of injury seen in the S3 segments of the proximal tubules. Cellular concentrations are high in the nuclear and microsomal fractions,[69] with quantitatively the greatest concentrations of cisplatin in the protein fraction of the cytosol associated with the sulfhydryl rich metallothioneins.[263] Levi et al.[263] demonstrated that following cisplatin administration *in vivo* there was a marked fall in

protein bound sulfhydryl groups. The binding to sulfhydryl groups suggests that glutathione dependent transferases may be important in the modulation and/or mediation of cisplatin nephrotoxicity. It has been suggested that either an active platinum metabolite binds to the sulfhydryl group, or alternatively the platinum metabolite(s) inhibits oxidative metabolism, preventing regeneration of reducing equivalents necessary to maintain the reduced sulfhydryl groups.[263] Exogenous reduced glutathione, at a high dose, has been shown to reduce cisplatin-induced nephrotoxicity,[554] further supporting the role of binding to sulfhydryl groups as well as the generation of free oxygen radicals is important in mediating toxicity. Depletion of mitochondrial GSH has been shown to be an early and critical step in cisplatin-induced cell injury which results from oxidative stress to the mitochondria.[544] Kruidering and colleagues[244] using porcine proximal tubular cells, have demonstrated that cisplatin specifically affected mitochondrial function by inhibition of the enzymatic complexes I to IV of the respiratory chain with decreased intracellular ATP levels as a consequence. GSH reductase activity was also impaired leading to reduced intracellular GSH levels.[244] Alterations in mitochondrial function will also lead to increased oxidative stress.

Thus the formation of reactive oxygen species may be one of the early signals that contribute to the activation of various intra-cellular signalling pathways leading to cellular injury. A number of experimental models (*in vitro* and *in vivo*) have demonstrated renoprotective effects for a number of different antioxidants including vitamin E, N-acetyl cysteine, and dimethylthiourea (DMTU).[207,371]

Recent studies have demonstrated several pathways by which cisplatin-induced apoptosis occurs (Figure 85.7)[78,371] that include the extrinsic pathway mediated by death receptors such as Fas and TNFα, the intrinsic pathway via mitochondrial-dependent pathways[10,224,380] and the endoplasmic reticulum (ER) stress pathway.[371] In the extrinsic pathway, the binding of ligands to the major death receptors Fas and TNFα receptors leads to activation of caspase 8 and subsequent downstream pathways leading to apoptosis. It has been shown that cisplatin upregulates the expression of Fas and Fas ligand in both lymphocytes and proximal tubular epithelial cells.[280] TNFα plays a major role in the inflammatory response associated with cisplatin injury, which may be the major route of subsequent injury rather than the activation of the extrinsic pathway.

Experimental evidence suggests that the intrinsic pathway via mitochondrial injury is the major pro-apoptotic pathway in cisplatin injury. Bax activation,

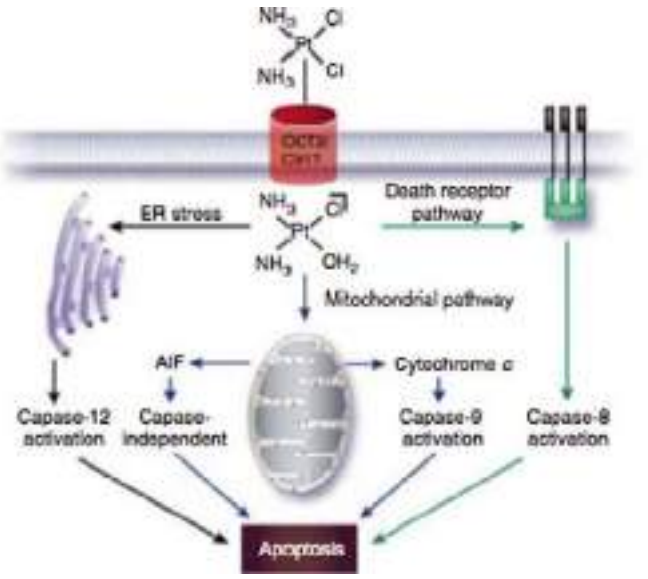

FIGURE 85.7 Apoptotic pathways activated by cisplatin in renal tubular epithelial cells. *(Used with permission from the Nature Publishing Company (Pablo & Dong).*[371])

mitochondrial release of cytochrome c and activation of caspase 9 are key steps in the pathway.[371]

The third pathway is via endoplasmic reticulum stress with activation of caspase 12[285] and more recently a role for COX-2 and membrane bound prostaglandin E synthase 1 in mediating cisplatin nephrotoxicity has been demonstrated.[205] In addition cisplatin may induce reactive oxygen species in microsomes via cytochrome P450 activation.[285]

Renal cells mount a cytoprotective response to oxidative stress. In an hypoxic setting, up-regulation of hypoxic–inducible factor 1α (HIF-1α) plays an important protective role against injury. Cisplatin has been shown to suppress HIF-1α in cell culture models. Downstream mediators of HIF-1α actions include heme-oxygenase 1, vascular endothelial growth factor and erythropoietin, all of which have been demonstrated to provide a degree of protection against cisplatin-induced nephrotoxicity.[424,511] Therefore HIF-1α is a potential target for protection against cisplatin nephrotoxicity.

DNA fragmentation has been observed in both apoptotic and necrotic pathways related to cisplatin injury, suggesting a common link at the level of cell death endonucleases. Basnakian and colleagues, using a deoxyribonuclease 1 (DNase 1) knock out mouse model, recently demonstrated that DNase 1 is important in mediating cisplatin-induced DNA fragmentation, tubular necrosis and possibly tubular necrosis.[19] They demonstrated that the inactivation of DNase 1 was protective against cisplatin-induced DNA

fragmentation. Another important step in the cellular response to DNA damage is activation of p53. A number of studies have demonstrated that p53 is rapidly phosphorylated and induced prior to tubular cell apoptosis. It is thought that activated p53 mediates its action through increased transcription of target genes. Studies have shown that p53 activation co-localises with apoptosis and nephrotoxicity can be ameliorated in p53 deficient mice.[206,510] Interventions that reduce cisplatin-induced nephrotoxicity have been shown to reduce apoptosis and decrease p53 activation.[206,207]

In cisplatin-induced nephrotoxicity, there is an intense inflammatory response to injury and experimental studies have demonstrated that TNFα is a key regulator of the inflammatory response. Inhibition of TNFα results in a marked amelioration of cisplatin injury. Of interest, is recent evidence that renal tubular cells contribute significantly to TNFα production during cisplatin nephrotoxicity.[543] This in conjunction with the studies by Linkerman[280] who demonstrated a close crosstalk between proximal tubular epithelial cells and distal tubular epithelial cell, suggest that the local production of TNFα by renal cells plays an important role in regulating cellular response to injury including apoptosis or necrosis pathways, referred to as fratricide.[423]

Cisplatin nephrotoxicity appears to be dependent on renal tubular uptake and probable conversion to more toxic intermediates. Nephrotoxicity is probably secondary to alterations in cellular mitochondrial function, generation of reactive oxygen species and the balance between the activation of cell death pathways and cell survival signals and inflammation.[224,371]

ACETAMINOPHEN NEPHROTOXICITY

Acetaminophen (paracetamol) is an antipyretic and analgesic agent that is freely available as a proprietary medicine and is the most widely used analgesic in the United States. Acetaminophen is the major metabolite of phenacetin, which has been used in compound analgesics. Both agents, either alone or in combination with other analgesics, have been implicated in the pathogenesis of analgesic nephropathy.[425] In addition, Sandler et al.[425] demonstrated a significant association between excessive acetaminophen intake and the subsequent development of chronic renal failure. The renal handling of phenacetin and acetaminophen exemplifies the heterogeneity of renal anatomical, biochemical, and physiological characteristics that influence the development of acute and chronic nephrotoxicity.[499] Phenacetin is metabolised extensively to acetaminophen by the liver and gut. Only very low concentrations of the parent compound enter the systemic circulation. Phenacetin is filtered at the glomerulus and undergoes passive reabsorption along the nephron at a rate equivalent to water, related to the lipid solubility of the drug.[105–107] Acetaminophen is moderately lipid soluble and it is filtered at the glomerulus with passive diffusion of the non-ionic form. Clearance is independent of plasma concentrations or tubular reabsorption. Reabsorption is not localised to a particular nephron segment.[105–107] Acetaminophen clearance is related to the rate and the concentration gradient generated between intracellular/interstitial compartments and the tubular fluid. Under conditions of antidiuresis, acetaminophen increases in concentration in the inner medulla, conversely diuresis results in a diminution of the concentration gradient, with the concentration of acetaminophen being the same as that of the cortex. The clearance of phenacetin is increased by changes in urine flow rate directly proportional to the increase in urinary flow.[105–107] The accumulation of acetaminophen in the medulla is important in the subsequent development of chronic nephrotoxicity. Renal metabolism of acetaminophen is essential in the development of nephrotoxicity[337,349–351] and is linked to the proportional conversion of acetaminophen to its non toxic and toxic metabolites. The generation of non-toxic conjugated metabolites is potentially rate limited and increases in renal concentrations of acetaminophen will favour the formation of toxic metabolites. The distribution of the enzymes involved in the metabolism of acetaminophen is important in the development and localisation of the renal injury in acute and chronic nephrotoxicity.[327] The predominant pathways for acetaminophen metabolism involve the $NADPH^+$-dependent cytochrome P-450 mixed function oxidases located in the renal cortex and the $NADPH^+$-independent prostaglandin H synthase (prostaglandin endoperoxidase synthetase system), consisting of a fatty acid cyclooxygenase and prostaglandin hydroperoxidase, localised predominantly in the inner medulla.[327]

Acute Nephrotoxicity

This occurs clinically in the context of an acute overdose of acetaminophen but is not always associated with acute hepatic toxicity.[108] The concentration of acetaminophen in the kidney is important in the development of acute nephrotoxicity.[106] Acute toxicity is dependent on metabolic activation of acetaminophen to reactive metabolites. This has been shown to be a prerequisite for the development of acute tubular necrosis which is confined predominantly to the renal cortex.[349,353] Following an acute overdose, there is insufficient GSH generated to bind all the metabolites generated by cytochrome P450 mixed function oxidases and intracellular reduced glutathione stores become

depleted. Reactive metabolites bind covalently to intracellular constituents, as well as causing depletion of cellular GSH and lipid peroxidation, producing cell damage and eventual cell death.[108] In the renal cortex, acetaminophen may be deacetylated to p-aminophenol, which is five to 10 times more nephrotoxic.[59,349,351] Deacetylase activity is predominantly located in the renal cortex and is significantly more active than in the liver.[59,108] Cytochrome P-450, prostaglandin H synthase, and possibly other peroxidases can convert acetaminophen and p-aminophenol into reactive intermediates through peroxidative reactions with the formation of semiquinoneimines [N-acetyl-p-benzoquinoneimine (NAPQI)], quinoneimines, or p-benzoquineimines (PQI).[108,326,337] In the absence of GSH and other reducing equivalents, acetaminophen and p-aminophenol may undergo catalytic conversion mediated by mixed function oxidases, peroxidation by cytochrome P-450 or prostaglandin H synthase, as well as auto oxidation of p-aminophenol to reactive arylating intermediates.[108] Cytochrome P-450 mediated peroxidative activation of both acetaminophen and p-aminophenol can continue to occur despite the depletion of cellular GSH and $NADPH^+$.[486] The arylation of renal macromolecules and subsequent cellular damage has been postulated as the initiating event in acetaminophen-induced acute nephrotoxicity.[352] The toxicity of acetaminophen occurs only after the depletion of cellular GSH. GSH protects against toxicity induced by acetaminophen metabolites by several potential mechanisms. GSH may form a glutathione conjugate with NAPQI, which will then be excreted.[350,396] GSH can react with NAPQI to reform acetaminophen.[350,396] GSH may protect against lipid peroxidation due to further reactions of NAPQI. Recent evidence also suggests a possible nephrotoxic role of p-aminophenol glutathione S-conjugates and other hepatic metabolites.[236,479] These S-conjugates after γ-glutamyl transpeptidase dependant cleavage are translocated into renal tubular epithelial cells where p-aminophenol derived S-conjugates accumulate as has been demonstrated for toxic S-conjugates from other xenobiotics.[429]

GSH is a prerequisite for the activity of glutathione peroxidases, which protect the cell from peroxidative injury. Depletion of GSH by acetaminophen and p-aminophenol reactive intermediates would prevent glutathione peroxidase activity, increase lipid peroxidation, and enhance cytochrome P-450 mediated peroxidase activation of acetaminophen and p-aminophenol.[108] Acute acetaminophen nephrotoxicity involves the metabolic activation by cytochrome P-450, mixed function oxidases, deacetylase, and prostaglandin H synthase with the generation of reactive intermediates. When the cellular protective mechanisms, predominantly GSH and GSH-related enzymes, cannot detoxify the reactive intermediates, tissue damage and subsequent acute tubular necrosis occur.

Chronic Nephrotoxicity

With chronic administration, acetaminophen achieves a higher concentration in the cells of the renal inner medulla compared to the renal cortex and plasma.[106] This relatively higher concentration is important in the subsequent development of chronic nephrotoxicity. The prostaglandin H synthase enzyme complex, which appears to be the main mediator of chronic nephrotoxicity, is predominantly located in the inner medulla.[540,541] The hydroperoxidase component reduces the hydroperoxy group of PGG_2 to the alcohol producing the endoperoxide PGH_2, with the oxidation of a suitable electron donor.[540,541] Acetaminophen has shown to act as a suitable substrate in this enzyme reaction.[35,326–328,543] Mohandas et al.[327,328] have demonstrated *in vitro*, using rabbit renal cortical and medullary microsomes, that the prostaglandin synthesis is enhanced by acetaminophen at low concentrations, comparable to those that would be achieved during chronic ingestion (up to O.5 mM), and inhibited at higher concentrations (as would be seen in acute overdose situations). More recently, similar results were demonstrated using human renal cortical, outer and inner medullary microsomes.[153] The prostaglandin hydroperoxidase component of the enzyme complex converts acetaminophen to its reactive metabolite probably by a one electron oxidation reaction and hydrogen abstraction to form the phenoxy radical of acetaminophen, which then undergoes further oxidation to the more reactive intermediate NAPQI.[329] This metabolite reacts rapidly with GSH with the regeneration of acetaminophen or the formation of a stable conjugate. The sharing of the conversion of PGG_2 to PGH_2 by both glutathione peroxidase and prostaglandin hydroperoxidase would influence the extent of co-oxidative activation of acetaminophen, since depletion of GSH by binding to NAPQI would decrease glutathione peroxidase participation in this reaction as opposed to prostaglandin hydroperoxidase which does not require GSH as a substrate. The increased prostaglandin hydroperoxidase activity would increase the co-oxidation of acetaminophen and formation of active metabolites.[329] The cellular concentration of GSH is critical in preventing damage initiated by the reactive acetaminophen metabolites. The metabolite NAPQI may form a conjugate or is reduced back to acetaminophen with the production of oxidised glutathione (GSSG).[328] GSSG is reduced by glutathione reductase requiring $NADPH^+$. Thus, depletion of cellular GSH may occur due to decreased availability of $NADPH^+$, low activity of

glutathione reductase in the renal medulla, or the movement of excess GSSG out of the cell, in addition to conjugation with metabolites.[328] In addition, extracellular GSSG is not readily available to the renal inner medulla cells due to very low levels of gamma glutamyl transpeptidases on the cell membranes as opposed to high enzyme concentrations in renal cells in the cortex.[328]

More recently, it has been demonstrated that acetaminophen may cause direct toxicity to renal inner medullary cells. Cai and colleagues[55] using passage 1 rat inner medullary collecting duct (p1rIMCD) cells maintained in a osmotic environment that represents the osmolality of the inner medulla *in vivo*, demonstrated a toxic effect of acetaminophen and caffeine. Acetaminophen (0.5−2.0 mM), either alone or in combination with caffeine or salicylic acid induced proliferation of p1rICD cells when they were confluent. This was in contrast to an inhibitory effect of acetaminophen on cell growth if the cells were subconfluent. Normally there is little proliferation of inner medullary cells *in vivo* and proliferating inner medullary cells have a reduced tolerance for hyperosmolality.[55] Thus it would appear that acetaminophen-induced proliferation appears to sensitize the cells to toxicity, which was demonstrated by evidence of DNA damage and apoptosis. Other workers have also suggested that acetaminophen induced renal cell injury may be mediated via an apoptotic process.

Lorz and colleagues[290] demonstrated that acetaminophen can induce apoptosis in murine tubular cells that was not mediated via the Fas Fas-ligand pathway or mitochondrial injury. Rather, apoptosis was associated with a decrease in antiapoptotic Bcl-xL protein levels and evidence of increased endoplasmic reticulum stress.[290]

Compound analgesics containing aspirin, caffeine and phenacetin (or its major metabolite, acetaminophen) have a synergistic effect in the development of chronic nephrotoxicity. Aspirin inhibits the action of cyclooxygenase but not prostaglandin hydroperoxidase in the prostaglandin synthase complex.[542] Clinically little or no aspirin reaches the kidney[141] as aspirin is deacetylated to salicylate. Salicylate, as well as depleting renal glutathione levels increasing the potential for oxidative injury, potentiates acetaminophen effects on renal inner medullary cell proliferation and susceptibility to hyperosmotic injury.[55] Likewise caffeine can potentiate acetaminophen induced cellular injury.[55] Caffeine influences a number of pathways involved in cellular response to DNA damage. Caffeine also blocks p53 activation in response to DNA damage as well as blocking DNA repair.[55,546]

Clearly, acetaminophen, either alone or in combination with other agents can have significant effects on renal cellular function leading to nephrotoxicity. These may be mediated via intracellular metabolic pathways producing reactive metabolites and/or by direct effects on cell survival.

AMINOGLYCOSIDES

Aminoglycosides are an important group of antibiotics that are widely prescribed in the treatment of life-threatening gram-negative infections. Nephrotoxicity remains the major limitation to their clinical use. Aminoglycosides consist of two or more amino sugars joined in glycoside linkage to a hexose nucleus, usually in a central position. At physiologic pH, they are polycations with a high degree of polarity and water solubility and have no significant binding to plasma proteins. Autoradiographic studies have demonstrated rapid proximal tubular uptake within six hours of administration of tritiated gentamicin.[451] Only a small percentage of the filtered aminoglycoside (about 5%) is taken up by the proximal tubular cells, yet the renal cortical concentrations exceed the plasma or tissue concentrations by two to five fold. The majority of renal aminoglycoside accumulation occurs by active transport into the proximal tubular cells following binding to the luminal membranes.[518] A smaller proportion is taken up across the basolateral membrane,[220,221] but this may be more important in the mediation of cellular toxicity, as it allows for drug exposure to intracellular organelles such as mitochondria and microsomes. Aminoglycosides have been demonstrated to cause multiple structural, functional, and metabolic alterations within renal proximal tubular epithelial cells. These alterations are evident within 90 minutes following the single administration of an aminoglycoside. It is probable that nephrotoxicity is the combined result of these insults which compromise cellular structural and functional integrity (Figure 85.8).[220,221,289]

The cationic aminoglycosides bind to the anionic phospholipids, predominantly the phosphoinositols, in the brush border membrane.[426] The drug-receptor complex is pinocytosed with subsequent translocation to intracellular lysosomes.[131] The more acidic pH of the lysosomes increases the binding affinity of the aminoglycosides to the phospholipids. The aminoglycosides have been shown to inhibit the action of phospholipases both *in vitro* and *in vivo*, preventing the degradation of the phospholipids and release of inositol triphosphate.[131,254,255,281,297,401]

Aminoglycosides have also been demonstrated to inhibit renal protein kinase C activity.[170] Inhibition of protein kinase C activity may be due to decreased substrate availability due to inhibition of phosphoinositol metabolism or a direct effect on the activation of the

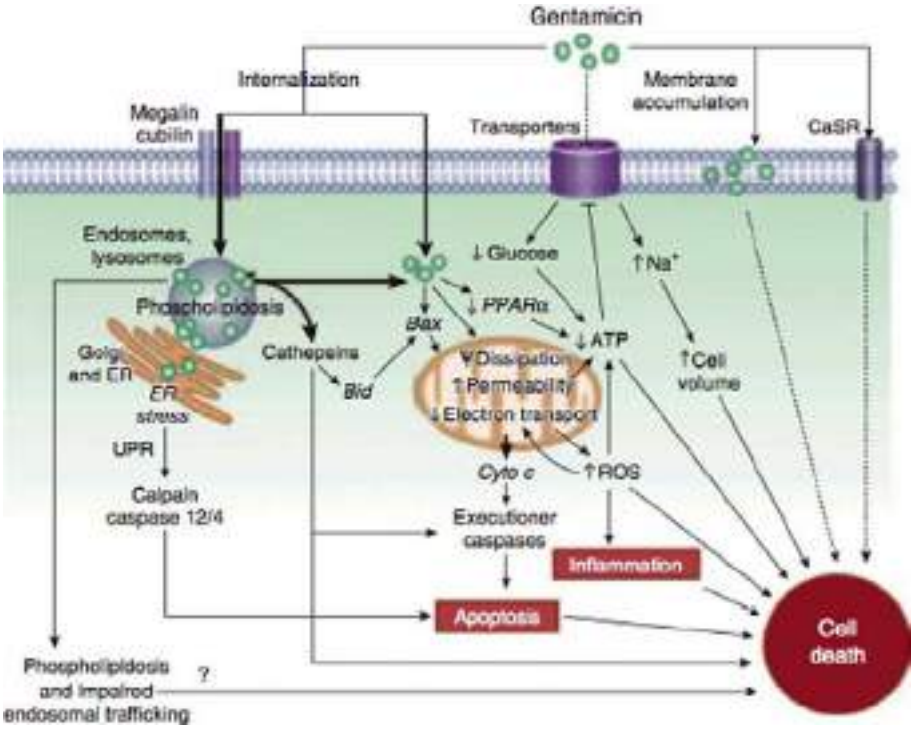

FIGURE 85.8 Mechanisms and cell signaling pathways underlying the cytotoxic effect of gentamicin. *(Used with permission from the Nature Publishing Company. Lopez-Novoa et al.*[289])

protein kinase C complex. Aminoglycoside-induced inhibition of phospholipid metabolism has been shown to occur not only within lysosomes but also involves other cellular constituents.[221,401,402] The net effect would be the impairment of the phosphoinositol cascade and second messenger pathway which may be an early event in aminoglycoside nephrotoxicity.[402]

The degree of aminoglycoside binding to the phospholipids, particularly in relationship to the ester bond split by the phospholipases, is postulated to be critical in the inhibition of phospholipid metabolism.[36,37] Alterations in membrane phospholipids probably result in the modification of both apical and basolateral membrane transport functions including decreased calcium transport, organic acid and base transport, decreased sodium/potassium ATPase and adenyl cyclase activity, ultimately impairing the control of cellular integrity.[196,220,221,297,515]

Gentamicin interacts with megalin (a giant multiligand endocytic receptor, localised to the apical membrane of proximal tubular epithelial cells) to gain entry into the cells, but can inhibit early endosomal fusion which may in part explain the toxic vacuolation in tubular cells that occurs with aminoglycoside toxicity.[178] Of interest, is the observation that megalin-knockout mice accumulate very little gentamicin compared to wild-type mice, further supporting a role for megalin-mediated endocytosis as the main mechanism of gentamicin accumulation in proximal tubular epithelium.[428] Megalin receptor-mediated endocytosis requires functional GTP-binding proteins that in turn require prenylation by isoprenoid products. Antione and colleagues have demonstrated that statins by inhibiting the formation of isoprenoids provide protection against aminoglycoside-induced accumulation and cytotoxicity in proximal tubule cells in culture.[9] This possible pleiotrophic action of statins in reducing megalin-mediated uptake of nephrotoxins and hence reducing proximal tubule cell injury needs to be explored with well-constructed clinical trials.

Aminoglycosides may access the intracellular cytosol via endosomal degradation or disruption. Aminoglycosides have been shown to bind to mitochondrial membranes and inhibit oxidative phosphorylation in renal cortical mitochondria *in vivo* and *in vitro*.[515] This is probably mediated by alterations in mitochondrial membrane permeability and mitochondrial calcium transport, which would produce alterations in mitochondrial respiration[452,513–515] and increased release of cytochrome c.[334] Increases in cytosolic cytochrome c concentrations will stimulate pro-apoptotic pathways with subsequent cell death. Several investigators have demonstrated increased markers of apoptosis in various animal models of aminoglycoside nephrotoxicity which was also associated with an increase in tubular and peritubular proliferation.[111,112,131]

Alterations in intracellular calcium transport, ATP synthesis, and mitochondrial permeability, are associated with endoplasmic reticulum stress and the

production of reactive oxygen species. *In vitro*, gentamicin has been demonstrated to enhance the generation of hydrogen peroxide by mitochondria[497] with the probable generation of other reactive oxygen species. Free oxygen radicals interact with numerous intracellular processes including peroxidation of membrane phospholipids, which has been demonstrated in aminoglycoside nephrotoxicity. Hydroxyl radical scavengers and iron chelators are protective against gentamicin induced acute renal failure.[497] However, the use of antioxidants (vitamin E and diphenyl-phenylenediamine) prevented gentamicin-induced lipid peroxidation but did not prevent the development of acute renal failure.[404,405] This suggests that lipid peroxidation is a consequence of toxicity[405] but does not exclude the interaction of hydroxyl radicals with other intracellular constituents in initiating cellular damage.

More recently Morales and colleagues have demonstrated that metformin (administered before gentamicin) substantially reduces gentamicin-induced mitochondrial respiratory chain dysfunction, in particular, reducing the changes in mitochondrial permeability transition, decreasing the release of cytochrome c and formation of reactive oxygen species, despite high tissue concentrations of gentamicin.[334] Co-administration of polyaspartic acid can also reduce aminoglycoside (gentamicin) nephrotoxicity despite higher intracellular concentrations of gentamicin.[143,195,403] This suggests that binding and intracellular uptake of aminoglycosides alone is not sufficient to produce cell damage.[143] Bennett et al. have demonstrated that aminoglycoside-induced inhibition of microsomal protein synthesis may be important in the generation of renal cell toxicity and a critical mechanism in determining the cellular ability to recover from the nephrotoxic insult.[29]

Tubular injury alone is probably insufficient to explain the significant reduction in GFR that occurs with aminoglycoside nephrotoxicity. There is good experimental evidence that aminoglycosides have direct effects on glomerular and vascular function with alterations in mesangial and endothelial cell contractility leading to a reduction in GFR as well as constriction of vascular smooth muscle cells leading to a reduction in renal blood flow.[289,304] In addition, the local cellular responses will enhance an inflammatory response which will produce an amplification of tubular, glomerular and vascular injury further exacerbating the renal injury.[289]

Chronic administration, for six months, of low-dose gentamicin has been shown to produce a mild chronic tubulointerstitial nephritis with progressive renal failure in rats.[195] Following cessation of the drug, interstitial inflammation intensified with a further decline in renal function, suggesting that gentamicin was inhibiting the reparative response (DNA and protein synthesis) of the tubular epithelium.[195] Alternatively, the chronic exposure to gentamicin can lead to enhanced proximal tubular cell apoptosis, and an ongoing inflammatory response resulting in chronic interstitial fibrosis. This raises the possibility that nephrotoxicity from aminoglycosides is inevitable and only in severe cases, where there has been marked renal cell injury, will the changes be observed clinically by the current rather insensitive clinical indices of renal function.

With the advent of sensitive urinary biomarkers of tubular injury as discussed above, it is to be hoped that monitoring of the urinary biomarkers will detect aminoglycoside toxicity earlier and minimise the risk of long-term injury.

LITHIUM

Lithium is a therapeutic agent used to treat patients with bipolar (manic depressive) illness and successfully alleviates both manic and depressive symptoms in 70−80% of patients. In fact, Timmer and Sands[474] estimate that about 1 in 1000 Americans are prescribed lithium at some time. However, chronic lithium administration has also been associated for many years with several different forms of renal injury. An analysis of several studies published from 1979 to 1986, comprising some 1172 patients,[34] revealed that the most prevalent renal effect of lithium reported was impairment of renal concentrating ability, which was estimated to be present in at least 54% of 1105 unselected patients on chronic lithium therapy. This defect translated into overt polyuria and polydipsia in up to 20% of cases.[34] Initially the decrease in urinary concentrating ability, which is resistant to the action of arginine vasopressin (AVP), is usually reversible following cessation of lithium administration. Of greater concern is the development of a progressive impairment of urinary concentrating ability in patients on long-term maintenance lithium therapy.[26] Markowitz et al.[298] reviewed the clinical features of 24 patients with biopsy-proven lithium toxicity, resulting from long-term treatment for bipolar disorder. This functional lesion is not usually readily reversible, is associated with a chronic focal interstitial fibrosis on renal biopsy, and may ultimately lead to renal failure.[298]

Complex mechanisms may be involved in lithium-induced changes in tubular cell water permeability, but the proximate cause is a loss of the ability to modulate the permeability, to water, of the apical cell membranes of the renal cortical and medullary collecting tubules. As a consequence of the loss of collecting duct permeability a hypo-osmotic urine is delivered to the medullary collecting tubule whose capacity to reabsorb water

(5% of the filtered water load) is limited. Thus voluminous dilute urine is produced which is manifest clinically as polyuria.

Rats given lithium therapy for up to 35 days became polyuric, losing weight and producing a large volume of dilute urine, a condition which was only partially reversed by water deprivation or by sustained treatment with AVP.[299] Semi-quantitative immunoblotting and studies by immunofluorescence and immunogold labelling revealed a massive reduction in aquaporin 2 (AQP2) expression in the lithium-treated animals. Water deprivation led to a small upregulation of AQP2, mainly in intracellular vesicles, while AVP infusion led to an accumulation of AQP2 largely in the apical membranes of collecting duct cells.[299] Chronic lithium therapy in the rat was associated with a reduction of AQP2 gene expression and product[249] along with altered cellular organization in collecting ducts characterized by a reduced fraction of principal cells, and increased number of intercalated cells.[71,72] These effects are likely to be important in lithium-induced nephrogenic diabetes insipidus.

Walker and colleagues recently demonstrated a reduction in urinary concentrating ability, associated with a decrease in urinary AQP2 excretion and urinary cAMP excretion, following lithium ingestion for four weeks in healthy human volunteers.[505] These changes are consistent with results obtained from animal models of lithium induced nephrogenic diabetes insipidus. In addition, in another study, they demonstrated a reduction in AQP2 expression in the cortical collecting tubules of human renal biopsies obtained from patients with lithium induced nephropathy.[22]

Lithium can readily substitute for sodium on several transport proteins that normally transport sodium, thus providing for lithium entry into tubular cells.[158,437] Lithium is a poor substitute for Na^+/K^+ ATPase thus allowing lithium to accumulate intracellularly. The amiloride-sensitive epithelial sodium channel (ENaC), co-expressed with AQP2 in the collecting duct, is critically involved in sodium homeostasis. Chronic lithium treatment is associated with a concomitant increase in urinary sodium excretion, and studies examining the expression of a number of sodium transporters in the rat kidney demonstrated a highly segment-specific down regulation of βENaC and γENaC in the cortical and outer medullary collecting ducts[355] but ENaC in the distal convoluted tubule, connecting tubule and inner medullary collecting duct are not modified by lithium.[72,355] Likewise there is no down regulation of the more proximal sodium transporters (NHE3, Na-K-ATPase, Na-K-2Cl cotransporter).[249] More recent studies by Christensen and colleagues using a specific cortical collecting duct ENaC knock out mouse model demonstrated that these mice did not develop lithium-induced NDI.[72] Of interest was the fact the ENaC expression, allowing lithium uptake, was still present in the adjacent cortical connecting tubular cells in these knock out mice. The exact mechanism of how segment-specific lithium uptake mediates NDI still needs greater clarification.

Earlier studies had shown that lithium inhibits the action of vasopressin at steps both proximal and distal to the intracellular formation of cAMP.[103,137] Within the cell, the principal action of lithium is thought to inhibit cAMP transduction pathways by competing with Mg for activation of G proteins which inhibit the activation of vasopressin-sensitive adenyl cyclase.[249] It has also been suggested that lithium may alter the balance between the formation of diacyl glycerol, with subsequent activation of protein kinase C, and the release of inositol triphosphate with subsequent mobilisation of intracellular calcium.[2] The phosphorylating activity of protein kinase C could in turn regulate the activation of adenyl cyclase and membrane transport function.[2] Bisphosphate nucleotidase activity which removes the 3′-phosphate from 3′−5′ bisphosphate nucleosides has a role in regulating salt tolerance. The presence of high levels of bisphosphate nucleotidase in the kidney and its role in sodium trafficking suggest a potential role also in lithium handling. It has been proposed that inhibition of human bisphosphate nucleotidase may contribute to lithium-induced nephrotoxicity.[455]

Alterations in adenyl cyclase activity and cAMP formation will impact on AVP receptor-stimulated regulation of aquaporin translocation and possibly (long term) aquaporin expression. cAMP activates protein kinase A by phosphorylation which in turn phosphorylates AQP2. It has recently been elegantly demonstrated that this is essential for the trafficking of AQP2 to the apical membrane.[2,299,300,356,358] Phosphorylation of AQP2 by other kinases in particular glycogen synthase kinase 3β (GSK3β), may also participate in the regulation of AQP2 trafficking. These effects are shown in a cartoon (Figure 85.9) adapted from Nielsen et al., and Grunfeld and Rossier.[160,357]

AQP2 gene expression is in part regulated via a cAMP response element in the 5′ flanking region of the AQP2 gene. Longer term, lithium via inhibition of adenylyl cyclase activity leads to the down regulation of cAMP-response element binding protein (CREB) which in turn down-regulates AQP2 gene expression via the cAMP response element.[269,299,300]

However a more recent study has demonstrated that the down regulation of AQP2 mRNA is by decreased gene transcription but it is independent of adenylate cyclase activity and it is proposed that glycogen synthase kinase 3β (GSK3β) (a serine/threonine protein kinase) may play a critical role.[269] GSK3β has been

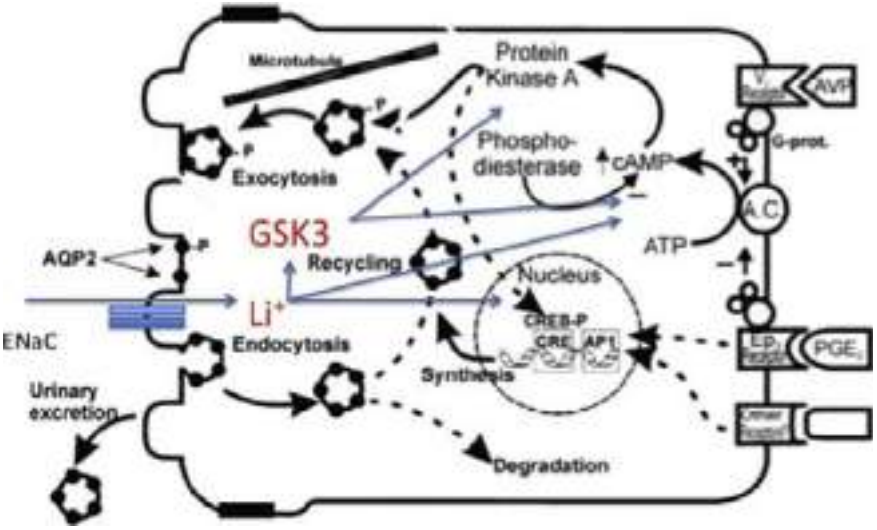

FIGURE 85.9 Pathways by which lithium modulates aquaporin 2 synthesis, phosphorylation and translocation to apical membrane in the principal cell in the collecting duct. Lithium (Blue lines) either directly modulates adenylyl cyclase activity or lithium inhibits GSK3β[160] which in turn modulates adenylyl cyclase pathways. *(Adapted from Nielsen et al.[357] with permission American Physiology Society.)*

demonstrated to mediate the renal response to vasopressin by modulating adenylate cyclase activity and cAMP generation.[407] Lithium at concentrations (10−25 mM) that can be achieved within collecting duct cells has been demonstrated to increase the amount of phosphorylated GSK3β (inactivated form) but not modifying the total amount of GSK3β.[238] Inactivation of GSK3β by lithium is associated with subsequent down-regulation of AQP2 expression.[238]

Battle and colleagues first demonstrated that amiloride can attenuate the polyuria associated with lithium-induced nephrogenic diabetes insipidus.[20] Amiloride blocks ENaC reducing lithium absorption in the distal convoluted tubule. Experimental animal studies[23,238,249,359] confirm that amiloride reduces transcellular lithium transport, and intracellular accumulation of lithium. This is associated with reduced phosphorylation and inactivation of GSK3β (238) along with increased AQP2 expression.[23,238] In addition to the direct effects in the distal convoluting tubule, amiloride largely restores the medullary concentrating gradient which is associated with upregulation of not only AQP2, but urea transporters (UT-A1 and UT-B) along with repletion of the medullary osmolytes critical for regulating the medullary osmotic gradient.[23] Presumably this is associated with restoring the cellular responsiveness to AVP, which regulates not only AQP2 expression but also regulates urea transporter expression. At a clinical level, amiloride has been demonstrated to significantly improve urinary concentrating ability in patients who had well established nephrogenic diabetes insipidus consistent with an improvement in the medullary concentration gradient.[24]

In patients on long-term lithium treatment for bipolar disorder, with biopsy-proven lithium toxicity, the histology demonstrates a chronic focal interstitial fibrosis, which may ultimately lead to renal failure.[298] The loss of nephrons and tubular damage with lithium induced nephropathy, is associated with a reduction in AQP2 expression in the cortical collecting tubules of human renal biopsies.[22] Electron microscopy has demonstrated that the cellular damage consists of swollen cells with increased numbers of mitochondria, swollen and damaged endoplasmic reticulum and vacuolation of the apical membranes with prominent accumulation of glycogen granules in the cytoplasm. The accumulation of glycogen correlated with the lithium-induced inhibition of AVP mediated activation of adenyl cyclase and alterations in glycogen synthesis. These lesions were associated with areas of fibrosis, dilated tubules and desquamation of tubular cells.

Earlier studies were not able to delineate the role of lithium-induced apoptosis compared to lithium-induced necrosis in mediating cell death and subsequent fibrosis. Controversy exists as to whether or not these lesions predispose to the development of a chronic focal interstitial nephritis as a consequence of long-term lithium therapy.[204] Lithium, at high concentrations (20 mmol/l), has been shown to produce apoptosis in neural tissue and other types of cell cultures[238,545] but there have been no studies in renal cell culture models. More recently, Walker and colleagues have established a long-term chronic model of lithium-induced interstitial fibrosis.[25] Preliminary studies demonstrate the TGFβ expression is markedly upregulated, especially in the medullary region but there is no associated inflammatory infiltrate. It is tempting to speculate that with active cellular update of lithium via sodium transport pathways that high intra-cellular concentrations can be achieved in both proximal and distal tubular epithelial cells, which in turn could

initiate cell to cell cross talk regulating apoptosis and a proinflammatory response as has recently been demonstrated for cisplatin nephrotoxicity.[280,423]

The link between lithium, sodium transport in the cortical collecting cells and subsequent lithium-induced nephrogenic diabetes insipidus is now well established.[70,72,238,249] However, the pathogenesis of the lithium-induced chronic interstitial nephritis still remains to be clearly elucidated.

Conclusion

This chapter has highlighted the importance of the kidney's unique functional organization, from a subcellular level to tissue level, in the development of drug nephrotoxicity. The heterogeneity of renal-tubular epithelial cell function and metabolism is the initial determinant in the development of nephrotoxicity. While these toxicants produce localized and specific injury to target cells in the kidney by specific mechanisms, many if not all of the final common pathways of toxicant injury are shared with ischemia-reperfusion injury.

The concentration of the drug and/or its metabolites within the tubular epithelial cells plays a critical role in the generation of toxicity. This may be modified by the tubular secretion and/or reabsorption of the drug, the intrarenal distribution of specific enzyme systems important in drug metabolism, and the potential generation of toxic metabolites. The final expression of nephrotoxicity will be dependent on the availability of intracellular mechanisms essential for maintaining cellular integrity and the cellular reparative response to injury. Thus, the pathophysiology of acute toxicant-induced kidney injury includes a complex interplay among specific cellular injury, inflammation, and altered renal hemodynamics.

References

[1] Adams JM, Cory S. The Bcl-2 protein family: arbiters of cell survival. Science 1998;281:1322–6.

[2] Agre P. Aquaporin water channels in kidney. J Am Soc Nephrol 2000;11:764–77.

[3] Alejandro V, Scandling Jr JD, Sibley RK, Dafoe D, Alfrey E, Deen W, et al. Mechanisms of filtration failure during postischemic injury of the human kidney. A study of the reperfused renal allograft. J Clin Invest 1995;95:820–31.

[4] Allen J, Winterford C, Axelsen RA, Gobe GC. Effects of hypoxia on morphological and biochemical characteristics of renal epithelial cell and tubule cultures. Ren Fail 1992;14:453–60.

[5] Allis JL, Endre ZH, Radda GK. 87Rb, 23Na and 31P nuclear magnetic resonance spectroscopy of the perfused rat kidney. Ren Physiol Biochem 1989;12:171–80.

[6] Andoh TF, Gardner MP, Bennett WM. Protective effects of dietary L-arginine supplementation on chronic cyclosporine nephrotoxicity. Transplantation 1997;64:1236–40.

[7] Andrade L, Vieira JM, Safirstein R. How cells die counts. Am J Kidney Dis 2000;36:662–8.

[8] Andreucci M, Michael A, Kramers C, Park KM, Chen A, Matthaeus T, et al. Renal ischemia/reperfusion and ATP depletion/repletion in LLC-PK(1) cells result in phosphorylation of FKHR and FKHRL1. Kidney Int 2003;64:1189–98.

[9] Antione D, Srivastava A, Pirmohamed M, Park BK. Statins inhibit aminoglycoside accumulation and cytotoxicity to renal proximal tubule cells. Biochem Pharmacol 2010;79:647–54.

[10] Arany I, Safirstein RL. Cisplatin nephrotoxicity. Semin Nephrol 2003;23:460–4.

[11] Ashkenazi A, Dixit VM. Death receptors: signaling and modulation. Science 1998;281:1305–8.

[12] Ashworth SL, Wean SE, Campos SB, Temm-Grove CJ, Southgate EL, Vrhovski B, et al. Renal ischemia induces tropomyosin dissociation-destabilizing microvilli microfilaments. Am J Physiol Renal Physiol 2004;286:F988–96.

[13] Atkinson SJ, Hosford MA, Molitoris BA. Mechanism of actin polymerization in cellular ATP depletion. J Biol Chem 2004;279:5194–9.

[14] Bagnasco S, Good D, Balaban R, Burg M. Lactate production in isolated segments of the rat nephron. Am J Physiol 1985;248:F522–6.

[15] Bantle JP, Nath KA, Sutherland DE, Najarian JS, Ferris TF. Effects of cyclosporine on the renin-angiotensin-aldosterone system and potassium excretion in renal transplant recipients. Arch Intern Med 1985;145:505–8.

[16] Barbier O, Jacquillet G, Tauc M, Cougnon M, Poujeol P. Effect of heavy metals on, handling by, the kidney. Nephron Physiol 2005;99:105–10.

[17] Barros LF, Hermosilla T, Castro J. Necrotic volume increase and the early physiology of necrosis. Comp Biochem Physiol A Mol Integr Physiol 2001;130:401–9.

[18] Basile DP, Liapis H, Hammerman MR. Expression of bcl-2 and bax in regenerating rat renal tubules following ischemic injury. Am J Physiol 1997;272:F640–7.

[19] Basnakian AG, Apostolov EO, Yin X, Napirei M, Mannherz HG, Shah SV. Cisplatin nephrotoxicity is mediated by deoxyribonuclease 1. J Am Soc Nephrol 2005;16:697–702.

[20] Batlle DC, von Riotte AB, Gaviria M, Grupp M. Amelioration of polyuria by amiloride in patients receiving long-term lithium therapy. N Engl J Med 1985;312:408–14.

[21] Baxter CR, Duggin GG, Willis NS, Hall BM, Horvath JS, Tiller DJ. Stimulation of renin release from rat renal cortical slices by cyclosporin A. Res Commun Chem Pathol Pharmacol 1984;43:417–23.

[22] Bedford JJ, Leader JP, Walker RJ. Aquaporin expression in normal human kidney and in renal disease. J Am Soc Nephrol 2003;14:2581–7.

[23] Bedford JJ, Leader JP, Jing R, Walker LJ, Klein JD, Sands JM, et al. Amiloride restores renal medullary osmolytes in lithium-induced nephrogenic diabetes insipidus. Am J Physiol Renal Physiol 2008;294:F812–20.

[24] Bedford JJ, Weggery S, Ellis G, McDonald FJ, Joyce PJ, Leader JP, et al. Lithium-induced nephrogenic diabetes insipidus: renal effects of amiloride. Clin J Am Soc Nephrol 2008;3:1324–31.

[25] Bedford JJ, Davis G, Leader JP, Gobe G, Walker RJ. Lithium induced chronic interstitial fiibrosis. Nephrology 2010;15 (Suppl 4):68.

[26] Bendz H, Sjodin I, Toss G, Berglund K. Hyperparathyroidism and long-term lithium therapy: a cross-sectional study and the effect of lithium withdrawal. J Intern Med 1996;240:349–65.

[27] Benigni A, Chiabrando C, Piccinelli A, Perico N, Gavinelli M, Furci L, et al. Increased urinary excretion of thromboxane B2

and 2,3-dinor-TxB2 in cyclosporin A nephrotoxicity. Kidney Int 1988;34:164–74.
[28] Benigni A, Remuzzi G. Endothelin in the progressive renal disease of glomerulopathies. Miner Electrolyte Metab 1995;21: 283–91.
[29] Bennett WM, Mela-Riker LM, Houghton DC, Gilbert DN, Buss WC. Microsomal protein synthesis inhibition: an early manifestation of gentamicin nephrotoxicity. Am J Physiol 1988;255: F265–9.
[30] Bonegio R, Lieberthal W. Role of apoptosis in the pathogenesis of acute renal failure. Curr Opin Nephrol Hypertens 2002;11:301–8.
[31] Bonventre JV. Mechanisms of ischemic acute renal failure. Kidney Int 1993;43:1160–78.
[32] Bonventre JV. Molecular response to cytotoxic injury: role of inflammation, MAP kinases, and endoplasmic reticulum stress response. Semin Nephrol 2003;23:439–48.
[33] Bonventre JV, Zuk A. Ischemic acute renal failure: an inflammatory disease? Kidney Int 2004;66:480–5.
[34] Boton R, Gaviria M, Battle DC. Prevalence, pathogenesis, and treatment of renal dysfunction associated with chronic lithium therapy. Am J Kidney Dis 1987;10:329–45.
[35] Boyd JA, Eling TE. Prostaglandin endoperoxide synthetase-dependent cooxidation of acetaminophen to intermediates which covalently bind *in vitro* to rabbit renal medullary microsomes. J Pharmacol Exp Ther 1981;219:659–64.
[36] Brasseur R, Carlier MB, Laurent G, Claes PJ, Vanderhaeghe HJ, Tulkens PM, et al. Interaction of streptomycin and streptomycylamine derivatives with negatively charged lipid layers. Correlation between binding, conformation of complexes and inhibition of lysosomal phospholipase activities. Biochem Pharmacol 1985;34:1035–47.
[37] Brasseur R, Laurent G, Ruysschaert JM, Tulkens P. Interactions of aminoglycoside antibiotics with negatively charged lipid layers. Biochemical and conformational studies. Biochem Pharmacol 1984;33:629–37.
[38] Brenner BM, Beeuwkes 3rd R. The renal circulations. Hosp Pract 1978;13:35–46.
[39] Brezis M, Greenfeld Z, Shina A, Rosen S. Angiotensin II augments medullary hypoxia and predisposes to acute renal failure. Eur J Clin Invest 1990;20:199–207.
[40] Brezis M, Rosen S, Silva P, Epstein FH. Renal ischemia: a new perspective. Kidney Int 1984;26:375–83.
[41] Brodsky SV, Yamamoto T, Tada T, Kim B, Chen J, Kajiya F, et al. Endothelial dysfunction in ischemic acute renal failure: rescue by transplanted endothelial cells. Am J Physiol Renal Physiol 2002;282:F1140–9.
[42] Buendia B, Santa-Maria A, Courvalin JC. Caspase-dependent proteolysis of integral and peripheral proteins of nuclear membranes and nuclear pore complex proteins during apoptosis. J Cell Sci 1999;112:1743–53.
[43] Burdmann EA, Andoh TF, Nast CC, Evan A, Connors BA, Coffman TM, et al. Prevention of experimental cyclosporin-induced interstitial fibrosis by losartan and enalapril. Am J Physiol 1995;269:F491–9.
[44] Burdmann EA, Andoh TF, Yu L, Bennett WM. Cyclosporine nephrotoxicity. Semin Nephrol 2003;23:465–76.
[45] Burne-Taney MJ, Ascon DB, Daniels F, Racusen L, Baldwin W, Rabb H. B cell deficiency confers protection from renal ischemia reperfusion injury. J Immunol 2003;171:3210–5.
[46] Burne-Taney MJ, Kofler J, Yokota N, Weisfeldt M, Traystman RJ, Rabb H. Acute renal failure after whole body ischemia is characterized by inflammation and T cell-mediated injury. Am J Physiol Renal Physiol 2003;285:F87–94.
[47] Burne-Taney MJ, Yokota N, Rabb H. Persistent renal and extrarenal immune changes after severe ischemic injury. Kidney Int 2005;67:1002–9.
[48] Burne-Taney MJ, Yokota-Ikeda N, Rabb H. Effects of combined T- and B-cell deficiency on murine ischemia reperfusion injury. Am J Transplant 2005;5:1186–93.
[49] Burns AT, Davies DR, McLaren AJ, Cerundolo L, Morris PJ, Fuggle SV. Apoptosis in ischemia/reperfusion injury of human renal allografts. Transplantation 1998;66:872–6.
[50] Burns TF, El-Deiry WS. The p53 pathway and apoptosis. J Cell Physiol 1999;181:231–9.
[51] Bush KT, George SK, Zhang PL, Nigam SK. Pretreatment with inducers of ER molecular chaperones protects epithelial cells subjected to ATP depletion. Am J Physiol 1999;277:F211–8.
[52] Bush KT, Keller SH, Nigam SK. Genesis and reversal of the ischemic phenotype in epithelial cells. J Clin Invest 2000;106: 621–6.
[53] Bush KT, Tsukamoto T, Nigam SK. Selective degradation of E-cadherin and dissolution of E-cadherin-catenin complexes in epithelial ischemia. Am J Physiol Renal Physiol 2000;278: F847–52.
[54] Buss WC, Stepanek J, Queen SA. Association of tissue-specific changes in translation elongation after cyclosporin with changes in elongation factor 2 phosphorylation. Biochem Pharmacol 1994;48:1459–69.
[55] Cai Q, Dmitrieva NI, Michea LF, Rocha G, Ferguson D, Burg MB. Toxicity of acetaminophen, salicylic acid, caffeine for first-passage rat renal inner medullary collecting duct cells. J Pharmacol Exp Ther 2003;306:35–42.
[56] Calne R, Rolles K, White DJG, Thiru S, Evans D, McMaster P, et al. Cyclosporin A initially as the only immunosuppressive in 34 recipients of cadaveric organs: 33 kidneys. 2 pancreases and 2 livers. Lancet 1979;2:1033–6.
[57] Cantley LG, Spokes K, Clark B, McMahon EG, Carter J, Epstein FH. Role of endothelin and prostaglandins in radiocontrast-induced renal artery constriction. Kidney Int 1993;44:1217–23.
[58] Carmago S, Shah SV, Walker PD. Meprin, a brush-border enzyme, plays an important role in hypoxic/ischemic acute renal tubular injury in rats. Kidney Int 2002;61:959–66.
[59] Carpenter HM, Mudge GH. Acetaminophen nephrotoxicity: studies on renal acetylation and deacetylation. J Pharmacol Exp Ther 1981;218:61–167.
[60] Castaneda MP, Swiatecka-Urban A, Mitsnefes MM, Feuerstein D, Kaskel FJ, Tellis V, et al. Activation of mitochondrial apoptotic pathways in human renal allografts after ischemiareperfusion injury. Transplantation 2003;76:50–4.
[61] Caterson R, Etheredge S, Snitch P, Duggin G. Mechanisms of renal excretion of cisdichlorodiamine platinum. Res Commun Chem Pathol Pharmacol 1983;41:255–64.
[62] Chan BBK, Kern JA, Flanagan TL, Kron IL, Tribble CG. Effects of *in vivo* cyclosporine adminstration on endothelium-dependent responses in isolated vascular rings. Circulation 1992;86:295.
[63] Chan HM, Satoh M, Zalups RK, Cherian MG. Exogenous metallothionein and renal toxicity of cadmium and mercury in rats. Toxicology 1992;76:15–26.
[64] Chen Y, Cai J, Anders MW, Stevens JL, Jones DP. Role of mitochondrial dysfunction in S-(1,2-dichlorovinyl)-l-cysteine-induced apoptosis. Toxicol Appl Pharmacol 2001;170:172–80.
[65] Chiao H, Kohda Y, McLeroy P, Craig L, Housini I, Star RA. Alpha-melanocyte-stimulating hormone protects against renal injury after ischemia in mice and rats. J Clin Invest 1997;99: 1165–72.

[66] Chiao H, Kohda Y, McLeroy P, Craig L, Linas S, Star RA. Alpha-melanocyte-stimulating hormone inhibits renal injury in the absence of neutrophils. Kidney Int 1998;54:765–74.
[67] Chien CT, Lee PH, Chen CF, Ma MC, Lai MK, Hsu SM. De novo demonstration and co-localization of free-radical production and apoptosis formation in rat kidney subjected to ischemia/reperfusion. J Am Soc Nephrol 2001;12:973–82.
[68] Chiou WL, Hsu FH. Pharmacokinetics of creatinine in man and its implications in the monitoring of renal function and in dosage regimen modifications in patients with renal insufficiency. J Clin Pharmacol 1975;15:427–34.
[69] Choie DD, Longnecker DS, del Campo AA. Acute and chronic cisplatin nephropathy in rats. Lab Invest 1981;44:397–402.
[70] Christensen BM, Marples D, Kim YH, Wang W, Frokiaer J, Nielsen S. Changes in cellular composition of kidney collecting duct cells in rats with lithium-induced NDI. Am J Physiol Cell Physiol 2004;286:C952–64.
[71] Christensen BM, Kim YH, Kwon TH, Nielsen S. Lithium treatment induces a marked proliferation of primarily principal cells in rat kidney inner medullary collecting duct. Am J Physiol Renal Physiol 2006;291:F39–48.
[72] Christensen BM, Zuber AM, Loffing J, Stehle J-C, Deen PMT, Rossier BC, et al. (alpha) ENaC-mediated lithium absorption promotes nephrogenic diabetes insipidus. J Am Soc Nephrol 2011;22:253–61.
[73] Cohen GM, Sun XM, Snowden RT, Dinsdale D, Skilleter DN. Key morphological features of apoptosis may occur in the absence of internucleosomal DNA fragmentation. Biochem J 1992;286:331–4.
[74] Conger J, Robinette J, Villar A, Raij L, Shultz P. Increased nitric oxide synthase activity despite lack of response to endothelium-dependent vasodilators in postischemic acute renal failure in rats. J Clin Invest 1995;96:631–8.
[75] Cowley Jr AW, Mori T, Mattson D, Zou AP. Role of renal NO production in the regulation of medullary blood flow. Am J Physiol Regul Integr Comp Physiol 2003;284:R1355–69.
[76] Cowley Jr AW, Roman RR. Countercurrent exchange in the renal medulla. Am J Physiol Regul Integr Comp Physiol 2003;284:R1151.
[77] Cross M, Endre ZH, Stewart-Richardson P, Cowin GJ, Westhuyzen J, Duggleby RG, et al. 23Na-NMR detects hypoxic injury in intact kidney: increases in sodium inhibited by DMSO and DMTU. Magn Reson Med 1993;30:465–75.
[78] Cummings BS, Schnellmann RG. Cisplatin-induced renal cell apoptosis: caspase 3-dependent and -independent pathways. J Pharmacol Exp Ther 2002;302:8–17.
[79] Cuttle L, Zhang XJ, Endre ZH, Winterford C, Gobe GC. Bcl-X (L) translocation in renal tubular epithelial cells *in vitro* protects distal cells from oxidative stress. Kidney Int 2001;59: 1779–88.
[80] Daemen MA, Denecker G, van't Veer C, Wolfs TG, Vandenabeele P, Buurman WA. Activated caspase-1 is not a central mediator of inflammation in the course of ischemia-reperfusion. Transplantation 2001;71:778–84.
[81] Daemen MA, van't Veer C, Denecker G, Heemskerk VH, Wolfs TG, Clauss M, et al. Inhibition of apoptosis induced by ischemia-reperfusion prevents inflammation. J Clin Invest 1999;104:541–9.
[82] Daemen MA, van de Ven MW, Heineman E, Buurman WA. Involvement of endogenous interleukin-10 and tumor necrosis factor-alpha in renal ischemia-reperfusion injury. Transplantation 1999;67:792–800.
[83] Dagher PC. Apoptosis in ischemic renal injury: roles of GTP depletion and p53. Kidney Int 2004;66:506–9.
[84] Dagher PC. Modeling ischemia *in vitro*: selective depletion of adenine and guanine nucleotide pools. Am J Physiol Cell Physiol 2000;279:C1270–7.
[85] Daley-Yates PT, McBrien DC. Cisplatin metabolites in plasma, a study of their pharmacokinetics and importance in the nephrotoxic and antitumour activity of cisplatin. Biochem Pharmacol 1984;33:3063–70.
[86] Daley-Yates PT, McBrien DC. The renal fractional clearance of platinum antitumour compounds in relation to nephrotoxicity. Biochem Pharmacol 1985;34:1423–8.
[87] Danial NN, Korsmeyer SJ. Cell death: critical control points. Cell 2004;116:205–19.
[88] Dash BC, El-Deiry WS. Cell cycle checkpoint control mechanisms that can be disrupted in cancer. Methods Mol Biol 2004;280:99–161.
[89] De Greef KE, Ysebaert DK, Dauwe S, Persy V, Vercauteren SR, Mey D, et al. Anti-B7–1 blocks mononuclear cell adherence in vasa recta after ischemia. Kidney Int 2001;60:1415–27.
[90] De Greef KE, Ysebaert DK, Ghielli M, Vercauteren S, Nouwen EJ, Eyskens EJ, et al. Neutrophils and acute ischemia-reperfusion injury. J Nephrol 1998;11:110–22.
[91] De Greef KE, Ysebaert DK, Persy V, Vercauteren SR, De Broe ME. ICAM–1 expression and leukocyte accumulation in inner stripe of outer medulla in early phase of ischemic compared to HgCl2-induced ARF. Kidney Int 2003;63:1697–707.
[92] DeLong ER, DeLong DM, Clarke-Pearson DL. Comparing the areas under two or more correlated receiver operating characteristic curves: a nonparametric approach. Biometrics 1988; 4:837–45.
[93] Del Moral RG, Olmo A, Osuna A, Aguilar M, Carvia R, Becerrra P, et al. Role of P-glycoprotein in chronic cyclosporine nephrotoxicity and its relationship to intrarenal angiotensin deposits. Transplant Proc 1998;30:2014–6.
[94] Dempsey EC, Newton AC, Mochly-Rosen D, Fields AP, Reyland ME, Insel PA, et al. Protein kinase C isozymes and the regulation of diverse cell responses. Am J Physiol Lung Cell Mol Physiol 2000;279:L429–38.
[95] Devarajan P, Mishra J, Supavekin S, Patterson LT, Steven Potter S. Gene expression in early ischemic renal injury: clues towards pathogenesis, biomarker discovery, novel therapeutics. Mol Genet Metab 2003;80:365–76.
[96] di Mari JF, Davis R, Safirstein RL. MAPK activation determines renal epithelial cell survival during oxidative injury. Am J Physiol 1999;277:F195–203.
[97] Dieperink H, Leyssac PP, Kemp E, Starklint H, Frandsen NE, Moller J, et al. Nephrotoxicity of cyclosporine A in humans: effects on glomerular filtration and tubular reabsorption rates. Eur J Clin Invest 1987;7:493–6.
[98] Dieterle F, Perentes E, Cordier A, Roth DR, Verdes P, Grenet O, et al. Urinary clusterin, cystatin C, beta2-microglobulin and total protein as markers to detect drug-induced kidney injury. Nature Biotechnology 2010;28(5):463–9.
[99] Dobyan DC, Levi J, Jacobs C, Kosek J, Weiner MW. Mechanism of cis-platinum nephrotoxicity. II. Morphologic observations. J Pharmacol Exp Ther 1980;213:551–6.
[100] Dong Z, Saikumar P, Weinberg JM, Venkatachalam MA. Internucleosomal DNA cleavage triggered by plasma membrane damage during necrotic cell death. Involvement of serine but not cysteine proteases. Am J Pathol 1997;151:1205–13.
[101] Donohoe JF, Venkatachalam MA, Bernard DB, Levinsky NG. Tubular leakage and obstruction after renal ischemia: structural-functional correlations. Kidney Int 1978;13:208–22.
[102] Douglas JB, Healy JK. Nephrotoxic effects of amphotericin B, including renal tubular acidosis. Am J Med 1969;46:154–62.

[103] Dousa TP. Interaction of lithium with vasopressin-sensitive cyclic AMP system of human renal medulla. Endocrinology 1974;95:1359–66.
[104] Du C, Fang M, Li Y, Li L, Wang X. Smac, a mitochondrial protein that promotes cytochrome c-dependent caspase activation by eliminating IAP inhibition. Cell 2000;102:33–42.
[105] Duggin GG, Mudge GH. Analgesic nephropathy: renal distribution of acetaminophen and its conjugates. J Pharmacol Exp Ther 1976;199:1–9.
[106] Duggin GG, Mudge GH. Effect of acute diuresis on the renal excretion of phenacetin and its major metabolites. J Pharmacol Exp Ther 1978;207:584–93.
[107] Duggin GG, Mudge GH. Renal tubular transport of paracetamol and its conjugates in the dog. Br J Pharmacol 1975;54: 359–66.
[108] Duggin GG, Walker RJ, Mohandas J. Mechanisms of paracetamol-induced acute toxicity in the renal cortex. New York: Marcel Dekker; 1990.
[109] Edelstein CL, Ling H, Wangsiripaisan A, Schrier RW. Emerging therapies for acute renal failure. Am J Kidney Dis 1997;30:S89–95.
[110] Edelstein CL, Shi Y, Schrier RW. Role of caspases in hypoxia-induced necrosis of rat renal proximal tubules. J Am Soc Nephrol 1999;10:1940–9.
[111] El Mouedden M, Laurent G, Mingeot-Leclercq MP, Taper HS, Cumps J, Tulkens PM. Apoptosis in renal proximal tubules of rats treated with low doses of aminoglycosides. Antimicrob Agents Chemother 2000;44:665–75.
[112] El Mouedden M, Laurent G, Mingeot-Leclercq MP, Tulkens PM. Gentamicin-induced apoptosis in renal cell lines and embryonic rat fibroblasts. Toxicol Sci 2000;56:229–39.
[113] El-Mas MM, Mohy El-Din MM, El-gowilly SM, Sharabi FM. Regional and endothelial differences in cyclosporine attenuation of adenosine receptor-mediated vasorelaxations. J Cardiovasc Pharmacol 2004;43:562–73.
[114] El-Mas MM, Mohy El-Din MM, El-Gowilly SM, Sharabi FM. Relative roles of endothelial relaxing factors in cyclosporine-induced impairment of cholinergic and beta-adrenergic renal vasodilations. Eur J Pharmacol 2004;487:149–58.
[115] Elfarra AA, Jakobson I, Anders MW. Mechanism of S-(1,2-dichlorovinyl)glutathione-induced nephrotoxicity. Biochem Pharmacol 1986;35:283–8.
[116] Elfarra AA, Lash LH, Anders MW. Metabolic activation and detoxication of nephrotoxic cysteine and homocysteine S-conjugates. Proc Natl Acad Sci U S A 1986;83:2667–71.
[117] Elzinga LW, Rosen S, Bennett WM. Dissociation of glomerular filtration rate from tubulointerstitial fibrosis in experimental chronic cyclosporine nephropathy: role of sodium intake. J Am Soc Nephrol 1993;4:214–21.
[118] Enari M, Sakahira H, Yokoyama H, Okawa K, Iwamatsu A, Nagata S. A caspase-activated DNase that degrades DNA during apoptosis, its inhibitor ICAD. Nature 1998;391:43–50.
[119] Endre ZH, Ratcliffe PJ, Tange JD, Ferguson DJ, Radda GK, Ledingham JG. Erythrocytes alter the pattern of renal hypoxic injury: predominance of proximal tubular injury with moderate hypoxia. Clin Sci 1989;76:19–29.
[120] Endre ZH, Solez K. Anatomical and functional imaging of transplant acute renal failure. Transpl Rev 1995;9:147–58.
[121] Endre ZH, Walker RJ, Pickering JW, Shaw GM, Frampton CM, Henderson SJ, et al. Early intervention with erythropoietin does not affect the outcome of acute kidney injury (the EARLYARF trial). Kidney International 2010;77:1020–30.
[122] Endre ZH, Pickering JW, Walker RJ, Devarajan P, Edelstein CL, Bonventre JV, et al. Improved performance of urinary biomarkers of acute kidney injury in the critically ill by stratification for injury duration and baseline renal function. Kidney International 2011;79(10):1119–30.
[123] Endre ZH, Westhuyzen J. Early detection of acute kidney injury: emerging new biomarkers. Nephrology 2008;13 (2):91–8.
[124] Endre Z, Pickering J. New markers of acute kidney injury: giant leaps and baby steps. Clinical Biochemistry Reviews 2011;32:121–4.
[125] Eppel GA, Denton KM, Malpas SC, Evans RG. Nitric oxide in responses of regional kidney perfusion to renal nerve stimulation and renal ischaemia. Pflugers Arch 2003;447: 205–13.
[126] Eun HM, Pak CY, Kim CJ, McArthur RG, Yoon JW. Role of cyclosporin A in macromolecular synthesis of beta-cells. Diabetes 1987;36:952–8.
[127] Evans RG, Eppel GA, Anderson WP, Denton KM. Mechanisms underlying the differential control of blood flow in the renal medulla and cortex. J Hypertens 2004;22:1439–51.
[128] Fantuzzi G, Dinarello CA. Interleukin-18 and interleukin-1 beta: two cytokine substrates for ICE (caspase-1). J Clin Immunol 1999;19:1–11.
[129] Farnsworth A, Hall BM, Ng ABP, Duggin GG, Horvath JS, Shiel AGR, et al. Renal biopsy morphology in renal transplantation: a comparative study of the light microscopic appearances of biopsies from patients treated with cyclosporin A or azathioprine prednisolone and antilymphocytic globulin. Am J Surg Pathol 1984;8:243–52.
[130] Feldenberg LR, Thevananther S, del Rio M, de Leon M, Devarajan P. Partial ATP depletion induces Fas- and caspase-mediated apoptosis in MDCK cells. Am J Physiol 1999;276: F837–46.
[131] Feldman S, Wang MY, Kaloyanides GJ. Aminoglycosides induce a phospholipidosis in the renal cortex of the rat: an early manifestation of nephrotoxicity. J Pharmacol Exp Ther 1982;220:514–20.
[132] Ferreira L, Quiros Y, Sancho-Martínez SM, García-Sánchez O, Raposo C, López-Novoa JM, et al. Urinary levels of regenerating islet-derived protein III β and gelsolin differentiate gentamicin from cisplatin-induced acute kidney injury in rats. Kidney Int 2011;79:518–28.
[133] Fischer G, Wittmann-Liebold B, Lang K, Kiefhaber T, Schmid FX. Cyclophilin and peptidyl-prolyl cis-trans isomerase are probably identical proteins. Nature 1989;337:476–8.
[134] Fish EM, Molitoris BA. Alterations in epithelial polarity and the pathogenesis of disease states. N Engl J Med 1994;330: 1580–8.
[135] Flo TH, Smith KD, Sato S, Rodriguez DJ, Holmes MA, Strong RK, et al. Lipocalin 2 mediates an innate immune response to bacterial infection by sequestrating iron. Nature 2004;432 (7019):917–21.
[136] Force T, Bonventre JV. Growth factors and mitogen-activated protein kinases. Hypertension 1998;31:152–61.
[137] Forrest JNJ, Cohen AD, Torretti J, Himmelhoch JM, Epstein FH. On the mechanism of lithium-induced diabetes insipidus in man and the rat. J Clin Invest 1974;53:1115–23.
[138] Fraser A, Evan G. A license to kill. Cell 1996;85:781–4.
[139] Garcon G, Leleu B, Zerimech F, Marez T, Haguenoer JM, Furon D, et al. Biologic markers of oxidative stress and nephrotoxicity as studied in biomonitoring of adverse effects of occupational exposure to lead and cadmium. J Occup Environ Med 2004;46:1180–6.
[140] Gardner MP, Houghton DC, Andoh TF, Lindsley J, Bennett WM. Clinically relevant doses and blood levels produce experimental cyclosporine nephrotoxicity when combined with nitric oxide inhibition. Transplantation 1996;61:1506–12.

[141] Gaspari F, Perico N, Locatelli M, Corna D, Remuzzi G, Garattini S. Renal handling of aspirin in the rat. J Pharmacol Exp Ther 1989;251:295–304.
[142] Gibbons GH, Pratt RE, Dzau VJ. Vascular smooth muscle cell hypertrophy vs. hyperplasia. Autocrine transforming growth factor-beta 1 expression determines growth response to angiotensin II. J Clin Invest 1992;90:456–61.
[143] Gilbert DN, Wood CA, Kohlhepp SJ, Kohnen PW, Houghton DC, Finkbeiner HC, et al. Polyaspartic acid prevents experimental aminoglycoside nephrotoxicity. J Infect Dis 1989;159:945–53.
[144] Gleyzer N, Vercauteren K, Scarpulla RC. Control of mitochondrial transcription specificity factors (TFB1M and TFB2M) by nuclear respiratory factors (NRF-1 and NRF-2) and PGC–1 family coactivators. Mol Cell Biol 2005;25:1354–66.
[145] Gobe G, Zhang XJ, Cuttle L, Pat B, Willgoss D, Hancock J, et al. Bcl-2 genes and growth factors in the pathology of ischaemic acute renal failure. Immunol Cell Biol 1999;77:279–86.
[146] Gobe G, Zhang XJ, Willgoss DA, Schoch E, Hogg NA, Endre ZH. Relationship between expression of Bcl-2 genes and growth factors in ischemic acute renal failure in the rat. J Am Soc Nephrol 2000;11:454–67.
[147] Gobe GC, Endre ZH. Cell death in toxic nephropathies. Semin Nephrol 2003;23:416–24.
[148] Goldberg HJ, Wong PY, Cole EH, Levy GA, Skorecki KL. Dissociation between the immunosuppressive activity of cyclosporine derivatives and their effects on intracellular calcium signaling in mesangial cells. Transplantation 1989;47:731–3.
[149] Goldstein RS, Noordewier B, Bond JT, Hook JB, Mayor GH. cis-Dichlorodiammineplatinum nephrotoxicity: time course and dose response of renal functional impairment. Toxicol Appl Pharmacol 1981;60:163–75.
[150] Goligorsky MS, Brodsky SV, Noiri E. Nitric oxide in acute renal failure: NOS versus NOS. Kidney Int 2002;61:855–61.
[151] Goligorsky MS, Brodsky SV, Noiri E. NO bioavailability, endothelial dysfunction, acute renal failure: new insights into pathophysiology. Semin Nephrol 2004;24:316–23.
[152] Goligorsky MS, Lieberthal W, Racusen L, Simon EE. Integrin receptors in renal tubular epithelium: new insights into pathophysiology of acute renal failure. Am J Physiol 1993;264:F1–8.
[153] Goodin MG, Walker RJ, Rosengren RJ. Renal PGE2 production in the human and rat following phenacetin, acetaminophen and p-aminophenol. Res Commun Chem Pathol Pharmacol 2002;111:153–66.
[154] Goodsaid FM, Blank M, Dieterle F, Harlow P, Hausner E, Sistare F, et al. Novel biomarkers of acute kidney toxicity. Clin Pharmacol Ther 2009;86:490–6.
[155] Goodsaid FM, Frueh FW, Mattes W. Strategic paths for biomarker qualification. Toxicology 2008;245:219–23.
[156] Goodsaid F, Frueh F. Biomarker qualification pilot process at the US Food and Drug Administration. AAPS J 2007;9:E105–8.
[157] Gorospe M, Cirielli C, Wang X, Seth P, Capogrossi MC, Holbrook NJ. p21(Waf1/Cip1) protects against p53-mediated apoptosis of human melanoma cells. Oncogene 1997;14:929–35.
[158] Greger R. Possible sites of lithium transport in the nephron. Kidney Int 1990;39(Suppl 28):S26–30.
[159] Gross A, Yin XM, Wang K, Wei MC, Jockel J, Milliman C, et al. Caspase cleaved BID targets mitochondria and is required for cytochrome c release, while BCL-XL prevents this release but not tumor necrosis factor-R1/Fas death. J Biol Chem 1999;274:1156–63.
[160] Grunfeld JP, Rossier BC. Lithium nephrotoxicity revisited. Nat Clin Pract Neph 2009;5:270–6.
[161] Guan Z, Willgoss D, Rahgozar M, Gobé G, Endre Z. Nitric oxide (NO) antagonises renal autoregulation after ischaemia-reperfusion injury. Nephrology 2004;9(1):A32.
[162] Gueler F, Rong S, Park JK, Fiebeler A, Menne J, Elger M, et al. Postischemic acute renal failure is reduced by short-term statin treatment in a rat model. J Am Soc Nephrol 2002;13:2288–98.
[163] Ha HC, Snyder SH. Poly(ADP-ribose) polymerase is a mediator of necrotic cell death by ATP depletion. Proc Natl Acad Sci U S A 1999;96:13978–82.
[164] Haase M, Bellomo R, Devarajan P, Schlattmann P, Haase-Fielitz A, Group, NGAL metaanalysis investigator group. Accuracy of neutrophil gelatinase-associated lipocalin (NGAL) in diagnosis and prognosis in acute kidney injury: a systematic review and meta-analysis. Am J Kidney Dis 2009;54(6):1012–24.
[165] Haase M, Devarajan P, Haase-Fielitz A, Bellomo R, Cruz DN, Wagener G, et al. The outcome of neutrophil gelatinase-associated lipocalin-positive subclinical acute kidney injury a multicenter pooled analysis of prospective studies. J Am Coll Cardiol 2011;57:1752–61.
[166] Haase-Fielitz A, Bellomo R, Devarajan P, Bennett M, Story D, Matalanis G, et al. The predictive performance of plasma neutrophil gelatinase-associated lipocalin (NGAL) increases with grade of acute kidney injury. Nephrol Dial Transpl 2009;24:3349–54.
[167] Hagar H, Ueda N, Shah SV. Endonuclease induced DNA damage and cell death in chemical hypoxic injury to LLC-PK1 cells. Kidney Int 1996;49:355–61.
[168] Hagar H, Ueda N, Shah SV. Role of reactive oxygen metabolites in DNA damage and cell death in chemical hypoxic injury to LLC-PK1 cells. Am J Physiol 1996;271:F209–15.
[169] Hagar H, Ueda N, Shah SV. Tyrosine phosphorylation in DNA damage and cell death in hypoxic injury to LLC-PK1 cells. Kidney Int 1997;51:1747–53.
[170] Hagiwara M, Inagaki M, Kanamura K, Ohta H, Hidaka H. Inhibitory effects of aminoglycosides on renal protein phosphorylation by protein kinase C. J Pharmacol Exp Ther 1988;244:355–60.
[171] Halestrap AP. Mitochondrial permeability: dual role for the ADP/ATP translocator? Nature 2004;430:983.
[172] Halestrap AP, Clarke SJ, Javadov SA. Mitochondrial permeability transition pore opening during myocardial reperfusion—a target for cardioprotection. Cardiovasc Res 2004;61:372–85.
[173] Hall BM, Tiller DJ, Duggin GG, Horvath JS, Farnsworth A, May J, et al. Post-transplant acute renal failure in cadaver renal recipients treated with cyclosporine. Kidney Int 1985;28:178–86.
[174] Hallett MA, Dagher PC, Atkinson SJ. Rho GTPases show differential sensitivity to nucleotide triphosphate depletion in a model of ischemic cell injury. Am J Physiol Cell Physiol 2003;285:C129–38.
[175] Hammerman MR. Growth factors and apoptosis in acute renal injury. Curr Opin Nephrol Hypertens 1998;7:419–24.
[176] Hammerman MR. The growth hormone-insulin-like growth factor axis in kidney re-revisited. Nephrol Dial Transplant 1999;14:1853–60.
[177] Hammerman MR. Recapitulation of phylogeny by ontogeny in nephrology. Kidney Int 2000;57:742–55.
[178] Hammond TG, Majewski RR, Kaysen JH, Goda FO, Navar GL, Pontillon F, et al. Gentamicin inhibits rat renal cortical homotypic endosomal fusion: role of megalin. Am J Physiol 1997;272:F117–23.
[179] Han WK, Bailly V, Abichandani R, Thadhani R, Bonventre JV. Kidney Injury Molecule-1 (KIM-1): a novel biomarker for

human renal proximal tubule injury. Kidney Int 2002;62: 237–44.
[180] Hara Y, Wakamori M, Ishii M, Maeno E, Nishida M, Yoshida T, et al. LTRPC2 Ca2 + -permeable channel activated by changes in redox status confers susceptibility to cell death. Mol Cell 2002;9:163–73.
[181] Harriman JF, Liu XL, Aleo MD, Machaca K, Schnellmann RG. Endoplasmic reticulum Ca(2 +) signaling and calpains mediate renal cell death. Cell Death Differ 2002;9:734–41.
[182] Harris RC. Cyclooxygenase-2 in the kidney. J Am Soc Nephrol 2000;11:2387–94.
[183] Harrison-Bernard LM, Navar LG. Renal cortical and medullary microvascular blood flow autoregulation in rat. Kidney Int Suppl 1996;57:S23–9.
[184] Hauser IA, Schaeffeler E, Gauer S, Scheuermann EH, Wegner B, Gossmann J, et al. ABCB1 genotype of the donor but not of the recipient is a major risk factor for cyclosporine-related nephrotoxocity after renal transplantation. J Am Soc Nephrol 2005;16:1501–11.
[185] Haylor JL, Morcos SK. Endothelin antagonism and contrast nephropathy. Kidney Int 2000;58:2239.
[186] Healy E, Dempsey M, Lally C, Ryan MP. Apoptosis and necrosis: mechanisms of cell death induced by cyclosporine A in a renal proximal tubular cell line. Kidney Int 1998;54:1955–66.
[187] Hellberg PO, Kallskog O, Wolgast M. Nephron function in the early phase of ischemic renal failure. Significance of erythrocyte trapping. Kidney Int 1990;38:432–9.
[188] Hellberg PO, Kallskog OT, Ojteg G, Wolgast M. Peritubular capillary permeability and intravascular RBC aggregation after ischemia: effects of neutrophils. Am J Physiol 1990;258: F1018–25.
[189] Hengartner MO. The biochemistry of apoptosis. Nature 2000;407:770–6.
[190] Henry MA, Harris PJ, Naughton RJ, Walker LL, Skinner SL, Tange JD. Filtration failure induced by p-aminophenol in rats is due to raised intratubular pressure and not changes in glomerular function. Clin Exp Pharmacol Physiol 1990;17:613–26.
[191] Herceg Z, Wang ZQ. Failure of poly(ADP-ribose) polymerase cleavage by caspases leads to induction of necrosis and enhanced apoptosis. Mol Cell Biol 1999;19:5124–33.
[192] Herzog C, Kaushal GP, Haun RS. Generation of biologically active interleukin-1beta by meprin B. Cytokine 2005;31: 394–403.
[193] Heyman SN, Brezis M, Epstein FH, Spokes K, Silva P, Rosen S. Early renal medullary hypoxic injury from radiocontrast and indomethacin. Kidney Int 1991;40:632–42.
[194] Hladunewich MA, Corrigan G, Derby GC, Ramaswamy D, Kambham N, Scandling JD, et al. A randomized, placebo-controlled trial of IGF-1 for delayed graft function: a human model to study postischemic ARF. Kidney Int 2003;64: 593–602.
[195] Houghton DC, Lee D, Gilbert DN, Bennett WM. Chronic gentamicin nephrotoxicity. Continued tubular injury with preserved glomerular filtration function. Am J Pathol 1986;123:183–94.
[196] Humes HD, Sastrasinh M, Weinberg JM. Calcium is a competitive inhibitor of gentamicin-renal membrane binding interactions and dietary calcium supplementation protects against gentamicin nephrotoxicity. J Clin Invest 1984;73:134–47.
[197] Hvidberg V, Jacobsen C, Strong RK, Cowland JB, Moestrup SK, Borregaard N. The endocytic receptor megalin binds the iron transporting neutrophil-gelatinase-associated lipocalin with high affinity and mediates its cellular uptake. FEBS Letters 2005;579:773–7.
[198] Ichihara A, Imig JD, Navar LG. Cyclooxygenase-2 modulates afferent arteriolar responses to increases in pressure. Hypertension 1999;34:843–7.
[199] Ichimura T, Hung CC, Yang SA, Stevens JL, Bonventre JV. Kidney injury molecule-1: a tissue and urinary biomarker for nephrotoxicant-induced renal injury. Am J Physiol Renal Physiol 2004;286:F552–63.
[200] Ichimura T, Asseldonk EJPV, Humphreys BD, Gunaratnam L, Duffield JS, Bonventre JV. Kidney injury molecule-1 is a phosphatidylserine receptor that confers a phagocytic phenotype on epithelial cells. J Clin Invest 2008;118:1657–68.
[201] Irmler M, Thome M, Hahne M, Schneider P, Hofmann K, Steiner V, et al. Inhibition of death receptor signals by cellular FLIP. Nature 1997;388:190–5.
[202] Jaber BL, Pereira BJ, Bonventre JV, Balakrishnan VS. Polymorphism of host response genes: implications in the pathogenesis and treatment of acute renal failure. Kidney Int 2005;67:14–33.
[203] Jackson NM, Hsu CH, Visscher GE, Venkatachalam MA, Humes HD. Alterations in renal structure and function in a rat model of cyclosporine nephrotoxicity. J Pharmacol Exp Ther 1987;242:749–56.
[204] Jacobsen NO, Olesen OV, Thomsen K, Ottosen PD, Olsen S. Early changes in renal distal convoluted tubules and collecting ducts of lithium-treated rats: light microscopy, enzyme histochemistry, 3H-thymidine autoradiography. Lab Invest 1982;46: 298–305.
[205] Jia Z, Wang N, Aoyagi T, Wang H, Liu H, Yang T. Amelioration of cisplatin nephrotoxiicity by genetic or pharmacologic blockade of prostaglandin synthesis. Kidney Int 2011;79:77–88.
[206] Jiang M, Dong Z. Regulation and pathological role of p53 in cisplatin nephrotoxicity. J Pharmacol Exp Ther 2008;327: 300–7.
[207] Jiang M, Wei Q, Pabla N, Dong G, Wang CY, Yang T, et al. Effects of hydroxyl radical scavenging on cisplatin-induced p53 activation, tubular cell apoptosis and nephrotoxicity. Biochem Pharmcol 2007;73:1499–510.
[208] Johnson DW, Saunders HJ, Johnson FJ, Huq SO, Field MJ, Pollock CA. Cyclosporin exerts a direct fibrogenic effect on human tubulointerstitial cells: roles of insulin-like growth factor I, transforming growth factor beta1, platelet-derived growth factor. J Pharmacol Exp Ther 1999;89:535–42.
[209] Johnson DW, Saunders HJ, Johnson FJ, Huq SO, Field MJ, Pollock CA. Fibrogenic effects of cyclosporin A on the tubulointerstitium: role of cytokines and growth factors. Exp Nephrol 1999;7:470–8.
[210] Johnson DW, Pat B, Vesey DA, Guan Z, Endre Z, Gobe GC. Delayed administration of darbepoietin or erythropoietin protects against ischemic acute renal injury and failure. Kidney Int 2006;69:1806–13.
[211] Johnson RJ, Alpers CE, Yoshimura A, Lombardi D, Pritzl P, Floege J, et al. Renal injury from angiotensin II-mediated hypertension. Hypertension 1992;19:464–74.
[212] Jones TW, Chopra S, Kaufman JS, Flamenbaum W, Trump BF. Cis-diamminedichloroplatinum (II)-induced acute renal failure in the rat. Correlation of structural and functional alterations. Lab Invest 1985;52:363–74.
[213] Joza N, Kroemer G, Penninger JM. Genetic analysis of the mammalian cell death machinery. Trends Genet 2002;18: 142–9.
[214] Joza N, Susin SA, Daugas E, Stanford WL, Cho SK, Li CY, et al. Essential role of the mitochondrial apoptosis-inducing factor in programmed cell death. Nature 2001;410:549–54.

[215] Justo P, Lorz C, Sanz A, Egido J, Ortiz A. Intracellular mechanisms of cyclosporin A-induced tubular cell apoptosis. J Am Soc Nephrol 2003;14:3072–80.
[216] Kadkhodaee M, Endre ZH, Towner RA, Cross M. Hydroxyl radical generation following ischaemia-reperfusion in cell-free perfused rat kidney. Biochim Biophys Acta 1995;1243:169–74.
[217] Kadkhodaee M, Hanson GR, Towner RA, Endre ZH. Detection of hydroxyl and carbon-centred radicals by EPR spectroscopy after ischaemia and reperfusion of the rat kidney. Free Radic Res 1996;25:31–42.
[218] Kahan BD. Cyclosporine nephrotoxicity: pathogenesis, prophylaxis, therapy, prognosis. Am J Kidney Dis 1986;8:323–31.
[219] Kakoki M, Hirata Y, Hayakawa H, Suzuki E, Nagata D, Tojo A, et al. Effects of tetrahydrobiopterin on endothelial dysfunction in rats with ischemic acute renal failure. J Am Soc Nephrol 2000;11:301–9.
[220] Kaloyanides GJ. Drug-phospholipid interactions: role in aminoglycoside nephrotoxicity. Ren Fail 1992;14:351–7.
[221] Kaloyanides GJ. Metabolic interactions between drugs and renal tubulointerstitial cells: role in nephrotoxicity. Kidney Int 1991;39:531–40.
[222] Kang DH, Kanellis J, Hugo C, Truong L, Anderson S, Kerjaschki D, et al. Role of the microvascular endothelium in progressive renal disease. J Am Soc Nephrol 2002;13:806–16.
[223] Kaushal GP. Role of caspases in renal tubular epithelial cell injury. Semin Nephrol 2003;23:425–31.
[224] Kaushal GP, Kaushal V, Hong X, Shah SV. Role and regulation of activation of caspases in cisplatin-induced injury to renal tubular epithelial cells. Kidney Int 2001;60:1726–36.
[225] Kaushal GP, Ueda N, Shah SV. Role of caspases (ICE/CED 3 proteases) in DNA damage and cell death in response to a mitochondrial inhibitor, antimycin A. Kidney Int 1997;52:438–45.
[226] Kelly KJ, Plotkin Z, Vulgamott SL, Dagher PC. P53 mediates the apoptotic response to GTP depletion after renal ischemia-reperfusion: protective role of a p53 inhibitor. J Am Soc Nephrol 2003;14:128–38.
[227] Kelly KJ, Williams Jr WW, Colvin RB, Bonventre JV. Antibody to intercellular adhesion molecule 1 protects the kidney against ischemic injury. Proc Natl Acad Sci U S A 1994;91:812–6.
[228] Kerr JF, Gobe GC, Winterford CM, Harmon BV. Anatomical methods in cell death. Methods Cell Biol 1995;46:1–27.
[229] Kerr JF, Winterford CM, Harmon BV. Apoptosis. Its significance in cancer and cancer therapy. Cancer 1994;73:2013–26.
[230] Kerr JF, Wyllie AH, Currie AR. Apoptosis: a basic biological phenomenon with wide-ranging implications in tissue kinetics. Br J Cancer 1972;26:239–57.
[231] Klaassen CD, Liu J, Choudhuri S. Metallothionein: an intracellular protein to protect against cadmium toxicity. Annu Rev Pharmacol Toxicol 1999;39:267–94.
[232] Klassen RB, Crenshaw K, Kozyraki R, Verroust PJ, Tio L, Atrian S, et al. Megalin mediates renal uptake of heavy metal metallothionein complexes. Am J Physiol Renal Physiol 2004;287:F393–403.
[233] Klausner JM, Paterson IS, Goldman G, Kobzik L, Rodzen C, Lawrence R, et al. Postischemic renal injury is mediated by neutrophils and leukotrienes. Am J Physiol 1989;256:F794–802.
[234] Kleinstreuer N, David T, Plank MJ, Endre Z. Dynamic myogenic autoregulation in the rat kidney: a whole-organ model. Am J Physiol-Renal Physiol 2008;294(6):F1453–64.
[235] Kleyman TR, Roberts C, Ling BN. A mechanism for pentamidine-induced hyperkalemia: inhibition of distal nephron sodium transport. Ann Intern Med 1995;122:103–6.
[236] Klos C, Koob M, Kramer C, Dekant W. p-aminophenol nephrotoxicity: biosynthesis of toxic glutathione conjugates. Toxicol Appl Pharmacol 1992;115:98–106.
[237] Kong T, Eltzschig HK, Karhausen J, Colgan SP, Shelley CS. Leukocyte adhesion during hypoxia is mediated by HIF-1-dependent induction of beta2 integrin gene expression. Proc Natl Acad Sci U S A 2004;101:10440–5.
[238] Kortenoeven MLA, Li Y, Shaw S, Gaeggeler HP, Rossier BC, Wetzels JFM, et al. Amioride blocks lithium entry through the sodium channel thereby attenuating the resultant nephrogenic diabetes insipdius. Kidney Int 2009;76:44–53.
[239] Kothakota S, Azuma T, Reinhard C, Klippel A, Tang J, Chu K, et al. Caspase-3-generated fragment of gelsolin: effector of morphological change in apoptosis. Science 1997;278:294–8.
[240] Koziolek M, Riess R, Geiger H, Thevenod F, Hauser IA. Expression of multidrug resistance P-glycoprotein in kidney allografts from cyclosporine A treated patients. Kidney Int 2001;60:156–66.
[241] Kroemer G, Dallaporta B, Resche-Rigon M. The mitochondrial death/life regulator in apoptosis and necrosis. Annu Rev Physiol 1998;60:619–42.
[242] Krueger A, Baumann S, Krammer PH, Kirchhoff S. FLICE-inhibitory proteins: regulators of death receptor-mediated apoptosis. Mol Cell Biol 2001;21:8247–54.
[243] Krueger A, Schmitz I, Baumann S, Krammer PH, Kirchhoff S. Cellular FLICE-inhibitory protein splice variants inhibit different steps of caspase-8 activation at the CD95 death-inducing signaling complex. J Biol Chem 2001;276:20633–40.
[244] Kruidering M, Van de Water B, de Heer E, Mulder GJ, Nagelkerke JF. Cisplatin-induced nephrotoxicity in porcine proximal tubular cells: mitochondrial dysfunction by inhibition of complexes I to IV of the respiratory chain. J Pharmacol Exp Ther 1997;280:638–49.
[245] Kuang E, Wan Q, Li X, Xu H, Liu Q, Qi Y. ER Ca2 + depletion triggers apoptotic signals for endoplasmic reticulum (ER) overload response induced by overexpressed reticulon 3 (RTN3/HAP). J Cell Physiol 2005;204:549–59.
[246] Kurtz A, Della Bruna R, Kuhn K. Cyclosporine A enhances renin secretion and production in isolated juxtaglomerular cells. Kidney Int 1988;33:947–53.
[247] Kurtz A, Pfeilschifter J, Kuhn K, Koch KM. Cyclosporin A inhibits PGE2 release from vascular smooth muscle cells. Biochem Biophys Res Commun 1987;147:542–9.
[248] Kuznetsov G, Bush KT, Zhang PL, Nigam SK. Perturbations in maturation of secretory proteins and their association with endoplasmic reticulum chaperones in a cell culture model for epithelial ischemia. Proc Natl Acad Sci U S A 1996;93:8584–9.
[249] Kwon T-H, Laursen UH, Marples D, Maunsbach AB, Knepper MA, Frokiaer J, et al. Altered expression of renal AQPs and Na^+ transporters in rats with lithium-induced NDI. Am J Physiol 2000;279:F552–74.
[250] Laiho KU, Shelburne JD, Trump BF. Observations on cell volume, ultrastructure, mitochondrial conformation and vital-dye uptake in Ehrlich ascites tumor cells. Effects of inhibiting energy production and function of the plasma membrane. Am J Pathol 1971;65:203–30.
[251] Lannigan R, Kark R, Pollak VE. The effect of a single intravenous injection of aminonucleoside of puromycin on the rat kidney: a light- and electron-microscope study. J Pathol Bacteriol 1962;83:357–62.
[252] Lassus P, Opitz-Araya X, Lazebnik Y. Requirement for caspase-2 in stress-induced apoptosis before mitochondrial permeabilization. Science 2002;297:1352–4.
[253] Lau AH. Apoptosis induced by cisplatin nephrotoxic injury. Kidney Int 1999;56:1295–8.

[254] Laurent G, Carlier MB, Rollman B, Van Hoof F, Tulkens P. Mechanism of aminoglycoside-induced lysosomal phospholipidosis: *in vitro* and *in vivo* studies with gentamicin and amikacin. Biochem Pharmacol 1982;31:3861–70.

[255] Laurent G, Kishore BK, Tulkens PM. Aminoglycoside-induced renal phospholipidosis and nephrotoxicity. Biochem Pharmacol 1990;40:2383–92.

[256] Laursen UH, Pihakaski-Maunsbach K, Kwon TH, Ostergaard Jensen E, Nielsen S, Maunsbach AB. Changes of rat kidney AQP2 and Na,K-ATPase mRNA expression in lithium-induced nephrogenic diabetes insipidus. Nephron Exp Nephrol 2004;97:e1–16.

[257] Leaf A. Cell swelling. A factor in ischemic tissue injury. Circulation 1973;48:455–8.

[258] Lee HT, Emala CW. Protein kinase C and G(i/o) proteins are involved in adenosine- and ischemic preconditioning-mediated renal protection. J Am Soc Nephrol 2001;12:233–40.

[259] Lee N, MacDonald H, Reinhard C, Halenbeck R, Roulston A, Shi T, et al. Activation of hPAK65 by caspase cleavage induces some of the morphological and biochemical changes of apoptosis. Proc Natl Acad Sci U S A 1997;94:13642–7.

[260] Lee SY, Jo SK, Cho WY, Kim HK, Won NH. The effect of alpha-melanocyte-stimulating hormone on renal tubular cell apoptosis and tubulointerstitial fibrosis in cyclosporine A nephrotoxicity. Transplantation 2004;78:1756–64.

[261] Leichtweiss HP, Lubbers DW, Weiss C, Baumgartl H, Reschke W. The oxygen supply of the rat kidney: measurements of intrarenal pO2. Pflugers Arch 1969;309:328–49.

[262] Lerman LO, Bentley MD, Fiksen-Olsen MJ, Strick DM, Ritman EL, Romero JC. Pressure dependency of canine intrarenal blood flow within the range of autoregulation. Am J Physiol 1995;268:F404–9.

[263] Levi J, Jacobs C, Kalman SM, McTigue M, Weiner MW. Mechanism of cis-platinum nephrotoxicity. I. Effects of sulfhydryl groups in rat kidneys. J Pharmacol Exp Ther 1980;213:545–50.

[264] Li C, Yang CW, Park JH, Lim SW, Sun BK, Jung JY, et al. Pravastatin treatment attenuates interstitial inflammation and fibrosis in a rat model of chronic cyclosporine-induced nephropathy. Am J Physiol Renal Physiol 2004;286:F46–57.

[265] Li LY, Luo X, Wang X. Endonuclease G is an apoptotic DNase when released from mitochondria. Nature 2001;412:95–9.

[266] Li P, Nijhawan D, Budihardjo I, Srinivasula SM, Ahmad M, Alnemri ES, et al. Cytochrome c and dATP-dependent formation of Apaf-1/caspase-9 complex initiates an apoptotic protease cascade. Cell 1997;91:479–89.

[267] Li S, Bhatt R, Megyesi J, Gokden N, Shah SV, Portilla D. PPARalpha ligand ameliorates acute renal failure by reducing cisplatin-induced increased expression of renal endonuclease G. Am J Physiol Renal Physiol 2004;287:F990–8.

[268] Li S, Wu P, Yarlagadda P, Vadjunec NM, Proia AD, Harris RA, et al. PPAR alpha ligand protects during cisplatin-induced acute renal failure by preventing inhibition of renal FAO and PDC activity. Am J Physiol Renal Physiol 2004;286:F572–80.

[269] Li Y, Shaw S, Kamsteeg EJ, Vandewalle A, Deen PM. Development of lithium-induced nephrogenic diabetes insipidus is dissociated from adenylyl cyclase activity. J Am Soc Nephrol 2006;17:1063–72.

[270] Lieberthal W. Biology of ischemic and toxic renal tubular cell injury: role of nitric oxide and the inflammatory response. Curr Opin Nephrol Hypertens 1998;7:289–95.

[271] Lieberthal W, Koh JS, Levine JS. Necrosis and apoptosis in acute renal failure. Semin Nephrol 1998;18:505–18.

[272] Lieberthal W, Levine JS. Mechanisms of apoptosis and its potential role in renal tubular epithelial cell injury. Am J Physiol 1996;271:F477–88.

[273] Lieberthal W, McKenney JB, Kiefer CR, Snyder LM, Kroshian VM, Sjaastad MD. Beta1 integrin-mediated adhesion between renal tubular cells after anoxic injury. J Am Soc Nephrol 1997;8:175–83.

[274] Lieberthal W, Menza SA, Levine JS. Graded ATP depletion can cause necrosis or apoptosis of cultured mouse proximal tubular cells. Am J Physiol 1998;274:F315–27.

[275] Lieberthal W, Nigam SK. Acute renal failure. I. Relative importance of proximal vs. distal tubular injury. Am J Physiol 1998;275:F623–31.

[276] Lieberthal W, Nigam SK. Acute renal failure. II. Experimental models of acute renal failure: imperfect but indispensable. Am J Physiol Renal Physiol 2000;278:F1–12.

[277] Lieberthal W, Triaca V, Levine J. Mechanisms of death induced by cisplatin in proximal tubular epithelial cells: apoptosis vs. necrosis. Am J Physiol 1996;270:F700–8.

[278] Lieberthal W, Wolf EF, Rennke HG, Valeri CR, Levinsky NG. Renal ischemia and reperfusion impair endothelium-dependent vascular relaxation. Am J Physiol 1989;256: F894–900.

[279] Linas SL, Shanley PF, Whittenburg D, Berger E, Repine JE. Neutrophils accentuate ischemia-reperfusion injury in isolated perfused rat kidneys. Am J Physiol 1988;255:F728–35.

[280] Linkermann A, Himmerkus N, Rölver L, Keyser KA, Steen P, Bräsen JH, et al. Renal tubular Fas ligand mediates fratricde in cisplatin-induced acute kidney failure. Kidney Int 2011;79: 169–78.

[281] Lipsky JJ, Lietman PS. Aminoglycoside inhibition of a renal phosphatidylinositol phospholipase C. J Pharmacol Exp Ther 1982;220:287–92.

[282] Liss P, Carlsson P-O, Nygren A, Palm F, Hansell P. Et-A receptor antagonist BQ123 prevents radiocontrast media-induced renal medullary hypoxia. Acta Radiologica 2003;44:111–7.

[283] Litterst CL. Cisplatinum: a review, with special reference to cellular and molecular interactions. Agents Actions 1984;15: 520–4.

[284] Liu H, Baliga R. Cytochrome P450 2E1 null mice provide novel protection against cisplatin-induced nephrotoxicity and apoptosis. Kidney Int 2003;63:1687–96.

[285] Liu H, Baliga R. Endoplasmic reticulum stress-associated caspase 12 mediates cisplatin-induced LLC-PK1 cell apoptosis. J Am Soc Nephrol 2005;16:1985–92.

[286] Liu X, Godwin ML, Nowak G. Protein kinase C-alpha inhibits the repair of oxidative phosphorylation after S-(1,2-dichlorovinyl)-L-cysteine injury in renal cells. Am J Physiol Renal Physiol 2004;287:F64–73.

[287] Liu X, Rainey JJ, Harriman JF, Schnellmann RG. Calpains mediate acute renal cell death: role of autolysis and translocation. Am J Physiol Renal Physiol 2001;281:F728–38.

[288] Liu X, Van Vleet T, Schnellmann RG. The role of calpain in oncotic cell death. Annu Rev Pharmacol Toxicol 2004;44: 349–70.

[289] Lopez-Novoa J, Quiros Y, Vicente L, Morales AI, Lopez-Hernandez FJ. New insights into the mechanism of aminoglycoside nephrotoxicity: an integrative point of view. Kidney Int 2011;79:33–45.

[290] Lorz C, Justo P, Sanz A, Subira D, Egido J, Ortiz A. Paracetamol-induced renal tubular injury: a role for ER stress. J Am Soc Nephrol 2004;15:380–9.

[291] Los M, Mozoluk M, Ferrari D, Stepczynska A, Stroh C, Renz A, et al. Activation and caspase-mediated inhibition of PARP: a

molecular switch between fibroblast necrosis and apoptosis in death receptor signaling. Mol Biol Cell 2002;13:978–88.
[292] Luo X, Budihardjo I, Zou H, Slaughter C, Wang X. Bid, a Bcl2 interacting protein, mediates cytochrome c release from mitochondria in response to activation of cell surface death receptors. Cell 1998;94:481–90.
[293] Maeno E, Ishizaki Y, Kanaseki T, Hazama A, Okada Y. Normotonic cell shrinkage because of disordered volume regulation is an early prerequisite to apoptosis. Proc Natl Acad Sci U S A 2000;97:9487–92.
[294] Majid DS, Godfrey M, Navar LG. Pressure natriuresis and renal medullary blood flow in dogs. Hypertension 1997;29: 1051–7.
[295] Majno G, Joris I. Apoptosis, oncosis, and necrosis. An overview of cell death. Am J Pathol 1995;146:3–15.
[296] Mandic A, Hannson J, Linder S. Cisplatin induces endoplasmic reticulum stress and nucleus-independent apoptotic signaling. J Biol Chem 2003;278:9100–6.
[297] Marche P, Olier B, Girard A, Fillastre JP, Morin JP. Aminoglycoside-induced alterations of phosphoinositide metabolism. Kidney Int 1987;31:59–64.
[298] Markowitz GS, Radhakrishnan J, Kambham N, Valeri AM, Hines WH, D'Agati VD. Lithium nephrotoxicity: a progressive combined glomerular and tubulointerstitial nephropathy. J Am Soc Nephrol 2000;11:1439–48.
[299] Marples D, Christensen S, Christensen EI, Ottosen PD, Nielsen S. Lithium-induced downregulation of aquaporin-2 water channel expression in rat kidney medulla. J Clin Invest 1995;95:1838–45.
[300] Marples D, Frokiaer J, Nielsen S. Long-term regulation of aquaporins in the kidney. Am J Physiol 1999;276:F331–9.
[301] Martin DR, Lewington AJ, Hammerman MR, Padanilam BJ. Inhibition of poly(ADP-ribose) polymerase attenuates ischemic renal injury in rats. Am J Physiol Regul Integr Comp Physiol 2000;279:R1834–40.
[302] Martin SJ, Finucane DM, Amarante-Mendes GP, O'Brien GA, Green DR. Phosphatidylserine externalization during CD95-induced apoptosis of cells and cytoplasts requires ICE/CED-3 protease activity. J Biol Chem 1996;271:28753–6.
[303] Martin SJ, O'Brien GA, Nishioka WK, McGahon AJ, Mahboubi A, Saido TC, et al. Proteolysis of fodrin (non-erythroid spectrin) during apoptosis. J Biol Chem 1995;270: 6425–8.
[304] Martinez-Salgado C, Lopez-Hernandez F, et al. Glomerular nephrotoxicity of aminoglycosides. Toxicol Appl Pharmacol 2007;223:86–98.
[305] Marumo T, Nakaki T, Hishikawa K, Suzuki H, Kato R, Saruta T. Cyclosporin A inhibits nitric oxide synthase induction in vascular smooth muscle cells. Hypertension 1995;25:764–8.
[306] Mason J, Takabatake T, Olbricht C, Thurau K. The early phase of experimental acute renal failure. III. Tubologlomerular feedback. Pflugers Arch 1978;373:69–76.
[307] Mason J, Welsch J, Torhorst J. The contribution of vascular obstruction to the functional defect that follows renal ischemia. Kidney Int 1987;31:65–71.
[308] Masson M, Rolli V, Dantzer F, Trucco C, Schreiber V, Fribourg S, et al. Poly(ADP-ribose) polymerase: structure-function relationship. Biochimie 1995;77:456–61.
[309] Mattson DL, Lu S, Roman RJ, Cowley Jr AW. Relationship between renal perfusion pressure and blood flow in different regions of the kidney. Am J Physiol 1993;264:R578–83.
[310] McNulty S, Fonfria E. The role of TRPM channels in cell death. Pflugers Arch 2005;451:235–42.
[311] Meagher LC, Savill JS, Baker A, Fuller RW, Haslett C. Phagocytosis of apoptotic neutrophils does not induce macrophage release of thromboxane B2. J Leukoc Biol 1992;52:269–73.
[312] Megyesi J, Andrade L, Vieira Jr JM, Safirstein RL, Price PM. Coordination of the cell cycle is an important determinant of the syndrome of acute renal failure. Am J Physiol Renal Physiol 2002;283:F810–6.
[313] Megyesi J, Andrade L, Vieira Jr JM, Safirstein RL, Price PM. Positive effect of the induction of p21WAF1/CIP1 on the course of ischemic acute renal failure. Kidney Int 2001;60: 2164–72.
[314] Megyesi J, Safirstein RL, Price PM. Induction of p21WAF1/CIP1/SDI1 in kidney tubule cells affects the course of cisplatin-induced acute renal failure. J Clin Invest 1998;101: 777–82.
[315] Megyesi J, Udvarhelyi N, Safirstein RL, Price PM. The p53-independent activation of transcription of p21 WAF1/CIP1/SDI1 after acute renal failure. Am J Physiol 1996;271:F1211–6.
[316] Meldrum KK, Meldrum DR, Sezen SF, Crone JK, Burnett AL. Heat shock prevents simulated ischemia-induced apoptosis in renal tubular cells via a PKC-dependent mechanism. Am J Physiol Regul Integr Comp Physiol 2001;281:R359–64.
[317] Melnikov VY, Ecder T, Fantuzzi G, Siegmund B, Lucia MS, Dinarello CA, et al. Impaired IL-18 processing protects caspase-1-deficient mice from ischemic acute renal failure. J Clin Invest 2001;107:1145–52.
[318] Melnikov VY, Faubel S, Siegmund B, Lucia MS, Ljubanovic D, Edelstein CL. Neutrophil-independent mechanisms of caspase-1– and IL-18–mediated ischemic acute tubular necrosis in mice. J Clin Invest 2002;110:1083–91.
[319] Melnikov VY, Faubel S, Siegmund B, Lucia MS, Ljubanovic D, Edelstein CL. Neutrophil-independent mechanisms of caspase-1- and IL-18-mediated ischemic acute tubular necrosis in mice. J Clin Invest 2002;110:1083–91.
[320] Meyer-Lehnert H, Schrier RW. Cyclosporine A enhances vasopressin-induced Ca2 + mobilization and contraction in mesangial cells. Kidney Int 1988;34:89–97.
[321] Mishra J, Ma Q, Prada A, Mitsnefes M, Zahedi K, Yang J, et al. Identification of neutrophil gelatinase-associated lipocalin as a novel early urinary biomarker for ischemic renal injury. J Am Soc Nephrol 2003;14:2534–43.
[322] Mishra J, Dent C, Tarabishi R, Mitsnefes MM, Ma Q, Kelly C, et al. Neutrophil gelatinase-associated lipocalin (NGAL) as a biomarker for acute renal injury after cardiac surgery. Lancet 2005;365:1231–8.
[323] Mishra J, Mori K, Ma Q, Kelly C, Barasch J, Devarajan P. Neutrophil gelatinase-associated lipocalin: a novel early urinary biomarker for cisplatin nephrotoxicity. Am J Nephrol 2004;24:307–15.
[324] Mistry P, Lee C, McBrien DC. Intracellular metabolites of cisplatin in the rat kidney. Cancer Chemother Pharmacol 1989;24:73–9.
[325] Miura K, Goldstein RS, Pasino DA, Hook JB. Cisplatin nephrotoxicity: role of filtration and tubular transport of cisplatin in isolated perfused kidneys. Toxicology 1987;44:147–58.
[326] Mohandas J, Duggin GG, Horvath JS, Tiller DJ. Metabolic oxidation of acetaminophen (paracetamol) mediated by cytochrome P–450 mixed-function oxidase and prostaglandin endoperoxide synthetase in rabbit kidney. Toxicol Appl Pharmacol 1981;61:252–9.
[327] Mohandas J, Duggin GG, Horvath JS, Tiller DJ. Regional differences in peroxidatic activation of paracetamol (acetaminophen) mediated by cytochrome P450 and prostaglandin endoperoxide synthetase in rabbit kidney. Res Commun Chem Pathol Pharmacol 1981;34:69–80.
[328] Mohandas J, Marshall JJ, Duggin GG, Horvath JS, Tiller DJ. Differential distribution of glutathione and glutathione-related

enzymes in rabbit kidney. Possible implications in analgesic nephropathy. Biochem Pharmacol 1984;33:1801–7.
[329] Moldeus P, Andersson B, Rahimtula A, Berggren M. Prostaglandin synthetase catalyzed activation of acetaminophen. Biochem Pharmacol 1982;31:1363–8.
[330] Molitoris BA. Actin cytoskeleton in ischemic acute renal failure. Kidney Int 2004;66:871–83.
[331] Molitoris BA, Leiser J, Wagner MC. Role of the actin cytoskeleton in ischemia-induced cell injury and repair. Pediatr Nephrol 1997;11:761–7.
[332] Molitoris BA, Sutton TA. Endothelial injury and dysfunction: role in the extension phase of acute renal failure. Kidney Int 2004;66:496–9.
[333] Moochhala SM, Renton KW. Inhibition of hepatic microsomal drug metabolism by the immunosuppressive agent cyclosporin A. Biochem Pharmacol 1986;33:1499–503.
[334] Morales A, Detaile D, Prieto M, Puente A, Briones E, Arévalo M, et al. Metformin prevents experimental gentamicin-induced nephropathy by a mitochonria-dependent pathway. Kidney Int 2010;77:861–9.
[335] Mori K, Lee HT, Rapoport D, Drexler IR, Foster K, Yang J, et al. Endocytic delivery of lipocalin-siderophore-iron complex rescues the kidney from ischemia-reperfusion injury. J Clin Invest 2005;115:610–21.
[336] Morris Jr SM, Kepka-Lenhart D, McGill RL, Curthoys NP, Adler S. Specific disruption of renal function and gene transcription by cyclosporin A. J Biol Chem 1992;267:13768–71.
[337] Mudge GH, Gemborys MW, Duggin GG. Covalent binding of metabolites of acetaminophen to kidney protein and depletion of renal glutathione. J Pharmacol Exp Ther 1978;206:218–26.
[338] Murray BM, Paller MS. Beneficial effects of renal denervation and prazosin on GFR and renal blood flow after cyclosporine in rats. Clin Nephrol 1986;25(Suppl 1):S37–9.
[339] Murray BM, Paller MS, Ferris TF. Effect of cyclosporine administration on renal hemodynamics in conscious rats. Kidney Int 1985;28:767–74.
[340] Muzio M, Chinnaiyan AM, Kischkel FC, O'Rourke K, Shevchenko A, Ni J. FLICE, a novel FADD-homologous ICE/CED-3-like protease, is recruited to the CD95 (Fas/APO–1) death—inducing signaling complex. Cell 1996;85:817–27.
[341] Myers BD. Cyclosporine nephrotoxicity. Kidney Int 1986;30:964–74.
[342] Myers BD, Ross J, Newton L, Luetscher J, Perlroth M. Cyclosporine-associated chronic nephropathy. N Engl J Med 1984;311:699–705.
[343] Myers BD, Sibley R, Newton L, Tomlanovich SJ, Boshkos C, Stinson E, et al. The long-term course of cyclosporine-associated chronic nephropathy. Kidney Int 1988;33:590–600.
[344] Nagai J, Takano M. Molecular aspects of renal handling of aminoglycosides and strategies for preventing the nephrotoxicity. Drug Metab Pharmacokinet 2004;19:159–70.
[345] Nakagawa T, Zhu H, Morishima N, Li E, Xu J, Yankner BA, et al. Caspase-12 mediates endoplasmic-reticulum-specific apoptosis and cytotoxicity by amyloid-beta. Nature 2000;403:98–103.
[346] Nankivell BJ, Borrows RJ, Fung CL, O'Connell PJ, Chapman JR, Allen RD. Calcineurin inhibitor nephrotoxicity: longitudinal assessment by protocol histology. Transplantation 2004;78:557–65.
[347] Nejat M, Pickering JW, Walker RJ, Westhuyzen J, Shaw GM, Frampton CM, et al. Urinary cystatin C is diagnostic of acute kidney injury and sepsis, and predicts mortality in the intensive care unit. Crit Care 2010;14(3):R85.
[348] Nejat M, Hill JV, Pickering JW, Edelstein CL, Devarajan P, Endre ZH. Albuminuria increases cystatin C excretion: implications for urinary biomarkers. Nephrol Dial Transplant 2011;:10.1093/ndt/gfr [(epub)]
[349] Newton JF, Bailie MB, Hook JB. Acetaminophen nephrotoxicity in the rat. Renal metabolic activation *in vitro*. Toxicol Appl Pharmacol 1983;70:433–44.
[350] Newton JF, Braselton Jr WE, Kuo CH, Kluwe WM, Gemborys MW, Mudge GH, et al. Metabolism of acetaminophen by the isolated perfused kidney. J Pharmacol Exp Ther 1982;221:76–9.
[351] Newton JF, Hoefle D, Gemborys MW, Mudge GH, Hook JB. Metabolism and excretion of a glutathione conjugate of acetaminophen in the isolated perfused rat kidney. J Pharmacol Exp Ther 1986;237:519–24.
[352] Newton JF, Yoshimoto M, Bernstein J, Rush GF, Hook JB. Acetaminophen nephrotoxicity in the rat. I. Strain differences in nephrotoxicity and metabolism. Toxicol Appl Pharmacol 1983;69:291–306.
[353] Newton JF, Yoshimoto M, Bernstein J, Rush GF, Hook JB. Acetaminophen nephrotoxicity in the rat. II. Strain differences in nephrotoxicity and metabolism of p-aminophenol, a metabolite of acetaminophen. Toxicol Appl Pharmacol 1983;69:307–18.
[354] Nguyen MT, Dent CL, Ross GF, Harris N, Manning PB, Mitsnefes MM, et al. Urinary aprotinin as a predictor of acute kidney injury after cardiac surgery in children receiving aprotinin therapy. Pediatr nephrol 2008;23:1317–26.
[355] Nielsen J, Kwon TH, Praetorius J, Kim YH, Frokiaer J, Knepper MA, et al. Segment-specific ENaC downregulation in kidney of rats with lithium-induced NDI. Am J Physiol Renal Physiol 2003;285:F1198–209.
[356] Nielsen S, Frokiaer J, Marples D, Kwon TH, Agre P, Knepper MA. Aquaporins in the kidney: from molecules to medicine. Physiol Rev 2002;82:205–44.
[357] Nielsen S, Kwon T-H, Frokiaer J, Knepper MA. Key roles of renal aquaporins in water balance and water balance disorders. News Physiol Sci 2000;15:136–43.
[358] Nielsen S, Kwon TH, Christensen BM, Promeneur D, Frokiaer J, Marples D. Physiology and pathophysiology of renal aquaporins. J Am Soc Nephrol 1999;10:647–63.
[359] Nielsen J, Kwon TH, Frøkiaer J, Knepper MA, Nielsen S. Lithium induced NDI in rats is associated with loss of a-ENaC regulation by aldosterone in CCD. Am J Physiol Renal Physiol 2006;290:F1222–33.
[360] Nigam S, Lieberthal W. Acute renal failure. III. The role of growth factors in the process of renal regeneration and repair. Am J Physiol Renal Physiol 2000;279:F3–11.
[361] Nishizuka Y, Nakamura S. Lipid mediators and protein kinase C for intracellular signalling. Clin Exp Pharmacol Physiol Suppl 1995;22:S202–3.
[362] Nogae S, Miyazaki M, Kobayashi N, Saito T, Abe K, Saito H, et al. Induction of apoptosis in ischemia-reperfusion model of mouse kidney: possible involvement of Fas. J Am Soc Nephrol 1998;9:620–31.
[363] Nony PA, Schnellmann RG. Mechanisms of renal cell repair and regeneration after acute renal failure. J Pharmacol Exp Ther 2003;304:905–12.
[364] Nowak G. Protein kinase C mediates repair of mitochondrial and transport functions after toxicant-induced injury in renal cells. J Pharmacol Exp Ther 2003;306:157–65.
[365] Nowak G. Protein kinase C-alpha and ERK1/2 mediate mitochondrial dysfunction, decreases in active Na + transport, cisplatin-induced apoptosis in renal cells. J Biol Chem 2002;277:43377–88.
[366] Oberbauer R, Rohrmoser M, Regele H, Muhlbacher F, Mayer G. Apoptosis of tubular epithelial cells in donor

kidney biopsies predicts early renal allograft function. J Am Soc Nephrol 1999;10:2006–13.
[367] Okada Y, Maeno E, Shimizu T, Manabe K, Mori S, Nabekura T. Dual roles of plasmalemmal chloride channels in induction of cell death. Pflugers Arch 2004;448:287–95.
[368] Okamura H, Tsutsi H, Komatsu T, Yutsudo M, Hakura A, Tanimoto T, et al. Cloning of a new cytokine that induces IFN-gamma production by T cells. Nature 1995;378:88–91.
[369] Okusa MD. The inflammatory cascade in acute ischemic renal failure. Nephron 2002;90:133–8.
[370] Ozer JS, Dieterle F, Troth S, Perentes E, Cordier A, Verdes P, et al. A panel of urinary biomarkers to monitor reversibility of renal injury and a serum marker with improved potential to assess renal function. Nature Biotechnology 2010;28:486–94.
[371] Pabla N, Dong G. Cisplatin nephrotoxicity: mechanisms and renoprotective strategies. Kidney Int 2008;73:994–1007.
[372] Padanilam BJ. Cell death induced by acute renal injury: a perspective on the contributions of apoptosis and necrosis. Am J Physiol Renal Physiol 2003;284:F608–27.
[373] Padanilam BJ. Induction and subcellular localization of protein kinase C isozymes following renal ischemia. Kidney Int 2001;59:1789–97.
[374] Pallet N, Bouvier N, Bendjallabah A, Rabant M, Flinois JP, Hertig A, et al. Cyclosporine-induced endoplasmic reticulum stress triggers tubular phenotypic changes and death. Am J Transplant 2008;8:2283–96.
[375] Pallet N, Bouvier N, Legendre C, Beaune P, Thervet E, Choukroun G, Martinez F. Antiapoptotic properties of recombinant human erythropoietin protects against tubular cyclosporine toxicity. Pharmacol Res 2010;61:71–5.
[376] Paragas N, Qiu A, Zhang Q, Samstein B, Deng SX, Schmidt-Ott KM, et al. The Ngal reporter mouse detects the response of the kidney to injury in real time. Nature Medicine 2011;17:216–22.
[377] Parikh CR, Jani A, Melnikov VY, Faubel S, Edelstein CL. Urinary interleukin-18 is a marker of human acute tubular necrosis. Am J Kidney Dis 2004;43:405–14.
[378] Park KM, Kramers C, Vayssier-Taussat M, Chen A, Bonventre JV. Prevention of kidney ischemia/reperfusion-induced functional injury, MAPK and MAPK kinase activation, inflammation by remote transient ureteral obstruction. J Biol Chem 2002;277:2040–9.
[379] Park JW, Bae EH, Kim IJ, Ma SK, Choi C, Lee J, et al. Paricalcitol attenuates cyclosporine-induced kidney injury in rats. Kidney Int 2010;77:1076–85.
[380] Park MS, De Leon M, Devarajan P. Cisplatin induces apoptosis in LLC-PK1 cells via activation of mitochondrial pathways. J Am Soc Nephrol 2002;13:858–65.
[381] Parrish J, Li L, Klotz K, Ledwich D, Wang X, Xue D. Mitochondrial endonuclease G is important for apoptosis in C. elegans. Nature 2001;412:90–4.
[382] Pencina MJ, D'Agostino RB, Vasan RS. Evaluating the added predictive ability of a new marker: from area under the ROC curve to reclassification and beyond. Statistics In Medicine 2008;27:157–72.
[383] Perico N, Remuzzi G. Role of platelet-activating factor in renal immune injury and proteinuria. Am J Nephrol 1990;10:98–104.
[384] Perico N, Rossini M, Imberti O, Malanchini B, Cornejo RP, Gaspari F, et al. Thromboxane receptor blockade attenuates chronic cyclosporine nephrotoxicity and improves survival in rats with renal isograft. J Am Soc Nephrol 1992;2:1398–404.
[385] Perico N, Zoja C, Benigni A, Ghilardi F, Gualandris L, Remuzzi G. Effect of short-term cyclosporine administration in rats on renin-angiotensin and thromboxane A2: possible relevance to the reduction in glomerular filtration rate. J Pharmacol Exp Ther 1986;239:229–35.
[386] Perraud AL, Fleig A, Dunn CA, Bagley LA, Launay P, Schmitz C, et al. ADP-ribose gating of the calcium-permeable LTRPC2 channel revealed by Nudix motif homology. Nature 2001;411:595–9.
[387] Perraud AL, Takanishi CL, Shen B, Kang S, Smith MK, Schmitz C, et al. Accumulation of free ADP-ribose from mitochondria mediates oxidative stress-induced gating of TRPM2 cation channels. J Biol Chem 2005;280:6138–48.
[388] Pfielschifter J, Ruegg UT. Cyclosporine A augments angiotensin II stimulated rise in intracellular free calcium in vascular smooth muscle cells. Biochem J 1987;248:883–7.
[389] Pichler RH, Franceschini N, Young BA, Hugo C, Andoh TF, Burdmann EA, et al. Pathogenesis of cyclosporine nephropathy: roles of angiotensin II and osteopontin. J Am Soc Nephrol 1995;6:1186–96.
[390] Pickering JW, Endre ZH. GFR shot by RIFLE: errors in staging acute kidney injury. Lancet 2009;373:1318–9.
[391] Poluha W, Poluha DK, Chang B, Crosbie NE, Schonhoff CM, Kilpatrick DL, et al. The cyclin-dependent kinase inhibitor p21 (WAF1) is required for survival of differentiating neuroblastoma cells. Mol Cell Biol 1996;16:1335–41.
[392] Pombo CM, Bonventre JV, Avruch J, Woodgett JR, Kyriakis JM, Force T. The stress-activated protein kinases are major c-Jun amino-terminal kinases activated by ischemia and reperfusion. J Biol Chem 1994;269:26546–51.
[393] Portilla D. Energy metabolism and cytotoxicity. Semin Nephrol 2003;23:432–8.
[394] Portilla D. Role of fatty acid beta-oxidation and calcium-independent phospholipase A2 in ischemic acute renal failure. Curr Opin Nephrol Hypertens 1999;8:473–7.
[395] Portilla D, Dai G, Peters JM, Gonzalez FJ, Crew MD, Proia AD. Etomoxir-induced PPA Ralpha-modulated enzymes protect during acute renal failure. Am J Physiol Renal Physiol 2000;278:F667–75.
[396] Potter DW, Hinson JA. Reactions of N-acetyl-p-benzoquinoneimine with reduced glutathione, acetaminophen and NADPH. Mol Pharmacol 1986;30:33–41.
[397] Price PM, Megyesi J, Safirstein RL. Cell cycle regulation: repair and regeneration in acute renal failure. Semin Nephrol 2003;23:449–59.
[398] Rabb H, Daniels F, O'Donnell M, Haq M, Saba SR, Keane W, et al. Pathophysiological role of T lymphocytes in renal ischemia-reperfusion injury in mice. Am J Physiol Renal Physiol 2000;279:F525–31.
[399] Racusen LC, Solez K, Colvin RB, Bonsib SM, Castro MC, Cavallo T, et al. The Banff 97 working classification of renal allograft pathology. Kidney Int 1999;55:713–23.
[400] Ramaswamy D, Corrigan G, Polhemus C, Boothroyd D, Scandling J, Sommer FG, et al. Maintenance and recovery stages of postischemic acute renal failure in humans. Am J Physiol Renal Physiol 2002;282:F271–80.
[401] Ramsammy LS, Josepovitz C, Kaloyanides GJ. Gentamicin inhibits agonist stimulation of the phosphatidylinositol cascade in primary cultures of rabbit proximal tubular cells and in rat renal cortex. J Pharmacol Exp Ther 1988;247:989–96.
[402] Ramsammy LS, Josepovitz C, Lane B, Kaloyanides GJ. Effect of gentamicin on phospholipid metabolism in cultured rabbit proximal tubular cells. Am J Physiol 1989;256:C204–13.
[403] Ramsammy LS, Josepovitz C, Lane BP, Kaloyanides GJ. Polyaspartic acid protects against gentamicin nephrotoxicity in the rat. J Pharmacol Exp Ther 1989;250:149–53.
[404] Ramsammy LS, Josepovitz C, Ling KY, Lane BP, Kaloyanides GJ. Effects of diphenyl-phenylenediamine on gentamicin-induced lipid peroxidation and toxicity in rat renal cortex. J Pharmacol Exp Ther 1986;238:83–8.

[405] Ramsammy LS, Josepovitz C, Ling KY, Lane BP, Kaloyanides GJ. Failure of inhibition of lipid peroxidation by vitamin E to protect against gentamicin nephrotoxicity in the rat. Biochem Pharmacol 1987;36:2125–32.
[406] Randle PJ. Metabolic fuel selection: general integration at the whole-body level. Proc Nutr Soc 1995;54:317–27.
[407] Rao R, Patel S, Hao C, Woodgett J, Harris R. GSK3beta mediates renal response to vasopression by modulating adenylate cyclase activity. J Am Soc Nephrol 2010;21:428–37.
[408] Rao RV, Castro-Obregon S, Frankowski H, Schuler M, Stoka V, del Rio G, et al. Coupling endoplasmic reticulum stress to the cell death program. An Apaf-1-independent intrinsic pathway. J Biol Chem 2002;277:21836–42.
[409] Ratcliffe PJ, Endre ZH, Scheinman SJ, Tange JD, Ledingham JG, Radda GK. 31P nuclear magnetic resonance study of steady-state adenosine 5′- triphosphate levels during graded hypoxia in the isolated perfused rat kidney. Clin Sci 1988;74:437–48.
[410] Ravagnan L, Roumier T, Kroemer G. Mitochondria, the killer organelles and their weapons. J Cell Physiol 2002;192:131–7.
[411] Reimer KA, Ganote CE, Jennings RB. Alterations in renal cortex following ischemic injury. 3. Ultrastructure of proximal tubules after ischemia or autolysis. Lab Invest 1972;26: 347–63.
[412] Ribeiro L, de Assuncao e Silva F, Kurihara RS, Schor N, Mieko E, Higa S. Evaluation of the nitric oxide production in rat renal artery smooth muscle cells culture exposed to radiocontrast agents. Kidney Int 2004;65:589–96.
[413] Rich T, Allen RL, Wyllie AH. Defying death after DNA damage. Nature 2000;407:777–83.
[414] Romanov V, Noiri E, Czerwinski G, Finsinger D, Kessler H, Goligorsky MS. Two novel probes reveal tubular and vascular Arg-Gly-Asp (RGD) binding sites in the ischemic rat kidney. Kidney Int 1997;52:93–102.
[415] Rouse RL, Zhang J, Stewart SR, Rosenzweig BA, Espandiari P, Sadrieh NK. Comparative profile of commercially available urinary biomarkers in preclinical drug-induced kidney injury and recovery in rats. Kidney Int 2011;79:1186–97.
[416] Ruegg CE. The renal proximal tubule: factors influencing toxicity and ischaemic injury. In: Goldstein R, editor. Renal toxicity. New York: Elsevier; 1997. p. 245–62.
[417] Ruegg CE, Mandel LJ. Bulk isolation of renal PCT and PST. II. Differential responses to anoxia or hypoxia. Am J Physiol 1990;259:F176–85.
[418] Saad SY, Najjar TA, Daba MH, Al-Rikabi AC. Inhibition of nitric oxide synthase aggravates cisplatin-induced nephrotoxicity: effect of 2-amino–4-methylpyridine. Chemotherapy 2002;48:309–15.
[419] Sabolic I, Herak-Kramberger CM, Brown D. Subchronic cadmium treatment affects the abundance and arrangement of cytoskeletal proteins in rat renal proximal tubule cells. Toxicology 2001;165:205–16.
[420] Sabolic I, Ljubojevic M, Herak-Kramberger CM, Brown D. Cd-MT causes endocytosis of brush-border transporters in rat renal proximal tubules. Am J Physiol Renal Physiol 2002;283: F1389–402.
[421] Safirstein R, Miller P, Guttenplan JB. Uptake and metabolism of cisplatin by rat kidney. Kidney Int 1984;25:753–8.
[422] Safirstein R, Winston J, Goldstein M, Moel D, Dikman S, Guttenplan J. Cisplatin nephrotoxicity. Am J Kidney Dis 1986;8:356–67.
[423] Safirstein R. Am I my brother's keeper?: fratricide in the kidney. Kidney Int 2011;79:149–50.
[424] Salahudeen AK, Haider N, Jenkins J, Joshi M, Patel H, Huang H, et al. Antiapoptotic properties of erythropoiesis-stimulating proteins in models of cisplatin-induced acute kidney injury. Am J Physiol Renal Physiol 2008;294:F1354–65.
[425] Sandler DP, Smith JC, Weinberg CR, Buckalew VM, Dennis VW, Blythe WB, et al. Analgesic use and chronic renal failure. N Engl J Med 1989;320:1238–43.
[426] Sastrasinh M, Knauss TC, Weinberg JM, Humes HD. Identification of the aminoglycoside binding site in rat renal brush border membranes. J Pharmacol Exp Ther 1982;222: 350–8.
[427] Schlichting CL, Schareck WD, Weis M. Dendritic cell adhesion is enhanced on endothelial cells preexposed to calcineurin inhibitors. J Cardiovasc Pharmacol 2005;46:250–4.
[428] Schmitz C, Hilpert J, Jacobsen C, Boensch C, Christensen EI, Luft FC, et al. Megalin deficiency offers protection from renal aminoglycoside accumulation. J Biol Chem 2002;277:618–22.
[429] Schnellmann RG, Moks TJ, Mandel LJ, Lau SS. 2-bromohydroquinone-induced toxicity to rabbit proximal tubules: role of biotransformation, glutathione and covalent bonding. Toxicol Appl Pharmacol 1989;99:19–27.
[430] Schumer M, Colombel MC, Sawczuk IS, Gobe G, Connor J, O'Toole KM, et al. Morphologic biochemical, molecular evidence of apoptosis during the reperfusion phase after brief periods of renal ischemia. Am J Pathol 1992;140:831–8.
[431] Schurek HJ, Jost U, Baumgartl H, Bertram H, Heckmann U. Evidence for a preglomerular oxygen diffusion shunt in rat renal cortex. Am J Physiol 1990;259:F910–5.
[432] Schurek HJ, Kriz W. Morphologic and functional evidence for oxygen deficiency in the isolated perfused rat kidney. Lab Invest 1985;53:145–55.
[433] Schwarz C, Gruber U, Oberbauer R. Pathophysiology of acute renal failure at the cellular level. Wien Klin Wochenschr 2000;112:5–15.
[434] Schwarz C, Hauser P, Steininger R, Regele H, Heinze G, Mayer G, et al. Failure of BCL-2 up-regulation in proximal tubular epithelial cells of donor kidney biopsy specimens is associated with apoptosis and delayed graft function. Lab Invest 2002;82:941–8.
[435] Serino F, Grevel J, Napoli KL, Kahan BD, Strobel HW. Generation of oxygen free radicals during the metabolism of cyclosporine A: a cause-effect relationship with metabolism inhibition. Mol Cell Biochem 1993;122:101–12.
[436] Seth R, Yang C, Kaushal V, Shah SV, Kaushal GP. p53-dependent caspase-2 activation in mitochondrial release of apoptosis-inducing factor and its role in renal tubular epithelial cell injury. J Biol Chem 2005;280:31230–9.
[437] Shahabi V, van Rossum GDV. Transport pathways for therapeutic concentrations of lithium in rat liver. J Membr Biol 1999;172:101–11.
[438] Sharp DA, Lawrence DA, Ashkenazi A. Selective knockdown of the long variant of cellular FLICE inhibitory protein augments death receptor-mediated caspase-8 activation and apoptosis. J Biol Chem 2005;280:19401–9.
[439] Sharples EJ, Patel N, Brown P, Stewart K, Mota-Philipe H, Sheaff M, et al. Erythropoietin protects the kidney against the injury and dysfunction caused by ischemia-reperfusion. J Am Soc Nephrol 2004;15:2115–24.
[440] Shehata M, Cope GH, Johnson TS, Raftery AT, el Nahas AM. Cyclosporine enhances the expression of TGF-beta in the juxtaglomerular cells of the rat kidney. Kidney Int 1995;48:1487–96.
[441] Shemesh O, Golbetz H, Kriss JP, Myers BD. Limitations of creatinine as a filtration marker in glomerulopathic patients. Kidney Int 1985;28:830–8.
[442] Sheridan AM, Bonventre JV. Cell biology and molecular mechanisms of injury in ischemic acute renal failure. Curr Opin Nephrol Hypertens 2000;9:427–34.

[443] Sheridan AM, Bonventre JV. Pathophysiology of ischemic acute renal failure. Contrib Nephrol 2001;132:7–21.
[444] Shi Y. Mechanisms of caspase activation and inhibition during apoptosis. Mol Cell 2002;9:459–70.
[445] Shihab FS, Andoh TF, Tanner AM, Yi H, Bennett WM. Expression of apoptosis regulatory genes in chronic cyclosporine nephrotoxicity favors apoptosis. Kidney Int 1999;56: 2147–59.
[446] Shihab FS, Bennett WM, Yi H, Andoh TF. Expression of vascular endothelial growth factor and its receptors Flt–1 and KDR/Flk–1 in chronic cyclosporine nephrotoxicity. Transplantation 2001;72:164–8.
[447] Shimizu A, Yamanaka N. Apoptosis and cell desquamation in repair process of ischemic tubular necrosis. Virchows Arch B Cell Pathol Incl Mol Pathol 1993;64:171–80.
[448] Shimizu S, Narita M, Tsujimoto Y. Bcl-2 family proteins regulate the release of apoptogenic cytochrome c by the mitochondrial channel VDAC. Nature 1999;399:483–7.
[449] Siegel NJ, Devarajan P, Van Why S. Renal cell injury: metabolic and structural alterations. Pediatr Res 1994;36:129–36.
[450] Sigmon DH, Beierwaltes WH. Influence of nitric oxide derived from neuronal nitric oxide synthase on glomerular filtration. Gen Pharmacol 2000;34:95–100.
[451] Silverblatt FJ, Kuehn C. Autoradiography of gentamicin uptake by the rat proximal tubule cell. Kidney Int 1979;15:335–45.
[452] Simmons CF, Bogusky RT, Humes HD. Inhibitory effects of gentamicin on renal mitochondrial oxidative phosphorylation. J Pharmacol Exp Ther 1980;214:709–15.
[453] Skorecki KL, Rutledge WP, Schrier RW. Acute cyclosporine nephrotoxicity—prototype for a renal membrane signalling disorder. Kidney Int 1992;42:1–10.
[454] Somersan S, Bhardwaj N. Tethering and tickling: a new role for the phosphatidylserine receptor. J Cell Biol 2001;155:501–4.
[455] Spiegelberg BD, Xiong JP, Smith JJ, Gu RF, York JD. Cloning and characterization of a mammalian lithium-sensitive bisphosphate 3′-nucleotidase inhibited by inositol 1,4-bisphosphate. J Biol Chem 1999;274:13619–28.
[456] Stacchiotti A, Borsani E, Rodella L, Rezzani R, Bianchi R, Lavazza A. Dose-dependent mercuric chloride tubular injury in rat kidney. Ultrastruct Pathol 2003;27:253–9.
[457] Star RA. Intrarenal localization of nitric oxide synthase isoforms and soluble guanylyl cyclase. Clin Exp Pharmacol Physiol 1997;24:607–10.
[458] Steinmann B, Bruckner P, Superti-Furga A. Cyclosporin A slows collagen triple-helix formation *in vivo*: indirect evidence for a physiologic role of peptidyl-prolyl cis-trans-isomerase. J Biol Chem 1991;266:1299–303.
[459] Summers WK, Jamison RL. The no reflow phenomenon in renal ischemia. Lab Invest 1971;25:635–43.
[460] Supavekin S, Zhang W, Kucherlapati R, Kaskel FJ, Moore LC, Devarajan P. Differential gene expression following early renal ischemia/reperfusion. Kidney Int. 2003;63: 1714–24.
[461] Susin SA, Daugas E, Ravagnan L, Samejima K, Zamzami N, Loeffler M, et al. Two distinct pathways leading to nuclear apoptosis. J Exp Med 2000;192:571–80.
[462] Susin SA, Lorenzo HK, Zamzami N, Marzo I, Snow BE, Brothers GM, et al. Molecular characterization of mitochondrial apoptosis-inducing factor. Nature 1999;397:441–6.
[463] Sutton TA, Mang HE, Campos SB, Sandoval RM, Yoder MC, Molitoris BA. Injury of the renal microvascular endothelium alters barrier function after ischemia. Am J Physiol Renal Physiol 2003;285:F191–8.
[464] Sutton TA, Molitoris BA. Mechanisms of cellular injury in ischemic acute renal failure. Semin Nephrol 1998;18:490–7.
[465] Takada M, Nadeau KC, Shaw GD, Marquette KA, Tilney NL. The cytokine-adhesion molecule cascade in ischemia/reperfusion injury of the rat kidney. Inhibition by a soluble P-selectin ligand. J Clin Invest 1997;99:2682–90.
[466] Takada M, Nadeau KC, Shaw GD, Tilney NL. Prevention of late renal changes after initial ischemia/reperfusion injury by blocking early selectin binding. Transplantation 1997;64: 1520–5.
[467] Takahashi N, Hayano T, Suzuki M. Peptidyl-prolyl cis-trans isomerase is the cyclosporin A-binding protein cyclophilin. Nature 1989;337:473–5.
[468] Takiguchi M, Cherrington NJ, Hartley DP, Klaassen CD, Waalkes MP. Cyproterone acetate induces a cellular tolerance to cadmium in rat liver epithelial cells involving reduced cadmium accumulation. Toxicology 2001;165:13–25.
[469] Tariq M, Morais C, Sobki S, Al Sulaiman M, Al Khader A. N-acetylcysteine attenuates cyclosporin-induced nephrotoxicity in rats. Nephrol Dial Transplant 1999;14:923–9.
[470] Thadhani R, Pascual M, Bonventre JV. Acute renal failure. N Engl J Med 1996;334:1448–60.
[471] Thornberry NA. Caspases: a decade of death research. Cell Death Differ 1999;6:1023–7.
[472] Thornberry NA, Lazebnik Y. Caspases: enemies within. Science 1998;281:1312–6.
[473] Thurau K, Boylan JW. Acute renal success. The unexpected logic of oliguria in acute renal failure. Am J Med 1976;61:308–15.
[474] Timmer RT, Sands JM. Lithium intoxication. J Am Soc Nephrol 1999;10:666–74.
[475] Tonomura Y, Tsuchiya N, Torii M, Uehara T. Evaluation of the usefulness of urinary biomarkers for nephrotoxicity in rats. Toxicology 2010;273:53–9.
[476] Tonshoff B, Kaskel FJ, Moore LC. Effects of insulin-like growth factor I on the renal juxtamedullary microvasculature. Am J Physiol 1998;274:F120–8.
[477] Trump BF, Berezesky IK, Lipsky MM, Jones TW. Heterogeneity of the nephron: significance to nephrotoxicity. In: Bach PH, Lock EA, editors. Renal heterogeneity and target cell toxicity. Chichester, UK: John Wiley & Sons; 1985. p. 31–42.
[478] Trump BF, Goldblatt PJ, Stowell RE. Studies of mouse liver necrosis *in vitro*. Ultrastructural and cytochemical alterations in hepatic parenchymal cell nuclei. Lab Invest 1965;14: 1969–99.
[479] Trumper L, Monosterolo LA, Ellias MM. Nephrotoxicity of acetaminophen in male wistar rats: role of hepatically derived metabolites. J Pharmacol Exp Ther 1996;279:548–54.
[480] Tsukamoto T, Nigam SK. Tight junction proteins form large complexes and associate with the cytoskeleton in an ATP depletion model for reversible junction assembly. J Biol Chem 1997;272:16133–9.
[481] Tsuruya K, Ninomiya T, Tokumoto M, Hirakawa M, Masutani K, Taniguchi M, et al. Direct involvement of the receptor-mediated apoptotic pathways in cisplatin-induced renal tubular cell death. Kidney Int 2003;63:72–82.
[482] Ueda N, Kaushal GP, Shah SV. Apoptotic mechanisms in acute renal failure. Am J Med 2000;108:403–15.
[483] Ueda N, Shah SV. Role of endonucleases in renal tubular epithelial cell injury. Exp Nephrol 2000;8:8–13.
[484] Vaidya VS, Ozer JS, Dieterle F, Collings FB, Ramirez V, Troth S, et al. Kidney injury molecule-1 outperforms traditional biomarkers of kidney injury in preclinical biomarker qualification studies: supplementary data. Nature Biotech 2010;28:478–85.
[485] Vaidya VS, Ozer JS, Dieterle F, Collings FB, Ramirez V, Troth S, et al. Kidney injury molecule-1 outperforms

traditional biomarkers of kidney injury in preclinical biomarker qualification studies. Nature Biotechnology 2010;28: 478–85.
[486] van de Straat R, Vromans RM, Bosman P, De Vries J, Vermeulen NPE. Cytochrome P–45r0 mediated oxidation of substrates by electron transfer: role of oxygen radicals and 1- and 2-electron oxidation of paracetamol. Chem Biol Interact 1988;64:267–80.
[487] Van Vleet TR, Schnellmann RG. Toxic nephropathy: environmental chemicals. Semin Nephrol 2003;23:500–8.
[488] Varfolomeev EE, Ashkenazi A. Tumor necrosis factor: an apoptosis JuNKie? Cell 2004;116:491–7.
[489] Vaux DL. Toward an understanding of the molecular mechanisms of physiological cell death. Proc Natl Acad Sci U S A 1993;90:786–9.
[490] Vaux DL, Silke J. HtrA2/Omi, a sheep in wolf's clothing. Cell 2003;115:251–3.
[491] Vaux DL, Weissman IL, Kim SK. Prevention of programmed cell death in Caenorhabditis elegans by human bcl-2. Science 1992;258:1955–7.
[492] Velazquez H, Perazella MA, Wright FS, Ellison DH. Renal mechanism of trimethoprim-induced hyperkalemia. Ann Intern Med 1993;119:296–301.
[493] Verhagen AM, Ekert PG, Pakusch M, Silke J, Connolly LM, Reid GE, et al. Identification of DIABLO, a mammalian protein that promotes apoptosis by binding to and antagonizing IAP proteins. Cell 2000;102:43–53.
[494] Vesey DA, Cheung C, Pat B, Endre Z, Gobe G, Johnson DW. Erythropoietin protects against ischaemic acute renal injury. Nephrol Dial Transplant 2004;19:348–55.
[495] Vieira Jr JM, Noronha IL, Malheiros DM, Burdmann EA. Cyclosporine-induced interstitial fibrosis and arteriolar TGF-beta expression with preserved renal blood flow. Transplantation 1999;68:1746–53.
[496] Wada T, Pippin JW, Marshall CB, Griffin SV, Shankland SJ. Dexamethasone prevents podocyte apoptosis induced by puromycin aminonucleoside: role of p53 and Bcl-2–related family proteins. J Am Soc Nephrol 2005;16:2615–25.
[497] Walker PD, Shah SV. Gentamicin enhanced production of hydrogen peroxide by renal cortical mitochondria. Am J Physiol 1987;253:C495–9.
[498] Walker R, Weggery S, Bedford J, McDonald F, Ellis G, Leader J. Lithium-induced reduction in urinary concentrating ability and urinary aquaporin 2 (AQP2) excretion in healthy volunteers. Kidney Int 2005;67:291–4.
[499] Walker RJ, Fawcett JP. Drug nephrotoxicity: the significance of cellular mechanisms. Prog in Drug Res 1993;41:3–45.
[500] Walker RJ, Lazzaro VA, Duggin GG, Horvath JS, Tiller DJ. Cyclosporin A inhibits protein kinase C activity: a contributing mechanism in the development of nephrotoxicity? Biochem Biophys Res Commun 1989;160:409–15.
[501] Walker RJ, Lazzaro VA, Duggin GG, Horvath JS, Tiller DJ. Evidence that alterations in renal metabolism and lipid peroxidation may contribute to cyclosporine nephrotoxicity. Transplantation 1990;50:487–92.
[502] Walker RJ, Lazzaro VA, Duggin GG, Horvath JS, Tiller DJ. Structure-activity relationships of cyclosporines. Inhibition of angiotensin II-stimulated prostaglandin release in cultured rat mesangial cells. Transplantation 1990;50:343–5.
[503] Walker RJ, Lazzaro VA, Duggin GG, Horvath JS, Tiller DJ. Structure-activity relationships of cyclosporines. Toxicity in cultured renal tubular epithelial cells. Transplantation 1989;48: 321–7.
[504] Walker RJ, Lazzaro VA, Duggin GG, Horvath JS, Tiller DJ. Synergistic toxicity of cyclosporin A and streptomycin in renal epithelial cell cultures. Res Commun Chem Pathol Pharmacol 1988;62:447–60.
[505] Walker RJ, Weggery S, Bedford JJ, McDonald FJ, Ellis G, Leader JP. Lithium induced reduction in urinary concentrating ability and urinary aquaporin 2 (AQP2) excretion in healthy volunteers. Kidney Int 2005;67:291–4.
[506] Wang A, Holcslaw T, Bashore TM, Freed MI, Miller D, Rudnick MR, et al. Exacerbation of radiocontrast nephrotoxicity by endothelin receptor antagonism. Kidney Int 2000;57:1675–80.
[507] Wang A, Schwab SJ. Reply from the authors. Kidney Int 2000;58:2239.
[508] Wang W, Reeves WB, Ramesh G. Netrin-1 and kidney injury. I. Netrin-1 protects against ischemia-reperfusion injury of the kidney. Am J Physiol Renal Physiol 2008;294:F739–47.
[509] Watarai Y, Morita K, Shimoda N, Miura M, Yoshioka M, Togashi H, et al. Effect of tacrolimus and cyclosporine on renal microcirculation and nitric oxide production. Transplant Proc 2004;36:2130–2.
[510] Wei Q, Dong G, Yang T, Megyesi J, Price PM, Dong Z. Activation and involvement of p53 in cisplatin-induced nephrotoxocity. Am J Physiol Renal 2007;293:F1282–91.
[511] Weidemann A, Bernhardt WM, Klanke B, Daniel C, Buchholz B, Câmpean V, et al. HIF activation protects from acute kidney injury. J Am Soc Nephrol 2008;19:486–94.
[512] Weight SC, Nicholson ML. Nitric oxide and renal reperfusion injury: a review. Eur J Vasc Endovasc Surg 1998;16: 98–103.
[513] Weinberg JM. The role of cell calcium overload in nephrotoxic renal tubular cell injury. Am J Kidney Dis 1986;8:284–91.
[514] Weinberg JM, Davis JA, Venkatachalam MA. Cytosolic-free calcium increases to greater than 100 micromolar in ATP-depleted proximal tubules. J Clin Invest 1997;100:713–22.
[515] Weinberg JM, Harding PG, Humes HD. Mechanisms of gentamicin-induced dysfunction of renal cortical mitochondria. II. Effects on mitochondrial monovalent cation transport. Arch Biochem Biophys 1980;205:232–9.
[516] Westenfelder C. Earlier diagnosis of acute kidney injury awaits effective therapy. Kidney Int 2011;79:1159–61.
[517] Westhuyzen J, Endre ZH, Reece G, Reith DM, Saltissi D, Morgan TJ. Measurement of tubular enzymuria facilitates early detection of acute renal impairment in the intensive care unit. Nephrol Dial Transpl 2003;18:543–51.
[518] Williams PD, Hottendorf GH, Bennett DB. Inhibition of renal membrane binding and nephrotoxicity of aminoglycosides. J Pharmacol Exp Ther 1986;237:919–25.
[519] Wirthensohn G, Guder WG. Renal lipid metabolism. Miner Electrolyte Metab 1983;9:203–11.
[520] Wirthensohn G, Guder WG. Renal substrate metabolism. Physiol Rev 1986;66:469–97.
[521] Wu H, Craft ML, Wang P, Wyburn KR, Chen G, Ma J, et al. IL-18 contributes to renal damage after ischemia-reperfusion. J Am Soc Nephrol 2008;19:2331–41.
[522] Wu X, Molinaro C, Johnson N, Casiano CA. Secondary necrosis is a source of proteolytically modified forms of specific intracellular autoantigens: implications for systemic autoimmunity. Arthritis Rheum 2001;44:2642–52.
[523] Wu XC, Richards NT, Johns EJ. Role of erythropoietin and nitric oxide in modulating the tone of human renal interlobular and subcutaneous arteries from uraemic subjects. Clin Sci (Colch) 1999;97:639–47.
[524] Wyllie A. Apoptosis. An endonuclease at last. Nature 1998;391: 20–1.
[525] Wyllie AH. Glucocorticoid-induced thymocyte apoptosis is associated with endogenous endonuclease activation. Nature 1980;284:555–6.

[526] Wyllie AH, Kerr JF, Currie AR. Cell death: the significance of apoptosis. Int Rev Cytol 1980;68:251–306.
[527] Xu K, Tavernarakis N, Driscoll M. Necrotic cell death in C. elegans requires the function of calreticulin and regulators of Ca^{2+} release from the endoplasmic reticulum. Neuron 2001;31:957–71.
[528] Yamamoto T, Tada T, Brodsky SV, Tanaka H, Noiri E, Kajiya F, et al. Intravital videomicroscopy of peritubular capillaries in renal ischemia. Am J Physiol Renal Physiol 2002;282:F1150–5.
[529] Yang CW, Faulkner GR, Wahba IM, Christianson TA, Bagby GC, Jin DC, et al. Expression of apoptosis-related genes in chronic cyclosporine nephrotoxicity in mice. Am J Transplant 2002;2:391–9.
[530] Yang CW, Kim YS, Kim J, Kim YO, Min SY, Choi EJ, et al. Oral supplementation of L-arginine prevents chronic cyclosporine nephrotoxicity in rats. Exp Nephrol 1998;6:50–6.
[531] Ylikoski J, Xing-Qun L, Virkkala J, Pirvola U. Blockade of c-Jun N-terminal kinase pathway attenuates gentamicin-induced cochlear and vestibular hair cell death. Hear Res 2002;166: 33–43.
[532] Yonezawa A, Inui KI. Organiic cation transporter OCT/SLC22A and (H +)/organic cation trnasporter MATE?SLC47A are key molecules for nephrotoxicity of platinum agents. Biochem Pharmcol 2011;81:563–8.
[533] Young BA, Burdmann EA, Johnson RJ, Alpers CE, Giachelli CM, Eng E, et al. Cellular proliferation and macrophage influx precede interstitial fibrosis in cyclosporine nephrotoxicity. Kidney Int 1995;48:439–48.
[534] Ysebaert DK, De Greef KE, De Beuf A, Van Rompay AR, Vercauteren S, Persy VP, et al. T cells as mediators in renal ischemia/reperfusion injury. Kidney Int 2004;66:491–6.
[535] Yu SW, Wang H, Poitras MF, Coombs C, Bowers WJ, Federoff HJ, et al. Mediation of poly(ADP-ribose) polymerase-1–dependent cell death by apoptosis-inducing factor. Science 2002;297:259–63.
[536] Yu Y, Jin H, Holder D, Ozer JS, Villarreal S, Shughrue P, et al. Urinary biomarkers trefoil factor 3 and albumin enable early detection of kidney tubular injury. Nature Biotech 2010;28:470–7.
[537] Zager RA, Fuerstenberg SM, Baehr PH, Myerson D, Torok-Storb B. An evaluation of antioxidant effects on recovery from postischemic acute renal failure. J Am Soc Nephrol 1994;4: 1588–97.
[538] Zalups RK. Molecular interactions with mercury in the kidney. Pharmacol Rev 2000;52:113–43.
[539] Zalups RK, Ahmad S. Molecular handling of cadmium in transporting epithelia. Toxicol Appl Pharmacol 2003;186: 163–88.
[540] Zenser TV, Davis BB. Enzyme systems involved in the formation of reactive metabolites in the renal medulla: cooxidation via prostaglandin H synthase. Fundam Appl Toxicol 1984;4:922–9.
[541] Zenser TV, Mattammal MB, Herman CA, Joshi S, Davis BB. Effect of acetaminophen on prostaglandin E2 and prostaglandin F2alpha synthesis in the renal inner medulla of rat. Biochim Biophys Acta 1978;542:486–95.
[542] Zenser TV, Mattammal MB, Rapp NS, Davis BB. Effect of aspirin on metabolism of acetaminophen and benzidine by renal inner medulla prostaglandin hydroperoxidase. J Lab Clin Med 1983;101:58–65.
[543] Zhang B, Ramesh G, Norbury CC, Reeves WB. Cisplatin-induced nephrotoxicity is mediated by tumor necrosis factor-[alpha] produced by renal parenchymal cells. Kidney Int 2007;72:37–44.
[544] Zhang JG, Lindup WE. Cisplatin nephrotoxicity: decreases in mitochondrial protein sulphydryl concentration and calcium uptake by mitochondria from rat renal cortical slices. Biochem Pharmacol 1994;47:1127–35.
[545] Zhang WV, Jullig M, Connolly AR, Stott NS. Early gene response in lithium chloride induced apoptosis. Apoptosis 2005;10:75–90.
[546] Zhou BB, Chaturvedi P, Spring K, Scott SP, Johanson RA, Mishra R, et al. Caffeine abolishes the mammalian g2/M DNA damage checkpoint by inhibiting ataxia-telangiectasia-mutated kinase activity. J Biol Chem 2000;275:10342–8.
[547] Zhou J, Alcorn D, Harris PJ, Mendelsohn FAO. Localisation and properties of angiotensin II receptors in rat kidney. Kidney Int 1993;44(Suppl 42):S40–6.
[548] Ziegler K, Frimmer M, Fritzsch G, Koepsell H. Cyclosporin binding to a protein component of the renal Na^{+}-D-glucose cotransporter. J Biol Chem 1990;265:3270–7.
[549] Zoja C, Angioletti S, Donadelli R, Zanchi C, Tomasoni S, Binda E, et al. Shiga toxin-2 triggers endothelial leukocyte adhesion and transmigration via NF-kappaB dependent up-regulation of IL-8 and MCP-1. Kidney Int 2002;62:846–56.
[550] Zou AP, Cowley Jr. AW. Nitric oxide in renal cortex and medulla. An *in vivo* microdialysis study. Hypertension 1997;29:194–8.
[551] Zou H, Henzel WJ, Liu X, Lutschg A, Wang X. Apaf-1, a human protein homologous to C. elegans CED-4, participates in cytochrome c-dependent activation of caspase-3. Cell 1997;90:405–13.
[552] Zou H, Li Y, Liu X, Wang X. An APAF-1.cytochrome c multimeric complex is a functional apoptosome that activates procaspase-9. J Biol Chem 1999;274:11549–56.
[553] Zuk A, Bonventre JV, Brown D, Matlin KS. Polarity, integrin, extracellular matrix dynamics in the postischemic rat kidney. Am J Physiol 1998;275:C711–31.
[554] Zunino F, Pratesi G, Micheloni A, Cavalletti E, Sala F, Tofanetti O. Protective effect of reduced glutathione against cisplatin-induced renal and systemic toxicity and its influence on the therapeutic activity of the antitumor drug. Chem Biol Interact 1989;70:89–101.

CHAPTER

86

Role of Glomerular Mechanical Stress in the Pathogenesis of Chronic Kidney Disease

Clarice Kazue Fujihara and Roberto Zatz

Renal Division, Department of Clinical Medicine, Faculty of Medicine of the University of São Paulo, Brazil

DETERMINANTS OF GLOMERULAR ULTRAFILTRATION AND HOW THEY ARE INFLUENCED BY THE GLOMERULAR ARTERIOLES

The notion that derangements of glomerular dynamics may exert a deleterious effect and play a role in the pathogenesis of chronic kidney disease (CKD) is relatively recent, having been first postulated in a coherent way in the early 1980s.[1,2] This formulation was made possible after the determinants of glomerular ultrafiltration were directly measured in micropuncture experiments, and theoretically analyzed by Brenner, Deen and co-workers in the late 1960s and early 1970s.[3,4]

The ultrafiltration process at each glomerulus is governed by four independent physical determinants:[4] the first and most important of them is the glomerular transcapillary hydraulic pressure difference, ΔP, defined by the expression, $\Delta P = P_{GC} - P_{BS}$, where P_{GC} represents the glomerular intracapillary hydraulic pressure and P_{BS} denotes the hydraulic pressure in Bowman's space. The second determinant is the plasma protein concentration at the afferent arteriole (C_A), which is nearly identical to the systemic plasma protein concentration and determines the oncotic force that opposes filtration. The third determinant is the initial glomerular plasma flow (Q_A); and the fourth determinant is the glomerular hydraulic conductance coefficient (K_f). Variations of ΔP and Q_A cause changes in the same direction in SNGFR, whereas the relationship between SNGFR and K_f is more complex: although a decrease of K_f below normal lowers SNGFR, an increase of K_f has limited effect on ultrafiltration. A more detailed description of these determinants, of their individual effects, and of the relationship between them is given in Chapter 21.

Two of the determinants of ultrafiltration, ΔP and Q_A, are directly affected by variations of the afferent (R_A) and efferent (R_E) arteriolar resistances, as well as by changes in systemic blood pressure. The deep influence of these vessels on the dynamics of ultrafiltration derives from the unusual arrangement of the glomerular microcirculation, with the capillary loops interposed between the afferent and efferent arteriolar resistors (Fig. 86.1). If we assume the hydraulic pressure at the end of the efferent arteriole (P_E) to be much lower than the mean arterial pressure (MAP), and neglect the effect of fluid escape from the glomerular capillaries through ultrafiltration, the glomerular intracapillary hydraulic pressure (P_{GC}) can be approximated by:

$$P_{GC} = MAP \times R_E / (R_A + R_E) \qquad (86.1)$$

It becomes clear from this ultra-simplified equation that P_{GC}, and therefore ΔP, varies simultaneously with MAP and with the ratio between R_E and the total glomerular arteriolar resistance. An arterial pressure elevation, with R_A and R_E kept constant, would be accompanied, still in accordance with Equation 86.1, by a proportional elevation of P_{GC}. Such situation is seldom observed, because autoregulatory mechanisms make R_A change in the same direction as the change of MAP or, more specifically, of the renal perfusion

Seldin and Giebisch's The Kidney, Fifth Edition.
DOI: http://dx.doi.org/10.1016/B978-0-12-381462-3.00086-0

© 2013 Elsevier Inc. All rights reserved.

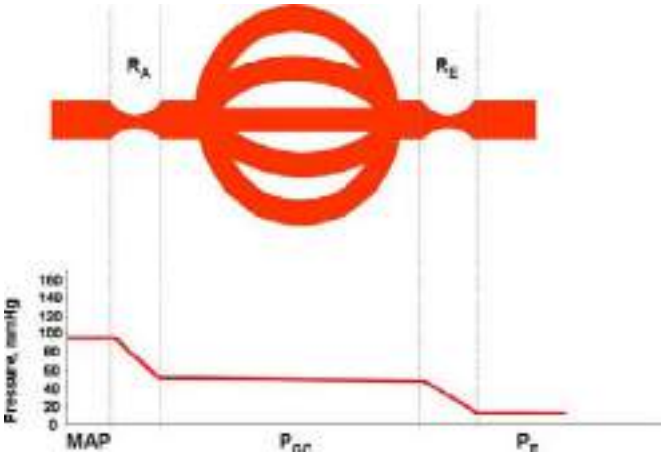

FIGURE. 86.1 Schematic representation of the glomerular microcirculation. MAP, mean arterial pressure; R_A, afferent arteriolar resistance; R_E, efferent arteriolar resistance; P_{GC}, glomerular hydraulic pressure; P_E, hydraulic pressure at the end of the efferent arteriole.

pressure (Chapters 21 and 24). On the other hand, changes in the glomerular arteriolar resistances can deeply influence SNGFR and its determinants. A decrease in R_A, with MAP kept constant, will elevate P_{GC}, still as predicted by Equation 86.1, whereas the opposite will occur if R_A increases. The consequences of changing the preglomerular resistance are not limited to the P_{GC}, since in a hydraulic system consisting of series resistors, such as the glomerular microcirculation, variations of one of the resistances will always promote reciprocal variations of flow. Specifically, Q_A can be approximated by the expression:

$$Q_A = MAP/(R_A + R_E) \times (1 - Ht) \qquad (86.2)$$

where Ht denotes the arterial hematocrit. Thus, a decrease of R_A will augment Q_A, while the reverse will occur if R_A increases. Since as noted above an analogous relationship exists between R_A and P_{GC}, and since SNGFR is a direct function of both Q_A and ΔP,[4] it follows that variations of R_A always promote changes of SNGFR in the opposite direction.

The effect of R_E on SNGFR is more complex than that of R_A, because of the peculiar location of the efferent resistor. An increase of R_E tends to increase P_{GC} (and ΔP), approaching its value to that of MAP, as predicted by Equation 86.1. Conversely, a decrease of R_E tends to bring P_{GC} close to zero, or more precisely, to the low pressure of the postglomerular microcirculation. On the other hand, an increase of R_E, as in the case of R_A, tends to diminish Q_A, as predicted by Equation 86.2, while the opposite will be seen with a decrease in R_E. Thus changes of R_E promote opposite effects in P_{GC} (and ΔP) and Q_A. If R_E is brought to very low values, ΔP may fall to critical levels (close to the plasma oncotic pressure), reducing SNGFR to values that approach zero, regardless of the value of Q_A. As R_E increases above these critically low values, SNGFR rises very steeply, since the positive effect on P_{GC} (and ΔP) largely compensates its initially small negative effect on Q_A. This effect reaches a maximum at R_E values that are within the normal range, since further efferent vasoconstriction will promote no additional increase of SNGFR and may even diminish it, because Q_A will be reduced in such a way as to offset the elevation of P_{GC}.

In view of the above considerations, it becomes clear that the pre and postglomerular resistors exert quite different functions. The monotonic inverse relationship between R_A and the SNGFR renders the afferent resistance ideally suited to function as a regulator of the glomerular microcirculation. Indeed, variations of R_A can entirely account for renal *autoregulation*, which keeps GFR, renal plasma flow and ΔP within narrow ranges in the face of wide variation of systemic blood pressure.[5] Although variations of R_E appear unsuited to intervene in the process of regulation of the glomerular microcirculation, the efferent arteriole is essential for the glomerular ultrafiltration process to occur. The mere existence of the efferent arteriole, acting as a "postcapillary sphincter," allows the glomerular capillaries to maintain much higher hydraulic pressures than in other microcirculatory territories, which is a physical requirement for high-grade ultrafiltration to occur. If R_E is decreased to critically low values, which may happen for instance in patients with bilateral renal artery stenosis treated with inhibitors of the renin-angiotensin system or angiotensin II receptor blockers, a catastrophic fall of SNGFR occurs, and acute renal failure can ensue.[6]

The GFR is Fairly Constant Under Physiologic Conditions—But There are Exceptions

Under physiologic conditions, there is little need for the GFR to vary very much, since the balance of water and solutes such as sodium, chloride and potassium is achieved by the action of the tubules, especially at the final portions of the nephron. In fact, GFR is tightly controlled by autoregulatory mechanisms, which involve mostly variations of the afferent arteriolar resistance, more suitable to this task, as pointed out earlier. These variations of R_A are thought to be achieved by local myogenic reflexes and by signals generated at the macula densa.[5,7]

In states of decreased effective arterial volemia such as in dehydration, the GFR can be brought to very low values, even in the absence of kidney injury, as part of the organism's effort to conserve salt and water. Such an effect is accomplished by arteriolar vasoconstriction and mesangial cell contraction, with consequent reduction of K_f.[8,9]

In contrast with the promptness with which GFR can be reduced whenever necessary, there is usually little need to promote a substantial *increase* of the GFR. However, there are a few notable exceptions to this rule. Expansion of the extracellular volume, besides promoting tubular rejection of fluid and electrolytes, can increase GFR through the action of atrial natriuretic peptides.[10,11] Ingestion of a single protein-rich meal can acutely increase the GFR by 30–50% in humans and in laboratory animals,[12,13] an effect that can be replicated by intravenous infusion of amino acids in rats,[14–16] and that is thought to represent an adaptation to the need to excrete the protein catabolites more readily.[1,17] A sustained increase of GFR, of similar magnitude as in the acute experiments, can be obtained by chronic feeding of a high-protein diet.[18–20] This change in GFR involves approximately proportional dilatation of both the afferent and efferent arterioles and consequent augmentation of Q_A, without elevation of P_{GC} and ΔP, as predicted by Equation 86.1.[20,21] Normal pregnancy is another physiologic situation characterized by augmented GFR.[22–24] As with high-protein feeding, the GFR increase observed during pregnancy is due to commensurate decreases of R_A an R_E, resulting in increased Q_A without elevation of ΔP.[23,24] These changes are entirely reversible, but will recur with every subsequent pregnancy in the same individual, with no cumulative effect.[25]

Single Nephron Hyperfiltration is a Prominent Feature of Chronic Kidney Disease

From the original description of chronic kidney disease (CKD) by Richard Bright in the XIXth century until the 1950s, it was generally believed that the kidneys affected by chronic disease simply ceased to function as a whole, thereafter becoming essentially unable to maintain homeostasis or to adapt to that unfavorable condition. In 1952, Robert Platt proposed that the functional disturbances encountered in renal disease result from progressive reduction in the number of functioning nephrons rather than from the separate impairment of glomerular or tubular functions of all nephrons.[26] He suggested that, as the number of nephrons diminishes, the remaining units undergo functional hypertrophy, in such a way that impairment of renal function is easily overlooked initially, becoming apparent only at relatively advanced stages of the disease. Bricker and colleagues[27,28] carried this concept a step further by showing that, in an experimental model of CKD, glomerular and tubular functions decreased in parallel, but function per nephron was increased, suggesting that whole nephrons were indeed disappearing as functional units, forcing the surviving nephrons to undergo vicarious hypertrophy. Bricker and coworkers coined the expression *intact nephron hypothesis* to define this concept, which has survived, with some modifications, up to the present day.

In the 1920s and 1930s, Addis had already postulated that increased "workload" to the kidneys, originating from excess protein intake and/or unilateral kidney removal, led to compensatory functional and structural hypertrophy of the remaining renal tissue.[29] The nephron hypertrophy implied by the intact nephron hypothesis was in keeping with this notion of compensatory whole kidney hypertrophy. However, it was not until the early 1980s that a detailed physiologic basis was constructed to explain the mechanisms by which this nephron adaptation might take place. In 1981, Hostetter, Rennke and Brenner[30] demonstrated that five-sixths renal ablation (by removal of the right kidney and infarction of two thirds of the contralateral one), standardized a few years earlier by Shimamura[31] as a model of progressive glomerulopathy, promoted a striking increase of SNGFR, confirming the earlier predictions of compensatory nephron hyperfiltration upon loss of renal parenchyma. These investigators went on to demonstrate that hyperfiltration was due to the combination of systemic hypertension with a pronounced dilatation of the glomerular microvessels, especially the afferent arteriole. As a consequence of this predominant decrease of R_A, and in keeping with Equations 86.1 and 86.2, there were marked increases of Q_A, P_{GC} and ΔP, leading to a corresponding increase of SNGFR, partially offset by a mild reduction of K_f. Similar results were later reported by the same group in a different model of glomerular injury, the DOC-salt model, in which uninephrectomy is associated with dietary salt overload and mineralocorticoid excess.[32]

Glomerular Hyperfiltration in Diabetes Mellitus

Renal mass reduction is not the only pathologic instance in which SNGFR is chronically increased. In type 1 diabetic patients not yet afflicted by the long-term complications of the disease, but in which metabolic control is poor, GFR tends to increase by 30 to 40% compared to the normal population, an abnormality that is accompanied by a proportional increase in kidney size.[33–35] Renal hypertrophy involves mostly the enlargement of glomeruli, whose size may double, although tubular hypertrophy is also prominent in these subjects. Although the mechanisms responsible for the renal hypertrophy in diabetes are presently unknown, a physiological basis for hyperfiltration in this setting is well established. In 1981, Hostetter and coworkers[36] showed that in rats made diabetic with streptozotocin there is vasodilatation of both the

afferent and efferent arterioles, with ample predominance of the former, in a similar manner as in compensatory single nephron hyperfiltration. As a consequence, both Q_A and ΔP are increased, thus promoting hyperfiltration even in the absence of systemic hypertension. These findings were later confirmed in the same laboratory[37,38] and elsewhere.[39–41] In diabetic patients, hyperfiltration and hyperperfusion can be easily demonstrated, but direct determination of P_{GC} is not possible. However, indirect estimates obtained from measurement of filtration fraction suggest that glomerular hypertension does accompany human diabetes as well.[42,43]

A large body of evidence indicates that glomerular hyperfiltration also occurs in patients with type 2 diabetes mellitus;[44–46] although its prevalence is lower than among type 1 diabetic patients,[47] and its very existence was questioned in some earlier reports.[48,49] Hyperfiltration has also been shown in experimental models of type 2 diabetes.[50,51] It must be noted that analysis of renal hemodynamics in these patients is clouded by the concomitant occurrence of cardiovascular abnormalities, which tend to compromise large arteries, including the renal arteries and their branches, along with the cardiac function. In addition, the exact time of onset of type 2 diabetes is often uncertain, allowing diabetic and/or ischemic nephropathy to develop, and GFR to decline substantially from initially elevated levels.

THE "HYPERFILTRATION HYPOTHESIS" AND THE PROGRESSIVE NATURE OF CHRONIC KIDNEY DISEASE

The consistent finding that nephron hyperfiltration antecedes, and even predicts, the development of renal injury in clinical and experimental CKD prompted the hypothesis, formulated by Brenner and coworkers, that a causal relationship existed between abnormal glomerular hemodynamics and the development of progressive glomerular damage. In the original version of this *hyperfiltration hypothesis*,[1] it was postulated that the presence of heightened flows *and* pressures at the glomerular capillaries would promote mechanical aggression to the fragile capillary walls, triggering a process of progressive injury of the glomerular tuft that would eventually result in its complete destruction. In addition, the concept of compensatory nephron hyperfunction implied that glomerular dropout would impose an ever-increasing burden on the remaining units, aggravating the existing mechanical stress and closing a vicious circle that would perpetuate the process of renal parenchymal destruction.

Besides offering a plausible explanation for the well-known progressive behavior of CKD, the hyperfiltration hypothesis formulated in the early 1980s fitted well with a series of findings reported elsewhere. A few years earlier, Steffes and coworkers[52] had demonstrated that the severity of diabetic nephropathy was aggravated in rats also subjected to uninephrectomy, presumably through exacerbation of hyperfiltration in the remaining kidney. In a prior study of the same laboratory, it had been shown that in diabetic rats subjected to unilateral renal artery clipping, diabetic nephropathy was prevented in the clipped side, and aggravated in the contralateral kidney.[53] Accordingly, ipsilateral protection from diabetic nephropathy in patients with unilateral renal artery stenosis has been reported.[54,55]

The practical implications of the hyperfiltration hypothesis were evident, since it opened the tangible possibility that chronic damage to the renal parenchyma by diabetes or progressive nephron loss could be treated by maneuvers aimed at lessening the associated abnormalities of glomerular dynamics. A few seminal studies developed by Brenner and associates showed that this goal was indeed attainable. Hostetter et al.[30] showed that the early structural abnormalities associated with 5/6 nephrectomy in rats were abrogated by administration of a low-protein diet, a maneuver that normalized SNGFR, Q_A and ΔP. Zatz and associates[20] obtained similar amelioration of glomerular dynamics, and equal renoprotection, in diabetic rats that received a low-protein diet for one year. These observations appeared to confirm the hyperfiltration hypothesis and, at the same time, the possibility of changing the natural course of CKD by measures distinct from treatment of hypertension or the metabolic disturbance of diabetes, then the only therapeutic resources available.

Glomerular Hypertension is the Relevant Pathogenic Factor Linking Hyperfiltration to Glomerular Damage

Although the hyperfiltration hypothesis initially seemed to explain convincingly the clinical and experimental findings obtained theretofore, it was soon challenged by a series of apparently inconsistent observations. The predictive value of GFR in relation to diabetic nephropathy was not confirmed in a number of clinical studies.[56,57] In addition, long-term observations in subjects that had undergone uninephrectomy showed only mild and non-progressive proteinuria and arterial hypertension,[58,59] or even no abnormality at all,[60] compared with the general population. Likewise, no renal injury was associated even with

multiple successive pregnancies in rats, in which GFR is expectedly increased,[25] a finding in keeping with clinical observations in multiparous women.[61] Other studies showed that it was possible to ameliorate glomerular injury in the 5/6 renal ablation model without reducing GFR.[62] Other attempts at preventing the progression of CKD, though successful, were not entirely consistent with the hyperfiltration hypothesis. In rats subjected to five-sixths nephrectomy and treated with the then brand new ACE inhibitor, enalapril, the associated glomerulosclerosis was largely prevented. However, enalapril failed to normalize GFR or Q_A, although it did normalize glomerular pressure.[63,64] Similar results were subsequently reported in the streptozotocin-diabetes model,[37–38] and confirmed elsewhere. In view of these results, it was no longer possible to bundle together glomerular hyperfiltration, hyperperfusion and hypertension as a pathogenic mechanism of chronic glomerular injury. It became necessary to modify the hyperfiltration hypothesis to reconcile it with the evidence that glomerular hypertension, rather than the hypertension/hyperperfusion/hypertension trio, represented the actual physical mechanism promoting long-term glomerular capillary injury. The designation "Hyperfiltration hypothesis," though still widely employed, should therefore be replaced by more precise expressions such as "Hemodynamic hypothesis," or "Hemodynamic theory."

THE IMPORTANCE OF GLOMERULAR HYPERTROPHY AND THE CONCEPT OF MECHANICAL AGGRESSION

During the second half of the 1980s, a series of clinical and experimental observations showed that enlargement of the glomerular tuft, a "nonhemodynamic" abnormality, was consistently associated with the development of progressive glomerular injury.[65–69] Several of these studies suggested that the development of glomerulosclerosis was more closely associated with glomerular hypertrophy than with glomerular hypertension. A study in proteinuric pediatric patients showed that glomerular size predicted the development of focal and segmental glomerulosclerosis,[70] while several experimental observations showed either the development of glomerulosclerosis without glomerular hypertension or the converse.[66–69] These observations gave rise to a "hypertrophy theory," which was initially regarded by many as a better alternative to the hemodynamic theory. However, evidence obtained during subsequent years failed to lend support to this "hypertrophy theory." Some of these studies corroborated the earlier observations of a tight association between glomerular hypertension and glomerular injury.[37,39,71] In others, the relationship between glomerular hypertrophy and glomerular injury was rather inconsistent.[72–74] However, it became clear, in the years that ensued, that the hypertrophy and hemodynamic theories were not at all irreconcilable, and that the two mechanisms must act in concert, rather than separately, to promote glomerular injury. The physical basis for such interaction becomes apparent when we consider the local forces that act on the glomerular filtration surface, shown in simplified form in Fig. 86.2. The presence of a transcapillary hydraulic pressure difference, ΔP, imposes a continuous mechanical stretch to the glomerular wall. According to Laplace's law,[65] the wall tension, T, equals the product of the pressure gradient, ΔP, and the capillary radius, R. An elevation of ΔP will promote a proportional increase of T and, therefore, of the mechanical stretch to which the components of the glomerular wall are subjected.[65] On the other hand, enlargement of the glomerular tuft will increase the capillary radius, R, augmenting T in exactly the same way as would an elevation of ΔP. Thus, while glomerular hypertension can conceivably promote capillary damage in the absence of tuft hypertrophy, mechanical injury to the glomerular capillary wall can in principle occur without elevation of ΔP. Accordingly, it is hardly surprising that the association of the two abnormalities can accelerate glomerular injury.[75,76]

Cellular Mechanisms by Which Mechanical Stretch Can Injure the Glomerular Wall

Stretching of the glomerular capillary wall by intracapillary hypertension or tuft hypertrophy would be expected to promote only localized, non-progressive injury if the resulting physical forces were the only factors at operation. However, the glomerular tuft is not constituted solely by inert elements such as collagen fibers: injury to endothelial cells, mesangial cells and podocytes trigger a series of events that together conspire to extend and amplify the initial mechanical aggression, as will be discussed in the paragraphs that follow.

FIGURE. 86.2 Schematic and simplified representation of the wall tension, T, generated by the glomerular transcapillary pressure difference (ΔP) at the walls of a cylindrical capillary with radius R. According to Laplace's law, T is directly proportional to both parameters.

Endothelial cells are sensitive to mechanical strain, undergoing changes of shape and increasing their rate of proliferation when exposed to axial stretch *in vitro*.[77] Subjecting these cells to prolonged strain *in vivo* may result in severe damage,[78] which can even promote disintegration or detachment, leading to local denudation of the glomerular basement membrane, with consequent exposure of extracellular matrix constituents to the circulatory stream. The resulting activation/aggregation of platelets, with fibrin accumulation, may favor the formation of intracapillary microthrombi, leading to luminal obliteration.[72] With subsequent organization of this material, the glomerular tuft can become partially or totally fibrotic.[72] Microaneurysms, which have been reported in several experimental models characterized by severe glomerular hypertension, may undergo a similar process of organization.[32,79,80]

The *mesangial cells* possess a complex cytoskeleton[81] that may be affected by mechanical stretch transmitted from the capillary filtration surface.[82] A number of *in vitro* experiments have brought evidence that, when subjected to such strain, cultured mesangial cells undergo a series of phenotype changes, increasing their proliferative activity and synthesizing a number of molecules involved in inflammatory phenomena—cytokines, growth factors, adhesion molecules and cyclooxygenase products.[83–87] In addition, mechanical stretch stimulates the production of collagen fibers,[87] thus favoring the development of fibrosis and contributing to the progressive destruction of the glomerular tuft. Heightened intracapillary pressure can promote additional mesangial injury by driving circulating macromolecules, including immunoglobulins and complement components, into the mesangial region, where they may accumulate, thus contributing to irritate the mesangial cells and to maintain an inflammatory environment at a local level.[88] Such movement is facilitated by the fact that the mesangial region is not covered by glomerular basement membrane, being separated from the circulatory stream only by the fenestrated endothelial layer.[82]

Among the native glomerular cells, the *podocytes* are perhaps the most likely to suffer phenotypic changes upon exposure to mechanical strain. These cells lie amidst a very complex molecular setup, with a myriad of intricate connections between cytoskeleton constituents, such as actin, myosin and α-actinin, and those of the slit membrane, such as nephrin and p-cadherin.[82,89,90] Conceivably, any disturbance of such a delicate arrangement can disrupt this complicated structure, leading to simplification of the foot processes, rupture of the slit membrane, and impairment of the glomerular barrier function, with ensuing proteinuria.[91,92] Because podocytes are terminally differentiated cells, they possess limited proliferative capacity, being unable to adapt to the increased capillary dimensions imposed by glomerular hypertension and/or hypertrophy.[93–95] Thus, the inevitable mechanical strain associated with these conditions can promote podocyte rupture, death by apoptosis or necrosis, and detachment from the basement membrane, resulting in denudation of its outermost aspect.[96–98] The latter is likely to favor the fixation of the glomerular tuft to the parietal layer of Bowman's capsule, leading to the formation of synechiae, from which a local process of sclerosis may arise and spread to a glomerular segment, to the whole tuft, and/or to the adjacent interstitium.[93–95,99] Additional damage can result from leakage to the interstitium, through this adhesion spot, of plasma ultrafiltrate, with limited hindrance to the passage of proteins, given the local absence of foot processes or slit membranes. This "misdirected filtration" (Fig. 86.3)[100,101] may lead to accumulation of fluid relatively rich in protein at the vicinity of the glomerulus or, if abundant enough, around extensive parts of the respective tubular segments. Inflammation and

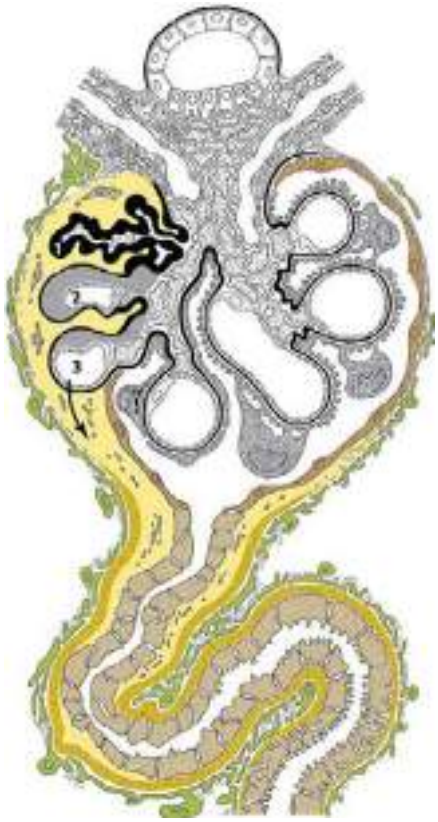

FIGURE. 86.3 Schematic illustration of the consequences of localized podocyte loss, with capillary loops adhering to Bowman's capsule and becoming hyalinized, while fluid leaking through the damaged glomerular walls infiltrates between the nephron (glomerular tuft and tubule) and the adjacent interstitium. Organization of this material may lead to progressive destruction of the nephron. (*Reproduced with permission from ref. [100].*)

subsequent organization of this initially amorphous layer may lead to ensheathing of substantial parts of that particular nephron, which can eventually be sectioned by the fibrotic process, and even disintegrate.[99,100]

As mentioned earlier, mechanical strain of the podocyte layer may lead to disruption of the glomerular filtration barrier, with the passage of large amounts of protein to the urinary space and the appearance of proteinuria, a well-known hallmark of glomerular injury. As a consequence, the protein reabsorption rate of the proximal tubular cells increases markedly, in an attempt at recovering the filtered protein, thus limiting the urinary protein loss. To perform this task, cells must digest the reabsorbed protein, intensifying the formation of endosomes and the synthesis of proteolytic enzymes. Several investigators believe that prolonged exposure of proximal tubular cells to this situation can trigger a process of interstitial fibrosis, which contributes strongly to accelerate the progression of the nephropathy. A number of clinical studies[102–104] support this hypothesis by showing a direct relationship between the proportion of patients with glomerulopathies that progress to end-stage renal disease and the level of proteinuria at the time of diagnosis.

Although other investigators note that these findings could merely reflect a natural association between the intensity of proteinuria and the severity of the underlying glomerular disease,[105] numerous experimental studies have provided more direct evidence that abnormal passage of proteins to the urinary space can indeed favor interstitial inflammation and fibrosis. When cultured in albumin-rich medium, proximal tubular cells produce significant amounts of cytokines and chemokines.[106–109] Accordingly, interstitial fibrosis, inflammation, and markers of oxidative stress were found in association with heavy proteinuria in congenital nephrotic syndrome.[110] Together, these findings indicate that glomerular injury with impairment of the filtration barrier can be indirectly propagated to the interstitium, amplifying the resulting renal damage. However, there is evidence that this mechanism may be of limited importance or may become active only at advanced stages of CKD. In two experimental models of proteinuric CKD, Kriz[99] showed that chronic injury was confined to individual nephrons, rather than being disseminated, as would be expected if increased glomerular passage of proteins were a major pathogenic factor in this setting. In addition, Theilig and coworkers[111] studied mutant mice in which proximal reabsorption of protein was severely limited due to deficient expression of megalin, an essential element for protein endocytosis to work properly. Although the presence of inflammatory markers did associate with protein uptake, tubulointerstitial injury correlated with glomerular damage to the parental glomerular tuft, rather than to the local inflammatory activity. Thus, despite evidence favoring the inflammatory effect of filtered protein, the role of impairment of the glomerular barrier in the pathogenesis of interstitial fibrosis in CKD remains open to question.

From Stretch-Induced Injury to Progressive Nephropathy: the Role of Inflammation

As remarked earlier, progressive nephron loss promotes or aggravates mechanical strain in the remaining units, thus contributing to the establishment of a vicious cycle that leads to further nephron destruction. An additional crucial factor for CKD perpetuation is the presence of inflammatory events, a common denominator to all cellular mechanisms discussed in the preceding paragraphs. The participation of inflammatory phenomena in the pathogenesis of nephropathies of *immunologic* injury has been known for decades.[112] Tissue infiltration by macrophages and fibroblasts has been regarded as a natural follow-up of such events as activation of T-lymphocytes and of the complement cascade.[113] Evidence obtained since the late 1980s in human nephropathies and, especially, in experimental models of CKD, showed that these phenomena are also important as promoters of chronic renal injury not mediated by immune mechanisms, especially those induced by mechanical strain. The presence of inflammatory cells has been described in several models of progressive renal injury, such as streptozotocin-induced diabetes mellitus,[114–116] aging nephropathy,[117–119] chronic NO inhibition,[120–122] experimental nonimmune nephrotic syndrome[123] and protein-overload proteinuria.[124]

Floege and coworkers[125–127] reported that, in rats with 5/6 renal ablation, by far the most widely utilized CKD model, renal interstitial lymphocyte infiltration, activated by unknown mechanisms, can be observed a few days after renal mass removal, when sclerosing glomerular lesions are still scarce. In the following days, the renal interstitium is progressively invaded by macrophages, while the intensity of the lymphocyte infiltration decreases. These findings were subsequently corroborated in other laboratories.[128–131] In addition, a surge of cell proliferation, mostly located at the tubulointerstitial compartment, is noted in these rats a few days after renal ablation, decreasing after two weeks, but persisting for at least two months.[128,127] The identity of these cells is uncertain, although it is conceivable that part of this proliferative activity may be related to the generation of myofibroblasts from either interstitial fibroblasts or tubular cells, the latter through epithelial-to-mesenchymal transdifferentiation.[132–134]

The recruitment of inflammatory cells into the renal parenchyma, and the proliferation of resident glomerular and tubular cells are crucially dependent on the production of inflammatory mediators. The presence in the renal parenchyma of a number of cytokines, chemokines and growth factors, such as interleukin-1, RANTES, fractalkine, TGF-β, MCP-1, TNF-α, and adhesion molecules, among many others, have been associated with several clinical conditions and experimental models of CKD,[107,114,135–139] along with evidence of activation of the intricate and often redundant intracellular pathways involved in the synthesis of these molecules.[132,140–143] An extensive analysis of the participation of these systems in the pathogenesis of CKD would transcend the scope of this chapter. Additional discussion of this subject can be found in Chapters 82, 87 and 90.

The importance of inflammatory phenomena in the pathogenesis of CKD is further highlighted by the protective effect exerted by anti-inflammatory agents. Fujihara and coworkers[128] reported that concomitant administration of mycophenolate mofetil (MMF), a specific inhibitor of lymphocyte proliferation, strongly attenuated renal inflammation and prevented glomerular and interstitial injury in the remnant kidney model, a finding also reported, almost simultaneously, by Romero and coworkers.[131] Renal protection by MMF monotherapy was also described in streptozotocin-induced diabetic rats[41] and in the chronic NO inhibition model,[120] and was strongly enhanced by association with a depressor of the renin-angiotensin system.[129,144–149] Interestingly, administration of non-steroidal anti-inflammatories exerted a protective effect in the remnant kidney model[130,150–152] and in experimental diabetes mellitus.[153] However, this class of drug is contraindicated in CKD due to the risk of precipitating a catastrophic fall of GFR (see below).

THE IMMENSE PATHOGENIC IMPORTANCE OF ANGIOTENSIN II IN CKD

As detailed in Chapter 15, Ang II is a potent vasoconstrictor agent, which binds to the AT-1 receptor, abundant in smooth muscle and mesangial cells.[154] By virtue of its vascular effects, Ang II contributes to the maintenance of blood pressure, especially in states of dehydration. This effect is strongly reinforced by the action of Ang II on sodium conservation, as a result of its effects on both the nephron itself, enhancing sodium reabsorption, and the adrenals, stimulating the release of aldosterone. At the glomerular microcirculation, Ang II constricts both the afferent and efferent arterioles.[154] However, this vasoconstrictor effect was shown to be disproportionally intense at the efferent arteriole,[155,156] a finding confirmed by *in vitro* studies of isolated afferent and efferent arterioles.[157,158] The reasons for this asymmetry are unclear, and may be related to the finding that Ang II stimulates vasoconstriction of the afferent arterioles through activation of voltage-gated (L-type) calcium channels, whereas Ang II–mediated vasoconstriction of the efferent arteriole depends mainly on mobilization of calcium from intracellular stores.[159–161] Ang II also promotes contraction of the mesangial cells,[9,162] with a consequent reduction of the glomerular K_f. The predominant efferent vasoconstriction leads to an elevation of P_{GC}. However, since K_f decreases, and since Q_A is depressed due to the arteriolar vasoconstriction, the SNGFR remains relatively constant during Ang II infusions,[163,155] with consequent increase of the filtration fraction (FF). Recent evidence has shown that the renin-angiotensin system is much more complex than originally thought, and that novel components of this system may have physiologic importance. Angiotensin 1–7, a heptapeptide generated by the action of angiotensin I converting enzyme 2 (ACE2), exerts a vasodilatory effect and may modulate the action of Ang II.[164] Likewise, activation of the AT2 receptor by Ang II can initiate a series of events that culminate in vasodilatation and natriuresis, thus antagonizing the vasoconstrictor/antinatriuretic effects elicited by Ang II binding to the AT1 receptor.[164] However, the exact physiologic role of angiotensin 1–7, the AT2 receptor and other, less known components of the renin-angiotensin system is presently unclear.

Chronic nephron loss tends to promote extracellular expansion due to a natural limitation to sodium excretion.[165,166] In this setting, there is a trend toward renal vasodilatation, while the circulating levels of renin and angiotensin II tend to be depressed, reflecting inhibition of renal renin release to the circulation.[165] On the other hand, abundant evidence has been amassed in the past two decades that a large number of organs and tissues, including the kidneys, possess all the components of the renin-angiotensin system, being able to produce Ang II locally in an independent fashion.[167–169] The combination of renal arteriolar vasodilatation with local production of Ang II, which as noted above acts preferentially on R_E, may result in disproportionate decrease of R_A, leading to simultaneous increases of Q_A and ΔP and, as a result, to single nephron hyperfiltration.

In diabetes mellitus, the circulating levels of renin and angiotensin II tend to be reduced,[37,170] which might favor hyperperfusion and hyperfiltration in these individuals. On the other hand, there is evidence that the renin-angiotensin system may be activated at the intrarenal level in early experimental diabetes,[171,172]

which may help to explain the relatively modest fall in R_E observed in this condition, which favors, as we have seen, the elevation of P_{GC}, hence glomerular injury. The reasons for the local and systemic derangement of the renin-angiotensin system in diabetes mellitus are yet to be elucidated.

The intrinsic action of Ang II on glomerular hemodynamics in CKD and in early diabetes mellitus is unveiled by the striking effect of treatment with angiotensin-converting enzyme inhibitors (ACEIs) or angiotensin II receptor type 1 blockers (ARBs), which promote dilatation of afferent and efferent arterioles, as well as normalization of glomerular pressure,[37–39,63,64,173,174] without significant changes of SNGFR. Thus it is beyond doubt that Ang II exerts a pathogenic effect on the glomerulus, which may favor the installation of tuft injury by the mechanisms discussed above. However, the scope of action of Ang II is now known to largely transcend the hemodynamic sphere, characterizing this octapeptide as a potent proinflammatory cytokine.[175,176] Chronic systemic Ang II infusion in rats was shown to promote not only arterial hypertension, but also glomerular and interstitial infiltration by mononuclear cells and severe renal fibrosis.[177,178] Ang II was subsequently shown to influence cell proliferation,[179,180,181] and the synthesis of a number of cytokines, chemokines, growth factors and adhesion molecules, all of which exert an obvious pathogenic impact on the progression of CKD, such as RANTES,[182] MCP-1,[176,183] osteopontin,[184] tumor necrosis factor-α (TNF-α),[178] CTGF[185] and PDGF,[186] among others. These actions are largely mediated by Ang II binding to the AT1 receptor,[179,187,188] which stimulates several intracellular pathways linked to inflammation, especially the NF-κB cascade[176,189] and the MAPK and Stat/Jnk pathways.[143,187] One of the main proinflammatory effects of Ang II is mediated by its strong stimulation of TGF-β, a well-known promoter of fibrosis in the renal tissue, as well as in other territories.[190,191] Furthermore, *in vitro* exposure of mesangial cells to Ang II can increase the production of superoxide anions and induce oxidative stress, a well-known promoter of inflammation.[192] Likewise, *in vivo* Ang II infusion enhances the production of oxidation markers such as thiobarbituric acid–reactive substances and protein carbonyl,[193] as well as 8-iso prostaglandin F2α.[194] Ang II can further contribute to CKD by one of its classical nonhemodynamic actions, the production of aldosterone by the adrenals. Aldosterone has been shown to increase collagen IV synthesis by mesangial cells,[195] and to facilitate the progression of CKD in the renal and myocardial tissue, independent of Ang II.[196,197] Plasma aldosterone concentrations are strikingly elevated in partially nephrectomized rats.[196,198] Conversely, mineralocorticoid receptor blockade, alone or associated with ACE inhibitors or Ang II receptor blockers, reduces glomerulosclerosis and proteinuria in several CKD models, further suggesting a pathogenic role for the stimulation of the mineralocorticoid receptor.[199,200] Ang II can provide additional contribution to renal damage by increasing glomerular permeability,[201–203] thus promoting tubulointerstitial damage through the mechanisms discussed earlier. An important evidence of the pathogenic role of Ang II is the demonstration, by immunohistochemistry and/or by immunofluorescence, that Ang II associates with infiltrating cells at inflamed areas of the renal interstitium in several models of CKD,[128,130,131,204] as well as in biopsy material obtained from CKD patients.[205,206] In these studies, the intensity of tissue infiltration by Ang II-positive cells correlated directly with the extent and severity of interstitial inflammation. A more direct link between Ang II and glomerular mechanical strain was unraveled by the finding that, when subjected to cyclical stretching, mesangial cells upregulate components of the renin-angiotensin system.[207–209] Thus, the glomerular action of Ang II may lead to a vicious cycle, in that Ang II elevates P_{GC}, which promotes mechanical stress, stimulating further Ang II production and setting in motion its many pro-inflammatory actions.

Given the plethora of hemodynamic and nonhemodynamic actions of Ang II, it is far from surprising that treatment with ACE inhibitors or Ang II receptor blockers prevents or attenuates renal injury in several forms of clinical and experimental CKD.[37,63,64,80,174,210–212] Although several promising novel therapeutic strategies have been proposed in the past two decades, administration of depressors of the renin-angiotensin system remains a mainstay of the therapy of CKD, along with diuretics, other antihypertensives and glycemic control in diabetics. However, CKD patients who receive these drugs still progress to ESRD, albeit at a slower rate,[210–212] particularly when treatment is initiated at advanced stages of the disease. The reasons why the protection offered by these drugs is incomplete are obscure. It is likely that several of the complex and interrelated intracellular pathways that culminate in the synthesis of inflammatory mediators are activated by physical and chemical events distinct from the Ang II-AT1 interaction, such as oxidative stress and the binding of a number of cytokines and growth factors to specific receptors. Of particular interest is the recent discovery that prorenin, once regarded as an inert precursor of renin, binds to a specific receptor, undergoing a nonproteolytic conformational change that enables prorenin to cleave angiotensinogen to angiotensin I.[213,214] In addition, binding of prorenin to this receptor activates several intracellular proinflammatory pathways.[215,216] This receptor can also be activated by renin through the binding of an epitope

shared with prorenin. For this reason, this receptor became known as the (pro)renin receptor.[214,217] Recent evidence suggests that blockade of this receptor with a specific antagonist prevents the progression of experimental diabetic nephropathy,[218] suggesting that this may become a new strategy in the management of CKD.

THE ROLE OF OTHER VASOACTIVE COMPOUNDS IN GLOMERULAR MECHANICAL STRAIN

Circulating Catecholamines and Renal Sympathetic Innervation

As with Ang II, the glomerular microcirculation is exquisitely sensitive to the vasoconstrictor activity of the sympathetic system and of its circulating mediators. Different from Ang II, however, norepinephrine induces vasoconstriction of both afferent and efferent arterioles,[156,157,219] an effect thought to be mediated by α-adrenergic receptors[219] and to depend at least in part on variations of intracellular calcium, especially at the efferent arterioles.[161] Acute catecholamine action results in systemic hypertension and, given the proportionate increases in pre- and postglomerular resistances, a corresponding elevation of glomerular pressure. Because the overall resistance of the glomerular microcirculation increases, glomerular blood flow is diminished. The net result of these changes is, as observed with Ang II, maintenance of GFR at relatively constant levels.[156] In addition to its direct effect on the glomerular vessels, the renal sympathetic inflow has been long known to stimulate renin exocytosis from the juxtaglomerular cells through activation of β1-adrenergic receptors, an effect that enhances the sympathetic action on blood pressure, sodium reabsorption, and the glomerular microcirculation,[220] and can contribute to cause glomerular injury through the mechanisms discussed above. Recent studies indicate that sympathetic activity and, in particular, the sympathetic inflow to the kidneys, are enhanced in CKD.[221] Increased renal sympathetic stimulation has been implicated in the pathogenesis of hypertension in CKD[222] and in the remnant kidney model,[223] while renal denervation has been shown to lower systemic blood pressure in murine hypertension, underlining the important influence exerted by the sympathetic innervation on the renal vasculature and on sodium reabsorption.[220,224] Additional complexity derives from the finding of two types of sympathetic nerve fibers in the kidney,[225] with differential innervation of the afferent and efferent arterioles.

Nitric Oxide

Nitric oxide (NO) was originally identified about a quarter century ago as a powerful endogenous vasodilator produced from L-arginine by endothelial cells, under the action of NO synthases (NOS), and soon proven to be responsible for the vasodilator effect of compounds such as acetylcholine, histamine and bradykinin.[226,227] Besides being a potent vasodilator, NO inhibits cell proliferation and platelet aggregation, which helps to preserve the endothelial integrity.[228,229] Although NO was originally described as a product of the endothelial cells, it became soon clear that it can be synthesized by mesangial cells, smooth muscle cells, tubular cells and leukocytes, among other cell types.[230–232] Because NO is very diffusible and highly reactive, it quickly combines with other free radicals or is taken away by hemoglobin.[233] In view of these characteristics, which are shared by other reactive species such as superoxide, NO has a short-lived effect, confined to the immediate surroundings of the cells in which it is produced, and must be generated uninterruptedly if it is to play any significant physiologic role.

A number of experimental studies suggest that continuous NO production is fundamental for the circulatory system to function properly. Acute intravenous administration of unselective NOS inhibitors promotes a quick and marked elevation of systemic blood pressure, in addition to a pronounced constriction of renal microvessels,[234–236] while P_{GC} rises and Q_A and K_f are decreased. As a result of these opposing changes, the SNGFR is little affected. These findings are strongly reminiscent of the effect of acute Ang II infusions,[155,156] and suggest that NO may be needed as a modulator of the effect of Ang II and other vasoconstrictors.[237] The individual role of the main isoforms of NOS is unclear. Acute selective inhibition of neuronal NOS (nNOS), which is strongly expressed at the macula densa,[238,239] lowers GFR without affecting blood pressure or renal blood flow.[240] Parallel results were obtained after perfusion of the macula densa with a NO synthase inhibitor.[241] These findings suggest a regulatory role for nNOS. However, chronic nNOS inhibition was reported to raise blood pressure without changing GFR.[242] Inhibition of the inducible isoform of NO synthase (iNOS) has not been reported to promote consistent changes of renal or systemic hemodynamics under physiologic conditions,[243,244] being more closely related to the operation of the innate immunity and of inflammatory mechanisms.[243,245,246] The current evidence suggests that the endothelial NOS isoform (eNOS) accounts for most of the modulation of renal and systemic hemodynamics ascribed to NO.[247]

Chronic inhibition of NO production promotes abnormalities of glomerular hemodynamics that are

qualitatively similar to those elicited by acute NO inhibition,[80,248] with the development of severe and progressive systemic and glomerular hypertension, besides intense renal vasoconstriction. After a few weeks of treatment, these rats exhibit glomerular ischemic and sclerotic injury, renal interstitial inflammation and vascular damage suggestive of malignant hypertension. Together, these findings indicate that NO exerts an indispensable tonic vasodilatation on renal and systemic microvessels, and that its absence may lead to severe cardiovascular and renal injury.

Evidence obtained in several studies suggests that changes in NO production can participate in the pathogenesis of deranged glomerular dynamics in CKD. Administration of inhibitors of NO synthase limits the hyperfiltration observed in experimental diabetes mellitus, suggesting that excessive renal production NO may be one of the mediators of the associated renal hemodynamic derangement.[249–251] In subnephrectomized rats, 24-hour urinary excretion of nitrites and nitrates, taken as a surrogate marker of NO production, is significantly decreased.[252,253] Similarly, in humans with chronic kidney disease (CKD), Schmidt and Baylis showed that urinary nitrites/nitrates excretion is diminished.[254] These observations suggest that CKD is a state of NO deficiency. One of the possible causes of impaired NO synthesis in CKD is the abnormal production in the circulation of a potent endogenous competitive inhibitor of NOS, asymmetric dimethyl-L-arginine (ADMA). The presence of this compound was demonstrated in animal models of CKD,[255,256] as well as in CKD patients.[254,257–259] The finding of elevated ADMA levels at early phases of CKD suggests that subtle degrees of NO deficiency may be one of the primary factors causing glomerular hemodynamic dysfunction and leading to progression of renal injury. On the other hand, inhibition of NO aggravates kidney injury in subnephrectomized rats,[79,260] in association with glomerular and peritubular endothelial cell loss,[260] with consequent development of microthrombosis and glomerulosclerosis.[79] Conversely, in partially nephrectomized rats, administration of the substrate for NO synthesis, L-arginine, prevented the decrease of GFR and renal blood flow, and reduced the severity of glomerulosclerosis.[261] These observations suggest that endogenous NO still exerts a protective role even after the development of CKD, and point to a potential therapeutic use of NO-releasing drugs,[262] although solid evidence in favor of this concept is lacking.

Prostanoids

Prostanoids are 20-carbon compounds derived from arachidonic acid through the action of two cyclooxygenase (COx) isoforms, COx-1, said to be "constitutive," and COx-2, initially considered as being "inducible." Subsequent research showed that both isoforms are active in normal subjects and should be considered "constitutive".[263–265] Although acute administration of vasodilator prostanoids such as prostacyclins and PGE2 can induce the synthesis of cyclic AMP and exert a pronounced effect on glomerular circulation and on sodium excretion,[8,266] acute inhibition of prostaglandin synthesis in normal rats does not affect GFR or glomerular hemodynamics,[267,268] indicating little tonic activity of these compounds.[269] Likewise, the use of COx inhibitors as anti-inflammatories or painkillers usually promotes little or no change of renal function in most individuals,[270] although adverse cardiovascular and renal effects such as sodium retention, hypertension and vascular injury may occur in a minority of patients treated chronically with these compounds.[271]

Although the effects of COx inhibitors in normal subjects are relatively mild, the vasodilator prostanoids exert an important physiologic role by modulating the action of the renal sympathetic innervation and of circulating vasoconstrictors such as catecholamines and Ang II.[8,163,272] For this reason, the use of COx inhibitors in situations in which there is exacerbation of vasoconstrictor activity, such as in states of volume depletion or contraction of the effective arterial volume, may promote exaggerated vasoconstriction and even the development of acute kidney injury.[271,272]

The thromboxanes, the main representative of which is Thromboxane A2, are potent renal vasoconstrictors, which act through activation of phospholipase C and elevation of the intracellular calcium levels, antagonizing the effects of the vasodilator prostanoids. The thromboxanes also have an important function in hemostasis through platelet activation. Despite the intensity of their vascular effects, the thromboxanes, as in the case of vasodilator prostanoids, exert little effect on renal hemodynamics under physiologic conditions.[273]

A number of observations suggest that vasodilator prostanoids may participate in the pathogenesis of CKD and early diabetic nephropathy by mediating at least part of the attending hemodynamic changes. The renal expression of COx-2 is increased in experimental diabetes mellitus,[153] and may contribute to the renal vasodilatation observed in this condition.[274] Likewise, renal mass ablation increases fractional urinary excretion of both vasodilator and vasoconstrictor prostaglandins in rodents.[267,268,275,276] In partially nephrectomized rats, indomethacin lowers both SNGFR and renal blood flow.[267,268] Together, these observations suggest that increased activity of cyclooxygenase derivatives may contribute to maintain the glomerular hemodynamic

changes encountered in CKD models. However, a different picture emerges when the synthesis of prostanoids is blocked on a chronic basis in rats with renal ablation. Chronic treatment of subnephrectomized rats with either an unselective or a COx-2 selective cyclooxygenase inhibitor, starting on the day following renal mass removal, led to a mild fall in glomerular pressure,[150,151] without change of GFR. Two months after renal ablation, renal injury was markedly attenuated in rats treated with the COx inhibitors. These observations suggest that prostanoids can act as mediators of progressive kidney injury through nonhemodynamic mechanisms, possibly related to inhibition of renal inflammatory mechanisms. These findings are difficult to translate into clinical practice, however, because, as just noted, increased prostanoid synthesis may be one of the mediators of single nephron hyperfiltration in CKD patients. Therefore, COx inhibition may abrogate this adaptive mechanism, leading to a sudden and dangerous fall of GFR in a substantial proportion of these subjects,[272] a finding that is paralleled in experimental models of CKD.[275] Thus, the use of COx inhibitors is better avoided in CKD.

Endothelin

Endothelin (ET), synthesized mostly, but not exclusively, by endothelial cells, is the most potent known vasoconstrictor. Experimental evidence indicates that ET constricts the afferent and efferent arterioles in proportion, without a clear predominance of one or another.[277–279] As a result, Q_A falls, while P_{GC} remains approximately constant, although higher doses may raise glomerular pressure.[280] Despite its vasoconstrictor potency, the physiologic role of ET in the regulation of the renal microcirculation is uncertain, because acute or chronic administration of ET inhibitors has little effect on glomerular microcirculation and renal function.[281] Equally unclear is the participation of ET in CKD. In rats subjected to partial nephrectomy, Benigni and coworkers reported an increase in the urinary excretion of the best-known ET isoform, ET-1,[282] and in the expression of the ET-1 gene.[283] Moreover, thrombin stimulated ET-1 secretion in glomeruli isolated from remnant kidneys, an effect that was absent in glomeruli isolated from intact kidneys,[282] raising the possibility that endothelins are involved in the alterations of glomerular hemodynamics seen after nephron loss. These investigators also showed that treatment with an ET inhibitor was renoprotective in the remnant kidney model, although a hemodynamic mechanism for this effect was not demonstrated.[284] In streptozotocin diabetic rats, chronic ET receptor blockade caused glomerular vasodilatation and limited hyperfiltration, despite a simultaneous increase of renal plasma flow, suggesting that glomerular pressure was reduced, although direct measurement of this parameter was not performed. In the long run, diabetic nephropathy was largely prevented in treated rats.[285]

Atrial Natriuretic Peptide

Atrial natriuretic peptide (ANP) is released mostly from the atrial wall, usually in response to extracellular volume expansion. As a result, the kidneys excrete a large amount of sodium, which tends to bring the hemodynamic status back to normal. This potent natriuretic effect stems from hemodynamic and nonhemodynamic renal actions. ANP promotes dilatation of the afferent arteriole and constriction of the efferent arteriole,[10,11] a unique effect among vasoactive substances, with resulting elevation of P_{GC} despite a concomitant fall of arterial pressure, which reflects systemic vasodilatation. Since Q_A is also increased due to the predominance of the afferent dilatation, SNGFR increases, augmenting the amount of sodium that reaches the tubules.[10] ANP may also inhibit renal sodium reabsorption by direct action and/or by promoting disproportionate medullary hyperperfusion[286–288] thus amplifying the natriuretic effect of glomerular hyperfiltration.

The participation of ANP in the pathogenesis of the glomerular hemodynamic changes associated with CKD and diabetes is unclear. The plasma concentration of atrial natriuretic peptide (ANP) is elevated in partially nephrectomized rats on high-salt, but not on low-salt diets,[289] suggesting a potential role of ANP in the adaptive increase of single-nephron sodium excretion in this model of chronic kidney injury. In experimental diabetes, the plasma levels of atrial natriuretic peptide are elevated, and may contribute to the attending renal hemodynamic abnormalities.[290,291]

The Metabolic Derangement Itself May Promote Hyperfiltration in Diabetes Mellitus

Besides the possible role of prostaglandins and nitric oxide, discussed above, the glomerular hemodynamic abnormalities observed in early diabetes may be influenced by factors more directly related to the attending metabolic derangement. Acute glucose infusions have been reported to increase GFR in normal men,[292] and in diabetic subjects,[293] raising the possibility that hyperglycemia itself may promote hyperfiltration in diabetes. Other contributing factors may be the excessive production of some hormones that deeply influence carbohydrate metabolism, such as growth hormone[294] and glucagon.[274]

GENETIC AND ENVIRONMENTAL FACTORS CAUSING GLOMERULAR INJURY THROUGH MECHANICAL STRAIN

Nephron Number at Birth

The rate of progression of CKD shows enormous variability among individuals. In some patients GFR declines at over 10 mL/min/1,73 m^2/year, leading to the need for renal replacement therapy in a few years; other patients lose renal function at a rate that barely exceeds that expected from normal aging, while in others still CKD does not progress at all.[295] Apart from differences in the genetic background, one of the reasons for such variability may be that the number of nephrons at birth differs widely among individuals, ranging from 210,000 to 1,825,000 per kidney, with an average of 600,000–800,000.[296–298] Brenner and colleagues postulated that the fraction of the population possessing few nephrons at birth is predisposed to hypertension and renal damage in adult life compared with those with a normal or increased nephron endowment.[299,300] Several lines of evidence have provided support for this hypothesis. In a recent autopsy study, Keller et al. found a 50% reduction in the number of nephrons in hypertensive subjects, compared with matched normotensives, all of whom had died in accidents.[301] Of note, little signs of glomerular obsolescence were found in hypertensive subjects, ruling out the hypothesis that nephron deficiency was caused by hypertension, rather than causing it. In addition, glomerular volume was twice as high in hypertensive as in normotensive subjects, indicating compensatory growth. Expectedly, less subtle nephron number reduction at birth is also associated with renal injury in adulthood. Subjects with unilateral renal agenesis develop proteinuria and focal segmental sclerosis is often encountered in the solitary kidney.[59,302] In oligomeganephronia, a congenital disorder characterized by developmental arrest of the metanephric renal blastema, the total nephron number at birth is reduced to 20–25% of normal. These subjects develop proteinuria and glomerulosclerosis, reaching end-stage CKD during adolescence.[303,304]

The association of congenital reduction of the nephron number with progressive renal injury in adults is also observed in rodents, although genetic factors may modify this relationship.[305,306] Several investigators demonstrated that Ang II is essential for proper nephrogenesis, and that administration of ACE inhibitors or AT-1 receptor blockers to rat pups during the first three weeks after birth, before nephron formation is completed, led to severe reduction of the nephron number at weaning, followed by progressive CKD during adult life.[307–309] These findings were later extended by Machado and coworkers,[310] who showed that these rats developed glomerular enlargement and intracapillary hypertension at three months of age, as well as systemic hypertension, severe glomerulosclerosis and extensive interstitial inflammation at 10 months of age. Arterial hypertension and/or CKD are also associated with spontaneous congenital limitation of nephron number. In the rat model of male hypogonadism (hgn/hgn) with bilaterally hypoplastic kidneys, an 80% reduction of nephron number is associated with glomerular hypertension, hyperfiltration, proteinuria, glomerulosclerosis and progressive renal insufficiency.[311] Spontaneously hypertensive rats (SHR), Dahl salt-sensitive rats, Milan hypertensive rats and Munich Wistar Fromter rats have fewer nephrons than their respective normotensive counterparts, Wistar Kyoto rats, Dahl salt-resistant rats, Milan normotensive rats and Wistar rats.[312–315] Conversely, PVG/c rats exhibit a higher number of nephrons and develop no renal disease compared to Wistar rats.[316,317]

Although the concept that nephron number reduction at birth predisposes to CKD appears well founded, the relationship between nephron loss during adult life and the subsequent development of renal injury appears to be less clear-cut. Extensive nephrectomy—for example, in cases of renal tumors—does associate with proteinuria, progressive renal injury, and eventual need for renal replacement therapy.[318–320] However, as noted earlier in this chapter, lower grade renal mass reduction is not consistently associated with the development of CKD. Veterans who had lost a kidney due to trauma during the Second World War failed to show an increased prevalence of renal disease and progression of proteinuria 45 years later.[321] Moreover, individuals who donate a kidney for transplantation show no serious long-term renal problems apart from mild proteinuria.[58,322,323] This apparent incongruence between the consequences of congenital and acquired nephron loss is echoed in experimental studies. Ikoma and coworkers found that in rats that underwent renal ablation during maturational growth renal injury is more severe than in adult animals subjected to identical procedure.[324] Similar results were obtained by Okuda et al.[325] The reason for the striking influence of the time when nephrons are lost is unclear, and may relate to a complex relationship between nephron number and the ability to remodel the extracellular matrix.[326]

Obesity

Morbid obesity is associated with focal segmental glomerulosclerosis, an association known as obesity-related glomerulopathy (ORG).[327–329] This disease

seems to be both histologically and clinically distinct from idiopathic focal segmental glomerulosclerosis (FSGS). In ORG, a lower percentage of glomeruli is affected by segmental sclerosis, the degree of foot process effacement is less severe, glomerulomegaly is always present,[327] and edema is absent despite nephrotic-range proteinuria.[330] As in other conditions that may cause CKD, ORG is associated with a state of hyperfiltration and renal hyperperfusion,[331,332] although ΔP has not been determined in these subjects. In severely obese patients without overt kidney disease, Chagnac and coworkers found that renal blood flow and GFR decreased following gastroplasty and a decrease of BMI from 48 to 32.1 kg/m^2.[333,334] In addition to the increased risk of *de novo* development of CKD, excessive body weight is also a risk factor for CKD in patients with kidney mass reduction, such as after uninephrectomy,[335] kidney transplantation[336,337] or severe renal mass reduction,[338] suggesting that the effects of massive weight increase add to other insults to promote renal injury.

The renal impact of obesity has also been studied in animal models. Henegar and colleagues studied dogs with obesity induced by a high-fat diet, a model that mimics the neurohormonal changes in the early stages of human obesity.[339] Renal plasma flow and GFR were increased in these animals, an abnormality that was accompanied by glomerular hypertrophy, increased mesangial matrix, and thickening of glomerular basement membrane.[339] In another animal model, the Zucker obese rat, an initial increase of GFR was noted, followed by normalization and subsequent decrease of GFR, in association with progressive albuminuria and glomerulosclerosis.[340] In other studies of obese Zucker rats, GFR at 26 weeks of age was significantly higher than in lean Zucker rats, underlining once again the relationship between obesity and hyperfiltration. Of note, ΔP, which as noted earlier is the most important hemodynamic factor of glomerular damage, was also elevated in these rats.[341,342] These differences disappeared when obese Zucker rats were fed the same food amount as given to the lean controls.[343] Thus, massive obesity can initiate or aggravate glomerular disease, at least in part, by promoting alterations in glomerular hemodynamics and glomerular size. The mechanisms by which these abnormalities take place are currently unknown.

Tobacco

According to the MRFIT study, which included over 300,000 men, smoking increases the risk of end-stage renal kidney disease (ESRD) in the general male population. Compared to nonsmokers, the relative risk was 1.69 in heavy smokers.[344] In a longitudinal study over 18.5 years of over 2500 healthy subjects, the risk of ESRD was elevated in smokers (odds ratio [OR] 1.42).[345] The importance of smoking in the development of renal diseases is further illustrated by the observation in a large cross-sectional population study that current cigarette smoking was associated with a hazard ratio for CKD of 2.4 in men and 2.9 in women.[346] Smoking also increases the risk of nephropathy in diabetic[347] and nondiabetic patients.[348,349]

The mechanisms by which smoking could promote renal damage have not been fully clarified. Acute smoking as compared to sham smoking causes sympathetic activation[350,351] with a rise of blood pressure and heart rate, which, as discussed earlier, may have been transmitted to the glomerular microcirculation and stimulated the production of renin. Recent evidence suggests that a hemodynamic basis for the deleterious effect of tobacco on the kidneys may indeed exist. Acute smoking has been recently reported to relax renal arteries.[352] Hyperfiltration was more prevalent in current smokers than in former smokers or nonsmokers in a cohort of healthy subjects.[353] Similar findings were reported in over 7000 healthy Japanese men.[354] These results were reproduced in db/db mice, in which nicotine intake was associated with glomerular hypertrophy.[355] Thus, mechanical strain to the glomerular tuft may contribute to the glomerular damage caused by tobacco smoking.

Protein Intake

As discussed earlier, increased protein intake promotes glomerular hyperfiltration and hyperperfusion in healthy rats, without elevating P_{GC}.[21,20] In the long run, high-protein diet promotes only mild glomerular injury in healthy rats.[20] However, high-protein diets tend to augment P_{GC} and glomerular size, and may accelerate the progression of renal injury, in experimental models of CKD.[20,356] Thus, excess protein may predispose to renal damage, and become especially deleterious in the setting of established renal disease. On the other hand, as noted above, dietary protein restriction has been shown to limit or prevent both glomerular hemodynamic abnormalities and chronic renal injury in a variety of experimental models of CKD.[20,30,357,358]

The mechanisms by which the dietary protein content interferes with the glomerular microcirculation remain unclear, and may involve the action of vasoactive agents such as kinins,[359] vasodilatory prostanoids[360] and nitric oxide.[361] Recently, a transcriptional regulator, the Kruppel-like factor 15 (KLF-15) has been shown to inhibit the development of renal fibrosis, and

to be downregulated by high-protein intake.[362] Thus protein intake may influence the development of CKD by a double mechanism: (1) by interfering with glomerular hemodynamics through the mediation of vasoactive compounds; (2) by modulating cell mechanisms that conduce to the development of renal fibrosis. Additional benefit of low-protein diets may result from the phosphorus restriction that inevitably accompanies such regimens.[363]

Despite these consistent experimental data, it remains uncertain whether dietary protein can initiate or aggravate human renal disease,[364–367] although some clinical studies indicate that protein excess does increase GFR.[360,368] On the other hand, a series of clinical studies tested the use of low-protein diets as a possible therapeutic measure in the management of CKD. However, although several of these studies showed a protective effect of dietary protein restriction in patients with CKD,[369–372] large randomized trials, such as the Modification of Diet in Renal Disease (MDRD) study, failed to unequivocally demonstrate that the administration of a low-protein diet improve renal survival in this setting.[373–375] In fact, protein restriction in CKD may pose a therapeutic dilemma, since it is necessary to carefully balance the possible beneficial effects of this maneuver against the risk of promoting protein malnutrition,[376,377] which is a matter of considerable concern in view of the high mortality associated with reduced body weight in dialysis patients. Thus the current evidence does not favor protein restriction as a therapeutic maneuver to slow the progression of CKD, nor does it emphatically prohibit protein-rich diets, although dietary protein excess is generally avoided.

Pregnancy

As pointed out earlier, pregnancy is associated with glomerular hyperfiltration and hyperperfusion, but not hypertension, a finding in keeping with the lack of association between repetitive pregnancies and the development of CKD. However, the rate of decline of renal function associated with CKD may be hastened in gravid women in whom GFR is already compromised at the onset of pregnancy.[378,379] The mechanisms underlying this pathogenic interaction between pregnancy and CKD are unknown. It is conceivable that the renal vasodilatation associated with pregnancy aggravates the glomerular hypertension that may be associated with CKD, although data on renal and glomerular hemodynamics under these conditions are lacking. The reader is referred to Chapter 81 for a more detailed discussion on the complex relationship between pregnancy and renal disease.

PREVENTING THE PROGRESSION OF CKD BY TREATMENT OF THE GLOMERULAR HEMODYNAMIC DERANGEMENT

Based on the above considerations, it is only natural that several therapeutic measures intended to prevent or detain the progression of CKD target the mechanisms of glomerular mechanical aggression discussed in the preceding paragraphs. The most obvious of these is the treatment of arterial hypertension. In most glomeruli of most subjects with essential hypertension, afferent arteriolar contraction, mediated by myogenic reflexes and/or by signals originated from the macula densa, protects the glomeruli from transmission of the elevated blood pressure, thus preventing mechanical strain and keeping SNGFR constant.[380,381] This mechanism may fail in a fraction of the glomeruli, which may undergo sclerosis,[382] while other units may become ischemic due to arteriolar injury,[383] leading to the development of "benign" nephrosclerosis in a fortunately small proportion of these patients. Autoregulation is deficient in CKD and in diabetes mellitus, as shown in a number of experimental studies, thus contributing to accelerate the progression of renal injury.[384–386] Accordingly, lowering blood pressure in CKD patients is expected to promote a proportional decrease in glomerular pressure, thus contributing to attenuate the progression of the disease.

As discussed above, inhibition of the RAS by ACEI or ARB became one of the current cornerstones of the pharmacological treatment of CKD, in view of both its hemodynamic and nonhemodynamic effects. For this reason, therapy with these drugs is said to exert renoprotection that is independent of their antihypertensive action. A similar consideration holds for sympatholytic agents, which may exert significant renoprotection even at doses that do not lower blood pressure.[387,388]

Since a large proportion of CKD patients still progress to ESRD despite being treated with inhibitors of the RAS, the use of higher doses of these compounds, or varying combinations between an ARB, an ACE inhibitor and, more recently, a renin inhibitor, have been proposed.[389–392] An alternative measure, supported by clinical and experimental evidence, is to associate a mineralocorticoid receptor antagonist, such as spironolactone or eplerenone, to an ARB or ACE inhibitor.[200,393] However, whether any of these regimens offers real advantages over the conventional therapeutic schemes is currently undetermined.[392,394]

Because a more extensive review of the therapeutics of CKD would be beyond the scope of this chapter, the reader is referred to clinically focused textbooks,

reviews and websites for more detailed analysis of the current clinical guidelines for the management of CKD patients, and of the most relevant clinical trials that provide the scientific support for these strategies.

MECHANICAL STRETCH IN THE PATHOGENESIS OF IMMUNE-MEDIATED GLOMERULONEPHRITIS

As pointed out earlier, hemodynamic stress of the glomerular capillary walls can trigger a sequence of inflammatory events that are in many respects indistinguishable from those evoked by immune-mediated glomerulonephritides. Several observations suggest that, on the other hand, the latter can promote glomerular hypertension, thus increasing the severity of the aggression to the renal parenchyma. Maddox and associates[395] showed that both glomerular plasma flow and glomerular intracapillary pressure were augmented in the early autologous phase of rat nephrotoxic serum nephritis, an experimental model for Goodpasture's syndrome. Similar findings were reported in the same model by Sakai et al.[396] Yoshioka and coworkers[397] observed elevated glomerular pressure in rats with passive Heymann's nephritis, an experimental model for membranous glomerulonephritis, showing in addition that proteinuria was acutely increased by maneuvers that aggravated glomerular hypertension. In patients with IgA nephropathy, Konichi et al.[398] showed that the estimated glomerular pressure correlated directly with the degree of glomerulosclerosis. Indirect evidence also supports the existence of glomerular hypertension in immune-mediated renal disease. Woo et al.[399] showed less severe renal injury in patients with the II ACE genotype than in those with the ID or DD genotypes, in all likelihood due to less renal ACE activity and, possibly, less severe glomerular hypertension, along with lesser manifestations of the nonhemodynamic effects of AII discussed earlier. Accordingly, treatment with inhibitors of the renin-angiotensin system ameliorated proteinuria and renal injury in clinical[400] and experimental[401] glomerulonephritis, prompting the recommendation, by several investigators, that ACE inhibitors or AII receptor blockers be used in this setting.[400–403]

GLOMERULAR HEMODYNAMICS AND THE CLINICAL TRANSLATION OF EXPERIMENTAL DATA: A WORD OF CAUTION

Knowledge about the vast majority of the mechanisms discussed in this chapter was obtained through animal studies. A large portion of these mechanisms is indeed shared by humans and animals, particularly rodents, largely justifying the widespread use of experimental models of CKD to mimic human disease. However, important differences exist that may preclude direct application of data generated by experimental work to the clinical context. For instance, unilateral nephrectomy is known to cause substantial proteinuria in rodents, being used as an experimental model of CKD,[88,95] whereas removal of one kidney in humans, as noted earlier in this chapter, leads to only mild abnormalities.[58,322,323] Another example of the disparity between human and animal disease is given by the differing responses to RAS inhibition, discussed earlier: whereas treatment reduces spectacularly proteinuria and glomerular injury in rats with renal mass removal or diabetic nephropathy,[38,64] the human response is frequently incomplete and, all too often, complicated by hyperkalemia and/or GFR decline, forcing the cessation of treatment.[404] Despite the enthusiasm that bench data may evoke, generation of clinical evidence remains mandatory before information thus obtained can be effectively applied.

SUMMARY AND CONCLUSIONS

The mechanisms discussed in this chapter are represented in a simplified manner in Fig. 86.4. Mechanical strain to the glomerular walls can be caused by intracapillary hypertension and/or tuft hypertrophy, both of which are associated with several instances of progressive renal disease. Capillary stretch can damage endothelial cells, mesangial cells and podocytes, setting off a chain of events that culminate in the development of glomerulosclerosis and interstitial fibrosis. Inflammatory events, such as leukocyte infiltration and local production of cytokines, chemokines and growth factors, play a crucial role in the translation of stretch-induced cell injury to progressive scarring of the renal tissue. Activation of the renin-angiotensin system plays a crucial role in this process, favoring both mechanical strain and inflammatory phenomena. Genetic and environmental factors, such as nephron number at birth, obesity, use of tobacco and protein intake can worsen the mechanical stretch to the glomeruli, contributing to an acceleration of the progression of the disease. Nephron dropout resulting from the combined action of all these factors aggravates the compensatory functional and anatomical hypertrophy of the remaining units, leading to further mechanical strain and establishing a positive feedback loop that perpetuates and intensifies the destruction of the renal parenchyma. Although a number of potential therapeutic targets has been uncovered in the past two decades, lowering of

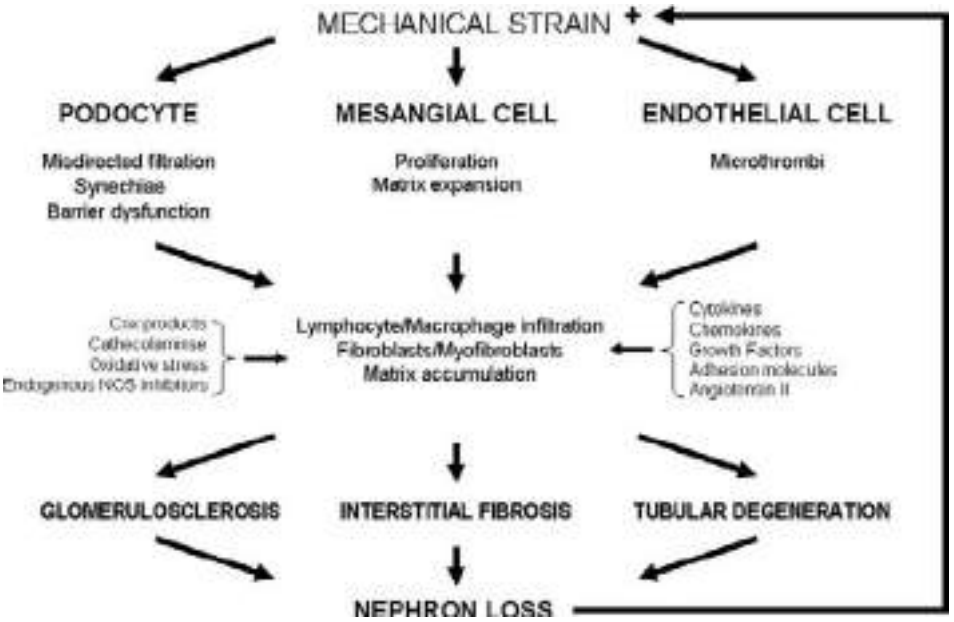

FIGURE. 86.4 Simplified schematic of the factors involved in progressive renal injury initiated by glomerular mechanical strain.

blood pressure, inhibition of the renin-angiotensin system and, in diabetic patients, strict metabolic control remain the best options in the effort to halt mechanical strain to the glomerulus and/or the development and propagation of its deleterious effects.

References

[1] Brenner BM, Meyer TW, Hostetter TH. Dietary protein intake and the progressive nature of kidney disease: the role of hemodynamically mediated glomerular injury in the pathogenesis of progressive glomerular sclerosis in aging, renal ablation, and intrinsic renal disease. N Engl J Med 1982;307:652–9.

[2] Hostetter TH, Rennke HG, Brenner BM. The case for intrarenal hypertension in the initiation and progression of diabetic and other glomerulopathies. Am J Med 1982;72:375–80.

[3] Brenner BM, Troy JL, Daugharty TM. The dynamics of glomerular ultrafiltration in the rat. J Clin Invest 1971;50:1776–80.

[4] Deen WM, Robertson CR, Brenner BM. A model of glomerular ultrafiltration in the rat. Am J Physiol 1972;223:1178–83.

[5] Robertson CR, Deen WM, Troy JL, et al. Dynamics of glomerular ultrafiltration in the rat. 3. Hemodynamics and autoregulation. Am J Physiol 1972;223(5):1191–2000.

[6] Hricik DE, Browning PJ, Kopelman R, et al. Captopril-induced functional renal insufficiency in patients with bilateral renal-artery stenoses or renal-artery stenosis in a solitary kidney. N Engl J Med 1983;308:373–6.

[7] Balint P, Szocs E, Tarjan E, et al. Autoregulation of renal circulation in mannitol-loaded dogs. Int Urol Nephrol 1975;7:65–78.

[8] Schor N, Ichikawa I, Brenner BM. Mechanisms of action of various hormones and vasoactive substances on glomerular ultrafiltration in the rat. Kidney Int 1981;20:442–51.

[9] Skorecki KL, Ballermann BJ, Rennke HG, et al. Angiotensin II receptor regulation in isolated renal glomeruli. Fed Proc 1983;42:3064–70.

[10] Dunn BR, Ichikawa I, Pfeffer JM, et al. Renal and systemic hemodynamic effects of synthetic atrial natriuretic peptide in the anesthetized rat. Circ Res 1986;59:237–46.

[11] Marin-Grez M, Fleming JT, Steinhausen M. Atrial natriuretic peptide causes pre-glomerular vasodilatation and post-glomerular vasoconstriction in rat kidney. Nature 1986;324:473–6.

[12] Bosch JP, Lauer A, Glabman S. Short-term protein loading in assessment of patients with renal disease. Am J Med 1984;77:873–9.

[13] Levine MM, Kirschenbaum MA, Chaudhari A, et al. Effect of protein on glomerular filtration rate and prostanoid synthesis in normal and uremic rats. Am J Physiol 1986;251:F635–41.

[14] Castellino P, Coda B, DeFronzo RA. Effect of amino acid infusion on renal hemodynamics in humans. Am J Physiol 1986;251: F132–40.

[15] Meyer TW, Ichikawa I, Zatz R, et al. The renal hemodynamic response to amino acid infusion in the rat. Trans Assoc Am Physicians 1983;96:76–83.

[16] Tolins JP, Raij L. Effects of amino acid infusion on renal hemodynamics. Role of endothelium-derived relaxing factor. Hypertension 1991;17:1045–51.

[17] Jamison RL. Dietary protein, glomerular hyperemia, and progressive renal failure. Ann Intern Med 1983;99:849–51.

[18] Bergstrom J, Ahlberg M, Alvestrand A. Influence of protein intake on renal hemodynamics and plasma hormone concentrations in normal subjects. Acta Med Scand 1985;217:189–96.

[19] Hostetter TH, Meyer TW, Rennke HG, et al. Chronic effects of dietary protein in the rat with intact and reduced renal mass. Kidney Int 1986;30:509–17.

[20] Zatz R, Meyer TW, Rennke HG, et al. Predominance of hemodynamic rather than metabolic factors in the pathogenesis of diabetic glomerulopathy. Proc Natl Acad Sci USA 1985;82:5963–7.

[21] Ichikawa I, Purkerson ML, Klahr S, et al. Mechanism of reduced glomerular filtration rate in chronic malnutrition. J Clin Invest 1980;65:982–8.

[22] Atherton JC, Pirie SC. The effect of pregnancy on glomerular filtration rate and salt and water reabsorption in the rat. J Physiol 1981;319:153–64.

[23] Baylis C. The mechanism of the increase in glomerular filtration rate in the twelve-day pregnant rat. J Physiol 1980;305:405–14.

[24] Dunlop W. Serial changes in renal haemodynamics during normal human pregnancy. Br J Obstet Gynaecol 1981;88:1–9.

[25] Baylis C, Rennke HG. Renal hemodynamics and glomerular morphology in repetitively pregnant aging rats. Kidney Int 1985;28:140–5.
[26] Platt R. Structural and functional adaptation in renal failure. Br Med J 1952;1:1313–7.
[27] Bricker NS, Morrin PA, et al. The pathologic physiology of chronic Bright's disease. An exposition of the "intact nephron hypothesis". Am J Med 1960;28:77–98.
[28] Bricker NS. On the meaning of the intact nephron hypothesis. Am J Med 1969;46:1–11.
[29] Walter F, Addis T. Organ work and organ weight. J Exp Med 1939;69:467–83.
[30] Hostetter TH, Olson JL, Rennke HG, et al. Hyperfiltration in remnant nephrons: a potentially adverse response to renal ablation. Am J Physiol 1981;241:F85–93.
[31] Shimamura T, Morrison AB. A progressive glomerulosclerosis occurring in partial five-sixths nephrectomized rats. Am J Pathol 1975;79:95–106.
[32] Dworkin LD, Hostetter TH, Rennke HG, et al. Hemodynamic basis for glomerular injury in rats with desoxycorticosterone-salt hypertension. J Clin Invest 1984;73:1448–61.
[33] Levin NW, Silveira E, Cortes P, et al. Relation of renal growth to diabetic glomerulosclerosis. Lancet 1975;1:1120–1.
[34] Mogensen CE, Andersen MJ. Increased kidney size and glomerular filtration rate in untreated juvenile diabetes: normalization by insulin-treatment. Diabetologia 1975;11:221–4.
[35] Stalder G, Schmid R. Severe functional disorders of glomerular capillaries and renal hemodynamics in treated diabetes mellitus during childhood. Ann Paediatr 1959;193:129–38.
[36] Hostetter TH, Troy JL, Brenner BM. Glomerular hemodynamics in experimental diabetes mellitus. Kidney Int 1981;19:410–5.
[37] Anderson S, Rennke HG, Garcia DL, et al. Short and long term effects of antihypertensive therapy in the diabetic rat. Kidney Int 1989;36:526–36.
[38] Zatz R, Dunn BR, Meyer TW, et al. Prevention of diabetic glomerulopathy by pharmacological amelioration of glomerular capillary hypertension. J Clin Invest 1986;77:1925–30.
[39] Fujihara CK, Padilha RM, Zatz R. Glomerular abnormalities in long-term experimental diabetes. Role of hemodynamic and nonhemodynamic factors and effects of antihypertensive therapy. Diabetes 1992;41:286–93.
[40] Stackhouse S, Miller PL, Park SK, et al. Reversal of glomerular hyperfiltration and renal hypertrophy by blood glucose normalization in diabetic rats. Diabetes 1990;39:989–95.
[41] Utimura R, Fujihara CK, Mattar AL, et al. Mycophenolate mofetil prevents the development of glomerular injury in experimental diabetes. Kidney Int 2003;63:209–16.
[42] Ditzel J, Junker K. Abnormal glomerular filtration rate, renal plasma flow, and renal protein excretion in recent and short-term diabetics. Br Med J 1972;2:13–9.
[43] Vittinghus E, Mogensen CE. Albumin excretion and renal haemodynamic response to physical exercise in normal and diabetic man. Scand J Clin Lab Invest 1981;41:627–32.
[44] Ishida K, Ishibashi F, Takashina S. Comparison of renal hemodynamics in early non-insulin-dependent and insulin-dependent diabetes mellitus. J Diabet Complications 1991;5:143–5.
[45] Lebovitz HE, Palmisano J. Cross-sectional analysis of renal function in black Americans with NIDDM. Diabetes Care 1990;13:1186–90.
[46] Silveiro SP, Friedman R, Gross JL. Glomerular hyperfiltration in NIDDM patients without overt proteinuria. Diabetes Care 1993;16:115–9.
[47] Jerums G, Premaratne E, Panagiotopoulos S, et al. The clinical significance of hyperfiltration in diabetes. Diabetologia 2010;53:2093–104.
[48] Mogensen CE, Schmitz A, Christensen CK. Comparative renal pathophysiology relevant to IDDM and NIDDM patients. Diabetes Metab Rev 1988;4:453–83.
[49] Ritz E, Hasslacher C, Tschope W. Diabetic nephropathy—are there differences between type I and type II? Miner Electrolyte Metab 1990;16:69–72.
[50] Bivona BJ, Park S, Harrison-Bernard LM. Glomerular filtration rate determinations in conscious type II diabetic mice. Am J Physiol Renal Physiol 2011;300:F618–25.
[51] Uriu K, Kaizu K, Qie YL, et al. Renal hemodynamics in Otsuka Long-Evans Tokushima fatty rat, a model rat of spontaneous non-insulin-dependent diabetes mellitus with obesity. J Lab Clin Med 1999;134:483–91.
[52] Steffes MW, Brown DM, Mauer SM. Diabetic glomerulopathy following unilateral nephrectomy in the rat. Diabetes 1978;27:35–41.
[53] Mauer SM, Steffes MW, Azar S, et al. The effects of Goldblatt hypertension on development of the glomerular lesions of diabetes mellitus in the rat. Diabetes 1978;27:738–44.
[54] Berkman J, Rifkin H. Unilateral nodular diabetic glomerulosclerosis (Kimmelstiel-Wilson): report of a case. Metabolism 1973;22:715–22.
[55] Beroniade VC, Lefebvre R, Falardeau P. Unilateral nodular diabetic glomerulosclerosis: recurrence of an experiment of nature. Am J Nephrol 1987;7:55–9.
[56] Lervang HH, Jensen S, Brochner-Mortensen J, et al. Early glomerular hyperfiltration and the development of late nephropathy in type 1 (insulin-dependent) diabetes mellitus. Diabetologia 1988;31:723–9.
[57] Viberti GC, Jarrett RJ, Wiseman MJ. Predicting diabetic nephropathy. N Engl J Med 1984;311:1256–7.
[58] Hakim RM, Goldszer RC, Brenner BM. Hypertension and proteinuria: long-term sequelae of uninephrectomy in humans. Kidney Int 1984;25:930–6.
[59] Zucchelli P, Cagnoli L, Casanova S, et al. Focal glomerulosclerosis in patients with unilateral nephrectomy. Kidney Int 1983;24:649–55.
[60] Robitaille P, Mongeau JG, Lortie L, et al. Long-term follow-up of patients who underwent unilateral nephrectomy in childhood. Lancet 1985;1:1297–9.
[61] Gumus II, Uz E, Bavbek N, et al. Does glomerular hyperfiltration in pregnancy damage the kidney in women with more parities? Int Urol Nephrol 2009;41:927–32.
[62] Purkerson ML, Joist JH, Yates J, et al. Inhibition of thromboxane synthesis ameliorates the progressive kidney disease of rats with subtotal renal ablation. Proc Natl Acad Sci USA 1985;82:193–7.
[63] Anderson S, Meyer TW, Rennke HG, et al. Control of glomerular hypertension limits glomerular injury in rats with reduced renal mass. J Clin Invest 1985;76:612–9.
[64] Anderson S, Rennke HG, Brenner BM. Therapeutic advantage of converting enzyme inhibitors in arresting progressive renal disease associated with systemic hypertension in the rat. J Clin Invest 1986;77:1993–2000.
[65] Daniels BS, Hostetter TH. Adverse effects of growth in the glomerular microcirculation. Am J Physiol 1990;258:F1409–16.
[66] Fogo A, Yoshida Y, Glick AD, et al. Serial micropuncture analysis of glomerular function in two rat models of glomerular sclerosis. J Clin Invest 1988;82:322–30.
[67] Lax DS, Benstein JA, Tolbert E, et al. Effects of salt restriction on renal growth and glomerular injury in rats with remnant kidneys. Kidney Int 1992;41:1527–34.
[68] O'Donnell MP, Kasiske BL, Cleary MP, et al. Effects of genetic obesity on renal structure and function in the Zucker rat. II. Micropuncture studies. J Lab Clin Med 1985;106:605–10.

[69] Yoshida Y, Fogo A, Ichikawa I. Glomerular hemodynamic changes vs. hypertrophy in experimental glomerular sclerosis. Kidney Int 1989;35:654–60.
[70] Fogo A, Hawkins EP, Berry PL, et al. Glomerular hypertrophy in minimal change disease predicts subsequent progression to focal glomerular sclerosis. Kidney Int 1990;38:115–23.
[71] Falk SA, Buric V, Hammond WS, et al. Serial glomerular and tubular dynamics in thyroidectomized rats with remnant kidneys. Am J Kidney Dis 1991;17:218–27.
[72] Fujihara CK, Limongi DM, Falzone R, et al. Pathogenesis of glomerular sclerosis in subtotally nephrectomized analbuminemic rats. Am J Physiol 1991;261:F256–64.
[73] Kimura K, Tojo A, Hirata Y, et al. Morphometric analysis of renal arterioles in subtotally nephrectomized rats. J Lab Clin Med 1993;122:273–83.
[74] Meyer TW, Rennke HG. Progressive glomerular injury after limited renal infarction in the rat. Am J Physiol 1988;254: F856–62.
[75] Fujihara CK, Limongi DM, De Oliveira HC, et al. Absence of focal glomerulosclerosis in aging analbuminemic rats. Am J Physiol 1992;262:R947–54.
[76] Miller PL, Rennke HG, Meyer TW. Glomerular hypertrophy accelerates hypertensive glomerular injury in rats. Am J Physiol 1991;261:F459–65.
[77] Lee YU, Hayman D, Sprague EA, et al. Effects of axial stretch on cell proliferation and intimal thickness in arteries in organ culture. Cell Mol Bioeng 2010;3:286–95.
[78] Olson JL, de Urdaneta AG, Heptinstall RH. Glomerular hyalinosis and its relation to hyperfiltration. Lab Invest 1985;52:387–98.
[79] Fujihara CK, De Nucci G, Zatz R. Chronic nitric oxide synthase inhibition aggravates glomerular injury in rats with subtotal nephrectomy. J Am Soc Nephrol 1995;5:1498–507.
[80] Ribeiro MO, Antunes E, De Nucci G, et al. Chronic inhibition of nitric oxide synthesis. A new model of arterial hypertension. Hypertension 1992;20:298–303.
[81] Cortes P, Mendez M, Riser BL, et al. F-actin fiber distribution in glomerular cells: structural and functional implications. Kidney Int 2000;58:2452–61.
[82] Kriz W, Elger M, Mundel P, et al. Structure-stabilizing forces in the glomerular tuft. J Am Soc Nephrol 1995;5:1731–9.
[83] Akai Y, Homma T, Burns KD, et al. Mechanical stretch/relaxation of cultured rat mesangial cells induces protooncogenes and cyclooxygenase. Am J Physiol 1994;267:C482–90.
[84] Harris RC, Haralson MA, Badr KF. Continuous stretch-relaxation in culture alters rat mesangial cell morphology, growth characteristics, and metabolic activity. Lab Invest 1992;66:548–54.
[85] Ishida T, Haneda M, Maeda S, et al. Stretch-induced overproduction of fibronectin in mesangial cells is mediated by the activation of mitogen-activated protein kinase. Diabetes 1999;48:595–602.
[86] Krepinsky JC, Li Y, Chang Y, et al. Akt mediates mechanical strain-induced collagen production by mesangial cells. J Am Soc Nephrol 2005;16:1661–72.
[87] Riser BL, Cortes P, Zhao X, et al. Intraglomerular pressure and mesangial stretching stimulate extracellular matrix formation in the rat. J Clin Invest 1992;90:1932–43.
[88] Grond J, Schilthuis MS, Koudstaal J, et al. Mesangial function and glomerular sclerosis in rats after unilateral nephrectomy. Kidney Int 1982;22:338–43.
[89] Reiser J, Kriz W, Kretzler M, et al. The glomerular slit diaphragm is a modified adherens junction. J Am Soc Nephrol 2000;11:1–8.
[90] Ruotsalainen V, Ljungberg P, Wartiovaara J, et al. Nephrin is specifically located at the slit diaphragm of glomerular podocytes. Proc Natl Acad Sci USA 1999;96:7962–7.
[91] Cooper ME, Mundel P, Boner G. Role of nephrin in renal disease including diabetic nephropathy. Semin Nephrol 2002;22:393–8.
[92] Jalanko H, Patrakka J, Tryggvason K, et al. Genetic kidney diseases disclose the pathogenesis of proteinuria. Ann Med 2001;33:526–33.
[93] Floege J, Kriz W, Schulze M, et al. Basic fibroblast growth factor augments podocyte injury and induces glomerulosclerosis in rats with experimental membranous nephropathy. J Clin Invest 1995;96:2809–19.
[94] Fries JW, Sandstrom DJ, Meyer TW, et al. Glomerular hypertrophy and epithelial cell injury modulate progressive glomerulosclerosis in the rat. Lab Invest 1989;60:205–18.
[95] Nagata M, Kriz W. Glomerular damage after uninephrectomy in young rats. II. Mechanical stress on podocytes as a pathway to sclerosis. Kidney Int 1992;42:148–60.
[96] Kihara I, Tsuchida S, Yaoita E, et al. Podocyte detachment and epithelial cell reaction in focal segmental glomerulosclerosis with cellular variants. Kidney Int Suppl 1997;63:S171–6.
[97] Laurens W, Battaglia C, Foglieni C, et al. Direct podocyte damage in the single nephron leads to albuminuria in vivo. Kidney Int 1995;47:1078–86.
[98] Petermann AT, Hiromura K, Blonski M, et al. Mechanical stress reduces podocyte proliferation in vitro. Kidney Int 2002;61:40–50.
[99] Kriz W, Hosser H, Hahnel B, et al. From segmental glomerulosclerosis to total nephron degeneration and interstitial fibrosis: a histopathological study in rat models and human glomerulopathies. Nephrol Dial Transplant 1998;13: 2781–98.
[100] Kriz W, Hartmann I, Hosser H, et al. Tracer studies in the rat demonstrate misdirected filtration and peritubular filtrate spreading in nephrons with segmental glomerulosclerosis. J Am Soc Nephrol 2001;12:496–506.
[101] Kriz W, Hosser H, Hahnel B, et al. Development of vascular pole-associated glomerulosclerosis in the Fawn- hooded rat. J Am Soc Nephrol 1998;9:381–96.
[102] Iseki K, Ikemiya Y, Iseki C, et al. Proteinuria and the risk of developing end-stage renal disease. Kidney Int 2003; 63:1468–74.
[103] Keane WF. Proteinuria: its clinical importance and role in progressive renal disease. Am J Kidney Dis 2000;35:S97–105.
[104] Ruggenenti P, Perna A, Mosconi L, et al. Urinary protein excretion rate is the best independent predictor of ESRF in non-diabetic proteinuric chronic nephropathies. "Gruppo Italiano di Studi Epidemiologici in Nefrologia" (GISEN). Kidney Int 1998;53:1209–16.
[105] Hirschberg R, Wang S. Proteinuria and growth factors in the development of tubulointerstitial injury and scarring in kidney disease. Curr Opin Nephrol Hypertens 2005;14:43–52.
[106] Donadelli R, Abbate M, Zanchi C, et al. Protein traffic activates NF-kB gene signaling and promotes MCP-1-dependent interstitial inflammation. Am J Kidney Dis 2000;36:1226–41.
[107] Donadelli R, Zanchi C, Morigi M, et al. Protein overload induces fractalkine upregulation in proximal tubular cells through nuclear factor kappaB- and p38 mitogen-activated protein kinase-dependent pathways. J Am Soc Nephrol 2003;14:2436–46.
[108] Morii T, Fujita H, Narita T, et al. Increased urinary excretion of monocyte chemoattractant protein-1 in proteinuric renal diseases. Ren Fail 2003;25:439–44.

[109] Wang Y, Chen J, Chen L, et al. Induction of monocyte chemoattractant protein-1 in proximal tubule cells by urinary protein. J Am Soc Nephrol 1997;8:1537–45.
[110] Kuusniemi AM, Lapatto R, Holmberg C, et al. Kidneys with heavy proteinuria show fibrosis, inflammation, and oxidative stress, but no tubular phenotypic change. Kidney Int 2005;68:121–32.
[111] Theilig F, Kriz W, Jerichow T, et al. Abrogation of protein uptake through megalin-deficient proximal tubules does not safeguard against tubulointerstitial injury. J Am Soc Nephrol 2007;18:1824–34.
[112] Cameron JS. Bright's disease today: the pathogenesis and treatment of glomerulonephritis–I. Br Med J 1972;4:87–90.
[113] Rovin BH, Schreiner GF. Cell-mediated immunity in glomerular disease. Annu Rev Med 1991;42:25–33.
[114] Sugimoto H, Shikata K, Hirata K, et al. Increased expression of intercellular adhesion molecule-1 (ICAM-1) in diabetic rat glomeruli: glomerular hyperfiltration is a potential mechanism of ICAM-1 upregulation. Diabetes 1997;46:2075–81.
[115] Teles F, Machado FG, Ventura BH, et al. Regression of glomerular injury by losartan in experimental diabetic nephropathy. Kidney Int 2009;75:72–9.
[116] Young BA, Johnson RJ, Alpers CE, et al. Cellular events in the evolution of experimental diabetic nephropathy. Kidney Int 1995;47:935–44.
[117] Mei C, Zheng F. Chronic inflammation potentiates kidney aging. Semin Nephrol 2009;29:555–68.
[118] Thomas SE, Anderson S, Gordon KL, et al. Tubulointerstitial disease in aging: evidence for underlying peritubular capillary damage, a potential role for renal ischemia. J Am Soc Nephrol 1998;9:231–42.
[119] Vlassara H, Torreggiani M, Post JB, et al. Role of oxidants/inflammation in declining renal function in chronic kidney disease and normal aging. Kidney Int Suppl 2009;:S3–11.
[120] Fujihara CK, Malheiros DMAC, Noronha IL, et al. Mycophenolate mofetil reduces renal injury in the chronic nitric oxide synthase inhibition model. Hypertension 2001;37:170–5.
[121] Fujihara CK, Sena CR, Malheiros DM, et al. Short-term nitric oxide inhibition induces progressive nephropathy after regression of initial renal injury. Am J Physiol Renal Physiol 2006;290:F632–40.
[122] Luvara G, Pueyo ME, Philippe M, et al. Chronic blockade of NO synthase activity induces a proinflammatory phenotype in the arterial wall: prevention by angiotensin II antagonism. Arterioscler Thromb Vasc Biol 1998;18:1408–16.
[123] Diamond JR, Pesek-Diamond I. Sublethal X-irradiation during acute puromycin nephrosis prevents late renal injury: role of macrophages. Am J Physiol 1991;260:F779–86.
[124] Eddy AA. Interstitial nephritis induced by protein-overload proteinuria. Am J Pathol 1989;135:719–33.
[125] Floege J, Alpers CE, Burns MW, et al. Glomerular cells, extracellular matrix accumulation, and the development of glomerulosclerosis in the remnant kidney model. Lab Invest 1992;66:485–97.
[126] Floege J, Burns MW, Alpers CE, et al. Glomerular cell proliferation and PDGF expression precede glomerulosclerosis in the remnant kidney model. Kidney Int 1992;41:297–309.
[127] Kliem V, Johnson RJ, Alpers CE, et al. Mechanisms involved in the pathogenesis of tubulointerstitial fibrosis in 5/6-nephrectomized rats. Kidney Int 1996;49:666–78.
[128] Fujihara CK, Malheiros DMAC, Zatz R, et al. Mycophenolate mofetil attenuates renal injury in the rat remnant kidney. Kidney Int 1998;54:1510–9.
[129] Fujihara CK, Noronha IL, Malheiros DMAC, et al. Combined mycophenolate mofetil and losartan therapy arrests established injury in the remnant kidney. J Am Soc Nephrol 2000;11:283–90.
[130] Goncalves AR, Fujihara CK, Mattar AL, et al. Renal expression of COX-2, ANG II, and AT1 receptor in remnant kidney: strong renoprotection by therapy with losartan and a nonsteroidal anti-inflammatory. Am J Physiol Renal Physiol 2004;286:F945–54.
[131] Romero F, Rodriguez-Iturbe B, Parra G, et al. Mycophenolate mofetil prevents the progressive renal failure induced by 5/6 renal ablation in rats. Kidney Int 1999;55:945–55.
[132] Carvajal G, Rodriguez-Vita J, Rodrigues-Diez R, et al. Angiotensin II activates the Smad pathway during epithelial mesenchymal transdifferentiation. Kidney Int 2008;74:585–95.
[133] Ng YY, Huang TP, Yang WC, et al. Tubular epithelial-myofibroblast transdifferentiation in progressive tubulointerstitial fibrosis in 5/6 nephrectomized rats. Kidney Int 1998;54:864–76.
[134] Takakuta K, Fujimori A, Chikanishi T, et al. Renoprotective properties of pirfenidone in subtotally nephrectomized rats. Eur J Pharmacol 2010;629:118–24.
[135] Mezzano SA, Droguett MA, Burgos ME, et al. Overexpression of chemokines, fibrogenic cytokines, and myofibroblasts in human membranous nephropathy. Kidney Int 2000;57:147–58.
[136] Sanz AB, Justo P, Sanchez-Nino MD, et al. The cytokine TWEAK modulates renal tubulointerstitial inflammation. J Am Soc Nephrol 2008;19:695–703.
[137] Schiller B, Moran J. Focal glomerulosclerosis in the remnant kidney model—an inflammatory disease mediated by cytokines. Nephrol Dial Transplant 1997;12:430–7.
[138] Taal MW, Zandi-Nejad K, Weening B, et al. Proinflammatory gene expression and macrophage recruitment in the rat remnant kidney. Kidney International 2000;58:1664–76.
[139] Yamamoto T, Nakamura T, Noble NA, et al. Expression of transforming growth factor beta is elevated in human and experimental diabetic nephropathy. Proc Natl Acad Sci USA 1993;90:1814–8.
[140] An WS, Kim HJ, Cho KH, et al. Omega-3 fatty acid supplementation attenuates oxidative stress, inflammation, and tubulointerstitial fibrosis in the remnant kidney. Am J Physiol Renal Physiol 2009;297:F895–903.
[141] Fujihara CK, Antunes GR, Mattar AL, et al. Chronic inhibition of nuclear factor-kappaB attenuates renal injury in the 5/6 renal ablation model. Am J Physiol Renal Physiol 2007;292:F92–9.
[142] Ng YY, Hou CC, Wang W, et al. Blockade of NFkappaB activation and renal inflammation by ultrasound-mediated gene transfer of Smad7 in rat remnant kidney. Kidney Int Suppl 2005;:S83–91.
[143] Tharaux PL, Chatziantoniou C, Fakhouri F, et al. Angiotensin II activates collagen I gene through a mechanism involving the MAP/ER kinase pathway. Hypertension 2000;36:330–6.
[144] Hamar P, Peti-Peterdi J, Razga Z, et al. Coinhibition of immune and renin-angiotensin systems reduces the pace of glomerulosclerosis in the rat remnant kidney. J Am Soc Nephrol 1999;10 (Suppl. 11):S234–8.
[145] Moscoso-Solorzano GT, Mastroianni-Kirsztajn G, Ozaki KS, et al. Synergistic effect of mycophenolate mofetil and angiotensin-converting enzyme inhibitor in patients with chronic allograft nephropathy. Braz J Med Biol Res 2009;42:445–52.
[146] Noris M, Azzollini N, Pezzotta A, et al. Combined treatment with mycophenolate mofetil and an angiotensin II receptor

antagonist fully protects from chronic rejection in a rat model of renal allograft. J Am Soc Nephrol 2001;12:1937–46.
[147] Remuzzi G, Zoja C, Gagliardini E, et al. Combining an antiproteinuric approach with mycophenolate mofetil fully suppresses progressive nephropathy of experimental animals. J Am Soc Nephrol 1999;10:1542–9.
[148] Rodriguez-Iturbe B, Quiroz Y, Shahkarami A, et al. Mycophenolate mofetil ameliorates nephropathy in the obese Zucker rat. Kidney Int 2005;68:1041–7.
[149] Wu YG, Lin H, Qian H, et al. Renoprotective effects of combination of angiotensin converting enzyme inhibitor with mycophenolate mofetil in diabetic rats. Inflamm Res 2006;55:192–9.
[150] Fujihara CK, Antunes GR, Mattar AL, et al. Cyclooxygenase-2 (COX-2) inhibition limits abnormal COX-2 expression and progressive injury in the remnant kidney. Kidney Int 2003;64:2172–81.
[151] Fujihara CK, Malheiros DMAC, Donato JL, et al. Nitroflurbiprofen, a new nonsteroidal anti-inflammatory, ameliorates structural injury in the remnant kidney. Am J Physiol 1998;274:F573–9.
[152] Wang JL, Cheng HF, Shappell S, et al. A selective cyclooxygenase-2 inhibitor decreases proteinuria and retards progressive renal injury in rats. Kidney International 2000;57:2334–42.
[153] Cheng HF, Wang CJ, Moeckel GW, et al. Cyclooxygenase-2 inhibitor blocks expression of mediators of renal injury in a model of diabetes and hypertension. Kidney Int 2002;62:929–39.
[154] Arendshorst WJ, Brannstrom K, Ruan X. Actions of angiotensin II on the renal microvasculature. J Am Soc Nephrol 1999;10 (Suppl. 11):S149–61.
[155] Blantz RC, Konnen KS, Tucker BJ. Angiotensin II effects upon the glomerular microcirculation and ultrafiltration coefficient of the rat. J Clin Invest 1976;57:419–34.
[156] Myers BD, Deen WM, Brenner BM. Effects of norepinephrine and angiotensin II on the determinants of glomerular ultrafiltration and proximal tubule fluid reabsorption in the rat. Circ Res 1975;37:101–10.
[157] Edwards RM. Segmental effects of norepinephrine and angiotensin II on isolated renal microvessels. Am J Physiol 1983;244: F526–34.
[158] Yuan BH, Robinette JB, Conger JD. Effect of angiotensin II and norepinephrine on isolated rat afferent and efferent arterioles. Am J Physiol 1990;258:F741–50.
[159] Carmines PK, Navar LG. Disparate effects of Ca channel blockade on afferent and efferent arteriolar responses to ANG II. Am J Physiol 1989;256:F1015–20.
[160] Conger JD, Falk SA. KCl and angiotensin responses in isolated rat renal arterioles: effects of diltiazem and low-calcium medium. Am J Physiol 1993;264:F134–40.
[161] Inscho EW, Imig JD, Cook AK. Afferent and efferent arteriolar vasoconstriction to angiotensin II and norepinephrine involves release of Ca2 + from intracellular stores. Hypertension 1997;29:222–7.
[162] Foidart J, Sraer J, Delarue F, et al. Evidence for mesangial glomerular receptors for angiotensin II linked to mesangial cell contractility. FEBS Lett 1980;121:333–9.
[163] Baylis C, Brenner BM. Modulation by prostaglandin synthesis inhibitors of the action of exogenous angiotensin II on glomerular ultrafiltration in the rat. Circ Res 1978;43:889–98.
[164] Ferrario CM, Varagic J. The ANG-(1–7)/ACE2/mas axis in the regulation of nephron function. Am J Physiol Renal Physiol 2010;298:F1297–305.
[165] Jackson B, Hodsman P, Johnston CI. Changes in the renin-angiotensin system, exchangeable body sodium, and plasma and atrial content of atrial natriuretic factor during evolution of chronic renal failure in the rat. Am J Hypertens 1988;1:298–300.
[166] Taverner D, Bing RF, Swales JD, et al. Hypertension produced by chemical renal medullectomy or partial nephrectomy in the rat: comparison of renal function and plasma volume. J Hypertens Suppl 1984;2:S367–9.
[167] Burns KD, Homma T, Harris RC. The intrarenal renin-angiotensin system. Semin Nephrol 1993;13:13–30.
[168] Kobori H, Nangaku M, Navar LG, et al. The intrarenal renin-angiotensin system: from physiology to the pathobiology of hypertension and kidney disease. Pharmacol Rev 2007;59:251–87.
[169] Vaziri ND, Bai Y, Ni Z, et al. Intra-renal angiotensin II/AT1 receptor, oxidative stress, inflammation, and progressive injury in renal mass reduction. J Pharmacol Exp Ther 2007;323:85–93.
[170] Christiansen JS, Giese J, Damkjaer M, et al. The renin-angiotensin system and kidney function during initial insulin treatment in diabetic man. Scand J Clin Lab Invest 1988;48:451–6.
[171] Anderson S, Jung FF, Ingelfinger JR. Renal renin-angiotensin system in diabetes: functional, immunohistochemical, and molecular biological correlations. Am J Physiol 1993;265: F477–86.
[172] Correa-Rotter R, Hostetter TH, Rosenberg ME. Renin and angiotensinogen gene expression in experimental diabetes mellitus. Kidney Int 1992;41:796–804.
[173] Fujihara CK, Velho M, Malheiros DMAC, et al. An extremely high dose of losartan affords superior renoprotection in the remnant model. Kidney Int 2005;67:1913–24.
[174] Lafayette RA, Mayer G, Park SK, et al. Angiotensin II receptor blockade limits glomerular injury in rats with reduced renal mass. J Clin Invest 1992;90:766–71.
[175] Hisada Y, Sugaya T, Yamanouchi M, et al. Angiotensin II plays a pathogenic role in immune-mediated renal injury in mice. J Clin Invest 1999;103:627–35.
[176] Ruiz-Ortega M, Bustos C, Hernandez-Presa MA, et al. Angiotensin II participates in mononuclear cell recruitment in experimental immune complex nephritis through nuclear factor-kappa B activation and monocyte chemoattractant protein-1 synthesis. J Immunol 1998;161:430–9.
[177] Johnson RJ, Alpers CE, Yoshimura A, et al. Renal injury from angiotensin II-mediated hypertension. Hypertension 1992;19:464–74.
[178] Ruiz-Ortega M, Ruperez M, Lorenzo O, et al. Angiotensin II regulates the synthesis of proinflammatory cytokines and chemokines in the kidney. Kidney Int Suppl 2002;:12–22.
[179] Nataraj C, Oliverio MI, Mannon RB, et al. Angiotensin II regulates cellular immune responses through a calcineurin-dependent pathway. J Clin Invest 1999;104:1693–701.
[180] Wolf G, Haberstroh U, Neilson EG. Angiotensin II stimulates the proliferation and biosynthesis of type I collagen in cultured murine mesangial cells. Am J Pathol 1992;140:95–107.
[181] Wolf G, Wenzel UO. Angiotensin II and cell cycle regulation. Hypertension 2004;43:693–8.
[182] Wolf G, Ziyadeh FN, Thaiss F, et al. Angiotensin II stimulates expression of the chemokine RANTES in rat glomerular endothelial cells. Role of the angiotensin type 2 receptor. J Clin Invest 1997;100:1047–58.
[183] Hilgers KF, Hartner A, Porst M, et al. Monocyte chemoattractant protein-1 and macrophage infiltration in hypertensive kidney injury. Kidney Int 2000;58:2408–19.
[184] Giachelli CM, Pichler R, Lombardi D, et al. Osteopontin expression in angiotensin II-induced tubulointerstitial nephritis. Kidney Int 1994;45:515–24.

[185] Ruperez M, Ruiz-Ortega M, Esteban V, et al. Angiotensin II increases connective tissue growth factor in the kidney. Am J Pathol 2003;163:1937–47.
[186] Tanaka R, Sugihara K, Tatematsu A, et al. Internephron heterogeneity of growth factors and sclerosis—modulation of platelet-derived growth factor by angiotensin II. Kidney Int 1995;47:131–9.
[187] Godeny MD, Sayyah J, VonDerLinden D, et al. The N-terminal SH2 domain of the tyrosine phosphatase, SHP-2, is essential for Jak2-dependent signaling via the angiotensin II type AT1 receptor. Cell Signal 2007;19:600–9.
[188] Ruiz-Ortega M, Lorenzo O, Ruperez M, et al. Angiotensin II activates nuclear transcription factor kappaB through AT(1) and AT(2) in vascular smooth muscle cells: molecular mechanisms. Circ Res 2000;86:1266–72.
[189] Lee FT, Cao Z, Long DM, et al. Interactions between angiotensin II and NF-kappaB-dependent pathways in modulating macrophage infiltration in experimental diabetic nephropathy. J Am Soc Nephrol 2004;15:2139–51.
[190] Ruiz-Ortega M, Egido J. Angiotensin II modulates cell growth-related events and synthesis of matrix proteins in renal interstitial fibroblasts. Kidney Int 1997;52:1497–510.
[191] Wolf G. Link between angiotensin II and TGF-beta in the kidney. Miner Electrolyte Metab 1998;24:174–80.
[192] Jaimes EA, Galceran JM, Raij L. Angiotensin II induces superoxide anion production by mesangial cells. Kidney Int 1998;54:775–84.
[193] Haugen EN, Croatt AJ, Nath KA. Angiotensin II induces renal oxidant stress in vivo and heme oxygenase-1 in vivo and in vitro. *Kidney Int JID - 0323470* 2000;58:144–52.
[194] Kawada N, Imai E, Karber A, et al. A mouse model of angiotensin II slow pressor response: role of oxidative stress. J Am Soc Nephrol 2002;13:2860–8.
[195] Diah S, Zhang GX, Nagai Y, et al. Aldosterone induces myofibroblastic transdifferentiation and collagen gene expression through the Rho-kinase dependent signaling pathway in rat mesangial cells. Exp Cell Res 2008;314:3654–62.
[196] Greene EL, Kren S, Hostetter TH. Role of aldosterone in the remnant kidney model in the rat. J Clin Invest 1996;98:1063–8.
[197] Pitt B, Zannad F, Remme WJ, et al. The effect of spironolactone on morbidity and mortality in patients with severe heart failure. Randomized aldactone evaluation study investigators. N Engl J Med 1999;341:709–17.
[198] Quan ZY, Walser M, Hill GS. Adrenalectomy ameliorates ablative nephropathy in the rat independently of corticosterone maintenance level. Kidney Int 1992;41:326–33.
[199] Lea WB, Kwak ES, Luther JM, et al. Aldosterone antagonism or synthase inhibition reduces end-organ damage induced by treatment with angiotensin and high salt. Kidney Int 2009;75:936–44.
[200] Piecha G, Koleganova N, Gross ML, et al. Regression of glomerulosclerosis in subtotally nephrectomized rats: effects of monotherapy with losartan, spironolactone, and their combination. Am J Physiol Renal Physiol 2008;295:F137–44.
[201] Langham RG, Kelly DJ, Cox AJ, et al. Proteinuria and the expression of the podocyte slit diaphragm protein, nephrin, in diabetic nephropathy: effects of angiotensin converting enzyme inhibition. Diabetologia 2002;45:1572–6.
[202] Mayer G, Lafayette RA, Oliver J, et al. Effects of angiotensin II receptor blockade on remnant glomerular permselectivity. Kidney Int 1993;43:346–53.
[203] Miceli I, Burt D, Tarabra E, et al. Stretch reduces nephrin expression via an angiotensin II-AT(1)-dependent mechanism in human podocytes: effect of rosiglitazone. Am J Physiol Renal Physiol 2010;298:F381–90.
[204] Graciano ML, RdC Cavaglieri, Delle H, et al. Intrarenal renin-angiotensin system is upregulated in experimental model of progressive renal disease induced by chronic inhibition of nitric oxide synthesis. J Am Soc Nephrol 2004;15:1805–15.
[205] Bahiense-Oliveira M, Mattar AL, Malheiros DM, et al. Interstitial expression of angiotensin II and AT1 receptor are increased in patients with progressive glomerulopathies. J Renin Angiotensin Aldosterone Syst 2010;11:158–64.
[206] Mezzano S, Droguett A, Burgos ME, et al. Renin-angiotensin system activation and interstitial inflammation in human diabetic nephropathy. Kidney Int Suppl 2003;:S64–70.
[207] Durvasula RV, Petermann AT, Hiromura K, et al. Activation of a local tissue angiotensin system in podocytes by mechanical strain. Kidney Int 2004;65:30–9.
[208] Ichihara A, Sakoda M, Kurauchi-Mito A, et al. Involvement of (pro)renin receptor in the glomerular filtration barrier. J Mol Med 2008;86:629–35.
[209] Yatabe J, Sanada H, Yatabe MS, et al. Angiotensin II type 1 receptor blocker attenuates the activation of ERK and NADPH oxidase by mechanical strain in mesangial cells in the absence of angiotensin II. Am J Physiol Renal Physiol 2009;296: F1052–60.
[210] Brenner BM, Cooper ME, de Zeeuw D, et al. Effects of Losartan on renal and cardiovascular outcomes in patients with type 2 diabetes and nephropathy. N Engl J Med 2001;345:861–9.
[211] Lewis EJ, Hunsicker LG, Bain RP, et al. The effect of angiotensin-converting-enzyme inhibition on diabetic nephropathy. The collaborative study group. N Engl J Med 1993;329:1456–62.
[212] Lewis EJ, Hunsicker LG, Clarke WR, et al. Renoprotective effect of the angiotensin-receptor antagonist irbesartan in patients with nephropathy due to type 2 diabetes. N Engl J Med 2001;345:851–60.
[213] Nguyen G. Renin, (pro)renin and receptor: an update. Clin Sci (Lond) 2011;120:169–78.
[214] Nguyen G, Muller DN. The biology of the (pro)renin receptor. J Am Soc Nephrol 2010;21:18–23.
[215] Huang J, Matavelli LC, Siragy HM. Renal (pro)renin receptor contributes to development of diabetic kidney disease through transforming growth factor-beta1—connective tissue growth factor signalling cascade. Clin Exp Pharmacol Physiol 2011;38:215–21.
[216] Nguyen G, Delarue F, Burckle C, et al. Pivotal role of the renin/prorenin receptor in angiotensin II production and cellular responses to renin. J Clin Invest 2002;109:1417–27.
[217] Nguyen G, Contrepas A. Physiology and pharmacology of the (pro)renin receptor. Curr Opin Pharmacol 2008;8:127–32.
[218] Takahashi H, Ichihara A, Kaneshiro Y, et al. Regression of nephropathy developed in diabetes by (Pro)renin receptor blockade. J Am Soc Nephrol 2007;18:2054–61.
[219] Edwards RM, Trizna W. Characterization of alpha-adrenoceptors on isolated rabbit renal arterioles. Am J Physiol 1988;254:F178–83.
[220] Schweda F, Friis U, Wagner C, et al. Renin release. Physiology (Bethesda) 2007;22:310–9.
[221] Masuo K, Lambert GW, Esler MD, et al. The role of sympathetic nervous activity in renal injury and end-stage renal disease. Hypertens Res 2010;33:521–8.
[222] Campese VM, Krol E. Neurogenic factors in renal hypertension. Curr Hypertens Rep 2002;4:256–60.
[223] Yuhara M, Ikeda T, Toya Y, et al. Participation of the sympathetic nervous system in hypertension in rats with subtotal renal ablation. J Hypertens 1989;7:443–6.

[224] Schlaich MP, Sobotka PA, Krum H, et al. Renal denervation as a therapeutic approach for hypertension: novel implications for an old concept. Hypertension 2009;54:1195–201.
[225] Denton KM, Luff SE, Shweta A, et al. Differential neural control of glomerular ultrafiltration. Clin Exp Pharmacol Physiol 2004;31:380–6.
[226] Ignarro LJ, Buga GM, Wood KS, et al. Endothelium-derived relaxing factor produced and released from artery and vein is nitric oxide. Proc Natl Acad Sci USA 1987;84:9265–9.
[227] Palmer RM, Ferrige AG, Moncada S. Nitric oxide release accounts for the biological activity of endothelium-derived relaxing factor. Nature 1987;327:524–6.
[228] Ingram A, Parbtani A, Thai K, et al. Dietary supplementation with L-arginine limits cell proliferation in the remnant glomerulus. Kidney Int 1995;48:1857–65.
[229] Salvemini D, De Nucci G, Gryglewski RJ, et al. Human neutrophils and mononuclear cells inhibit platelet aggregation by releasing a nitric oxide-like factor. Proc Natl Acad Sci USA 1989;86:6328–32.
[230] McLay JS, Chatterjee P, Nicolson AG, et al. Nitric oxide production by human proximal tubular cells: a novel immunomodulatory mechanism? Kidney Int 1994;46:1043–9.
[231] Shultz PJ, Tayeh MA, Marletta MA, et al. Synthesis and action of nitric oxide in rat glomerular mesangial cells. Am J Physiol 1991;261:F600–6.
[232] Stuehr DJ, Gross SS, Sakuma I, et al. Activated murine macrophages secrete a metabolite of arginine with the bioactivity of endothelium-derived relaxing factor and the chemical reactivity of nitric oxide. J Exp Med 1989;169:1011–20.
[233] Beckman JS, Koppenol WH. Nitric oxide, superoxide, and peroxynitrite: the good, the bad, and ugly. Am J Physiol 1996;271: C1424–37.
[234] Deng A, Baylis C. Locally produced EDRF controls preglomerular resistance and ultrafiltration coefficient. Am J Physiol 1993;264:F212–5.
[235] Yukimura T, Yamashita Y, Miura K, et al. Renal effects of the nitric oxide synthase inhibitor, L-NG-nitroarginine, in dogs. Am J Hypertens 1992;5:484–7.
[236] Zatz R, De Nucci G. Effects of acute nitric oxide inhibition on rat glomerular microcirculation. Am J Physiol 1991;261: F360–3.
[237] De Nicola L, Blantz RC, Gabbai FB. Nitric oxide and angiotensin II. Glomerular and tubular interaction in the rat. J Clin Invest 1992;89:1248–56.
[238] Bachmann S, Bosse HM, Mundel P. Topography of nitric oxide synthesis by localizing constitutive NO synthases in mammalian kidney. Am J Physiol 1995;268:F885–98.
[239] Mundel P, Bachmann S, Bader M, et al. Expression of nitric oxide synthase in kidney macula densa cells. Kidney Int 1992;42:1017–9.
[240] Sigmon DH, Beierwaltes WH. Influence of nitric oxide derived from neuronal nitric oxide synthase on glomerular filtration. Gen Pharmacol 2000;34:95–100.
[241] Wilcox CS, Welch WJ, Murad F, et al. Nitric oxide synthase in macula densa regulates glomerular capillary pressure. Proc Natl Acad Sci U S A 1992;89:11993–7.
[242] Ollerstam A, Pittner J, Persson AEG, et al. Increased blood pressure in rats after long-term inhibition of the neuronal isoform of nitric oxide synthase. J Clin Invest 1997;99:2212–8.
[243] Fujihara CK, Mattar AL, Vieira Jr. JM, et al. Evidence for the existence of two distinct functions for the inducible NO synthase in the rat kidney: effect of aminoguanidine in rats with 5/6 ablation. J Am Soc Nephrol 2002;13:2278–87.
[244] Tian N, Gannon AW, Khalil RA, et al. Mechanisms of salt-sensitive hypertension: role of renal medullary inducible nitric oxide synthase. Am J Physiol Regul Integr Comp Physiol 2003;284:R372–9.
[245] Furusu A, Miyazaki M, Abe K, et al. Expression of endothelial and inducible nitric oxide synthase in human glomerulonephritis. Kidney Int 1998;53:1760–8.
[246] Markewitz BA, Michael JR, Kohan DE. Cytokine-induced expression of a nitric oxide synthase in rat renal tubule cells. J Clin Invest 1993;91:2138–43.
[247] Huang PL, Huang Z, Mashimo H, et al. Hypertension in mice lacking the gene for endothelial nitric oxide synthase. Nature 1995;377:239–42.
[248] Baylis C, Mitruka B, Deng A. Chronic blockade of nitric oxide synthesis in the rat produces systemic hypertension and glomerular damage. J Clin Invest 1992;90:278–81.
[249] Komers R, Allen TJ, Cooper ME. Role of endothelium-derived nitric oxide in the pathogenesis of the renal hemodynamic changes of experimental diabetes. Diabetes 1994;43:1190–7.
[250] Komers R, Lindsley JN, Oyama TT, et al. Role of neuronal nitric oxide synthase (NOS1) in the pathogenesis of renal hemodynamic changes in diabetes. Am J Physiol Renal Physiol 2000;279:F573–83.
[251] Mattar AL, Fujihara CK, Ribeiro MO, et al. Renal effects of acute and chronic nitric oxide inhibition in experimental diabetes. Nephron 1996;74:136–43.
[252] Aiello S, Noris M, Todeschini M, et al. Renal and systemic nitric oxide synthesis in rats with renal mass reduction. Kidney Int 1997;52:171–81.
[253] Ashab I, Peer G, Blum M, et al. Oral administration of L-arginine and captopril in rats prevents chronic renal failure by nitric oxide production. Kidney Int 1995;47:1515–21.
[254] Schmidt RJ, Baylis C. Total nitric oxide production is low in patients with chronic renal disease. Kidney Int 2000; 58:1261–6.
[255] Ueda S, Yamagishi S, Matsumoto Y, et al. Involvement of asymmetric dimethylarginine (ADMA) in glomerular capillary loss and sclerosis in a rat model of chronic kidney disease (CKD). Life Sci 2009;84:853–6.
[256] Wagner L, Riggleman A, Erdely A, et al. Reduced nitric oxide synthase activity in rats with chronic renal disease due to glomerulonephritis. Kidney Int 2002;62:532–6.
[257] Kielstein JT, Boger RH, Bode-Boger SM, et al. Marked increase of asymmetric dimethylarginine in patients with incipient primary chronic renal disease. J Am Soc Nephrol 2002;13:170–6.
[258] Schwedhelm E, Boger RH. The role of asymmetric and symmetric dimethylarginines in renal disease. Nat Rev Nephrol 2011;7:275–85.
[259] Vallance P, Leone A, Calver A, et al. Accumulation of an endogenous inhibitor of nitric oxide synthesis in chronic renal failure. Lancet 1992;339:572–5.
[260] Kang DH, Nakagawa T, Feng L, et al. Nitric oxide modulates vascular disease in the remnant kidney model. Am J Pathol 2002;161:239–48.
[261] Reyes AA, Purkerson ML, Karl I, et al. Dietary supplementation with L-arginine ameliorates the progression of renal disease in rats with subtotal nephrectomy. Am J Kidney Dis 1992;20:168–76.
[262] Benigni A, Zoja C, Noris M, et al. Renoprotection by nitric oxide donor and lisinopril in the remnant kidney model. Am J Kidney Dis 1999;33:746–53.
[263] Guan Y, Chang M, Cho W, et al. Cloning, expression, and regulation of rabbit cyclooxygenase-2 in renal medullary interstitial cells. Am J Physiol 1997;273:F18–26.
[264] Harris RC, McKanna JA, Akai Y, et al. Cyclooxygenase-2 is associated with the macula densa of rat kidney and increases with salt restriction. J Clin Invest 1994;94:2504–10.

[265] Komhoff M, Grone HJ, Klein T, et al. Localization of cyclooxygenase-1 and -2 in adult and fetal human kidney: implication for renal function. Am J Physiol 1997;272:F460–8.
[266] Baylis C, Deen WM, Myers BD, et al. Effects of some vasodilator drugs on transcapillary fluid exchange in renal cortex. Am J Physiol 1976;230:1148–58.
[267] Nath KA, Chmielewski DH, Hostetter TH. Regulatory role of prostanoids in glomerular microcirculation of remnant nephrons. Am J Physiol 1987;252:F829–37.
[268] Pelayo JC, Shanley PF. Glomerular and tubular adaptive responses to acute nephron loss in the rat. Effect of prostaglandin synthesis inhibition. J Clin Invest 1990;85:1761–9.
[269] Gullner HG, Gill Jr. JR, Bartter FC, et al. The role of the prostaglandin system in the regulation of renal function in normal women. Am J Med 1980;69:718–24.
[270] Brater DC. Anti-inflammatory agents and renal function. Semin Arthritis Rheum 2002;32:33–42.
[271] Cheng HF, Harris RC. Cyclooxygenases, the kidney, and hypertension. Hypertension 2004;43:525–30.
[272] Dunn MJ. Nonsteroidal antiinflammatory drugs and renal function. Annu Rev Med 1984;35:411–28.
[273] Zipser RD. Effects of selective inhibition of thromboxane synthesis on renal function in humans. Am J Physiol 1985;248: F753–6.
[274] Tuttle KR, Puhlman ME, Cooney SK, et al. Effects of amino acids and glucagon on renal hemodynamics in type 1 diabetes. Am J Physiol Renal Physiol 2002;282:F103–12.
[275] Kirschenbaum MA, Serros ER. Effect of prostaglandin inhibition on glomerular filtration rate in normal and uremic rabbits. Prostaglandins 1981;22:245–54.
[276] Stahl RA, Kudelka S, Paravicini M, et al. Prostaglandin and thromboxane formation in glomeruli from rats with reduced renal mass. Nephron 1986;42:252–7.
[277] Badr KF, Murray JJ, Breyer MD, et al. Mesangial cell, glomerular and renal vascular responses to endothelin in the rat kidney. Elucidation of signal transduction pathways. J Clin Invest 1989;83:336–42.
[278] Edwards RM, Trizna W, Ohlstein EH. Renal microvascular effects of endothelin. Am J Physiol 1990;259:F217–21.
[279] Lanese DM, Yuan BH, McMurtry IF, et al. Comparative sensitivities of isolated rat renal arterioles to endothelin. Am J Physiol 1992;263:F894–9.
[280] King AJ, Brenner BM, Anderson S. Endothelin: a potent renal and systemic vasoconstrictor peptide. Am J Physiol 1989;256: F1051–8.
[281] Fujihara CK, De Nucci G, Zatz R. Physiologic role of ETA receptors in the regulation of renal hemodynamics in normal and salt-depleted rats. J Cardiovasc Pharmacol 1995;26(Suppl. 3):S466–9.
[282] Benigni A, Perico N, Gaspari F, et al. Increased renal endothelin production in rats with reduced renal mass. Am J Physiol 1991;260:F331–9.
[283] Orisio S, Benigni A, Bruzzi I, et al. Renal endothelin gene expression is increased in remnant kidney and correlates with disease progression. Kidney Int 1993;43:354–8.
[284] Benigni A, Zoja C, Corna D, et al. A specific endothelin subtype A receptor antagonist protects against injury in renal disease progression. Kidney Int 1993;44:440–4.
[285] Ding SS, Qiu C, Hess P, et al. Chronic endothelin receptor blockade prevents both early hyperfiltration and late overt diabetic nephropathy in the rat. J Cardiovasc Pharmacol 2003;42:48–54.
[286] Kiberd BA, Larson TS, Robertson CR, et al. Effect of atrial natriuretic peptide on vasa recta blood flow in the rat. Am J Physiol 1987;252:F1112–7.
[287] Takezawa K, Cowley Jr. AW, Skelton M, et al. Atriopeptin III alters renal medullary hemodynamics and the pressure-diuresis response in rats. Am J Physiol 1987;252:F992–1002.
[288] van de SA, Jamison RL. Micropuncture study of the effect of ANP on the papillary collecting duct in the rat. Am J Physiol 1988;254:F477–83.
[289] Smith S, Anderson S, Ballermann BJ, et al. Role of atrial natriuretic peptide in adaptation of sodium excretion with reduced renal mass. J Clin Invest 1986;77:1395–8.
[290] Ortola FV, Ballermann BJ, Anderson S, et al. Elevated plasma atrial natriuretic peptide levels in diabetic rats. Potential mediator of hyperfiltration. J Clin Invest 1987;80:670–4.
[291] Perico N, Benigni A, Gabanelli M, et al. Atrial natriuretic peptide and prostacyclin synergistically mediate hyperfiltration and hyperperfusion of diabetic rats. Diabetes 1992;41:533–8.
[292] Brochner-Mortensen J. The glomerular filtration rate during moderate hyperglycemia in normal man. Acta Med Scand 1973;1-2:31–7.
[293] Wiseman MJ, Mangili R, Alberetto M, et al. Glomerular response mechanisms to glycemic changes in insulin-dependent diabetics. Kidney Int 1987;31:1012–8.
[294] Muntzel M, Hannedouche T, Niesor R, et al. Long-term effects of a somatostatin analogue on renal haemodynamics and hypertrophy in diabetic rats. Clin Sci (Lond) 1992;83:575–81.
[295] Mitch WE, Walser M, Buffington GA, et al. A simple method of estimating progression of chronic renal failure. Lancet 1976;2:1326–8.
[296] Dunnill MS, Halley W. Some observations on the quantitative anatomy of the kidney. J Pathol 1973;110:113–21.
[297] Hoy WE, Douglas-Denton RN, Hughson MD, et al. A stereological study of glomerular number and volume: preliminary findings in a multiracial study of kidneys at autopsy. Kidney Int Suppl 2003;:S31–7.
[298] Nyengaard JR, Bendtsen TF. Glomerular number and size in relation to age, kidney weight, and body surface in normal man. Anat Rec 1992;232:194–201.
[299] Brenner BM, Garcia DL, Anderson S. Glomeruli and blood pressure. Less of one, more the other? Am J Hypertens 1988;1:335–47.
[300] Brenner BM, Mackenzie HS. Nephron mass as a risk factor for progression of renal disease. Kidney Int Suppl 1997;63:S124–7.
[301] Keller G, Zimmer G, Mall G, et al. Nephron number in patients with primary hypertension. N Engl J Med 2003;348:101–8.
[302] Kiprov DD, Colvin RB, McCluskey RT. Focal and segmental glomerulosclerosis and porteinuria associated with unilateral renal agenesis. Lab Invest 1982;46:275–81.
[303] Carter JE, Lirenman DS. Bilateral renal hypoplasia with oligomeganephronia. Oligomeganephronic renal hypoplasia. Am J Dis Child 1970;120:537–42.
[304] McGraw M, Poucell S, Sweet J, et al. The significance of focal segmental glomerulosclerosis in oligomeganephronia. Int J Pediatr Nephrol 1984;5:67–72.
[305] Esposito C, He CJ, Striker GE, et al. Nature and severity of the glomerular response to nephron reduction is strain-dependent in mice. Am J Pathol 1999;154:891–7.
[306] He C, Zalups RK, Henderson DA, et al. Molecular analysis of spontaneous glomerulosclerosis in Os/ + mice, a model with reduced nephron mass. Am J Physiol 1995;269:F266–73.
[307] Friberg P, Sundelin B, Bohman SO, et al. Renin-angiotensin system in neonatal rats: induction of a renal abnormality in response to ACE inhibition or angiotensin II antagonism. Kidney Int 1994;45:485–92.
[308] Spence SG, Zacchei AG, Lee LL, et al. Toxicokinetic analysis of losartan during gestation and lactation in the rat. Teratology 1996;53:245–52.

[309] Tufro-McReddie A, Romano LM, Harris JM, et al. Angiotensin II regulates nephrogenesis and renal vascular development. Am J Physiol 1995;269:F110–5.
[310] Machado FG, Poppi EP, Fanelli C, et al. AT1 blockade during lactation as a model of chronic nephropathy: mechanisms of renal injury. Am J Physiol Renal Physiol 2008;294:F1345–53.
[311] Suzuki H, Tokuriki T, Saito K, et al. Glomerular hyperfiltration and hypertrophy in the rat hypoplastic kidney as a model of oligomeganephronic disease. Nephrol Dial Transplant 2005;20:1362–9.
[312] Azar S, Johnson MA, Hertel B, et al. Single-nephron pressures, flows, and resistances in hypertensive kidneys with nephrosclerosis. Kidney Int 1977;12:28–40.
[313] Fassi A, Sangalli F, Maffi R, et al. Progressive glomerular injury in the MWF rat is predicted by inborn nephron deficit. J Am Soc Nephrol 1998;9:1399–406.
[314] Menini S, Ricci C, Iacobini C, et al. Glomerular number and size in Milan hypertensive and normotensive rats: their relationship to susceptibility and resistance to hypertension and renal disease. J Hypertens 2004;22:2185–92.
[315] Skov K, Nyengaard JR, Korsgaard N, et al. Number and size of renal glomeruli in spontaneously hypertensive rats. J Hypertens 1994;12:1373–6.
[316] Grond J, Beukers JY, Schilthuis MS, et al. Analysis of renal structural and functional features in two rat strains with a different susceptibility to glomerular sclerosis. Lab Invest 1986;54:77–83.
[317] Weening JJ, Beukers JJ, Grond J, et al. Genetic factors in focal segmental glomerulosclerosis. Kidney Int 1986;29:789–98.
[318] Argueso LR, Ritchey ML, Boyle Jr. ET, et al. Prognosis of children with solitary kidney after unilateral nephrectomy. J Urol 1992;148:747–51.
[319] Lent V, Harth J. Nephropathy in remnant kidneys: pathological proteinuria after unilateral nephrectomy. J Urol 1994;152:312–6.
[320] Novick AC, Gephardt G, Guz B, et al. Long-term follow-up after partial removal of a solitary kidney. N Engl J Med 1991;325:1058–62.
[321] Narkun-Burgess DM, Nolan CR, Norman JE, et al. Forty-five year follow-up after uninephrectomy. Kidney Int 1993;43:1110–5.
[322] Miller IJ, Suthanthiran M, Riggio RR, et al. Impact of renal donation. Long-term clinical and biochemical follow-up of living donors in a single center. Am J Med 1985;79:201–8.
[323] Saran R, Marshall SM, Madsen R, et al. Long-term follow-up of kidney donors: a longitudinal study. Nephrol Dial Transplant 1997;12:1615–21.
[324] Ikoma M, Yoshioka T, Ichikawa I, et al. Mechanism of the unique susceptibility of deep cortical glomeruli of maturing kidneys to severe focal glomerular sclerosis. Pediatr Res 1990;28:270–6.
[325] Okuda S, Motomura K, Sanai T, et al. High incidence of glomerular sclerosis in rats subjected to uninephrectomy at young age. Nephron 1988;49:240–4.
[326] Arnould C, Lelievre-Pegorier M, Ronco P, et al. MMP9 limits apoptosis and stimulates branching morphogenesis during kidney development. J Am Soc Nephrol 2009;20:2171–80.
[327] Kambham N, Markowitz GS, Valeri AM, et al. Obesity-related glomerulopathy: an emerging epidemic. Kidney Int 2001;59:1498–509.
[328] Mathew AV, Okada S, Sharma K. Obesity related kidney disease. Curr Diabetes Rev 2011;7:41–9.
[329] Praga M, Morales E. Obesity, proteinuria and progression of renal failure. Curr Opin Nephrol Hypertens 2006;15:481–6.
[330] Praga M, Hernandez E, Morales E, et al. Clinical features and long-term outcome of obesity-associated focal segmental glomerulosclerosis. Nephrol Dial Transplant 2001;16:1790–8.
[331] Chagnac A, Weinstein T, Korzets A, et al. Glomerular hemodynamics in severe obesity. Am J Physiol Renal Physiol 2000;278: F817–22.
[332] Porter LE, Hollenberg NK. Obesity, salt intake, and renal perfusion in healthy humans. Hypertension 1998;32:144–8.
[333] Bueter M, Dubb SS, Gill A, et al. Renal cytokines improve early after bariatric surgery. Br J Surg 2010;97:1838–44.
[334] Chagnac A, Weinstein T, Herman M, et al. The effects of weight loss on renal function in patients with severe obesity. J Am Soc Nephrol 2003;14:1480–6.
[335] Praga M, Hernandez E, Herrero JC, et al. Influence of obesity on the appearance of proteinuria and renal insufficiency after unilateral nephrectomy. Kidney Int 2000;58:2111–8.
[336] Meier-Kriesche HU, Arndorfer JA, Kaplan B. The impact of body mass index on renal transplant outcomes: a significant independent risk factor for graft failure and patient death. Transplantation 2002;73:70–4.
[337] Modlin CS, Flechner SM, Goormastic M, et al. Should obese patients lose weight before receiving a kidney transplant? Transplantation 1997;64:599–604.
[338] Gonzalez E, Gutierrez E, Morales E, et al. Factors influencing the progression of renal damage in patients with unilateral renal agenesis and remnant kidney. Kidney Int 2005;68:263–70.
[339] Henegar JR, Bigler SA, Henegar LK, et al. Functional and structural changes in the kidney in the early stages of obesity. J Am Soc Nephrol 2001;12:1211–7.
[340] Kasiske BL, Cleary MP, O'Donnell MP, et al. Effects of genetic obesity on renal structure and function in the Zucker rat. J Lab Clin Med 1985;106:598–604.
[341] Park SK, Kang SK. Renal function and hemodynamic study in obese Zucker rats. Korean J Intern Med 1995;10:48–53.
[342] Schmitz PG, O'Donnell MP, Kasiske BL, et al. Renal injury in obese Zucker rats: glomerular hemodynamic alterations and effects of enalapril. Am J Physiol 1992;263:F496–502.
[343] Maddox DA, Alavi FK, Santella RN, et al. Prevention of obesity-linked renal disease: age-dependent effects of dietary food restriction. Kidney Int 2002;62:208–19.
[344] Klag MJ, Whelton PK, Randall BL, et al. End-stage renal disease in African-American and white men. 16-year MRFIT findings. JAMA 1997;277:1293–8.
[345] Fox CS, Larson MG, Leip EP, et al. Predictors of new-onset kidney disease in a community-based population. JAMA 2004;291:844–50.
[346] Haroun MK, Jaar BG, Hoffman SC, et al. Risk factors for chronic kidney disease: a prospective study of 23,534 men and women in Washington county, Maryland. J Am Soc Nephrol 2003;14:2934–41.
[347] Sawicki PT, Didjurgeit U, Muhlhauser I, et al. Smoking is associated with progression of diabetic nephropathy. Diabetes Care 1994;17:126–31.
[348] Orth SR, Stockmann A, Conradt C, et al. Smoking as a risk factor for end-stage renal failure in men with primary renal disease. Kidney Int 1998;54:926–31.
[349] Stengel B, Couchoud C, Cenee S, et al. Age, blood pressure and smoking effects on chronic renal failure in primary glomerular nephropathies. Kidney Int 2000;57:2519–26.
[350] Cryer PE, Haymond MW, Santiago JV, et al. Norepinephrine and epinephrine release and adrenergic mediation of smoking-associated hemodynamic and metabolic events. N Engl J Med 1976;295:573–7.

[351] Ritz E, Benck U, Franek E, et al. Effects of smoking on renal hemodynamics in healthy volunteers and in patients with glomerular disease. J Am Soc Nephrol 1998;9:1798–804.
[352] Halmai R, Szijarto IA, Feher E, et al. Cigarette smoke elicits relaxation of renal arteries. Eur J Clin Invest 2011;41:195–202.
[353] Sauriasari R, Sakano N, Wang DH, et al. C-reactive protein is associated with cigarette smoking-induced hyperfiltration and proteinuria in an apparently healthy population. Hypertens Res 2010;33:1129–36.
[354] Ishizaka N, Ishizaka Y, Toda E, et al. Association between cigarette smoking and chronic kidney disease in Japanese men. Hypertens Res 2008;31:485–92.
[355] Hua P, Feng W, Ji S, et al. Nicotine worsens the severity of nephropathy in diabetic mice: implications for the progression of kidney disease in smokers. Am J Physiol Renal Physiol 2010;299:F732–9.
[356] Adams LG, Polzin DJ, Osborne CA, et al. Influence of dietary protein/calorie intake on renal morphology and function in cats with 5/6 nephrectomy. Lab Invest 1994;70:347–57.
[357] Barretti P, Soares V. Importance of early and continuous use of protein restriction on the progression of adriamycin nephropathy. Ren Fail 1999;21:603–13.
[358] Brenner BM. Nephron adaptation to renal injury or ablation. Am J Physiol 1985;249:F324–37.
[359] Jaffa AA, Silva RH, Kim B, et al. Modulation of renal kallikrein production by dietary protein in streptozotocin-induced diabetic rats. J Am Soc Nephrol 1996;7:721–7.
[360] Vanrenterghem YF, Verberckmoes RK, Roels LM, et al. Role of prostaglandins in protein-induced glomerular hyperfiltration in normal humans. Am J Physiol 1988;254:F463–9.
[361] Tolins JP, Shultz PJ, Westberg G, et al. Renal hemodynamic effects of dietary protein in the rat: role of nitric oxide. J Lab Clin Med 1995;125:228–36.
[362] Gao X, Huang L, Grosjean F, et al. Low-protein diet supplemented with ketoacids reduces the severity of renal disease in 5/6 nephrectomized rats: a role for KLF15. Kidney Int 2011;79:987–96.
[363] Kalantar-Zadeh K, Gutekunst L, Mehrotra R, et al. Understanding sources of dietary phosphorus in the treatment of patients with chronic kidney disease. Clin J Am Soc Nephrol 2010;5:519–30.
[364] Bernstein AM, Treyzon L, Li Z. Are high-protein, vegetable-based diets safe for kidney function? A review of the literature. J Am Diet Assoc 2007;107:644–50.
[365] Lentine K, Wrone EM. New insights into protein intake and progression of renal disease. Curr Opin Nephrol Hypertens 2004;13:333–6.
[366] Martin WF, Armstrong LE, Rodriguez NR. Dietary protein intake and renal function. Nutr Metab (Lond) 2005;2:25.
[367] Pecoits-Filho R. Dietary protein intake and kidney disease in Western diet. Contrib Nephrol 2007;155:102–12.
[368] Knight EL, Stampfer MJ, Hankinson SE, et al. The impact of protein intake on renal function decline in women with normal renal function or mild renal insufficiency. Ann Intern Med 2003;138:460–7.
[369] Ihle BU, Becker GJ, Whitworth JA, et al. The effect of protein restriction on the progression of renal insufficiency. N Engl J Med 1989;321:1773–7.
[370] Rosman JB, ter Wee PM, Meijer S, et al. Prospective randomised trial of early dietary protein restriction in chronic renal failure. Lancet 1984;2:1291–6.
[371] Walker JD, Bending JJ, Dodds RA, et al. Restriction of dietary protein and progression of renal failure in diabetic nephropathy. Lancet 1989;2:1411–5.
[372] Zeller K, Whittaker E, Sullivan L, et al. Effect of restricting dietary protein on the progression of renal failure in patients with insulin-dependent diabetes mellitus. N Engl J Med 1991;324:78–84.
[373] Klahr S, Levey AS, Beck GJ, et al. The effects of dietary protein restriction and blood-pressure control on the progression of chronic renal disease. Modification of diet in renal disease study group. N Engl J Med 1994;330:877–84.
[374] Locatelli F, Alberti D, Graziani G, et al. Prospective, r.andomised, multicentre trial of effect of protein restriction on progression of chronic renal insufficiency. Northern Italian cooperative study group. Lancet 1991;337:1299–304.
[375] Wingen AM, Fabian-Bach C, Schaefer F, et al. Randomised multicentre study of a low-protein diet on the progression of chronic renal failure in children. European study group of nutritional treatment of chronic renal failure in childhood. Lancet 1997;349:1117–23.
[376] Franch HA, Mitch WE. Navigating between the Scylla and Charybdis of prescribing dietary protein for chronic kidney diseases. Annu Rev Nutr 2009;29:341–64.
[377] Kopple JD, Levey AS, Greene T, et al. Effect of dietary protein restriction on nutritional status in the modification of diet in renal disease study. Kidney Int 1997;52:778–91.
[378] Imbasciati E, Pardi G, Capetta P, et al. Pregnancy in women with chronic renal failure. Am J Nephrol 1986;6:193–8.
[379] Jones DC, Hayslett JP. Outcome of pregnancy in women with moderate or severe renal insufficiency. N Engl J Med 1996;335:226–32.
[380] Hayashi K, Epstein M, Loutzenhiser R. Pressure-induced vasoconstriction of renal microvessels in normotensive and hypertensive rats. Studies in the isolated perfused hydronephrotic kidney. Circ Res 1989;65:1475–84.
[381] Hsu CH, Slavicek JM. The effect of renal perfusion pressure on renal vascular resistance in the spontaneously hypertensive rat. Pflugers Arch 1982;393:340–3.
[382] Loutzenhiser R, Griffin K, Williamson G, et al. Renal autoregulation: new perspectives regarding the protective and regulatory roles of the underlying mechanisms. Am J Physiol Regul Integr Comp Physiol 2006;290:R1153–67.
[383] Sealey JE, Blumenfeld JD, Bell GM, et al. On the renal basis for essential hypertension: nephron heterogeneity with discordant renin secretion and sodium excretion causing a hypertensive vasoconstriction-volume relationship. J Hypertens 1988;6: 763–77.
[384] Bidani AK, Schwartz MM, Lewis EJ. Renal autoregulation and vulnerability to hypertensive injury in remnant kidney. Am J Physiol 1987;252:F1003–10.
[385] Hashimoto Y, Ideura T, Yoshimura A, et al. Autoregulation of renal blood flow in streptozocin-induced diabetic rats. Diabetes 1989;38:1109–13.
[386] Parving HH, Kastrup H, Smidt UM, et al. Impaired autoregulation of glomerular filtration rate in type 1 (insulin-dependent) diabetic patients with nephropathy. Diabetologia 1984; 27:547–52.
[387] Amann K, Koch A, Hofstetter J, et al. Glomerulosclerosis and progression: effect of subantihypertensive doses of alpha and beta blockers. Kidney Int 2001;60:1309–23.
[388] Hausberg M, Tokmak F, Pavenstadt H, et al. Effects of moxonidine on sympathetic nerve activity in patients with end-stage renal disease. J Hypertens 2010;28:1920–7.
[389] Kanno Y, Takenaka T, Nakamura T, et al. Add-on angiotensin receptor blocker in patients who have proteinuric chronic kidney diseases and are treated with angiotensin-converting enzyme inhibitors. Clin J Am Soc Nephrol 2006;1:730–7.

[390] Parving HH, Persson F, Lewis JB, et al. Aliskiren combined with losartan in type 2 diabetes and nephropathy. N Engl J Med 2008;358:2433–46.
[391] Toto R, Palmer BF. Rationale for combination angiotensin receptor blocker and angiotensin-converting enzyme inhibitor treatment and end-organ protection in patients with chronic kidney disease. Am J Nephrol 2008;28:372–80.
[392] Werner C, Poss J, Bohm M. Optimal antagonism of the Renin-Angiotensin-aldosterone system: do we need dual or triple therapy?. Drugs 2010;70:1215–30.
[393] Navaneethan SD, Nigwekar SU, Sehgal AR, et al. Aldosterone antagonists for preventing the progression of chronic kidney disease: a systematic review and meta-analysis. Clin J Am Soc Nephrol 2009;4:542–51.
[394] Yusuf S, Teo KK, Pogue J, et al. Telmisartan, ramipril, or both in patients at high risk for vascular events. N Engl J Med 2008;358:1547–59.
[395] Maddox DA, Bennett CM, Deen WM, et al. Determinants of glomerular filtration in experimental glomerulonephritis in the rat. J Clin Invest 1975;55:305–18.
[396] Sakai T, Harris Jr. FH, Marsh DJ, et al. Extracellular fluid expansion and autoregulation in nephrotoxic serum nephritis in rats. Kidney Int 1984;25:619–28.
[397] Yoshioka T, Rennke HG, Salant DJ, et al. Role of abnormally high transmural pressure in the permselectivity defect of glomerular capillary wall: a study in early passive Heymann nephritis. Circ Res 1987;61:531–8.
[398] Konishi Y, Imanishi M, Okamura M, et al. Relationship of renal histological damage to glomerular hypertension in patients with immunoglobulin A nephropathy. Journal of Hypertension 2000;18:103–9.
[399] Woo KT, Lau YK, Zhao Y, et al. Disease progression, response to ACEI/ATRA therapy and influence of ACE gene in IgA nephritis. Cell Mol Immunol 2007;4:227–32.
[400] Bedogna V, Valvo E, Casagrande P, et al. Effects of ACE inhibition in normotensive patients with chronic glomerular disease and normal renal function. Kidney Int 1990;38:101–7.
[401] Hutchinson FN, Schambelan M, Kaysen GA. Modulation of albuminuria by dietary protein and converting enzyme inhibition. Am J Physiol 1987;253:F719–25.
[402] Duran-Barragan S, McGwin Jr. G, Vila LM, et al. Angiotensin-converting enzyme inhibitors delay the occurrence of renal involvement and are associated with a decreased risk of disease activity in patients with systemic lupus erythematosus—results from LUMINA (LIX): a multiethnic US cohort. Rheumatology (Oxford) 2008;47:1093–6.
[403] Praga M, Gutierrez E, Gonzalez E, et al. Treatment of IgA nephropathy with ACE inhibitors: a randomized and controlled trial. J Am Soc Nephrol 2003;14:1578–83.
[404] Titan SM, Vieira M, Dominguez WV, et al. ACEI and ARB combination therapy in patients with macroalbuminuric diabetic nephropathy and low socioeconomic level: a double-blind randomized clinical trial. Clin Nephrol 2011; 76:273–83.

This page intentionally left blank

CHAPTER

87

Role of Proteinuria in the Progression of Renal Disease

Mauro Abbate[1], *Daniela Macconi*[1], *Giuseppe Remuzzi*[1,2] *and Carla Zoja*[1]

[1]'Mario Negri' Institute for Pharmacological Research, Centro Anna Maria Astori, Bergamo, Italy

[2]Division of Nephrology and Dialysis, Ospedali Riuniti di Bergamo, Bergamo, Italy

INTRODUCTION

Chronic progressive nephropathies, independent of the type of the initial insult, have in common persistently high levels of urinary protein excretion, chronic tubulointerstitial lesions, and glomerular sclerosis. It has become clear that in otherwise comparable groups of patients, those with higher levels of proteinuria are at a greater risk of progression. It has been long known that the severity of tubular interstitial damage is highly correlated to the degree of deterioration of renal failure, even better than the glomerular lesions do. The recognition that proteinuria is an independent predictor and a possible contributor of progression rather than just a marker of the severity of glomerular damage represents a major change in our concepts of progressive kidney disease. Proteinuria is enlisted among modifiable risk factors of progressive renal insufficiency, and antiproteinuric treatments are consistently renoprotective. Proteinuria reduction must therefore be considered as a target of therapeutic intervention in managing the patient with a chronic proteinuric nephropathy.

Among the cellular mechanisms that may contribute to determine progression, proteins that gain access to the glomerular filtrate as a consequence of altered glomerular permeability reach the Bowman's space and the tubular lumen and act as trigger of interstitial inflammatory and fibrotic reactions through the tubular synthesis of bioactive mediators. *In vitro* studies using polarized proximal tubular epithelial cells as a model system to mimic the effects of prolonged exposure to proteins have highlighted specific mechanisms underlying renal cell activation and renal interstitial injury.

The main focus of this chapter is on pathways of interstitial inflammation and fibrosis activated by ultrafiltered proteins that play major roles in the multifactorial process ultimately responsible for kidney scarring and loss of function (Figure 87.1).

Historical Perspective

A relentless decline in glomerular filtration rate can follow initial insults to the kidney through a process termed as 'renal disease progression' by nephrologists since 1982.[1] Studies in the early 19th and 20th centuries[2,3] contributed to link a disparate body of knowledge about patients with albuminuria and pathological evidence of diseased kidneys. By summarizing his concept in term of renal 'osmotic work', Addis calculated how this work would vary with the amount of proteins in the diet and suggested that dietary protein restriction could possibly help patients with renal impairment.[4]

When glomerular permeability is altered, as occurs in many glomerular diseases, considerable quantities of circulating proteins are abnormally filtered in the urinary space. Volhard and Fahr[5] and subsequently Mollendorf and Stohr[6] provided the early descriptions of hyalin droplets in the cytoplasm of proximal tubular cells and suggested that they reflected renal damage related to severe proteinuria. It was then proposed that such changes could represent the initial phase of activation of cellular pathways leading to cell necrosis.[7] The appearance of droplets was also

Seldin and Giebisch's The Kidney, Fifth Edition.
DOI: http://dx.doi.org/10.1016/B978-0-12-381462-3.00087-2

© 2013 Elsevier Inc. All rights reserved.

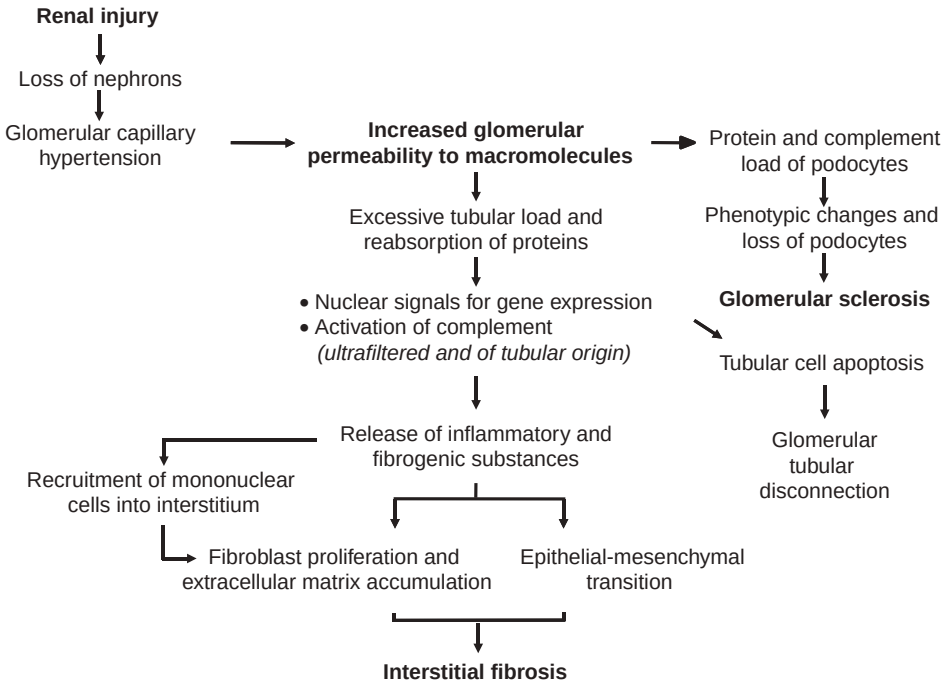
Renal injury
Loss of nephrons
Glomerular capillary hypertension
Increased glomerular permeability to macromolecules
Protein and complement load of podocytes
Excessive tubular load and reabsorption of proteins
Phenotypic changes and loss of podocytes
• Nuclear signals for gene expression
• Activation of complement
(ultrafiltered and of tubular origin)
Glomerular sclerosis
Tubular cell apoptosis
Release of inflammatory and fibrogenic substances
Glomerular tubular disconnection
Recruitment of mononuclear cells into interstitium
Fibroblast proliferation and extracellular matrix accumulation
Epithelial-mesenchymal transition
Interstitial fibrosis

FIGURE 87.1 Schematic representation of the events that lead to chronic tubulointerstitial damage and glomerular sclerosis in proteinuric nephropathy.

suggested to be associated with impairment of normal reabsorbption and degradation of plasma proteins by proximal tubular cells.[8]

Hints about a possible association between proteinuria and renal function impairment formally emerged in the late 1970s. Cameron and colleagues showed that among patients with focal and segmental glomerulosclerosis those with nephrotic syndrome progressed more rapidly than those who had never been nephrotics.[9] This was also true for mesangiocapillary glomerulonephritis[9] and membranous nephropathy.[10] Their speculation was that during the course of prolonged nephrotic syndrome intracapillary platelet thrombi induced segmental sclerosis, or that these glomerular lesions were a consequence of proteinuria. These observations were in agreement with previous findings that none of patients with focal and segmental glomerulosclerosis who responded to corticosteroid treatment with reduction of proteinuria developed renal failure.[11]

In 1981 Brenner and associates introduced the concept that glomerular hemodynamic changes (glomerular hyperfiltration) ensuing as compensatory adaptation to nephron loss can cause progressive deterioration of remaining nephrons. Instrumental in clarifying the pathophysiology of renal adaptation to nephron loss was the model of renal ablation in the rat.[12] After removal of a critical portion of renal mass, remnant nephrons undergo sudden hypertrophy with concomitant lowering of arteriolar resistance and increased glomerular plasma flow. Since the vascular tone drops more in afferent arterioles than in the efferent ones, glomerular capillary hydraulic pressure rises and more filtrate is formed per nephron. While such changes serve to enhance the filtration capacity of remaining nephron units, thus minimizing the functional consequences of nephron loss, they are ultimately detrimental. Therapies that attenuate such adaptive changes limit GFR decline and structural damage. In harmony with the data obtained in animal studies, clinical studies showed markedly reduced rates of GFR decline in patients with diabetes receiving antihypertensive agents.[13,14] Elevated intraglomerular capillary pressure was suggested to act as a noxious stimulus to glomerular cells.[15] Studies of mathematical models of the glomerular filtering membrane documented that the high glomerular capillary pressure acted to enlarge the radii of the pores perforating the glomerular membrane by a mechanism at least partly mediated by angiotensin II.[16] This impairs the size-selective function of the barrier resulting in protein ultrafiltration. The association of protein ultrafiltration and progression of renal disease was underscored by Mathiesen and coworkers[17] who reported that in diabetic patients the higher the microalbuminuria the faster the rate of GFR decline.

In 1986, it was suggested for the first time that proteins abnormally filtered through the glomerular capillary might have intrinsic renal toxicity that is relevant to the progression of renal damage.[18] In the kidneys of proteinuric rats with adriamycin nephrosis, the accumulation of filtered proteins in the cytoplasm of proximal tubular cells and in luminal casts was associated with focal breaking of the tubular basement membrane

and extravasation of the tubular content into the renal interstitium. Aging is associated with progressive proteinuria and glomerulosclerosis, which lead to the renal insufficiency of certain strains of rats. The severity of proteinuria predicted the development of glomerulosclerosis and tubulointerstitial changes.[19] Implications of these studies were that the enhanced protein uptake may activate proximal tubular epithelial cells to promote the accumulation of inflammatory cells into the interstitium, in turn responsible for renal scarring.[20] Studies using animal models and pharmacologic manipulations found that the dysfunction of the glomerular capillary barrier to proteins can precede the onset of structural lesions in the absence of glomerular hemodynamic changes, consistent with the possibility that—at least in certain settings—protein load of the nephron may contribute independently to progressive renal damage before maladaptive hemodynamic changes can take place or be measurable within the glomerulus.[21,22]

Cause-and-effect relationships between enhanced transtubular protein passage and interstitial inflammation were investigated by Eddy in a rat model of protein overload.[23] Repeated injections of albumin increased the permeability of the glomerular barrier leading to proteinuria and tubular changes, including the accumulation of injected albumin in intracellular droplets of tubular cells. These changes occurred in advance of heavy infiltration of macrophages and T lymphocytes into the renal interstitium. Excessive proteinuria was also induced in rats by transplanting a pituitary tumor (MtT SA5) that causes liver hyperplasia with both overproduction and abnormally high urinary excretion of albumin, followed by tubular damage and interstitial inflammation.[24] Models of protein overload contributed to suggest that the pathogenic potential of ultrafiltered plasma proteins is not confined to pathways underlying tubular and interstitial damage. The availability of cultured cells with features of differentiated podocytes revived investigation on the effects of plasma proteins on the function of glomerular epithelial cells,[25,26] currently recognized to play a key role in the progression of lesions toward glomerular sclerosis. Plasma proteins that are filtered accumulate as protein droplets within podocytes from the early stages of non-immunologically-induced glomerular damage. At the same stage, podocytes show signs of dedifferentiation and injury.[25] These abnormalities are likely to play role in the development of glomerular sclerotic lesions. They will be discussed in the light of findings indicating another important pathway, i.e., the activation of complement upon excess protein ultrafiltration.

Tubular Handling of Proteins

Proteins that reach the tubular lumen are reabsorbed in the proximal segments by receptor-mediated endocytosis, via two multiligand-binding receptors, megalin and cubilin.[27] Megalin, a 600-kDa transmembrane glycoprotein belonging to the low density-lipoprotein receptor family, represents the most abundant endocytic receptor in the proximal tubule, being concentrated in clathrin-coated pits (CCPs) and vesicles in the brush border region.[28,29] It binds different ligands including albumin, hormones such as insulin, angiotensin II and prolactin, and vitamin-binding proteins. Megalin's endocytic function is regulated by the G protein–mediated signaling pathway that includes Gαi3, GAIP and GIPC, the latter interacting with the cytoplasmic tail of megalin[30] (Figure 87.2). This portion contains recognition motifs for intracellular adaptor proteins and protein kinases involved in endocytosis, apical sorting of receptor, and signaling.[27]

Among adaptor proteins, Disabled protein 2 (Dab2) colocalizes with megalin in CCPs and vesicles of renal proximal tubules where it binds the second endocytic motif of megalin, and, by interacting with the motor protein nonmuscle myosin heavy chain IIA, regulates trafficking of megalin through the endocytic/recycling pathway[31] (Figure 87.2). Suboptimal trafficking of megalin in Dab2 knockout mice leads to decreased megalin levels, possibly due to increased protein shedding and degradation, and impaired endocytosis as documented by urinary loss of megalin ligand.[32] Association of motor proteins with adaptor proteins is now emerging to be instrumental for renal proximal tubular endocytosis. Myosin VI (Myo6) is highly expressed in the brush border where it associates with the CCP via its tail domain binding to Dab2 (Figure 87.2). Myo6 functional null mice show increased urinary albumin excretion, similar to megalin- and cubilin-deficient animals, and reduced and delayed endocytic uptake and trafficking of horseradish peroxidase consistent with impaired endocytosis.[33] This defect is associated with structural and phenotypic changes of tubular cells and fibrosis.

The expression and subcellular distribution of megalin is controlled by the chaperone receptor-associated protein RAP that prevents ligand–induced endoplasmic reticulum (ER) retention and degradation of the receptor and is possibly involved in its proper folding[27] (Figure 87.2). RAP knockout mice are characterized by both reduced expression of megalin and its preferential subcellular distribution to the ER. RAP deficiency is also associated with leakage of proteins in urines due to impaired megalin-dependent tubular reabsorption. Pro-inflammatory and pro-fibrotic mediators such as transforming growth factor beta (TGF-β) and angiotensin II[34,35] as well as nephrotoxicants[36] also down-regulate megalin expression in proximal tubular cells.

Cubilin or intrinsic-factor B12 receptor, is a 460-kDa peripheral membrane protein that binds albumin,

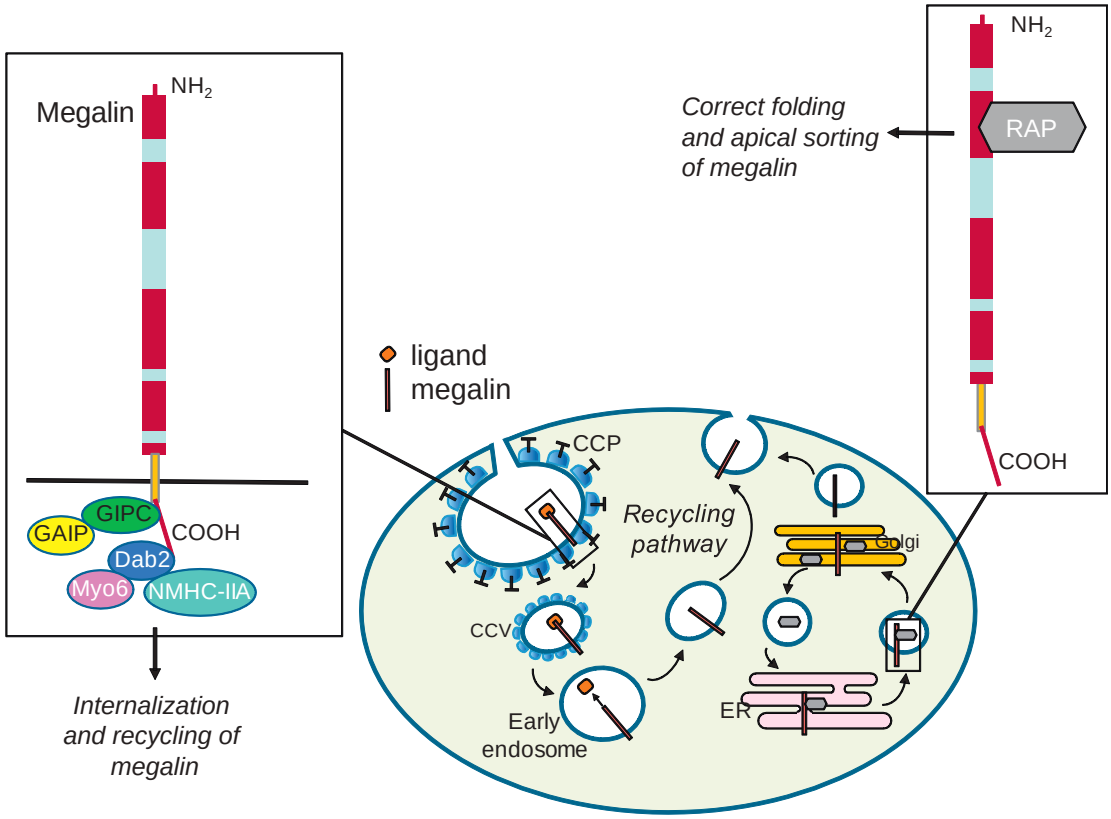

FIGURE 87.2 Regulation of trafficking and apical sorting of megalin. Megalin is associated with CCPs in the brush border of the renal proximal tubular cell. Through its cytoplasmic tail it interacts with the G protein GIPC and the adaptor protein Dab2, both regulating the endocytic/recycling pathway of the receptor. GIPC interacts with GAIP, and Dab2 binds the motor proteins NMHC-IIA and Myo6, which contribute to megalin's endocytic function. RAP binds megalin within the extracellular domain with the effect of regulating the receptor processing by proper folding, and prevents its retention in the ER due to early binding of ligands. This leads to correct transport of megalin through the Golgi and subsequent apical sorting to the brush border. Abbreviations: CCPs, clathrin-coated pits; CCV, clathrin-coated vesicle; Dab2, Disabled protein 2; ER, endoplasmic reticulum; GAIP, Gα interacting protein; GIPC, GAIP interacting protein, C terminus; Myo6, myosin 6; NMHC-IIA, nonmuscle myosin heavy chain IIA; RAP, receptor-associated protein.

transferrin, IgG light chains and RAP, but lacks the sites for interaction with adaptor proteins or other mediators of clathrin-dependent endocytosis.[28,29] Since megalin binds cubilin with high affinity, it has been hypothesized that megalin mediates endocytosis and intracellular trafficking of cubilin.[37] *In vitro*, the uptake of the cubilin-specific ligands, including transferrin, was inhibited both by anti-megalin antibodies and by megalin anti-sense oligonucleotides.[38–40] Furthermore, in megalin-deficient mice transferrin accumulates on the luminal membrane of the proximal tubule without being internalized.[38] Cubilin binds amnionless (AMN), a 50-kD transmembrane protein that is required for membrane targeting and may permit internalization of cubilin.[27] Patients with Imerslund-Grasbesk syndrome (IGS), a rare autosomal recessive disease caused by inheritable cubilin or AMN gene defect, show reduced protein reabsorption and proteinuria. Consistently, inappropriate apical membrane insertion of cubilin in the proximal tubule leads to proteinuria in a model of IGS in dogs with a mutation of the AMN gene. Kidney specific AMN knockout mice also show increased urinary excretion of transferrin.[41]

The generation of mice with the genetic ablation of cubilin, with or without ablation of megalin, disclosed a mutual dependency of cubilin and AMN to form a functional membrane receptor complex.[42] Cubilin is indispensable for albumin reabsorption in renal proximal tubule under physiological conditions, whereas megalin drives the internalization of cubilin-albumin complexes.[42]

Megalin undergoes regulated intramembrane proteolysis with protease-mediated ectodomain shedding, producing a membrane–associated C-terminal fragment, which is in turn the substrate for the γ-secretase activity of a multimolecular complex of proteins, including the so-called presenilins, that release the C-terminal soluble cytosolic domain predicted to target the nucleus. In the rat kidney, the brush border exhibits both γ-secretase activity and presenilin-1 expression.[43]

In a cell line derived from opossum proximal tubule (OK cells), metalloprotease activity sheds the ectodomain of megalin, producing a membrane-bound megalin COOH-terminal fragment with the same size as a major fragment of megalin found in the kidney.[43] This fragment is further cleaved by γ-secretase into a soluble intracellular domain leading to down-regulation of megalin and Na^+/H^+ exchanger 3 (NHE-3) transcripts.[44] This domain does not affect megalin expression and endocytic function *in vivo* at least under physiological conditions, although a regulatory effect on renal gene transcription under stress cannot be excluded.[45]

Reduced expression of megalin is a common feature to settings of proteinuria and defective tubular uptake of filtered proteins, such as early stages of experimental diabetes or polycystic kidney disease, Fanconi syndrome and Dent's disease in humans.[41] Dent's disease is caused by a mutation of the gene CLCN5 encoding the 2 chloride (Cl^-)/proton (H^+) exchanger ClC-5. Inactivating mutations of ClC-5 in Dent's disease and the deletion of CLCN5 in knockout mice lead to low-molecular-weight proteinuria due to reduced endocytic uptake of filtered proteins in the proximal tubule. This defect was initially attributed to impaired acidification of apical endosomes in these cells,[46–48] but subsequent data indicate selective loss of expression of megalin and cubilin at the brush border as a major cause of defective protein endocytosis in this disease.[49] Along this line, reduced megalin and cubilin levels have been found in tubules with the uncoupling E211A (unc) mutation that converts CLC-5 into a pure Cl^- conductor. Despite maintaining active endosomal acidification, $ClCN5^{unc}$ mice show impaired proximal tubular endocytosis and resultant low-molecular-weight proteinuria as found in CLC-5 knockout mice and in patients with Dent's disease.[50] These results indicate that endosomal chloride-proton exchange rather than chloride conductance is crucial for tubular endocytosis (Figure 87.3).

During receptor-mediated endocytosis, ligand-receptor complexes are internalized and transported via clathrin-coated vesicles to early endosomes where they dissociate. The receptor is sorted to the plasma membrane (recycling pathway) and the endocytosed proteins are transported further into the degradative pathway. The endocytic pathway is regulated by a protein network. The inositol 5′-phosphatase OCRL -whose mutations are responsible for *OculoCerebroRenal Syndrome of Lowe*, an X-linked disorder characterized by cataract, mental retardation, and renal Fanconi syndrome- is present throughout the early endocytic pathway including CCPs and interacts with adaptor molecules involved in the early endocytic traffic of receptors in brain and kidney.[51] On peripheral early endosomes OCRL binds the Rab5 effector APPL1, an adaptor/signaling protein that binds several transmembrane receptors and also the adaptor protein GIPC (Figure 87.3). Since GIPC directly binds megalin (see above), loss of the interaction of OCRL with APPL1 due to disease mutation may have a causal role in the reabsorptive defect of kidney resulting in low-molecular-weight proteinuria in Lowe syndrome patients and in a subset of Dent's disease patients.

Another protein, the transporter NHE-3 contributes to the early phase of the apical endocytic pathway at least in part due to its involvement in endocytic vesicle fusion.[52] NHE-3 is associated with megalin and dipeptidyl IV in proximal tubule endosomes where it also participates in the acidification process[48] (Figure 87.3). Acidification of endosomal compartment is crucial not only for ligand-receptor dissociation and receptor recycling, but also for a correct protein endocytic trafficking from early to late endosomes, and finally lysosomes. The acidification of proximal tubule endosomes is driven by the vacuolar H^+-ATPase (V-ATPase), an electrogenic pump that translocates protons from the cytoplasm to the endosomal lumen and in conjunction with a parallel chloride conductance generates the acidic milieu of the endosomal compartment[53] (Figure 87.3). V-ATPase acts as an endosomal pH sensor that recruits the small GTPase Arf6 (ADP-ribosylation factor) and its cognate GDP/GTP exchange factor ARNO (ADP-ribosylation factor nucleotide site opener) from the cytosol to the endosomal membranes by direct binding these proteins upon vesicle acidification (Figure 87.3). Interaction of both Arf6 and ARNO with V-ATPase allows correct vesicular trafficking from early to late endosomes. By contrast, inhibition of V-ATPase or uncoupling of endosomal acidification impairs V-ATPase/ARNO/Arf6 interaction leading to accumulation of endocytosed proteins in early endosomes, and ultimately, to inhibition of endocytosis.[53] An intact actin cytoskeleton is important for correct assembly and function of the V-ATPase.[53] The disorganization of the actin cytoskeleton induced by statins through reduced prenylation of the small GTP-binding proteins results in a defect of albumin endocytosis in proximal tubular cells.[54,55]

Protein Overload Activates Phenotypic Changes in Cultured Proximal Tubular Cells

Insights into mechanisms linking the excess traffic of plasma proteins and interstitial injury have come from *in vitro* studies using polarized proximal tubular cells as a model to assess effects of apical exposure to proteins (Figure 87.4). Challenge of cultured proximal tubular cells with high concentrations of proteins

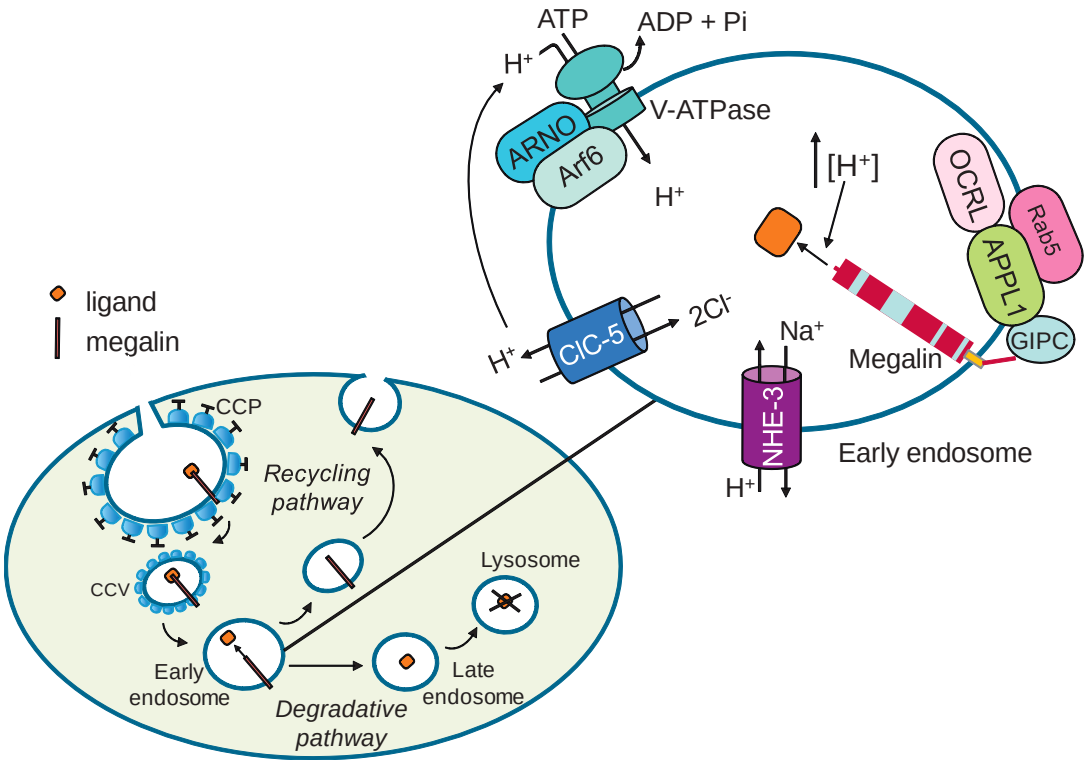

FIGURE 87.3 Regulation of endocytic pathway in the renal proximal tubular cell. Upon binding of ligand (i.e., albumin) to megalin in CCPs, ligand-receptor complexes are internalized and transported via clathrin-coated vesicles to early endosomes where they dissociate. Megalin is sorted to the plasma membrane (recycling pathway) and the endocytosed proteins are transported further into the degradative pathway. Acidification of intracellular lumen of the early endosome involves NHE-3 and V-ATPase with counter ion being provided by CLC-5. Upon acidification, Arf6 and ARNO are recruited to the endosomal membrane and both interact with V-ATPase driving the vesicular trafficking of endocytosed proteins from early to late endosomes. Interaction of the inositol 5′-phosphatase OCRL with the rab5 effector APPL1, which binds GIPC regulates the early steps of the endocytic traffic of megalin. Abbreviations: Arf6, ADP-ribosylation factor; APPL1, Adaptor Protein containing pleckstrin homology domain, PTB domain and Leucine zipper motif 1; ARNO, ADP-ribosylation factor nucleotide site opener; CCPs, clathrin-coated pits; CCV, clathrin-coated vesicle; CLC-5, 2 chloride (Cl^-)/proton (H^+) exchanger; NHE-3, Na^+/H^+ exchanger 3; OCRL, oculocerebrorenal syndrome of Lowe; V-ATPase, vacuolar H^+-ATPase.

(delipidated or lipid-enriched albumin, IgG and transferrin) induced the synthesis of the vasoconstrictor peptide endothelin-1,[56] a mediator of progressive renal injury due to its ability to stimulate renal cell proliferation and extracellular matrix production and to attract monocytes. Monocyte chemoattractant protein-1 (MCP-1 or CCL2) and Regulated upon Activation, Normal T cell Expressed and Secreted (RANTES or CCL5), potent chemoattractants for monocytes/macrophages and T-lymphocytes, were upregulated in proximal tubular cells challenged with albumin and other plasma proteins.[57,58] Albumin overload also induced tubular gene expression and production of the C-X-C chemokine interleukin-8 (IL-8), a potent chemoattractant for neutrophils and lymphocytes.[59] Endothelin-1 and chemokines induced by plasma proteins were released mainly toward the basolateral compartment of the cell, which is indicative of a directional secretion potentially responsible for the tubulointerstitial inflammatory reaction as found in proteinuric nephropathies. Co-culture systems of proximal tubular epithelial cells and monocytes/T cells proved useful to document that the release of MCP-1 and RANTES upon apical exposure of tubular cells to albumin was further increased in the presence of monocytes or T cells, either through a cell-to-cell contact mechanism or mediated by soluble factors such as interleukin-1 and tumor necrosis factor.[60] Moreover, the conditioned medium of tubular cells activated by albumin induced distinct patterns of chemokine receptor expression on T cells or monocytes, thereby implying that different arrays of chemokines may mediate the chemotactic activity of leukocytes in the tubulointerstitium during the proteinuric state.

Protein overload promotes the tubular expression of fractalkine/CX3CL1, a cell-membrane anchored chemokine that serves as an adhesive molecule to promote firm adhesion of mononuclear cells expressing the specific receptor CX3CR1, in addition to functioning in its cleaved soluble form as a chemoattractant. Upregulation of fractalkine mRNA and increased

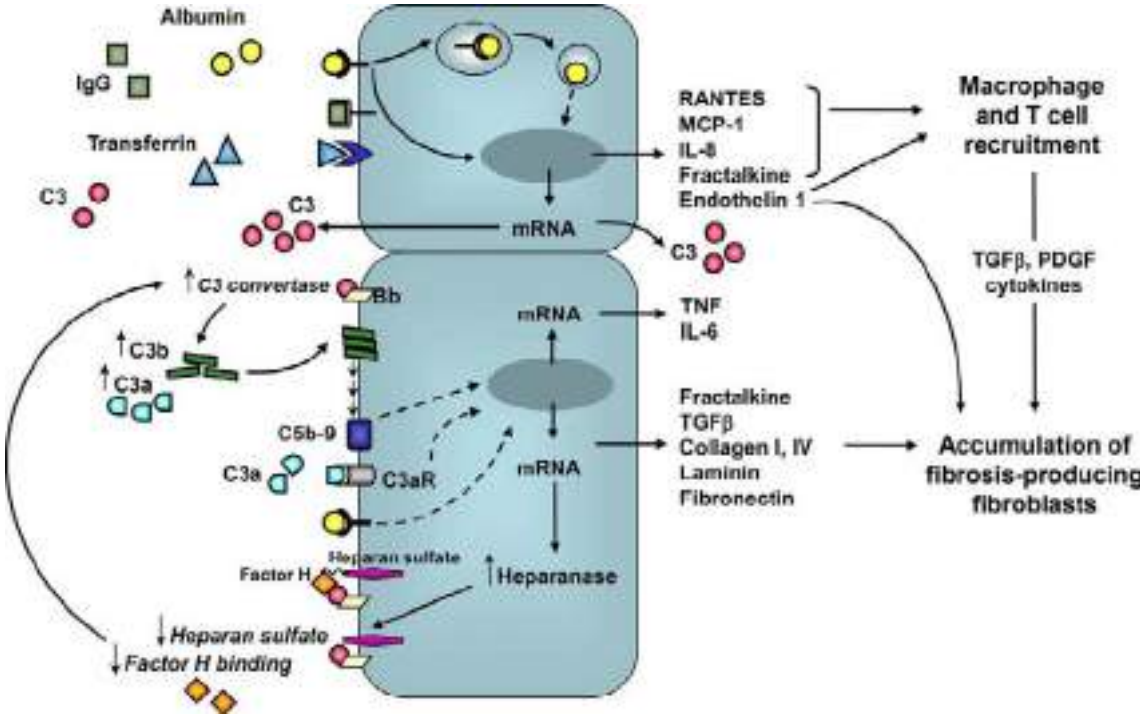

FIGURE 87.4 Cellular mechanisms of injury underlying the activation of inflammatory and fibrogenic pathways by proximal tubular cells in response to excess load of filtered plasma proteins that occurs in chronic proteinuric nephropathies.

synthesis of both membrane-bound and soluble forms of the protein occurred upon stimulation of human proximal tubular cells with albumin.[61] In a murine model of protein overload proteinuria, fractalkine mRNA was overexpressed in the kidney, and fractalkine staining was detected in tubular epithelial cells in a focal distribution.[61] Treatment of mice with an antibody against CX3CR1 limited the accumulation of monocytes/macrophages in the renal interstitium. These data suggest that in proteinuric conditions, fractalkine overproduction might contribute to direct mononuclear cells into the peritubular interstitium and possibly enhance their adhesive property.

TGFβ is a profibrogenic cytokine capable of directly stimulating the proliferation of fibroblasts and the synthesis of matrix proteins, in addition to exerting indirect stimulatory effects via inflammatory infiltrating cells. TGFβ acts as a key stimulus for epithelial-to-mesenchymal transition (EMT), by which tubular cells acquire features of fibroblasts.[62] High concentrations of albumin induced in cultured proximal tubular cells the transcription of the TGFβ gene resulting in the enhanced release of the cytokine in the cell supernatant.[63,64] Albumin upregulated TGFβ receptor type II expression in proximal tubular cells, which became more susceptible to the matrix-stimulatory actions of TGFβ.[65] Albumin stimulated the accumulation of extracellular collagen type IV, laminin, and fibronectin by proximal tubular cells through a post-transcriptional mechanism.[66] A reduced degradation could be responsible for the increased accumulation of extracellular matrix protein components, as indicated by induction of tissue inhibitors of metalloproteinases (TIMP)-1 and TIMP-2, in response to albumin.[66]

Advances have been made in clarifying the mechanisms of albumin-induced TGFβ production in proximal tubular cells. *In vitro*, albumin-induced secretion of TGFβ1 by proximal tubular cells could occur in the absence of albumin endocytosis.[67] Thus two cell lines, opossum kidney (OK) proximal tubular cells and HKC-8 proximal tubular cells, which display different degrees of endocytosis, produced an equivalent amount of TGFβ1 when exposed to albumin. Moreover, inhibiting albumin endocytosis in OK cells with two agents with different mechanisms of action as EIPA (a sodium/hydrogen exchanger-3 inhibitor) or simvastatin (a 3-hydroxy-3-methylglutaryl CoA reductase inhibitor) did not reduce albumin-induced TGF-β1 secretion. On the other hand, RAP, a known inhibitor of binding of albumin to megalin, inhibited albumin endocytosis but it did not affect TGFβ1 production, suggesting that albumin-induced secretion of TGFβ1 is not via megalin signaling.[67] Along this line, further studies showed that primary cultures of mouse proximal tubular cells exhibited substantial albumin endocytosis that could be similarly inhibited by both statins

and thiazolinediones, but only statins had the ability to limit albumin-stimulated MCP-1 production.[68] It was concluded that inhibition of albumin endocytosis alone was insufficient to attenuate chemokine production and therefore to protect proximal tubular cells from the toxic effects of albumin.[69]

The contact between tubular cells and interstitial matrix is operated by specialized adhesion molecules, the integrins. They are α/β transmembrane heterodimers that mediate adhesion of the basal surface of cells to the underlying substratum by recognizing extracellular matrix components and by interacting with different cytoskeletal molecules. *In vitro* these molecules are clustered in specialized structures, called focal contacts. In tubular cells the expression of integrins can be regulated by cytokines, including TGFβ, that either directly influence mRNA transcription of integrins or modulate the synthesis of interstitial matrix and the consequent rearrangement of integrins at focal contacts.[70] On the other hand, matrix proteins can modulate integrin expression and via integrin-generated signals, regulate the synthesis, degradation and organization of the matrix itself. Therefore, alterations in the expression and/or functional status of tubular cell integrins may play roles in the events leading to tubulointerstitial fibrosis. In cultured tubular cells the addition of albumin increased membrane expression of αvβ5 integrin which became organized in typical focal contacts dose-fashion related.[71]

The Role of Proteinuria in Tubular Apoptosis

Protein overload is a stimulus for apoptosis. A dose- and time-dependent induction of apoptosis by albumin was demonstrated in cultured proximal tubular cells as revealed by internucleosomal DNA fragmentation, morphological changes including cell shrinkage and nuclear condensation, and plasma membrane alterations.[72] Apoptosis in this setting was associated with activation of Fas-FADD-caspase 8 pathway, suggesting activation via the extrinsic pathway of apoptosis. Peroxisome proliferator activated receptor (PPAR)-γ[73] is also implicated in molecular mechanisms underlying albumin-induced apoptosis. **A**lbumin-bound fatty acids stimulated PPAR-γ in primary cultures of human proximal tubular cells and caused apoptosis that could be blocked by PPAR response element decoy oligonucleotides. Moreover, transfection experiments revealed that the transient overexpression of PPAR-γ in tubular cells resulted in enhanced apoptosis.[73] In HKC-8 human proximal tubular cells, albumin-induced apoptosis was mainly mediated by the intrinsic pathway of apoptosis, characterized by Bax translocation to mitochondria and cytochrome *c* release from the organelles.[74] This pathway was recently confirmed in rat proximal tubular cells by inhibition with Bcl-2 transfection and was found to be mediated by protein kinase C-delta (PKC-δ), a novel subfamily member of PKC serine/threonine protein kinases.[75]

Albumin-dependent signaling and albumin endocytosis appear to act as interrelated processes regulating the fate of proximal tubular cells *in vitro*. Megalin may behave as a sensor molecule that determines whether the cells will be protected from or injured by albumin, pending on the protein concentration. On one hand, low concentrations of albumin lead to activation of serine/threonine kinase PKB and phosphorylation of Bad protein, which inhibits apoptosis.[76] On the other hand, albumin overload decreased the expression of megalin on the plasma membrane that was associated with a reduction of PKB activity and Bad phosphorylation, favoring apoptosis.[77] As well as albumin load of tubular cells, a balance has also been suggested between the induction of a NF-kB dependent, Bcl-xL mediated anti-apoptotic pathway and the induction of AP-1 mediated clusterin overexpression that instead, by inhibiting the pathway, would favor a switch from inflammatory phenotype to apoptotic injury.[78]

Multiple pathways of apoptosis can be activated in renal tubular cells during proteinuric kidney diseases. Apoptotic responses to protein load were documented in the rat model of albumin overload proteinuria, showing increased numbers of terminal dUTP nick-end labeling positive apoptotic cells both in the tubulointerstitial compartment and in glomeruli.[79] In tubuli, most of the positive cells were found in profiles expressing angiotensin II type 2 (AT2) receptor. Findings of reduced phosphorylation of ERK and Bcl-2 were suggested to reflect an AT2 receptor-mediated mechanism underlying tubular cell apoptosis.[79] Proximal tubular cell apoptosis may contribute to glomerular-tubule disconnection and atrophy in response to proteinuria in rats with accelerated passive Heymann nephritis.[80] Another study, in agreement with results obtained using cultured proximal tubular cells, showed PKC-δ overexpression and tubular apoptosis in kidneys of mice upon albumin overload, whereas PKC-δ knockout mice were protected.[75] Levels of proteinuria remained comparable, indicating lower susceptibility to apoptosis rather than differences in protein exposure. Mechanistically, PKC-δ could promote apoptosis by activation of apoptotic genes, phosphorylation of caspases, interaction with apoptotic regulators, remodeling of cell membranes, or interference with mitochondrial function possibly including ER-mitochondrial crosstalk during ER-stress-induced apoptosis. ER stress has been demonstrated both in proximal tubular cells *in vitro* and in kidneys of rats with albumin-overload or puromycin aminonucleoside-nephrosis.[81]

Apoptotic cells were also detected both in proximal and distal tubular profiles in biopsy specimens of patients with primary focal segmental glomerulosclerosis. A positive correlation was found between proteinuria and incidence of tubular cell apoptosis, which was identified as a strong predictor of outcome in these patients.[82] Albumin exposure caused the activation of the Fas pathway and apoptosis in cultured Madin-Darby canine kidney epithelial (distal/collecting) cells, hence extending to the distal nephron the pro-apoptotic potential of enhanced protein load.[82] Besides promoting tubulo-glomerular disconnection at proximal level, tubular apoptosis could create and sustain a local proinflammatory microenvironment via release of molecules that serve as danger signals by dying cells. Danger-associated molecular patterns (DAMPs) trigger inflammation by engaging Toll-like receptors (TLR) and nucleotides-binding domains, leucin-rich, repeat-containing proteins (NLRs). Engaged NLR form complexes with apoptosis-associated proteins to produce macromolecular complexes termed inflammasomes that cleave proinflammatory cytokines to their mature forms.[83] A role for inflammasomes in progressive renal disease has been recently shown in NLRP3 $^{-/-}$ mice that were protected from injury and fibrosis of unilateral ureteral obstruction. Increased expression of NLRP3 was also detected in kidney biopsy specimens of patients with progressive kidney diseases.[84]

Intracellular Signaling of Protein Overload

In vitro studies have documented that protein overload activates signal transduction cascades in proximal tubular cells resulting in transcriptional upregulation of proinflammatory and fibrogenic molecules.[85]

Molecular mechanisms leading to chemokine gene induction as a consequence of enhanced protein uptake have been identified. Nuclear transcription factors such as NF-kB have attracted attention as candidate pathways and are seen as a potential target of therapeutic intervention against proteinuria-induced tubulointerstitial injury. The NF-kB/Rel family includes homodimeric or heterodimeric complexes designated as p50, p52, p65, c-rRel and RelB.[86,87] The prototype NF-kB is composed of p50-p65 subunits. NF-kB proteins normally exist in the cytoplasm bound to the inhibitory protein IkBα. Upon cell activation by different stimuli, such as cytokines, viruses and oxidants, IkBα is phosphorylated by the IkB kinase (IKK) complex, ubiquitinated and degraded, allowing NF-kB translocation into the nucleus for binding to DNA motifs in gene promoters. In cultured proximal tubular cells albumin dose-dependently enhanced NF-kB activity resulting in upregulation of RANTES, MCP-1 and IL-8.[58,59,88] The role of NF-kB activation in chemokine mRNA induction by protein overload was supported by experiments showing that adenovirus-mediated gene transfer of IkBα or the dominant negative mutant of IkB kinase-2 (IKK-2) which fails to phosphorylate IkBα, reduced upregulation of fractalkine mRNA in proximal tubular cells exposed to albumin.[61] Reactive oxygen species (ROS) served as second messengers in protein overload-induced NF-kB activation.[89] Albumin and IgG caused a rapid and sustained generation of hydrogen peroxide (H_2O_2) in human proximal tubular cells, and antioxidants while preventing hydrogen peroxide production, almost abolished the enhanced NF-kB activity induced by both proteins.[89] Oxidant generation is upstream regulated by protein kinase C (PKC) which, once activated, translocates from the cytoplasm to cell membrane to mediate ROS production and NF-kB activation. Inhibitors of PKC prevented hydrogen peroxide generation, NF-kB activation,[89] and MCP-1 and IL-8 gene upregulation induced by albumin, suggesting a cascade of signals from PKC-dependent oxygen radical generation to nuclear translocation of NF-kB and consequent gene upregulation.[89,90]

NF-kB transcriptional activity also depends on mitogen-activated protein kinase (MAPK) cascade pathways that transduce external stress stimuli into intracellular responses.[91] In human proximal tubular cells albumin caused rapid phosphorylation of p38 MAPK.[61] Treatment with a specific p38 inhibitor resulted in inhibition of the transcription of NF-kB promoter/luciferase reporter gene construct, consistent with a role of p38 as regulator in this pathway. The p38 blockade limited the overexpression of fractalkine mRNA and protein induced by albumin.[61] Moreover, activation of the MAPK signaling pathway was involved in albumin-stimulated TGFβ-1 gene expression and protein secretion in rat proximal tubular cells.[64] Strong and rapid activation of p44/42 MAPK was detected following cell exposure to albumin. A specific MAPK inhibitor abolished the increase of TGFβ-1 mRNA induced by albumin.

There is evidence in mouse proximal tubular cells that albumin activated extracellular signal-regulated kinase (ERK) and that blockade of ERK activation by a specific inhibitor of the mitogen-activated protein kinase kinase (MEK), the immediate upstream regulator of ERK, partially reduced albumin-induced MCP-1 expression, inhibited the increase in AP-1 and NF-kB DNA-binding activity, and prevented the degradation of IkB in albumin treated cells.[92] It has been shown that in a proximal tubular epithelial cell line engineered to constitutively express heme oxygenase-1 (HO-1) MCP-1 production in response to albumin was

reduced and that this inhibitory effect involved mechanisms that are distal to the activation of ERK and are associated with a suppressive effect on NF-kB activation.[93] Another study showed that high concentrations of albumin stimulated ERK via an EGF-receptor-dependent pathway.[94] The mechanism underlying albumin-induced stimulation of EGF-R is undefined. Based on the observations that EGF-like activators of EGF-R exist as transmembrane precursors that must undergo ectodomain cleavage to release the soluble EGF-activating fragment, and that the extracellular domain of megalin has 17 EGF-type repeats, it has been suggested that abnormal EGF activation could result from ectodomain shedding of megalin occurring from proximal tubular cells in the pathological setting of proteinuria.[69] In addition, it has also been proposed that transactivation of EGF-R by G-protein-coupled receptors could in part be regulated by PKC and c-Src, that activate ERK and are stimulated by albumin.[69] Moreover, in primary cultured proximal tubular cells albumin stimulated DNA synthesis by Ca^{2+}/PKC as well as the EGFR-dependent p44/42 MAPK and NK-kB signal pathways.[95]

The activation of the Janus kinase/signal transducer and activator of transcription (JAK/STAT) pathway is an important mechanism converting cytokine and growth factor signals into gene expression programs that regulate cell proliferation and survival.[96] The evidence that albumin activated JAK/STAT in murine proximal tubular cells[97] led to the suggestion that albumin may stimulate proximal tubular cells in the manner of a cytokine.[98] The activation of STAT was also observed after treatment of the cells with apotransferrin, one of the major components of plasma proteins consisting of transferrin not saturated with iron. Findings that albumin and apotransferrin induced in tubular cells the upregulation of intracellular ROS generation and that antioxidants prevented albumin-induced phosphorylation of STAT suggested that STAT activation could occur by way of the ROS generating system.[97]

Among genes differentially regulated by excess proteins in proximal tubular cells of mice with protein overload proteinuria, glia maturation factor-B (GMF-B), a 17-kD intracellular protein originally purified from the brain, that regulates the life/death signaling by activating p38 was identified.[99] Proximal tubular cells engineered to overexpress GMF-B acquired susceptibility to cell death under sustained oxidative stress through p38 pathway activation. H_2O_2 stimulation persisted in GMF-B overexpressing cells in which the H_2O_2-generating enzyme, CuZn-SOD, was upregulated, and the H_2O_2-reducing enzymes glutathione peroxidase and catalase were down-regulated.

In Vivo *Evidence for Proinflammatory and Profibrogenic Signaling in Tubular Cells Activated by Proteinuria*

Proinflammatory signals. Studies of experimental models of kidney disease or injury, followed by further investigation in human nephropathies, have shown that activation of transcription factors and overexpression of chemokines can indeed be elicited by the proteinuric condition contributing to the development of progressive renal damage. In rats with protein-overload proteinuria the upregulation of MCP-1 and osteopontin in tubular epithelial cells was closely associated with an interstitial inflammatory reaction.[100] In this model, enhanced renal NF-kB activity was localized preferentially to tubular epithelial cells.[101] In rats with 5/6 nephrectomy, the increased urinary protein excretion over time was attended by a remarkable increase in NF-kB activity in the remnant kidney.[102] Strong nuclear staining for the p50 NF-kB subunit was visualized in proximal tubular cells and in sparse cells within the renal interstitium. A progressive increase in renal expression of MCP-1 gene occurred over time concomitant to the activation of NF-kB. Tubular MCP-1 mRNA upregulation became detectable at stages that preceded the accumulation of monocytes/macrophages and T lymphocytes in the remnant kidney interstitium, suggesting MCP-1 dependent recruitment of the cells. In other animal models of proteinuric nephropathies, renal MCP-1 overexpression preceded or coincided with the interstitial infiltration of mononuclear cells.[90,100] The administration of a neutralizing anti-MCP-1 antibody to rats with tubulointerstitial nephritis significantly decreased macrophage infiltration, strenghtening the possibility that MCP-1 is functionally important in eliciting an interstitial inflammatory response.[90] The possibility that excess protein load and reabsorption by proximal tubular cells could indeed play a role in the development of interstitial inflammation and fibrosis was supported by results of analysis of time course and sites of protein accumulation and interstitial infiltration by macrophages and MHC-II-positive cells in the rat models of 5/6 nephrectomy[103,104] and passive Heymann nephritis.[103] A link was also observed between excess plasma protein reabsorption by proximal tubuli and the expression of osteopontin, a cytokine responsible for the attraction of mononuclear cells. Osteopontin was detected in cells of proximal tubuli congested with ultrafiltered proteins, and the sites of colocalization revealed a strict relationship with adjacent infiltrates.[103] If the interstitial inflammatory reaction ensued as a consequence of excessive ultrafiltration and proximal tubular reabsorption of proteins that also promoted NF-kB activation and chemokine synthesis, limiting the enhanced

protein traffic should also limit the biological effect of excessive tubular protein reabsorption and should slow renal disease progression. The best strategy to reduce protein traffic both in experimental animals and humans relies on ACE inhibitors effectively employed to slow the pace of progression of renal disease.[105,106] ACE inhibitor given to rats with a remnant kidney reduced urinary protein excretion and at the same time almost suppressed NF-kB DNA-binding activity and reduced MCP-1 mRNA expression and interstitial inflammatory cell infiltrates.[102] Similar effects were observed in the immune model of passive Heymann nephritis.[102] The decrease of NF-kB activation was associated with down-regulation of MCP-1 expression and reduction of interstitial inflammation.

In line with the possibility that NF-kB activation has a role in tubulointerstitial injury in proteinuric rats, there are data showing that in rats with adriamycin-induced nephropathy, chronic treatment with the putative NF-kB inhibitor pyrrolidine dithiocarbamate (PDTC), initiated at the time of overt proteinuria, suppressed cortical NF-kB activation and markedly reduced interstitial monocyte infiltration.[107] Chronic inhibition of NF-kB with PDTC also attenuated renal inflammation and injury in rats with 5/6 nephrectomy.[108] The mechanism by which PDTC inhibits NF-kB is unclear. It can directly impede the degradation of IkB or it may act through its antioxidant properties to inhibit the stimulatory effect of oxidative stress on NF-kB system. Although in the above models no major side effects were observed, studies on the clinical toxicity and safety of PDTC and other NF-kB inhibitors are needed before considering their potential use against renal disease progression. Systemic inhibition of NF-kB might have unwanted effects on the induction of genes critically regulating inflammatory and immunologic responses. Several conventional therapies in clinical use, including ACE inhibitors, AT1 receptor antagonists, glucocorticoids and hydroxymethyl glutaryl-CoA reductase inhibitors, are able to modulate NF-kB activation, but data on specific NF-kB inhibition in human disease are still lacking.[109]

To more specifically inhibit NF-kB activation, a recombinant adenovirus vector expressing the truncated form of IkBα that lacks the phosphorylation sites essential for the activation of NF-kB, was injected into renal arteries of rats with protein overload proteinuria.[110] This maneuver prevented NF-kB activation in tubular cells and attenuated the interstitial infiltration of mononuclear cells, interstitial edema, and fibrosis. These data suggest the possibility of using gene therapy targeting NF-kB as a means of interrupting the process of tubulointerstitial injury.

Specific blockade of the MCP-1/CCR2 signaling pathways attenuated interstitial nephritis induced by protein overload proteinuria. A hydrodynamic-based gene transfer technique was used to introduce naked plasmid encoding 7ND (a MCP-1 antagonist) into the left kidney of rats subsequently given repeated injections of bovine serum albumin.[111] Anti-MCP-1 gene therapy reduced interstitial inflammation and fibrosis and tubular damage, and limited the number of apoptotic cells in the treated kidney but not in the contralateral one. Finding that 7ND acted locally would envision a potential therapeutic application for this strategy against tubulointerstitial injury in the clinical setting.

Analysis of renal biopsy specimens from patients with severe proteinuria revealed NF-kB activation in tubular epithelial cells, which significantly correlated with the magnitude of proteinuria. There was a concomitant upregulation of proinflammatory chemokines, MCP-1, RANTES and osteopontin, found mainly in tubular epithelial cells, with the strongest expression in patients with progressive nephropathy.[109,112,113] NF-kB activation and MCP-1 upregulation in proximal tubular cells were also shown in patients with diabetic nephropathy.[114] A relationship between proteinuria and MCP-1 mediated interstitial damage was documented in a prospective study of patients who underwent renal biopsy for chronic kidney disease.[115] Furthermore, transcriptome analysis by complementary DNA microarray of renal proximal tubular epithelial cells isolated by laser capture microdissection from patients with proteinuric nephropathies revealed more than 160 differentially expressed genes, including those encoding for signal transduction, cell cycle control, intracellular transport and metabolism.[116]

Profibrogenic signal. Interstitial fibrosis represents the final common pathway of any form of progressive renal disease.[117] There is general consensus that fibroblasts within fibrotic tubulointerstitium proliferate[118,119] and that fibrosis-generating myofibroblasts – i.e, activated matrix secreting cells with features and gene patterns of smooth muscle cells – are an hallmark of the process.[119–121] In proteinuric settings, protein load and reabsorption by proximal tubular cells initiate or enhance fibrogenesis by at least two mechanisms. First, proximal tubular epithelial cells have the potential to interact directly with the adjacent interstitial fibroblasts via paracrine mechanisms. Indeed, proximal tubular cells by their ability to synthesize platelet derived growth factor (PDGF) and TGFβ1 stimulated renal cortical fibroblasts in coculture to grow and synthesize collagen.[122] On the other hand, the proinflammatory activation of tubular cells fosters local recruitment of macrophages and lymphocytes that by releasing TGFβ, PDGF and other cytokines[123] stimulate interstitial cells to produce excess matrix. That both the tubular paracrine

pathway and the inflammatory cell-mediated pathway are activated after the onset of proteinuria was suggested by findings that in remnant kidneys of rats, cells expressing the myofibroblast-associated marker α-smooth muscle actin (α-SMA) were first detectable in the interstitial areas and colocalized with macrophages surrounding proximal tubular cells that were engaged in excess protein reabsorption.[104] TGFβ mRNA was upregulated in proximal tubular cells in parallel with the nearby accumulation of inflammatory cells and α-SMA positive cells. Treatment of rats with remnant kidney with an ACE inhibitor limited excess protein accumulation and interstitial inflammatory cell infiltration and also abrogated abnormal TGFβ1 gene expression in tubular cells, and myofibroblast formation.[104]

In addition to the activation of interstitial cells, the fibrogenic reaction involved a phenotypic reversal of tubular epithelial cells termed as EMT.[119] The epithelial cells can be induced by several stimuli to become α-SMA expressing myofibroblasts. A huge number of studies have documented the abnormal expression of α-SMA and other myofibroblast markers in the renal tubule both in human and experimental nephropathies (for review, see [124]). Urinary proteins from nephrotic patients with focal segmental sclerosis, or to a lesser extent from patients with minimal change disease, induced cultured proximal tubular cells to express EMT-related patterns including α-SMA and vimentin via ERK1/2 and p38 pathway.[125] In remnant kidneys, α-SMA expression was also found in focal areas both in the context of the tubular epithelium and in peritubular microvascular cells with features of endothelium following the onset of proteinuria and TGFβ overexpression.[104] However, the primary source(s) of activated fibroblasts or myofibroblasts even in experimental settings are not clear.[119] Evidence was provided both for EMT in tubular epithelium[126,127] and endothelial-mesenchymal-transition.[128] Complete EMT appears difficult to detect as compared to intermediate phenotypic EMT stages.[119] Fate-tracing studies of epithelial cells in non-proteinuric mouse models failed to identify myofibroblasts originating from the epithelium.[129–131] A more predominant role is emerging for mesenchyme-derived stromal cells of the developing kidney that mature into perivascular pericytes in the adult kidney.[129]

TGFβ remains the most important cytokine for renal fibrogenesis. It has also been identified as the best characterized stimulus for EMT in renal tubular cells. Studies have focused on the signaling pathways which are activated during TGFβ-induced EMT. TGFβ caused Smad2 phosphorylation in a tubular epithelial cell line, and overexpression of the inhibitory Smad protein, Smad7, inhibited TGFβ − induced Smad2 activation, thereby preventing EMT and collagen synthesis.[132,133] An endogenous antagonist of TGFβ1−induced EMT has been identified as bone morphogenic protein-7 (BMP-7), a member of TGFβ superfamily whose genetic deletion in mice leads to severe impairment of kidney development.[134] BMP-7 reversed TGFβ1−induced EMT through a Smad-dependent reinduction of E-cadherin, an adhesive junction protein serving to maintain the structural integrity and polarity of epithelial cells.[135] Systemic administration of recombinant BMP-7 repaired severely damaged renal tubular epithelial cells and reversed renal injury in mice with nephrotoxic serum nephritis.[135] Investigation of a candidate mechanism downstream of BMP-7 suggested a role for *TRPS1* (whose mutations cause tricho-rhino-pharyngeal syndrome) acting as an essential regulator of nephron development.[136] Trps1 was found in proximal tubular epithelial cells of mice and its expression was reduced by ureteral obstruction. Trps haploinsufficiency promoted interstitial fibrosis via increased phosphorylation of Smad3 and decreased Smad7 protein. *In vitro* studies using proximal tubular cells suggested that the mechanisms underlying both TGFβ1−induced EMT and fibrosis were related to reduction of amount of Smad7 protein through ubiquitin-mediated degradation.[136] Other mediators that may critically contribute to fibrogenesis include PDGF[137] and endothelin-1[138] able to activate α-SMA gene expression in renal fibroblasts and vascular smooth muscle cells, respectively. IL18[139] and parathyroid hormone-related protein[140] were found to promote EMT *in vitro* and to contribute to interstitial fibrosis in murine models of ureteral obstruction.

Growth factors in the ultrafiltrate, such as hepatocyte growth factor (HGF) and TGFβ1 itself, may contribute to the induction of fibrosis *in vivo*.[141] In rats with glomerular proteinuria due to diabetic nephropathy, HGF and TGFβ were both detected in proximal tubular fluid and their receptors were upregulated in apical tubular membranes. In cultured proximal tubular cells, the exposure to ultrafiltrate rich in HGF and TGFβ induced the expression of fibronectin and PDGF as well as the basolateral secretion of MCP-1 and RANTES. The latter by interacting with macrophages in the renal interstitium caused them to secrete TGFβ which in turn, stimulated the expression of collagen type I and II, and fibronectin by interstitial myofibroblasts. Proximal tubular fluid from proteinuric, diabetic rats also increased the expression of connective tissue growth factor (CTGF) in tubular cells.[142] Interestingly, CTGF induces moderate pro-fibrogenic activity and raises the expression of fibronectin in proximal tubular cells as well as extracellular matrix proteins in renal fibroblasts.

Thus, a multitude of profibrotic cytokines are generated as a consequence of glomerular inflammation and are conveyed with proteins into the tubular urine to amplify interstitial injury. Evidence indicates that glomerular proinflammatory cytokines combined with massive proteinuria are major determinants of subsequent tubulo-interstitial injury and progressive kidney failure in experimental and human glomerulonephritis. An elegant experiment, however, yielded data to dissect the role of glomerular inflammation from that of protein toxicity. Besides closed nephrons the kidney of a primitive amphibium, the axolotl, contains nephrons with ciliated peritoneal funnels (nephrostomes) that have free access to the peritoneal fluid.[143] Injection of albumin into the peritoneal cavity caused selective uptake of proteins in tubular epithelial cells of nephrons with nephrostomes. As a consequence, protein and lipid droplets massively accumulated in the tubular cells. Furthermore, tubular lumen dilatation occurred and progressive focal accumulation of fibrous tissue was noted around protein-storing tubules, with the presence of fibronectin and TGFβ both in the tubular epithelial cells and in interstitial cells. Thus, protein loading *in vivo* directly induces tubulointerstitial activation and interstitial fibrosis, in the absence of glomerular inflammatory lesions. In this respect, myosin 1e (myo1e) knockout mice are a novel interesting model of glomerular disease, due to the disruption of a podocyte associated molecular motor protein that evolves to progressive tubulointerstitial injury.[144] Early ultrastructural glomerular changes consisting of increased thickness of glomerular basement membrane and effacement of podocyte foot processes were detected in 1−3 week old mice and were followed by albuminuria, formation of protein droplets, and accumulation of immunoglobulin and C3 in proximal tubular cells. Tubular changes were associated with excess deposition of collagen V and fibronectin in the periglomerular and peritubular interstitium, that could be related to proteinuria-associated signaling, in the absence of any evidence of immune or inflammatory glomerular disease.[144] Another report basing on an albumin-tracing analysis on serial sections of kidneys of OVE26 diabetic mice showed significant internephron heterogeneicity with sharp localization of albumin-staining to proximal tubuli showing various degrees of injury from minimal protein droplet formation to ultrastructural damage and dilatation. Similar findings were obtained in biopsy samples of proteinuric patients. The intensity of positive staining was dependent on the level of albuminuria and immunoglobulin and C3 stained in albumin positive tubules. Connections were visualized between albumin-leaking glomeruli and tubuli accumulating albumin, either prior to or in association with the onset of fibrosis. Collectively these findings favor the possibility that both progressive injury within individual nephrons and consequent scarring were directly related to worsening of proteinuria of glomerular origin.[145]

The Pathogenic Role of the Complement System in Renal Disease Progression

Intrarenal activation of complement. In physiologic states with an intact glomerular filtration barrier, the epithelial cells of the adult nephron are exposed to tightly regulated amounts of serum-derived complement proteins. C3 is an essential factor of both the classical and alternative pathways of complement activation that lead to the formation of C5b-9 membrane attack complex. Renal tubular epithelial cells appear most susceptible to effects of C5b-9 formation because of a relative lack of membrane-bound complement regulators such as membrane cofactor protein (CD46), decay-accelerating factor or CD55 and CD59 on apical surface.[146,147] *In vitro*, proximal tubular cells activated exogenous complement via alternative pathway leading to fixation of C5b-9 on cell surface[148] followed disruption of the network of actin stress fibers, and cytolysis. Increased production of superoxide anion, H_2O_2, and proinflammatory cytokines such as IL-6 and TNFβ was also observed.[149]

Deposition and intracellular accumulation of complement in proximal tubular cells was seen both in experimental models, such as protein overload proteinuria,[23] renal mass ablation[150,151] and aminonucleoside nephrosis,[152] and in patients with nonselective proteinuria. C5b-9 is a mediator of interstitial inflammation and fibrosis in experimental animals. Thus, in rats with severe nephrotic syndrome induced by aminonucleoside of puromycin the congenital absence of C6 markedly attenuated both complement dependent interstitial inflammation and renal dysfunction.[153] In C6-deficient rats with 5/6 nephrectomy a marked improvement of tubulointerstitial injury and function in respect with normocomplementemic rats was demonstrated.[154] Complement deposition greatly augments interstitial inflammation and fibrosis in the context of enhanced proximal tubular uptake of proteins. In the rat remnant kidney,[151] the intracellular C3 staining colocalized with IgG in proximal tubules in a stage closely preceding the appearance of inflammation. Protein accumulation in proximal tubular cells was followed by local recruitment of infiltrating mononuclear cells as well as by peritubular accumulation of myofibroblasts.[104] The amidation of C3 by ammonia in the presence of high protein catabolism was suggested to contribute to luminal formation of C5b-9[155] and generation of a monocyte-activating factor (amidated

C3).[150,156] Treatment with ACE inhibitor prevented proteinuria and, at the same time, limited both the tubular accumulation of C3 and IgG and interstitial inflammation.[151] The pivotal role of complement as a mediator of progressive tubulointerstitial damage seems to require an environment of protein-enriched ultrafiltrate. In the absence of proteinuria C5b-9 alone did not modify the evolution of tubulointerstitial disease[157] that showed similar degrees of severity among three distinct models of non-proteinuric disease regardless of whether the animals were from breeding pairs with normal complement activity or C6-deficiency.[157]

The presence of C3 in the tubular ultrafiltrate is recognized as a major promoter of injury in proteinuric nephropathies. C3 deficient mice were significantly protected against protein overload-induced renal injury.[158] This protective effect was explained by the absence of circulating C3, as indicated by kidney transplant studies showing that C3 deficient mice recipients of a wild-type kidney developed only mild proteinuria and tubulointerstitial injury upon protein load. Moreover, the treatment of wild-type mice with ACE inhibitor therapy in this model limited the amount of plasma proteins and C3 filtered, the accumulation of C3 by proximal tubular cells, and the degree of renal inflammation. The interaction between complement and other proteins in the ultrafiltrate and its functional consequences on tubular cells have been analyzed *in vitro* (Figure 87.4). Plasma protein overload of human proximal tubular cells (HK-2) renders the cells prone to activate complement. Addition of albumin or transferrin to HK-2 cells caused increased apical deposition of exogenous serum-derived C3, and, if added together, they additively increased fractalkine and TGFβ mRNA expression.[159] Enhanced C3 deposition was blocked by incubation with the wide-range inhibitor of complement activation, soluble complement receptor-1 (sCR1), but not by inhibitors of classic or lectin pathways, consistent with a disruptive interference by plasma proteins on the regulation of alternative pathway C3 convertase. The main regulator of this pathway is factor H, a 150-KDa soluble protein that binds to heparan sulfate on cell surface. The density of heparan sulfate was reduced by protein load via stimulation of heparanase synthesis, thereby reducing factor H binding and enhancing the serum-dependent complement activation potential of the cells.[159] The impact of factor H binding on renal tubule function is difficult to establish *in vivo*, particularly in human disease. Evidence in mice lacking other important complement regulators including either factor D or CD59 is in support of a role of alternative pathway in accelerating tubulointerstitial injury of adriamycin nephropathy.[160] Collectively these data provide links between proteinuria, uncontrolled activation of complement, and phenotypic changes of tubular cells that may underlie renal inflammatory cell infiltration and fibrosis.

Renal parenchymal tissues express a limited repertoire of receptors, including CR1, CR3, CD88, that may directly bind complement proteins present in the ultrafiltrate. The receptor for the complement anaphylotoxin C3a is highly expressed both by normal murine and human kidney epithelial cells. Among target genes, TGFβ[161] and collagen I[162] were upregulated by activated C3a, suggesting the induction of pathways underlying inflammation and fibrosis. In kidneys of proteinuric mice with adriamycin nephrosis a topographic relationship was found between the deposition of C3 and the enhanced expression of collagen type IV and its intracellular chaperone heat shock protein 47 at sites of tubulointerstitial damage.[163] The gene expression of collagen and heat shock protein 47 was also upregulated in primary cultures of mouse proximal tubular epithelial cells stimulated with C5b-9, further suggesting that complement activation on tubular cells can act directly to stimulate the profibrotic process associated with tubulointerstitial damage.[163] Other genes, such as pyrin (a gene responsible for familial Mediterranean fever) and Gulp were negatively regulated in tubular cells exposed to C3a, possibly reflecting modulatory effects on the inflammatory response and, respectively, on the clearance of apoptotic bodies.[162] Tubular epithelial cells exposed to either serum proteins or C3a also adopt phenotypic and functional characteristics of mesenchymal cells, with decreased expression of E-cadherin and increased expression of both α-SMA protein and collagen I mRNA.[164] These effects were prevented by cell treatment with a C3a receptor antagonist. Importantly, C3a receptor deficient mice were less susceptible to develop interstitial collagen I and α-SMA overexpression and kidney dysfunction, and to die, when subjected to adriamycin-induced proteinuria, in respect to wild-type mice.[164] A C5a receptor dependent, TGFβ1 mediated pathway has been shown to play major role in the pathogenesis of interstitial fibrosis induced in mice by unilateral ureteral ligation.[165]

Complement Activation and Proteinuria-Associated Progressive Glomerular Injury

Experimental models have been instrumental to identifying the role of complement in the progression of glomerular lesions in proteinuric disease. Abnormal fixation of C3 by immunohistology was detected in podocytes and glomerular epithelial cell areas in early stage of proteinuric disease in the remnant kidney in rats[25] and in the protein overload model in mice.[158] C3 colocalized with other plasma proteins that were filtered

as a consequence of their abnormal passage across the glomerular capillary wall. Podocytes showed signs of dedifferentiation and injury with loss of synaptopodin and *de novo* expression of desmin, followed by glomerular TGFβ overexpression and development of sclerotic lesions. The antiproteinuric treatment with ACE inhibitor mitigated all these changes.[25] Moreover, the exposure of cultured podocytes to protein overload also caused synaptopodin loss, actin rearrangement, and TGFβ overexpression. The conditioned medium of albumin-stimulated podocytes was able to induce a myofibroblast-like phenotypic change of cultured mesangial cells to express α-SMA. The role of C3 in the presence of other excess plasma proteins to enhance glomerular epithelial cell injury of proteinuric disease was further addressed directly in the protein overload model. C3 deficient mice were protected from podocyte injury and sclerosis, largely because of the lack of systemically-derived C3, as confirmed by transplantation experiments using wild-type donor kidneys.[158]

Other recent studies have consistently shown the importance of C3[160] and C3a[164] in the pathogenesis of glomerulosclerosis in experimental animals. The mechanisms by which complement can become activated and mediate the progression of glomerular injury in the above models are yet unknown. Because podocytes normally express complement inhibitory molecules such as complement receptor 1 or its mouse analogue factor H,[166] perturbed complement regulation can be pivotal. Indeed, the lack of either the alternative pathway regulator, factor D, or the membrane-bound regulator of membrane attack complex, CD59, was associated with worse glomerular injury in mice with adriamycin nephrosis,[160] whereas the lack of the alternative pathway factor B was associated with less severe albuminuria in the early stage of injury.[167] Future studies in this field will be important in view of potential therapeutic implications. Antibodies capable of blocking complement activation, including an anti-C5 antibody, are approved for use in humans. Given the role of permselective dysfunction in allowing both access of complement proteins to the glomerular and tubular ultrafiltrate and the activation of complement in the renal tubular and interstitial compartment, an antiproteinuric treatment might be most beneficial if combined with inhibitors of circulating and/or serum-derived complement. The consideration of alternative cellular sources of C3, such as the tubular cell itself, will be important for determining additional pharmacologic and molecular targets. Small molecule receptor inhibitors under development for human use may better block the actions of the C3a and C5a cleavage products and their unwanted consequences on the renal parenchyma.

Role of locally synthesized complement. In addition to activating exogenous complement, proximal tubular epithelial cells can synthesize a number of complement components including C3, C4, factor B, and C5.[168] The exposure of cultured tubular epithelial cells to total serum proteins at the apical surface upregulated C3 mRNA expression and protein biosynthesis.[169] The enhanced secretion of the protein was predominantly at the basolateral site. Serum fractionation experiments identified the substance(s) responsible for such effects in the molecular size range of 30 to 100 kD. This fraction contains proteins that pass across the glomerular barrier during proteinuric states, including albumin and transferrin. However, the addition of albumin alone did not reproduce the effects observed with whole serum, whereas after incubation with apical transferrin, C3 mRNA was overexpressed and both apical and basolateral C3 secretion increased.[170] A similar degree of C3 upregulation was obtained using iron-poor transferrin, or apotransferrin as stimuli, indicating that the synthesis of C3 in proximal tubular cells is upregulated by the protein rather than the iron moiety accounting for observed effects. Despite the documented role of C3 of non-renal cell origin as demonstrated in mice with protein overload proteinuria, the additional finding of marked C3 mRNA upregulation in tubular cells in the same model would reflect the functional engagement of C3 synthesis also contributing to tubulointerstitial injury.[158] Studies in nonproteinuric settings of ischemia-reperfusion or allograft injury strongly support this possibility. In this respect, complement activation may directly regulate the immunologic response. Of important note, the local synthesis of C3 may stimulate transmigration of T cells across tubular epithelial cells.[171] This pathway involves direct action of tissue C3 with infiltrating T cells expressing C3 receptors and is a candidate target of lymphocyte inhibitory agents, such as mofetil mycophenolate, shown to be effective if combined with antiproteinuric therapy against primary non-immune disease characterized by tubular deposition of complement.[151,172] Intrarenal effects of local complement activation have been recently reviewed.[173] Whether similar mechanisms may be recruited within glomeruli is not known. Incidentally, cyclosporine A, another immunosuppressant drug, showed the peculiar action of blocking calcineurin-mediated dephosphorylation of synaptopodin to preserve podocyte function, possibly accounting for its ability to induce remission of proteinuria in patients with proteinuric glomerulopathies.[174] Novel drugs more safely combining antiproteinuric and lymphocyte inhibitory actions might represent a valid tool to simultaneously protect both the glomerular epithelium and the tubular interstitial compartment from the deleterious effects of both plasma protein/C3 load and local activation of complement in the long-term.

Proteinuria Triggers Immune Response

The accumulation of immune-competent cells such as T lymphocytes and dendritic cells (DC) in the renal parenchyma is a common finding of proteinuric nephropathies even in the absence of an immune insult.[172,175] As antigen presenting cells, DC can initiate immune response or tolerance. The outcome depends on context. The current view is that immunity is controlled by internal communication between the tissue, where DC are resident, and the immune-competent cells, so that tolerance is maintained by the healthy organ, whereas immunity can be stimulated by a distressed organ.[176] In proteinuric nephropathies abnormal filtration of proteins that causes distress of renal proximal tubular cells ensues an inflammatory environment that might enable DC, in close contact with the tubular epithelium, to become immunogenic towards normally ignored self-antigens. It has been documented that through the concerted action of renal proximal tubular cells and DC, albumin is processed into antigenic peptides, thus triggering an immune response[177] (Figure 87.5). Proteolysis of excess autologous albumin by proximal tubular cells *in vitro* generated N terminal fragments, the most abundant being albumin 1 to 24 aminoacids (Alb1-24). This peptide was then taken up by DC and further processed, by a proteasome-dependent pathway, into antigenic peptides that bore binding motifs for MHC class I and activated syngeneic $CD8^+$ T cells. Studies in a rat model of proteinuria secondary to renal mass reduction confirmed the functional role of Alb1-24 processing by renal DC in inducing immune response. Dendritic cells were found to accumulate in the renal parenchyma of proteinuric rats one week after surgery. At four weeks a decrease in the percentage of DC in the kidney was paralleled by an enhancement of these cells in the renal draining lymph nodes, suggesting migration of DC from the renal interstitium. The $CD8^+$ T cells isolated from renal lymph nodes from renal mass reduction rats were already activated at the first encounter, when incubated with Alb1-24-pulsed DC, suggesting that they were pre-sensitized to the albumin peptide *in vivo* during the course of the disease. By contrast, the *in vivo* treatment with the proteasome inhibitor bortezomib, that prevents the formation of peptides for recognition by $CD8^+$ T cells, made these cells resistant to activation by Alb1-24-pulsed DC either in a primary or secondary culture. These findings provide a link among proteinuria, autoimmunity, and renal disease progression.[177]

Role of Protein-Bound Lipids

Beside proteins themselves, fatty acids carried by filtered albumin have been advocated as trigger of

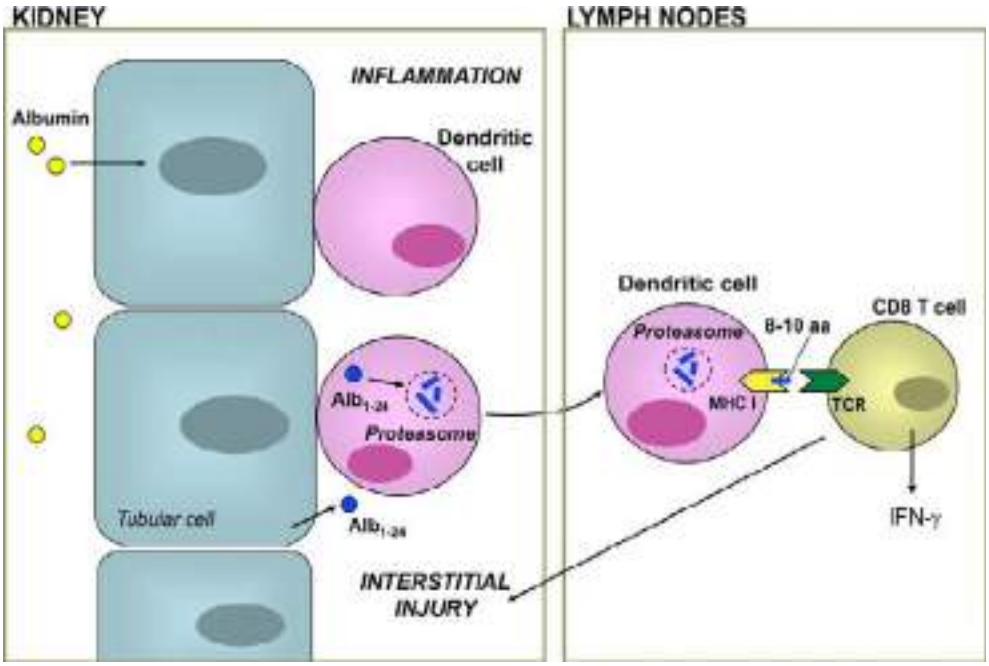

FIGURE 87.5 Proteasomal processing of albumin fragment by renal dendritic cells generates antigenic peptides. The inflammatory environment caused by distressed renal tubuli exposed to protein load favors dendritic cell (DC) accumulation and activation in the peritubular interstitium. Albumin is cleaved by proximal tubular cells into Alb1-24 that is taken up by DC and processed into 8 to 10 aminoacid peptides with a size compatible with MHC-I binding. DC migrate to the renal lymph node and present antigenic peptides within MHC-I to naive $CD8^+$ T cells leading to their activation. Activated T cells then reenter the kidney where they propagate renal damage (Ref. 177).

tubulointerstitial injury. In rats with overload proteinuria a potent chemotactic lipid was isolated from the urine, which attracted monocytes but not neutrophils.[178] Consistently, incubation of isolated proximal tubuli with albumin caused the release of a lipid factor chromatographically indistinguishable from that isolated from proteinuric urine.[179] This inflammatory lipid was not released after exposure of proximal tubuli to delipidated albumin, indicating that the synthesis of chemoattractant lipid is a consequence of tubular metabolism of fatty acid-bearing albumin. Rats injected with fatty acid-carrying BSA developed macrophage infiltration and apoptosis to a greater extent than those receiving fatty acid-depleted albumin.[180] Similar results were obtained in mice transgenic for human liver-type fatty acid binding protein, that in human proximal tubular cells was shown to bind free fatty acids in the cytoplasm and to carry them to mitochondria or peroxisomes for metabolism by beta-oxidation.[181] These mice developed less macrophage infiltration and a tendency to reduced tubulointerstitial damage than the wild-type control, possibly suggesting that intracellular accumulation of overloaded free-fatty acids can be regulated so as to modulate cell activation.

Studies in cultured proximal tubular cells have contributed to differentiate the effects of individual fatty acids (palmitate, stearate, oleate, and linoleate) on cell toxicity and fibronectin production. Oleate and linoleate were identified as the most profibrogenic and tubulotoxic fatty acids.[182]

By comparing effects of BSA alone or loaded with oleic acid, it has been shown that fatty acids accentuated albumin-induced oxidative stress and inflammatory cytokine expression in proximal tubular cells by increasing mitochondrial ROS and impairing protective antioxidant responses.[183] In human proximal tubular cells albumin repleted with fatty acids (rBSA) and defatted albumin complexed with linoleic acid (LA/dBSA) induced more apoptosis than defatted albumin alone.[184] Interestingly, fatty acid-bound BSA increased the number of lipid droplets (LDs)-organelles that store esterified fatty acids and the LD-associated proteins adipocyte differentiation-related protein and TIP47, that favor LD formation. Knockdown of adipocyte differentiation-related protein or TIP47 by RNA interference enhanced the induction of apoptosis by both rBSA and LA/dBSA, leading to suggestions that LDs and LD-associated proteins could protect tubular cells from fatty acid-induced apoptosis by sequestering free fatty acids.[184]

An additional pathogenic pathway has been linked to a form of low density lipoprotein modified by hypochlorous acid (HOCL), found to accumulate in tubular epithelial cells in settings of injury.[185] Hypochlorous acid/hypochlorite is a major oxidant generated from H_2O_2 by myeloperoxidase during oxydative burst. In the HK-2 proximal tubular cell line, hypochlorite-modified low density lipoprotein caused a rapid increase in the expression of several genes encoding for proteins engaged in control of cell proliferation and apoptosis (Gadd153), ROS metabolism (HO-1, cytochrome b5 reductase), tissue remodeling and inflammation (CTGF, VCAM1, IL-1β, MMP7, VEGF).[185]

SUMMARY

Experimental studies have established that a loss of selectivity of the glomerular filtration barrier causes excess transglomerular and tubular passage of plasma proteins which are potentially toxic to renal epithelial cells. This knowledge was derived by studies of models of progressive kidney disease including protein overload proteinuria, immune-mediated PHN and renal mass reduction in rats that leads to increased glomerular capillary hydraulic pressure and perfusion pressure resulting in capillary stretching and enhanced passage of proteins in the urine. Protein overload and reabsorption by proximal tubular cells can activate intracellular signaling pathways underlying the release of mediators into the interstitium. Chemokines attract mononuclear cells which together with activated tubular epithelial cells initiate fibrosis via TGFβ/growth factor mediated proliferation of fibroblasts and deposition of excess extracellular matrix. Complement activation is a stimulus for inflammation and fibrosis in experimental models of proteinuric nephropathies. Proteinuria acts both as a source of filtered complement and as a likely permissive factor by favoring both local synthesis and uncontrolled activation of complement via alternative pathway. A mechanism of interstitial injury in proteinuric diseases is mediated by immune cell activation through the interaction of renal proximal tubular cells and dendritic cells processing albumin into antigenic peptides. The glomerular epithelium is an important target of toxicity by filtered proteins and complement possibly fueling a vicious cycle of abnormal permeability, capillary injury, adhesion of tuft to Bowman's capsule, and sclerosis. ACE inhibitors/angiotensin II receptor blocking agents exert beneficial effects acting upstream at glomerular level to ameliorate the integrity of the glomerular barrier. A large body of clinical data is available from the past two decades to support the concept that proteinuria is both a marker of renal disease and a risk factor for human renal disease progression.[186–189] Clinical trials have suggested a tight link between the specific antiproteinuric action of ACE inhibitors/angiotensin II receptor blocking agents and their superior ability to limit GFR decline as compared to other

antihypertensive drugs, despite similar effect on blood pressure.[190] Therapeutic approaches have been devised on top of angiotensin II blockers based on experimental data demonstrating that combinations of therapies targeted to reduce proteinuria may retard renal disease progression more efficiently than single drugs.[191] Thus, the "Remission Clinic Program" uses all available pharmacological tools and lifestyle rules to reduce urinary proteins in patients with chronic kidney disease and heavy proteinuria despite ACE inhibitor therapy.[192] Advances in these areas will hopefully improve current protocols to prevent both proteinuria and its consequences on the renal parenchyma and kidney dysfunction in the long term.

Acknowledgment

The Authors thank Drs. Monica Locatelli and Antonella Piccinelli for advice in preparing the figures and Manuela Passera for helping in final text preparation.

References

[1] Brenner BM, Meyer TW, Hostetter TH. Dietary protein intake and the progressive nature of kidney disease: the role of hemodynamically mediated glomerular injury in the pathogenesis of progressive glomerular sclerosis in aging, renal ablation, and intrinsic renal disease. N Engl J Med 1982;307:652–9.

[2] Bright R. Reports of medical cases, selected with a view of illustratingthe symptoms and cure of diseases by a reference to morbid anatomy. Longman, Rees and Orme, London: Brown & Green; 1827.

[3] Addis T, Oliver J. In: Hoeber P, editor. The renal lesion in Bright's disease. New York: 1931.

[4] Addis T. The osmotic work of the kidney and the treatment of glomerular nephritis. Trans Assoc Am Phys 1940;55:223–9.

[5] Volhard F, Fahr TH. Die Bright'sche Nierenkrankheit. [Table II] Berlin: Julius Springer; 1914.

[6] Mollendorf W, Stohr P. Lehrbuch der Histologie. Jena: Fischer; 1924. p. 343.

[7] Allen AC. In: Grune & Stratton GA, editor. The kidney, medical and surgical diseases. New York: 1951 p. 207.

[8] Oliver J, Macdowell M, Lee YC. Cellular mechanisms of protein metabolism in the nephron. I. The structural aspects of proteinuria: tubular absorption, droplet formation, and the disposal of proteins. J Exp Med 1954;99:589–604.

[9] Cameron JS, Turner DS, Ogg GS, Chantler C, Williams DG. The long-term prognosis of patients with focal segmental glomerulosclerosis. Clin Nephrol 1978;10:213–8.

[10] Row PG, Cameron JS, Turner DR, Evans DJ, White RH, Ogg CS, et al. Membranous nephropathy. Long-term follow-up and association with neoplasia. Q J Med 1975;44:207–39.

[11] Habib R. Editorial: focal glomerular sclerosis. Kidney Int 1973;4:355–61.

[12] Hostetter TH, Olson JL, Rennke HG, Venkatachalam MA, Brenner BM. Hyperfiltration in remnant nephrons: a potentially adverse response to renal ablation. Am J Physiol 1981;241: F85–93.

[13] Mogensen CE, Christensen C, Beck-Nielsen H. Early changes in kidney function, blood pressure and the stages in diabetic nephropathy. In: Keen H, Legrain M, editors. In prevention and treatment of diabetic nephropathy. Boston: MTP Press LTD; 1983. p. 57–83.

[14] Parving HH, Andersen AR, Smidt UM, Svendsen PA. Early aggressive antihypertensive treatment reduces rate of decline in kidney function in diabetic nephropathy. Lancet 1983;1:1175–9.

[15] Anderson S, Meyer TW, Rennke HG, Brenner BM. Control of glomerular hypertension limits glomerular injury in rats with reduced renal mass. J Clin Invest 1985;76:612–9.

[16] Bohrer MP, Deen WM, Robertson CR, Brenner BM. Mechanism of angiotensin II-induced proteinuria in the rat. Am J Physiol 1977;233:F13–21.

[17] Mathiesen ER, Hommel E, Giese J, Parving HH. Efficacy of captopril in postponing nephropathy in normotensive insulin dependent diabetic patients with microalbuminuria. Br Med J 1991;303:81–7.

[18] Bertani T, Cutillo F, Zoja C, Broggini M, Remuzzi G. Tubulointerstitial lesions mediate renal damage in adriamycin glomerulopathy. Kidney Int 1986;30:488–96.

[19] Bertani T, Zoja C, Abbate M, Rossini M, Remuzzi G. Age-related nephropathy and proteinuria in rats with intact kidneys exposed to diets with different protein content. Lab Invest 1989;60:196–204.

[20] Remuzzi G, Bertani T. Is glomerulosclerosis a consequence of altered glomerular permeability to macromolecules? Kidney Int 1990;38:384–94.

[21] Remuzzi A, Puntorieri S, Battaglia C, Bertani T, Remuzzi G. Angiotensin converting enzyme inhibition ameliorates glomerular filtration of macromolecules and water and lessens glomerular injury in the rat. J Clin Invest 1990;85:541–9.

[22] Remuzzi G, Bertani T. Pathophysiology of progressive nephropathies. N Engl J Med 1998;339:1448–56.

[23] Eddy AA. Interstitial nephritis induced by protein-overload proteinuria. Am J Pathol 1989;135:719–33.

[24] Mori H, Yamashita H, Nakanishi C, Koizumi K, Makino S, Kishimoto Y, et al. Proteinuria induced by transplantable rat pituitary tumor MtT SA5. Model for homologous protein overload proteinuria. Lab Invest 1986;54:636–44.

[25] Abbate M, Zoja C, Morigi M, Rottoli D, Angioletti S, Tomasoni S, et al. Trasforming growth factor-β1 is up-regulated by podocytes in response to excess intraglomerular passage of proteins. Am J Pathol 2002;161:2179–93.

[26] Morigi M, Buelli S, Angioletti S, Zanchi C, Longaretti L, Zoja C, et al. In response to protein load podocytes reorganize cytoskeleton and modulate endothelin-1 gene: implication for permselective dysfunction of chronic nephropathies. Am J Pathol 2005;166:1309–20.

[27] Christensen EI, Verroust PJ, Nielsen R. Receptor-mediated endocytosis in renal proximal tubule. Pflugers Arch 2009;458:1039–48.

[28] Verroust P, Birn H, Nielsen R, Kozyraki R, Christensen EI. The tandem endocytic receptors megalin and cubilin are important proteins in renal pathology. Kidney Int 2002;62:745–56.

[29] Christensen EI, Gburek J. Protein reabsorption in renal proximal tubule-function and dysfunction in kidney pathophysiology. Pediatr Nephrol 2004;19:714–21.

[30] Lou X, Mcquistan T, Orlando RA, Farquhar MG. GAIP, GIPC and Gαi3 are concentrated in endocytic compartments of proximal tubule cells: putative role in regulating megalin's function. J Am Soc Nephrol 2002;13:918–27.

[31] Hosaka K, Takeda T, Iino N, Hosojima M, Sato H, Kaseda R, et al. Megalin and nonmuscle myosin heavy chain IIA interact with the adaptor protein Disabled-2 in proximal tubule cells. Kidney Int 2009;75:1308–15.

[32] Nagai J, Christensen EI, Morris SM, Willnow TE, Cooper JA, Nielsen R. Mutually dependent localization of megalin and Dab2 in the renal proximal tubule. Am J Physiol Renal Physiol 2005;289:F569–76.
[33] Gotoh N, Yan Q, Du Z, Biemesderfer D, Kashgarian M, Mooseker MS, et al. Altered renal proximal tubular endocytosis and histology in mice lacking myosin-VI. Cytoskeleton (Hoboken) 2010;67:178–92.
[34] Russo LM, del Re E, Brown D, Lin HY. Evidence for a role of transforming growth factor (TGF)-beta1 in the induction of postglomerular albuminuria in diabetic nephropathy: amelioration by soluble TGF-beta type II receptor. Diabetes 2007;56:380–8.
[35] Hosojima M, Sato H, Yamamoto K, Kaseda R, Soma T, Kobayashi A, et al. Regulation of megalin expression in cultured proximal tubule cells by angiotensin II type 1A receptor- and insulin-mediated signaling cross talk. Endocrinology 2009;150:871–8.
[36] Gena P, Calamita G, Guggino WB. Cadmium impairs albumin reabsorption by downregulating megalin and ClC5 channels in renal proximal tubule cells. Environ Health Perspect 2010; [In Press].
[37] Moestrup SK, Kozyraki R, Kristiansen M, Kaisen JH, Rasmussen HH, Brault D, et al. The intrinsic factor-vitamin B12 receptor and target of teratogenic antibodies is a megalin-binding peripheral membrane protein with homology to developmental proteins. J Biol Chem 1998;273:5235–42.
[38] Kozyraki R, Fyfe JC, Verroust PJ, Jacobsen C, Dautry-Varsat A, Gburek J, et al. Megalin-dependent cubilin-mediated endocytosis is a major pathway for the apical uptake of transferrin in polarized epithelia. Proc Natl Acad Sci U S A 2001;98:12491–6.
[39] Kozyraki R, Fyfe J, Kristiansen M, Gerdes C, Jacobsen C, Cui S, et al. The intrinsic factor-vitamin B12 receptor, cubilin, is a high-affinity apolipoprotein A-I receptor facilitating endocytosis of high-density lipoprotein. Nat Med 1999;5:656–61.
[40] Hammad SM, Barth JL, Knaak C, Argraves WS. Megalin acts in concert with cubilin to mediate endocytosis of high density lipoproteins. J Biol Chem 2000;275:12003–8.
[41] Nielsen R, Christensen EI. Proteinuria and events beyond the slit. Pediatr Nephrol 2010;25:813–22.
[42] Amsellem S, Gburek J, Hamard G, Nielsen R, Willnow TE, Devuyst O, et al. Cubilin is essential for albumin reabsorption in the renal proximal tubule. J Am Soc Nephrol 2010;21:1859–67.
[43] Zou Z, Chung B, Nguyen T, Mentone S, Thomson B, Biemesderfer D. Linking receptor-mediated endocytosis and cell signaling: evidence for regulated intramembrane proteolysis of megalin in proximal tubule. J Biol Chem 2004;279:34302–10.
[44] Li Y, Cong R, Biemesderfer D. The COOH terminus of megalin regulates gene expression in opossum kidney proximal tubule cells. Am J Physiol Cell Physiol 2008;295:C529–37.
[45] Christ A, Terryn S, Schmidt V, Christensen EI, Huska MR, Andrade-Navarro MA, et al. The soluble intracellular domain of megalin does not affect renal proximal tubular function in vivo. Kidney Int 2010;78:473–7.
[46] Piwon N, Gunther W, Schwake M, Bosl MR, Jentsch TJ. ClC-5 Cl^- -channel disruption impairs endocytosis in a mouse model for Dent's disease. Nature 2000;408:369–73.
[47] Wang SS, Devuyst O, Courtoy PJ, Wang XT, Wang H, Wang Y, et al. Mice lacking renal chloride channel, CLC-5, are a model for Dent's disease, a nephrolithiasis disorder associated with defective receptor-mediated endocytosis. Hum Mol Genet 2000;9:2937–45.
[48] Marshansky V, Ausiello DA, Brown D. Physiological importance of endosomal acidification: potential role in proximal tubulopathies. Curr Opin Nephrol Hypertens 2002;11:527–37.
[49] Christensen EI, Devuyst O, Dom G, Nielsen R, Van Der Smissen P, Verroust P, et al. Loss of chloride channel ClC-5 impairs endocytosis by defective trafficking of megalin and cubilin in kidney proximal tubules. Proc Natl Acad Sci U S A 2003;100:8472–7.
[50] Novarino G, Weinert S, Rickheit G, Jentsch TJ. Endosomal chloride-proton exchange rather than chloride conductance is crucial for renal endocytosis. Science 2010;328:1398–401.
[51] Erdmann KS, Mao Y, McCrea HJ, Zoncu R, Lee S, Paradise S, et al. A role of the Lowe syndrome protein OCRL in early steps of the endocytic pathway. Dev Cell 2007;13:377–90.
[52] Gekle M, Freudinger R, Mildenberger S. Inhibition of Na+-H+ exchanger-3 interferes with apical receptor-mediated endocytosis via vesicle fusion. J Physiol 2001;531:619–29.
[53] Marshansky V, Futai M. The V-type H+-ATPase in vesicular trafficking: targeting, regulation and function. Curr Opin Cell Biol 2008;20:415–26.
[54] Sidaway JE, Davidson RG, McTaggart F, Orton TC, Scott RC, Smith GJ, et al. Inhibitors of 3-hydroxy-3-methylglutaryl-CoA reductase reduce receptor-mediated endocytosis in opossum kidney cells. J Am Soc Nephrol 2004;15:2258–65.
[55] Verhulst A, D'Haese PC, De Broe ME. Inhibitors of HMG-CoA reductase reduce receptor-mediated endocytosis in human kidney proximal tubular cells. J Am Soc Nephrol 2004;15:2249–57.
[56] Zoja C, Morigi M, Figliuzzi M, Bruzzi I, Oldroyd S, Benigni A, et al. Proximal tubular cell synthesis and secretion of endothelin-1 on challenge with albumin and other proteins. Am J Kidney Dis 1995;26:934–41.
[57] Wang Y, Chen J, Chen L, Tay YC, Rangan GK, Harris DC. Induction of monocyte chemoattractant protein-1 in proximal tubule cells by urinary protein. J Am Soc Nephrol 1997;8:1537–45.
[58] Zoja C, Donadelli R, Colleoni S, Figliuzzi M, Bonazzola S, Morigi M, et al. Protein overload stimulates RANTES production by proximal tubular cells depending on NF-kB activation. Kidney Int 1998;53:1608–15.
[59] Tang S, Leung JCK, Abe K, Wah Chan K, Chan LYY, Mao Chan T, et al. Albumin stimulates interleukin-8 expression in proximal tubular epithelial cells in vitro and in vivo. J Clin Invest 2003;111:515–27.
[60] Lai KN, Leung JC, Chan LY, Guo H, Tang SC. Interaction between proximal tubular epithelial cells and infiltrating monocytes/T cells in the proteinuric state. Kidney Int 2007;71:526–38.
[61] Donadelli R, Zanchi C, Morigi M, Buelli S, Batani C, Tomasoni S, et al. Protein overload induces fractalkine upregulation in proximal tubular cells through nuclear factor kappaB- and p38 mitogen-activated protein kinase-dependent pathways. J Am Soc Nephrol 2003;14:2436–46.
[62] Garcia-Sanchez O, Lopez-Hernandez FJ, Lopez-Novoa JM. An integrative view on the role of TGF-beta in the progressive tubular deletion associated with chronic kidney disease. Kidney Int 2010;77:950–5.
[63] Yard BA, Chorianopoulos E, Herr D, van der Woude FJ. Regulation of endothelin-1 and transforming growth factor-beta1 production in cultured proximal tubular cells by albumin and heparan sulphate glycosaminoglycans. Nephrol Dial Transplant 2001;16:1769–75.
[64] Zhao J, Tramontano A, Makker SP. Albumin-stimulated TGFbeta-1 in renal tubular cells is associated with activation of MAP kinase. Int Urol Nephrol 2007;39:1265–71.
[65] Wolf G, Schroeder R, Ziyadeh FN, Stahl RA. Albumin upregulates the type II transforming growth factor-beta receptor in cultured proximal tubular cells. Kidney Int 2004;66:1849–58.

[66] Stephan JP, Mao W, Filvaroff E, Cai L, Rabkin R, Pan G. Albumin stimulates the accumulation of extracellular matrix in renal tubular epithelial cells. Am J Nephrol 2004;24:14–9.
[67] Diwakar R, Pearson AL, Colville-Nash P, Brunskill NJ, Dockrell ME. The role played by endocytosis in albumin-induced secretion of TGF-beta1 by proximal tubular epithelial cells. Am J Physiol Renal Physiol 2007;292:F1464–70.
[68] Chana RS, Sidaway JE, Brunskill NJ. Statins but not thiazolidinediones attenuate albumin-mediated chemokine production by proximal tubular cells independently of endocytosis. Am J Nephrol 2008;28:823–30.
[69] Baines RJ, Brunskill NJ. The molecular interactions between filtered proteins and proximal tubular cells in proteinuria. Nephron Exp Nephrol 2008;110:e67–71.
[70] Wu C, Dedhar S. Integrin-linked kinase (ILK) and its interactors: a new paradigm for the coupling of extracellular matrix to actin cytoskeleton and signaling complexes. J Cell Biol 2001;155:505–10.
[71] Peruzzi L, Trusolino L, Amore A, Gianoglio B, Cirina P, Basso G, et al. Tubulointerstitial responses in the progression of glomerular diseases: albuminuria modulates alpha v beta 5 integrin. Kidney Int 1996;50:1310–20.
[72] Erkan E, De Leon M, Devarajan P. Albumin overload induces apoptosis in LLC-PK(1) cells. Am J Physiol Renal Physiol 2001;280:F1107–14.
[73] Arici M, Chana R, Lewington A, Brown J, Brunskill NJ. Stimulation of proximal tubular cell apoptosis by albumin-bound fatty acids mediated by peroxisome proliferator activated receptor-γ. J Am Soc Nephrol 2003;14:17–27.
[74] Erkan E, Devarajan P, Schwartz GJ. Mitochondria are the major targets in albumin-induced apoptosis in proximal tubule cells. J Am Soc Nephrol 2007;18:1199–208.
[75] Li X, Pabla N, Wei Q, Dong G, Messing RO, Wang CY, et al. PKC-delta promotes renal tubular cell apoptosis associated with proteinuria. J Am Soc Nephrol 2010;21:1115–24.
[76] Song G, Ouyang G, Bao S. The activation of Akt/PKB signaling pathway and cell survival. J Cell Mol Med 2005;9:59–71.
[77] Caruso-Neves C, Pinheiro AA, Cai H, Souza-Menezes J, Guggino WB. PKB and megalin determine the survival or death of renal proximal tubule cells. Proc Natl Acad Sci U S A 2006;103:18810–5.
[78] Takase O, Minto AW, Puri TS, Cunningham PN, Jacob A, Hayashi M, et al. Inhibition of NF-kappaB-dependent Bcl-xL expression by clusterin promotes albumin-induced tubular cell apoptosis. Kidney Int 2008;73:567–77.
[79] Tejera N, Gomez-Garre D, Lazaro A, Gallego-Delgado J, Alonso C, Blanco J, et al. Persistent proteinuria up-regulates angiotensin II type 2 receptor and induces apoptosis in proximal tubular cells. Am J Pathol 2004;164:1817–26.
[80] Benigni A, Gagliardini E, Remuzzi A, Corna D, Remuzzi G. Angiotensin-converting enzyme inhibition prevents glomerular-tubule disconnection and atrophy in passive Heymann nephritis, an effect not observed with a calcium antagonist. Am J Pathol 2001;159:1743–50.
[81] Ohse T, Inagi R, Tanaka T, Ota T, Miyata T, Kojima I, et al. Albumin induces endoplasmic reticulum stress and apoptosis in renal proximal tubular cells. Kidney Int 2006;70:1447–55.
[82] Erkan E, Garcia CD, Patterson LT, Mishra J, Mitsnefes MM, Kaskel FJ, et al. Induction of renal tubular cell apoptosis in focal segmental glomerulosclerosis: roles of proteinuria and fas-dependent pathways. J Am Soc Nephrol 2005;16:398–407.
[83] Mariathasan S, Monack DM. Inflammasome adaptors and sensors: intracellular regulators of infection and inflammation. Nat Rev Immunol 2007;7:31–40.
[84] Vilaysane A, Chun J, Seamone ME, Wang W, Chin R, Hirota S, et al. The NLRP3 inflammasome promotes renal inflammation and contributes to CKD. J Am Soc Nephrol 2010;21:1732–44.
[85] Abbate M, Zoja C, Remuzzi G. How does proteinuria cause progressive renal damage? J Am Soc Nephrol 2006;17:2974–84.
[86] Barnes PJ, Karin M. Nuclear factor-kB - A pivotal transcription factor in chronic inflammatory diseases. N Engl J Med 1997;336:1066–71.
[87] Baldwin AS. The transcription factor NF-kB and human disease. J Clin Invest 2001;107:3–11.
[88] Wang Y, Rangan GK, Tay Y-C, Harris DCH. Induction of monocyte chemoattractant protein-1 by albumin is mediated by nuclear factor kB in proximal tubule cells. J Am Soc Nephrol 1999;10:1204–13.
[89] Morigi M, Macconi D, Zoja C, Donadelli R, Buelli S, Zanchi C, et al. Protein overload-induced NF-kB activation in proximal tubular cells requires H_2O_2 through a PKC-Dependent pathway. J Am Soc Nephrol 2002;13:1179–89.
[90] Tang WW, Qi M, Warren JS, Van GY. Chemokine expression in experimental tubulointerstitial nephritis. J Immunol 1997;159:870–6.
[91] Ono K, Han J. The p38 signal transduction pathway. Activation and function. Cell Signal 2000;12:1–13.
[92] Takaya K, Koya D, Isono M, Suimoto T, Suguya T, Kashiwagi A, et al. Involvement of ERK pathway in albumin-induced MCP-1 expression in mouse proximal tubular cells. Am J Physiol Renal Physiol 2003;284:F1037–45.
[93] Murali NS, Ackerman AW, Croatt AJ, Cheng J, Grande JP, Sutor SL, et al. Renal upregulation of HO-1 reduces albumin-driven MCP-1 production: implications for chronic kidney disease. Am J Physiol Renal Physiol 2007;292:F837–44.
[94] Reich H, Tritchler D, Herzenberg AM, Kassiri Z, Zhou X, Gao W, et al. Albumin activates ERK via EGF receptor in human renal epithelial cells. J Am Soc Nephrol 2005;16:1266–78.
[95] Lee YJ, Han HJ. Albumin-stimulated DNA synthesis is mediated by Ca2+/PKC as well as EGF receptor-dependent p44/42 MAPK and NF-kappaB signal pathways in renal proximal tubule cells. Am J Physiol Renal Physiol 2008;294:F534–41.
[96] Rawlings JS, Rosler KM, Harrison DA. The JAK/STAT signaling pathway. J Cell Sci 2004;117:1281–3.
[97] Nakajima H, Takenaka M, Kaimori JY, Hamano T, Iwatani H, Sugaya T, et al. Activation of the signal transducer and activator of transcription signaling pathway in renal proximal tubular cells by albumin. J Am Soc Nephrol 2004;15:276–85.
[98] Brunskill NJ. Albumin signals the coming of age of proteinuric nephropathy. J Am Soc Nephrol 2004;15:504–5.
[99] Kaimori JY, Takenaka M, Nakajima H, Hamano T, Horio M, Sugaya T, et al. Induction of glia maturation factor-beta in proximal tubular cells leads to vulnerability to oxidative injury through the p38 pathway and changes in antioxidant enzyme activities. J Biol Chem 2003;278:33519–27.
[100] Eddy AA, Giachelli CM. Renal expression of genes that promote interstitial inflammation and fibrosis in rats with protein-overload proteinuria. Kidney Int 1995;47:1546–57.
[101] Gomez-Garre D, Largo R, Tejera N, Fortes J, Manzarbeitia F, Egido J. Activation of nuclear factor kB in tubular epithelial cells of rats with intense proteinuria: role of angiotensin II and endothelin-1. Hypertension 2001;37:1171–8.
[102] Donadelli R, Abbate M, Zanchi C, Corna D, Tomasoni S, Benigni A, et al. Protein traffic activates NF-kB gene signaling and promotes MCP-1-dependent interstitial inflammation. Am J Kidney Dis 2000;36:1226–41.
[103] Abbate M, Zoja C, Corna D, Capitanio M, Bertani T, Remuzzi G. In progressive nephropathies, overload of tubular cells with filtered proteins translates glomerular permeability

dysfunction into cellular signals of interstitial inflammation. J Am Soc Nephrol 1998;9:1213–24.
[104] Abbate M, Zoja C, Rottoli D, Corna D, Tomasoni S, Remuzzi G. Proximal tubular cells promote fibrogenesis by TGF-β1-mediated induction of peritubular myofibroblasts. Kidney Int 2002;61:2066–77.
[105] Perico N, Benigni A, Remuzzi G. Present and future drug treatments for chronic kidney diseases: evolving targets in renoprotection. Nat Rev Drug Discov 2008;7:936–53.
[106] Ruggenenti P, Schieppati A, Remuzzi G. Progression, remission, regression of chronic renal diseases. Lancet 2001;357:1601–8.
[107] Rangan GK, Wang Y, Tay Y-C, Harris DCH. Inhibition of nuclear factor-kB activation reduces cortical tubulointerstitial injury in proteinuric rats. Kidney Int 1999;56:118–34.
[108] Fujihara CK, Antunes GR, Mattar AL, Malheiros DM, Vieira Jr. JM, Zatz R. Chronic inhibition of nuclear factor-kappaB attenuates renal injury in the 5/6 renal ablation model. Am J Physiol Renal Physiol 2007;292:F92–9.
[109] Sanz AB, Sanchez-Nino MD, Ramos AM, Moreno JA, Santamaria B, Ruiz-Ortega M, et al. NF-kappaB in renal inflammation. J Am Soc Nephrol 2010;21:1254–62.
[110] Takase O, Hirahashi J, Takayanagi A, Chikaraishi A, Marumo T, Ozawa Y, et al. Gene transfer of truncated IkBa prevents tubulointerstitial injury. Kidney Int 2003;63:501–13.
[111] Shimizu H, Maruyama S, Yuzawa Y, Kato T, Miki Y, Suzuki S, et al. Anti-monocyte chemoattractant protein-1 gene therapy attenuates renal injury induced by protein-overload proteinuria. J Am Soc Nephrol 2003;14:1496–505.
[112] Mezzano SA, Droguett MA, Burgos ME, Ardiles LG, Aros CA, Caorsi I, et al. Overexpression of chemokines, fibrogenic cytokines, and myofibroblasts in human membranous nephropathy. Kidney Int 2000;57:147–58.
[113] Mezzano SA, Barria M, Droguett MA, Burgos ME, Ardiles LG, Flores C, Egido J. Tubular NF-kB and AP-1 activation in human proteinuric renal disease. Kidney Int 2001;60:1366–77.
[114] Mezzano S, Aros C, Droguett A, Burgos ME, Ardiles L, Flores C, et al. NF-kappaB activation and overexpression of regulated genes in human diabetic nephropathy. Nephrol Dial Transplant 2004;19:2505–12.
[115] Eardley KS, Cockwell P. Macrophages and progressive tubulointerstitial disease. Kidney Int 2005;68:437–55.
[116] Rudnicki M, Eder S, Perco P, Enrich J, Scheiber K, Koppelstatter C, et al. Gene expression profiles of human proximal tubular epithelial cells in proteinuric nephropathies. Kidney Int 2007;71:325–35.
[117] Iwano M, Neilson EG. Mechanisms of tubulointerstitial fibrosis. Curr Opin Nephrol Hypertens 2004;13:279–84.
[118] Lin SL, Kisseleva T, Brenner DA, Duffield JS. Pericytes and perivascular fibroblasts are the primary source of collagen-producing cells in obstructive fibrosis of the kidney. Am J Pathol 2008;173:1617–27.
[119] Zeisberg M, Duffield JS. Resolved: EMT produces fibroblasts in the kidney. J Am Soc Nephrol 2010;21:1247–53.
[120] Desmoulière A, Geinoz A, Gabbiani F, Gabbiani G. Transforming growth factor-beta1 induces alpha-smooth muscle actin expression in granulation tissue myofibroblasts and in quiescent and growing cultured fibroblasts. J Cell Biol 1993;122:103–11.
[121] Muchaneta-Kubara EC, El-Nahas M. Myofibroblast phenotypes expression in experimental renal scarring. Nephrol Dial Transplant 1997;12:904–15.
[122] Johnson DW, Saunders HJ, Baxter RC, Field MJ, Pollock CA. Paracrine stimulation of human renal fibroblasts by proximal tubule cells. Kidney Int 1998;54:747–57.
[123] Eddy AA. Role of cellular infiltrates in response to proteinuria. Am J Kidney Dis 2001;37(Suppl. 2):S25–9.
[124] Liu Y. New insights into epithelial-mesenchymal transition in kidney fibrosis. J Am Soc Nephrol 2010;21:212–22.
[125] Wen Q, Huang Z, Zhou SF, Li XY, Luo N, Yu XQ. Urinary proteins from patients with nephrotic syndrome alters the signalling proteins regulating epithelial-mesenchymal transition. Nephrology (Carlton) 2010;15:63–74.
[126] Higgins DF, Kimura K, Bernhardt WM, Shrimanker N, Akai Y, Hohenstein B, et al. Hypoxia promotes fibrogenesis in vivo via HIF-1 stimulation of epithelial-to-mesenchymal transition. J Clin Invest 2007;117:3810–20.
[127] Zeisberg M, Kalluri R. Fibroblasts emerge via epithelial-mesenchymal transition in chronic kidney fibrosis. Front Biosci 2008;13:6991–8.
[128] Zeisberg EM, Potenta SE, Sugimoto H, Zeisberg M, Kalluri R. Fibroblasts in kidney fibrosis emerge via endothelial-to-mesenchymal transition. J Am Soc Nephrol 2008;19:2282–7.
[129] Humphreys BD, Lin SL, Kobayashi A, Hudson TE, Nowlin BT, Bonventre JV, et al. Fate tracing reveals the pericyte and not epithelial origin of myofibroblasts in kidney fibrosis. Am J Pathol 2010;176:85–97.
[130] Li L, Zepeda-Orozco D, Black R, Lin F. Autophagy is a component of epithelial cell fate in obstructive uropathy. Am J Pathol 2010;176:1767–78.
[131] Koesters R, Kaissling B, Lehir M, Picard N, Theilig F, Gebhardt R, et al. Tubular overexpression of transforming growth factor-beta1 induces autophagy and fibrosis but not mesenchymal transition of renal epithelial cells. Am J Pathol 2010;177:632–43.
[132] Li JH, Zhu HJ, Huang XR, Lai KN, Johnson RJ, Lan HY. Smad7 inhibits fibrotic effect of TGF-beta on renal tubular epithelial cells by blocking Smad2 activation. J Am Soc Nephrol 2002;13:1464–72.
[133] Lan HY, Mu W, Tomita N, Huang XR, Li JH, Zhu HJ, et al. Inhibition of renal fibrosis by gene transfer of inducible Smad7 using ultrasound-microbubble system in rat UUO model. J Am Soc Nephrol 2003;14:1535–48.
[134] Klahr S. The bone morphogenetic proteins (BPMs). Their role in renal fibrosis and renal function. J Nephrol 2003;16:179–85.
[135] Zeisberg M, Hanai J-i, Sugimoto H, Mammoto T, Charytan D, Strutz F, et al. BMP-7 counteracts TGF-β1- induced epithelial-to-mesenchymal transition and reverses chronic renal injury. Nat Med 2003;7:964–9.
[136] Gai Z, Zhou G, Gui T, Itoh S, Oikawa K, Uetani K, et al. Trps1 haploinsufficiency promotes renal fibrosis by increasing Arkadia expression. J Am Soc Nephrol 2010;21:1468–76.
[137] Tang WW, Ulich TR, Lacey DL, Hill DC, Qi M, Kaufman SA, et al. Platelet-derived growth factor-BB induces renal tubulointerstitial myofibroblast formation and tubulointerstitial fibrosis. Am J Pathol 1996;148:1169–80.
[138] Andrawis NS, Wang E, Abernethy DR. Endothelin-1 induces an increase in total protein synthesis and expression of the smooth muscle alpha-actin gene in vascular smooth muscle cells. Life Sciences 1996;59:523–8.
[139] Bani-Hani AH, Leslie JA, Asanuma H, Dinarello CA, Campbell MT, Meldrum DR, et al. IL-18 neutralization ameliorates obstruction-induced epithelial-mesenchymal transition and renal fibrosis. Kidney Int 2009;76:500–11.
[140] Ardura JA, Rayego-Mateos S, Ramila D, Ruiz-Ortega M, Esbrit P. Parathyroid hormone-related protein promotes epithelial-mesenchymal transition. J Am Soc Nephrol 2010;21:237–48.
[141] Hirschberg R, Wang S. Proteinuria and growth factors in the development of tubulointerstitial injury and scarring in kidney disease. Curr Opin Nephrol Hypertens 2005;14:43–52.

[142] Wang SN, Hirschberg R. Growth factor ultrafiltration in experimental diabetic nephropathy contributes to interstitial fibrosis. Am J Physiol Renal Physiol 2000;278:F554–60.
[143] Gross ML, Hanke W, Koch A, Ziebart H, Amann K, Ritz E. Intraperitoneal protein injection in the axolotl: the amphibian kidney as a novel model to study tubulointerstitial activation. Kidney Int 2002;62:51–9.
[144] Krendel M, Kim SV, Willinger T, Wang T, Kashgarian M, Flavell RA, et al. Disruption of Myosin 1e promotes podocyte injury. J Am Soc Nephrol 2009;20:86–94.
[145] Kralik PM, Long Y, Song Y, Yang L, Wei H, Coventry S, et al. Diabetic albuminuria is due to a small fraction of nephrons distinguished by albumin-stained tubules and glomerular adhesions. Am J Pathol 2009;175:500–9.
[146] Ichida S, Yuzawa Y, Okada H, Yoshioka K, Matsuo S. Localization of the complement regulatory proteins in the normal human kidney. Kidney Int 1994;46:89–96.
[147] Nangaku M. Complement regulatory proteins in glomerular diseases. Kidney Int 1998;54:1419–28.
[148] Biancone L, David S, Della Pietra V, Montrucchio G, Cambi V, Camussi G. Alternative pathway activation of complement by cultured human proximal tubular epithelial cells. Kidney Int 1994;45:451–60.
[149] David S, Biancone L, Caserta C, Bussolati B, Cambi V, Camussi G. Alternative pathway complement activation induces proinflammatory activity in human proximal tubular epithelial cells. Nephrol Dial Transplant 1997;12:51–6.
[150] Nath KA, Hostetter MK, Hostetter TH. Pathophysiology of chronic tubulo-interstitial disease in rats: interactions of dietary acid load, ammonia, and complement component C3. J Clin Invest 1985;76:667–75.
[151] Abbate M, Zoja C, Rottoli D, Corna D, Perico N, Bertani T, et al. Antiproteinuric therapy while preventing the abnormal protein traffic in proximal tubule abrogates protein and complement-dependent interstitial inflammation in experimental renal disease. J Am Soc Nephrol 1999;10:804–13.
[152] Nomura A, Morita Y, Maruyama S, et al. Role of complement in acute tubulointerstitial injury of rats with aminonucleoside nephrosis. Am J Pathol 1997;151:539–47.
[153] Nangaku M, Pippin J, Couser WG. Complement membrane attack complex (C5b-9) mediates interstitial disease in experimental nephrotic syndrome. J Am Soc Nephrol 1999;10:2323–31.
[154] Nangaku M, Pippin J, Couser WG. C6 mediates chronic progression of tubulointerstitial damage in rats with remnant kidneys. J Am Soc Nephrol 2002;13:928–36.
[155] Rangan GK, Pippin JW, Couser WG. C5b-9 regulates peritubular myofibroblast accumulation in experimental focal segmental glomerulosclerosis. Kidney Int 2004;66:1838–48.
[156] Isenman DE, Kells DI, Cooper NR, Muller-Eberhard HJ, Pangburn MK. Nucleophilic modification of human complement protein C3: correlation of conformational changes with acquisition of C3b-like functional properties. Biochemistry 1981;20:4458–67.
[157] Rangan GK, Pippin JW, Coombes JD, Couser WG. C5b-9 does not mediate chronic tubulointerstitial disease in the absence of proteinuria. Kidney Int 2005;67:492–503.
[158] Abbate M, Zoja C, Corna D, Rottoli D, Zanchi C, Azzollini N, et al. Complement-mediated dysfunction of glomerular filtration barrier accelerates progressive renal injury. J Am Soc Nephrol 2008;19:1158–67.
[159] Buelli S, Abbate M, Morigi M, Moioli D, Zanchi C, Noris M, et al. Protein load impairs factor H binding promoting complement-dependent dysfunction of proximal tubular cells. Kidney Int 2009;75:1050–9.
[160] Turnberg D, Lewis M, Moss J, Xu Y, Botto M, Cook HT. Complement activation contributes to both glomerular and tubulointerstitial damage in adriamycin nephropathy in mice. J Immunol 2006;177:4094–102.
[161] Peake PW, O'Grady S, Pussell BA, Charlesworth JA. C3a is made by proximal tubular HK-2 cells and activates them via the C3a receptor. Kidney Int 1999;56:1729–36.
[162] Braun MC, Reins RY, Li TB, Hollmann TJ, Dutta R, Rick WA, et al. Renal expression of the C3a receptor and functional responses of primary human proximal tubular epithelial cells. J Immunol 2004;173:4190–6.
[163] Abe K, Li K, Sacks SH, Sheerin NS. The membrane attack complex, C5b-9, up regulates collagen gene expression in renal tubular epithelial cells. Clin Exp Immunol 2004;136:60–6.
[164] Tang Z, Lu B, Hatch E, Sacks SH, Sheerin NS. C3a mediates epithelial-to-mesenchymal transition in proteinuric nephropathy. J Am Soc Nephrol 2009;20:593–603.
[165] Boor P, Konieczny A, Villa L, Schult AL, Bucher E, Rong S, et al. Complement C5 mediates experimental tubulointerstitial fibrosis. J Am Soc Nephrol 2007;18:1508–15.
[166] Alexander JJ, Wang Y, Chang A, Jacob A, Minto AW, Karmegam M, et al. Mouse podocyte complement factor H: the functional analog to human complement receptor 1. J Am Soc Nephrol 2007;18:1157–66.
[167] Lenderink AM, Liegel K, Ljubanovic D, Coleman KE, Gilkeson GS, Holers VM, et al. The alternative pathway of complement is activated in the glomeruli and tubulointerstitium of mice with adriamycin nephropathy. Am J Physiol Renal Physiol 2007;293:F555–64.
[168] Zhou W, Marsh JE, Sacks SH. Intrarenal synthesis of complement. Kidney Int 2001;59:1227–35.
[169] Tang S, Sheerin NS, Zhou W, Brown Z, Sacks SH. Apical proteins stimulate complement synthesis by cultured human proximal tubular epithelial cells. J Am Soc Nephrol 1999;10:69–76.
[170] Tang S, Neng Lai K, Mao Chan T, Lan HY, Ho SK, Sacks SH. Transferrin but not albumin mediates stimulation of complement C3 biosynthesis in human proximal tubular epithelial cells. Am J Kidney Dis 2001;37:94–103.
[171] Li K, Patel H, Farrar CA, Hargreaves RE, Sacks SH, Zhou W. Complement activation regulates the capacity of proximal tubular epithelial cell to stimulate alloreactive T cell response. J Am Soc Nephrol 2004;15:2414–22.
[172] Remuzzi G, Zoja C, Gagliardini E, Corna D, Abbate M, Benigni A. Combining an antiproteinuric approach with mycophenolate mofetil fully suppresses progressive nephropathy of experimental animals. J Am Soc Nephrol 1999;10:1542–9.
[173] Vieyra MB, Heeger PS. Novel aspects of complement in kidney injury. Kidney Int 2010;77:495–9.
[174] Faul C, Donnelly M, Merscher-Gomez S, Chang YH, Franz S, Delfgaauw J, et al. The actin cytoskeleton of kidney podocytes is a direct target of the antiproteinuric effect of cyclosporine A. Nat Med 2008;14:931–8.
[175] Remuzzi A, Gagliardini E, Donadoni C, Fassi A, Sangalli F, Lepre MS, et al. Effect of angiotensin II antagonism on the regression of kidney disease in the rat. Kidney Int 2002;62:885–94.
[176] Matzinger P. The danger model: a renewed sense of self. Science 2002;296:301–5.
[177] Macconi D, Chiabrando C, Schiarea S, Aiello S, Cassis L, Gagliardini E, et al. Proteasomal processing of albumin by renal dendritic cells generates antigenic peptides. J Am Soc Nephrol 2009;20:123–30.
[178] Kees-Folts D, Sadow JL, Schreiner GF. Tubular catabolism of albumin is associated with the release of an inflammatory lipid. Kidney Int 1994;45:1697–709.

[179] Schreiner GF. Renal toxicity of albumin and other lipoproteins. Curr Opin Nephrol Hypertens 1995;4:369–73.
[180] Thomas ME, Harris KPG, Walls J, Furness PN, Brunskill NJ. Fatty acids exacerbate tubulointerstitial injury in protein-overload proteinuria. Am J Physiol Renal Physiol 2002;283:F640–7.
[181] Kamijo A, Sugaya T, Hikawa A, Okada M, Okumura F, Yamanouchi M, et al. Urinary excretion of fatty acid-binding protein reflects stress overload on the proximal tubules. Am J Pathol 2004;165:1243–55.
[182] Arici M, Brown J, Williams M, Harris KP, Walls J, Brunskill NJ. Fatty acids carried on albumin modulate proximal tubular cell fibronectin production: a role for protein kinase C. Nephrol Dial Transplant 2002;17:1751–7.
[183] Ishola Jr. DA, Post JA, van Timmeren MM, Bakker SJ, Goldschmeding R, Koomans HA, et al. Albumin-bound fatty acids induce mitochondrial oxidant stress and impair antioxidant responses in proximal tubular cells. Kidney Int 2006;70:724–31.
[184] Urahama Y, Ohsaki Y, Fujita Y, Maruyama S, Yuzawa Y, Matsuo S, et al. Lipid droplet-associated proteins protect renal tubular cells from fatty acid-induced apoptosis. Am J Pathol 2008;173:1286–94.
[185] Porubsky S, Schmid H, Bonrouhi M, Kretzler M, Malle E, Nelson PJ, et al. Influence of native and hypochlorite-modified low-density lipoprotein on gene expression in human proximal tubular epithelium. Am J Pathol 2004;164:2175–87.
[186] Iseki K, Iseki C, Ikemiya Y, Fukiyama K. Risk of developing end-stage renal disease in a cohort of mass screening. Kidney Int 1996;49:800–5.
[187] Ruggenenti P, Perna A, Mosconi L, Matalone M, Pisoni R, Gaspari F, et al. Proteinuria predicts end-stage renal failure in non-diabetic chronic nephropathies. The "Gruppo Italiano di Studi Epidemiologici in Nefrologia" (GISEN). Kidney Int Suppl 1997;63:S54–7.
[188] Ruggenenti P, Perna A, Mosconi L, Pisoni R, Remuzzi G. Urinary protein excretion rate is the best independent predictor of ESRF in non-diabetic proteinuric chronic nephropathies. "Gruppo Italiano di Studi Epidemiologici in Nefrologia" (GISEN). Kidney Int 1998;53:1209–16.
[189] Cravedi P, Ruggenenti P, Remuzzi G. Proteinuria should be used as a surrogate in CKD. Nat Rev Nephrol 2012;8:301–6.
[190] Remuzzi G, Benigni A, Remuzzi A. Mechanisms of progression and regression of renal lesions of chronic nephropathies and diabetes. J Clin Invest 2006;116:288–96.
[191] Zoja C, Corna D, Camozzi D, Cattaneo D, Rottoli D, Batani C, et al. How to fully protect the kidney in a severe model of progressive nephropathy: a multidrug approach. J Am Soc Nephrol 2002;13:2898–908.
[192] Ruggenenti P, Perticucci E, Cravedi P, Gambara V, Costantini M, Sharma SK, et al. Role of remission clinics in the longitudinal treatment of CKD. J Am Soc Nephrol 2008;19:1213–24.

This page intentionally left blank

CHAPTER

88

The Inflammatory Response to Ischemic Acute Renal Injury

Christopher Y. Lu

Division of Nephrology, Department of Internal Medicine, University of Texas, Southwestern Medical Center, Dallas, Texas, USA

INTRODUCTION

Acute ischemia reperfusion injury (IRI) is a major cause of acute kidney injury (AKI).[1] A major conceptual insight is that the total amount of renal injury is the result of not only the initial ischemic insult, by the ensuing responses. This simple insight has profound clinical implications: it suggests that therapy after the initial insult has already occurred may ameliorate the course of AKI (see Figure 88.1). Some of these responses are maladaptive. Examples include inappropriate intrarenal hemodynamics, altered mitochondrial and other metabolic functions,[2–4] endothelial dysfunction,[5,6] and tubular obstruction and back-leak.[7] Other responses are reparative. Examples include the production of growth factors such as Wnt7.[8]

In addition to the above, IRI elicits an inflammatory response. Some components of this inflammatory response exacerbate injury, other components mediate repair. In either case, inflammation is a major determinant of the ultimate outcome of ischemic AKI. A complete understanding of the inflammatory response to IRI—the composition and functions of the leukocytes, the stimuli that elicit inflammation, and the regulation of inflammation—remain a fundamental unsolved problem in renal disease. The goal of this chapter to provide a perspective on our rapidly growing insights into the inflammatory response to IRI.

In addition to its importance for injury of the native kidney, the inflammatory response to IRI is important for transplantation. Ischemic injury to the allograft inevitably accompanies organ harvesting, the cold storage, and the warm ischemia during the surgical creation of the vascular anastomoses between allograft and recipient. In addition, for brain dead donors, the donor kidneys are damaged by the hemodynamic instability resulting from the trauma that causes brain death. The leukocytes recruited to the allograft by ischemia exacerbate rejection. This is predicted by the "danger" theory of immunology where injury elicits inflammation, the leukocytes detect non-self at the site of injury (infectious pathogens or the allograft), and then develop an immune response against the non-self.[9–13] The relation of this "injury response" to rejection has previously been reviewed.[14–23]

An inflammatory response is also elicited by chronic injuries in common human diseases such as progressive renal failure from diabetes and hypertension.[24–26] Understanding the inflammatory response to the "single hit" model of acute ischemia may aid our understanding of the more complicated chronic diseases. The goal of this chapter is to review our current understanding of this rapidly evolving field. Although complement and gene activation by hypoxia/reactive oxygen species are important, our focus will be on the nature of the inflammation and its regulation by injured and dying cells.

Most studies of the inflammatory response to renal ischemia have involved rodents. The potential difficulties in extrapolating such studies to the clinical setting have been discussed previously.[27–29] Although inflammation is not a prominent feature of human ischemic acute renal failure, leukocytes are present.[30] The susceptibility of patients to acute renal failure may correlate with polymorphisms of pro- and anti-inflammatory genes;[31] and this further supports a role of inflammation in the pathogenesis of human disease. Biopsy studies during ischemic acute renal failure of native human kidneys are limited, but post-anastomosis

Seldin and Giebisch's The Kidney, Fifth Edition.
DOI: http://dx.doi.org/10.1016/B978-0-12-381462-3.00088-4

© 2013 Elsevier Inc. All rights reserved.

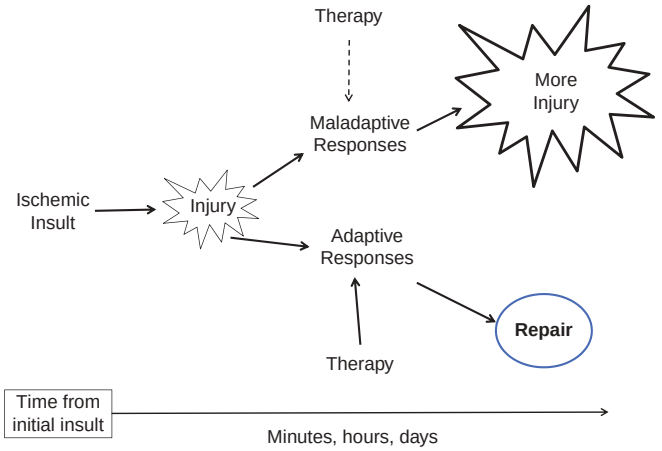

FIGURE 88.1 Injury after ischemic AKI is the sum result of the initial insult, subsequent maladaptive, and adaptive responses. Original figure.

biopsies of renal allografts are increasingly common. Most such biopsies indicate inflammation, particularly in deceased, compared to living, donors.[32–36] Furthermore, intraoperative biopsies have also indicated expression of pro-inflammatory genes.[37–40] Such inflammation may be a response to ischemic injury to the allograft due to the hypotension associated with the trauma that caused brain death, due to the cold storage, and due to the warm ischemia during creation of the vascular anastomoses. In addition, inflammation in the cadaver kidneys was also caused by neurohormonal effects of brain death.[41] Inflammation during these intraoperative biopsies are not due to rejection because there is no time for immune recognition of the transplant. Furthermore, biopsies of kidneys between identical twins, where there is no allo-recognition, also shows inflammation that must be due to ischemic injury occurring during the transplant process.[42]

Some argued that injury and damage to kidney is not the major contributor to most cases of human ischemic AKI.[43] Instead the major factor is abnormal renal microvascular function and use of oxygen.[2] Indeed, in those rare cases where the kidney is biopsied, the morphologic injury by conventional staining techniques are minimal. However, the longterm maladaptive effects of ischemic AKI suggests that injury does occur and the kidney never completely recovers from this injury. Indeed, recurrent episodes of ischemic AKI may be a major contributor to the current epidemic of CKD.[44,45]

The medullary thick ascending limb and the S3 straight proximal tubule in the outer medulla are the tubules most vulnerable to ischemic injury in both rodents and humans.[29,46–50] This is the area with the greatest inflammation.[51,52] Although the outer medulla is the injured earliest and after the least ischemia, longer periods of ischemia result in the injury of the cortex also.[43] Because different structures in the kidney may be injured depending on the intensity of ischemia, and because these structures produce different cytokines, chemokines, and other regulatory molecules in response to IRI, renal IRI may be a family of diseases rather than a single entity. Thus, the length of ischemia time, or the temporature of ischemia may modify the inflammatory response to IRI.[53]

The inflammatory response to acute ischemia of the heart, and brain have been more intensively studied than ischemic acute renal failure because of the greater clinical incidence of coronary artery disease and stroke. Where renal studies are not available, we will review studies from these and other non-renal organs. Although the general principles may be the same in these various organs, the particular mechanisms of the inflammatory response to ischemic injury may be different in different organs. For example, blocking the pro-inflammatory cytokine interleukin 1α and β ameliorates ischemic injury of the rodent brain[54] and heart,[55] but has no effect on ischemic acute renal failure.[56]

LEUKOCYTES IN INJURED, ISCHEMIC TISSUES: FRIEND, AND FOE.

Over a decade ago, anti-inflammatory agents were shown to ameliorate ischemic acute renal failure.[57,58] These studies demonstrated the maladaptive effects of the inflammatory response to injury. Recent studies elucidate greater detail about which leukocytes are involved and how they regulate renal IRI.

Mononuclear phagocytes—monocytes, macrophages and dendritic cells: The relationship of the various members of the mononuclear phagocyte family—monoctye, macrophages, and dendritics, and there various subsets—is complex.[59–63] Various mononuclear phagocytes participate in ischemic AKI. Some exacerbate injury. Others facilitate repair.

These leukocytes exacerbate the early phases of ischemic injury.[52,64,65] Macrophages appear within hours after ischemic injury in both mice and rats; these macrophages are located adjacent to the vasa rectae of the outer medulla.[52,66] This is the region of the rodent kidney that is most vulnerable to ischemic injury,[29,67,68] and where there is endothelial injury[69] and expression of both B7 and adhesion molecules.[51,52]

Elimination of this early macrophage infiltrate prevented the increased interleukin 6[64,70] that occurs after renal ischemia.[71,72] The former exacerbate ischemic renal injury because its elimination by transgenic knockout, or anti-interleukin-6 antibodies[66,73] ameliorates renal injury. *In situ* hybridization shows that interleukin 6 is produced by macrophages in the

ischemic kidneys; the construction of bone marrow chimeras where renal parenchymal cells or macrophages have their IL6 gene knocked out showed that the greatest injury occurred when macrophages were capable of making interleukin 6.[66] Macrophages are also capable of producing a number of other molecules that might exacerbate ischemic acute renal failure. However, as discussed below, what cytokines are produced by which renal cells, and which cytokines have harmful versus helpful effects remain to be clearly delineated.

In these studies, there was an early infiltration of macrophages in the absence of neutrophils. This sequence of macrophages then neutrophils contradicts the classical paradigm which proposes that neutrophils infiltrate first, and produce molecules that recruit monocytes subsequently.[74] However, recent data indicate that monocytes can infiltrate tissues early and, in some cases, in the absence of neutrophils.[75] In the lung[76,77] and liver,[78] macrophage inflammation may precede neutrophilic inflammation. This may also occur in ischemic acute renal failure. Furthermore, the nature of renal cell death during ischemic AKI may regulate the type of inflammation. Apoptosis generally recruit macrophages, but necrosis recruits neutrophils. We discuss the various types of cell death and their effects in inflammation later in this chapter.

In addition to this early infiltrate, there is also a late infiltrate of macrophages and related dendritic cells during the first weeks after acute ischemic injury.[79–82] Large numbers of these leukocytes are still present after the recovery of glomerular filtration has already occurred. The contribution of these leukocytes to renal injury and repair is not known. On the one hand, they may contribute to chronic injury. On the other hand, some macrophage subpopulations participate in tissue repair, perhaps through the secretion of growth factors such as Wnt7b or anti-inflammatory cytokines such as interleukin 10.[8,83–92] These macrophages have many attributes of "M2" macrophages present late after infections.[93]

Macrophage infiltration into the outer medulla is regulated by endothelia. Endothelia are the border between the vasculature and the renal interstitium. Thus, the quantity and composition of leukocyte traffic from blood into the renal interstitial spaces is regulated by proinflammatory genes expressed by endothelia.[94–97] Ischemic endothelia in the outer medulla do increase their expression of pro-inflammatory ICAM-1 (CD54) and B7. 1 (CD80).[51,52,98,99] In addition, endothelial expression of P-selectin (CD62P) and VCAM-1 (CD106) also contribute to the inflammatory response to renal ischemia,[100–103] but the precise anatomical location is not known. Inactivation of ICAM-1 and selectins via antibodies, antisense oligonucleotides, or transgenic knockout ameliorates inflammation and injury after acute ischemia.[98,103–107]

Furthermore, macrophage infiltration into the ischemic kidney is regulated by MCP 1, a chemokine that attracts macrophages are expressed by the ischemic kidneys.[108] Transgenic knockout of the receptor for MCP 1 (CCR2)[109] or administration of a truncated, inhibitory form of MCP 1[110] both ameliorate ischemic injury and inflammation.

In addition, macrophages may be recruited by molecules released by necrotic or apoptotic cells. This will be discussed in later sections of this chapter. Finally, blocking B7 on ischemic endothelia decreases macrophage infiltration and ischemic renal injury.[111,112] CD28, the ligand for B7, is not known to be expressed by macrophages, but is expressed by T cells. This suggests a role for T cells in ischemic acute renal failure (see below).

Neutrophils: In contrast to the early infiltration of macrophages, some studies report that there is a later infiltrate of neutrophils.[100,113] The role of these neutrophils is not clear. Early reports[98,114] suggested that elimination of these neutrophils with antibodies ameliorated ischemic injury. But this may have reflected the use of polyclonal antibodies that actually recognized both neutrophils and macrophages.[115] Recent data using monoclonal antibodies for neutrophils are controversial. Some,[116] but not others,[117,118] find that deleting neutrophils ameliorated ischemic injury. One difficulty in these studies is the use of the monoclonal antibody for Ly6C/G (Gr1). Although Ly6C/G is highly expressed on neutrophils, it is also expressed, albeit weakly, on some subsets of monocyte/ macrophages.[119]

Renal parenchymal cells produce the neutrophil chemokines KC and MIP 2,[108,116] the murine analogs for human interleukin 8, as well G-CSF that would stimulate neutrophil production by the bone marrow.[113] In one study, antibody to the neutrophil chemokines KC and MIP 2[116] decreased neutrophilic infiltration and also ameliorated ischemic injury. However, antibody to the receptor for these chemokines CXCR2 unexpectedly exacerbated injury.[120] These results need to be reconciled. One possibility is that these chemokines have both maladaptive and adaptive functions; in addition to regulating neutrophilic inflammation, KC and MIP 2 may also regulate the differentiation of renal tubular cells during the repair process after injury.[121,122]

Those advocating a role for neutrophils point out that, in addition to releasing toxic molecules that might injure the kidney, neutrophils are now known to produce cytokines, chemokines, and other regulatory molecules.[123] By producing these molecules, neutrophils may regulate any subsequent inflammation and repair.[124] Those, who find no role for neutrophils in renal injury, might argue that the presence of neutrophils in tissue does not necessary indicate that these

neutrophils are activated. Thus, ectopic gene expression of the neutrophil chemokine KC results in a neutrophilic infiltrate but no tissue damage, presumably because the neutrophils are not activated to produce toxic molecules.[125] This neutrophil infiltration may be regulated by NK T cells.[126,127]

Lymphocytes: Small numbers of T cells are found in kidneys after renal ischemia.[52,128] The role of these T cells is not understood. On the one hand, elimination of T cells via the foxn1 mutation (nude mice) ameliorated injury. FTY720, an immunosuppressive drug that traps lymphocytes in lymph nodes, inhibits ischemic acute renal injury.[129] But, on the other hand, elimination of all classical T cells via mutation of the TCRα chain[128] or via mutation of the rag gene (scid mice)[130] did not inhibit. There is further controversy when elimination of specific subsets of T cells was examined. On the one hand, eliminating CD4 T cells with monoclonal antibodies[128,131] did not ameliorate injury, but elimination with transgenic knockout[101] did. Similar controversy surrounds the role of CD8 T cells. On the one hand, transgenic knockout of CD8 did not ameliorate ischemic injury;[101] however, anti-CD8 antibodies used in combination with anti-CD4 antibodies did.[131] B-lymphocytes may also contribute to ischemic AKI.[132] This is discussed further in the section on complement and "natural" antibodies.

The role of lymphocytes in ischemic injury is further complicated by observations suggesting that T cells ameliorate injury in some models. These studies fall into three groups: those involving CD4 T cells, those involving interferon gamma, and those involving "unconventional" $\gamma\delta$ T cells.

Some CD4 T cells may ameliorate injury. CD4 knockout results in decreased HGF production and increased tubular apoptosis after ureteral obstruction.[133,134] Nude mice with no classical T cells have increased injury after optic nerve injury, and injection of such T cells improves repair.[135] CD4 T cells play a dual role of exacerbating and inhibiting inflammation after ischemic hepatic injury.[136]

Interferon gamma may play a dual function. Interferon gamma is a cytokine associated with ischemic injury, and produced in quantity by T cells. Interferon gamma exacerbates ischemic acute renal failure in some models.[101,137] However, there are interferon gamma dependent pathways of tissue repair.[138,139] Whether or not there are such pathways in the kidney is not known.

Recent data suggest that unconventional T cells recognize injured tissues. Thus, some T cells with $\gamma\delta$ T cell receptors recognized stressed epithelia and release keratinocyte growth factors that facilitate repair.[140] Whether or not such T cells are present in the ischemic kidney is not known. NK T cells also participate in ischemic AKI[126,127] and some NKT cell regulate inflammation during AKI.[141–143]

THE PROINFLAMMATORY EFFECTS OF INJURY—DAMPS, STERILE INFLAMMATION, AND THE "DANGER/ DAMAGE" HYPOTHESIS

Although the above shows that the inflammatory response to ischemia may an important determinant of the extent of injury and repair, how ischemic injury is translated into inflammation is a major outstanding question. Approaches to addressing this question are reviewed in the remainder of this chapter. Several concepts and terms need to be defined before beginning our discussion. A major recent concept is that injury itself is proinflammatory. The proinflammatory signals are generated in several ways. Molecules, normally residing within cells, elicit inflammation when they are released into the extracellular space or are expressed on cell surfaces. In addition, enzymes released by injured cells or leukocytes convert extracellular matrix molecules into proinflammatory signals. Finally, intracellular stress may generate proinflammatory signals. Altogether these proinflammatory molecules have been called "danger (or damage)-associated molecular pattern" molecules (DAMPS) or Alarmins. This inflammatory response to injury has been called the "danger" response or "sterile" inflammation to differentiate it from the inflammatory response to infections.[144–150]

The biology of DAMPS, their receptors, and their regulation of injury, of the inflammatory response to injury, and of repair remain to be completely elucidated. The biology is complex because the receptors are promiscuous and interact with numerous DAMPS, because each DAMP interacts with multiple receptors, because DAMPS interact with each other, and because the cellular response to a DAMP is unique to the cell and its microenvironment. We review our current understanding of this rapidly evolving field with the humble realization that this understanding will certainly change in the future.

TLR4 AND HMGB1

During ischemic AKI, the best characterized receptor for DAMPS is TLR4. TLR4 is best known as the receptor for endotoxin produced by gram negative bacteria, and mediates the inflammatory response against these bacteria.[151,152] It is one member of a family of "pattern recognition receptors" that recognize molecules produced by pathogens. In addition to endotoxin, these molecules include viral DNA, viral RNA, and sugar molecules

unique to yeast. The TLR's are present on most leukocytes of the "innate" immune response—macrophages and neutrophils.[153–155] They are critical for the immediate inflammatory response against infections.[13]

A major discovery was the insight that TLR4 not only recognizes endotoxin, but also recognizes DAMPS.[148,156–163] These molecules are called "endogenous" because they are produced by mammalian cells and to differentiate them from endotoxin, the "exogenous" TLR4 ligand that is produced by gram negative bacteria.

Striking confirmation for the importance of TLR4 in ischemic disease were experiments comparing inflammation and injury in wildtype mice versus TLR4 deficient mutant mice after ischemia to the heart,[164,165] liver,[166–168] lung,[169] and kidney.[170–175] In all of these studies, mutant mice with non-functional TLR4 are protected from ischemic injury. Furthermore, human mutations that inactivate TLR4 ameliorate post-transplant ischemic AKI.[173]

HMGB1 is released from injured cells and is the best documented DAMP ligand for TLR4 during ischemic AKI. The HMGB1-TLR4 interaction is one of the few DAMP-TLR4 interactions that have been confirmed by biophysical studies.[176] Furthermore, HMGB1 has a proven role in ischemic AKI. Its expression increases in both murine ischemic AKI,[170,177] and biopsies of human renal transplant grafts that had ischemic AKI during the transplant process.[173] Antibodies that inactivate HMGB1 ameliorate murine ischemic AKI.[177,178] Altogether this data show HMGB1 has maladaptive functions during ischemic AKI.

Within four hours reperfusion, reactive oxygen species produced during ischemia reperfusion[179–181] increase endothelial expression of TLR4. HMGB1 released from injured renal tubulesbind the endothelial TLR4, and cause increased adhesion molecule expression.[150] These adhesion molecules facilitate the immigration of leukocytes into the injured outer medulla.[98,104,182–184] HMGB1 binds to TLR4 on these leukocytes, including macrophages, and stimulates the production of maladaptive interleukin 6.[174] In addition, the HMGB1 also stimulates TLR4 on tubules and stimulates the production of maladaptive chemokines and cytokines.[178] See review[185] and Figure 88.2.

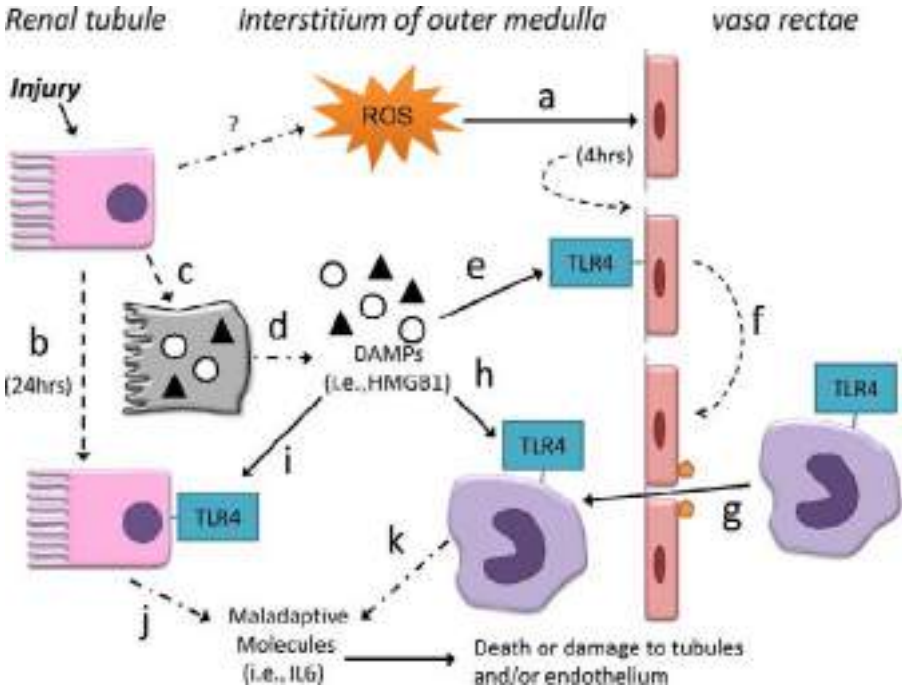

FIGURE 88.2 The structure of HMGB1. TLR4-HMGB1 in Ischemic AKI. In response to reactive oxygen species (ROS) released during ischemia/ reperfusion, endothelia of the vasa rectae express TLR4 within four hours after reperfusion (a). Renal tubules also express TLR4, but only after 24 hours following reperfusion; renal tubular TLR4 expression is a response to interferon gamma and TNFα (b). Injury also increases renal tubular production of endogenous TLR4 ligands such as HMGB1 (b), and severely injured cells release these ligands into the extracellular space (d). These extracellular TLR4-ligands trigger maladaptive responses. They activate TLR4 on endothelial cells (e) which in turn, express adhesion molecules (f) that facilitate diapedesis of monocytes (macrophages) from blood into the renal interstitial space (g). The endogenous TLR4-ligands (HMGB1) then activate TLR4 on macrophages (h), and tubules (i). The activated macrophages and tubules release maladaptive molecules such as interleukin 6 (j & k) that exacerbate injury. From Lu CY, Winterberg PD, Chen J, Hartono JR. Acute kidney injury: a conspiracy of toll-like receptor 4 on endothelia, leukocytes, and tubules. *Pediatr Nephrol 2011*. http://www.ncbi.nlm.nih.gov/pubmed/22033798.

The Complex Biology of HMGB1 and TLR4—Promiscous Molecules with Promiscous Partners and Multiple Biologic Effects

Although the HMGB1–TLR4 interaction in ischemic AKI is well documented in the above experiments, much remains to be learned.

The biology of HMGB1 is complex. HMGB1 is expressed by all eukaryotic cells and is highly conserved through evolution. It was originally described as a nuclear protein that enables interactions between DNA and nuclear proteins that regulate transcription. However, in the late 1990's a search for mediators of shock revealed that HMGB1 elicited lethal inflammation.[186] Antibodies against HMGB1 prevented shock. Subsequent experiments showed that HMGB1 was released by necrotic cells, and actively secreted by leukocytes of the innate immune response. The little inflammation seen after apoptosis, as opposed to necrosis, may result from sequestration of HMGB1 within the nucleus of apoptotic cells. The various protein domains HMGB1 have unique functions as shown in Figure 88.3. The A and B boxes bind to DNA, and the C box is negatively charged. The proinflammatory effect of HMGB1 may be reproduced by recombinant B box. Recombinant A box peptide is a specific antagonist of the proinflammatory effects. Thus, there is therapeutic potential in using these genetically engineered peptides to either increase or decrease inflammation.[187]

HMGB1 is post-translationally modified both enzymatically and by reactive oxygen species. It also binds endotoxin and nucleic acids. These may change its biological activity.[187–189]

HMGB1 has seven known receptors in addition to TLR4.[176] In addition to TLR4, only one other receptor, RAGE,[190,191] has been studied in ischemic AKI. RAGE is thought not to participate in ischemic AKI in mice because its transgenic knockout does not affect disease.[192]

The biology of TLR4 is also complex. In addition to HMGB1 it binds to other DAMPS. These include oxidation products resulting from reactive oxygen species produced during ischemia reperfusion,[193,194] extracellular matrix components and heat shock proteins as discussed below.

After tissue injury, the extracellular matrix is degraded into low molecular weight fragments. Two of these fragments, heparan sulfate and hyaluronan, activate TLR4,[162,163,195,196] and may participate in ischemic AKI. Low molecular weight heparan sulfates are

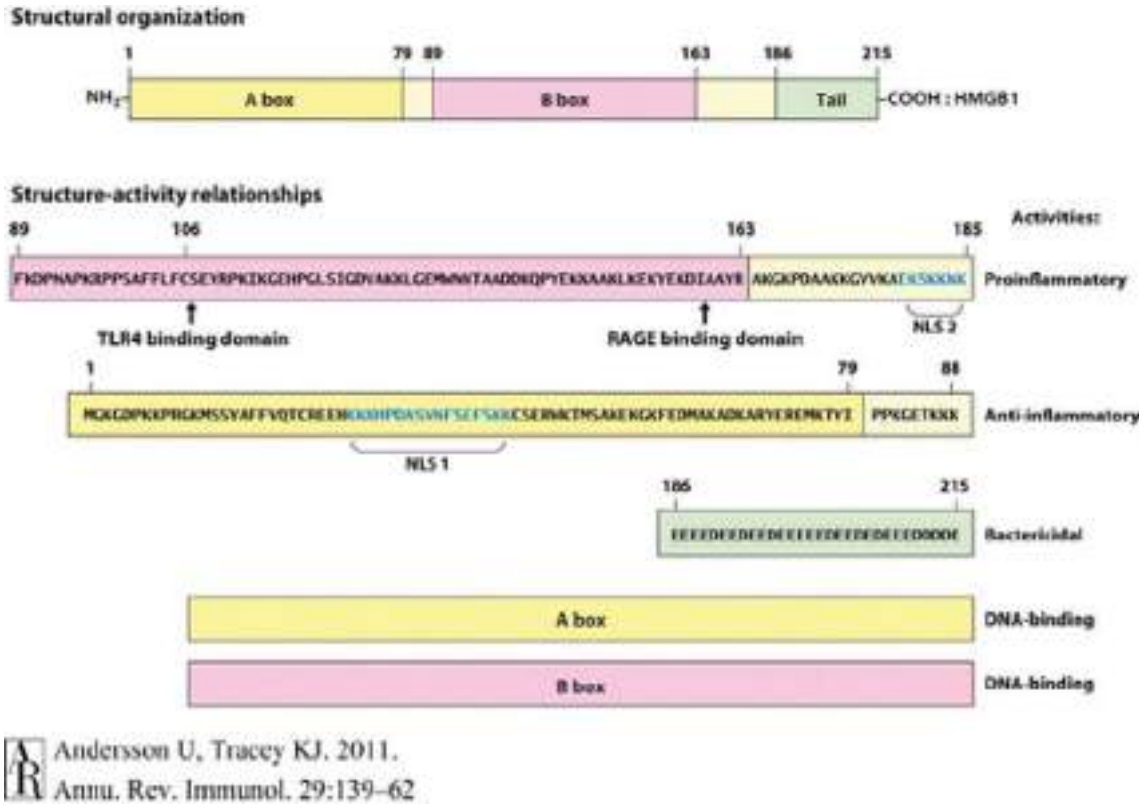

FIGURE 88.3 Structure function of HMGB1. From article cited in text.

released when neutrophil elastase degrades heparan sulfate proteoglycans in the extracellular matrix (see review[197]). Inhibition of neutrophil elastase ameliorated ischemic acute renal failure in rodents, possibly by inhibiting the production of heparan sulfate fragments.[198] Hyaluronan increases in the ischemic kidney.[199] Low molecular weight hyaluronans are released when hyaluronidases from tubules and leukocyes degrade the extracellular matrix. Small hyaluronans stimulate renal tubular cells to produce MCP-1 (a macrophage chemokine), and TNFα (a proinflammatory cytokine) *in vitro*.[200] Biglycan is another extracellular matrix component that may stimulate TLR4 after tissue injury.[201]

Heat shock proteins (Hsp's) are major candidates for being the TLR4 ligands during ischemic AKI: different intracellular and extracellular functions during ischemic AKI?

Hsp70. 1 and Hsp70. 3 are two members of the murine heat-shock-70 family. They are over 95% identical to each other.[202–207] Gp96 is the heat shock protein of the endoplasmic reticulum.[207,208] The murine and human Hsp's are highly homologous.

Although these Hsp's have well known intracellular cytoprotective effects, they also have extracellular functions as cytokines, and particularly as TLR4-ligands.[148,156–161] Indeed, Hsp's have been used as adjuvants in an attempt to immunize experimental subjects against cancer.[209]

Intracellular Heat Shock Proteins are Cytoprotective

Hsp's70. 1 and 70. 3 expressions in the nucleus and cytoplasm is increased after cell stress. Gp96 expression is increased as well.[207,208] These proteins have also been implicated in renal ischemic injury. Within one hour of renal ischemia, Hsp's70. 1 and 70.3 increase by 5x in the S3 segment of the proximal tubule,[210–213] and gp96 increases in both the S3 segment and the loop of Henle.[213] Therefore, increased intracellular Hsp's70. 1 & 3 and gp96 may be part of a cytoprotective mechanism during ischemic ARF (for example[214] and see reviews [215–218]).

Extracellular heat shock proteins may be endogenous TLR4-ligands that recruit inflammatory responses during ischemic ARF.

There is also mounting evidence that extracellular Hsp's act as cytokines, and the term "chaperokine" was coined to highlight their dual functions.[219] Most importantly, extracellular Hsp's activate TLR4 to recruit an inflammatory response.[10–12,158,220] The possibility that extracellular Hsp's may have a harmful proinflammatory role in ARF was proposed in a theoretical paper.[221]

Source of Extracellular Hsp's

Since Hsp's are normally intracellular proteins, the question of how Hsp's are released into the extracellular space during injury needs to be addressed. There are several possibilities.

Firstly, leakage from cells *with* morphologically evident injury (necrosis). Hsp's may be released from severely injured and therefore leaky cells. Since Hsp's are abundant proteins, and their cytokine functions are likely to require very low extracellular concentrations, a small amount of leakage may trigger the self-amplifying inflammatory mechanisms that induce further injury during the "extension" phase of ischemic ARF. Such necrosis would result in the release of intracellular heat shock proteins into the extracellular space where they could activate the endothelium and leukocytes.

Secondly, release from cells *without* evident morphologic injury. Several such mechanisms have been proposed: One is the secretion of Hsp's by stressed cells[156,157] or cells activated by cytokines. A second mechanism is the release of "exosomes." Exosomes are formed by a process of "reverse" endocytosis. These small particles contain Hsp's and they activate macrophages and dendritic cells (see review[209,222–224]). A third mechanism is the expression of membrane bound Hsp's. Although Hsp's normally reside in the cytoplasm, endoplasmic reticulum, or mitochondria, they may redistribute to the cell surface after stress.[225–227] Such cell surface Hsp's activate leukocytes.[228] Altogether there is ample evidence to support the possibility that Hsp's from injured renal tubular cells could stimulate TLR4 in the absence of morphologic features of cell death that are detectable by light microscopy.

Other endogenous molecules also interact with TLR4, but they are less well studied than HMGB1, Hsp's and extracellular matrix components discussed above. Fibronectin IIIA is a variant fibronectin that is produced by stressed cells,[229] and is increased during ischemic ARF.[230] β-defensin is found in kidneys stressed by infection,[231] but β-defensin production during ischemic ARF has not previously been examined. Hsp60 is not known to increase after renal ischemia, but might still be released during ischemic ARF and stimulate TLR4.[161] Tamm Horsfall protein may also be a TLR4 ligand.[232,233] See review.[234] Not only does TLR4 bind to numerous ligands, each ligand may trigger unique biological effects.

Thus, endotoxin and the endogenous TLR4-ligands have different interactions with the TLR4 receptor. Endotoxin interacts with TLR4 in two ways: first, soluble endotoxin may bind the TLR4-MD2 heterodimer.[235] Second, endotoxin may form lipid micelles that

intercalate into cell membrane and then bind TLR4.[236–239] In contrast, all of the endogenous TLR4 ligands identified so far are soluble molecules. Although the hydrophobicity of these ligands may be important,[9] they are unlikely to directly intercalate into the membrane bilayer. Furthermore, some endogenous TLR4 ligands also bind other cell surface receptors in addition to activating TLR4. For example: Hsp's 70. 1 & 3 and gp96 bind cell surface CD40[240] and CD91.[241]

Because endotoxin and the endogenous TLR4-ligands have different modes of interaction with the TLR4 receptor, it is not surprising that they elicit different responses *in vitro*[242] and in a model of autoimmunity *in vivo*.[243]

Of particular importance for this discussion is the different effect of endotoxin and ischemia on the kidney. Both injure the kidney, but in different ways. When care is taken to prevent hypotension, endotoxin decreases GFR by over 70% in the absence of apoptosis, inflammation, and other morphological changes; this injury is not affected by transgenic knockout of inducible nitric oxide synthase (iNOS).[244] In contrast, murine ischemic ARF, which is accompanied by the release of endogenous TLR4-ligands, is characterized by profound morphologic injury and inflammation (see for example review[245]). Unlike normotensive endotoxin ARF, ischemic ARF is ameliorated by transgenic knockout of iNOS.[246,247]

When hypotension is not controlled, endotoxin causes glomerular, in addition to tubular, injury. In contrast, ischemic ARF with release of endogenous ligands, injures tubules, but not glomeruli.[248] Other data shows that systemic endotoxin injures the kidney by increasing the production of extrarenal TNFα.[249]

Note that ARF induced by endotoxin differs from ischemic ARF in another fundamental way: endotoxin is injected systemically and induces massive cytokine production in many organs; on the other hand, during ischemia the postulated TLR4 ligands are released locally in the kidney.

Another example of differences between endotoxin and endogenous TLR4 ligands is a model of autoimmune isletis where endotoxin alone induced diabetes, but Hsp's 70.1 and 70.3 (both endogenous TLR4 ligands) required additional activating anti-CD40 to induce diabetes.[243] Still another relevant example is the TLR4-dependent abilities of LPS to decrease, but HMGB1, another TLR4 ligand, to increase, the carcinogenicity of croton oil.[250]

In addition to differences between the response of TLR4 to endotoxin versus DAMPS, individual DAMPS may each elicit a unique response through TLR4.[251]

As discussed above, TLR4 recognizes both DAMPs and endotoxin produced by bacteria. Microbial products, such as endotoxin, have hydrophobic domains; these domains are also found on proteins denatured during cellular injury, and on DAMPs such as HMGB1 that are released into the extracellular space. Because DAMP receptors appeared early during evolution,[252,253] they may have evolved to recognize injury, organize repair, and then later acquired a host-defense role by recognizing microbes.[9] However, the responses to infection and repair have different goals. After recognizing microbes, TLR4 triggers an aggressive inflammatory response where elimination of the pathogen is the overwhelming priority, and collateral damage to self tissue by toxic microbicidal molecules is an acceptable price for survival of the organism; ultimately, repair occurs after cure of the infection. In contrast, sterile injury such as ischemia/ reperfusion, has tissue repair as the priority. The initial maladaptive inflammation may reflect the fact that tissue injury and infection often occur together, especially after trauma and disruption of the skin. A "shoot first, ask questions later" strategy may have evolved because an initial inflammatory response against the possibility of infection best served survival despite some collateral tissue damage. A fundamental question is how, after either infection or sterile injury, the mononuclear phagocytes change from aggressively proinflammatory (maladaptive for ischemic injury) to reparative.[254] This question may be answered, at least in part, by the presence of CD24-Siglec 10 on mammalian but not bacterial cel surfaces.[255,256] CD24/ Siglec 10 binds DAMPSand turns off the TLR4 response. Bacteria do not express CD24/ Siglec 10 and the TLR4 response would therefore not be inhibited. See Figure 88.4.

Less widely appreciated are recent studies showing that TLR4 participates in repair of non-infectious colitis.[257–265] Some types of non-infectious pulmonary injury,[196,266–269] skin wounding[270] and partial hepatectomy.[271] Whether TLR4 has similar repair functions in the kidney is not known.

Other Multi-Ligand Receptors for other Multi-Receptor DAMPS may Detect Ischemic Injury?

In addition to TLR4, a number of other receptors recognize DAMPS. These recognize injury by a number of pathways including the detection of reactive oxygen species, uric acid, glycolipids, and intracellular stress.[126,146,272,273] These receptors include

CD91: This is also a receptor for heat shock proteins[241,274,275] released by injured cells. It has been targeted as a means of increasing immunity against tumors. In addition to binding heat shock proteins, CD91 also binds α2-macroglobulin,[276,277] collectin and calreticulin,[278] and is known as LDL receptor related protein.[279] These recognize injury by a number of pathways including the detection of reactive oxygen

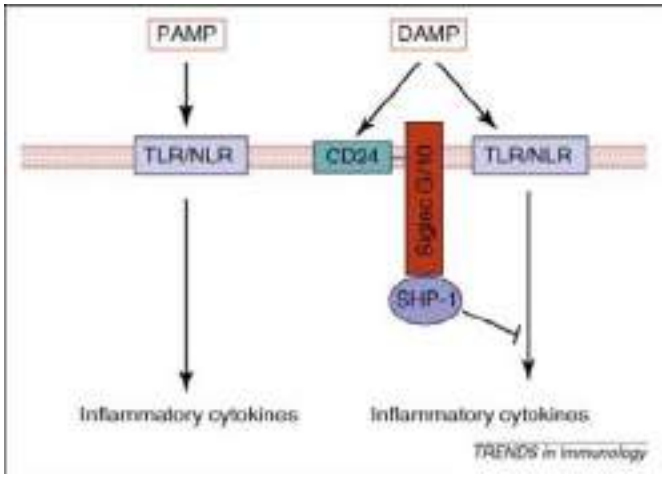

FIGURE 88.4 CD24/ Siglec 10 prevent excessive inflammation after stimulation of TLR4. Pathogen-associated molecular pattern molecules (PAMP), such as endotoxin associated with bacteria, elicits a vigorous response. In contrast, damage-associated molecular pattern molecules (DAMP), such as HMGB1, elicit a response which is inhibited by CD24/ Siglec/10 on the host cell. *(From Liu Y, Chen GY, Zheng P. CD24-Siglec G/10 discriminates danger- from pathogen-associated molecular patterns. Trends Immunol 2009; 30: 557-561. http://www.ncbi.nlm.nih.gov/entrez/query.fcgi?cmd = Retrieve&db = PubMed&dopt = Citation&list_uids = 19786366 PMCID 2788100.)*

species, uric acid, glycolipids, and intracellular stress.[126,146,272,273]

TLR2: TLR2 is related to TLR4 and may also recognize Hsp's.[152,280,281] Mice with non-functional TLR2 are protected from ischemic renal failure.[272,273,282] Renal tubules express both TLR2 and TLR4 after severe ischemic injury.[283,284] TLR2 may also be important in ischemic injury to the liver[285] and heart.[286]

RAGE: Although RAGE is best known as the receptor for advanced glycation endproducts and for its contribution to the secondary complications of diabetes mellitus, including diabetic nephropathy,[287–290] RAGE also detects molecules released by injured cells, and triggers an inflammatory response.

Uric acid: Weibel Paladi bodies, NALP3, and Pyronecrosis. Uric acid is released from injured cells.[146] During ischemic AKI this may induce endothelia to release proinflammatory Weibel-Palade bodies.[291] Uric acid may also activate Nlrp3,[273] possibly by activating the inflammasome and triggering pyronecrosis.[292]

Complement: Renal IRI does activate complement. Tubular injury decreases expression of basolateral expression of Crry, the murine homolog of human MCP (membrane cofactor protein) and DAF (decay accelerating factor); Crry normally prevents amplification of the alternative complement pathway after "C3 tickover".[293] In the absence of basolateral Crry during renal IRI, alternative complement activation continues unrestrained and renal tubular injury results.[294,295]

Why there should be so many ways to detect molecules released by injured cells is not clear. Do all injured cells release the same molecules, are different molecules released after different types of death and injury, do different molecules and receptors elicit different inflammatory responses? In very broad strokes, we will discuss the different modes of programmed cell death and the different inflammation elicited by different types of death later in the chapter. However, a profound understanding of these questions remains to be elucidated by future research.

WHEN DEATH IS NO ACCIDENT: NECROSIS AS A PROGRAMMED EVENT

The above section shows that molecules released from necrotic cells elicit an inflammatory response. Necrosis is often considered accidental death. However, a growing body of data indicates that necrosis may also be a programmed event.[296–301] This suggests that when inflammation is desirable, a cell may be programmed to die a necrotic death, and thus release the pro-inflammatory molecules discussed above.

Poly (ADP-Ribose) Polymerase [PARP] and Programmed Necrosis

The PARP's are a family of 18 genes. PARP-1 regulates necrosis.[302–304] That an enzyme regulates necrosis indicates that death is no accident, but is programmed. Pharmacologic inhibition of PARP ameliorates ischemic acute renal injury in rodents.[305,306] Transgenic knockout of PARP-1 also decreases injury after acute renal ischemia.[307,308] Inhibition of PARP-1 also ameliorates ischemic injury of the brain and liver.

The best known function of PARP-1 is to repair DNA damage, such as occurs in response to oxidative stress during ischemic acute renal failure. Renal PARP-1 levels increase during ischemic acute renal failure.[305,309]

It is not intuitively obvious why such a repair enzyme should be required for necrosis. One possibility is that, in the face of massive DNA damage, PARP depletes intracellular NAD^+ and thus ATP stores. This leads to necrosis, especially in the setting of mitochondrial damage as discussed later in this section.[310–312] However, necrosis is not necessarily correlated with intracellular energy stores in all model systems. Another possibility is that PARP-1 enhances the activity of NFκB and other pro-inflammatory transcription factors. PARP may also increase mitochondrial release of AIF.

Some suggest that caspases degrade PARP and thus direct cell death down an apoptotic pathway.[313]

However, there is decreased ischemic acute renal injury in mice expressing a genetically engineered PRAP-1 that cannot be degraded by caspases.[314]

Cyclophilin D, Mitochondria, and Programmed Necrosis

Another argument that necrosis is regulated comes from studies of mice with transgenic knockout of cyclophilin D. Such mice have decreased necrosis during ischemic acute renal failure.[315–317] Cerebral ischemia was similarly ameliorated in these knockout animals.[318] These results extend data that cyclosporine, by inhibiting cyclophilin D, ameliorates ischemic injury in some tissues.[319,320]

Cyclophilin D regulates the mitochondrial permeability transition pore, and the subsequent release of mitochondrial molecules that regulate cell death. The above data suggest an important role for mitochondria in regulating necrosis.[319,321,322] Whether opening this pore results in necrosis or apoptosis may depend upon several factors. One is the length of time that the pore is open—transient opening might result in apoptosis; longer opening, necrosis.[323] In addition the availability of ATP may switch the mitochondrial signal from necrosis to apoptosis.[321] This is in line with data showing that lower, more prolonged decreases in ATP are associate with necrosis, while shorter and lesser ATP depletion result in necrosis in renal cells,[324] and that lesser oxidant injury also leads to apoptosis instead of necrosis.[325,326] Finally, intracellular pH also regulates. The return of the pH from acidic to more alkaline levels with reperfusion makes necrosis more likely.[321]

Additional Examples of Programmed Necrosis *in Vivo*

We will now review three additional striking examples of the importance of programmed necrosis *in vitro*.

One example is the host defense against murine vaccinia virus. This virus protects itself by preventing apoptotic programs within infected host cells. In mice with wild type TNFR2, infected cells die by programmed TNFα-mediated necrosis, and elicit a protective inflammatory response. Mice with TNFR2 knockout have a reduced programmed necrosis and thus reduced antiviral inflammatory response and decreased viral clearance.[327]

The second example is the difference between cerulean pancreatitis in rats versus mice. The worse outcome in the latter is due to greater programmed necrosis. Rats have high apoptosis and low necrosis and thus a better clinical outcome. Mice have low apoptosis and high necrosis and thus a worse outcome with more inflammation. This difference was due to different function of the X-linked inhibitor of caspases (XIAP) in these two species. There was less inhibition of caspases, and thus less inhibition of apoptosis, in the rat by XIAP.[328]

The third example is the exacerbation of shock when apoptosis is inhibited in mice given TNFα. In this case, switching programmed cell death from apoptosis to necrosis had fatal consequences.[329]

AFTER THE SUICIDE, DISPOSAL OF THE CORPSE: REGULATION OF INFLAMMATION BY MACROPHAGES AFTER THEY PHAGOCYTOSE APOPTOTIC CELLS

Apoptosis occurs during ischemic acute renal failure.[330–335] The goal of this discussion is not the regulation of this apoptosis but rather the effect of apoptosis on inflammation. In other words, we discuss phagocytic clearance of the apoptotic cells before their loss of membrane integrity and leakage of the proinflammatory molecules discussed in the previous section. Such clearance is regulated by "eat me," "don't eat me," "come get me" signals.

The surface of the apoptotic cell has "eat me" signals that trigger phagocytosis by macrophages. A major signal is phosphatidylserine that has somehow "flipped" from the intracellular leaflet to the extracellular leaflet of the plasma membrane where it is recognized by macrophage receptors including the phosphatidylserine receptor after bridging by Annexin I. Other less well understood interactions between apoptotic cell and macrophage also contribute to the "eat me" signal. These include sites also capable of binding collectins such as mannose binding protein, C1q, C3b/bi, oxidized LDL, and thrombospondin 1. In addition, the apoptotic cell surface has decreased "don't eat me" signals such as CD31. Furthermore, phosphatidylcholine on apoptotic cell surfaces is cleaved by phospholipase A2 to form lysophosphatidyl choline which is the best understood chemoattractant "come get me" signal issued by apoptotic cells to macrophages. [See review[336]].

Under many circumstances, macrophages, which have engulfed apoptotic cells, release anti-inflammatory molecules that prevent further inflammation (for example [337,338]). The phosphatidylserine receptor on macrophages may trigger the release of inhibitory cytokines, but this begs the question of why this receptor is not triggered when macrophage phagocytose necrotic debris, including phosphatidylserine on the intracellular side of cell membrane fragments.[339] In the absence of a receptor for phosphatidylserine, macrophages cannot ingest apoptotic cells, and the

lungs of such mice fill with cellular debris and inflammation.[340,341] This may reflect the consequences of overwhelming the phagocytotic system with too many apoptotic corpses as perhaps occurs during ischemic acute renal failure.[332] This situation may reflect "post-apoptotic necrosis" and the release of proinflammatory mediators.

However, there are a number of experimental circumstances where phagocytosis of apoptotic cells results in the release of pro-inflammatory molecules by macrophages, and where ingestion of necrotic debris results in the release of anti-inflammatory molecules. This may reflect the influence of cytokines in the microenvironment,[342] or the redox potential of the microenvironment that can oxidize phospholipids and turn them into macrophage activating signals.[343,344]

Efferocytosis is the phagocytosis of apoptotic cells and does not cause the release of proinflammatory cytokines. If efferocytosis cannot dispose of all the apoptotic cells, then some will degenerate and release DAMPS.[345–347] Increasing efferocytos by injections of MFG-E8 (milk fat globule-EGF factor 8/ lactadherin) ameliorates ischemic AKI in rodents;[348,349] MFG-E8 is a "bridging molecule" that links the apoptotic cells to phagocytes, and thus increases efferocytosis.[350]

SUMMARY

The ultimate amount of injury during ischemic AKI is the result, not only of the ischemic insult, but also of the resulting inflammation. In this chapter, we have summarized the current understanding of the major inflammatory processes during ischemic AKI.

References

[1] Havasi A, Borkan SC. Apoptosis and acute kidney injury. Kidney Int 2011; <http://www.ncbi.nlm.nih.gov/pubmed/21562469>

[2] Legrand M, Mik EG, Johannes T, Payen D, Ince C. Renal hypoxia and dysoxia after reperfusion of the ischemic kidney. Mol Med 2008;14:502–16 <http://www.ncbi.nlm.nih.gov/entrez/query.fcgi?cmd = Retrieve&db = PubMed&dopt = Citation&list_uids = 18488066>PMCID 2386087

[3] Feldkamp T, Park JS, Pasupulati R, Amora D, Roeser NF, Venkatachalam MA, et al. Regulation of the mitochondrial permeability transition in kidney proximal tubules and its alteration during hypoxia-reoxygenation. Am J Physiol Renal Physiol 2009;297:F1632–46 <http://www.ncbi.nlm.nih.gov/entrez/query.fcgi?cmd = Retrieve&db = PubMed&dopt = Citation&list_uids = 19741014>PMCID 2801335

[4] Brooks C, Wei Q, Cho SG, Dong Z. Regulation of mitochondrial dynamics in acute kidney injury in cell culture and rodent models. J Clin Invest 2009;119:1275–85 <http://www.ncbi.nlm.nih.gov/entrez/query.fcgi?cmd = Retrieve&db = PubMed&dopt = Citation&list_uids = 19349686>

[5] Basile DP, Friedrich JL, Spahic J, Knipe NL, Mang HE, Leonard EC, et al. Impaired endothelial proliferation and mesenchymal transition contribute to vascular rarefaction following acute kidney injury. Am J Physiol Renal Physiol 2011;2011:F721–33 <http://www.ncbi.nlm.nih.gov/pubmed/21123492>

[6] Goligorsky MS, Patschan D, Kuo MC. Weibel-Palade bodies–sentinels of acute stress. Nat Rev Nephrol 2009;5:423–6 <http://www.ncbi.nlm.nih.gov/entrez/query.fcgi?cmd = Retrieve&db = PubMed&dopt = Citation&list_uids = 19556996>

[7] Schrier RW, Wang W, Poole B, Mitra A. Acute renal failure: definitions, diagnosis, pathogenesis, and therapy. J Clin Invest 2004;114:5–14 [PMID: 15232604]

[8] Lin SL, Li B, Rao S, Yeo EJ, Hudson TE, Nowlin BT, et al. Macrophage Wnt7b is critical for kidney repair and regeneration. Proc Natl Acad Sci U S A 2010;107:4194–9 <http://www.ncbi.nlm.nih.gov/entrez/query.fcgi?cmd = Retrieve&db = PubMed&dopt = Citation&list_uids = 20160075>

[9] Seong SY, Matzinger P. Hydrophobicity: an ancient damage-associated molecular pattern that initiates innate immune responses. Nat Rev Immunol 2004;4:469–78 <http://www.ncbi.nlm.nih.gov/entrez/query.fcgi?cmd = Retrieve&db = PubMed&dopt = Citation&list_uids = 15173835>

[10] Gallucci S, Matzinger P. Danger signals: SOS to the immune system. Curr Opin Immunol 2001;13:114–9.

[11] Matzinger P. The danger model: a renewed sense of self. Science 2002;296:301–5.

[12] Matzinger P. Tolerance, danger, and the extended family. Annual Review Immunology 1994;12:991–1045.

[13] Medzhitov R, Janeway Jr. C. Innate immunity. N Engl J Med 2000;343:338–44 [PM:10922424].

[14] Halloran PF, Homik J, Goes N, Lui SL, Urmson J, Ramassar V, et al. The "injury response": a concept linking nonspecific injury, acute rejection, and long-term transplant outcomes. Transplant Proc 1997;29:79–81.

[15] Nadeau KC, Azuma H, Tilney NL. Cytokines in the pathophysiology of acute and chronic allograft rejection. Transplant Rev 1996;10:99–107.

[16] Orosz CG, Bergese SD, Wakely E, Xia D, Gordillo GM, VanBuskirk AM. Acute versus chronic graft rejection: related manifestations of allosensitization in graft recipients. Transplant Rev 1997;11:38–50.

[17] Samaniego M, Baldwin WM, Sanfilippo F. Delayed graft function: immediate and late impact. Curr Opin Nephrol Hypertens 1997;6:533–7.

[18] Land W, Messmer K. The impact of ischemia/ reperfusion injury on specific and non-specific, early and late chronic events after organ transplantation. Transplant Rev 1996;10:108–27.

[19] Land WG. Emerging role of innate immunity in organ transplantation Part II: potential of damage-associated molecular patterns to generate immunostimulatory dendritic cells. Transplant Rev (Orlando) 2011; <http://www.ncbi.nlm.nih.gov/pubmed/22074784>

[20] Lu CY, Penfield JG, Kielar ML, Vazquez MA, Jeyarajah DR. Hypothesis: is renal allograft rejection initiated by the response to injury sustained during the transplant process? Kidney Int 1999;55:2157–68 <http://www.ncbi.nlm.nih.gov/pubmed/10354265>

[21] Boros P, Bromberg JS. New cellular and molecular immune pathways in ischemia/reperfusion injury. Am J Transplant 2006;6:652–8 <http://www.ncbi.nlm.nih.gov/entrez/query.fcgi?cmd = Retrieve&db = PubMed&dopt = Citation&list_uids = 16539620>

[22] LaRosa DF, Rahman AH, Turka LA. The innate immune system in allograft rejection and tolerance. J Immunol 2007;178:7503–9 <http://www.ncbi.nlm.nih.gov/entrez/query.fcgi?cmd = Retrieve&db = PubMed&dopt = Citation&list_uids = 17548582>

[23] Kim IK, Bedi DS, Denecke C, Ge X, Tullius SG. Impact of innate and adaptive immunity on rejection and tolerance. Transplantation 2008;86:889–94.

[24] Tuttle KR. Linking metabolism and immunology: diabetic nephropathy is an inflammatory disease. J Am SocNephrol 2005;16:1537–8.

[25] Remuzzi G, Bertani T. Pathophysiology of progressive nephropathies. N Engl J Med 1998;339:1448–56.

[26] Rodriguez-Iturbe B, Vaziri ND, Herrera-Acosta J, Johnson RJ. Oxidative stress, renal infiltration of immune cells, and salt-sensitive hypertension: all for one and one for all. AJP - Renal Physiol 2004;286:F606–16.

[27] Nigam SK, Lieberthal W, Hammerman MR, Safirstein R, Harris RC. Acute renal failure. III. The role of growth factors in the process of renal regeneration and repair. Am J Physiol Renal Physiol 2000;279:F3–11.

[28] Molitoris BA, Weinberg JM, Venkatachalam MA, Lieberthal W, Nigam SK, Zager RA, et al. Acute renal failure. II. Experimental models of acute renal failure: imperfect but indispensable. Am J Physiol 2000;278:F1–12 <http://www.ncbi.nlm.nih.gov/entrez/query.fcgi?cmd = Retrieve&db = PubMed&dopt = Citation&list_uids = 10644651>

[29] Lieberthal W, Nigam SK, Bonventre JV, Brezis M, Siegel N, Rosen S, et al. Acute renal failure. I. Relative importance of proximal vs. distal tubular injury. Am J Physiol 1998;275: F623–31 <http://www.ncbi.nlm.nih.gov/entrez/query.fcgi?cmd = Retrieve&db = PubMed&dopt = Citation&list_uids = 9815122>

[30] Marcussen N, Lai R, Olsen TS, Solez K. Morphometric and immunohistochemical investigation of renal biopsies from patients with transplant ATN , native ATN , or acute graft rejection. Transplant Proc 1996;28:470–6 <http://www.ncbi.nlm.nih.gov/entrez/query.fcgi?cmd = Retrieve&db = PubMed&dopt = Citation&list_uids = 8644316>

[31] Jaber BL, Pereira BJ, Bonventre JV, Balakrishnan VS. Polymorphism of host response genes: implications in the pathogenesis and treatment of acute renal failure. Kidney Int 2005;67:14–33.

[32] Hoffmann SC, Kampen RL, Amur S, Sharaf MA, Kleiner DE, Hunter K, et al. Molecular and immunohistochemical characterization of the onset and resolution of human renal allograft ischemia-reperfusion injury. Transplantation 2002;74:916–23 <http://www.ncbi.nlm.nih.gov/entrez/query.fcgi?cmd = Retrieve&db = PubMed&dopt = Citation&list_uids = 12394831>

[33] Koo DD, Fuggle SV. Impact of ischemia/ reperfusion injury and early inflammatory responses in kidney transplantation. Transplant Rev 2000;14:210–24.

[34] Koo DD, Welsh KI, Roake JA, Morris PJ, Fuggle SV. Ischemia/ reperfusion injury in human kidney transplantation: an immunohistochemical analysis of changes after reperfusion. Am J Pathol 1998;153:557–66 <http://www.ncbi.nlm.nih.gov/entrez/query.fcgi?cmd = Retrieve&db = PubMed&dopt = Citation&list_uids = 9708815>

[35] Turunen AJ, Lindgren L, Salmela KT, Kyllonen LE, Makisalo H, Siitonen SM, et al. Association of graft neutrophil sequestration with delayed graft function in clinical renal transplantation. Transplantation 2004;77:1821–6.

[36] Gaber LW, Gaber AO, Tolley EA, Hathaway DK. Prediction by postrevascularization biopsies of cadaveric kidney allografts of rejection, graft loss, and preservation nephropathy. Transplant 1992;53:1219–25.

[37] Avihingsanon Y, Ma N, Pavlakis M, Chon WJ, Uknis ME, Monaco AP, et al. On the intraoperative molecular status of renal allografts after vascular reperfusion and clinical outcomes. J Am SocNephrol 2005;16:1542–8 <http://www.ncbi.nlm.nih.gov/entrez/query.fcgi?cmd = Retrieve&db = PubMed&dopt = Citation&list_uids = 15888558>

[38] Hauser P, Schwarz C, Mitterbauer C, Regele HM, Muhlbacher F, Mayer G, et al. Genome-wide gene-expression patterns of donor kidney biopsies distinguish primary allograft function. Lab Invest 2004;84:353–61 <http://www.ncbi.nlm.nih.gov/entrez/query.fcgi?cmd = Retrieve&db = PubMed&dopt = Citation&list_uids = 14704720>

[39] Schwarz C, Regele H, Steininger R, Hansmann C, Mayer G, Oberbauer R. The contribution of adhesion molecule expression in donor kidney biopsies to early allograft dysfunction. Transplantation 2001;71:1666–70.

[40] Araki M, Fairchild R, et al. The clinical impact of chemokine and receptor gene expression during ischemia/reperfusion injury in renal allografts. Am J Transpl 2004;8:74.

[41] Pratschke J, Wilhelm MJ, Kusaka M, Basker M, Cooper DK, Hancock WW, et al. Brain death and its influence on donor organ quality and outcome after transplantation. Transplant 1999;67:343–8.

[42] Porter KA, Heptinstall RH. Renal transplantation. Pathology of the Kidney, vol. 4. Boston: Little, Brown & Co.; 1992 [pp. 1799-1934]

[43] Rosen S, Stillman IE. Acute tubular necrosis is a syndrome of physiologic and pathologic dissociation. J Am Soc Nephrol 2008;19:871–5 <http://www.ncbi.nlm.nih.gov/pubmed/18235086>

[44] Venkatachalam MA, Griffin KA, Lan R, Geng H, Saikumar P, Bidani AK. Acute kidney injury: a springboard for progression in chronic kidney disease. Am J Physiol Renal Physiol 2010;298:F1078 <http://www.ncbi.nlm.nih.gov/pubmed/20200097>

[45] Kelly KJ, Dominguez JH. Rapid progression of diabetic nephropathy is linked to inflammation and episodes of acute renal failure. Am J Nephrol 2010;32:469–75 <http://www.ncbi.nlm.nih.gov/entrez/query.fcgi?cmd = Retrieve&db = PubMed&dopt = Citation&list_uids = 20956853>

[46] Kashgarian M. Acute tubular necrosis an ischemic renal injury [edn] In: 5th edition Jennette JC, Olsen JC, Schwartz MM, Silva FG, editors. Heptinstall's pathology of the kidney, vol. 5th. Philadelphia New York: Lippincott - Raven; 1999; p. 863–89.

[47] Lucke B. Lower nephron nephrosis. Mil Surg 1946;99:371–96.

[48] Oliver J, Mac DM, Tracy A. The pathogenesis of acute renal failure associated with traumatic and toxic injury; renal ischemia, nephrotoxic damage and the ischemic episode. J Clin Invest 1951;30:1307–439 <http://www.ncbi.nlm.nih.gov/entrez/query.fcgi?cmd = Retrieve&db = PubMed&dopt = Citation&list_uids = 14897900>

[49] Solez K. Pathogenesis of acute renal failure. Int Rev Exp Pathol 1983;24:277–333 <http://www.ncbi.nlm.nih.gov/entrez/query.fcgi?cmd = Retrieve&db = PubMed&dopt = Citation&list_uids = 6840997>

[50] Brezis M, Rosen S, Silva P, Epstein FH. Renal ischemia: a new perspective. Kidney Int 1984;26:375–83 <http://www.ncbi.nlm.nih.gov/entrez/query.fcgi?cmd = Retrieve&db = PubMed&dopt = Citation&list_uids = 6396435>

[51] De Greef KE, Ysebaert DK, Persy V, Vercauteren SR, De Broe ME. ICAM-1 expression and leukocyte accumulation in inner stripe of outer medulla in early phase of ischemic compared to HgCl2-induced ARF. Kidney Int 2003;63:1697–707 <http://

www.ncbi.nlm.nih.gov/entrez/query.fcgi?cmd = Retrieve&db = PubMed&dopt = Citation&list_uids = 12675845>
[52] De Greef KE, Ysebaert DK, Dauwe SE, Persy VP, Vercauteren S, Mey D, et al. Anti-B7-1 blocks mononuclear cell adherence in vasa recta after ischemia. Kidney Int 2001;60:1415–27 <http://www.ncbi.nlm.nih.gov/entrez/query.fcgi?cmd = Retrieve&db = PubMed&dopt = Citation&list_uids = 11576355>
[53] Fukuzawa N, Schenk AD, Petro M, Nonomura K, Baldwin 3rd WM, Fairchild RL. High renal ischemia temperature increases neutrophil chemoattractant production and tissue injury during reperfusion without an identifiable role for CD4 T cells in the injury. Transpl Immunol 2009;22:62–71 <http://www.ncbi.nlm.nih.gov/pubmed/19664707> PMCID 2783467
[54] Boutin H, LeFeuvre RA, Horai R, Asano M, Iwakura Y, Rothwell NJ. Role of IL-1alpha and IL-1beta in ischemic brain damage. J Neurosci 2001;21:5528–34.
[55] Shito M, Wakbayashi G, Ueda M, Shimazu M, Shirasugi N, Endo M, et al. Interleukin 1 receptor blockade reduces tumor necrosis factor production, tissue injury, and mtality after hepatic iscehmia reperfusion in e rat. Transplant 1997;63:143–8.
[56] Haq M, Norman J, Saba SR, Ramirez G, Rabb H. Role of IL-1 in renal ischemic reperfusion injury. J Am Soc Nephrol 1998;9:614–9.
[57] Valentin JF, Bruijn JA, Paul LC. Donor treatment with mycophenolate mofetil: protection against ischemia-reperfusion injury in the rat. Transplant 2000;69:344–50.
[58] Ventura CG, Coimbra TM, de Campos SB, de CI, Yu L, Seguro AC. Mycophenolate mofetil attenuates renal ischemia/reperfusion injury. J Am Soc Nephrol 2002;13:2524–33.
[59] Geissmann F, Manz MG, Jung S, Sieweke MH, Merad M, Ley K. Development of monocytes, macrophages, and dendritic cells. Science 2010;327:656–61 <http://www.ncbi.nlm.nih.gov/entrez/query.fcgi?cmd = Retrieve&db = PubMed&dopt = Citation&list_uids = 20133564>
[60] Velazquez P, Dustin ML, Nelson PJ. Renal dendritic cells: an update. Nephron Exp Nephrol 2009;111:e67–71 <http://www.ncbi.nlm.nih.gov/entrez/query.fcgi?cmd = Retrieve&db = PubMed&dopt = Citation&list_uids = 19276627>
[61] Hochheiser K, Tittel A, Kurts C. Kidney dendritic cells in acute and chronic renal disease. Int J Exp Pathol 2010; <http://www.ncbi.nlm.nih.gov/entrez/query.fcgi?cmd = Retrieve&db = PubMed&dopt = Citation&list_uids = 20681979>
[62] Mosser DM, Edwards JP. Exploring the full spectrum of macrophage activation. Nat Rev Immunol 2008;8:958–69 <http://www.ncbi.nlm.nih.gov/entrez/query.fcgi?cmd = Retrieve&db = PubMed&dopt = Citation&list_uids = >
[63] Geissmann F, Gordon S, Hume DA, Mowat AM, Randolph GJ. Unravelling mononuclear phagocyte heterogeneity. Nat Rev Immunol 2010;10:453–60 <http://www.ncbi.nlm.nih.gov/entrez/query.fcgi?cmd = Retrieve&db = PubMed&dopt = Citation&list_uids = 20467425>
[64] Jo SK, Sung SA, Cho WY, Go KJ, Kim HK. Macrophages contribute to the initiation of ischaemic acute renal failure in rats. Nephrol Dial Transplant 2006; <http://www.ncbi.nlm.nih.gov/entrez/query.fcgi?cmd = Retrieve&db = PubMed&dopt = Citation&list_uids = 16410269>
[65] Day YJ, Huang L, Ye H, Linden J, Okusa MD. Renal ischemia-reperfusion injury and adenosine 2a receptor-mediated tissue protection: the role of macrophages. AJP - Renal Physiol 2004.
[66] Kielar ML, John R, Bennett M, Richardson JA, Shelton JM, Chen L, et al. Maladaptive role of IL-6 in ischemic acute renal failure. J Am Soc Nephrol 2005;16:3315–25 <http://www.ncbi.nlm.nih.gov/entrez/query.fcgi?cmd = Retrieve&db = PubMed&dopt = Citation&list_uids = 16192425>
[67] Molitoris BA, Sutton TA. Endothelial injury and dysfunction: role in the extension phase of acute renal failure. Kidney Int 2004;66:496–9 <http://www.ncbi.nlm.nih.gov/pubmed/15253696>
[68] Basile DP, Donohoe D, Roethe K, Osborn JL. Renal ischemic injury results in permanent damage to peritubular capillaries and influences long-term function. Am J Physiol Renal Physiol 2001;281:F887–99 <http://www.ncbi.nlm.nih.gov/pubmed/11592947>
[69] Molitoris BA, Sandoval R, Sutton TA. Endothelial injury and dysfunction in ischemic acute renal failure. Crit Care Med 2002;30:S235–40.
[70] Li L, Okusa MD. Macrophages, dendritic cells, and kidney ischemia-reperfusion injury. Semin Nephrol 2010;30:268–77 < http://www.ncbi.nlm.nih.gov/entrez/query.fcgi?cmd = Retrieve&db = PubMed&dopt = Citation&list_uids = 20620671 PMCID 2904394 >
[71] Lemay S, Rabb H, Postler G, Singh AK. Prominent and sustained up-regulation of gp130 - signaling cytokines and of the chemokine MIP 2 in murine renal ischemia—reperfusion injury. Transplant 2000;69:959–63.
[72] Takada M, Nadeau KC, Shaw GD, Marquette KA, Tilney NL. The cytokine-adhesion molecule cascade in ischemia/ reperfusion injury the rat kidney—inhibition by a soluble P-selectin ligand. J Clin Invest 1997;99:2682–90.
[73] Patel NS, Chatterjee PK, Di Paola R, Mazzon E, Britti D, De Sarro A, et al. Endogenous interleukin-6 enhances the renal injury, dysfunction, and inflammation caused by ischemia/reperfusion. J Pharmacol Exp Ther 2005;312:1170–8 <http://www.ncbi.nlm.nih.gov/entrez/query.fcgi?cmd = Retrieve&db = PubMed&dopt = Citation&list_uids = 15572648>
[74] Hurst SM, Wilkinson TS, McLoughlin RM, Jones S, Horiuchi S, Yamamoto N, et al. Il-6 and its soluble receptor orchestrate a temporal switch in the pattern of leukocyte recruitment seen during acute inflammation. Immunity 2001;14:705–14.
[75] Henderson RB, Hobbs JA, Mathies M, Hogg N. Rapid recruitment of inflammatory monocytes is independent of neutrophil migration. Blood 2003;102:328–35.
[76] Maus UA, Waelsch K, Kuziel WA, Delbeck T, Mack M, Blackwell TS, et al. Monocytes are potent facilitators of alveolar neutrophil emigration during lung inflammation: role of the CCL2-CCR2 axis. J Immunol 2003;170:3273–8.
[77] Maus UA, Koay MA, Delbeck T, Mack M, Ermert M, Ermert L, et al. Role of resident alveolar macrophages in leukocyte traffic into the alveolar air space of intact mice. Am J Physiol Lung Cell Mol Physiol 2002;282:L1245–52.
[78] Gregory SH, Wing EJ. Neutrophil-Kupffer-cell interaction in host defenses to systemic infections. Immunol Today 1998;19:507–10.
[79] Penfield JG, Wang Y, Li S, Kielar ML, Sicher SC, Jeyarajah DR, et al. Transplant surgery injury recruits recipient MHC class II-positive leukocytes into the kidney. Kidney Int 1999;56:1759–69 <http://www.ncbi.nlm.nih.gov/entrez/query.fcgi?cmd = Retrieve&db = PubMed&dopt = Citation&list_uids = 10571784>
[80] Penfield JG, Dawidson IA, Ar'Rajab A, Kielar ML, Jeyarajah DR, Lu CY. Syngeneic renal transplantation increases the number of renal dendritic cells in the rat. Transpl Immunol 1999;7:197–200 <http://www.ncbi.nlm.nih.gov/entrez/query.fcgi?cmd = Retrieve&db = PubMed&dopt = Citation&list_uids = 10638831>
[81] Shoskes DA, Parfrey NA, Halloran PF. Increased major histocompatibility complex antigen expression in unilateral ischemic acute tubular necrosis in the mouse. Transplant 1990;49:201–7.

[82] Heemann UW, Tullius SG, Tamatami T, Miyasaka M, Milford E, Tilney NL. Infiltration patterns of macrophages and lymphocytes in chronically rejecting rat kidney allografts. TransplInt 1994;7:349–55.
[83] Duffield JS, Forbes SJ, Constandinou CM, Clay S, Partolina M, Vuthoori S, et al. Selective depletion of macrophages reveals distinct, opposing roles during liver injury and repair. J Clin Invest 2005;115:56–65 <http://www.ncbi.nlm.nih.gov/entrez/query.fcgi?cmd = Retrieve&db = PubMed&dopt = Citation&list_uids = 15630444>
[84] Wilson HM, Walbaum D, Rees AJ. Macrophages and the kidney. Curr Opin Nephrol Hypertens 2004;13:285–90.
[85] Park JE, Barbul A. Understanding the role of immune regulation in wound healing. Am J Surg 2004;187:11S–6S.
[86] Saville LR, Pospisil CH, Mawhinney LA, Bao F, Simedrea FC, Peters AA, et al. A monoclonal antibody to CD11d reduces the inflammatory infiltrate into the injured spinal cord: a potential neuroprotective treatment. J Neuroimmunol 2004;156:42–57.
[87] Duffield JS. The inflammatory macrophage: a story of Jekyll and Hyde. Clin Sci (Lond) 2003;104:27–38.
[88] Humes HD. Potential molecular therapy for acute renal failure. Cleve Clin J Med 1993;60:166–8 [PM: 8443951]
[89] Basile DP, Rovak JM, Martin DR, Hammerman MR. Increased transforming growth factor-beta 1 expression in regenerating rat renal tubules following ischemic injury. Am J Physiol 1996;270:F500–9 <http://www.ncbi.nlm.nih.gov/entrez/query.fcgi?cmd = Retrieve&db = PubMed&dopt = Citation&list_uids = 8780254>
[90] Lee S, Huen S, Nishio H, Nishio S, Lee HK, Choi BS, et al. Distinct macrophage phenotypes contribute to kidney injury and repair. J Am Soc Nephrol 2011;22:317–26 http://www.ncbi.nlm.nih.gov/entrez/query.fcgi?cmd = Retrieve&db = PubMed&dopt = Citation&list_uids = 21289217 PMCID 3029904
[91] Lassen S, Lech M, Rommele C, Mittruecker HW, Mak TW, Anders HJ. Ischemia reperfusion induces IFN regulatory factor 4 in renal dendritic cells, which suppresses postischemic inflammation and prevents acute renal failure. J Immunol 2010;185:1976–83 <http://www.ncbi.nlm.nih.gov/entrez/query.fcgi?cmd = Retrieve&db = PubMed&dopt = Citation&list_uids = 20601597>
[92] Afzali B, Mitchell P, Lechler RI, John S, Lombardi G. Translational mini-review series on Th17 cells: induction of interleukin-17 production by regulatory T cells. Clin Exp Immunol 2010;159:120–30 http://www.ncbi.nlm.nih.gov/entrez/query.fcgi?cmd = Retrieve&db = PubMed&dopt = Citation&list_uids = 19912251 PMCID 2810380
[93] Mantovani A, Sica A, Locati M. Macrophage polarization comes of age. Immunity 2005;23:344–6 <http://www.ncbi.nlm.nih.gov/entrez/query.fcgi?cmd = Retrieve&db = PubMed&dopt = Citation&list_uids = 16226499>
[94] Springer TA. Traffic signals for lymphocyte recirculation and leukocyte emigration. Cell 1994;76:301.
[95] Butcher EC, Picker LJ. Lymphocyte homing and homeostasis. Science 1996;272:60–6.
[96] Imhof BA, Aurrand-Lions M. Adhesion mechanisms regulating the migration of monocytes. Nat RevImmunol 2004;4:432–44.
[97] Dustin M. A supercode for inflammation. Immunity 2004;20:361–2.
[98] Kelly KJ, Williams Jr. WW, Colvin RB, Bonventre JV. Antibody to intercellular adhesion molecule 1 protects the kidney against ischemic injury. Proc Natl Acad Sci USA 1995;91:812–6 <http://www.ncbi.nlm.nih.gov/pubmed/7904759>
[99] Rabb H, Mendiola CC, Saba SR, Dietz JR, Smith CW, Bonventre JV, et al. Antibodies to ICAM 1 protect kidneys in severe ischemic reperfusion injury. Biochem Biophys Res Commun 1995;211:67–73.
[100] Miura M, Fu X, Zhang QW, Remick DG, Fairchild RL. Neutralization of Gro alpha and macrophage inflammatory protein-2 attenuates renal ischemia/reperfusion injury. Am J Pathol 2001;159:2137–45 <http://www.ncbi.nlm.nih.gov/pubmed/11733364>
[101] Burne MJ, Daniels F, El Ghandour A, Mauiyyedi S, Colvin RB, O'Donnell MP, et al. Identification of the CD4(+) T cell as a major pathogenic factor in ischemic acute renal failure. J Clin Invest 2001;108:1283–90 [PM:11696572]
[102] Nemoto T, Burne MJ, Daniels F, O'Donnell MP, Crosson J, Berens K, et al. Small molecule selectin ligand inhibition improves outcome in ischemic acute renal failure. Kidney Int 2001;60:2205–14.
[103] Takada M, Nadeau KC, Shaw GD, Tilney NL. Prevention of late renal changes after initial ischemia/reperfusion injury by blocking early selectin binding. Transplant 1997;64:1520–5.
[104] Rabb H, Mendiola CC, Dietz J, Saba SR, Issekutz TB, Abanilla F, et al. Role of CD11a and CD11b in ischemic acute renal failure in rats. Am J Physiol 1994;267:F1052–8 http://www.ncbi.nlm.nih.gov/pubmed/7810691
[105] Burne MJ, Rabb H. Pathophysiological contributions of fucosyltransferases in renal ischemia reperfusion injury. J Immunol 2002;169:2648–52 [PM: 12193737]
[106] Gasser M, Waaga AM, Kist-van Holthe JE, Lenhard SM, Laskowski I, Shaw GD, et al. Normalization of brain death-induced injury to rat renal allografts by recombinant soluble P-selectin glycoprotein ligand. J Am Soc Nephrol 2002;13:1937–45.
[107] Dragun D, Tullius SG, Park JK, Maasch C, Lukitsch I, Lippoldt A, et al. ICAM-1 antisense oligodesoxynucleotides prevent reperfusion injury and enhance immediate graft function in renal transplantation. Kidney Int 1998;54:590–602.
[108] Safirstein R, Megyesi J, Saggi SJ, Price PM, Poon M, Rollins BJ, et al. Expression of cytokine-like genes JE and KC is increased during renal ischemia. Am J Physiol 1991;261:F1095–100.
[109] Furuichi K, Wada T, Iwata Y, Kitagawa K, Kobayashi K, Hashimoto H, et al. CCR2 signaling contributes to ischemia-reperfusion injury in kidney. J Am Soc Nephrol 2003;14:2503–15.
[110] Furuichi K, Wada T, Iwata Y, Kitagawa K, Kobayashi K, Hashimoto H, et al. Gene therapy expressing amino-terminal truncated monocyte chemoattractant protein-1 prevents renal ischemia-reperfusion injury. J Am SocNephrol 2003;14:1066–71.
[111] De Greef KE, Ysebaert DK, Vercauteren SR, Persy VP, De Broe ME. Upregulation of B7-1 and B7-2 along the vasa recta after renal ischemia/reperfusion injury. Am J Transplantation 2001;1:A484.
[112] Takada M, Chandraker A, Ndeau KC, Sayegh M, Tilney NL. The role of the B7 costimulatory pathway in experimental cold ischemia/ reperfusion injury. J Clin Invest 1997;100:1199–203.
[113] Zhang Y, Woodward VK, Shelton JM, Richardson JA, Link DC, Zhou XJ, et al. Ischemia/ reperfusion induces G-CSF gene expression by renal medullary thick ascending limb cells in vivo and in vitro. Am J Physiol Renal Physiol 2004;286:F1193–201 <http://www.ncbi.nlm.nih.gov/entrez/query.fcgi?cmd = Retrieve&db = PubMed&dopt = Citation&list_uids = 14734360>
[114] Lauriat S, Linas SL. The role of neutrophils in acute renal failure. Semin Nephrol 1998;18:498–504.

[115] De Greef KE, Ysebaert DK, Ghielli M, Vercauteren S, Nouwen EJ, Eyskens EJ, et al. Neutrophils and acute ischemia-reperfusion injury. J Nephrol 1998;11:110–22.
[116] Miura M, Fu X, Zhang Q, Remick DG, Fairchild RL. Neutralization of kc and macrophage inflammatory protein-2 attenuates renal ischemia/reperfusion injury. Am J Transplantation 2001;1:A1292.
[117] Melnikov VY, Faubel S, Siegmund B, Lucia MS, Ljubanovic D, Edelstein CL. Neutrophil-independent mechanisms of caspase-1- and IL-18-mediated ischemic acute tubular necrosis in mice. J Clin Invest 2002;110:1083–91.
[118] de Vries B, Kohl J, Leclercq WK, Wolfs TG, van Bijnen AA, Heeringa P, et al. Complement factor C5a mediates renal ischemia-reperfusion injury independent from neutrophils. J Immunol 2003;170:3883–9 <http://www.ncbi.nlm.nih.gov/pubmed/12646657>
[119] Taylor PR, Gordon S. Monocyte heterogeneity and innate immunity. Immunity 2003;19:2–4.
[120] Araki M, Fairchild RL, et al. [1461] Role of cxcr2 in renal ischemia/reperfusion injury. Am J Transpl 2004;41461.
[121] Grone HJ, Cohen CD, Grone E, Schmidt C, Kretzler M, Schlondorff D, et al. Spatial and temporally restricted expression of chemokines and chemokine receptors in the developing human kidney. J Am Soc Nephrol 2002;13:957–67.
[122] Luan J, Furuta Y, Du J, Richmond A. Developmental expression of two CXC chemokines, MIP-2 and KC, and their receptors. Cytokine 2001;14:253–63.
[123] Scapini P, Lapinet-Vera JA, Gasperini S, Calzetti F, Bazzoni F, Cassatella MA. The neutrophil as a cellular source of chemokines. Immunol Rev 2000;177:195–203.
[124] El Sawy T, Fahmy NM, Fairchild RL. Chemokines: directing leukocyte infiltration into allografts. Curr Opin Immunol 2002;14:562–8 <http://www.sciencedirect.com/science/article/B6VS1-46FPX4V-4/2/4e0a4d735561dc88bca8f9ca7c344907>
[125] Mehrad B, Wiekowski M, Morrison BE, Chen SC, Coronel EC, Manfra DJ, et al. Transient lung-specific expression of the chemokine KC improves outcome in invasive aspergillosis. Am J RespirCrit Care Med 2002;166:1263–8.
[126] Li L, Huang L, Vergis AL, Ye H, Bajwa A, Narayan V, et al. IL-17 produced by neutrophils regulates IFN-gamma-mediated neutrophil migration in mouse kidney ischemia-reperfusion injury. J Clin Invest 2010;120:331–42 <http://www.ncbi.nlm.nih.gov/entrez/query.fcgi?cmd = Retrieve&db = PubMed&dopt = Citation&list_uids = 20038794> [PMCID 2798679]
[127] Li L, Huang L, Sung SS, Lobo PI, Brown MG, Gregg RK, et al. NKT cell activation mediates neutrophil IFN-{gamma} production and renal ischemia-reperfusion injury. J Immunol 2007;178:5899–911 <http://www.ncbi.nlm.nih.gov/entrez/query.fcgi?cmd = Retrieve&db = PubMed&dopt = Citation&list_uids = 17442974>
[128] Faubel SG, Ljubanovic D, Poole B, Dursun B, Cushing S, He Z, et al. Peripheral CD4 T cell depletion is not sufficient to prevent ischemic acute renal failure. Transplantation 2005;80:643–9.
[129] Dragun D, Bohler T, Nieminen-Kelha M, Waiser J, Schneider W, Haller H, et al. FTY720-induced lymphocyte homing modulates post-transplant preservation/reperfusion injury. Kidney Int 2004;65:1076–83.
[130] Park P, Haas M, Cunningham PN, Bao L, Alexander JJ, Quigg RJ. Injury in renal ischemia-reperfusion is independent from immunoglobulins and T lymphocytes. Am J Physiol Renal Physiol 2002;282:F352–7.
[131] Yokota N, Daniels F, Crosson J, Rabb H. Protective effect of T cell depletion in murine renal ischemia-reperfusion injury. Transplant 2002;74:759–63 [PM: 12364852].
[132] Burne-Taney MJ, Ascon DB, Daniels F, Racusen L, Baldwin W, Rabb H. B cell deficiency confers protection from renal ischemia reperfusion injury. J Immunol 2003;171:3210–5 <http://jimmunol.org/content/171/6/3210.abstract>
[133] Rouschop KM, Sewnath ME, Claessen N, Roelofs JJ, Hoedemaeker I, van der NR, et al. CD44 deficiency increases tubular damage but reduces renal fibrosis in obstructive nephropathy. J Am Soc Nephrol 2004;15:674–86.
[134] Florquin S, Rouschop KM. Reciprocal functions of hepatocyte growth factor and transforming growth factor-beta1 in the progression of renal diseases: a role for CD44?. Kidney Int Suppl 2003;S15–20.
[135] Kipnis J, Mizrahi T, Hauben E, Shaked I, Shevach E, Schwartz M. Neuroprotective autoimmunity: naturally occurring CD4 + CD25 + regulatory T cells suppress the ability to withstand injury to the central nervous system. Proc Natl Acad Sci USA 2002;99:15620–5.
[136] Caldwell CC, Okaya T, Martignoni A, Husted T, Schuster R, Lentsch AB. Divergent functions of CD4 + T lymphocytes in acute liver inflammation and injury after ischemia-reperfusion. Am J Physiol Gastrointest Liver Physiol 2005;289:G969–76 [PM:16002566]
[137] Yokota N, Burne-Taney M, Racusen L, Rabb H. Contrasting roles for STAT4 and STAT6 signal transduction pathways in murine renal ischemia-reperfusion injury. Am J Physiol Renal Physiol 2003;285:F319–25.
[138] Cario E, Becker A, Sturm A, Goebell H, Dignass AU. Peripheral blood mononuclear cells promote intestinal epithelial restitution in vitro through an interleukin-2/interferon-gamma-dependent pathway. Scand J Gastroenterol 1999;34:1132–8.
[139] Ahdieh M, VandenBos T, Youakim A. Lung epithelial barrier function and wound healing are decreased by IL-4 and IL-13 and enhanced by IFN-gamma. AJP - Cell Physiol 2001;281:C2029–38.
[140] Jameson J, Ugarte K, Chen N, Yachi P, Fuchs E, Boismenu R, et al. Role for Skin gamma delta T Cells in Wound Repair. Science 2002;296:747–9.
[141] Lai LW, Yong KC, Lien YH. Pharmacologic recruitment of regulatory T cells as a therapy for ischemic acute kidney injury. Kidney Int 2011; http://www.ncbi.nlm.nih.gov/pubmed/22189844
[142] Kinsey GR, Huang L, Vergis AL, Li L, Okusa MD. Regulatory T cells contribute to the protective effect of ischemic preconditioning in the kidney. Kidney Int 2010;: <http://www.ncbi.nlm.nih.gov/entrez/query.fcgi?cmd = Retrieve&db = PubMed&dopt = Citation&list_uids = 20164824>
[143] Linfert D, Chowdhry T, Rabb H. Lymphocytes and ischemia-reperfusion injury. Transplant Rev (Orlando) 2009;23:1–10 <http://www.ncbi.nlm.nih.gov/entrez/query.fcgi?cmd = Retrieve&db = PubMed&dopt = Citation&list_uids = 19027612> PMCID 2651229
[144] Matzinger P. Friendly and dangerous signals: is the tissue in control? Nat Immunol 2007;8:11–3 <http://www.ncbi.nlm.nih.gov/entrez/query.fcgi?cmd = Retrieve&db = PubMed&dopt = Citation&list_uids = 17179963>
[145] Oppenheim JJ, Tewary P, de la Rosa G, Yang D. Alarmins initiate host defense. Adv Exp Med Biol 2007;601:185–94 <http://www.ncbi.nlm.nih.gov/entrez/query.fcgi?cmd = Retrieve&db = PubMed&dopt = Citation&list_uids = 17713005>

[146] Rock KL, Latz E, Ontiveros F, Kono H. The sterile inflammatory response. Annu Rev Immunol 2010;28:321–42 <http://www.ncbi.nlm.nih.gov/entrez/query.fcgi?cmd = Retrieve&db = PubMed&dopt = Citation&list_uids = 20307211>

[147] Mollen KP, Anand RJ, Tsung A, Prince JM, Levy RM, Billiar TR. Emerging paradigm: toll-like receptor 4-sentinel for the detection of tissue damage. Shock 2006;26:430–7 <http://www.ncbi.nlm.nih.gov/entrez/query.fcgi?cmd = Retrieve&db = PubMed&dopt = Citation&list_uids = 17047512>

[148] Takeda K, Kaisho T, Akira S. Toll-like receptors. Annu Rev Immunol 2003;21:335–76.

[149] Shigeoka AA, Holscher TD, King AJ, Hall FW, Kiosses WB, Tobias PS, et al. TLR2 is constitutively expressed within the kidney and participates in ischemic renal injury through both MyD88-dependent and -independent pathways. J Immunol 2007;178:6252–8 <http://www.ncbi.nlm.nih.gov/entrez/query.fcgi?cmd = Retrieve&db = PubMed&dopt = Citation&list_uids = 17475853>

[150] Chen J, John R, Richardson JA, Shelton JM, Zhou XJ, Wang Y, et al. Toll-like receptor 4 regulates early endothelial activation during ischemic acute kidney injury. Kidney Int 2011;79:288–99 <http://www.ncbi.nlm.nih.gov/pubmed/20927041> PMCID pmc journal in process

[151] Beutler B, Hoebe K, Du X, Ulevitch RJ. How we detect microbes and respond to them: the Toll-like receptors and their transducers. J Leukoc Biol 2003;74:479–85 <http://www.ncbi.nlm.nih.gov/entrez/query.fcgi?cmd = Retrieve&db = PubMed&dopt = Citation&list_uids = 12960260>

[152] Akira S, Takeda K. Toll-like receptor signalling. Nat Rev Immunol 2004;4:499–511.

[153] Iwasaki A, Medzhitov R. Toll-like receptor control of the adaptive immune responses. Nat Immunol 2004;5:987–95.

[154] Matsuguchi T, Takagi K, Musikacharoen T, Yoshikai Y. Gene expressions of lipopolysaccharide receptors, toll-like receptors 2 and 4, are differently regulated in mouse T lymphocytes. Blood 2000;95:1378–85.

[155] Liew FY, Komai-Koma M, Xu D. A toll for T cell costimulation. Ann Rheum Dis 2004;63(Suppl 2):ii 76–8.

[156] Asea A, Kraeft SK, Kurt-Jones EA, Stevenson MA, Chen LB, Finberg RW, et al. HSP70 stimulates cytokine production through a CD14-dependant pathway, demonstrating its dual role as a chaperone and cytokine. Nat Med 2000;6:435–42.

[157] Asea A, Rehli M, Kabingu E, Boch JA, Bare O, Auron PE, et al. Novel signal transduction pathway utilized by extracellular HSP70: role of toll-like receptor (TLR) 2 and TLR4. J Biol Chem 2002;277:15028–34.

[158] Beg AA. Endogenous ligands of Toll-like receptors: implications for regulating inflammatory and immune responses. Trends Immunol 2002;23:509–12 <http://www.sciencedirect.com/science/article/B6W7H-46VBFWM-1/1/0610c6f1293b9ec628681d96f6c3f60f>

[159] Vabulas RM, Ahmad-Nejad P, Ghose S, Kirschning CJ, Issels RD, Wagner H. HSP70 as endogenous stimulus of the Toll/interleukin-1 receptor signal pathway. J Biol Chem 2002;277:15107–12.

[160] Vabulas RM, Braedel S, Hilf N, Singh-Jasuja H, Herter S, Ahmad-Nejad P, et al. The endoplasmic reticulum-resident heat shock protein Gp96 activates dendritic cells via the Toll-like receptor 2/4 pathway. J Biol Chem 2002;277:20847–53.

[161] Vabulas RM, Wagner H, Schild H. Heat shock proteins as ligands of toll-like receptors. Curr Top Microbiol Immunol 2002;270:169–84.

[162] Johnson GB, Brunn GJ, Kodaira Y, Platt JL. Receptor-mediated monitoring of tissue well-being via detection of soluble heparan sulfate by Toll-like receptor 4. J Immunol 2002;168:5233–9.

[163] Johnson GB, Brunn GJ, Platt JL. Cutting edge: an endogenous pathway to systemic inflammatory response syndrome (SIRS)-Like reactions through toll-like receptor 4. J Immunol 2004;172:20–4.

[164] Oyama J, Blais Jr. C, Liu X, Pu M, Kobzik L, Kelly RA, et al. Reduced myocardial ischemia-reperfusion injury in toll-like receptor 4-deficient mice. Circulation 2004;109:784–9.

[165] Chong AJ, Shimamoto A, Hampton CR, Takayama H, Spring DJ, Rothnie CL, et al. Toll-like receptor 4 mediates ischemia/reperfusion injury of the heart. J Thorac Cardiovasc Surg 2004;128:170–9.

[166] Peng Y, Gong JP, Liu CA, Li XH, Gan L, Li SB. Expression of toll-like receptor 4 and MD-2 gene and protein in Kupffer cells after ischemia-reperfusion in rat liver graft. World J Gastroenterol 2004;10:2890–3.

[167] Wu HS, Zhang JX, Wang L, Tian Y, Wang H, Rotstein O. Toll-like receptor 4 involvement in hepatic ischemia/reperfusion injury in mice. Hepatobiliary Pancreat Dis Int 2004;3:250–3.

[168] Zhai Y, Shen XD, O'Connell R, Gao F, Lassman C, Busuttil RW, et al. Cutting Edge: TLR4 activation mediates liver ischemia/reperfusion inflammatory response via IFN regulatory factor 3-dependent MyD88-independent pathway. J Immunol 2004;173:7115–9 <http://www.ncbi.nlm.nih.gov/entrez/query.fcgi?cmd = Retrieve&db = PubMed&dopt = Citation&list_uids = 15585830>

[169] Barsness KA, Arcaroli J, Harken AH, Abraham E, Banerjee A, Reznikov L, et al. Hemorrhage-induced acute lung injury is TLR-4 dependent. Am J Physiol RegulIntegr Comp Physiol 2004;287:R592–9 <http://www.ncbi.nlm.nih.gov/entrez/query.fcgi?cmd = Retrieve&db = PubMed&dopt = Citation&list_uids = 15072965>

[170] Wu H, Chen G, Wyburn KR, Yin J, Bertolino P, Eris JM, et al. TLR4 activation mediates kidney ischemia/reperfusion injury. J Clin Invest 2007;117:2847–59 <http://www.ncbi.nlm.nih.gov/entrez/query.fcgi?cmd = Retrieve&db = PubMed&dopt = Citation&list_uids = 17853945>

[171] Pulskens WP, Teske GJ, Butter LM, Roelofs JJ, van der Poll T, Florquin S, et al. Toll-like receptor-4 coordinates the innate immune response of the kidney to renal ischemia/reperfusion injury. PLoS ONE 2008;3:e3596 <http://www.ncbi.nlm.nih.gov/entrez/query.fcgi?cmd = Retrieve&db = PubMed&dopt = Citation&list_uids = 18974879>

[172] Rusai K, Sollinger D, Baumann M, Wagner B, Strobl M, Schmaderer C, et al. Toll-like receptors 2 and 4 in renal ischemia/reperfusion injury. Pediatr Nephrol 2010;25:853–60 <http://www.ncbi.nlm.nih.gov/entrez/query.fcgi?cmd = Retrieve&db = PubMed&dopt = Citation&list_uids = 20130923>

[173] Kruger B, Krick S, Dhillon N, Lerner SM, Ames S, Bromberg JS, et al. Donor Toll-like receptor 4 contributes to ischemia and reperfusion injury following human kidney transplantation. Proc Natl Acad Sci U S A 2009;106:3390–5 <http://www.ncbi.nlm.nih.gov/entrez/query.fcgi?cmd = Retrieve&db = PubMed&dopt = Citation&list_uids = 19218437> PMCID 2651292

[174] Chen J, Hartono J, John R, Bennett M, Zhou X, Wang Y, et al. Interleukin 6 production by leukocytes during ischemic acute kidney injury is regulated by TLR4. Kidney Int 2011;80:504–15 <http://www.ncbi.nlm.nih.gov/pubmed/21633411> PMCID pmc journal in progress

[175] John R, Chen L, Bennett M, Richardson JA, Zhou XJ, Shelton JM, et al. Potential roles for collecting duct and endothelial

TLR4 in murine ischemic acute renal injury. Under Review 2006.

[176] Yang H, Hreggvidsdottir HS, Palmblad K, Wang H, Ochani M, Li J, et al. A critical cysteine is required for HMGB1 binding to Toll-like receptor 4 and activation of macrophage cytokine release. Proc Natl Acad Sci U S A 2010;107:11942–7 <http://www.ncbi.nlm.nih.gov/entrez/query.fcgi?cmd = Retrieve&db = PubMed&dopt = Citation&list_uids = 20547845>

[177] Li J, Gong Q, Zhong S, Wang L, Guo H, Xiang Y, et al. Neutralization of the extracellular HMGB1 released by ischaemic damaged renal cells protects against renal ischaemia-reperfusion injury. Nephrol Dial Transplant 2010;26:469–78 <http://www.ncbi.nlm.nih.gov/entrez/query.fcgi?cmd = Retrieve&db = PubMed&dopt = Citation&list_uids = 20679140>

[178] Wu H, Ma J, Wang P, Corpuz TM, Panchapakesan U, Wyburn KR, et al. HMGB1 Contributes to kidney ischemia reperfusion injury. J Am Soc Nephrol 2010;21:1878–90 <http://www.ncbi.nlm.nih.gov/entrez/query.fcgi?cmd = Retrieve&db = PubMed&dopt = Citation&list_uids = 20847143>

[179] Li C, Jackson RM. Reactive species mechanisms of cellular hypoxia-reoxygenation injury. Am J Physiol Cell Physiol 2002;282:C227–41 <http://www.ncbi.nlm.nih.gov/entrez/query.fcgi?cmd = Retrieve&db = PubMed&dopt = Citation&list_uids = 11788333>

[180] Chandel NS, Maltepe E, Goldwasser E, Mathieu CE, Simon MC, Schumacker PT. Mitochondrial reactive oxygen species trigger hypoxia-induced transcription. Proc Natl Acad Sci USA 1998;95:11715–20.

[181] Nath KA, Norby SM. Reactive oxygen species and acute renal failure. Am J Med 2000;109:665–78 <http://www.ncbi.nlm.nih.gov/entrez/query.fcgi?cmd = Retrieve&db = PubMed&dopt = Citation&list_uids = 11099687>

[182] Kelly KJ, Williams Jr. WW, Colvin RB, Meehan SM, Springer TA, Gutierrez-ramos JC, et al. Intercellular adhesion molecule-1-deficient mice are protected against ischemic renal injury. J Clin Invest 1996;97:1056–63 <http://www.ncbi.nlm.nih.gov/pubmed/8613529>

[183] Kiew LV, Munavvar AS, Law CH, Azizan AN, Nazarina AR, Sidik K, et al. Effect of antisense oligodeoxynucleotides for ICAM-1 on renal ischaemia-reperfusion injury in the anaesthetised rat. J Physiol 2004;557:981–9 <http://www.ncbi.nlm.nih.gov/pubmed/15047774> PMCID 1665139

[184] Haller H, Dragun D, Miethke A, Park JK, Weis A, Lippoldt A, et al. Antisense oligonucleotides for ICAM 1 attenuate reperfusion injury and renal failure in the rat. Kidney Int 1996;50:473–80 <http://www.ncbi.nlm.nih.gov/pubmed/8840275>

[185] Lu CY, Winterberg PD, Chen J, Hartono JR. Acute kidney injury: a conspiracy of toll-like receptor 4 on endothelia, leukocytes, and tubules. Pediatr Nephrol 2011;: <http://www.ncbi.nlm.nih.gov/pubmed/22033798>

[186] Wang H, Bloom O, Zhang M, Vishnubhakat JM, Ombrellino M, Che J, et al. HMG-1 as a late mediator of endotoxin lethality in mice. Science 1999;285:248–51.

[187] Andersson U, Tracey KJ. HMGB1 is a therapeutic target for sterile inflammation and infection. Annu Rev Immunol 2011;29: <http://www.ncbi.nlm.nih.gov/entrez/query.fcgi?cmd = Retrieve&db = PubMed&dopt = Citation&list_uids = 21219181>

[188] Bianchi ME, Celona B. Ancient news: HMGBs are universal sentinels. J Mol Cell Biol 2010;2:116–7 <http://www.ncbi.nlm.nih.gov/pubmed/20031963>

[189] Tang D, Kang R, Zeh 3rd HJ, Lotze MT. High-mobility group box 1, oxidative stress, and disease. Antioxid Redox Signal 2011;14:1315–35 <http://www.ncbi.nlm.nih.gov/pubmed/20969478> PMCID 3048826

[190] Dumitriu IE, Baruah P, Manfredi AA, Bianchi ME, Rovere-Querini P. HMGB1: guiding immunity from within. Trends Immunol 2005;26:381–7 [PM:15978523]

[191] Lotze MT, Tracey KJ. High-mobility group box 1 protein (HMGB1): nuclear weapon in the immune arsenal. Nat Rev Immunol 2005;5:331–42 [PM:15803152]

[192] Dessing MC, Pulskens WP, Teske GJ, Butter LM, van der Poll T, Yang H, et al. RAGE does not contribute to renal injury and damage upon ischemia/reperfusion-induced injury. J Innate Immun 2011; <http://www.ncbi.nlm.nih.gov/pubmed/22067944>

[193] Miller YI, Choi SH, Wiesner P, Fang L, Harkewicz R, Hartvigsen K, et al. Oxidation-specific epitopes are danger-associated molecular patterns recognized by pattern recognition receptors of innate immunity. Circ Res 2011;108:235–48 <http://www.ncbi.nlm.nih.gov/pubmed/21252151> PMCID 3075542

[194] Gill R, Tsung A, Billiar T. Linking oxidative stress to inflammation: toll-like receptors. Free Radic Biol Med 2010;48:1121–32 <http://www.ncbi.nlm.nih.gov/entrez/query.fcgi?cmd = Retrieve&db = PubMed&dopt = Citation&list_uids = 20083193>

[195] Taylor KR, Trowbridge JM, Rudisill JA, Termeer CC, Simon JC, Gallo RL. Hyaluronan fragments stimulate endothelial recognition of injury through TLR4. J BiolChem 2004;279:17079–84 <http://www.ncbi.nlm.nih.gov/entrez/query.fcgi?cmd = Retrieve&db = PubMed&dopt = Citation&list_uids = 14764599>

[196] Jiang D, Liang J, Fan J, Yu S, Chen S, Luo Y, et al. Regulation of lung injury and repair by Toll-like receptors and hyaluronan. Nat Med 2005;11:1173–9 <http://www.ncbi.nlm.nih.gov/entrez/query.fcgi?cmd = Retrieve&db = PubMed&dopt = Citation&list_uids = 16244651>

[197] Kawabata K, Hagio T, Matsuoka S. The role of neutrophil elastase in acute lung injury. EurJ Pharmacol 2002;451:1–10.

[198] Linas SL, Whittenburg D, Parsons PE, Repine JE. Mild renal ischemia activates primed neutrophils to cause acute renal failure. Kidney Int 1992;42:610–6.

[199] Johnsson C, Tufveson G, Wahlberg J, Hallgren R. Experimentally-induced warm renal ischemia induces cortical accumulation of hyaluronan in the kidney. Kidney Int 1996;50:1224–9 <http://www.ncbi.nlm.nih.gov/entrez/query.fcgi?cmd = Retrieve&db = PubMed&dopt = Citation&list_uids = 8887281>

[200] Wuthrich RP. The proinflammatory role of hyaluronan-CD44 interactions in renal injury. Nephrol Dial Transplant 1999;14:2554–6 <http://www.ncbi.nlm.nih.gov/entrez/query.fcgi?cmd = Retrieve&db = PubMed&dopt = Citation&list_uids = 10534482>

[201] Schaefer L, Babelova A, Kiss E, Hausser HJ, Baliova M, Krzyzankova M, et al. The matrix component biglycan is proinflammatory and signals through Toll-like receptors 4 and 2 in macrophages. J Clin Invest 2005;115:2223–33 <http://www.ncbi.nlm.nih.gov/entrez/query.fcgi?cmd = Retrieve&db = PubMed&dopt = Citation&list_uids = 16025156>

[202] Gunther E, Walter L. Genetic aspects of the hsp70 multigene family in vertebrates. Experientia 1994;50:987–1001.

[203] Hunt CR, Gasser DL, Chaplin DD, Pierce JC, Kozak CA. Chromosomal localization of five murine HSP70 gene family members: Hsp70-1, Hsp70-2, Hsp70-3, Hsc70t, and Grp78. Genomics 1993;16:193–8.

[204] Cornell LD, Colvin RB. Chronic allograft nephropathy. Curr Opin Nephrol Hypertens 2005;14:229–34 <http://www.ncbi.

nlm.nih.gov/entrez/query.fcgi?cmd = Retrieve&db = PubMed&dopt = Citation&list_uids = 15821415>
[205] Peelman LJ, Van de Weghe AR, Coppieters WR, Van Zeveren AJ, Bouquet YH. Complete nucleotide sequence of a porcine HSP70 gene. Immunogenetics 1992;35:286–9.
[206] Walter L, Rauh F, Gunther E. Comparative analysis of the three major histocompatibility complex-linked heat shock protein 70 (Hsp70) genes of the rat. Immunogenetics 1994;40:325–30.
[207] Robert J, Menoret A, Basu S, Cohen N, Srivastava PR. Phylogenetic conservation of the molecular and immunological properties of the chaperones gp96 and hsp70. Eur J Immunol 2001;31:186–95.
[208] Maki RG, Old LJ, Srivastava PK. Human homologue of murine tumor rejection antigen gp96: 5′-regulatory and coding regions and relationship to stress-induced proteins. Proc Natl Acad Sci USA 1990;87:5658–62.
[209] Zitvogel L, Casares N, Pequignot MO, Chaput N, Albert ML, Kroemer G. Immune response against dying tumor cells. Adv Immunol 2004;84:131–79.
[210] Van Why SK, Hildebrandt F, Ardito T, Mann AS, Siegel NJ, Kashgarian M. Induction and intracellular localization of HSP-72 after renal ischemia. Am J Physiol 1992;263:F769–75.
[211] Emami A, Schwartz JH, Borkan SC. Transient ischemia or heat stress induces a cytoprotectant protein in rat kidney. Am J Physiol 1991;260:F479–85.
[212] Schober A, Muller E, Thurau K, Beck FX. The response of heat shock proteins 25 and 72 to ischaemia in different kidney zones. Pflugers Arch 1997;434:292–9.
[213] Morita K, Wakui H, Komatsuda A, Ohtani H, Miura AB, Itoh H, et al. Induction of heat-shock proteins HSP73 and HSP90 in rat kidneys after ischemia. Ren Fail 1995;17:405–19.
[214] Mao H, Wang Y, Li Z, Ruchalski KL, Yu X, Schwartz JH, et al. HSP72 interacts with paxillin and facilitates the reassembly of focal adhesions during recovery from ATP depletion. J Biol Chem 2004;279:15472–80 <http://www.ncbi.nlm.nih.gov/entrez/query.fcgi?cmd = Retrieve&db = PubMed&dopt = Citation&list_uids = 14718530>
[215] Van Why SK, Siegel NJ. Heat shock proteins in renal injury and recovery. Curr Opin Nephrol Hypertens 1998;7:407–12.
[216] Beck FX, Neuhofer W, Muller E. Molecular chaperones in the kidney: distribution, putative roles, and regulation. AJP - Renal Physiol 2000;279:F203–15.
[217] Kelly KJ, Baird NR, Greene AL. Induction of stress response proteins and experimental renal ischemia/reperfusion. Kidney Int 2001;59:1798–802.
[218] Bonventre JV. Kidney ischemic preconditioning. Curr Opin Nephrol Hypertens 2002;11:43–8.
[219] Asea A. Chaperokine-induced signal transduction pathways. ExercImmunol Rev 2003;9:25–33.
[220] Wallin RP, Lundqvist A, More SH, von Bonin A, Kiessling R, Ljunggren HG. Heat-shock proteins as activators of the innate immune system. Trends Immunol 2002;23:130–5.
[221] Land W. Allograft injury mediated by reactive oxygen species: from conserved proteins of Drosophila to acute and chronic rejection of human transplants. Part III: Interaction of (oxidative) stress-induced heat shock proteins with Toll-like receptor-bearing cells of innate immunity and its consequences forthe development of acute and chronic allograft rejection. Transplant Rev 2003;17:67–86.
[222] Skokos D, Botros HG, Demeure C, Morin J, Peronet R, Birkenmeier G, et al. Mast cell-derived exosomes induce phenotypic and functional maturation of dendritic cells and elicit specific immune responses in vivo. J Immunol 2003;170:3037–45.
[223] Wubbolts R, Leckie RS, Veenhuizen PT, Schwarzmann G, Mobius W, Hoernschemeyer J, et al. Proteomic and biochemical analyses of human B cell-derived exosomes. Potential implications for their function and multivesicular body formation. J Biol Chem 2003;278:10963–72.
[224] Morelli AE, Larregina AT, Shufesky WJ, Sullivan ML, Stolz DB, Papworth GD, et al. Intracellular Sorting and Processing of Exosomes by Dendritic Cells. Blood 2004;104:3257–66.
[225] Wand-Wurttenberger A, Schoel B, Ivanyi J, Kaufmann SH. Surface expression by mononuclear phagocytes of an epitope shared with mycobacterial heat shock protein 60. Eur J Immunol 1991;21:1089–92.
[226] Soltys BJ, Gupta RS. Cell surface localization of the 60 kDa heat shock chaperonin protein (hsp60) in mammalian cells. Cell Biol Int 1997;21:315–20.
[227] Soltys BJ, Gupta RS. Immunoelectron microscopic localization of the 60-kDa heat shock chaperonin protein (Hsp60) in mammalian cells. Exp Cell Res 1996;222:16–27.
[228] Gross C, Koelch W, DeMaio A, Arispe N, Multhoff G. Cell surface-bound heat shock protein 70 (Hsp70) mediates perforin-independent apoptosis by specific binding and uptake of granzyme B. J Biol Chem 2003;278:41173–81.
[229] Okamura Y, Watari M, Jerud ES, Young DW, Ishizaka ST, Rose J, et al. The extra domain A of fibronectin activates Toll-like receptor 4. J Biol Chem 2001;276:10229–33.
[230] Zuk A, Bonventre JV, Matlin KS. Expression of fibronectin splice variants in the postischemic rat kidney. AJP - Ren Physiol 2001;280:F1037–53.
[231] Biragyn A, Ruffini PA, Leifer CA, Klyushnenkova E, Shakhov A, Chertov O, et al. Toll-like receptor 4-dependent activation of dendritic cells by beta-defensin 2. Science 2002;298:1025–9.
[232] Saemann MD, Weichhart T, Zeyda M, Staffler G, Schunn M, Stuhlmeier KM, et al. Tamm-Horsfall glycoprotein links innate immune cell activation with adaptive immunity via a Toll-like receptor-4-dependent mechanism. J Clin Invest 2005;115:468–75 <http://www.ncbi.nlm.nih.gov/entrez/query.fcgi?cmd = Retrieve&db = PubMed&dopt = Citation&list_uids = 15650774>
[233] El-Achkar TM, McCracken R, Rauchman M, Heitmeier MR, Al-Aly Z, Dagher PC, et al. Tamm-Horsfall protein-deficient thick ascending limbs promote injury to neighboring S3 segments in an MIP-2-dependent mechanism. Am J Physiol Renal Physiol 2011;300:F999–1007 <http://www.ncbi.nlm.nih.gov/pubmed/21228114>
[234] Rosin DL, Okusa MD. Dangers within: DAMP responses to damage and cell death in kidney disease. J Am Soc Nephrol 2011;22:416–25 <http://www.ncbi.nlm.nih.gov/pubmed/21335516>
[235] Nishitani C, Mitsuzawa H, Hyakushima N, Sano H, Matsushima N, Kuroki Y. The Toll-like receptor 4 region Glu24-Pro34 is critical for interaction with MD-2. Biochem Biophys Res Commun 2005;328:586–90.
[236] Triantafilou M, Triantafilou K. Lipopolysaccharide recognition: CD14, TLRs and the LPS-activation cluster. Trends Immunol 2002;23:301–4 <http://www.ncbi.nlm.nih.gov/entrez/query.fcgi?cmd = Retrieve&db = PubMed&dopt = Citation&list_uids = 12072369>
[237] Triantafilou M, Morath S, Mackie A, Hartung T, Triantafilou K. Lateral diffusion of Toll-like receptors reveals that they are transiently confined within lipid rafts on the plasma membrane. J Cell Sci 2004;117:4007–14.
[238] Underhill DM. Toll-like receptors: networking for success. Eur J Immunol 2003;33:1767–75.
[239] Muller M, Scheel O, Lindner B, Gutsmann T, Seydel U. The role of membrane-bound LBP, endotoxin aggregates, and the

MaxiK channel in LPS-induced cell activation. J Endotoxin Res 2003;9:181–6.
[240] Becker T, Hartl FU, Wieland F. CD40, an extracellular receptor for binding and uptake of Hsp70-peptide complexes. J Cell Biol 2002;158:1277–85.
[241] Stebbing J, Savage P, Patterson S, Gazzard B. All for CD91 and CD91 for all. J Antimicrob Chemother 2004;53: 1–3.
[242] Termeer C, Benedix F, Sleeman J, Fieber C, Voith U, Ahrens T, et al. Oligosaccharides of Hyaluronan activate dendritic cells via toll-like receptor 4. J Exp Med 2002;195:99–111.
[243] Millar DG, Garza KM, Odermatt B, Elford AR, Ono N, Li Z, et al. Hsp70 promotes antigen-presenting cell function and converts T-cell tolerance to autoimmunity in vivo. Nat Med 2003;9:1469–76 <http://www.ncbi.nlm.nih.gov/entrez/query.fcgi?cmd = Retrieve&db = PubMed&dopt = Citation&list_uids = 14625545>
[244] Knotek M, Rogachev B, Wang W, Ecder T, Melnikov V, Gengaro PE, et al. Endotoxemic renal failure in mice: Role of tumor necrosis factor independent of inducible nitric oxide synthase. Kidney Int 2001;59:2243–9.
[245] Bonventre JV, Zuk A. Ischemic acute renal failure: an inflammatory disease? Kidney Int 2004;66:480–5 <http://www.ncbi.nlm.nih.gov/pubmed/15253693>
[246] Noiri E, Peresleni T, Miller F, Goligorsky MS. In vivo targeting of inducible NO synthase with oligodeoxynucleotides protects rat kidney against ischemia. J Clin Invest 1996;97:2377–83 <http://www.ncbi.nlm.nih.gov/entrez/query.fcgi?cmd = Retrieve&db = PubMed&dopt = Citation&list_uids = 8636419> PMCID 8636419
[247] Ling H, Edelstein C, Gengaro P, Meng X, Lucia S, Knotek M, et al. Attenuation of renal ischemia-reperfusion injury in inducible nitric oxide synthase knockout mice. Am J Physiol Renal Physiol 1999;277:F383–90 <http://www.ncbi.nlm.nih.gov/entrez/query.fcgi?cmd = Retrieve&db = PubMed&dopt = Citation&list_ uids = 10484522> PMCID 10484522
[248] Donnahoo KK, Meng X, Ao L, Ayala A, Shames BD, Cain MP, et al. Differential cellular immunolocalization of renal tumour necrosis factor-alpha production during ischaemia versus endotoxaemia. Immunology 2001;102:53–8 <http://www.ncbi.nlm.nih.gov/entrez/query.fcgi?cmd = Retrieve&db = PubMed&dopt = Citation&list_uids = 11168637>
[249] Cunningham PN, Wang Y, Guo R, He G, Quigg RJ. Role of toll-like receptor 4 in endotoxin-induced acute renal failure. J Immunol 2004;172:2629–35.
[250] Mittal D, Saccheri F, Venereau E, Pusterla T, Bianchi ME, Rescigno M. TLR4-mediated skin carcinogenesis is dependent on immune and radioresistant cells. EMBO J 2010; <http://www.ncbi.nlm.nih.gov/entrez/query.fcgi?cmd = Retrieve&db = PubMed&dopt = Citation&list_uids = 20526283>
[251] Midwood K, Sacre S, Piccinini AM, Inglis J, Trebaul A, Chan E, et al. Tenascin-C is an endogenous activator of Toll-like receptor 4 that is essential for maintaining inflammation in arthritic joint disease. Nat Med 2009;15:774–80 <http://www.ncbi.nlm.nih.gov/entrez/query.fcgi?cmd = Retrieve&db = PubMed&dopt = Citation&list_uids = 19561617>
[252] Spear AM, Loman NJ, Atkins HS, Pallen MJ. Microbial TIR domains: not necessarily agents of subversion? Trends Microbiol 2009;17:393–8 <http://www.ncbi.nlm.nih.gov/entrez/query.fcgi?cmd = Retrieve&db = PubMed&dopt = Citation&list_uids = 19716705>
[253] Gauthier ME, Du Pasquier L, Degnan BM. The genome of the sponge Amphimedon queenslandica provides new perspectives into the origin of Toll-like and interleukin 1 receptor pathways. Evol Dev 2010;12:519–33 <http://www.ncbi.nlm.nih.gov/entrez/query.fcgi?cmd = Retrieve&db = PubMed&dopt = Citation&list_uids = 20883219>
[254] Barton GM. A calculated response: control of inflammation by the innate immune system. J Clin Invest 2008;118:413–20 <http://www.ncbi.nlm.nih.gov/entrez/query.fcgi?cmd = Retrieve&db = PubMed&dopt = Citation&list_uids = 18246191>
[255] Chen GY, Tang J, Zheng P, Liu Y. CD24 and Siglec-10 selectively repress tissue damage-induced immune responses. Science 2009;323:1722–5 <http://www.ncbi.nlm.nih.gov/entrez/query.fcgi?cmd = Retrieve&db = PubMed&dopt = Citation&list_uids = 19264983>
[256] Liu Y, Chen GY, Zheng P. CD24-Siglec G/10 discriminates danger- from pathogen-associated molecular patterns. Trends Immunol 2009;30:557–61 <http://www.ncbi.nlm.nih.gov/entrez/query.fcgi?cmd = Retrieve&db = PubMed&dopt = Citation&list_uids = 19786366> PMCID 2788100
[257] Ungaro R, Fukata M, Hsu D, Hernandez Y, Breglio K, Chen A, et al. A novel Toll-like receptor 4 antagonist antibody ameliorates inflammation but impairs mucosal healing in murine colitis. Am J Physiol Gastrointest Liver Physiol 2009;296: G1167–79 <http://www.ncbi.nlm.nih.gov/entrez/query.fcgi?cmd = Retrieve&db = PubMed&dopt = Citation&list_uids = 19359427>
[258] Rakoff-Nahoum S, Paglino J, Eslami-Varzaneh F, Edberg S, Medzhitov R. Recognition of commensal microflora by toll-like receptors is required for intestinal homeostasis. Cell 2004;118:229–41 <http://www.ncbi.nlm.nih.gov/entrez/query.fcgi?cmd = Retrieve&db = PubMed&dopt = Citation&list_uids = 15260992>
[259] Putnins EE, Sanaie AR, Wu Q, Firth JD. Induction of keratinocyte growth factor 1 Expression by lipopolysaccharide is regulated by CD-14 and toll-like receptors 2 and 4. Infect Immun 2002;70:6541–8 <http://www.ncbi.nlm.nih.gov/entrez/query.fcgi?cmd = Retrieve&db = PubMed&dopt = Citation&list_uids = 12438323> PMCID 132971
[260] Sanale AR, Firth JD, Uitto VJ, Putnins EE. Keratinocyte growth factor (KGF)-1 and -2 protein and gene expression in human gingival fibroblasts. J Periodontal Res 2002;37:66–74 <http://www.ncbi.nlm.nih.gov/entrez/query.fcgi?cmd = Retrieve&db = PubMed&dopt = Citation&list_uids = 11842940>
[261] Sugiyama A, Ogawa T, Daikuhara Y, Takada H. Enhancement of hepatocyte growth factor (scatter factor) production by human gingival fibroblasts in culture stimulated with Porphyromonas gingivalis fimbriae. J Med Microbiol 2000;49:319–25 <http://www.ncbi.nlm.nih.gov/entrez/query.fcgi?cmd = Retrieve&db = PubMed&dopt = Citation&list_uids = 10755625>
[262] Yoshioka T, Morimoto Y, Iwagaki H, Itoh H, Saito S, Kobayashi N, et al. Bacterial lipopolysaccharide induces transforming growth factor beta and hepatocyte growth factor through toll-like receptor 2 in cultured human colon cancer cells. J Int Med Res 2001;29:409–20 <http://www.ncbi.nlm.nih.gov/entrez/query.fcgi?cmd = Retrieve&db = PubMed&dopt = Citation&list_uids = 11725828>
[263] Spix JK, Chay EY, Block ER, Klarlund JK. Hepatocyte growth factor induces epithelial cell motility through transactivation of the epidermal growth factor receptor. Exp Cell Res 2007;313:3319–25 <http://www.ncbi.nlm.nih.gov/entrez/query.fcgi?cmd = Retrieve&db = PubMed&dopt = Citation&list_uids = 17643426> PMCID 2128736
[264] Hsu D, Fukata M, Hernandez YG, Sotolongo JP, Goo T, Maki J, et al. Toll-like receptor 4 differentially regulates epidermal growth factor-related growth factors in response to intestinal mucosal injury. Lab Invest 2010;90:1295–305 <http://www.

ncbi.nlm.nih.gov/entrez/query.fcgi?cmd = Retrieve&db = PubMed&dopt = Citation&list_uids = 20498653>
[265] Zeng F, Singh AB, Harris RC. The role of the EGF family of ligands and receptors in renal development, physiology and pathophysiology. Exp Cell Res 2009;315:602–10 <http://www.ncbi.nlm.nih.gov/entrez/query.fcgi?cmd = Retrieve&db = PubMed&dopt = Citation&list_uids = 18761338> PMCID 2654782
[266] Zhang X, Shan P, Jiang G, Cohn L, Lee PJ. Toll-like receptor 4 deficiency causes pulmonary emphysema. J Clin Invest 2006;116:3050–9 <http://www.ncbi.nlm.nih.gov/entrez/query.fcgi?cmd = Retrieve&db = PubMed&dopt = Citation&list_uids = 17053835> PMCID 1616193
[267] Qureshi ST, Zhang X, Aberg E, Bousette N, Giaid A, Shan P, et al. Inducible activation of TLR4 confers resistance to hyperoxia-induced pulmonary apoptosis. J Immunol 2006;176:4950–8 <http://www.ncbi.nlm.nih.gov/entrez/query.fcgi?cmd = Retrieve&db = PubMed&dopt = Citation&list_uids = 16585591>
[268] Zhang X, Shan P, Qureshi S, Homer R, Medzhitov R, Noble PW, et al. Cutting edge: TLR4 deficiency confers susceptibility to lethal oxidant lung injury. J Immunol 2005;175:4834–8 <http://www.ncbi.nlm.nih.gov/entrez/query.fcgi?cmd = Retrieve&db = PubMed&dopt = Citation&list_uids = 16210584>
[269] Paun A, Fox J, Balloy V, Chignard M, Qureshi ST, Haston CK. Combined Tlr2 and Tlr4 deficiency increases radiation-induced pulmonary fibrosis in mice. Int J Radiat Oncol Biol Phys 2010;77:1198–205.
[270] Goren I, Allmann N, Yogev N, Schurmann C, Linke A, Holdener M, et al. A transgenic mouse model of inducible macrophage depletion: effects of diphtheria toxin-driven lysozyme M-specific cell lineage ablation on wound inflammatory, angiogenic, and contractive processes. Am J Pathol 2009;175:132–47 <http://www.ncbi.nlm.nih.gov/entrez/query.fcgi?cmd = Retrieve&db = PubMed&dop = Citation&list_uids = 19528348>
[271] Campbell JS, Riehle KJ, Brooling JT, Bauer RL, Mitchell C, Fausto N. Proinflammatory cytokine production in liver regeneration is Myd88-dependent, but independent of Cd14, Tlr2, and Tlr4. J Immunol 2006;176:2522–8 <http://www.ncbi.nlm.nih.gov/entrez/query.fcgi?cmd = Retrieve&db = PubMed&dopt = Citation&list_uids = >
[272] Shigeoka AA, Kambo A, Mathison JC, King AJ, Hall WF, da Silva Correia J, et al. Nod1 and nod2 are expressed in human and murine renal tubular epithelial cells and participate in renal ischemia reperfusion injury. J Immunol 2010; 184:2297–304 <http://www.ncbi.nlm.nih.gov/entrez/query.fcgi?cmd = Retrieve&db = PubMed&dopt = Citation&list_uids = 20124104>
[273] Shigeoka AA, Mueller JL, Kambo A, Mathison JC, King AJ, Hall WF, et al. An inflammasome-independent role for epithelial-expressed nlrp3 in renal ischemia-reperfusion injury. J Immunol 2010; <http://www.ncbi.nlm.nih.gov/entrez/query.fcgi?cmd = Retrieve&db = PubMed&dopt = Citation&list_uids = 20962258>
[274] Basu S, Binder RJ, Ramalingam T, Srivastava PK. CD91 is a common receptor for heat shock proteins gp96, hsp90, hsp70, and calreticulin. Immunity 2001;14:303–13.
[275] Binder RJ, Han DK, Srivastava PK. CD91: a receptor for heat shock protein gp96. Nat Immunol 2000;1:151–5.
[276] Bhattacharjee G, Misra UK, Gawdi G, Cianciolo G, Pizzo SV. Inducible expression of the alpha2-macroglobulin signaling receptor in response to antigenic stimulation: a study of second messenger generation. J Cell Biochem 2001;82:260–70.
[277] Misra UK, Gawdi G, Gonzalez-Gronow M, Pizzo SV. Coordinate regulation of the alpha(2)-macroglobulin signaling receptor and the low density lipoprotein receptor-related protein/alpha(2)-macroglobulin receptor by insulin. J Biol Chem 1999;274:25785–91.
[278] Gardai SJ, Xiao YQ, Dickinson M, Nick JA, Voelker DR, Greene KE, et al. By binding SIRPalpha or calreticulin/CD91, lung collectins act as dual function surveillance molecules to suppress or enhance inflammation. Cell 2003;115:13–23 <http://www.ncbi.nlm.nih.gov/entrez/query.fcgi?cmd = Retrieve&db = PubMed&dopt = Citation&list_uids = 14531999>
[279] Herz J, Hui DY. Lipoprotein receptors in the vascular wall. Curr Opin Lipidol 2004;15:175–81.
[280] Kirschning CJ, Schumann RR. TLR2: cellular sensor for microbial and endogenous molecular patterns. Curr Top Microbiol Immunol 2002;270:121–44.
[281] Sabroe I, Read RC, Whyte MK, Dockrell DH, Vogel SN, Dower SK. Toll-like receptors in health and disease: complex questions remain. J Immunol 2003;171:1630–5 <http://www.ncbi.nlm.nih.gov/entrez/query.fcgi?cmd = Retrieve&db = PubMed&dopt = Citation&list_uids = 12902458>
[282] Leemans JC, Stokman G, Claessen N, Rouschop KM, Teske GJ, Kirschning CJ, et al. Renal-associated TLR2 mediates ischemia/reperfusion injury in the kidney. J Clin Invest 2005;115:2894–903 <http://www.ncbi.nlm.nih.gov/entrez/query.fcgi?cmd = Retrieve&db = PubMed&dopt = Citation&list_uids = 16167081>
[283] Kim BS, Lim SW, Li C, Kim JS, Sun BK, Ahn KO, et al. Ischemia-reperfusion injury activates innate immunity in rat kidneys. Transplantation 2005;79:1370–7 <http://www.ncbi.nlm.nih.gov/entrez/query.fcgi?cmd = Retrieve&db = PubMed&dopt = Citation&list_uids = 15912106>
[284] Wolfs TG, Buurman WA, van Schadewijk A, de Vries B, Daemen MA, Hiemstra PS, et al. In vivo expression of Toll-like receptor 2 and 4 by renal epithelial cells: IFN-gamma and TNF-alpha mediated up-regulation during inflammation. J Immunol 2002;168:1286–93 <http://www.ncbi.nlm.nih.gov/entrez/query.fcgi?cmd = Retrieve&db = PubMed&dopt = Citation&list_uids = 11801667>
[285] Zhang JX, Wu HS, Wang H, Zhang JH, Wang Y, Zheng QC. Protection against hepatic ischemia/reperfusion injury via downregulation of toll-like receptor 2 expression by inhibition of Kupffer cell function. World J Gastroenterol 2005;11:4423–6 [PM:16038046].
[286] Shishido T, Nozaki N, Yamaguchi S, Shibata Y, Nitobe J, Miyamoto T, et al. Toll-like receptor-2 modulates ventricular remodeling after myocardial infarction. Circulation 2003;108:2905–10.
[287] Wendt T, Tanji N, Guo J, Hudson BI, Bierhaus A, Ramasamy R, et al. Glucose, glycation, and RAGE: implications for amplification of cellular dysfunction in diabetic nephropathy. J Am Soc Nephrol 2003;14:1383–95.
[288] Nawroth P, Bierhaus A, Marrero M, Yamamoto H, Stern DM. Atherosclerosis and restenosis: is there a role for RAGE? Curr Diab Rep 2005;5:11–6 [PM:15663911].
[289] Jensen LJ, Ostergaard J, Flyvbjerg A. AGE-RAGE and AGE Cross-link interaction: important players in the pathogenesis of diabetic kidney disease. Horm Metab Res 2005;37(Suppl 1):26–34 [PM:15918107].
[290] Bohlender JM, Franke S, Stein G, Wolf G. Advanced glycation end products and the kidney. AJP - Renal Physiol 2005;289: F645–59 [PM:16159899].
[291] Rabadi MM, Kuo MC, Ghaly T, Rabadi SM, Weber M, Goligorsky MS, et al. Interaction between uric acid and

HMGB1 translocation and release from endothelial cells. Am J Physiol Renal Physiol 2011; <http://www.ncbi.nlm.nih.gov/pubmed/22189943>

[292] Iyer SS, Pulskens WP, Sadler JJ, Butter LM, Teske GJ, Ulland TK, et al. Necrotic cells trigger a sterile inflammatory response through the Nlrp3 inflammasome. Proc Natl Acad Sci U S A 2009;106:20388–93 <http://www.ncbi.nlm.nih.gov/entrez/query.fcgi?cmd=Retrieve&db=PubMed&dopt=Citation&list_uids=19918053> PMCID 2787135

[293] Ricklin D, Hajishengallis G, Yang K, Lambris JD. Complement: a key system for immune surveillance and homeostasis. Nat Immunol 2010;11:785–97 <http://www.ncbi.nlm.nih.gov/pubmed/20720586> PMCID 2924908

[294] Thurman JM, Renner B. Dynamic control of the complement system by modulated expression of regulatory proteins. Lab Invest 2011;91:4–11 <http://www.ncbi.nlm.nih.gov/pubmed/20921948>

[295] Bao L, Wang Y, Chang A, Minto AW, Zhou J, Kang H, et al. Unrestricted C3 activation occurs in Crry-deficient kidneys and rapidly leads to chronic renal failure. J Am Soc Nephrol 2007;18:811–22 <http://www.ncbi.nlm.nih.gov/pubmed/17229915>

[296] Lockshin RA, Zakeri Z. Caspase-independent cell death? Oncogene 2004;23:2766–73 [PM: 15077140]

[297] Edinger AL, Thompson CB. Death by design: apoptosis, necrosis and autophagy. Curr OpinCell Biol 2004;16:663–9 <http://www.ncbi.nlm.nih.gov/entrez/query.fcgi?cmd=Retrieve&db=PubMed&dopt=Citation&list_uids=15530778>

[298] Vercammen D, Brouckaert G, Denecker G, Van de CM, Declercq W, Fiers W, et al. Dual signaling of the Fas receptor: initiation of both apoptotic and necrotic cell death pathways. J Exp Med 1998;188:919–30 [pm:9730893].

[299] Leist M, Jaattela M. Four deaths and a funeral: from caspases to alternative mechanisms. Nat Rev Mol Cell Biol 2001;2:589–98 [PM:11483992].

[300] Proskuryakov SY, Konoplyannikov AG, Gabai VL. Necrosis: a specific form of programmed cell death? Exp Cell Res 2003;283:1–16 [PM:12565815].

[301] Kitanaka C, Kuchino Y. Caspase-independent programmed cell death with necrotic morphology. Cell Death Differ 1999;6:508–15 [PM: 10381653].

[302] Devalaraja-Narashimha K, Singaravelu K, Padanilam BJ. Poly (ADP-ribose) polymerase-mediated cell injury in acute renal failure. Pharmacol Res 2005;52:44–59.

[303] Ame JC, Spenlehauer C, de Murcia G. The PARP superfamily. Bioessays 2004;26:882–93 [PM: 15273990]

[304] Boulares AH, Zoltoski AJ, Sherif ZA, Jolly P, Massaro D, Smulson ME. Gene knockout or pharmacological inhibition of poly(ADP-ribose) polymerase-1 prevents lung inflammation in a murine model of asthma. Am J Respir Cell Mol Biol 2003;28:322–9.

[305] Martin DR, Lewington AJ, Hammerman MR, Padanilam BJ. Inhibition of poly(ADP-ribose) polymerase attenuates ischemic renal injury in rats. Am J Physiol Regul Integr Comp Physiol 2000;279:R1834–40.

[306] Chatterjee PK, Chatterjee BE, Pedersen H, Sivarajah A, McDonald MC, Mota-Filipe H, et al. 5-Aminoisoquinolinone reduces renal injury and dysfunction caused by experimental ischemia/reperfusion. Kidney Int 2004;65:499–509 [PM:14717920]

[307] Patel NS, Cortes U, Di Poala R, Mazzon E, Mota-Filipe H, Cuzzocrea S, et al. Mice lacking the 110-kD isoform of poly (ADP-Ribose) glycohydrolase are protected against renal ischemia/reperfusion injury. J Am Soc Nephrol 2005;16:712–9 <http://www.ncbi.nlm.nih.gov/entrez/query.fcgi?cmd=Retrieve&db=PubMed&dopt=Citation&list_uids=15677308>

[308] Zheng J, Devalaraja-Narashimha K, Singaravelu K, Padanilam BJ. Poly(ADP-ribose) polymerase-1 gene ablation protects mice from ischemic renal injury. AJP - Renal Physiol 2005;288: F387–98.

[309] Chatterjee PK, Zacharowski K, Cuzzocrea S, Otto M, Thiemermann C. Inhibitors of poly (ADP-ribose) synthetase reduce renal ischemia-reperfusion injury in the anesthetized rat in vivo. FASEB J 2000;14:641–51 [PM: 10744621].

[310] Ha HC, Snyder SH. Poly(ADP-ribose) polymerase is a mediator of necrotic cell death by ATP depletion. Proc Natl Acad Sci USA 1999;96:13978–82 [pm: 10570184].

[311] Alano CC, Ying W, Swanson RA. Poly(ADP-ribose) polymerase-1-mediated cell death in astrocytes requires NAD+ depletion and mitochondrial permeability transition. J Biol Chem 2004;279:18895–902.

[312] Szabo C, Dawson VL. Role of poly(ADP-ribose) synthetase in inflammation and ischaemia-reperfusion. Trends Pharmacol Sci 1998;19:287–98.

[313] Los M, Mozoluk M, Ferrari D, Stepczynska A, Stroh C, Renz A, et al. Activation and caspase-mediated inhibition of PARP: a molecular switch between fibroblast necrosis and apoptosis in death receptor signaling. Mol Biol Cell 2002;13:978–88 [pm:11907276]

[314] Petrilli V, Herceg Z, Hassa PO, Patel NS, Di Paola R, Cortes U, et al. Noncleavable poly(ADP-ribose) polymerase-1 regulates the inflammation response in mice. J Clin Invest 2004;114:1072–81 [PM: 15489954].

[315] Baines CP, Kaiser RA, Purcell NH, Blair NS, Osinska H, Hambleton MA, et al. Loss of cyclophilin D reveals a critical role for mitochondrial permeability transition in cell death. Nature 2005;434:658–62 <http://www.ncbi.nlm.nih.gov/pubmed/15800627>

[316] Nakagawa T, Shimizu S, Watanabe T, Yamaguchi O, Otsu K, Yamagata H, et al. Cyclophilin D-dependent mitochondrial permeability transition regulates some necrotic but not apoptotic cell death. Nature 2005;434:652–8 <http://www.ncbi.nlm.nih.gov/pubmed/15800626>

[317] Schneider MD. Cyclophilin D: knocking on death's door. Sci STKE 2005;2005:e26 [PM:15942033].

[318] Schinzel AC, Takeuchi O, Huang Z, Fisher JK, Zhou Z, Rubens J, et al. Cyclophilin D is a component of mitochondrial permeability transition and mediates neuronal cell death after focal cerebral ischemia. Proc Natl Acad Sci USA 2005;102:12005–10 [PM: 16103352].

[319] Kim JS, Ohshima S, Pediaditakis P, Lemasters JJ. Nitric oxide: a signaling molecule against mitochondrial permeability transition- and pH-dependent cell death after reperfusion. Free Radic Biol Med 2004;37:1943–50 [PM: 15544914].

[320] Yoshimoto T, Siesjo BK. Posttreatment with the immunosuppressant cyclosporin A in transient focal ischemia. Brain Res 1999;839:283–91 [PM: 10519051].

[321] Kim JS, He L, Lemasters JJ. Mitochondrial permeability transition: a common pathway to necrosis and apoptosis. Biochem Biophys Res Commun 2003;304:463–70 [PM: 12729580].

[322] Malhi H, Gores GJ, Lemasters JJ. Apoptosis and necrosis in the liver: a tale of two deaths? Hepatology 2006;43:S31–44 [PM: 16447272].

[323] Halestrap A. Biochemistry: a pore way to die. Nature 2005;434:578–9 [PM: 15800609]

[324] Lieberthal W, Menza SA, Levine JS. Graded ATP depletion can cause necrosis or apoptosis of cultured mouse

proximal tubular cells. Am J Physiol 1998;274:F315–27 [pm: 9486226]
[325] Leist M, Single B, Naumann H, Fava E, Simon B, Kuhnle S, et al. Inhibition of mitochondrial ATP generation by nitric oxide switches apoptosis to necrosis. Exp Cell Res 1999;249:396–403 [PM: 10366439].
[326] Lelli Jr. JL, Becks LL, Dabrowska MI, Hinshaw DB. ATP converts necrosis to apoptosis in oxidant-injured endothelial cells. Free Radic Biol Med 1998;25:694–702 [pm: 9801070].
[327] Chan FK, Shisler J, Bixby JG, Felices M, Zheng L, Appel M, et al. A role for tumor necrosis factor receptor-2 and receptor-interacting protein in programmed necrosis and antiviral responses. J Biol Chem 2003;278:51613–21 [PM: 14532286].
[328] Mareninova OA, Sung KF, Hong P, Lugea A, Pandol SJ, Gukovsky I, et al. Cell death in pancreatitis: caspases protect from necrotizing pancreatitis. J Biol Chem 2006;281:3370–81 [PM: 16339139].
[329] Cauwels A, Janssen B, Waeytens A, Cuvelier C, Brouckaert P. Caspase inhibition causes hyperacute tumor necrosis factor-induced shock via oxidative stress and phospholipase A2. Nat Immunol 2003;4:387–93 [PM: 12652297].
[330] Castaneda MP, Swiatecka-Urban A, Mitsnefes MM, Feuerstein D, Kaskel FJ, Tellis V, et al. Activation of mitochondrial apoptotic pathways in human renal allografts after ischemiareperfusion injury. Transplant 2003;76:50–4.
[331] Daemen MA, de Vries B, Buurman WA. Apoptosis and inflammation in renal reperfusion injury. Transplant 2002;73: 1693–700.
[332] Kelly KJ, Sandoval RM, Dunn KW, Molitoris BA, Dagher PC. A novel method to determine specificity and sensitivity of the TUNEL reaction in the quantitation of apoptosis. AJP - Cell Physiol 2003;284:C1309–18 <http://www.ncbi.nlm.nih.gov/pubmed/12676658>
[333] Basile DP, Liapis H, Hammerman MR. Expression of bcl-2 and bax in regenerating rat renal tubules following ischemic injury. Am J Physiol 1997;272:F640–7 <http://www.ncbi.nlm.nih.gov/entrez/query.fcgi?cmd = Retrieve&db = PubMed&dopt = Citation&list_uids = 9176375>
[334] Ueda N, Kaushal GP, Shah SV. Apoptotic mechanisms in acute renal failure. Am J Med 2000;108:403–15.
[335] Bonegio R, Lieberthal W. Role of apoptosis in the pathogenesis of acute renal failure. Curr Opin Nephrol Hypertens 2002;11:301–8.
[336] Lauber K, Blumenthal SG, Waibel M, Wesselborg S. Clearance of apoptotic cells: getting rid of the corpses. Mol Cell 2004;14:277–87 <http://www.ncbi.nlm.nih.gov/entrez/query.fcgi?cmd = Retrieve&db = PubMed&dopt = Citation&list_uids = 15125832>
[337] Huynh ML, Fadok VA, Henson PM. Phosphatidylserine-dependent ingestion of apoptotic cells promotes TGF-beta1 secretion and the resolution of inflammation. J Clin Invest 2002;109:41–50.
[338] Savill J, Dransfield I, Gregory C, Haslett C. A blast from the past: clearance of apoptotic cells regulates immune responses. Nat Rev Immunol 2002;2:965–75.
[339] Henson PM, Bratton DL, Fadok VA. The phosphatidylserine receptor: a crucial molecular switch? Nat Rev Mol Cell Biol 2001;2:627–33.
[340] Savill J, Gregory C, Haslett C. Cell biology. Eat me or die. Science 2003;302:1516–7 <http://www.ncbi.nlm.nih.gov/entrez/query.fcgi?cmd = Retrieve&db = PubMed&dopt = Citation&list_uids = 14645835>
[341] Li MO, Sarkisian MR, Mehal WZ, Rakic P, Flavell RA. Phosphatidylserine receptor is required for clearance of apoptotic cells. Science 2003;302:1560–3 <http://www.ncbi.nlm.nih.gov/entrez/query.fcgi?cmd = Retrieve&db = PubMed&dopt = Citation&list_uids = 14645847>
[342] Gregory CD, Devitt A. The macrophage and the apoptotic cell: an innate immune interaction viewed simplistically? Immunology 2004;113:1–14 [PM: 15312130].
[343] Chang MK, Binder CJ, Miller YI, Subbanagounder G, Silverman GJ, Berliner JA, et al. Apoptotic cells with oxidation-specific epitopes are immunogenic and proinflammatory. J Exp Med 2004;200:1359–70.
[344] Bratton DL, Henson PM. Autoimmunity and apoptosis: refusing to go quietly. Nat Med 2005;11:26–7.
[345] Poon IK, Hulett MD, Parish CR. Molecular mechanisms of late apoptotic/necrotic cell clearance. Cell Death Differ 2010;17:381–97 <http://www.ncbi.nlm.nih.gov/pubmed/20019744>
[346] Tabas I. Macrophage death and defective inflammation resolution in atherosclerosis. Nat Rev Immunol 2010;10:36–46 <http://www.ncbi.nlm.nih.gov/pubmed/19960040> PMCID 2854623
[347] Peter C, Wesselborg S, Herrmann M, Lauber K. Dangerous attraction: phagocyte recruitment and danger signals of apoptotic and necrotic cells. Apoptosis 2010;15:1007–28 <http://www.ncbi.nlm.nih.gov/pubmed/20157780>
[348] Matsuda A, Wu R, Jacob A, Komura H, Zhou M, Wang Z, et al. Protective effect of milk fat globule-epidermal growth factor-factor VIII after renal ischemia-reperfusion injury in mice. Crit Care Med 2011;39:2039–47 <http://www.ncbi.nlm.nih.gov/pubmed/21666453> PMCID 3158289
[349] Harrois A, Duranteau J. Acute kidney injury: clear the kidney of apoptotic debris!. Crit Care Med 2011;39:2180–1 <http://www.ncbi.nlm.nih.gov/pubmed/21849826>
[350] Matsuda A, Jacob A, Wu R, Zhou M, Nicastro JM, Coppa GF, et al. Milk fat globule-EGF factor VIII in sepsis and ischemia-reperfusion injury. Mol Med 2011;17:126–33 <http://www.ncbi.nlm.nih.gov/pubmed/20882259> PMCID 3022991.

CHAPTER

89

Catalytic (Labile) Iron in Kidney Disease

Mohan Rajapurkar[1], *Radhakrishna Baliga*[2] *and Sudhir V. Shah*[3]

[1]Department of Nephrology, Muljibhai Patel Urological Hospital, Gujarat, India

[2]Department of Pediatrics, University of Mississippi Medical Center, Mississippi, USA

[3]Division of Nephrology, Department of Internal Medicine, University of Arkansas for Medical Sciences and Renal Section, Medicine Service Central Arkansas Veterans Healthcare System, Little Rock, Arkansas, USA

INTRODUCTION

Despite advances in understanding the pathophysiology of acute kidney injury (AKI) and chronic kidney disease, treatment for kidney disease remains unsatisfactory. In this chapter, we briefly recount the importance of acute kidney injury and chronic kidney disease, then provide a brief description of labile iron, and, finally, summarize the role of labile iron in acute and chronic kidney disease. The availability of iron chelators provides new therapeutic tools to prevent and/or treat kidney disease.

Acute kidney injury is an independent risk factor for morbidity and mortality. A modest increase (0.3 mg/dL) in serum creatinine is associated with high in-hospital mortality,[1,2] and AKI is associated with post-hospital discharge mortality[3,4] and progression to end-stage kidney disease (ESKD).[5,6]

Chronic kidney disease (CKD) affects approximately 10-15% of the adult population worldwide,[7,8] is an independent risk factor for cardiovascular disease,[9] and carries a high economic cost.[10] There is a worldwide increase in the incidence and prevalence of diabetes, which is the most common cause of CKD. These observations, coupled with the increasing incidence of end-stage kidney disease despite the use of angiotensin receptor blockers (ARBs) and the multiplier effect of CKD on cardiovascular disease, indicate a major importance of CKD as a global public health problem. The failure of recent studies to halt diabetic nephropathy highlights an urgent need[11] for new therapeutic modalities to halt progression of kidney disease.

DEFINITION OF CATALYTIC (LABILE) IRON AND ITS IMPORTANCE IN TISSUE INJURY

Iron is the most abundant transitional metal in the body. The term "labile iron pool" was first used to denote a transient iron pool of low-molecular-weight, weakly chelated iron that passes through the cell.[12,13] Methodological approaches for detection of this pool of iron ions are based on the use of metal chelators.[14] Critical to iron's importance in biological processes is its ability to cycle reversibly between its ferrous and ferric oxidation states. This precise property, which is essential for its functions, also makes it very dangerous, because free iron can catalyze the formation of free radicals that can damage the cell. Thus, from a pathophysiological standpoint, the broadest definition of a labile iron pool is that it consists of chemical forms that can participate in redox cycling, and is therefore often referred to as catalytic iron.[15]

The catalytic iron pool[15,16] is estimated to be less than 100 mg compared to the total iron in the body, which is approximately 4 g. In most cells iron homeostasis consists of iron uptake, utilization, and storage. The process of iron uptake is carried out by a transferrin receptor (TFR) and a divalent metal transporter 1

Seldin and Giebisch's The Kidney, Fifth Edition.
DOI: http://dx.doi.org/10.1016/B978-0-12-381462-3.00089-6

© 2013 Elsevier Inc. All rights reserved.

(DMT1, also called DCT1; NRAMP2), whereas ferritin is an intracellular, iron-sequestering protein. Studies are beginning to yield information on the pathways of iron transport, its export from the cell via the divalent iron ion exporter ferroportin 1,[17] and its regulatory mechanisms including hepcidin.[18] Since uptake and storage of iron is carried out by different proteins, the pool of accessible iron ions constitutes a crossroad of metabolic pathways of iron-containing compounds.

Studies using a variety of methods have begun to define intracellular distribution of labile iron (for reviews see Kruszewski[14] and Esposito[19]). Using several techniques including laser scanning microscopy, the concentration and distribution of chelatable iron has been estimated to be about 5.0 to 15 μM in the cytoplasm and subcellular organelles including mitochondria and nuclei.[20] *In vivo*, most of the iron is bound to heme or non-heme protein and does not directly catalyze the generation of hydroxyl radicals or a similar oxidant.[15] The bleomycin-detectable iron assay measures catalytic iron and is based on the observation that the anti-tumor antibiotic bleomycin, in the presence of catalytic iron, binds to and degrades DNA with the formation of a product that reacts with thiobarbituric acid to form a chromogen. Thus the assay detects iron complexes capable of catalyzing free-radical reactions in biological samples.[21,22] The binding of the bleomycin-iron complex to DNA makes the reaction site-specific and antioxidants rarely interfere. The bleomycin assay detects only "free" iron and not iron bound to specific transport proteins or to enzymes.

The ability of iron to participate in redox cycling makes it potentially hazardous by enabling it to participate in the generation of powerful oxidant species such as hydroxyl radical (metal-catalyzed Haber-Weiss reaction, below) and/or reactive iron-oxygen complexes such as ferryl or perferryl ion.[15] In several systems, the amount of free-radical generation is related to the amount of labile iron present[23] (Figure 89.1).

$$Fe^{3+} + O_2^{\bullet} \rightarrow Fe^{2+} + O_2$$
$$Fe^{2+} + H_2O_2 \rightarrow Fe^{3+} + {}^{-}OH + {}^{\bullet}OH$$
$$H_2O_2 + O_2^{\bullet} \xrightarrow{Fe^{3+}} {}^{-}OH + {}^{\bullet}OH + O_2$$

Iron also has a major role in lipid peroxidation, either directly or indirectly (through hydroxyl radicals or forming a perferryl ion) in which there is oxidative reaction of polyunsaturated lipids by removing hydrogen atoms from polyunsaturated fatty acids.[15]

A major advancement in understanding the important role of iron in the pathophysiology of tissue injury is the recognition that iron plays a role even in the absence of systemic iron overload. It is now known that specific defects in cellular iron metabolism and/or an increase in catalytic iron may be important in several disease processes not associated with iron overload.[17,24] In Friedreich's ataxia, there is an improper processing of iron because of the deficiency of the iron-chaperone protein frataxin, resulting in accumulation of iron in the mitochondria.[24] Deficiencies in pantothenate kinase, a key enzyme in coenzyme A synthesis, leads to iron depositions and brain damage.[24] In addition to these specific defects in cellular iron, there is now overwhelming evidence that increased catalytic iron from subcellular or other sources participates in tissue injury in a wide variety of common disease states. This has been demonstrated in many disease states including acute and chronic kidney disease, acute myocardial infarction, and neurodegenerative disorders.[25] In large part, the evidence consists of demonstrating an increase in catalytic iron and the ability of iron chelators to provide a protective effect, thus establishing a cause-effect relationship (Table 89.1).

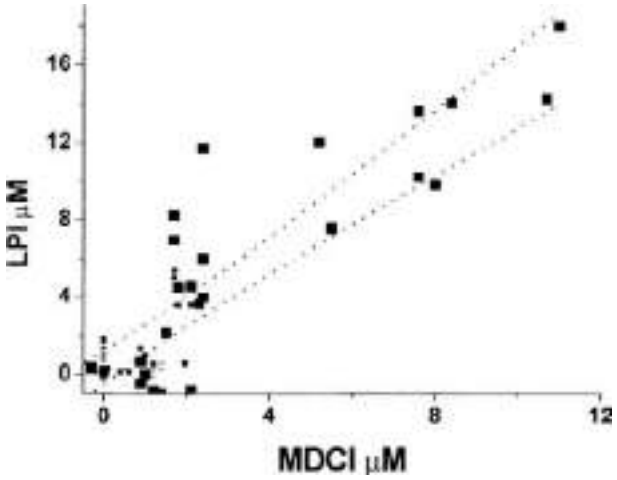

FIGURE 89.1 Labile plasma iron (LPI) in sera from thalassemic patients and its correlation with mobilizer-dependent chelatable iron (MDCI).

ROLE OF CATALYTIC IRON IN ACUTE KIDNEY INJURY

Catalytic Iron in Myoglobinuric Acute Kidney Injury

The first causative association of acute kidney injury with muscle injury (rhabdomyolysis) was described during the Battle of Britain.[26] We now recognize that the spectrum of etiologies for rhabdomyolysis, myoglobinuria, and renal failure has been expanded with the recognition of both traumatic and nontraumatic causes.[27] The most widely used model of myoglobinuric acute kidney injury is produced by subcutaneous or intramuscular injection of hypertonic glycerol.[28]

There are a number of studies that indicate a role for catalytic iron in rhabdomyolysis. There is a marked and specific increase in catalytic iron content in myoglobinuric acute kidney injury[29] (Figure 89.2). In addition, studies from different investigators have shown functional and histological protection in models of myoglobinuric acute kidney injury[12,30,31] (Fig. 89.2).

Because myoglobin is rich in heme iron, the prevailing dogma is that myoglobin from the muscle serves as an important source of iron in glycerol-induced acute kidney injury. However, several studies indicate that cytochrome P450 can also serve as a rich source of iron.[32] Cytochrome P450 is a heme-containing enzyme that can generate reactive oxygen metabolites. Baliga et al. have shown that cytochrome P450 is a significant source of catalytic iron in glycerol-induced acute renal failure, and inhibitors of cytochrome P450 provide significant protection.[29]

TABLE 89.1 Catalytic (Labile) Iron

What is catalytic iron?
- A transient iron pool of low-molecular-weight, weakly chelated iron that passes through the cell
- The broadest definition of labile iron pool (LIP) is that it consists of chemical forms that can participate in redox cycling (catalytic iron)
- LIP is less than 3% (70–90 mg) of total cellular iron (3–5 g)

Evidence for its participation in disease states:
- LIP (catalytic iron) is increased in disease states
- Iron chelators have a protective effect, establishing a cause-effect relationship

Catalytic iron is a common theme of cellular injury in disease states of:
- Acute and chronic kidney disease
- Acute myocardial infarction
- Neurodegenerative disorders

Catalytic Iron in Cisplatin-Induced Nephrotoxicity

The mechanism of cisplatin nephrotoxicity is not well known. Baliga et al. have shown that the exposure of LLC-PK$_1$ cells to cisplatin results in a significant increase in catalytic iron released into the medium (Figure 89.3). In addition, two iron chelators significantly protected against cisplatin-induced cytotoxicity (Fig. 89.3). In an *in vivo* study, rats treated with cisplatin have a marked increase in catalytic iron (Figure 89.4). An iron chelator provided marked functional (as measured by blood urea nitrogen and creatinine) (Fig. 89.4) and histological protection against cisplatin-induced acute kidney injury.[33]

Baliga et al. have also examined potential sources of catalytic iron in cisplatin-induced nephrotoxicity.[34] Using CYP2E1null (CYP2E1$^{-/-}$) mice, Liu and Baliga have demonstrated a pivotal role of CYP2E1 in cisplatin-induced nephrotoxicity (Figure 89.5, Table 89.2).[35] Incubation of CYP2E1$^{-/-}$ kidney slices with cisplatin results in a significant decrease in the generation of reactive oxygen metabolites and attenuation of cytotoxicity as compared to that of wild-type mice (CYP2E1$^{+/+}$). CYP2E1-null mice had marked functional and histological protection against cisplatin-induced renal injury, thus demonstrating the importance of cytochrome P450 2E1 in cisplatin nephrotoxicity. Taken together, these data support a critical role for iron in mediating tissue injury via hydroxyl radical (or a similar oxidant) in this model of nephrotoxicity.

Catalytic Iron in Gentamicin Nephrotoxicity

The mechanisms of gentamicin nephrotoxicity remain unknown.

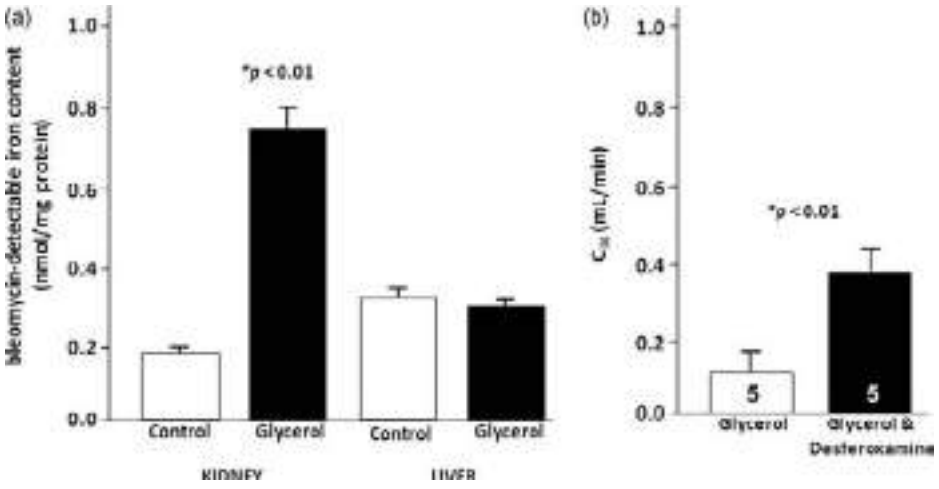

FIGURE 89.2 Glycerol-induced acute renal failure. Panel a. Bleomycin-detectable iron content in the kidneys and in the liver. Panel b. Effect of deferoxamine on glycerol-induced renal failure.

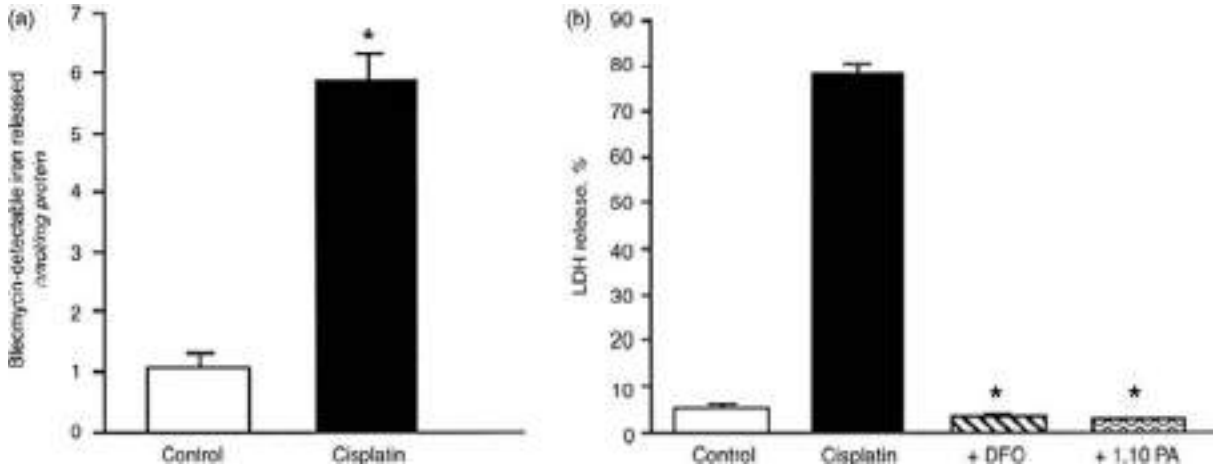

FIGURE 89.3 *In vitro* evidence suggesting a role for iron in cisplatin-induced nephrotoxicity. Panel A. Effect of cisplatin on catalytic iron released as measured by bleomycin-detectable iron in LLC-PK1 cells. Panel B. Effect of iron chelators on cisplatin-induced cytotoxicity as measured by lactate dehydrogenase (LDH) release in LLC-PK1 cells.

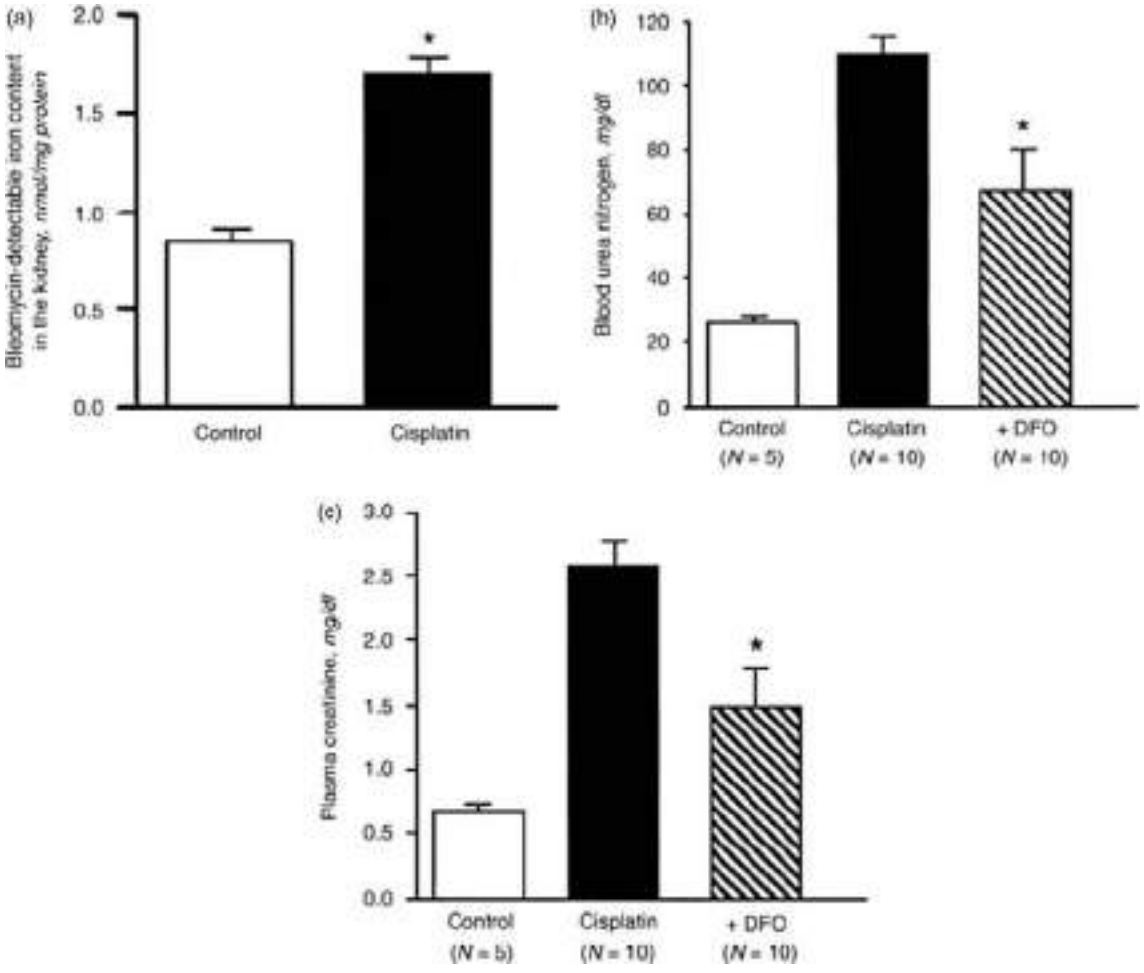

FIGURE 89.4 Cisplatin-induced acute kidney injury. Catalytic iron in the kidney (a) and the effect of the iron chelator deferoxamine (DFO) as measured by blood urea nitrogen (b) and plasma creatinine (c).

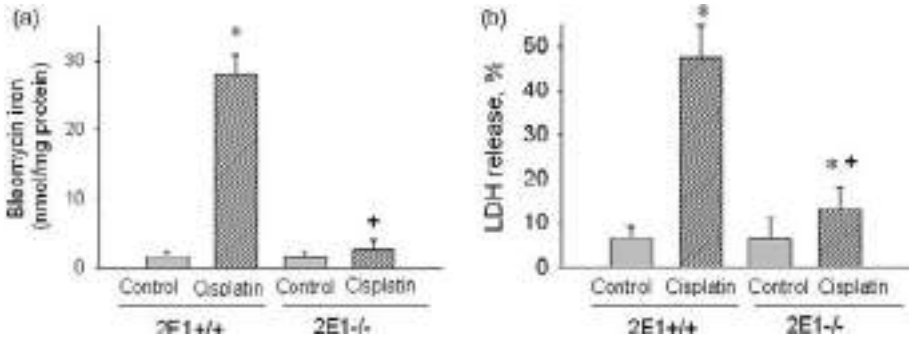

FIGURE 89.5 *In vitro* study using kidney slices from CYP2E1 +/+ and CYP2E1 − / − mice. Panel a. Catalytic iron release from kidney slices exposed to cisplatin. Panel b. Cytotoxicity of cisplatin to kidney slices as measured by lactate dehydrogenase (LDH) release.

TABLE 89.2 Renal Function and Catalytic Iron

	Blood Urea Nitrogen mg/dL	Serum Creatinine mg/dL	Creatinine Clearance mL/hour	Catalytic Iron nmol/mg Protein
CYP2E1 + / +				
Sham ($N = 6$ to 9)	17 ± 2	0.27 ± 0.02	7.21 ± 0.9	11.47 ± 0.18
Cisplatin ($N = 8$ to 14)	69 ± 2[a]	1.55 ± 0.23[a]	1.02 ± 0.2[a]	38.98 ± 3.88[a]
CYP2E1 − / −				
Sham ($N = 6$)	15 ± 3	0.27 ± 0.02	7.71 ± 0.5	6.54 ± 0.96
Cisplatin ($N = 10$)	32 ± 4[a,b]	0.47 ± 0.06[b]	6.24 ± 0.8[b]	12.08 ± 1.33[b]

[a] $P < 0.05$ *compared to the respective control.*
[b] $P < 0.05$ *compared to* CYP2e1 + / + *mice treated with cisplatin.*
Values are mean ± SE.
There is no significant difference in the control values between *CYP2e1* + / + and *CYP2e1* − / − .

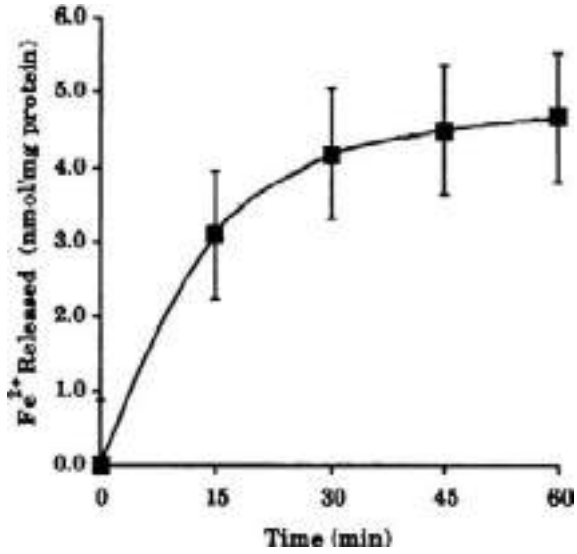

FIGURE 89.6 Time course of gentamicin-induced iron release from rat renal cortical mitochondria.

Gentamicin-Induced Mobilization of Iron from Renal Cortical Mitochondria

A source of iron not previously considered is iron-rich mitochondria, which contain heme as well as non-heme iron. Ueda et al. demonstrated that rat renal mitochondria incubated with gentamicin results in a time- and dose-dependent iron release as measured by the formation of the iron-bathophenanthroline complex FeII (BPS)3[36] (Figure 89.6). In addition, it was shown that gentamicin-induced iron mobilization from mitochondria is mediated by hydrogen peroxide. Direct addition of hydrogen peroxide to mitochondria results in release of iron. These results demonstrate that gentamicin induces the release of iron from mitochondria and that this is mediated through the generation of hydrogen peroxide. These results also indicate that mitochondria should be considered as a potential source of iron for the generation of other oxidant species or initiation of lipid peroxidation in other models of tissue injury.

Evidence Suggesting a Role for Iron in Gentamicin-Induced Acute Renal Failure in Rats

Superoxide and hydrogen peroxide may interact (with trace metals such as iron as the redox agent) to generate highly reactive and unstable oxidizing species including the hydroxyl radical. Several studies have in fact shown that agents that enhance the generation of hydrogen peroxide and superoxide anion by mitochondria also enhance generation of the hydroxyl radical. Walker et al. demonstrated that hydroxyl radical scavengers and iron chelators provide a marked protective effect on renal function in gentamicin-induced acute

renal failure in rats.[37] Data collected from several experiments are depicted in Figure 89.7. In addition, histological evidence of damage is markedly reduced by the interventional agents. Additional support for a role of iron-catalyzed free-radical generation has been provided by demonstrating that gentamicin-induced generation of hydroxyl radicals is reduced by iron chelators *in vitro*[38] and iron supplementation enhances gentamicin nephrotoxicity *in vivo*.[39,40] Taken together, it appears that reactive oxygen metabolites and catalytic iron play an important role in gentamicin nephrotoxicity.

Catalytic Iron in Contrast-Media-Associated Nephrotoxicity

Subjects undergoing either an intravenous pyelogram or a renal arteriogram have a marked increase in urinary catalytic iron accompanied by evidence of tubular injury, documented by an increase in urinary alkaline phosphatase and N-acetyl-β-glucosaminidase[13] (Figure 89.8). Since the effect of catalytic iron is to increase oxidative stress, unsurprisingly there is experimental evidence for the role of oxidants in contrast-induced acute kidney injury.[41–43] In human studies Efrati et al. reported an increase in urinary F2-isoprotane levels after coronary angiography,[44] and Drager et al. reported a several-fold increase in urinary isoprostane compared to the control group after cardiac catheterization.[45]

These human studies indicate an association between catalytic iron and oxidative stress with contrast-induced nephropathy, but they do not establish a cause-effect relationship. Although there do not appear to be any satisfactory animal models of contrast-induced acute kidney injury,[46] Vari et al., utilizing a multi-insult model,[47] examined the effect of an iron chelator on renal function. An infusion of contrast was associated with a significant decrease in creatinine clearance, which was prevented in rabbits pretreated with an iron chelator, suggesting an important role of catalytic iron in this model[48] (Table 89.3).

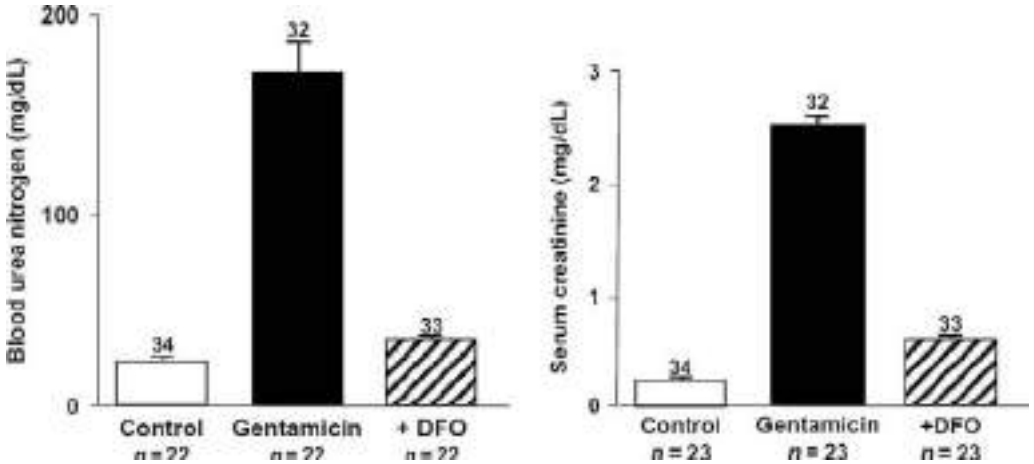

FIGURE 89.7 Effect of deferoxamine in gentamicin-induced acute renal failure.

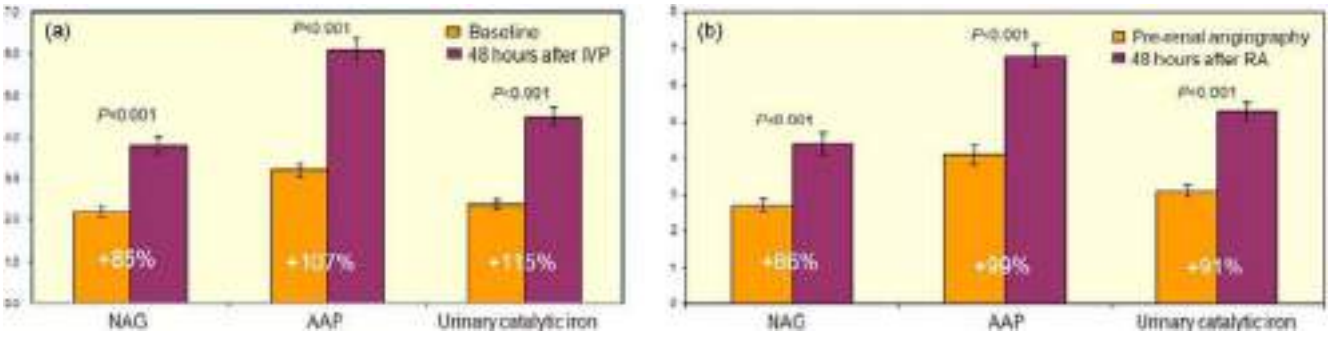

FIGURE 89.8 Catalytic iron and measures of renal injury after administration of contrast. Panel a. Intravenous pyelogram. Panel b. Renal angiogram.

TABLE 89.3 Animal Model of Contrast-Induced Nephropathy

	Group 1 Saline only		Group 2 DFO	
	Pre-	Post-	Pre-	Pre-
CCR (mL/min)	8.64 ± 1	4.96 ± 1.5[a]	11.6 ± 1.5	10.2 ± 1.6

[a] $P \leq 1$; *pre- versus post-contrast infusion.*

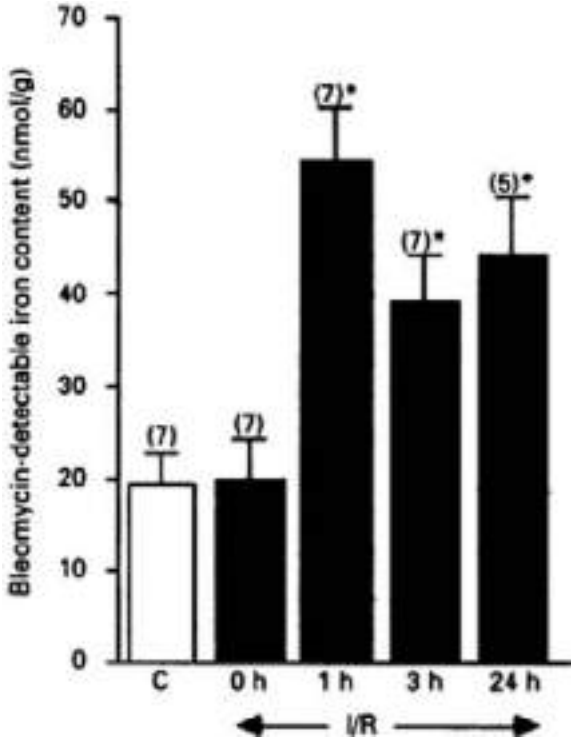

FIGURE 89.9 Bleomycin-detectable iron in plasma urea nitrogen in the kidneys of rats after ischemia and various periods of reperfusion.

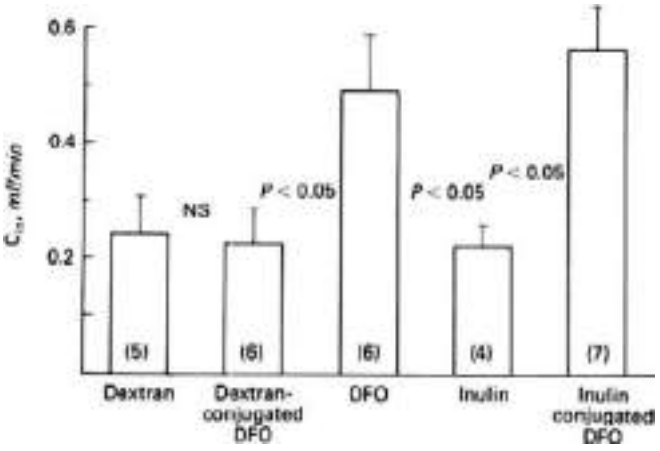

FIGURE 89.10 Effect of an iron chelator on renal function after ischemia.

Catalytic Iron in Ischemia-Reperfusion Injury

Ischemia-reperfusion is an important cause of acute kidney injury. In this section, evidence for the role of catalytic iron in this injury is reviewed. In addition, we briefly describe the role of catalytic iron in cardiac ischemia-reperfusion injury to provide supportive evidence for these mechanisms in cellular injury.

There is a marked increase in catalytic iron after ischemia-reperfusion injury[49] (Figure 89.9), and an iron chelator has been shown to be protective[50,51] (Figure 89.10). The amount of circulating redox-active iron has been shown to increase significantly in an experimental model of ischemia-reperfusion injury, and an infusion of apotransferrin (but not iron-saturated apotransferrin) results in a dose-dependent improvement in renal function following reperfusion.[52] In addition, studies related to neutrophil gelatinase-associated lipocalin (NGAL),[53,54] which is an important iron-transporting and -translocating compound, provide evidence for the importance of iron in acute kidney injury.[55] NGAL is one of the most upregulated genes and proteins in the kidney following ischemic insult,[55] and infusion of NGAL protein has been demonstrated to be protective of renal ischemia-reperfusion injury.[54]

There is a 30-fold increase in catalytic iron during experimental cardiac ischemic injury.[56] This increase in the cellular catalytic iron pool is associated with severe oxidative stress.[56–58] Two iron chelators, deferiprone and deferoxamine, have been demonstrated to protect against experimental cardiac ischemia-reperfusion injury,[59–61] and iron loading has been demonstrated to further increase cardiac ischemia-reperfusion injury.[59] It is of great therapeutic significance that deferoxamine has also been shown to improve outcomes in humans following coronary artery bypass graft surgery.[62] Taken together, the body of scientific and clinical data supporting the importance of the role of iron in the pathogenesis of ischemic injury is compelling.

CATALYTIC IRON IN CHRONIC KIDNEY DISEASE

Catalytic Iron in Experimental Glomerular Disease

Several studies have examined the role of iron in models of leukocyte-dependent and -independent glomerular disease. In an anti-glomerular basement membrane antibody model, a well-characterized model of complement- and neutrophil-dependent glomerular injury, Boyce et al. reported that an iron chelator

significantly attenuates proteinuria[63] (Figure 89.11). The ability of glomerular cells to generate oxidants suggests that they may act as important mediators of injury in glomerular diseases that lack infiltrating leukocytes. A single intravenous injection of puromycin aminonucleoside in rats results in an animal model of minimal change disease. Ueda et al. have shown that catalytic iron (measured as bleomycin-detectable iron) is markedly increased in glomeruli from nephrotic rats, and that an iron chelator prevents an increase in catalytic iron and provides complete protection against proteinuria[64,65] (Figure 89.12).

Cytochrome P450 appears to be a source of this catalytic iron, at least in part. Baliga et al. have demonstrated that cytochrome treatment of PAN results in a significant loss of glomerular cytochrome P-450 content accompanied by a marked increase in catalytic iron. The loss of CYP content can be prevented by CYP inhibitors, which also prevent the rise in catalytic iron. Administration of CYP inhibitors also resulted in a marked decrease in proteinuria.[66] In an *in vitro* study using glomerular epithelial cells (GEC), CYP inhibitors also markedly prevented a PAN-induced increase in catalytic iron (Figure 89.13) and hydroxyl radical formation accompanied by significant protection against PAN-induced cytotoxicity. Taken together these data indicate that CYP, a group of heme protein, may serve as a significant source of this catalytic iron. In addition, they have shown with *in vivo* and *in vitro* studies that cytochrome P450 2B1, an isozyme present in the glomerulus, is a source of catalytic iron that participates in glomerular injury in this model.[67,68]

Passive Heymann nephritis, induced by a single intravenous injection of anti-Fx1A, is a complement-dependent model of membranous nephropathy in humans. The role of iron in this model has been delineated by demonstration of an increase in catalytic iron, both *in vivo* and *in vitro*, and reduction in proteinuria by either an iron chelator or an iron-deficient diet[30,69] (Figure 89.14).

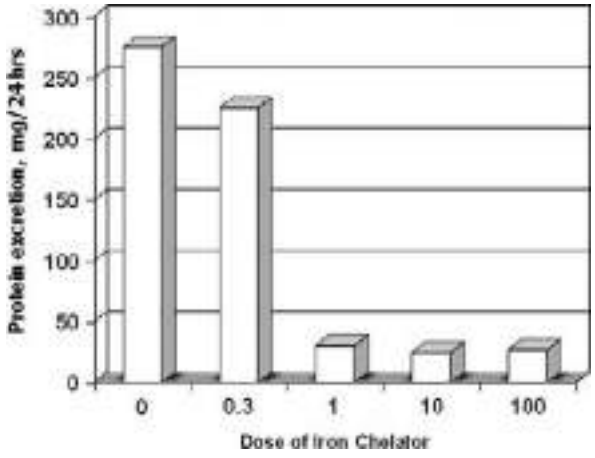

FIGURE 89.11 Effect of an iron chelator on proteinuria in anti-GBM antibody disease.

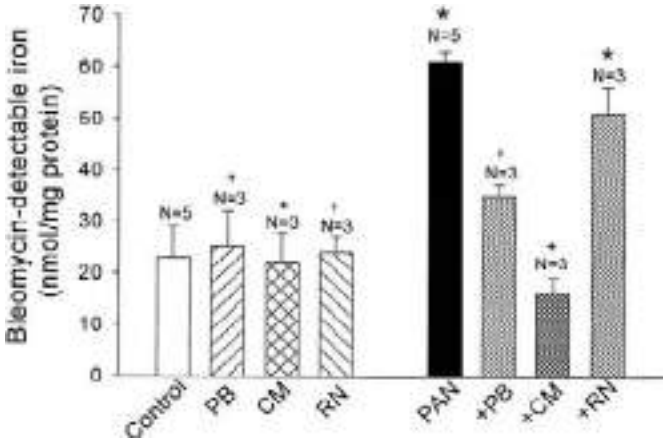

FIGURE 89.13 Role of cytochrome P-450 in PAN-induced glomerular epithelial cell release of catalytic iron.

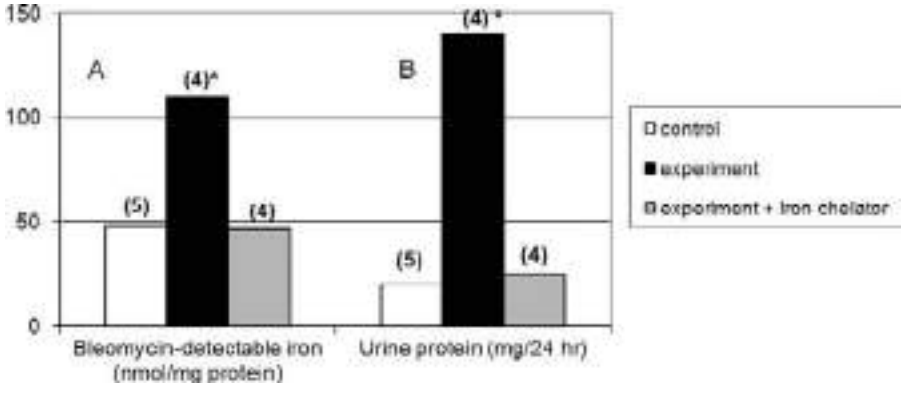

FIGURE 89.12 Effect of an iron chelator on bleomycin-detectable iron in (a) glomeruli and (b) proteinuria from rats injected with puromycin aminonucleoside.

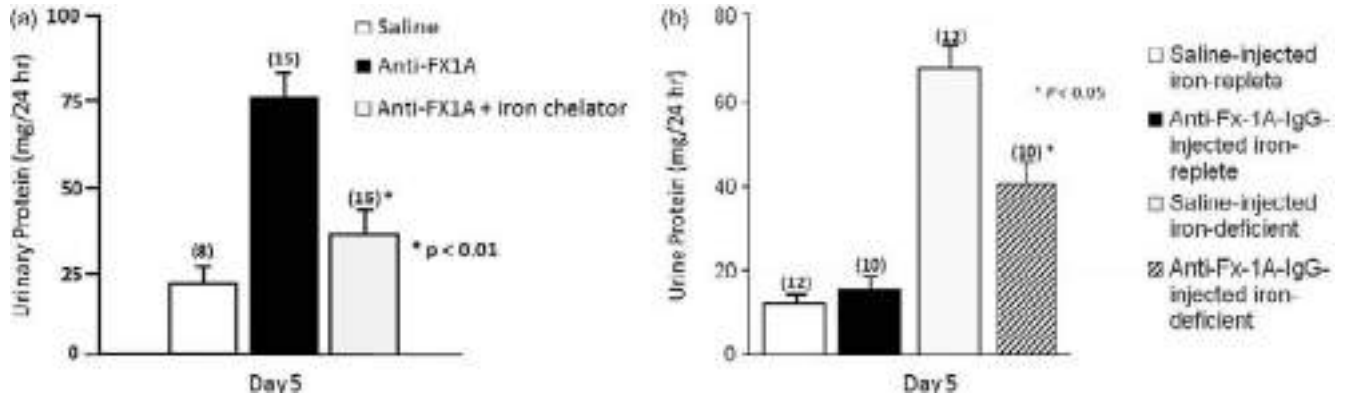

FIGURE 89.14 Effect of an iron chelator (Panel a) and an iron-deficient diet (Panel b) on proteinuria in the Passive Heymann Nephritis model of membranous nephropathy.

Role of Iron in Experimental Progressive Kidney Disease

A major determinant of the degree and rate of progression of renal failure is the severity of the tubular interstitial injury. Several lines of evidence support the role of iron in progressive renal disease. These include demonstration of increased iron in the kidney; enhanced oxidant generation, which provides a mechanism by which iron can be mobilized; and the beneficial effect of iron-deficient diets and iron chelators. Rats with proteinuria have increased iron content in proximal tubular cells, which is the only independent predictor of both functional and structural damage.[70] Similarly, in a remnant kidney model of progressive kidney disease, there is a substantial iron accumulation associated with increased evidence of lipid peroxidation. The sources of increased iron in the kidney have not been well-delineated, but Alfrey et al. have suggested that urinary transferrin provides a potential source of iron.[71,72]

Several studies have demonstrated an important role of iron in progressive kidney disease. An iron chelator significantly reduces iron accumulation and tubular damage in the rat remnant kidney, a model for progressive renal disease.[73] Remuzzi et al. have shown that rats fed an iron-deficient diet have a significant reduction in proteinuria and develop less glomerulosclerosis.[74] It was reported that an iron-deficient diet (Figure 89.15) or iron chelators prevent the development of tubulointerstitial disease and renal functional deterioration in nephrotoxic serum nephritis.[72,75]

Catalytic Iron in Human Disease

While there is substantial evidence for the role of oxidants and iron derived from models of glomerular disease as well as progressive renal failure, there is little information on the potential role of these mechanisms in human disease. There are many differences

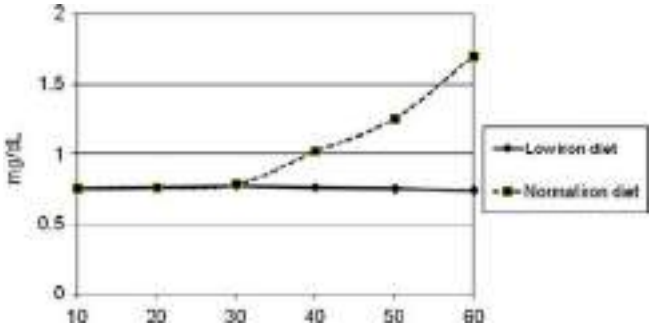

FIGURE 89.15 Effect of a low-iron diet in halting progression of kidney disease. Feeding a low-fat diet to rats with nephrotoxic serum nephritis prevented a rise in serum creatinine and provided histological protection.

between animal models and glomerular disease in humans. For example, the animal model of minimal change disease is a toxic model whereas the mechanism of minimal change disease in humans is not known. Similarly, the anti-Fx1A antibody, which is used for the animal model of membranous nephropathy, has been difficult to demonstrate in human membranous nephropathy. Indeed, the lessons from animal models of acute kidney injury have been disappointing when attempting to translate to human disease. However, although the information from human studies is limited, it does appear to support the notion that mechanisms observed in animal models may be applicable to human disease.

Catalytic Iron in Diabetic Nephropathy

Early in the course of diabetic kidney disease in humans there is an increase in urinary iron excretion.[76] Our data demonstrate that patients with overt diabetes have a marked increase in urinary catalytic iron (Figure 89.16A). Urinary catalytic iron is not merely a reflection of albuminuria, because patients with

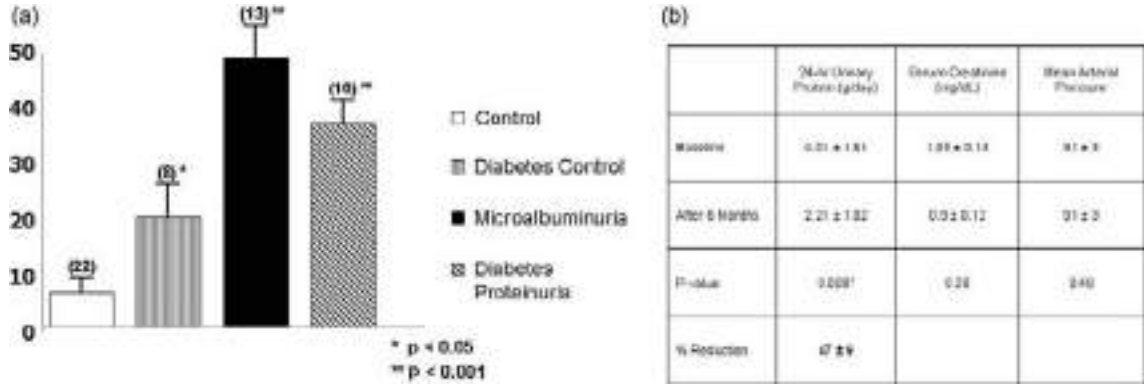

FIGURE 89.16 Urinary catalytic iron in patients with diabetic nephropathy (Panel a) and the effect of the iron chelator deferiprone on proteinuria (Panel b).

microalbuminuria also have a marked and highly significant increase in urinary catalytic iron. Some patients in the diabetic control group who do not have microalbuminuria have high catalytic iron, leading us to postulate that urinary catalytic iron precedes the onset of microalbuminuria and may predict patients at risk for diabetic nephropathy.

Adult patients with a diagnosis of diabetes mellitus and significant abnormal albumin excretion but with serum creatinine levels <1.2 mg/dL were included in a single-center, single-arm, open-label, proof-of-concept study to evaluate the safety and efficacy of the oral iron chelator deferiprone in reducing albuminuria.[77] Patients received standard of care and enalapril, which was kept constant throughout the study. Deferiprone, an oral iron chelator, was administered in a daily dose of ~50 mg/kg in three divided doses for nine months. There were 37 patients (21 males and 16 females) enrolled in the study, with a mean age of 51.27 (± 1.67) years. Deferiprone did not affect the blood glucose control as measured by HbA1c.The administration of deferiprone resulted in a significant decrease in the albumin-to-creatinine ratio, as shown in Figure 89.16, Panel B. There was no significant effect on renal function as measured by serum creatinine. The calculated mean arterial blood pressure (MAP) declined from a baseline value of 100.78 ± 1.7 to 97 ± 0.6 at three months ($p = 0.2$), but remained relatively stable from then on to 6 months (96.24 ± 0.7; $p = 0.6$) and 9 months. Future randomized, double-blind trials, with careful monitoring of safety issues, may lead to use of a new class of agents for the treatment of diabetic nephropathy.

Catalytic Iron in Progression

Using the urinary catalytic iron assay described before, we have shown a marked increase in patients who have biopsy-proven glomerulonephritis (Figure 89.17A). In addition, Nankivell et al. have reported increased iron content in patients with chronic kidney disease.[78]

We conducted a single-center, prospective, single-arm, open-label, proof-of-concept study to evaluate the safety and efficacy of an oral iron chelator, deferiprone, in patients with biopsy-proven glomerulonephritis. We enrolled 15 patients with biopsy-proven idiopathic glomerulonephritis who had persistent proteinuria despite treatment with steroids and/or cyclophosphamides. Secondary glomerulonephritis was ruled out by appropriate serologic tests. Two patients complained of severe nausea and vomiting after administration of the first dose of the drug and did not participate in the study.

The thirteen patients who completed the study were considered for analysis. Of the remaining 13 subjects there were six males. The age at study entry was 26.76 ± 4 years; four were pediatric subjects. Among the 13 patients, four had membranous nephropathy, three had focal segmental glomerulosclerosis (FSGS), three had diffuse proliferative glomerulonephritis, two had mesangial proliferation, and one had chronic sclerosing glomerulonephritis. These patients had persistent proteinuria despite receiving steroids (seven subjects) or steroids and cyclophosphamides (six subjects).

All patients were monitored clinically and with laboratory evaluation for the evidence of development of adverse effects of deferiprone. Three patients noticed dark coloration of urine during administration of the medication. No patients developed arthritis. No patients developed agranulocytosis. Bilirubin and SGOT and SGPT were not significantly different from baseline at the end of the study. Deferiprone therapy reduced the proteinuria from 4.05 ± 0.46 g/day (range 1.2–6.5) to 2.21 ± 1.61 g/day by six months, an overall reduction of 47 ± 9% (Figure 89.1). Seven of 13 subjects had >50% improvement in proteinuria and three had <600 mg/day proteinuria after therapy. As shown in Figure 89.17, Panels B, C, and D, treatment with the iron chelator significantly decreased the amount of

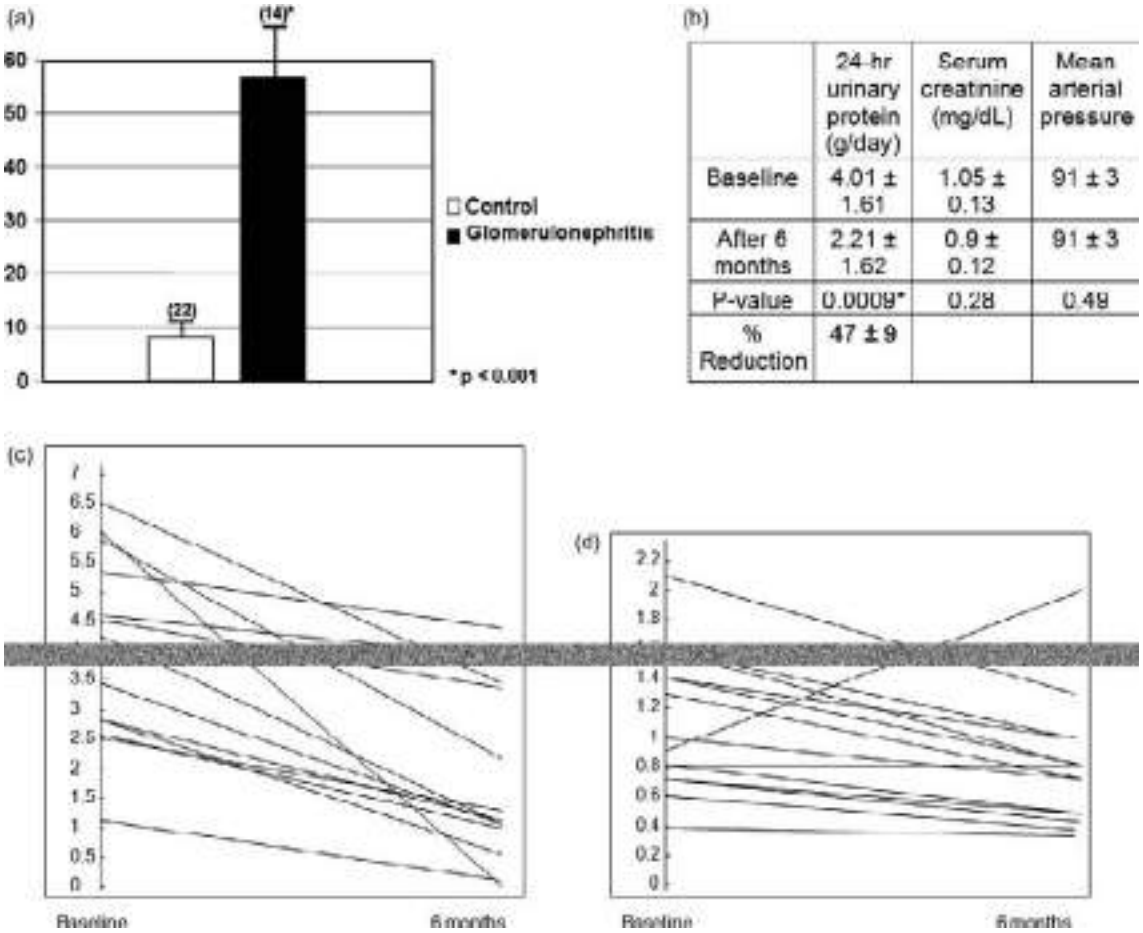

	24-hr urinary protein (g/day)	Serum creatinine (mg/dL)	Mean arterial pressure
Baseline	4.01 ± 1.61	1.05 ± 0.13	91 ± 3
After 6 months	2.21 ± 1.62	0.9 ± 0.12	91 ± 3
P-value	0.0009*	0.28	0.49
% Reduction	47 ± 9		

FIGURE 89.17 Urinary catalytic iron in patients with biopsy-proven glomerulonephritis (Panel a); effect of deferiprone on urinary protein and serum creatinine in patients with steroid-resistant glomerulonephritis (Panel b). Panels c and d depict individual patient data.

total urinary protein in patients with glomerulonephritis.[79] Serum creatinine was 1.10 ± 0.15 before and 0.90 ± 0.10 (n = 11) at the end of the study period. Our data indicate an increase of catalytic iron in patients with glomerulonephritis and that treatment with an oral iron chelator leads to a reduction in proteinuria.

There is at least one published study in the literature in which the effect of a metal chelator on progressive kidney disease has been examined. Lin et al. have shown that chelation therapy with ethylenediaminetetraacetic acid (EDTA) in patients with chronic renal insufficiency results in a reduced rate of decline in the glomerular filtration rate[80] (Figure 89.18). The authors attribute the beneficial effect to the chelation of lead, which also participates in the Fenton reaction. However, given the affinity constants for iron and lead, the large experimental evidence for the role of iron in kidney disease, and the demonstrated efficacy of EDTA in enhancing excretion of urinary iron, we believe that the beneficial effects are more likely to be explained by the chelation of iron rather than lead.[81]

CONCLUDING COMMENTS

One has to be cautious in extrapolating results from animal studies to humans. The results from clinical trials in acute kidney injury based on animal models have not been encouraging. These studies to prevent or treat acute kidney injury using atrial natriuretic peptide,[82,83] insulin-like growth factor,[84,85] thyroxine,[86,87] and furosemide[88,89] have yielded negative results. Nonetheless, evidence that catalytic iron appears to be involved in a variety of models of acute kidney injury suggests that it may be a common mechanism of tissue injury (Table 89.4). Additionally, limited human data support the possibility of similar pathophysiological mechanisms in humans. Demonstration of an increase in catalytic iron in humans and the availability of iron chelators with a favorable side-effect profile for short-term use make them attractive for evaluating their efficacy and safety in preventing or treating acute kidney injury.

There are several points from animal and human studies related to halting progression with a metal

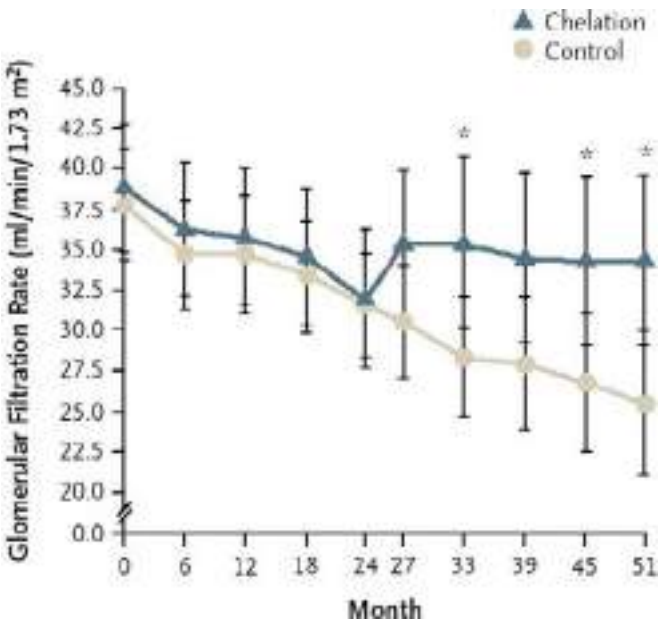

FIGURE 89.18 Estimated mean (±2 SE) glomerular filtration rate according to time in the EDTA chelation group (N = 31) and the control group (N = 30) during the observation and intervention periods.

TABLE 89.4 Catalytic Iron in Models of Acute Kidney Injury

	Genta-micin	Cisplatin	Ischemia-Reperfusion	Myoglobin	Contrast
Oxidative Stress	Yes	Yes	Yes	Yes	Yes
Catalytic Iron	Yes	Yes	Yes	Yes	Yes
Iron Chelator (protective effect)	Yes	Yes	Yes	Yes	Yes

chelator that are worth noting. Based on animal studies, it is conceivable that iron chelators may provide a beneficial effect, not only by reducing proteinuria but also by directly preserving the tubulointerstitial region, independent of its effect on proteinuria. Bicarbonate supplementation was shown to slow the rate of progression of renal failure to ESRD without reducing proteinuria.[90] In an open-label trial, pirfenidone was shown to slow the loss of kidney function in patients with focal segmental sclerosis with no reduction in proteinuria.[91] In a model of diabetic nephropathy, pirfenidone was shown to reduce generation of reactive oxidant species and significantly reduce mesangial matrix expansion without affecting albuminuria. In studies by Alfrey, an iron-deficient diet or iron chelator provided both functional and histological protection against progression in a model of nephrotoxic serum without affecting proteinuria.[71,75] Similarly, in a study by Lin et al., EDTA provided protection against progression without reducing urinary protein.[80] Thus, clinical studies targeted toward halting progression should focus not only on short-term studies on proteinuria, but they need be of sufficient duration to evaluate the effect on renal function.

The evidence reviewed suggests the possibility of using iron chelators to halt the progression of kidney disease. As a practical matter, the long-term use required for chronic kidney disease makes oral iron chelators more attractive than parenteral medications. Of the two oral iron chelators currently approved for human use in iron overload states, deferasirox has been shown to have some nephrotoxicity[92] but may nonetheless be potentially beneficial in patients with kidney disease. Deferiprone (1,2-dimethyl-3-hydroxypyridin-4-1) has been approved for treatment of iron overload states in Europe, India, and recently North America. In addition to its suitability for long-term treatment (because of oral administration), the high-membrane permeability of deferiprone is well documented, as shown by its capacity to access and deplete intracellular iron pools.[24] In addition, a recent study has demonstrated its ability to remove labile iron from nuclei, endosomes, and mitochondria.[24] The major adverse effect reported so far in several thousand patients receiving deferiprone for periods of up to 14 years is transient agranulocytosis in less than 1% of patients. Based on the collective evidence to date, randomized, controlled, double-blind trials may be warranted to evaluate the efficacy and safety of iron chelators to halt progression of chronic kidney disease.

References

[1] Chertow GM, Burdick E, Honour M, Bonventre JV, Bates DW. Acute kidney injury, mortality, length of stay, and costs in hospitalized patients. J Am Soc Nephrol 2005;16(11):3365–70.
[2] Mehta RL, Kellum JA, Shah SV, Molitoris BA, Ronco C, Warnock DG, et al. Acute kidney injury network (AKIN): report of an initiative to improve outcomes in acute kidney injury. Crit Care 2007;11(2):R31.
[3] Lafrance J-P, Miller DR. Acute kidney injury associates with inreased long-term mortality. J Am Soc Nephrol 2010;21: 345–52.
[4] Hobson CE, Yavas S, Segal MS, Schold JD, Tribble CG, Layon AJ, et al. Acute kidney injury is associated with increased long-term mortality after cardiothoracic surgery. Circulation 2009;119:2444–53.
[5] Hsu C. Linking the population epidemiology of acute renal failure, chronic kidney disease and end-stage renal disease. Curr Opin Nephrol Hypertens 2007;16:221–6.
[6] Triverio P-A, Martin P-Y, Romand J, Pugin J, Perneger T, Saudan P. Long-term prognosis after acute kidney injury requiring renal replacement therapy. Nephrol Dial Transplant 2009;24(7):2186–9.
[7] Coresh J, Selvin E, Stevens LA, Manzi J, Kusek JW, Eggers P, et al. Prevalence of chronic kidney disease in the United States. JAMA 2007;298(17):2038–47.
[8] Xue JL, Ma JZ, Louis TA, Collins AJ. Forecast of the number of patients with end-stage renal disease in the United States to the year 2010. J Am Soc Nephrol 2001;12:2753–8.

[9] Sarnak MJ, Levey AS, Schoolwerth AC, Coresh J, Culleton BF, Hamm LL, et al. Kidney disease as a risk factor for development of cardiovascular disease: a statement from the American heart association councils on kidney in cardiovascular disease, high blood pressure research, clinical cardiology, and epidemiology and prevention. Circulation 2003;108(17):2154–69.
[10] Szczech LA, Lazar IL. Projecting the United States ESRD population: Issues regarding treatment of patients with ESRD. Kidney Int 2004;66(Suppl. 90):S3–7.
[11] Lambers Heerspink H, Greene T, Lewis JB, Raz I, Rohde RD, Hunsicker LG, et al. Effects of sulodexide in patients with type 2 diabetes and persistent albuminuria. Nephrol Dial Transplant 2007;23(6):1946–54.
[12] Zager RA. Combined mannitol and deferoxamine therapy for myohemoglobinuric renal injury and oxidant tubular stress. Mechanistic and therapeutic implications. J Clin Invest 1992;90:711–9.
[13] Rajapurkar M, Gang S, Hegde U, Gohel K, Shah SV. Study of urinary catalytic (bleomycin-detectable) iron following radiocontrast exposure in healthy kidney donors [abstract]. J Am Soc Nephrol 2007;18:575A.
[14] Kruszewski M. The role of labile iron pool in cardiovascular diseases. Acta Biochim Pol 2004;51(2):471–80.
[15] Halliwell B, Gutteridge JM. Role of free radicals and catalytic metal ions in human disease: an overview. Methods Enzymol 1990;186:1–85.
[16] Kakhlon O, Cabantchik ZI. The labile iron pool: characterization, measurement, and participation in celullar processes. Free Rad Biol Med 2002;33(8):1037–46.
[17] Andrews NC. Forging a field: the golden age of iron biology. Blood 2008;112(2):219–30.
[18] Ganz T, Nemeth E. Hepcidin and disorders of iron metabolism. Annu Rev Med 2011;62:347–60.
[19] Esposito BP, Breuer W, Slotki I, Cabantchik ZI. Labile iron in parenteral iron formulations and its potential for generating plasma nontransferrin-bound iron in dialysis patients. Euro J Clin Invest 2002;32(Suppl. 1):42–9.
[20] Lai CC, Huang WH, Klevay LM, Gunning III WT, Chiu TH. Antioxidant enzyme gene transcription in copper-deficient rat liver. Free Radic Biol Med 1996;21:233–40.
[21] Gutteridge JMC, Rowley DA, Halliwell B. Superoxide-dependent formation of hydroxyl radicals in the presence of iron salts. Detection of 'free' iron in biological systems by using bleomycin-dependent degradation of DNA. Biochem J 1981;199: 263–5.
[22] Gutteridge JMC, Cao W, Chevion M. Bleomycin-detectable iron in brain tissue. Free Rad Res Comm 1991;11(6):317–20.
[23] Esposito BP, Breuer W, Sirankapracha P, Pootrakul P, Hershko C, Cabantchik I. Labile plasma iron in iron overload: redox activity and susceptibility to chelation. Blood 2003;102(7): 2670–7.
[24] Sohn YS, Breuer W, Munnich A, Cabantchik ZI. Redistribution of accumulated cell iron: a modality of chelation with therapeutic implications. Blood 2008;111(3):1690–9.
[25] Boddaert N, Le Quan Sang KH, Rötig A, Leroy-Willig A, Gallet S, Brunelle F, et al. Selective iron chelation in Friedreich ataxia: biologic and clinical implications. Blood 2007;110(1):401–8.
[26] Bywaters EGL, Beall D. Crush injuries with impairment of renal function. Br Med J 1941;1:427–32.
[27] Gabow PA, Kaehny WD, Kelleher SP. The spectrum of rhabdomyolysis. Medicine 1982;61(3):141–52.
[28] Hostetter TH, Wilkes BM, Brenner BM. Renal circulatory and nephron function in experimental acute renal failure. In: 1st ed. Brenner BM, Lazarus JM, editors. Acute renal failure, Vol 1. Philadelphia: W.B. Saunders Company; 1983. p. 99–115.
[29] Baliga R, Zhang Z, Baliga M, Shah SV. Evidence for cytochrome P-450 as a source of catalytic iron in myoglobinuric acute renal failure. Kidney Int 1996;49:362–9.
[30] Shah SV. Evidence suggesting a role for hydroxyl radical in passive Heymann nephritis in rats. Am J Physiol 1988;254(23):F337–44.
[31] Paller MS. Hemoglobin- and myoglobin-induced acute renal failure in rats: role of iron in nephrotoxicity. Am J Physiol 1988;255(24):F539–44.
[32] Paller MS, Jacob HS. Cytochrome P-450 mediates tissue-damaging hydroxyl radical formation during reoxygenation of the kidney. Proc Natl Acad Sci USA 1994;91:7002–6.
[33] Baliga R, Zhang Z, Baliga M, Ueda N, Shah SV. *In vitro* and *in vivo* evidence suggesting a role for iron in cisplatin-induced nephrotoxicity. Kidney Int 1998;53:394–401.
[34] Baliga R, Zhang Z, Baliga M, Ueda N, Shah SV. Role of cytochrome P-450 as a source of catalytic iron in cisplatin-induced nephrotoxicity. Kidney Int 1998;54:1562–9.
[35] Liu H, Baliga R. Cytochrome P450 2E1 null mice provide novel protection against cisplatin-induced nephrotoxicity and apoptosis. Kidney Int 2003;63:1687–96.
[36] Ueda N, Guidet B, Shah SV. Gentamicin-induced mobilization of iron from renal cortical mitochondria. Am J Physiol 1993;265 (34):F435–9.
[37] Walker PD, Shah SV. Evidence suggesting a role for hydroxyl radical in gentamicin-induced acute renal failure in rats. J Clin Invest 1988;81:334–41.
[38] Yang CL, Du XH, Han YX. Renal cortical mitochondria are the source of oxygen free radicals enhanced by gentamicin. Renal Failure 1995;17(1):21–6.
[39] Kays SE, Crowell WA, Johnson MA. Iron supplementation increases gentamicin nephrotoxicity in rats. J Nutr 1991;121:1869–75.
[40] Ben Ismail TH, Ali BH, Bashir AA. Influence of iron, deferoxamine and ascorbic acid on gentamicin-induced nephrotoxicity in rats. Gen Pharmacol 1994;25(6):1249–52.
[41] Parvez Z, Rahman MA, Moncada R. Contrast media-induced lipid peroxidation in the rat kidney. Invest Radiol 1989;24:697–702.
[42] Bakris GL, Lass N, Gaber AO, Jones JD, Burnett Jr JC. Radiocontrast medium-induced declines in renal function: a role for oxygen free radicals. Am J Physiol 1990;258:F115–20 [Renal Fluid Electrolyte Physiol 27].
[43] Yoshioka T, Fogo A, Beckman JK. Reduced activity of antioxidant enzymes underlies contrast media-induced renal injury in volume depletion. Kidney Int 1992;41:1008–15.
[44] Efrati S, Dishy V, Averbukh M, Blatt A, Krakover R, Weisgarten J, et al. The effect of N-acetylcysteine on renal function, nitric oxide, and oxidative stress after angiography. Kidney Int 2003;64(6):2182–7.
[45] Drager LF, Andrade L, Barros De Toledo JF, Laurindo FR, Machado Cesar LA, Seguro AC. Renal effects of N-acetylcysteine in patients at risk for contrast nephropathy: decrease in oxidant stress-mediated renal tubular injury. Nephrol Dial Transplant 2004;19(7):1803–7.
[46] Sandler CM. Contrast-agent-induced acute renal dysfunction–is iodixanol the answer? N Engl J Med 2003;348(6):551–3.
[47] Vari RC, Natarajan LA, Whitescarver SA, Jackson BA, Ott CE. Induction, prevention and mechanisms of contrast media-induced acute renal failure. Kidney Int 1988;33(3):699–707.
[48] Hanss BG, Valencia SH, Shah SV, Vari RC. The iron chelator deferoxamine prevents contrast media induced acute renal failure in the rabbit [abstract]. J Am Soc Nephrol 1990;1(4):612.
[49] Baliga R, Ueda N, Shah SV. Increase in bleomycin-detectable iron in ischaemia/reperfusion injury to rat kidneys. Biochem J 1993;291(3):901–5.
[50] Paller MS, Hedlund BE. Role of iron in postischemic renal injury in the rat. Kidney Int 1988;34:474–80.

[51] Huang H, He Z, Roberts II LJ, Salahudeen AK. Deferoxamine reduces cold-ischemic renal injury in a syngeneic kidney transplant model. Am J Transplant 2003;3:1531–7.
[52] de Vries B, Walter SJ, von Bonsdorff L, Wolfs TG, van Heurn LW, Parkkinen J, et al. Reduction of circulating redox-active iron by apotransferrin protects against renal ischemia-reperfusion injury. Transplantation 2004;77(5):669–75.
[53] Yang T, Brittenham GM, Dong W-Q, Levy MN, Obejero-Paz CA, Kuryshev YA, et al. Deferoxamine prevents cardiac hypertrophy and failure in the gerbil model of iron-induced cardiomyopathy. J Lab Clin Med 2003;142(5):332–40.
[54] Mishra J, Mori K, Ma Q, Kelly C, Yang J, Mitsnefes M, et al. Amelioration of ischemic acute renal injury by neutrophil gelatinase-associated lipocalin. J Am Soc Nephrol 2004;15:3073–82.
[55] Devarajan P. Update on mechanisms of ischemic acute kidney injury. J Am Soc Nephrol 2006;17(6):1503.
[56] Voogd A, Sluiter W, van Eijk HG, Koster JF. Low molecular weight iron and the oxygen paradox in isolated rat hearts. J Clin Invest 1992;90:2050–5.
[57] Nath KA, Norby SM. Reactive oxygen species and acute renal failure. Am J Med 2000;109:555–78.
[58] Kruszewski M. Labile iron pool: the main determinant of cellular response to oxidative stress. Mutat Res 2003;531:81–92.
[59] van der Kraaij AMM, Mostert LJ, van Eijk HG, Koster JF. Iron-load increases the susceptibility of rat hearts to oxygen reperfusion damage. Protection by the antioxidant (+)-cyanidanol-3 and deferoxamine. Circulation 1988;78:442–9.
[60] van der Kraaij AMM, van Eijk HG, Koster JF. Prevention of postischemic cardiac injury by the orally active iron chelator 1,2-dimethyl-3-hydroxy-4-pyridone (L1) and the antioxidant (+)-cyanidanol-3. Circulation 1989;80:158–64.
[61] Nicholson SC, Squier M, Ferguson DJP, Nagy Z, Westaby S, Evans RD. Effect of desferrioxamine cardioplegia on ischemia-reperfusion in isolated rat heart. Ann Thorac Surg 1997;63:1003–11.
[62] Paraskevaidis JA, Iliodromitis EK, Vlahakos D, Tsiapras DP, Nikolaidis A, Marathias A, et al. Deferoxamine infusion during coronary artery bypass grafting ameliorates lipid peroxidation and protects the myocardium against reperfusion injury: immediate and long-term significance. Euro Heart J 2005;26(3):263–70.
[63] Boyce NW, Holdsworth SR. Hydroxyl radical mediation of immune renal injury by desferrioxamine. Kidney Int 1986;30: 813–7.
[64] Ueda N, Baliga R, Shah SV. Role of "catalytic" iron in an animal model of minimal change nephrotic syndrome. Kidney Int 1996;49:370–3.
[65] Thakur V, Walker PD, Shah SV. Evidence suggesting a role for hydroxyl radical in puromycin aminonucleoside-induced proteinuria. Kidney Int 1988;34:494–9.
[66] Liu H, Shah SV, Baliga R. Cytochrome P-450 as a source of catalytic iron in minimal change nephrotic syndrome in rats. Am J Physiol Renal Physiol 2001;280:F88–94.
[67] Liu H, Bigler SA, Henegar JR, Baliga R. Cytochrome P450 2B1 mediates oxidant injury in puromycin-induced nephrotic syndrome. Kidney Int 2002;62(3):868–76.
[68] Tian N, Arany I, Waxman DJ, Baliga R. Cytochrome P450 2B1 gene silencing attenuates puromycin aminonucleoside-induced cytotoxicity to glomerular epithelial cells. Kidney Int 2010;78(2): 182–90.
[69] Baliga R, Ueda N, Shah SV. Kidney iron status in passive Heymann nephritis and the effect of iron deficient diet. J Am Soc Nephrol 1996;7:1183–8.
[70] Harris DC, Tay C, Nankivell BJ. Lysosomal iron accumulation and tubular damage in rat puromycin nephrosis and ageing. Clin Exp Pharmacol Physiol 1994;21(2):73–81.
[71] Alfrey AC. Toxicity of tubule fluid iron in the nephrotic syndrome. Am J Physiol 1992;263(32):F637–41.
[72] Cooper MA, Buddington B, Miller NL, Alfrey AC. Urinary iron speciation in nephrotic syndrome. Am J Kidney Dis 1995;25(2): 314–9.
[73] Nankivell BJ, Chen J, Boadle RA, Harris DCH. The role of tubular iron accumulation in the remnant kidney. J Am Soc Nephrol 1994;4:1598–607.
[74] Remuzzi A, Puntorieri S, Brugnetti B, Bertani T, Remuzzi G. Renoprotective effect of low iron diet and its consequence on glomerular hemodynamics. Kidney Int 1991;39:647–52.
[75] Alfrey AC, Froment DH, Hammond WS. Role of iron in the tubulo-interstitial injury in nephrotoxic serum nephritis. Kidney Int 1989;36:753–9.
[76] Howard RL, Buddington B, Alfrey AC. Urinary albumin, transferrin and iron excretion in diabetic patients. Kidney Int 1991; 40:923–6.
[77] Rajapurkar MM, Alam MG, Bhattacharya A. Novel treatment for diabetic nephropathy [abstract]. J Am Soc Nephrol 2007;18:329A.
[78] Nankivell BJ, Boadle RA, Harris DCH. Iron accumulation in human chronic renal disease. Am J Kidney Dis 1992;20(6): 580–4.
[79] Rajapurkar MM, Baliga R, Shah SV. Treatment of patients with glomerulonephritis with an oral iron chelator [abstract]. J Am Soc Nephrol 2007;18:57–58A.
[80] Lin J-L, Lin-Tan D-T, Hsu K-H, Yu C-C. Environmental lead exposure and progression of chronic renal diseases in patients without diabetes. N Engl J Med 2003;348(4):277–86.
[81] Owda AK, Alam MG, Shah SV. Environmental lead exposure and chronic renal disease. N Engl J Med 2003;348(18): 1810.
[82] Nakamoto M, Shapiro JI, Shanley PF, Chan L, Schrier RW. *In vitro* and *in vivo* protective effect of atriopeptin III on ischemic acute renal failure. J Clin Invest 1987;80(3):698–705.
[83] Allgren RL, Marbury TC, Rahman SN, Weisberg LS, Fenves AZ, Lafayette RA, et al. Anaritide in acute tubular necrosis. N Eng J Med 1997;336(12):828–34.
[84] Ding H, Kopple JD, Cohen A, Hirschberg R. Recombinant human insulin-like growth factor-I accelerates recovery and reduces catabolism in rats with ischemic acute renal failure. J Clin Invest 1993;91:2281–7.
[85] Hirschberg R, Kopple J, Lipsett P, Benjamin E, Minei J, Albertson T, et al. Multicenter clinical trial of recombinant human insulin-like growth factor I in patients with acute renal failure. Kidney Int 1999;55:2423–32.
[86] Siegel NJ, Gaudio KM, Katz LA, Reilly HF, Ardito TA, Hendler FG, et al. Beneficial effect of thyroxin on recovery from toxic acute renal failure. Kidney Int 1984;25:906–11.
[87] Acker CG, Singh AR, Flick RP, Bernadini J, Greenberg A, Johnson JP. A trial of thyroxine in acute renal failure. Kidney Int 2000;57:293–8.
[88] Heyman SN, Brezis M, Greenfeld Z, Rosen S. Protective role of furosemide and saline in radiocontrast-induced acute renal failure in the rat. Am J Kidney Dis 1989;14(5):377–85.
[89] Solomon R, Werner C, Mann D, D'Elia J, Silva P. Effects of saline, mannitol, and furosemide on acute decreases in renal function induced by radiocontrast agents. N Engl J Med 1994; 331 (21):1416–20.
[90] de Brito-Ashurst I, Varagunam M, Raftery MJ, Yaqoob MM. Bicarbonate supplementation slows progression of CKD and improves nutritional status. J Am Soc Nephrol 2009;20:2075–84.
[91] Cho ME, Smith DC, Branton MH, Penzak SR, Kopp JB. Pirfenidone slows renal function decline in patients with focal segmental glomerulosclerosis. Clin J Am Soc Nephrol 2007;2:906–13.
[92] Cohen AR. New advances in iron chelation therapy. Hematology Am Soc Hematol Educ Program 2006;:42–7.

CHAPTER

90

Chronic Kidney Disease: Pathophysiology and the Influence of Dietary Protein

Biruh T. Workeneh and William E. Mitch

Department of Medicine (Division of Nephrology), Baylor College of Medicine, Houston, Texas, USA

INTRODUCTION

The concept of chronic kidney disease (CKD) continues to evolve from a common pathway initiated by unrelated diseases into a number of complications and adaptations that affect the function of virtually every organ. Key concepts are that these complications increase in severity as glomerular filtration rate (GFR) declines and their severity can be modified by modifying the diet and by treating each part of the syndrome of CKD. This concept of CKD allows for individual variations in the manifestations of the complications of CKD related to the primary kidney disease and/or an individual's genetic and environmental background. The increasing number of patients with CKD[1] and especially the growing number of elderly, diabetic, and minority populations, leads to morbidity and mortality concerns as well as the increasing costs of treating patients with end-stage renal disease (ESRD) when dialysis or transplantation are required to sustain life. Recent information underlines the necessity of employing established methods of treating CKD and preventing its complications. At least three groups of investigators have evaluated the hypothesis that "early dialysis" should be initiated in CKD patients.[2–7] Their analyses demonstrated that early dialysis does not improve survival, clinical outcomes or quality of life.

The flood of new information about the pathophysiology of CKD (e.g., hypertension, the renin-angiotensin system, renal hypertrophy, electrolyte disturbances, nephron adaptations, and mineral metabolism, among others) has created separate fields of study. There also has been identification of mechanisms associated with the complications of CKD such as the contribution of the gastrointestinal tract to the generation of uremic toxins, the influence of erythropoietin on morbidity and mortality, the abnormalities in protein metabolism and the potential role that acid accumulation plays in the progression of CKD. Epidemiologic reports have emphasized the risks of CKD patients for the development of cardiovascular diseases and a link with the impending world wide increase in diabetes. These reports also emphasize that new strategies for slowing progression of CKD and mitigating its complications (e.g., cardiovascular disease, death) must be developed since a randomized, clinical trial has confirmed earlier reports indicating that initiating dialysis "early" does not improve mortality expectations of CKD patients.[6] Our major focuses are the pathophysiology of progressive CKD and the role of the diet in counteracting CKD complications. The latter focus is relevant because successful implementation of dietary measures can blunt the severity of complications of CKD and recent findings show that this type of therapy is safe.

MEASUREMENT AND NATURAL HISTORY OF CKD

Assessment of Glomerular Filtration Rate

The "gold standard" for assessing the amount of residual kidney function and the rate of loss of kidney function is the GFR. The measurement of GFR is classically, the urinary clearance of inulin, a 5200 Da polysaccharide which is filtered by the glomerulus, is neither reabsorbed nor filtered and has no extrarenal clearance (i.e., no metabolism or elimination by other organs). Unfortunately, measuring inulin clearance is cumbersome and expensive: trained personnel are

Seldin and Giebisch's The Kidney, Fifth Edition.
DOI: http://dx.doi.org/10.1016/B978-0-12-381462-3.00090-2

© 2013 Elsevier Inc. All rights reserved.

required to infuse inulin in order to achieve a prolonged, steady-state plasma concentration and for obtaining precisely timed urine collection.[8,9] In addition, the measurement of inulin is difficult.[10] To minimize errors due to retained urine in the bladder, patients are given a water load and sonography can be used to confirm completeness of bladder emptying. To minimize changes in renal perfusion, patients should remain supine or be seated, standing only to void.[11–13] Despite these precautions, the coefficient of variation of inulin clearance ranges from 5–10 ml/min per 1.73 m^2 in subjects with nearly "normal" GFR values; the variability is higher in patients with CKD.[10] Sources of this error include variation in the steady-state concentration of inulin; since the common practice is to collect urine after two to three hours which may be insufficient time for complete distribution of inulin and hence, produces a degree of variability in the plasma inulin concentration. This is the reason that the inulin clearance calculated from the rate of inulin infusion (mg/min) divided by the plasma inulin concentration consistently exceeds inulin clearance calculated from the urinary excretion. The alternative explanation is that there is an extrarenal clearance of inulin and there is no concurrence why the two means of calculation differ.

To reduce the analytic error due to difficulties in measuring inulin in blood and urine, radiolabeled compounds that are cleared predominantly by glomerular filtration have been used. Generally, these compounds (e.g., 125I-iothalamate) are gamma-emitters so the error from variable quenching of beta-emitting compounds (e.g., 14C-inulin) is minimized. Fortunately, there is concordance between the clearances of inulin and 125I-iothalamate (or other radiolabeled compounds) over a wide range of GFR.[9,13] To avoid the error related to incomplete urine collections, GFR has also been calculated from the plasma disappearance of an injected compound (e.g., radiolabeled compounds or compounds like iothalamate which can be measured by spectrophotometry). This method is based on the assumption that the plasma and renal clearance will be insignificantly different because there is minimal extrarenal clearance of the compound. There are at least two other assumptions: (1) that the plasma clearance is constant when blood is sampled; and (2) the duration of blood sampling must be sufficiently prolonged to ensure that the terminal, steady-state period of monoexponential loss of plasma radioactivity with time is present. The latter requirement is especially important for patients with advanced CKD because hours may be required to reach a constant.[8] In patients with severe CKD, there also may be a small extrarenal clearance (e.g., intestinal secretion) which would not be detected while there can be a delay in distribution of the GFR marker in patients with ascites or edema.

The radionuclide agents most commonly used to assess GFR is Tc-99m-DTPA and ^{125}I-iothalamate in the U.S. and ^{51}Cr-EDTA in Europe. Overall, the correlation of these radionuclide markers and urinary inulin clearance is high ($r > 0.9$ in most published studies) as is the use of nonradioactive iodinated compounds, such as iohexol.[14] In addition, some have advocated estimating the entire plasma disappearance curve from a single plasma sample obtained after only a few hours following injection of a GFR marker. Unfortunately, this technique is decidedly less accurate compared to the multiple sampling techniques, especially when there is renal insufficiency.[8,14–18] Lastly, gamma cameras have been used to estimate GFR from the disappearance of labeled GFR markers but this technique has errors greater than plasma-based techniques (up to 20% error). An advantage of this technique is it can provide an estimate of GFR in individual kidneys.

SERUM CREATININE

A single value of serum creatinine (SCr) is an unreliable estimate of creatinine clearance (or GFR) because it is a function of creatinine production and its clearance by the kidney and extrarenal means. Creatinine production is emphasized because it is directly proportional to lean body mass and hence, a muscular individual will have a higher serum creatinine than one who has lost muscle mass, even though they have the same creatinine clearance (CCr).[19] Three other caveats are important in evaluating GFR from the serum creatinine. First, the rate of creatinine production is not constant, despite the fact that lean body mass does not vary (at least over short periods). In part, this occurs because creatine in meat is converted to creatinine by cooking extensively.[20] Secondly, the kidney not only filters but also secretes creatinine and hence consistently exceeds GFR by a variable amount.[21–23] Third, creatinine is degraded, presumably by bacteria in the gastrointestinal tract. This extrarenal clearance is small and averages 0.04 liters/kg/day. Consequently, it is difficult to detect until renal clearance is depressed. Specifically, creatinine removal by extrarenal creatinine clearance (i.e., a method of clearing the blood that does not depend on excretion by the kidney) affects estimates of creatinine production when SCr rises to ~6 mg/dL. At this level, the amount of creatinine degraded is significant and should be considered in interpretation of estimates of SCr in CKD patients. The amount of creatinine degraded in mg/kg/day can be calculated as 0.042 l/kg/d x serum creatinine in mg/L.[21]

The inaccuracies in estimating GFR from SCr can be compounded by practices in the Clinical Laboratory. If the SCr standards are 1, 4, and 10 mg/dl, the accuracy

TABLE 90.1 Most Commonly Used Creatinine-Based Approximations of GFR

Name of Equation	Formula
Cockcroft-Gault CCr[25]	Men: CCr = [(14-age) × weight (kg)]/ SCr × 72; Women: CCr = ([(14-age) × weight (kg)]/SCr × 72) × 0.85
MDRD Study Equation[26]	GFR (mL/min/1.73 m^2) = 186 × $(S_{cr})^{-1.154}$ × $(Age)^{-0.203}$ × (0.742 if female) × (1.212 if African-American)
IDMS-Traceable MDRD Study Equation[27]	GFR (mL/min/1.73 m^2) = 175 × $(S_{cr})^{-1.154}$ × $(Age)^{-0.203}$ × (0.742 if female) × (1.212 if African American)
CKD-Epidemiology group (CKD-EPI)[28]	GFR (mL/min/1.73 m^2) = 141 × min(Scr/k, 1)^a × max(Scr/k, 1)$^{-1.209}$ × 0.993^{Age} × 1.018 [if female] × 1.159 [if black]
Schwartz Equation[29]	GFR (mL/min/1.73 m^2) = k (Height in cm)/Serum creatinine; k = 0.33 in preemie infants; 0.45 in term infants to 1 year of age; 0.55 in children to 13 years of age and adolescent females; 0.70 in adolescent males

of measuring SCr in the normal range (typically less than 1.2 mg/dl) will be compounded.[24] Variability among clinical laboratories in the calibration of serum creatinine assays introduces another error in GFR estimates especially at high SCr levels. Efforts are underway to institute national standardization of creatinine using values determined by isotope-dilution mass spectrometry (IDMS). Selected equations used to estimate the GFR from SCr yield results that are satisfactory as long as the patient is in the steady state and the SCr exceeds 2 mg/dl[25–29] (Table 90.1; Fig. 90.1). Although it can be clinically useful, the practice of estimating GFR from SCr often introduces a significant degree of inaccuracy.

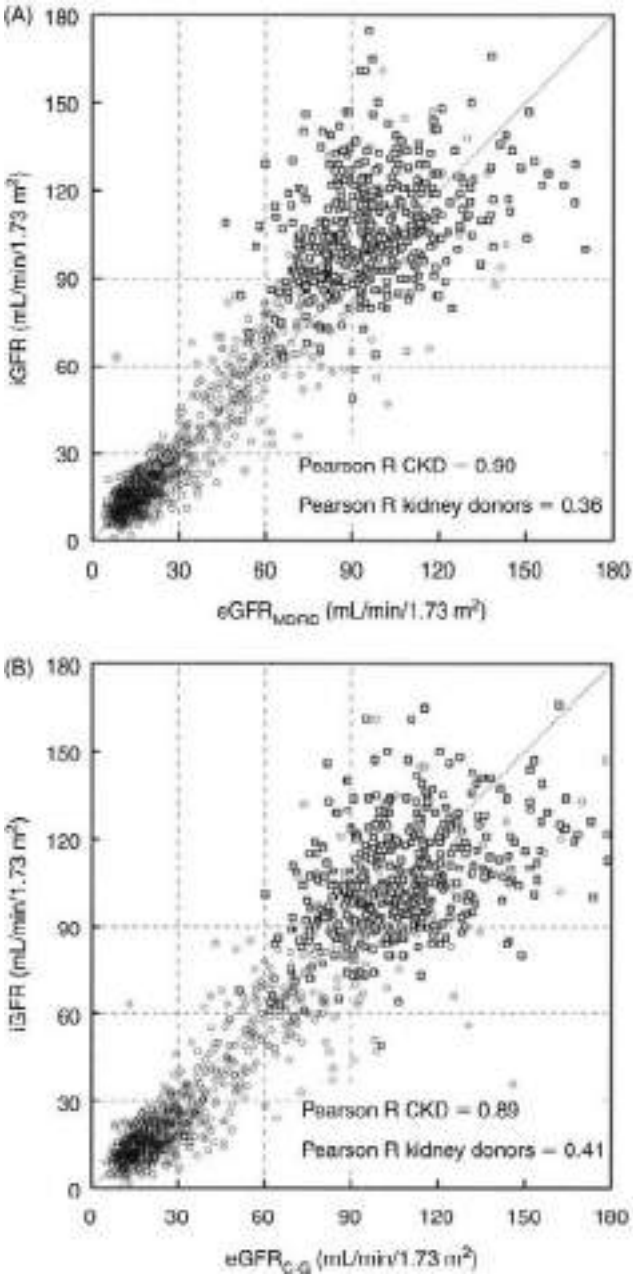

FIGURE 90.1 Association of estimated GFR with measured iGFR in outpatients with chronic kidney disease (*circles*) and potential kidney donors (*squares*). **(A)** Association of iGFR with $eGFR_{MDRD}$. **(B)** Association of iGFR with eGFRCG. Dotted lines subclassify the GFR on the basis of the Kidney Disease Outcomes Quality Initiative stages. eGFR is plotted on the horizontal axis, and iGFR on the vertical axis. *(With permission from Poggio ED, Wang X, Greene T, Van Lente F, Hall PM. Performance of the modification of diet in renal disease and Cockcroft-Gault Equations in the estimation of GFR in health and in chronic kidney disease. J Am Soc Nephrol 2005;16:459–466).*

CREATININE CLEARANCE

Since creatinine is secreted by proximal tubule cells, the 24-hour endogenous CCr usually exceeds inulin clearance but with advanced CKD, values of CCr and GFR become numerically closer even though the percentage difference between CCr and GFR increases.[10,22,30,31] Using CCr as an estimate of GFR presents difficulties including the inconvenience of obtaining an accurate 24-hour urine collection. In addition, 24-hour CCr values have a high coefficient of variation: in one study of 119 healthy ambulatory subjects, the coefficient of variation was 26% and others reports that the variability varies from 6% to 22%.[21,22,32] One reason for this variability is the day-to-day differences in creatinine excretion;[20,23,32,33] among hospitalized patients, it varies by at least 10%.[19,25,34] These problems have prompted some investigators to recommend abandoning the 24-hour CCr as an index of CKD

severity.[35] The same caveats apply to calculating the average of the 24-hour creatinine and urea clearances to estimate GFR, even though this average value corresponds closely to inulin clearance.[30]

Another strategy is to measure CCr after giving cimetidine to inhibit creatinine secretion and hence, improve the estimate of GFR. Generally, 1.2 g of cimetidine completely suppresses creatinine secretion and lower doses yield incomplete blockade. Reportedly, with water loading and carefully timed urine collections, the cimetidine-adjusted CCr procedure yields values that have a coefficient of variation of approximately 8% in patients with GFR values ranging from 12 to 150 ml/min.[36] Although this technique avoids using radioactive markers, it does require trained personnel to improve the accuracy of urine and blood collections.

FORMULAS FOR ESTIMATNG GFR

Cockcroft-Gault Formula

Frustration with the variability of the 24-hour CCr has led to the widespread practice of estimating CCr from SCr. The equations rely on an estimated daily rate of creatinine production (and hence, excretion in the steady state). The widely used Cockcroft-Gault formula (Table 90.1) is based on a value of creatinine production form the age, weight, and gender of the patient. However, it was derived from results obtained in "normal, hospitalized" patients, and hence, may not be appropriate for patients with CKD.[25,37] It also does not include a value for extrarenal clearance (see above) although for SCr values below 6 mg/dL, this variable has a minimal impact on the estimates of creatinine production. Creatinine production in milligrams per kilograms per day has also been estimated as 28−0.2 A, and for women, as 23.8−0.17 A where A is the age of the subject in years.[25,37] Besides using these equations to estimate CCr and hence, GFR, some investigators have calculated creatinine production as a means of estimating loss of muscle mass. Since there are no independent means of evaluating muscle mass, the reliability of this method is unknown. Regardless, creatinine production in mg/kg/day in men can be predicted as $(28-0.2A)+(0.04\times SCr\times 10)$ and for women, as $(23.8-0.17\times SCr\times 10)$. Using these formulas, the measured 24-hour CCr of uremic adults with stable serum creatinine values above 8 mg/dl was estimated to within 1.5 ml/min.[37] It is important to recognize the assumptions underlying these estimates (and those accompanying the Cockcroft-Gault equation): they were derived from a homogenous cohort of predominantly Caucasian males without kidney disease and may not be appropriate for individuals of other races or groups. This shortcoming was uncovered when the MDRD formulas were studied in patients in China and Japan. Secondly, the Cockroft and Gault equation can systematically overestimate the GFR because of tubular secretion of creatinine.

MDRD Formula

The Modification of Diet in Renal Disease (MDRD) Study was a multicenter, randomized, controlled trial to evaluate the effectiveness of dietary protein restriction plus strict blood pressure control on the progression of renal insufficiency. The outcome was based on measurements of GFR estimated from urinary clearances of ^{125}I-iothalamate. Many other variables were collected (e.g., age, gender, weight, serum albumin, serum creatinine, etc.) and used to develop equations that predicted the measured ^{125}I-iothalamate clearance.[38] The initial MDRD equation was found to yield a correlation of $r^2 = 91\%$ (Table 90.1; Eq. 90.1). In this equation, SUN is serum urea nitrogen and UUN is urine urea nitrogen. A revised MDRD equation (Table 90.1; Eq. 90.2) is based on demographic assessments and serum variables only (yielding a maximal R2 of 90.3%). The most widely used modified MDRD equation was derived to avoid including serum values of albumin and urea nitrogen (Table 90.1; Eq. 90.3). The latter equation has almost the same predictive ability and its use is fully supported by the National Kidney Disease Education Program (NKDEP) of the National Institutes of Health (NIH), the National Kidney Foundation (NKF), and the American Society of Nephrology (ASN). In fact, it is widely used as a means of estimating the severity of kidney disease based on a conclusion that patients with an estimated GFR below 60 ml/min/1.73 m^2 have a high risk of progressive CKD and should be treated to postpone or avoid ESRD.

There are caveats associated with using the MDRD equation: firstly, the equations were derived from results of measurements in only two ethnic groups, Caucasian and African Americans. Subsequent reports indicate that the equation does not accurately estimate GFR in Chinese, Japanese and Brazilian patients.[39−42] In short, the ability of these equations to predict an individual's GFR from SCr, etc. in other races/ethnicities will introduce errors. Furthermore, a recent analysis uncovered that measurements of the urinary clearance of ^{125}I-iothalamate (the reference GFR in the MDRD Study) had stable average values, but substantial variability across visits.[43] Although it is known that GFR in individuals varies throughout the day and that repeated measures of GFR may better reflect an individual's true GFR, there is inherent variability in GFR

measured using iothalamate. This analysis points to another difficulty in interpreting GFR values and the severity of kidney disease based on SCr plus other factors present in an individual patient. An important factor is the age of the patient because those of >65−70 years comprised a small fraction of the MDRD study group and very few of ≥80 years were studied. It is critical to recognize that aged patients may have a depressed GFR even when SCr is within reference range. Regardless, the MDRD equation overestimates eGFR in the elderly. Besides the inaccuracies associated with different ethnic groups, there are serious deficiencies in the predictive value of these equations in people with obesity and normal kidney function.[39,44,476]

In a study of adults from the Netherlands, Vervoort et al. compared the inulin clearance of 46 controls and 46 uncomplicated diabetic patients with predicted GFRs based on the MDRD and Cockcroft-Gault equations.[45] The difference between predicted values and the measured GFR was significant (the Cockcroft-Gault formula had a 9.0 ml/min/1.73 m^2 difference while the MDRD equation had a 10.7 ml/min/1.73 m^2 difference from the measured inulin clearance). Secondly, Lin et al. found that the MDRD equation is decidedly less accurate in subjects without kidney disease when compared to GFR measured as 99mTc clearance; the MDRD equation systematically underestimated GFR while the Cockcroft-Gault formula overestimated the GFR. The Schwartz formula is commonly used to estimate GFR in children. Other equations used in estimating the GFR in CKD patients are listed in Table 90.1.

In summary, the GFR can be predicted from formulas that are based on SCr and characteristics of a patient with CKD.[24] The prediction equations exhibit errors and must be used with an understanding of the sources of variability, including the influence of obesity, race and age. Specifically, no single equation will reproducibly predict the GFR of an individual patient and this is especially true for subjects with minimal loss of kidney function or aged patients. Presumably, standardization of the measurement of creatinine and the use of a range of "standards" in a creatinine assay will be associated with improvements in the accuracy of the equations. But, it also is clear that GFR varies from hour to hour and is not constant day to day. These shortcomings do not invalidate the calculations because the estimation of GFR provides a means of identifying patients at risk for developing increasingly severe renal insufficiency and a method for detecting differences in rates of loss of kidney function (see below).

CKD-EPI Formula

The estimated GFR based on the MDRD equation has increased the awareness of CKD in both physicians and patients. There is, however, concern about assigning a CKD diagnosis if there is no kidney disease.[46] The concern has prompted The Chronic Kidney Disease Epidemiology Collaboration (CKD-EPI) to derive another designed to improve the detection of CKD in adults with early/moderate kidney disease.[28] This new equation (Table 90.1) is based on a method of measuring creatinine that is traceable to standards established by isotope dilution mass spectroscopy (IDMS) and in patients with normal or mildly decreased GFR, it appears to yield a more accurate estimate of GFR compared to the MDRD Study equation. Importantly, when the CKD-EPI equation was used to analyze the NHANES database, it was concluded that the prevalence of CKD in U.S. adults was 11.5% compared to the estimate of 13.1% derived with the MDRD Study equation. Although this difference may seem small, the number of individuals predicted to have CKD would change from roughly 26 down to 23 million and thus may have significant public health implications.

Estimation of GFR from Cystatin C Concentration

Cystatin C is a low molecular-weight protein (13,000 Da) that is produced by all nucleated cells and acts to inhibit cysteine proteases. It has been used as an estimate of the severity of CKD because a high level of cystatin C is associated cardiovascular disease and may even be more closely associated than SCr.[47−49] As a marker of GFR, however, it has shortcomings. A factor that estimates glomerular filtration should be produced as a constant rate, should not be removed by organs other than the kidney, and should be measured by a reliable method. Cystatin C fulfills some but not all of these requirements. Reportedly, the production rate of cystatin C is unaffected by age, gender, and muscle mass, while creatinine production is affected by all three.[50] However, cystatin C production was not estimated using standard techniques but rather indirect estimates of production. Moreover, reports indicate that smoking, evidence of inflammation, and catabolic conditions affect cystatin C production.[50,51] Second, although cystatin C is filtered through the glomerulus and is reabsorbed and catabolized by the proximal tubule,[52] it is not known if other epithelial cells absorb and degrade cystatin C; it is evident that the extrarenal clearance of cystatin C is substantial.[50] Third, cystatin C measurements employ an antibody-based technique, and there is controversy concerning which method is "most accurate."[47] Conclusions about the impact of CKD as assessed by serum cystatin C in patients is principally based on the conclusion that measured GFR

has a higher correlation coefficient with serum cystatin C compared to GFR estimated from the reciprocal of serum creatinine.[47,48] For example, in adults over 65 years of age living in four different areas in the US, it was found that in a comparison with serum creatinine, a high serum cystatin C level was correlated more closely with the number of deaths and cardiovascular events (stroke, myocardial infarction and congestive heart failure) occurring seven years later.[53] Although it is known that CKD is associated with cardiovascular disease, the association between serum cystatin C and stroke, myocardial infarction and congestive heart failure, could be related to factors affecting cystatin C production and elimination that are independent of kidney function since there was no information about events and treatments occurring in the seven-year interval following the initial, baseline measurement. Thus, serum levels of cystatin C may be a harbinger of future adverse events but whether this can be attributed to CKD is unsettled. A related question is whether cystatin C accurately reflects the rate of loss of kidney function in patients with progressive renal insufficiency. Some have reported that serum cystatin C does reflect changes in GFR,[54] but others conclude that the reciprocal of serum cystatin C is inferior or that there is no statistical difference between the analysis of changes in reciprocal serum creatinine and serum cystatin C.[55] The association between serum cystatin C and GFR is more complex during pregnancy[56] and in infants and children.[55,57–59] It was proposed that serum cystatin C may have a higher sensitivity for detecting a low GFR compared to serum creatinine in patients with cirrhosis but in patients with chronic liver disease, neither serum cystatin C nor creatinine reliably predicts the GFR.[60] The role of cystatin C continues to evolve but to date, it lacks evidence for being a precise measure of kidney function.

Estimation of GFR from Other Substances

β-2-microglobulin is another endogenous protein that undergoes glomerular filtration plus reabsorption and metabolism by the proximal tubule. Like serum cystatin C, the serum β-2 microglobulin has been suggested to be more sensitive to an early decrease in GFR compared to serum creatinine.[61] However, the influence of extrarenal clearance and constant production are unsettled and tubule degradation of the protein rises when urine is acidic, so patients should be given sodium bicarbonate to raise the urine pH above 7 if β-2 microglobulin is used to monitor kidney function. Even less fully investigated markers include beta-trace protein[62] and tryptophan glycoconjugate[63] and additional experiments are needed before they can be recommended as a method of monitoring kidney function.

In conclusion, the most accurate estimate of kidney function is the measurement of GFR using inulin, radionucleotide-labelled compounds, or iodinated compounds like iodothalamate. Results of studies from large groups of patients indicate that the MDRD equation can be used but it is important to remember its limitations. They include variations that are associated with different ages, races, etc. as well as those associated with the measurement of serum creatinine. Other strategies for estimating the degree of dysfunction of the kidney include the CCr that has been estimated from predictions of creatinine production and serum cystatin C. The latter has been used to evaluate the risks of adverse outcomes of kidney disease, including cardiovascular disease. But, there are problems with using serum cystatin C as an estimate of kidney function since its production depends on several factors and there is the potential for extrarenal clearance of cystatin C. To screen populations or even individuals for the presence of CKD, the MDRD equation has been most widely evaluated and provides a reasonable approximation. During long-term followup evaluations, it should be remembered that serum creatinine is the major factor that changes with renal insufficiency so determining the rate of loss of estimated GFR with time is subject to the same influences as evaluating changes in the reciprocal of serum creatinine with time (see below). In diagnosing CKD, a combination of techniques along with sound judgment about the influence of variables such as age, gender, diet, etc. should be employed since CKD is a progressive disease associated with increased mortality.

EPIDEMIOLOGY OF CHRONIC KIDNEY DISEASE

End-Stage Renal Disease

The epidemiology of ESRD is based largely on information from the United States Renal Data System (USRDS), a geographically comprehensive, population-based ESRD registry that collects information from all Medicare-eligible patients (~90% of all incident U.S. patients) at the start of dialysis, and at death or transplantation. Despite the robust information contained in the USRDS, it should be remembered that there are legitimate concerns about the accuracy of the primary cause of kidney disease, comorbid conditions, and the causes of death present in the yearly report. The concerns arise because diagnoses are left to the judgment of the treating nephrologist who often does not have a tissue diagnosis. For example, few ESRD patients who

have hypertension listed as the cause of kidney failure have in fact, satisfied uniform diagnostic criteria for this diagnosis making it possible that other diseases led to ESRD. There are similar concerns about the accuracy of comorbid conditions[64] and causes of death.[65]

Undeniably, USRDS data indicate there has been substantial growth in the number of patients enrolled in the Medicare-supported ESRD program: there were roughly 10,000 beneficiaries in 1973 and over 86,000 a decade later but by 2009, the prevalence of ESRD in the US had grown to approximately 527,000. Moreover, in 1980, the incidence rate for ESRD compiled after adjustment for age, race/ethnicity and gender was 76 cases per million (18,000 patients). In 2002, the rate was 338 cases per million (102,000 patients) but by 2007, the rate was 361 cases per million (110,000 patients).[66] The seemingly relentless increase in the incidence of ESRD has declined from 8% per year in 1980 to below 1.5% per year in the years after 2000. This encouraging change may represent improvements in preventive care or some unidentified factors.

In the 2009 USRDS report, the primary cause of ESRD was diabetes, afflicting 54% of new patients, yielding an incidence rate of 155 per million population. In contrast, the incidence of ESRD from hypertension or other kidney diseases has not increased. The diabetes-associated incidence rate is 36% higher than a decade ago and it parallels the rising prevalence of diabetes in the general population: increasing from 5% in the 1988–1994 era to 7.6% during 2003–2006. The increase in diabetes and CKD is especially prevalent in African and Native American populations. Besides diabetes, other ESRD-associated epidemiologically relevant factors include aging of the dialysis patients. From 1999–2009, the prevalent ESRD population of 20–40 years of age has risen 9.7%. Among those 40–60 year of age, the prevalence had risen 54% and 61% for those beyond 70 years. Besides age, the incidence of ESRD is clearly racial-dependent; in 2007, the incident rates in African Americans and Native Americans were 3.7 and 1.8 times greater, respectively, than the rate in whites while the rate in the Hispanic population is 1.5 times higher than that of non-Hispanics. Among African Americans, the rate of new ESRD cases in 2007 reached 998 per million population or 3.7 times greater than the rate of 273 among whites. Likewise, in 2007, Hispanic patients had an incidence rate of 508 per million population (1.5 times greater than in non-Hispanic patients). Thus, the annual increase in incidence ESRD may be leveling but these racial factors may still increase the number of ESRD patients because of demographic trends; similar factors present in developing countries may also be active and increase the number of ESRD patients.[67]

Definition of CKD

Guidelines from the U.S. National Kidney Foundation (NKF) have led to a widely adopted framework for defining CKD.[68] CKD is a nonspecific term that does not indicate the cause of kidney disease but it is useful for improving communications with investigators, practitioners and the public. CKD is defined as kidney injury and/or impaired kidney function lasting 3 or more months.[69] Kidney injury is signified by the presence of microalbuminuria or proteinuria, abnormalities in the urinary sediment (RBC, RBC casts, WBC, WBC casts, tubular cells, cellular casts, granular casts, oval fat bodies, fatty casts, or free fat) and/or abnormal radiographic evidence and of course, evidence from kidney biopsies. CKD is categorized into five stages according to the level of the estimated GFR (see Table 90.2). All patients with CKD are increased cardiovascular risk, but those with an estimated GFR ≤ 60 ml/min/1.73 m^2 are also at higher risk for a progressive decline in kidney function and as GFR declines, pathophysiologic changes increase in complexity and management becomes more varied and increasingly specialized.[69] The NKF guidelines attempted to tie the stages of CKD to specific clinical abnormalities and suggested treatment goals. In Stages 1 and 2, efforts are needed to adjust dietary factors, control blood pressure and glycemia. It is also suggested that inhibitors of the renin-angiotensin-aldosterone system (RAAS) should be used to conserve kidney function and reduce the risk of death and cardiovascular disease. In Stage 3 CKD, efforts are increased to detect and manage anemia and renal bone disease while the diet is controlled to prevent the accumulation of unexcreted waste products. These products include the myriad of compounds associated with the metabolism of a high protein diet (e.g., guanidines, middle molecules, etc.) and ions (sodium, acid, phosphates, etc.) but moderate to severe kidney disease, dietary adjustments are needed because the damaged kidney does not eliminate these metabolites. In Stage 4 CKD, attention to the same

TABLE 90.2 National Kidney Foundation Staging of CKD

Stage	Description	GFR (ml/min)
1	Kidney damage (marked by proteinuria or abnormal urine sediment)	> = 90
2	Early kidney disease	60–89
3	Moderate kidney disease	30–59
4	Advanced kidney disease	15–29
5	Established renal failure	<15 or dialysis

topics is needed and the patient should be introduced to options for treating ESRD; if hemodialysis is chosen, the patient should be evaluated for placement of a vascular access. At this stage, it is especially important to adjust medication doses for the loss of kidney function. In Stage 5 CKD, the pathophysiologic and metabolic functions become more difficult to manage and the clinician will need special training and skills to maximize therapy. The importance of managing the complications of advanced CKD is emphasized because the alternative option of initiating dialysis "early" (i.e., before uremic symptoms are present) has been tested repeatedly and found to be wanting in terms of improving mortality/morbidity.[2,4–6]

Unfortunately, many patients are unaware of the presence of CKD and the factors needed to treat CKD appropriately. In one study, patient awareness of CKD was only 22% of patients in Stage 3 and 44.5% of those with Stage 4 CKD (these dismal percentages were independent of race/ethnicity, gender, or age.[70,71]) Undoubtedly, the lack of awareness contributes to the development of complications of CKD in those with advanced CKD including anemia, bone disease, loss of muscle mass, abnormalities in serum electrolytes, etc.[7,72] Similar shortcomings of managing CKD are present in primary care practices and Nephrology clinics.[73,74] Even when it is recognized that a therapy target has not been met, clinicians can fail to change management, a behavior present in other chronic conditions and known as "clinical inertia".[74]

Epidemiology of CKD

Population-based studies of epidemiologic factors and CKD are largely based on the National Health and Nutrition Survey (NHANES). This survey includes results from representative samples of the U.S. population that were collected by the National Center for Health Statistics of the Centers for Disease Control and Prevention.[75–77] For example, the prevalence of Stages 1 to 4 CKD estimated from the NHANES data that was collected between1999 to 2004 was found to be 13.1% (approximately, 26.3 million people) and varies according to the stage of CKD.[78] As expected from information about the epidemiology of patients with ESRD (see above), the prevalence of CKD is greater among diabetic subjects vs patients without diabetes (40.2% vs 15.4%). Data from the NHANES III survey of those in different stages of CKD also identify significant racial and gender discrepancies. Based on analyses of serum creatinine values, evidence from both diabetic and nondiabetic subjects reveal that a GFR below 60 ml/min/1.73 m^2 was present in 5% of non-Hispanic whites, 3.4% of non-Hispanic blacks, 1% of Mexican Americans, and 2.2% of other race/ethnic groups.[76] Among black and white NHANES III participants with a comparable prevalence of CKD, it was estimated that the risk of developing ESRD for African Americans was fivefold greater compared to other populations even when results were controlled for differences in age, gender, and the presence of diabetes. Analyses of this database revealed that the prevalence of proteinuria in the U.S. population aged 20 years and older was present in those without impaired kidney function.[76] In men of this age group, a random albumin/creatinine ratio of 17 to 250 mg/g (or 25 to 355 mg/g for women was) was present in 10.5% of the population; this was also present in 63.2% of the people on reexamination two months later. Overt proteinuria (an albumin/creatinine ratio >250 mg/g for men and 355 mg/g for women was found in 1.1% of the U.S. population, including 0.5% of individuals with an estimated GFR >90 ml/min/1.73 m^2, 1.2% of whom had an estimated GFR between 60 and 89 ml/min/1.73 m^2, and 7.2% of those with a GFR between 15 and 30 ml/min/1.73 m^2. Evaluation of the NHANES III data indicated that increasing age affected the prevalence of proteinuria (urine albumin/creatinine ratio) and diabetes was the most frequently associated diagnosis while hypertension was the second most common abnormality.[76] The staging of CKD also affected proteinuria since nonhypertensive, nondiabetic people with an estimated GFR between 30 and 60 ml/min/1.73 m^2 and aged 60 to 79 years had a prevalence of albuminuria of 20.6% compared to 14.1% among individuals with an estimated GFR >60 ml/min/1.73 m^2.

High-Risk Populations

Patients with hypertension, diabetes mellitus, and cardiovascular disease, and family members of patients with ESRD are at high risk of developing CKD (Fig. 90.2). Screening and health promotion can be cost-effective in such high-risk groups.[79]

Hypertension. From the NHANES III results, the serum creatinine increased as the severity of hypertension rose.[80–82] It is still not settled whether nonmalignant hypertension is a primary cause of ESRD or whether hypertension is caused by pre-existing kidney disease.[83]

Diabetes. The USRDS has identified diabetes as the most common cause of ESRD, accounting for nearly 54% of all new cases of ESRD (USRDS ADR 2009). In a population-based study of Rochester, Minnesota, the risk of developing diabetic nephropathy among individuals with type 2 diabetes mellitus but no kidney disease, the incidence was 133 per 100,000 person-years.[84] The cumulative incidence of diabetic nephropathy was similar for type 1 and type 2 diabetes mellitus: the 20-year cumulative risks were 27% for type 2 and 28% for type diabetes mellitus.[85] Although there seems to

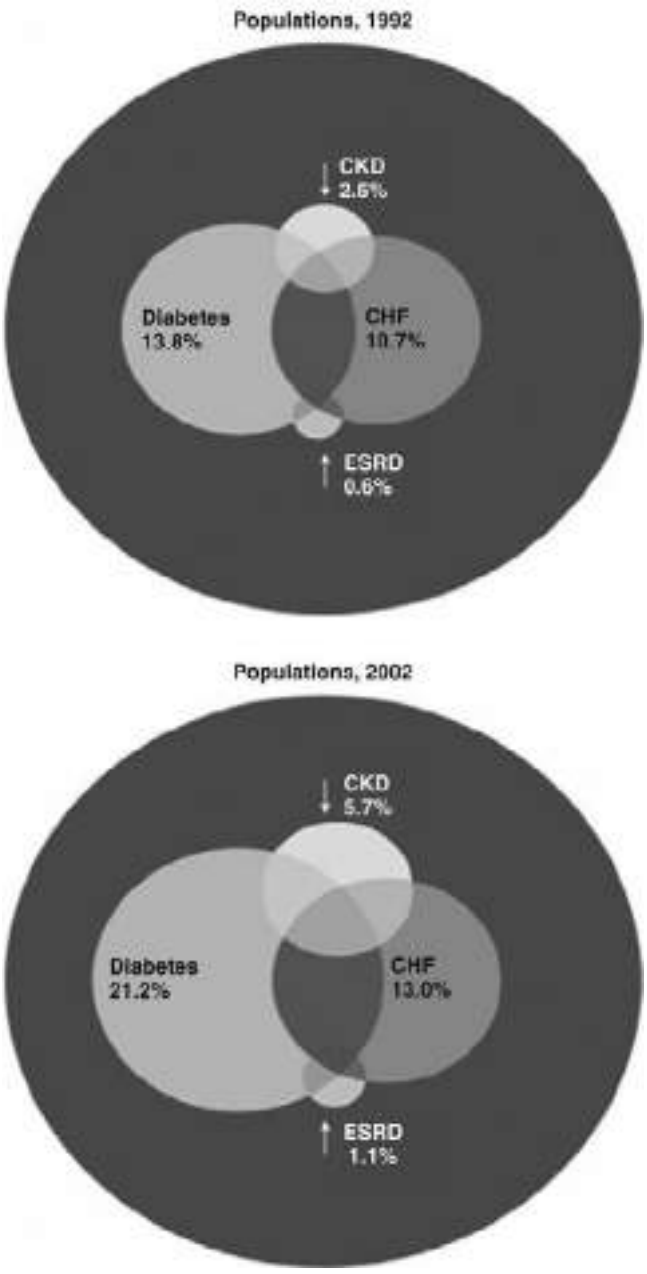

FIGURE 90.2 Distribution of patient counts in the CKD, CHF, DM, and ESRD populations. Populations were estimated from the 5% Medicare sample, and include patients surviving the entire cohort year (1992, 2002) with Medicare as the primary payor, plus period-prevalent end-stage renal disease (ESRD) patients for 1993 and 2003. Diagnoses were determined from claims in 1992 and 2002. Patients with ESRD in the 5% sample were excluded, as they are counted in the ESRD population. *(From United States Renal Data System. 2005 annual data report: atlas of end-stage renal disease in the United States. Bethesda, MD: National Institutes of Health, National Institute of Diabetes and Digestive and Kidney Diseases; 2005.)*

be a declining incidence of diabetic nephropathy among individuals with type 1 diabetes mellitus (attributable to improved detection and care)[86,87] but not for those with type 2 diabetes.

Cardiovascular Disease. CKD is associated with an increased risk of cardiovascular disease and adverse outcomes from it.[88] Reports from more than 28 study populations reveal that cardiovascular disease patients had evidence of impaired kidney function; the average prevalence was 29.9%.[88] The Valsartan in Acute Myocardial Infarction Trial (VALIANT) trial of participants evaluated from 0.5 to 12 days following an acute myocardial infarction complicated by heart failure and/or left ventricular dysfunction revealed that 11.3% had an estimated GFR < 45 ml/min/1.73 m^2 and the overall prevalence of impaired kidney function was 33.5%.[89] The baseline characteristics of the 1,120,295 participants in the Kaiser Permanente Renal Registry in Northern California aged 20 years and older revealed that the prevalence of an estimated GFR below 60 ml/min/1.73 m^2 was 6.4% of subjects with a history of diabetes mellitus, 7.5% of those with hypertension, 10.5% of those with coronary heart disease, and 12.5% of those with cerebrovascular disease.[90] Other studies have essentially confirmed these associations.[91]

Family History of ESRD. Individuals with a family history of ESRD have an increased prevalence of hypertension, diabetes, and CKD. Bergman et al. screened the first-degree relatives of patients with hypertensive ESRD and found that 65% of those in participating families had evidence of kidney disease, including those with a serum creatinine of ≥ 1.4 mg/dL.[92] The same relationships occur in Canada.[93]

Clinical Outcomes of CKD

Mortality. An analysis of nearly 28,000 health plan members with CKD defined as estimated GFR values below 90 ml/min per 1.73 m^2 on two occasions separated by at least 90 days revealed that during the ensuing five years, the cumulative risk of ESRD for CKD Stages 2, 3, and 4 were, respectively, 1.1%, 1.3%, and 19.9%, and the risk of death was 19.5%, 24.3%, and 45.7%.[94] In another analysis of a large sample of patients, Go et al. found that the risk of all-cause mortality increased with decreasing GFR.[95] In those with an estimated GFR of ≥ 60 ml/min per 1.73 m^2 there were 0.76 deaths per 100 person-years but 4.76 deaths per 100 person-years when the estimated GFR was 30–44 ml/min per 1.73 m^2 and 11.36 deaths per 100 person-years for individuals with a GFR 15–29 ml/min per 1.73 m^2.

CVD Disease. Pre-existing cardiovascular disease in CKD patients increases the risk of morbidity and mortality.[96] In a screening of 185 publications involving more than 550,000 subjects, 96% concluded there is a positive relationship between the presence of cardiovascular disease and CKD.[97] Specifically, among

individuals with an estimated GFR of 15–60 ml/min per 1.73 m^2, the rate of myocardial infarction or fatal coronary heart disease was 13.9 per 1000 person-years vs 6.5 per 1000 person-years when the GFR was >60 ml/min per 1.73 m^2.[98]

Natural History of CKD

The most accurate measure of kidney function is a measured GFR but as discussed, this is cumbersome so various equations have been used to estimate the GFR and hence, evaluate the loss of GFR as indicative of lost kidney function. Besides kidney disease, one factor affecting GFR is the decline that occurs with advancing age in many but not all patients. This "renal senescence" was associated a 20–25% decrease in GFR after 60 years of age and as many as two-thirds of normal adults over age 40 years are predicted to have such a decrease in GFR despite the absence of obvious kidney disease;[99] in the remaining third of adults, GFR remains stable.[100] Histologically, aging yields interstitial expansion and glomerular sclerosis and reabsorption. Fortunately, this abnormality rarely progresses to ESRD. In contrast, kidney damage from various diseases leads to manifestations of CKD plus continued loss of function, commonly known as "progression." Notably, progression occurs even when the disease that initially damaged the kidneys is no longer active (e.g., obstructive uropathy or cortical necrosis following obstetric accidents.[101] The rate of progression varies widely as some CKD patients (including those with diabetic nephropathy) do not progress over periods as long as three years.[102,103] Since these reports indicated there was improved control of blood sugar and blood pressure, this could have accounted in part for the improvement in progression. Attention to such factors may have contributed to the lack of progression found in ~15% of patients who participated in the closely monitored Modification of Diet in Renal Disease Study [MDRD], despite having GFR values between 13 and 24 ml/min/1.73 m^2.[104]

Patient-specific characteristics that have been related to the occurrence and progression of kidney disease are shown in Table 90.3.[88,91,105–130] Some of these factors were uncovered in results from the MDRD Study and are expected (e.g., African American race/ethnicity, increased mean arterial blood pressure, baseline urine protein excretion, polycystic kidney disease) while others are not obvious (e.g., lower baseline levels of serum transferrin and HDL cholesterol). The utility of these factors is not obvious although they may serve as a stimulus for clinical trials. Two caveats should be remembered: first, the MDRD Study included a large number of patients with polycystic kidney disease but virtually none with diabetes making it difficult to extend the findings to other populations of CKD patients. Secondly, if risk factors do play an important role in determining the rate of loss of GFR, the implication is that the progression of CKD in individual patients is unpredictable. This is incorrect since the rate of loss of GFR in most patients, including those with diabetes is linear and hence, predictable.

TABLE 90.3 Risk Factors for Chronic Kidney Disease Progression

Older age[105]
Race and ethnicity[106,107]
Dietary protein intake[108,109]
Gender[110]
Lower birth weight[111]
Low socioeconomic status[112]
Smoking[113]
Alcohol[114,115]
Lead and other heavy metals{7881}}
Analgesic abuse[117]
Sugar-sweetened beverages[118]
Illicit drug use[88]
Poverty and access to health care[88]
Obesity and metabolic syndrome[119,120]
Biomarkers
Oxidative stress/carbonyl stress[121]
Insulin resistance[122]
Hyperlipidemia[123]
Hyperuricemia[124]
Proteinuria[125,126]
Anemia[127]
NOS/ADMA[128,129]
Aldosterone[130]
Sympathetic nervous system activation[475]

Assessment of Rate of Progression of Renal Insufficiency

Before it was recognized that the course of CKD in most individual patients is predictable, the prognosis for CKD patients was estimated from analyses of the average time for patients with similar degrees of CKD to reach the stage requiring dialysis or to reach a predetermined degree of renal insufficiency.[131–133] The breakthrough in identifying that progression of CKD was not chaotic was based on the determination that

individual CKD patients experience a loss of renal function with time is linear, constant and predictable.[134,135] The recognition that individual patients have a characteristic rate of loss of kidney function arose from the finding that the reciprocal of serum creatinine (SCr^{-1}) declines linearly with time in most patients. For example, about 80% of the patients reported by Rutherford et al.[136] or by Coresh et al.[137] had linear slopes in plots of changes in SCr^{-1} with time. The implication of this finding was that GFR declines linearly with time and therefore that creatinine clearance will decline linearly with time. These conclusions were confirmed by Viberti and colleagues who measured GFR sequentially in studies of patients with diabetic nephropathy[138] and by Barsotti and colleagues who measured CCr sequentially in patients with different types of non-diabetic kidney disease.[139] Results from the MDRD Study of patients with non-diabetic kidney diseases confirmed that GFR is lost in a linear fashion with time in larger numbers of patients.[140] In a group of patients with progressive diabetic nephropathy, the SCr^{-1} declined linearly with time as renal insufficiency advanced but the rate varied almost 40-fold[102] ! The conclusion is that individual patients exhibit a specific rate of loss of kidney function and hence, the rate of loss must be determined individually; it can not be assumed that a particular kidney disease has a "characteristic" rate of loss of GFR or CCr or SCr^{-1} with time[22,134,140] (Fig. 90.3). Considering the complexity of CKD, it is not surprising that some patients will have periods in which there are deviations from linearity and a "break-point" in the SCr^{-1} plot with time was reported in as many as 32% of 77 patients.[141] The clinical relevance of finding such a breakpoint was not reported, but is likely associated with new insults or acute perturbations in kidney function. In contrast, Coresh et al. found significant breakpoints in only 19% of a series of 67 patients who had sequential measurements that were made until ESRD was required.[137] There have been few reports comparing the rates of progression by measuring GFR and SCr^{-1} in the same patient. In one such study, the rate of loss of GFR in 17 selected patients was compared to changes in their plots of SCr^{-1} with time, four had progressive loss of SCr^{-1} but stable GFR values.[142] But, two of these four patients had to begin dialysis and one actually experienced a sharp increase in GFR while SCr^{-1} remained stable. When rates of progression were evaluated during different treatment periods, 9 of 22 periods exhibited a statistical difference between the slopes of estimated SCr^{-1} and DTPA clearance. In two of these periods, GFR remained stable while changes in the SCr^{-1} values of clearance suggested progression and in two other periods, the estimated SCr^{-1} method suggested faster progression. These results are difficult to interpret but as with any test, caution must be used when interpreting results since in 4 of 22 periods, the SCr^{-1} estimate yielded an inappropriate conclusion based on the measured GFR. A practical implication of these results would be that the physician caring for a CKD patients should investigate why the rate of loss of kidney function (GFR, CCr or SCr^{-1}) deviates from linearity.

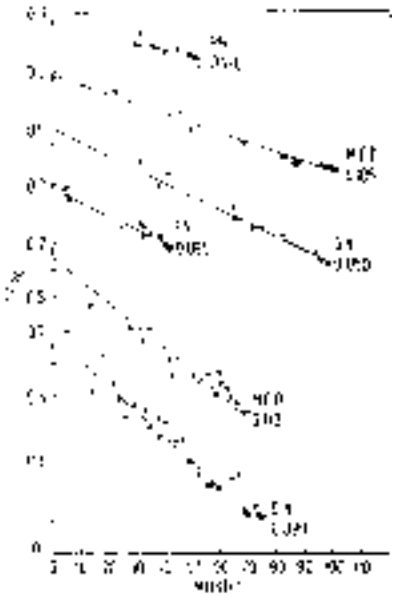

FIGURE 90.3 Rate of loss of residual renal function with time in patients with pyelonephritis (PN), medullary cystic disease (MCD), and glomerulonephritis (GN), estimated as changes in the reciprocal of serum creatinine concentration ($1/S_{cr}$). The unit divisions of the ordinate have been changed so that the curves can be displayed on the same plot numbers that refer to final measured value for $1/S_{cr}$. *(With permission from Mitch WE, Buffington GA, Lemann J, et al. A simple method of estimating progression of chronic renal failure.* Lancet *1976;2:1326–1328.)*

In estimating the rate of progression, it is suggested that GFR should be measured at least four times over two or more years.[143] This can be cumbersome because of the costs and complexities of measuring GFR. To circumvent this difficulty in trials directed at evaluating the effectiveness of therapy, another outcome has been used, the time required for serum creatinine to double. Unless large numbers of patients are studied, this method can be misleading because the rate of loss of GFR varies so widely even in patients with the same disease.[102]

For clinical evaluations, the SCr^{-1} vs time plot is a simple alternative of obtaining repetitive GFR measurements. Alternatively, the modified MDRD equation (see above) is widely recommended as a means of monitoring the course of renal insufficiency; inspection of this equation reveals that it is essentially a plot of relatively constant values (ethnicity, age, gender)

multiplied by SCr^{-1}. The reasons for the popularity of these methods are first, the measurement of serum creatinine is being standardized in most clinical laboratories, prior values are widely available and the values are reproducible (the day-to-day coefficient of variation in CKD patients with relatively advanced CKD is only 6.5%[144]). Second, SCr^{-1} (like GFR and CCr) declines linearly with time in most patients with progressive CKD.[22,134,137] Another alternative is to monitor changes in serum cystatin C but there are interpretative problems with this approach.

Do changes in SCr^{-1} with time spontaneously slow as GFR falls to low levels? Analyses of small groups of patients have not settled this question. There have been reports of either acceleration or slowing of changes in SCr^{-1} in patients with advanced CKD.[145,146] Results from the AASK (African-American Study of Kidney Disease) trial suggested that patients with hypertensive nephrosclerosis had accelerated loss of GFR but the interpretation is complicated because the rapid loss of GFR was largely confined to those treated with ramipril but not in those treated with amlodipine or metoprolol.[147] Thus, certain treatments or possibly changes in processes causing nephrosclerosis may indeed, change the loss rate of loss of GFR so it is no longer constant. Besides these factors, results from the AASK trial also uncovered an accelerated loss of GFR in those patients assigned to a mean blood pressure goal of 102 mm Hg at least when compared to MDRD study patients who were enrolled with a similar blood pressure goal and no dietary restriction.[140] These variations in response seem to point to a difference characteristics of the patient population (e.g., possibly genetic) or in the pathophysiology of nephrosclerosis. For example, it was recently reported that the rate of loss of GFR in participants in the AASK trial was not improved by lowering the blood pressure to $\leq 140/80$.[148,149] The caveat is that patients with higher degrees of proteinuria might have a more beneficial response.

There are other reasons why creatinine-based methods (SCr^{-1}, estimated CCr, or MDRD GFR) could yield an inaccurate estimate of the rate of loss of residual renal function. First, it is well known that creatinine secretion accounts for differences between CCr and GFR and any method of estimating CCr method will not correct for secretion.[31,146] Second, as discussed earlier, creatinine production exceeds creatinine excretion because there is extrarenal elimination of creatinine (presumably degradation by gastrointestinal bacteria[150]). Fortunately, there is a method for correcting CCr for the creatinine extrarenal clearance because there is evidence that the extrarenal clearance is constant.[37,51] Using a constant value of 0.04 liters/kg/day for the extrarenal clearance, it can be shown that the linear decline in CCr of patients with CKD is compatible with a linear decline in the SCr^{-1}.[22,139] It should be pointed out, however, that it is not known whether extrarenal CCr is constant throughout the course of CKD. A more important confounder is the problem of dietary factors, especially variations in the amount of meat eaten. Meat, like other muscle, contains creatine, so varying meat in the diet varies the size of the creatine pool. Cooking meat converts a portion of the creatine to creatinine, so the larger creatine pool will increase the amount of creatinine that is excreted.[20] In contrast, an abrupt reduction in meat intake decreases the creatine and creatinine pools, and this will lower serum creatinine at least as long as CCr is constant. On the other hand, if GFR falls, then serum creatinine will rise. When the meat content of the diet is relatively constant, any change induced by varying dietary meat and hence, creatine intake, is at best short-lived because the conversion of creatine to creatinine in muscle (and other cells) is quite slow; the turnover of the endogenous creatine pool averages only 1.7% per day.[20,151,152] Thus, a new steady state of creatinine production after a sustained change in meat intake will occur in approximately four months.[22,37] In practical terms, if dietary protein is reduced to any extent, a change in serum creatinine should not be used as an indication that the loss of GFR has been identified until at least four months have passed. Finally, there is the problem that raising dietary protein acutely increases GFR and, hence, CCr.[153] This alone has virtually no effect on changes in SCr−1 but will affect GFR if the measurement occurs shortly after a meal.[154] On the other hand, results from the MDRD indicate that a prolonged decrease in dietary protein (or blood pressure) can be associated with a sustained fall in GFR that is due to hemodynamic factors. This decrease in GFR does not signify a loss of kidney function because GFR rises following resumption of a higher protein intake.[140] In summary, changes in serum creatinine alone should be discarded as a method of estimating the GFR, and hence, the degree of kidney damage. For an individual patient, however, changes in the slope of SCr^{-1} can be used to screen and detect patients who are progressing, or determine if there has been a sudden change in clinical status. Ideally, changes in SCr−1 should not be used to determine if a new therapy slows progression; changes in GFR should be measured more accurately.

The emphasis should be on evaluating the course of renal insufficiency in an individual patient. It is well known that variation of rates of progression among patients is high: Jones et al.[102] reported that patients with diabetic nephropathy had rates varying as much as 20-fold, and Walser[143] found that changes in 99mTc-DTPA clearance in 34 patients with different causes of CKD varied from −0.96 to +0.64 ml/min/month.

According to these results, about 15% of CKD patients may not show any progression (at least during the period of observation). These results emphasize why clinical trials with no attempt to initially screen patients to exclude those with no evidence of progressive loss of GFR will be at risk of studying an inadequate number of subjects and thereby leading to incorrect conclusions.

PATHOPHYSIOLOGY OF CKD

The pathophysiology of CKD is varied depending on underlying injury and the response to injury is complex involving interplay of hemodynamic and biochemical processes that affect the glomerular capillaries and tubulointerstitium. In this section we will focus largely on common pathways of renal injury and waste products of protein metabolism, which are among the most important determinants of progression and uremia. To retain the larger view of the pathophysiology generated by loss of renal function, we will discuss the role of other uremic toxins, including hormonal changes. We will touch briefly on other crucial factors such as sodium and 1,25 hydroxyvitamin D3 affecting the development of CKD; these are discussed in other chapters.

Hyperfiltration Theory

Thomas Addis was a pioneering nephrologist who came to Stanford University in the first half of the twentieth century. He introduced and developed the concept of osmotic work by progressively nephrectomizing rats to varying degrees, feeding them diets with varying amounts of protein. He used renal ablation (1 and 5/6 nephrectomy) as a model of kidney disease and showed that when he progressive reduced the kidney volume in rats, the kidney hypertrophied.[155] He observed that the more renal mass that was removed the greater the remnant kidney grew in relation. He hypothesized the kidneys hypertrophied because of the increased osmotic work that the remnant kidney had to undertake. His work led to speculation about the mechanism by which protein restriction preserved renal function and inspired further work in this field. The question reduced renal mass was revived by Brenner, Deen and others who found a way to study the hemodynamic changes that take place in animal models of CKD.[156] The discovery of Munich-Wistar rats, a unique breed that had superficial glomeruli that was accessible using micropuncture techniques, was especially useful in characterizing the pathophysiology of CKD. Investigators found that characteristic hemodynamic changes take place in the glomerular capillaries of nephrectomized rats, namely increased glomerular plasma flow and increased hydraulic pressure, which accounted for the observed rise in single nephron GFR (SNGFR). This increase in glomerular capillary hydraulic pressure (glomerular hypertension) causes injury, which results in progressive glomerulosclerosis. Investigators found that glomerular hypertension was result of renal adaptation of nephron loss (due to any cause) and that a final common pathway resulting in progressive nephron loss occurred once glomerular number was reduced below a critical threshold.[157,158] The hyperfiltration theory is generally accepted as the cause for progressive renal failure in CKD and therapies targeting glomerular hypertension (e.g., ACE inhibitors) as an intervention to retard progression have been pursued with success.

Hemodynamic Mechanisms of Progression

Systemic hypertension. Arterial hypertension arises in the course of most cases of chronic renal insufficiency, and generally increases as renal damage progresses. Most but not all clinical studies suggest that blood pressure control can sharply reduce the rate of loss of renal function and all studies demonstrate important reductions in cardiovascular mortality. The role of sodium intake on blood pressure and mechanisms of hypertension-related renal damage are discussed in detail elsewhere (Chapter 88), but it is important to recognize the primary role that sodium retention plays in the hypertension seen in CKD. While population studies strongly suggest increases in blood pressure when sodium intake is increased, healthy subjects do not invariably increase blood pressure and GFR.[159] However, an increase in salt intake not only raises blood pressure in humans with mild CKD but also increases GFR (see below). In addition to sodium, dietary influences on blood pressure include protein, calcium, potassium, and trace minerals, and the complex interaction of these factors explains the blood pressure reduction with the Dietary Approaches in Systolic Hypertension (DASH) diet.[160]

In experimental kidney disease, there is an association between an increase in dietary protein and a higher blood pressure, and lowering dietary protein has been effective in reducing systemic arterial pressure in mineralocorticoid-induced hypertension in rats.[161] In other forms of experimental hypertension, dietary protein restriction has not been so clearly associated with a reduced systemic pressure. The systemic hypertension that develops in rats following subtotal nephrectomy or in the two-kidney, one-clip renovascular hypertension model persists even when dietary

protein is severely restricted.[162] In several models of CKD, dietary protein restriction diminishes renal injury, but there has been no consistent decrease in blood pressure, indicating that the beneficial effects of protein restriction do not necessarily depend directly on reducing salt or eliminating some unidentified factor or compound that raises blood pressure.

Similarly, for humans with essential hypertension, there is no clear cause-effect relationship between protein intake and arterial pressure.[163] Notably, when adults with CKD and hypertension are examined, systemic blood pressure has not been consistently reduced by restriction of dietary protein intake, similar to the results found in rats with CKD from subtotal nephrectomy.[140,164–167] The caveat is that a high-protein diet is generally associated with a high salt intake, and this could certainly raise the blood pressure of hypertensive CKD patients. However, raising the vegetable and dairy protein content of a DASH diet does not impair the effect on blood pressure lowering.[168] The observation that the role of dietary protein on blood pressure in CKD appears to increase as GFR falls[169] suggests that either alterations in diseased nephrons create sensitivity to dietary protein or that other dietary-derived compounds accumulated in CKD (e.g., phosphorous, acid, uric acid, or other uremic toxins) cause hypertensive effects. Of these compounds, uric acid is most clearly associated with hypertension (see below). Recent reports emphasize that diets that are uncontrolled for phosphates or salt will negate the beneficial effects of angiotensin converting enzymes on the progression of CKD.[169a,169b] These reports emphasize the importance of the design of a diet for patients with CKD.

Other hemodynamic effects. The neurohumoral basis for the hemodynamic responses of normal and diseased nephrons to changes in dietary protein is unknown but there are several candidates. For example, infusion of amino acids causes vasodilatation; somatostatin blocks this response.[176,177] The changes induced by somatostatin could be secondary to many hormones, including glucagon, because plasma glucagon levels rise with oral protein feeding or intravenous amino acids while intravenous infusion of glucagon to achieve blood levels that are similar to those observed following an amino acid infusion does provoke a rise in GFR and renal blood flow in humans.[178] This response to glucagon, however, appears to depend at least in part on prostaglandin (PG) synthesis because the simultaneous administration of a cyclooxygenase inhibitor and either amino acids or glucagon blunts the expected increase in GFR and renal blood flow. Several cyclooxygenase-dependent products could be the mediator in these studies; at least urinary excretion of PGE and the prostacyclin metabolite, PGF1α, are quite variable following dietary protein loads, making it unlikely that these compounds are the sole mediators of renal vasodilatation. Another renal vasodilator system, the endothelium-derived relaxing factor or nitric oxide, could be involved since blocking of the synthesis of nitric oxide does cause renal vasoconstriction in the rat.[129,179] Moreover, the renal vasodilatation that occurs with amino acid infusion appears to be particularly susceptible to nitric oxide synthase blockade, suggesting that nitric oxide is a major factor affecting the renal hemodynamic response to dietary protein. In fact, a chronic increase in protein intake by normal rats increases both GFR and the excretion of metabolites of nitric oxide.[180] The stimulus for nitric oxide production is uncertain but some suggest that it is arginine, the substrate for nitric acid production.[181,182] However, infusion of amino acids other than arginine also causes renal vasodilatation, emphasizing the complexity of this response.

In rats with diseased kidneys, raising dietary protein increases GFR by raising renal blood flow, but also by increasing areteriolar tone.[165] The major mediator of the rise in efferent resistance is initiated by renin secretion activating the intrinsic, intrarenal angiotensin-converting enzyme activity. This raises angiotensin II to cause efferent arteriolar vasoconstriction. Notably, dietary protein stimulates renin and angiotensin-converting enzyme expression in the kidney.[165,183] The response is more complicated than prolonged stimulation of the efferent arteriole,[184,185] and may involve production of another intrarenal hemodynamic mediator such as endothelin.[165,186] When glomerular capillary pressure or the diameter of glomerular capillaries increases, the tension in the capillary walls will rise, and constriction of the efferent arteriole constriction will also augment the increase in wall tension. This increase in mechanical stress could cause or at least predispose to sclerosis.

Do similar events occur in other animal models of CKD? Similar events do occur, at least partially. Following subtotal nephrectomy, cats fed a high-protein diet (51.7% protein) develop more serious kidney injury than cats fed a more restricted diet (27.6% protein).[187] At least over the short term, the cats fed a high-protein diet do not have loss of GFR. Baboons subjected to a partial nephrectomy and fed 25% protein did lose GFR at a faster rate than animals fed 8% protein; the degree of histologic damage was not reported.[188]

Plasma aldosterone levels also increase with dietary protein and this could induce a fibrotic response in the kidney.[186,189] Hostetter and colleagues studied the subtotal nephrectomy CKD model in rats treated with aldosterone inhibitors and found that the treated rats had less kidney damage.[190] In recent studies, they have found that aldosterone treatment over only 3 days will

stimulate TGF-β expression independently of the degree of hypertension.[191] Thus, aldosterone should be added to the list of factors causing kidney damage in CKD.

Uric Acid

Another accumulated product that has toxic properties and is associated with a high-protein diet is uric acid. A 12-year population study of 47,150 previously normal men led to the conclusion that diets containing high levels of meat or seafood are associated with an increased risk of gout.[170] The mechanism for this effect was not identified. Besides gout, Johnson and colleagues have emphasized the toxicity of uric acid. They point out that the gene encoding urate oxidase was lost by primates millions of years ago leading to plasma uric acid levels that are substantially higher in humans compared to rodents, and other animals.[171] Johnson et al. also point out that hyperuricemia predisposes humans to hypertension, through sodium retention and possibly a renin-dependent mechanism. They showed that when rodents are given an inhibitor of uricase and/or allopurinol, there is an important association between the plasma level of uric acid and hypertension and the rate of loss of residual renal function.[172,173] Importantly, they found that serum uric acid levels in untreated, otherwise normal adolescents with hypertension are highly correlated with systolic blood pressure ($r^2 > 0.8$). In a randomized, controlled crossover trial of 30 hypertensive adolescents Feig et al. showed that patients treated with allopurinol treatment resulted in significant reduction in blood pressure by a mean systolic pressure reduction of −6.9 mmHg (95% CI −4.5 to −9.3 mmHg) and mean diastolic change of −5.1 mmHg (95%CI −2.5 to −7.8 mmHg).[174]

Identifying the impact of uric acid on progression of renal insufficiency is difficult because the serum uric acid level in these patients do not rise to the level that would be predicted from their degree of lost kidney function. This occurs because bacteria in the gastrointestinal tract extensively metabolize uric acid and hence, it is difficult to link the serum uric acid to dietary protein or to rates of loss of kidney function.[175] On the other hand, the plasma uric acid level of patients with CKD is above the concentration that has been shown to be associated with hypertension and possibly kidney damage.[171] For the same reason, the degree to which dietary protein restriction will reduce the level of serum uric acid in CKD patients has not been established. Potential mechanisms that cause the nephrotoxicity of uric acid have been explored. In rats given an inhibitor of urate oxidase, there is only a slight rise in serum uric acid (1−2 mg/dl) but this is associated with the development of a primary arteriolopathy which is independent of hypertension; this abnormality is largely corrected by allopurinol treatment.[173] Similarly prepared rats were found to have glomerular hyperfiltration, an abnormality that was prevented by allopurinol administration. Other mechanisms might involve impairment of nitric oxide. Both normal and CKD rats (subtotal nephrectomy) exhibit collagen deposition, macrophage infiltration, and an increase in juxtaglomerular renin content, but there also is a decrease in the macula densa expression of neuronal nitric oxide synthase. It is proposed that uric acid decreases nitric oxide synthesis in endothelial cells, possibly through peroxynitrite production and oxidative injury.[129,171] The scientific evidence suggests that uric acid could have a role in the development of hypertension and possibly kidney disease progression. At present, additional information is needed before we can recommend the use of uric acid to protect against progression of CKD. Certainly, acute or chronic gouty attacks should be treated.

Progression of Experimental Renal Damage and Dietary Protein

There is a body of evidence that suggests proteinuria is toxic to the kidney. This is relevant because high-protein diets potentiate proteinuria. For example, it has been proposed that filtration and subsequent reabsorption of albumin by proximal tubule cells can excite inflammatory responses, including expression of NF-κB, a transcription factor that is heavily involved in mediating inflammatory responses.[192,193] Clinical support for this formulation comes from results of a multicenter trial (RENAAL): when proteinuria was successfully suppressed, there was a decrease in the risk of both kidney failure and major cardiovascular events such as stroke, congestive heart failure, and death.[194,195] The relevance to the amount of protein eaten is that dietary protein restriction suppresses proteinuria and will add to the effectiveness of the antiproteinuric response to ACEIs.[196–198]

The beneficial effects of dietary therapy in order to limit renal injury in experimental models of CKD have been recognized for more than 65 years (Table 90.4).[199]

TABLE 90.4 Experimental Models of Renal Diseases Improved by Dietary Protein Restriction

Subtotal nephrectomy
Nephrotoxic serum nephritis
Doxorubicin nephrosis
Deoxycorticosterone acetate (DOCA)-salt hypertension
Spontaneous hypertension with reduced renal mass
Salt-sensitive hypertension with glomerulonephritis
Diabetes mellitus
Spontaneous glomerular sclerosis of aging
Antitubular basement membrane nephritis

Identification of the mechanisms responsible for the effectiveness of dietary therapy requires integrating the separate contributions of dietary protein, phosphates, salt, and/or unexcreted metabolic waste products that cause ongoing kidney damage. This identification would be useful not only to understand how diet affects the kidney, but also because it could lead to more specific therapies that would act to preserve kidney function. The mechanisms by which components of the diet affect kidney function are probably not mutually exclusive. We will focus on the dietary protein derived largely from meat as is typical in a Western diet. There are some intriguing data suggesting that diets of different protein sources might be less nephrotoxic in early CKD, but there is insufficient human evidence to judge this question at this time.[109] Later in CKD, the high phosphorous content of vegetable and dairy protein sources makes these diets poorly tolerated.[169]

Nephrotoxic Compounds Derived from Dietary Protein

When speaking to patients and the lay public, we often explain the manifestations of kidney disease in terms of poisons that accumulate in bodily fluids as renal function (GFR) falls. The appealing simplicity of this concept is based on the role of the kidney as the principal clearance mechanism for water-soluble waste. In this concept, the symptoms progress with declining GFR because of the decreased clearance of substances (often called "uremic toxins") that cause specific signs or symptoms of CKD.[200] In 1905, Folin pointed out that the principal metabolic response to an increase or a decrease in dietary protein content is a parallel change in urea excretion.[201] Using somewhat more sophisticated techniques, the same relationship between protein intake and urea production has been demonstrated repeatedly in normal adults and patients with CKD.[202–204] This occurs because protein ingested is metabolized in the gastrointestinal tract to peptides and amino acids. These peptides and amino acids are further degraded in the gastrointestinal tract or liver, yielding an enormous number of nitrogen-containing products that must be excreted by the kidney in addition to the newly synthesized proteins. Thus, if kidney function is impaired, it follows that the products arising from the metabolism of dietary protein will accumulate in patients in direct proportion to the amount of protein eaten and in inverse proportion to the degree of kidney failure. Accumulation of unexcreted compounds not only causes metabolic abnormalities but also can damage the injured kidney. A more categorical discussion of protein-derived uremic toxins follows in the next section.

Progression of renal disease can similarly be seen to be caused by accumulation of these toxins. While it is theoretically possible that there is one toxin that explains progression of renal disease or certain signs and symptoms, the interaction of many toxins is thought to be required in most circumstances. For example, a combination of waste products of protein metabolism (urea, magnesium, acetoin, 2, 3-butylene-glycol, sulfate, creatinine, p-cresol, and guanidine) impair oxidative metabolism in slices of cerebral cortex, but when studied separately at the same concentration, each agent has no effect.[205] Certain signs or symptoms that do not increase progressively as GFR fails can be explained by a threshold model. Furthermore, if a threshold can be identified, the threshold concentrations can define criteria for adequacy of renal replacement therapy. While simple in theory, the large number of potential uremic toxins makes such calculations difficult. In 2003, the European Uremic Toxin Work Group (Eutox) published a structured review of the literature identifying 90 known compounds that are accumulated in CKD that have toxic potential. Since then 25 additional retention solutes have been identified, thus suggesting the uremic syndrome is produced by complex biochemical interactions of a number of retained solutes.[206]

Bergstrom has proposed definitive criteria for determining if a proposed chemical (organic or inorganic) compound is a uremic toxin: (1) the chemical identity of the compound should be known; (2) the concentration should be higher in tissue or plasma from uremic patients than in that from normal subjects; (3) the concentration should correlate with specific uremic signs or symptoms and be improved by the removal of substance; and (4) the toxicity of the compound in tissue, cells, or a test system should be demonstrated at the concentration found in tissue or fluids from uremic patients.[207] Given the complex nature of renal excretion, few compounds have been found that meet all criteria.

Urea

The possibility that urea itself might be toxic has been tested, albeit with some challenges, since the half-life of urea is short with normal kidney function is difficult to test the toxicity of urea.[200] Nephrectomized dogs, treated with peritoneal dialysis and a dialysate supplemented with urea, achieved BUN values between 173 and 224 mg/dl and developed weakness, anorexia, and decreased attentiveness.[208] Continued therapy was followed by vomiting, hemorrhagic diarrhea, hypothermia, and death. In humans, no apparent toxicity was seen when chronic dialysis patients were dialyzed against urea-supplemented dialysate.[209] However, when the urea concentration was gradually

increased in the dialysate of stable long-term hemodialysis patients to obtain a steady state BUN between 140 and 200 mg/dl for several weeks, most patients experienced malaise, weakness, lethargy, and a bleeding diathesis.[210] Thus, some symptoms of uremia, such as nausea, vomiting, malaise, and bleeding, may be due to urea intoxication; other uremic symptoms cannot be provoked by even high urea concentrations. Thus, urea seems to be clinically important only at very high concentrations. Consistent with this idea, there is little direct effect of high urea on cellular function. Urea suppresses inducible nitric oxide synthesis in mouse macrophages and stimulates macrophage proliferation in a dose-dependent fashion.[211] This response could be relevant to the proliferation of macrophages within atherosclerotic lesions.

One possible explanation for this high degree of tolerance to urea is that its decomposition may be required for direct toxicity. Urea can also be spontaneously decomposed to form ammonia or cyanate adducts. Cyanate can condense with NH_2-terminal amino and amide lysine groups on proteins to alter the tertiary structure of proteins; enzyme activity can change. This explains why CKD is associated with carbamylation of many proteins. The consequences of this process are not settled; protein carbamylation has been reported to aggravate the uremic syndrome and may decrease the activity of insulin.[212] As discussed below, carbamylation may enhance oxidation and formation of advanced glycosylation end products. A variety of lipids may also be carbamylated to form toxins.[200] For example, 3-carboxy-4-methyl-5-propyl-2-furaproprionic (CMPF) acid has been demonstrated to be a major cause of altered drug protein binding in uremia.[213] Finally, urea is converted to ammonia and carbon dioxide, principally by bacterial urease. Systemic blood ammonia levels are minimally elevated in uremia, largely because the resulting ammonia diffuses across intestinal epithelia to portal blood and is reconverted to urea in the liver.[214,215] Thus, at high concentrations urea is toxic, but is insufficient to completely account for the uremic syndrome.

Other Toxic Metabolites of Protein

A major difficulty in identifying uremic toxins occurs because most compounds produce toxic effects in concert with other compounds or after secondary modification.[200] Widespread and variable secondary modification of organic molecules by carbamylation, glycosylation, and oxidization in uremia often influences their toxicity.[212,216] Rather than trying to identify individual toxins, the toxins should be considered in broader categories. The most important group is the products of protein metabolism. These include not only nitrogen containing compounds, but also metabolic acidosis and phosphorous.[169] However, any substance with decreased clearance can meet these criteria including bacterial products, electrolytes (e.g., sodium), cytokines, and hormones.[200]

Not all manifestations of chronic kidney disease are caused by water-soluble toxins easily cleared by hemodialysis or peritoneal dialysis.[206] Inadequate removal of toxins can lead to complications even with seemingly adequate dialysis: the inability to clear sufficient sodium in conventional hemodialysis leads to extracellular volume expansion, cardiac dilatation, sympathetic nervous system activation, and inflammatory cytokine production. But even with ideal dialysis therapy, there is increasing evidence that other aspects of renal function may still drive complications of CKD. The best examples of this are the hormones erythropoietin (EPO) and 1,25 hydroxyvitamin D3, where the kidney acts as a major source of production. Larger molecules (both so-called middle molecules (0.5−3.0 kD) and larger polypeptides) including many hormones and cytokines, are destroyed by the kidney and their levels rise as GFR declines. The kidney is metabolically active playing a secondary role in glucose production, lactic acid metabolism, and arginine metabolism. These metabolic functions of the kidney may not be crucial in the normal, resting state, but may regulate major adaptations in liver disease, oxidative stress, and regional ischemia.

The principal example of metabolic disorders is the accumulation of unexcreted acid arising from the metabolism of certain amino acids (e.g., sulfur-containing amino acids and others). Metabolic acidosis leads to several metabolic abnormalities including an increase in the breakdown of protein and essential amino acids, insulin resistance, and abnormalities in endocrine function and bone metabolism.[217−221] An example of a toxin accumulated by CKD patients is indoxyl sulfate, which arises from the breakdown of tryptophan.[222] When given to rodents that serve as models of glomerular sclerosis, indoxyl sulfate (or indole compounds) accelerates the degree of kidney damage.[223,224] The mechanism underlying this toxic effect is complex and may involve expression of TGF-β in the kidney, but how TGF-β is stimulated and whether other toxic mechanisms are involved is unknown.[225] The link to dietary protein is that accumulation of indoxyl sulfate in uremic rats and CKD patients can be reduced by restricting dietary protein.[226] This should not be surprising because the amino acid, tryptophan, is the precursor of indoxyl sulfate. Another means of lowering indoxyl sulfate is by ingestion of a sorbent to increase its extrarenal clearance, and there are clinical trials assessing if this strategy as a means of preventing uremic toxicity.[226,227]

Besides these compounds, other potentially toxic metabolites of dietary protein can affect kidney

function indirectly. For example, excess dietary protein will increase the accumulation of phenylalanine metabolites in patients with renal insufficiency, and at least in dialysis patients, phenylacetic acid accumulates and inhibits the expression of inducible nitric oxide synthase.[228] This inhibitory effect could increase atherosclerosis, one of the major problems caused by kidney failure. The metabolism of amino acid derivatives, like the metabolism of creatinine, is complex in patients with renal insufficiency.[51,175] Metabolism of these (and other) compounds makes it difficult to predict how the serum/plasma level of these compounds will change or how abnormalities caused by accumulation of the metabolites will respond to dietary protein restriction. Regardless, it is clear that dietary protein restriction will decrease the accumulation of any of these products.

Guanidino-Containing Compounds

Guanidino compounds are strong organic bases that bear the amidino group; these compounds accumulate in the sera and tissues of uremic patients.[200,229,230] Dietary protein is the ultimate source of the nitrogen in guanidino compounds, and their excretion rises with increased protein intake.[231,232] However, urinary excretion of guanidine compounds in CKD patients is higher than that of control subjects even when protein intake is the same. Because the extrarenal clearance of these compounds is negligible, it follows that CKD increases the production of guanidino compounds. The biochemical pathways in which guanidino compounds are synthesized are largely unknown. Arginine can be converted into amidino groups *in vivo*, and urinary excretion of both methylguanidine and guanidinosuccinic acid rise when dietary protein is increased, but whether this is attributable to an increase in arginine accumulation is unknown. Besides arginine levels, there are other factors regulating their production. Kopple et al.[231] reported that three CKD patients with a constant protein intake had increased excretion of guanidinosuccinic acid with an intercurrent illness. Most synthesis of guanidine-containing compounds from arginine is likely to occur in the liver, because there is a high activity of glycine transamidinase and a low rate of arginine export by hepatocytes.[233] Arginine turnover in normal adults includes a relatively large nonexchangeable pool in the liver that could serve as a source of guanidino compounds, and perfusion of rat liver with L-[guanidino-14 C] arginine yields a progressive increase of 14 C-guanidinosuccinic acid.[234] Ingestion of L-[guanidino-15 N] arginine by uremic patients yielded 15N-methylguanidine at levels that initially exceeded that present in creatinine, consistent with (methylguanidine) being a precursor of creatinine.[235] This result supports the hypothesis that arginine may be degraded to form methylguanidine and a-aminobutyric acid. High concentrations of creatinine or its immediate precursor, guanidinoacetic acid decreases utilization of arginine to form guanidinoacetic acid. The increased availability of arginine may lead to donation of its amidino group to form other compounds, such as guanidinosuccinic acid, methylguanidine, γ-guanidinobutyric acid, and guanidinopropionic acid.[236] Regardless of the mechanism, the concentration of guanidino compounds in tissue and plasma increases as renal function declines, and their concentrations are best correlated with the amount of protein eaten.

Difficulty measuring plasma and tissue concentrations of guanidino compounds has caused much of the controversy surrounding the importance of candidate uremic toxins.[200] Because there is great variation among species in levels of guanidino compounds, human studies will be considered here.[237] Plasma levels as high as 8 to 10 mM can occur in uremic patients, but corresponding tissue levels have not been extensively studied, so it is difficult to verify toxicity. Methylguanidine has been detected in the cerebrospinal fluid of uremic patients, but not in normal subjects or experimental animal models of renal failure.[238] *In vitro*, high doses of methylguanidine cause autohemolysis, defects in erythrocyte metabolism, and inhibit salivary and exocrine pancreatic secretion.[239] Likewise, guanidinopropionic acid, guanidinoacetic acid, or γ-guanidinobutyric acid can cause autohemolysis of red blood cells, possibly related to inhibition of glucose-6-phosphate dehydrogenase.[240] Clinically, plasma levels of these compounds in uremic patients can be shown to be inversely correlated with the erythrocyte glutathione concentration, suggesting they induce a loss of the protective effect of glutathione against hemolysis. Other guanidino compounds may have neurotoxic effects: guanidine and methylguanidine have been related to peripheral neuropathy, and γ-guanidinobutyric acid, taurocyamine, homoarginine, and α-keto-δ-guanidinovaleric acid lower the seizure threshold of experimental animals.[241] The concentrations of guanidine compounds in serum, urine, and cerebrospinal fluid of nondialyzed patients with renal insufficiency were as much as 100-fold higher in the cerebrospinal fluid of uremic patients, and these compounds can induce experimental convulsions at concentrations found in uremic brain.[242,243] Based on biochemical and electrophysiologic measurements *in vitro*, the central nervous system excitatory effects of uremic guanidino compounds could be explained by inhibition of γ-aminobutyric acid (GABA) receptors, selective activation of N-methyl-D-aspartate (NMDA)

receptors by guanidinosuccinic acid, and an intrinsic depolarizing response.[244]

ADMA and Other Arginine Derivatives

Related compounds derived from arginine can inhibit NO synthase: asymmetric dimethylarginine (ADMA) inhibits this enzyme and some, but not all, investigators feel that ADMA accumulates in patients with impaired renal excretion.[245,246] Interpretation is difficult because plasma concentrations of ADMA are higher in patients with vascular disease and even asymptomatic hypercholesterolemia.[247,248] A recent report found a GFR-dependent increase in the serum concentration of ADMA and related compounds in CKD patients, but also found that patients with both CKD and cardiovascular disease had even higher levels.[246] Clearance of ADMA by hemodialysis is lower than expected for its molecular weight, suggesting that there is binding to plasma proteins. For example, two groups found only a 20% reduction in ADMA concentrations during dialysis.[245]

In experimental animals, accumulation of ADMA is associated with a concentration-dependent pressor and bradycardic response and vasoconstriction in mesenteric and hindquarter vessels.[249] In CKD patients, loss of the vasodilating properties of NO (e.g., because of a high ADMA level) could aggravate hypertension and accelerate the progression of renal failure.[250] A positive correlation between plasma levels of ADMA and mean arterial blood pressure has been noted and possibly an inverse relationship between progression of CKD and nitrate excretion.[251] Despite the suggestive higher levels in cardiovascular disease patients and the appropriate physiologic responses, there are no studies showing whether ADMA causes cardiovascular disease or cardiovascular disease increases ADMA.[246] Besides changing hemodynamic responses, NO depletion may cause anorexia in hemodialysis patients as administration of N-nitro-L-arginine, an inhibitor of NO synthesis, reduced the food intake of rats. Another possibility is that it raised the ornithine concentration because ornithine can inhibit protein ingestion in a dose-dependent manner.[252]

Products of Bacterial Metabolism

Uremic toxins can be synthesized by gut bacteria and absorption of bacterial products could be high because of increased permeability of the gastrointestinal mucosa.[200,253] The gut (mainly colon) has come forth as a major source of the generation of various metabolic wastes.[254,255] Nutrients that escape digestion/absorption in the small bowel become substrates for bacterial metabolism—there are more bacterial cells in the colon than there are cells in the whole human body. Moreover, there is bacterial overgrowth in the gastrointestinal tracts of uremic patients so it is possible that these bacteria contribute to the accumulation of "uremic toxins.[257]" Bacteria use the nutrients for their own metabolism, as well as generating short chain fatty acids, which are absorbed and used as energy. This constitutes about 3% of our total energy source, which is not a vital source of calories in modern societies, but in evolutionary terms or when food is scarce, this extra energy may be essential. Intestinal bacteria generate nitrogenous wastes and aromatic compounds (e.g., phenols, indoles, aliphatic amines) from protein metabolism and are cleared mainly by the kidneys. Bacteria derived uremic toxins include indoxyl sulfate, hippuric acid, p-cresol, and 3-carboxy-4-methyl-5-propyl-2-furanpropionic acid.[256] The evidence that bacterial products contribute to altered mental status in uremia is indirect: administration of nonabsorbable antibiotics to two patients with uremic encephalopathy resulted in a marked improvement in asterixis, myoclonus, mental alertness, and electroencephalographic abnormalities, coinciding with a decline in serum amine levels.[257] Some of these bacterial products are directly derived from amino acids; others are derived from compounds rich in muscle, such as creatinine, lecithin, and choline.

Aromatic amines. Tryptophan has been suggested as one of the major precursors of this class of uremic toxins.[200] Tryptophan undergoes deamination and decarboxylation by gut bacteria, yielding a variety of metabolites that include indole, indoxyl, skatole, skatoxyl, indican, and indoleacetic acid. Aromatic amines also result from bacterial metabolism of tyrosine, phenylalanine, or tryptophan.[258,259] Several indole compounds are high in the plasma of uremic subjects and can inhibit oxidative metabolism in brain slices.[260] Moreover, patients with uremic encephalopathy have high concentrations of tryptophan, 5-hydroxyindoleacetic acid, and homovanillic acid in their cerebrospinal fluid.[261,262] The pathogenic significance of this association is unclear, but 5-hydroxyindoleacetic acid is a precursor of the neurotransmitter serotonin, as well as indoxyl sulfate.[261,262] The potential nephrotoxicity of indol sulfate was discussed above. Uremic rats fed a proprietary resin that absorbs such compounds were found to have greatly reduced plasma and urinary levels of indoxyl sulfate, but more interestingly, there were improvements in several metabolic pathways, even though the degree of azotemia was unchanged.[222] The administration of this resin was associated with increased food intake, leading to the suggestion that other toxins causing anorexia were removed. Indoxyl sulfate can inhibit the deiodination of T4 to T3 in cultured hepatocytes.[263] Most if not all of the breakdown products of the aromatic amino acids, including

tryptophan, have been shown to interfere with the binding of drugs to serum proteins.

Aromatic amines could contribute to uremic encephalopathy by serving as false neurotransmitters.[258,259] Infusion of phenol or p-cresol into dogs results in a variety of neurologic symptoms, and conjugated phenols can inhibit ATPases and ion transport systems, leading to changes in intracellular ionic composition and abnormal cellular metabolism.[264] It is known that p-cresol can inactivate β-hydroxylase, a key enzyme in the transformation of dopamine to norepinephrine.[265] P-cresol is also associated with decreased bactericidal free-radical formation by activated macrophages[266] and reduces vascular endothelial function.[267]

Aliphatic amines. Aliphatic amines come from different sources: monomethylamine is thought to be derived from the metabolism of creatinine through sarcosine, whereas bacterial metabolism of choline and lecithin produce tertiary methylamines, which are absorbed and oxidized or demethylated to form secondary methylamines.[200,257,268] These compounds can be absorbed by the gut and taken up by the muscle of the animal and finally eaten by humans. For example, trimethylamine-N-oxide (TMAO) is readily absorbed from dietary fish, and is promptly excreted by normal adults, but accumulates in CKD patients.[269]

Secondary methylamines are high in blood, cerebrospinal fluid, and brain tissue, as well as in duodenal aspirates.[257,270] This may reflect the greater density of bacteria in the small intestines of uremic patients or the higher choline levels in the plasma of uremic patients Niwa has identified high levels of derivatives of hydroxyphenolic acids, including p-hydroxybenzoic acid and p-hydroxyphenylacetic acid and precursors of phenol and p-cresol, in the sera of hemodialysis patients; the levels were proportional to dietary protein intake.[222]

Toxins not derived from dietary protein. Finally, not all bacterial products that are potential uremic toxins are synthesized from amino acids or other substances in meat. Low-molecular-weight polyamines necessary for the synthesis of nucleic acid and cell growth include putrescine, spermidine, and spermine. These factors can be synthesized in mammalian tissues, and cadaverine and putrescine are formed by intestinal bacteria in a reaction that decarboxylates lysine and ornithine.[271] *In vitro* experiments indicate that spermine can inhibit erythropoiesis, whereas in hemodialysis patients, the serum spermine levels vary inversely with the hematocrit.

Evidence for Protein Restriction in CKD

For more than 100 years, it has been known that dietary protein restriction decreases the BUN and the severity of uremic symptoms.[200,272] Dietary manipulations in the form of protein restriction were the standard of care to alleviate the symptoms of uremia prior to the widespread availability of dialysis. Presumably this maneuver lowered the generation rates of nitrogenous waste solutes. When dialysis became readily available to treat advanced uremia, efforts to reduce uremic solute production by restricting the diet were largely abandoned. However, studies that manipulated dietary intake of protein provide important insight into the uremic syndrome. Cotton and Knochel demonstrated the toxic consequences of excess dietary protein by measuring abnormalities in the resting membrane potential of skeletal muscle fibers in patients with advanced uremia.[273] After six weeks of intensive dialysis, uremic symptoms improved, and the skeletal muscle resting membrane potentials returned to normal.[274,275] When the investigators reduced the frequency of their dialysis treatments, anorexia, nausea, and vomiting developed in four of six patients, and the muscle membrane potential fell. On the same reduced dialysis schedule, the diet was switched from 1 g of protein per kilogram per day to 0.5 g/kg/day plus a supplement of essential amino acids. With the reduced amount of dietary protein, five of six patients had normal membrane potential values in skeletal muscle (the remaining patient did not comply with the dietary restriction) and in all patients, uremic symptoms resolved.[273] We have discussed some of these protein-derived toxins in the section on progression of renal disease, especially uric acid. We will not discuss acidosis separately here, because it influences a variety of systems and will be discussed in detail in the section on endocrine abnormalities.

Besides reducing nitrogen intake, a low-protein diet is generally associated with a reduction in phosphorus and sodium intake. The potential benefit of lowering salt intake in hypertensive CKD patients is obvious, but benefits of dietary phosphate restriction are less obvious. A low-phosphate diet can mitigate the progressive renal disease that occurs after subtotal nephrectomy or experimental glomerulonephritis in the rat,[276] but interpreting these results is complicated because there are studies in which dietary protein but not phosphorus was varied, and it was concluded that dietary protein restriction without phosphate restriction can be beneficial.[277] On the other hand, dietary phosphate restriction without simultaneous protein restriction is capable of reducing progressive experimental renal disease. The mechanism whereby phosphate restriction reduces renal injury is uncertain. Four possibilities have been suggested. First, dietary phosphate restriction can reduce GFR so that its effect could occur by diminishing hyperperfusion in residual nephrons. Second, severe dietary phosphate restriction leads to defects in inflammatory responses and

dysfunction of leukocytes, which could reduce damage. However, the degree of phosphate restriction for this response is too severe to be used clinically. Third, intrarenal deposition of calcium phosphate crystals could be reduced by dietary restriction of phosphates as demonstrated histologically in 1937.[278] Fourth, phosphate restriction could minimize renal hypermetabolism (i.e., oxygen and glucose consumption).[279] Clearly, these mechanisms are not mutually exclusive, and all may contribute to the beneficial effects of phosphate restriction.

In summary, while there is confusion surrounding the identity of uremic toxins derived from animal protein, there is no shortage of candidate molecules. It is likely that many toxins contribute to any given pathophysiologic response. It is clear that the degree of uremic toxicity is roughly related to protein intake; the most severe symptoms occur in the patients with the highest protein intake; and most symptoms decline in severity when dietary protein intake is reduced or are removed through dialysis. However, there are pathophysiologic responses that do not respond to these maneuvers, suggesting that restricting dietary protein by itself is not sufficient for conservative management of uremia.

Larger Uremic Toxins

It is clear that not all compounds accumulated in CKD are small molecules derived from metabolism of dietary precursors for which urea is a surrogate marker.[200] For example, uremic neuropathy has been linked to accumulation of so-called "middle molecules" weighing between 500 and 3000 Daltons (0.5−3 kD).[280] Just like the smaller toxins, much of the controversy about the clinical importance of accumulating middle molecules stems from difficulties in identifying compounds present at low concentrations in fluid that is as chemically complex as plasma. It is also clear that the 3-kD cut-off for defining middle molecules is arbitrary, and larger protein molecules may cause uremic toxicity by similar mechanisms.

Middle Molecules

Most of the data on middle molecules derives from studies on fractions of uremic plasma. When the plasma ultrafiltrates from uremic patients or urine from normal adults were injected intraperitoneally into rats, their appetites fell sharply, whereas injections of normal saline or ultrafiltrates of plasma from normal adults did not alter feeding behavior.[281] It was concluded that one or more factors eliminated by the kidney accumulate in the body fluids of patients with renal failure and suppress appetite. Ultrafiltrate subfractions with molecular weights of 1−5 kD and 5−10 kD obtained from uremic patients were also shown to inhibit the hunger for carbohydrates and proteins in a dose-dependent manner.[282] Similar results occurred after direct injection of the middle molecule fractions into the lateral brain ventricles of rats, suggesting that specific brain receptors or neurotransmitters control feeding.[280] These results were site- and route-specific because intravenous injection of the same uremic ultrafiltrate subfractions had no effect on feeding behavior nor was the sexual behavior of the rats altered.[283] The authors concluded that middle molecules contained in plasma from uremic patients or from urine of normal adults act in both the brain and the splanchnic region to inhibit food intake.

Similar studies have implicated middle molecules in the impairment of immune responses and abnormalities in lipoprotein metabolism associated with uremia. Middle molecule fractions of uremic serum inhibited lymphocyte proliferation by 50% and decreased production of interleukin-2, a cytokine that stimulates T-lymphocyte proliferation.[284] Middle molecules also cause polymorphonuclear leukocyte dysfunction in uremia. Serum samples containing middle molecules can inhibit chemotaxis, oxidative metabolism, intracellular bacterial killing, and other polymorphonuclear leukocyte functions.[285−287] Middle molecule fractions from serum of uremic patients directly inhibit apolipoprotein A-I (apo A-I) production in hepatoma cells.[288] Since apo A-I is the structural protein for HDL, this mechanism could contribute to the lower HDL levels seen in CKD and ESRD patients.

What is the chemical identity of these molecules? Specific toxic responses to molecules identified thus far are unknown, although β2-microglobulin, which accumulates in the plasma of patients with renal failure, is the major constituent of amyloid-like deposits that accumulate in dialysis-related secondary amyloidosis.[289] Small polypeptides accumulate in the plasma of uremic patients; at least 38 ninhydrin-positive (i.e., amines or amino-containing peptides) have been isolated from dialysate, while peptide-bound, N-substituted amino acids are present in excess amounts in the plasma of uremic patients.[290] Abiko and associates isolated four peptides from the plasma of patients with severe uremia that were characterized as peptide fragments of plasma proteins that are eliminated or metabolized by the normal kidney.[291,292] Similarly, Chu and colleagues identified six middle molecules weighing between 800 and 2015 Daltons that accumulate in the serum of uremic patients but are excreted by healthy subjects.[293]

A number of these substances may be circulating hormones or cytokines accumulating in uremic patients—and we will discuss hormonal changes in a

separate section—but one class of possible middle molecule uremic toxins is inflammatory cytokines. The half-lives of circulating cytokines are elevated due to decreased glomerular filtration and proximal tubular uptake and destruction. How clinically relevant decreased destruction of small inflammatory cytokines is in CKD is unknown, and most well-studied cytokines are above the 3 kDa used by some to describe middle molecules. For example, elevated TNF-α and IL-6 plasma levels have been noted in CKD and ESRD.[49] However, cytokines often act in a paracrine fashion, so that circulating levels may not correlate with tissue action. In one study monocyte levels had a much smaller increase than in plasma.[294] Inflammation and oxidative stress clearly play a major role in increasing the production of these cytokines, accounting for the marked variability seen among patients and studies. Some cytokines do have important circulating responses. For example, reports suggest that IL-6 has important circulating effects to promote inflammation.[49] On multivariate analysis, serum creatinine was the sole determinant of IL-6 levels in a group of CKD patients.[295] The IL-6 circulating receptor, a binding protein that increases plasma half-life, also increased with declining GFR. However, these results suggest, but do not prove, that decreased renal clearance may increase plasma levels of this circulating cytokine.

The relative importance of larger versus smaller uremic toxins is not entirely known. Dialysis efficiently corrects the uremic syndrome, suggesting that low-molecular-weight solutes are most important. However, the high mortality of dialysis patients suggests that major abnormalities remain. A carefully performed study did not show a survival advantage (except in the subgroup of the patients who had been on dialysis the longest) of a larger hemodialyzer-membrane pore size (high flux dialysis) designed to clear some middle molecules.[296] Caution should be used in the interpretation of dialysis studies to determine the importance of small versus middle molecules, because of the distinction between dialyzability and elimination. For instance, inorganic phosphorous is readily cleared through dialysis membranes, but is removed poorly because of its large volume of distribution and slow release from its intracellular stores. Larger molecular weight fractions of plasma are also cleared efficiently by the kidney, but not with dialysis, even when high-flux membranes are used. Suggestions have been made that continuous dialysis or bioartificial kidneys may remove these molecules more successfully, but data remain limited. Overall, the data suggest that larger uremic toxins have the potential for enhancing morbidity associated with the uremic syndrome, but it is not clear what approach may be best for their removal.

Advanced Carbamylation, Oxidation, and Glycosylation Products

In the discussion on urea, we pointed out that modification of peptide and protein substrates by carbamylation probably accounted for some of the toxic effects of this molecule. Modification of protein substrates by carbamylation is a possible mechanism for formation of middle molecule and larger uremic toxins related to dietary protein intake. While proteins can be directly modified by oxidation and glycosylation, carbamylated proteins can have enhanced reactivity with oxygen and glucose accelerating formation of these products.

Oxidation

While carbamylation, glycosylation, oxidation, and nitrosolation of proteins are all probably important mechanisms for generating toxins, oxidant and glucose modification has a high correlation with cardiovascular disease. Generation of oxidant species is a normal enzymatic process example, xanthine oxidase, NAD(P)H oxidase, endothelial nitric oxide synthase (NOS), as well as by transition metals, such as iron.[297] Activated leukocytes and other phagocytic cells generate reactive oxidation species such as hydrogen peroxide or hydroxyl radicals. Antioxidant defenses include superoxide dismutase, catalase, glutathione peroxidase, trace metal scavengers and nonenzymatic substances such as melatonin, tocopherol, ascorbic acid, carotenoids, and flavonoids. The structure of proteins is altered by oxidation of specific amino acid residues such as tyrosine resulting in cross-linking, aggregation, or fragmentation of proteins following reactions with reactive oxygen species including advanced oxidation protein products.[216,298] An imbalance between reactive oxygen radical production and antioxidant defense occurs in uremia, although the mechanisms are not entirely clear.[297] Possible causes include changes in diet to reduce the intake of antioxidant compounds in fruits and vegetables, retention of circulating oxidant molecules, and intercurrent inflammatory illnesses. Dietary protein intake does not appear to influence oxidative stress.[299]

Advanced oxidation products can be found even in the early stages of renal insufficiency, but increase sharply with progressive loss of renal function. These products are at high concentrations in dialysis patients, forming protein aggregates, and there is a positive correlation between the levels of oxidation products and inflammatory markers such as TNF-α and its soluble receptor.[298] Because these compounds have been linked to the development of atherosclerosis,[283] formation of these products could be linked to cardiovascular disease.

Glycosylation. Advanced glycosylation end products (AGE) form from glucose modification of proteins, and are associated with toxicity in diabetes mellitus. While insulin resistance and reduced removal of small proteins are thought to contribute to AGE formation in CKD, they are not believed to be the only mechanisms.[300] Glucose can interact with proteins that have been modified by carbamylation to form AGEs. The toxic properties of AGEs have been well studied in the diabetes literature.[301] Needless to say, they may contribute to similar end-organ dysfunction in patients with CKD, including increased progression of renal disease. The role of AGEs may explain, in part, the synergistic effects of decreased GFR and diabetes on uremic signs, symptoms, and end-organ damage. Furthermore, the potential that this modification could interact with protein carbamylation and oxidation products to additively impair protein function must be considered.

Homocysteine and cysteine-homocysteine.One interaction between amino acids and oxidative stress is the formation of homocysteine derivatives. Homocysteine, a sulfur-containing amino acid derived from the metabolism of methionine or cysteine, is rapidly oxidized creating a special class of uremic toxins.[200] Homocysteine is found in the plasma and in erythrocytes and cells of the liver and other organs.[302–304] In plasma from CKD patients, the levels of sulfur-containing amino acids, including homocysteine, are high; the mechanism for these abnormalities is unknown. Accumulation of homocysteine is a potentially severe complication because of the association between homocysteine levels and cardiovascular disease. By convention, plasma or serum total homocysteine refers to the sum of homocysteine and its disulfide derivatives whether they exist in the bound or the free-state. Studies in rats and humans suggest that the kidney eliminates about 70% of the daily homocysteine burden and this indicates why homocysteinemia levels are high in predialysis as well as renal transplant patients[305,306] It is postulated that homocysteine plays a role in the excessive cardiovascular risk associated with CKD.[307] Homocysteine is metabolized by reactions that include transsulfuration or remethylation. In transsulfuration, homocysteine is degraded to cystathione and then to cysteine and other sulfur-containing compounds, including glutathione, taurine, hydrogen sulfide, and sulfate. In remethylation, homocysteine is methylated through the action of methylenetetrahydrofolate reductase. Folic acid is the major cofactor for this enzyme and a deficiency of folic acid leads to increases in homocysteine. Vitamin B6 is a cofactor involved in transsulfuration and vitamin B12 is involved in remethylation. Treatment of homocysteine excess with folic acid has shown some value in subjects with normal renal function, but was not proven effective in a clinical trial in dialysis and pre-dialysis patients.[308,309] This result has led to speculation about a folate-independent pathway for the hyperhomocysteinemia seen in ESRD.

Alterations in Endocrine Function

Many characteristic features of uremia result from the extensive disruption of endocrine systems. Clearly, hormones predominately produced by the kidney, such as EPO and 1,25-$(OH)_2D_3$, are found in progressively reduced concentrations as CKD worsens.[69] However, more subtle disruption occurs in endocrine systems that have no renal production. Accumulation of nitrogenous waste, phosphate and other inorganic acids, and the effect of other hormonal systems affect endocrine systems, which is addressed in Chapter 91. In the discussion below we will limit our focus to endocrine abnormalities that affect nutritional status and protein turnover.

Insulin

Patients with CKD exhibit significant abnormalities of glycemic control. These include an alteration of peripheral glucose utilization, a subnormal response to insulin, and elevated plasma insulin.[310] The increase in insulin levels is generally attributed to the decreased insulin catabolism secondary to renal dysfunction. Insulin requirements decline in diabetic subjects with advancing CKD, because most insulin catabolism is mediated by the kidneys. The plasma *t1/2* of insulin increases significantly when the creatinine clearance decreases to less than 30 ml/min.[311] Plasma levels of both C-peptide and proinsulin are increased in individuals with CKD. Although serum insulin levels also are increased, clinically significant hypoglycemia is not observed except with the use of endogenous hypoglycemia agents.[310] Glucose tolerance tests in uremic individuals are marked by elevated glucose levels and hyperinsulinemia, even if diabetes mellitus is not present. In addition, there is decreased insulin-mediated glucose uptake by forearm tissues, and patients with renal failure metabolize less glucose in response to infused insulin than normal subjects. In euglycemic or hyperglycemic clamp studies, the late responses to glucose and insulin are quite characteristic of peripheral insulin resistance.[312] Hepatic glycogenolysis appears to occur at normal or increased rates, but it is less sensitive to insulin than that in nonuremic subjects.[313]

The defect in insulin responsiveness appears to reside primarily in skeletal muscle, which represents the vast bulk of glucose-dependent metabolic tissue.

This peripheral unresponsiveness to insulin in uremia has been examined in detail. The number of insulin receptors appears to be normal or increased, and the binding affinity for insulin of the receptors is not affected in uremia.[314] However, the degradation of the hormone-receptor complexes occurs at slower rates than normal.[315] The findings together define the insulin resistance to be a post-receptor event. Thus, uremia-associated resistance to the action of insulin in muscle has been linked to abnormalities in insulin signaling, but it is not known which step(s) in the signaling pathway is abnormal.[316] In normal cells, activation of the insulin receptor following insulin binding induces auto phosphorylation of the β-subunit to stimulate the activity of a tyrosine kinase that subsequently phosphorylates other substrates.[317] The major substrates are the insulin-receptor substrates (IRS-1 and IRS-2), which after phosphorylation acts as a scaffold to bring together enzymes critical for subsequent insulin events, including phosphatidylinositol- 3-kinase (PI3-K).[318] The PI3-K complex is a heterodimer composed of an 86-kD (p85) regulatory subunit and a 110-kD (p110) catalytic subunit. The p85 regulatory subunit can form stable high-affinity complexes with the p110 catalytic subunit, but the amount of these cellular complexes and the amounts of the subunits are differentially regulated by stimuli like glucocorticoids.[319] For example, Giorgino and coworkers reported that stimulation of expression of the p85 subunit of PI3-K following glucocorticoid treatment was associated with reduced IRS-1−associated PI3-K activity.[320] They speculated that the excess of p85 competed with the p85-p110 complex for binding to phosphorylated IRS-1. The reduced amount of IRS-1 associated p110 catalytic subunit resulted in decreased PI3-K activity. This would partially explain the insulin resistance associated with glucocorticoid administration. Since glucocorticoids are increased in uremia, insulin resistance may occur via a similar mechanism. Just as with glucocorticoid treatment, the quantity of p85 was substantially increased in muscle of chronically uremic rats.[200]

Acidosis also has the potential induce insulin resistance. Acidosis does not alter islet cell secretion of insulin, but does induce resistance to insulin action in peripheral tissues; reversal of acidosis improves the sensitivity of glucose metabolism to insulin.[321] One possible mechanism of acidosis is to increase glucocorticoids. Bailey and colleagues also found that correction of acidosis with sodium bicarbonate improved insulin stimulated PI3-K activation in rats.[322] In muscle cell culture models without elevated glucocorticoids, acidosis by itself causes decreases in insulin stimulated PI3-K, without the typical glucocorticoid-mediated changes in the quantity of p85 subunits.[323] This suggests that in uremia acidosis induces insulin resistance at the level of PI3-K by glucocorticoid-dependent and -independent pathways. It is not clear if these same mechanisms may be important earlier in CKD where frank acidosis is not present, but the transient acid loads increase amino-acid mobilization from muscle.

Several other factors have been found to be at least partially responsible for the decreased insulin sensitivity. As discussed above, PTH excess impairs the response to insulin.[324] Suppression of PTH levels by the administration of 1,25-$(OH)_2D_3$ improves glucose metabolism.[325] Additional factors associated with uremia that could aggravate insulin resistance include angiotensin II, TNF-α, and chronic insulin stimulation.[326,327] The relative contributions of these factors are unknown.

In uremia, the counter-regulatory hormones of carbohydrate metabolism are also affected. Plasma glucagons levels are elevated.[328] Both active hormone and inactive precursors and metabolites are found in greater than normal concentrations. In contrast to insulin, the cellular response to glucagons is normal or only slightly depressed. On the other hand, glucagon binding by receptors and the post-receptor cyclic adenosine monophosphate (cAMP) response to glucagon are both subnormal in uremia.[329]

Growth Hormone/IGF-1

Growth hormone levels increase in renal failure.[330] Renal failure does not decrease the clearance of growth hormone so the production of growth hormone must be greater than normal. Thus, the high serum levels result from abnormally increased growth hormone secretion. Despite excess growth hormone, growth retardation is nearly universal in children with renal failure, beginning by the time the GFR decreases to about 50 ml/min/1.73 m^2. Resistance to the action of IGF-1 is thought to be, in part, due to the accumulation of circulating binding proteins that reduce the free fraction (i.e., the active fraction) of the hormone.[331,332] In the case of growth hormone, there are circulating proteins that bind growth hormone, and receptor density is reduced, especially in acidotic patients.[332a]

The administration of exogenous growth hormone may stimulate growth; even though increased hormone levels are already present.[333] These data suggest that there is resistance to growth hormone action. Based on these results, Schaefer and colleagues investigated whether a post-receptor defect in growth hormone signaling caused of growth hormone resistance in uremic rats.[334] There was a marked reduction in phosphorylation of the JAK/STAT signal transduction pathway in liver tissue isolated from uremic rats and an increase in the corresponding suppressor protein. Thus, they

found impairment in the intracellular signal transduction pathway of growth hormone that could contribute to the growth hormone resistance found in patients with CKD.

Acidosis reduces growth hormone release from the pituitary and this leads to lower levels of IGF-1 production.[335] The response to an infusion of physiological concentrations of growth hormone may be very mildly impaired in acidosis, but larger concentrations completely reverse the effects of acidosis. Two factors appear to blunt the response to administered growth hormone: first, the density of IGF-1 receptors in muscle is lowered by acidemia; and secondly there is a defect in the signaling that results from the binding of IGF-1.[335] Since insulin and IGF signal through the same IRS proteins, the mechanisms that impair insulin signaling should also impair IGF-1 signaling. With correction of acidosis IGF-1 in uremic subjects, IGF-1 resistance does not improve to the same extent as insulin resistance, suggesting that separate mechanisms also play a role.[336,337]

It has recently been shown that administration of super-physiological doses of growth hormone reduces renal nitrogen loss. As discussed in the section on nitrogen metabolism in uremia, IGF-1 and insulin are major determinants of amino acid release from the muscle. Abnormalities in insulin and IGF-1 play an important role in the growth suppression seen in children with uremia and acidosis.[338] Despite normal levels of circulating growth hormone and IGF-1, growth retardation is common in uremic children.[339]

Leptin and Other Energy-Related Hormones

Plasma levels of leptin, a 16-kDa protein hormone that regulates appetite and energy expenditure, rise during CKD. Leptin is produced in adipose cells and in skeletal muscle.[340] When fat stores are large, the level of leptin is high and acts to suppress appetite but changes in serum leptin levels can occur within hours of fasting and are out of proportion to corresponding changes in body fat.[341] Leptin production is increased by hormones that have altered metabolism in CKD including glucocorticoids and proinflammatory cytokines (e.g., IL-1 and TNF-α).[340] Thus, inflammation would ordinarily be expected to stimulate leptin production, but this relationship may not hold in uremia.[342] CRP levels actually show an inverse correlation with leptin in ESRD. Leptin levels also increase markedly in conditions of insulin resistance.[343] Because leptin is a small peptide, it is partly cleared by the kidney, and with kidney damage, leptin clearance is reduced. Transplantation reduces leptin to control levels.[344] Some results suggest mechanisms besides clearance may also increase leptin levels in uremia. Clearly, leptin levels in patients with advanced renal failure increase up to fourfold in plasma when compared with controls of similar body composition.[345] In addition, uremic patients have decreased protein binding of leptin and nearly all their circulating leptin is in the free, biologically active form.

While human mutations as well as animal studies make it clear that absence of leptin activity can result in obesity,[341,346] the role of elevated leptin levels in driving anorexia or in regulating body mass is less clear, especially in CKD. Leptin binds its receptor in the hypothalamus, especially in the areas most associated with regulation of appetite and body weight.[340] Leptin suppresses neural pathways associated with hunger including neurons that produce neuropeptide Y and agouti related peptide.[347] For example, a decline in leptin levels yields a reciprocal increase in the production of by the hypothalamus which stimulates appetite. Thus, increased leptin should bias the system toward anorexia and weight loss. However, other peripheral energy-related hormones also influence similar signaling. Ghrelin is released an empty stomach, stimulates neuropeptide Y release from hypothalamic neurons and appetite while, PYY_{3-36} released from a full intestine, has the opposite effect. Plasma ghrelin levels also rise with CKD possibly partly offsetting leptin-induced hypothalamic signaling.[348] Insulin and neural inputs also have complicated regulation of this system. Leptin levels correlate very well with insulin resistance in many populations including ESRD. Clinical studies confirm that regulation of this system is complex in ESRD.[349] While there are high levels in ESRD, both leptin and ghrelin plasma levels seem to modulate appropriately with food intake and do seem to correlate appropriately with body mass and composition in ESRD patients. Even though regulation of leptin may be occurring, the extent to which this system is responsible for anorexia and weight loss in uremia remains to be determined.

Mechanism(s) in animal models of CKD with poor appetite had abnormal signaling processes in the third ventricular region of the hypothalamus.[347] Their appetite improved when the agouti-related peptide were injected into this area because this peptide blocks the anorexia-producing receptor, melanocortin receptor-4. It has been proposed that anorexia was caused by high levels of the negative regulator of appetite, leptin, because they found that CKD-associated anorexia was eliminated in db/db mice that do not express the leptin receptor. There are complementary possibilities. For example, Mamoun and colleagues reported that a circulating factor with a molecular weight of 1−5 kDa could be isolated from the plasma of dialysis patients and would cause anorexia when injected into rats.[283]

This is of interest because another anorexiogenic hormone produced by the intestine, PYY_{3-36}, has an estimated molecular weight of 3.9 kDa, raising the possibility that accumulation of PYY_{3-36} could contribute to the anorexia of uremia.[350] In fact, injection of PYY_{3-36} into animals or patients produces anorexia. Finally, the report by Cheung et al.[347] is of interest because the events they found to occur in mice with CKD also occur in animal models of cancer and sepsis.[350] This provides additional results for a common pathway leading to loss of protein stores in uremia and other catabolic conditions (see below).

Leptin can act directly on T cells to stimulate inflammatory responses[351] and is required for full cell-mediated immunity in mice.[340] Hyperleptinemia correlates with some inflammatory markers (e.g., IL-6) in ESRD patients, but inversely correlates with CRP.[342] Immunodepletion of leptin in uremic serum restored normal neutrophil chemotaxis in an *in vitro* study, but addition of leptin to normal serum did not hamper chemotaxis.[352] Once again it appears that leptin's effects are being modulated by other factors in uremic serum. Leptin stimulates glomerular endothelial and mesangial cell proliferation.[353] Because leptin increases extracellular matrix production in both cell types, it is interesting to note that infusion of leptin into normal rats for three weeks fostered the development of focal glomerulosclerosis and resulted in proteinuria. Thus, leptin may influence sympathetic activity, bone mineralization, inflammation, and glomerular disease, but the clinical importance of these findings remains to be determined.

INFLUENCE OF DIETARY THERAPY IN PATIENTS WITH CHRONIC KIDNEY DISEASE

Uremia and Anorexia

It was reported as early as 1869 that dietary manipulation can improve uremic symptoms and, at least in some patients, dietary protein restriction can change the course of renal insufficiency at least in some patients.[272,354–356] It seems curious, therefore, that this strategy is not more widely used. Perhaps, its use would increase if there were not the concern that dietary protein restriction will increase the risk of developing malnutrition and hence, compromise the patient's prognosis after dialysis therapy is initiated. The intakes of protein, calories and other nutrients that are required to prevent malnutrition in CKD are known[357] and compliance with the diet can be monitored by 24 hour urine collections for urea nitrogen measurements.[202,203] Therefore, it has been possible to evaluate the risk of loosing protein stores with low-protein diets in CKD patients. The National Institutes of Health Modification of Diet in Renal Disease Study (MDRD) was a multicenter study of the impact of low-protein diets in CKD patients.[140] Throughout this study, patients were examined for evidence of malnutrition. Despite reports that some patients spontaneously reduce their dietary protein with progressive CKD, malnutrition is rare when a properly monitored diet is used to treat patients even when GFR is below 10 ml/min.[358–360] This point is emphasized because of the suggestion that a decrease in protein in the diet of a CKD patient is a signal to start dialysis.[2] It is axiomatic that if little or no attention is given to the diet severe metabolic disturbances will develop, including metabolic acidosis, hyperphosphatemia, low values of serum proteins, and so on.[3] With proper attention, these problems do not occur: CKD patients (average GFR 18 ml/min) were given a restrictive diet plus a supplement of essential amino acid analogues and followed for one year.[361] The patients were found to be in neutral nitrogen balance, had no acidosis, and normal values of serum phosphorus and albumin. Walser et al. evaluated 76 patients with GFR values $\leq$15 ml/min and followed them for a median of 1 year while they ate a low-protein diet.[358] Weight did not decline and average serum biochemistry values were: HCO_3^-, 22 mM; phosphorus, 5.6 mg/dl; and albumin, 4.1 g/dl. Aparicio and colleagues reported similar outcomes in 239 CKD patients followed for an average of 29.6 months.[359] There was no decline in weight or body mass index and average values of serum HCO_3^- and albumin were 24 mM and 3.9 g/dl respectively. A few reports indicate that prolonged use of low-protein diets by CKD patients does not impair their survival after beginning dialysis.[137,362] MDRD patients assigned to different diets were examined repeatedly for the presence of malnutrition during an average of 2.2 years.[363] The average values of "nutritional indices" (including weight and serum proteins) of those given low-protein diets remained within the normal range. There were small, statistically significant decreases in certain parameters in each of the groups eating protein-restricted diets but only two patients had to withdraw from the MDRD because of abnormalities in nutritional status values. Finally, Aparicio and colleagues examined the outcomes of dietary protein restriction in 203 CKD patients treated for an average duration of 33.1 months.[6] The number of patients is comparable to that participating in the MDRD Study. The outcome of these patients after they began treatment with dialysis or kidney transplantation was superior to that of CKD patients who were not treated by dietary restriction. This is of interest considering the report of Menon et. al.[364] They examined the outcome of CKD patients

treated in the MDRD study and concluded that treatment with ketoacids increased the risk of death in these patients. There are numerous problems with this report: (1) the therapies, complications, etc. of patients during the ~7 years from the end of the MDRD study until death were not evaluated; (2) ketoacid therapy was stopped at the end of the MDRD study nor was the outcome of those patients who complied with the ketoacid therapy during the two year trial. (3) This outcome was the opposite of that published by Chauveau et al.[6]

We emphasize these results because they document the safety of dietary therapy in terms of nutritional measurements. They also underscore the need to use strategies to delay the need for dialysis.[365] This is necessary because dialysis it will not be possible to offer dialysis therapy for all the patients who will develop kidney failure throughout the world. Most importantly, the survival of CKD patients is not improved by instituting dialysis at higher levels of renal insufficiency.[4–6] This points out why strategies must be developed to avoid or delay the development of end-stage renal disease.

Since there is evidence that low-protein diets do not compromise nutritional status if the diets are properly designed and if compliance is monitored,[202,355] we will address factors that could adversely affect nutritional status. One such factor is the mechanisms that decrease appetite of CKD and dialysis patients. This is a problem because there are reports that the protein and calorie intakes of CKD patients decreases as renal insufficiency becomes more severe and many dialysis patients will have decreased appetite.[366,367] Concern about this type of report plus the constellation of hypoalbuminemia, loss of weight and anthropometric evidence for loss of lean body mass has been ascribed to malnutrition or "uremic malnutrition." The specter of this syndrome has even prompted the suggestion that dialysis should be initiated "early" (e.g., creatinine clearance 20 ml/min) in order to avoid the development of malnutrition.[2] This diagnosis is incorrect because malnutrition is defined as abnormalities that arise from an inadequate amount of food or an abnormal composition of the diet. In CKD, however, there are several other mechanisms that can cause these abnormalities and they provide persuasive reasons why there is loss of weight, hypoalbuminemia, and so on.[368–370] Identifying mechanisms for a loss of protein stores is not simply pedantic or formalistic because a diagnosis of malnutrition implies that simply eating more protein can correct the abnormalities.[368,370] On the contrary, it has been known for over 130 years that eating too much protein will aggravate the symptoms of CKD leading to the constellation of findings that is termed "uremia.[272]" The critical questions are whether

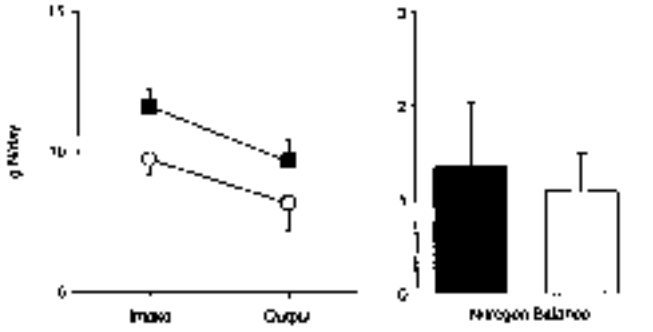

FIGURE 90.4 Nitrogen balance results in control subjects (*open symbols*) and nephrotic patients (*closed symbols*) fed 0.8 g of protein per kilogram per day plus 1 g per gram of proteinuria. The intake and output values of nitrogen were not different and nitrogen balance was mildly positive in both groups. *(With permission from Maroni BJ, Staffeld C, Young VR, et al. Mechanisms permitting patients with the nephrotic syndrome achieve nitrogen equilibrium with a protein-restricted diet. J Clin Invest 1997;99:2479–2487.)*

long-term therapy with low-protein diets leads to loss of protein stores, and at what point dialytic therapies improve survival compared to adequate conservative therapy. We will address the first question in detail, but the latter question still requires adequate controlled trials in diverse populations.

It has been repeatedly demonstrated that protein-restricted diets will maintain nutritional status: early studies demonstrated that neutral nitrogen balance was achieved during long-term therapy with low-protein diets; normal values of serum albumin were also present.[361,371–373] There is a report that a regimen of 0.3 g protein/kg/day plus a supplement of ketoacids increased the serum albumin level in CKD patients who had hypoalbuminemia.[374] Even for nephrotic patients, there is evidence that protein restricted diets are safe and that they improve the metabolic consequences of CKD[375–377] (Fig. 90.4). What then causes the loss of lean body mass and low values of serum proteins in CKD patients?

Abnormalities in Protein Turnover in Uremia

Body weights of dialysis patients are often low for the patient's height and are coupled with anthropometric evidence for loss of muscle mass plus low values of serum proteins.[207,378,379] Lack of attention to the diet does cause serious problems in patients with moderate CKD: Hakim and Lazarus reported biochemical measurements in 911 outpatients who were treated for up to seven years with received minimal attention to their diets.[380] When serum creatinine exceeded 5 mg/dl, one-third of patients had serum bicarbonate levels below 15 mM, hyperphosphatemia (values >7 mg/dl) and severe azotemia (BUN >120 mg/dl). These values

are rare even when CKD is advanced if patients are instructed about the design of diets and progress with this intervention is monitored.[358,359,361,373,381–384]

To what extent is excess dietary protein responsible for abnormal protein stores found in some CKD patients? In young rats with CKD, feeding a high-protein diet stunted linear growth and weight gain and led to very high levels of serum urea nitrogen (BUN).[385] CKD rats fed lower amounts of protein exhibited improved utilization of dietary protein to promote growth and decreased the BUN. Since acid is generated from the metabolism of sulfur-containing amino acids, phosphoproteins and phospholipids, a high protein diet would not only raise the BUN but also reduce serum bicarbonate. This is relevant because studies of rats as well as CKD patients have demonstrated that acidosis stimulates the catabolism of protein and amino acids and these reports led Bergstrom to conclude that acidosis is the only demonstrable uremic toxin.[207,221,386–388]

CKD is commonly associated with evidence of inflammation identified by the presence of increased levels of circulating cytokines.[49] In addition, high circulating levels of acute phase reactant proteins not only indicate the presence of inflammation but also are closely linked to subnormal levels of serum albumin in hemodialysis patients.[389,390] Experimental studies have demonstrated that injection of TNF-α or IL-6 can cause muscle protein wasting but the mechanism for this effect only recently was identified. Zhang et al. infused angiotensin II into mice and found increased production of both IL-6 and serum amyloid A, an acute phase reactant protein.[391] These events were accompanied by an increase in muscle protein breakdown and muscle atrophy. Their investigations showed that the inflammatory increase in IL-6 and serum amyloid A levels acted synergistically to impair IGF-1 signaling in muscle. The result was stimulation of muscle protein breakdown. These results not only show how inflammation can cause muscle atrophy but also demonstrate that some acute phase reactant proteins actually impair muscle metabolism. What is the mechanism by which metabolic acidosis and/or inflammatory cytokines cause a loss of protein stores? The answer involves understanding two metabolic principles: (1) the daily turnover rate of protein is quite large; and (2) metabolic responses are activated to prevent loss of protein stores when dietary protein is restricted. For example, in a 70 kg adult eating 1 g protein/kg/day, protein turnover is approximately 280 g of protein each day (i.e., four times the protein intake of 1 g per kilogram per day).[51,392] Therefore, even a small but sustained decrease in protein synthesis or increase in protein degradation will cause a major loss of lean body mass.

Mechanisms that Regulate Body Protein Stores

An increase or decrease in protein intake activates robust metabolic responses to maintain lean body mass: rates of amino acid and protein synthesis and degradation are adjusted rapidly and precisely to prevent loss of body protein stores. A major metabolic response is the rapid suppression of essential amino acids (EAA) degradation to ensure that an adequate supply of EAA is available for protein synthesis. When EAA degradation is suppressed to its minimum level, another mechanism is activated which suppresses protein degradation and increases protein synthesis (a less robust response).[393] These changes are detectable when the quantity of dietary protein is just adequate for achieving nitrogen balance; the World Health Organization (WHO) has determined that this amount of dietary protein is the minimum daily requirement or $\sim$0.6 g of protein per kilogram of ideal body weight per day.[394] These changes in EAA and protein metabolism are demonstrable in normal adults and in CKD patients as long as there are no complicating illnesses such as acidosis.[361,382,395] The same adaptive responses occur in patients with the nephrotic syndrome treated with 0.8 g protein/kg/day but the responses are keyed to a "net intake of protein" (the difference between actual intake and urinary losses).[375] Fortunately, the responses are not only precise, but they also occur rapidly and hence, are able to prevent changes in body protein stores when dietary protein changes. In CKD patients with metabolic acidosis or increased cytokine production, these metabolic responses are impaired and dietary protein restriction leads to loss of lean body mass.[396]

There is abundant evidence that metabolic acidosis causes amino acid and protein catabolism in infants, children, normal adults and CKD patients (Table 90.5).[221,386,387,397–404] The fate of essential amino acids is difficult to measure with the exception of the, branched-chain amino acids (BCAA), which are measured from the decarboxylation of the carbonyl group. In addition, BCAA are important components of muscle protein and the correction of acidosis raises their levels in plasma and muscle. In a rat model of CKD, Hara et al. identified the mechanism for the accelerated breakdown of BCAA in muscle.[220] They found that the mechanism reducing the levels of valine, leucine, and isoleucine was an increase in the activity of branched-chain ketoacid dehydrogenase (BCKAD), the rate-limiting enzyme that irreversibly oxidizes BCAA. They also showed that the low levels of BCAAs were corrected simply by adding sodium bicarbonate to the diet. The increase in BCKAD activity was found to result from an increase in the fraction of the enzyme in the dephosphorylated—and hence, its activated form.[405] There also are increased levels of the

TABLE 90.5 Metabolic Acidosis Induces Protein and Amino Acid Catabolism in Infants, Children and Adults

Subjects Investigated	Measurements	Outcome of Trial
Infants[397]	Low-birth-weight, acidotic infants were given $NaHCO_3$ or NaCl	$NaHCO_3$ supplement improved growth
Children with chronic kidney disease[398]	Children with CKD had protein degradation measured	Protein loss was approximately twofold higher with serum HCO_3 <16 mM vs 22 mM
Normal adults[399]	Acidosis induced and amino acid and protein metabolism measured	Acidosis increased amino acid and protein degradation
Normal adults[400]	IAcidosis induced and nitrogen balance and albumin synthesis measured	Acidosis induced negative nitrogen balance and suppressed albumin synthesis
Chronic kidney disease[401]	Nitrogen balance before and after acidosis treatment	$NaHCO_3$ improved nitrogen balance
Chronic kidney disease[221]	Essential amino acid and protein degradation before and after acidosis treatment	$NaHCO_3$ suppressed amio acid and protein degradation
Chronic kidney disease[402]	Muscle protein degradation and degree of acidosis	Proteolysis was proportional to acidosis and blood cortisol
Hemodialysis[387]	Protein degradation before and after acidosis treatment	$NaHCO_3$ decreased protein degradation
Hemodialysis[403]	Serum albumin before and after acidosis treatment	$NaHCO_3$ increased serum albumin
Continuous ambulatory Peritoneal dialysis[386]	Protein degradation before and after acidosis treatment	$NaHCO_3$ decreased protein degradation
Continuous ambulatory peritoneal dialysis[404]	Weight and muscle mass before and after acidosis treatment	Raising dialysis buffer increased weight and muscle mass

messenger RNAs (mRNAs) encoding E1a, E1b, and E2 subunits of the enzyme, implying that the expression of BCKAD is increased in response to acidosis. The biochemical triggers for these responses of BCKAD are complex because the expression and activation of BCKAD depend on both acidification and glucocorticoids.[388,406]

In humans as well, metabolic acidosis stimulates BCAA degradation: normal adults fed NH4Cl to induce acidosis raised their levels of leucine oxidation by 25%.[399] Likewise, when CKD patients were given sodium bicarbonate to raise their serum bicarbonate levels from16 to 21 mM, the rates of leucine oxidation decreased by 29%.[221] These changes are significant because muscle biopsies of hemodialysis patients revealed low free levels of BCAA and the levels increased to normal when the patients were given sodium bicarbonate.[407] Likewise, Mochizuki[408] reported that low levels of BCAAs in the plasma of acidotic CKD patients increased substantially when acidosis was treated. Acute uremia that is not complicated by acidosis is also associated with increased BCAA catabolism in muscle by unknown mechanisms.[409] Thus, acidosis stimulates the breakdown of essential amino acids and this in turn could reduce protein synthesis in muscle and potentially other organs.

Metabolic acidosis also stimulates protein degradation in muscle and hence, will block the second adaptive response to dietary protein restriction, the ability to suppress protein degradation when protein intake is restricted to minimal levels.[410] May et al.[411] studied acidotic, CKD rats and found their nitrogen excretion was 22% higher than in sham-operated, pair-fed rats. The mechanism causing the nitrogen losses was a 90% increase in the rate of muscle protein degradation. The critical experiment showed that correcting acidosis with dietary sodium bicarbonate eliminated the increase in muscle protein degradation.

Mechanisms that Degrade Muscle Protein

In muscle cells, a low pH activates the ATP-ubiquitin-proteasome system (UPS) to degrade protein.[51,323] The UPS initially acts to conjugate a chain of ubiquitins to proteins that are destined for degradation; these protein are then degraded in a very large structure, the 26S proteasome which consists of many subunits.[412] ATP is also required to remove the ubiquitins and to unfold the substrate protein and inject it into the central tunnel of the proteasome where it is degraded. Ubiquitin is present in the cytoplasm and nuclei of all cells and is a member of the heat-shock family of proteins. Degradation of proteins in the 26S proteasome yields peptides that are split to form amino acids by cytoplasmic peptidases or the peptides are used in the process of antigen recognition.[412] The UPS is responsible for degrading the bulk of proteins in all cells and hence, its activity is highly regulated. This regulation principally occurs by the availability and action of specific E3 ubiquitin conjugating enzymes. There about 1000 of these enzymes which are able to recognize specific proteins that are destined for degradation and transfer the activated ubiquitin to the

substrate protein. In the case of muscle, the specific E3 enzymes are atrogin-1 or MAFbx and MuRF1 and their expression rises sharply in conditions associated with accelerated muscle protein degradation. When the atrogin-1/MAFbx gene was knocked out in mice, the increase in protein degradation stimulated by muscle denervation was reduced by ~50%.[413] Notably, the expression of atrogin-1/MAFbx and a number of other genes in muscle of rats with various catabolic conditions, including uremia, starvation, cancer, or insulin deficiency rises sharply.[414] These reports suggest that catabolic conditions, including CKD, activate a catabolic program of gene expression leading to muscle atrophy. In fact, experiments in rats with CKD have demonstrated that there is increased transcription of the genes encoding components of the UPS, including ubiquitin and subunits of the 26S proteasome.[217]

Experimental models of metabolic acidosis as well as CKD with associated metabolic acidosis have demonstrated that the UPS plays the critical role in the production of muscle atrophy in these conditions.[217,415] These results are reminiscent of the increase in the mRNAs that encode subunits of branched chain ketoacid dehydrogenase in muscle of acidotic rats.[405] Because the UPS is responsible for the breakdown of the bulk of proteins in all cells and the regulation of the half lives of so proteins that influence transcription and biochemical reactions, its mechanisms have been extensively studied and its discoverers Hershko, Ciechanover and Rose were awarded the 2005 Nobel Prize in Chemistry.

Activation of the UPS is responsible for the excessive protein degradation that occurs in response to diabetes, starvation, denervation, burns, sepsis, and cancer as well as metabolic acidosis.[51] Because the UPS is the key to the loss of muscle mass that occurs in all of these catabolic conditions, triggers to its activation have been sought. It has been speculated that the development of muscle wasting in CKD is initiated by inflammation.[49] As noted above, there is evidence that inflammation can activate muscle protein degradation but this process is complicated and does not depend on a direct influence of inflammatory markers. Instead, the activation of the UPS and protein degradation occurs when insulin- or IGF-1-induced cellular signaling is impaired.[391] In fact, the influence of NF-κB, the transcription factor that is activated by inflammatory cytokines, is not to stimulate expression of proteasome subunits in muscle cells but rather to suppress transcription of proteasome subunit genes by a mechanism that involves glucocorticoids.[416] In contrast, the transcription of the ubiquitin gene is stimulated by activation of the Sp1 transcription factor.[417] In short, the increase in expression of genes encoding components of the ubiquitin-proteasome system in catabolic conditions such as uremia cannot be explained by activation of a single transcription factor.

Other proteases besides the UPS participate when muscle proteins are being degraded. This was uncovered when it was shown that the UPS rapidly degrades actin or myosin but degrades actomyosin or myofibrils only slowly. This means that the complex structure of muscle is first cleaved yielding substrates for the UPS. This initial cleavage is performed by caspase-3.[396,418] In the process of cleaving actomyosin or myofibrils, caspase-3 leaves a characteristic "footprint" in muscle, a 14-kDa actin fragment in muscle that can be recognized by Western blotting. As with activation of the UPS, impaired insulin or IGF-1 cell signaling stimulates caspase-3 activity; in muscle of insulin-deficient rats, the 14-kDa actin fragment accumulates and protein degradation is accelerated.[419] Another demonstration of the integration of mechanisms that degrade muscle protein is the influence of caspase-3 on activity of the UPS. It was found that caspase-3 increases proteolytic activity of the 26S proteasome by altering subunits of the proteasome.[420]

The cell signaling mechanism activating caspase-3 and the UPS depends on the presence of defects in downstream signaling of the insulin/IGF-1 pathway. Whent there is suppression of the activity of phosphatidylinositol 3-kinase (PI3K) and Akt[419] there is reduced phosphorylation of the Forkhead transcription factor, FOXO. This factor can then enter the nucleus to increase the expression of the key E3 conjugating enzyme, atrogin-1/MAFbx. This response is responsible for stimulating muscle protein degradation. There are still important responses and processes that regulate muscle protein turnover, but these steps are relevant to patients with CKD. First, it was shown that correction of the metabolic acidosis of patient being treated by chronic ambulatory peritoneal dialysis resulted in an increase in body weight and evidence for suppression of the UPS.[256] Second, it was demonstrated that the 14 kD actin fragment in muscle biopsies was proportional to the rate of protein degradation measured in patients who had muscle wasting from severe osteoarthritis.[421] In addition, the density of the 14 kD actin fragment decreased in muscle biopsies of hemodialysis patients when they were trained in endurance exercise (i.e., bicycle pedaling); this beneficial response was not present in control patients or those trained in resistance exercise.

There is abundant clinical evidence that acidosis causes protein losses in uremic patients (Table 90.5). Papadoyannakis et al.[401] showed that treating CKD patients with sodium bicarbonate improved their nitrogen balance. Williams and colleagues[422] studied acidotic CKD patients who were eating a high-protein diet and reported that the rate of protein degradation

did not decrease appropriately when the patients were switched to a low-protein diet. This response was attributed to interference with adaptive responses to decreasing dietary protein and was corrected by giving sodium bicarbonate. Using a similar strategy, Reaich et al.[221] found that the rate of protein degradation was high in acidotic, CKD patients. When the patients were given sodium bicarbonate, partial correction of acidosis decreased protein degradation by 28% but when given an equimolar amount of sodium as sodium chloride, proteolysis increased again. The presence of metabolic acidosis in CAPD or hemodialysis patients increases protein breakdown and correction of acidosis significantly reduces the rate of protein breakdown.[386,387,423,424] Similar responses can be detected in subjects with normal kidney function. Induction of metabolic acidosis in otherwise normal adults increases protein breakdown and causes negative nitrogen.[399,400] Moreover, if premature infants, children with renal tubular acidosis, or elderly women are treated to correct acidosis, their growth in the first two cases or the estimate of nitrogen balance improves in the last case.[397,425,426] This benefit extends to increasing serum albumin. Ballmer et al.[400] reported that creating metabolic acidosis in normal adults reduced their rate of albumin synthesis and Movelli et al.[403] reported that correcting metabolic acidosis in hemodialysis patients increase the concentration of serum albumin.

Acidosis also causes important changes in hormone responses. For example, Krapf and colleagues have reported that induction of metabolic acidosis in otherwise normal adults will impair the function of growth hormone and thyroid hormone and the conversion of vitamin D to its most active form, 1,25 $(OH)_2$ cholecalciferol.[337,427] Consequently, acidosis could interact to impair the ability of CKD patients to maintain protein stores by indirect mechanisms. One of the most well documented abnormalities in hormones is insulin resistance. It can occur in CKD patients who have serum creatinine values as low as 2.4 mg/dL.[428] The presence of insulin resistance is a trigger of muscle protein breakdown because it stimulates the activity of both casapase-3 and the UPS.[418,429,430] Fortunately, there is evidence that restricting dietary protein can improve the insulin sensitivity of CKD patients.[431,432]

Despite these well-documented reports of acidosis-induced catabolism in animals and humans, results from a cross sectional analysis of dialysis patients led the authors to conclude that acidosis is benign.[433] There are several problems with this conclusion. First, a cause-effect relationship cannot be established by results from cross-sectional studies.[434] Second, a single serum bicarbonate measurement is insufficient evidence of acidosis. This occurs because there can be loss of CO_2 during processing of the blood sample giving a falsely low HCO_3 level.[435] We recommend that even mild degrees of acidosis should be corrected to prevent interruption of the critical adaptive responses to changes in the diet. Otherwise, the patients will be at risk of loosing protein stores, including albumin.

In summary, uremic patients can lose protein stores if the adaptive metabolic responses that are required to maintain lean body mass are blocked when dietary protein is restricted. This has been demonstrated in normal subjects and CKD patients with acidosis. Another cause of lost body stores is the presence of inflammation or insulin resistance. Whether uremic toxins besides acid induce muscle wasting is unknown. Fortunately, acidosis and insulin insensitivity are improved by a low-protein diet and this may explain why eating a low-protein diet will improve the nutritional state of CKD patients.[358,359,377]

Assessment of Dietary Compliance

Since adequate but not excessive protein intake is required for optimal patient outcomes, monitoring dietary compliance is essential. The classic report by Folin[201] showed that a change in urea excretion is the principal response that occurs when the amount of protein in the diet is raised or lowered. This relationship has been repeatedly confirmed and provides the basis for methods directed at assessing compliance with low-protein diets.[202,203,371,372,436] In short, a change in the steady-state rate of urea excretion indicates that the amount of protein in the diet has changed. Methods devised to estimate dietary protein intake can be used repeatedly to evaluate how the diet affects the symptoms of kidney disease as well as assessing compliance with a dietary prescription.[202,203,363] The accuracy of the method is based on two facts. First, urea production is directly proportional to protein intake. Second, the half-life of urea in normal adults is approximately seven hours, so virtually all the urea that is synthesized following a change in the amount of protein in the diet is excreted within a day. To utilize the method optimally, it is important to emphasize that steady-state conditions must be present. Specifically, if kidney function is increasing or decreasing this introduces an error because the amount of urea excreted will depend not only on changes in the amount of protein eaten but also on the change in urea clearance. Fortunately, it is possible to determine if steady-state conditions are present, it is only necessary to measure body weight and the serum urea nitrogen (SUN). If both are stable, then the patient is in the steady state. Even if weight and/or SUN are not constant, the method can be used to estimate the change in the body pool of urea nitrogen as will be explained.

It is important to define certain elements of urea turnover in order to understand the basis for this

method of estimating dietary protein. First, the rate of urea production actually exceeds the steady-state rate of urea excretion in both normal and uremic subjects.[437] This occurs because there is an extrarenal clearance of urea that is due to urea degradation by bacterial ureases present in the gastrointestinal tract.[437–440] Fortunately, the amount of urea degraded does not cause a net decrease in urea excreted or accumulated in body fluids because the urea degraded is simply recycled and used to synthesize more urea.[437] Physiologically, this is important because it demonstrates there is no benefit to urea recycling. Previously, it was believed that the ammonia nitrogen arising from the degradation of urea can contribute substantially to the synthesis of amino acids in the liver, ultimately, providing a source of amino acids that could be used to synthesize proteins with an improvement in the nutritional status of uremic patients.[441] However, it was shown that ammonia nitrogen arising from urea breakdown is simply used to synthesize more urea and hence does not improve protein synthesis or nitrogen balance.[437,440] Because recycling of urea nitrogen does not change the rate of net urea production, this net urea production closely parallels dietary nitrogen.[202,371,442] Fortunately, net urea production is easily calculated even when weight and SUN are changing because the concentration of urea is equal throughout body water.[189,437] Since water represents ~60% of body weight in nonedematous patients, changes in the urea nitrogen pool can be calculated by multiplying 60% of body weight (in kilograms) by the serum urea nitrogen concentration (in grams per liter). The net production of urea, generally termed the urea appearance rate (UNA), is calculated as the change in the urea nitrogen pool (positive or negative) plus the amount of urea nitrogen excreted in the urine. Clearly, when serum urea nitrogen and weight are stable, there is no urea nitrogen accumulation and the urea appearance rate equals the urea nitrogen excretion rate (Table 90.6).

Non-Urea Nitrogen

Fortunately, the contribution of non-urea nitrogen excretion (i.e., the nitrogen that is excreted in feces and in urinary uric acid, creatinine, peptides, and unmeasured nitrogenous products) can be estimated even more easily than urea nitrogen. The non-urea nitrogen varies minimally over a large range of dietary protein and averages 0.031 g of nitrogen per kilogram ideal body weight per day (Fig. 90.5).[202–204] This average value was based on results from CKD patients who had 5 g/day or less of proteinuria (if proteinuria exceeds 5 g per day, an additional amount of nitrogen equivalent to the urinary loss of protein nitrogen should be added to non-urea nitrogen excretion). To assess the accuracy of this equation for estimating dietary protein intake, we examined results from more than 70 nitrogen-balance measurements of CKD patients and found no significant correlation between dietary nitrogen and either fecal nitrogen or the sum of all forms of non-urea nitrogen excretion. Thus, compliance with a prescribed amount of dietary protein is evaluated by converting the prescribed amount to its nitrogen equivalent by multiplying it by 0.16 (protein is 16% nitrogen). If nitrogen balance is assumed to be

TABLE 90.6 Estimating Dietary Compliance Using Urea metabolism

1. A 70-year-old man with a urea clearance of 10 ml/min weighs 70 kg (CKD stage 5). He is prescribed a diet containing 0.8 g of protein per kilogram per day, which meets the daily allowance of protein recommended by the World Health Organization. Since protein is 16% nitrogen, he is eating 9 g nitrogen daily. His nonurea nitrogen excretion is 70 kg. His serum urea nitrogen (SUN) and weight are unchanging. A 24-hour urine collection contains 6.5 g of urea nitrogen. His non-urea nitrogen excretion is 0.031 g nitrogen per kilogram per day or 2.17 g nitrogen per day. His total nitrogen excretion is 8.7 nitrogen per day indicating he is compliant with the prescribed diet ($8.7 \times 6.25 = 54$ g protein per day (1 gram nitrogen equals 6.25 g protein).
2. cA 60-year-old woman with stage 5 chronic kidney disease is admitted to the hospital for plastic surgery. She weighs 60 kg and is eating a diet of 40 g per day (the minimum daily protein requirement (equivalent to 6.4 g nitrogen/day since protein is 16% nitrogen). She is excreting 4.5 g of urea nitrogen per day and her non-urea nitrogen is 1.9 gN/day ($60 \text{ kg} \times 0.031$ gN/Kg). Therefore, her total daily nitrogen excretion is 4.5 g urea nitrogen + 1.9 non-urea nitrogen ~6.4 gN per day. Subsequently, her SUN rose from 50 to 60 mg/dl. This represents an additional increase in nitrogen production ($10 \text{ mg/dL} \times 36$ L of body water or an excess of 3.6 gN above the pre-surgery value (this would not be rapidly excreted by patients with advanced or stage 5 CKD). Because her nitrogen excretion exceeds her protein nitrogen intake, her diet should be reviewed and a stool sample for blood should be collected (to exclude GI bleeding).

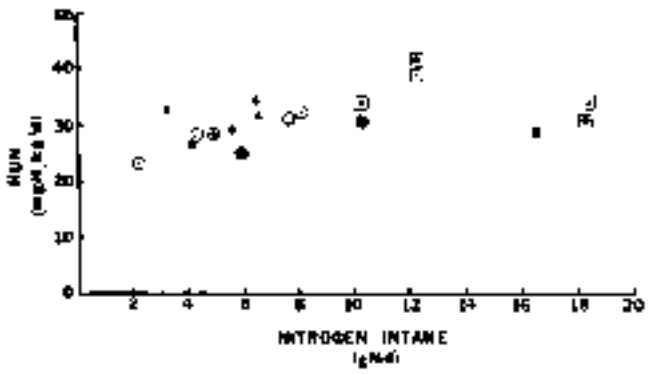

FIGURE 90.5 Calculated values of total non-urea nitrogen excretion (NUN) in normal subjects (*solid symbols*) and patients with chronic renal failure. The average value for patients not being treated by dialysis is 0.031 g of nitrogen per kilogram per day. *(With permission from Maroni BJ, Steinman T, Mitch WE. A method for estimating nitrogen intake of patients with chronic renal failure. Kidney Int 1985;27:58–65).*

zero, then nitrogen intake will be equal to nitrogen excretion and the latter can be calculated as the sum of the urea appearance rate plus 0.031 g of nitrogen per kilogram per day.[202] If the total amount of waste nitrogen produced is the same as the amount of protein in the prescribed diet, then the patient is compliant with the diet. But, if waste nitrogen production is greater or lesser than the amount of nitrogen in the prescribed diet, the patient should meet with a skilled dietician to uncover why the patient is not being compliant with the prescribed diet. The caveat to using method is that it is unreliable in patients who are receiving total parenteral nutrition or eating completely digestible foods (e.g., astronauts). In these cases, non-urea nitrogen excretion will be less than 0.031 g of nitrogen per kilogram per day.[443] The method could also be inaccurate when assessing patients with severe catabolic illnesses or for those being treated with glucocorticoids or medicines that affect protein turnover in the body (e.g., anticancer drugs or growth hormone, and so on). This is important because patients being treated with glucocorticoids, or those with severe catabolic conditions will break down body protein stores to increase nitrogen excretion more than that derived from dietary protein.

In summary, the amount of nitrogen-containing waste products produced each day can be calculated from changes in body weight and SUN plus the 24-hour excretion of urea nitrogen and 0.031 g of nitrogen per kilogram per day. This is valuable because the amount of waste nitrogen produced is equal to nitrogen intake in stable patients. Since protein is 16% nitrogen, the prescribed nitrogen intake can be compared to the amount of nitrogen excreted and if the values differ by more than 20%, then reasons for noncompliance or reasons for nitrogen balance to be negative should be investigated.[354]

These calculations can also be used to evaluate calorie intake. Although this calculation is not as accurate as that of dietary protein, the principle is similar. Specifically, a skilled dietician can determine the percentage of calories that are derived from dietary protein so the calorie intake can be estimated from the calculated protein intake based on urea excretion. It is important to monitor calorie intake regularly for two reasons: first, an insufficient intake of calories will reduce the utilization of dietary protein, increasing the risk of losing protein stores. Second, there is evidence that CKD patients frequently "under-report" their calorie intake.[444–446] It is important to make these calculations so that the adequacy of a patient's actual intake can be evaluated. Moreover, advising a patient about his/her degree of compliance will help them participate in their therapy.

Other methods of assessing protein intake including dietary histories have been exhaustively reviewed:[447] dietary interviews not only provide less accurate estimates of actual intake but their reliability is questionable when interviews are used repeatedly (patients quickly learn to give the expected responses about dietary habits). At least two groups have compared estimates of energy intake obtained from food records with those based on anthropometric and oxygen consumption measurements.[444,445] The evaluations indicated that the intakes of calories based on dietary records are gross underestimates of actual energy intake. For these reasons, we recommend that dietary compliance be evaluated from measurements of urea nitrogen production plus an estimate of non-urea nitrogen excretion.

DIETARY PROTEIN RESTRICTION AND PROGRESSION OF RENAL INSUFFICIENCY

Clinical trials have been used to examine whether reducing dietary protein can influence the nutritional status and the loss of kidney function in CKD patients. Some of the published studies are of low methodological quality because they were based on a retrospective analysis, enrolled only a small number of patients or had serious design flaws. Overall, we examined more than eighty trials and identified ten randomized controlled trials[140,164,422,448–454] and five meta-analyses that were studied to assess if dietary protein restriction would slow the progression of CKD.[455–459] We also reviewed recent studies to assess whether dietary protein restriction (as part of an integrated treatment program for CKD patients) is nutritionally sound and does not jeopardize survival following a kidney transplant or initiation of dialysis therapy.[460] Generally, the trials were based on estimating changes in serum creatinine or the degree of proteinuria. The problems with this strategy are that several factors can modify creatinine metabolism and/or influence the degree of proteinuria (see discussions of creatinine metabolism and proteinuria). Second, restricting protein intake to treat the complications of CKD can change the rate of loss of kidney function by mechanisms not directly related to protein metabolism. For example, a low protein diet will also limit dietary salt intake to reduce the severity of hypertension and slow the progression of CKD. Alternatively, reducing protein intake could limit the accumulation and hence the toxicity of metabolic products such as indoxyl sulfate.

Efficacy of Protein Restriction in Non-Diabetic Kidney Disease

There are clinical trials which satisfy requirements for a high quality report.[458] The Northern Italian

Cooperative Study Group analyzed 456 patients who were designated as NKF-defined Stage CKD patients.[450] Patients were randomly prescribed 0.6 g/kg/day (LPD) or 1 g/kg/day (control group) plus at least 30 kcal/kg/day and followed for at least two years. Based on urea nitrogen excretion, the amount of protein eaten can be estimated: the control group ate an average of 0.90 g protein/kg/day while the low protein group ingested an average of 0.78 g protein/kg/day and there was substantial overlap in the protein ingested by the two patient groups.[202] The primary outcome, "renal survival," was defined as the start of dialysis or the doubling of serum creatinine and there was only a borderline difference between control and LPD groups; slightly fewer of the LPD patients group reached the endpoint ($p = 0.059$). Because the difference in protein intake was so small, it can not be concluded that the trial tested the hypothesis that "eating a low protein diet will slow the loss of kidney function."

The Modification of Diet in Renal Disease Study (MDRD) examined in a 2×2 design how different levels of protein intake and two levels of blood pressure control influenced changes in GFR measured using urinary collections of injected ^{125}I-iothalamate.[140] In Study A (Stages 3 CKD) 585 patients were randomly assigned to a standard diet of >1 g protein/kg/day or a diet containing 0.6 g protein/kg/day; targeted mean blood pressures were 105 or 92 mmHg. In Study B, 255 CKD patients (Stage 4 CKD) were randomly assigned diets of 0.6 g protein/kg/day or 0.3 g protein/kg/day supplemented with a ketoacid/essential amino acid mixture; blood pressure goals were the same as in Study A. There were no control patients eating an unrestricted diet. The actual protein intakes in Study A averaged 1.11 or 0.73 g protein/kg/day and in Study B, they averaged 0.69 or 0.46 g protein/kg/day plus the ketoacids/amino acids mixture.[202] After analyzing the results, it was concluded that in Study A, the loss of GFR in the two groups was not different. In Study B, the rate of GFR loss was somewhat higher in the group ingesting 0.69 g protein/kg/day compared to the rate in patients assigned to the 0.46 g protein/kg/day plus ketoacids/amino acids diet ($p = 0.07$). While these conclusions were consistent with a negative outcome, there are caveats. First, patients assigned to the restricted diet in Study A had an initial decrease in GFR during the first four months. This was assigned to the lower protein intake producing a hemodynamic reduction in glomeruli.[154] Subsequently, these patients had a slower loss of GFR than those assigned to the unrestricted diet. If the initial physiologic response is ignored (because it did not arise from kidney damage), then the low protein diet led to a significantly slower loss of GFR; there also was a significant improvement in "kidney survival" ($p = 0.009$). Secondly, the rate of loss of GFR in the unrestricted dietary protein group was lower than predicted and hence an additional three month follow-up should have been added before determining whether decreasing dietary protein influences the progression of CKD. For example, there was no protective effect of intensive insulin treatment in the U. S. NIH-sponsored Diabetes Control and Complications Trial (DCCT) on the protective effect of strict blood glucose control on the progression of kidney disease initially. After two years of observation, however, a benefit of glucose control was established and after four years of therapy, the development of microalbuminuria or macroalbuminuria/proteinuria was significantly reduced. In fact, secondary analyses of results of the MDRD trial, although less robust did identify slowing of progression during the trial.[461] For example, when the hypothesis that *eating a low-protein diet* slowed the loss of kidney function was tested, the reduced protein intake measured in Study B patients was associated with significant ($P = 0.011$) slowing of the loss of kidney function.[462] There also was reduced frequency of renal death (death or initiation of dialysis; $p = 0.001$). Indeed, for every reduction of 0.2 g /kg/d of protein intake there was a 1.15 mL/min/yr reduction in the rate of loss of GFR and there was a 49% reduction in the frequency of renal deaths. Notably, the benefit from eating a low-protein diet seemed to be linearly related to slowing of progression; stated another way, a progressive reduction in the amount of protein in the diet protects the kidney to a greater degree suggesting that there is no single level of dietary protein which will that provide benefits for all patients. Third, there was no apparent benefit of restricting dietary protein or controlling blood pressure in patients with polycystic kidney disease. This caveat is relevant because patients with polycystic kidney disease constituted ~25 percent of all patients in the MDRD Study and the presence of this group would prevent documentation of slowed progression in a trial lasting only 2.2 years. In short, inclusion of patients with CKD could have obscured beneficial responses of the diet in patients with other types of kidney disease.[140] Despite these caveats, the intention-to-treat analysis of the MDRD study results showed no statistically significant benefit of dietary protein restriction on the rate of decline in GFR.

In a smaller study lasting only 18 months, Williams et al. analyzed the effects of three dietary interventions in 95 patients with stage 4-5 CKD.[422] Patients were randomly to diets containing 0.6 g protein/kg/day and 800 mg phosphate, 1000 mg phosphate/day plus phosphate binders or to an unrestricted intake of protein and phosphates. Dietary compliance was estimated from diet records and urea excretion, yielding average levels of 0.7, 1.02 and 1.14 g protein/kg/day and 815,

1000 and 1400 mg phosphorus per day, respectively. Although there was a minor loss of weight in the low protein and low phosphate groups (−1.3 and −1.6 kg respectively) there were no differences in the decrease in repeated measures of creatinine clearance over time. There also were no differences in the numbers of patients who died or began dialysis therapy. Shortcomings of the study included a limited number of patients and the problems of detecting differences in creatinine clearances assessed over a relatively short period. For these reasons, no conclusions about the influence of the diets on progression of kidney disease can be reliably made.

Cianciaruso et al. studied patients with stage 4-5 CKD when they were randomly assigned to protein intakes of 0.55 or 0.80 g/kg/day.[453] The study lasted 18 months and included 212 CKD patients assigned to the lower protein intake and 211 who were prescribed the higher level of dietary protein. In the two groups, there was a significant ($p < 0.05$) difference in urea nitrogen production and hence, the average protein intakes. The protein-restricted group ate 0.72 while those assigned to the higher protein diet ate 0.92 g protein/kg/day ($p < 0.05$) but serum phosphorus, parathyroid hormone and bicarbonate levels were not different. In contrast, values of urinary excretion of urea, sodium and phosphate were all reduced in the low-protein diet patients yet the authors found no differences in body composition or nutritional indices (principally, serum albumin) between the two groups. Notably, if the results were analyzed on an intention-to-treat basis, 13 patients assigned to the 0.8 g protein/kg/day diet vs 9 assigned to 0.55 g protein/kg/day died or had to begin dialysis.

Di Iorio et al. evaluated 20 patients assigned to a very low protein intake supplemented with ketoacids and assessed whether the diet would affect the efficiency of erythropoietin therapy during two years.[452] Actual protein intakes of the two groups were 0.49 g/kg/day plus a supplement of ketoacids compared to 0.79 g/kg/day. Interestingly, only two patients assigned to the very low protein plus ketoacid regimen began dialysis compared to seven such outcomes in those assigned to the higher dietary protein ($p < 0.05$). Erythropoietin responsiveness was also improved in the low protein diet subjects and the improvement was inversely related to the serum parathyroid hormone and the decrease in serum phosphorus.[452]

Ihle and colleagues, studied 72 Australian patients with stage 4-5 CKD over 18 months.[164] They were randomly assigned to a unlimited protein diet or to 0.4 g protein/kg/day and actual protein intakes based on urea excretion values were 0.6 g/kg/day vs 0.8 g protein/kg/day.[202] The GFR (^{51}Cr-EDTA clearance) was measured every 6 months; it progressively declined only in subjects assigned to the higher protein intake. This adverse outcome was confirmed by a higher number of patients who had to begin dialysis ($p < 0.05$). The authors reported that patients in the protein-restricted group lost weight but there were no differences in other anthropometric measures or serum albumin. There was no analysis of differences in energy intake as a reason for weight loss.

Jungers et al. reported the outcomes of dietary protein manipulation in only 19 stage 5 CKD patients.[449] Ten patients were randomly assigned to a very low protein diet (0.4 g protein/kg/day) supplemented with ketoacids while 9 were assigned to a conventional low protein diet of 0.6 g protein/kg/day. The actual amount of dietary protein, however, differed by only 0.2 g/kg/day. Seven of the 9 patients assigned to the 0.6 g protein/kg/day had to begin dialysis vs 5 of 10 patients assigned to the ketoacid regimen ($p = 0.20$). The small number of patients limits conclusions from this report.

Malvy et al. studied 50 stage 4-5) randomly assigned patients prescribed a very low protein diet (0.3 g protein/kg/day) supplemented with ketoanalogues (Ketosteril®, 0.17 g/kg/day) or a diet containing 0.65 g protein/kg/day diet.[451] The outcome tested depended on differences between the diets in terms of the time until creatinine clearance decreased below 5 ml/min/1.73 m^2 or until a patient began dialysis. There was no significant difference in this measure of "renal survival" but the study was underpowered to test the hypothesis adequately. Patients in the very low protein/ketoacid group but not in the higher protein diet lost 2.7 kg of both fatty tissue and lean body mass during the three year study. Interestingly, the time for patients to reach a GFR of ≤ 15 ml/min/1.73 m^2 was different: for the 0.65 g protein/kg/day group it yielded a "half-life" before renal death of 9 months compared to 21 months for those assigned to the more restricted diet/ketoacid regimen. Although delaying the need for dialysis is undoubtedly a beneficial response, it is difficult to interpret the results because there was no control group assigned to an unrestricted diet.

Mircescu et al. evaluated the clinical course of 53 stage 4-5 CKD patients over 60 weeks.[454] They randomly assigned 26 patients to a diet of 0.6 g protein/kg/day and 27 to a 0.3 g protein/kg/day diet supplemented with ketoacids. Actual protein intakes were estimated to be 0.59 ± 0.08 and 0.32 ± 0.07 g protein/kg/day respectively. There were no deaths but 7 of the 26 patients assigned to the 0.6 g protein/kg/d diet required dialysis compared to only 1 of 27 in the very low protein/ketoacid group ($p = 0.06$). The more restrictive diet decreased serum phosphorus values ($p < 0.05$) but no differences in nutritional status and no significant difference in the loss of GFR estimated from serum creatinine. Again, the number of patients studied was too few to determine if dietary protein restriction slowed progression of CKD (in fact, the authors estimated that approximately 100 patients per

group would be required to identify if the diets produced a significant difference in progression of CKD).

Rosman et al. evaluated the influence of dietary protein restriction in 247 stage 3–5 CKD patients after two or four years.[166,448] There was a control group assigned to an unrestricted diet yielding stage 3 CKD patients eating 0.90–0.95 g/kg/day and stage 4–5 CKD patients eating 0.70–0.80 g/kg/day. After two years, there was significant slowing of progression of kidney failure but only in male patients (again, patients with polycystic kidney disease had no benefit). After four years, patients assigned to the protein-restricted diet had beneficial responses calculated as kidney survival and/or the percentage of patients who did not require dialysis (60% vs 30%, $p < 0.025$).[448] It is not clear whether patients prescribed the unrestricted diet had to begin dialysis because of increasing uremic symptoms. Regardless, the beneficial effect of low protein diet on the decline in GFR of patients prescribed the low protein diet was evident. Notably, there were no signs of malnutrition and the authors concluded that compliance was reasonable.

Brunori et al. examined 56 elderly IFtalian patients with Stage 5 CKD when they were treated with a protein-restricted diet or dialysis.[463] The patients were randomly assigned to begin dialysis therapy or treatment with a very low protein diet (0.3 g protein/kg/day) supplemented with ketoacids. After one year, the survival rates were comparable (83.7% in the dialysis group and 87.3% in the low protein diet; $p = 0.6$). When the results were evaluated by an intention-to-treat analysis (including those in the diet-restricted group who were switched to dialysis), there was a continuous benefit of the protein-restricted diet over time. Specifically, patients assigned to dialysis had a 50% higher degree of hospitalization. It was concluded that the low protein diet plus ketoacids did not impair survival compared to maintenance dialysis (Fig. 90.6).

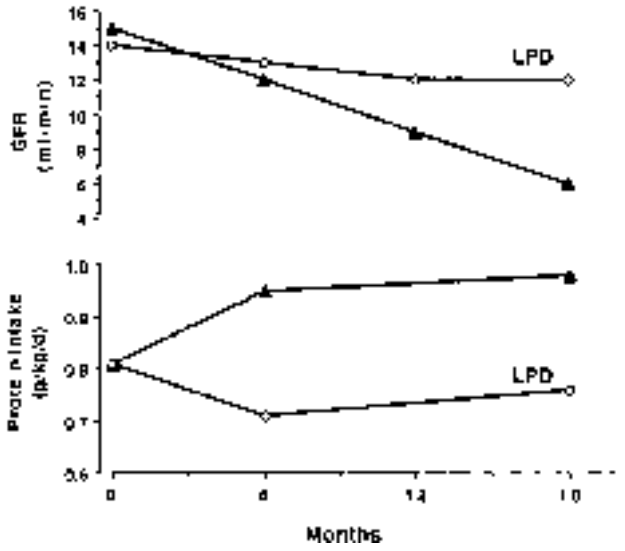

FIGURE 90.6 Changes in glomerular filtration rate (GFR) measured as the plasma clearance of 51Cr-EDTA in patients prescribed a protein-restricted diet (open circles) or an unrestricted diet (open triangles). The calculated level of dietary protein based on urea excretion is also shown. The low-protein regimen significantly reduced the decline in GFR. LPD, low-protein diet. *(Figure based on results from Ihle et al.[164] and is reproduced with permission from Mitch WE, Klahr S, eds, Nutrition and the Kidney. Second ed. Boston: Little, Brown; 1993:254.)*

Efficacy of Protein Restriction in Diabetic Kidney Disease

In diabetic, CKD patients, the benefits from dietary protein restriction have been tested but generally, only over brief periods of time. Consequently, surrogate analyses have been based to examine if there is efficacy of protein-restricted diets in terms of progression of CKD or changes in nutritional factors. The surrogate outcomes include changes in the degree of microalbuminuria or proteinuria and/or changes in creatinine clearance or serum creatinine (converted into an estimate of GFR). Besides the brief treatment periods, ACE inhibitor use was not distributed equally yielding important differences in the control of blood pressure.

Zeller et al. compared a diet containing 1 g protein/kg/d or 0.6 g protein/kg/d in 36 type 1 diabetic, CKD patients treated for an average of 35 months.[167] Changes in creatinine clearance and iothalamate clearance were measured and protein intakes were monitored from urea excretion: they averaged 1.08 vs 0.72 g protein/kg/day. The low-protein diet led to a significant ($p < 0.02$) reduction in the loss of GFR compared to results with the control diet. There was no indication that nutritional status was compromised by the low-protein diet.

The longest randomized trial of dietary responses in patients with Type 1 diabetes and CKD was reported by Hansen et al.[464] Patients were prescribed their usual diet or assigned to one containing 0.6 g protein/kg/day (actual protein intakes were 1.02 and 0.89 g/kg/day) over a four year trial. The degree of proteinuria was not different with the two diets but the frequency of renal death (i.e., end-stage renal disease) was 36% lower in patients consuming the protein-restricted diet and after adjustment for cardiovascular disease, the benefits in terms of renal deaths were even more significant ($p = 0.01$) for the low-protein diets.

Meta-Analyses of Reports Concerning CKD Progression and Low-Protein Diets

Meta-analysis is an alternative approach that to clinical research because it is a means of artificially raising

the number of subjects studied if the clinical trials are methodologically acceptable and address a common question. Meta-analyses can help to identify responses found in each original study that exhibit a tendency towards resolving a question but are insufficiently powered to determine if there is a statistically significant response when the outcomes are combined. Results and conclusions from large, randomized trials are considered to yield "level one" evidence while evidence from meta-analyses is considered to be equal to outcomes from smaller randomized trials. Meta-analyses are generally based on a so-called systematic review of the scientific literature, ensuring the most exhaustive collection of trials; they include searches of international databases as well. As noted, the most rigorous criteria for selecting or rejecting a report for analysis is to include only randomized, controlled trials because they are generally believed to produce more reliable results than those arising from non-randomized controlled trials.[457] Based on the identified problems with the planning and interpretations of the MDRD study results (see above), several meta-analyses have addressed the question of whether low-protein diets slow the loss of kidney function. The most frequent outcome in the analyzed trials is 'renal death' defined as a patient's death or the need to start dialysis;[455,456,465] alternatively, the rate of decline in kidney function[457] or changes in the degree of proteinuria[459] have been used.

In one of these meta-analyses, Kasiske et al. analyzed published results of clinical trials addressing whether low-protein diets reduced the loss of estimated GFR; they included a total of more than 1900 patients. It was concluded that these diets were positive since they prevented a loss of 0.53 ml/min GFR per year ($p < 0.05$).[457] This degree of protection was less than the amount reported by Fouque and colleagues.[458]

Meta-analyses of this question in diabetic patients have produced opposing views. Pedrini et al. found that low-protein diets reduced the risk of developing combined criteria of microalbuminuria and declining renal function by 44% ($p < 0.001$).[456] A more recent meta-analysis was based on eight randomized trials with a total of 519 patients, 253 in the low-protein diet group and 266 in the control group.[459] When analyzed by changes in GFR or creatinine clearance, no difinitive outcome was noted concerning differences in death or need for dialysis. Proteinuria did decrease significantly ($p = 0.003$), glycosylated hemoglobin improved (mean reduction, 0.31%, $p = 0.005$) and there was evidence for improved insulin sensitivity. However, the difference in protein intake between the control and experimental diets was small, 1.27 *vs* 0.91 g protein/kg/day ($p = 0.04$) and in six of the eight studies evaluated, the average estimated GFR values were above 69 ml/min. There are limits to this report: both type I and II diabetic patients were evaluated with some studies addressing only patients with early renal impairement (e.g., isolated microalbuminuria and no renal insufficiency (i.e., CKD stages 1 or 2) while another report consisted only patients with macroalbuminuria. The duration of trials only ≤ 12 months in four trials and the total number of patients might have been too small to assess all the measures tested.

Fouque and Laville performed their meta-analysis using results of ten randomized, controlled trials of the influence of low protein diets in slowing the loss of kidney function in non-diabetic CKD patients.[458] The outcome criterion was renal death. In their analysis, the genders of patients and their kidney diseases were equally distributed between control and diet-restricted patient groups, thereby avoiding the need to evaluate independent causes for more rapid losses of kidney function. The outcomes of 1002 patients assigned to dietary protein restriction were compared to the outcomes of 998 patients who were assigned to higher protein intakes (Fig. 90.7). Overall, 113 "renal deaths" occurred in the low-protein diet group compared to 168 patients with renal death in the control group. These outcomes reveal a 0.68 odds ratio for renal death in the low protein group compared to the control group (95% confidence interval, 0.55−0.84; $p = 0.0002$). The authors concluded that eating low protein diets can result in a 32% reduction in patient death or the need to start dialysis therapy when compared to unrestricted diets. Another method of expressing the results is to calculate the number of patients "needed to treat" or NNT in order to compare the outcomes of a treatment in different studies; this method tends to homogenize the results when absolute event risks are quite different between studies.[466] The NNT is the number of patients that would have to be treated for one year in order to spare one major event (e.g., death, kidney failure, or even hospitalization). Fouque and Laville concluded that the NNT with a low protein diet varied from 2 to 56 for each study.[458] Notably, the variability in the NNT mainly depends on the risk for renal death present at inclusion of the study and the degree of impairment in renal function; this follows because the absolute risk of renal death will be greater in subjects with more impaired kidney function.[449,451] Thus, the 2−56 NNT values are acceptable for evaluating primary and secondary prevention for a treatment, especially since the costs of therapy with a low protein diet is far below that of dialysis or transplant therapy. To illustrate the difference, consider that the reduction in mortality associated with prescribing a statin uncovered in the 4S trial (NNT = 30) or in the WOSCOPS study (NNT = 111) is in the range of that found with the low-protein diet.[467]

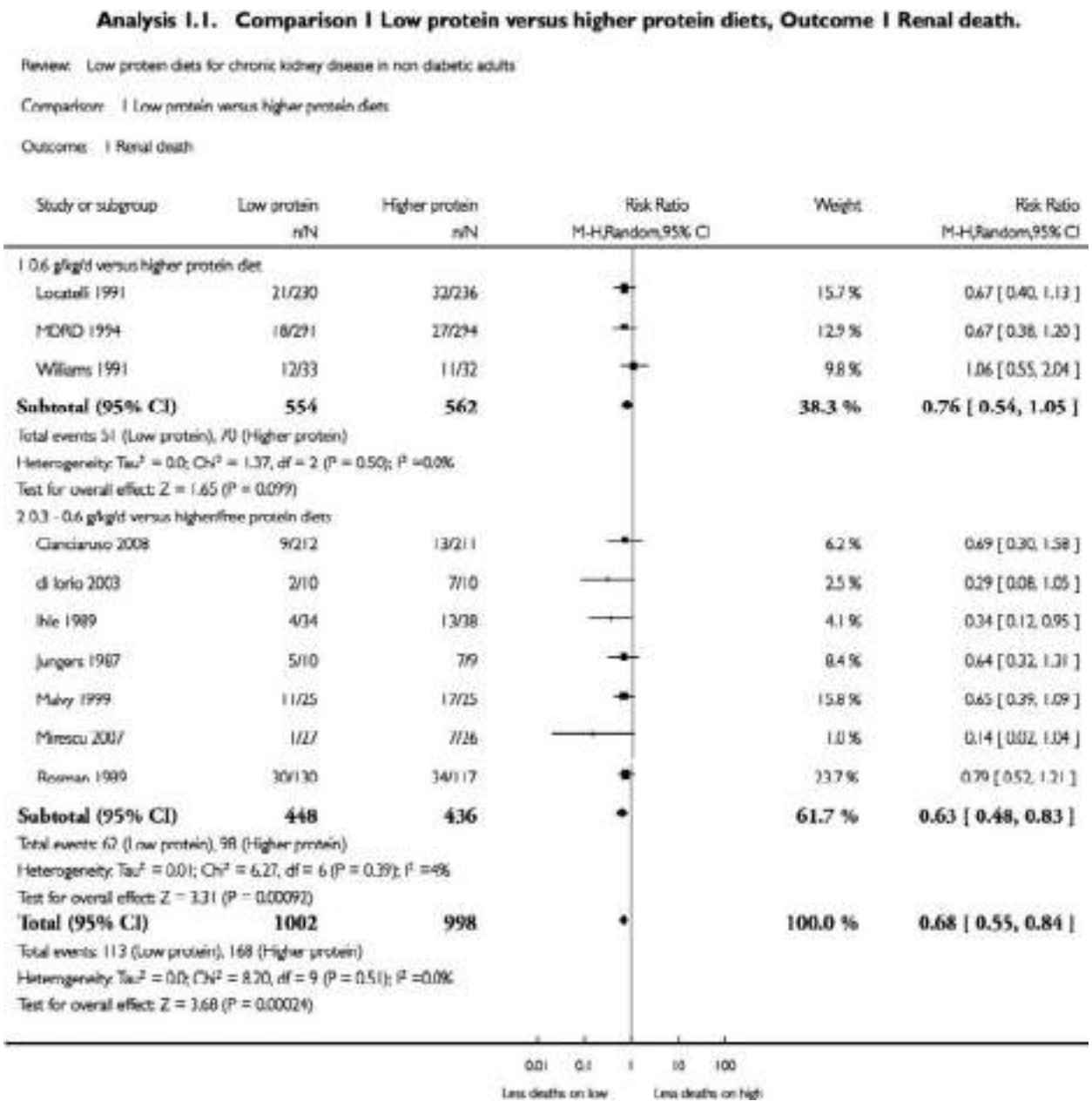
Analysis 1.1. Comparison 1 Low protein versus higher protein diets, Outcome 1 Renal death.
Review: Low protein diets for chronic kidney disease in non diabetic adults
Comparison: 1 Low protein versus higher protein diets
Outcome: 1 Renal death
Study or subgroup
Low protein n/N
Higher protein n/N
Risk Ratio M-H,Random,95% CI
Weight
Risk Ratio M-H,Random,95% CI
1 0.6 g/kg/d versus higher protein diet
Locatelli 1991 21/230 32/236 15.7 % 0.67 [0.40, 1.13]
MDRD 1994 18/291 27/294 12.9 % 0.67 [0.38, 1.20]
Williams 1991 12/33 11/32 9.8 % 1.06 [0.55, 2.04]
Subtotal (95% CI) 554 562 38.3 % 0.76 [0.54, 1.05]
Total events: 51 (Low protein), 70 (Higher protein)
Heterogeneity: Tau² = 0.0; Chi² = 1.37, df = 2 (P = 0.50); I² =0.0%
Test for overall effect: Z = 1.65 (P = 0.099)
2 0.3 - 0.6 g/kg/d versus higher/free protein diets
Cianciaruso 2008 9/212 13/211 6.2 % 0.69 [0.30, 1.58]
di Iorio 2003 2/10 7/10 2.5 % 0.29 [0.08, 1.05]
Ihle 1989 4/34 13/38 4.1 % 0.34 [0.12, 0.95]
Jungers 1987 5/10 7/9 8.4 % 0.64 [0.32, 1.31]
Malvy 1999 11/25 17/25 15.8 % 0.65 [0.39, 1.09]
Mircescu 2007 1/27 7/26 1.0 % 0.14 [0.02, 1.04]
Rosman 1989 30/130 34/117 23.7 % 0.79 [0.52, 1.21]
Subtotal (95% CI) 448 436 61.7 % 0.63 [0.48, 0.83]
Total events: 62 (Low protein), 98 (Higher protein)
Heterogeneity: Tau² = 0.01; Chi² = 6.27, df = 6 (P = 0.39); I² =4%
Test for overall effect: Z = 3.31 (P = 0.00092)
Total (95% CI) 1002 998 100.0 % 0.68 [0.55, 0.84]
Total events: 113 (Low protein), 168 (Higher protein)
Heterogeneity: Tau² = 0.0; Chi² = 8.70, df = 9 (P = 0.51); I² =0.0%
Test for overall effect: Z = 3.68 (P = 0.00024)
0.01 0.1 1 10 100
Less deaths on low
Less deaths on high

FIGURE 90.7 Meta-analysis of randomized clinical trials of low-protein diets for non-diabetic and diabetic kidney disease. Low protein diets for chronic renal failure in non-diabetic adults (Cochrane Review). *(With permission from Fouque D, Laville M. (Cochrane Database Syst Rev, Cochrane Database Syst Rev. 2009 Jul 8;(3):CD001892). B. Robertson L, Waugh N, Robertson A. Protein restriction for diabetic renal disease (Cochrane Database Syst Rev. 2007 Issue 4 CD002181).)*

Thus, the meta-analysis technique, by increasing the number of observations, can reduce the incidence of renal death or increasing the time until dialysis is required. The conclusion stands in sharp contrast to the suggestion that dialysis be "started early".[2,3] As noted, results from controlled trials of early start dialysis have demonstrated that this practice does not offer patients any survival benefit.[4–6,137,460] It is worth noting that only two evaluations of the influence of the diet on the loss of kidney function were actually based on GFR measurements in patients with more advanced CKD: the report of Ihle et al. showed a protective effect and results from the MDRD study yielded a benefit that was nearly significant benefit ($p = 0.07$).[140,164] In contrast to outcomes with this precise measure of kidney function, there is abundant evidence that these diets can reduce the accumulation of unexcreted, metabolic products while maintaining nutritional status and consequently, can delay the need to begin dialysis therapy.

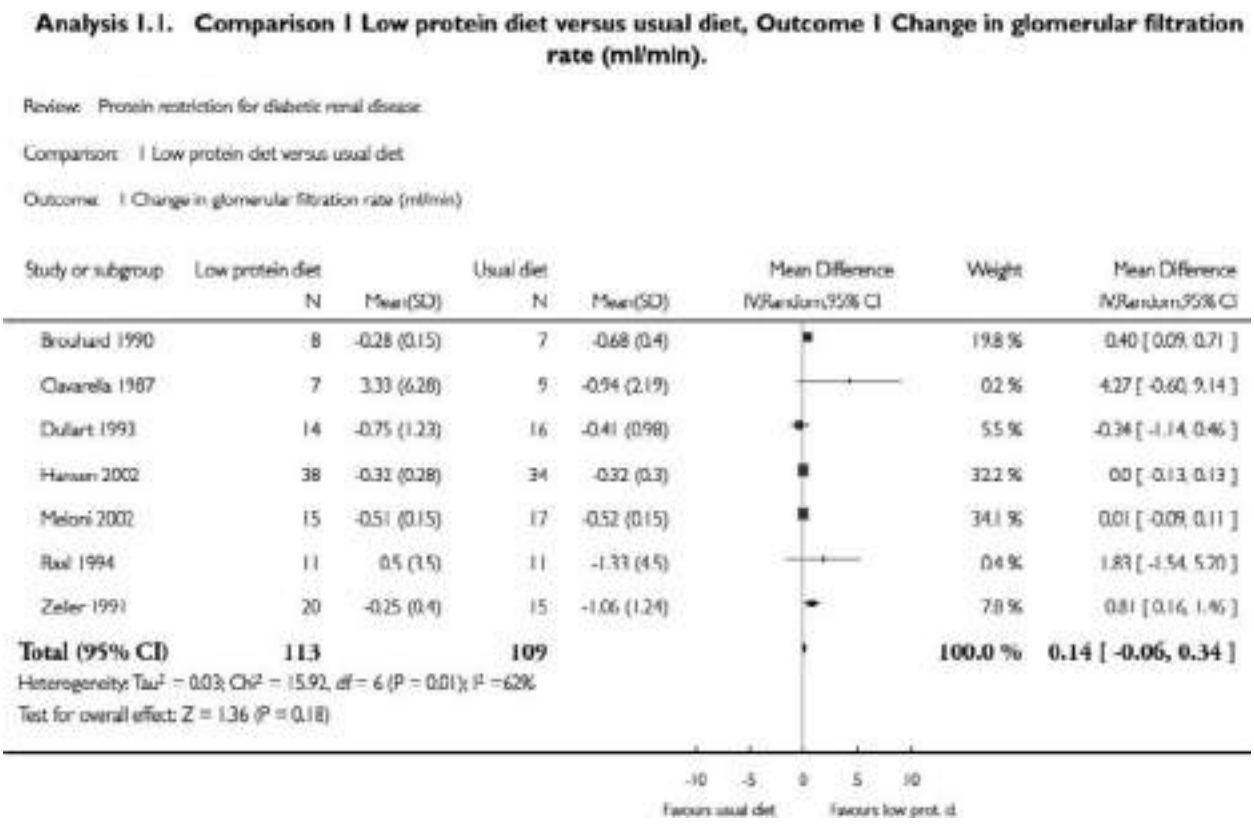
Analysis 1.1. Comparison 1 Low protein diet versus usual diet, Outcome 1 Change in glomerular filtration rate (ml/min).
Review: Protein restriction for diabetic renal disease
Comparison: 1 Low protein diet versus usual diet
Outcome: 1 Change in glomerular filtration rate (ml/min)
Study or subgroup
Low protein diet
N
Mean(SD)
Usual diet
N
Mean(SD)
Mean Difference
IV,Random,95% CI
Weight
Mean Difference
IV,Random,95% CI
Brouhard 1990 8 -0.28 (0.15) 7 -0.68 (0.4) 19.8 % 0.40 [0.09, 0.71]
Clavarella 1987 7 3.33 (6.28) 9 -0.94 (2.19) 0.2 % 4.27 [-0.60, 9.14]
Dullaart 1993 14 -0.75 (1.23) 16 -0.41 (0.98) 5.5 % -0.34 [-1.14, 0.46]
Hansen 2002 38 -0.32 (0.28) 34 -0.32 (0.3) 32.2 % 0.0 [-0.13, 0.13]
Meloni 2002 15 -0.51 (0.15) 17 -0.52 (0.15) 34.1 % 0.01 [-0.09, 0.11]
Rasi 1994 11 0.5 (1.5) 11 -1.33 (4.5) 0.4 % 1.83 [-1.54, 5.20]
Zeller 1991 20 -0.25 (0.4) 15 -1.06 (1.24) 7.8 % 0.81 [0.16, 1.46]
Total (95% CI) 113 109 100.0 % 0.14 [-0.06, 0.34]
Heterogeneity: Tau² = 0.03; Chi² = 15.92, df = 6 (P = 0.01); I² =62%
Test for overall effect: Z = 1.36 (P = 0.18)
-10
-5
0
5
10
Favours usual diet
Favours low prot. d

FIGURE 90.7 (Continued)

Our discussion of the pathophysiology and treatment of patients with CKD is based on a seemingly simple concept, namely that the cause of the morbidity and mortality occurring in CKD patients results from a reduced ability to excrete nitrogenous, non-nitrogen-containing metabolites and ions. It follows that restricting the precursor of treatment reduces signs and symptoms of CKD and is nutritionally safe as long as there is no complicating factor such as acidosis, infection, and so on (Fig. 90.7). Thus, dietary manipulation in a treatment program that includes monitoring protein and calorie intake in consultation with a dietician[202,468] should be a mainstay of therapy for all patients. The observation that protein intake voluntarily decreases as renal insufficiency progresses is not a signal for increasing in dietary protein because high-protein diets will simply increase the degree of uremia (including hyperphosphatemia, aggravate hypertension, etc.) and it will not raise serum proteins.[377,385] On the contrary, a well-designed protein-restricted diet usually increases serum albumin.[469] Regardless of an effect on progression, a low-protein diet could delay the need for dialysis by ameliorating uremic symptoms while maintaining nutritional status. Two publications provide strong evidence for the long-term safety of this approach.[358] Patients in these studies were followed for an average of 1.5–2 years after GFR had decreased to 10–13 ml/min. Nutritional status was well maintained while they ate protein-restricted diets and dialysis was not required. Clearly, successful implementation of dietary therapy requires the motivation of both the patient and the physician. The principal, if not the only disadvantage of such therapy (assuming that it is successful in eliminating uremic symptoms), is the dietary restriction that it entails, but it is reasonable to expect that dialysis therapy will be significantly delayed.

Metabolic Acidosis and Progression

The kidneys are responsible for clearing fixed acids that are generated from protein intake and metabolic acidosis is a common complication seen in progressive kidney disease.[470] There have been a number of studies that have suggested that correction of acidosis can modify the course of CKD. Shah et al. studied 5422 patients with a baseline eGFR <60 mL/min/1.73 for at least four years.[471] Kidney progression was defined as a 30% decrease in eGFR or a doubling of serum creatinine. Kidney failure developed in a significantly higher rate in those patients with serum bicarbonate <22 mM

compared to those with serum bicarbonate of 25 mM. Kovesdy et al. found that serum bicarbonate was related to all-cause mortality in patients with moderate to advanced CKD.[472] In a randomized, controlled trial, 134 Stage 4 CKD patients (CrCl 15–30 ml/min per 1.73 m^2) and serum bicarbonate 16–20 mM were assigned to receive oral bicarbonate or a placebo.[473] Over two years, fewer patients in the bicarbonate group developed rapid progression and ESRD developed less frequently ($p < 0.001$). Recently, Majahan and colleagues reported results from a randomized, placebo-controlled trial in which CKD patients were given sodium citrate[474] and showed that there was significantly reduced loss of estimated GFR.

CONCLUSIONS

Based on the pathophysiology of CKD, it is clear that multiple, adverse effects products of protein metabolism can be minimized by careful dietary planning to reduce protein intake. A clinician ignores dietary therapy at his or her patient's peril because the consequences in terms of the generation of symptoms and acceleration of the rate of loss of kidney function are predictable. It is also clear that treatment with an optimal amount of dietary protein is only part of conservative management. As we have discussed and has been covered elsewhere in this textbook, preventing acidosis, limiting the accumulation of phosphates and sodium, controlling blood pressure, repleting EPO and vitamin D, and inhibiting the activation of the sympathetic nervous system and renin-angiotensin-aldosterone systems have the potential to improve outcomes both in conjunction with and independent of optimal dietary protein intake. While there are differences of opinion in how best to implement these measures, they form the basis of the National Kidney Foundation's clinical practice guidelines on the conservative management of CKD. The epidemiology of CKD reminds us not only of the societal importance of addressing this issue, but also of the many comorbid conditions that complicate management. In short, the conservative management of CKD must take into account other comorbidities. For example, inflammation from infection, cardiac failure, malignancy, or poorly controlled diabetes can change requirements for dietary protein. Still, the safety of conservative therapy, and the availability of reliable methods for judging compliance and its effects combined with its potential for ameliorating many symptoms of CKD indicate that conservative therapy should be offered to all patients unless a transplant will be immediately available or there are complications that require initiation of dialysis therapy.

References

[1] Coresh J, Selvin E, Stevens LA, et al. Prevalence of chronic kidney disease in the United States. JAMA 2007;298(17):2038–47.

[2] Hakim RM, Lazarus JM. Initiation of dialysis. J Am Soc Nephrol 1995;6:1319–20.

[3] Mehrotra R, Nolph KD. Treatment of advanced renal failure: low-protein diets or timely initiation of dialysis. Kidney Int 2000;58:1381–8.

[4] Beddhu S, Samore MH, Roberts MS, et al. Impact of timing of initiation of dialysis on mortality. J Am Soc Nephrol 2003;14:2305–12.

[5] Traynor JP, Simpson K, Geddes CC, Deighan CJ, Fox JG. Early initiation of dialysis fails to prolong survival in patients with end-stage renal failure. J Am Soc Nephrol 2002;13:2125–32.

[6] Cooper BA, Branley P, Bulfone L, et al. A randomized, controlled trial of early versus late initiation of dialysis. N Engl J Med 2010;363(7):609–19.

[7] Korevaar JC, Jansen MA, Dekker FW, Boeschoten EW, Bossuyt PM, Krediet RT. Evaluation of DOQI guidelines: early start of dialysis treatment is not associated with better health-related quality of life. National kidney foundation-dialysis outcomes quality initiative. Am J Kidney Dis 2002;39(1):108–15.

[8] Gaspari F, Guerini E, Perico N, Mosconi L, Ruggenenti P, Remuzzi G. Glomerular filtration rate determined from a single plasma sample after intravenous iohexol injection: is it reliable? J Am Soc Nephrol 1996;7:2689–93.

[9] Perrone RD, Steinman TI, Beck GJ, et al. Utility of radioisotopic filtration markers in chronic renal insufficiency: simultaneous comparison of 125I-iothalamate, 169Yb-DPTA, 99mTc-DTPA and inulin. Am J Kid Dis 1990;16:224–35.

[10] Bauer JH, Brooks CS, Burch RN. Clinical appraisal of creatinine clearance as a measurement of glomerular filtration rate. Am J Kid Dis 1982;2:337–46.

[11] Myers BD, Nelson RG, Williams GW, et al. Glomerular function in Pima Indians with noninsulin-dependent diabetes mellitus of recent onset. J Clin Invest 1991;88:524–30.

[12] Nelson RG, Bennett PH, Beck GJ, et al. Development and progression of renal disease in Pima Indians with non-insulin-dependent diabetes mellitus. N Engl J Med 1996;335:1636–42.

[13] Rehling M, Moller ML, Thamdrup B, Lund JO, Trap-Jensen J. Simultaneous measurement of renal clearance and plasma clearance of 99mTc-labelled diethylenetriaminepenta-acetate, 51Cr-labelled ethylenediaminetetra-acetate and inulin in man. Clin Sci 1984;66:613–9.

[14] Gaspari F, Perico N, Matalone M, et al. Precision of plasma clearance of iohexol for estimation of GFR in patients with renal disease. J Am Soc Nephrol 1998;9:310–3.

[15] Frennby B, Sterner G, Almen T, Hagstam KE, Hultberg B, Jacobsson L. The use of iohexol clearance to determine GFR in patients with severe chronic renal failure: a comparison between different clearance techniques. Clin Nephrol 1995;43:35–46.

[16] Gaspari F, Perico N, Remuzzi G. Measurement of glomerular filtration rate. Kidney Int 1997;52(Suppl. 63):S151–4.

[17] Li Y, Lee HB, Blaufox MD. Single-sample methods to measure GFR with technetium-99M-DTPA. J Nucl Med 1997;38:1290–5.

[18] Sambataro M, Thomaseth K, Pacini G, et al. Plasma clearance of 51Cr-EDTA provides a precise and convenient technique for measurement of glomerular filtration rate in diabetic humans. J Am Soc Nephrol 1996;7:118–27.

[19] Forbes GB, Bruining GS. Urinary creatinine excretion and lean body mass. Am J Clin Nutr 1978;29:1359–66.

[20] Bleiler RE, Schedle HP. Creatinine excretion: variability and relationships to diet and body size. J Lab Clin Med 1962;59:945–55.

[21] Mitch WE, Walser M. A proposed mechanism for reduced creatinine excretion in severe chronic renal failure. Nephron 1978;21:248–54.
[22] Mitch WE. Measuring the rate of progression of renal insufficiency. In: Mitch WE, editor. The progressive nature of renal disease. 2nd ed. New York: Churchill Livingstone; 1992. p. 203–22.
[23] Morgan DB, Dillon S, Payne RB. The assessment of glomerular function: creatinine clearance or plasma creatinine? Postgrad Med J 1978;54:302–10.
[24] Coresh J, Astor BC, McQuillan G, et al. Calibration and random variation of the serum creatinine assay as critical elements of using equations to estimate glomerular filtration rate. Am J Kidney Dis 2002;39(5):920–9.
[25] Cockcroft DW, Gault MH. Prediction of creatinine clearance from serum creatinine. Nephron 1975;16:31–41.
[26] Levey AS, Greene T, Kusek J, Beck GJ, Group MS. A simplified equation to predict glomerular filtration rate from serum creatinine. J Am Soc Nephrol 1999;130:461–70 [11, A155]
[27] Levey AS, Coresh J, Greene T, et al. Using standardized serum creatinine values in the modification of diet in renal disease study equation for estimating glomerular filtration rate. Ann Intern Med 2006;145(4):247–54.
[28] Levey AS, Stevens LA, Schmid CH, et al. A new equation to estimate glomerular filtration rate. Ann Intern Med 2009;150 (9):604–12.
[29] Schwartz GJ, Haycock GB, Edelmann Jr CM, Spitzer A. A simple estimate of glomerular filtration rate in children derived from body length and plasma creatinine. Pediatrics 1976;58:259–63.
[30] Lubowitz H, Slatopolsky E, Shankel S, Rieselbach RE, Bricker NS. Glomerular filtration rate: determination in patients with chronic renal disease. JAMA 1967;199:252–6.
[31] Shemesh O, Golbetz H, Kriss JP, Myers BD. Limitations of creatinine as a filtration marker in glomerulopathic patients. Kidney Int 1985;28:830–8.
[32] Doolan PD, Alpen EL, Theil GB. A clinical appraisal of the plasma concentration and endogenous clearance of creatinine. Am J Med 1962;32:56–79.
[33] Kelly RA, Mitch WE. Creatinine uric acid and other nitrogenous waste products: clinical implication of the imbalance between their production and elimination in uremia. Sem Nephrol 1983;3:286–94.
[34] Heymsfield SB, Arteaga C, McManus C, Smith J, Moffitt S. Measurement of muscle mass in humans: validity of the 24-hour urinary creatinine method. Am J Clin Nutr 1983;37:478–98.
[35] Payne RB. Creatinine clearance: a redundant clinical investigation. Ann Clin Biochem 1986;23:243–50.
[36] Hellerstein S, Berenbom M, Alon US, Warady BA. Creatinine clearance following cimetidine for estimation of glomerular filtration rate. Ped Nephrol 1998;12:49–54.
[37] Mitch WE, Walser M. A proposed mechanism for reduced creatinine excretion in severe chronic renal failure. Nephron 1978;21:248–59.
[38] Levey AS, Bosch JP, Lewis JB, Greene T, Rogers N, Roth D. A more accurate method to estimate glomerular filtration rate from serum creatinine: a new predition equation. Ann Intern Med 1999;130:461–70.
[39] Zuo L, Ma YC, Zhou YH, Wang M, Xu GB, Wang HY. Application of GFR-estimating equations in Chinese patients with chronic kidney disease. Am J Kid Dis 2005;45(3):463–72.
[40] Ma YC, Zuo L, Chen JH, et al. Modified glomerular filtration rate estimating equation for Chinese patients with chronic kidney disease. J Am Soc Nephrol 2006;17(10):2937–44.
[41] Horio M, Imai E, Yasuda Y, Watanabe T, Matsuo S. Modification of the CKD epidemiology collaboration (CKD-EPI) equation for Japanese: accuracy and use for population estimates. Am J Kidney Dis 2010;56(1):32–8.
[42] Soares AA, Eyff TF, Campani RB, et al. Performance of the CKD Epidemiology Collaboration (CKD-EPI) and the modification of diet in renal disease (MDRD) study equations in healthy South Brazilians. Am J Kidney Dis 2010;55(6):1162–3.
[43] Kwong YT, Stevens LA, Selvin E, et al. Imprecision of urinary iothalamate clearance as a gold-standard measure of GFR decreases the diagnostic accuracy of kidney function estimating equations. Am J Kidney Dis 2010;56(1):39–49.
[44] Lin J, Knight EL, Hogan ML, Singh AK. A comparison of prediction equations for estimating glomerular filtration rate in adults without kidney disease. J Am Soc Nephrol 2003;14:2573–80.
[45] Vervoort G, Willems HL, Wetzels JF. Assessment of glomerular filtration rate in healthy subjects and normoalbuminuric diabetic patients: validity of a new MDRD prediction equation. Nephrol Dial Transpl 2002;17:1909–13.
[46] Stevens LA, Coresh J, Feldman HI, et al. Evaluation of the modification of diet in renal disease study equation in a large diverse population. J Am Soc Nephrol 2007;18(10):2749–57.
[47] Dharnidharka VR, Kwon C, Stevens G. Serum cystatin C is superior to serum creatinine as a marker of kidney function: a meta-analysis. Am J Kid Dis 2002;40:221–6.
[48] Mussap M, Dalla Vestra M, Fioretto P, et al. Cystatin C is a more sensitive marker than creatinine for the estimation of GFR in type 2 diabetic patients. Kidney Int 2002;61:1453–61.
[49] Stenvinkel P, Ketteler M, Johnson RJ, et al. IL-10, IL-6, and TNF-alpha: central factors in the altered cytokine network of uremia—the good, the bad, and the ugly. Kidney Int 2005;67 (4):1216–33.
[50] Sjostrom P, Tidman M, Jones I. Determination of the production rate and non-renal clearance of cystatin C and estimation of the glomerular filtration rate from the serum concentration of cystatin C in humans. Scand J Clin Lab Invest 2005;65:111–24.
[51] Mitch WE, Goldberg AL. Mechanisms of muscle wasting: the role of the ubiquitin-proteasome system. N Engl J Med 1996;335:1897–905.
[52] Jacobsson B, Lignelid H, Bergerheim USR. Transthyretin and cystatin C are catabolized in proximal tubular epithelial cells and the proteins are not useful as markers for renal cell carcinomas. Histopathology 1995;26:559–64.
[53] Shlipak MG, Sarnak MJ, Katz R, et al. Cystatin C and the risk of death and cardiovascular events among elderly persons. N Engl J Med 2005;352(20):2049–60.
[54] Tian S, Kusano E, Ohara T, et al. Cystatin C measurement and its practical use in patients with various renal diseaes. Clin Nephrol 1997;48:104–8.
[55] Oddoze C, Morange S, Portugal H, Bertrand Y, Dussoi Y. Cystatin C is not more sensitive than creatinine for detecting renal impairment in patients with diabetes. Am J Kid Dis 2001;38:310–6.
[56] Strevens H, Wide-Swensson D, Torffvit O, Grubb A. Serum cystatin C for assessment of glomerular filtration rate in pregnant and non-pregnant women. Indications of altered filtration process in pregnancy. Scand J Clin Lab Invest 2002;62:141–7.
[57] Galli G, Rufini V, Vellante C, D'errico G, Piraccini R. Estimation of glomerular filtration rate with 99Tc(m)-DTPA: A comparative assessment of simplified methods. Nucl Med Commun 1997;18:634–41.
[58] Hjorth L, Wiebe T, Karpman D. Correct evaluation of renal glomerular filtration rate requires clearance assays. Pediatr Nephrol 2002;17:847–51.

[59] Krieser D, Rosenberg AR, Kainer G, Daya N. The relationship between serum creatinine, serum cystatin C and glomerular filtration rate in pediatric renal transplant recipients: a pilot study. Pediatr Transplant 2002;6:392–5.
[60] Poge U, Gerhardt T, Stoffel-Wagner B, Klehr HU, Sauerbruch T, Woitas RP. Calculation of glomerular filtration rate based on cystatin C in cirrhotic patients. Nephrol Dial Transplant 2006;21 (3):660–4.
[61] Bianchi C, Donadio C, Tramonti G, Consani C, Lorusso P, Rossi G. Reappraisal of serum beta 2-microglobulin as a marker of GFR. Ren Fail 2001;23:419–29.
[62] Giessing M. Beta-trace protein as indicator of glomerular filtration rate. Urology 1999;54:940–1.
[63] Takahira R, Yonemura K, Yonekawa O, et al. Tryptophan glycoconjugate as a novel marker of renal function. Am J Med 2001;110:192–7.
[64] Longenecker JC, Coresh J, Klag MJ, et al. Validation of comorbid conditions on the end-stage renal disease medical evidence report: the CHOICE study. Choices for healthy outcomes in caring for ESRD. J Am Soc Nephrol 2000;11(3):520–9.
[65] Rocco MV, Yan G, Gassman J, et al. Comparison of causes of death using HEMO Study and HCFA end-stage renal disease death notification classification systems. The national institutes of health-funded hemodialysis. Health care financing administration. Am J Kidney Dis 2002;39(1):146–53.
[66] Division of Kidney UaHDNN. USRDS 2009 annual data report: atlas of end-stage renal disease in the United States. Bethesda: NIH; 2003.
[67] Flegal KM, Carroll MD, Duczmarski RJ, Johnson CL. Overweight and obesity in the United States: prevalence and trends. Int J Obes Relat Metab Disord 1998;22:39–47.
[68] Hsu CY, Chertow GM. Chronic renal confusion: insufficiency, failure, dysfunction, or disease. Am J Kidney Dis 2000;36 (2):415–8.
[69] National Kidney Foundation. K/DOQI clinical practice guidelines for chronic kidney disease: evaluation, classification, and stratification. Am J Kidney Dis 2005;45(Suppl. 3):S1–153.
[70] Coresh J, Byrd-Holt D, Astor BC, et al. Chronic kidney disease awareness, prevalence, and trends among U.S. adults, 1999 to 2000. J Am Soc Nephrol 2005;16(1):180–8.
[71] Nickolas TL, Frisch GD, Opotowsky AR, Arons R, Radhakrishnan J. Awareness of kidney disease in the US population: findings from the national health and nutrition examination survey (NHANES) 1999 to 2000. Am J Kidney Dis 2004;44 (2):185–97.
[72] Obrador GT, Ruthazer R, Arora P, Kausz AT, Pereira BJG. Prevalence and factors associated with suboptimal care before initiation of dialysis in the United States. J Am Soc Nephrol 1999;10:1793–800.
[73] Kausz AT, Khan SS, Abichandani R, Kazmi WHOGT, Ruthazer R, Pereira BJG. Management of patients with chronic renal insufficiency in the northeastern United States. J Am Soc Nephrol 2001;12:1501–7.
[74] Lafayette RA, Lai G. Examining chronic kidney disease management in a single center. Clin Nephrol 2004;62(4):260–6.
[75] Clase CM, Garg AX, Kiberd BA. Prevalence of low glomerular filtration rate in nondiabetic Americans: third national health and nutrition examination survey (NHANES III). J Am Soc Nephrol 2002;13(5):1338–49.
[76] Garg AX, Kiberd BA, Clark WF, Haynes RB, Clase CM. Albuminuria and renal insufficiency prevalence guides population screening: results from the NHANES III. Kidney Int 2002;61 (6):2165–75.
[77] Haffner SM, Lehto S, Ronnemaa T, Pyorala K, Laakso M. Mortality from coronary heart disease in subjects with type 2 diabetes and in nondiabetic subjects with and without prior myocardial infarction. N Engl J Med 1998;339:229–34.
[78] Snyder JJ, Foley RN, Collins AJ. Prevalence of CKD in the United States: a sensitivity analysis using the national health and nutrition examination survey (NHANES) 1999–2004. Am J Kidney Dis 2009;53(2):218–28.
[79] Akbari A, Swedko PJ, Clark HD, et al. Detection of chronic kidney disease with laboratory reporting of estimated glomerular filtration rate and an educational program. Arch Intern Med 2004;164(16):1788–92.
[80] Vupputuri S, Batuman V, Muntner P, et al. Effect of blood pressure on early decline in kidney function among hypertensive men. Hypertension 2003;42(6):1144–9.
[81] Walker WG, Neaton JD, Cutler JA, Neuwirth R, Cohen JD. Renal function change in hypertensive members of the multiple risk factor intervention trial. Racial and treatment effects. The MRFIT research group. JAMA 1992;268(21):3085–91.
[82] Brancati FL, Whelton PK, Randall BL, Neaton JD, Stamler J, Klag MJ. Risk of end-stage renal disease in diabetes mellitus: a prospective cohort study of men screened for MRFIT. JAMA 1997;278:2069–74.
[83] Hsu CY. Does non-malignant hypertension cause renal insufficiency? Evidence-based perspective. Curr Opin Nephrol Hypertens 2002;11(3):267–72.
[84] Humphrey LL, Ballard DJ, Frohnert PP, Chu CP, O'Fallon WM, Palumbo PJ. Chronic renal failure in non-insulin-dependent diabetes mellitus. A population-based study in Rochester, Minnesota. Ann Intern Med 1989;111(10):788–96.
[85] Hasslacher C, Ritz E, Wahl P, Michael C. Similar risks of nephropathy in patients with type I or type II diabetes mellitus. Nephrol Dial Transplant 1989;4(10):859–63.
[86] Andersen AR, Christiansen JS, Andersen JK, Kreiner S, Deckert T. Diabetic nephropathy in type 1 diabetes: an epidemiological study. Diabetologia 1983;25:496–501.
[87] Bojestig M, Arnqvist HJ, Hermansson G, Karlberg BE, Ludvigsson J. Declining incidence of nephropathy in insulin-dependent diabetes mellitus. N Engl J Med 1994;330(1):15–8.
[88] McClellan WM. Epidemiology and risk factors for chronic kidney disease. Med Clin North America 2005;89:419–45.
[89] Anavekar NS, McMurray JJ, Velazquez EJ, et al. Relation between renal dysfunction and cardiovascular outcomes after myocardial infarction. N Engl J Med 2004;351(13):1285–95.
[90] Manjunath G, Tighiouart H, Ibrahim H, et al. Level of kidney function as a risk factor for atherosclerotic cardiovascular outcomes in the community. J Am Coll Cardiol 2003;41(1):47–55.
[91] Perry Jr HM, Miller JP, Fornoff JR, et al. Early predictors of 15-year end-stage renal disease in hypertensive patients. Hypertension 1995;25(4 Pt 1):587–94.
[92] Bergman S, Key BO, Kirk KA, Warnock DG, Rostand SG. Kidney disease in the first-degree relatives of African-Americans with hypertensive end-stage renal disease. Am J Kidney Dis 1996;27:341–6.
[93] O'Dea DF, Murphy SW, Hefferton D, Parfrey PS. Higher risk for renal failure in first-degree relatives of white patients with end-stage renal disease: a population-based study. Am J Kidney Dis 1998;32(5):794–801.
[94] Keith DS, Nichols GA, Gullion CM, Brown JB, Smith DH. Longitudinal follow-up and outcomes among a population with chronic kidney disease in a large managed care organization. Arch Intern Med 2004;164(6):659–63.
[95] Go AS, Chertow GM, Fan D, McCulloch CE, Hsu CY. Chronic kidney disease and the risks of death, cardiovascular events, and hospitalization. N Engl J Med 2004;351(13):1296–305.
[96] Satko SG, Freedman BI. The familial clustering of renal disease and related phenotypes. Med Clin North Am 2005;89(3):447–56.

[97] Vanholder R, Massy Z, Argiles A, Spasovski G, Verbeke F, Lameire N. Chronic kidney disease as cause of cardiovascular morbidity and mortality. Nephrol Dial Transplant 2005;20 (6):1048–56.
[98] Weiner DE, Tabaabai S, Tighiouart H, et al. Cardiovascular outcomes and all-cause mortality: exploring the interaction between CKD and cardiovascular disease. Am J Kid Dis 2006;48:392–401.
[99] Lindeman RD, Tobin J, Shock NW. Longitudinal studies on the rate of decline in renal function with age. J Am Geriatr Soc 1985;33:278–85.
[100] Lindeman RD. Overview: renal physiology and pathophysiology of aging. Am J Kid Dis 1990;16:275–82.
[101] Kleinknecht D, Grunfeld JP, Gomez PC, Moreau J-F, Garcia-Torrez R. Diagnostic procedures and long-term prognosis in bilateral renal cortical necrosis. Kidney Int 1973;4:390.
[102] Jones RH, Hayakawa H, MacKay JD, Parsons V, Watkins PF. The progression of diabetic nephropathy. Lancet 1979;1:1105–6.
[103] Toto RD, Mitchell HC, Smith RD, Lee H-C, McIntire D, Pettinger WA. "Strict" blood pressure control and progression of renal disease in hypertensive nephrosclerosis. Kidney Int 1995;48:851–9.
[104] Hunsicker LG, Adler S, Caggiula A, et al. Predictors of the progression of renal disease in the modification of diet in renal disease study. Kidney Int 1997;51:1908–19.
[105] Goetz FC, Jacobs Jr DR, Chavers B, Roel J, Yelle M, Sprafka JM. Risk factors for kidney damage in the adult population of Wadena, Minnesota. A prospective study. Am J Epidemiol 1997;145(2):91–102.
[106] Rostand SG. US minority groups and end-stage renal disease: a disproportionate share. Am J Kidney Dis 1992;19(5):411–3.
[107] Pugh JA, Stern MP, Haffner SM, Eifler CW, Zapata M. Excess incidence of treatment of end-stage renal disease in Mexican Americans. Am J Epidemiol 1988;127(1):135–44.
[108] Knight EL, Stampfer MJ, Hankinson SE, Spiegelman D, Curhan GC. The impact of protein intake on renal function decline in women with normal renal function or mild renal insufficiency. Ann Intern Med 2003;138:460–7.
[109] Wrone EM, Carnethon MR, Palaniappan L, Fortmann SP. Association of dietary protein intake and microalbuminuria in healthy adults: third national health and nutrition examination survey. Am J Kidney Dis 2003;41(3):580–7.
[110] Neugarten J, Acharya A, Silbiger SR. Effect of gender on the progression of nondiabetic renal disease: a meta-analysis. J Am Soc Nephrol 2000;11(2):319–29.
[111] Lackland DT, Bendall HE, Osmond C, Egan BM, Barker DJ. Low birth weights contribute to high rates of early-onset chronic renal failure in the Southeastern United States. Arch Intern Med 2000;160(10):1472–6.
[112] Perneger TV, Whelton PK, Klag MJ. Race and end-stage renal disease. Socioeconomic status and access to health care as mediating factors. Arch Intern Med 1995;155(11):1201–8.
[113] Orth SR, Ritz E, Schrier RW. The renal risks of smoking. Kidney Int 1997;51(6):1669–77.
[114] Perneger TV, Whelton PK, Puddey IB, Klag MJ. Risk of end-stage renal disease associated with alcohol consumption. Am J Epidem 1999;150:1275–81.
[115] Knight EL, Stampfer MJ, Rimm EB, Hankinson SE, Curhan GC. Moderate alcohol intake and renal function decline in women: a prospective study. Nephrol Dial Transplant 2003;18 (8):1549–54.
[116] Muntner P, He J, Vupputuri S, Coresh J, Batuman V. Blood lead and chronic kidney disease in the general United States population: results from NHANES III. Kidney Int 2003;63 (3):1044–50.
[117] Perneger TV, Whelton PK, Klag MJ. Risk of kidney failure associated with the use of acetaminophen, aspirin, and nonsteroidal anti-inflammatory drugs. N Engl J Med 1994;331:1675–9.
[118] Curhan GC, Forman JP. Sugar-sweetened beverages and chronic disease. Kidney Int 2010;77(7):569–70.
[119] Abrass CK. Overview: obesity: what does it have to do with kidney disease? J Am Soc Nephrol 2004;15(11):2768–72.
[120] Bagby SP. Obesity-initiated metabolic syndrome and the kidney: a recipe for chronic kidney disease? J Am Soc Nephrol 2004;15(11):2775–91.
[121] Haugen E, Nath KA. The involvement of oxidative stress in the progression of renal injury. Blood Purif 1999;17 (2–3):58–65.
[122] Kurella M, Lo JC, Chertow GM. Metabolic syndrome and the risk for chronic kidney disease among nondiabetic adults. J Am Soc Nephrol 2005;16(7):2134–40.
[123] Massy ZA, Ma JZ, Louis TA, Kasiske BA. Lipid-lowering therapy in patients with renal disease. Kidney Int 1995;48:188–98.
[124] Johnson RJ, Segal MS, Srinivas T, et al. Essential hypertension, progressive renal disease, and uric acid: a pathogenetic link? J Am Soc Nephrol 2005;16(7):1909–19.
[125] Iseki K, Ikemiya Y, Iseki C, Takishita S. Proteinuria and the risk of developing end-stage renal disease. Kidney Int 2003;63 (4):1468–74.
[126] Remuzzi G, Bertani T. Pathophysiology of progressive nephropathies. N Engl J Med 1998;339:1448–56.
[127] Gouva C, Nikolopoulos P, Ioannidis JP, Siamopoulos KC. Treating anemia early in renal failure patients slows the decline of renal function: a randomized controlled trial. Kidney Int 2004;66(2):753–60.
[128] Boger RH, Zoccali C. ADMA: a novel risk factor that explains excess cardiovascular event rate in patients with end-stage renal disease. Atheroscler Suppl 2003;4(4):23–8.
[129] Modlinger PS, Wilcox CS, Aslam S. Nitric oxide, oxidative stress and progression of chronic renal failure. Sem Nephrol 2004;24:354–65.
[130] Ibrahim HN, Hostetter TH. Aldosterone in renal disease. Curr Opin Nephrol Hypertens 2003;12:159–64.
[131] Ahlman J. Incidence of chronic renal insufficiency. A study of the incidence and pattern of renal insufficiency in adults during 1966-1971 in Gothenberg. Acta Med Scand 1975;582:3–50.
[132] Johnson WJ, O'Kane HO, Elveback LR. Survival of patients with end-stage renal disease. Mayo Clinic Proceedings 1973;48:18.
[133] Maher JF, Nolph KD, Bryan CW. Prognosis of advanced chronic renal failure. I. Unpredictability of survival and reversibility. Ann Intern Med 1974;81:43–7.
[134] Mitch WE, Buffington GA, Lemann J, Walser M. A simple method of estimating progression of chronic renal failure. Lancet 1976;2:1326–8.
[135] Mitch WE. The influence of the diet on the progression of renal failure. Ann Rev Med 1984;35:249–64.
[136] Rutherford WE, Blondin J, Miller JP, Greenwalt AS, Vavra JD. Chronic progressive renal disease. Kidney Int 1977;11:62–72.
[137] Coresh J, Walser M, Hill S. Survival on dialysis among chronic renal failure patients treated with a supplemented low-protein diet before dialysis. J Am Soc Nephrol 1995;6:1379–85.
[138] Viberti GC, Bilous RW, Mackintosh BS, Keen H. Monitoring glomerular function in diabetic nephropathy. Am J Med 1983;74:256–64.
[139] Barsotti G, Guiducci A, Ciardella F, Giovannetti S. Effects on renal function of a low-nitrogen diet supplemented with essential amino acids and ketoanalogues and of hemodialysis and free protein supply in patients with chronic renal failure. Nephron 1981;27:113–7.

[140] Klahr S, Levey AS, Beck GJ, et al. The effects of dietary protein restriction and blood-pressure control on the progression of chronic renal failure. N Engl J Med 1994;330:878–84.
[141] Shah BV, Levey AS. Spontaneous changes in the rate of decline in reciprocal serum creatinine: errrors in predicting the progression of renal disease from extrapolation of the slope. J Am Soc Nephrol 1992;2:1186–91.
[142] Walser M, Drew HH, LaFrance ND. Creatinine measurements often yield false estimates of progression in chronic renal failure. Kidney Int 1988;34:412–8.
[143] Walser M. Progression of chronic renal failure in man. Kidney Int 1990;37:1195–210.
[144] Fraser CG, Williams P. Short-term biological variation of plasma analytes in renal disease. Clin Chem 1983;29:508–10.
[145] Gretz N, Manz F, Strauch M. Predictability of the progression of chronic renal failure. Kidney Int 1983;24(Suppl. 15):2–5.
[146] Oksa H, Pasternack A, Luomala M, Sirvio M. Progression of chronic renal failure. Nephron 1983;35:31–4.
[147] Lewis J, Greene T, Appel L, et al. Comparison of iothalamate-GFR and serum creatinine-based outcomes: acceleration in the rate of GFR decline in the African American study of kidney disease. J Am Soc Nephrol 2004;15:3175–83.
[148] Wright Jr JT, Bakris G, Greene T, et al. Effect of blood pressure lowering and antihypertensive drug class on progression of hypertensive kidney disease: results from the AASK trial. JAMA 2002;288(19):2421–31.
[149] Appel LJ, Wright Jr JT, Greene T, et al. Intensive blood-pressure control in hypertensive chronic kidney disease. N Engl J Med 2010;363(10):918–29.
[150] Jones JD, Burnett PC. Creatinine metabolism in humans with decreased renal function: creatinine deficit. Clin Chem 1974;20:1204–12.
[151] Crim MC, Calloway DH, Margen S. Creatinine metabolism in men: creatine pool size and turnover in relation to creatine intake. J Nutr 1976;106:371–81.
[152] Levey AS, Beck GJ, Bosch JP, et al. Short-term effects of protein intake, blood pressure and antihypertensive therapy on glomerular filtration rate in the modification of diet in renal disease study. J Am Soc Nephrol 1996;7:2097–109.
[153] Lew SQ, Bosch JP. Effect of diet on creatinine clearance and excretion in young and elderly healthy subjects and in patients with renal disease. J Am Soc Nephrol 1991;2:856–65.
[154] Hostetter TH. Human renal response to a meat meal. Am J Physiol 1986;19:F613–8.
[155] Addis T, Lippman RW, Lew W, Poo LJ, Wong W. Effect of dietary protein consumption upon body growth and organ size in the rat. Am J Physiol 1951;165(2):491–6.
[156] Deen WM, Maddox DA, Robertson CR, Brenner BM. Dynamics of glomerular ultrafiltration in the rat. VII. Response to reduced renal mass. Am J Physiol 1974;227(3):556–62.
[157] Brenner BM, Meyer TW, Hostetter TH. Dietary protein intake and the progressive nature of kidney disease: the role of hemodynamically mediated glomerular injury in the pathogenesis of progressive glomerular schlerosis in aging, renal ablation, and intrinsic renal disease. N Engl J Med 1982;307:652–9.
[158] Hostetter TH, Olson JL, Rennke HG, Venkatachalam MA, Brenner BM. Hyperfiltration in remnant nephrons: a potentially adverse response to renal ablation. Am J Physiol 1981;241:F85–93.
[159] Mallamaci F, Leonardis D, Bellizzi V, Zoccali C. Does high salt intake cause hyperfiltration in patients with essential hypertension? J Hum Hypertens 1996;10:157–61.
[160] Sacks FM, Svetkey LP, Vollmar WM, et al. Effects on blood pressure of reduced dietary sodium and the dietary approaches to stop hypertension (DASH) diet. N Engl J Med 2001;344:3–10.
[161] Dworkin LD, Hostetter TH, Rennke HG, Brenner BM. Hemodynamic basis for glomerular injury in rats with desoxycorticosterone salt hypertension. J Clin Invest 1984;73:1448–61.
[162] Nath KA, Kren SM, Hostetter TH. Dietary protein restriction in established renal injury in the rat. Selective role of glomerular capillary pressure in progressive glomerular dysfunction. J Clin Invest 1986;78(5):1199–205.
[163] Stamler J, Elliott MB, Kesteloot H, et al. Inverse relation of dietary protein markers with blood pressure: findings for 10020 men and women in the intersalt study. Circulation 1996;94:1629–34.
[164] Ihle BU, Becker GJ, Whitworth JA, Charlwood RA, Kincaid-Smith PS. The effect of protein restriction on the progression of renal insufficiency. N Engl J Med 1989;321:1773–7.
[165] Rosenberg ME, Swanson JE, Thomas BL, Howtetter TH. Glomerular and hormonal responses to dietary protein intake in human renal disease. Am J Physiol 1987;253:F1083–90.
[166] Rosman JB, Meijer S, Sluiter WJ, Ter Wee PM, Piers-Becht TP, Donker AJM. Prospective randomised trial of early dietary protein restriction in chronic renal failure. Lancet 1984;2:1291–5.
[167] Zeller KR, Whittaker E, Sullivan L, Raskin P, Jacobson HR. Effect of restricting dietary protein on the progression of renal failure in patients with insulin-dependent diabetes mellitus. N Engl J Med 1991;324:78–83.
[168] Appel LJ, Sacks FM, Carey VJ, et al. Effects of protein, monounsaturated fat, and carbohydrate intake on blood pressure and serum lipids: results of the OmniHeart randomized trial. JAMA 2005;294(19):2455–64.
[169] Mitch WE. Beneficial responses to modified diets in treating patients with chronic kidney disease. Kidney Int Suppl 2005; April(94):S133–5.
[169a] Vegter S, Perna A, Postma MJ, et al. Sodium intake, ACE inhibition and progression to ESR. J Am Soc Nephrol 2012;23:165–73.
[169b] Zoccali C, Ruggenenti P, Perna A, et al. Phosphate may promote CKD progression and attenuate renoprotective effect of ACE inhibition. J Am Soc Nephrol 2011;22:1923–30.
[170] Choi HK, Atkinson K, Karlson EW, Willett W, Curhan G. Purine-rich foods, dairy and protein intake and the risk of gout in men. N Engl J Med 2004;350:1093–103.
[171] Feig DI, Nakagawa T, Karumanchi SA, et al. Hypothesis: uric acid, nephron number and the pathogenesis of essential hypertension. Kidney Int 2004;66:281–7.
[172] Kang D-H, Nakagawa T, Feng L, et al. A role for uric acid in the progression of renal disease. J Am Soc Nephrol 2002;13:2888–98.
[173] Mazzali M, Kanellis J, Han H, et al. Hyperuricemia induces a primary renal arteriolopathy in rats by a blood pressure-independent mechanism. Am J Physiol 2002;282:F991–7.
[174] Feig DI, Soletsky B, Johnson RJ. Effect of allopurinol on blood pressure of adolescents with newly diagnosed essential hypertension: a randomized trial. JAMA 2008;300(8):924–32.
[175] Mitch WE. Effects of intestinal flora on nitrogen metabolism in patients with chronic renal failure. Am J Clin Nutr 1978;31:1594–600.
[176] Castellino P, Giordano C, Perna A, DeFronzo RA. Effects of plasma amino acid and hormone levels on renal hemodynamics in humans. Am J Physiol 1988;255:F444–9.
[177] Meyer TW, Ichikawa I, Zatz R, Brenner BM. The renal hemodynamic response to amino acid infusion in the rat. Trans Assoc Am Physicians 1983;96:76–83.
[178] Hirschberg RR, Zipser RD, Slomowitz LA, Kopple JD. Glucagon and prostaglandins are mediators of amino acid-induced rise in renal hemodynamics. Kidney Int 1988;33:1147–55.

[179] Kone BC. Nitric oxide in renal health and disease. Am J Kid Dis 1997;30:311–33.
[180] Tolins JP, Shultz PJ, Westberg G, Raij L. Renal hemodynamic effects of dietary protein in the rat: role of nitric oxide. J Lab Clin Med 1995;125:228–36.
[181] Arnal J-F, Munzel T, Venema RC, et al. Interactions between L-arginine and L-glutamine change endothelial NO production: an effect independent of NO synthase substrate availability. J Clin Invest 1995;95:2565–72.
[182] Narita I, Border WA, Ketteler M, Ruoslahti E, Noble NA. L-arginine may mediate the therapeutic effects of low protein diets. Proc Natl Acad Sci USA 1995;92:4552–6.
[183] Paller MS, Hostetter TH. Dietary protein increases plasma renin activity and reduces pressor reactivity to angiotensin II. Am J Physiol 1986;251:F34–9.
[184] Baboolal K, Meyer TW. The effect of acute angiotensin II blockade on renal function in rats with reduced renal mass. Kidney Int 1994;46(980):985.
[185] Mitch WE, Collier VU, Walser M. Creatinine metabolism in chronic renal failure. Clin Sci 1980;58:327–35.
[186] Ibrahim HN, Rosenberg ME, Greene EL, Kren S, Hostetter TH. Aldosterone is a major factor in the progression of renal disease. Kidney Int 1997;63(Suppl. 63):S115–9.
[187] Adams LG, Polzin DJ, Osborne CA, O'Brien TD, Hostetter TH. Influence of dietary protein/calorie intake on renal morphology and function in cats with 5/6 nephrectomy. Lab Invest 1994;70:347–57.
[188] Bourgoignie JJ, Gavellas G, Sabnis SG, Antonovych TT. Effect of protein diets on the renal function of baboons (Papio hamadryas) with remnant kidneys: a 5-year follow-up. Am J Kid Dis 1994;23:199–204.
[189] Mitch WE, Wilcox CS. Disorders of body fluids, sodium and potassium in chronic renal failure. Am J Med 1982;72:536–50.
[190] Greene EL, Kren S, Hostetter TH. Role of aldosterone in the remnant kidney model in the rat. J Clin Invest 1996;98:1063–8.
[191] Juknevicius I, Segal Y, Kren S, Lee R, Hostetter TH. Effect of aldosterone on renal transforming growth factor-beta. Am J Physiol 2004;286:F1059–62.
[192] Zoja C, Benigni A, Remuzzi G. Cellular responses to protein overload: key event in renal disease progression. Curr Opin Nephrol Hypertens 2004;13:31–7.
[193] Zoja C, Donadelli R, Colleoni S, et al. Protein overload stimulates RANTES production by proximal tubular cells depending on NF-kB activation. Kidney Int 1998;53:1608–15.
[194] De Zeeuw D, Remuzzi G, Parving H-H, et al. Proteinuria, a target for renoprotection in patients with type 2 diabetic nephropathy: lessons from RENAAL. Kidney Int 2004;65:2309–20.
[195] De Zeeuw D, Remuzzi G, Parving H-H, et al. Proteinuria, a therapeutic target for cardiovascular protection in type 2 diabetic patients with nephropathy. Circulation 2004;110:921–7.
[196] Aparicio M, Bouchet JL, Gin H, et al. Effect of a low-protein diet on urinary albumin excretion in uremic patients. Nephron 1988;50:288–91.
[197] Gansevoort RT, De Zeeuw D, De Jong PE. Additive antiproteinuric effect of ACE inhibition and a low-protein diet in human renal disease. Nephrol Dial Transpl 1995;10:497–504.
[198] Ruilope LM, Casal MC, Praga M, et al. Additive antiporteinuric effect of converting enzyme inhibition and a low protein diet. J Am Soc Nephrol 1992;3:1307–11.
[199] Chanutin A, Ludewig S. Experimental renal insufficiency produced by partial nephrectomy. V. Diets containing whole dried meat. Arch Int Med 1936;58:60–80.
[200] Bailey JL, Mitch WE. Pathophysiology of uremia. In: Brenner BM, Rector FC, editors. The kidney. 6th ed. New York: W.B. Saunders; 1999 [In press]
[201] Folin O. Laws governing the clinical composition of urine. Am J Physiol 1905;13:67–115.
[202] Maroni BJ, Steinman T, Mitch WE. A method for estimating nitrogen intake of patients with chronic renal failure. Kidney Int 1985;27:58–65.
[203] Masud T, Manatunga A, Cotsonis G, Mitch WE. The precision of estimating protein intake of patients with chronic renal failure. Kidney Int 2002;62:1750–6.
[204] Rafoth RS, Onstad GR. Urea synthesis after oral protein loading in man. J Clin Invest 1975;56:1170–4.
[205] Lascelles PT, Taylor WH. The effect upon tissue respiration *in vitro* of metabolites which accumulate in uremic coma. Clin Sci 1966;31:403–13.
[206] Vanholder RC, Glorieux G, De SR, De Deyn PP. Low water-soluble uremic toxins. Adv Ren Replace Ther 2003;10 (4):257–69.
[207] Bergstrom J. Why are dialysis patients malnourished ? Am J Kid Dis 1995;26:229–41.
[208] Grollman EF, Grollman A. Toxicity of urea and its role in the pathogensis of uremia. J Clin Invest 1959;38:749.
[209] Merrill JP, Legrain M, Hoigne R. Observations on the role of urea in uremia. Am J Med 1953;14:519–20.
[210] Johnson WJ, Hagge WH, Wagoner RD, Dinapolu RP, Rosevear JW. Effects of urea loading in patients with far-advanced renal failure. Mayo Clinic Proc 1972;47:21–9.
[211] Moeslinger T, Friedl R, Volv I, et al. Urea induces macrophage proliferation by inhibition of inducible nitric oxide synthesis. Kidney Int 2002;56:581–8.
[212] Kraus LM, Jones MR, Kraus AP. Essential carbamoyl-amino acids *in vivo* in patients with end-stage renal disease managed by continuous ambulatory peritoneal dialysis: isolation, identification and quantitation. J Lab Clin Med 1998;131:425–31.
[213] Depner TA, Gulyassy PF. Plasma protein binding in uremia: extraction and characterization of an inhibitor. Kidney Int 1980;18:86–94.
[214] Tizianello A, DeFerrari G, Garibotto G, Gurreri G, Robaudo C. Renal metabolism of amino acids and ammonia in subjects with normal renal function and in patients with chronic renal insufficiency. J Clin Invest 1980;65:1162–73.
[215] Walser M. Urea metabolism in chronic renal failure. J Clin Invest 1974;53:1385–92.
[216] Witko-Sarsat V, scamps-Latscha B. Advanced oxidation protein products: novel uraemic toxins and pro-inflammatory mediators in chronic renal failure?. Nephrol Dial Transplant 1997;12(7):1310–2.
[217] Bailey JL, Wang X, England BK, Price SR, Ding X, Mitch WE. The acidosis of chronic renal failure activates muscle proteolysis in rats by augmenting transcription of genes encoding proteins of the ATP-dependent, ubiquitin-proteasome pathway. J Clin Invest 1996;97:1447–53.
[218] Bushinsky DA. The contribution of acidosis to renal osteodystrophy. Kidney Int 1995;47:1816–32.
[219] DeFronzo RA, Beckles AD. Glucose intolerance following chronic metabolic acidosis in man. Am J Physiol 1979;236: E328–34.
[220] Hara Y, May RC, Kelly RA, Mitch WE. Acidosis, not azotemia, stimulates branched-chain amino acid catabolism in uremic rats. Kidney Int 1987;32:808–14.
[221] Reaich D, Channon SM, Scrimgeour CM, Daley SE, Wilkinson R, Goodship THJ. Correction of acidosis in humans with CRF decreases protein degradation and amino acid oxidation. Am J Physiol 1993;265:E230–5.
[222] Niwa T. Organic acids and the uremic syndrome: protein metabolite hypothesis in the progression of chronic renal failure. Sem Nephrol 1996;16:167–82.

[223] Niwa T, Ise M, Miyazaki T. Progression of glomerular sclerosis in experimental uremic rats by administration of indole, a precursor of indoxyl sulfate. Am J Neph 1994;14:207–12.
[224] Niwa T, Ise M. Indoxyl sulfate, a circulating uremic toxin, stimulates the progression of glomerular sclerosis. J Lab Clin Med 1994;124:96–104.
[225] Miyazaki T, Ise M, Seo H, Niwa T. Indoxyl sulfate increases the gene expression of TGF-Beta-1, TIMP-1 and Pro-alpha-1 collagen in uremic rat kidneys. Kidney Int 1997;52(Suppl. 62): S15–22.
[226] Niwa T, Tsukushi S, Ise M, et al. Indoxyl sulfate and progression of renal failure-effects of a low-protein diet and oral sorbent on indoxyl sulfate production in uremic rats and undialyzed uremic patients. Min Elect Metab 1997;23:179–84.
[227] Niwa T, Nomura T, Sugiyama S, Miyazaki T, Tsukushi S, Tsutsui S. The protein metabolite hypothesis, a model for the progression of renal failure—an oral adsorbent lowers indoxyl sulfate levels in undialyzed uremic patients. Kidney Int 1997;52(Suppl. 62):S23–8.
[228] Kalantar-Zadeh K, Horwich TB, Oreopoulos A, et al. Risk factor paradox in wasting diseases. Curr Opin Clin Nutr Metab Care 2007;10(4):433–42.
[229] Ando A, Orita Y, Tsubakihara R, et al. The effect of low protein diet and surplus of essential amino acids on the serum concentrations and the urinary excretion of methyl-guanidine and guanidinosuccinic acid in chronic renal failure. Nephron 1979;24:161–9.
[230] Marescau B, Deshumkh DR, Kockx M, et al. Guanidino compounds in serum, urine, liver, kidney, and brain of man and some ureotelic animals. Metabolism 1992;41:526–32.
[231] Kopple JD, Gordon SI, Wang M, Swenseid ME. Factors affecting serum and urinary guanidinosuccinic acid levels in normal and uremic subjects. J Lab Clin Med 1977;90:303–11.
[232] Yokozawa T, Fujitsuka N, Oura H. Studies on the precursor of methylguanidine in rats with renal failure. Nephron 1991;58:90–4.
[233] Brusilow S, Tinker T, Batshaw ML. Amino acid acylation: a mechanism of nitrogen excretion in inborn errors of urea synthesis. Sci 1980;207:659–61.
[234] Castillo L, DeRojas TC, Chapman TE, et al. Splanchnic metabolism of dietary arginine in relation to nitric oxide synthesis in normal adult man. Proc Natl Acad Sci 1993;90:193–7.
[235] Orita Y, Tsubakihara Y, Ando A, et al. Effect of arginine or creatinine administration on the urinary excretion of methylguanidine. Nephron 1978;22:328–36.
[236] Cohen BD. Guanidinosuccinic acid in uremia. Arch Int Med 1970;126:846–50.
[237] Giovannetti S, Balestri PL, Barsotti G. Methylguanidine in uremia. Arch Int Med 1973;131:709–13.
[238] Orita Y, Ando A, Tsubakihara Y. Tissue and blood cell concentration of methylguanidine in rats and patients with chronic renal failure. Nephron 1981;27:35–9.
[239] Giovannetti S, Dioni L, Balestri PL, Biagini M. Evidence that guanidines and some related compounds cause hemolysis in chronic uremia. Clin Sci 1968;34:141–8.
[240] Shainkin-Kestenbaum R, Giatt Y, Berlyne GM. The toxicity of guanidino compounds in the rat blood cell in uremia and the effect of hemodialysis. Nephron 1982;31:20–3.
[241] Marescau B, Hiramatsu M, Mori A. alpha-keto-d-guanidinovaleric acid induced electroencephalographic, epileptiform discharges in rabbits. Neurochem Pathol 1983;1:203–11.
[242] DeDeyn PP, Marescau B, Cuykens JJ, Van Gorp L, Lowenthal A, De Potter WP. Guanidino compounds in serum and cerebrospinal fluid of non-dialyzed patients with renal insufficiency. Clin Chim Acta 1987;167:81–8.
[243] Marescau B, Nagel G, Possemiers I, et al. Guanidino compounds in serum and urine of nondialyzed patients with chronic renal insufficiency. Metabolism 1997;46:1024–37.
[244] D'Hooge R, DeDeyn PP, van de Vijver G, Antoons G, Raes A, Van Bogaert PP. Uraemic guanidino compounds inhibit y-amino-butyric acid-evoked whole-cell currents in mouse spinal cord neurons. Neurosci Lett 1999;265:83–6.
[245] Anderstam B, Katzaraki K, Bergstrom J. Serum levels of NG, NG-dimethyl -L-arginine, a potential endogenous nitric oxide inhibitor in dialysis patients. J Am Soc Nephrol 1997;8:1437–42.
[246] Fleck C, Schweitzer F, Karge E, Busch M, Stein G. Serum concentrations of asymmetric (ADMA) and symmetric (SDMA) dimethylarginine in patients with chronic kidney diseases. Clin Chim Acta 2003;336(1–2):1–12.
[247] Boger RH, Bode-Boger SM, Thiele W, Junker W, Alexander K, Frolich JC. Biochemical evidence for impaired nitric oxide synthesis in patients with peripheral arterial occlusive disease. Circulation 1997;95:2068–74.
[248] Boger RH, Bode-Boger SM, Szuba T, et al. Asymmetric dimethylarginine (ADMA): a novel risk factor for endothelial dysfunction: its role in hypercholesterolemia. Circulation 1998;98:1842–7.
[249] Gardiner SM, Kemp PA, Bennett R, Palmer RM, Moncado S. Regional and cardiac haemodynamic effects of NG, NG-dimethyl-L-arginine and their reversibility by vasodilators in conscious rats. Br J Pharm 1993;110:1457–64.
[250] Reyes AA, Karl IE, Kissane J, Klahr S. L-Arginine administration prevents glomerular hyperfiltration and decreases proteinuria in diabetic rats. J Am Soc Nephrol 1993;4:1039–45.
[251] Miyazaki H, Matsuoka H, Cook JPUM, Ueda S, Okuda S, Imaizumi T. Endogenous nitric oxide synthase inhibitor: a novel marker of atherosclerosis. Circulation 1999;99:1141–6.
[252] Mamoun A-H, Bergstrom J, Soderstein P. Cholecystokinin octapeptide inhibits carbohydrate but not protein intake. Am J Physiol 1987;273:R972–80.
[253] Magnusson M, Magnusson K, Sundqvist T, Denneberg T. Increased intestinal permeability to differently sized polyethylene glycols in uremic rats: effects of low- and high-protein diets. Nephron 1990;56:306–11.
[254] Schepers E, Glorieux G, Vanholder R. The gut: the forgotten organ in uremia? Blood Purif 2010;29(2):130–6.
[255] Evenepoel P, Meijers BK, Bammens BR, Verbeke K. Uremic toxins originating from colonic microbial metabolism. Kidney Int Suppl 2009;December(114):S12–9.
[256] Pickering WP, Price SR, Bircher G, Marinovic AC, Mitch WE, Walls J. Nutrition in CAPD: serum bicarbonate and the ubiquitin-proteasome system in muscle. Kidney Int 2002;61:1286–92.
[257] Simenhoff ML, Burke JF, Sankkonen JJ, Wesson LG, Schaedler RW. Amine metabolism and the small bowel in uremia. Lancet 1976;2:818–22.
[258] Noree L-O, Bergstrom J. Treatment of chronic uremic patients with protein-poor diet and oral supply of essential amino acids. Clin Nephrol 1975;3(5):195–203.
[259] Walser M, Hill SB. Free and protein-bound tryptophan in serum of untreated patients with chronic renal failure. Kidney Int 1993;44:1366–71.
[260] Byrd DJ, Berthold HW, Trefz KF, et al. Indolic tryptophan metabolism in uraemia. Proc Eur Dial Transplant Assoc 1976;12:347–54.
[261] Niwa T, Miyazaki T, Hashimoto N, et al. Suppressed serum and urine levels of indoxyl sulfate by oral sorbent in experimental uremic rats. Am J Neph 1992;12:201–6.
[262] Siassi F, Wang M, Chan W, Swenseid ME. Brain serotonin turnover in chronically uremic rats. Am J Physiol 1977;232: E526–8.

[263] Lim CF, Bernard BF, DeJong M, Doctor R, Krenning EP, Hennemann G. A furan fatty acid and indoxyl sulfate are the putative inhibitors of thyroxine hepatocyte transport in uremia. J Clin Endo Metab 1993;76:318–24.
[264] Wardle EN. Phenols, phenolic acids and sodium-potassium ATPases. J Mol Med 1978;3:319.
[265] Goodhart PJ, DeWolf WE, Kruse LI. Mechanism based inactivation of dopamine beta-hydroxylase by p-cresol and related alkyl phenols. Biochemistry 1987;26:2576–83.
[266] Vanholder R, DeSmet R, Waterloos MA, et al. Mechanisms of uremic inhibition of phagocytic reactive species production: characterization of the role of p-cresol. Kidney Int 1995;47:510–7.
[267] Dou L, Bertrand E, Cerini C, et al. The uremic solutes p-cresol and indoxyl sulfate inhibit endothelial proliferation and wound repair. Kidney Int 2004;65(2):442–51.
[268] Simenhoff ML, Saukkonen JJ, Burke JF, Wesson LG, Schaedler RW, Gordon SJ. Bacterial populations of the small bowel in uremia. Nephron 1978;22:63–8.
[269] Bell JD, Lee JA, Lee HA, Sadler PJ, Wilkie DR, Woodham RH. Nuclear magnetic resonance studies of blood plasma and urine from patients with chronic renal failure: Identification of trimethylamine-N-oxide. Biochim Biophys Acta 1991;1096:101–7.
[270] Simenhoff ML, Milne MD, Asatoor AM, Zilva JF. Retention of aliphatic amines in uremia. Clin Sci 1963;25:65–77.
[271] Saito A, Takaji T, Chung TG, Ohta K. Serum levels of polyamines in patients with chronic renal failure. Kidney Int 1983;24 (Suppl. 16):S234–7.
[272] Beale LS. Kidney diseases, urinary deposits and calculous disorders; their nature and treatment. 3rd ed. Phildelphia: Lindsay and Blakiston; 1869.
[273] Cotton JR, Knochel JP. Correction of uremic cellular injury with a protein-restricted, amino acid-supplemented diet. Am J Kid Dis 1985;5:233–8.
[274] Bilbrey GL, Carter NW, White MG, Schilling JF, Knochel JP. Potassium deficiency in chronic renal failure. Kidney Int 1973;4:423–30.
[275] Cotton JR, Woodward T, Carter NW, Knochel JP. Resting skeletal muscle membrane potential as an index of uremic toxicity. J Clin Invest 1979;63:501–8.
[276] Lumlertgul G, Burke TJ, Gillum DM, et al. Phosphate depletion arrests progression of chronic renal failure independent of protein intake. Kidney Int 1986;29:658–66.
[277] Hostetter TH, Meyer TW, Rennke HG, Brenner BM. Chronic effects of dietary protein in the rat with intact and reduced renal mass. Kidney Int 1986;30:509–17.
[278] Donohue W, Spingarn C, Pappenheimer AM. The calcium content of the kidney as related to parathyroid function. J Exp Med 1937;66:697–701.
[279] Harris DCH, Chan L, Schrier RW. Remnant kidney hypermetabolism and progression of chronic renal failure. Am J Physiol 1988;254:F267–76.
[280] Bergstrom J. Anorexia in dialysis patients. Sem Nephrol 1996;16:222–9.
[281] Anderstam B, Mamoun A-H, Bergstrom J, Sodersten P. Middle-sized molecule fractions isolated from uremic ultrafiltrate and normal urine inhibit ingestive behavior in the rat. J Am Soc Nephrol 1996;7:2453–60.
[282] Mamoun AH, Anderstam B, Sodersten P, Lindholm B, Bergstrom J. Influence of peritoneal dialysis solutions with glucose and amino acids on ingestive behavior in rats. Kidney Int 1996;49:1276–82.
[283] Mamoun AH, Sodersten P, Anderstam B, Bergstrom J. Evidence of splanchnic-brain signalling in inhibition of ingestive behaviour by middle molecules. J Am Soc Nephrol 1999;10:309–14.
[284] Severini G, Diana L, DiGiovannandrea R, Sagliaschi G. Influence of uremic middle molecules on *in vitro* stimulated lymphocytes and interleukin-2 production. ASAIO Trans 1996;42:64–7.
[285] Balke N, Holtkamp U, Horl WH, Hempelmann U. Inhibition of degranulation of human polymorphonuclear leukocytes by complement factor D. FEBS Lett 1995;371:300–2.
[286] Haag-Weber M, Mai B, Horl WH. Isolation of a granulocyte inhibitory protein from uraemic patients with homology of B-2-microglobulin. Nephrol Dial Transpl 1994;9:382–8.
[287] Horl WH, Haag-Weber M, Georgopoulos A, Block LH. Physiochemical characterization of a polypeptide present in uremic serum that inhibits the biological activity of polymorphonuclear cells. Proc Natl Acad Sci USA 1990;87:6353–7.
[288] Bellomo G, Venanzi S, Verdura C, Saronio P, Esposito A, Timio M. Association of uric acid with change in kidney function in healthy normotensive individuals. Am J Kid Dis 2010;56:264–72.
[289] Gejyo F, Homma N, Arakawa M. Long-term complications of dialysis: pathogenic factors with special reference to amyloidosis. Kidney Int 1993;43(Suppl. 41):S78–82.
[290] Lubash GD, Stenzel KH, Rubin AL. Nitrogenous compounds in hemodialysate. Circulation 1964;30:848–52.
[291] Abiko T, Kumikawa M, Higuchi H, Sekono H. Identification and synthesis of a heptapeptide in uremic fluid. Biochem Biophys Res Comm 1978;84:184–94.
[292] Abiko T, Kumikawa M, Ishizaki M, Takahashi H, Sekino H. Identification and synthesis of a tripeptide in coecum fluid of a uremic patient. Biochem Biophys Res Com 1978;83:357–64.
[293] Chu J, Yuan Z, Liu X, Wu Q, Mi H, He B. Separation of six uremic middle molecular compounds by high performance liquid chromatography and analysis by matrix-assisted laser desorption/ionization time-of-flight mass spectrometry. Clin Chim Acta 2001;311:95–107.
[294] Himmelfarb J, Le P, Klenzak J, Freedman S, McMenamin ME, Ikizler TA. Impaired monocyte cytokine production in critically ill patients with acute renal failure. Kidney Int 2004;66 (6):2354–60.
[295] Bolton CH, Downs LG, Victory JG, et al. Endothelial dysfunction in chronic renal failure: roles of lipoprotein oxidation and pro-inflammatory cytokines. Nephrol Dial Transplant 2001;16 (6):1189–97.
[296] Eknoyan G, Beck GJ, Cheung AK, et al. Effect of dialysis dose and membrane flux in maintenance hemodialysis. N Engl J Med 2002;347:2010–9.
[297] Horl WH, Cohen JJ, Harrington JT, Madias NE, Zusman CJ. Atherosclerosis and uremic retention solutes. Kidney Int 2004;66(4):1719–31.
[298] Himmelfarb J, McMonagle E, McMenamin E. Plasma protein thiol oxidation and carbonyl formation in chronic renal failure. Kidney Int 2000;58:2571–8.
[299] Petzke KJ, Elsner A, Proll J, Thielecke F, Metges CC. Long-term high protein intake does not increase oxidative stress in rats. J Nutr 2000;130(12):2889–96.
[300] Miyata T, Wada Y, Cai Z, et al. Implication of an increased oxidative stress in the formation of advanced glycation end products in patients with end-stage renal failure. Kidney Int 1997;51:1170–81.
[301] Rajan V, Mitch WE. Ubiquitin, proteasomes and proteolytic mechanisms activated by kidney disease. Biochim Biophys Acta 2008;1782(12):795–9.
[302] Christensen B, Refsum H, Vintermyr O, Ueland PM. Homocysteine export from cells cultured in the presence of

physiological or superfluous levels of methionine: methionine loading of non-transformed, proliferating and quiescent cells in culture. J Cell Physiol 1991;146:52–62.

[303] Finkelstein JD, Kyle WR, Harris BJ. Methionine metabolism in mammals: regulation of homocysteine methyltransferases in rat tissues. Arch Biochem Biophys 1971;146:84–92.

[304] Kang SS, Wong PWK, Malinow MR. Hyperhomocyst(e)inemia as a risk factor for occlusive vascular disease. Ann Rev Nutr 1992;12:259–78.

[305] Bostom AG, Lathrop L. Hyperhomocysteinemia in end-stage renal disease: prevalence, etiology, and potential relationship to arteriosclerotic outcomes. Kidney Int 1997;52:10–20.

[306] Kang SS, Wong PWK, Cook HY, Norusis M, Messer JV. Protein-bound homocyst(e)ine: a possible risk factor for coronary heart disease. J Clin Invest 1986;77:1482–6.

[307] Gupta A, Robinson K. Hyperhomocysteinaemia and end stage renal disease. J Nephrol 1997;10:77–84.

[308] Stam F, van GC, Ter Wee PM, Jakobs C, de MK, Stehouwer CD. Effect of folic acid on methionine and homocysteine metabolism in end-stage renal disease. Kidney Int 2005;67 (1):259–64.

[309] Jamison RL, Hartigan P, Kaufman JS, et al. Effect of homocysteine lowering on mortality and vascular disease in advanced chronic kidney disease and end-stage renal disease: a randomized controlled trial. JAMA 2007;298(10):1163–70.

[310] DeFronzo RA, Alvestrand A, Smith D, Hendler R. Insulin resistance in uremia. J Clin Invest 1981;67:563–8.

[311] Navalesi R, Pilo A, Lenzi S, Donato L. Insulin metabolism in chronic uremia and in the anephric state: effect of the dialytic treatment. J Clin Endocrinol Metab 1975;40(1):70–85.

[312] DeFronzo RA, Tobin JD, Rowe JW, Andres R. Glucose intolerance in uremia. J Clin Invest 1978;62:425–30.

[313] Kalhan SC, Ricanati ES, Tserng KY, Savin SM. Glucose turnover in chronic uremia: increased recycling with diminished oxidation of glucose. Metabolism 1983;32(12):1155–62.

[314] Bak JF, Schmitz O, Sorensen SS, Frokjaer J, Kjaer T, Pedersen O. Activity of insulin receptor kinase and glycogen synthase in skeletal muscle from patients with chronic renal failure. Acta Endo 1989;121:744–50.

[315] Kauffman JM, Caro JF. Insulin resistance in uremia: characterization of insulin action, binding, and processing in isolated hepatocytes from chronic uremic rats. J Clin Invest 1983;71:698–708.

[316] Cecchin F, Ittoop O, Sinha MK, Caro JF. Insulin resistance in uremia: insulin receptor kinase activity in liver and muscle from chronic uremic rats. Am J Physiol 1988;254:E394–401.

[317] White MF, Kahn CR. The insulin signaling system. J Biol Chem 1994;269:1–4.

[318] Saad MJA, Araki E, Miralpeix M, Rothenberg PL, White MF, Kahn CR. Regulation of insulin receptor substrate-1 in liver and muscle of animal models of insulin resistance. J Clin Invest 1992;90:1839–49.

[319] Folli F, Saad MJA, Backer JM, Kahn CR. Regulation of phosphatidylinositol 3-kinase activity in liver and muscle of animal models of insulin-resistant and insulin-deficient diabetes mellitus. J Clin Invest 1993;92:1787–94.

[320] Giorgino F, Pedrini MT, Matera L, Smith RJ. Specific increase in p85a expression in response to dexamethasone is associated with inhibition of insulin-like growth factor-1 stimulated phophatidylinositol 3-kinase activity in cultured muscle cells. J Biol Chem 1997;272:7455–63.

[321] Mak RHK. Insulin resistance but IGF-1 sensitivity in chronic renal failure. Am J Physiol 1996;271:F114–9.

[322] Bailey JL, Price SR, Zheng B, Hu Z, Mitch WE. Chronic kidney disease causes defects in signaling through the insulin receptor substrate/phosphatidylinositol 3-kinase/Akt pathway: implications for muscle atroply. J Am Soc Nephrol 2006;17:1388–94.

[323] Franch HA, Raissi S, Wang X, Zheng B, Bailey JL, Price SR. Acidosis impairs insulin receptor substrate-1-associated phosphoinositide 3-kinase signaling in muscle cells: consequences on proteolysis. Am J Physiol 2004;287:F700–6.

[324] Akmal M, Massry SG, Goldstein DA, Fanti P, Weisz A, DeFronzo RA. Role of parathyroid hormone in the glucose intolerance of chronic renal failure. J Clin Invest 1985;75:1037–44.

[325] Mak RH. Intravenous 1,25 dihydroxycholecalciferol corrects glucose intolerance in hemodialysis patients. Kidney Int 1992;41(4):1049–54.

[326] Folli F, Kahn CR, Hansen H, Bouchie JL, Feener EP. Angiotensin II inhibits insulin signaling in aortic smooth muscle cells at multiple levels: A potential role for serine phosphorylation in insulin/angiotensin II crosstalk. J Clin Invest 1997;100:2158–69.

[327] Hotamisligil GS, Peraldi P, Budavari A, Ellis R, White MF, Spielgelman BM. IRS-1-mediated inhibition of insulin receptor tyrosine kinase activity in TNF-a- and obesity-induced insulin resistance. Sci 1996;271:665–8.

[328] Bilbrey GL, Falonna GR, White MG, Knochel JP. Hyperglucagonemia of renal failure. J Clin Invest 1974;53:841–7.

[329] Dighe RR, Rojas FJ, Birnbaumer L, Garber AJ. Glucagon-stimulable adenylyl cyclase in rat liver. Effects of chronic uremia and intermittent glucagon administration. J Clin Invest 1984;73(4):1004–12.

[330] Mehls O, Ritz E, Hunziker EB, Tonshoff B, Heinrich U. Role of growth hormone in growth failure in uremia. Kidney Int 1988;34:118–26.

[331] Jones JI, Clemmons DR. Insulin-like growth factors and their binding proteins: biological actions. Endocr Rev 1995;16:3–34.

[332] Haffner D, Blum WF, Heinrich U, Mehls O, Tonshoff B. Impaired postprandial regulation of insulin-like growth factor binding protein-1 in children with chronic renal failure. J Clin Endocrinol Metab 1997;82(9):2832–5.

[332a] Baumannn G. Growth hormone binding protein and free growth hormone in chronic renal failure. Pediatric Nephrol 1996;10:328–30.

[333] Mehls O, Schaefer F, Tonshoff B, Wuhl E. Effectiveness of growth hormone treatment in short children with chronic renal failure. J Pediatr 2002;141:147–8.

[334] Schaefer F, Chen Y, Tsao T, Nouri P, Rabkin R. Impaired JAK-STAT signal transduction contributes to growth hormone resistance in chronic uremia. J Clin Invest 2001;108:467–75.

[335] Ding H, Gao X-L, Hirschberg R, Vadgama JV, Kopple JD. Impaired actions of insulin-like growth factor-1 on protein synthesis and degradation in skeletal muscle of rats with chronic renal failure: evidence for a postreceptor defect. J Clin Invest 1996;97:1064–75.

[336] Bereket A, Wilson TA, Kolasa AJ, Fan J, Lang CH. Regulation of the insulin-like growth factor system by acute acidosis. Endocrin 1996;137:2238–45.

[337] Brungger M, Hulter HN, Krapf R. Effect of chronic metabolic acidosis on the growth hormone/IGF-1 endocrine axis: new cause of growth hormone insensitivity in humans. Kidney Int 1997;51:216–21.

[338] Hanna JD, Krieg Jr RJ, Scheinman JI, Chan JC. Effects of uremia on growth in children. Semin Nephrol 1996;16 (3):230–41.

[339] Fouque D, Peng SC, Kopple JD. Impaired metabolic response to recombinant insulin-like growth factor-I in dialysis patients. Kidney Int 1995;47:876–83.

[340] Otero M, Lago R, Lago F, et al. Leptin, from fat to inflammation: old questions and new insights. FEBS Lett 2005;579 (2):295–301.
[341] Caro JF, Sinha MK, Kolaczynski JW, Zhang PL, Considine RV. Leptin: the tale of an obesity gene. Diabetes 1996;45 (11):1455–62.
[342] Don BR, Rosales LM, Levine NW, Mitch WE, Kaysen GA. Leptin is a negative acute phase protein in chronic hemodialysis patients. Kidney Int 2001;59:1114–20.
[343] Kolaczynski JW, Considine RV, Ohannesian J, et al. Responses of leptin to short-term fasting and refeeding in humans: a link with ketogenesis but not ketones themselves. Diabetes 1996;45:1511–5.
[344] El HW, Chauveau P, Barthe N, Merville P, Potaux L, Aparicio M. Serum leptin, body fat, and nutritional markers during the six months post-kidney transplantation.. Metabolism 2004;53 (5):614–9.
[345] Sharma K, Considine RV. The Ob protein (leptin) and the kidney. Kidney Int 1998;53:1483–7.
[346] Montague CT, Farooqi IS, Whitehead JP , et al. Congenital leptin deficiency is associated with severe early-onset obesity in humans. Nature 1997;387(6636):903–8.
[347] Cheung W, Yu PX, Cone RD, Marks DL, Mak RH. Role of leptin and melanocortin signaling in uremia-associated cachexia. J Clin Invest 2005;115:1659–65.
[348] Perez-Fontan M, Cordido F, Rodriguez-Carmona A, Peteiro J, Garcia-Naveiro R, Garcia-Buela J. Plasma ghrelin levels in patients undergoing haemodialysis and peritoneal dialysis. Nephrol Dial Transplant 2004;19(8):2095–100.
[349] Rodriguez AE, Pecoits-Filho R, Heimburger O, Lindholm B, Nordfors L, Stenvinkel P. Associations between plasma ghrelin levels and body composition in end-stage renal disease: a longitudinal study. Nephrol Dial Transplant 2004;19(2):421–6.
[350] Mitch WE. Cachexia in chronic kidney disease: a link to defective central nervous system control of appetite. J Clin Invest 2005;115:1476–9.
[351] Mancuso P, Canetti C, Gottschalk A, Tithof PK, Peters-Golden M. Leptin augments alveolar macrophage leukotriene synthesis by increasing phospholipase activity and enhancing group IVC iPLA2 (cPLA2gamma) protein expression. Am J Physiol Lung Cell Mol Physiol 2004;287(3):L497–502.
[352] Ottonello L, Gnerre P, Bertolotto M, et al. Leptin as a uremic toxin interferes with neutrophil chemotaxis. J Am Soc Nephrol 2004;15(9):2366–72.
[353] Wolf G, Chen SC, Han DC, Ziyadeh FJ. Leptin and renal disease. Am J Kid Dis 2002;39:1–11.
[354] Maroni BJ, Mitch WE. Role of nutrition in prevention of the progression of renal disease. Ann Rev Nutr 1997;17:435–55.
[355] Mitch WE, Remuzzi G. Diets for patients with chronic kidney disease, still worth prescribing. J Am Soc Nephrol 2004;15:234–7.
[356] Franch HA, Mitch WE. Navigating between the Scylla and Charybdis of prescribing dietary protein for chronic kidney diseases. Annu Rev Nutr 2009;29:341–64.
[357] Masud T, Mitch WE. Requirements for protein, calories and fat in the predialysis patient. In: Mitch WE, Ikizler TA, editors. Handbook of nutrition and the kidney. 6th ed. Philadelphia: Lippincott-Williams & Wilkins; 2010. p. 92–108.
[358] Walser M, Hill S. Can renal replacement be deferred by a supplemented very-low protein diet?. J Am Soc Nephrol 1999;10:110–6.
[359] Aparicio M, Chauveau P, dePrecigout V, Bouchet J-L, Lasseur C, Combe C. Nutrition and outcome on renal replacement therapy of patients with chronic renal failure treated by a supplemented very low protein diet. J Am Soc Nephrol 2000;11:719–27.
[360] Aparicio M, Chauveau P, Combe C. Low protein diets and outcome of renal patients. J Nephrol 2001;14:433–9.
[361] Tom K, Young VR, Chapman T, Masud T, Akpele L, Maroni BJ. Long-term adaptive responses to dietary protein restriction in chronic renal failure. Am J Physiol 1995;268:E668–77.
[362] Chauveau P, Barthe N, Rigalleau V, et al. Outcome of nutritional status and body composition of uremic patients on a very low protein diet. Am J Kid Dis 1999;34:500–7.
[363] Kopple JD, Levey AS, Greene T, et al. Effect of dietary protein restriction on nutritional status in the modification of diet in renal disease (MDRD) study. Kidney Int 1997;52:778–91.
[364] Menon V, Kopple JD, Wang X, et al. Effect of a very lowlow-protein diet on outcomes: long-term follow-up of the modification of diet in renal disease (MDRD) study. Am J Kid Dis 2008;53:208–17.
[365] Ruggenenti P, Schieppati A, Remuzzi G. Progression, remission, regression of chronic renal diseases. Lancet 2001;357:1601–8.
[366] Ikizler TA, Greene JH, Wingard RL, Hakim RM, Parker RA. Spontaneous dietary protein intake during progression of chronic renal failure. J Am Soc Nephrol 1995;6:1386–91.
[367] MDRD Study Group, Kopple JD, Greene T, et al. Relationship between nutritional status and the glomerular filtration rate: results from the MDRD study. Kidney Int 2000;57:1688–703.
[368] Kloppenburg WD, Stegeman CA, Hovinga TK, et al. Effect of prescribing a high protein diet and increasing the dose of dialysis on nutrition in stable chronic haemodialysis patients: a randomized, controlled trial. Nephrol Dial Transpl 2004;19:1212–23.
[369] Mitch WE. Malnutrition: a frequent misdiagnosis for hemodialysis patients. J Clin Invest 2002;110:437–9.
[370] Stenvinkel P, Heimburger O, Lindholm B. Wasting, but not malnutrition, predicts cardiovascular mortality in end-stage renal disease. Nephrol Dial Transpl 2004;19:2181–3.
[371] Cottini EP, Gallina DL, Dominguez JM. Urea excretion in adult humans with varying degrees of kidney malfunction fed milk, egg or an amino acid mixture: assessment of nitrogen balance. J Nutrition 1973;103:11–9.
[372] Kopple JD, Coburn JW. Metabolic studies of low protein diets in uremia: I. Nitrogen and potassium. Medicine 1973;52:583–94.
[373] Mitch WE, Abras E, Walser M. Long-term effects of a new ketoacid-amino acid supplement in patients with chronic renal failure. Kidney Int 1982;22:48–53.
[374] Walser M. Does prolonged protein restriction preceding dialysis lead to protein malnutrition at the onset of dialysis? Kidney Int 1993;44:1139–44.
[375] Maroni BJ, Staffeld C, Young VR, Manatunga A, Tom K. Mechanisms permitting nephrotic patients to achieve nitrogen equilibrium with a protein-restricted diet. J Clin Invest 1997;99:2479–87.
[376] Walser M, Hill S, Tomalis EA. Treatment of nephrotic adults with a supplemented, very low-protein diet. Am J Kid Dis 1996;28:354–64.
[377] Walser M, Mitch WE, Maroni BJ, Kopple JD. Should protein be restricted in predialysis patients? Kidney Int 1999;55:771–7.
[378] Lim VS, Kopple JD. Protein metabolism in patients with chronic renal failure: role of uremia and dialysis. Kidney Int 2000;58:1–10.
[379] Qureshi AR, Alvestrand A, Danielsson A, et al. Factors predicting malnutrition in hemodialysis patients: a cross-sectional study. Kidney Int 1998;53:773–82.
[380] Hakim RM, Lazarus JM. Biochemical parameters in chronic renal failure. Am J Kid Dis 1988;9:238–47.
[381] Kopple JD, Sorensen MK, Coburn JW, Gordon S, Rubini ME. Controlled comparison of 20-g and 40-g protein diets in the treatment of chronic uremia. Am J Clin Nutr 1968;21:553–64.

[382] Masud T, Young VR, Chapman T, Maroni BJ. Adaptive responses to very low protein diets: the first comparison of ketoacids to essential amino acids. Kidney Int 1994;45:1182–92.
[383] Walser M, Hill S, Ward L. Progression of chronic renal failure on substituting a ketoacid supplement for an amino acid supplement. J Am Soc Nephrol 1992;2:1178–85.
[384] Walser M, Hill SB, Ward L, Magder L. A crossover comparison of progression of chronic renal failure: ketoacids versus amino acids. Kidney Int 1993;43:933–9.
[385] Meireles CL, Price SR, Pererira AML, Carvalhaes JTA, Mitch WE. Nutrition and chronic renal failure in rats: what is an optimal dietary protein? J Am Soc Nephrol 1999;10:2367–73.
[386] Graham KA, Reaich D, Channon SM, et al. Correction of acidosis in CAPD decreases whole body protein degradation. Kidney Int 1996;49:1396–400.
[387] Graham KA, Reaich D, Channon SM, Downie S, Goodship THJ. Correction of acidosis in hemodialysis decreases whole-body protein degradation. J Am Soc Nephrol 1997;8:632–7.
[388] May RC, Bailey JL, Mitch WE, Masud T, England BK. Glucocorticoids and acidosis stimulate protein and amino acid catabolism *in vivo*. Kidney Int 1996;49:679–83.
[389] Aukema HM, Housini I, Rawling JM. Dietary soy protein effects on inherited polycystic kidney disease are influenced by gender and protein level. J Am Soc Nephrol 1999;10:300–8.
[390] Kaysen GA, Dubin JA, Muller H-G, Rosales L, Levin NW, Mitch WE. Inflammation and reduced albumin synthesis associated with stable decline in serum albumin in hemodialysis patients. Kidney Int 2004;65:1408–15.
[391] Zhang L, Du J, Hu Z, et al. IL-6 and serum amyloid A synergy mediates angiotensin II-induced muscle wasting. J Am Soc Nephrol 2009;20(3):604–12.
[392] Motil KJ, Matthews DE, Bier DM, Burke JF, Munro HN, Young VR. Whole-body leucine and lysine metabolism: response to dietary protein intake in young men. Am J Physiol 1981;240: E712–21.
[393] Matthews DE, Motil KS, Rohrbaugh DR, Burke JF, Young VR, Bier DM. Measurements of leucine metabolism in man from a primed continuous infusion of [1-13C]leucine. Am J Physiol 1980;238:E473–9.
[394] National Research Council. Recommended dietary allowances. 10th ed. Washington, D.C.: National Academy Press; 1989.
[395] Goodship THJ, Mitch WE, Hoerr RA, Wagner DA, Steinman TI, Young VR. Adaptation to low-protein diets in renal failure: leucine turnover and nitrogen balance. J Am Soc Nephrol 1990;1:66–75.
[396] Du J, Mitch WE. Identification of pathways controlling muscle protein metabolism in uremia and other catabolic conditions. Curr Opin Nephrol Hypertens 2005;14:378–82.
[397] Kalhoff H, Diekmann L, Kunz C, Stock GJ, Manz F. Alkali therapy versus sodium chloride supplement in low birthweight infants with incipient late metabolic acidosis. Acta Paediatr 1997;86:96–101.
[398] Boirie Y, Broyer M, Gagnadoux MF, Niaudet P, Bresson J-L. Alterations of protein metabolism by metabolic acidosis in children with chronic renal failure. Kidney Int 2000;58:236–41.
[399] Reaich D, Channon SM, Scrimgeour CM, Goodship THJ. Ammonium chloride-induced acidosis increases protein breakdown and amino acid oxidation in humans. Am J Physiol 1992;263:E735–9.
[400] Ballmer PE, McNurlan MA, Hulter HN, Anderson SE, Garlick PJ, Krapf R. Chronic metabolic acidosis decreases albumin synthesis and induces negative nitrogen balance in humans. J Clin Invest 1995;95:39–45.
[401] Papadoyannakis NJ, Stefanides CJ, McGeown M. The effect of the correction of metabolic acidosis on nitrogen and protein balance of patients with chronic renal failure. Am J Clin Nutr 1984;40:623–7.
[402] Garibotto G, Russo R, Sofia A, et al. Skeletal muscle protein synthesis and degradation in patients with chronic renal failure. Kidney Int 1994;45:1432–9.
[403] Movilli E, Zani R, Carli O, et al. Correction of metabolic acidosis increases serum albumin concentration and decreases kinetically evaluated protein intake in hemodialysis patients: a prospective study. Nephrol Dial Transpl 1998;13:1719–22.
[404] Stein A, Moorhouse J, Iles-Smith H, et al. Role of an improvement in acid-base status and nutrition in CAPD patients. Kidney Int 1997;52:1089–95.
[405] England BK, Greiber S, Mitch WE, et al. Rat muscle branched-chain ketoacid dehydrogenase activity and mRNAs increase with extracellular acidemia. Am J Physiol 1995;268:C1395–400 [Cell Physiol. 37]
[406] Wang X, Jurkovitz C, Price SR. Regulation of branched-chain ketoacid dehydrogenase flux by extracellular pH and glucocorticoids. Am J Physiol 1997;272:C2031–6.
[407] Lofberg E, Wernerman J, Anderstam B, Bergstrom J. Correction of metabolic acidosis in dialysis patients increases branched-chain and total essential amino acid levels in muscle. Clin Nephrol 1997;48:230–7.
[408] Mochizuki T. The effect of metabolic acidosis on amino and keto acid metabolism in chronic renal failure. Jap J Nephrol 1991;33:213–24.
[409] Price SR, Reaich D, Marinovic AC, et al. Mechanisms contributing to muscle wasting in acute uremia: Activation of amino acid catabolism. J Am Soc Nephrol 1998;9:439–43.
[410] May RC, Kelly RA, Mitch WE. Metabolic acidosis stimulates protein degradation in rat muscle by a glucocorticoid-dependent mechanism. J Clin Invest 1986;77:614–21.
[411] May RC, Kelly RA, Mitch WE. Mechanisms for defects in muscle protein metabolism in rats with chronic uremia: The influence of metabolic acidosis. J Clin Invest 1987;79:1099–103.
[412] Lecker SH, Goldberg AL, Mitch WE. Protein degradation by the ubiquitin-proteasome pathway in normal and disease states. J Am Soc Nephrol 2006;17:1807–19.
[413] Bodine SC, Latres E, Baumhueter S, et al. Identification of ubiquitin ligases required for skeletal muscle atrophy. Sci 2001;294:1704–8.
[414] Lecker SH, Jagoe RT, Gomes M, et al. Multiple types of skeletal muscle atrophy involve a common program of changes in gene expression. FASEB J 2004;18:39–51.
[415] Giardini O, Taccone-Gallucci M, Lubrano R, et al. Evidence of red blood cell membrane lipid peroxidation in haemodialysis patients. Nephron 1984;36:235–7.
[416] Du J, Mitch WE, Wang X, Price SR. Glucocorticoids induce proteasome C3 subunit expression in L6 muscle cells by opposing the suppression of its transcription by NF-kB. J Biol Chem 2000;275:19661–6.
[417] Marinovic AC, Zheng B, Mitch WE, Price SR. Ubiquitin expression in muscle cells is increased by glucocorticoids through a mechanism involving Sp1 and MEK1. J Biol Chem 2002;277:16673–81.
[418] Du J, Wang X, Meireles CL, et al. Activation of caspase 3 is an initial step triggering muscle proteolysis in catabolic conditions. J Clin Invest 2004;113:115–23.
[419] Lei HH, Perneger TV, Klag MJ, Whelton PK, Coresh J. Familial aggregation of renal disease in a population-based case-control study. J Am Soc Nephrol 1998;9(7):1270–6.
[420] Wang XH, Zhang L, Mitch WE, LeDoux JM, Hu J, Du J. Caspase-3 cleaves specific proteasome subunits in skeletal muscle stimulating proteasome activity. J Biol Chem 2010;285:3527–32.

[421] Workeneh B, Rondon-Berrios H, Zhang L, et al. Development of a diagnostic method for detecting increased muscle protein degradation in patients with catabolic conditions. J Am Soc Nephrol 2006;17:3233–9.
[422] Williams PS, Stevens ME, Fass G, Irons L, Bone JM. Failure of dietary protein and phosphate restriction to retard the rate of progression of chronic renal failure: a prospective, randomized, controlled trial. Quart J Med 1991;81:837–55.
[423] Szeto C-C, Chow K-M. Metabolic acidosis and malnutrition in dialysis patients. Sem Dialysis 2004;17:371–5.
[424] Szeto C-C, Wong TY, Chow K-M, Leung C-B, Li PK-T. Oral sodium bicarbonate for the treatment of metabolic acidosis in peritoneal dialysis patients: a randomized placebo-control trial. J Am Soc Nephrol 2003;14:2119–26.
[425] Frassetto L, Morris RC, Sebastian A. Potassium bicarbonate reduces urinary nitrogen excretion in postmenopausal women. J Clin Endocrinol Metab 1997;82:254–9.
[426] McSherry E, Morris RC. Attainment of normal stature with alkali therapy in infants and children with classic renal tubular acidosis. J Clin Invest 1978;61:509–14.
[427] Brungger M, Hulter HN, Krapf R. Effect of chronic metabolic acidosis on thyroid hormone homeostasis in humans. Am J Physiol 1997;272:F648–53.
[428] Kobayashi S, Maesato K, Moriya H, Ohtake T, Ikeda T. Insulin resistance in patients with chronic kidney disease. Am J Kid Dis 2005;45:275–80.
[429] Lee SW, Dai G, Hu Z, Wang X, Du J, Mitch WE. Regulation of muscle protein degradation: coordinated control of apoptotic and ubiquitin-proteasome systems by phosphatidylinositol 3 kinase. J Am Soc Nephrol 2004;15:1537–45.
[430] Wang XH, Hu Z, Hu JP, Du J, Mitch WE. Insulin resistance accelerates muscle protein degradation: activation of the ubiquitin-proteasome pathway by defects in muscle cell signaling. Endocrin 2006;147:4160–8.
[431] Aparicio M, Potaux L, de Precigout V, Bouchet JL, Aubertin J. Low protein and low phosphorus diet in patients with chronic renal failure: influence on glucose tolerance and tissue insulin sensitivity. Metabolism 1987;36:1080–5.
[432] Rigalleau V, Blanchetier V, Combe C, et al. A low-protein diet improves insulin sensitivity of endogenous glucose production in predialytic uremic patients. Am J Clin Nutr 1997;65:1512–6.
[433] Uribarri J, Levin NW, Delmez J, et al. Association of acidosis and nutritional parameters in hemodialysis patients. Am J Kid Dis 1999;34:493–9.
[434] Mitch WE. Getting beyond cross-sectional studies of abnormal nutritional indices in dialysis patients. Am J Clin Nutr 2003;77:760–1.
[435] Kirschbaum BB. Spurious metabolic acidosis in hemodialysis patients. Am J Kid Dis 2000;35:1068–71.
[436] Dalla Libera L, Ravara B, Angelini A, et al. Beneficial effects on skeletal muscle of the angiotensin II type 1 receptor blocker Ibesartan in experimental heart failure. Circulation 2001;103:2195–200.
[437] Mitch WE, Lietman PS, Walser M. Effects of oral neomycin and kanamycin in chronic renal failure: I. urea metabolism. Kidney Int 1977;11:116–22.
[438] Gibson JA, Park NJ, Sladen GE, Dawson AM. The role of the colon in urea metabolism in man. Clin Sci 1976;50:51–9.
[439] Jones EA, Smallwood RA, Craigie A, Rosenoer VM. The enterohepatic circulation of urea nitrogen. Clin Sci 1969;37:825–36.
[440] Mitch WE, Walser M. Effects of oral neomycin and kanomycin in chronic uremic patients. II. Nitrogen balance. Kidney Int 1977;11:123–7.
[441] Giordano C. Use of exogenous and endogenous urea for protein synthesis in normal and uremic subjects. J Lab Clin Med 1963;62:231–46.
[442] Kopple JD, Gao X, Qing DP. Dietary protein, urea nitrogen appearance and total nitrogen appearance in chronic renal failure and CAPD patients. Kidney Int 1997;52:486–94.
[443] Loder PB, Kee AJ, Horsburgh R, Jones M, Smith RC. Validity of urinary urea nitrogen as a measure of total urinary nitrogen in adult patients requiring parenteral nutrition. Crit Care Med 1989;17:309–12.
[444] Avesani CM, Kamimura MA, Draibe SA, Cuppari L. Is energy intake underestimated in nondialyzed chronic kidney disease patients? J Ren Nutr 2005;15(1):159–65.
[445] Kloppenburg WD, De Jong PE, Huisman RM. The contradiction of stable body mass despite low reported dietary energy intake in chronic haemodialysis patients. Nephrol Dial Transpl 2002;17:1628–33.
[446] Martin LJ, Su W, Jones PJ, Lockwood GA, Tritchler DL, Boyd NF. Comparison of energy intakes determined by food records and doubly labeled water in women participating in a dietary-intervention trial. Am J Clin Nutr 1996;63:483–90.
[447] Bingham SA. The dietary assessment of individuals: methods, accuracy, new techniques and recommendations. Nutr Abstr Rev 1987;57:705–42.
[448] Rosman JB, Langer K, Brandl M, et al. Protein-restricted diets in chronic renal failure: a four year follow-up shows limited indications. Kidney Int 1989;36:S96–102.
[449] Jungers P, Chauveau P, Ployard F, Lebkiri B, Ciancioni C, Man NK. Comparison of ketoacids and low protein diet on advanced chronic renal failure progression. Kidney Int 1987;22:67–71.
[450] Locatelli F, Alberti D, Graziani G, Buccianti G, Redaelli B, Giangrande A. Prospective, randomised, multicentre trial of effect of protein restriction on progression of chronic renal insufficiency. Lancet 1991;337:1299–304.
[451] Malvy D, Maingourd C, Pengloan J, Bagros P, Nivet H. Effects of severe protein restriction with ketoanalogues in advanced renal failure. J Am Coll Nutr 1999;8:481–6.
[452] Di Iorio BR, Minutolo R, De Nicola L, et al. Supplemented very low protein diet ameliorates responsiveness to erythropoietin in chronic renal failure. Kidney Int 2003;64:1822–8.
[453] Cianciaruso B, Pota A, Pisani A, et al. Metabolic effects of two low protein diets in chronic kidney disease stage 4–5—a randomized controlled trial. Nephrol Dial Transplant 2008;23 (2):636–44.
[454] Mircescu G, Garneata L, Stancu SH, Capusa C. Effects of a supplemented hypoproteic diet in chronic kidney disease. J Ren Nutr 2007;17(3):179–88.
[455] Fouque D, Laville M, Boissel JP, Chifflet R, Labeeuw M, Zech PY. Controlled low protein diets in chronic renal insufficiency: meta-analysis. Br Med J 1992;304:216–20.
[456] Pedrini MT, Levey AS, Lau J, Chalmers TC, Wang PH. The effect of dietary protein restriction on the progression of diabetic and nondiabetic renal diseases: a meta-analysis. Ann Intern Med 1996;124:627–32.
[457] Kasiske BL, Lakatua JDA, Ma JZ, Louis TA. A meta-analysis of the effects of dietary protein restriction on the rate of decline in renal function. Am J Kid Dis 1998;31:954–61.
[458] Fouque D, Laville M. Low protein diets for chronic renal failure in non-diabetic adults (Cochrane Review). Cochrane Database Syst Rev 2009;:10.1002/14651858.CD001892.pub3 [3, Art. No.: CD001892]
[459] Pan Y, Guo LL, Jin HM. Low-protein diet for diabetic nephropathy: a meta-analysis of randomized controlled trials. Am J Clin Nutr 2008;88:660–6.

[460] Chauveau P, Couzi L, Vendrely B, et al. Long-term outcome on renal replacement therapy in patients who previously received a keto acid-supplemented very-low-protein diet. Am J Clin Nutr 2009;90:969–74.

[461] Levey AS, Greene T, Beck GJ, et al. Dietary protein restriction and the progression of chronic renal disease: what have all the results of the MDRD study shown? J Am Soc Nephrol 1999;10:2426–39.

[462] Levey AS, Adler S, Caggiula AW, et al. Effects of dietary protein restriction on the progression of advanced renal disease in the modification of diet in renal disease study. Am J Kid Dis 1996;27:652–63.

[463] Brunori G, Viola BF, Parrinello G, et al. Efficacy and safety of a very-low-protein diet when postponing dialysis in the elderly: a prospective randomized multicenter controlled study. Am J Kidney Dis 2007;49(5):569–80.

[464] Hansen HP, Tauber-Lassen E, Jensen BR, Parving HH. Effect of dietary protein restriction on prognosis in patients with diabetic nephropathy. Kidney Int 2002;62:220–8.

[465] Fouque D, Wang P, Laville M, Boissel JP. Low protein diets delay end-stage renal disease in non diabetic adults with chronic renal failure. Nephrol Dial Transpl 2000;15:1986–92.

[466] Altman DG, Andersen PK. Calculating the number needed to treat for trials where the outcome is an event. Brit Med J 1999;319:1492–5.

[467] Skolbekken JA. Communicating the risk reduction achieved by cholesterol reducing drugs. Brit Med J 1998;316:1956–8.

[468] Rosman JB, Donker-Willenborg MA. Dietary compliance and its assessment in the Groningen trial on protein restriction in chronic renal failure. Contrib Nephrol 1990;81:95–101.

[469] Yeh S-S, Schuster MW. Geriatric cachexia: the role of cytokines. Am J Clin Nutr 1999;70:183–97.

[470] Eustace JA, Astor B, Muntner PM, Ikizler TA, Coresh J. Prevalence of acidosis and inflammation and their association with low serum albumin in chronic kidney disease. Kidney Int 2004;65(3):1031–40.

[471] Shah SN, Abramowitz M, Hostetter TH, Melamed ML. Serum bicarbonate levels and the progression of kidney disease: a cohort study. Am J Kidney Dis 2009;54(2):270–7.

[472] Kovesdy CP, Anderson JE, Kalantar-Zadeh K. Association of serum bicarbonate levels with mortality in patients with non-dialysis-dependent CKD. Nephrol Dial Transplant 2009;24 (4):1232–7.

[473] de Brito-Ashurst I, Varagunam M, Raftery MJ, Yaqoob MM. Bicarbonate supplementation slows progression of CKD and improves nutritional status. J Am Soc Nephrol 2009;20 (9):2075–84.

[474] Mahajan A, Simoni J, Sheather SJ, Broglio KR, Rajab MH, Wesson DE. Daily oral sodium bicarbonate preserves glomerular filtration rate by slowing its decline in early hypertensive nephropathy. Kidney Int 2010;78(3):303–9.

[475] Esler MD, Krum H, Sobotka PA, Schlaich MP, Schmieder RE, Bohm M. Renal sympathetic denervation in patients with treatment-resistant hypertension (The Symplicity HTN-2 Trial): a randomised controlled trial. Lancet 2010;376 (9756):1903–9.

[476] Verhave J, Fesler P, Rinstein J, Callar G, Mimran A. Estimation of renal function in subjects with normal serum creatinine levels: influence of age and body mass index. Am J Kidney Dis 2005;46:233–41.

CHAPTER

91

Management of Calcium and Bone Disease in Renal Patients

L. Darryl Quarles

Division of Nephrology, Department of Medicine, Associate Dean for Research, College of Medicine, Memphis, Tennessee, USA

INTRODUCTION

We have made significant advances in understanding of the pathogenesis and treatment of secondary hyperparathyroidism in chronic kidney disease (CKD). These include: (1) the discovery of the calcium-sensing receptor CaSR and the development of calcimimetics to target this receptor to suppress PTH secretion and production;[1] (2) the recognition that metabolic derangements in calcium and phosphate have a significant impact on morbidity and mortality,[1] possibly through effects on vascular calcification; (3) the discovery of the FGF23-bone kidney axis, where FGF23 produced by osteoblasts/osteocytes suppresses $1,25(OH)_2D$ production as an early adaptive response to the loss of kidney function,[2] (4) the finding that elevated serum FGF23 concentration is an important predictor of mortality and progression of kidney disease;[3] (5) the development of less hypercalcemic and hyperphosphatemic vitamin D analogs with the potential of reduced toxicity;[4] (6) the recognition of the possible importance of nutritional vitamin D deficiency on innate immune function; and (7) the availability of non-calcium containing phosphate binders.[5] The National Kidney Foundation Kidney Disease Outcomes Quality Initiative (KDOQI™) and more recently KDIQGO have also provided guidelines for earlier interventions and management of mineral metabolism disorders in CKD.[6,7] These new pharmacological agents and treatment paradigms offers the potential to more effectively and safely manage disordered mineral metabolism in patients with CKD.

Parathyroid Gland Disease versus Mineral Metabolism Disorders in CKD

Secondary hyperparathyroidism is an adaptive response to the loss of kidney function. Progressive parathyroid gland disease (i.e., hypertrophy and hyperplasia) and pathological consequences of elevated serum PTH levels have dominated the clinical focus of disordered mineral metabolism in CKD. PTH actions are mediated through PTH receptor (PTH1R) in the kidney, whose activation inhibits renal Pi reabsorption, decreases renal tubular calcium excretion and increases $1,25(OH)_2D_3$ production. Activation of PTH1R in osteoblasts in bone stimulates bone formation and osteoclastic bone resorption.[8] Chronic elevation of PTH in SHPT leads to increased bone remodeling which plays crucial role in mineral homeostasis by providing access to the stores in bones Ca and Pi. Thus, PTH is a calcemic hormone that maintains serum calcium levels by stimulating $1,25(OH)_2D$ production, renal calcium conservation and bone calcium efflux. The phosphaturic actions of PTH permit excretion of phosphate that accompanies the gastrointestinal absorption and bone efflux of calcium.

It is clinically important to prevent and treat secondary hyperparathyroidism, since increments in PTH (typically levels that exceed the 400–600 pg/ml range) are associated with increased mortality in CKD.[1,9,10] In addition, elevated PTH is associated with progressive parathyroid disease leading to tertiary hyperparathyroidism that may require parathryoidectomy[11] and high cortical bone remodeling leading to an increase in the risk of bone fractures.[12]

In spite of the importance of PTH, the recognition that hyperphosphatemia, vascular calcifications and

Seldin and Giebisch's The Kidney, Fifth Edition.
DOI: http://dx.doi.org/10.1016/B978-0-12-381462-3.00091-4

© 2013 Elsevier Inc. All rights reserved.

different treatment strategies may have a greater impact upon survival of patients with CKD has lead to a broadening of our conceptualization of hyperparathyroidism and "renal osteodystrophy" to include other metabolic abnormalities, termed, Chronic Kidney Disease—Mineral and Bone Disorder (CKD-MBD).[7] CKD-MBD describes a clinical syndrome that includes multiple metabolic/endocrine abnormalities, parathyroid gland dysfunction, bone disease, and unique CKD associated cardiovascular risk factors as well as other adverse clinical outcomes, such as fractures, vascular and soft tissue calcifications.

Because of the integration and interdependence of the calcium, phosphate, vitamin D and PTH axis, it is difficult to elucidate the primary or proximate causes of secondary hyperparathyroidism in CKD. Hyperphosphatemia, $1,25(OH)_2D_3$ and hypocalemia, acting through distinct molecular mechanisms, act in concert to cause secondary hyperparathyroidism in CKD. However, elevations of FGF23 and secondary suppression of $1,25(OH)_2D$ production may the initial abnormality in CKD that leads to increments in PTH, which may further stimulate FGF23 levels.[2,13] Nevertheless, suppression of PTH, while minimizing hyperphosphatemia, providing adequate vitamin D replacement, and maintaining bone health, remains the major goal of therapy. Different strategies to achieve this are based on different molecular targets for the available therapies that include, phosphate binders, vitamin D analogues and calcimimetics.

Molecular Targets for Suppressing Parathyroid Gland Function in CKD

Role of Hyperphosphatemia

A decline in GFR and reduced renal phosphate excretion is associated with increased PTH secretion by the parathyroid glands in CKD. In patients on maintenance hemodialysis, increased levels of serum phosphate strongly predict the degree of serum PTH elevation.[14] The importance of phosphate is also supported by the observation that phosphate restriction can attenuate the development of secondary hyperparathyroidism in CKD.[15] The stimuli linking hyperphosphatemia and increments in PTH are likely to be both direct and indirect. The molecular mechanism mediating the direct effects of phosphate on the parathyroid gland, however, are poorly understood.[16] Increments in media phosphate concentrations increases PTH synthesis in parathyroid cell cultures,[17–19] regulates PTH message stability,[16] and dietary restriction of phosphorus retards the development of hyperparathyroidism.[20] Phosphorus also modulates parathyroid growth and hypertrophy through activation of MAPK (mitogen activated protein kinases), TGF-alpha, and cyclin dependent kinases.[21] To date, no specific receptors, transporters or other molecular targets have been identified that mediate direct effects of phosphate on the parathyroid gland function.

Indirect effects of hyperphosphatemia on parathyroid gland function have greater experimental support, and are potentially mediated via FGF23, $1,25(OH)_2D_3$, and calcium, acting on their respective receptors in the parathyroid gland. Phosphate loading can also decrease $1,25(OH)_2D_3$ production by the kidney,[22] which in turn can decrease dietary absorption of calcium, thereby regulating parathyroid gland function indirectly through both the calcium sensing receptor and the vitamin D receptor.[23]

Vitamin D Receptor and the Role of 1, 25$(OH)_2D_3$ Deficiency

Decrements in both 25(OH)D and $1,25(OH)_2D$ occur early in the course of CKD-MBD. Low levels of vitamin D are associated with increased mortality in CKD and treatment in vitamin D analogs are believed to have a survival benefit.[24] ($1,25(OH)_2$) acts on the vitamin D receptor (VDR) in the parathyroid gland to suppress PTH transcription, but not PTH secretion, whereas calcitriol acts on the small intestines to increase active transport of both calcium and phosphate. Reductions in serum $1,25(OH)_2D$ levels play a central role in the pathogenesis of secondary hyperparathyroidism. Cross sectional studies of patients with CKD show that serum 1, 25(OH) $_2D_3$ levels decline as a function of the severity of renal impairment. Increments in PTH are inversely correlated with serum 1, 25 $(OH)_2D_3$ levels below GFRs of 60 ml/min/m^2. Low levels of 1,25 $(OH)_2D$ stimulate PTH though both loss of direct effects of $1,25(OH)_2D_3$ on vitamin D receptors (VDR) in the parathyroid glands and due to reductions in gastrointestinal absorption of calcium, which leads inhibition of the calcium sensing receptor (CaSR) in the parathyroid gland.

Nutritional deficiency of vitamin D as measured by low circulating $25(OH)D_3$ levels, is also common in patients with CKD, likely due to poor nutritional status, inadequate exposure to sunlight and chronic illness.[25] The negative correlation between serum PTH concentrations and 25(OH) vitamin D, the precursor to $1,25(OH)_2D_3$, is well established in the general population,[26] and may also contribute to secondary hyperparathyroidism in stage 3 and 4 CKD.

Role of the Calcium Sensing Receptor (CaSR) and Hypocalcemia

Calcium acting through CaSR is the major regulator of PTH transcription, secretion, and parathyroid gland

hyperplasia. From a biological standpoint, calcium and CaSR are more important that phosphate and 1,25 $(OH)_2D_3$ acting through the vitamin D receptor (VDR) in regulating parathyroid gland function. This conclusion is supported by mouse genetic approaches that have evaluated the phenotype in CaR, VDR, and 1 α-hydroxylase deficient mice has overlapping functions with CaR.[27–31] For example, secondary hyperparathyroidism and bone abnormalities in VDR-deficient mice can be corrected by normalizing serum calcium concentrations, whereas increased 1,25 $(OH)_2D_3$ levels is not sufficient to normalize PTH secretion and parathyroid gland growth in the absence of CaR. These mouse genetic studies are potentially important in setting the theoretical basis for selecting therapeutic strategies that target CaR as the dominant target in the parathyroid gland function, compared to VDR and phosphate.

Role of the FGF23-FGF Receptor/Klotho Signaling Network

FGF23, is a novel phosphaturic hormone produced by bone[32] is important in regulating phosphate homeostasis. Elevations in circulating FGF23 levels are one of the earliest abnormalities in CKD-MBD and are strongly associated with increased all-cause mortality.[33–34] Elevations of FGF23 inversely correlate with GFR.[35–38] Patients with end-stage renal disease (ESRD) have markedly elevated levels of FGF23 that parallels with degree of hyperphosphatemia[39] and SHPT.[40,41] FGF23 interacts with FGF receptors (FGFR) in the presence of the members of Klotho family of proteins.[42–43] The mechanism of increased FGF23 in CKD is poorly understood. The increase in serum FGF23 is not explained by reduced FGF23 clearance; and the proximate stimulus in early CKD that leads to increments in FGF23 are not clear. Nevertheless, FGF23 production is likely increased to counteract Pi retention due to reduced nephron mass by promoting urinary Pi excretion.[2] Elevations in FGF23 precede increments in PTH in CKD[44] and animal studies show that blockade of FGF23 by neutralizing antibodies lead to normalization of 1,25$(OH)_2D_3$ and PTH levels in models of CKD.[45] The effects of FGF23 on parathyroid gland function, however, are controversial. While some studies suggest that FGF23 promotes parathyroid gland hyperplasia,[46] other studies indicate that FGF23 directly suppresses PTH secretion via activation of FGF receptor/klotho complexes located in the parathyroid gland,[47] thereby explaining the apparent paradox between elevated FGF23 in patients with CKD and hyperparathyroidism. Additional studies will be needed to understand the direct effects of FGF23 in the pathogenesis secondary hyperparathyroidism.

Clinical Manifestations of Disordered Mineral Metabolism in CKD

The major abnormalities in CKD-MBD that require treatment are parathyroid gland dysfunction (i.e., increase PTH secretion and parathyroid gland hyperplasia), metabolic bone disease, and vascular calcifications/non-traditional cardiovascular risk.

Parathyroid Gland Abnormalities

Parathyroid disease in CKD is a progressive disorder characterized by increased PTH secretion as well as by an increase in the number of the PTH-secreting chief cells (hyperplasia). Disease progress correlates with hypocalcemia, hyperphosphatemia and duration of renal failure.[14,48] Unless adequately treated, secondary hyperparathyroidism inexorably progresses, with the frequency of parathyroidectomy proportional to the number of years of renal replacement therapy. The difficulty in treating hyperparathyroidism is due in part to massive hyperplasia and adenomatous transformation of the parathyroid gland that occur as a result of the chronic stimulation of PTH production in CKD. As the hyperplastic parathyroid glands enlarge, increments in basal, calcium-independent PTH secretion contributes to the elevated circulating PTH levels, although the glands retain responsiveness to calcium-mediated PTH suppression, i.e., normal set point.[49] With further progress there is adenomatous transformation along with reductions in CaR and VDR,[50] resulting in a right-ward shift in the set point typically associated with marked elevations of PTH and spontaneous hypercalcemia.

Renal Osteodystrophies

Bone disease in CKD is classically defined by bone histological analysis that assesses bone formation and resorption (rate of turnover or remodeling) and the presence or absence of a superimposed mineralization defect (osteomalacia). The major classifications include osteitis fibrosa (high turnover due to PTH stimulation of osteoblasts that are coupled to osteoclastic mediated bone resorption), osteomalacia (defective mineralization), and adynamic bone disease (low turnover due to low PTH and/or excessive treatment with vitamin D).[51] Symptomatic musculoskeletal disease, particularly tendon rupture, bone pain, muscle pain and weakness, and periarticular pain have decreased because of the success in suppressing PTH and the use of purer water to generate dialysate. Nevertheless, hip fractures occur 4-times more often in stage 5 CKD patients compared to the general population.[52] Attempts to link the type of histological bone disease or a specific level of PTH to increased fracture risk have been inconclusive. The utility of bone mineral density measurements to measure fracture risk have not been validated in CKD. Bone

biopsy after tetracycline labeling remains the standard for diagnosing bone disease in CKD. The use of bone biopsies, however, is diminishing because of cost and its invasiveness. Recent analysis of a cross section of patients with CKD found racial differences in the type of bone disease in CKD.[53] In this regard, whites exhibit low turnover whereas blacks have a greater prevalence of high turnover bone disease. A greater reliance is being placed on assessment of PTH and serum markers of bone turnover, which provide imprecise measures of bone disease.

The pathogenesis of the different forms of renal osteodystrophy is complex and not completely understood. PTH is the predominant factor controlling bone remodeling in CKD. In addition, the presence of C-terminal PTH fragments, which constitute 80% of circulating PTH, could potentially compete with PTH for type I PTH/PTHrP receptor or activate a novel C-PTH receptor with biological effects opposite to those of human PTH(1−84).[54] Whether the assessment of the PTH-(1−84)/C-PTH fragment ratio adds to the prediction of the underlying bone disease remains to be determined.[55] Active vitamin analogues also target osteoblasts and chondrocytes in vitro, but it has been difficult to separate the direct effects of vitamin D on bone and growth plate from that of PTH and calcium. Mouse genetic approaches to delete the VDR and 1α-hydroxylase suggest an independent role of Vitamin D in the growth plate and action in concert with calcium and PTH to activate osteoblasts and osteoclasts.[31,56]

The type of bone disease can influence serum calcium and phosphate levels. High bone turnover states contribute to elevated serum calcium and phosphate levels through increased release from bone, whereas low turnover states can also make patients more susceptible to developing hypercalcemia after dietary loads or vitamin D therapy, due to the diminished buffering capacity for calcium resulting from the diminished bone remodeling.[57] Adynamic bone disease may increase the risk of vascular and soft tissue calcifications, possibly due to limited calcium buffering capacity or to a calcium surfeit state.[58] An inverse relationship between vascular calcification and bone density is also found in stage 5 CKD.[59] Other examples of the impact of bone turnover on serum calcium and phosphate in ESRD are hungry bone syndrome following parathyroidectomy, hyercalcemina observed with immobilization, and hypocalcemia following treatment with anti-resorptive therapies.

Vascular Calcifications, Disordered Mineral Metabolism and Cardiovascular Disease/Morbidity and Mortality

Disordered bone and mineral metabolism in CKD contributes to calcification of soft tissues, particularly vessels, heart valves and skin. Vascular calcifications are very prevalent in CKD[60] and cardiovascular disease accounts for approximately half of all deaths in dialysis patients.[61] Several types of vascular calcification have been described in patients in CKD,[62,63] including intimal/atherosclerotic/fibrotic calcification, medial calcification, heart valve calcification, and calciphylaxis/calcific uremic arteriolopathy. First, intimal calcification occurs as focal calcification associated with lipid-laden foam cells seen in atherosclerotic plaques. Atherosclerotic/fibrotic calcification can have components of endochondral bone formation in the vessel wall. These calcifications may increase plaque fragility and risk for plaque rupture, or alternatively might stabilize the plaque, or merely represent an epiphenomena of atherosclerotic disease. Second, medial calcification is diffuse calcification that is not associated with atherosclerotic plaques and occurs in the media of vessels. Medial calcification, also called "Monckeberg's sclerosis," is seen with aging, diabetes, and with progressive renal failure. Valvular calcification represents the third major type of vascular calcification. This is a dystrophic calcification that is also associated with atherosclerotic disease.[64,65] There is a strong association between cardiac valve calcifications and vascular calcifications.

Calciphylaxis/calcific uremic arteriolopathy is the fourth type of calcification that results from amorphous calcium phosphate deposition in the vessel lumen leading to occlusion and tissue necrosis. The pathogenesis of calciphylaxis is not clear, but is associated with obesity, older age, female gender, diabetes mellitus, warfarin use, recent trauma, and calcium ingestion. Recently, studies in mice lacking fetuin, a calcium phosphate binding protein, have provided potential insights into the pathogenesis of this disorder. Fetuin binds to calcium phosphate to facilitate the clearing of this complex from the circulation. The absence of fetuin results in soft tissue calcification in mouse models. Low fetuin levels, which can be caused by inflammation, have been identified in dialysis patients with vascular calcifications and increased cardiovascular mortality.[66−68] Treatment of calciphylaxis with phosphate binders and parathyroidectomy typically are ineffective. Case reports suggest that sodium thiosulfate treatment can improve calciphylaxis-calcific uremic arteriolopathy.[69]

Coronary artery and vascular calcifications increase as a function of the number of years on renal replacement therapy and successful renal transplantation can lead to significant reductions in coronary artery calcifications by six months.[70] There is debate regarding whether the intimal calcification, which has predictive power in diagnosing coronary artery disease in non-uremic population, has the same significance in end stage renal disease. Traditional "non-uremic" factors,

TABLE 91.1 Clinical Practice Guidelines for Bone Metabolism and Disease in CKD

CKD Stage	GFR Range(ml/min/1.73 m^2)	Recommended Serum Values			
		Phosphorus (mg/dL)	Calcium (corrected) (mg/dL)	Ca X P (mg^2/dL^2)	Intact PTH (pg/ml)
3*	30 – 59	2.7 – 4.6	8.4 – 10.2		35 – 70
4*	15 – 29	2.7 – 4.6	8.4 – 10.2		70 – 110
5*	<15, dialysis	3.5 – 5.5	8.4 – 9.5	<55	150 – 300
KDOQI*		Normal range	8.4 – 10		130 – 585
KDIGO#		3.5 – 6	8.4 – 10		60 – 180
JSDT+					

Modified from National Kidney Foundation DOQI™ Kidney Disease Outcomes Quality Initiative[77]; KDIGO-Kidney Disease: Improving Global Outcomes#[77], and Japanese Society of Dialysis Therapy (JSDT) +[78].*

such as hypertension, diabetes, and hyperlipidemia, may account for the increase in risk of cardiovascular disease. Interestingly, a multicenter, randomized, double-blind, prospective study of atorvastatin in type 2 diabetes mellitus CKD 5 showed that a 42% reduction in low-density lipoprotein cholesterol was not associated with a reduction in composite of death from cardiac causes, nonfatal myocardial infarction, and stroke.[71] Treatments to reduce cardiovascular mortality in non-dialysis patients may not be as effective in stage V CDK patients. Unique factors associated with renal failure may have a greater importance. Epidemiological data implicate hyperphosphatemia and elevated Ca X P product as being risk factors for increased mortality.[1]

Medial calcification of blood vessels had been thought to be of little clinical significance for many years, but its effect to increase blood vessel stiffness and reduce vascular compliance resulting in a widened pulse pressure, increased afterload, and left ventricular hypertrophy are potential mechanisms whereby vascular calcification could contribute to cardiovascular morbidity. In addition, retrospective analysis indicates that the presence of intimal and medial calcification are both associated with increased all-cause mortality and cardiovascular mortality in patients with ESRD.[72]

While hyperphosphatemia is believed to be the major the major cause of vascular calcification, it has not been proven that strategies to prevent hyperphosphatemia or efforts to maintain neutral phosphate homeostasis will prevent vascular calcifications in CKD.

Treatment Goals: K/DOQI™ Guidelines for Mineral Metabolism in CKD

Clinical practice guidelines for bone metabolism and disease in stage 3, 4, and 5 CKD have been developed by the National Kidney Foundation Kidney Disease Outcomes Quality Initiative (KDOQI™) (Table 91.1).[6] The K/DOQI recommendations are influenced by the compelling evidence that elevated serum phosphorus and calcium x phosphorus product contribute to increased mortality[73] and the belief that excessive calcium loading may increase the risk of cardiovascular calcification.[5] The K/DOQI guidelines recommend attaining serum calcium, phosphorus, Ca X P product and PTH levels in a range that permits control of metabolic bone disease while limiting the potential toxicity of increased Ca X P product. The respective upper limit for serum phosphate in stage 5 CKD is 5.5 mg/dl, the corrected serum calcium is 9.5 mg/dL (corrected serum calcium = 0.8 x (4 − g/dL of serum albumin), and the Ca X P product <55 and intact PTH 300 pg/ml).

Retrospective data provide support for these recommendations. Most recently, analysis of the DOPPS database found that all-cause mortality and cardiovascular mortality were significantly and independently associated with serum concentrations of phosphorus, calcium, calcium-phosphorus product, and PTH.[74] Cardiovascular mortality was significantly associated with the serum concentrations of phosphorus, calcium (RR 1.14, P <0.0001), calcium-phosphorus product (RR 1.05, P <0.0001), and PTH (RR 1.02, P = 0.03). It is worth noting, however, that prospective studies demonstrating the benefit of attaining the recommended biochemical parameters or the adverse effects on mortality of excessive calcium exposure have not been performed or have not fully validated the K/DOQI recommendations. For example, the DCOR study, which enrolled 2103 adult hemodialysis patients who were randomly assigned to either sevelamer or calcium-based phosphate binders, found a 9 percent reduction in the risk of death from all causes in the sevelamer group compared to patients using calcium-based phosphate binders, but the result was not statistically significant (p = 0.30). Ganesh et al also did not find serum calcium or calcium based binders to be associated with higher cardiovascular mortality.[75]

In spite of wide adoption of these Kidney Disease Outcomes Quality Initiative (KDOQI)[76] guidelines in the United States, it is difficult to achieve the KDOQI guidelines. In a survey of hemodialysis facilities (N = 307) and patients (N = 17,236) participating in the Dialysis Outcomes and Practice Patterns Study (DOPPS) in the United States, Europe, and Japan from 1996 to 2001, 8% of patients were below lower target range and 52% were above upper target range for serum phosphorus; 9% were below and 50% were above for albumin-corrected calcium; 44% were above and 51% were below for calcium-phosphorus product; and 27% were above for intact PTH.[74] Because of this and other considerations, differing views of what represents adequate control of PTH and alternative clinical practice guidelines have been proposed, such as Kidney Disease: Improving Global Outcomes (KDIGO),[77] and Japanese Society of Dialysis Therapy (JSDT).[78] KDOQI PTH targets between 150 and 300 pg/ml is based on the estimated levels of PTH to maintain normal bone remodeling, with the higher than normal range reflecting the resistance to PTH actions and assessment of circulating inactive PTH fragments in dialysis patients.[79] The emphasis of changes in PTH and higher (i.e., >600 pg/ml) threshold PTH concentrations in the KDIGO recommendations reflects the variability in existing PTH assays in measuring bioactive PTH and the recognitions that only high PTH values are associated with increased mortality. In contrast, JSTA uses PTH concentrations in the normal range for the general population in CKD, which emphasizes the prevention of progressive parathyroid gland hyperplasia.[80] Other differences in these guidelines include more stringent control of serum phosphate and increasing the upper limit for serum calcium from 9.5 to 10 mg/dL in the KDIGO recommendations.

The guidelines for the lower phosphate, higher calcium and lower PTH values recommended for stage 3 and 4 CKD are largely best estimates that were available at the time the guidelines were formulation. Recent retrospective observations also suggest that hyperphosphatemia is a risk factor for mortality in predialysis patients as well.[81] Several studies support the fact that declining GFR is independently associated with the development of atherosclerotic cardiovascular disease independent of other risk factors.[82–84]

Treatment Strategies

The goals of treatment are to adequately control biochemistries (i.e., Ca, P, Ca x P, and PTH as recommended by the K/DOQI), prevent parathyroid gland hyperplasia, normalize bone remodeling, and prevent soft-tissues and vascular calcifications. To achieve these goals combinations therapy is needed, including phosphate binders, calcium supplementation, active vitamin D analogues, and calcimimetics. There are two major treatment paradigms using various drugs in different combinations. One approach uses titration of active vitamin D analogues (i.e., calcitriol paracalcitol, doxercalciferol) to achieve suppression of PTH. The other strategy uses titration of calcimimetics to suppress PTH. Both strategies require phosphate binders to control serum phosphate. The calcimimetic strategy does not require use of active vitamin D treatment, but is typically used in combination with a fixed low dose active vitamin D analog.

There have been numerous clinical trials comparing use of vitamin D analogous alone and in combination with calcimimetics both in incident and prevalent dialysis patients.[85,86] Several generalizations can be made from these studies. First, incident HD patients are more responsive to either strategy than prevalent patients with more severe hyperparathyroidism. In the groups with milder degree of hyperparathyroidism, cinacalcet HCl HCl tends to oversuppress PTH.[87,88] Second, cinacalcet HCl HCl based treatments are superior in suppressing PTH than treatment strategies using phosphate binders and vitamin D analogs in prevalent hemodialysis patients. Third, treatment strategies using active vitamin D analogs increase serum calcium and phosphate levels, whereas strategies that use cinacalcet HCl HCl in combination with low fixed doses of vitamin D results in lowering of both serum calcium and phosphate levels,[89] making it easier to achieve KDOQI targets.[90] Fourth, vitamin D treatment increases, whereas use of cinacalcet HCl-based strategies has no effect on or may lower serum FGF23 concentrations.[91] Fifth, there is indirect evidence, based on the persistently high rate of parathyroidectomies in patients treated with active vitamin D analog compared to the reduction in parathryoidectomies associated with calcimimetic treatment, that activation of CaSR is more effective than activation of VDR in preventing the progression of hyperparathryoidism. Sixth, the persistently high rate of vascular calcification and mortality in ESRD patients also suggest that the current use of phosphate binders in combination with vitamin D analogs is not adequately addressing these complications. Although animal studies indicate an effect of cinacalcet HCl HCl to reduce vascular calcifications, clinical trials failed to observe a significant difference between strategies using active vitamin D analogues compared to cinacalcet HCl HCl.[92] Seventh, cinacalcet HCl HCl based treatment regimens are associated with reduced fractures in retrospective analysis of phase three trials.[93] Finally, whether different treatment strategies affect mortality remains unknown, although initial studies favor an effect of cinacalcet

TABLE 91.2 Effects of Dialysis Modality, Phosphate Binders and Vitamin D on Estimated Phosphorus Balance in Stage V CKD

Subject/Treatment	Intake (g/wk)[a]	Absorption (g/wk)[c]	Bound (g/wk)[b]	Output (g/wk)[d]	Approximate Balance (g/wk)
Normal	5.9	4.7		4.7	0
ESRD	5.9	3.5		0	+3.5
HD	5.9	3.5		2.8	+0.7
Binders[b]	5.9	2.4	1.1	2.8	−0.4
Binders + VitD	5.9	3.6	1.1	2.8	+0.8
SNHD	5.9	3.5		5.3	−1.8
PD	5.9	3.5		2.3	+1.2
Binders	5.9	2.4	1.1	2.3	+0.1
Binders + VitD	5.9	3.6	1.1	2.3	+1.3

[a] *Assumes dietary phosphorus of 800–900 mg/day*
[b] *Assumes two calcium carbonate tablets (1250 mg; 1000 mg elemental calcium) three times each day or three calcium acetate tablets (667 mg; 507 mg elemental calcium) three times each day with meals for all patients*
[c] *Assumes 60% absorption in ESRD patients and 80% absorption in normal subjects and calcitriol treated ESRD patients*
[d] *Assumes no residual renal function in ESRD patients.*
ESRD (end stage renal disease), HD (hemodialysis 3 times per week), PD (peritoneal dialysis), SNHD (slow nocturnal hemodialysis 6 nights per week).

HCl HCl to improve all-cause mortality.[94] There is an ongoing prospective clinical trial to address this question.[95]

Management of Hyperphosphatemia

Hyperphosphatemia develops in CKD when compensatory increments in PTH and FGF23 fail to offset the reduction in phosphate excretion due to diminished GRF. While dietary sources of phosphate is the major contributing factor to hyperphosphatemia in patients with ESRD, treatment with active vitamin D analogues further increases the gastrointestinal absorption of phosphate and calcium leading to elevated serum phosphate and calcium levels[96] (Table 91.2). Early in the disease process, CKD 3 and 4, initial management with dietary phosphate restriction can be effective. During these early stages, there is still capacity for renal excretion of phosphate, and a neutral phosphorus balance can be achieved if the diet is adequately restricted. However, frequently by late CKD 4 and certainly by CKD 5, dietary restriction is inadequate, and other methods for achieving phosphorus balance are necessary. Hemodialysis and peritoneal dialysis have a limited capacity for phosphorus removal (Table 91.2), and this net removal is usually not enough with thrice weekly dialysis to maintain a neutral phosphorus balance, especially when vitamin D is needed (Table 91.2). Therefore, use of phosphate binders with limited doses or less hyperphosphatemic vitamin D analogs are required to achieve neutral phosphate balance.

Dietary phosphate restriction, while theoretically attractive based on results of limiting phosphate intake in animal models of CKD, it is difficult to achieve in clinical practice due to the high amounts of phosphate in processed foods and the risk of inadequate dietary protein with phosphate restricted diets. Therefore, phosphate binders are required to control serum phosphate levels. Phosphate binders are the first line in medical management of hyperphosphatemia in CKD 5. Phosphate binders may need to be started in earlier stages of CKD before serum phosphate is elevated; the efficacy of early use of phosphate binder to limit a positive phosphate balance on serm PTH and FGF23 elevations have produced inconclusive results.[97] Three categories of phosphate binders exist, trivalent cations, divalent cations, and synthetic resin polyallylamine hydrochloride (sevelamer).

Trivalent cations, such as aluminum and lanthanum carbonate, are the most potent phosphate binder on a per weight basis.[98] Aluminum use as a phosphate binder, however, has been discontinued because of potential bone and CNS toxicity. Lanthanium carbonate has been shown to be an effective phosphate binder in clinical trials,[99] and has been recently approved for use as a phosphate binder. Current safety data look encouraging (e.g., no evidence of bone and CNS toxicity), but there is some systemic absorption of lanthanum, and studies are needed that evaluate potential long-term safety.[100] Calcium based products, calcium carbonate and calcium acetate, are the mainstay of treatment, but high calcium loads and risk of vascular calcifications lead to the K/DOQI recommendation to limit the total calcium intake to 2 grams per day. Recently, the risk of calcium loading has been reevaluated,[101] and greater amounts of oral calcium may be tolerated, especially in the absence of high dose vitamin D therapy. The CARE study, which is the only

prospective trial to directly compare the efficacy of calcium acetate with sevelamer showed that the calcium based binder was more effect in controlling serum phosphorus and CaxP product than sevelamer, although calcium acetate treatment resulted in higher calcium levels.[101] Poly-allylamine (sevelamer) is a non-metal and non-calcium based phosphorus binder that is a less potent than trivalent and divalent cations. However, sevelamer has been shown to reduce the development of vascular calcifications.[5] The Treat-to-Goal study demonstrated slower development of coronary and aortic calcification with sevelamer compared to calcium based binders, and the D-COR study, showed marginal survival benefit in subgroup analysis (i.e., patient over 65 years of age and treatment greater than two years, but no survival advantage in the entire sevelamer group). Poly-allylamines also lower LDL, which is probably due to its ability to bind bile acids akin to cholestyramine.[5,101,102]

It is common to use combinations of calcium and non-calcium phosphate binders to achieve control of serum phosphate in stage V CKD. Also, phosphate binders containing magnesium and iron are also under development. In addition efforts to block the active transport of phosphate across the intestinal epithelium might also reduce phosphate absorption. Therapies that target Npt2b, the sodium-phosphate contrasporter in the intestines are under development. Two other approaches may reduce active phosphate transport, including reduction of dose of active vitamin D and its analogs and treatment with niacin. Since use of active vitamin D analogs increases gastrointestinal calcium and phosphate absorption, the use of lower doses of active vitamin D analogs may lead to lower Pi absorption by the GI tract, and lower serum Pi. Niacin is converted into niacinamide during its metabolism and reduces intestinal transport of Pi via inhibition of Npt2b. Both, niacin and niacinamide are available, but niacinamide may be better tolerated since it does not cause vasodilatation or flushing. Niacinamide has been shown in small clinical trials effectively reduce serum Pi levels in hemodialysis patients,[103,104] as well as peritoneal dialysis patients.[105]

Use of phosphate binders alone is not sufficient to treat secondary hyperparathyroidism in stage V CKD, and therapy with vitamin D and/or calcimimetics are needed.

Role of Vitamin D Analogs

Treatment with 1,25-dihydroxyvitamin D_3 (calcitriol) or an active vitamin D analog (calcitriol, paricalcitol, doxercalciferol, and alfacalcidol) have been the major intervention to treat secondary hyperparathyroidism in CKD stage V. There is no uniform agreement regarding the route, dose, and type of active vitamin D analog that should be given, with oral vitamin D predominating in Europe and Asia and intravenous vitamin D administration the mainstay in the U.S. Available vitamin D_2 analogs, such as paricalcitol, may cause less hypercalcemia and hyperphosphatemia than calcitriol, although the mechanisms for this effect are not clear. In preclinical studies, *paricalcitol* induced less hypercalcemia than calcitriol in vitamin D–deficient rats, in spite of having similar intestinal and bone-mediated calcimimetic actions.[4] Some studies, however, have failed to observe major differences in the propensity of paricalcitol and calcitriol to induce hypercalcemia and hyperphosphatemia, indicating that all forms of currently available vitamin D analogs retain the side effect of increasing the Ca X P product, if given in sufficient dosages.[106,107] Moreover, activate vitamin D analogs elevate FGF23 levels,[2] which is a strong biomarker for mortality in CKD.[33] There have been no prospective, long-term trials comparing the efficacy and safety of the various vitamin D analogs. Alphacalcidol is a 1-alpha hydroxylated "low affinity" analogue that is hydroxylated by the liver to become the active drug that targets the vitamin D receptor. In spite of the effects of active vitamin D analogs to worsen hyperphosphatemia and stimulate FGF23, there is also data suggesting that treatment with active vitamin D may offer a survival benefit and paricalcitol may offer a survival advantage over calcitriol.[108] The survival effects of active vitamin D therapy may be dose dependent, with the survival advantage occurring with low dose and possible untoward effects associated with higher doses. Finally the potential of vitamin D to promote vascular calcifications in animal models has not been fully explored in the clinical setting. In a uremic rat model, calcitriol resulted in an increase in Ca X P production and aortic calcification.[109]

Until the institution of bundled payments in ESRD, the major factors influencing the use of vitamin D analogues were reimbursement. There have been no prospective studies that compare different vitamin D analogues or which attempt to determine the optimal dose of these agents. Since treatment with vitamin D analogues in CKD stage V make it difficult to achieving K/DOQI guidelines[110] and do not appear to eliminate the progression of parathyroid gland hyperplasia and rates of parathyroidectomy rates.[111] Significant parathyroid disease often persists following successful renal transplantation who have been managed with vitamin D based regimens, as evidenced by the frequent need for parathyroidectomy in this patient population.[112]

Use of vitamin D therapy in earlier stages of renal failure is controversial, in spite of the evidence of decreased 1, 25$(OH)_2D_3$ occurs early, in CKD stage 3 and 4, since calcium supplementation and phosphate binders can be effective in this setting. In addition,

elevations of FGF23 occur early in CKD and appear to suppress 1,25(OH)$_2$D synthesis, suggesting that reductions of 1,25(OH)$_2$D in early CKD is an adaptive response. This observation, along with the related observation that treatment with activate vitamin D analogues increases serum FGF23, raises concerns about use of active vitamin D analogs in early CKD.

On the other hand, vitamin D deficiency (defined by a serum 25(OH)D $<$ 20 ng/ml) is common in CKD.[113] Treatment with ergocalciferol or cholecalciferol to correct the deficiency of vitamin D along with phosphate binders to offset the loss of renal phosphate excretion may provide the most rational approach to manage patients with CKD 3 and 4. The standard of care is to treat individuals with serum 25 (OH)D concentrations $<$20 ng/mL (50 nmol/L) with 50,000 international units (units) of vitamin D_2 or D_3 orally once per week for six to eight weeks, followed by 800 units of vitamin D daily to maintain the target 25 (OH)D level.[114] Patients with CKD may be resistant to standard treatment with vitamin D_2 and D_3, requiring high doses to achieve 25(0H)D levels above 30 ng/ml.[115] Cholecalciferol treatment has been shown to regulate vitamin D receptor response in circulating monocytes in ESRD.[116] Treatment with Active vitamin D analogues, such as calcitriol, alfacalcidol, doxercalciferol, and paricalcitrol, can be reserved for patients who do not respond to phosphate binders and nutritional vitamin D supplementation.

Role of Calcimimetics

Calcimimetics offers an alternative approach to treating secondary hyperparathyroidism without raising calcium or using active vitamin D analogs. Calcimimetics are calcium-receptor sensing agonists that act on the parathyroid gland's CaSR by allosterically increasing the sensitivity of the receptor to calcium. Cinacalcet HCl HCl or (αR)-(−)-α -methyl-*N*-[3-[3-[trifluoromethylphenyl]propyl]-1-napthalenemethanamine hydrochloride has been approved for the treatment of secondary hyperparathyroidism in stage 5 CKD[117] as well as for primary hyperparathyroidism. In addition to directly suppressing PTH secretion and gene transcription through CaSR activation, calcimimetics have been shown to attenuate parathyroid gland hyperplasia in animal models of secondary hyperparathyroidism,[118] substantiating the role of CaSR in regulating parathyroid cell proliferation.

Results from several large clinical trials indicate that treatment with cinacalcet HCl hydrochloride (Sensipar®/Mimpara®) effectively lowers plasma PTH levels in hemodialysis patients with inadequately controlled secondary hyperparathyroidism despite previous management with vitamin D sterols and phosphate-binding agents.[85,86,95,119] Treatment with cinacalcet HCl HCl caused significant decreases in PTH without elevating serum calcium or phosphorus. In fact, there was a modest reduction in serum calcium and phosphate in protocols using calcimimetics in conjunction with standard therapy. The reduction in calcium and phosphate may be due to alterations in bone flux of these ions. The use of cinacalcet HCl HCl allowed more patients (approximately 41%) to attain the PTH and Ca X P values recommended by the KDOQI™ guidelines compared to less than 10% treated with phosphate binders and vitamin D analogues alone.[119] Treatment with cinacalcet HCl HCl also permits a reduction in doses of active vitamin D sterols while maintaining control of serum PTH. Calcimimetics are potent suppressors of PTH, and as a result use of cinacalcet HCl HCl can result in oversuppression of PTH and well as symptomatic hypocalcemia. In addition, cinacalcet HCl HCl is associated with increased nausea and vomiting, which limits its use in some patients. Only oral forms of cinacalcet HCl HCl are currently available, therefore, cinacalcet HCl HCl is currently outside of the bundled reimbursement for ESRD.

Calcimimetics also are effective in reducing PTH in CKD, but are associated with increased serum phosphate due to the loss of the phosphaturic effects of PTH and the lack of effects of cinacalect to stimulate FGF23.[120]

Specific Recommendations for Treatment

A possible algorithm is shown in Table 91.3 that takes into consideration advantages and disadvantages of calcium and non-calcium based phosphate binders, active vitamin D analogs, and calcimimetics.

Step 1: After measuring serum calcium, albumin, phosphate and intact PTH, begin therapy in all patients with phosphate of $>$5.5 mg/dl a phosphate binder. Calcium-based phosphate binder, either calcium carbonate or calcium acetate versus non-calcium containing phosphate binder. Calcium-based phosphate binders can be taken with meals at doses up to 1500 mg elemental calcium per day. Calcium carbonate has 500 mg of elemental calcium in a 1250 mg tablet; calcium acetate has 169 mg of elemental calcium in one 667 mg tablet. If serum phosphate remains greater than 5.2 mg/dl on maximal doses of calcium binders, then a non-calcium phosphate binder can be added. If there are vascular calcifications and unusual risk of cardiovascular disease in older patients, sevelamer, might be the treatment of choice, based on the treat to goal and D-Cor studies. In addition, concomitant use of active vitamin analogs favors use on non-calcium based binders, whereas the use of cinacalcet HCl HCl favors the use of calcium binders. Thus, the algorithm limits calcium exposure in patient receiving concomitant high

TABLE 91.3 Treatment Algorithm for Secondary Hyperparathyroidism in stage 5D CKD

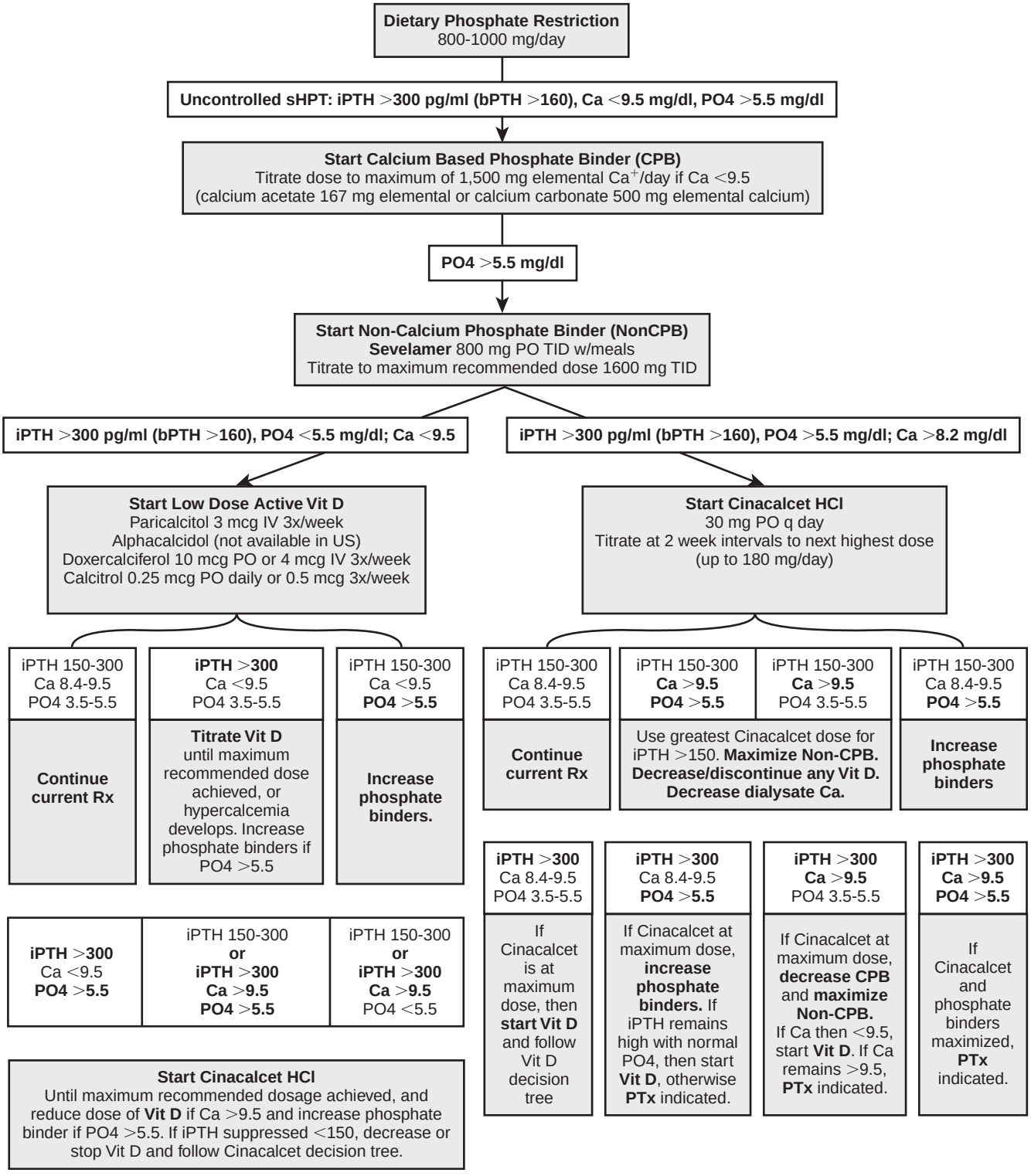

dose therapy with vitamin D, but liberalizes calcium intake in hypocalemic patients treated with cinacalcet HCl HCl.

Step 2: Assess 25(OH)D levels. Treatment of vitamin D insufficiency should be considered if 25(OH)D levels are less than 20 ng/ml. Ergocalciferol or cholecalciferol should be administered to increase serum 25(OH)D levels to the 30 and 50 ng/ml (50−125 nM/L), regardless of serum PTH levels. If active vitamin D analogs are to be used to suppress PTH, correction of 25(OH)D levels may be superfluous, since active vitamin D analogs stimulate the innate immune responses similar to normalizing serum 25(OH)D.[116]

Step 3: Assess PTH levels. If PTH is greater than 300 pg/ml in the setting of phosphate binder therapy, then initiation of low dose, physiological replacement doses of active vitamin D analogs in doses equivalent to ~0.5 ug of calcitriol is recommended. If hyperphosphatemia develops after starting or increasing vitamin D, increments in the dose of phosphate binders, reductions in active vitamin D or institution of cinacalcet HCl HCl should be considered.

Step 4: If PTH values are greater than 300 pg/ml and serum calcium concentrations are above 8.2 mg/dl, on phosphate binders and low-dose active vitamin D therapy, cinacalcet HCl should be started at a dose of 30 mg/day and titrated upwards to suppress PTH in to the range of 150−300 pg/ml. Alternatively, active vitamin D analog doses can be titrated upward to achieve suppression of PTH if serum calcium and phosphate are respectively less than 9.5 mg/dL and 5 mg/dL.

Current clinical trials support the use of the cinacalcet HCl algorithm for patients with more severe hyperparathyroidism and elevated serum phosphate levels. This approach suppresses PTH without raising serum calcium and phosphate, whereas titration of active vitamin D tends to increase both calcium and phosphate (especially at high doses), making it difficult to achieve the K/DOQI endpoints. Cinacalcet HCl HCl should also be considered if hypercalcemia develops with treatment with Vitamin D. Calcium based phosphate binder may be preferred when using cinacalcet HCl HCl, since serum calcium levels are lower by calcimimetics. If hypocalcemia persists, consideration should be given to titrating upward the active vitamin D therapy. Patients with persistent hyperparathyroidism, in spite of maximal doses of cinacalcet HCl HCl and vitamin D should undergo parathyroidectomy. An open labeled trial comparing cinacalcet HCl HCl titration versus an active vitamin D titration,[85] similar to the proposed treatment paradigm, found that use of cinacalcet HCl HCl resulted in better control of serum PTH and phosphate concentrations than vitamin D titration. On the other hand, patients with milder forms of hyperparathyroidism, either a cinacalcet HCl or active vitamin D analog titration can reduce PTH levels to the 150 to 300 pg/ml range.[88] The ultimate choice between the initial use of cinacalcet HCl HCl versus active vitamin D analog titration involves patient compliance, ability to tolerate the gastrointestinal side effects of cinacalcet HCl, relative greater efficacy in optimizing serum calcium, phosphate and PTH with cinacalcet HCl, the differential costs of medications and reimbursement, and pending data on the effects on these different approaches to reduce mortality and morbidity in ESRD.

References

[1] Block GA, Klassen PS, Lazarus JM, Ofsthun N, Lowrie EG, Chertow GM. Mineral metabolism, mortality, and morbidity in maintenance hemodialysis. J Am Soc Nephrol 2004;15 (8):2208−18.

[2] Quarles LD. The bone and beyond: "Dem bones" are made for more than walking. Nat Med 2011;17(4):428−30.

[3] Wolf M. Forging forward with 10 burning questions on FGF23 in kidney disease. J Am Soc Nephrol 2010;21(9):1427−35.

[4] Brown AJ, Finch J, Takahashi F, Slatopolsky E. Calcemic activity of 19-Nor-1,25(OH)(2)D(2) decreases with duration of treatment. J Am Soc Nephrol 2000;11(11):2088−94.

[5] Chertow G. Long term effects of sevelamer hydrochloride on the calcium x phosphate product and lipid profile of haemodialysis patients. Nephrol Dial Transplant 1999;14:2907−14.

[6] K/DOQI Clinical practice guidelines for cardiovascular disease in dialysis patients. Am J Kidney Dis 2005;45(3 Pt 2):16-153.

[7] Wetmore JB, Quarles LD. Calcimimetics or vitamin D analogs for suppressing parathyroid hormone in end-stage renal disease: time for a paradigm shift? Nat Clin Pract Nephrol 2009;5 (1):24−33.

[8] Murray TM, Rao LG, Divieti P, Bringhurst FR. Parathyroid hormone secretion and action: evidence for discrete receptors for the carboxyl-terminal region and related biological actions of carboxyl- terminal ligands. Endocr Rev 2005;26(1):78−113.

[9] Kalantar-Zadeh K, Kuwae N, Regidor DL, Kovesdy CP, Kilpatrick RD, Shinaberger CS, et al. Survival predictability of time-varying indicators of bone disease in maintenance hemodialysis patients. Kidney Int 2006;70(4):771−80.

[10] Uhlig K, Berns JS, Kestenbaum B, Kumar R, Leonard MB, Martin KJ, et al. KDOQI US commentary on the 2009 KDIGO clinical practice guideline for the diagnosis, evaluation, and treatment of CKD-mineral and bone disorder (CKD-MBD). Am J Kidney Dis 2010;55(5):773−99.

[11] Li S, Chen YW, Peng Y, Foley RN, Peter St WL. Trends in parathyroidectomy rates in US hemodialysis patients from 1992 to 2007. Am J Kidney Dis 2011;57(4):602−11.

[12] Nickolas TL, Stein E, Cohen A, Thomas V, Staron RB, McMahon DJ, et al. Bone mass and microarchitecture in CKD patients with fracture. J Am Soc Nephrol 2010;21(8):1371−80 [PMCID: 2938588].

[13] Isakova T, Wahl P, Vargas GS, Gutierrez OM, Scialla J, Xie H, et al. Fibroblast growth factor 23 is elevated before parathyroid hormone and phosphate in chronic kidney disease. Kidney Int 2011;79(12):1370−8 [PMCID: 3134393].

[14] Indridason OS, Pieper CF, Quarles LD. Predictors of short-term changes in serum intact parathyroid hormone levels in hemodialysis patients: role of phosphorus, calcium, and gender. J Clin Endocrinol Metab 1998;83(11):3860−6.

[15] Slatopolsky E, Bricker NS. The role of phosphorus restriction in the prevention of secondary hyperparathyroidism in chronic renal disease. Kidney Int 1973;4(2):141–5.
[16] Silver J, Levi R. Regulation of PTH synthesis and secretion relevant to the management of secondary hyperparathyroidism in chronic kidney disease. Kidney Int Suppl 2005;95:S8–12.
[17] Qunibi W. Treatment of hyperphosphatemia in hemodialysis patients: the calcium acetate renagel evaluation (CARE Study). Kidney Int 2004;65:1914–26.
[18] Slatopolsky E. Phosphorus restriction prevents parathyroid gland growth high phosphorus directly stimulates pth secretion in vitro. J Clin Invest 1996;97:2534–40.
[19] Almaden Y. Direct effect of phosphorus on PTH secretion from whole rat parathyroid glands in vitro. J Bone Miner Res 1996;11:970–6.
[20] Takahashi F. Hyperplasia of the parathyroid gland without secondary hyperparathyroidism. Kidney International 2002;61 (4):1332–8.
[21] Slatopolsky E. Role of phosphorus in the pathogenesis of secondary hyperparathyroidism. Am J Kidney Dis 2001;2(1 Suppl.):S54–7.
[22] Tenenhouse HS, Martel J, Gauthier C, Zhang MY, Portale AA. Renal expression of the sodium/phosphate cotransporter gene, Npt2, is not required for regulation of renal 1 alpha-hydroxylase by phosphate. Endocrinology 2001;142(3):1124–9.
[23] Brautbar N, Levine BS, Walling MW, Coburn JW. Intestinal absorption of calcium: role of dietary phosphate and vitamin D. Am J Physiol 1981;241(1):G49–53.
[24] Wolf M, Shah A, Gutierrez O, Ankers E, Monroy M, Tamez H, et al. Vitamin D levels and early mortality among incident hemodialysis patients. Kidney Int 2007;72(8):1004–13.
[25] Gonzalez EA, Sachdeva A, Oliver DA, Martin KJ. Vitamin D insufficiency and deficiency in chronic kidney disease. A single center observational study. Am J Nephrol 2004;24(5):503–10.
[26] Holick MF, Siris ES, Binkley N, Beard MK, Khan A, Katzer JT, et al. Prevalence of Vitamin D inadequacy among postmenopausal North American women receiving osteoporosis therapy. J Clin Endocrinol Metab 2005;90(6):3215–24.
[27] Garner S, Pi M, Tu Q, Quarles LD. Rickets in cation-sensing receptor-deficient mice: an unexpected skeletal phenotype. Endocrinology 2001;142:3996–4005.
[28] Kostakis A. Parathyroidectomy in the treatment of secondary hyperparathyroidism in chronic renal failure. Int Surg 1997;82:85–6.
[29] Kovacs C. Regulation of murine fetal-placental calcium metabolism by the calcium-sensing receptor. J Clin Investig 1998;101:2812–20.
[30] Li Y. Normalization of mineral ion homeostasis by dietary means prevents hyperparathyroidism, rickets, and osteomalacia, but not alopecia in vitamin d receptor-ablated mice. Endocrinology 1998;139:4391–6.
[31] Panda DK, Miao D, Bolivar I, Li J, Huo R, Hendy GN, et al. Inactivation of the 25-hydroxyvitamin D 1alpha-hydroxylase and vitamin D receptor demonstrates independent and interdependent effects of calcium and vitamin D on skeletal and mineral homeostasis. J Biol Chem 2004;279(16):16754–66.
[32] Quarles LD. Evidence for a bone-kidney axis regulating phosphate homeostasis. J Clin Invest 2003;112(5):642–6.
[33] Gutierrez OM, Mannstadt M, Isakova T, Rauh-Hain JA, Tamez H, Shah A, et al. Fibroblast growth factor 23 and mortality among patients undergoing hemodialysis. N Engl J Med 2008;359(6):584–92 [PMCID: 2890264].
[34] Jean G, Terrat JC, Vanel T, Hurot JM, Lorriaux C, Mayor B, et al. High levels of serum fibroblast growth factor (FGF)-23 are associated with increased mortality in long haemodialysis patients. Nephrol Dial Transplant 2009;24(9):2792–6.
[35] Gutierrez O, Isakova T, Rhee E, Shah A, Holmes J, Collerone G, et al. Fibroblast growth factor-23 mitigates hyperphosphatemia but accentuates calcitriol deficiency in chronic kidney disease. J Am Soc Nephrol 2005;16(7):2205–15.
[36] Larsson T, Nisbeth U, Ljunggren O, Juppner H, Jonsson KB. Circulating concentration of FGF-23 increases as renal function declines in patients with chronic kidney disease, but does not change in response to variation in phosphate intake in healthy volunteers. Kidney Int 2003;64(6):2272–9.
[37] Westerberg PA, Linde T, Wikstrom B, Ljunggren O, Stridsberg M, Larsson TE. Regulation of fibroblast growth factor-23 in chronic kidney disease. Nephrol Dial Transplant 2007;22 (11):3202–7.
[38] Ix JH, Shlipak MG, Wassel CL, Whooley MA. Fibroblast growth factor-23 and early decrements in kidney function: the heart and soul study. Nephrol Dial Transplant 2010;25(3):993–7 [PMCID: 2902926].
[39] Weber TJ, Liu S, Indridason OS, Quarles LD. Serum FGF23 levels in normal and disordered phosphorus homeostasis. J Bone Miner Res 2003;18(7):1227–34.
[40] Komaba H, Goto S, Fujii H, Hamada Y, Kobayashi A, Shibuya K, et al. Depressed expression of Klotho and FGF receptor 1 in hyperplastic parathyroid glands from uremic patients. Kidney Int 2010;77(3):232–8.
[41] Weber TJLS, Indridason OS, Quarles LD. Serum FGF23 levels in normal and disordered phosphorus homeostasis. J Bone Miner Res 2003;18:1227–34.
[42] Kurosu H, Yamamoto M, Clark JD, Pastor JV, Nandi A, Gurnani P, et al. Suppression of aging in mice by the hormone Klotho. Science 2005;309(5742):1829–33 [PMCID: 2536606].
[43] Tsujikawa H, Kurotaki Y, Fujimori T, Fukuda K, Nabeshima Y. Klotho, a gene related to a syndrome resembling human premature aging, functions in a negative regulatory circuit of vitamin D endocrine system. Mol Endocrinol 2003;17(12):2393–403.
[44] Isakova T, Gutierrez O, Shah A, Castaldo L, Holmes J, Lee H, et al. Postprandial mineral metabolism and secondary hyperparathyroidism in early CKD. J Am Soc Nephrol 2008;19 (3):615–23 [PMCID: 2391049]
[45] Hasegawa H, Nagano N, Urakawa I, Yamazaki Y, Iijima K, Fujita T, et al. Direct evidence for a causative role of FGF23 in the abnormal renal phosphate handling and vitamin D metabolism in rats with early-stage chronic kidney disease. Kidney Int 2010;78(10):975–80.
[46] Wetmore JB, Santos PW, Mahnken JD, Krebill R, Menard R, Gutta H, et al. Elevated FGF23 levels are associated with impaired calcium-mediated suppression of PTH in ESRD. J Clin Endocrinol Metab 2011;96(1):E57–64 [PMCID: 3038477].
[47] Galitzer H, Ben-Dov IZ, Silver J, Naveh-Many T. Parathyroid cell resistance to fibroblast growth factor 23 in secondary hyperparathyroidism of chronic kidney disease. Kidney Int 2010;77 (3):211–8.
[48] Chertow GM, Plone M, Dillon MA, Burke SK, Slatopolsky E. Hyperparathyroidism and dialysis vintage. Clin Nephrol. 2000;54(4):295–300.
[49] Indridason OS, Heath III H, Khosla S, Yohay DA, Quarles LD. Non-suppressible parathyroid hormone secretion is related to gland size in uremic secondary hyperparathyroidism. Kidney Int 1996;50(5):1663–71.
[50] Fukuda N, Tanaka H, Tominaga Y, Fukagawa M, Kurokawa K, Seino Y. Decreased 1,25-dihydroxyvitamin D3 receptor density is associated with a more severe form of parathyroid hyperplasia in chronic uremic patients. J Clin Invest 1993;92(3):1436–43.
[51] Parfitt AM. Renal bone disease: a new conceptual framework for the interpretation of bone histomorphometry. Curr Opin Nephrol Hypertens 2003;12(4):387–403.

[52] Ball AMGD, Sherrard D, Weiss NS, Emerson SS, Seliger SL, Kestenbaum BR, et al. Risk of hip fracture among dialysis and renal transplant recipients. JAMA 2002;288:3014–8.
[53] Malluche HH, Mawad HW, Monier-Faugere MC. Renal osteodystrophy in the first decade of the new millennium: analysis of 630 bone biopsies in black and white patients. J Bone Miner Res 2011;26(6):1368–76.
[54] Divieti P, Geller AI, Suliman G, Juppner H, Bringhurst FR. Receptors specific for the carboxyl-terminal region of parathyroid hormone on bone-derived cells: determinants of ligand binding and bioactivity. Endocrinology 2005;146(4):1863–70.
[55] Monier-Faugere MC, Geng Z, Mawad H, Friedler RM, Gao P, Cantor TL, et al. Improved assessment of bone turnover by the PTH-(1-84)/large C-PTH fragments ratio in ESRD patients. Kidney Int 2001;60(4):1460–8.
[56] Goltzman D, Miao D, Panda DK, Hendy GN. Effects of calcium and of the Vitamin D system on skeletal and calcium homeostasis: lessons from genetic models. J Steroid Biochem Mol Biol 2004;89-90(1-5):485–9.
[57] Frazao JM, Messa P, Mellotte GJ, Geiger H, Hagen EC, Quarles LD, et al. Cinacalcet HCl reduces plasma intact parathyroid hormone, serum phosphate and calcium levels in patients with secondary hyperparathyroidism irrespective of its severity. Clin Nephrol 2011;76(3):233–43.
[58] Goldsmith D, Ritz E, Covic A. Vascular calcification: a stiff challenge for the nephrologist: does preventing bone disease cause arterial disease? Kidney Int 2004;66(4):1315–33.
[59] London GM, Marty C, Marchais SJ, Guerin AP, Metivier F, de Vernejoul MC. Arterial calcifications and bone histomorphometry in end-stage renal disease. J Am Soc Nephrol 2004;15 (7):1943–51.
[60] Goodman WG, Goldin J, Kuizon BD, Yoon C, Gales B, Sider D, et al. Coronary-artery calcification in young adults with end-stage renal disease who are undergoing dialysis. N Engl J Med 2000;342(20):1478–83.
[61] McClellan WM, Chertow GM. Beyond Framingham: cardiovascular risk profiling in ESRD. J Am Soc Nephrol 2005;16 (6):1539–41.
[62] Towler DA. Vascular calcification in ESRD: Another cloud appears in the perfect storm–but highlights a silver lining? Kidney Int 2004;66(6):2467–8.
[63] Parfitt AM. Soft-tissue calcification in uremia. Arch Intern Med 1969;124(5):544–56.
[64] Kajbaf S, Veinot JP, Ha A, Zimmerman D. Comparison of surgically removed cardiac valves of patients with ESRD with those of the general population. Am J Kidney Dis 2005;46(1):86–93.
[65] Wang AY, Ho SS, Wang M, Liu EK, Ho S, Li PK, et al. Cardiac valvular calcification as a marker of atherosclerosis and arterial calcification in end-stage renal disease. Arch Intern Med 2005;165(3):327–32.
[66] Schafer C, Heiss A, Schwarz A, Westenfeld R, Ketteler M, Floege J, et al. The serum protein alpha 2-Heremans-Schmid glycoprotein/fetuin-A is a systemically acting inhibitor of ectopic calcification. J Clin Invest 2003;112(3):357–66.
[67] Ketteler M, Bongartz P, Westenfeld R, Wildberger JE, Mahnken AH, Bohm R, et al. Association of low fetuin-A (AHSG) concentrations in serum with cardiovascular mortality in patients on dialysis: a cross-sectional study. Lancet 2003;361(9360):827–33.
[68] Heiss A, DuChesne A, Denecke B, Grotzinger J, Yamamoto K, Renne T, et al. Structural basis of calcification inhibition by alpha 2-HS glycoprotein/fetuin-A. Formation of colloidal calciprotein particles. J Biol Chem 2003;278(15):13333–41.
[69] Cicone JS, Petronis JB, Embert CD, Spector DA. Successful treatment of calciphylaxis with intravenous sodium thiosulfate. Am J Kidney Dis 2004;43(6):1104–8.
[70] Abedi SA, Tarzamni MK, Nakhjavani MR, Bohlooli A. Effect of renal transplantation on coronary artery calcification in hemodialysis patients. Transplant Proc 2009;41(7):2829–31.
[71] Wanner C, Krane V, Marz W, Olschewski M, Mann JF, Ruf G, et al. Atorvastatin in patients with type 2 diabetes mellitus undergoing hemodialysis. N Engl J Med 2005;353(3):238–48.
[72] London GM, Guerin AP, Marchais SJ, Metivier F, Pannier B, Adda H. Arterial media calcification in end-stage renal disease: impact on all-cause and cardiovascular mortality. Nephrol Dial Transplant 2003;18(9):1731–40.
[73] Block G. Association of serum phosphorus and calcium x phosphorus product with mortality risk in chronic hemodialysis patients: A national study. Am J Kidney Dis 1998;31:607–17.
[74] Young EW, Albert JM, Satayathum S, Goodkin DA, Pisoni RL, Akiba T, et al. Predictors and consequences of altered mineral metabolism: the dialysis outcomes and practice patterns study. Kidney Int 2005;67(3):1179–87.
[75] Ganesh S. Association of elevated serum PO4, Ca x PO4 product, and parathyroid hormone with cardiac mortality risk in chronic hemodialysis patients. J Am Soc Nephrol 2001;12:2131–8.
[76] K/DOQI clinical practice guidelines for bone metabolism and disease in chronic kidney disease. Am J Kidney Dis 2003;42(4 Suppl. 3):S1–201.
[77] KDIGO clinical practice guideline for the diagnosis, evaluation, prevention, and treatment of Chronic Kidney Disease-Mineral and Bone Disorder (CKD-MBD). Kidney Int Suppl. 2009(113):S1–130.
[78] Kazama JJ. Japanese society of dialysis therapy treatment guidelines for secondary hyperparathyroidism. Ther Apher Dial 2007;11(Suppl. 1):S44–7.
[79] Quarles LD, Lobaugh B, Murphy G. Intact parathyroid hormone overestimates the presence and severity of parathyroid-mediated osseous abnormalities in uremia. J Clin Endocrinol Metab 1992;75(1):145–50.
[80] Nakai S, Akiba T, Kazama J, Yokoyama K, Fukagawa M, Tominaga Y, et al. Effects of serum calcium, phosphorous, and intact parathyroid hormone levels on survival in chronic hemodialysis patients in Japan. Ther Apher Dial 2008;12(1):49–54.
[81] Kestenbaum B, Sampson JN, Rudser KD, Patterson DJ, Seliger SL, Young B, et al. Serum phosphate levels and mortality risk among people with chronic kidney disease. J Am Soc Nephrol 2005;16(2):520–8.
[82] Foley RN, Murray AM, Li S, Herzog CA, McBean AM, Eggers PW, et al. Chronic kidney disease and the risk for cardiovascular disease, renal replacement, and death in the United States medicare population, 1998 to 1999. J Am Soc Nephrol 2005;16 (2):489–95.
[83] Manjunath G, Tighiouart H, Ibrahim H, MacLeod B, Salem DN, Griffith JL, et al. Level of kidney function as a risk factor for atherosclerotic cardiovascular outcomes in the community. J Am Coll Cardiol 2003;41(1):47–55.
[84] Tornig J, Amann K, Ritz E, Nichols C, Zeier M, Mall G. Arteriolar wall thickening, capillary rarefaction and interstitial fibrosis in the heart of rats with renal failure:the effects of ramipril, nifedipine and moxonidine. J Am Soc Nephrol 1996;7 (5):667–75.
[85] Messa P, Macario F, Yaqoob M, Bouman K, Braun J, von Albertini B, et al. The OPTIMA study: assessing a new cinacalcet HCl (Sensipar/Mimpara) treatment algorithm for secondary hyperparathyroidism. Clin J Am Soc Nephrol 2008;3(1):36–45 [PMCID: 2390975].
[86] Chertow GM, Blumenthal S, Turner S, Roppolo M, Stern L, Chi EM, et al. Cinacalcet HCl hydrochloride (Sensipar) in hemodialysis patients on active vitamin D derivatives with controlled PTH and elevated calcium x phosphate. Clin J Am Soc Nephrol 2006;1(2):305–12.

[87] Ketteler M, Martin KJ, Cozzolino M, Goldsmith D, Sharma A, Khan S, et al. Paricalcitol versus cinacalcet HCl plus low-dose vitamin D for the treatment of secondary hyperparathyroidism in patients receiving haemodialysis: study design and baseline characteristics of the IMPACT SHPT study. Nephrol Dial Transplant 2011.

[88] Fishbane S, Shapiro WB, Corry DB, Vicks SL, Roppolo M, Rappaport K, et al. Cinacalcet HCl HCl and concurrent low-dose vitamin D improves treatment of secondary hyperparathyroidism in dialysis patients compared with vitamin D alone: the ACHIEVE study results. Clin J Am Soc Nephrol 2008;3(6):1718–25 [PMCID: 2572296].

[89] Block GA, Zeig S, Sugihara J, Chertow GM, Chi EM, Turner SA, et al. Combined therapy with cinacalcet HCl and low doses of vitamin D sterols in patients with moderate to severe secondary hyperparathyroidism. Nephrol Dial Transplant 2008;23(7):2311–8.

[90] Urena P, Jacobson SH, Zitt E, Vervloet M, Malberti F, Ashman N, et al. Cinacalcet HCl and achievement of the NKF/K-DOQI recommended target values for bone and mineral metabolism in real-world clinical practice–the ECHO observational study. Nephrol Dial Transplant 2009;24(9):2852–9.

[91] Wetmore JB, Liu S, Krebill R, Menard R, Quarles LD. Effects of cinacalcet HCl and concurrent low-dose vitamin D on FGF23 levels in ESRD. Clin J Am Soc Nephrol 2010;5(1):110–6 [PMCID: 2801647].

[92] Raggi P, Chertow GM, Torres PU, Csiky B, Naso A, Nossuli K, et al. The ADVANCE study: a randomized study to evaluate the effects of cinacalcet HCl plus low-dose vitamin D on vascular calcification in patients on hemodialysis. Nephrol Dial Transplant 2011;26(4):1327–39.

[93] Cunningham J, Danese M, Olson K, Klassen P, Chertow GM. Effects of the calcimimetic cinacalcet HCl HCl on cardiovascular disease, fracture, and health-related quality of life in secondary hyperparathyroidism. Kidney Int 2005;68(4):1793–800.

[94] Block GA, Zaun D, Smits G, Persky M, Brillhart S, Nieman K, et al. Cinacalcet HCl hydrochloride treatment significantly improves all-cause and cardiovascular survival in a large cohort of hemodialysis patients. Kidney Int 2010;78(6):578–89.

[95] Chertow GM, Pupim LB, Block GA, Correa-Rotter R, Drueke TB, Floege J, et al. Evaluation of Cinacalcet HCl therapy to lower cardiovascular events (EVOLVE): rationale and design overview. Clin J Am Soc Nephrol 2007;2(5):898–905.

[96] Kilpatrick RD, Danese MD, Belozeroff V, Smirnakis K, Goodman WG, Rothman KJ. The association of vitamin D use with hypercalcemia and hyperphosphatemia in hemodialysis patients: a case-crossover study. Pharmacoepidemiol Drug Saf 2011;20(9):914–21.

[97] Ketteler M, Petermann AT. Phosphate and FGF23 in early CKD: on how to tackle an invisible foe. Nephrol Dial Transplant 2011;26(8):2430–2.

[98] Finn W. Phosphorus binders: relative potency of available agents. Medscape Nephrology 2005.

[99] Joy MS, FWL-SG. Randomized, double-blind, placebo-controlled, dose-titration, phase III study assessing the efficacy and tolerability of lanthanum carbonate: a new phosphate binder for the treatment of hyperphosphatemia 2003;42(1):96–107.

[100] Lacour BLA, Auchere D, Ruellan N, de Serre Patey NM, Drueke TB. Chronic renal failure is associated with increased tissue deposition of lanthanum after 28-day oral administration. Kidney Int 2005;67:1062–9.

[101] Nolan C. Phosphate binder therapy for attainment of K/DOQI bone metabolism guidelines. Kidney Int 2005;68(Suppl. 96):S7–14.

[102] Cozzolino M. The effects of sevelamer hydrochloride and calcium carbonate on kidney calcification in uremic rats. J Am Soc Nephrol 2002;13:2299–308.

[103] Cheng SC, Young DO, Huang Y, Delmez JA, Coyne DW. A randomized, double-blind, placebo-controlled trial of niacinamide for reduction of phosphorus in hemodialysis patients. Clin J Am Soc Nephrol 2008;3(4):1131–8 [PMCID: 2440276].

[104] Takahashi Y, Tanaka A, Nakamura T, Fukuwatari T, Shibata K, Shimada N, et al. Nicotinamide suppresses hyperphosphatemia in hemodialysis patients. Kidney Int 2004;65(3):1099–104.

[105] Young DO, Cheng SC, Delmez JA, Coyne DW. The effect of oral niacinamide on plasma phosphorus levels in peritoneal dialysis patients. Perit Dial Int 2009;29(5):562–7.

[106] Sprague SM, Llach F, Amdahl M, Taccetta C, Batlle D. Paricalcitol versus calcitriol in the treatment of secondary hyperparathyroidism. Kidney Int 2003;63(4):1483–90.

[107] Steddon SJ, Schroeder NJ, Cunningham J. Vitamin D analogues: how do they differ and what is their clinical role? Nephrol Dial Transplant 2001;16(10):1965–7.

[108] Teng M, Wolf M, Lowrie E, Ofsthun N, Lazarus JM, Thadhani R. Survival of patients undergoing hemodialysis with paricalcitol or calcitriol therapy. N Engl J Med 2003;349(5):446–56.

[109] Henley C, Colloton M, Cattley RC, Shatzen E, Towler DA, Lacey D, et al. 1,25-Dihydroxyvitamin D3 but not cinacalcet HCl HCl (Sensipar/Mimpara) treatment mediates aortic calcification in a rat model of secondary hyperparathyroidism. Nephrol Dial Transplant 2005;20(7):1370–7.

[110] Moe SM, Chertow GM, Coburn JW, Quarles LD, Goodman WG, Block GA, et al. Achieving NKF-K/DOQI bone metabolism and disease treatment goals with cinacalcet HCl HCl. Kidney Int 2005;67(2):760–71.

[111] Foley RN, Li S, Liu J, Gilbertson DT, Chen SC, Collins AJ. The fall and rise of parathyroidectomy in U.S. hemodialysis patients, 1992 to 2002. J Am Soc Nephrol 2005;16(1):210–8.

[112] Malberti F, Marcelli D, Conte F, Limido A, Spotti D, Locatelli F. Parathyroidectomy in patients on renal replacement therapy: an epidemiologic study. J Am Soc Nephrol 2001;12(6):1242–8.

[113] Andress D. Vitamin D treatment in chronic kidney disease. Semin Dial 2005;18:315–21.

[114] Dawson-Hughes B, Heaney RP, Holick MF, Lips P, Meunier PJ, Vieth R. Estimates of optimal vitamin D status. Osteoporos Int 2005;16(7):713–6.

[115] Zisman AL, Hristova M, Ho LT, Sprague SM. Impact of ergocalciferol treatment of vitamin D deficiency on serum parathyroid hormone concentrations in chronic kidney disease. Am J Nephrol 2007;27(1):36–43.

[116] Stubbs JR, Idiculla A, Slusser J, Menard R, Quarles LD. Cholecalciferol supplementation alters calcitriol-responsive monocyte proteins and decreases inflammatory cytokines in ESRD. J Am Soc Nephrol 2010;21(2):353–61 [PMCID: 2834546].

[117] Nemeth EF, Heaton WH, Miller M, Fox J, Balandrin MF, Van Wagenen BC, et al. Pharmacodynamics of the type II calcimimetic compound cinacalcet HCl HCl. J Pharmacol Exp Ther 2004;308(2):627–35.

[118] Colloton M, Shatzen E, Miller G, Stehman-Breen C, Wada M, Lacey D, et al. Cinacalcet HCl HCl attenuates parathyroid hyperplasia in a rat model of secondary hyperparathyroidism. Kidney Int 2005;67(2):467–76.

[119] Block GA, Martin KJ, de Francisco AL, Turner SA, Avram MM, Suranyi MG, et al. Cinacalcet HCl for secondary hyperparathyroidism in patients receiving hemodialysis. N Engl J Med 2004;350(15):1516–25.

[120] Charytan CCJ, Chonchol M, Herman J, Lien YH, Liu W, Klassen PS, et al. Cinacalcet HCl hydrochloride is an effective treatment for secondary hyperparathyroidism in patients with CKD not receiving dialysis. Am J Kidney Dis 2005;46:58–67.

CHAPTER

92

Hematopoiesis and the Kidney

Armin Kurtz, Roland H. Wenger and Kai-Uwe Eckardt

Institute of Physiology, University of Regensburg, Regensburg, Germany
Institute of Physiology, University of Zurich, Zurich, Switzerland
Department of Nephrology and Hypertension, Friedrich-Alexander-University Erlangen-Nuremberg, Erlangen, Germany

INTRODUCTION

During ontogeny, hematopoiesis—comprising erythropoiesis, granulocytopoiesis, and thrombopoiesis—is initiated in the blood islands of the yolk sac before the development of the kidneys. Later during gestation, at a time when hematopoiesis is fully established in the bone marrow, the kidney starts to play an important role in the control of erythro- and thrombopoiesis. This control is achieved through renal production of the hematopoietic growth factors erythropoietin and thrombopoietin. Thus, in addition to its role in waste excretion and water and electrolyte homeostasis, the kidney is also important in tissue oxygenation and coagulation.

With the exception of the growth period, the circulating red blood cell (RBC) mass, and hence the oxygen-carrying capacity of the blood, is normally fairly constant. Since the erythron is a continuously regenerating organ, a daily production of 20 ml of red blood cells is required in human adults to compensate for the physiologic demise of 120-day-old erythrocytes. In addition, when increased blood loss occurs or the oxygen saturation of hemoglobin falls, the bone marrow is capable of increasing this normal production rate of red blood cells three- to five-fold within a few days, and even up to seven-fold under chronic conditions. Similarly, the number of circulating platelets is kept constant (although in a wider range than red blood cells), and any decrease of platelet number results in activation of thrombocytopoiesis.

The predominant and essential regulators of red cell and platelet formation, erythropoietin and thrombopoietin are true hormones that are produced outside the bone marrow, and mainly in the kidney and in the liver.

This chapter is designed to summarize current knowledge about the specific role of the kidney in the humoral control of hematopoiesis both under physiologic and pathophysiologic conditions.

ERYTHROPOIESIS

Erythropoietin

Background

More than hundred years ago after the relationship between high altitude and inadequate tissue oxygenation was realized, it was postulated that hypoxia accounts for the adaptive increase in red cell mass that occurs during altitude exposure. While it was primarily believed that low oxygen pressure directly stimulates the bone marrow, the existence of a plasma factor regulating erythropoiesis was inferred from experiments in the early twentieth century,[1] and the term "erythropoietin" was coined to describe this putative factor.[2] However, it took another 50 years until convincing evidence was obtained for humoral oxygen-dependent control of erythropoiesis. At that time, Erslev[3] was able to stimulate erythropoiesis in rabbits temporarily through the injection of plasma from anemic donor animals, and Reissman[4] observed increased red cell formation in parabiotic rats kept at normal levels of oxygen when their partners were maintained in a hypoxic atmosphere. Surprisingly, it was found that—in addition to insufficient oxygen supply—the transition metal cobalt is also capable of inducing erythropoietin formation *in vivo*.[5] Systemic organ ablation analysis then revealed that the capability of the organism to

Seldin and Giebisch's The Kidney, Fifth Edition.
DOI: http://dx.doi.org/10.1016/B978-0-12-381462-3.00092-6

© 2013 Elsevier Inc. All rights reserved.

elaborate erythropoietin in response to anemia or to cobalt is markedly attenuated in bilaterally nephrectomized rats.[6] This was the starting point to consider a direct regulatory role of the kidney for erythropoiesis and a complement to the observation made much earlier that patients with kidney disease are usually anemic.[7] Nevertheless, the knowledge about erythropoietin remained rather limited, and erythropoietin was considered as an "elusive" hormone. This becomes understandable because the plasma concentration in healthy mammals is around a few femtomoles per milliliter. Continuous efforts to purify erythropoietin from the plasma of anemic animals have therefore not been successful, but provided very helpful information about the physicochemical properties of erythropoietin. Using the information that erythropoietin is a heat-stable acidic glycoprotein, Miyake et al.[8] then succeeded to purify human erythropoietin to apparent homogeneity from about 2500 liters of urine of patients suffering from severe aplastic anemia and obtained a few milligrams of the hormone. These small amounts allowed them to determine critical amino acid sequences, and with the help of recombinant DNA techniques, two groups independently succeeded to clone the human erythropoietin gene in 1985.[9,10] The knowledge of the genomic and complementary DNA sequence of erythropoietin and the availability of pure recombinant erythropoietin initiated a burst of activity leading to a greatly improved knowledge base about erythropoietin itself—action, regulation, and clinical use—and overall this work confirmed the important role of the kidneys as the primary site of erythropoietin production.

Structure of Erythropoietin

To the present, evidence for the existence of erythropoietin has been obtained for mammals. Whether *erythropoietin* also exists in lower organisms or in all vertebrates is not yet known. Evidence for erythropoietin genes was also reported for teleosts including fugu, zebra fish and trout.[11] Interestingly, this gene was found to be mainly expressed in the kidney, which is also an erythropoietic organ in these teleost fish.[12] Recently also erythropoietin of Xenopous laevis has been characterized.[13] The amino acid sequences of erythropoietin in mammals show a high degree of interspecies similarity. First, erythropoietin is generally synthesized as pre-erythropoietin that contains a typical endoplasmatic leader sequence of 25–27 amino acid residues that is cleaved off during intracellular processing. Second, the size of native erythropoietin is similar if not identical among species and comprises 165–167 amino acids. It was shown that the carboxy-terminal arginine of human erythropoietin is deleted from the molecule,[14] so that the 165 amino acids may be the species-independent length of circulating erythropoietin. Third, the overall structure of the molecule is highly conserved.[15,16] For example, out of 15 amino acid replacements between human and monkey and 41 replacements between human and mouse, roughly 50% are conservative. The high sequence conservation also explains the interspecies cross-reactivity of erythropoietin. From bioassays for erythropoietin, it is known that human, rat, monkey, dog, and rabbit erythropoietin are active in the mouse, and human erythropoietin also stimulates erythropoiesis in ewes, cats, and dogs. In keeping with the high degree of conservation, erythropoietin also shows no homology with other known proteins,[9,10] with the exception only of thrombopoietin.

Erythropoietin has a four-helical bundle structure with two disulfide bonds[17] (Fig. 92.1). One disulfide bridge between cys 7 and cys 161 links the N-terminus and the carboxy-terminus of the molecule together, generating a long loop. This disulfide bridge is fully conserved in mammals[16] and it appears therefore as if

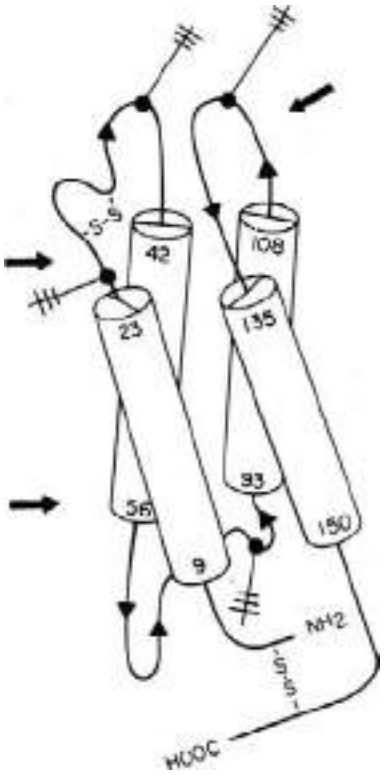

FIGURE 92.1 Predicted three-dimensional structure of the human erythropoietin molecule. The molecule appears as a four-helix structure, with four antennas of sugar side chains and two intramolecular loops formed by disulfide bridges. *(From Goldwasser E. The structure-function relationship of erythropoietin. In: Erslev AJ, Adamson JW, Eschbach JW, Winearls CG, eds, Erythropoietin: Molecular, Cellular, and Clinical Biology. Baltimore: Johns Hopkins University Press; 1991: pp. 41–52.)*

formation of the long loop is essential for the biologic activity of erythropoietin.

Erythropoietin is heavily glycosylated and different carbohydrate chains attached to the molecule contribute more than 40% to the total molecular weight of 30,400 Daltons. The protein backbone contains three highly conserved sites of N-glycosylation, to which sugar side chains are attached (Asn 24, 38, 83).[16,18] In addition, human but not mouse erythropoietin also contains a serine (Ser 126) as a possible O-linked glycosylation site, which bears a small oligosaccharide chain.

The oligosaccharide structures of recombinant human and native urinary erythropoietin have been determined[19,20] and were found to be rather similar. On average, one molecule of recombinant human erythropoietin contains 3 fructose, 10 mannose, 13 galactose, 16 N-acetylglucose, and 13 sialic acid molecules. The major component of the O-linked sugar is a disialyl chain.[21] The N-linked side chains are predominantly organized as tetra-antennaries (about 80%) and to a minor extent only as tri- (15%) or bi-antennaries (1–6%).[20,22] All of these saccharides are sialylated, although to a different extent. The distribution of different sugar chains varies at each glycosylation site. Chains at position Asn-38 are more heavily sialylated and less frequently of biantennary structure than those at Asn-24. Oligosaccharides at position Asn-83 are relatively homogenous tetra-antennary chains without polylactosaminyl repeats.[19] The glycosylation of erythropoietin results in slight heterogeneity of erythropoietin molecules. Interestingly, clear differences were found in the distribution of oligosaccharide components of urinary erythropoietin among individuals.[22]

The carbohydrates appear to be of considerable importance for the biologic activity of the hormone. Removal of the terminal sialic acids also increases the biologic activity of erythropoietin *in vitro* about two- to three-fold.[23] The carbohydrate moieties of erythropoietin therefore appear not to be essential for binding of erythropoietin to its receptor or the subsequent cellular signaling and may even inhibit both steps. However, *in vivo* the carbohydrate moiety is essential for the availability of erythropoietin for its target structures. Full deglycosylation abolishes the *in vivo* activity of erythropoietin, and removal of terminal sialic acids inactivates the hormone by shortening its biologic half-life in the circulation from about six hours to a few minutes.[23,24] The liver contains asialo-glycoprotein receptors that clear glycoproteins with free galactosyl residues from the circulation, and clearance through these receptors presumably causes the dramatic shortening of the biologic half-life of asialo-erythropoietin *in vivo*.[23,24] How and where this modified erythropoietin and the fully deglycosylated erythropoietin are cleared from the circulation is not yet known.

Biologic Effects of Erythropoietin

Hematopoiesis: Erythropoietin is absolutely necessary for erythropoiesis, particularly for the later stages of erythroid differentiation, and therefore is essential for life. Mice with disrupted erythropoietin or erythropoietin receptor genes[25–27] die from anemia at an embryonic stage of 12–13 days after fertilization because they cannot develop definitive erythropoiesis.

Erythropoiesis appears as a hierarchy of cell divisions and cell differentiations starting from the pluripotent stem and ending with the erythrocyte as a highly differentiated and specialized cell (Fig. 92.2). The pluripotent stem cell, which has the capability for self-renewal, feeds into three hematopoietic lineages, namely the megakaryocytic pathway, the granulocyte-macrophage pathway, and the erythroid pathway. For the erythroid lineage cells can be identified morphologically by specific markers at the state of the proerythroblast, which develops into the basophilic erythroblast and begins to produce hemoglobin. Downstream of the erythroblast stages, the erythroid lineage is not regulated significantly by erythropoietin, nor does the commitment of pluripotent stem cells into the erythroid lineage require erythropoietin.[28] The self-renewal of committed early erythroid progenitors is induced by the receptor tyrosine kinase c-ErbB,[29] whereas the downstream initiation of the erythroid differentiation program is then regulated by c-Kit and erythropoietin receptors. Thus, the main action

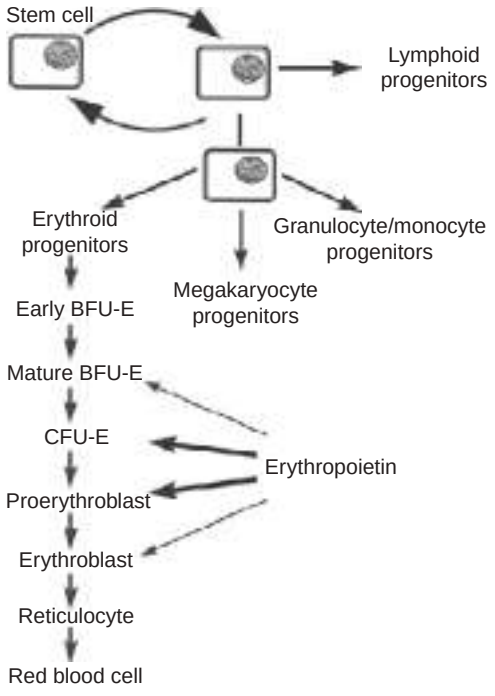

FIGURE 92.2 Schematic demonstration of differentiation steps of erythropoiesis and the action sites of erythropoietin.

of erythropoietin for erythropoiesis occurs on erythroid progenitors at stages between early committed erythroid precursors on the one side and the proerythroblasts on the other. Information about growth and differentiation of these cells has predominantly been obtained with cell cultures of hemopoietic cells. From those experiments, the existence of a rather early erythroid progenitor was inferred that was termed burst-forming unit erythroid (BFU-E), which has an abundance of about 0.01% among the nucleated cells of the bone marrow. Within 1 week of cell culture, a burst containing multiple subcolonies in clusters with up to 104 cells develops from one BFU-E. Hypertransfusion and acute erythropoietic stress have only a transient effect on BFU-E, suggesting that this progenitor cell is not dependent on ambient levels of erythropoietin for maintenance of its numbers. *In vitro*, the early divisions of this progenitor and the development of erythroid bursts essentially require interleukins, in particular IL-3, but are independent on erythropoietin. Final maturation and hemoglobinization of the cells of the burst are erythropoietin dependent. Hemoglobin synthesis begins at the stage of the proerythroblast and the cell population at this stage is considered as the main target for erythropoietin. *In vitro*, these cells are reflected by the colony-forming unit erythroid (CFU-E). In the normal bone marrow, about 0.1−0.2% of nucleated cells are CFU-E. The cells have limited proliferative potential, probably not more than six or seven cell divisions. Thus, CFU-E-derived colonies generally contain 60 to 120 hemoglobinized cells. Colony formation *in vitro* is essentially dependent on erythropoietin, and is positively modulated by insulin-like growth factor I.[30] CFU-E has the highest density of erythropoietin receptors within the normal erythroid precursor population, and is very sensitive toward erythropoietin. *In vivo*, the abundance of CFU-E is dependent on erythropoietin, such that the number of CFU-E increases during bleeding or hemolytic anemia and also in response to erythropoietin injection, whereas hypertransfusion-induced polycythemia results in a 70−80% reduction in the number of CFU-E in marrow and spleen. In summary, erythropoietin acts on erythropoiesis mainly by regulating the pool size of CFU-E, which then undergoes terminal differentiation into erythrocytes.

Expansion and maturation of the CFU-E pool implies three major effects of erythropoietin. First, erythropoietin increases the survival rate of erythroid progenitors and in line with this assumption evidence has been elaborated that erythropoietin prevents apoptosis in erythroid precursors.[31] Second, erythropoietin actively induces mitosis in erythroid precursors[32] with a preceding stimulation of RNA polymerase activity and subsequent DNA synthesis[33] and cell division. Third, erythropoietin initiates differentiating events such as the expression of globin chains, hemoglobin synthesis, transferrin receptor synthesis, and the synthesis of integral erythrocyte membrane proteins.[34] After induction by erythropoietin hemoglobin synthesis persists and becomes independent of the presence of erythropoietin. High doses of erythropoietin also stimulate platelet formation[35,36] and erythropoietin binding sites have been reported on megakaryocytes.[37] In view of the structural similarity between erythropoietin and thrombopoietin, one could imagine that this effect is at least in part due to cross-activation of the thrombopoietin receptor by erythropoietin.

Effects of erythropoietin unrelated to hematopoiesis: A steadily increasing number of reports clearly indicates that erythropoietin is involved in a number of effects outside the hemopoietic tissues, such as on the vasculature, the brain, the myocardium and else. There it may stimulate proliferation and inhibit apoptosis. For more detailed information, the reader is referred to recent reviews on this topic.[38−42]

Erythropoietin Receptor

Distribution: The biologic effect of erythropoietin is mediated by specific binding sites at the surface of its target cells. Erythropoietin binding sites have been identified on erythroid precursors, on megakaryocytes,[37] endothelial cells,[43−45] in distinct areas of the brain,[46] cultured neurons,[47] and placenta.[48]

The expression of the erythropoietin receptor is crucial for definitive erythropoiesis *in vivo*, since disruption of erythropoietin receptor gene leads to death around embryonic day 13. Primitive erythropoiesis in the yolk sac, however, proceeds in the absence of erythropoietin receptors. Erythropoietin receptors are also not required for erythroid lineage commitment nor for the proliferation and differentiation of BFU-E to CFU-E, but they are crucial *in vivo* for the proliferation and survival of CFU-E progenitors and their irreversible terminal differentiation. In line with this functional dependence, erythropoietin receptors are mainly found on erythroid precursors of the CFU-E stage. Nonetheless, compared with other cell surface receptors, CFU-E express a comparatively small number of erythropoietin receptors with 800−1200 binding sites per cell. The binding sites appear to occur with two distinct affinities, a high-affinity one with a dissociation constant below 100 pmol/liter and a low-affinity one with a dissociation constant higher than 300 pmol/liter. Binding sites with both affinities can be found on the same cell, and it is thought that the erythropoietic activity is mainly mediated via the high affinity binding site, because cells lacking these binding sites fail to differentiate in response to erythropoietin.

Erythropoietin receptor gene and protein: Erythropoietin binds and activates a high-affinity receptor (EpoR) present on the surface of immature erythroid cells,[49,50] exerting four known effects on erythroid progenitors, namely maintenance of viability, promotion of cell division, increase of hemoglobin synthesis, and fostering of morphological maturation. No other cytokine receptors can replace the erythropoietin receptor, because mice homozygous for deletions of the EPO or EPO receptor genes die at embryonic day 12.5 owing to severe anemia.[28] In these mice, erythropoiesis progresses through the BFU-E stage, but terminates at the colony forming unit-erythroid (CFU-E) and erythrocytes are not formed, demonstrating an absolute requirement of the EPO receptor for later stages of red blood cell development.[28] The EPO receptor belongs to the cytokine receptor superfamily.[51,52] Cytokine receptor signal transduction is mediated by cytoplasmic protein tyrosine kinases of the JAK family, found associated with individual receptor subunits (Fig. 92.3).[53]

The erythropoietin receptor genes exist as single copies and encompass eight exons.[50,54–56] In all species the cDNA encode with a high degree of interspecies homology a 507–amino acid protein of 55 kDa, which is modified by glycosylation and phosphorylation to 72–78 kDa.[57]

The EPO receptor does not have an intrinsic enzymatic activity; however, numerous signaling proteins

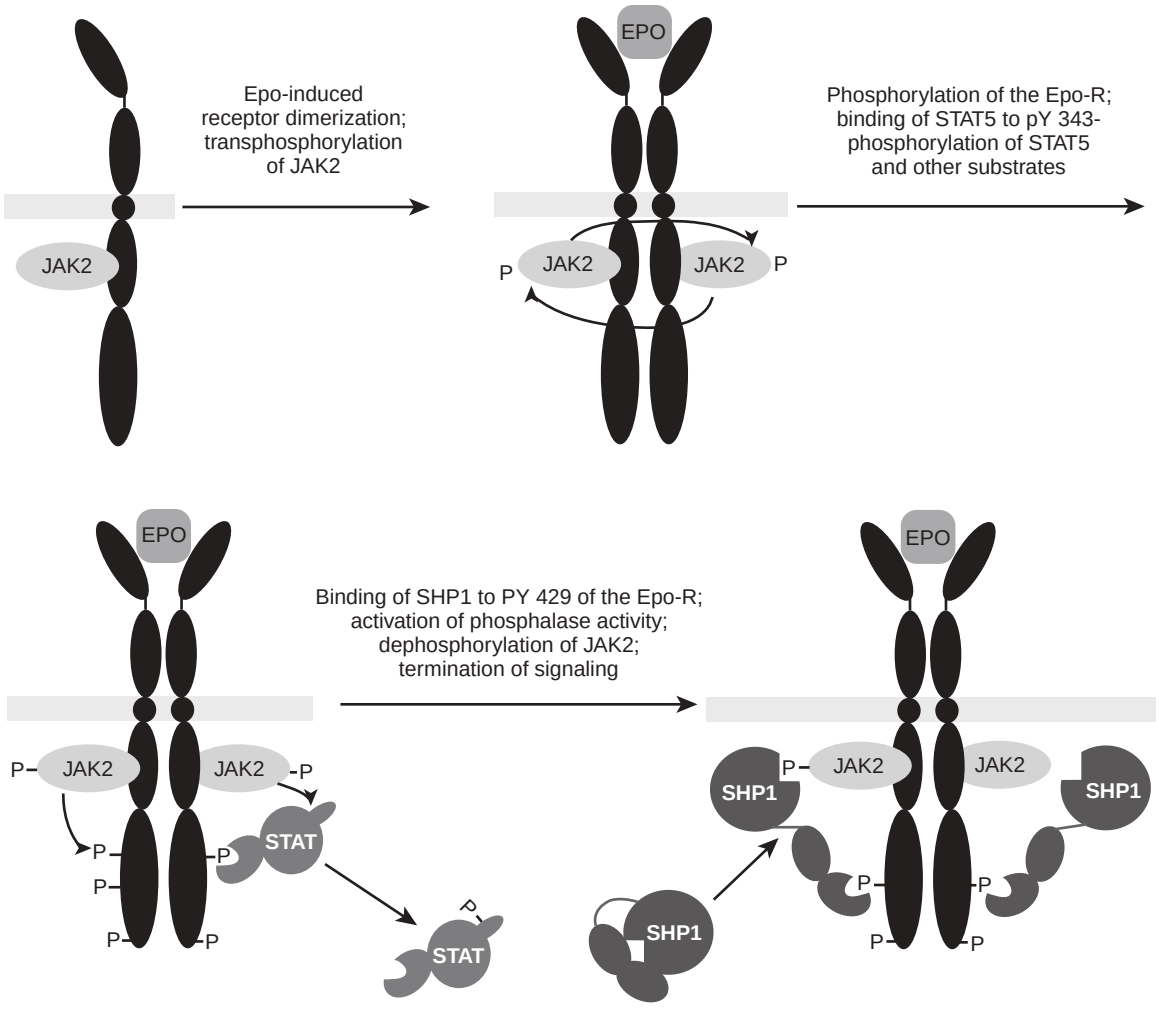

FIGURE 92.3 Model for activation and inactivation of the erythropoietin receptor. Binding of EPO induces receptor dimerization and auto- or trans-phosphorylation of the Janus family kinase, JAK2. JAK2 or another kinase then phosphorylates several tyrosine residues in the EpoR, creating docking sites for the SH2 domains of several signal transduction proteins, including STAT5. Once bound to the EpoR, STAT5 and other signaling proteins become phosphorylated and activated; phosphorylated STAT5 dissociates from the receptor, dimerizes, moves to the nucleus, and activates gene expression. The protein tyrosine phosphatase, SHP1, binds to a segment of the EPO receptor containing phosphotyrosine 429. Binding induces activation of the phosphatase, removal of the activating phosphate from JAK2, and termination of signal transduction. *(With permission from Stefan N, Constantinescu SN, Ghaffari S, Lodish HF. The erythropoietin receptor: structure, activation and intracellular signal transduction. Trends Endocrinol Metab 1999;10:18–23.)*

and the receptor itself are phosphorylated as a result of EPO stimulation. Like other members of the cytokine receptor family, such as receptors for growth hormone, prolactin, granulocyte colony-stimulating factor (G-CSF) and thrombopoietin, EpoR forms ligand-induced homodimers. EPO binding results in homodimerization of EpoR chains, which is critical for Jak2 (associated with the EpoR cytoplasmic tail) activation and the initiation of intracellular signaling.[58] JAK2 is rapidly phosphorylated in response to EPO stimulation. JAK2 is the primary kinase responsible for phosphorylation of the EPO receptor[58,59] and is essential for erythropoiesis.[60,61]

Erythropoietin receptor modifications: Mutations in the extracellular domain of the EpoR within the dimer interface renders the receptor constitutively active[62] as a result of the formation of an intermolecular disulfide bond.[58] The carboxyterminal end of the erythropoietin receptor appears to contain an inhibitory signaling element.[62] A hereditary truncation of the erythropoietin receptor at the COOH end has been discovered that is associated with increased affinity of the receptor and with erythrocytosis.[63,64] Similar to other members of the hematopoietin receptor family such as interleukins or thrombopoietin,[65] a naturally occurring soluble form of the membrane-bound receptor for erythropoietin has been found in the serum.[66] It has a molecular mass of 34 kD, is related to the extracellular domain of the erythropoietin receptor, and increased concentrations are found with enhanced erythropoiesis.[66] The physiological role of these soluble receptors and potential modes of action, however, are not yet understood.

Regulation of Erythropoietin Production

Sites of erythropoietin production: During fetal life the liver appears to be the predominant site of erythropoietin production. This has been shown for sheep and rats,[67,68] and the relevance of the liver for erythropoietin formation in the human fetus may be assumed from the fact that the cDNA for human erythropoietin has been cloned from human fetal liver.[9] Investigations in fetal sheep[69] revealed that the kidneys are also significant production sites for erythropoietin, particularly during the first half of gestation. In sheep and rat, a predominance of hepatic erythropoietin formation was found to last beyond birth,[68,70–72] whereas in mice the majority of erythropoietin mRNA has been observed in the kidneys from mid-gestation on.[73] An analysis performed in rats revealed that the kidney steadily increases its capacity for erythropoietin mRNA expression from birth on until adulthood, whereas the hepatic erythropoietin mRNA concentration changes less dramatically postpartum and even decreases when adulthood has been reached.[71]

The kidney overtakes hepatic erythropoietin mRNA three weeks after birth. Although species differences in the timing of the switch and the degree of contribution of the liver to total body EPO mRNA content exist,[69] the switch is undoubtedly found in humans as well.[74]

The reasons for the postnatal increase of renal erythropoietin formation may be related to the fact that in some species the kidney is not fully mature at birth. Once the kidney has gained its full function for waste excretion and salt and water homeostasis, the maximal capacity for erythropoietin has been reached. Apparently changes of organ oxygenation are not a major trigger for the switch from liver to kidney.[75] Based on experiments in anephric animals, the adult liver was generally assumed to contribute no more than about 15% to erythropoietin production.[6,67,68] However, this experimental approach may underestimate the hepatic contribution in intact organisms, because hepatic erythropoietin mRNA accumulation was found to be reduced after bilateral nephrectomy.[71] In intact adult rats erythropoietin mRNA amounts to about 30−40% of the total under conditions of severe hypoxic stimulation.[71,76] However, the hepatic contribution depends on the severity of the stimulus applied and is less significant, that is, below 20% of the total under mild hypoxia. This suggests that the liver is less sensitive in terms of hypoxia-induced erythropoietin formation than the kidneys, and it might help to explain why the liver, despite its large potential for erythropoietin mRNA expression, does not compensate for failure of the renal production site.

Cellular production sites in the kidney: In contrast to a number of other hormones, erythropoietin does not appear to be stored in the cells producing it. Consequently, almost no erythropoietin can be extracted from the liver and kidney of normoxic animals.[77–79] Attempts to localize erythropoietin by means of immunohistochemistry in normoxic and hypoxic animals have revealed inconclusive results. In situ hybridization studies localized erythropoietin mRNA to peritubular cells in the renal cortex.[80–82] Likely, peritubular interstitial fibroblasts are production sites for erythropoietin.[80] In this context colocalization was demonstrated for erythropoietin mRNA and the enzyme 5′-ectonucleotidase,[83] which is expressed on peritubular fibroblasts, but not on endothelial cells[84] (Fig. 92.4). The same conclusion about the peritubular fibroblast as production site for erythropoietin has been reached in an elegant approach of marker gene expression in mice bearing a transgene of erythropoietin/SV-40 T. In response to anemia or hypoxia the expression of the EPO-TAg gene was induced, and SV-40 T antigen accumulated in nuclei of peritubular cortical fibroblasts expressing 5′-nucleotidase, but not in other peritubular cell types.[85] Erythropoietin gene expression has been demonstrated in interstitial,

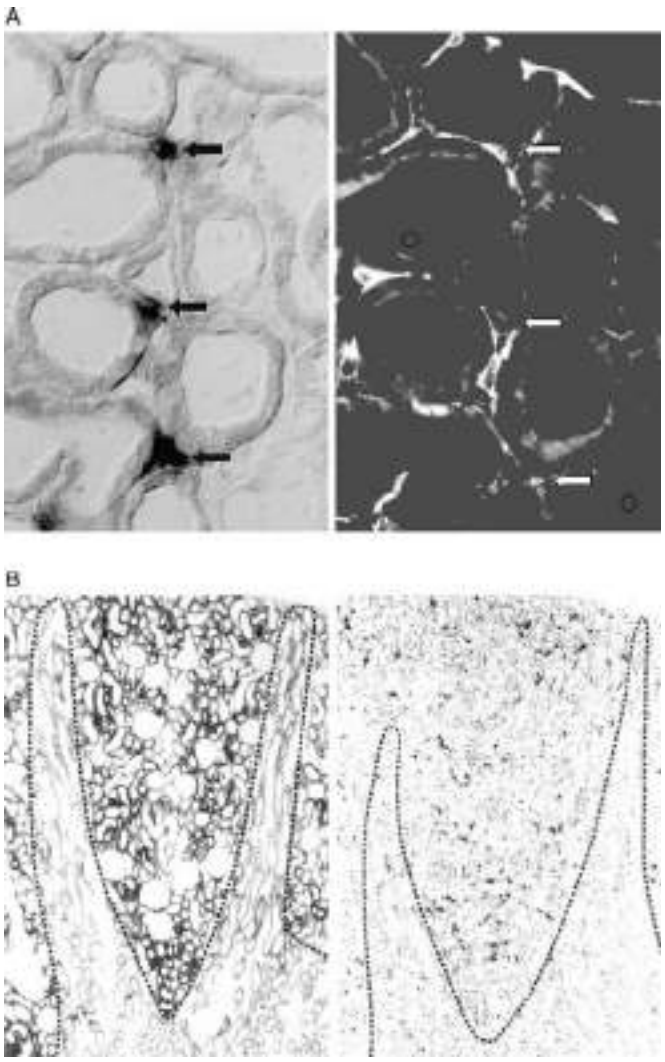

FIGURE 92.4 A: Detailed localization of erythropoietin-producing cells in the kidney. Combined in situ hybridization and immunohistochemistry on the same tissue section taken from anemic rat renal cortex. Left: Demonstration of erythropoietin mRNA. Right: Double-labeling on the same tissue section with antibody to 5′-ectonucleotidase. Cells positively stained with either technique are indicated by arrowheads. Only a minor proportion of 5′-ectonucleotidase-positive interstitial cells reveal erythropoietin mRNA expression. Double-labeled cells typically lie in angles between adjacent tubules, or between vessels and tubules. (Magnification × 800.) (*Courtesy of S. Bachmann, Berlin.*) B: Topography of the production of erythropoietin in the rat kidney. Left: The cortical labyrinth is well visualized using an enzyme histochemical technique for 5′-nucleotidase, with the strong reaction seen as black deposits in the proximal convoluted tubule and in the fibroblasts. Right: In situ hybridization of erythropoietin-mRNA in the kidney of an anemic rat. The comparison of the two micrographs shows that hybridization took place in the cortical labyrinth (delimited with a dotted line), but not in the medullary rays or in the outer medulla. (Magnification: A ~ ×62, B ~ ×95.) *(With permission from LeHir M, Eckardt KU, Kaissling B, Koury ST, Kurtz A. Structure–function correlations in erythropoietin formation and oxygen sensing in the kidney. KlinWochenschr 1991;69:567–575.)*

nonendothelial cells in normal human kidneys,[86] as well as in the walls of renal cysts of patients with polycystic kidney disease.[87] Similarly, renal erythropoietin has been localized in cortical interstitial cells in monkey[88] and sheep.[89] Although fibroblasts are widely distributed in the kidney both in the cortex and in the medulla, erythropoietin production appears to be confined to a special subset of fibroblasts in particular locations. Thus, cells expressing erythropoietin mRNA are generally not found in the inner renal medulla.[80,82,90] At least in rats, they are not present in the outer medulla, and within the renal cortex they have almost exclusively been found in the cortical labyrinths created by the convoluted tubules, and not in the medullary rays.[90] Even under severe hypoxia, however, only a minority of interstitial fibroblasts in the peritubular cortical labyrinth express erythropoietin mRNA.[83,91]

In addition, there are reports about enhanced expression of erythropoietin mRNA in human hypernephromas, and in one tumor, erythropoietin mRNA was clearly localized to epithelial tumor cells,[92] indicating that tubular cells may acquire the ability to produce erythropoietin with malignant transformation.

Cellular production sites in the liver: Within the liver at least two different cell types can express the erythropoietin gene. In situ hybridization in anemic rats demonstrated erythropoietin mRNA in hepatocytes, as well as in an interstitial cell type.[93] Similarly, in severely anemic mice transfected with the human erythropoietin gene, human erythropoietin mRNA was mainly localized to hepatocytes and to a lesser extent to an interstitial cell type, while endogenous mouse erythropoietin mRNA was not demonstrable in these animals.[94] That hepatocytes are a site of erythropoietin production was further confirmed by mRNA analysis in cells isolated from hypoxic rat livers, and the observation that in freshly isolated hepatocytes from normoxic animals erythropoietin mRNA expression can be stimulated by hypoxia *in vitro*.[95]

In contrast, the abovementioned mice bearing a erythropoietin SV-40 T gene construct were found to express the T40 antigen in Ito cells of the liver following stimulation by hypoxia or anemia,[96] indicating that these perisinusoidal cells represent the nonparenchymal cell population that produces erythropoietin in the liver. Moreover, in isolated Ito cells in culture, erythropoietin mRNA expression can be induced by hypoxia.[97] Interestingly, the Ito cells of the liver share similarities with the renal peritubular cells expressing the erythropoietin gene. In particular, the Ito cells, like the peritubular fibroblasts in the renal cortex, express 5′-ectonucleotidase.[98]

Other cellular production sites: Apart from liver and kidneys, small amounts of erythropoietin mRNA have also been observed in other organs such as the

lung, spleen, heart, and bone marrow.[99] In these organs, erythropoietin mRNA expression is stimulated by anemia or hypoxia and thus apparently regulated like in the kidney and the liver (see below). The physiological relevance of erythropoietin formation in organs other than liver and kidney is probably a para/autocrine one such as in the bone marrow. For the heart, EPO appears to be necessary for proper cardiac morphogenesis,[27] and might protect the myocardium from ischemia reperfusion injury.[70]

EPO expression in the reproductive tract[100–103] and in the brain[99,102,104–106] has been extensively considered. EPO is expressed in the central nervous system in the human fetus early in gestation,[104,107] suggesting a central role for normal brain development.[108] In addition, EPO has been found to be neuroprotective, particularly in situations of insufficient oxygen supply to the brain.[109–111] For the female reproductive tract, regulated expression of EPO in the uterus[103] and the oviduct of the mouse[101] has been found. The human endometrium expresses EPO throughout the menstrual cycle, with higher levels in the secretory than in the proliferative phase.[112] Along the same lines, estrogens stimulate EPO expression in the mouse oviduct and uterus,[101,103] but neither in the brain nor in the kidney.[113] Functionally, EPO appears to play an important role for endometrial angiogenesis and thus reproductive function.[103] EPO mRNA expression has been found in the human, murine, and ovine placenta, as well as on both the maternal and the fetal sides.[73,114–116] In addition, EPO exerts a trophic effect on the fetal gastrointestinal tract when taken up enterally from the amniotic fluid.[117]

Physiological determinants regulating erythropoietin production: Numerous experimental and clinical studies have developed the concept that circulating erythropoietin levels in turn are related to a balance of tissue oxygen supply and oxygen need. As a consequence, erythropoietin appears to carefully adapt red blood cell formation to meet the oxygen requirements of the organism. Comparing the role of both oxygen supply and demand for erythropoietin concentrations, the influence of oxygen supply appears to be of major importance. It has been established that reductions of oxygen supply either by anemia or by a fall of the arterial oxygen tension are by far the most powerful stimuli for elevations of the circulating erythropoietin concentration. Apart from these classic stimuli, it was recognized early on that the pharmacological application of certain transition metals, in particular cobalt[5] induces significant and reproducible elevations of circulating erythropoietin levels.

Effect of arterial oxygen tension: Both hypobaric normobaric hypoxia stimulate erythropoietin levels to a similar extent indicating that, it is a decline in alveolar oxygen tension and consequently a fall in arteriolar oxygen tension that stimulate erythropoietin levels.[118] Following a sudden fall of inspiratory, and subsequently, arterial oxygen tension plasma, erythropoietin levels start to rise after 60–90 minutes and then increase approximately linearly. The slope of this increase is dependent on the severity of hypoxia, a maximum value is reached between 12 and 24 hours in rodents[119–123] and within 48 hours in humans;[119,124] thereafter, erythropoietin declines to a steady-state level that is well below peak concentration, but still elevated above baseline and inversely related to the severity of hypoxia (Fig. 92.5A). Since the decline of plasma erythropoietin levels, which occurs long before an increase in red cell mass, proceeds in parallel with decreases in renal and hepatic erythropoietin mRNA levels,[123] it is reasonable to assume that the production of erythropoietin is downregulated during prolonged hypoxia. It has been excluded in this context that the downregulation of erythropoietin production is causally related to erythropoietin itself in the sense of a negative feedback,[123] and it is likely therefore that a desensitization of the cellular oxygen sensing mechanism occurs during continuous hypoxia (see below). Once plasma erythropoietin concentrations have moved out of the normal range, they are inversely related to the alveolar or arterial oxygen tension at any time after onset of hypoxia.[123,125]

The influence of oxygen tension on plasma erythropoietin concentrations is quite characteristic in the way that a lowering of the oxygen tension to about half of the normal value only exerts a rather small effect on circulating erythropoietin levels. A fall of inspiratory oxygen tensions below this threshold then induces an almost exponential increase of plasma erythropoietin concentration in humans and in laboratory animals.[123,125] The arterial oxygen tension, however, does not appear to directly influence erythropoietin levels, since the stimulation of plasma erythropoietin by inspiratory hypoxia is attenuated by polycythemia.[118,126] In conclusion, it appears therefore that the effect of the oxygen tension on erythropoietin concentrations is indirectly mediated by a process essentially involving the number of red blood cells.

Effect of blood oxygen-carrying capacity: The relevance of the red cell count for the plasma erythropoietin concentration is known based on numerous observations that anemias of various etiology (with the exception of renal anemia) are associated with elevated plasma erythropoietin levels, while states of primary polycythemia move in parallel with subnormal erythropoietin concentrations.[127,128] In principle, anemia could lead to an elevation of plasma erythropoietin levels by reduction of the oxygen-carrying capacity of the blood, as well as by the fall of the number of circulating red blood cells per se. This latter possibility is not trivial

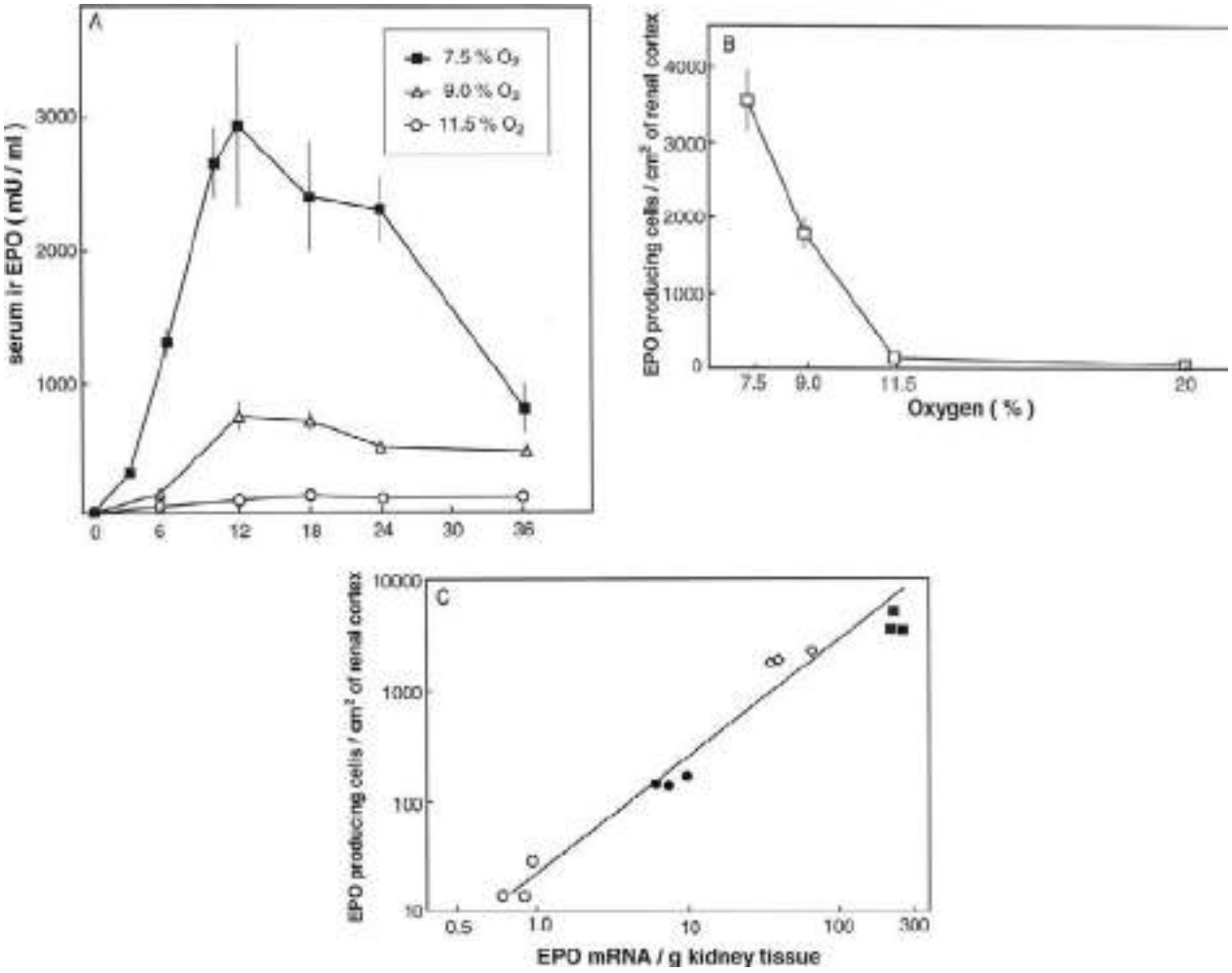

FIGURE 92.5 A: Influence of the oxygen tension on serum erythropoietin levels in rats. Time-dependent change in serum immunoreactive erythropoietin in rats exposed to different oxygen concentrations in a normobaric atmosphere. Total gas pressure was kept constant by balance nitrogen. *(With permission from Eckardt KU, Dittmer J, Neumann R, et al. Decline of erythropoietin formation at continuous hypoxia is not due to feedback inhibition. Am J Physiol 1990;258:1432–1437.)* B: Oxygen dependency of the number of erythropoietin-expressing cells in rat kidney cortex. Relationship between the number of erythropoietin producing cells per square centimeter of renal cortex and oxygen concentrations in rats exposed to different oxygen concentrations in a normobaric atmosphere for 8 hours. *(With permission from Eckardt KU, Koury ST, Tan CC, et al. Distribution of erythropoietin producing cells in rat kidneys during hypoxic hypoxia. Kidney Int 1993;43:815–823.)* C: Correlation between number of erythropoietin-expressing cells in kidney cortex and whole-kidney erythropoietin mRNA. Relationship between the number of erythropoietin-producing cells per square centimeter of renal cortex in one kidney and erythropoietin mRNA concentrations in the contralateral kidney in individual animals studied under normoxic conditions or after 8 hours exposure to hypoxia of various levels of severity. Hollow circles, 20% O_2; solid circles, 11.5% O_2; hollow squares, 9% O_2; solid squares, 7.5% O_2. The number of erythropoietin-producing cells correlated linearly with tissue concentrations of erythropoietin mRNA. *(With permission from Eckardt KU, Koury ST, Tan CC, et al. Distribution of erythropoietin producing cells in rat kidneys during hypoxic hypoxia. Kidney Int 1993;43:815–823.)*

since, for example, plasma thrombopoietin levels appear to be regulated by the number of circulating platelets (see below). Therefore, the demonstration that a reduction of the oxygen-carrying capacity of the blood in the presence of a normal red cell count—for example, by carbon monoxide inhalation[129]—stimulates erythropoietin levels to a similar extent as anemia was an important confirmation that anemia influences erythropoietin production mainly through changes of the oxygen-carrying capacity of the blood. Again, the efficacy of carbon monoxide to increase plasma erythropoietin levels is dependent on the hematocrit/hemoglobin concentration in a way that it is less effective during polycythemia and exaggerated during anemia.[118]

The time course of changes of plasma erythropoietin in response to an acute reduction of the oxygen-carrying capacity of the blood induced by blood loss or carbon monoxide inhalation is rather similar to that seen with acute arterial hypoxia.[118] Plasma erythropoietin concentrations start to rise after about 60–90 minutes, reach a

maximum value after about 20 hours, and then decline to a steady-state level.[130] As with the influence of the oxygen tension on plasma erythropoietin levels, the effect of the oxygen-carrying capacity of blood on erythropoietin is not a linear one. The sensitivity of changes erythropoietin levels toward changes in hematocrit/hemoglobin concentration greatly decreases with increasing hematocrit/hemoglobin concentration, which becomes apparent when considering the plasma erythropoietin–hematocrit/hemoglobin relationship during the steady-state phase of chronic anemias (Fig. 92.6). In humans and in laboratory animals, a fall of the hematocrit/hemoglobin concentration down to 70% of the normal value induces only a moderate increases erythropoietin levels. If the hemoglobin concentration decreases further, erythropoietin levels begin to increase exponentially.[131–133] Nonetheless, significant elevations of plasma erythropoietin concentrations are measurable when hematocrit/hemoglobin are only slightly reduced from normal, such as following the donation of one unit of red blood cells.[130,134] An increase in hemoglobin concentration above the normal value, such as during polycythemia rubra vera or hypertransfusion, significantly lowers serum erythropoietin levels, but does not fully suppress them.[127,135,136]

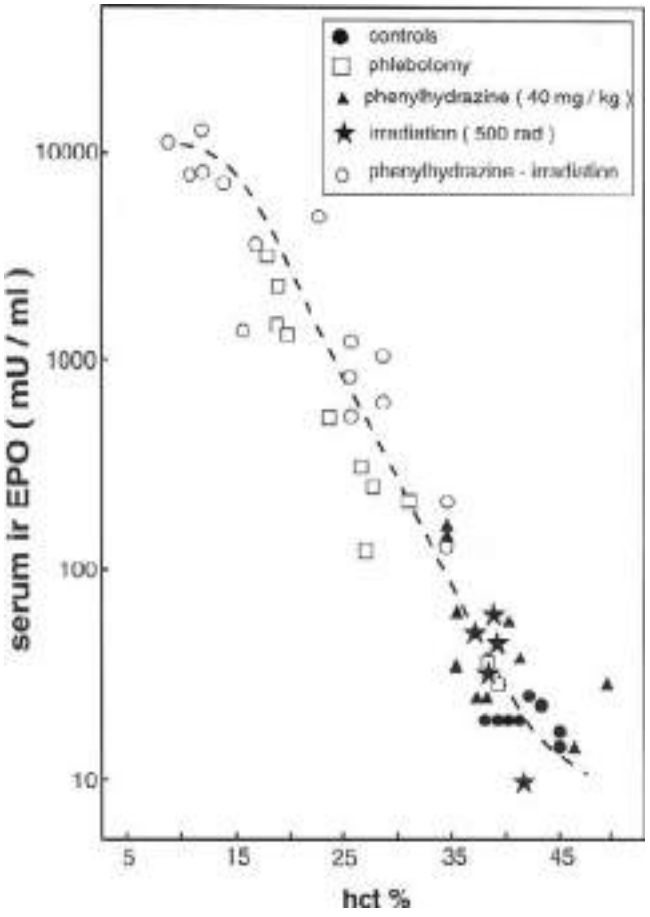

FIGURE 92.6 Relationship between hematocrit and plasma erythropoietin in rats. Anemia was induced by various maneuvers as indicated. *(With permission, from LeHir M, Eckardt KU, Kaissling B, Koury ST, Kurtz A. Structure–function correlations in erythropoietin formation and oxygen sensing in the kidney. Klin Wochenschr 1991;69:567–575.)*

Effect of hemoglobin oxygen affinity: Another parameter relevant for plasma erythropoietin levels that is linked to hemoglobin function is the oxygen affinity of the hemoglobin, which primarily determines oxygen release in the tissues. It has been observed that an increase of the hemoglobin oxygen affinity which impairs oxygen release to the tissues increases erythropoietin levels, while a decrease of the oxygen affinity attenuates the rise of erythropoietin levels in response to hypoxia.[137]

All of the findings mentioned above converge to the oxygen availability to the tissues as common denominator governing circulating erythropoietin levels, because this value depends on the concentration of hemoglobin molecules available for oxygen transport, on the arterial oxygen tension determining the degree of oxygen saturation of hemoglobin, and on the oxygen affinity of the hemoglobin which finally determines the oxygen release from the hemoglobin. The fact that erythropoietin levels are only weakly affected by reductions of the arterial oxygen tension or hemoglobin concentration down to 50–70% of the normal values but then increase exponentially may be explained by the characteristic dissociation of oxygen from the heterotetrameric hemoglobin, which allows sufficient oxygen supply to the tissues down to a significant reduction of the oxygen content of the arterial blood. The observations that maneuvers interfering with oxygen delivery to the tissues and administration of transition metals such as cobalt and nickel increase plasma erythropoietin levels remained without sufficient explanation for a long time. In contrast to the effects of hypoxia and of carbon monoxide is the stimulatory effect of cobalt, which is not dependent on the hematocrit/hemoglobin concentration,[118] suggesting that the effect of cobalt is not mediated by changes of the oxygen availability to the tissues. As outlined in detail below, a hypothesis has been developed that links the effects of cobalt and of hypoxia in a common model of oxygen sensing.

Additional physiological determinants involved in oxygen-dependent epo production?: Using a transgenic mouse model to modify keratinocytes, Johnson and coworkers suggested that the skin might be involved in systemic oxygen sensing by hypoxia induced vasodilation and redirection of the blood flow towards the skin, leading to renal hypoperfusion and increased Epo production.[138] This putative mechanism is difficult to reconcile with the fact that other modalities leading to increased perfusion of the skin, such as heat exposure,

must not alter renal Epo production and erythropoiesis. Subsequent to this study, it has been hypothesized that hair follicles in the skin itself could be a relevant source of circulating Epo.[139] However, in studies with human volunteers no difference in the hypoxic increase in circulating Epo could be observed between subjects exposed to either systemic hypobaric hypoxia or inspiratory normobaric hypoxia of identical oxygen partial pressures, suggesting that extracutaneous hypoxia does not cause a physiologically relevant change in circulating Epo (C. Lundby, Zürich, Switzerland, personal communication). It has also been suggested that the brain releases an as yet unidentified factor upon hypoxia that triggers renal Epo production.[140]

Astrocytes have been reported to represent another cell type responding to hypoxia with increased Epo synthesis in the human brain.[105] While it was believed that Epo cannot cross the blood-brain-barrier, it was reported that astrocyte-derived Epo accounts for up to 50% of circulating Epo in mice following acute hypoxic exposure.[141] This conclusion was derived from astrocyte-specific deletion of oxygen sensing which resulted in a 50% reduction of hypoxic Epo levels compared to wild-type mice.[141] However, when human subjects were exposed to normobaric hypoxia, increases in blood Epo levels were similar in *arteria brachialis* and *vena jugularis*, suggesting that the brain does not substantially contribute to total circulating Epo (C. Lundby, Zürich, Switzerland, personal communication).

Linkage between erythropoietin secretion and rate of erythropoietin gene transcription: Hypoxia, anemia, and cobalt increase erythropoietin mRNA abundance, and changes of plasma erythropoietin levels correlate closely with the amount of erythropoietin mRNA in kidney and liver.[90,91,142–145] Several lines of evidence suggest that erythropoietin producing cells do not develop stores of the hormone that can be rapidly released upon challenge. Thus, almost no erythropoietin can be extracted from the liver and kidney of normoxic animals.[77–79] It takes a delay of at least 1 hour between an acute stimulation of erythropoietin and the first measurable rise of erythropoietin in the plasma.[118,146] Several attempts to localize erythropoietin in the kidneys of normoxic animals failed to produce specific results. It is rather likely therefore that erythropoietin secretion into the bloodstream is directly triggered by the rate of de novo synthesis of the protein. Thus far, no evidence has been elaborated on how erythropoietin synthesis could be regulated on the ribosomal level; it is assumed now that erythropoietin synthesis is primarily determined by the number of mRNA copies available for translation. Steady-state mRNA levels in general result from a balance of gene transcription rate and the rate of mRNA degradation. Although there is some information that erythropoietin mRNA stability may be enhanced during hypoxia[147] and an erythropoietin mRNA-binding protein has been identified,[148] it is more or less accepted that cellular erythropoietin mRNA levels are mainly determined by the transcriptional activity of the erythropoietin gene. In summary, the erythropoietin secretion rate into the circulation is likely determined by the rate of erythropoietin gene transcription.

Survival of erythropoietin in the circulation: Considerable differences among species of the biologic half-life of erythropoietin in the circulation have been observed. In rats erythropoietin half-life is around two hours,[123,149,150] in dogs,[150] in sheep around nine hours,[151] and around eight hours in rabbits.[152] In humans the survival of erythropoietin is rather variable, and for human recombinant erythropoietin a number of studies have reported averaged half-lives at 4–11 hours. The mean half-life of endogenous erythropoietin in healthy humans was determined to be 5–6 hours.[125] There is no information about a physiologically relevant regulation of erythropoietin survival in the circulation; in particular, hypoxia does not appear to affect the plasma clearance of erythropoietin.[123] Even kidney function appears not to influence the half-life of erythropoietin in the plasma significantly,[149,151,153] although a small proportion of the hormone appears each day in the urine. It is furthermore conceivable that the target cells of EPO contribute to its plasma half-life, since receptor-bound EPO is internalized and degraded. Supportive of this idea are observations that at a given hematocrit, plasma levels of EPO are lower in hyper-regenerative than in hyporegenerative anemias, and that for hyper-regenerative anemias such as sickle-cell anemia, half-life times for erythropoietin appears to be rather short.

Taken together, the survival rate of erythropoietin displays a rather high degree if intra- and inter-species variability, but appears not to be regulated in states of elevated or suppressed plasma erythropoietin concentrations.

Recruitment of erythropoietin-expressing kidney cells: Under normoxic conditions, renal (and also hepatic) erythropoietin mRNA abundance is low. After acute onset of hypoxia or anemia, erythropoietin mRNA levels start to increase within 30–60 minutes, and after termination of hypoxia, erythropoietin mRNA levels decline with a half-life time of around 1–2 hours.[145] The rise of erythropoietin mRNA levels precedes and parallels the increase of erythropoietin plasma levels.[118,145] The increase of whole-organ erythropoietin mRNA abundance could in principle result from an acceleration of erythropoietin gene transcription in a fixed number of cells, recruitment of erythropoietin expression cells, or a combination of both. For the kidney, good evidence has been elaborated for the latter possibility. Thus, the number of erythropoietin-

expressing peritubular cells increases strikingly during anemia[91] and hypoxia[90] (Fig. 92.5B). In the kidneys of normoxic animals, only a few erythropoietin mRNA-expressing cells are found, preferentially in the deep cortex at the cortico-medullary junction. With increasing severity of hypoxic or anemic stress, an almost exponential increase occurs in the number or erythropoietin-expressing peritubular fibroblasts cells, which are recruited in direction to the superficial cortex.[90,91] By that the number of erythropoietin-expressing cells increases several hundred-fold in response to hypoxia or anemia. Considering the ratio of whole-organ erythropoietin mRNA and number of erythropoietin-expressing cells reveals that there is a certain regulation of erythropoietin mRNA per cell, but that the increase of the number of cells that start to express erythropoietin is by far the more relevant mechanism to account for the rise of whole-kidney erythropoietin mRNA, and consequently, plasma erythropoietin levels (Fig. 92.5B).[90,91] Therefore, regulation of erythropoietin production in the kidney appears mainly as an "on-off" switch of erythropoietin gene transcription by renal peritubular fibroblasts. In addition, cobalt administration increases the number of erythropoietin-expressing cells in the kidney.[90] In contrast to the effects seen during hypoxia or anemia, is the recruitment induced by cobalt, which is zonally less organized.

In the liver it appears as if it is an up- and down-regulation of erythropoietin gene expression in certain hepatocytes, rather than a recruitment of erythropoietin-expressing cells, that accounts for the increase of hepatic erythropoietin mRNA in response to anemia.[94] A gradual upregulation of erythropoietin mRNA in hepatocytes would also be supported by *in vitro* findings with primary cultures of hepatocytes or hepatoma cells (Fig. 92.7).

Evidence for local oxygen sensing in control of erythropoietin production: Oxygen-sensitive chemoreceptors are well known in the carotid body, and they are responsible for hemodynamic and respiratory adaptations to hypoxia. The regulation of erythropoietin appears to be independent of these systemic oxygen sensors; instead, it appears to be regulated by local oxygen sensing in liver and kidneys. Thus, ablation of the arterial chemoreceptors does not significantly alter erythropoietin production in response to hypoxia.[154] Moreover, with respect to the renal production of erythropoietin, renal denervation has been found not to influence the expression of erythropoietin in response to hypoxia or anemia.[155,156] On the other hand, there is consistent evidence that in isolated perfused kidneys taken from normoxic animals, erythropoietin gene expression[157] and erythropoietin protein secretion[158,159] can be induced by lowering the oxygen

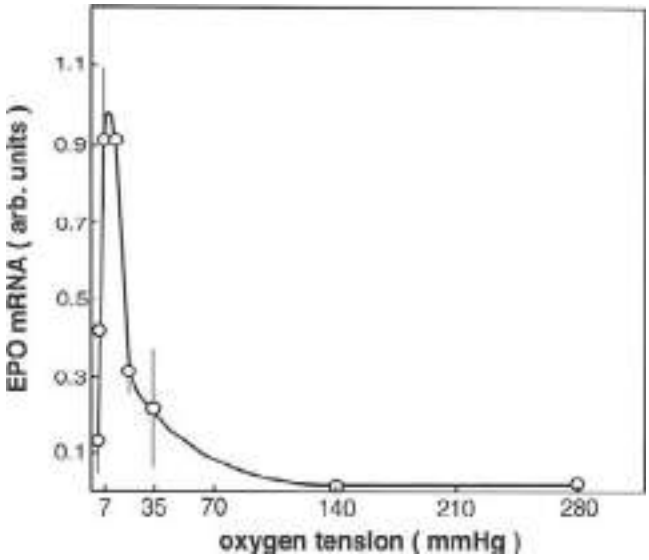

FIGURE 92.7 Oxygen dependency of erythropoietin mRNA in primary cultured rat hepatocytes. Freshly isolated rat hepatocytes were plated on gas permeable culture supports and were exposed to different oxygen concentration in a normobaric atmosphere for 3 hours as described in Eckardt et al.[104] Erythropoietin mRNA levels were standardized to β-actin mRNA levels and are given as arbitrary units.

tension of the perfusate, with rather similar characteristics of the *in vivo* situation. Thus, it appears that the essential events by which systemic hypoxia or anemia stimulate peritubular erythropoietin gene transcription occur within the kidneys itself. This does not rule out the possibility that renal erythropoietin production may in addition be modulated by extrarenal factors (see below).

Because erythropoietin production is stimulated in a similar fashion by a fall of the arterial oxygen tension, by a reduction of the oxygen-carrying capacity of the blood, and by an impairment of oxygen delivery from the hemoglobin, it is likely that the common denominator for these effects is a reduction of the oxygen availability to the peritubular tissue. A measurable parameter that results from the oxygen availability in conjunction with the local oxygen consumption is the local oxygen tension. In addition to oxygen availability, oxygen consumption is of relevance for erythropoietin production. This may be derived from observations that hormonal modulation of the metabolic rate exerts a major role in erythropoietin production. Thus, even upon hypoxic exposure, erythropoietin production in hypophysectomized animals may be as low as in nephrectomized animals.[160,161] Similarly, starvation also attenuates erythropoietin production.[122] On the other hand, hormones stimulating energy turnover such as growth hormone,[162] insulin-like growth factor I,[163] thyroid hormone,[164,165] and androgens[166,167]

enhance hypoxia-induced erythropoietin formation. Indeed, the renal cortical fibroblasts expressing erythropoietin are in close anatomical contact with proximal tubular cells,[83] which have a high metabolic rate. Since circumstantial evidence suggests that the oxygen regulation of erythropoietin production in the kidneys is dependent on transport activity of the proximal tubule,[168] it is conceivable that proximal tubule cells generate a sink of the oxygen tension around the neighbored fibroblasts.

Attempts to isolate erythropoietin-expressing fibroblasts and to study the regulation of erythropoietin gene regulation in these cells *in vitro*, however, have not been successful thus far. In mice bearing an erythropoietin SV-40T antigen construct transgene, renal fibroblasts expressing the T antigen could be isolated and cultured. In contrast to the *in vivo* situation, however, the cells did not increase their erythropoietin mRNA or T-antigen expression in response to hypoxia.[85]

In principle, the pericellular oxygen tension can directly trigger erythropoietin gene expression. Thus, in cultures of hepatoma cells,[169] hepatocytes,[95] astrocytes,[106] and liver Ito cells,[97] a prominent effect of the pericellular oxygen tension on erythropoietin gene expression can be demonstrated, in a fashion rather similar to that expected from *in vivo* data (Fig. 92.7).

Oxygen Supply to Kidney and Oxygen Sensor Function of Renal Cortex

At first glance, the location of an oxygen (tension) sensor in the kidney appears somewhat surprising, since the volume of oxygen transported to the kidney cortex is rather large compared to its oxygen consumption. Considering the comparatively low oxygen extraction rate of 8-10%, one might conclude that the kidney cortex generally is luxuriously supplied with oxygen. On the other hand, not only does the oxygen sensor governing erythropoietin gene transcription appear to reside within the kidney, but clinical experience also teaches that the kidney is an organ rather susceptible to hypoxic injury. The explanation for both these putative discrepancies probably resides in the unique architecture of intrarenal vessels. Since arterial and venous vessels run counter-currently over long distances in close association, it is assumed that a shunt diffusion of oxygen occurs between arterial and venous vessels, which lowers arterial oxygen pressure. While shunt diffusion of oxygen in postglomerular vessels is thought to be responsible for the high vulnerability of the thick ascending limb to ischemia,[170,171] shunt diffusion in preglomerular vessels, in particular interlobular vessels, might explain the oxygen sensitivity of cortical structures relevant for erythropoietin production. Support for this concept comes from measurements of oxygen tension in the renal cortex well below the venous PO_2 of the kidney.[172,173] Moreover, it has been demonstrated that preglomerular oxygen tensions at the kidney surface are much lower than those in the systemic circulation, this difference increasing greatly with rising oxygen tension and decreasing hemoglobin concentrations.[174] It should be noted that assuming major oxygen shunting along interlobular vessels would predict an oxygen gradient from the corticomedullary junction to the subcapsular cortex, while the distribution of erythropoietin-expressing cells displays just the opposite direction, with the majority of signals in situ hybridizations being located in the inner part of the cortex.[90,91] Thus, additional parameters are required to explain the particular distribution of erythropoietin-expressing cells. In particular, in the lower cortex the peritubular tissue frequently receives blood returning from the medulla or cortical medullary rays. Since these structures already extract a substantial amount of oxygen, oxygen delivery to the inner part of the cortex may be lower than in other cortical areas. Similarly, oxygen delivery to the midcortical peritubular cells may be somewhat reduced, because it also receives blood returning from the medullary rays, while in the superficial cortex postglomerular blood directly reaches the peritubular tissue. Another factor that has to be taken into account is that shunt diffusion is not limited to oxygen; it also (in the opposite direction) affects carbon dioxide, thereby trapping it in the outermost subcapsular zone.[175,176] Since carbon dioxide attenuates erythropoietin production by a pH-related mechanism,[121] an accumulation of carbon dioxide might at least partially counterbalance the effect of low oxygen tensions in the outer cortex. Consideration of all of these issues suggests that the main physiologic role of oxygen shunting occurring in the cortex could be an amplifying mechanism for the stimulation of erythropoietin production, which operates predominantly during states of anemia and less during arterial hypoxia. Assuming that the renocortical oxygen consumption is more or less unaltered during anemia, the oxygen tension in the primary capillary effluate leaving the parenchyma will be decreased in comparison with the nonanemic state. This decrease in venous oxygen tension will increase the driving force for oxygen shunting between interlobular arteries and veins, and in consequence further lowers the arterial oxygen tension of the blood entering the renocortical parenchyma.

In any case, the high oxygen sensitivity of the renocortical peritubular tissue is also substantiated by the observation that apart from erythropoietin expression, other events occur in the peritubular region of the renal cortex. Thus, within 1 week following the onset of anemia, a marked hypertrophy of peritubular fibroblasts in the cortical labyrinth of rat kidneys was found, with

an increased activity of 5′-ectonucleotidase on the surface of these cells.[84]

CELLULAR OXYGEN SENSING REGULATING ERYTHROPOIETIN GENE TRANSCRIPTION

Erythropoietin Gene

Gene promoter: There is only a single copy of the erythropoietin gene, and no evidence exists for an erythropoietin gene family or any pseudogenes. The human erythropoietin gene has been mapped to the long arm of chromosome 7,[177] and the mouse gene has been mapped to chromosome 5.[178]

The basic organization of the erythropoietin genes in different species is similar and consists of five exons and four introns.[9,10,179] The most conserved region between the genes has a high sequence homology, and is located directly upstream from putative transcriptional start sites. The first intron also shows interspecies homologies. In contrast, the size and sequence of the second, third, and fourth introns are highly divergent among species.

There is evidence for multiple start sites for erythropoietin gene transcription.[180] Within the putative promoter region for the human erythropoietin gene, apart from steroid hormone response elements,[181] none of the classical sequences has been identified. Two complementary approaches have been undertaken to localize cis-acting DNA sequences responsible for tissue- and stimulus-specific regulation of erythropoietin gene expression. First, the generation of transgenic mice carrying erythropoietin gene constructs of different length, and second, the expression of gene constructs incorporating different sections of the erythropoietin gene and its flanking sequence in cell lines. It turned out, that the regulation of the erythropoietin gene by the same parameters requires different gene sequences for liver and kidney, in a way that the physiologic regulation of the erythropoietin gene is managed within −0.4 kb of the 5′-sequence and 0.7 kb of the 3′region, while an essential regulator element for the renal expression of erythropoietin resides between −12 and −8 kb in the 5′-region[180,182] (Fig. 92.8).

Gene enhancer: The minimal erythropoietin (EPO) promoter encompasses 117 bp 5′ to the transcription start site and has no oxygen-regulated element. Proteins interacting with a 17 bp (nt −61 to −45) sequence synergize with transcription factors (HAF) binding to the 3′ enhancer of the EPO gene.[183] HAF is the murine homologue of Sart-1, a 125-kDa human protein recognized by cytotoxic T lymphocytes. HAF likely acts in conjunction with other transcription factors to modulate O_2-dependent EPO expression.[183] Some negative cis-acting elements exist in the promoter that also repress EPO expression. Two GATA sites have been extensively studied with respect to oxygen sensitivity, tissue specificity, and also their potential role during ontogeny.[184,185] Increased expression and binding of GATA-2 were found at high oxygen tensions and overexpression of GATA-2 and -3 suppressed EPO expression.[185]

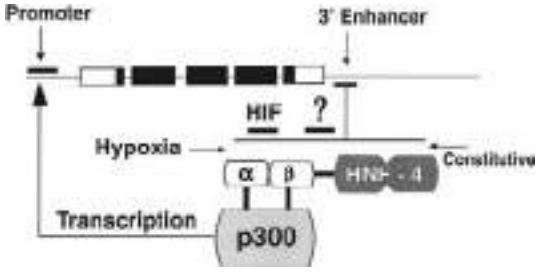

FIGURE 92.8 Organization of the erythropoietin gene. The erythropoietin gene is schematically illustrated with five exons (rectangles) and the coding regions (black). During hypoxia the HIF-1 heterodimer is stabilized and binds to a site on the 3′-enhancer. Downstream of this site, the nuclear receptor HNF-4 binds constitutively to the direct repeat (DR-2) site and also to the β-subunit of HIF-2. Both HIF-subunits bind to the transcriptional activator p300, providing a mechanism for triggering the erythropoietin gene promoter to transcribe the mRNA. Between the HIF-2 and HNF-4 binding sites, an essential sequence with an as yet unknown mechanism of operation is located. *(Modified with permission from Huang LE, H V, Arany Z, Kranic D, Galson D, Tendler D, Livingston DM, Bunn HF. Erythropoietin gene regulation depnds on heme-dependent oxygen sensing and assembly of interacting transcription factors. Kidney Int 1997;51:548−552.)*

The EPO 5′-promoter is only a weak promoter. However, it shows hypoxic inducibility and acts synergistically in concert with a 3′-enhancer[31] to achieve a 1000-fold stimulation *in vivo*. A 50-bp hypoxia response element (HRE) has been identified in the human gene within the untranslated 3′-sequence, 116 bp downstream of the erythropoietin RNA polyadenylation site. This sequence conveys oxygen-regulated expression on a variety of heterologous promoters *in vitro*[186−188] and acts in a position- and orientation-independent way, and thus fulfills the criteria of a classical eukaryotic enhancer. A similar enhancer, with highly conserved sequences, has been located at an equivalent position in the mouse gene. Within this EPO enhancer, three defined sites are important for the response to hypoxia. At the 5′ end, the sequence CACGTGCT was the first to be identified as a "hypoxia inducible factor" (HIF) binding site (HBS). Two protein complexes were identified, one bound constitutively and the other (HIF) was present only in hypoxic cells.[189] Components of the constitutive complex are ATF-1 and CREB-1, but the role for hypoxia-regulated EPO expression has not yet been settled for these

factors.[189] In contrast, intact HBS and HIF bindings are indispensable for hypoxia-induced EPO expression.

The second essential area within the erythropoietin HRE located downstream of the HBS encompasses the core sequence 5′-CACAG-3′. Mutation of this site abrogates hypoxia-inducible activity of the enhancer, but so far no protein bound to this repeat has been identified.

A third and more distal area in the EPO enhancer is a direct repeat of two steroid receptor half-sites separated by two base pairs (DR-2 site).[181] This DR-2 site is also absolutely required for hypoxic regulation of the EPO gene.[190] DR-2 sites bind nuclear receptors for hormones, but none of the known ligands such as thyroxine and vitamin D significantly influence EPO expression through this site.[181] However, screening for orphan receptors revealed specific binding of hepatocyte nuclear factor-4 (HNF4) that significantly enhances EPO gene expression in response to hypoxia.[190] It was further hypothesized that HNF4 may play an important role for tissue-specific expression of EPO.

Hypoxia-inducible transcription factor: The critical hypoxia-inducible protein binding at the most proximal 9 bp area (5′-TACGTGCT-3′) of this enhancer was initially termed hypoxia-inducible factor-1 (HIF-1),[189] and is a heterodimeric protein consisting of a HIF-1α and a HIF-1β subunit.[191,192] The HIF-1 binding motif is also found in other genes activated by hypoxia, such as, for example, vascular endothelial growth factor (VEGF) or enzymes of the glycolytic pathway—enolase, pyruvate kinase, and lactate dehydrogenase —indicating a widespread oxygen-sensitive system.[193,194]

HIF-β (120 kD) is the aryl hydrocarbon receptor nuclear translocator (ARNT),[191] and HIF-1α (91−94 kD)[192] is a member of the group of basic-helix-loop-helix proteins containing a PAS domain. Assembly of an active HIF complex is a multistep process involving regulated synthesis, processing, and stabilization of HIF-1, nuclear localization, dimerization, and interaction with transcriptional coactivators.

The discovery of two human cell lines (HepG2 and Hep3B) that produce *in vitro* erythropoietin in a fashion inversely related to the pericellular oxygen tension[169] was an enormous step forward for investigating the mechanisms along which a fall of the oxygen tension (hypoxia) could stimulate erythropoietin gene transcription on the cellular level. It turned out that hypoxia signaling likely follows a novel nonclassical pathway (Fig. 92.9).

This exciting novel pathway was unraveled by milestone publications within the last few years, emphasizing a central mediator role of the HIF-1α subunit. It turned out that the HIF-1 protein contained two groups of oxygen-sensitive domains, those determining protein stability (oxygen degradation domain [ODD]), and

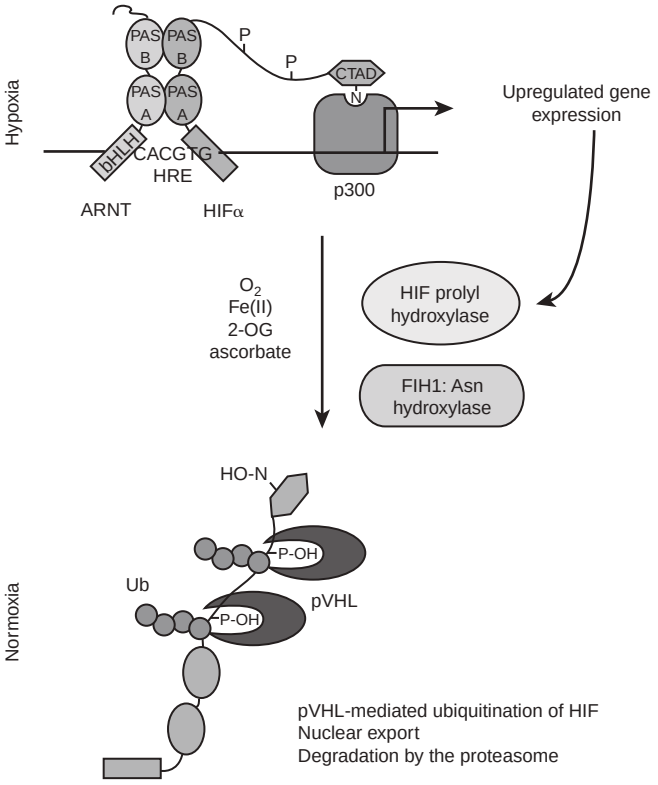

FIGURE 92.9 Hypoxia-mediated regulation of HIF stabilization and activation. Under normoxic conditions (bottom), two proline residues within the oxygen degradation domain of the HIF-α subunit are modified by HIF-prolyl hydroxylases, allowing for HIF recognition by a protein-ubiquitin ligase complex containing pVHL, and leading to HIF-α degradation by the proteasome. Meanwhile, the asparaginyl hydroxylase FIH-1 modifies the CTAD of the HIF-α, blocking its interaction with transcriptional coactivators such as p300. When oxygen levels decrease, both prolyl and asparaginyl hydroxylation are blocked. HIF-α accumulates and interacts with the HIF-β subunit (ARNT) and the larger transcriptional machinery, thereby promoting transcription of downstream HIF target genes. *(With permission from Bruick RK. Oxygen sensing in the hypoxic response pathway: regulation of the hypoxia-inducible transcription factor. Genes Dev 2003;17: 2614−2623.)*

those regulating transactivity (NH_2-terminal and COOH-terminal transactivating domains), which are independently regulated by oxygen.[195,196] In addition, cellular localization of HIF-1α also appears to be O_2 dependent, because translocation from the cytosol to the nucleus is increased under hypoxia.[197]

While steady-state levels of HIF-1α and HIF-1ß mRNA are not significantly affected by hypoxia, the cellular HIF-1α protein content increases greatly under hypoxia.[198] The hypoxia inducibility of the HIF-1 complex is solely achieved by hypoxic accumulation of the α-protein subunit, since the β-subunit is constitutively expressed. In normoxic cells, HIF-1α is barely detectable due to rapid degradation via the ubiquitin proteasome pathway.[199,200] HIF-1α is continuously synthesized irrespective of the oxygenation status of the cells, providing a

very rapid response of HIF-1α accumulation when hypoxia occurs, simply by blocking the degradation of the protein, and allows an almost instantaneous response to hypoxia by accumulation of HIF-1 without activating the transcriptional/translational machinery.[201]

Proteolytic regulation of HIF-1α and HIF-2α is critically dependent on the von Hippel-Lindau tumor suppressor protein (pVHL), with pVHL functioning as the substrate recognition component of a multicomponent ubiquitin E3 ligase.[202–204] VHL protein binds to the two oxygen-dependent degradation domains (ODD) of HIF-1α, which confer oxygen-dependent instability on the HIF-1α protein.[200,205,206] The HIF–pVHL protein interaction is suppressed by the classical HIF-activating stimuli of cobaltous ions, iron chelation, and hypoxia. The interaction sites for pVHL within the two HIF ODDs contain the amino acid proline within the LxxLxP motif for hydroxylation.[207] It was confirmed that the interaction between HIF-1α and pVHL is regulated by enzymatic hydroxylation of these specific prolyl residues (for human HIF-1, at Pro 402 and at Pro 564).[207–209] Since the only previously characterized mammalian prolyl hydroxylases (pro-collagen prolyl hydroxylases) are 2-oxoglutarate-dependent oxygenases, it was predicted that the HIF prolyl hydroxylases would also belong to this family of enzymes.

Subsequently, in mammalian cells, three isoforms were identified, termed prolyl hydroxylase domain (PHD) enzymes (PHD1-PHD3), and shown to hydroxylate HIF-α *in vitro*.[210,211] These enzymes have an absolute requirement for dioxygen as cosubstrate. The overall reaction results in insertion of one oxygen atom into the HIF-α peptide substrate at the prolyl residue, the other generating succinate from 2-OG with the release of CO_2. Relatively labile binding of Fe(II) at the 2-His-1-carboxylate centre results in striking sensitivity to inhibition by iron chelators and metals such as Co_{II} that can exchange for Fe_{II} at this site. As predicted, the activity of the recombinant PHD enzymes is strongly inhibited by cobaltous ions, and iron chelation. Furthermore, reactions conducted in a controlled oxygen environment showed that the activity of the purified enzyme is strikingly sensitive to graded levels of hypoxia *in vitro*.[211] Thus, the properties of these nonhaem iron enzymes fit those of the postulated ferroprotein sensor underlying the classic characteristics of the erythropoietin/HIF response. The activity of PHDs depends on the availability of oxygen and thus qualifies these enzymes as O_2 sensors. Recently, the O_2 affinity has been determined and suggests appropriate sensitivity in the physiological relevant PO_2 range.[212] Under hypoxia, activity of the enzymes is greatly reduced, the specific proline residues in HIF-α are no longer hydroxylated, and HIF-α subunits can accumulate to activate HIF-1-dependent genes such as EPO. HIF-1α and HIF-2α also contain two transactivation domains (TADs): an N-terminal TAD overlapping the ODD, and a C-terminal TAD that is distinct from the ODD[196,205,206] and manifests oxygen-regulated interaction with p300/CBP.[195,213] The C-TAD is modulated by an O_2-sensitive hydroxylation on the asparagine residue 803 in human HIF-1α.[214] Here, hydroxylation of asparagine under high oxygen pressure inhibits recruitment of the transcriptional coactivator CBP/p300[199,215] necessary for hypoxic HIF-1 activity. This asparagine hydroxylase had been identified earlier as factor inhibiting HIF-1 (FIH-1), because its interaction hydroxylation of asparagine N803 inhibited the transactivity of HIF-1.[216] It has also been reported that FIH interacts with pVHL and forms a ternary complex with the HIF-α C-TAD.[216] Although interaction with pVHL is not an absolute requirement for FIH activity,[199,212] these findings fit well with studies of HIF-dependent transcription in pVHL-defective cells. Upregulation of HIF-target gene expression in such cells is essentially complete,[203,217,218] which implies that all oxygen-dependent controls of HIF, and not just proteolytic regulation, are disabled in the absence of VHL. This suggests that VHL is intimately involved with the hypoxia response, its functions extending beyond those of an E3 ligase. FIH-1-like PHDs turned out to be a 2-oxoglutarate-dioxygenase requiring O_2 and iron for its function.[212,219] It is of note that PHDs and FIH-1 are localized in different cellular compartments[220] and display differences in O_2 affinities.[221,222] Numerous pieces of evidence point to a further mode of HIF regulation involving oxygen-dependent nuclear/cytoplasmic localization of HIF-α.[207] In normoxia, HIF-1α levels are low and subcellular localization cannot be directly observed. However, overexpression of HIF- or HIF-1α–GFP fusion proteins that are less rapidly degraded yields detectable protein in normoxic cells and several,[197,223] although not all,[224] studies have observed that this protein shifts to the nucleus only in hypoxia, implying a distinct oxygen-regulated step. Interestingly, as with the other modes of HIF regulation, the effect of hypoxia is mimicked by iron chelators, which suggests that subcellular localization is also regulated by the same or similar Fe_{II}- and 2-OG–dependent oxygenases.[197] The underlying mechanisms of this effect still have to be clarified.

To date, analyses of the regulatory mechanisms underlying HIF activation by hypoxic and nonhypoxic stimuli have emphasized the involvement of different types of pathway and different modes of HIF activation. Whilst proteolysis of HIF-subunits is strikingly oxygen dependent,[187,225,226] is the rate of HIF-1 translation largely independent of oxygen,[227] but is responsive to growth factor and oncogenic stimulation.[228–230] Phosphorylation cascades such as the mitogen-activated

protein kinase (MAPK) and phosphoinositide-3 kinase (PI3K) pathways are activated by growth factor stimulation, and amplify the HIF response to hypoxia by post-translational[231,232] as well as translational controls.[228–230]

HIF-1α is ubiquitously expressed, but is not the only member of this subfamily of PAS proteins. HIF-2α[233–236] and HIF-3α[237] partly overlap with HIF-1α in their expression pattern, but assignment of specific functions to the different HIF-αs has not yet been achieved. Knockout mice for HIF-1α and HIF-2α significantly differ in their phenotype. Whereas HIF-1α -/- mice die around midgestation due to severe cardiovascular and central nervous system malformations,[238] HIF-2α -/- mice display different phenotypes, probably related to the genetic background.[239–241] Although all of these mice die soon after birth, no clear conclusions regarding defects in EPO expression can be drawn from these animals. In contrast, heterozygous HIF-1α knockout mice developed normally but, among other impaired physiological responses to hypoxia, these mice had delayed erythrocytosis on exposure to hypoxia,[242] apparently suggesting a dominant role for HIF-1α for EPO regulation.

First evidence that HIF-2α rather than HIF-1α might regulate renal Epo synthesis came from descriptive studies demonstrating *in situ* overlapping of HIF-2α but not HIF-1α with the peritubular, interstitial EPO producing cells.[243] Similar results have been reported using chemical PHD inhibition.[244] The critical role of HIF-2α was further confirmed by RNAi experiments in liver-derived hepatoma.[245]

Such a central role of HIF-2α hypothesis would be supported by a study on the retinopathy of prematurity to which expression of EPO in the retina significantly contributes.[246] In this study, HIF-2α knockdown, that is, reduction of HIF-2α expression to about one-fifth of the normal level, lowered EPO expression induced by relative hypoxia that was not compensated by unchanged HIF-1α accumulation.[246] In addition, in two cell lines producing EPO that express both HIF-1α and HIF-2α, downregulation of HIF-2α but not HIF-1α by siRNAs blunted the EPO response.[245] These results were subsequently confirmed in a hepatic HIF-2α knock-out mouse model.[247] Quite surprisingly, an independent HIF-2α global knock-out mouse strain turned out to be viable and these mice were indeed anemic with decreased renal Epo expression.[248] Conditional global deletion of HIF-2α but not HIF-1α also resulted in anemia in adult mice.[249] Finally, a kidney-specific conditional knock-out mouse model confirmed the non-redundant role of HIF-2α in oxygen-regulated Epo gene expression.[250]

Together, plasma erythropoietin concentrations are regulated by an effective negative feedback loop, in which the kidney integrates a number parameters such as arterial oxygen tension, oxygen-carrying capacity of the blood and metabolic rate to one signal, namely, the pericellular oxygen tension in the cortex, which then is transduced by the hydroxylation of prolyl and aspargyl residues into a stabilization and activation of HIF-α protein, which in turn triggers in concert with HIF-β the transcriptional activity of the erythropoietin gene (Fig. 92.10).

Dysregulated EPO gene expression by PHD2, VHL or HIF-2α mutations in familial erythrocytosis: In contrast to worms and insects, in vertebrates both the PHD oxygen sensors and the HIFα transcription factor subunits are encoded by three distinct but related genes. All three PHD family members are expressed in the kidney.[251] The physiological relevance of a potential fourth family member, called PH-4, is less clear: HIFα seems to be regulated under PH-4 overexpression conditions only.[252,253] There exist three related genes even for HIF-β/ARNT (i.e. ARNT2, ARNTL and ARNTL2) and all of them seem to be able to interact with HIF-2α, at least *in vitro*.[254] However, whether these additional ARNT family members play any role for Epo gene expression is currently unknown. Regarding the

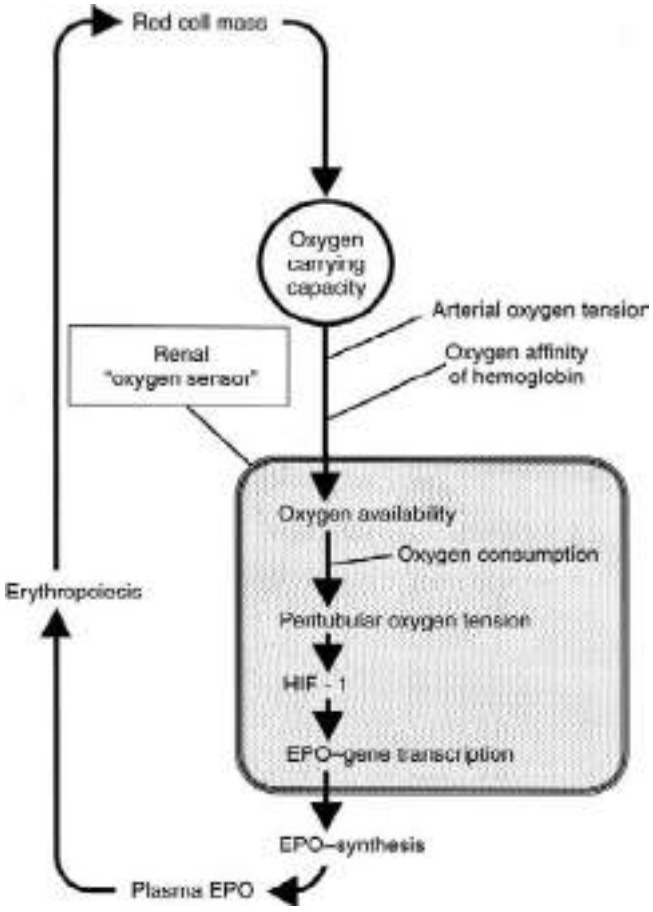

FIGURE 92.10 Negative feedback loop controlling the renal production of erythropoietin.

PHD and HIFα gene families, the question arises which family member(s) is/are responsible for oxygen-regulated Epo gene expression. Mouse gene targeting and human hereditary diseases provided genetic answers to this question.

Two independent inducible PHD2 knock-out mouse models showed increased erythropoiesis and angiogenesis as well as evidence for dilated cardiomyopathy and premature death.[255–257] These findings are in line with *in vitro* data demonstrating that PHD2 is the main oxygen sensor responsible for normoxic HIFα turnover.[258] Consistently, systemic PHD2 but not PHD1 or PHD3 knock-out mice die during embryonic development.[259] Only when all three PHDs are deleted simultaneously in a conditional knock-out mouse model, even the liver can become a rich source of Epo expression.[260] A further confirmation for the major role PHD2 is playing in oxygen-regulated Epo synthesis *in vivo* comes from the identification of gene mutations that cause familial erythrocytosis: the affected amino acids identified up to date confer residues P317, R371 and H374 of PHD2.[261–263] Neither PHD1 nor PHD3 mutations in familial erythrocytosis have been reported so far.

Due to its nature as a tumor suppressor, a large number of mutations in the human VHL gene were known before its role as HIFα E3 ubiquitin ligase was discovered. In accordance with its essential and non-redundant role in normoxic HIFα degradation it did not come as a surprise that such mutations can also cause erythrocytosis.[264] Interestingly, Chuvash polycythemia is caused by a pVHL R200W mutation in the absence of cancer.[265] A number of additional pVHL mutations causing congenital erythrocytosis have been identified thereafter.[266–268] Finally, a genetically altered mouse model recapitulated the polycythemic phenotype.[269]

As already mentioned before HIF-2 rather than HIF-1 is the physiological regulator of EPO gene transcription. Support to this conclusion is provided by the identification of HIF-2α P534L, M535V, M535I, G537W, G537R and D539E mutations that cause human familial erythrocytosis.[270–276] No HIF-1α or HIF-3α mutations have been reported so far to be involved in erythrocytosis.

Altogether, there is now compelling evidence that the oxygen sensing pathway regulating renal and hepatic Epo synthesis consists of the PHD2-VHL-HIF-2 axis.

Negative feedback loops and cross-talks of the Phd-Vhl-Hif oxygen signaling pathway: Although the main players for Epo gene regulation have been identified, there is clearly more complexity in the oxygen signaling pathway. Of particular physiologically importance are negative feedback mechanisms that limit or actually downregulate Epo induction under chronically hypoxic conditions. It is well known that hypoxically induced plasma Epo levels decrease clearly before the hematocrit is increased, excluding an early negative feedback loop via the subsequent increase in blood oxygen content.[119] The drop in plasma Epo is paralleled by a drop in renal Epo protein and mRNA levels and is independent of changes in extracellular Epo levels.[122,123] These findings suggest one or several negative feedback loop(s) intrinsic to the PHD-VHL-HIF axis controlling renal Epo synthesis.

Of note, the ratios between the levels of PHDs and HIFs are interconnected. If either one is upregulated it overcomes the function of the other. As well as an increase in PHD synthesis leads to HIFα degradation, an increase in HIFα synthesis leads to its own stabilization by saturating the degradation machinery. Even under hyperoxic conditions the PHDs are not fully active,[221] and a further decrease in the oxygenation as well as a decrease in the PHD levels allows for the stabilization of HIFα.[277–280] This feature explains why regulation of the PHD levels is of physiological relevance: the slightest up- or downregulation of PHD abundance and/or activity potentially affects HIF-2-dependent Epo expression. A very likely, albeit unproven, mechanism regulating Epo production hence might consist of the HIF-dependent transcriptional increase in PHD levels. PHD2 and PHD3, but not PHD1 or FIH, are HIF target genes induced under hypoxic conditions.[211,258,281–287] Hypoxically increased PHD2 and PHD3 in turn downregulate HIF-2α protein and hence Epo mRNA levels. This model shows a biphasic response, with an early PHD3 and a late PHD2 induction, and it allows for ongoing oxygen sensing, suggesting that it could easily adapt to both acute and chronic changes in oxygenation.[277–280]

There exist a large number of additional mechanisms regulating PHD and HIF abundance and activity, but due to the lack of appropriate renal cell culture models, their role in Epo gene regulation remains largely unknown. Basically, PHDs are regulated on three levels: transcription, protein abundance/stability and enzymatic activity. Up to date, little is known about the tissue-specific and growth factor-induced PHD transcription. Estradiol is known to induce PHD1 gene expression,[288,289] and TGF-β1 has been shown to inhibit PHD2 gene expression.[290] Whether these data are relevant to the sex-specific and developmentally regulated Epo gene expression is currently unknown. PHD protein abundance and activity can further be regulated by protein-protein interactions as well as by cellular metabolites and other small molecules. More than a dozen different proteins have been identified to interact with PHDs, all of them representing candidate Epo regulators, but none of them have ever been tested for Epo regulation (for an overview see[291]).

Cellular small molecule regulating PHD enzymatic activity include the redox-active substances ascorbate,

transition metals, nitric oxide and other reactive oxygen species.[292–298] Transition metal ions, such as cobalt, nickel and manganese, are very well known to induce Epo gene expression both *in vitro* and *in vivo*.[299,300] The discovery of the PHD oxygen sensors finally provided the molecular explanation for their function. Cellular metabolites that potently inhibit PHD activity are the Krebs cycle intermediates succinate and fumarate.[301–303] Germline mutations of the genes encoding fumarate hydratase (FH) or succinate dehydrogenase (SDH) result in the accumulation of fumarate and succinate, respectively, two potent inhibitors of PHD activity.[304,305] Moreover, mutations in the gene encoding isocitrate dehydrogenase-1 (IDH-1) lead to a decrease in the PHD co-substrate 2-oxoglutarate and an increase in HIF-1α levels.[306] Thus, the PHDs link oxygen sensing with mitochondrial metabolism. However, whether Krebs cycle enzyme mutations contribute to dysregulated Epo gene expression, for instance in familial erythrocytosis, is a major focus of ongoing research.

Modulation of Renal Erythropoietin Production

Renal perfusion: Renal erythropoietin production is not significantly changed unless renal perfusion is reduced to less than 10% of its normal value.[307,308] This may explain why renal artery stenosis is only rarely associated with erythrocytosis.

Although not yet proven, a likely explanation for the insensitivity of erythropoietin production toward changes of renal blood flow may arise from the fact that in the kidney oxygen consuming function and renal blood flow are directly linked. A fall of renal perfusion will decrease glomerular filtration and will lower the workload of the proximal tubule leading to a reduced oxygen demand of the proximal tubule. Thus, in spite of the fact that a decline of renal perfusion will lower the oxygen delivery to the cortical interstitium, it will not necessarily lower the pericellular oxygen tension, because the oxygen demand is also reduced in this situation. Because of this relationship, the kidney is in fact an "ideal" organ to sense changes in the systemic oxygen delivery independent of the renal perfusion.

Acid–base state: A physiological parameter that can effectively modulate renal erythropoietin production is the acid–base state of the organism, in a way that hypercarbia inhibits erythropoietin production while hypocarbia enhances it.[309–311] It was confirmed that not only respiratory but also metabolic acidosis markedly attenuates the stimulation of erythropoietin in response to arterial hypoxia or to a reduction of the oxygen-carrying capacity of the blood by an effect related to the hypoxia triggering of erythropoietin production.[121] The mechanisms of this pH sensitivity of oxygen sensing in the control of erythropoietin production have not yet been clarified.

Blood viscosity: In addition, blood viscosity appears to be a determinant for the efficacy of hypoxia to stimulate renal erythropoietin production. Patients with hypergammaglobulinemia may develop anemia that is not always explained by displacement of erythroid progenitors in the bone marrow, and that is characterized by plasma erythropoietin concentrations that are relatively low for the degree of anemia.[312,313] In fact, an inverse correlation between erythropoietin production and plasma viscosity unrelated to kidney function was found for those patients.[314] Plasma exchange experiments in rats showed that the renal expression of erythropoietin mRNA in response to anemia was inversely related to plasma viscosity.[314] Although the mechanism for this marked influence of plasma viscosity is not yet understood, it may provide an additional mechanism along which the circulating red cells mass could exert influence on the renal production of erythropoietin. Since it is well established that the packed red cell volume is the major determinant for whole-blood viscosity *in vivo*, it is conceivable that a fall of blood viscosity during anemia contributes to the enhancement of erythropoietin production, while an increase of viscosity during polycythemia would support inhibition of erythropoietin production.

Inflammatory cytokines: Based on the observation that chronic inflammatory diseases can lead to anemia and that plasma erythropoietin levels are relatively low in those patients, the possibility has been considered that inflammatory cytokines might exert an effect on erythropoietin production.[315] Indeed, it was found that interleukin-1 and tumor necrosis factor (TNF-α) potently suppress hypoxia-induced erythropoietin production and erythropoietin mRNA accumulation in cultured hepatoma cells.[316,317] This notion was confirmed in isolated perfused rat kidneys, where TNF-α attenuated hypoxia-induced erythropoietin production.

Iron Metabolism and Epo Gene Regulation

Of major physiologically relevance is the cross-talk between the oxygen and iron signalling pathways. Increased Epo production is futile unless sufficient iron is available for incrased erythropoiesis, the major iron consuming process of our body. Therefore, iron metabolism is directly regulated by oxygen supply and Epo production is directly regulated by iron availability. The most obvious possible cross-talk between the two pathways would be the strict requirement of the PHD oxygen sensors for iron.[298,318] Indeed, iron chelators are known for a long time to induce HIFα protein stability and HIF-dependent target gene induction, including Epo gene expression.[319,320]

PLASMA ERYTHROPOIETIN CONCENTRATION AND REQUIREMENT FOR ERYTHROPOIESIS

In healthy humans, the plasma erythropoietin concentration ranges independently of gender between 10–20 mU/ml with rather moderate diurnal variations.[321] Very similar values are measured in laboratory animals. Erythropoietin concentrations are given in terms of a biologic activity resulting from a comparison with an international reference standard.

Given a specific biologic activity of between 130,000 U/mg of protein for urinary erythropoietin and 200,000 U/mg of protein for pure human recombinant erythropoietin,[8] normal plasma concentrations in humans are then calculated to around 10 pmol/liter. In view of the absolute dependency of definitive erythropoiesis on erythropoietin, it follows that an insufficient formation of erythropoietin can be a major reason for anemia. To determine whether erythropoietin formation is appropriate or not, it is not sufficient to consider plasma erythropoietin levels alone. Since erythropoietin formation is mainly triggered by the oxygen delivery to the renal cortex, erythropoietin formation relative to the oxygen availability reflected by the hemoglobin concentration is the more reliable parameter to estimate the appropriateness of erythropoietin production. In laboratory animals, hemoglobin concentration can be changed under more controlled conditions, and those experiments have established an inverse semilogarithmic relationship between plasma concentration of erythropoietin and hemoglobin concentration, or the hematocrit, that is not dependent on the maneuver used to lower hemoglobin concentration such as irradiation, bleeding, or induction of hemolysis (Fig. 92.6). A very similar inverse semilogarithmic relationship is also found in humans suffering from regenerative, hemolytic, or iron-deficiency anemias (Fig. 92.11).[131,132] Depending on the degree of anemia, plasma erythropoietin concentrations can certainly increase up to 1000-fold, that is, up to 10 nmol/liter. The physiological reasons of such high plasma concentrations of erythropoietin are difficult to understand in view of the fact that the dissociation constant of the erythropoietin receptor is in the range of 10–50 pmol/liter, and that those concentrations are sufficient to stimulate CFU-E proliferation *in vitro* (see above). Studies in humans have shown that only moderate elevations of plasma erythropoietin concentrations are required to effectively stimulate erythropoiesis. This is most evident in patients suffering from renal anemia in which hemoglobin levels can be triggered to almost any extent by the subcutaneous administration of recombinant erythropoietin. Upon subcutaneous administration of erythropoietin, plasma erythropoietin concentrations, however, only rarely exceed a level of 100 pmol/liter. Thus, the reasons for the highly exaggerated plasma erythropoietin concentrations seen during severe anemia and severe arterial hypoxia are not yet understood. In more complex forms of anemia, such as postsurgery forms, or during chronic inflammation or tumor disease, the characteristic inverse relationship between plasma concentrations of erythropoietin and hemoglobin/hematocrit flattens,[322–324] suggesting that erythropoietin production is in appropriately low in those patients. In chronic renal disease, a positive relationship between plasma erythropoietin concentration and the hemoglobin concentration appears, indicating insufficient erythropoietin formation (Fig. 92.11).[132] In the latter instance, plasma erythropoietin concentrations reflect its efficacy on erythropoiesis rather than the efficacy of the renal oxygen erythropoietin sensor to regulate erythropoietin production in response to changes of the oxygen availability.

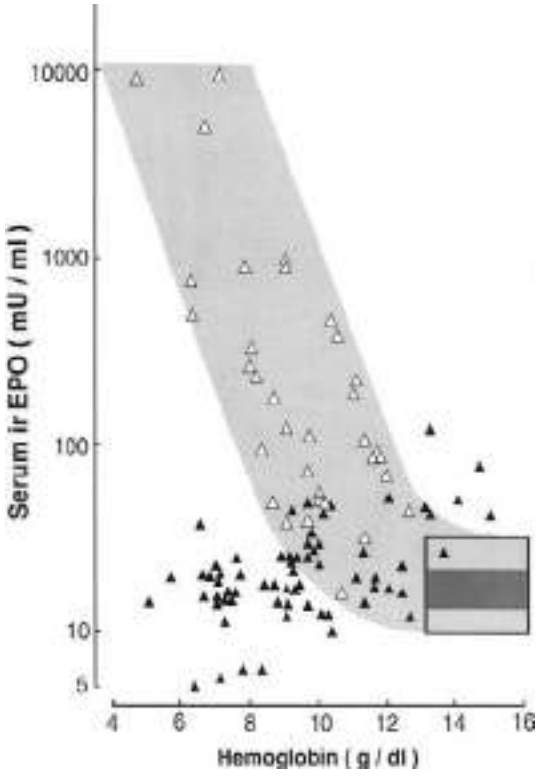

FIGURE 92.11 Relationship between serum immunoreactive (ir) EPO levels and hemoglobin concentration in patients with hypo- and hyper-regenerative nonrenal anemias (black triangles) and in patients with chronic renal failure (white triangles) (excluding patients with polycystic kidney disease). The rectangle depicts the interquartile range (dark stippled) and 95% confidence range of EPO levels in non-anemic healthy adults. *(With permission from Kurtz A, Eckardt KU. Erythropoietin production in chronic renal disease before and after transplantation. Contrib Nephrol 1990;87:15–25.)*

RENAL ANEMIA

Pathophysiology

Since the association of kidney disease with anemia was first documented in 1836,[7] anemia has been recognized as a characteristic symptom of chronic renal failure. This anemia is usually normocytic and normochromic, and develops almost invariably and largely independent of the underlying kidney disease when the creatinine clearance decreases to less than 20–30 ml/min.[325,326] It was an early observation that patients with renal failure lack the increase in serum erythropoietin levels that normally occurs as a response to reduced hemoglobin levels.[131,327] All three causes that can lead to anemia in general, namely, hemolysis, blood loss, and mainly impaired erythropoiesis, play a role in the pathogenesis of renal anemia. Although the contribution of hemolysis and blood loss to the anemia of patients with renal diseases is variable, and in selected patients may become predominant factors, both mechanisms are usually of a severity that can be compensated for by a moderate increase in the red cell production rate. Characteristically, however, erythropoiesis in renal failure is not enhanced, despite the persistence of anemia, as reflected by a lack of an appropriate increase in the number of reticulocytes and in iron kinetic studies. The determinants of this lack of response are therefore key elements in the pathogenesis of renal anemia.

Erythropoietin production during renal disease: Numerous investigators have demonstrated that endogenous erythropoietin production is severely blunted in patients with renal failure, and that erythropoietin levels do not rise appropriately for the degree of anemia (Fig. 92.11). It is also clear, however, that the erythropoietin deficiency is relative, rather than absolute, since levels in uremics are usually within or slightly above the normal range of nonanemic individuals. Even anephric patients maintain some basal erythropoietin production, which is presumably of hepatic origin.[328,329]

The reason for the inadequate production of erythropoietin relative to the degree of anemia is far from being understood. Although it might be assumed that renal disease implies damage to the cellular production sites of the hormone, the issue is more complex. When patients with chronic renal failure experience acute blood loss or hemolysis superimposed on their preexisting anemia, marked increases in circulating erythropoietin levels have been observed,[330] whereas conversely, red cell transfusions lead to a slight reduction in serum EPO.[327,329] Erythropoietin levels in patients with renal anemia also rise when oxygen supply is further compromised by a reduction in the arterial oxygen saturation of hemoglobin.[330] Although the response may be subnormal, these increases in erythropoietin under acute hypoxia are often of a magnitude that would certainly be sufficient to correct renal anemia, if they persisted.

These oxygen-dependent changes of plasma erythropoietin in patients with renal failure may in part reflect alterations in hepatic synthesis of the hormone. In general, the quantitative role of the liver for erythropoietin production in humans remains unknown, but a substantial hepatic contribution to the total erythropoietin mRNA expression has been found in anemic and hypoxic rats,[71,76] and hepatic erythropoietin mRNA accumulation was found not to be reduced in uremic animals.[76] Furthermore, in patients with renal anemia serum, erythropoietin and erythropoiesis can be transiently enhanced during episodes of viral and toxic hepatitis.[331] Although the mechanisms stimulating erythropoietin in inflamed and/or regenerating liver tissue have not been clarified, such observations suggest that the hepatic capacity for erythropoietin production would in principle be sufficient to compensate for inappropriately low renal synthesis.

Additional evidence indicates that a substantial production capacity for erythropoietin can also be maintained in diseased kidneys. A marked increase in erythropoietin mRNA has been found in remnant-kidney five-sixths nephrectomized rats after hypoxic exposure.[76] In experimental models of local renal tissue, injury expression of the erythropoietin gene was found to be reduced, but not abolished in areas of tubular atrophy and interstitial fibrosis.[97] Data about erythropoietin production in human diseased kidneys are sparse, but in patients developing erythrocytosis after successful kidney transplantation, selective measurements of erythropoietin in the veins draining the transplant and the endogenous kidneys have revealed an elevated erythropoietin production in the end-stage kidneys, which probably maintains the inappropriate increase in red cell production.[332,333]

In summary, it appears that in chronic renal failure, a considerable production capacity for erythropoietin is preserved, and that some feedback control of erythropoietin production is still operative, although the mechanisms linking erythropoietin production to the degree of anemia are disturbed. Given the evidence discussed above indicating that transport capacity of tubular cells plays a role in the control of erythropoietin production, it is conceivable that a reduction of tubular function contributes to inhibition of the normal erythropoietin response. Moreover, some evidence suggests that erythropoietin production in diseased kidneys may be inhibited by immunomodulatory cytokines, as mentioned earlier.[316,317]

Although erythropoietin production is generally unrelated to the etiology of renal failure, cystic kidney disease provides an interesting exception. Autosomal dominant polycystic kidney disease is a genetically determined structural and functional disorder that leads to chronic renal failure in the adult. The degree of anemia in patients with end-stage polycystic kidney disease is generally less severe than usual, and occasionally patients may become polycythemic.[334] In addition, acquired cysts in end-stage kidneys and single cysts may lead to erythrocytosis.[335,336] Plasma erythropoietin concentrations in patients with autosomal dominant polycystic kidney disease are, on average, twofold greater than in end-stage renal disease of noncystic origin,[334] and significant arteriovenous concentration differences for erythropoietin exist in polycystic kidneys.[87] The mechanisms by which cysts may stimulate erythropoietin production have not been resolved, although it is conceivable that compression and remodeling of pericystic tissue leads to regional hypoxia. In the cyst walls of patients with autosomal polycystic kidney disease, interstitial cells have been shown to express erythropoietin mRNA,[87] and cysts derived from proximal, but not those derived from distal tubules, may contain high concentrations of erythropoietin that are on average four-fold above the plasma concentration.[87] It has also been shown that single cysts derived from proximal tubules can contain high concentrations of erythropoietin,[337] indicating that erythropoietin formation is linked to the phenomenon of cysts formation itself rather than to the genetic abnormalities in polycystic kidney disease.

Therapy of Renal Anemia with rhEPO

Large multicenter trials have unequivocally shown that rhEPO is a highly effective therapy for renal anemia, with approximately 95% of patients responding. Primarily, rhEPO was used in dialysis patients only, but it is equally effective in predialysis patients and, importantly, was found not to accelerate the progression of renal failure in this population.[338,339] It appears rational therefore to start rhEPO therapy once a significant anemia develops, irrespective of whether renal replacement therapy is already necessary. Initial phase I clinical trials with rhEPO demonstrated that, depending on the dose of rhEPO, a steep increase in hemoglobin levels can be achieved within few weeks.[340,341] However, a very rapid correction of anemia is generally not necessary, not cost effective, and may be associated with a higher incidence of side effects. Thus, while initially doses of up to 1500 IU/kg of body weight per week were used, it is meanwhile recommended to use 75–120 IU/kg per week in order to achieve and maintain a hemoglobin value of 11 g/dl. The dose requirement in individual patients is quite variable, probably as a reflection of the complexity of the pathophysiology of renal anemia. In cases of primary treatment failure and when the response to rhEPO declines during therapy, the factors mentioned above that interfere with EPO efficacy should be evaluated. The majority of patients require iron supplementation to achieve an optimal effect with EPO therapy, and parenteral iron is frequently superior to oral supplements.[342] As outlined above, some effects of erythropoietin are unrelated to hematopoiesis. Those effects have to be taken into account for side effects of treatment with recombinant erythropoietin.

PHD Inhibitors as Future Therapeutics?

Albeit not fully understood regarding renal Epo production, the wealth of novel insights into the basic mechanisms of oxygen sensing and signalling opened new routes towards the treatment of diseases related to oxygen sensing. In kidney failure, oxygen consumption is decreased, resulting in increased tissue pO_2, decreased renal Epo production and anemia. Kidney dialysis patients hence need lifelong Epo treatments. Pharmaceutical interference with protein hydroxylase enzymatic activity proved to be efficient *in vitro* and beneficial for the treatment of a number of diseases in animal models *in vivo*, including tissue ischemia, kidney injury and transplantation.[244,343–346] Protein hydroxylase inhibitors also stimulated Epo production in mouse and rhesus macaque models.[254,347] Clinical phase II studies are being conducted to test the safety and efficacy of protein hydroxylase inhibitors in the treatment of patients with renal anemia. The near future will answer the question as to whether the currently available inhibitors of the oxygen sensing protein hydroxylases are sufficiently efficient and specific to serve as novel therapy strategies for the treatment of anemia caused by renal disease.

Erythropoietin Production after Renal Allotransplantation

Prior to the availability of rhEPO, renal allotransplantation has been the only way to definitely correct renal anemia. Hemoglobin concentrations usually normalize within a few weeks following successful renal allotransplantation. If one accepts that it is mainly an inappropriate erythropoietin production that leads to anemia in end-stage renal disease (ESRD), then consideration of erythropoietin production after renal transplantation becomes interesting. In fact, provided immediate excretory graft function, plasma erythropoietin levels rise

within 3–4 days after transplantation.[348–350] When hemoglobin concentrations subsequently have normalized, plasma erythropoietin declines to normal values.[351] These findings suggest that the transplant is capable of registering the anemia of ESRD and of responding with an increase in erythropoietin production. The oxygen dependency of erythropoietin formation becomes even more obvious when patients experience acute blood loss in the post-transplant period.[349] Regarding the mechanisms responsible for a disturbance of erythropoietin production during kidney failure, the analysis of erythropoietin formation after transplantation is of particular interest in those cases where the graft initially lacks excretory function. In this situation, erythropoietin formation was found to be rather unpredictable and variable. In some cases, temporal increases occur and plasma erythropoietin levels may display an irregular spiking pattern with no relationship to hemoglobin concentrations.[349] In others, no evidence for erythropoietin production by transplanted kidney is obtained at all, and a reduction in hemoglobin concentrations does not evoke an increase in erythropoietin. As soon as excretory function commences, erythropoietin production increases in primary inactive kidneys, or stabilizes in those cases where inconsistent elevations occurred during graft failure. In both instances, erythropoietin levels after onset of excretory function reach the values typical for cases with immediate graft function.[349] Irrespective of the different behavior of erythropoietin formation in individual cases, it appears as if during kidney failure the production capacity for erythropoietin may be preserved, but becomes decoupled from oxygen-dependent regulation. Furthermore, the temporal concurrence between the onset of excretory renal function and a regular oxygen dependency of erythropoietin formation in all cases may indicate that ongoing excretory function in the kidney is a prerequisite for the regulation of erythropoietin. This may have to do with the oxygen consumption of proximal tubules, which apparently is of relevance for the oxygen sensing.

Post-Transplant Polycythemia

In about 10% of the patients undergoing successful renal allotransplantation, a polycythemia develops, which in turn may give rise to thromboembolic complications.[352] Plasma erythropoietin concentrations in these patients were reported to be elevated,[333,353] and in some cases serial determinations showed as sustained elevation of erythropoietin after transplantation despite an increase in hemoglobin.[351] As to the question about the source of erythropoietin in these patients, both the native kidneys left in situ and the graft have to be considered. In some instances, an association with rejection, artery stenosis,[354] or hydronephrosis of the transplanted kidney has been reported. Extirpation of native kidneys has been found to cure post-transplant polycythemia,[355,356] suggesting a substantial role of the native kidneys as a source of inappropriate erythropoietin secretion.[357] This clinical inference is supported by multiple site estimates in post-transplant patients with polycythemia, demonstrating significant arteriovenous concentration differences for erythropoietin in the native kidneys.[332,353] At first view, it appears somewhat contradictory that after transplantation erythropoietin formation by diseased kidneys appears to induce polycythemia, whereas before transplantation erythropoietin formation was inappropriately low resulting in anemia. Although not yet proven, one may assume that the removal of uremia by the working graft and or suppression of inflammation by immunosuppressants play a major role. In any case, it appears also in the situation of post-transplant polycythemia the native kidneys have defect in adapting erythropoietin production appropriately to the oxygen availability. Interestingly, the enhanced formation of erythropoietin by the native kidneys can be lowered by theophyilline by a mechanism that is not yet understood.[358]

THROMBOCYTOPOIESIS

Platelet Formation

Like red cells, platelets derive from the pluripotent stem cells (Fig. 92.12). Due to mechanisms that are not well understood, stem cells become committed to the megakaryocytic pathway ending up with the platelets. Between the committed stem cells and the megakaryocyte as the histologically clearly identifiable differentiation state, there lie a number of cell divisions and differentiation steps. Under the influence of a variety of stimuli, the committed cells give rise to the earliest detectable progenitor, the megakaryocyte colony–forming unit (CFU-M), which is close to the megakaryocyte. When acted upon by appropriate regulatory substances, the CFU-M may be triggered to differentiate and to pro-liferate. During this period of development, these cells retain the normal diploid complement of DNA, and some cytoplasmic maturation does begin to occur as mitotic amplification proceeds including the accumulation of acetylcholinesterase activity, a cytochemical marker specific for megakaryocytes. Mitosis ceases in these early progenitor cells shortly after the appearance of acetylcholinesterase activity, as a result of this early cytoplasmic maturation. Cessation of mitotic activity does, however, not halt DNA synthesis. Rather, DNA synthesis

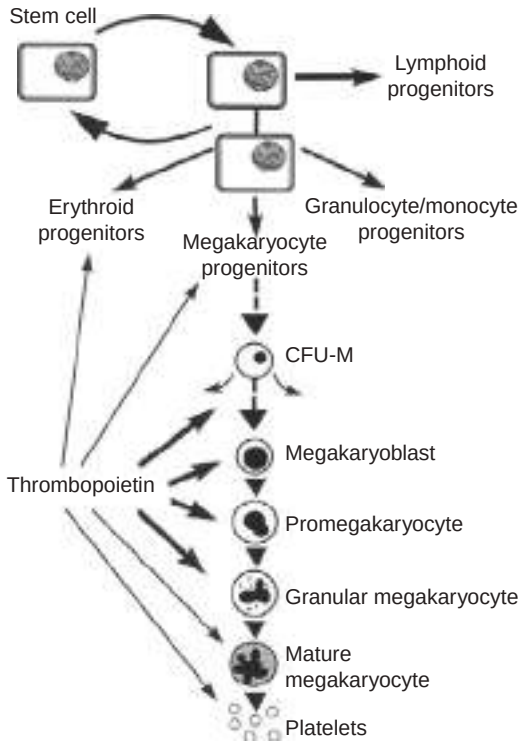

FIGURE 92.12 Schematic demonstration of differentiation steps of platelet formation and the action sites of thromobopoietin.

continues to occur in the form of nuclear endoreduplication. It is this unique megakaryocyte characteristic that allows these cells to become polyploid. Early megakaryocytes begin to form platelet granules and to form cytoplasmic invaginations that ultimately build up the platelet demarcation membrane system. Increasing cell ploidy is accompanied by increases in cell size, nuclear lobulation, cytoplasmic granulation, and changes in RNA content. As the ploidy level increases, the megakaryocyte progenitors enter the terminal stages of differentiation and become morphologically recognizable at the level of light microscopy. Platelet formation is initiated when pseudopodia are extended out of the megakaryocyte and penetrate the bone marrow sinusoids. The pseudopodia then fracture in the sinusoidal lumen and the fragments are carried to the lung. Either during passage to the lung or in the lung itself, the megakaryocyte fragment becomes a platelet, as organization of the microtubular and dense tubular systems induces its typical discoid shape.

Platelet formation appears to be controlled at least by two main factors. One is thrombopoietin, which increases DNA synthesis in young megakaryocytes, increases the number of immediate megakaryocyte precursors, augments their differentiation into mature megakaryocytes, increases the ploidy of megakaryocytes and platelet volume.[359] Although thrombopoietin seems to be the primary regulator of megakaryocyte development and platelet production,[360–362] a specific megakaryocyte-stimulating activity (Meg-CSA) that is regulated independently from thrombopoietin has also been suggested.[363]

Current models also suggest that early acting megakaryocyte colony stimulating factors, such as IL-3 or c-kit ligand are required for expansion of hematopoietic progenitors into cells capable of responding to late-acting megakaryocyte potentiators, including IL-6, IL-1,[364] and thrombopoietin. All together, it appears as if thrombopoietin is the primary and main regulator of megakaryocyte development and platelet production.

THROMBOPOIETIN

Historical Development

Initial studies concerning the regulation of megakaryocytopoiesis conclusively demonstrated a relationship between peripheral blood platelet numbers and alterations in their production. These alterations, which were manifested by the changes in megakaryocyte number, size, mitotic index, and ploidy values, appeared to be similar in both human and animal species. By analogy to the effect of erythropoietin on erythropoiesis, it was postulated that all of these effects were under the control of a single humoral regulatory substance designated thrombopoietin, which could be assayed by its ability to raise platelet counts in recipient animals.[365] It was recognized that plasma taken from thrombocytopenic patients or animals was able to increase platelet count or 35S-incorporation into platelets in healthy recipients. Attempts were made to purify thrombopoietin from the plasma of thrombopenic animals, however, were not met with great success. By chance it was found that the culture medium conditioned by the human embryonic kidney cell line (HEK) contained activity that was thrombopoietic both *in vivo* and *in vitro*.[366] The breakthrough came in 1994 when three groups reported the cloning of the thrombopoietin gene and demonstrated that thrombopoietin was a novel protein.[367–369] Important for the cloning strategy was the previous finding that platelets express the c-mpl proto-oncogene product, which was found to belong to the cytokine receptor superfamily.[370–372] Ingeniously anticipating that this receptor could be the thrombopoietin receptor, an assumption that was subsequently confirmed, affinity purification of thrombopoietin with the help of c-mpl was possible. The cloning of the thrombopoietin gene not only gave information about the structure of thrombopoietin and provided molecular tools for further investigations, but also led to the production of recombinant

thrombopoietin, which is available now for clinical trials in the treatment of thrombocytopenia.

Thrombopoietin Structure

Thrombopoietin has a predicted molecular mass of 35 kD.[367,369] Human full-length recombinant thrombopoietin has 332 residues. cDNAs for human, dog, and mouse are highly conserved and contain open reading frames for proteins of 353, 352, and 356 amino acids, respectively, including predicted 21 As signal peptides.[367,368] The protein backbone contains 6 N-carbohydrate linkage sites[368] and one O-carbohydrate linkage site to which complex carbohydrates are bound.[373] At the N-terminus, thrombopoietin has a high similarity to erythropoietin. Similar to the erythropoietin protein, the thrombopoietin protein probably contains two disulfide bonds (Cys 7−151 and Cys 29−85) that thus form a looped molecule.

Earlier attempts to purify thrombopoietic activities from HEK cells or from plasma or urine of thrombopenic beings led to activities with apparent molecular masses of around 30 kD and smaller sizes. In addition, thrombopoietic activity purified from canine or porcine thrombopenic plasma by binding to c-mpl appeared to be smaller than expected, namely with masses of 30, 25, and 20 kD,[367,368] but was found to have the same amino terminus as 25-kD thrombopoietin. It appears likely therefore that native thrombopoietin is cleaved into smaller products. This assumption is compatible with the fact that thrombopoietin contains two dibasic−amino acid sequences at positions 153−154 and 245-246, which could serve as potential processing sites. Although the cleavage mechanism is not yet understood, recent evidence suggests that thrombin could be involved in the physiologic cleavage of thrombopoietin.[374] However, in the circulation as well as in cell culture, this characteristic cleavage of thrombopoietin appears to occur.

Taken together, it appears as if thrombopoietin is produced as a glycoprotein with a protein backbone of around 330 amino acids, which physiologically becomes cleaved into a smaller fragments with a main size of around 30 kD. The fragments are biologically active and they share the same N-terminus, indicating that the N-terminus is essential for transmitting the biologic activity.

Thrombopoietin Gene

Controversial information has been reported about the structure of the thrombopoietin gene. While there is consensus that the human thrombopoietin gene contains a single copy on chromosome 3q26−28,[375−377] variable information exists about the length and organization of the gene. One group reported that the human thrombopoietin gene encompasses 6.2 kb with six exons and five introns,[376,377] whereas others found that the human thrombopoietin gene spans over 8 kb, consisting of seven exons and six introns.[375] Evidence suggests the existence of RNA splice variants for thrombopoietin.[369] The promoter region of the thrombopoietin gene contains no canonical TATA box. Investigations of regulating the thrombopoietin promoter have just begun. Early results suggest that the Ets transcription factor could play a role in its regulation.[378]

Thrombopoietin Receptor

Analysis of a leukemogenic retrovirus genome revealed the existence of a region coding for the so-called c-mpl proto-oncogene, which was expressed in hematopoietic tissue, and shared strong structural analogies with the hematopoietin superfamily.[372] Subsequently, it was shown that the c-mpl protein transduces a proliferative signal in hemopoietic cells.[371] Demonstration that oligodesoxynucleotides antisense to c-mpl specifically inhibited *in vitro* megakaryopoiesis led then to the assumption that c-mpl is the physiologic receptor for thrombopoietin.[370] c-Mpl-deficient mice have a marked (85%) decrease of platelet count and megakaryocytes, but have normal amounts of other hematopoietic cell types.[379,380] C-mpl is found in early progenitors of the various lineages and particularly in cells of the megakaryocytic lineage including platelets. This is a major difference compared to erythropoietin receptors, which are mainly expressed in late erythroid progenitors (CFU-E) and then decline and are absent from red blood cells.

Like other members of the hematopoietin/cytokine receptor superfamily, C-mpl consists of one extracellular domain, a single transmembrane domain and a cytosolic region.[381] Essential for the signaling are less than 100 amino acids of the cytoplasmic tail proximal to the transmembrane domain.[382] This region contains two boxes that are essential for tyrosine phosphorylation induced by thrombopoietin, and the thrombopoietin receptor itself is a substrate for phosphorylation.[383] Similar to the erythropoietin receptor, the signaling mechanism essentially starts with the receptor association and activation of Janus-kinase 2 (JAK2) and subsequent activation of STAT proteins.[382−385] The C-terminus of the c-mpl intracellular domain was found to be required for induction of Shc phosphorylation and c-fos mRNA accumulation, suggesting also involvement of the Ras signal transduction pathway.[382] In addition, the MAP kinase pathway becomes activated by thrombopoietin.[386] Finally, it has been found that thrombopoietin like erythropoietin activates phosphatidylinositol-3-kinase,[387] which causes an as yet unknown signaling pathway in megakaryocytes.

In addition to the membrane-anchored thrombopoietin receptor, a soluble form of the thrombopoietin receptor exists, of smaller size, and which has biologic

activity probably by associating with the target cells.[65] The binding characteristics of the thrombopoietin/MGDF receptor suggest the existence of a single affinity binding site with a dissociation constant of around 190 pmol/liter and about 30 binding sites per platelet.[388] The number of thrombopoietin binding sites on megakaryocytes is presumably higher but has not yet been determined.

Thrombopoietin Action

Mouse thrombopoietin activates human mpl, and human thrombopoietin activates mouse mpl, indicating the absence of strict species specificity.[389] Thrombopoietin increases megakaryocyte number and size in the bone marrow.[390] Thrombopoietin *in vivo* also increases DNA content of mouse bone marrow megakaryocytes indicating the induction of polyploidization.[391] Recombinant thrombopoietin also supports *in vitro* megakaryocyte formation, and acts at late stage of development to increase megakaryocyte size, polyploidization, and expression of differentiation markers. *In vivo* recombinant thrombopoietin stimulates platelet production by expanding the number of megakaryocytes and their progenitors in marrow and spleen. Transgenic mice overexpressing human thrombopoietin exhibit chronic thrombocytosis.[392] Conversely, animals with a disrupted thrombopoietin gene have low numbers of platelets and megakaryocytes. Thrombopoietin is therefore the major physiological regulator of both proliferation and differentiation of hematopoietic progenitor cells into mature megakaryocytes.[393] In addition to acting as a proliferation and differentiation factor, it has also been suggested that thrombopoietin suppresses apoptosis and behaves as a survival factor for megakaryocytes.[394,395] Interestingly, thrombopoietin appears not to be essential for a very late step in thrombocytopoiesis, namely proplatelet formation.[396]

Apart from these effects of thrombopoietin on late thrombopoiesis, however, thrombopoietin appears—in contrast to the action of erythropoietin—to also exert influence on early progenitors of different lineages. Thus, recombinant thrombopoietin increases not only the number circulating platelets but also the number CFU-M in primates.[397] Furthermore, thrombopoietin synergizes with stem cell factor or interleukin-3 to act on early multipotential hemopoietic progenitors.[398] The hematopoietic progenitor cell compartment responds to thrombopoietin as a whole, and therefore thrombopoietin can stimulate BFU-E, CFU-GM, and CFU-Mk formation *in vivo*.[399,400] Since erythroid progenitors respond to thrombopoietin, thrombopoietin can therefore augment erythropoiesis in states of bone marrow failure[401] by enhancing the effect of erythropoietin on early progenitors.[402] Physiologically increased levels of thrombopoietin, however, do not stimulate erythropoiesis.[403] Similarly, physiologically increased levels of erythropoietin do not stimulate thrombopoiesis,[403] while high doses of recombinant erythropoietin stimulate platelet production in mice[36] by synergizing with thrombopoietin to stimulate proliferation of CFU-M[404] or by cross-activation of the thrombopoietin receptor.

The existence of thrombopoietin receptors on circulating platelets in contrast to the lack of erythropoietin receptors on circulating red blood cells, suggests that thrombopoietin could also exert effects in mature platelets. In fact, there is accumulating evidence to suggest that thrombopoietin by itself does not change platelet activity, but substantially enhances platelet activation induced by ADP, thrombin, or other factors.[405–407]

Sites of Thrombopoietin Production

Given that the human embryonic kidney (HEK) cell line produces thrombopoietin activity, it was assumed that the kidney is a major site of thrombopoietin production.[366,408] Studies in nephrectomized animals, however, produced inconsistent results. Only one study reported a lack of response of platelet production in thrombocytopenic nephrectomized rats.[409] From a more clinical point of view, it can be noted that anephric patients on regular dialysis who are not treated with rhEPO are severely anemic, but not regularly thrombocytopenic.[410] It appeared reasonable therefore to conclude that other organs such as the liver[411] are able to compensate for the lack of renal thrombopoietin production. This assumption was confirmed by the finding that liver and kidney are the main sites of thrombopoietin mRNA expression in the body,[368,369] while thrombopoietin mRNA abundance is greater in the liver than in kidneys. In situ hybridization localized thrombopoietin mRNA to proximal tubules and hepatocytes, with no signal in renal peritubular cells.[412] From these findings, it appears as if liver and therein hepatocytes are the main site of thrombopoietin mRNA expression.[413] Apart from kidney and liver thrombopoietin, mRNA is found in spleen and bone marrow,[414] albeit at substantially lower levels. Some evidence has been provided to suggest that thrombopoietin produced by stromal cells in a hematopoietic environment stimulates proliferation and maturation of megakaryocytes.[415]

Regulation of Plasma Thrombopoietin Levels

The data about the plasma concentration of thrombopoietin are as yet rather scarce. It was reported that in healthy humans, plasma thrombopoietin concentrations are around 0.7 fmol/liter with no gender difference or age dependency,[416] which is consistent with another report that normal values are below 150 pg/ml.[417] Plasma thrombopoietin levels are increased during

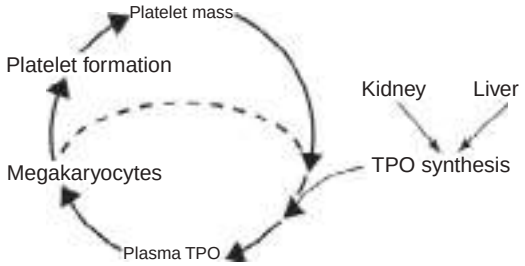

FIGURE 92.13 Negative feedback regulation of plasma thrombopoietin concentration.

thrombocytopenic states of different etiology. Up to know highest levels of thrombopoietin were reported for patients with aplastic anemia in which values up to 18 fmol/ml[418] or 4000 pg/ml[417] were measured.

Thrombopoietin levels are usually inversely related to the number of circulating platelets, in striking similarity to the relationship between plasma erythropoietin levels and red cell counts. As for erythropoietin, liver and kidney as the main production sites for thrombopoietin apparently do not contain significant stores of preformed hormone, since successful isolation of thrombopoietin from organs has not yet been reported. One may infer that thrombopoietin secretion into the bloodstream is mainly determined by the rate of de novo synthesis in liver and kidney. In marked contrast to the regulation of the erythropoietin gene, however, changes in platelet counts have no effect on thrombopoietin mRNA levels in liver, kidney, and spleen,[414,419] although a certain upregulation may occur in the bone marrow during thrombocytopenia.[412,414] The lack of relationship between thrombopoietin mRNA levels in the organs mainly responsible for thrombopoietin production and the circulating thrombopoietin level strongly suggests that the regulation does not occur at the level of its mRNA, and that the production rate either depends on regulation at the post-transcriptional level or that changes in circulating thrombopoietin levels do not reflect changes in its production rate. Although a post-translational regulation cannot be excluded, the evidence currently available favors the idea that changes in circulating thrombopoietin levels are mainly regulated by thrombopoietin metabolism rather than by alterations of its production. From the observation that plasma thrombopoietin changes reciprocally with changes of platelet counts, it was postulated that platelet mass may directly play a role in regulating the circulating levels of thrombopoietin (Fig. 92.13).[420] Evidence was in fact provided that thrombopoietin levels are directly determined by the number of circulating platelets,[393] because they bind thrombopoietin to the c-mpl receptor,[421] and internalize and metabolize thrombopoietin.[419,421,422] Moreover, megakaryocytes appear to affect thrombopoietin levels and to contribute to thrombopoietin degradation.[422,423] In line with this inference, it has been reported that megakaryocyte mass is an essential determinant of circulating thrombopoietin levels,[417] and it is assumed that not only platelets but also megakaryocytes must be involved in the regulation of the level of circulating thrombopoietin.[424,425] In patients with aplastic anemia, however, no direct correlation between thrombopoietin levels and the degree of thrombocytopenia was found,[426] suggesting that parameters different from circulating platelets (and number of megakaryocytes) also influence plasma thrombopoietin levels.

FUTURE ASPECTS

Although understanding the role of the kidney in hematopoiesis has been significantly expanded in recent years, some obvious questions are still unanswered. Thus, it will be interesting to learn why only a special subset of interstitial fibroblasts around proximal tubules elaborate EPO. Furthermore, the reasons for why renal cells producing EPO in situ do not do so *in vitro* have to be clarified, as well as those underlying the observation that a number of extrarenal cells (primary cultures and cell lines) express EPO in an inverse fashion with the oxygen tension. Understanding how the renal oxygen sensor controlling erythropoietin production works will also help in learning why, in chronic renal disease, erythropoietin production is decoupled from oxygen availability, since significant production capacity of the kidney to elaborate erythropoietin appears to be preserved.

References

[1] Carnot MP, deFlandre MC, Bouchard M. Physiologie sur l'activite hemopoietique du serum au cours de la regeneration du sang. C R Acad Sci 1906;143:384–6.
[2] Bonsdorff E. On the presence of erythropoietins in the plasma from sheep foetuses during the latter half of gestation. Acta Physiol Scand 1949;18(1):51–62.
[3] Erslev AJ. Physiologic control of red cell production. Blood 1955;10(9):954–61.
[4] Reissmann KR. Studies on the mechanism of erythropoietic stimulation in parabiotic rats during hypoxia. Blood 1950;5(4):372–80.
[5] Goldwasser E, Jacobson LO, Fried W, Plzak LF. Studies on erythropoiesis. V. The effect of cobalt on the production of erythropoietin. Blood 1958;13(1):55–60.
[6] Jacobson LO, Goldwasser E, Fried W, Plzak L. Role of the kidney in erythropoiesis. Nature 1957;179(4560):633–4.
[7] Bright R. reports on medical cases London. 1827.
[8] Miyake T, Kung CK, Goldwasser E. Purification of human erythropoietin. J Biol Chem 1977;252(15):5558–64.

[9] Jacobs K, Shoemaker C, Rudersdorf R, et al. Isolation and characterization of genomic and cDNA clones of human erythropoietin. Nature 1985;313(6005):806–10.
[10] Lin FK, Suggs S, Lin CH, et al. Cloning and expression of the human erythropoietin gene. Proc Natl Acad Sci U S A 1985;82 (22):7580–4.
[11] Chu CY, Cheng CH, Yang CH, Huang CJ. Erythropoietins from teleosts. Cell Mol Life Sci 2008;65(22):3545–52.
[12] Shiels A, Wickramasinghe SN. Expression of an erythropoietin-like gene in the trout. Br J Haematol 1995;90(1):219–21.
[13] Nogawa-Kosaka N, Hirose T, Kosaka N, et al. Structural and biological properties of erythropoietin in Xenopus laevis. Exp Hematol 2010;38(5):363–72.
[14] Recny MA, Scoble HA, Kim Y. Structural characterization of natural human urinary and recombinant DNA-derived erythropoietin. Identification of des-arginine 166 erythropoietin. J Biol Chem 1987;262(35):17156–63.
[15] Suliman HB, Majiwa PA, Feldman BF, Mertens B, Logan-Henfrey L. Cloning of a cDNA encoding bovine erythropoietin and analysis of its transcription in selected tissues. Gene 1996;171(2):275–80.
[16] Wen D, Boissel JP, Tracy TE, et al. Erythropoietin structure-function relationships: high degree of sequence homology among mammals. Blood 1993;82(5):1507–16.
[17] Cheetham JC, Smith DM, Aoki KH, et al. NMR structure of human erythropoietin and a comparison with its receptor bound conformation. Nat Struct Biol 1998;5(10):861–6.
[18] Egrie JC, Strickland TW, Lane J, et al. Characterization and biological effects of recombinant human erythropoietin. Immunobiology 1986;172(3–5):213–24.
[19] Sasaki H, Ochi N, Dell A, Fukuda M. Site-specific glycosylation of human recombinant erythropoietin: analysis of glycopeptides or peptides at each glycosylation site by fast atom bombardment mass spectrometry. Biochemistry 1988;27(23): 8618–26.
[20] Takeuchi M, Takasaki S, Miyazaki H, et al. Comparative study of the asparagine-linked sugar chains of human erythropoietins purified from urine and the culture medium of recombinant Chinese hamster ovary cells. J Biol Chem 1988;263(8):3657–63.
[21] Sato H, Ohkubo M, Nagaoka T. Levels of serum colony-stimulating factors (CSFs) in patients on long-term haemodialysis. Cytokine 1994;6(2):187–94.
[22] Tsuda E, Goto M, Murakami A, et al. Comparative structural study of N-linked oligosaccharides of urinary and recombinant erythropoietins. Biochemistry 1988;27(15):5646–54.
[23] Goldwasser E, Kung CK, Eliason J. On the mechanism of erythropoietin-induced differentiation. 13. The role of sialic acid in erythropoietin action. J Biol Chem 1974;249(13):4202–6.
[24] Lukowsky WA, Painter RH. Studies on the role of sialic acid in the physical and biological properties of erythropoietin. Can J Biochem 1972;50(8):909–17.
[25] Lin CS, Lim SK, D'Agati V, Costantini F. Differential effects of an erythropoietin receptor gene disruption on primitive and definitive erythropoiesis. Genes Dev 1996;10(2):154–64.
[26] Wu H, Liu X, Jaenisch R, Lodish HF. Generation of committed erythroid BFU-E and CFU-E progenitors does not require erythropoietin or the erythropoietin receptor. Cell 1995;83(1):59–67.
[27] Wu H, Lee SH, Gao J, Liu X, Iruela-Arispe ML. Inactivation of erythropoietin leads to defects in cardiac morphogenesis. Development 1999;126(16):3597–605.
[28] Wu H, Klingmuller U, Besmer P, Lodish HF. Interaction of the erythropoietin and stem-cell-factor receptors. Nature 1995;377 (6546):242–6.
[29] Mellitzer G, Wessely O, Decker T, Meinke A, Hayman MJ, Beug H. Activation of Stat 5b in erythroid progenitors correlates with the ability of ErbB to induce sustained cell proliferation. Proc Natl Acad Sci U S A 1996;93(18):9600–5.
[30] Sawada K, Krantz SB, Dessypris EN, Koury ST, Sawyer ST. Human colony-forming units-erythroid do not require accessory cells, but do require direct interaction with insulin-like growth factor I and/or insulin for erythroid development. J Clin Invest 1989;83(5):1701–9.
[31] Koury MJ, Bondurant MC. Erythropoietin retards DNA breakdown and prevents programmed death in erythroid progenitor cells. Science 1990;248(4953):378–81.
[32] Spivak JL, Pham T, Isaacs M, Hankins WD. Erythropoietin is both a mitogen and a survival factor. Blood 1991;77(6): 1228–33.
[33] Gross M, Goldwasser E. On the mechanism of erythropoietin-induced differentiation. VII. The relationship between stimulated deoxyribonucleic acid synthesis and ribonucleic acid synthesis. J Biol Chem 1970;245(7):1632–6.
[34] Koury MJ, Bondurant MC, Atkinson JB. Erythropoietin control of terminal erythroid differentiation: maintenance of cell viability, production of hemoglobin, and development of the erythrocyte membrane. Blood Cells 1987;13(1–2):217–26.
[35] Berridge MV, Fraser JK, Carter JM, Lin FK. Effects of recombinant human erythropoietin on megakaryocytes and on platelet production in the rat. Blood 1988;72(3):970–7.
[36] McDonald TP, Cottrell MB, Clift RE, Cullen WC, Lin FK. High doses of recombinant erythropoietin stimulate platelet production in mice. Exp Hematol 1987;15(6):719–21.
[37] Fraser JK, Tan AS, Lin FK, Berridge MV. Expression of specific high-affinity binding sites for erythropoietin on rat and mouse megakaryocytes. Exp Hematol 1989;17(1):10–6.
[38] Cariou A, Andre S, Claessens YE. Extra-hematopoietic effects of erythropoietin. Cardiovasc Hematol Disord Drug Targets 2008;8 (3):173–8.
[39] Gassmann M, Heinicke K, Soliz J, Ogunshola OO. Non-erythroid functions of erythropoietin. Adv Exp Med Biol 2003;543:323–30.
[40] Jelkmann W, Wagner K. Beneficial and ominous aspects of the pleiotropic action of erythropoietin. Ann Hematol 2004;83 (11):673–86.
[41] Maiese K, Li F, Chong ZZ. New avenues of exploration for erythropoietin. JAMA 2005;293(1):90–5.
[42] Noguchi CT, Wang L, Rogers HM, Teng R, Jia Y. Survival and proliferative roles of erythropoietin beyond the erythroid lineage. Expert Rev Mol Med 2008;10:e36.
[43] Anagnostou A, Lee ES, Kessimian N, Levinson R, Steiner M. Erythropoietin has a mitogenic and positive chemotactic effect on endothelial cells. Proc Natl Acad Sci U S A 1990;87 (15):5978–82.
[44] Anagnostou A, Liu Z, Steiner M, et al. Erythropoietin receptor mRNA expression in human endothelial cells. Proc Natl Acad Sci U S A 1994;91(9):3974–8.
[45] Yamaji R, Okada T, Moriya M, et al. Brain capillary endothelial cells express two forms of erythropoietin receptor mRNA. Eur J Biochem 1996;239(2):494–500.
[46] Digicaylioglu M, Bichet S, Marti HH, et al. Localization of specific erythropoietin binding sites in defined areas of the mouse brain. Proc Natl Acad Sci U S A 1995;92(9):3717–20.
[47] Morishita E, Masuda S, Nagao M, Yasuda Y, Sasaki R. Erythropoietin receptor is expressed in rat hippocampal and cerebral cortical neurons, and erythropoietin prevents in vitro glutamate-induced neuronal death. Neuroscience 1997;76 (1):105–16.
[48] Sawyer ST, Krantz SB, Sawada K. Receptors for erythropoietin in mouse and human erythroid cells and placenta. Blood 1989;74(1):103–9.
[49] Krantz SB. Erythropoietin. Blood 1991;77(3):419–34.

[50] Youssoufian H, Longmore G, Neumann D, Yoshimura A, Lodish HF. Structure, function, and activation of the erythropoietin receptor. Blood 1993;81(9):2223–36.
[51] Bazan JF. Structural design and molecular evolution of a cytokine receptor superfamily. Proc Natl Acad Sci U S A 1990;87 (18):6934–8.
[52] Cosman D, Lyman SD, Idzerda RL, et al. A new cytokine receptor superfamily. Trends Biochem Sci 1990;15(7):265–70.
[53] Ihle JN. Cytokine receptor signalling. Nature 1995;377 (6550):591–4.
[54] D'Andrea AD, Lodish HF, Wong GG. Expression cloning of the murine erythropoietin receptor. Cell 1989;57(2):277–85.
[55] Jones SS, D'Andrea AD, Haines LL, Wong GG. Human erythropoietin receptor: cloning, expression, and biologic characterization. Blood 1990;76(1):31–5.
[56] Winkelmann JC, Penny LA, Deaven LL, Forget BG, Jenkins RB. The gene for the human erythropoietin receptor: analysis of the coding sequence and assignment to chromosome 19p. Blood 1990;76(1):24–30.
[57] Sawyer ST, Hankins WD. The functional form of the erythropoietin receptor is a 78-kDa protein: correlation with cell surface expression, endocytosis, and phosphorylation. Proc Natl Acad Sci U S A 1993;90(14):6849–53.
[58] Watowich SS, Hilton DJ, Lodish HF. Activation and inhibition of erythropoietin receptor function: role of receptor dimerization. Mol Cell Biol 1994;14(6):3535–49.
[59] Witthuhn BA, Quelle FW, Silvennoinen O, et al. JAK2 associates with the erythropoietin receptor and is tyrosine phosphorylated and activated following stimulation with erythropoietin. Cell 1993;74(2):227–36.
[60] Neubauer H, Cumano A, Muller M, Wu H, Huffstadt U, Pfeffer K. Jak2 deficiency defines an essential developmental checkpoint in definitive hematopoiesis. Cell 1998;93(3): 397–409.
[61] Parganas E, Wang D, Stravopodis D, et al. Jak2 is essential for signaling through a variety of cytokine receptors. Cell 1998;93 (3):385–95.
[62] Yoshimura A, Longmore G, Lodish HF. Point mutation in the exoplasmic domain of the erythropoietin receptor resulting in hormone-independent activation and tumorigenicity. Nature 1990;348(6302):647–9.
[63] de la Chapelle A, Traskelin AL, Juvonen E. Truncated erythropoietin receptor causes dominantly inherited benign human erythrocytosis. Proc Natl Acad Sci U S A 1993;90(10):4495–9.
[64] Longmore GD. Erythropoietin receptor mutations and Olympic glory. Nat Genet 1993;4(2):108–10.
[65] Ku H, Hirayama F, Kato T, et al. Soluble thrombopoietin receptor (Mpl) and granulocyte colony-stimulating factor receptor directly stimulate proliferation of primitive hematopoietic progenitors of mice in synergy with steel factor or the ligand for Flt3/Flk2. Blood 1996;88(11):4124–31.
[66] Baynes RD, Reddy GK, Shih YJ, Skikne BS, Cook JD. Serum form of the erythropoietin receptor identified by a sequence-specific peptide antibody. Blood 1993;82(7):2088–95.
[67] Fried W. The liver as a source of extrarenal erythropoietin production. Blood 1972;40(5):671–7.
[68] Zanjani ED, Ascensao JL, McGlave PB, Banisadre M, Ash RC. Studies on the liver to kidney switch of erythropoietin production. J Clin Invest 1981;67(4):1183–8.
[69] Moritz KM, Lim GB, Wintour EM. Developmental regulation of erythropoietin and erythropoiesis. Am J Physiol 1997;273(6 Pt 2):R1829–44.
[70] Carmena AO, Howard D, Stohlman Jr. F. Regulation of erythropoiesis. XXII. Erythropoietin production in the newborn animal. Blood 1968;32(3):376–82.
[71] Eckardt KU, Ratcliffe PJ, Tan CC, Bauer C, Kurtz A. Age-dependent expression of the erythropoietin gene in rat liver and kidneys. J Clin Invest 1992;89(3):753–60.
[72] Schooley JC, Mahlmann LJ. Extrarenal erythropoietin production by the liver in the weanling rat. Proc Soc Exp Biol Med 1974;145(3):1081–3.
[73] Koury MJ, Bondurant MC, Graber SE, Sawyer ST. Erythropoietin messenger RNA levels in developing mice and transfer of 125I-erythropoietin by the placenta. J Clin Invest 1988;82(1):154–9.
[74] Dame C, Fahnenstich H, Freitag P, et al. Erythropoietin mRNA expression in human fetal and neonatal tissue. Blood 1998;92 (9):3218–25.
[75] Flake AW, Harrison MR, Adzick NS, Zanjani ED. Erythropoietin production by the fetal liver in an adult environment. Blood 1987;70(2):542–5.
[76] Tan CC, Eckardt KU, Ratcliffe PJ. Organ distribution of erythropoietin messenger RNA in normal and uremic rats. Kidney Int 1991;40(1):69–76.
[77] Fried W, Barone-Varelas J, Berman M. Detection of high erythropoietin titers in renal extracts of hypoxic rats. J Lab Clin Med 1981;97(1):82–6.
[78] Jelkmann W, Bauer C. Demonstration of high levels of erythropoietin in rat kidneys following hypoxic hypoxia. Pflugers Arch 1981;392(1):34–9.
[79] Sherwood JB, Goldwasser E. Extraction of erythropoietin from normal kidneys. Endocrinology 1978;103(3):866–70.
[80] Koury ST, Bondurant MC, Koury MJ. Localization of erythropoietin synthesizing cells in murine kidneys by in situ hybridization. Blood 1988;71(2):524–7.
[81] Kurtz A, Eckardt KU, Neumann R, Kaissling B, Le Hir M, Bauer C. Site of erythropoietin formation. Contrib Nephrol 1989;76:14–20 [discussion 1–3].
[82] Lacombe C, Da Silva JL, Bruneval P, et al. Peritubular cells are the site of erythropoietin synthesis in the murine hypoxic kidney. J Clin Invest 1988;81(2):620–3.
[83] Bachmann S, Le Hir M, Eckardt KU. Co-localization of erythropoietin mRNA and ecto-5'-nucleotidase immunoreactivity in peritubular cells of rat renal cortex indicates that fibroblasts produce erythropoietin. J Histochem Cytochem 1993;41(3):335–41.
[84] Le Hir M, Eckardt KU, Kaissling B. Anemia induces 5'-nucleotidase in fibroblasts of cortical labyrinth of rat kidney. Ren Physiol Biochem 1989;12(5–6):313–9.
[85] Maxwell PH, Osmond MK, Pugh CW, et al. Identification of the renal erythropoietin-producing cells using transgenic mice. Kidney Int 1993;44(5):1149–62.
[86] Liapis H, Roby J, Birkland TP, Davila RM, Ritter D, Parks WC. In situ hybridization of human erythropoietin in pre- and postnatal kidneys. Pediatr Pathol Lab Med 1995;15(6):875–83.
[87] Eckardt KU, Mollmann M, Neumann R, et al. Erythropoietin in polycystic kidneys. J Clin Invest 1989;84(4):1160–6.
[88] Fisher JW, Koury S, Ducey T, Mendel S. Erythropoietin production by interstitial cells of hypoxic monkey kidneys. Br J Haematol 1996;95(1):27–32.
[89] Darby IA, Evans BA, Fu P, Lim GB, Moritz KM, Wintour EM. Erythropoietin gene expression in fetal and adult sheep kidney. Br J Haematol 1995;89(2):266–70.
[90] Eckardt KU, Koury ST, Tan CC, et al. Distribution of erythropoietin producing cells in rat kidneys during hypoxic hypoxia. Kidney Int 1993;43(4):815–23.
[91] Koury ST, Koury MJ, Bondurant MC, Caro J, Graber SE. Quantitation of erythropoietin-producing cells in kidneys of mice by in situ hybridization: correlation with hematocrit, renal erythropoietin mRNA, and serum erythropoietin concentration. Blood 1989;74(2):645–51.

[92] Da Silva JL, Lacombe C, Bruneval P, et al. Tumor cells are the site of erythropoietin synthesis in human renal cancers associated with polycythemia. Blood 1990;75(3): 577–82.
[93] Schuster SJ, Koury ST, Bohrer M, Salceda S, Caro J. Cellular sites of extrarenal and renal erythropoietin production in anaemic rats. Br J Haematol 1992;81(2):153–9.
[94] Koury ST, Bondurant MC, Koury MJ, Semenza GL. Localization of cells producing erythropoietin in murine liver by in situ hybridization. Blood 1991;77(11):2497–503.
[95] Eckardt KU, Pugh CW, Ratcliffe PJ, Kurtz A. Oxygen-dependent expression of the erythropoietin gene in rat hepatocytes in vitro. Pflugers Arch 1993;423(5–6):356–64.
[96] Maxwell PH, Ferguson DJ, Osmond MK, et al. Expression of a homologously recombined erythopoietin-SV40 T antigen fusion gene in mouse liver: evidence for erythropoietin production by Ito cells. Blood 1994;84(6):1823–30.
[97] Maxwell PH, Ferguson DJ, Nicholls LG, et al. Sites of erythropoietin production. Kidney Int 1997;51(2):393–401.
[98] Schmid TC, Loffing J, Le Hir M, Kaissling B. Distribution of ecto-5′-nucleotidase in the rat liver: effect of anaemia. Histochemistry 1994;101(6):439–47.
[99] Fandrey J, Bunn HF. In vivo and in vitro regulation of erythropoietin mRNA: measurement by competitive polymerase chain reaction. Blood 1993;81(3):617–23.
[100] Kobayashi T, Yanase H, Iwanaga T, Sasaki R, Nagao M. Epididymis is a novel site of erythropoietin production in mouse reproductive organs. Biochem Biophys Res Commun 2002;296(1):145–51.
[101] Masuda S, Kobayashi T, Chikuma M, Nagao M, Sasaki R. The oviduct produces erythropoietin in an estrogen- and oxygen-dependent manner. Am J Physiol Endocrinol Metab 2000;278(6):E1038–44.
[102] Tan CC, Eckardt KU, Firth JD, Ratcliffe PJ. Feedback modulation of renal and hepatic erythropoietin mRNA in response to graded anemia and hypoxia. Am J Physiol 1992;263(3 Pt 2): F474–81.
[103] Yasuda Y, Masuda S, Chikuma M, Inoue K, Nagao M, Sasaki R. Estrogen-dependent production of erythropoietin in uterus and its implication in uterine angiogenesis. J Biol Chem 1998;273(39):25381–7.
[104] Dame C, Bartmann P, Wolber E, Fahnenstich H, Hofmann D, Fandrey J. Erythropoietin gene expression in different areas of the developing human central nervous system. Brain Res Dev Brain Res 2000;125(1–2):69–74.
[105] Marti HH, Wenger RH, Rivas LA, et al. Erythropoietin gene expression in human, monkey and murine brain. Eur J Neurosci 1996;8(4):666–76.
[106] Masuda S, Okano M, Yamagishi K, Nagao M, Ueda M, Sasaki R. A novel site of erythropoietin production. Oxygen-dependent production in cultured rat astrocytes. J Biol Chem 1994;269(30):19488–93.
[107] Juul SE, Anderson DK, Li Y, Christensen RD. Erythropoietin and erythropoietin receptor in the developing human central nervous system. Pediatr Res 1998;43(1):40–9.
[108] Yu X, Shacka JJ, Eells JB, et al. Erythropoietin receptor signalling is required for normal brain development. Development 2002;129(2):505–16.
[109] Bernaudin M, Marti HH, Roussel S, et al. A potential role for erythropoietin in focal permanent cerebral ischemia in mice. J Cereb Blood Flow Metab 1999;19(6):643–51.
[110] Sakanaka M, Wen TC, Matsuda S, et al. In vivo evidence that erythropoietin protects neurons from ischemic damage. Proc Natl Acad Sci U S A 1998;95(8):4635–40.
[111] Siren AL, Fratelli M, Brines M, et al. Erythropoietin prevents neuronal apoptosis after cerebral ischemia and metabolic stress. Proc Natl Acad Sci U S A 2001;98(7):4044–9.
[112] Yokomizo R, Matsuzaki S, Uehara S, Murakami T, Yaegashi N, Okamura K. Erythropoietin and erythropoietin receptor expression in human endometrium throughout the menstrual cycle. Mol Hum Reprod 2002;8(5):441–6.
[113] Chikuma M, Masuda S, Kobayashi T, Nagao M, Sasaki R. Tissue-specific regulation of erythropoietin production in the murine kidney, brain, and uterus. Am J Physiol Endocrinol Metab 2000;279(6):E1242–8.
[114] Conrad KP, Benyo DF, Westerhausen-Larsen A, Miles TM. Expression of erythropoietin by the human placenta. FASEB J 1996;10(7):760–8.
[115] Kim MJ, Bogic L, Cheung CY, Brace RA. Expression of erythropoietin mRNA, protein and receptor in ovine fetal membranes. Placenta 2001;22(10):846–51.
[116] Westgren M, Ek S, Remberger M, Ringden O, Stangenberg M. Cytokines in fetal blood and amniotic fluid in Rh-immunized pregnancies. Obstet Gynecol 1995;86(2):209–13.
[117] Juul SE, Ledbetter DJ, Joyce AE, et al. Erythropoietin acts as a trophic factor in neonatal rat intestine. Gut 2001;49(2):182–9.
[118] Kurtz A, Eckardt KE, Tannahill L, Bauer C. Regulation of erythropoietin production. Contrib Nephrol 1988;66:1–16.
[119] Abbrecht PH, Littell JK. Plasma erythropoietin in men and mice during acclimatization to different altitudes. J Appl Physiol 1972;32(1):54–8.
[120] Caro J, Erslev AJ. Biologic and immunologic erythropoietin in extracts from hypoxic whole rat kidneys and in their glomerular and tubular fractions. J Lab Clin Med 1984;103 (6):922–31.
[121] Eckardt KU, Kurtz A, Bauer C. Triggering of erythropoietin production by hypoxia is inhibited by respiratory and metabolic acidosis. Am J Physiol 1990;258(3 Pt 2):R678–83.
[122] Jelkmann W. Temporal pattern of erythropoietin titers in kidney tissue during hypoxic hypoxia. Pflugers Arch 1982;393 (1):88–91.
[123] Eckardt KU, Dittmer J, Neumann R, Bauer C, Kurtz A. Decline of erythropoietin formation at continuous hypoxia is not due to feedback inhibition. Am J Physiol 1990;258(5 Pt 2):F1432–7.
[124] Reynafarje C, Ramos J, Faura J, Villavicencio D. Humoral control of erythropoietic activity in man during and after altitude exposure. Proc Soc Exp Biol Med 1964;116:649–50.
[125] Eckardt KU, Boutellier U, Kurtz A, Schopen M, Koller EA, Bauer C. Rate of erythropoietin formation in humans in response to acute hypobaric hypoxia. J Appl Physiol 1989;66 (4):1785–8.
[126] Necas E, Neuwirt J. Feedback regulation by red cell mass of the sensitivity of the erythropoietin-producing organ to hypoxia. Blood 1970;36(6):754–63.
[127] Erslev AJ, Caro J. Pure erythrocytosis classified according to erythropoietin titers. Am J Med 1984;76(1):57–61.
[128] Le Hir M, Eckardt KU, Kaissling B, Koury ST, Kurtz A. Structure-function correlations in erythropoietin formation and oxygen sensing in the kidney. Klin Wochenschr 1991;69 (13):567–75.
[129] Syvertsen GR, Harris JA. Erythropoietin production in dogs exposed to high altitude and carbon monoxide. Am J Physiol 1973;225(2):293–9.
[130] Miller ME, Cronkite EP, Garcia JF. Plasma levels of immunoreactive erythropoietin after acute blood loss in man. Br J Haematol 1982;52(4):545–9.
[131] Cotes PM. Immunoreactive erythropoietin in serum. I. Evidence for the validity of the assay method and the

physiological relevance of estimates. Br J Haematol 1982;50 (3):427–38.
[132] Erslev AJ, Wilson J, Caro J. Erythropoietin titers in anemic, nonuremic patients. J Lab Clin Med 1987;109(4):429–33.
[133] Garcia JE, Senent C, Pascual C, et al. Anaphylactic reaction to recombinant human erythropoietin. Nephron 1993;65 (4):636–7.
[134] Lorentz A, Jendrissek A, Eckardt KU, Schipplick M, Osswald PM, Kurtz A. Serial immunoreactive erythropoietin levels in autologous blood donors. Transfusion 1991;31(7):650–4.
[135] Cotes PM, Dore CJ, Yin JA, et al. Determination of serum immunoreactive erythropoietin in the investigation of erythrocytosis. N Engl J Med 1986;315(5):283–7.
[136] Rege AB, Brookins J, Fisher JW. A radioimmunoassay for erythropoietin: serum levels in normal human subjects and patients with hemopoietic disorders. J Lab Clin Med 1982;100 (6):829–43.
[137] Lechermann B, Jelkmann W. Erythropoietin production in normoxic and hypoxic rats with increased blood O_2 affinity. Respir Physiol 1985;60(1):1–8.
[138] Boutin AT, Weidemann A, Fu Z, et al. Epidermal sensing of oxygen is essential for systemic hypoxic response. Cell 2008;133(2):223–34.
[139] Paus R, Bodo E, Kromminga A, Jelkmann W. Erythropoietin and the skin: a role for epidermal oxygen sensing? Bioessays 2009;31(3):344–8.
[140] von Wussow U, Klaus J, Pagel H. Is the renal production of erythropoietin controlled by the brain stem? Am J Physiol Endocrinol Metab 2005;289(1):E82–6.
[141] Weidemann A, Kerdiles YM, Knaup KX, et al. The glial cell response is an essential component of hypoxia-induced erythropoiesis in mice. J Clin Invest 2009;119(11):3373–83.
[142] Schuster SJ, Badiavas EV, Costa-Giomi P, Weinmann R, Erslev AJ, Caro J. Stimulation of erythropoietin gene transcription during hypoxia and cobalt exposure. Blood 1989;73(1):13–6.
[143] Beru N, McDonald J, Lacombe C, Goldwasser E. Expression of the erythropoietin gene. Mol Cell Biol 1986;6(7):2571–5.
[144] Bondurant MC, Koury MJ. Anemia induces accumulation of erythropoietin mRNA in the kidney and liver. Mol Cell Biol 1986;6(7):2731–3.
[145] Schuster SJ, Wilson JH, Erslev AJ, Caro J. Physiologic regulation and tissue localization of renal erythropoietin messenger RNA. Blood 1987;70(1):316–8.
[146] Clemons GK, De Manincor D, Fitzsimmons SL, Garcia JF. Immunoreactive erythropoietin studies in hypoxic rats and the role of the salivary glands. Exp Hematol 1987;15(1):18–23.
[147] Goldberg MA, Gaut CC, Bunn HF. Erythropoietin mRNA levels are governed by both the rate of gene transcription and posttranscriptional events. Blood 1991;77(2):271–7.
[148] Rondon IJ, MacMillan LA, Beckman BS, et al. Hypoxia upregulates the activity of a novel erythropoietin mRNA binding protein. J Biol Chem 1991;266(25):16594–8.
[149] Steinberg SE, Garcia JF, Matzke GR, Mladenovic J. Erythropoietin kinetics in rats: generation and clearance. Blood 1986;67(3):646–9.
[150] Fu JS, Lertora JJ, Brookins J, Rice JC, Fisher JW. Pharmacokinetics of erythropoietin in intact and anephric dogs. J Lab Clin Med 1988;111(6):669–76.
[151] Mladenovic J, Eschbach JW, Koup JR, Garcia JF, Adamson JW. Erythropoietin kinetics in normal and uremic sheep. J Lab Clin Med 1985;105(6):659–63.
[152] Roh BL, Paulo LG, Thompson J, Fisher JW. Plasma disappearance of 125 I-labeled erythropoietin in anesthetized rabbits. Proc Soc Exp Biol Med 1972;141(1):268–70.
[153] Kindler J, Eckardt KU, Ehmer B, et al. Single-dose pharmacokinetics of recombinant human erythropoietin in patients with various degrees of renal failure. Nephrol Dial Transplant 1989;4(5):345–9.
[154] Hansen AJ, Fogh J, Mollgard K, Sorensen SC. Evidence against erythropoietin production by the carotid body. Respir Physiol 1973;18(1):101–6.
[155] Beynon G. The influence of the autonomic nervous system in the control of erythropoietin secretion in the hypoxic rat. J Physiol 1977;266(2):347–60.
[156] Eckardt KU, LeHir M, Tan CC, Ratcliffe PJ, Kaissling B, Kurtz A. Renal innervation plays no role in oxygen-dependent control of erythropoietin mRNA levels. Am J Physiol 1992;263(5 Pt 2):F925–30.
[157] Ratcliffe PJ, Jones RW, Phillips RE, Nicholls LG, Bell JI. Oxygen-dependent modulation of erythropoietin mRNA levels in isolated rat kidneys studied by RNase protection. J Exp Med 1990;172(2):657–60.
[158] Pagel H, Jelkmann W, Weiss C. Isolated serum-free perfused rat kidneys release immunoreactive erythropoietin in response to hypoxia. Endocrinology 1991;128(5):2633–8.
[159] Scholz H, Schurek HJ, Eckardt KU, Kurtz A, Bauer C. Oxygen-dependent erythropoietin production by the isolated perfused rat kidney. Pflugers Arch 1991;418(3):228–33.
[160] Halvorsen S, Roh BL, Fisher JW. Erythropoietin production in nephrectomized and hypophysectomized animals. Am J Physiol 1968;215(2):349–52.
[161] Peschle C, Rappaport IA, Magli MC, et al. Role of the hypophysis in erythropoietin production during hypoxia. Blood 1978;51(6):1117–24.
[162] Halvorsen S. Effects of growth hormone on erythropoiesis in the intact rabbit and the polycythemic mouse. Acta Physiol Scand 1966;66(1):203–13.
[163] Kurtz A, Zapf J, Eckardt KU, Clemons G, Froesch ER, Bauer C. Insulin-like growth factor I stimulates erythropoiesis in hypophysectomized rats. Proc Natl Acad Sci U S A 1988;85 (20):7825–9.
[164] Fandrey J, Pagel H, Frede S, Wolff M, Jelkmann W. Thyroid hormones enhance hypoxia-induced erythropoietin production in vitro. Exp Hematol 1994;22(3):272–7.
[165] Peschle C, Zanjani ED, Gidari AS, McLaurin WD, Gordon AS. Mechanism of thyroxine action on erythropoiesis. Endocrinology 1971;89(2):609–12.
[166] Alexanian R. Erythropoietin and erythropoiesis in anemic man following androgens. Blood 1969;33(4):564–72.
[167] Fried W, Jonasson O, Lang G, Schwartz F. The hematologic effect of androgen in uremic patients. Study of packed cell volume and erythropoietin responses. Ann Intern Med 1973;79 (6):823–7.
[168] Eckardt KU, Kurtz A, Bauer C. Regulation of erythropoietin production is related to proximal tubular function. Am J Physiol 1989;256(5 Pt 2):F942–7.
[169] Goldberg MA, Glass GA, Cunningham JM, Bunn HF. The regulated expression of erythropoietin by two human hepatoma cell lines. Proc Natl Acad Sci U S A 1987;84(22):7972–6.
[170] Brezis M, Rosen S, Silva P, Epstein FH. Selective vulnerability of the medullary thick ascending limb to anoxia in the isolated perfused rat kidney. J Clin Invest 1984;73(1):182–90.
[171] Schurek HJ, Kriz W. Morphologic and functional evidence for oxygen deficiency in the isolated perfused rat kidney. Lab Invest 1985;53(2):145–55.
[172] Aukland K, Krog J. Renal oxygen tension. Nature 1960;188:671.
[173] Lubbers DW, Baumgartl H. Heterogeneities and profiles of oxygen pressure in brain and kidney as examples of the pO2

distribution in the living tissue. Kidney Int 1997;51 (2):372–80.
[174] Schurek HJ, Jost U, Baumgartl H, Bertram H, Heckmann U. Evidence for a preglomerular oxygen diffusion shunt in rat renal cortex. Am J Physiol 1990;259(6 Pt 2):F910–5.
[175] DuBose Jr. TD, Bidani A. Kinetics of CO_2 exchange in the kidney. Annu Rev Physiol 1988;50:653–67.
[176] Sohtell M. CO_2 along the proximal tubules in the rat kidney. Acta Physiol Scand 1979;105(2):146–55.
[177] Law ML, Cai GY, Lin FK, et al. Chromosomal assignment of the human erythropoietin gene and its DNA polymorphism. Proc Natl Acad Sci U S A 1986;83(18):6920–4.
[178] Watkins PC, Eddy R, Hoffman N, et al. Regional assignment of the erythropoietin gene to human chromosome region 7pter–q22. Cytogenet Cell Genet 1986;42(4):214–8.
[179] Shoemaker CB, Mitsock LD. Murine erythropoietin gene: cloning, expression, and human gene homology. Mol Cell Biol 1986;6(3):849–58.
[180] Semenza GL, Dureza RC, Traystman MD, Gearhart JD, Antonarakis SE. Human erythropoietin gene expression in transgenic mice: multiple transcription initiation sites and cis-acting regulatory elements. Mol Cell Biol 1990;10(3):930–8.
[181] Blanchard KL, Acquaviva AM, Galson DL, Bunn HF. Hypoxic induction of the human erythropoietin gene: cooperation between the promoter and enhancer, each of which contains steroid receptor response elements. Mol Cell Biol 1992;12 (12):5373–85.
[182] Semenza GL, Koury ST, Nejfelt MK, Gearhart JD, Antonarakis SE. Cell-type-specific and hypoxia-inducible expression of the human erythropoietin gene in transgenic mice. Proc Natl Acad Sci U S A 1991;88(19):8725–9.
[183] Gupta M, Mungai PT, Goldwasser E. A new transacting factor that modulates hypoxia-induced expression of the erythropoietin gene. Blood 2000;96(2):491–7.
[184] Dame C, Sola MC, Fandrey J, et al. Developmental changes in the expression of transcription factors GATA-1, -2 and -3 during the onset of human medullary haematopoiesis. Br J Haematol 2002;119(2):510–5.
[185] Imagawa S, Yamamoto M, Miura Y. Negative regulation of the erythropoietin gene expression by the GATA transcription factors. Blood 1997;89(4):1430–9.
[186] Beck I, Ramirez S, Weinmann R, Caro J. Enhancer element at the 3′-flanking region controls transcriptional response to hypoxia in the human erythropoietin gene. J Biol Chem 1991;266 (24):15563–6.
[187] Pugh CW, Tan CC, Jones RW, Ratcliffe PJ. Functional analysis of an oxygen-regulated transcriptional enhancer lying 3′ to the mouse erythropoietin gene. Proc Natl Acad Sci U S A 1991;88 (23):10553–7.
[188] Semenza GL, Nejfelt MK, Chi SM, Antonarakis SE. Hypoxia-inducible nuclear factors bind to an enhancer element located 3′ to the human erythropoietin gene. Proc Natl Acad Sci U S A 1991;88(13):5680–4.
[189] Semenza GL, Wang GL. A nuclear factor induced by hypoxia via de novo protein synthesis binds to the human erythropoietin gene enhancer at a site required for transcriptional activation. Mol Cell Biol 1992;12(12):5447–54.
[190] Galson DL, Tsuchiya T, Tendler DS, et al. The orphan receptor hepatic nuclear factor 4 functions as a transcriptional activator for tissue-specific and hypoxia-specific erythropoietin gene expression and is antagonized by EAR3/COUP-TF1. Mol Cell Biol 1995;15(4):2135–44.
[191] Wang GL, Semenza GL. Purification and characterization of hypoxia-inducible factor 1. J Biol Chem 1995;270(3):1230–7.
[192] Wang GL, Jiang BH, Rue EA, Semenza GL. Hypoxia-inducible factor 1 is a basic-helix-loop-helix-PAS heterodimer regulated by cellular O2 tension. Proc Natl Acad Sci U S A 1995;92 (12):5510–4.
[193] Ratcliffe PJ, Ebert BL, Firth JD, et al. Oxygen regulated gene expression: erythropoietin as a model system. Kidney Int 1997;51(2):514–26.
[194] Semenza GL. HIF-1: mediator of physiological and pathophysiological responses to hypoxia. J Appl Physiol 2000;88 (4):1474–80.
[195] Ema M, Hirota K, Mimura J, et al. Molecular mechanisms of transcription activation by HLF and HIF1alpha in response to hypoxia: their stabilization and redox signal-induced interaction with CBP/p300. EMBO J 1999;18(7):1905–14.
[196] O'Rourke JF, Tian YM, Ratcliffe PJ, Pugh CW. Oxygen-regulated and transactivating domains in endothelial PAS protein 1: comparison with hypoxia-inducible factor-1alpha. J Biol Chem 1999;274(4):2060–71.
[197] Kallio PJ, Okamoto K, O'Brien S, et al. Signal transduction in hypoxic cells: inducible nuclear translocation and recruitment of the CBP/p300 coactivator by the hypoxia-inducible factor-1alpha. EMBO J 1998;17(22):6573–86.
[198] Wood SM, Gleadle JM, Pugh CW, Hankinson O, Ratcliffe PJ. The role of the aryl hydrocarbon receptor nuclear translocator (ARNT) in hypoxic induction of gene expression. Studies in ARNT-deficient cells. J Biol Chem 1996;271(25):15117–23.
[199] Sang N, Fang J, Srinivas V, Leshchinsky I, Caro J. Carboxyl-terminal transactivation activity of hypoxia-inducible factor 1 alpha is governed by a von Hippel-Lindau protein-independent, hydroxylation-regulated association with p300/CBP. Mol Cell Biol 2002;22(9):2984–92.
[200] Huang LE, Gu J, Schau M, Bunn HF. Regulation of hypoxia-inducible factor 1alpha is mediated by an O2-dependent degradation domain via the ubiquitin-proteasome pathway. Proc Natl Acad Sci U S A 1998;95(14):7987–92.
[201] Jewell UR, Kvietikova I, Scheid A, Bauer C, Wenger RH, Gassmann M. Induction of HIF-1alpha in response to hypoxia is instantaneous. FASEB J 2001;15(7):1312–4.
[202] Cockman ME, Masson N, Mole DR, et al. Hypoxia inducible factor-alpha binding and ubiquitylation by the von Hippel-Lindau tumor suppressor protein. J Biol Chem 2000;275 (33):25733–41.
[203] Maxwell PH, Wiesener MS, Chang GW, et al. The tumour suppressor protein VHL targets hypoxia-inducible factors for oxygen-dependent proteolysis. Nature 1999;399(6733):271–5.
[204] Ohh M, Park CW, Ivan M, et al. Ubiquitination of hypoxia-inducible factor requires direct binding to the beta-domain of the von Hippel-Lindau protein. Nat Cell Biol 2000;2(7):423–7.
[205] Jiang BH, Zheng JZ, Leung SW, Roe R, Semenza GL. Transactivation and inhibitory domains of hypoxia-inducible factor 1alpha. Modulation of transcriptional activity by oxygen tension. J Biol Chem 1997;272(31):19253–60.
[206] Pugh CW, O'Rourke JF, Nagao M, Gleadle JM, Ratcliffe PJ. Activation of hypoxia-inducible factor-1; definition of regulatory domains within the alpha subunit. J Biol Chem 1997;272 (17):11205–14.
[207] Masson N, Willam C, Maxwell PH, Pugh CW, Ratcliffe PJ. Independent function of two destruction domains in hypoxia-inducible factor-alpha chains activated by prolyl hydroxylation. EMBO J 2001;20(18):5197–206.
[208] Ivan M, Haberberger T, Gervasi DC, et al. Biochemical purification and pharmacological inhibition of a mammalian prolyl hydroxylase acting on hypoxia-inducible factor. Proc Natl Acad Sci U S A 2002;99(21):13459–64.

[209] Jaakkola P, Mole DR, Tian YM, et al. Targeting of HIF-alpha to the von Hippel-Lindau ubiquitylation complex by O2-regulated prolyl hydroxylation. Science 2001;292(5516):468–72.
[210] Bruick RK, McKnight SL. A conserved family of prolyl-4-hydroxylases that modify HIF. Science 2001;294(5545):1337–40.
[211] Epstein AC, Gleadle JM, McNeill LA, et al. C. elegans EGL-9 and mammalian homologs define a family of dioxygenases that regulate HIF by prolyl hydroxylation. Cell 2001;107(1):43–54.
[212] Hewitson KS, McNeill LA, Riordan MV, et al. Hypoxia-inducible factor (HIF) asparagine hydroxylase is identical to factor inhibiting HIF (FIH) and is related to the cupin structural family. J Biol Chem 2002;277(29):26351–5.
[213] Bhattacharya S, Michels CL, Leung MK, Arany ZP, Kung AL, Livingston DM. Functional role of p35srj, a novel p300/CBP binding protein, during transactivation by HIF-1. Genes Dev 1999;13(1):64–75.
[214] Lando D, Peet DJ, Gorman JJ, Whelan DA, Whitelaw ML, Bruick RK. FIH-1 is an asparaginyl hydroxylase enzyme that regulates the transcriptional activity of hypoxia-inducible factor. Genes Dev 2002;16(12):1466–71.
[215] Arany Z, Huang LE, Eckner R, et al. An essential role for p300/CBP in the cellular response to hypoxia. Proc Natl Acad Sci U S A 1996;93(23):12969–73.
[216] Mahon PC, Hirota K, Semenza GL. FIH-1: a novel protein that interacts with HIF-1alpha and VHL to mediate repression of HIF-1 transcriptional activity. Genes Dev 2001;15 (20):2675–86.
[217] Gnarra JR, Zhou S, Merrill MJ, et al. Post-transcriptional regulation of vascular endothelial growth factor mRNA by the product of the VHL tumor suppressor gene. Proc Natl Acad Sci U S A 1996;93(20):10589–94.
[218] Iliopoulos O, Levy AP, Jiang C, Kaelin Jr. WG, Goldberg MA. Negative regulation of hypoxia-inducible genes by the von Hippel-Lindau protein. Proc Natl Acad Sci U S A 1996;93 (20):10595–9.
[219] Lando D, Peet DJ, Whelan DA, Gorman JJ, Whitelaw ML. Asparagine hydroxylation of the HIF transactivation domain a hypoxic switch. Science 2002;295(5556):858–61.
[220] Metzen E, Berchner-Pfannschmidt U, Stengel P, et al. Intracellular localisation of human HIF-1 alpha hydroxylases: implications for oxygen sensing. J Cell Sci 2003;116(Pt 7):1319–26.
[221] Hirsila M, Koivunen P, Gunzler V, Kivirikko KI, Myllyharju J. Characterization of the human prolyl 4-hydroxylases that modify the hypoxia-inducible factor. J Biol Chem 2003;278 (33):30772–80.
[222] Koivunen P, Hirsila M, Gunzler V, Kivirikko KI, Myllyharju J. Catalytic properties of the asparaginyl hydroxylase (FIH) in the oxygen sensing pathway are distinct from those of its prolyl 4-hydroxylases. J Biol Chem 2004;279(11):9899–904.
[223] Kallio PJ, Wilson WJ, O'Brien S, Makino Y, Poellinger L. Regulation of the hypoxia-inducible transcription factor 1alpha by the ubiquitin-proteasome pathway. J Biol Chem 1999;274 (10):6519–25.
[224] Hofer T, Desbaillets I, Hopfl G, Gassmann M, Wenger RH. Dissecting hypoxia-dependent and hypoxia-independent steps in the HIF-1alpha activation cascade: implications for HIF-1alpha gene therapy. FASEB J 2001;15(14):2715–7.
[225] Huang LE, Arany Z, Livingston DM, Bunn HF. Activation of hypoxia-inducible transcription factor depends primarily upon redox-sensitive stabilization of its alpha subunit. J Biol Chem 1996;271(50):32253–9.
[226] Sutter CH, Laughner E, Semenza GL. Hypoxia-inducible factor 1alpha protein expression is controlled by oxygen-regulated ubiquitination that is disrupted by deletions and missense mutations. Proc Natl Acad Sci U S A 2000;97(9):4748–53.
[227] Gorlach A, Camenisch G, Kvietikova I, Vogt L, Wenger RH, Gassmann M. Efficient translation of mouse hypoxia-inducible factor-1alpha under normoxic and hypoxic conditions. Biochim Biophys Acta 2000;1493(1–2):125–34.
[228] Karni R, Dor Y, Keshet E, Meyuhas O, Levitzki A. Activated pp60c-Src leads to elevated hypoxia-inducible factor (HIF)-1alpha expression under normoxia. J Biol Chem 2002;277 (45):42919–25.
[229] Laughner E, Taghavi P, Chiles K, Mahon PC, Semenza GL. HER2 (neu) signaling increases the rate of hypoxia-inducible factor 1alpha (HIF-1alpha) synthesis: novel mechanism for HIF-1-mediated vascular endothelial growth factor expression. Mol Cell Biol 2001;21(12):3995–4004.
[230] Treins C, Giorgetti-Peraldi S, Murdaca J, Semenza GL, Van Obberghen E. Insulin stimulates hypoxia-inducible factor 1 through a phosphatidylinositol 3-kinase/target of rapamycin-dependent signaling pathway. J Biol Chem 2002;277 (31):27975–81.
[231] Conrad PW, Freeman TL, Beitner-Johnson D, Millhorn DE. EPAS1 trans-activation during hypoxia requires p42/p44 MAPK. J Biol Chem 1999;274(47):33709–13.
[232] Zundel W, Schindler C, Haas-Kogan D, et al. Loss of PTEN facilitates HIF-1-mediated gene expression. Genes Dev 2000;14 (4):391–6.
[233] Ema M, Taya S, Yokotani N, Sogawa K, Matsuda Y, Fujii-Kuriyama Y. A novel bHLH-PAS factor with close sequence similarity to hypoxia-inducible factor 1alpha regulates the VEGF expression and is potentially involved in lung and vascular development. Proc Natl Acad Sci U S A 1997;94(9):4273–8.
[234] Flamme I, Frohlich T, von Reutern M, Kappel A, Damert A, Risau W. HRF, a putative basic helix-loop-helix-PAS-domain transcription factor is closely related to hypoxia-inducible factor-1 alpha and developmentally expressed in blood vessels. Mech Dev 1997;63(1):51–60.
[235] Hogenesch JB, Chan WK, Jackiw VH, et al. Characterization of a subset of the basic-helix-loop-helix-PAS superfamily that interacts with components of the dioxin signaling pathway. J Biol Chem 1997;272(13):8581–93.
[236] Tian H, McKnight SL, Russell DW. Endothelial PAS domain protein 1 (EPAS1), a transcription factor selectively expressed in endothelial cells. Genes Dev 1997;11(1):72–82.
[237] Gu YZ, Moran SM, Hogenesch JB, Wartman L, Bradfield CA. Molecular characterization and chromosomal localization of a third alpha-class hypoxia inducible factor subunit, HIF3alpha. Gene Expr 1998;7(3):205–13.
[238] Kotch LE, Iyer NV, Laughner E, Semenza GL. Defective vascularization of HIF-1alpha-null embryos is not associated with VEGF deficiency but with mesenchymal cell death. Dev Biol 1999;209(2):254–67.
[239] Compernolle V, Brusselmans K, Acker T, et al. Loss of HIF-2alpha and inhibition of VEGF impair fetal lung maturation, whereas treatment with VEGF prevents fatal respiratory distress in premature mice. Nat Med 2002;8(7):702–10.
[240] Peng J, Zhang L, Drysdale L, Fong GH. The transcription factor EPAS-1/hypoxia-inducible factor 2alpha plays an important role in vascular remodeling. Proc Natl Acad Sci U S A 2000;97 (15):8386–91.
[241] Tian H, Hammer RE, Matsumoto AM, Russell DW, McKnight SL. The hypoxia-responsive transcription factor EPAS1 is essential for catecholamine homeostasis and protection against heart failure during embryonic development. Genes Dev 1998;12(21):3320–4.
[242] Yu AY, Shimoda LA, Iyer NV, et al. Impaired physiological responses to chronic hypoxia in mice partially deficient for hypoxia-inducible factor 1alpha. J Clin Invest 1999;103(5):691–6.

[243] Rosenberger C, Mandriota S, Jurgensen JS, et al. Expression of hypoxia-inducible factor-1alpha and -2alpha in hypoxic and ischemic rat kidneys. J Am Soc Nephrol 2002;13(7): 1721–32.

[244] Paliege A, Rosenberger C, Bondke A, et al. Hypoxia-inducible factor-2alpha-expressing interstitial fibroblasts are the only renal cells that express erythropoietin under hypoxia-inducible factor stabilization. Kidney Int 2010;77(4):312–8.

[245] Warnecke C, Zaborowska Z, Kurreck J, et al. Differentiating the functional role of hypoxia-inducible factor (HIF)-1alpha and HIF-2alpha (EPAS-1) by the use of RNA interference: erythropoietin is a HIF-2alpha target gene in Hep3B and Kelly cells. FASEB J 2004;18(12):1462–4.

[246] Morita M, Ohneda O, Yamashita T, et al. HLF/HIF-2alpha is a key factor in retinopathy of prematurity in association with erythropoietin. EMBO J 2003;22(5):1134–46.

[247] Rankin EB, Biju MP, Liu Q, et al. Hypoxia-inducible factor-2 (HIF-2) regulates hepatic erythropoietin in vivo. J Clin Invest 2007;117(4):1068–77.

[248] Scortegagna M, Ding K, Zhang Q, et al. HIF-2alpha regulates murine hematopoietic development in an erythropoietin-dependent manner. Blood 2005;105(8):3133–40.

[249] Gruber M, Hu CJ, Johnson RS, Brown EJ, Keith B, Simon MC. Acute postnatal ablation of Hif-2alpha results in anemia. Proc Natl Acad Sci U S A 2007;104(7):2301–6.

[250] Kapitsinou PP, Liu Q, Unger TL, et al. Hepatic HIF-2 regulates erythropoietic responses to hypoxia in renal anemia. Blood. 2010; 116:3039–3048.

[251] Schodel J, Klanke B, Weidemann A, et al. HIF-prolyl hydroxylases in the rat kidney: physiologic expression patterns and regulation in acute kidney injury. Am J Pathol 2009;174 (5):1663–74.

[252] Koivunen P, Tiainen P, Hyvarinen J, et al. An endoplasmic reticulum transmembrane prolyl 4-hydroxylase is induced by hypoxia and acts on hypoxia-inducible factor alpha. J Biol Chem 2007;282(42):30544–52.

[253] Oehme F, Ellinghaus P, Kolkhof P, et al. Overexpression of PH-4, a novel putative proline 4-hydroxylase, modulates activity of hypoxia-inducible transcription factors. Biochem Biophys Res Commun 2002;296(2):343–9.

[254] Safran M, Kim WY, O'Connell F, et al. Mouse model for noninvasive imaging of HIF prolyl hydroxylase activity: assessment of an oral agent that stimulates erythropoietin production. Proc Natl Acad Sci U S A 2006;103(1):105–10.

[255] Minamishima YA, Moslehi J, Bardeesy N, Cullen D, Bronson RT, Kaelin Jr. WG. Somatic inactivation of the PHD2 prolyl hydroxylase causes polycythemia and congestive heart failure. Blood 2008;111(6):3236–44.

[256] Takeda K, Aguila HL, Parikh NS, et al. Regulation of adult erythropoiesis by prolyl hydroxylase domain proteins. Blood 2008;111(6):3229–35.

[257] Takeda K, Cowan A, Fong GH. Essential role for prolyl hydroxylase domain protein 2 in oxygen homeostasis of the adult vascular system. Circulation 2007;116(7):774–81.

[258] Berra E, Benizri E, Ginouves A, Volmat V, Roux D, Pouyssegur J. HIF prolyl-hydroxylase 2 is the key oxygen sensor setting low steady-state levels of HIF-1alpha in normoxia. EMBO J 2003;22(16):4082–90.

[259] Takeda K, Ho VC, Takeda H, Duan LJ, Nagy A, Fong GH. Placental but not heart defects are associated with elevated hypoxia-inducible factor alpha levels in mice lacking prolyl hydroxylase domain protein 2. Mol Cell Biol 2006;26 (22):8336–46.

[260] Minamishima YA, Kaelin Jr WG. Reactivation of hepatic EPO synthesis in mice after PHD loss. Science Jul 23;329(5990):407.

[261] Ladroue C, Carcenac R, Leporrier M, et al. PHD2 mutation and congenital erythrocytosis with paraganglioma. N Engl J Med 2008;359(25):2685–92.

[262] Percy MJ, Furlow PW, Beer PA, Lappin TR, McMullin MF, Lee FS. A novel erythrocytosis-associated PHD2 mutation suggests the location of a HIF binding groove. Blood 2007;110 (6):2193–6.

[263] Percy MJ, Zhao Q, Flores A, et al. A family with erythrocytosis establishes a role for prolyl hydroxylase domain protein 2 in oxygen homeostasis. Proc Natl Acad Sci U S A 2006;103 (3):654–9.

[264] Wiesener MS, Seyfarth M, Warnecke C, et al. Paraneoplastic erythrocytosis associated with an inactivating point mutation of the von Hippel-Lindau gene in a renal cell carcinoma. Blood 2002;99(10):3562–5.

[265] Ang SO, Chen H, Hirota K, et al. Disruption of oxygen homeostasis underlies congenital Chuvash polycythemia. Nat Genet 2002;32(4):614–21.

[266] Bento MC, Chang KT, Guan Y, et al. Congenital polycythemia with homozygous and heterozygous mutations of von Hippel-Lindau gene: five new Caucasian patients. Haematologica 2005;90(1):128–9.

[267] Pastore YD, Jelinek J, Ang S, et al. Mutations in the VHL gene in sporadic apparently congenital polycythemia. Blood 2003;101(4):1591–5.

[268] Perrotta S, Nobili B, Ferraro M, et al. Von Hippel-Lindau-dependent polycythemia is endemic on the island of Ischia: identification of a novel cluster. Blood 2006;107(2):514–9.

[269] Hickey MM, Lam JC, Bezman NA, Rathmell WK, Simon MC. von Hippel-Lindau mutation in mice recapitulates Chuvash polycythemia via hypoxia-inducible factor-2alpha signaling and splenic erythropoiesis. J Clin Invest 2007;117(12):3879–89.

[270] Furlow PW, Percy MJ, Sutherland S, et al. Erythrocytosis-associated HIF-2alpha mutations demonstrate a critical role for residues C-terminal to the hydroxylacceptor proline. J Biol Chem 2009;284(14):9050–8.

[271] Gale DP, Harten SK, Reid CD, Tuddenham EG, Maxwell PH. Autosomal dominant erythrocytosis and pulmonary arterial hypertension associated with an activating HIF2 alpha mutation. Blood 2008;112(3):919–21.

[272] Martini M, Teofili L, Cenci T, et al. A novel heterozygous HIF2AM535I mutation reinforces the role of oxygen sensing pathway disturbances in the pathogenesis of familial erythrocytosis. Haematologica 2008;93(7):1068–71.

[273] Percy MJ, Beer PA, Campbell G, et al. Novel exon 12 mutations in the HIF2A gene associated with erythrocytosis. Blood 2008;111(11):5400–2.

[274] Percy MJ, Furlow PW, Lucas GS, et al. A gain-of-function mutation in the HIF2A gene in familial erythrocytosis. N Engl J Med 2008;358(2):162–8.

[275] van Wijk R, Sutherland S, Van Wesel AC, et al. Erythrocytosis associated with a novel missense mutation in the HIF2A gene. Haematologica 2010;95(5):829–32.

[276] Perrotta S, Della Ragione F. The HIF2A gene in familial erythrocytosis. N Engl J Med 2008;358(18):1966 [author reply -7]

[277] Ginouves A, Ilc K, Macias N, Pouyssegur J, Berra E. PHDs overactivation during chronic hypoxia "desensitizes" HIFalpha and protects cells from necrosis. Proc Natl Acad Sci U S A 2008;105(12):4745–50.

[278] Khanna S, Roy S, Maurer M, Ratan RR, Sen CK. Oxygen-sensitive reset of hypoxia-inducible factor transactivation response: prolyl hydroxylases tune the biological normoxic set point. Free Radic Biol Med 2006;40(12):2147–54.

[279] Minamishima YA, Moslehi J, Padera RF, Bronson RT, Liao R, Kaelin Jr. WG. A feedback loop involving the Phd3 prolyl

hydroxylase tunes the mammalian hypoxic response in vivo. Mol Cell Biol 2009;29(21):5729–41.
[280] Stiehl DP, Wirthner R, Koditz J, Spielmann P, Camenisch G, Wenger RH. Increased prolyl 4-hydroxylase domain proteins compensate for decreased oxygen levels. Evidence for an autoregulatory oxygen-sensing system. J Biol Chem 2006;281 (33):23482–91.
[281] Aprelikova O, Chandramouli GV, Wood M, et al. Regulation of HIF prolyl hydroxylases by hypoxia-inducible factors. J Cell Biochem 2004;92(3):491–501.
[282] Cioffi CL, Liu XQ, Kosinski PA, Garay M, Bowen BR. Differential regulation of HIF-1 alpha prolyl-4-hydroxylase genes by hypoxia in human cardiovascular cells. Biochem Biophys Res Commun 2003;303(3):947–53.
[283] D'Angelo G, Duplan E, Boyer N, Vigne P, Frelin C. Hypoxia up-regulates prolyl hydroxylase activity: a feedback mechanism that limits HIF-1 responses during reoxygenation. J Biol Chem 2003;278(40):38183–7.
[284] del Peso L, Castellanos MC, Temes E, et al. The von Hippel Lindau/hypoxia-inducible factor (HIF) pathway regulates the transcription of the HIF-proline hydroxylase genes in response to low oxygen. J Biol Chem 2003;278(49):48690–5.
[285] Marxsen JH, Stengel P, Doege K, et al. Hypoxia-inducible factor-1 (HIF-1) promotes its degradation by induction of HIF-alpha-prolyl-4-hydroxylases. Biochem J 2004;381(Pt 3): 761–7.
[286] Metzen E, Stiehl DP, Doege K, Marxsen JH, Hellwig-Burgel T, Jelkmann W. Regulation of the prolyl hydroxylase domain protein 2 (phd2/egln-1) gene: identification of a functional hypoxia-responsive element. Biochem J 2005;387(Pt 3):711–7.
[287] Pescador N, Cuevas Y, Naranjo S, et al. Identification of a functional hypoxia-responsive element that regulates the expression of the egl nine homologue 3 (egln3/phd3) gene. Biochem J 2005;390(Pt 1):189–97.
[288] Appelhoff RJ, Tian YM, Raval RR, et al. Differential function of the prolyl hydroxylases PHD1, PHD2, and PHD3 in the regulation of hypoxia-inducible factor. J Biol Chem 2004;279 (37):38458–65.
[289] Seth P, Krop I, Porter D, Polyak K. Novel estrogen and tamoxifen induced genes identified by SAGE (Serial Analysis of Gene Expression). Oncogene 2002;21(5):836–43.
[290] McMahon S, Charbonneau M, Grandmont S, Richard DE, Dubois CM. Transforming growth factor beta1 induces hypoxia-inducible factor-1 stabilization through selective inhibition of PHD2 expression. J Biol Chem 2006;281(34):24171–81.
[291] Wenger RH, Hoogewijs D. Regulated oxygen sensing by protein hydroxylation in renal erythropoietin-producing cells. Am J Physiol Renal Physiol Jun;298(6):F1287–96.
[292] Berchner-Pfannschmidt U, Yamac H, Trinidad B, Fandrey J. Nitric oxide modulates oxygen sensing by hypoxia-inducible factor 1-dependent induction of prolyl hydroxylase 2. J Biol Chem 2007;282(3):1788–96.
[293] Gerald D, Berra E, Frapart YM, et al. Jun D reduces tumor angiogenesis by protecting cells from oxidative stress. Cell 2004;118(6):781–94.
[294] Hirsila M, Koivunen P, Xu L, Seeley T, Kivirikko KI, Myllyharju J. Effect of desferrioxamine and metals on the hydroxylases in the oxygen sensing pathway. FASEB J 2005;19 (10):1308–10.
[295] Knowles HJ, Raval RR, Harris AL, Ratcliffe PJ. Effect of ascorbate on the activity of hypoxia-inducible factor in cancer cells. Cancer Res 2003;63(8):1764–8.
[296] Martin F, Linden T, Katschinski DM, et al. Copper-dependent activation of hypoxia-inducible factor (HIF)-1: implications for ceruloplasmin regulation. Blood 2005;105(12):4613–9.
[297] Metzen E, Zhou J, Jelkmann W, Fandrey J, Brune B. Nitric oxide impairs normoxic degradation of HIF-1alpha by inhibition of prolyl hydroxylases. Mol Biol Cell 2003;14(8): 3470–81.
[298] Nytko KJ, Spielmann P, Camenisch G, Wenger RH, Stiehl DP. Regulated function of the prolyl-4-hydroxylase domain (PHD) oxygen sensor proteins. Antioxid Redox Signal 2007;9(9): 1329–38.
[299] Goldberg MA, Dunning SP, Bunn HF. Regulation of the erythropoietin gene: evidence that the oxygen sensor is a heme protein. Science 1988;242(4884):1412–5.
[300] Sandner P, Gess B, Wolf K, Kurtz A. Divergent regulation of vascular endothelial growth factor and of erythropoietin gene expression in vivo. Pflugers Arch 1996;431(6):905–12.
[301] Dalgard CL, Lu H, Mohyeldin A, Verma A. Endogenous 2-oxoacids differentially regulate expression of oxygen sensors. Biochem J 2004;380(Pt 2):419–24.
[302] Lu H, Dalgard CL, Mohyeldin A, McFate T, Tait AS, Verma A. Reversible inactivation of HIF-1 prolyl hydroxylases allows cell metabolism to control basal HIF-1. J Biol Chem 2005;280 (51):41928–39.
[303] Selak MA, Armour SM, MacKenzie ED, et al. Succinate links TCA cycle dysfunction to oncogenesis by inhibiting HIF-alpha prolyl hydroxylase. Cancer Cell 2005;7(1):77–85.
[304] Isaacs JS, Jung YJ, Mole DR, et al. HIF overexpression correlates with biallelic loss of fumarate hydratase in renal cancer: novel role of fumarate in regulation of HIF stability. Cancer Cell 2005;8(2):143–53.
[305] Pollard PJ, Briere JJ, Alam NA, et al. Accumulation of Krebs cycle intermediates and over-expression of HIF1alpha in tumours which result from germline FH and SDH mutations. Hum Mol Genet 2005;14(15):2231–9.
[306] Zhao S, Lin Y, Xu W, et al. Glioma-derived mutations in IDH1 dominantly inhibit IDH1 catalytic activity and induce HIF-1alpha. Science 2009;324(5924):261–5.
[307] Fisher JW, Samuels AI. Relationship between renal blood flow and erythropoietin production in dogs. Proc Soc Exp Biol Med 1967;125(2):482–5.
[308] Pagel H, Jelkmann W, Weiss C. A comparison of the effects of renal artery constriction and anemia on the production of erythropoietin. Pflugers Arch 1988;413(1):62–6.
[309] Cohen RA, Miller ME, Garcia JF, Moccia G, Cronkite EP. Regulatory mechanism of erythropoietin production: effects of hypoxemia and hypercarbia. Exp Hematol 1981;9(5):513–21.
[310] Wolf-Priessnitz J, Schooley JC, Mahlmann LJ. Inhibition of erythropoietin production in unanesthetized rabbits exposed to an acute hypoxic-hypercapnic environment. Blood 1978;52 (1):153–62.
[311] Zucali JR, Lee M, Mirand EA. Carbon dioxide effects on erythropoietin and erythropoiesis. J Lab Clin Med 1978;92(4):648–55.
[312] Ludwig H, Fritz E, Kotzmann H, Hocker P, Gisslinger H, Barnas U. Erythropoietin treatment of anemia associated with multiple myeloma. N Engl J Med 1990;322(24):1693–9.
[313] Taylor J, Mactier RA, Stewart WK, Henderson IS. Effect of erythropoietin on anaemia in patients with myeloma receiving haemodialysis. BMJ 1990;301(6750):476–7.
[314] Singh A, Eckardt KU, Zimmermann A, et al. Increased plasma viscosity as a reason for inappropriate erythropoietin formation. J Clin Invest 1993;91(1):251–6.
[315] Jelkmann W, Wolff M, Fandrey J. Modulation of the production of erythropoietin by cytokines: in vitro studies and their clinical implications. Contrib Nephrol 1990;87:68–77.
[316] Faquin WC, Schneider TJ, Goldberg MA. Effect of inflammatory cytokines on hypoxia-induced erythropoietin production. Blood 1992;79(8):1987–94.

[317] Jelkmann W, Pagel H, Wolff M, Fandrey J. Monokines inhibiting erythropoietin production in human hepatoma cultures and in isolated perfused rat kidneys. Life Sci 1992;50(4):301–8.
[318] McNeill LA, Flashman E, Buck MR, et al. Hypoxia-inducible factor prolyl hydroxylase 2 has a high affinity for ferrous iron and 2-oxoglutarate. Mol Biosyst 2005;1(4):321–4.
[319] Wang GL, Semenza GL. Desferrioxamine induces erythropoietin gene expression and hypoxia-inducible factor 1 DNA-binding activity: implications for models of hypoxia signal transduction. Blood 1993;82(12):3610–5.
[320] Wanner RM, Spielmann P, Stroka DM, et al. Epolones induce erythropoietin expression via hypoxia-inducible factor-1 alpha activation. Blood 2000;96(4):1558–65.
[321] Cotes PM, Brozovic B. Diurnal variation of serum immunomoreactive erythropoietin in a normal subject. Clin Endocrinol (Oxf) 1982;17(4):419–22.
[322] Clemens J, Spivak JL. Serum immunoreactive erythropoietin during the perioperative period. Surgery 1994;115(4):510–5.
[323] Miller CB, Jones RJ, Piantadosi S, Abeloff MD, Spivak JL. Decreased erythropoietin response in patients with the anemia of cancer. N Engl J Med 1990;322(24):1689–92.
[324] Spivak JL, Barnes DC, Fuchs E, Quinn TC. Serum immunoreactive erythropoietin in HIV-infected patients. JAMA 1989;261 (21):3104–7.
[325] Caro J, Erslev AJ. Uremic inhibitors of erythropoiesis. Semin Nephrol 1985;5(2):128–32.
[326] Chandra M, Clemons GK, McVicar M, et al. Serum erythropoietin levels and hematocrit in end-stage renal disease: influence of the mode of dialysis. Am J Kidney Dis 1988;12(3):208–13.
[327] Caro J, Brown S, Miller O, Murray T, Erslev AJ. Erythropoietin levels in uremic nephric and anephric patients. J Lab Clin Med 1979;93(3):449–58.
[328] Naets JP, Garcia JF, Tousaaint C, Buset M, Waks D. Radioimmunoassay of erythropoietin in chronic uraemia or anephric patients. Scand J Haematol 1986;37(5):390–4.
[329] Walle AJ, Wong GY, Clemons GK, Garcia JF, Niedermayer W. Erythropoietin-hematocrit feedback circuit in the anemia of end-stage renal disease. Kidney Int 1987;31(5):1205–9.
[330] Chandra M, Clemons GK, McVicar MI. Relation of serum erythropoietin levels to renal excretory function: evidence for lowered set point for erythropoietin production in chronic renal failure. J Pediatr 1988;113(6):1015–21.
[331] Klassen DK, Spivak JL. Hepatitis-related hepatic erythropoietin production. Am J Med 1990;89(5):684–6.
[332] Aeberhard JM, Schneider PA, Vallotton MB, Kurtz A, Leski M. Multiple site estimates of erythropoietin and renin in polycythemic kidney transplant patients. Transplantation 1990;50 (4):613–6.
[333] Dagher FJ, Ramos E, Erslev AJ, Alongi SV, Karmi SA, Caro J. Are the native kidneys responsible for erythrocytosis in renal allorecipients? Transplantation 1979;28(6):496–8.
[334] Chandra M, Miller ME, Garcia JF, Mossey RT, McVicar M. Serum immunoreactive erythropoietin levels in patients with polycystic kidney disease as compared with other hemodialysis patients. Nephron 1985;39(1):26–9.
[335] Koplan JP, Sprayregan S, Ossias AL, Zanjani ED. Erythropoietin-producing renal cyst and polycythemia vera. Clarification of their relationship. Am J Med 1973;54 (6):819–24.
[336] Shalhoub RJ, Rajan U, Kim VV, Goldwasser E, Kark JA, Antoniou LD. Erythrocytosis in patients on long-term hemodialysis. Ann Intern Med 1982;97(5):686–90.
[337] Franek E, Kokot F, Wiecek A, et al. Erythropoietin concentration in cyst fluid in patients with simple renal cysts. Nephron 1994;67(4):431–5.
[338] Eschbach JW, Kelly MR, Haley NR, Abels RI, Adamson JW. Treatment of the anemia of progressive renal failure with recombinant human erythropoietin. N Engl J Med 1989;321 (3):158–63.
[339] Roth D, Smith RD, Schulman G, et al. Effects of recombinant human erythropoietin on renal function in chronic renal failure predialysis patients. Am J Kidney Dis 1994;24(5):777–84.
[340] Eschbach JW, Egrie JC, Downing MR, Browne JK, Adamson JW. Correction of the anemia of end-stage renal disease with recombinant human erythropoietin. Results of a combined phase I and II clinical trial. N Engl J Med 1987;316(2):73–8.
[341] Winearls CG, Oliver DO, Pippard MJ, Reid C, Downing MR, Cotes PM. Effect of human erythropoietin derived from recombinant DNA on the anaemia of patients maintained by chronic haemodialysis. Lancet 1986;2(8517):1175–8.
[342] Horl WH, Cavill I, MacDougall IC, Schaefer RM, Sunder-Plassmann G. How to diagnose and correct iron deficiency during r-huEPO therapy—a consensus report. Nephrol Dial Transplant 1996;11(2):246–50.
[343] Bernhardt WM, Gottmann U, Doyon F, et al. Donor treatment with a PHD-inhibitor activating HIFs prevents graft injury and prolongs survival in an allogenic kidney transplant model. Proc Natl Acad Sci U S A 2009;106(50):21276–81.
[344] Fraisl P, Aragones J, Carmeliet P. Inhibition of oxygen sensors as a therapeutic strategy for ischaemic and inflammatory disease. Nat Rev Drug Discov 2009;8(2):139–52.
[345] Katschinski DM. In vivo functions of the prolyl-4-hydroxylase domain oxygen sensors: direct route to the treatment of anaemia and the protection of ischaemic tissues. Acta Physiol (Oxf) 2009;195(4):407–14.
[346] Song YR, You SJ, Lee YM, et al. Activation of hypoxia-inducible factor attenuates renal injury in rat remnant kidney. Nephrol Dial Transplant;25(1):77–85.
[347] Hsieh MM, Linde NS, Wynter A, et al. HIF prolyl hydroxylase inhibition results in endogenous erythropoietin induction, erythrocytosis, and modest fetal hemoglobin expression in rhesus macaques. Blood 2007;110(6):2140–7.
[348] Besarab A, Caro J, Jarrell BE, Francos G, Erslev AJ. Dynamics of erythropoiesis following renal transplantation. Kidney Int 1987;32(4):526–36.
[349] Eckhardt KU, Frei U, Kliem V, Bauer C, Koch KM, Kurtz A. Role of excretory graft function for erythropoietin formation after renal transplantation. Eur J Clin Invest 1990;20(5): 563–72.
[350] Rejman AS, Grimes AJ, Cotes PM, Mansell MA, Joekes AM. Correction of anaemia following renal transplantation: serial changes in serum immunoreactive erythropoietin, absolute reticulocyte count and red-cell creatine levels. Br J Haematol 1985;61(3):421–31.
[351] Sun CH, Ward HJ, Paul WL, Koyle MA, Yanagawa N, Lee DB. Serum erythropoietin levels after renal transplantation. N Engl J Med 1989;321(3):151–7.
[352] Davis HP. Polycythaemia following renal transplantation. J R Soc Med 1987;80(8):475–6.
[353] Thevenod F, Radtke HW, Grutzmacher P, et al. Deficient feedback regulation of erythropoiesis in kidney transplant patients with polycythemia. Kidney Int 1983;24(2):227–32.
[354] Bacon BR, Rothman SA, Ricanati ES, Rashad FA. Renal artery stenosis with erythrocytosis after renal transplantation. Arch Intern Med 1980;140(9):1206–11.
[355] Friman S, Nyberg G, Blohme I. Erythrocytosis after renal transplantation; treatment by removal of the native kidneys. Nephrol Dial Transplant 1990;5(11):969–73.
[356] Ianhex LE, Da Fonseca JA, Chocair PR, Maspes V, Sabbaga E. Polycythemia after kidney transplantation: influence of the

native kidneys on the production of hemoglobin. Urol Int 1977;32(5):382–92.
[357] Martino R, Oliver A, Ballarin JM, Remacha AF. Postrenal transplant erythrocytosis: further evidence implicating erythropoietin production by the native kidneys. Ann Hematol 1994;68 (4):201–3.
[358] Bakris GL, Sauter ER, Hussey JL, Fisher JW, Gaber AO, Winsett R. Effects of theophylline on erythropoietin production in normal subjects and in patients with erythrocytosis after renal transplantation. N Engl J Med 1990;323(2): 86–90.
[359] McDonald TP. Regulation of megakaryocytopoiesis by thrombopoietin. Ann N Y Acad Sci 1987;509:1–24.
[360] Kaushansky K, Lok S, Holly RD, et al. Promotion of megakaryocyte progenitor expansion and differentiation by the c-Mpl ligand thrombopoietin. Nature 1994;369(6481):568–71.
[361] Kaushansky K, Broudy VC, Lin N, et al. Thrombopoietin, the Mp1 ligand, is essential for full megakaryocyte development. Proc Natl Acad Sci U S A 1995;92(8):3234–8.
[362] Wendling F, Maraskovsky E, Debili N, et al. cMpl ligand is a humoral regulator of megakaryocytopoiesis. Nature 1994;369 (6481):571–4.
[363] Hunt P, Li YS, Nichol JL, et al. Purification and biologic characterization of plasma-derived megakaryocyte growth and development factor. Blood 1995;86(2):540–7.
[364] Ishibashi T, Kimura H, Shikama Y, et al. Interleukin-6 is a potent thrombopoietic factor in vivo in mice. Blood 1989;74 (4):1241–4.
[365] De Gabriele G, Penington DG. Regulation of platelet production: "hypersplenism" in the experimental animal. Br J Haematol 1967;13(3):384–93.
[366] McDonald TP, Clift R, Lange RD, Nolan C, Tribby II, Barlow GH. Thrombopoietin production by human embryonic kidney cells in culture. J Lab Clin Med 1975;85(1):59–66.
[367] Bartley TD, Bogenberger J, Hunt P, et al. Identification and cloning of a megakaryocyte growth and development factor that is a ligand for the cytokine receptor Mpl. Cell 1994;77 (7):1117–24.
[368] de Sauvage FJ, Hass PE, Spencer SD, et al. Stimulation of megakaryocytopoiesis and thrombopoiesis by the c-Mpl ligand. Nature 1994;369(6481):533–8.
[369] Lok S, Kaushansky K, Holly RD, et al. Cloning and expression of murine thrombopoietin cDNA and stimulation of platelet production in vivo. Nature 1994;369(6481):565–8.
[370] Methia N, Louache F, Vainchenker W, Wendling F. Oligodeoxynucleotides antisense to the proto-oncogene c-mpl specifically inhibit in vitro megakaryocytopoiesis. Blood 1993;82(5):1395–401.
[371] Skoda RC, Seldin DC, Chiang MK, Peichel CL, Vogt TF, Leder P. Murine c-mpl: a member of the hematopoietic growth factor receptor superfamily that transduces a proliferative signal. EMBO J 1993;12(7):2645–53.
[372] Souyri M, Vigon I, Penciolelli JF, Heard JM, Tambourin P, Wendling F. A putative truncated cytokine receptor gene transduced by the myeloproliferative leukemia virus immortalizes hematopoietic progenitors. Cell 1990;63(6): 1137–47.
[373] Hoffman RC, Andersen H, Walker K, et al. Peptide, disulfide, and glycosylation mapping of recombinant human thrombopoietin from ser1 to Arg246. Biochemistry 1996;35 (47):14849–61.
[374] Kato T, Oda A, Inagaki Y, et al. Thrombin cleaves recombinant human thrombopoietin: one of the proteolytic events that generates truncated forms of thrombopoietin. Proc Natl Acad Sci U S A 1997;94(9):4669–74.
[375] Chang MS, McNinch J, Basu R, et al. Cloning and characterization of the human megakaryocyte growth and development factor (MGDF) gene. J Biol Chem 1995;270(2):511–4.
[376] Foster DC, Sprecher CA, Grant FJ, et al. Human thrombopoietin: gene structure, cDNA sequence, expression, and chromosomal localization. Proc Natl Acad Sci USA 1994;91(26): 13023–7.
[377] Sohma Y, Akahori H, Seki N, et al. Molecular cloning and chromosomal localization of the human thrombopoietin gene. FEBS Lett 1994;353(1):57–61.
[378] Kamura T, Handa H, Hamasaki N, Kitajima S. Characterization of the human thrombopoietin gene promoter. A possible role of an Ets transcription factor, E4TF1/GABP. J Biol Chem 1997;272(17):11361–8.
[379] Carver-Moore K, Broxmeyer HE, Luoh SM, et al. Low levels of erythroid and myeloid progenitors in thrombopoietin-and c-mpl-deficient mice. Blood 1996;88(3):803–8.
[380] Gurney AL, Carver-Moore K, de Sauvage FJ, Moore MW. Thrombocytopenia in c-mpl-deficient mice. Science 1994;265 (5177):1445–7.
[381] Vigon I, Florindo C, Fichelson S, et al. Characterization of the murine Mpl proto-oncogene, a member of the hematopoietic cytokine receptor family: molecular cloning, chromosomal location and evidence for a function in cell growth. Oncogene 1993;8(10):2607–15.
[382] Gurney AL, Wong SC, Henzel WJ, de Sauvage FJ. Distinct regions of c-Mpl cytoplasmic domain are coupled to the JAK-STAT signal transduction pathway and Shc phosphorylation. Proc Natl Acad Sci U S A 1995;92(12):5292–6.
[383] Drachman JG, Griffin JD, Kaushansky K. The c-Mpl ligand (thrombopoietin) stimulates tyrosine phosphorylation of Jak2, Shc, and c-Mpl. J Biol Chem 1995;270(10):4979–82.
[384] Miyakawa Y, Oda A, Druker BJ, et al. Thrombopoietin induces tyrosine phosphorylation of Stat3 and Stat5 in human blood platelets. Blood 1996;87(2):439–46.
[385] Pallard C, Gouilleux F, Benit L, et al. Thrombopoietin activates a STAT5-like factor in hematopoietic cells. EMBO J 1995;14 (12):2847–56.
[386] Yamada M, Komatsu N, Okada K, Kato T, Miyazaki H, Miura Y. Thrombopoietin induces tyrosine phosphorylation and activation of mitogen-activated protein kinases in a human thrombopoietin-dependent cell line. Biochem Biophys Res Commun 1995;217(1):230–7.
[387] Sattler M, Salgia R, Durstin MA, Prasad KV, Griffin JD. Thrombopoietin induces activation of the phosphatidylinositol-3′ kinase pathway and formation of a complex containing p85PI3K and the protooncoprotein p120CBL. J Cell Physiol 1997;171(1):28–33.
[388] Broudy VC, Lin NL, Sabath DF, Papayannopoulou T, Kaushansky K. Human platelets display high-affinity receptors for thrombopoietin. Blood 1997;89(6):1896–904.
[389] Gurney AL, Kuang WJ, Xie MH, Malloy BE, Eaton DL, de Sauvage FJ. Genomic structure, chromosomal localization, and conserved alternative splice forms of thrombopoietin. Blood 1995;85(4):981–8.
[390] McDonald TP, Kalmaz GD. Effects of thrombopoietin on the number and diameter of marrow megakaryocytes of mice. Exp Hematol 1983;11(2):91–7.
[391] McDonald TP, Jackson CW. Thrombopoietin derived from human embryonic kidney cells stimulates an increase in DNA content of murine megakaryocytes in vivo. Exp Hematol 1990;18(7):758–63.
[392] Zhou W, Toombs CF, Zou T, Guo J, Robinson MO. Transgenic mice overexpressing human c-mpl ligand exhibit chronic thrombocytosis and display enhanced recovery from 5-

fluorouracil or antiplatelet serum treatment. Blood 1997;89 (5):1551–9.
[393] de Sauvage FJ, Carver-Moore K, Luoh SM, et al. Physiological regulation of early and late stages of megakaryocytopoiesis by thrombopoietin. J Exp Med 1996;183(2):651–6.
[394] Borge OJ, Ramsfjell V, Veiby OP, Murphy Jr. MJ, Lok S, Jacobsen SE. Thrombopoietin, but not erythropoietin promotes viability and inhibits apoptosis of multipotent murine hematopoietic progenitor cells in vitro. Blood 1996;88 (8):2859–70.
[395] Ritchie A, Vadhan-Raj S, Broxmeyer HE. Thrombopoietin suppresses apoptosis and behaves as a survival factor for the human growth factor-dependent cell line, M07e. Stem Cells 1996;14(3):330–6.
[396] Choi ES, Hokom MM, Chen JL, et al. The role of megakaryocyte growth and development factor in terminal stages of thrombopoiesis. Br J Haematol 1996;95(2):227–33.
[397] Farese AM, Hunt P, Boone T, MacVittie TJ. Recombinant human megakaryocyte growth and development factor stimulates thrombocytopoiesis in normal nonhuman primates. Blood 1995;86(1):54–9.
[398] Itoh R, Katayama N, Kato T, et al. Activity of the ligand for c-mpl, thrombopoietin, in early haemopoiesis. Br J Haematol 1996;94(2):228–35.
[399] Kaushansky K, Lin N, Grossmann A, Humes J, Sprugel KH, Broudy VC. Thrombopoietin expands erythroid, granulocyte-macrophage, and megakaryocytic progenitor cells in normal and myelosuppressed mice. Exp Hematol 1996;24(2): 265–9.
[400] Young JC, Bruno E, Luens KM, Wu S, Backer M, Murray LJ. Thrombopoietin stimulates megakaryocytopoiesis, myelopoiesis, and expansion of CD34 + progenitor cells from single CD34 + Thy-1 + Lin- primitive progenitor cells. Blood 1996;88 (5):1619–31.
[401] Kaushansky K, Broudy VC, Grossmann A, et al. Thrombopoietin expands erythroid progenitors, increases red cell production, and enhances erythroid recovery after myelosuppressive therapy. J Clin Invest 1995;96(3):1683–7.
[402] Kobayashi M, Laver JH, Kato T, Miyazaki H, Ogawa M. Recombinant human thrombopoietin (Mpl ligand) enhances proliferation of erythroid progenitors. Blood 1995;86(7): 2494–9.
[403] Evatt BL, Spivak JL, Levin J. Relationships between thrombopoiesis and erythropoiesis: with studies of the effects of preparations of thrombopoietin and erythropoietin. Blood 1976;48 (4):547–58.
[404] Broudy VC, Lin NL, Kaushansky K. Thrombopoietin (c-mpl ligand) acts synergistically with erythropoietin, stem cell factor, and interleukin-11 to enhance murine megakaryocyte colony growth and increases megakaryocyte ploidy in vitro. Blood 1995;85(7):1719–26.
[405] Chen J, Herceg-Harjacek L, Groopman JE, Grabarek J. Regulation of platelet activation in vitro by the c-Mpl ligand, thrombopoietin. Blood 1995;86(11):4054–62.
[406] Ezumi Y, Takayama H, Okuma M. Thrombopoietin, c-Mpl ligand, induces tyrosine phosphorylation of Tyk2, JAK2, and STAT3, and enhances agonists-induced aggregation in platelets in vitro. FEBS Lett 1995;374(1):48–52.
[407] Montrucchio G, Brizzi MF, Calosso G, Marengo S, Pegoraro L, Camussi G. Effects of recombinant human megakaryocyte growth and development factor on platelet activation. Blood 1996;87(7):2762–8.
[408] McDonald TP. Role of the kidneys in thrombopoietin production. Exp Hematol 1976;4(1):27–31.
[409] McDonald TP, Kalmaz GD. Nephrectomy abolishes the increase in small acetylcholinesterase-positive immature rat megakaryocytes induced by acute thrombocytopenia. Proc Soc Exp Biol Med 1983;174(1):131–6.
[410] Ebbe S. Experimental and clinical megakaryocytopoiesis. Clin Haematol 1979;8(2):371–94.
[411] Siemensma NP, Bathal PS, Penington DG. The effect of massive liver resection on platelet kinetics in the rat. J Lab Clin Med 1975;86(5):817–33.
[412] Sungaran R, Markovic B, Chong BH. Localization and regulation of thrombopoietin mRNa expression in human kidney, liver, bone marrow, and spleen using in situ hybridization. Blood 1997;89(1):101–7.
[413] Shimada Y, Kato T, Ogami K, et al. Production of thrombopoietin (TPO) by rat hepatocytes and hepatoma cell lines. Exp Hematol 1995;23(13):1388–96.
[414] McCarty JM, Sprugel KH, Fox NE, Sabath DE, Kaushansky K. Murine thrombopoietin mRNA levels are modulated by platelet count. Blood 1995;86(10):3668–75.
[415] Nagahisa H, Nagata Y, Ohnuki T, et al. Bone marrow stromal cells produce thrombopoietin and stimulate megakaryocyte growth and maturation but suppress proplatelet formation. Blood 1996;87(4):1309–16.
[416] Ishiguro A, Nakahata T, Muraoka K, et al. Effects and serum levels of thrombopoietin in a case of chronic thrombocytopenia with achondroplasia. Int J Hematol 1997;66(1):99–102.
[417] Emmons RV, Reid DM, Cohen RL, et al. Human thrombopoietin levels are high when thrombocytopenia is due to megakaryocyte deficiency and low when due to increased platelet destruction. Blood 1996;87(10):4068–71.
[418] Tahara T, Usuki K, Sato H, et al. A sensitive sandwich ELISA for measuring thrombopoietin in human serum: serum thrombopoietin levels in healthy volunteers and in patients with haemopoietic disorders. Br J Haematol 1996;93(4):783–8.
[419] Stoffel R, Wiestner A, Skoda RC. Thrombopoietin in thrombocytopenic mice: evidence against regulation at the mRNA level and for a direct regulatory role of platelets. Blood 1996;87(2):567–73.
[420] Kuter DJ, Rosenberg RD. The reciprocal relationship of thrombopoietin (c-Mpl ligand) to changes in the platelet mass during busulfan-induced thrombocytopenia in the rabbit. Blood 1995;85(10):2720–30.
[421] Fielder PJ, Gurney AL, Stefanich E, et al. Regulation of thrombopoietin levels by c-mpl-mediated binding to platelets. Blood 1996;87(6):2154–61.
[422] Hitchcock IS, Chen MM, King JR, Kaushansky K. YRRL motifs in the cytoplasmic domain of the thrombopoietin receptor regulate receptor internalization and degradation. Blood 2008;112 (6):2222–31.
[423] Stefanich E, Senn T, Widmer R, Fratino C, Keller GA, Fielder PJ. Metabolism of thrombopoietin (TPO) in vivo: determination of the binding dynamics for TPO in mice. Blood 1997;89 (11):4063–70.
[424] Cohen-Solal K, Villeval JL, Titeux M, Lok S, Vainchenker W, Wendling F. Constitutive expression of Mpl ligand transcripts during thrombocytopenia or thrombocytosis. Blood 1996;88 (7):2578–84.
[425] Ichikawa N, Ishida F, Shimodaira S, Tahara T, Kato T, Kitano K. Regulation of serum thrombopoietin levels by platelets and megakaryocytes in patients with aplastic anaemia and idiopathic thrombocytopenic purpura. Thromb Haemost 1996;76(2):156–60.
[426] Marsh JC, Gibson FM, Prue RL, et al. Serum thrombopoietin levels in patients with aplastic anaemia. Br J Haematol 1996;95 (4):605–10.

CHAPTER

93

Individualizing the Dialysate to Address Electrolyte Disturbances in the Dialysis Patient

Biff F. Palmer

Professor of Internal Medicine, Department of Internal Medicine, Division of Nephrology
University of Texas Southwestern Medical School

INTRODUCTION

The goal of dialysis in patients with end-stage renal disease is to restore the composition of the body's fluid environment to normal. Dialysis is performed by creating an artificial situation in which the blood is separated from a disposable second solution (the dialysate) by a semipermeable membrane (the dialyzer or the peritoneal membrane). Solutes will diffuse from the blood through the membrane in proportion to their membrane permeability and the concentration gradient. The physician is able to decrease or prevent removal of a solute by adding it to the dialysate, thereby decreasing the concentration gradient for diffusive movement. One may also introduce solute into the dialysate in a concentration in excess of that usually found in the plasma water so that diffusive movement of this solute into the patient is favored. This chapter focuses on the changes that take place in electrolytes and acid–base during hemodialysis and peritoneal dialysis.

SODIUM

Hemodialysis

The patient with end-stage renal disease is dependent on dialysis to remove sodium from the body in an amount that matches sodium intake so that balance can be maintained. Sodium is free to cross the dialysis membrane primarily by the process of diffusion, and to a lesser extent by convection. The concentration of sodium in the dialysate plays a pivotal role in determining whether sodium balance is maintained at a level that avoids volume overload and yet provides adequate cardiovascular stability during the procedure.

As dialysis has evolved, there has been continued interest in adjusting the dialysate sodium concentration in an attempt to improve the tolerability of the procedure. In the early days of dialysis, a low-sodium dialysate was typically utilized to reduce the complications (such as hypertension and congestive heart failure) of chronic volume overload. However, with reduced dialysis treatment times it became apparent that such therapy contributed to hemodynamic instability by exacerbating the decline in plasma osmolality (particularly early in the dialysis procedure) and intravascular volume. Subsequent studies demonstrated that raising dialysate sodium to between 139 and 144 mEq/liter was associated with improved hemodynamic stability and general tolerance to the procedure.[19,74,175]

There was concern that an increased dialysate sodium concentration would produce a dipsogenic effect resulting in increased weight gain and poor blood pressure control. Studies addressing this issue confirmed that a higher-dialysate sodium modestly increased interdialytic weight gain. However, this excess weight was found to be readily removed with improved tolerance to ultrafiltration.[74]

Seldin and Giebisch's The Kidney, Fifth Edition.
DOI: http://dx.doi.org/10.1016/B978-0-12-381462-3.00093-8

© 2013 Elsevier Inc. All rights reserved.

More recently, there has been interest in varying the concentration of sodium in the dialysate during the procedure so as to minimize the potential complications of a high-sodium solution while retaining the beneficial hemodynamic effects.[154] A high dialysate sodium concentration is used initially with a progressive reduction toward isotonic or hypotonic levels by the end of the procedure. This method allows for a diffusive Na influx early in the session in order to prevent the rapid decline in plasma osmolality due to the efflux of urea and other small-molecular-weight solutes. During the remainder of the procedure, when the reduction in osmolality accompanying urea removal is less abrupt the lower dialysate Na level minimizes the development of hypertonicity and any resultant excessive thirst, fluid gain, and hypertension in the interdialytic period (Figure 93.1).

As outlined in Table 93.1, several studies have compared the hemodynamic and symptomatic effects of a dialysate in which the sodium concentration is varied during the procedure to that in which the sodium concentration is fixed. Dumler et al. used a dialysate sodium of 150 mEq/liter during the initial 3 hours of dialysis at the time of ultrafiltration. The dialysate sodium was decreased to 130 mEq/liter for the last hour.[49] The control group was dialyzed against sodium concentration fixed at 140 mEq/liter. Use of the high/low sodium hemodialysis was associated with a smaller decline in systolic pressure and fewer symptomatic hypotensive episodes.

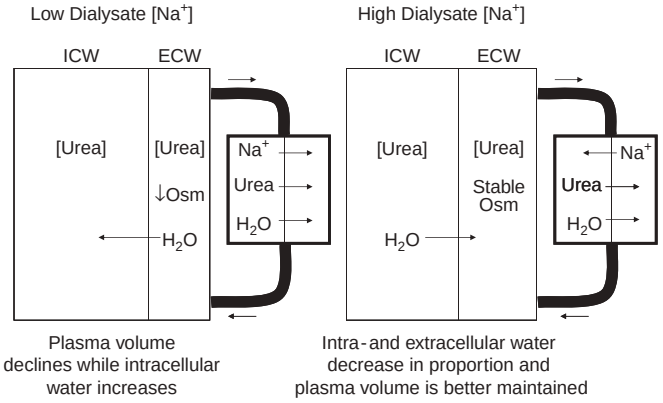

FIGURE 93.1 Use of a low sodium dialysate is more commonly associated with intradialytic hypotension. In the initial period of dialysis the extracellular urea concentration falls creating an osmotic driving force for water movement into the cell due to the higher intracellular urea concentration. This drop in extracellular osmolality and movement of water into the intracellular space is exacerbated in the setting of a low dialysate Na concentration. As a result plasma volume falls and the risk of hypotension increases. A high sodium dialysate helps to minimize the development of extracellular hyposmolality allowing for better refilling of the intravascular compartment. Plasma volume remains better preserved and the risk of hypotension is reduced.

Other investigators have varied dialysate sodium according to a sodium-gradient protocol in which the sodium is set to decrease from a high to a low level over the course of a dialysis session. The mixed results from these experiences are outlined in Table 93.1. Raja et al.[145] and Daugirdas et al.[37] found no measurable benefit. Acchiardo et al.[1] found a reduction in hypotensive episodes, and Sandowski et al. had similar results in young patients.[152] The linear and step sodium modeling programs have been found to be better in lowering the risk of intradialytic headache compared to the exponential program. The linear program was the only individual program that alleviated interdialytic cramps. The most striking reduction in the risk for post-treatment hypotension occurred with the step program.

Differences in the incidence of symptomatic hypotension during dialysis or in the degree of interdialytic weight gain between the fixed and variable sodium protocols have been difficult to demonstrate. Levin et al. studied a group of patients who were specifically selected because of the frequent occurrence of symptoms upon dialysis—such as headaches, cramps, and lightheadedness.[104] In a crossover trial, these patients were assigned either to a fixed sodium dialysate and a constant rate of ultrafiltration or to a gradient protocol in which the initial sodium concentration and ramping pattern were individually adjusted to minimize thirst. Use of patient-specific sodium gradient profiles was associated with improvement in all patients with headache and in 70% of patients with lightheadedness. The majority of patients reported an increase in thirst, but there were no differences in interdialytic weight gain or in pre-dialysis and postdialysis mean arterial pressure.

Utilizing a more general dialysis population, Sang et al. compared a linear or step sodium gradient (155−140 mEq/liter) protocol to a fixed sodium dialysate (140 mEq/liter).[156] In this study, sodium modeling was associated with a significant reduction in cramps and symptomatic hypotension. However, these benefits were followed by increasing thirst, fatigue, and weight gain between dialysis sessions—as well as by a higher predialysis blood pressure. The authors concluded that only 22% of patients had a significant benefit from the modeling programs. Finally, a study by Movilli et al.[122] found improved blood volume preservation by using a pattern of high-to-low sodium change (160−133 mEq/liter). The changes in blood pressure were similar between this high-to-low variation and conventional dialysis.

In summary, the available data suggest that in most chronic dialysis patients changing the dialysate Na during the course of treatment offers little advantage over a constant dialysate Na of between 140 and

TABLE 93.1 Summary of Recent Studies Examining Effects of Na Gradient Protocols

Study (reference)	Design	Intervention	Results
Dumler et al.,[49]	10 patients, crossover design	Fixed (140) vs high (150)/low (130), Uf only with 150	50% decrease in cramping episodes (no statistical comparison possible)
Raja et al.,[145]	10 patients, crossover design	Fixed (135 and 140) vs high (145)/low (135) vs low (135)/high (145)	No difference in hypotensive episodes between high/low and 140, but both better than 135 and low/high protocols
Daugirdas et al.,[37]	7 patients, crossover design	Fixed (143,135) vs gradient (160 to 133)	No difference in hypotensive episodes or cramps among 3 groups
Acchiardo et al.,[1]	39 patients, crossover design	Fixed (140) *vs* gradient (149 to 140 linear, exponential, step)	50% reduction in hypotensive episodes and cramps with gradient protocol
Sandowski et al.,[152]	16 patients (16–32 years of age), crossover design	Fixed (138) *vs* gradient (149 to 138, linear, exponential, step)	Decrease in intra- and interdialytic morbidity with gradient, no differences in symptomatic hypotension
Levin et al.,[104]	11 symptomatic patients and 5 asymptomatic patients, crossover design	Fixed (140) *vs* ramped Na (155–160 to 140) and Uf, each individually tailored	Significant decrease in dialysis morbidity with ramped protocol
Sang et al.,[156]	23 patients, crossover design	Fixed (140) *vs* gradient (155 to 140, linear or step)	Decrease in cramps and hypotension with gradient but only 22% of patients with significant benefit

145 mEq/liter. The inability to clearly demonstrate a superiority of Na modeling may be due to the fact that the time-averaged concentration of Na was similar in many of the comparative studies. For example, a linear decline in dialysate Na from 150 to 140 mEq/liter will produce approximately the same postdialysis serum Na as occurs when a dialysate Na of 145 mEq/liter is used throughout the procedure. In addition, the optimal time-averaged Na concentration (whether administered in a modeling protocol or with a fixed dialysate concentration) is likely to vary from patient to patient (as well as in the same patient) during different treatment times.[159] This variability is supported by studies demonstrating wide differences in the month-to-month pre-dialysis Na concentration in otherwise stable dialysis patients.[57]

Nevertheless, in selected patients Na modeling may be of benefit (Table 93.2). Patients initiating dialysis with marked azotemia are often deliberately dialyzed so as to decrease the urea concentration slowly over the course of several days in order to avoid the development of the dialysis disequilibrium syndrome. The use of a high-/low-Na dialysate in these patients may minimize fluid shifts into the intracellular compartment and decrease the tendency for neurologic complications. Na modeling may also be beneficial in patients suffering frequent intradialytic hypotension, cramping, nausea, vomiting, fatigue, or headache. In such patients, the modeling protocol can be individually tailored to minimize increased thirst, weight gain, and hypertension.

TABLE 93.2 Indications and Contraindications for use of Na Modeling (high/low programs)

A. Indications

- Intradialytic hypotension
- Cramping
- Initiation of hemodialysis in setting of severe azotemia
- Hemodynamically unstable patient (as in intensive care unit setting)

B. Contraindications

- Intradialytic development of hypertension
- Large interdialytic weight gain induced by high Na dialysate
- Hypernatremia

Combining dialysate Na profiling with a varying rate of ultrafiltration may provide additional benefit in particularly symptomatic patients.[169,198] Ultrafiltration profiling is the deliberate use of a high rate of ultrafiltration in the initial part of the treatment when the volume of interstitial fluid available for vascular refilling is maximal and then sequentially decreasing the rate so as to parallel the anticipated fall in interstitial fluid volume. Use of this combined approach may be of particular benefit in ensuring hemodynamic stability in patients with acute renal failure in the intensive care unit.[132]

When prescribing a Na gradient protocol it is important to monitor the patient for evidence of a progressive increase in total body Na. Use of a low-dialysate

Na during the terminal phase of the procedure does not necessarily guarantee negative Na balance. In some patients, a high/low Na protocol can lead to large interdialytic weight gain or cause intradialytic hypertension (Table 93.2). Such adverse effects are more likely to occur when the time-averaged Na concentration is greater than the pre-dialysis serum Na concentration. In one report, this complication was avoided when the time-averaged Na concentration was kept 0.5–0.8 mmol/liter lower than the patient's pre-dialysis serum sodium concentration.[168,93]

A Na gradient protocol can be administered in such a way that the amount of Na exchanged is the same as with a fixed Na dialysate while better preserving blood volume during ultrafiltration. Coli et al., has described a procedure termed profiled hemodialysis.[32–34,181] This technique is based on a mathematical model in which baseline patient characteristics are used to construct a patient-specific sodium profile dialysate prior to each treatment. Initial experience with this procedure has shown improved cardiovascular hemodynamics when compared to a fixed dialysate sodium concentration despite the same total mass of sodium being removed.[33,34]

In hypertensive patients, adjusting the protocol to achieve negative Na balance may be of therapeutic benefit in the long-term control of blood pressure. In this regard, Flanigan et al. recently compared a fixed dialysate Na of 140 mEq/liter to a gradient protocol in which the dialysate Na was lowered in an exponential fashion from 155 to 135 mEq/liter and then held constant at 135 mEq/liter for the final half-hour of the procedure.[58] Ultrafiltration was discontinued during the final half hour of the session. Use of the variable Na dialysate permitted a 50% reduction in the dose of antihypertensive medication without significant changes in pre-dialysis blood pressure or interdialytic weight gain. Although not specifically measured, use of the terminal low-sodium period likely caused a decrease in the total-body exchangeable Na—thus accounting for improved blood pressure control in Na-sensitive patients. Several other trials have noted a modest reduction in the dialysate Na can be an effective maneuver in lowering blood pressure in dialysis patients.

Sodium loading during the dialysis procedure by stimulating thirst can result in expansion of extracellular fluid volume and cause increased cardiac output and blood pressure. Volume independent mechanisms may also play a role in the hypertensive effect of a salt load.[15] For example, increased sympathetic outflow has been linked to hypernatremia in the Dahl salt-sensitive rat. Increased brain Na and osmolality is associated with increased angiotensin II levels. In addition to potential vasoconstrictive and vasculotoxic effects, angiotensin II stimulates sympathetic outflow by binding to AT_1 receptors centrally. *In vitro*, high medium Na concentration results in hypertrophy of cardiac myocytes and vascular smooth muscle cells.[65] Increased medium Na also leads to endothelial cell stiffness and decreased nitric oxide production in the presence of aldosterone.[127] Taken together these observations suggest sodium overload and hypernatremia induced by a high dialysate Na concentration may play an important role in hypertension and abnormal vascular function in dialysis patients.

The ability to achieve neutral sodium balance requires the dialysate sodium concentration to be individualized such that with each treatment a constant end-session plasma sodium concentration is reached. In dialysis patients, interdialytic sodium and water loads vary from one patient to another and from treatment to treatment. Water balance can be achieved by making total ultrafiltrate volume equal to interdialytic weight gain. If over time end-dialysis weight and plasma sodium concentration are kept constant (assuming no change in sodium distribution volume), one can assume that the patient will be in sodium balance. As currently practiced, dialysate sodium concentrations (whether fixed or varied) are not chosen with the primary aim of achieving sodium balance. In fact, pre-dialysis serum sodium levels may vary between 125 and 147 mEq/liter in dialysis patients, but for any individual patient the standard deviation of the pre-dialysis serum sodium value is less than or equal to 2.5 mEq/liter.[56,96] As a result, a dialysate sodium concentration that achieves neutral sodium balance for one patient may cause salt loading when applied to another. This approach risks a pathologic excess in the total sodium mass, which over time can lead to clinical manifestations of volume overload such as hypertension and congestive heart failure.

To properly calculate the dialysate sodium concentration required to maintain sodium balance, measurement of plasma water sodium concentration at the beginning of the treatment is required. Hemodynamics were recently compared in 27 patients dialyzed against dialysate Na set at 138 mEq/liter versus dialysate Na set to match the average pre-dialysis Na concentration multiplied by the Donnan coefficient of 0.95 (individualized Na dialysate).[39] This latter step was undertaken to better approximate the ionic concentration of Na rather than its total concentration. The ionic concentration of Na better reflects the amount available for movement across a dialysis membrane because a small amount of total Na is unavailable for diffusive flux due to Donnan effects and complexes formed with certain anions. Use of the individualized Na dialysate was associated with less interdialytic weight gain, decreased thirst, and improved blood pressure control.

The ionic activity of sodium can also be measured through the use of conductivity measurements. Locatelli et al. have recently described the use of a biofeedback system that allows for the automatic determination of plasma water and dialysate conductivity such that blood sampling can be avoided.[108–110] With these measurements—along with session time, desired weight loss, and expected end-treatment plasma water conductivity—the dialysate conductivity is automatically adjusted in order to achieve the prescribed final plasma water conductivity. Application of this conductivity kinetic model to patients treated with a variant of hemodiafiltration achieves near-zero hydrosodium balance and improves intradialytic cardiovascular stability.[109] Such techniques may also be useful in patients with a low pre-dialysis Na concentration who are prone to positive sodium balance when dialyzed against a fixed dialysate Na.[120] Newer technology will allow for plasma water and dialysate conductivity to be measured repetitively during the procedure, allowing automatic adjustment of the dialysate sodium online throughout the procedure.[21,113,139]

With increased ability to individualize the dialysate sodium concentration, one can envision a scenario in which a patient initiated on hemodialysis is initially treated with a dialysate sodium concentration designed to achieve negative sodium balance. Once the patient becomes normotensive or requires minimal amounts of antihypertensive medication, the dialysate sodium can be adjusted on a continual basis to ensure that sodium balance is maintained. In this manner, management of sodium balance would be made similar to management of fluid intake. Achieving the optimal total body sodium content will likely become just as important as determining an accurate dry weight.

Peritoneal Dialysis

Ultrafiltration in peritoneal dialysis is achieved by instilling into the peritoneal cavity a fluid that is hyperosmolar relative to plasma. The creation of this osmotic gradient results in net movement of free water into the peritoneal cavity. The degree of hypertonicity, the dwell time, and peritoneal transport characteristics are the main determinants of volume removal. The magnitude of ultrafiltration is determined clinically by subtracting the volume of fluid instilled in the peritoneal cavity from the effluent volume.

The osmotic driving force of peritoneal dialysate can be adjusted by changing the dialysate glucose concentration. A 1.5% glucose dialysate is only slightly hypertonic to plasma, and small volumes of ultrafiltration will be expected. In contrast, ultrafiltration rates of up to one liter per hour have been obtained with a 4.25% solution. The osmolality of the infused dialysate declines over time due to the movement of water into the peritoneal cavity and the absorption of glucose from the peritoneal cavity. Due to a sieving coefficient across the peritoneal membrane of less than one, the sodium concentration in the ultrafiltrate during peritoneal dialysis is usually less than the extracellular fluid. As a result, there is a tendency for water loss and the development of hypernatremia. Commercially available peritoneal dialysates have a sodium concentration of 132 mEq/liter to compensate for this tendency toward dehydration. This effect is most pronounced with increasing frequency of exchanges and with increasing dialysate glucose concentrations. Use of the more hypertonic solutions with frequent cycling can result in significant dehydration and hypernatremia. As a result of stimulated thirst, water intake and weight may increase—resulting in a vicious cycle.

There are three components that determine sodium transport in peritoneal dialysis. The components that account for removal of sodium from the body are diffusion (due to the concentration gradient between blood and dialysate) and convection (due to ultrafiltration). Acting to oppose sodium removal is peritoneal absorption. Lymphatic and intestinal tissue fluid absorption leads to the convective movement of sodium from the dialysate to blood. There is a strong positive correlation between net ultrafiltration volume and the total mass of sodium removed from the body.[187] Ultrafiltration not only increases sodium removal by convection but increases the diffusive flux by secondarily increasing the concentration gradient from blood to dialysate. The more favorable gradient results from the sodium-sieving effect such that the fluid entering the peritoneal space is hypotonic and dilutes the dialysate sodium concentration.

The use of a peritoneal solution containing the standard sodium concentration of 132 mEq/liter creates a relatively small concentration gradient for sodium diffusion. As a result, more sodium is removed by convection compared to diffusion.[90–97] Differences in osmolality of the solutions utilized and dwell time account for the variability in sodium removal among the different modalities of peritoneal dialysis. Automated forms of peritoneal dialysis (APD) are characterized by rapid exchanges and short dwell times. Although hypertonic exchanges during APD lead to a more pronounced fall in dialysate sodium concentration, there is little time available for diffusion. It is for this reason that sodium removal in APD is lower than chronic ambulatory peritoneal dialysis, in which dwell times are much longer. Patients treated with APD may achieve adequate ultrafiltration with hypertonic solutions but have inadequate sodium removal.

Sodium and water removal is more difficult to achieve in patients with increased membrane permeability. These patients have increased diastolic blood pressures and are prone to volume overload. In addition, patient and technique survival may be decreased in this setting. Sodium transport in this patient group is characterized by a high peritoneal absorption rate and a decreased ultrafiltration rate. The diffusive flux of sodium is not significantly different in these patients.[187] Typically, such high-transport patients are placed on APD to minimize dialysate dwell time. An alternative strategy that could be utilized is to lower the sodium concentration in the dialysate. Studies examining ultrafiltration and sodium kinetics using a dialysate sodium concentration of either 102 mmol/liter (383 mOsm/kg) or 105 mmol/L (348 mOsm/kg) have shown that a low-sodium dialysate is more effective in the removal of excess sodium compared to a conventional sodium solution.[79,102]

Enhanced sodium removal may be the result of an increased diffusive flux of sodium or may be secondary to enhanced convective transport due to the higher glucose concentrations used in low-sodium solutions. Alternatively, the decreased sodium concentration in the dialysate may contribute to less sodium absorption. In short-term clinical trials, use of a low-sodium dialysate (98 mmol/liter and 120 mEq/liter) has been shown effective in reducing both body weight and blood pressure in volume-overloaded patients on chronic ambulatory peritoneal dialysis.[92,124,125] Limited data also suggest that this strategy may be of use in patients receiving APD.[90–92]

An additional strategy for enhancing sodium removal and preventing volume overload in patients with increased membrane permeability is to substitute icodextran for glucose as the osmotic agent.[118,185] Icodextran is a glucose polymer that is isosmolar to plasma but still capable of generating an ultrafiltrate through the process of colloid osmosis. This process is based on the principle that water is transported from capillaries in the direction of impermeable large solutes rather than down an osmotic gradient (as occurs with glucose-containing solutions). Water movement occurs through small pores, whereas in the osmotic effect of glucose water movement is primarily through ultrasmall transcellular pores. Sodium sieving does not occur with icodextran as a result of this difference.

In a six-hour dwell, the 7.5% icodextran solution generates an ultrafiltrate volume that is higher than that generated by 1.5% dextrose—despite having a lower osmolality (285 *vs* 347 mOsm/kg). With prolonged dwell times of 8–12 hours, the icodextran solution provides equivalent or higher ultrafiltrate volumes than that generated by the 4.25% dextrose solution (486 mOsm/kg).[138] In prospective randomized studies, use of icodextran has been found more effective in reducing extracellular water[95] and in removing sodium[38] compared to standard glucose solutions. The ability to maintain a colloid osmotic pressure for prolonged periods makes this solution ideal for overnight dwells in patients on continuous ambulatory peritoneal dialysis and for daytime dwells for those on automated peritoneal dialysis regimens.

In patients with ultrafiltration failure who would otherwise be transferred to hemodialysis, use of icodextran has been shown to extend the time that patients remain on peritoneal dialysis by many months.[26] In addition use of icodextran is associated with less weight gain, improved lipid control, and less hyperinsulinemia as compared with dextrose-containing solutions. It is likely that icodextran will become the preferred agent for the long dwell in most peritoneal dialysis patients.

POTASSIUM

Regulation of Potassium in Renal Disease

Acute kidney injury may lead to marked decreases in distal delivery of salt and water which may secondarily decrease distal K^+ secretion. For this reason, hyperkalemia tends to occur more commonly in oliguric renal failure. Hyperkalemia is much less common in non-oliguric renal failure since distal delivery of salt and water is plentiful.

Chronic kidney disease is more complicated than acute renal failure. In addition to the decreased GFR and secondary decrease in distal delivery, there is nephron dropout and a smaller number of collecting ducts to secrete K^+. However, this is counterbalanced by an adaptive process in which the remaining nephrons develop an increased ability to excrete K^+. In a study of normokalemic patients with stage 4 chronic kidney disease, the fractional excretion of K^+ was 126% compared with 26% in normal controls.[195] The fractional excretion of Na^+ in the two groups was 2.3% and 15%, respectively. Following the intravenous administration of amiloride, the fractional excretion of K^+ decreased by 87% in the patients with chronic kidney disease compared with 19.5% in control patients. These findings support the idea that patients with chronic kidney disease are able to maintain a normal serum K^+ concentration through an adaptive increase in renal K^+ secretion that is largely amiloride sensitive.

Once a patient reaches end-stage renal disease the capacity for renal potassium excretion is no longer present. Interestingly, despite this limitation, total body potassium (in particular, intracellular potassium) in patients with end-stage renal disease is low or

normal.[17,20,119] The low intracellular potassium content has been attributed to decreased activity of the Na,K-ATPase, which is a characteristic finding in uremia.[28,196] Studies in red blood cells taken from uremic patients have shown that the diminished activity of the pump can be reversed when cells are incubated in normal plasma. There is also an improvement in the activity of the pump following dialysis.[28,80,97,144] Red blood cells taken from normal individuals and incubated in uremic plasma acquire the defect.

Decreased potassium concentration, increased sodium concentration, and decreased resting membrane potential have been demonstrated in skeletal muscle from uremic patients.[35] After seven weeks of hemodialysis, these physiologic parameters were restored to normal. These observations suggest the presence of a circulating inhibitor of the Na^+,K^+-ATPase in some uremic patients.[84] In other patients, there may be a decrease in the number of pump sites rather than decreased activity. A decrease in pump activity or a decrease in the total number of pumps may account for the impaired extrarenal potassium disposal reported in some uremic patients.

In the absence of renal function, the cellular uptake of potassium becomes an important defense against the development of hyperkalemia. Studies of patients on dialysis have shown a defect in this extrarenal mechanism of potassium disposal.[3,7,55] Fernandez et al. compared the disposition of an oral potassium load (0.25 mEq/kg/body weight) in a group of dialysis patients and in normal controls.[55] The normal controls excreted 67% of the potassium load within 3 hours and translocated 51% of the retained potassium intracellularly. In contrast, the dialysis patients did not excrete any of the potassium and only 21% of the retained potassium was translocated intracellularly. The increment in plasma potassium was significantly different between the two groups. The plasma potassium concentration increased by 1.06 mEq/liter in the dialysis patients, whereas only a 0.39-mEq/liter increase was noted in the control group. The impairment in potassium disposal persists even when the potassium load is accompanied by oral glucose, although glucose-induced stimulation of insulin attenuates the maximal rise in potassium levels.[3]

In patients with renal failure, a significant proportion of daily potassium excretion occurs via the gastrointestinal tract. Gastrointestinal losses are important in maintaining potassium balance in chronic dialysis patients because hemodialysis removes approximately 80−100 mEq/treatment (300 mEq/week), yet dietary potassium intake is usually 400−500 mEq/week. In a balance study performed in patients already on peritoneal dialysis, 25% of the daily potassium intake was lost via the feces.[71,72] The amount of potassium excreted in the stools correlates directly with the wet stool weight.[79,80] Therefore, constipation should be avoided because it will decrease the gastrointestinal elimination of potassium and increase the tendency toward hyperkalemia.[174]

The mechanism of the increased gastrointestinal potassium loss is not known. The process appears to be due to active secretion, as it is unrelated to plasma potassium or total body potassium.[114,135,185] In fact, hemodialysis patients continue to have enhanced rectal potassium secretion even after dialysis—their plasma potassium being less than that of controls. Potassium transport in the large intestine was recently studied in patients with end-stage renal disease using a rectal dialysis technique.[116] Rectal potassium secretion was found to be three fold greater in end-stage renal disease patients as compared to control patients with normal renal function. When barium (a potassium channel inhibitor) was placed in the lumen, colonic potassium secretion was reduced by 45% in the end-stage renal disease patients while no effect was seen in the control group. Immunostaining using an antibody directed to the α-subunit of the high conductance potassium channel protein revealed greater expression of the channel in surface colonocytes and crypt cells in the end-stage renal disease patients while only a low levels of expression was observed in the control group. These data are consistent with increased expression of potassium channels as the mechanism for the adaptive increase in colonic potassium secretion in patients with end-stage renal disease.

Elevated levels of plasma aldosterone may play an important role in stimulating the gastrointestinal excretion and cellular uptake of potassium in patients with end-stage renal disease.[5] Exogenous administration of mineralocorticoids has been shown to decrease the serum potassium in anuric dialysis patients, presumably by increasing colonic potassium excretion.[78] In a prospective study, fludrocortisone administered at 0.1 mg/d was compared with no treatment in 21 hyperkalemic hemodialysis patients.[47] At the end of 10 months, the serum K^+ concentration in the two groups was not statistically different. However, there was a decrease in serum K^+ compared with pretreatment values in patients who received the drug.

A recent study examined the effects of glycyrrhetinic acid food supplementation on the serum K concentration in a group of maintenance hemodialysis patients.[50] This substance inhibits the enzyme 11β-hydroxysteroid dehydrogenase II which is found not only in the principal cells of the renal collecting duct but also epithelial cells in the colon. This enzyme converts cortisol to cortisone thereby ensuring the mineralocorticoid receptor remains free to only interact with aldosterone since cortisone has no affinity for the receptor. In 9 of 10

patients given the supplement there was a persistent decrease in measured predialysis serum potassium concentration. In addition, treatment with the supplement significantly decreased the frequency of severe hyperkalemia. These beneficial effects occurred without weight gain or increases in systemic blood pressure suggesting glycyrrhetinic acid supplementation may be of benefit in enhancing colonic K secretion and minimizing the risk of hyperkalemia in dialysis patients.

Angiotensin-converting enzyme inhibitors and angiotensin receptor blockers have both been reported to cause hyperkalemia in patients treated with hemodialysis and peritoneal dialysis.[94,142] The development of hyperkalemia with these drugs may be due to decreased colonic potassium excretion resulting from lower circulating levels of aldosterone or decreased activity of angiotensin II. In this regard, enhanced colonic potassium excretion in renal failure has been attributed to upregulation of angiotensin II receptors in the colon—suggesting that angiotensin II has a direct effect in stimulating colonic potassium excretion.[70] Blocking the mineralocorticoid receptor with spironolactone given at a dose of 25 mg/day does not raise the serum potassium concentration in hemodialysis patients.[155]

Hemodialysis

Dialysis is required to maintain normal or near-normal serum potassium concentrations in patients with end-stage renal disease. The removal of excess potassium by dialysis is achieved by the use of a dialysate with a potassium concentration lower than that of plasma, creating a gradient favoring potassium removal. Its rate is largely a function of this gradient.[51] Typically, one should not expect more than about 80−100 mEq of potassium removal even with the use of a potassium-free dialysate. Plasma potassium concentration falls rapidly in the early stages of dialysis, but as the plasma concentration falls potassium removal becomes less efficient. Because potassium is freely permeable across the dialysis membrane, movement of potassium from the intracellular space to the extracellular space appears to be the limiting factor in potassium removal. Factors that importantly dictate the distribution of potassium between these two spaces include changes in acid−base status, tonicity, glucose and insulin concentration, and catecholamine activity (Table 93.3).

The movement of potassium between the intra- and extra-cellular spaces is influenced by changes in acid−base balance that occur during the dialysis procedure.[89,173] Extracellular alkalosis causes a shift of potassium into cells, whereas acidosis results in potassium efflux from cells. During a typical dialysis, there is net addition of base to the extracellular space—which promotes cellular uptake of potassium and therefore attenuates the removal of potassium during dialysis. With routine dialysis, the change in blood pH is of small magnitude and the effect on potassium removal is not profound.

TABLE 93.3 Factors Affecting Potassium Removal during Hemodialysis

A. Shifts K into cell thereby ↓ dialytic K removal
• Exogenous insulin
• Glucose containing dialysate vs glucose free dialysate
• Beta agonists
• Correction of metabolic acidosis during dialysis
B. Shifts K to extracellular space or impairs cell K uptake thereby ↑ dialytic K removal
• Beta blockers
• Alpha adrenergic receptor stimulation
• Hypertonicity

By contrast, dialysis in patients who are acidotic will result in less potassium removal because potassium is shifted into cells as the serum bicarbonate rises. Weigand et al. described five patients in whom the serum potassium concentration decreased during dialysis even though the dialysate potassium concentration was higher than the original serum potassium concentration.[189] The decline in potassium concentration occurred in association with a marked rise in pH. In one patient, the decline in potassium concentration was of such magnitude that she became quadriplegic and developed respiratory failure. There appears to be no difference in potassium removal whether acetate or bicarbonate is chosen as the dialysate buffer.

Conversely, the serum potassium concentration can influence the net addition of base. Redaelli et al. found that a potassium-free dialysate was associated with less bicarbonate uptake compared to a dialysate that contained a potassium concentration of 2 mEq/liter.[147] It was postulated that a lower potassium dialysate that results in a high plasma-to-dialysate potassium concentration gradient causes less hydrogen ion movement from the intracellular space to the extracellular space and hence less downward titration of the extracellular bicarbonate concentration. As a result, the concentration gradient favoring diffusion of bicarbonate from the dialysate to the extracellular space is reduced. This relationship should be considered when dialyzing an acidotic patient.

Insulin is known to stimulate the cellular uptake of potassium, and it can therefore influence the amount of potassium removal during dialysis. This effect of

insulin was demonstrated in studies comparing potassium removal using glucose-containing and glucose-free dialysates.[161,188] The use of a glucose-free dialysate was found to result in greater amounts of potassium removal when compared to patients treated with a glucose-containing bath. The use of a glucose-free dialysate would be expected to result in lower levels of insulin. As a result, there is increased movement of potassium to the extracellular space—where it becomes available for dialytic removal.

Changes in plasma tonicity can affect the distribution of potassium between the intra- and extra-cellular spaces.[173] Administration of hypertonic saline or mannitol is sometimes used in the treatment of hypotension during dialysis. These agents would be expected to favor potassium removal during dialysis because the resultant increased tonicity would favor potassium movement into the extracellular space. There are no studies addressing whether there is any significant clinical benefit with this approach.

Beta-adrenergic stimulation is known to shift potassium into cells and thus lower the extracellular concentration. Inhaled beta stimulants have been reported to be effective in the acute treatment of hyperkalemia. Thus, such therapy prior to dialysis may lower the total amount of potassium removed during the dialytic procedure. Allon et al. found that the cumulative dialytic potassium removal was significantly lower in patients treated with nebulized albuterol 30 minutes prior to the procedure compared to patients in whom the albuterol treatment was omitted.[4]

Alterations in serum potassium concentration during dialysis can conceivably have important effects on systemic hemodynamics. A decrease in serum potassium concentration during hemodialysis would be predicted to increase systemic vascular resistance. Hypokalemia has been shown to increase resistance in skeletal muscle, skin, and coronary vascular beds—possibly through effects on the electrogenic Na-K pump in the sarcolemmal membranes of vascular smooth muscle cells.[22] In addition, decreased serum potassium concentration may enhance the sensitivity of the vasculature to endogenous pressor hormones.[105]

Despite the potential for hypokalemia to increase systemic vascular resistance, Pogglitsch et al. found that the incidence of hypotensive episodes were in fact reduced when supplemental potassium was administered during the final 30 minutes of dialysis.[141] One explanation for this seemingly paradoxical finding rests on the known interaction between hypokalemia and the autonomic nervous system. For example, hypokalemia has been found to be associated with dysautonomia in patients with hyperaldosteronism.[18] It is reasonable to speculate that in patients with advanced renal failure, who already have a propensity for autonomic insufficiency, a fall in plasma potassium may uncover or cause impairment in sympathetic responses.[73]

In support of this suggestion, Henrich et al. found that hypokalemic dialysis was accompanied by a fall in plasma catecholamine concentration compared to dialysis in which serum potassium concentration was held constant.[75] Moreover, despite similar reductions in blood pressure the isokalemic dialysis group had a significant increase in heart rate after dialysis and the hypokalemic group demonstrated no significant change. Further studies are needed to investigate the effects of fluctuations in serum potassium concentration during dialysis on the autonomic nervous system.

Changes in serum potassium concentration during dialysis may also influence systemic hemodynamics through effects on myocardial performance. Dialysis is associated with an increase in contractility, which can be attributed to an increase in ionized serum calcium. Increased ionized calcium is most closely related to improved ventricular contractility, but modifying effects of concomitant decreases in potassium may also be important. Haddy et al. have demonstrated that the inotropic effect of increased serum calcium concentration is enhanced by simultaneous decreases in plasma potassium concentration.[67] In this regard, Wizemann et al. found that improvement in myocardial contractility during a series of isovolemic dialysis maneuvers was related to a simultaneous increase in plasma calcium and a decrease in plasma potassium concentration.[193] In the presence of an elevated plasma potassium concentration, a high plasma calcium concentration failed to exert a significant inotropic effect.

An increase in peripheral vascular resistance secondary to the development of hypokalemia could have potential detrimental effects on dialysis efficiency. This decrease in efficiency would result from decreased blood flow to urea-rich tissues (such as skeletal muscle) and in effect increase the amount of body-wide recirculation. In support of this possibility, Dolson et al. found that a dialysate potassium concentration of 1.0 mmol/liter compared to 3.0 mmol/liter resulted in lower values for both the urea reduction ratio and Kt/V in 14 patients with end-stage renal disease.[45] By contrast, Zehnder et al. found no effect of dialysate potassium on dialysis adequacy.[197] Although more studies are needed in this area, it is likely that any effect of a low dialysate potassium concentration to decrease dialysis adequacy is small in magnitude. In addition, increasing the dialysate potassium concentration to improve dialysis adequacy will increase the risk of hyperkalemia during the interdialytic period.

Most patients dialyzed with a fixed potassium dialysate tolerate the procedure well and do not suffer from complications of hypokalemia or hyperkalemia.

Nevertheless, there are clinical conditions in which an individualized dialysate potassium concentration may be useful. Patients with underlying heart disease, particularly in the setting of digoxin therapy, are prone to arrhythmias as hypokalemia develops toward the end of a typical treatment. The risk of arrhythmias is also increased in the early stages of a dialysis session, when the plasma potassium concentration may still be normal but rapidly declining.[146] The sudden reduction in the plasma potassium concentration during the initial portions of the dialysis procedure has recently been shown to unfavorably alter the QTc (a marker of risk of ventricular arrhythmias) even in dialysis patients without obvious heart disease.[36,112] Patients who have suffered a cardiac arrest in the dialysis unit are more likely to have been dialyzed against a 0- or 1.0-mEq/liter potassium dialysate compared to patients without this complication.[85]

With these considerations in mind, Redaelli et al. have studied the effects of modeling the dialysate potassium concentration in such a way as to minimize the initial rapid decline in the plasma potassium concentration.[148] Patients with frequent intradialytic premature ventricular complexes were dialyzed using a dialysate with a fixed (2.5 mEq/liter) potassium level or one with an exponentially declining potassium level (from 3.9 to 2.5 mEq/liter) that maintained a constant blood-to-dialysate potassium gradient of 1.5 mEq/liter throughout the procedure. In the fixed dialysate group, the blood-to-dialysate potassium gradient decreased over the treatment from 3.0 /liter to 1.4 mEq/liter. The variable potassium dialysate decreased premature ventricular complexes—a finding most evident during the first hour of the procedure. The total drop in the serum potassium concentration was no different between the fixed and variable potassium dialysate groups.

In addition to decreasing arrhythmias, maintenance of a constant blood-to-dialysate potassium concentration may prove useful in patients who tend to develop worsening hypertension during the course of the dialysis procedure. Hypokalemia increases resistance in skeletal muscle, skin, and coronary vascular beds—possibly through effects on the electrogenic Na-K pump in the sarcolemmal membranes of vascular smooth muscle cells.[22] In addition, decreased serum potassium concentration may enhance the sensitivity of the vasculature to endogenous presser hormones.[105] In chronic dialysis patients, postdialysis rebound hypertension is greater with a 1.0-mEq/liter than with a 3.0-mEq/liter potassium dialysate.[46] Although not yet studied, preventing the initial rapid decline in the plasma potassium concentration with a ramped dialysate potassium may help attenuate the hypertensive response some patients exhibit toward the end of a dialysis treatment.

In summary, due to the kinetics of potassium movement from the intra- to the extra-cellular space one can expect only up to 70−90 mEq of potassium to be removed during a typical dialysis session. As a result, one should not overestimate the effectiveness of the dialytic procedure in the treatment of severe hyperkalemia. The total amount removed will exhibit considerable variability and will be influenced by changes in acid−base status, changes in tonicity, changes in glucose and insulin concentration, and catecholamine activity. Given the tendency for the plasma potassium to rise in the immediate postdialysis time period, the most efficient way of removing excess potassium stores would be to prescribe two- to three-hour periods of dialysis separated by several hours.

Studies examining the hemodynamic effect of potassium fluxes during hemodialysis are limited. More importantly, deliberate alterations in dialysate potassium concentration to effect hemodynamic stability would not be without risk. Use of low-potassium dialysate concentration may contribute to arrhythmias, especially in those patients with underlying coronary artery disease or those taking digoxin. On the other hand, use of dialysate with high potassium concentration may predispose patients to pre-dialysis hyperkalemia. In patients at high risk for arrhythmias on dialysis, modeling the dialysate potassium concentration so as to maintain a constant blood-to-dialysate potassium gradient throughout the procedure may be of clinical benefit.

Peritoneal Dialysis

Potassium is cleared by peritoneal dialysis at a rate similar to that of urea. With continuous ambulatory peritoneal dialysis (CAPD) and 10 liters of drainage per day, approximately 35−46 mEq of potassium is removed per day. Daily potassium intake is usually greater than this amount, and yet significant hyperkalemia is uncommon in these patients. Presumably, potassium balance is maintained by increased colonic secretion of potassium and by some residual renal excretion. Given these considerations, potassium is not routinely added to the dialysate.

Maximal removal of potassium with peritoneal dialysis is approximately 10 mEq/hr even in the setting of severe hyperkalemia.[24] It should be noted that removal rates with Kayexalate enemas far exceed this value and may approach 30 mEq/hr. In patients undergoing frequent exchanges, hypokalemia may develop. In these instances, potassium can be added to the dialysate to achieve a final concentration of 2−3 mEq/liter. This is particularly important in patients receiving digoxin because the development of hypokalemia can precipitate arrhythmias.

CLINICAL DISORDERS OF POTASSIUM IN THE DIALYSIS PATIENT

Hypokalemia

In the hemodialysis patient hypokalemia can be a sign of poor oral intake and severe malnourishment. On occasion hypokalemia can result from K^+ binding in the gastrointestinal tract. Although not a dialysis patient, a serum K^+ concentration of 0.9 mmol/L was found in a three year old girl following several days of oral and rectal administration of bentonite given as a home remedy for the treatment of constipation.[16] Bentonite, also called montmorillonite or fuller's earth, is a type of clay primarily composed of hydrated aluminum silicate. Clay eating (geophagia) can be a manifestation of pica and has been reported to cause hypokalemic paralysis during pregnancy and in the postpartum period.[178,179] Clay eating is also practiced by some dialysis patients and should be considered in the setting of unexplained hypokalemia.

Cation exchange resins are frequently used to manage hyperkalemia in patients with chronic kidney disease. Abuse of these resins can result in hypokalemia, hypomagnesemia, and occasionally metabolic alkalosis.[27] The most commonly used resin is sodium polystyrene sulfonate but calcium polystyrene sulfonate is also available. Following the oral administration of these drugs sodium or calcium is released from the resin in exchange for hydrogen H^+ in the gastric juice. As the resin passes through the rest of the gastrointestinal tract H^+ is exchanged for other cations such as potassium which is present in greater quantities particularly in the colon. The affinity of different cations for these resins is as follows: $Ca^+ > Mg^+ > K^+ > Na^+ >$ and H^+. In addition to differences in affinity and concentration, cation binding to the resin is influenced by duration of exposure primarily dictated by gut transit time.

The primary complication of using sodium polystyrene sulfonate is the development of sodium overload. The absorption of liberated sodium from the resin can lead to hypertension, congestive heart failure, and occasionally hypernatremia. Since the resin also binds divalent cations, hypomagnesemia and hypocalcemia can also develop when using this agent. Decreased plasma levels of magnesium and calcium are more likely to occur in patients taking diuretics or those with poor nutrition. Use of the resin can also lead to metabolic alkalosis when administered with antacids or phosphate binders such as magnesium hydroxide or calcium carbonate. As magnesium and calcium binds to the resin, the base is free to be absorbed into the systemic circulation. Chronic use of the resin can also be associated with small and large bowel ulcerations.

Hyperkalemia

Inadequate dialysis is an important consideration in the workup of hyperkalemia. Frequently missed treatments or shortening of the treatment time on a repetitive basis are frequent causes. In patients who are deemed to be otherwise compliant, one should consider recirculation within the vascular access as a potential cause of the disorder.

Dietary indiscretion is one of the most common reasons for hyperkalemia in the dialysis patient. In the presence of normal renal and adrenal function it is difficult to ingest sufficient K^+ in the diet to produce hyperkalemia. Rather, dietary intake of K^+ as a contributor to hyperkalemia is usually observed in the setting of impaired kidney function. Dietary sources particularly enriched with K^+ include melons, citrus juice, and commercial salt substitutes containing potassium (reviewed in Ref.[133]). Other hidden sources of K^+ reported to cause life threatening hyperkalemia include raw coconut juice (K^+ concentration of 44.3 mmol/L) and Noni juice.[6,7] While clay ingestion can cause hypokalemia due to binding in the gastrointestinal tract, river bed clay is K^+ enriched (100 mEq K^+ in 100 gm clay) and can cause life threatening hyperkalemia in chronic kidney disease patients. Ingestion of burnt match heads (cautopyreiophagia) can also be a hidden source of K^+. This activity was found to add an additional 80 mmol of K^+ to one dialysis patient's daily intake and produced a plasma K^+ concentration of 8 mmol/liter.

Hyperkalemia can also occur as an iatrogenic complication in the hospital setting. A 16-day-old infant with newly diagnosed maple syrup urine disease was placed on continuous venovenous hemofiltration to treat markedly elevated levels of leucine, isoleucine, and valine.[13] To treat a decrease in serum K^+, a 10 ml vial containing 20 mEq KCl was injected into a 5 liter bag of replacement fluid. Within four minutes, ventricular premature beats developed that rapidly deteriorated into ventricular fibrillation. The serum K^+ concentration was 9.6 mEq/l. The rapid development of hyperkalemia was attributed to injecting the KCl into the dependent portion of the hanging 5-liter bag though a port immediately adjacent to the exit port. As a result of poor mixing, the concentrated KCl was immediately delivered into the patient, resulting in life-threatening hyperkalemia.

Severe hemolysis can produce an endogenous K^+ load sufficient to cause hyperkalemia, particularly in the setting of impaired renal function. A chronic dialysis patient with a prosthetic aortic valve developed severe hemolysis and hyperkalemia, following the abrupt onset of atrioventricular nodal reentrant tachycardia.[136] The hemolysis and release of K^+ was attributed to fragmentation of red blood cells by the

prosthetic value due to the hemodynamic turbulence brought on by the arrhythmia.

Blood transfusions can be a contributing factor in the development of hyperkalemia. The risk of transfusion-associated hyperkalemia is related to not only the number of red blood cell transfusions but also the rapidity in which the units are given. Concomitant conditions such as low cardiac output, metabolic acidosis, hypocalcemia, hyperglycemia, and hypothermia increase this risk.[167]

Whole blood and PRBC are stored in anticoagulant preservative solution and have a shelf-life of approximately 35 d. The duration of storage can be extended to 42 d through the addition of an additive solution which contains varying concentrations of adenine, dextrose, and other substances.[12] During storage, K^+ leaks into the supernatant due to aging of red blood cell membranes and decreased synthesis of adenosine triphosphate. The magnitude of this leak increases with duration of storage.

Irradiation of blood to inactivate T-lymphocytes and minimize the risk of graft-versus-host disease enhances K^+ leakage from red cells due to subtle membrane injury. Depending on the conditions, the supernatant of stored red blood cell units may contain more than 60 mEq/l of K^+. If fresh PRBCs are unavailable, the risk of post transfusion hyperkalemia can be minimized by washing the cells and decreasing the amount of additive solution. These maneuvers are of particular use in neonatal patients undergoing surgery for congenital heart disease who require irradiated blood due to the concomitant presence of cell-mediated immunodeficiency disorders.[176]

Renin-angiotensin system blockers are frequently used to treat hypertension in patients with end-stage renal disease. Hyperkalemia is a potential concern with these drugs even in the functionally anephric patient to the extent that aldosterone levels fall and colonic K^+ excretion decreases. Indeed, a small number of patients undergoing dialysis have been described who developed hyperkalemia in association with ACEI and ARB therapy. By contrast, this complication did not occur in a prospective crossover study of 69 maintenance hemodialysis patients treated with either ACEI or ARB therapy alone or in combination.[68]

Acid–Base

During the course of advancing renal failure, the ability of the kidney to regenerate consumed bicarbonate becomes progressively impaired. As a result, daily acid production leads to a fall in serum bicarbonate concentration. In the long term, the serum bicarbonate concentration eventually stabilizes despite continuing positive acid balance. A stable, though low, serum bicarbonate concentration is maintained at the expense of other buffer stores such as bone bicarbonate. The goal of dialysis in acid–base balance is to transfer sufficient base to the patient to neutralize metabolic acid production and thus correct the metabolic acidosis and prevent depletion of body buffer stores. Base transfer across the dialysis membrane has been achieved using bicarbonate- or acetate-containing dialysate.

Hemodialysis

The early use of bicarbonate as the base in dialysis solutions required a cumbersome system in which CO_2 was continuously bubbled through the dialysate to lower pH in order to prevent the precipitation of calcium and magnesium salts. As a result, in the 1960s acetate became the standard dialysate buffer used to correct uremic acidosis and to offset the diffusive losses of bicarbonate during hemodialysis.

Acetate was an effective buffer in dialysis patients because it is metabolized to bicarbonate primarily in muscle and liver. However, over the next several years reports began to accumulate linking routine use of acetate with cardiovascular instability and hypotension during dialysis. This intolerance to acetate was found to be particularly common in patients with decreased muscle mass where acetate influx would be expected to exceed the capability of converting acetate to bicarbonate.[186] In particular, critically ill patients undergoing acute hemodialysis (especially with the use of large surface area dialyzers) were found to exhibit vascular instability when exposed to acetate in dialysis fluid. Acetate intolerance became more of an issue with the introduction of high-efficiency dialyzers in the 1980s. In this setting, accumulation of acetate was associated with nausea, vomiting, fatigue, decreased myocardial contractility, peripheral vasodilation, and arterial hypoxemia. A more detailed discussion of acetate dialysate is available in the third edition of this book and elsewhere[134] (Table 93.4).

Given these observations, bicarbonate-containing dialysate began to reemerge as the principal dialysate buffer—especially as advances in biotechnology made the use of bicarbonate dialysate less expensive and less cumbersome to use. Producing bicarbonate dialysate requires a specifically designed system that mixes a bicarbonate concentrate and an acid concentrate with purified water. The acid concentrate contains a small amount of either lactic or acetic acid, and all the calcium and magnesium. The exclusion of these cations from the bicarbonate concentrate prevents the precipitation of magnesium and calcium carbonate that would otherwise occur in the setting of a high-bicarbonate

TABLE 93.4 Mechanisms by which Acetate Buffer Contributes to Hemodynamic Instability

Directly decreases peripheral vascular resistance (in approximately 10% of patients)
• Stimulates release of the vasodilator compound, interleuken 1
• Induction of metabolic acidosis via bicarbonate loss through the dialyzer
• Associated with arterial hypoxemia and increases in oxygen consumption
• ? Myocardial effects of acetate

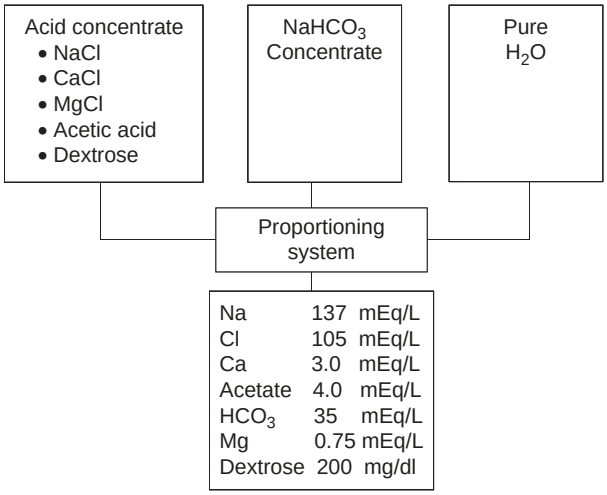

FIGURE 93.2 Use of a bicarbonate dialysate requires a proportioning system that mixes a bicarbonate concentrate with an acid concentrate and purified water. Calcium and magnesium are kept separate from the bicarbonate concentrate to prevent precipitation.

concentration. During the mixing procedure, the acid in the acid concentrate will react with an equimolar amount of bicarbonate to generate carbonic acid and carbon dioxide. The generation of carbon dioxide causes the pH of the final solution to fall to approximately 7.0–7.4. This more acidic pH, as well as the lower concentrations of calcium and magnesium in the final mixture, allows for these ions to remain in solution. The final concentration of bicarbonate in the dialysate is generally fixed in the range of 33–38 mmol/liter (Figure 93.2).

The use of a bicarbonate dialysate is associated with a number of potential complications.[103,184] The liquid bicarbonate concentrate can be responsible for microbial contamination of the final dialysate, largely because the bicarbonate concentrate is an excellent bacterial growth medium. This complication can be minimized by short storage time and by filtration of the concentrate during the production procedure. Use of a bicarbonate cartridge can further minimize this complication. This device allows for the bicarbonate concentrate to be produced on-line by passing water through a column containing powdered bicarbonate. The concentrate is produced and proportioned immediately before mixing with the acid concentrate. Hypoxemia may occur during bicarbonate dialysis when high concentrations of bicarbonate are used. This complication appears to be the result of suppressed ventilation secondary to the increase in pH and serum bicarbonate concentration. In addition, excessively high levels of bicarbonate in the dialysate may result in acute metabolic alkalosis—causing mental confusion, lethargy, weakness, and cramps.

The factors that determine bicarbonate requirements in hemodialysis patients include acid production during the interdialytic period, the removal of organic anions during the hemodialysis procedure, and the buffer deficit of the body. Because these factors are likely to vary from patient to patient, there is increasing interest in individualizing the dialysate bicarbonate concentration. The optimal level of dialysate bicarbonate would be a concentration low enough to prevent significant alkalosis in the postdialytic period and yet high enough to prevent predialysis acidosis.[6,11] The need for individualization is highlighted in data from the first 1000 patients randomized in the HEMO study (Hemodialysis Study Group).[180] Using a set dialysate bicarbonate concentration of 35 mEq/liter, the mean pre-dialysis plasma bicarbonate concentration was 21.6 mEq/liter. However, in 25% of patients the predialysis bicarbonate concentration was less than 19 mEq/liter.

Maintaining a pre-dialysis total CO2 concentration greater than 23 mmol/liter can be achieved in most patients by individually adjusting the dialysate bicarbonate concentration. Oettinger et al. found that 75% of patients exceeded this level with a dialysate bicarbonate concentration of 42 mmol/liter.[130] Use of this high-bicarbonate dialysate did not result in progressive alkalemia, even in patients beginning the study with a normal predialysis total CO_2 using a standard bicarbonate dialysate concentration of 36 mmol/liter. In addition, the high-bicarbonate dialysate did not cause hypoxia or hypercarbia or alter the pre-dialysis calcium, ionized calcium, or phosphorus.

Using high-bicarbonate dialysate may improve nutrition and bone metabolism.[131] Graham et al. examined protein turnover in a group of chronic dialysis patients in whom dialysate bicarbonate concentration was increased from 35 to 40 mmol/liter. Supplemental oral bicarbonate therapy was given to two patients whose predialysis tCO_2 concentration did not exceed 23 mmol/liter.[63] The mean tCO_2 concentration increased from 18.5 to 24.8 mmol/liter during the high-bicarbonate dialysate. Correction of the acidosis was

associated with a significant decrease in protein degradation, as suggested by leucine kinetic studies. In a similarly designed study, these investigators found an increase in the sensitivity of the parathyroid glands to calcium in patients using a dialysate bicarbonate concentration of 35–40 mmol/liter.[64]

Another strategy that may be effective in improving the acidosis of chronic dialysis patients is to use citric acid in place of acetic acid in the acid concentrate. In a recent study of 22 patients, use of citric acid decreased the number of patients with a pre-dialysis bicarbonate concentration less than 23 mEq/liter from 14 to 7.[2] Use of the citric acid dialysate was also associated with an increased delivered dose of dialysis, an effect postulated to be due to improved membrane permeability resulting from citrate's local anticoagulant effect. Improved membrane permeability with greater diffusive flux of bicarbonate from dialysate to blood or metabolism of citrate to bicarbonate in liver and muscle are the most likely explanations for the improvement in bicarbonate concentration.

The bicarbonate concentration used in most dialysis centers is set at 35 mmol/liter and is rarely adjusted. Given the increasing evidence that correction of chronic acidosis is of clinical benefit, clinical practice guidelines now recommend that the midweek predialysis plasma bicarbonate level be no less than 22 mmol/liter. In addition to increasing the dialysate bicarbonate concentration, supplemental oral bicarbonate therapy will be required in some patients to achieve this goal. Substitution of citric acid for acetic acid in the acid concentrate is a maneuver worthy of further investigation.

Prospective and retrospective studies have demonstrated that use of sevelamer hydrochloride is associated with significantly lower predialysis total CO_2 as compared to calcium containing phosphate binders.[143,170] Some of this difference may be the effect of decreased intake of potential alkali (calcium acetate or carbonate) in patients prescribed sevelamer. However the chemical structure and mechanism of action of sevelamer suggests the drug may directly lead to an acid load to the patient.[23,194] For this reason close attention should be paid to changes in total CO_2 following the prescription of sevelamer. In some patients supplemental bicarbonate may be required to keep total CO_2 at goal. In a study of 20 hemodialysis patients raising the dialysate bicarbonate concentration to 40 mEq/L was effective in correcting both acidosis and hyperkalemia over a 24 month period despite the ongoing use of this non-calcium containing phosphate binder.[126] To overcome this adverse effect on acid-base balance sevelamer is now produced and marketed as sevelamer carbonate.[14] This form of the drug does not adversely affect the serum bicarbonate concentration.

Peritoneal Dialysis

The buffer present in most commercially available peritoneal dialysate solutions is lactate. In patients with normal hepatic function, lactate is rapidly converted to bicarbonate such that each mM of lactate absorbed generates 1 mM of bicarbonate. Even with the most vigorous peritoneal dialysis, there is no appreciable accumulation of circulating lactate.[151] The rapid metabolism of lactate to bicarbonate maintains the high dialysate-to-plasma lactate gradient necessary for continued absorption. This absorption may be somewhat less with use of dialysate containing higher concentrations of dextrose. Under these conditions, increased ultrafiltrate formation may dilute the concentration of lactate in the peritoneal cavity and therefore decrease the concentration gradient for diffusion. Lactate is normally provided as a racemic mixture of the dextro and levo isomers in approximately equal concentrations. There is some evidence that the natural isomer (L-lactate) is more rapidly absorbed than the D-isomer (D-lactate).[151]

The pH of commercially available peritoneal dialysis solutions is purposely made acidic by adding hydrochloric acid in order to prevent dextrose caramelization during the sterilization procedure. Once instilled into the abdomen, the pH of the solution rises to values greater than 7.0. The acidic nature and buffer composition of currently available solutions further contributes to the bioincompatibility of peritoneal dialysate.[31,53]

To address this issue, neutral pH solutions buffered with bicarbonate or with a mixture of bicarbonate and lactate have been introduced into clinical practice.[61] Until recently, bicarbonate was not able to be used as the buffer in peritoneal dialysis solutions because calcium and magnesium would precipitate in the presence of bicarbonate in the setting of an alkaline pH. Omitting magnesium and calcium from the dialysate was not an option because patients undergoing chronic peritoneal dialysis would develop deficits of these divalent cations. These limitations have largely been overcome by the development of a two-chamber dialysate bag in which one chamber contains the bicarbonate or buffer and the other contains a solution with calcium and magnesium. The system is designed so that the two solutions are mixed just prior to entering the patient, thus avoiding the problem of precipitation. In addition to having a neutral pH, there are fewer glucose degradation products because the bicarbonate is sterilized separately from the other components of the solution.

In a recent randomized trial of 106 patients, a pH-neutral bicarbonate-/lactate-based peritoneal dialysis solution was compared to the conventional acidic lactate buffered solution in which markers of peritoneal membrane integrity and inflammation were

examined.[82,83] At the end of 6 months, patients treated with the pH-neutral solution had a significantly greater increase in dialysate CA 125 (a marker of viability and cell mass of the mesothelium). The same group also had a significantly greater decrease in dialysate hyaluronan (a marker of inflammation in the peritoneal cavity). The pH-neutral solution is associated with less inflow pain, and no adverse effect has been demonstrated on peritoneal transport.[82,83] Use of the pH-neutral solution has also been shown to result in long-term improvement in peritoneal macrophage function compared to conventional solutions.[83] Similar benefits have been found with this solution in patients receiving automated forms of peritoneal dialysis.[59]

The dual-chamber bag has also been used to separate glucose from the other solution components. The advantage of this setup is that glucose can be sterilized at a much lower pH compared to a single chamber bag and as a result the formation of glucose degradation products is markedly reduced. Mixing of the two components at the time of abdominal installation effectively raises the pH. The application of this solution has been studied in a randomized trial of 80 patients.[149] Compared to conventional treatment, patients treated with the study solution had significantly greater dialysate CA 125 and significantly lower dialysate hyaluronan. Over a 24-month follow-up there were no adverse effects on parameters of peritoneal transport (Table 93.5).

Metabolic Alkalosis

The discussion to this point has focused on the development and treatment of metabolic acidosis in patients with end-stage renal disease. These patients are also prone to the development of metabolic alkalosis due to an inability to excrete alkaline loads. Even in patients with mild reductions in renal function exogenous administration of bicarbonate can lead to metabolic alkalosis due to decreased bicarbonate clearance. Decreased renal function is a critical event in the pathogenesis of milk-alkali syndrome. In this syndrome consumption of large quantities of milk and calcium containing antacids result in hypercalcemia and metabolic alkalosis.[8] Self-administration of large quantities of antacids containing $NaHCO_3$ can occur as a manifestation of pica during pregnancy or for self-treatment of abdominal pain.[6,7] Volume depletion or renal insufficiency increases the risk of severe metabolic alkalosis in this setting.

A moderate degree of metabolic alkalosis may be present post-dialysis, and more so with bicarbonate-buffered dialysate and especially if the concentration of the bicarbonate buffer exceeds 35 mEq/liter. End-stage renal disease patients are more susceptible to alkalosis developing as a consequence by vomiting or nasogastric suction. Excessive consumption of oral bicarbonate (a teaspoon of baking soda contains 40 mm of bicarbonate) is not an infrequent cause of metabolic alkalosis among the dialysis population.

Extensive use of crack cocaine has been implicated as a cause of metabolic alkalosis in a dialysis patient.[44] Cocaine hydrochloride is the salt form of the drug. This form is not suitable for smoking because the temperature at which it vaporizes is very close to the temperature at which it burns. By contrast, cocaine base "free base" vaporizes at a low temperature making it more suitable for smoking. Free base is made by dissolving cocaine hydrochloride in water and then adding an alkali. In this patient, the source of the alkali was "Draino" which contains NaOH. The chemical reaction produces a precipitate composed of three components: (1) excess NaOH, (2) a white powder often referred to as "the cut" containing talc or baking soda added to increase the weight and thus the street value of the preparation and (3) the free base cocaine. On two separate occasions following extensive crack cocaine use this patient developed a serum bicarbonate concentration of >40 mEq/L. Presumably the cocaine preparation contained a considerable quantity of base and the alkali load was unable to be excreted to the presence of renal failure.

Net gain of HCO_3^- can occur in the setting of massive transfusion due to administration of citrate found in packed red blood cells. A similar situation can complicate plasmapheresis when citrate containing fresh frozen plasma is used as a replacement fluid.[111,121,123,137] The use of citrate for the purpose of regional anticoagulation in patients undergoing

TABLE 93.5 Advantages and Disadvantages of new Peritoneal Dialysis Solutions

Solution	Advantage	Disadvantage
Icodextran	Sustained ultrafiltration in overnight dwell in CAPD, long dwell in APD, and during peritonitis, avoids effects of glucose absorption, iso-osmotic	Skin reactions (<10%), maltose accumulation
Amino acids	Improves malnutrition	Azotemia and metabolic acidosis
Bicarbonate and bicarbonate/lactate buffer	Improved biocompatibility due to neutral pH, ↓ glucose degradation products	Two chamber bags to separate Ca and Mg from bicarbonate
Glucose sterilized separately at lower pH	Improved biocompatibility, ↓ glucose degradation products	Two chamber bag required

continuous renal replacement therapy can cause metabolic alkalosis.[30,42,88] Citrate is rapidly metabolized to bicarbonate by the liver and skeletal muscle. The risk for alkalosis during citrate regional anticoagulation can be lowered by using anticoagulant citrate dextrose formula A (ACD-A) because this formulation produces 33% less bicarbonate in comparison to hypertonic trisodium citrate.

In the absence of renal function, no route exists for elimination of extra bicarbonate. A bicarbonate dialysate can be fashioned with a lower than normal amount of buffer so that the serum bicarbonate may be decreased.[60] An acetate-buffered dialysate may also be used. In this situation, the larger than normal bicarbonate transmembrane gradient will favor increased loss of buffer and (because the rate of acetate metabolism is already near maximal) the net effect should be a decrease in plasma bicarbonate. If the patient is not overly symptomatic or having respiratory or cardiovascular compromise, one may simply choose to wait for normal endogenous acid production to titrate the excessive amount of bicarbonate.

Conversely, if cardiopulmonary function is compromised an intravenous infusion of hydrochloric acid can be given. In general, HCl can be safely administered as a 0.15-0.25 normal solution in normal saline or D5W given through a central line. Due to the sclerosing properties of HCl, it is imperative that the position of the central line in the superior vena cava be verified by chest x-ray prior to initiating infusion. Infusion rates should be no more than 0.2 mmol per kilogram of body weight per hour. One should use a bicarbonate space of 50% of ideal body weight when calculating the amount of HCl to be given. As an example, to reduce the plasma bicarbonate from 50 to 40 mmol/L in a 70 kilogram patient the amount of HCl required is 350 mmol ($10 \times 70 \times 0.5$). If the physician wishes, the HCl can be added to an amino acid solution in TPN and given centrally.

If patients are not ill enough to warrant the risk of central venous catheterization and the infusion of intravenous hydrochloric acid, they probably do not need their alkalosis corrected acutely. Administration of ammonium chloride is not recommended because the ammonium will tend to increase urea nitrogen levels. Arginine chloride is not recommended because of the possibility of inducing hyperkalemia.[25]

CALCIUM

Hemodialysis

During the course of advancing chronic kidney disease, there is a tendency for patients to develop hypocalcemia. The pathophysiology is multifactorial and includes increased tissue deposition due to phosphate retention and the resultant increase in the calcium-phosphate solubility product. Decreased circulating levels of $1,25(OH)_2$ vitamin D lead to decreased absorption of calcium from the gastrointestinal tract. In addition, low vitamin D levels as well as hyperphosphatemia impair the ability of parathyroid hormone to mobilize calcium from bone. Finally, patients with chronic kidney disease are prescribed phosphate-restricted diets that by necessity are also low in calcium.

In the setting of chronic kidney disease, more than 60% of plasma calcium is not protein bound and is subject to forces leading to movement across the dialysis membrane. Calcium diffusion into the body can either be positive or negative, depending on the concentration gradient established across the membrane. The net flux of calcium is also influenced by a component of convective loss that occurs during ultrafiltration. Given these considerations, the goal of dialytic therapy for many years was to choose a dialysate calcium concentration that would result in a net flux of calcium into the patient. A dialysate calcium concentration of 3.5 mEq/liter (1.75 mmol/liter) became relatively standard because this concentration usually prevented intradialytic calcium losses.

Raising the dialysate calcium concentration has been associated with beneficial effects on indices of metabolic bone disease. Wing showed that raising the dialysate concentration of calcium from 2.5 to 3 mEq/liter arrested the biochemical and radiographic changes of hyperparathyroidism.[192] Metacarpal bone thickness was found to be stable with use of a dialysate calcium concentration of 3.5 mEq/liter, whereas thickness declined over time in patients dialyzed with a 2.5-mEq/liter calcium bath. Use of a high-dialysate calcium concentration has also been shown to reduce parathyroid hormone levels to a greater extent than does a low-calcium dialysate. As discussed in more detail in material following, use of vitamin D analogues has largely supplanted upward adjustments in the dialysate calcium concentration for purposes of treating secondary hyperparathyroidism. However, this strategy may be useful in carefully selected patients.[69]

A limitation of using higher dialysate calcium concentrations is the development of hypercalcemia. This complication has become more common with the widespread use of calcium-containing phosphate binders as a substitute for aluminum and the wider use of high doses of intravenous $1,25(OH)_2$ vitamin D to treat secondary hyperparathyroidism. As a result, the typical dialysate calcium concentration has generally fallen from that used several years ago.

Using a dialysate calcium concentration of 2.5 mEq/liter, Slatapolsky et al. were able to control the serum phosphorus in 21 patients with calcium carbonate at an average daily dose of 10.5 g with no instances of hypercalcemia.[165] In an earlier study utilizing a dialysate calcium concentration of 3.5 mEq/liter, large doses of calcium carbonate were also effective in controlling the serum phosphorus—but only at the expense of several instances of hypercalcemia.[166] The beneficial effect of combining high-dose calcium-containing phosphate binders with a low dialysate calcium concentration has been confirmed by other investigators.[157] In a similar manner, Van der Merwe et al. treated patients with secondary hyperparathyroidism with high-dose oral calcitriol combined with a low-calcium dialysate concentration.[182] During the course of the study, there was a significant fall in the parathyroid hormone level and alkaline phosphatase concentration without the development of hypercalcemia.

Despite the enthusiasm for use of low-calcium dialysate, some recent studies have emphasized that such an approach requires careful monitoring to ensure that the patient does not develop negative calcium balance or worsening secondary hyperparathyroidism.[177] Argiles et al. found that serum immunoreactive parathyroid hormone (iPTH) levels increased significantly in patients treated with a 2.5-mEq/liter dialysate calcium bath compared to a control group of patients dialyzed with dialysate calcium of 3.0 mEq/liter.[8] This increase in iPTH occurred despite 2.4-fold more oral $CaCO_3$ ingested in the low-dialysate calcium group. Although the increase in oral calcium intake was not sufficient to prevent the stimulation in iPTH, subsequent treatment with 1,25 $(OH)_2$ vitamin D was effective in reversing the rise in iPTH levels.

Similar results were reported by Fernandez et al. in a group of patients sequentially dialyzed against a 3.5-/liter and then a 2.5-mEq/liter Ca bath.[54] While on the low-calcium dialysate, there was a significant increase in serum iPTH and serum alkaline phosphatase levels. These changes occurred despite the fact that oral calcium carbonate was administered at doses ranging from 3 to 6 g/day while on the low-calcium dialysate. As determined by clearance studies, the authors suggested that the low-calcium dialysate resulted in negative calcium balance—which in turn contributed to the worsening hyperparathyroidism. Furthermore, the maintenance of a normal serum calcium concentration noted in the study occurred at the expense of PTH-induced calcium mobilization from bone. Utilizing measurements of total and ionized calcium in serum and in spent dialysate, Argiles et al. have confirmed that a 2.5-mEq/liter calcium dialysate is associated with negative calcium balance.[10] Based on the potential of a 2.5-mEq/liter dialysate calcium to cause negative calcium balance and to worsen secondary hyperparathyroidism, these authors now utilize a dialysate calcium of at least 3.0 mEq/liter in the majority of chronic dialysis patients.[9]

In addition to effects on metabolic bone disease, varying the dialysate calcium concentration can affect hemodynamic stability during dialysis. Maynard et al. studied 12 patients in a prospective crossover trial and found that a high dialysate calcium concentration (3.75 mEq/liter) was associated with significantly less fall in systolic blood pressure and in mean arterial pressure than a low-calcium dialysate (2.75 mEq/liter).[117] In a double-blind prospective study, Sherman et al. studied 20 patients who underwent alternate hemodialysis with dialysate calcium concentrations of 2.5 and 3.5 mEq/liter.[160] The use of a low dialysate calcium concentration was associated with a minor but statistically significant reduction in mean blood pressure during hemodialysis. This effect may become clinically important in patients with congestive heart failure. One study found that a 3.5 mEq/liter Ca dialysate offered clear hemodynamic benefits over a 2.5-mEq/liter dialysate in patients with an ejection fraction less than 40%.[183]

In patients prone to intradialytic hypotension who are at risk for hypercalcemia, dialysate calcium profiling can be utilized as a strategy to improve hemodynamic stability and yet minimize the potential for hypercalcemia.[99] In one study, patients were dialyzed for 4 hours in which the dialysate calcium concentration was set low (1.25 mmol/liter) for the first two hours and then increased to 1.75 mmol/liter for the last two hours.[99] Use of the varying dialysate calcium concentration was associated with greater hemodynamic stability compared to a fixed dialysate calcium concentration of either 1.25 or 1.5 mmol/liter. This hemodynamic benefit was accomplished via an increase in cardiac output. At the end of three weeks, there was no difference in the pre-dialysis ionized calcium concentration among the three groups.

Changes in serum calcium concentration may influence blood pressure through alterations in either systemic vascular resistance or the determinants of cardiac output, or both. In an attempt to determine the physiologic mechanisms for calcium-induced changes in systemic arterial pressure, Fellner et al. studied hemodynamic variables that determine arterial blood pressure as a function of changes in dialysate calcium concentration.[52] Eight patients underwent hemodialysis three times within a single week with dialysate calcium concentrations of 1.0, 3.5, or 5.0 mEq/liter. As in previous studies, changes in blood calcium concentration correlated directly with blood pressure. In addition, higher levels of calcium augmented left ventricular stroke volume and cardiac

output while leaving total vascular resistance unchanged. It was concluded that alterations in blood calcium concentration affected blood pressure primarily through changes in left ventricular output rather than in peripheral vascular tone.

In addition to changes in ionized calcium concentration, hemodialysis leads to alterations in several factors that could conceivably be responsible for the observed changes in ventricular function. Henrich et al.[76] performed a series of dialysis maneuvers to determine the contribution of dialyzable toxins, ionized calcium, and acidemia to left ventricular performance during routine hemodialysis. The dialysate of each maneuver was adjusted to produce three effects: isovolemic dialysis in which neither ionized calcium nor bicarbonate was allowed to increase (this procedure tested the effects of uremic toxin removal), isovolemic dialysis during which ionized calcium increased but bicarbonate was held constant, and isovolemic dialysis in which bicarbonate increased but ionized calcium was kept constant.

Echocardiographic studies showed that left ventricular end-diastolic and end-systolic volumes decreased and ejection fraction and velocity of circumferential shortening increased only in the procedure in which plasma-ionized calcium increased. This study suggested that the rise in ionized calcium is a major element in the observed improvement in myocardial contractility. Similar findings were recently reported by Lang et al.[101] Using dialysates differing only in calcium concentration, myocardial contractility was shown to correlate directly with plasma ionized calcium. The mechanism by which increases in ionized calcium seen during hemodialysis led to enhanced ventricular function is not known.

In summary, the dialysate calcium concentration has implications with regard to metabolic bone disease and hemodynamic stability. As with the other dialysate constituents, the calcium concentration should be individually tailored to the patient[106] (Table 93.6). In patients prone to intradialytic hypotension, avoidance of a low dialysate calcium concentration may be of benefit. On the other hand, the use of a lower calcium concentration in the dialysate will allow the use of increased doses of calcium-containing phosphate binders and will lessen any dependence on aluminum-containing binders. In addition, use of 1,25 $(OH)_2$ vitamin D can be liberalized so as to reduce circulating

TABLE 93.6 Considerations when Individualizing Components of the Dialysate

Dialysate component	Advantage	Disadvantage
Na: Increased	More hemodynamic stability Less cramping	Dipsogenic effect, Increased interdialytic weight gain, ? chronic hypertension
Decreased (rarely used)	Less interdialytic weight gain	Intradialytic hypotension and cramping more common
Ca: Increased	Suppression of PTH, promotes hemodynamic stability	Hypercalcemia with Vitamin D and Ca containing phosphate binders
Decreased	Permits greater use of vitamin D and calcium containing phosphate binders	Potential for negative calcium balance, stimulation of PTH, slight decrease in hemodynamic stability
K: Increased	Less arrhythmias in setting of digoxin or coronary heart disease, Less rebound hypertension	Limited by hyperkalemia
Decreased (ramped dialysate K ideal, prevents rapid initial decline in plasma K)	Greater dietary intake of K with less hyperkalemia? improvement in myocardial contractility	Increased arrhythmias, may exacerbate autonomic insufficiency
HCO_3: Increased	Corrects chronic acidosis thereby benefits nutrition and bone metabolism	Post-dialysis metabolic alkalosis
Decreased	Less metabolic alkalosis	Potential for chronic acidosis
Mg: Increased	? Less arrhythmias ? Hemodynamic benefit	Hypermagnesemia
Decreased	Permits use of Mg containing phosphate binders	Hypomagnesemia
PO_4 (rarely added to dialysate)	Treats or prevents hypophosphatemia in malnourished, chronic disease state, overdose setting, daily dialysis	Hyperphosphatemia

levels of parathyroid hormone with less fear of inducing hypercalcemia. However, when using low dialysate calcium concentrations (< 3.0 mEq/liter) one needs to monitor patients closely to ensure that negative calcium balance does not develop and that iPTH levels remain in an acceptable range.[115,150] This latter issue will become increasingly important as calcium-free phosphate binders such as sevelamer and lanthanum are more frequently used.[29,43]

One other critical consideration in the discussion of dialysate calcium is the description of calcium loading as being a factor in the development and progression of vascular calcification.[126] To date there is no consensus guidelines for the integrated prescription of dietary calcium and phosphorus, choice of phosphate binders, vitamin D analogs, calcimimetics, and dialysate calcium in hemodialysis patients. The most recent Improving Global Outcomes (KDIGO) Clinical Practice Guideline suggests using a dialysate calcium concentration between 2.5 and 3.0 mEq/L (1.25 and 1.5 mmol/l).[48,62] The working group in making this recommendation felt this concentration would provide near-normal calcium balance for most patients. The pros and cons of this recommendation continue to be debated.[48,62] Further research is needed to define the optimal mix of dialysate calcium concentration, dose of vitamin D, amount of calcium and non calcium containing phosphate binder, and use of the calcimimetic agent cinacalcet.

Peritoneal Dialysis

To avoid negative calcium balance and to potentially suppress circulating parathyroid hormone, commercially available peritoneal dialysis solutions evolved to contain a calcium concentration of 3.5 mEq/liter (1.75 mmol/liter). This concentration is equal to or slightly greater than the ionized concentration in the serum of most patients. As a result, there is net calcium absorption in most patients when using a conventional dialysis regime such as $3 \times 1.5\%$ and $1 \times 4.5\%$ glucose solutions.[191] When ultrafiltration volume is high, as occurs with use of 4.25% dextrose concentration at high rates of exchange, net transfer of calcium can be reversed such that calcium balance becomes negative. In this setting, the convective flux of calcium exceeds the diffusive flux such that net calcium balance can become negative.[164]

As the use of calcium-containing phosphate binders has increased, hypercalcemia has become a common problem when utilizing the 3.5 mEq/liter calcium dialysate. This complication has been particularly common in patients treated with peritoneal dialysis because these patients have a much greater incidence of adynamic bone disease compared to hemodialysis patients.[162] In fact, the continual positive calcium balance associated with the 3.5 mEq/liter solution has been suggested as a contributing factor in the development of this lesion. The low bone turnover state typical of this disorder impairs the accrual of administered calcium, contributing to the development of hypercalcemia. As a result, there has been increased interest in using a strategy similar to that employed in hemodialysis; namely, lower the calcium content of the dialysate. This strategy can allow for increased usage of calcium-containing phosphate binders as well as more liberal use of 1,25 $(OH)_2$ vitamin D in order to effect decreases in the circulating level of parathyroid hormone. In this manner, the development of hypercalcemia can be minimized.

Several studies have confirmed that a stable serum calcium concentration can be maintained when using low-calcium dialysis solutions.[81,190] In a large randomized controlled multicenter trial, Weinreich et al. studied 103 stable CAPD patients in a comparison of 1.0 and 1.75 mmol/liter calcium solutions over six months.[190] Aluminum-containing binders were given in place of $CaCO_3$ in cases of hypercalcemia. In the low-calcium group, serum calcium levels were maintained within the normal range—with a threefold reduction in the incidence of hypercalcemia and significant reduction in the need for $Al(OH)_3$ compared to the conventional dialysate. One concern with use of a low-calcium dialysate is that parathyroid hormone levels might be stimulated. However, in this study PTH levels remained within the desired range. In addition, there was no radiologic evidence of renal osteodystrophy or demineralization of bones.

More recently, Johnson et al. reported data from a randomized prospective double-blind trial in 45 CAPD patients comparing treatment with 1.25 and 1.75 mmol/liter dialysate calcium over 12 months.[81] In this study, the low-calcium dialysate was associated with less hypercalcemia and at the same time permitted larger quantities of calcitriol and $CaCO_3$ to be prescribed. Increased use of these agents, however, may explain why use of $Al(OH)_3$ could not be reduced in the low-calcium group. Increased doses of calcitriol can preserve the need for $Al(OH)_3$ by increasing intestinal calcium absorption and thereby limiting the maximum dose of $CaCO_3$ that could be used, and by increasing phosphate absorption—thereby increasing the total dose of phosphate binders required for satisfactory phosphate control. In addition, PTH levels increased in the low-calcium group but returned toward baseline after the first six months of the study. Bone mineralization studies showed no differences between the two groups.

Sanchez et al. performed a one-year randomized multicenter study comparing the effects of a 1.25 versus a 1.75 mmol/liter calcium-containing solution on bone histology.[153] The patients assigned to the low-calcium solution had a greater increase in serum parathyroid hormone, but there was no differences noted in bone histology between the two groups.

In summary, peritoneal dialysis solutions are widely available with a calcium concentration of either 1.25 or 1.75 mmol/liter. The decision to use one concentration or the other should be made on an individual basis. The majority of patients can be treated with a dialysis solution that contains 1.75 mmol/liter calcium. On the other hand, a low dialysate calcium solution offers a valuable therapeutic option to treat patients with increased doses of calcium-containing phosphate binders and calcitriol with a much lower incidence of hypercalcemia. Close monitoring of patients is required when using a low-calcium solution to ensure that secondary hyperparathyroidism is not exacerbated. This is particularly so in patients who are questionably compliant with their calcium-containing phosphate binders or when sevelamer or lanthanum is used as the primary phosphate binder. Monitoring of bone mineralization is also indicated with long-term use of low-calcium dialysate.

MAGNESIUM

Hemodialysis

The usual concentration of magnesium in the dialysate is 0.5–1.0 mEq/liter and is only rarely manipulated. In an attempt to minimize the development of hypercalcemia and calcium loading associated with the use of calcium-containing phosphate binders and vitamin D, there has been interest in using magnesium-containing compounds as a phosphate binder.[171,172] The use of oral magnesium requires the use of a low-magnesium dialysate concentration to avoid the development of hypermagnesemia.

Depending on which magnesium salt is used, this strategy has had variable success.[66,129] Use of oral $Mg(OH)_3$ in association with a magnesium-free dialysate had little or no effect on phosphate and increased mean serum magnesium to 4.3 mg/dl. In addition, diarrhea was a frequent side effect. More favorable results have been reported with oral $MgCO_3$. Donovan et al. reported good control of the serum phosphorus level using oral $MgCO_3$ and a magnesium-free dialysate.[128] On this regimen, diarrhea was mild and transient and the serum concentration of magnesium did not change. More recently, Kelber et al. examined the feasibility of using a magnesium-free dialysate in the setting of high-efficiency dialysis.[86] Despite the use of oral $MgCO_3$, patients developed severe muscle cramping that was immediately relieved by adding magnesium back to the dialysate. It was determined that measured magnesium removal exceeded the estimated predialysis extracellular fluid magnesium pool. By contrast, dialysate magnesium of 0.6 mg/dl in combination with oral $MgCO_3$ was well tolerated.

Use of this latter regimen was then examined in a prospective randomized crossover study.[40] Patients were studied while taking $MgCO_3$ and half the usual dose of $CaCO_3$ along with dialysate magnesium of 0.6 mg/dl, and again while ingesting $CaCO_3$ given in the usual dose with dialysate magnesium of 1.8 mg/dl. There was no difference in the serum concentrations of phosphorus, calcium, or magnesium between the two phases of the study. In addition, the $MgCO_3$-low $CaCO_3$ regimen permitted a greater amount of intravenous calcitriol to be used without the development of hypercalcemia. It was concluded that use of oral $MgCO_3$ as a phosphate binder and a low dialysate magnesium concentration may be a useful strategy in patients.

The dialysate magnesium has also been varied in an attempt to obtain better hemodynamic stability in the setting of a low dialysate calcium concentration.[100] Lowering the dialysate calcium concentration from 1.75–1.25 mmol/liter in the setting of a dialysate magnesium concentration of 0.25 mmol/liter results in deleterious effects on mean arterial pressure, cardiac index, and stroke volume. These hemodynamic effects are prevented by raising the dialysate magnesium concentration from 0.25 to 0.75 mmol/liter even though the dialysate calcium concentration is kept low.

Peritoneal Dialysis

Initially, the standard peritoneal dialysis solution contained 1.5 mEq/liter magnesium. The concentration has since been lowered to 0.5 mEq/liter to lessen the frequency of hypermagnesmia that was observed with the higher magnesium concentration. As discussed with hemodialysis, a lower dialysate magnesium concentration may allow use of magnesium salts as an additional calcium-free phosphate binder.

Dialysate Phosphate

In patients with mild to moderate hyperphosphatemia, hemodialysis has been estimated to remove 250–325 mg/day of phosphorus when extrapolated to an average week.[41,77] Because a diet that provides adequate protein may provide approximately 900 mg of phosphorus daily, it follows that dialysis cannot provide adequate control of phosphate by itself. Rather,

management of hyperphosphatemia requires a combination of dietary restriction, oral phosphate binders, and dialysis.

The limited ability of dialysis to remove phosphorus is primarily related to the kinetics of phosphorus distribution within the body, and not to inadequate clearance across the dialyzer.[98] In a typical dialysis session, the rate of phosphorus removal is greatest during the initial stages of the procedure and then progressively declines to a low constant level toward the end of the treatment. This decline is due to the decrease in plasma concentration and the slow efflux of phosphorus from the intracellular space and/or mobilization from bone stores. Although dialysis membranes differ with respect to plasma clearance of phosphate, it is the slow transfer of phosphorus to the extracellular space (where it becomes accessible for dialytic removal) that is the most important factor limiting phosphorus removal.[158,163]

There are only a few situations in which one might consider adding phosphorus to the dialysate (Table 93.6). Hypophosphatemia can be an occasional finding in the chronic dialysis patient who is malnourished and suffering from some chronic disease state. In such patients, adding phosphorus to the dialysate may be an effective means of treating hypophosphatemia without having to utilize a parenteral route of administration. The phosphate must be added to the bicarbonate component of a dual proportioning system to avoid the precipitation of calcium phosphate that would result from addition to the calcium-containing acid concentrate. Kaye et al. described three hypophosphatemic dialysis patients treated by adding phosphorus to the dialysate in a single proportioning system.[87] In these patients, phosphate was added to a bicarbonate concentrate that contained no calcium. To avoid hypocalcemia, calcium was infused into the venous drip chamber as a 10% $CaCl_2$ solution. A final phosphate concentration of 1–2 mmol/liter was found effective in correcting the hypophosphatemia by the end of a four-hour session.

Another situation in which addition of phosphate to the dialysate may be useful is in the setting of an overdose. In a patient with normal renal function and a normal serum phosphate concentration, use of a phosphate-free dialysate will commonly result in hypophosphatemia. In most circumstances, the hypophosphatemia is of short duration and is of little clinical consequence. However, some intoxications may increase the risk for complications of hypophosphatemia such that addition of phosphate to the dialysate may be warranted.

Due to the slow equilibration of phosphorus between the intravascular and intracellular space, long frequent hemodialysis sessions are more effective in removing dialysis.[107] In fact, hypophosphatemia has been noted in some patients treated with prolonged daily nocturnal hemodialysis.[140] In this setting, adding phosphate to the dialysate may prove useful as a means of normalizing the serum phosphate concentration.

References

[1] Acchiardo SR, Hayden AJ. Is Na modeling necessary in high flux dialysis? Trans Am Soc Artif Organs 1991;37:M135–7.

[2] Ahmad S, Callan R, Cole J, Blagg C. Dialysate made from chemicals using citric acid increases dialysis dose. Am J Kidney Dis 2000;35:493–9.

[3] Allon M, Dansby L, Shanklin N. Glucose modulation of the disposal of an acute potassium load in patients with end-stage renal disease. Am J Med 1993;94:475–82.

[4] Allon M, Shanklin N. Effect of albuterol treatment on subsequent dialytic potassium removal. Am J Kidney Dis 1995;26:607–13.

[5] Allon M. Treatment and prevention of hyperkalemia in end-stage renal disease. Kidney Int 1993;43:1197–209.

[6] Alpern RJ, Sakhaee K. The clinical spectrum of chronic metabolic acidosis: homeostatic mechanisms produce significant morbidity. Am J Kidney Dis 1997;29:291–302.

[7] Alvo M, Krsulovic P, Fernandez V, et al. Effect of a simultaneous potassium and carbohydrate load on extrarenal K homeostasis in end-stage renal failure. Nephron 1989;53:133–7.

[8] Argiles A, Kerr PG, Canaud B, et al. Calcium kinetics and the long-term effects of lowering dialysate calcium concentration. Kidney Int 1993;43:630–40.

[9] Argiles A, Mion CM. Low-calcium dialysate worsens secondary hyperparathyroidism. J Am Soc Nephrol 1996;7:635–6.

[10] Argiles A, Mion CM. Calcium balance and intact PTH variations during haemodiafiltration. Nephrol Dial Transplant 1995;10:2083–9.

[11] Bailey JL. Metabolic acidosis and protein catabolism: mechanisms and clinical implications. Miner Electrolyte Metab 1998;24:13–9.

[12] Bansal I, Calhoun B, Joseph C, Pothiawala M, Baron B. A comparative study of reducing the extracellular potassium concentration in red blood cells by waching and by reduction of additive solution. Transfusion 2007;47:248–50.

[13] Bar-Joseph G, Tarabia M, Halberthal M, et al. Mysterious hyperkalemia and cardiac arrest in a newborn infant undergoing continuous ven-venous hemofiltration dialysis: question. Pediatr Nephrol 2008;23:1053–4.

[14] Barna MM, Kapoian T, O'Mara NB. Sevelamer carbonate. Ann Pharmacother 2010;44:127–34.

[15] Bealer S. Increased dietary sodium alters neural control of blood pressure during Ang II infusion. Am J Physiol Heart Circ Physiol 2003;284:H559–65.

[16] Bennett A, Stryjewski G. Severe hypokalemia caused by oral and rectal administration of bentonite in a pediatric patient. Pediatr Emerg Care 2006;22:500–2.

[17] Bergstrom J, Alvestrand A, Furst P, Hultman E, Widstam-Attorps U. Muscle intracellular electrolytes in patients with chronic uremia. Kidney Int 1983;24(Suppl. 16):S153–60.

[18] Biglieri EG, McIlray MB. Abnormalities of renal function and circulatory reflexes in primary aldosteronism. Circulation 1966;33:78–86.

[19] Bihaphala S, Bell AJ, Bennett CA, et al. Comparison of high and low-sodium bicarbonate and acetate dialysis in stable chronic hemodialysis patients. Clin Nephrol 1985;23:179–83.

[20] Bilbrey GL, Carter NW, White MG, et al. Potassium deficiency in chronic renal failure. Kidney Int 1973;4:423–30.
[21] Bosetto A, Bene B, Petitclerc T. Sodium management by dialysis conductivity. Adv Renal Replace Ther 1999;6: 243–54.
[22] Brace RA, Anderson DK, Chen W-T, et al. Local effects of hypokalemia on coronary resistance and myocardial contractile force. Am J Physiol 1974;227:590–7.
[23] Breznia B, Qunibi W, Nolan C. Acid loading during treatment with sevelamer hydrochloride:mechanisms and clinical implications. Kidney Intl 2004;66(Suppl. 90):S39–45.
[24] Brown ST, Ahearn DJ, Nolph KD. Potassium removal with peritoneal dialysis. Kidney Int 1973;4:67.
[25] Bushinsky DA, Gennari FJ. Life-threatening hyperkalemia induced by arginine. Ann Intern Med 1978;89:632.
[26] Chaudhary K, Khanna R. Biocompatible peritoneal dialysis solutions: do we have one? Clin J Am Soc Nephrol 2010;5: 723–32.
[27] Chen CC, Chen CA, Chau T, Lin SH. Hypokalaemia and hypomagnesaemia in an oedematous diabetic patient with advanced renal failure. Nephrol Dial Transplant 2005;20(10):2271–3 [Epub].
[28] Cheng J-T, Kahn T, Kaji DM. Mechanism of alteration of sodium potassium pump of erythrocytes from patients with chronic renal failure. J Clin Invest 1984;74:1811–20.
[29] Cizman B. Hyperphosphataemia and treatment with sevelamer in haemodialysis patients. Nephrol Dial Transplant 2003;18: v47–9.
[30] Cointault O, Kamar N, Bories P, et al. Regional citrate anticoagulation in continuous venovenous haemodiafiltration using commercial solutions. Nephrol Dial Trans 2004;19: 171–8.
[31] Coles G. Towards a more physiologic solution for peritoneal dialysis. Semin Dial 1995;8:333–5.
[32] Coli L, Bonomini M, La Manna GL, et al. Clinical use of profiled hemodialysis. Int J Artif Organs 1998;22:724–30.
[33] Coli L, La Manna G, Dalmastri V, et al. Evidence of profiled hemodialysis efficacy in the treatment of intradialytic hypotension. Int J Artif Organs 1998;21:398–402.
[34] Coli L, Ursino M, Dalmastri V, et al. A simple model applied to selection of the sodium profile during profiled hemodialysis. Nephrol Dial Trans 1998;13:404–16.
[35] Cotton JR, Woodard T, Carter NW, Knochel JP. Resting skeletal muscle membrane potential as an index of uremic toxicity. J Clin Invest 1979;63:501–6.
[36] Cupisti A, Galetta F, Caprioli R, et al. Potassium removal increases the QTc interval dispersion during hemodialysis. Nephron 1999;82:122–6.
[37] Daugirdas JT, Al-Kudsi RR, Ing TS, et al. A double-blind evaluation of sodium gradient hemodialysis. Am J Nephrol 1985;5: 163–8.
[38] Davies SJ, Woodrow G, Donovan K, et al. Icodextrin improves the fluid status of peritoneal dialysis patients: results of a double-blind randomized controlled trial. J Am Soc Nephrol 2003;14:2338–44.
[39] dePaula FM, Peixoto AJ, Pinto LV, et al. Clinical consequences of an individualized dialysate sodium presecription in hemodialysis patients. Kidney Int 2004;66:1232–8.
[40] Delmez JA, Kelber J, Norword KY, Giles KS, Slatopolsky E. Magnesium carbonate as a phosphorus binder: a prospective, controlled, crossover study. Kidney Int 1996;49:163–7.
[41] DeSoi CA, Umans J. Does the dialysis prescription influence phosphate removal. Semin Dial 1995;8:201–3.
[42] De Vos J, Hombrouckx R. Citrate anticoagulation and adverse events. EDTNA ERCA J 2003;29:112–3 ,117.
[43] D'Haese PC, Spasovski GB, Sikole A, et al. A multicenter study on the effects of lanthanum carbonate (Fosrenol) and calcium carbonate on renal bone disease in dialysis patients. Kidney Int Suppl 2003;85:S73–8.
[44] Diskin CJ, Stokes TJ, Dansby LM, Radcliff L, Carter TB. Recurrent metabolic alkalosis and elevated troponins after crack cocaine use in a hemodialysis patient. Clin Exp Nephrol 2006;10:156–8.
[45] Dolson GM, Androgue HJ. Low dialysate [K^+] decreases efficiency of hemodialysis and increases urea rebound. J Am Soc Nephrol 1998;9:2124–8.
[46] Dolson G, Ellis K, Bernardo M, Prakash R, et al. Acute decreases in serum potassium augment blood pressure. Am J Kidney Dis 1995;26:321–6.
[47] Dong-Min K, Chung J, Yoon S, Kim H. Effect of fludrocortisones acetate on reducing serum potassium levels in patients with end-stage renal disease undergoing haemodialysis. Nephrol Dial Transplant 2007;22:3273–6.
[48] Drueke TB, Touam M. Calcium balance in haemodialysis—do not lower the dialysate calcium concentration too much (con part). Nephrol Dial Transplant 2009;24:2990–3.
[49] Dumler F, Grondin G, Levin NW. Sequential high/low sodium hemodialysis: an alternative to ultrafiltration. Trans Am Soc Artif Intern Organs 1979;25:351–3.
[50] Farese S, Kruse A, Pasch A, et al. Glycyrrhetinic acid food supplementation lowers serum potassium concentration in chronic hemodialysis patients. Kidney Int 2009;76:877–84.
[51] Feig PV, Shook A, Sterns RS. Effect of potassium removal during hemodialysis on the plasma potassium concentration. Nephron 1981;27:25.
[52] Fellner SK, Lang RM, Neumann A, et al. Physiological mechanisms for calcium-induced changes in systemic arterial pressure in stable dialysis patients. Hypertension 1989;13: 213–8.
[53] Feriani M. Buffers: bicarbonate, lactate and pyruvate. Kidney Int 1996;50:S75–80.
[54] Fernandez E, Borras M, Pais B, et al. Low-calcium dialysate stimulates parathormone secretion and its long-term use worsens secondary hyperparathyroidism. J Am Soc Nephrol 1995;6: 132–5.
[55] Fernandez J, Oster JR, Perez GO. Impaired extrarenal disposal of an acute oral potassium load in patients with endstage renal disease on chronic hemodialysis. Miner Electrolyte Metab 1986;12:125–9.
[56] Flanigan M. Dialysate composition and hemodialysis hypertension. Semin Dial 2004;17:279–83.
[57] Flanigan MJ. Role of sodium in hemodialysis. Kidney Int 2000;76(Suppl. 76):S72–8.
[58] Flanigan MJ, Khairullah QT, Lim VS. Dialysate sodium delivery can alter chronic blood pressure management. Am J Kidney Dis 1997;29:383–91.
[59] Fusshoeller A, Plail M, Grabensee B, et al. Biocompatibility pattern of a bicarbonate/lactate-buffered peritoneal dialysis fluid in APD: a prospective, randomized study. Nephrol Dial Transplant 2004;19:2101–6.
[60] Gerhardt RE, Koethe JD, Glickman JD, et al. Acid dialysate correction of metabolic alkalosis in renal failure. Am J Kidney Dis 1995;25:343–5.
[61] Gokal R. Peritoneal dialysis in the 21st century: an analysis of current problems and future developments. J Am Soc Nephrol 2002;13(Suppl. 1):S104–16.
[62] Gotch FA, Kotanko P, Thijssen S, Levin NW. The KDIGO guideline for dialysate calcium will result in an increased incidence of calcium accumulation in hemodialysis patients. Kidney Int 2010;78:343–50.

[63] Graham KA, Reaich D, Channon SM, et al. Correction of acidosis in hemodialysis decreases whole-body protein degradation. J Am Soc Nephrol 1997;8:632–7.
[64] Graham KA, Hoenich NA, Tarbit M, et al. Correction of acidosis in hemodialysis patients increases the sensitivity of the parathyroid glands to calcium. J Am Soc Nephrol 1997;8:627–31.
[65] Gu J, Anand V. Soidum induces hypertrophy of cultured myocardial myoblasts and vascular smooth muscle cells. Hypertension 1998;31:1083–7.
[66] Guillot AP, Hood VL, Runge CF, et al. The use of magnesium-containing phosphate binders in patients with end-stage renal disease on maintenance hemodialysis. Nephron 1982;30:114–7.
[67] Haddy FJ, Scott JB, Emerson TE, et al. Effects of generalized changes in plasma electrolyte concentration and osmolarity on blood pressure in the anesthetized dog. Circ Res 1969;24:I59–74.
[68] Han S, Won Y, Yi J, Kim H. No impact of hyperkalaemia with renin-angiotensin system blockade in maintenance haemodialysis patients. Nephrol Dial Transplant 2007;22:1150–5.
[69] Haris A, Richardson RMA. Biochemical effects of high dialysate calcium in hemodialysis patients with hyperparathyroidism: a 10 month study. ASAIO J 2003;49:70–3.
[70] Hatch M, Freel RW, Vaziri ND. Local up-regulation of colonic angiotensin II receptors enhances potassium excretion in chronic renal failure. Am J Physiol Renal Physiol 1998;274(43):F275–82.
[71] Hayes Jr CP, Robinson RR. Fecal potassium excretion in patients on chronic intermittent hemodialysis. Trans Am Soc Artif Intern Organs 1965;11:242.
[72] Hayes Jr CP, McLeod ME, Robinson RR. An extrarenal mechanism for the maintenance of potassium balance in severe chronic renal failure. Trans Assoc Am Phys 1967;80:207.
[73] Henrich WL. Hemodynamic instability during hemodialysis. Kidney Int 1986;30:605–12.
[74] Henrich WL, Woodard TD, McPhaul JJ. The chronic efficacy and safety of high sodium dialysate: double-blind, crossover study. Am J Kidney Dis 1982;2:349–53.
[75] Henrich WL, Katz FH, Molinoff PB, et al. Competitive effects of hypokalemia and volume depletion on plasma renin activity, aldosterone and catecholamine concentrations in hemodialysis patients. Kidney Int 1977;12:279–84.
[76] Henrich WL, Hunt JM, Nixon JV. Increased ionized calcium and left ventricular contractility during hemodialysis. N Engl J Med 1984;310:19–23.
[77] Hou SH, Zhao J, Ellman CF, Hu J, Griffin Z, Spiegel DM, et al. Calcium and phosphorus fluxes during hemodialysis with low calcium dialysate. Am J Kidney Dis 1991;18:217–24.
[78] Imbriano LJ, Durham JH, Maesaka JK. Treating interdialytic hyperkalemia with fludrocortisone. Semin Dial 2003;16:5–7.
[79] Imholz AL, Koomen GC, Struijk DG, Arisz L, Krediet RT. Fluid and solute transport in CAPD patients using ultralow sodium dialysate. Kidney Int 1994;46:333–40.
[80] Izumo H, Izumo S, DeLuise M, et al. Erythrocyte Na,K pump in uremia: acute correction of a transport defect by hemodialysis. J Clin Invest 1984;74:581–8.
[81] Johnson D, Rigby R, McIntyre H, Brown A, Freeman J. A randomized trial comparing 1.25 mmol/l calcium dialysate to 1.75 mmol/l calcium dialysate in CAPD patients. Nephrol Dial Transplant 1996;11:88–93.
[82] Jones S, Holmes C, Krediet R, MacKenzie R, et al. Bicarbonate/lactate-based peritoneal dialysis solution increases cancer antigen 125 and decreases hyaluronic acid levels. Kidney Int 2001;59:1529–38.
[83] Jones S, Holmes C, MacKenzie R, et al. Continuous dialysis with bicarbonate/lactate- buffered peritoneal dialysis fluids results in a long-term improvement in ex vivo peritoneal macrophage function. J Am Soc Nephrol 2002;13(Suppl. 1):S97–103.
[84] Kaji D, Kahn T. Na^+-K^+ pump in chronic renal failure. Am J Physiol 1987;252:F785–93.
[85] Karnick JA, Young BS, Lew NL, et al. Cardiac arrest and sudden death in dialysis units. Kidney Int 2001;60:350–7.
[86] Kelber J, Slatopolsky E, Delmez JA. Acute effects of different concentration of dialysate magnesium during high-efficiency dialysis. Am J Kidney Dis 1994;24:453–60.
[87] Kaye M, Vasillevsky M, Barber E. Correction of hypophosphatemia in patients on hemodialysis using a calcium-free dialysate with added phosphate. Clin Nephrol 1991;35:130–3.
[88] Kelleher SP, Schulman G. Severe metabolic alkalosis complicating regional citrate hemodialysis. Am J Kidney Dis 1987;9:235.
[89] Ketchersid TL, Van Stone JC. Dialysate potassium. Semin Dial 1991;4:46–51.
[90] Khandewal M, Kothari J, Krishnan M, et al. Volume expansion and sodium balance in peritoneal dialysis patients. Part I: recent concepts in pathogenesis. Adv Perit Dial 2003;19:36–43.
[91] Khandewal M, Kothari J, Krishnan M, et al. Volume expansion and sodium balance in peritoneal dialysis patients. Part II: newer insights in management. Adv Perit Dial 2003;19:44–52.
[92] Khandewal M, Oreopoulos DG. Is there a need for low sodium dialysis solution for peritoneal dialysis patients? Adv Perit Dial 2004;20:156–62.
[93] Kim MJ, Song J, Kim G, et al. Optimization of dialysate sodium profiling haemodial. Nephrology (Carlton) 2003;8:S16–22.
[94] Knoll GA, Sahgal A, Nair RC, et al. Renin-angiotensin system blockade and the risk of hyperkalemia in chronic hemodialysis patients. Am J Med 2002;112:110–4.
[95] Konings C, Kooman JP, Schonck M, et al. Effect of icodextrin on volume status, blood pressure and echocardiographic parameters: a randomized study. Kidney Int 2003;63:1556–63.
[96] Kooman JP, van der Sande F, Leunissen K, et al. Sodium balance in hemodialysis therapy. Semin Dial 2003;16:351–5.
[97] Kramer HJ, Gospodinov D, Kruck D. Functional and metabolic studies on red blood cell sodium transport in chronic uremia. Nephron 1976;16:344–58.
[98] Kuhlmann MK. Phosphate elimination in modalities of hemodialysis and peritoneal dialysis. Blood Purif 2010;29:137–44.
[99] Kyriazis J, Glotsos J, Bilirakis L, et al. Dialysate calcium profiling during hemodialysis: use and clinical implications. Kidney Int 2002;61:276–87.
[100] Kyriazis J, Kalogeropoulou K, Bilirakis L, et al. Dialysate magnesium level and blood pressure. Kidney Int 2004;66:1221–31.
[101] Lang RB, Fellner SK, Neumann A, et al. Left ventricular contractility varies directly with blood ionized calcium. Ann Intern Med 1988;108:524–9.
[102] Leypoldt JK, Charney DI, Cheung AK, et al. Ultrafiltration and solute kinetics using low sodium peritoneal dialysate. Kidney Int 1995;48:1959–66.
[103] Leunissen KML, Kooman JP, van Kuijk WHM, et al. Bicarbonate dialysis: a review and future perspectives. Semin in Dial 1994;7:186–91.
[104] Levin A, Goldstein MB. The benefits and side effects of ramped hypertonic sodium dialysis. J Am Soc Nephrol 1996;7:242–6.
[105] Linas SL. The role of potassium in the pathogenesis and treatment of hypertention. Kidney Int 1991;39:771–86.
[106] Lindley EJ. Should dialysate calcium concentration be standardised or individualised? J Ren Care 2009;35(Suppl. 1):101–6.

[107] Lindsay RM, Alhejalli F, Nesrallah G, et al. Calcium and phosphate balance with quotidian hemodialysis. Am J Kidney Dis 2003;42:S24–9.
[108] Locatelli F, Covic A, Chazot C, et al. Optimal composition of the dialysate, with emphasis on its influence on blood pressure. Nephrol Dial Transplant 2004;19:785–96.
[109] Locatelli F, Andrulli S, Di Filippo S, et al. Effect of on-line conductivity plasma ultrafiltrate kinetic modeling on cardiovascular stability of hemodialysis patients. Kidney Int 1998;53: 1052–60.
[110] Locatelli F, Manzoni C, Di Filippo S, et al. On-line monitoring and convective treatment modalities: short-term advantages. Nephrol Dial Transplant 1999;14(Suppl. 3):92–7.
[111] Lohr JW, Slusher S, Diederich D. Safety of regional citrate hemodialysis in acute renal failure. Am J Kidney Dis 1989;13:104.
[112] Lorincz I, Matyus J, Zilahi Z. QT dispersion in patients with end-stage renal failure and during hemodialysis. J Am Soc Nephrol 1999;10:1297–302.
[113] Manlucu J, Gallo K. Lowering postdialysis plasma sodium (conductivity) to increase sodium removal in volume expanded hemodialysis patients: a pilot study using a biofeedback software system. 2010;56:69–76.
[114] Martin RS, Panese S, Virginillo M, et al. Increased secretion of potassium in the rectum of humans with chronic renal failure. Am J Kidney Dis 1986;8:105.
[115] McIntyre CW. Calcium balance during hemodialysis. Semin Dial 2008;21:38–42.
[116] Mathialahan T, Maclennan KA, Sandle LN, Verbeke C, Sandle GI. Enhanced large intestinal potassium permeability in end-stage renal disease. J Pathol 2005;206:46–51.
[117] Maynard JC, Cruz C, Kleerekoper M, Levin NW. Blood pressure response to changes in serum ionized calcium during hemodialysis. Ann Intern Med 1986;104:358–61.
[118] Mistry C, Gokal R, Peers E, the MIDAS Study Group. A randomized multicenter clinical trial comparing isosmolar Icodextrin with hyperosmolar glucose solutions in CAPD. Kidney Int 1994;46:496–503.
[119] Montanari A, Graziani G, Borghi L, Cantaluppi A, Simoni I, Lorenzano E, et al. Skeletal muscle water and electrolytes in chronic renal failure: effects of long-term regular dialysis treatment. Nephron 1985;39:316–20.
[120] Moret K, Hassell D, Kooman JP, et al. Ionic mass balance and blood volume preservation during a high, standard, and individualized dialysate sodium concentration. Nephrol Dial Transplant 2002;17:1463–9.
[121] Morgera S, Scholle C, Voss G, et al. Metabolic complications during regional citrate anticoagulation continuous venovenous hemodialysis: single-center experience. Nephron Clin Pract 2004;97:c131–6.
[122] Movilli E, Camerini C, Viola BF, et al. Blood volume changes during three different profiles of dialysate sodium variation with similar intradialytic sodium balances in chronic hemodialyzed patients. Am J Kidney Dis 1997;30:58–63.
[123] Nagai Y, Itabashi M, Mizutani M, Ogawa T, Yumura W, Tsuchiya K, et al. A Case report of uncompensated alkalosis induced by daily plasmapheresis in a patient with thrombotic thrombocytopenic purpura. Ther Apher Dial 2007;12(1):86–90.
[124] Nakayama M, Kawaguchi Y, Yokoyama K, et al. Antihypertensive effect of low Na concentration (120 mEq/l) solution for CAPD patients. Clin Nephrol 1994;41:357–63.
[125] Nakayama M, Yokoyama K, Kubo H, et al. The effect of ultralow sodium dialysate in CAPD: a kinetic and clinical analysis. Clin Nephrol 1996;45:188–93.
[126] Navaneethan SD, Palmer SC, Craig JC, Elder GJ, Strippoli GF. Benefits and harms of phosphate binders in CKD: a systematic review of randomized controlled trials. Am J Kidney Dis 2009;54:619–37.
[127] Oberleithner H, Riethmuller C. Plasma sodium stiffens vascular endothelium and reduces nitric oxide release. Proc Natl Acad Sci USA 2007;104:16281–6.
[128] O'Donovan R, Hammer M, Baldwin D, et al. Substitution of aluminum salts by magnesium salts in control of dialysis hyperphosphataemia. Lancet 1986;1:880–2.
[129] Oe PL, Lips P, van der Meulen J, et al. Long-term use of magnesium hydroxide as a phosphate binder in patients on hemodialysis. Clin Nephrol 1987;28:180–5.
[130] Oettinger CW, Olive JC. Normalization of uremic acidosis in hemodialysis patients with a high bicarbonate dialysate. J Am Soc Nephrol 1993;3:1804–7.
[131] Oh MS, Uribarri J. What unique acid–base considerations exist in dialysis patients? Semin Dial 2004;17:351–4.
[132] Paganini EP, Moreno DSL, Kozlowski L, et al. The effect of sodium and ultrafiltration modeling on plasma volume changes and haemodynamic stability in intensive care patients receiving haemodialysis for acute renal failure: a prospective, stratified, randomized, cross-over study. Nephrol Dial Trans 1996;11:32–7.
[133] Sterns R, Palmer BF. Fluid, electrolyte and acid–base disturbances. NephSAP 2007;6:210–80.
[134] Palmer BF. The effect of dialysate composition on systemic hemodynamics. Semin Dial 1992;5:54–60.
[135] Panese S, Martin RS, Virginillo M, et al. Mechanism of enhanced transcellular potassium-secretion in man with chronic renal failure. Kidney Int 1987;31:1377.
[136] Papadogiannakis A, Xydakis D, Sfakianaki M, Kostakis K, Zouridakis A. An unusual cause of severe hyperkalemia in a dialysis patient. J Cardiovasc Med 2007;8:541–3.
[137] Pearl RG, Rosenthal MH. Metabolic alkalosis due to plasmapheresis. Am J Med 1985;79:391.
[138] Pecoitis-Filho R, Mujais S, Lindholm B. Future of icodextran as an osmotic agent in peritoneal dialysis. Kidney Int 2002;62 (Suppl. 81):S80–7.
[139] Petitclerc T. Recent developments in conductivity monitoring of haemodialysis session. Nephrol Dial Trans 1999;14: 2607–13.
[140] Pierratos A, Ouwendyk M, Francoeur R, et al. Nocturnal hemodialysis: three-year experience. J Am Soc Nephrol 1998;9:859–68.
[141] Pogglitsch H, Holzer H, Waller J, Pristautz H, Leopold H, Katschnigg H. The cause of inadequate haemodynamic reactions during ultradiffusion. Proc Eur Dial Transplant Assoc 1978;8:245–52.
[142] Prakdeekitcharoen B, Leelasa-nguan P. Effects of an ACE inhibitor or angiotensin receptor blocker on potassium in CAPD patients. Am J Kidney Dis 2004;44:738–46.
[143] Qunibi W, Hootkins R, McDowell L, et al. Treatment of hyperphosphatemia in hemodialysis patients: the calcium acetate renalgel evaluation (CARE Study). Kidney Intl 2004;65: 1914–26.
[144] Quarello F, Boero R, Guarena C, et al. Acute effects of hemodialysis on erythrocyte sodium fluxes in uremic patients. Nephron 1985;41:22–5.
[145] Raja R, Kramer M, Barber K, et al. Sequential changes in dialysate sodium (DNa) during hemodialysis. Trans Am Soc Artif Intern Organs 1983;24:649–51.
[146] Redaelli B. Electrolyte modeling in haemodialysis: potassium. Nephrol Dial Transplant 1996;11:39–41.

[147] Redaelli B, Sforzini S, Bonoldi L, et al. Potassium removal as a factor limiting the correction of acidosis during dialysis. Proc EDTA 1982;19:366.
[148] Redaelli B, Locatelli F, Limido D, et al. Effect of a new model of hemodialysis potassium removal on the control of ventricular arrhythmias. Kidney Int 1996;50:609–17.
[149] Rippe B, Simonsen O, Heimburger O, et al. Long-term clinical effects of a peritoneal dialysis fluid with less glucose degradation products. Kidney Int 2001;59:348–57.
[150] Ritz E, Passlick-Deetjen J, Lippert J. What is the appropriate dialysate calcium concentration for the dialysis patient? Nephrol Dial Transplant 1996;11:91–5.
[151] Rubin J, Adair C, Johnson B, et al. Stereospecific lactate absorption during peritoneal dialysis. Nephron 1982;31:224.
[152] Sadowski RH, Allred EN, Jabs K. Sodium modeling ameliorates intradialytic and interdialytic symptoms in young hemodialysis patients. J Am Soc Nephrol 1993;4:1192–8.
[153] Sanchez C, Lopez-Barea F, Sanchez-Cabezudo J, et al. Low VS standard calcium dialysate in peritoneal dialysis: differences in treatment, biochemistry and bone histomorphometry. A randomized multicentre study. Nephrol Dial Transplant 2004;19: 1587–2593.
[154] Santos SF, Peixoto AJ. Revisiting the dialysate sodium prescription as a tool for better blood pressure and interdialytic weight gain management in hemodialysis patients. Clin J Am Soc Nephrol 2008;3:522–30.
[155] Saudan P, Mach F, Perneger T, et al. Safety of low-dose spironolactone administration in chronic haemodialysis patients. Nephrol Dial Transplant 2003;18:2359–63.
[156] Sang GLS, Kovithavongs C, Ulan R, et al. Sodium ramping in hemodialysis: a study of beneficial and adverse effects. Am J Kidney Dis 1997;29:669–77.
[157] Sawyer N, Noonan K, Altmann P, et al. High-dose calcium carbonate with stepwise reduction in dialysate calcium concentration: effective phosphate control and aluminium avoidance in haemodialysis patients. Nephrol Dial Trans 1989;4: 105–9.
[158] Schuck O, Kaslikova J. Kinetics of phosphorus during hemodialysis and the calculation of its effective dialysis clearance. Clin Nephrol 1997;47:379–83.
[159] Sherman RA. Intradialytic hypotension: an overview of recent, unresolved and overlooked issues. Semin Dial 2002;15:141–3.
[160] Sherman RA, Bialy GB, Gazinski B, et al. The effect of dialysate calcium levels on blood pressure during hemodialysis. Am J Kidney Dis 1986;8:244–7.
[161] Sherman RA, Hwang ER, Bernholc AS, et al. Variability in potassium removal by hemodialysis. Am J Nephrol 1986;6: 284.
[162] Sherrard D, Hercz G, Pei Y, et al. The spectrum of bone disease in end-stage renal failure—an evolving disorder. Kidney Int 1993;43:436–42.
[163] Shinaberger JH, Miller JH, von Albertini B, et al. Phosphate removal by conventional dialysis, high efficiency dialysis, and high flux hemodiafiltration. Kidney Int 1987;31:245.
[164] Simonsen O, Venturoli D, Wieslander A, et al. Mass transfer of calcium across the peritoneum at three different peritoneal dialysis flud Ca^{2+} and glucose concentrations. Kidney Int 2003;64:208–15.
[165] Slatopolsky E, Weerts C, Norwood K, et al. Long term effects of calcium carbonate and 2.5 mEq/liter calcium dialysate on mineral metabolism. Kidney Int 1989;36:897.
[166] Slatopolsky E, Weerts C, Lopez-Hilker S, et al. Calcium carbonate as a phosphate binder in patients with chronic renal failure undergoing dialyais. N Engl J Med 1986;315:157.
[167] Smith H, Farrow S, Ackerman J, Stubbs J, Sprung J. Cardiac arrests associated with hyperkalemia during red blood cell transfusion: a case series. Anesth Analg 2008;106 (4):1062–9.
[168] Song J, Lee S, Suh C, Kim M. Time-averaged concentration of dialysate sodium relates with sodium load and interdialytic weight gain during sodium-profiling hemodialysis. Am J Kidney Dis 2002;40:291–301.
[169] Song JH, Park GH, Lee SY, Lee SW, Lee SW, Kim M-J. Effect of sodium balance and the combination of ultrafiltration profile during sodium profiling hemodialysis on the maintenance of the quality of dialysis and sodium and fluid balances. J Am Soc Nephrol 2005;16:237–46.
[170] Sonikian M, Pani I, Iliopoulos A, Koutala K, Marioli S, Vlassopoulos D. Metabolic acidosis aggravation and hyperkalemia in hemodialysis patients treated by sevelamer hydrochloride. Ren Fail 2005;27:143–7.
[171] Spiegel DM, Farmer B. Long-term effects of magnesium carbonate on coronary artery calcification and bone mineral density in hemodialysis patients: a pilot study. Hemodial Int 2009;13:453–9.
[172] Spiegel DM. The role of magnesium binders in chronic kidney disease. Semin Dial 2007;20:333–6.
[173] Spital A, Sterns RH. Potassium homeostasis in dialysis patients. Semin Dial 1988;1:14–20.
[174] Sugarman A, Brown RS. The role of aldosterone in potassium tolerance: studies in anephric humans. Kidney Int 1988;34:397.
[175] Swartz RD, Somermeyer MG, Hsu C-H. Preservation of plasma volume during hemodialysis depends on dialysate osmolality. Am J Nephrol 1982;2:189–94.
[176] Swindell C, Barker T, McGuirk S, et al. Washing of irradiated red blood cells prevents hyperkalaemia suring cardiopulmonary bypass in neonates and infants undergoing surgery for complex congenital heart disease. Eur J Cardiothorac Surg 2007;31:659–64.
[177] Toussaint N, Cooney P, Kerr PG. Review of dialysate calcium concentration in hemodialysis. Hemodial Int 2006;10: 326–37.
[178] Trivedi TH, Daga GL, Yeolekar ME. Geophagia leading to hypokalemic quadriparesis in a popartum patient. J Assoc Physicians India 2005;53:205–7.
[179] Ukaonu C, Hill DA, Christensen F. Hypokalemic myopathy in pregnancy caused by clay ingestion. Obstet Gynecol 2003;102: 1169–71.
[180] Uribarri J, Levin NW, Delmez J, Depner J, Ornt D, et al. Association of acidosis and nutritional parameters in hemodialysis patients. Am J Kidney Dis 1999;34:493–9.
[181] Ursino M, Coli L, Brighenti C, et al. Mathematical modeling of solute kinetics and body fluid changes during profiled hemodialysis. Int J Artif Organs 1999;22:94–107.
[182] Van der Merwe WM, Rodger RSC, Grant AC, et al. Low calcium dialysate and high-dose oral calcitriol in the treatment of secondary hyperparathyroidism in haemodialysis patients. Nephrol Dial Transplant 1990;5:874–7.
[183] van der Sande FM, Cheriex EC, van Kuijk WH, Leunissen KM. Effect of dialysate calcium concentrations on intradialytic blood pressure course in cardiac-compromised patients. Am J Kidney Dis 1998;32:125–31.
[184] Van Stone JC. Bicarbonate dialysate: still more to learn. Semin Dial 1994;7:168–9.
[185] Vanholder R, Lameire N. Osmotic agents in peritoneal dialysis. Kidney Int 1996;50:S86–91.
[186] Velez RL, Woodard TD, Henrich WL. Acetate and bicarbonate hemodialysis in patients with and without autonomic dysfunction. Kidney Int 1984;26:59–65.

[187] Wang T, Waniewski J, Heimburger O, et al. A quantitative analysis of sodium transport and removal during peritoneal dialysis. Kidney Int 1997;52:1609–16.
[188] Ward RA, Wathen RL, Williams TE, et al. Hemodialysate composition and intradialytic metabolic, acid base and potassium changes. Kidney Int 1987;32:129.
[189] Weigand C, Davin T, Raig L, et al. Life threatening hypokalemia during hemodialysis. Trans Am Soc Artif Internal Organ 1975;25:416.
[190] Weinreich T, Deetjen J, Ritz E, et al. Low dialysate calcium in continuous ambulatory peritoneal dialysis: a randomized controlled multicenter trial. Am J Kidney Dis 1995;25: 452–60.
[191] Weinreich T. Low or high calcium dialysate solutions in peritoneal dialysis? Kidney Int 1996;50:S92–6.
[192] Wing AJ. Optimum calcium concentration of dialysis fluid for maintenance haemodialysis. BMJ 1968;4:145.
[193] Wizemann V, Kramer W, Bechthold A, Thormann J. Acute effects of dialysis on myocardial contractility: influence of cardiac status and calcium/potassium ratio. Contrib Nephrol 1986;52:60–8.
[194] Wrong O, Harland C. Sevelamer-induced acidosis. Kidney Int 2005;67:776–7.
[195] Yeyati N, Fellet A, Arranz C, Balaszczuk A, Adrogue H. Amiloride-sensitive and amiloride insensitive kaliuresis in advance chronic kidney disease. J Nephrol 2008;21:93–8.
[196] Zannad F, Royer RJ, Kessler M, et al. Cation transport in erythrocytes of patients with renal failure. Nephron 1982;32:347–50.
[197] Zehnder C, Gutzwiller J, Huber A, et al. Low-potassium and glucose-free dialysis maintains but enhances potassium removal. Nephrol Dial Transplant 2001;16:78–84.
[198] Zhou YL, Liu HL, Duan XF, Yao Y, Sun Y, Liu Q. Impact of sodium and ultrafiltration profiling on haemodialysis-related hypotension. Nephrol Dial Transplant 2006;21: 3231–7.

CHAPTER

94

Homeostasis of Solute and Water by the Transplanted Kidney

J. Harold Helderman[1], *Heidi Schaefer*[1], *Anthony J. Langone*[1] *and Simin Goral*[2]

[1]Vanderbilt University Medical Center, Nashville, Tennessee, USA

[2]Hospital of the University of Pennsylvania, Philadelphia, Pennsylvania, USA

INTRODUCTION

The transplanted kidney is a healthy organ responding to a multiplicity of complex and variant clinical experiences and insults. There is no single model to adequately explain the manner in which solutes are handled by the transplanted kidney or the physiologic derangements that might be encountered. There is an ordered sequence of transplant events that can be isolated and provide the impetus for unique alterations in function that can be delineated. The hemodynamic state of the donor prior to harvesting can adversely affect early function of the graft. Perioperative circumstances, including the effects of warm and cold ischemia on the donor kidney, produce functional abnormalities similar to those intentionally produced by investigators examining ischemic acute renal failure.[42,99,151] Intraoperative factors including hypotension, blood loss, and technical damage establish conditions capable of deranging the function of the transplant. Additionally, the transplanted kidney, both early and several months after engraftment, is a denervated organ with all the consequences to tubular function attendant upon that state.[30,32] The use of newer immunosuppressive agents, which directly alter physiologic function of the kidney, also affects the performance of the new graft.

The placement of a functioning allograft in a setting in which ischemic effects have been minimized and engraftment has been uncomplicated may result in the passage of salt and water during the early post-transplant period. The nature and amount of salt and water are a function of volume and osmolar loads imposed by the azotemic state, which presents excess solute loads and stimuli for the elaboration of saluretic hormones.[37,92,116,128,155] The effect of other comorbid disorders associated with uremia, such as secondary hyperparathyroidism, which may persist post-transplant, can alter the handling of such solutes as calcium, phosphorus, hydrogen ion, and bicarbonate even when excretory function is excellent.[31]

The maintenance of a functioning allograft depends on forestalling immunologically mediated assault. For all but identical twins, transplant recipients are maintained on immunosuppressive medications, some of which may have an impact on salt and water regulation. For example, many recipients receive corticosteroids early in the transplant period regardless of the additional immunosuppressive medicines during the maintenance regimen. These drugs have profound effects on sodium, chloride, potassium, and water regulation.[58] Other immunosuppressive agents including calcineurin inhibitors and rapamycin may alter renal transplant tubular function.[35] Since the early 1980s, calcineurin inhibitors have been the mainstay of maintenance immunosuppression in the allograft recipient. Both cyclosporine and tacrolimus have the ability to profoundly alter renal blood flow and thus renal function[50,203] through reduced glomerular filtration with resultant effects on the handling of sodium, potassium hydrogen and uric acid.[203] Rapamycin, one of the newer agents to be added to the armamentarium may also lead to tubular dysfunction and altered solute transport.[7] On this background, immunologic assault in the form of acute and chronic rejection can profoundly alter the handling of salt and water by the transplanted kidney, possibly related to effector cells or their released cytokines.[96,133]

Seldin and Giebisch's The Kidney, Fifth Edition.
DOI: http://dx.doi.org/10.1016/B978-0-12-381462-3.00094-X

© 2013 Elsevier Inc. All rights reserved.

This review, updated from its previous version, first explores the intrinsic capacity of the transplanted kidney to modulate solute and water, and to maintain the internal milieu in homeostatic balance. By using the classic observations of Bricker et al.[30,31,32] and more recent studies of tubular function that minimize warm ischemia and avoid the confounding variables of immunosuppressive drugs and rejection, the handling of solutes and water by the denervated transplanted organ will be characterized.

The remainder of this review deals with the various derangements of solute and water handling observed clinically after successful engraftment. These separate syndromes will be explained employing clinical data and observations in the human. When experimental data from transplant or related fields of research derived from animal models are applicable, they will be discussed and placed in proper context in an attempt to explain the etiology of or the physiologic basis that underlies the clinical syndromes.

The effect of immunosuppressive therapies on renal function and metabolic derangements has been extensively studied. This revised chapter makes a special effort to explicate the impact of these potent agents, particularly that of calcineurin inhibitors and rapamycin. Those experiments that reveal the multiplicity of effects of these agents in general are reviewed in an attempt to suggest a unifying theory as to their physiologic consequences.

INTRINSIC CAPACITY OF THE DENERVATED TRANSPLANTED ISOGRAFT

To observe the intrinsic capacity of the transplanted kidney to maintain solute and water homeostasis, an experiment must be designed to minimize the effects of ischemia related to harvest, the solute load that the azotemic patient presents to the new kidney, the use of immunosuppressive medications, and the effects of rejection. These criteria were best met by the classic renal autotransplantation studies reported by Bricker et al.[32] in the dog. These researchers left one kidney intact, excised the contralateral kidney, and retransplanted it into a discreet hemibladder. In this two-kidney autotransplantation model in nonuremic animals, renal hemodynamics, maximal concentration and dilution capacity, response to vasopressin, sodium, and potassium excretion, response to modulation of plasma volume by hypertonic and isotonic infusion, and the response to mercurial diuretics were studied. When renal hemodynamics had returned to normal after surgery in the transplanted kidney, the measured tubular functions were virtually equal in the just transplanted kidney to those observed in the contralateral, undisturbed kidney. Sodium excretion rates factored for respective solute loads were also equivalent to the contralateral, undisturbed kidney as was the ability to maximally concentrate or dilute the urine after several days. This study illustrates the ability of the denervated autotransplanted kidney to maintain normal solute and water balance.

In healthy individuals, head-out water immersion increases sodium excretion.[63] Interestingly, in renal denervated dogs, the natriuretic response to head-out water immersion is completely abolished, suggesting a major role for the renal nervous system for this response.[140] Yet, despite renal denervation, it has been shown that patients with well-functioning renal transplants of less than two months duration are capable of a normal natriuretic response to head-out water immersion.[174] This observation suggests that renal nerve activity is not essential for a normal natriuretic response to head-out water immersion in renal transplant recipients. When six renal transplant recipients were compared to, six normal individuals subjected to head-out water immersion, it was demonstrated that the denervated, transplanted kidneys of the six recipients were able to maintain a sodium excretory response to head-out water immersion identical to that obtained in the normal controls.[49] These studies, taken together with the earlier reports, illustrate that the denervated autotransplanted kidney is able to maintain normal solute and water balance.

More precise experimental observations about renal tubular function in the transplanted kidney were made in the studies of Muller-Suur et al.[145] and Norlen et al.[152] These investigators used a rat model in which recipient animals underwent bilateral nephrectomy just prior to isotransplantation. Using standard micropuncture techniques to assess tubular function, Muller-Suur et al.[145] were able to show that five minutes after reestablishment of circulation to the donor kidney that had suffered the least amount of cold ischemia, there was no statistical difference in the single-nephron glomerular filtration rate (GFR) of the transplant compared to the untransplanted normal kidney (13.4 nl/min per 100 g of body weight vs 14.1). After an initial polyuric phase related to solute load, a phenomenon discussed later, the passage of sodium and potassium into the urine was equivalent in the transplant to that of the normal, untransplanted kidney. Norlen et al.[152] measured proximal tubule reabsorptive capacity using micropuncture techniques in a similar experimental rat model. They demonstrated that there was normal proximal tubular fluid reabsorption (TF/P inulin ratio of 2.1 [$\pm$ 0.4]) as well as normal whole-kidney function and normal single-nephron GFR. These studies show that bulk solute handling by the denervated,

isotransplanted kidney is normal on a whole-kidney clearance basis. These nonrejecting grafts can maintain a relatively undisturbed total GFR, single-nephron GFR, and proximal tubular absorptive capacity as determined by micropuncture.

The functional integrity of the more distal nephron segments as well as the intrinsic capacity of the transplanted kidney to exhibit tubuloglomerular (T-G) feedback was investigated further by Muller-Suur et al.[145] in the rat isotransplant model. Two experimental paradigms were employed. In the first, the isograft was punctured in the presence of the normal contralateral kidney; in the second, the puncture occurred in the solitary isograft after contralateral nephrectomy. In contrast to the observations by Norlen et al.[152] the investigators found that the whole-kidney GFR of the transplanted kidney fell approximately 40% when the contralateral kidney was left in place. Yet when the remnant kidney was removed, the GFR in the isotransplant rose toward but not entirely to the two-kidney control value. These animals were then studied 15 hours after isotransplantation at a time when single-nephron GFR had risen essentially to normal in order to measure the effects of T-G feedback. There was normal urine flow rate, normal sodium and potassium excretion, a normal TF/P inulin, and a slightly reduced GFR. When unilateral nephrectomy was performed, urine flow and sodium/potassium excretion rates increased in both the transplanted kidney and in the control. Interestingly, T-G feedback was found to be intact, permitting appropriate modulation of GFR in response to solute load by the transplanted kidney when the contralateral, normal kidney was in place. An increase in osmotic and solute load that would occur after the contralateral kidney was removed would be expected to have produced a substantial reduction in GFR if no other compensatory mechanisms were at play. In the actual experimental situation, the single remaining transplanted kidney demonstrated a decreased sensitivity of the T-G feedback mechanism, measured as a shift in the T-G set-point (Fig. 94.1). This attenuation of the feedback sensitivity set-point allowed the GFR to rise toward normal rather than fall in the transplanted single kidney to maintain normal clearance despite the increased solute load reaching the macula densa. Muller-Surr et al.[145] advanced the hypothesis that increased interstitial pressure and volumes to which the transplanted kidney is exposed after contralateral nephrectomy explains resetting of T-G feedback. In summary, the isotransplanted kidney, when studied with a functioning renal remnant, retains its capacity to modulate GFR to solute load, but resets the T-G feedback set-point to maintain GFR in the face of increased bulk blood flow when placed in an environment devoid of additional functioning nephron mass represented by a normal remnant kidney.

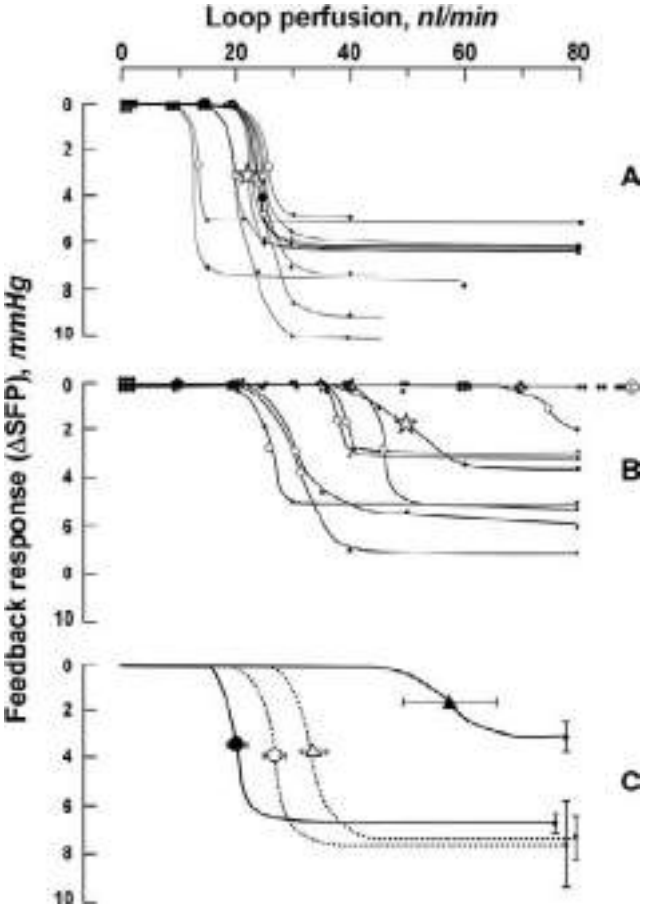

FIGURE 94.1 Feedback responses (change in stop-flow pressure [SFP]) (ordinates) to different loop perfusion rates (abscissa) in kidneys 1 day after transplantation. A: Data on single experiments. The open circles indicate the graphically determined turning points. B: As in A, but after uninephrectomy. One individual tubule was studied both before and up to 30 minutes after unilateral nephrectomy. This tubule is marked by an asterisk in A and B. C: Mean curves from A and B for transplanted kidneys (solid lines) and for control kidneys (broken lines). Note the shift to the left in transplanted (closed circles) kidneys compared with controls (open circles), and to the right after uninephrectomy in controls (closed triangles) and transplanted (Δ) animals. *(From Muller-Suur R, Norlen BJ, Persson AEG. Resetting of tubuloglomerular feedback in rat kidneys after unilateral nephrectomy. Kidney Int 1980;18:48–50.)*

Kidney transplantation between identical twins provides an interesting clinical counterpart to the rat and dog isograft studies. Bricker et al.[30] analyzed the intrinsic capacity of the human kidney allograft to maintain solute and water homeostasis in the original set of identical twins transplanted at the then Peter Bent Brigham Hospital (now Brigham & Women's Hospital) in Boston in 1954, an advance in clinical medicine recognized for the Nobel Prize of 1990. Recipients of an identical twin kidney allograft require no

immunosuppressive therapy and rarely exhibit rejection. When compared to the remaining kidney function of the identical donor sibling, the transplanted organ was able to maintain an equivalent filtration fraction and showed a normal ability to concentrate and dilute urine as well as to acidify and to alkalinize the urine when challenged. Further, the allograft could increase and decrease the rate of sodium excretion in the face of load, to respond to various volume- and drug-related stimuli, and to retain the capacity to alter filtration fraction and renal blood flow acutely while maintaining extracellular fluid volume and composition. One can conclude from isograft studies in animals and from the observations in identical twin human allografts that the transplanted denervated kidney retains the capacity to modulate solute and maintain volume homeostasis.[30,78]

ISCHEMIA ATTENDANT TO HARVEST, PRESERVATION, AND ENGRAFTMENT

Experimental models and clinical observation demonstrate that the transplanted kidney has the intrinsic capacity to maintain solute and water homeostasis. Unfortunately, the allograft in clinical settings is exposed to injurious environmental pressures to which it must respond by modifications of physiologic function. This section of the chapter will attempt to isolate several of the insults to which the functioning allograft is exposed and reveal the means by which the transplant has successfully responded to these challenges or delineate the derangements that flow from unsuccessful responses.

Although every attempt is made to minimize the ischemic effect of kidney transplantation by paying scrupulous attention to donor management, to conditions of harvest, organ preservation, and to conditions of engraftment, some degree of ischemic injury is a uniform phenomenon. Even in the early studies of Bricker et al.[32] of autotransplantation in the dog, an initial drop in GFR and renal plasma flow that normalized several days after surgery was observed. This initial drop in GFR was felt to be due to tissue ischemia induced by the operative procedure and did not have any lasting effects on kidney function as revealed by their measurements.

Muller-Suur et al.[145] also noted important consequences of early ischemia in their Munich-Wistar rat isograft model. They observed that even in the group of animals that received the least amount of protocol-determined cold ischemia prior to implantation, a group able to maintain normal single-nephron GFR, there still were increases in urine flow rate with diminished urinary concentration (approximately 100 mOsm/kg) during the first three hours postoperatively, thought a consequence of surgical ischemic injury. During this initial polyuric phase, there was an additional increase in sodium and potassium excretion paralleling the enhanced urine flow rate. An initial polyuria and the formation of hypotonic urine, even when GFR is normal, were felt to be a universal consequence of the unavoidable ischemia of the transplantation event.

These findings have been confirmed in reperfusion studies in renal allografts in humans.[5] Alejandro et al., noted that in the ensuing hours of post-transplant, fractional excretion of rates of sodium were elevated to $>20\%$ with an impairment of urinary concentrating ability even in those with normofiltration. Although significant tubular dysfunction occurred, by morphometric analysis, only $\sim 2\%$ of proximal tubular cells exhibited necrosis and obstruction of the tubular lumen. Unlike studies in the native kidney[157] and supporting the work of others,[192] this points away from an important contribution of tubular obstruction to postischemic injury in the transplanted allograft.

In turn, it has been suggested that afferent arteriolar constriction with an attendant fall in the glomerular perfusion pressure is the primary mechanism by which glomerular filtration is affected in the freshly transplanted kidney.[5] One contributing mechanism may be that the high fraction of filtered sodium reaching the macula densa mediates afferent vasoconstriction via tubulo-glomerular feedback. In patients with persistent hypofiltration post-transplantation, loss of polarity of proximal tubular cells with redistribution of cytoskeletal proteins including Na^+/K^+-ATPase, fodrin and ankyrin from the basolateral membrane to the cytoplasm has been noted[4,119] with subsequent impairment of proximal tubular sodium reabsorption.

In addition to tubuloglomerular feedback, vascular mediators are felt to contribute to a state of afferent arteriolar vasoconstriction. With sustained injury and delayed function of the transplant, both elevation in plasma renin activity and endothelin-1 levels have been observed.[5] In addition, there appears to be resistance of afferent arterioles to the vasodilator actions of endogenous atrial natruiretic peptide, which is present in excess.[220] Thus, postischemic allograft injury appears to be accompanied by an imbalance that favors constrictor hormones over those that dilate the afferent arteriole with a resultant depression in GFR by lowering of glomerular perfusion pressure.

Urinary exosomes released into the urine by fusion of the outer membrane of multivesicular bodies with the apical plasma membrane of renal epithelial cells[101,168] are shown to include membrane and cytosolic proteins, which have the characteristics of all renal tubule epithelial cells, podocytes, and transitional epithelial from the urinary collecting system.

Importantly, several of these proteins found in urinary exosomes have been implicated in various kidney diseases and suggest that the examination of urinary endosomes may allow for a non-invasive measurement of site-specific biomarkers.[167]

Several studies have demonstrated changes in excretion of urinary exosomal Na^+/H^+ exchanger isoform 3 (NHE3)[60] and fetuin-A[234] after renal ischemia/reperfusion. NHE3, a sodium transporter protein in the proximal tubule, was present in the urine within 24 hours after renal allograft transplantation with levels returning to undetectable 48 hours after transplantation relating to a marked improvement in renal function.[60] Conversely, NHE3 levels were not increased in the urine in the setting of acute allograft rejection. This data suggests that NHE3 may be a temporal marker of renal ischemia/reperfusion injury. Urinary exosomal fetuin-A levels have been shown to be increased after ischemia/reperfusion in allograft recipients[234,193] but also in donor patients[193] suggesting this may be a response to a change in renal hemodynamics and not specific to renal ischemia/perfusion injury.

The excretion of urinary exosomal aquaporin-1 has been studied both in animal models and in human allograft recipients. Aquaporin-1 is a water channel protein abundantly expressed in renal epithelial cells of the proximal tubules and the descending limb. It is known that renal ischemia/reperfusion in the native kidney leading to acute kidney injury is associated with decreased renal aquaporin-1 expression[80] with subsequent data showing a decreased abundance of urinary exosomal aquaporin-1 in Sprague-Dawley rats subjected to unilateral renal ischemia/reperfusion as well as a renal transplant recipient at two and six days after renal transplantation despite a dramatic decrease in the plasma creatinine concentration following the operation.[193] There was no decrease in urinary exosomal aquaporin-1 excretion in both animal models of nephrotic syndrome and patients with proteinuria. These data suggest that urinary exosomal aquaporin-1 may be a useful urinary biomarker to predict post-transplant acute kidney injury related to ischemia/reperfusion injury. Follow-up studies in larger sets of patients will be needed to confirm these findings and validate the utility of the role of urinary exosomal proteins in the detection of renal/ischemia reperfusion injury.

Norlen et al.[151] used microsphere injection techniques to evaluate alterations in intrarenal blood flow during varying lengths of warm and cold ischemia of the renal transplant. Analysis of cross sections of rat kidney showed that microspheres injected during the reperfusion phase after two hours of cold ischemia showed no areas of preferential blood flow. Longer degrees of ischemia (12–16 hours) resulted in poor filling of the medulla. Except for the polyuric phase, which always seems to accompany such ischemia, there was no functional or structural abnormality after two hours of cold ischemia. On the other hand, after 12–16 hours of cold ischemia, there were dilated and collapsed tubules interspersed with morphologically "normal" tubules. The dilated tubules exhibited no glomerular filtration and were thought a consequence of obstruction by swollen epithelial cells in the corticomedullary region. This study provides anatomic correlates to the ischemic engraftment and preservation procedures.

The different studies in animals taken together show that short-term ischemia may derange volume homeostasis and concentration ability. Longer periods of ischemia may result in delayed reperfusion of the corticomedullary region, possibly due to cellular swelling in that area.[151] The effect of the more prolonged ischemia to the transplant is a fall in GFR and an early loss of concentrating ability of the tubule. These alterations are potentially reversible spontaneously and may lead to no long-term sequelae. Clinically, the absence of urine formation after surgery suggests longer ischemic injury, whereas some element of the universally encountered polyuria is a consequence of shorter periods of ischemia.

Most data, however, would suggest that early ischemia/reperfusion injury of short duration does not lead to untoward long-term consequence to the allograft. Prolonged injury on the other hand, may contribute to late renal allograft deterioration and failure.[89,148,211] To evaluate the association between initial ischemia/reperfusion injury occurring secondary to organ retrieval, storage, and transplantation and late renal allograft deterioration and failure, Azuma et al.[11] studied the patterns of proteinuria, cellular infiltration, cytokine expression, and glomerular sclerosis over time in 344 Lewis and Fischer rats after 45 minutes of warm ischemia of a singe kidney. Intracellular adhesion molecule I, endothelin, and major histocompatibility complex (MHC) class II expression were found to be upregulated within two to five days after the injury, which enhances the antigen load presented to the recipient and the appropriate signal pathways to enhance antigen recognition, culminating in a drive for additional acute and later chronic rejection. In the animals, proteinuria developed after 8 weeks, and glomerulosclerosis, arterial obliteration, and interstitial fibrosis occurred after 16 weeks. These data suggest that early ischemia and reperfusion, if severe enough, may not only contribute to early dysfunction but also to late renal deterioration and chronic rejection. Further studies are needed for better understanding of the factors mediating these abnormalities.

ALLOGRAFT IN THE AZOTEMIC SOLUTE-LOADED RECIPIENT

Clinical observations teach that the placement of a functioning allograft into an azotemic patient leads to copious urine formation. The typical diuretic phase postoperatively has been attributed to several potential etiologies. As has been previously discussed, ischemia per se affects the concentrating ability of the nephron.[145] Solutes that accumulate in azotemic patients, even in the face of adequate dialysis, can induce an osmotic diuresis when GFR is adequate.[128,155] Additionally, the administration of loop diuretics such as furosemide and osmotic diuretics such as mannitol during the transplant operation will contribute to this polyuric phase. Lastly, the etiologic role of atrial natriuretic peptide (ANP) as the basis for some of this polyuric phase has been suggested by observations in humans and studies on animals using a volume-overloaded ischemic kidney model and measurements of that peptide in early clinical transplant experience.[37]

During the immediate postoperative period, the diuresis that frequently occurs can be profound and, if not followed assiduously with appropriate replacement therapy, can be life threatening.[128] In their study of six patients after native nephrectomy and transplantation, Ogden et al.[155] observed diuresis of 5−14 liters over the first 24 hours after transplantation. The diuresis was osmotic, with the osmolar clearance of electrolytes accounting for more than 50% of the total solute clearance. Although these patients were relatively hyperosmolar due to retained blood urea nitrogen (BUN), their osmotic diuresis post-transplant was not primarily driven by urea but by electrolytes, principally sodium. Swenson et al.[199] studied sodium balance in four patients who had undergone kidney isotransplantation and found negative sodium balance of 150−1000 mEq during the immediate postoperative period. They found that the rate of sodium loss correlated with pretransplant overexpansion of extracellular space (ECS) and that water excretion was more a function of sodium than urea excretion. Additionally, they observed hypovolemia related to this osmotic diuresis in several patients with postural hypotension and tachycardia when urine output was inadequately replaced. These data suggest that the osmotic diuresis may be a result of an inability to retain filtered sodium when required and not merely of the presence of increased filtered loads.

As was discussed in the previous section, the ischemic insult of transplantation alters the ability of the tubule to concentrate urine, in particular the proximal tubule. This occurs even in the optimal setting of live donor transplantation whereby ischemia is minimized. In a study of eight renal allograft recipients of live donor kidneys, Bugge et al.[33] noted a high fractional excretion of sodium during the first hour after surgery correlating with a high urinary excretion of N-acetyl-ß-glucosaminidase. NAG is a lysosomal enzyme found in high concentrations in renal tubules, especially in the S3 segment of the proximal tubule. The data taken together suggest that it is the defect in proximal tubular transport contributing to the post-transplant osmotic diuresis that hitherto was thought to be a consequence of solute loads presented to disordered cortical collecting tubules.

Diuretics, including both osmotic and loop, given during the perioperative period also contribute to the post-transplant polyuria. Mannitol has been shown to reduce the frequency of postsurgical acute renal failure after renal transplantation.[213] It has been suggested that the combination of mannitol and volume expansion gives better protection than volume expansion alone, but the mechanism for this protective effect is not known. By its osmotic activity, mannitol increases plasma volume expansion, decreases systemic and renal vascular resistance, and counteracts swelling of tubular cells. All of these properties of mannitol may contribute to its protective effect against ischemic renal injury. Loop diuretics reduce sodium reabsorption and oxygen consumption in the thick ascending limb of Henle, and simultaneously, increase the oxygen availability for the S3 segment of the proximal tubule that may protect against ischemic injury.[94]

One might infer that the correct clinical response to the expansion component of the diuresis would be to restrict perioperative volume loads. In fact, such inference is absolutely false, as it has been shown that challenges of hypervolemia during renal transplantation decrease the post-transplant period of dysfunction due to postsurgical acute renal failure.[38] It has long been known that salt loading prior to ischemia or nephrotoxic insults delimits the physiologic display of injury; the transplant condition is not different in this regard. Some have hypothesized that the protective effect of volume expansion may be due to released atrial natriuretic factor (ANF). One argument is that the intrinsic hypervolemia of the transplant recipient at the time of surgery and the additional volume loads imposed by the transplant team generate high levels of ANF, which protect the nephron from ischemic injury, an unavoidable consequence of the surgical event. Measurements of pulmonary artery pressure (PAP), pulmonary wedge pressure (PWP), and central venous pressure (CVP) as an estimate of systemic volemia in seventeen patients during allograft placement were compared with levels of ANF. Although it was difficult to statistically relate measures of these parameters of volume status to

markedly elevated levels of ANF, there was a clear positive correlation between the changes in ANF and acute changes in central volemia (Fig. 94.2). This study suggests that during transplantation ANF is elevated at the time of surgery and its release is facilitated by therapeutic volume challenges. Additional data by Nyberg et al.[154] and Plum et al.[170] lend further support to this view. In a study of 14 patients undergoing live donor kidney transplantation, Nyberg et al. showed that ANF levels rose significantly after transplantation and volume expansion and by stepwise multiple linear regression analysis was the strongest determinant of post-transplant diuresis. Similar findings were also reported by Plum et al. in the early post-transplant period.

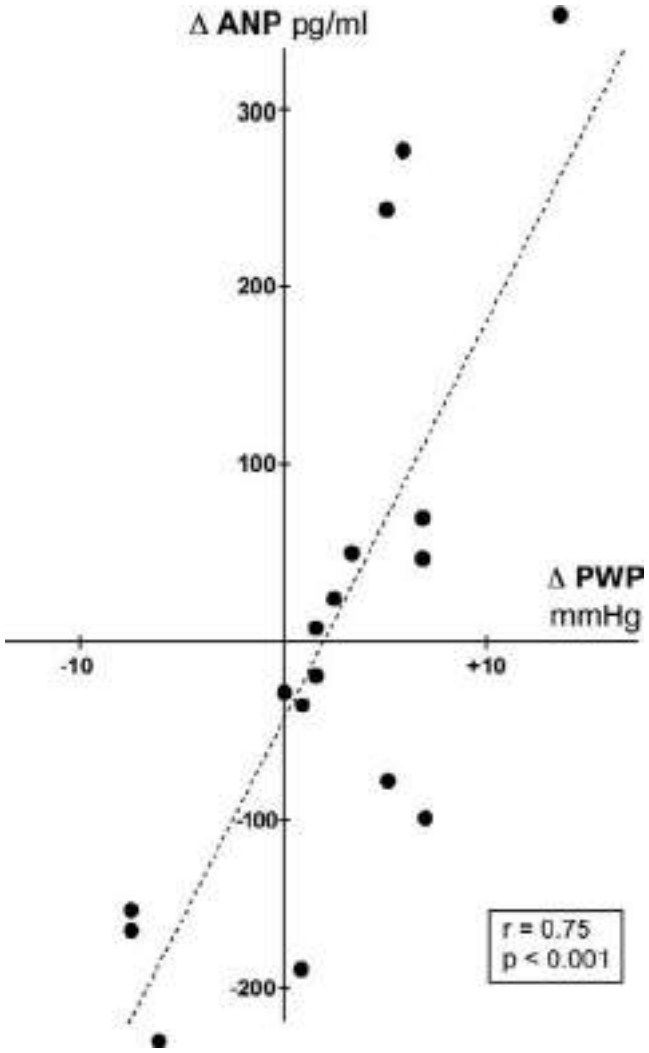

FIGURE 94.2 Correlation between atrial natriuretic factor (ANF) and pulmonary wedge pressure (PWP) variations during renal transplantation. *(From Gianello P, Squifflet JP, Carlier M, et al. Beneficial effect of atrial natriuretic factor on ischemically injured kidneys in the rat. Transplantation 1989;48:9–14.)*

The protective role of ANF on the ischemic injury of transplantation has been suggested by animal models. By using an ischemic renal injury rat model, Gianello et al.[76] investigated whether the atrial natruiretic peptide by itself was able to improve early renal function after an ischemic injury. In a group of Wistar rats subjected to right nephrectomy and left renal artery occlusion for 30 minutes followed by a two hour infusion of rat atrial natruiretic peptides, there was a significant improvement in early recovery of renal function as compared to those rats who received isotonic saline alone. There was a notable increase in urinary flow rate, sodium excretion and improvement In GFR recovery. A similar experiment confirmed and extended these observations in a dog model[77] showing protective ANF effects with low doses of human exogenous ANF. It is worth noting in both animal models, a striking increase in GFR after ANF infusion. In the intact kidney, the enhanced GFR induced by ANF results from a hemodynamic effect as noted by vasodilation of the preglomerular afferent arteriole and constriction of the efferent artery. It has been hypothesized that a similar mechanism of action of ANF is involved in the ischemically injured kidney model.

In addition to the glomerular effects, ANF also considerably improves natriureisis and fractional sodium reabsorption rates suggesting that ANF may also have direct tubular effects and may be direct or mediated by an inhibition of the renin-angiotensin-aldosterone system.

These experiments in animals show that volume expansion and the resultant diuresis is protective of recovery after ischemic renal injury. This conclusion is corroborated by studies in renal transplant recipients who have improved graft function after perioperative volume expansion.[38] The onset of a rapid osmotic diuresis after transplantation heralds a rapid recovery and all attempts should be made to augment the early and copious formation of urine through volume expansion and diuretics. There is evidence to suggest that the protective nature of volume expansion leading to early renal recovery from surgical injury may be partially related to ANF release.

In addition to hypervolemia-induced release of ANF, there is evidence that glucocorticoids, a standard concomitant of clinical transplantation, directly stimulate ANF release and by doing so provide further protection to the renal transplant against ischemic injury. Eight healthy men were studied by Weidmann et al.[224] in a cross-over, "blinded" study of the effect of prednisone (50 mg/day for nine days) on ANF while on a diet containing 130 mmol of sodium and 75 mmol of potassium. During the prednisone therapy period, there was no change in sodium balance, blood pressure, or weight compared with the placebo period.

Over the nine-day study period, the mean supine ANF was nearly threefold greater during prednisone intake than during placebo intake in controls. Confirmatory studies in Sprague-Dawley rats by Gardner et al.[74] showed that rats injected with dexamethasone, 1 mg/day, for one to two days while water deprived, exhibited a twofold increase in ANF. These animals were then killed and slot-blot analysis of atrial cells by using a cDNA probe for ANF showed 1.5-fold to two-fold increase in mRNA for ANF in those animals treated with steroids. These findings suggest that glucocorticoids directly stimulate ANF synthesis by atrial cells. Although not directly studied in transplantation, the early use of glucocorticoids in that setting may enhance the release of ANF in the early post-transplant period, play some part in the observed initial polyuria, and serve as a protective therapeutic maneuver against perioperative ischemia.

Although it has been shown in animal models of acute ischemic renal failure that ANF ameliorates renal damage, administration of synthetic ANF in humans following renal transplantation in attempts to promote initial graft function have not shown any beneficial effects. In a prospective, double-blind study by Sands et al.[186] 10 pairs of cadaveric kidneys were transplanted into 20 recipients. Upon revascularization of the allograft, paired recipients received either humanized ANF or placebo administered intravenously as a 50-μg bolus, followed by a 4-hour infusion at 0.1 μg/kg/min. Renal allograft function was determined both by serum creatinine and measurements of GFR by (125I)iothalamate. No significant differences were noted in renal allograft function between the two groups. Similar results have been obtained by others.[175,191] These results do not mean that ANF plays no role in preserving renal function after transplantation as extracellular volume expansion is a major stimulus for endogenous ANF secretion. It suggests that hANF alone is not superior to conventional extracellular volume expansion.

The early diuretic phase after transplantation is important for the long-term outcome of the graft.[36] Although there is suggestion that the early diuretic phase is related to impairment of function in the concentrating segment and proximal tubule, the impairment is transient, with no long-term sequelae. The osmotic load provided by the azotemic state and the perioperative volume expansion with resultant additional solute loads presented to the kidney, all contribute to diuresis directly and further stimulate ANF, which is responsible for an additional component of urine formation. Every attempt should be made to facilitate post-transplant diuresis, which improves immediate graft function, enhances the rapid recovery of the transplant recipient, helps to make the early management period less difficult for the transplant team, and culminates in a substantial increase in graft survival.

SOLUTE REGULATION DURING REJECTION

The most unique syndrome that a transplanted kidney must deal with is that of acute rejection. Derangements of renal function, which characterize this immune assault on the allograft, include not only a decrease in the GFR but also altered solute excretion. The diminution of sodium concentration in the urine has even been used by some as a useful clue to the diagnosis of acute rejection.[64,90,97,156] Renal retention of sodium reflects intrarenal ischemia, the final result of the immunologic assault on the transplanted allograft. In general terms, renal inflammation with organ swelling and edema can extrinsically reduce renal blood flow. More precise mechanisms responsible for physiologic dysfunction during rejection are doubtless at play and are worthy of a great deal of study. Acute cellular rejection of the kidney is associated with the release of monokines from activated T lymphocytes and from monocytes, which are in great measure responsible for the changes one calls inflammation. One important cytokine released is interleukin-2 (IL-2).[48] Although not formally studied in kidney transplantation, patients who are receiving supraphysiologic doses of IL-2 for immunotherapy of metastatic melanoma or renal cell carcinoma exhibit functional changes in solute handling similar to those encountered during acute rejection.[75,171,202,223] IL-2 regimens result in systemic hypotension due to systemic vasodilatation associated with azotemia and low urinary excretion rates of sodium. Although the amount of systemic IL-2 released during rejection is insufficient to cause systemic hypotension, the local release of the cytokine into the renal circulation may be sufficient to vasodilate renal beds directly or indirectly, open endothelial tight junctions, and contribute to the edema and high intrarenal pressures thought to be responsible for extrinsic reduction in total renal blood flow and sodium avidity.

Another cytokine, tumor necrosis factor (TNF), is found to be elevated during acute rejection episodes.[133] In a group of prospectively monitored transplant recipients, TNF elevation was diagnostic of rejection in half of the cases. Even when not diagnostic of acute allograft rejection alone, elevated TNF measured during rejection amplifies the importance of cytokines during the immunologic assault. The effects of human TNF on glomerular histology in rabbits given doses of 0.08, 0.8, and 80 g/kg/liter for five hours were studied by Bertani et al.[23] At the 0.8g/kg/liter dose

administered, there was leukocyte infiltration of glomerular capillaries as well as inflammatory cells within the glomerular capillaries. At the dose of 8 g/kg/hr, there was renal failure accompanied by the leukocyte infiltration with fibrin accumulation. The effects of TNF on renal vascular resistance released during acute rejection may mediate the observed endothelial damage.

Inflammatory prostanoids of the vasoconstrictive variety released from activated monocytes infiltrating the allograft have been implicated in the reduction of renal blood flow and impaired excretory function of rejection. The role of arachidonic acid metabolites in the transplant physiologic derangement during acute rejection has been studied by Coffman et al.[45] using a rat allograft model between inbred rat strains (Lewis rat donors to Brown-Norway recipients). Associated with the histologic evidence of cellular rejection based on interstitial and perivascular infiltrates of mononuclear cells and the reduction of inulin clearance rates, there was an increase in the production of thromboxane B2 (TXB2) without a correlative increase in prostaglandin E2 (PGE2) or 6-ketoPGF1α (the stable metabolite of prostacyclin [PGI2]) (Fig. 94.3). Attempts at reversal of the cellular rejection by using cyclophosphamide resulted in improvements in the clearance of inulin as well as in a reduction in the urinary levels of TXB2. Additionally, the use of a thromboxane synthetase inhibitor resulted in an improvement in GFR and renal blood flow during acute cellular rejection episodes when administered before an immune assault on the organ.[45] The fact that a thromboxane synthetase inhibitor did not completely ameliorate the detrimental effects of the acute cellular rejection suggests that other factors also may be at play during rejection. In another study by Munger et al.[146] kidneys were transplanted from Munich Wistar (MW) rats to syngeneic controls and MHC-incompatible recipients to evaluate the effects of surgery and acute rejection on glomerular hemodynamics by clearance and micropuncture techniques. A significant decrease in both single-nephron GFR and glomerular capillary pressure was found in animals with acute rejection. Micropuncture studies showed that the principal derangement in renal microvascular function during acute rejection is intense preglomerular vasoconstriction. Interestingly, the glomerular histology was normal, suggesting that locally acting vasoconstrictor influences such as TXA2 and leukotrienes were most likely responsible for the depressed renal function.

A recent study by Velic et al.[214] examined the effect of transplant rejection on the functional activity and regulation of transporters involved in sodium reabsorption in the proximal tubule using a rat allograft model of acute rejection without immunosuppression.

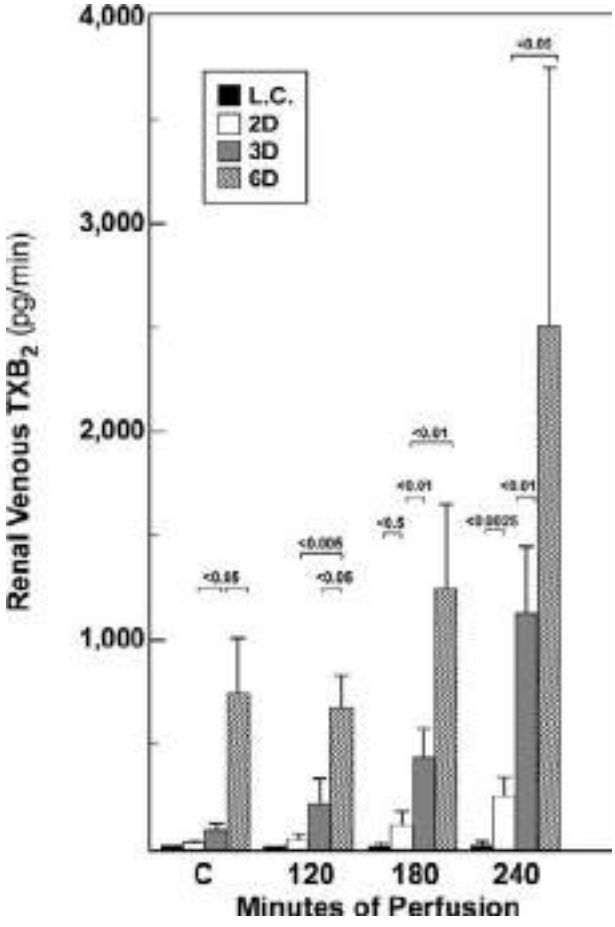

FIGURE 94.3 Renal venous thromboxane B2 (TXB2) production by ex vivo perfused Lewis control kidneys (L.C.) and 2-d (2D), 3-d (3D), and 6-d (6D) allografts. The control period (C) represents renal TXB2 production determined for all groups before bradykinin stimulation. Renal TXB2 production by all groups also is indicated after 120, 180, and 240 minutes of bradykinin stimulation (1 μg given as a bolus every 30 minutes). Bars represent mean plus standard error of the mean (SEM). Statistically significant differences between groups are indicated by brackets with the corresponding p value. *(From Coffman TM, Yarger WE, Klotman PE. Functional role of thromboxane production by acutely rejecting renal allografts in rats. J Clin Invest 1985;75:1242–1248.)*

In those kidneys with histologic evidence of acute rejection, downregulation of mRNA and protein levels for Na + /H + exchanger type-3 (NHE-3) were noted, independent of ischemia.

In follow-up, the same group extended their experiments to the distal nephron to further characterize the role of rejection on expression and function of transporters and receptors.[215] In the cortical collecting duct, mRNA expression and function of the epithelial Na^+-channel (ENaC) and mRNA and protein expression of the water-channel AQP2 were downregulated. To differentiate between possible effects of acute rejection and those directly related with the transplant process

such as denervation or ischemia/reperfusion, syngeneic transplantations were performed. Whole kidney mRNA and protein expression of ENaC and AQP2 remain unchanged. Addition of cyclosporine abolished the downregulation of both channels, again supporting the notion that these changes are the result of acute rejection. Both studies show that in models of acute rejection, transporters important in Na^+ reabsorption and consecutively solute and volume reabsorption may lead to a significant decrease in energy consumption and represent a period of adaptation by the kidney to support recovery of the stressed organ and protect it from further non-immunologic and immunologic damages.

These studies taken together suggest that changes in expression of proteins involved in tubular transport may be subjected to rejection-associated mechanisms. This is a fertile area for future research and may provide therapeutic targets for the accelerated recovery of acute rejection of the allograft, and therefore, the prognosis of the renal transplant.

In summary, true rejection is a state of low GFR, intrarenal vasoconstriction, and sodium avidity related to the immune activity within the graft that often persists beyond the abrogation of the cellular infiltration or humoral assault on the tissue. This may reflect the consequences of inflammatory mediators released by various infiltrating cells and adaptive tubular regulation of solute transport. This is a fertile area for future research and may provide therapeutic targets for the accelerated recovery of acute rejection of the allograft, and therefore, the prognosis of the renal transplant.

RENAL TUBULAR ACIDOSIS ASSOCIATED WITH ISCHEMIA AND REJECTION

Renal tubular acidosis (RTA) is the most commonly encountered group of tubular abnormalities found after successful renal transplantation and may cause profound changes in acid base balance.[20,107] One can describe various types of renal tubular acidosis including proximal RTA, Fanconi syndrome, distal RTA and Type IV RTA with hyporeninemic hyperaldosteronism, some of which may overlap and vary as a function of time during the lifespan of the allograft. For example, proximal RTA and Fanconi syndrome have been noted to occur early in the post-transplant period and resolve spontaneously suggesting that this may be in part attributable to acute ischemic renal failure related to the harvest procedure. Other types of renal tubular acidosis, particularly distal RTA may appear months to years after the transplant and are due to chronic rejection or drug-induced nephrotoxicity, including calcineurin inhibitors. Secondary hyperparathyroidism, obstructive uropathy and urinary tract infections may also contribute to the pathogenesis of RTA. Chronic RTA following transplantation is important as it may interfere with bone metabolism and at times lead to nephrocalcinosis and nephrolithiasis.

The presence of hyperchloremic, nonanion gap acidosis in the transplant patient was first described by Massry et al. in 1967.[130] In their case, hyperchloremic acidosis appeared on day 33 after successful transplantation when GFR was improving and the serum potassium was 3.3 mEq/liter, chloride was 1215 mEq/liter, and plasma bicarbonate was 15 mEq/liter. Additionally, this patient had glycosuria, aminoaciduria, and hyperphosphaturia along with the metabolic acidosis, suggesting a complete Fanconi syndrome due to proximal tubular dysfunction. The clinical picture was best defined as a dual effect located in the distal and the proximal tubule, in part because of the failure to acidify the urine, even with administration of exogenous acid coupled to the Fanconi syndrome. Better[24] additionally showed that when excess buffer base was provided to the distal nephron, this patient was unable to generate a steep hydrogen ion gradient, indicating that there was a distal tubular defect in transporting hydrogen ions either into the lumen from the tubular cell or from the blood into the lumen. In the report of Rubini et al. from 1967,[182] an early post-transplant tubular dysfunction similar to the Fanconi syndrome with spontaneous resolution was observed. Rubini et al.[182] also suggested that distal tubular dysfunction was found along with the Fanconi syndrome, arguing that the form of RTA observed in the early post-transplant period is a mixed disorder of proximal and distal tubular dysfunction perhaps the result of ischemic injury encountered during the harvest and engraftment procedure.

The impact of high circulating levels of parathyroid hormone (PTH) of the recipient on proximal tubular acidification may contribute to the early post-transplant RTA as shown by studies of Arruda et al.[9] in dogs in which PTH was infused acutely. Animals receiving a human PTH infusion of 1 U/min or a bolus of 100 U followed by a continuous infusion of 5 U/min exhibited an increase in bicarbonate excretion and an increase in urinary pH. The increase in urine pH was associated with an increase in total titratable acid due to an increase in proximal tubular rejection of phosphate. The next acid excretion remained unchanged during the bicarbonaturia due to a decrease in ammonia excretion. The urine−blood (U-B) PCO2 ratio remained stable during the study period, suggesting the distal tubular ability to secrete H^+ was not altered by the PTH infusion.

Purer forms of distal tubular acidosis are the types of acid–base disorders most likely to persist after transplant and can become a clinical problem requiring intervention. In a study by Better et al.[24] six patients not receiving cyclosporine were shown to have urinary acidification defects after successful cadaveric transplant. All these patients showed an inability to create a steep gradient for hydrogen ion exchange in the distal tubule. Follow-up studies done over the next 15 months showed that each patient was able to acidify the urine and excrete titratable acid, in spite of the development of chronic transplant rejection in two patients. Indeed, Better et al.[24] concluded that neither rejection nor the immunosuppressive medications used at the time of their study played an important role in the urinary acidification defect that they were observing in transplant recipients. They argued that the defect observed was truly the result of ischemic injury attendant on the transplantation event and organ retrieval, which slowly resolves over time.

The natural history of RTA after renal transplantation has been best described in studies by Wilson and Siddiqui[230] in 32 patients prospectively studied for one to three years with repetitive urinary acidification testing. The authors argued that there are two clinical pictures of RTA after renal transplantation. Fourteen of the 32 patients initially had a distal RTA with an inability to reduce the urine pH below 5.3 in the face of systemic acidosis. Ten other patients initially had a systemic, hyperchloremic acidosis with depressed serum bicarbonate levels but with a normal ability to acidify the urine in the face of the acidosis. In this latter group, two patients had clearly demonstrable proximal tubular bicarbonate wasting. The presumed proximal bicarbonate wastage and the hyperchloremic acidosis disappeared or improved with time in seven of the ten patients. Partial distal defects of hydrogen ion transport with a persistent acidification defect remained in nine of the 14 patients with distal lesions. They concluded that initially after surgery, a wide variety of tubular transport defects may be found from pure forms of proximal RTA, sometimes with a complete Fanconi syndrome, to distal RTA, although a mixed defect was most commonly encountered. With a resumption of normal organ function, there is a fairly rapid recovery of the proximal tubular acidification capacity. In most patients, a distal acidification defect remains for a greater length of time with ultimate resolution in most. Those with persistent distal lesions become a management problem with respect to potassium homeostasis and healing of the metabolic bone disease of renal failure, which requires the careful attention of the astute clinician.

A second group of patients will develop new defects in renal tubular acidification because of the immunologic complications of rejection. Wilson and Siddiqui[230] also described the new appearance of a distal tubular acidification defect in patients who had no previous abnormalities of acid–base tubular homeostasis, which they suspected was due to superimposed renal rejection. Batlle et al.[18] directly studied the role of chronic rejection on hyperchloremic metabolic acidosis. In five of six carefully studied patients with chronic rejection, urine pH could not be acidified below 5.5, and the U-B PCO2 difference was not increased after a sodium sulfate buffer base infusion. A tubular defect of distal hydrogen ion secretion was found to account for this inability to acidify the urine. These investigators emphasized the development of interstitial infiltrates by round cells characteristic of chronic rejection in five of these six patients, who ultimately lost renal function. A similar pathologic picture, with the infiltration of round cells into the parenchyma associated with the development of RTA, is seen in other states of immune activation and renal infiltration by immune cells such as in Sjögren syndrome. The distal RTA of Sjögren syndrome may result from an absence of the H^+-ATPase pump, a key enzyme in distal urinary acidification by the intercalated cells of collecting ducts,[16,46] and it has been hypothesized that this deficiency may also account for the RTA of kidney transplant rejection. Jordan et al.[102] studied six kidney transplant patients with biopsy proven rejection and two control patients physiologically and by immunohistochemistry. Impaired ammonium excretion as well as impaired proton secretion with reduction in urinary PCO_2 was noted in those patients with rejection. In none of the patients was there a total absence of intercalated cell H^+-ATPase staining as seen in Sjögren syndrome, but there was an inverse relationship between the abundance of H^+-ATPase staining and degree of scarring. A direct relationship was noted in the abundance of H^+-ATPase-stained intercalated cells and 100/plasma creatinine. It may be that the tubulitis of rejection not only affects H^+-ATPase-mediated acidification by individual intercalated cells but also, via disruption of tubular anatomy, reduces the transepithelial voltage leading to defective ammonium excretion and a distal RTA. The development of secondary distal RTA may be an early sign of the immunologic process that leads to rejection.

In summary, renal tubular acidoses that affect all portions of the nephron can be observed after successful renal transplantation. Proximal tubular defects including the complete Fanconi syndrome are found most often in the perioperative period. The proximal tubular abnormality resolves as the transplant function improves. Distal tubular defects of acidification are encountered both early and late after successful renal transplantation and are the most common lesions encountered. These lesions can persist throughout the

functional life of the kidney, although they usually recede at a slower rate than the early proximal RTA. These defects have been described in patients before the introduction of calcineurin inhibitors to the immunosuppressive protocol. The nature of RTA in the transplant patient will be revisited in our discussion of the impact of immunosuppressive medications on renal function. Ischemic injury related to organ retrieval and placement has been described as the cause for the abnormalities seen early after transplantation. A second, spontaneously appearing distal RTA is seen in patients whose graft is undergoing rejection. The development of distal RTA may be an early sign that a transplant is having an immunologic insult.

SYNDROMES OF POTASSIUM HANDLING

After successful renal transplantation, potassium transport was generally normal in the precyclosporine era.[117] Postoperatively, if one did encounter a problem with potassium homeostasis, hypokalemia was frequently observed.[24,130] The most common cause for this hypokalemia is polyuria and inadequate replacement during the diuretic phase, as was discussed earlier in this chapter.[128,199] A large osmotic diuresis drives potassium into the urine and limits the tubular capacity to modulate potassium. In addition, a distal RTA and the use of relatively high doses of steroids early in the postsurgical period may contribute to the hypokalemia. These circumstances aside, persistent hypokalemia has been found to be uncommon after the immediate postoperative period.

Hyperkalemia also has been described after renal transplantation in the absence of impaired filtration, significant acidosis, potassium supplementation, or calcineurin inhibitor use. DeFronzo et al.[53] observed clinical hyperkalemia in 23 of 75 patients in the first three months following successful transplantation. Four patients of this group were studied in detail to ascertain the mechanism for their hyperkalemia. As would be expected after a successful renal transplant, these patients responded appropriately to volume and sodium challenges with respect to the renin-angiotensin-aldosterone axis. Increased distal delivery of solute achieved by a loop diuretic, by a carbonic anhydrase inhibitor, or by bicarbonate infusion did not enhance potassium excretion, suggesting that a distal sodium-potassium exchanger was defective. Therapeutic challenge with 9-fluorohydrocortisone also failed to reduce serum potassium. The failure to enhance potassium excretion by increasing the solute delivery and the impaired mineralocorticoid response pointed to impaired distal tubular potassium transport as the etiology for the observed hyperkalemia. Thiazide diuretics were able to diminish the serum potassium level and enhance potassium excretion, suggesting that this defect was not structural. Indeed, studies of these patients showed that hyperkalemia disappeared with time, further suggesting that the distal tubular defects of potassium transport may resolve as transplant function improves.

The presence of the syndrome of pseudohypoaldosteronism originally described by DeFronzo et al.[53] remains controversial, with confirmation by some and rejection by others.[96] The quoted rate of occurrence of 30% has been most vigorously challenged. In one supporting study of a 56-year-old woman with hyperkalemia, Uribarri et al.[210] found diminished kaliuresis and a marked kaliuretic response to 9-fluorohydrocortisone after successful renal transplantation. Other clinicians pointed to hypoaldosteronism in patients related to adrenal failure and renal transplantation.[178] In two such patients, low plasma renin and aldosterone levels in the salt-restricted, volume-contracted, upright posture were absent. When challenged with 9-fluorohydrocortisone, these patients had a normal kaliuretic response. Several other reports of transient hypoaldosteronism supported this initial observation by Perez and Oster[162] and Rosenbaum et al.[179] These studies suggested that after transplantation, impaired secretion of potassium from the distal tubule may appear to be due either to direct tubular dysfunction or to mineralocorticoid deficiency. This pseudohypoaldosteronism is observed early in the post-transplant period and resolves spontaneously. The functional defect can be corrected with thiazide diuretics. The hyperkalemia of true hypoaldosteronism also can appear after transplantation and responds to replacement therapy.

It is important to emphasize that although potassium-handling defects were interesting before the use of calcineurin inhibitors, their clinical significance was trivial. With the introduction of cyclosporine and tacrolimus into the immunosuppressive armamentarium, the problem of hyperkalemia has become more prominent. A complete discussion of the effect of calcineurin-inhibitor immunosuppressants on tubular handling of potassium is the subject of a later section of this chapter.

MINERAL METABOLISM STATES AFTER TRANSPLANT

Renal transplant handling of elements related to mineral metabolism is perhaps the most complex of the matters discussed in this chapter. The alterations in hormonal status and in the synthesis of regulators of these elements provided by the azotemic milieu coupled to the circumstances that surround surgery and

early patient management added to the intrinsic transplant properties contribute to several different distinct syndromes found in a temporal sequence (Table 94.1). Patients may be hypercalcemic, eucalcemic, or hypocalcemic. They may be hypophosphatemic and/or hypomagnesemic. Parathyroid gland function may be normal or exhibit persistent secondary hyperparathyroidism or rarely autonomous function (tertiary hyperparathyroidism). Renal hydroxylation of vitamin D may be subnormal early or normal late. The tubule may intrinsically leak phosphate, calcium or magnesium. This section attempts to isolate these factors and provide a context for understanding the impact of renal transplantation on renal metabolic bone disease.

Almost all allograft recipients have some degree of secondary hyperparathyroidism, which may be unmasked, when the transplant is placed. Serum PTH concentrations decrease progressively during the first three to six months after grafting;[103] however, 1 year after transplantation, resolution of hyperparathyroidism is incomplete in 50% of recipients.[125] Pretransplant factors associated with persistent secondary hyperparathyroidism after kidney transplantation include duration of dialysis, parathyroid gland size, and the development of nodular hyperplasia of parathyroid glands.[110] Due to the long lifespan of parathyroid cells of approximately 20 years and the cell renewal rate of approximately 5% per year, the process of involution of the parathyroid glands may take from a few months to several years. Incomplete normalization of renal function, suboptimal levels of calcitriol and decreased intestinal calcium absorption secondary to corticosteroid therapy also may contribute to the high PTH concentrations after transplant.[207] In great measure, the impact of persistent hyperfunction of the gland characterizes renal handling of ions important for mineral metabolism in transplant recipients.

TABLE 94.1 Mineral Metabolic States After Transplant

Hypercalemia
Persistent secondary hyperparathyroidism
Tertiary hyperparathyroidism
Tubular phosphate leak
Calcium-containing antacids
Low or normal calcemia
Early
High-dose steroids
1,25-dihydroxy vitamin D
Late
Normal renal function
Tubular calcium leak
Hypophosphatemia
Early
Persistent secondary hyperparathyroidism
High-dose steroids
Antacids
Late
Persistent secondary hyperparathyroidism
Tubular phosphate leak
Hypomagnesemia
Early
High-dose steroids
Diuretics
Late
Cyclosporine A

During the initial period of graft function, hypercalcemia is commonly observed due to the effect of hyperparathyroidism.[137] High PTH concentrations stimulate the renal production of calcitriol leading to increased intestinal calcium absorption and improved skeletal mobilization of calcium. Additional factors contributing to the resolution of the skeletal resistance to PTH include correction of uremia and normalization of serum phosphorus levels, thus facilitating the release of calcium due to osteoclastic bone resorption. Finally, resorption of soft tissue calcifications can contribute to the post-transplant hypercalcemia.

Transient hypercalcemia post-transplant is common, and spontaneous resolution occurs in most cases within one year after grafting. In approximately 5–10% of recipients, hypercalcemia persists beyond the first year but resolves gradually within two to five additional years.[129] Such persistent mild hypercalcemia is usually well tolerated and not associated with untoward effects on the allograft. If severe hypercalcemia (>12 mg/dl) is encountered post-transplant, complications including renal dysfunction, nephrocalcinosis, pancreatitis and vascular calcifications become significant risks and may require elective parathyroidectomy.

During the initial period of graft function, hypercalcemia is commonly observed due to the effect of hyperparathyroidism.[137] Despite elevated PTH levels, the gland retains its capacity to respond to short-term administration of calcium by downregulation of PTH formation and release.[134] The higher levels of ionized calcium required to suppress PTH secretion show that the parathyroid gland has an altered "calcium stat" (Fig. 94.4). In spite of successful renal transplantation, the parathyroid gland continued to require a higher threshold of ionized calcium to suppress function

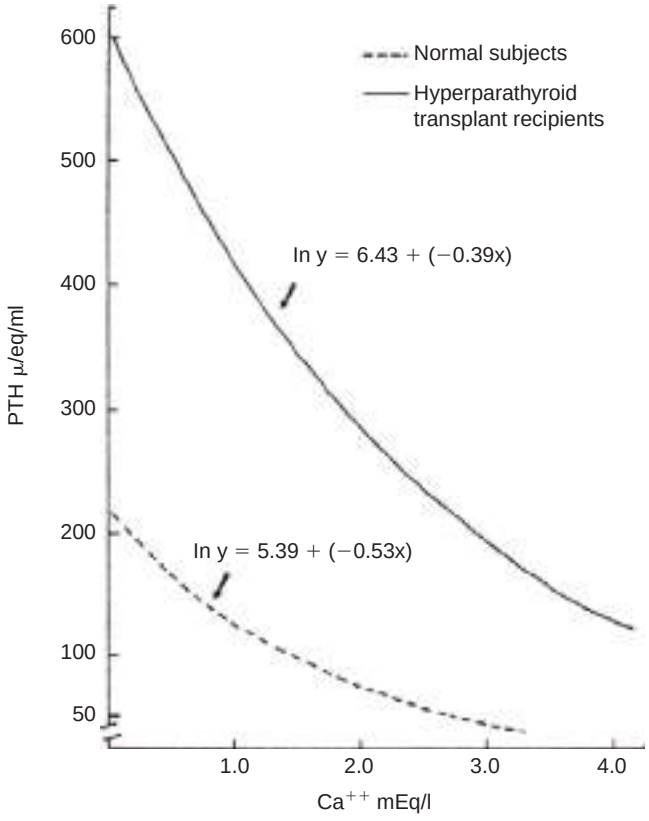

FIGURE 94.4 Parathyroid gland responsive to calcium infusion in renal transplant recipient compared with normal. *(With permission from American Society for Clinical Nutrition, McCarron DA, Bennett WM, Muther RS, Barry JM, Krutzik S. Post transplantation hyperparathyroidism: demonstration of retained control of parathyroid function by ionized calcium. Am J Clin Nutr 1980;33:1536–1540.)*

completely.[134] In this circumstance, the higher serum calcium sometimes found in these patients is a consequence of an appropriate response to the fixedly elevated PTH concentration and reset threshold. Other potential causes for hypercalcemia include calcium-containing antacids used to prevent the ulcerogenic potential of high-dose steroids used during the early post-transplant period.[184] Additionally, if serum calcium levels are unable to reach the new set-point for gland suppression parathyroid hyperfunction will continue.[135] There is also the potential for the loss of suppressive ability that calcium has on parathyroid gland function. This conversion from what is called "secondary" to what has been labeled "tertiary" hyperparathyroidism can occur before the transplant surgery or thereafter, but is a rare event. If allowed to continue without surgical reduction in gland mass, tertiary hyperparathyroidism can cause persistent hypercalcemia and hypophosphatemia at a cost primarily to bone mineralization.[135]

Normal or even low levels of serum calcium after successful transplantation in the face of elevated PTH have also been encountered. Confounding variables that characterize the early post-transplant period, which can impair gut absorption of calcium, include high doses of steroids used to prevent rejection[88] and inadequate hydroxylation of vitamin D by the transplant.[184] That the "normal" or low levels of calcium often persist in the setting of persistent elevation of PTH levels, even when gut absorption of calcium returns toward normal as prednisone is reduced and the graft hydroxylation of vitamin D normalizes, suggests the presence of additional alterations in calcium metabolism. By using isotopic calcium excretion studies, Sakhaee et al.[184] were able to show that a primary tubular calcium leak occurred in such patients in spite of normal or even elevated PTH levels, normal 1,25-dihydroxy vitamin D levels, and normal intestinal absorption of calcium. This primary calcium leak provides a persistent stimulus for PTH generation, explaining the measured abnormalities, in part, years after successful transplantation in some patients.

Of all the reported electrolyte abnormalities that follow renal transplantation, hypophosphatemia is the most commonly encountered,[82,93,127,222] occurring in up to 93% of patients during the first few months after transplantation.[67] Although this phenomenon is usually limited to the early post-transplant period, hypophosphatemia may persist for more than 10 years.[69] Traditionally, several pathogenic factors have been implicated in the development of post-transplant hypophosphatemia including persistent hyperparathyroidism, relative deficiency of calcitriol, use of glococorticoids. Pabico and McKenna[158] reconfirmed the findings of McCarron et al.[134,135] with respect to responsiveness of the parathyroid glands to calcium infusions and extended those findings to examine tubular handling of phosphate. Despite an elevated parathyroid hormone level in the six study patients, an infusion of 15 mg/kg of ionized calcium over 3 hours raised serum calcium into the normal range, lowered serum PTH toward normal levels, and diminished urinary cyclic AMP appropriately. Serum phosphorus rose commensurate with an increase in tubular reabsorption of phosphorous (TRP) reflecting the relationship between TRP and PTH levels. Parfitt et al.[161] confirmed the possibility that a primary leak of phosphorus existed in their study of a group of transplant patients with normal serum calcium, slightly elevated parathyroid hormone level, and normal urinary cyclic AMP, but high tubular rejection rates of phosphorus as a function of glomerular filtration rate. These two studies make several points in general and about phosphorus as a function of glomerular filtration rate. These two studies make several points in general and about

phosphate handling in particular. Transplant impact on mineral metabolism is complex. In most, there is persistent hyperparathyroidism even after successful renal transplantation, whichh is responsive to calcium infusion albeit with a higher calcium stat or setpoint. Second, phosphorous handling by the tubule in some reflects PTH levels and in others reflects a primary tubular leak as clearly shown by Graf et al.[82]

These effects may be compounded by the use of immunosuppressive, antacid and diuretic drugs. Micropuncture studies performed on Sprague-Dawley rats by Frick et al.[72] suggest that glucocorticoids may cause an increased tubular rejection of phosphorus in the proximal tublule. Rats receiving a diet stable in calcium and phosphorus infused with a modified Ringer's lactate solution, which contained an increased dose of inorganic phosphorus, while receiving 0.03 mg/kg/min of hydrocortisone 90 minutes before micropuncture reabsorbed only 29% of the filtered phosphorus load in the proximal convoluted tubule, as opposed to 41% proximal tubule reabsorption in a control group. Another confounding variable in the equation of post-transplant hypophosphatemia is the frequent, often indiscriminate use of antacids. These agents bind phosphate in the gut lumen and prevent absorption.[184] The decreased intestinal absorption magnifies the hypophosphatemia owing to the PTH effect at the tubule and to the intrinsic tubular phosphorus leak. It has become clear in the face of recent data, that none of these factors can explain hypophosphatemia in its entirety. Recently, a new family of phosphorus-regulating hormones termed "phosphatonins" have been described that may play an important role in the pathophysiology of phosphorus wasting in the post-transplant period.

Although elevated PTH levels are noted in the majority of patients after kidney transplantation, a growing body of evidence suggests that it is not the primary cause of defective renal phosphorus reabsoprtion. In one study, identical serium PTH levels were observed in post-transplant recipients with normal and low serum phosphorus concentrations.[180] In addition, suppression of PTH levels with intravenous calcium infusion failed to normalize serum phosphorus concentration and fractional excretion of phosphorus in those sujbects with hypophosphatemia. Further support suggesting a non-PTH humoral mechanism in the development of hypophosphatemia came from an in-vitro study using opossum kidney cells incubated with sera from end-stage renal disease, chronic kidney disease and recipents both "early" (two weeks to one month) and "late" (9 to 12 months) post-kidney transplant.[83] Sodium-dependent phosphorus transport was measured by radioactive phosphorus flux. There was significant inhibition of Na^+-dependent phosphorus transport in those with ESRD, CKD and early post-transplant which persisted following the addition of a bovine PTH inhibitor. It was hypothesized that a humorally mediated adaptation mechanism maintains phosphorus homeostasis in renal failure by inhibiting phosphorus transport and sodium/phosphorus activity along the proximal tubule. Persistence of this putative circulating factor for some time following successful transplantation could therefore lead to hypophosphatemia accompanied by increased phosphaturia. Exciting work by several groups[13,67] have suggested that fibroblast growth factor-23 (FGF-23) may be one such factor.

FGF-23 induces phosphaturia and inhibits renal 1-α hydroxylase leading to decreased calcitriol synthesis.[189] Recent studies have shown that FGF-23 levels increase as CKD progresses and contribute to the declining calcitriol levels observed.[86,121] In a prospective longitudinal study of 27 patients undergoing living donor kidney transplantation, 85% developed hypophosphatemia, including one who had previously undergone parathyroidectomy.[13] Although FGF-23 levels decreased after transplantation, the levels remained significantly above mean levels reported in healthy individuals. FGF-23 was independently associated with serum phosphate, urinary excretion of phosphate and calcitriol levels. PTH was not independently associated with any of these parameters. This data has been corroborated by others[67,66] and the term "tertiary hyperphosphatonsim" coined. In longitudinal follow-up of renal transplant recipients, FGF-23 declined over time with regression of renal phosphorus wasting.[66] Taken together, it is reasonable to conclude that high FGF-23 levels that developed as a compensatory mechanism with worsening kidney function, persist post-transplant and contribute to the hypophosphatemia and phosphaturia noted in the early-transplant period. Other phosphatoninins have recently been described including secreted frizzled related protein-4 (sFRP-4), matrix extracellular phosphoglycoprotein (MEPE) and FGF-7.[22,181] Their physiologic role in kidney transplant recipients remains to be determined.

Hypophosphatemia may be compounded by the use of immunosuppressive, antacid and diuretic drugs. Micropuncture studies performed on Sprague-Dawley rats by Frick et al.[72] suggest that glucocorticoids may cause an increased tubular rejection of phosphorus in the proximal tubule. Rats receiving a diet stable in calcium and phosphorus infused with a modified Ringer's lactate solution, which contained an increased dose of inorganic phosphorus, while receiving 0.03 mg/kg/min of hydrocortisone 90 minutes before micropuncture reabsorbed only 29% of the filtered phosphorus load in the proximal convoluted tubule, as opposed to 41% proximal tubule reabsorption in a

control group. Another confounding variable in the equation of post-transplant hypophosphatemia is the frequent, often indiscriminate use of antacids. These agents bind phosphate in the gut lumen and prevent absorption.[184] The decreased intestinal absorption magnifies the hypophosphatemia owing to the PTH effect at the tubule and to the intrinsic tubular phosphorus leak.

Clinically, patients may present with muscle weakness and osteomalacia when the plasma phosphate concentration is below 1.4 mg/dl. Although severe phosphate depletion with phosphate concentrations below 0.9 mg/dl is rare, it may lead to hemolytic anemia, rhabdomyolysis, decreased myocardial contractility, and respiratory failure. Oral phosphate supplements are capable of normalizing the serum phosphate concentrations after transplantation. Furthermore, the administration of neutral phosphate increases net acid excretion and may lead to a more rapid recovery of the latent metabolic acidosis observed during the early post-transplant period.

Both hypercalcemia and hypophosphatemia are metabolic conditions that may have profound effects on urinary acidification and systemic acid–base status. Studies in animals and humans show that acute infusion of synthetic PTH results in increased proximal tubular bicarbonate wasting and decreased net acid excretion.[9] In a study of artificially induced hyperparathyroidism in normal humans, which is analogous to placing a healthy allograft in a patient with hyperparathyroidism, Hulter and Peterson[98] showed that normal healthy male patients who were fed a stable diet and infused with synthetic PTH at a dose of 6800 U/mg for a period of 12–13 days exhibited a transient, early, mild hyperchloremic metabolic acidosis due to inhibition of proximal tubule bicarbonate regeneration and to a decrease in net titratable acid excretion. When a new steady state was achieved in which net acid returned to normal and plasma bicarbonate levels were elevated, the acidosis was terminated, and subjects were left in a mild metabolic alkalosis. These results oppose the clinical observation that hyperparathyroidism is associated with persistent metabolic acidosis. Although high serum levels of PTH can transiently produce metabolic acidosis because of bicarbonate rejection and a decrease in net acid excretion, the renal or extrarenal mechanism that propagates this metabolic acidosis related to persistently elevated PTH remains uncertain.

Alterations in magnesium homeostasis after transplantation can also be directly related to hyperfunction of the parathyroid gland.[187] This having been said, multiplicities of factors that make up the transplant experience alter the direct relation between excess PTH and magnesium level. Variations in serum levels of magnesium are importantly related to magnesium intake. The protein and caloric malnutrition frequently encountered before and after transplantation is a contributor to magnesium homeostasis.[221] During the early post-transplant period, steroid therapy[130] and diuresis[130] contribute to the hypomagnesaemia. Additionally, hypercalcemia can reduce tubular reabsorption of magnesium, leading to magnesium wasting.[130] Although hypomagnesemia is commonly seen after transplant, it has rarely been of clinical consequence until the use of calcineurin inhibitors. The effects of the calcineurin inhibitors on the handling of magnesium will be discussed later in the chapter.

In summary, the disorders of divalent ion metabolism after transplantation are a function of three factors. The first factor relates to the background into which a working renal transplant is placed, with nutritional status and even more important, persistence of secondary hyperparathyroidism. The second factor is that drugs used after transplant affect the modulation of divalent ions. Finally, the third factor is that intrinsic abnormalities of tubular handling of calcium and phosphorus by recently identified phosphatonins can impair the maintenance of normal mineral metabolite levels and worsen any single abnormality. Taken together, all can synergistically contribute to the development of osteodystrophy and increased cumulative incidence of fractures post-kidney transplant.

HANDLING OF URATE AFTER TRANSPLANT

Hyperuricemia is a common complication of renal transplant with gout affecting approximately 2–13% of patients.[43] Several factors may contribute to the high prevalence of hyperuricemia and gout. Renal allograft recipients are prone to hypertension and edema, and diuretics are frequently used in their management. Both loop and thiazide diuretics reduce uric acid excretion, presumably by causing mild volume depletion with consequent enhancement of proximal tubular reabsorption. Also, loop agents may compete with uric acid for secretion by the proximal organic acid transporter. Delayed graft function or the development of chronic allograft nephropathy may contribute to the impaired excretion of uric acid. However, a correlation between serum creatinine or creatinine clearance and serum urate levels has not always been found.[81,226] When uric acid handling was examined in patients with functioning kidney transplants in the period before widespread use of calcineurin inhibitors, no consistent abnormalities in fractional reabsorption or excretion of uric acid emerged arguing against any specific impairment in uric acid excretion inherent to the

transplant itself.[24] It is clear that the greatest risk of hyperuricemia and gout can be attributed to the use of calcineurin inhibitors. The mechanisms by which cyclosporine and tacrolimus contribute to the altered handling of uric acid by the transplanted kidney will be discussed in subsequent sections.

RENAL TRANSPORT AND IMMUNOSUPPRESSIVE DRUGS

Successful allograft transplantation requires acceptance of the grafted tissue by the immune system of the host. For nearly all patients, some form of immunosuppressive medicine to maintain graft survival is required. Although an array of physiologic derangements can be a consequence of immunosuppressive therapy, most patients with successful transplants exhibit essentially normal renal functional characteristics. Studies by Lewis et al.[123] and Blaufox et al.[29] in recipients of live-related transplants after bilateral nephrectomy revealed normal exchangeable sodium and potassium in spite of immunosuppressive therapy with prednisone and azathioprine. Balance studies on both high (200 mEq/day) and low (10 mEq/day) sodium diets showed balance was achieved in all patients within four days. Almost all studies that have examined the renin-angiotensin-aldosterone system in nonhypertensive renal transplant recipients with stable graft function have found that the conventional immunosuppressive protocol of prednisone and azathioprine do not affect the kidney's ability to modulate plasma renin activity when GFR is maintained.[28,84,105,112,113,196]

Having just delineated the general failure to relate tubular transport abnormalities to drug regimens in the past, one must yet uncover those instances of pathophysiology that flow directly from drug therapy. Glucocorticoids have been the backbone of the various regimens used to prevent rejection of the allograft and frequently are employed to reverse the process once underway. Since most patients are maintained on glucocorticoids in the initial post-transplant period, the impact of these agents on renal function is important. No direct studies have been undertaken to define the effects of glucocorticoids on renal allograft transplant function. One must posit a set of drug related changes based indirectly on studies in normal subjects. Studies by Connell et al.[47] of renal function in such normal humans who receive cortisol at a dose of 50 mg every 6 hours over five days showed an increase in GFR to 113% based on insulin clearance. This increase was not found when creatinine clearance was measured.[47] They proposed that the increase in creatinine turnover due to cortisol limited the usefulness of creatinine as a measure of GFR.[47] The exact cause for this increase in GFR induced by glucocorticoids is unknown, but micropuncture studies in rats show that both pre- and postglomerular arterioles are vasodilated, suggesting that the exuberant GFR is a consequence of increased glomerular flow.[19] The cortical collecting tubule responds to the mineralocorticoid activity of the high-dose prednisone, the form of steroid almost exclusively employed in transplantation, by reabsorbing sodium in exchange for potassium and hydrogen ions.[107] The nephron escapes from the sodium retention by decreasing sodium reabsorption in segments other than the cortical collecting tubule.[103] The escape is characterized by increased renal arterial pressure transmitted to the microcirculation, which contributes to decreased sodium reabsorption, by the proximal tubule.[87] The relationship of steroids to calcium absorption in the gut, phosphorus wasting in the kidney, and potassium handling has been previously discussed.

Antibodies directed to lymphoid elements are directly used to induce graft acceptance along with glucocorticoids during initiation of immunosuppression therapy and to reverse episodes of rejection. Polyclonal preparations have no known direct effect on tubular function. On the other hand, initial doses of the monoclonal preparation OKT3 result in a wave of IL-2 and TNF release, which alters intra renal blood flow and can produce systemic hypotension and a pre-renal state that can result in a fall in GFR and fall in fractional excretion of sodium if severe enough.[1,164] One can observe in treated patients an actual increase in serum creatinine, an increase in filtration fraction, and pathologic synergy with other nephrotoxins. The powerful capacity of the drug to reverse acute rejection has generated a search to block the physiologic derangements rather than abandon the use of this agent. Early studies with blockade of TNF have shown great promise.[70]

The introduction of the potent calcineurin inhibitor agents such as Cyclosporine A and tacrolimus have so greatly improved graft survival as to make their use almost ubiquitous for maintenance of renal as well as extrarenal organ transplants. These agents have profound effects on renal physiology, coloring greatly the function of the kidney already altered by circumstances of engraftment. The effects of the calcineurin inhibitors on the kidney are observed when the kidney is the engrafted organ, but functional alterations in renal function are described in patients receiving these agents for extrarenal organ transplantation as well.[160] A complete discussion of the renal effects of the calcineurin inhibitors then is essential to any full discussion of the impact of immunosuppressive drug therapy on transplant physiologic function.

Cyclosporine A is a profound regulator of renal blood flow and of glomerular filtration rate.[50] Cyclosporine A universally reduces the glomerular filtration rate in all patients receiving the drug whether for transplantation or for disorders in which the immune system is thought to play a role.[55,63,188] Using glomerular micropuncture, Barros et al.[15] have demonstrated that acute intravenous administration of cyclosporine A at a dose of 50 mg/kg in the Munich-Wistar rat causes intense efferent arteriolar vasoconstriction. Additionally, there is an increase in afferent arteriolar resistance, which results in an increase in mean glomerular capillary hydrostatic pressure. These findings coupled to a fall in glomerular ultra-filtration coefficient culminate in a fall in both single nephron and total glomerular filtration rates. Although effective renal blood flow decreases, Barros et al.[15] found that the filtration fraction increases or does not seem to be altered suggesting to those investigators that the major site of action of cyclosporine is at the efferent arteriole.

Some have dismissed the findings of Barros et al.[15] because of the high dose (50 mg/kg) of cyclosporine A used. But the rat is resistant to cyclosporine and doses of this magnitude are required for immunosuppression. Unfortunately, these doses lead to whole animal dysfunction, characterized by anorexia, weight loss, and volume depletion, which color the interpretation of many rat studies.[204] Micropuncture studies performed by Thomson et al.[206] used pair-fed controls and plasma volume expansion to minimize these effects of cyclosporine A. In male Munich-Wistar rats receiving cyclosporine A at a dose of 30 mg/kg for 8 days prior to study, Thomson et al.[206] were still able to demonstrate an important decrease in single-nephron GFR and in glomerular capillary hydrostatic pressure gradient without a substantial change in glomerular ultrafiltration coefficient (LpA). The partitioning of resistance between afferent (AR) and efferent (ER) arterioles in the cyclosporine A–treated rats showed a higher AR-ER ratio than compared to their controls. In contrast to the conclusions of Barros et al.[15] Thomson et al.[206] concluded that the hemodynamic changes related to cyclosporine A are focused at increases in afferent arteriolar resistance.

Using a similar pair-fed control study, English et al.[62] measured the effect of chronic cyclosporine A dosage of 50 mg/kg in male Fisher rats on glomerular filtration rate, fractional sodium and lithium excretions, as well as on arteriolar diameter by vascular perfusion cast examination (Fig. 94.5). After 14 days of cyclosporine A, there was a decrease in GFR and luminal diameter of the afferent arterioles as measured by scanning electron microscopy decreasing to 8.9 (± 0.4) as compared to 13.5 (± 0.4) in pair-fed controls. The study further supports the theory that the afferent arteriole is the major site of cyclosporine A vasoconstriction. Thus, cyclosporine acutely and chronically reduces GFR owing to its impact on the elements of glomerular hemodynamics. Vasoconstriction of all contractile elements can be found with the effect on the afferent arteriole of largest magnitude.

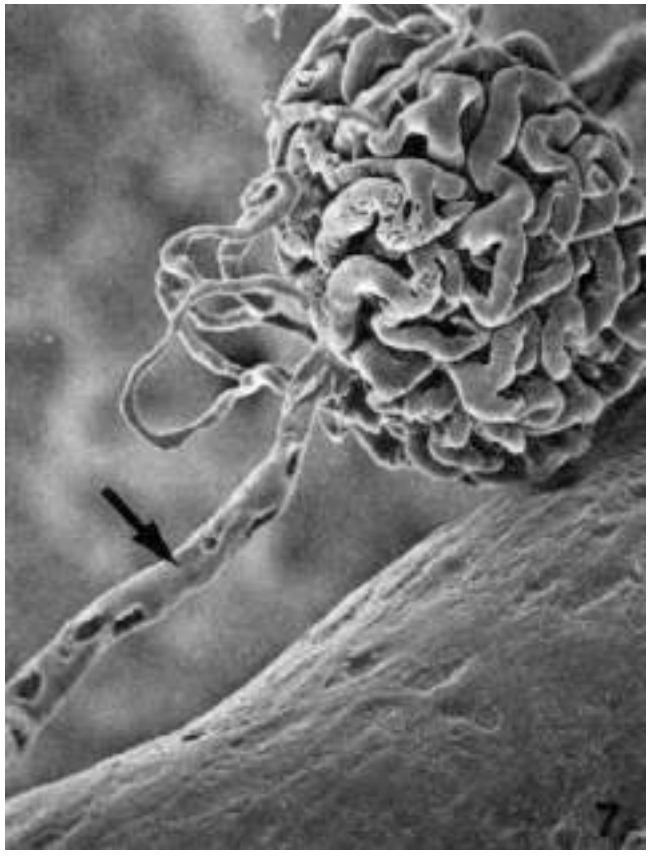

FIGURE 94.5 After 14 days of cyclosporine treatment, the entire length of an afferent arteriole (arrow) shows narrowing. *(From English J, Evan A, Houghton DC, Bennett WM. Cyclosporine induced acute renal dysfunction in the rat: evidence of arteriolar vasoconstriction with preservation of tubular function. Transplantation 1987;44:135–141.)*

In addition to drug-induced reductions in GFR is the almost universally encountered decline in renal blood flow. The exact cause of this decrease in renal blood flow is uncertain, but several possible mechanisms can be discerned from well-described cyclosporine effects. The renal blood flow may be constrained because of (1) the acute stimulation of the renin-aldosterone-angiotensin axis; (2) alterations in arachidonic acid metabolism; (3) increase in T-G feedback; (4) endothelin release; (5) stimulation of the autonomic nervous system (Table 94.2). Perico et al.[163,165] proposed that the infusion of cyclosporine A at a dose of 25 mg/kg for 20 or 45 days in rats resulted in an increase in plasma renin activity associated with a fall in GFR. There is also direct renin release by rat

TABLE 94.2 Potential Mechanisms of Cyclosporine A–Induced Renal Blood Flow Impairment

Renin–aldosterone–angiotensin axis
Arachidonic acid metabolism
Tubuloglomerular feedback
Endothelin release
Autonomic nervous system

juxtaglomerular cells grown in culture after cyclosporine A exposure confirming activation of this system after acute administration of drug.[118] The importance of cyclosporine A stimulation acutely of the renin-aldosterone-angiotensin axis is further supported by the micropuncture studies by Barros et al.[15] in which cyclosporine A effects on GFR and renal blood flow were markedly ameliorated when an angiotensin converting enzyme inhibitor was infused. Because angiotensin converting enzyme inhibition did not completely abrogate the glomerular hemodynamic effects of cyclosporine A, the authors suggest that the renin-aldosterone-angiotensin axis is only partially responsible for the fall in renal plasma flow and GFR. Taken together, these studies suggest that during the acute phase of cyclosporine A effect on the tubule, there is an increase in the activity of the renin-aldosterone-angiotensin axis. The actual contribution of this system to the reduction in effective renal plasma flow is currently in debate.

There is no uniformity of view with respect to the etiologic role of the renin-aldosterone-angiotensin axis in cyclosporine-induced reduction in GFR, however, Dieperink et al.[56] in Copenhagen confirmed that rats treated with cyclosporine A at a dose of 25 mg/kg for 13 days prior to the study exhibited an appropriate fall in GFR and renal plasma flow, but they failed to reproduce the salutary effect of captopril on renal plasma flow or glomerular filtration as compared to untreated cohorts. Furthermore, studies attempting to stimulate the renin-aldosterone-angiotensin axis by diuretics or low salt intake show a blunted response in renin plasma activity in the face of cyclosporine A use.[51,91,195] Weir et al.[225] showed in normal healthy humans that an acute infusion of cyclosporine A at a dose of 4 mg/kg resulted in an appropriate reduction in GFR from 108.8 (± 2.5) ml/min to 9.1 (± 2.2) ml/min, a dose that led to no significant changes in renal plasma flow or systemic blood pressure. It was noted that during the period of reduced GFR, there was no change in plasma renin activity, angiotensin II, or aldosterone levels compared to the controls.

A second theory advanced to explain the fall in GFR after cyclosporine A administration is attributed to an increase in T-G feedback that has been measured.[79] Histologic studies of kidneys after cyclosporine A administration in both rats and humans show a hypertrophy of juxtaglomerular cells after cyclosporine A administration.[217] A mechanism for the increase in T-G feedback has been proposed by Gnutzmann et al.[79] based on micropuncture studies of the thick ascending limb of the loop of Henle in Munich-Wistar rats receiving an acute infusion of cyclosporine A at a dose of 15 mg/kg. Gnutzmann et al.[79] found an increased delivery of sodium and chloride to the thick ascending limb and the early distal tubule, which should be sensed by the macula densa adjacent to the thick ascending limb stimulating the T-G feedback mechanism in order to decrease GFR.[79]

The third theory advanced to explain the manner in which cyclosporine A alters renal blood flow is related to the ability of the drug to alter eicosanoid synthesis leading to an increased generation of the vasoconstrictor metabolites.[20] In a postischemic denervated rat model in which cyclosporine A was administered at a dose of 50 mg/kg over 12–14 days, Coffman et al.[44] uncovered an increase in the renal excretion of TXB2 associated with a fall in the clearance of insulin and in renal blood flow. There was no associated increase in PGE2 excretion during this period of decreased renal blood flow. Additionally, when arachidonic acid was perfused to stimulate eicosanoid production during the cyclosporine A–induced altered physiology there was an increased production of TXB2 in both the study and control animals, but the PGE2 production was also greatly increased in the cyclosporine A–treated animals as compared to controls (Fig. 94.6).[44] This suggests that the cyclosporine A–induced inhibition of PGE2 production can be overcome by increased concentrations of the precursor. These results are corroborated by studies in humans by Weir et al.[225] in which acute infusion of cyclosporine A (4 mg/kg over a six-hour period) resulted in a reduction of the GFR without affecting renal plasma flow as would be suggested by predominant vasoconstriction at the locus of the afferent arterial associated with an increase in urinary excretion of the TXA2 metabolite TXB2 without a correlative increase in 6-keto prostaglandin F1A.[225] During the period of study, there was no measured increase in circulating levels of TXB2, suggesting that the increased urinary levels of this TXA2 metabolic originated from the kidney.[225] In another study by Petric and colleagues, it has been demonstrated that urinary TXB2 excretion increased significantly following cyclosporine administration in Sprague-Dawley rats.[167] A concomitant rise in proximal tubular sodium reabsorption was observed as well as an increase in the excretion of urinary PGE2 and 6-keto-prostaglandin F2I without a change in plasma levels. Functional

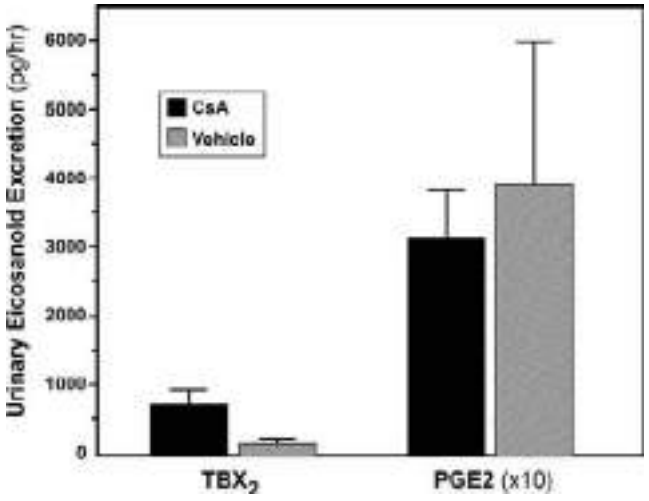

FIGURE 94.6 Urinary excretion of thromboxane B2 (TXB2) was significantly elevated in rats treated with cyclosporine versus controls ($p < 0.025$). There was no difference in prostaglandin E2 (PGE2) excretion in cyclosporine-treated rats when compared with controls. The measured levels of PGE2 are 10 times the values graphically represented *(Adapted from Coffman TM, Carr DR, Yarger WE, Klotman PE. Evidence that renal prostaglandin and thromboxane production is stimulated in chronic cyclosporine nephrotoxicity. Transplantation 1987;43:282–285.)*

changes accompanied to these biochemical changes were a decrease in renal blood flow, and in the clearance of creatinine and urea. Renal morphology showed severe vacuolization and necrosis confined to the proximal tubular region of the cortex.

The exact source of the altered eicosanoid production related to cyclosporine toxicity is unclear but may reflect cyclosporine A alteration of immune cell metabolism rather than of the graft itself. Cyclosporine A has been shown to increase thromboxane production in inflammatory cells aspirated from renal allografts[177] as well as in vascular endothelial cells[150] while decreasing prostaglandin production in isolated glomerular cells grown in culture.[194] Various experimental drugs that further block thromboxane synthesis[190] or stimulate intrinsic prostacyclin synthesis while inhibiting thromboxane production[200] have been shown to reduce cyclosporine nephrotoxicity. The blunted response in PGE2 excretion associated with an increase in thromboxane B2 excretion in cyclosporine A–treated rats as a function of increase renal vascular resistance when compared to controls suggests that cyclosporine A causes a shift in arachidonic acid metabolism from the production of prostaglandins such as PGE2 and prostacyclin to the vasoconstricting TXA2.[44]

The role of the very potent vasoconstrictor peptide endothelin in renal transplantation was explained by Badr et al.[12] who showed that infusion of endothelin at a dose of 10 pmol/min decreased renal blood flow by 40% in micropunctured rats associated with sharp increases in afferent arteriolar resistance (65%) and efferent arteriolar resistance (82%) accompanied by a reduction in ultrafiltration coefficient to a third of its preinfusion value. There is marked similarity between the endothelin effect on glomerular hemodynamics and the picture presented by Badr et al.[12] for that of acute cyclosporine A infusion. Kon et al.[164] were able to show in Munich-Wistar rats receiving high-dose cyclosporine infusion a substantial increase in circulating endothelin of almost 30-fold associated with the expected fall in single-nephron GFR. When a rabbit antiporcine endothelin serum was infused concomitantly with cyclosporine A, thus blocking the endothelin receptor sites, there was no significant difference in single-nephron glomerular filtration as compared to preinfusion levels. Further supporting these tantalizing findings relating endothelin-induced alterations in renal function to cyclosporine A was the study of Perico et al.[164] using the isolated perfused rat kidney model. A rabbit anti-rat endothelin antibody given prior to cyclosporine A infusion blunted reductions in renal blood flow and GFR in this second model (Fig. 94.7). To close the intellectual loop, Kon et al.[164] in cows and Bunchman and Brookshire[34] were also able to inhibit the release of endothelin by concomitant calcium channel blockade, angiotensin converting enzyme inhibition, and cyclooxygenase inhibition.[164] These studies taken together point strongly to endothelin as a partial culprit in the acute, early reduction in renal blood flow associated with cyclosporine A toxicity, and possible mechanisms to explain the clinical observations relating cyclosporine A toxicity sparing effects of certain treatments. It remains to be seen if the more chronic reduction in GFR found with cyclosporine A use can be related as well to endothelin.

A discussion of the effect of cyclosporine A on renal blood flow would not be complete without mentioning direct stimulation of the sympathetic nervous system. In the use of cyclosporine A for nonrenal transplants or other immune disorders, such direct stimulation may add importantly to those causes of reduction in GFR and renal blood flow already discussed. Denervation, a consequence of renal transplant surgery, protects the renal transplant from this cyclosporine A effect as shown by Moss et al.[141] Using a unilateral denervation rat model, they were able to show that acute infusion of cyclosporine A 10 mg/kg resulted in an increase in afferent renal nerve activity by 82% associated with a fall in effective renal blood flow in the innervated side without any noticeable alterations in the denervated side.[141] Murray and Paller[147] were able to reproduce the observation that denervation protects the kidney from cyclosporine A–induced alterations in renal blood flow associated with sympathetic activation, and

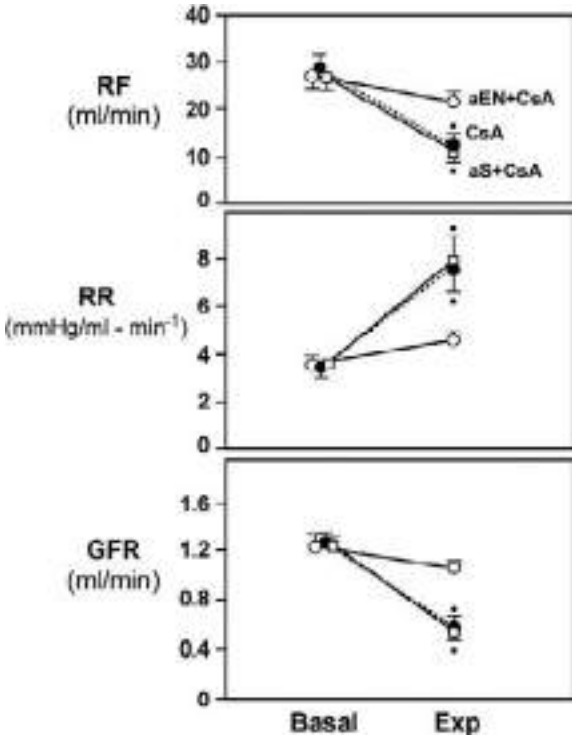

FIGURE 94.7 Effect of cyclosporine (CsA) on renal function parameters in isolated kidneys preexposed to antiendothelin antibody (aEN), nonimmunized rabbit serum (aS), or vehicle. Data represent average values of the two control clearance periods (basal) and the four experimental periods after challenging the kidney with CsA. Values expressed as mean plus standard deviation. $p < 01$, versus aEN+++CsA. *(From Perico N, Dadan J, Remuzzi G. Endothelin mediates the renal vasoconstriction induced by cyclosporine in the rat. J Am Soc Nephrol 1990;1:76–83.)*

they were able to prevent some of the fall in renal blood flow to the innervated kidney through a chemical sympathectomy using an adrenergic antagonist. The decrease in effective renal blood flow that cyclosporine A may induce as a result of the activation of the sympathetic nervous system would therefore not be experienced by the kidney immediately after transplantation. Cyclosporine A–induced activation of the sympathetic nervous system may be an additional mechanism by which renal blood flow is reduced when that drug is used for autoimmune disease or for transplantation other than the kidney. Cyclosporine A may alter renal hemodynamics through the stimulated sympathetic nervous system remotely after transplantation either through hyper responsiveness to adrenergic receptors within the chronically denervated kidney or through regeneration of renal innervation.[141,147] The isolated perfused rat kidney was used to study the acute effects of cyclosporine A and its metabolites by Roby et al.[176] Metabolite levels can greatly exceed parent drug levels, especially in patients with abnormal liver function. Interestingly, all of the metabolites caused significant reductions in GFR, some even in very low concentrations, which may be an important and unrecognized factor in cyclosporine-induced nephrotoxicity. Cyclosporine metabolites did not increase tubular potassium reabsorption.

Renal tubular acidification capacity was studied in 12 patients treated with cyclosporine for idiopathic uveitis and in 5 patients with idiopathic uveitis not treated with cyclosporine, thus with intact native kidney function.[2] After intravenous bicarbonate loading fractional excretion was similar in both groups indicating normal proximal tubular acidification function. Plasma renin activity, plasma aldosterone and transtubular potassium gradient were similar in both groups. On the other hand, distal hydrogen ion secretion evaluated by the ability to increase U-B PCO2 in highly alkaline urine was impaired in cyclosporine-treated patients as compared to controls suggesting a distal acidification defect associated with cyclosporine therapy. Quereda and colleagues studied the response of urinary acidification parameters and electrolytes to furosemide administration in nine psoriatic patients treated with low-dose cyclosporine (5 mg/kg).[173] The post-furosemide urinary pH decrease and ammonium and titratable acid increase were significantly lower in cyclosporine-treated patients suggesting an abnormal distal tubular response to furosemide and a possible alteration in the H^+-ATPase pump associated with cyclosporine use.

In addition to the striking changes in renal blood flow and GFR, cyclosporine A may have direct effects on renal tubular transport capacity thought to be a consequence of cellular toxicity.[138] There are well-described morphological changes in the proximal tubular cells related to high concentrations of cyclosporine A in rats and humans such as tubular inclusions by isometric, ubiquitous vacuolization, and tubular microcalcifications.[138,216] Whiting et al.[229] evaluated evidence of functional correlates to observe cellular alterations due to cyclosporine A by measuring levels of urinary excretion of enzymes released from injured tubular cells. The lysosomal hydrolase, N-acetyl-β-D-glucosaminidase (NAG) is found in the urine of humans and rats exhibiting clinical features of cyclosporine A toxicity. The proximal tubule brush border enzyme G-glutamyltranspeptidase (gGT) has also been found in the urine at excess after cyclosporine A toxicity in rats. The increase in NAG enzymuria occurs prior to the fall in renal function or the presence of structural abnormalities that can be seen by biopsy.[229]

There is no consensus as to whether there is any physiologic correlation to the proximal tubule morphologic changes associated with cyclosporine A excess.[139] Extensive examination of salt and water handling by

the proximal tubule while under the influence of cyclosporine A has been undertaken. To study the ability of the proximal tubule to reabsorb sodium and water, lithium clearance studies have been employed to provide a measurement of isosmotic tubular fluid delivery from the end of the proximal tubule to the loop of Henle.[205] Lithium, which is not handled by the loop of Henle or the distal tubule, has thus been taken as a measure of proximal tubular function during cyclosporine A therapy. Dieperink et al.[55] first looked at the clearance of lithium as a function of proximal tubular transport in rats chronically receiving cyclosporine A at a dose of 50 mg/kg/day for 13 days. In these animals, falls in the clearance of inulin and to a greater extent the clearance of lithium were found, suggesting an increase in fractional tubular reabsorption by the proximal tubule. They propose that the increase in fractional tubular reabsorption of the proximal tubule is the result of lower ultrafiltration pressure related to cyclosporine A.[55] Human studies performed by Vincent et al.[219] using clearance of lithium as a measure of proximal tubule function showed that there was an increase in the renal vascular resistance associated with a fall in the clearance of lithium in the early post-transplant period after cyclosporine A administration. They also theorized that the proximal tubule is able to increase renal reabsorption in the face of cyclosporine A–induced alterations in glomerular hemodynamics. With a model of chronic cyclosporine nephropathy in the uninephrectomized salt-depleted rat, the relationship between renal functional impairment and structural changes was studied by Elzinga and colleagues.[61] Groups of uninephrectomized rats maintained on a salt-depleted or salt-repleted diet were treated with cyclosporine. Although GFR was similarly depressed in cyclosporine-treated animals on either diet, tubulointerstitial injury was largely confined to cyclosporine-treated rats on salt-depleted diet. Despite the apparent recovery of renal function after cyclosporine withdrawal, the degree of tubular atrophy and interstitial fibrosis did not improve indicating that once structural damage is established, the withdrawal of cyclosporine does not lead to its reversal. In addition, although the mechanism is unclear, this study demonstrates the importance of sodium depletion in promoting cyclosporine-induced tubulointerstitial injury.

Whiting and Simpson[228] repeated the study by Dieperink et al.[55] with several technical changes. They used creatinine as a measure of GFR and allowed for the continual availability of water during the lithium infusion study periods. These investigators were able to reproduce the decrease in the clearance of lithium as well as the increase in fractional reabsorption of sodium. They noted the fall in total clearance of sodium and potassium as well as the fall in absolute reabsorption of sodium, potassium, and water distal to the proximal tubule. As opposed to Dieperink et al.[55] Whiting and Simpson[228] felt that the increased fractional reabsorption of the proximal tubule associated with cyclosporine toxicity was due to a direct but undefined tubular defect distal to the proximal tubule independent of the well-defined hemodynamic alterations of the drug. In their human studies, Propper et al.[172] showed that in cyclosporine A–treated patients with stable graft function several months after transplant, there was a persistent decrease in the clearance of lithium compared to their azathioprine-treated cohorts and to untreated subjects. They additionally noted a much lower absolute reabsorption of sodium and water in the distal nephron compared to the azathioprine-treated group. Whiting et al.[227] theorized that increased proximal tubular reabsorption was the result of cyclosporine A toxicity at a site downstream from the proximal tubule, which resulted in decreased sodium reabsorption with subsequent increase in tubuloglomerular feedback. The decreased absolute reabsorption of sodium from the distal tubule as seen in rats and humans would be sensed by the juxtaglomerular apparatus and cause afferent arteriolar constriction with resultant decrease in GFR and proximal tubule sodium avidity. The studies of Dieperink et al.[55] and Vincent et al.,[219] and those of Whiting et al.[227] differ in their proposed mechanisms for cyclosporine A–induced increase in proximal tubular reabsorption; yet all agree that the proximal tubule transport function is not directly a consequence of tubular drug toxicity.

Tacrolimus, another calcineurin inhibitor agent commonly employeed in renal transplantation with a similar mechanism of immunosuppresion but on entirely different molecular structure, shares much of the vasoconstrictive properties of cyclosporine. The impact of this agent on the renin-angiotensin-aldosterone axis remains similarly time dependent with early stimulation of renin and endothelin and late inhibition. Sodium avidity by the proximal tubule remains the rule although a rate sodium wasting syndrome related to hyporesponsive of the distal nephron to aldosterone has been reported by Sakamoto and colleagues.[183]

Clinical syndromes that derive from altered renal transport support the experimental thesis that the proximal tubule responds appropriately to the hemodynamic alterations induced by cyclosporine A and distal tubular transport reflecting direct cellular toxicity of the drug (Fig. 94.8). For example, the clinical observation of mild and sometimes symptomatic hyperuricemia in patients receiving cyclosporine A after renal transplantation can be related primarily to hemodynamic changes. The first studies to suggest the relationship between cyclosporine and hyperuricemia were

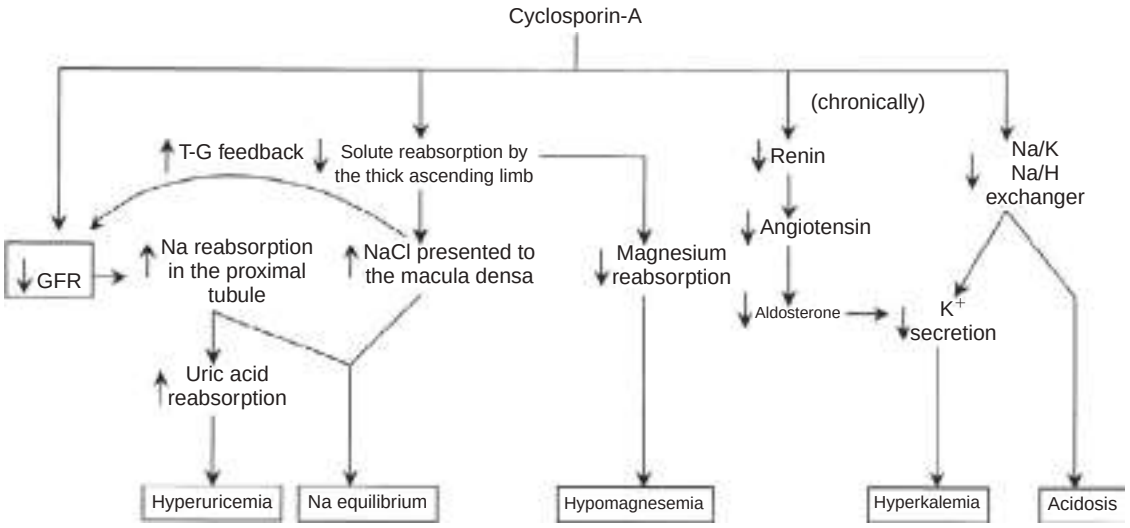

FIGURE 94.8 Diagrammatic representation of cyclosporine effects on the nephron with corresponding clinical syndromes.

those of Chapman et al.[40] who reviewed the Oxford experience of high-dose cyclosporine A in 1983–1985. Patients (n = 62) receiving a mean dose of cyclosporine A of 17.5 mg/kg/day had serum uric acid levels nearly 12 times that of their azathioprine- and prednisone-treated cohorts. The increase in serum uric acid was felt to reflect the decreased filtration fraction exhibited uniformly by the cyclosporine-treated group. Unfortunately, this study did not account for the possibility of increased uric acid turnover or for the alterations in uric acid metabolism related to other commonly used drugs post-transplant that may have interfered with uric acid excretion. Versluis et al.[218] studied 23 patients receiving cyclosporine A at a dose titrated to maintain a predetermined therapeutic level while in a metabolic ward measuring urinary and fractional excretion of uric acid before and after removal of cyclosporine A in a protocol designed to convert to an azathioprine dominated regimen. In those patients with successful removal of the cyclosporine A, the serum uric acid levels fell without a significant change in fractional clearance of uric acid. When stratified for the serum creatinine, the mean uric acid level was significantly higher during cyclosporine A therapy as compared to that after conversion to azathioprine for any given level of GFR. Although Versluis et al.[218] carefully accounted for metabolic alterations that change uric acid production rates, the GFR observations are weak in that they rely on serum creatinine as its measure of GFR. Creatinine clearance is a poor measure of true glomerular filtration rates during cyclosporine A treatment as tubular secretion of creatinine through the aromatic acid and base pathway is fully intact despite sharp constraints on glomerular filtration. Creatinine clearance thus overestimates GFR and calls into question conclusions reached in studies such as Versluis et al.[218] in which GFR is so improperly measured.[21,159] These two clinical studies highlight the interpretative dilemma between cyclosporine A–induced electrolyte abnormalities as a function of hemodynamics alterations or direct tubular toxicity. Flaws in study design required new observations to solve this dilemma.

A study in 19 pediatric renal transplant recipients demonstrated that patients with hyperuricemia had lower 51-EDTA, PAH, and urate clearances and serum urate concentration correlated with cyclosporine dose and inversely with urate, and lithium clearances.[120] Urate clearance showed a significant positive correlation with lithium clearance and an inverse correlation with fractional proximal tubular reabsorption. These data supported the idea for proximal tubular urate reabsorption rather than decreased secretion as one of the mechanisms in cyclosporine-induced hyperuricemia. In another study by Zurcher et al.[235] 82 cyclosporine-treated patients (50 bone marrow transplant recipients and 32 renal transplant recipients) and 28 healthy, living, related kidney donors were prospectively followed for up to two years. Plasma uric acid levels, inulin clearances, and fractional clearances of uric acid were examined. After one year of cyclosporine treatment, hyperuricemia was found in 36% of bone marrow transplant patients, in 53% of renal transplant patients, and 30% of living-related kidney donors. The GFR at one year, measured by inulin clearance, was identical in the cyclosporine-treated groups and slightly higher in the living-related kidney donors. The fractional clearance of uric acid did not change

significantly over time, suggesting that there is no evidence for impaired tubular handling of uric acid induced by a cyclosporine-specific tubulo-toxic effect. Hyperuricemia in cyclosporine-treated patients is thought to be a consequence of cyclosporine-induced diminished renal function.

The effects of calcium channel (amlodipine) and angiotensin converting enzyme (perindopril) blockade on glomerulotubular function in cyclosporine-treated renal allograft recipients were evaluated in a randomized, double-blind crossover fashion.[188] Both drugs maintained GFR and effective renal plasma flow and lowered mean arterial pressure to a similar extent. Sodium clearance and fractional excretion of sodium were not affected by either drug. Interestingly, output of fluid from the proximal tubules measured as clearance of lithium and uric acid was higher after amlodipine. Consequently, distal absolute reabsorption of sodium was higher and serum uric acid was lower after amlodipine in comparison with perindopril.

Although it has been difficult to rigorously prove that cyclosporine A has a direct toxic effect on proximal tubular transport function in the face of prior assumptions based on morphologic expectations, the physiologic and clinical evidence for isolated and specific cyclosporine A–induced transplant defects in more distal structures of the nephron are stronger. We have already reviewed the manner in which sodium and volume handling exhibited by the whole kidney during cyclosporine use is a function of, in part, a normal response of the proximal nephron to reduced GFR and to, in part, a function of a disordered loop. Additional specific defects exist in the loop of Henle in response to cyclosporine A. In one study of a segmental analysis of nephron function in cyclosporine A–treated animals, most measurements of transport appeared unaltered by the drug but a hint of defective loop and thick limb function was offered.[144] This hint was fleshed out by Gnutzmann et al.[79] who performed micropuncture experiments on Munich-Wistar rats after a 10-day course of cyclosporine A at 15 mg/kg or after a single intravenous infusion of 5 mg/kg of cyclosporine A. They reported an increase of luminal sodium chloride concentration in the thick ascending limb of Henle as a consequence of decreased limb transport diluting capacity.[79] They theorized that the impaired sodium chloride absorption in the thick limb provides stimulus to the macula densa that culminates in excitement in T-G feedback signals and lowering GFR. This study is a micropuncture counterpart to the clinical observations of Whiting et al.[227] who argued that the increased absorption of sodium by the proximal tubule is a consequence of constrained GFR and flows from a compensatory response to distal tubular defects created by the drug. The effect of chronic cyclosporine administration on volume regulation was also studied in mongrel dogs.[41] Dogs were given either cyclosporine or vehicle on a constant sodium diet. It has been demonstrated that cyclosporine administration induced a chronic state of avid sodium retention with associated activation of renin-angiotensin-aldosterone system and suppression of circulating atrial natriuretic factor. In addition, the ability of the kidney to acutely excrete sodium in response to saline volume expansion was attenuated because of the enhanced tubular reabsorption of sodium.

A second example of a precise transport defect in the distal nephron related to cyclosporine A derives from clinical and basic studies of magnesium handling. Exploring potential transport defects from serum measurements or even whole-kidney clearance studies for magnesium is fraught with interpretative errors. As discussed earlier in this chapter, PTH excess, diuretic use, and the use of osmotic agents drive serum magnesium downward. Patients receiving cyclosporine A for maintenance of bone marrow grafts are more instructive in that these confounding variables are not in play. A clear decline in serum magnesium levels in general, and an increase in urinary magnesium excretion in particular, once cyclosporine A is initiated, strongly suggest a direct drug-related transport derangement in renal magnesium handling.[104] Cyclosporine infusion in rats also culminates in plasma magnesium reduction, a consequence of urinary wasting of magnesium that resolves completely upon cessation of cyclosporine A, which is strong evidence that the abnormalities are a direct consequence of this drug.[231] When Nozue and colleagues determined the serum and tissue levels of magnesium in cyclosporine-treated Sprague-Dawley rats, they found that serum magnesium levels were significantly lower in the cyclosporine-treated groups than in the control group.[153] Serum magnesium concentration fell in a dose-dependent manner. Interestingly, urinary magnesium excretion was inappropriately increased and there was no significant difference between the control and cyclosporine-treated groups with regard to total urinary excretion of magnesium indicating the impaired renal conservation of magnesium. On the other hand, magnesium content in the kidney, muscle, and liver was significantly higher in the cyclosporine-treated group than in the control group, which suggested a role for intracellular migration of magnesium on cyclosporine-induced hypomagnesemia. Calcineurin inhibitors appear to transiently increase intracellular calcium levels in mouse distal convoluted tubule cells (MDCT). In addition, calcineurin inhibitors, inhibit PTH stimulated magnesium entry in MDCT cells resulting in wasting.[109]

Tacrolimus has been associated with more profound magnesium wasting than cyclosporine, with lower

serum levels and higher dietary requirements.[10] It is thought that the calcineurin inhibitors in general, and tacrolimus in particular, block the basolateral sodium-potassium pump in the loop of Henle decreasing an otherwise lumen-positive gradient resulting in decreased paracellular magnesium reabsorption.[10] The result is an inappropriately high fractional excretion of magnesium despite low serum concentrations. The hypomagnesemia independent of diuretic use or diarrhea may also be a consequence of tacrolimus use. This effect is believed one of direct tubular transport functional alterations not explained by the confounding variables of tissue distribution of the cation or by parathyroid hormone status.[126] Serum magnesium levels correlate inversely with serum tacrolimus levels and creatinine clearance. Magnesium replacement doesn't appear to influence the fractional excretion of magnesium[149]

Tacrolimus decreases intracellular magnesium in osteoblast cells by inhibiting activation of the extracellular signal-regulated kinases (ERK). Tacrolimus effects on intracellular magnesium and ERK may partially explain some of its untoward effects on bone metabolism.[100]

Hypomagnesemia has been shown to be an independent predictor of new onset diabetes after transplantation. It has long been known that diabetics have lower serum magnesium levels than non diabetics.[106] Although one can reason that low magnesium levels are a consequence of the diabetic state due to osmotic diuresis or impaired magnesium absorption in the thick ascending limb due to insulin resistance, there appears to be an independent and direct effect of low magnesium on insulin sensitivity that improves with supplementation.[112]

The use of sirolumus results in hypomagnesemia as well. Sirolimus use leads to an increased transtubular potassium gradient (compared to cyclosporine) leading to hypokalemia and tubular dysfuction resulting in polyuria and hypomagnesemia. Sirolimus decreases the expression of NKCC2 in the thick ascending limb (the princial sodium transporter), reduces aquaporin-2 expression and increases the expression of TRPM6 (Mg permeable channel on the apical membrane of the distal convoluted tubule). Rosiglitazone prevents sirolimus induced hypokalemia and hypomagnesemia by increasing the protein expression of sodium transporters and aquaporin-2.[52]

The best characterized transport defect associated with cyclosporine is that of potassium with hyperkalemia, the consequence of a well-recognized disorder of electrolyte excretion during this form of immunosuppressive therapy either in kidney transplant recipients or following its uses in autoimmune diseases.[57,71] Mineralocorticoid status of the transplant recipient is an important controlling influence on potassium handling by the graft as discussed earlier. Interestingly, there is a dialectical response of the renin-angiotensin-aldosterone axis to cyclosporine A administration. Acutely after cyclosporine A intravenous infusions in normals and in the first days of cyclosporine use in animals and humans, renin is directly stimulated leading to increases in aldosterone. After chronic administration and for the bulk of the time a patient keeps the transplant, renin responsiveness is reduced and a state of hypoaldosteronism is common. This reduction in renin response in patients receiving cyclosporine A raises the possibility that reductions in distal tubular sodium/potassium exchange, a function of this relative aldosterone deficiency, account for the majority of clinical instances of hyperkalemia.[14] Chan et al.[39] compared 20 renal allograft recipients receiving cyclosporine A in doses of 10 mg/kg/day to a group of 17 patients given azathioprine immunosuppression, observing that the fractional excretion of potassium is lower than would be predicted by the decrement in GFR related to cyclosporine A alone. These data support the concept of distal tubular reduction in sodium/potassium exchange. Deppe and colleagues[54] studied the principal and intercalated cell properties of the distal nephron in order to investigate the influence of cyclosporine A on key plasma membrane ion transport systems. It has been demonstrated that cyclosporine A decreased the activities of Na^+,K^+-ATPase and Na^+-K^+-2Cl cotransporter in cells of the distal nephron thereby contributing to the hyperkalemia observed in patients treated with cyclosporine A.[122,208,232]

In addition to the mineralocorticoid state of the transplant recipient, other derangements in potassium handling produced by cyclosporine have been proposed. Batlle et al.[17] in their detailed analysis of acidification highlight defects in the distal tubule that extend to potassium. Accompanying an impaired ability to secrete hydrogen ions distally were decreases in potassium excretion, failure to excrete a potassium load, and failure to increase the fractional excretion of potassium in the face of increased plasma potassium concentration, findings confirmed by micropuncture.[17,159] They proposed that cyclosporine A causes a voltage-dependent defect in hydrogen ion and potassium excretion that is clinically evident in patients receiving cyclosporine A as hyperkalemic, metabolic acidosis.[39]

Just as the immunosuppressive mechanism of action of tacrolimus is similar to that of cyclosporine, much of the toxicity profile is similar as well, including neurotoxicity, nephrotoxicity, and hypertension. It has been demonstrated in rat kidneys that tacrolimus blocks the angiotensin II–induced activation of Na^+,K^+-ATPase, which is an enzyme that is present in the basolateral membrane of all renal tubular cells.[8] Na^+,K^+-ATPase

plays a pivotal role for sodium reabsorption and subsequently for regulation of blood pressure. Studies demonstrated that tacrolimus is as nephrotoxic as cyclosporine A, it also induces both morphologic and biochemical changes in animal models. Animals treated with 10 mg/kg/day of tacrolimus intraperitoneally were found to have juxtaglomerular apparatus hyperplasia and juxtaglomerular cell transformation with vascular changes.[233] While the urinary excretion of TXB2 was significantly high, urinary excretion of 6-keto-PGF1A was low, which reflected increased production of TXA2 leading to glomerular vasoconstriction. The cellular enlargement of juxtaglomerular cells along with a decrease in renal cortical blood flow has also been shown by Ueda et al. using the hydrogen ion clearance method.[209] In an *in vitro* model, using electrical resistance pulse sizing technique, Lieberman and colleagues demonstrated that tacrolimus causes a dose-dependent contraction of isolated glomeruli that can be inhibited by blockade of calcium channels.[124] In addition, tacrolimus was found to have a direct cytotoxic effect on cultured porcine proximal tubular epithelial cells,[143] as well as periodic-acid-Schiff (PAS) stain positive large granules and vacuolar changes in the convoluted part of the proximal tubules in rats.[233] It also has been shown to inhibit porcine[136] and human[27] proximal tubular cell proliferation in a dose-dependent manner, which was thought to be a contributing factor along with altered prostaglandin metabolism and enhanced endothelin secretion in tacrolimus-induced nephrotoxicity.[142]

Hyperkalemia may be more frequent with tacrolimus use than cyclosporine.[95] *In vitro*, cyclosporine inhibits the activity of the $Na^+/K^+/2Cl^-$ cotransporter whereas tacrolimus stimulates the activity of the cotransporter which should increase serum concentrations of potassium.[3] In addition to common mechanisms that have been described, tacrolimus inhibits calcium-dependent exocytosis of catecholamines from adrenal chromaffin cells, which may lead to potassium shifting out of cells contributing to elevated plasma concentrations.[132] Additionally there appears to be a differential effect on potassium channel currents between the undecapeptide immunosuppressant cyclosporine and the two macrolide antibiotic agents, sirolimus and tacrolimus. Both of the macrolides enter cells to bind with a carrier protein the class of which are called immunophilins. The precise immunophilin utilized by the macrolides, called the FK-binding protein (FKBP), is different from that for cyclosporine and has a unique role in potassium homeostasis prolonging the mean opening time of the channel enhancing serum potassium concentrations.[201] Both of the macrolides increase the action potential duration prolonging recovery from inactivation of potassium channels responsible for repolarization in mouse ventricles.[59] Interestingly, all three of the immunosuppressants inhibit insulin release through disordered regulation of the ATP-sensitive potassium channel further contributing to cellular shifts in potassium favoring hyperkalemia.[73]

Both cyclosporine and tacrolimus impair tubular reabsorption of phosphate after kidney transplantation. One study suggests that tacrolimus treated patients exhibit significantly faster recovery from the drug impairment related tubular phosphate reabsorption than with cyclosporine. The effects on phosphate wasting with cyclosporine is still seen two years after renal transplantation.[68]

The array of transport abnormalities that might be encountered after using the newest class of immunosuppressants—which inhibit the mammalian target of rapamycin or mTOR—are not yet understood. Some of the effects of the main agent in this class sirolimus share transport alterations with its chemical cousin tacrolimus as a function of its macrolide structure as discussed with respect to potassium channel deviations. Uric acid handling appears to be unaffected,[85] while the potassium effects seem to involve the KFBP alteration of channel function and insulin secretory inhibition. It has been recognized for sometime that renal allografts have impaired phosphate handling and sirolimus may prolong renal phosphate leak resulting in low serum phosphate concentrations the first weeks after renal transplantation.[198] Sirolimus appears to promote hypophosphatemia by inhibiting the intestinal phosphate transporter as well as regulating the major renal tubular phosphate transporter (NaPi-IIa) resulting in phosphaturia independent of serum phosphorous concentrations. Kemp and colleagues using both a xenopus oocyte recorder system *in vitro* and a murine *in vitro* model confirmed the inhibition of the NaPi-IIa phosphate transporter through inhibition of the serum—and glucocorticois—inducible kinase. There is also inhibition of Hg FGT23 probably responding to direct tubular wasting of phosphorous. In time 1,2 $(OH)_2D3$ increases due to stimulation of 1 alpha-hydroxylase by cellular phosphate depletion. This increase in vitamin D leads to increased intestinal absorption of phosphate despite on going renal wasting of phosphorous with sirolimus. Serum concentrations of phosphate will normalize as a result.[108]

In summary, the universal employ of novel immunosuppressant agents with complex molecular mechanisms of action has uncovered an array of renal physiologic derangements in the successfully renal engrafted patient. Sodium handling, uric acid metabolism, homeostasis of divalent cations, potassium balance, acid−base alteration have become important accretions to the appropriate clinical management of

the renal transplant recipient who will enjoy dwindling numbers of rejection episodes and prolonged allograft survival. A clear understanding of normal renal physiology and the manner in which standard drug regimens alter transport from normality has become an essential component of renal transplant management.

References

[1] Abramowicz D, Schandene L, Goldman M, Crusiaux A, Vereerstraeten P, De Pauw L, et al. Release of tumor necrosis factor, *interleukin*-2, and gamma-interferon in serum after injection of OKT3 monoclonal antibody in kidney transplant recipients. Transplantation 1989;47(4):606–8.

[2] Aguilera S, Deray G, Desjobert H, Benhmida M, Le Hoang P, Jacobs C. Effects of cyclosporine on tubular acidification function in patients with idiopathic uveitis. Am J Nephrol 1992;12 (6):425–30.

[3] Aker S, Heering P, Kinne-Saffran E, Deppe C, Grabensee B, Kinne RK. Different effects of cyclosporine A and FK506 on potassium transport systems in MDCK cells. Exp Nephrol 2001;9(5):332–40.

[4] Alejandro VS, Nelson WJ, Huie P, Sibley RK, Dafoe D, Kuo P, et al. Postischemic injury, delayed function and Na + /K (+)-ATPase distribution in the transplanted kidney. Kidney Int 1995;48(4):1308–15.

[5] Alejandro V, Scandling Jr JD, Sibley RK, Dafoe D, Alfrey E, Deen W, et al. Mechanisms of filtration failure during postischemic injury of the human kidney. A study of the reperfused renal allograft. J Clin Invest 1995;95(2):820–31.

[6] Ambuhl PM, Meier D, Wolf B, Dydak U, Boesiger P, Binswanger U. Metabolic aspects of phosphate replacement therapy for hypophosphatemia after renal transplantation: impact on muscular phosphate content, mineral metabolism, and acid/base homeostasis. Am J Kidney Dis 1999;34(5): 875–83.

[7] Andoh TF, Burdmann EA, Fransechini N, Houghton DC, Bennett WM. Comparison of acute rapamycin nephrotoxicity with cyclosporine and FK506. Kidney Int 1996;50(4):1110–7.

[8] Aperia A, Holtback U, Syren ML, Svensson LB, Fryckstedt J, Greengard P. Activation/deactivation of renal Na + ,K (+)-ATPase: a final common pathway for regulation of natriuresis. FASEB J 1994;8(6):436–9.

[9] Arruda JA, Nascimento L, Westenfelder C, Kurtzman NA. Effect of parathyroid hormone on urinary acidification. Am J Physiol 1977;232(5):F429–33.

[10] Arthur JM, Shamim S. Interaction of cyclosporine and FK506 with diuretics in transplant patients. Kidney Int 2000;58 (1):325–30.

[11] Azuma H, Nadeau K, Takada M, Mackenzie HS, Tilney NL. Cellular and molecular predictors of chronic renal dysfunction after initial ischemia/reperfusion injury of a single kidney. Transplantation 1997;64(2):190–7.

[12] Badr KF, Murray JJ, Breyer MD, Takahashi K, Inagami T, Harris RC. Mesangial cell, glomerular and renal vascular responses to endothelin in the rat kidney. Elucidation of signal transduction pathways. J Clin Invest 1989;83(1):336–42.

[13] Bahn I, Shah A, Holmes J, Isakova T, Gutierrez O, Burnett SM, et al. Post-transplant hypophosphatemia: Tertiary "Hyper-Phosphatoninism?". Kidney Int 2006;70(8):1486–94 [Epub 2006 Aug 30]

[14] Bantle JP, Nath KA, Sutherland DE, Najarian JS, Ferris TF. Effects of cyclosporine on the renin-angiotensin-aldosterone system and potassium excretion in renal transplant recipients. Arch Intern Med 1985;145(3):505–8.

[15] Barros EJ, Boim MA, Ajzen H, Ramos OL, Schor N. Glomerular hemodynamics and hormonal participation on cyclosporine nephrotoxicity. Kidney Int 1987;32(1):19–25.

[16] Bastani B, Haragsim L, Gluck S, Siamopoulos KC. Lack of H-ATPase in distal nephron causing hypokalaemic distal RTA in a patient with Sjogren's syndrome. Nephrol Dial Transplant 1995;10(6):908–9.

[17] Batlle DC, Gutterman C, Tarka J, Prasad R. Effect of short-term cyclosporine A administration on urinary acidification. Clin Nephrol 1986;25(Suppl. 1):S62–9.

[18] Batlle DC, Mozes MF, Manaligod J, Arruda JA, Kurtzman NA. The pathogenesis of hyperchloremic metabolic acidosis associated with kidney transplantation. Am J Med 1981;70(4):786–96.

[19] Baylis C, Handa RK, Sorkin M. Glucocorticoids and control of glomerular filtration rate. Semin Nephrol 1990;10(4):320–9.

[20] Bennett WM, Elzinga L, Kelley V. Pathophysiology of cyclosporine nephrotoxicity: role of eicosanoids. Transplant Proc 1988;20(Suppl 3):628–33.

[21] Berg KJ, Gjellestad A, Nordby G, Rootwelt K, Djoseland O, Fauchald P, et al. Renal effects of trimethoprim in ciclosporin- and azathioprine-treated kidney-allografted patients. Nephron 1989;53(3):218–22.

[22] Berndt T, Craig TA, Bowe AE, Vassiliadis J, Reczek D, Finnegan R, et al. Secreted frizzled-related protein 4 is a potent tumor-derived phosphaturic agent. J Clin Invest 2003;112(5):785–94.

[23] Bertani T, Abbate M, Zoja C, Corna D, Perico N, Ghezzi P, et al. Tumor necrosis factor induces glomerular damage in the rabbit. Am J Pathol 1989;134(2):419–30.

[24] Better OS, Chaimowitz C, Naveh Y, Stein A, Nahir AM, Barzilai A, et al. Syndrome of incomplete renal tubular acidosis after cadaver kidney transplantation. Ann Intern Med 1969;71 (1):39–46.

[25] Better OS. Tubular dysfunction following kidney transplantation. Nephron 1980;25(5):209–13.

[26] Bhan I, Shah A, Holmes J, Isakova T, Gutierrez O, Burnett SM, et al. Post-transplant hypophosphatemia: Tertiary "Hyper-Phosphatoninism?" Kidney Int 2006;70(8):1486–94.

[27] Blaehr H, Andersen CB, Ladefoged J. Acute effects of FK506 and cyclosporine A on cultured human proximal tubular cells. Eur J Pharmacol 1993;228(5–6):283–8.

[28] Blaufox MD, Birbari AE, Hickler RB, Merrill JP. Peripheral plasma renin activity in renal-homotransplant recipients. N Engl J Med 1966;275(21):1165–8.

[29] Blaufox MD, Lewis EJ, Jagger P, Lauler D, Hickler R, Merrill JP. Physiologic responses of the transplanted human kidney. N Engl J Med 1969;280(2):62–6.

[30] Bricker NS, Guild WR, Merrill JP, Reardan JB. Studies on the functional capacity of a denervated homotransplanted kidney in an identical twin with parallel observations in the donor. J Clin Invest 1956;35(12):1364–80.

[31] Bricker NS, Slatopolsky E, Reiss E, Avioli LV. Calcium, phosphorus, and bone in renal disease and transplantation. Arch Intern Med 1969;123(5):543–53.

[32] Bricker NS, Straffon RA, Mahoney EP, Merrill JP. The functional capacity of the kidney denervated by autotransplantation in the dog. J Clin Invest 1958;37(2):185–93.

[33] Bugge JF, Hartmann A, Osnes S, Bentdal O, Stenstrom J. Immediate and early renal function after living donor transplantation. Nephrol Dial Transplant 1999;14(2):389–93.

[34] Bunchman TE, Brookshire CA. Cyclosporine stimulated synthesis of endothelin by human endothelial cells in tissue culture. Kidney Int 1990;37:365.

[35] Butler Jr HE, Morgan JM, Smythe CM. Mercaptopurine and acquired tubular dysfunction in adult nephrosis. Arch Intern Med 1965;116(6):853–6.
[36] Canafax DM, Torres A, Fryd DS, Heil JE, Strand MH, Ascher NL, et al. The effects of delayed function on recipients of cadaver renal allografts. A study of 158 patients randomized to cyclosporine or ALG-azathioprine. Transplantation 1986;41(2): 177–81.
[37] Carlier M, Gianello P, Squifflet JP, Donckier J, Ketelslegers JM, Alexandre GP. Correlation between atrial natriuretic peptide levels and cardiac filling pressures in renal transplant recipients. Transplantation 1989;48(4):700–2.
[38] Carlier M, Squifflet JP, Pirson Y, Gribomont B, Alexandre GP. Maximal hydration during anesthesia increases pulmonary arterial pressures and improves early function of human renal transplants. Transplantation 1982;34(4):201–4.
[39] Chan MK, Wong KK, Cheng KP, Li MK. Clinical prevalence and significance of electrolyte disorders in cyclosporine A-treated patients. Transplant Proc 1988;20(Suppl. 3): 705–8.
[40] Chapman JR, Griffiths D, Harding NG, Morris PJ. Reversibility of cyclosporin nephrotoxicity after three months' treatment. Lancet 1985;1(8421):128–30.
[41] Ciresi DL, Lloyd MA, Sandberg SM, Heublein DM, Edwards BS. The sodium retaining effects of cyclosporine. Kidney Int 1992;41(6):1599–605.
[42] Clapp JR, Robinson RR. Functional characteristics of the transplanted kidney. Arch Intern Med 1969;123(5):531–6.
[43] Clive DM. Renal transplant-associated hyperuricemia and gout. J Am Soc Nephrol 2000;11(5):974–9.
[44] Coffman TM, Carr DR, Yarger WE, Klotman PE. Evidence that renal prostaglandin and thromboxane production is stimulated in chronic cyclosporine nephrotoxicity. Transplantation 1987;43 (2):282–5.
[45] Coffman TM, Yarger WE, Klotman PE. Functional role of thromboxane production by acutely rejecting renal allografts in rats. J Clin Invest 1985;75(4):1242–8.
[46] Cohen EP, Bastani B, Cohen MR, Kolner S, Hemken P, Gluck SL. Absence of H(+)-ATPase in cortical collecting tubules of a patient with Sjogren's syndrome and distal renal tubular acidosis. J Am Soc Nephrol 1992;3(2):264–71.
[47] Connell JM, Whitworth JA, Davies DL, Lever AF, Richards AM, Fraser R. Effects of ACTH and cortisol administration on blood pressure, electrolyte metabolism, atrial natriuretic peptide and renal function in normal man. J Hypertens 1987;5(4): 425–33.
[48] Cornaby A, Simpson M, Vann Rice R, Dempsey R, Madras P, Jenkins R, et al. Interleukin 2 levels and urine cytology distinguish between cyclosporine toxicity and rejection in renal and liver allograft recipients. Transplant Proc 1988;20(Suppl. 3):827–30.
[49] Coruzzi P, Musiari L, Mossini GL, Ceriati R, Mutti A. The renin-aldosterone system and renal function in kidney transplantation. Clin Nephrol 1994;41(4):225–9.
[50] Curtis JJ, Laskow DA. Cyclosporine-induced nephrotoxicity: pathophysiology of decreased blood flow. Transplant Proc 1988;20(Suppl. 3):540–3.
[51] Curtis JJ, Luke RG, Jones P, Diethelm AG. Hypertension in cyclosporine-treated renal transplant recipients is sodium dependent. Am J Med 1988;85(2):134–8.
[52] da Silva CA, de Bragança AC, Shimizu MH, Sanches TR, Fortes MA, Giorgi RR, et al. Rosiglitazone prevents sirolimus-induced hypomagnesemia, hypokalemia, and downregulation of NKCC2 protein expression. Am J Physiol Renal Physiol 2009;297:F916–22.
[53] DeFronzo RA, Goldberg M, Cooke CR, Barker C, Grossman RA, Agus ZS. Investigations into the mechanisms of hyperkalemia following renal transplantation. Kidney Int 1977;11(5):357–65.
[54] Deppe CE, Heering PJ, Tinel H, Kinne-Saffran E, Grabensee B, Kinne RK. Effect of cyclosporine A on Na + /K(+)-ATPase, Na + /K + /2Cl- cotransporter, and H + /K(+)-ATPase in MDCK cells and two subtypes, C7 and C11. Exp Nephrol 1997;5 (6):471–80.
[55] Dieperink H, Leyssac PP, Kemp E, Steinbruckl D, Starklint H. Glomerulotubular function in cyclosporine A treated rats. Clin Nephrol 1986;25(Suppl. 1):S70–4.
[56] Dieperink H, Leyssac PP, Starklint H, Jorgensen KA, Kemp E. Antagonist capacities of nifedipine, captopril, phenoxybenzamine, prostacyclin and indomethacin on cyclosporin A induced impairment of rat renal function. Eur J Clin Invest 1986;16(6): 540–8.
[57] Dieterle A, Abeywickrama K, von Graffenried B. Nephrotoxicity and hypertension in patients with autoimmune disease treated with cyclosporine. Transplant Proc 1988;20 (Suppl. 4):349–55.
[58] Dietl P, Good D, Stanton B. Adrenal corticosteroid action on the thick ascending limb. Semin Nephrol 1990;10(4):350–64.
[59] DuBell WH, Lederer WJ, Rogers TB. K(+) currents responsible for repolarization in mouse ventricle and their modulation by FK-506 and rapamycin. Am J Physiol Heart Circ Physiol 2000;278(3):H886–97.
[60] Du Cheyron D, Daubin C, Poggioli J, Ramakers M, Houillier P, Charbonneau P, et al. Urinary measurement of NA + /H + exchanger Isoform 3 (NHE3) protein as new marker of tubule Injury In critically Ill patients with ARF. Am J Kidney Dis 2003;42(3):497–506.
[61] Elzinga LW, Rosen S, Bennett WM. Dissociation of glomerular filtration rate from tubulointerstitial fibrosis in experimental chronic cyclosporine nephropathy: role of sodium intake. J Am Soc Nephrol 1993;4(2):214–21.
[62] English J, Evan A, Houghton DC, Bennett WM. Cyclosporine-induced acute renal dysfunction in the rat. Evidence of arteriolar vasoconstriction with preservation of tubular function. Transplantation 1987;44(1):135–41.
[63] Epstein M. Renal effects of head-out water immersion in humans: a 15-year update. Physiol Rev 1992;72(3):563–621.
[64] Espinel CH, Mendez-Picon G, Currier C, Novello A, Helfrich GB, Lee HM. FE Na effective in early diagnosis of acute rejection after kidney transplantation. Proc Clin Dial Transplant Forum 1979;9:256–9.
[65] Evenpoel P, Claes K, Kuypers D, Maes B, Bammens B, Vanrenterghem Y. Natural history of parathyroid function and calcium metabolism after kidney transplantation: a single-centre study. Nephrol Dial Transplant 2004;19(5):1281–7.
[66] Evenepoel P, Meijers BK, de Jonge H, Naesens M, Bammens B, Claes K, et al. Recovery of hyperphosphatoninism and renal phosphorus wasting one year after successful renal transplantation. Clin J Am Soc Nephrol 2008;3(6):1829–36 [Epub 2008 Oct 15].
[67] Evenepoel P, Naesens M, Claes K, Kuypers D, Vanrenterghem Y. Tertiary 'hyperphosphatoninism' accentuates hypophosphatemia and suppresses calcitriol levels in renal transplant recipients. Am J Transplant 2007;7(5):1193–2000 [Epub 2007 Mar 12]
[68] Falkiewics K, Kaminska D, Nahaczewska W, Boratvnska M, Owczarek H, Klinger M, et al. Renal function and tubular phosphate handling in long-term cyclosporine and tacrolimus based immunosuppression in kidney transplantation. Transplant Proc 2006;38(1):119–22.
[69] Felsenfeld AJ, Gutman RA, Drezner M, Llach F. Hypophosphatemia in long-term renal transplant recipients:

effects on bone histology and 1,25-dihydroxycholecalciferol. Miner Electrolyte Metab 1986;12(5-6):333–41 -362

[70] Ferran C, Sheehan K, Schreiber R, Bach JF, Chatenoud L. Anti-TNF abrogates the cytokine-related anti-CD3 induced syndrome. Transplant Proc 1991;23(1 Pt 1):849–50.

[71] Foley RJ, Van Buren CT, Hamner R, Weinmann EJ. Cyclosporine associated hyperkalemia. Transplant Proc 1983; 15(Suppl 1):2726–9.

[72] Frick A, Durasin I, Neuweg M. Glucocorticoid-induced inhibition of the reabsorption of inorganic phosphate in the proximal tubule in the absence of parathyroid hormone. Adv Exp Med Biol 1984;178:81–6.

[73] Fuhrer DK, Kobayashi M, Jiang H. Insulin release and suppression by tacrolimus, rapamycin and cyclosporin A are through regulation of the ATP-sensitive potassium channel. Diabetes Obes Metab 2001;3(6):393–402.

[74] Gardner DG, Hane S, Trachewsky D, Schenk D, Baxter JD. Atrial natriuretic peptide mRNA is regulated by glucocorticoids in vivo. Biochem Biophys Res Commun 1986;139 (3):1047–54.

[75] Geertsen PF, von der Maase H, Olsen NV, Fogh-Andersen N, Nielsen SL, Leyssac PP. Renal haemodynamics, sodium and water reabsorption during continuous intravenous infusion of recombinant interleukin-2. Clin Sci (Lond) 1998;95(1):73–81.

[76] Gianello P, Poelaert D, Ramboux A, Squifflet JP, Berbinschi A, Donckier J, et al. Beneficial effect of atrial natriuretic factor on ischemically injured kidneys in rats. Transplant Proc 1988;20 (5):921–2.

[77] Gianello P, Squifflet JP, Carlier M, Jamart J, Pirson Y, Mahy B, et al. Evidence that atrial natriuretic factor is the humoral factor by which volume loading or mannitol infusion produces an improved renal function after acute ischemia. An experimental study in dogs. Transplantation 1989;48(1):9–14.

[78] Ginn Jr HR, Unger AM, Hume DM, Schilling JA. Human renal transplantation: an investigation of the functional status of the denervated kidney after successful homotransplantation in identical twins. J Lab Clin Med 1960;56:1–13.

[79] Gnutzmann KH, Hering K, Gutsche HU. Effect of cyclosporine on the diluting capacity of the rat kidney. Clin Nephrol 1986;25(Suppl. 1):S51–6.

[80] Gong H, Wang W, Kwon TH, Jonassen T, Li C, Ring T, et al. EPO and alpha-MSH prevent ischemia/reperfusion-induced down-regulation of AQPs and sodium transporters in rat kidney. Kidney Int 2004;66(2):683–95.

[81] Gores PF, Fryd DS, Sutherland DE, Najarian JS, Simmons RL. Hyperuricemia after renal transplantation. Am J Surg 1988;156 (5):397–400.

[82] Graf H, Kovarik J, Stummvoll HK, Wolf A, Pinggera WF. Handling of phosphate by the transplanted kidney. Proc Eur Dial Transplant Assoc 1979;16:624–9.

[83] Green J, Debby H, Lederer E, Levi M, Zajicek HK, Bick T. Evidence for a PTH-independent humoral mechanism in post-transplant hypophosphatemia and phosphaturia. Kidney Int 2001;60(3):1182–96.

[84] Greene Jr JA, Vander AJ, Kowalczyk RS. Plasma renin activity and aldosterone excretion after renal homotransplantation. J Lab Clin Med 1968;71(4):586–95.

[85] Groth CG, Backman L, Morales JM, Calne R, Kreis H, Lang P, et al. Sirolimus (rapamycin)-based therapy in human renal transplantation: similar efficacy and different toxicity compared with cyclosporine. Sirolimus European renal transplant study group. Transplantation 1999;67(7):1036–42.

[86] Gutierrez O, Isakova T, Rhee E, Shah A, Holmes J, Collerone G, et al. Fibroblast growth factor-23 mitigates hyperphosphatemia but accentuates calcitriol deficiency in chronic kidney disease. J Am Soc Nephrol 2005;16(7):2205–15 [Epub 2005 May 25].

[87] Haas JA, Knox FG. Mechanisms for escape from the salt-retaining effects of mineralocorticoids: role of deep nephrons. Semin Nephrol 1990;10(4):380–7.

[88] Hahn TJ, Halstead LR, Teitelbaum SL, Hahn BH. Altered mineral metabolism in glucocorticoid-induced osteopenia. Effect of 25-hydroxyvitamin D administration. J Clin Invest 1979;64 (2):655–65.

[89] Halloran PF, Aprile MA, Farewell V, Ludwin D, Smith EK, Tsai SY, et al. Early function as the principal correlate of graft survival. A multivariate analysis of 200 cadaveric renal transplants treated with a protocol incorporating antilymphocyte globulin and cyclosporine. Transplantation 1988;46 (2):223–8.

[90] Hansen HE, Skov PE. The functional pattern of the transplanted living-donor kidney during the early posttransplant period. Acta Med Scand 1974;196(6):507–12.

[91] Heering P, Westhoff A, Bach D, Sprenger KB, Passlick J, Helmchen U, et al. Renin-aldosterone system and renal function under cyclosporine A. Transplant Proc 1988;20(Suppl 3):556–62.

[92] Henderson LW, Nolph KD, Puschett JB, Goldberg M. Proximal tubular malfunction as a mechanism for diuresis after renal homotransplantation. N Engl J Med 1968;278(9):467–73.

[93] Herdman RC, Michael AF, Vernier RL, Kelly WD, Good RA. Changes in phosphorus excretion and renal function after human renal homotransplantation. Nephron 1968;5(3):170–84.

[94] Heyman SN, Rosen S, Epstein FH, Spokes K, Brezis ML. Loop diuretics reduce hypoxic damage to proximal tubules of the isolated perfused rat kidney. Kidney Int 1994;45(4):981–5.

[95] Higgins R, Ramaiyan K, Dasgupta T, Kanji H, Fletcher S, Lam F, et al. Hyponatraemia and hyperkalaemia are more frequent in renal transplant recipients treated with tacrolimus than with cyclosporin. Further evidence for differences between cyclosporin and tacrolimus nephrotoxicities. Nephrol Dial Transplant 2004;19(2):444–50.

[96] Hollenberg NK, Birtch A, Rashid A, Mangel R, Briggs W, Epstein M, et al. Relationships between intrarenal perfusion and function: serial hemodynamic studies in the transplanted human kidney. Medicine (Baltimore) 1972;51(2):95–106.

[97] Hong CD, Kapoor BS, First MR, Pollak VE, Alexander JW. Fractional excretion of sodium after renal transplantation. Kidney Int 1979;16(2):167–78.

[98] Hulter HN, Peterson JC. Acid–base homeostasis during chronic PTH excess in humans. Kidney Int 1985;28(2):187–92.

[99] Jacobsen IA. Renal transplantation in the rabbit: a model for preservation studies. Lab Anim 1978;12(2):63–70.

[100] Jeon SH, Kim SJ, Kang HS. Immunosuppressant FK-506 decreases the intracellular magnesium in the human osteoblast cell by inhibiting the ERK 1/2 pathway. Life Science 2009;84(1-2):23–7.

[101] Johnstone RM. Exosome biological significance: A concise review. Blood Cells Mol Dis 2006;35(2):315–21 [Epub 206 Feb 17].

[102] Jordan M, Cohen EP, Roza A, Adams MB, Johnson C, Gluck SL, et al. An immunocytochemical study of H+ ATPase in kidney transplant rejection. J Lab Clin Med 1996;127(3):310–4.

[103] Julian BA, Quarles LD, Niemann KM. Musculoskeletal complications after renal transplantation: pathogenesis and treatment. Am J Kidney Dis 1992;19(2):99–120.

[104] June CH, Thompson CB, Kennedy MS, Loughran Jr TP, Deeg HJ. Correlation of hypomagnesemia with the onset of cyclosporine-associated hypertension in marrow transplant patients. Transplantation 1986;41(1):47–51.

[105] Kalbfleisch JH, Hebert LA, Lemann Jr J, Piering WF, Beres JA. Habitual excessive dietary salt intake and blood pressure levels in renal transplant recipients. Am J Med 1982;73(2): 205–10.

[106] Kao WH, Folsom AR, Nietro FJ, Mo JP, Watson RL, Brancati FL. Serum and dietary magnesium and the risk for type 2 diabetes mellitus. The atherosclerosis risk in communities study. *Arch Int Med* 159:2151–59.

[107] Katz AI. Corticosteroid regulation of NaK-ATPase along the mammalian nephron. Semin Nephrol 1990;10(4):388–99.

[108] Kempe DS, Dermaku-Sopjani M, Frohlich H, Sopjani M, Umback A, Puchchakavala G, et al. Rapamycin-induced phosphaturia. Nephrol Dial Transplant 2010;25:2938–44.

[109] Kim SJ, Kang HS, Jeong CW, Park SY, Kim IS, Kim NS, et al. Immunosuppressants inhibit hormone-stimulated magnesium uptake in mouse distal convoluted tubule cells. Biochm Biophys Res Commun 2006;34(3):742–8.

[110] Koch Nogueira PC, David L, Cochat P. Evolution of secondary hyperparathyroidism after renal transplantation. Pediatr Nephrol 2000;14(4):342–6.

[111] Kon VSM, Inagami T, et al. Cyclosporine causes endothelin dependent acute renal failure. Kidney Int 1990;37:486.

[112] Kornerup HJ, Pedersen EB. Plasma renin, plasma aldosterone and exchangeable sodium in normotensive and hypertensive kidney transplant recipients with and without transplant renal artery stenosis. Acta Med Scand 1977;202(6):509–16.

[113] Kornerup HJ, Pedersen EB. Plasma renin, plasma aldosterone and exchangeable sodium in normotensive and hypertensive kidney transplant recipients with and without transplant renal artery stenosis. Acta Med Scan 1977;37(4):295–301.

[114] Kornerup HJ. The significance of body sodium content in hypertension following renal transplantation: exchangeable sodium and plasma renin concentration before and after renal transplantation. Scand J Clin Lab Invest 1977;37(4): 295–301.

[115] Kotanko P, Margreiter R, Pfaller W. Graft ischemia correlates with urinary excretion of the proximal marker enzyme fructose-1 6-bisphosphatase in human kidney transplantation. Nephron 1997;77(1):62–7.

[116] Kramer HJ, Goldman R, Gonick HC. Salt-losing syndromes following renal transplantation. Am J Med 1972;53(3):368–76.

[117] Kritikou P, Kamvyssi-Dea S, Hadjiyannakis E, Tavormina V. Changes of serum potassium during experimental bilateral nephrectomy and renal transplantation. Panminerva Med 1977;19(5):361–4.

[118] Kurtz A, Della Bruna R, Kuhn K. Cyclosporine A enhances renin secretion and production in isolated juxtaglomerular cells. Kidney Int 1988;33(5):947–53.

[119] Kwon O, Corrigan G, Myers BD, Sibley R, Scandling JD, Dafoe D, et al. Sodium reabsorption and distribution of Na + /K + -ATPase during postischemic Injury to the renal allograft. Kidney Int 1999;55(3):963–75.

[120] Laine J, Holmberg C. Mechanisms of hyperuricemia in cyclosporine-treated renal transplanted children. Nephron 1996;74(2):318–23.

[121] Larsson T, Nisbeth U, Ljunggren O, Jüppner H, Jonsson KB. Circulating concentration of FGF-23 increases as renal function declines in patients with chronic kidney disease, but does not change in response to variation in phosphate intake in healthy volunteers. Kidney Int 2003;64(6):2272–9.

[122] Lea JP, Sands JM, McMahon SJ, Tumlin JA. Evidence that the inhibition of Na + /K(+)-ATPase activity by FK506 involves calcineurin. Kidney Int 1994;46(3):647–52.

[123] Lewis BMGE, DeTar B. Pendelluft: fact or fiction? J Clin Invest 1966;45:1040.

[124] Lieberman KV, Lin WG, Reisman L. FK 506 is a direct glomeruloconstrictor, as determined by electrical resistance pulse sizing (ERPS). Transplant Proc 1991;23(6):3119–20.

[125] Lobo PI, Cortez MS, Stevenson W, Pruett TL. Normocalcemic hyperparathyroidism associated with relatively low 1:25 vitamin D levels post-renal transplant can be successfully treated with oral calcitriol. Clin Transplant 1995;9(4):277–81.

[126] Lote CJ, Thewles A, Wood JA, Zafar T. The hypomagnesaemic action of FK506: urinary excretion of magnesium and calcium and the role of parathyroid hormone. Clin Sci (Lond) 2000;99 (4):285–92.

[127] Madsen S, Olgaard K, Lund B, Lund B, Sorensen OH. Pathogenesis of hypophosphataemia in kidney necrograft recipients: a controlled trial. Proc Eur Dial Transplant Assoc 1979;16:618–23.

[128] Magee JH, Hume DM, Kauffman HM, Bower JD. Massive diuresis following renal homotransplantation. Proc Soc Exp Biol Med 1964;116:480–3.

[129] Massari PU. Disorders of bone and mineral metabolism after renal transplantation. Kidney Int 1997;52(5):1412–21.

[130] Massry SG, Coburn JW, Chapman LW, Kleeman CR. The acute effect of adrenal steroids on the interrelationship between the renal excretion of sodium, calcium, and magnesium. J Lab Clin Med 1967;70(4):563–70.

[131] Massry SG, Preuss HG, Maher JF, Schreiner GE. Renal Tubular acidosis after cadaver kidney homotransplantation. Studies on mechanism. Am J Med 1967;42(2):284–92.

[132] Matsumura C, Kuwashima H, Kimura T. Differential effects of FK506 and cyclosporin A on catecholamine release from bovine adrenal chromaffin cells. Auton Autacoid Pharmacol 2004;24(3):55–61.

[133] Maury CP, Teppo AM. Raised serum levels of cachectin/tumor necrosis factor alpha in renal allograft rejection. J Exp Med 1987;166(4):1132–7.

[134] McCarron DA, Bennett WM, Muther RS, Barry JM, Krutzik S. Posttransplantation hyperparathyroidism: demonstration of retained control of parathyroid function by plasma ionized calcium. Am J Clin Nutr 1980;33(7):1536–40.

[135] McCarron DA, Muther RS, Lenfesty B, Bennett WM. Parathyroid function in persistent hyperparathyroidism: relationship to gland size. Kidney Int 1982;22(6):662–70.

[136] McCauley J, Farkus Z, Prasad SJ, Plummer HA, Murray SA. Cyclosporine and FK 506 induced inhibition of renal epithelial cell proliferation. Transplant Proc 1991;23(6):2829–30.

[137] McPhaul Jr JJ, McIntosh DA, Hammond WS, Park OK. Autonomous secondary (renal) parathyroid hyperplasia. N Engl J Med 1964;271:1342–5.

[138] Mihatsch MJ, Ryffel B, Hermle M, Brunner FP, Thiel G. Morphology of cyclosporine nephrotoxicity in the rat. Clin Nephrol 1986;25(Suppl. 1):S2–8.

[139] Mihatsch MJ, Thiel G, Ryffel B. Histopathology of cyclosporine nephrotoxicity. Transplant Proc 1988;20(Suppl. 3):759–71.

[140] Miki K, Hayashida Y, Sagawa S, Shiraki K. Renal sympathetic nerve activity and natriuresis during water immersion in conscious dogs. Am J Physiol 1989;256(2 Pt 2):R299–305.

[141] Moss NG, Powell SL, Falk RJ. Intravenous cyclosporine activates afferent and efferent renal nerves and causes sodium retention in innervated kidneys in rats. Proc Natl Acad Sci U S A 1985;82(23):8222–6.

[142] Moutabarrik A, Ishibashi M, Fukunaga M, Kameoka H, Kawaguchi N, Takano Y, et al. FK506-induced kidney tubular cell injury. Transplantation 1992;54(6):1041–7.

[143] Moutabarrik A, Ishibashi M, Fukunaga M, Kameoka H, Takano Y, Kokado Y, et al. FK 506 mechanism of nephrotoxicity: stimulatory effect on endothelin secretion by cultured

kidney cells and tubular cell toxicity *in vitro*. Transplant Proc 1991;23(6):3133–6.
[144] Muller-Suur R, Davis SD. Effect of cyclosporine A on renal electrolyte transport: whole kidney and Henle loop study. Clin Nephrol 1986;25(Suppl. 1):S57–61.
[145] Muller-Suur R, Norlen BJ, Persson AE. Resetting of tubuloglomerular feedback in rat kidneys after unilateral nephrectomy. Kidney Int 1980;18(1):48–57.
[146] Munger KA, Coffman TM, Griffiths RC, Fogo A, Badr KF. The effects of surgery and acute rejection on glomerular hemodynamics in the transplanted rat kidney. Transplantation 1993;55 (6):1219–24.
[147] Murray BM, Paller MS. Beneficial effects of renal denervation and prazosin on GFR and renal blood flow after cyclosporine in rats. Clin Nephrol 1986;25(Suppl. 1):S37–9.
[148] Najarian JS, Gillingham KJ, Sutherland DE, Reinsmoen NL, Payne WD, Matas AJ. The impact of the quality of initial graft function on cadaver kidney transplants. Transplantation 1994;57(6):812–6.
[149] Navaneethan SD, Sankarasubbaiyan S, Gross MD, Jeevanantham V, Monk RD. Tacrolimus-associated hypomagnesemia in renal transplant recipients. Transplant Proc 2006;38 (5):1320–2.
[150] Neild GH, Rocchi G, Imberti L, Fumagalli F, Brown Z, Remuzzi G, et al. Effect of Cyclosporin A on prostacyclin synthesis by vascular tissue. Thromb Res 1983;32(4):373–9.
[151] Norlen BJ, Engberg A, Kallskog O, Wolgast M. Intrarenal hemodynamics in the transplanted rat kidney. Kidney Int 1978;14(1):1–9.
[152] Norlen BJ, Muller-Suur R, Persson AE. Tubulo-glomerular feedback response and excretory characteristics of the transplanted rat kidney. Scand J Urol Nephrol 1978;12(1):27–33.
[153] Nozue T, Kobayashi A, Sako A, Satoh T, Kodama T, Yamazaki H, et al. Evidence that cyclosporine causes both intracellular migration and inappropriate urinary excretion of magnesium in rats. Transplantation 1993;55(2):346–9.
[154] Nyberg G, Herlitz H, Bjorck S, Karlberg I, Hedner T, Hedner J. Acute and long-term changes in plasma levels of atrial natriuretic factor in patients with renal replacement therapy. Transpl Int 1990;3(4):195–8.
[155] Ogden DA, Sitprija V, Holmes JH. Function of the renal homograft in man immediately after transplantation. Am J Med 1965;38:873–82.
[156] Ogden DA. Donor and recipient function 2 to 4 years after renal homotransplantation. A paired study of 28 cases. Ann Intern Med 1967;67(5):998–1006.
[157] Oliver J, Macdowell M, Tracy A. The pathogenesis of acute renal failure associated with traun and toxic injury; renal ischemia, nephrotoxic damage and the ischemic episode. J Clin Invest 1951;30(12:1):1305–51.
[158] Pabico RC, McKenna BA. Metabolic problems in renal transplant patients. Persistent hyperparathyroidism and hypophosphatemia: effects of Intravenous calcium infusion. Transplant Proc 1988;20(Suppl 1):438–42.
[159] Pachon J, Lorber MI, Bia MJ. Effects of H2-receptor antagonists on renal function in cyclosporine-treated renal transplant patients. Transplantation 1989;47(2):254–9.
[160] Palestine AG, Austin III HA, Nussenblatt RB. Renal tubular function in cyclosporine-treated patients. Am J Med 1986;81 (3):419–24.
[161] Parfitt AM, Kleerekoper M, Cruz C. Reduced phosphate reabsorption unrelated to parathyroid hormone after renal transplantation: implications for the pathogenesis of hyperparathroidism in chronic renal failure. Miner Electrolyte Metab 1986;12(5-6):356–62.
[162] Perez GO, Oster JR. Hyporeninemic hypoaldosteronism after renal transplantation. South Med J 1977;70(3):363–4.
[163] Perico N, Benigni A, Bosco E, Rossini M, Orisio S, Ghilardi F, et al. Acute cyclosporine A nephrotoxicity in rats: which role for renin-angiotensin system and glomerular prostaglandins?. Clin Nephrol 1986;25(Suppl. 1):S83–8.
[164] Perico N, Dadan J, Remuzzi G. Endothelin mediates the renal vasoconstriction induced by cyclosporine in the rat. J Am Soc Nephrol 1990;1(1):76–83.
[165] Perico N, Zoja C, Benigni A, Ghilardi F, Gualandris L, Remuzzi G. Effect of short-term cyclosporine administration in rats on renin-angiotensin and thromboxane A2: possible relevance to the reduction in glomerular filtration rate. J Pharmacol Exp Ther 1986;239(1):229–35.
[166] Peters DH, Fitton A, Plosker GL, Faulds D. Tacrolimus. A review of its pharmacology, and therapeutic potential in hepatic and renal transplantation. Drugs 1993;46(4):746–94.
[167] Petric R, Freeman D, Wallace C, McDonald J, Stiller C, Keown P. Effect of cyclosporine on urinary prostanoid excretion, renal blood flow, and glomerulotubular function. Transplantation 1988;45(5):883–9.
[168] Pisitkun T, Johnstone R, Knepper MA. Discovery of urinary biomarkers. Mol Cell Proteomics 2006;5(10):1760–71 [Epub 2006 Jul 12].
[169] Pisitkun T, Shen RF, Knepper MA. Identification and proteomic profiling of exosome in human urine. Proc Natl Acad Sci USA 2004;101(36):13368–73 [Epub 2004 Aug 23]
[170] Plum J, Scholtz W, Grabensee B. Atrial natriuretic peptide in renal transplantation. Horm Res 1996;46(2):74–82.
[171] Ponce P, Cruz J, Travassos J, Moreira P, Oliveira J, Melo-Gomes E, et al. Renal toxicity mediated by continuous infusion of recombinant interleukin-2. Nephron 1993;64(1):114–8.
[172] Propper DJ, Whiting PH, Mackay J, Catto GR. Glomerulotubular function in long-term renal allograft recipients. A comparison of conventional therapy with cyclosporine. Transplantation 1990;50(1):72–5.
[173] Quereda C, Soria C, Gallego N, Sabater J, Pascual J, Orofino L, et al. Urinary acidification response to furosemide administration in patients on low-dose cyclosporine therapy. Am J Nephrol 1993;13(2):107–14.
[174] Rabelink TJ, van Tilborg KA, Hene RJ, Koomans HA. Natriuretic response to head-out immersion in humans with recent kidney transplants. Clin Sci (Lond) 1993;85(4):471–7.
[175] Ratcliffe PJ, Richardson AJ, Kirby JE, Moyses C, Shelton JR, Morris PJ. Effect of intravenous infusion of atriopeptin 3 on immediate renal allograft function. Kidney Int 1991;39(1): 164–8.
[176] Roby KA, Shaw LM. Effects of cyclosporine and its metabolites in the isolated perfused rat kidney. J Am Soc Nephrol 1993;4 (2):168–77.
[177] Rogers TS, Elzinga L, Bennett WM, Kelley VE. Selective enhancement of thromboxane in macrophages and kidneys in cyclosporine-induced nephrotoxicity. Dietary protection by fish oil. Transplantation 1988;45(1):153–6.
[178] Roll D, Licht A, Rosler A, Durst AL, Kleeman CR, Czaczkes JW. Transient hypoaldosteronism after renal allotransplantation. Isr J Med Sci 1979;15(1):29–34.
[179] Rosenbaum R, Hoffsten PE, Cryer P, Klahr S. Hyperkalemia after renal transplantation. Occurrence in a patient with insulin-dependent diabetes. Arch Intern Med 1978;138 (8):1270–2.
[180] Rosenbaum RW, Hruska KA, Korkor A, Anderson C, Slatopolsky E. Decreased phosphate reabsorption after renal transplantation: Evidence for a mechanism independent of calcium and parathyroid hormone. Kidney Int 1981;19(4):568–78.

[181] Rowe PS. The wrickkened pathways of FGF23, MEPE and PHEX. Crit Rev Oral Biol Med 2004;15(5):264–81.
[182] Rubini ME, Agre KL, Mims MM, Koppel MH, Coburn JW. Curious tubular syndromes after homotransplantation. Clin Res 1967;16:167.
[183] Sakamoto K, Yamada K, Arita S, Hamaguchi K, Kashiwabara H, Yokoyama T. Sodium-losing nephropathy and distal tubular damage of transplant kidneys with FK506 administration. Transplant Proc 1995;27(1):826–8.
[184] Sakhaee K, Brinker K, Helderman JH, Bengfort JL, Nicar MJ, Hull AR, et al. Disturbances in mineral metabolism after successful renal transplantation. Miner Electrolyte Metab 1985;11 (3):167–72.
[185] Sakhaee JH. Kidney transplantation: mineral metabolism complications. New York: Marcel Dekker; 1997.
[186] Sands JM, Neylan JF, Olson RA, O'Brien DP, Whelchel JD, Mitch WE. Atrial natriuretic factor does not improve the outcome of cadaveric renal transplantation. J Am Soc Nephrol 1991;1(9):1081–6.
[187] Schwartz GH, David DS, Riggio RR, Saville PD, Whitsell JC, Stenzel KH, et al. Hypercalcemia after renal transplantation. Am J Med 1970;49(1):42–51.
[188] Sennesael JJ, Lamote JG, Violet I, Tasse S, Verbeelen DL. Divergent effects of calcium channel and angiotensin converting enzyme blockade on glomerulotubular function in cyclosporine-treated renal allograft recipients. Am J Kidney Dis 1996;27(5):701–8.
[189] Shimada T, Hasegawa H, Yamazaki Y, Muto T, Hino R, Takeuchi Y, et al. FGF-23 is a potent regulator of vitamin D metabolism and phosphate homeostasis. J Bone Miner Res 2004;19(3):429–35.
[190] Smeesters C, Chaland P, Giroux L, Moutquin JM, Etienne P, Douglas F, et al. Prevention of acute cyclosporine A nephrotoxicity by a thromboxane synthetase inhibitor. Transplant Proc 1988;20(Suppl 3):658–64.
[191] Smits P, Huysmans F, Hoitsma A, Tan A, Koene R. The effect of alpha-human atrial natriuretic peptide on the incidence of acute renal failure in cadaveric kidney transplantation. Transpl Int 1989;2(2):73–7.
[192] Solez K, Racusen LC, Marcussen N, Slatnik I, Keown P, Burdick JF, et al. Morphology of ischemic acute renal failure, normal function, and cyclosporine toxicity in cyclosporine-treated renal allograft recipients. Kidney Int 1993;43 (5):1058–67.
[193] Sonoda H, Yokota-Ikeda N, Oshikawa S, Kanno Y, Yoshinaga K, Uchida K, et al. Decreased abundance of urinary exosomal aquaporin-1 in renal ischemia-reperfusion injury. Am J Physiol Renal Physiol 2009;297(4):F1006–16 [Epub 2009 Jul 29].
[194] Stahl RA, Kudelka S. Chronic cyclosporine A treatment reduces prostaglandin E2 formation in isolated glomeruli and papilla of rat kidneys. Clin Nephrol 1986;25(Suppl. 1):S78–82.
[195] Stanek B, Kovarik J, Rasoul-Rockenschaub S, Silberbauer K. Renin-angiotensin-aldosterone system and vasopressin in cyclosporine-treated renal allograft recipients. Clin Nephrol 1987;28(4):186–9.
[196] Sufrin G, Kirdani R, Sandberg AA, Murphy GP. Studies of renin-aldosterone axis in stable normotensive and hypertensive renal allograft recipients. Urology 1978;11(1):46–52.
[197] Suthanthiran M, Fotino M, Riggio RR, Cheing JS, Stenzel KH. OKT-3 Associated adverse reactions: mechanistic basis and therapeutic options. Am J Kidney Dis 1967;14(Suppl 2):39–44.
[198] Schwarz C, Bohmig GA, Steininger R, Mayer G, Oberhauer R. Impaired phosphate handling of renal allografts is aggravated under rapamycin-based immunosuppresion. Nephrol Dial Transplant 2001;16(2):378–82.
[199] Swenson RS, Kountz SL, Cohn R, Maffly RH. Posttransplant natriuresis. Clin Res 1967;15:115.
[200] Teraoka S, Sanaka T, Takahashi K, Toma H, Yamaguchi Y, Yagisawa T, et al. Stimulation of intrinsic prostacyclin synthesis and inhibition of thromboxane production to minimize cyclosporine nephrotoxicity. Transplant Proc 1988;20(Suppl 3):638–45.
[201] Terashima A, Nakai M, Hashimoto T, Kawamata T, Taniguchi T, Yasuda M, et al. Single-channel activity of the Ca2 + -dependent K + channel is modulated by FK506 and rapamycin. Brain Res 1998;786(1-2):255–8.
[202] Textor SC, Margolin K, Blayney D, Carlson J, Doroshow J. Renal, volume, and hormonal changes during therapeutic administration of recombinant interleukin-2 in man. Am J Med 1987;83(6):1055–61.
[203] Thiel G, Mihatsch MJ, Stahl RA, Hermle M, Brunner FP. Cyclosporine A nephrotoxicity in Goldblatt renovascular hypertension in rats. Clin Nephrol 1986;25(Suppl. 1):S199–204.
[204] Thiel G. Experimental cyclosporine A nephrotoxicity: an international workshop. April 24–26, 1985, Basle. Clin Nephrol 1986;25(Suppl 1):S1–210.
[205] Thomsen K. Lithium clearance: a new method for determining proximal and distal tubular reabsorption of sodium and water. Nephron 1984;37(4):217–23.
[206] Thomson SC, Tucker BJ, Gabbai F, Blantz RC. Functional effects on glomerular hemodynamics of short-term chronic cyclosporine in male rats. J Clin Invest 1989;83(3):960–9.
[207] Torres A, Lorenzo V, Salido E. Calcium metabolism and skeletal problems after transplantation. J Am Soc Nephrol 2002;13 (2):551–8.
[208] Tumlin JA, Sands JM. Nephron segment-specific inhibition of Na + /K(+)-ATPase activity by cyclosporin A. Kidney Int 1993;43(1):246–51.
[209] Ueda D, Tajima A, Ohtawara Y, Ishikawa A, Nakano M, Ushiyama T, et al. Influence of FK 506 on renal blood flow. Transplant Proc 1991;23(6):3121–2.
[210] Uribarri J, Oh MS, Butt KM, Carroll HJ. Pseudohypoaldosteronism following kidney transplantation. Nephron 1982;31(4):368–70.
[211] van ESA, Hermans J, van Bockel JH, Persijn GG, van Hooff JP, de Graeff J. Effect of warm ischemia time and HLA (A and B) matching on renal cadaveric graft survival and rejection episodes. Transplantation 1983;36(3):255–8.
[212] Van Laecke S, Van Biesen W, Verbeke F, De Bacquer D, Peeters P, Vanholder R. Post-transplantation hypomagnesemia and its relation with immunosuppression as predictors of new-onset diabetes after transplantation. Am J of Transplant 2009;9:2140–9.
[213] van Valenberg PL, Hoitsma AJ, Tiggeler RG, Berden JH, van Lier HJ, Koene RA. Mannitol as an indispensable constituent of an intraoperative hydration protocol for the prevention of acute renal failure after renal cadaveric transplantation. Transplantation 1987;44(6):784–8.
[214] Velic A, Hirsch JR, Bartel J, Thomas R, Schroter R, Stegemann H, et al. Renal transplantation modulates expression and function of receptors and transporters of rat proximal tubules. J Am Soc Nephrol 2004;15(4):967–77.
[215] Velic A, Gabriëls G, Hirsch JR, Schröter R, Edemir B, Paasche S, et al. Acute rejection after rat renal transplantation leads to downregulation of NA + and water channels in the collecting duct. Am J Transplant 2005;5(6):1276–85.
[216] Verani R. Cyclosporine nephrotoxicity in the Fischer rat. Clin Nephrol 1986;25(Suppl. 1):S9–13.

[217] Verpooten GA, Wybo I, Pattyn VM, Hendrix PG, Giuliano RA, Nouwen EJ, et al. Cyclosporine nephrotoxicity: comparative cytochemical study of rat kidney and human allograft biopsies. Clin Nephrol 1986;(Suppl 1):S18–22.

[218] Versluis DJ, Wenting GJ, Jeekel J, Weimar W. The influence of cyclosporine A on proximal tubular function in renal allografts. Transplant Proc 1988;20(Suppl 3):686–90.

[219] Vincent HH, Wenting GJ, Versluis DJ, Weimar W, Schalekamp MA. Impaired fractional excretion of lithium: an early marker of cyclosporine-induced changes in renal hemodynamics. Transplant Proc 1988;20(Suppl. 3):681–5.

[220] Vinot O, Bialek J, Canaan-Kühl S, Scandling Jr JD, Dafoe D, Alfrey E, et al. Endogenous ANP In Postichemic acute renal allograft failure. Am J Physiol 1995;269(1Pt2):F125–33.

[221] Wacker WE, Parisi AF. Magnesium metabolism. N Engl J Med 1968;278(12):658–63.

[222] Ward HN, Pabico RC, McKenna BA, Freeman RB. The renal handling of phosphate by renal transplant patients: correlation with serum parathyroid hormone (SPTH), cyclic 3′,5′-adenosine monophosphate (cAMP) urinary excretion, and allograft function. Adv Exp Med Biol 1977;81:173–81.

[223] Webb DE, Austin III HA, Belldegrun A, Vaughan E, Linehan WM, Rosenberg SA. Metabolic and renal effects of interleukin-2 immunotherapy for metastatic cancer. Clin Nephrol 1988;30 (3):141–5.

[224] Weidmann P, Matter DR, Matter EE, Gnadinger MP, Uehlinger DE, Shaw S, et al. Glucocorticoid and mineralocorticoid stimulation of atrial natriuretic peptide release in man. J Clin Endocrinol Metab 1988;66(6):1233–9.

[225] Weir MR, Klassen DK, Shen SY, Sullivan D, Buddemeyer EU, Handwerger BS. Acute effects of intravenous cyclosporine on blood pressure, renal hemodynamics, and urine prostaglandin production of healthy humans. Transplantation 1990;49 (1):41–7.

[226] West C, Carpenter BJ, Hakala TR. The incidence of gout in renal transplant recipients. Am J Kidney Dis 1987;10 (5):369–72.

[227] Whiting PH, Propper DJ, Simpson JG, McKay J, Jones MC, Catto GR. The use of lithium clearance measurements to assess renal tubular function in experimental and clinical cyclosporine nephrotoxicity. Transplant Proc 1988;20 (Suppl. 3):675–80.

[228] Whiting PH, Simpson JG. Lithium clearance measurements as an indication of cyclosporin A nephrotoxicity in the rat. Clin Sci (Lond) 1988;74(2):173–8.

[229] Whiting PH, Thomson AW, Simpson JG. Cyclosporine and renal enzyme excretion. Clin Nephrol 1986;25(Suppl. 1):S100–4.

[230] Wilson DR, Siddiqui AA. Renal tubular acidosis after kidney transplantation. Natural history and significance. Ann Intern Med 1973;79(3):352–61.

[231] Wong NL, Dirks JH. Cyclosporin-induced hypomagnesaemia and renal magnesium wasting in rats. Clin Sci (Lond) 1988;75 (5):509–14.

[232] Wu MS, Yang CW, Bens M, Peng KC, Yu HM, Vandewalle A. Cyclosporine stimulates $Na+-K+-Cl-$ cotransport activity in cultured mouse medullary thick ascending limb cells. Kidney Int 2000;58(4):1652–63.

[233] Yamada K, Sugisaki Y, Akimoto M, Yamanaka N. FK 506-induced juxtaglomerular apparatus hyperplasia and tubular damage in rat kidney—morphologic and biologic analysis. Transplant Proc 1992;24(4):1396–8.

[234] Zhou H, Pisikun T, Aponte A, Yuen PS, Hoffert JD, Yasuda H, et al. Exosomal Fetuin-A identified by proteomics: a novel urinary biomarker for detecting acute kidney injury. Kidney Int 2006;70(10):1847–57 [Epub 2006 Oct 4]

[235] Zurcher RM, Bock HA, Thiel G. Hyperuricaemia in cyclosporin-treated patients: GFR-related effect. Nephrol Dial Transplant 1996;11(1):153–8.

This page intentionally left blank

CHAPTER

95

Renal Disposition of Drugs and Translation to Dosing Strategies

Pär Matsson, Kathleen M. Giacomini and D. Craig Brater

Uppsala University, Department of Pharmacy, Uppsala, Sweden
University of California San Francisco, Department of Bioengineering and Therapeutic Sciences, San Francisco, California, USA
Indiana University School of Medicine, Department of Medicine, Indianapolis, Indiana, USA

INTRODUCTION

Numerous drugs are eliminated by the kidney. For others, polar metabolites are formed by metabolism or conjugation (usually in the liver)—that are then excreted by the kidney. Renal impairment thereby leads to the accumulation of drugs and their metabolites. For many drugs, doses must be adjusted to attain concentrations similar to those obtained in patients with normal renal function. Renal dysfunction can also affect distribution of drugs, primarily by effects on protein binding. Last, changes in renal function can affect response to drugs independent of any change in disposition.

Several general characteristics of a drug allow prediction as to whether renal dysfunction is likely to affect its disposition sufficiently to mandate changes in drug dosing (Table 95.1).[1–2] If a drug has a wide therapeutic index, accumulation in patients with renal insufficiency to concentrations several-fold higher than in patients with normal renal function has little, if any, consequence, and dose adjustment can be ignored. For example, a number of penicillin derivatives and many cephalosporins are primarily eliminated by the kidney but can accumulate with little risk. Toxic accumulation of these drugs can sometimes occur, but usually only with massive doses in patients with compromised excretion.

The amount of a drug or active metabolite excreted in the urine can allow predictions as to the potential for clinically important drug or metabolite accumulation in patients with renal insufficiency. In general, if about 40% or more of a drug dose is excreted in urine, dose adjustment will be needed in patients with renal insufficiency—assuming the drug in question has a sufficiently narrow therapeutic index to be of concern. An exception to this rule of thumb is drugs with the potential for undergoing a "futile cycle," which refers to the fact that the metabolic route serves to form a reservoir for parent drug. Thus, the metabolic step is "futile" (see the section on metabolism). With such agents, little (if any) drug itself is normally excreted in the urine—yet renal insufficiency can result in its accumulation in plasma. The mechanism of this effect, and the few drugs to which it applies, are discussed in material following. It is also important to note that some drugs are metabolized to active metabolites in which case, both drug and metabolite are pharmacologically potent. Further, some drugs are pro-drugs, which are themselves inactive, but are converted to active compounds (e.g., clopidogrel or irnotecan). For these drugs, the focus of dosing adjustment should be on the active compounds.

It should be apparent from the foregoing that for drugs that have not been explicitly studied in patients with renal insufficiency one can make reasonable predictions as to the need for adjusting therapy. Although lack of quantitative guidelines makes dose adjustments tentative, a worse problem is ignoring the need to do so. When no information concerning the relevant characteristics of a drug is available, one therapeutic strategy is to use a drug of the same class—but with no

Seldin and Giebisch's The Kidney, Fifth Edition.
DOI: http://dx.doi.org/10.1016/B978-0-12-381462-3.00095-1

© 2013 Elsevier Inc. All rights reserved.

TABLE 95.1 General Characteristics of Drug That Predict Important Influences of Renal Function

Characteristics	Implications
Therapeutic index	If the drug has a wide therapeutic index, its accumulation poses negligible risk.
Protein binding	A high degree of binding (>90%) to albumin makes displacement likely in uremic patients. A high degree of binding to either albumin or α1-acid glycoprotein means little drug is available for removal by dialysis.
Amount of drug excreted in the urine unchanged	If ≥40% of a drug is excreted in the urine unchanged, it is highly likely to accumulate in patients with renal insufficiency.
Active metabolites excreted in the urine	The metabolites can accumulate, with attendant effects.
Volume of distribution	A small volume of distribution (that of total body water or less; that is, ≤0.7 liter/kg) means the drug may be accessible for dialytic removal if it is not highly protein bound. A large volume of distribution means little if any removal by dialysis.

dependence on the kidney for elimination. For example, if a clinician wishes to prescribe a cardio-selective beta-adrenergic antagonist to a patient with renal insufficiency one alternative is to administer atenolol in a modified dose. Another option is to administer metoprolol, which is eliminated by the liver and needs no dose adjustment in patients with renal insufficiency.[2] The converse would apply to patients with liver disease. However, there is a growing body of literature that suggests that drug metabolism may be altered in patients with renal dysfunction,[3–6] and increasingly the U.S. Food and Drug Administration is requiring studies of the effects of renal dysfunction on new drugs that are cleared by non-renal routes.[7] Therefore, some caution should be exercised in simply switching a patient from a drug predominantly eliminated by the kidney to a drug with a predominant nonrenal elimination.

ROLE OF THE KIDNEY IN DRUG DISPOSITION

Most drugs are excreted via the kidneys, either in the form of the unchanged drug molecule or after conversion of the parent drug into polar metabolites. Mechanisms by which the kidney excretes drugs are analogous to its normal physiologic processes of glomerular filtration, active secretion, and active and passive reabsorption. Below, the processes of importance for the handling of drugs are briefly described. Effects on any of these processes, e.g., through interactions between concomitantly administered drugs or through renal disease, can mandate changes in drug dosing. The influence of altered kidney function on systemic drug disposition, and corresponding dosing strategies are discussed in more detail in subsequent sections.

Glomerular Filtration

The glomerulus offers no barrier to filtration of the unbound fraction of most drugs.[8–9] Glomerular pores allow passage of molecules up to molecular weights of about 65,000 Daltons, and the vast majority of xenobiotics (including many biologic agents) are approximately two orders of magnitude smaller than this. Exceptions include larger proteins and dextran. Dextran is a good example of the role of molecular size; it can be administered as several different preparations, the size of which determines their ability to be filtered.[10] Thus, dextran 1 (MW=1000) is freely filtered and is eliminated rapidly by the kidney—with a half-life of elimination of about 2 hours.[11] In contrast, dextran 70 is too large to be filtered and is eliminated slowly by metabolism. It is detectable in plasma for 4 to 6 weeks.[11–12] Dextran 40 is a mixture of both higher- and lower-molecular-weight species so that the smaller dextrans are freely filtered and eliminated quickly, with selective retention of the larger components.[10–11]

For drugs freely filtered at the glomerulus, such as aminoglycoside antibiotics, renal elimination can be quite rapid. For many other drugs, binding to serum proteins restricts filtration and thus only the unbound fraction can be filtered and renal excretion, depending on the extent of binding, may be negligible. The limits to glomerular filtration of a drug, then, are usually not the glomerular barrier itself but factors that prevent filtration—predominantly binding to macromolecules too large to be filtered.

Secretion and Reabsorption

The overall renal drug clearance is determined by the relative importance of filtration, secretion of drug into the primary urine, and reabsorption back into the blood. It follows that secretion must occur if the rate of excretion is higher than that of filtration, and conversely, if the rate of excretion is lower than the filtration rate, the drug is by necessity reabsorbed.

Secretion: The classical method described for assessing drug secretion by the kidney was that of Cross and Taggart, using incubations of renal cortical slices.[13]

The sine qua non for secretion was a slice-to-medium–concentration ratio greater than unity. Numerous more sophisticated methods for characterizing secretion have since evolved, including microperfusion of isolated nephron segments, use of isolated proximal tubular cells or vesicles derived from peritubular or luminal membranes of proximal tubules, and cellular expression systems for detailed studies of drug transport by specific membrane transporters.[14–16]

Drugs gain access to secretory sites via the peritubular capillary. If 20% of renal plasma flow is filtered, the remaining 80% of flow reaches sites of secretion. This process is active because an uphill concentration gradient can be generated. Moreover, depriving the proximal tubule of energy also inhibits movement of drugs from the peritubular to the tubular side of the cell.[8,17] The energy for active secretion is ultimately obtained from ATP hydrolysis, either directly driving transmembrane drug flux (i.e., primary active transport), or generating concentration gradients across the cell membranes that, in turn, drive the solute flux (secondary active transport). In the latter case, energy is generated by peritubular sodium-potassium exchange via Na^+,K^+-ATPase.[8,18–19]

The efficiency of secretion is quite impressive. For example, secretion occurs for many drugs that are highly protein bound (such as furosemide).[20] For this and other drugs, the affinity for transport exceeds that for binding. As such, binding to plasma proteins actually facilitates elimination by increasing the amount of drug in the plasma and thereby delivering it to secretory sites.[21] That this is the case has been demonstrated in studies with analbuminemic rats. Administration of furosemide to these animals results in very low plasma concentrations of diuretic because without albumin binding the drug distributes widely outside the vascular space. Consequently, only small amounts are delivered to secretory sites and little is excreted into the urine. Administration of albumin in this setting binds furosemide, keeping it in the vascular space so that more diuretic reaches secretory sites (where more can be secreted into the urine).[21] A similar effect has been shown to occur in humans.[21–22]

Reabsorption: The kidney is capable of both active and passive reabsorption of drugs. Various membrane transporters mediate active luminal-to-abluminal flux of substrate drugs, whereas passive drug reabsorption is the consequence of concentration differences between the primary urine and the blood in the peritubular capillaries, that in turn results either from active drug secretion or, typically, from the reabsorption of water along the nephron. Passive reabsorption relies on diffusion of drugs across the lipid bilayers of the renal tubule epithelium and favors nonpolar drugs. For passive diffusion of drugs that are weak acids or bases, the nonionized form of the drug will be passively reabsorbed since it can cross the tubular membranes. Hence, for both weak acids and bases, urine pH can influence passive reabsorption, and urine pH can be manipulated to reduce passive reabsorption and enhance renal elimination. For example, in the case of patients with aspirin overdose, sodium bicarbonate is administered to alkalinize the urine. In the alkaline urine, salicylate is present predominately in the ionized form and is therefore not reabsorbed.

Renal Drug Transporters

While energy-dependent solute transport in the kidney was demonstrated almost a century ago,[23] the roles of transport proteins in the renal handling of drugs remain an active area of research. The human genome contains more than four hundred membrane transporters classified into the ATP-Binding Cassette (ABC) and Solute Carrier (SLC) gene families, in addition to the numerous aquaporins and ion channels that serve the same purpose of facilitating transmembrane solute flux. Here, we limit the discussion to ABC and SLC membrane transporters that are known to transport drug molecules across the membranes of renal cells, either in the secretory or the reabsorptive direction (Figure 95.1). Data on the clinical relevance of the various membrane transporters continues to emerge, and additional members are likely involved in the renal transport of some drugs. In this section we focus on the function and expression of renal drug transporters under physiological

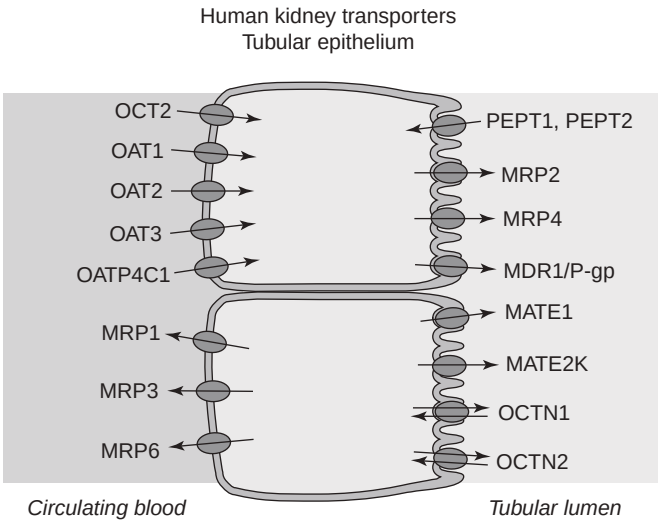

FIGURE 95.1 Cellular localization of clinically important drug transporters in renal epithelia.

conditions, whereas the effects of renal disease is discussed in more detail below (See: Influence of Renal Disease on Drug Disposition and Response).

Early studies defined two separate transport systems for organic solutes in the kidneys, with broad substrate specificities towards organic anions and organic cations, respectively.[17] During the past decades, a large number of distinct transport proteins have been identified as contributors to these transport systems, and functionally characterized with respect to their substrate specificities, cellular localization, genetic variation, and so on. The historical categorization based on substrate charge is, however, not directly mirrored in the assignment of transporters to different gene families based on similarity in amino acid sequence. While substrate specificities often are shared within subfamilies of structurally similar transporters, members of both the anion and the cation systems are found across multiple subfamilies in the ABC and SLC gene families, and some subfamilies contain both anion and cation transporting members.

ABC transporters: The human ABC gene family contains 49 distinct protein coding genes, divided into seven families (ABCA−ABCG) based on amino acid sequence similarity.[24,25] All members contain a highly conserved ATP-binding region, and utilize energy from ATP hydrolysis to drive efflux of substrate molecules from the inside to the outside of cells. ABC transporters of importance for renal drug transport include P-glycoprotein (P-gp/ABCB1) and several members of the Multidrug Resistance Associated Protein (MRP/ABCC) subfamily. P-gp is by far the most well-characterized drug transporter, and has been shown to transport many structurally diverse compounds, typically of a lipophilic and uncharged or weakly basic character (Table 95.2).[24,25] P-gp is expressed in the luminal membrane of proximal tubule epithelium and appears to play a role in the renal clearance of digoxin.[26]

The MRP/ABCC family consists of thirteen transporters, many of which have been shown to accept drugs as substrates, in particular anionic drugs and compounds conjugated with sulfate, glucuronide and glutathione moieties (Table 95.2).[27−31] In the kidney proximal tubule epithelium, MRP2/ABCC2 and MRP4/ABCC4 are expressed in the luminal membrane and mediate secretion of substrates to the urine.[27,30−36] MRP6/ABCC6 is also expressed in the kidney proximal tubules, but is instead localized to the basolateral membrane.[36−38] Expression of MRP1/ABCC1 and MRP3/ABCC3 is highest in more distal parts of the nephron, including the thick ascending loop of Henle, distal tubuli and collecting duct, where their expression in the basolateral membrane suggests involvement in the reabsorption of organic anions.[28,36,39−40] Based on in vivo studies in knockout mice, MRP4 appears to be important in the renal clearance of tenofovir and adefovir, two anti-viral drugs.[41]

SLC transporters: More than 350 human membrane transporters are categorized to the SLC gene family.[42] In contrast to the ABC family, transport by SLCs is not directly coupled to ATP hydrolysis, but is instead dependent on concentration gradients of the transported substrate or of co- or counter-transported ions

TABLE 95.2 Transporters of Emerging Clinical Importance in the Renal Handling of Drugs

Transporter[a]	Gene Symbol	Selected Substrates
P-gp (MDR1)	ABCB1	Digoxin, doxorubicin, irinotecan, loperamide, paclitaxel, ritonavir, saquinavir, vinblastine
MRP1	ABCC1	Daunorubicin, doxorubicin, etoposide, leukotriene C4, methotrexate, saquinavir
MRP2 (cMOAT)	ABCC2	Methotrexate, statins, olmesartan, valsartan, glutathione and glucuronide conjugates
MRP3	ABCC3	Fexofenadine, methotrexate, glucuronide conjugates
MRP4	ABCC4	Adefovir, cyclic AMP, dehydroepiandrosterone sulphate, methotrexate, tenofovir, topotecan
MRP6	ABCC6	Leukotriene C4, BQ123
OCT2	SLC22A2	Amantadine, amiloride, cimetidine, cisplatin, histamin, metformin, serotonin
OCTN1	SLC22A4	Carnitine, pyrilamine, quinidine, verapamil
OCTN2	SLC22A5	Carnitine, cephaloridine, quinidine, verapamil
OAT1	SLC22A6	Acyclovir, adefovir, cidofovir, ciprofloxacin, lamivudine, methotrexate, tenofovir, zalcitabine, zidovudine
OAT2	SLC22A7	Allopurinol, bumetanide, dehydroepiandrosterone sulfate, estrone-3-sulfate, 5-fluorouracil
OAT3	SLC22A8	Bumetanide, cefaclor, ceftizoxime, furosemide, NSAIDs, estrone-3-sulfate
OAT4	SLC22A11	Bumetanide, NSAIDs, tetracycline, urate, zidovudine,
OATP4C1 (OATP-H)	SLCO4C1	Digoxin, estrone sulfate, methotrexate sitagliptin
PepT1	SLC15A1	Amoxicillin, captopril, cephalexin, cefadroxil, enalapril, glycylsarcosine, valacyclovir, dipeptides, tripeptides
PepT2	SLC15A2	Amoxicillin, captopril, cephalexin, cefadroxil, enalapril, glycylsarcosine, valacyclovir, dipeptides, tripeptides

[a]*Alternative transporter symbols in parentheses*

or small endogenous molecules. The SLC family contains many of the transporters necessary for cellular nutrient uptake, including glucose transporters in the SLC2 and SLC5 subfamilies and amino acid transporters in the SLC1, SLC3, SLC6, SLC7, SLC36 and SLC38 subfamilies. Many of these are expressed along the nephron, where they have the important function of limiting the loss of essential nutrients to the urine. The di/tripeptide transporters PepT1/SLC15A1 and PepT2/SLC15A2 have a corresponding role in nutrient reabsorption, but also accept some peptidomimetic drugs as substrates, including β-lactam antibiotics like cephalexin and amoxicillin and angiotensin converting enzyme inhibitors like enalapril and fosinopril (Table 95.2).[43–46]

The SLC subfamilies with the most extensive evidence for a role in drug disposition are the organic anion (OAT) and organic cation (OCT) transporter family SLC22, the organic anion transporting polypeptide family OATP/SLCO, and the recently discovered multidrug and toxic compound extrusion family MATE/SLC47. The SLC22 family contains a mixture of structurally similar organic anion and organic cation transporters.[47] In the kidney proximal tubule, OCT2/SLC22A2 is the primary transporter mediating cellular uptake of organic cations from the blood. Substrates are typically low molecular weight cations, and include drugs such as metformin, amiloride, procainamide, oxaliplatin and varenicline (Table 95.2).[48–51] Recently, MATE1/SLC47A1 and MATE2-K/SLC47A2 were identified as luminal exporters of organic cations in the proximal tubuli, and overlapping substrate and inhibitor specificities between the MATEs and OCT2 have led to the hypothesis that these form a complementary transport system for tubular secretion of small organic cations.[51–58]

Renal organic anion transporters include OAT1–3/SLC22A6–8 and OAT4/SLC22A11. OAT1, 2 and 3 are expressed on the abluminal membrane of proximal tubule cells and mediate cellular uptake of anionic drugs such as para-aminohippuric acid, acyclovir, ciprofloxacin, methotrexate, ceftizoxime, and furosemide (Table 95.2).[47,59–61] OAT4 is expressed on the luminal membrane, and is involved in urate homeostasis and in the reabsorption and/or secretion of anionic drugs.[62,63] In addition to the SLC22s, members of the OATP/SLCO family have been shown to transport numerous anionic drugs. In the kidney, the most prominent member is OATP4C1/SLCO4C1.[61,64] In comparison to the hepatic OATPs 1B1, 1B3 and 2B1, OATP4C1 is so far much less studied. It mediates uptake from the blood into the proximal tubule cells, and substrate drugs include digoxin, estrone sulfate, methotrexate and sitagliptin.[64–66]

Two other transporters in the SLC22 family have been implicated in renal drug elimination: OCTN1 (SLC22A4) and OCTN2 SLC22A5), which transports carnitine in the kidney.[67,68] Mice with mutations in OCTN2 eliminate the model organic cation tetraethylammonium by renal excretion at about half the rate of their wild-type littermates.[67]

Interindividual differences: Genetic variation in membrane transporters can result in increased or diminished drug transport. Such variation has been catalogued as part of genome-wide studies[69–71] and in greater detail in gene family-focused efforts.[72] Many commonly occurring genetic variants in important drug transporters have been characterized in cellular expression systems and some have also been shown to affect the in vivo disposition and pharmacological effect of substrate drugs. For example, torsemide renal clearance was correlated with genetic variation in OAT4/SLC22A11,[73] and a common genetic variant (A270S) in OCT2/SLC22A2 was shown to result in changes in metformin clearance in multiple populations.[74–76]

Several heritable diseases have genetic variants that result in non-functional transporters as their underlying cause. For example, Dubin-Johnson syndrome, which manifests as hyperbilirubinemia, is caused by mutations in MRP2/ABCC2 that reduces biliary excretion of bilirubin.[77–79] The effects of Dubin-Johnson syndrome on renal drug handling is much less studied, but the pharmacokinetics of drugs that utilize MRP2/ABCC2 in their renal excretion may be affected in Dubin-Johnson patients.

In addition to genetic variants that cause direct functional effects by altering or truncating the amino acid sequence, mutations in regulatory genomic regions can have functional effects, by altering expression levels of the transporter. In fact, natural interindividual variation in transporter expression levels can be significant. In liver samples from 110 patients, MRP2/ABCC2 levels varied more than 300-fold,[80] and expression level differences may thus have effects on drug disposition on par with or even greater than many coding region variants. Data on inter-individual differences in renal transporter expression is scarce, but such variation may ultimately affect the disposition of renally cleared drugs.

Renal Metabolism

The kidney has the capacity to metabolize numerous drugs and proteins.[81] The proximal nephron has high levels of glucuronyl transferases, sulfotransferases, and peptidases.[8] The ability of the kidney to conjugate drugs via the transferases has been demonstrated unequivocally in animals, but data in man are fragmentary and less direct. Renal glucuronidation may be substantial. For example, approximately 20% of an

intravenous dose of furosemide and 50% of a dose of morphine may be glucuronidated by the kidney.[82,83]

When glucuronide is conjugated to a xenobiotic, the chemical bond between the two can be either an ether (e.g., phenolic) or an ester (e.g., carboxylic). The latter is called an "acyl-glucuronide." Ether-linked glucuronides are chemically stable and are for the most part excreted in the urine. In contrast, acyl-glucuronides are unstable under physiologic conditions such that the glucuronide can deconjugate back to the parent compound. In addition, the glucuronic acid moiety can migrate to other parts of the molecule (acyl migration).[84]

One implication of this chemical instability is analytical. Consider, for example, that one wishes to measure the amount of a drug excreted in the urine. If not just drug but its acyl-glucuronide is excreted, one must be certain that the metabolite does not deconjugate *ex vivo*—causing a falsely elevated measure of the parent drug. To avoid this phenomenon, samples of urine must be stabilized quickly in acidic buffer (e.g., using 75 μl of 17 M glacial acetic acid in a 20-ml urine aliquot is sufficient).[83,85]

A second implication of acyl-glucuronide formation is the possibility of a futile cycle of drug metabolism (Fig. 95.2). In patients with normal renal function, circulating acyl-glucuronide conjugates that are formed in the liver are readily eliminated in the urine. In patients with renal insufficiency, however, renal excretion is decreased and the conjugate accumulates in plasma—where it can spontaneously hydrolyze to reform the parent compound (Fig. 95.2). This phenomenon leads to a paradox in which a drug may accumulate in patients with renal insufficiency even though negligible amounts of parent drug are eliminated in the urine in patients with normal renal function.

Clofibrate,[86,87] diflunisal,[88,89] and some of the arylpropionic NSAIDs[90–93] have been shown to undergo a futile cycle. It would seem prudent to avoid drugs undergoing acyl-glucuronide conjugation in patients with renal insufficiency, or to at least use them very cautiously in such patients.

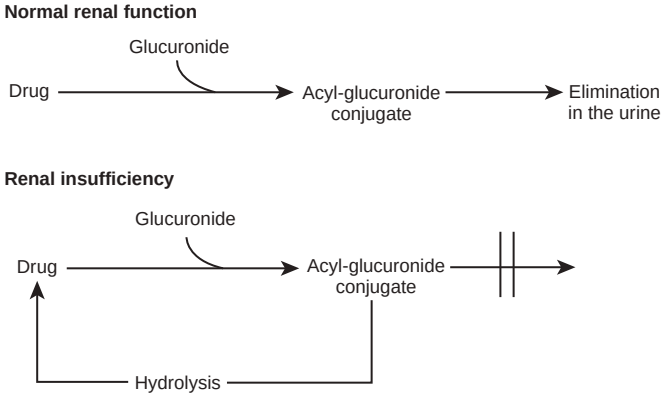

FIGURE 95.2 Schematic illustration of a futile cycle of drug elimination.

The proximal nephron also contains mixed-function cytochrome P450 oxidases (CYP), but in lower amounts than the liver. Interestingly, isoforms of CYP appear to be differentially regulated in the kidney relative to the liver.[94] The relative contribution of renal compared to hepatic metabolism is unknown.[8,81]

The kidney is able to metabolize proteins, such as insulin and other biologic agents—including interleukins, superoxide dismutase (SOD), and likely many others.[95,96] In patients with normal renal function, up to 50% of insulin elimination occurs via renal metabolism. This component of overall elimination diminishes in patients with renal insufficiency and accounts at least in part for the decreased insulin requirement as a patient's renal function deteriorates.[97] Many biologic proteins, such as SOD, are small enough to be freely filtered by the glomerulus. They are then metabolized by the peptidases of the proximal tubule. When renal function declines, renal metabolism is decreased and the substance can accumulate.

Proximal tubule dipeptidases also metabolize imipenem.[98] As such, if imipenem alone is administered to patients, all antibacterial effect in the urine is lost. To attain efficacy for urinary tract infections, imipenem is administered with cilastatin—which inhibits the dipeptidases, allowing sufficient amounts of unchanged imipenem in the urine to kill bacteria.[98]

Overall, then, the kidney is metabolically active toward drugs in a variety of ways. Unfortunately, renal metabolic contributions to drug elimination in man have been inadequately explored and thus clinical implications are for the most part speculative.

In addition to the metabolic roles of the kidney described previously, the kidney excretes many drug metabolites formed in the liver. Renal insufficiency does not necessarily mean that drug metabolites will accumulate because other excretory pathways exist, such as biliary excretion. In addition, many drug metabolites presumably have no effects. On the other hand, there are numerous examples of metabolite accumulation in which the metabolites are pharmacologically active (Table 95.3).[99,100] Some of the metabolites listed exert pharmacologic effects similar to those of the parent compound (e.g., primidone).[101] Others account for all of the pharmacologic activity, the parent compound having no effect (e.g., enalapril).[102] In other examples, the metabolite has a different pharmacologic profile from the parent drug. For example, normeperidine excites the CNS and can cause seizures in contrast to the sedating effect of the parent compound meperidine.[103,104]

It should be apparent that in order to safely use drugs with active metabolites in patients with renal

TABLE 95.3 Active Metabolites of Drugs that can Accumulate in Patients with Renal Insufficiency

Drug	Active Metabolite
ANALGESICS	
Codeine	Morphine-6-glucuronide
Meperidine	Normeperidine
Morphine	Morphine-6-glucuronide
Propoxyphene	Norpropoxyphene
ANESTHETICS AND DRUGS USED DURING ANESTHESIA	
Atracurium	Laudanoside
Cisatracurium	Laudanoside
Pancuronium	3-OH pancuronium
Remifentanil	Carboxylic acid metabolite
Vecuronium	3-Desacetylvecuronium
ANTIANXIETY AGENTS, SEDATIVES, AND HYPNOTICS	
Buspirone	1-(2-Pyrimidinyl)-piperazine (1-PP)
Midazolam	α-Hydroxymidazolam
ANTICOAGULANTS, ANTIFIBRINOLYTICS, AND ANTIPLATELET AGENTS	
Sulfinpyrazone	Thioether metabolite
ANTICONVULSANTS	
Oxcarbazepine	10,11-Dihydro-10-hydroxycarbamazepine (HYCZ)
Primidone	Phenylethylmalonamide
Valproic acid	Not identified
ANTIHISTAMINES	
Cimetidine	Cimetidine sulfoxide
Ebastine	Carebastine
Hydroxyzine	Cetirizine
Ketotifen	Desmethylketotifen
Nizatidine	N2-monodesmethylnizatidine
ANTI-INFLAMMATORY AGENTS	
Diacerein	Rhein
Oxaprozin	Two hydroxylated metabolites
ANTIMICROBIAL AGENTS/ANTIBACTERIALS	
Cephalosporins	
Cefotaxime	Desacetylcefotaxime
Cefoxitin	Decarbamoylcefoxitin
Cephalothin	Desacetylcephalothin
Cephapirin	Desacetylcephapirin
SULFONAMIDES	
Sulfamethoxazole	Acetyl metabolite
Sulfisoxazole	Acetyl metabolite
URINARY BACTERIOSTATICS	
Nalidixic acid	7-hydroxynalidixic acid
ANTINEOPLASTICS AND ANTIMETABOLITES	
Cyclophosphamide	4-Hydroxycyclophosphamide
	Aldophosphamide
Ifosfamide	4-Hydroxyifosfamide
	Aldoifosfamide
	Isofosforamide
	Acrolein
	Chloracetaldehyde (oral dosing)
ANTISPASTICITY AGENTS	
Dantrolene	Hydroxy and amino metabolites
CARDIOVASCULAR AGENTS	
ANTIARRHYTHMICS	
Disopyramide	Mono-N-desisopropyl-disopyramide (MND)
Flecainide	Meta-O-dealkylflecainide
Lorcainide	Norlorcainide
Procainamide	N-acetylprocainamide (NAPA)
ANTIHYPERTENSIVES	
Acebutolol	N-acetylacebutolol (diacetolol)
Captopril	Mixed disulfides with endogenous thiols
Delapril	5-Hydroxyindane diacid
Losartan	E3174
Methyldopa	Methyldopamine
Metoprolol	α-Hydroxymetoprolol
Minoxidil	Minoxidil sulfate
Nebivolol	β-Hydroxy metabolites
Nitroprusside	Thiocyanate
Pinacidil	Pinacidil-N-oxide
CARDIAC INOTROPES	
Digitoxin	Digoxin
Enoximone	Piroximone

(*Continued*)

TABLE 95.3 (*Continued*)

Drug	Active Metabolite
Flosequinan	7-Fluoro-1-methyl-3-methylsulfinyl-4-quinolone (flosequinoxan)
BLOOD LIPID-LOWERING AGENTS	
Clofibrate	Parachlorophenoxyisobutyric acid (CPIB)
Lovastatin	β-Hydroxy acid
Simvastatin	β-Hydroxy acid
DIURETICS	
Triamterene	Sulfuric ester of hydroxytriamterene
HYPOGLYCEMIC AGENTS	
Acetohexamide	Hydroxyhexamide
Tolbutamide	Hydroxytolbutamide
	Carboxytolbutamide
HYPOURICEMIC AGENTS	
Allopurinol	Oxipurinol
PSYCHOTHERAPEUTIC AGENTS	
Acamprosate	Acetyl-homotaurine
Resperidone	9-Hydroxyresperidone
Tianeptine	Not characterized
Venlafaxine	0-Desmethylvenlafaxine
SYMPATHOMIMETICS	
Dolasetron	R + -hydroxydolasetron

insufficiency one must know the pharmacologic profile of the parent drug and its metabolite(s). One should try to avoid such drugs in patients with renal disease.

INFLUENCE OF DRUGS AND RENAL DISEASE ON DRUG DISPOSITION AND RESPONSE

Inter-individual variation in drug disposition among patients can lead to too high or too low systemic plasma levels and is a major factor in the safe and effective use of drugs. Variation may be associated with gender, age, concurrent drugs (drug-drug interactions) and disease. This section focuses on drug-drug interactions that occur in the kidney and on the effect of renal disease on drug disposition. The recent publication of a whitepaper co-authored by an International Transporter Consortium focused on the role of transporters in drug development and highlighted transporter based drug-drug interactions.[105] Among the interactions described were drug interactions that occur in the kidney and that may contribute to drug toxicity. Clinicians should be aware of these interactions as they may interfere with rational drug therapy. With the molecular identity of many drug transporters, there is an emerging appreciation of the mechanisms that underlie renal drug-drug interactions. Similarly, with the advent of sensitive analytical methods and metabolomic studies, a new appreciation for the molecular mechanisms involved in renal disease induced changes in drug absorption and disposition has emerged. Further, advances in physiologic based pharmacokinetics have led to an increased understanding of the mechanisms by which renal disease may affect drug disposition.[106] In this section, drug-drug interactions in the kidney are described first, followed by the effect of renal disease on drug disposition. New information is highlighted and where possible mechanistic explanations of how drug interactions or disease effects occur are included.

Influence of Drug-Drug Interactions on Renal Pharmacokinetics

Drug-drug interactions are important from a drug safety point of view. In fact, of the drugs withdrawn from the market because of drug safety issues, many are associated with clinical drug-drug interactions.[107] Considerable information is available on drug-drug interactions that occur in the liver and for which one drug alters the metabolism of a second drug. In contrast, there are comparably few studies of drug-drug interactions in the kidney. The recent identification, characterization and localization of a number of ABC and SLC transporters in the kidney have led to increasing recognition of the potential importance of drug-drug interactions in the kidney. With the availability of recombinant human renal transporters expressed in continuous cell lines, it is now possible to determine the potential of various drugs to inhibit the renal transport of other drugs. The concentration of a drug that inhibits transport in cellular assays can be compared to its clinical concentrations to determine whether a potential drug-drug interaction is likely to occur *in vivo*. *In vivo* drug-drug interactions can be investigated in healthy populations or in patients to determine the magnitude of the interaction and whether dosing adjustments will be needed when drugs are administered concomitantly.

The magnitude of effect of a concomitant drug on the systemic blood levels of another drug depends on the following factors. First, the fraction of the dose of the affected drug that is eliminated in the kidney is an important factor. If the fraction is low, renal drug-drug interactions will be unimportant to the overall elimination of the drug. In contrast, for drugs for which a high fraction of the dose is eliminated in the kidney, renal

drug-drug interactions may potentially be important. In particular, an interacting drug may inhibit the entire secretory component of renal elimination of the affected drug. If renal secretion constitutes, for example one-half of the renal clearance of the affected drug, then an interacting drug may reduce the renal clearance of the affected drug by one-half. Thus, to estimate the potential importance of a drug-drug interaction in the kidney, a comparison of the net secretory clearance to the total renal clearance of the drug should be made. Net secretory clearance is equal to total renal clearance minus filtration clearance, which in turn is equal to GFR x fraction unbound. So, for example, if a drug has a renal clearance of 50 ml/min and a fraction unbound of 0.01, then in a patient with a GFR of 100 ml/min, the net secretory clearance would be equal to 50 ml/min minus 0.01*100 ml/min or 49 ml/min. Thus a major portion of the renal clearance would be tubular secretion.

Drug-drug interactions in the kidney are often charge specific. That is, weakly acidic drugs will inhibit the renal elimination of other weakly acidic drugs and basic drugs will inhibit other weak bases. There are however a few drug-drug interactions that are not charge selective. Below clinical drug-drug interactions in the kidney are described for acidic drugs and basic drugs.

TABLE 95.4 Selected Examples of Clinical Drug–Drug Interactions Occurring in the Kidney in which the Renal Elimination is Inhibited by More than 25%

Organic Anion Transport Mediated Drug–Drug Interactions		
Affected Drug	Inhibitor	Reference
Cefamandole	Probenecid	118
Cidofovir	Probenecid	119
Ciprofloxacin	Probenecid	173
Cisplatin	Probenecid	174
Famotidine	Probenecid	175
Furosemide	Probenecid	176
Nafcillin	Probenecid	177
Zidovudine	Probenecid	178
ORGANIC CATION TRANSPORT MEDIATED DRUG-DRUG INTERACTIONS		
Metformin	Cimetidine	179
Procainamide	Cimetidine	180
Quinidine	Cimetidine	181
Triamterene	Ranitidine	182
Zidovudine	Cimetidine	183

Clinical Drug-Drug Interactions Involving Acidic Drugs

As noted previously, many organic anions or weak acids are eliminated in the kidney by renal tubular secretion. In general, OAT1 and OAT3, localized to the basolateral membrane of proximal tubule cells, mediate the first step in the tubular secretion of organic anions. On the apical membrane, ABC transporters, including MRP2 and MRP4, transport acidic drugs into the tubule fluid for excretion. OAT4, on the luminal membrane, is thought to function primarily in reabsorption of anionic drugs, but may participate in secretion. In clinical studies, identification of the specific transporter involved in an interaction is often difficult given that most inhibitors can affect multiple transporters and are not selective for a single transporter. The major drug that has been shown to inhibit renal organic anion secretion is the uricosuric agent, probenecid.[108] Clinical examples of drug-drug interactions with probenecid are shown in Table 95.4 and include a number of cephalosporins[109] and anti-viral agents.[110] In general these drug-drug interactions result in higher systemic blood levels and may cause potential toxicities of the affected drug. Probenecid itself is not substantially eliminated in the kidney; therefore its renal disposition is not altered during the drug-drug interaction. Probenecid has long been used to extend therapeutic plasma levels of penicillins by reducing its renal clearance.[111] It is notable that probenecid has been shown to protect the kidney from the nephrotoxic antiviral drug, cidofovir. In fact, the approved cidofovir label contains the following warning:[112]

> "Renal impairment is the major toxicity of Vistide (cidofovir). Cases of acute renal failure resulting in dialysis and/or contributing to death have occurred with as few as one or two doses of Vistide. To reduce possible nephrotoxicity, intravenous prehydration with normal saline and administration of probenecid must be used with each Vistide infusion."

While not completely understood, evidence suggests that the mechanism of the cidofovir renal toxicity is related to high drug concentrations in proximal tubule cells. Co-administration with probenecid leads to a redirection of cidofovir elimination to almost exclusively involve glomerular filtration, a markedly decreased cellular accumulation, and the prevention of clinical signs of nephrotoxicity.[110] Thus, probenecid exemplifies that drug-drug interactions in the kidney can have pronounced effects on drug levels, and that inhibitors of renal drug transport can be exploited in drug therapy.

Clinical Drug-Drug Interactions Involving Cationic Drugs

Many hydrophilic organic cations are eliminated by renal secretion. Notable examples include the anti-

diabetic drug metformin[113] and the anti-viral drug, zidovudine.[114,115] Other examples are listed in Table 95.4. OCT2 is thought to mediate the first step in tubular secretion of organic cations across the basolateral membrane.[50] On the apical membrane, two transporters are thought to be involved: MATE1 and MATE2-K.[51,52,58] Whereas OCT2 is a facilitative transporter that mediates drug transport in accordance with the electrochemical gradient, MATE1 and MATE2-K appear to be proton exchangers. That is, these transporters efflux their cationic substrates in an apparent electroneutral exchange with protons. Although other inhibitors of tubular secretion of organic cations have been described, cimetidine is the major perpetrator of renal drug-drug interactions that involve organic cations. Until recently, it was thought that the cimetidine mediated renal drug-drug interaction occurred at OCT2; however, recent studies have shown that cimetidine is actually a more potent inhibitor of MATE1.[57] Thus, in vivo, cimetidine may inhibit renal transport of organic cations at MATE1 and not at OCT2.

Digoxin is a neutral compound, which is eliminated primarily in the kidney with a small component of tubular secretion. P-glycoprotein (ABCB1) appears to mediate its renal secretion and a number of P-glycoprotein inhibitors including verapamil,[116] ritonavir,[117] itraconazole[118] and quinidine[119] have been found to inhibit its tubular secretion.

INFLUENCE OF RENAL DISEASE ON DRUG DISPOSITION AND RESPONSE

As illustrated in Fig. 95.3, the concentration of a drug in plasma is influenced by a number of factors—each of which, including processes that are not directly associated with the kidneys, may be affected by renal disease. This can lead to altered drug disposition and ultimately to toxic accumulation of drugs or the loss of pharmacological effect. The dose and dosing interval of a drug are controlled by the physician, and altering them is the only method of compensating for alterations in drug disposition in the patient.

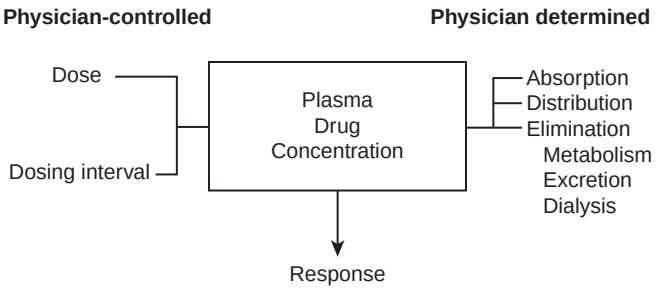

FIGURE 95.3 Determinants of plasma drug concentration and response.

Absorption

By several theoretical mechanisms, renal disease could affect drug absorption. Altered intestinal motility could change rates of gastric emptying of medications to small intestinal absorption sites. Changed regional distribution of blood flow could affect absorption from intramuscular or subcutaneous sites. Such effects on drug absorption remain speculative. Based on current data, clinicians may assume that drug absorption is not changed in patients with renal insufficiency.

Although not strictly an absorptive process, first-pass metabolism by the intestinal mucosa and liver influences the systemic availability of a drug after oral dosing. By largely uncharacterized mechanisms, renal insufficiency can also diminish non-renal (presumably hepatic) elimination of some drugs. For drugs with substantial first-pass elimination, such inhibition of hepatic metabolism could cause greater bioavailability. This mechanism may account for the apparent increase in propoxyphene bioavailability in patients with severe renal insufficiency.[120] Because this phenomenon has not been described with other drugs, clinicians should not extrapolate these findings to all drugs that undergo first-pass elimination.

Distribution

Systemic pH can affect distribution of drugs into tissues. A pH favoring the non-ionized form of a weak acid or base can facilitate its distribution out of plasma and into tissues. This phenomenon has been demonstrated to occur with salicylate. Being a weak acid, a more acidic systemic pH increases the relative amount of non-ionized salicylate and increases the amount reaching the central nervous system (CNS) and toxicity.[121,122] Presumably the acidemia of uremia would increase access of salicylate into the CNS. A similar phenomenon has not been described with other drugs, although this area is little studied.

Protein binding of highly bound drugs is another major determinant of drug distribution. Many acidic drugs, such as nonsteroidal anti-inflammatory drugs (NSAIDs), thiazide and loop diuretics, penicillins, and others bind predominantly to albumin—whereas basic compounds such as lidocaine, propranolol, tricyclic antidepressants, and so on typically bind to the acute-phase reactant α1-acid glycoprotein.[123–126] Patients with renal insufficiency accumulate endogenous organic acids that are normally excreted by the kidney,

and these compounds are able to displace acidic drugs from albumin binding sites.[127–129] The likelihood that such an effect will be important is a function of the degree of binding of the drug. Generally, for drugs bound less than 90% the magnitude of effect is so small as to be irrelevant. In contrast, drugs bound more than 90% may be importantly affected by changes in binding. For example, NSAIDs are more than 99% bound to albumin.[11] Thus, less than 1% is free in plasma and constitutes the active moiety. In uremia, what may appear to be a trivial decrease in binding from 99 to 98% actually results in a doubling of the free unbound concentration from 1 to 2%—a magnitude of change that may be clinically important. In contrast, only about 50% of methotrexate is bound to albumin.[97] A decrease in binding to 45% would have only a minor, clinically negligible effect on unbound methotrexate concentrations.

A frequent misconception is that such an effect results in increased concentrations of unbound pharmacologically active drug, causing an enhanced effect—including toxicity. In the majority of instances, however, there is no increase in concentration of unbound drug and therefore no change in response unless caused by other factors.[130–133] The reason unbound drug concentrations are unchanged is that for many drugs with low total clearance (obeying so-called "restrictive" elimination, in which unbound clearance equals intrinsic clearance), clearance of total drug from plasma from all routes of elimination is directly related to the fraction of unbound drug,[134] calculated as:

$$\text{CL total} = \text{fu} \times \text{CLu}$$

where CL is clearance, fu is fraction unbound, and CLu is unbound clearance. Thus, if displacement from albumin causes the unbound fraction to increase, total clearance increases proportionally but unbound or intrinsic clearance is unchanged—resulting in maintenance of the unbound concentration and pharmacologic effect at its previous level. This similar unbound concentration occurs at a lower total drug concentration. Thus, the fraction that is unbound is increased but the concentration unbound is unchanged.[130–133]

This scenario is true for acidic drugs that are highly protein bound and have low total clearances when displaced from albumin binding sites in uremia. Some other drugs have high organ clearances and extraction rates such that their clearance is less dependent on protein binding but partially or totally dependent on organ blood flow. In this case, unbound clearance will decline as the fraction unbound increases so that unbound drug concentrations increase despite, in some cases, an unchanged total drug concentration.[133] Here, the opposite problem exists in that a dosage adjustment may be necessary even though total drug concentration changes little (if at all).

The degree of protein binding can also allow one to predict the potential for dialytic removal of a drug. A high degree of binding means only small amounts of drug are free in plasma and can be removed by the dialysis procedure. Drugs, either acidic or basic, that are more than 90% bound to plasma proteins will have negligible removal by dialytic procedures except hemoperfusion techniques.

The binding changes described previously can influence the calculation of distribution volume. If calculated based on total drug concentration, the volume of distribution may become larger when binding decreases—particularly for drugs that distribute extensively into intracellular sites and therefore have large volumes of distribution.[130–133] This observation alone can lead to the false conclusion that loading doses need to be increased. In contrast, the distribution volume of the unbound pharmacologically active drug is essentially unchanged—meaning that no adjustment of loading dose should be made. For drugs with smaller volumes of distribution, particularly those restricted to extracellular sites, the total volume of distribution may be insensitive to changes in protein binding. However, there would be almost proportional changes in the unbound volume of distribution, and consequently loading doses should be adjusted.[133]

Unfortunately, the medical literature concerning changes in drug disposition in patients with renal insufficiency is replete with data ignoring unbound drug concentrations. For highly bound drugs, if disposition parameters for total drug (clearance and volume of distribution) are the only values reported—and if these values are increased in patients with renal insufficiency—one must be suspicious that the effect is solely due to displacement from binding. The implication of this conclusion is that disposition parameters for unbound drug are unchanged and that no alteration in dosing is indicated. Clinicians and scientists should be alert to the potential for misinformation from a good deal of the medical literature concerning drugs subject to this phenomenon.

Reductions in protein binding in uremic patients, or with the hypoalbuminemia of nephrotic syndrome, can lead to misinterpretation of serum concentrations of phenytoin owing to the mechanisms discussed previously.[130] In both clinical conditions, binding of phenytoin is decreased. Unbound concentrations are unchanged, although total concentrations are diminished.[130,132] If plasma concentrations of phenytoin are obtained in a patient, the clinical laboratory reports total concentration—a value that could be misinterpreted as being too low even though unbound concentrations are within the therapeutic range. If the misled clinician increased the dose of phenytoin in an attempt to attain a total concentration in the usual therapeutic

range, so doing would also increase the unbound concentration of phenytoin and could result in toxicity. This problem can be avoided by measuring unbound concentrations. Alternatively, one can redefine the therapeutic range for uremic and hypoalbuminemic patients.[135]

Displacement from protein binding in patients with renal insufficiency has therefore been a misunderstood and misinterpreted phenomenon.[130–135] This mechanism is too often cited as causal of altered response to drugs in patients with renal disease. However, because unbound drug concentrations often do not change this mechanism cannot explain altered response to drugs in many uremic patients. Moreover, displacement from binding does not necessarily mandate a change in drug dosing. Clinicians should avoid false conclusions regarding drug disposition from what may be incomplete data in the medical literature; namely, studies of highly bound drugs that quantify only total and not unbound concentrations. The clinical setting in which this phenomenon is most apparent is use of phenytoin in uremic or hypoalbuminemic patients, as described previously.[135]

Digoxin represents a drug for which volume of distribution decreases as renal function diminishes:[136]

$$\text{Volume of distribution (liters/kg)} = 3.84 + 0.0446\ \text{CLcr (ml/min)}.$$

The mechanism of this effect is unknown, but the magnitude is sufficient to mandate dose adjustment. Because volume of distribution influences the loading dose of a drug (as opposed to the maintenance dose), this effect is important only in patients to whom a loading dose is administered. From the previous equation, it should be apparent that the loading dose of digoxin for a patient with end-stage renal disease should be approximately half that of a patient with normal renal function.

Elimination

Both glomerular filtration and active secretion are typically reduced in patients with renal insufficiency, with possible implication for dosing strategies. Renal failure is accompanied by elevated levels of metabolic products that would normally be renally excreted, and that have been associated with multiple pathologies in uremic patients including neuropathy, hypertension, cardiac failure and increased bleeding.[137–140] The molecular identities of these uremic toxins are largely unknown, but elevated levels of, e.g., hippuric acid, indoxyl sulfate, guanidino succinate, trans-aconitate, and 3-carboxy-4-methyl-5-propyl-2-furanpropanoic acid (CMPF) have been demonstrated in plasma from uremic patients, and have been demonstrated to cause some of the pathological processes in model systems of renal failure.[141]

It has long been appreciated that constituents of uremic serum can affect renal transport processes. Serum from uremic patients inhibited the uptake of the model organic anion para-aminohippuric acid (PAH) in kidney slices and isolated renal tubules from rat and rabbit,[142–144] and, more recently, CMPF was shown to affect renal PAH uptake, likely through competitive inhibition of the OAT1 and OAT3 transporters[145–149] Similarly, indoxyl sulfate is accumulated in the proximal tubuli of uremic rats, as well as in OAT1/3-expressing human proximal tubuli cells,[150] and may thus compete with tubular uptake of substrate drugs.

In addition to direct inhibition by uremic toxins, several studies demonstrate altered expression of membrane transporters in models of renal disease. For example, decreased expression of OCT2, OAT1, OAT3 and MATE1 have been observed in rats with chronic renal failure.[55,151–155] In contrast, renal expression of the efflux transporters P-gp and MRP2 were increased in such rats,[156,157] possibly as a mechanism of protection from toxic accumulation in proximal tubuli cells.

Notably, the effects of accumulated uremic toxins are not limited to transporters in the kidney. An increasing body of literature demonstrates effects of renal disease on transporter function and expression also in other organs, including the intestine and liver.[6,158–162] Inhibition of hepatic drug-metabolizing enzymes has also been demonstrated, including the Cytochrome P450s CYP2C9, CYP2C19 and CYP3A4.[3,4,163,164] These extra-renal effects have important implications for drug therapy in renal disease, since dosing changes may be necessary also for drugs that undergo extensive hepatic metabolism or are cleared through biliary excretion. In line with the evidence for extra-renal pharmacokinetic effects of renal disease, the U. S. Food and Drug Administration (FDA) now recommends performing pharmacokinetic studies in patients with varying stages of renal impairment, for all chronically administered drugs, regardless of clearance pathway.[7]

Drug Response

Even if the plasma concentration of a drug in a patient with renal insufficiency is identical to that of a patient with normal renal function, response may differ. For example, the effect of pindolol to block exercise-induced increases in heart rate and its effects to decrease plasma renin activity were greater in uremic patients than in normal volunteers despite similar serum concentrations of this beta-adrenergic antagonist.[165] As such, an approximate fourfold greater

plasma concentration was required in healthy subjects to cause the same effect on heart rate as in uremic patients. The mechanism of this enhanced response is unknown.

Unfortunately, comparable studies are not available with the host of drugs used commonly in patients with renal insufficiency. Clinicians must therefore use caution when using drugs in patients with renal disease in addition to adjusting doses to compensate for changes in disposition.

Dialysis

Just as dialytic procedures are used to remove accumulated endogenous end products of metabolism, they can remove drugs and their metabolites. With some drugs, the amount removed is sufficient to require supplemental dosing—or in poisoning settings is helpful in speeding the elimination of the toxin(s).

Drugs restricted to the extracellular, and particularly the plasma, compartment are accessible to removal by hemodialysis unless precluded by protein binding. Drugs with small volumes of distribution on the order of total body water or less (i.e., about 0.7 liter/kg) are likely but not necessarily restricted to the extracellular space, whereas a large volume of distribution often implies wide disbursement of drug throughout tissues. A drug with a small volume of distribution and low-protein binding (e.g., aminoglycoside antibiotics) would be predicted to be substantially removed by dialytic procedures and likely require supplemental dosing after dialysis. In contrast, a drug with a large volume of distribution may pass through a dialysis membrane. However, so little of the drug is in the plasma relative to overall body stores that the amount removed is negligible.

The best method of calculating drug clearance by peritoneal or hemodialysis is to actually measure how much drug is removed. So doing serves as an integrated function of dialyzer clearance throughout the entire procedure.[166,167] The calculation is as follows:

$$\text{Dialyzer clearance} = \text{Total amount of drug recovered in the dialysate}/\text{Duration of dialysis} \times \text{drug concentration at the midpoint of dialysis.}$$

The drug concentration at the midpoint of dialysis can be measured by a single determination or preferably from a regression of serial samples obtained during the dialytic procedure. The considerations cited previously apply to conventional hemodialysis. Removal of drugs by continuous arteriovenous hemofiltration (CAVH) or continuous venovenous hemofiltration (CVVH) may differ from conventional hemodialysis in two ways. First, the pore size of the membrane is larger—allowing drugs of about 5000 angstroms to be freely filtered. Thus, a drug such as vancomycin (the size of which limits conventional dialytic removal) is readily removed by these filtration techniques. Second, other than large-molecular-weight compounds, essentially all of the unbound drug in plasma can be removed by these methods. Thus, drug clearance by ultrafiltration is equal to the unbound fraction times the ultrafiltration rate. This value can be used to estimate whether supplementary drug dosing needs to be given, and if so the amount.

Hemoperfusion techniques allow removal of substantially greater amounts of some drugs than can be accomplished with other methods. In fact, some of these methods are so efficient that all of the drug entering the dialysis cartridge is removed. In other words, the effluent drug concentration is zero.[168–170] It is important to emphasize, however, that this efficient removal from blood may still not remove a clinically important amount of drug from the body. For example, if only 1% of the total amount of drug in the body is circulating (even if hemoperfusion removes all of the circulating drug), 99% of it is still left in body reservoirs inaccessible to the dialyzer. As soon as dialysis is stopped, these reservoirs serve to refill the circulating compartment such that decrements in circulating drug concentrations caused by hemoperfusion are only transient. This concept clearly applies to drugs with large volumes of distribution and accounts for the lack of efficacy of hemoperfusion in treating poisoning with highly lipid-soluble sedative-hypnotics having large volumes of distribution (e.g., glutethimide and methaqualone with volumes of distribution of 2.7 and 6 liters per kilogram, respectively).

Dialytic removal of many drugs has been quantified in clinical studies. Table 95.5 outlines current data that can be used to derive clinical dosing guidelines.[2] For drugs having negligible removal, no dosing regimen adjustment is needed over and above that which occurs due to the patient's level of renal function. In contrast, for drugs having removal of potentially important amounts a supplemental dose equal to the amount removed can be given at the conclusion of hemodialysis. In patients treated with peritoneal dialysis, the dosing regimen can be increased to compensate for the amount of drug removed by the dialytic procedure. Interestingly, most drugs are negligibly removed by peritoneal dialysis (Table 95.5). This observation is in contrast to the substantial absorption of many drugs that occurs when administered with the peritoneal dialysate.[171] For example, although only 20–25% of a dose of an aminoglycoside antibiotic is removed by peritoneal dialysis, in contrast instillation of these drugs into the peritoneum results in 50% or more being absorbed systemically.

TABLE 95.5 Removal of Drugs by Dialysis: Percentage of Dose Removed During Session of Hemodialysis or 24 Hours of CAPD

Drug	Hemodialysis	CAPD
ANALGESICS		
Meperidine	Negligible	Negligible
Methadone	Negligible (<1%)	Negligible (<1%)
Nalmefene	Negligible (3.3%)	—
Propoxyphene	Negligible	Negligible
Salicylates	Negligible	Negligible
Tilidine	Negligible (<1%)	—
Tramadol	Negligible (7%)	—
ANESTHETICS AND DRUGS USED DURING ANESTHESIA		
Gallamine	Considerable	Considerable
ANTIANXIETY AGENTS, SEDATIVES, AND HYPNOTICS		
Buspirone	Negligible	—
Chloral Hydrate	Negligible	—
Ethchlorvynol	Negligible	—
Glutethimide	Negligible	—
Meprobamate	Negligible	—
Methaqualone	Negligible	—
Oxazepam	Negligible	—
Phenobarbital	Negligible	—
Zopiclone	Negligible	—
ANTICHOLINERGICS AND CHOLINERGICS		
Cisapride	Negligible	—
Metoclopramide	Negligible	—
Pirenzipine	11–15%	—
ANTICOAGULANTS, ANTIFIBRINOLYTICS, AND ANTIPLATELET AGENTS		
Warfarin	Negligible	Negligible
LMW heparins	Negligible	—
ANTICONVULSANTS		
Gabapentin	50%	—
Ethosuximide	45%	—
Levetiracetam	25–50%	—
Phenytoin	Negligible	Negligible
Primidone	30%	—
Topiramate	50%	—
Valproic Acid	Negligible (1%)	Negligible
ANTIHISTAMINES		
Cetirizine	—	Negligible (9%)
Cimetidine	10–20%	Negligible (1.6%)
Famotidine	Negligible (6–16%)	Negligible (4.5%)
Fexofenadine	Negligible (<1.7%)	—
Levocabastine	Negligible (11%)	—
Loratadine	Negligible	—
Nizatidine	Negligible (10%)	—
Ranitidine	50–60%	Negligible (<1%)
ANTI-INFLAMMATORY AGENTS		
Anakinra	Negligible	Negligible
Azapropazone	Negligible	Negligible
Bromfenac	Negligible	—
Leflunomide	Negligible	Negligible
Lornoxicam	Negligible	—
Nabumetone	Negligible	—
Oxaprozin	Negligible	Negligible
Penicillamine	30%	—
Sulindac	Negligible	—
ANTIMICROBIAL AGENTS/ANTIBACTERIALS		
Aminoglycosides		
Aminoglycosides	50%	20–25%
Spectinomycin	50%	—
Carbapenems		
Biapenem	90%	—
Imipenem	80–90%	Negligible
Meropenem	50–70%	—
Cephalosporins		
Cefaclor	33%	—
Cefadroxil	50%	—
Cefamandole	50%	Negligible (5%)
Cefazolin	50%	20%
Cefdinir	—	Negligible (1.4–7.2%)
Cefipime	40–70%	26%
Cefixime	Negligible (1.6%)	Negligible
Cefmenoxime	16–51%	Negligible (<10%)
Cefmetazole	60%	—

(*Continued*)

TABLE 95.5 (*Continued*)

Drug	Hemodialysis	CAPD
Cefodizime	50%	Negligible (15%)
Cefonicid	Negligible	Negligible (6.5%)
Cefoperazone	Negligible	Negligible
Ceforanide	20–50%	—
Cefotaxime	60%	Negligible (5%)
Cefotetan	Negligible (5–9%)	—
Cefotiam	30–40%	—
Cefoxitin	50%	Negligible
Cefpirome	32–48%	Negligible (12%)
Cefpodoxime	50%	—
Cefprozil	55%	—
Cefroxadine	50%	—
Cefsulodin	60%	—
Ceftazidime	50%	Negligible
Ceftibuten	39%	—
Ceftizoxime	50%	Negligible (16%)
Ceftriaxone	40%	Negligible (4.5%)
Cefuroxime	—	20%
Cephacetrile	50%	—
Cephalexin	50–75%	30%
Cephalothin	50%	—
Cephapirin	20%	—
Macrolide Antibiotics		
Clindamycin	Negligible	Negligible
Dirithromycin	Negligible	—
Lincomycin	Negligible	Negligible
Monobactams		
Aztreonam	40%	Negligible
Carumonam	51%	—
Moxalactam	30–50%	Negligible (15–20%)
Nitromidazoles		
Metronidazole	45%	Negligible (10%)
Ornidazole	42%	Negligible (6%)
Tinidazole	40%	—
Oxazolindiones		
Linezolid	33%	—
Penicillins	—	—

(*Continued*)

TABLE 95.5 (*Continued*)

Drug	Hemodialysis	CAPD
Amdinocillin	32–70%	Negligible (< 4%)
Amoxicillin	30%	—
Ampicillin	40%	—
Azlocillin	30–45%	—
Carbenicillin	50%	—
Cloxacillin	Negligible	—
Dicloxacillin	Negligible	—
Methicillin	Negligible	—
Mezlocillin	20–25%	24%
Nafcillin	Negligible	—
Oxacillin	Negligible	—
Penicillin	50%	—
Piperacillin	30–50%	Negligible (6%)
Temocillin	50%	Negligible
Ticarcillin	50%	Negligible
Polymyxins		
Colistin	Negligible	Negligible
Quinolones		
Ciprofloxacin	Negligible (2%)	Negligible (0.4–1.6%)
Enoxacin	Negligible	—
Fleroxacin	Negligible (3–7%)	Negligible (< 10%)
Gatifloxacin	Negligible (14%)	Negligible (11%)
Levofloxacin	Negligible	Negligible
Lomefloxacin	Negligible	—
Norfloxacin	Negligible	—
Ofloxacin	Negligible (15–25%)	Negligible (4–6%)
Pefloxacin	—	Negligible
Temafloxacin	Negligible (9.4%)	—
Streptogramins		
Quinupristin-dalfopristin	—	Negligible
Sulfonamides		
Sulfamethoxazole	50%	Negligible (8%)
Trimethorprim	50%	Negligible (7%)
Tetracyclines		
Doxycycline	Negligible	Negligible
Minocycline	Negligible	Negligible

(*Continued*)

TABLE 95.5 (*Continued*)

Drug	Hemodialysis	CAPD
Vancomycin	Negligible	Negligible (15–20%)
Teicoplanin	Negligible	Negligible (5%)
ANTIFUNGALS		
Amphotericin B	Negligible	—
Fluconazole	40%	Negligible (18%)
Flucytosine	50%	—
Itraconazole	Negligible	Negligible
Ketoconazole	Negligible	Negligible
Miconazole	Negligible	Negligible
ANTIMALARIALS		
Chloroquine	Negligible	—
Mefloquine	Negligible	—
Quinine	Negligible	—
ANTITUBERCULOUS AGENTS		
Ethambutol	Negligible (12%)	—
Isoniazid	75%	—
Para-aminosalicylic acid	50%	—
ANTIVIRAL AGENTS		
Abacavir	24%	—
Acyclovir	60%	Negligible (< 10%)
Amantadine	Negligible	—
Cidofovir	50%	Negligible
Didanosine	20–67%	Negligible
Foscarnet	27–58%	—
Ganciclovir	Negligible	—
Lamivudine	Negligible	—
Ribavirin	Negligible (8%)	—
Vidarabine	50%	—
Zidovudine	Negligible	Negligible
ANTINEOPLASTICS AND ANTIMETABOLITES		
Cyclophosphamide	30–60%	—
Etoposide	Negligible	—
Methotrexate	Negligible	—
Paclitaxel	Negligible	—
ANTI-ULCER AGENTS AND ANTACIDS		
Lansoprazole	Negligible	—
Omeprazole	Negligible	—
Pantoprazole	Negligible	—
Rabeprazole	Negligible	—
BRONCHODILATORS		
Dyphylline	28%	—
Theophylline	40%	—
Zileuton	Negligible (0.5%)	—
CARDIOVASCULAR AGENTS		
Antianginal Agents		
Amlodipine	Negligible	Negligible
Bepridil	Negligible	—
Diltiazem	—	Negligible (< 0.1%)
Felodidine	Negligible	—
Isradipine	Negligible	—
Nifedipine	Negligible (< 1%)	Negligible
Antiarrhythmics		
Acecainide (NAPA)	50%	Negligible
Amiodarone	Negligible	—
Bretylium	Negligible	—
Cibenzoline	Negligible	—
Disopyramide	Negligible (2–4%)	—
Flecainide	Negligible (1%)	Negligible
Lorcainide	Negligible (8–12%)	—
Mexiletine	Negligible	Negligible
Procainamide	Negligible	Negligible (< 5%)
Propafenone	Negligible	—
Quinidine	Negligible (< 1%)	—
Recainam	Negligible (9%)	—
Sematilide	20–25%	—
Sotalol	40–57%	—
Tocainide	25%	Negligible (2%)
Antihypertensives		
Acebutolol	Negligible	—
Atenolol	50%	—
Buflomedil	Negligible (3.4–6.7%)	—
Candesartan	Negligible (0.2%)	—
Captopril	35–40%	Negligible (< 1%)
Carvedilol	Negligible	—

(*Continued*)

TABLE 95.5 (*Continued*)

Drug	Hemodialysis	CAPD
Cilazapril	Negligible (14%)	—
Clonidine	Negligible	—
Diazoxide	Negligible	—
Doxazosin	Negligible	—
Enalapril	50%	—
Erbesartan	Negligible	—
Esmolol	Negligible	Negligible
Fosinopril	—	Negligible (2%)
Guanfacine	Negligible	—
Irbesartan	Negligible	—
Ketansirin	Negligible	—
Labetalol	Negligible (2–5%)	Negligible (0.14%)
Lisinopril	50–60%	—
Losartan	Negligible	—
Metoprolol	Negligible	—
Minoxidil	24–43%	—
Nadolol	50%	—
Omapatrilat	Negligible	—
Perindopril	55%	—
Quinapril	Negligible (5.4%)	Negligible (2.6%)
Ramipril	Negligible	—
Urapadil	Negligible (6.5%)	—
Cardiac Inotropes		
Digoxin	Negligible	Negligible (8%)
FaB	Negligible	Negligible
Lipid-Lowering Agents		
Bezafibrate	Negligible	Negligible (1.6%)
Clofibrate	Negligible	—
Fenofibrate	Negligible	—
Gemfibrozil	Negligible	—
Pravastatin	Negligible	—
HORMONAL AGENTS		
Epoeitin	—	Negligible (2.3%)
HYPOGLYCEMIC AGENTS		
Repaglinide	Negligible	—
Rosiglitazone	Negligible	—
HYPOURICEMIC AGENTS		
Allopurinol (Oxipurinol)	40%	—
PSYCHOTHERAPEUTIC AGENTS		
Citalopram	Negligible (<1%)	—
Lithium	Considerable	Considerable
Olanzepine	Negligible	—
Sertindole	Negligible (<0.1%)	—
Sertraline	Negligible	—
Tianeptine	Negligible	—
STEROIDS		
Prednisone	Negligible	—
MISCELLANEOUS		
Cyclosporine	Negligible	—
Mycophenolate	Negligible	—
Sulbactam	—	Negligible
Tazobactam	30–50%	Negligible (11–13%)

CAPD, continuous ambulatory peritoneal dialysis.

DOSING RECOMMENDATIONS IN PATIENTS WITH RENAL INSUFFICIENCY

Loading Dose

In some clinical conditions, a rapid response to a drug is desired. Attainment of steady-state serum concentrations requires four to five times the drug half-life. If this time is too long for the clinical setting, a loading dose strategy needs to be employed. The loading dose of a drug that is needed is a function of its volume of distribution:

$$\text{Loading dose} = \text{desired concentration} \times \text{volume of distribution.}$$

Values for volume of distribution can be found in standard reference texts, but these sources often ignore changes in this parameter that may occur in patients with renal disease. For example, the volume of distribution of digoxin in patients with end-stage renal disease is about half that of patients with normal renal function.[136] Thus, such patients require a loading dose half that of those without renal disease to attain identical concentrations.

TABLE 95.6 Volume of Distribution of Drugs in Patients with Renal Disease, V_d (liters/kilogram)[a]

Drug	Normal Renal Function	ESRD
ANALGESICS		
Codeine	3.5–6.0	7.3
Nalmefene	8.2	17.1
Salicylate	0.15	Increase (no change)[b]
ANESTHETICS AND DRUGS USED DURING ANESTHESIA		
Thiopental	1.9–2.2[12]	3.0[12]
ANTIANXIETY AGENTS		
Abecarnil	14	19 (no change)
Oxazepam	0.6–2.0	Increase (no change)
ANTICOAGULANTS, ANTIFIBRINOLYTICS, AND ANTIPLATELET AGENTS		
Sulfinpyrazone	0.06	Increase (no change)
Warfarin	0.11–0.20	Increase (no change)
ANTICONVULSANTS		
Phenytoin	0.5–1.0	Increase (no change)
Valproate	0.2–0.4	Increase (no change)
ANTIHISTAMINES		
Roxatidine	3.2	2.0
ANTI-INFLAMMATORY AGENTS		
Anakinra	0.11	0.17
Celecoxib	5.7–7.1	Increase (no change)
Diflunisal	0.10–0.13	0.27 (no change)
Oxaprozin	0.07–0.25	(Decrease)
ANTIMICROBIAL AGENTS/ANTIBACTERIALS		
Cephalosporins		
Cefazolin	0.11–0.14	0.17
Cefoxitin	0.27	Increase
Macrolide Antibiotics		
Erythromycin	0.6–0.8	1.2
Penicillins		
Azlocillin	0.18	0.3
Timocillin	0.15–0.24	Increase (no change)
Quinolones		
Norfloxacin	3.2	1.7
ANTIFUNGALS		
Amphotericin	1.6–4	Increase (no change)
Miconazole	2–3	Decrease
BRONCHODILATORS		
Albuterol	2.0–2.5	0.8
CARDIOVASCULAR AGENTS		
Antihypertensives		
Moxonidine	1.8–3	2.4
Cardiac Inotropes		
Digitoxin	0.73	Increase (no change)
Digoxin	Vd = 3.84 + 0.0446 CLCr	
Blood Lipid-Lowering Agents		
Acifran	0.5	Decrease to one-third normal
Clofibrate	0.14	Increase (no change)
HORMONAL AGENTS		
Insulin-like growth factor	0.15	0.07–0.09
MISCELLANEOUS		
Bendazac	0.18	Increase (no change)

[a]*Data in parentheses pertain to unbound drug.*
CLCr, creatinine clearance; ESRD, end-stage renal disease; Vd, volume of distribution.

TABLE 95.7 Methods of Adjusting Dosing Regimens in Patients with Renal Insufficiency

- Variable frequency (or interval) method: Individual doses are the same as in patients with normal renal function are administered at more widely spaced intervals.
- Variable dose method: The same dosing interval as in patients with normal renal function is used. Individual doses are diminished. One regimen is designed to attain the same average drug concentration as in patients with normal renal function. An alternative regimen attains the same peak concentrations.
- Kunin method: Half the dose used in patients with normal renal function is administered every half-life.
- Combination method: Both the dosing interval and individual doses are altered.

Table 95.6 lists drugs for which changes in volume of distribution have been documented in patients with renal disease.[2] For those drugs that are highly protein bound, notation is made as to whether the distribution volume of the pharmacologically active unbound drug concentration is altered. In most instances, where unbound drug has been measured there is no change

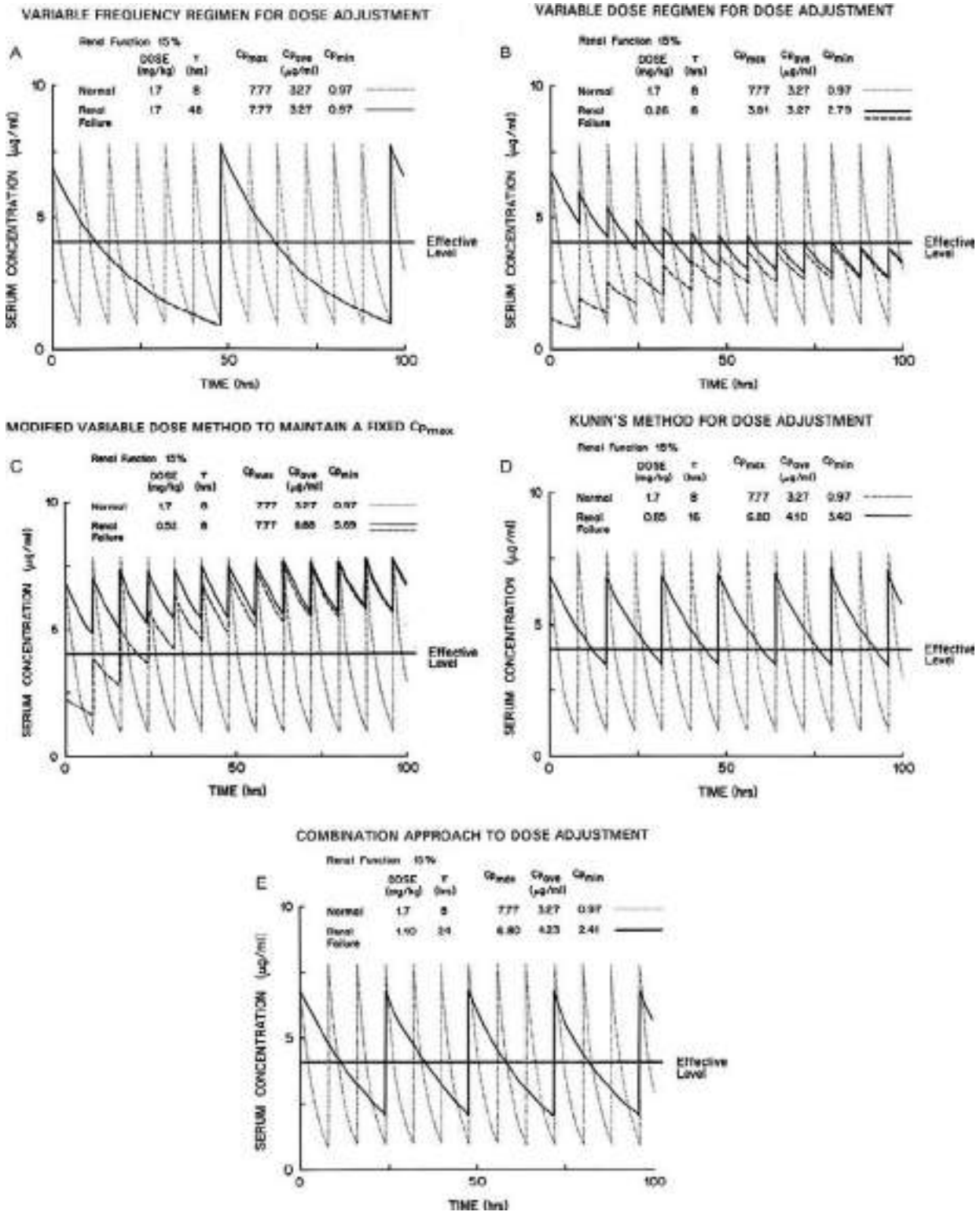
VARIABLE FREQUENCY REGIMEN FOR DOSE ADJUSTMENT
A
Renal Function 15%
DOSE (mg/kg) τ (hrs) $C_{P_{max}}$ $C_{P_{ave}}$ (μg/ml) $C_{P_{min}}$
Normal 1.7 8 7.77 3.27 0.97
Renal Failure 1.7 48 7.77 3.27 0.97
SERUM CONCENTRATION (μg/ml)
Effective Level
TIME (hrs)
VARIABLE DOSE REGIMEN FOR DOSE ADJUSTMENT
B
Renal Function 15%
DOSE (mg/kg) τ (hrs) $C_{P_{max}}$ $C_{P_{ave}}$ (μg/ml) $C_{P_{min}}$
Normal 1.7 8 7.77 3.27 0.97
Renal Failure 0.26 8 3.81 3.27 2.79
SERUM CONCENTRATION (μg/ml)
Effective Level
TIME (hrs)
MODIFIED VARIABLE DOSE METHOD TO MAINTAIN A FIXED $C_{P_{max}}$
C
Renal Function 15%
DOSE (mg/kg) τ (hrs) $C_{P_{max}}$ $C_{P_{ave}}$ (μg/ml) $C_{P_{min}}$
Normal 1.7 8 7.77 3.27 0.97
Renal Failure 0.52 8 7.77 6.66 5.69
SERUM CONCENTRATION (μg/ml)
Effective Level
TIME (hrs)
KUNIN'S METHOD FOR DOSE ADJUSTMENT
D
Renal Function 15%
DOSE (mg/kg) τ (hrs) $C_{P_{max}}$ $C_{P_{ave}}$ (μg/ml) $C_{P_{min}}$
Normal 1.7 8 7.77 3.27 0.97
Renal Failure 0.65 16 6.80 4.10 3.40
SERUM CONCENTRATION (μg/ml)
Effective Level
TIME (hrs)
COMBINATION APPROACH TO DOSE ADJUSTMENT
E
Renal Function 15%
DOSE (mg/kg) τ (hrs) $C_{P_{max}}$ $C_{P_{ave}}$ (μg/ml) $C_{P_{min}}$
Normal 1.7 8 7.77 3.27 0.97
Renal Failure 1.10 24 6.80 4.23 2.41
SERUM CONCENTRATION (μg/ml)
Effective Level
TIME (hrs)

FIGURE 95.4 Schematic representation of the serum concentration versus time profiles of a hypothetical drug that depends on the kidney for elimination that is obtained by different methods of dose adjustment in patients with renal function 15% of normal. Stippled curves represent concentrations in patients with normal renal function. Solid curves represent concentrations in patients with renal insufficiency. Dashed curves in B and C represent concentrations when a loading dose is administered. Dosing regimens and peak, average, and trough serum concentrations are provided in each panel. See text for discussion of individual panels. *(Adapted from Chennavasin P, Brater DC. Nomograms for drug use in renal disease. Clin Pharmacokinet 1981;6:193–214.)*

TABLE 95.8 Maintenance Doses in Patients with Renal Insufficiency (Relative to Normal Dose)

CREATININE CLEARANCE (ML/MIN)			
Drug	>50	20–50	<20
ANALGESICS			
Butorphanol	—	—	1/2
Codeine	—	—	1/2
Meperidine	—	Avoid	Avoid
Metamizol	—	—	1/3
Morphine	—	Avoid	Avoid
Nalmefene	—	—	1/2
Propoxyphene	—	Avoid	Avoid
Tramadol	—	—	1/2
ANESTHETICS AND DRUGS USED DURING ANESTHESIA			
Alcuronium	—	—	1/3
4-Aminopyridine	—	Avoid	Avoid
Cisatracurium	—	Avoid	Avoid
Doxacurium	—	—	1/2
Gallamine	—	—	1/8
Metocurine	—	—	1/3
Pancuronium	—	—	1/5
Pipecuronium	—	—	1/2
D-Tubocurarine	—	—	1/2
Vecuronium	—	—	Avoid
ANTIANXIETY AGENTS			
Acamprosate	—	1/2	1/3
Buspirone	—	1/2	1/4
ANTICHOLINERGICS AND CHOLINERGICS			
Metoclopramide	—	1/2	1/4
Neostigmine	—	1/2	1/3
Pirenzipine	—	—	1/2
Pyridostigmine	1/2	1/3	1/5
ANTICOAGULANTS, ANTIFIBRINOLYTICS, AND ANTIPLATELET AGENTS			
Bivalirudin	—	—	1/4
Desirudin	—	—	1/6
Iloprost	—	—	1/2
Lamifiban	—	—	1/10
LMW heparins	—	—	1/2
Lotrafiban	—	—	1/2
Sulotroban	1/2	1/5	1/20
Tirofiban	—	—	1/2
Tranexamic acid	1/2	1/4	1/8
ANTICONVULSANTS			
Felbamate	—	—	1/2
Gabapentin	1/2	1/4	1/8
Levetiracetam	—	1/2	1/3
Oxcarbazepine	—	—	1/2
Pregabalin	1/2	1/3	1/6
Primidone	—	—	Avoid
Topiramate	—	—	1/2
Vigabatrin	—	1/2	1/4
ANTIHISTAMINES			
Cetirizine	—	—	1/3
Cimetidine	—	1/2	1/6
Ebastine	—	—	1/2
Emedastine	—	—	2/3
Famotidine	1/2	1/3	1/5
Fexofenadine	—	—	1/2
Levocabastine	—	—	1/3
Nizatidine	1/2	1/4	1/4
Ranitidine	1/2	1/3	1/4
Roxatidine	3/4	1/2	1/4
ANTI-INFLAMMATORY AGENTS			
Anakinra	—	—	1/5
Azapropazone	1/2	1/5	1/10
Diacerein	—	—	1/2
Diflunisal	—	—	1/2
Indobufen	—	1/2	1/3
Ketoprofen	—	—	1/2
Ketorolac	—	—	1/2
Oxaprozin	—	2/3	1/2
Penicillamine	—	Avoid	Avoid
Tiaprofenic acid	—	—	1/2
Ximoprofen	—	1/2	1/3
ANTIMICROBIAL AGENTS/ANTIBACTERIALS			
Aminoglycosides	1/3	1/2	1/4
Carbapenems			
Biapenem	—	—	1/5

(*Continued*)

TABLE 95.8 (*Continued*)

Imipenem	—	1/2	1/4
Meropenem	2/3	1/3	1/6
Cephalosporins			
Cefaclor	—	1/2	1/4
Cefadroxil	1/2	1/4	1/8
Cefamandole	1/2	1/3	1/4
Cefazolin	1/2	1/4	1/6
Cefdinir	—	—	1/10
Cefditorin pivoxil	—	—	1/3
Cefepime	2/3	1/5	1/8
Cefetamet	1/2	1/4	1/8
Cefixime	—	1/2	1/3
Cefmenoxime	1/2	1/4	1/6
Cefmetazole	2/3	1/2	1/3
Cefodizime	—	—	1/2
Cefonicid	1/2	1/5	1/10
Ceforanide	1/2	1/3	1/5
Cefotaxime	—	1/2	1/4
Cefotetan	1/2	1/4	1/10
Cefotiam	—	3/4	1/2
Cefoxitin	1/2	1/4	1/6
Cefpirome	—	1/2	1/4
Cefpodoxime	—	1/4	1/8
Cefprodoxime	1/2	1/3	1/5
Cefprozil	—	—	1/2
Cefroxadine	—	1/2	1/4
Cefsulodin	1/2	1/4	1/10
Ceftazidime	1/2	1/5	1/10
Ceftibuten	—	1/2	1/6
Ceftizoxime	1/2	1/4	1/10
Cefuroxime	—	1/2	1/4
Cephacetrile	1/2	1/4	1/10
Cephalexin	—	1/3	1/10
Cephalothin	2/3	1/2	1/6
Cephapirin	—	1/2	1/3
Cephradine	—	1/3	1/10
Loracarbef	1/2	1/4	1/10
Chloramphenicol and Thiamphenicol			
Thiamphenicol	1/2	1/3	1/10

(*Continued*)

TABLE 95.8 (*Continued*)

Macrolide Antibiotics			
Clarithromycin	—	—	1/3
Lincomycin	—	1/2	1/3
Roxithromycin	—	—	1/2
Telithromycin	—	—	1/2
Monobactams			
Aztreonam	1/2	1/3	1/4
Carumonam	2/3	1/3	1/6
Moxalactam	1/2	1/3	1/10
Penicillins			
Amdinocillin	—	1/2	1/4
Amoxicillin	—	1/2	1/6
Ampicillin	1/2	1/4	1/10
Azlocillin	—	1/2	1/4
Carbenicillin	1/3	1/5	1/10
Methicilin	—	1/2	1/4
Mezlocillin	1/2	1/4	1/8
Penicillin	—	1/5	1/8
Piperacillin	—	1/2	1/3
Ticarcillin	1/2	1/3	1/4
Timocillin	—	1/2	1/4
Polymyxins			
Colistin	1/2	1/3	1/6
Polymyxin B	Avoid	Avoid	Avoid
Quinolones			
Ciprofloxacin	—	—	1/2
Fleroxacin	3/4	1/2	1/3
Gatifloxacin	—	—	1/4
Gemifloxacin	—	—	1/2
Levofloxacin	—	1/4	Avoid
Lomefloxacin	—	—	1/6
Norfloxacin	—	—	1/2
Ofloxacin	—	—	1/2
Rufloxacin	—	—	2/3
Sparfloxacin	—	—	1/2
Sulfonamides			
Sulfamethoxazole	—	—	1/2
Sulfisoxazole	3/4	1/2	1/4
Trimethoprim	—	—	1/2

(*Continued*)

TABLE 95.8 (*Continued*)

Tetracyclines			
Tetracycline	—	1/3	1/10
Urinary Bacteriostatics			
Cinoxacin	—	—	1/10
Fosfomycin	—	—	1/4
Nalidixic acid	Avoid	Avoid	Avoid
Nitrofurantoin	Avoid	Avoid	Avoid
Vancomycin-Like Agents			
Teicoplanin	—	1/2	1/3
Vancomycin	2/3	1/2	1/10
ANTIFUNGALS			
Fluconazole	—	1/2	1/3
Flucytosine	1/2	1/3	1/4
Miconazole	—	—	1/3
Terbinafine	—	—	1/2
ANTIHELMINTHICS			
Diethylcarbamazine	—	—	Avoid
ANTIMALARIALS			
Chloroquine	1/2	1/5	1/10
Quinine	—	1/2	1/3
ANTITUBERCULOUS AGENTS			
Ethambutol	—	1/2	1/3
Isoniazid	—	—	1/2
ANTIVIRAL AGENTS			
Acyclovir	—	1/2	1/5
Amantadine	1/2	1/5	1/10
Cidofovir	1/2	1/5	1/10
Didanosine	—	—	1/3
Emtricitabine	1/2	1/3	1/4
Entecavir	1/2	1/4	1/10
Foscarnet	—	—	Avoid
Ganciclovir	1/2	1/5	1/10
Lamivudine	—	1/3	1/10
Oseltamivir	—	—	Avoid
Penciclovir	—	1/2	1/4
Ribavirin	—	—	1/3
Rimantadine	—	—	1/2
Stavudine	—	1/5	1/10
Zalcitabine	—	1/2	1/4
Zanamivir	—	1/5	1/10
Zidovudine	—	—	1/2
ANTINEOPLASTIC AGENTS			
Bleomycin	—	—	1/2
Capecitabine	—	3/4	Avoid
Carboplatin	—	1/2	1/3
Etoposide	—	1/2	1/3
Exemestane	—	—	1/3
Methotrexate	—	Undefined	Undefined
Oxaliplatinin	—	—	1/2
Pentostatin	—	—	1/2
Ralitrexed	—	1/2	Avoid
Topotecan	—	—	1/4
ANTISPASTICITY AGENTS			
Baclofen	—	Undefined	Undefined
Dantrolene	—	Undefined	Undefined
Tizanidine	—	—	1/4
ANTIULCER AGENTS			
Bismuth	—	Avoid	Avoid
BISPHOSPHONATES			
All	Avoid	Avoid	Avoid
BRONCHODILATORS			
Albuterol	—	—	1/3
Dyphylline	—	Undefined	Undefined
Enprofylline	—	Undefined	Undefined
Prenalterol	—	Undefined	Undefined
Terbutaline	—	Undefined	Undefined
Tiotropium	1/2	1/5	1/10
CARDIOVASCULAR AGENTS			
Antianginal Agents			
Isradipine	—	—	1/4
Lercanidipine	—	—	1/2
Ranolazine	—	—	1/2
Antiarrhythmics			
Acecainide [N-acetylprocainamide (NAPA)]	—	1/2	1/4
Bretylium	—	—	1/5
Cibenzoline	—	1/2	1/3

(*Continued*)

TABLE 95.8 (*Continued*)

Disopyramide	—	1/2	1/5
Dofetilide	—	1/2	Avoid
Flecainide	—	—	1/3
Procainamide	—	—	(See Acecainide)
Recainam	—	1/2	1/4
Sematilide	1/2	1/4	1/4
Sotalol	—	1/3	1/8
Tocainide	—	3/4	1/2
Antihypertensives			
Acebutolol	—	1/2	1/3
Atenolol	—	1/2	1/4
Betaxolol	—	—	1/2
Benazepril	—	—	1/4
Bisoprolol	—	1/2	1/3
Bosentan	—	—	1/2
Buflomedil	—	—	1/2
Candesartan	—	—	1/2
Captopril	1/2	1/6	1/12
Carteolol	—	1/2	1/4
Celiprolol	—	Undefined	Undefined
Cetamolol	—	—	1/3
Cilazapril	3/4	1/2	1/4
Clonidine	—	1/2	1/3
Delapril	—	—	1/3
Diazoxide	—	2/3	1/2
Enalapril	—	1/3	1/5
Eposartan	—	—	2/3
Fosinopril	—	—	1/2
Guanadrel	1/2	1/5	1/10
Imidapril	—	—	1/2
Lisinopril	—	1/2	1/4
Methyldopa	—	—	1/2
Metoprolol	—	—	1/2
Minoxidil	—	—	1/2
Moexipril	—	—	1/2
Moxonidine	—	—	1/3
Nebivolol	—	—	1/2
Nadolol	3/4	1/2	1/4
Olmesartan	—	—	1/3
Pentopril	—	Avoid	Avoid
Perindopril	—	—	1/10
Pinacidil	—	—	1/2
Quinapril	1/2	1/4	1/8
Ramipril	—	2/3	1/3
Rilmenidine	2/3	1/3	1/5
Spirapril	—	—	1/3
Temocapril	—	—	1/2
Trandolapril	—	—	1/3
Valsartan	—	—	2/3
Cardiac Inotropes			
Digoxin	1/2	1/3	1/5
Flosequinan	—	—	1/3
Milrinone	1/3	1/4	1/10
Piroximone	—	—	1/2
Blood Lipid-Lowering Agents			
Acifran	—	Avoid	Avoid
Bezafibrate	2/3	1/3	1/6
Cerivastatin	—	—	2/3
Ciprofibrate	—	—	1/2
Clofibrate	1/2	Avoid	Avoid
Fenofibrate	—	—	1/6
Lovastatin	—	—	1/2
DRUG FOR COGNITIVE IMPAIRMENT			
Memantine	—	—	1/2
DRUGS FOR ERECTILE DYSFUNCTION			
Sildenafil	—	—	1/2
Tadalafil	—	1/2	1/4
HORMONAL AGENTS			
Goserelin	—	—	1/4
Lanreotide	—	—	1/2
Octreotide	—	—	1/2
Triptorelin	—	—	1/2
HYPOGLYCEMIC AGENTS			
Acetohexamide	—	Avoid	Avoid
Chlorpropamide	—	Avoid	Avoid
Insulin	—	—	2/3

(*Continued*)

TABLE 95.8 (*Continued*)

Metformin	Avoid	Avoid	Avoid
Repaglinide	—	—	1/3
Saxagliptin	—	1/2	1/4
Tolrestat	—	—	1/2
HYPOURICEMIC AGENTS			
Allopurinol	2/3	1/3	1/6
Colchicine	—	—	1/2
IMMUNOSUPPRESANTS			
Anakinra	—	—	1/4
PSYCHOTHERAPEUTIC AGENTS			
Acamprosate	—	Avoid	Avoid
Amisulpride	—	—	1/2
Bupropion	—	—	1/3
Milnacipran	—	1/2	1/4
Mirtazapine	—	—	2/3
Paliperidone	—	—	1/3
Quetiapine	—	—	3/4
Reboxetine	—	—	2/3
Remoxipride	—	—	1/2
Resperidone	—	—	2/3
Sulpiride	2/3	1/2	1/4
Tianeptine	—	—	1/3
Venlafaxine	—	—	1/2
SYMPATHOMIMETICS			
Almotriptan	—	—	1/2
Dolasetron	—	—	1/2
Pramipexole	—	—	1/4
Selegiline	—	—	1/6
MISCELLANEOUS			
Dextran 40	—	—	Avoid
EDTA	—	1/2	1/4
Iodixanol	—	—	1/10
Sulbactam	—	—	1/5
Tazobactam	—	—	1/4
Varenicline	—	—	1/4

and therefore no change in loading dose is required. As discussed previously, adjusting therapy based on findings from total concentration of highly bound drugs can lead to errors. Clinicians should be alert that an increase in volume of distribution of total drug when the drug is highly bound to albumin often means no change in terms of unbound drug. Cognizance of this phenomenon should avoid misinterpretation of incomplete data in the scientific literature.

Maintenance Dose

Once it is determined that a maintenance dose of drug needs modification in patients with renal insufficiency, several methods of changing the dosing regimen can be employed (Table 95.7).[172] With most drugs, any of the methods listed in Table 95.7 can be utilized and the choice depends on such factors as ease of the regimen for the patient and size of individual doses relative to tablet strength. In contrast, for drugs for which it is important to achieve specified target peak and trough serum concentrations (e.g., antiarrhythmics or anticonvulsants) the dosing methods differ considerably.

The schematics shown in Fig. 95.4 illustrate the differences in dosing methods in terms of peak and trough serum concentrations attained.[172] The interrupted curves in this figure represent serum concentration profiles of an illustrative drug in an average patient with normal renal function. Values for peak and trough concentrations and the dosing regimen are shown in the figure. The solid curves represent serum concentrations in a patient with renal function 15% of normal. Each panel illustrates a different dosing method. It is important to note that the average drug concentration attained with the variable frequency method and with the first variable dose method is the same as in patients with normal renal function. Keeping the average concentration the same is an adequate goal with the majority of drugs, and thus one of these two simple methods can be employed in most settings.

For drugs where peak and trough as well as average concentration is important the simple methods of dose adjustment are flawed. Thus, the variable frequency method shown in Fig. 95.4A could result in prolonged periods of time with sub-therapeutic serum concentrations. The variable dose method shown in Fig. 95.4B, if used without an initial loading dose, may never result in therapeutic peak concentrations. When a loading dose is given, therapeutic concentrations are initially attained. However, when steady state is reached concentrations become sub-therapeutic. Moreover, trough concentrations with this dosing regimen may be higher than desirable and cause toxicity. Thus, in patients with severe renal insufficiency, the variable dose method could result in diminished efficacy and enhanced toxicity. It should be apparent that the two simplest methods of dose adjustment, although adequate for many if not most drugs, may be seriously

flawed for other drugs where attainment of specific peak and trough serum drug concentrations is required for maximal benefit.

Because of the flaws with simple dose adjustment methods, other strategies have been explored. Fig. 95.4C depicts a method designed to attain target peak concentrations while maintaining the same dosing interval as in patients with normal renal function. But this regimen may be unsuitable for some drugs owing to the very high trough concentrations that occur. For other drugs (such as cephalosporin or penicillin antibiotics) for which maintenance of peak concentrations is critical but there is little concern about elevated trough concentrations, this regimen would be acceptable. Kunin's method for dose adjustment is shown in Fig. 95.4D. Its merits and flaws are similar to those of the regimen in Fig. 95.4C and may therefore be appropriate for some drugs, but it is inappropriate for others.

The combination approach of adjusting both the dose and the dosing interval (Fig. 95.4E) is a compromise aimed at a minor decrease in peak concentration, a modest increase in trough concentration, and a dosing interval that is of less concern in terms of duration of time with potentially sub-therapeutic drug concentrations.

The disposition of many drugs has been studied in patients with renal insufficiency. From such data, dosing guidelines can be derived based on a patient's level of renal function[2] (Table 95.8). Once the table is used to decide the amount of dose adjustment required, the concepts explored in the previous discussion of Fig. 95.4 can be used to decide the method of dose adjustment. These data can then be coupled with those from Table 95.5 in patients receiving dialysis.

References

[1] Brater DC. Drug dosing in patients with impaired renal function. Clin Pharmacol Ther 2009;86:483–9.

[2] UpToDate. Waltham, MA: 2010.

[3] Frye RF, Matzke GR, Alexander ACM, Palevsky P, Rault R, Branch RA. Effect of renal insufficiency on CYP activity. Clin Pharmacol Ther 1996;59:155.

[4] Dreisbach AW, Japa S, Gebrekal AB, Mowry SE, Lertora JJ, Kamath BL, et al. Cytochrome P4502C9 activity in end-stage renal disease. Clin Pharmacol Ther 2003;73:475–7.

[5] Dreisbach AW, Lertora JJ. The effect of chronic renal failure on hepatic drug metabolism and drug disposition. Semin Dial 2003;16:45–50.

[6] Nolin TD, Naud J, Leblond FA, Pichette V. Emerging evidence of the impact of kidney disease on drug metabolism and transport. Clin Pharmacol Ther 2008;83:898–903.

[7] U. S. Food and Drug Administration. Guidance for industry: pharmacokinetics in patients with impaired renal function—study design, data analysis, and impact on dosing and labeling, <http://www.fda.gov>; 2010.

[8] Besseghir K, Roch-Ramel F. Renal excretion of drugs and other xenobiotics. Ren Physiol 1987;10:221–41.

[9] Prescott LF. Mechanisms of renal excretion of drugs (with special reference to drugs used by anaesthetists). Br J Anaesth 1972;44:246–51.

[10] Data JL, Nies AS. Drugs five years later: dextran 40. Ann Intern Med 1974;81:500–4.

[11] Klotz U, Kroemer H. Clinical pharmacokinetic considerations in the use of plasma expanders. Clin Pharmacokinet 1987;12:123–35.

[12] Walkley JW, Tillman J, Bonnar J. The persistence of dextran 70 in blood plasma following its infusion, during surgery, for prophylaxis against thromboembolism. J Pharm Pharmacol 1976;28:29–31.

[13] Cross RJ, Taggart JV. Renal tubular transport: accumulation of p-aminohippurate by rabbit kidney slices. Am J Physiol 1950;161:181–90.

[14] Grundemann D, Gorboulev V, Gambaryan S, Veyhl M, Koepsell H. Drug excretion mediated by a new prototype of polyspecific transporter. Nature 1994;372:549–52.

[15] Masuda S, Saito H, Inui KI. Interactions of nonsteroidal anti-inflammatory drugs with rat renal organic anion transporter, OAT-K1. J Pharmacol Exp Ther 1997;283:1039–42.

[16] Saito H, Masuda S, Inui K. Cloning and functional characterization of a novel rat organic anion transporter mediating basolateral uptake of methotrexate in the kidney. J Biol Chem 1996;271:20719–25.

[17] Pritchard JB, Miller DS. Renal secretion of organic anions and cations. Kidney Int 1996;49:1649–54.

[18] Burckhardt G, Ullrich KJ. Organic anion transport across the contraluminal membrane–dependence on sodium. Kidney Int 1989;36:370–7.

[19] Shimada H, Moewes B, Burckhardt G. Indirect coupling to Na + of p-aminohippuric acid uptake into rat renal basolateral membrane vesicles. Am J Physiol 1987;253:F795–801.

[20] Hall S, Rowland M. Influence of fraction unbound upon the renal clearance of furosemide in the isolated perfused rat kidney. J Pharmacol Exp Ther 1985;232:263–8.

[21] Inoue M, Okajima K, Itoh K, Ando Y, Watanabe N, Yasaka T, et al. Mechanism of furosemide resistance in analbuminemic rats and hypoalbuminemic patients. Kidney Int 1987;32:198–203.

[22] Sjostrom PA, Odlind BG, Beermann BA, Karlberg BE. Pharmacokinetics and effects of frusemide in patients with the nephrotic syndrome. Eur J Clin Pharmacol 1989;37:173–80.

[23] Marshall EK, Vickers L. The mechanism of the elimination of phenolsulphonphtalein by kidney-a proof of secretion by the convoluted tubules. Bull Johns Hopkins Hosp 1923;34:1–6.

[24] Borst P, Elferink RO. Mammalian ABC transporters in health and disease. Annu Rev Biochem 2002;71:537–92.

[25] Glavinas H, Krajcsi P, Cserepes J, Sarkadi B. The role of ABC transporters in drug resistance, metabolism and toxicity. Curr Drug Deliv 2004;1:27–42.

[26] Stephens RH, O'Neill CA, Warhurst A, Carlson GL, Rowland M, Warhurst G. Kinetic profiling of P-glycoprotein-mediated drug efflux in rat and human intestinal epithelia. J Pharmacol Exp Ther 2001;296:584–91.

[27] Chen C, Klaassen CD. Rat multidrug resistance protein 4 (Mrp4, Abcc4): molecular cloning, organ distribution, postnatal renal expression, and chemical inducibility. Biochem Biophys Res Commun 2004;317:46–53.

[28] Kool M, van der Linden M, de Haas M, Scheffer GL, de Vree JM, Smith AJ, et al. MRP3, an organic anion transporter able to transport anti-cancer drugs. Proc Natl Acad Sci U S A 1999;96:6914–9.

[29] Kruh GD, Belinsky MG. The MRP family of drug efflux pumps. Oncogene 2003;22:7537–52.
[30] Leslie EM, Deeley RG, Cole SP. Multidrug resistance proteins: role of P-glycoprotein, MRP1, MRP2, and BCRP (ABCG2) in tissue defense. Toxicol Appl Pharmacol 2005;204:216–37.
[31] Ritter CA, Jedlitschky G, Meyer zu Schwabedissen H, Grube M, Kock K, Kroemer HK. Cellular export of drugs and signaling molecules by the ATP-binding cassette transporters MRP4 (ABCC4) and MRP5 (ABCC5). Drug Metab Rev 2005;37:253–78.
[32] Rius M, Thon WF, Keppler D, Nies AT. Prostanoid transport by multidrug resistance protein 4 (MRP4/ABCC4) localized in tissues of the human urogenital tract. J Urol 2005;174:2409–14.
[33] Schaub TP, Kartenbeck J, Konig J, Spring H, Dorsam J, Staehler G, et al. Expression of the MRP2 gene-encoded conjugate export pump in human kidney proximal tubules and in renal cell carcinoma. J Am Soc Nephrol 1999;10:1159–69.
[34] Toyoda Y, Hagiya Y, Adachi T, Hoshijima K, Kuo MT, Ishikawa T. MRP class of human ATP binding cassette (ABC) transporters: historical background and new research directions. Xenobiotica 2008;38:833–62.
[35] van Aubel RA, Smeets PH, Peters JG, Bindels RJ, Russel FG. The MRP4/ABCC4 gene encodes a novel apical organic anion transporter in human kidney proximal tubules: putative efflux pump for urinary cAMP and cGMP. J Am Soc Nephrol 2002;13:595–603.
[36] van de Water FM, Masereeuw R, Russel FG. Function and regulation of multidrug resistance proteins (MRPs) in the renal elimination of organic anions. Drug Metab Rev 2005;37:443–71.
[37] Beck K, Hayashi K, Dang K, Hayashi M, Boyd CD. Analysis of ABCC6 (MRP6) in normal human tissues. Histochem Cell Biol 2005;123:517–28.
[38] Scheffer GL, Hu X, Pijnenborg AC, Wijnholds J, Bergen AA, Scheper RJ. MRP6 (ABCC6) detection in normal human tissues and tumors. Lab Invest 2002;82:515–8.
[39] Peng KC, Cluzeaud F, Bens M, Duong Van Huyen JP, Wioland MA, Lacave R, et al. Tissue and cell distribution of the multidrug resistance-associated protein (MRP) in mouse intestine and kidney. J Histochem Cytochem 1999;47:757–68.
[40] Zelcer N, Saeki T, Reid G, Beijnen JH, Borst P. Characterization of drug transport by the human multidrug resistance protein 3 (ABCC3). J Biol Chem 2001;276:46400–7.
[41] Imaoka T, Kusuhara H, Adachi M, Schuetz JD, Takeuchi K, Sugiyama Y. Functional involvement of multidrug resistance-associated protein 4 (MRP4/ABCC4) in the renal elimination of the antiviral drugs adefovir and tenofovir. Mol Pharmacol 2007;71:619–27.
[42] Hediger MA, Romero MF, Peng JB, Rolfs A, Takanaga H, Bruford EA. The ABCs of solute carriers: physiological, pathological and therapeutic implications of human membrane transport proteinsIntroduction. Pflugers Arch 2004;447:465–8.
[43] Daniel H, Kottra G. The proton oligopeptide cotransporter family SLC15 in physiology and pharmacology. Pflugers Arch 2004;447:610–8.
[44] Daniel H, Rubio-Aliaga I. An update on renal peptide transporters. Am J Physiol Renal Physiol 2003;284:F885–92.
[45] Kamal MA, Keep RF, Smith DE. Role and relevance of PEPT2 in drug disposition, dynamics, and toxicity. Drug Metab Pharmacokinet 2008;23:236–42.
[46] Li M, Anderson GD, Phillips BR, Kong W, Shen DD, Wang J. Interactions of amoxicillin and cefaclor with human renal organic anion and peptide transporters. Drug Metab Dispos 2006;34:547–55.
[47] Dresser MJ, Leabman MK, Giacomini KM. Transporters involved in the elimination of drugs in the kidney: organic anion transporters and organic cation transporters. J Pharm Sci 2001;90:397–421.
[48] Fujita T, Urban TJ, Leabman MK, Fujita K, Giacomini KM. Transport of drugs in the kidney by the human organic cation transporter, OCT2 and its genetic variants. J Pharm Sci 2006;95:25–36.
[49] Jonker JW, Schinkel AH. Pharmacological and physiological functions of the polyspecific organic cation transporters: OCT1, 2, and 3 (SLC22A1-3). J Pharmacol Exp Ther 2004;308:2–9.
[50] Okuda M, Saito H, Urakami Y, Takano M, Inui K. cDNA cloning and functional expression of a novel rat kidney organic cation transporter, OCT2. Biochem Biophys Res Commun 1996;224:500–7.
[51] Zhang S, Lovejoy KS, Shima JE, Lagpacan LL, Shu Y, Lapuk A, et al. Organic cation transporters are determinants of oxaliplatin cytotoxicity. Cancer Res 2006;66:8847–57.
[52] Yokoo S, Yonezawa A, Masuda S, Fukatsu A, Katsura T, Inui K. Differential contribution of organic cation transporters, OCT2 and MATE1, in platinum agent-induced nephrotoxicity. Biochem Pharmacol 2007;74:477–87.
[53] Otsuka M, Matsumoto T, Morimoto R, Arioka S, Omote H, Moriyama Y. A human transporter protein that mediates the final excretion step for toxic organic cations. Proc Natl Acad Sci U S A 2005;102:17923–8.
[54] Masuda S, Terada T, Yonezawa A, Tanihara Y, Kishimoto K, Katsura T, et al. Identification and functional characterization of a new human kidney-specific H + /organic cation antiporter, kidney-specific multidrug and toxin extrusion 2. J Am Soc Nephrol 2006;17:2127–35.
[55] Nishihara K, Masuda S, Ji L, Katsura T, Inui K. Pharmacokinetic significance of luminal multidrug and toxin extrusion 1 in chronic renal failure rats. Biochem Pharmacol 2007;73:1482–90.
[56] Tanihara Y, Masuda S, Sato T, Katsura T, Ogawa O, Inui K. Substrate specificity of MATE1 and MATE2-K, human multidrug and toxin extrusions/H(+)-organic cation antiporters. Biochem Pharmacol 2007;74:359–71.
[57] Matsushima S, Maeda K, Inoue K, Ohta KY, Yuasa H, Kondo T, et al. The inhibition of human multidrug and toxin extrusion 1 is involved in the drug-drug interaction caused by cimetidine. Drug Metab Dispos 2009;37:555–9.
[58] Tsuda M, Terada T, Mizuno T, Katsura T, Shimakura J, Inui K. Targeted disruption of the multidrug and toxin extrusion 1 (mate1) gene in mice reduces renal secretion of metformin. Mol Pharmacol 2009;75:1280–6.
[59] Motohashi H, Sakurai Y, Saito H, Masuda S, Urakami Y, Goto M, et al. Gene expression levels and immunolocalization of organic ion transporters in the human kidney. J Am Soc Nephrol 2002;13:866–74.
[60] Sakurai Y, Motohashi H, Ueo H, Masuda S, Saito H, Okuda M, et al. Expression levels of renal organic anion transporters (OATs) and their correlation with anionic drug excretion in patients with renal diseases. Pharm Res 2004;21:61–7.
[61] Sekine T, Miyazaki H, Endou H. Molecular physiology of renal organic anion transporters. Am J Physiol Renal Physiol 2006;290:F251–61.
[62] Minematsu T, Hashimoto T, Usui T, Kamimura H. Characterization of renal tubular apical efflux of zonampanel, an alpha-amino-3-hydroxy-5-methylisoxazole-4-propionate receptor antagonist, in humans. Xenobiotica 2008;38: 1191–202.
[63] Shima JE, Komori T, Taylor TR, Stryke D, Kawamoto M, Johns SJ, et al. Genetic variants of human organic anion transporter 4 demonstrate altered transport of endogenous substrates. Am J Physiol Renal Physiol 2010;299:F767–775.

[64] Mikkaichi T, Suzuki T, Onogawa T, Tanemoto M, Mizutamari H, Okada M, et al. Isolation and characterization of a digoxin transporter and its rat homologue expressed in the kidney. Proc Natl Acad Sci U S A 2004;101:3569–74.
[65] Chu XY, Bleasby K, Yabut J, Cai X, Chan GH, Hafey MJ, et al. Transport of the dipeptidyl peptidase-4 inhibitor sitagliptin by human organic anion transporter 3, organic anion transporting polypeptide 4C1, and multidrug resistance P-glycoprotein. J Pharmacol Exp Ther 2007;321:673–83.
[66] Toyohara T, Suzuki T, Morimoto R, Akiyama Y, Souma T, Shiwaku HO, et al. SLCO4C1 transporter eliminates uremic toxins and attenuates hypertension and renal inflammation. J Am Soc Nephrol 2009;20:2546–55.
[67] Ohashi R, Tamai I, Nezu Ji J, Nikaido H, Hashimoto N, Oku A, et al. Molecular and physiological evidence for multifunctionality of carnitine/organic cation transporter OCTN2. Mol Pharmacol 2001;59:358–66.
[68] Urban TJ, Brown C, Castro RA, Shah N, Mercer R, Huang Y, et al. Effects of genetic variation in the novel organic cation transporter, OCTN1, on the renal clearance of gabapentin. Clin Pharmacol Ther 2008;83:416–21.
[69] The International HapMap Project. Nature 2003;426: 789–96.
[70] A haplotype map of the human genome. Nature 2005;437: 1299–320.
[71] Frazer KA, Ballinger DG, Cox DR, Hinds DA, Stuve LL, Gibbs RA, et al. A second generation human haplotype map of over 3.1 million SNPs. Nature 2007;449:851–61.
[72] Kroetz DL, Yee SW, Giacomini KM. The pharmacogenomics of membrane transporters project: research at the interface of genomics and transporter pharmacology. Clin Pharmacol Ther 2010;87:109–16.
[73] Vormfelde SV, Schirmer M, Hagos Y, Toliat MR, Engelhardt S, Meineke I, et al. Torsemide renal clearance and genetic variation in luminal and basolateral organic anion transporters. Br J Clin Pharmacol 2006;62:323–35.
[74] Chen Y, Li S, Brown C, Cheatham S, Castro RA, Leabman MK, et al. Effect of genetic variation in the organic cation transporter 2 on the renal elimination of metformin. Pharmacogenet Genomics 2009;19:497–504.
[75] Song IS, Shin HJ, Shim EJ, Jung IS, Kim WY, Shon JH, et al. Genetic variants of the organic cation transporter 2 influence the disposition of metformin. Clin Pharmacol Ther 2008;84: 559–62.
[76] Wang ZJ, Yin OQ, Tomlinson B, Chow MS. OCT2 polymorphisms and in-vivo renal functional consequence: studies with metformin and cimetidine. Pharmacogenet Genomics 2008;18: 637–45.
[77] Keitel V, Nies AT, Brom M, Hummel-Eisenbeiss J, Spring H, Keppler D. A common Dubin-Johnson syndrome mutation impairs protein maturation and transport activity of MRP2 (ABCC2). Am J Physiol Gastrointest Liver Physiol 2003;284: G165–74.
[78] Nies AT, Keppler D. The apical conjugate efflux pump ABCC2 (MRP2). Pflugers Arch 2007;453:643–59.
[79] Toh S, Wada M, Uchiumi T, Inokuchi A, Makino Y, Horie Y, et al. Genomic structure of the canalicular multispecific organic anion-transporter gene (MRP2/cMOAT) and mutations in the ATP-binding-cassette region in Dubin-Johnson syndrome. Am J Hum Genet 1999;64:739–46.
[80] Meier Y, Pauli-Magnus C, Zanger UM, Klein K, Schaeffeler E, Nussler AK, et al. Interindividual variability of canalicular ATP-binding-cassette (ABC)-transporter expression in human liver. Hepatology 2006;44:62–74.
[81] Anders MW. Metabolism of drugs by the kidney. Kidney Int 1980;18:636–47.
[82] Jacqz E, Ward S, Johnson R, Schenker S, Gerkens J, Branch RA. Extrahepatic glucuronidation of morphine in the dog. Drug Metab Dispos 1986;14:627–30.
[83] Smith DE, Lin ET, Benet LZ. Absorption and disposition of furosemide in healthy volunteers, measured with a metabolite-specific assay. Drug Metab Dispos 1980;8:337–42.
[84] Faed EM. Properties of acyl glucuronides: implications for studies of the pharmacokinetics and metabolism of acidic drugs. Drug Metab Rev 1984;15:1213–49.
[85] Iwakawa S, Suganuma T, Lee SF, Spahn H, Benet LZ, Lin ET. Direct determination of diastereomeric carprofen glucuronides in human plasma and urine and preliminary measurements of stereoselective metabolic and renal elimination after oral administration of carprofen in man. Drug Metab Dispos 1989;17:414–9.
[86] Gugler R, Kurten JW, Jensen CJ, Klehr U, Hartlapp J. Clofibrate disposition in renal failure and acute and chronic liver disease. Eur J Clin Pharmacol 1979;15:341–7.
[87] Meffin PJ, Zilm DM, Veenendaal JR. Reduced clofibric acid clearance in renal dysfunction is due to a futile cycle. J Pharmacol Exp Ther 1983;227:732–8.
[88] Erikson LO, Wahlin-Boll E, Odar-Cederlof I, Lindholm L, Melander A. Influence of renal failure, rheumatoid arthritis and old age on the pharmacokinetics of diflunisal. Eur J Clin Pharmacol 1989;36:165–74.
[89] Verbeeck R, Tjandramaga TB, Mullie A, Verbesselt R, Verberckmoes R, de Schepper PJ. Biotransformation of diflunisal and renal excretion of its glucuronides in renal insufficiency. Br J Clin Pharmacol 1979;7:273–82.
[90] Advenier C, Roux A, Gobert C, Massias P, Varoquaux O, Flouvat B. Pharmacokinetics of ketoprofen in the elderly. Br J Clin Pharmacol 1983;16:65–70.
[91] Aronoff GR, Ozawa T, DeSante KA, Nash JF, Ridolfo AS. Benoxaprofen kinetics in renal impairment. Clin Pharmacol Ther 1982;32:190–4.
[92] Sallustio BC, Purdie YJ, Birkett DJ, Meffin PJ. Effect of renal dysfunction on the individual components of the acyl-glucuronide futile cycle. J Pharmacol Exp Ther 1989;251: 288–94.
[93] Stafanger G, Larsen HW, Hansen H, Sorensen K. Pharmacokinetics of ketoprofen in patients with chronic renal failure. Scand J Rheumatol 1981;10:189–92.
[94] Haehner BD, Gorski JC, Vandenbranden M, Wrighton SA, Janardan SK, Watkins PB, et al. Bimodal distribution of renal cytochrome P450 3A activity in humans. Mol Pharmacol 1996;50:52–9.
[95] Aoyama K, Uchida T, Takanuki F, Usui T, Watanabe T, Higuchi S, et al. Pharmacokinetics of recombinant human interleukin-11 (rhIL-11) in healthy male subjects. Br J Clin Pharmacol 1997;43:571–8.
[96] Tsao C, Greene P, Odlind B, Brater DC. Pharmacokinetics of recombinant human superoxide dismutase in healthy volunteers. Clin Pharmacol Ther 1991;50:713–20.
[97] Rabkin R, Simon NM, Steiner S, Colwell JA. Effect of renal disease on renal uptake and excretion of insulin in man. N Engl J Med 1970;282:182–7.
[98] Barza M. Imipenem: first of a new class of beta-lactam antibiotics. Ann Intern Med 1985;103:552–60.
[99] Drayer DE. Pharmacologically active drug metabolites: therapeutic and toxic activities, plasma and urine data in man, accumulation in renal failure. Clin Pharmacokinet 1976;1: 426–43.
[100] Verbeeck RK, Branch RA, Wilkinson GR. Drug metabolites in renal failure: pharmacokinetic and clinical implications. Clin Pharmacokinet 1981;6:329–45.

[101] Streete JM, Berry DJ, Newberry JE, Crome P. Pharmacokinetics of phenylethylmalonamide (PEMA) in elderly men. Eur J Clin Pharmacol 1987;33:431–4.
[102] Davies RO, Gomez HJ, Irvin JD, Walker JF. An overview of the clinical pharmacology of enalapril. Br J Clin Pharmacol 1984;18 (Suppl. 2):215S–29S.
[103] Odar-Cederlof I, Boreus LO, Bondesson U, Holmberg L, Heyner L. Comparison of renal excretion of pethidine (meperidine) and its metabolites in old and young patients. Eur J Clin Pharmacol 1985;28:171–5.
[104] Szeto HH, Inturrisi CE, Houde R, Saal S, Cheigh J, Reidenberg MM. Accumulation of normeperidine, an active metabolite of meperidine, in patients with renal failure of cancer. Ann Intern Med 1977;86:738–41.
[105] International Transporter Consortium, Giacomini KM, Huang SM, Tweedie DJ, Benet LZ, Brouwer KL, et al. Membrane transporters in drug development. Nat Rev Drug Discov 2010;9:215–36.
[106] Rowland M, Balant L, Peck C. Physiologically based pharmacokinetics in drug development and regulatory science: a workshop report (Georgetown University, Washington, DC, May 29-30, 2002). AAPS J 2004;6:56–67.
[107] Giacomini KM, Krauss RM, Roden DM, Eichelbaum M, Hayden MR, Nakamura Y. When good drugs go bad. Nature 2007;446:975–7.
[108] Li M, Anderson GD, Wang J. Drug-drug interactions involving membrane transporters in the human kidney. Expert Opin Drug Metab Toxicol 2006;2:505–32.
[109] Griffith RS, Black HR, Brier GL, Wolny JD. Effect of probenecid on the blood levels and urinary excretion of cefamandole. Antimicrob Agents Chemother 1977;11:809–12.
[110] Cundy KC. Clinical pharmacokinetics of the antiviral nucleotide analogues cidofovir and adefovir. Clin Pharmacokinet 1999;36:127–43.
[111] Beyer KH, Russo HF, Tillson EK, Miller AK, Verwey WF, Gass SR. 'Benemid,' p-(di-n-propylsulfamyl)-benzoic acid; its renal affinity and its elimination. Am J Physiol 1951;166: 625–40.
[112] Lalezari JP, Kuppermann BD. Clinical experience with cidofovir in the treatment of cytomegalovirus retinitis. J Acquir Immune Defic Syndr Hum Retrovirol 1997;14(Suppl. 1): S27–31.
[113] Sambol NC, Chiang J, O'Conner M, Liu CY, Lin ET, Goodman AM, et al. Pharmacokinetics and pharmacodynamics of metformin in healthy subjects and patients with noninsulin-dependent diabetes mellitus. J Clin Pharmacol 1996;36: 1012–21.
[114] Aiba T, Sakurai Y, Tsukada S, Koizumi T. Effects of probenecid and cimetidine on the renal excretion of 3′-azido-3′-deoxythymidine in rats. J Pharmacol Exp Ther 1995;272: 94–9.
[115] Chatton JY, Munafo A, Chave JP, Steinhauslin F, Roch-Ramel F, Glauser MP, et al. Trimethoprim, alone or in combination with sulphamethoxazole, decreases the renal excretion of zidovudine and its glucuronide. Br J Clin Pharmacol 1992;34: 551–4.
[116] Pedersen KE, Dorph-Pedersen A, Hvidt S, Klitgaard NA, Nielsen-Kudsk F. Digoxin-verapamil interaction. Clin Pharmacol Ther 1981;30:311–6.
[117] Ding R, Tayrouz Y, Riedel KD, Burhenne J, Weiss J, Mikus G, et al. Substantial pharmacokinetic interaction between digoxin and ritonavir in healthy volunteers. Clin Pharmacol Ther 2004;76:73–84.
[118] Jalava KM, Partanen J, Neuvonen PJ. Itraconazole decreases renal clearance of digoxin. Ther Drug Monit 1997;19:609–13.
[119] Hager WD, Fenster P, Mayersohn M, Perrier D, Graves P, Marcus FI, et al. Digoxin-quinidine interaction Pharmacokinetic evaluation. N Engl J Med 1979;300:1238–41.
[120] Gibson TP, Giacomini KM, Briggs WA, Whitman W, Levy G. Propoxyphene and norpropoxyphene plasma concentrations in the anephric patient. Clin Pharmacol Ther 1980;27: 665–70.
[121] Hill JB. Experimental salicylate poisoning: observations on the effects of altering blood pH on tissue and plasma salicylate concentrations. Pediatrics 1971;47:658–65.
[122] Hill JB. Salicylate intoxication. N Engl J Med 1973;288: 1110–3.
[123] Jusko WJ, Gretch M. Plasma and tissue protein binding of drugs in pharmacokinetics. Drug Metab Rev 1976;5: 43–140.
[124] Tiula E, Tallgren LG, Neuvonen PJ. Serum protein binding of phenytoin, diazepam and propranolol in chronic renal diseases. Int J Clin Pharmacol Ther Toxicol 1987;25: 545–52.
[125] Vallner JJ. Binding of drugs by albumin and plasma protein. J Pharm Sci 1977;66:447–65.
[126] Vanholder R, Van Landschoot N, De Smet R, Schoots A, Ringoir S. Drug protein binding in chronic renal failure: evaluation of nine drugs. Kidney Int 1988;33:996–1004.
[127] Depner TA, Gulyassy PF. Plasma protein binding in uremia: extraction and characterization of an inhibitor. Kidney Int 1980;18:86–94.
[128] Gulyassy PF, Bottini AT, Stanfel LA, Jarrard EA, Depner TA. Isolation and chemical identification of inhibitors of plasma ligand binding. Kidney Int 1986;30:391–8.
[129] Reidenberg MM, Drayer DE. Alteration of drug-protein binding in renal disease. Clin Pharmacokinet 1984;9(Suppl. 1): 18–26.
[130] Greenblatt DJ, Sellers EM, Koch-Weser J. Importance of protein binding for the interpretation of serum or plasma drug concentrations. J Clin Pharmacol 1982;22:259–63.
[131] Klotz U. Pathophysiological and disease-induced changes in drug distribution volume: pharmacokinetic implications. Clin Pharmacokinet 1976;1:204–18.
[132] MacKichan JJ. Protein binding drug displacement interactions fact or fiction? Clin Pharmacokinet 1989;16:65–73.
[133] Tozer TN. Concepts basic to pharmacokinetics. Pharmacol Ther 1981;12:109–31.
[134] Wilkinson GR. Clearance approaches in pharmacology. Pharmacol Rev 1987;39:1–47.
[135] Reidenberg MM, Affrime M. Influence of disease on binding of drugs to plasma proteins. Ann N Y Acad Sci 1973;226: 115–26.
[136] Sheiner LB, Rosenberg B, Marathe VV. Estimation of population characteristics of pharmacokinetic parameters from routine clinical data. J Pharmacokinet Biopharm 1977;5: 445–79.
[137] Dzurik R, Spustova V, Krivosikova Z, Gazdikova K. Hippurate participates in the correction of metabolic acidosis. Kidney Int Suppl 2001;78:S278–81.
[138] Niwa T, Ise M. Indoxyl sulfate, a circulating uremic toxin, stimulates the progression of glomerular sclerosis. J Lab Clin Med 1994;124:96–104.
[139] Niwa T, Tsukushi S, Ise M, Miyazaki T, Tsubakihara Y, Owada A, et al. Indoxyl sulfate and progression of renal failure: effects of a low-protein diet and oral sorbent on indoxyl sulfate production in uremic rats and undialyzed uremic patients. Miner Electrolyte Metab 1997;23:179–84.
[140] Sun H, Frassetto L, Benet LZ. Effects of renal failure on drug transport and metabolism. Pharmacol Ther 2006;109:1–11.

[141] Niwa T, Ise M, Miyazaki T. Progression of glomerular sclerosis in experimental uremic rats by administration of indole, a precursor of indoxyl sulfate. Am J Nephrol 1994;14: 207–12.
[142] Hook JB, Munro JR. Specificity of the inhibitory effect of "uremic" serum on p-aminohippurate transport. Proc Soc Exp Biol Med 1968;127:289–92.
[143] Preuss HG, Massry SG, Maher JF, Gilliece M, Schreiner GE. Effects of uremic sera on renal tubular P-aminohippurate transport. Nephron 1966;3:265–73.
[144] White AG. Uremic serum inhibition of renal paraaminohippurate transport. Proc Soc Exp Biol Med 1966;123:309–10.
[145] Deguchi T, Ohtsuki S, Otagiri M, Takanaga H, Asaba H, Mori S, et al. Major role of organic anion transporter 3 in the transport of indoxyl sulfate in the kidney. Kidney Int 2002;61: 1760–8.
[146] Deguchi T, Takemoto M, Uehara N, Lindup WE, Suenaga A, Otagiri M. Renal clearance of endogenous hippurate correlates with expression levels of renal organic anion transporters in uremic rats. J Pharmacol Exp Ther 2005;314: 932–8.
[147] Enomoto A, Niwa T. Roles of organic anion transporters in the progression of chronic renal failure. Ther Apher Dial 2007;11 (Suppl. 1):S27–31.
[148] Enomoto A, Takeda M, Taki K, Takayama F, Noshiro R, Niwa T, et al. Interactions of human organic anion as well as cation transporters with indoxyl sulfate. Eur J Pharmacol 2003;466: 13–20.
[149] Henderson SJ, Lindup WE. Renal organic acid transport: uptake by rat kidney slices of a furan dicarboxylic acid which inhibits plasma protein binding of acidic ligands in uremia. J Pharmacol Exp Ther 1992;263:54–60.
[150] Taki K, Nakamura S, Miglinas M, Enomoto A, Niwa T. Accumulation of indoxyl sulfate in OAT1/3-positive tubular cells in kidneys of patients with chronic renal failure. J Ren Nutr 2006;16:199–203.
[151] Aoyama I, Enomoto A, Niwa T. Effects of oral adsorbent on gene expression profile in uremic rat kidney: cDNA array analysis. Am J Kidney Dis 2003;41:S8–14.
[152] Ji L, Masuda S, Saito H, Inui K. Down-regulation of rat organic cation transporter rOCT2 by 5/6 nephrectomy. Kidney Int 2002;62:514–24.
[153] Jin QR, Shim WS, Choi MK, Tian GY, Song IS, Yang SG, et al. Decreased urinary secretion of belotecan in folic acid-induced acute renal failure rats due to down-regulation of Oat1 and Bcrp. Xenobiotica 2009;39:711–21.
[154] Monica Torres A, Mac Laughlin M, Muller A, Brandoni A, Anzai N, Endou H. Altered renal elimination of organic anions in rats with chronic renal failure. Biochim Biophys Acta 2005;1740:29–37.
[155] Schneider R, Sauvant C, Betz B, Otremba M, Fischer D, Holzinger H, et al. Downregulation of organic anion transporters OAT1 and OAT3 correlates with impaired secretion of para-aminohippurate after ischemic acute renal failure in rats. Am J Physiol Renal Physiol 2007;292: F1599–605.
[156] Huang ZH, Murakami T, Okochi A, Yumoto R, Nagai J, Takano M. Expression and function of P-glycoprotein in rats with glycerol-induced acute renal failure. Eur J Pharmacol 2000;406:453–60.
[157] Laouari D, Yang R, Veau C, Blanke I, Friedlander G. Two apical multidrug transporters, P-gp and MRP2, are differently altered in chronic renal failure. Am J Physiol Renal Physiol 2001;280:F636–45.
[158] Franke RM, Sparreboom A. Inhibition of imatinib transport by uremic toxins during renal failure. J Clin Oncol 2008;26:4226–7 [author reply 4227–8].
[159] Naud J, Michaud J, Boisvert C, Desbiens K, Leblond FA, Mitchell A, et al. Down-regulation of intestinal drug transporters in chronic renal failure in rats. J Pharmacol Exp Ther 2007;320:978–85.
[160] Naud J, Michaud J, Leblond FA, Lefrancois S, Bonnardeaux A, Pichette V. Effects of chronic renal failure on liver drug transporters. Drug Metab Dispos 2008;36:124–8.
[161] Nolin TD, Frye RF, Matzke GR. Hepatic drug metabolism and transport in patients with kidney disease. Am J Kidney Dis 2003;42:906–25.
[162] Sun H, Huang Y, Frassetto L, Benet LZ. Effects of uremic toxins on hepatic uptake and metabolism of erythromycin. Drug Metab Dispos 2004;32:1239–46.
[163] Dowling TC, Briglia AE, Fink JC, Hanes DS, Light PD, Stackiewicz L, et al. Characterization of hepatic cytochrome p4503A activity in patients with end-stage renal disease. Clin Pharmacol Ther 2003;73:427–34.
[164] Nolin TD, Appiah K, Kendrick SA, Le P, McMonagle E, Himmelfarb J. Hemodialysis acutely improves hepatic CYP3A4 metabolic activity. J Am Soc Nephrol 2006;17: 2363–7.
[165] Galeazzi RL, Gugger M, Weidmann P. beta blockade with pindolol: differential cardiac and renal effects despite similar plasma kinetics in normal and uremic man. Kidney Int 1979;15:661–8.
[166] Gibson TB, Nelson HA. Drug kinetics and artificial kidneys. Clin Pharmacokinet 1977;2:403–26.
[167] Gibson TP, Matusik E, Nelson LD, Briggs WA. Artificial kidneys and clearance calculations. Clin Pharmacol Ther 1976;20:720–6.
[168] Hoy WE, Gibson TP, Rivero AJ, Jain VK, Talley TT, Bayer RM, et al. XAD-4 resin hemoperfusion for digitoxic patients with renal failure. Kidney Int 1983;23:79–82.
[169] Rosenbaum JL, Kramer MS, Raja R. Resin hemoperfusion for acute drug intoxication. Arch Intern Med 1976;136:263–6.
[170] Winchester JF, Gelfand MC, Tilstone WJ. Hemoperfusion in drug intoxication: clinical and laboratory aspects. Drug Metab Rev 1978;8:69–104.
[171] Somani P, Shapiro RS, Stockard H, Higgins JT. Unidirectional absorption of gentamicin from the peritoneum during continuous ambulatory peritoneal dialysis. Clin Pharmacol Ther 1982;32:113–21.
[172] Chennavasin P, Brater DC. Nomograms for drug use in renal disease. Clin Pharmacokinet 1981;6:193–214.
[173] Jaehde U, Sorgel F, Reiter A, Sigl G, Naber KG, Schunack W. Effect of probenecid on the distribution and elimination of ciprofloxacin in humans. Clin Pharmacol Ther 1995;58: 532–41.
[174] Jacobs C, Coleman CN, Rich L, Hirst K, Weiner MW. Inhibition of cis-diamminedichloroplatinum secretion by the human kidney with probenecid. Cancer Res 1984;44: 3632–5.
[175] Inotsume N, Nishimura M, Nakano M, Fujiyama S, Sato T. The inhibitory effect of probenecid on renal excretion of famotidine in young, healthy volunteers. J Clin Pharmacol 1990;30:50–6.
[176] Chennavasin P, Seiwell R, Brater DC, Liang WM. Pharmacodynamic analysis of the furosemide-probenecid interaction in man. Kidney Int 1979;16:187–95.
[177] Waller ES, Sharanevych MA, Yakatan GJ. The effect of probenecid on nafcillin disposition. J Clin Pharmacol 1982;22:482–9.

[178] Hedaya MA, Elmquist WF, Sawchuk RJ. Probenecid inhibits the metabolic and renal clearances of zidovudine (AZT) in human volunteers. Pharm Res 1990;7:411–7.

[179] Somogyi A, Stockley C, Keal J, Rolan P, Bochner F. Reduction of metformin renal tubular secretion by cimetidine in man. Br J Clin Pharmacol 1987;23:545–51.

[180] Somogyi A, McLean A, Heinzow B. Cimetidine-procainamide pharmacokinetic interaction in man: evidence of competition for tubular secretion of basic drugs. Eur J Clin Pharmacol 1983;25:339–45.

[181] Hardy BG, Schentag JJ. Lack of effect of cimetidine on the metabolism of quinidine: effect on renal clearance. Int J Clin Pharmacol Ther Toxicol 1988;26:388–91.

[182] Muirhead M, Bochner F, Somogyi A. Pharmacokinetic drug interactions between triamterene and ranitidine in humans: alterations in renal and hepatic clearances and gastrointestinal absorption. J Pharmacol Exp Ther 1988;244:734–9.

[183] Fletcher CV, Henry WK, Noormohamed SE, Rhame FS, Balfour Jr HH. The effect of cimetidine and ranitidine administration with zidovudine. Pharmacotherapy 1995;15:701–8.

Index

Note: Page numbers followed by "*f*" and "*t*" refer to figures and tables, respectively.

A

A kinase anchoring proteins (AKAPs), 393–394, 417
  function in kidney transport processes, 418–419
  water transport in, 418
ABC superfamily
  ABC1 in, 149, 2447–2448
  ABCC2 in, 2433–2434
  ABCC4, 2434–2435
  ABCC6, 2429–2430
  ATP hydrolysis and, 149
Abortion, septic, 2714
Absorbance, in intracellular pH measurement, 1775–1776
Absorption-limited kinetics, 1368
ACE inhibitors, 429, 430*f*, 728
  bradykinin and, 429
  functions of, 429–431
  glomerular filtration rate and, 2585
  homologs of, 429
  hyperkalemia due to, 1762
  inhibitors, *see* ACE inhibitors
  mechanism of action of, 437–438
  for preeclampsia-eclampsia, 2741*t*
  somatic, 429
  testicular, 429
Acetaminophen, nephrotoxicity of, 2911–2913
Acetate-buffered dialysate, 3140
Acetazolamide
  absorption, by GI tract, 1361
  adverse effects, 1361
  calcium reabsorption and, 2238–2239
  clinical use, 1361–1362
  and potassium excretion, 1358
  for salicylate poisoning, 2078
Acetoacetic acid, in ketogenesis, 2064, 2066–2067
Acetone, in ketogenesis, 2067–2068
Acetyl-CoA
  in ketogenesis, 2065–2066, 2067*f*, 2068*f*
  in pyruvate metabolism, 2069*f*, 2070
Acetyl-CoA carboxylase (ACC), 161
Acetylsalicylate transporters, 2436
Acid load, *see* Net endogenous acid production
Acid loading
  chronic inhibition of, 1805
  mechanisms of, 1791–1796
Acid production, endogenous, 2051
Acid–base balance, *see also* pH
  acid excretion in, 919–920, 2061–2062, 2062*f*
  acid sources in, 308–312, 2050
  amino acids in, 311
  ammonium ions in, 1995–1997, 2051, 2054
  in brain interstitial fluid, 1988
  breathing in, 1990
  in cerebrospinal fluid, 1988
  chemoreceptors in, 1979
  in erythropoiesis, 3105
  gastrointestinal absorption in, 312–315
    calculation of, 313–315, 2052
  gut in, 2052
  hepatorenal interactions in, 2051–2052, 2051*f*
  measurement of, 307–308
  net acid excretion in, 307–308
  organic acid in, 309
  pH in, 1979, *see also* pH
  phosphate in, 2054
  phosphoric acid in, 309–310
  potassium transport and, 1689*f*, 1690*f*, 1691–1693, 1691*f*, 1700, 1745
    extrarenal, 1638–1641
  in pregnancy, 2701–2702, 2709*f*
  renal regulation of, 2053–2054
  renal tubular acidification in, 1917–1941, *see also* Renal tubular acidification
  sulfuric acid in, 308–309
  systemic processes in, 2050–2054, 2050*f*
  ureagenesis and, 2051–2052, 2051*f*
Acid–base disorders, 2113, *see also* Metabolic acidosis; Metabolic alkalosis; Respiratory acidosis; Respiratory alkalosis
Acid–base transporters
  in distal nephron, 1943–1959
  intracellular pH and, 1789–1791
  in loop of Henle and thick ascending limb, 1941–1943
  in proximal tubule, 1917–1941
Acid-generating diet, metabolic acidosis and, 2062
Acidic aminoaciduria, 2419
Acidification
  in cell volume regulation, 127
  postnatal development of, 917–920
Acidosis, 2497, *see also* Acid–base balance; Metabolic acidosis; Renal tubular acidosis; Respiratory acidosis
  in acute kidney injury, 2562
Acid(s)
  bone buffering of, in metabolic acidosis, 315–316
  excretion of, 919–920, 2061–2062, 2062*f*
    postnatal renal acidification and, 919–920
  extrusion of
    chronic inhibition of, 1805–1806
    mechanisms of, 1796–1804, 1796*f*, 1798*f*, 1799*f*, 1801*f*
  gastrointestinal absorption of, 312–315
  inorganic, metabolism of, 2062–2063
  organic
    metabolism of, 2062–2063
    potassium balance and, 1639–1640
  production of
    in acid–base balance, 2061–2062, 2062*f*
  titratable, 307–308
    excretion of, postnatal renal acidification and, 919–920
Acid-sensing ion channel (ASIC), 984–985
  structure of, 244*f*
Acquired immunodeficiency syndrome
  lactic acidosis in, 2073
Actin, 6, *see also* Cytoskeleton
  in apical microvilli, 8–9, 8*f*
  in cell volume regulation, 126
α-actinin, 13, 2868
α-actinin-4, 738
Active water transport, 1087
Activin
  and fibroblast growth factor, 873
Actomyosin cytoskeleton, 6
Acute Dialysis Quality Initiatives (ADQI), 2527
Acute fatty liver of pregnancy, 2715
Acute glomerulonephritis (AGN), 2763
  disorders mimicking, 2764*t*
Acute interstitial nephritis (AIN), 2531–2532
Acute intracellular acid load, 1804, 1805*f*
Acute kidney disease, *see* Renal failure, acute
Acute kidney injury (AKI), 1357
  apoptosis in, 2551–2556
    caspases in, 2553–2554
    heat shock proteins in, 2555–2556
    heme oxygenase in, 2556

Acute kidney injury (AKI) (*Continued*)
kinase-mediated pathways in, 2555
mitochondria in, 2554
oxidative stress in, 2556–2557
reactive oxygen species in, 2556–2557
receptor-mediated pathways in, 2554
stress response in, 2555–2556
biomarkers, 2513, 2536
area under the receiver-operating characteristic curve (AUC-ROC), 2516–2518
characteristics of promising, 2515*t*
combinations, 2522–2523
desirable characteristic of, 2513–2514, 2514*t*
differentiation from chronic kidney disease (CKD), 2514
interleukin-18 (IL-18), 2522
kidney injury molecule 1 *(Kim-1)*, 2521
limitations of existing studies, 2523
liver-type fatty acid binding protein (L-FABP), 2522
neutrophil gelatinase-associated lipocalin (NGAL), 2514–2521
novel, for early diagnosis, 2521*t*
novel, for predicting outcome, 2521*t*
temporal sequence of, 2523
in terms of prognostic abilities, 2514
blood tests in, 2561
causes of, 2529, 2530*f*
interstitial, 2531–2532
prerenal azotemia as, 2529–2531
cell necrosis in, 2551–2552, 2553*f*
potassium metabolism and, 1646–1647
classification, 2527–2528
clinical course, 2560–2561
clinical features, 2560
clinical overview of, 2527–2534
coagulation abnormalities in, 2545–2546
complications of, 2561–2563, 2564*f*
acidosis, 2562
fluid overload, 2561
hyperkalemia, 2561–2562
hypermagnesemia, 2563
hyperphosphatemia, 2562–2563
hyperuricemia, 2562
hypocalcemia, 2562–2563
hyponatremia, 2561
malnutrition, 2563
uremia, 2562
cross-talk amongst organs in, 2559–2560
cytokines in, 2549
cytoskeletal alterations in, 2538–2540, 2539*f*
definition, 2527–2528
differential diagnosis of, 2561*t*, 2562*t*
endothelial cell injury in, 2544–2545
endothelial cell therapy for, 2566–2567
endothelin-1 in, 2544
endotoxin in, 2535*t*, 2536, 2989
epidermal growth factors, 2558
erythropoietin in, 2564–2565
experimental models of, 2535*t*, 2536
extension phase of, 2536–2537
GFR in, 2527
glomerular changes in, 2538
growth factors in, 2558–2559
growth hormone in, 2558
hemoglobin in, 2533
hepatocyte growth factors in, 2558
human, biopsies of, 2548
incidence, 2528
inflammation in, 2546–2549, 2547*f*
insulin-like growth factor 1 in, 2558
interstitial edema in, 2542
intrinsic/intra-renal, 2531–2534
ischemic, 2542–2543, 2985
ATP depletion in, 166
inflammation in, 2985, *see also* Inflammation
mitochondrial reperfusion injury in, 166
pathophysiology of, 166
preconditioning for, 2563–2564
junctional defects in, 2540–2541
leukocytes and, 2546–2549
light chains and, 2533–2534
long-term effects, 2559–2560
loop diuretics and, 1368
macrophages, 2548
management of, 2563–2567
microvascular changes in, 2542
microvascular insult in, 2542–2544
models of, 2534–2536, 2535*t*
morphological changes of, 2536–2538
myoglobin in, 2533
pathophysiological categories of, drugs based on, 2532*t*
pathophysiology of, 2536–2542, 2537*f*
permeability alterations in, 2540–2541
platelet activating factor (PAF) in, 2550
post-renal, 2531
prevention of, 2563–2567
protein C in, 2545
protein p21 in, 2559
radiocontrast induced nephropathy, 2532–2533
in rhabdomyolysis, 2533
RIFLE criteria, 2527, 2528*t*
risk factors, 2528–2529, 2529*t*
in sepsis, 2549–2557
signaling in, 2555
stem cells in, 2565–2566
thromboxane in, 2550
toll-like receptors (TLRs) in, 2550–2551, 2988–2993
transforming growth factor β in, 2558
tubular epithelial cell injury in, 2536–2538
tubular obstruction in, 2541–2542
tubular regeneration in, 2557–2560
urinary indices in, 2561, 2561*t*
VEGF in, 2558–2559
Acute Kidney Injury Network (AKIN), 2527, 2528*t*
Acute metabolic acidosis, bone buffering in, 315–316
Acute nephritis
major causes, 2764*t*
Acute nephrotoxicity, 2911–2912
Acute post-streptococcal glomerulonephritis (APSGN)
clinical presentation, 2765
general characteristics, 2767*t*
group A streptococci, 2763
infections associated with, 2764*t*
neutrophils associated with, 2764–2765
pathogenesis, 2763–2764
enzymatic modification of IgG, 2763–2764
potential mechanisms, 2764*t*
pathology, 2764–2765
prognosis, 2765
treatment and prevention, 2765
penicillin G, 2765
Acute renal failure (ARF), *see* Renal failure, acute
Acute respiratory acidosis, causes of, 2115*t*
Acute respiratory alkalosis, causes of, 2128*t*
Acute tubular necrosis (ATN), 2482–2483, 2536, *see also* Acute kidney injury (AKI)
nitric oxide in, 2543–2544
Acyclovir, transporters for, 2435–2436, 2435*f*
Acyl-glucuronide formation, 3190
Adapter proteins, 54
Adaptins, 30
Addison disease, 2093
hyperkalemia in, 1758–1759
hyponatremia in, 1520
Adefovir, transporters for, 2435–2436, 2435*f*
Adenine, structure of, 513*f*
Adenine receptors, 511–512, 513*f*, 527
Adenoma
adrenal, metabolic alkalosis and, 2022
villous, metabolic alkalosis and, 2036
Adenomatous polyposis coli (APC) tumor suppressor, 21
Adenosine, 767–768
ATP as precursor for, 769
in blood flow regulation, 832–833, 833*f*, 834*f*
formation of, blocking, 768–769
in renin release, 783–784
renin secretion and, 517
structure, 512, 513*f*
Adenosine receptors
and dopamine receptors, 564
Adenosine-5′-triphosphate (ATP), *see* ATP
Adenyl cyclase, in signaling, 370*f*, 371
Adenylyl cyclase, 545–547
Adherens junctions, 4–7, 627
in acute kidney injury, 2540
formation of, 7, 8*f*
in kidney disease, 362
in signaling, 380–381, 383*f*
structure and function of, 7–8
structure and localization of, 361
Adhesion molecules
epithelial cells polarization mechanisms and, 16–19, 17*f*, 18*f*
Na,K-ATPase in, 75
in vasculitis, 2824–2828, 2825*t*
endothelial cell-selective adhesion molecule (ESAM), 2824–2825
matrix molecules, 2825–2826
monocytes, 2825–2826
platelet/endothelial cell adhesion molecule-1 (PECAM-1) (CD31), 2824–2825

ADMA (asymmetric dimethylarginine), as uremic toxin, 3039–3041
ADP, in mitochondrial respiration, 158–159
ADP/ATP ratio, potassium transport and, 1666
Adrenal adenoma, metabolic alkalosis and, 2022
Adrenal cortex hypertension, 1346–1347
Adrenal hyperplasia, metabolic alkalosis and, 2022
Adrenal insufficiency, 2093–2094, 2095*f*
  hypercalcemia in, 2291
Adrenal steroids, *see also* Glucocorticoids
  biosynthesis of, 2093, 2095*f*
  potassium transport and, 1682–1685, 1683*f*, 1684*f*
Adrenergic receptors
  and dopamine receptors, 564
Adrenoceptors, in renal function, 454
  α-adrenoceptors, 453–454
  α_1-adrenoceptors, 453
  α_2-adrenoceptors, 453–454
  β-adrenoceptors, 453
  β_2-adrenoceptors, 453–454
Adrenocortical hormones
  primary deficiency of, 2093
Adrenocorticotropin (ACTH), 1244–1245
Adrenogenital syndrome, 2093–2094
  metabolic alkalosis in, 2039
Adrenomedullin (ADM), 829–830
  in acute renal failure, 1264
  biological effects, 1255–1256
  in cirrhosis, 1302–1303
  in hemodialysis, 1261
α-Adrenoceptors
  in renal function, 453–454
  renorenal reflexes and, 474–475
α_1-Adrenoceptors
  in renal function, 453
  renorenal reflexes and, 474–475
α_2-Adrenoceptors
  in renal function, 453–454
  renorenal reflexes and, 475
Adult kidney
  cellular proliferation in, 960–963, 961*f*
    aging and, 963
    injuries and, 961–963, 962*f*, 963*f*
  diseased, cells in, 972–973
  endothelial cells of, 960
  epithelial cells of, 959–960
  papillary label-retaining cells, 965, 965*f*
  podocytes, 967–968
  repair, stem cells and, 973–975
  stem cells in, 963–969
    sites harboring, 969–970
  stromal cells of, 960
Advanced carbamylation products, as uremic toxins, 3042
Advanced glycation products
  in diabetic nephropathy, 2617–2621
Advanced glycosylation products, as uremic toxins, 3042
Advanced oxidation products, as uremic toxins, 3042
AE4 (SLC4A9 Gene), 1852–1853
Afferent arterioles, 596–597, 597*f*, 617–618, 617*f*, 618*f*, 619*f*
  wall structure of, 599–600, 599*f*
Afferent renal nerves, *see also* Renorenal reflexes
  overview, 468
  stimulation of, 469
African Americans
  potassium balance in, 1647
Agalsidase, for Fabry disease, 2862
Aging
  and cellular proliferation in adult kidney, 963
Agrin
  in glomerular basement membrane, 904
AIDS
  lactic acidosis in, 2073
AKAP proteins, *see* A kinase anchoring proteins (AKAPs)
Akt, functions of, 389, 390*f*
Alarmins, 2988
Albright's hereditary osteodystrophy, 2297
Albumin
  albumin receptors, endocytosis of, 2462
  Amadori, in diabetic nephropathy, 2617
  calcium concentration and, 2273
  endocytosis of, 2460–2461
  epithelial-mesenchymal transition (EMT), 2466–2467
    distal to the proximal tubule, 2466–2467
  glomerular cells, uptake in, 2460
  glomerular filtration of, 2460, *see also* Glomerular capillary wall
    rate of, 2459–2463
  induced renal tubular and interstitial damage, 2464–2466
    apoptosis, 2464–2465
    ER-stress, 2465–2466
  interstitial inflammation and fibrosis, 2466
  lysosomal degradation of, 2463
  metabolism of, 2457–2459
    pathways of, retrieval, 2463
  and nephrotic syndrome, 2467
  properties of, 2457–2459
  reabsorption in, 2464*f*
  regulation of, 2462–2463
  in renal proximal tubule, 2460–2461
  renal tubular metabolism of
    rate of, 2463–2467
  transcapillary escape rate for, 2457–2459
  transport of, 817, 2457–2459
  transtubular recovery of, 2463–2464
  tubular albumin uptake, 2460–2461
Albumin-dependent signaling, 2968
Albuminuria, 2457, *see also* Proteinuria
  in cardiovascular disease, 2467–2468
  in congenital nephrotic syndrome, 2459–2460
  in diabetes mellitus, 2468–2469
  in diabetic nephropathy, 2608, 2608*t*
  endocytosis in, 2460–2461
  glomerular basement membrane in, 2459
  in hypertension, 2467–2468
  in Imerslund-Gräsbeck disease, 2460–2461
  mechanisms of, 2467–2469
  nephrin in, 2459–2460
  plasma albumin in, 2458*f*
  in pregnancy, 2707
  renin-angiotensin system in, 2462–2463
Albuterol, for hyperkalemia, 1765
Alcohol use/abuse
  hyponatremia in, 1514
  ketoacidosis in, 2068
  metabolic acidosis in, 2068, 2074–2077, 2080*t*
  withdrawal in, hypophosphatemia in, 2380
Alcoholic ketoacidosis, 2068–2069, 2075, 2080*t*
Aldehyde dehydrogenase activity (ALDH), 966–967
Aldose reductase, hypernatremia and, 1546–1547, 1548*f*
Aldosterone, 1391, *see also* Mineralocorticoids; Renin-angiotensin-aldosterone system (RAAS)
  biosynthesis of, 431–432, 2093, 2095*f*
    drugs inhibiting, 1762
    inherited disorders of, hyperkalemia due to, 1759
  biphasic stimulation of Na,K-ATPase and, 78, 79*f*
  in blood flow regulation, 829
  in cirrhosis, 1301
  vs. cortisol, 1181
  deficiency of
    causes of, 2092–2093, 2096*f*
    21-hydroxylase deficiency and, 2093–2094
    hyporeninemic, 2094–2096
    primary, 2093
    secondary, 2093–2094
  and ENaC, 392–393, 393*f*, 1002, 1185–1194
    activation of, 1199–1202
  functions of, 431–432
  and 11β-HSD2, 1197–1198
  and hypertension, 1329–1330
  in hypokalemia, 1733–1734
  imbalances of, sodium balance in, 304
  low-potassium diet and, 1681
  mechanisms of action, 1194–1203
  in metabolic alkalosis, 2028, 2038
  and Na,K-ATPase, 1193–1194
  in non-ASDN cells, 1184–1185
  in potassium transport, 1192–1193, 1669–1670, 1682–1685, 1683*f*, 1684*f*, 1699–1700
    extrarenal, 1641–1642
    metabolic acidosis and, 1692–1693, 1700
    urine flow rate and, 1685
  in pregnancy, 2700, 2702*f*, 2708, 2709*f*
  in proximal tubule, 1940
  release of, angiotensin in, 438
  renal salt reabsorption, 1215–1216
  in renal tubular acidification, 2092–2093, 2093*f*
  in renin-angiotensin system, 431–432
  secretion
    ANP and, 1252
    GRA and, 1216–1218, 1217*f*
  in sodium reabsorption, 392, 393*f*

Aldosterone (*Continued*)
and sodium transport, 1167–1169, 1185–1194
in sodium transport, 392, 393*f*
Aldosterone resistance, in pseudohypoaldosteronism, 2096–2097
Aldosterone sensitive distal nephron (ASDN), 355, 649, 1181–1184
cells, 1181–1182
sodium transport across, 1183–1184
and Wnk kinases, 355
Aldosterone-induced proteins (AIPs), 1379–1380
Aldosterone-producing adenoma, and hypertension, 1218–1220
Aldosterone-regulated RNA, 1202–1203
Aldosteronism
glucocorticoid-suppressible, metabolic alkalosis in, 2039
hypokalemia and, 1699–1700
Alfacalcidol, for hyperparathyroidism, 3080–3081, 3082*t*
Aliphatic amines, as uremic toxins, 3040
Alkali
in complex mixtures, calculation of, 313–315
gastrointestinal absorption of, 312–315
Alkali therapy, 2126
for distal renal tubular acidosis, 2091, 2091*t*
for lactic acidosis, 2074
for metabolic acidosis, 2101
for proximal renal tubular acidosis, 2091, 2091*t*
for salicylate poisoning, 2077
Alkalinization, in cell volume regulation, 127
Alkalosis, *see also* Acid–base balance; Metabolic alkalosis; Respiratory alkalosis
definition of, 2021
gastric, 2035
All-trans-retinoic acid (ATRA), 944
Alpha-mercaptopropionylglycine, for hypercystinuria, 2341–2342
Alport syndrome, 731, 731*f*, 2847–2857
anti-GBM disease in, 2766
anti-glomerular basement membrane in, 2853
autosomal dominant, 2852, 2852*t*
autosomal recessive, 2852–2853, 2852*t*
clinical features of, 2847–2849
diagnosis of, 2855–2856
diffuse leiomyomatosis in, 2849
end-stage renal disease in, 2847–2848
genetic testing for, 2855–2856
genotype-phenotype correlations in, 2853
glomerular basement membrane defects in, 2854–2855
hearing loss in, 2848
hematuria in, 2847, 2854–2855
medical therapy for, 2856–2857
ocular defects in, 2848
pathology of, 2849–2850, 2849*f*, 2850*f*
proteinuria in, 2847
transplantation for, 2856
X-linked, 2852, 2852*t*
Alstrom Syndrome (ALMS), 340
Altered perfusion pressure, myogenic response to, 516
Aluminum carbonate, metabolic alkalosis and, 2034
Amadori albumin, in diabetic nephropathy, 2617
Ambiguous genitalia, in Denys-Drash syndrome, 2871
Amiloride, 254, 983, 1380–1381
adverse effects, 1381–1382
binding site, 990–991
clinical use, 1381
hyperkalemic renal tubular acidosis due to, 2097–2098
for Liddle syndrome, 1723
magnesium balance and, 2144–2145
for nephrolithiasis, 2322
pharmacokinetics, 1381
potassium excretion and, 1694
structure of, 1377*f*
Amiloride test, 2505–2506
Amiloride-sensitive sodium channel, *see* ENaC (amiloride-sensitive sodium channel)
Amino acid(s)
in acid–base balance, 311
anionic, 2411, 2413
aromatic, 2415
catabolism of, in metabolic acidosis, 3048–3049, 3049*t*
cationic, 2411–2413
in cell volume regulation, 124
filtration and reabsorption, 2405–2406
along nephron, 2405
cellular model, 2409*f*
glomerular fluid filtration rate (GFR), 2405
plasma and urine concentration and fractional excretion of, 2406*t*
imino and small neutral, 2410–2411
neutral, 2412
organic osmolytes, 1545–1546, 1551*f*
in pregnancy, 2699–2700
reabsorption by kidney proximal tubules, 2407–2410
renal metabolism and interorgan exchange of, 2414
supplemental, in low-protein diet, 3054
transport of free, 2406–2407
functional role of, 2407
human genome organization (HUGO) classification, 2406–2407
molecular identification, 2406–2407
solute carriers (SLC) gene nomenclature, 2406–2407
transporter selectivity for, 2407
transporters involved in basolateral efflux of
SLC7A13 (AGT1), 2413
SLC7A12 (Asc-2), 2413
Slc7a10 (Asc-1) and SLC3A2 (4F2hc), 2413
SLC43A2 (LAT4), 2412
SLC7A8 (LAT2) and SLC3A2 (4F2*hc*), 2412
SLC38A3 (SNAT3, SN1), 2412
SLC16A10 (TAT1), 2412
SLC6A6 (TauT1), 2413–2414
SLC7A7 (y^+LAT1) and SLC3A2 (4F2*hc*), 2412–2413
transporters involved in luminal uptake of
SLC36A1 and 2 (PAT1 and PAT2), 2407, 2410–2411
SLC15A1 and SLC15A2 (PEPT1 and PEPT2), 2411–2412
SLC6A18 (B^0AT3), 2410
SLC6A19 (B^0AT1), 2407, 2410
SLC7A9 ($b^{0,+}AT$), 2407, 2411
SLC1A1 (EAAC1/EAAT3), 2411
SLC3A1 (rBAT), 2411
SLC6A20 (SIT-1), 2407, 2411
Aminoacidurias
cystinuria, 2416–2417
dicarboxylic aminoaciduria, 2419
genetically elucidated in human, 2416*t*
hartnup disorder, 2418
iminoglycinuria, 2418–2419
lysinuric protein intolerance, 2417–2418
Aminoglycosides
hypomagnesemia due to, 2157
nephrotoxicity of, 2913–2915
Amino-terminus, 988–989
Ammonia transporters, 2007–2009, 2011*f*
Ammonium, urinary
urine anion gap and, 2500, 2502*f*
Ammonium acid urate stones, 2312*t*
Ammonium chloride loading test, 2503–2504
Ammonium ion(s), production/secretion of
in acid–base balance, 1995–1997, 2051, 2054
in anion exchange regulation, 1885–1886
collecting duct permeability to, 2009–2010
excretion of
bicarbonate production and, 1996, 1996*f*
in metabolic acidosis, 1997–1998, 2009–2012
postnatal renal acidification and, 919–920
potassium excretion and, 1693, 1693*f*
steps in, 2007–2009, 2011*f*
future research directions for, 2012
luminal acidification and, 2010
in metabolic acidosis, excretion of, 1997–1998, 2000, 2009–2012
production/secretion of, 1995
acute regulation of, 1997–1999
in metabolic acidosis, 1997–1999, 2007–2008, 2011*f*, 2012
pathways of, 1997
potassium balance and, 2007–2008
in proximal tubule, 2007–2008, 2011*f*
rate of, 2012
reabsorption of, in thick ascending limb of Henle, 2008–2009
re-entry in collecting duct, 2009–2011, 2011*f*
transport of, 2007–2009, 2011*f*
in thick ascending limb, 1154

Amnionless (AMN), 633–634, 2460–2462, 2461*f*, 2963–2964
AMP-activated protein kinase (AMPK), 161, 2673–2674
Amphotericin B
  hypomagnesemia due to, 2159
Ampicillin, transporters for, 2431–2432
Amyloidosis, 2790, 2792
Anatomy, *see* Renal anatomy
ANCA-mediated vasculitis, *see* Anti-neutrophil cytoplasmic antibodies (ANCA)-mediated vasculitis
Anemia
  in acute kidney injury, 2563
    acidosis, 2562
    fluid overload, 2561
    hyperkalemia, 2561–2562
    hypermagnesemia, 2563
    hyperphosphatemia, 2562–2563
    hyperuricemia, 2562
    hypocalcemia, 2562–2563
    hyponatremia, 2561
    malnutrition, 2563
    uremia, 2562
  in chronic renal failure, 3107–3108
    historical perspective on, 3107–3108
    impaired erythropoiesis in, 3107–3108
    pathophysiology of, 3107–3108
    PHD inhibitors as future therapeutics, 3108
    with rhEPO, 3108
    uremic inhibitors of erythropoiesis in, 3107
  erythropoietin in, 3106*f*, 3107–3109
  lactic acidosis in, 2072
Anesthesia, chemoreceptors and, 1981
Aneurysms, intracranial, in polycystic kidney disease, 2650
Angiitis, 2818, 2821*f*, 2830–2832, *see also* Leukocytoclastic angiitis; Vasculitis
Angiogenesis
  in preeclampsia-eclampsia, 2734–2735, 2738–2740
Angiography, for renal artery stenosis, 2580
Angioplasty, renal artery, 2595–2596, 2595*t*
Angiopoietins, glomerular endothelial cells, 725–726
Angiotensin I (AI), 1215–1216
Angiotensin II (AII), 728, 1215–1216, 1218–1219, *see also* Renin-angiotensin system
  in aldosterone release, 438
  ammonium ion production and secretion and, 2008
  in antidiuretic hormone regulation, 1449
  biphasic effect on Na,K-ATPase, 77
  in blood flow regulation, 828–829, 829*f*
  in brain, 466–467
  in diabetic nephropathy, 2618–2620
  dopamine receptors and, 564–565
  and ENaC regulation, 1003
  epithelial effects of, 438
  glomerular filtration rate and, 2585
  and glomerulosclerosis, 1329
  and hypertension, 1328
  in intracellular pH regulation, 1813–1814
  nitric oxide and, 438
  in preeclampsia-eclampsia, 2732–2734
  in pregnancy, 2711
  in renal function, 454–455
  renal hemodynamic effects of, 1329
  in renal tubular acidification
    in distal nephron, 1959
    in proximal tubule, 1940
  in renal tubular hypertrophy, 948
  in renin regulation, 391, 392*f*, *see also* Renin-angiotensin system
  renorenal reflexes and, 474
  in sodium excretion, 1287–1288, 1290, 1290*f*, 1291*f*
  in sodium transport, in proximal tubule, 1113–1114
  in solute transport, 440
  in thirst regulation, 1455
  tubular effects of, 439–440
    in loop of Henle, 440
    in proximal tubule, 439
  in urea transport, 1494
  in vascular smooth muscle regulation, 391, 392*f*
  in water transport, 439
Angiotensin receptor antagonists
  hyperkalemia due to, 1762
Angiotensin receptor(s), 372, 372*f*, 378*f*, 429–431, 436
  in medullary circulation, 438
  and dopamine receptors
    AT_1R, 564–565
    AT_2R, 565–566
Angiotensin-converting enzyme (ACE), *see* ACE inhibitors
Angiotensinogen, 427–429, 430*f*
Anion channels
  CaCC, 1030–1033, 1031*f*
  CFTR, 1026–1030, 1027*f*
  classes of, 1020–1039, 1020*f*
  in human kidney, 1039–1041, 1040*f*
    ADPKD, 1039–1041
    Bartter's syndrome, 1039
  overview, 1019–1020
  volume-regulated, 1034–1035, 1034*f*
Anion exchange resins, in acid–base balance, 313, 313*t*
Anion exchangers
  chronic regulation of, 1886–1888
  deficiency diseases of erythrocytes involving, 1888
  developmental regulation of, 1886–1888
  localization of, function and, 1864–1865, 1867*f*, 1868*f*
  pH regulation of, 1885
  phosphorylation of, 1884
  SLC4, 1861, *see also* SLC transporters
Anion gap (AG), 2063–2064
  decreased, causes of, 2063–2064, 2064*t*
  increased, 2064*f*
  measurement of, 2063
  in plasma, 2498–2499
  significance of, 2063
  urine, 2499–2502, 2502*t*
Anion gap acidosis, 2063–2064
  causes of, 2065*t*
  hyperchloremic, 2063–2064, 2064*f*, 2065*t*
  ketoacidosis, 2064
  pathophysiology of, 2063
  in poisoning, 2074–2101
  uremic, 2064
Anion transport inhibitor
  SITS, 1095
Anion(s), organic
  definition of, 2425
  secretion of, 2425–2426
Anoikis, in renal cancer, 386–387
Anorexia, in chronic kidney disease, 3046–3047
Antacids, metabolic alkalosis and, 2034
Anterior lenticonus, in Alport syndrome, 2848
Anti-angiotensin receptor-1 antibodies, in preeclampsia-eclampsia, 2735
Antiarrhythmics
  transporters for, 2441
Antibiotics
  beta-lactam, transporters for, 2435, 2435*f*
  hypomagnesemia due to, 2159
  for urinary tract infections, in pregnancy, 2713
Antibodies, *see also* Immune
  antiangiotensin receptor-1, in preeclampsia-eclampsia, 2735
  anti-glomerular basement membrane in vasculitis, 2818
Anticonvulsants
  for eclampsia, 2741, 2742*t*
  hypocalcemia due to, 2298
  vitamin D and, 2298
Antidiabetic agents, transporters for, 2441
Antidiuretic hormone (ADH), 1382
  anatomic considerations for, 1443–1444, 1443*f*
  angiotensin and, 1449
  aquaporins and, 393–394, 1417–1420, 1418*f*
  biosynthesis of, 1444–1445, 1444*f*, 1543*f*, 1571–1572
  cellular actions of, 1574*f*, 1575*f*, 1576–1578, 1577*f*
  chemistry of, 1442–1443, 1443*f*
  clearance of, 1451–1452
  in diabetes insipidus, 1571–1578
  distribution of, 1451–1452
  effects of, 1445*f*, 1452–1454
  and ENaC regulation, 1002
  glucopenia and, 1449
  hypernatremia and, 1542–1544, *see also* Diabetes insipidus
  hypodipsia and, 1581–1582, 1581*f*
  hypokalemia and, 1732
  in hyponatremia, 2487–2488
  inappropriate secretion of
    aquaporins in, 1428
    causes of, 1518*t*, 1520–1523
    chronic volume expansion in, 306
    demeclocycline for, 1556*t*, 1557
    pathophysiology of, 1517–1520, 1518*t*, 1522*f*
  medullary blood flow and, 827–828, 827*f*
  Na,K-ATPase stimulation and, 78–79, 79*f*

Antidiuretic hormone (ADH) (*Continued*)
in pregnancy, 1450, 1588, 2702, 2703*f*
quantitation of, 1445–1446
in renal tubular acidification, 1958
and sodium transport, 1169
secretion of
age and, 1450
control of, 1542–1544, 1543*f*
drugs affecting, 1451, 1451*t*
emetic stimulation of, 1449
hemodynamic effects on, 1448–1449, 1448*f*
nonosmotic stimulation of, 1575
osmotic stimulation of, 1446–1448, 1572–1575
in signaling, 333–334, 334*f*
sodium handling and, 1291
thick ascending limb of Henle and, 1473
potassium transport in, 1671
sodium transport in, 1156, 1156*t*, 1157*t*, 1158–1159
thirst and, in osmoregulation, 1456–1457
urea transporters and, 1492–1493
in water excretion, aquaporin-2 and, 2484–2491, 2485*f*
Antidiuretic hormone antagonists
for polycystic kidney disease, 2671
Anti-GBM disease, 2765–2768
antibodies from patients, 2766
linear staining of IgG, 2767*f*
pathogenesis, 2766
following renal transplantation, 2766
therapy for, 2768*t*
Antigens, *see under* Immune
Antigen-presenting cells, dendritic cells as, 607
Anti-glomerular basement membrane antibodies
for anti-glomerular basement membrane glomerulonephritis, 2856
in vasculitis, 2818
Anti-glomerular basement membrane glomerulonephritis
posttransplant, 2856
Antihypertensives
in pregnancy
for chronic hypertension, 2743
for preeclampsia-eclampsia, 2722, 2741*t*, 2742*t*
Antineoplastic agents
hypomagnesemia due to, 2157
Antineutrophil cytoplasmic autoantibody, immunogenesis of, 2840–2842
Anti-neutrophil cytoplasmic antibodies (ANCA)-mediated vasculitis, 2766
therapy for, 2768
Antineutrophil cytoplasmic autoantibody vasculitis, 2818, 2821*f*, 2833–2842, *see also* Vasculitis, small-vessel, inflammation in
after immunization with myeloperoxidase, 2839–2840
animal models of, 2837–2839
anti-myeloperoxidase IgG in, 2835–2837, 2838*f*, 2839–2840
anti-myeloperoxidase lymphocytes in, 2837–2839, 2838*f*
antineutrophil cytoplasmic autoantibody, immunogenesis of, 2840–2842
diagnosis of, 2834, 2835*f*, 2835*t*
inflammation in, 2818–2822, 2822*f*, 2825*t*, 2826*f*
myeloperoxidase in, 2834–2837, 2835*t*
pathogenesis of, 2818–2824, 2835–2837
sites of, 2833–2834
Antiporters, 53–54, 56, 58–59
anion
SLC4, 1861, *see also* SLC transporters
Antiviral agents
hypomagnesemia due to, 2159
transporters for
organic anion, 2435–2436, 2435*f*
Apatite stones, 2312*t*
APC tumor suppressor, *see* Adenomatous polyposis coli (APC) tumor suppressor
Apical brush border membrane, 8
Apical junctional complex, 18
Apical membrane, epithelial, 11
patch-clamp studies of, 204–205
potassium recycling and, 1669
renal potassium channels and, 1672*f*, 1673–1675
potassium conductance in, 1148–1150, 1149*f*
potassium transport and, 1665, 1666*f*, 1669
potassium-chloride cotransport and, 1675
sodium channel in, 1161
Apical microvilli, 8–11
Apoptosis
in acute kidney injury, 2551–2556, 2994
caspases in, 2553–2554
heat shock proteins in, 2555–2556
heme oxygenase in, 2556
kinase-mediated pathways in, 2555
mitochondria in, 2554
oxidative stress in, 2556–2557
reactive oxygen species in, 2556–2557
receptor-mediated pathways in, 2554
stress response in, 2555–2556
in atherosclerotic renal artery stenosis, 2588
in cell volume regulation, 131–132, 132*f*
in drug-induced injury, 2894–2901, 2897*f*
macrophages in, 2994–2995
and mesangial proliferation, 939
PI 3-K signaling in, 389, 390*f*
$p27^{Kip1}$and, 939
prevention, during renal development, 879–880
proteinuria in, 2968–2969
in renal ischemia, 166, 2994
Apparent mineralocorticoid excess (AME), 1197–1198, 1220–1221, 1344
Application of vasopressin, 453–454, 1025
AQP1 channels
enhancement of exchanger efficiency and, 812–814
Aquaglyceroporins, 107–108, 107*f*, 108*t*, 1410, 1412–1416, 1413*t*
Aquaporin-1 (AQP1)
deficiency of, 1411–1412
discovery of, 1406–1407
distribution of, 1410–1411, 1410*f*
functions of, 1412
structure of, 1407, 1409*f*
Aquaporin-2 (AQP2), 2275
in arginine vasopressin-dependent water excretion, 2484–2491, 2485*f*
calcium transport and, 1421–1422
cytoskeleton and, 1421–1422
diabetes insipidus and, 1424–1425
in hypercalcemia, 1425–1426
in hypokalemia, 1425–1426
loss-of-function mutations of, 1582–1585
measurement of, 1592
targeting receptors and, 1422–1423
in urinary tract obstruction, 1426
vasopressin regulation of, 1417–1421, 1418*f*
Aquaporin(s), 95, 106–107, 1407–1410
in cell volume regulation, 123
dysregulation of, in water balance disorders, 1424
expression of, long-term regulation of, 1423–1424
functions of, 1407–1410, 1412–1415, 1413*t*, 1414*t*, 1415*f*, 1416*f*
localization of, 1412–1415, 1413*t*, 1414*t*, 1415*f*, 1416*f*
in renal failure, 1426–1427
structure of, 1407–1410
urinary concentrating defects and, 1424–1427
vasopressin regulation of, 1417–1420, 1418*f*
Aquaretics, 1382–1383
clinical use, 1382–1383
mechanism of action, 1382
Arachidonic acid, 487
epoxyeicosatrienoic acids and, 488
metabolism, 488
enzymes mediating, 488
metabolites
in blood flow regulation, 834–837, 836*f*
phospholipase-mediated release, 487–488
in ROMK phosphorylation, 1609
Arcuate artery
anatomy of, 595–596, 596*f*, 601*f*
connective tissue of, 608, 608*f*
Arcuate vein, anatomy of, 595–596, 596*f*, 600, 601*f*
Arginine, in acid–base balance, 311
Arginine vasopressin, 1382, *see also* Antidiuretic hormone (ADH)
secretion, hyponatremia and, 2487
water excretion, 2484–2491
Arginine-based uremic toxins, 3039–3041
βARK, in signaling, 371–372
Aromatic amines, as uremic toxins, 3039–3040
Aromatic amino acid decarboxylase (AADC), 540–542
Arp2/3, 7–8
Arrestin, in signaling, 372
Arrhythmias
in hypokalemia, 1719

in metabolic alkalosis, 2033
Arterial baroreceptors, 1286–1287, *see also* Baroreceptors
Arterial blood pH, *see also* pH
ventilation and, 1979
Arterial oxygen tension, in erythropoietin production, 3094, 3095*f*, 3098*f*, 3099
Arterioles, *see also* Microvascular; Renal vessels
afferent, 596–597, 597*f*, 599, 617–618, 617*f*, 618*f*, 619*f*
efferent, 617–618, 617*f*, 618*f*, 619*f*
cortical, 599, 599*f*
juxtamedullary, 596–598, 597*f*, 598*f*
wall structure of, 599–600, 599*f*
Arteriosclerosis, *see* Atherosclerotic renal artery stenosis
Arteritis, 2817–2818, *see also* Polyarteritis nodosa; Vasculitis
giant cell, 2817–2818, 2819*t*, 2820*f*, 2827
necrotizing, 2821*f*
Arthus reaction, in immune complex vasculitis, 2828–2830
Ascending thin limb of Henle, 635, 636*f*, 639, 640*f*
calcium transport in, 2230, 2231*t*
water transport in, 1472–1473
Ascending vasa recta (AVR), 282
Ascites
effective vascular volume in, 302–303
overflow theory of, 302–303
proANP gene in, 1250
sodium retention in, 301–302, 1292–1294
Aspirin
overdose of, 2077–2078, 2081*t*
for preeclampsia prophylaxis, 2739
AT receptors, *see* Angiotensin receptor(s)
AT1 autoantibodies, in preeclampsia-eclampsia, 2735
Atheroemboli, 2587
Atherosclerosis, 2586–2587
chronic kidney disease and, 3076
Atherosclerotic renal artery stenosis, 2577–2578
adaptive responses to, 2584–2585, 2584*f*
angiography for, 2580
apoptosis in, 2588
atheroemboli and, 2587
blood flow in, 2587
clinical presentations of, 2578–2579
diagnosis of, 2579–2581, 2579*f*
duplex ultrasonography for, 2580
epidemiology of, 2577–2578
fibrogenic factors in, 2588
functional testing, 2580–2581
hemodynamic changes in, 2581–2583, 2582*f*, 2583*f*
inflammation in, 2588
intracellular milieu, 2588
medical management of, 2593–2599
mortality rate, 2578
natural history of, 2590–2591
overview of, 2577–2578
oxidative stress in, 2587–2588
pathophysiology of, 2583–2584
issues associated with, 2588–2589
renal pathology in, 2589–2590
revascularization for
angioplasty in, 2595–2596, 2595*t*
indications, 2578
results of, 2594*t*, 2595, 2595*t*
stenting in, 2596–2598, 2596*f*
utilization trends for, 2578
shear stress in, 2587
treatment strategy of, 2591–2593
vasoconstrictors, imbalance of, 2587
ATP, 768–769
cellular content of, determinants of, 153–154
as chemoreceptor, 1985
depletion of, in acute ischemia, 155
distribution along nephron segments, 154–158
and ENaC regulation, 1001
extracellular, in blood flow regulation, 833–834, 835*f*
hydrolysis of, 143–158, 147*f*
ABC superfamily and, 149
H-ATPase in, 149, 150*f*
H,K-ATPase in, 147*f*, 148, 150*f*
Na,K-ATPase in, 145–147, 147*f*, 150*f*, 158*f*, 159–161
nucleotide receptors and, 511, 531
in polycystic kidney disease, 529–530
in potassium transport, 164, 1672–1673
as precursor for adenosine, 769
production of
ATP hydrolysis in, 143–144, 146*f*
coupled with transport, 158–162
fatty acid oxidation in, 151, 152*f*
gluconeogenesis in, 152*f*, 153
glycolysis in, 152–153, 152*f*
ketone body metabolism in, 151–152, 152*f*
mitochondrial oxidative phosphorylation in, 149–150, 150*f*, 151*f*
pathophysiological states in, 165–167
sodium transport in, 143–144
tricarboxylic acid cycle in, 151
in sodium transport, 143–144, 159–161, 1101
structure of, 513*f*
tubuloglomerular feedback, 516–517
ATP-binding cassette (ABC)
proteins, 54, 57, 1151*f*, 1612*f*
superfamily, *see* ABC superfamily
transporters, 3188
ATP synthases, 67
ATP/ADP ratio, potassium transport and, 1666
ATPases
Ca^{2+}-ATPases (SERCA and PMCA), 67–68
ion transporting, 48
ion-motive, 67, *see also* Ion pumps
ATPγS, 512
AT1-receptor antagonists, for preeclampsia-eclampsia, 2741*t*
ATP-binding casette superfamily, *see* ABC superfamily
Atrial natriuretic peptide (ANP), *see also* Natriuretic hormones
in acute renal failure, 1260–1264
and aldosterone secretion, 1252
anatomical studies, 1241–1242
antiproliferative/anticancer properties of, 1265
in breast cancer, 1266, 1266*t*
cerebral salt wasting and, 1521–1523
in cirrhosis, 1302–1303
in congestive heart failure, 1291–1292
dopamine receptors and, 565–566
and ERK 1/2 activation, 1268
family of, 1243
historical overview of, 1241–1243
and MEK 1/2 activation, 1268
and natriuresis, 1251–1252
in nephrotic syndrome, 1309
postnatal, in sodium transport, 917
physiological studies, 1242–1243
in pregnancy, 2709
receptors, *see* Natriuretic peptide receptors (NPR)
receptors per cell, 1258–1259
renal actions of, 1252
sodium excretion and, 1291–1292, 1301
structure of, 1242*f*
vascular effects of, 837–838
and vasodilation, 1251
Atrial natriuretic peptide prohormone, 1243
amino acid sequence of, 1245, 1246*f*
gastrointestinal processing of, 1257
renal processing of, 1246–1247
synthesis of, 1243
Autoantibodies
against angiotensin receptor-1, in preeclampsia-eclampsia, 2735
antineutrophil cytoplasmic immunogenesis of, 2840–2842
in vasculitis, 2834–2837, 2835*t*
AT1, in preeclampsia-eclampsia, 2735
Autocrine/paracrine regulation, and dopamine receptors, 557
Autoimmune hypoparathyroidism, calcium-sensing receptor mutations in, 2192
Autoimmune regulator gene, 2296
Autoregulation
altered perfusion pressure, 516
blood flow, *see also* Blood flow
pressure natriuresis and, 826–827, 826*f*
of blood flow, 516
in neonates, 911
tubuloglomerular feedback in, 516–517, 770–771
Autosomal dominant focal segmental glomerulosclerosis, 2868–2870
Autosomal dominant polycystic kidney disease (ADPKD), 631–632, 1039–1041, *see also* Polycystic kidney disease
epithelial cell polarity and, 33–34
Autosomal dominant traits, 1213
Autosomal recessive PHA I, 1226–1227
Autosomal recessive steroid-resistant nephrotic syndrome, 2865–2866
Autosomal-dominant hypoparathyroidism, 2149
Avβ3 integrin, 740

Axonemal microtubules, 323
Azotemia
  intrinsic renal, 2531
  prerenal, and acute kidney injury, 2529–2531, 2560

B

Backflux, sodium, across tight junction, 1107–1108
Bacterial infections
  in cirrhotic renal failure, 2635–2636
  treatment of, *see* Antibiotics
Bacterial infusion model, of acute kidney injury, 2535*t*
Bacterial metabolism, uremic toxins from, 3039–3040
Bacterial peritonitis, in cirrhotic renal failure, 2635–2636
Bacteriuria, in pregnancy, 2713
Balloon distention, atria, 1242–1243
Bardet–Biedl Syndrome (BBS), 326–327, 340
Barium, potassium metabolism and, 1647
Baroreceptors, 463–464
  in congestive heart failure, 1286–1287
  in extracellular volume control, 1286–1287
  high-pressure, 463–464, 1286–1287
  low-pressure, 464, 1286–1287
  in renin regulation, 434–436
Bartter syndrome (BS), 1039, 1227–1230, 1720–1722
  antenatal, 2146
    with sensorineural deafness, 2146
  calcium receptors in, 2196–2197
  calcium transport in, 2232
  calcium-sensing receptor and, 1229–1230, 2196–2197
  classic, 2146–2148
  CLCNKB gene and, 1228–1229
  clinical presentation, 1721–1722
  diagnosis of, 1229
  genetic and molecular biology, 1720–1721
  hypercalciuria in, 2320
  hypokalemia in, 1671, 1720–1722
  hypomagnesemia in, 2148
  magnesium balance in, 2145
  metabolic alkalosis in, 2037
  NKCC2 mutations and, 1047, 1228
  pathogenesis of, 1721
  pathophysiology, 1721
  ROMK in, 1228, 1614–1615
  salt wasting in, 1310
  with sensorineural deafness, 1229
  urinary sodium/chloride excretion in, 2480–2481, 2480*t*
Bartter syndrome type II, 254–256
Bartter syndrome type III, 248–250
Bartter syndrome type IV, 250–251
Bartter-like syndromes, 2146
Barttin, 234–235, 250–251
Basal body and centrosomes, 322
Basement membrane, 11–13, *see also* Glomerular basement membrane (GBM)
Basic fibroblast growth factor (bFGF), 937–938
Basolateral calcium efflux, regulation of, 2230, 2232*f*
Basolateral Cl channels
  of distal convoluted tubule cells, 1162
Basolateral endocytosis, role of, 634–635
Basolateral interdigitations, 630
Basolateral K channels
  of distal convoluted tubule cells, 1162
  in TAL, 1150–1152, 1151*f*, 1152*f*
Basolateral membrane, 11–13, 630–631
  Cl^--selective channels in, 1152–1153
  electrogenic NA^+ pump, 1161–1162
  KCl symport, 1153–1154
  of macula densa cells, 516–517
  patch-clamp studies of, 205, 1672*f*, 1673–1675
  PDZ protein complexes at, 414–417, 415*f*, 417*f*
  potassium conductance and, 1665–1667, 1666*f*, 1669–1671
  potassium ion channels in, 1672–1673, 1672*f*, 1675
  potassium transport in, 1665, 1666*f*, 1669–1671
  sodium transport in, 1100–1101
Basolateral transport of amino acids, 2408–2409
  SLC7A13 (AGT1), 2413
  SLC7A12 (Asc-2), 2413
  Slc7a10 (Asc-1) and SLC3A2 (4F2hc), 2413
  SLC43A2 (LAT4), 2412
  SLC7A8 (LAT2) and SLC3A2 (4F2*hc*), 2412
  SLC38A3 (SNAT3, SN1), 2412
  SLC16A10 (TAT1), 2412
  SLC6A6 (TauT1), 2413–2414
  SLC7A7 (y^+LAT1) and SLC3A2 (4F2*hc*), 2412–2413
BBSome, ciliary targeting and, 326–327
BCECF, in intracelullar pH measurement, 1777–1778
Bcl-2 proteins
  in acute kidney injury, 2555
  in drug-induced injury, 2897–2898
Bed rest, hypercalcemia in, 2292
Beer drinkers' potomania, 1514
Benign prostatic hyperplasia, obstructive uropathy due to, *see* Obstructive uropathy
Bentonite, 3135
Benzylpenicillin, transporters for, 2435, 2435*f*
Bernard, Claude, 451
Best Vitelliform Macular Dystrophy (BVMD), 1037
Bestrophin, 1037–1038
Beta blockers, for preeclampsia-eclampsia, 2741*t*
Beta-2 microglobulin, glomerular filtration rate and, 3026
Beta-lactam antibiotics, transporters for, 2435, 2435*f*
Beta-OH butyric acid, in ketogenesis, 2064, 2066–2067
Bicarbonate, *see also* Acid–base balance; Sodium bicarbonate
  in extracellular fluid
    distribution of, 2022–2023, 2022*f*
    in metabolic alkalosis, 2022–2023, 2022*f*
  in metabolic acidosis, 2049–2050
  in metabolic alkalosis, *see also* Metabolic alkalosis
    excess, 2025–2027
    excretion of, 2022–2024, 2022*f*
    redistribution in extracellular fluid, 2022–2023, 2022*f*
    renal reabsorption of, 2023–2025, 2029–2032
  production of, 2053
  reabsorption of, 2053
    glutamine catabolism and, 1996, 1996*f*
    in pregnancy, 2702, 2703*f*
    in renal tubular acidification, 1917–1941, *see also* Renal tubular acidosis
    in thick ascending limb of Henle, 2008–2009
Bicarbonate absorption, V-ATPases in, 84
Bicarbonate dialysate, 3137, 3137*f*
Bicarbonate excretion
  mechanism of enhanced, 1843
Bicarbonate reabsorption
  thick ascending limb of Henle, 641–642
Bicarbonate transport
  in cell volume regulation, 129, 130*f*
  in distal nephron, 1943–1959
  in loop of Henle and thick ascending limb, 1941–1943
  postnatal renal acidification and, 917–919
  in proximal tubule, 1917–1941
    chloride transport and, 1092–1095
    potassium transport and intracellular pH and, 1794
    sodium co-transport, 1095–1097
    sodium transport and intracellular pH and, 1793–1794
  in renal tubular acidification, 1917–1941, *see also* Renal tubular acidification
  in thick ascending limb
    chloride transport and, 1154
Bilateral adrenal hyperplasia, metabolic alkalosis and, 2022
Biochemical buffering, intracellular, 1788–1789
Biomarkers
  role in acute kidney injury, 2536
Biopsies, of human AKI, 2548
Biopsy, renal, in pregnancy, 2712
Bisphosphonates, 2210
  for hypercalcemia, 2293–2294
  for hyperparathyroidism, 2288–2289
BK_{Ca} channels, 235
Bladder
  intestinal, chronic metabolic acidosis and, 2099
  obstruction, *see* Obstructive uropathy
Bleeding
  uterine, in pregnancy, 2714
Blood clotting, *See* Coagulation; Coagulopathy
Blood flow, 803, *see also* Renal blood flow
  angiotensin II in, 437–438
  microvascular, *see* Microvascular blood flow

postnatal development of, 911
regulation of, 391, 392*f*
Blood pressure, *see also* Hypertension; Hypotension
calcium and, 3141–3142
in chronic renal failure, 2718
potassium depletion and, 1733
in pregnancy, 2718, *see also* Hypertension; Preeclampsia-eclampsia
in chronic renal failure, 2718
classification of, 2726–2727
measurement of, 2725–2726
regulation of, 2725
regulation of, 1213–1214
dopamine and, 566
renin-angiotensin system in, 432, 433*f*
variation in, 1214
Blood viscosity, in erythropoiesis, 3105
Bohr factor, 2061
BOLD magnetic resonance imaging, 167
Bone
in acid–base balance, 2052–2053, 2053*f*
calcium storage in, 2273
in metabolic acidosis, 315–316, 2059, 2062
parathyroid hormone effects on, 2249, 2260–2261, 2260*f*, 3074–3075
vitamin D and, 2281
Bone buffering
in acute metabolic acidosis, 315–316
in chronic metabolic acidosis, 315
Bone disease, *see also* Renal osteodystrophy
in hyperparathyroidism, 3075–3076
treatment of, 3078–3083, 3082*t*
Bone marrow-derived stem cells, 974–975
Bone morphogenetic protein (BMP), 871–872
gremlin, 875–876
neuropeptide Y and, 873
Bowel diseases
ileostomy, 2338
obesity bypass procedures and bariatric surgery, 2337–2338
small bowel resection, 2336–2337
Bowman, William, 693
Bowman space, 616, 617*f*
Bowman's capsule (BC), 349*f*, 352
anatomy of, 616, 617*f*
hyperplasia of, 968
parietal epithelium of, 617*f*, 626–627
PEC of, 967
Boyle–Van't Hoff equation, 103, 103*f*
Bradykinin
angiotensin-converting enzyme and, 429
renorenal reflexes and, 475
in sodium excretion, 1302
sympatho-excitatory effects, 475
Brain angiotensin II, in renal system, 466–467
autonomic control, 466–467
dietary sodium intake and, 467
Brain function, *see also* Cerebral
in eclampsia, 2730–2731
in extracellular volume control, 1286–1287
in hyponatremia, 1524, 1525*f*, 1526*f*
in SIADH, 1521–1523
Brain interstitial fluid
flow of, 1988–1989
pH of, 1987*f*, 1988–1990
potassium in, 1989
Brain natriuretic peptide (BNP), 1243–1244, *see also* Natriuretic hormones
in acute renal failure, 1264
anti-cancer effects, 1265
biological effects, 1254–1255
cerebral salt wasting and, 1521–1523
in hemodialysis, 1261
prohormone gene, 1250–1251
sodium excretion and, 1291–1292
cirrhosis and, 1302–1303
Braking phenomenon, diuretics and, 1389
Branching morphogenesis
ureteric bud, 873–878, 874*t*
BrdU-labeled cells, 964
Breast cancer
atrial natriuretic peptide in, 1266, 1266*t*
hypercalcemia in, 2290
Breathing, *see also* Respiration; Ventilation
during anesthesia, 1981
chemoreceptors in, 1979, *see also* Chemoreceptors
in pH regulation, 1990
Brn1 gene, 872
Brush border, 8–11, 629–630
Brush border membrane, apical, 8, 629–630
Brush border membrane vesicles
in glucose reabsorption, 2396
in phosphate reabsorption, 2351, 2361
Brushite stones, 2312*t*
BSC1/NKCC2 transporter, in metabolic acidosis, 2008–2009
Buffering, intracellular, 1781–1783, 1786*f*
measurement of, 1789–1791, 1790*f*
Bumetanide, *see also* Loop diuretics
calcium reabsorption and, 2239
transporters for, 2432, 2436–2437, 2436*f*
BUMPT-306 line, 15
Burst-forming unit erythroid, 3089–3090, 3089*f*

C

Ca^{2+} recovery
thick ascending limb of Henle in, 642–643
Ca × Pi product, in dialysis, calcimimetics and, 2206–2207
Ca^{2+}-activated Cl^- channel, 1020, 1030–1033, 1031*f*, 1037
Ca^{2+}-ATPase, 147–148
in ion transport, 60–61
structure and function of, 67–68
Cadherins, 7–8, 737–738, 899
in signaling, 380–381, 383*f*
Caenorhabditis elegans, 18–19
as model systems for cilia, 335–336
Calbindin, 2254, 2257
Calcifediol, 2299–2300
Calcific uremic arteriolopathy, *see* Calciphylaxis
Calcifications
vascular, in chronic kidney disease, 3076–3077
Calcimimetics
bone effects of, 2206–2207
Ca x Pi product and, 2206–2207
in chronic kidney disease, 2207–2208
for hyperparathyroidism, 2205–2206, 2294, 3081, 3082*t*
parathyroid carcinoma, 2208
for polycystic kidney disease, 2671
Calcineurin, 743
Calcineurin inhibitors, *see also* Cyclosporine; Tacrolimus
hyperkalemia due to, 1764
hypomagnesemia due to, 2157–2158
renal effects of, 3166–3167, 3168*f*, 3170*f*, 3173*f*
in transplantation, 3151
Calciphylaxis, 2210, 3076
Calcitonin, 2277
in calcium balance, 2261, 2283
for hypercalcemia, 2293
in potassium reabsorption, 1670
secretion of, 2261
Calcitonin gene-related peptide (CGRP), 468–469, 472*f*, 473–474, 476*f*
Calcitonin receptor, 2261
Calcitriol, 2299
for chronic hypocalcemic treatment, 2299–2300
for hyperparathyroidism, 3080
in idiopathic hypercalciuria, 2319*f*, 2320
Calcium
absorption of, in idiopathic hypercalciuria, 2319*f*, 2320
and blood pressure, 3141–3142
chemical forms of, 2225–2226, 2226*f*
circulating, 2273
complexed, 2225–2226, 2226*f*
disturbances in hemodialysis, 3140–3143
disturbances in peritoneal dialysis, 3143–3144
and ENaC regulation, 999
excretion of, 2226–2227, 2250, 2250*f*
effects of CAI on, 1358
effects of diuretics on, 1356*t*
in hypophosphatemia, 2236–2237
extracellular fluid of, 2273
functions of, 2225, 2273
ionized, 2225–2226, 2226*f*
metabolism of, *see* Calcium balance
in polycystic kidney disease, 2666–2667, 2671
in proANP gene expression, 1249
protein-bound, 2225–2226, 2226*f*
reabsorption of, 2226–2227, 2250, 2250*f*
in connecting tubule, 2234
in cortical collecting ducts, 2200–2201, 2233*f*, 2234–2235
in distal collecting tubule, 2200
in distal convoluted tubule, 2232–2234, 2232*f*
diuretics and, 2238–2239
energetics of, 2228, 2230–2231
in Gitelman's syndrome, 2234
in glomerulus, 2227–2228, 2228*f*
in loop of Henle, 2230–2232
parathyroid hormone in, 2235
in proximal tubule, 2195–2196, 2228, 2228*f*, 2231*f*
rate of, 2227

Calcium (*Continued*)
sites of, 2228, 2228*f*
in thick ascending limb of Henle, 2196–2199, 2196*f*, 2197*f*, 2230–2232, 2231*f*
reference ranges for, 294*t*, 2249–2250, 2250*t*
in renin regulation, 436
serum
concentration of, 2225–2227, 2226*f*, 2249–2250, 2250*t*
constituents of, 2249
reference ranges for, 294*t*, 2249–2250, 2250*t*
total, 2273
in signaling, 2273
structure of, 2225–2226
supplemental
for preeclampsia prophylaxis, 2739
transport
distal convoluted tubule diuretics, 1373–1374, 1373*f*
loop diuretics and, 1365
ultrafilterable, 2225–2228, 2226*f*
Calcium acetate
for hyperparathyroidism, 3082*t*
for hyperphosphatemia, 3079*t*, 3081–3083, 3082*t*
Calcium balance, 2225, 2273–2283
acid–base balance and, 2236
calcimimetics in, 2205–2206
calcitonin in, 2249, 2261
calcium-sensing receptor in, *see* Calcium-sensing receptor
calculation of, 2227
derangements of, *See* Hypercalcemia; Hypocalcemia
extracellular fluid volume and, 2236
hypercalcemia, 2237
in hyperparathyroidism, 3074–3075
in hypophosphatemia, 2236–2237
magnesium balance and, 2143–2144, 2149–2150
in metabolic acidosis, 2037, 2051–2052, 2051*f*, 2058
overview of, 2226–2227, 2227*f*, 2249–2250, 2250*f*
parathyroid hormone in, 2205–2206, 2235, 2249, 2258–2261, 2258*f*, 2274
phosphate depletion, 2236–2237
posttransplant, 3162–3163, 3164*f*, 3165
potassium transport and, 1669, 1673–1674
in pregnancy, 2700, 2700*t*, 2701*f*
reference ranges for, 294*t*, 2226, 2249–2250, 2250*t*
renal mechanisms in, 2257
tubule reabsorption maximum in, 2227
vitamin D in, 2249–2258
Calcium carbonate
for hyperparathyroidism, 3082*t*
for hyperphosphatemia, 3079*t*, 3081–3083, 3082*t*
Calcium channel blockers, patch-clamp studies of, 202–203
Calcium channels, 219*t*, *see also* Calcium ion channels
microvascular permeability, 285–286
Calcium chloride
in acid–base balance, 312
for hypocalcemia, 2299
Calcium fluxes
basolateral, regulation of, 2230, 2232*f*
Calcium gluconate, for hypocalcemia, 2299
Calcium ion channels, 2167–2168
in cell volume regulation, 122, 123*f*, 126, 128*f*, 129, 130*f*
epithelial, 2170–2172, 2170*f*, 2254, 2255*f*, 2257
androgens and, 2176–2177
biophysical properties of, 2171–2172
calmodulin and, 2177–2178, 2178*f*
cDNA of, 2170, 2170*f*
dietary calcium and, 2177
distribution of, 2170–2171, 2171*f*
estrogens and, 2176–2177
gating of, 821–822, 822*t*, 2173
ion selectivity of, 2172–2173, 2173*f*
kallikrein, 2177
80K-H and, 2179
klotho, 2176
modulation of, 2173–2174
molecular structure of, 2174–2175
parathyroid hormone and, 2176
pH and, 2174
pharmacology of, 2174
primary protein structure of, 2170, 2170*f*
Rab11a and, 2179
rectification of, 2173
regulation of, 2175–2182
by auxiliary proteins, 2177–2179
by diuretics, 2180–2181
by immunosuppressives, 2180
S100A10 and, 2178
tacrolimus and, 2180
vitamin D and, 2175–2176
WNK, 2179
non-voltage-dependent, 2168
segmental, 2168*t*
selectivity of, 2168*t*
store-operated, 822
TRP, 822
TRPC, 2168, 2168*t*, 2169*f*
TRPM, 2168–2169, 2168*t*, 2169*f*
TRPP, 2168*t*, 2169, 2169*f*
TRPV4, 2168*t*, 2169–2170, 2169*f*
TRPV5, 2168*t*, 2169*f*, 2170–2172
TRPV6, 2168*t*, 2169*f*, 2170–2171
voltage-dependent, 2167–2168
voltage-gated, 821–822, 822*t*
Calcium metabolism
integrated regulation of, 2283–2284
Calcium oxalate stones, 2312
idiopathic hypercalciuria and, 2319–2322
inhibitors of, 2318–2319
risk factors for, 2319*f*
Calcium permeability
TRPC6 channels, 236–237
TRPV5 channels, 237–238
Calcium phosphate stones, 2312, 2312*t*
idiopathic hypercalciuria and, 2319–2322
risk factors for, 2319*f*
Calcium reabsorption
in CNT and DCT, 649
Calcium salts
in acid–base balance, 312
Calcium sensing receptor, 2273–2276
Calcium signaling, podocytes, 743
calcineurin, 743
synaptopodin, 743
TRPC6, 743
Calcium transport, 48
acid–base balance and, 2236
along nephron, 2226–2235
in Bartter syndrome, 2232
calbindin in, 2254, 2257
calcium efflux regulation in, 2234
in calcium-sensing receptor, 2237
cellular mechanisms of, 2233–2234
in clinical hypercalcemia, 2237–2240
in collecting tubule, 2233*f*, 2234–2235, 2235*t*
in connecting tubule, 2234
in distal convoluted tubule, 2232–2234, 2232*f*
diuretics and, 2238–2239
extracellular fluid volume and, 2236
in Gitelman syndrome, 2234
in glomerulus, 2227–2228, 2228*f*
in hypercalcemia, 2237
in hypophosphatemia, 2236–2237
intestinal, vitamin D in, 2254–2256, 2254*f*, 2255*f*
in loop of Henle, 2230–2232, 2231*f*, 2231*t*, 2235*t*
in descending and ascending thin limb, 2230
in descending thin limb, 2235*t*
in thick ascending limb, 2230–2232, 2231*t*, 2235*t*
phosphate depletion, 2236–2237
in proximal convoluted tubule, 2228, 2229*f*, 2235*t*
in proximal straight tubule, 2228–2229, 2229*f*
regulation of, 2235–2240, 2235*t*
parathyroid hormone in, 2235
renal calcium transport, 2235–2236
vitamin D in, 2254–2256, 2254*f*, 2255*f*
renal osteodystrophy and, 2238
transepithelial, cellular mechanisms of, 2254–2256, 2255*f*
Calcium-sensing receptor (CaSR), 1151–1152, 1152*f*, 2187–2190
agonists for, 2187–2189, 2188*f*
superagonism and, 2189
autoantibodies to
in hyperparathyroidism, 2296
in hypoparathyroidism, 2296
in autosomal-dominant hypoparathyroidism, 2149–2150
and Bartter syndrome, 1229–1230
binding partners, 2190
calcium transport in, 2237
in cartilage, 2202–2203
and c-cell function, 2194
in collecting duct, 2200–2201
in colon, 2204
in cortical collecting duct, 2200–2201

developmental regulation of, 2202
in distal convoluted tubule, 2200
extracellular ionic strength and, 2187–2188
in familial hypocalciuric hypercalcemia, 2149–2150
as G protein-coupled receptor, 2187
and gastrointestinal tract, 2203–2204
in hyperparathyroidism, 3073–3075
and kidney function, 2194–2202
L-amino acids and, 2187–2188
ligand binding to, 2188–2189, 2188*f*
in magnesium balance, 2141, 2144, 2145*f*, 2149–2150
modulation in secondary hyperparathyroidism, 2204–2207
mutations of, 2191–2192, 2196–2197
in neonatal severe hyperparathyroidism, 2149–2150
in osteitis fibrosa, 2206–2207
in osteoblasts, 2203
in osteoclasts, 2203
overview, 2187, 2190–2191
in parathyroid, 2191–2194, 2192*f*
regulation, 2258–2259
pH and, 2187–2188
polyamines and, 2187–2188
preproPTH gene, 2193
promiscuous of, 2189–2190
properties of, 2187
regulation, 2190
and renin secretion, 2201–2202
in secondary hyperparathyroidism, 2204–2207
and skeleton, 2202–2203
in small intestine, 2204
in stomach, 2203–2204
structure of, 2188*f*
in thick ascending limb of Henle, 2196–2199, 2196*f*, 2197*f*
Venus flytrap model of, 2188–2189, 2188*f*
vitamin D and, 2193–2194
Calcium-sensing receptor agonists, for hyperparathyroidism, 3081, 3082*t*
Calculi, 294*t*, *see also* Nephrolithiasis
Calgranulin, as stone inhibitor, 2319
Calmodulin, 67–68
calcium ion channels and, 2177–2178, 2178*f*
Caloric intake, estimation of, 3053
Calyx
anatomy of, 595, 596*f*
in pregnancy, 2689, 2691*f*
cAMP
in intracellular pH regulation, 1813–1814
in polycystic kidney disease, 2667, 2671–2672
in renin regulation, 436–437
in sodium chloride transport regulation, 1109–1111, 1110*f*
cAMP-protein kinase A (PKA), 474
Cancer
atrial natriuretic peptide in, 1265
BNP/CNP and, 1265
chemotherapy for
hypomagnesemia due to, 2157
hypercalcemia in, 2290
fibroblast growth factor 23 in, 2381
hypophosphatemia in, 2381
lactic acidosis in, 2073
osteomalacia in, 2253–2254
hypophosphatemia in, 2380
proANP gene in, 1266
proximal renal tubular acidosis in, 2085
Ras-MAPK pathway in, 1266–1268, 1267*f*
SIADH in, 1520
urodilatin and, 1265
Candidiasis, disseminated, hypercalcemia in, 2290–2291
Capillaries, *see also* Microvascular; Renal vessels
anatomy of, 597–598, 597*f*
glomerular, 617–618, 618*f*, 621*f*, *see also* Glomerulus
wall structure of, 600, 600*f*
Capillary endothelial cells in, 2459
Captopril
for hypertension, in pregnancy, 2743
Carbamazepine, for diabetes insipidus, 1561
Carbamylation products, as uremic toxins, 3042
Carbicarb, 2126
Carbon anhydrase II deficiency, renal tubular acidosis in, 2082–2083
Carbon dioxide, *see also* Hypercapnia; Hypocapnia
dissociation curve, in metabolic acidosis, 2061
intracellular pH and, 1781–1783, 1782*f*
transport
failure, 2116–2117
overproduction of, 2116
ventilation and, 1979–1980
Carbon monoxide (CO)
in blood flow regulation, 832
poisoning, lactic acidosis in, 2071–2072
Carbonic anhydrase
anion exchange and, 1882–1884
in renal tubular acidification
in distal tubule, 1953–1954
postnatal, 920
in proximal tubule, 1930–1931
Carbonic anhydrase inhibitors (CAI), 1357–1362, 1358*f*
adverse effects, 1361
calcium reabsorption and, 2239
clinical use, 1361–1362
effects on calcium excretion, 1358
mechanism of action, 1358–1361, 1359*f*, 1360*f*
pharmacokinetics, 1361
renal hemodynamics, 1361
urinary electrolyte excretion and, 1356*t*, 1357–1362
Carboplatin, hypomagnesemia due to, 2157
Carboxyl-terminus, 992
Carcinogenesis
epithelial cell polarity and, 32
Cardiac arrest model, of acute kidney injury, 2534–2536, 2535*t*
Cardiac arrhythmias, *see* Arrhythmias
Cardiac dysfunction, *see also* Heart disease
in preeclampsia-eclampsia, 2729–2730
Cardiac ischemia-reperfusion injury
role of iron, 3013
Cardiac output, in congestive heart failure, 1287
Cardiac steroids, 72
interaction with Na,K-ATPase, 72
Cardiomyopathy, *see* Congestive heart failure (CHF)
Cardiovascular baroreceptors, 463–464
high pressure, 463–464
low pressure, 464
Cardiovascular disease, *see also* Cardiac; Heart disease; Hypertension; Vascular
albuminuria in, 2467–2468
chronic kidney disease and, 3029, 3076–3077
in dialysis, 3076–3077
mortality in, 3029–3030
Cardiovascular dysfunction, *see also* Hypertension
in dialysis patients, calcimimetics for, 2206–2207
Carnitine-acylcarnitine translocase, 151*f*
Carotid body
chemoreceptors in, 1980–1981, *see also* Chemoreceptors
function of, 1980–1981
location of, 1980
Carrier-mediated transport, 58–59, 60*f*
Cartilage
and bone
parathyroid hormone-related protein, 2282, 2282*f*
calcium-sensing receptor in, 2202–2203
CASK proteins, 414–416, 415*f*
Caspases
in apoptosis
in acute kidney injury, 2553–2554
in drug-induced injury, 2895–2896, 2897*f*, 2898
Catabolism, in metabolic acidosis, 3048–3053, 3049*t*
Catalytic iron pool, 3007–3008, 3009*t*, *see also* Labile (catalytic) iron, in kidney disease
bleomycin-detectable iron assay measures of, 3008
renal function and, 3011*t*
Catecholamines
in hypokalemia, 1719
in intracellular pH regulation, 1813
in metabolic acidosis, 2060
in nephrotic syndrome, 1304–1305, 1308
in phosphate balance, 2374
in potassium transport, 1634–1638, 1635*f*, 1694–1695, 1744
in renal tubular acidification, in proximal tubule, 1941
in sodium transport, 917
Catenin(s), 737–738
β form of, 7–8
glomerular parietal epithelium, 744
in signaling, 381, 383*f*
Cation channels, nonselective, 822

Cation exchange resins
in acid–base balance, 313
for hyperkalemia, 1766–1767
Cation leak syndromes, red cell, SLC4 in, 1876*t*
Cation(s), organic
definition of, 2425
reabsorption of, 2437–2438
secretion of, 2425–2426, 2437–2438
Caudal ventrolateral medulla (CVLM), 466–467
Caveolae intracellulares, 265
C-cell function, 2194
c-Src activity in PKD, 2672
CD2-associated protein (CD2AP), 899–900
CD11/CD18
in vasculitis, 2823–2824
Cd24 protein, 967
CD45, in T-cell activation, 377, 378*f*
CD45 receptor phosphatase, in signaling, 377, 378*f*
CD59, as stone inhibitor, 2319
CD91, in ischemic inflammation, 2992–2993
CD95, in acute kidney injury, 2554
Cd133, glycoprotein, 963–964, 966–967
CD151, 740
Cell adhesion
Na,K-ATPase in, 75
molecules, in vasculitis, 2824–2828
proteins, 628
Cell culture models, in renal development, 866–867
Cell cycle
podocyte and, 940–944, 941*f*
regulatory proteins, 935–936
in renal hyperplasia/hypertrophy, 934–937, 934*f*
stopping, 936–937
Cell death, programmed, *see* Apoptosis
Cell membrane, *see* Plasma membrane
Cell migration, PI 3-K signaling in, 389–390, 390*f*
Cell necrosis, in acute kidney injury, 1646–1647, 2551–2552, 2553*f*
Cell proliferation, PI 3-K signaling in, 389, 390*f*
Cell signaling, *see also* Signaling
by Na,K-ATPase, 75
Cell type-specific sorting
epithelial cells polarization, 28–29
Cell volume
changes in, quantification of, 103, 103*f*
determinants of, 122, 122*f*
extracellular osmolality and, 104, 1544–1552, 1544*t*
neuromuscular excitability and, 129–130
regulation of, 121, 128*f*
apoptosis in, 131–132, 132*f*
bicarbonate concentration in, 128
cell migration in, 131
cell proliferation and, 131, 131*f*
drugs and, 128
energy depletion and, 128–129
epithelial transport in, 129
genetic factors in, 125
glycogen metabolism in, 124, 130
hormones in, 129, 130*f*
hydrogen ion concentration in, 128
hypernatremia and, 1544–1545, 1544*t*, 1545*t*
hypotonic hyponatremia and, 1523–1524
ion transport in, 122, 122*f*, 129
metabolic pathways in, 124–125, 130–131
necrosis in, 126
neurotransmitters in, 129
organic acids in, 128
osmolarity in, 127
osmolytes in, 124
hypernatremia and, 1545–1547, 1546*f*, 1547*f*, 1547*t*, 1548*f*
potassium ion concentration in, 127
protein metabolism in, 124
signaling in, 125–127, 130*f*
toxins and, 128
urea in, 128
solute amount and, 104
Cell–cell interactions
cell–substratum interactions and, 17–18
epithelial cells polarization mechanisms and, 16–19, 17*f*, 18*f*
Cell-location signaling, 380–382, 381*f*, 383*f*, *see also* Signaling
cell-cell interactions in, 380–381, 383*f*
cell-matrix interactions in, 380, 381*f*
Cell-specific markers, 944
Cell–substratum interactions
cell–cell interactions and, 17–18
Cell-surface receptors, 369–383, *see also* Receptor(s); Signaling
Cellular cable analysis, 189–191
Cellular potassium depletion
hypokalemia and, 2160
Cellular respiration, solute transport and, 158–159
Central core assumption, 1481, 1482*f*
Central diabetes insipidus, 1555, 1555*t*
Central nervous system, 466–467, *see also* Brain; Neurological
in eclampsia, 2730–2731
in extracellular volume control, 1286–1287
renal nerves and, 466–467
brain angiotensin II, 466–467
central processing, 466
in SIADH, 1521–1523
Centrosomes and basal bodies, 322, 322*f*
Cephalosporins, transporters for, 2435, 2435*f*
Cerebral edema, in eclampsia, 2731
Cerebral salt wasting, 1311, 1311*f*, 1521–1523
Cerebrospinal fluid
blood-brain barrier and, 1988
choroid plexus secretion of, 1988
composition, 2120, 2133
interstitial fluid and, 1988–1989
pH of, 1987*f*, 1988–1990
chemoreceptors in, 1987*f*, 1988–1990
potassium in, 1989
Cerebrovascular disease
chronic kidney disease in, 3029
proANP gene in, 1249
Cesium, potassium metabolism and, 1647
Cetuximab, 237
CFTR channel, *see* Cystic fibrosis transmembrane conductance regulator (CFTR) channel
cGMP (guanosine cyclic 3′,5′-monophosphate)
nitric oxide and potassium transport and, 1675
in pregnancy, 2695
Channel blockers, patch-clamp studies of, 203
Channel gating, 229–230
modeling, 232–233
regulation of, 231–232
types, 230–231
Channel-inducing factor (CHIF), 2154
Channels, *see* Ion channels
Charge barrier, glomerular filtration, 746
endothelial surface layer as, 746
GBM as, 746
Charge selectivity
glomerular capillary wall permeability and, 2459
Chemical buffering, intracellular, 1787–1788
Chemical driving force, in ion transport, 48, 1085–1087
Chemoattractants
in vasculitis, 2821–2822
Chemokines, 2901
in vasculitis, 2821–2822
Chemoreceptors
in alveolar ventilation, 1979
anesthetics and, 1981
central, 1981–1983
arousal states and, 1986
cerebrospinal fluid pH and, 1987*f*, 1988–1990
cholinergic, 1984
distribution of, 1981–1983, 1982*f*
diversity of, 1979
early studies of, 1981
evolution of, 1986
functions of, 1985
glutamatergic, 1982*f*, 1983–1984
noradrenergic neurons as, 1982*f*, 1984
vs. peripheral, 1986–1988
primary sites for, 1979
putative, 1983–1985
serotonergic neurons as, 1983
peripheral, 1980–1981
vs. central, 1986–1988
rapid-response, 1987–1988
Chemotherapy
hypomagnesemia due to, 2157
Children, *see also* Congenital; Infants; Neonates
treatment of, 1594
Chlamydomonas Reinhardtii, as model systems for cilia, 335
Chloride
balance, in metabolic alkalosis, 2028, 2031
channels, 219*t*
in basolateral membrane, 1152–1153
and dopamine, 542
excretion of
assessment of, 2479–2481, 2480*t*

effects of diuretics on, 1356*t*
transport
chloride/base exchange in, 1092–1095, 1093*f*, 1094*f*
loop diuretics and, 1363–1365, 1365*f*
urinary, in volume status assessment, 2479–2481, 2480*t*
Chloride intracellular channels (CLICs), 1038–1039
Chloride ion channels, 822–823
in cell volume regulation, 128*f*, 129, 130*f*
luminal membrane, 1089
Chloride transporters, 1097–1099, 1098*f*
in cell volume regulation, 122, 123*f*
potassium-coupled, 1669, 1671, 1675
Chloride/OH exchange, in renal tubular acidification, in proximal tubule, 1922–1923
Chloridorrhea, congenital, 2480
Chlorothiazide
calcium reabsorption and, 2240
magnesium balance and, 2144–2145
Chlorpropamide
for diabetes insipidus, 1561, 1594
for hypernatremia, 1561
Chlorthalidone, for nephrolithiasis, 2322
Cholecalciferol, 2299–2300
Cholecystokinin receptors
dopamine receptors and, 566
Cholesterol, *see* Lipid(s)
Cholestyramine, for enteric hyperoxaluria, 2337
Cholinergic receptors, as chemoreceptors, 1984
Chondroitin sulfate
in glomerular basement membrane, 904
as stone inhibitor, 2319
Choroid plexus, cerebrospinal fluid secretion from, 1988
Chronic kidney disease, 3021, *see also* Renal failure
angiotensin II, role of, 2940–2942
anorexia in, 3046–3047
calcimimetics in, 2207–2208
cardiovascular disease and, 3029, 3076–3077
in cerebrovascular disease, 3029
clinical correlates of, 3029–3030
coronary artery disease and, 3029, 3076–3077
definition of, 3027–3028
determinants of glomerular ultrafiltration, 2933–2936, 2934*f*
arteriolar resistances and, 2933–2934
in diabetes mellitus, 2935–2936
glomerular transcapillary hydraulic pressure difference, 2933
independent physical determinants, 2933
initial glomerular plasma flow, 2933
under physiologic conditions, 2934–2935
plasma protein concentration, 2933
single nephron hyperfiltration, 2935
development of glomerular hypertrophy, 2937–2940
cellular mechanism leading to, 2937–2939
role of inflammation, 2939–2940
in diabetes mellitus, 3028–3029, *see also* Diabetes mellitus (DM); Diabetic nephropathy
dietary management of, 3035*t*, 3046–3053
protein restriction in, 3033, 3040–3041, 3046–3060, *see also* Low-protein diet
end-stage renal disease in, 3026–3027, *see also* End-stage renal disease (ESRD)
epidemiology of, 3028
erythropoietin in, 3037, 3055
experimental models, 2948
glomerular filtration rate in, 2940–2942
assessment of, 3021–3022, 3032, *see also* Glomerular filtration rate
linear decline in, 3031*f*, 3032
renal function and, 3030–3033
variability in, 3030–3032
glomerular mechanical strain, 2942–2944
atrial natriuretic peptide (ANP), action of, 2944
circulating mediators for, 2942
endothelin (ET), action of, 2944
genetic and environmental factors, 2945–2947
metabolic derangement, 2944
NO synthases (NOS), action of, 2942–2943
prostanoids, action of, 2943–2944
glucocorticoids in, 3043–3044
growth hormone in, 3044–3045
hormones in, 3043
hyperfiltration hypothesis, 2936–2937
hyperperfusion and hypertension as a pathogenic mechanism, 2936–2937
practical implications of, 2936
hyperparathyroidism in, 3055, 3074, *see also* Hyperparathyroidism
in hypertension, 3028
inflammatory phenomena in, 2940
insulin in, 3051
insulin-like growth factor in, 3044–3045
leptin in, 3045–3046
metabolic acidosis in, 3046–3047, 3049
mineral metabolism in, 3076–3077
mortality in, 3029–3030
number of nephrons, 2945
obesity and, 2945–2946
overview of, 3021
parathyroid hormone in, 3055, 3074–3075
pathophysiology of, 3033–3046
phosphate balance in, 3040–3041
pregnancy and, 2947
progression of, 3027–3028, 3027*t*, 3033–3046, 3059–3060, *see also* Renal disease
assessment of, 3030–3033
meta-analyses and, 3056–3059
risk factors for, 3030, 3030*t*
protein intake and, 2946–2947
protein metabolism in, in muscle, 3049–3053
risk factors for, 3028–3030, 3030*t*
smoking and, 2946
staging of, 3027–3028, 3027*t*
therapeutic measures for glomerular mechanical aggression, 2947–2948
uremic toxins in, 3038–3039, *see also* Uremic toxins
vascular calcifications in, 3076–3077
vitamin D in, 3051
Chronic lithium toxicity, 1844
Chronic metabolic acidosis, bone buffering in, 315
Chronic nephrotoxicity, 2912–2913
Chronic obstructive pulmonary disease (COPD)
Ca^{2+}-activated Cl^- channels (CLCA) and, 1037
lactic acidosis in, 2071
Chronic pyelonephritis, in pregnancy, 2719*t*
Chronic respiratory acidosis, causes of, 2115*t*
Chronic ureteral obstruction, 1844
Churg-Strauss syndrome, 2820*f*, 2833–2834, 2835*t*
Chvostek's sign, in hypocalcemia, 2299
Cidofovir, transporters for, 2435–2436, 2435*f*
Cilia, 11, 319, 2651–2653
and Canonical Wnt Signaling, 331–332
and Hedgehog signaling, 334
and Jak/STAT Signaling, 329–330
mechanisms of, 325–326
and mechanosensation, 329
model systems for, 336*f*
mTOR, 332–333
and non-canonical Wnt/planar cell polarity (PCP) signaling, 330–331
primary single, 631–632
in polycystic kidney disease, 2651–2653, 2651*f*
in signaling, 382–383
signaling in nephron, 328–334
transport and trafficking, 324–327
ciliary targeting and BBsome, 326–327
Intraflagellar Transport (IFT), 324–325
vesicular trafficking of transmembrane proteins, 326
ultrastructure and components, 322–324
centrosomes and basal bodies, 322
cilia membrane, 324
ciliary axoneme, 322–323
ciliary necklace, 323
transition fibers, 323–324
transition zone, 323
and Vasopressin signaling, 333–334
Cilia membrane, 324
Ciliary axoneme, 322–323
Ciliary necklace, 323
Ciliary pocket, 327–328
Ciliogenesis, 327–328
and cell cycle, 327
and cilia disease, 335–337
cilia extension, 327–328
growth control, 328
model systems for
Caenorhabditis Elegans, 335–336
Chlamydomonas Reinhardtii, 335
Danio rerio, 336–337
Mus Musculus, 337

Ciliogenesis (*Continued*)
transcriptional control of, 327
"Ciliopathies," 319, 320*t*
Cimetidine transporters, 2441
Cinacalcet, 2274
bone effects of, 2206–2207
Ca × Pi product and, 2206
for hyperparathyroidism, 2205, 2294, 3081, 3082*t*
Cingulins, 6
Cip/Kip family, of proteins, 936–937
Circadian rhythms, potassium excretion and, 1696*f*, 1698
Cirrhosis
aldosterone in, 1301
aquaporins in, 1427–1428
balance concept in, 1299, 1299*f*
effector mechanisms in, 1299–1303
endothelin in, 1303
hepatorenal syndrome in, 2635, 2635*t*
hyperdynamic circulation in, 1296–1299
hyponatremia in, 1517
kallikrein–kinin system in, 1302
metabolic alkalosis in, 2034
natriuretic hormones in, 1302–1303
proANP gene in, 1250
prostaglandins in, 1302
renal failure in
approach to, 2635–2639
bacterial infections and, 2635–2636
definition of, 2633–2639
drug-induced, 2638–2639
epidemiology of, 2634–2639
etiology, 2634–2639, 2634*f*, 2634*t*
evaluation of patients with, 2635*t*
hypovolemia-induced, 2636
liver transplantation, 2641
management of, 2639–2641, 2639*f*
sodium retention in, 1292–1303, 1303*f*
treatment of, 1303
sympathetic nervous system in, 1300–1301
transjugular intrahepatic portosystemic shunt for, 2640–2641
Cisplatin
hypomagnesemia due to, 2157
nephrotoxicity of, 2903, 2909–2911
Citrate
low urine, in nephrolithiasis, 2323
in metabolic acidosis, 2060–2061, 2060*f*
for nephrolithiasis prophylaxis, 2323
as stone inhibitor, 2318–2319
C-kit, stem cell factor receptor, 960
Cl^- channels (CLC), 57–58, 1020
bestrophin, 1037–1038
CFTR as, 1026–1030, 1027*f*
ClC-2, 1023
CLCA, 1037
CLC-K channels, 1024–1025
function of, 1025–1026
CLIC, 1038–1039
exchangers, 1024
GABA/GABAC, 1035–1039
in human kidney, 1039–1041, 1040*f*
ADPKD, 1039–1041
Bartter's syndrome, 1039
overview, 1019
tweety (human homolog hTTYH3), 1036–1037
VDAC, 1036
Clathrin-coated pits/vesicles, 30
Claudins, 6, 222, 350–351, 628, 2151
functional domains of, 350–351, 352*f*
localization of, 353*f*
Clay eating (geophagia), 3135
ClC-1, Cl^- channel, 1023
ClC-2, Cl^- channel, 1023
ClC channels, architecture of, 230, 239–245, 239*f*
channel gating, 241
Cl^- permeation pathway, 240–241
ENaC/Deg channels
architecture of, 242
gate in, 245
permeation pathway in, 242–245
selectivity filter of, 241*f*
topology and structure of, 218*f*
CLCAs, *see* Ca^{2+}-activated Cl^- channels (CLCAs)
CLC-K channels, 1024–1025
function of, 1025–1026
CLCN5, ClC-5 gene, 1024
CLDN16 gene, 2150–2151
Clinical hypercalcemia
calcium transport in, 2237–2240
Clofibrate, 3190
Clotting, *See* Coagulation; Coagulopathy
CNNM2 mutations
magnesium balance, 2155
Coagulation
abnormalities, in acute kidney injury, 2545–2546
Coagulopathy
in preeclampsia, 2730
Coarse grained models, of renal development, 868
Cockcroft-Gault formula, 3023*t*, 3024
Cold ischemia-warm reperfusion model, 2534, 2535*t*
Collagen
in glomerular basement membrane, 618–619
type IV
in Alport syndrome, 2853, 2854*f*
genetics and biochemistry of, 2850–2852, 2851*t*, 2852*t*, 2854*f*
in glomerular basement membrane, 902–903
structure of, 2850–2852, 2850*t*
type XVIII, in glomerular basement membrane, 904
Collagen IV, 12
Collecting duct (CD), *see also* Cortical collecting duct (CCD); Medullary collecting duct
anatomy of, 1143–1144
calcium-sensing receptor in, 2200–2201
Collecting tubules
calcium reabsorption in, 2234–2235
Collectrin, 429
Colon, *see also* Intestinal
in acid–base balance, 312–315, 2052
calcium-sensing receptor in, 2204
villous adenoma of, metabolic alkalosis and, 2036
Colonic H,K-ATPase, 69
Colony-forming unit erythroid, 3089–3090, 3091*f*
Colony-forming unit megakaryocyte, 3109–3110
COLXVIII, 746
Comma-shaped bodies, epithelial cells, 860
Complement, in tubulointerstitial injury, 2973–2975
Complex polyuropolydipsic syndrome, 1587
Computed tomography
in polycystic kidney disease, 2646*f*, 2647
Computed tomography angiography (CTA)
for renal artery stenosis, 2579–2580
Condensates, 13–14
Congenital adrenal enzyme deficiencies, 2093–2094
Congenital adrenal hyperplasia (CAH), 1343
17-α-hydroxylase deficiency, 1220
11-β-hydroxylase deficiency and, 1220
salt-wasting, causes of, 1226
steroid 21-hydroxylase deficiency and, 1225–1226
Congenital chloride diarrhea, 2480
metabolic alkalosis in, 2036
Congenital enzyme deficiencies, metabolic acidosis in, 2079–2080, 2080*t*, 2081*t*
Congenital hyper-reninemic hypoaldosteronism, 1225
Congenital nephrotic syndrome of Finnish type, 2863–2865
albuminuria in, 2459–2460
Congenital organic acidoses, 2079–2080, 2080*t*, 2081*t*
Congestive heart failure (CHF), 1286–1292, 1288*f*
afferent sensing mechanisms in, 1286–1287, 1288*f*
aquaporins in, 1427
cardiac output in, 1287
effector mechanisms in, 1287–1292
endothelin in, 1292
hyponatremia in, 1517
metabolic alkalosis in, 2034
natriuretic hormones in, 1264–1265, 1291–1292
nitric oxide in, 1292
proANP gene expression in, 1250
prostaglandins in, 1291
renal sodium retention and, nephron sites of, 1287–1288
renin-angiotensin-aldosterone system in, 1289–1290
sympathetic nervous system in, 1290–1291
Conivaptan, for hyponatremia, 1528–1529
Conn Syndrome, 1346–1347
and hypertension, 1218–1220
Connecting tubule, calcium reabsorption in
Connecting tubule (CNT), 643–658, 1216–1220
anatomy, 644*f*, 645*f*, 646*f*, 648
anatomy of, 1143
calcium reabsorption, 649, 2234
cell organization, 648–649, 648*f*

electophysiologic considerations, 1160–1163, 1161*f*, 1161*t*
ENaC at apical membrane of, 1164–1165
Na,K-ATPase control in, 78–79
overview, 643
potassium transport, 650, 1662, 1663*f*, 1672–1675, 1672*f*
control of, 1677
sodium reabsorption, 649–650
sodium transport in, 1163–1170
Connective tissue, periarterial, 608–610, 608*f*, 609*f*
Connective tissue growth factor, in fibrogenesis, 2972
Connexins, 824–825
Connexons, 5
Contractile ability of mesangial cells, 730
Contraction alkalosis, 2026–2027
Contrast-media-associated nephrotoxicity
animal model, 3013*t*
role of iron, 3012, 3013*t*
Coronary artery disease
calcifications in, 3076
in chronic kidney disease, 3076–3077
renal artery stenosis in, *see* Atherosclerotic renal artery stenosis
Cortical collecting duct (CCD), 643–658, 1216–1220, 2200–2201
in acid–base transport, 1945–1948, 1946*f*
anatomy of, 601–602, 602*f*, 644*f*, 645*f*, 646*f*, 1143–1144
in ASDN, 1181–1182
calcium transport in, 2200–2201, 2234–2235
calcium-sensing receptor in, 2200–2201
cells, 610, 651*f*
dopamine receptors and, 559
electrophysiologic and transport properties of, 1165*t*
in mineralocorticoid resistance, 2096–2098
Na,K-ATPase control in, 78–79
overview, 643, 650
potassium secretion in, 1662, 1663*f*
antidiuretic hormone and, 1692*f*, 1693–1694
transport mechanisms and, 1672–1673, 1672*f*
transtubular potassium gradient and, 1753
potassium transport in, control of, 1677, 1678*f*
sodium reabsorption in, 651–652
sodium retention and, 1301, 1311*f*
sodium transport in, 1165–1166
oxygen consumption and, 144, 146*f*
substrate preferences in, 154*f*, 157
urea permeability of, 1470*t*, 1471*t*, 1473–1474
urine flow rate in, 1747
vasopressin-regulated water and urea reabsorption in, 652–653
water permeability of, 1470*t*, 1471*t*, 1473–1474
aquaporins and, 1417
Cortical efferent arterioles, 599, 599*f*
Cortical labyrinth, anatomy of, 595, 596*f*
Cortical microcirculation, 803–804, 804*f*, 805*f*, 806*f*
measurement of, 818–819, 818*f*, 819*t*
Cortical necrosis, in pregnancy, 2715
Cortical radial artery
anatomy of, 595–596, 597*f*
connective tissue of, 608, 608*f*
Cortical radial vein, anatomy of, 595–596, 597*f*
Corticosteroid-resistant nephrotic syndrome, autosomal recessive, 2865–2866
Corticosteroids, *see also* Glucocorticoids; Mineralocorticoids
in transplantation, renal effects of, 3163
Corticotrophin-releasing hormone (CRH), 1247–1248
Cortisol, aldosterone vs.., 1181
Cotransporters, 48, 53–54, 58–59
electrogenic sodium borate, 1851–1852
Countercurrent exchange
of solutes and water, 668–669
Countercurrent multiplication, medullary, 810, 1474–1488, 1475*f*, *see also* Urine concentration
Countertransporters, 48, 53–54
anion
SLC4, 1861, *see also* SLC4
Coupled transport, 52–53, 53*f*
COX, *see* Cyclooxygenase (COX)
COX-1, *see* Cyclooxygenase-1 (COX-1)
COX-2, *see* Cyclooxygenase-2 (COX-2)
Cranionectodermal dysplasia (CED), 341
Creatine, homeostatic mechanisms for, 309
Creatine-P to ATP, conversion of, 310–311
Creatinine
homeostatic mechanisms for, 297
serum, glomerular filtration rate and, 3022–3023
Creatinine clearance
Cockcroft-Gault formula for, 3022–3023
glomerular filtration rate and, 3022–3023
Cre-loxP, 866
Crescent formation, 744
Crescentic GN, 2765–2766
Crest kidney, 595
Crohn's disease, 6
Cross-talk, epithelial transport, 1666
Crumbs complex, 19
Cryoglobulinemia in APSGN, 2765
Cryoglobulinemic vasculitis, 2818*t*, 2819*t*, 2820*f*, 2821–2822, 2828–2832, *see also* Vasculitis
animal models, 2831–2832
hepatitis-induced, 2830–2831
mediators, 2831
CTR transporters, 1873*f*, 1876*t*
C-type natriuretic peptide (CNP), 1243–1244
in acute renal failure, 1264
anti-cancer effects, 1265
biological effects, 1255
circulating concentrations, 1255
Cubilin, 633–634, 2461–2462, 2461*f*
tubular reabsorption of, 2963–2964
Cushing syndrome, 1347
metabolic alkalosis in, 2039
CXCR4/CXCR7/CXCL12 axis
glomerular endothelial cells, 727–728
Cyanide poisoning, metabolic acidosis in, 2072
Cyclic adenosine monophosphate, *see* cAMP
Cyclic guanosine monophosphate, *see* cGMP
Cyclic 3′5′-guanosine monophosphate (cyclic GMP), 1246, 1248*f*, 1256
Cyclin B-Cdc2, 936, 936*f*
Cyclin E-Cdk2, 936
Cyclin-dependent kinases (Cdks), 935–936, 935*f*
inhibitors
and mesangial cell proliferation, 938–945
as negative regulators, 936–937
in mesangial cell proliferation, 938
Cyclins, and cell cycle, 935–936
Cyclooxygenase (COX), 607, 775
as homodimers, 488–489
isoforms of, 489
peroxidase activity of, 488–489
Cyclooxygenase-1 (COX-1), 489
in medullary interstitial cells, 489
Cyclooxygenase-2 (COX-2), 489, 642
administration of, 782–783
in cardiovascular homeostasis, 489
in collecting duct, 489
diabetic nephropathy and, 496
expression of, MD cells and, 759
inhibitors, hyperkalemia and, 1762
proteinuria and, 496–497
renal dysgenesis, 489
renal inflammation and, 496
and renin, 781–782
Cyclophilin D, in programmed necrosis, 2994
Cyclosporine
glomerular filtration rate and, 3168
hyperkalemia due to, 3176
hypomagnesemia due to, 2157–2158
nephrotoxicity of, 2903–2909, 2906*f*, 2908*f*, 3170, 3175
potassium transport and, 3174–3175
renal blood flow and, 3169*t*, 3170–3171
renal effects of, 3161, 3167, 3168*f*, 3170*f*, 3173*f*
renal tubular acidification and, 3171
renal tubular acidosis due to, 2098
solute transport and, 3151, 3173*f*, 3175
thromboxane and, 3168–3169, 3170*f*
in transplant immunosuppression, 3159–3160, 3168, 3168*f*, 3170*f*, 3173*f*
Cyp4a12, 2673
Cystatin C
glomerular filtration rate and, 3025–3026
Cysteine-homocysteine, as uremic toxin, 3043
Cysteinyl (cys) leukotrienes, 497
Cystic fibrosis (CF), 998, *see also* Cystic fibrosis transmembrane conductance regulator (CFTR) channel
Cystic fibrosis transmembrane conductance regulator (CFTR) channel, 54, 57, 163–164, 2672
as CLC, 1026–1030, 1027*f*

Cystic fibrosis transmembrane conductance regulator (CFTR) channel (*Continued*)
and ENaC regulation, 998–999, 1029
and endocytosis, 1030
in human kidney, 1028
as regulator of ROMK, 1029, 1611–1613
as regulator of SLC26A, 1030
Cystic kidney disease, *see also* Polycystic kidney disease
cilia in, 2651–2653
non-motile cilia in, 382
polycystin in, 382
Cystine stones, 2312, 2312*t*, 2341–2342, 2341*t*
Cystinosis
in pregnancy, 2721
proximal renal tubular acidosis in, 2084
Cystinuria, 2341–2342, 2341*t*, 2416–2417
Cystitis, in pregnancy, 2713
Cystoskeleton, 382, *see also* Actin; Myosin
Cyst(s)
hepatic, 2649, 2671–2672, 2674
in PKD, 2646–2647
formation of, 2646–2647
TNF expression, 2673
prostaglandin E2 (PGE2) accumulation in, 2673
renal, *see* Polycystic kidney disease
treatment for, in PKD
cystic fibrosis transmembrane conductance regulator (CFTR), 2672
Metformin, 2672–2674
NS-398, 2673
pioglitazone, 2674
signal transducers and activators of transcription (Stats) inhibitors, 2674
Src inhibitor SKI-606 and, 2672
SU-5416 inhibitor and, 2672
Cytochrome P450, 776, 3009
vascular effects of, 836–837, 836*f*
Cytochrome P450 monooxygenases (CYP450), 498
Cytokines
in acute kidney injury, 2549
in erythropoiesis, 3105
in preeclampsia-eclampsia, 2732
in vasculitis, 2821–2822
Cytomegalovirus infection, hypercalcemia in, 2290–2291
Cytoskeletal alterations, in AKI, 2538–2540, 2539*f*
Cytoskeleton
aquaporin-2 and, 1421–1422
in cell volume regulation, 126
epithelial, 8–13
Na,K-ATPase interaction with, 75
Cytosol, solute concentrations in, 1087–1088
Cytosolic base, chloride exchange with, 1092–1095, 1093*f*, 1094*f*

D

Danger/damage hypothesis, 2988
Danger/damage-associated molecular pattern molecules (DAMPS), 2988
Danio rerio, as model systems for cilia, 336–337
Dapagliflozin, 2400–2401
DARPP-32, 547–548
phosphorylation, 547–548
dDAVP, *see* Desmopressin
Deafness
in Alport syndrome, 2848
in Bartter syndrome, 2146
distal renal tubular acidosis and, 2087
Decay accelerating factor (DAF), 760
Defensin, 2991
Deferiprone, 3016–3017
Dehydrocholesterol, 2252*f*
metabolism of, 2253*f*
nomenclature for, 2250–2251
structure of, 2251*f*, 2252*f*
in vitamin D synthesis, 2251
Dehydration, *See* Fluid balance; Hypovolemia
Dehydration tests, *see* Water deprivation tests
Demeclocycline
diabetes insipidus due to, 1556*t*, 1557
for hyponatremia, 1528
Demyelination, osmotic, hyponatremia and, 1526–1527
Dendritic cells
in acute kidney injury
ischemic, 2987
interstitial, 607–608
Dendroaspis natriuretic peptide (DNP)
in acute renal failure, 1264
biological effects, 1256
Dense apical tubules (DAT), 632–634
Dense Deposit Disease, *see* Idiopathic MPGN
Dent's disease, 2467
epithelial cell polarity and, 33
hypercalciuria in, 2320
proximal renal tubular acidosis in, 2084
Denys-Drash syndrome, 2871–2873
Deoxyribonucleic acid (DNA)
synthesis
and cell growth measurement, 934
Depolarization, MD cells, 769–770
Descending thin limb of Henle
anatomy of, 635–640, 636*f*
calcium transport in, 2230, 2235*t*
of long loops, 635–640, 636*f*, 637*f*, 638*f*
potassium transport in, 1667–1668, 1668*f*
of short loops, 612, 616*f*, 635–640, 636*f*
substrate preferences in, 155–156
urea permeability of, 1467*f*, 1468, 1468*f*, 1469*t*
Desmocollins, 4–5
Desmogleins, 4–5
Desmoplakins, 4–5
Desmopressin
in diabetes insipidus
in diagnosis, 1589, 1593*t*
in treatment, 1561, 1591, 1594
in pregnancy, 1585, 2702–2703, 2704*f*
Desmosomes, 4–5, 361–362, 627
in acute kidney injury, 2540
in kidney disease, 362
structure and localization of, 361–362
Development, renal, *see* Renal development
Deubiquitinating enzyme (DUB)
and ENaC regulation, 995
DHR domains, *see* PDZ proteins
Diabetes insipidus, 393–394, 1555
antidiuretic hormone in, 1571–1578
aquaporin-2 in, 1424–1425
carriers of, 1591–1592
central, 1555
causes of, 1555*t*
treatment of, 1559–1561
clinical features of, 1579–1582, 1580*t*
direct tests for, 1591
drug-induced, 1557
hypernatremia in, 1555–1556
indirect tests for, 1590–1591
laboratory findings in, 1592–1593, 1593*t*
magnetic resonance imaging in, 1593
nephrogenic, 1556, 1556*t*, 1582
acquired, 1587–1589, 1588*t*
aquaporin-2 in, 1425
aquaporin-2 in, 1424–1425
clinical features of, 1582
expression studies of, 1584–1585
historical perspective on, 1582
lithium-induced, 1425
population genetics of AVPR2 mutations, 1583–1584
treatment of, 1561
neurogenic, autosomal recessive, 1578, 1580*t*
autosomal dominant, 1580–1581
autosomal recessive, 1578, 1580–1581
perinatal testing for, 1591–1592
polyuria in, 1555, 2490–2491, 2490*f*
in pregnancy, 1588–1589, 2704
treatment of, 1594
early, 1591–1592
water deprivation tests in, 1589–1590
water excretion in, 1578
in Wolfram syndrome, 1581
Diabetes mellitus (DM), 2399
albuminuria in, 2468–2469
blocking renal glucose reabsorption as a treatment for, 2399–2401
glomerular ultrafiltration in, 2935–2936
lactic acidosis in, 2072
low-protein diet in, 3056
and mesangial cells, 946
metabolic acidosis in, 130, 2069, 2072
metabolic derangement and hyperfiltration in, 2944
organic cation transporters in, 2445–2446
phosphate balance in, 2360, 2373
and podocytes, 946–947
pregnancy in, 2719*t*, 2720
renal disease in, *see* Diabetic nephropathy
urea transporters in, 1493–1494
Diabetic ketoacidosis, 2068
cell volume in, 130
Diabetic kidney disease
protein restriction in, 3056
Diabetic lactic acidosis, 2072
Diabetic nephropathy
advanced glycation end products in, 2617–2621
albuminuria in, 2608, 2608*t*
Amadori albumin in, 2617

cellular/molecular mechanisms in, 2613–2617, 2613*t*
clinical course of, 2607–2609, 2607*f*, 2608*t*
epidemiology of, 2605–2607, 3028–3029
genetic risk factors, 2606–2607, 2606*t*
glomerular filtration rate in, 2608, 2608*t*
glucose uptake/metabolism in, 2614–2615
hemodynamic changes in, 2613–2614
hexosamine biosynthetic pathway in, 2615
hyperfiltration, 2608, 2608*t*
hypertension in, 2608, 2608*t*
hypertrophy of, 946
hypoxia and, 2621
low-protein diet in, 3056
metabolic syndrome in, 2621–2622
obesity in, 2621–2622
overview of, 2605
oxidative stress in, 2616–2617
podocytes in, 2611–2613
polyol pathway in, 2615
in pregnancy, 2719*t*, 2720
protein glycation in, 2617
protein kinase C in, 2616
regression of, 2622
renal pathology in, 2609–2611
renin-angiotensin-aldosterone system in, 2618–2620
risk factors, 2606–2607, 2606*t*
role of iron, 3015–3016
signaling in, 2616
stages of, 2607–2609, 2607*f*, 2608*t*
transforming growth factor β in, 2620–2621
Diacylglycerol, phospholipase C-mediated production of, 384, 385*f*
Dialysate sodium concentration, 3126*f*
disturbances in hemodialysis, 3125
Dialysis, *see also* Hemodialysis; Peritoneal dialysis
anemia and, 3107–3109, *see also* Anemia
Ca × Pi product in, 2206
calcimimetics for, 2206
cardiovascular complications of, 3076
chronic kidney disease and, 2207
for ethylene glycol poisoning, 2074–2075
for hyperkalemia, 1767
hyperparathyroidism in, 2206–2207
for lactic acidosis, 2074
for methanol poisoning, 2075–2076
in pregnancy, 2722
in acute renal failure, 2715
protein metabolism in, 3046–3047
in muscle, 3049–3053
for salicylate poisoning, 2078
Diaphragms, glomerular endothelial cells, 722
Diarrhea, 2499
congenital chloride, 2480
metabolic alkalosis in, 2036
hyperchloremic acidosis in, 2098
urinary sodium/chloride excretion in, 2480, 2480*t*
Dicarboxylic aminoaciduria, 2419
Diclofenac transporters, 2436
DIDMOAD (Wolfram syndrome), 1581
Diet, *see also* Nutritional; Starvation
in chronic kidney disease, 3046–3053
high-potassium, 1679*f*, 1680, 1681*f*, 1699
potassium excretion and, 1679*f*, 1680, 1681*f*
cooperative factors modulating, 1699
potassium reabsorption and, 1670
high-protein
intracellular pH and, 1815
low-phosphate, 3040–3041
low-potassium, 1680, 1681*f*, 1682*f*
potassium excretion and, 1680, 1681*f*, 1682*f*
aldosterone and, 1700
low-protein, *see* Low-protein diet
low-sodium
for nephrogenic diabetes insipidus, 1553–1554
metabolic acidosis and, 2061–2062
thirst and, 1456, 1457*f*
uric acid in, 2324
Diffuse leiomyomatosis, in Alport syndrome, 2849
Diffuse mesangial sclerosis (DMS), 2782
Diffusion, 266
facilitated, 58–59
in ion transport, 47, 49–50, 50*f*, 223, 1664
Diffusion coefficients, 266
"Diffusion limited" transport, 283
Diffusional permeability, 266–267
Diffusive water permeability coefficient
osmotic water transport across lipid vs. porous membranes, 98–99
Diflunisal, 3190
Dihydrotachysterol
metabolism of, 2251–2254
1,25-Dihydroxyvitamin D, 2299, *see also* Vitamin D
active form of, 2277
skeletal effects of, 2275–2276
Dilution acidosis, 2100
Dinitrophenol poisoning, metabolic acidosis in, 2072
Dinucleotides, 512
Disease progression, *see* Renal disease, progression of
Distal appendages, 322
Distal convoluted tubule (DCT), 559, 640, 643–658, 1354, 1370–1377, 1371*f*, *see also* Renal tubular; Tubular
in acid–base transport, 1944–1945
adverse effects, 1376–1377
anatomy of, 1143
in ASDN, 1181–1182
calcium reabsorption in, 649, 2232–2234, 2232*f*
parathyroid hormone in, 2235
calcium-sensing receptor in, 2200
calcium transport and, 1373–1374, 1373*f*
clinical use, 1369*t*, 1375–1376
dopamine receptors and, 559
dysfunctions of NaCl reabsorption in, 647–648
electophysiologic considerations, 1160–1163, 1161*f*, 1161*t*
magnesium reabsorption in, 2142–2143, 2145*f*
magnesium transport and, 1373–1374, 1373*f*
mechanism of action, 1371–1373
Mg^{2+} transport in, 647
overview, 643
paracellular pathway in, 628
DCT 2, 647
pharmacokinetics, 1375
potassium transport in, 650, 1661–1662, 1663*f*, 1671–1675, 1672*f*
antidiuretic hormone and, 1692*f*, 1693–1694
control of, 1677
renal hemodynamics, 1374–1375
salt reabsorption in, 1049, 1050*f*
sodium chloride transport in, 1371–1373, 1372*f*
postnatal developmental of, 915–916, 916*f*
sodium reabsorption, 649–650
sodium retention in, 1288
sodium transport in, 1160–1163
regulation of, 1162–1163
steroid hormones and, 1162–1163
structure and function of, 644–647, 644*f*, 645*f*, 646*f*
substrate preferences in, 154*f*, 157
urinary electrolyte excretion and, 1356*t*, 1370–1377
water excretion and, 1370–1377
Distal renal tubular acidosis, *see* Renal tubular acidosis, distal
Distal diuretics
magnesium balance and, 2144–2145
Distal tubule
collecting, calcium-sensing receptor, 2200
redistribution of renal blood flow to, 1251–1252
Diuresis
osmotic, in hypernatremia, 1554
Diuretics
action, general principles of, 1383–1385, 1384*f*
adaptations to, 1385–1394
chronic, 1385, 1389
epithelial hypertrophy/hyperplasia and, 1390–1394, 1391*f*, 1392*f*, 1393*f*
immediate, 1385–1394
physical factors, 1389
renin-angiotensin-aldosterone system, 1390
short-term, 1385–1389, 1387*f*
sympathetic renal nerve activity and, 1389–1390
aquaretics, 1382–1383
calcium transport and, 2180–2181, 2238–2239
for cirrhosis, 1303
distal
in magnesium balance, 2144–2145
for hypercalcemia, 2293
hypercalcemia due to, 2292
hyperkalemic renal tubular acidosis due to, 2097–2098
hyponatremia due to, 1514–1515
loop, 764, 764*f*, 1362–1366, 1363*f*, 2142

Diuretics (*Continued*)
metabolic alkalosis due to, 2036, 2480
for nephrogenic diabetes insipidus, 1554
osmotic, 1354–1357, 1355*f*, 1356*t*
urinary electrolyte excretion and, 1355–1357, 1356*t*
overview, 1353–1354
potassium excretion and, 1695–1696, 1696*f*
potassium transport and, 1670–1671
potassium-sparing, 1377–1382, 1377*f*, 1695–1696, 2240
for preeclampsia prophylaxis, 2738
for proximal renal tubular acidosis, 2091
proximal tubule, *see* Carbonic anhydrase inhibitors (CAI)
resistance to, 1385–1394
cirrhosis and, 1303
salt transport sensitive to, 1354, 1355*f*
sodium balance and, 307
thiazide, 1370–1377
transporters for, 2436–2437, 2436*f*
Divalent cation transporter
in intracellular pH regulation, 1795–1796
Diverticular disease, in polycystic kidney disease, 2650
d-lactic acidosis, 2080
DNA-binding domain (DBD), 1194–1195
DOCK180, in PI 3-K signaling, 389
Docking proteins, *see* Scaffolding proteins
Dolichos biflorus, 861
Donnai Barrow's syndrome, 2467
Donnan potential, 1082
Dopamine, 1844
age-dependent production of, 543
and blood pressure regulation, 566
dietary influence of, 542–544
chloride, 542
sodium intake, 542
sodium loading, 543
endogenous, 539
gender and, 543
historical perspective, 539
hypertension and, 544
in invertebrate, 539
metabolism, 542
monoamine oxidase (MAO), 542
Na,K-ATPase control by, 76–77, 77*f*
overview, 540
pharmacological doses, 540
in phosphate balance, 2359, 2374, 2374*f*
in potassium balance, 1636–1637
in renal function, 453
in sodium balance, 1114–1115
transporters, 542
in vertebrates, 539
in water regulation, 540
Dopamine β-hydroxylase (DBH), 542
Dopamine receptors
adenosine receptors and, 564
adenylyl cyclase and, 545–547
adrenergic receptors and, 564
angiotensin II and, 564–565
angiotensin receptors and
AT_1R, 564–565
AT_2R, 565–566
atrial natriuretic peptide (ANP) and, 565–566
autocrine/paracrine regulation and, 557
basolateral membrane, 560–561
and blood pressure regulation, 566
cholecystokinin receptors and, 566
cortical collecting duct, 559
distal convoluted tubule, 559
D_2-like receptors, 546
D_1R, 549–550
D_2R, 550
D_3R, 550
D_4R, 550
D_5R, 550
endothelin receptors and, 566
hypertension and, 568–569
inflammation and, 568
insulin and insulin receptors and, 567
ion channels, 547
ion transport, 557–558
moderate volume expansion, 557–558
loop of Henle, 558–559
luminal membrane, 558
medullary collecting duct, 559–560
membrane microdomains, 549
mineralocorticoid receptor and, 567
mutant mice, 562–563
phospholipase C and, 545, 547
phospholipase D and, 545
prolactin and, 567
prostaglandins and, 567
protein kinase A (PKA), 545
protein kinase C (PKC), 545–546
recycling, 548–549
renal distribution of, 545
renal hemodynamics, 552–554
D_1-like receptors, 552
D_2-like receptors, 552–553
glomerular filtration, 553–554
tubuloglomerular feedback, 554
ROS and, 567–568
signaling, 371–372, 544–545
sodium loading on, 548
subtypes, 544
interactions, 563
vascular receptors
D_1-like receptors, 551
D_2-like receptors, 551
Dopamine regulation
of ion channels, 547
mitogen-activated protein kinases, 547
Dosing strategy for patients with renal insufficiency
loading dose, 3201–3208
Doxercalciferol, for hyperparathyroidism, 3078, 3081, 3082*t*
D-Prostanoid receptors, 494–495
Driving force, in ion transport, 47–49, 1085–1087
Drosophila melanogaster, 18–19
Drug disposition
calculating drug clearance, 3197
drug-drug interactions, 3192–3193
acidic drugs, 3193
cationic drugs, 3193–3194
effect of renal disease, 3194–3200
absorption, 3194
clearance of total drug, 3195
degree of protein binding, 3195
during dialysis, 3197–3200
distribution, 3194–3196
drug response, 3196–3197
elimination, 3196, 3198*t*
during hemoperfusion techniques, 3197
maintenance doses, 3204*t*, 3208–3209
volume of distribution of drugs, 3202*t*
glomerular pores, 3186
inter-individual variation in drug disposition, 3192
organic anion transporters in, 2425–2428
organic cation transporters in, 2437–2449
reabsorption of drugs, 3187
by renal metabolism, 3189–3192
active metabolites, 3191*t*
roles of transport proteins, 3187–3189
ABC transporters, 3188
genetic variation, 3189
MRP/ABCC family, 3188
SLC transporters, 3188–3189
secretion of drugs, 3186–3187
Drug-drug interactions, influence on renal pharmacokinetics, 3192–3193
Drug-related renal injury, *see* Nephrotoxic agents
Dubin-Johnson syndrome, 2433–2434, 3189
Duplex ultrasonography, for renal artery stenosis, 2580
Dyes, intracellular, for pH measurement, 1777–1778
Dynamin, 987
Dyslipidemia
preeclampsia-eclampsia and, 2740
Dysmorphic RBCs in APSGN, 2765
Dysrhythmias, *see* Arrhythmias
Dystrobrevin, 416–417
Dystroglycan, 740
Dystrophin-associated protein complex, 416–417, 417*f*
Dystrophin-glycoprotein complex (DGC), 740

E

EAST/SeSAME syndrome, 2148–2149
E-cadherins, 7–8, 18, 20–21
Eccentric hypertrophy, 2725
Eclampsia, *see also* Preeclampsia-eclampsia
late postpartum, 2728
Econazole, epithelial calcium ion channels and, 2174
Ecto-enzymes, 512
Ectonucleotidases, 513*f*, 526–528, 527*t*, 528*f*
alkaline phosphatase, 527
catalytic activities of, 526–527, 527*t*
distribution of, 528*f*
ecto-50-nucleotidase, 527
NPP, 527
NTPDases, 527
Edema
cerebral, in eclampsia, 2731
flash pulmonary, 2578–2579

formation of, peripheral capillary mechanisms of, in nephrotic syndrome, 1306–1307, 1306*t*, 1308*f*
hyponatremia and, 1517
interstitial, in acute kidney injury, 2542
metabolic alkalosis and, 2034
nephrotic, sodium retention in, 303
primary, 1284
pulmonary
in preeclampsia, 2729
secondary, 1284
Effective arterial blood volume (EABV), 1284–1286, 1286*f*, 2478
cirrhotic renal salt retention and, 1296, 1297*f*
in metabolic alkalosis, 2033–2038, 2035*f*
Effective arterial volume (EAV), 2529
Effective renal plasma flow, in pregnancy, 2691–2699, 2717
in preeclampsia, 2737
Effective vascular volume
in ascites, 302–303
assessment of, sodium intake/output in, 301–302
in chronic hypernatremia, 306–307
sodium balance and, 306–307
Efferent arterioles, 596–597, 597*f*, 617–618, 617*f*, 618*f*, 619*f*
cortical, 599, 599*f*
juxtamedullary, 596–598, 597*f*, 598*f*
wall structure of, 599–600, 599*f*
Efferent renal nerves, 1389–1390
Efferocytosis, 2995
Efficacy of Vasopressin Antagonist in Heart Failure Outcome Study with Tolvaptan (EVEREST), 1383
Eicosanoids
in cell volume regulation, 126
in cyclosporine toxicity, 3169–3170, 3170*f*
overview, 487
in tubuloglomerular feedback adaptation, 775–776
Eicosapentanoic acid
for preeclampsia, 2739
Electrodiffusion, 49–51, 50*f*, 51*f*
Electrogenic sodium borate cotransporter, 1851–1852
Electrolyte balance, 291
deficit/excess limits in, 294
external, 2477–2478
in hyperaldosteronism, 304
in hypoaldosteronism, 303–304
internal, 2477
mechanisms of, 2477–2478, 2479*f*
principles of, 291
reference values for, 294*t*
restoration of
infinite gain control mechanism in, 297–298, 299*f*
input-output processes in, 295–297, 296*f*, 297*f*
mechanisms of, 293*f*
misconceptions about, 298–303
models of, 295–297, 296*f*, 297*f*
overview of, 291
principles of, 291
in salt-losing nephropathy, 300
sequence of events in, 291, 293*f*
set point for sodium excretion in, 299
speed of, 293–294
steady-state, 304, 2477–2478
storage capacity in, 291–293
Electrolyte-free water clearance, 2485–2486
in hyponatremia assessment, 2488–2489, 2488*t*, 2489*t*
Electron microscopy
tight junction, 5–6
Electron motive force, 177–178
Electroneutral co-transporter, 1047
Electroneutral potassium bicarbonate cotransporter, 1794
Electrophysiology, epithelial, *see* Epithelial electrophysiology
Ellsworth-Howard test, 2297–2298
Embryonic stem (ES) cells, 18–19
Emetic stimuli, in antidiuretic hormone regulation, 1449
Emx2 gene, 871
ENaC (amiloride-sensitive sodium channel), *see also* Epithelial Na^+ channel (ENaC)
activity, 251–254
Liddle's syndrome, 254
PHA-I, 251–254
aldosterone and, 392, 393*f*
amiloride-sensitive sodium channel, 649
channels, 236
drugs affecting, hyperkalemia due to, 1763
regulation of, 392
ENaC regulatory complex (ERC), 1203
ENaC/Deg channels
architecture of, 242
gate in, 245
permeation pathway in, 242–245
Enalapril, 3016
for hypertension, in pregnancy, 2743
Endocytosis
basolateral, role of, 634–635
CFTR and, 1030
of megalin, 2462
receptor-mediated, 633–634, 633*f*
and recycling, renal transport protein function regulation by, 24–25
in renal epithelial cells, V-ATPases in, 85–86
Endoplasmic reticulum (ER), 986
stress, 2465–2466
Endothelial cells
of adult kidney, 960
glomerular, 620*f*, 621*f*, 622, 622*f*, 623*f*
origin of, 893–894
proliferation, 945
recruitment and differentiation, 894–896
injury, 2536–2537
in AKI, 2544–2545, 2566–2567
in vasculitis, 2819–2821, 2822*f*
Endothelial glycocalyx, 272
Endothelial NO synthase (eNOS), 728, 2543
Endothelial surface layer
as glomerular filtration barrier, 746
Endothelin
in cirrhosis, 1303
in congestive heart failure, 1292
and ENaC regulation, 1003
endothelin-A (ETA) receptors, 476–477
endothelin-B (ETB) receptors, 476
and hypertension, 1330–1332
in metabolic acidosis, 2059
in pregnancy, 2696
in renal transplantation, 3168–3169
in renal tubular acidification
in distal nephron, 1958
in proximal tubule, 1940
renorenal reflexes, 476–477
in sodium handling, 1292
in vasoconstriction, 837
Endothelin-1 (ET-1), 728
role, in acute kidney injury, 2544
Endothelin-A (ETA) receptors, 476–477
Endothelin-B (ETB) receptors, 476
Endothelium
continuous, 264
fenestrated, 264, 264*f*
in preeclampsia-eclampsia, 2732
Endothelium-derived relaxing factors
in pregnancy, 2695–2696
Endotoxin
in acute kidney injury, 2535*t*, 2536, 2989
TLR4 and, 2988–2989
End-stage renal disease (ESRD), 2578, *see also* Chronic kidney disease; Renal failure, chronic; Uremia
in Denys-Drash syndrome, 2873
epidemiology of, 3026–3027
in Fabry disease, 2859–2863
renal replacement therapy for, *See* Dialysis; Renal transplantation
Energy consumption, 143–158, 147*f*
ABC superfamily and, 149
ATP hydrolysis and, 149
H,K-ATPase in, 147*f*, 148, 150*f*
Na,K-ATPase in, 145–147, 147*f*, 150*f*, 158*f*, 159–161
in solute transport, 48, 143
Energy production
ATP hydrolysis in, 143–144, 146*f*
coupled with transport, 158–162
fatty acid oxidation in, 151, 152*f*
gluconeogenesis in, 152*f*, 153
glycolysis in, 152–153, 152*f*
ketone body metabolism in, 151–152, 152*f*
mitochondrial
oxidative phosphorylation in, 149–150, 150*f*, 151*f*
sodium transport in, 143–144
tricarboxylic acid cycle in, 151
Entactin, in glomerular basement membrane, 620
Enteric hyperoxaluria, 2336
Enzyme deficiencies, congenital, lactic acidosis in, 2069–2070, 2072
Eosinophils
associated with APSGN, 2764–2765
Ephrin B2 ligand, 730
Ephrin-eph molecules, glomerular endothelial cells, 726–727
Epidermal growth factor (EGF)

Epidermal growth factor (EGF) (*Continued*)
in acute kidney injury, 2558
receptors for, 375
in renal development, 876
Epidermal growth factor receptor (EGFR) antibodies, 2158
Epilepsy, *see* Seizures
Epinephrine
in phosphate balance, 2374
in potassium balance, 1633, 1635*f*, 1637
Epithelial calcium channel, *see* Calcium ion channels, epithelial
Epithelial cell(s), 627, 891
adherens junctions in, 4
of adult kidney, 959–960
apical microvilli of, 8–11
basolateral membrane of, *see* Basolateral membrane
cell–cell adhesive relationships, 4
cilia of, 11
cultures
on permeable filter supports, 15*f*
two- and three-dimensional, 16*f*
electrophysiology of, *see* Epithelial electrophysiology
endocytosis in, V-ATPases in, 85–86
gap junctions of, 4–5, 382, 627
junctional complex of, 4–13, 627
basement membrane, 11–13
basolateral plasma membrane, 11
lateral interdigitating folds in, 630
morphology of, 4–13
parietal, *see* Parietal epithelial cell (PEC)
PDZ proteins in, 405, 407*f*
physiology of, 4–13
polarization of, 1
biogenesis of, 13–34
carcinogenesis and, 32
Dent's disease and, 33
intrinsic machinery, 19–21, 20*f*
ischemic injury and, 32–33
mechanisms, 16–21, 17*f*, 18*f*, 20*f*
morphological characteristics of, 4–13
nature and physiologic implications, 3–4
Oculo Cerebral Renal Syndrome of Lowe and, 33
polycystic kidney disease and, 33–34
potassium ion channels and, 1675
renal disease and, 32–34
sorting pathways, 21–32, 22*f*, *see also* Sorting pathways, epithelial cells polarization
two- and three-dimensional cultures, 16*f*
in vitro models of, 14–21, 14*f*, 15*f*, 16*f*
of ureteric bud, 862–864
Epithelial electrophysiology, 177
change in electron motive force vs. potential in, 210
general equivalent circuit in, 178, 178*f*, 190*f*
basic equations for, 208–210
intracellular measurements in, 188–196
in basolateral membrane, 194*f*
cell membrane potential, 188–189
cellular cable analysis in, 191–195
electrogenic potential, 195–196
individual membrane resistance, 189–191, 190*f*, 192*f*, 192*t*, 194*t*
ion substitution experiments in, 195
membrane selectivity, 195
Na/K pump current, 195–196
luminal membrane and, 1088–1095
Na/K pump contribution to membrane potential and, 211–212
overview of, 177–179
partial ionic conductance equations for, 210–211
patch-clamp analysis in, 197
in apical membranes, 204–205
in basolateral membranes, 205, 207*f*, 1672–1673, 1672*f*
of channel number, 201–202, 202*t*
of channel pharmacology, 203, 204*f*
of channel selectivity, 199–200, 201*f*
in isolated cells, 205–206
noise analysis in, 206–208, 208*f*
of open and closed times, 202–203
of open probability, 200–201, 202*t*
parameters measured by, 198–199
single-channel, 198–201
principles of, 177–179
transepithelial measurements in, 179–188
impedance analysis in, 187–188
interpretation of, 182
membrane selectivity and, 187
paracellular selectivity and, 186–187
resistance, 179
paracellular, 186–187
short-circuit current technique in, 184–186, 185*t*
typical results for, 180*t*, 181–182
voltage, 179, 180*f*, 1154–1155
active transport and, 182–183, 183*f*
with circulating current, 183–184
diffusion potentials and, 183, 184*f*
estimation of membrane parameters from, 186–188
in open-circuit tubules, 179–181
technical problems in, 186
in voltage-clamped tubules, 181–182
Epithelial flux equation, 1085
Epithelial Na^+ channel (ENaC), 56–57, 163–164, *see also* ENaC (amiloride-sensitive sodium channel)
activation of, 1199–1202
aldosterone and, 1185–1194
at apical membrane of CNT, 1164
biochemical characteristics of, 983–984
biogenesis, 986, 987*f*
cation permeation and selectivity, 992–993
cellular localization of, 987–988
CFTR as regulator of, 989
electrophysiologic characteristics, 983, 984*f*
ENaC/Degenerin gene family, 984–985, 984*f*
function of, 985–986, 985*f*
gating mechanisms, 993
and human disorders, 1003–1004
intracellular trafficking of, 986–987, 987*f*
and Liddle's syndrome, 994, 1003, 1189–1192
molecular characteristics of, 983–984
overview, 983–988
and PHA I, 1192
PKA effect on, 1002
pore, structure of, 990–992, 990*f*
regulation, 993–1003
aldosterone and, 1002
angiotensin II and, 1003
ATP and, 1001
calcium and, 999
CFTR, 998–999
endothelin, 1003
extracellular Na^+, 1001
GR and, 1196–1197
insulin and, 1002–1003
intracellular Na^+, 1000–1001
kinases in, 995–997
lipids and, 1000
methyltransferases and, 999
MR and, 1196–1197
nitric oxide and, 1000
pH and, 999–1000
PPAR and, 1001
proteases and, 997–998
of sodium transport, 1167, 1168*f*
syntaxins in, 998
ubiquitination and deubiquitination in, 994–995
vasopressin and, 1002
and sodium balance, 1166–1167
structure of, 985–986, 985*f*
subunits, 984–986, 985*f*
functional domains, 988–992
and Liddle syndrome, 1222, 1222*f*
proteolysis of, 997–998
Epithelial transport, 1082–1087
in cell volume regulation, 129
cross-talk in, 1666
flux adjustment in, 1082–1084, 1082*t*, 1083*f*, 1084*f*, 1085*f*
paracellular, 628, 628*f*, 1102–1109
lateral intercellular space, 1102–1105, 1103*f*
peritubular membrane, 1095–1100
tight junctions in, 1106–1109, 1108*f*
transcellular, 628–631
cytosolic concentrations and, 1087–1088
luminal membrane, 1088–1095
transport forces, 1085–1087
Epithelial-to-mesenchymal transition (EMT), 973, 2466–2467, 2972
Epithelium, 627–632
adherens junctions in, 6–8, 627
barrier function of, 5
basolateral membrane domain, 630–631
of intermediate tubule, 632–633, 638*f*
junctional complex of, 4–13, 627
luminal membrane domain, 628–630
overview, 627–631, 627*f*
papillary surface, permeability properties of, 1471*t*, 1474
paracellular pathway, 628, 628*f*
proximal tubule, 632–633
of thick ascending limb of Henle, 640, 641*f*
transcellular pathway, 628–631
Eplerenone, 1380
hyperkalemia due to, 1763

Epoxygenases
vascular effects of, 836–837
E-Prostanoid receptors, 491
EP_1 receptor, 491–492
antagonists, 491
cDNA, 491
in collecting duct, 491
renin-angiotensin system, 491–492
EP_2 receptor, 492
cDNA, 492
mRNA expression, 492
in renal medullary interstitial cells, 492
EP_3 receptor, 492–493
antagonists, 493
cAMP, 492
in collecting duct, 493
splice variants, 492
EP_4 receptor, 493
cDNA, 493
in controlling blood pressure, 493
in glomerular podocytes, 493
in hyperkalemia, 493
in hyporeninemic hypoaldosteronism, 493
mRNA, 493
Epstein syndrome, 2870–2871
Equlibrative nucleoside transporters (ENT), 768–769
ER associated degradation (ERAD), 986
Ergocalciferol, 2299–2300
ERK MAPK signaling pathway, 386–387
Erythrocyte cation leak syndromes, SLC4 in, 1876*t*
Erythrocytes, anion exchanger deficiency diseases of, 1888
Erythropoiesis, 3087–3100, 3089*f*
burst-forming unit erythroid in, 3089–3090, 3089*f*
in chronic renal failure, 3107, *see also* Anemia
colony-forming unit erythroid in, 3089–3090, 3089*f*
erythropoietin requirements for, 3106
overview of, 3087–3088
posttransplant, 3108–3109
Erythropoietin
in acute kidney injury, 2564–2565
in anemia, 3106*f*, 3107–3109, *see also* Anemia
biological effects of, 3089–3090, 3089*f*
n chronic kidney disease, 3033, 3055, 3107
clearance rate for, 3097
early studies of, 3087–3088
plasma concentration of, 3093
measurement of, 3106
reference ranges for, 3106
regulation of, 3100–3105, 3100*f*
production of
acid–base balance in, 3105
arterial oxygen tension in, 3094, 3095*f*, 3098*f*, 3099
blood oxygen-carrying capacity and, 3094–3095, 3096*f*
blood viscosity in, 3105
in chronic renal failure, 3107
gene expression and, 3097
hemoglobin oxygen affinity and, 3096
hepatocyte recruitment in, 3093
HIF-1 in, 3100–3105, 3101*f*
hormones in, 3105
inflammatory cytokines in, 3105
iron metabolism and epo gene regulation, 3105
modulators of, 3105
overview of, 3087–3088
oxygen sensor in, 3099–3100
oxygen-dependent epo production, 3096–3097
phases of, 3089–3090, 3089*f*
posttransplant, 3108–3109
rate of, 3097
regulation of, 3094, 3100–3105, 3101*f*
renal perfusion and, 3105
signaling in, 3100–3105, 3101*f*
sites of, 3092–3093, 3093*f*
receptor, 3090–3092, 3091*f*
recombinant, 3087–3088
for renal anemia, 3107–3109
replacement, for chronic kidney disease, 3037
structure of, 3088–3089, 3088*f*
Erythropoietin gene, 3100*f*
cloning of, 3087–3088
structure of, 3088–3089, 3100*f*
transcription of, 3097
Erythropoietin-producing cells, recruitment of, 3097–3098
ES cells, *see* Embryonic stem (ES) cells
"Escape" from sodium retention, 1347
Escherichia coli, 54
Espin, 10
Essential amino acids, *see* Amino acid(s)
Estrogen
calcium ion channels and, 2176–2177
for hyperparathyroidism, 2288–2289
in pregnancy, renal hemodynamics and, 2694
Ethacrynic acid
calcium reabsorption and, 2239
Ethanol, for methanol poisoning, 2075
Ethylene glycol poisoning, 2076–2077
Etidronate, for hypercalcemia, 2293–2294
Etilefrine, transporters for, 2441
Etv4/5 gene, 871
Eubicarbonatemic metabolic acidosis, 2061–2062, 2062*t*
Exchangers, 48, 53–54, 58–59
anion
SLC4, *see* SLC4
Excitatory reflexes, in injured/diseased kidneys, 478–479
Exercise-related lactic acidosis, 2073
hypernatremia in, 1553–1554, 1554*t*
Exocyst, 18
Extracellular calcium-sensing receptor, *see* Calcium-sensing receptor
Extracellular domain (ECD), 989–990
Extracellular fluid volume (ECFV), *see also* Fluid balance
afferent control of, 1286–1287
afferent sensing mechanisms and, 1286–1287
effector mechanisms regulating, 1287–1292
renal tubular acidification and, 1938
sodium balance and, 2477–2478, 2479*f*
TGF adaptations, 772–773
Extracellular matrix (ECM)
in renal development, 876
Extracellular signal-regulated kinase (ERK), 996, 1194, 2969–2970
ERK ½ kinase, 1268
Extracorporeal shockwave lithotripsy (ESWL), 2331
Extraglomerular mesangium (EGM), 659, 661*f*, 662, 759–760
expression patterns, 760
MD cells vs.,, 759
morphology, 759–760
Extrarenal loss
in hypokalemia, 1719–1720
Eya1 gene, 869–870
Eye anomalies, in Alport syndrome, 2848
Ezrin/radixin/moesin (ERM) proteins, 10
in cell volume regulation, 127

F

Fabry disease, 2848*t*, 2859–2863
in children, 2862–2863
Facilitated diffusion, 58–59
FAK, in signaling, 386–387
Falciparum malaria, 2789
Familial hypekalemia hypertension (FHH)
sodium-coupled cation chloride co-transporters and, 1225–1227
Familial hyperaldosteronism
KCNJ5 mutation and, 1218–1220
Familial hyperaldosteronism type I, 1342
Familial hyperaldosteronism type II, 1343
Familial hypocalciuric hypercalcemia, 2149–2150
calcium-sensing receptor mutations and, 2209
Familial Hypocalciuric Hypercalcemia (FHH), 2289
Familial hypomagnesemia with hypercalciuria and nephrocalcinosis, 2150–2151
Familial Mediterranean fever, in pregnancy, 2720
Familial proximal renal tubular acidosis, 1840–1841
Familial renal glycosuria (FRG), 2398–2399
Fanconi syndrome, 2467
low-molecular-weight proteinuria in, 2467
pathophysiology of, 165
proximal renal tubular acidosis in, 2083–2084
in transplant recipients, 3160
Fanconi-Bickel syndrome, 2399
Fastigial nucleus, chemoreceptors in, 1982, 1982*f*, 1985
FAT1, 738
Fatty acid(s), 488
in ATP production, 151, 152*f*
in ketogenesis, 2064–2068, 2066*f*, 2067*f*
preference for, in proximal tubule, 154
in proteinuria, 2976–2977

Fc receptors, 26
in antineutrophil cytoplasmic autoantibody vasculitis, 2836–2837
in immune complex vasculitis, 2829
Fechtner syndrome, 2870–2871
Fenestrae, glomerular endothelial cells, 722
FGF-23, 3165
FGHNTIDAVP peptide, 1059–1061
Fibrillin1, in renal development, 878
Fibrin, in vasculitis, 2825–2826, 2826*f*
Fibroblast growth factor (FGF)
activin and, 873
external, 2477–2478
as growth factor, in renal development, 874
internal, 2477
steady-state, 2477–2478
Fibroblast growth factor 7, in phosphate balance, 2369–2370, 2377
Fibroblast growth factor 23 (FGF-23), 2277, 2359, 2361–2362
in hypercalcemia of malignancy, 2381
in hyperparathyroidism, 2381
for hypophosphatemia, 2359
hypophosphatemic syndromes relating to, 2362–2363
in phosphate balance, 2253–2254, 2369–2370, 2375–2376, 2376*f*
Fibroblasts, 972–973
interstitial, 602–605, 604*f*, 605*f*
cortical, 604*f*, 605–606, 605*f*
extracellular matrix, 605
lipid droplets, 605
medullary, 606–607, 606*f*, 607*f*
peritubular, 604*f*, 605
Fibrogenesis, proteinuria and, 2971–2972
Fibromuscular dysplasia (FMD), 2585–2586
Fibronectin, 13
in acute ischemic injury, 2991
in glomerular basement membrane, 618–619
Fibrous dysplasia, hypophosphatemia in, 2381
Fick's second law of diffusion, 50
Filtration barrier, glomerular, 624*f*, 625–626
Fimbrin, 10
First transmembrane domain (TM1), 989
Fish, renal progenitors in, 971, 972*f*
Fish oil, for preeclampsia prophylaxis, 2739
Flash pulmonary edema, 2578–2579
Flk-1, in preeclampsia-eclampsia, 2732–2734, 2733*f*
Flt-1, in preeclampsia-eclampsia, 2738
Flufenamate, transporters for, 2436
Fluid, interstitial, drainage of, 608–610, 608*f*
Fluid balance, *see also* Hypervolemia; Hypovolemia; Water transport
antidiuretic hormone in, 2484–2491, 2485*f*
aquaporins in, 1427–1428
assessment of
electrolyte-free-water clearance in, 2486–2487
free-water clearance in, 2486–2487
in hyponatremia, 2487–2488
plasma osmolality in, 2485–2486
urinary chloride in, 2479–2481, 2480*t*
urinary sodium in, 2479–2481, 2480*t*
urine osmolality in, 2485–2486, 2486*t*
dietary sodium in, 2478, 2479*f*
mechanisms of, 2477–2478, 2479*f*
hypernatremia and, 1541–1542, 1543*f*
potassium transport and, 1683*f*, 1687–1691
in pregnancy, 1587–1588, 2702–2708, 2703*f*, 2706*f*
in chronic renal failure, 2718
renal aquaporins and, dysregulation of, 1424
renin-angiotensin-aldosterone system and, 1289–1290
in transplanted kidney, 3151, *see also* Renal transplantation
Fluid intake
limits on, 299
reference values for, 294*t*
Fluid management, *see also* Diuretics
dilution acidosis in, 2100
in hypernatremia, 1559–1561
Fluid mosaic model, of plasma membrane, 46, 46*f*
Fluid movements through microvascular walls, 276–279
changes in microvascular pressure, 277–278
plasma oncotic pressure, 279
Starling forces, 276–277
Fluid transport, *see* Water transport
Fluorescence, in intracellular pH measurement, 1776
Fluorescent activated cell sorting (FACS) and assessment of hyperplasia, 934
4-Fluoro-4-deoxy-dapagliflozin, 2401
Flurbiprofen, transporters for, 2436
Flux, ion, 47
tight junctional, 1106–1107
Fmn1 gene, 871
Focal adhesion kinase (FAK), 13
Focal adhesions, in signaling, 380, 386
Focal glomerulosclerosis, in pregnancy, 2719*t*, 2720
Focal segmental glomerulosclerosis (FSGS), 2779*f*
classification, 2781*t*
diagnosis, 2781
proteinuria in, 2781
heroin-induced, 2792
idiopathic, 2781
prognosis and clinical course of, 2781
pathology, 2781–2782
scarring, 2781
pathophysiology, 2782–2783
associated with sporadic, 2782
gene mutations, 2782
T cells, role of, 2782–2783
prognosis, 2781
treatment, 2783
angiotensin receptor antagonists (ARBs), 2783
angiotensin-converting enzyme (ACE) inhibitors, 2783
corticosterioids, 2783
cyclophosphamide, 2783
cyclosporine, 2783
non-specific therapy, 2783
prednisone, 2783
rituxamab, 2783
Fodrin, 8–9
Fomepizole, for methanol poisoning, 2075
Food(s), *see* Diet
Foxc2, 735
in podocyte differentiation, 898
Foxc1 gene, 870
Foxd1 gene, 871–872
F-Prostanoid receptors, 494
Fractalkine, 2966–2967
Fractional excretion
of lithium, 2484
of potassium, 2495–2496, 2495*f*, 2496*t*
of sodium, 2481–2483
of urea, 2483–2484
Fractures, pathological
diet-related metabolic acidosis and, 2062
in idiopathic hypercalciuria, 2320–2321
in nephrolithiasis, 2320–2321
Frasier syndrome, 2871–2873
Free-water clearance (FWC), 2486–2487
Freeze-fracture electron microscopy, 347
Friedreich's ataxia, 3008
Frizzled receptor, 381–382
Frizzled-related protein
in phosphate balance, 2253–2254, 2369–2370, 2376–2377, 2377*f*
in renal development, 875
Fructosuria, in pregnancy, 2699
F-type ATPases, 67, 82
Furosemide, *see also* Loop diuretics
calcium ion channels and, 2180
calcium reabsorption and, 2239
epithelial calcium and, 2180
loop diuretics, 1367–1368, 1368*t*
potassium excretion and, 1695, 1696*f*
test, 2505
transporters for, 2436*f*, 2437
Fusion–fission hypothesis, 273
FXYD2, 2154
FXYD4, 2154
FXYD proteins
in Na,K-ATPase and H,K-ATPases, 70–71
function and interaction with α- and β-subunits, 70–71
isoforms, 70
Fz receptor, 381–382

G

GABA, Cl^- channel, 1035–1039
GAC mRNA, in metabolic acidosis, 2001
Gap junctions, 4–5, 627
and connexin hemichannels, 356–360
podocyte slit diaphragms, 382
in signaling, 382
structure and biochemical composition, 356
glomerulus and juxtaglomerular apparatus, 357–358
renal localization, 357–358
roles in renal pathology, 360
tubule function, 359–360
tubules, 358
physiological function in, 358–360

tubuloglomerular feedback and renin secretion, 358–359
vascular conduction and myoendothelial communication, 358
vasculature, 357
Gastric alkalosis, 2035
Gastric H,K-ATPase, 80–82
Gastrointestinal absorption, in acid–base balance, 312–315, 2052
calculation of, 313–315
Gastrointestinal bleeding
renal anemia and, 3089–3090
Gastrointestinal (GI) tract
and acetazolamide, 1361
and methazolamide, 1361
Gastrointestinal hyperchloremic acidosis, 2098–2099
Gastrointestinal tract
calcium-sensing receptor and, 2203–2204
GAT-1, 28
GAT-3, 28
GATA 4, transcription factor, 1250
Gating mechanisms, 48, 54–56
ENaC, 993
Gender and dopamine, 543
Gene knockout studies, of TRPV5 channel, 2181–2182
Genes knockout technology, 865–866
limitation of, 865–866
Genetic Information Nondiscrimination Act (GINA), 2645–2646
Genetic testing, for Alport syndrome, 2855–2856
Genetically modified mice, 865–866
Genetics
ambiguous, in Denys-Drash syndrome, 2871–2873
Na,K-ATPase, 73
Genitourinary developmental molecular anatomy project (GUDMAP), 867
Genome-wide association studies (GWAS), 1214, 1232
Gentamicin
hypomagnesemia due to, 2157
nephrotoxicity of, 2903–2904, 2913–2914, 2914*f*
Gentamicin nephrotoxicity
role of iron, 3009–3010
Gestational hypertension, 2727, *see also* Pregnancy
Giant cell arteritis, 2817–2818, 2819*t*, 2820*f*, 2827, *see also* Vasculitis
Git1, in signaling, 377
Gitelman syndrome (GS), 1230–1231, 1722–1723, 2148
calcium reabsorption in, 2234
clinical presentation, 1722–1723
genetic and molecular biology, 1722
hypokalemia in, 1722–1723
hypomagnesemia in, 2148
metabolic alkalosis in, 2037
NCC and, 1047, 1067–1068
pathogenesis of, 1722
pathophysiology, 1722
salt wasting in, 1310
Glia maturation factor-B, in proteinuria, 2970
Glial cell line-derived neurotrophic factor (GDNF), 862
as growth factor, in renal development, 874
regulation, transcription factors and, 869–870
restriction of, 872
sprouty (Spry), 873
GLGF repeats, *see* PDZ proteins
Glomerular arterioles, 616–617, 618*f*
Glomerular basement membrane (GBM), 616–620, 618*f*, 730–732, 891–893, 901–904
in albuminuria, 2459
in Alport syndrome, 2847, 2849–2850, 2849*f*
type IV collagen in, 2853–2855, 2853*t*, 2854*f*
antibodies to
for anti-glomerular basement membrane nephritis, 2856
in vasculitis, 2818
as charge barrier, 746
charge selectivity and, 2459
collagen IV in, 902–903
description, 730–732
glomerular cell interactions with, mediation of, 904–905
laminin, 730–731, 901–904
heterotrimers, 730–731
mutation, 731
matrix proteins of, in signaling, 380, 381*f*
nidogen, 732, 903
podocytes, 739–740
α3β1 integrin, 739–740
CD151, 740
dystroglycan, 740
dystrophin-glycoprotein complex (DGC), 740
integrin-linked kinase, 740
αvβ3 integrin, 740
proteoglycans, 732, 903–904
in thin membrane nephropathy, 2857–2858
type IV collagen in, 731–732, 2850
in Alport syndrome, 2853–2855, 2853*t*, 2854*f*
mutations, 731
Glomerular capillaries, 617–618, 618*f*, 693, 694*f*, 722
structure-based models of, 712–715
width of, 626
Glomerular capillary pressure, 765–766
Glomerular capillary wall
in Alport syndrome, 2849, 2849*f*, 2850*f*
permeability of
charge selectivity and, 2459
Glomerular cell hypertrophy, 945–947
compensatory, 947
Glomerular disease
inherited, 2848*t*
Alport syndrome, 2847–2857
autosomal dominant focal segmental glomerulosclerosis, 2868–2870
autosomal recessive steroid-resistant nephrotic syndrome, 2848*t*, 2865–2866
congenital nephrotic syndrome of Finnish type, 2863–2865
Denys-Drash syndrome, 2871–2873
Epstein syndrome, 2870–2871
Fabry disease, 2859–2863
Fechtner syndrome, 2870–2871
Frasier syndrome, 2871–2873
G6PD deficiency, 2863
nail-patella syndrome, 2873–2874
Pierson syndrome, 2858–2859
of podocyte gene regulation, 2871–2874
of podocyte skeleton, 2868–2871
sialidosis, 2863
storage diseases, 2848*t*, 2859–2863
thin basement membrane nephropathy, 2857–2858
Glomerular endothelial cells, 722–728
description, 722
diaphragms, 722
fenestrae, 722
functional maintenance of, 722–728
angiopoietins, 725–726
CXCR4/CXCR7/CXCL12 axis, 727–728
ephrin-eph molecules, 726–727
Pdgfb/Pdgfbr, 723
Tgfb1, 724–725
Vegfa, 723–724
luminal side of, 722
origin of, 893–894
peripheral portions of, 722
recruitment and differentiation, 894–896
as vasoregulators source, 728
Glomerular endotheliosis, in preeclampsia-eclampsia, 2735–2736
Glomerular filtration
of calcium, 2227–2228
filtration pressure equilibrium, 697–698
hydraulic permeability, 695–696
hydrostatic pressure, 699–700
of magnesium, 2139
membrane permeability, 693–694
micropuncture, 695–701, 697*t*
nephron plasma flow, 699
pore theory and, 702–707
advective transport, 704
fiber matrix theory and, 707
Fick's law of diffusion, 702
glomerulus experiments, 705–706
and hydrodynamic flow, 703–704
Kedem-Katchalsky flux, 702, 705
restricted diffusion, 704–707
sieving curves, 706–707
steric hindrance, 703
Stokes' law, 702
Stokes-Einstein radius, 702–703
renal blood flow and, 695
renal plasma flow (RPF), 695
SNGFR, *see* Single nephron glomerular filtration rate (SNGFR)
systemic plasma protein concentration, 699
theoretical consideration, 693–694
ultrafiltration coefficient, 697–698

Glomerular filtration barrier, 744–746, 2459–2460
albumin sieving, 708–709
charge barrier, 746
endothelial surface layer as, 746
GBM as, 746
charge selectivity, 708–711
endothelial glycocalyx, 709–711
theory, 708–709
electron micrograph of, 2459*f*
endothelial cells in, 2459
overview, 744
pore theory and, 702–707
advective transport, 704
fiber matrix theory and, 707
Fick's law of diffusion, 702
glomerulus experiments, 705–706
and hydrodynamic flow, 703–704
Kedem-Katchalsky flux, 702, 705
restricted diffusion, 704–707
sieving curves, 706–707
steric hindrance, 703
Stokes' law, 702
serial membrane models, 711–712
size barrier, 744–745
Glomerular filtration rate (GFR)
ACE inhibitors and, 2585
in acute kidney injury (AKI), 2527
angiotensin II and, 2585
assessment of, 3021–3022, 3024–3026
beta-2 microglobulin in, 3026
Cockcroft-Gault formula for, 3023*t*, 3024
creatinine clearance in, 3023–3024, 3023*t*, 3030–3031
from cystatin C concentration, 3025–3026
inulin in, 3021–3022
MDRD formulas for, 3023*t*, 3024
methods of, 3021–3022
from plasma clearance, 3023–3024
serum creatinine in, 3022–3023, 3035*t*
atrial natriuretic peptide (ANP) and, 1252
in calcium reabsorption, 2227, 2228*f*
corticosteroids and, 3163
cyclosporine and, 3168
in diabetic nephropathy, 2608, 2608*t*
dietary protein and, 3033–3034
fractional excretion of potassium, 2495–2496, 2495*f*, 2496*t*
and free amino acids, 2405
in metabolic alkalosis, 2027
postnatal development and, 911–912, 912*f*
potassium balance and, 1660–1663
in preeclampsia-eclampsia, 2737
in pregnancy, 2691–2699, 2709–2710, 2717, 2723
measurement of, 2711–2712
renin-angiotensin system in, 437
serum creatinine and, 3023–3024
sodium excretion and, 2481–2483
sodium reabsorption and
in proximal tubule, 913
sodium retention and, 1287–1288
in transplant recipients, 3152–3153, 3153*f*
vascular smooth muscle and, 391, 392*f*
Glomerular hilum, 721–722
Glomerular hydraulic pressure
intracapillary, 2933
mean arterial pressure, 2933–2934
transcapillary, 2933
Glomerular hyperfiltration, dietary protein and, 3035
Glomerular hyperplasia, 937–938, 937*f*, 938*f*
podocytes and, *see* Podocytes
Glomerular hypertension, 942, 2936–2937
Glomerular injury, 744
crescent formation, 744
glomerular permeability, 744
glomerulosclerosis, 744
Glomerular mesangium, 618
Glomerular parietal epithelium, 743–744
β-catenin/Wnt signaling, 744
description, 743
in glomerular injury, 744
crescent formation, 744
glomerular permeability, 744
glomerulosclerosis, 744
podocytes, 743–744
Glomerular permeability, 744
Glomerular plasma flow (GPF), 766
Glomerular receptors, 551–552
in juxtaglomerular apparatus, 551–552
Glomerular sclerosis, 729
Glomerular tuft, 616–617, 618*f*, 619*f*, 721
cells of, 620–625
filtration barrier, 625–626
folding pattern, 626
and mesangial cells, 728
parietal epithelium of Bowman's capsule, 626–627
stability of, 626, 626*f*
Glomerulonephritis, *see also* Glomerular disease
antineutrophil cytoplasmic autoantibody, *see* Antineutrophil cytoplasmic autoantibody vasculitis
anti-glomerular basement membrane
albuminemia in, 2466
posttransplant, 2856
in pregnancy, 2718–2719, 2719*t*
Glomerulosclerosis, 744
Glomerulotubular balance, 1119–1121, 1119*f*, 1120*f*
proximal tubule reabsorption and postnatal developmental and, 912–913
Glomerulus
anatomy of, 616–627, 617*f*
architecture, 616–618
calcium reabsorption in, 2227–2228, 2228*f*
capillary loops, development of, 721, 722*f*, 892, 893*f*
cell growth in, 933
development of, 881–882
diameter of, 616
function, 721–722
glomerular basement membrane (GBM), 618–620
glomerular tuft, cells of, 620–625
filtration barrier, 625–626
parietal epithelium of Bowman's capsule, 626–627
stability of, 626, 626*f*
morphogenesis, 891–893
structure, 721–722
Glucagon
in cell volume regulation, 129, 130*f*
in ketogenesis, 2064–2065
in potassium transport, 1633–1634, 1694
in renal tubular acidification, 1958
Glucocorticoid receptor (GR), 1182–1183, 1194–1196
for ENaC regulation, 1196–1197
post-translational modifications, 1195
Glucocorticoid-remediable aldosteronism (GRA)
and aldosterone secretion, 1216–1218, 1217*f*
treatment options for, 1218
Glucocorticoids, 1163
adrenal
biosynthesis of, 2093, 2095*f*
potassium transport and, 1682–1685, 1683*f*, 1684*f*
biosynthesis of, 2093–2094, 2095*f*
in chronic kidney disease, 3043–3044
for glomerular hyperplasia, 944
in intracellular pH regulation, 1812–1813
in metabolic acidosis, 2056, 2060
in muscle protein metabolism, 3052–3053
pharmaceutical, *see* Corticosteroids
in potassium transport, 1685–1686
in proANP gene expression, 1247–1248
in renal tubular acidification, 1941
in urea transporter regulation, 1493
Glucocorticoid-suppressible aldosteronism, metabolic alkalosis in, 2039
Glucopenia
antidiuretic hormone in, 1449
thirst in, 1455
Glucose, 154–155
in cell volume regulation, 124
in hypernatremia, 1554
homeostasis
diabetes mellitus (DM), 2399
overview of, 2393
transporters in, 2393
hyperuricuria and, 2322
metabolism of
PI 3-K signaling in, 388, 390, 390*f*
in pregnancy, 2699
reabsorption of, 2393
blocking of, as treatment for diabetes, 2399–2401
hSGLT2 in, 2398
sodium-dependent glucose transporters and, 2394–2397
transporters in, *see* Glucose transporters
Glucose transporters, 2393, *see also* Sodium-dependent glucose transporters (SGLTs)
facilitated (GLUT), 2393
in diabetic nephropathy, 2614–2615
sodium-glucose co-transport, 1089–1090
Glucose-galactose malabsorption (GGM), 2393–2394
Glucose-6-phosphate dehydrogenase (G6PDH), 758–759
deficiency, 2863

Glucosuria
in pregnancy, 2699
GLUT transporters
in diabetic nephropathy, 2614–2615
Glutamate
in acid–base balance, 311
in metabolic acidosis, in acute state, 1997–1998
Glutamate dehydrogenase, in acid–base balance, 1996
Glutamate transporters, in intracellular pH regulation, 1795
Glutamatergic neurons, as chemoreceptors, 1982*f*, 1983–1984
Glutaminase, in metabolic acidosis, 2001–2002
Glutamine
in ammonium ion production, 1995–1996
in bicarbonate production, 1995–1996
in metabolic acidosis, 2051–2052
in acute state, 1997–1998, 1998*f*
in chronic state, 1999–2005, 1999*f*
Glutamine transporters
in ammoniagenesis, 1997
Glutamine/glutamate renal transport metabolism, 2414
Glutathione (GSH) metabolism, 2415–2416
Glycation products, as uremic toxins, 3042
Glycine receptor (GlyR) Cl^- channels, 1035–1036
Glycocalyx, 264–265
Glycogen, in cell volume regulation, 124–125
Glycogen storage diseases, 2863
Glycophospholipid, 26–27
Glycoproteins
decay accelerating factor, 760
Glycosaminoglycan (GAG) chains, 607, 746, 877
Glycosphingolipid-rich membrane domains
epithelial cells polarization, 31
Glycosylation products, as uremic toxins, 3042
Glycosylphosphotidyl inositol (GPI) lipids, 24
Glypican 3 (Gpc3) gene, 877–878
Goldman–Hodgkin–Katz (GHK) Voltage Equation, 225–227
Golgi complex, 21
Gonadal dysgenesis, in Denys-Drash syndrome, 2871
Gonadal hormones, *see* Sex hormones
Goodpasture syndrome, 2765–2768, 2948
clinical presentation, 2767
laboratory findings, 2767
pulmonary hemorrhage, 2767
α3(IV) collagen, 2766
C-terminal and N-terminal domains, 2766
genetic susceptibility, 2766
pathology, 2766
peak incidence, 2765–2766
in pregnancy, 2719*t*, 2720
prognosis and therapy, 2767–2768
azathioprine, 2768
corticosteroids and immunosuppressive therapy, 2767–2768
cyclophosphamide, 2768
plasmapheresis, 2767
survival rates, 2767
pulmonary inflammation associated with, 2766
tubulointerstitial nephritis in, 2766
Goormaghtigh cells, *see* Extraglomerular mesangium (EGM)
Gordon syndrome, 1344, 1747, 1759–1760, 2097
Gout, *see also* Hyperuricemia
posttransplant, 3166–3167
gp330, 10–11
G6PD deficiency, 2863
G-protein-coupled receptor(s)
adenyl cyclase and, 370*f*, 371
amplification of, 371
arginine vasopressin, 371–372
calcium-sensing receptor, 2187
class C, 2187
dopamine, 371–372
inhibition of, 371
ligand binding to, 370, 370*f*
MAPK signaling and, 372–373, 372*f*
phospholipase C signaling and, 372–373, 372*f*
in polycystic kidney disease, 2667–2668
structure of, 369–370, 370*f*
G-proteins, in cell volume regulation, 127
Granular cells
functional aspects, 760–761
in juxtaglomerular apparatus, 760–761
morphology, 760
in renin synthesis, 432–433
Granules, atrial
structure of, 1241–1242
Granulomatous disease
hypercalcemia in, 2290–2291
hypernatremia in, 1557–1558
Green fluorescent protein (GFP), 23
in intracellular pH measurement, 1778
Gremlin, in renal development, 875–876
GRK2, in signaling, 371
Growth arrest specific gene 6 (Gas6), 937–938
Growth factor(s)
in acute kidney injury, 2558–2559
in cell volume regulation, 129
in disease progression, 2973–2975
in fibrogenesis, 2971–2972
in intracellular pH regulation, 1816–1817
in mesangial cells proliferation, 730, 937–938
in phosphate balance, 2253–2254, 2359, 2369–2370, 2373, 2375–2376
in preeclampsia-eclampsia, 2733*f*, 2734–2735
receptors, 374, 374*f*, 2559
in renal development, 375, 874
EGF, 876
FGF, 874
GDNF, 874
HGF, 876
IGF, 876
pleiotrophin, 875
secreted frizzled-related proteins in, 875
TGFβ, 875
WNT2b, 875
in tubulointerstitial disease, 2971–2972
in vitamin D metabolism, 2253–2254
Growth hormone (GH)
in acute kidney injury, 2558
in chronic kidney disease, 3044–3045
in metabolic acidosis, 2059
in phosphate balance, 2373
Growth/differentiation factor 11 (Gdf11), 873
GSK1016790A, 2671
GTPases, in acute kidney injury, 2540
Guanidino-containing compounds, as uremic toxins, 3038–3039
Guanosine diphosphate (GDP)
cyclic
nitric oxide and potassium transport and, 1675
in pregnancy, 2695
in signaling, 370, 370*f*
Guanosine monophosphate (GMP)
in pregnancy, 2695
Guanosine triphosphate (GTP), in signaling, 370, 370*f*
Guanylin
biological effects, 1256–1257
in hemodialysis, 1261
Gut, in acid–base balance, 2052

H

HA protein, 25–26
Haldane effect, 2061
Harboyan syndrome, 1852
Hartnup disease, 1997
Hartnup disorder, 2418
H-ATPase, 48, 60
in hydrogen ion transport, 1919, 1948–1950, 1954, 1956
structure of, 1949*f*
Hearing loss
in Alport syndrome, 2848
in Bartter syndrome, 2146
distal renal tubular acidosis and, 2087
Heart disease, *see also* Cardiac; Cardiovascular
albuminuria in, 2467–2468
chronic kidney disease in, 3029
in polycystic kidney disease, 2650
Heart failure, *see* Congestive heart failure (CHF)
Heat shock proteins (Hsp)
in acute kidney injury
in apoptosis, 2555–2556, 2991
in inflammation, 2991
extracellular, sources of, 2991–2992
intracellular, cytoprotective actions of, 2991
Heavy metal poisoning, phosphate balance in, 2361
Hedgehog signaling and cilia, 334, 335*f*
HELLP syndrome, preeclampsia-eclampsia and, 2715
Hematocrit, intrarenal, 817–818
Hematological cancer, *see* Cancer
Hematopoiesis, 3087–3100

Hematopoiesis (*Continued*)
erythropoiesis in, 3087–3100, *see also* Erythropoiesis
future aspects of, 3113
overview of, 3087–3100
thrombocytopoiesis in, 3109–3110
Hematuria
in Alport syndrome, 2847, 2854–2855
in APSGN, 2765
in pregnancy, 2707
Heme oxygenase, in acute kidney injury, 2556
Hemodialysis, 1261, *see also* Dialysis
electrolyte disturbances in
bicarbonate requirements in, 3137
bicarbonate-containing dialysate, 3136–3138, 3137*f*
calcium, 3140–3143
incidence of symptomatic hypotension during, 3126
intolerance to acetate, 3136
magnesium, 3144
phosphorus, 3144–3145
potassium, 3132–3134, 3136–3138
sodium, 3125–3129
standard dialysate buffer used, 3136
for ethylene glycol poisoning, 2076
for hyperkalemia, 1767
for lactic acidosis, 2074
for methanol poisoning, 2074, 2076
in pregnancy, in acute renal failure, 2716
for salicylate poisoning, 2078
Hemodynamic probes, 2581–2583
Hemoglobin
in AKI, 2533
Hemolytic anemia, *see also* Anemia
in chronic renal failure, 3089–3090
Hemolytic-uremic syndrome (HUS) and thrombotic thrombocyto-penic purpura (TTP), 2793
associated with Shiga toxin-producing *E. coli*, 2774
atypical form of, 2774–2775
drug-induced HUS/TTP, 2793
metalloprotease ADAMTS13 dysfunction, 2774
pathophysiology of, 2775*t*
von Wildebrand factor (vWF) multimers, 2774
Hemorrhage
uterine, in pregnancy, 2714
Hemoxygenases -1 and -2 (HO-1, HO-2)
in blood flow regulation, 832
Henle's loop, *see* Loop of Henle
Henoch-Schönlein purpura, 2832–2833, *see also* Vasculitis
in pregnancy, 2719*t*, 2720
Heparan, 30
Heparan sulfate
in acute ischemic injury, 2990–2991
in glomerular basement membrane, 619
as stone inhibitor, 2319
Heparin
hyperkalemia due to, 1763
for preeclampsia prophylaxis, 2739
Hepatic cysts, 2649, 2671–2672, 2674
Hepatic disease, *see* Liver disease/dysfunction
Hepatic fibrosis, 2790
Hepatitis B virus (HBV) infection
clinical presentation and natural history, 2788
proteinuria, 2788
diagnosis, 2788
immune complex vasculitis in, 2830
pathology, 2788
pathophysiology, 2788
treatment, 2788
adenine arabinoside (vidarabine), 2788
glucocorticoid hormones, 2788
interferon-α therapy, 2788
3TC (lamivudine, Epivir), 2788
Hepatitis C virus (HCV) infection, 2787–2788
clinical presentation, 2787
membranoproliferative glomerulonephritis (MPGN), 2787
physical findings, 2787
natural history, 2787
pathology, 2787
mesangial proliferation, 2787
with non-cryoglobulinemic MPGN, 2787
pathophysiology, 2787
treatment, 2787–2788
interferon-α treatment, 2787–2788
rituximab, 2788
Hepatocyte growth factor (HGF), 867
in acute kidney injury, 2558
in fibrosis, 2972
receptors for, 375
in renal development, 876
Hepatocyte nuclear factor (Hnf)-1, 872
Hepatocyte nuclear factor 1β (HNF1β), 2156
Hepatorenal syndrome (HRS)
in cirrhosis, 2635, 2635*t*, 2637–2638, 2637*f*
management of, 2639–2640
liver transplantation and, 2641
vasoconstrictors, 2639–2640, 2640*t*
prevention of, 2641–2642
Hereditary nephritis, in pregnancy, 2719*t*, 2721
Hereditary spherocytosis, 1888
anion exchanger mutations in, 1876*t*
Heterodimeric amino acid transporters (HAT), 2411
Heterodimeric nucleotide receptors, 512
Hexosamine biosynthetic pathway
in diabetic nephropathy, 2615
Heymann nephritis, 2779, 2970–2971
HIFs, *see* Hypoxia-inducible transcription factors (HIFs)
High Mobility Group Box 1 (HMGB1), 2989
biology of, 2990–2993
structure function of, 2989*f*
High pressure baroreceptors, 463–464
High-density lipoproteins, *see* Lipid(s)
High-potassium diet
potassium excretion and, 1679*f*, 1680
cooperative factors modulating, 1699
potassium reabsorption and, 1670
High-protein diet
intracellular pH and, 1815
and tubuloglomerular feedback, 772
Histidine, in acid–base balance, 311
Histone deacetylases (HDACs), 2674
Histotopography, medullary, 611*f*, 615–616
HIV infection
lactic acidosis in, 2073
HIV-associated nephropathy (HIVAN), 2785–2786
clinical presentation, 2785
neutrophil gelatinase-associated lipocalin (NGAL), 2785
proliferative glomerulonephritis with immune complex deposition, 2785
proteinuria, 2785
renal insufficiency, 2785
thrombotic microangiopathies with renal involvement, 2785
natural history, 2785
pathology, 2785
podocyte markers, 2785
pathophysiology, 2786
CD4 counts, 2786
treatment, 2786
ACE inhibitor therapy, 2786
ARB therapy, 2786
highly active antretroviral therapy (HAART), 2786
H,K-ATPases, 27–28, 48, 60–61, 148
in acid–base transport, 1950
ATP hydrolysis and, 148
α-subunit, 69
isoforms, 69
structure, 69
β-subunit, 69–70
functional role, 70
isoforms, 69–70
structure and α–β interaction, 70
β-subunit of, 28
colonic, 81–82
distribution along nephron, 1950
FXYD proteins, 70–71
function and interaction with α- and β-subunits, 70–71
isoforms, 70
gastric, 80–82
genetics, 73
ion transport, 71–72, 72*f*
in kidney, 12
pharmacology, 72–73
in potassium depletion, 1680–1682, 1681*f*
in potassium reabsorption, 1676
properties, 71–73
structure of, 68–71
vacuolar (V-ATPases), 28–29
Homocysteine, as uremic toxin, 3043
Hormone(s)
in cell volume regulation, 129, 130*f*
in chronic kidney disease, 3043
in erythropoiesis, 3105
in intracellular pH regulation, 1812–1814
in potassium transport, 1745
Hox genes, 869
Human anti-GBM antibodies, 2766
Human disease genes, 1213–1214
Human immunodeficiency virus infection
lactic acidosis in, 2073

Human mesenchymal stem cells (hMSC), 974
Human renal ciliopathies, 337–341
  Alstrom Syndrome (ALMS), 340
  Bardet–Biedl Syndrome (BBS), 340
  Jeune Asphyxiating Thoracic Dystrophy (ATD), 340–341
  Joubert Syndrome (JBTS), 339
  Meckel–Gruber Syndrome (MKS), 339–340
  Nephronophthisis (NPHP), 338
  Orofaciodigital Syndrome Type 1 (OFD1), 340
  overlapping genes of, 338*f*
  Polycystic Kidney Disease (PKD), 338
  Sensenbrenner Syndrome, 341
Hyaluronan, in acute ischemic injury, 2990–2991
Hyaluronic acid (HA)
  in branching morphogenesis, 878
Hydralazine, for preeclampsia-eclampsia, 2741*t*, 2742*t*
Hydraulic permeability coefficient, 96–97
Hydrochloric acid (HCl), 3140
  in metabolic alkalosis, 2035
Hydrochlorothiazide
  for diabetes insipidus, 1594
  for preeclampsia-eclampsia, 2741*t*
  transporters for, 2434
Hydrogen
  excretion of
    in bicarbonate production, 2021
    routes of, 2021
  loss of, in metabolic alkalosis, 2026
  secretion of, in renal tubular acidification, 1917–1941, *see also* Renal tubular acidification
Hydrogen leak, in renal tubular acidification, 1923–1924, 1923*f*, 1928
Hydrogen transport
  apical membrane mechanisms of, 1917–1918
  in distal nephron, 1943–1959
  H-ATPase in, 1797–1798, 1919, 1948–1950, 1954, 1956
  H,K-ATPase in, 48, 148, 1797–1798, *see also* H,K-ATPase
  in loop of Henle and thick ascending limb, 1941–1943
  Na/H antiporter in, 1109–1111, 1110*f*, 1919–1921, 1921*f*
  passive movement in, forces affecting, 1779–1780
  potassium balance and, 1638–1639
  primary active, 1919
  in proximal tubule, 1917–1941
  in renal tubular acidification, 1917, *see also* Renal tubular acidification
  secondary active, 1918–1921, 1921*f*
  tertiary active, 1918, 1921–1922
Hydronephrosis
  split hydronephrotic kidney and, 820–821, 821*f*
Hydrophilic solutes, microvascular permeability to, 814, 815*t*
Hydroxy-3-methylglutaryl-CoA (HMG-CoA), in albumin metabolism, 2967–2968
25-Hydroxycalciferol, in metabolic acidosis, 2058–2059
20-Hydroxyeicosatetraenoic acid (20-HETE), 498, 499*f*, 2673
  and TGF response, 776
  vascular effects of, 836
11-β-Hydroxylase deficiency
  and congenital adrenal hyperplasia, 1220
17-α-hydroxylase deficiency
  and congenital adrenal hyperplasia, 1220
21-Hydroxylase deficiency, 2093–2094
11-β-Hydroxysteroid-dehydrogenase type 2 (11β-HSD2)
  aldosterone receptors and, 1197–1198, 1685–1686, 1686*f*
1,25-Hydroxyvitamin D
  in chronic kidney disease, 3033
  production of, 2276
25-Hydroxyvitamin D
  metabolism of, 2251–2254, 2256
  production of, 2251–2254
25-Hydroxyvitamin D_3
  metabolism of, 2252*f*, 2253*f*
  production of, 2252*f*
  structure of, 2252*f*
Hyperaldosteronism
  hypokalemia and, 1699–1700
  metabolic alkalosis in, 2022
  in pregnancy, 2700–2701, 2702*f*
Hypercalcemia, 2275
  aquaporin-2 in, 1425–1426
  calcium metabolism, 2284–2290
  calcium transport in, 2237–2240
  calcium-sensing receptor mutations in, 2191–2192
  causes of, 2284*t*, 2290
  clinical presentation of, 2285
  drug-induced, 2292–2293
  in endocrine disorders, 2291
  familial hypocalciuric, 2149–2150, 2289–2290
    calcium-sensing receptor mutations and, 2209
  familial hypocalciuric hypercalcemia (FHH), 2289
  in granulomatous disease, 2290–2291
  and hyperparathyroidism following renal transplantation, 2207–2208
  in hypoparathyroidism, metabolic acidosis and, 2038
  in immobilization, 2292
  of malignancy, 2290
    fibroblast growth factor 23 in, 2381
    hypophosphatemia in, 2381
  in milk-alkali syndrome, 2291
  posttransplant, 3163, 3164*f*, 3166
  primary hyperparathyroidism (PHP), 2285–2289
  in renal failure, 2292–2293
  symptoms and signs of, 2285*t*
  treatment of, 2293–2294
  urea transport in, 1494
  urine concentrating ability in, 1554
Hypercalciuria
  hypocalcemic, 2320
  idiopathic, 2319–2322, 2319*f*
  in metabolic acidosis, 2058
  in nephrolithiasis, 2319–2322, 2319*f*
  thiazide diuretics, 2322
Hypercapnia
  chemoreceptors in, 1987–1988, *see also* Chemoreceptors
  chronic, 1815
  intracellular pH in, 1807
  metabolic alkalosis and, 2033, 2036–2037
  primary, *see* Respiratory acidosis
  respiratory acidosis, 2120–2121
Hypercatabolism, cell volume and, 130
Hyperchloremic acidosis, 2064, 2064*f*, 2065*t*, 2066*f*, 2081, 2098–2099
  with anion gap acidosis, 2064, 2066*f*
  gastrointestinal, 2098–2099
  posthypocapnic, 2099–2100
Hyperemesis gravidarum, 2714
Hyperfiltration
  in diabetic nephropathy, 2608, 2608*t*
Hyperfiltration theory, 3033
Hypergammaglobulinemia in APSGN, 2765
Hyperglycemia
  hyponatremia and, 1530
  and mesangial cells, 946
  tubuloglomerular feedback and, 774
Hyperkalemia, 1741, 3136
  in acute kidney injury, 2561–2562
  in Addison disease, 1758–1759
  in aldosterone biosynthesis disorders, 1759
  ammonium ion production in, 2007–2008, 2012
  assessment of, 2492–2498
  cardiac effects of, treatment of, 1764–1765
  causes of, 1758–1764, 1758*t*
  clinical evaluation of, 1753–1758
  cyclosporine-induced, 3176
  drug-induced, 1644–1645, 1758*t*, 1762
  evaluation, urinary indices in, 2494–2496
  in Gordon syndrome, 1759–1760
  in hyporeninemic hypoaldosteronism, 1759–1761, 2094–2096
  in metabolic acidosis, 2057–2058, 2092–2093, 2093*f*
  potassium in, 3135–3136
  in pseudohypoaldosteronism
    type I, 1759
    type II, 1759–1760
  in respiratory acidosis, 1640–1641
  tacrolimus-induced, 3176
  treatment of, 1764–1765
Hyperkalemic periodic paralysis, 1761–1762
Hyperkalemic renal tubular acidosis, 2092–2093
Hyperlipidemia, *see* Dyslipidemia
Hypermagnesemia, *see also* Magnesium balance
  in acute kidney injury, 2563
Hypernatremia, chronic
  causes of, 1546, 1547*t*, 1553–1554
  cellular response to, 1544–1552

Hypernatremia, chronic (*Continued*)
chronic
effective vascular volume in, 306–307
recovery from, 1546
classification of, 1553–1559, 1557*t*, 1559*t*
clinical features of, 1559, 1559*t*
essential, 1557–1558
fluid balance and, 1541–1542, 1543*f*
generation of, 1542
in granulomatous disease, 1557–1558
hypodipsia and, 1581–1582, 1581*f*
natriuretic effect of, 306
osmolytes in, 1545–1547, 1546*f*, 1547*f*, 1547*t*, 1548*f*
outcome in, 1561–1563, 1562*t*, 1563*t*
plasma sodium concentration and, 1541–1542
severe, risk of, 1561–1563, 1563*t*
thirst and, 1544
transient, 1552
treatment of, 1559–1561
volume depletion in, 306
volume regulation in, 1544–1545, 1544*t*, 1545*t*
Hypernatremia, *see* Sodium balance
Hyperosmolarity, potassium metabolism and, 1646
Hyperoxaluria
enteric, 2336
primary, 2338
Hyperparathyroid jaw-tumor syndrome, 2286
Hyperparathyroidism
calcium-sensing receptor agonists for, 3081, 3082*t*
calcium-sensing receptor mutations and, 2205, 2209
diagnosis of, 2288
fibroblast growth factor 23 in, 2381
and hypercalcemia following renal transplantation, 2207–2208
primary, 2285–2289
adenomas and, 2285–2289
familial, 2285–2289
genetic factors in, 2285–2289
in MEN syndromes, 2286
pathophysiology of, 2285–2289
renal osteodystrophy in, 3075–3076
secondary, 3075–3077
calcimimetics for, 3081
calcitriol in, 3073, 3078
calcitriol therapy for, 3078, 3082*t*
calcium-sensing receptor in, 2204–2207, 3073–3075
in chronic renal failure, 3075–3077
in dialysis, 2206–2207
FGF23-FGF receptor/Klotho signaling network, 3075
hyperphosphatemia in, 3073, 3083
hypocalcemia in, 3074–3076
hypophosphatemia in, 2382
neonatal severe, 2149–2150, 2209
nephrolithiasis in, 2333–2335
osteitis fibrosa and, 2206–2207
parathyroid gland abnormalities in, 3075
posttransplant, 3162–3163
skeletal complications of, 2249, 2260–2261, 2260*f*
treatment of, 2209, 3078–3083, 3082*t*
vitamin D analogues for, 3078–3079, 3081, 3082*t*
vitamin D in, 3074
Hyperphosphatemia, 2382, *see also* Phosphate balance
in acute kidney injury, 2562–2563
in chronic kidney disease, 3074, 3083
in renal failure, 2382
secondary, treatment of, 3081, 3082*t*
in tumoral calcinosis, 2382
Hyperplasia
of Bowman's capsule, 968
renal, *see* Renal hyperplasia
Hyperprostaglandin E syndrome, *see* Bartter syndrome (BS)
Hypertension, 1214, *see also* Mendelian hypertension
albuminuria in, 2467–2468
aldosterone effects, 1329–1330
AME and, 1220–1221
and atrial natriuretic peptide (ANP), 1335–1336
in chronic renal failure, 2718, 3028
classification for treatment, 1319–1320
prehypertension, 1319
primary, 1320
Conn's syndrome and, 1218–1220
in diabetic nephropathy, 2608, 2608*t*
and dopamine, 544, 568–569
early-onset, mineralocorticoid receptor in, 431
and eicosanoids, 1335
and endothelin, 1330–1332
end-stage renal disease and, 3028–3029
essential, genetic studies of, 1231–1232
genetic casues, 1341–1344, 1343*t*
gestational, 2727
glomerular, *see* Glomerular hypertension
glomerular capillary filtration coefficient in, 1324
GRA and, 1216–1218, 1217*f*
in hyperparathyroidism, 2287–2288
incidence rate, 1319
and inflammatory cytokines, 1334–1335
Liddle syndrome and, 1222–1223
low-phosphate diet for, 3040–3041
malignant, 3028
mendelian, 1216–1225, 1216*f*
metabolic alkalosis and, 2038–2040
metabolic syndrome relating to, 1341
monogenic disorders relating to, 1342–1344
natriuretic peptide hormones and, 1249–1250
neural and hormonal mechanisms of, 1326–1336
obesity and, 1327–1328
resetting of baroreceptor reflexes in, 1327
SNS activity, 1327–1328
and nitric oxide (NO), 1332–1333
pheochromocytomas and, 1249–1250
in polycystic kidney disease, 2648
in pregnancy, 1221, 2724
causes of, 2727
in chronic renal failure, 2718
classification of, 2726–2727
diagnosis of, 2725–2727
gestational, 2727
in preeclampsia-eclampsia, 2727–2735, *see also* Preeclampsia-eclampsia
treatment of, 2742
primary essential, 1336–1341
proANP gene in, 1249
protein intake and, 3034
regulation methods, 1320–1322
renal-body fluid feedback mechanism, 1321–1322
vasoconstrictors, 1321–1322
renal denervation in, 451
renal mechanisms of, 1322–1326
renin–angiotensin–aldosterone system, 1328–1329
renovascular, *see* Renovascular hypertension (RVH)
salt-insensitive, 1323–1325
secondary casues, 1344–1349
sodium intake and, *see* Salt-sensitivity hypertension
Hyperthyroidism, hypercalcemia in, 2291
Hypertonic NaCl, 771–772
Hypertonic solutions, 104
Hypertrophy, renal, *see* Renal hypertrophy
Hyperuricemia
in acute kidney injury, 2562
cyclosporine-induced, 3173–3174, 3173*f*
organic cation transporters in, 2445–2446
posttransplant, 3166–3167
in preeclampsia, 2740–2742
Hyperventilation
in metabolic acidosis, 1980–1981, 1981*f*, 2054–2055, 2055*f*, 2056*f*, 2057*f*
Hypervolemia, *see also* Fluid balance
in syndrome of inappropriate antidiuretic hormone secretion, 306
Hypoaldosteronism, hyporeninemic, 1759–1761, 2094–2096
Hypocalcemia, 2275, 2294–2300
acquired hypoparathyroidism, 2296
in acute kidney injury, 2562–2563
calcium concentration in, 2294
causes of, 2294–2295, 2295*t*
clinical features of, 2295*t*
clinical presentation of, 2294
diagnosis and treatment, 2296
in hyperparathyroidism, 3073–3075
in hypomagnesemia, 2151–2153, 2299
in hypoparathyroidism, 2295–2297, 2295*t*
hypoparathyroidism and, 2295–2297
neonatal, 2295*t*
in pancreatitis, 2299
physiological response to, 2255*f*
posttransplant, 3162–3163
in pseudohypoparathyroidism, 2297–2298
treatment of, 2299–2300
vitamin D deficiency and, 2295*t*, 2298
Hypocalcemic hypercalciuria, 2320
Hypocalciuria

in Gitelman syndrome, 2148, 2234
in isolated dominant hypomagnesemia, 2154
Hypocapnia
in acid–base balance, 1807–1808, 2055–2056, 2056*f*, 2057*f*
adverse effects of, 2135
central-nervous-system–mediated, 2129
chemoreceptors in, 1987–1988, *see also* Chemoreceptors
metabolic acidosis and, 2099–2100
primary, *see* Respiratory alkalosis
respiratory alkalosis, 2127–2128
secondary physiologic response, 2130–2132
Hypodipsia, 1552
hypernatremia and, 1581–1582, 1581*f*
Hypodipsia-hypernatremia syndrome, causes of, 1557–1558, 1557*t*
Hypokalemia
aldosterone in, 1733–1734
ammonium ion production in, 2007–2008, 2012
antidiuretic hormone in, 1732
aquaporin-2 in, 1425–1426
assessment of, 2492–2498
associated with intracellular shift, 1719
in Bartter syndrome, 1671, 1720–1722
blood pressure and, 1733
catecholamines in, 1634–1638, 1719
causes of, 1717, 2497
collecting duct dysfunctions
sodium uptake, 1729
diagnosis, 2496–2497
distal tubule dysfunctions
bicarbonate absorption, 1728
potassium secretion, 1729
sodium chloride transport, 1728
evaluation, urinary indices in, 2494–2496
experimental studies, 1724–1725
extrarenal loss from body, 1719–1720
in Gitelman syndrome, 1722–1723
and glucose intolerance, 1734–1735
human studies, 1725–1726
hyperaldosteronism and, 1699
hyperuricuria and, 2320
hypomagnesemia and, 1643–1644, 2160
in hypothermia, 1647
insulin-related, 1631–1633, 1633*f*
intracellular pH in, 1815
in Liddle syndrome, 1723
loop diuretics and, 1369
loop of Henle dysfunctions
bicarbonate and ammonium absorption, 1728
sodium chloride transport, 1728
metabolic acidosis and, 2098
metabolic alkalosis and, 1640, 2025–2032, 2037
polyuria in, 1556
posttransplant, 3162
potassium depletion in, 1630–1631, 1631*f*
potassium excretion in, 1680–1682, 1681*f*, 1682*f*
potassium in, 3135
potassium repletion for, 1631
proton secretion, 1729–1732
potassium excretion, 1730–1731
urea uptake, 1731
urinary concentrating defect, 1731–1732
proximal tubule dysfunctions
ammonia production and excretion, 1727
ammoniagenesis, 1727
bicarbonate reabsorption, 1726–1727
hypocitraturia, 1727
serum phosphate (Pi) concentration, 1727
sodium chloride transport, 1726
renal changes, 1724–1733
renal tubular acidification in, 1937–1938, 1958
renal tubular acidosis and, 2081–2088
respiratory alkalosis and, 1640–1641
systemic effects of, 1733
tubular fluid K^+ concentration, 1718
urea transport in, 1494
urinary potassium excretion, assessment of, 1718–1719
Hypokalemic hyperchloremic acidosis, 2098–2099
Hypomagnesemia
with abnormal renal salt handling, 2146–2149
acquired, 2157–2160
in Bartter syndrome, 2148
cyclosporine-induced, 3174
drug-induced, 2157
familial, with hypercalciuria and nephrocalcinosis, 2150–2151
in Gitelman syndrome, 2148
hypocalcemia and, 2151–2153, 2299
hypokalemia and, 1643–1644, 2160
hypoparathyroidism and, 2299
hypophosphatemia and, 2159
isolated dominant, 2153–2155
CNNM2, 2155
FXYD2, 2153–2154
KNCA1, 2154–2155
isolated recessive, 2156
metabolic acidosis and, 2058, 2159
metabolic alkalosis and, 2037
mitochondrial, 2156–2157
posttransplant, 3174
with secondary hypocalcemia, 2151–2153
tacrolimus-induced, 3175
Hyponatremia, *see also* Sodium balance
in acute kidney injury, 2561
antinatriuretic effect of, 306
assessment, electrolyte-free water clearance in, 2488–2489, 2488*t*, 2489*t*
distal convoluted tubule diuretics and, 1376
diuretic-induced, 1514–1515
drug-induced, nondiuretic, 1520–1521
evaluation of, 2487–2488
hemodynamic causes of, 1516–1517
hypertonic, 1530–1531
hypotonic
adaptations to, 1523–1526
classification of, 1512–1513, 1513*f*, 1513*t*
pathogenesis of, 1512–1513
treatment of, 1527–1529, 1529*f*
hypoxia and, 1525–1526
isotonic, 1530–1531
non-hypotonic, 1530–1531, 1531*f*
causes of, 1511, 1512*t*
rapid correction of, effects of, 1526
treatment
loop diuretics and, 1368–1369
vasopressin-receptor antagonists and, 1382
vasopressin escape in, 1428
water restriction in, 1527–1528
Hypoparathyroidism, 2295–2297
autoimmune, calcium-sensing receptor mutations in, 2192
autosomal-dominant, 2149
diagnosis of, 2296
hypercalcemia in, metabolic acidosis and, 2038
hypomagnesemia and, 2295–2296
with secondary hypocalcemia, 2151–2153
laboratory findings in, 2297–2298
vs. pseudohypoparathyroidism, 2297–2298
secondary
calcimimetics in, 2205–2206, 2209
calcium-sensing receptor mutations in, 2209
parathyroidectomy for, 2207
treatment of, 2209
Hypoperfusion model, of acute kidney injury, 2534–2536, 2535*t*
Hypophosphatemia, 2378–2381, 3145, *see also* Phosphate balance
in alcohol withdrawal, 2380
calcium balance in, 2236–2237
causes of, 2378–2381, 2379*t*
clinical manifestations of, 2378–2381
in fibrous dysplasia, 2381
hypomagnesemia and, 2159
in McCune-Albright syndrome, 2381
in metabolic acidosis, 2058
phosphatonins in, 2253–2254
posttransplant, 3164–3165
pseudohypophosphatemia and, 2379*t*
in refeeding syndrome, 2380
in renal transplantation, 2380
in respiratory alkalosis, 2378–2381, 2379*f*
in rickets, 2380–2381
in sepsis, 2379–2380
sodium-phosphate cotransporter in, 2354, 2361
in tumor-induced osteomalacia, 2380
vitamin D deficiency and, 2298
Hypophosphatemic rickets
autosomal dominant, 2380–2381
X-linked, 2381
Hypophosphatemic syndromes
related to reduced FGF23, 2363
relating to elevated FGF23, 2362–2363
Hyporeninemic hypoaldosteronism, 1759–1761, 2094–2096
Hypotension
in hypocalcemia, 2299
mendelian, *see* Mendelian hypotension

Hypothermia, hypokalemia in, 1647
Hypothyroidism, urea transport in, 1495
Hypotonic hyponatremia, *see also* Hyponatremia
  adaptations to, 1523–1526
  classification of, 1512–1513, 1513*f*, 1513*t*
  pathogenesis of, 1512–1513
  treatment of, 1527–1529, 1529*f*
Hypotonic solutions, 104
Hypovolemia, 561, 2705, *see also* Fluid balance
  defense mechanisms against, 1542–1544, 1543*f*
  in hypernatremia, 306, 1542–1544, 1553
    with low total-body sodium, 1553–1554
    with normal total-body sodium, 1554–1558, 1558*t*
  in hyponatremia, 1516
  prerenal azotemia and, 2530
Hypovolemia-induced renal failure, 2636
Hypoxemia
  lactic acidosis and, 2071
  in metabolic acidosis, 2061
Hypoxia, *see also* Ischemia
  antidiuretic hormone and, 1449
  and diabetic nephropathy, 2621
  erythropoietin production in, 3098–3099
  hyponatremia and, adaptation to, 1525–1526
  intracellular pH in, 1810–1811
  in metabolic alkalosis, 2033
  nephrotoxic agents and, 2890–2891
Hypoxia-inducible transcription factors (HIFs), 968
  in endothelial development, 895
Hypoxia-inducible transcription factor-1 (HIF-1), 3100–3105, 3101*f*

I

Ibuprofen, transporters for, 2436
ICAM, in inflammation, 2901
Idiopathic calcium oxalate stone
  apatite nucleation, 2326–2327, 2328*f*
  CaSR and, 2327–2328
  formation, 2324–2330, 2325*f*
  growth on plaque, 2325–2326, 2327*f*, 2328
  pathology, 2324–2331
  phenotype, 2330
  in practice, 2331
Idiopathic calcium phosphate stone formers, 2330–2331
  clinical and histopathological features, 2330–2331
  in practice, 2331
Idiopathic calcium stones
  metabolic abnormalities, 2319
Idiopathic hyperaldosteronism, 1347
Idiopathic hypercalciuria, 2319–2322, 2319*f*
Idiopathic MPGN, 2771–2773
  clinical presentation, 2773, 2773*t*
    sub-nephrotic proteinuria in, 2773
  incidence, 2771
  laboratory findings, 2773
  pathogenesis, 2772, 2773*t*
    nephritic autoantibodies in, 2772
  pathology, 2771–2772, 2774*t*
    Burkholder variant, 2771–2772
    dense intramembranous deposits, 2771–2772
    silver stains, 2772*f*
    type I electron micrograph, 2772*f*
    type II and type III, 2771–2772
  treatment, 2773
    calcineurin inhibitor, 2773
    mycophenolate mofetil, 2773
    prednisolone, 2773
    steroids, 2773
Idiopathic postpartum renal failure, 2715
IgA nephropathy (IgAN), 2763
  biomarkers and treatment, 2770–2771
  clinical presentation, 2770
    loin pain, 2770
  incidence, 2768–2769
    ethnic difference, 2768–2769
  pathogenesis, 2769–2770
    cellular immunity, role of, 2769
    decreased clearance of IgA-containing complexes, impact of, 2769
    podocyte injury, 2769
  pathology, 2770
  prognosis, 2770
    adverse prognosis factors, 2771*t*
IgG Fc receptor
  in antineutrophil cytoplasmic autoantibody vasculitis, 2836–2837
  in immune complex vasculitis, 2829
IgG receptor, in immune complex vasculitis, 2829
Ileostomy, 2338
IMCD-3 cells, 1203
Imerslund-Gräsbeck's syndrome, 2467
  albuminuria in, 2460–2461
Iminoglycinuria, 2418–2419
Immobilization, hypercalcemia in, 2291
Immune-complex-mediated vasculitis, 2828–2830, *see also* Vasculitis
  Arthus reaction in, 2828–2830
  cryoglobulinemic, 2818*t*, 2819*t*, 2820*f*, 2821–2822, 2828–2832
  early studies of, 2828–2829
  hepatitis B-induced, 2830
  hepatitis C-induced, 2830–2831
  pathogenesis of, 2828–2830
  small-vessel
    immune-complex-mediated, 2828–2830, *see also* Immune-complex-mediated vasculitis
Immune-mediated glomerulonephritides, 2948
Immunoglobulin G receptor
  in antineutrophil cytoplasmic autoantibody vasculitis, 2836–2837
  in immune complex vasculitis, 2829
Immunoglobulin(s), *see* Antibodies
Immunoreactive parathyroid hormone (iPTH) levels in dialysis patients, 3141
Immunosuppression
  hypomagnesemia due to, 2157–2158
  renal effects of
    with cyclosporine, 3167, 3168*f*, 3170*f*, 3173*f*, *see also* Cyclosporine
    with tacrolimus, 3167, *see also* Tacrolimus
  transplant, 3151, 3159–3160, 3168
    cyclosporine in, 3159–3160, 3168, 3168*f*, 3170*f*, 3173*f*
    tacrolimus in, 3174–3175
Impedance analysis, 187–188
In vitro growth behavior, stem cells, 964
In vivo growth behavior, stem cells, 964–965
Inborn errors of metabolism, metabolic acidosis in, 2069, 2079–2080, 2081*t*
Independence principle, 49
Indian Hedgehog (IHH), 2282
Indomethacin
  for diabetes insipidus, 1594
  transporters for, 2436
Indoprofen, transporters for, 2436
Indoxyl sulfate, from dietary protein, 3037
Inducible nitric oxide synthase (iNOS), 728, 1000, 2543, 2550
Infants, *see also* Children; Congenital; Neonates
  renal development in, 911
  water intoxication in, 1514
Infection (struvite) stones, 2312, 2312*t*, 2344–2345
Inflammation
  in acute ischemic injury, 2985
    CD91 in, 2992–2993
    defensin in, 2991
    endotoxin in, 2988–2989
    fibronectin in, 2991
    heat shock proteins in, 2991
    heparan sulfate in, 2990–2991
    hyaluronan in, 2990–2991
    leukocytes in, 2986–2988
    macrophages in, 2985, 2994–2995
    neutrophils in, 2987
      proinflammatory effects, 2988
    overview of, 2985–2986
    poly(ADP-ribose) polymerase in, 2993–2994
    programmed necrosis in, 2993–2994
    proinflammatory molecules in, 2988–2993
    RAGE in, 2993
    Toll-like receptors in, 2988–2993
  in acute kidney injury, 2546–2549, 2547*f*
  in atherosclerotic renal artery stenosis, 2588
  in preeclampsia-eclampsia, 2735
  in proteinuria, 2973–2974
INK4 proteins, 936
Inner medulla, 612, 665
  passive mechanism hypothesis for, 1480–1481
Inner medullary collecting duct (IMCD), 643–644, 650–653, 652*f*
  in acid–base transport, 1947–1948
  anatomy of, 1144
  ANP in, 1252
  calcium-sensing receptor in, 2201, 2201*f*
  potassium reabsorption in, 1676
  sodium transport in, 1166, 1167*t*
    rate of, 1181–1182
  substrate preferences in, 154*f*, 157–158

water and urea permeability of, 1471*t*, 1474
Inner stripe of outer medulla, 611*f*, 612, 612*f*, 614*f*, 616*f*, 665
potassium reabsorption in, 1676
Inorganic acids, *see also* Acid(s)
metabolism of, 2062–2063
Inorganic phosphate (Pi) transport, 634, *see also* Phosphate
Inositol triphosphate, phospholipase C-mediated production of, 384, 385*f*
Insulin
in cell volume regulation, 129, 130*f*
in chronic kidney disease, 3051
and ENaC regulation, 1002–1003
for hyperkalemia, 1765
in ketogenesis, 2064–2065
lactic acidosis due to, 2072
in magnesium balance, 2143–2144
Na,K-ATPase control by, 76
in phosphate balance, 2360–2361, 2373
in potassium balance, 1631–1633, 1633*f*, 1694, 1745
in renal tubular acidification, 1941
and sodium transport, 1169–1170
Insulin resistance
in chronic kidney disease, 3043–3044, 3051
preeclampsia-eclampsia and, 2740
Insulin signaling, 743
Insulin-like growth factor (IGF)
in chronic kidney disease, 3044–3045
in phosphate balance, 2373
in renal development, 876
Insulin-like growth factor I (IGF-1)
in acute kidney injury, 2558
Intact nephron hypothesis, 2935
Intake and output, *see also* Fluid; Urine
limits on, 299–300
reference values for, 294*t*
$\alpha_3\beta_1$ Integrin, 739–740
Integrin-linked kinase, 740
Integrins, 13, 729–730
in proteinuria, 2968
in signaling, 380, 381*f*
Intercalated cells (IC cells), 653–658
in acid–base transport, 1943–1944, 1944*f*
consistent structural features of, 653–654, 653*f*
disruption of characteristic genes, 658
distribution of, 658
in potassium reabsorption, 1674*f*, 1675
potassium depletion and, 1678–1679, 1682*f*
proteins, 654–658, 654*t*
subtypes
non A-non B, 654*t*, 657–658
type A, 654–656, 654*t*, 655*f*, 656*f*
type B, 654*t*, 656–657
V-ATPases in, 84–85
Intercellular junctions, 347
adherens junctions
in kidney disease, 362
structure and localization of, 361
desmosomes, 361–362
in kidney disease, 362
structure and localization of, 361–362
gap junctions and connexin hemichannels, 356–360
structure and biochemical composition, 356
tight junctions, 347–356
biochemical composition, 348–351
dysfunction in ischemic acute kidney injury, 355–356
physiological functions, 348
physiology of, 351–355
structure, 347–348
Interleukin-18 (IL-18)
as AKI biomarker, 2522
Interleukin(s)
in drug-induced injury, 2901
Interlobular artery, anatomy of, 595–596, 597*f*, 600
Interlobular vein, anatomy of, 595–596, 597*f*
Interlukin 18 (IL-18), 2536
Intermediate filaments, *see* Cytoskeleton
Intermediate junctions, *see* Adherens junctions
Intermediate tubule
anatomy of, 635–640, 636*f*
ascending thin limbs of, 635–640, 636*f*, 640*f*
descending thin limb of
of long loops, 635–640, 636*f*, 637*f*, 638*f*
of short loops, 612, 616*f*, 635–640, 636*f*
Interspace model, and proximal tubule, 1104*t*, 1105
Interstitial edema, in acute kidney injury, 2542
Interstitial fibrosis
in pregnancy, 2737–2738
Interstitial fluid
brain
flow of, 1988–1989
pH of, 1987*f*, 1988–1990
drainage of, 608–610, 608*f*
Interstitial hydrostatic pressure, 279–282
interstitial oncotic pressure, 279–280
steady-state fluid uptake into microvessels associated with absorptive epithelia, 281–282
transient and steady-state fluid movements through microvascular walls, 280–281
Interstitial inflammation and fibrosis, 2466
Interstitial oncotic pressure, 279–280
Interstitial pressure, TGF and, 777
Interstitial space
defined, 602
Interstitium, 602–608
anatomy of, 602–608
cellular constituents, 602
defined, 602
dendritic cells of, 607–608
fibroblasts of, 602–608, *see also* Fibroblasts
lymphocytes, 608
macrophages, 608
volume fraction, 602
Intestinal bladder, chronic metabolic acidosis and, 2099
Intestinal transport, of calcium, vitamin D in, 2254–2256, 2254*f*, 2255*f*
Intestines
in acid–base balance, 312–315, 2052
in metabolic alkalosis, 2037
Intracellular adhesion molecules, in vasculitis, 2824
Intracellular shift
in hypokalemia, 1719
Intracranial aneurysms, in polycystic kidney disease, 2650
Intraflagellar Transport (IFT) and IFT motors, 323*t*, 324–325
Intrarenal arteries, *see also* Arcuate artery; Cortical radial artery
connective tissue of, 608–610, 608*f*, 609*f*
Intrarenal hematocrit, 817–818
Intrinsic renal azotemia
causes of, 2531
Inulin concentration
glomerular filtration rate and, 3021–3022
Invertebrates
proANP gene in, 1261–1262
renal progenitors in, 971–972
Ion carriers, *see* Transporters
Ion channels, 47–48, 52, 54–58, 55*f*, 217
adaptation of Ohm's Law to biological systems, 224–227
architecture of, 821–825, 822*t*
biophysical properties, 223–233
vs. carriers and pumps, 62–63
in cell signaling, 217
channel gate, 229–230
modeling, 232–233
regulation of, 231–232
types, 230–231
Cl^--selective, 57–58
definition of, 197
and dopamine receptors, 547
drug effects on, patch-clamp studies of, 203, 204*f*
electrophysiological studies of, 177, *see also* Epithelial electrophysiology
function of, 234–238, 238*f*
CLC channels and barttin (BSND), 234–235
KCNA channels, 235
KCNJ channels, 235–236
KCNK channels, 236
KCNM channels, 235
SCNN channels, 236
TRP channels, 236–238
functional expression of, 218*f*
gated, 197
Goldman–Hodgkin–Katz (GHK) Voltage Equation, 225–227
K^+-selective, 56, 57*f*
ligand-gated, 1035–1036
Na^+-selective, 56–57
Nernst equation, 225–227
number of, determination of, 200, 201*f*, 202*t*
open and closed times of, determination of, 202–203
open probability of, determination of, 200–201, 201*f*, 202*t*

Ion channels (*Continued*)
passive diffusion, 223
patch-clamp recording of, 197, 199*f*, *see also* Patch-clamp analysis
single-channel, 198–201, 200*f*, 201*f*
permeation, 228–229, 228*f*
and gating of, 993
pore block, 233
pumps transformation into, 63
with recognized function, 219*t*
recording with patch-clamp electrophysiology, 223–224
rectification, 232
selectivity of, 227–228, 228*f*
assessment of, 195
determination of, 199–200, 201*f*
structure of, 238–248
ClC channels, 239–245
ROMK gating, 247–248
in water transport, 109
Ion concentration, intracellular vs. extracellular, 45–46
Ion flux, 47
Ion pores, 47–48, 52, 54–55, 55*f*
Ion pumps, 47–48, 54, 60–63, 61*f*, 62*f*, 67, 144–149, *see also* ATPases
channels vs.,, 62–63
H/K, *see* H,K-ATPase
Na/K, *see* Na,K-ATPase
transformation into channel, 63
Ion substitution experiments, 195, 764–765, 765*f*
Ion transport, 45, 557–558
active
primary, 48, 53
secondary, 48, 53–54, 53*f*
ATPases in, 48, 144–149
at blood-brain barrier, 1988
calcium, 48
carrier-mediated, 58–59, 60*f*
in cell volume regulation, 122, 122*f*, 123*f*
cotransport (symport), 48, 53–54
countertransport (antiport), 48, 53–54
coupled, 52–53, 53*f*
diffusion in, 49–50, 50*f*
driving force in, 47–49
electrodiffusion in, 49–51, 50*f*, 51*f*
energetics of, 48, 143, *see also* ATP, hydrolysis of; ATP, production of
flux in, 47
gating, 48, 54–56
H,K-ATPases, 71–72, 72*f*
hydrogen, 48
intracellular ATP and, 158*f*, 159–161
ion pumps in, 144–149, *see also* Ion pumps
ion-exchange, 48
kinetics, and bumetanide affinity of NKCC1, 1057*t*
mechanisms, 48–54
membrane permeability and, 47–48, 50, 50*f*
moderate volume expansion, 557–558
Na,K-ATPase, 71–72, 72*f*
overview, 45
passive, 48–53
coupled transport, 52–53, 53*f*
diffusion in, 49–50, 50*f*
electrodiffusion in, 49–51, 50*f*, 51*f*
kinetics of, 52, 52*f*
mediated, 47, 51–52
pathways and mechanisms, 49–53
solubility diffusion, 47, 49, 52
thermodynamics of, 52
sodium, 47–48, 52–53
substrate utilization to, 1155–1156
transepithelial
electrophysiological analysis of, 177, *see also* Epithelial electrophysiology
transmembrane, 45
Ion transport proteins, 47–48, 54–63
channels for, 47–48, 52, 54–58, 55*f*, *see also* Ion channels
comparisons, 62–63
functionally different, in same family, 63
pores, 47–48, 52, 54–55, 55*f*
pumps, 47–48
structure–function correlations in, 63*f*
transporters (carriers), 47–48, 52, 54, 58–60, 59*f*
Ion-motive ATPases, 67, *see also* Ion pumps*specific types*
overview, 67
IP receptor, 495
Iron, deficiency of, *see* Anemia
Iron metabolism and epo gene regulation, 3105
in erythropoiesis, 3105
Iron-catalyzed free-radical generation, 3011–3012
Iron-deficient diet, 3015
Irrigant absorption syndrome, 1530–1531, 1531*f*
Ischemia, *see also* Hypoxia
acute
ATP depletion in, 166
inflammation in, 2985, *see also* Inflammation
mitochondrial reperfusion injury in, 166
pathophysiology of, 166
in acute kidney injury, 2542–2543
apoptosis in, 166
chronic, pathophysiology of, 166–167
Ischemia-reperfusion injury, endothelial cells in, 2891–2893
lactic acidosis and, 2071
necrosis in, 165–166
in renal allograft, 3152–3154
uteroplacental, in preeclampsia-eclampsia, 2731, 2732*f*
Ischemic injury
epithelial cell polarity and, 32–33
Ischemic nephropathy (IN)
adaptive responses to, 2584–2585, 2584*f*
atheroemboli and, 2587
atherosclerotic, *see* Atherosclerotic renal artery stenosis
clinical presentations of, 2578–2579
diagnosis of, 2579–2581, 2579*f*
global renal atrophy of, 2583
inflammation in, 2985, *see also* Inflammation
natural history of, 2590–2591
necrosis in, 2993–2994
oxidative stress in, 2587–2588
pathophysiology of, 2583–2584
issues associated with, 2588–2589
renal pathology in, 2589–2590
shear stress in, 2587
treatment strategy of, 2591–2593
vasoconstrictors, imbalance of, 2587
Ischemic preconditioning, for acute kidney injury prevention, 2563–2564
Isoforms
nitric oxide synthase, 2543
Isolated dominant hypomagnesemia, 2153–2155
Isolated perfused kidney technique, 2463, 2534, 2535*t*
Isolated recessive hypomagnesemia (IRH), 2156, 2158
Isoprenylcysteine carboxylmethyltransferase (PCMTase), 999
Isopropyl alcohol poisoning, metabolic acidosis in, 2068
Isoproterenol
in magnesium balance, 2143–2144
in renal tubular acidification, in distal nephron, 1958–1959
Isotonic solutions, 104
Isotonic transport, 1084

J

Jak/STAT signaling
and cilia, 329–330, 330*f*
in proteinuria, 2970
Jeune Asphyxiating Thoracic Dystrophy (ATD), 340–341
JNK signaling pathway, 388
Joubert Syndrome (JBTS), 339
Junctional adhesion molecules (JAMs), 18, 20–21
Junctional complexes, 4–13, 627
Juxtaglomerular apparatus (JGA), 516, 757, *see also* Tubuloglomerular feedback (TGF)
anatomy of, 617*f*, 658–659, 659*f*
cellular elements of, 757–761, 758*f*, *see also* Extraglomerular mesangium (EGM); Granular cells; Macula densa (MD) cells
components of, 433*f*
nerves of, 610
renin secretion in, 518
renin synthesis in, 432–433, 433*f*, 436
in tubuloglomerular feedback, 761–763
Juxtamedullary efferent arterioles, 596–598, 597*f*, 598*f*, 599*f*
Juxtamedullary nephron preparation, 820, 821*f*
Juxtamesangial portion, 721–722

K

K^+ channels, 56, 57*f*
architecture of, 245–247
TGF response and, 764
Kaliurea, in pregnancy, 2700–2701, 2702*f*
Kaliuresis
aldosterone-induced, 1685, 1693
sodium-induced, 1690–1691

Kaliuretic peptide, 1245
activation of MEK 1/2, 1267, 1268*f*
mechanisms of action, 1252–1253, 1253*f*
Kallikrein, 2177
Kallikrein–kinin system
sodium excretion and, 1302
cirrhosis and, 1302
Kawasaki disease, 2818, 2818*t*, 2819*t*, 2820*f*, *see also* Vasculitis
KCNA channels, 235
KCNA1 mutations
magnesium balance, 2154–2155
KCNA10 channel, 1617
KCNJ channels, 235–236
KCNJ5 mutation
and familial hyperaldosteronism, 1218–1220
KCNK channels, 236
KCNM channels, 235
KCNQ1 channel, 1616–1617
Kearns–Sayre syndrome, lactic acidosis in, 2073
Ketoacidosis, 2064
alcoholic, 2068–2069, 2075
causes of, 2064
diabetic, 2068
in inborn errors of metabolism, 2064, 2069, 2077, 2081*t*
ketogenesis and, 2064–2068, 2066*f*, 2067*f*, 2068*f*
pathophysiology of, 2064–2068
in starvation, 2068
treatment of, 2100
Ketoacids, supplemental, in low-protein diet, 3054
Ketogenesis, 2064–2068, 2066*f*, 2067*f*, 2068*f*
Ketoglutarate, in metabolic acidosis, in acute state, 1997
Ketone bodies
metabolism, 151–152
preference for, in proximal tubule, 151–152
Ketoprofen, transporters for, 2436
KGA mRNA, in metabolic acidosis, 2001
Ki67, cellular proliferation marker, 969–970
Kidney, *see also* Renal
anatomy of, 593, *see also* Renal anatomy
calcium sensing receptor, 2275
erythropoietin production in, 3092, 3093*f*
functional aspects, 633–635
reabsorption of water and solutes, 634–635
receptor-mediated endocytosis, 633–634, 633*f*
sodium proton exchange, 634
H,K-ATPases in, 80–82
IMCD transport, 1849
morphological types of, 595
mTAL transport in, 1849
Na,K-ATPase in, 75–80
control by dopamine and parathormone, 76–77, 77*f*
control by insulin, 76
regulation in proximal tubule, 76–77
reniculus, 595
SLC4A7 gene disruption in mouse, 1849
structure-function correlations of, 631
primary single cilia, 631–632
proximal tubule, 632–635
unipapillary, 595, 596*f*
vitamin D, 2281
Kidney function
calcium-sensing receptor and, 2194–2202
Kidney injury molecule 1 (KIM-1),, 2521, 2536
Kidney stones, *see* Nephrolithiasis
Kidney transplantation, 2768
Kimmelstiel-Wilson lesion, 2610–2611
Kinase receptors
serine/threonine, 375–376, 376*f*, 384
in signaling, 374–375, 374*f*, 376*f*
tyrosine kinase, 374*f*, 375
Kinase(s)
cyclin-dependent, 935–936, 935*f*
inhibitors, as negative regulators, 936–937
and regulation of ENaC, 995–997
in ROMK regulation, 1609–1610
Kir channels, 230, 235–236
Klotho, 635, 2176
mutations of, 2362
Krebs cycle
in ketogenesis, 2065–2066
in lactate metabolism, 2070
Kreisler (Mafb), 735
in podocyte differentiation, 898
Kv1.3 channel, 1617

L

Label-retaining cells (LRC), 964
papillary, 965, 965*f*, 966*f*
Labetalol, for preeclampsia-eclampsia, 2741*t*, 2742*t*
Labile (catalytic) iron, in kidney disease
in cardiac ischemia-reperfusion injury, 3013, 3013*f*
in cisplatin nephrotoxicity, 3009, 3010*f*
in cisplatin-induced acute kidney injury, 3010*f*
in contrast-media-associated nephrotoxicity, 3012, 3013*t*
definition, 3007–3008
in diabetic nephropathy, 3015–3016
in experimental glomerular disease, 3013–3014
in experimental progressive kidney disease, 3015
in gentamicin nephrotoxicity, 3009–3010
in gentamicin-induced renal mitochondria, 3011
evidence in rat models, 3011–3012
in human disease, 3015
in myoglobinuric acute kidney injury, 3008–3009
in progression, 3016–3017
in redox cycling, 3008
Lacis cells, Extraglomerular mesangial (EGM) cells
Lactate
metabolism of, 2065*f*, 2069–2070, 2069*f*
preference for, in proximal tubule, 152–153
Lactate dehydrogenase, 2070
Lactic acid, metabolism of, 2065*f*, 2069–2070, 2069*f*
Lactic acidosis, 2065*f*, 2069–2070, 2074
causes of, 2071–2074, 2080*t*
in diabetes mellitus, 2072–2073
d-type, 2080
hypernatremia in, 1552
in inborn errors of metabolism, 2079–2080
ischemia and, 2071
pathophysiology of, 2065*f*, 2069–2070, 2069*f*, 2074
pyruvate in, 2069–2070
treatment of, 2074, 2100
Lactosuria, in pregnancy, 2699
Lamina densa (LD), 12, 2459*f*
Lamina lucida, 12
Lamina rara externa (LRE), 2459*f*
Lamina rara interna (LRI), 2459*f*
Laminin, 12, 18, 30, 730–731, 877
glomerular basement membrane and, 901–902
heterotrimers, 730–731
mutation, 731
L-amino acids, 2274
Lamins
in drug-induced injury, 2895–2896
in glomerular basement membrane, 618–619
Lamivudine, transporters for, 2441
Lanthanum carbonate, *see also* Phosphate binders
for hyperparathyroidism, 3081
LARG, in vascular smooth muscle regulation, 391
Large pores water flow, 97–98, 98*f*
Large-volume paracentesis, for cirrhosis, 1303
L-arginine synthesis, 2414–2415
by proximal tubule cells, 2415
Laser-Doppler method, for blood flow measurement, 819
Late postpartum eclampsia, 2728
Lateral interdigitating folds, 630
Laxative abuse, 2497
L-citrulline, 2414–2415
L-3,4-dihydroxyphenylalanine (L-DOPA), 541–542
AADC and, 540–542
plasma, 540–541
renal tubular uptake, 541
sodium intake and, 542
sources of, 540–541
LDL receptor, 26
"Leak pathway," 6
Lei Gong Teng, 2671
Leprosy-associated nephrotic syndrome, 2790
Leptin
in chronic kidney disease, 3045–3046
Leukemia, *see also* Cancer
hypercalcemia in, 2292
Leukemia-associated Rho guanine nucleotide exchange factor (LARG)
in vascular smooth muscle regulation, 391
Leukocyte adhesion molecules, in vasculitis, 2822*f*, 2824–2826, 2825*t*

Leukocyte(s)
and acute kidney injury, 2546–2549
in inflammation
in acute ischemic injury, 2986–2988
in vasculitis, 2822–2826, 2825*t*
Leukocytoclastic angiitis, 2821*f*
Leukotriene A4 (LTA4), 497
Leukotriene receptor B4, 497–498
Leukotrienes, 497
cysteinyl (cys), 497–498
leukocytes and, 497
5-lipoxygenase in, 497
synthetic pathway, 497*f*
L-glycine, 2415
Liddle syndrome (LS), 254, 1343–1344, 1723
clinical presentation, 1723
ENaC and, 994, 1003, 1189–1192
genetic and molecular biology, 1723
and hypertension, 1222–1223
hypokalemia in, 1723
metabolic alkalosis in, 2040
pathogenesis of, 1723
pathophysiology, 1723
treatment of, 1723
Lidocaine, transporters for, 2441
Ligand-binding domain (LBD), 1194–1195
Ligand-binding receptor domains, 369
Ligand-gated ion channel (LGIC), 1035–1036
Light chains, acute kidney injury due to, 2533–2534
Lim1 gene, 870
Limb deformity (ld) gene, 871
Lin-7/CASK/SAP-97 complex proteins, 414–416, 415*f*
Lin-7 isoforms, 415–416
Lipase
in ketogenesis, 2064–2065, 2066*f*
Lipid bilayer, 5, 45
Lipid rafts, 46
Lipid(s)
elevated serum, *see* Dyslipidemia
and ENaC regulation, 1000
in ketogenesis, 2065, 2066*f*, 2067*f*, 2068*f*
in proteinuria, 2976–2977
Lipocalin PGD synthase (L-PGDS), 494
Lipolysis, in ketogenesis, 2065, 2066*f*, 2067*f*, 2068*f*
Lipoxins
for glomerular hyperplasia, 940
Lipoxygenase, eicosanoids and, 497–498
12/15-Lipoxygenase-derived products, 498
Lithium
diabetes insipidus due to, 1557
aquaporin-2 in, 1425
fractional excretion of, 2484
hypercalcemia due to, 2292
nephrotoxicity of, 2915–2918, 2917*f*
polyuria due to, 1557, 2491
urine concentration and, 1495
Lithotripsy, extracorporeal shock wave, 2331
Liver
in acid–base balance, 2050
acute fatty, pregnancy, 2715
erythropoietin production in, 3093
Liver cirrhosis
sodium retention in, Na,K-ATPase induction and, 79–80
Liver disease/dysfunction
lactic acidosis in, 2073
polycystic, 2649–2650
in preeclampsia, 2730
urea nitrogen in, 301
Liver transplantation (LT), 2641
Liver-type fatty acid binding protein (L-FABP), 2522
LL5, 21
LLC-PK cells, 30
LLC-PK1 cells, 14
Lmx1b, 735
in podocyte differentiation, 897
Loading dose of a drug, 3201–3208
Locus ceruleus, chemoreceptors in, 1982, 1982*f*, 1985
Long transient receptor potential channel 2, 2899
Long-acting natriuretic peptide (LANP), 1244–1245
and ERK 1/2 activation, 1268
mechanisms of action, 1252–1253, 1253*f*
and MEK 1/2 activation, 1268
receptor, 1260
and stroke, 1249
Loop diuretics, 764, 764*f*, 1362–1366, 1363*f*, 1368, 1368*t*, 2505, 3194–3195
adverse effects of, 1368–1370
calcium reabsorption and, 2239
and calcium transport, 1365
and chloride transport, 1363–1365, 1365*f*
clinical use, 1368, 1369*t*
dose-response curve, 1364*f*
for hyponatremia, 1528
magnesium balance and, 2142
and magnesium transport, 1365
mechanisms of action, 1363–1366, 1365*f*
NKCC1, 1051
NKCC2, 1049–1053, 1055–1056
oxygenation, 1366–1370
pharmacokinetics, 1368, 1368*t*
potassium excretion and, 1695, 1696*f*
potassium transport and, 1670–1671
renal hemodynamics and, 1366–1370
renin secretion, 1365–1366, 1366*f*
and sodium transport, 1363–1365, 1365*f*
systemic hemodyanamics, 1367–1370
urinary electrolyte excretion and, 1356*t*, 1362–1363
Loop of Henle, 4, 558–559, 1356, *see also* Ascending thin limb of Henle; Descending thin limb of Henle; Thick ascending limb of Henle's loop (TAL)
acid–base transport in, 1941–1943
anatomy of, 1143–1144
calcium transport in, 2230–2232
calcium-sensing receptor in, 2196–2199, 2196*f*, 2197*f*
collecting ducts and, 615
defined, 1363
dopamine receptors and, 558–559
effects, on MD NaCl concentration, 763
flow, and preglomerular resistance, 766
length of, 600, 602*f*
magnesium reabsoprtion in, 2140–2142, 2141*t*, 2142*f*, 2145*f*
potassium transport in, 1667–1668, 1668*f*, 1670–1671
sodium retention and, 1288–1289, 1300, 1303
sodium transport in, 1144–1160
oxygen consumption and, 154*f*, 155–156
substrate preferences in, 154*f*, 155–156
Low pressure baroreceptors, 464
Low slat diet, 3053
Low-calcium dialysate, 3141
Low-density lipoproteins, *see* Lipid(s)
Lower body negative pressure (LBNP), 460
Lowe's syndrome, proximal renal tubular acidosis in, 2084
Low-phosphate diet, 3040–3041
Low-potassium diet
potassium excretion and, 1680, 1681*f*, 1682*f*
aldosterone and, 1700
Low-protein diet, *see also* Protein(s), dietary
amino acid/ketoacid supplements in, 3054
in chronic kidney disease, 3040–3041, 3046–3060
clinical trials of, 3056–3057, 3059*f*
compliance with, 3051–3052
disease progression and, 3056–3059, 3059*f*
in diabetes mellitus, 3056
efficacy of, 3056, 3059*f*
indications for, 3056
protein stores and, 3047–3049
types of, 3050–3051
urea transporters and, 1493
Lowry method, 695–696
L-phenylalanine, 2415
L-serine, 2415
L-tyrosine, 2415
Ludwig, Carl, 693
Luminal glycocalyx, 272
Luminal membrane, 558, 628–630
chloride ion channels, 1089
and dopamine receptors, 558
potassium transport across
antidiuretic hormone and, 1692*f*, 1694
salt and water balance and, 1683*f*, 1687–1691
sodium channels, 1089
transport pathways across, 1088–1095, 1094*f*
Lung cancer, *see also* Cancer
hyponatremia in, 1520
Lung disease/dysfunction
SIADH in, 1520
LX4211, 2401
Lymphatics, 608–610
Lymphocytes, *see also* T cell(s)
associated with APSGN, 2764–2765
interstitial, 608
Lysinuric protein intolerance, 2417–2418
Lysosomes, in albumin metabolism, 2461

M

Macrophages
in acute kidney injury
ischemic, 2986, 2994–2995

in AKI, 2548
in tubulointerstitial disease, 608
in vasculitis, 2819–2821
Macula densa (MD) cells, 757–759, *see also* Juxtaglomerular apparatus
anatomy, 659–663
and ATP, 768
cells of, 659, 659*f*
and COX-2 expression, 759
depolarization, 769–770
vs. EGM cells, 759
expression pattern of, 759*t*
functional aspects, 659–663, 660*f*, 661*f*, 662*f*
morphology, 757
NaCl concentration
effects, on SNGFR, 763, 763*f*
loop of Henle flow and, 763
NaCl transport, 757–758, 758*f*, 769–770
renin and, 432, 433*f*, 434
and renin secretion, 778–785
Madin-Darby canine kidney (MDCK) cells, 2463–2464
cell line, 6, 14, 14*f*, 17–19
Magnesium
calcium-sensing receptor and, 2187–2190
disturbances in hemodialysis, 3144
excretion of
effects of diuretics on, 1356*t*
in peritoneal dialysis, 3144
supplemental
gastrointestinal toxicity of, 2152–2153
for hypomagnesemia with secondary hypocalcemia, 2151, 2153
transport
distal convoluted tubule diuretics, 1373–1374, 1373*f*
loop diuretics and, 1365
Magnesium balance, 2139
in Bartter's syndrome, 2145
calcium balance and, 2143–2144
calcium-sensing receptor in, 2141, 2144, 2145*f*, 2149–2150, 2187
CNNM2 mutations, 2155
cyclosporine and, 3173*f*, 3174
distal convoluted tubule in, 2142–2145
distal diuretics and, 2157
glomerular filtration in, 2139
hormones in, 2141, 2143–2144
KCNA1 mutations, 2154–2155
loop diuretics and, 2142
loop of Henle in, 2140–2142, 2142*f*
metabolic acidosis and, 2058
metabolic alkalosis and, 2036
posttransplant, 3174
potassium balance and, 1643–1644
proximal tubule in, 2139, 2140*f*
reference values for, 294*t*
tacrolimus and, 3175
Magnesium carbonate, metabolic alkalosis and, 2034
Magnesium channels, 219*t*
Magnesium reabsorption via TRPM6, 237
Magnesium sulfate
for eclampsia, 2741, 2742*t*
for hypocalcemia, 2299
Magnetic resonance angiography (MRA)
for renal artery stenosis, 2579–2580
Magnetic resonance imaging
BOLD, 167
in diabetes insipidus, 1593
in hypernatremia, 1549–1552, 1551*f*, 1552*f*, 1553*f*, 1553*t*, 1554*f*
in intracellular pH measurement, 1779
in polycystic kidney disease, 2646*f*, 2647
Major facilitator superfamily (MFS), 59
structure of, 2443*f*
Malaria, 2789
falciparum, 2789
infection with *P. falciparum*, 2789
infection with *P. malariae*, 2789
quartan, 2789
Malate-aspartate shuttle, 151*f*
Malignant hypertension, 3028
Malnutrition, 3047
in acute kidney injury, 2563
metabolic alkalosis in, 2038, 2073
Malpighi, Marcello, 693
MALS/Veli proteins, 415–416
Maltase, 10–11
Mammalian target of rapamycin (mTOR), 389
and cilia, 332–333, 333*f*
inhibitors, 2672–2673
in polycystic kidney disease, 2668–2669
Mammals
CLC Cl^- channels, 1021–1026, 1022*f*
pharmacology of, 1023
Mannitol, 1354–1355
in cell volume regulation, in hypernatremia, 1554
clinical use, 1357
effect on GFR, 1356–1357
intravenous administration of, 1357
mechanism of action, 1356
pharmacokinetics, 1357
renal hemodynamics, 1356–1357
MAP kinase kinase (MKK-1)/(MEK-1), 1267–1268
MAP kinases
in drug-induced injury, 2900–2901
MAPK signaling pathway, 386–388, 387*f*
activation of, 380
ERK, 386, 387*f*
G-protein-coupled receptors in, 372–373
JNK, 388
kinase receptors in, 375–376, 388
Mast cells, renin and, 434
MATE2-K, 2447
Matrix extracellular phosphoglycoprotein, in phosphate balance, 2369–2370, 2377
Matrix metalloproteinases
in pregnancy, 2696–2698, 2697*f*
in vascular smooth muscle regulation, 391
in vasculitis, 2825–2827, 2827*f*
Maxi-potassium channel, 1615–1616
calcium-sensitive, 1674–1675
McCune-Albright syndrome, hypophosphatemia in, 2381
Monocyte chemoattractant-1 (MCP-1), , in proteinuria, 2970–2971
MDR1, 2447–2448
MDRD formulas, for glomerular filtration rate, 3023*t*, 3024–3025, 3032
Mechanical ventilation, 2124–2125
Mechanistic target of rapamycin, 741–742
Mechanosensation and cilia, 329, 329*f*
Mechanosensory nerves, 469
α-adrenoceptors, 474–475
angiotensin II, 474
bradykinin, 475
endothelin, 476–477
impairment of, 477–478
pathophysiological conditions, 477–479
physiological conditions, 470–477
prostaglandin E_2 (PGE_2), 474
cAMP-protein kinase A (PKA), 474
receptors, 474
substance P and, 468*f*, 471–474
CGRP and, 473
functional support for, 473
TRPV1 and, 473–474
Meckel–Gruber Syndrome (MKS), 339–340
Medullary collecting duct
anatomy of, 602, 602*f*, 616
dopamine receptors and, 559–560
inner (IMCD), 643–644
substrate preferences in, 154*f*, 157–158
water and urea permeability of, 1471*t*, 1474
outer (OMCD), 643–644
substrate preferences in, 154*f*, 157
water and urea permeability of, 1470*t*, 1474
in potassium reabsorption, 1674*f*, 1676
potassium depletion and, 1682*f*
in potassium transport, 1668
ratio of loops of Henle, 615
Medullary microcirculation, 804–809, 806*f*, 807*f*, 808*f*, 809*f*, 827–828, 827*f*
measurement of, 818–819, 818*f*, 819*t*
Medullary raphe, chemoreceptors in, 1982, 1982*f*, 1985
Medullary thick ascending limb, *see* Thick ascending limb of Henle
Megakaryocyte growth and differentiation factor, 3109–3110
Megakaryocytes, in thrombopoiesis, 3109–3110
Megalin, 10–11, 633–634, 2461, 2461*f*
in albuminuria, 2460–2461
tubular reabsorption of, 2963, 2964*f*
in tubulointerstitial disease, 2963, 2965
MEK inhibitors
in MAPK pathway activation, 385
PD184352, 2672
U0126, 2672
Melanocyte-stimulating hormones (MSHs), 1258
Mitochondrial encephalopathy, lactic acidosis, and stroke-like episodes (MELAS) syndrome, 2073
Melastatin-like TRPM2, 2899
Membrane microdomains, dopamine receptors and, 549
Membrane permeability, 47–48, 50, 50*f*
aquaporins and, 106–107, 107*f*, 108*t*

Membrane permeability (*Continued*)
cell type and, 104–105
cell volume and, 121, *see also* Cell volume
descending vasa recta hydraulic conductivity and, 812, 813*f*
luminal, 1088–1095
osmotic equilibrium and, 95–96, 96*f*
Membrane proteins
of apical membrane, 8–11
of basolateral membrane, 11
peripheral, 4–5
of tight junctions, 6
Membrane trafficking
Na,K-ATPase regulation and, 74–75
Membrane-associated guanylate kinase (MAGUK) proteins, 31, 407–408
Membranoproliferative glomerulonephritis, 2763, 2791
Membranous nephropathy (MN), 2775–2780, 2779*f*
clinical presentation, 2776–2777
with fibrocellular crescents (RPGN), 2776
proteinuria as a surrogate marker, 2777
thrombosis, 2777
diagnosis, 2777
associated with other systemic diseases, 2777
drug-induced, 2792–2793
genetic susceptibility, 2779
HLA B18 expression, 2779
HLA DR3 expression, 2779
malignancy-associated, 2790–2791
clinical presentation, 2790–2791
pathology, 2791
pathophysiology, 2791
treatment, 2791
natural history, 2776–2777
progress to ESRD, 2777
pathology, 2777–2778
C5b-9 staining, 2778
pathophysiology, 2778–2779
systemic diseases associated with, 2776*t*
treatment, 2779–2780
chlorambucil plus prednisone, 2780
corticosteroids, 2780
cyclophosphamide plus prednisone, 2780
cyclosporine, 2780
diuretics, 2780
methylprednisolone, 2780
mycophenolate mofetil (MMF), 2780
rituximab, 2780
Multiple endocrine neoplasia (MEN) syndromes, hyperparathyroidism in, 2286
Mendelian hypertension, 1216–1225, 1216*f*, *see also* Hypertension
Mendelian hypotension
congenital adrenal hyperplasia, 1225–1226
salt-wasting, causes of, 1226
congenital hyper-reninemic hypoaldosteronism, 1225
Mendelian traits, 1213
2 meSADP, 512, 518
Mesangial cells, 861
contractile ability of, 730
description, 728
diabetes and, 946
extraglomerular, *see* Extraglomerular mesangium (EGM)
in GBM, 621*f*, 626
glomerular development and, 881–882
glomerular tuft and, 728
growth factors, 730
mesangial matrix and, 728–729
origin of, 882
proliferation, 937–938, 937*f*
and apoptosis, 939
role of Cdks in, 938
therapeutic inhibition of, 939–940
signaling molecules in, 729–730
ephrin B2, 730
integrins, 729–730
Pdgfb, 730
vasoactive factors, 730
Mesangial matrix, and mesangial cells, 728–729
Mesangiocapillary GN, 2771
Mesangioproliferative glomerulonephritis, 496
Mesangium, 517
development of, 896–897
Mesenchymal stem cells (MSC), 960, 968–969
human, 974
kidney repair by, 974
Mesenchymal-to-epithelial transformation (MET), 860
Mesonephros, development of, 859
Metabolic acidosis
acute, 2049–2050
adaptation to
acute, 1997–1998, 2049
chronic, 1999–2005, 2049–2050
in adrenal insufficiency, 2093–2094
age-related, 2062*f*, 2062*t*
alcohol-related, 2068–2069, 2074–2077
ammonium ions in
anion gap, 2063–2064
excretion of, 1997–1998, 2009–2012
production of, 1997–1999, 2007–2008, 2011*f*, 2012
secretion of, 2006–2008
in anemia, 2072
assessment of
urinary indices in, 2480*t*, 2481
bone changes in, 315–316, 2059, 2062
calcium balance in, 2037, 2051–2052, 2051*f*, 2058
in cancer, 2073
carbon dioxide dissociation curve in, 2061
in carbon monoxide poisoning, 2071–2072
catecholamines in, 2060
chronic, 1814–1815, 1999–2005, 2049–2050
after urinary diversion, 2099
treatment of, 2100–2101
urea production in, 2051–2052, 2051*f*
in chronic kidney disease, 3046–3049, 3049*t*, 3059–3060
citrate metabolism in, 2060–2061, 2060*f*
in clinical disorders, 2062–2074
in congenital tubulopathies, 2037
in cyanide poisoning, 2072
definition of, 2049–2050
in diabetes mellitus, 2069, 2072
in diarrhea, 2098
diet-related, 2062
dilution, 2100
endothelin in, 2059
erythropoiesis in, 3105
in ethylene glycol poisoning, 2076–2077
eubicarbonatemic, 2061–2062, 2062*t*
evaluation of, 2498–2506
plasma anion gap, 2498–2499
urinary indices in, 2499
exercise-related, 2073
gastrointestinal–ureteral connections in, 2099
glucocorticoids in, 2056, 2060
growth hormone in, 2059
Haldane effect in, 2061
hyperchloremic, 2064, 2064*f*, 2065*t*, 2066*f*, 2081, 2098–2099
anion gap in, 2064, 2066*f*
gastrointestinal, 2098–2099
posthypocapnic, 2099–2100
hyperkalemia and, 2092–2093
hypokalemia and, 2098
hypomagnesemia and, 2159
hypoparathyroid hypercalcemia and, 2038
hyporeninemic hypoaldosteronism and, 2094–2096
hypoxemia in, 2061
in inborn errors of metabolism, 2069, 2079–2080
intracellular pH in, 1806
ketoacidosis, 2064
lactic, 1552, 2065*t*, 2069–2070, 2074
local vs. systemic effects in, 2061
in methanol poisoning, 2075–2076
in mineralocorticoid deficiencies, 2092–2093, 2094*t*
mitochondrial glutaminase in, 2001–2002
mixed anion gap-hyperchloremic, 2064, 2066*f*
NHE3 in, 2006–2007
nitrogen balance in, 2056–2057
organic vs. inorganic acid metabolism and, 2062–2063
overview of, 2049
oxygen dissociation curve in, 2061
in paraldehyde poisoning, 2077
pathophysiology of, 2011–2012
in patients with end-stage renal disease, 3139–3140
PEPCK in, 1999–2000, 1999*f*, 2004–2005
phosphate balance in, 2058, 2361
in poisoning, 2071–2072, 2074–2101
poorly absorbed anions and, 2037
post-fasting, 2037–2038
potassium balance and, 1691–1693, 1700, 2007–2008, 2012, 2057–2058
in primary adrenocortical deficiency, 2093
protein metabolism in, 2056–2057, 3047–3053, 3049*t*
in muscle, 3049–3053, 3049*t*

renal growth and, 2061
renal tubular, *see* Renal tubular acidosis
in salicylate poisoning, 2077–2078, 2081*t*
signaling in, 2005–2007
SN1 transporter in, 1999, 1999*f*
sodium balance in, 2057
thyroid hormones in, 2059
trade-off hypothesis for, 2061–2062, 2062*f*
treatment of, 2100–2101
uremic, 2078–2079
urinary sodium/chloride excretion in, 2479–2481, 2480*t*
ventilation in, 1980–1981, 1981*f*, 2054–2056, 2055*f*, 2056*f*, 2057*f*
in wasting syndrome, 2056
Metabolic alkalosis, 2021
adaptation to
chronic, 2027–2029
respiratory response in, 2022*f*, 2023
systemic response in, 2022–2024, 2022*f*
adrenal adenoma and, 2022
adrenal hyperplasia and, 2022
in adrenogenital syndromes, 2039
adverse effects of, 2033, 2033*t*
aldosterone in, 2028, 2038–2040
antacids and, 2034
approach to patient in, 2032–2033
in Bartter syndrome, 2037
bicarbonate in
excess, 2025–2027
excretion of, 2022–2024, 2022*f*
redistribution in extracellular fluid, 2022–2023, 2022*f*
renal reabsorption of, 2023–2025, 2029–2032
chloride balance in, 2028, 2031
chronic, 1814–1815
in cirrhosis, 2034
clinical significance of, 2040
in congenital chloride diarrhea, 2036
in congestive heart failure, 2034
contraction, 2027
in Cushing syndrome, 2039
decreased glomerular filtration rate in, 2027
definition of, 2021
in a dialysis patient, 3139–3140
distal convoluted tubule diuretics and, 1376
distal nephron acidification in, 2030–2031
diuretic-induced, 2036, 2481
in edematous patients, 2034
effective arterial blood volume in, 2033–2038, 2035*f*
with exogenous bicarbonate gain, 2033–2034
extracellular fluid in
bicarbonate distribution in, 2022–2023, 2022*f*
composition of, 2021
decrease in, 2028
increase in, 2022–2023, 2022*f*
future research directions for, 2041
gastric, 2035
generation phase of, 2021–2022
in Gitelman syndrome, 2037
history in, 2032–2033
hydrochloric acid in, 2035
hydrogen loss in, 2026
in hyperaldosteronism, 2022
with hypertension, 2038–2040
in hypomagnesemia, 2037
intracellular pH in, 1806
intrinsic tubular defect, 2031–2032
laboratory findings in, 2032
in Liddle syndrome, 2040
loop diuretics and, 1369–1370
maintenance phase of, 2021–2022
management of, 2032
mechanisms of, 2025–2032
in milk alkali syndrome, 2034
mineralocorticoids in, 2028–2030, 2038–2040
overview of, 2021–2022
pathophysiology of, 2025–2027, 2041
physical examination in, 2032–2033
post-hypercapneic, 2036–2037
potassium balance in, 1640, 1691, 1693, 1700, 2025–2032, 2037
presentation of, 2032
proximal tubule in, 2029–2030, 2030*f*
renin in, 2038
salt intake and, 2025, 2031
in starvation, 2037–2038, 2068
thick ascending limb of Henle in, 2030
ventilation in, 1980–1981, 1981*f*
without exogenous bicarbonate gain, 2035
Metabolic pathways
in ATP hydrolysis, 143–149
in ATP production, 149–154
cell volume and, 130–131
fatty acid oxidation, 151
gluconeogenetic, 153
glycolytic, 152–153
impaired, metabolite output and, 301
ketone body, 151–152
mitochondrial oxidative, 158–159
mitochondrial oxidative, 149–151, 150*f*, 151*f*, 152*f*
in renal transport, 154–165, 154*f*
coupling mechanisms for, 158–162
energy production pathways in, 149–154
substrate preference along nephron segments and, 154
tricarboxylate acid cycle, 154
Metabolic substrates
preference for, 154–158, 154*f*
in cortical collecting duct, 157
in distal convoluted tubule, 157
in loop of Henle, 155–156
in medullary collecting ducts, 157–158
in proximal tubule, 153–155
utilization of, ion transport and, 1155–1156
Metabolic syndrome
in chronic kidney disease, 3051
in diabetic nephropathy, 2621–2622
preeclampsia-eclampsia and, 2740
Metalloproteases (MMPs), 878
Metanephric mesenchymal cells, 960
Metanephric mesenchyme (MM)
induction
molecules involved in, 880–881, 880*t*
and tubulogenesis, 878–881
isolated culture of, 864–867, 865*f*, 866*f*
unidentified signals from, 873
Metanephros, development of, 859–861, 860*f*
transcription factors in, 868–872
Metformin, 2672–2674
lactic acidosis due to, 2072
transporters for, 2441
Methanol poisoning, 2075–2076
Methazolamide
absorption, by GI tract, 1361
Methyldopa, for preeclampsia-eclampsia, 2741*t*
α,β-Methylene adenosine 5′-diphosphate (MADP), 768–769
Methylprednisolone, *see* Corticosteroids
Methyltransferases
and ENaC regulation, 999
Mg^{2+} recovery
thick ascending limb of Henle in, 642–643
Mg^{2+} transport
in distal convoluted tubule, 642–643
Mg-ATP
interaction with Na,K-ATPase, 73
Michaelis–Menten equation, 52
Microalbuminuria, *see* Albuminuria
Microfilaments, in apical microvilli, 9–10
Microperfusion in *in vitro*, 820, 820*f*
Microscopic polyangiitis, 2833–2834, 2835*t*, 2839–2840
Microtubule-organizing center (MTOC), 322
Microtubule(s), 634, *see also* Cytoskeleton; Renal tubular; Tubular
in cell volume regulation, 126
in epithelial polarization, 8*f*
Microtubule-associated (MAP) kinases, *see* MAP kinases
Microvascular blood flow, *see also* Blood flow
regulation of
adenosine in, 832–833, 833*f*, 834*f*
adrenomedullin in, 829–830
aldosterone in, 829
angiotensins in, 828–829, 829*f*
antidiuretic hormones in, 827–828, 827*f*
arachidonic acid metabolites in, 834–837, 836*f*
autoregulation, 826–827, 826*f*
carbon monoxide in, 832
cytochrome P-450 metabolites in, 836–837, 836*f*
endothelins in, 837
extracellular ATP in, 833–834, 835*f*
hemoxygenases -1 and -2 in, 832
natriuretic peptide in, 837–838
nitric oxide in, 830–831
pressure natriuresis and, 826–827, 826*f*
purinoceptors in, 832–834, 833*f*, 834*f*, 835*f*
reactive oxygen species in, 831–832
Microvascular blood flow and solute transport, 283–285
Microvascular exchange, 810–812
AQP1 water channels and, 812–814

Microvascular exchange (*Continued*)
coupling of fluid and solute transport during ultrafiltration, 275–276
of fluid and solutes by convection and diffusion, 275–287
fluid movements through microvascular walls, 276–279
increases in microvascular permeability, 285–286
measuring, 286–287
interstitial hydrostatic pressure, 279–282
microvascular blood flow and solute transport, 283–285
starling forces in, 810–812
starling pressures and local lymph flow, 282–283
Microvascular permeability, 263–275
to lipophilic solutes, 267
permeability coefficients to macromolecules, 269–272
permeability coefficients to small hydrophilic molecules, 267–269
porous membranes, passive transport and permeability coefficients of, 265–272
of small hydrophilic solutes, 814, 815*t*
small hydrophilic solutes and water, 272–273
macromolecules, 273–275
ultrastructural features, 264–265
continuous endothelium, 264
fenestrated endothelium, 264, 264*f*
to urea, 814–815, 817*f*
Microvascular walls
endothelium in
fenestrated, 599*f*, 600
fluid movement through, *see* Microvascular exchange
structure of, 599–600, 599*f*, 600*f*
Microvasculature, 803
anatomy of, 595–600, 596*f*, 597*f*, 598*f*, 599*f*, 600*f*, 803–804, 804*f*, 805*f*, 806*f*, 807*f*, 808*f*, 809*f*
cortical, 803–804, 804*f*, 805*f*, 806*f*
measurement of, 818–819, 818*f*, 819*t*
medullary, 804–809, 806*f*, 807*f*, 808*f*, 809*f*
reactivity of, measurement of, 820–821, 820*f*, 821*f*
transport functions and properties of, 809–817
vasoactivity of, 821–822, 822*t*, 823*t*
Microvilli, apical, 8–11
Middle molecules, as uremic toxins, 3041–3042
Milk-alkali syndrome, 2034
hypercalcemia in, 2291
Mineralocorticoid receptor (MR), 431, 1194–1196, 1215–1216
activation of, mutations and, 1216–1220
ASDN cells and, 1182–1183
for ENaC regulation, 1196–1197
in TAL, 1184–1185
Mineralocorticoids, *see also* Aldosterone; Renin
biosynthesis of, 2093–2094, 2095*f*
deficiency of
causes of, 2092–2093, 2094*t*
renal tubular acidosis and, 2092–2093
in metabolic alkalosis, 2028–2030, 2038–2040
in potassium transport, 1682–1685, 1683*f*, 1684*f*
in pregnancy, 2700
in proANP gene expression, 1248
renal resistance to, 2096–2098
in renal tubular acidification, 1957
in salt wasting, 1310–1311
in sodium reabsorption, 392
in sodium transport
TAL, 1159–1160
Minimal change disease (MCD)
clinical presentation, 2783–2784
concomitant tubulointerstitial disease, 2783–2784
episodes of acute kidney injury, 2783–2784
hypertension, 2783–2784
diagnostic test, 2784
malignancy-associated, 2791–2792
natural history, 2783–2784
non-steroidal anti-inflammatory drug (NSAID)-induced, 2792–2793
pathology, 2784
pathophysiology, 2784
T cell activation, 2784
in pregnancy, 2719*t*, 2720
treatment, 2784–2785
chlorambucil, 2784–2785
cyclophosphamide, 2784–2785
cyclosporine, 2784–2785
prednisone, 2784
Mints, 415
Mitochondria
in apoptosis, AKI, 2554
in programmed necrosis, 2994
reperfusion injury in, 166
Mitochondrial carriers, 149–150, 151*f*
Mitochondrial cytopathies, 165
Mitochondrial encephalomyopathies, lactic acidosis in, 2073
Mitochondrial glutaminase, in metabolic acidosis, 2001–2002
Mitochondrial hypomagnesemia, 2156–2157
Mitochondrial oxidative phosphorylation, 149–150, 150*f*, 151*f*, 152*f*, 158–159
regulation of, 158–159
Mitochondrial respiration, 149–150, 150*f*
disorders of, 165
regulation of, 158–159
solute transport and, 158–159
Mitogen-activated protein kinase kinase (MEK), 2969–2970
Mitogen-activated protein kinase (MAPK), 328, 547, *see also* MAPK signaling pathway
in polycystic kidney disease, 2668
Mitogenic factors, in cell volume, 131
Molar Tooth Malformation (MTM), 339
Molecular coupling, 52–53
Molecular sieving, 272
Monckeberg's sclerosis, 3076
Monoamine oxidase (MAO), 542
Monocarboxylate transporters
intracellular pH and, 1802–1803
Monocytes
in acute kidney injury
ischemic, 2987
associated with APSGN, 2764–2765
in vasculitis, 2819–2821, 2824–2827
Montmorillonite, 3135
Mortality rate
atherosclerotic renal artery stenosis, 2578
MRP1, 2430
MRP3, 2430
MRP6, 2429–2430
MRP/ABCC family, 3188
mTOR, *see* Mammalian target of rapamycin (mTOR)
Muddybrown granular casts, 2537
Multidrug and toxin extrusion 1 transporter (MATE1), 2446–2447
Multidrug resistance (MDR) family, 23–24
Multidrug resistance-associated proteins
MRP1, 2430
MRP2, 2433–2434
MRP3, 2430
MRP4, 2434–2435
MRP6, 2429–2430
Multiple myeloma, *see also* Cancer
hypercalcemia in, 2290
proximal renal tubular acidosis in, 2084
Mus Musculus, as model systems for cilia, 337
Muscle contraction, signaling in, 391, 392*f*
Muscle function
in hypocalcemia, 2294
Muscle protein metabolism, in chronic kidney disease, 3049–3053
Muscle wasting
in chronic kidney disease, 3049–3053
Mutant mice, 562–563
D_1R, 562
D_2R, 562
D_3R, 562
D_4R, 562–563
D_5R, 563
Myc gene, 871
Mycobacterial diseases with renal manifestations, 2790
membranous nephropathy attributed to *M. tuberculosis* and *M. leprae*, 2790
Myeloma, *see* Multiple myeloma
Myeloperoxidase, in antineutrophil cytoplasmic autoantibody vasculitis, 2834–2837, 2835*t*
Myocardial contractility, 2134
Myoclonic epilepsy with ragged fibers, lactic acidosis in, 2073
Myofibrils, 760
Myofibroblasts, 972–973
Myoglobin, in AKI, 2533
Myoglobinuric acute kidney injury
role of iron, 3008–3009
Myosin, 760
in apical microvilli, 8–9
Myosin light chain kinase (MLCK), 6
in vascular smooth muscle regulation, 391, 392*f*

Myosin light-chain phosphatase (MLCP), in vascular smooth muscle regulation, 391, 392*f*
Myosin VI, 2963

N

n-3 polyunsaturated fatty acids, 488
Na^+ gradient hypothesis, 53–54
Na^+-selective channels, 56–57
NaBC1 (SLC4A11 gene), 1851
Na^+-Ca^{2+} exchangers, 54
N-acetyl-β-D-glucosaminidase (NAG), 2536, 3012
Na^+-Cl^- co-transporter (NCC), 645–646, 1047
  analysis of, 1062*t*
  cDNA sequence, 1051–1052
  functional characterization of, 1054–1055, 1055*t*
  and Gitelman's syndrome, 1047, 1067–1068
  phosphorylation of, 1066*t*
  physiological roles of, 1070
  physiology of, 1048–1051
  regulation of, 1059–1067
  structure function relationship issues in, 1056–1059, 1058*f*
  thiazide-sensitive, 1049, 1051–1052, 1054–1055, 1055*t*
  transepithelial ion transport by, 1050*f*
NaCl reabsorption
  dysfunctions, in distal convoluted tubule, 647–648
  thick ascending limb of Henle role in, 641
    bicarbonate reabsorption, 641–642
    Mg^{2+} and Ca^{2+} recovery, 642–643
NAD(P)H, 455–456
Nafamostat mesylate, hyperkalemia due to, 1764
Na^+-glucose co-transporters, 54
Nail-patella syndrome, 2873–2874
Na,K-ATPase, 145–147, 147*f*, 162–165, 221–222
  active NaCl transport and, 765
  aldosterone and, 78, 79*f*, 1193–1194
  angiotensin II, biphasic effect of, 77
  in ascending thin limb of Henle, 1472–1473
  ATP hydrolysis and, 145–147, 147*f*, 150*f*, 158*f*, 159–161
  basolateral membrane domain, 630–631
  in basolateral membrane domain, 1665, 1666*f*
  cardiac steroid interaction with, 72
  in cell adhesion, 75
  cell signaling by, 75
  control
    in collecting duct, 78–79
    by dopamine and parathormone, 76–77, 77*f*
    by insulin, 76
  functions, 75
  FXYD proteins, 70–71
    function and interaction with α- and β-subunits, 70–71
    isoforms, 70
  genetics, 73
  induction of
    liver cirrhosis and, 79–80
    nephrotic syndrome and, 79–80
  ion transport, 48, 52–53, 60–61, 71–72, 72*f*
  in kidney, 75–80
    control by dopamine and parathormone, 76–77, 77*f*
    control by insulin, 76
    regulation in proximal tubule, 76–77
  MD cells, 758
  Mg-ATP interaction with, 73
  modulation of, 1111–1113, 1112*f*
  in peritubular membrane, 1099–1100, 1100*f*
  pharmacology, 72–73
  postnatal development of, 913–914, 914*f*
  potassium transport by, 1638–1639, 1665, 1666*f*, 1741
    sodium-coupled, 1665–1667, 1666*f*, 1668*f*
  properties, 71–73
  protein kinase C and, 384–385
  regulation of, 73–75
    potassium deprivation and, 1681
    in proximal tubule, 76–77
    by sodium availability, 79
    in thick ascending limb of Henle's loop, 77–78
  sodium transport by, 1099–1100
  structure of, 68–71
  structure-function correlations, 631
  substrates, 73–75
    interaction with cytoskeleton, 75
    membrane trafficking, 74–75
    post-translational modifications, 74
    synthesis and degradation, 74
  α-subunit, 69
    isoforms, 69
    structure, 69
  β-subunit, 69–70, 145–146
    functional role, 70
    isoforms, 69–70
    structure and α–β interaction, 70
  vasopressin and, 78–79, 79*f*
Na^+:K^+:2Cl^- co-transporter 1 (NKCC1)
  loop-diuretic sensitive, 1051
  physiological roles of, 1070
  regulation of, 1059–1067
  structure function relationship issues in, 1056–1059
  ubiquitous bumetanide-sensitive, 1053
Na^+:K^+:2Cl^- co-transporter 2 (NKCC2), 163, 1047, 1354
  analysis of, 1065*t*
  and Bartter syndrome, 1047, 1068–1069, 1228
  functional characterization of, 1054–1055
  inhibitors of, 1159
  loop-diuretic-sensitive, 1049–1053, 1055–1056
  phosphorylation of, 1066*t*
  phylogenetic analysis, 1053–1054
  physiological pathways, regulation in TAL, 1159
  physiological roles of, 1070
  regulation of, 1059–1067
  and sodium transport, 1147–1148
  structure function relationship issues in, 1056–1059
  transepithelial ion transport by, 1050*f*
  variants, 1057
NaPi-IIa, 635
Natriuresis
  ANP-induced, 1251–1252
  mechanisms of action, 1252–1253
  in metabolic acidosis, 2057
  pressure
    autoregulation and, 826–827, 826*f*
  urodilatin in, 1254
Natriuretic hormones, *see also* Atrial natriuretic peptide (ANP)
  biological effects of, 1251–1258
  in congestive heart failure, 1264–1265
  degradation, by kidney, 1260
  and hypertension, 1249–1250
  list of, 1244*t*
  molecular biology of, 1245–1246
  origination from prohormones, 1244
  overview, 1241
  renal transplantation and, 1261
  secretion of, 1251
Natriuretic peptide
  vascular effects of, 837–838
Natriuretic peptide receptors (NPR), 1258–1260
  active receptor, 1259
  clearance receptor, 1259
NBCe1 function
  in the kidney, 1843–1847
  molecular regulation of, 1844–1846
  various organs, 1844
NBCe2 function
  functional properties, 1846–1847
  hypertension, 1847
  structural variants and tissue distribution, 1846
  targeted disruption in mouse, 1847
NCBE/NBCn2 (SLC4A10 Gene), 1850–1851
NCCα gene, 1051–1052
NCCβ gene, 1051–1052
Nck adaptor proteins, in slit diaphragm, 900
NDCBE (SLC4A8 gene), 1849–1850
Near silent channel, 994
Near-equilibrium theory, 159
Near-isosmotic transport model, 114, 114*f*
Necrosis
  cyclophilin D in, 2994
  mitochondria in, 2994
  poly(ADP-ribose) polymerase in, 2993–2994
  programmed, 2993–2994
    animal models of, 2994
    poly(ADP-ribose) polymerase in, 2993–2994
  in renal ischemia, 165–166, 2993–2994
Necrotizing arteritis, 2818–2819, 2821*f*
Nectins, 18, 20–21
Necturus maculosus, 2460
Nedd4-2 protein, and ENaC regulation, 994–995, 995*f*, 1199–1202, 1201*f*, 1202*f*

Neobladder, chronic metabolic acidosis and, 2099
Neonatal severe hyperparathyroidism, 2149–2150
  calcium-sensing receptor mutations and, 2191–2192
Neonates, *see also* Infants
  potassium transport, 1696–1697
  renal development in, 911
    autoregulation, 911
    distal tubule NaCl transport, 915–916, 916*f*
    glomerular filtration rate, 911–912, 912*f*
    glomerulotubular balance, 912–913
    induction of nephron maturation, 920–921
    Na^+/K^+-ATPase activity, 913–914, 914*f*
    paracellular transport, developmental changes in, 914–915
    phosphate transport, 921–923
    potassium transport, 923
    proximal tubule NaCl transport, 914
    proximal tubule volume reabsorption, 913
    renal acidification, 917–920
    renal blood flow, 911
    sodium chloride transport, 912–916, 913*f*
    sodium transport regulation, 916–917
    urinary concentrating and diluting ability, 924–925
Neph proteins, 736–737
Nephrin, 736, 898–899, 899*f*
  in albuminuria, 2459–2460
Nephritis, *see also* Glomerulonephritis; Inflammation; Pyelonephritis
  hereditary, in pregnancy, 2719*t*, 2721
  Heymann, 2970–2971
Nephrocalcinosis, in hyperparathyroidism, 2287
Nephrogenic diabetes insipidus (NDI), 1025, *see also* Diabetes insipidus, nephrogenic
Nephrogenic syndrome of inappropriate antidiuretic hormone, *see* Syndrome of inappropriate antidiuretic hormone secretion (SIADH)
Nephrogenic zone, 971
Nephrolithiasis, 2311
  ammonium acid urate stones in, 2312*t*
  apatite stones in, 2312*t*
  calcium oxalate stones in, 2312, 2312*t*
    inhibitors of, 2318–2319
    risk factors for, 2319*f*
  calcium phosphate (brushite) stones in, 2312, 2312*t*
    calcium/oxalate molar ratio and, 2318
    phytate and, 2318
    pyrophosphate and, 2318
  calcium sources in, 2319–2322, 2319*f*
  cell crystal interactions in, 2318
    inhibitors of, 2318–2319
  clinical manifestations of, 2312–2313
  crystal types in, 2313
  cystine stones in, 2312, 2341–2342, 2341*t*
  diagnosis of, 2313
  evolutionary aspects of, 2319
  gender differences in, 2315
  in hyperparathyroidism, 2333–2335
  low urine citrate and, 2323
  pain in, 2312
  pathologic fractures and, 2320–2321
  in pregnancy, 2719*t*, 2721–2722, 2721*f*
  radiographic findings in, 2312–2313
  recurrence of, 2313
  risk factors for, 2319*f*
  stone composition in, 2311–2312
    supersaturation and, 2314–2315, 2315*f*
  stone formation in
    alternative nucleation mechanisms in, 2314–2315
    inhibitors of, 2318–2319
    supersaturation in, 2314–2315
  stone size and passage in, 2312–2313
  struvite stones in, 2312, 2312*t*, 2344–2345
  supersaturation in, 2314–2315
    control of, 2315–2318
    stone composition and, 2314–2315, 2315*f*
    upper limit of metastability and, 2314, 2314*f*, 2318
    urinary solute traffic and, 2316, 2316*f*
    urine pH and, 2317, 2317*f*
    water reabsorption and, 2315–2316, 2316*f*
  uric acid stones in, 2312, 2324
    risk factors for, 2319*f*
  urinalysis in, 2313
  X-linked hereditary, proximal renal tubular acidosis in, 2084
Nephron number
  association of congenital reduction and, 2945
  at birth, 2945
  in hypertensive subjects, 2945
  in oligomeganephronia, 2945
Nephron tubules
  formation, molecules involved in, 880–881, 880*t*
  regulation, transcription factors in, 872
Nephronophthisis (NPHP), 338
Nephron(s), 959
  anatomy of, 600–602, 602*f*
  development
    S-shaped stage of, 891
    vesicle stage of, 891, 892*f*
  epithelial cells of, 3, *see also* Epithelial cell(s)
  postnatal maturation of, induction of, 618–620
  renal sodium retention sites in, 1287–1288
  short- vs. long-looped, 600–602, 602*f*
  substrate preference along segments of, 154–158, 154*f*, *see also* Metabolic substrates, preference for
Nephrotic agents
  and acute nephrotoxicity, 2911–2912
  and chronic nephrotoxicity, 2912–2913
Nephrotic injury, biomarkers of
  in acetaminophen (paracetamol)-induced injury, 2911–2913
  in cisplatin-induced injury, 2909–2911
  in cyclosporin A-induced injury, 2904–2909
  detection of histological injury, 2903
  induced, 2902
  legal framework, 2902
  NGAL, 2904
  sensitivity, specificity and time course of, 2902–2903
  serum creatinine and urea (BUN), 2901–2902
  tubular enzymes, 2902
  upregulated, 2904
  urinary, 2902–2903
Nephrotic proteinuria, 2765
Nephrotic syndrome, 2459–2460, 2765, 2770, 2773
  and albuminuria, 2467
  aquaporins in, 1428
  atrial natriuretic peptide in, 1309
  autosomal-recessive steroid-resistant, 2865–2866
  blood volume in, 1304
  clinical manifestation, 2775
  defined, 2775
  in Denys-Drash syndrome, 2871
  edema formation in, 1306–1307, 1306*t*, 1308*f*
  infectious causes
    hepatitis C virus (HCV) infection, 2787–2788
    HIV-associated nephropathy (HIVAN), 2785–2786
  plasma volume in, 1304
  proximal renal tubular acidosis in, 2085
  renin-angiotensin-aldosterone system in, 1307–1308
  secondary, 2785
  sodium retention in, 303, 1303–1309, 1306*t*, 1308*f*
    mechanism of, 1305*t*, 1307
    Na,K-ATPase induction and, 79–80
  steroid-sensitive, 2782–2783
  sympathetic nervous system in, 1308–1309
Nephrotoxic acute tubular necrosis, *see* Acute tubular necrosis
Nephrotoxic agents
  acetaminophen, 2911–2913
  aminoglycosides, 2913–2915
  apoptosis due to, 2901
  aspirin, 2077–2078, 2081*t*
  cell injury pathways in, 2894–2895
  cellular susceptibility to, 2889–2892
    renal blood flow and, 2890–2892
  cellular targets of, 2892–2893
  cirrhotic renal failure and, 2638–2639
  cisplatin, 2903, 2909–2911
  cyclosporine, 2903–2909, 2906*f*, 2908*f*, 3170, 3175
  diabetes insipidus due to, 1556, 1556*t*
  endothelial dysfunction and, 2891, 2894
  hyperkalemia due to, 1644–1646, 1758*t*, 1762
  in imaging studies, 2891
  inflammation due to, 2900–2901
  ischemic injury due to, 2892–2893
    apoptosis due to, 2894–2901
  lethal injuries, 2895–2901
  lithium, 2915–2918, 2917*f*

necrosis due to, 2894–2895, 2898–2899
outcome determinants for, 2890*f*
proximal tubular effects of, 2889–2890, 2892
salicylates, 2077–2078, 2081*t*
salt wasting due to, 1310
sublethal injuries, 2893–2894
in transplant immunosuppression, 3170–3171
transport-based selectivity and, 2892–2893
Nernst equation, 225–227
Nernst–Planck equation, 50–51
Nerves
anatomy of, 609*f*, 610
disorders of
in SIADH, 1521–1523
efferent renal, 1389–1390
in phosphate balance, 2374
in sodium balance, 917
Net acid excretion, 2061–2062, 2062*f*
measurement of, 307–308
Net endogenous acid production, 2050–2051
reference ranges for, 2050
Net flux, ion, 47
Net water transport, 95, 103–104, *see also* Water transport
N-ethylmaleimide (NEM), 274–275
Neurogenic diabetes insipidus, *see also* Diabetes insipidus
autosomal dominant, 1580–1581
autosomal recessive, 1578, 1580–1581
clinical features of, 1579–1582, 1580*t*
Neurological dysfunction, in SIADH, 1521–1523
Neuronal NOS (nNOS), 2543
Neuropeptide Y (Npy)
and BMP, 873
Neurotransmitters, 453
in cell volume regulation, 129
dopamine as, 453, 539, *see also* Dopamine
noradrenaline, 453
Neutral amino acids, 635
Neutrophil gelatinase-associated lipocalin (NGAL), 2514–2521, 2536, 2904, 3013
biological role of, 2515
for differential diagnosis of AKI, 2519
for early prediction of AKI
after cardiac surgery, 2517*t*
in critical care settings, 2518*t*
severity, 2519*t*
in enhancing the epithelial phenotype, 2515
limitations as AKI biomarker, 2520–2521
mRNA expression, 2514–2515
pathophysiology, 2514–2516
physiology, 2514–2516
in predicting delayed graft function (DGF) complications, 2518
for the prediction of AKI and its severity, 2516–2519
for prognosis of AKI, 2519–2520
siderophore-chelating property of, 2514–2515
Neutrophils
associated with APSGN, 2764–2765
in inflammation
in acute ischemic injury, 2987
lymphocytes in, 2988
in vasculitis, 2818–2821, 2824, 2827
N-glycans, 986
NHE3
in metabolic acidosis, 2006–2009
as Na/H antiporter, 1109–1111, 1110*f*, 1920–1921, 1921*f*, 1935, 1936*f*
glucocorticoids and, 1941
NHERF proteins, 408–409, 409*f*
in epithelial transport, 409–414
NHERF1, 410–411
NHERF2, 411–412
NHERF3, 412
NHERF4, 412
sodium transport and, 1109–1110
Niches, stem cells, 970
Nidogen, 12, 732
in glomerular basement membrane, 903
Nifedipine, for preeclampsia-eclampsia, 2741*t*, 2742*t*
Nitric oxide (NO), 455, 2414–2415, *see also* Oxidative stress
in acute tubular necrosis, 2543–2544
angiotensin II and, 438
in basolateral potassium transport, 1675
in congestive heart failure, 1292
and ENaC regulation, 1000
functions of, 165
and hypertension, 1332–1333
as inhibitors of NKCC2, 1159
in microvascular function, 830–831
nephrotoxic drugs and, 2890–2891, 2905, 2908
oxygen consumption and, 165
in pregnancy, 2695
in renin regulation, 434, 780–781
in sodium transport, 1115–1117, 1292
in tubuloglomerular feedback adaptation, 776–777
uric acid nephrotoxicity and, 3035
Nitric oxide synthase (NOS), 455
isoforms, 2543
NOS I/nNOS, 758–759
Nitrogen, *see also* Urea
excretion of
in chronic kidney disease, 3052–3053
in dietary compliance assessment, 3052–3053
Nitrogen balance, in metabolic acidosis, 2056–2057
Nitroprusside, for preeclampsia-eclampsia, 2742*t*
Nitroprusside reaction, in ketogenesis, 2066–2067
NMR spectroscopy, *see* Nuclear magnetic resonance (NMR) spectroscopy
Nmyc1 gene, 871
Noise analysis, in patch-clamp analysis, 206–208, 208*f*
Non A-non B IC cells, 654*t*, 657–658
Non-canonical Wnt/planar cell polarity (PCP) signaling and cilia, 330–331, 332*f*
Non-diabetic kidney disease
protein restriction in, 3053–3056
Noninvasive positive pressure ventilation, 2124
Nonsteroidal antiinflammatory drugs (NSAIDS), 3190, 3194–3195
cirrhotic renal failure and, 2638–2639
hyperkalemia and, 1762
transporters for, 2436
Noradrenaline
in renal function, 453
Noradrenergic neurons, as chemoreceptors, 1982*f*, 1984
Norepinephrine, 1843
in congestive heart failure, 1290
Notch family, 735–736
Notch2, in podocyte differentiation, 898
Notch proteins
in signaling, 377–378, 379*f*
NPT1, 2431–2432
NPT4, 2432
NTCP transporter, 1865–1871, 1867*f*, 1868*f*, 1869*t*
Nuclear magnetic resonance (NMR) spectroscopy, 1087
Nucleotide receptors, 164–165
agonists, 512
antagonists, 512–514
autoregulation
altered perfusion pressure, myogenic response to, 516
blood flow, 516
tubuloglomerular feedback in, 516–517
in blood flow regulation, 832–834, 833*f*, 834*f*, 835*f*
physiological responses to, 514
in polycystic kidney disease, 529–530, 529*f*, 530*f*
P2X, 511
P2Y, 511–512
dinucleotides, 512
heterodimeric, 512
renal effects of, 514–531
in collecting duct, 521
in distal tubule, 520–521
in glomerulus, 514–516, 516*f*
in loop of Henle, 519–520
in potassium, 522
in proximal tubule, 518–519
in sodium, 522–523
vascular, 514–516, 515*f*, 516*f*
in water, 521–522
in renal inflammation, 530–531, 530*f*
in renin release, 517–518
Nucleotide release, 523–525
cilium in, 525
mechanism of, 525–526
Nucleotide-binding domains (NBD), 1026
Nucleotides
ectonucleotidases, 513*f*, 526–528, 527*t*, 528*f*
extracellular, in renal function, 511, 531
in ROMK regulation, 1611–1613
secretion of, *see* Nucleotide release
Nucleus tractus solitarius (NTS), 466
chemoreceptors in, 1982–1983, 1982*f*, 1985
Nutrition, *See* Diet; Starvation
Nutritional supplements

Nutritional supplements (*Continued*)
for preeclampsia prophylaxis, 2740
Nutritional support, refeeding syndrome
hypophosphatemia in, 2380

O

OAT1, OAT3 and OAT4, 3193
2′3′-*O*-(4-benzoylbenzoyl)ATP (BzATP), 512
Obesity, in diabetic nephropathy, 2621–2622
Obesity bypass procedures and bariatric surgery, 2337–2338
Obesity hypertension, 1337–1341
kidney injury, 1340–1341
Leptin's stimulatory effect on SNS activity, 1338
mineralocorticoid receptor MR activation in, 1339–1340
RAAS activation, 1338–1339
SNS activation, 1337–1338
visceral, 1340
Obstructive nephropathy, *see* Obstructive uropathy
Obstructive uropathy
aquaporin-2 in, 1426
in pregnancy, 2690
tubuloglomerular feedback, 773
Occludin, 6, 349, 628
Occlusion, 58
Ochratoxin A, 167
OCT2, 3193–3194
17-Octadecynoic acid (ODYA), 776
Octreotide
for polycystic kidney disease, 2671–2672
Ocular defects, in Alport syndrome, 2848
Oculo Cerebral Renal Syndrome of Lowe, 33
Oculocerebral syndrome, proximal renal tubular acidosis in, 2084
Ohm's Law
ion channels and, 224–227
Oligopeptide(s), 2405–2406, 2410–2412
metabolism, 2411–2412, 2415–2416
Omeprazole, in H,K-ATPase inhibition, potassium reabsorption and, 1676
Oncogenes, intracellular pH and, 1817
Oncogenic osteomalacia, 2253–2254
Oncosis, 2898–2899
Oncotic pressure
sodium transport and, 1108–1109
Oncotic pressure, 276
OPC-31260, for polycystic kidney disease, 2671
Organ culture, 861, 862*f*
Organellar buffering, intracellular, 1789
Organelles
pH measurement in, 1778
Organic acids, *see also* Acid(s)
in acid–base balance, 309
in meat, 311–312
metabolism of, 2062–2063
in potassium balance, 1639–1640
Organic anion transporters (OAT), 635, 2425–2430, 2437*f*
for antiviral drugs, 2435–2436, 2435*f*
distribution of, 2426*f*
for diuretics, 2436–2437, 2436*f*
drug–drug interactions at, 2448
future research directions for, 2449
isoforms of, 1384
kidney-specific, 2429
for β-lactam antibiotics, 2435, 2435*f*
multidrug resistance-associated proteins, 2429–2430, 2433–2435
for nonsteroidal anti-inflammatory drugs, 2436
organic anion transporting polypeptide (OATP4C1), 2429
overview of, 2426
properties of, 2425–2426
sodium-dependent phosphate, 2431–2432
types of, 2426, 2426*f*
urate anion transporter 1, 2431
voltage sensitive urate anion transporter 1, 2431–2432
Organic anion transporting polypeptide (OATP4C1), 2429
Organic anion-chloride exchangers, 1791–1793
Organic anion(s)
definition of, 2425
secretion of, 2425–2426
Organic cation transporters (OCT), 635, 2430, 2437–2449
MDR1, 2447–2448
alternating access model of, 2444, 2444*f*
in chronic renal failure, 2445–2446
cloning and functions of, 2438
common transport characteristics of, 2441
in diabetes, 2445–2446
distribution of, 2437*f*
expression and main functions of, 2438–2441, 2439*t*
expression and renal functions of, 2446
future research directions for, 2449
high-affinity binding sites in, 2442–2444
in hyperuricemia, 2445–2446
ligand specificities of, 2441–2442
mutations in, 2448–2449
overview of, 2437–2438
phosphorylation of, 2445
polymorphisms in, 2448–2449
regulation of, 2445–2446
long-term, 2445
under pathological conditions, 2445–2446
short-term, 2444–2445
substrate binding region of, 2442
substrates for, 2441
transport mechanisms of, 2444, 2444*f*
Organic cation(s)
definition of, 2425
reabsorption of, 2437–2438
secretion of, 2425–2426, 2437–2438
Orofaciodigital Syndrome Type 1 (OFD1), 340
Oropharyngeal effect
antidiuretic hormone and, 1450
thirst and, 1455–1456
Osmolality, 96
extracellular, cell volume and, 104, 1544*t*, 1545–1547
plasma, 1542, 2485–2486
antidiuretic hormone secretion and, 1543–1544, 1543*f*
in pregnancy, 2702–2706
urine, 1463, 2485–2486, 2486*t*, 2491
in hypernatremia, 1559
in thin descending limb, 1471
Osmolar gap
urine, 2502–2503
Osmolytes
in cell volume regulation, 124, 1544*t*, 1545–1547, 1545*t*, 1549*t*
in hypernatremia, 1545–1547, 1546*f*, 1547*f*, 1547*t*, 1548*f*
in hyponatremia, 1523–1524
osmoprotective, 1488–1489, 1489*f*
Osmotic coefficient, 96
Osmotic demyelination, hyponatremia and, rapid correction of, 1526
Osmotic diuretics, 1354–1357, 1355*f*, 1356*t*, *see also* Diuresis
adverse effects, 1357
clinical use, 1357
in hypernatremia, 1554
mechanism of action, 1356
pharmacokinetics, 1357
renal hemodynamics, 1356–1357
urinary electrolyte excretion and, 1355–1357, 1356*t*
Osmotic equilibrium, 95–96, 96*f*
Osmotic permeability coefficient, 96–97
diffusive water permeability coefficient vs., 98–99
Osmotic pressure, 95–96
Osmotic reflection coefficient, 265–266
Osmotic transport, 95–98, *see also* Water transport, osmotic
Osteitis fibrosa, *see also* Renal osteodystrophy
in hyperparathyroidism, 2286–2287
Osteoblasts
calcium-sensing receptor in, 2203
Osteoclasts
calcium-sensing receptor in, 2203
Osteomalacia
oncogenic, 2253–2254
pseudofractures in, 2298–2299
tumor-induced hypophosphatemia in, 2380
Osteoporosis
chronic metabolic acidosis and, 2062
in hyperparathyroidism, 2279, 2286–2287
Osteoprotegerin (OPG), 2279
Ototoxicity
loop diuretics and, 1370
Ouabain-like factors, 1258
Outer medullary collecting duct (OMCD), 643–644, 650–653
in acid–base transport, 1947
anatomy of, 1144
potassium reabsorption in, 1676
potassium depletion and, 1682*f*
sodium transport in, 1166, 1167*t*
rate of, 1181–1182
substrate preferences in, 154*f*, 157
water and urea permeability of, 1470*t*, 1474
Outer stripe of outer medulla, 611*f*, 612, 612*f*, 614*f*, 665–668, 666*f*

concentrating mechanism in, 1478–1479
mechanism, 664*f*, 666–667
potassium reabsorption in, 1676
solutes dragging by flow to deeper medullary levels, 664*f*, 667–668
Outwardly rectifying currents (ORCC), 1026
Ovalocytosis, 1889
Ovarian vein, dilation of, in pregnancy, 2690
Overdistention syndrome, in pregnancy, 2690–2691, 2691*f*
Overflow theory, of ascites, 302–303
Oxacalcitriol, for hyperparathyroidism, 3082*t*
Oxaliplatin, transporters for, 2441
Oxidants, *See* Oxidative stress; Reactive oxygen species (ROS)
Oxidation, products of, *see* Reactive oxygen species (ROS)
Oxidative phosphorylation, mitochondrial, 149–150, 150*f*, 151*f*, 152*f*, 158–159
in ATP production, 149–150, 150*f*, 151*f*
regulation of, 158–159
Oxidative stress
in acute kidney injury, 2556–2557
in blood flow regulation, 831
in chronic kidney disease, 3043
in diabetic nephropathy, 2616–2617
in preeclampsia-eclampsia, 2735
in renal artery stenosis, 2587–2588
Oxygen administration, 2123–2124
Oxygen consumption
cellular components of, 145*f*
nitric oxide and, 165
Oxygen dissociation curve, in metabolic acidosis, 2061
Oxygen metabolites, *see* Reactive oxygen species (ROS)
Oxygen sensor
in erythropoietin production, 3099–3100
location of, 3099–3100
signaling of, 3099–3100, 3101*f*
Oxygen tension, in erythropoietin production, 3094–3096, 3095*f*, 3098, 3098*f*
Oxygenation, loop diuretics and, 1366–1370

P

P2 receptors, 164, 511–514
agonists, 512
antagonists, 512–514
physiological responses to, 514
P2X, 511
P2Y, 511–512
dinucleotides, 512
heterodimeric, 512
P38 MAPK signaling pathway, 388
Pain
in nephrolithiasis, 2312
in polycystic kidney disease, 2648–2649
PAK, in signaling, 386–388
Palitoxin (PTX), 63
PALS proteins, 416
Pamidronate
for hypercalcemia, 2293–2294
hypomagnesemia due to, 2159
Pancreatitis, in hyperparathyroidism, 2287–2288
PAN-induced cytotoxicity, 3014, 3014*f*
Papillary label-retaining cells, 965, 965*f*, 966*f*
Papillary peristalsis, urine concentration and, 1486–1488
Par complex, 19
Paracalcitriol, for hyperparathyroidism, 3082*t*
Paracellin, in magnesium balance, 2151
Paracellular pathway, 5
in distal convoluted tubule, 628, 647
epithelial transport, 628, 628*f*, 1087, 1102–1109
lateral intercellular space, 1102–1105, 1103*f*
Paracellular transport
postnatal developments and, 914–915
Paracentesis, large-volume, for cirrhosis, 1303
Paracrine regulation, dopamine in, *see* Dopamine
Parathormone (PTH), *see* Parathyroid hormone
Parathyroid adenoma
hyperparathyroidism and, 2285–2289
Parathyroid carcinoma, 2208
Parathyroid glands
vitamin D and, 2281
Parathyroid hormone, 2258–2261
assays for, 2288, 2291
biosynthesis of, 2258–2259
in calcium balance, 2187–2188, 2235, 2258–2261, 2258*f*, 2274
calcium channels and, 2176
calcium homeostasis, 2276–2279
in calcium transport, 2235
in chronic kidney disease, 3044, 3055, 3074, *see also* Hyperparathyroidism
functions of, 2274
in hypercalcemia, 2275
in hypocalcemia, 2275
imbalances of, *See* Hyperparathyroidism; Hypoparathyroidism
in intracellular pH regulation, 1813–1814
in magnesium balance, 2143, 2145*f*
in metabolic acidosis, 2058
metabolism of, 2288
Na,K-ATPase control by, 76–77, 77*f*
in phosphate balance, 2358–2359, 2370, 2370*f*, 2372–2373
in pseudohypoparathyroidism, 2297–2298
receptors, 373, 2259
recombinant, for hypoparathyroidism, 2296–2297
regulation of, 2258–2259
calcium-sensing receptor in, 2191–2193, 2192*f*, 2258–2259
vitamin D in, 2193–2194, 2258–2259, 2258*f*
renal effects of, 2259
in renal tubular acidification
in distal nephron, 1958
in proximal tubule, 1941
secretion of, 2258–2259
skeletal effects of, 2249, 2260–2261, 2260*f*, 2275–2276
stone formation and, 2333–2335
in transplant recipients, 3164–3165
Parathyroid hormone-related protein (PTHrP), 2276, 2281–2283
cartilage and bone, 2282, 2282*f*
mammary gland, 2282
Parathyroidectomy, for hyperparathyroidism, 2288
Par1b, 21
Paricalcitriol, for hyperparathyroidism, 3080
Parietal basement membrane, 617*f*, 626–627
Parietal epithelial cell (PEC), 943
of Bowman's capsule, 967
proliferation, 944
PARP, in drug-induced injury, 2901
Pars recta, *see* Thick ascending limb of Henle
Partial ionic conductance, equations for, 210–211
Passive Heymann nephritis (PHN) model, 941–942, 2970–2971
Patch-clamp analysis, 197
in apical membranes, 204–205, 1672*f*, 1673
potassium recycling and, 1669
renal potassium channels and, 1672*f*, 1673–1675
in basolateral membranes, 205, 207*f*, 1672*f*, 1673–1675
of channel number, 201–202, 202*t*
of channel pharmacology, 203, 204*f*
of channel selectivity, 199–200, 201*f*
in isolated cells, 205–206
luminal membrane, 1088–1095
noise analysis in, 206–208, 208*f*
molecular identification of ion channels, 207–208, 209*t*
of open and closed times, 202–203
of open probability, 200–201, 202*t*
parameters measured by, 198–199
in peritubular membranes, 1101
single-channel, 198–201
Patch-clamp electrophysiology
ion channel activity recording, 223–224, 224*f*
Pathological fractures
diet-related metabolic acidosis and, 2062
in idiopathic hypercalciuria, 2320–2321
in nephrolithiasis, 2320–2321
Pattern recognition receptors, 2988–2989
Pax gene, 869
Paxillin, 13, 380, 386
Pbx1 gene, 872
PDK1, in PI 3-K signaling, 389, 390*f*
PDZ domain, 54
PDZ domain-containing proteins
epithelial cells polarization, 31–32
PDZ proteins, 6, 405
basolateral membrane, 414–417
binding of, regulation of, 405
classification of, 405, 406*f*
functions of, 407
Lin-7 isoforms, 415–416
Lin-7/CASK/SAP-97 complex, 414–416, 415*f*
MAGUK, 407–408
polarized expression in epithelial cells, 407, 407*f*
structure of, 405–406, 406*f*

PDZ proteins (*Continued*)
Veli/MALS, 415–416
Péclet number, 275–276
Pelvic extensions, 595, 596*f*
Penicillin, 3194–3195
transporters for, 2435
Pentamidine, hyperkalemia due to, 1763
Peptic ulcers
in hyperparathyroidism, 2287–2288
Peptide hormones, renal hemodynamics and, 2694–2695
Peptide transporters
in intracellular pH regulation, 1795–1796
Peptides, *See* Oligopeptide(s); Protein(s)
Percutaneous transluminal renal angioplasty (PTRA), 2595–2596, 2595*t*
Perfusion-absorption balance, glomerulotubular
postnatal development and, 912–913
Periarterial connective tissue, 608–610, 608*f*, 609*f*
Periarteritis nodosa, pregnancy in, 2719*t*, 2720
Pericentriolar material, 322
Pericytes, 968–969
Peripheral membrane proteins, 4–5
Peristalsis, papillary, urine concentration and, 1486–1488
Peritoneal dialysate, 3129
Peritoneal dialysis, *see also* Dialysis
automated forms of, 3129–3130
for ethylene glycol poisoning, 2076
for lactic acidosis, 2074
for methanol poisoning, 2074, 2076
peritoneal dialysate solutions, 3138
pH-neutral bicarbonate-/lactate-based, 3138–3139
and potassium concentration, 3134
in pregnancy, in acute renal failure, 2716
for salicylate poisoning, 2078
and sodium concentration, 3129–3130
solutions, advantages and disadvantages, 3139*t*
Peritoneovenous shunting, for ascites, 1294, 1297–1299
Peritubular fibroblasts, 604*f*, 605
Peritubular membrane, transport pathways, 1095–1100
chloride transporters, 1097–1099, 1098*f*
Na,K-ATPase, 1099–1100, 1100*f*
sodium bicarbonate co-transport, 1095–1097
Perlecan, in glomerular basement membrane, 903–904
Permeability
epithelial, 110–111, 111*t*
membrane, 47–48, 50, 50*f*, *see also* Membrane permeability
"Permeability limited" transport, 283–285
Permeation, 228–229, 228*f*
Permissive hypercapnia, 2124–2125
Peroxisome proliferator activated receptor (PPAR), 1001, 2899–2900, 2968
P-glycoprotein, 2447, 3194
ATP hydrolysis and, 149
pH, *see also* Acid–base balance
anion exchange regulation by, 1885
of brain interstitial fluid, 1988–1990
of cerebrospinal fluid, 1988
chemoreceptors in, 1987*f*, 1988–1990
chemoreceptors and, 1979, *see also* Chemoreceptors
and ENaC regulation, 999–1000
factors influencing, 1804
growth factors and, 1816–1817
intracellular, 1773
acid–base transport systems and, 1789–1791
acid-extrusion mechanisms and, 1796–1804, 1796*f*, 1798*f*, 1799*f*, 1801*f*
acid-loading mechanisms and, 1791–1796, 1792*f*
carbon dioxide effects on, 1781–1783, 1782*f*
luminal/peritubular, in acid–base transport, 1931–1932, 1938
measurement of
magnetic resonance imaging in, 1779
pH-sensitive dyes in, 1775–1779
pH-sensitive microelectrodes in, 1774–1775
weak acid and base distribution in, 1775, 1775*f*
monocarboxylate transporters and, 1802–1803
oncogenes and, 1817
regulation of
breathing in, 1990
buffering in, 1781–1783, 1786*f*, 1790*f*, 1792*f*
complexity of, 1773
disturbances in, 1803–1804, 1805*f*
energetics of, 1781, 1781*f*
forces affecting charged weak acids/bases in, 1780–1781
forces affecting hydrogen ions in, 1779–1780
fundamental law of, 1803–1804
molecular mechanisms of, 1774
steady-state, factors influencing, 1804, 1804*f*
temperature effects on, 1809–1810
threshold of, 1798
weak acid/base effects on, 1775, 1775*f*, 1781–1783, 1782*f*, 1783*f*
in ROMK regulation, 1613
urinary, acetazolamide and, 1362
urine, *see* Urine pH
ventilation and, 1979, *see also* Chemoreceptors
Pharmacology, *see under* Drug
PHC signaling pathway, 372–373, 372*f*, 375, 384–386, 385*f*
Phenylethanolamine-*N*-methyl transferase (PNMT), 542
Phenytoin
for eclampsia, 2741, 2742*t*
transporters for, 2441
Pheochromocytoma, 1348
and hypertension, 1249–1250
Phlorizin
in renal glucose reabsorption inhibition, 2394, 2399–2400, 2400*f*
Phosphatases, receptor-like, in signaling, 377, 378*f*
Phosphate, *see also* Phosphorus
in acid–base balance, 2054
dietary
physiological response to, 2360, 2371–2372
restriction of, in chronic kidney disease, 3040–3041
excretion of
effects of diuretics on, 1356*t*
genetic alterations, 2361–2363, 2362*t*
for hyperparathyroidism, 2288
Klotho, mutations of, 2362
in mitochondrial respiration, 159
proximal tubular reabsorption of, 2351–2352
in acidosis, 2361
age-related changes in, 2361
apical entry in, 2351–2352
basolateral exit in, 2352
in diabetes, 2360–2361
in fasting, 2360–2361
gene products in, 2352–2357
in heavy metal poisoning, 2361
regulation of, 2358–2361
serum concentrations of, reference ranges for, 2378, 2378*t*
sodium-phosphate cotransporters in, 2351–2357, 2371
SLC34 mutations cotransporters, 2361–2363
as stone inhibitor, 2318
structure-function relationships, 2356–2357
transport mechanisms, 2354–2356
in vitamin D biosynthesis, 2370*f*
Phosphate balance
in acidosis, 2361
age-related changes in, 2361
atrial natriuretic factor in, 2359–2360
catecholamines in, 2374
derangements of, *See* Hyperphosphatemia; Hypophosphatemia
dietary phosphate in, 2360, 2370–2372, 2371*f*
dopamine in, 2359, 2374, 2374*f*
fibroblast growth factors in, 2369–2370
genetic alterations, 2361–2363, 2362*t*
in heavy metal poisoning, 2361
insulin in, 2360–2361, 2373
Klotho, mutations of, 2362
matrix extracellular phosphoglycoprotein in, 2369–2370
membrane lipids in, 2360
in metabolic acidosis, 2059, 2361
nitric oxide in, 2359–2360
parathyroid hormone in, 2358–2359, 2370, 2370*f*, 2372–2373
phosphate excretion in, 2371*f*
phosphatonins in, 2253–2254, 2369–2370, 2375, *see also* Phosphatonins
posttransplant, 3164–3165
in potassium depletion, 2360
reabsorption in, 2351–2352
regulation of, 2358–2361, 2369–2370

renal nerves in, 2374
serotonin in, 2374
SLC34 mutations cotransporters, 2361–2363
structure-function relationships, 2356–2357
transport mechanisms, 2354–2356
vitamin D in, 2369–2370, 2370*f*, 2373
Phosphate binders
for hyperphosphatemia, 3077, 3079*t*, 3081, 3082*t*
for renal osteodystrophy, 3078, 3079*t*, 3081
Phosphate restriction and phosphate depletion, 2159–2160
Phosphate transport
postnatal development of, 620–625
sodium-coupled, *see* Sodium-phosphate cotransporter
through apical membrane, 2351–2352
through basolateral membrane, 2352
Phosphate-wasting disorders, 2209–2210
Phosphatidylinositol 4,5-bisphosphate, 20–21, 47
in cell volume regulation, 126
and ENaC, 989, 1000
in molecular regulation of NBCe1 function and membrane expression, 1844–1846
Phosphatidylinositol 3-kinase (PI3K), 935, 1002–1003
Phosphatidylinositol (3,4,5)P_3 (PIP3), 20–21
Phosphatonins, 2369–2370, 2375
fibroblast growth factor 7, 2369–2370, 2377
fibroblast growth factor 23, 2253–2254, 2369–2370, 2375–2376, 2376*f*
for hypophosphatemia, 2359
secreted frizzled-related protein, 2253–2254, 2369–2370, 2376–2377, 2377*f*
in vitamin D metabolism, 2253–2254
Phosphoenolpyruvate carboxykinase (PEPCK)
in metabolic acidosis, 1999, 1999*f*, 2004–2005
production of, 1995
Phosphoinositide 3-kinase, 1002–1003
signaling pathway, 389–390, 390*f*
Phosphoinositide 4,5-bisphosphate, 255–256
Phosphoinositides, in ROMK regulation, 1613–1614
Phospholipase A2s (PLA_2), 487–488
in cell volume regulation, 126
receptors, 488
Phospholipase C
and dopamine receptors, 545, 547
signaling pathway, 372–373, 372*f*, 375, 384–386, 385*f*
Phospholipase D, and dopamine receptors, 545
Phospholipid bilayer, 45–47
Phospholipids, 46
Phosphoric acid, in acid–base balance, 309–310
Phosphorus, *see also* Phosphate
functions of, 2369
metabolism of, 2369–2370
reference values for, 294*t*
Phytate, as stone inhibitor, 2318
Pierson syndrome, 731, 2858–2859
Pi/OH exchanger, 151*f*
PIP3, *see also* Phosphatidylinositol (3,4,5)P_3 (PIP3)
in PI 3-K signaling, 388
Piretanide, calcium reabsorption and, 2239
PKC family, 2900
Placenta, in preeclampsia-eclampsia, 2731–2732, 2732*f*
Placental growth factor, in preeclampsia–eclampsia, 2734, 2738–2740
Placental lactogen, 2694
Plants, proANP gene in, 1261–1262
Plaque and deposits, quantities of, 2342–2343
physiological correlates of, 2343–2344
Plasma, anion gap in, 2498–2499
Plasma albumin, 2458*f*
Plasma electrolyte composition, 2120
during respiratory acidosis, 2120
during respiratory alkalosis, 2121
Plasma membrane, *see also* Membrane
epithelial
apical, 8–11, 629–630
basolateral, 11–13
microvillar, 10–11
fluid mosaic model, 46, 46*f*
function of, 46–48
ionic asymmetry, 45
lipid bilayer of, 5, 45
permeability of, 47–48, 50, 50*f*, *see also* Membrane permeability
reabsorption of water and solutes, 80–82
structure of, 45–47, 46*f*
V-ATPases in, 83–84
Plasma membrane Ca^{2+} pump (PMCA pump), 61, 67–68, 148, 2233–2234, 2254, 2255*f*, 2257
isoforms of, 2233–2234
Plasma oncotic pressure, 279
Plasma osmolality, 1542
antidiuretic hormone secretion and, 1543–1544, 1543*f*
urine osmolality and, 2485–2486, 2486*t*
Plasma sodium
sodium excretion and, 2481–2483
Plastin-1, 10
Platelet activating factor (PAF)
in AKI, 2550
Platelet-derived growth factor (PDGF), 937–938, 2971–2972
receptors for, 374
Platelet-derived growth factor B (Pdgfb), 723
Platelets, production of, 3109–3110, 3110*f*
PLC signaling pathway, 375
Pleiotrophin, in renal development, 875
PLX5568 inhibitor, 2672
PMCA
PMCA pump, *see* Plasma membrane Ca^{2+} pump (PMCA pump)
Pod1 gene, 872
in podocyte differentiation, 897–898
Podocalyxin, 622, 741, 967
Podocin, 736, 899
Podocyte gene regulation, disorders of, 2871–2874
Podocyte slit diaphragm, disorders of, 2848*t*, 2863–2867
Podocytes, 721
adult kidney, 967–968
and cell cycle, 940–944, 941*f*
cell cycle proteins and, 943–944
diabetes and, 946–947
in diabetic nephropathy, 2611–2613
differentiation, glomerulogenesis and, 897–898
Foxc2, 898
kreisler/Mafb, 898
Lmx1b in, 897
Notch2, 898
Pod1/Tcf21 in, 897–898
WT-1 in, 897
GBM and, 739–740
CD151, 740
dystroglycan, 740
dystrophin-glycoprotein complex (DGC), 740
α3β1 integrin, 739–740
αvβ3 integrin, 740
integrin-linked kinase, 740
glomerular, 622*f*, 623, 623*f*
glomerular parietal epithelium, 743–744
metabolism, 741–742
calcium signaling, 743
insulin signaling, 743
mTOR, 741–742
morphology, 732–733
negative charge on, 741
podocalyxin, 741
precursors, 733–734
sialyation defects and, 741
slit diaphragm (SD) assembly, 736
α-actinin-4, 738
cadherin and catenins, 737–738
FAT1, 738
Neph proteins, 736–737
nephrin, 736
podocin, 736
Rho GTPases, 738–739
transcription factors
Foxc2, 735
Kreisler (Mafb), 735
Lmx1b, 735
Notch, 735–736
Tcf21, 735
Wt-1, 734–735
Poisoning
heavy metal, phosphate balance in, 2361
metabolic acidosis in, 2071–2072, 2074–2101
Polarity protein complexes, 19
Poly(ADP-ribose) polymerase (PARP)
in drug-induced injury, 2899–2901
in programmed necrosis, 2993–2994
Poly-allylamine, *see also* Phosphate binders
for hyperparathyroidism, 3079–3080, *see also* Phosphate binders

Polyarteritis nodosa, 2818, 2819*t*, 2820*f*, 2830, *see also* Vasculitis
Polycystic kidney disease, 338
  cardiac manifestations in, 2650
  cell cycle in, 2669–2671
  cellular pathways in, 2664–2671
  clinical manifestations of, 2649–2651
  cysts in, 2646–2648
    formation of, 2647–2648, 2671
  diagnosis of, 2645–2646, 2646*f*
  diverticular disease in, 2650
  epidemiology of, 2645
  epithelial cell polarity and, 33–34
  extrarenal/extrahepatic cysts in, 2649–2651
  genetic factors in, 2653–2659
    in cyst formation, 2653–2657, 2655*f*
    in disease progression, 2655*f*, 2657–2658
    gene protein products and, 2659–2664
    genotype-phenotype correlations in, 2658–2659
  genetic testing for, 2647
  hypertension in, 2648
  imaging studies in, 2646*f*, 2647–2648
  metabolic acidosis in, 2061
  modifier effects in, 2659
  natural history of, 2647–2648
  non-motile cilia in, 382
  nucleotide receptors in, 529–530, 530*f*
  pain in, 2648–2649
  peroxisome proliferator activated receptors (PPARs), role of, 2674
  polycystic liver disease and, 2649–2650
  polycystins in, 382, 2659–2671, 2665*f*
  in pregnancy, 2719*t*, 2720–2721
  renal failure in, 2649
  signaling in
    calcium in, 2666–2667, 2671
    cAMP in, 2667, 2671–2672
    cell cycle in, 2665*f*, 2669–2671
    C-terminal cleavage in, 2669–2671
    G-protein-coupled receptors in, 2667–2668
    mammalian target of rapamycin in, 2668–2669
    mitogen-activated protein kinase/extracellular regulated kinase in, 2668
    planar cell polarity pathway in, 2664, 2666
    Wnt pathway in, 2664–2666
  treatment, 2671–2675
    AMP-activated protein kinase (AMPK), 2673–2674
    calcimimetics, 2671
    cell division cycle 25A (Cdc25A) regulator, 2674
    curcumin, 2674
    cyclins and cyclin dependent kinases (CDK), 2674
    E-prostanoid (EP) receptor activation, 2673
    Genz-123346, 2675
    glucosylceramide (GlcCer), 2675
    glycosphingolipids, 2675
    GSK1016790A, 2671
    HET-0016, 2673
    histone deacetylases (HDACs), 2674
    lactosylceramide (LacCer), 2675
    MEK inhibitors
      PD184352, 2672
      U0126, 2672
    menadione, 2674
    mTOR inhibitors, 2672–2673
    N-(4-hydroxyphenyl) retinamide (HPR), 2674
    NS-398, 2673
    OPC-31260, 2671
    pioglitazone, 2674
    PLX5568 inhibitor, 2672
    R-568, 2671
    roscovitine, 2674
    rosiglitazone, 2674
    sirolimus, 2673
    SKI-606, 2672
    somatostatin, 2665*f*, 2671
    sphingolipids, 2675
    Src kinase inhibitors, 2672
    SU-5416, 2672
    thiazolidinediones, 2674
    tolvaptan, 2671
    TRAM-34, 2672
    trichostatin A (TSA), 2674
    valproic acid, 2674
    vasopressin V2 receptor (VPV2R) antagonists, 2671
  vascular manifestations in, 2650
Polycystic liver disease
  isolated, 2650–2651
  with polycystic kidney disease, 2649–2650
Polycystin-1 (PC-1), 382, 631–632, 2659–2660, 2665*f*, 2666–2671
Polycystin-2 (PC-2), 382, 631–632, 2662–2664, 2665*f*, 2666, 2669
Polycythemia
  posttransplant, 3108–3109
Polydipsia, 2491, 2492*f*
  in nephrogenic diabetes insipidus, 1587–1588
  primary, 1587–1588
  psychotic, 1513–1514
Polymeric immunoglobulin receptor (pIgR), 23–24
Polyuria, *see also* Diabetes insipidus
  assessment of, 1589–1592, 2490–2491, 2490*f*
  hypernatremia and, 1556, 1559, 1561
  hypokalemia and, 1556
  lithium and, 2491
  in sickle cell disease, 1557
Polyuropolydipsic syndrome, 1587
"Pore pathway," 6
Pore theory, 702–707
  advective transport, 704
  fiber matrix theory and, 707
  Fick's law of diffusion, 702
  glomerulus experiments, 705–706
  and hydrodynamic flow, 703–704
  Kedem-Katchalsky flux, 702, 705
  restricted diffusion, 704–707
  sieving curves, 706–707
  steric hindrance, 703
  Stokes' law, 702
  Stokes-Einstein radius, 702–703
Pores, *see* Ion pores
Porins, 55
Positive pressure breathing, *see* Mechanical ventilation
Post-diuretic NaCl retention, 1386–1389, 1387*f*
Posttransplant anti-glomerular basement membrane nephritis, 2856
Potassium
  in acid–base balance, 3136
  and beta-adrenergic stimulation, 3133
  in brain interstitial fluid, 1989
  in cerebrospinal fluid, 1989
  dietary sources of, 2492, 2493*t*
  disorders
    clinical approach to, 2496–2498
    evaluation of, 2492–2498
  distribution of, 1659
  disturbances in hemodialysis, 3132–3134, 3136–3138
  excretion of
    acetazolamide and, 1358
    acid–base balance and, 1689*f*, 1690*f*, 1691–1693, 1691*f*
    ammonium excretion and, 1693, 1693*f*
    assessment of, 1752–1753
    circadian rhythm of, 1696*f*, 1698
    diuretics and, 1695, 1696*f*
    drugs interfering with, 1762
    effects of diuretics on, 1356*t*
    enhancement of, 1765
    external potassium balance and, 1660–1671, 1661*t*, 1663*f*
    fractional, 2495–2496, 2495*f*, 2496*t*
    integrated regulation of homeostasis and, 1698–1700
    internal potassium balance and, 1659–1660, 1660*f*
    potassium intake and, 1662, 1677–1678
    sodium intake and, 1683*f*, 1687–1691
    urinary, 2493–2495, 2494*f*
  homeostatic mechanisms for, 293, 296, *see also* Potassium balance
  in hyperkalemia, 3135–3136
  in hypokalemia, 3135
  in phosphate balance, 2360
  recycling of, 1667–1668
  reference values for, 294*t*
  regulation of, 1659–1671, 1661*t*, 1663*f*
    in renal disease, 3130–3132
  secretion of, 1672–1673, 1672*f*
    antidiuretic hormone and, 1692*f*, 1694
    glucocorticoids and, 1685–1686
    mineralocorticoids and, 1682–1685, 1683*f*, 1684*f*
    transtubular potassium gradient and, 1753
  supplemental, for distal renal tubular acidosis, 2091
Potassium balance
  acid–base balance and, 1638–1641
  ammonium ion production and, 2007–2008, 2012
  assessment of, 2492–2498
  barium and, 1647

cell necrosis and, 1646–1647
cesium and, 1647
in chronic renal failure, 1642–1643
cyclosporine and, 3176–3177
dopamine in, 1636–1637
external, 1660–1671, 1661*t*, 1663*f*
glomerular filtration rate in, 1660–1661, 1663
hypothermia and, 1647
insulin in, 1631–1633, 1633*f*
internal, 1659–1660, 1660*f*
magnesium balance and, 1643–1644
in metabolic acidosis, 2007–2008, 2012, 2037, 2057–2058
in metabolic alkalosis, 2025–2032
posttransplant, 3176–3177
in pregnancy, 2700–2701, 2701*f*
in proximal renal tubular acidosis, 2082
in proximal tubule cells, 1665
regulation of, 1742*f*, 1743–1745
renal tubular acidification and, 1937–1938
ROMK in, 1673–1675, 1747
low-potassium diet and, 1678–1679, 1681*f*
tacrolimus and, 3176–3177
thyroid hormones in, 1638
transtubular potassium gradient in, 1753
Potassium channels, 219*t*
Potassium chloride, in hyponatremia treatment, 1528
Potassium citrate, for nephrolithiasis, 2323
Potassium conductance
apical, sodium transport and, 1148–1150, 1149*f*
basolateral, sodium transport and, 1665–1667, 1666*f*, 1668*f*
Potassium homeostasis
feedback control, 1717
feedforward control, 1717–1718
and glucose intolerance, 1734–1735
renal changes in deficiency, 1724–1733
Potassium intake
high, 1679*f*, 1680, 1699
low, 1677–1678, 1681*f*, 1682*f*
potassium excretion and, 1661, 1677–1678
potassium reabsorption and, in loop of Henle, 1670
restricted, aldosterone and, 1699–1700
Potassium ion channels, 823–824, 823*t*, 1606*f*, 1615–1619, 1673–1675, 1674*f*, 1741–1743, 1742*f*, 1743*f*
ATP-sensitive, 164
basolateral, 1675
calcium balance and, 1669, 1673–1674
in cell volume regulation, 122, 123*f*, 125–126, 128*f*, 129–130, 130*f*
potassium secretion and, 1662, 1663*f*
ROMK, 394–395
AKAPs and, 419
isoforms of, 1604–1605, 1606*f*
localization of, 1605, 1606*f*
phosphorylation of, 1608–1609
pore characteristics of, 1605–1614, 1610*f*
in potassium balance, 1673–1675, 1747
low-potassium diet and, 1678–1679, 1681*f*
regulation of, 1608–1614, 1610*f*
structure of, 1601–1604, 1602*f*
ubiquitination and, 1611
WNK and, 1609–1610
two-pore, 1619
Potassium loading, potassium excretion and, 1678–1680, 1678*f*, 1679*f*
Potassium phosphate, in acid–base balance, 312–313
Potassium reabsorption, 1674*f*, 1675–1676
acid–base balance and, 1693
diuretics and, 1670–1671
in loop of Henle, 1668, 1670–1671
mechanisms of, 1664, 1666*f*
potassium depletion and, 1678–1679, 1682*f*
Potassium transport, 1661*t*, 1662
acid–base balance and, 1638–1641, 1689*f*, 1690*f*, 1691–1693, 1691*f*, 1745
active, 1664
aldosterone in, 1192–1193
antidiuretic hormone and, 1692*f*, 1693–1694
ATP in, 164
ATP/ADP ratio and, 1666
catecholamines and, 1634–1638, 1635*f*, 1694–1695, 1744
in CNT and DCT, 650
in connecting tubule, 1672–1675, 1672*f*, 1677
cooperative factors in, 1698–1700
in cortical collecting duct, 1672–1675, 1672*f*, 1677, 1678*f*
in distal convoluted tubule, 1671–1675, 1672*f*, 1677
diuretics and, 1695–1696, 1696*f*
driving force in, 1741, 1742*f*, 1743*f*
drugs affecting, 1762
glomerular filtration rate and, 1662–1663
glucagon and, 1694
hormones affecting, 1745
insulin and, 1631–1633, 1633*f*, 1694, 1745
in loop of Henle, 1667–1668, 1668*f*
postnatal development of, 625–626, 1696–1697
in proximal tubule, 1665, 1666*f*, 1677
salt and water balance and, 1683*f*, 1687–1691
sodium reabsorption and, 1699
in thick ascending limb, 1668–1671, 1670*f*, 1671*f*, 1677
through apical membrane, 1665, 1666*f*, 1669
through basolateral membrane, 1665, 1666*f*
in transplant recipients, 3162
Potassium transporters, 1665, 1666*f*
sodium-coupled, 1665–1667, 1666*f*, 1668*f*
Potassium-bicarbonate cotransporter electroneutral, 1794
Potassium-chloride cotransporter, 1671–1675
Potassium-sodium cotransporters, 1665–1667, 1666*f*, 1668*f*
Potassium-sparing diuretics, 1377–1382, 1377*f*, *see also* Diuretics
adverse effects, 1381–1382
calcium reabsorption and, 2240
clinical use, 1381
mechanism of action, 1378–1381
pharmacokinetics, 1381
urinary electrolyte excretion, 1377–1382, 1378*f*
Pramipexole, transporters for, 2441
Precursor cells, *see* Stem cells
Precursor prohormone pro-opiomelanocortin (POMC), 1258
Prednisone, *see also* Corticosteroids
in transplantation, renal effects of, 3157–3158
Pre-eclampsia, 1348–1349
Preeclampsia-eclampsia, 2727–2735
angiogenesis in, 2734–2735, 2738–2740
anti-angiotensin receptor-1 antibodies in, 2735
cardiac dysfunction in, 2729–2730
central nervous system in, 2730–2731
circulating factors in, 2732–2734
clinical spectrum of, 2727–2728
coagulopathy in, 2730
differential diagnosis of, 2727
endothelial dysfunction in, 2732–2734
epidemiology of, 2727
glomerular endotheliosis in, 2735–2736
glomerular filtration rate in, 2737
HELLP syndrome and, 2715
hepatic dysfunction in, 2730
hyperlipidemia and, 2740
hypertension in, 2729
long-term risk for, 2740
treatment of, 2740, 2741*t*, 2742*t*
inflammation in, 2735
kidney in
functional changes in, 2737
morphological changes in, 2735–2737
late postpartum eclampsia, 2728
management of, 2740–2743
drug therapy in, 2740–2743, 2741*t*, 2742*t*
induced delivery in, 2740–2743
metabolic syndrome and, 2740
oxidative stress in, 2735
pathogenesis of, 2728–2729
pathophysiology of, 2729
placenta in, 2731–2732, 2732*f*
predictors of, 2738–2740
prevention of, 2738–2739
prognosis for, 2739–2740
risk factors for, 2738–2740
seizures in, 2728, 2731
severity of, 2728
sFlt-1, 2732–2734, 2733*f*
in trisomy 13, 2727
urate clearance in, 2740–2742
vascular endothelial growth factor in, 2734
Preferential bicarbonate reabsorption, 1084
Pregnancy, 2689–2691
acid–base balance in, 2701–2702, 2709*f*
acute fatty liver of, 2715
acute renal failure in, 2714
after urologic surgery, 2719*t*
albuminuria in, 2707
amino acids in, 2699–2700
anatomic changes in, 2689–2691, 2691*f*

Pregnancy (*Continued*)
antidiuretic hormone in, 1450, 1588, 2702, 2703*f*
bacteriuria in, 2713
bicarbonate in, 2701–2702, 2703*f*
blood pressure in
abnormal, *See* Preeclampsia-eclampsia; Pregnancy
classification of, 2726–2727
measurement of, 2725–2726
normal values for, 2725
regulation of, 2725
calcium balance in, 2700*t*
cGMP in, 2695
chronic pyelonephritis in, 2719*t*
chronic renal failure in, 2716–2724
causes of, 2718–2723, 2719*t*
outcome of, 2723
pathophysiology of, 2717–2718
prognosis of, 2716–2724, 2717*f*
treatment of, 2722–2723
collecting system in, 2691*f*
cystinosis in, 2721
diabetes insipidus in, 1588, 2704
diagnosis of, 2725–2727
dialysis in, 2722
in acute renal failure, 2714
effective renal plasma flow in, 2691–2699, 2717
in preeclampsia, 2737
endothelin in, 2696
endothelium-derived relaxing factors in, 2695–2696
extracellular volume in, 2693
familial Mediterranean fever in, 2720
fluid balance in, 2707–2708
in chronic renal failure, 2718
focal glomerulosclerosis in, 2719*t*, 2720
fructosuria in, 2699
glomerular filtration rate in, 2691–2699, 2709–2710, 2717, 2723
measurement of, 2711–2712
in preeclampsia, 2737
glomerulonephritis in, 2718–2719, 2719*t*
glucosuria in, 2699
Goodpasture syndrome in, 2719*t*, 2720
HELLP syndrome in, 2715
hematuria in, 2712
Henoch-Schönlein purpura in, 2719*t*, 2720
hydronephrosis, 2689, 2690*f*
hyperemesis gravidarum in, 2714
hypertension in, 1221, 2724
causes of, 2727, 2727*t*
in chronic renal failure, 2718, 2741*t*
classification of, 2726–2727
diagnosis of, 2725–2727
gestational, 2727
in preeclampsia-eclampsia, 2727–2735, *see also* Preeclampsia-eclampsia
lactosuria in, 2699
matrix metalloproteinases in, 2696–2698, 2697*f*
minimal change disease in, 2719*t*, 2720
nitric oxide in, 2695
nonosmotic stimulus for AVP secretion in, 2705–2706
normal cardiovascular changes in, 2724–2743
obstructive uropathy in, 2690
osmoregulation in, 2702–2706
ovarian vein syndrome in, 2690
overdistention syndrome in, 2690–2691, 2691*f*
peptide hormones in, 2694–2695
periarteritis nodosa in, 2719*t*, 2720
polycystic kidney disease in, 2719*t*, 2720–2721
potassium balance in, 2700–2701, 2700*t*, 2701*f*
preeclampsia-eclampsia in, 2727–2735, *see also* Preeclampsia-eclampsia
prostaglandins in, 2695
proteinuria in, 2707, 2717
reflux nephropathy in, 2720
renal biopsy in, 2712
renal cortical necrosis in, 2714–2715
renal disorders in, 2711–2716
patient evaluation in, 2711–2712
prognosis of, 2716–2724, 2717*f*
renal hemodynamics in, 2691–2699, 2717, 2718*f*, 2723
renal size in, 2689, 2690*f*, 2691
renal transplantation in, 2722–2723
renal tubular function in, 2699–2702
renal weight in, 2689, 2690*f*
scleroderma in, 2719*t*, 2720
septic abortion in, 2714
sex hormones, 2694
sodium balance in, 2700–2701, 2700*t*, 2701*f*, 2702*f*, 2708–2710, 2709*f*
systemic lupus erythematosus in, 2719–2720, 2719*t*
tuberous sclerosis in, 2721
ureteral dilation in, 2690, 2691*f*
uric acid in, 2700
urinary acidification in, 2702
urinary stasis, 2689, 2690*f*
urinary tract infections in, 2713–2714
urine concentration/dilution in, 2705–2706
urine sediment in, 2712
urine tests in, 2691–2692
urolithiasis in, 2719*t*, 2721–2722, 2721*f*
uterine hemorrhage in, 2714
uterine vein dilation in, 2690
von Hippel–Lindau disease in, 2721
Wegener granulomatosis in, 2719*t*, 2720
weight gain in, 2706–2707, 2706*t*
xylosuria in, 2699
Prerenal azotemia
and acute kidney injury, 2529–2531, 2560
Pressure natriuresis
autoregulation and, 826–827, 826*f*
Primary aldosteronism, 1346–1347
Primary Ciliary Dyskinesia, 319
Primary cilium, 11, 319
ultrastructure of, 322*f*
Primary essential hypertension, 1336–1341
obesity and overweight risk factors, 1337–1341
Primary hypercapnia, 2113, *see also* Respiratory acidosis
Primary hyperoxaluria, 2338
Primary hyperparathyroidism (PHP), 2285–2289
cause of, 2286
clinical presentation, 2286
complications of, 2287*t*
diagnosis of, 2288
management of, 2288
non-surgical management of, 2289*t*
Primary single cilia, 631–632
Principal cell, polarity of, 3–4
Proadrenomedullin N-terminal 20 peptide (PAMP)
biological effects, 1255–1256
in hemodialysis, 1261
ProANP gene, 1245
in cancer, 1266
in congestive heart failure, 1250
expression, enhancement of
calcium and, 1249
glucocorticoids and, 1247–1248
mechanical stretch and, 1247
mineralocorticoids and, 1248
thyroid hormones and, 1247
in invertebrates, 1261–1262
localization of, 1250
mechanism of action, 1246, 1248*f*
in plants, 1261–1262
tissue-specific expression of, 1245–1246, 1247*f*
transgenic/knockout mice, 1249
upregulation, and human diseases, 1249–1250
Procainamide, transporters for, 2441
Progesterone
in pregnancy, renal hemodynamics and, 2694
Programmed cell death, *see* Apoptosis
Programmed necrosis, 2993–2994
Proliferative glomerulonephritis, 2791
Pronephric duct, 859
Pronephros, development of, 859
Prostacyclin (PGI_2), 495
in renal tubular acidification, 1959
Prostaglandin F synthesis, 493–494
Prostaglandin 9-ketoreductase (PG9KR), 494
Prostaglandin(s)
in cirrhosis, 1302
in congestive heart failure, 1291
in magnesium balance, 2141*t*, 2143–2144
in pregnancy, 2695
prostaglandin D_2, 494
prostaglandin E_2, 2143–2144
PGE receptors, 474
renorenal reflexes, 474
renal inflammation and, 496
in renin regulation, 435, 781–783
in sodium transport regulation, 1291
transport of, 495–496
vascular effects of, 835–836, 836*f*
Prostanoid synthases, 490
Prostanoids, 488–489
biologic effects, 490
biosynthesis, 496
cellular expression of, 490
diabetic nephropathy and, 496

DP receptors, 494–495
EP receptors, 490–493
FP receptors, 494
G-protein coupled receptors, 490
IP receptors, 495
prostacyclin (PGI_2), 495
prostaglandin E2, 490–491
thromboxane A_2 (TxA_2), 495
TP receptors, 495
Proteases, 997–998
Proteasomes, in muscle protein metabolism, 3049–3053, 3049*t*
Protein C, in acute kidney injury, 2545
Protein Data Bank (PDB), 55
Protein kinase(s), *see* Kinase(s)
Protein kinase A (PKA)
dopamine receptors and, 545
effect on ENaC, 1002
Npy and BMP through, 873
in ROMK phosphorylation, 1608–1609, 1610*f*
in sodium ion transport, 1109, 1110*f*
in water reabsorption, 393–394
Protein kinase B (PKB), 935
Protein kinase C (PKC)
in album metabolism, 2464–2465
in diabetic nephropathy, 2616
dopamine receptors, 545–546
in ROMK phosphorylation, 1608–1609
in signaling, 372, 384–385
in T-cell activation, 384
Protein p21, in acute kidney injury, 2559
Protein p21-associated kinase, in signaling, 386–388
Protein restriction
in diabetic kidney disease, 3056
in non-diabetic kidney disease, 3053–3056
Protein tyrosine phosphatases, in signaling, 377, 378*f*
Proteinases
extracellular, in renal development, 878
in vasculitis, 2825–2827, 2827*f*
Protein(s)
body stores of, in low-protein diet, 3048–3049
catabolism of, in metabolic acidosis, 3049–3053, 3049*t*
cell cycle regulatory, 935–936
Cip/Kip family, 936–937
dietary
in disease progression, 3035–3036
glomerular filtration rate and, 3053
guanidino-containing compounds from, 3038–3039
health effects of, 2061–2062
hypertension and, 3033
intake assessment for, 3052–3053
intracellular pH and, 1815
nephrotoxic compounds from, 3036
non-urea nitrogen from, 3052–3053
renal hemodynamics and, 3033–3036
renal hypertrophy and, 3021
restriction of, *see* Low-protein diet
urea from, 3036–3038, 3051–3052, 3052*f*
urea transporters and, 1493
uremic toxins from, 3036
glycated, in diabetic nephropathy, 2617
INK4, 936
membrane
of apical membrane, 8–11
of basolateral membrane, 11
peripheral, 4–5
of tight junctions, 6
metabolism of
in cell volume regulation, 124, 126
in chronic kidney disease, 3046–3060
in dialysis, 3046–3047
in metabolic acidosis, 2056–2057, 3047–3053, 3049*t*
phosphorylation of, in cell volume regulation, 126
toxic metabolites of, 3037–3038
tubular reabsorption of, 2963
Proteinuria, 2464, *see also* Albuminuria
in acute post-streptococcal glomerulonephritis, 2765
in Alport syndrome, 2847
in apoptosis, 2968–2969
in congenital nephrotic syndrome, 2462
in disease progression, 2961
complement and, 2973–2975
early studies of, 2961–2965
events in, 2962*f*
overview of, 2961–2973
signaling in, 2969–2973
tubular injury in, 2963–2965, 2970–2975
fibrogenesis and, 2971–2972
in Heyman nephritis, 2970–2971
immune response, triggering, 2976–2977
inflammation in, 2973–2974
lipids in, 2976–2977
in pregnancy, 2707, 2717
receptor-associated protein deficiency in, 2963
renal injury from, 3052–3053
Proteinuria-associated progressive glomerular injury, 2974–2975
Proteoglycans, 12, 732, 877–878
in glomerular basement membrane, 620, 903–904
Proteolytic cleavage-activated receptors, 377–379, 378*f*
Prothrombin F1 fragment, as stone inhibitor, 2319
Proton gradients, sodium transport and, 1090–1092, 1091*f*
Proton-pump inhibitors (PPIs), 2158–2159
Proximal convoluted tubule
bicarbonate transport in
postnatal renal acidification and, 917–919
calcium reabsorption in, 2228, 2228*f*
epithelial cells of, 1
potassium transport in, 1661, 1663*f*
control of, 1677
direction of, 1663–1667
magnitude of, 1663–1667
mechanism of, 1665, 1666*f*
sodium transport in
oxygen consumption and, 144
substrate preference in, 154–155, 154*f*
Proximal renal tubular acidosis, 1840–1841, *see also* Renal tubular acidosis, proximal
Proximal tubule, 352–354, 632–635, 2393, *see also* Glucose, reabsorption in; Renal tubular; Tubular
ammonium ion secretion in, 2007–2008
calcium transport in, 2229–2230, 2235*t*
calcium-sensing receptor in, 2195–2196
convoluted, *see* Proximal convoluted tubule
dopamine and, 1114–1115
drug transporters in basolateral membrane of, 2427–2428
epithelium, morphology of, 632–633
function of, 1081
glucose reabsorption in, 2394, 2395*f*
interspace model to, 1104*t*, 1105
in metabolic alkalosis, 2029–2030, 2030*f*
Na,K-ATPase regulation in, 76–77, 1099–1100
NaCl reabsorption, 353
net fluxes across, 1082–1084, 1082*t*, 1083*f*, 1084*f*, 1085*f*
organic anion reabsorption in, 2425–2426, 2426*f*
organic cation reabsorption in, 2437–2438, 2437*f*
overview, 1081–1082
paracellular pathway
across tight junction, 1106–1109, 1108*f*
lateral intercellular space, 1102–1105, 1103*f*
permeability properties of, 1086, 1086*t*
phosphate reabsorption in, 2351–2352
protein reabsorption in, proteinuria and, 2964
redistribution of renal blood flow to, 1251–1252
sodium chloride transport in
maturation of, 913
sodium retention and, 1288–1290, 1300
sodium transport in, 1371
sodium-bicarbonate cotransport in, 1095–1097
sodium-glucose co-transport in, 1089–1090
straight
calcium reabsorption in, 2228–2229, 2228*f*
potassium transport in, 1661
transcellular pathway, 1087–1102
cytosolic concentrations, 1087–1088
luminal membrane, 1088–1095
peritubular membrane, 1095–1100
transcellular water reabsorption, 634
transport forces, 1085–1087
water reabsorption in
maturation of, 913
water transport in, 1085–1087, 1371
Proximal tubule, 558
PSD-95, 407
Pseudofractures
in osteomalacia, 2298–2299
Pseudohypoaldosteronism, 2096
posttransplant, 3162

Pseudohypoaldosteronism (*Continued*)
type I, 1759
type II, 1759–1760
Pseudohypoaldosteronism type I (PHA I), 1226–1227
autosomal recessive, 1226–1227
and ENaC, 1192
Pseudohypoaldosteronism type II (PHAII), 1163, 1223–1225, 1344
sodium-coupled cation chloride co-transporters and, 1225–1227
Pseudohyponatremia, 1530
Pseudohypoparathyroidism, 2297–2298
Pseudo-solvent drag, 102
Psychogenic polydipsia
self-induced water intoxication in, 1513–1514
P-type ATPases, 60, 61*f*, 67
ATP hydrolysis and, 145
structure and conserved motifs, 67, 68*f*
Pulmonary disorders, SIADH in, 1520
Pulmonary edema
flash, 2578–2579
in preeclampsia, 2729
Pulmonary ventilation, chemical stimulus for, 2114
Pumps, *see* Ion pumps
Purinergic receptors, *see* Nucleotide receptors
Purinoceptors
in blood flow regulation, 832–834, 833*f*, 834*f*, 835*f*
P2X receptors, 511, 1985, *see also* Nucleotide receptors
$P2X_7$ receptors, 511
in polycystic kidney disease, 529–530
in renal inflammation, 528–531
P2Y receptors, 511–512
dinucleotides, 512
heterodimeric, 512
Pyelonephritis, in pregnancy, 2713
Pyranine-based dyes, in intracellular pH measurement, 1778
Pyridoxine
for ethylene glycol poisoning, 2076
for hyperoxaluria, 2338
for primary hyperoxaluria, 2338
Pyrophosphate, as stone inhibitor, 2318
Pyruvate metabolism, 2069–2070, 2069*f*

Q

Quartan malaria, 2789
in children, 2789
nephropathy associated with, 2789
Quinidine, transporters for, 2441

R

R-568, for polycystic kidney disease, 2671
Race
potassium balance and, 1647
Radiation, in vitamin D production, 2251
Radiocontrast induced nephropathy (CIN), 2532–2533, 2891
Radiography
of kidney stones, 2312–2313
Raf, in MAPK signaling, 385, 388
RAGE
in diabetic nephropathy, 2618
in ischemic inflammation, 2993
RANKL, vitamin D and, 2281
Rapamycin
for polycystic kidney disease, 2669
in transplantation, solute transport and, 3151
Ras mitogen-activated protein kinase (Ras-MAPK) pathway
in cancer, 1266–1268, 1267*f*
Ras oncogene, cell volume and, 131*f*
Reactive oxygen species (ROS)
in acute kidney injury, 2556–2557
in blood flow regulation, 831–832
dopamine receptors, 567–568
nephrotoxic drugs and, 2897*f*, 2898–2901, 2910–2911, 2914–2915
in preeclampsia-eclampsia, 2735
in renal function, 455–456
as uremic toxins, 3042
uric acid nephrotoxicity and, 3036
Receiver-operator curves (ROC), 2579–2580, 2579*f*
Receptor tyrosine kinases, 374–375, 374*f*
in MAPK signaling, 386, 387*f*
Receptor-like phosphatases, in signaling, 377–379, 378*f*
Receptor-mediated endocytosis, 633–634, 633*f*
Receptor(s), 375–376, 376*f*, 1985, *see also* Baroreceptors
angiotensin, 372, 372*f*, 429–431, 436–437
in medullary circulation, 438
in aquaporin-2 channels, 1422–1423
arginine vasopressin, 371–372
atrial natriuretic peptides, *see* Natriuretic peptide receptors (NPR)
calcitonin, 2261
calcium sensing, 2187–2190, 2273–2276
cell-surface, 369–383, *see also* Signaling
cholinergic, 1984
c-kit, 960
classification of, 370–376
dopamine, 371
epidermal growth factor, 374
erythropoietin, 3090–3092, 3091*f*
Fc
in antineutrophil cytoplasmic autoantibody vasculitis, 2836–2837
in immune complex vasculitis, 2829
Frizzled, 381–382
G-protein-coupled, 369–376, 374*f*, *see also* G-protein-coupled receptor(s)
glucocorticoid, 1182–1183, 1194–1196
growth factor, 374–375, 374*f*, 2559
hepatocyte growth factor, 375
heterologous desensitization and, 371
homologous desensitization and, 371
IgG, in immune complex vasculitis, 2829
IGF1, ureteric bud and, 876
IgG Fc, *see* Receptor(s)
kinase, 374–375, 374*f*, *see also* Kinase receptors
serine/threonine, 375–376, 376*f*, 384
in signaling, 374–375, 374*f*, 376*f*
tyrosine kinase, 374–375, 374*f*
ligand-binding domains of, 369
long-acting natriuretic peptide, 1260
mineralocorticoid, 431, 1194–1196, 1215–1216
activation of, mutations and, 1216–1220
ASDN cells and, 1182–1183
in TAL, 1184–1185
NPR-A, 1259
NPR-C, 1259
nucleotide, 164–165
parathyroid hormone, 373, 2259
pattern recognition, 2988–2989
peroxisome proliferator-activated, 2899–2900
platelet-derived growth factor, 374
protein tyrosine phosphatase, 377, 378*f*
proteolytic cleavage-activated, 377–379, 378*f*
purinergic, *see* Nucleotide receptors
Ret tyrosine kinase, 375
retinoic acid, in renal development, 872
serine/threonine, 375–376, 376*f*, 385
in PI 3-K signaling, 389, 390*f*
in signaling, 369–383, *see also* Signaling
thrombopoietin, 3111–3112
toll-like
in acute kidney injury, 2988–2993
endotoxin and, 2991
transactivation of, 373
vascular endothelial growth factor, 374
vessel dilator, 1260
vitamin D, 2254
Recombinant erythropoietin, 3087–3088
for renal anemia, 3107
Recombinant thrombopoietin, 3111
Red cell cation leak syndromes, SLC4 in, 1876*t*
Red cell(s)
anion exchanger deficiency diseases of, 1888
production of, *See* Erythropoiesis; Erythropoietin
Refeeding syndrome, hypophosphatemia in, 2380
Reflection coefficient, 276
Reflux nephropathy, in pregnancy, 2719*t*, 2720
Regression
of diabetic nephropathy, 2622
Regulated on activation normal T cell expressed and secreted (RANTES), 2466
Regulatory volume decrease (RVD), 1034–1035
Relaxin, in pregnancy, 2694
Remission Clinic Program, 2977–2978
Renal amyloidosis, 2792
Renal anatomy
cortex, 610–612, 611*f*, 612*f*, 613*f*
crest kidney, 595
epithelium, *see* Epithelium
glomerulus, 616–627, 617*f*
histotopography and, 611*f*, 615–616
interstitium, 602–608

medulla, 595, 596*f*, 612–616, *see also* Renal medulla
multipapillary kidney, 595, 596*f*
nephron and collecting duct system, 600–602
nerves, 609*f*, 610
periarterial connective tissue and lymphatics, 608–610
in pregnancy, 2689–2691, 2691*f*
reniculus kidney, 595
segments of, 603*f*
terminology of, 603*f*
topographical relationships in, 610–616
unipapillary kidney, 595, 596*f*
urine concentrating mechanism and, 1464–1469, 1464*t*, 1465*f*, 1466*f*, 1467*f*
vascular, 595–600, 596*f*, 597*f*, 598*f*, 599*f*, 600*f*
Renal anemia, *see* Anemia
Renal artery, anatomy of, 595–596
Renal artery angioplasty, 2595–2596, 2595*t*
Renal artery constriction/aortic coarctation, 1345
Renal artery revascularization
angioplasty in, 2595–2596, 2595*t*
indications, 2578
results of, 2594*t*, 2595, 2595*t*
stenting in, 2596–2598, 2596*f*
utilization trends for, 2578
Renal artery stenosis, 2596–2598, 2596*f*
atherosclerotic, *see* Atherosclerotic renal artery stenosis
causes of, 2590*t*
clinical syndromes associated with, 2589*t*
ischemic nephropathy in, *see* Ischemic nephropathy (IN)
severity, 2592
sonographically determined resistance index in, 2581–2583
revascularization for, *see* Renal artery revascularization
Renal biopsy, in pregnancy, 2712
Renal blood flow (RBF), 803, 2542–2543
angiotensin II in, 437
cyclosporine and, 3169*t*, 3170–3171
denervation, 456–457
intra-renal haemodynamics, 457
measurement, 457
sympathetic nerve stimulation, 457
nephrotoxic drug effects and, 2890–2892
osmotic diuretics and, 1356
postnatal development of, 911
redistribution, to proximal and distal tubules, 1251–1252
regional, measurement of, 818–819, 818*f*, 819*t*
regulation of, 391, 392*f*
renin-angiotensin system and, 437–438
sympathetic nerves, 456
Renal calcium transport, 2235–2236
Renal calculi, *see* Nephrolithiasis
Renal calyx
anatomy of, 595, 596*f*
in pregnancy, 2689, 2691*f*
Renal channelopathies, 249*t*
Renal colic, in nephrolithiasis, 2312
Renal corpuscle, *see* Glomerulus
Renal cortex, *see also* Cortical
anatomy of, 595, 596*f*, 610–612, 611*f*, 612*f*, 613*f*
capillary uptake of tubular reabsorbate and, 809–810
macromolecules transport in, 816–817
Renal cortical necrosis, in pregnancy, 2714–2715
Renal cysts and diabetes syndrome, 2155
Renal denervation, 451
Renal development
apoptosis prevention during, 879–880
cell culture models, 866–867
cell-locating signaling in, 380–382, 381*f*, 383*f*
coarse grained models of, 868
ECM in, 876
experimental approaches to, 861–867
extracellular proteinases in, 878
fibrillin1 in, 878
gene knockout technology, 865–866
glomerular basement membrane, 901–904
glomerular capillaries in, *see* Glomerulus
glomerular development, 881–882
growth factors in, 874
EGF, 876
FGF, 874
GDNF, 874
glomerular development and, 894–895
HGF, 876
IGF, 876
pleiotrophin, 875
secreted frizzled-related proteins in, 875
TGFβ, 875
WNT2b, 875
laminin in, 877
mesangial, 896–897
mesonephros in, 859
metanephros in, 859–861, 860*f*
molecular approaches to, 867–868, 867*f*, 868*f*
overview, 859, 860*f*
postnatal, 911
potassium transport and, 1698–1699
pronephros in, 859
proteoglycans in, 877–878
retinoic acid in, 872
termination of, 882
transcription factors in, 868–872
tubulogenesis in, 878–881, 880*t*
tyrosine kinase receptors in, 375, 377
vascular development, 881–882
Renal dialysis, *see* Dialysis
Renal disease
epithelial cell polarity and, 32–34
hyperfiltration theory, 3033
in pregnancy, 2711–2716
progression of, 3056–3059
apoptosis in, 2968–2969
complement in, 2973–2975
dietary protein and, 3035–3036
fibrogenesis in, 2971–2972
hemodynamic mechanisms of, 3033–3036
in hypertension, 3033
low-protein diet and, 3056–3059, *see also* Low-protein diet
in diabetes mellitus, 3056
protein-bound lipids in, 2976–2977
proteinuria in, 2961
uric acid in, 3035
Renal drug disposition, *see* Drug disposition
Renal dysfunction
severity and acuity of, 2593
Renal epithelium, *see* Epithelium
Renal failure
acute, *see also* Acute kidney disease
ADM in, 1264
aquaporins in, 1426–1427
BNP in, 1264
CNP in, 1264
DNP in, 1264
hypercalcemia in, 2292–2293
natriuretic hormones in, 1260–1264
in pregnancy, 2714
salt wasting in, 1310
urodilatin in, 1262–1263
vessel dilator in, 1263–1264, 1263*f*
chronic, *see also* Chronic kidney disease
anemia in, 3107–3108
aquaporins in, 1427
atherosclerotic renal artery stenosis and, *see* Atherosclerotic renal artery stenosis
bleeding in, anemia due to, 3107
diabetes insipidus in, 1556
end-stage renal disease in, 3026–3027, *see also* End-stage renal disease
hypercalcemia in, 2292–2293
hyperparathyroidism in, 3075–3077
hyperphosphatemia in, 2382
idiopathic postpartum, 2715
metabolic acidosis in, 2079
organic cation transporters in, 2445–2446
in polycystic kidney disease, 2649
potassium metabolism in, extrarenal, 1642–1643
in pregnancy, 2716–2724, *see also* Pregnancy
progression of, *see* Renal disease
uremic toxins in, 3038–3039
Renal glycosuria, familial, *see* Familial renal glycosuria (FRG)
Renal hemodynamics, 552–554, *see also* Glomerular hypertension; Renal blood flow (RBF)
D_1-like receptors, 552
D_2-like receptors, 552–553
dietary protein and, 3033–3036
in disease progression, 3033–3036
glomerular filtration, 553–554
renin-angiotensin system in, 437–438, *see also* Renin-angiotensin system
tubuloglomerular feedback, 554
Renal hyperplasia
assessment of, FACS and, 934, 937–945
cell cycle and, 934–937
cell growth, measurement of, 934
defined, 933

Renal hyperplasia (*Continued*)
in diuretic resistance, 1390–1394, 1391*f*, 1392*f*, 1393*f*
glomerular, 937–938, 937*f*, 938*f*
intracellular pH in, 1815
in metabolic acidosis, 2061
overview, 933–934
tubular, 945
Renal hypertrophy, 945–947
cell cycle and, 934–937, 934*f*
cell growth, measurement of, 934
defined, 933–934
in diuretic resistance, 1390–1394, 1391*f*, 1392*f*, 1393*f*
glomerular, 945–947
overview, 933–934
tubular, 947–951, 949*t*, 950*t*
Renal hypoperfusion, *See* Hypoxia; Ischemia
Renal inflammation, *see also* Inflammation
dopamine receptors, 568
Renal innervation, 451
efferent innervation, 451–452, 452*f*
para-vertebral ganglia, 451–452
pre-ganglionic nerve fibers, 451–452
intrinsic innervation, 452
neuro-effector junctions, 452, 453*f*
Renal insufficiency
chronic, hyperkalemia in, 1758
Renal interstitium, *see* Interstitium
Renal ion channels, 217
with recognized function, 219*t*
Renal ischemia, *see* Ischemia
Renal isoforms
of V-ATPases, 83
Renal lymphatics, 608–610, 608*f*
Renal medulla, *see also* Medullary
anatomy of, 595, 596*f*, 612–616
complex-type, 613–615, 613*f*
countercurrent exchange of solutes and water, 668–669
countercurrent multiplication in, 810, 1474–1488, 1475*f*, *see also* Urine concentration
countercurrent solute-water exchange in, 1476
histotopography of, 611*f*
inner, 612, 665
passive mechanism hypothesis for, 1480–1481
macromolecules transport in, 816–817
mass balance in, 1479–1480
outer, 611*f*, 612
inner stripe of, 611*f*, 612, 614*f*, 616*f*, 665
potassium reabsorption in, 1676
outer stripe of, 611*f*, 612, 612*f*, 614*f*, 665–668, 666*f*
potassium reabsorption in, 1676
potassium recycling in, 1667–1668
simple-type, 613–615, 613*f*
urea recycling, 669–670
in urine concentration, 663–670
vascular bundles of, 612, 612*f*, 614*f*
Renal medullary interstitial cells (RMIC), 806–807
Renal morphogenesis, 959–960
Renal nerves, *see also* Nerves; Renorenal reflexes
analysis, 462–463
central nervous system, 466–467
brain angiotensin II, 466–467
central processing, 466
electrical stimulation, 461–463
efferent activity, 461
haemodynamics, 462
stimuli, 461–462, 462*f*
functionalities, 460–461
men, neural regulation in, 468
reflex regulation, 463–466
cardiovascular baroreceptors, 463–464
higher cortical centers, 465
selective functions, 465–466
somatosensory system, 464
visceral system, 464–465
Renal osteodystrophy, 2249
calcium transport and, 2238
in hyperparathyroidism, 3075–3076
treatment of, 3079*t*, 3081–3083, 3082*t*
Renal outer medullary potassium channel (ROMK), *see* ROMK
Renal pelvis
anatomy of, 595, 596*f*
in pregnancy, 2689, 2691*f*
Renal plasma flow, *see also* Renal hemodynamics
in pregnancy, 2691–2699, 2717
in preeclampsia, 2737
Renal replacement therapy (RRT), 2527, 2641
Renal salt homeostasis
overview of, 1214–1216, 1215*f*
Renal transplant rejection, 1844
Renal transplantation
for Alport syndrome, 2856
calcium balance after, 3162–3163, 3164*f*
in congenital nephrotic syndrome of Finnish type, 2863–2865
endothelin in, 3168–3169
erythropoiesis after, 3108–3109
hypercalcemia and hyperparathyroidism following, 2207–2208
hyperuricemia after, 3166–3167
hypophosphatemia in, 2380
immunosuppression in, 3151, 3175
cyclosporine in, 3167, 3168*f*, 3170*f*, 3173*f*
tacrolimus in, 3174–3175
magnesium balance in, 3174
natriuretic hormones in, 1261
phosphate balance after, 3164–3165
polycythemia after, 3109
potassium balance after, 3157–3158
in pregnancy, 2722–2723
solute and water regulation after
animal studies of, 3153
in azotemic solute-loaded recipient, 3156–3158
glomerular filtration rate and, 3152–3153
immunosuppression and, 3151, 3175
ischemia and, 3154–3155
in rejection, 3158–3160
renal tubular acidosis and, 3160
twin studies of, 3153–3154
tubular function in, 3152, 3153*f*
Renal transport, *See* Ion transport; Solute transport; Water transport
Renal transport proteins, types of, 221*f*
Renal tubular acidification, 1917–1941
aldosterone in, 2092–2093, 2093*f*
ammonia excretion and, 919–920
carbonic anhydrase in, 920
cyclosporine and, 3171
defects in, *see* Renal tubular acidosis
in distal nephron, 919, 1943–1959
angiotensin II in, 1959
antidiuretic hormone in, 1958
basolateral chloride channels in, 1951
basolateral hydrogen extrusion in, 1952–1953
carbonic anhydrase in, 1953–1954
chloride delivery in, 1957–1959
cortical collecting duct in, 1944*f*, 1945–1948, 1946*f*, 1954–1957
distal tubule in, 1944–1945, *see also* Renal tubular acidosis
endothelin in, 1958
H-ATPase in, 1948–1950, 1949*f*, 1956
H,K-ATPase in, 1950
inner medullary collecting duct in, 1947–1948
isoproterenol in, 1958–1959
mineralocorticoids in, 1957–1958
models of, 1944*f*
NHE3 in, 1938–1941
outer medullary collecting duct in, 1947
parathyroid hormone in, 1958
peritubular and luminal pH in, 1954–1957
potassium depletion and, 1958–1959
prostacyclin in, 1959
regulation of, 1954–1957
sodium delivery in, 1957–1959
transepithelial voltage in, 1957–1959
postnatal development of, 917–920
in proximal tubule, 917–919, 1917–1941
aldosterone in, 1940
angiotensin II in, 1940
apical membrane mechanisms in, 1917–1918, 1918*f*, 1923*f*
basolateral membrane mechanisms in, 1924–1927
carbonic anhydrase in, 1930–1931
catecholamines in, 1941
chloride/OH exchange in, 1922–1923, 1927–1928, 1929*f*
defects in, 2081–2083
electrogenic sodium-bicarbonate cotransport in, 1924–1927, 1935
endothelin in, 1940
extracellular fluid volume and, 1938
glucocorticoids in, 1941
H-ATPase in, 1919
hydrogen leak in, 1923–1924, 1923*f*, 1928
hydrogen secretion vs. bicarbonate absorption in, 1917–1918
insulin, 1941
luminal bicarbonate and pH and, 1931–1932

luminal flow rate and, 1932–1933
luminal pH and, 1931–1932
Na/H antiporter in
apical-membrane, 1919, 1921*f*, 1923
basolateral-membrane, 1924–1927, 1935, 1935*f*
NHE3 in, 1917–1918, 1920–1921, 1921*f*, 1935, 1935*f*
parathyroid hormone in, 1938
in potassium depletion, 1937–1938
primary active, 1919
secondary active, 1918–1919, 1921*f*
tertiary active, 1918, 1921–1922
regulation of, 1931–1933
titratable acid and, 919–920
in transplant recipients, 3161
Renal tubular acidosis, 2335–2336, *see also* Metabolic acidosis
distal
anion exchanger absence in, 1896–1897
autosomal dominant, 2086
causes of, 2086*t*
diagnosis of, 2088–2090
generalized, 2092–2093
with hearing loss, 2087
hyperkalemic, 2092–2093
hypokalemic, 2085–2086
pathophysiology of, 2011–2012, 2030–2031
primary/inherited, 2086–2087
proximal, 2012, 2083
vs. distal, 2012
recessive, anion exchanger and, 1893*f*
salt wasting in, 1310
secondary, 2087–2088
SLC4 mutations in, 1880–1881, 1889–1896, 1892*f*, 1893*f*
treatment of, 2090–2091
familial proximal, 1840–1841
hyperkalemic, 2092–2093
cortical collecting duct abnormalities and, 2096
drug-induced, 2096–2098, 2096*f*
in hyporeninemic hypoaldosteronism, 2094–2096
in mineralocorticoid resistance, 2096
primary, 2093
in primary adrenocortical deficiency, 2093
in pseudohypoaldosteronism, 2096
secondary, 2096
hypokalemic
distal (classic), 2085–2086
proximal, 2081–2088
inherited mixed, 2083
potential mutant-specific therapy, 1843
proximal, 2081–2083
autosomal dominant, 2083, 2086
autosomal recessive, 2087
causes of, 2083*t*
diagnosis of, 2088, 2090
with distal type, 2083
hypokalemic, 2081–2088
with ocular abnormalities, 2083
pathophysiology of, 2081–2083, 2082*f*
primary, 2083
salt wasting in, 1310
secondary, 2083–2085
treatment of, 2091
in transplant recipients, 3160
Renal tubular and interstitial damage, albumin induced, 2464–2466
apoptosis, 2464–2465
ER-stress, 2465–2466
Renal tubular apoptosis, ischemic, 165–166
Renal tubular hypertrophy, 947–951, 949*t*, 950*t*
angiotensin II, 948
transforming growth factor β, 947–948
Renal tubular necrosis, ischemic, 165–166
Renal tubular system, 1181–1182, 1182*f*
Renal tubular uptake, of L-DOPA, 541
Renal tubule(s), *see also* Tubular
cell types of, 603*f*
connecting, *see* Connecting tubule (CNT)
distal convoluted, *see* Distal convoluted tubule (DCT)
intermediate tubule, 603*f*, 635–640, 636*f*, *see also* Intermediate tubule
nerves of, 610
neuronal influences on, 610
in pregnancy, 2699–2702
proximal, 603*f*, *see also* Proximal tubule
segmentation of, 603*f*
terminology for, 603*f*
Renal vein, anatomy of, 595–596
Renal vessels
anatomy of, 595–600, 596*f*, 597*f*, 598*f*, 599*f*, 600*f*
development of, 881–882
nerves accompanying, 610
specialized fornices of, 595, 596*f*
wall structure of, 599–600, 599*f*
Reniculus kidney, 595
Renin, *see also* Mineralocorticoids; Renin-angiotensin system
in angiotensin synthesis, 427, 432
biosynthesis of, 427, 432–433, 437
deficient, hypoaldosteronism and, 1759–1761
granular cells in, 432–433, 433*f*
mast cells in, 434
cellular release of, 436–437
cyclooxygenase-2 and, 781–782
deficiency of, hypoaldosteronism and, 2094–2096
expression of
in connecting tubule, 433–434
extrarenal, 434
functions of, 427–428
gene expression for, 437
in metabolic alkalosis, 2038
in pregnancy, 2700–2701, 2702*f*, 2708–2710, 2709*f*
regulation of, 432–438
adenosine in, 783–784
baroreceptors in, 433–434
calcium in, 436
cAMP in, 436–437
macula densa in, 432, 433*f*, 434
nitric oxide in, 434, 780–781
prostaglandins in, 435, 781–783
short-loop feedback in, 436
sympathetic nerve activation in, 436
secretion of, 778–785
ion specificity and, 779–780
loop diuretics and, 1365–1366, 1366*f*
organic compounds and, 780
in signaling, 427–428
sources of, 432–434
Renin release, 458–460
granular cells, 458–459
exocytosis, 459–460
intracellular signaling pathways
adenyl cyclase, 459
cAMP, 458–460, 459*f*
cytosolic calcium, 458–459
L-type calcium channel, 459
mRNA, 458–460
nerves' stimulation, 459–460
neural and non-neural interactions, 460
Renin secretion
calcium-sensing receptor and, 2201–2202
Renin-angiotensin system, 427–432, 474
in albuminuria, 2462–2463
aldosterone in, 431–432
angiotensin receptors in, 429–431
angiotensin-converting enzyme in, 429, 430*f*
angiotensinogen in, 428–429, 430*f*
in blood pressure regulation, 432, 433*f*
components of, 427–432
cyclosporine effects on, 3172
functions of, 437–438
integrated actions of, 432
overview of, 427
renal hemodynamics and, 437–438
glomerular microcirculation in, 437
renal epithelium in, 438–440
renal medullary circulation in, 438
tubular function in, 440
renin in, 427–428, 430*f*, 432–438, *see also* Renin
in tubuloglomerular feedback adaptation, 774–775
Renin-angiotensin-aldosterone system (RAAS), 728, 2530
in congestive heart failure, 1289–1290
cyclosporine effects on, 3172
in diabetic nephropathy, 2618–2620
disorders
renal salt loss, 1225–1227
renal salt reabsorption, 1215–1216, 1215*f*
urodilatin and, 1254
in diuretic adaptation, 1390
drugs interfering with, 1762–1764
in extracellular fluid balance, 1289–1290, 1291*f*
genetic disorders of, 1216–1221
hypertension, 1328–1329
kaliuretic peptide and, 1253
LANP, 1253, 1253*f*
in nephrotic syndrome, 1307–1308
in postnatal sodium transport, 916–917
in pregnancy, 2700–2701, 2702*f*, 2708–2710, 2709*f*
sodium excretion and, 1307–1309

Renoguanylin, biological effects of, 1256–1257
Renorenal reflexes, 469–479
  dorsal rhizotomy (DRX), 469–470
  efferent and afferent nerves, 471
  excitatory reflexes, in injured/diseased kidneys, 478–479
  mechanosensory nerves, 469
    α-adrenoceptors, 474–475
    angiotensin II, 474
    bradykinin, 475
    cAMP-protein kinase A (PKA), 474
    CGRP and, 473
    endothelin, 476–477
    impairment of, 477–478
    natriuretic nature of, 470–471
    pathophysiological conditions, 477–479
    PGE receptors, 474
    physiological conditions, 470–477
    prostaglandin E_2 (PGE_2), 474
    substance P and, 468*f*, 471–474
    TRPV1 and, 473–474
  overview, 469
Renovascular hypertension (RVH), 1345
  diagnosis of, 2579–2580, 2579*f*
  revascularization for, *see also* Renal artery revascularization
Reperfusion injury, mitochondrial, 166
Resistance index, in renal artery stenosis, 2581–2583
Respiration, *see also* Breathing; Ventilation
  mitochondrial, 149–150, 150*f*
    disorders of, 165
    regulation of, 158–159
    solute transport and, 158–159
Respiratory acidosis
  cerebrospinal fluid composition, 2120
  diagnosis of, 2123
  hemodynamic consequences of, 2121–2122
  intracellular pH during, 1806–1807, 2120
  management of, 2123–2126
    alkali therapy, 2126
    assisted ventilation, 2124–2125
    oxygen administration, 2123–2124
    pulmonary function improvement, 2125
  and metabolic acidosis, 2126–2127
  and metabolic alkalosis, 2127
  mixed acid–base disorders associated with, 2126–2127
    respiratory acidosis and metabolic acidosis, 2126–2127
    respiratory acidosis and metabolic alkalosis, 2127
  pathophysiologic effects and clinical manifestations of, 2120–2123
    cardiovascular, 2121–2122
    immune response, 2122
    neurologic, 2120–2121
    renal and metabolic, 2123
    respiratory, 2122
    skeletal, 2123
  pathophysiology, 2113–2120
    carbon dioxide transport, failure, 2116–2117
    function of respiratory muscles, 2114–2115
    overproduction of CO_2, 2116
    plasma electrolyte composition, 2120
    pulmonary ventilation, chemical stimulus for, 2114
    secondary physiologic response, 2117–2120
  potassium metabolism in, 1640–1641
  primary hypercapnia, 2113, *see also* Respiratory acidosis
Respiratory alkalosis, 2127
  definition of, 2021
  diagnosis of, 2135
  hypophosphatemia in, 2378–2381, 2379*f*
  intracellular pH during, 1807, 2133
  management of, 2135
  mixed acid–base disorders associated with, 2135–2136
  pathophysiologic effects and clinical manifestations of, 2133–2135
  pathophysiology, 2127–2133
  posthypocapnic hyperchloremic acidosis in, 2099–2100
  potassium balance in, 1640–1641
Respiratory compensation, in metabolic acidosis, 1980–1981, 1981*f*, 2055, 2055*f*, 2056*f*, 2057*f*
Respiratory control index, 158–159
Respiratory dysfunction
  SIADH in, 1520
Respiratory muscles, function of, 2114–2115
Ret tyrosine kinase receptor, 375
Retinoblastoma protein (pRb), 935–936
Retinoic acid (RA)
  for glomerular hyperplasia
    mesangial, 940
    podocyte, 944
  hypercalcemia due to, 2292
Retinoic acid receptor genes, in renal development, 872
Retrotrapezoid nucleus, chemoreceptors in, 1982–1983, 1982*f*, 1985
Rhabdomyolysis, 3008
  AKI in, 2533
RhBG, in ammonium transport, 2009–2011
RhCG, in ammonium transport, 2009–2011
Rho GTPases, 738–739
  in acute kidney injury, 2540
Rho kinase, in vascular smooth muscle regulation, 391
Rhodamine-based dyes, in intracellular pH measurement, 1778
Rhubidium-86 methodology, 457
Rickets
  autosomal dominant hypophosphatemic, 2380–2381
  vitamin D-dependent, 2298–2299
  X-linked hypophosphatemic, 2381
RNA, aldosterone-regulated, 1202–1203
Robo2 gene, 872
ROMK, 227, 235, 394–395, 1606*f*, 2492, *see also* Renal outer medullary potassium channel (ROMK)
  AKAPs and, 419
  CFTR as regulator of, 1029
  gating, molecular basis of, 247–248
  isoforms of, 1604–1605, 1606*f*
  localization of, 1605, 1606*f*
  molecular basis of rectification in, 246–247
  phosphorylation of, 1608–1609
  pore characteristics of, 1605–1614, 1610*f*
  in potassium balance, 1673–1675, 1747
    low-potassium diet and, 1678–1679, 1681*f*
  regulation of, 1608–1614, 1610*f*
  selectivity and permeation, 245–246
  structure of, 1601–1604, 1602*f*
  ubiquitination and, 1611
  WNK and, 1609–1610
Roscovitine
  for glomerular hyperplasia
    mesangial, 940
    podocyte, 944
  for polycystic kidney disease, 2674
Rostral aspect of ventral respiratory group, chemoreceptors in, 1982–1983, 1982*f*, 1985
Rostral ventrolateral medulla (CVLM), 466–467
Rough endoplasmic reticulum (RER), 21
Rubbing alcohol poisoning, metabolic acidosis in, 2068
Ruthenium red, epithelial calcium ion channels and, 2174

S

SAGE (Serial Analysis of Gene Expression), 1203
Salicylate overdose, 2077–2078, 2081*t*
Salicylate transporters, 2436
Salicylates, for preeclampsia prophylaxis, 2738–2739
Sall1 gene, 870
Salt, *See* Sodium; Sodium chloride
Salt intake
  fluid and electrolyte balance and, 2478, 2479*f*
  in metabolic alkalosis, 2025, 2031
  in nephrolithiasis, 2322
  potassium excretion and, 1683*f*, 1687–1691
Salt wasting, 1309–1311
  in acute renal failure, 1310
  in Bartter syndrome, 1310
  cerebral, 1311, 1311*f*, 1521–1523
  in chronic kidney disease, 1309–1310
  in Gitelman syndrome, 1310
  mineralocorticoids and, 1310–1311
  in renal tubular disorders, 1310
Salt-losing nephropathy, sodium balance in, 300
Salt-sensitivity hypertension
  increased renal tubular sodium reabsorption, 1325
  nephron loss, 1325
  and organ injury, 1326
  significance, 1325–1326
SAP-97 proteins, 414–416, 415*f*
Sarcoidosis, hypercalcemia in, 2290–2291
Sca-1, stem cell marker, 963–964
Scaffolding proteins, 405
  AKAP, 417

dystrophin-associated, 416–417, 417*f*
NHERF, 408–409, 409*f*
overview of, 405
PDZ, 405
in signaling, 373, 380
in MAPK pathway, 386–388
SCH-28080, in H,K-ATPase inhibition potassium reabsorption and, 1676
Schistosomiasis, 2789–2790
Scleroderma, pregnancy in, 2719*t*, 2720
SCNN channels, 236
Scribble complex, 19
Second transmembrane domain (TM2), 990–992
Secondary hyperparathyroidism
calcium-sensing receptor modulation in, 2204–2207
Secreted frizzled-related protein (sFRPs)
in phosphate balance, 2253–2254, 2369–2370, 2376–2377, 2377*f*
in renal development, 875
Seizures
eclamptic, 2728, 2731, *see also* Preeclampsia-eclampsia
hypernatremia due to, 1554*t*, 1559
treatment of, 2742, 2742*t*
Self-organizing map (SOM), 867, 868*f*
Semipermeable membranes, osmotic equilibrium and, 95–96, 96*f*
Sensenbrenner Syndrome, 341
Sepsis
acute kidney injury in, 2549–2557
hypophosphatemia in, 2379–2380
Septic abortion, 2714
Septins, 21
SERCA, 67–68
SERCA1a, 61–62
Serine proteinases, in vasculitis, 2825–2827, 2827*f*
Serine/threonine receptors, 375–376, 376*f*, 386–388
in PI 3-K signaling, 389, 390*f*
Serotonergic neurons, as chemoreceptors, 1983
Serotonin, in phosphate balance, 2374
Serum sickness vasculitis, 2828, *see also* Vasculitis
SeSAME disease, 1150–1151
SeSAME/EAST syndrome, 1231
Set point hypothesis, 299
Sevelamer, *see also* Phosphate binders
for hyperparathyroidism, 3079, 3081–3083, 3082*t*
Sex hormones
antidiuretic hormone and, 1450
biosynthesis of, 2093–2094, 2095*f*
in pregnancy, renal hemodynamics and, 2694
sFlt-2, in preeclampsia-eclampsia, 2740
SGLT2 transporters, 634
SH2 domains, tyrosine kinase receptors and, 374–376
Shank proteins, 413–414, 413*f*
Shear stress, in renal artery stenosis, 2587
Shock wave lithotripsy, 2341
Shohl's solution, for distal renal tubular acidosis, 2091
Short-circuit current technique, 184–186, 185*t*
Sialidosis, 2863
Sickle cell disease, polyuria in, 1557
Side Population discrimination assay, stem cells, 965–966
Side population (SP) cells, 965–966
Signal transducer and activator of transcription (STAT), 2466
Signaling, 369–383
in acute kidney injury, 2555
adenyl cyclase in, 370, 370*f*
adherens junctions in, 380–381, 383*f*
in albumin metabolism, 2465*f*
arachidonic acid, 2673
calcium-sensing receptor in, 2189–2190
catenins in, 381, 383*f*
in cell volume regulation, 130–131, 130*f*
cell-location, 380–382, 381*f*, 383*f*
cell-cell interactions in, 380–381, 383*f*
cell-matrix interactions in, 380, 381*f*
cilia in, 382–383
cross-talk in, 386–388
cyclic AMP, 2671–2672
in diabetic nephropathy, 2616
downregulation in, 371
effector proteins in, 390–391
ERK MAPK pathway in, 386
in erythropoiesis, 3100–3105, 3101*f*
first messengers in, 369
focal adhesions in, 380, 386
gap junctions in, 381–382
in glomerular filtration rate regulation, 391, 392*f*
glomerular vascular smooth muscle and, 391
G-protein coupled receptor, 2667–2668
heterologous desensitization in, 371
homologous desensitization in, 371
integrins in, 380, 381*f*
JAK/STAT pathway in, 2970
JNK pathway in, 388
MAPK pathway in, 386–388, 387*f*
of MAPK (Ras/Raf/MEK/ERK) inhibitors, 2672
in metabolic acidosis, 2005–2007, 2011–2012
in muscle protein metabolism, 3049–3053
Notch proteins in, 377–378, 379*f*
overview of, 369
PHC pathway in, 372–373, 372*f*, 375–376, 384–386, 385*f*
PI 3-K pathway in, 389–390, 390*f*
PLC pathway in, 376
in polycystic kidney disease, 2664–2666
protein tyrosine phosphatases in, 377–379, 378*f*
in proteinuria, 2969–2973
receptor transactivation in, 373
receptor-like phosphatases in, 377–379, 378*f*
receptors in, 369–383, *see also* Receptor(s)
G-protein-coupled, 370–376, 370*f*, 372*f*
kinase, 373, 374*f*, 376*f*
protein tyrosine phosphatase, 377–379, 378*f*
proteolytic cleavage-activated, 377–379, 378*f*
renin-angiotensin system in, 427–428
scaffolding proteins in, 380, 405, *see also* Scaffolding proteins
signal amplification in, 370–371
at slit diaphragm, 900–901
smads in, 376
in solute transport, 158, 158*f*, 164, 391–395
Src pathway in, 375, 380
transforming growth factor β receptor in, 376, 376*f*
in vasoconstriction, 391, 392*f*
in water transport, 393–394
WNK kinases in, 395
Wnt pathway in, 381–382
in polycystic disease, 2664–2666
Singer-Nicholson fluid-mosaic model, 46, 46*f*
Single nephron filtration fraction (SNFF) and GPF estimation, 766
Single nephron glomerular filtration rate (SNGFR), 696, 700–701, 950, 1361
distal tubule flow perturbations on, effects of, 761–762
lat proximal flow rate and, 761*f*
MD NaCl Concentration on, effects of, 763, 763*f*
Single nucleotide polymorphisms (SNPs), 1214
in organic cation transporters, 2428
Single-channel recording, 198–201, 200*f*, 201*f*
Single-file pore water flow, 98
Sirolimus, 2673
SITS, anion transport inhibitor, 1095
Six1/2 gene, 869–870
Skeleton
calcium-sensing receptor and, 2202–2203
SKI-606, 2672
Skin, vitamin D metabolism in, 2251
SLC transporters, 3188–3189, *see also* Transporters
SLC4, 1862*f*, 1863–1864
acute regulation of, 1885–1886
anion conductance and, 1882
anion exchange C-terminal transmembrane domain, binding proteins and, 1873–1875, 1873*f*, 1876*t*
anion exchange deficiency and, 1888
anion exchange domain structure of, alternative transcripts and, 1863–1864, 1863*f*, 1864*f*, 1866*f*
anion translocation pathway and, 1881–1882
C-terminal cytoplasmic tail of, 1882–1884
cytoplasmic domain, binding proteins and, 1865–1871, 1867*f*, 1868*f*, 1869*t*
mechanisms of anion exchange and, 1873–1880
pharmacology of, 1880–1881
Slc4 sodium-driven bicarbonate transporters
AE4 (SLC4A9 gene), 1852–1853
dendrogram of, 1838*f*
functional categorization of, 1837–1839

Slc4 sodium-driven bicarbonate transporters (*Continued*)
NaBC1 (*SLC4A11* Gene), 1851
NBCe2
functional properties, 1846–1847
hypertension, 1847
structural variants and tissue distribution, 1846
targeted disruption in mouse, 1847
NBCE-1 function
in the kidney, 1843–1847
molecular regulation of, 1844–1846
various organs, 1844
NCBE/NBCn2 (SLC4A10 gene), 1850–1851
NDCBE (SLC4A8 gene), 1849–1850
sodium bicarbonate cotransporters
electrogenic, 1839–1843
Slc4 sodium-driven bicarbonate transporters
electroneutral, 1847–1849
targeted disruption of, 1841–1842
SLC12 gene family
as gene encoding NKCC2, 1053–1054
phylogenetic tree of, 1047–1048, 1048*f*
SLC17A1, 2431–2432
SLC17A3, 2432
SLC20 proteins, 2355–2357
SLC22A4, 2446
SLC22A5, 2446
SLC22A6, 2427–2428
SLC22A7, 2428
SLC22A8, 2428–2430
SLC22A9, 2430
SLC22A12, 2431
SLC22A13, 2430–2431
SLC22A19, 2430
SLC26 family, 1094, 1861–1863
SLC 34, 2354–2356
SLC47A1, 2446–2447
SLC47A2, 2447
SLCO1A1, 2432–2433
SLCO1A3, 2432–2433
SLCO4C1, 2429
SLGT1, 634
Slit diaphragm (SD), of podocytes
α-actinin-4, 738
assembly mechanisms, 900
cadherin and catenins, 737–738
components, 898–900
disorders of, 2848*t*, 2863–2867
FAT1, 738
formation of, 898–901
Neph proteins, 736–737
nephrin, 736
podocin, 736
Rho GTPases, 738–739
signaling at, 900–901
Slit2 protein, 872
Smads, 376
Small bowel resection, 2336–2337
Small intestine, *see also* Intestinal
in acid–base balance, 312–315, 2052
calcium-sensing receptor in, 2204
Small ventral surface cells, as chemoreceptors, 1985
Smith, Homer, 451, 695
α Smooth muscle actin (αSMA), 972
SN1 transporter, in metabolic acidosis, 1999, 1999*f*
SNAP-Tag, 23
SNARE proteins, 32
in ENaC regulation, 998
in water transport, 394
Sodium, *see also* Na
availability, Na,K-ATPase expression regulation and, 79
concentration in peritoneal dialysis, 3129–3130
dietary, *see* Salt intake
disturbances in hemodialysis, 3125–3129
excretion of
antidiuretic hormone and, 1291
assessment of, 2478–2484, 2480*t*
atrial natriuretic peptide and, 1291–1292
effective vascular volume and, 301–302
fractional, 2481–2483
kallikrein–kinin system and, 1302
prostaglandins and, 1291
renin-angiotensin-aldosterone system and, 1291*f*, 1307–1309
sympathetic pathways for, 1284, 1286–1291, 1288*f*, 1291*f*, 1295–1296, 1300–1301, 1308–1309
loading during dialysis, 3128
modeling, 3127–3128
plasma
body fluid tonicity and, 1511
fluid balance and, 1541–1542
reference values for, 294*t*
storage capacity for, 294
total body, in hypernatremia classification, 1553–1559, 1557*t*, 1558*t*
urinary
in volume status assessment, 2478–2484, 2480*t*
Sodium balance, *see also* Electrolyte balance
diuretics and, 306
dopamine in, 1114–1115
effective vascular volume and, 306–307
in hyperaldosteronism, 304
in hypoaldosteronism, 303–304
impaired, *See* Hypernatremia, chronic; Hyponatremia
mechanisms for, 292–293, 296, 304, 2478
in metabolic acidosis, 2057
ontogenetic factors in, 2361
potassium transport and, 1683*f*, 1687–1691
in pregnancy, 2700–2701, 2700*t*, 2701*f*, 2702*f*, 2708–2710, 2709*f*
set point for, 299–300
sodium intake/output and, *see* Sodium
in transplant recipients, 3151
Sodium bicarbonate, *see also* Bicarbonate
for distal renal tubular acidosis, 2089–2090, 2091*t*
for hyperkalemia, 1765
for lactic acidosis, 2074
for metabolic acidosis, 2099–2100
for proximal renal tubular acidosis, 2090–2091, 2091*t*
for salicylate poisoning, 2078
Sodium bicarbonate co-transport, 1095–1097
Sodium bicarbonate cotransporters
electrogenic, 1839–1843
additional lessons from mice, 1843
familial proximal renal tubular acidosis, 1840–1841
inhibitors, 1840
missense mutations, 1841–1842
NBCe1 (SLC4A4 Gene), 1839–1843
potential mutant-specific therapy, 1841–1842
structural variants, 1839
topological and structural properties, 1839–1840
electroneutral, 1847–1849
expression pattern, 1847–1848
functional properties, 1849
PDZ binding proteins, 1848
structural variants, 1847
systemic factors affecting NBCN1 expression in organs, 1848
intracellular pH and, 1793–1794
in renal tubular acidification, 1924–1927, 1935
Sodium channel blockers
patch-clamp studies of, 203
urinary electrolyte excretion and, 1356*t*
Sodium channels, 219*t*, *see also* Sodium ion channels
Sodium chloride, *see also* Salt
in hyponatremia treatment, 1528
Sodium chloride retention, post-diuretic, 1386–1389, 1387*f*
Sodium chloride transport, *see also* Chloride transport; Sodium transport
distal tubule, 1371–1373, 1372*f*
maturation of, 915–916, 916*f*
glomerulotubular balance, 912–913
paracellular, developmental changes in, 914–915
postnatal development and, 912–916, 913*f*
proximal tubule
maturation of, 913
regulation of, 1109–1121
sodium retention and, 1288–1290, 1299–1300
Sodium intake
in effective vascular volume, 301–302
potassium excretion and, 1683*f*, 1687–1691
sodium balance and, 1283–1284
Sodium ion channels, amiloride-sensitive, *see also* ENaC
in cell volume regulation, 122, 123*f*, 128*f*, 129, 130*f*
luminal membrane, 1089
mineralocorticoid-induced, 1685
Sodium phosphate, in acid–base balance, 312–313
Sodium polystyrene sulfonate, 3135
Sodium proton exchange, 634, 1090–1092, 1091*f*
Sodium pump targeting
epithelial cells polarization, 23–24
Sodium reabsorption
aldosterone in, 392, 393*f*

in CCD, 651–652
in CNT and DCT, 649–650
potassium transport and, 1699
prostaglandins and, 1291, 1302
proximal tubular glomerulotubular balance and, 912–913
Sodium retention
aquaporins in, 1427–1428
in ascites, 301–302, 1292–1294
in cirrhosis, 1292–1303
in congestive heart failure, 1286–1292, 1288*f*
edema in, 1284
effective arterial blood volume and, 1284–1286, 1286*f*
glomerular filtration rate and, 1287–1288
in hyperaldosteronism, 304
in nephrotic edema, 303
in nephrotic syndrome, 1303–1309, 1306*t*, 1308*f*
renal mechanisms for, 1287–1288
Sodium sulfate infusion test, 2504
Sodium transport, *see also* Ion transport; Na, K-ATPase; Sodium balance
across ASDN cells, 1183–1184
across tight junction, 1106–1109, 1108*f*
aldosterone and, 392, 393*f*, 1167–1169
angiotensin in, 1113–1114
ATP in, 1101
atrial natriuretic peptide in, 917, 1291–1292
in basolateral membrane, 1100–1101
catecholamines in, 917
in connecting tubule, 1163–1170
in cortical collecting duct, 1165–1166
cyclosporine and, 3173*f*, 3175
in descending thin limb of Henle, 1469–1474, 1469*t*
in distal convoluted tubule, 1160–1163
regulation of, 1162–1163
steroid hormones and, 1162–1163
diuretic-sensitive, 1354, 1355*f*
gluconeogenesis in, 153
heterogeneity along nephron, 146*f*
heterogeneity among nephron, 144
in inner medullary collecting duct, 1166, 1167*t*
insulin and, 1169–1170
loop diuretics and, 1363–1365, 1365*f*
in loop of Henle, 1144–1160
by Na,K-ATPase, 1099–1100
Na,K-ATPase in, 145–147
NHE3 in, 1109–1111, 1110*f*
nitric oxide in, 1115–1117
in outer medullary collecting duct, 1166, 1167*t*
oxygen consumption and, 143–144, 144*f*, 146*f*
postnatal regulation of, 916–917
in proximal tubule, 1371
regulation
aldosterone and, 1185–1194
ENaC and, 1167, 1168*f*
renal nerves in, 917, 1113
renin-angiotensin-aldosterone axis in, 916–917
signaling in, 391, 393*f*
substrate utilization and, 1155–1156
in thick ascending limb of Henle's loop, 144, 146*f*, 1145–1154, 1146*t*, 1147*f*
ADH and, 1156, 1156*t*, 1157*t*, 1158–1159
regulation of, 1156–1160
vasopressin and, 1169
Sodium wastage, *see* Salt wasting
Sodium-chloride cotransporter
in epithelial transport of potassium, 1669
Sodium-coupled solute transport, 634
Sodium-dependent glucose transporters (SGLTs), 2393
cellular and molecular physiology of, 2393–2394, 2396*f*
genetic ablation of, 2397–2398
inhibitors, 2400
and renal glucose reabsorption, 2394–2397
Sodium-glucose co-transport, 1089–1090
Sodium-hydrogen exchanger (NHE), 634, 1353–1354
intracellular pH and, 1798
in metabolic acidosis, 1999–2000, 1999*f*
NHE3 as, 1109–1111, 1110*f*, 1920–1921, 1921*f*, 1935, 1935*f*, 1936*f*
in renal tubular acidification, 1109–1111, 1110*f*, 1919, 1921*f*
apical-membrane, 1919, 1921*f*, 1923
basolateral-membrane, 1924–1927, 1933–1941
in loop of Henle, 1942
in thick ascending limb, 1154
Sodium-phosphate cotransporter, 2351–2357, 2371, 2371*f*
age-related changes in, 2361
in diabetes, 2360–2361
genetic alterations leading to imbalance of Pi, 2361–2363, 2362*t*
in heavy metal poisoning, 2361
ontogenetic factors in, 2361
regulation of, 2358–2361
atrial natriuretic factor in, 2359–2360
dietary phosphate in, 2360
dopamine in, 2359
insulin in, 2360–2361
membrane lipid composition in, 2360
nitric oxide in, 2359–2360
parathyroid hormone in, 2358–2359
potassium in, 2360
in renal handling of Pi, 2354
SLC34 mutations cotransporters, 2361–2363
structure-function relationships, 2356–2357
transport mechanisms, 2354–2356
type I, 2352–2353, 2352*f*
type II, 2352*f*, 2353–2354
type IIa, 2352*f*, 2353, 2353*f*
endocytosis of, 2358
function of, 2353
in hypophosphatemia, 2361
protein-protein interactions of, 2356*f*, 2357–2358
structure of, 2353–2354, 2353*f*
type IIb, 2352*f*, 2353, 2355, 2358
type IIc, 2352*f*, 2353–2354
type III, 2352*f*, 2354
Sodium-phosphate transporter, 2432
Sodium-potassium cotransporter, 1665–1667, 1666*f*, 1668*f*
Sodium-potassium pump, *see* Na,K-ATPase
Solubility diffusion transport, 47, 49
Solute carrier (SLC) 26A, 1033–1034
CFTR as regulator of, 1030
Solute reflection coefficients
osmotic water transport across lipid vs. porous membranes, 101–102
Solute sodium symporters (SSS), 59–60
Solute transport, *see also* Ion transport; Transporters
across microvascular walls, 810–812
angiotensin II in, 440
ATP hydrolysis in, 143–149
coupled with water transport, 1102–1109, 1103*f*
cyclosporine and, 3173*f*, 3175
electrophysiological analysis of, 177, *see also* Epithelial electrophysiology
energetics of, 143, *see also* Adenosine-5′-triphosphate (ATP)
energy production pathways in, 149–154
fatty acid oxidation in, 151, 152*f*
gluconeogenesis in, 152*f*, 153
glycolysis in, 152–153, 152*f*
ketone body metabolism in, 151–152, 152*f*
metabolic processes in, 149–165, *see also* Metabolic pathways
mitochondrial oxidative phosphorylation in, 149–150, 150*f*, 151*f*, 152*f*
mitochondrial respiration and, 158–159
oxygen consumption and, 143–144, 145*f*, 146*f*
regulation of, by AMPK, 162
signaling in, 158, 158*f*, 164, 369, 391–395, *see also* Signaling
in transplanted kidney, 3151, *see also* Renal transplantation
Whittam model of, 158, 158*f*
Solutes
reabsorption of, 634–635
Solute-solvent coupling
in transepithelial water transport, 112–115
Solute-water countercurrent exchange
in urine concentration, 1476
Solutions
hypertonic, 104
hypotonic, 104
isotonic, 104
Solvent drag, 102, 115–116
in potassium reabsorption, 1663–1664
Somatosensory system, and renal nerves, 464
Somatostatin
for polycystic kidney disease, 2665*f*, 2671
Sonographically determined resistance index, in renal artery stenosis, 2581–2583
Sorbitol, as osmolyte, 1546–1547, 1548*f*
Sorting pathways, epithelial cells polarization, 21–32, 22*f*
cell type-specific sorting: patterns, 28–29

Sorting pathways, epithelial cells polarization (*Continued*)
glycosphingolipid-rich membrane domains, 31
mechanisms, 29–30
PDZ domain-containing proteins, 31–32
renal transport protein function regulation by endocytosis and recycling, 24–25
sodium pump targeting, 23–24
sorting signals, 25–28
technical approaches, 22–23
tyrosine-based motifs and adaptors, 30–31
Sorting signals
epithelial cells polarization, 25–28
Southeast Asian ovalocytosis, 1889
Sox genes, 871
Specialized fornices, 595, 596*f*
Spectrin, non-erythroid, 8–9
Spherocytosis, hereditary, 1889
anion exchanger mutations in, 1876*t*
Spinal cord injury, hyponatremia after, 1517
Spironolactone, 1377, 1380
adverse effects, 1381–1382
clinical use, 1381
pharmacokinetics, 1381
structure of, 1377*f*
urinary electrolyte excretion and, 1356*t*
Split hydronephrotic kidney, 820–821, 821*f*
Spontaneous bacterial peritonitis (SBP)
in cirrhotic renal failure, 2635–2636
Sprouty (Spry), 873
Src kinase inhibitors, 2672
Src signaling pathway, 375, 380
Src-homology 2 domains, 380
S-shaped bodies, epithelial cells, 860, 879–880
S-shaped stage, of nephrons development, 891–892, 892*f*
Standing-gradient hypothesis, of water transport, 113–114, 113*f*
Starling, Ernest Henry, 693
Starling forces, 276–277
Starling pressures, 276
microvascular exchange and, 810–812
proximal tubular solute transport and, 1306
and local lymph flow, 282–283
Starvation
metabolic alkalosis in, 2037–2038, 2068
refeeding syndrome in, hypophosphatemia in, 2380
Statin drugs
mechanism of action of, 2967–2968
Stellate vein, anatomy of, 595–596, 596*f*
Stem cells
in acute kidney injury, 2565–2566
in adult kidney, 963–969
sites harboring, 969–970
bone marrow-derived, 974–975
factor receptor, 960
function, 965–967
and kidney repair, 973–975
markers, 963–964
mesenchymal, *see* Mesenchymal stem cells (MSC)
niches, 970
in non-mammals, 971–972, 972*f*
Side Population discrimination assay in, 965–966
in vitro growth, 964
in vivo growth, 964–965
Stents, renal artery, 2596–2598, 2596*f*
Steroid hormones
in NaCl transport in distal convoluted tubule, 1162–1163
Steroid 21-hydroxylase deficiency
and congenital adrenal hyperplasia, 1225–1226
Steroid-resistant nephrotic syndrome, autosomal recessive, 2865–2866
Steroids, cardiac, *see* Cardiac steroids
Steroids, endogenous, *See* Glucocorticoids; Mineralocorticoids
Steroids, exogenous, *see* Corticosteroids
Steroid-sensitive nephrotic syndrome, 2782–2783
Stomach
in acid–base balance, 312–315
calcium-sensing receptor in, 2203–2204
Stones, *see* Nephrolithiasis
Stop flow pressure (P_{SF}), 765–766
mean responses of, 768*f*
Storage disorders, 2848*t*, 2859–2863
Stress response, *see also* Oxidative stress
in acute kidney injury, 2555–2556
antidiuretic hormone in, 1449–1450
Stroke
LANP and, 1249
proANP gene in, 1249
Stroma
development, transcription factors and, 871–872
Stromal cells
of adult kidney, 960
Struvite stones, 2312, 2312*t*, 2344–2345
"Studs," 653–654
SU-5416, 2672
Sub-distal appendages, 322
Substance P, 468*f*, 471–474
CGRP and, 473
functional support for, 473
TRPV1 and, 473–474
Sulfuric acid
in acid–base balance, 308–309
production of, 315–316
Sulindac, transporters for, 2434
Sun exposure
in vitamin D production, 2251
Supersaturation
in nephrolithiasis, 2314–2315, 2314*f*, 2315*f*
pH and, 2317
Surreptitious vomiting, 2497
Sympathetic nerves, in renal function, 451
activation of, 456
efferent innervation, 451–452, 452*f*
para-vertebral ganglia, 451–452
pre-ganglionic nerve fibers, 451–452
intrinsic innervation, 452
neuro-effector junctions, 452, 453*f*
Sympathetic nervous system
in cirrhosis, 1300–1301
in congestive heart failure, 1290–1291
in nephrotic syndrome, 1308–1309
Symporters, 48, 53–54, 58–59
structure, 59–60, 61*f*
Synaptopodin, 743
Syndrome of hyporeninemic hypoaldosteronism, 1759–1761
Syndrome of inappropriate antidiuretic hormone secretion (SIADH), 1382, 1523
aquaporins in, 1428
causes of, 1518*t*, 1520–1523
chronic volume expansion in, 306
demeclocycline for, 1557
pathophysiology of, 1517–1520, 1518*t*, 1522*f*
postoperative, 1521, 1522*f*
Syntaxins
in ENaC regulation, 998
Syntrophin, 416–417, 417*f*
Syphilis associated with glomerular disease, 2789
System L transporters, 1997
Systemic lupus erythematosus, pregnancy in, 2719–2720, 2719*t*
Systemic sclerosis, pregnancy in, 2719*t*, 2721

T

T cell(s)
activation of
CD45 in, 377, 378*f*
protein kinase C in, 384–386
in focal segmental glomerulosclerosis (FSGS), 2782–2783
in Goodpasture's syndrome, 2766
minimal change disease (MCD), 2784
in vasculitis, 2818–2821, 2827
Tacrolimus
hypomagnesemia due to, 2158
renal effects of, 3167
in transplant immunosuppression, 3174–3175
in transplantation, solute transport and, 3151
Takayasu arteritis, 2817–2818, 2818*t*, 2819*t*, 2820*f*, 2827, *see also* Vasculitis
Talin, 13
Tamm Horsfall protein
as stone inhibitor, 2325–2326
Tamm-Horsfall glycoprotein (THP), 643
TASK-2, 236
Tau, 623–624
Tcf21, 735
in podocyte differentiation, 897–898
Temperature
antidiuretic hormone secretion and, 1450
intracellular pH and, 1809–1810
Tetany, in hypocalcemia, 2294
Thermodynamic coupling, 52–53
Thiamine, for ethylene glycol poisoning, 2076
Thiazide diuretics, 1370–1377, 3194–3195
calcium reabsorption and, 2239–2240
hypercalcemia due to, 2292
potassium excretion and, 1695
for proximal renal tubular acidosis, 2091

Thiazide-sensitive Na^+:Cl^- co-transporter, 1049
functional properties, 1054–1055, 1055*t*
molecular biology of, 1051–1054
physiology of, 1049
Thick ascending limb of Henle's loop, 612, 615, 640–643, 1024–1025
acid–base transport in, 1941–1943
ammonium ion reabsoprtion in, 2008–2009
anatomy of, 1143–1144
Bartter syndrome, 1227–1230, 1227*f*
basolateral K channels in, 1150–1152, 1151*f*, 1152*f*
calcium reabsorption in, 2228*f*, 2230–2232, 2231*f*
in Bartter syndrome, 2232
calcium-sensing receptor in, 2196–2199, 2196*f*, 2197*f*
cells, 640, 641*f*, 642*f*, 757–758
renin secretion in, 778–779, 778*f*
Cl^- channels in, 1152–1153
in metabolic alkalosis, 2030
MR expression in, 1184–1185
NaCl absorption in, 1145–1154, 1146*t*, 1147*f*
ADH and, 1156, 1156*t*, 1157*t*, 1158–1159
regulation of, 1156–1160
Na,K-ATPase regulation in, 77–78
physiological pathways for NKCC2 regulation in, 1159
potassium transport in, 1661–1662, 1663*f*, 1677
control of, 1677
diuretics and, 1695–1696, 1696*f*
mechanisms of, 1668–1671, 1670*f*, 1671*f*
role in NaCl reabsorption, 641
bicarbonate reabsorption, 641–642
Mg^{2+} and Ca^{2+} recovery, 642–643
salt reabsorption in, NKCC2 and, 1049–1051
sodium-hydrogen exchanger in, 1154
sodium transport in
oxygen consumption and, 144, 146*f*
substrate preferences in, 156
urea permeability of, 1470*t*, 1473
water permeability of, 1470*t*, 1473
Thick ascending loop of Henle
calcium sensing receptor, 2275
Thin ascending limb of loop of Henle
sodium transport by, 1144, 1145*t*
Thin basement membrane nephropathy, 2857–2858
Thin descending limb of loop of Henle
sodium transport by, 1144, 1145*t*
Thin limbs of loop of Henle, *See* Ascending thin limb of Henle; Descending thin limb of Henle
Thirst, 1454, *see also* Hypodipsia; Polydipsia
age and, 1456
anatomic aspects of, 1455
definition of, 1454
effects of, 1456
hypernatremia and, 1544, 1552, 1557–1558, 1557*t*
in osmoregulation, 1456–1457
quantitation of, 1454
regulation of, 1455
antidiuretic hormone and, 1543*f*, 1544
in pregnancy, 1589, 2702–2703
Three-compartment model, of water transport, 112, 113*f*
Threonine-286 (Thr-286), 935
Thrombocytopenia, in preeclampsia, 2730
Thrombocytopoiesis, 3109–3110
regulation of, 3109–3110
site of, 3109–3110
Thrombopoietin
action, 3112
effects of, 3110–3111
plasma concentration of, 3110–3111, 3110*f*
production of, 3112
structure of, 3111
Thrombopoietin gene, 3111
Thrombopoietin receptor, 3111–3112
Thrombosis, in preeclampsia, 2730
Thrombotic microangiopathy (TMA), *see also* Hemolytic-uremic syndrome (HUS) and thrombotic thrombocyto-penic purpura (TTP)
clinical presentation, 2775
incidence, 2774
laboratory features, 2775
pathology, 2775
pathophysiology, 2774–2775
sporadic forms, 2773
systemic disease and conditions associated, 2774*t*
treatment, 2775
corticosteroids, 2775
eculizumab, 2775
plasma exchange therapy, 2775
rituximab, 2775
Thromboxane (TAX)
in AKI, 2550
cyclosporine and, 3170, 3170*f*
Thromboxane A_2 (TxA_2), 495
Thromboxane receptor (TP), 495
diabetic nephropathy, 496
Thromboxane synthase (TxAS), 495
Thromboxane (TP), 775
Thyroid disease, hypercalcemia in, 2291
Thyroid hormones
in chronic kidney disease, 3044
in intracellular pH regulation, 1813
in metabolic acidosis, 2059
in potassium balance, 1638
in proANP gene expression, 1247
Thyrotoxicosis, hypercalcemia in, 2292
Thyroxine, *see also* Thyroid hormones
in metabolic acidosis, 2059
Tight junctions, 4–5, 220–221, 347–356, 627
in acute kidney injury, 2540
biochemical composition, 348–351
claudins, 350–351
functional domains of, 350–351
occludin, 349
tricellulin, 349
dysfunction in ischemic acute kidney injury, 355–356
in epithelial transport, 627, 1106–1109, 1108*f*
formation of, 7
freeze-fracture morphology of, 351*f*
membrane proteins of, 6
physiological functions, 348
fence function, 348
gate function, 348
physiology of, 351–355
aldosterone-sensitive distal nephron, 355
and WNK kinases, 355
Bowman's capsule, 349*f*, 352
proximal tubule, 352–354
NaCl reabsorption, 353
reabsorption of other cations, 354
thick ascending limb of Henle, 354–355
water reabsorption, 354
structure, 347–348
general structure, 347
regional differences in, 347–348
glomerulus, 347
renal tubule, 347–348
structure and functions of, 5–7
in thick ascending limb of Henle, 640–641
Timeless gene, 871
TIPS, for cirrhosis, *see* Transjugular intrahepatic portosystemic shunt (TIPS), for cirrhosis
Titratable acids, 307–308
excretion of, postnatal renal acidification and, 919–920
TLR4
HMGB1 and, 2990–2993, 2990*f*
TMEM16 protein family
CaCC, 1020
TMEM16A, 58
TMEM16B, 58
Toll-like receptors (TLR)
in acute kidney injury, 2988–2993
in AKI, 2550–2551
endotoxin and, 2988–2989, 2991
in ischemic inflammation, 2993
Tolvaptan
for hyponatremia, 1528–1529
for polycystic kidney disease, 2671
Tonicity-responsive enhancer, 1548–1549
Torsemide
calcium reabsorption and, 2239
loop diuretics, 1368, 1368*t*
Trade-off hypothesis, 2061–2062, 2062*f*
TRAM-34, 2672
Trans Golgi Network (TGN), 21–22
Transcellular movement, 220–221
Transcellular pathway, for epithelial transport, 628–631, 1087–1102
cytosolic concentrations, 1087–1088
luminal membrane, 1088–1095
peritubular membrane, 1095–1100
Transcription factors
and GDNF regulation, 869–870
hypoxia-inducible, in endothelial development, 895
in metanephrogenesis, 868–872
in nephron tubules regulation, 872
podocytes
Foxc2, 735
Kreisler (Mafb), 735

Transcription factors (*Continued*)
Lmx1b, 735
Notch, 735–736
Tcf21, 735
Wt-1, 734–735
and stroma development, 871–872
and ureteric bud, 870–871
Transepithelial resistance (TER), 348
Transepithelial transport
electrophysiological analysis of, 177, *see also* Epithelial electrophysiology
paracellular pathway, 628, 628*f*, 1087, 1102–1109
solute, *see* Solute transport
transcellular pathway, 628–631, 1087–1102
water, 110–116, *see also* Water transport
water reabsorption, 634
Transplantation, *see* Renal transplantation
Transport, *See* Ion transport; Solute transport; Water transport
Transforming growth factor α (TGFα), 876
Transforming growth factor β (TGFβ), 13, 376, 376*f*, 935–936
in acute kidney injury, 2558
in album metabolism, 2462–2463
in diabetic nephropathy, 2620–2621
in fibrogenesis, 2972
in ischemia-reperfusion injury, 2890–2891
and mesangial cells, 946
in proteinuria, 2967
in renal development, 875
and renal failure, 2649
tubular cell hypertrophy, 947–948
Transgenic/knockout mice, proANP gene and, 1249
Transient receptor potential vanilloid type 1 (TRPV1), 473–474
Transition fibers, 323–324
Transition zone, in cilia, 322*f*, 323
Transjugular intrahepatic portosystemic shunt (TIPS), for cirrhosis, 1294, 2640–2641
Transmembrane domains (TMD), 1026
Transmission electron microscopy, 347
Transport proteins, 629
Transporters, 47–48, 52, 54, 58–60, 59*f*
anion exchangers, 1861
antiporters (exchangers), 48
in cell volume regulation, 122–124
channels vs.,, 62–63
cotransporters, 48
regulation of, 391–395
aquaporin-2 in, 393–394
ENaC in, 391, 393*f*
ROMK in, 394–395
SLC4, 1850–1853
symporters, 48
in water transport, 109–110
Transtubular potassium gradient (TTKG), 1753, 2495–2496
Traveler's diarrhea, 1256
Triamterene, 1380–1381
adverse effects, 1381–1382
clinical use, 1381
hyperkalemic renal tubular acidosis and, 2097–2098
pharmacokinetics, 1381
potassium excretion and, 1695
structure of, 1377*f*
Tricarboxylate carrier (exchanger), 151*f*
Tricarboxylic acid cycle, 151, 155
Tricellulin, 349
Triglycerides, *see* Lipid(s)
Triiodothyronine, *see also* Thyroid hormones
in metabolic acidosis, 2059
Trimethoprim, hyperkalemia due to, 1763
Trinitrophenyl-ATP (TNP-ATP), 514
Triptolide, for polycystic kidney disease, 2665*f*, 2671
Tromethamine, 2126
Trousseau's sign, in hypocalcemia, 2299
TRP channels, 236–238, 822
architecture of, 245–247
TRPC6, 236–237, 743
TRPM6, 237, 900
TRPV4, 237
TRPV5, 237–238
TRPC channels, 2168, 2168*t*, 2169*f*
TRPM2, 2899
TRPM6, 256–257, 2142–2143, 2145, 2151–2152
TRPM channels, 2168–2169, 2168*t*, 2169*f*
TRPP channels, 2168*t*, 2169, 2169*f*
TRPV4 channels, 649, 2168*t*, 2169–2170, 2169*f*
TRPV5 channels, 2168*t*, 2169*f*, 2170–2171, *see also* Calcium ion channels
in knockout mice, 2181–2182
TRPV6 channels, 2168*t*, 2169*f*, 2170–2171, *see also* Calcium ion channels
Tuberculosis, hypercalcemia in, 2290–2291
Tuberous sclerosis, in pregnancy, 2721
Tubular albuminuria and animal models, 2468*t*
Tubular epithelial cell injury, in AKI, 2536–2538
Tubular obstruction, in AKI, 2541–2542
Tubular renal hyperplasia, 945
Tubular transport, neuronal influences on, 610
Tubule epithelium, 218–223
active transport, 221–222
barrier function, 218–220
disequilibrium, importance of, 222
emergent properties, 222
equivalent circuit of, 220*f*
facilitative diffusion, 221
ion transport, 223
polarized, 221
protein-mediated transport, 221
restrictive diffusion, 221
simple diffusion, 221
transport and transporters, types of, 221–222
transport routes across, 220–221
urine flows in, 222–223
Tubules, *See under* Renal tubular; Renal tubule(s)
Tubulogenesis, 878–881, 880*t*
Tubuloglomerular feedback (TGF), 516–517, 761–763
adaptations
eicosanoids, 775–776
extracellular fluid volume, 772–773
hyperglycemia, 774
nitric oxide, 776–777
renal mass, loss of, 773–774
renin-angiotensin system, 774–775
unilateral ureteral obstruction, 773
in autoregulation, 770–771
high-protein diet and, 772
hypertonic NaCl, 771–772
interstitial pressure, 777
K channel blockade and, 764
loop diuretics and, 764, 764*f*
oscillations, 762–763
renin secretion and, 1365–1366, 1366*f*
resetting, 772
responses
NaCl transport and, 764–765
sensitivity, 772
Tubuloinfundibular peptide of 39 amino acids (TIP39), 2276
Tubulointerstitial disease, *see also* Interstitial
apoptosis in, 2968–2969
complement in, 2973–2975
fatty acids in, 2976–2977
fibrogenesis in, 2971–2972
proteinuria in, 2965–2968, *see also* Proteinuria
Tubulointerstitial fibrosis
in pregnancy, 2720
Tubulointerstitial nephritis, 2766
Tubulopathies, 248–257
Bartter syndrome type II, 254–256
Bartter syndrome type III, 248–250
Bartter syndrome type IV, 250–251
TRPM6, 256–257
Tubulovascular cross-talk, 438
Tubulovesicular elements (TVEs), 27–28
Tumor lysis syndrome, hyperkalemia in, 1745
Tumor necrosis factor (TNF), 6
Tumoral calcinosis, hyperphosphatemia in, 2382
Tumor-induced osteomalacia (TIO), 2209–2210
hypophosphatemia in, 2380
Tumor(s), *see also* Cancer
osteomalacia and, 2253–2254
renin-secreting, metabolic alkalosis and, 2022
Tweety genes, 1036–1037
Two-photon microscopy
filtration fraction by, 2460
for glomerular sieving coefficient, 2460
Type 1 diabetes mellitus (T1DM), 2399
Type 1 ligands, 2274
Type 2 diabetes mellitus (T2DM), 2399
Type A IC cells, 654–656, 654*t*, 655*f*, 656*f*
Type B IC cells, 654*t*, 656–657
Type I K-ATPase activity, 80–82
Type III K-ATPase activity, 81–82
Type IV collagen, 731–732
mutations, 731

Tyrosine kinase, in ROMK
phosphorylation, 1610–1611
Tyrosine-based motifs and adaptors
epithelial cells polarization, 31

U
Ubiquitin, in muscle protein metabolism, 3049–3050
Ubiquitination, in ROMK regulation, 1611
UCH-L3, deubiquitinating enzyme, 995
UDP, 511–512, 513*f*
structure of, 513*f*
Ulcers, peptic
in hyperparathyroidism, 2287–2288
Ultrasonography
of parathyroid gland, 2288
of polycystic kidney disease, 2647
of renal artery stenosis, 2580
Unfolded protein response (UPR), 2465–2466
Unilateral ureteral obstruction (UUO), 773, 972
Uniporter, 58–59
Uracil receptors, 512, 513*f*
URAT1, 2431
Urate anion transporter 1, 2431
Urate clearance, in preeclampsia, 2737
Urea
cell volume in, 131
in cell volume regulation, 128
as dietary compliance indicator, 3051–3052, 3052*f*
from dietary protein, 3036–3038
fractional excretion of, 2483–2484
in hypernatremia, 1554
for hyponatremia, 1528
nephrotoxicity of, 3036
plasma osmolality and, 1542
production of
from dietary protein, 3036–3038, 3051–3052, 3052*f*
in metabolic acidosis, 2051–2052, 2051*f*
recycling of
potassium transport and, 1670
urine concentration and, 1496–1497
as uremic toxin, 3037
Urea appearance rate, 3051–3052
Urea nitrogen
decreased, in liver disease, 301
Urea permeability
in thick ascending limb, 1473
in thin descending limb, 1465–1467, 1469–1474, 1469*t*
Urea recycling, 669–670
Urea transport
across microvascular walls, 814–815, 817*f*
active, 1496
facilitated, rapid regulation of, 1490–1492
Urea transporters
abundance of, factors regulating, 1493–1495
active, 1492
facilitated, 1489–1490, 1490*t*
genetic knockout of, 1495–1496
long-term regulation of, 1492–1496
Uremia, *see also* Chronic kidney disease; End-stage renal disease (ESRD); Renal failure, chronic
and anorexia., 3046–3047
in acute kidney injury, 2562
cell volume in, 131
Uremic acidosis, 2078–2079
Uremic toxins, 3038–3039
ADMA, 3039–3041
advanced carbamylation products, 3042
aliphatic amines, 3040
arginine derivatives, 3039–3041
aromatic amines, 3039–3040
from bacterial metabolism, 3039–3040
cysteine-homocysteine, 3043
glycosylation products, 3042
guanidino-containing compounds, 3038
homocysteine, 3043
identification of, 3033
larger, 3041
middle molecules, 3041
non-protein-derived, 3040
from protein metabolism, 3036
reactive oxygen species, 3042
urea, 3036–3038
Uremic-anion gap acidosis, 2064
Ureteral dilation, in pregnancy, 2690, 2691*f*
Urethral obstruction, *see* Obstructive uropathy
Ureteric bud (UB)
branching morphogenesis, 873–878, 874*t*
ECM for, 876, 877*f*
epithelial cells of, 862–864
and IGF1 receptor, 876
isolated culture of, 862–864, 864*f*
overgrowth of, 872–873
regulation, transcription factors and, 870
survival/branching, transcription factors and, 871
Ureterosigmoidostomy, metabolic acidosis after, 2099
Uric acid
cyclosporine and, 3172–3173, 3173*f*
from dietary protein, 3035
dietary sources of, 2324, 3035
elevated urine, 2324
homeostatic mechanisms for, 296–297
nephrotoxicity of, 3036
in pregnancy, 2700
in stones, 2339–2341
in transplant recipients, 3166–3167
Uric acid nephropathy, 2533–2534, 3036
Uric acid stones, 2312, 2324
risk factors for, 2319*f*
Urinalysis
in pregnancy, 2691–2692
Urinary acidification
in pregnancy, 2702
Urinary chloride, in volume status assessment, 2479–2481, 2480*t*
Urinary concentrating ability, in neonates, 924–925
Urinary diversion, chronic metabolic acidosis after, 2099
Urinary indices, 2478–2484
in acute kidney injury, 2561, 2561*t*
aquaporin-2 excretion, 2484–2491, 2485*f*
in evaluation of hypokalemia and hyperkalemia, 2494–2496
in evaluation of metabolic acidosis, 2499
in metabolic acidosis, 2480*t*, 2481
in nephrolithiasis, 2313
pH, *see* Urine pH
sodium excretion, 2479–2481, 2480*t*
specimen collection for, 2478–2479
in volume status assessment, 2478–2484, 2480*t*
vomiting and, 2480
in water excretion disorders, 2484–2491
Urinary sodium, in volume status assessment, 2479–2481, 2480*t*
Urinary tract infections
in pregnancy, 2713–2714
Urine
anion gap, 2499–2502, 2502*t*
blood in
in Alport syndrome, 2847, 2854–2855
in pregnancy, 2711–2712
composition, assessment of, 2478–2484
osmolar gap, 2502–2503
potassium excretion, 2493–2495, 2494*f*
protein fragments in, 2463
Urine acidification
V-ATPase in, 83–84
Urine collection
methods of, 2478–2479
spot vs. timed, 2481–2484, 2481*t*, 2482*f*
Urine concentrating capacity, 1463
postnatal development of, 924–925, 1497–1498
Urine concentration
anatomic aspects of, 1464–1469, 1464*t*, 1465*f*, 1466*f*, 1467*f*
in collecting duct, 1476–1477
countercurrent multiplication in, 1474–1476, 1475*f*, 1478
central core assumption and, 1481, 1482*f*
countercurrent multiplier hypothesis of, 1478
medullary mass balance in, 1479–1480
outer medulla and, 1478–1479
countercurrent solute-water exchange in, 1476
defects in, diabetes insipidus and, 1424–1427, 1578
diabetes insipidus and, 1557
mechanisms of
computer simulations of, 1481–1485, 1482*f*
in neonates, 1497–1498
osmoprotective osmolytes and, 1488–1489, 1489*f*
in pregnancy, 2705–2706
sickle cell disease and, 1557
urea recycling in, 1496–1497, 1496*f*
urea transport in, 1489–1492, 1490*t*
Urine dilution
in neonates, 924–925
in pregnancy, 1589, 2705–2706
Urine flow rate, 2485–2486
aldosterone-induced kaliuresis and, 1685
in cortical collecting duct, 1747

Urine osmolality, 1463, 2485–2486, 2486*t*, 2491
in diabetes insipidus, 1593
in hypernatremia, 1559
in thin descending limb, 1471
Urine output
limits on, 299–300
reference values for, 294*t*
Urine oxalate, 2323
Urine pH
regulation of, 2317, 2317*f*
supersaturation and, 2317
Urine potassium, 1668, *see also* Potassium
Urine sediment, in pregnancy, 2712
Urine supersaturation
in nephrolithiasis, 2314, 2314*f*, 2315*f*
pH and, 2317
Urine volume
elevated, 2490–2491
in hypernatremia, 1559
Urodilatin
in acute renal failure, 1262–1263
anti-cancer effects, 1265
localization, in kidney, 1254
in natriuresis, 1254
and renin-angiotensin-aldosterone system, 1254
in vasodilation, 1254
Uroguanylin
biological effects, 1256–1257
in hemodialysis, 1261
Urolithiasis, *see* Nephrolithiasis
Usp2-45, 1200
Uterine hemorrhage, in pregnancy, 2714
Uterine veins, dilation of, in pregnancy, 2690
Uteroplacental ischemia, in preeclampsia-eclampsia, 2731, 2732*f*
UTP, 511–512, 513*f*
structure of, 513*f*
Utrophin, 416

V

V2 antagonists
for hyponatremia, 1528–1529, 1529*f*
Vacuolar apparatus, 632
Vacuolar H-ATPase (V-ATPase), 67, 163
in bicarbonate absorption, 84
in endocytosis in renal epithelial cells, 85–86
in intercalated cells, 84–85
isoforms, 83
mechanism of action, 82–86
multiple functions, 83–86
overview, 82
renal isoforms, 83
structure, 82–86
in urine acidification, 83–84
Vacuolar-vesicular organelles (VVOs), 285
Van't Hoff's law, 265–266
Vasa recta, 597*f*, 598
ascending, 612
solute transport across, 815–816
descending, 612
hydraulic conductivity of, osmotic water permeability and, 812, 813*f*
solute transport across, hydrophilic, 814, 815*t*
urea transport across, 814–815, 817*f*
water transport across, 810–816, 811*t*
in inner medulla, 616, 616*f*
in outer medulla, 612
wall structure of, 599–600, 599*f*
Vascular bundles, medullary
in inner medulla, 616, 616*f*
in outer medulla, 612, 612*f*
Vascular calcifications, in chronic kidney disease, 3076–3077
Vascular cell adhesion molecule (VCAM), in inflammation, 2901
Vascular dropout, 2545–2546
Vascular endothelial growth factor (VEGF), 945
in acute kidney injury, 2558–2559
in glomerular endothelial development, 894–895
in preeclampsia-eclampsia, 2734
receptors for, 374
Vascular receptors
D_1-like receptors, 551
D_2-like receptors, 551
Vascular smooth muscle
glomerular filtration rate and, 391
regulation of, 391, 392*f*
Vascular smooth muscle cell (VSMC), 357, 2550
Vasculature, *See under* Microvascular; Renal vessels
Vasculitis, 2792, 2818*t*
ANCA-mediated, 2766
classification of, 2817–2818, 2818*t*, 2820*f*
definitions of, 2819*t*
Henoch-Schönlein, 2832–2833
large-vessel, 2817–2818, 2819*t*, 2820*f*
medium-sized vessel, 2818, 2819*t*, 2820*f*
selectin-mediated rolling in, 2822–2823
serum sickness, 2828
small-vessel, 2818–2824, 2820*f*
antineutrophil cytoplasmic autoantibody, 2833–2842, *see also* Antineutrophil cytoplasmic autoantibody vasculitis
chemoattractants in, 2821–2822
chemokines in, 2821–2822
cytokines in, 2821–2822
endothelial cells in, 2819–2821, 2822*f*, 2825*t*
inflammation in, 2818–2821, 2821*f*, 2822*f*, 2825*t*
integrin-mediated adhesion and diapedesis in, 2823–2824, 2825*t*
leukocyte adhesion molecules in, 2822*f*, 2824–2826, 2825*t*
leukocytes in, 2818–2826, 2825*t*
selectin-mediated rolling in, 2825*t*
tissue injury mechanisms in, 2826–2828
types of, 2819*t*, 2820*f*
Vasculogenesis, for glomerular capillaries, 722
Vasoconstriction
angiotensin II in, 437
endothelin in, 837
regulation of, 391, 392*f*
Vasoconstrictor
dopamine as, *see* Dopamine
imbalance of, 2587
and management of hepatorenal syndrome, 2639–2640, 2640*t*
Vasodilation
ANP and, 1251
in cirrhotic renal failure, 1297–1299
LANP and, 1252
urodilatin in, 1254
Vasopressin (ADH) signaling, 333–334, 334*f*
cilium mechanism
Vasopressin V2 receptor (VPV2R) antagonists, for polycystic kidney disease, 2671
Vasopressin-receptor antagonists, 1382–1383
clinical use, 1382–1383
in hyponatremia treatment, 1382
Vasopressin-regulated water and urea reabsorption
in CCD, 652–653
VEGFR-1 and VEGFR-2 ribozyme treatment, 2672
Veli/MALS proteins, 415–416
Veno-arteriolar response, 278
Ventilation
during anesthesia, 1981
carbon dioxide levels and, 1979–1980
carotid body in, 1980–1981
chemoreceptors in, 1979, *see also* Chemoreceptors
in metabolic acidosis, 1980–1981, 1981*f*, 2054–2056, 2055*f*, 2056*f*, 2057*f*
in metabolic alkalosis, 2022*f*, 2023
in pH regulation, 1990
Ventilatory support, *see* Mechanical ventilation
Ventral respiratory group, rostral aspect of, chemoreceptors in, 1982–1983, 1982*f*, 1985
Vesicle stage, of nephrons development, 891, 892*f*
Vesicular monoamine transporters (VMATs), 542
sodium loading, 543
Vesicular stomatitis virus (VSV), 14–15
Vessel dilator, *see also* Natriuretic hormones
and ERK 1/2 activation, 1268
and MEK 1/2 activation, 1267, 1268*f*
receptor, 1260
Videomicroscopy, in microvascular measurements, 818–819
Villin, 9–10
Villous adenoma, metabolic alkalosis and, 2036
Vinculin, 13
Visceral system, and renal nerves, 464–465
Vitamin A, overdose of, hypercalcemia in, 2292
Vitamin D
absorption of, 2254–2256, 2254*f*, 2255*f*
actions of
intestinal, 2254–2256
renal, 2256–2258
skeletal, 2281

active form of, 2277
biosynthesis of, 2250–2254, 2252*f*, 2253*f*
phosphate in, 2370*f*
in calcium balance, 2143, 2250–2258, 2281
calcium homeostasis regulator, 2279–2281
calcium-sensing receptor and, 2193–2194
in chronic kidney disease, 3051
deficiency of
anticonvulsant-induced, 2298
clinical manifestations of, 2298–2299
in hyperparathyroidism, 3074
hypocalcemia and, 2298–2299
hypophosphatemia and, 2298
treatment of, 2298
for hyperparathyroidism, 2193–2194, 3080–3081
intestinal, 2280–2281
kidney and, 2281
in magnesium balance, 2143
metabolism of, 2251–2254, 2252*f*, 2273–2274
to 25-hydroxyvitamin D, 2251
to 25-hydroxyvitamin D_3, 2252*f*
nomenclature for, 2250–2251
overdose of, hypercalcemia in, 2292
parathyroid glands, 2281
in parathyroid hormone regulation, 2258–2259, 2258*f*
in phosphate balance, 2369–2370, 2370*f*, 2373
photochemical production of, 2251
production of
renal, 2251–2254, 2252*f*
RANKL and, 2281
serum concentration of, 2251
sources of, 2298
structure of, 2251*f*, 2252*f*
supplemental, *see also* Calcitriol
for hyperparathyroidism, 3080–3081
transport of, 2254–2256, 2255*f*
Vitamin D analogues, for hyperparathyroidism, 3080–3081, 3082*t*
Vitamin D binding protein (DBP), 2280
Vitamin D metabolites, 2251*f*
metabolism of, 2251–2254, 2252*f*
structure of, 2251*f*, 2252*f*
Vitamin D receptor (VDR), 2252–2253, 2277, 2280
intestinal, 2280–2281
in phosphate balance, 2373
Vitamin D-dependent rickets, 2299
Vitronectin, 13
Voltage-dependent anion-selective channel (VDAC), 1036
Volume depletion, *see* Hypovolemia
Volume expansion, *see* Hypervolemia
Volume fraction, interstitial, 602
Volume status, *see* Fluid balance
Volume-regulated anion channels (VRAC), 1034–1035, 1034*f*
Vomiting
in pregnancy, 2714
urinary sodium/chloride in, 2480
von Gierke disease, lactic acidosis in, 2073
von Hippel–Lindau disease, in pregnancy, 2721
von Hippel–Lindau gene, 968
VSV G protein, 21–22, 25–26
V-type ATPase, *see also* Ion pumps
ATP hydrolysis and, 148–149

W

Warfarin, 937–938
Warm ischemia-reperfusion renal clamp model, 2534, 2535*t*
Wasting syndrome, metabolic acidosis in, 2056
Water
intake/output of, *see also* Intake and output
reference values for, 294*t*
reabsorption of, 634–635
in proximal tubule
in lateral intercellular space, 1102–1105, 1103*f*
maturation of, 913
signaling in, 393–394
total body, 1542
plasma sodium concentration and, 1541–1542
reference values for, 294*t*
Water deprivation tests, in diabetes insipidus, 1589–1590
Water excretion
in diabetes insipidus, 1578
disorders, evaluation of, 2484–2491
hemodynamic regulation of, 1512
interstitial osmolality and, 2484
medullary blood flow and, 827–828, 827*f*
osmotic regulation of, 1511–1512
potassium excretion and, 1683*f*, 1687–1691
urine osmolality and, 1464
vasopressin-dependent defects in, 1515–1516
vasopressin-independent defects in, 1514–1515
Water intoxication, with maximally dilute urine, 1513–1514
Water pores, 106–107, 107*f*, 108*t*
Water regulation, dopamine in, 540
Water restriction, *see also* Fluid management
in hyponatremia, 1527–1528
Water transport, 95, 561
across microvascular walls, 815–816
active, 1087, 1104–1105
AKAPs in, 418
angiotensin II in, 439
aquaporins in, 106–107, 107*f*, 108*t*, 393–394, 1407–1410
cotransporters in, 109–110
coupled with solute transport, 109–110, 1102–1105, 1103*f*
cyclosporine and, 3172, 3173*f*
intracellular, 102–110
in animal cells, 103–104
Boyle–Van't Hoff equation, 103, 103*f*
cell volume and, 104, *see also* Cell volume
pathways for, 105–110, 106*f*
ion channel size and, 109
net, 95, 103–104
osmotic
across lipid vs. porous membranes, 96–99, 98*f*, 99*f*, 101–102, 101*f*
membrane permeability and, 95–96, 96*f*, 812, 813*f*
in cortical collecting duct, 1470*t*, 1471*t*, 1473–1474
solubility diffusion in, 97
solute reflection coefficients and, 101–102
solvent drag and, 102, 115–116
overview, 95
in pregnancy, 1589, 2702–2706
principles, 95–102
in proximal tubule, 1085–1087
distal diuretics and, 1371
signaling in, 393–394
solubility diffusion in, 97
in thin ascending limb, 1472
transepithelial, 110–116
in cell volume regulation, 129
characteristics, 110
epithelial asymmetry in, 115
mechanisms of, 111–112, 113*f*, 114*f*
near-isosmotic transport model, 114, 114*f*
pathways for, 115–116
permeabilities and, 110–111, 111*t*
solute recirculation in, 114
solute-solvent coupling in, 112–115
standing-gradient hypothesis for, 113–114, 113*f*
three-compartment model of, 112, 113*f*
transcellular vs. paracellular, 115–116
unstirred layer effects and, 99–101, 100*f*
in transplanted kidney, 3151, *see also* Renal transplantation
Wegener granulomatosis, 2818*t*, 2834, 2835*t*, 2839–2841, *see also* Vasculitis
in pregnancy, 2719*t*, 2720
Weight gain, in pregnancy, 2706–2707, 2706*t*
White blood cells, *see* Leukocyte(s)
Whole embryonic kidney organ culture, 861, 862*f*
Wilms tumor, in Denys-Drash syndrome, 2871–2873
Wilm's tumor suppressor protein 1 (WT-1), 944
in podocyte differentiation, 897
WKY rat, dopamine and, 543
WNK kinases, 395, 2179
potassium transport and ROMK channel, 1609–1610
Wnt signaling pathway, 381–382
in cilium, 331*f*
glomerular parietal epithelium, 744
in polycystic disease, 2664–2666
in renal development, 875
Wolffian duct, 859
GDF11, 873
isolated culture of, 862, 862*f*, 863*f*
outgrowth of ureteric bud from, 872–873
Wolfram syndrome, 1581, *see also* Diabetes insipidus
Wt-1 mRNA, 734–735
Wt1 gene, 870

X

X11s, 415
Xenopus laevis oocytes, 1054
Xenopus oocytes, 983–984, 998
  CaCC and, 1031
X-linked diabetes insipidus, 1555
X-linked hereditary nephrolithiasis syndrome, proximal renal tubular acidosis in, 2084
X-linked hypophosphatemia (XLH), 2209–2210
X-linked hypophosphatemic rickets, 2381
X-linked inhibitor of caspases (XIAP), 2994
Xylosuria, in pregnancy, 2699

Z

Zebrafish
  kidney of, progenitor cells in, 971, 972*f*
Zidovudine
  transporters for, 2435–2436, 2435*f*
Zinc-α^2-glycoprotein (Zag), 963
Zoledronate, for hypercalcemia, 2293–2294
Zonula adherens, *see* Adherens junctions
Zonula occludens, *see* Tight junctions
Zonula occludens-1 (ZO-1), 899
  in epithelial polarization, 6
Zonula occludentes, 1106